JMIR Medical Informatics

Impact Factor (2023): 3.1
Volume 13 (2025) ISSN 2291-9694 Editor in Chief: Christian Lovis, MD, MPH, FACMI

Contents

Reviews

Trends and Trajectories in the Rise of Large Language Models in Radiology: Scoping Review (e78041)
Adhari Al Zaabi, Rashid Alshibli, Abdullah AlAmri, Ibrahim AlRuheili, Syaheerah Lutfi. 27

Predictive Performance of Radiomics-Based Machine Learning for Colorectal Cancer Recurrence Risk: Systematic Review and Meta-Analysis (e78644)
Yuan Sun, Bo Li, Chuanlan Ju, Liming Hu, Huiyi Sun, Jing An, Tae-Hun Kim, Zhijun Bu, Zeyang Shi, Jianping Liu, Zhaolan Liu. 44

Using Large Language Models for Chronic Disease Management Tasks: Scoping Review (e66905)
Henry Serugunda, Ouyang Jianquan, Hasifah Kasujja Namatovu, Paul Ssemaluulu, Nasser Kimbugwe, Christopher Garimoi Orach, Peter Waiswa. 63

Acceptability, Needs, Concerns, and Barriers to Digital-Based Interventions for the Prevention of Mother-to-Child Transmission of HIV: Systematic Review and Qualitative Meta-Aggregation (e64816)
Sidik Maulana, Kusman Ibrahim, Rachel Arbing, Iqbal Pramukti, Annisa Nugrahani, Luh Armini, Muhammad Iqhrammullah, Wei-Ti Chen. . . 86

Validation of Telehealth Outcome Categories for Patient Safety: Systematic Literature Review (e75486)
Sari Palojoki, Lasse Lehtonen, Riikka Vuokko. 101

Diagnostic Prediction Models for Primary Care, Based on AI and Electronic Health Records: Systematic Review (e62862)
Liesbeth Hunik, Asma Chaabouni, Twan van Laarhoven, Tim Olde Hartman, Ralph Leijenaar, Jochen Cals, Annemarie Uijen, Henk Schers. . 112

Performance of Natural Language Processing for Information Extraction From Electronic Health Records Within Cancer: Systematic Review (e68707)
Simon Dahl, Martin Bøgsted, Tomer Sagi, Charles Vesteghem. 127

The Role of AI in Cardiovascular Event Monitoring and Early Detection: Scoping Literature Review (e64349)
Luis Elvas, Ana Almeida, Joao Ferreira. 141

Comparing Diagnostic Accuracy of Clinical Professionals and Large Language Models: Systematic Review and Meta-Analysis (e64963)
Guxue Shan, Xiaonan Chen, Chen Wang, Li Liu, Yuanjing Gu, Huiping Jiang, Tingqi Shi. 154

Using Large Language Models to Enhance Exercise Recommendations and Physical Activity in Clinical and Healthy Populations: Scoping Review (e59309)
Xiangxun Lai, Jiacheng Chen, Yue Lai, Shengqi Huang, Yongdong Cai, Zhifeng Sun, Xueding Wang, Kaijiang Pan, Qi Gao, Caihua Huang. . . 170

XSL•FO
RenderX

Machine Learning and Deep Learning Techniques for Prediction and Diagnosis of Leptospirosis: Systematic Literature Review (e67859)
Suhila Sawesi, Arya Jadhav, Bushra Rashrash. . . . 184

Preclinical Cognitive Markers of Alzheimer Disease and Early Diagnosis Using Virtual Reality and Artificial Intelligence: Literature Review (e62914)
María Scribano Parada, Fátima González Palau, Sonia Valladares Rodríguez, Mariano Rincon, Maria Rico Barroeta, Marta García Rodriguez, Yolanda Bueno Aguado, Ana Herrero Blanco, Estela Díaz-López, Margarita Bachiller Mayoral, Raquel Losada Durán. . . . 203

Current Landscape and Future Directions for Mental Health Conversational Agents for Youth: Scoping Review (e62758)
Jinkyung Park, Vivek Singh, Pamela Wisniewski. . . . 224

The Use of Machine Learning for Analyzing Real-World Data in Disease Prediction and Management: Systematic Review (e68898)
Norah Alhumaidi, Doni Dermawan, Hanin Kamaruzaman, Nasser Alotaiq. . . . 249

Current Landscape and Future Directions Regarding Generative Large Language Models in Stroke Care: Scoping Review (e76636)
XingCe Zhu, Wei Dai, Richard Evans, Xueyu Geng, Aruhan Mu, Zhiyong Liu. . . . 271

Evidence for the Use of Patient-Reported Outcome Measures in the Treatment of Patients With Noncommunicable Diseases: Systematic Review (e66160)
Marie Villumsen, Benedikte von Osmanski, Kirsten Lomborg, Kirstine Benthien. . . . 295

Large Language Models in Critical Care Medicine: Scoping Review (e76326)
Tongyue Shi, Jun Ma, Zihan Yu, Haowei Xu, Rongxin Yang, Minqi Xiong, Meirong Xiao, Yilin Li, Huiying Zhao, Guilan Kong. . . . 312

Number of Publications on New Clinical Prediction Models: A Bibliometric Review (e62710)
Banafsheh Arshi, Laure Wynants, Eline Rijnhart, Kelly Reeve, Laura Cowley, Luc Smits. . . . 1907

Predictive Value of Frailty on Outcomes of Patients With Cirrhosis: Systematic Review and Meta-Analysis (e60683)
Wen-Zhen Tang, Sheng-Rui Zhu, Shu-Tian Mo, Yuan-Xi Xie, Zheng-Ke-Ke Tan, Yan-Juan Teng, Kui Jia. . . . 2538

Pharmacoepidemiologic Research Based on Common Data Models: Systematic Review and Bibliometric Analysis (e72225)
Yongqi Zheng, Meng Zhang, Conghui Wang, Ling Gao, Junqing Xie, Peng Shen, Yexiang Sun, Mengling Feng, Seng You, Feng Sun. . . . 3835

Smart Contracts and Shared Platforms in Sustainable Health Care: Systematic Review (e58575)
Carlos Marino, Claudia Diaz Paz. . . . 3850

Original Papers

Coagulation Risk Prediction in Patients With Liver Failure: Integrated Meta-Analysis and Machine Learning Model Study (e76348)
Hao Wang, Tao He, Liang Ren, Tingjun Zhang. . . . 337

Optimizing an Electronic Health Record System Used to Help Health Care Professionals Comply With a Standardized Care Pathway for Heart Failure During the Transition From Hospital To Chronic Care: Qualitative Semistructured Interview Study (e63665)
Marta Font, Nadia Davoody. . . . 435

XSL•FO
RenderX

Interpretable Artificial Intelligence Analysis of Functional Magnetic Resonance Imaging for Migraine Classification: Quantitative Study (e72155)
Guohao Li, Hao Yang, Li He, Guojun Zeng. . . . 457

Cost-Benefit Analysis of Preventing Acute Care Use in Oncology Patients Following Systemic Therapy Using Medicare Claims Data: Retrospective Cohort Study (e77891)
Sara Keller, Maximilian Schuessler, Behzad Naderalvojoud, Tina Seto, Lu Tian, Mohana Roy, Tina Hernandez-Boussard. . . . 528

Implementing Electronic Health Records in Philippine Primary Care Settings: Mixed-Methods Pilot Study (e63036)
Anton Elepaño, Carol Tan-Lim, Mark Javelosa, Regine De Mesa, Mia Rey, Josephine Sanchez, Leonila Dans, Antonio Dans. . . . 581

Artificial Intelligence–Based Computerized Digit Vigilance Test in Community-Dwelling Older Adults: Development and Validation Study (e73038)
Gong-Hong Lin, Dorothy Bai, Yi-Jing Huang, Shih-Chieh Lee, Mai Vu, Tsu-Hsien Chiu. . . . 602

Estimating 10-Year Cardiovascular Disease Risk in Primary Prevention Using UK Electronic Health Records and a Hybrid Multitask BERT Model: Retrospective Cohort Study (e76659)
Tianyi Liu, Lei Lu, Yanzhong Wang, Andrew Krentz, Vasa Curcin. . . . 613

Automated Chronic Obstructive Pulmonary Disease Phenotyping and Control Assessment in Primary Care: Retrospective Multicenter Study Using the Seleida Model (e74932)
José Maya Viejo, Fernando Navarro Ros. . . . 633

Scalable Big Data Platform With End-to-End Traceability for Health Data Monitoring in Older Adults: Development and Performance Evaluation (e81701)
Ander Cejudo, Yone Tellechea, Amaia Calvo, Aitor Almeida, Cristina Martín, Andoni Beristain. . . . 656

A Weighted Voting Approach for Traditional Chinese Medicine Formula Classification Using Large Language Models: Algorithm Development and Validation Study (e69286)
Zhe Wang, Keqian Li, Suyuan Peng, Lihong Liu, Xiaolin Yang, Keyu Yao, Heinrich Herre, Yan Zhu. . . . 675

Federated Analysis With Differential Privacy in Oncology Research: Longitudinal Observational Study Across Hospital Data Warehouses (e59685)
Théo Ryffel, Perrine Créquit, Maëlle Baillet, Jason Paumier, Yasmine Marfoq, Olivier Girardot, Thierry Chanet, Ronan Sy, Louise Bayssat, Julien Mazières, Vincent Vuiblet, Julien Ancel, Maxime Dewolf, François Margraff, Camille Bachot, Jacek Chmiel. . . . 686

Estimating Nurse Workload Using a Predictive Model From Routine Hospital Data: Algorithm Development and Validation (e71666)
Paul Meredith, Christina Saville, Chiara Dall'Ora, Tom Weeks, Sue Wierzbicki, Peter Griffiths. . . . 698

Retracted: A Dynamic Adaptive Ensemble Learning Framework for Noninvasive Mild Cognitive Impairment Detection: Development and Validation Study (e60250)
Aoyu Li, Jingwen Li, Yishan Hu, Yan Geng, Yan Qiang, Juanjuan Zhao. . . . 710

Applying Robotic Process Automation to Monitor Business Processes in Hospital Information Systems: Mixed Method Approach (e59801)
Adam Park, Se Jung, Ilha Yune, Ho-Young Lee. . . . 729

Extracting Multifaceted Characteristics of Patients With Chronic Disease Comorbidity: Framework Development Using Large Language Models (e70096)
Junyan Zhang, Junchen Zhou, Liqin Zhou, Zhichao Ba. . . . 744

Automated Literature Screening for Hepatocellular Carcinoma Treatment Through Integration of 3 Large Language Models: Methodological Study (e76252)
Chen Pan, Wei Lu, Bingliang Chen, Gang Zhang, Zhiming Yang, Jingcheng Hao. . . . 764

XSL•FO
RenderX

Understanding Health Information Systems Utilization Across Public Health Centers in Indonesia: Cross-Sectional Study (e68613)
Dewi Aisyah, Agus Setiawan, Chyntia Mayadewi, Alfiano Lokopessy, Zisis Kozlakidis, Logan Manikam. 777

Nurses' Experience Regarding Barriers to Providing Internet Plus Continuous Nursing: Mixed Methods Study (e65445)
Huanhuan Huang, Zhiyu Chen, Lijuan Chen, Xingyao Du, Qi Huang, Wenbi Jia, Qinghua Zhao. 792

Health Information Systems' Support for Management and Changing Work: Survey Study Among Physicians (e65913)
Tarja Heponiemi, Lotta Virtanen, Emma Kainiemi, Petra Saukkonen, Jarmo Reponen, Tinja Lääveri. 803

Construction and Application of an Information Closed-Loop Management System for Maternal and Neonatal Access and Exit Rooms: Non Randomized Controlled Trial (e66451)
Shafeng Jia, Naifeng Zhu, Jia Liu, Niankai Cheng, Ling Jiang, Jing Yang. 814

Correlation Between Diagnosis-Related Group Weights and Nursing Time in the Cardiology Department: Cross-Sectional Study (e65549)
Chen Lv, Yi-Hong Gong, Xiu-Hua Wang, Jun An, Qian Wang, Jing Han, Xiao-Feng Chen. 826

The Perceptions of Potential Prerequisites for Artificial Intelligence in Danish General Practice: Vignette-Based Interview Study Among General Practitioners (e63895)
Natasha Jørgensen, Camilla Merrild, Martin Jensen, Thomas Moeslund, Kristian Kidholm, Janus Thomsen. 837

Identifying and Optimizing Factors Influencing the Implementation of a Fast Healthcare Interoperability Resources Accelerator: Qualitative Study Using the Consolidated Framework for Implementation Research–Expert Recommendations for Implementing Change Approach (e66421)
Jane Li, Emma Maddock, Michael Hosking, Kate Ebrill, Jeremy Sullivan, Kylynn Loi, Danielle Tavares-Rixon, Rajiv Jayasena, Grahame Grieve, Alana Delaforce. 847

Health Care Professionals' Perspectives on Implementing Patient-Accessible Electronic Health Records in Primary Care: Qualitative Study (e64982)
Irene Muli, Åsa Cajander, Isabella Scandurra, Maria Hägglund. 863

Ensuring General Data Protection Regulation Compliance and Security in a Clinical Data Warehouse From a University Hospital: Implementation Study (e63754)
Christine Riou, Mohamed El Azzouzi, Anne Hespel, Emeric Guillou, Gouenou Coatrieux, Marc Cuggia. 880

Analyzing Sleep Behavior Using BERT-BiLSTM and Fine-Tuned GPT-2 Sentiment Classification: Comparison Study (e70753)
Yihan Deng, Julia van der Meer, Athina Tzovara, Markus Schmidt, Claudio Bassetti, Kerstin Denecke. 893

Large Language Model Versus Manual Review for Clinical Data Curation in Breast Cancer: Retrospective Comparative Study (e73605)
Young-Joon Kang, Hocheol Lee, Jae Yi, Hyobin Kim, Chang Yoon, Jong Baek, Yong-seok Kim, Ye Jeon, Jiyoung Rhu, Su Lim, Hoon Choi, Se Oh. 915

An Extraction Tool for Venous Thromboembolism Symptom Identification in Primary Care Notes to Facilitate Electronic Clinical Quality Measure Reporting: Algorithm Development and Validation Study (e63720)
John Novoa-Laurentiev, Mica Bowen, Avery Pullman, Wenyu Song, Ania Syrowatka, Jin Chen, Michael Sainlaire, Frank Chang, Krissy Gray, Purushottam Panta, Luwei Liu, Khalid Nawab, Shadi Hijjawi, Richard Schreiber, Li Zhou, Patricia Dykes. 929

XSL•FO
RenderX

Natural Language Processing and ICD-10 Coding for Detecting Bleeding Events in Discharge Summaries: Comparative Cross-Sectional Study (e67837)
Frederic Gaspar, Mehdi Zayene, Claire Coumau, Elliott Bertrand, Marie Bettex, Marie Le Pogam, Chantal Csajka. 942

A Machine Learning Approach for Identifying People With Neuroinfectious Diseases in Electronic Health Records: Algorithm Development and Validation (e63157)
Arjun Singh, Shadi Sartipi, Haoqi Sun, Rebecca Milde, Niels Turley, Carson Quinn, G Harrold, Rebecca Gillani, Sarah Turbett, Sudeshna Das, Sahar Zafar, Marta Fernandes, M Westover, Shibani Mukerji. 958

Identifying Transportation Needs in Ophthalmology Clinic Notes Using Natural Language Processing: Retrospective, Cross-Sectional Study (e69216)
Lauren Wasser, Hai-Wei Liang, Chenyu Li, Julie Cassidy, Pooja Tallapaneni, Hunter Osterhoudt, Yanshan Wang, Andrew Williams. 971

Large Language Model–Enhanced Drug Repositioning Knowledge Extraction via Long Chain-of-Thought: Development and Evaluation Study (e77837)
Hongyu Kang, Jiao Li, Li Hou, Xiaowei Xu, Si Zheng, Qin Li. 983

Clinical Information Extraction From Notes of Veterans With Lymphoid Malignancies: Natural Language Processing Study (e63908)
Lu He, Matthew Moldenhauer, Kai Zheng, Helen Ma. 1004

Automated Esophageal Cancer Staging From Free-Text Radiology Reports: Large Language Model Evaluation Study (e75556)
Yao Yao, Xingxing Cen, Lu Gan, Jiehui Jiang, Min Wang, Yinghui Xu, Junyi Yuan. 1015

Large Language Models as a Consulting Hotline for Patients With Breast Cancer and Specialists in China: Cross-Sectional Questionnaire Study (e66429)
Hui Liu, Jialun Peng, Lu Li, Ao Deng, XiangXin Huang, Guobing Yin, Haojun Luo. 1029

Toward Cross-Hospital Deployment of Natural Language Processing Systems: Model Development and Validation of Fine-Tuned Large Language Models for Disease Name Recognition in Japanese (e76773)
Seiji Shimizu, Tomohiro Nishiyama, Hiroyuki Nagai, Shoko Wakamiya, Eiji Aramaki. 1041

Predicting Drug–Side Effect Relationships From Parametric Knowledge Embedded in Biomedical BERT Models: Methodological Study With a Natural Language Processing Approach (e67513)
Woohyuk Jeon, Minjae Park, Doyeon An, Wonshik Nam, Ju-Young Shin, Seunghee Lee, Suehyun Lee. 1053

Performance of Natural Language Processing versus International Classification of Diseases Codes in Building Registries for Patients With Fall Injury: Retrospective Analysis (e66973)
Atta Taseh, Souri Sasanfar, Michelle Chan, Evan Sirls, Ara Nazarian, Kayhan Batmanghelich, Jonathan Bean, Soheil Ashkani-Esfahani. . . .
1 0 6 7

Automated Radiology Report Labeling in Chest X-Ray Pathologies: Development and Evaluation of a Large Language Model Framework (e68618)
Abdullah Abdullah, Seong Kim. 1079

Identifying Patient-Reported Outcome Measure Documentation in Veterans Health Administration Chiropractic Clinic Notes: Natural Language Processing Analysis (e66466)
Brian Coleman, Kelsey Corcoran, Cynthia Brandt, Joseph Goulet, Stephen Luther, Anthony Lisi. 1092

Performance Improvement of a Natural Language Processing Tool for Extracting Patient Narratives Related to Medical States From Japanese Pharmaceutical Care Records by Increasing the Amount of Training Data: Natural Language Processing Analysis and Validation Study (e68863)
Yukiko Ohno, Tohru Aomori, Tomohiro Nishiyama, Riri Kato, Reina Fujiki, Haruki Ishikawa, Keisuke Kiyomiya, Minae Isawa, Mayumi Mochizuki, Eiji Aramaki, Hisakazu Ohtani. 1108

XSL•FO
RenderX

Improving Systematic Review Updates With Natural Language Processing Through Abstract Component Classification and Selection: Algorithm Development and Validation (e65371)
Tatsuki Hasegawa, Hayato Kizaki, Keisho Ikegami, Shungo Imai, Yuki Yanagisawa, Shuntaro Yada, Eiji Aramaki, Satoko Hori. 1125

Improving Phenotyping of Patients With Immune-Mediated Inflammatory Diseases Through Automated Processing of Discharge Summaries: Multicenter Cohort Study (e68704)
Adam Remaki, Jacques Ung, Pierre Pages, Perceval Wajsburt, Elise Liu, Guillaume Faure, Thomas Petit-Jean, Xavier Tannier, Christel Gérardin. 1140

Improving Large Language Models' Summarization Accuracy by Adding Highlights to Discharge Notes: Comparative Evaluation (e66476)
Mahshad Koohi Habibi Dehkordi, Yehoshua Perl, Fadi Deek, Zhe He, Vipina Keloth, Hao Liu, Gai Elhanan, Andrew Einstein. 1158

Generative Models and Sentence Transformers for the Recognition and Normalization of Continuous and Discontinuous Phenotype Mentions: Model Development and Evaluation (e68558)
Areej Alhassan, Viktor Schlegel, Monira Aloud, Riza Batista-Navarro, Goran Nenadic. 1175

Model for Predicting Serious Hematological Adverse Events in Individuals With Ovarian Cancer Receiving Poly (Adenosine Diphosphate Ribose) Polymerase Inhibitor Treatment: Prospective Cohort Study (e72994)
Xiaotong Lian, Yu Lei. 1191

Large Language Model–Based Critical Care Big Data Deployment and Extraction: Descriptive Analysis (e63216)
Zhongbao Yang, Shan-Shan Xu, Xiaozhu Liu, Ningyuan Xu, Yuqing Chen, Shuya Wang, Ming-Yue Miao, Mengxue Hou, Shuai Liu, Yi-Min Zhou, Jian-Xin Zhou, Linlin Zhang. 1205

Comparative Analysis of Outcomes of Influenza and COVID-19 Admissions Among Children With Asthma: A Nationwide Retrospective Cohort Study Using the US National Readmissions Database (e73047)
Ying-Chen Chen, Chia-Pi Cheng, Po-Cheng Chen, Jinn-Li Wang, Chia-Chen Wu, Ying-Chun Lu. 1218

Evaluating the Body Roundness Index as a Novel Digital Biomarker for Psoriasis Risk Prediction: Cross-Sectional Study (e75727)
Pengfei Wen, Xiaoyan Wang, Xiaoxue Zhuo, Siliang Xue. 1230

An Intelligent Trial Eligibility Screening Tool Using Natural Language Processing With a Block-Based Visual Programming Interface: Development and Usability Study (e80072)
Ya-Han Hu, Yi-Ying Cheng, Chung-Ching Lan, Yu-Hsiang Su, Sheng-Feng Sung. 1245

Deep Learning–Based Early Warning Systems in Hospitalized Patients at Risk of Code Blue Events and Length of Stay: Retrospective Real-World Implementation Study (e72232)
Ji-hyun Kim, Eun Cho, Yuhyun Choi, Joo-Yun Won, Se Cheon, Young Kim, Ki-byung Lee, Kwang Kim, Ho Kim, Taeyong Sim. 1260

Using Machine Learning to Predict-Then-Optimize Elective Orthopedic Surgery Scheduling to Improve Operating Room Utilization: Retrospective Study (e70857)
Johnathan Lex, Aazad Abbas, Jacob Mosseri, Jay Singh Toor, Michael Simone, Bheeshma Ravi, Cari Whyne, Elias Khalil. 1272

Optimizing Loop Diuretic Treatment for Mortality Reduction in Patients With Acute Dyspnea Using a Practical Offline Reinforcement Learning Pipeline for Health Care: Retrospective Single-Center Simulation Study (e69145)
Jung Lee, Shengpu Tang, Michael Sjoding, Jenna Wiens. 1284

XSL•FO
RenderX

Development and Validation of an Extra Spindle Pole Bodies–like 1–Based Diagnostic and Prognostic Model for Hepatitis B Virus–Related Hepatocellular Carcinoma: Retrospective Cohort Study (e78354)
Lu-Huai Feng, Hengkai Liang, Bobin Hu, Lu Wei, Qingmei Li, Tumei Su, Qianbing Yin, Yanfei Feng, Long Huang, Hongqian Liang, Minghua Su, Jianning Jiang. . . . 1298

Development and Validation of a Predictive Model for Severe Tubular Atrophy/Interstitial Fibrosis in Patients with IgA Nephropathy: Multicenter Retrospective Study (e78761)
Caizheng Yu, Zhitong Niu, Qin Fang, Qing Lei. . . . 1317

Comparative Analysis of Generative Artificial Intelligence Systems in Solving Clinical Pharmacy Problems: Mixed Methods Study (e76128)
Lulu Li, Pengqiang Du, Xiaojing Huang, Hongwei Zhao, Ming Ni, Meng Yan, Aifeng Wang. . . . 1331

Cardiorenal Interorgan Assessment via a Novel Clustering Method Using Dynamic Time Warping on Electrocardiogram: Model Development and Validation Study (e73353)
Sally Zhao, Zhan Ye, Bhavna Adhin, Matti Vuori, Jari Laukkanen, FinnGen, Sudeshna Fisch. . . . 1344

Assessing the Role of Large Language Models Between ChatGPT and DeepSeek in Asthma Education for Bilingual Individuals: Comparative Study (e65365)
Yaxin Liu, Fangfei Yu, Xiaofei Zhang, Xiaohan Tong, Kui Li, Weikuan Gu, Baiquan Yu. . . . 1361

AI-Driven Integrated System for Burn Depth Prediction With Electronic Medical Records: Algorithm Development and Validation (e68366)
Md Rahman, Mohamed Masry, Surya Gnyawali, Yexiang Xue, Gayle Gordillo, Juan Wachs. . . . 1374

Enhancing Surgery Scheduling in Health Care Settings With Metaheuristic Optimization Models: Algorithm Validation Study (e57231)
João Lopes, Tiago Guimarães, Júlio Duarte, Manuel Santos. . . . 1385

The Construction and Application of a Clinical Decision Support System for Cardiovascular Diseases: Multimodal Data-Driven Development and Validation Study (e63186)
Shumei Miao, Pei Ji, Yongqian Zhu, Haoyu Meng, Mang Jing, Rongrong Sheng, Xiaoliang Zhang, Hailong Ding, Jianjun Guo, Wen Gao, Guanyu Yang, Yun Liu. . . . 1395

Convolutional Neural Network Models for Visual Classification of Pressure Ulcer Stages: Cross-Sectional Study (e62774)
Changbin Lei, Yan Jiang, Ke Xu, Shanshan Liu, Hua Cao, Cong Wang. . . . 1408

Predicting Clinical Outcomes at the Toronto General Hospital Transitional Pain Service via the Manage My Pain App: Machine Learning Approach (e67178)
James Skoric, Anna Lomanowska, Tahir Janmohamed, Heather Lumsden-Ruegg, Joel Katz, Hance Clarke, Quazi Rahman. . . . 1422

Effect of Uncertainty-Aware AI Models on Pharmacists' Reaction Time and Decision-Making in a Web-Based Mock Medication Verification Task: Randomized Controlled Trial (e64902)
Corey Lester, Brigid Rowell, Yifan Zheng, Zoe Co, Vincent Marshall, Jin Kim, Qiyuan Chen, Raed Kontar, X Yang. . . . 1437

Expectations of Intensive Care Physicians Regarding an AI-Based Decision Support System for Weaning From Continuous Renal Replacement Therapy: Predevelopment Survey Study (e63709)
Benjamin Popoff, Sandie Cabon, Marc Cuggia, Guillaume Bouzillé, Thomas Clavier. . . . 1451

Proposal for Using AI to Assess Clinical Data Integrity and Generate Metadata: Algorithm Development and Validation (e60204)
Caroline Bönisch, Christian Schmidt, Dorothea Kesztyüs, Hans Kestler, Tibor Kesztyüs. . . . 1469

XSL•FO
RenderX

Performance of an Electronic Health Record–Based Automated Pulmonary Embolism Severity Index Score Calculator: Cohort Study in the Emergency Department (e58800)
Elizabeth Joyce, James McMullen, Xiaowen Kong, Connor O'Hare, Valerie Gavrila, Anthony Cuttitta, Geoffrey Barnes, Colin Greineder. 1483

Diagnostic Decision-Making Variability Between Novice and Expert Optometrists for Glaucoma: Comparative Analysis to Inform AI System Design (e63109)
Faisal Ghaffar, Nadine Furtado, Imad Ali, Catherine Burns. 1492

Improving AI-Based Clinical Decision Support Systems and Their Integration Into Care From the Perspective of Experts: Interview Study Among Different Stakeholders (e69688)
Godwin Giebel, Pascal Raszke, Hartmuth Nowak, Lars Palmowski, Michael Adamzik, Philipp Heinz, Marianne Tokic, Nina Timmesfeld, Frank Brunkhorst, Jürgen Wasem, Nikola Blase. 1506

Deep Learning and Image Generator Health Tabular Data (IGHT) for Predicting Overall Survival in Patients With Colorectal Cancer: Retrospective Study (e75022)
Seo Oh, Youngho Lee, Jeong-Heum Baek, Woongsang Sunwoo. 1521

Machine Learning–Based Prediction of In-Hospital Falls in Adult Inpatients: Retrospective Observational Multicenter Study (e75958)
Takuya Nishino, Kotone Matsuyama, Yasuo Miyagi, Nari Tanabe, Fumiko Yamaguchi, Hiroki Ito, Shizuka Soh, Ayako Yano, Masako Mizuno, Katsuhito Kato, Hiroshige Jinnouchi, Chol Kim, Yosuke Ishii, Hiroki Yamaguchi, Yukihiro Kondo. 1537

Online Clinical Calculator for Predicting 28-Day Mortality in Older Adult Patients With Sepsis-Associated Encephalopathy: Retrospective Study Using MIMIC-IV (e76417)
Guangyong Jin, Menglu Zhou, Jiayi Chen, Mengyuan Diao, Wei Hu. 1553

Comparison of Risk Factors, Their Interaction Patterns, and Scoring Systems for Liver Cancer Between Patients With and Those Without Diabetes: Retrospective Cohort Study Using Electronic Health Records and Tree-Structured Algorithms (e72239)
Sarah Yau, Chi Hung, Eman Leung, Albert Lee, Eng Yeoh. 1570

Named Entity Recognition for Chinese Cancer Electronic Health Records—Development and Evaluation of a Domain-Specific BERT Model: Quantitative Study (e76912)
Junbai Chen, Butian Zhao, Xiaohan Tian, Zhengkai Zou, Ruojia Wang, Jiarui Wu, Songxing Du, Fengying Guo. 1583

Unsupervised Coverage Sampling to Enhance Clinical Chart Review Coverage for Computable Phenotype Development: Simulation and Empirical Study (e72068)
Zigui Wang, Jillian Hurst, Chuan Hong, Benjamin Goldstein. 1600

Leveraging Machine Learning and Robotic Process Automation to Identify and Convert Unstructured Colonoscopy Results Into Actionable Data: Proof-of-Concept Study (e73504)
Elizabeth Stevens, Jager Hartman, Paul Testa, Ajay Mansukhani, Casey Monina, Amelia Shunk, David Ranson, Yana Imberg, Ann Cote, Dinesha Prabhu, Adam Szerencsy. 1616

Label Accuracy in Electronic Health Records and Its Impact on Machine Learning Models for Early Prediction of Gestational Diabetes: 3-Step Retrospective Validation Study (e72938)
Mark Germaine, Amy O'Higgins, Brendan Egan, Graham Healy. 1627

Co-Opetition Strategies of Superior and Subordinate Hospitals for Integration of Electronic Health Records Within the Medical Consortiums in China Based on Two-Party Evolutionary Game Theory: Mixed Methods Study (e70866)
Shenghu Tian, Rong Jiang, Jianfeng Yao, Yu Chen. 1639

XSL•FO
RenderX

Bridging Global Frameworks and Local Practice: Quantitative Evaluation of Electronic Health Record Safety in Kuwait's Public Hospitals (e70782)
Anwar AlHussainan, Dari Alhuwail. . . . 1650

Relationship Between Stroke Knowledge, Health Information Literacy, and Health Self- Management Among Patients with Stroke: Multicenter Cross-Sectional Study (e63956)
Mengxue Zeng, Yanhua Liu, Ying He, Wenxia Huang. . . . 1667

Implementation of an Integrated, Clinical Decision Support Tool at the Point of Antihypertensive Medication Refill Request to Improve Hypertension Management: Controlled Pre-Post Study (e70752)
John Matulis 3rd, Jason Greenwood, Michele Eberle, Benjamin Anderson, David Blair, Rajeev Chaudhry. . . . 1678

Biases in Race and Ethnicity Introduced by Filtering Electronic Health Records for "Complete Data": Observational Clinical Data Analysis (e67591)
Jose Acitores Cortina, Yasaman Fatapour, Kathleen Brown, Undina Gisladottir, Michael Zietz, Oliver Bear Don't Walk IV, Danner Peter, Jacob Berkowitz, Nadine Friedrich, Sophia Kivelson, Aditi Kuchi, Hongyu Liu, Apoorva Srinivasan, Kevin Tsang, Nicholas Tatonetti. . . . 1686

Electronic Health Record Use Patterns Among Well-Being Survey Responders and Nonresponders: Longitudinal Observational Study (e64722)
Daniel Tawfik, Tait Shanafelt, Mohsen Bayati, Jochen Profit. . . . 1698

Linking Electronic Health Record Prescribing Data and Pharmacy Dispensing Records to Identify Patient-Level Factors Associated With Psychotropic Medication Receipt: Retrospective Study (e63740)
Peng Wu, Jillian Hurst, Alexis French, Michael Chrestensen, Benjamin Goldstein. . . . 1711

Large-Scale Evaluation and Liver Disease Risk Prediction in Finland's National Electronic Health Record System: Feasibility Study Using Real-World Data (e62978)
Viljami Männikkö, Janne Tommola, Emmi Tikkanen, Olli-Pekka Hätinen, Fredrik Åberg. . . . 1724

Clinician Attitudes and Perceptions of Point-of-Care Information Resources and Their Integration Into Electronic Health Records: Qualitative Interview Study (e60191)
Marlika Marceau, Sevan Dulgarian, Jacob Cambre, Pamela Garabedian, Mary Amato, Diane Seger, Lynn Volk, Gretchen Jackson, David Bates, Ronen Rozenblum, Ania Syrowatka. . . . 1738

Service Users' Perspectives on an Integrated Electronic Care Record in Mental Health Care: Qualitative Vignette and Interview Study (e64162)
Timothy Kariotis, Megan Prictor, Kathleen Gray, Shanton Chang. . . . 1752

Identifying People Living With or Those at Risk for HIV in a Nationally Sampled Electronic Health Record Repository Called the National Clinical Cohort Collaborative: Computational Phenotyping Study (e68143)
Eric Hurwitz, Cara Varley, A Anzolone, Vithal Madhira, Amy Olex, Jing Sun, Dimple Vaidya, Nada Fadul, Jessica Islam, Lesley Jackson, Kenneth Wilkins, Zachary Butzin-Dozier, Dongmei Li, Sandra Safo, Julie McMurry, Pooja Maheria, Tommy Williams, Shukri Hassan, Melissa Haendel, Rena Patel, The National Clinical Cohort Collaborative (N3C) Consortium. . . . 1771

Genotype Distribution and Migration Patterns of Hepatitis C Virus in Shandong Province, China: Molecular Epidemiology and Phylogenetic Study (e60207)
Lin Lin, Guoyong Wang, Lianzheng Hao, Tingbin Yan. . . . 1790

Effectiveness of the Facility for Elderly Surveillance System (FESSy) in Two Public Health Center Jurisdictions in Japan: Prospective Observational Study (e58509)
Junko Kurita, Motomi Hori, Sumiyo Yamaguchi, Aiko Ogiwara, Yurina Saito, Minako Sugiyama, Asami Sunadori, Tomoko Hayashi, Akane Hara, Yukari Kawana, Youichi Itoi, Tamie Sugawara, Yoshiyuki Sugishita, Fujiko Irie, Naomi Sakurai. . . . 1807

Health Information Exchange Usage in Japan: Content Analysis of Audit Logs (e65575)
Jun Suzumoto, Yukiko Mori, Tomohiro Kuroda. . . . 1818

XSL•FO
RenderX

The Impact of Data Control and Delayed Discounting on the Public's Willingness to Share Different Types of Health Care Data: Empirical Study (e66444)
Dongle Wei, Pan Gao, Yunkai Zhai. . . . 1838

Influences on Emergency Clinician Use of Health Information Exchange: Interview Study (e75865)
Brian Dixon, Umesh Ghimire, Benjamin Richter, Corinne Bowditch, Saurabh Rahurkar, John Finnell, Joshua Vest. . . . 1852

Predicting Metabolic Dysfunction–Associated Fatty Liver Disease Phenotypes Among Adults: 2-Stage Contrastive Learning Method (e75747)
Sizhe Chen, Da Xu, Derek Hu, Paul Hu, Ting-Shuo Huang. . . . 1866

Methods for Addressing Missingness in Electronic Health Record Data for Clinical Prediction Models: Comparative Evaluation (e79307)
Jean Digitale, Deborah Franzon, Mark Pletcher, Charles McCulloch, Efstathios Gennatas. . . . 1886

Patients' Experienced Usability and Satisfaction With Digital Health Solutions in a Home Setting: Instrument Validation Study (e63703)
Susan Oudbier, Ellen Smets, Pythia Nieuwkerk, David Neal, S Nurmohamed, Hans Meij, Linda Dusseljee-Peute. . . . 1915

Imputation and Missing Indicators for Handling Missing Longitudinal Data: Data Simulation Analysis Based on Electronic Health Record Data (e64354)
Molly Ehrig, Garrett Bullock, Xiaoyan Leng, Nicholas Pajewski, Jaime Speiser. . . . 1931

Use of the FHTHWA Index as a Novel Approach for Predicting the Incidence of Diabetes in a Japanese Population Without Diabetes: Data Analysis Study (e64992)
Jiao Wang, Jianrong Chen, Ying Liu, Jixiong Xu. . . . 1946

Leveraging GPT-4o for Automated Extraction and Categorization of CAD-RADS Features From Free-Text Coronary CT Angiography Reports: Diagnostic Study (e70967)
Youmei Chen, Mengshi Dong, Jie Sun, Zhanao Meng, Yiqing Yang, Abudushalamu Muhetaier, Chao Li, Jie Qin. . . . 1957

Extracting Symptoms of Complex Conditions From Online Discourse (Subreddit to Symptomatology): Lexicon-Based Approach (e70940)
Bushra Hossain, Sarah Preum, Md Rabbi, Rifat Ara, Mohammed Ali. . . . 1970

Interpretable Machine Learning Model for Predicting and Assessing the Risk of Diabetic Nephropathy: Prediction Model Study (e64979)
Yili Wen, Zhiqiang Wan, Huiling Ren, Xu Wang, Weijie Wang. . . . 1989

Holistic Influence of Multimodal Medical Crowdfunding Affordances on Charitable Crowdfunding Outcome: Systematic Multimodel Analysis Study (e75563)
Yuxuan Du, Yujin Yang, Zihe Li, Jiaolong Xue. . . . 2010

Multisource Coherence Analysis of the First European Multicenter Cohort Study for Cancer Prevention in People Experiencing Homelessness: Data Quality Study (e73596)
Antonio Blasco-Calafat, Vicent Blanes-Selva, Tobias Fragner, Ascensión Doñate-Martínez, Tamara Alhambra-Borrás, Julia Gawronska, Lee Smith, Juan Garcia-Gomez, Igor Grabovac, Carlos Sáez. . . . 2032

The State of Practice About Security in Telemedicine Systems in Chile: Exploratory Study (e77395)
Gaston Marquez, Michelle Pacheco, Priscilla Vergara, Felix Liberona, May Chomalí, Eric Rojas. . . . 2044

Medical Science Data Value Evaluation Model: Mixed Methods Study (e63544)
Dandan Wang, Yaning Liu. . . . 2059

XSL•FO
RenderX

Assessing Internet Quality Across Public Health Centers in Indonesia: Cross-Sectional Evaluation Study (e65940)
Dewi Aisyah, Agus Setiawan, Alfiano Lokopessy, Chyntia Mayadewi, M Endryantoro, Viktor Wibowo, Sarah Disviana, Indra Laksana, Mohammad Aviandito, Zisis Kozlakidis, Logan Manikam. . . . 2074

Toward Interoperable Digital Medication Records on Fast Healthcare Interoperability Resources: Development and Technical Validation of a Minimal Core Dataset (e64099)
Eduardo Salgado-Baez, Raphael Heidepriem, Renate Delucchi Danhier, Eugenia Rinaldi, Vishnu Ravi, Akira-Sebastian Poncette, Iris Dahlhaus, Daniel Fürstenau, Felix Balzer, Sylvia Thun, Julian Sass. . . . 2092

Predicting Unplanned Readmission Risk in Patients With Cirrhosis: Complication-Aware Dynamic Classifier Selection Approach (e63581)
Zixin Shi, Linjun Huang, Xiaomei Xu, Kexue Pu, Qingpeng Zhang, Haolin Wang. . . . 2103

A Validation Tool (VaPCE) for Postcoordinated SNOMED CT Expressions: Development and Usability Study (e67984)
Tessa Ohlsen, Viola Hofer, Josef Ingenerf. . . . 2122

Taxonomy Portraits: Deciphering the Hierarchical Relationships of Medical Large Language Models (e72918)
Radha Nagarajan, Vanessa Klotzman, Midori Kondo, Sandip Godambe, Adam Gold, John Henderson, Steven Martel. . . . 2135

An Ontology for Digital Medicine Outcomes: Development of the Digital Medicine Outcomes Value Set (DOVeS) (e67589)
Benjamin Rosner, Matthew Horridge, Guillen Austria, Tiffany Lee, Andrew Auerbach. . . . 2146

Assessing Data Quality in Heterogeneous Health Care Integration: Simulation Study of the AIDAVA Framework (e75275)
Jens Declerck, Ömer Kılıç, Ensar Emir Erol, Shervin Mehryar, Dipak Kalra, Isabelle de Zegher, Remzi Celebi. . . . 2157

Effects of the National Institutes of Health Stroke Scale and Modified Rankin Scale on Predictive Models of 30-Day Nonelective Readmission and Mortality After Ischemic Stroke: Cohort Study (e69102)
Mai Nguyen-Huynh, Janet Alexander, Zheng Zhu, Melissa Meighan, Gabriel Escobar. . . . 2172

Predicting Postoperative Stress Urinary Incontinence After Prolapse Surgery via Machine Learning and Regression Models: Development and Validation Study (e76021)
Minna Su, Shuyu Wang, Xiaochun Liu. . . . 2183

Attitudes Toward Common Data Models Among Chinese Biomedical Professionals: Cross-Sectional Survey (e77603)
Yexian Yu, Yongqi Zheng, Meng Zhang, Junqing Xie, Seng You, Mengling Feng, Siyan Zhan, Feng Sun. . . . 2200

Simulation of Clinical Visits as a Novel Approach to Evaluate Digital Health in Multiple Sclerosis: Simulation Study (e67845)
Riley Bove, Luca Capezzuto, Imogen West, Simon Dryden, Saira Ghafur, Jack Halligan, Stanislas Hubeaux, Agne Kazlauskaite. . . . 2216

Organizing Telemonitoring—Decision-Making Between Centralized and Distributed Models in the Netherlands, Using the Non-Adoption, Abandonment, Scale-Up, Spread, and Sustainability (NASSS) Framework: Case Study (e69349)
Nienke Elferink, Manon Roest, Anne Weggelaar, Marleen de Mul. . . . 2233

Home Monitoring Delivered Through the Emergency Department for Outpatients With COVID-19: COVID19@Home Aachen Pilot Cohort Study (e58364)
Lukas Niekrenz, Christian Hübel, Christopher Plata, Henning Biermann, Claas Leber, Lisa Schütze, Svea Holtz, Susanne Köhler, Kim Deutsch, Nurlan Dauletbayev, Sebastian Kuhn, Beate Müller, Christian Cornelissen, Rembert Koczulla, Gernot Rohde, Claus Vogelmeier, Jörg Brokmann, Michael Dreher. . . . 2248

XSL•FO
RenderX

Benefits and Limitations of Teledermatology in German Correctional Facilities: Cross-Sectional Analysis (e58712)
Brigitte Stephan, Kathrin Gehrdau, Christina Sorbe, Matthias Augustin, Martin Scherer, Anne Kis. . . . 2257

Networked Behaviors Associated With a Large-Scale Secure Messaging Network: Cross-Sectional Secondary Data Analysis (e66544)
Laura Baratta, Linlin Xia, Daphne Lew, Elise Eiden, Y Wu, Noshir Contractor, Bruce Lambert, Sunny Lou, Thomas Kannampallil. . . . 2265

Investigating the Role of Wearable Devices in Facilitating Telehealth Adoption Among the Aging Population: Mediation Analysis of US National Data (e68559)
Ruijing Wang, Onur Asan, Ting Liao. . . . 2280

Public Attitudes Toward Violence Against Doctors: Sentiment Analysis of Chinese Users (e63772)
Yuwen Zheng, Meirong Tian, Jingjing Chen, Lei Zhang, Jia Gao, Xiang Li, Jin Wen, Xing Qu. . . . 2295

Copy Tools in the Electronic Health Record: Perceptions, Implications, and Future Directions (e78502)
Sky Corby, Joan Ash, Rebecca Jungbauer, Gretchen Scholl, Sarah Florig, Vishnu Mohan, Jeffrey Gold. . . . 2318

Competition or Complementarity Among Telemedicine Tools in Ambulatory Care Practice: Cross-Sectional Analysis (e75246)
Xiang Liu, Avijit Sengupta. . . . 2332

Regulatory Insights From 27 Years of Artificial Intelligence/Machine Learning–Enabled Medical Device Recalls in the United States: Implications for Future Governance (e67552)
Wei-Pin Chen, Wei-Guang Teng, C Kuo, Yu-Jui Yen, Jian-Yu Lian, Matthew Sing, Peng-Ting Chen. . . . 2356

Impact of Diagnostic Stewardship on Urine Culture Ordering in Saudi Arabia: Prospective Pre- and Postintervention Study (e68044)
Ahlam Alghamdi, Afrah Alkazemi, Alnada Ibrahim, Mohammed Alraey, Mohammed Alaboud, Isra Farooqi, Mohammad Aatif Khan, Asem Allam, Mohammed Alwadai, Renad Alyahya, Ohoud Alzahrani, Hajar AlQahtani, Amir Mohareb, Muneerah Aleissa. . . . 2374

Process for Quality Management of Electronic Medical Records–Based Data: Case Study Using Real Colorectal Cancer Data (e73884)
NaYoung Park, Kyungmin Na, Woongsang Sunwoo, Jeong-Heum Baek, Youngho Lee, Suehyun Lee, Hyekyung Woo. . . . 2382

Patient Perspectives on Digital Technology and Experiences of Computerized History-Taking for Chest Pain Management in the Emergency Department: CLEOS-CPDS Prospective Cohort Study (e65568)
Kaisa Fritzell, Helge Brandberg, Jonas Spaak, Sabine Koch, Carl Sundberg, David Zakim, Thomas Kahan, Kay Sundberg. . . . 2404

Alert Reduction and Telemonitoring Process Optimization for Improving Efficiency in Remote Patient Monitoring Programs: Framework Development Study (e66066)
Job van Steenkiste, Niki Lupgens, Martijn Kool, Daan Dohmen, Iris Verberk-Jonkers. . . . 2416

Real-Time, Risk-Based Clinical Trial Quality Management in China: Development of a Digital Monitoring Platform (e64114)
Min Jiang, Shuhua Zhao, Yun Mei, Zhiying Fu, Yannan Yuan, Jie Ai, Yuan Sheng, Ying Gong, Jingjing Chen. . . . 2428

A Novel Framework to Assess Clinical Information in Digital Health Technologies: Cross-Sectional Survey Study (e58125)
Kayode Fadahunsi, Petra Wark, Nikolaos Mastellos, Ana Neves, Joseph Gallagher, Azeem Majeed, Josip Car. . . . 2438

XSL•FO
RenderX

Acceptance of Electronic Medical Records and Associated Factors Among Health Care Workers in Northwest Ethiopia: Cross-Sectional Study (e72030)
Asmamaw Tsehay, Kholofelo Matlhaba. . . . 2452

Fusion of X-Ray Images and Clinical Data for a Multimodal Deep Learning Prediction Model of Osteoporosis: Algorithm Development and Validation Study (e70738)
Jun Tang, Xiang Yin, Jiangyuan Lai, Keyu Luo, Dongdong Wu. . . . 2467

Using a Large Language Model for Breast Imaging Reporting and Data System Classification and Malignancy Prediction to Enhance Breast Ultrasound Diagnosis: Retrospective Study (e70924)
Su Miaojiao, Liang Xia, Zeng Xian Tao, Hong Zhi Liang, Cheng Sheng, Wu Songsong. . . . 2482

Deep Learning Radiomics Model Based on Computed Tomography Image for Predicting the Classification of Osteoporotic Vertebral Fractures: Algorithm Development and Validation (e75665)
Jiayi Liu, Lincen Zhang, Yousheng Yuan, Jun Tang, Yongkang Liu, Liang Xia, Jun Zhang. . . . 2494

Rapid Liver Fibrosis Evaluation Using the UNet-ResNet50-32 × 4d Model in Magnetic Resonance Elastography: Retrospective Study (e80351)
Pei-Yuan Su, Han-Jie Shih, Jia-Lang Xu. . . . 2511

Evaluating Multiple Input Strategies of Large Language Models for Gallbladder Polyps on Ultrasound: Comparative Study (e71178)
Lin Jiang, Jiaqian Yao, Zebang Yang, Fuqiu Tang, Xin Zheng, Xiaoer Zhang, Xiaoyan Xie, Ming Xu, Tongyi Huang. . . . 2522

Integrating Health Care Data in an Informatics for Integrating Biology & the Bedside (i2b2) Model Persisted Through Elasticsearch: Design, Implementation, and Evaluation in a French University Hospital (e65753)
Romain Griffier, Fleur Mougin, Vianney Jouhet. . . . 2554

Large Separable Kernel Attention–Driven Multidimensional Feature Cross-Level Fusion Classification Network of Knee Cartilage Injury: Algorithm Development and Validation (e79748)
Lirong Zhang, Hang Yu, Yating Yang. . . . 2572

Evaluating the Accuracy of the Frysian Questionnaire for Differentiation of Musculoskeletal Complaints for Triage of Musculoskeletal Diseases: Algorithm Development and Validation Study (e77345)
Tjardo Maarseveen, Floor Reimann, Ahmed al Hasan, Annemarie Schilder, Dan Zhang, Freke Wink, Lidy Hendriks, Rachel Knevel, Reinhard Bos. . . . 2588

Predicting 30-Days Hospital Readmission for Patients with Heart Failure Using Electronic Health Record Embeddings: Comparative Evaluation (e73020)
Prabin Shakya, Ayush Khaneja, Kavishwar Wagholikar. . . . 2603

Prognostic Value of the Charlson Comorbidity Index for Mortality and Machine Learning–Based Prediction in Critically Ill Patients with Paralytic Ileus: Retrospective Cohort Study (e76003)
Hui Feng, Fuhai Zhou, Yi Shen, Zhen Wang, Yiyang Yuan, Wenshan Jing, Zhou Zheng, Hui Peng, Qingsheng Yu. . . . 2611

Survival Prediction for Postoperative Patients With Kidney Cancer Based on Computed Tomography Radiomics: Retrospective Cohort Study (e73162)
Guizhen He, Liwen Lai, Guoan Yu, Haowen Pang, Xiaohui Yu, Huaiwen Zhang, Qingxiu Zhu, Yingzi Lv. . . . 2633

Multimodal Multitask Learning for Predicting Depression Severity and Suicide Risk Using Pretrained Audio and Text Embeddings: Methodology Development and Application (e66907)
Ya-Han Hu, Ruei-Yan Wu, Min-Yi Su, I-Li Lin, Cheng-Che Shen. . . . 2646

Predicting Delayed Extubation After General Anesthesia in Postanesthesia Care Unit Patients Using Machine Learning: Model Development Study (e72602)
Jianwei Luo, Shaoman Lin, Liman Wang, Huanfan Ji, Jingcong Zheng, Tingkang Wang, Lin Chen, Ziqi Lin, Zhongqi Liu, Ning Liufu. . . . 2663

XSL•FO
RenderX

Detection of Polyphonic Alarm Sounds From Medical Devices Using Frequency-Enhanced Deep Learning: Simulation Study (e35987)
Kazumasa Kishimoto, Tadamasa Takemura, Osamu Sugiyama, Ryosuke Kojima, Masahiro Yakami, Goshiro Yamamoto, Tomohiro Kuroda. . . 2 6 7 7

Predicting Waiting Times for Medical Tasks in a Pediatric Hospital Using Machine Learning: Comprehensive, Retrospective, Real-World Study (e77297)
Lin Guo, Rui Tang, Jia Wang, Si Zheng, Yin Zeng, Jun Hou, Mo Dong, Jiao Li, Ying Cui. . . . 2689

Machine Learning and Shapley Additive Explanations Value Integration for Predicting the Prognostic of Anti-N-Methyl-D-Aspartate Receptor Encephalitis: Model Development and Evaluation Study (e75020)
Jia Wang, Haotian Wu, Han Cai, YingXiang Wang, Jian Gu. . . . 2703

Predicting Lymph Node Metastasis in Rectal Cancer: Development and Validation of a Machine Learning Model Using Clinical Data (e73765)
Wei Hou, Chuangwei Li, Zhen Wang, Wanqin Wang, Shouhong Wan, Bingbing Zou. . . . 2720

Interpretable Machine Learning Model for Pulmonary Hypertension Risk Prediction: Retrospective Cohort Study (e74117)
Hongxia Jiang, Han Gao, Dexin Wang, Qingli Zeng, Xiaojun Hao, Zhenshun Cheng. . . . 2741

Interpretable Machine Learning for Predicting Adverse Pregnancy Outcomes in Gestational Diabetes: Retrospective Cohort Study (e71539)
Jiaxi Li, Xiali Liu, Shenyang He, Yan Ren. . . . 2764

Real-Time Estimation of Arterial Partial Pressure of Carbon Dioxide in Patients Undergoing General Anesthesia: Predictive Modeling Study (e64855)
Ah Lee, Jun Lee, Sooyoung Yoo, Ho-Young Lee, Hyun Kim. . . . 2779

Using Wearable Device and Machine Learning to Predict Mood Symptoms in Bipolar Disorder: Development and Usability Study (e66277)
Chia-Tung Wu, Ming Hsieh, I-Ming Chen, Lian-Yin Jhao, Ding-Shan Liu, Ssu-Ming Wang, Chia-Ting Wu, Yi-Ling Chien. . . . 2792

Prediction of Insulin Resistance in Nondiabetic Population Using LightGBM and Cohort Validation of Its Clinical Value: Cross-Sectional and Retrospective Cohort Study (e72238)
Ting Peng, Rujia Miao, Hao Xiong, Yanhui Lin, Duzhen Fan, Jiayi Ren, Jiangang Wang, Yuan Li, Jianwen Chen. . . . 2804

Development and Validation of a Predictive Model for Activities of Daily Living Dysfunction in Older Adults: Retrospective Analysis of Data From the China Health and Retirement Longitudinal Study (e73030)
Fangbo Lin, Chao Liu, Hua Liu. . . . 2822

A Responsible Framework for Assessing, Selecting, and Explaining Machine Learning Models in Cardiovascular Disease Outcomes Among People With Type 2 Diabetes: Methodology and Validation Study (e66200)
Yang Yang, Che-Yi Liao, Esmaeil Keyvanshokooh, Hui Shao, Mary Weber, Francisco Pasquel, Gian-Gabriel Garcia. . . . 2837

Enhancing the Predictions of Cytomegalovirus Infection in Severe Ulcerative Colitis Using a Deep Learning Ensemble Model: Development and Validation Study (e64987)
Jeong Kim, A Choe, Ju Byeon, Yehyun Park, Eun Song, Seong-Eun Kim, Eui Jeong, Rena Lee, Jin Kim, So Ahn, Sung Jung. . . . 2852

Leveraging AI to Drive Timely Improvements in Patient Experience Feedback: Algorithm Validation (e60900)
Mustafa Khanbhai, Catalina Carenzo, Sarindi Aryasinghe, David Manton, Erik Mayer. . . . 2869

XSL•FO
RenderX

Combining Machine Learning With Real-World Data to Identify Gaps in Clinical Practice Guidelines: Feasibility Study Using the Prospective German Stroke Registry and the National Acute Ischemic Stroke Guidelines (e69282)
Sandrine Müller, Susanne Diekmann, Markus Wenzel, Horst Hahn, Johannes Tuennerhoff, Ulrike Ernemann, Florian Hennersdorf, German Stroke Registry Investigators, Max Westphal, Sven Poli. . . . 2887

Autoencoder-Based Representation Learning for Similar Patients Retrieval From Electronic Health Records: Comparative Study (e68830)
Deyi Li, Aditi Shukla, Sravani Chandaka, Bradley Taylor, Jie Xu, Mei Liu. . . . 2908

Predictive Modeling of Osteonecrosis of the Femoral Head Progression Using MobileNetV3_Large and Long Short-Term Memory Network: Novel Approach (e66727)
Gang Kong, Qi Zhang, Dan Liu, Jingbo Pan, Kegui Liu. . . . 2925

A Machine Learning–Based Prognostication Model Enhances Prediction of Early Hepatic Encephalopathy in Patients With Noncancer-Related Cirrhosis: Multicenter Longitudinal Cohort Study in Taiwan (e71229)
Hsin-Yu Chen, Yiu-Hua Cheng, Wei-Chung Yeh, Yi-Chuan Chen, Yi-Wen Tsai. . . . 2939

Probability-Based Early Warning for Seasonal Influenza in China: Model Development Study (e73631)
Jinzhao Cui, Ting Zhang, Yifeng Shen, Xiaoli Wang, Liuyang Yang, Xuefeng Huang, Qiang Huang, Yu Yang, Weizhong Yang, Zhongjie Li. . . . 2 9 5 5

Machine Learning–Based Analysis of Lifestyle Risk Factors for Atherosclerotic Cardiovascular Disease: Retrospective Case-Control Study (e74415)
Hye-Jin Kim, Heeji Choi, Hyo-Jung Ahn, Seung-Ho Shin, Chulho Kim, Sang-Hwa Lee, Jong-Hee Sohn, Jae-Jun Lee. . . . 2967

Tongue Image–Based Diagnosis of Acute Respiratory Tract Infection Using Machine Learning: Algorithm Development and Validation (e74102)
Qianzi Che, Yuanming Leng, Wei Yang, Xihao Cao, Zhongxia Wang, Lizheng Liu, Feibiao Xie, Ruilin Wang. . . . 2980

Prediction of Mini-Mental State Examination Scores for Cognitive Impairment and Machine Learning Analysis of Oral Health and Demographic Data Among Individuals Older Than 60 Years: Cross-Sectional Study (e75069)
Alper Idrisoglu, Johan Flyborg, Sarah Nauman Ghazi, Elina Mikaelsson Midlöv, Helén Dellkvist, Anna Axén, Ana Dallora. . . . 2994

Experience of Cardiovascular and Cerebrovascular Disease Surgery Patients: Sentiment Analysis Using the Korean Bidirectional Encoder Representations from Transformers (KoBERT) Model (e65127)
Hocheol Lee, Yu Hwang, Ye Kim, Yukyung Park, Heui Jo. . . . 3007

Enhancing Antidiabetic Drug Selection Using Transformers: Machine-Learning Model Development (e67748)
Hisashi Kurasawa, Kayo Waki, Tomohisa Seki, Eri Nakahara, Akinori Fujino, Nagisa Shiomi, Hiroshi Nakashima, Kazuhiko Ohe. . . . 3019

Transformer-Based Language Models for Group Randomized Trial Classification in Biomedical Literature: Model Development and Validation (e63267)
Elaheh Aghaarabi, David Murray. . . . 3033

A Risk Warning Model for Anemia Based on Facial Visible Light Reflectance Spectroscopy: Cross-Sectional Study (e64204)
Yahan Zhang, Yi Chun, Hongyuan Fu, Wen Jiao, Jizhang Bao, Tao Jiang, Longtao Cui, Xiaojuan Hu, Ji Cui, Xipeng Qiu, Liping Tu, Jiatuo Xu. 3 0 4 1

Predicting Agitation-Sedation Levels in Intensive Care Unit Patients: Development of an Ensemble Model (e63601)
Pei-Yu Dai, Pei-Yi Lin, Ruey-Kai Sheu, Shu-Fang Liu, Yu-Cheng Wu, Chieh-Liang Wu, Wei-Lin Chen, Chien-Chung Huang, Guan-Yin Lin, Lun-Chi Chen. . . . 3060

XSL•FO
RenderX

Development and Validation of a Machine Learning Algorithm for Predicting Diabetes Retinopathy in Patients With Type 2 Diabetes: Algorithm Development Study (e58107)
Sunyoung Kim, Jaeyu Park, Yejun Son, Hojae Lee, Selin Woo, Myeongcheol Lee, Hayeon Lee, Hyunji Sang, Dong Yon, Sang Rhee. 3075

Predicting Readmission Among High-Risk Discharged Patients Using a Machine Learning Model With Nursing Data: Retrospective Study (e56671)
Eui Oh, Sunyoung Oh, Seunghyeon Cho, Mir Moon. 3089

Performance of Artificial Intelligence Chatbots on Ultrasound Examinations: Cross-Sectional Comparative Analysis (e63924)
Yong Zhang, Xiao Lu, Yan Luo, Ying Zhu, Wenwu Ling. 3103

Robust Automated Harmonization of Heterogeneous Data Through Ensemble Machine Learning: Algorithm Development and Validation Study (e54133)
Doris Yang, Doudou Zhou, Steven Cai, Ziming Gan, Michael Pencina, Paul Avillach, Tianxi Cai, Chuan Hong. 3116

Development and Validation of a Machine Learning Method Using Vocal Biomarkers for Identifying Frailty in Community-Dwelling Older Adults: Cross-Sectional Study (e57298)
Taehwan Kim, Jung-Yeon Choi, Myung Ko, Kwang-il Kim. 3128

Interpretable Machine Learning Model for Predicting Postpartum Depression: Retrospective Study (e58649)
Ren Zhang, Yi Liu, Zhiwei Zhang, Rui Luo, Bin Lv. 3142

The Social Construction of Categorical Data: Mixed Methods Approach to Assessing Data Features in Publicly Available Datasets (e59452)
Theresa Willem, Alessandro Wollek, Theodor Cheslerean-Boghiu, Martha Kenney, Alena Buyx. 3162

Machine Learning–Based Risk Factor Analysis and Prediction Model Construction for the Occurrence of Chronic Heart Failure: Health Ecologic Study (e64972)
Qian Xu, Xue Cai, Ruicong Yu, Yueyue Zheng, Guanjie Chen, Hui Sun, Tianyun Gao, Cuirong Xu, Jing Sun. 3177

Identification of Clusters in a Population With Obesity Using Machine Learning: Secondary Analysis of The Maastricht Study (e64479)
Maik Beuken, Melanie Kleynen, Susy Braun, Kees Van Berkel, Carla van der Kallen, Annemarie Koster, Hans Bosma, Tos Berendschot, Alfons Houben, Nicole Dukers-Muijrers, Joop van den Bergh, Abraham Kroon, Maastricht Study Management, Iris Kanera. 3195

An Interpretable Model With Probabilistic Integrated Scoring for Mental Health Treatment Prediction: Design Study (e64617)
Anthony Kelly, Esben Jensen, Eoin Grua, Kim Mathiasen, Pepijn Van de Ven. 3210

Identification of Patients With Congestive Heart Failure From the Electronic Health Records of Two Hospitals: Retrospective Study (e64113)
Daniel Sumsion, Elijah Davis, Marta Fernandes, Ruoqi Wei, Rebecca Milde, Jet Veltink, Wan-Yee Kong, Yiwen Xiong, Samvrit Rao, Tara Westover, Lydia Petersen, Niels Turley, Arjun Singh, Stephanie Buss, Shibani Mukerji, Sahar Zafar, Sudeshna Das, Valdery Junior, Manohar Ghanta, Aditya Gupta, Jennifer Kim, Katie Stone, Emmanuel Mignot, Dennis Hwang, Lynn Trotti, Gari Clifford, Umakanth Katwa, Robert Thomas, M Westover, Haoqi Sun. 3234

Daily Automated Prediction of Delirium Risk in Hospitalized Patients: Model Development and Validation (e60442)
Kendrick Shaw, Yu-Ping Shao, Manohar Ghanta, Valdery Junior, Eyal Kimchi, Timothy Houle, Oluwaseun Akeju, Michael Westover. 3245

Prediction of Snacking Behavior Involving Snacks Having High Levels of Saturated Fats, Salt, or Sugar Using Only Information on Previous Instances of Snacking: Survey- and App-Based Study (e57530)
Shaima Dammas, Tillman Weyde, Katy Tapper, Gerasimos Spanakis, Anne Roefs, Emmanuel Pothos. 3258

XSL•FO
RenderX

Prediction of Spontaneous Breathing Trial Outcome in Critically Ill-Ventilated Patients Using Deep Learning: Development and Verification Study (e64592)
Hui-Chiao Yang, Angelica Hao, Shih-Chia Liu, Yu-Cheng Chang, Yao-Te Tsai, Shao-Jen Weng, Ming-Cheng Chan, Chen-Yu Wang, Yeong-Yuh Xu. . . . 3281

Machine Learning for the Prediction of Acute Kidney Injury in Critically Ill Patients With Coronary Heart Disease: Algorithm Development and Validation (e72349)
Yike Li, Mingyang Xiao, Yaqian Li, Lulu Lv, Shanshan Zhang, Yuhui Liu, Juan Zhang. . . . 3298

Intelligent Prediction Platform for Sepsis Risk Based on Real-Time Dynamic Temporal Features: Design Study (e74940)
Mingwei Zhang, Ming Zhong, Yunzhang Cheng, Tianyi Zhang. . . . 3315

Trajectory-Ordered Objectives for Self-Supervised Representation Learning of Temporal Healthcare Data Using Transformers: Model Development and Evaluation Study (e68138)
Ali Amirahmadi, Farzaneh Etminani, Jonas Björk, Olle Melander, Mattias Ohlsson. . . . 3327

A Machine Learning Model for Predicting Sarcopenia Among Middle-Aged Adults: Development and External Validation (e75760)
Hye Chong. . . . 3346

A Machine Learning Algorithm With an Oversampling Technique in Limited Data Scenarios for the Prediction of Present and Future Restorative Treatment Need: Development and Validation Study (e75117)
Elina Väyrynen, Otso Tirkkonen, Henna Tiensuu, Jaakko Suutala, Vuokko Anttonen, Marja-Liisa Laitala, Katri Kukkola, Saujanya Karki. . . . 3357

An Artificial Intelligence–Based Framework for Predicting Emergency Department Overcrowding: Development and Evaluation Study (e73960)
Orhun Vural, Bunyamin Ozaydin, Khalid Aram, James Booth, Brittany Lindsey, Abdulaziz Ahmed. . . . 3372

Synthetic Tabular Data Generation Under Horizontal Federated Learning Environments in Acute Myeloid Leukemia: Case-Based Simulation Study (e74116)
Imanol Isasa, Mikel Catalina, Gorka Epelde, Naiara Aginako, Andoni Beristain. . . . 3390

Evaluation of Machine Learning Model Performance in Diabetic Foot Ulcer: Retrospective Cohort Study (e71994)
Veerle van Velze, Hendrico Burger, Tim van der Steenhoven, Hani Al-Ers, Lauren Goncalves, Daniël Eefting, Willem-Jan de Jong, Harm Smeets, Janna Welleweerd, Joost van der Vorst, Sandy Uchtmann, Robert Rissmann, Jaap Hamming, Lampros Stergioulas, Koen van der Bogt. . . . 3421

Prediction of Postoperative Venous Thromboembolism in Patients With Traumatic Brain Injury: Model Development and Validation Study (e78655)
Jiang Zheng, Qiling Jiang, Yusheng Zhan, Yanming Tang, Xiaohui Du, Guangrong Xiang, Yufang Ouyang, Hong Fu. . . . 3438

Risk Prediction of Major Adverse Cardiovascular Events Within One Year After Percutaneous Coronary Intervention in Patients With Acute Coronary Syndrome: Machine Learning–Based Time-to-Event Analysis (e81778)
Hong-Jae Choi, Changhee Lee, Hack-Lyoung Kim, Youn-Jung Son. . . . 3452

Identifying Key Variances in Clinical Pathways Associated With Prolonged Hospital Stays Using Machine Learning and ePath Real-World Data: Model Development and Validation Study (e71617)
Saori Tou, Koutarou Matsumoto, Asato Hashinokuchi, Fumihiko Kinoshita, Yasunobu Nohara, Takanori Yamashita, Yoshifumi Wakata, Tomoyoshi Takenaka, Hidehisa Soejima, Tomoharu Yoshizumi, Naoki Nakashima, Masahiro Kamouchi. . . . 3466

Unsupervised Characterization of Temporal Dataset Shifts as an Early Indicator of AI Performance Variations: Evaluation Study Using the Medical Information Mart for Intensive Care-IV Dataset (e78309)
David Fernández-Narro, Pablo Ferri, Alba Gutiérrez-Sacristán, Juan García-Gómez, Carlos Sáez. . . . 3479

XSL•FO
RenderX

Automated Speech Analysis for Screening and Monitoring Bipolar Depression: Machine Learning Model Development and Interpretation Study (e79093)
Sooyeon Min, Tae-Sung Yeum, Daun Shin, Sang Rhee, Hyunju Lee, Han-Sung Lee, Seongmin Park, Jihwa Lee, Yong Ahn. 3493

A Machine Learning Approach to Predicting Mortality Risk in Chemotherapy-Treated Lung Cancer: Machine Learning Model Development and Validation (e72424)
Jianjun Zou, Jinyi Huang, Katie Lu, Ao Lin, Chen Xie, Jinrong Zhang, Boqi Rao, Zhi Li, Dongming Xie, Ling Lu, Feng Luo, Jinbin Chen, Lei Yang, Fuman Qiu, Xin Zhang, Yibin Deng, Jiachun Lu. 3510

A Machine Learning Model Based on Clinical Factors to Predict the Efficacy of First-Line Immunochemotherapy for Patients With Advanced Gastric Cancer: Retrospective Study (e82533)
Xu Cheng, Ping Li, Enqing Meng, Xinyi Wu, Hao Wu. 3526

Predicting Left Ventricular Ejection Fraction Recovery After Percutaneous Coronary Intervention in Patients With Chronic Coronary Syndrome by Using Interpretable Machine Learning Models: Retrospective Study (e77839)
Jiayi Ding, Guanqi Lyu, Masaharu Nakayama, Kotaro Nochioka, Jun Takahashi, Satoshi Yasuda, Tetsuya Matoba, Takahide Kohro, Naoyuki Akashi, Hideo Fujita, Yusuke Oba, Tomoyuki Kabutoya, Kazuomi Kario, Yasushi Imai, Arihiro Kiyosue, Yoshiko Mizuno, Takamasa Iwai, Yoshihiro Miyamoto, Masanobu Ishii, Kenichi Tsujita, Taishi Nakamura, Hisahiko Sato, Ryozo Nagai. 3544

Prescription Refill Adherence Before and After Patient Portal Registration in Among General Practice Patients in England Using the Clinical Practice Research Datalink: Longitudinal Observational Study (e50294)
Abrar Alturkistani, Thomas Beaney, Geva Greenfield, Ceire Costelloe. 3581

Innovative Integration of 4D Cardiovascular Reconstruction and Hologram: Framework Development of a New Visualization Tool for Coronary Artery Bypass Grafting Planning (e72237)
Shuo Wang, Tong Ren, Nan Cheng, Li Zhang, Rong Wang. 3594

Assessment of a Digital Platform for Routine Outcome Monitoring in Psychotherapy: Usability Study and Thematic Analysis (e75885)
Mattia Olive, Antonino La Tona, Gianluca Lo Coco, Angelo Compare, Joseph Cafazzo, Cristina Masella. 3610

A Unique Way to Axe the Fax Through Using Business Automation Workflow to Expedite eReferral Adoption, Bridging eReferral, and Fax: Proof-of-Concept Study (e62983)
Zhigang Tian, Kayla Wierts, Lirije Hyseni, Beth Gerritsen, Kim Lynch, Russell Buchanan, Mohamed Alarakhia. 3622

Incorporating Generative AI Into a Health Informatics Curriculum to Build 21st Century Competencies: Multisite Pre-Post Study (e76507)
Freddie Seba, Miriam Isola, Laura Mills, Mohan Zalake, Jacob Krive. 3635

Bibliometric Insights Into the Infodemic: Global Research Trends and Policy Responses: Quantitative Research (e76378)
Sijia Wang, Linan Zhang, Yang Liu, Xin Feng, Shipeng Ren. 3656

Deep Learning Approaches for Classifying Children With and Without Autism Spectrum Disorder Using Inertial Measurement Unit Hand Tracking Data: Comparative Study (e73440)
John Mutersbaugh, Wan-Chun Su, Anjana Bhat, Amir Gandjbakhche. 3681

A Machine Learning Approach to Differentiate Cold and Hot Syndrome in Viral Pneumonia Integrating Traditional Chinese Medicine and Modern Medicine: Machine Learning Model Development and Validation (e64725)
Xiaojie Jin, Yanru Wang, Jiarui Wang, Qian Gao, Yuhan Huang, Lingyu Shao, Jiali Zhao, Jintian Li, Ling Li, Zhiming Zhang, Shuyan Li, Yongqi Liu. 3695

XSL•FO
RenderX

Detection and Analysis of Circadian Biomarkers for Metabolic Syndrome Using Wearable Data: Cross-Sectional Study (e69328)
Jeong-Kyun Kim, Sujeong Mun, Siwoo Lee. . . . 3715

Enhancing Oral Health Diagnostics With Hyperspectral Imaging and Computer Vision: Clinical Dataset Study (e76148)
Paul Römer, Jean-Jacques Ponciano, Katharina Kloster, Fabia Siegberg, Bastian Plaß, Shankeeth Vinayahalingam, Bilal Al-Nawas, Peer Kämmerer, Thomas Klauer, Daniel Thiem. . . . 3732

Autonomous International Classification of Diseases Coding Using Pretrained Language Models and Advanced Prompt Learning Techniques: Evaluation of an Automated Analysis System Using Medical Text (e63020)
Yan Zhuang, Junyan Zhang, Xiuxing Li, Chao Liu, Yue Yu, Wei Dong, Kunlun He. . . . 3747

YOLOv12 Algorithm-Aided Detection and Classification of Lateral Malleolar Avulsion Fracture and Subfibular Ossicle Based on CT Images: Multicenter Study (e79064)
Jiayi Liu, Peng Sun, Yousheng Yuan, Zihan Chen, Ke Tian, Qian Gao, Xiangsheng Li, Liang Xia, Jun Zhang, Nan Xu. . . . 3763

Performance of ChatGPT-4o, Claude 3 Opus, and DeepSeek-R1 in BI-RADS Category 4 Classification and Malignancy Prediction From Mammography Reports: Retrospective Diagnostic Study (e80182)
Xingwei Dai, Man Ke, Dixing Xie, Mengting Mei, Si Wei, Yi Dai, Ronghua Yan. . . . 3777

Assessing Total Hip Arthroplasty Outcomes and Generating an Orthopedic Research Outcome Database via a Natural Language Processing Pipeline: Development and Validation Study (e64705)
Nicholas Mast, Clara Oeste, Dries Hens. . . . 3791

Data Interoperability in COVID-19 Vaccine Trials: Methodological Approach in the VACCELERATE Project (e65590)
Salma Malik, Zoi Dorothea, Christos Argyropoulos, Sophia Themistocleous, Alan Macken, Olena Valdenmaiier, Frank Scheckenbach, Elena Bardach, Andrea Pfeiffer, Katherine Loens, Jordi Ochando, Oliver Cornely, Jacques Demotes-Mainard, Sergio Contrino, Gerd Felder. . . . 3801

Toward a Domain-Overarching Metadata Schema for Making Health Research Studies FAIR (Findable, Accessible, Interoperable, and Reusable): Development of the NFDI4Health Metadata Schema (e63906)
Haitham Abaza, Aliaksandra Shutsko, Sophie Klopfenstein, Carina Vorisek, Carsten Schmidt, Claudia Brünings-Kuppe, Vera Clemens, Johannes Darms, Sabine Hanß, Timm Intemann, Franziska Jannasch, Elisa Kasbohm, Birte Lindstädt, Matthias Löbe, Katharina Nimptsch, Ute Nöthlings, Marisabel Ocanto, Tracy Osei, Ines Perrar, Manuela Peters, Tobias Pischon, Ulrich Sax, Matthias Schulze, Florian Schwarz, Carolina Schwedhelm, Sylvia Thun, Dagmar Waltemath, Atinkut Zeleke, Wolfgang Müller, Martin Golebiewski. . . . 3818

Analysis of Retinal Thickness in Patients With Chronic Diseases Using Standardized Optical Coherence Tomography Data: Database Study Based on the Radiology Common Data Model (e64422)
ChulHyoung Park, So Lee, Da Lee, Seoyoon Choi, Seng You, Ja Jeon, Sang Park, Rae Park. . . . 3872

Developing a SNOMED CT–Based Value Set to Document Symptoms and Diagnoses for Adverse Drug Events: Mixed Methods Study (e70167)
Erica Lau, Linda Bird, Anthony Lau, Yau-Lam Chau, Katherine Butcher, Susan Buchkowsky, Kira Gossack-Keenan, Cheryl Sadowski, Corinne Hohl. . . . 3887

Detecting Redundant Health Survey Questions by Using Language-Agnostic Bidirectional Encoder Representations From Transformers Sentence Embedding: Algorithm Development Study (e71687)
Sunghoon Kang, Hyewon Park, Ricky Taira, Hyeoneui Kim. . . . 3900

Building a Standardized Cancer Synoptic Report With Semantic and Syntactic Interoperability: Development Study Using SNOMED CT and Fast Healthcare Interoperability Resources (FHIR) (e76870)
Jieun Hwang, Alexander Goel, Brian Rous, George Birdsong, Paul Seegers, Stefan Dubois, Thomas Rüdiger, Walter Campbell. . . . 3914

XSL•FO
RenderX

Clinical Trial Schedule of Activities Specification Using Fast Healthcare Interoperability Resources Definitional Resources: Mixed Methods Study (e71430)
Andrew Richardson, Patrick Genyn. . . . 3926

Effect of Smartphone-Based Messaging on Interns and Nurses at an Academic Medical Center: Observational Study (e66859)
Sankirth Madabhushi, Andrew Nguyen, Katie Hsia, Sucharita Kher, William Harvey, Jennifer Murzycki, Daniel Chandler, Michael Davis. . . . 3942

Performance of the Large Language Models on the Chinese National Nurse Licensure Examination: Cross-Sectional Evaluation Study (e78279)
Longhui Xu, Xiao Cong, Renxiu Wang, Na Li, Xinru Liu, Ronghui Wang, Cuiping Xu. . . . 3952

Enabling Just-in-Time Clinical Oncology Analysis With Large Language Models: Feasibility and Validation Study Using Unstructured Synthetic Data (e78332)
Peter May, Julian Greß, Christoph Seidel, Sebastian Sommer, Markus Schuler, Sina Nokodian, Florian Schröder, Johannes Jung. . . . 3965

Enhancing Large Language Models With AI Agents for Chronic Gastritis Management: Comprehensive Comparative Study (e73857)
Shurui Wang, Qing Ye. . . . 3980

Development of a Large-Scale Dataset of Chest Computed Tomography Reports in Japanese and a High-Performance Finding Classification Model: Dataset Development and Validation Study (e71137)
Yosuke Yamagishi, Yuta Nakamura, Tomohiro Kikuchi, Yuki Sonoda, Hiroshi Hirakawa, Shintaro Kano, Satoshi Nakamura, Shouhei Hanaoka, Takeharu Yoshikawa, Osamu Abe. . . . 3994

Large Language Models for Automating Clinical Trial Criteria Conversion to Observational Medical Outcomes Partnership Common Data Model Queries: Validation and Evaluation Study (e71252)
Kye Lee, Sujung Jang, Grace Kim, Sukyoung Park, Doeun Kim, Oh Kwon, Jae-Ho Lee, Young-Hak Kim. . . . 4013

Performance of Large Language Models in the Non-English Context: Qualitative Study of Models Trained on Different Languages in Chinese Medical Examinations (e69485)
Zhong Yao, Liantan Duan, Shuo Xu, Lingyi Chi, Dongfang Sheng. . . . 4029

Language Models for Multilabel Document Classification of Surgical Concepts in Exploratory Laparotomy Operative Notes: Algorithm Development Study (e71176)
Jeremy Balch, Sasank Desaraju, Victoria Nolan, Divya Vellanki, Timothy Buchanan, Lindsey Brinkley, Yordan Penev, Ahmet Bilgili, Aashay Patel, Corinne Chatham, David Vanderbilt, Rayon Uddin, Azra Bihorac, Philip Efron, Tyler Loftus, Protiva Rahman, Benjamin Shickel. . . . 4040

Clinical Performance and Communication Skills of ChatGPT Versus Physicians in Emergency Medicine: Simulated Patient Study (e68409)
ChulHyoung Park, Min An, Gyubeom Hwang, Rae Park, Juho An. . . . 4055

Evaluation of ChatGPT-4 as an Online Outpatient Assistant in Puerperal Mastitis Management: Content Analysis of an Observational Study (e68980)
Fatih Dolu, O uzhan Ay, Aydın Kupeli, Enes Karademir, Muhammed Büyükavcı. . . . 4069

Optimizing Thyroid Nodule Management With Artificial Intelligence: Multicenter Retrospective Study on Reducing Unnecessary Fine Needle Aspirations (e71740)
Jia-Hui Ni, Yun-Yun Liu, Chao Chen, Yi-Lei Shi, Xing Zhao, Xiao-Long Li, Bei-Bei Ye, Jing-Liang Hu, Li-Chao Mou, Li-Ping Sun, Hui-Jun Fu, Xiao-Xiang Zhu, Yi-Feng Zhang, Lehang Guo, Hui-Xiong Xu. . . . 4080

Application of Large Language Models in Complex Clinical Cases: Cross-Sectional Evaluation Study (e73941)
Yuanheng Huang, Guozhen Yang, Yahui Shen, Huiguo Chen, Weibin Wu, Xiaojun Li, Yonghui Wu, Kai Zhang, Jiannan Xu, Jian Zhang. . . . 4094

XSL•FO
RenderX

Benchmarking the Confidence of Large Language Models in Answering Clinical Questions: Cross-Sectional Evaluation Study (e66917)
Mahmud Omar, Reem Agbareia, Benjamin Glicksberg, Girish Nadkarni, Eyal Klang. 4105

Identifying Patient-Reported Care Experiences in Free-Text Survey Comments: Topic Modeling Study (e63466)
Brian Steele, Paul Fairie, Kyle Kemp, Adam D'Souza, Matthias Wilms, Maria Santana. 4113

Transforming Informed Consent Generation Using Large Language Models: Mixed Methods Study (e68139)
Qiming Shi, Katherine Luzuriaga, Jeroan Allison, Asil Oztekin, Jamie Faro, Joy Lee, Nathaniel Hafer, Margaret McManus, Adrian Zai. 4124

Diagnosis of Chronic Kidney Disease Using Retinal Imaging and Urine Dipstick Data: Multimodal Deep Learning Approach (e55825)
Youngmin Bhak, Yu Lee, Joonhyung Kim, Kiwon Lee, Daehwan Lee, Eun Jang, Eunjeong Jang, Christopher Lee, Eun Kang, Sehee Park, Hyun Han, Sang Nam. 4135

Classifying Unstructured Text in Electronic Health Records for Mental Health Prediction Models: Large Language Model Evaluation Study (e65454)
Nicholas Cardamone, Mark Olfson, Timothy Schmutte, Lyle Ungar, Tony Liu, Sara Cullen, Nathaniel Williams, Steven Marcus. 4152

The Transformative Potential of Large Language Models in Mining Electronic Health Records Data: Content Analysis (e58457)
Amadeo Wals Zurita, Hector Miras del Rio, Nerea Ugarte Ruiz de Aguirre, Cristina Nebrera Navarro, Maria Rubio Jimenez, David Muñoz Carmona, Carlos Miguez Sanchez. 4163

Development and Evaluation of a Mental Health Chatbot Using ChatGPT 4.0: Mixed Methods User Experience Study With Korean Users (e63538)
Boyoung Kang, Munpyo Hong. 4178

Qwen-2.5 Outperforms Other Large Language Models in the Chinese National Nursing Licensing Examination: Retrospective Cross-Sectional Comparative Study (e63731)
Shiben Zhu, Wanqin Hu, Zhi Yang, Jiani Yan, Fang Zhang. 4196

Evaluating and Enhancing Japanese Large Language Models for Genetic Counseling Support: Comparative Study of Domain Adaptation and the Development of an Expert-Evaluated Dataset (e65047)
Takuya Fukushima, Masae Manabe, Shuntaro Yada, Shoko Wakamiya, Akiko Yoshida, Yusaku Urakawa, Akiko Maeda, Shigeyuki Kan, Masayo Takahashi, Eiji Aramaki. 4208

InfectA-Chat, an Arabic Large Language Model for Infectious Diseases: Comparative Analysis (e63881)
Yesim Selcuk, Eunhui Kim, Insung Ahn. 4224

Performance Assessment of Large Language Models in Medical Consultation: Comparative Study (e64318)
Sujeong Seo, Kyuli Kim, Heyoung Yang. 4243

Extracting Pulmonary Embolism Diagnoses From Radiology Impressions Using GPT-4o: Large Language Model Evaluation Study (e67706)
Mohammed Mahyoub, Kacie Dougherty, Ajit Shukla. 4260

Summarizing Online Patient Conversations Using Generative Language Models: Experimental and Comparative Study (e62909)
Rakhi Nair, Matthias Hartung, Philipp Heinisch, Janik Jaskolski, Cornelius Starke-Knäusel, Susana Veríssimo, David Schmidt, Philipp Cimiano.
4 2 7 4

Exploring the Potential of Electroencephalography Signal–Based Image Generation Using Diffusion Models: Integrative Framework Combining Mixed Methods and Multimodal Analysis (e72027)
Chi-Sheng Chen, Shao-Hsuan Chang, Che-Wei Liu, Tung-Ming Pan. 4292

XSL•FO
RenderX

Efficient Detection of Stigmatizing Language in Electronic Health Records via In-Context Learning: Comparative Analysis and Validation Study (e68955)
Hongbo Chen, Myrtede Alfred, Eldan Cohen. . . . 4312

Human-Machine Agreement in Medical Ethics: Patient Autonomy Case-Based Evaluation of Large Language Models (e77061)
Vamshi Mugu, Brendan Carr, Ashish Khandelwal, Mike Olson, John Schupbach, John Zietlow, T Vu, Alex Chan, Christopher Collura, John Schmitz. . . . 4343

Medical Feature Extraction From Clinical Examination Notes: Development and Evaluation of a Two-Phase Large Language Model Framework (e78432)
Manal Abumelha, Abdullah AL-Ghamdi, Ayman Fayoumi, Mahmoud Ragab. . . . 4351

A Vision-Language–Guided Multimodal Fusion Network for Glottic Carcinoma Early Diagnosis: Model Development and Validation Study (e74902)
Zhaohui Jin, Yi Shuai, Yun Li, Mianmian Chen, Yumeng Liu, Wenbin Lei, Xiaomao Fan. . . . 4376

Heterogeneous Network With Multiview Path Aggregation: Drug–Target Interaction Prediction Study Design (e74974)
Haixue Zhao, Kui Yao, Yunjiong Liu, Chao Che, Lin Tang. . . . 4387

Evaluating and Improving Syndrome Differentiation Thinking Ability in Large Language Models: Method Development Study (e75103)
Chunliang Chen, Xinyu Wang, Ming Guan, Wenjing Yue, Yuanbin Wu, Ya Zhou, Xiaoling Wang. . . . 4401

Hypertension Medication Recommendation via Synergistic and Selective Modeling of Heterogeneous Medical Entities: Development and Evaluation Study of a New Model (e74170)
Ke Zhang, Zhichang Zhang, Yali Liang, Wei Wang, Xia Wang. . . . 4409

Leveraging Retrieval-Augmented Large Language Models for Dietary Recommendations With Traditional Chinese Medicine's Medicine Food Homology: Algorithm Development and Validation (e75279)
Hangyu Sha, Fan Gong, Bo Liu, Runfeng Liu, Haofen Wang, Tianxing Wu. . . . 4426

Patient Attitudes Toward Ambient Voice Technology: Preimplementation Patient Survey in an Academic Medical Center (e77901)
Gary Leiserowitz, Jeff Mansfield, Scott MacDonald, Melissa Jost. . . . 4445

Viewpoints

Gaps and Pathways to Success in Global Health Informatics Academic Collaborations: Reflecting on Current Practices (e67326)
Elizabeth Campbell, Felix Holl, Oliver Bear Don't Walk IV, Badisa Mosesane, Andrew Kanter, Hamish Fraser, Amanda Joseph, Judy Gichoya, Kabelo Mauco, Sansanee Craig. . . . 360

Resilience in the Face of Disruption: Viewpoint on the CrowdStrike Incident in July 2024 (e69958)
Christopher Dennis, Christopher Evans, Kathleen Duckworth, Misty Skinner, John Hanna, Tanya Thompson, Donette Herring, Richard Medford.
3 6 9

Integration of Data and Information Systems Into the Health Data Strategy (e70066)
Martin Komenda, Jakub Gregor, Daniel Klimeš, Tomáš Pavlík, Milan Blaha, Vladimíra T šitelová, Ond ej Májek, Ond ej Ngo, Renata Chloupková, Karel Hejduk, Lenka Šnajdrová, Ji í Jarkovský, Jan Mužík, Petra R ži ková, Vlastimil Válek, Ladislav Dušek. . . . 378

XSL•FO
RenderX

Digital Health Innovations to Catalyze the Transition to Value-Based Health Care (e57385)
Lan Zhang, Christopher Bullen, Jinsong Chen. 390

Digital Representation of Patients as Medical Digital Twins: Data-Centric Viewpoint (e53542)
Stanislas Demuth, Jérôme De Sèze, Gilles Edan, Tjalf Ziemssen, Françoise Simon, Pierre-Antoine Gourraud. 398

Developing an Intelligent Mobile Clinic—A Medical Vehicle for Improve Access to Healthcare in Remote Areas: Evidence From China (e59103)
Xinlei Chen, Xufang Huang, Yimiao Xu, Jiabin Xu, Yanan Wang, Xinyue Ren, Xuebo Zhu, Xiaoge Xie, Yeqin Yang. 411

Artificial Intelligence (AI) and Emergency Medicine: Balancing Opportunities and Challenges (e70903)
Félix Amiot, Benoit Potier. 421

AI-Driven Integration of Deep Learning With Lung Imaging, Functional Analysis, and Blood Gas Metrics for Perioperative Hypoxemia Prediction (e73995)
Kecheng Huang, Chujun Wu, Rongpeng Pi, Jieyu Fang. 428

Implementation Reports

Development of a New Electronic Death Certificate and Death Management Module Integrated Into the Health Information System of a Tertiary Hospital in Mali: Implementation Report (e62949)
Mahmoud Cissé, Mahamoudane Niang, Abdrahamane Anne, Mariam Sidibé, Dramane Traoré, Abdoulaye Traoré, Idrissa Traoré, Cheick Bagayoko. 473

Lessons Learned From Building a Data Platform for Longitudinal, Analytical Use Cases and Scaling to 77 German Hospitals: Implementation Report (e69853)
Markus Bockhacker, Peter Martens, Clara von Münchow, Sarah Löser, Rosita Günther, Ralf Kuhlen, Olaf Kannt, Sebastian Ortleb. 480

Real-World Evaluation of AI-Driven Diabetic Retinopathy Screening in Public Health Settings: Validation and Implementation Study (e67529)
Mona Duggal, Anshul Chauhan, Vishali Gupta, Ankita Kankaria, Deepmala Budhija, Priyanka Verma, Vaibhav Miglani, Preeti Syal, Gagandeep Kaur, Lakshay Kumar, Naveen Mutyala, Rishabh Bezbaruah, Nayanshi Sood, Ashleigh Kernohan, Geeta Menon, Luke Vale. 492

Enhancing Efficiency and User Experience of Digital Community Health Worker Payments in Zanzibar: Implementation Report (e65325)
Lee Pyne-Mercier, Krishna Jafa, Susan Maigua, Jennifer Muli, Elijah Gichinga, Antony Khaemba, Nitusima Kataraia, Aisha Mohammed, Frank Kamangadazi Tembo, Imran Esmail, Giulia V R Besana, Heiko Hornung, Ali Makame Zubeir. 504

A Bilingual On-Premises AI Agent for Clinical Drafting: Implementation Report of Seamless Electronic Health Records Integration in the Y-KNOT Project (e76848)
Hanjae Kim, So-Yeon Lee, Seng You, Sookyung Huh, Jai-Eun Kim, Sung-Tae Kim, Dong-Ryul Ko, Ji Kim, Jae Lee, Joon Lim, Moo Park, Kang Lee. 515

Creation and Implementation of an Electronic Sexual Assault Record at the Geneva University Hospital (e66764)
Sara Cottler-Casanova, Laurène Rimondi, Monique Lamuela Naulin, Tony Fracasso, Jasmine Abdulcadir. 539

Implementation of WHO SMART Guidelines-Digital Adaptation Kits in Pathfinder Countries in Africa: Processes and Early Lessons Learned (e58858)
Rosemary Muliokela, Kuwani Banda, Abdulaziz Hussen, Sarai Malumo, Andrew Kashoka, Angel Mwiche, Innocent Chiboma, Maria Barreix, Muyereka Nyirenda, Zvanaka Sithole, Natschja Ratanaprayul, Berhanu Endehabtu, Hanna Telake, Adane Weldeab, William Probert, zge Tunçalp, Ernest Maya, Mulatu Woldetsadik, Binyam Tilahun, Chris Guure, Kafui Senya, Lale Say, Tigest Tamrat. 550

XSL•FO
RenderX

Dolodoc, an App to Leverage Self-Management of Chronic Pain: Design, Development, and Implementation Report (e71597)
Frederic Ehrler, Julie Guebey, Jessica Rochat, Laetitia Gosetto, Benno Rehberg, Christian Lovis, Aude Molinard-Chenu. 560

Leveraging Interoperable Electronic Health Record (EHR) Data for Distributed Analyses in Clinical Research: Technical Implementation Report of the HELP Study (e68171)
Julia Palm, Kutaiba Saleh, André Scherag, Danny Ammon. 568

Patient-Centered Outpatient Process Optimization System Based on Intelligent Guidance in a Large Tertiary Hospital in China: Implementation Report (e60219)
Xiaoyi Wang, Rujia Zhang, Zhihong Gao, Mengxuan Xia, Songjia Zhang, Lizheng Ge, Yuyang Zhu, Haojie Jin, Shenglian Pan, Manman Zheng, Chun Chen, Xiangyang Zhang. 590

Short Paper

Virtual Transition of Care Clinics and Associated Readmission Rates: 3-Year Retrospective Cohort Study (e73495)
Sarah Horman, Milla Kviatkovsky, Edward Castillo, Patricia Maysent, Chad VanDenBerg, John Bell, Christopher Longhurst. 2312

Letters to the Editor

Authors' Reply: Involving Health, Technology, and Financial Stakeholders in Co-Designing Digital Pathways for Value-Based Care (e86837)
Jinsong Chen, Christopher Bullen, Lan Zhang. 3557

Involving Health, Technology, and Financial Stakeholders in Co-Designing Digital Pathways for Value-Based Care (e84885)
Pieter Vandekerckhove, Benjamin Harris, Louis Koizia, Steven Howard. 3559

Code Error in "Diagnostic Classification and Prognostic Prediction Using Common Genetic Variants in Autism Spectrum Disorder: Genotype-Based Deep Learning" (e66556)
Catriona Miller, Theo Portlock, Denis Nyaga, Greg Gamble, Justin O'Sullivan. 3561

The Anemia Risk Warning Model Based on a Noninvasive Method: Key Insights and Clarifications (e73297)
Jiaqi Wei, Nana Zheng, Depei Wu. 3563

Authors' Reply: The Anemia Risk Warning Model Based on a Noninvasive Method: Key Insights and Clarifications (e74333)
Yahan Zhang, Yi Chun, Liping Tu, Jiatuo Xu. 3565

Data Contamination in AI Evaluation (e80987)
Alaeddin Acar. 3567

Author's Reply: "Data Contamination in AI Evaluation" (e82057)
ChulHyoung Park, Min An, Gyubeom Hwang, Rae Park, Juho An. 3569

XSL•FO
RenderX

Corrigenda and Addendas

Correction: Patients' Experienced Usability and Satisfaction With Digital Health Solutions in a Home Setting: Instrument Validation Study (e73416)
Susan Oudbier, Ellen Smets, Pythia Nieuwkerk, David Neal, S Nurmohamed, Hans Meij, Linda Dusseljee-Peute. . . . 3571

Correction: Distributed Statistical Analyses: A Scoping Review and Examples of Operational Frameworks Adapted to Health Analytics (e71249)
Félix Camirand Lemyre, Simon Lévesque, Marie-Pier Domingue, Klaus Herrmann, Jean-François Ethier. . . . 3573

Correction: Relationship Between Stroke Knowledge, Health Information Literacy, and Health Self-Management Among Patients With Stroke: Multicenter Cross-Sectional Study (e80547)
Mengxue Zeng, Yanhua Liu, Ying He, Wenxia Huang. . . . 3575

Correction: Toward a Domain-Overarching Metadata Schema for Making Health Research Studies FAIR (Findable, Accessible, Interoperable, and Reusable): Development of the NFDI4Health Metadata Schema (e78151)
Haitham Abaza, Aliaksandra Shutsko, Sophie Klopfenstein, Carina Vorisek, Carsten Schmidt, Claudia Brünings-Kuppe, Vera Clemens, Johannes Darms, Sabine Hanß, Timm Intemann, Franziska Jannasch, Elisa Kasbohm, Birte Lindstädt, Matthias Löbe, Katharina Nimptsch, Ute Nöthlings, Marisabel Ocanto, Tracy Osei, Ines Perrar, Manuela Peters, Tobias Pischon, Ulrich Sax, Matthias Schulze, Florian Schwarz, Carolina Schwedhelm, Sylvia Thun, Dagmar Waltemath, Atinkut Zeleke, Wolfgang Müller, Martin Golebiewski. . . . 3577

Correction: The Roles of Electronic Health Records for Clinical Trials in Low- and Middle-Income Countries: Scoping Review (e84394)
JMIR Publications Editorial Office. . . . 3579

Editorial

AI Scribes in Health Care: Balancing Transformative Potential With Responsible Integration (e80898)
Tiffany Leung, Andrew Coristine, Arriel Benis. . . . 3649

Research Letters

The Advanced Reasoning Capabilities of Large Language Models for Detecting Contraindicated Options in Medical Exams (e68527)
Yuichiro Yano, Mizuki Ohashi, Taiju Miyagami, Hirotake Mori, Yuji Nishizaki, Hiroyuki Daida, Toshio Naito. . . . 3939

GPT-3.5 Turbo and GPT-4 Turbo in Title and Abstract Screening for Systematic Reviews (e64682)
Takehiko Oami, Yohei Okada, Taka-aki Nakada. . . . 3948

Commentary

From Context to Care: Rethinking Stigma Detection in Clinical Language Models (e82484)
Shefali Haldar, Oliver Bear Don't Walk IV, Sadia Akter. . . . 4372

XSL•FO
RenderX

Expression of Concern

Expression of Concern: A Dynamic Adaptive Ensemble Learning Framework for Noninvasive Mild Cognitive Impairment Detection: Development and Validation Study (e75352) 4442

Retractions

Retraction: "Diagnostic Classification and Prognostic Prediction Using Common Genetic Variants in Autism Spectrum Disorder: Genotype-Based Deep Learning" (e76833)
JMIR Editorial Office. 4443

Retraction: "A Dynamic Adaptive Ensemble Learning Framework for Noninvasive Mild Cognitive Impairment Detection: Development and Validation Study" (e77635)
JMIR Editorial Office. 4444

XSL•FO
RenderX

Trends and Trajectories in the Rise of Large Language Models in Radiology: Scoping Review

Adhari Al Zaabi[1]; Rashid Alshibli[2]; Abdullah AlAmri[2]; Ibrahim AlRuheili[2]; Syaheerah Lebai Lutfi[3]

[1]Human and Clinical Anatomy Department, College of Medicine and Health Sciences, Sultan Qaboos University, P.O. Box 35, Al Khodh, Muscat, Oman

[2]College of Medicine and Health Sciences, Sultan Qaboos University, Muscat, Oman

[3]Medical Education and Informatics Department, College of Medicine and Health Sciences, Sultan Qaboos University, Muscat, Oman

Corresponding Author:
Adhari Al Zaabi
Human and Clinical Anatomy Department, College of Medicine and Health Sciences, Sultan Qaboos University, P.O. Box 35, Al Khodh, Muscat, Oman

Abstract

Background: The use of large language models (LLMs) in radiology is expanding rapidly, offering new possibilities in report generation, decision support, and workflow optimization. However, a comprehensive evaluation of their applications, performance, and limitations across the radiology domain remains limited.

Objective: This review aimed to map current applications of LLMs in radiology, evaluate their performance across key tasks, and identify prevailing limitations and directions for future research.

Methods: A scoping review was conducted in accordance with the framework by Arksey and O'Malley framework and the PRISMA-ScR (Preferred Reporting Items for Systematic Reviews and Meta-Analyses extension for Scoping Reviews) guidelines. Three databases—PubMed, ScopusCOPUS, and IEEE Xplore—were searched for peer-reviewed studies published between January 2022 and December 2024. Eligible studies included empirical evaluations of LLMs applied to radiological data or workflows. Commentaries, reviews, and technical model proposals without evaluation were excluded. Two reviewers independently screened studies and extracted data on study characteristics, LLM type, radiological use case, data modality, and evaluation metrics. A thematic synthesis was used to identify key domains of application. No formal risk-of-bias assessment was performed, but a narrative appraisal of dataset representativeness and study quality was included.

Results: A total of 67 studies were included. (n/N, %)GPT-4 was the most frequently used model (n=28, 42%), with text-based corpora as the primary type of data used (n=43, 64%). Identified use cases fell into three thematic domains: (1) decision support (n=39, 58%), (2) report generation and summarization (n=16, 24%), and (3) workflow optimization (n=12, 18%). While LLMs demonstrated strong performance in structured-text tasks (eg, report simplification with >94% accuracy), diagnostic performance varied widely (16%-86%) and was limited by dataset bias, lack of fine tuning, and minimal clinical validation. Most studies (n=53, 79.1%) had single-center, proof-of-concept designs with limited generalizability.

Conclusions: LLMs show strong potential for augmenting radiological workflows, particularly for structured reporting, summarization, and educational tasks. However, their diagnostic performance remains inconsistent, and current implementations lack robust external validation. Future work should prioritize prospective, multicenter validation of domain-adapted and multimodal models to support safe clinical integration.

(JMIR Med Inform 2025;13:e78041) doi:10.2196/78041

KEYWORDS

large language models; GPT-4; scoping review; natural language processing; report generation; clinical decision support; workflow optimization; artificial intelligence; AI; radiology

Introduction

The integration of artificial intelligence (AI) into health care has accelerated over the past decade, with large language models (LLMs) emerging as transformative tools for natural language processing in clinical contexts. Built on transformer architectures, models such as GPT-4, bidirectional encoder representations from transformers (BERT), and Text-to-Text Transfer Transformer (T5) have demonstrated high performance in text-based tasks such as summarization, classification, and information extraction across general and clinical domains [1].

Radiology is inherently data intensive and text rich, making it an ideal domain for the application of LLMs. These models can support a wide range of tasks, including automated report

XSL•FO
RenderX

generation, structured documentation, code assignment, and even preliminary diagnostic reasoning from clinical narratives [2-5] Despite the growing number of pilot studies, there is no unified synthesis evaluating the practical effectiveness, integration readiness, and safety implications of LLMs in real-world radiology settings.

Several prior scoping reviews have investigated the use of LLMs in radiology, but these have typically focused on specific application domains. For example, Reichenpfader et al [6] performed conducted a scoping review focused exclusively on information extraction from radiology reports. Their analysis highlighted that most approaches relied on encoder-based transformer models such as BERT, that datasets were often small and single center, and that performance varied substantially by annotation quality and task definition. They concluded that, while information extraction is promising, generalizability and external validation are lacking [6,7]. Busch et al [8] conducted a narrative overview of approximately 10 studies specifically addressing structured reporting in radiology. They emphasized the potential of GPT-3.5 and GPT-4 to transform free text into structured templates and discussed opportunities for multilingual structured reporting adoption. Their analysis was conceptual, with limited systematic synthesis across tasks. Nakaura et al [9] traced the evolution of deep learning and transformer architectures in radiology; explained key limitations such as hallucinations, bias, and lack of explainability; and emphasized the risks of premature deployment in clinical decision support. Their review highlighted proof-of-concept applications, including report generation, translation of radiology reports into plain language, exam preparation, and early feasibility of protocol selection and research support [9].

Unlike these prior reviews that were narrowly focused on single use cases (information extraction or patient-facing report simplification), our study systematically mapped the full spectrum of LLM applications across radiology—including decision support, report generation, workflow optimization, and education. Furthermore, our work integrated both generative and nongenerative transformer models, multimodal applications, and educational and operational use cases. This broader lens allowed us to identify converging themes; quantify distribution across modalities; and highlight gaps in validation, equity, and clinical integration. Accordingly, this review aimed to systematically map the applications of LLMs in radiology; evaluate their reported outcomes; and provide a thematic synthesis of emerging use cases, methodological trends, and future research priorities.

Methods

Study Design

This scoping review was conducted in accordance with the methodological framework proposed by Arksey and O'Malley [10] and adhered to the PRISMA-ScR (Preferred Reporting Items for Systematic Reviews and Meta-Analyses extension for Scoping Reviews) checklist (Checklist 1) to ensure methodological transparency and reproducibility.

Eligibility Criteria (PICOS-Based)

Eligibility criteria were defined using the population, intervention, comparator, outcomes, and study designPICOS framework (Table 1). We included peer-reviewed empirical studies evaluating LLM applications in radiology workflows using models such as GPT-3 and GPT-4, BERT, or domain-specific transformers. Reviews, opinion pieces, and conference abstracts were excluded. Only English-language studies published between January 2022 and December 2024 were included due to resource limitations, which we acknowledge may restrict the generalizability of the findings.

Table . Eligibility criteria for study selection structured using the PICOS framework (population, intervention, comparator, outcomes, study design) with additional filtering criteria related to language and publication date.

PICOS domain or criterion	Inclusion criteria	Exclusion criteria
Population	Studies involving radiology professionals, radiological workflows, or radiology-related data	Studies unrelated to radiology or without reference to radiological applications
Intervention	Use or evaluation of LLMs[a], including GPT-3 and GPT-4, BERT[b], or custom transformer models	Studies using general AI[c] models without a language modeling component
Comparator	—[d]	—
Outcomes	Reported outcomes related to LLM performance, feasibility, integration, or limitations in radiology	Studies lacking outcome data or reporting only theoretical frameworks without application
Study design	Peer-reviewed empirical studies (qualitative, quantitative, or mixed methods)	Reviews, editorials, opinion pieces, letters, and conference abstracts
Language	English	Non-English
Publication date	Published between January 2022 and December 2024	Published before 2022 or after December 2024

[a]LLM: large language model.

[b]BERT: bidirectional encoder representations from transformers.

[c]AI: artificial intelligence.

[d]Not applicable (scoping review design).

XSL•FO
RenderX

Information Sources and Search Strategy

The databases were selected to ensure coverage across clinical (PubMed), multidisciplinary (Scopus), and technical and engineering (IEEE Xplore) domains. The search combined MeSH (Medical Subject Headings) and free-text terms related to LLMs ("large language model," "GPT," "BERT," and "transformer-based AI") and radiology ("radiology," "medical imaging," and "diagnostic imaging").

Database-specific search strings tailored to syntax and operators are provided in Multimedia Appendix 1. Gray literature (eg, arXiv and medRxiv) and conference proceedings were excluded, which may have limited capture of emerging non–peer-reviewed work. Furthermore, the use of MeSH terms in PubMed was optimized but may not have fully captured all relevant variations due to evolving terminology in this rapidly developing field. These limitations may have affected the comprehensiveness of the search and should be considered when interpreting the findings.

Study Selection

All retrieved records were imported into Rayyan [11] (Qatar Computing Research Institute), a web-based tool designed to facilitate systematic and scoping review workflows. Rayyan facilitated duplicate removal and blinded screening. Two reviewers (AA and IR) independently screened titles and abstracts and assessed full texts against the eligibility criteria. Disagreements were resolved through consensus or, if needed, by a third reviewer (RS). To ensure calibration, an initial pilot screening was conducted, and a random 20% sample of the included studies was cross-checked. The study selection process is presented in the PRISMA (Preferred Reporting Items for Systematic Reviews and Meta-Analyses) 2020 flow diagram.

Data Extraction Strategy

A structured data extraction form was developed and piloted on a sample of 5 studies. The following data were collected:

- Publication details (year, country, and journal)
- LLM type (eg, GPT-3.5, GPT-4, BERT, or domain-specific models)
- Radiology use case (eg, classification, report generation, decision support)
- Data modalities (text, images, multimodal, or radiology information systems [RISs])
- Evaluation metrics (eg, accuracy, bilingual evaluation understudy [BLEU], recall-oriented understudy for gisting evaluation [ROUGE], Matthews correlation coefficient, area under the curve, and F_1-score)
- Dataset characteristics (size, source, and multicenter vs single center)
- Reported outcomes and limitations

Data extraction was conducted independently by 2 reviewers. A random 20% subset was cross-checked for accuracy, with discrepancies resolved through consensus.

Secondary Data Extraction and Thematic Classification

Data Extraction and Coding

A hybrid thematic analysis was conducted. Initially, themes were extracted manually by 3 independent raters who analyzed and categorized the data. An interrater reliability measure (percentage of agreement) was applied to ensure consistency across raters. Subsequently, GPT-4 was used to assist with clustering recurring patterns using a zero-shot prompt. The prompt applied was as follows: "Act as a pseudo analyst, read this file (Excel file with the raw data), and label abstracts with relevant codes. Provide a summary of recurring themes."

The outputs generated by GPT-4 were then compared and triangulated with the manually derived results by an additional expert reviewer, who was provided with (1) the original raw Microsoft Excel file and (2) GPT-4's preliminary coding and theme map. Discrepancies between manual and AI-assisted outputs were discussed in a consensus meeting, and revisions were made to finalize the thematic framework.

It should be noted that GPT-4 was not used during the initial manual theme extraction, which was conducted independently by the 3 student raters. The use of GPT-4 in the subsequent phase was intended to support rather than replace human analytical judgment and ensure that AI-generated outputs were critically appraised before integration.

Theme Development

Through inductive synthesis, the extracted codes were grouped into broader categories that reflected the primary ways in which LLMs are currently being explored in radiology. After multiple rounds of refinement, three overarching themes were established: (1) decision support, including diagnostic support, case prioritization, and aiding clinical judgments; (2) report generation, encompassing drafting, summarization, and improving clarity or standardization of radiology reports; and (3) workflow optimization, referring to efficiency gains such as automating routine tasks, assisting communication, and integrating radiology processes into clinical workflows.

This thematic classification was not predetermined but derived from recurring patterns across the reviewed material. GPT-4 was used as a supporting tool to enhance coding efficiency and cross-check clustering of concepts, whereas the final themes were reviewed, validated, and confirmed manually by the research team.

By systematically identifying and categorizing these themes, the analysis provided a structured synthesis of the literature while ensuring methodological transparency and reproducibility.

Narrative Quality Assessment

Although a formal risk-of-bias assessment was not performed in accordance with scoping review methodology, a narrative appraisal revealed several recurring limitations in the included studies. Many were small-scale, single-institution implementations or proof-of-concept projects, with limited external validation. Most lacked robust methodological

XSL•FO
RenderX

descriptions or standardized evaluation metrics, making cross-study comparisons challenging.

In terms of dataset size and representativeness, several studies relied on relatively small or synthetic datasets, often drawn from publicly available repositories rather than real-world clinical systems. This raises concerns about generalizability. Geographically, a substantial proportion of the studies originated from North America, Europe, and China, indicating potential regional bias in the development and evaluation of LLMs for radiology. There was limited representation from low- and middle-income countries, which may affect the global applicability of the findings.

Critical Reflection on Methodology

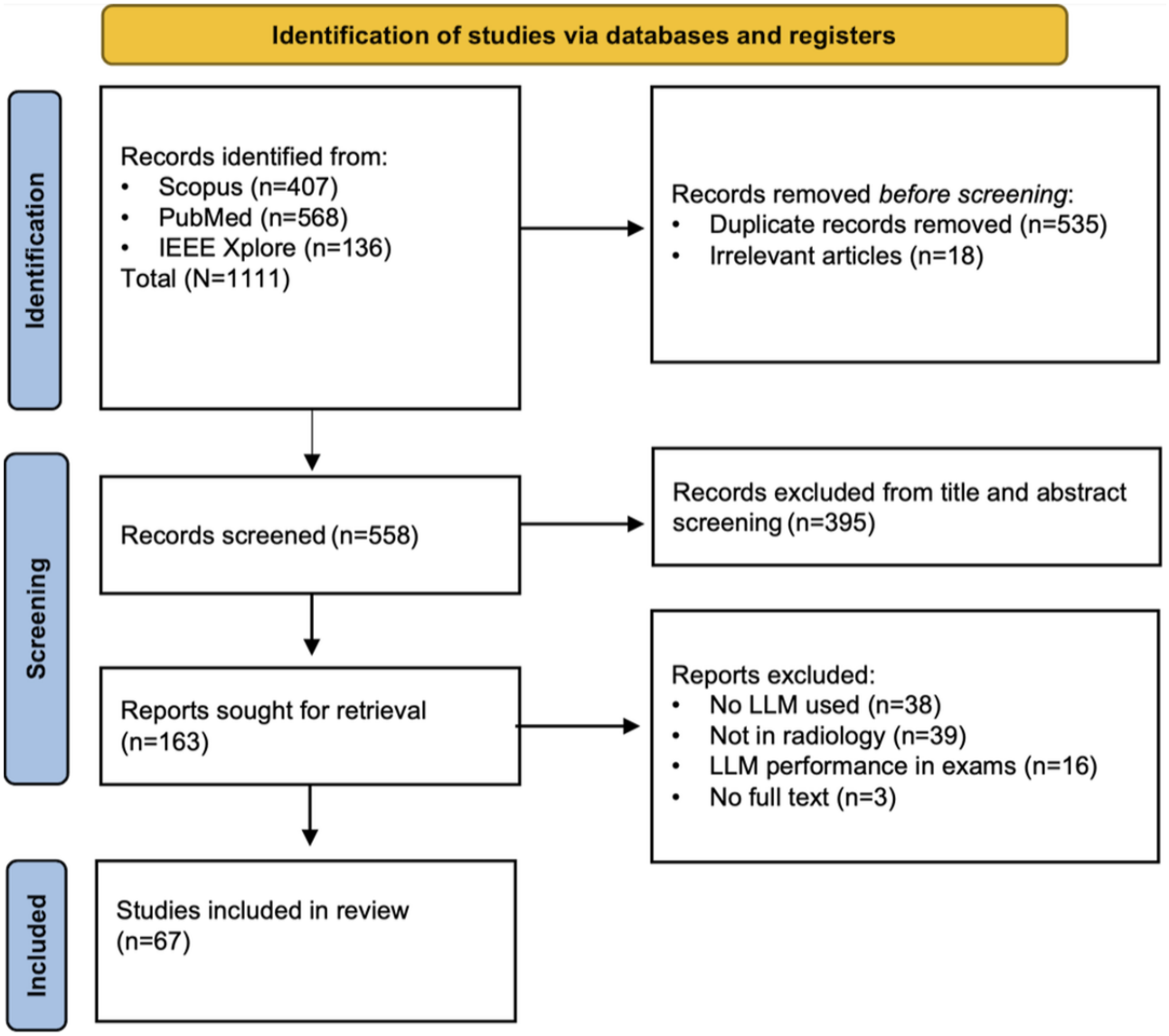
This review used a rigorous and transparent methodology; however, certain limitations must be acknowledged. Restriction to English-language studies and the exclusion of gray literature may have limited comprehensiveness. The fast pace of LLM development also means that new studies may have emerged since the search was conducted. Finally, thematic synthesis, while appropriate for mapping breadth, is interpretive and may introduce subjectivity despite the use of calibration and consensus procedures.

Results

Overview of the Included Studies

A total of 1111 records were retrieved from Scopus (n=407, 36.6%), PubMed (n=568, 51.1%), and IEEE Xplore (n=136, 12.2%). Of these 1111 records, after removing 535 (48.2%) duplicates and 18 (1.6%) irrelevant records, 558 (50.2%) studies remained. Following title and abstract screening, 163 full-text articles were reviewed, and 67 (41.1%) met the inclusion criteria (Figure 1). A summary of all included articles is presented in Multimedia Appendix 2.

Figure 1. PRISMA (Preferred Reporting Items for Systematic Reviews and Meta-Analyses) 2020 flow diagram detailing the study selection process for the included records across databases. LLM: large language model.

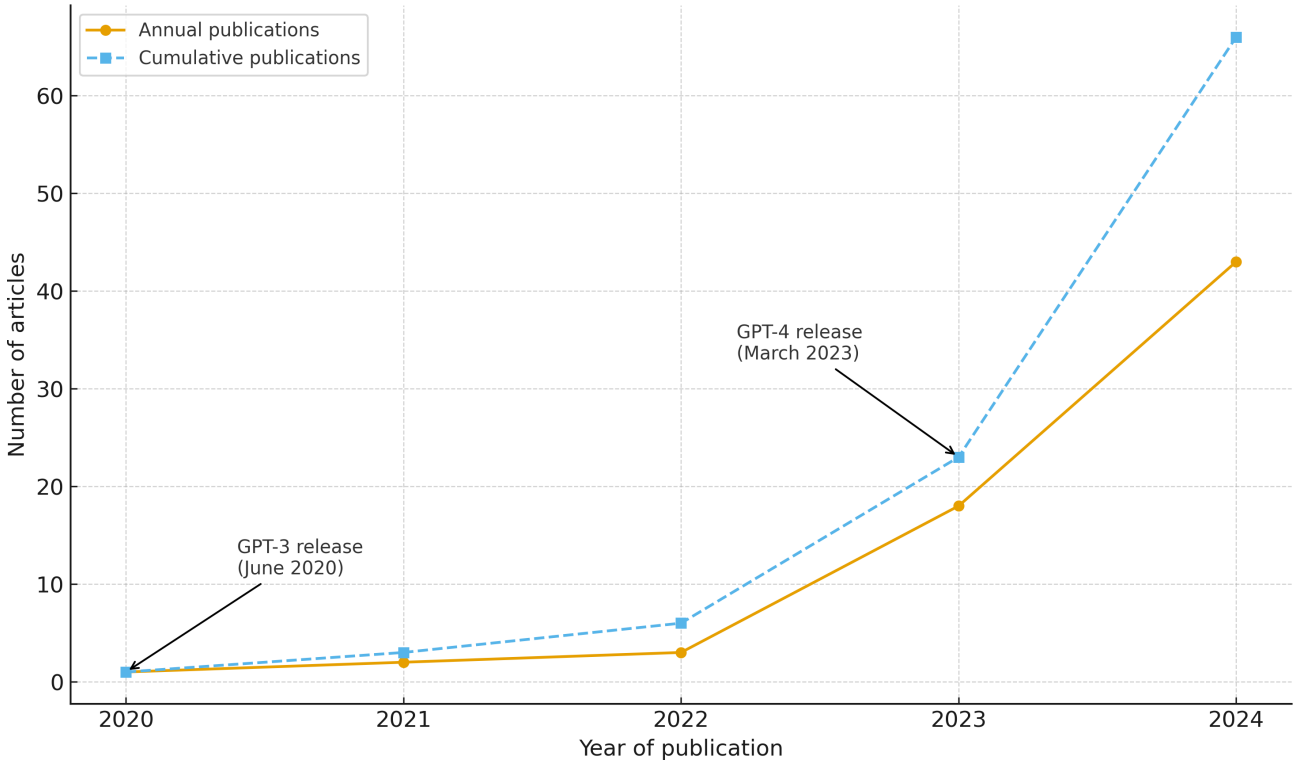


Most studies (44/67, 65.7%) were published in 2024, reflecting a sharp rise in interest following the release of GPT-4 in March 2023 (Figure 2). Geographically, the United States contributed the most studies (24/67, 35.8%), followed by Japan (10/67,

XSL•FO
RenderX

14.9%) and Germany (10/67, 15%). Very few studies originated from low- and middle-income countries, and a few studies assessed non–English-language corpora (Multimedia Appendix 2).

Figure 2. Annual and cumulative number of publications applying large language models in radiology (2020 - 2024). Data derived from the included studies (N=67). Milestones for the release of GPT-3 (June 2020) and GPT-4 (March 2023) are annotated.



Types of LLMs and Implementation Approaches

GPT-4 was the most frequently studied model (28/67, 42%), followed by GPT-3.5 (14/67, 21%). A smaller proportion (n/N, %)used BERT-based models such as CheXbert and BioBERT or domain-specific variants, including Radiology-Llama2 and RadSpaT5. Multimodal models capable of integrating text and images were reported in 17.9% (12/67) of the studies, although few underwent clinical validation.

Regarding input data, 64% (43/67) of the studies used text-based corpora such as radiology reports, request forms, or quizzes; 15% (10/67) analyzed images; 18% (12/67) used multimodal datasets; and 3% (2/67) used either RIS data or exam question datasets (Multimedia Appendix 3). Of the 67 studies, 56 (84%) used English-language corpora (English language only: n=50, 89%; mixed English+another language: n=6, 11%), and 11 (16%) used only corpora in non-English languages (German: n=4, 36%; Japanese: n=4, 36%; Italian: n=2, 18%; French: n=1, 9%). Most studies (53/67, 79%) were single center, whereas 21% (14/67) were multicenter.

Imaging Modalities and Radiological Subspecialties

Imaging modality use varied across the studies (Figures 3 and 4). Multimedia Appendix 4 shows the distribution of the 67 studies across various radiology subspecialties. The most represented field was thoracic imaging with 24% (16/67) of the studies, followed by general radiology (13/67, 19%) and oncologic imaging (11/67, 16%).

XSL•FO
RenderX

Figure 3. Imaging modalities used, stratified by data type (N=67). Most studies relied on text-only data (yellow), with fewer using image-only (blue) or multimodal text+image datasets (green) datasets. CT: computed tomography; MRI: magnetic resonance imaging; PET: positron emission tomography.

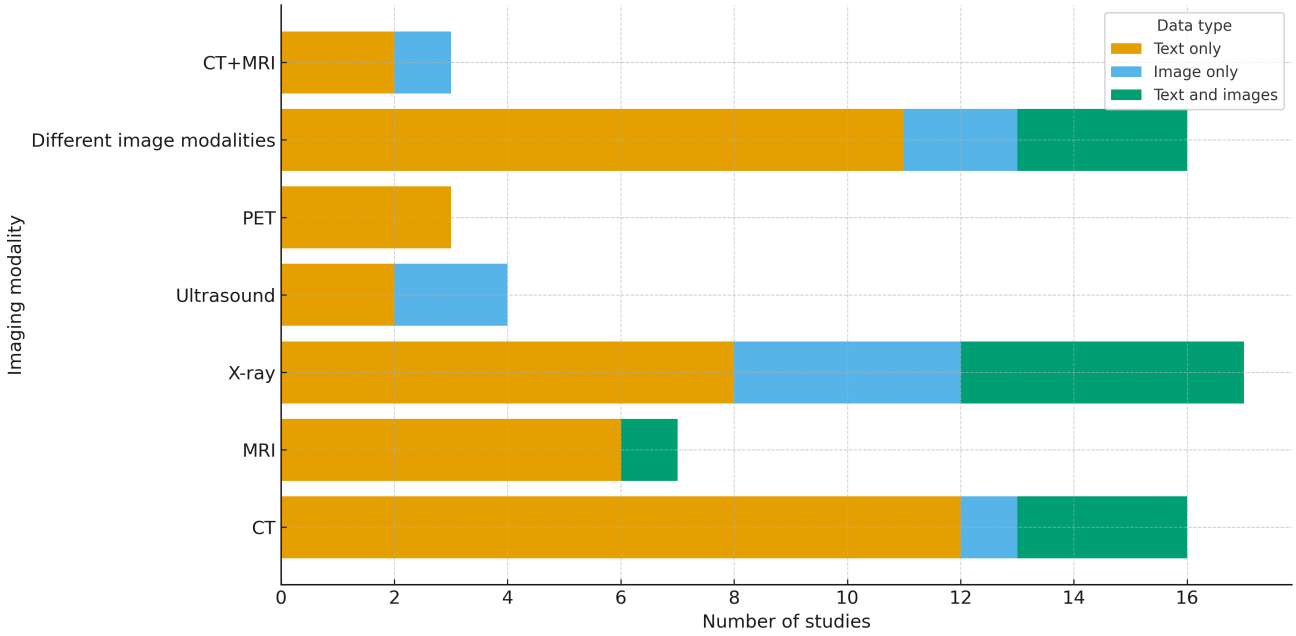
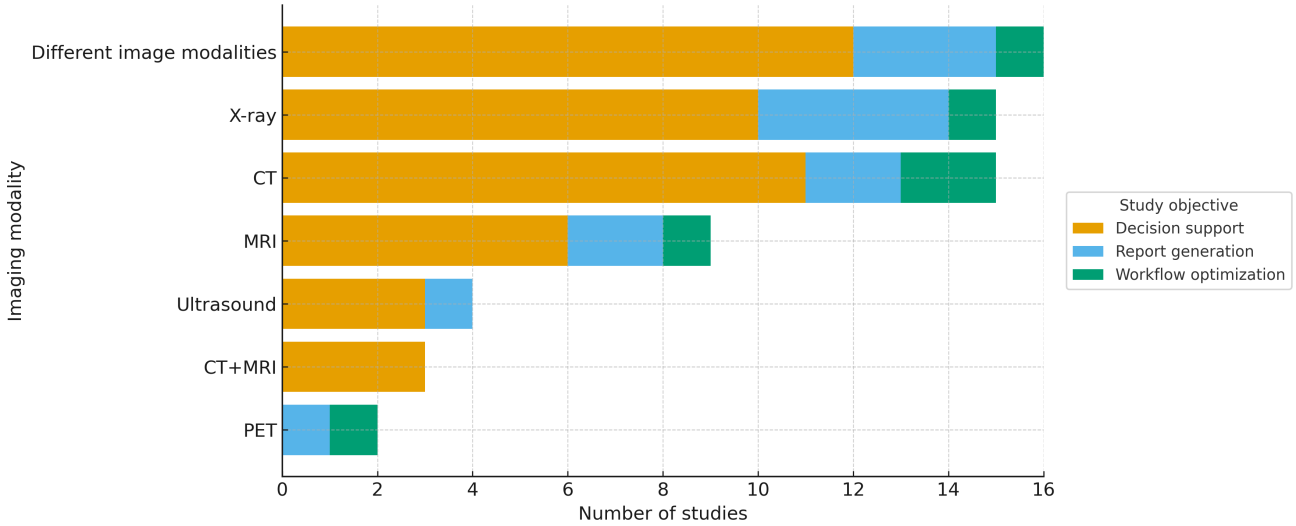


Figure 4. Imaging modality by study objective (N=67). Decision support (yellow) predominated, followed by report generation (blue) and workflow optimization (green). Positron emission tomography (PET) and ultrasound were the least represented. CT: computed tomography; MRI: magnetic resonance imaging.



Thematic Domains of Application

Overview

Table 2 shows the 3 thematic domains that emerged (detailed thematic domains and models are presented in Multimedia Appendix 5).

XSL•FO
RenderX

Table . Thematic classification of large language model applications in radiology across the 67 included studies (2022 - 2024).

Theme and subtheme	Articles
Decision support	
Classification	• Blankemeier et al [12] • Chambon et al [13] • Fervers et al [14] • Haver et al [15] • Olivato et al [16] • Putelli et al [17] • Santos et al [18] • Sehanobish et al [19] • Suzuki et al [20] • Wu et al [21] • Zhang et al [22]
Diagnosis from clinical cases	• Danu et al [23] • Horiuchi et al [24] • Horiuchi et al [25] • Kurokawa et al [26] • Wada et al [27]
Diagnosis from images	• Elek et al [28] • Khare et al [29] • Pachade et al [30] • Busch et al [31] • Silva et al [32] • Wu et al [33] • Kottlors et al [34] • Overgaard Olesen et al [35] • Lee et al [36] • Reith et al [37] • Horiuchi et al [38]
Extracting information from reports	• Mukherjee et al [39] • Bressem et al [4] • Tan et al [40] • Tay et al [41] • Russe et al [42] • Le Guellec et al [43] • Lybarger et al [44] • Dada et al [45] • Sun et al [46] • Bhayana et al [47]
Summarization	• Wu and Bibault [48]
Report generation	
Generating the report	• Danu et al [49] • Hasani et al [50] • Ji et al [51] • López-Úbeda et al [52] • Mallio et al [53] • Moezzi et al [54] • Nakaura et al [55] • Selivanov et al [56] • Shentu and Al Moubayed [57] • Soleimani et al [58] • Woźnicki et al [59] • Wu et al [60] • Bhayana et al [61] • Tie et al [62]
Summarization	• Karn et al [63]
Quality of complex reports	• Zhu et al [64]

XSL•FO
RenderX

Theme and subtheme	Articles
Decision support	
Workflow optimization	
Selecting appropriate modality from radiology order	• Gertz et al [65]
Image quality	• Chen et al [66]
Exam questions	• Mistry et al [67]
Summarization	• Nishio et al [68]
Classification	• Yasaka et al [69] • Huemann et al [70] • Kanzawa et al [71]
User interface improvement	• Zhang et al [72]
Identification of reports containing recommendations	• Abbasi et al [73]
Detection of errors	• Kathait et al [74]
Simplification of reports for patients	• Sarangi et al [75]
Answering patient questions	• Rogasch et al [76]

Theme 1: AI-Assisted Clinical Decision Support

Four subthemes emerged from this theme.

Classification Tasks

Across radiology classification tasks, domain-tuned transformers remained the most reliable, whereas general LLMs were mixed. BERT-style models standardized the Thyroid Imaging Reporting and Data System and matched or exceeded radiologists for chest x-ray report extraction [18,22], with added interpretability and effectiveness in Italian reports [17]. GPT-3.5 and GPT-4 underperformed or were inconsistent for the Liver Imaging Reporting and Data System and tumor node metastasis staging [14,20], although structured Reporting and Data System categorization showed promise [21]. The multimodal GPT-4V struggled to describe Breast Imaging Reporting and Data System features [15], whereas specialized models such as RadBERT and a 3D vision language model (Merlin) achieved strong document-level COVID-19 classification and surpassed other models. Overall, BERT-family and domain-adapted approaches are currently more dependable than generic LLMs for clinical deployment.

Diagnosis From Clinical Cases

Across clinical case diagnosis, general LLMs remained inconsistent and typically trailed expert radiologists. GPT-4 reached approximately 50% overall accuracy on neuroradiology cases of the week, performing far worse on central nervous system tumors (16%) than on non–central nervous system tumors (62%) [23]. In musculoskeletal cases, text-only GPT-4 was roughly at the resident level but below board-certified radiologists, whereas GPT-4V lagged further [23]. On challenging cases from the Freiburg Neuropathology Case Conference, both GPT-4 and GPT-4V underperformed compared to radiologists [24]. Among Anthropic models, Claude 3.5 Sonnet outperformed Claude 3 Opus, with accuracy improving when both clinical history and imaging were provided, yet differential diagnosis listing remained limited [26]. Targeted prompt engineering and confidence thresholds measurably boosted GPT-4 Turbo's diagnostic accuracy, highlighting the value of workflow tuning [27]

Diagnosis From Images

General LLMs were promising but not yet dependable. GPT-4 (via Bing) was able to recognize basic computed tomography (CT) and magnetic resonance imaging (MRI) features but lacked diagnostic reliability [28]. Multimodal and domain-tuned models fared better: mmBERT set a new visual question answering state of the art with interpretable attention maps [29], and self-supervised Contrastive Language-Image Pretraining improved large-vessel occlusion detection over supervised baselines [30]. GPT-4V showed potential across subspecialties but should complement clinicians, not replace them [31], and GPT-3.5 showed variable accuracy and should be considered as supplementary—not stand-alone—for dental panoramic radiographs [32]. Pairing LLMs with image-to-text modules boosted diagnostic performance in thyroid ultrasound [33]. For differential diagnosis, GPT-4 reached 68.8% concordance with experts (93.8% of outputs were acceptable), with best results in neuroradiology and chest x-rays, yet task performance varied [34] and remained limited for specific findings such as pulmonary congestion [35]. Broadly, LLMs were able to propose differentials but were not reliable for independent use [38]; specialized vision models such as KARA-CXR currently outperform ChatGPT in chest x-ray interpretation [36]. GPT-4, even with single-shot prompts, identified incidental findings with high precision and recall from CT scans. In contrast,

XSL•FO
RenderX

multimodal LLMs remain inadequate for pediatric image interpretation [37].

Extracting Information From Reports

Domain-tuned transformers consistently excelled. BERT variants, especially RadBERT, surpassed other text report classifiers with less annotation in extracting findings from intensive care chest radiograph reports [4], and SpERT achieved high anatomy-linked extraction [44]. Large clinical models also performed strongly: GatorTron reached high accuracy for cancer disease response [40], and an information extraction pipeline inferred metastatic sites accurately and explainably [41]. The open-source Vicuna showed excellent accuracy on emergency brain MRI reports without additional training [43].

Theme 2: LLMs for Report Generation and Quality

In total, 22.4% (15/67) of the studies examined LLMs for generating, structuring, or evaluating radiology reports, falling into 2 streams.

Text to Text

These systems converted free text into structured outputs or summaries: T5 and SciFive performed relation extraction to produce clinician-interpretable structured reports [54], fine-tuned T5 yielded near-expert MRI conclusions in Spanish [52], and Llama 2-70B locally structured reports with approximate human accuracy but variable semantics across languages and findings [59]. GPT-4 improved standardization and generated reports with higher clarity and conciseness than those of human reports but lower diagnostic precision [50,55,58]. It produced the most reliable report templates versus Perplexity, GPT-3.5, and Bing [53]. PEGASUS generated clinically acceptable personalized positron emission tomography (PET) impressions [62].

Image to Text

These pipelines enhanced captioning and paired reports. CXR-IRGen outperformed baselines for chest x-ray image-report pairs [54,57], and a Bloomz-7B1 2-step model (image→abnormality→report) was promising and has potential to reduce workload [49]. GPT-4 consistently emerged as the most robust model across multiple benchmarks [55,58], offering both high readability and coherence, although challenges in diagnostic precision and handling rare findings remain. All 4 studies in this theme showed that LLMs matched or exceeded baseline performance metrics such as BLEU, ROUGE, and Consensus-Based Image Description Evaluation for radiology report generation [49,51,56,57]. Integration of domain-adaptive training or prompt tuning improved model performance, underscoring the importance of radiology-specific fine-tuning.

Theme 3: Clinical Workflow Optimization

total of 17.9% (12/67) of the studies evaluated how LLMs can optimize various nondiagnostic tasks in clinical workflows. This theme included 6 subthemes.

Summarization and Simplification

LLMs supported patient - facing and clinician - to - clinician communication. GPT-3.5 reliably simplified radiology reports into plain language while preserving salient clinical details [75]. Text-to-text transformers (eg, RadSpaT5 and T5) achieved expert-level abstractive summaries, producing accurate report conclusions in most cases [68].

Classification of Reports

Fine-tuned BERT models accurately categorized brain MRI reports into treatment-related groups and identified lung cancer pretreatment cases with performance comparable to that of human experts [69,71]. Domain-adapted variants (BioClinicalBERT and RadBERT) further improved PET and CT report classification, highlighting the value of specialty-specific pretraining [70].

Error Detection and Recommendation Extraction

LLMs showed high precision in identifying diagnostic inaccuracies and extracting actionable recommendations. The Augmented Transformer Assisted Radiology Intelligence model, which integrates both vision and language processing, significantly outperformed traditional natural language processing approaches in detecting laterality errors within reports [74]. A BERT-based model identified reports containing recommendations for additional imaging with high precision and recall, enabling automated recommendation extraction [73].

Radiology Protocol Selection and Answering Patient Queries

GPT-4 accurately selected imaging modalities and protocols from referral forms, indicating potential to streamline protocoling tasks [65]. It also answered common patient questions regarding PET and CT preparation and reporting as a supplementary education tool [76].

User Interface Enhancement

User interface enhancement was explored through models such as ChatUI-RIS, which improved the usability of RISs by offering a more intuitive interface and enhanced learning experiences, particularly for trainees and junior radiologists [72].

Image Quality Assessment and Educational Use

Multimodal LLMs with visual understanding (eg, IQAGPT) provided effective CT image quality assessment [66]. For education, GPT-4 generated high-quality board-style multiple-choice questions (ie, questions at the level of those on a board examination) and rationales for radiology curricula [67].

Model Performance Across Applications

Performance varied widely across tasks (Table 3; the full metrics can be found in Multimedia Appendices 2 and 6). Models fine-tuned on domain-specific corpora (eg, RadBERT, BioClinicalBERT, and Japanese BERT variants) consistently outperformed general-purpose LLMs in structured classification and report-based tasks, often achieving accuracies of >95% [69,71,73].

XSL•FO
RenderX

Table . Summary of performance ranges across the included studies. The lowest and highest reported values are shown where available. Data were extracted from Multimedia Appendices 2-4 (N=67).

Task or application domain and metric	Reported range
Classification	
Accuracy (%)	83 - 97
F_1-score	0.66 - 1.00
AUC[a]	0.84 - 0.99
Diagnostic reasoning from clinical cases	
Accuracy (%)	16 - 50
Diagnosis from images	
Accuracy (%)	25 - 84
Match rate (%)	48-62
Concordance (%)	66.7-68.8
Information extraction from radiology reports	
Accuracy (%)	83-97
F_1-score	0.66 - 1.00
AUC	0.84-0.99
Report generation and summarization	
F_1-score	0.29-0.88
Accuracy (%)	67-89
Clinical acceptability (physician rated; %)	89
BLEU[b] or ROUGE[c] scores	Variable, generally modest (BLEU: 0.46 - 0.74; ROUGE-L[d]: 0.37 - 0.61)
Similarity score (%)	98.9-99.3
Quality assessment	
Accuracy (%)	70.2-98.3

[a]AUC: area under the curve.

[b]BLEU: bilingual evaluation understudy.

[c]ROUGE: recall-oriented understudy for gisting evaluation.

[d]ROUGE-L: recall-oriented understudy for gisting evaluation based on the longest common subsequence.

In contrast, performance for diagnostic reasoning and image-based tasks remained modest. For instance, GPT-4V achieved only 27% to 35% accuracy in primary and differential diagnoses [31], and GPT-4 variants reached <25% accuracy in case-based diagnostic challenges [23].

Text-based applications such as error detection [74] and structured report inference [18,73] approached human-level accuracy (≥95%). Image-focused tasks yielded lower values, with rank-1 accuracy as low as 25% [32], area under the curve values between 0.80 and 0.83 [30,33], and F_1-scores below 0.30 in some generative settings [57].

Report generation and simplification tasks demonstrated variable performance depending on evaluation metrics. While BLEU and ROUGE scores remained modest, physician-rated acceptability and utility scores were encouraging [62,77], suggesting that automated metrics may underestimate clinical usability. GPT-4 also showed superior performance in exam question generation [67] and summarization [75].

Discussion

Principal Findings

Overview

This scoping review provides the first comprehensive synthesis of LLM applications across all domains of radiology. By mapping 67 studies, we identified 3 main areas of application: clinical decision support, report generation, and workflow optimization. There is evidence suggesting that LLMs are most reliable in structured tasks such as classification, information extraction, and educational support, whereas diagnostic reasoning and visual interpretation remain underdeveloped.

Decision Support

GPT-based and BERT models showed strong performance in structured classification tasks such as the Thyroid Imaging Reporting and Data System, the Liver Imaging Reporting and Data System [14,15,18,21], fracture coding [42], and tumor node metastasis staging [20], particularly when domain-specific

XSL•FO
RenderX

BERT variants were fine-tuned on radiology data. These models frequently matched or exceeded human performance in multilingual and specialty-specific contexts. In contrast, diagnostic reasoning tasks involving clinical cases or direct image interpretation showed limited and inconsistent performance. General-purpose GPT-4 and GPT-4V models achieved variable accuracy across case-based and imaging tasks, underscoring the immaturity of current multimodal reasoning [15,24,25,27,31].

Report Generation

Transformer models such as T5, PEGASUS, and GPT-4 generated radiology reports that were linguistically coherent and frequently rated as clinically acceptable. Physician-rated outcomes often aligned GPT-4 reports with radiologist-written impressions. However, hallucinations and factual inaccuracies persist, particularly in rare or ambiguous cases. Automated linguistic metrics (BLEU and ROUGE) did not always correlate with clinical usability, highlighting the importance of human-centered evaluation. Without factuality scoring and domain-specific safeguards, unsupervised deployment of report generation tools remains premature.

Workflow Optimization

While our thematic synthesis identified distinct application domains, we acknowledge that the "workflow optimization" category is intentionally broad. It encompasses a range of nondiagnostic use cases, including patient education, radiology report simplification, imaging protocol selection, and user interface enhancement. This thematic grouping reflects the expanding role of LLMs in supporting communication, training, and clinical efficiency beyond core diagnostic tasks. Although its breadth may resemble a "catch-all," we believe that it accurately represents the dynamic and evolving integration of LLMs into radiological practice. Notably, the most reliable use cases for near-term clinical integration were concentrated in workflow support tasks. These included report simplification, protocol selection [73], error identification [74], and RIS user interface enhancement [72]. Such tasks rely primarily on structured reasoning and language fluency rather than on complex diagnostic inference, making them especially suitable for early implementation. Specialized tools such as Augmented Transformer Assisted Radiology Intelligence (for error detection) [74] and ChatUI-RIS (for user interface enhancement) [72] outperformed general-purpose LLMs, reinforcing the value of domain adaptation. Educational uses such as generating board-style multiple-choice questions also proved effective, with high user satisfaction and accuracy [67]. Taken together, these low-risk, high-utility functions offer a promising entry point for safe and meaningful adoption of LLMs in radiology.

Emerging Trends

Two developments were particularly noteworthy. First, multimodal LLMs integrating text and image inputs are moving toward context-aware systems but continue to show high variability in performance and lack prospective validation. Second, domain-specific models such as Radiology-Llama2 and RadSpaT5 demonstrate stronger alignment with radiological terminology but remain underrepresented. Broader external validation and adoption of these models could improve interpretability and clinical fidelity.

Methodological Limitations of the Evidence

Several methodological gaps were consistently observed across the literature. Most studies relied on retrospective, single-center datasets, frequently limited to chest radiographs or neuroradiology, restricting generalizability. Sample sizes were often small, and only 22% of the studies (15/67) reported external validation. Publication bias is likely as studies with positive results may be preferentially published. Heterogeneous reporting of metrics further complicates benchmarking, and the absence of standardized evaluation frameworks for radiology-specific tasks prevents direct comparison across studies.

Equity and Global Applicability

The predominance of English-language publications and Western data sources poses a significant barrier to equitable implementation. Without multilingual evaluation datasets and cross-regional external validation, performance estimates risk being skewed toward English-language and high-resource settings. Ensuring equity and inclusivity in model development and validation is essential for global relevance.

Recommendations and Future Work

Future research should prioritize the following areas:

1. Data and validation; assemble diverse, multicenter, and multilingual datasets to improve generalizability. Conduct prospective evaluations across clinical environments.
2. Evaluation standards; develop radiology-specific factuality and safety benchmarks and ensure standardized reporting of performance and bias assessments.
3. Human factors; implement human-in-the-loop frameworks for oversight, error mitigation, and usability evaluation.
4. Governance; establish clear regulatory guidance and accountability standards to ensure transparency and safety in clinical use.

Limitations

This scoping review has several limitations that should be acknowledged to aid interpretation and guide future research.

First, the search strategy, while designed to be comprehensive, was limited to 3 databases: PubMed, Scopus, and IEEE Xplore. These were selected to capture clinical, biomedical, and technical literature; however, this may have excluded relevant studies indexed in other databases (eg, Embase or Web of Science) or reported in gray literature sources such as arXiv and medRxiv or key conference proceedings (eg, NeurIPS and Medical Image Computing and Computer-Assisted Intervention). This limitation may have led to the omission of emerging or unpublished work.

Second, although efforts were made to use both free-text and controlled vocabulary (eg, MeSH terms in PubMed), the evolving and inconsistent terminology used to describe LLMs may have affected search sensitivity. Terms such as "GPT," "LLM," or "transformer-based AI" may not have been uniformly used across all relevant publications. While the search was

XSL•FO
RenderX

iteratively refined and detailed strategies are included in Multimedia Appendix 1 to improve reproducibility, some studies may have been inadvertently missed due to terminology mismatch.

Third, only English-language articles were included. This decision was made to ensure consistency in interpretation and quality appraisal; however, it introduces language bias and may have excluded valuable contributions from non–English-speaking regions, particularly in a globally active research field such as AI.

Fourth, consistent with the framework by Arksey and O'Malley [10], we did not include a formal quality assessment of the included studies. While appropriate for scoping reviews, future systematic reviews could integrate AI-specific appraisal tools (eg, the Minimum Information About Clinical Artificial Intelligence Modeling checklist and Checklist for Artificial Intelligence in Medical Imaging) to enhance interpretability. Importantly, the performance ranges reported across the studies (Table 3) should be approached with caution due to the heterogeneity of study designs, evaluation metrics, datasets, and model versions. Many included studies had proof-of-concept or single-institution designs with limited generalizability. Without standardized benchmarks or head-to-head comparisons, the reported values are best interpreted as illustrative of the field's current status rather than definitive benchmarks.

Publication bias is a potential concern, particularly given the rapid growth and high visibility of LLM research. Studies with positive or novel findings may be more likely to be published and indexed, whereas negative or inconclusive results may be underrepresented. Although publication bias was not formally assessed, this limitation should be considered when interpreting the results.

Fifth, while thematic synthesis is useful for structuring a heterogeneous literature, it is inherently interpretive. We mitigated bias by having 2 reviewers code independently and resolve discrepancies through consensus; however, subjective judgment may still have influenced the final thematic map. In addition, studies that addressed multiple tasks were assigned to a single primary category to avoid duplication. Certain subthemes—such as classification—appear under 2 overarching themes (decision support and workflow optimization). This placement reflects differences in the primary intent (eg, classifying reports and images to support diagnosis vs to streamline workflow), as detailed in the Results section. Finally, while the initial thematic analysis was conducted manually by human researchers, GPT-4 was later used as a supportive tool to assist in clustering and cross-verifying patterns. Given that GPT-4 is a generative and nondeterministic model, the reproducibility of its suggested outputs cannot be fully guaranteed. Therefore, this hybrid approach may introduce potential bias and variability, which should be considered when interpreting the thematic synthesis.

Conclusions

The integration of LLMs into radiology is accelerating but remains uneven across application domains. Structured tasks such as classification and information extraction are approaching maturity, whereas diagnostic reasoning and multimodal interpretation require substantial improvement. Safe clinical deployment will depend not only on technical performance but also on rigorous validation, global inclusivity, and ethical governance.

Acknowledgments

The authors would like to thank the librarian at Sultan Qaboos University for assistance in refining the search strategy and supporting the review process. The authors used ChatGPT (OpenAI; accessed July 2025) to assist with language refinement and proofreading. All scientific interpretations were conducted by the authors.

Funding

This research received no specific grant from any funding agency in the public, commercial, or not-for-profit sectors.

Data Availability

All data generated or analyzed during this study are included in this published article and its supplementary information files.

Authors' Contributions

Conceptualization: AAZ
Data curation: AAZ, SL
Formal analysis: AAZ
SLMethodology: AAZ, IR, RS, AAA
Project administration: AAZ
Supervision: AAZ
Visualization: IR
Writing—original draft: AAZ, SL
Writing—review and editing: AAZ, SL

XSL•FO
RenderX

Conflicts of Interest

None declared.

Multimedia Appendix 1
Full search strategies.
[DOCX File, 14 KB - medinform_v13i1e78041_app1.docx]

Multimedia Appendix 2
Summary of all the included articles.
[XLSX File, 43 KB - medinform_v13i1e78041_app2.xlsx]

Multimedia Appendix 3
Data modalities used across the included studies (N=67): text-only (eg, radiology reports, cases, and request forms), image-only (eg, x-ray, computed tomography, and magnetic resonance imaging), multimodal (text + images), and system or metadata sources (eg, radiology information system) sources.
[PNG File, 44 KB - medinform_v13i1e78041_app3.png]

Multimedia Appendix 4
Distribution of radiology studies by subspecialty (N=67). This chart illustrates the number of studies conducted in each radiology subspecialty. Thoracic imaging, general radiology, and oncologic imaging were the most frequently studied areas.
[PNG File, 111 KB - medinform_v13i1e78041_app4.png]

Multimedia Appendix 5
Summary of the extracted themes from the included articles (N=67).
[XLSX File, 44 KB - medinform_v13i1e78041_app5.xlsx]

Multimedia Appendix 6
Reported performance metrics of large language model (LLM) applications in radiology across the included studies (N=67).
[DOCX File, 211 KB - medinform_v13i1e78041_app6.docx]

Checklist 1
PRISMA-ScR checklist.
[DOCX File, 87 KB - medinform_v13i1e78041_app7.docx]

References

1. Kotkar AD, Mahadik RS, More PG, Thorat SA. Comparative analysis of transformer-based large language models (LLMs) for text summarization. Presented at: 2024 1st International Conference on Advanced Computing and Emerging Technologies (ACET); Aug 23-24, 2024. [doi: 10.1109/ACET61898.2024.10730348]
2. Bluethgen C, Van Veen D, Zakka C, et al. Best practices for large language models in radiology. Radiology 2025 Apr;315(1):e240528. [doi: 10.1148/radiol.240528] [Medline: 40298602]
3. Zaki HA, Aoun A, Munshi S, Abdel-Megid H, Nazario-Johnson L, Ahn SH. The application of large language models for radiologic decision making. J Am Coll Radiol 2024 Jul;21(7):1072-1078. [doi: 10.1016/j.jacr.2024.01.007] [Medline: 38224925]
4. Bressem KK, Adams LC, Gaudin RA, et al. Highly accurate classification of chest radiographic reports using a deep learning natural language model pre-trained on 3.8 million text reports. Bioinformatics 2021 Jan 29;36(21):5255-5261. [doi: 10.1093/bioinformatics/btaa668] [Medline: 32702106]
5. Sterling NW, Brann F, Frisch SO, Schrager JD. Patient-readable radiology report summaries generated via large language model: safety and quality. J Patient Exp 2024;11. [doi: 10.1177/23743735241259477]
6. Reichenpfader D, Müller H, Denecke K. A scoping review of large language model based approaches for information extraction from radiology reports. NPJ Digit Med 2024 Aug 24;7(1):222. [doi: 10.1038/s41746-024-01219-0] [Medline: 39182008]
7. Reichenpfader D, Müller H, Denecke K. Large language model-based information extraction from free-text radiology reports: a scoping review protocol. BMJ Open 2023 Dec 9;13(12):e076865. [doi: 10.1136/bmjopen-2023-076865] [Medline: 38070902]
8. Busch F, Hoffmann L, Dos Santos DP, et al. Large language models for structured reporting in radiology: past, present, and future. Eur Radiol 2025 May;35(5):2589-2602. [doi: 10.1007/s00330-024-11107-6] [Medline: 39438330]

XSL•FO
RenderX

9. Nakaura T, Ito R, Ueda D, et al. The impact of large language models on radiology: a guide for radiologists on the latest innovations in AI. Jpn J Radiol 2024 Jul;42(7):685-696. [doi: 10.1007/s11604-024-01552-0] [Medline: 38551772]
10. Arksey H, O'Malley L. Scoping studies: towards a methodological framework. Int J Soc Res Methodol 2005;8(1):19-32. [doi: 10.1080/1364557032000119616]
11. Faster systematic literature reviews. Rayyan. URL: https://www.rayyan.ai/ [accessed 2025-11-10]
12. Blankemeier L, Cohen JP, Kumar A. Merlin: a vision language foundation model for 3D computed tomography. Res Sq. Preprint posted online on Jun 28, 2024. [doi: 10.48550/arXiv.2406.06512] [Medline: 38978576]
13. Chambon P, Cook TS, Langlotz CP. Improved fine-tuning of in-domain transformer model for inferring COVID-19 presence in multi-institutional radiology reports. J Digit Imaging 2023 Feb;36(1):164-177. [doi: 10.1007/s10278-022-00714-8] [Medline: 36323915]
14. Fervers P, Hahnfeldt R, Kottlors J, et al. ChatGPT yields low accuracy in determining LI-RADS scores based on free-text and structured radiology reports in German language. Front Radiol 2024 Jul 5;4:1390774. [doi: 10.3389/fradi.2024.1390774] [Medline: 39036542]
15. Haver HL, Bahl M, Doo FX, et al. Evaluation of multimodal ChatGPT (GPT-4V) in describing mammography image features. Can Assoc Radiol J 2024 Nov;75(4):947-949. [doi: 10.1177/08465371241247043] [Medline: 38581353]
16. Olivato M, Putelli L, Arici N, Emilio Gerevini A, Lavelli A, Serina I. Language models for hierarchical classification of radiology reports with attention mechanisms, BERT, and GPT-4. IEEE Access 2024;12:69710-69727. [doi: 10.1109/ACCESS.2024.3402066]
17. Putelli L, Gerevini AE, Lavelli A, Mehmood T, Serina I. On the behaviour of BERT's attention for the classification of medical reports. Presented at: Italian Workshop on Explainable Artificial Intelligence 2022; Nov 28 to Dec 3, 2022 URL: https://ceur-ws.org/Vol-3277/paper2.pdf [accessed 2025-11-11]
18. Santos T, Kallas ON, Newsome J, Rubin D, Gichoya JW, Banerjee I. A fusion NLP model for the inference of standardized thyroid nodule malignancy scores from radiology report text. AMIA Annu Symp Proc 2022 Feb 21;2021:1079-1088. [Medline: 35308953]
19. Sehanobish A, Kannan K, Abraham N, Das A, Odry B. Meta-learning pathologies from radiology reports using variance aware prototypical networks. Presented at: Proceedings of the 2022 Conference on Empirical Methods in Natural Language Processing; Dec 7-11, 2022. [doi: 10.18653/v1/2022.emnlp-industry.34]
20. Suzuki K, Yamada H, Yamazaki H, Honda G, Sakai S. Preliminary assessment of TNM classification performance for pancreatic cancer in Japanese radiology reports using GPT-4. Jpn J Radiol 2025 Jan;43(1):51-55. [doi: 10.1007/s11604-024-01643-y] [Medline: 39162781]
21. Wu Q, Wu Q, Li H, et al. Evaluating large language models for automated reporting and data systems categorization: cross-sectional study. JMIR Med Inform 2024 Jul 17;12:e55799. [doi: 10.2196/55799] [Medline: 39018102]
22. Zhang Y, Liu M, Hu S, et al. Development and multicenter validation of chest X-ray radiography interpretations based on natural language processing. Commun Med (Lond) 2021 Oct 28;1:43. [doi: 10.1038/s43856-021-00043-x] [Medline: 35602222]
23. Horiuchi D, Tatekawa H, Shimono T, et al. Accuracy of ChatGPT generated diagnosis from patient's medical history and imaging findings in neuroradiology cases. Neuroradiology 2024 Jan;66(1):73-79. [doi: 10.1007/s00234-023-03252-4] [Medline: 37994939]
24. Horiuchi D, Tatekawa H, Oura T, et al. Comparing the diagnostic performance of GPT-4-based ChatGPT, GPT-4V-based ChatGPT, and radiologists in challenging neuroradiology cases. Clin Neuroradiol 2024 Dec;34(4):779-787. [doi: 10.1007/s00062-024-01426-y] [Medline: 38806794]
25. Horiuchi D, Tatekawa H, Oura T, et al. ChatGPT's diagnostic performance based on textual vs. visual information compared to radiologists' diagnostic performance in musculoskeletal radiology. Eur Radiol 2025 Jan;35(1):506-516. [doi: 10.1007/s00330-024-10902-5] [Medline: 38995378]
26. Kurokawa R, Ohizumi Y, Kanzawa J, et al. Diagnostic performances of Claude 3 Opus and Claude 3.5 Sonnet from patient history and key images in Radiology's "Diagnosis Please" cases. Jpn J Radiol 2024 Dec;42(12):1399-1402. [doi: 10.1007/s11604-024-01634-z] [Medline: 39096483]
27. Wada A, Akashi T, Shih G, et al. Optimizing GPT-4 turbo diagnostic accuracy in neuroradiology through prompt engineering and confidence thresholds. Diagnostics (Basel) 2024 Jul 17;14(14):1541. [doi: 10.3390/diagnostics14141541] [Medline: 39061677]
28. Elek A, Ekizalioğlu DD, Güler E. Evaluating Microsoft Bing with ChatGPT-4 for the assessment of abdominal computed tomography and magnetic resonance images. Diagn Interv Radiol 2025 Apr 28;31(3):196-205. [doi: 10.4274/dir.2024.232680] [Medline: 39155793]
29. Khare Y, Bagal V, Mathew M, Devi A, Priyakumar UD, Jawahar CV. MMBERT: multimodal BERT pretraining for improved medical VQA. Presented at: 2021 IEEE 18th International Symposium on Biomedical Imaging (ISBI); Apr 13-16, 2021. [doi: 10.1109/ISBI48211.2021.9434063]
30. Pachade S, Datta S, Dong Y, et al. Self-supervised learning with radiology reports, a comparative analysis of strategies for large vessel occlusion and brain CTA images. Presented at: 2023 IEEE 20th International Symposium on Biomedical Imaging (ISBI); Apr 18-21, 2023. [doi: 10.1109/ISBI53787.2023.10230623]

XSL•FO
RenderX

31. Busch F, Han T, Makowski MR, Truhn D, Bressem KK, Adams L. Integrating text and image analysis: exploring GPT-4V's capabilities in advanced radiological applications across subspecialties. J Med Internet Res 2024 May 1;26:e54948. [doi: 10.2196/54948] [Medline: 38691404]
32. Silva TP, Andrade-Bortoletto MFS, Ocampo TSC, et al. Performance of a commercially available generative pre-trained transformer (GPT) in describing radiolucent lesions in panoramic radiographs and establishing differential diagnoses. Clin Oral Investig 2024 Mar 9;28(3):204. [doi: 10.1007/s00784-024-05587-5] [Medline: 38459362]
33. Wu SH, Tong WJ, Li MD, et al. Collaborative enhancement of consistency and accuracy in US diagnosis of thyroid nodules using large language models. Radiology 2024 Mar;310(3):e232255. [doi: 10.1148/radiol.232255] [Medline: 38470237]
34. Kottlors J, Bratke G, Rauen P, et al. Feasibility of differential diagnosis based on imaging patterns using a large language model. Radiology 2023 Jul;308(1):e231167. [doi: 10.1148/radiol.231167] [Medline: 37404149]
35. Overgaard Olesen AS, Miger KC, Nielsen OW, Grand J. How does ChatGPT-4 match radiologists in detecting pulmonary congestion on chest X-ray? J Med Artif Intell 2024;7:18. [doi: 10.21037/jmai-24-26]
36. Lee KH, Lee RW, Kwon YE. Validation of a deep learning chest X-ray interpretation model: integrating large-scale AI and large language models for comparative analysis with ChatGPT. Diagnostics 2023 Dec 30;14(1):90. [doi: 10.3390/diagnostics14010090] [Medline: 38201398]
37. Reith TP, D'Alessandro DM, D'Alessandro MP. Capability of multimodal large language models to interpret pediatric radiological images. Pediatr Radiol 2024 Sep;54(10):1729-1737. [doi: 10.1007/s00247-024-06025-0] [Medline: 39133401]
38. Sarangi PK, Irodi A, Panda S, Nayak DS, Mondal H. Radiological differential diagnoses based on cardiovascular and thoracic imaging patterns: perspectives of four large language models. Indian J Radiol Imaging 2023 Dec 28;34(2):269-275. [doi: 10.1055/s-0043-1777289] [Medline: 38549881]
39. Mukherjee P, Hou B, Lanfredi RB, Summers RM. Feasibility of using the privacy-preserving large language model vicuna for labeling radiology reports. Radiology 2023 Oct;309(1):e231147. [doi: 10.1148/radiol.231147] [Medline: 37815442]
40. Tan RS, Lin Q, Low GH, et al. Inferring cancer disease response from radiology reports using large language models with data augmentation and prompting. J Am Med Inform Assoc 2023 Sep 25;30(10):1657-1664. [doi: 10.1093/jamia/ocad133] [Medline: 37451682]
41. Tay SB, Low GH, Wong GJ, et al. Use of natural language processing to infer sites of metastatic disease from radiology reports at scale. JCO Clin Cancer Inform 2024 May;8:e2300122. [doi: 10.1200/CCI.23.00122] [Medline: 38788166]
42. Russe MF, Fink A, Ngo H, et al. Performance of ChatGPT, human radiologists, and context-aware ChatGPT in identifying AO codes from radiology reports. Sci Rep 2023 Aug 30;13(1):14215. [doi: 10.1038/s41598-023-41512-8] [Medline: 37648742]
43. Le Guellec B, Lefèvre A, Geay C, et al. Performance of an open-source large language model in extracting information from free-text radiology reports. Radiol Artif Intell 2024 Jul;6(4):e230364. [doi: 10.1148/ryai.230364] [Medline: 38717292]
44. Lybarger K, Damani A, Gunn M, Uzuner OZ, Yetisgen M. Extracting radiological findings with normalized anatomical information using a span-based BERT relation extraction model. AMIA Jt Summits Transl Sci Proc 2022 May 23;2022:339-348. [Medline: 35854739]
45. Dada A, Ufer TL, Kim M, et al. Information extraction from weakly structured radiological reports with natural language queries. Eur Radiol 2024 Jan;34(1):330-337. [doi: 10.1007/s00330-023-09977-3] [Medline: 37505252]
46. Sun D, Hadjiiski L, Gormley J, et al. Outcome prediction using multi-modal information: integrating large language model-extracted clinical information and image analysis. Cancers (Basel) 2024 Jun 29;16(13):2402. [doi: 10.3390/cancers16132402] [Medline: 39001463]
47. Bhayana R, Elias G, Datta D, Bhambra N, Deng Y, Krishna S. Use of GPT-4 with single-shot learning to identify incidental findings in radiology reports. AJR Am J Roentgenol 2024 Mar;222(3):e2330651. [doi: 10.2214/AJR.23.30651] [Medline: 38197759]
48. Wu DJ, Bibault JE. Pilot applications of GPT-4 in radiation oncology: summarizing patient symptom intake and targeted chatbot applications. Radiother Oncol 2024 Jan;190:109978. [doi: 10.1016/j.radonc.2023.109978] [Medline: 37913954]
49. Danu MD, Marica G, Karn SK, et al. Generation of radiology findings in chest X-ray by leveraging collaborative knowledge. Procedia Comput Sci 2023;221:1102-1109. [doi: 10.1016/j.procs.2023.08.094]
50. Hasani AM, Singh S, Zahergivar A, et al. Evaluating the performance of Generative Pre-trained Transformer-4 (GPT-4) in standardizing radiology reports. Eur Radiol 2024 Jun;34(6):3566-3574. [doi: 10.1007/s00330-023-10384-x] [Medline: 37938381]
51. Ji J, Hou Y, Chen X, Pan Y, Xiang Y. Vision-language model for generating textual descriptions from clinical images: model development and validation study. JMIR Form Res 2024 Feb 8;8:e32690. [doi: 10.2196/32690] [Medline: 38329788]
52. López-Úbeda P, Martín-Noguerol T, Escartín J, Luna A. Automatic generation of conclusions from neuroradiology MRI reports through natural language processing. Neuroradiology 2024 Apr;66(4):477-485. [doi: 10.1007/s00234-024-03312-3] [Medline: 38381144]
53. Mallio CA, Sertorio AC, Bernetti C, Beomonte Zobel B. Large language models for structured reporting in radiology: performance of GPT-4, ChatGPT-3.5, Perplexity and Bing. Radiol Med 2023 Jul;128(7):808-812. [doi: 10.1007/s11547-023-01651-4] [Medline: 37248403]

XSL•FO
RenderX

54. Moezzi SA, Ghaedi A, Rahmanian M, Mousavi SZ, Sami A. Application of deep learning in generating structured radiology reports: a transformer-based technique. J Digit Imaging 2023 Feb;36(1):80-90. [doi: 10.1007/s10278-022-00692-x] [Medline: 36002778]
55. Nakaura T, Yoshida N, Kobayashi N, et al. Preliminary assessment of automated radiology report generation with generative pre-trained transformers: comparing results to radiologist-generated reports. Jpn J Radiol 2024 Feb;42(2):190-200. [doi: 10.1007/s11604-023-01487-y] [Medline: 37713022]
56. Selivanov A, Rogov OY, Chesakov D, Shelmanov A, Fedulova I, Dylov DV. Medical image captioning via generative pretrained transformers. Sci Rep 2023 Mar 13;13(1):4171. [doi: 10.1038/s41598-023-31223-5] [Medline: 36914733]
57. Shentu J, Al Moubayed N. CXR-IRGen: an integrated vision and language model for the generation of clinically accurate chest X-ray image-report pairs. Presented at: 2024 IEEE/CVF Winter Conference on Applications of Computer Vision (WACV); Jan 3-8, 2024. [doi: 10.1109/WACV57701.2024.00513]
58. Soleimani M, Seyyedi N, Ayyoubzadeh SM, Kalhori SR, Keshavarz H. Practical evaluation of ChatGPT performance for radiology report generation. Acad Radiol 2024 Dec;31(12):4823-4832. [doi: 10.1016/j.acra.2024.07.020] [Medline: 39142976]
59. Woźnicki P, Laqua C, Fiku I, et al. Automatic structuring of radiology reports with on-premise open-source large language models. Eur Radiol 2025 Apr;35(4):2018-2029. [doi: 10.1007/s00330-024-11074-y] [Medline: 39390261]
60. Wu W, Li M, Wu J, Ni M, Yuan H. Learning to generate radiology findings from impressions based on large language model. Presented at: 2023 IEEE International Conference on Big Data (BigData); Dec 15-18, 2023. [doi: 10.1109/BigData59044.2023.10386916]
61. Bhayana R, Nanda B, Dehkharghanian T, et al. Large language models for automated synoptic reports and resectability categorization in pancreatic cancer. Radiology 2024 Jun;311(3):e233117. [doi: 10.1148/radiol.233117] [Medline: 38888478]
62. Tie X, Shin M, Pirasteh A, et al. Personalized impression generation for PET reports using large language models. J Imaging Inform Med 2024 Apr;37(2):471-488. [doi: 10.1007/s10278-024-00985-3] [Medline: 38308070]
63. Karn SK, Ghosh R, Kusuma P, Farri O. shs-nlp at RadSum23: domain-adaptive pre-training of instruction-tuned LLMs for radiology report impression generation. Presented at: 22nd Workshop on Biomedical Natural Language Processing and BioNLP Shared Tasks; Jul 13, 2023. [doi: 10.18653/v1/2023.bionlp-1.57]
64. Zhu Q, Chen X, Jin Q. Leveraging professional radiologists' expertise to enhance LLMs' evaluation for radiology reports. arXiv. Preprint posted online on Jan 29, 2024 URL: https://pmc.ncbi.nlm.nih.gov/articles/PMC11188146/ [accessed 2025-11-12] [doi: 10.48550/arXiv.2401.16578]
65. Gertz RJ, Bunck AC, Lennartz S, et al. GPT-4 for automated determination of radiological study and protocol based on radiology request forms: a feasibility study. Radiology 2023 Jun;307(5):e230877. [doi: 10.1148/radiol.230877] [Medline: 37310247]
66. Chen Z, Hu B, Niu C, et al. IQAGPT: computed tomography image quality assessment with vision-language and ChatGPT models. Vis Comput Ind Biomed Art 2024 Aug 5;7(1):20. [doi: 10.1186/s42492-024-00171-w] [Medline: 39101954]
67. Mistry NP, Saeed H, Rafique S, Le T, Obaid H, Adams SJ. Large language models as tools to generate radiology board-style multiple-choice questions. Acad Radiol 2024 Sep;31(9):3872-3878. [doi: 10.1016/j.acra.2024.06.046] [Medline: 39013736]
68. Nishio M, Matsunaga T, Matsuo H, et al. Fully automatic summarization of radiology reports using natural language processing with large language models. Inform Med Unlocked 2024;46:101465. [doi: 10.1016/j.imu.2024.101465]
69. Yasaka K, Kanzawa J, Kanemaru N, Koshino S, Abe O. Fine-tuned large language model for extracting patients on pretreatment for lung cancer from a picture archiving and communication system based on radiological reports. J Imaging Inform Med 2025 Feb;38(1):327-334. [doi: 10.1007/s10278-024-01186-8] [Medline: 38955964]
70. Huemann Z, Lee C, Hu J, Cho SY, Bradshaw TJ. Domain-adapted large language models for classifying nuclear medicine reports. Radiol Artif Intell 2023 Sep 27;5(6):e220281. [doi: 10.1148/ryai.220281] [Medline: 38074793]
71. Kanzawa J, Yasaka K, Fujita N, Fujiwara S, Abe O. Automated classification of brain MRI reports using fine-tuned large language models. Neuroradiology 2024 Dec;66(12):2177-2183. [doi: 10.1007/s00234-024-03427-7] [Medline: 38995393]
72. Zhang L, Shu J, Hu J, et al. Exploring the potential of large language models in radiological imaging systems: improving user interface design and functional capabilities. Electronics 2024;13(11):2002. [doi: 10.3390/electronics13112002]
73. Abbasi N, Lacson R, Kapoor N, et al. Development and external validation of an artificial intelligence model for identifying radiology reports containing recommendations for additional imaging. Am J Roentgenol 2023 Sep;221(3):377-385. [doi: 10.2214/AJR.23.29120] [Medline: 37466185]
74. Kathait AS, Garza-Frias E, Sikka T, et al. Assessing laterality errors in radiology: comparing generative artificial intelligence and natural language processing. J Am Coll Radiol 2024 Oct;21(10):1575-1582. [doi: 10.1016/j.jacr.2024.06.014] [Medline: 38960083]
75. Sarangi PK, Lumbani A, Swarup MS, et al. Assessing ChatGPT's proficiency in simplifying radiological reports for healthcare professionals and patients. Cureus 2023 Dec 21;15(12):e50881. [doi: 10.7759/cureus.50881] [Medline: 38249202]
76. Rogasch JM, Metzger G, Preisler M, et al. ChatGPT: can you prepare my patients for [18F]FDG PET/CT and explain my reports? J Nucl Med 2023 Dec 1;64(12):1876-1879. [doi: 10.2967/jnumed.123.266114] [Medline: 37709536]

XSL•FO
RenderX

77. Butler JJ, Acosta E, Kuna MC, et al. Decoding radiology reports: artificial intelligence-large language models can improve the readability of hand and wrist orthopedic radiology reports. Hand (N Y) 2025 Oct;20(7):1144-1152. [doi: 10.1177/15589447241267766] [Medline: 39138809]

Abbreviations

AI: artificial intelligence
BERT: bidirectional encoder representations from transformers
BLEU: bilingual evaluation understudy
CT: computed tomography
LLM: large language model
MeSH: Medical Subject Headings
MRI: magnetic resonance imaging
PET: positron emission tomography
PRISMA: Preferred Reporting Items for Systematic Reviews and Meta-Analyses
PRISMA-ScR: Preferred Reporting Items for Systematic Reviews and Meta-Analyses extension for Scoping Reviews
RIS: radiology information system
ROUGE: recall-oriented understudy for gisting evaluation
T5: Text-to-Text Transfer Transformer

Edited by A Coristine; submitted 25.05.25; peer-reviewed by D Reichenpfader, J Zhang; revised version received 30.10.25; accepted 31.10.25; published 09.12.25.

Please cite as:
Al Zaabi A, Alshibli R, AlAmri A, AlRuheili I, Lutfi SL
Trends and Trajectories in the Rise of Large Language Models in Radiology: Scoping Review
JMIR Med Inform 2025;13:e78041
URL: https://medinform.jmir.org/2025/1/e78041
doi:10.2196/78041

© Adhari Al Zaabi, Rashid Alshibli, Abdullah AlAmri, Ibrahim AlRuheili, Syaheerah Lebai Lutfi. Originally published in JMIR Medical Informatics (https://medinform.jmir.org), 9.12.2025. This is an open-access article distributed under the terms of the Creative Commons Attribution License (https://creativecommons.org/licenses/by/4.0/), which permits unrestricted use, distribution, and reproduction in any medium, provided the original work, first published in JMIR Medical Informatics, is properly cited. The complete bibliographic information, a link to the original publication on https://medinform.jmir.org/, as well as this copyright and license information must be included.

XSL•FO
RenderX

Predictive Performance of Radiomics-Based Machine Learning for Colorectal Cancer Recurrence Risk: Systematic Review and Meta-Analysis

Yuan Sun[1,2], PhD; Bo Li[3], MMed; Chuanlan Ju[4], MMed; Liming Hu[5], MMed; Huiyi Sun[6], PhD; Jing An[7], PhD; Tae-Hun Kim[8], PhD; Zhijun Bu[1], PhD; Zeyang Shi[1], MMed; Jianping Liu[1], PhD; Zhaolan Liu[1], PhD

[1]Centre for Evidence-based Chinese Medicine, Beijing University of Chinese Medicine, No.11 East Beisanhuan Road, Heping Street, Chaoyang District, Beijing, China

[2]Department of Public Health, Shandong College of Traditional Chinese Medicine, Yantai, China

[3]Preventive Medicine Association, Yantai Center for Disease Control and Prevention, Yantai, China

[4]Department of Public Health, Yantai Hospital of Traditional Chinese Medicine, Yantai, China

[5]Department of Spleen, Stomach, Liver and Gallbladder, Dongfang Hospital, Beijing University of Chinese Medicine, Beijing, China

[6]Department of Spleen, Stomach, Liver and Gallbladder, Dongzhimen Hospital, Beijing University of Chinese Medicine, Beijing, China

[7]Department of Spleen and Stomach, The Third Affiliated Hospital of Beijing University of Chinese Medicine, Beijing, China

[8]Korean Medicine Clinical Trial Center, Kyung Hee University Korean Medicine Hospital, Seoul, Republic of Korea

Corresponding Author:
Zhaolan Liu, PhD
Centre for Evidence-based Chinese Medicine, Beijing University of Chinese Medicine, No.11 East Beisanhuan Road, Heping Street, Chaoyang District, Beijing, China

Abstract

Background: Predicting colorectal cancer (CRC) recurrence risk remains a challenge in clinical practice. Owing to the widespread use of radiomics in CRC diagnosis and treatment, some researchers recently explored the effectiveness of radiomics-based models in forecasting CRC recurrence risk. Nonetheless, the lack of systematic evidence of the efficacy of such models has hampered their clinical adoption.

Objective: This study aimed to explore the value of radiomics in predicting CRC recurrence, providing a scholarly rationale for developing more specific interventions.

Methods: Overall, 4 databases (Embase, PubMed, the Cochrane Library, and Web of Science) were searched for relevant articles from inception to January 1, 2025. We included studies that developed or validated radiomics-based machine learning models for predicting CRC recurrence using computed tomography or magnetic resonance imaging and provided discriminative performance metrics (c-index). Nonoriginal articles, studies that did not develop a model, and those lacking clear outcome measures were excluded from the study. The quality of the included original studies was assessed using the Radiomics Quality Score. A bivariate mixed-effects model was used to conduct a meta-analysis in which the c-index values with 95% CI were pooled. For the meta-analysis, subgroup analyses were conducted separately on the validation and training sets.

Results: This meta-analysis included 17 original studies involving 4600 patients with CRC. The quality of the identified studies was low (mean Radiomics Quality Score 13.23/36, SD 2.56), with limitations in prospective design and biological validation. In the validation set, the c-index values based on clinical features, radiomics features, and radiomics features combined with clinical features were 0.73 (95% CI 0.68 - 0.79), 0.80 (95% CI 0.75 - 0.85), and 0.83 (95% CI 0.79 - 0.87), respectively. In the internal validation set, the c-index values based on clinical features, radiomics features, and radiomics features+clinical features were 0.70 (95% CI 0.61 - 0.79), 0.83 (95% CI 0.78 - 0.88), and 0.83 (95% CI 0.78 - 0.88), respectively. Finally, in the external validation set, the c-index values based on clinical features, radiomics features, and radiomics features combined with clinical features were 0.76 (95% CI 0.70 - 0.83), 0.75 (95% CI 0.66 - 0.83), and 0.83 (95% CI 0.78 - 0.88), respectively.

Conclusions: Radiomics-based machine learning models, especially those integrating radiomics and clinical features, showed promising predictive performance for CRC recurrence risk. However, this study has several limitations, such as moderate study quality, limited sample size, and high heterogeneity in modeling approaches. These findings suggest the potential clinical value of integrated models in risk stratification and their potential to enhance personalized treatment, though further high-quality prospective studies are warranted.

Trial Registration: PROSPERO CRD420250656632; https://www.crd.york.ac.uk/PROSPERO/view/CRD420250656632

XSL•FO
RenderX

(JMIR Med Inform 2025;13:e78644) doi:10.2196/78644

KEYWORDS

colorectal cancer; radiomics; meta-analysis; clinical prediction model; PRISMA; Preferred Reporting Items for Systematic Reviews and Meta-Analyses

Introduction

Colorectal cancer (CRC) is ranked as the third most prevalent malignancy and the second most common cause of cancer-related deaths worldwide [1,2]. According to the International Agency for Research on Cancer, there were 1,926,100 (9.6%) new CRC cases and 903,900 (9.3%) CRC-related deaths in 2022 alone [2], highlighting CRC as a major public health concern. Although notable developments have been reported for targeted therapies, adjuvant chemotherapy, as well as radical surgery, cases of tumor recurrence are still a major issue leading to poor survival outcomes [3]. Therefore, early identification of CRC recurrence risk in clinical practice and the development of precise interventions would be imperative for improved clinical outcomes.

Machine learning (ML) and radiomics have recently gained widespread attention in oncological diagnoses and treatments, including in CRC [4,5]. Radiomics is an interdisciplinary technology that quantitatively analyzes high-dimensional features in medical images (eg, computed tomography [CT], magnetic resonance imaging [MRI], and positron emission tomography) to mine pathological information not visible to the naked eye. It entails segmenting regions of interest (ROIs) from medical images, extracting predefined mathematical features, and integrating them with ML or deep learning (DL) algorithms to generate interpretable clinical prediction models [6]. This technique has been extensively documented in the literature for cancer diagnosis and survival prediction [7-9]. Specifically within CRC, several studies have explored radiomics for recurrence prediction [10], using various image modalities including CT and MRI.

However, the available primary studies adopt diverse methodologies, using different imaging protocols, segmentation methods, feature extraction techniques, and model validation approaches. Therefore, the findings from such studies are inconsistent, making the clinical translation of individual models challenging. Although some reviews have summarized the application of radiomics in CRC management [11,12], none have specifically synthesized and quantitatively evaluated the predictive performance of radiomics-based ML models for CRC recurrence risk through meta-analysis. In addition, most of the previous reviews failed to discuss how integrative modeling, combined with radiomic and clinical variables, facilitates clinical decision-making to mitigate recurrence and improve patient management.

In this meta-analysis, we aimed to systematically assess the predictive performance of radiomics-based ML models on the risk of CRC recurrence, focusing on models incorporating both imaging and clinical features. In addition, we explored whether integrated approaches offer superior predictive accuracy compared to models using either data type alone. By comprehensively evaluating the existing evidence and its limitations, this study aims to provide robust evidence that can inform the development of effective, personalized intervention strategies for CRC.

Methods

Study Registration

This study was submitted to PROSPERO (International Prospective Register of Systematic Reviews; ID: CRD420250656632) and adhered to the PRISMA (Preferred Reporting Items for Systematic Reviews and Meta-Analyses) guidelines.

Eligibility Criteria

The inclusion and exclusion criteria for study selection are summarized in Textbox 1.

Textbox 1. Inclusion and exclusion criteria.

Inclusion criteria

- Studies enrolling patients with colorectal cancer with no requirement for cancer staging and metastatic resections.
- Studies involving radiomics-based machine learning (ML) predictive models and imaging data (magnetic resonance imaging and computed tomography)–based radiomics models.
- Studies published in English.

Exclusion criteria

- Meta-analyses, reviews, guidelines, expert opinions, and conference abstracts.
- Studies that performed variance factor analysis but did not construct a grammatical ML model.
- Studies without clearly defined endpoint metrics that could make it difficult to assess ML predictive accuracy.
- Studies that only performed image segmentation without constructing a full model.

XSL•FO
RenderX

Data Sources and Search Strategy

We systematically searched 4 databases (Web of Science, Cochrane Library, Embase, and PubMed) from inception to 1 January 2025. The search strategy involved a combination of Medical Subject Heading terms and free-text words. Detailed search strategies are provided in Table S1 in Multimedia Appendix 1 [10,13-28]. The search had no regional restrictions.

Study Selection and Data Extraction

The literature retrieved from the searched databases was imported into EndNote software (Clarivate). After eliminating redundant entries, the remaining articles were systematically screened based on titles and abstracts to discard references that did not meet the predetermined eligibility requirements. The full texts of the remnant studies were screened to obtain additional relevant studies.

Data extracted included titles, year of publication, first author, study type, country, patient sources, study design, treatment regimen, outcome definitions, radiomics source, segmentation method, number of imaging investigators, ROI segmentation software, number of cases and total number of outcome events in the validation and training sets, type of model used, variable screening method, modeling variables, overfitting assessment, and model rating metrics.

Two authors (YS and BL) independently selected the studies and extracted the data, with a third researcher (JA) consulted to resolve any disputes. The interrater agreement between the 2 independent reviewers during the study selection process was excellent, with a Cohen κ value of 0.895.

Study Quality and Risk-of-Bias Assessment

This meta-analysis included studies that used radiomics-based ML models to predict CRC recurrence risk. The Radiomics Quality Score (RQS) was used to determine the reporting completeness and methodological robustness of the included articles [29]. This 16-item scoring system, with a maximum score of 36, is specifically designed to facilitate radiomics studies that encompass various aspects, including image protocol quality, multiple segmentation processes, phantom studies across all scanners, imaging conducted at multiple time points, feature reduction techniques, and multivariable analyses incorporating nonradiomics features. In addition, it addresses the detection and discussion of biological correlates, cut-off analyses, discrimination statistics, calibration statistics, and prospective studies registered in trial databases. Furthermore, the system emphasizes the importance of validation, comparison against established “gold standards,” potential clinical use, cost-effectiveness analyses, and adherence to principles of open science and data sharing. Existing radiological studies are challenging to evaluate within the RQS framework, as they often lack phantom studies across different scanners, imaging at multiple time points, identification and discussion of biological correlates, prospective trial registration, and cost-effectiveness analyses.

Two investigators (YS and CJ) administered the RQS measure and cross-checked the results upon completion. A third investigator (HS) was consulted to resolve any disputes.

Synthesis Methods

This meta-analysis aimed to synthesize the discrimination metrics (c-index) for evaluating the overall accuracy of ML models. For primary studies with 95% CI values or SEs for c-index values, the standard errors were estimated using Debray et al [30] methodological framework. Heterogeneity across studies was evaluated quantitatively using the I^2 index. The restricted maximum likelihood method was used to estimate between-group variance, which is recommended for its improved performance in handling heterogeneity, particularly when the number of studies is limited [31]. Given significant heterogeneity (defined as I^2>50%), a random-effects model was adopted for meta-analysis, and sensitivity analyses were performed. Publication bias was assessed through funnel plot asymmetry analysis and Egger test. Subgroup analyses were conducted to further detect possible sources of heterogeneity. Subgroup analyses were conducted based on imaging modality (CT vs MRI) and dataset type (training vs validation sets). The meta-analysis was conducted in Stata 15 (StataCorp LLC). In addition, to calculate the 95% prediction intervals, which estimate the range within which the true effect of a future study would be expected to fall, we used R software (version 4.4.3; R Development Core Team).

Quality of the Evidence (Grading of Recommendations, Assessment, Development, and Evaluation Assessment)

The GRADE (Grading of Recommendations, Assessment, Development, and Evaluation) approach was used to determine the overall certainty of evidence for our primary outcome (predictive performance measured by c-index) [32]. Given that the included studies were observational in design, the initial evidence level was low. Therefore, we evaluated the evidence across the 5 GRADE domains (risk of bias [RoB], inconsistency, indirectness, imprecision, and publication bias), creating a final certainty rating for each model comparison.

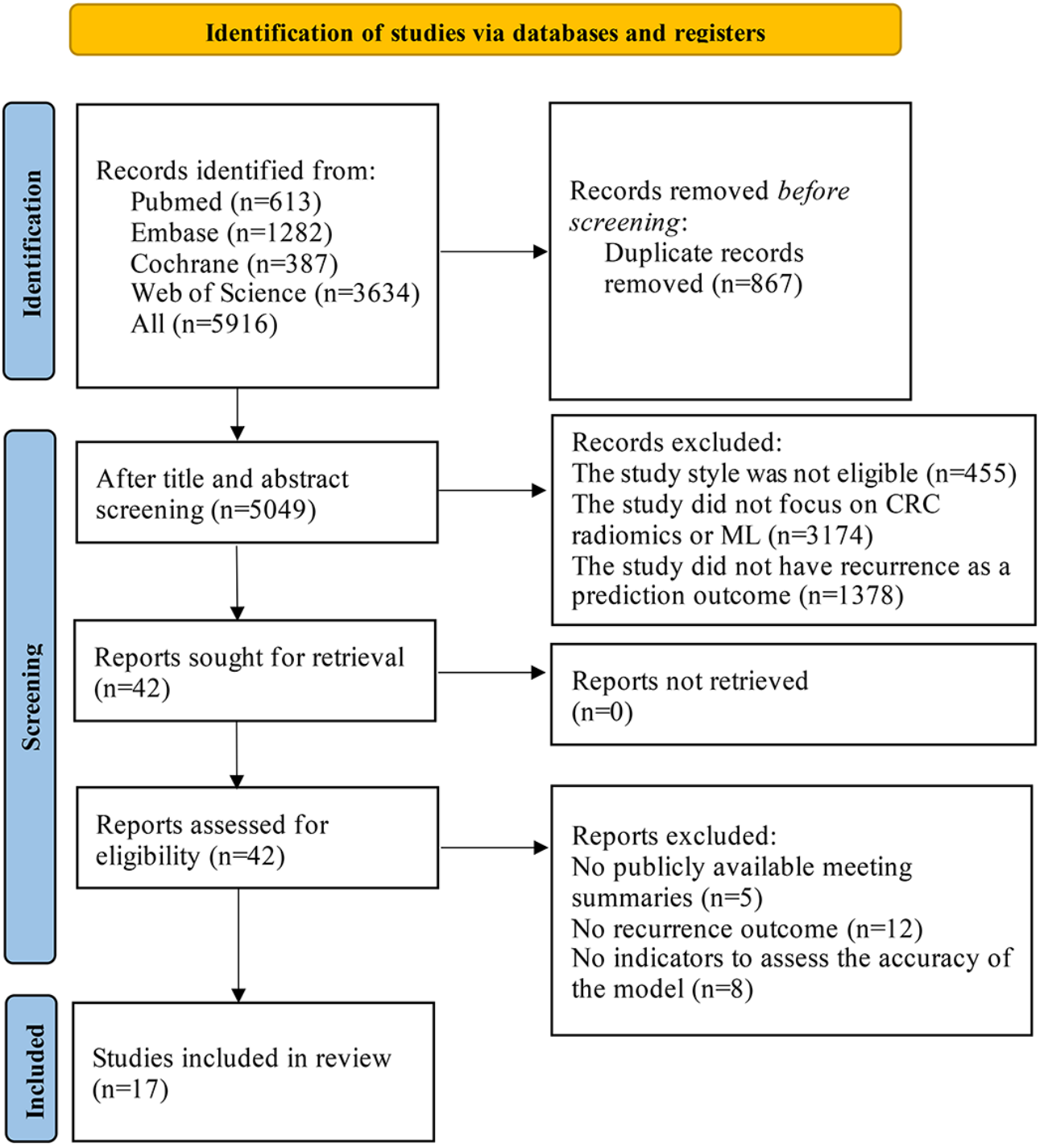
Results

Study Selection

The initial search of the 4 databases yielded 5916 articles, of which 5049 remained after removing duplicates. Two reviewers independently assessed the title and abstract of all remaining articles, of which 5007 were excluded due to inconsistencies with the study goals. Reasons for exclusion were primarily nonrelevant study type (eg, reviews), not focusing on CRC radiomics or ML, or not having recurrence as a prediction outcome. The remaining articles were further subjected to a careful full-text review, after which 25 articles (5 conference abstracts, 12 articles without CRC recurrence endpoints, and 8 articles missing indicators for assessing model accuracy) were removed. Therefore, only 17 articles [10,13-28] were included in the study’s analyses. Figure 1 shows the study selection process.

XSL•FO
RenderX

Figure 1. PRISMA (Preferred Reporting Items for Systematic Reviews and Meta-Analyses) flowchart of the study selection procedure for this systematic review and meta-analysis. CRC: colorectal cancer; ML: machine learning.



Features of the Included Study

This meta-analysis included 17 studies (involving 4600 patients with CRC) [10,13-28], which were published between 2019 and 2025. All 17 studies were cohort investigations, of which 12 were conducted in China [10,13-15,17,18,20,21,23,25-27], and the rest were conducted in Canada [16], France [24], South Korea [28], the Netherlands [19], and the United States [22]. Furthermore, 8 [16,20,22,23,25-28] and 9 [10,13-15,17-19,21,24] studies were single- and multicenter investigations, respectively. In addition, 7 [16-18,20,23-25], 9 [10,13-15,19,21,22,26,28], and 1 [27] studies involved patients with CRC, rectal cancer, and colon cancer, respectively. The included studies encompassed patients from stage I to IV, with the majority involving stages II and III. Most patients underwent curative-intent surgery, and 2 [18,20] studies specifically included cases with resectable metastases. All studies conducted radiomics analysis, of which 8 [13-15,19,21,22,26,28] and 9 [10,16-18,20,23-25,27] were based on MRI and CT images, respectively. Only 1 included study applied a DL model [16], while the remaining used diverse traditional ML algorithms [10,13-15,17-28]. Regarding the number of researchers involved in image segmentation, 2 studies [24,28] had only 1 imaging researcher, 9 studies [10,13,14,17-21,23] had 2 researchers

XSL•FO
RenderX

working together, 4 studies [15,22,25,26] had 3 researchers working together, and 2 studies [16,27] did not report the number of imaging researchers. Regarding the segmentation software used for ROI regions, ITK-SNAP and 3D Slicer were used in 8 [10,13-15,17,18,20,21] and 3 studies [20,24,25], respectively, with the rest of the studies using The Medical Imaging Interaction Toolkit (MITK) [16], Gold LX [22], INFINITE PACS [23], Radcloud radiomics platform, and the Eclipse system. Two studies [16,27] did not perform validation set partitioning, 1 study [22] performed 5-fold cross-validation, and 8 studies [10,13-15,17-21,25] had a separate external validation cohort [10,13-15,17-19,21], of which 5 studies [13-15,17,18] had 2 cohorts (internal and external). In 14 studies [10,13-21,23-25,28], clinical factors were combined with radiomics features to construct models, while the rest of the studies developed models using radiomics features or clinical factors alone [22,26,27]. Table S2 in Multimedia Appendix 1 [10,13-28] shows the basic characteristics of the included studies. Table S4 in Multimedia Appendix 1 [10,13-28] shows essential data for pooled analysis.

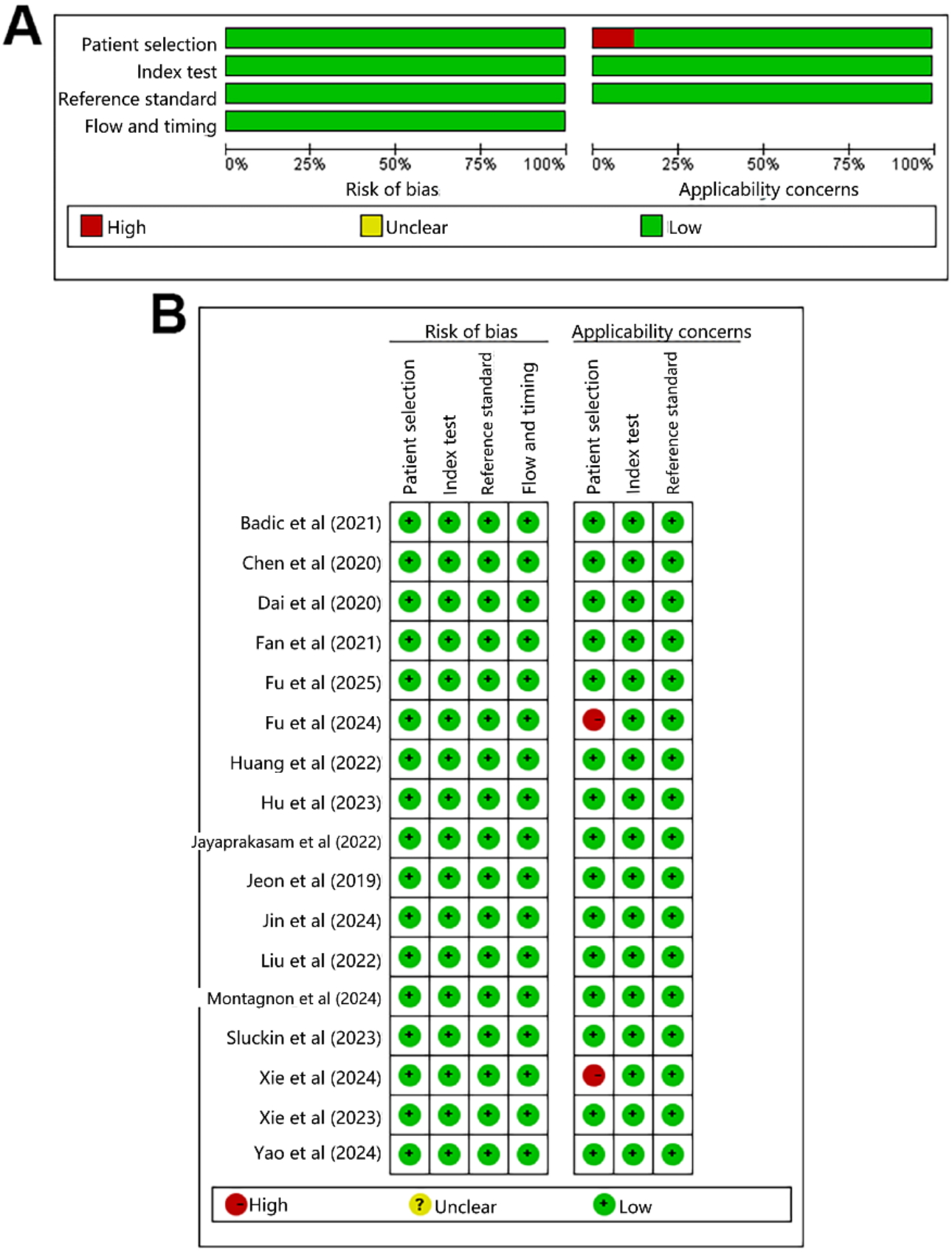
Study Quality and RoB Assessment

The average and median RQS scores of all 17 studies were 13.23 (SD 2.56) and 13 (IQR 6-16), respectively. All studies had "Image protocol quality," "Discrimination statistics," and "Cut-off analyses" items. In addition, 16 [10,14-28] out of 17 studies (94%) had "Calibration statistics" and "Validation" items [10,13-26,28]. On the other hand, 13 [10,13-15,17-23,25,26] out of 17 studies (77%) conducted "Multiple segmentations." Fourteen [10,13-21,23-25,27,28] out of 17 studies (82%) performed multivariable analysis and incorporated nonradiomics features [10,13,14,16-18,21-28], potentially yielding a more holistic model. A total of 11 [10,13,15,17-21,26-28] out of 17 studies (65%) reported potential clinical use and generated clinical decision curves. Two [15,16] studies provided open science and data access, and only 1 study [23] detected and discussed biological correlations. There were no phantom studies, and none of the studies used the comparison to the "gold standard," adjustment for multiple testing or feature reduction, prospective designs, imaging at multiple time points, or cost-effectiveness analysis. Supplementary material provides the detailed RQS scores for all included studies (Table S3 in Multimedia Appendix 1) [10,13-28].

The RoB and concerns regarding applicability for each included study were rigorously assessed using the Quality Assessment of Diagnostic Accuracy Studies (QUADAS-2) tool [33]. Notably, the included studies were cohort studies, and most of them were not excluded, which avoided the low RoB in case selection. Furthermore, considering that the included studies primarily used supervised ML with clearly defined outcomes, they had a low RoB. The implementation and interpretation of gold standards were performed by using clear criteria for recurrence, and the blinding did not influence outcomes; hence, the RoB was minimal. In addition, there was low RoB in case selection, given that known gold standards were applied. However, given that both studies enrolled cases of CRC-related metastases, there was a high RoB in the clinical applicability. A traffic-light plot summarizing the QUADAS-2 assessment for each study is presented in Figure 2.

XSL•FO
RenderX

Figure 2. Traffic-light plot summarizing the Quality Assessment of Diagnostic Accuracy Studies-2 assessment [10,13-28].



XSL•FO
RenderX

Meta Analysis

Training Set

In total, 8 studies [10,13-15,18-20,25] compared models constructed to predict recurrence based on clinical factors, and a c-index of 0.73 (95% CI 0.69 - 0.78; GRADE=low) was obtained using a random-effects model (Figure 3A; Table S5 in Multimedia Appendix 1) [10,13-28]. Furthermore, 13 radiomics-based ML models had a pooled c-index of 0.83 (95% CI 0.77 - 0.89; GRADE=very low, due to inconsistency; Figure 3B; Table S5 in Multimedia Appendix 1) [10,13-28]. The c-index values of the CT-based and MRI-based radiomics summaries were 0.84 (95% CI 0.74 - 0.94; GRADE=very low, due to inconsistency) and 0.81 (95% CI 0.71 - 0.91; GRADE=very low, due to inconsistency), respectively. In addition, 12 studies [10,13-21,25,27] developed ML models based on radiomics features plus clinical features, with a pooled c-index of 0.82 (95% CI 0.72 - 0.91; GRADE=very low, due to inconsistency; Figure 3C; Table S5 in Multimedia Appendix 1) [10,13-28].

XSL•FO
RenderX

Figure 3. (**A**) Forest plot of c-index meta-analysis of machine learning (ML) constructed based on clinical features to predict colorectal cancer (CRC) recurrence in the training set. (**B**) Forest plot of c-index meta-analysis for ML to predict CRC recurrence based on radiomics features in the training set. (**C**) Forest plot of c-index meta-analysis of ML based on radiomics combined with clinical features to predict CRC recurrence in the training set [10,13-22,25-28]. CT: computed tomography; MRI: magnetic resonance imaging.

XSL•FO
RenderX

Validation Set

Eight studies [10,13-15,18-20,25] compared models constructed to predict recurrence based on clinical factors, and a pooled c-index of 0.73 (95% CI 0.68 - 0.79; GRADE=very low, due to inconsistency) was obtained using a random-effects model (Figure 4A; Table S5 in Multimedia Appendix 1) [10,13-28]. Publication bias was not detected by the Egger test (*P*=.11) and funnel plot (Multimedia Appendix 2). Furthermore, 16 radiomics features–based ML models had a pooled c-index of 0.80 (95% CI 0.75 - 0.85; GRADE=very low, due to inconsistency; Figure 4B; Table S5 in Multimedia Appendix 1) [10,13-28]. Publication bias was not detected by Egger test (*P*=.73) and funnel plot (Multimedia Appendix 3). The c-index values of the CT-based and MRI-based radiomic summaries were 0.83 (95% CI 0.80 - 0.87; GRADE=low) and 0.78 (95% CI 0.70 - 0.86; GRADE=very low, due to inconsistency), respectively. In addition, ML models based on radiomics features plus clinical features had a pooled c-index of 0.83 (95% CI 0.79 - 0.87; GRADE=very low, due to inconsistency; Figure 4C; Table S5 in Multimedia Appendix 1) [10,13-28]. Publication bias was detected by the Egger test (*P*=.01) and funnel plot (Multimedia Appendix 4).

XSL•FO
RenderX

Figure 4. (**A**) Forest plot of c-index meta-analysis of machine learning constructed based on clinical features to predict colorectal cancer (CRC) recurrence in the validation set. (**B**) Forest plot of c-index meta-analysis for machine learning to predict CRC recurrence based on radiomics features in the validation set. (**C**) Forest plot of c-index meta-analysis of machine learning based on radiomics combined with clinical features to predict CRC recurrence in the validation set [10,13-21,23-28]. CT: computed tomography; MRI: magnetic resonance imaging.

XSL•FO
RenderX

Internal Validation Set

Overall, 6 studies [13-15,18,20,25] compared models constructed to predict recurrence based on clinical factors, and a pooled c-index of 0.70 (95% CI 0.61 - 0.79; GRADE=very low, due to inconsistency) was obtained using the random-effects model (Multimedia Appendix 5; Table S5 in Multimedia Appendix 1) [10,13-28]. Furthermore, 9 radiomics features–based ML models had a pooled c-index of 0.83 (95% CI 0.78 - 0.88; GRADE=very low, due to inconsistency; Multimedia Appendix 6; Table S5 in Multimedia Appendix 1) [10,13-28]. The c-index values for the CT-based and MRI-based models were 0.84 (95% CI 0.80 - 0.88; GRADE=low) and 0.82 (95% CI 0.71 - 0.92; GRADE=very low, due to inconsistency), respectively. In addition, ML models based on radiomics features plus clinical features had a pooled c-index of 0.83 (95% CI 0.78 - 0.88; GRADE=very low, due to inconsistency; Multimedia Appendix 7; Table S5 in Multimedia Appendix 1) [10,13-28].

External Validation Set

A total of 5 studies [10,14,15,18,19] compared models constructed to predict recurrence based on clinical factors and a pooled c-index of 0.76 (95% CI 0.70 - 0.83; GRADE=very low, due to inconsistency) was obtained using the random-effects model (Multimedia Appendix 8; Table S5 in Multimedia Appendix 1) [10,13-28]. Furthermore, 7 ML models established using radiomics features showed a pooled c-index of 0.75 (95% CI 0.66 - 0.83; GRADE=very low, due to inconsistency; Multimedia Appendix 9; Table S5 in Multimedia Appendix 1) [10,13-28], while that of MRI-based radiomics models was 0.74 (95% CI 0.62 - 0.85; GRADE=very low, due to inconsistency) and that for CT-based was 0.79 (95% CI 0.71 - 0.88; GRADE=low). In addition, the ML models derived from radiomics features plus clinical features had a pooled c-index of 0.83 (95% CI 0.78 - 0.88; GRADE=low; Multimedia Appendix 10; Table S5 in Multimedia Appendix 1) [10,13-28].

Sensitivity Analysis

The robustness of the pooled estimates was determined using leave-one-out sensitivity analyses applied to the validation set results. It was observed that, while the point estimate of the pooled c-index showed minor fluctuations upon the sequential removal of each study, the overall estimates remained stable and within a consistent range. The results of the sensitivity analysis are visualized in Figure 5.

XSL•FO
RenderX

Figure 5. Sensitivity analysis on the validation sets based on clinical features, radiomics features, and combined clinical and radiomics features [10,13-15,17-21,23-26,28].

XSL•FO
RenderX

Discussion

Principal Findings

This meta-analysis systematically evaluated and compared the predictive performance of different radiomics-based ML models for CRC recurrence risk. We postulated that models integrating both radiomic features and clinical variables may show superior predictive accuracy compared to either modality alone. The results revealed that the integrated models achieved the highest pooled c-index of 0.83 (95% CI 0.79 - 0.87) in the validation set, outperforming models based solely on radiomics features (c-index: 0.80; 95% CI 0.75 - 0.85) or clinical features (c-index: 0.73; 95% CI 0.68 - 0.79). Collectively, the findings of this study underscore the complementary value of combining quantitative imaging biomarkers with clinical data to enhance recurrence risk stratification in patients with CRC.

Notably, research on cancer diagnosis has seen a proliferation of systematic reviews and meta-analyses, particularly concerning CRC diagnosis, treatment response, and prognosis [34,35]. While this reflects the high clinical interest in radiomics, it also underscores the challenge of demonstrating novel and impactful contributions. Our study addresses a specific and clinically pertinent niche within this saturated field. Unlike previous reviews that often focus on a broader diagnostic or prognostic scope, this meta-analysis provides a dedicated quantitative synthesis focused exclusively on ML-based models for recurrence risk prediction. More importantly, we placed a particular emphasis on evaluating the incremental value of integrating radiomics with clinical features, a comparative approach that is less commonly the central focus of existing reviews. Therefore, we believe this work offers a nuanced and actionable insight: that the future of radiomics in clinical decision-making may lie not in replacing clinical factors, but in synergistically combining with them. This promising finding, however, should be considered in light of the detected publication bias, which indicates that the literature may lack smaller studies with negative results. Therefore, there is an urgent need for prospective validation studies in the future to confirm these promising findings.

Comparison to Prior Work

Multiple reviews and meta-analyses have reported the clinical use of potential biomarkers in predicting CRC recurrence postsurgery [36,37]. Nonetheless, the predictive value of radiomics remains inadequately assessed. Several studies have constructed different clinical prediction models for CRC recurrence risk. For instance, Alinia constructed a predictive model and validated its predictive efficacy using 7 ML algorithms based solely on clinicopathological features (eg, disease stage and treatment type) in a cohort of 284 patients with CRC [38]. In addition, Mohammadian Rad predicted recurrence risk using a gradient-boosting model that combined clinicopathological features (eg, carcinoembryonic antigen level) and demographic data [39]. Furthermore, Seong et al [40] integrated unstructured textual information from colonoscopy reports with clinical data for CRC risk stratification.

Despite their good predictive results, these studies had some limitations, which could be attributed to several factors. First, the performance of the models based on clinical data alone in predicting CRC recurrence risk was lower than that of the fusion model integrating radiomics features, highlighting the significance of combining imaging features for an improved predictive ability. Second, colonoscopy is highly invasive and relies largely on the endoscopist's experience and skill level; hence, its images are mainly based on morphological features, which lack quantitative analysis of deep infiltration or the tumor's metastatic potential, thus limiting the model's clinical applicability. Conversely, radiomics can extract hundreds of quantitative features (eg, texture and grayscale covariance matrix) from CT and MRI, among other images, reflecting tumor heterogeneity more comprehensively and providing a more reliable individualized treatment basis.

Herein, the CT and MRI images were predominantly used to predict CRC recurrence risk. Notably, there were no significant differences between the CT and MRI radiomics-based prediction models in the validation set. Nonetheless, MRI radiomics studies often require integrated multisequence image segmentation and feature extraction, whereas CT radiomics is usually based on a single modality (eg, enhanced CT) and features a relatively simplified process. In other words, MRI image segmentation has a greater workload [41]. Given that there is no significant difference in the predictive value between the 2, CT-based radiomics, despite its simplicity, can still be considered in the future in constructing radiomics-based ML prediction models.

Selecting ML algorithms remains a notable challenge when constructing radiomics-based predictive models, especially for image-processing tasks. Notably, ML models could be influenced by traditional ML and DL algorithms [42]. Traditional ML relies on the (manual) segmentation of images, image texture screening for model construction, and model validation. When extracting and screening image textures, some of the image information may be lost, somewhat impacting the model's accuracy [43]. On the other hand, DL can intelligently segment images or be trained directly on segmented images. Furthermore, it incorporates the extraction and screening of image texture features into the training process, maximizing image information retention and providing better accuracy [44,45]. Here, manual segmentation was used owing to the few enrolled studies. Therefore, future studies should further explore the application of DL methods in constructing radiomics-based predictive models, potentially improving image recognition.

The role of clinical and demographic characteristics is particularly important when constructing prediction models based on radiomics, as they can accurately reflect disease progression. Some studies reported a significant correlation between laboratory test results and tumor staging and prognosis information, including tumor markers [46,47]. In addition, social factors such as marital status and family income were markedly linked to the prognosis of patients with tumors [48,49]. These studies highlight the potential significance of screening and incorporating meaningful clinical and sociodemographic characteristics when constructing radiomics-based prediction models. To effectively integrate these multimodal models into clinical practice, future efforts should focus on developing interoperable digital health platforms that can seamlessly combine radiomic features with real-time clinical and

XSL•FO
RenderX

demographic data. Such systems should be designed to interface with existing electronic health records, support automated image analysis, and generate interpretable risk scores that can be readily used by clinicians for personalized recurrence risk assessment. In addition, implementation studies are needed to evaluate the usability, workflow integration, and clinical impact of these tools in routine care settings.

When constructing a clinical prediction model, validation is often conducted both internally and externally. For internal validation, both the training and validation sets are often derived from the same dataset and split through random sampling, among other methods [50]. Notably, internal validation often has limitations on the model's interpretation and generalizability, especially in radiomics research that is highly dependent on images. Consequently, external validation, which involves datasets from different sources, is often recommended [51]. Herein, internal and external validation performances were assessed separately, revealing that the latter exhibited desirable prediction accuracy.

The significant statistical heterogeneity observed in our meta-analysis, while addressed by the use of a random-effects model, warrants a deeper qualitative discussion regarding its potential sources. The methodological diversity across the included studies likely introduced substantial variability that influences the interpretation of our pooled estimates. For instance, differences in imaging protocols (eg, CT vs MRI, scanner manufacturers, and contrast-enhancement phases) directly affect radiomics feature values, making it challenging to harmonize models across studies. Variations in patient characteristics, such as the inclusion of different cancer stages (I-IV), alter the underlying recurrence risk profiles of the cohorts. Simpler models, such as logistic regression, offer high interpretability but may fail to capture intricate, nonlinear relationships in the radiomics data. In contrast, more complex traditional ML algorithms (eg, random forest and support vector machines) can model these nonlinearities and often achieve higher accuracy, albeit at the cost of increased computational demand and potential overfitting if not properly regularized. While DL models hold the promise of end-to-end feature learning and potentially superior performance by automatically discovering relevant patterns from image data, they were scarcely represented in our included studies and require large datasets to train effectively. Finally, the definition of the recurrence outcome itself varied, encompassing disease-free survival, local recurrence, or time-to-recurrence, each capturing a slightly different clinical endpoint. Despite the methodological heterogeneity, our meta-analysis offers a comprehensive and robust synthesis of the current evidence. The fact that a consistently strong discriminative performance (c-index >0.80) was maintained across such varied technical and clinical contexts is a key finding, underscoring the robustness of radiomics-based prediction for CRC recurrence.

Study Limitations

Despite its valuable insights, this study had some limitations. First, the number of eligible studies was limited, which constrained more granular subgroup analyses. In addition, the geographic origin of the evidence base was imbalanced, with 12 of the 17 included studies conducted in China. While this provides a robust assessment within that specific context, it may limit the generalizability of our findings to other populations with different genetic backgrounds, ethnicities, and healthcare systems (eg, in terms of screening protocols, treatment strategies, and staging criteria). Therefore, further multinational studies are advocated to validate the broader applicability of these radiomics models and to investigate potential geographic or ethnic variations in their performance. Second, the limited number of studies resulted in even less data for the subgroup analysis of images, possibly affecting result interpretation. Third, although subgroup analyses based on the image source (CT vs MRI) were performed in the validation set, thereby explaining some of the heterogeneity, there was significant heterogeneity. This likely reflects the clinical and methodological diversity across studies, including differences in imaging protocols, patient characteristics, model types, clinical variables, and recurrence definitions. These factors, compounded by the limited number of studies, make it difficult to quantitatively identify other potential sources of heterogeneity and highlight the challenges in achieving standardized validation across independent cohorts. Furthermore, regarding reproducibility, only 2 studies provided open-source code or datasets. This lack of transparency prevents independent validation of the proposed models and limits the clinical translation of our findings. In the future, researchers should promote open science practices by sharing code and data where possible to facilitate verification and build upon existing work. Finally, the assessment of model performance was primarily based on the c-index due to inconsistent reporting of calibration metrics (eg, Brier score and calibration slope) and time-dependent discrimination measures (eg, time-dependent–area under the curve) across studies. While the c-index provides valuable evidence of the models' ability to stratify risk, this assessment should be complemented by future evaluations of calibration to ensure the accuracy of predicted probabilities for individual patients. Establishing robust calibration will be a crucial next step in translating these promising discriminative models into reliable clinical tools. These aspects represent important limitations that should be addressed in future studies with larger and more standardized datasets.

Conclusions

This study demonstrates that ML models based on radiomics and incorporating clinical features exhibit superior performance in predicting the risk of CRC recurrence, with a significantly higher discriminative ability (c-index) than models relying only on a single data source. This finding highlights the significant value of multimodal data fusion in improving prediction accuracy. However, most of the existing studies use traditional ML methods that rely on manual feature extraction and screening, which may lead to information loss and limited model generalization ability. Future studies should further explore the potential of end-to-end feature learning methods, such as DL, to improve model robustness and clinical translational value by automatically extracting high-level image features and reducing manual intervention, and prioritize prospective, multicenter validation with standardized protocols and explainable AI to facilitate clinical adoption.

XSL•FO
RenderX

Funding

This work was supported by the National Natural Science Foundation of China (grant 82374298), Backup Leader Support Program of Beijing University of Chinese Medicine (90010960920033), and High-level Chinese Medicine Key Discipline of the Double-tier Supporting Support Bureau - Evidence-based Medicine in Chinese Medicine (90010951310169).

Data Availability

The datasets generated during and analyzed during this study are included in this published article and its supplementary information files.

Authors' Contributions

Conceptualization, methodology, and software: YS and BL
Data curation, writing – original draft preparation: YS
Data curation: CJ, HS, JA, ZB, and ZS
Supervision: LH
Writing – review and editing: THK, JL, and ZL

Conflicts of Interest

None declared.

Multimedia Appendix 1
Data detailing the literature search strategies, characteristics of included studies, methodological quality assessments, and essential data for the meta-analysis.
[DOC File, 368 KB - medinform_v13i1e78644_app1.doc]

Multimedia Appendix 2
Funnel plot based on clinical features in the validation set.
[PNG File, 90 KB - medinform_v13i1e78644_app2.png]

Multimedia Appendix 3
Funnel plot based on radiomics features in the validation set.
[PNG File, 102 KB - medinform_v13i1e78644_app3.png]

Multimedia Appendix 4
Funnel plot based on radiomics combined with clinical features in the validation set.
[PNG File, 101 KB - medinform_v13i1e78644_app4.png]

Multimedia Appendix 5
Forest plot of c-index meta-analysis of machine learning constructed based on clinical features to predict colorectal cancer recurrence in the internal validation set.
[PNG File, 144 KB - medinform_v13i1e78644_app5.png]

Multimedia Appendix 6
Forest plot of c-index meta-analysis for machine learning to predict colorectal cancer recurrence based on radiomics features in the internal validation set.
[PNG File, 252 KB - medinform_v13i1e78644_app6.png]

Multimedia Appendix 7
Forest plot of c-index meta-analysis of machine learning based on radiomics combined with clinical features to predict colorectal cancer recurrence in the internal validation set.
[PNG File, 263 KB - medinform_v13i1e78644_app7.png]

Multimedia Appendix 8
Forest plot of c-index meta-analysis of machine learning constructed based on clinical features to predict colorectal cancer recurrence in the external validation set.

XSL•FO
RenderX

[PNG File, 160 KB - medinform_v13i1e78644_app8.png]

Multimedia Appendix 9
Forest plot of c-index meta-analysis for machine learning to predict colorectal cancer recurrence based on radiomics features in the external validation set.
[PNG File, 231 KB - medinform_v13i1e78644_app9.png]

Multimedia Appendix 10
Forest plot of c-index meta-analysis of machine learning based on radiomics combined with clinical features to predict colorectal cancer recurrence in the external validation set.
[PNG File, 232 KB - medinform_v13i1e78644_app10.png]

Checklist 1
PRISMA checklist.
[PDF File, 174 KB - medinform_v13i1e78644_app11.pdf]

References

1. Sung H, Ferlay J, Siegel RL, et al. Global cancer statistics 2020: GLOBOCAN estimates of incidence and mortality worldwide for 36 cancers in 185 countries. CA Cancer J Clin 2021 May;71(3):209-249. [doi: 10.3322/caac.21660] [Medline: 33538338]
2. Bray F, Laversanne M, Sung H, et al. Global cancer statistics 2022: GLOBOCAN estimates of incidence and mortality worldwide for 36 cancers in 185 countries. CA Cancer J Clin 2024;74(3):229-263. [doi: 10.3322/caac.21834] [Medline: 38572751]
3. Mahar AL, Compton C, Halabi S, Hess KR, Weiser MR, Groome PA. Personalizing prognosis in colorectal cancer: a systematic review of the quality and nature of clinical prognostic tools for survival outcomes. J Surg Oncol 2017 Dec;116(8):969-982. [doi: 10.1002/jso.24774] [Medline: 28767139]
4. Wang Q, Xu J, Wang A, et al. Systematic review of machine learning-based radiomics approach for predicting microsatellite instability status in colorectal cancer. Radiol Med 2023 Feb;128(2):136-148. [doi: 10.1007/s11547-023-01593-x] [Medline: 36648615]
5. Zhang M, Zhang Y, Zhao L, et al. Development and multi-center validation of a machine learning Model for advanced colorectal neoplasms screening. Comput Biol Med 2025 May;190:110066. [doi: 10.1016/j.compbiomed.2025.110066] [Medline: 40157315]
6. Liu X, Elbanan MG, Luna A, et al. Radiomics in abdominopelvic solid-organ oncologic imaging: current status. AJR Am J Roentgenol 2022 Dec;219(6):985-995. [doi: 10.2214/AJR.22.27695] [Medline: 35766531]
7. Meng Y, Yang Y, Hu M, Zhang Z, Zhou X. Artificial intelligence-based radiomics in bone tumors: technical advances and clinical application. Semin Cancer Biol 2023 Oct;95(75-87):75-87. [doi: 10.1016/j.semcancer.2023.07.003] [Medline: 37499847]
8. Ferro A, Bottosso M, Dieci MV, et al. Clinical applications of radiomics and deep learning in breast and lung cancer: a narrative literature review on current evidence and future perspectives. Crit Rev Oncol Hematol 2024 Nov;203:104479. [doi: 10.1016/j.critrevonc.2024.104479] [Medline: 39151838]
9. Chen K, Qu Y, Han Y, Li Y, Gao H, Zheng D. Performance of Machine learning in diagnosing KRAS (Kirsten Rat Sarcoma) mutations in colorectal cancer: systematic review and meta-analysis. J Med Internet Res 2025 Jul 18;27:e73528. [doi: 10.2196/73528] [Medline: 40680189]
10. Xie Z, Zhang Q, Wang X, et al. Development and validation of a novel radiomics nomogram for prediction of early recurrence in colorectal cancer. Eur J Surg Oncol 2023 Dec;49(12):107118. [doi: 10.1016/j.ejso.2023.107118] [Medline: 37844471]
11. Vicini S, Bortolotto C, Rengo M, et al. A narrative review on current imaging applications of artificial intelligence and radiomics in oncology: focus on the three most common cancers. Radiol Med 2022 Aug;127(8):819-836. [doi: 10.1007/s11547-022-01512-6] [Medline: 35771379]
12. Huang W, Tao Z, Younis MH, Cai W, Kang L. Nuclear medicine radiomics in digestive system tumors: concept, applications, challenges, and future perspectives. VIEW (Beijing) 2023 Dec;4(6):20230032. [doi: 10.1002/VIW.20230032] [Medline: 38179181]
13. Fu S, Xia T, Li Z, et al. Baseline MRI-based radiomics improving the recurrence risk stratification in rectal cancer patients with negative carcinoembryonic antigen: a multicenter cohort study. Eur J Radiol 2025 Jan;182:111839. [doi: 10.1016/j.ejrad.2024.111839] [Medline: 39591940]
14. Yao X, Zhu X, Deng S, et al. MRI-based radiomics for preoperative prediction of recurrence and metastasis in rectal cancer. Abdom Radiol (NY) 2024 Apr;49(4):1306-1319. [doi: 10.1007/s00261-024-04205-y] [Medline: 38407804]

XSL•FO
RenderX

15. Xie PY, Zeng ZM, Li ZH, et al. MRI-based radiomics for stratifying recurrence risk of early-onset rectal cancer: a multicenter study. ESMO Open 2024 Oct;9(10):103735. [doi: 10.1016/j.esmoop.2024.103735] [Medline: 39368416]
16. Montagnon E, Cerny M, Hamilton V, et al. Radiomics analysis of baseline computed tomography to predict oncological outcomes in patients treated for resectable colorectal cancer liver metastasis. PLoS ONE 2024;19(9):e0307815. [doi: 10.1371/journal.pone.0307815] [Medline: 39259736]
17. Jin Z, Zou Q, Zhou T, Xue T. Preoperative prediction of early recurrence in patients with BRAF mutant colorectal cancer using a intergrated nomogram. Sci Rep 2024 Oct 25;14(1):25320. [doi: 10.1038/s41598-024-77256-2] [Medline: 39455810]
18. Fu S, Chen D, Zhang Y, et al. A CT-based radiomics tumor quality and quantity model to predict early recurrence after radical surgery for colorectal liver metastases. Clin Transl Oncol 2025 Mar;27(3):1198-1210. [doi: 10.1007/s12094-024-03645-8] [Medline: 39153176]
19. Sluckin TC, Hekhuis M, Kol SQ, et al. A deep learning framework with explainability for the prediction of lateral locoregional recurrences in rectal cancer patients with suspicious lateral lymph nodes. Diagnostics (Basel) 2023 Sep 29;13(19):3099. [doi: 10.3390/diagnostics13193099] [Medline: 37835842]
20. Hu H, Chi JC, Zhai B, Guo JH. CT-based radiomics analysis to predict local progression of recurrent colorectal liver metastases after microwave ablation. Medicine (Baltimore) 2023 Dec 29;102(52):e36586. [doi: 10.1097/MD.0000000000036586] [Medline: 38206750]
21. Liu Z, Wang Y, Shen F, et al. Radiomics based on readout-segmented echo-planar imaging (RS-EPI) diffusion-weighted imaging (DWI) for prognostic risk stratification of patients with rectal cancer: a two-centre, machine learning study using the framework of predictive, preventive, and personalized medicine. EPMA J 2022 Dec;13(4):633-647. [doi: 10.1007/s13167-022-00303-3] [Medline: 36505889]
22. Jayaprakasam VS, Paroder V, Gibbs P, et al. MRI radiomics features of mesorectal fat can predict response to neoadjuvant chemoradiation therapy and tumor recurrence in patients with locally advanced rectal cancer. Eur Radiol 2022 Feb;32(2):971-980. [doi: 10.1007/s00330-021-08144-w] [Medline: 34327580]
23. Huang YC, Tsai YS, Li CI, et al. Adjusted CT image-based radiomic features combined with immune genomic expression achieve accurate prognostic classification and identification of therapeutic targets in stage III colorectal cancer. Cancers (Basel) 2022 Apr 8;14(8):1895. [doi: 10.3390/cancers14081895] [Medline: 35454802]
24. Badic B, Da-Ano R, Poirot K, et al. Prediction of recurrence after surgery in colorectal cancer patients using radiomics from diagnostic contrast-enhanced computed tomography: a two-center study. Eur Radiol 2022 Jan;32(1):405-414. [doi: 10.1007/s00330-021-08104-4] [Medline: 34170367]
25. Fan S, Cui X, Liu C, et al. CT-based radiomics signature: a potential biomarker for predicting postoperative recurrence risk in stage II colorectal cancer. Front Oncol 2021;11:644933. [doi: 10.3389/fonc.2021.644933] [Medline: 33816297]
26. Chen F, Ma X, Li S, et al. MRI-based radiomics of rectal cancer: assessment of the local recurrence at the site of anastomosis. Acad Radiol 2021 Nov;28 Suppl 1:S87-S94. [doi: 10.1016/j.acra.2020.09.024] [Medline: 33162318]
27. Dai W, Mo S, Han L, et al. Prognostic and predictive value of radiomics signatures in stage I‐III colon cancer. Clinical & Translational Med 2020 Mar;10(1):288-293. [doi: 10.1002/ctm2.31] [Medline: 32508036]
28. Jeon SH, Song C, Chie EK, et al. Delta-radiomics signature predicts treatment outcomes after preoperative chemoradiotherapy and surgery in rectal cancer. Radiat Oncol 2019 Mar 12;14(1):43. [doi: 10.1186/s13014-019-1246-8] [Medline: 30866965]
29. Lambin P, Leijenaar RTH, Deist TM, et al. Radiomics: the bridge between medical imaging and personalized medicine. Nat Rev Clin Oncol 2017 Dec;14(12):749-762. [doi: 10.1038/nrclinonc.2017.141] [Medline: 28975929]
30. Debray TP, Damen JA, Riley RD, et al. A framework for meta-analysis of prediction model studies with binary and time-to-event outcomes. Stat Methods Med Res 2019 Sep;28(9):2768-2786. [doi: 10.1177/0962280218785504] [Medline: 30032705]
31. Langan D, Higgins JPT, Jackson D, et al. A comparison of heterogeneity variance estimators in simulated random-effects meta-analyses. Res Synth Methods 2019 Mar;10(1):83-98. [doi: 10.1002/jrsm.1316] [Medline: 30067315]
32. Almadi MA, Barkun A, Martel M. Plastic vs. self-expandable metal stents for palliation in malignant biliary obstruction: a series of meta-analyses. Am J Gastroenterol 2017 Feb;112(2):260-273. [doi: 10.1038/ajg.2016.512] [Medline: 27845340]
33. Whiting PF, Rutjes AWS, Westwood ME, et al. QUADAS-2: a revised tool for the quality assessment of diagnostic accuracy studies. Ann Intern Med 2011 Oct 18;155(8):529-536. [doi: 10.7326/0003-4819-155-8-201110180-00009] [Medline: 22007046]
34. Maqbool M, Khan A, Shahzad A, et al. Predictive biomarkers for colorectal cancer: a state-of-the-art systematic review. Biomarkers 2023 Sep;28(6):562-598. [doi: 10.1080/1354750X.2023.2247185] [Medline: 37585692]
35. Zhang Y, Song K, Zhou Y, et al. Accuracy and long‐term effectiveness of established screening modalities and strategies in colorectal cancer screening: an umbrella review. Intl Journal of Cancer 2025 Jul;157(1):126-138. [doi: 10.1002/ijc.35381] [Medline: 39998407]
36. Wang R, Zhao A, Cao N, Li Z, Zhang G, Liu F. The value of circulation tumor DNA in predicting postoperative recurrence of colorectal cancer: a meta-analysis. Int J Colorectal Dis 2020 Aug;35(8):1463-1475. [doi: 10.1007/s00384-020-03667-y] [Medline: 32572601]

XSL•FO
RenderX

37. You YN, Rustin RB, Sullivan JD. Oncotype DX(®) colon cancer assay for prediction of recurrence risk in patients with stage II and III colon cancer: a review of the evidence. Surg Oncol 2015 Jun;24(2):61-66. [doi: 10.1016/j.suronc.2015.02.001] [Medline: 25770397]
38. Alinia S, Asghari-Jafarabadi M, Mahmoudi L, Roshanaei G, Safari M. Predicting mortality and recurrence in colorectal cancer: comparative assessment of predictive models. Heliyon 2024 Mar 30;10(6):e27854. [doi: 10.1016/j.heliyon.2024.e27854] [Medline: 38515707]
39. Mohammadian Rad N, Sosef O, Seegers J, et al. Prognostic models for colorectal cancer recurrence using carcinoembryonic antigen measurements. Front Oncol 2024;14:1368120. [doi: 10.3389/fonc.2024.1368120] [Medline: 38873251]
40. Seong D, Choi YH, Shin SY, Yi BK. Deep learning approach to detection of colonoscopic information from unstructured reports. BMC Med Inform Decis Mak 2023 Feb 7;23(1):28. [doi: 10.1186/s12911-023-02121-7] [Medline: 36750932]
41. Mukherjee T, Pournik O, Arvanitis TN. Magnetic resonance imaging (MRI) radiomics in paediatric neuro-oncology: a systematic review of clinical applications, feature interpretation, and biological insights in the characterisation and management of childhood brain tumours. Digit Health 2025;11:20552076251336285. [doi: 10.1177/20552076251336285] [Medline: 40297347]
42. Wang T, Chen R, Fan N, et al. Machine learning and deep learning for diagnosis of lumbar spinal stenosis: systematic review and meta-analysis. J Med Internet Res 2024 Dec 23;26:e54676. [doi: 10.2196/54676] [Medline: 39715552]
43. Maniaci A, Lavalle S, Gagliano C, et al. The integration of radiomics and artificial intelligence in modern medicine. Life (Basel) 2024 Oct 1;14(10):1248. [doi: 10.3390/life14101248] [Medline: 39459547]
44. Liang H, Hu M, Ma Y, et al. Performance of deep-learning solutions on lung nodule malignancy classification: a systematic review. Life (Basel) 2023 Sep 14;13(9). [doi: 10.3390/life13091911] [Medline: 37763314]
45. Demircioğlu A. Are deep models in radiomics performing better than generic models? A systematic review. Eur Radiol Exp 2023 Mar 15;7(1):11. [doi: 10.1186/s41747-023-00325-0] [Medline: 36918479]
46. Liu Z, Zhang J, Wang H, et al. MRI-based radiomics feature combined with tumor markers to predict TN staging of rectal cancer. J Robot Surg 2024 May 29;18(1):229. [doi: 10.1007/s11701-024-01978-8] [Medline: 38809383]
47. Tan Y, Liu R, Xue JW, Feng Z. Construction and validation of artificial intelligence pathomics models for predicting pathological staging in colorectal cancer: using multimodal data and clinical variables. Cancer Med 2024 Apr;13(7):e6947. [doi: 10.1002/cam4.6947] [Medline: 38545828]
48. Zhu S, Lei C. Association between marital status and all-cause mortality of patients with metastatic breast cancer: a population-based study. Sci Rep 2023 Jun 5;13(1):9067. [doi: 10.1038/s41598-023-36139-8] [Medline: 37277464]
49. Yao A, Liu Z, Rao H, Shen Y, Wang C, Xie S. Exploration of the optimal number of regional lymph nodes removed for resected N0 NSCLC patients: a population-based study. Front Oncol 2022;12:1011091. [doi: 10.3389/fonc.2022.1011091] [Medline: 36249000]
50. Liu Y, Li M, Chen H, et al. Diagnostic precision in thyroid-associated ophthalmopathy using multi-center radiomics with 99mTc-DTPA SPECT/CT. Sci Rep 2024 Oct 28;14(1):25810. [doi: 10.1038/s41598-024-76018-4] [Medline: 39468140]
51. Ge L, Wu J, Jin Y, Xu D, Wang Z. Noninvasive assessment of tumor histological grade in invasive breast carcinoma based on ultrasound radiomics and clinical characteristics: a multicenter study. Technol Cancer Res Treat 2024;23:15330338241257424. [doi: 10.1177/15330338241257424] [Medline: 38780506]

Abbreviations

CRC: colorectal cancer
CT: computed tomography
DL: deep learning
GRADE: Grading of Recommendations, Assessment, Development, and Evaluation
ML: machine learning
MRI: magnetic resonance imaging
PRISMA: Preferred Reporting Items for Systematic Reviews and Meta-Analyses
PROSPERO: International Prospective Register of Systematic Reviews
RoB: risk of bias
ROI: region of interest
RQS: Radiomics Quality Score

XSL•FO
RenderX

Edited by A Coristine; submitted 06.06.25; peer-reviewed by LK Chua, L Zhou; revised version received 27.10.25; accepted 27.10.25; published 28.11.25.

Please cite as:
Sun Y, Li B, Ju C, Hu L, Sun H, An J, Kim TH, Bu Z, Shi Z, Liu J, Liu Z
Predictive Performance of Radiomics-Based Machine Learning for Colorectal Cancer Recurrence Risk: Systematic Review and Meta-Analysis
JMIR Med Inform 2025;13:e78644
URL: https://medinform.jmir.org/2025/1/e78644
doi:10.2196/78644

© Yuan Sun, Bo Li, Chuanlan Ju, Liming Hu, Huiyi Sun, Jing An, Tae-Hun Kim, Zhijun Bu, Zeyang Shi, Jianping Liu, Zhaolan Liu. Originally published in JMIR Medical Informatics (https://medinform.jmir.org), 28.11.2025. This is an open-access article distributed under the terms of the Creative Commons Attribution License (https://creativecommons.org/licenses/by/4.0/), which permits unrestricted use, distribution, and reproduction in any medium, provided the original work, first published in JMIR Medical Informatics, is properly cited. The complete bibliographic information, a link to the original publication on https://medinform.jmir.org/, as well as this copyright and license information must be included.

XSL•FO
RenderX

Using Large Language Models for Chronic Disease Management Tasks: Scoping Review

Henry Mukalazi Serugunda[1], MSc, MBA; Ouyang Jianquan[2], PhD; Hasifah Kasujja Namatovu[3], PhD; Paul Ssemaluulu[4], PhD; Nasser Kimbugwe[5], PhD; Christopher Garimoi Orach[6], PhD; Peter Waiswa[7], PhD

[1]Department of Information Technology, School of Computing and Informatics Technology, Makerere University, Kampala, Uganda

[2]School of Computer Science and School of Cyberspace, Xiangtan University, Engineering Building, 2nd Floor, Yuhu District, Xiangtan, Hunan, China

[3]Department of Information Systems, School of Computing and Informatics Technology, Makerere University, Kampala, Uganda

[4]Department of Computer Science, Faculty of Computing and Library Science, Kabale University, Kabale, Uganda

[5]Department of Networks, School of Computing and Informatics Technology, Makerere University, Kampala, Uganda

[6]Department of Community Health and Behavioral Sciences, School of Public Health, College of Health Sciences, Makerere University, Kampala, Uganda

[7]Department of Health Policy Planning and Management, School of Public Health, College of Health Sciences, Makerere University, Kampala, Uganda

Corresponding Author:
Ouyang Jianquan, PhD
School of Computer Science and School of Cyberspace, Xiangtan University, Engineering Building, 2nd Floor, Yuhu District, Xiangtan, Hunan, China

Abstract

Background: Chronic diseases present significant challenges in health care, requiring effective management to reduce morbidity and mortality. While digital technologies like wearable devices and mobile applications have been widely adopted, large language models (LLMs) such as ChatGPT are emerging as promising technologies with the potential to enhance chronic disease management. However, the scope of their current applications in chronic disease management and associated challenges remains underexplored.

Objective: This scoping review investigates LLM applications in chronic disease management, identifies challenges, and proposes actionable recommendations.

Methods: A systematic search for English-language primary studies on LLM use in chronic disease management was conducted across PubMed, IEEE Xplore, Scopus, and Google Scholar to identify articles published between January 1, 2023, and January 15, 2025. Of the 605 screened records, 29 studies met the inclusion criteria. Data on study objectives, LLMs used, health care settings, study designs, users, disease management tasks, and challenges were extracted and thematically analyzed using the Preferred Reporting Items for Systematic Reviews and Meta-Analyses extension for Scoping Reviews guidelines.

Results: LLMs were primarily used for patient-centered tasks, including patient education and information provision (18/29, 62%) of studies, diagnosis and treatment (6/29, 21%), self-management and disease monitoring (8/29, 28%), and emotional support and therapeutic conversations (4/29, 14%). Practitioner-centered tasks included clinical decision support (8/29, 28%) and medical predictions (6/29, 21%). Challenges identified include inaccurate and inconsistent LLM responses (18/29, 62%), limited datasets (6/29, 21%), computational and technical (6/29, 21%), usability and accessibility (9/29, 31%), LLM evaluation (5/29, 17%), and legal, ethical, privacy, and regulatory (10/29, 35%). While models like ChatGPT, Llama, and Bard demonstrated use in diabetes management and mental health support, performance issues were evident across studies and use cases.

Conclusions: LLMs show promising potential for enhancing chronic disease management across patient and practitioner-centered tasks. However, challenges related to accuracy, data scarcity, usability, and ethical concerns must be addressed to ensure patient safety and equitable use. Future studies should prioritize the integration of LLMs with low-resource platforms, wearable and mobile technologies, developing culturally and age-appropriate interfaces, and establishing robust regulatory and evaluation frameworks to support safe, effective, and inclusive use in health care.

(JMIR Med Inform 2025;13:e66905) doi:10.2196/66905

KEYWORDS

chronic diseases; disease management; artificial intelligence in health care; large language models; natural language processing; NLP; generative pre-trained transformer; GPT

XSL•FO
RenderX

Introduction

Chronic diseases, such as diabetes, heart disease, asthma, lung disease, depression, hypertension, Alzheimer disorder, and cancer, are a significant global burden on health care systems [1-3]. These conditions often lead to long-term health issues and have profound physical, psychological, and social impacts on patients [1,2]. Chronic diseases demand continuous, personalized care, often resource-intensive and difficult to scale [1]. Therefore, disease management, which encompasses screenings, regular check-ups, monitoring, coordination of treatment, medication adherence, lifestyle modifications, and patient education, is crucial for improving patient outcomes, enhancing quality of life, and reducing the overall burden on health care systems [1]. However, the resource-intensive nature of personalized, continuous care often makes it inaccessible to many patients, particularly in underserved populations where limited access to health care professionals and resources creates significant barriers to effective disease management [3].

In recent years, the use of digital technologies such as wearable devices [4], mobile apps [5], and chatbots [6,7] has grown significantly in the management of chronic diseases. These have mainly been used for health care tasks, including patient education, symptom monitoring, and medication management [4-7]. The recent emergence of large language models (LLMs) such as GPT, Palm, Llama, and LaMDA [8-11] has demonstrated growing potential in health care applications. These models have been applied in health care for tasks such as personalized treatment recommendations, medical diagnosis, medical record summarization, and interpretation of clinical data to support clinical decision-making and disease management [12-16].

Chronic disease management requires continuous monitoring, patient education, treatment coordination, and personalized care strategies [1]. Recent advancements in LLMs have introduced new possibilities for improving these tasks. For instance, ChatGPT has been explored in providing personalized health advice, enhancing patient engagement, and supporting symptom monitoring [12,13]. In diabetes management, GPT-based models have been investigated for interpreting continuous glucose monitoring data, providing personalized lifestyle recommendations [17], and assessing individualized risk profiles for complications such as retinopathy [17]. Beyond diabetes, LLMs such as LLaMA and GPT have been investigated for mental health support [18], blood pressure measurement using wearable bio signals [19], management of sickle cell anemia [20], and dissemination of information on inflammatory bowel diseases to patients and health care professionals [21].

Despite these applications, several challenges affect the effectiveness of LLMs in chronic disease management, including inaccurate responses, limited and biased datasets, and ethical concerns [17,22,23]. These issues raise concerns regarding the accuracy, reliability, and clinical applicability of LLM-generated recommendations [24]. Given these challenges, a comprehensive review is essential to assess the current applications, identify key limitations, and propose strategies to enhance the effectiveness and safety of LLMs in chronic disease care. While existing reviews explore LLMs in general health care, this scoping review uniquely focuses on their role in chronic disease management. It synthesizes evidence across patient- and practitioner-centered applications, domain-specific challenges, and provides actionable recommendations. Specifically, this review aims to evaluate the current applications of LLM in chronic disease management tasks, identify key challenges, and provide actionable recommendations to address identified challenges.

Methods

Search Strategy and Information Sources

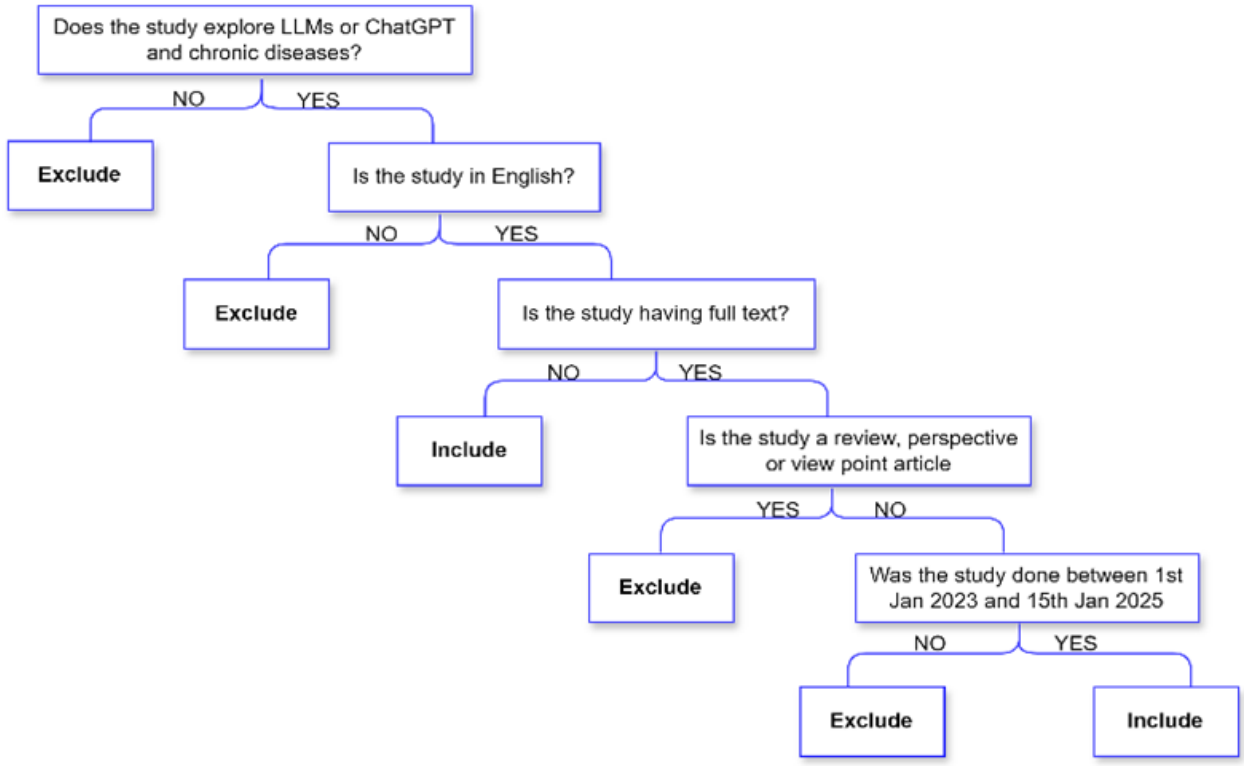
This scoping review explored the use of LLMs in chronic disease management following the PRISMA-ScR (Preferred Reporting Items for Systematic Reviews and Meta-Analyses Extension for Scoping Reviews) [25]. A comprehensive search was conducted in PubMed, Scopus, IEEE Xplore, and Google Scholar, selected for their coverage of peer-reviewed medical, technical, and AI-related research. Google Scholar was included to capture a broad range of academic publications, including preprints and conference papers that may not be covered by traditional databases. Search terms included combinations of “Large language models,” “LLMs,” “ChatGPT,” “chronic diseases,” and “chronic disease management.” The search targeted both published and unpublished English-language articles from January 1, 2023, to January 15, 2025, ensuring a focus on recent advancements in LLM applications in health care.

Article Selection

Studies were included if they focused on applications of LLM in chronic disease management, provided full-text access, were published in English, and appeared between January 2023 and January 15, 2025. Exclusion criteria eliminated nonprimary research (reviews, editorials, viewpoints, and commentaries), abstracts without full text, non-English publications, and articles outside the date range. To capture emerging research and potentially studies, reputable non-peer–reviewed preprints from established repositories such as arXiv and medRxiv were included. Figure 1 illustrates the eligibility screening process with a decision tree.

XSL•FO
RenderX

Figure 1. Decision tree for assessing article eligibility. The exclusion of certain publication types was necessary to ensure the review focused on primary research and empirical studies that directly address the application of large language models in chronic disease management.



Data Extraction and Synthesis

The data from selected studies were extracted into a structured form that captured study objectives, the LLMs used, health care settings, study designs, disease management tasks, identified challenges, evaluation methods, and target users. These extracted data points were selected to ensure a structured and objective analysis aligned with the study's aims. Study objectives provided insight into the intended applications of LLMs in chronic disease management, while health care settings contextualized their use across clinical and patient-centered environments. Study design and evaluation methods were included to assess methodological rigor and the validity of findings. In addition, data on LLM models, disease management tasks, and key challenges enabled a systematic evaluation of current applications, limitations, and areas for future research.

The Mixed Methods Appraisal Tool (MMAT, version 2018) [26] was used to perform a formal methodological quality assessment. The MMAT was selected due to its flexibility in evaluating diverse study designs included in the review. Two reviewers independently appraised each study using the 5 criteria relevant to its methodological design, with discrepancies resolved through discussion and reached consensus on final ratings. Consistent with scoping review methodology, the studies were not excluded based on quality, but results inform the interpretation of findings [25]. The findings from the included studies were synthesized and presented in alignment with the study objectives. A thematic analysis approach was used to categorize qualitative insights, grouping findings into patient-centered tasks, practitioner-centered tasks, and challenges. Discrepancies in data interpretation were resolved through consensus among the reviewers. Reference management and citation generation were conducted using Mendeley.

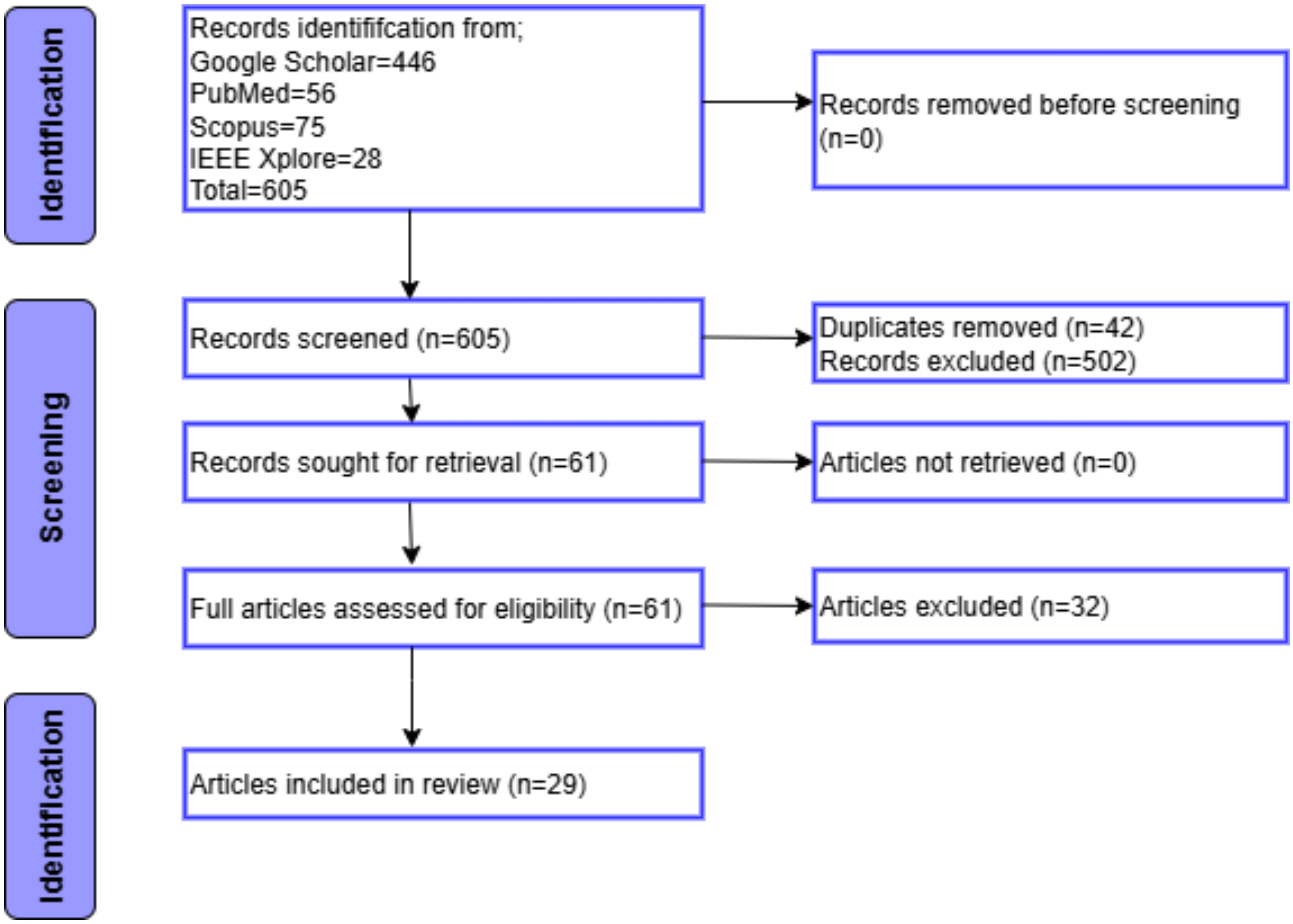
Results

Included Studies

The PRISMA flow diagram (Figure 2) outlines each stage of the study selection process. The PRISMA-ScR framework was followed to ensure transparency and reproducibility, incorporating detailed search strategies and clearly defined exclusion criteria. A total of 446 records were identified from Google Scholar, 75 from Scopus, 56 from PubMed, and 28 from IEEE Xplore. After removing duplicates, 242 unique records underwent title and abstract screening, resulting in 61 articles for full-text review. Following the application of eligibility criteria, 29 articles were included in the final analysis.

XSL•FO
RenderX

Figure 2. PRISMA (Preferred Reporting Items for Systematic Reviews and Meta-Analyses) flowchart.



Characteristics of Included Articles

Table 1 provides the characteristics of the 29 articles included in this scoping review. The articles were categorized based on publication type, with the majority of the studies being journal articles (n=18), followed by conference papers (n=8), and preprints (n=3). The studies used a variety of research designs, including experimental (n=10), qualitative research (n=3), comparative studies (n=4), cross-sectional study (n=2), case study (n=1), observational (n=3), retrospective cohort designs (n=3), mixed methods (n=1), pilot study (n=1), and prospective study (n=1). Table 1 provides more details on the characteristics of the reviewed studies.

XSL•FO
RenderX

Table . Study characteristics (n=29).

Study	Country	Article category	Study objective	Health care setting	Study design	Evaluation
Montagna et al [6]	Italy	Conference paper	To design and implement a system architecture for a chatbot-based home blood pressure monitoring solution.	Home care setting	Experimental (system design and prototype development)	Human evaluation
Yang et al [16]	China	Preprint	To explore the application of a fine-tuned model-based outpatient treatment support system for treating patients with diabetes and to evaluate its effectiveness and potential value.	Clinical (West China Hospital) home care	Experimental (fine-tuning)	Human evaluation and automated evaluation metrics
Raghu et al [17]	India	Journal article	To evaluate the ability of ChatGPT to predict the diabetic retinopathy risk.	—[a]	Comparative study	Human evaluation
Song et al [18]	The Republic of Korea	Preprint	To investigate the experiences of individuals using LLM[b] chatbots for mental health support.	Korea Advanced Institute of Science and Technology	Qualitative study	Human evaluation
Liu et al [19]	China	Conference paper	Explore the use of LLMs for cuffless blood pressure measurement using wearable bio signals	Home care settings	Experimental (cuffless blood pressure measurement using LLMs)	Human evaluation
Ogundare et al [20]	Nigeria	Conference paper	To investigate the potential of LLMs in ambulatory devices for sickle cell anemia management.	Home care setting	Case study	Automated evaluation metrics
Cankurtaran et al [21]	Turkey	Journal article	To evaluate the performance of ChatGPT within the context of inflammatory bowel disease.	—	Cross-sectional study	Human evaluation
Wang et al [22]	China	Conference paper	To enhance the diagnosis and treatment of depression.	Clinical and home-care settings	Experimental (pre-training and fine-tuning)	Human evaluation
Abdullahi et al [23]	Germany	Journal article	To explore the potential of three popular Large Language Models in medical education to enhance the diagnosis of rare and complex diseases.	Home care setting	Qualitative study	Human evaluation and automated evaluation metrics

XSL•FO
RenderX

Study	Country	Article category	Study objective	Health care setting	Study design	Evaluation
Al Anezi [24]	Saudi Arabia	Journal article	To analyze the use of ChatGPT as a virtual health coach for chronic disease management.	Home care setting	Quasi-experimental design	Human evaluation
Athavale et al [27]	United States	Journal article	To assess whether chatbots could assist with answering patient questions and electronic health record inbox management	Clinical (Division of Vascular Surgery, Stanford University School of Medicine in Palo Alto)	Experimental (chatbot assistance in chronic venous disease management)	Human evaluation
Soto-Chávez et al [28]	Colombia	Journal article	To evaluate the reliability and readability of Spanish chronic disease information presented to ChatGPT	—	Cross-sectional study	Human evaluation
Abbas et al [29]	Pakistan	Journal article	To assess the predictive accuracy of ChatGPT-assisted machine learning models for various chronic diseases.	Clinical (Tertiary hospital)	Observational study	Automated evaluation metrics
Anderson et al [30]	United States	Conference paper	The study aims to discover and rank novel relationships between various aspects of this condition.	—	Experimental	Human evaluation and automated evaluation metrics
Ding et al [31]	Taiwan	Conference paper	To develop and evaluate Large Language Multimodal Models that integrate clinical notes and laboratory test results for predicting the risk of chronic diseases, particularly type 2 diabetes mellitus	Clinical (Eastern Memorial Hospital in Taiwan	Retrospective cohort study	Automated evaluation metrics
Jairoun et al [32]	Malaysia	Journal article	To investigate the benefits and risks associated with the application of ChatGPT in managing diabetes and metabolic illnesses	—	Qualitative study	Human evaluation
Mondal and Naskar [33]	India	Journal article	To evaluate GPT-4's competency in reviewing diabetic patient management plans compared to expert reviews.	General medical setting	Comparative study	Human evaluation and automated evaluation metrics

XSL•FO
RenderX

Study	Country	Article category	Study objective	Health care setting	Study design	Evaluation
Liu et al [34]	N/S[a]	Journal article	To leverage LLMs and multi-prompt engineering for chronic disease management, specifically for detecting mental disorders through user-generated textual content.	Online platforms	Experimental (few-shot learning)	Automated evaluation metrics
Liao et al [35]	Taiwan	Conference paper	To develop an EHR-based chronic disease prediction platform using LLMs for diabetes, heart disease, and hypertension.	Clinical (Far Eastern Memorial Hospital, Taiwan)	Retrospective cohort study	Automated evaluation metrics
Ding et al [36]	Taiwan	Journal article	Predict new-onset type 2 diabetes using large language multimodal models with EHR data	Clinical (Far Eastern Memorial Hospital, Taiwan)	Retrospective cohort study	Automated evaluation metrics
Dao et al [37]	Ireland and Singapore	Conference paper	Design and evaluate an AI chatbot system using GPT-3.5 for proactive diabetes prevention	Community-based setting	Experimental (AI design and evaluation)	Automated evaluation metrics
Khan [38]	United States	Journal article	Assess the efficacy of ChatGPT in facilitating self-management strategies for diabetic patients.	Outpatient diabetes care	Observational study	Human evaluation
Mondal et al [39]	India	Journal article	To evaluate the effectiveness of ChatGPT, an LLM, in providing answers to queries related to lifestyle-related diseases or disorders	Clinical and academic settings	Observational study	Human evaluation
Young et al [40]	United States	Journal article	Assess LLMs' capacity to deliver age-appropriate explanations of chronic pediatric conditions to enhance patient understanding.	Clinical (Boston Children's Hospital)	Pilot study	Human evaluation
Li et al [41]	China	Journal article	Develop DeepDR-LLM, an integrated AI system for primary diabetes care and diabetic retinopathy (DR) screening	Low-resource primary care settings	Experimental	Human evaluation and automated evaluation metrics
Ying et al [42]	China	Preprint	To evaluate the feasibility and utility of ChatGPT in diabetes education using retrospective and real-world patient questions.	Outpatient setting	Mixed methods	Human evaluation

XSL•FO
RenderX

Study	Country	Article category	Study objective	Health care setting	Study design	Evaluation
Li et al [43]	China	Journal article	To evaluate the performance of LLMs in diabetes-related queries and their potential to assist in diabetes training for primary care physicians	Primary diabetes care, endocrinology, and diabetes management.	Prospective study	Human evaluation and automated evaluation metrics
Hussain and Grundy [44]	Australia	Journal article	Evaluate the responses of ChatGPT models to queries from diabetes patients, assessing their accuracy, biases, and limitations in providing self-management advice.	Home care setting	Comparative study	Human evaluation
Wang et al [45]	China	Journal article	To evaluate the potential of the RISE framework to improve LLMs' performance in accurately and safely responding to diabetes-related inquiries.	Home care setting	Comparative study	Human evaluation

[a]Not available.

[b] LLM: large language model.

As shown in Table 1, most studies were conducted in China (7/29, 24%) and the United States (4/29, 14%), with limited representation of low-resource settings. Experimental designs were predominant (10/29, 35%), and nearly half of the studies (14/29, 48%) focused on diabetes management. The studies primarily focused on adult populations (28/29, 96%), with only 1 study (1/29, 4%) specifically addressing pediatric applications. Human evaluation was the most common evaluation method (16/29, 55%), followed by automated evaluation metrics (10/29, 35%) used in prototype evaluation, with some studies using both approaches (3/29, 10%). Studies were carried out in diverse health care settings, with home care settings (10/29, 35%) and clinical settings (9/29, 31%) being the most common. This diversity in study characteristics reflects the broad application of LLMs across various health care contexts for chronic disease management.

Methodological Quality Assessment

Using the Mixed Methods Appraisal Tool [26], the studies were categorized as quantitative descriptive studies (19/29, 66%), comprizing observational, cross-sectional, case study, system development, prototype evaluation, and comparative analyses. Quantitative nonrandomized studies (3/29, 10%) included retrospective cohort and quasi-experimental designs, qualitative studies (5/29, 17%), and 2 studies with mixed methods design (2/29, 7%). Of the 29 studies, 18 studies (62.1%) were classified as high quality (meeting ≥4 of 5 criteria), 9 studies (31.1%) as moderate quality (meeting 2 - 3 criteria), and 2 studies (6.9%) as low quality (meeting ≤1 criterion). The most common methodological limitations identified across studies included inadequate sampling strategy descriptions, limited participant demographic reporting, use of synthetic clinical data, and lack of external validation. Detailed quality appraisal results for each study are provided in Multimedia Appendix 1. Table 2 provides an overview of the LLM types, users, tasks, and challenges identified across the included studies.

XSL•FO
RenderX

Table . Large language model tasks and challenges (N=29).

Study	LLM[a]	Users	Disease management tasks	Challenges
Montagna et al [6]	GPT-3	Individuals with hypertension	Patient engagement blood pressure monitoring and management.	• The incorrect way patients measure their blood pressure
Yang et al [16]	ChatGLM-6B	Patients diagnosed with diabetes	Treatment recommendations, suggesting appropriate laboratory tests, and medication	• Inadequate understanding of complex medical records • The small size of the training data
Raghu et al [17]	ChatGPT	Practitioner (ophthalmologist)	Patient education, medical reports: diagnoses and predictions	• Incorrect information, privacy and protection of patient data
Song et al [18]	ChatGPT Llama	Individuals who have used LLM chatbots for mental health support	• Providing emotional support, engaging in therapeutic conversations, and offering recommendations tailored to individual contexts. • Addressing specific stressors or challenges faced by individuals.	• Cultural Misalignments: Participants noted that recommendations from LLM chatbots often felt like they were translated from stereotypical American responses. • Linguistic Biases: Participants often felt compelled to use English when interacting with LLM chatbots. • Therapeutic Misalignment.
Liu et al [19]	Gemma-7B, Mistral-7B, Yi-6B, MedAlpaca-7B, LLaMA2-7B, LLaMA3-8B, Qwen2-7B, PalmyraMed-20B, PMCLLaMA13B, OpenBioLLM-8B	Patients with hypertension	Cardiovascular disease management via cuffless blood pressure measurement.	• Dataset imbalances diminish accuracy • Privacy concerns in real-world deployment • Need for calibration to mitigate individual variability
Ogundare et al [20]	Unspecified	Sickle cell patients and clinicians	Assessing anemia severity in real-time, predicting time to vaso-occlusive episodes, and communicating with emergency personnel.	• Creation of a reliable non-invasive tool for angiogenic level assessment, development of a biophysics model, and practical considerations of LLM communication with emergency personnel
Cankurtaran et al [21]	ChatGPT	Inflammatory bowel disease patients and health care professionals.	• Tailored responses, educational resources • monitoring and follow-up, patient empowerment • Decision support	• Insufficient responses • Limited scope of knowledge (up-to-date information)
Wang et al [22]	LLaMA-7B, ChatGLM-6B Alpaca.	Individuals with depression.	Diagnosis and treatment of depression	• Absence of pretraining data sets on depression • Hallucination problem • Evaluation methodologies emphasize predictive performance and lack • Quantification of the impact on patient treatment

XSL•FO
RenderX

Study	LLM[a]	Users	Disease management tasks	Challenges
Abdullahi et al [23]	Bard ChatGPT 3.5 and GPT-4	• Physicians • Medical Students Resident Nurses • Nurse Practitioners	• Clinical Decision Support • Medical Education • Disease Diagnosis	• Inconsistency in Responses, LLMs do not always explicitly indicate their level of uncertainty due to Limited Scope, Sample Size, and knowledge. ChatGPT-3.5 and GPT-4 were limited to health care data available up to 2021 • LLMs may generate different responses for the same prompt
Al Anezi [24]	ChatGPT	Outpatients with chronic diseases	• Providing information about patient conditions, treatment plans, and medication schedules. Reminders for medication intake, appointments, or lifestyle adjustments. • Assisting in behavior change efforts by providing evidence-based strategies, personalized goal-setting techniques, and reminders for healthy habits. • Identifying barriers to behavior change and exploring solutions to overcome them. • Monitoring blood pressure, blood glucose levels, or weight and providing feedback based on shared data.	• Limited physical examination, Lack of human connection and empathy • Complexity of individual cases • Privacy and security concerns • Legal and ethical challenges, language and cultural barriers, technical limitations, diagnostic limitations, and lack of reliability and trust • Ineffectiveness in emergencies
Athavale et al [27]	ChatGPT 4.0	Patient	Answered administrative and non-complex medical questions well, and electronic health record inbox management. Answering complex medical questions	• Hallucinations • Need for extensive supervised training by subject experts • No regulatory approval
Soto-Chávez et al [28]	ChatGPT	Patients with chronic diseases using the Spanish language	Evaluating the reliability and readability of ChatGPT-generated patient information on chronic diseases in Spanish.	• ChatGPT was trained in English, which affects the accuracy of responses in Spanish • Lower reliability on chronic diseases like heart failure and chronic kidney disease
Abbas et al [29]	GPT-3.5	Machine Learning engineers, clinical researchers	Chronic disease prediction	• lack of longitudinal data • limited generalizability
Anderson et al [30]	GPT (Generative Pre-trained Transformer)	Practitioners	Discover and rank novel relationships between various aspects of chronic lower back pain.	

XSL•FO
RenderX

Study	LLM[a]	Users	Disease management tasks	Challenges
				• The GPT-based approach took around half an hour to process approximately 500 pairs, making it computationally intensive. • Achieving strong agreement among human evaluators
Ding et al [31]	MedAlpaca	• Patients with early diabetes • Patients with multiclass chronic diseases	Early prediction of diabetes Prediction of multiclass chronic diseases	• Lower positive rates when using only laboratory blood values • Missing tests for most patients when using only laboratory blood values. • Integrating multimodal data from clinical notes and laboratory test results • Difficulty in model explainability for early disease prediction
Jairoun et al [32]	ChatGPT	diabetes and metabolic illnesses, endocrinologists and diabetologists	Patient support and education Tailored treatment	• Diagnostic mistakes • Patient data security and privacy • Limitations on generalizability • Integration difficulties and workflow errors, and Compliance with laws and regulations • Absence of empathy and human contact
Mondal et al [33]	GPT-4	Health care professionals	Reviewing and evaluating diabetes management plans for guideline adherence	• GPT-4's difficulties in handling complex clinical judgments, such as medication adjustments and treatment modifications in varied clinical scenarios
Liu et al [34]	GPT-2 and T5	Patients with mental disorders	Detection of mental disorders (depression, anorexia, pathological gambling, self-harm) through user-generated textual content.	• Need for personalized prompts to capture individual user characteristics. • Integration of medical knowledge into prompts for accurate detection. • Handling noisy and lengthy user-generated content. Few-shot learning with minimal labeled data
Liao et al [35]	BERT BiomedBERT Flan-T5-large-770M GPT-2	Physicians, health care providers	Prediction of chronic diseases (diabetes, heart disease, hypertension) using EHR data.	

XSL•FO
RenderX

Study	LLM[a]	Users	Disease management tasks	Challenges
				• Difficulty in classifying diseases with lower positive rates (eg, hypertension) • Need for interpretability in model predictions • Integration of multimodal data (clinical notes and blood test results) for accurate predictions
Ding et al [36]	BERT, Roberta, Biomed-BERT, Flan-T5, GPT-2	Researchers, health care professionals	Predict new-onset T2DM, early detection, and risk assessment	• Handling multimodal data, missing values, and model interpretability
Dao et al [37]	GPT-3.5	Individuals at risk of diabetes or with prediabetes	Instant Q&A and advice Personalized reminders Data analysis for tailored guidance Health resource aggregation Emotional support	• Engagement barriers in prevention programs (eg, transportation, personal responsibilities) • Lack of research on AI in diabetes prevention • Need for reliable, context-aware AI responses
Khan [38]	ChatGPT	Diabetic patients	Real-time education and support Blood glucose monitoring guidance Medication adherence advice Lifestyle/diet recommendations Emergency detection	• Inaccuracies in medical information (eg, insulin storage guidelines, trial data mix-ups) • Lack of emotional support/empathy • Limited to pre-2021 knowledge • Difficulty distinguishing medical terminologies • Low adoption among older adults
Mondal et al [39]	ChatGPT-4	Patients and health care professionals	Answering patient questions (causes, symptoms, treatment, diet) Providing information on managing Crohn's disease (CD) and ulcerative colitis (UC). Addressing professional queries (classification, diagnosis, disease activity, prognostic markers, complications)	• Insufficient elaboration on medical agents and surgical indications • Inadequate information for patients. ChatGPT provided different answers to the same question across sessions • Lower reliability/usefulness scores for patient-directed questions compared to professional-focused ones. • Outdated information
Young et al [40]	GPT-4 Gemini 1.0 Ultra	Pediatric patients, health care providers, and caregivers	Generating explanations for chronic conditions	• Age-appropriateness discrepancies between models (GPT-4 versus Gemini) • Lack of direct feedback from pediatric patients; reliance on clinician evaluations.

XSL•FO
RenderX

Study	LLM[a]	Users	Disease management tasks	Challenges
li et al [41]	LLaMA	Primary care physicians	Individualized diabetes management recommendations	• Underdiagnosis and poor primary diabetes management
Ying et al [42]	GPT-3.5	Physicians, laypersons, and type 2 diabetes patients	Diabetes education and personalized Q&A support	• Lower real-world performance, variability by prompt, trust, and safety concerns
Li et al [43]	ChatGPT-3.5 ChatGPT-4.0 Google Bard MedGPT LlaMA2-7B	Researchers Primary care physicians	Answering diabetes-related exam questions and assisting in diabetes training.	• Poor performance in both Chinese and English diabetes-related questions • LLMs may provide misleading explanations and difficulty with multiple-choice and case analysis questions
Hussain and Grundy [44]	ChatGPT-3.5 ChatGPT-4	Diabetes patients and health care providers	Patient education, treatment recommendations, insulin management, dietary advice	• Inaccuracies in medical advice • Lack of personalization • Failure to recognize regional variations • Incorrect assumptions about blood glucose units limitations in addressing complex patient histories
Wang et al [45]	GPT-4 Anthropic Claude 2 Google Bard	• Clinicians • Diabetes patients	Responding to diabetes-related inquiries and providing accurate and comprehensive information for diabetes self-management.	• Lack of specialized medical knowledge in commercially available LLMs • Susceptibility to generating inaccurate or misleading information • Need for real-time, domain-specific knowledge to improve accuracy and reliability • Ensuring responses are safe, accurate, and understandable for patients

[a] LLM: large language model.

As shown in Table 2, GPT models were the most commonly used (14/29, 48%), followed by LLaMA variants (5/29, 17%), the Bard model (3/29, 10%), and BERT-based models (2/29, 7%). LLMs were primarily used for patient education and information provision (18/29, 62%), with most studies targeting patients (18/29, 62%) rather than health care providers (11/29, 38%). Inaccurate and inconsistencies in responses (18/29, 62 %) were the most frequently reported challenge across studies.

Objective 1: The Tasks in Chronic Disease Management Performed by LLMs

Our literature synthesis revealed that LLMs have significant potential to improve various chronic disease management tasks. The tasks identified have been broadly categorized into patient-centered tasks and practitioner-centered tasks.

Patient-Centered Tasks

Patient Education and Information Provision

Eighteen studies (n=18) delved into the use of LLMs in providing health information to enhance patient health literacy [16,17,21,23,24,27,28,32,33,37-41]. Key applications included using ChatGPT to provide personalized guidance on diabetes management [16,38,39,42], educational content for diabetic retinopathy and inflammatory bowel disease patients [17,21], generating age-appropriate explanations of chronic pediatric conditions [40], and supporting physician training in diabetes management [43]. In addition, LLMs supported treatment adherence through tools like ChatGPT and GPT-3.5, offering tailored medication reminders, appointment scheduling, and strategies for behavior change [24,37]. For Spanish-speaking

XSL•FO
RenderX

populations, ChatGPT was evaluated for reliability and readability of chronic disease information [28], while multiple ChatGPT versions were assessed for regional variations in diabetes education quality [44].

Diagnosis and Treatment

Six studies (n=6) examined the role of LLMs in assisting with diagnosis and treatment recommendations. These studies explored the potential of LLMs to suggest appropriate laboratory tests, generating differential diagnoses and medication options tailored to the individual patient's condition [16,22,32,34]. Notable applications included enhancing depression diagnosis and treatment through fine-tuning of models like LLaMA-7B and ChatGLM-6B [22], supporting the diagnosis of rare and complex diseases [23], and detecting mental disorder patterns through analysis of user-generated content [34]. Furthermore, integrating AI-driven diagnostic and treatment capabilities with diabetes management systems showed particular promise in low-resource primary care settings [41].

Self-Management and Disease Monitoring

Eight studies (n=8) addressed using LLMs for self-management and disease monitoring. These studies explored how LLMs provide guidance on managing chronic conditions, promote patient engagement, and support home disease monitoring [6,18,20,21,24,37,38,42]. Key applications included developing chatbot architectures for home blood pressure monitoring [6], creating cuffless blood pressure measurement systems using wearable biosignals [19], and assessing real-time disease severity in sickle cell anemia [20]. LLMs also demonstrated value in detecting emergencies such as hypoglycemic episodes in diabetic patients and guiding appropriate actions [38]. Additional applications encompassed monitoring tools for inflammatory bowel disease management [21], personalized reminders for diabetes prevention [37], and comprehensive health parameter tracking with feedback based on patient-shared data [24]. These implementations highlight the potential of LLMs to enhance patient self-management through continuous monitoring and timely intervention guidance.

Emotional Support and Therapeutic Conversations

Four studies (n=4) explored the role of LLMs in providing emotional support and engaging in therapeutic conversations for patients managing chronic diseases. The review identified several key applications, including investigating LLM chatbots for mental health support with tailored recommendations addressing specific stressors [18], evaluating ChatGPT as a virtual health coach identifying barriers to behavior change [24], assessing GPT-3.5's emotional support capabilities in proactive diabetes prevention [37], and examining ChatGPT's ability to provide coping strategies for diabetic patients [38].

Practitioner-Centered Tasks

Clinical Decision Support

Eight studies (n=8) investigated the use of LLMs for clinical decision support. The review identified several key applications, including generating personalized medical reports with treatment options and diagnostic procedures for conditions like diabetic retinopathy [17] and inflammatory bowel disease [21], assessing LLMs' diagnostic accuracy compared with human experts in rare and complex diseases [23], and exploring potential use for electronic health record inbox management [27]. Other applications included using GPT to discover and rank novel relationships between aspects of chronic lower back pain [30], evaluating diabetes management plans using GPT-4 [33], disease classification and prognosis [39], and evaluating LLMs' competency in answering diabetes-related exam questions for physician training [43].

Medical Predictions

Six studies (n=6) explored the predictive capabilities of LLMs in chronic disease management. The review identified several key applications, including predicting diabetic retinopathy risk [17], developing ChatGPT-assisted machine learning models for chronic disease classification [29], and integrating multimodal data from electronic health records and laboratory tests to predict new-onset type 2 diabetes [31,36]. Additional applications included creating an EHR-based prediction platform for diabetes, heart disease, and hypertension [35] and implementing integrated AI systems for diabetes risk assessment in primary care settings [41].

LLMs in chronic disease management are predominantly utilized for patient education and information provision, accounting for (18/29) of reported applications. Self-management and disease monitoring and clinical decision support each account for 28% (8/29) of applications. Diagnosis and treatment tasks, along with medical predictions, both constitute 21% (6/29) of applications, while emotional support and therapeutic conversations account for 14% (4/29). Percentages exceed 100% due to thematic overlaps where individual studies addressed multiple tasks.

LLMs in chronic disease management are predominantly utilized for patient education and information provision, accounting for (18/29) of reported applications. Self-management and disease monitoring and clinical decision support each account for 28% (8/29) of applications. Diagnosis and treatment tasks, along with medical predictions, both constitute 21% (6/29) of applications, while emotional support and therapeutic conversations account for 14% (4/29). Percentages exceed 100% due to thematic overlaps where individual studies addressed multiple tasks.

Objective 2: Challenges Associated With Using LLMs for Chronic Disease Management

The challenges identified and presented in Table 2 were categorized as follows.

Inaccurate and Inconsistencies in Responses

Eighteen studies (n=18) highlighted issues with hallucinations, diagnostic errors, and unreliable outputs [6,16,17,21-23,27-29,32-34,38,39,42-45]. The review identified several key challenges, including hallucinations where models like ChatGPT and LLaMA generate reasonable but factually incorrect information [22,45], diagnostic errors in conditions ranging from depression to inflammatory bowel disease [21,32,44], and inconsistent responses to identical prompts without indicating uncertainty levels [23,39,42]. In addition,

XSL•FO
RenderX

models demonstrated limited understanding of complex medical records [16], struggled with regional variations in medical practice [44], provided insufficient elaboration on medical treatments [39], and showed difficulty distinguishing medical terminologies [38]. Further challenges included lower reliability in the Spanish language for specific chronic conditions like heart failure and chronic kidney disease [28] as well as limited generalizability due to restricted training populations [29,32]. These inaccuracies stem from erroneous input data, such as incomplete or incorrect test results [6,21,22,27,31].

Limited Datasets and Knowledge

Six studies (n=6) identified challenges related to limited datasets and knowledge cutoffs in LLM applications for chronic disease management. The review highlighted several key limitations, including scarcity of disease-specific datasets [16,22], dataset imbalances affecting predictions for conditions like hypertension [19], and knowledge limitations that restrict LLM awareness of the current medical guidelines [21,23,39].

Computational and Technical Challenges

Six studies (n=6) highlight significant computational and technical challenges in deploying LLMs for chronic disease management. The review identified several key limitations, including resource-intensive processing that results in prolonged training time in resource-constrained environments [30]. In addition, technical challenges include integrating multimodal data from clinical notes and laboratory results [31,36], ensuring model explainability for early disease prediction [35], and handling noisy user-generated content in mental health applications [31,34]. Further challenges involve difficulties in integrating LLMs into clinical workflows [32] and managing complex clinical judgments, such as medication adjustments and treatment modifications [33].

Usability and Accessibility Concerns

Nine studies (n=9) identified usability and accessibility concerns surrounding LLMs in chronic disease management tasks. Notably, the restriction to textual inputs limits use for tasks involving multimodal diagnostic tasks [28,40] language and cultural misalignments [18,28], while age-inappropriate outputs pose challenges for pediatric care [40]. In addition, poor interpretability of model predictions for early disease prediction and risk assessment [31,35,36]. Additional challenges included a lack of empathy and ineffectiveness in emergencies [24,29], digital literacy gaps restricting adoption among older adults [29,38]. Furthermore, these studies also noted how insufficient transparency in model decision-making processes hindered trust and clinical acceptance [35,36].

LLM Evaluation

Five studies (n=5) noted challenges involving LLM evaluation. Notable challenges identified included that automated evaluation metrics primarily focus on predictive performance and fail to assess the impact on patient treatment outcomes [22], difficulties in achieving consensus among human evaluators when assessing LLM outputs [30], discrepancies between model performance in test environments versus real-world applications [42], difficulties in consistently evaluating language models across different diabetes-related tasks [43], and significant variations in age-appropriateness scoring between different LLM platforms [40].

Legal, Ethical, Privacy, and Regulatory Concerns

Ten studies (n=10) identified legal, ethical, privacy, and regulatory challenges of using LLMs in chronic disease management. The review highlighted several critical concerns, including privacy and data security vulnerabilities [17,19,24,27,28,32], absence of regulatory approval and standardized guidelines [27], and compliance issues with health care laws across different jurisdictions [27,32]. In addition, language and cultural barriers posed additional challenges, particularly for non-English speakers [18,28], while bias and equity issues stemming from limited training data diversity raised concerns about health care disparities [24,32,42]. Studies also noted ethical challenges around accountability for errors [24], lack of transparency in decision-making [22,27], and limitations in addressing complex ethical dilemmas in clinical care [44,45].

The most prevalent challenge identified was inaccurate and inconsistent responses, reported in 62% (18/29) of studies. Legal, ethical, privacy, and regulatory concerns followed, appearing in 35% (10/29) of studies. Usability and accessibility issues were noted in 31% (9/29) of studies. Computational and technical limitations, as well as dataset and knowledge constraints, were each reported in 21% (6/29) of studies. Additionally, 17% (5/29) of studies highlighted limitations in evaluation methodologies.

Discussion

Principal Findings

This scoping review presents 3 significant findings from the 29 included studies (n=29): (1) LLMs are mostly used for both patient-centered (18/29, 62%) and practitioner-centered (11/29, 38%) tasks, with patient education and information provision emerging as the major application (18/29, 62%); (2) despite promising applications, significant challenges still exist, particularly regarding LLM response accuracy (18/29, 62% of studies), ethical concerns (10/29, 35%), and usability issues (9/29, 31%); and (3) methodological quality varies considerably across studies, with journal articles demonstrating higher quality (13/18, 72%) compared with conference papers (3/8, 38%) and preprints (1/3, 33%). These findings highlight both the considerable promise and significant limitations of current LLM applications in chronic disease management, which are examined in detail below.

Chronic Disease Management Tasks

Chronic disease management is an approach to managing chronic illnesses involving screenings, regular check-ups, monitoring, coordination of treatment, medication adherence, lifestyle modifications, and patient education [1]. The findings from this scoping review reveal an increasing interest in leveraging LLMs like ChatGPT to support both patient-centered and practitioner-centered tasks [6,16,22-24,30,31].

XSL•FO
RenderX

Patient-Centered Tasks

The majority of the studies (18/29, 62%) focused on patient-centered tasks, reflecting the emphasis on patient active engagement in chronic disease management [3,46]. Patients' active engagement enables them to monitor their symptoms, disease progress, weight, and adverse drug effects, and adhere to medication and visits [3,46]. This review found that LLMs support various patient-centered applications, including patient education and information provision, disease monitoring and self-management, emotional support and therapeutic conversations, and diagnosis and treatment assistance.

Patient education and information provision emerged as the most prominent application (18/29, 62%), with LLMs providing health information about conditions, treatment plans, and medication schedules [16,17,21,23,24,27,28,32,33,37-41]. With the right health information, individuals with chronic diseases can easily self-manage their conditions. Diagnosis and treatment applications accounted for (6/29, 21%). Studies experimented using LLMs to suggest laboratory tests, for diagnosis, and for medication generation tailored to individual patient conditions [16,22,23,32,34,41]. However, using LLMs for diagnostic and treatment has been criticized due to concerns about hallucinations and misinterpretations of clinical guidelines [22,23], highlighting the need for continued research to ensure patient safety. Therefore, LLM usage should not replace health practitioners but instead serve as complementary tools.

Self-management and disease monitoring applications (8/29, 28%) demonstrated how LLMs can facilitate home-based monitoring of various physiological parameters [6,19-21,24,37,38,42]. Recent studies have highlighted that patient engagement with health monitoring technologies is crucial for improving health outcomes in chronic disease management [47]. Studies have also shown that wearable technologies integrated with LLMs provide real-time patient-centered health data that can better inform self-management decision-making [48]. However, ensuring consistent long-term engagement is still a challenge.

Emotional support and therapeutic conversations (4/29, 14%) represented an emerging application area [18,24,37,38]. Studies showed that LLMs can provide psychological support through tailored recommendations addressing specific stressors [18], identifying barriers to behavior change [24], and offering coping strategies for patients with diabetes [38]. Emotional support is increasingly recognized as essential in chronic disease management [49], which helps patients overcome psychological barriers to treatment adherence and lifestyle modifications.

Practitioner-Centered Tasks

Practitioner-centered tasks (11/29, 38%) mainly revolved around clinical decision support and medical predictions. Clinical decision support applications (8/29, 28%) provided health care practitioners with actionable information to enhance decision-making. Studies demonstrated that LLMs can generate personalized medical reports, generate treatment recommendations, and support diagnostic processes that assist health care specialists in making informed decisions [17,21]. However, while LLMs enhance diagnostic efficiency, concerns regarding inconsistent outputs pose barriers to clinical adoption. Medical prediction applications account for (7/29, 24%) of LLM use in chronic disease management, showing strong potential for early disease detection and risk stratification. By integrating structured and unstructured clinical data, such as lab results, clinical notes, and imaging, LLMs enable more comprehensive and accurate predictive models compared with traditional methods [17,29,31,34-36].

Notably, real-time risk assessment tools, like the ambulatory device developed for sickle cell anemia management [20], demonstrate how LLMs can predict complications before symptoms appear. However, challenges relating to medical accuracy still limit their seamless integration into clinical workflows [6,16,17,21-23,27]. A significant emerging trend is the development of retrieval-augmented generation (RAG) frameworks that enhance prediction accuracy by dynamically incorporating up-to-date medical knowledge [22,35,50-53]. Future advancements should focus on seamless integration of LLMs with existing medical systems, wearable health technologies, and mobile health applications to improve interoperability and trustworthiness.

Methodological Quality and Strength of Evidence

The methodological quality assessment revealed notable trends that should be considered while interpreting the results of this scoping review. High-quality studies (18/29, 62%) were not uniformly distributed across LLM application tasks, studies examining medical prediction applications [29,31,35,36] and patient education and information provision [28,32,38,39] had significantly stronger methodological rigor. Studies investigating emotional support showed mixed quality, with some high-quality qualitative research [18,24], a quantitative descriptive study [37] alongside a moderate-quality mixed study [38]. Notably, self-management and disease monitoring studies showed significant methodological heterogeneity, with quality ratings ranging from low to high.

Journal articles demonstrated a substantially higher proportion of high-quality studies (13/18, 72%) compared with conference papers (3/8, 38%) and preprints (1/3, 33%), suggesting that peer-review processes enhance methodological quality. The identified common limitations, including inadequate sampling strategies, limited participant demographic reporting, and insufficient methodological transparency, were more prevalent in lower-tier publication sources, including conference papers and preprints. Quantitative descriptive studies, especially those focused on system design and prototype testing (10/29, 34.5%), showed mixed quality ratings ranging from low to high, with a common limitation being the use of synthetic data, lack of clinical validation, as they commonly prioritized technical utility. These methodological patterns significantly influence the reliability of the findings.

Challenges and Corresponding Recommendations

This section discusses the key challenges identified in the review and presents corresponding recommendations to mitigate these issues. Each challenge is followed by practical solutions to enhance the applicability of LLMs in chronic disease management.

XSL•FO
RenderX

Inaccurate Data and Inconsistencies in Responses

Inaccurate and inconsistent responses emerged as a significant challenge (18/29, 62%), primarily due to poor data quality, inherent biases in training datasets, and the limited scope of knowledge constrained by the model's training cutoff [6,22,23,31]. Given that LLM performance is intrinsically linked to data quality, flawed datasets inevitably propagate errors in outputs, a manifestation of the "garbage in, garbage out" principle [54-56]. The issue of biases in AI models has gathered significant attention in recent literature [54-56], prompting possible migration strategies [57-59]. These limitations carry critical implications for health care, as erroneous LLM outputs may lead to incorrect clinical decisions, posing significant risks to patient safety [8,12]. Hence, researchers are exploring technical solutions such as advancing domain-specific fine-tuning techniques [60,61], leveraging retrieval-augmented generation (RAG) frameworks [22,50-52], and refining outputs through reinforcement learning (RL) and prompt engineering techniques [62-64]. In addition, implementing expert validation protocols has emerged as a crucial safeguard to ensure adherence to evidence-based practice.

Limited Datasets

The scarcity of high-quality datasets for chronic diseases accounted for (6/29, 21%). Studies highlighted limitations and narrow coverage of publicly accessible clinical training datasets due to data privacy and institutional restrictions [16,19,21-23,39]. Given that experimental studies often require substantial model training datasets, the absence of adequate data poses a significant challenge to the effectiveness and success of these studies. Therefore, to address this gap, synthetic datasets and data augmentation techniques have been explored by studies [15,65]. However, these methods risk amplifying pre-existing biases in source data [54-56]. Therefore, dataset validation is essential to ensure quality, collaborative partnerships with health care institutions to access real-world clinical datasets and knowledge distillation techniques, where smaller models can be trained on outputs from larger, clinically validated models, reducing dependency on raw data volume, can be explored [66].

Computational Resources and Technical Challenges

The computational demands of training LLMs for health care applications remain a significant challenge (6/29, 21%). Consequently, low computing resources approaches, such as quantization, parameter-efficient fine-tuning (PEFT) techniques like Low-Rank Adaptation (LORA), Quantized LoRA (QLORA), Weight-Decomposed Low-Rank Adaptation, and REFT [67-73], are evolving and are popularly used in fine-tuning LLMs in low-resource computing environments. In addition, adapter-based tuning methods provide lightweight alternatives by injecting trainable adapter layers into frozen pretrained models, enabling task-specific fine-tuning without updating the entire model parameters [74,75]. Building on these advances, the development of lightweight LLMs optimized for mobile devices presents a promising direction for extending AI-based chronic disease management to resource-constrained settings [76].

Usability and Accessibility Concerns

Usability and accessibility concerns accounted for (9/29, 31%), including issues with text-only interfaces for some LLMs, cultural misalignments, and outputs ill-suited for pediatric or elderly populations [18,28,40]. While studies highlighted text-only interfaces as a critical limitation of LLMs in health care [28,40], recent advances in multimodal architectures have addressed this gap. These models now integrate and interpret diverse data modalities, including medical images, audio, and structured documents, while generating composite textual and visual outputs [31,77-79]. In addition, having dynamic and simplified interfaces to accommodate low-digital-literacy users, pediatric users, and for different cultural and language settings could further improve LLM usability and adaptation.

Legal, Ethical Issues, and Regulatory Issues

Legal, ethical, and regulatory concerns (10/29, 35%) remain a key issue in LLM adoption in health care. Studies identified data privacy, biases, misinformation, responsibility, and accountability for LLM-generated content as key concerns. Although several AI frameworks have been proposed, the absence of standardized guidelines and regulatory approvals creates significant gaps [27,80-82]. This regulatory vacuum risks inconsistent model development and validation practices, unaddressed ethical dilemmas regarding accountability for AI-generated recommendations, and potential mismatches between rapidly evolving LLM capabilities and static health care regulations [27,83]. Addressing these ethical concerns requires standard guidelines and rules to ensure responsible use in health care settings[84]. Therefore, future efforts must prioritize the development of a comprehensive regulatory framework.

LLM Evaluation

Evaluation gaps accounted for (5/29, 17%), reflecting critical shortcomings in current methodologies for assessing LLM performance in clinical contexts. The existing automated evaluation metrics mainly focus on predictive performance using metrics such as accuracy and F_1-scores that lack medical and treatment knowledge [22,85]. These metrics may produce misleading conclusions if not appropriately selected [85]. Furthermore, human evaluation, although valuable, introduces subjectivity and interrater variability, yet the absence of a standardized LLM evaluation framework makes attaining consensus among human raters challenging [30,85]. A promising direction involves a hybrid evaluation approach that integrates human expert reviews with automated metrics. Future efforts should prioritize the development of standardized LLM evaluation frameworks tailored to health care settings. Table 3 summarizes the challenges associated with applying LLMs in chronic disease management with proposed recommendations.

XSL•FO
RenderX

Table . Key challenges and recommendations.

Challenge	Key observations	Recommendation
Inaccurate and inconsistent responses	Hallucinations, inconsistent responses, outdated knowledge	Adopting RAG frameworks, fine-tuning, and prompt engineering. RL, expert validation of LLM-generated recommendations
Limited datasets	Scarcity of datasets, missing data, and dataset imbalances.	Use synthetic data, data augmentation, partnerships with health care institutions, knowledge distillation
Computational demands	High computational demands	Adopt PEFT (LORA and QLORA), quantization use lightweight models for mobile devices
Ethical and privacy concerns	Privacy concerns, language and cultural barriers, and lack of regulatory oversight	Develop a regulatory framework
Usability issues	Restriction to textual inputs, lack of empathy, ineffectiveness in emergencies Age-appropriate interaction	Use multimodal LLMs. Dynamic interfaces to accommodate low-digital-literacy users, age-appropriate interaction modes customize to different cultural settings Integrate with wearable devices and mobile health apps
Evaluation challenges	Predictive performance metrics, subjectivity, and interrater variability	Develop a standardized LLM evaluation framework for health care.

Limitations of the Study

Although quality assessment was conducted using MMAT, studies were not excluded based on their methodological rigor. As a result, including moderate and low-quality studies may have influenced the reliability and consistency of the reviewer's findings. The varied methodological designs across studies may have affected the interpretation of results and conclusions drawn. Furthermore, the review was limited to only English-language publications, which may have introduced language bias and limited the generalizability of our findings, particularly in contexts where LLMs are being adapted to local languages or integrated into culturally specific health care practices. The exclusion of databases such as Embase and Web of Science may have limited the comprehensiveness of the search. Future research can consider broader database coverage and non-English sources to enhance diversity and scope.

Implications for Practice and Future Research

This scoping review reveals several critical implications for the integration of LLMs in chronic disease management. First, it is essential to address the accuracy issues identified in 18/29, 62% of studies. This calls for both technical solutions (domain-specific fine-tuning, reinforcement learning (RL), and retrieval-augmented generation (RAG) frameworks [61,64]) and nontechnical solutions (expert validation and collaborative partnerships with health care institutions to access and use real-world clinical data). Second, enhancing accessibility across diverse patient populations requires developing culturally adapted LLM interfaces, implementing age-appropriate interaction modes [40], and integrating with low-resource platforms such as SMS-based systems and lightweight mobile apps for various populations [76]. Third, robust governance frameworks must be established to address the ethical, legal, and privacy concerns noted in 10/29, 35% of studies to ensure regulatory compliance.

Finally, future research should focus on multimodal LLMs that can synthesize diverse data inputs from wearable devices and mobile health applications for holistic patient monitoring [19,31,35] and develop resource-efficient deployment techniques. The predominance of diabetes-focused studies (14/29, 48%) highlights a potential research gap in addressing other prevalent chronic conditions. Similarly, there is a research gap in age-inclusive LLM design, given the overwhelming focus on adult populations (28/29, 96%) and the lack of pediatric studies. Addressing these gaps would enhance the clinical relevance and equitable application of LLMs across the full spectrum of chronic disease management.

Conclusion

This scoping review highlights the growing potential of LLMs in supporting chronic disease management through patient education, diagnosis and treatment, emotional support, self-management support, decision support, and prediction tasks. While LLMs offer promising capabilities, their effective integration into health care still requires addressing key challenges related to accuracy, accessibility, usability, and ethical and privacy concerns. Future research should focus on integrating LLMs with mobile and wearable technologies, creating culturally and age-appropriate interfaces, and exploring integration with low-resource platforms. Addressing these research gaps will ensure equitable and safe use of LLMs across diverse health care settings.

Acknowledgments

The authors acknowledge the valuable inputs of the reviewers and the editor, and the support of Mr. Bazekketa Datson of Ndejje University, Faculty of Science and Computing, for illustrating the figures used in this scoping review. The authors did not receive any funding for this review study. During the preparation of this work, the authors used Grammarly to improve the readability

XSL•FO
RenderX

and language of the paper. After using this tool, the authors reviewed and edited the content as needed and took full responsibility for the content of the publication.

Authors' Contributions

SHM contributed to conceptualization, methodology, data extraction and analysis, writing-original draft, and writing-review and editing. OJ managed conceptualization, methodology, data extraction and analysis, and writing-review and editing. HKN handled data extraction and analysis and review and editing. CGO, PS, PW, and NK contributed to review and critical input.

Conflicts of Interest

None declared.

Multimedia Appendix 1
Detailed methodological quality appraisal results for each included study using the Mixed Methods Appraisal tool (MMAT).
[DOCX File, 78 KB - medinform_v13i1e66905_app1.docx]

Checklist 1
PRISMA-ScR checklist.
[PDF File, 154 KB - medinform_v13i1e66905_app2.pdf]

References

1. Bardhan I, Chen H, Karahanna E. Connecting systems, data, and people: a multidisciplinary research roadmap for chronic disease management. MIS Q 2020 Mar 1;44(1):185-200. [doi: 10.25300/MISQ/2020/14644]
2. Hacker K. The burden of chronic disease. Mayo Clinic Proceedings: Innovations, Quality & Outcomes 2024 Feb;8(1):112-119. [doi: 10.1016/j.mayocpiqo.2023.08.005]
3. Holmen H, Larsen MH, Sallinen MH, et al. Working with patients suffering from chronic diseases can be a balancing act for health care professionals - a meta-synthesis of qualitative studies. BMC Health Serv Res 2020 Feb 10;20(1):98. [doi: 10.1186/s12913-019-4826-2] [Medline: 32039723]
4. Xie Y, Lu L, Gao F, et al. Integration of artificial intelligence, blockchain, and wearable technology for chronic disease management: a new paradigm in smart healthcare. CURR MED SCI 2021 Dec;41(6):1123-1133. [doi: 10.1007/s11596-021-2485-0] [Medline: 34950987]
5. Jiménez-Muñoz L, Gutiérrez-Rojas L, Porras-Segovia A, Courtet P, Baca-García E. Mobile applications for the management of chronic physical conditions: a systematic review. Intern Med J 2022 Jan;52(1):21-29. [doi: 10.1111/imj.15081] [Medline: 33012045]
6. Montagna S, Ferretti S, Klopfenstein LC, Florio A, Pengo MF. Data decentralisation of LLM-based chatbot systems in chronic disease self-management. GoodIT '23: Proceedings of the 2023 ACM Conference on Information Technology for Social Good 2023 Sep 6:205-212. [doi: 10.1145/3582515.3609536]
7. Haque A, Chowdhury M, Soliman H. Transforming chronic disease management with chatbots: key use cases for personalized and cost-effective care. 2023 Presented at: 2023 Sixth International Symposium on Computer, Consumer and Control (IS3C); Jun 30 to Jul 3, 2023; Taichung, Taiwan p. 367-370. [doi: 10.1109/IS3C57901.2023.00104]
8. Reddy S. Evaluating large language models for use in healthcare: a framework for translational value assessment. Informatics in Medicine Unlocked 2023;41(May):101304. [doi: 10.1016/j.imu.2023.101304]
9. Huang X, Lian J, Lei Y, Yao J, Lian D, Xie X. Recommender AI agent: integrating large language models for interactive recommendations. arXiv. Preprint posted online on Jan 30, 2024 URL: https://arxiv.org/abs/2308.16505 [accessed 2025-08-24]
10. Snoswell CL, Snoswell AJ, Kelly JT, Caffery LJ, Smith AC. Artificial intelligence: augmenting telehealth with large language models. J Telemed Telecare 2025 Jan;31(1):150-154. [doi: 10.1177/1357633X231169055] [Medline: 37041736]
11. Khan MA, Mohammad N. A review on large language models: architectures, applications, taxonomies, open issues and challenges. TechRxiv. Preprint posted online on Sep 27, 2023. [doi: 10.36227/techrxiv.24171183.v1]
12. Yang R, Tan TF, Lu W, Thirunavukarasu AJ, Ting DSW, Liu N. Large language models in health care: development, applications, and challenges. Health Care Sci 2023 Aug;2(4):255-263. [doi: 10.1002/hcs2.61] [Medline: 38939520]
13. Sharma P, Parasa S. ChatGPT and large language models in gastroenterology. Nat Rev Gastroenterol Hepatol 2023 Aug;20(8):481-482. [doi: 10.1038/s41575-023-00799-8] [Medline: 37253794]
14. Karabacak M, Margetis K. Embracing large language models for medical applications: opportunities and challenges. Cureus 2023 May;15(5):e39305. [doi: 10.7759/cureus.39305] [Medline: 37378099]
15. Latif A, Kim J. Evaluation and analysis of large language models for clinical text augmentation and generation. IEEE Access 2024 Apr;12:1-1. [doi: 10.1109/ACCESS.2024.3384496]
16. Yang H, li J, liu S, Liu J. Exploring the potential of large language models in personalized diabetes treatment strategies. In Review. Preprint posted online on 2023. [doi: 10.21203/rs.3.rs-3995740/v1]

XSL•FO
RenderX

17. Raghu K, S T, S Devishamani C, M S, Rajalakshmi R, Raman R. The utility of ChatGPT in diabetic retinopathy risk assessment: a comparative study with clinical diagnosis [response to letter]. Clin Ophthalmol 2024;18:313-314. [doi: 10.2147/OPTH.S461186] [Medline: 38317795]
18. Song I, Pendse SR, Kumar N. The typing cure: experiences with large language model chatbots for mental health support. arXiv. Preprint posted online on May 9, 2025 URL: https://arxiv.org/abs/2401.14362
19. Liu Z, Chen C, Cao J, et al. Large language models for cuffless blood pressure measurement from wearable biosignals. BCB '24: Proceedings of the 15th ACM International Conference on Bioinformatics, Computational Biology and Health Informatics :1-11. [doi: 10.1145/3698587.3701447]
20. Ogundare O, Sofolahan S. Large language models in ambulatory devices for home health diagnostics: a case study of sickle cell anemia management. arXiv. Preprint posted online on May 5, 2023. [doi: 10.1007/978-3-031-40971-4_42]
21. Cankurtaran RE, Polat YH, Aydemir NG, Umay E, Yurekli OT. Reliability and usefulness of ChatGPT for inflammatory bowel diseases: an analysis for patients and healthcare professionals. Cureus 2023 Oct;15(10):e46736. [doi: 10.7759/cureus.46736] [Medline: 38022227]
22. Wang X, Liu K, Wang C. Knowledge-enhanced pre-training large language model for depression diagnosis and treatment. Presented at: 2023 IEEE 9th International Conference on Cloud Computing and Intelligent Systems (CCIS); Aug 12-13, 2023; Dali, China p. 532-536. [doi: 10.1109/CCIS59572.2023.10263217]
23. Abdullahi T, Singh R, Eickhoff C. Learning to make rare and complex diagnoses with generative AI assistance: qualitative study of popular large language models. JMIR Med Educ 2024 Feb 13;10:e51391. [doi: 10.2196/51391] [Medline: 38349725]
24. Al-Anezi FM. Exploring the use of ChatGPT as a virtual health coach for chronic disease management. Learn Health Syst 2024 Jul;8(3):e10406. [doi: 10.1002/lrh2.10406] [Medline: 39036525]
25. Tricco AC, Lillie E, Zarin W, et al. PRISMA extension for scoping reviews (PRISMA-ScR): checklist and explanation. Ann Intern Med 2018 Oct 2;169(7):467-473. [doi: 10.7326/M18-0850] [Medline: 30178033]
26. Hong QN, Fàbregues S, Bartlett G, et al. The Mixed Methods Appraisal Tool (MMAT) version 2018 for information professionals and researchers. EFI 2018;34(4):285-291. [doi: 10.3233/EFI-180221]
27. Athavale A, Baier J, Ross E, Fukaya E. The potential of chatbots in chronic venous disease patient management. JVS Vasc Insights 2023;1:100019. [doi: 10.1016/j.jvsvi.2023.100019] [Medline: 37701430]
28. Soto-Chávez MJ, Bustos MM, Fernández-Ávila DG, Muñoz OM. Evaluation of information provided to patients by ChatGPT about chronic diseases in Spanish language. Digit Health 2024;10:20552076231224603. [doi: 10.1177/20552076231224603] [Medline: 38188865]
29. Abbas S, Iftikhar M, Shah MM, Khan SJ. ChatGPT-assisted machine learning for chronic disease classification and prediction: a developmental and validation study. Cureus 2024 Dec;16(12):e75851. [doi: 10.7759/cureus.75851] [Medline: 39822450]
30. Anderson P, Lin D, Davidson J, et al. Bridging domains in chronic lower back pain: large language models and ontology-driven strategies for knowledge graph construction. bioRxiv. Preprint posted online on Mar 14, 2024. [doi: 10.1101/2024.03.11.584505]
31. Ding JE, Thao PNM, Peng WC, et al. Large language multimodal models for 5-year chronic disease cohort prediction using EHR data. arXiv. Preprint posted online on Aug 29, 2024 URL: https://arxiv.org/abs/2403.04785
32. Jairoun AA, Al-Hemyari SS, Shahwan M, Al-Qirim T, Shahwan M. Benefit-risk assessment of ChatGPT applications in the field of diabetes and metabolic illnesses: a qualitative study. Clin Med Insights Endocrinol Diabetes 2024;17:11795514241235514. [doi: 10.1177/11795514241235514] [Medline: 38495947]
33. Mondal A, Naskar A. Artificial intelligence in diabetes care: evaluating GPT-4's competency in reviewing diabetic patient management plan in comparison to expert review. Endocrinology (including Diabetes Mellitus and Metabolic Disease). p. 2024. [doi: 10.1101/2024.04.12.24305732]
34. Liu H, Zhang W, Xie J, et al. Few-shot learning for chronic disease management: leveraging large language models and multi-prompt engineering with medical knowledge injection. Proceedings of the 58th Hawaii International Conference on System Sciences 2025. [doi: 10.24251/HICSS.2025.084] [Medline: 38681743]
35. Liao C, Kuo WT, Hu IH, et al. EHR-based mobile and web platform for chronic disease risk prediction using large language multimodal models. CIKM '24: Proceedings of the 33rd ACM International Conference on Information and Knowledge Management 2024 Oct 21:5244-5248. [doi: 10.1145/3627673.3679227]
36. Ding JE, Thao PNM, Peng WC, et al. Large language multimodal models for new-onset type 2 diabetes prediction using five-year cohort electronic health records. Sci Rep 2024 Sep 6;14(1):20774. [doi: 10.1038/s41598-024-71020-2] [Medline: 39237580]
37. Dao D, Teo JYC, Wang W, Nguyen HD. LLM-powered multimodal AI conversations for diabetes prevention. 2024 Jun 10 Presented at: ICMR '24: International Conference on Multimedia Retrieval; Phuket, Thailand p. 1-6 URL: https://dl.acm.org/doi/proceedings/10.1145/3643479 [accessed 2025-09-02]
38. Khan M. Assessing the efficacy of ChatGPT in facilitating self-management strategies among diabetic patients section. European Chemical Bulletin 2023;12(10):10490-10502 [FREE Full text]
39. Mondal H, Dash I, Mondal S, Behera JK. ChatGPT in answering queries related to lifestyle-related diseases and disorders. Cureus 2023 Nov. [doi: 10.7759/cureus.48296]

XSL•FO
RenderX

40. Young CC, Enichen E, Rao A, et al. Pilot study of large language models as an age-appropriate explanatory tool for chronic pediatric conditions. medRxiv. Preprint posted online on Aug 7, 2024. [doi: 10.1101/2024.08.06.24311544]
41. Li J, Guan Z, Wang J, et al. Integrated image-based deep learning and language models for primary diabetes care. Nat Med 2024 Oct;30(10):2886-2896. [doi: 10.1038/s41591-024-03139-8] [Medline: 39030266]
42. Ying Y, Wang Y, Yuan S, et al. Exploration of ChatGPT application in diabetes education based on multi-dataset. medRxiv. Preprint posted online on Sep 27, 2023. [doi: 10.1101/2023.09.27.23296144]
43. Li H, Jiang Z, Guan Z, et al. Large language models for diabetes training: a prospective study. Sci Bull Sci Found Philipp 2025 Mar;70(6):934-942. [doi: 10.1016/j.scib.2025.01.034]
44. Hussain W, Grundy J. Advice for diabetes self-management by ChatGPT models: challenges and recommendations. arXiv. Preprint posted online on Jan 14, 2025 URL: https://arxiv.org/abs/2501.07931
45. Wang D, Liang J, Ye J, et al. Enhancement of the performance of large language models in diabetes education through retrieval-augmented generation: comparative study. J Med Internet Res 2024 Nov 8;26:e58041. [doi: 10.2196/58041] [Medline: 39046096]
46. Eaton C, Vallejo N, McDonald X, et al. User engagement with mHealth interventions to promote treatment adherence and self-management in people with chronic health conditions: systematic review. J Med Internet Res 2024 Sep 24;26:e50508. [doi: 10.2196/50508] [Medline: 39316431]
47. Cheikh-Moussa K, Mira JJ, Orozco-Beltran D. Improving engagement among patients with chronic cardiometabolic conditions using mHealth: critical review of reviews. JMIR Mhealth Uhealth 2020 Apr 8;8(4):e15446. [doi: 10.2196/15446] [Medline: 32267239]
48. Mattison G, Canfell O, Forrester D, et al. The influence of wearables on health care outcomes in chronic disease: systematic review. J Med Internet Res 2022 Jul 1;24(7):e36690. [doi: 10.2196/36690] [Medline: 35776492]
49. Laranjo L, Dunn AG, Tong HL, et al. Conversational agents in healthcare: a systematic review. J Am Med Inform Assoc 2018 Sep 1;25(9):1248-1258. [doi: 10.1093/jamia/ocy072] [Medline: 30010941]
50. Lewis P, Perez E, Pictus A, et al. Retrieval-augmented generation for knowledge-intensive NLP tasks. arXiv. Preprint posted online on Apr 12, 2021. [doi: 10.48550/arXiv.2005.11401]
51. Zakka C, Chaurasia A, Shad R, et al. Almanac: retrieval-augmented language models for clinical medicine. Res Sq 2023 May 2:rs.3.rs-2883198. [doi: 10.21203/rs.3.rs-2883198/v1] [Medline: 37205549]
52. Wang Y, Ma X, Chen W. Augmenting black-box llms with medical textbooks for clinical question answering. arXiv. Preprint posted online on Feb 23, 2025. [doi: 10.48550/arXiv.2309.02233]
53. Xiong G, Jin Q, Lu Z, Zhang A. Benchmarking retrieval-augmented generation for medicine. Findings of the Association for Computational Linguistics ACL 2024 2024:6233-6251. [doi: 10.18653/v1/2024.findings-acl.372]
54. Li H, Moon JT, Purkayastha S, Celi LA, Trivedi H, Gichoya JW. Ethics of large language models in medicine and medical research. Lancet Digit Health 2023 Jun;5(6):e333-e335. [doi: 10.1016/S2589-7500(23)00083-3] [Medline: 37120418]
55. Navigli R, Conia S, Ross B. Biases in large language models: origins, inventory, and discussion. J Data and Information Quality 2023 Jun 30;15(2):1-21. [doi: 10.1145/3597307]
56. Liang PP, Wu C, Morency LP, Salakhutdinov R. Towards understanding and mitigating social biases in language models. arXiv. Preprint posted online on Jun 24, 2021. [doi: 10.48550/arXiv.2106.13219] [Medline: 34545335]
57. Verma S, Ernst M, Just R. Removing biased data to improve fairness and accuracy. arXiv. Preprint posted online on Feb 5, 2021. [doi: 10.48550/arXiv.2102.03054]
58. Kim E, Lee J, Choo J. BiaSwap: removing dataset bias with bias-tailored swapping augmentation. 2021 Presented at: 2021 IEEE/CVF International Conference on Computer Vision (ICCV); Oct 10-17, 2021; Montreal, QC, Canada p. 14972-14981. [doi: 10.1109/ICCV48922.2021.01472]
59. Ernst JS, Marton S, Brinkmann J, et al. Bias mitigation for large language models using adversarial learning. 2023 Presented at: CEUR Workshop on Fairness and Bias in AI; Krakow, Poland URL: https://ceur-ws.org/Vol-3523/paper11.pdf [accessed 2025-08-24]
60. Li Y, Li Z, Zhang K, Dan R, Jiang S, Zhang Y. ChatDoctor: a medical chat model fine-tuned on a Large Language Model Meta-AI (LLaMA) using medical domain knowledge. Cureus 2023 Jun;15(6):e40895. [doi: 10.7759/cureus.40895] [Medline: 37492832]
61. Alghanmi I, Espinosa-Anke L, Schockaert S. Self-supervised intermediate fine-tuning of biomedical language models for interpreting patient case descriptions. Proceedings of the 29th International Conference on Computational Linguistics 2022 [FREE Full text]
62. Heston TF, Khun C. Prompt engineering in medical education. IME 2023;2(3):198-205. [doi: 10.3390/ime2030019]
63. Meskó B. Prompt engineering as an important emerging skill for medical professionals: tutorial. J Med Internet Res 2023 Oct 4;25:e50638. [doi: 10.2196/50638] [Medline: 37792434]
64. Wang J, Shi E, Yu S, et al. Prompt engineering for healthcare: methodologies and applications. arXiv. Preprint posted online on Apr 23, 2024. [doi: 10.48550/arXiv.2304.14670]
65. Sarker S, Qian L, Dong X. Medical data augmentation via chatgpt: a case study on medication identification and medication event classification. arXiv. Preprint posted online on Jun 10, 2023 URL: https://arxiv.org/abs/2306.07297

XSL•FO
RenderX

66. Yang C, Zhu Y, Lu W, et al. Survey on knowledge distillation for large language models: methods, evaluation, and application. ACM Trans Intell Syst Technol 2024. [doi: 10.1145/3699518]
67. Liao B, Meng Y, Monz C. Parameter-efficient fine-tuning without introducing new latency. 2023 Presented at: Proceedings of the 61st Annual Meeting of the Association for Computational Linguistics (Volume 1 p. 4242-4260. [doi: 10.18653/v1/2023.acl-long.233]
68. Ding N, Qin Y, Yang G, et al. Parameter-efficient fine-tuning of large-scale pre-trained language models. Nat Mach Intell 2023;5(3):220-235. [doi: 10.1038/s42256-023-00626-4]
69. Liu H, Tam D, Muqeeth M, et al. Few-shot parameter-efficient fine-tuning is better and cheaper than in-context learning. arXiv. Preprint posted online on Aug 26, 2022. [doi: 10.48550/arXiv.2205.05638]
70. Hu E, Shen Y, Wallis P, et al. LoRA: low-rank adaptation of large language models. arXiv. Preprint posted online on Oct 16, 2021. [doi: 10.48550/arXiv.2106.09685]
71. Dettmers T, Pagnoni A, Holtzman A, Zettlemoyer L. QLoRA: efficient finetuning of quantized LLMs. arXiv. Preprint posted online on May 23, 2023. [doi: 10.48550/arXiv.2305.14314]
72. Liu SY, Wang CY, Yin H, et al. DoRA: weight-decomposed low-rank adaptation. arXiv. Preprint posted online on Jul 9, 2024. [doi: 10.48550/arXiv.2402.09353]
73. Wu Z, Arora A, Wang Z, et al. ReFT: representation finetuning for language models. arXiv. Preprint posted online on May 22, 2024. [doi: 10.48550/arXiv.2404.03592]
74. Houlsby N, Giurgiu A, Jastrzebski S, et al. Parameter-efficient transfer learning for NLP. arXiv. Preprint posted online on Jun 13, 2019. [doi: 10.48550/arXiv.1902.00751]
75. Li XL, Liang P. Prefix-tuning: optimizing continuous prompts for generation. Proceedings of the 59th Annual Meeting of the Association for Computational Linguistics and the 11th International Joint Conference on Natural Language Processing (Volume 1). Preprint posted online on Jan, 2021. [doi: 10.18653/v1/2021.acl-long.353]
76. Wang X, Dang T, Kostakos V, Jia H. Efficient and personalized mobile health event prediction via small language models. 2024 Dec 4 Presented at: Proceedings of the 30th Annual International Conference on Mobile Computing and Networking (MobiCom '24) p. 2353-2358. [doi: 10.1145/3636534.3698123]
77. Meskó B. The impact of multimodal large language models on health care's future. J Med Internet Res 2023 Nov 2;25:e52865. [doi: 10.2196/52865] [Medline: 37917126]
78. Belyaeva A, Cosentino J, Hormozdiari F, et al. Multimodal llms for health grounded in individual-specific data. arXiv. Preprint posted online on Jul 20, 2023. [doi: 10.48550/arXiv.2307.09018]
79. Gemini Team Google. Gemini: a family of highly capable multimodal models. arXiv. Preprint posted online on May 9, 2025. [doi: 10.48550/arXiv.2312.11805]
80. Ali H, Qadir J, Alam T, Househ M, Shah Z. ChatGPT and large language models in healthcare: opportunities and risks. 2023 Presented at: IEEE International Conference on Artificial Intelligence, Blockchain, and Internet of Things (AIBThings). [doi: 10.1109/AIBThings58340.2023.10291020]
81. Nasir S, Khan RA, Bai S. Ethical framework for harnessing the power of AI in healthcare and beyond. IEEE Access 2024;12:31014-31035. [doi: 10.1109/ACCESS.2024.3369912]
82. Goirand M, Austin E, Clay-Williams R. Implementing ethics in healthcare AI-based applications: a scoping review. Sci Eng Ethics 2021 Sep 3;27(5):5. [doi: 10.1007/s11948-021-00336-3] [Medline: 34480239]
83. Meskó B, Topol EJ. The imperative for regulatory oversight of large language models (or generative AI) in healthcare. NPJ Digit Med 2023 Jul 6;6(1):120. [doi: 10.1038/s41746-023-00873-0] [Medline: 37414860]
84. Lareyre F, Raffort J. Ethical concerns regarding the use of large language models in healthcare. EJVES Vasc Forum 2024;61:1. [doi: 10.1016/j.ejvsvf.2023.10.003] [Medline: 38025830]
85. Reddy S, Rogers W, Makinen VP, et al. Evaluation framework to guide implementation of AI systems into healthcare settings. BMJ Health Care Inform 2021 Oct;28(1):1-7. [doi: 10.1136/bmjhci-2021-100444] [Medline: 34642177]

Abbreviations

LLM: large language model
PRISMA-ScR: Preferred Reporting Items for Systematic Reviews and Meta-Analyses Extension for Scoping Reviews
RAG: retrieval augmented generation
RL: reinforcement learning

XSL•FO
RenderX

Edited by A Castonguay; submitted 26.09.24; peer-reviewed by A Jafarizadeh, ST Arasteh; revised version received 06.05.25; accepted 23.05.25; published 29.09.25.

Please cite as:
Serugunda HM, Jianquan O, Kasujja Namatovu H, Ssemaluulu P, Kimbugwe N, Garimoi Orach C, Waiswa P
Using Large Language Models for Chronic Disease Management Tasks: Scoping Review
JMIR Med Inform 2025;13:e66905
URL: https://medinform.jmir.org/2025/1/e66905
doi:10.2196/66905

©Henry Mukalazi Serugunda, Ouyang Jianquan, Hasifah Kasujja Namatovu, Paul Ssemaluulu, Nasser Kimbugwe, Christopher Garimoi Orach, Peter Waiswa. Originally published in JMIR Medical Informatics (https://medinform.jmir.org), 29.9.2025. This is an open-access article distributed under the terms of the Creative Commons Attribution License (https://creativecommons.org/licenses/by/4.0/), which permits unrestricted use, distribution, and reproduction in any medium, provided the original work, first published in JMIR Medical Informatics, is properly cited. The complete bibliographic information, a link to the original publication on https://medinform.jmir.org/, as well as this copyright and license information must be included.

XSL•FO
RenderX

Acceptability, Needs, Concerns, and Barriers to Digital-Based Interventions for the Prevention of Mother-to-Child Transmission of HIV: Systematic Review and Qualitative Meta-Aggregation

Sidik Maulana[1], MSN, RN; Kusman Ibrahim[2], RN, PhD; Rachel H A Arbing[3], MSc, MPH; Iqbal Pramukti[4], RN, PhD; Annisa Dewi Nugrahani[5,6], MD, MBiomed; Luh Nik Armini[7], PhD; Muhammad Iqhrammullah[8], MSc, MPH, PhD; Wei-Ti Chen[3], RN, CNM, PhD

[1]Doctoral Study Program of Nursing, Faculty of Nursing, Universitas Padjadjaran, Sumedang, Indonesia

[2]Department of Medical-Surgical Nursing, Faculty of Nursing, Universitas Padjadjaran, Jl. Ir. Soekarno KM.21, Hegarmanah, Jatinangor, Sumedang, Indonesia

[3]Joe C. Wen School of Nursing, University of California Los Angeles, Los Angeles, CA, United States

[4]Department of Community Health Nursing, Faculty of Nursing, Universitas Padjadjaran, Sumedang, Indonesia

[5]Doctoral Study Program of Medicine, Faculty of Medicine, Universitas Padjadjaran, Bandung, Indonesia

[6]Department of Obstetrics and Gynecology, Faculty of Medicine, Universitas Padjadjaran, Hasan Sadikin General Hospital, Bandung, Indonesia

[7]Department of Midwifery, Faculty of Medicine, Universitas Pendidikan Ganesha, Singaraja, Indonesia

[8]Department of Chemistry, Faculty of Mathematics and Natural Sciences, Universitas Syiah Kuala, Banda Aceh, Indonesia

Corresponding Author:
Kusman Ibrahim, RN, PhD
Department of Medical-Surgical Nursing, Faculty of Nursing, Universitas Padjadjaran, Jl. Ir. Soekarno KM.21, Hegarmanah, Jatinangor, Sumedang, Indonesia

Abstract

Background: Digital-based interventions have the potential to support initiatives for the prevention of mother-to-child HIV transmission (PMTCT). Nevertheless, reviews to explore experiences and perspectives toward digital-based interventions in mothers living with HIV remain limited.

Objective: The aim of the study was to explore the experiences and perspectives toward digital-based interventions in promoting PMTCT services in mothers living with HIV.

Methods: This study conducted a systematic review and qualitative meta-aggregation and adhered to the PRISMA (Preferred Reporting Items for Systematic Reviews and Meta-Analysis) and the Joanna Briggs Institute (JBI) Reviewer's Manual. Electronic databases such as Scopus, PubMed, the Cumulative Index to Nursing and Allied Health Literature (CINAHL), and Wiley Online Library were systematically searched on July 5, 2024. The eligibility criteria included qualitative studies that focus on mothers living with HIV and health care providers, exploring their experiences and attitudes toward digital-based interventions for the PMTCT of HIV. The quality of the studies was assessed using the JBI Critical Appraisal tools for qualitative research and the Mixed Methods Appraisal Tool (MMAT) for mixed methods studies. The meta-aggregation was used to synthesize findings from included qualitative studies.

Results: The 8 included studies (3 qualitative and 5 mixed-methods studies) were conducted in Kenya, South Africa, and India and evaluated mobile-based interventions such as SMS, phone calls, and mobile apps. The findings were synthesized into overarching themes: (1) positive acceptability of digital-based intervention for PMTCT services; (2) the need for integrating education, support systems, and reminders into digital-based intervention among mothers living with HIV; (3) concerns about confidentiality; and (4) personal, interpersonal, and health care–related barriers to care adherence. These themes were divided into 9 categories, including perceived satisfaction, improved adherence, the need for education, support systems, reminders, concerns about their privacy, lack of family support, financial constraints, and negative provider attitudes.

Conclusion: Although most included studies were limited, their findings highlight the insight that the integration of digital-based interventions is perceived as acceptable and beneficial in strengthening PMTCT services delivery among mothers living with HIV. Mobile-based tools were valued for delivering education and reminders and facilitating communication with providers. However, concerns about confidentiality and persistent structural barriers must be addressed. To strengthen PMTCT services, it is essential to integrate user-centered digital tools into maternal care, supported by policies that ensure data privacy and equitable access.

XSL•FO
RenderX

(JMIR Med Inform 2025;13:e64816) doi:10.2196/64816

KEYWORDS

attitude; digital health intervention; HIV; mother-to-child transmission; acceptability; systematic review; HIV transmission; patient experiences; qualitative; meta-analysis; patient needs education; support

Introduction

Since the onset of the epidemic, an estimated 88.4 million individuals are living with HIV, and approximately 42.3 million have died from HIV-related causes [1]. By the end of 2023, around 39.9 million individuals were living with HIV globally [1]. Although the global HIV prevalence among adults aged 15 - 49 years is approximately 0.8%, the burden of the epidemic varies significantly across regions and countries [1]. Pregnant and breastfeeding women, particularly in high-risk areas, remain a vulnerable group for HIV transmission [2]. HIV can be transmitted from a mother living with HIV to her child during pregnancy, childbirth, or breastfeeding [3,4]. Furthermore, pregnancies complicated by HIV infection are associated with an increased risk of miscarriage [5]. Numerous studies have shown that, without treatment, maternal HIV infection significantly raises the likelihood of stillbirth, premature birth, low birth weight, and infants being small for their gestational age [2,5-7].

Mother-to-child transmission (MTCT) of infectious diseases remains a significant global public health concern, with the prevention of HIV transmission from mother to child being one of the most pressing challenges [8]. In 2013, the World Health Organization (WHO) recommended lifelong antiretroviral therapy (ART) for all pregnant and breastfeeding women, and since 2016, also recommended its use before conception, as part of its strategy to prevent mother-to-child HIV transmission (PMTCT) [9]. To accelerate progress, the WHO Regional Office for Southeast Asia developed the “Regional Framework for Triple Elimination of MTCT in Asia and the Pacific 2018 - 2030” aiming for zero new infections in children by 2030 [10]. Supporting this initiative, WHO released the third edition of its global guidelines, which detail the standards and procedures for validating the elimination of MTCT of HIV, syphilis, and hepatitis B (triple elimination). These guidelines provide uniform targets and criteria for evaluating national progress toward the elimination of one or more of these infections [10,11].

The PMTCT program is the standard of care for mothers living with HIV, which aims to enhance both maternal and infant outcomes [12]. It includes the integration of ART during pregnancy to manage HIV viremia, support retention in care, and reduce the risk of vertical transmission [13]. Continued engagement during the postpartum period is crucial for maintaining retention and achieving viral suppression, which are essential for optimal long-term health outcomes [14]. Providing ART during pregnancy and extending prophylaxis to infants during the first 6 weeks of breastfeeding has been shown to significantly reduce the risk of MTCT [15]. However, despite ongoing efforts, treatment coverage for mothers living with HIV and their children remains below the Joint United Nations Program on HIV/AIDS (UNAIDS) 95-95-95 targets for 2030 [11,16]. These gaps highlight the urgent need for effective strategies to expand access to evidence-based interventions, particularly for pregnant women, to ensure timely treatment and improve health outcomes [16].

Digital-based interventions, such as mobile health (mHealth) and telemedicine, have emerged as promising tools to support PMTCT services [17-22]. Digital-based interventions involve the use of telecommunications technologies to deliver health services remotely, encompassing a range of platforms including text messaging, websites, mobile apps, and health-related devices. Over the past decade, the integration of digital health technologies into the standard of care has grown rapidly across the continuum of HIV care [23-25]. There is growing interest in leveraging these tools to improve maternal and child health outcomes [26,27]. In low- and middle-income countries (LMIC), digital-based interventions offer innovative solutions to persistent barriers in HIV care, such as a shortage of trained health care providers, limited infrastructure, and high out-of-pocket costs for facility-based services [28]. During the HIV epidemic, digital-based interventions were widely adopted and improved provider-patient and interprovider communication, overcoming disparities in global HIV responses [29,30].

Despite the growing interest in digital-based interventions for PMTCT, evidence regarding their acceptability remains limited. Many studies have reported positive outcomes, such as increased uptake of HIV testing and adherence to ART [19,20,27,31,31-33]. Nevertheless, the feasibility and experimental aspects have often been overlooked [19,20,27,31,31-33]. A recent systematic review of 27 studies on text messaging and phone call interventions for HIV care and treatment in LMICs found showed significant favorable effects on ART adherence and increase in retention in care [34]. In addition, a meta-analysis of phone-based interventions integrating into PMTCT services showed a moderate improvement in ART [35]. These findings highlight the importance of integrating qualitative perspectives into digital-based interventions to better understand the experiences, preferences, and barriers faced by mothers living with HIV. Nurses and other health care professionals play a critical role in delivering ongoing support and personalized education through digital platforms. This approach not only fosters mothers living with HIV engagement, but also bridges the gap between technological innovation and practical, person-centered care, thereby improving maternal and their children’s health outcomes.

Understanding the feasibility of integrating digital-based interventions into PMTCT services is essential for their successful implementation. While quantitative studies provide valuable evidence on effectiveness, qualitative studies are equally important to understand the acceptability, usability, and contextual relevance of these interventions within the target population. Therefore, there is a pressing need for review studies

XSL•FO
RenderX

that synthesize the experiences and perspectives of both mothers living with HIV and health care providers regarding integrating digital-based interventions into PMTCT services. This study explored the acceptability, perceived needs, and barriers related to digital-based interventions used in antenatal care (ANC) services, HIV testing, and ART adherence to support the PMTCT services. Specifically, this study aimed to: (1) identify the barriers and facilitators to the uptake and use of these interventions, (2) assess their acceptability among mothers living with HIV and health care providers, and (3) understand the treatment-related needs of mothers living with HIV.

Methods

Study Design

The study used a systematic review and qualitative meta-aggregation. The study adheres to the PRISMA (Preferred Report Items for Systematic Review and Meta-Analysis; see Checklist 1) and the Joanna Briggs Institute (JBI) Reviewer's Manual [36,37]. Meta-aggregation, based on the philosophical traditions of pragmatism and Husserlian transcendental phenomenology, aims to produce generalizable recommendations to guide practitioners and policymakers [37,38].

Eligibility Criteria

Inclusion criteria were established for this study according to the PCC (population, content, and context) framework. The population of interest consisted of mothers living with HIV and their health care providers. The content experiences and perspectives toward integrating digital-based interventions into PMTCT of HIV. Studies that reported on both positive and negative experiences and perspectives were included. Context was defined as any type of digital-based intervention (synchronous and asynchronous), such as text messaging, mobile health apps, telemedicine, or internet-based programs.

The exclusion criteria were quantitative studies of articles published in nonpeer-reviewed journals. Conference abstracts, posters, editorials, commentaries, and reviews were excluded. The articles not written in English were excluded. In addition, no date restrictions were applied to ensure the inclusion of all relevant studies regardless of their publication year. All database searches were conducted on July 5, 2024.

Search Strategy and Study Selection

A comprehensive search of multiple databases was conducted to identify relevant studies. Scopus, PubMed, Medline, the Cumulative Index to Nursing and Allied Health Literature (CINAHL), and Wiley Online Library were searched from their inception up to 5 July 2024. The search strategy was developed using a combination of keywords and Medical Subject Headings (MeSH) terms related to digital-based interventions and MTCT of HIV. The search terms used were ([HIV OR "Human Immunodeficiency Virus" OR "Human Immunodeficiency Viruses"] AND ["Digital technology" OR "mobile health" OR mhealth OR ehealth OR telehealth OR telemedicine OR telenursing OR "mobile apps" OR "mobile application"] AND ["medication adherence" OR adherence OR "medication nonadherence" OR "medication compliance" OR "medication noncompliance"]). See Multimedia Appendix 1 for the search strategy. Additional relevant studies were identified through snowballing searches, using the "related articles" feature and the reference lists of the included articles. A total of 2 independent reviewers (SM and ADN) assessed all articles for eligibility, with any discrepancies resolved through consultation with a third reviewer (LNA). Studies were included if they contained original qualitative data on the experiences and perspectives of mothers living with HIV, health care providers, or other relevant stakeholders of digital-based interventions in PMTCT services.

Data Extraction and Quality Appraisal

A total of 2 reviewers conducted data extraction independently using a standardized tabulation table. The table included study details such as author and year, study design, country, participant characteristics, model of digital technology, superordinate themes, subordinate themes, and quotes. Reviewers independently evaluated the studies, considering potential sources of bias, the research questions, the appropriateness of methodology, data collection, ethical considerations, rigor, data analysis, and findings. Any discrepancies between the authors were resolved through discussion and consensus.

The quality of the included studies was assessed using the JBI Critical Appraisal tools for qualitative research, and the Mixed Methods Appraisal Tool (MMAT; version 2018) for mixed methods studies [38,39]. The use of both tools was necessary due to the inclusion of qualitative and mixed methods studies. The JBI checklist is designed to evaluate the methodological validity of studies and to determine the extent to which a study has addressed the possibility of bias in its design, conduct, and analysis [38]. The MMAT is a comprehensive tool that allows for the simultaneous appraisal of qualitative, quantitative, and mixed methods studies [39]. It includes criteria tailored to assess the methodological quality of mixed methods research, such as the integration of the qualitative and quantitative components, the coherence between the research question and methodological approach, and the adequacy of the data collection and analysis methods. The authors assigned a total score to each study and divided them into three categories of quality: high (≥75%), some concerns (50% - 74%), and low (≤49%).

Data Synthesis

Following the JBI Reviewer's Manual, the study used a 3-step meta-aggregation approach to synthesize qualitative study findings [38]. Initially, 2 reviewers independently and repeatedly analyzed the reports of the selected studies, extracting findings and illustrative examples from the results sections. They identified themes, metaphors, and concepts described by the original authors. The credibility of the findings was then assessed and categorized as unequivocal, credible, or unsupported, based on how well the findings matched their supporting illustrations. Second, the reviewers independently grouped the unequivocal or credible findings into categories based on similar meanings. They discussed any differences and clarified the descriptions of the categories until they reached a consensus. Finally, they created synthesized findings by summarizing the categories that shared common features.

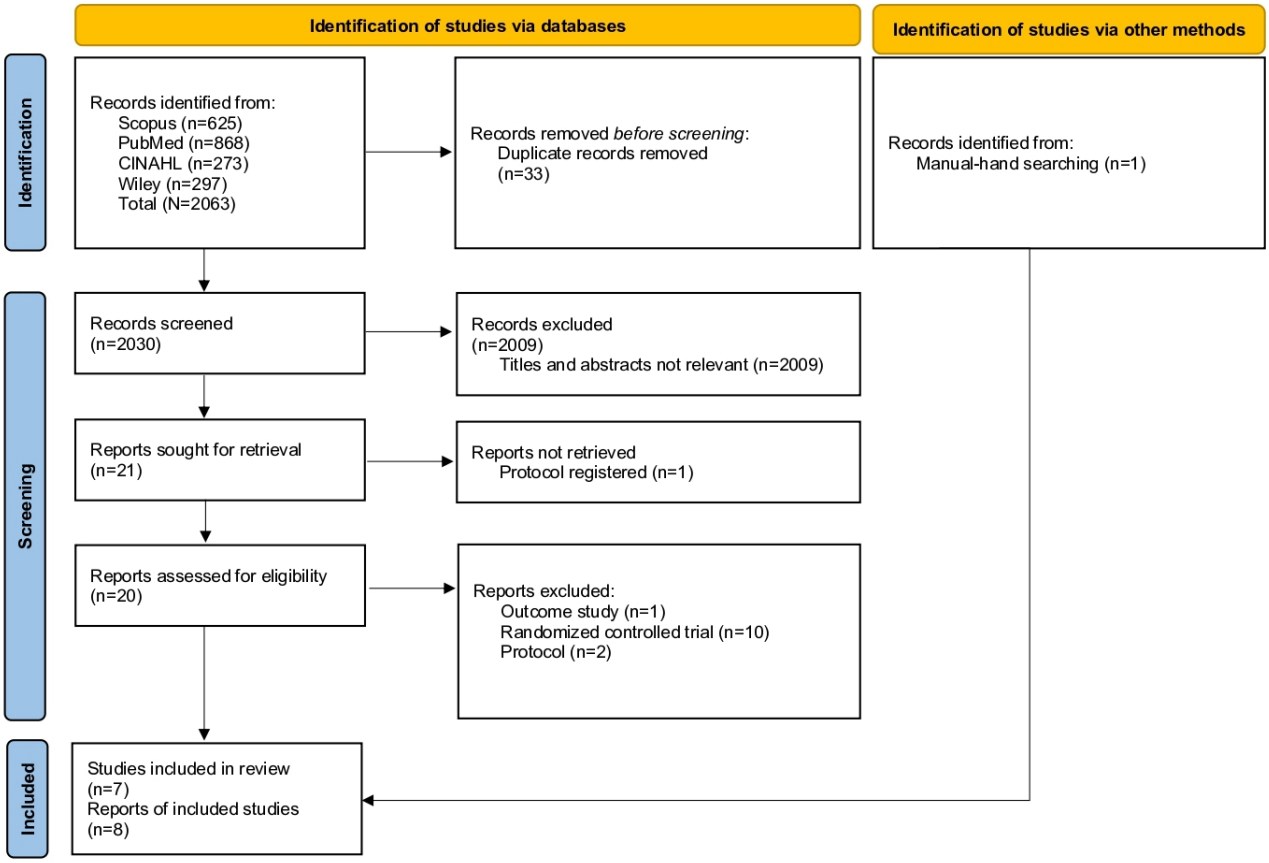
XSL•FO
RenderX

Results

Study Selection

A total of 2063 records were identified through database searches, including Scopus (n=625), PubMed (n=868), CINAHL (n=273), and Wiley Online Library (n=297). After removing 33 duplicates, 2030 records remained for title and abstract screening. Of these, 2009 records were excluded because they did not meet the inclusion criteria (eg, not focused on PMTCT, not HIV-related, not involving digital-based interventions, or not qualitative in design). These records are reported collectively as "not relevant" in the PRISMA flow diagram, resulting in 21 reports identified for full-text retrieval. Among these 21, one study was a registered protocol or rationale paper without complete study findings and therefore excluded from the eligibility assessment. Thus, 20 full-text articles were assessed for eligibility. After full-text review, 13 studies were excluded due to reasons such as reporting outcomes only (n=1), being randomized controlled trials (n=10), and protocol studies (n=2). Consequently, 7 studies met the inclusion criteria and were included in the synthesis. An additional study was identified through snowballing, bringing the total to 8 studies included in the final synthesis. A detailed breakdown of the study selection process and exclusion reasons is presented in the PRISMA flow diagram (see Figure 1) [40-47].

Figure 1. PRISMA (Preferred Reporting Items for Systematic Reviews and Meta-Analysis) flow diagram of the study selection process. Adapted from Page et al [36] (The PRISMA 2020 statement: an updated guideline for reporting systematic reviews).



Characteristics and Quality of Included Studies

Included studies were diverse in terms of the study design, study location, and digital-based intervention model used. Among the 8 studies included, 3 were qualitative studies [41,43,44] and 5 used mixed methods [40,42,45-47]. The studies were conducted in Kenya, South Africa, and India and aligned with areas with high HIV prevalence. Digital-based interventions evaluated in these studies included mobile SMS, mobile phone calls, and mobile apps. The maternal age distribution of the study participants ranged from 18 to 32 years old. The diversity of study designs and intervention models included provided an understanding of the experiences and perspective toward digital-based interventions that addressed PMTCT of HIV (see Table 1).

XSL•FO
RenderX

Table . Characteristics of included studies.

Study	Design	Country	Number of participants	Model	Maternal age, Median (IQR[a])	Code
Ronen et al (2018) [41]	Qualitative study	Kenya	87[b]	Mobile SMS	26	S1
Nachega et al (2016) [42]	Mixed methods	South Africa	20[b]	Mobile SMS	18 - 30	S2
Van Heerden et al (2013) [40]	Mixed methods	South Africa	12[b], 16[c]	MPAPI[d]	27	S3
Fairbanks et al (2018) [43]	Qualitative study	Kenya	87[b], 15[c], 30[e]	Mobile SMS	26 (23 - 32)	S4
Okal et al (2022) [44]	Qualitative study	Kenya	27[b]	Mobile-phone call	N/A[f]	S5
Dean et al (2012) [46]	Mixed methods	South Africa	7[b], 2[e]	Mobile group-SMS	18	S6
Suryavanshi et al (2020) [45]	Mixed methods	India	15[b], 15[e]	Mobile SMS	23	S7
Simpson et al (2021) [47]	Mixed methods	Zambia	43[b]	Mobile group-SMS	22 (21 - 24)	S8

[a]Median (IQR) reported only where the studies reported it.

[b]Pregnant women participants for interview or focus group discussion.

[c]Male partner participants for interview or focus group discussion.

[d]MPAPI: mobile phone-assisted personal interview.

[e]Health care provider participants for interview or focus group discussion.

[f]Not available.

Furthermore, the characteristics of the intervention model in the included studies are presented in Table 2. The interventions predominantly used mobile phone technology, including SMS-based messaging, voice calls, and mobile applications. Messaging formats ranged from unidirectional updates to interactive, bidirectional communication, enabling users to engage more actively with the system. Some interventions used group messaging platforms or private phone calls, while others relied on mobile apps specifically designed for maternal and child health support. The content of these interventions varied widely, covering areas such as appointment reminders, early infant diagnosis follow-up, counseling on ART and PMTCT, educational messages on pregnancy, breastfeeding, and disclosure, as well as support for general health and well-being. Many models also incorporated treatment adherence support and emotional or social support mechanisms. These services primarily targeted pregnant, postpartum, and breastfeeding women. They were delivered by a range of providers, including nurses, general practitioners, HIV specialists, nutritionists, trained mentors, and community health workers.

XSL•FO
RenderX

Table . Characteristics of the intervention model.

Characteristic	Number of studies, n	Reference
Intervention platform		
Mobile text–based	6	[41-43,45-47]
Mobile call phone	1	[44]
Mobile app	1	[40]
Media delivery		
Unidirectional SMS	3	[41,43,45]
Bidirectional SMS	2	[41,43]
Unspecified SMS media	1	[43]
Mobile group chat	2	[46,47]
Private phone call	1	[44]
Mobile app	1	[40]
Type of intervention delivered		
Assessment and data collection	4	[40,44-46]
Reminder (unspecified)	1	[41]
Reminder for ANC[a] visit	1	[44]
Reminder to clients scheduled appointment	1	[44]
Reminder for EID[b]	1	[44]
ART[c] counseling	1	[44]
Adherence counseling	1	[44]
PMTCT[d] counseling (eg, EID)	2	[41,47]
Education (unspecified)	1	[47]
Education related to pregnancy	1	[46]
Education related to PMTCT (eg, breastfeeding, ART, and EID)	2	[45,46]
Education related to general health and well-being	1	[46]
Education related to disclosure	1	[45]
Treatment support	3	[42,44,46]
Social support	3	[41,46,47]
Target group		
Pregnant women	8	[40-47]
Postpartum and breastfeeding women	6	[40-42,44,45,47]
Target provider group		
Clinical nurse and general practitioner	3	[41,44,47]
Specialist (HIV physician, obstetrician, or gynecologist)	2	[46,47]
Nutritionist	1	[47]
Trained mentor or facilitator	2	[46,47]
CHW[e] (includes outreach worker)	2	[44,45]

[a]ANC: antenatal care.

[b]EID: early infant diagnosis.

[c]ART: antiretroviral therapy.

XSL•FO
RenderX

[d]PMTCT: prevention of mother-to-child transmission.

[e]CHW: community health worker.

Quality Appraisal

Based on the quality assessment of the included qualitative studies, a study was categorized as "Low" and another 2 were categorized as "Some concerns" (see Multimedia Appendix 2). The analysis revealed that most biases were identified in the research components related to alignment between the research methodology and the question or objectives, methods used to collect data, data analysis, and the interpretation of results.

The MMAT assessment revealed that while all studies clearly stated their research questions and collected sufficient data to address them, several methodological concerns were noted. In particular, the alignment between research questions and methodologies was often weak. The qualitative components showed unclear justification for the chosen approaches, and in the quantitative (nonrandomized and descriptive) components, issues such as limited sample representativeness, potential nonresponse bias, and inadequate statistical analyses were identified. Furthermore, the rationale for adopting a mixed methods design was frequently insufficient, with many studies failing to justify how combining methods addressed their research aims. These findings, detailed in the MMAT assessment matrix (see Multimedia Appendix 2), highlight the need for more rigorous methodological justification, especially in studies using mixed methods designs.

Study Outcome

A total of 4 synthesized findings emerged, and 9 categories from 17 findings of this study. Table 3 shows detailed information about findings, categories, and synthesized findings. Multimedia Appendix 3 shows detailed information with original quotes.

Table . Findings, categories, and synthesized findings. S5

Finding	Category (code[s])	**Synthesized findings**
Enhances knowledge	Perceived satisfaction (S1, S2, and S4-S8)	Acceptability of digital-based intervention for PMTCT[a] services: Mothers living with HIV have experienced positive acceptability, expressed good perceived satisfaction, and enhanced adherence (S1, S2, and S4-S7).
Enhances motivation		
Usefulness		
Easy to use		
Enhanced support system		
Helpful		
Promotes adherence	Improved adherence (S5-S7)	
Need information related to ART[b] side effects	Need for education (S1 and S2)	Need for integrating education, support system, and reminders into digital-based intervention among mothers living with HIV: Mothers living with HIV have expressed a desire for education related to prevention and care for themselves and their baby; support system; reminders (S1, S2, S4, and S8).
Need information related to MTCT[c]		
Need information related to infant prophylaxis		
Mothers living with HIV desire support group	Support systems (S2)	
Mothers living with HIV need reminders for medication and clinical visits	Reminders (S4)	
Other people may read the message	Concern about their privacy (S1 and S2)	Concern about confidentiality: Mothers living with HIV are concerned about their privacy (S1 and S2).
Family caregiver is indifferent.	Lack of family support (S5)	Personal, interpersonal, and healthcare-related barriers to care adherence: Mothers living with HIV express that they face barriers related to family support, financial, and provider attitudes during the program (S5).
Visit to clinic when women have money	Financial constraints (S5)	
Women do not have money for meals		
Providers were displeased and even argued with mothers living with HIV	Negative provider attitudes (S5)	

[a]PMTCT: prevention of mother-to-child transmission.

[b]ART: antiretroviral therapy.

[c]MTCT: mother-to-child transmission.

Synthesis 1: Acceptability of Digital-Based Intervention for PMTCT Services

The findings of this study explored the acceptability of using digital-based interventions to deliver health information among mothers living with HIV. The findings revealed that the use of digital-based interventions was perceived as acceptable by the participants. Perceived satisfaction emerged as the central theme, with participants expressing that the information delivered through digital-based interventions was helpful and informative. The content included messages on pregnancy nutrition, the importance of breastfeeding, and reassurance about the

XSL•FO
RenderX

possibility of giving birth to a healthy baby despite being HIV positive [41-47]. Another prominent theme was motivation, as participants described feeling encouraged and supported by health care providers who maintained regular phone contact [41,44]. The usefulness of mobile phones was also emphasized, with participants reporting that these tools facilitated data collection and task completion at work [40,43,44]. The ease of use of mobile phones was another major theme, with participants finding them easy to operate and flexible to interact with [40,43]. Therefore, the use of mobile phones was highly acceptable and perceived as helpful, informative, and supportive by mothers living with HIV [44].

This study yielded several findings related to care adherence among mothers living with HIV. Participants reported that counseling services remotely played a supportive role in reminding them to attend clinic appointments, adhere to medication regimens, and follow appropriate infant feeding practices [44,45]. Specifically, participants reported that counselors encouraged regular clinic visits for medication and infant weight monitoring and provided guidance on exclusive breastfeeding for the first 6 months and the importance of avoiding supplemental water [44]. Participants also reported adherence to the recommended immunization schedule [44]. These findings suggest that digital-based intervention services were both acceptable and effective in enhancing adherence to maternal and child health recommendations. In addition, the previously mentioned quotes by Suryavanshi et al [45] reported that reminder messages helped the women to remember to go get medications, demonstrating the positive impact of the counseling service on adherence to medication regimens. Another participant from Suryavanshi and colleague's [45] study expressed their care commitment by keeping track of medication and testing schedules even without reminders [45]. These findings highlight the role of digital-based intervention in fostering a sense of responsibility and self-management among participants.

Synthesis 2: The Need for Integrating Education, Support System, and Reminders Into Digital-Based Intervention Among Mothers Living With HIV

This study revealed that mothers living with HIV have specific needs related to digital-based interventions, particularly in education, support systems, and reminders. In terms of education, participants expressed a desire to receive information on ART side effects [41,42], MTCT of HIV [41], infant prophylaxis [41], and the importance of medication adherence [43]. In terms of support systems, mothers living with HIV found that receiving information about peer support groups helped reduce feelings of isolation and fostered a sense of belonging [42]. In addition, digital reminders were perceived as effective tools for improving adherence to clinical appointments and medication schedules [43].

Synthesis 3: Concerns About Confidentiality

Concerns related to the digital integration of treatment emerged as a key theme in this study, with confidentiality identified as a prominent subtheme. Participants expressed concerns about the privacy of their HIV status and potential for stigma and discrimination if their status was disclosed [41,42]. For example, some mothers living with HIV were uncomfortable receiving SMS messages about their treatment in the presence of others who were unaware of their HIV status, fearing that this could lead to unintentional disclosure and social repercussions [41]. Similarly, some participants expressed concerns about taking ART in public places, where their status could be revealed to others unaware of their status [42].

Synthesis 4: Personal, Interpersonal, and Health Care-Related Barriers to Care Adherence

The findings of this study revealed that limited family support, financial constraints, and negative provider attitudes influenced access and use of HIV care integrated with digital-based interventions among mothers living with HIV. In terms of lack of family support, participants reported that having support from their family members was crucial in encouraging them to attend clinic appointments [37]. Some participants expressed how their family members would encourage them to seek treatment when they were feeling unwell. Financial barriers also emerged as a major concern, as some participants delayed treatment due to insufficient funds for transportation or medication, often relying on family members for financial assistance [37]. Furthermore, provider attitudes impacted service use, with participants reporting experiences of disrespect or poor communication from health care providers that led them to miss appointments or avoid seeking care.

Discussion

Principal Findings

This study identified 4 key themes that reflect the experiences and perspectives of mothers living with HIV and health care providers regarding integration of digital-based interventions into PMTCT of HIV services. First, digital interventions were perceived as acceptable, supported by subthemes such as perceived satisfaction, ease of use, usefulness, increased motivation, and improved adherence to care. Second, mothers living with HIV expressed specific needs for education, support systems, and reminders. They desired information about ART side effects, MTCT, and infant prophylaxis. Subthemes also included the importance of peer support groups and timely reminders for clinic visits and medication use. Third, concerns about confidentiality emerged as a barrier, particularly the fear of unintended HIV status disclosure through text messages received in the presence of others. Finally, participants highlighted personal, interpersonal, and health system barriers that hindered digital care adherence. These included a lack of family support, financial hardship, and negative attitudes from health care providers.

The use of digital-based interventions in health care has grown rapidly in recent years, and this study highlights their benefits in promoting adherence to maternal and child health interventions [41-47]. These interventions have increasingly become a critical component of health care delivery, even in resource-limited settings, and are now embedded within modern society [48,49]. Although some mothers living with HIV expressed concerns about confidentiality, this study found that the integration of digital-based interventions into PMTCT of

XSL•FO
RenderX

HIV services enhanced their satisfaction with care and supported better adherence to treatment. This suggests the use of digital technology as an effective platform to reach and engage mothers living with HIV and their infants. As suggested previously, a high level of acceptability significantly determines successful linkage to and retention in care [50]. The findings align with the growing body of evidence on the usefulness of mobile technology in enhancing health care services across the HIV care continuum and among key populations [34,51-55].

The health care–related needs of mothers living with HIV, particularly in the context of digital-based interventions, primarily focus on education, support systems, and reminders [41-47]. This study found that mothers expressed a desire for digital-based interventions that provide educational content related to treatment, maternal health, and infant care [41]. These digital platforms can serve as valuable tools by delivering reliable information on health conditions, treatment options, medication usage, and self-care practices, thereby supporting improved health literacy and better health outcomes [56,57]. Empowering mothers with such knowledge enables them to make more informed decisions regarding their own health and that of their children.

Furthermore, mothers living with HIV, who often face complex medical and psychosocial challenges, frequently seek emotional and psychological support [58]. The theme of self-isolation frequently emerged in relation to experiences of HIV-related stigma and coping mechanisms [59]. Digital interventions that include support features, such as online communities, chat groups, or direct messaging with health care professionals can provide emotional support, reduce feelings of isolation, and foster a sense of belonging [60]. However, some participants may avoid participating in peer groups due to concerns about confidentiality.

Although mobile phone–based platforms, as digital-based interventions, were generally acceptable and facilitated care engagement, concerns specifically related to SMS were frequently reported [41,42]. These concerns were primarily driven by fears of unintended HIV status disclosure through visible text messages, particularly in shared phone settings or when notifications appeared on locked screens [41,42]. This contrast highlights that while the device itself was acceptable, the mode of digital communication, such as SMS, may introduce risks that affect trust and usability. Therefore, this is not a contradiction but rather a reflection of how acceptability is influenced by the specific design features of digital interventions.

Retention in care and adherence to treatment and care are essential for effectively managing mothers living with HIV and reducing the risk of vertical transmission through viral suppression [61,62]. In this study, mothers living with HIV frequently expressed the need for digital applications that provide timely reminders for taking and refilling medications, clinic appointments, and daily health routines. Such features can significantly enhance treatment adherence and contribute to improved health outcomes for both mothers living with HIV and their babies [55,63].

Although digital health interventions show promise in improving PMTCT outcomes, this study identified confidentiality as a major concern among mothers living with HIV [41,42]. This concern highlights the critical importance of protecting the privacy and confidentiality of health information for mothers living with HIV, especially their HIV status. This underscores the need for health care systems to protect the privacy of individuals' health information, particularly HIV status, by implementing robust privacy policies and upholding legal and ethical standards [64]. This includes securing medical records, limiting access to sensitive data, and obtaining informed consent before disclosing health information to others, including family members or partners.

Barriers to treatment, such as lack of family support, financial difficulties, and negative provider attitudes, are critical factors influencing access to and use of digital-based HIV care interventions among mothers living with HIV. Within the context of ANC, regular clinical visits are essential; however, limited family support and financial problems often make it difficult for mothers to undergo HIV testing and access necessary health care services [65]. The cost of transportation and medical services, combined with poverty-related issues such as food insecurity, further hinders treatment adherence [66]. In addition, partner notification and effective couples counseling are essential as an entry point to identify serodiscordant partners, facilitate mutual disclosure of HIV status, and link those living with HIV to appropriate care and treatment services [67].

A strategic approach involves encouraging national HIV program leaders to advocate long-term policy changes that support the home delivery of antiretrovirals [68]. In addition, targeted financial incentives—such as unconditional cash transfers—have been shown to improve access to care and support treatment adherence, including assistance with ART initiation and transportation to health care facilities [66]. To further address economic barriers, livelihood programs and vocational training, such as microcredit initiatives, can empower mothers living with HIV [66].

In addition, provider attitudes and communication styles can significantly influence the willingness of mothers living with HIV to seek health care services. When mothers living with HIV feel judged, disrespected, or misunderstood—whether during in-person visits or digital interactions—they may be hesitant to participate fully in care or may withhold important health information. Cultural competence and empathy are essential for building trust, particularly given the unique vulnerabilities and stigma often experienced by this population [69]. Negative provider attitudes can contribute to disparities in health care access, leading to reduced quality of care and poorer health outcomes for certain patient populations [69]. To address these challenges, health care professionals should receive training in cultural sensitivity, empathetic communication, and care tailored to mothers living with HIV—both in traditional and digital settings—to ensure that integration of digital-based interventions into PMTCT services is delivered in a supportive and inclusive manner [69].

XSL•FO
RenderX

Implications for Practices and Policies

These findings inform the design of future digital-based interventions for PMTCT of HIV by highlighting the importance of tailoring programs to the specific needs and preferences of both mothers living with HIV and health care providers. To address concerns around confidentiality, policies should ensure robust privacy protections, grounded in the ethical and legal standards of nursing and other health care professions [64]. In addition, government regulations should establish clear guidelines for evaluating the effectiveness and impact of digital health practice [70]. In addition, the national HIV program should consider implementing home delivery of antiretrovirals to address financial barriers. In addition, providing financial incentives to improve linkage to ANC and early infant diagnosis (EID), particularly among low-income populations [71,72], such as covering mobile data costs and offering transportation support for facility visits when ANC or EID is required.

Furthermore, international financial support has played a crucial role in advancing digital-based intervention for HIV care, including PMTCT initiatives. These contributions have supported progress in reducing new HIV infections and lowering maternal and infant mortality related to HIV. However, several major donor countries have announced substantial cuts to their aid budgets for the 2025 - 2026 period. This financial shift may jeopardize the sustainability of PMTCT programs, particularly in low-resource settings. Strategic investment in digital infrastructure is therefore essential to maintaining momentum toward achieving global health targets, especially in remote and underserved areas. The rapid expansion of mobile and communication technologies in LMICs presents an opportunity to optimize service delivery. Digital platforms, such as eHealth and mHealth, can support timely counseling, treatment adherence, follow-up, and remote monitoring for mothers living with HIV and their infants through SMS, video consultations, or online check-ins. Strengthening these systems aligns directly with Sustainable Development Goal 3, which aims to ensure healthy lives and promote well-being for all, including ending the HIV/AIDS epidemic and improving maternal and child health outcomes.

To enhance feasibility, delivery models for PMTCT digital interventions must be tailored to local digital infrastructures and user contexts, ensuring they integrate seamlessly with existing care pathways and uphold privacy standards. In low-connectivity settings, voice calls and SMS reminders offer widely accessible options, while in higher-connectivity areas, smartphone-based tools like apps or chatbots can support more interactive counseling, peer support, and data reporting [73]. These digital platforms should be interoperable with national health information systems to monitor ANC, ART adherence, and EID outcomes. Equitable implementation also demands backup delivery modes, for instance, offering SMS as an alternative for users without smartphones.

Limitations

Despite the valuable insights offered by this study, several limitations must be acknowledged to provide a balanced interpretation of the findings. First, methodological limitations were evident in the included studies, particularly regarding the alignment between philosophical underpinnings and research design. Many studies did not explicitly state the researcher's cultural or theoretical positioning, nor did they reflect on how the researcher may have influenced or been influenced by the research process—an important element in qualitative rigor [74] . Second, the scope of this study was limited to 4 electronic databases (eg, Scopus, PubMed, CINAHL, and Wiley), which may have resulted in the omission of relevant studies published elsewhere, including in scientific search engines (eg, Google Scholar and ScienceDirect) and in the gray literature. This limitation may reduce the comprehensiveness and inclusivity of the synthesized evidence. However, to minimize publication and selection bias, we supplemented our search with manual hand-searching [75,76]. Third, this study included only studies published in English, which may have excluded relevant evidence from non-English sources and introduced language bias.

Fourth, in some themes, the synthesis was informed by only a single primary study, which weakens the transferability and generalizability of the findings. Conclusions drawn from a single context are less robust and may not be applicable across diverse populations or settings. Fifth, considerable variation was observed in the types of digital technologies reported across studies, which may contribute to heterogeneity in outcomes. These differences, ranging from SMS reminders to mobile health apps, can impact the consistency and reliability of the synthesized conclusions. Sixth, the search strategy did not fully use database-specific indexing terms such as PubMed MeSH headings; although MeSH terms were consulted to inform keyword development, reliance on title and abstract keyword searches may have increased the risk of missing relevant studies.

Most interventions in the included studies relied on mobile phone text (SMS) and voice-call technologies. However, 2 SMS-based studies were rated as moderate or lower in quality [41,43], which may introduce potential bias in findings related to SMS delivery models. Also, advanced digital tools were less frequently used and may present different acceptability, usability, and concern profiles compared to simpler technologies. In addition, the barriers identified regarding the integration of digital-based interventions into PMTCT services were predominantly contextual rather than technical in nature. Rather than focusing on usability or platform-specific issues, the findings revealed broader systemic challenges related to the integration of digital interventions into existing health care services. Furthermore, few studies provided technical specifications about the mobile phones used, such as device types, operating systems, or internet requirements. This lack of detail limits our ability to assess disparities in access, particularly in low-resource settings where smartphone ownership, digital literacy, and mobile network coverage are often constrained. These factors should be explored in future research to strengthen the applicability of digital-based interventions for PMTCT of HIV in diverse and underserved contexts.

Conclusions

Findings from this study indicate that digital-based interventions, particularly mobile-based technologies, are highly acceptable

XSL•FO
RenderX

among mothers living with HIV and effectively support adherence to PMTCT-related services. Mothers living with HIV valued digital tools for delivering education, emotional support, and appointments or medication reminders. However, concerns regarding confidentiality and barriers such as limited family support, financial constraints, and provider attitudes were identified as significant challenges to digital intervention uptake. To improve PMTCT outcomes in HIV, future digital strategies must prioritize confidentiality, address women's expressed needs, and consider structural barriers.

Acknowledgments

We would like to express our heartfelt gratitude to Universitas Padjadjaran for providing a database to conduct this systematic review and meta-analysis. We also thank JMIR Medical Informatics for the article processing charges support. This study was supported by Universitas Padjadjaran under grant contract 4269/UN6.3.1/PT.00/2023.

Authors' Contributions

Conceptualization: SM, KI
Investigation: SM, ADN
Formal analysis: SM, ADN
Writing – review & editing: SM, KI, ADN, RHAA, IP, LNA, MI, W-TC
Author SM is the co-correspondence author, and can be reached at Jl. Ir. Soekarno KM.21, Hegarmanah, Jatinangor, Sumedang, 45363, Indonesia; sidik17001@mail.unpad.ac.id or sidik17001@gmail.com.

Conflicts of Interest

None declared.

Multimedia Appendix 1
Searching strategy.
[DOCX File, 14 KB - medinform_v13i1e64816_app1.docx]

Multimedia Appendix 2
Summary of synthesis finding, category, finding, and quotes.
[DOCX File, 29 KB - medinform_v13i1e64816_app2.docx]

Multimedia Appendix 3
Quality appraisal.
[DOCX File, 24 KB - medinform_v13i1e64816_app3.docx]

Checklist 1
PRISMA checklist.
[PDF File, 109 KB - medinform_v13i1e64816_app4.pdf]

References

1. Global HIV & AIDS statistics — fact sheet. UNAIDS. 2024. URL: https://www.unaids.org/en/resources/fact-sheet [accessed 2025-04-10]
2. Machekano R, Tiam A, Kassaye S, et al. HIV incidence among pregnant and postpartum women in a high prevalence setting. PLoS One 2018;13(12):e0209782. [doi: 10.1371/journal.pone.0209782] [Medline: 30592749]
3. Wudineh F, Damtew B. Mother-to-child transmission of HIV infection and its determinants among exposed infants on care and follow-up in Dire Dawa City, Eastern Ethiopia. AIDS Res Treat 2016;2016:3262746. [doi: 10.1155/2016/3262746] [Medline: 26989507]
4. Global Monitoring Framework and Strategy for the Global Plan towards the Elimination of New HIV Infections among Children by 2015 and Keeping Their Mothers Alive (EMTCT): UNAIDS. URL: http://apps.who.int/iris/bitstream/10665/75341/1/9789241504270_eng.pdf?ua=1 [accessed 2024-10-19]
5. Tukei VJ, Hoffman HJ, Greenberg L, et al. Adverse pregnancy outcomes among HIV-positive women in the era of universal antiretroviral therapy remain elevated compared with HIV-negative women. Pediatr Infect Dis J 2021 Sep 1;40(9):821-826. [doi: 10.1097/INF.0000000000003174] [Medline: 33990522]
6. Li H, Liu J, Tan D, et al. Maternal HIV infection and risk of adverse pregnancy outcomes in Hunan province, China. Medicine (Baltimore) 2020 Feb;99(8):e19213. [doi: 10.1097/MD.0000000000019213]

XSL•FO
RenderX

7. Rebnord T, Mmbaga BT, Sandøy IF, et al. Time trends in perinatal outcomes among HIV-positive pregnant women in Northern Tanzania: A registry-based study. PLOS ONE 2023;18(8):e0289740. [doi: 10.1371/journal.pone.0289740]
8. Njom Nlend AE. Mother-to-child transmission of HIV through breastfeeding improving awareness and education: a short narrative review. IJWH 2022 May 13;Volume 14:697-703. [doi: 10.2147/IJWH.S330715]
9. Drake AL, Wagner A, Richardson B, John-Stewart G. Incident HIV during pregnancy and postpartum and risk of mother-to-child HIV transmission: a systematic review and meta-analysis. PLoS Med 2014 Feb;11(2):e1001608. [doi: 10.1371/journal.pmed.1001608] [Medline: 24586123]
10. Regional Framework for the Triple Elimination of Mother-to-Child Transmission of HIV, Hepatitis b and Syphilis in Asia and the Pacific, 2018-2030: WHO Regional Office for the Western Pacific, World Health Organization; 2018. URL: https://apps.who.int/iris/handle/10665/274111
11. Armini LN, Setiawati EP, Arisanti N, Hilmanto D. Evaluation of process indicators and challenges of the elimination of mother-to-child transmission of HIV, syphilis, and hepatitis B in Bali Province, Indonesia (2019–2022): a mixed methods study. TropicalMed 2019 Mar;8(11):492. [doi: 10.3390/tropicalmed8110492]
12. Mutabazi JC, Zarowsky C, Trottier H. The impact of programs for prevention of mother-to-child transmission of HIV on health care services and systems in sub-Saharan Africa - A review. Public Health Rev 2017;38(1):28. [doi: 10.1186/s40985-017-0072-5] [Medline: 29450099]
13. Paredes R, Marconi VC, Lockman S, Abrams EJ, Kuhn L. Impact of antiretroviral drugs in pregnant women and their children in Africa: HIV resistance and treatment outcomes. J Infect Dis 2013 Jun 15;207 Suppl 2(Suppl 2):S93-100. [doi: 10.1093/infdis/jit110] [Medline: 23687295]
14. Adams JW, Brady KA, Michael YL, Yehia BR, Momplaisir FM. Postpartum engagement in HIV care: an important predictor of long-term retention in care and viral suppression. Clin Infect Dis 2015 Dec 15;61(12):1880-1887. [doi: 10.1093/cid/civ678] [Medline: 26265499]
15. Daniels B, Spooner E, Coutsoudis A. Getting to under 1% vertical HIV transmission: lessons from a breastfeeding cohort in South Africa. BMJ Glob Health 2022 Sep 20;7(9):1-5. [doi: 10.1136/bmjgh-2022-009927] [Medline: 36130776]
16. Mushamiri I, Belai W, Sacks E, Genberg B, Gupta S, Perry HB. Evidence on the effectiveness of community-based primary health care in improving HIV/AIDS outcomes for mothers and children in low- and middle-income countries: Findings from a systematic review. J Glob Health 2021;11:11001. [doi: 10.7189/jogh.11.11001] [Medline: 34327001]
17. John-Stewart G. eHealth and prevention of mother-to-child transmission of HIV. Curr HIV/AIDS Rep 2018 Aug;15(4):350-357. [doi: 10.1007/s11904-018-0408-x] [Medline: 29931467]
18. Coleman J, Bohlin KC, Thorson A, et al. Effectiveness of an SMS-based maternal mHealth intervention to improve clinical outcomes of HIV-positive pregnant women. AIDS Care 2017 Jul 3;29(7):890-897. [doi: 10.1080/09540121.2017.1280126]
19. Dryden-Peterson S, Bennett K, Hughes MD, et al. An augmented SMS intervention to improve access to antenatal CD4 testing and ART initiation in HIV-infected pregnant women: a cluster randomized trial. PLoS ONE 2015;10(2):e0117181. [doi: 10.1371/journal.pone.0117181] [Medline: 25693050]
20. Kebaya LMN, Wamalwa D, Kariuki N, Admani B, Ayieko P, Nduati R. Efficacy of Mobile phone use on adherence to Nevirapine prophylaxis and retention in care among the HIV-exposed infants in prevention of mother to child transmission of HIV: a randomized controlled trial. BMC Pediatr 2021 Dec;21(1):186. [doi: 10.1186/s12887-021-02660-w]
21. Kinuthia J, Ronen K, Unger JA, et al. SMS messaging to improve retention and viral suppression in prevention of mother-to-child HIV transmission (PMTCT) programs in Kenya: a 3-arm randomized clinical trial. PLoS Med 2021 May;18(5):e1003650. [doi: 10.1371/journal.pmed.1003650] [Medline: 34029338]
22. Odeny TA, Hughes JP, Bukusi EA, et al. Text messaging for maternal and infant retention in prevention of mother-to-child HIV transmission services: a pragmatic stepped-wedge cluster-randomized trial in Kenya. PLoS Med 2019 Oct;16(10):e1002924. [doi: 10.1371/journal.pmed.1002924] [Medline: 31577792]
23. Ibrahim K, Kahle EM, Christiani Y, Suryani S. Utilization of social media for the prevention and control of HIV/AIDS: a scoping review. J Multidiscip Healthc 2024;17:2443-2458. [doi: 10.2147/JMDH.S465905] [Medline: 38799010]
24. Mhando F, Nyankomo M, Hall C, et al. Digital intervention services to promote HIV self-testing and linkage to care services: a bibliometric and content analysis-global trends and future directions. Public Health Rev 2024;45:1606354. [doi: 10.3389/phrs.2024.1606354] [Medline: 38434540]
25. Shi H, Du J, Jin G, et al. Effectiveness of eHealth interventions for HIV prevention, testing and management: an umbrella review. Int J STD AIDS 2024 Sep;35(10):752-774. [doi: 10.1177/09564624241252457]
26. Finocchario-Kessler S, Brown M, Maloba M, et al. A pilot study to evaluate the impact of the HIV infant tracking system (HITSystem 2.0) on priority prevention of mother-to-child transmission (PMTCT) outcomes. AIDS Behav 2021 Aug;25(8):2419-2429. [doi: 10.1007/s10461-021-03204-0] [Medline: 33709212]
27. Sarna A, Saraswati LR, Okal J, et al. Cell phone counseling improves retention of mothers with HIV infection in care and infant HIV testing in Kisumu, Kenya: a randomized controlled study. Glob Health Sci Pract 2019 Jun;7(2):171-188. [doi: 10.9745/GHSP-D-18-00241] [Medline: 31142546]
28. Hoffer-Hawlik M, Moran A, Zerihun L, Usseglio J, Cohn J, Gupta R. Telemedicine interventions for hypertension management in low- and middle-income countries: A scoping review. PLoS One 2021;16(7):e0254222. [doi: 10.1371/journal.pone.0254222] [Medline: 34242327]

XSL•FO
RenderX

29. Mahmoud K, Jaramillo C, Barteit S. Telemedicine in low- and middle-income countries during the COVID-19 pandemic: a scoping review. Front Public Health 2022;10:914423. [doi: 10.3389/fpubh.2022.914423] [Medline: 35812479]
30. Kurniawan K, Yosep I, Maulana S, et al. Efficacy of online-based intervention for anxiety during COVID-19: a systematic review and meta-analysis of randomized controlled trials. Sustainability 2022;14(19):12866. [doi: 10.3390/su141912866]
31. Schwartz SR, Clouse K, Yende N, et al. Acceptability and feasibility of a mobile phone-based case management intervention to retain mothers and infants from an Option B+ program in postpartum HIV care. Matern Child Health J 2015 Sep;19(9):2029-2037. [doi: 10.1007/s10995-015-1715-0] [Medline: 25656728]
32. Pintye J, Rogers Z, Kinuthia J, et al. Two-way short message service (SMS) communication may increase pre-exposure prophylaxis continuation and adherence among pregnant and postpartum women in Kenya. Glob Health Sci Pract 2020 Mar 30;8(1):55-67. [doi: 10.9745/GHSP-D-19-00347] [Medline: 32139420]
33. Drake AL, Rothschild C, Jiang W, Ronen K, Unger JA. Utility of short message service (SMS) for remote data collection for HIV in low- and middle-income countries. Curr HIV/AIDS Rep 2020 Dec;17(6):654-662. [doi: 10.1007/s11904-020-00534-x] [Medline: 33010003]
34. Demena BA, Artavia-Mora L, Ouedraogo D, Thiombiano BA, Wagner N. A systematic review of mobile phone interventions (SMS/IVR/Calls) to improve adherence and retention to antiretroviral treatment in low-and middle-income countries. AIDS Patient Care STDS 2020 Feb;34(2):59-71. [doi: 10.1089/apc.2019.0181] [Medline: 32049555]
35. Shah R, Watson J, Free C. A systematic review and meta-analysis in the effectiveness of mobile phone interventions used to improve adherence to antiretroviral therapy in HIV infection. BMC Public Health 2019 Dec;19(1). [doi: 10.1186/s12889-019-6899-6]
36. Page MJ, McKenzie JE, Bossuyt PM, et al. The PRISMA 2020 statement: an updated guideline for reporting systematic reviews. BMJ 2021 Mar 29;372:n71. [doi: 10.1136/bmj.n71] [Medline: 33782057]
37. Lockwood C, Munn Z, Porritt K. Qualitative research synthesis: methodological guidance for systematic reviewers utilizing meta-aggregation. Int J Evid Based Healthc 2015 Sep;13(3):179-187. [doi: 10.1097/XEB.0000000000000062] [Medline: 26262565]
38. Hannes K, Lockwood C. Pragmatism as the philosophical foundation for the Joanna Briggs meta‐aggregative approach to qualitative evidence synthesis. J Adv Nurs 2011 Jul;67(7):1632-1642. [doi: 10.1111/j.1365-2648.2011.05636.x]
39. Hong QN, Fabregues S, Bartlett G, et al. The Mixed Methods Appraisal Tool (MMAT) version 2018 for information professionals and researchers. Education for Information 2018;34(4):285-291. [doi: 10.3233/EFI-1802]
40. van Heerden A, Norris S, Tollman S, Richter L, Rotheram-Borus MJ. Collecting maternal health information from HIV-positive pregnant women using mobile phone-assisted face-to-face interviews in Southern Africa. J Med Internet Res 2013 Jun 10;15(6):e116. [doi: 10.2196/jmir.2207] [Medline: 23748182]
41. Ronen K, Unger JA, Drake AL, et al. SMS messaging to improve ART adherence: perspectives of pregnant HIV-infected women in Kenya on HIV-related message content. AIDS Care 2018 Apr 3;30(4):500-505. [doi: 10.1080/09540121.2017.1417971]
42. Nachega J, Skinner D, Jennings L, et al. Acceptability and feasibility of mHealth and community-based directly observed antiretroviral therapy to prevent mother-to-child HIV transmission in South African pregnant women under Option B+: an exploratory study. PPA 2016;10:683. [doi: 10.2147/PPA.S100002]
43. Fairbanks J, Beima-Sofie K, Akinyi P, et al. You will know that despite being HIV positive you are not alone: qualitative study to inform content of a text messaging intervention to improve prevention of mother-to-child HIV transmission. JMIR Mhealth Uhealth 2018 Jul 19;6(7):e10671. [doi: 10.2196/10671] [Medline: 30026177]
44. Okal JO, Sarna A, Lango D, et al. Client experiences in a mobile-phone counseling intervention for enhancing access to prevention of mother to-child transmission (PMTCT) services in Kenya. Front Glob Womens Health 2022;3:785194. [doi: 10.3389/fgwh.2022.785194] [Medline: 35720809]
45. Suryavanshi N, Kadam A, Kanade S, et al. Acceptability and feasibility of a behavioral and mobile health intervention (COMBIND) shown to increase uptake of prevention of mother to child transmission (PMTCT) care in India. BMC Public Health 2020 May 24;20(1):752. [doi: 10.1186/s12889-020-08706-5] [Medline: 32448299]
46. Dean AL, Makin JD, Kydd AS, Biriotti M, Forsyth BWC. A pilot study using interactive SMS support groups to prevent mother-to-child HIV transmission in South Africa. J Telemed Telecare 2012 Oct;18(7):399-403. [doi: 10.1258/jtt.2012.120118]
47. Simpson N, Kydd A, Phiri M, et al. Insaka: mobile phone support groups for adolescent pregnant women living with HIV. BMC Pregnancy Childbirth 2021 Sep 30;21(1):663. [doi: 10.1186/s12884-021-04140-6] [Medline: 34592959]
48. Kaplan WA. Can the ubiquitous power of mobile phones be used to improve health outcomes in developing countries? Global Health 2006 May 23;2:9. [doi: 10.1186/1744-8603-2-9] [Medline: 16719925]
49. Olsen M, Campos M, Lohning A, et al. Mobile phones represent a pathway for microbial transmission: A scoping review. Travel Med Infect Dis 2020;35:101704. [doi: 10.1016/j.tmaid.2020.101704] [Medline: 32360322]
50. Sekhon M, Cartwright M, Francis JJ. Acceptability of healthcare interventions: an overview of reviews and development of a theoretical framework. BMC Health Serv Res 2017 Jan 26;17(1):88. [doi: 10.1186/s12913-017-2031-8] [Medline: 28126032]

XSL•FO
RenderX

51. DeNicola N, Grossman D, Marko K, et al. Telehealth interventions to improve obstetric and gynecologic health outcomes: a systematic review. Obstet Gynecol 2020 Feb;135(2):371-382. [doi: 10.1097/AOG.0000000000003646] [Medline: 31977782]
52. Bonett S, Li Q, Sweeney A, Gaither-Hardy D, Safa H. Telehealth models for PrEP delivery: a systematic review of acceptability, implementation, and impact on the PrEP care continuum in the United States. AIDS Behav 2024 Sep;28(9):2875-2886. [doi: 10.1007/s10461-024-04366-3] [Medline: 38856846]
53. Beecroft A, Vaikla O, Engel N, Duchaine T, Liang C, Pant Pai N. Evidence on digital HIV self-testing from accuracy to impact: updated systematic review. J Med Internet Res 2025 Mar 4;27:e63110. [doi: 10.2196/63110] [Medline: 40053740]
54. Yeh PT, Kennedy CE, Minamitani A, et al. Web-based service provision of HIV, viral hepatitis, and sexually transmitted infection prevention, testing, linkage, and treatment for key populations: systematic review and meta-analysis. J Med Internet Res 2022 Dec 22;24(12):e40150. [doi: 10.2196/40150] [Medline: 36548036]
55. Li D, Ma S, Dang B, Shi H, Wei Y, Wang X. Effectiveness of telemedicine for the prevention of mother-to-child transmission of HIV in low-income and middle-income countries: a systematic review and meta-analysis. Int J Infect Dis 2024 Jun;143:106981. [doi: 10.1016/j.ijid.2024.02.024] [Medline: 38458425]
56. Schnall R, Cho H, Mangone A, Pichon A, Jia H. Mobile health technology for improving symptom management in low income persons living with HIV. AIDS Behav 2018 Oct;22(10):3373-3383. [doi: 10.1007/s10461-017-2014-0] [Medline: 29299790]
57. Tesema N, Guillaume D, Francis S, Paul S, Chandler R. Mobile phone apps for HIV prevention among college-aged black women in atlanta: mixed methods study and user-centered prototype. JMIR Form Res 2023 Feb 23;7:e37987. [doi: 10.2196/37987] [Medline: 36821362]
58. Fauk NK, Merry MS, Mwanri L, Hawke K, Ward PR. Mental health challenges and the associated factors in women living with HIV who have children living with HIV in Indonesia: a qualitative study. Int J Environ Res Public Health 2022 Jun 4;19(11):6879. [doi: 10.3390/ijerph19116879] [Medline: 35682460]
59. Xie T, Yang JP, Simoni JM, et al. Unable to be a human being in front of other people: a qualitative study of self-isolation among people living with HIV/AIDS in China. J Clin Psychol Med Settings 2017 Dec;24(3-4):211-222. [doi: 10.1007/s10880-017-9513-z] [Medline: 29086186]
60. Yang C, Lai DWL, Sun Y, Ma CY, Chau AKC. Mobile application use and loneliness among older adults in the digital age: insights from a survey in Hong Kong during the COVID-19 pandemic. IJERPH 2022;19(13):7656. [doi: 10.3390/ijerph19137656]
61. Maulana S, Ibrahim K, Pramukti I, Amirah S, Hartantri Y. Retention in HIV care among Southeast Asian people living with HIV: A systematic review and meta-analysis. Belitung Nurs J 2025;11(3):264-277. [doi: 10.33546/bnj.3719]
62. WHO. Programmatic Update Use of Antiretroviral Drugs for Treating Pregnant Women and Preventing HIV Infection in Infants Executive Summary: WHO; 2012. URL: https://www.aidsdatahub.org/sites/default/files/resource/use-antiretroviral-drugs-treating-pregnant-women.pdf [accessed 2024-10-19]
63. Mwapasa V, Joseph J, Tchereni T, Jousset A, Gunda A. Impact of mother-infant pair clinics and short-text messaging service (SMS) reminders on retention of HIV-infected women and HIV-exposed infants in eMTCT care in Malawi: a cluster randomized trial. J Acquir Immune Defic Syndr 2017 Jun 1;75 Suppl 2:S123-S131. [doi: 10.1097/QAI.0000000000001340] [Medline: 28498181]
64. Nittari G, Khuman R, Baldoni S, et al. Telemedicine practice: review of the current ethical and legal challenges. Telemedicine and e-Health 2020 Dec;26(12):1427-1437. [doi: 10.1089/tmj.2019.0158] [Medline: 32049608]
65. Pandey S, Karki S. Socio-economic and demographic determinants of antenatal care services utilization in Central Nepal. Int J MCH AIDS 2014;2(2):212-219. [doi: 10.21106/ijma.27] [Medline: 27621975]
66. Swann M. Economic strengthening for HIV testing and linkage to care: a review of the evidence. AIDS Care 2018;30(sup3):85-98. [doi: 10.1080/09540121.2018.1476665] [Medline: 29985055]
67. Hampanda KM, Pelowich K, Freeborn K, et al. Strategies to increase couples HIV testing and counselling in sub-Saharan Africa: a systematic review. J Int AIDS Soc 2023 Mar;26(3):e26075. [doi: 10.1002/jia2.26075] [Medline: 36929284]
68. Hoke T, Bateganya M, Toyo O, et al. how home delivery of antiretroviral drugs ensured uninterrupted HIV treatment during COVID-19: experiences from Indonesia, Laos, Nepal, and Nigeria. Glob Health Sci Pract 2021 Dec 31;9(4):978-989. [doi: 10.9745/GHSP-D-21-00168] [Medline: 34933991]
69. Moudatsou M, Stavropoulou A, Philalithis A, Koukouli S. The role of empathy in health and social care professionals. Healthcare (Basel) 2020 Jan 30;8(1):26. [doi: 10.3390/healthcare8010026] [Medline: 32019104]
70. Komariah M, Maulana S, Platini H, Pahria T. A scoping review of telenursing's potential as a nursing care delivery model in lung cancer during the COVID-19 pandemic. J Multidiscip Healthc 2021;14(null):3083-3092. [doi: 10.2147/JMDH.S337732] [Medline: 34754196]
71. Yotebieng M, Thirumurthy H, Moracco KE, et al. Conditional cash transfers to increase retention in PMTCT care, antiretroviral adherence, and postpartum virological suppression: a randomized controlled trial. J Acquir Immune Defic Syndr 2016 Aug 1;72 Suppl 2(Suppl 2):S124-S129. [doi: 10.1097/QAI.0000000000001062] [Medline: 27355499]
72. Richterman A, Thirumurthy H. The effects of cash transfer programmes on HIV-related outcomes in 42 countries from 1996 to 2019. Nat Hum Behav 2022 Oct 1;6(10):1362-1371. [doi: 10.1038/s41562-022-01414-7]

XSL•FO
RenderX

73. Virtual interventions in response to HIV, sexually transmitted infections and viral hepatitis. : UNAIDS and WHO; 2022 URL: https://www.unaids.org/sites/default/files/media_asset/policy-brief_virtual-interventions_en.pdf [accessed 2024-10-19]
74. Yadav D. Criteria for good qualitative research: a comprehensive review. Asia-Pacific Edu Res 2022 Dec;31(6):679-689. [doi: 10.1007/s40299-021-00619-0]
75. Vassar M, Atakpo P, Kash MJ. Manual search approaches used by systematic reviewers in dermatology. J Med Libr Assoc 2016 Oct;104(4):302-304. [doi: 10.3163/1536-5050.104.4.009]
76. Gusenbauer M, Gauster SP. How to search for literature in systematic reviews and meta-analyses: a comprehensive step-by-step guide. Technol Forecast Soc Change 2025 Mar;212:123833. [doi: 10.1016/j.techfore.2024.123833]

Abbreviations

CINAHL: Cumulative Index to Nursing and Allied Health Literature
EID: early infant diagnosis
JBI: Joanna Briggs Institute
MeSH: Medical Subject Headings
MMAT: Mixed Methods Appraisal Tool
MTCT: mother-to-child transmission
PMTCT: prevention of mother-to-child transmission
PRISMA: Preferred Reporting Items for Systematic Reviews and Meta-Analysis

Edited by A Coristine; submitted 26.07.24; peer-reviewed by F Mawardi, MA Virtanen, N Nurleli; revised version received 21.08.25; accepted 21.08.25; published 09.10.25.

Please cite as:
Maulana S, Ibrahim K, Arbing RHA, Pramukti I, Nugrahani AD, Armini LN, Iqhrammullah M, Chen WT
Acceptability, Needs, Concerns, and Barriers to Digital-Based Interventions for the Prevention of Mother-to-Child Transmission of HIV: Systematic Review and Qualitative Meta-Aggregation
JMIR Med Inform 2025;13:e64816
URL: https://medinform.jmir.org/2025/1/e64816
doi:10.2196/64816

© Sidik Maulana, Kusman Ibrahim, Rachel H A Arbing, Iqbal Pramukti, Annisa Dewi Nugrahani, Luh Nik Armini, Muhammad Iqhrammullah, Wei-Ti Chen. Originally published in JMIR Medical Informatics (https://medinform.jmir.org), 9.10.2025. This is an open-access article distributed under the terms of the Creative Commons Attribution License (https://creativecommons.org/licenses/by/4.0/), which permits unrestricted use, distribution, and reproduction in any medium, provided the original work, first published in JMIR Medical Informatics, is properly cited. The complete bibliographic information, a link to the original publication on https://medinform.jmir.org/, as well as this copyright and license information must be included.

XSL•FO
RenderX

Validation of Telehealth Outcome Categories for Patient Safety: Systematic Literature Review

Sari Palojoki[1*], PhD; Lasse Lehtonen[2*], MD, PhD; Riikka Vuokko[1*], PhD

[1]Department for Steering of Healthcare and Social Welfare, Ministry of Social Affairs and Health, PO Box 33, Helsinki, Finland

[2]Diagnostic Centre, Hospital District of Helsinki and Uusimaa, Helsinki, Finland

[*]all authors contributed equally

Corresponding Author:
Sari Palojoki, PhD
Department for Steering of Healthcare and Social Welfare, Ministry of Social Affairs and Health, PO Box 33, Helsinki, Finland

Abstract

Background: Integrating telehealth into established care processes can be challenging. With the integration of telehealth into routine health care practices, there is a growing need to evaluate telehealth outcomes to understand its impact on health care delivery. However, existing literature on telehealth outcomes to support evaluation remains limited.

Objective: This study aimed to analyze recent research from the past decade to develop a categorization of telehealth outcomes. This study seeks to validate a defined set of telehealth outcome categories and examine the broader impact of digital transformation on health care delivery.

Methods: We built the telehealth outcome categories according to the existing literature. During the category-building process, we identified 2 main components: the patient safety outcomes of telehealth and the other care-related outcomes. To validate these categories, we conducted a literature search. The initial search yielded 65 unique articles. Following the screening process, we selected 15 articles for the review. In the review analysis, comprehensive data extraction points established a robust framework for evaluating the scope and impact of telehealth research across multiple dimensions.

Results: On the basis of the analysis, 6 patient safety outcome categories were identified: mortality, adverse effects and harm, complications, hospitalization and readmission, diagnostic and treatment errors, and medication safety. The 9 other care-related outcome categories include cost-effectiveness, access to care, and patient satisfaction. Despite a limited sample, the results on the patient safety outcomes of telehealth indicate a generally positive impact. Several studies have reported that telehealth services are associated with reduced adverse events, complications, and readmissions and enhanced monitoring of patient conditions. The reviewed articles did not include use cases covering all identified preliminary outcome categories, such as medication safety and privacy. However, the review supported patient safety categories being well suited to classifying telehealth outcomes. The other care-related outcomes were not so clearly defined and would require more case examples to support category building.

Conclusions: Further refinement of the main categories identified in this article is necessary to allow for the identification of specific areas and themes that warrant further research initiatives. Future research is essential to evaluate the true benefits and outcomes of telemedicine, offering deeper insights into its real-world impact.

(JMIR Med Inform 2025;13:e75486) doi:10.2196/75486

KEYWORDS

telehealth; telemedicine; outcome; patient safety; health care; literature review; PRISMA

Introduction

The expansion of telehealth signifies a fundamental transformation in the delivery of health care services. The increasing demand for accessible and efficient health care services, especially in light of demographic shifts such as aging populations and rising chronic disease prevalence, as well as a shortage of health care personnel, is among the drivers for the growing implementation of telehealth services. New technological advancements are expected to enhance health care delivery, resulting in more efficient, streamlined, and cohesive care processes [1-3].

Integrating telehealth into existing care processes can be challenging. It is crucial that the transition to telehealth applications is managed carefully to maximize the benefits for all stakeholders, including patients, health care providers, and the broader health care system. Ensuring patient safety is a fundamental priority in health care, and this concern is particularly prominent in the context of telehealth, where the lack of direct physical examinations and in-person interactions can introduce unique challenges and potential risks [3-5].

XSL•FO
RenderX

Despite the potential risks to patient safety, such as miscommunication and preventable harm due to missed or delayed diagnoses, telemedicine has in several studies improved clinical outcomes through timely interventions, reduced mortality, and shortened length of stay [1,4,6-9]. Concerns about the risks associated with telehealth remain, however, since, for example, real-time interactions via telehealth are becoming more common. To date, the literature about the patient safety outcomes of telehealth has not been sufficiently reviewed [4,9]. Although some research exists, comprehensive systematic reviews on alternative modes of delivering telehealth across various care settings remain limited [10].

Although patient safety remains a critical focal point, other outcomes such as clinical efficacy, patient and provider satisfaction, and cost-effectiveness are equally vital in assessing the overall success of telehealth initiatives. With the growing integration of telehealth into routine health care practices, the imperative to thoroughly evaluate these outcomes has become increasingly significant, necessitating a balanced and comprehensive approach to understanding telehealth's broader impact on health care delivery [11-15].

Given the limited scope of existing studies, a literary review could serve as a foundational step in validating telehealth outcomes. Consequently, this systematic review aims to analyze recent research from the past decade to establish a categorization of telehealth outcomes. By examining studies across diverse settings and populations, it seeks to validate a defined set of telehealth outcome categories and explore the broader impact of digital transformation on health care delivery.

Methods

Overview

The rationale for this study lies in the planning phase of an empirical telehealth study. We noticed a lack of comprehensive classifications for telehealth outcomes. Instead, we encountered various reports and studies describing telehealth outcomes and benefits in quite variable ways [eg, 4,16,17]. This led us to compile a categorization of telehealth outcomes based on the existing literature.

Our research question is as follows: Based on the findings of a literature review, can preliminary literature-based telehealth outcome types be systematically built and validated into a categorization?

Conceptualizing Telehealth Outcome Categories

We began by focusing on the core concepts and their definitions. The World Health Organization (WHO) describes telehealth as "the delivery of health care services, where distance is a critical factor, by all health-care professionals using information and communication technologies for the exchange of valid information for diagnosis, treatment, and prevention of disease and injuries, research and evaluation, and for the continuing education of health-care providers, all in the interests of advancing the health of individuals and their communities" [16].

Telehealth can be defined and understood in multiple ways. According to the WHO, telehealth includes 4 main categories: (1) health care consultations between patients and clinicians, (2) the remote monitoring of patient health or diagnostic data by clinicians, (3) the transmission of medical data to clinicians, and (4) case management consultations between clinicians [2,16]. However, for this review, our analysis is informed by the Organization for Economic Co-operation and Development (OECD) categorization [17], as it provides a more detailed classification of telehealth modalities. The classification emphasizes a technical perspective, distinguishing telemedicine as a subset of telehealth. Here, telehealth encompasses not only clinical services provided remotely but also includes broader applications such as distance learning. However, due to our search objective emphasizing patient safety and other care-related outcomes, specifically distance learning telehealth applications were not included in our review. In summary, in this study, we use telehealth as our primary concept, following the definition provided by the WHO [16], while also acknowledging the OECD's [17] distinction of telemedicine as a specific subset within the broader telehealth framework.

For patient safety outcomes, we identified the core concepts primarily based on the Agency for Healthcare Research and Quality (AHRQ) patient safety and quality indicators and monitoring tools, which provided a well-established starting point [18,19]. The patient safety and quality indicators are intended to help health care providers assess, for example, the incidence of adverse events and in-hospital complications and identify issues that might need further study. As a general principle, our aim was to create a generic-level category from individual disease-specific indicators, which are sometimes quite precise, to describe the phenomenon at a general level. Based on the AHRQ indicator materials, broad-level patient safety outcome categories were composed preliminarily as follows: adverse events and harm, diagnostic, treatment errors and complications, visits, hospitalization and readmission, and mortality outcomes. Medication safety was added to the categorization due to its overall importance and relevance in patient safety: medication errors occur throughout the medication use process. Harm due to medicines and therapeutic options accounted for nearly 50% of the overall preventable harm in medical care [20].

We also explored several other outcomes associated with telehealth, including patient and provider satisfaction, as well as cost-effectiveness, as defined in the existing literature. For categorizing the other outcomes, as a starting point, we agreed on using the OECD examples for telehealth impacts, which entail the following themes: continuity of care, improved care coordination, and timelines of care; patient-centered care and health literacy; improved quality of care; increased access to care; avoided travel and reduced costs; and increased knowledge sharing and learning [21].

To test and validate the emerging categories, we performed a literary review on telehealth outcomes. For this, we adhered to the PRISMA (Preferred Reporting Items for Systematic Reviews and Meta-Analyses) statement [10,22] to ensure the validity of our review process (Checklist 1).

XSL•FO
RenderX

Applying the Methodology

The literature search was conducted in July 2024 using the PubMed database, which was selected for its comprehensive coverage of the biomedical literature [23]. PubMed with MEDLINE records enables precise and systematic search strategies using Medical Subject Headings terms [24]. Given PubMed's extensive repository, no additional databases were queried. The search was documented in detail to allow for reproducibility.

The search strategy (see Textbox 1) was meticulously crafted based on the key concepts of the study: Telehealth serves as our primary concept in line with the WHO definition [[16]], although we also refer to the OECD's [17] classification. The search was limited to articles published in English and within the past 10 years.

Textbox 1. Search strategy and filters used.

((“patient safety” [Title/Abstract]) AND (“telemedicine” [Title/Abstract] OR

“telehealth” [Title/Abstract])) AND (outcome)

Filters: Abstract, Free full text, in the last 10 years, English

The initial search yielded 65 unique articles. In July 2024, the research team initiated the screening process by reviewing the titles and abstracts of all remaining articles. Following the test reading, the researchers convened to discuss and refine the inclusion and exclusion criteria, ensuring a shared understanding. We defined 3 inclusion criteria for the initial screening: an article must document telehealth use case, report patient safety-related outcomes, and be an original research article. During the screening, we identified 14 review articles. The research team decided to process these review articles separately from the original research articles based on the nature of our research questions [2,4,5,10,25-27]. At the same time, we recognized the importance of analyzing the review articles to ensure that we were fully informed by previous research and to support the development of our telehealth outcome categories.

The screening was conducted independently and in a blinded manner, with each researcher applying the criteria separately. Afterward, the results were compared. A match was identified when researchers selected the same option, while a nonmatch occurred if different alternatives were chosen or if a category was not recognized. In 1 borderline case, discussion was required to achieve consensus, but no particularly challenging situations arose. During the initial screening, 42 articles were excluded: 4 of these were due to a lack of telehealth context, 20 due to a lack of patient safety outcomes or other documented health care–related outcomes, and 4 because the paper did not qualify as a research paper (eg, poster).

Ultimately, 23 articles were subjected to a thorough screening process by the authors. For 2 articles, despite being designated as an open access publication, the full text of the article was not accessible. The research team thoroughly reviewed the full texts of the remaining 21 articles to assess their eligibility in July to August 2024. For the final eligibility assessment, the exclusion criteria were defined as follows: the study topic being out of scope or not addressing telehealth outcomes. At this stage, 2 articles were excluded for being out of scope, and an additional 5 articles were excluded for not addressing telehealth-related patient safety outcomes or other health care–related outcomes. Consequently, the eligibility of the identified review articles was also assessed, and 7 previous review articles were included in our study based on their reporting of telehealth outcomes.

The remaining 14 original research articles were systematically analyzed based on specific data extraction criteria following the final inclusion round. One of the included articles described a research protocol where potential result categories were identified. Therefore, our research team agreed to search for an article presenting the results of the study, and this article was included in the review. As a result of this, we had 15 eligible articles for data extraction. The extracted data included the publication year and the journal in which each study was published, providing insight into the academic context of the research. The country of origin of the research and the affiliations of the authors were also documented to assess the geographical distribution.

Each article was further evaluated based on its research goals and motivations, with a focus on the type of telehealth research conducted and whether it pertained to telemedicine or other relevant telehealth innovations. The phase of telehealth intervention within the overall health care process was inspected through 2 categories: prehospital care or posthospital care. Moreover, the clinical domain or specialty, including the specific department involved, was identified to pinpoint the areas of health care most engaged with telehealth solutions. The telehealth application, approach, or method documented in each study was examined to capture the diversity and specificity of the telehealth practices being reported.

Finally, the review recorded patient safety outcomes associated with telehealth interventions, alongside other health care–related outcomes. One of the analyzed articles did not report a specific patient safety outcome despite its research design, instead providing a general discussion on patient safety. Similarly, another article documented patient safety outcomes but did not report other outcomes. After careful consideration and discussion, the research team decided to include both studies due to their valuable content on telehealth outcomes. The content related to these articles is presented in the Results section. These comprehensive data extraction points provided a robust framework for assessing the scope and impact of telehealth research across various dimensions.

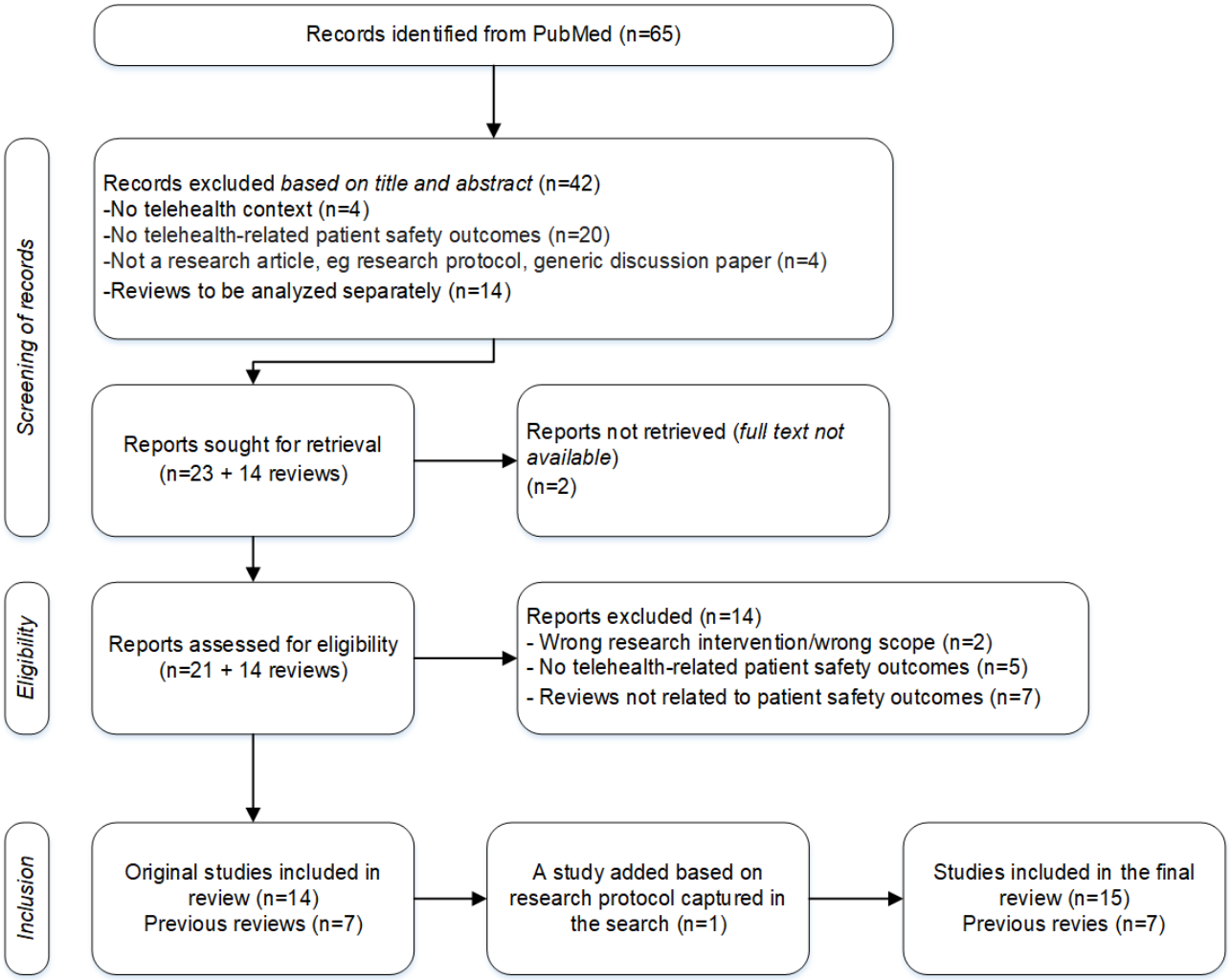
XSL•FO
RenderX

Results

Overview

In total, we analyzed the telehealth outcomes from 15 original articles encompassing 14 distinct studies [28-42]. In total, 2 separate publications addressed the same research topic and project but reported different stages of the study. One of the articles was published in 2016, whereas the remaining articles were published between 2019 and 2024. These articles appeared in 14 peer-reviewed journals and 1 National Health Service publication. The studies were conducted across various countries: 3 (20%) in the USA, 1 (6.7%) in both the USA and Italy, 2 (13.3%) in the Netherlands, 2 (13.3%) in Canada, and 1 (6.7%) in both Canada and Argentina. Other countries of origin included Denmark, the United Kingdom, France, the Republic of Korea, Israel, and Singapore. Regarding the research setting, the articles presented a diverse range of studies, including, for example, cohort studies, a feasibility study, and 2 (13.3%) qualitative studies. Notably, 1 of the articles was a study protocol that outlined preliminary outcome categories (Figure 1).

Figure 1. Flowchart of article identification, screening, and final inclusion.



When analyzing the focus of the telehealth intervention within the overall treatment process, it appeared that the research setting in 9 (60%) studies was posthospital [28-31,33,35,39,41,42] and in 6 (40%) was prehospital [32,34,36-38,40]. The clinical setting of the telehealth intervention was described in all studies at a minimum of specifying the patient group involved. These included 2 (13%) studies related to patients with heart failure [41,42], 2 related to high-risk pregnancy monitoring [37,40], and another 2 related to COVID-19, namely to patients with mild COVID-19 symptoms [33] and clinically healthy COVID-19 patients [34]. One study examined pediatric patients [35] and 1 specifically looked at infant patients with congenital heart disease [39]. One study considered patients in emergency care [38], and another considered remote triage of patients with stroke [32]. Other studies included patients undergoing radiotherapy [28], patients with respiratory tract infection [29], patients undergoing bariatric surgery [31], patients with ureteric colic [35], and chronically ill patients at home [30].

Regarding the telehealth approach implemented, several studies described the utilization of 2 or 3 telehealth approaches. Telemonitoring was used in 7 (46%) studies [29,30,34,37,40-42], store and forward telemedicine in 6 (40%) studies [28,30,33,34,36,40], and interactive telemedicine in 11 (73%) studies [28,29,31-39]. Telecare or assisted living at home was not included in any of these studies.

XSL•FO
RenderX

The Results on Category Building

As outlined in the methods chapter, we developed preliminary categories for telehealth outcomes based on existing categorizations. We used the AHRQ patient safety and quality indicators, along with reported telehealth impact descriptions, as a foundation for developing our telehealth outcome analysis categories [18,21]. To refine the emerging outcome categories, we first enriched them with case examples from the previous review articles identified in our literature search [2,4,5,10,25,26,36] and then standardized the terminology to ensure clearer and more consistent naming.

Our goal was to minimize the overlap between categories. At this stage, in light of the latest research, we decided to add 3 new outcome categories related to clinical outcomes, data protection, and ecological sustainability. The main results of the outcome category building, as used in our review analysis, are presented with references in Multimedia Appendix 1, which contains both key telehealth concepts and the outcome categorization with illustrative examples (on relevant themes in each category) based on previous research. Finally, the telehealth outcome categories are summarized in Textbox 2.

Using the defined set of telehealth outcome categories, we proceeded to analyze the 15 original articles that were included in the review. Detailed results can be found in Multimedia Appendix 2 and Multimedia Appendix 3, as well as in the following 2 result sections.

Textbox 2. The compiled telehealth outcome categories for our review.

1. Patient safety outcomes of telehealth
    a. Mortality outcomes
    b. Adverse effects and harm
    c. Complications
    d. Hospitalization and readmission
    e. Diagnostic and treatment errors
    f. Medication safety

1. Other health care–related outcomes of telehealth
    a. Clinical outcomes
    b. Cost-effectiveness
    c. Quality of care
    d. Access to care
    e. Management and process efficiency
    f. Patient satisfaction
    g. Provider satisfaction
    h. Privacy and confidentiality
    i. Ecological sustainability

The Results on Patient Safety Outcomes of Telehealth

The literature (5/15, 33%) provided references supporting our preliminary categorization of patient safety outcomes related to mortality [29,30,33,37,39]. The analysis of mortality outcomes across the studies suggests that telehealth services may be associated with a reduction in mortality rates for certain diseases. In 1 study, the mortality rate decreased from 16% to 9% [30]. The study on telehealth for infants with congenital heart disease reported no deaths [39], whereas the remaining 3 studies found that telehealth did not result in improved survival or mortality outcomes compared to traditional treatment methods [29,33,37].

The analyzed articles identified an adverse event outcome category that is closely linked to patient safety. Two (13.3%) studies [28,39] reported instances of adverse effects, near misses, or harm associated with telehealth. A study on fully remote radiation oncology care examined patient safety events, defined as staff-reported actual incidents and near misses that could impact patient care [28]. Of the 764 reported safety events, 763 (99.9%) did not reach patients or cause harm to patients, indicating that radiation oncology care provided by fully remote clinicians was safe, with no serious patient events. Another study found no missed events [39].

The reviewed articles supported the complications category, with this outcome identified in 3 (20%) studies [30,37,40]. Our findings suggest that complications among patients receiving telehealth services are relatively rare. In a study on a vital signs telemonitoring system as a regional solution in Italy, the occurrence of major complications decreased from 44% to 30% among the monitored patients [30]. A randomized controlled trial reported a composite of adverse perinatal outcomes as its primary outcome [37]. In the Netherlands, hospitals offering home-based monitoring and telemonitoring for high-risk

XSL•FO
RenderX

pregnancies reported improved patient safety as a key outcome of complication monitoring [40]. The category of diagnostic and treatment errors was identified in 3 (20%) studies [32,34,36]. While telehealth improves access to specialists, it may also contribute to misdiagnoses due to limitations in physical examinations and assessments, highlighting the need for enhanced diagnostic protocols [32,34,36].

The analysis of the papers revealed findings that supported our preliminary category of hospitalization and readmission outcomes in 9 (60%) studies [29-31,33,35,37,39-42]. Specifically, these studies suggest that telehealth has an impact on hospitalization and readmission rates. Notably, some studies reported that patients using telehealth services experienced lower readmission rates, likely due to improved management of chronic conditions and enhanced patient monitoring. An Italian study found a 4% reduction in readmissions within 21 days of discharge [30]. Similarly, a study on bariatric surgery patients reported no readmissions at 30/90 days posttelecare [31].

In 1 of the studies, authors do not demonstrate specific patient safety outcomes but that telemedicine used at triage does not compromise maintaining standard care for chest pain and increasing attention to patient comfort via analgesia. Telescreening in triage is both effective and safe, particularly when extending coverage into previously unstaffed hours. No safety concerns specific to telemedicine use (eg, diagnostic errors) were reported [38]. Despite its central importance to patient safety, medication safety is an aspect that was not addressed in the papers reviewed.

The Results of Other Health Care–Related Outcomes of Telehealth

Other health care–related outcome categories of telehealth were documented in all but 1 of the studies under review (14/15, 93%). Of the 9 outcome categories described in Multimedia Appendix 1 (see also Textbox 2) based on previous telehealth reviews, our reviewed analysis provided research evidence for 8 outcome categories. The category for clinical outcomes [26] was not reported in the studies included in our review, although previous reviews documented examples categorized tentatively as care-related outcomes for telehealth. Feasibility of the tentative outcome category would require more research examples.

The most common other outcome category in our review was cost-effectiveness, which was documented in 11 (73%) of the studies [28,29,31,32,34,37-42]. However, there was no unified way of documenting cost-effectiveness that enables a comparison of telehealth outcomes related to cost reduction. For example, in a telehealth case of radiation oncology, cost savings were calculated per patient [28], whereas another study explored how the intervention costs could be accurately calculated [29]. In this study, clinicians performed telehealth assessments for which average costs were calculated based on the type of contact (telemedicine assessment and domestic visit), number of self-measurements, and severity of alerts. Related to cost-effectiveness, other work-related and occupational benefits were reported [31], such as time saved and no requirement for absence from work to attend a care visit, as well as the possibility to arrange telehealth follow-ups at the workplace. In a telemonitoring case [39], avoidance of emergency department visits contributed to decreasing costs. In addition, indirect cost savings were related to no missed work and no need for transportation. In a COVID-19 telemonitoring case [34], a potential increase in costs and issues of reimbursement were reported, although with no apparent evidence. Another study [38] regarded telehealth costs and a lack of reimbursement as potential barriers to telehealth adoption. Similar reimbursement issues were reported in another case [40]. A high-risk pregnancy telemonitoring case identified patient satisfaction, health-related quality of life, and cost-effectiveness as secondary outcomes of the study [40]. In summary, the results indicate that cost-effectiveness includes many dimensions, especially with regard to telehealth outcomes.

The second most common other telehealth outcome category in our review was patient satisfaction, which was reported in 10 (66.7%) studies [28,29,31,34,35,37-40,42]. In a case of remote management of radiation oncology, nearly all of the patients (n=451, 97.6%) included in the study rated patient satisfaction as good to very good [28]. In a case of a 2-year follow-up after telehealth implementation [31], the satisfaction rate was 80%, with 33% of patients preferring to continue using the telehealth solution. However, 34% of patients felt insecure with telehealth monitoring in relation to health issues that may arise. In a telehealth implementation case [35], 93.1% (n=465) of patients reported satisfaction with the telehealth service. A telescreening case [38] suggested that, in general, patients were happy with telehealth, with a few exceptions. This finding is documented as similar to the evidence gathered from more formal patient satisfaction surveys. Related to patient satisfaction, access to care by remote monitoring was documented as a telehealth outcome only in 1 case [29].

In addition to patient satisfaction, care provider satisfaction was reported as a telehealth outcome in 5 (33%) of the studies [30-32,36,39]. In a case where provider satisfaction was reported, the care personnel were surveyed with 8 different questions to assess their level of satisfaction with the telehealth used in patient care [30]. In an infant congenital heart disease telemonitoring case [39], high levels of provider satisfaction were reported, with physicians expressing an interest in continuing with telemonitoring visits.

The fourth reported health care–related telehealth outcome category was quality of care, which was illustrated in 4 (27%) studies [37,40-42]. In a COVID-19-related telehealth monitoring case [34], the participating professionals reported the possibility to improve the quality of care due to data being measured and shared through the telehealth device. A high-risk pregnancy telemonitoring case [37] reported quality of care related to the advantages of monitoring from home, such as reduced stress and increased rest, including the possible reduction of costs. In a case related to older patients with heart failure [41], home monitoring was expected to improve comfort and quality of life as well as quality of care through the timely detection of possible patient deterioration.

The overall management and process efficiency outcomes related to telehealth were positive, with 4 (26.7%) studies

XSL•FO
RenderX

demonstrating improved operational efficiency and patient management [30,34,38,41]. A reduction in the burden on medical staff was documented as a positive outcome [34,36]. Better communication between members of the care team [41] was included in this category. However, the research evidence was partly ambiguous, stating that, for example, higher level patient compliance and workflow optimization would be beneficial [30].

A telehealth outcome categorized as ecological sustainability was documented in 1 of the studies as a result of less traveling by patients and professionals [28]. Similarly, patient privacy and confidentiality were documented in 1 of the studies [30]. One of the original articles [33] reported only patient safety–related outcomes and did not include other health care–related outcomes.

Discussion

Principal Findings

Digital transformation and advancements in medical technology, such as remote data exchange and mobile communication, are now reshaping health care. This shift is moving health care from an intermittent, acute care model to one that emphasizes continuous, integrated, and comprehensive care and potentially improving patient outcomes. However, previous research suggests that telehealth outcome measures should be standardized to assess and compare different telehealth implementations' and use cases' outcomes more easily [1,10,26]. Despite existing research in this area, an established typology for exploring telehealth outcomes appears to be lacking. Previous research explores telehealth, for example, as a communication means, focusing on its role in facilitating information exchange between patients and health care providers (eg, [11]). Few studies have directly compared different telehealth modalities (eg, [10]). Existing research tends to focus on specific providers or particular conditions [10,25,26,41]. Therefore, we aimed to examine recent research from the past decade to develop an initial categorization for telehealth outcomes.

We built the telehealth outcome categories by using the AHRQ patient safety and quality indicators with an added category for medication safety [18-20] for patient safety outcomes and the OECD telehealth impact categories [21] for other care-related outcomes. During the category building, we checked the overlap between the AHRQ patient safety and quality indicator-based categories and the OECD telehealth impact categories. As the patient safety indicators were described in more detail and were more established, we considered them as guidelines to achieve our data analysis categories for telehealth outcomes. The categories of both groupings were referred to in recent literature reviews, which is why previous reviews were used to further clarify the categories and to refine their naming. Based on a recent review, 3 additional care-related outcome categories were added, namely clinical outcomes, data protection, and ecological sustainability [4,21,25]. Finally, we had 6 outcome categories for patient safety and 9 for other health care–related outcomes (see Multimedia Appendix 1).

The review supported patient safety outcome categories being well suited for classifying telehealth outcomes. However, the medication safety [5,18] category was not met with results in the available study material. Similarly, for other health care–related outcome categories, all were supported with the review except 1 on the clinical outcomes [25]. However, these categories were not so clearly defined originally, and the research team discussed the boundaries and features of the categories to reach a shared interpretation of them. At the same time, the names of the categories were elaborated. Moreover, 2 of the categories were supported with only single examples within the reviewed articles. To summarize, the OECD telehealth impact categories are less clearly defined, being more descriptive and partially parallel to the AHRQ indicators.

On the basis of previous reviews, we decided to introduce new outcome categories related to data protection [4] and ecological sustainability [21]. While no comprehensive validation data were found for these categories in the reviewed literature, their inclusion highlights emerging areas of interest in telemedicine. These categories are particularly relevant, as data protection remains a key concern in health care and ecological sustainability (eg, the need for patient transportation in comparison to digital services) is gaining increasing attention in the context of health care practices [21,28].

The unique nature of telehealth requires patient safety practices specifically tailored to address the risks inherent in virtual care settings. Moreover, the ability to provide safe digital health services anytime and anywhere further underscores the need for robust patient safety practices. Seamless, secure, and universally accessible telehealth services depend on well-integrated safety measures that uphold patient trust while supporting care delivery. In this effort, telehealth outcome data can serve as a starting point for developing virtual care practices, helping to identify and prioritize the most urgent needs for strengthening patient safety measures.

Telehealth outcomes are not always consistent or well integrated, with factors such as device stability and reliability, patient education, accountability, and reimbursement issues impacting the effectiveness of remote patient monitoring [34,40]. While the cost-effectiveness of various telehealth interventions has been studied [28,29,31,32,34,37-42], there are limited data on their long-term efficiency compared to conventional medical practices. In addition, the cost of investment and ongoing maintenance, particularly when multiple stakeholders are involved, may pose significant challenges. Ensuring sustainable implementation requires addressing these financial and logistical barriers while optimizing resource allocation. Future research should focus on evaluating the long-term economic and operational impact of telehealth to guide decision-making and policy development, ultimately enhancing the integration and effectiveness of telehealth solutions.

Our results are significant from multiple perspectives. Our findings have the potential to offer valuable insights for health care providers, policymakers, and researchers, supporting future telemedicine implementations and policies to optimize both safety and other expected outcomes. Moreover, the results could contribute to future telehealth research by providing a systematic

XSL•FO
RenderX

approach for classifying and evaluating telehealth outcomes. Structured data on telehealth outcomes could benefit, for example, the assessment of long-term changes in delivering care [26].

By providing a structured approach, these results can shape the future of telehealth, support evidence-based decision-making, and enhance the integration of telehealth into routine care. Furthermore, the study has significant management implications as health care leaders seek to optimize technology resources to improve efficiency. A well-structured telehealth evaluation framework can contribute to ensuring that patient-centered care remains the cornerstone of medical practice, aligning technological advancements with high-quality, accessible, and equitable health care delivery.

Future research is suggested to focus on delineating its scope, establish clear inclusion criteria, and distinguish it from existing outcome categories to improve the reliability and reproducibility of telehealth outcome assessments. Regarding patient safety outcome categories, medication safety warrants further research, given its critical role in ensuring safe care in, for example, preventing adverse events [20]. In the context of building the outcome categorization, it is possible to consider conducting additional, focused literature searches on medication safety–related topics in the next phase of the study. When viewed more broadly from the perspective of telehealth research, future studies should prioritize identifying specific medication safety risks unique to telehealth settings, developing targeted assessment tools, and evaluating intervention strategies to mitigate these risks. To validate “other outcomes” requires also further refinement to enhance conceptual clarity and methodological consistency. In this review, for example, regarding ecological sustainability, because of its emerging nature, it may be necessary to revisit the theoretical foundations concerning conceptualization and factors before proceeding to examine the outcomes.

Limitations

One limitation of this study is the small number of articles included, which affects the applicability of the findings. More case studies are needed to further validate the results and strengthen the overall evidence base. Incorporating a greater variety of case studies would enhance the robustness of the conclusions drawn. In particular, despite the central importance of medication safety to overall patient safety, this critical aspect was not adequately addressed in the papers reviewed, highlighting a possible gap in the current literature. The same applies to ecological sustainability. Our literature review relied solely on PubMed, which can serve as a primary search tool according to peer-reviewed research [43]. It is, however, essential to acknowledge that the use of a single database may limit the comprehensiveness of the search in areas outside strict biomedicine or in multidisciplinary contexts. While PubMed is the largest biomedical database and citations in PubMed primarily stem from the biomedicine and health fields, and related disciplines such as life sciences, behavioral sciences, chemical sciences, and bioengineering, it has less coverage of fields such as social sciences. For future reviews with broader scope covering also, for example, social sciences, PubMed searches can be complemented with other scientific databases [24,43,44].

Conclusions

To conclude, preliminary validation based on the literature review supported patient safety outcome categories being well suited for classifying telehealth outcomes. Nevertheless, further refinement of the main categories identified in this article is necessary to allow for the identification of specific areas and themes that warrant further research initiatives. Future research would be critical for assessing the true benefits and outcomes of telemedicine, providing a deeper understanding of its real-world impact.

Acknowledgments

The study was supported by Finnish governmental research grant TYH2023406.

Data Availability

All data generated or analyzed during this study are included in this published article and its supplementary information files.

Authors' Contributions

Conceptualization: SP, LL, RV
Data curation: SP, RV
Formal analysis: SP, LL, RV
Funding acquisition: LL
Investigation: SP, LL, RV
Methodology: SP, LL, RV
Project administration: SP, RV
Resources: SP, LL, RV
Software: SP, RV
Supervision: SP, LL, RV
Validation: SP, LL, RV
Visualization: SP, RV

XSL•FO
RenderX

Writing – original draft: SP, LL, RV
Writing – review & editing: SP, LL, RV

Conflicts of Interest

None declared.

Multimedia Appendix 1
Key concepts and outcome categories for data analysis.
[DOCX File, 16 KB - medinform_v13i1e75486_app1.docx]

Multimedia Appendix 2
Characteristics of the publications.
[DOCX File, 24 KB - medinform_v13i1e75486_app2.docx]

Multimedia Appendix 3
Overview of the results.
[DOCX File, 27 KB - medinform_v13i1e75486_app3.docx]

Checklist 1
Preferred Reporting Items for Systematic Reviews and Meta-Analyses (PRISMA) checklist.
[DOCX File, 32 KB - medinform_v13i1e75486_app4.docx]

References

1. Neves AL, Burgers J. Digital technologies in primary care: implications for patient care and future research. Eur J Gen Pract 2022 Dec;28(1):203-208. [doi: 10.1080/13814788.2022.2052041] [Medline: 35815445]
2. Grygorian A, Montano D, Shojaa M, Ferencak M, Schmitz N. Digital health interventions and patient safety in abdominal surgery: a systematic review and meta-analysis. JAMA Netw Open 2024 Apr 1;7(4):e248555. [doi: 10.1001/jamanetworkopen.2024.8555] [Medline: 38669018]
3. WHO guideline: recommendations on digital interventions for health system strengthening. World Health Organization. 2019. URL: https://apps.who.int/iris/bitstream/handle/10665/311941/9789241550505-eng.pdf [accessed 2024-08-22]
4. Rosen M, Stewart CM, Kharrazi H, et al. Potential harms resulting from patient-clinician real-time clinical encounters using video-based telehealth: a rapid evidence review. In: Making Healthcare Safer IV: A Continuous Updating of Patient Safety Harms and Practices: Rockville (MD): Agency for Healthcare Research and Quality (US); 2023. [Medline: 38051800]
5. Sharifi Kia A, Rafizadeh M, Shahmoradi L. Telemedicine in the emergency department: an overview of systematic reviews. Z Gesundh Wiss 2022 Jan 27:1-15. [doi: 10.1007/s10389-021-01684-x] [Medline: 35103232]
6. Institute of Medicine (US) Committee on Quality of Health Care in America. In: Kohn LT, Corrigan JM, Donaldson MS, editors. To Err Is Human: Building a Safer Health System: Washington (DC): National Academies Press (US); 2000. [doi: 10.17226/9728] [Medline: 25077248]
7. Kahn JM, Le TQ, Barnato AE, et al. ICU telemedicine and critical care mortality: a national effectiveness study. Med Care 2016 Mar;54(3):319-325. [doi: 10.1097/MLR.0000000000000485] [Medline: 26765148]
8. Kopec IC. Impact of intensive care unit telemedicine on outcomes. Crit Care Clin 2019 Jul;35(3):439-449. [doi: 10.1016/j.ccc.2019.02.002] [Medline: 31076044]
9. Guise V, Anderson J, Wiig S. Patient safety risks associated with telecare: a systematic review and narrative synthesis of the literature. BMC Health Serv Res 2014 Nov 25;14:588. [doi: 10.1186/s12913-014-0588-z] [Medline: 25421823]
10. Byambasuren O, Greenwood H, Bakhit M, et al. Comparison of telephone and video telehealth consultations: systematic review. J Med Internet Res 2023 Nov 17;25:e49942. [doi: 10.2196/49942] [Medline: 37976100]
11. Kruse CS, Krowski N, Rodriguez B, Tran L, Vela J, Brooks M. Telehealth and patient satisfaction: a systematic review and narrative analysis. BMJ Open 2017 Aug 3;7(8):e016242. [doi: 10.1136/bmjopen-2017-016242] [Medline: 28775188]
12. Buvik A, Bergmo TS, Bugge E, Smaabrekke A, Wilsgaard T, Olsen JA. Cost-effectiveness of telemedicine in remote orthopedic consultations: randomized controlled trial. J Med Internet Res 2019 Feb 19;21(2):e11330. [doi: 10.2196/11330] [Medline: 30777845]
13. Gajarawala SN, Pelkowski JN. Telehealth benefits and barriers. J Nurse Pract 2021 Feb;17(2):218-221. [doi: 10.1016/j.nurpra.2020.09.013] [Medline: 33106751]
14. Totten AM, Hansen RN, Wagner J, Stillman L, Ivlev I, Davis-O'Reilly C, et al. Telehealth for Acute and Chronic Care Consultations: Agency for Healthcare Research and Quality. URL: https://www.ncbi.nlm.nih.gov/books/NBK547239 [accessed 2024-08-22]
15. World Health Organization. Global Strategy on Digital Health 2020-2025. URL: https://www.who.int/health-topics/digital-health [accessed 2024-08-22]

XSL•FO
RenderX

16. World Health Organization. Consolidated Telemedicine Implementation Guide. URL: https://www.who.int/publications/i/item/9789240059184 [accessed 2024-08-01]
17. OECD. The COVID-19 pandemic and the future of telemedicine. : OECD Health Policy Studies, OECD Publishing, Paris; 2023 Jan 17 URL: https://www.oecd.org/en/publications/the-covid-19-pandemic-and-the-future-of-telemedicine_ac8b0a27-en.html [accessed 2025-10-03] [doi: 10.1787/ac8b0a27-en]
18. AHRQ quality indicator tools for data analytics. Agency for Healthcare Research and Quality AHRQ. URL: https://www.ahrq.gov/data/qualityindicators/index.html [accessed 2024-08-22]
19. Weiner BJ, Alexander JA, Baker LC, Shortell SM, Becker M. Quality improvement implementation and hospital performance on patient safety indicators. Med Care Res Rev 2006 Feb;63(1):29-57. [doi: 10.1177/1077558705283122] [Medline: 16686072]
20. World Health Organization. Medication without Harm: Policy Brief ISBN 978-92-4-006276-4 (Electronic Version): World Health Organization; 2023. URL: https://www.who.int/publications/i/item/9789240062764 [accessed 2024-08-22]
21. Oliveira Hashiguchi T. Bringing health care to the patient: an overview of the use of telemedicine in OECD countries. : OECD Health Working Papers, No. 116, OECD Publishing, Paris; 2020 URL: https://doi.org/10.1787/8e56ede7-en [accessed 2025-10-03]
22. Page MJ, McKenzie JE, Bossuyt PM, et al. The PRISMA 2020 statement: an updated guideline for reporting systematic reviews. BMJ 2021 Mar 29;372:n71. [doi: 10.1136/bmj.n71] [Medline: 33782057]
23. Cooper C, Booth A, Varley-Campbell J, Britten N, Garside R. Defining the process to literature searching in systematic reviews: a literature review of guidance and supporting studies. BMC Med Res Methodol 2018 Aug 14;18(1):85. [doi: 10.1186/s12874-018-0545-3] [Medline: 30107788]
24. National center for biotechnology information. US National Library of Medicine [Internet]. URL: https://www.ncbi.nlm.nih.gov [accessed 2025-10-03]
25. Farzandipour M, Nabovati E, Sharif R. The effectiveness of tele-triage during the COVID-19 pandemic: a systematic review and narrative synthesis. J Telemed Telecare 2024 Oct;30(9):1367-1375. [doi: 10.1177/1357633X221150278] [Medline: 36683438]
26. Jonker P, van den Heuvel S, Hoeks S, Heijkoop È, Stolker RJ, Korstanje JW. Alternatives to the in-person anaesthetist-led preoperative assessment in adults undergoing low-risk or intermediate-risk surgery: a scoping review. Eur J Anaesthesiol 2023 May 1;40(5):343-355. [doi: 10.1097/EJA.0000000000001815] [Medline: 36876738]
27. Haimi M, Wheeler SQ. Safety in teletriage by nurses and physicians in the United States and Israel: narrative review and qualitative study. JMIR Hum Factors 2024 Mar 25;11:e50676. [doi: 10.2196/50676] [Medline: 38526526]
28. Cuaron JJ, McBride S, Chino F, et al. Patient safety and satisfaction with fully remote management of radiation oncology care. JAMA Netw Open 2024 Jun 3;7(6):e2416570. [doi: 10.1001/jamanetworkopen.2024.16570] [Medline: 38865123]
29. Sandreva T, Larsen MN, Rasmussen MK, et al. Transforming health care: investigating Influenzer, a novel telemedicine-supported early discharge program for patients with lower respiratory tract infection: a non-randomized feasibility study. J Telemed Telecare 2025 Sep;31(8):1138-1151. [doi: 10.1177/1357633X241254572] [Medline: 38780386]
30. Pietrantonio F, FADOI-OdC Group, Vinci A, et al. Intra- and extra-hospitalization monitoring of vital signs-two sides of the same coin: perspectives from LIMS and greenline-HT study operators. Sensors (Basel) 2023 Jun 7;23(12):5408. [doi: 10.3390/s23125408] [Medline: 37420575]
31. Daouadji-Ghazouani A, Aron-Wisnewsky J, Torcivia A, et al. Correction: follow-up, safety, and satisfaction with tele-bariatric follow-up implemented during the COVID-19 French lockdown: a 2-year follow-up study. OBES SURG 2023 Jun;33(6):1958-1959. [doi: 10.1007/s11695-023-06612-4] [Medline: 37099253]
32. Ramsay AI, Ledger J, Tomini SM, et al. Prehospital video triage of potential stroke patients in North Central London and East Kent: rapid mixed-methods service evaluation. Health Soc Care Deliv Res 2022 Sep;10(26):1-114. [doi: 10.3310/IQZN1725]
33. Pedretti A, Marquez Fosser S, Pasquinelli R, et al. Risk of readmission to the emergency department in mild COVID-19 outpatients with telehealth follow-up. Rev Fac Cien Med Univ Nac Cordoba 2021 Aug 23;78(3):249-256. [doi: 10.31053/1853.0605.v78.n3.32414] [Medline: 34617705]
34. Bae YS, Kim KH, Choi SW, Ko T, Lim JS, Piao M. Satisfaction and usability of an information and communications technology-based system by clinically healthy patients with COVID-19 and medical professionals: cross-sectional survey and focus group interview study. JMIR Form Res 2021 Aug 26;5(8):e26227. [doi: 10.2196/26227] [Medline: 34254946]
35. Ong CSH, Lu J, Tan YQ, Tan LGL, Tiong HY. Implementation of a ureteric colic telemedicine service: a mixed methods quality improvement study. Urology 2021 Jan;147:14-20. [doi: 10.1016/j.urology.2020.10.010] [Medline: 33091386]
36. Haimi M, Brammli-Greenberg S, Baron-Epel O, Waisman Y. Assessing patient safety in a pediatric telemedicine setting: a multi-methods study. BMC Med Inform Decis Mak 2020 Apr 3;20(1):63. [doi: 10.1186/s12911-020-1074-7] [Medline: 32245469]
37. van den Heuvel JFM, Ganzevoort W, De Haan-Jebbink JM, et al. Hospital care versus telemonitoring in high-risk pregnancy (HOTEL): study protocol for a multicentre non-inferiority randomised controlled trial. BMJ Open 2019 Oct 28;9(10):e031700. [doi: 10.1136/bmjopen-2019-031700] [Medline: 31662396]

XSL•FO
RenderX

38. Rademacher NJ, Cole G, Psoter KJ, et al. Use of telemedicine to screen patients in the emergency department: matched cohort study evaluating efficiency and patient safety of telemedicine. JMIR Med Inform 2019 May 8;7(2):e11233. [doi: 10.2196/11233] [Medline: 31066698]
39. Stagg A, Giglia TM, Gardner MM, et al. Initial experience with telemedicine for interstage monitoring in infants with palliated congenital heart disease. Pediatr Cardiol 2023 Jan;44(1):196-203. [doi: 10.1007/s00246-022-02993-y] [Medline: 36050411]
40. van den Heuvel JFM, Ayubi S, Franx A, Bekker MN. Home-based monitoring and telemonitoring of complicated pregnancies: nationwide cross-sectional survey of current practice in the Netherlands. JMIR Mhealth Uhealth 2020 Oct 28;8(10):e18966. [doi: 10.2196/18966] [Medline: 33112250]
41. TEC4Home Healthcare Innovation Community. Supporting heart failure patient transitions from acute to community care with home telemonitoring technology: a protocol for a provincial randomized controlled trial (TEC4Home). JMIR Res Protoc 2016 Dec 18;5(4):e198. [doi: 10.2196/resprot.5856]
42. Ho K, Novak Lauscher H, Cordeiro J, et al. Testing the feasibility of sensor-based home health monitoring (TEC4Home) to support the convalescence of patients with heart failure: pre-post study. JMIR Form Res 2021 Jun 3;5(6):e24509. [doi: 10.2196/24509] [Medline: 34081015]
43. Gusenbauer M, Haddaway NR. Which academic search systems are suitable for systematic reviews or meta-analyses? Evaluating retrieval qualities of Google Scholar, PubMed, and 26 other resources. Res Synth Methods 2020 Mar;11(2):181-217. [doi: 10.1002/jrsm.1378] [Medline: 31614060]
44. Bramer WM, Rethlefsen ML, Kleijnen J, Franco OH. Optimal database combinations for literature searches in systematic reviews: a prospective exploratory study. Syst Rev 2017 Dec 6;6(1):245. [doi: 10.1186/s13643-017-0644-y] [Medline: 29208034]

Abbreviations

AHRQ: Agency for Healthcare Research and Quality
OECD: Organization for Economic Co-operation and Development
PRISMA: Preferred Reporting Items for Systematic Reviews and Meta-Analyses
WHO: World Health Organization

Edited by A Benis; submitted 04.04.25; peer-reviewed by MA Zoubi, O Ahonen; revised version received 05.08.25; accepted 11.08.25; published 16.10.25.

Please cite as:
Palojoki S, Lehtonen L, Vuokko R
Validation of Telehealth Outcome Categories for Patient Safety: Systematic Literature Review
JMIR Med Inform 2025;13:e75486
URL: https://medinform.jmir.org/2025/1/e75486
doi:10.2196/75486

© Sari Palojoki, Lasse Lehtonen, Riikka Vuokko. Originally published in JMIR Medical Informatics (https://medinform.jmir.org), 16.10.2025. This is an open-access article distributed under the terms of the Creative Commons Attribution License (https://creativecommons.org/licenses/by/4.0/), which permits unrestricted use, distribution, and reproduction in any medium, provided the original work, first published in JMIR Medical Informatics, is properly cited. The complete bibliographic information, a link to the original publication on https://medinform.jmir.org/, as well as this copyright and license information must be included.

XSL•FO
RenderX

Diagnostic Prediction Models for Primary Care, Based on AI and Electronic Health Records: Systematic Review

Liesbeth Hunik[1], MSc, MD; Asma Chaabouni[1], MSc, MD; Twan van Laarhoven[2], PhD; Tim C Olde Hartman[1], PhD, MD; Ralph T H Leijenaar[3], PhD; Jochen W L Cals[3], Prof Dr; Annemarie A Uijen[1], PhD, MD; Henk J Schers[1], Prof Dr

[1]Department of Primary and Community Care, Research Institute for Medical Innovation, Radboudumc, Geert Grooteplein Zuid 21, Nijmegen, The Netherlands

[2]Institute for Computing and Information Science, Radboud University, Nijmegen, The Netherlands

[3]Department of Family Medicine, Care and Public Health Research Institute, Maastricht University, Maastricht, The Netherlands

Corresponding Author:
Liesbeth Hunik, MSc, MD
Department of Primary and Community Care, Research Institute for Medical Innovation, Radboudumc, Geert Grooteplein Zuid 21, Nijmegen, The Netherlands

Abstract

Background: Artificial intelligence (AI)–based diagnostic prediction models could aid primary care (PC) in decision-making for faster and more accurate diagnoses. AI has the potential to transform electronic health records (EHRs) data into valuable diagnostic prediction models. Different prediction models based on EHR have been developed. However, there are currently no systematic reviews that evaluate AI-based diagnostic prediction models for PC using EHR data.

Objective: This study aims to evaluate the content of diagnostic prediction models based on AI and EHRs in PC, including risk of bias and applicability.

Methods: This systematic review was performed according to the PRISMA (Preferred Reporting Items for Systematic Reviews and Meta-Analyses) guidelines. MEDLINE, Embase, Web of Science, and Cochrane were searched. We included observational and intervention studies using AI and PC EHRs and developing or testing a diagnostic prediction model for health conditions. Two independent reviewers (LH and AC) used a standardized data extraction form. Risk of bias and applicability were assessed using PROBAST (Prediction Model Risk of Bias Assessment Tool).

Results: From 10,657 retrieved records, a total of 15 papers were selected. Most EHR papers focused on 1 chronic health care condition (n=11, 73%). From the 15 papers, 13 (87%) described a study that developed a diagnostic prediction model and 2 (13%) described a study that externally validated and tested the model in a PC setting. Studies used a variety of AI techniques. The predictors used to develop the model were all registered in the EHR. We found no papers with a low risk of bias, and high risk of bias was found in 9 (60%) papers. Biases covered an unjustified small sample size, not excluding predictors from the outcome definition, and the inappropriate evaluation of the performance measures. The risk of bias was unclear in 6 papers, as no information was provided on the handling of missing data and no results were reported from the multivariate analysis. Applicability was unclear in 10 (67%) papers, mainly due to lack of clarity in reporting the time interval between outcomes and predictors.

Conclusions: Most AI-based diagnostic prediction models based on EHR data in PC focused on 1 chronic condition. Only 2 papers tested the model in a PC setting. The lack of sufficiently described methods led to a high risk of bias. Our findings highlight that the currently available diagnostic prediction models are not yet ready for clinical implementation in PC.

Trial Registration: PROSPERO CRD42022320002; https://www.crd.york.ac.uk/PROSPERO/view/CRD42022320002

(JMIR Med Inform 2025;13:e62862) doi:10.2196/62862

KEYWORDS

primary care; electronic health records; artificial intelligence; EHR; AI; systematic review; decision-making; AI-based diagnostic; applicability; assessment tool

XSL•FO
RenderX

Introduction

Background

The diagnostic process is a core task of general practitioners (GPs). However, making a diagnosis may be a challenging task given the diversity, complexity, and early presentation of symptoms. Clinical prediction models are intended to improve the diagnostic process [1]. These models can support the health care provider by predicting serious illness [2]. In the last years, the interest in artificial intelligence (AI) techniques for the development of prediction models has been growing [3,4]. AI-based prediction models could aid in decision-making for faster and more accurate diagnoses, with more diagnostic efficiency that can benefit patients' health [5-8]. Examples are prediction tools that can predict colorectal cancer in patients [9,10].

Clinical prediction models used to be built on data from large databases, such as data collected for research purposes, claim data, or data from electronic health records (EHRs) [11,12]. EHR data consist of structured data, which are data in standardized format, and unstructured data, which are free-text data. Primary care (PC) EHR data provide extensive and longitudinal data from a patient's health trajectory and changes over time. AI might prove to be a valuable method to extract clinically useful and actionable insight from this vast and complex source of patient data [13]. For that reason, AI has the potential to transform EHR data into a valuable tool for predicting diagnosis in daily PC practice.

Reviews on the value of AI in PC are scarce, and previous research had different aims. For example, Kueper et al [14] provided an overview of diagnostic prediction models based on AI in PC. However, the authors did not assess the quality of these diagnostic prediction models. Other research in this field explored AI systems in community-based primary health care [15] or focused on different machine learning (ML)–based diagnostic and prognostic models that predicted a health care condition [16]. As AI has the potential to support and improve the diagnostic process, high-quality and validated prediction models are crucial in order to ensure patient safety after clinical implementation. Although a variety of prediction models for PC have been developed, to our knowledge, there are currently no systematic reviews on AI-based diagnostic prediction models for PC using EHR data.

Objective

Evaluation of the content and quality assessment of AI-based diagnostic prediction models using EHRs in PC was largely lacking in current literature. Therefore, we systematically reviewed the literature in order to critically evaluate the content of these AI-based diagnostic prediction models, including risk of bias and applicability.

Methods

Study Design

We performed a systematic review according to the PRISMA (Preferred Reporting Items for Systematic Reviews and Meta-Analyses) guidelines [17] (the PRISMA checklist is provided in Checklist 1). The protocol for this study was registered in PROSPERO (nr: CRD42022320002). The research team included stakeholders such as practicing GPs, researchers, methodologists, and AI experts in the design, analysis, and reporting of the study.

Search Strategy and Study Selection

Our search was adapted from the search strategy developed by Kueper et al [14]. It combines two concepts including a wide range of different terms used to describe the concepts: (1) artificial intelligence and (2) primary care (for full search strategy, see Multimedia Appendix 1, part 1 [18-67]). EHRs were not part of the search strategy, because literature suggests that we might miss important studies when including EHRs or related terms in the search strategy [13]. We searched in the following databases: MEDLINE, Embase, Web of Science, and Cochrane. There were no restrictions concerning the publication date. The last search update was conducted on August 28, 2023. We focused on intervention and observational studies. We excluded systematic reviews, meta-analyses, case studies, editorials, protocols, and conference posters or abstracts. Full text had to be available to be selected for screening. The literature had to be written in English or Dutch. Duplicate publications were removed with EndNote 20.

Inclusion and Exclusion Criteria

Four inclusion criteria were used to select the papers: (1) primary care focus: this included PC data, models that were tested in a PC setting, or PC had to be specifically mentioned in the aim of the study; (2) diagnostic prediction model: models had to predict a health condition applicable during a GP's consultation; prediction models that identified a disease in a database, rather than predicting a disease for an individual, were excluded; (3) AI: this included all ML and deep learning techniques; we directed our focus to data-driven prediction models without using medical images as input data; and (4) EHR-based data: EHR data had to be used for the development or validation of the model. EHRs were defined as PC data from EHRs, medical records, or clinical notes. See Multimedia Appendix 1, part 2 [18-67], for the full screening guidance.

Title and abstract screening was done in management software Rayyan (rayyan.ai) by 2 independent reviewers (LH and LvdH). Conflicts were resolved by a third reviewer (AU). Full-text screening was done by the same independent reviewers. Conflicts were resolved by discussion, and if no consensus was reached, they were resolved by a third reviewer (AU). Backward citation searching was conducted on the included papers and finished on November 7, 2023.

Data Extraction and Quality Assessment

Data extraction of included papers was done by 2 independent reviewers (LH and AC). They used a standardized data extraction form adapted from the Checklist for Critical Appraisal and Data Extraction for Systematic Reviews of Prediction Modelling Studies (CHARMS) [68]. Basic information was extracted from all papers. The extraction of more detailed information was focused on EHR-based papers. For all papers (EHR and non-EHR papers), we extracted general information

XSL•FO
RenderX

(first author, year of publication, title, data source, and country of data source), study design (retrospective or prospective), and outcome (predicted health condition). For the EHR papers, we additionally extracted dataset information (name of the dataset and sample size: number of participants used for model training, testing, or validation), AI technique, and predictors (the potentially used predictors used to develop the model). Risk of bias and applicability were assessed using PROBAST (Prediction Model Risk of Bias Assessment Tool). This tool includes 20 signaling questions divided into 4 domains (participants, predictors, outcome, and analysis) [69,70]. Overall judgment (ie, low, unclear, or high) of risk of bias is based on the 4 domains. If 1 domain is considered to have a high risk of bias, the overall judgment is scored as a high risk of bias. If at least 1 domain is considered to have an unclear risk of bias (without a domain with high risk of bias), the overall judgment is scored as unclear risk of bias. Applicability concern was rated based on 3 domains (participants, predictors, and outcome) and an overall judgment of applicability (ie, low, unclear, or high) was also given with the same approach as the risk-of-bias scoring. Applicability evaluation depends on the review question [69], and we translated applicability assessment as usability of the diagnostic prediction model in a PC setting. Conflicts in data extraction between the 2 reviewers (LH and AC) were resolved by discussion, and if no consensus was reached, they were resolved by a third reviewer (TvL).

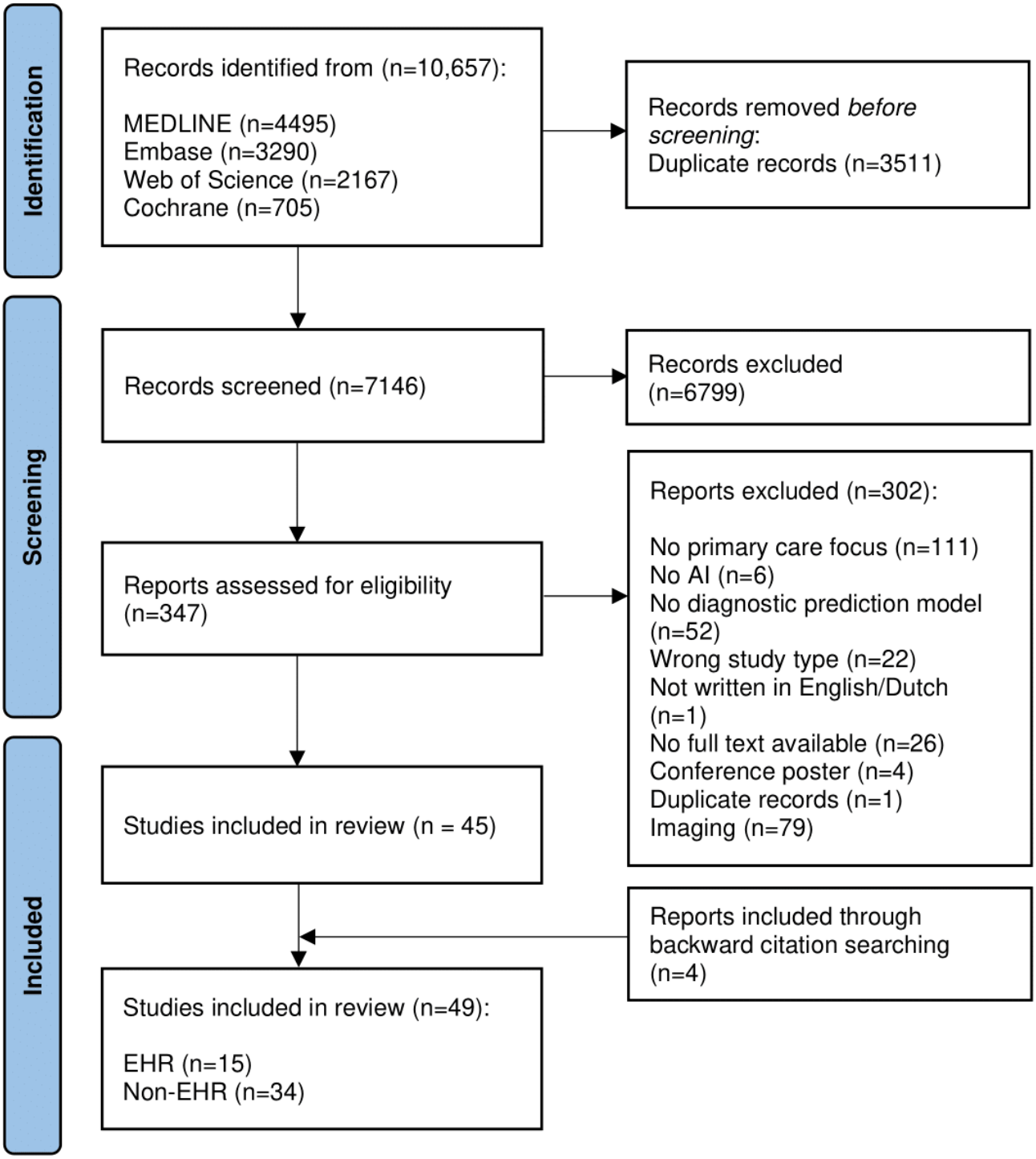
Results

Description of Included Studies

We retrieved 10,657 records using our search strategy. After duplicate removal, we conducted title and abstract screening on 7146 records. A total of 347 records met the eligibility criteria for full-text screening. After full-text screening, 45 records were included. Backward citation searching yielded an additional 4 papers. A total of 49 papers were thus included in the review (Figure 1). Of the included papers, we identified 15 EHR papers and 34 non-EHR papers. A detailed description of the 34 non-EHR papers can be found in Multimedia Appendix 1, part 3 [18-67]. The data used in these 34 papers were collected from different sources, including secondary care datasets (n=17), questionnaires (n=4), and the knowledge of different health care providers (n=5).

XSL•FO
RenderX

Figure 1. PRISMA (Preferred Reporting Items for Systematic Reviews and Meta-Analyses) flowchart of study selection. AI: artificial intelligence; EHR: electronic health record.



Overview of the EHR-Based Papers

Of the 15 EHR papers, 13 (87%) included the development of a prediction model [18-30]. In Table 1, the data extraction per paper can be found. The included EHR papers covered various outcomes, mostly chronic conditions (11/15, 73%) [19-28,31]. The most frequent predicted outcomes were dementia (3/15, 20%) [19,20,23], asthma (3/15, 20%), or chronic obstructive pulmonary disease (COPD) (3/15, 20%) [21,26,31]. Other study outcomes are shown in Table 1. All included papers used predictors registered in EHRs. Predictors included findings from clinical examination (n=6) [19,25,26,28,31,32], laboratory results (n=5) [21,22,25,28,32], and medication (n=4) [19,21,24,29]. All models used structured data.

Two papers externally validated and tested a prediction model in a PC setting [31,32]. One paper had a prospective approach and tested the diagnostic performance of a prediction model for asthma and COPD [31]. Ten papers (10/15, 67%) were published after 2020 [18,21-24,26,27,29,31,32]. Most data sources used in the studies originated from Europe (8/15, 53%) [18-22,24,27,31], followed by North America (5/15, 33%) [23,25,28,29,31,32] and Asia (2/15, 13%) [26,30].

XSL•FO
RenderX

Table . Extracted information from electronic health record papers.

Author, year	Country	Study type	Study design	Outcome	Dataset	Participants and inclusion criteria	Predictors	AI technique
Barnes et al (2020) [23]	United States	Developmental	Retrospective cohort study	To identify patients at high risk of unrecognized dementia	Data from Kaiser Permanente Washington	4330 participants aged at least 65 years, community member with no dementia	Demographics, diagnosis, vital signs, health care usage, medication	LR[a]
Briggs et al (2022) [22]	United Kingdom	Developmental	Nested case-control study	To predict risk of esophagogastric cancer	Data from General Practice Research Database	40,348 participants with esophagus or gastric cancer (7471 cases and 32,877 matched controls) diagnosed after 2000 (aged ≥40 years)	Demographics, symptoms, laboratory results	RF[b], SVM[c], LR, NB[d], XGBoost[e]
Dhanda et al (2023) [32]	United States	Developmental + Validation	Retrospective cohort study	To predict urine culture result without microscopy data to predict urinary tract infection	Data from emergency department (developmental phase). Data from primary care outpatient family medicine department at University of Kansas Medical Center (external validation)	80,859 participants (80,387 development, 472 external validation) with an ordered urinalysis and urine culture	Demographics, urine analysis, vital signs, symptoms, history of urinary tract infection, higher risk of clinical features	XGBoost, RF, NN[f]
Dros et al (2022) [24]	Netherlands	Developmental	Nested case-control study	To identify primary Sjögren syndrome	Data from Nivel Primary Care Database linked with Diagnosis Related Groups Information System dataset	930,590 participants (1411 cases, 1411 controls for training phase and all of the 929,179 controls for testing phase), with primary Sjögren syndrome from 2017	Demographics, diagnosis, medication, health usage	LR, RF
Ellertsson et al (2021) [18]	Iceland	Developmental	Retrospective cohort study	To diagnose common clinical headaches (cluster headache, migraine [with or without aura], tension headache)	Data from 15 primary Health Care of the Capital Area clinics	Unknown number of participants, 800 clinical notes from patients with 4 headache diagnoses from 2006 to 2020	Headache symptoms, sex, age, family history	RF

XSL•FO
RenderX

Author, year	Country	Study type	Study design	Outcome	Dataset	Participants and inclusion criteria	Predictors	AI technique
Ford et al (2019) [19]	United Kingdom	Developmental	Nested case-control study	To detect dementia	Data from Clinical Practice Research Datalink data	93,120 participants (46,560 cases with a dementia diagnosis code between 2000 and 2012, 46,560 controls)	Symptoms of physical or cognitive frailty, medical history, health care usage, ethnicity, family history of dementia, intoxications, BMI, blood pressure, psychological diagnoses, and treatment	RF, NB, SVM, NN
Jammeh et al (2018) [20]	United Kingdom	Developmental	Case-control study	To identify undiagnosed dementia	NHS Devon dataset with 18 participating GP[g] surgeries	3063 participants (850 cases with a dementia diagnosis code, 2213 controls)	Demographics, long-term conditions, and consultations	LR, RF, NB, SVM
Kocks et al (2023) [31]	Netherlands	Validation	Prospective observational study	To diagnose asthma, COPD[h], or asthma-COPD overlap	Data from Nivel Primary Care Database	116 cases, tested on 180 specialists from 9 countries (external validation) from patients aged ≥40 years, with complete data file	Symptoms, BMI, spirometry scores, smoking, diagnosis of chronic or allergic rhinitis, age at onset of respiratory disease	Multinomial LR
LaFreniere et al (2016) [25]	Canada	Developmental	Case-control study, nested is unclear	To predict hypertension	EHR data from Canadian Primary Care Sentinel Surveillance Network	379,027 participants (185,371 cases with hypertension, 193,656 controls with no hypertension and with no 8 specific chronic conditions)	Demographics, BMI, blood pressure, laboratory results	NN
Lin et al (2023) [26]	China	Developmental	Retrospective cohort study	To identify COPD	Public health data from EHRs and electronic medical records of Chinese residents	1875 participants with lung symptoms or chronic lung disease	Demographics, smoking, BMI, chronic cough, shortness of breath, biofuel use, and family history. Based on the questionnaire for COPD	18 methods, including: Decision tree, LR, discriminant analysis (linear and quadratic), SVM, gradient boosting classifiers, NN, Gaussian process classifier, KNN[i], NB

XSL•FO
RenderX

Author, year	Country	Study type	Study design	Outcome	Dataset	Participants and inclusion criteria	Predictors	AI technique
Mariani et al (2021) [21]	Netherlands	Developmental	Retrospective cohort study	To diagnose asthma and COPD or asthma-COPD overlap	Data from Dutch primary care laboratory in Groningen	3659 participants with asthma or COPD from 2007 to 2017	Demographics, symptoms, diagnosis, medication, laboratory results, referrals, spirometry results	SVM, RF, KNN
Nemlander et al (2023) [27]	Sweden	Developmental	Nested case-control study	To identify nonmetastatic colorectal cancer	Regional administrative health care database from Västra Götaland Region	2681 participants (542 cases with a cancer diagnosis, 2139 controls)	Nonmetastatic colorectal cancer stage, number of GP consultations, diagnosis codes	Stochastic gradient boosting
Perveen et al (2016) [28]	Canada	Developmental	Retrospective cohort study	To classify diabetes mellitus in 3 adult age groups	EHR data from Canadian Primary Care Sentinel Surveillance Network	4678 participants (377 cases of diabetes, 4301 controls with no diabetes) with all documented risk factors	Demographics blood pressure, laboratory results	Decision tree, bagging, ADAboost
Singh et al (2022) [29]	United States	Developmental	Retrospective cohort study	To predict anterior segment vision-threatening disease (asVTD)	EHRs of the University of Michigan	2942 participants with anterior segment eye complaint (133 cases with asVTD, 2809 controls) with PC notes with ophthalmologist visit	Demographics, history of eye problems, symptoms, medication	Elastic net LR
Su et al (2019) [30]	China	Developmental	Retrospective cohort study	Top 100 diagnoses (within general diagnoses)	National Hospital Ambulatory Medical Care Survey and the National Ambulatory Medical Care Survey	Unknown number of participants, top 100 diagnosis selected from 2,000,000 records	Demographics, symptoms, past medical history	NN

[a]LR: logistic regression.

[b]RF: random forest.

[c]SVM: support vector machine.

[d]NB: naïve Bayes.

[e]XGBoost: extreme gradient boosting.

[f]NN: neural network.

[g]GP: general practitioner.

[h]COPD: chronic obstructive pulmonary disease.

[i]KNN: K-nearest neighbors.

AI Technique

All of the included studies performed at least 1 supervised AI technique (Table 1). The most used AI techniques were random forest (9 papers), logistic regression (7 papers), support vector machines (5 papers), boosting algorithms (5 papers), neural networks (5 papers), and naïve Bayes (4 papers).

Quality Assessment: Risk of Bias

None of the studies assessed by the PROBAST tool had a low risk of bias. We found a high risk of bias in 9 studies (9/15, 60%) and an unclear risk of bias in 6 studies (6/15, 40%; Table 2). In Multimedia Appendix 1, part 4 [18-67], the full assessment of the PROBAST tool can be found.

XSL•FO
RenderX

Table . Risk of bias per domain using the Prediction model Risk Of Bias ASsessment Tool.

	Participants	Predictors	Outcome	Analysis	Overall
Barnes [23]	Low	Low	Low	Unclear	Unclear
Briggs et al [22]	Low	Unclear	Unclear	Unclear	Unclear
Dhanda et al [32]	High	Low	Unclear	Unclear	High
Dros et al [24]	Low	Low	Unclear	High	High
Ellertsson et al [18]	Low	Unclear	Low	High	High
Ford et al [19]	Unclear	Low	Low	Unclear	Unclear
Jammeh et al [20]	High	Unclear	Unclear	Unclear	High
Kocks et al [31]	Low	Low	High	High	High
LaFreniere et al [25]	Unclear	Low	Unclear	Unclear	Unclear
Lin et al [26]	Unclear	Low	Unclear	High	High
Mariani et al [21]	Unclear	Low	Unclear	Unclear	Unclear
Nemlander et al [27]	High	Low	Unclear	Unclear	High
Perveen et al [28]	Low	Unclear	High	High	High
Singh et al [29]	Low	Low	Unclear	High	High
Su et al [30]	Unclear	Unclear	Unclear	Unclear	Unclear

The most significant source of bias was found in the analysis domain. The main reasons for the high risk of bias in this domain were the insufficient number of participants with the outcome (5/15, 33%) [18,24,26,29,31] and irrelevant model performance measures that were used to evaluate the model (2/15, 13%) [28,31]. The main reasons for an unclear risk of bias in the analysis domain were lack of clarity on how missing data were handled (10/15, 67%) [18-20,22,23,27-30,32], and on how the predictors and their assigned weights in the final model correspond to results from the reported multivariate analysis (9/15, 60%) [18,20,21,25-30]. Although measures of calibration are not part of the signaling questions of the PROBAST, we noticed that only 4 papers (4/15, 27%) [22,23,29,32] used calibration to assess the performance of the model.

The second significant source of bias was found in the outcome domain. The main reasons for the high risk of bias in this domain were the determination of the predictors with a prior knowledge of the outcome (1/15, 7%) [31] and not excluding the predictors from the outcome definition (2/15, 13%). For example, Perveen et al [28] included fasting glucose levels to predict diabetes and Kocks et al [31] included spirometry findings to predict asthma and COPD. The 2 main reasons for an unclear risk of bias in the outcome domain were lack of clarity on the time interval between the outcome and the predictors (9/15, 60%) [20,24-30,32] and the lack of clarity on the outcome definition (7/15, 47%) [20-22,24,26,28,30].

The third domain with risk of bias was the participants domain. A high risk of bias in the participants domain was found because inclusion and exclusion criteria were not appropriate in 2 studies (2/15, 13%) as both studies excluded participants at high risk of the outcome [27,32]. Another reason for the high risk of bias was a nonappropriate data source that was used in 1 study [20] because the authors described the study as a case-control study although the study was not nested as recommended in the PROBAST guidelines [69,70]. The predictors domain was the domain with the lowest risk of bias. The lack of clarity that resulted in an unclear risk of bias covered mainly insufficient information on whether the predictors were defined and assessed in a similar way for all participants (4/15, 27%) [18,20,22,30].

Applicability

Overall, we found an unclear concern for applicability in 10 papers (10/15, 67%) and a low concern for applicability in 5 papers (5/15, 33%; Table 3). The unclear concern for applicability to our research question was mainly noticed in the outcome domain due to a lack of clarity in reporting the time interval between the outcomes and predictors (8/15, 53%) [20,25-30,32].

XSL•FO
RenderX

Table . Applicability per domain using the Prediction model Risk Of Bias Assessment Tool.

	Participants	Predictors	Outcome	Overall
Barnes et al [23]	Low	Low	Low	Low
Briggs et al [22]	Low	Unclear	Unclear	Unclear
Dhanda et al [32]	Low	Low	Unclear	Unclear
Dros et al [24]	Low	Low	Low	Low
Ellertsson et al [18]	Low	Unclear	Low	Unclear
Ford et al [19]	Low	Low	Low	Low
Jammeh et al [20]	Low	Unclear	Unclear	Unclear
Kocks et al [31]	Low	Low	Low	Low
LaFreniere et al [25]	Unclear	Low	Unclear	Unclear
Lin et al [26]	Unclear	Low	Unclear	Unclear
Mariani et al [21]	Low	Low	Low	Low
Nemlander et al [27]	Low	Low	Unclear	Unclear
Perveen et al [28]	Low	Unclear	Unclear	Unclear
Singh et al [29]	Low	Low	Unclear	Unclear
Su et al [30]	Unclear	Unclear	Unclear	Unclear

In the predictors domain we also found an unclear concern for applicability due to the lack of clarity in the definition of the included predictors (5/15, 33%) [18,20,22,28,30]. For example, 1 paper lacked information on how notes were annotated before they were used as predictors in the model [18]. The unclear concern for applicability in the participants' domain was mainly due to lack of information on inclusion and exclusion criteria (3/15, 20%) [25,26,30].

Discussion

Principal Results

We systematically reviewed the literature for studies about AI-based diagnostic prediction models for PC. These models were developed with different data sources, such as questionnaire data, secondary care data, or EHR data. Only 15 out of 49 models were developed using data from EHRs. Most of the models using EHR data focused on just 1 chronic condition. Merely 2 papers tested the model in a PC setting. All of the included studies performed at least 1 supervised AI technique, most often with random forest or logistic regression. Evaluation with the PROBAST guidelines showed an unclear to high risk of bias for all EHR papers. In most of the papers, we found unclear concerns about the applicability to our research question.

Comparison With Prior Work

To the best of our knowledge, only 2 reviews evaluated the risk of bias in clinical prediction models on a wide range of diseases in PC studies [15,16]. Most of the included studies in these reviews showed a high to unclear risk of bias, which is in line with our findings [15,16]. However, there appear to be differences in grading compared with Abdulazeem et al [16]. They considered incomplete reporting and the absence of external validation a high risk of bias, whereas in our systematic review, these points were considered as an unclear risk of bias and no risk of bias, respectively. The study by Abbasgholizadeh et al [15] did not report details on the reasons they coded subdomains as high or unclear risk of bias, for which reason we are unable to make a formal comparison with our results.

Systematic reviews evaluating AI-based clinical prediction models in other medical fields have followed the same grading criteria as we did and found similar flaws in the analysis domain as we did in our systematic review [71,72]. These similarities include the unjustified small sample size in EHR studies, inappropriate evaluation in the performance measures, and flaws in handling of missing data [71-73].

The most used AI techniques were random forest, logistic regression, support vector machines, boosting algorithms, and neural networks. In previous systematic reviews, random forest and support vector machines are also more often found as most used methodology [16,71,73-75]. This might be explained by the well-described strong performance and ease of interpretability of random forests and support vector machines, particularly when working with lower-quality structured data. Most PC EHRs are primarily used for clinical purposes, with secondary purposes for research [69]. Thus, the challenges associated with using such EHRs to develop prediction models have been widely documented and include missing values and inconsistencies in data entry [13]. These challenges are inherent to the data and should be addressed at the preprocessing stage. We did not find papers that used generative AI methods (such as large language models). Our retrieved papers developed or validated tools based only on structured data (numbers or codes such as laboratory results, vital signs, and diagnosis codes from International Classification of Primary Care or *ICD-10* [*International Statistical Classification of Diseases, Tenth Revision*]) rather than unstructured data or written text, where large language models work well on. Literature found it valuable

XSL•FO
RenderX

for the performance of the model to use unstructured data together with structured data for prognostic prediction models [76,77]. We think that future studies about diagnostic prediction tools will increasingly use generative AI methods, although it is still difficult to integrate them into clinical workflows [78].

In general, studies analyzing EHRs are subject to a high risk of bias, because these data are collected for clinical rather than research purposes [69]. Hence, clinical prediction models developed on EHRs are more difficult to reproduce and generalize, given the heterogeneity of coding systems and database infrastructures [16]. In line with models analyzed in previous studies [15,16,73], most of the clinical prediction models were not externally validated. Most of the studies developed in PC were performed in high-income countries and may not have taken into account regional or global differences in the availability of certain predictors [14-16]. For example, some predictors may not be easy to obtain in PC settings in low-income countries (eg, spirometry results for the prediction of asthma or COPD). Furthermore, the lack of stratified analyses in most studies implies that we cannot draw conclusions about how diagnostic models perform across different equity groups. Together, all these factors limit the generalizability of the clinical prediction models.

Strengths and Limitations

The main strength of the study is the extensive search strategy with no date limit in a large and diverse range of studies on AI prediction models in PC. Not including "EHR" in the search strategy added rigor to our study as a recent review suggests that important papers could have been missed when we included EHRs in the search strategy [13]. A second strength is that the findings on the risk of bias were carefully assessed by 2 independent reviewers (LH and AC) with experience in clinical PC, and the conflicts were discussed with other experts in the field of PC and AI. Unlike previous systematic reviews that found a high proportion of studies with a high concern of applicability to the research question [72], we noticed no high concern for applicability in any study. We believe that the findings shared in our review are highly reliable in highlighting the current situation of AI studies in PC using EHRs.

The main limitation of this study is the broad definition of the terminology for the search strategy, which may have prevented us from capturing all relevant studies. For example, we included all studies that used ML and deep learning techniques. Given the lack of a widely accepted definition of AI, other reviews use other criteria for AI or ML [71,73,75]. Similarly, given our definition of diagnostic prediction models, we considered a diagnostic prediction model to be a model that predicts a health condition during a GP's consultation. As a result, multiple prediction models that identified a disease in a database were excluded. The second limitation is the use of the PROBAST guidelines to determine the risk of bias and applicability in evaluating AI prediction models. Although the PROBAST guidelines are highly detailed and reliable in evaluating clinical prediction models [33], PROBAST has been criticized for being less specific and less applicable for AI-based models than traditional statistical methods. Considering this criticism, a protocol on the extension of PROBAST into PROBAST-Artificial Intelligence (PROBAST-AI) has been published with the aim to develop a PROBAST-AI tool to better support evaluation of prediction model studies that applied AI [3]. The PROBAST-AI tool has not yet been published.

Future Research and Practical Implications

The relevance of the applicability of prediction models in clinical practice should be the priority when developing clinical prediction models, as stated in a number of standardized frameworks designed for prediction model developers [79,80]. We found that only 2 models were tested in PC settings. Moreover, most studies included in this review predict chronic conditions. This is also seen in previous reviews evaluating clinical prediction models in PC [14,16]. However, in general, chronic conditions are not known to be difficult to diagnose in PC. Two examples from our included papers are the diagnosis of hypertension predicted on the variable high blood pressure [25] and the diagnosis of diabetes predicted on the variable high glucose levels [28]. These predictions might not be as useful in clinical practice, even if the model performance metrics are excellent. Nevertheless, chronic conditions are highly prevalent in PC and for conditions that are influenced by several and complex factors, prediction models may facilitate the diagnostic process for the GP. As most tools focused on predicting 1 condition, GPs would have to use many prediction tools side by side to predict the correct diagnosis in daily practice. All these findings highlight that involving more practicing GPs and asking what they need are important in developing clinical prediction models with a higher success rate of clinical implementation. We recommend involving relevant stakeholders in the early stages of the development of a new model.

To improve the methodology in future studies, our findings suggest that a special focus is required on reporting areas such as methods for internal validation, appropriate inclusion of participants, and a proper sample size calculation. A high risk of bias mainly found in the analysis and outcome domains should be alarming as this questions the methodology of the included papers. We found an unclear risk of bias and unclear concern for applicability in more than half of the included studies, mainly related to poor reporting, for example, about missing data. Missing data is known as a large challenge for EHR data [13], and extra attention should therefore be paid to reporting this. Researchers can benefit from the use of the TRIPOD (Transparent Reporting of a Multivariable Prediction Model for Individual Prognosis or Diagnosis) statement [81] and PROBAST guidelines in communicating their findings [3], particularly now that the TRIPOD-AI extension is released [82]. To enhance the applicability of the prediction model, we highlight the importance of clear reporting on the time interval between predictors and outcome, a clear definition of the outcome and predictors, and a clear description of the inclusion and exclusion criteria. Differences in recording between EHRs might lower the performance of the model in the external validation step, and external validation is a crucial step for generalizable and reliable models [76]. However, we found only 2 papers that performed external validation.

XSL•FO
RenderX

Conclusions

AI-based prediction models using EHR data are not yet ready for implementation into PC daily practice. The number of studies found was limited, and reproducibility and generalizability were insufficient. For a diagnostic prediction model to be used in PC, it is important that GPs and relevant stakeholders are involved in the development, that the model is externally validated, and that it is appropriately recorded.

Acknowledgments

This study was funded by ZonMw file number: 839150005. The authors would like to thank Lori van den Hurk for her help with the screening process.

Conflicts of Interest

None declared.

Multimedia Appendix 1
Search strategy, screening guidance, table with all included papers, PROBAST (Prediction Model Risk of Bias Assessment Tool) checklist, and references of appendix.
[DOCX File, 290 KB - medinform_v13i1e62862_app1.docx]

Checklist 1
PRISMA (Preferred Reporting Items for Systematic Reviews and Meta-Analyses) 2020 checklist.
[PDF File, 69 KB - medinform_v13i1e62862_app2.pdf]

References

1. van Smeden M, Reitsma JB, Riley RD, Collins GS, Moons KG. Clinical prediction models: diagnosis versus prognosis. J Clin Epidemiol 2021 Apr;132:142-145. [doi: 10.1016/j.jclinepi.2021.01.009] [Medline: 33775387]
2. Moons KGM, Royston P, Vergouwe Y, Grobbee DE, Altman DG. Prognosis and prognostic research: what, why, and how? BMJ 2009 Feb 23;338:b375. [doi: 10.1136/bmj.b375] [Medline: 19237405]
3. Collins GS, Dhiman P, Andaur Navarro CL, et al. Protocol for development of a reporting guideline (TRIPOD-AI) and risk of bias tool (PROBAST-AI) for diagnostic and prognostic prediction model studies based on artificial intelligence. BMJ Open 2021 Jul 9;11(7):e048008. [doi: 10.1136/bmjopen-2020-048008] [Medline: 34244270]
4. Goldstein BA, Navar AM, Carter RE. Moving beyond regression techniques in cardiovascular risk prediction: applying machine learning to address analytic challenges. Eur Heart J 2017 Jun 14;38(23):1805-1814. [doi: 10.1093/eurheartj/ehw302] [Medline: 27436868]
5. Liyanage H, Liaw ST, Jonnagaddala J, et al. Artificial intelligence in primary health care: perceptions, issues, and challenges. Yearb Med Inform 2019 Aug;28(1):41-46. [doi: 10.1055/s-0039-1677901] [Medline: 31022751]
6. Mistry P. Artificial intelligence in primary care. Br J Gen Pract 2019 Sep;69(686):422-423. [doi: 10.3399/bjgp19X705137] [Medline: 31467001]
7. Summerton N, Cansdale M. Artificial intelligence and diagnosis in general practice. Br J Gen Pract 2019 Jul;69(684):324-325. [doi: 10.3399/bjgp19X704165] [Medline: 31249070]
8. Lin S. A clinician's guide to artificial intelligence (AI): Why and how primary care should lead the health care AI revolution. J Am Board Fam Med 2022;35(1):175-184. [doi: 10.3122/jabfm.2022.01.210226] [Medline: 35039425]
9. Birks J, Bankhead C, Holt TA, Fuller A, Patnick J. Evaluation of a prediction model for colorectal cancer: retrospective analysis of 2.5 million patient records. Cancer Med 2017 Oct;6(10):2453-2460. [doi: 10.1002/cam4.1183] [Medline: 28941187]
10. Burnett B, Zhou SM, Brophy S, et al. Machine learning in colorectal cancer risk prediction from routinely collected data: a review. Diagnostics (Basel) 2023 Jan 13;13(2):301. [doi: 10.3390/diagnostics13020301] [Medline: 36673111]
11. Morgenstern JD, Buajitti E, O'Neill M, et al. Predicting population health with machine learning: a scoping review. BMJ Open 2020 Oct 27;10(10):e037860. [doi: 10.1136/bmjopen-2020-037860] [Medline: 33109649]
12. Obermeyer Z, Emanuel EJ. Predicting the future—big data, machine learning, and clinical medicine. N Engl J Med 2016 Sep 29;375(13):1216-1219. [doi: 10.1056/NEJMp1606181] [Medline: 27682033]
13. Goldstein BA, Navar AM, Pencina MJ, Ioannidis JPA. Opportunities and challenges in developing risk prediction models with electronic health records data: a systematic review. J Am Med Inform Assoc 2017 Jan;24(1):198-208. [doi: 10.1093/jamia/ocw042] [Medline: 27189013]
14. Kueper JK, Terry AL, Zwarenstein M, Lizotte DJ. Artificial intelligence and primary care research: a scoping review. Ann Fam Med 2020 May;18(3):250-258. [doi: 10.1370/afm.2518] [Medline: 32393561]

XSL•FO
RenderX

15. Abbasgholizadeh Rahimi S, Légaré F, Sharma G, et al. Application of artificial intelligence in community-based primary health care: systematic scoping review and critical appraisal. J Med Internet Res 2021 Sep 3;23(9):e29839. [doi: 10.2196/29839] [Medline: 34477556]
16. Abdulazeem H, Whitelaw S, Schauberger G, Klug SJ. A systematic review of clinical health conditions predicted by machine learning diagnostic and prognostic models trained or validated using real-world primary health care data. PLoS One 2023;18(9):e0274276. [doi: 10.1371/journal.pone.0274276] [Medline: 37682909]
17. Page MJ, McKenzie JE, Bossuyt PM, et al. The PRISMA 2020 statement: an updated guideline for reporting systematic reviews. BMJ 2021 Mar 29;372:n71. [doi: 10.1136/bmj.n71] [Medline: 33782057]
18. Ellertsson S, Loftsson H, Sigurdsson EL. Artificial intelligence in the GPs office: a retrospective study on diagnostic accuracy. Scand J Prim Health Care 2021 Dec;39(4):448-458. [doi: 10.1080/02813432.2021.1973255] [Medline: 34585629]
19. Ford E, Rooney P, Oliver S, et al. Identifying undetected dementia in UK primary care patients: a retrospective case-control study comparing machine-learning and standard epidemiological approaches. BMC Med Inform Decis Mak 2019 Dec 2;19(1):248. [doi: 10.1186/s12911-019-0991-9] [Medline: 31791325]
20. Jammeh EA, Carroll CB, Pearson SW, et al. Machine-learning based identification of undiagnosed dementia in primary care: a feasibility study. BJGP Open 2018 Jul;2(2):bjgpopen18X101589. [doi: 10.3399/bjgpopen18X101589] [Medline: 30564722]
21. Mariani S, Metting E, Lahr MMH, Vargiu E, Zambonelli F. Developing an ML pipeline for asthma and COPD: the case of a Dutch primary care service. Int J of Intelligent Sys 2021 Nov;36(11):6763-6790. [doi: 10.1002/int.22568]
22. Briggs E, de Kamps M, Hamilton W, Johnson O, McInerney CD, Neal RD. Machine learning for risk prediction of oesophago-gastric cancer in primary care: comparison with existing risk-assessment tools. Cancers (Basel) 2022 Oct 14;14(20):5023. [doi: 10.3390/cancers14205023] [Medline: 36291807]
23. Barnes DE, Zhou J, Walker RL, et al. Development and validation of eRADAR: a tool using EHR data to detect unrecognized dementia. J Am Geriatr Soc 2020 Jan;68(1):103-111. [doi: 10.1111/jgs.16182] [Medline: 31612463]
24. Dros JT, Bos I, Bennis FC, et al. Detection of primary Sjögren's syndrome in primary care: developing a classification model with the use of routine healthcare data and machine learning. BMC Prim Care 2022 Aug 9;23(1):199. [doi: 10.1186/s12875-022-01804-w] [Medline: 35945489]
25. LaFreniere D, Zulkernine F, Barber D, Martin K. Using machine learning to predict hypertension from a clinical dataset. Presented at: 2016 IEEE Symposium Series on Computational Intelligence (SSCI; Dec 6-9, 2016; Athens, Greece. [doi: 10.1109/SSCI.2016.7849886]
26. Lin X, Lei Y, Chen J, et al. A case-finding clinical decision support system to identify subjects with chronic obstructive pulmonary disease based on public health data. Tsinghua Sci Technol 2023 Jun;28(3):525-540. [doi: 10.26599/TST.2022.9010010]
27. Nemlander E, Ewing M, Abedi E, et al. A machine learning tool for identifying non-metastatic colorectal cancer in primary care. Eur J Cancer 2023 Mar;182(100-6):100-106. [doi: 10.1016/j.ejca.2023.01.011] [Medline: 36758474]
28. Perveen S, Shahbaz M, Guergachi A, Keshavjee K. Performance analysis of data mining classification techniques to predict diabetes. Procedia Comput Sci 2016;82:115-121. [doi: 10.1016/j.procs.2016.04.016]
29. Singh K, Thibodeau A, Niziol LM, et al. Development and validation of a model to predict anterior segment vision-threatening eye disease using primary care clinical notes. Cornea 2022 Aug 1;41(8):974-980. [doi: 10.1097/ICO.0000000000002877] [Medline: 34620768]
30. Su G, Wen J, Zhu Z, et al. An approach of integrating domain knowledge into data-driven diagnostic model. Stud Health Technol Inform 2019 Aug 21;264:1594-1595. [doi: 10.3233/SHTI190551] [Medline: 31438248]
31. Kocks JWH, Cao H, Holzhauer B, et al. Diagnostic performance of a machine learning algorithm (asthma/chronic obstructive pulmonary disease [COPD] differentiation classification) tool versus primary care physicians and pulmonologists in asthma, COPD, and asthma/COPD overlap. J Allergy Clin Immunol Pract 2023 May;11(5):1463-1474. [doi: 10.1016/j.jaip.2023.01.017] [Medline: 36716998]
32. Dhanda G, Asham M, Shanks D, et al. Adaptation and external validation of pathogenic urine culture prediction in primary care using machine learning. Ann Fam Med 2023;21(1):11-18. [doi: 10.1370/afm.2902] [Medline: 36690486]
33. Moons KGM, Altman DG, Reitsma JB, Collins GS, Transparent Reporting of a Multivariate Prediction Model for Individual Prognosis or Development Initiative. New guideline for the reporting of studies developing, validating, or updating a multivariable clinical prediction model: the TRIPOD statement. Adv Anat Pathol 2015 Sep;22(5):303-305. [doi: 10.1097/PAP.0000000000000072] [Medline: 26262512]
34. Ahmed MM, Sayed AM, El Abd D, et al. Diagnosis of coronavirus disease 2019 and the potential role of deep learning: insights from the experience of Cairo University Hospitals. J Int Med Res 2022 Jul;50(7). [doi: 10.1177/03000605221109392]
35. Ahmed MM, Sayed AM, Khafagy GM, et al. Accuracy of the traditional COVID-19 phone triaging system and phone triage-driven deep learning model. J Prim Care Community Health 2022;13(21501319221113544):21501319221113544. [doi: 10.1177/21501319221113544] [Medline: 35869692]
36. Basta M, John Simos N, Zioga M, et al. Personalized screening and risk profiles for mild cognitive impairment via a machine learning framework: implications for general practice. Int J Med Inform 2023 Feb;170(104966):104966. [doi: 10.1016/j.ijmedinf.2022.104966] [Medline: 36542901]

XSL•FO
RenderX

37. Blanes-Vidal V, Lindvig KP, Thiele M, Nadimi ES, Krag A. Artificial intelligence outperforms standard blood-based scores in identifying liver fibrosis patients in primary care. Sci Rep 2022 Feb 21;12(1):2914. [doi: 10.1038/s41598-022-06998-8] [Medline: 35190650]
38. Braido F, Santus P, Corsico AG, et al. Chronic obstructive lung disease "expert system": validation of a predictive tool for assisting diagnosis. Int J Chron Obstruct Pulmon Dis 2018;13(1747-53):1747-1753. [doi: 10.2147/COPD.S165533] [Medline: 29881264]
39. Brooks GJ, Ashton RE, Pethybridge RJ. DERMIS: a computer system for assisting primary-care physicians with dermatological diagnosis. Br J Dermatol 1992 Dec;127(6):614-619. [doi: 10.1111/j.1365-2133.1992.tb14875.x] [Medline: 1476920]
40. Cruz-Gutiérrez V, Posada-Zamora MA, Sánchez-López A. An efficient expert system for diabetes with a Bayesian inference engine. Adv Soft Comput, Micai 2016;10062:54-64. [doi: 10.1007/978-3-319-62428-0_5]
41. Dong W, Tse TYE, Mak LI, et al. Non-laboratory-based risk assessment model for case detection of diabetes mellitus and pre-diabetes in primary care. J Diabetes Investig 2022 Aug;13(8):1374-1386. [doi: 10.1111/jdi.13790] [Medline: 35293149]
42. Exarchos TP, Rigas G, Bibas A, et al. Mining balance disorders' data for the development of diagnostic decision support systems. Comput Biol Med 2016 Oct 1;77(240-8):240-248. [doi: 10.1016/j.compbiomed.2016.08.016] [Medline: 27619194]
43. Faris H, Habib M, Faris M, Elayan H, Alomari A. An intelligent multimodal medical diagnosis system based on patients' medical questions and structured symptoms for telemedicine. Inform Med Unlocked 2021;23:100513. [doi: 10.1016/j.imu.2021.100513]
44. Farmer N, Schilstra MJ. A knowledge-based diagnostic clinical decision support system for musculoskeletal disorders of the shoulder for use in a primary care setting. Shoulder Elbow 2012 Apr;4(2):141-151. [doi: 10.1111/j.1758-5740.2011.00165.x]
45. Farmer N. An update and further testing of a knowledge-based diagnostic clinical decision support system for musculoskeletal disorders of the shoulder for use in a primary care setting. J Eval Clin Pract 2014 Oct;20(5):589-595. [doi: 10.1111/jep.12153] [Medline: 24828447]
46. Grill E, Groezinger M, Feil K, Strupp M. Developing and implementing diagnostic prediction models for vestibular diseases in primary care. Stud Health Technol Inform 2016;228(735-9):735-739. [doi: 10.3233/978-1-61499-678-1-735] [Medline: 27577483]
47. Harabor V, Mogos R, Nechita A, et al. Machine learning approaches for the prediction of hepatitis B and C seropositivity. Int J Environ Res Public Health 2023 Jan 29;20(3):2380. [doi: 10.3390/ijerph20032380] [Medline: 36767747]
48. Heckerling PS, Canaris GJ, Flach SD, Tape TG, Wigton RS, Gerber BS. Predictors of urinary tract infection based on artificial neural networks and genetic algorithms. Int J Med Inform 2007 Apr;76(4):289-296. [doi: 10.1016/j.ijmedinf.2006.01.005] [Medline: 16469531]
49. Hejlesen OK, Olesen KG, Dessau R, Beltoft I, Trangeled M. Decision support for diagnosis of Lyme disease. Stud Health Technol Inform 2005;116(205-10):205-210. [Medline: 16160260]
50. Koch Nogueira PC, Venson AH, de Carvalho MFC, Konstantyner T, Sesso R. Symptoms for early diagnosis of chronic kidney disease in children—a machine learning-based score. Eur J Pediatr 2023 Aug;182(8):3631-3637. [doi: 10.1007/s00431-023-05032-x] [Medline: 37233777]
51. Liu X, Zhang W, Zhang Q, et al. Development and validation of a machine learning-augmented algorithm for diabetes screening in community and primary care settings: a population-based study. Front Endocrinol 2022;13:1043919. [doi: 10.3389/fendo.2022.1043919]
52. Maizels M, Wolfe WJ. An expert system for headache diagnosis: the Computerized Headache Assessment tool (CHAT). Headache 2008 Jan;48(1):72-78. [doi: 10.1111/j.1526-4610.2007.00918.x] [Medline: 17868352]
53. Pasic A, Pasic L, Pasic A. The artificial intelligence based diagnostic assistant—AIDA. Presented at: 2022 IEEE 21st Mediterranean Electrotechnical Conference (MELECON); Jun 14-16, 2022; Palermo, Italy p. 114-119. [doi: 10.1109/MELECON53508.2022.9843070]
54. Rahimi SA, Kolahdoozi M, Mitra A, et al. Quantum-inspired interpretable ai-empowered decision support system for detection of early-stage rheumatoid arthritis in primary care using scarce dataset. Mathematics 2022 Feb;10(3):496. [doi: 10.3390/math10030496]
55. Razzaki S, Baker A, Perov Y, Middleton K, Baxter J, Mullarkey D, et al. A comparative study of artificial intelligence and human doctors for the purpose of triage and diagnosis. arXiv. Preprint posted online on Jun 27, 2018. [doi: 10.48550/arXiv.1806.10698]
56. Salmeron JL, Rahimi SA, Navali AM, Sadeghpour A. Medical diagnosis of Rheumatoid Arthritis using data driven PSO–FCM with scarce datasets. Neurocomputing 2017 Apr;232:104-112. [doi: 10.1016/j.neucom.2016.09.113]
57. Sanaeifar A, Eslami S, Ahadi M, Kahani M, Vakili Arki H. DxGenerator: An improved differential diagnosis generator for primary care based on MetaMap and semantic reasoning. Methods Inf Med 2022 Dec;61(5-06):174-184. [doi: 10.1055/a-1905-5639] [Medline: 35858654]
58. Shen EX, Lord A, Doecke JD, et al. A validated risk stratification tool for detecting high-risk small bowel Crohn's disease. Aliment Pharmacol Ther 2020 Jan;51(2):281-290. [doi: 10.1111/apt.15550] [Medline: 31769537]

XSL•FO
RenderX

59. Suárez-Araujo CP, García Báez P, Cabrera-León Y, et al. A real-time clinical decision support system, for mild cognitive impairment detection, based on a hybrid neural architecture. Comput Math Methods Med 2021;2021(5545297):5545297. [doi: 10.1155/2021/5545297] [Medline: 34257699]
60. Tsoi KKF. Application of artificial intelligence on a symptom diagnostic platform for telemedicine a pilot case study. Presented at: 2019 IEEE International Conference on Systems, Man and Cybernetics (SMC); Oct 6-9, 2019; Bari, Italy p. 806-813 URL: https://ieeexplore.ieee.org/xpl/mostRecentIssue.jsp?punumber=8906183 [accessed 2025-08-12] [doi: 10.1109/SMC.2019.8914229]
61. Velickovski F, Ceccaroni L, Roca J, et al. Clinical Decision Support Systems (CDSS) for preventive management of COPD patients. J Transl Med 2014 Nov 28;12(Suppl 2):25471545. [doi: 10.1186/1479-5876-12-S2-S9] [Medline: 25471545]
62. Velu SR, Ravi V, Tabianan K. Data mining in predicting liver patients using classification model. Health Technol 2022 Nov;12(6):1211-1235. [doi: 10.1007/s12553-022-00713-3]
63. Xiao T, Wang C, Yang M, et al. Use of virus genotypes in machine learning diagnostic prediction models for cervical cancer in women with high-risk human papillomavirus infection. JAMA Netw Open 2023 Aug 1;6(8):e2326890. [doi: 10.1001/jamanetworkopen.2023.26890] [Medline: 37531108]
64. Yoshihara A, Yoshimura Noh J, Inoue K, et al. Prediction model of Graves' disease in general clinical practice based on complete blood count and biochemistry profile. Endocr J 2022 Sep 28;69(9):1091-1100. [doi: 10.1507/endocrj.EJ21-0741] [Medline: 35387949]
65. Yu C, Peng YY, Liu L, Wang X, Xiao Q. Leukemia can be effectively early predicted in routine physical examination with the assistance of machine learning models. J Healthc Eng 2022;2022:8641194. [doi: 10.1155/2022/8641194] [Medline: 36465253]
66. Zardab M, Balarajah V, Banerjee A, et al. Differentiating ductal adenocarcinoma of the pancreas from benign conditions using routine health records: a prospective case-control study. Cancers (Basel) 2023 Jan;15(1):280. [doi: 10.3390/cancers15010280]
67. Zhang H, Yin M, Liu Q, et al. Machine and deep learning-based clinical characteristics and laboratory markers for the prediction of sarcopenia. Chin Med J 2023;136(8):967-973. [doi: 10.1097/CM9.0000000000002633]
68. Moons KGM, de Groot JAH, Bouwmeester W, et al. Critical appraisal and data extraction for systematic reviews of prediction modelling studies: the CHARMS checklist. PLoS Med 2014 Oct;11(10):e1001744. [doi: 10.1371/journal.pmed.1001744] [Medline: 25314315]
69. Moons KGM, Wolff RF, Riley RD, et al. PROBAST: a tool to assess risk of bias and applicability of prediction model studies: explanation and elaboration. Ann Intern Med 2019 Jan 1;170(1):W1-W33. [doi: 10.7326/M18-1377] [Medline: 30596876]
70. Wolff RF, Moons KGM, Riley RD, et al. PROBAST: a tool to assess the risk of bias and applicability of prediction model studies. Ann Intern Med 2019 Jan 1;170(1):51-58. [doi: 10.7326/M18-1376] [Medline: 30596875]
71. Andaur Navarro CL, Damen JAA, Takada T, et al. Risk of bias in studies on prediction models developed using supervised machine learning techniques: systematic review. BMJ 2021 Oct 20;375:n2281. [doi: 10.1136/bmj.n2281] [Medline: 34670780]
72. Kareemi H, Vaillancourt C, Rosenberg H, Fournier K, Yadav K. Machine learning versus usual care for diagnostic and prognostic prediction in the emergency department: a systematic review. Acad Emerg Med 2021 Feb;28(2):184-196. [doi: 10.1111/acem.14190] [Medline: 33277724]
73. Andaur Navarro CL, Damen JAA, van Smeden M, et al. Systematic review identifies the design and methodological conduct of studies on machine learning-based prediction models. J Clin Epidemiol 2023 Feb;154:8-22. [doi: 10.1016/j.jclinepi.2022.11.015] [Medline: 36436815]
74. Rajkomar A, Dean J, Kohane I. Machine learning in medicine. N Engl J Med 2019 Apr 4;380(14):1347-1358. [doi: 10.1056/NEJMra1814259] [Medline: 30943338]
75. Christodoulou E, Ma J, Collins GS, Steyerberg EW, Verbakel JY, Van Calster B. A systematic review shows no performance benefit of machine learning over logistic regression for clinical prediction models. J Clin Epidemiol 2019 Jun;110:12-22. [doi: 10.1016/j.jclinepi.2019.02.004] [Medline: 30763612]
76. Seinen TM, Fridgeirsson EA, Ioannou S, et al. Use of unstructured text in prognostic clinical prediction models: a systematic review. J Am Med Inform Assoc 2022 Jun 14;29(7):1292-1302. [doi: 10.1093/jamia/ocac058] [Medline: 35475536]
77. Zhang D, Yin C, Zeng J, Yuan X, Zhang P. Combining structured and unstructured data for predictive models: a deep learning approach. BMC Med Inform Decis Mak 2020 Oct 29;20(1):280. [doi: 10.1186/s12911-020-01297-6] [Medline: 33121479]
78. Hager P, Jungmann F, Holland R, et al. Evaluation and mitigation of the limitations of large language models in clinical decision-making. Nat Med 2024 Sep;30(9):2613-2622. [doi: 10.1038/s41591-024-03097-1] [Medline: 38965432]
79. Liu Y, Chen PH, Krause J, Peng L. How to read articles that use machine learning: users' guides to the medical literature. JAMA 2019 Nov 12;322(18):1806-1816. [doi: 10.1001/jama.2019.16489] [Medline: 31714992]
80. Sujan M, Smith-Frazer C, Malamateniou C, et al. Validation framework for the use of AI in healthcare: overview of the new British standard BS30440. BMJ Health Care Inform 2023 Jun;30(1):e100749. [doi: 10.1136/bmjhci-2023-100749] [Medline: 37364922]

XSL•FO
RenderX

81. Collins GS, Reitsma JB, Altman DG, Moons KGM. Transparent Reporting of a multivariable prediction model for Individual Prognosis or Diagnosis (TRIPOD): the TRIPOD statement. J Clin Epidemiol 2015 Feb;68(2):134-143. [doi: 10.1016/j.jclinepi.2014.11.010] [Medline: 25579640]
82. Collins GS, Moons KGM, Dhiman P, et al. TRIPOD+AI statement: updated guidance for reporting clinical prediction models that use regression or machine learning methods. BMJ 2024 Apr 16;385:e078378. [doi: 10.1136/bmj-2023-078378] [Medline: 38626948]

Abbreviations

AI: artificial intelligence
CHARMS: Checklist for Critical Appraisal and Data Extraction for Systematic Reviews of Prediction Modelling Studies
COPD: chronic obstructive pulmonary disease
EHR: electronic health record
GP: general practitioner
***ICD-10*:** *International Statistical Classification of Diseases, Tenth Revision*
ML: machine learning
PC: primary care
PRISMA: Preferred Reporting Items for Systematic Reviews and Meta-Analyses
PROBAST: Prediction Model Risk of Bias Assessment Tool
PROBAST-AI: Prediction Model Risk of Bias Assessment Tool-Artificial Intelligence
TRIPOD: Transparent Reporting of a Multivariable Prediction Model for Individual Prognosis or Diagnosis

Edited by A Benis; submitted 03.06.24; peer-reviewed by B Delaney, D Chrimes, D Manuel; revised version received 06.06.25; accepted 09.06.25; published 22.08.25.

Please cite as:
Hunik L, Chaabouni A, van Laarhoven T, Olde Hartman TC, Leijenaar RTH, Cals JWL, Uijen AA, Schers HJ
Diagnostic Prediction Models for Primary Care, Based on AI and Electronic Health Records: Systematic Review
JMIR Med Inform 2025;13:e62862
URL: https://medinform.jmir.org/2025/1/e62862
doi:10.2196/62862

© Liesbeth Hunik, Asma Chaabouni, Twan van Laarhoven, Tim C olde Hartman, Ralph T H Leijenaar, Jochen W L Cals, Annemarie A Uijen, Henk J Schers. Originally published in JMIR Medical Informatics (https://medinform.jmir.org), 22.8.2025. This is an open-access article distributed under the terms of the Creative Commons Attribution License (https://creativecommons.org/licenses/by/4.0/), which permits unrestricted use, distribution, and reproduction in any medium, provided the original work, first published in JMIR Medical Informatics, is properly cited. The complete bibliographic information, a link to the original publication on https://medinform.jmir.org/, as well as this copyright and license information must be included.

XSL•FO
RenderX

Performance of Natural Language Processing for Information Extraction From Electronic Health Records Within Cancer: Systematic Review

Simon Dahl[1,2], MSc; Martin Bøgsted[1,2,3], PhD; Tomer Sagi[4], PhD; Charles Vesteghem[1,2,3], PhD

[1]Center for Clinical Data Science, Department of Clinical Medicine, Aalborg University, Selma Lagerløfs Vej 249, Gistrup, Denmark

[2]Center for Clinical Data Science, Research, Education and Innovation, Aalborg University Hospital, Aalborg, Denmark

[3]Clinical Cancer Research Centre, Department of Clinical Medicine, Aalborg University Hospital, Aalborg, Denmark

[4]Department of Computer Science, Aalborg University, Aalborg, Denmark

Corresponding Author:
Simon Dahl, MSc
Center for Clinical Data Science, Department of Clinical Medicine, Aalborg University, Selma Lagerløfs Vej 249, Gistrup, Denmark

Abstract

Background: Over the last decade, natural language processing (NLP) has provided various solutions for information extraction (IE) from textual clinical data. In recent years, the use of NLP in cancer research has gained considerable attention, with numerous studies exploring the effectiveness of various NLP techniques for identifying and extracting cancer-related entities from clinical text data.

Objective: We aimed to summarize the performance differences between various NLP models for IE within the context of cancer to provide an overview of the relative performance of existing models.

Methods: This systematic literature review was conducted using 3 databases (PubMed, Scopus, and Web of Science) to search for articles extracting cancer-related entities from clinical texts. In total, 33 articles were eligible for inclusion. We extracted NLP models and their performance by F_1-scores. Each model was categorized into the following categories: rule-based, traditional machine learning, conditional random field-based, neural network, and bidirectional transformer (BT). The average of the performance difference for each combination of categorizations was calculated across all articles.

Results: The articles covered various scenarios, with the best performance for each article ranging from 0.355 to 0.985 in F_1-score. Examining the overall relative performances, the BT category outperformed every other category (average F_1-score between 0.2335 and 0.0439). The percentage of articles on implementing BTs has increased over the years.

Conclusions: NLP has demonstrated the ability to identify and extract cancer-related entities from unstructured textual data. Generally, more advanced models outperform less advanced ones. The BT category performed the best.

(JMIR Med Inform 2025;13:e68707) doi:10.2196/68707

KEYWORDS

natural language processing; information extraction; clinical textual data; performance; F1-score; review; rule-based solutions; traditional machine learning; neural network; bidirectional transformer

Introduction

Electronic health records (EHRs) are increasingly being adopted by health care providers worldwide, as they offer numerous benefits [1]. This has led to an increase in the quantity of data stored in EHRs, consisting of both structured and unstructured data (eg, text, images, and time series). Unstructured textual data from discharge summaries, radiology reports, clinical notes, and patient histories provide valuable information about patients that may not be captured by structured data alone [2]. The extraction of clinical parameters from unstructured textual data, also known as information extraction (IE), has proven to be valuable in health care, such as in clinical research (eg, epidemiology) and decision support systems [3,4].

However, working with unstructured textual data presents several challenges to health care providers and researchers. The volume of free text makes manual extraction and analysis time-consuming and resource-heavy, thereby limiting their utility and requiring automated solutions. Moreover, the lack of standardization and consistency in formatting and terminology makes it difficult to accurately identify and extract the relevant information in an automated manner. Furthermore, free text is prone to spelling errors, resulting in inaccurate or harder-to-find

XSL•FO
RenderX

patient information for methods that rely on keyword extraction or other exact-match search techniques.

Natural language processing (NLP) techniques are well suited for extracting information from free text because of their ability to process, comprehend, and generate human language in a manner that allows for automatic extraction of structured information from free text. In recent years, NLP has gained considerable attention, with numerous studies exploring the effectiveness of various NLP techniques, notably for identifying and extracting cancer-related entities, such as smoking history [2], toxicities [5], and Gleason scores [6], which are only recorded as free text in clinical notes. These techniques are known as named entity recognition, or more generally, IE [7-9].

A variety of techniques and pipelines have been developed for IE from medical free texts, ranging from simple rule-based solutions to advanced machine learning approaches. Rule-based solutions allow domain experts to define a set of linguistic rules and patterns to be implemented to identify and extract relevant information from clinical notes and medical free-form texts. Studies have shown that rule-based approaches can outperform machine-learning models [10-13]. However, rule-based approaches are custom-made for specific datasets and use cases, require manual specification of rules by medical experts, and are therefore difficult to generalize [3]. Moreover, machine learning models allow for multiple methodologies and applications for different IE problems, solved by training specific traditional machine learning models such as support vector machines, decision trees, and neural networks (NNs). Recently, bidirectional transformers (BTs) such as large language models (LLM) have been identified as a possible tool for IE because of their strengths in pattern recognition, text summarization, and generation [14]. LLMs allow for pretraining on large text corpora, which enables them to learn linguistic patterns applicable to different IE tasks. Furthermore, LLMs show promising results for specific tasks because of the domain-specific fine-tuning of pretrained models [15].

Over the years, numerous models have been developed for various IE tasks, but their relative performance across different datasets remains largely unknown. Both rule-based and machine learning approaches often exhibit limited generalizability between tasks, and their results are frequently inconsistent when applied to different datasets. This inconsistency highlights the need for studies that investigate and compare the relative performance of these models.

To the best of our knowledge, no review has been conducted that summarizes the differences in the performance of various types of NLP models for IE within the context of cancer. This review provides an overview of the various NLP methods used for IE and compares them in terms of their performance.

Methods

This systematic review followed the Preferred Reporting Items for Systematic Reviews and Meta-Analyses (PRISMA) guidelines.

We searched 3 databases—PubMed, Scopus, and Web of Science—for relevant literature published between January 1, 2014, and April 19, 2024 (Multimedia Appendix 1). The following search criteria were used for the titles and abstracts:

("information extraction" OR "natural language processing" OR "nlp") AND (EHR OR notes OR reports) AND (cancer OR tumor OR oncology)

The inclusion criterion for articles was the application of 2 or more NLP models to extract identical cancer-related entities from the same unstructured medical text in EHR. Articles were excluded during title and abstract screening if they were as follows: (1) reviews; (2) articles that do not compare 2 or more NLP models; (3) articles whose purpose is not to extract information from free text from EHR; and (4) articles whose purpose is not to develop an NLP cancer-related application.

For further exclusion during the full-text screening, articles were excluded if they were defined as follows: (1) abstract only; (2) text classification without cancer entity extraction; (3) results within the article were not compatible; (4) no NLP application development; (5) not related to cancer IE from EHR; and (6) no comparison with other NLP methods within the article.

Using the exclusion criteria, one author (SCD) performed 2 rounds of article selection: title and abstract screening, followed by a full-text review. A second reviewer (CV) was consulted for unclear cases during the screening.

Data from each of the included articles were extracted by 2 authors (SCD and CV). Both authors independently categorized the NLP models and extracted their performance metrics. Any discrepancies in categorization were resolved through consensus guided by consideration of the primary architectural components of the model. Each model was categorized into the following groups: rule-based, traditional machine learning (ML), conditional random field (CRF)–based, NN, and BT.

The rule-based category includes IE models that use regular expressions (Regex), keywords, and dictionary matching. The CRF-based category includes linear CRF, except bidirectional long short-term memory-CRF, which is in the NN category. The NN category includes NNs, except for BTs, that belong to the BT category. Ensemble models are categorized as the most advanced part of the ensemble. For example, a rule-based model combined with a BT is categorized as a BT model (see Table 1). For articles that included both strict and relaxed keyword matching, the strict F_1-scores were extracted as the performance metric. For articles presenting both macro- and micro-averaged F_1-scores, macro-averaged F_1-scores were extracted.

XSL•FO
RenderX

Table . Method categorization of models.

Category	Included models	Articles using category	Total number of models implemented
Rule-based	• Regular expressions • keyword, term, and dictionary matching	[10-13,16-22] (n=11)	12
CRF[a]-based	• Linear CRF • CRF + Rule-based	[10,12,16-18,20,23,24] (n=8)	26
Bidirectional transformer	• BERT[b] • BlueBERT • BioBERT • CharBERT • Character-BERT • CancerBERT • RoBERTa • MBERT (multilingual BERT) • BETO • XLM-R • ClinicalBERT • XLNet • Bidirectional Transformer + Rule-based • Bidirectional Transformer + BiLSTM[c]-CRF	[11,15-17,21,23-33] (n=16)	60
Neural network	• BiGRU • BiRNN • CNN • LSTM • BiLSTM-CRF • RNN • MLP, • HAN, • SLA, • CNN + Rule-based	[15-20,24-26,28-43] (n=25)	83
Traditional machine learning	• SVM[d] • Random forest • Naïve Bayes • Extreme Gradient Boosting • AdaBoost	[13,22,27,30,34-43] (n=14)	39

[a]CRF: conditional random field.

[b]BERT: Bidirectional Encoder Representations from Transformers.

[c]BiLSTM: bidirectional long short-term memory.

[d]SVM: support vector machine.

To calculate the performance differences for all categories across the included articles, the following steps were executed for all categories.

The best-performing model for each category within each article was selected. The best-performing model within category c for article a is given by maxc,a:

$$\text{maxc,a} = \max(\text{Pc,m1,Pc,m2,}\ldots\text{,Pc,mn})$$

where P is the F_1 performance score of method m within category c. n is the number of methods within category c.

Having the best-performing categories within an article allows for calculation of the category difference for each combination of categories. Category differences for categories c^1 and c^2 within article a are given as category_diffc1,c2,a:

$$\text{category_diffc1,c2,a} = \text{maxc1,a} - \text{maxc2,a}$$

where maxc,a is the best performing model of category c in article a.

All performance differences of the same combination of categories were averaged across all the articles. The average of the category difference for all articles with combination c^1 and c^2 is given as performance_differencec1,c2 :

$$\text{performance_difference c1,c2} = \text{category_diff c1,c2,1} + \text{category_diff c1,c2,2} + \text{category_diff c1,c2,m}$$

XSL•FO
RenderX

where category_diffc1,c2,a is the category difference between c^1 and c^2 in article a. n is the number of articles with a specific category combination.

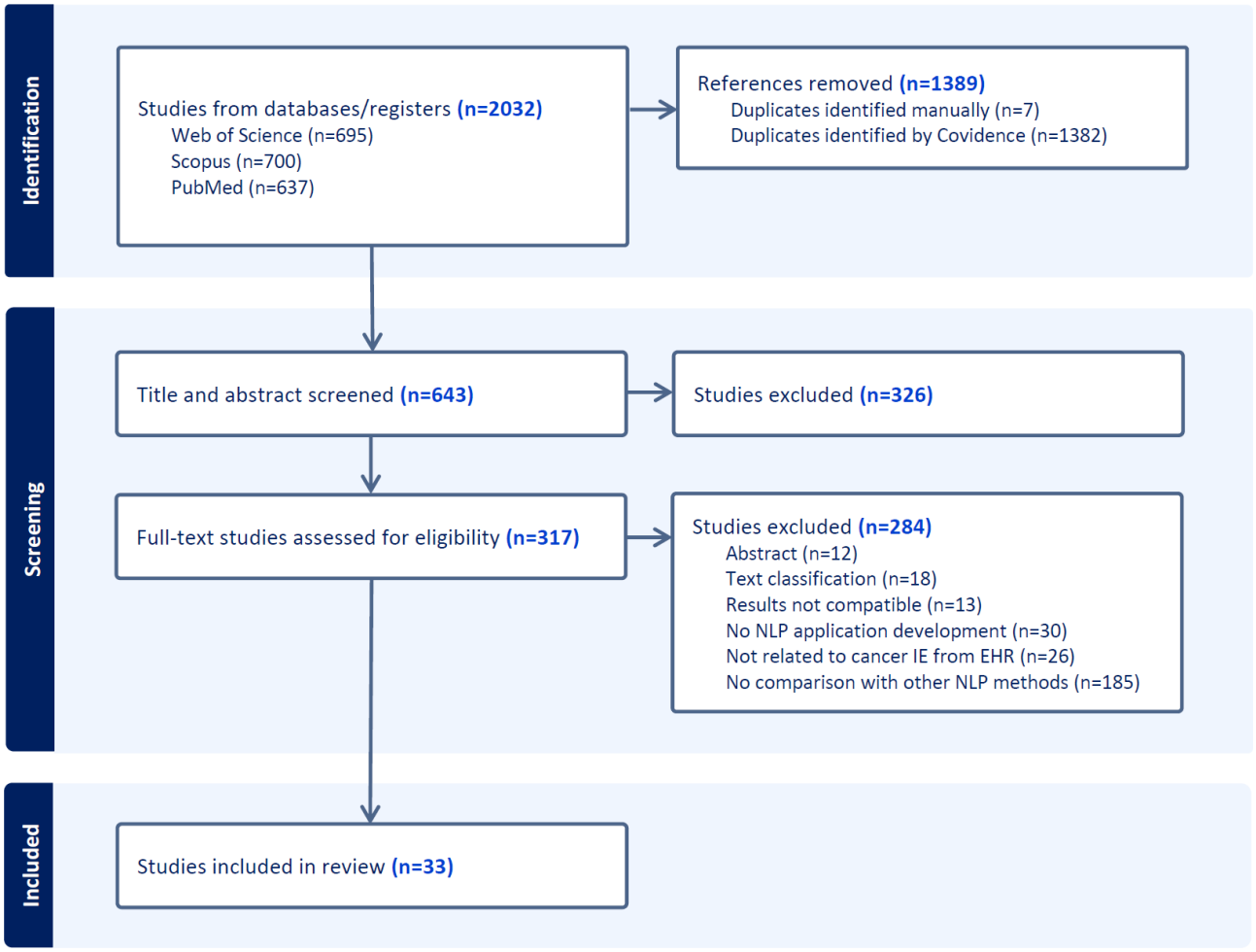
Statistical significance between categories for each category combination was determined using a t test (P<.05).

Results

Overview

The article selection process is detailed in a PRISMA flowchart, shown in Figure 1. A total of 2032 articles were identified through searches in Web of Science, Scopus, and PubMed.

Figure 1. The PRISMA (Preferred Reporting Items for Systematic Reviews and Meta-Analyses) flowchart for article selection.



In total, 33 articles were included in this review. The articles were published between 2018 and 2024. They compared at least 2 NLP models for cancer-related IE from unstructured medical texts in EHRs. The articles contained a total of 220 implementations of NLP models. Selecting only the best-performing models within each category of each article summarizes 74 implementations.

Models

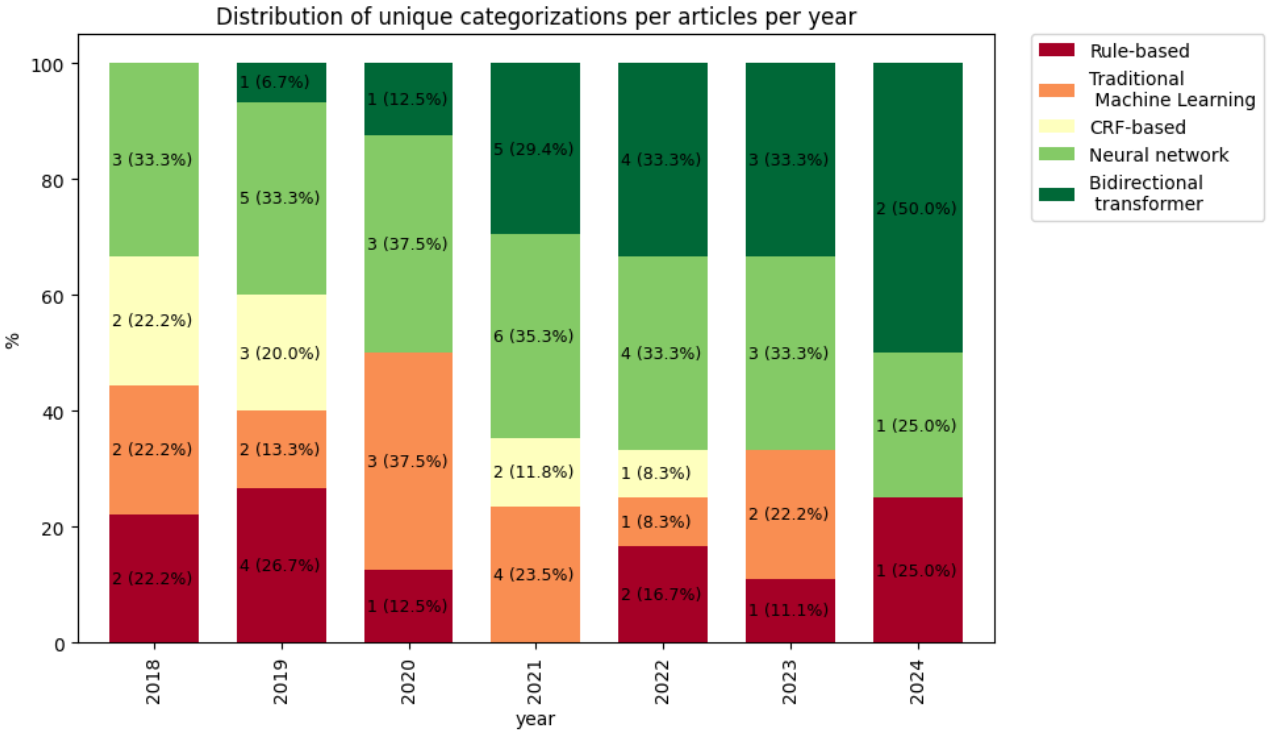
We categorized each NLP model as rule-based, CRF-based, BT, NN, and ML. Table 1 shows how each model was categorized and the articles in which the categories are contained.

Table 1 shows the categorization of the models, which articles contain the specific categories, and the total number of implemented models within each category.

The most frequently used category was NN, with 25 occurrences, followed by BT and ML with 16 and 11 occurrences, respectively. The most frequently implemented category was NN, with 83 implementations. The distribution of unique categorizations per year shows the variety of models that have been used throughout the years (see Figure 2). Notably, the percentage of articles on the implementation of BTs has increased over the years.

XSL•FO
RenderX

Figure 2. Distribution of unique categorizations per article per year. CRF: conditional random field.



Performance

The performance varied a lot according to specific use cases. Inspecting the best-performing models of the specific articles shows that a total of 5 rule-based models performed best in their articles, with F_1-scores in the range of 0.73-0.887 (see Table 2). ML did not perform best in any article despite being compared in 14 articles with a total of 39 different model implementations, and neither did CRF-based. In total, 14 articles showed that NN performed the best, with F_1-scores ranging from 0.3539 to 0.972. BT performed the best in 13 articles, with F_1-scores ranging from 0.6023 to 0.97. Looking at the raw F_1-scores, more advanced models outperformed less advanced ones.

XSL•FO
RenderX

Table . Article overview.

Article	Year	Title	Number of tested models (best performing F_1-score within category)
AAlAbdulsalam et al [10]	2018	Automated extraction and classification of cancer stage mentions from unstructured text fields in a central cancer registry	Rule-based=1 (0.887)[a]; CRF[b]-based=1 (0.882)
Alawad et al [36]	2018	Coarse-to-fine multi-task training of convolutional neural networks for automated information extraction from cancer pathology reports	ML[c]=1 (0.626); NN[d]=2 (0.752)[a]
Miao et al [20]	2018	Extraction of BI-RADS findings from breast ultrasound reports in Chinese using deep learning approaches	Rule-based=1 (0.848); CRF-based=1 (0.881); NN=2 (0.904)[a]
Qiu et al [35]	2018	Deep learning for automated extraction of primary sites from cancer pathology reports	ML=3 (0.640); NN=3 (0.701)[a]
Chen et al [12]	2019	Using natural language processing to extract clinically useful information from Chinese electronic medical records	Rule-based=1 (0.83)[a]; CRF=1 (0.8)
Coquet et al [19]	2019	Comparison of orthogonal NLP methods for clinical phenotyping and assessment of bone scan utilization among prostate cancer patients	Rule-based=1 (0.897); NN=3 (0.918)[a]
Dubey et al [37]	2019	Inverse regression for extraction of tumor site from cancer pathology reports	ML=5 (0.759)[a]; NN=2 (0.701)
Kim et al [18]	2019	A study of medical problem extraction for better disease management	Rule-based=2 (0.883); CRF-based=4 (0.926); NN=5 (0.929)[a]
Thompson et al [34]	2019	Relevant word order vectorization for improved natural language processing in electronic health records	ML=7 (0.788); NN=7 (0.858)[a]
Zhang et al [17]	2019	Extracting comprehensive clinical information for breast cancer using deep learning methods	Rule-based=1 (0.484); NN=1 (0.887); CRF-based=1 (0.837); BT[e]=1 (0.935)[a]
Alawad et al [40]	2020	Automatic extraction of cancer registry reportable information from free-text pathology reports using multitask convolutional neural networks	ML=2 (0.615); NN=3 (0.752)[a]
Odisho et al [28]	2020	Natural language processing systems for pathology parsing in limited data environments with uncertainty estimation	ML=4 (0.948); NN=2 (0.972)[a]
Osborne et al [11]	2020	Identification of cancer entities in clinical text combining transformers with dictionary features	Rule-based=1 (0.73)[a]; BT=7 (0.7)
Wu et al [38]	2020	Structured information extraction of pathology reports with attention-based graph convolutional network	ML=1 (0.74); NN=6 (0.803)[a]
Hu et al [28]	2021	Automatic extraction of lung cancer staging information from computed tomography reports: deep learning approach	NN=2 (0.773); BT=1 (0.81)[a]

XSL•FO
RenderX

Article	Year	Title	Number of tested models (best performing F_1-score within category)
Liu et al [24]	2021	Use of BERT (Bidirectional Encoder Representations from Transformers)-based deep learning method for extracting evidences in Chinese radiology reports: development of a computer-aided liver cancer diagnosis framework	CRF-based=1 (0.729); NN=1 (0.832); BT=1 (0.857)[a]
López-García et al [23]	2021	Detection of tumor morphology mentions in clinical reports in Spanish using transformers	CRF-based=1 (0.794); BT=18 (0.89)[a]
Lu et al [27]	2021	Natural language processing and machine learning methods to characterize unstructured patient-reported outcomes: validation study	ML=2 (0.365); BT=1 (0.602)[a]
Park et al [43]	2021	Improving natural language information extraction from cancer pathology reports using transfer learning and zero-shot string similarity	ML=4 (0.484); NN=5 (0.502)[a]
Rios et al [42]	2021	Assigning ICD-O-3 codes to pathology reports using neural multi-task training with hierarchical regularization	ML=3 (0.276); NN=12 (0.355)[a]
Wu et al [41]	2021	BioIE: biomedical information extraction with multi-head attention enhanced graph convolutional network	ML=1 (0.444); NN=5 (0.613)[a]
Yu et al [26]	2021	A study of social and behavioral determinants of health in lung cancer patients using transformers-based natural language processing models	BT=4 (0.879)[a]; NN=2 (0.844)
Bozkurt et al [13]	2022	Expanding the secondary use of prostate cancer real world data: automated classifiers for clinical and pathological stage	Rule-based=1 (0.87)[a]; ML=1 (0.723)
Fang et al [16]	2022	Extracting clinical named entity for pituitary adenomas from Chinese electronic medical records	Rule-based=1 (0.431); CRF-based=16 (0.904); NN=1 (0.899); BT=1 (0.913)[a]
Hu et al [29]	2022	Using natural language processing and machine learning to preoperatively predict lymph node metastasis for non-small cell lung cancer with electronic medical records: development and validation study	NN=1 (0.701); BT=2 (0.948)[a]
Pabón et al [25]	2022	Negation and uncertainty detection in clinical texts written in Spanish: a deep learning-based approach	NN=2 (0.788); BT=1 (0.823)[a]
Zhou et al [15]	2022	CancerBERT: a cancer domain-specific language model for extracting breast cancer phenotypes from electronic health records	NN=1 (0.834); BT=8 (0.876)[a]
Ansoborlo et al [22]	2023	Prescreening in oncology trials using medical records. Natural language processing applied on lung cancer multidisciplinary team meeting reports	Rule-based=1 (0.932)[a]; ML=1 (0.68)

XSL•FO
RenderX

Article	Year	Title	Number of tested models (best performing F_1-score within category)
Rohanian et al [32]	2023	Using bottleneck adapters to identify cancer in clinical notes under low-resource constraints	NN=3 (0.83); BT=8 (0.97)[a]
Seong et al [31]	2023	Deep learning approach to detection of colonoscopic information from unstructured reports	NN=3 (0.985)[a]; BT=2 (0.982)
Zitu et al [30]	2023	Generalizability of machine learning methods in detecting adverse drug events from clinical narratives in electronic medical records	ML=1 (0.69); NN=2 (0.763); BT=2 (0.778)[a]
Martín-Noguerol et al [33]	2024	Natural language processing deep learning models for the differential between high-grade gliomas and metastasis: what if the key is how we report them?	NN=3 (0.872)[a]; BT=1 (0.766)
Hu et al [21]	2024	Zero-shot information extraction from radiological reports using ChatGPT	Rule-based=1 (0.926); BT=2 (0.957)[a]

[a]This is the best F_1-score for the article.

[b]CRF: conditional random field.

[c]ML: traditional machine learning.

[d]NN: neural network.

[e]BT: bidirectional transformer.

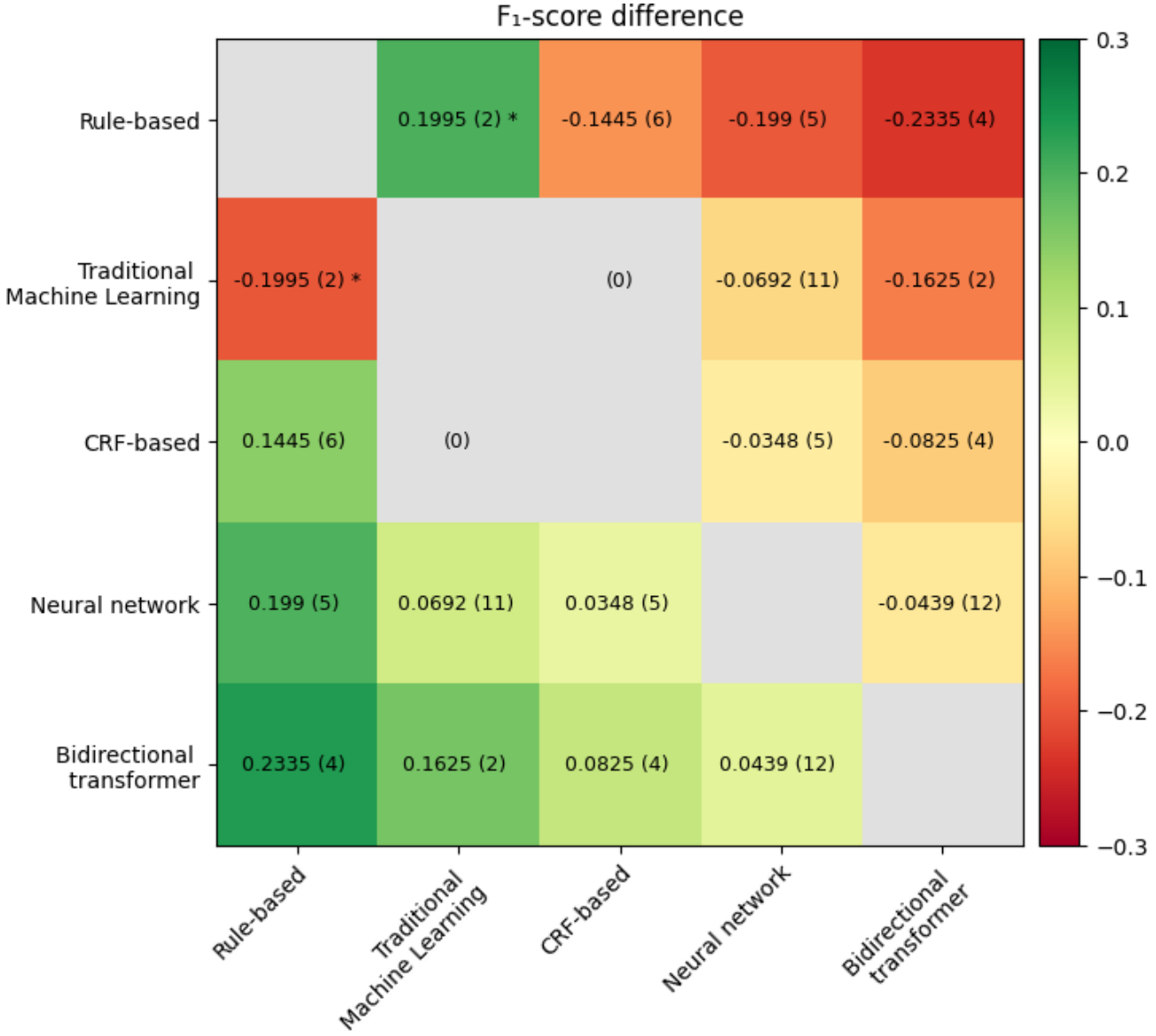
Table 2 shows each article and the number of models in each category within the article. Parentheses show the best F_1-score for each category. The best F_1-score for each article is marked by a footnote.

Some variations between the average F_1-score performance differences were observed (see Figure 3).

Our results show that more advanced models outperform less advanced ones. The largest difference between the category performance F_1-scores was observed between the BT category and the rule-based category. BT models were compared with rule-based models in 4 studies, yielding an average performance difference of 0.2335 in terms of F_1-score. BT was the best-performing category. NN outperformed CRF-based, ML, and rule-based models, while CRF-based outperformed rule-based models, and rule-based outperformed ML models. The only statistically significant difference between categories is observed when comparing rule-based and ML; see Multimedia Appendix 2 for *P* values.

XSL•FO
RenderX

Figure 3. Illustration of the average F_1-score performance differences for all combinations of the best model within each category. The parentheses indicate the number of comparisons between the categories. CRF: conditional random field. *P<.05.



Discussion

Principal Findings

This study provides an overview of the models used for IE in cancer and their performance in terms of the F_1-score. By including only articles with 2 or more NLP models for IE, we were able to evaluate the relative performance of each NLP within categories: rule-based, CRF-based, BT, NN, and ML.

The search string for this review combined keywords for techniques (IE and NLP), data sources (EHR, notes, reports), and the domain (cancer, tumor, and oncology) using Boolean operators to limit irrelevant results. The initial yield of 2032 articles suggests a reasonable balance, considering the stringent inclusion criteria. The "AND" clauses effectively limit the search while still including the relevant articles for the screening process. Although our search strategy included articles published from 01/01/2014, no articles prior to 2018 were included in the analysis. The reason for this discrepancy is not addressed within the scope of this review, which focused on quantifying performance differences between our categories. Notably, the most frequent reason for full-text exclusion was "No comparison with other NLP methods within the article (185 articles)." Arguing for common benchmark testing of the implemented NLP models.

Without considering a dataset or specific extraction entities, our results show that BT is the best performing category, followed by NN, CRF-based, rule-based, and ML in written order. We observed an increasing number of transformer-based models developed in recent years, with promising results. Our results highlight a pivotal moment in which BTs, such as language models, are on the verge of demonstrating their full potential in IE. Although transformers [44] and BERT [45] were introduced in 2017 and 2018, respectively, our literature review includes no articles using these technologies until 2019. This delay in time may reflect the time required for these models to become integrated into clinical research workflows. Surprisingly, rule-based solutions perform better than machine learning [13,22]. One explanation could be that rule-based solutions allow for the implementation of expert knowledge.

XSL•FO
RenderX

The lowest-performing articles in terms of F_1-score do not aim to show the best possible method for extraction, but rather how F_1-scores increase using hierarchical regularization when extracting ICD-O-3 codes [42]. Similarly, the study of Park et al [43] aims to show how to increase the F_1-score, using transfer learning and zero-shot string similarity, when the number of annotated pathology reports is limited.

Multiple reviews have been conducted within the scope of NLP in a clinical context with different aims. The review by Kreimeyer et al [46] aims to identify NLP systems capable of processing clinical free text and generating structured output, thereby compiling a list of NLP solutions in use. The review by Datta et al [47] defines relevant linguistic terms by organizing unstructured clinical text related to cancer into structured data using frame semantics. The review by Bilal et al [48] examines the current state-of-the-art literature on NLP applications in analyzing EHRs and clinical notes for cancer research, quantifying the number of studies for each cancer type and outlining the research challenges and future directions for NLP when analyzing EHRs and clinical notes in cancer research. However, no review has been conducted comparing the performance of NLP models for IE of cancer-related entities from clinical text, a gap relevant to clinical informatics and crucial for improving the accuracy of cancer-related data IE within EHRs. This is the first review to summarize and compare the performance of NLP models for IE of different cancer entities from unstructured text, offering insights for clinical researchers focused on leveraging EHR data for cancer care and research.

Strengths

One strength of our study was its ability to overcome the challenge of comparing low-performing models. By including only articles with 2 or more categories, we can determine the relative performance for each paper while neglecting low-performing models from papers that do not aim to beat state-of-the-art F_1-score. Our review shows how models can be categorized and how the categorizations perform compared to each other through different datasets and extraction entities. The performance differences observed in our included articles highlight the importance of selecting the appropriate NLP model for each health care application. Our categorizations allow all models to be included, even ensemble and hybrid models. Furthermore, our performance calculation uses the best-performing model for each category reported within each included article. This approach allows for the addition of multiple new categories to support the desired level of model performance granularity.

Limitations

A categorization strategy was required to categorize all models. Most models assign into well-defined and distinct categories. However, some could be assigned to multiple categories, notably bidirectional long short-term memory-CRF models. To present intelligible results, the number of categories had to be kept relatively low, neglecting model specificities. Increasing the number of categories would reduce the number of models in that category, making the results too anecdotal. Decreasing the number of categories would increase the number of times each categorization was compared, making the averaged F_1-scores less distinctive. Ideally, we would have wished for multiple studies implementing the same set of models and categorizations to avoid certain categorizations not being compared with every other category and to avoid certain combinations of categorizations occurring only once.

We selected the F_1-score as a metric for performance; precision or recall could also be used. However, extracting specific numbers from the confusion matrix can provide deeper insights. The included studies reported F_1-scores as a measure of performance. Although this is a practical method to generate 1 performance metric, its use has some limitations. In medical IE, one could argue that false negatives are worse than false positives, potentially leading to missed diagnoses or inappropriate treatment decisions, which is not considered in the F_1-score. While metrics such as AUC-ROC, precision-recall tradeoff, or specificity offer complementary insights, their calculation was limited by the inconsistent reporting of the necessary data. Furthermore, given the sensitive nature of EHR data and the need for clinical trust, future research should also prioritize evaluating the interpretability of IE models alongside traditional performance measures to allow clinicians to understand how cancer-related entities are being extracted and validated from EHR data.

Furthermore, our included studies neglected to address the handling of negation and spelling errors. Giorgia et al [49] showed that negations account for 66% of the errors. Another study stated that BERT fails completely to show a generalizable understanding of negation, raising questions about the aptitude of language models to learn this type of meaning [50]. In this study, BTs performed well; one could wish for a general approach to analyze the errors of each model instead of the general performance derived from the confusion matrix. Negation errors pose a significant challenge in EHR data and are critical in oncology, as a misidentified negated symptom or finding can alter clinical interpretation, treatment planning, and patient care.

Perspectives

The field of IE has evolved rapidly, and models, such as LLMs, have been successfully applied in the context of cancer IE, both in terms of model performance and operational efficiency [51]. LLM could allow for enhanced transferability and utility for different IE tasks on unstructured textual data. Using LLMs for IE on unstructured textual data seems feasible because of the variety of available pretrained models in different versions. Some might perform well out of the box or with minor domain-specific fine-tuning [15]. Generally, the evaluation of LLMs is challenging because of the lack of clarity regarding whether a public benchmark dataset has been used for training. However, when using data from EHRs, it is certain that they have not been used for training a public model.

Conclusions

NLP has demonstrated the ability to identify and extract cancer-related entities from unstructured medical textual data. Generally, most of the reviewed models showed excellent

XSL•FO
RenderX

performance in terms of the F_1-score, and more advanced models outperformed less advanced ones. The BT category performed the best, followed by NN. The use of BTs has increased in recent years. Rule-based applications for IE remain competitive in terms of performance in this specific context.

Acknowledgments

This study was supported solely by the institutional resources of the Center for Clinical Data Science at Aalborg University Hospital. We acknowledge the use of Covidence systematic review software (Veritas Health Innovation, Melbourne, Australia) for automatic identification and removal of duplicate articles.

Data Availability

The datasets used and analyzed in this study are available upon reasonable request from the corresponding author.

Authors' Contributions

All authors were involved in the conception and design of the study. SCD contributed to the collection and assembly of data. SCD and CV were involved in data analysis and interpretation. All authors contributed to manuscript writing, and all authors approved the final version of the manuscript.

Conflicts of Interest

None declared.

Multimedia Appendix 1
Search strategy.
[DOCX File, 12 KB - medinform_v13i1e68707_app1.docx]

Multimedia Appendix 2
Statistical significance of *t* test results.
[DOCX File, 14 KB - medinform_v13i1e68707_app2.docx]

Checklist 1
PRISMA 2020 checklist.
[PDF File, 67 KB - medinform_v13i1e68707_app3.pdf]

References

1. Evans RS. Electronic health records: then, now, and in the future. Yearb Med Inform 2016 May 20;Suppl 1(Suppl 1):S48-S61. [doi: 10.15265/IYS-2016-s006] [Medline: 27199197]
2. Ruckdeschel JC, Riley M, Parsatharathy S, et al. Unstructured data are superior to structured data for eliciting quantitative smoking history from the electronic health record. JCO Clin Cancer Inform 2023 Feb;7:e2200155. [doi: 10.1200/CCI.22.00155] [Medline: 36809022]
3. Landolsi MY, Hlaoua L, Ben Romdhane L. Information extraction from electronic medical documents: state of the art and future research directions. Knowl Inf Syst 2023;65(2):463-516. [doi: 10.1007/s10115-022-01779-1] [Medline: 36405956]
4. Spasić I, Livsey J, Keane JA, Nenadić G. Text mining of cancer-related information: review of current status and future directions. Int J Med Inform 2014 Sep;83(9):605-623. [doi: 10.1016/j.ijmedinf.2014.06.009] [Medline: 25008281]
5. Hong JC, Fairchild AT, Tanksley JP, Palta M, Tenenbaum JD. Natural language processing for abstraction of cancer treatment toxicities: accuracy versus human experts. JAMIA Open 2021 Feb 15;3(4):513-517. [doi: 10.1093/jamiaopen/ooaa064]
6. Yu S, Le A, Feld E, et al. A natural language processing-assisted extraction system for Gleason scores: development and usability study. JMIR Cancer 2021 Jul 2;7(3):e27970. [doi: 10.2196/27970] [Medline: 34255641]
7. Alkaitis MS, Agrawal MN, Riely GJ, Razavi P, Sontag D. Automated NLP extraction of clinical rationale for treatment discontinuation in breast cancer. JCO Clin Cancer Inform 2021 May;5(5):550-560. [doi: 10.1200/CCI.20.00139] [Medline: 33989016]
8. Benson R, Winterton C, Winn M, et al. Leveraging natural language processing to extract features of colorectal polyps from pathology reports for epidemiologic study. JCO Clin Cancer Inform 2023 Jan;7:e2200131. [doi: 10.1200/CCI.22.00131] [Medline: 36753686]
9. Si Y, Roberts K. A frame-based NLP system for cancer-related information extraction. AMIA Annu Symp Proc 2018;2018:1524-1533. [Medline: 30815198]

XSL•FO
RenderX

10. AAlAbdulsalam AK, Garvin JH, Redd A, Carter ME, Sweeny C, Meystre SM. Automated extraction and classification of cancer stage mentions from unstructured text fields in a central cancer registry. AMIA Jt Summits Transl Sci Proc 2018;2017:16-25. [Medline: 29888032]
11. Osborne JD, O'Leary T, Monte JD, Sasse K, Liang WH. Identification of cancer entities in clinical text combining transformers with dictionary features. In: CEUR Workshop Proceedings 2020, Vol. 2664:458-467.
12. Chen L, Song L, Shao Y, Li D, Ding K. Using natural language processing to extract clinically useful information from Chinese electronic medical records. Int J Med Inform 2019 Apr;124:6-12. [doi: 10.1016/j.ijmedinf.2019.01.004] [Medline: 30784428]
13. Bozkurt S, Magnani CJ, Seneviratne MG, Brooks JD, Hernandez-Boussard T. Expanding the secondary use of prostate cancer real world data: automated classifiers for clinical and pathological stage. Front Digit Health 2022;4:793316. [doi: 10.3389/fdgth.2022.793316] [Medline: 35721793]
14. Iannantuono GM, Bracken-Clarke D, Floudas CS, Roselli M, Gulley JL, Karzai F. Applications of large language models in cancer care: current evidence and future perspectives. Front Oncol 2023;13:1268915. [doi: 10.3389/fonc.2023.1268915] [Medline: 37731643]
15. Zhou S, Wang N, Wang L, Liu H, Zhang R. CancerBERT: a cancer domain-specific language model for extracting breast cancer phenotypes from electronic health records. J Am Med Inform Assoc 2022 Jun 14;29(7):1208-1216. [doi: 10.1093/jamia/ocac040] [Medline: 35333345]
16. Fang A, Hu J, Zhao W, et al. Extracting clinical named entity for pituitary adenomas from Chinese electronic medical records. BMC Med Inform Decis Mak 2022 Mar 23;22(1):72. [doi: 10.1186/s12911-022-01810-z] [Medline: 35321705]
17. Zhang X, Zhang Y, Zhang Q, et al. Extracting comprehensive clinical information for breast cancer using deep learning methods. Int J Med Inform 2019 Dec;132:103985. [doi: 10.1016/j.ijmedinf.2019.103985] [Medline: 31627032]
18. Kim Y, Meystre SM. A study of medical problem extraction for better disease management. Stud Health Technol Inform 2019 Aug 21;264:193-197. [doi: 10.3233/SHTI190210] [Medline: 31437912]
19. Coquet J, Bozkurt S, Kan KM, et al. Comparison of orthogonal NLP methods for clinical phenotyping and assessment of bone scan utilization among prostate cancer patients. J Biomed Inform 2019 Jun;94:103184. [doi: 10.1016/j.jbi.2019.103184] [Medline: 31014980]
20. Miao S, Xu T, Wu Y, et al. Extraction of BI-RADS findings from breast ultrasound reports in Chinese using deep learning approaches. Int J Med Inform 2018 Nov;119:17-21. [doi: 10.1016/j.ijmedinf.2018.08.009] [Medline: 30342682]
21. Hu D, Liu B, Zhu X, Lu X, Wu N. Zero-shot information extraction from radiological reports using ChatGPT. Int J Med Inform 2024 Mar;183:105321. [doi: 10.1016/j.ijmedinf.2023.105321] [Medline: 38157785]
22. Ansoborlo M, Gaborit C, Grammatico-Guillon L, Cuggia M, Bouzille G. Prescreening in oncology trials using medical records. Natural language processing applied on lung cancer multidisciplinary team meeting reports. Health Informatics J 2023;29(1):146045822211467. [doi: 10.1177/14604582221146709] [Medline: 36964666]
23. López-García G, Jerez JM, Ribelles N, Alba E, Veredas FJ. Detection of tumor morphology mentions in clinical reports in Spanish using transformers. In: Advances in Computational Intelligence 2021:24-35. [doi: 10.1007/978-3-030-85030-2_3]
24. Liu H, Zhang Z, Xu Y, et al. Use of BERT (Bidirectional Encoder Representations from Transformers)-based deep learning method for extracting evidences in chinese radiology reports: development of a computer-aided liver cancer diagnosis framework. J Med Internet Res 2021 Jan 12;23(1):e19689. [doi: 10.2196/19689] [Medline: 33433395]
25. Solarte Pabón O, Montenegro O, Torrente M, Rodríguez González A, Provencio M, Menasalvas E. Negation and uncertainty detection in clinical texts written in Spanish: a deep learning-based approach. PeerJ Comput Sci 2022;8:e913. [doi: 10.7717/peerj-cs.913] [Medline: 35494817]
26. Yu Z, Yang X, Dang C, et al. A study of social and behavioral determinants of health in lung cancer patients using transformers-based natural language processing models. AMIA Annu Symp Proc 2021;2021:1225-1233. [Medline: 35309014]
27. Lu Z, Sim JA, Wang JX, et al. Natural language processing and machine learning methods to characterize unstructured patient-reported outcomes: validation study. J Med Internet Res 2021 Nov 3;23(11):e26777. [doi: 10.2196/26777] [Medline: 34730546]
28. Hu D, Zhang H, Li S, Wang Y, Wu N, Lu X. Automatic extraction of lung cancer staging information from computed tomography reports: deep learning approach. JMIR Med Inform 2021 Jul 21;9(7):e27955. [doi: 10.2196/27955] [Medline: 34287213]
29. Hu D, Li S, Zhang H, Wu N, Lu X. Using natural language processing and machine learning to preoperatively predict lymph node metastasis for non-small cell lung cancer with electronic medical records: development and validation study. JMIR Med Inform 2022 Apr 25;10(4):e35475. [doi: 10.2196/35475] [Medline: 35468085]
30. Zitu MM, Zhang S, Owen DH, Chiang C, Li L. Generalizability of machine learning methods in detecting adverse drug events from clinical narratives in electronic medical records. Front Pharmacol 2023;14:1218679. [doi: 10.3389/fphar.2023.1218679] [Medline: 37502211]
31. Seong D, Choi YH, Shin SY, Yi BK. Deep learning approach to detection of colonoscopic information from unstructured reports. BMC Med Inform Decis Mak 2023 Feb 7;23(1):28. [doi: 10.1186/s12911-023-02121-7] [Medline: 36750932]

XSL•FO
RenderX

32. Rohanian O, Jauncey H, Nouriborji M, et al. Using bottleneck adapters to identify cancer in clinical notes under low-resource constraints. In: Proceedings of the 22nd Workshop on Biomedical Natural Language Processing and BioNLP Shared Tasks: Association for Computational Linguistics; 2023:62-78. [doi: 10.18653/v1/2023.bionlp-1.5]
33. Martín-Noguerol T, López-Úbeda P, Pons-Escoda A, Luna A. Natural language processing deep learning models for the differential between high-grade gliomas and metastasis: what if the key is how we report them? Eur Radiol 2024 Mar;34(3):2113-2120. [doi: 10.1007/s00330-023-10202-4] [Medline: 37665389]
34. Thompson J, Hu J, Mudaranthakam DP, et al. Relevant word order vectorization for improved natural language processing in electronic health records. Sci Rep 2019 Jun 25;9(1):9253. [doi: 10.1038/s41598-019-45705-y] [Medline: 31239489]
35. Qiu JX, Yoon HJ, Fearn PA, Tourassi GD. Deep learning for automated extraction of primary sites from cancer pathology reports. IEEE J Biomed Health Inform 2018 Jan;22(1):244-251. [doi: 10.1109/JBHI.2017.2700722] [Medline: 28475069]
36. Alawad M, Yoon HJ, Tourassi GD. Coarse-to-fine multi-task training of convolutional neural networks for automated information extraction from cancer pathology reports. Presented at: 2018 IEEE EMBS International Conference on Biomedical & Health Informatics (BHI); Mar 4-7, 2018; Las Vegas, NV, USA. [doi: 10.1109/BHI.2018.8333408]
37. Dubey AK, Yoon HJ, Tourassi GD. Inverse regression for extraction of tumor site from cancer pathology reports. Presented at: 2019 IEEE EMBS International Conference on Biomedical & Health Informatics (BHI); May 19-22, 2019; Chicago, IL, USA. [doi: 10.1109/BHI.2019.8834527]
38. Wu J, Tang K, Zhang H, Wang C, Li C. Structured information extraction of pathology reports with attention-based graph convolutional network. Presented at: 2020 IEEE International Conference on Bioinformatics and Biomedicine (BIBM); Dec 16-19, 2020; Seoul, South Korea. [doi: 10.1109/BIBM49941.2020.9313347]
39. Odisho AY, Park B, Altieri N, et al. Natural language processing systems for pathology parsing in limited data environments with uncertainty estimation. JAMIA Open 2020 Oct;3(3):431-438. [doi: 10.1093/jamiaopen/ooaa029] [Medline: 33381748]
40. Alawad M, Gao S, Qiu JX, et al. Automatic extraction of cancer registry reportable information from free-text pathology reports using multitask convolutional neural networks. J Am Med Inform Assoc 2020 Jan 1;27(1):89-98. [doi: 10.1093/jamia/ocz153] [Medline: 31710668]
41. Wu J, Zhang R, Gong T, Liu Y, Wang C, Li C. BioIE: biomedical information extraction with multi-head attention enhanced graph convolutional network. Presented at: 2021 IEEE International Conference on Bioinformatics and Biomedicine (BIBM); Dec 9-12, 2021; Houston, TX, USA. [doi: 10.1109/BIBM52615.2021.9669650]
42. Rios A, Durbin EB, Hands I, Kavuluru R. Assigning ICD-o-3 codes to pathology reports using neural multi-task training with hierarchical regularization. : ACM; 2021 Aug Presented at: BCB '21; Gainesville Florida p. 1-10. [doi: 10.1145/3459930.3469541]
43. Park B, Altieri N, DeNero J, Odisho AY, Yu B. Improving natural language information extraction from cancer pathology reports using transfer learning and zero-shot string similarity. JAMIA Open 2021 Jul;4(3):ooab085. [doi: 10.1093/jamiaopen/ooab085] [Medline: 34604711]
44. Vaswani A, Shazeer N, Parmar N, et al. Attention is all you need. arXiv. Preprint posted online on Jun 12, 2017. [doi: 10.48550/arXiv.1706.03762]
45. Devlin J, Chang MW, Lee K, Toutanova K. BERT: pre-training of deep bidirectional transformers for language understanding. arXiv. Preprint posted online on Oct 11, 2018. [doi: 10.48550/arXiv.1810.04805]
46. Kreimeyer K, Foster M, Pandey A, et al. Natural language processing systems for capturing and standardizing unstructured clinical information: a systematic review. J Biomed Inform 2017 Sep;73:14-29. [doi: 10.1016/j.jbi.2017.07.012] [Medline: 28729030]
47. Datta S, Bernstam EV, Roberts K. A frame semantic overview of NLP-based information extraction for cancer-related EHR notes. J Biomed Inform 2019 Dec;100:103301. [doi: 10.1016/j.jbi.2019.103301] [Medline: 31589927]
48. Bilal M, Hamza A, Malik N. NLP for analyzing electronic health records and clinical notes in cancer research: a review. J Pain Symptom Manage 2025 May;69(5):e374-e394. [doi: 10.1016/j.jpainsymman.2025.01.019] [Medline: 39894080]
49. Giorgia T, Johannes CS, Gerasimos S. A study of BERT's processing of negations to determine sentiment. : BNAIC/BeneLearn; 2021.
50. Ettinger A. What BERT is not: lessons from a new suite of psycholinguistic diagnostics for language models. Trans Assoc Comput Linguist 2020 Dec;8:34-48. [doi: 10.1162/tacl_a_00298]
51. Choi HS, Song JY, Shin KH, Chang JH, Jang BS. Developing prompts from large language model for extracting clinical information from pathology and ultrasound reports in breast cancer. Radiat Oncol J 2023 Sep;41(3):209-216. [doi: 10.3857/roj.2023.00633] [Medline: 37793630]

Abbreviations

BERT: Bidirectional Encoder Representations from Transformers
BT: bidirectional transformer
CRF: conditional random field
EHR: electronic health record
IE: information extraction

XSL•FO
RenderX

LLM: large language model
ML: machine learning
NLP: natural language processing
NN: neural network
PRISMA: Preferred Reporting Items for Systematic Reviews and Meta-Analyses

Edited by A Castonguay; submitted 12.11.24; peer-reviewed by A Chaturvedi, D Chrimes; revised version received 16.06.25; accepted 17.06.25; published 12.09.25.

Please cite as:
Dahl S, Bøgsted M, Sagi T, Vesteghem C
Performance of Natural Language Processing for Information Extraction From Electronic Health Records Within Cancer: Systematic Review
JMIR Med Inform 2025;13:e68707
URL: https://medinform.jmir.org/2025/1/e68707
doi:10.2196/68707

© Simon Dahl, Martin Bøgsted, Tomer Sagi, Charles Vesteghem. Originally published in JMIR Medical Informatics (https://medinform.jmir.org), 12.9.2025. This is an open-access article distributed under the terms of the Creative Commons Attribution License (https://creativecommons.org/licenses/by/4.0/), which permits unrestricted use, distribution, and reproduction in any medium, provided the original work, first published in JMIR Medical Informatics, is properly cited. The complete bibliographic information, a link to the original publication on https://medinform.jmir.org/, as well as this copyright and license information must be included.

XSL•FO
RenderX

The Role of AI in Cardiovascular Event Monitoring and Early Detection: Scoping Literature Review

Luis B Elvas[1,2], MSc; Ana Almeida[3], BSc; Joao C Ferreira[1,2], PhD

[1]Department of Logistics, Molde University College, Molde, Norway

[2]INESC INOV Rua Alves Redol, Lisbon, Portugal

[3]Instituto Universitário de Lisboa (ISCTE-IUL), ISTAR, Lisboa, Portugal

Corresponding Author:
Luis B Elvas, MSc
Department of Logistics, Molde University College, Molde, Norway

Abstract

Background: Artificial intelligence (AI) has shown exponential growth and advancements, revolutionizing various fields, including health care. However, domain adaptation remains a significant challenge, as machine learning (ML) models often need to be applied across different health care settings with varying patient demographics and practices. This issue is critical for ensuring effective and equitable AI deployment. Cardiovascular diseases (CVDs), the leading cause of global mortality with 17.9 million annual deaths, encompass conditions like coronary heart disease and hypertension. The increasing availability of medical data, coupled with AI advancements, offers new opportunities for early detection and intervention in cardiovascular events, leveraging AI's capacity to analyze complex datasets and uncover critical patterns.

Objective: This review aims to examine AI methodologies combined with medical data to advance the intelligent monitoring and detection of CVDs, identifying areas for further research to enhance patient outcomes and support early interventions.

Methods: This review follows the PRISMA (Preferred Reporting Items for Systematic Reviews and Meta-Analyses) methodology to ensure a rigorous and transparent literature review process. This structured approach facilitated a comprehensive overview of the current state of research in this field.

Results: Through the methodology used, 64 documents were retrieved, of which 40 documents met the inclusion criteria. The reviewed papers demonstrate advancements in AI and ML for CVD detection, classification, prediction, diagnosis, and patient monitoring. Techniques such as ensemble learning, deep neural networks, and feature selection improve prediction accuracy over traditional methods. ML models predict cardiovascular events and risks, with applications in monitoring via wearable technology. The integration of AI in health care supports early detection, personalized treatment, and risk assessment, possibly improving the management of CVDs.

Conclusions: The study concludes that AI and ML techniques can improve the accuracy of CVD classification, prediction, diagnosis, and monitoring. The integration of multiple data sources and noninvasive methods supports continuous monitoring and early detection. These advancements help enhance CVD management and patient outcomes, indicating the potential for AI to offer more precise and cost-effective solutions in health care.

(JMIR Med Inform 2025;13:e64349) doi:10.2196/64349

KEYWORDS

artificial intelligence; machine learning; cardiovascular diseases; cardiovascular events; health care; monitoring; early detection; AI; cardiovascular; literature review; medical data; detect; patient outcomes; neural network; ML model; mobile phone

Introduction

Artificial intelligence (AI) has revolutionized various aspects of our lives, showing exponential growth and advancements. The ubiquity of AI and its influence on nearly every facet of human life, from business and entertainment to technology, has not yet been fully realized in the field of medicine [1]. Despite these strides, machine learning (ML) in health care faces significant challenges, particularly in the realm of domain adaptation, where the goal is to apply ML models developed in one context to different but related health care settings. This is particularly crucial in health care, where the variability in patient demographics, disease prevalence, and health care practices across different regions and populations can affect the performance and reliability of ML models. Addressing these challenges is essential for ensuring that AI-driven technologies can be effectively and equitably applied across diverse health care environments [2].

The increasing availability of medical data, combined with advancements in AI techniques, creates new opportunities for

XSL•FO
RenderX

developing intelligent systems that can assist health professionals in the early detection and rapid intervention of cardiovascular events [3]. For instance, studies like Elvas et al [4] have demonstrated the capability of predictive models to anticipate myocardial ischemia incidents, enabling timely interventions and improving patient outcomes. One key advantage of AI in this context is its ability to analyze large volumes of complex data, uncovering patterns and correlations that might be missed by analysts [5,6]. This capability could be especially significant in the context of cardiology, the specific subject of our study, helping to provide a more comprehensive understanding of a patient's cardiovascular health.

Cardiovascular diseases (CVDs) remain the leading cause of mortality worldwide [7]. Globally, CVDs account for approximately 17.9 million deaths annually, representing 32% of all global deaths [8]. These conditions encompass a range of disorders affecting the heart and blood vessels, including coronary heart disease, rheumatic heart disease, congenital heart defects, and hypertension. The total number of CVD deaths and years of life lost are likely to increase as a result of population growth and aging [9], underscoring the critical need for effective methods to monitor and diagnose these conditions early.

The primary objective of this review is to address these gaps by conducting a comprehensive review of studies focusing on AI methodologies, in conjunction with medical data, that contributed to knowledge and progress in the intelligent monitoring, detection, prediction, and diagnosis of these kinds of diseases. Specially, this review aims to examine and synthesize current research on the application of AI and ML methodologies in CVD management. The study seeks to identify and evaluate various AI-driven approaches, including deep learning (DL) and ensemble methods, that have shown promise in improving the accuracy of CVD classification, risk assessment, and patient monitoring. Additionally, the review aims to highlight the potential of these technologies in enabling diverse treatment strategies, supporting health care professionals' decision-making processes, and ultimately enhancing patient outcomes. By assessing the current state of research, the review also intends to identify challenges, limitations, and areas for further investigation to guide future advancements in AI-driven cardiovascular care.

Despite the comprehensive nature of this review, it is important to acknowledge certain limitations and challenges that affected the search process. The review is confined to papers published between 2020 and 2024, which is a narrow year range, however, no papers were found outside of that range using that selected search query. Additionally, the search was limited to English-language publications, which may have resulted in the omission of valuable research published in other languages. One significant challenge is the variability in study quality across the selected literature. The rapidly evolving nature of AI and ML techniques in health care means that methodologies and reporting standards may vary considerably between studies, potentially affecting the comparability and generalizability of findings. Additionally, the integration of diverse AI methodologies presents a challenge in synthesizing results, as different approaches may have varying levels of interpretability and clinical applicability. The heterogeneity in data sources, sample sizes, and outcome measures across studies may also complicate the process of drawing cohesive conclusions. Furthermore, the field's fast-paced development means that some cutting-edge methodologies might be underrepresented in peer-reviewed literature at the time of this review. These limitations should be considered when interpreting the findings and their implications for clinical practice and future research directions in AI-driven cardiovascular care.

In summary, this literature review highlights the transformative potential of AI in health care, particularly in the domain of CVD. It underscored the significant global impact of CVD and the urgent need for improved methods of monitoring, detection, and early intervention. The review aims to explore how AI and ML techniques, when combined with extensive medical data, can advance our approach to managing cardiovascular health. By examining current methodologies and their practical implications, there were identified areas for further research and development. As health care evolves, incorporating intelligent systems may improve patient outcomes and support early interventions [10]. The potential for AI to transform cardiovascular health care is immense, offering the promise of more accurate diagnoses, personalized treatment plans, and improved patient outcomes.

Methods

The PRISMA (Preferred Reporting Items for Systematic Reviews and Meta-Analyses) methodology assisted the search by providing an organized structure and clear steps. Originally developed for medical research, PRISMA provides evidence-based guidelines to help authors transparently report their review process, methods, and findings [11].

This methodology ensures a rigorous literature review, providing a comprehensive overview of the current state of research on the use of AI in monitoring and detecting cardiovascular events in hospital settings.

The research conducted in May 2024 focused on literature related to the topic in review. The selection process involved developing a targeted search query, specifying the desired paper type, keywords, and subject areas. The search query was as follows:

("Machine Learning" OR "Data Analysis" OR "Artificial Intelligence" OR "AI" OR "Data Analytics") AND ("Cardiovascular events") AND ("Monitoring systems" OR "Early Detection" OR "Alert Systems") AND ("Hospital Data" OR "Medical Data" OR "Clinical Data" OR "Physiological Data") AND PUBYEAR>2017 AND PUBYEAR<2025 AND (LIMIT-TO (SRCTYPE , "j")) AND (LIMIT-TO (SUBJAREA , "COMP") OR LIMIT-TO (SUBJAREA , "ENGI") OR LIMIT-TO (SUBJAREA , "MATE") OR LIMIT-TO (SUBJAREA , "MATH")) AND (LIMIT-TO (DOCTYPE , "ar") OR LIMIT-TO (DOCTYPE , "re"))

The search was first applied on Scopus [12], and then, it was also attempted on the Web of Science website [13]. Textbox 1 illustrates the constructed search query, organized into sections based on keywords (Concepts, Population, Context, and Application). Additionally, specific limitations were defined,

XSL•FO
RenderX

including the publication year, document type, and subject areas. It should be noted that all the papers obtained through this search query were written in English.

Textbox 1. Process of keyword selection

Concepts (7,470,936 documents)

- Machine Learning
- Data Analysis
- Artificial Intelligence
- AI
- Data Analytics

Population (reduced to 23,858 documents)

- Hospital Data
- Medical Data
- Clinical Data
- Physiological Data

Context (reduced to 1601 documents)

- Monitoring systems
- Early Detection
- Alert Systems

Application (reduced to 248 documents)

- Cardiovascular events

Limitations (reduced to 64 documents)

- Date: 2017-2024
- Document Type: Article, Reviews
- Source Type: Journal
- Limited to: Computer Science, Mathematics, Engineering

The data publication year was limited to 2017 - 2024, because there were no papers, attending to the other limitations, outside of that range. This may be caused by the need to improve the health care system, combined with technological advances and available data, causing a lot of interest in this area, leading researchers to publish papers as a way of satisfying this need.

The search process yielded a progressive refinement of results, starting from an initial pool of 7,470,936 documents, then 1601 documents, culminating in a final selection of 64 relevant papers, after adding the limitations. This significant reduction reflects the effectiveness of our targeted search strategy and filtering process. The final set of 64 documents represents a focused collection of recent, relevant research in the application of AI to cardiovascular event monitoring and detection.

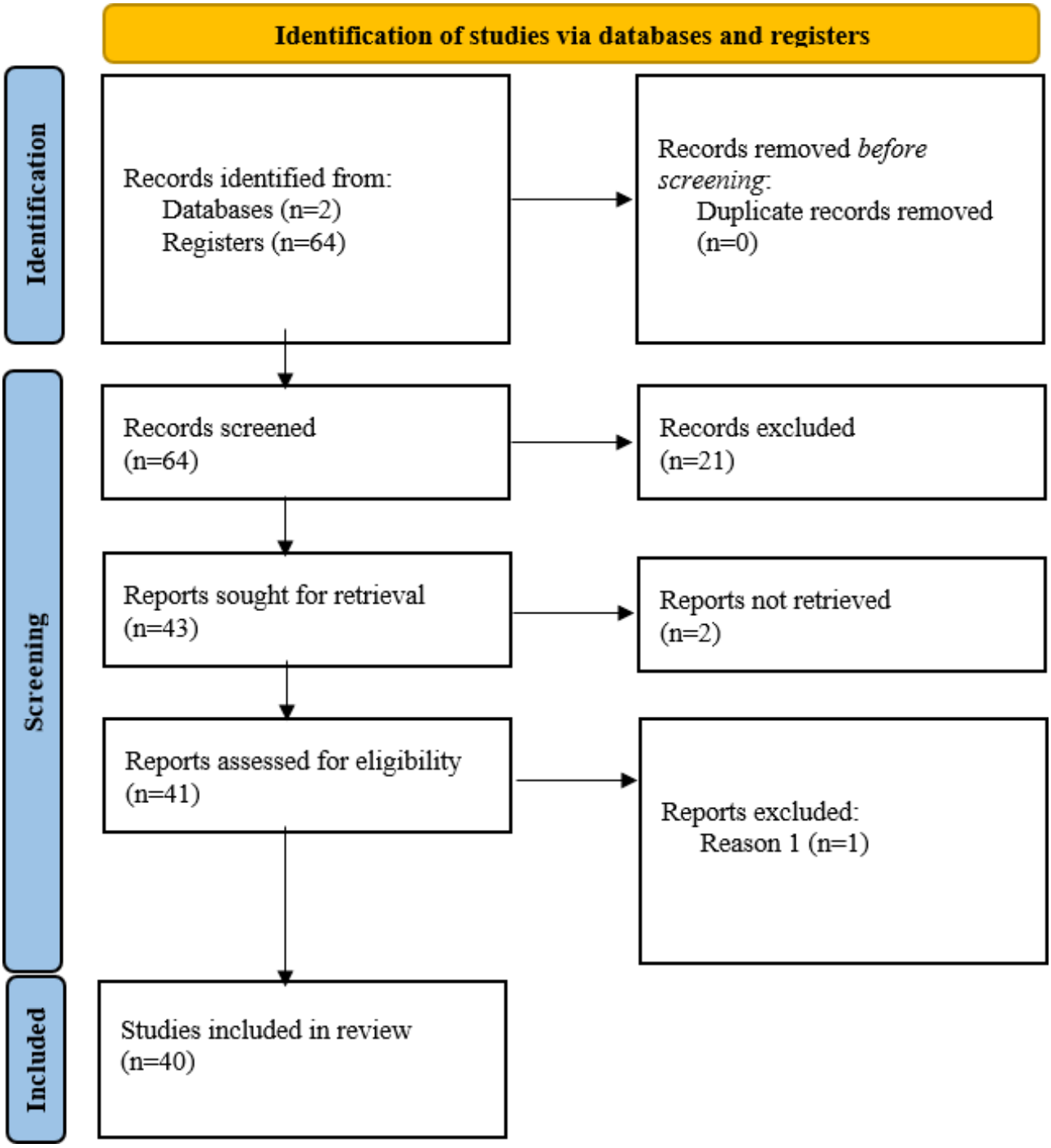
Results

Overview

All the papers that have been selected came from a selection process detailed in the PRISMA flow diagram (Figure 1).

XSL•FO
RenderX

Figure 1. PRISMA flow diagram with the state-of-the-art results. PRISMA: Preferred Reporting Items for Systematic Reviews and Meta-Analyses.



The first step in the process included the removal of duplicated records, and then, a second selection was made based on the title and abstract, where 21 papers did not meet the standards. Essentially, all papers that did not focus on CVDs or events were excluded. After that, the papers that could not be retrieved were removed. In the final step, after analyzing the papers in their entirety, a selection was made, where the papers that were not relevant and that did not meet the established goal would be eliminated. In practice, it meant that any paper that did not have ML applications for the monitoring, detection or diagnosis of cardiovascular events, and diseases were excluded.

As it is shown in Figure 1, 64 documents were retrieved initially, but, after the screening, 40 studies were left in total to include. All the papers selected for this review were published between 2020 and 2024.

The remaining papers selected for inclusion were then subjected to a detailed analysis to extract data. Key themes and concepts were identified through a keyword extraction process, allowing for the categorization of papers into relevant thematic areas. This initial categorization facilitated the identification of common trends across the literature. Subsequently, a deeper analysis was conducted, focusing on the specific methodologies, objectives, results, and conclusions of each study. This in-depth examination enabled a more nuanced understanding of the research landscape, allowing for the identification of recurring approaches, significant findings, and emerging trends in the

XSL•FO
RenderX

field of AI applications for CVD management. The results and discussion chapter were then constructed based on this comprehensive analysis, synthesizing the extracted data to present an overview of the current state of research in this domain.

Outcome Analysis

Overview

Analyzing the application goals keywords in Table 1, the one with the biggest representation was “Early Detection” present in 31 (78%) papers, followed by “Risk Assessment,” present in 14 (35%) of the final papers. On the topics identified in the remaining 40 studies, there was a clear winner approach, as shown in Table 1: “Machine Learning” which appeared in 28 (70%) papers; however, the other techniques referenced were also related to ML, such as “Classification” and “Predictive Analysis.”

Table . Absolute frequency of the identified application goals and identified techniques within the studies included.

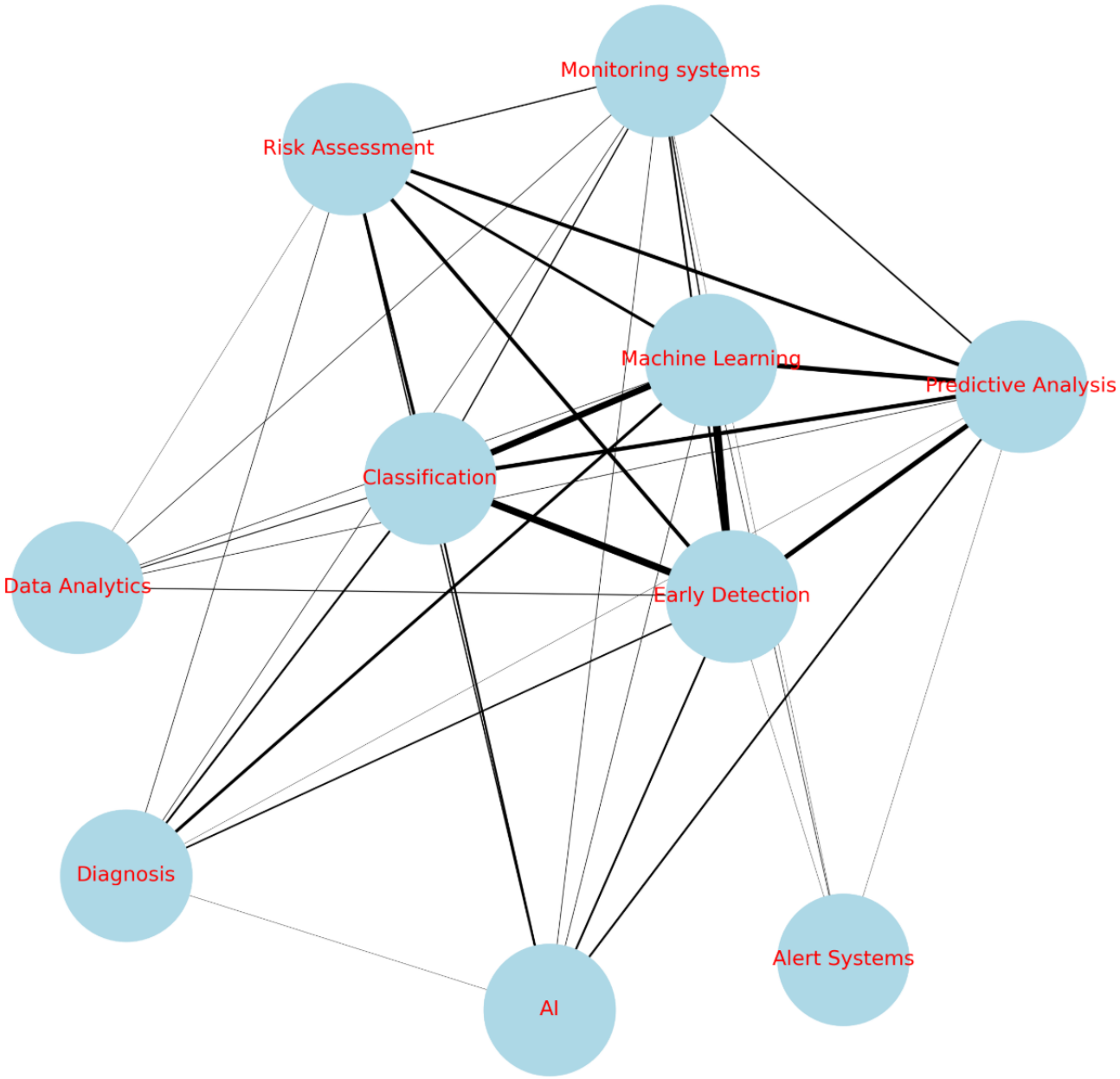
		Absolute frequency and percentage (n=40), n (%)
Application goals		
	Alert Systems	2 (5)
	Diagnosis	10 (25)
	Monitoring systems	11 (28)
	Risk Assessment	14 (35)
	Early Detection	31 (78)
Techniques		
	Data Analytics	3 (8)
	AI[a]	9 (23)
	Predictive Analysis	19 (48)
	Classification	24 (60)
	Machine Learning	28 (70)

[a]AI: artificial intelligence.

In Figure 2, we present a visual representation of keyword relationships constructed using Python. Our analysis focused on the existing relationships between keywords within the reviewed papers, specifically in the context of AI and cardiovascular event detection. The keyword relationships revealed in this analysis offer insights into current research trends and potential gaps in the field of AI applications for cardiovascular health.

XSL•FO
RenderX

Figure 2. Keyword network. AI: artificial intelligence.



Key Findings

Frequent Combination

As expected, the most common keyword combination across the papers is "Machine Learning" paired with "Early Detection." This combination appears 22 times, accounting for 57.5% of the papers. This strong association underscores a significant focus on developing predictive models for timely identification of cardiovascular risks. This trend suggests a shift toward more proactive health care strategies, where AI tools could potentially identify subtle indicators of cardiovascular issues before they become clinically apparent.

Additional Relationships

"Classification" correlates significantly with "Early Detection" and "Machine Learning." This could indicate an emphasis on developing nuanced categorization systems for cardiovascular conditions, potentially leading to more personalized treatment approaches.

A weaker relationship between "Predictive Analysis" and the concepts: "Machine Learning," "Early Detection," and "Classification" is also significant. This weaker but notable relationship hints at an emerging, more holistic approach to cardiovascular risk assessment. This could involve integrating diverse data sources and analytical methods for comprehensive, long-term health predictions.

Future Directions

Interestingly, the relative absence of strong connections to "Alert Systems" or specific CVDs suggests areas where research might be less developed, presenting opportunities for future studies.

These insights provide context for understanding the prevailing themes in the literature but also point to potential future directions in AI-driven cardiovascular care. They suggest a trajectory toward more integrated, proactive, and personalized

XSL•FO
RenderX

approaches in clinical practice, where AI tools could significantly enhance early detection, risk stratification, and treatment planning in cardiovascular medicine.

We organized the included references based on the specific topics they address, as outlined in Table 2. Recent years have witnessed significant growth in ML-based models and other innovative approaches, as evidenced by our evaluation of the selected studies.

Table . Papers by topic.

Topics	References	Papers (n=40), n (%)
Early Detection	[3,14-43]	31 (78)
Risk Assessment	[14,16,21,23,24,32,35-37,41,43-46]	14 (35)
Monitoring Systems	[17,24,35,37,39,40,46-50]	11 (28)
Diagnosis	[3,14,20,25,26,44,48,49,51,52]	10 (25)
Alert Systems	[38,50]	2 (5)

Early Detection of CVD

ML Techniques

Recent studies have explored various ML techniques for classifying CVDs. Rani et al [14], Ghasemieh et al [15], Prakash and Karthikeyan [26], and Nijaguna et al [48] present different approaches, each with its own merits:

- Rani et al [14] compared several algorithms, including Naïve Bayes, support vector machine, random forest (RF), and Adaboost. The RF model achieved the best results among these.
- Ghasemieh et al [15] introduced a stacking ensemble learner (SEL) algorithm. In addition to heart-related diagnoses, SEL can be applied for COVID-19-related diagnoses.
- Prakash and Karthikeyan [26] used a more complex Dual Layer Stacking Ensemble (DLSE) classification method. This ensemble approach helps in leveraging the strengths of different models to achieve better performance.
- Nijaguna et al [48] proposed a novel approach using a Selective Opposition strategy based on artificial rabbits optimization algorithm. This novel optimization algorithm is designed to handle the high-dimensional feature space of electrocardiogram (ECG) signals.

The first two studies [14,15] reported accuracy results in the range of 86% - 88%, while the last two [26,48] demonstrated improved performance, achieving accuracy scores above 90%. This progression suggests that more sophisticated ensemble methods and optimization strategies may yield better classification results for CVD.

Another set of papers highlights the promising applications of ML for the prediction of CVD. Theerthagiri and Vidya [21] and Theerthagiri [36] focus on CVD prediction using feature elimination techniques, both achieving accuracy values of 88%. Singh et al [27] compares several traditional ML algorithms for CVD prediction such as decision trees (DT), k-nearest neighbors (KNN), artificial neural networks, and Extreme Gradient Boosting (XGBoost). Among these, XGBoost demonstrated the best performance with an accuracy of 73%. While this accuracy is lower than in some other studies, it is worth noting that the comparison of multiple algorithms provides valuable insights into their relative strengths in CVD prediction.

In a more innovative approach, Safa et al [37] introduces a hybrid clustering–based disease assessment model. This model aims to monitor patients' cardiac and anatomic conditions, predict diseases and associated risks, and use a clustering approach to analyze patient data. The hybrid clustering–based disease assessment model achieved impressive results with prediction accuracy of up to 96% and lower error rates. This high accuracy suggests that hybrid approaches combining clustering with traditional ML techniques may offer significant improvements in CVD prediction.

Several studies focus on predicting and detecting specific cardiovascular conditions, demonstrating the versatility of ML in addressing various aspects of heart health.

Nasarian et al [19], Al-Ssulami et al [30], and Selvaraj et al [33] specifically address coronary artery disease (CAD) prediction and detection. Selvaraj et al [33] combines ML and image processing techniques for CAD prediction and detection. Using three classifiers (RF, gradient boosting tree, and multilayer perceptron [MLP]), it achieved scores higher than 95 in precision, recall, and F_1-score. Nasarian et al [19] introduces a Heterogeneous Hybrid Feature Selection algorithm, combined with the Synthetic Minority Oversampling Technique for data balancing. This approach achieved an accuracy of 80%. Al-Ssulami et al [30] pair a ML model with an augmented dataset approach for early CVD prediction. Using a DT classifier, they achieved 99.2% accuracy with the Cleveland dataset. These exceptionally high accuracy rates suggest that data augmentation could be a powerful tool in improving ML model performance for CVD prediction.

Daliri et al [29] explores a heptagonal reinforcement learning model for predicting sinus and nonsinus arrhythmias. However, the results indicate that the model's performance needs improvement, as the prediction accuracy was suboptimal. This highlights the challenges in applying reinforcement learning to complex medical prediction tasks and suggests areas for future research.

Itzhak et al [35] proposes a prediction model based on temporal abstraction and frequent temporal interval relational sequence patterns to predict acute hypotensive episodes. The approaches are to continuously predict "when" or "whether" an acute

XSL•FO
RenderX

hypertensive episode will occur. The model's performance to each prediction task was:

- "When" prediction: area under the receiver operating characteristic curve of 0.82, area under precision-recall curve of 0.07;
- "Whether" prediction: area under the receiver operating characteristic curve of 0.74, area under precision-recall curve of 0.71.

These results demonstrate the potential of temporal pattern analysis in predicting specific cardiovascular events, though the variation in performance metrics suggests that further refinement may be necessary.

DL Techniques

Recent research has explored various DL approaches for CVD classification and prediction. These studies demonstrate the potential of advanced DL techniques to significantly improve accuracy compared to conventional methods.

Dubey et al [28] and Manur et al [44] aim to classify CVD using different techniques: fuzzy deep convolutional network (FDCN) and a crow search optimization algorithm (CSOA), integrated with DL techniques, respectively. Both approaches significantly improve prediction accuracy compared to conventional classifiers, achieving scores above 95%.

Meanwhile, Nagarajan et al [52] discusses CVD classification through feature selection, using a genetic-based crow search algorithm with deep convolutional neural networks strategy. It reported an accuracy of 88.78% using all original features and 95.34% for extracted features, highlighting the critical role of feature selection and extraction in boosting the performance of DL models for classification tasks.

Abuhaija et al [41] uses various AI algorithms, such as MLP, ZeroR, and Naïve Bayes, to analyze, classify, and predict CVD. The MLP with backpropagation model achieved the highest performance, with an accuracy exceeding 95%. The MLP with backpropagation model proved to be accurate, rapid, and inexpensive medical decision-making. It has handled test datasets robustly and efficiently.

Nuryani et al [17] and Ghavidel et al [42] aim to predict and detect hypertension using convolution neural networks (CNN) and the need for cardiovascular surgery using deep neural networks, respectively. The first study achieved an F_1-score of 98.88, while the second reached a recall of 72%, which may vary depending on the dataset used.

In contrast, Abbas et al [18] uses both ML and DL techniques to identify heart abnormalities. The study uses algorithms such as KNN, RF, XGB, a Machine and Deep Learning–based Stacked Model, and DT for heart disease prediction. Among these, the Machine and Deep Learning–based Stacked Model achieved the highest accuracy, with a score of 94.14%. By gathering and growing more data, in this case, DL techniques better handled the prediction problem and produced better results.

Reviews

Parashar et al [31] explores the current state-of-the-art application of ML in the detection, categorization, and prediction of CVD and respiratory diseases. Key findings include the prevalent use of clinical features such as age, blood pressure (BP), and cholesterol for CVD prediction, and the dominance of CNN for feature selection. Challenges identified include the need for standardized frameworks, data privacy, and algorithm interpretability.

In Rani et al [3], researchers conclude that combining various ML algorithms (such as RF, support vector machine, XGBoost, AdaBoost, deep neural network or CNN, and KNN) with expert cardiologist input on feature prioritization and leveraging unstructured health care data can significantly enhance the accuracy of heart disease prediction systems. Collectively, these studies underscore the transformative potential of AI and ML in improving CVD classification accuracy.

Diagnosis of CVD

Some papers aim specifically at the diagnosis of these kinds of diseases. Al-Absi et al [20] presents a DL approach using the retinal image and dual-energy x-ray absorptiometry to diagnose CVD, achieving an accuracy of 78.3% in distinguishing between patients with CVD and controls. The findings suggest that integrating retinal images with dual-energy x-ray absorptiometry data improves the accuracy of CVD detection, while also highlighting the greater discriminatory power of fat content and bone mineral density over muscle mass and bone areas for CVD diagnosis. Chen et al [38] used self-supervised learning to pretrain generalized laboratory progress model with the aim of detecting CVD, which significantly improves the classification accuracy from 0.63 to 0.90. The results reveal that linear and Piecewise Cubic Hermite Interpolating Polynomial interpolation enhances self-supervised learning performance, by expanding the tolerance for periods of absence. This allows for less frequent patient returns and examinations, reducing travel and medical expenses, and suggests that patients can benefit from diminished frequency of visits and onerous examinations through sustainable estimation methods.

Also, Kakudi et al [25] explores ML methodologies for the diagnosis of metabolic syndrome (MetS). The findings provide valuable insights for researchers and health care practitioners into current trends and developments, suggesting that nonclinical methods could serve as early preventive tools for managing MetS and CVD.

Monitoring Patients

A certain number of publications focus on the use of ECG, BP, and wearable devices for monitoring cardiovascular health. Širaiy et al [39], Charlton et al [40], and Alugubelli et al [46] center around the use of wearable technology for monitoring cardiovascular health. These papers emphasize the role of wearable technology in providing continuous, noninvasive monitoring of cardiovascular parameters, contributing to early detection and management of heart conditions. Lyon et al [22] provides a literature review that describe the clinical applications and main ML methods currently used for ECG analysis, and Agham and Chaskar [49] provides a perspective of ML

XSL•FO
RenderX

approaches using cuffless BP for the generation of predictive models for continuous BP measurement. Pires et al [50] also aims to develop innovative solutions to empower patients with CVD, by providing them with personalized plans for treatment and increasing their ability for self-monitoring.

Varma et al [47] aimed to evaluate the current status of mobile health (mHealth) technologies, including AI-driven tools, in the monitoring and management of heart rhythm disorders. The paper reviewed various mHealth modalities, such as wearable devices, smartphone-based ECG, and photoplethysmography, and discussed their potential in detecting atrial fibrillation and other arrhythmias. The authors highlighted the role of predictive analytics in improving clinical decision-making and patient self-management. Despite the promising applications, the study noted several challenges, including data validation, integration into clinical practice, and cybersecurity concerns. The statement concluded that while mHealth holds significant potential for enhancing CVD management, particularly in arrhythmia detection, further research is needed to overcome operational barriers and optimize its integration into health care systems.

Risk Assessment

The papers presented in this paragraph collectively emphasize the application of advanced ML and AI techniques to improve CVD risk assessment and prediction. Faizal et al [16] and Jamthikar et al [45] highlight the superior performance of AI-based predictive models compared to traditional methods like the Global Registry of Acute Cardiac Events and thrombolysis in myocardial infarction, with AI frameworks incorporating noninvasive data for enhanced accuracy. Groccia et al [23] demonstrates the effectiveness of cost-sensitive models in predicting cardiovascular deterioration in patients with chronic heart failure, stressing the clinical importance of early detection. This last system achieved sensitivity scores of 65% and specificity scores of 55%. Similarly, Bostani et al [32] introduces a novel method combining reinforcement learning and MLPs for early risk detection in athletes, achieving an F_1-measure of 87.4% and a geometric mean of 89.6%. Navarrete et al [43] confirms that RF models perform well in predicting mortality risk in older adults, suggesting practical applications in health care settings. Gunasekaran et al [34] presents an Internet of Health care Things–integrated model that improves accuracy in CVD prediction, enhancing performance and data security. The presented model achieved an impressive accuracy of 97%. These findings collectively underscore the potential of AI and ML in transforming CVD risk prediction and management, providing more accurate, early, and cost-effective solutions.

Baek and Arzani [24] and Kadem et al [51] emphasize the transformative potential of integrating hemodynamic modeling, medical imaging, and ML in understanding cardiovascular anomalies and managing abdominal aortic aneurysms. Both highlight the importance of personalized medicine and data-driven approaches, particularly through physics-based ML models, in improving diagnostic accuracy and risk assessment. They address the need for extensive multisite and multimodal patient studies to validate these tools' benefits, accuracy, and safety. As computational power and data availability increase, these technologies are expected to enhance patient outcomes and reduce health care costs related to CVDs.

Discussion

Principal Findings

The literature review reveals significant advancements in the use of ML and DL techniques for the classification, prediction, and diagnosis of CVD and events. Techniques such as DLSE, FDCN, and CSOA have demonstrated high accuracy, surpassing 95%. Feature selection and elimination methods like Selective Opposition strategy based on artificial rabbits optimization, genetic-based crow search algorithm, and recursive feature elimination (RFE)–based gradient boosting further enhance prediction accuracy.

Some of the studies aim to predict the detection of CVD while others specify their ML algorithms to predict and manage specific conditions such as CAD, arrhythmia, hypertension, MetS, and abdominal aortic aneurysms.

Various studies highlight the importance of integrating multiple data sources and expert input to improve model performance. Wearable technologies and noninvasive methods are emphasized for continuous monitoring and early detection, showing promise in reducing health care costs and patient burden. Additionally, the application of AI in predicting emergency readmissions and the need for cardiovascular surgery underscores its potential to improve patient outcomes. Challenges identified include the need for standardized frameworks, data privacy, and algorithm interpretability.

Multimedia Appendix 1 provides a summary of the various AI methodologies and datasets used in CVD monitoring and prediction. The advantages of ensemble techniques like the SEL and the DLSE method lie in their ability to combine multiple models for improved accuracy, as evidenced by results ranging from 88% to over 95% accuracy. However, their complexity and interpretability present significant challenges that could hinder their adoption in clinical settings. Similarly, techniques like RFE and gradient boosting highlight the importance of feature selection in enhancing model precision, but the imbalanced nature of datasets used in some studies, such as the Nasarian CAD dataset, introduces limitations in the generalizability of results. The current literature often focuses on performance metrics like accuracy, precision, and F_1-score, without offering a robust analysis of the practical limitations of these systems, such as computational cost, scalability, or real-world clinical applicability.

The most frequently used datasets across the reviewed literature include the Cleveland Heart Disease dataset and the Cardiovascular Disease dataset. Some studies leverage datasets from Kaggle, which offer larger, publicly available cardiovascular data that span a variety of CVD conditions. These datasets are valuable for training more generalizable models, but they often demonstrate class imbalances, as seen in studies using RFE and gradient boosting.

Overall, these findings collectively underscore the potential of AI and ML in enhancing CVD risk assessment, prediction, and

XSL•FO
RenderX

management. The application of advanced methodologies such as ensemble learning and optimization strategies offers more accurate and early detection solutions, as evidenced by performance improvements across various datasets. However, the limitations in dataset diversity, model interpretability, and scalability highlight the ongoing need for more comprehensive real-world validations. Additionally, integrating discussions on the specific advantages, disadvantages, and performance measures of existing systems will further strengthen the understanding of their practical applications. Future research should focus on overcoming these challenges to develop more robust, cost-effective, and generalizable AI-driven solutions for cardiovascular health care.

Future Work

The future research prospects, across the studies referenced, suggest promising opportunities for integrating advanced technologies to improve CVD management. Combining multiomics data (genomics, proteomics, etc) with AI and Internet of Things could potentially enhance precision in disease detection, decision-making, and personalized care. Developing hybrid ML models using real-time and large datasets might improve heart disease prediction. Computational techniques for ECG analysis show the potential to uncover new biomarkers and enhance patient risk stratification. Wearable devices and remote monitoring systems could transform patient care by providing continuous, real-time health data. Addressing challenges such as data quality, standardization, and regulatory approval will be necessary to advance these innovations. Additionally, incorporating nonclinical models, evaluating diverse datasets, and leveraging advanced computational resources may be beneficial for developing effective and scalable solutions.

Conclusions

This literature review underscores the transformative potential of AI and ML in revolutionizing cardiovascular health care. Advanced AI-driven methodologies, including DLSE, FDCN, and CSOA, have demonstrated remarkable improvements in the detection, prediction, and management of CVD.

The integration of diverse data sources with these sophisticated algorithms enhances diagnostic accuracy, supports personalized treatment strategies, and enables early intervention efforts. Furthermore, the application of AI in wearable technologies shows great promise for continuous, noninvasive health monitoring, potentially improving patient outcomes while reducing health care costs.

These advancements represent a significant shift toward more proactive and personalized patient care, offering health care professionals powerful tools to support their decision-making processes. The high accuracy demonstrated by AI models in CVD classification and prediction suggests a future where cardiovascular events can be anticipated and prevented with greater precision.

However, the widespread adoption of AI in health care faces several challenges. These include the standardization of frameworks and protocols, ensuring robust data privacy and security measures, enhancing the interpretability and explainability of AI algorithms, validating AI models across diverse patient populations, and addressing ethical considerations in AI-driven health care.

Overcoming these obstacles could be crucial to realizing the full potential of AI-driven technologies in transforming cardiovascular care. Future research should focus on: (1) refining and optimizing AI models for improved accuracy and reliability; (2) integrating real-time data streams to enhance the applicability of AI in clinical settings; (3) conducting large-scale, multicenter studies to validate AI efficacy across different health care systems and patient demographics; (4) developing guidelines and best practices for the ethical implementation of AI in health care; and (5) exploring the synergies between AI and other emerging technologies to create more comprehensive health care solutions.

By addressing these challenges and pursuing these research directions, AI and ML have the potential to revolutionize cardiovascular health care on a global scale. The promise of more accurate, timely, and cost-effective solutions could significantly benefit both patients and health care providers, ultimately leading to improved cardiovascular health outcomes.

As we move forward, it is essential to maintain a balance between technological innovation and ethical considerations, ensuring that the advancements in AI-driven cardiovascular care are accessible, equitable, and centered on improving patient well-being. The integration of these technologies into clinical practice represents a significant step toward more proactive, personalized, and efficient cardiovascular care, aiming to improve global health outcomes.

Conflicts of Interest

None declared.

Multimedia Appendix 1
Summary of the paper's methods, used datasets, limitations, and performance measures.
[DOCX File, 19 KB - medinform_v13i1e64349_app1.docx]

Checklist 1
PRISMA-ScR checklist.
[PDF File, 118 KB - medinform_v13i1e64349_app2.pdf]

XSL•FO
RenderX

References

1. Kagiyama N, Shrestha S, Farjo PD, Sengupta PP. Artificial intelligence: practical primer for clinical research in cardiovascular disease. J Am Heart Assoc 2019 Sep 3;8(17):e012788. [doi: 10.1161/JAHA.119.012788] [Medline: 31450991]
2. Habehh H, Gohel S. Machine learning in healthcare. Curr Genomics 2021 Dec 16;22(4):291-300. [doi: 10.2174/1389202922666210705124359] [Medline: 35273459]
3. Rani P, Kumar R, Jain A, et al. An extensive review of machine learning and deep learning techniques on heart disease classification and prediction. Arch Computat Methods Eng 2024 Aug;31(6):3331-3349. [doi: 10.1007/s11831-024-10075-w]
4. Elvas LB, Nunes M, Ferreira JC, Dias MS, Rosário LB. AI-driven decision support for early detection of cardiac events: unveiling patterns and predicting myocardial ischemia. J Pers Med 2023 Sep 21;13(9):1421. [doi: 10.3390/jpm13091421] [Medline: 37763188]
5. Ogunpola A, Saeed F, Basurra S, Albarrak AM, Qasem SN. Machine learning-based predictive models for detection of cardiovascular diseases. Diagnostics (Basel) 2024 Jan;14(2):144. [doi: 10.3390/diagnostics14020144]
6. Sun X, Yin Y, Yang Q, Huo T. Artificial intelligence in cardiovascular diseases: diagnostic and therapeutic perspectives. Eur J Med Res 2023 Jul 21;28(1):242. [doi: 10.1186/s40001-023-01065-y] [Medline: 37475050]
7. Cardiovascular diseases. WHO. URL: https://www.who.int/health-topics/cardiovascular-diseases [accessed 2024-06-28]
8. Cardiovascular diseases (CVDs). WHO. URL: https://www.who.int/news-room/fact-sheets/detail/cardiovascular-diseases-(cvds) [accessed 2024-06-24]
9. Cardiovascular disease burden. Pan American Health Organization. URL: https://www.paho.org/en/enlace/cardiovascular-disease-burden [accessed 2024-06-24]
10. Gala D, Behl H, Shah M, Makaryus AN. The role of artificial intelligence in improving patient outcomes and future of healthcare delivery in cardiology: a narrative review of the literature. Healthcare (Basel) 2024 Jan;12(4):481. [doi: 10.3390/healthcare12040481]
11. PRISMA statement. URL: https://www.prisma-statement.org [accessed 2024-06-20]
12. Scopus Preview. URL: https://www.scopus.com/search/form.uri?display=basic&zone=header&origin=#basic [accessed 2024-06-20]
13. Web of Science. URL: https://www.webofscience.com/wos/woscc/basic-search [accessed 2024-06-20]
14. Rani P, Kumar R, Ahmed N, Jain A. A decision support system for heart disease prediction based upon machine learning. J Reliable Intell Environ 2021 Sep;7(3):263-275. [doi: 10.1007/s40860-021-00133-6]
15. Ghasemieh A, Lloyed A, Bahrami P, Vajar P, Kashef R. A novel machine learning model with Stacking Ensemble Learner for predicting emergency readmission of heart-disease patients. Decis Anal J 2023 Jun;7:100242. [doi: 10.1016/j.dajour.2023.100242]
16. Faizal ASM, Thevarajah TM, Khor SM, Chang SW. A review of risk prediction models in cardiovascular disease: conventional approach vs. artificial intelligent approach. Comput Methods Programs Biomed 2021 Aug;207:106190. [doi: 10.1016/j.cmpb.2021.106190] [Medline: 34077865]
17. Nuryani N, Utomo TP, Prabowo NA, Yazid M, Yunianto M. Advancing non-cuff hypertension detection: leveraging 1D convolutional neural network and time domain physiological signals. Int J Onl Eng 2024;20(5):78-100. [doi: 10.3991/ijoe.v20i05.45547]
18. Abbas S, Sampedro GA, Alsubai S, Almadhor A, Kim TH. An efficient stacked ensemble model for heart disease detection and classification. Comput Mater Contin 2023;77(1):665-680. [doi: 10.32604/cmc.2023.041031]
19. Nasarian E, Abdar M, Fahami MA, et al. Association between work-related features and coronary artery disease: a heterogeneous hybrid feature selection integrated with balancing approach. Pattern Recognit Lett 2020 May;133:33-40. [doi: 10.1016/j.patrec.2020.02.010]
20. Al-Absi HRH, Islam MT, Refaee MA, Chowdhury MEH, Alam T. Cardiovascular disease diagnosis from DXA scan and retinal images using deep learning. Sensors (Basel) 2022 Jun 7;22(12):4310. [doi: 10.3390/s22124310] [Medline: 35746092]
21. Theerthagiri P, Vidya J. Cardiovascular disease prediction using recursive feature elimination and gradient boosting classification techniques. Expert Syst 2022 Nov;39(9). [doi: 10.1111/exsy.13064]
22. Lyon A, Mincholé A, Martínez JP, Laguna P, Rodriguez B. Computational techniques for ECG analysis and interpretation in light of their contribution to medical advances. J R Soc Interface 2018 Jan;15(138):20170821. [doi: 10.1098/rsif.2017.0821] [Medline: 29321268]
23. Groccia MC, Guido R, Conforti D, et al. Cost-sensitive models to predict risk of cardiovascular events in patients with chronic heart failure. Information 2023;14(10):542. [doi: 10.3390/info14100542]
24. Baek S, Arzani A. Current state-of-the-art and utilities of machine learning for detection, monitoring, growth prediction, rupture risk assessment, and post-surgical management of abdominal aortic aneurysms. Appl Eng Sci 2022 Jun;10:100097. [doi: 10.1016/j.apples.2022.100097]
25. Kakudi HA, Kiong LC, Moy FM, Kau LC, Pasupa K. Diagnosis of metabolic syndrome using machine learning, statistical and risk quantification techniques: a systematic literature review. Malays J Comput Sci 2021;34(3):221-241. [doi: 10.22452/mjcs.vol34no3.1]
26. Prakash VJ, Karthikeyan NK. Dual-layer deep ensemble techniques for classifying heart disease. Inf Technol Control 2022;51(1):158-179. [doi: 10.5755/j01.itc.51.1.30083]

XSL•FO
RenderX

27. Singh E, Singh V, Rai A, Christopher I, Mishra R, Arikumar KS. Early detection of cardiovascular disease with different machine learning approaches. EAI Endorsed Trans IoT 2024;10. [doi: 10.4108/eetiot.5389]
28. Dubey AK, Sinhal AK, Sharma R. Heart disease classification through crow intelligence optimization-based deep learning approach. Int J Inf Technol 2024 Mar;16(3):1815-1830. [doi: 10.1007/s41870-023-01445-x]
29. Daliri A, Sadeghi R, Sedighian N, Karimi A, Mohammadzadeh J. Heptagonal Reinforcement Learning (HRL): a novel algorithm for early prevention of non-sinus cardiac arrhythmia. J Ambient Intell Human Comput 2024 Apr;15(4):2601-2620. [doi: 10.1007/s12652-024-04776-0]
30. Al-Ssulami AM, Alsorori RS, Azmi AM, Aboalsamh H. Improving coronary heart disease prediction through machine learning and an innovative data augmentation technique. Cogn Comput 2023 Sep;15(5):1687-1702. [doi: 10.1007/s12559-023-10151-6]
31. Parashar G, Chaudhary A, Pandey D. Machine learning for prediction of cardiovascular disease and respiratory disease: a review. SN Comput Sci 2024;5(1). [doi: 10.1007/s42979-023-02529-y]
32. Bostani A, Mirzaeibonehkhater M, Najafi H, et al. MLP-RL-CRD: diagnosis of cardiovascular risk in athletes using a reinforcement learning-based multilayer perceptron. Physiol Meas 2023 Dec 29;44(12). [doi: 10.1088/1361-6579/ad1459] [Medline: 38081126]
33. Selvaraj R, Satheesh T, Suresh V, Yathavaraj V. Optimized machine learning for CHD detection using 3D CNN-based segmentation, transfer learning and adagrad optimization. SSRG Int J Electr Electron Eng 2023;10(3):20-34. [doi: 10.14445/23488379/IJEEE-V10I3P103]
34. Gunasekaran K, Kumar VDA, Jayashree K. Prediction and risk analysis of cardio vascular diseases in IoHT by enhanced CHIO-based residual and dilated gated network with attention mechanism. Biomed Signal Process Control 2024 Aug;94:106222. [doi: 10.1016/j.bspc.2024.106222]
35. Itzhak N, Pessach IM, Moskovitch R. Prediction of acute hypertensive episodes in critically ill patients. Artif Intell Med 2023 May;139:102525. [doi: 10.1016/j.artmed.2023.102525] [Medline: 37100504]
36. Theerthagiri P. Predictive analysis of cardiovascular disease using gradient boosting based learning and recursive feature elimination technique. Intell Syst Appl 2022 Nov;16:200121. [doi: 10.1016/j.iswa.2022.200121]
37. Safa M, Pandian A, Gururaj HL, Ravi V, Krichen M. Real time health care big data analytics model for improved QoS in cardiac disease prediction with IoT devices. Health Technol 2023 Jun;13(3):473-483. [doi: 10.1007/s12553-023-00747-1]
38. Chen LC, Hung KH, Tseng YJ, et al. Self-supervised learning-based general laboratory progress pretrained model for cardiovascular event detection. IEEE J Transl Eng Health Med 2024;12:43-55. [doi: 10.1109/JTEHM.2023.3307794] [Medline: 38059127]
39. Širaiy B, Ilić V, Toskić L. Usability of wireless ECG body sensor for cardiac function monitoring during field testing. Meas Sci Rev 2021 Apr 1;21(2):55-60. [doi: 10.2478/msr-2021-0008]
40. Charlton PH, Kyriaco PA, Mant J, Marozas V, Chowienczyk P, Alastruey J. Wearable photoplethysmography for cardiovascular monitoring. Proc IEEE Inst Electr Electron Eng 2022 Mar 11;110(3):355-381. [doi: 10.1109/JPROC.2022.3149785] [Medline: 35356509]
41. Abuhaija B, Alloubani A, Almatari M, et al. A comprehensive study of machine learning for predicting cardiovascular disease using Weka and Statistical Package for Social Sciences tools. Int J Electr Comput Eng 2023;13(2):1891. [doi: 10.11591/ijece.v13i2.pp1891-1902]
42. Ghavidel A, Pazos P, Del Aguila Suarez R, Atashi A. Predicting the need for cardiovascular surgery: a comparative study of machine learning models. J Electron Electromed Eng Med Inform 2024;6(2):92-106. [doi: 10.35882/jeeemi.v6i2.359]
43. Navarrete JP, Pinto J, Figueroa RL, Lagos ME, Zeng Q, Taramasco C. Supervised learning algorithm for predicting mortality risk in older adults using cardiovascular health study dataset. Appl Sci (Basel) 2022;12(22):11536. [doi: 10.3390/app122211536]
44. Manur M, Pani A, Kumar P. A big data analysis using fuzzy deep convolution network based model for heart disease classification. Int J Intell Eng Syst 2021;14(2):147-156. [doi: 10.22266/ijies2021.0430.13]
45. Jamthikar AD, Gupta D, Saba L, et al. Artificial intelligence framework for predictive cardiovascular and stroke risk assessment models: A narrative review of integrated approaches using carotid ultrasound. Comput Biol Med 2020 Nov;126:104043. [doi: 10.1016/j.compbiomed.2020.104043]
46. Alugubelli N, Abuissa H, Roka A. Wearable devices for remote monitoring of heart rate and heart rate variability-what we know and what is coming. Sensors (Basel) 2022 Nov 17;22(22):8903. [doi: 10.3390/s22228903] [Medline: 36433498]
47. Varma N, Cygankiewicz I, Turakhia MP, et al. 2021 ISHNE/HRS/EHRA/APHRS collaborative statement on mHealth in arrhythmia management: digital medical tools for heart rhythm professionals: from the International Society for Holter and Noninvasive Electrocardiology/Heart Rhythm Society/European Heart Rhythm Association/Asia Pacific Heart Rhythm Society. Cardiovasc Digital Health J 2021;2:4-54. [doi: 10.1016/j.cvdhj.2020.11.004]
48. Nijaguna GS, Lal ND, Divakarachari PB, Prado RPD, Woźniak M, Patra RK. Feature selection using selective opposition based artificial rabbits optimization for arrhythmia classification on internet of medical things environment. IEEE Access 2023;11:100052-100069. [doi: 10.1109/ACCESS.2023.3312537]
49. Agham ND, Chaskar UM. Learning and non-learning algorithms for cuffless blood pressure measurement: a review. Med Biol Eng Comput 2021 Jun;59(6):1201-1222. [doi: 10.1007/s11517-021-02362-6] [Medline: 34085135]

XSL•FO
RenderX

50. Pires IM, Denysyuk HV, Villasana MV, et al. Mobile 5P-medicine approach for cardiovascular patients. Sensors (Basel) 2021 Oct 21;21(21):6986. [doi: 10.3390/s21216986] [Medline: 34770292]
51. Kadem M, Garber L, Abdelkhalek M, Al-Khazraji BK, Keshavarz-Motamed Z. Hemodynamic modeling, medical imaging, and machine learning and their applications to cardiovascular interventions. IEEE Rev Biomed Eng 2023;16:403-423. [doi: 10.1109/RBME.2022.3142058] [Medline: 35015648]
52. Nagarajan SM, Muthukumaran V, Murugesan R, Joseph RB, Meram M, Prathik A. Innovative feature selection and classification model for heart disease prediction. J Reliable Intell Environ 2022 Dec;8(4):333-343. [doi: 10.1007/s40860-021-00152-3]

Abbreviations

AI: artificial intelligence
BP: blood pressure
CAD: coronory artery disease
CNN: convolution neural network
CSOA: crow search optimization algorithm
CVD: cardiovascular diseases
DL: deep learning
DLSE: Dual Layer Stacking Ensemble
DT: decision tree
ECG: electrocardiogram
FDCN: fuzzy deep convolutional network
KNN: k-nearest neighbor
MetS: metabolic syndrome
mHealth: mobile health
ML: machine learning
MLP: multilayer perceptron
PRISMA: Preferred Reporting Items for Systematic Reviews and Meta-Analyses
RF: random forest
RFE: recursive feature elimination
SEL: stacking ensemble learner
XGB: Extreme Gradient Boosting

Edited by C Lovis; submitted 15.07.24; peer-reviewed by A Sharafeldeen, H Sattar; revised version received 08.12.24; accepted 25.12.24; published 06.03.25.

Please cite as:
Elvas LB, Almeida A, Ferreira JC
The Role of AI in Cardiovascular Event Monitoring and Early Detection: Scoping Literature Review
JMIR Med Inform 2025;13:e64349
URL: https://medinform.jmir.org/2025/1/e64349
doi:10.2196/64349

© Luis B Elvas, Ana Almeida, Joao C Ferreira. Originally published in JMIR Medical Informatics (https://medinform.jmir.org), 6.3.2025. This is an open-access article distributed under the terms of the Creative Commons Attribution License (https://creativecommons.org/licenses/by/4.0/), which permits unrestricted use, distribution, and reproduction in any medium, provided the original work, first published in JMIR Medical Informatics, is properly cited. The complete bibliographic information, a link to the original publication on https://medinform.jmir.org/, as well as this copyright and license information must be included.

XSL•FO
RenderX

Comparing Diagnostic Accuracy of Clinical Professionals and Large Language Models: Systematic Review and Meta-Analysis

Guxue Shan[1], BSc; Xiaonan Chen[1], BSc; Chen Wang[1], BSc; Li Liu[2], BMed; Yuanjing Gu[3], MNS; Huiping Jiang[4], BSc; Tingqi Shi[5], MPH

[1]Nanjing Drum Tower Hospital Clinical College of Nanjing University of Chinese Medicine, Nanjing, China

[2]Jiangsu Province Hospital of Chinese Medicine, Affiliated Hospital of Nanjing University of Chinese Medicine, Nanjing, China

[3]Department of Emergency, Nanjing Drum Tower Hospital, Nanjing, China

[4]Department of Nursing, Nanjing Drum Tower Hospital, Nanjing, China

[5]Department of Quality Management, Nanjing Drum Tower Hospital, Affiliated Hospital of Medical School, Nanjing University, 321 Zhongshan Road, Gulou District, Nanjing, China

Corresponding Author:
Tingqi Shi, MPH
Department of Quality Management, Nanjing Drum Tower Hospital, Affiliated Hospital of Medical School, Nanjing University, 321 Zhongshan Road, Gulou District, Nanjing, China

Abstract

Background: With the rapid development of artificial intelligence (AI) technology, especially generative AI, large language models (LLMs) have shown great potential in the medical field. Through massive medical data training, it can understand complex medical texts and can quickly analyze medical records and provide health counseling and diagnostic advice directly, especially in rare diseases. However, no study has yet compared and extensively discussed the diagnostic performance of LLMs with that of physicians.

Objective: This study systematically reviewed the accuracy of LLMs in clinical diagnosis and provided reference for further clinical application.

Methods: We conducted searches in CNKI (China National Knowledge Infrastructure), VIP Database, SinoMed, PubMed, Web of Science, Embase, and CINAHL (Cumulative Index to Nursing and Allied Health Literature) from January 1, 2017, to the present. A total of 2 reviewers independently screened the literature and extracted relevant information. The risk of bias was assessed using the Prediction Model Risk of Bias Assessment Tool (PROBAST), which evaluates both the risk of bias and the applicability of included studies.

Results: A total of 30 studies involving 19 LLMs and a total of 4762 cases were included. The quality assessment indicated a high risk of bias in the majority of studies, primary cause is known case diagnosis. For the optimal model, the accuracy of the primary diagnosis ranged from 25% to 97.8%, while the triage accuracy ranged from 66.5% to 98%.

Conclusions: LLMs have demonstrated considerable diagnostic capabilities and significant potential for application across various clinical cases. Although their accuracy still falls short of that of clinical professionals, if used cautiously, they have the potential to become one of the best intelligent assistants in the field of human health care.

(JMIR Med Inform 2025;13:e64963) doi:10.2196/64963

KEYWORDS

machine learning; ML; artificial intelligence; AI; large language model; LLM; natural language processing; algorithm; model; analytics; NLP; deep learning; clinical diagnosis; diagnosis; diagnostic accuracy; accuracy; systematic review

Introduction

The Google Brain research team has consistently aimed to push the boundaries of recurrent language models and encoder-decoder architectures. In 2017, Vaswani et al [1] introduced a novel and simple network architecture known as the Transformer. This architecture uses a new mechanism called “self-attention,” leading to significant advancements in the development and training of large language models (LLMs). These models possess advanced capabilities beyond extraction or summarization tasks and include natural language generation. Although there is no official definition of LLM, based on the literature [2,3], we define LLM as a model with over a billion parameters, designed for typical artificial intelligence (AI) applications.

Accurate clinical diagnosis is essential for patient treatment outcomes and survival rates. However, even when health care professionals gather extensive information and conduct

XSL•FO
RenderX

numerous observations and tests, absolute diagnostic accuracy cannot be guaranteed. Minimizing diagnostic uncertainty and making the most appropriate treatment decisions remain persistent clinical challenges [4,5]. As of May 2024, the US Food and Drug Administration has approved 882 medical devices that use AI or machine learning assistance. By June 2024, the National Medical Products Administration of China has approved 17 AI-assisted diagnostic devices. In the era of big data in health care, the integration of AI with clinical decision support is a developing trend [6]. Numerous experts and scholars have explored the application of specialized AI and software tools in clinical diagnosis, yet there is limited knowledge about the performance of LLMs in this context. Therefore, this study aims to comprehensively evaluate the performance and accuracy of LLMs in clinical diagnosis, providing references for their clinical application.

Methods

Overview

This systematic review was conducted following the Preferred Reporting Items for Systematic Reviews and Meta-Analysis of Diagnostic Test Accuracy Studies (PRISMA-DTA) statement [7]. Specific details can be found in Checklist 1.

Data Sources

A computer-assisted literature search of PubMed, Web of Science, Embase, CINAHL (Cumulative Index to Nursing and Allied Health Literature), CNKI (China National Knowledge Infrastructure), VIP, and SinoMed databases was performed from January 1, 2017, to the present. Search terms included controlled terms (MeSH [Medical Subject Heading] in PubMed and Emtree in Embase) and free-text terms. The following terms were used (including synonyms and closely related words) as index terms or free-text words: “large language model,” “medicine,” “diagnosis,” and “accuracy.” A search filter was applied to limit the results to humans. Only peer-reviewed cross-sectional studies and cohort studies were included. Multimedia Appendix 1 provides more details of the search strategy and study selection.

Selection Criteria

This review included studies meeting the following criteria: (1) investigated the application of LLMs in the initial diagnosis of human cases, (2) published between January 1, 2017, and the date of the search, (3) study type was either cross-sectional or cohort, (4) a primary source, and (5) written in English or Chinese.

An article was excluded if it (1) was a nonprimary source such as theses, conference papers, etc, (2) did not compare the diagnostic accuracy of clinical professionals in relevant departments with that of LLMs, (3) did not specify the type or scale of the LLM used for diagnosis, (4) did not have LLM independently conduct clinical case diagnoses, (5) was a duplicate publication, and (6) did not provide complete data or the full text could not be obtained.

Data Selection and Extraction

A total of 2 reviewers (GS and XC) independently reviewed the full texts of the eligible articles and extracted data. Any disagreements between the reviewers were discussed until a consensus was reached. The detailed characteristics extracted from each included study were: the first author and publication year, the country where the research was conducted, the study type, the study population, the source of cases, sample size, the LLMs used, control groups, and outcome measures.

Quality of Evidence and Risk of Bias

Due to the significant heterogeneity often present in the design and implementation of diagnostic accuracy studies, it is crucial to carefully assess the quality of the included studies. The Prediction Model Risk of Bias Assessment Tool (PROBAST) was used to evaluate the risk of bias and applicability of all included studies [8]. PROBAST assesses risk of bias across 4 domains: study participants, predictors, outcomes, and statistical analysis, while applicability is evaluated through the first 3 domains.

Given the complex structure and vast number of parameters in LLMs, they can be considered a “black box” to some extent, meaning that their internal workings and decision-making processes may not be entirely transparent or easily understood by humans [6]. Consequently, during the quality assessment, certain signal issues were excluded as they were unrelated to generative AI models [9].

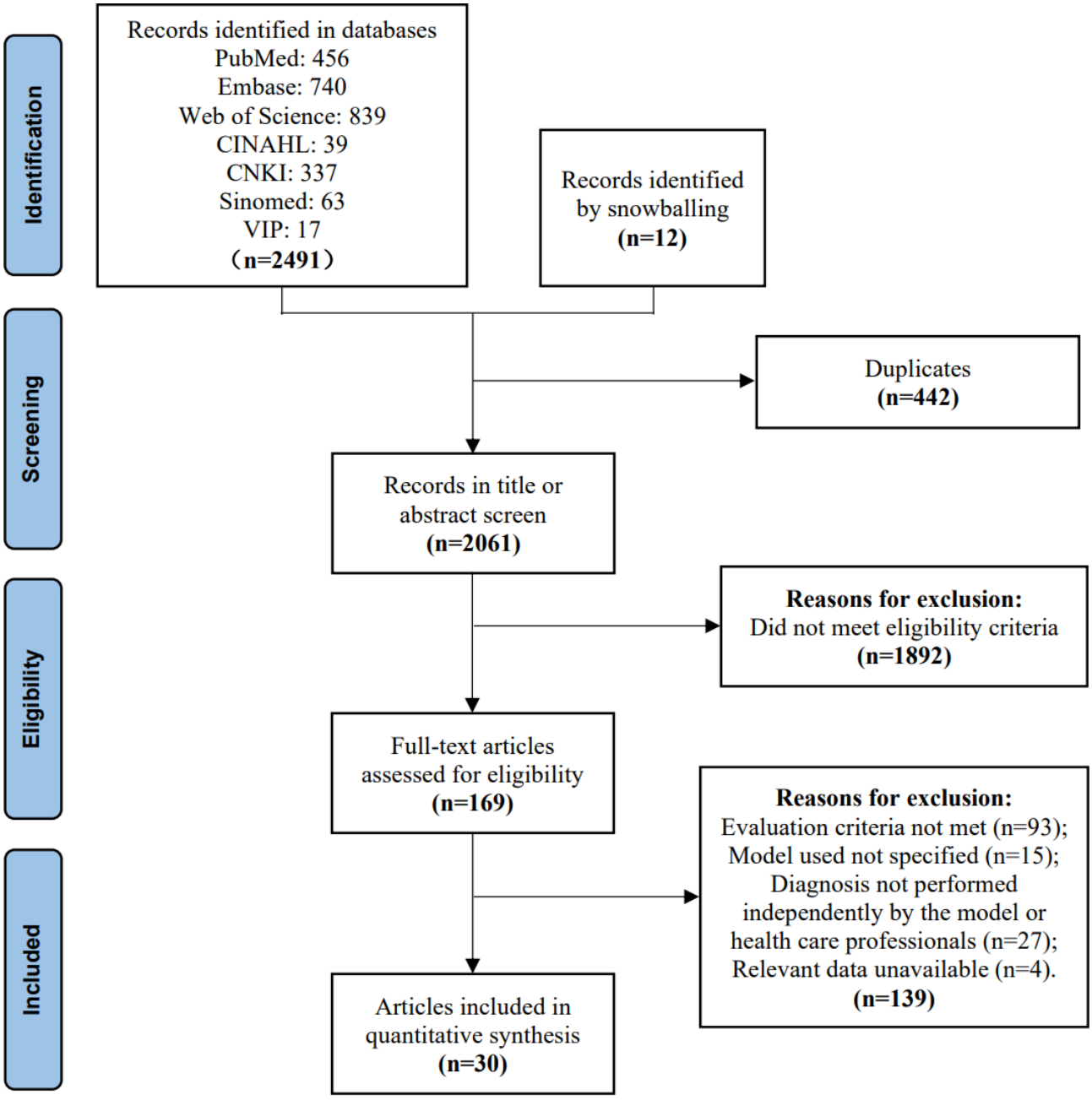
Results

Selection of Studies

A total of 2491 studies were found in the databases by 2 researchers independently following the predefined search strategies and data collection methods. An additional 12 articles were identified through reference tracing, bringing the total number of studies screened to 2503. Among these, 169 studies were read in full, resulting in 30 studies that met the inclusion criteria for synthesis. Reasons for exclusion at this stage were recorded and can be found in the flow diagram (see Figure 1).

XSL•FO
RenderX

Figure 1. Flow diagram. Papers identified in databases, title or abstract screened, read full text, and included in the synthesis. Reasons for exclusion are listed. CINAHL: Cumulative Index to Nursing and Allied Health Literature; CNKI: China National Knowledge Infrastructure.



Studies Characteristics

The 30 included studies [10-39] were concentrated within the past 3 years, with 12 published in 2023, 16 in 2024, and 2 in 2025. These studies cover a wide range of countries, primarily from Japan, the United States, and China. A total of 4762 cases were analyzed, involving 19 LLMs. The studies predominantly focused on GPT-3.5 (n=14) and GPT-4 (n=20) versions (OpenAI), extensively applied in assessing clinical diagnostic accuracy. In contrast, fewer studies addressed Google Bard (n=3), Bing (n=3), GPT-4o (n=2), and GPT-4V (n=2). The case diagnoses encompassed various fields, including ophthalmology (n=9), internal medicine (n=6), emergency medicine (n=3), and general medicine (n=3), among others. The control groups included at least 193 clinical professionals, ranging from resident doctors to medical experts with over 30 years of clinical experience, to compare their diagnostic capabilities with those of the LLMs. All included studies used LLMs for data testing purposes only and were not used for real-time diagnosis of clinical patients. Table 1 shows the basic characteristics of the included studies.

XSL•FO
RenderX

Table . Characteristics and results of the eligible studies.

Study	Year	Country	Study type	Subjects	Case source	Sample size	LLM[a]	Comparison group	Outcome measures
Zhang et al [10]	2024	China	Prospective study	Ophthalmology cases	Patient visit records	26	GPT-4o	Ophthalmologists	c[b], g[c]
Makhoul et al [11]	2024	Lebanon	Cross-sectional study	Otolaryngology cases	Published case reports	32	GPT-3.5	ENT[d] physicians, FM[e] specialists	a[f], b[g]
Pillai et al [12]	2023	The United States	Cross-sectional study	Autoimmune diseases cases	Published case reports	40	GPT-3.5 GPT-4 LLaMa 2	A certified internist	a[f], b[g]
Levin et al [13]	2024	Israel	Cross-sectional study	Neonatal cases	Developed by researchers	6	GPT-4 Claude-2.0	Certified neonatal nurse practitioners	c[b], g[c]
Lyons et al [14]	2023	The United States	Cross-sectional study	Ophthalmology cases	Developed by researchers	44	GPT-4 Bing	Ophthalmology physicians	b[g], d[h]
Sarangi et al [15]	2023	India	Cross-sectional study	General cases	Developed by researchers	120	GPT-3.5 Bard Bing	Radiology residents	a[f]
Paslı et al [16]	2024	Turkey	Prospective study	Emergency cases	Patient visit records	758	GPT-4	The ED[i] triage team	d[h]
Wang et al [17]	2024	China	Retrospective cohort study	Thyroid cases	Patient visit records	109	GPT-4	Thyroid doctors	c[b]
Huang et al [18]	2024	The United States	Cross-sectional study	Ophthalmology cases	Patient visit records	20	GPT-4	Subspecialists (in glaucoma or retina)	c[b], g[c]
Stoneham et al [19]	2023	UK	Retrospective study	Dermatology cases	Patient visit records	36	GPT-4	A dermatologist	a[f]
Hirosawa et al [20]	2023	Japan	Cross-sectional study	Internal medicine cases	Published case reports	52	GPT-3.5 GPT-4	GIM[j] physicians	a[f], b[g]
Horiuchi et al [21]	2025	Japan	Retrospective study	Musculoskeletal cases	Published case reports	106	GPT-4 GPT-4V	Radiologists	a[f], b[g]
Mitsuyama et al [22]	2024	Japan	Retrospective study	Brain tumors cases	Patient visit records	150	GPT-4	Radiologists	a[f], b[g]
Hirosawa et al [23]	2023	Japan	Retrospective cohort study	Internal medicine cases	Published case reports and developed by researchers	82	Bard	GIM[j] physicians	a[f], b[g]
Suh et al [24]	2024	Korea	Retrospective study	General cases	Published case reports	190	GPT-4V Gemini Pro Vision	Radiologists	b[g]
Fraser et al [25]	2023	The United States	Cross-sectional study	Emergency cases	Patient visit records	40	GPT-3.5 GPT-4	ED physician	a[f], b[g], d[h]
Hirosawa et al [26]	2023	Japan	Prospective study	Internal medicine cases	Developed by researchers	30	GPT-3.5	GIM[j] physicians	a[f], b[g]

XSL•FO
RenderX

Study	Year	Country	Study type	Subjects	Case source	Sample size	LLM[a]	Comparison group	Outcome measures
Shemer et al [27]	2024	Israel	Retrospective cohort study	Ophthalmology cases	Patient visit records	63	GPT-3.5	Ophthalmology residents and ophthalmologists	a[f], g[c]
Mohammadi et al [28]	2024	Iran	Retrospective study	Tibial plateau fracture cases	Retrospective study	111	GPT-4 GPT-4o	An ED physician and radiologist	f[k]
Arslan et al [29]	2025	Turkey	Prospective study	Emergency cases	Patient visit records	468	GPT-4 Copilot Pro	Triage nurses	d[h]
Rojas-Carabali et al [30]	2023	Singapore	Cross-sectional study	Ophthalmology cases	Developed by researchers	25	GPT-3.5 GPT-4	Ophthalmologists	a[f], b[g]
Kaya et al [31]	2024	Germany	Retrospective study	Myocarditis cases	Patient visit records	396	GPT-4	Radiologists	a[f], e[l]
Delsoz et al [32]	2024	The United States	Cross-sectional study	Ophthalmology cases	Published case reports	20	GPT-3.5 GPT-4	Cornea specialists	a[f]
Ming et al [33]	2024	China	Cross-sectional study	Ophthalmology cases	Published case reports	104	GPT-3.5 GPT-4	Ophthalmic residents	a[f], b[g]
Nakaura et al [34]	2024	Japan	Retrospective study	Internal medicine cases	Patient visit records	28	GPT-2 GPT-3.5 GPT-4	Radiologists	a[f], b[g]
Ito et al [35]	2023	Japan	Cross-sectional study	General cases	Published case reports	45	GPT-4	Emergency physicians	a[f], d[h]
Gunes et al [36]	2024	Turkey	Cross-sectional study	thoracic cases	Published case reports	124	10 LLMs including GPT-3.5/4 Claude 3 Opus…	Published case reports	a[f]
Delsoz et al [37]	2023	The United States	Cross-sectional study	Ophthalmology cases	Published case reports	11	GPT-3.5	Ophthalmology residents	a[f]
Liu et al [38]	2023	China	Prospective study	Ophthalmology cases	Patient visit records	1226	GPT-3.5	Ophthalmologists	e[l]
Li et al [39]	2024	China	Retrospective study	Abdominal cases	Patient visit records	300	ERNie, 4.0 Claude 3.5 Sonnet	Radiologists	c[b]

[a]LLM: large language model.

[b]Accuracy score.

[c]Other auxiliary indicators (such as diagnostic completeness, diagnostic time, number of answers, etc).

[d]ENT: ear, nose, and throat.

[e]FM: family medicine.

[f]Frequency of correct primary diagnosis (answer).

[g] Frequency of correct diagnosis in a differential diagnosis list.

[h]Triage accuracy.

[i]ED: emergency department.

[j]GIM: general internal medicine.

[k]AUC: area under the curve.

[l]F_1-score

Quality of Evidence and Risk of Bias

The included articles were evaluated using the PROBAST tool, with the results presented in Multimedia Appendix 2. Overall, 10/30 (33.3%) studies had a low risk of bias, while 20/30 (66.6%) exhibited a high risk of bias. Regarding applicability, majority of study had low applicability concerns. Due to ethical concerns and patient privacy issues associated with the use of

XSL•FO
RenderX

LLMs in clinical settings, most of the studies consist of retrospective studies with deidentified data and are limited to data testing. A total of 14 studies evaluated the diagnostic accuracy of models using small test sets. In addition, the "black box" nature of LLMs, whose training data are often undisclosed, complicates external evaluation and verification.

LLM Feature Analysis

Although a total of 19 different LLMs were used in the included studies, extracting the LLM with the best diagnostic performance in studies tested with multiple large models simultaneously, we found that the optimal LLM did not belong to the GPT series in only 6 studies. In 80% (24/30) of the studies, the researchers chose to obtain and use the corresponding LLMs directly on the official website by online access, which somewhat lowered the threshold for the use of the LLMs in the medical field and made it more accessible to the public. In total, 18 of the included studies specified the date of access or version of the LLM used. Retrieval-augmented generation (RAG) is a technique that combines information retrieval and generation to enhance task performance by incorporating relevant information into LLMs [40]. RAG was mentioned in 2 of the studies by further training of pretrained models specific to task datasets, and although RAG has been widely used in large model studies, it needs to be strengthened in the medical field. Specific details can be found in Table 2.

XSL•FO
RenderX

Table . Characteristics of the large language models (LLMs) in eligible studies.

Study	Optimal LLM[a] in research	Issuing company	Access mode	Date accessed (version)	Parameter settings	RAG[b]
Zhang et al [10]	GPT-4o	Open AI	__[c]	—	—	Unused
Makhoul et al [11]	GPT-3.5	—	Application-based ChatGPT 3.5	—	—	Unused
Pillai et al [12]	GPT-4	Open AI	Online access	August 12, 2023	—	Unused
Levin et al [13]	Claude-2.0	Anthropic	Platform developed by Anthropic (@Poe)	—	—	Unused
Lyons et al [14]	GPT-4	Open AI	Online access	March 19-24, 2023	—	Unused
Sarangi et al [15]	Bing	Microsoft	Search engine-based GPT-4	June 2023	—	Unused
Paslı et al [16]	GPT-4	Open AI	Online access	September 25, 2023	—	RAG
Wang et al [17]	GPT-4	—	Platform-based GPT-4 developed by researchers (ThyroAIGuide)	—	—	Unused
Huang et al [18]	GPT-4	Open AI	Online access	May 12, 2023	—	Unused
Stoneham et al [19]	GPT-4	Open AI	Online access	—	—	Unused
Hirosawa et al [20]	GPT-4	Open AI	Online access	April 10, 2023	—	Unused
Horiuchi et al [21]	GPT-4	Open AI	Online access	September 25, 2023	—	Unused
Mitsuyama et al [22]	GPT-4	Open AI	Online access	May 24, 2024	—	Unused
Hirosawa et al [23]	Bard	Google	Online access	June 8, 2023	—	Unused
Suh et al [24]	GPT-4V	Open AI	Online access	—	Temperature=1	Unused
Fraser et al [25]	GPT-3.5	Open AI	Online access	July 2023	—	Unused
Hirosawa et al [26]	GPT-3.5	Open AI	Online access	January 5, 2023	—	Unused
Shemer et al [27]	GPT-3.5	Open AI	Online access	March 2023	—	Unused
Mohammadi et al [28]	GPT-4o	Open AI	Online access	December 2023	—	Unused
Arslan et al [29]	GPT-4	Open AI	Online access	—	—	Unused
Rojas-Carabali et al [30]	GPT-4	Open AI	Online access	—	—	Unused
Kaya et al [31]	GPT-4	Open AI	Online access	March to July 2023	—	Unused
Delsoz et al [32]	GPT-4	Open AI	Online access	—	—	Unused
Ming et al [33]	GPT-4	Open AI	Online access	March 5-18, 2024	—	Unused
Nakaura et al [34]	Bing	Microsoft	Search engine-based GPT-4	—	—	Unused
Ito et al [35]	GPT-4	Open AI	Online access	March 15, 2023	—	Unused
Gunes et al [36]	Claude 3 Opus	Anthropic	Online access	May 2024	—	Unused
Delsoz et al [37]	GPT-3.5	Open AI	Online access	—	—	Unused
Liu et al [38]	GPT-3.5	Open AI	Online access	—	Temperature=0	Unused
Li et al [39]	Claude 3.5 Sonnet	Anthropic	Online access	June 13 to July 5, 2024	Temperature=1×10^{-10}	RAG

[a]LLM: large language model.

[b]RAG: retrieval-augmented generation.

XSL•FO
RenderX

[C]Not available.

Results of Diagnosis

The accuracy of the diagnoses made by the LLMs and the clinical professionals in the studies depends on the "standard answer" mentioned in the literature. The comparison is based on how their answers align with this standard. The "standard answer" in the included studies consists of the final diagnoses recorded in patient medical records or case reports, predetermined answers set by case developers, and diagnoses established by experienced clinical experts in the relevant departments.

Application of LLMs in Clinical Diagnosis

The most common model task was the free text task, which appeared in 19 articles, while only 1 article involved a choice task. English was used for input and output in all but 2 articles: one used Hebrew for prompting, and the other used Chinese to compare model diagnostic performance. In LLM, prompt is an input mode that guides the model to specific tasks or generates specific outputs, typically including elements such as instructions (task descriptions), context (background information), examples, input data, output instructions, and roles [41,42]. When LLMs are used for case diagnosis, the most frequently used elements are commands and input data, which primarily include patient basic information, complaints, medical history, physical examination, and laboratory tests. The output content mainly consists of diagnostic lists or triage recommendations. The diagnostic accuracy of health care professionals in each study was evaluated by investigators or experts in relevant fields.

In studies where multiple LLMs were used to diagnose sample cases, only the data for the model with the best diagnostic performance were recorded. Of these studies, 85% (24/30) reported that the ChatGPT series models demonstrated the best diagnostic performance. Several investigators noted that the diagnostic accuracy of GPT models was comparable with that of physicians and did not show significant differences. Specific details can be found in Multimedia Appendix 3.

Comparison of Diagnostic Accuracy Between LLMs and Health Care Professionals

Pooling the data revealed that 70% (21/30) of the studies used the frequency of correct diagnoses in model responses as the primary evaluation indicator of clinical diagnostic accuracy, excluding other auxiliary indicators. All accuracy results were expressed as percentages. For the optimal model, the accuracy of the primary diagnosis ranged from 25% to 97.8%, while triage accuracy ranged from 66.5% to 98%. In medical practice, the diagnostic agreement criterion is usually set at over 80%. The GPT series LLMs achieved diagnostic accuracy greater than 80% in clinical tasks across 3 studies in ophthalmology, 2 studies in general medicine, and 1 study each in radiology, emergency medicine, and general practice. Among the 7 studies focused on ophthalmic case diagnosis, the diagnostic performance was generally high, with 77.8% (7/9) of the large models showing diagnostic accuracy comparable with that of health care professionals.

In these cases, health care professionals received the same prompting words as the LLMs. In 60% (18/30) of the studies, control group participants were blinded to the true nature and goals of the study until it was completed. The diagnostic accuracy of health care professionals was compared with the outcomes of LLMs. The results showed that in 33.7% (20/30) of the studies, professionals had higher diagnostic accuracy than the models. In 33.3% (10/30) of the studies, the LLMs, specifically ChatGPT, had higher diagnostic accuracy than humans. The specific diagnostic accuracy comparisons are detailed in Table 3.

XSL•FO
RenderX

Table . Comparison of diagnostic accuracy between large language models (LLMs) and clinical professionals.

Specialty and study	Clinical professionals	Evaluation results (LLMs vs clinical professionals), %					
		a[a]	b[b]	c[c]	d[d]	e[e]	f[f]
Ophthalmology							
Zhang et al [10]	3	—[g]	—	55 vs 74.7	—	—	—
Lyons et al [14]	8	—	93 vs 95[h]	—	98.0 vs 86.0	—	—
Huang et al [18]	15	—	—	50.4 vs 50.3	—	—	—
Shemer et al [27]	6	68 vs 90	—	—	—	—	—
Rojas-Carabali et al [30]	5	64 vs 85.6	72 vs 89.6[h]	—	—	—	—
Delsoz et al [32]	3	85 vs 96.7	—	—	—	—	—
Ming et al [33]	3	59.6 vs 60.6	76 vs 65.4[h]	—	—	—	—
Delsoz et al [37]	3	72.7 vs 66.6	—	—	—	—	—
Liu et al [38]	2	—	—	—	—	80.1 vs 89.4	—
Internal medicine							
Hirosawa et al [20]	3	60 vs 50	81 vs 67[i]; 83 vs 75[j]	—	—	—	—
Mitsuyama et al [22]	5	73 vs 69.4	94 vs 81.6[h]	—	—	—	—
Hirosawa et al [23]	5	40.2 vs 64.6	53.7 vs 78[i]; 56.1 vs 82.9[j]	—	—	—	—
Hirosawa et al [26]	2	53.3 vs 93.3	83.3 vs 98.3[i]	—	—	—	—
Nakaura et al [34]	1	54 vs 100	96 vs 100[i]	—	—	—	—
Li et al [39]	5	—	—	93.8 vs 99.6	—	—	—
Emergency department							
Sinan Paslı et al [16]	Team	—	—	—	95.6 vs 92.8	—	—
Fraser et al [25]	3	40 vs 47	63 vs 69[h]	—	—	—	—
Arslan et al [29]	Team	—	—	—	66.5 vs 65.2	—	—
General medicine							
Sarangi et al [15]	2	53.3 vs 60.4	—	—	—	—	—
Suh et al [24]	8	—	48.9 vs 60.5[h]	—	—	—	—
Ito et al [35]	3	97.8 vs 91.1	—	—	66.7 vs 66.7	—	—
Orthopedics							

XSL•FO
RenderX

Specialty and study		Clinical professionals	Evaluation results (LLMs vs clinical professionals), %					
			a[a]	b[b]	c[c]	d[d]	e[e]	f[f]
	Horiuchi et al [21]	2	43 vs 47	58 vs 62.5[h]	—	—	—	—
	Mohammadi et al [28]	2	—	—	—	—	—	0.73 vs 0.74
Cardiothoracic								
	Kaya et al [31]	3	81 vs 91.3	—	—	—	85 vs 92.7	—
	Gunes et al [36]	2	70.3 vs 46.8	—	—	—	—	—
Otolaryngology								
	Makhoul et al [11]	20	—	70.8 vs 71.3[h]	—	—	—	—
Immunology								
	Pillai et al [12]	1	25 vs 47.5	45 vs 60[i]; 47.5 vs 75[j]	—	—	—	—
Neonatology								
	Levin et al [13]	32	—	—	70.8 vs 82.5	—	—	—
Thyroid								
	Wang et al [17]	40	—	—	73.6 vs 87.4	—	—	—
Dermatology								
	Stoneham et al [19]	1	56 vs 83	—	—	—	—	—

[a]Frequency of correct primary diagnosis (answer)

[b]Frequency of correct diagnosis in the 3, 5, or 10 differential diagnoses.

[c]Accuracy score

[d]Triage accuracy

[e]F_1-score.

[f]AUC: area under the curve.

[g]Not available.

[h]Frequency of correct diagnosis in the 3 differential diagnoses.

[i]Frequency of correct diagnosis in the 5 differential diagnoses.

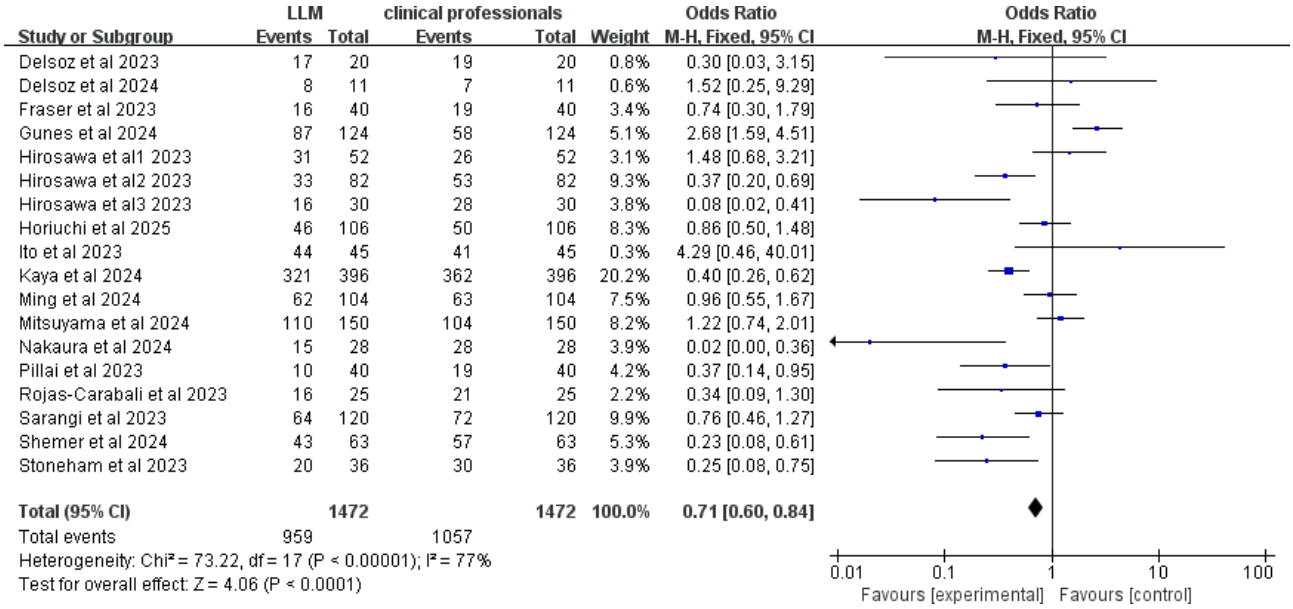
[j]Frequency of correct diagnosis in the 10 differential diagnoses.

Meta-Analysis

Although this paper synthesizes over 4000 clinical cases, these cases exhibit significant heterogeneity in terms of clinical departments, diagnostic methodologies, and evaluation metrics. Due to these inherent differences, only 18 studies that used primary diagnostic accuracy as the evaluation metric were included in a meta-analysis. The analysis revealed that clinical professionals generally outperformed LLMs in diagnostic accuracy across various conditions, as shown in Figure 2. The *P* value was less than 0.05, and the I^2 value was 77%, indicating significant heterogeneity among the studies. Sensitivity analysis did not significantly improve the heterogeneity. Subgroup analyses by clinical department showed reduced heterogeneity in ophthalmology-related research, yet results still favored the diagnostic accuracy of ophthalmology professionals over LLMs.

XSL•FO
RenderX

Figure 2. Forest plot comparing diagnostic accuracy of large language models (LLMs) and clinical professionals [37,32,25,36,20,23,26,21,35,31,33,22,34,12,30,15,27,19].



Discussion

Principal Findings

In this systematic review, we analyzed the diagnostic accuracy of LLMs compared with clinical professionals, encompassing various LLMs and common medical specialties. Although the results typically indicated superior diagnostic accuracy among professionals, this study compiled the methodologies, functionalities, and outcomes of using LLMs in medical diagnostics. It affirmed the diagnostic capabilities of generic LLMs, providing evidence for their potential as healthcare assistants.

Application of LLMs in Clinical Diagnosis Still in Exploratory Stage

This review includes only peer-reviewed and published literature, so the models examined in the included studies primarily use text-based input and output for diagnostic tasks. However, with the advancement of large models, multimodal capabilities have also been integrated [43]. Some preprint studies [44,45] have explored using GPT-4V, incorporating imaging data into input prompts. Notably, adding images to LLM did not improve diagnostic performance. In a study by Horiuchi et al [44], ChatGPT-4, which relied solely on text prompts, achieved higher diagnostic accuracy compared to GPT-4V, which combined text and images. Without few-shot learning, LLMs may struggle with image recognition and interpretation, sometimes leading to counterproductive outcomes.

Currently, the performance of general LLMs continues to improve, showing strong results in health care question answering, text classification, and clinical concept extraction [46]. However, these studies remain experimental and laboratory-based. Issues such as the interpretability of model responses and medical ethics pose significant challenges to applying these models in real clinical settings. Furthermore, the trust and acceptance of AI models by clinicians directly affect their adoption and implementation. Therefore, education and training programs are crucial for enhancing physicians' AI literacy [47].

Evolution of Artificial Intelligence in Clinical Diagnosis

The evolution of AI in clinical diagnosis has progressed from simple specialized systems to complex deep learning models. Early AI systems were based on fixed rules and expert knowledge bases. While these systems achieved some success in specific tasks, they had limited scalability and flexibility. The advancement of deep learning technologies, particularly the emergence of LLMs, has ushered AI applications in the health care sector into a new era [48,49].

LLM can learn from vast amounts of medical data to autonomously discover and summarize diagnostic rules, significantly enhancing diagnostic accuracy and reliability. The development of RAG technology and fine-tuning techniques has further enabled LLM to acquire advanced domain expertise and effectively perform specialized tasks.

Ethics of Artificial Intelligence in Clinical Diagnosis

Although the pace of artificial intelligence development is swift, its broad implementation in clinical settings continues to encounter numerous obstacles, including concerns over data privacy, accountability, and ethics. Consequently, numerous scholars [50-53] underscore the imperative of utmost caution in using these technologies. Advances in the future will necessitate not only technological innovations but also comprehensive enhancements in legal and ethical frameworks to ensure that AI technology is safely and effectively woven into clinical diagnostic processes. In deploying LLMs within actual clinical workflows, it is crucial to first guarantee the transparency of all used data and secure patients' informed consent. In addition, to tackle potential biases within AI models, periodic audits are advised to identify and amend any discrepancies. Furthermore, to safeguard patient safety and adhere to regulatory demands, medical institutions should work alongside legal and ethical experts to establish stringent guidelines and oversight mechanisms for AI use. For instance,

XSL•FO
RenderX

forming an ethics committee to assess and monitor AI applications could ensure compliance with ethical standards and legal requirements. These targeted measures are essential to surmount existing challenges and foster the successful incorporation of AI technologies in clinical diagnostics.

Application of LLMs in Specific Medical Fields

The application of LLMs in the medical field is gradually expanding, especially in imaging diagnosis, clinical decision support, and personalized treatment planning. Due to their specific needs and challenges, each medical field shows different ways and effects of LLMs' application.

Ophthalmology is one of the pioneers of LLMs' applications. In ophthalmic diagnosis, imaging data such as fundus images, retinal scans are typically complex, but LLMs excel in processing and analyzing these types of data [45,54]. Research has shown that LLMs can identify minor lesions in fundus images and diagnose conditions such as glaucoma and macular degeneration [55,56]. Ophthalmic diagnostics rely not only on imaging but also on additional data such as patients' genetic information and blood sugar levels. In the future, LLMs could integrate these multimodal data to achieve more accurate disease predictions through personalized treatment. Particularly in resource-limited areas, easily accessible LLMs with low usage thresholds could replace some ophthalmologists in preliminary screenings, further providing efficient diagnostic support in remote regions.

There are many internal medicine diseases that require long-term follow-up and monitoring. LLMs can process all historical data of patients simultaneously and updating personalized treatment plans, assisting clinical professionals in making more beneficial decisions [57-59]. In the future, LLMs will be paired with wearable devices to monitor patients' health in real time, predict potential risks through data analysis, and provide early intervention for patients with medical diseases, thereby reducing the incidence and recurrence of the disease.

In the fields of otolaryngology [60,61] and dermatology [62,63], LLMs have been used to analyze imaging data for detecting lesions in respective areas. The latest models now offer voice input features, allowing patients to use the model anytime and anywhere to help in the early detection of speech disorders and vocal cord issues. In the future, integrating voice recognition with physiological data can also assist physicians in more accurately locating lesion areas during otolaryngological surgeries, thus improving treatment efficacy. Furthermore, by combining images of skin lesions with patients' genetic data, LLMs can help predict the risk of dermatological conditions and provide early warnings.

Exploration of the Use of LLMs in Various Clinical Departments

Currently, extensive research in fields such as ophthalmology, internal medicine, and radiology has demonstrated the substantial potential of LLMs in clinical diagnostics and pathological analysis. These models have even been implemented in some hospitals. Many clinical professionals are actively exploring how to integrate these technologies into their daily diagnostic and treatment routines.

However, the application of LLMs in other specialized areas remains limited, and research in these fields appears to be lacking. Several reasons account for this disparity: First, the departments mentioned above primarily focus on diagnostic issues, providing rich training data for large models, especially in terms of imaging and case data. Second, the main challenges these departments face in clinical practice, such as accurate diagnosis and disease prediction, are areas where LLMs can excel. In contrast, other departments such as surgery, although also using imaging data, face complexities in surgical and procedural tasks that hinder the maturity of AI applications. Gynecology has seen some applications of image recognition, but lacks depth in research and sufficient data accumulation, making model training challenging. In addition, real-world factors such as data privacy protection and technology dissemination also restrict the application of large models in certain departments.

Future Directions

The "human-AI collaboration" model involves an initial diagnosis provided by AI, which is then reviewed and confirmed by clinicians. AI's capability to analyze clinical data in real time enables it to offer personalized monitoring plans based on the specific conditions of patients. This continuous tracking of patient health and treatment outcomes helps achieve the goals of personalized medicine and precise diagnosis [64,65]. In addition, AI can provide customized services and recommendations based on user preferences and backgrounds, enhancing user experience and effectiveness. This model combines the rapid processing capabilities of AI with the expert judgment of clinicians, improving the efficiency and reliability of clinical trials. It also enhances data analysis and patient management, offering significant advantages in cost reduction, resource use, and ensuring the reliability of trial results.

Although LLMs are not inherently designed for clinical diagnostic tasks, advancements in technology and data accumulation are expected to improve their performance in clinical settings. Techniques such as large-scale medical literature analysis, specific clinical data training, task-specific fine-tuning, personalized training for particular scenarios, and integration with APIs or other supplementary software tools are anticipated to enhance the diagnostic support and treatment recommendations provided by these models [66,67]. Hybrid models could be developed by combining rule-based clinical decision support systems with the pattern recognition capabilities of LLMs. For example, Vision China 2023 introduced Eye GPT [68], a system that integrates ophthalmic medical knowledge with LLM. This system aims to assist clinicians in disease diagnosis and improve medical efficiency by combining extensive ophthalmic information with powerful computational capabilities. This innovation in integrating large models with specialized clinical fields is expected to play a crucial role in future clinical applications and provide research directions for other medical specialties.

Limitations

This study has several limitations. First, the inclusion criteria restricted the review to studies comparing the diagnostic accuracy of LLMs with that of clinical health care professionals

XSL•FO
RenderX

using case groups. This limitation may affect the comprehensiveness of the review and introduce selection bias. In addition, there is no specialized tool for assessing the risk of bias in literature related to LLMs. Although PROBAST was used to evaluate the quality of the included studies, its focus on diagnostic accuracy may influence the evaluation results. Finally, significant heterogeneity among the studies was observed, with variations in outcome measures potentially related to differences in intervention subjects, prompt inputs, and information modalities. Further exploration of LLM diagnostic performance is needed through large-scale, multicenter, and high-quality cross-sectional and cohort studies.

Conclusions

This systematic review included 20 studies comparing the diagnostic accuracy of LLMs with that of health care professionals, encompassing various generative AI models and medical specialties. The findings indicate that while LLMs still have a long way to go in accurately diagnosing real-world clinical scenarios and currently lack the level of understanding of human experts, they undeniably possess significant potential as health care assistants. With ongoing advancements and optimizations in technology, it is anticipated that LLMs will play an increasingly important role in future clinical diagnostics.

Conflicts of Interest

None declared.

Multimedia Appendix 1
Details of the search strategy in PubMed.
[DOCX File, 15 KB - medinform_v13i1e64963_app1.docx]

Multimedia Appendix 2
Quality assessment of included studies.
[DOCX File, 23 KB - medinform_v13i1e64963_app2.docx]

Multimedia Appendix 3
Characteristics of large language models (LLMs) applied in clinical diagnostic studies.
[DOCX File, 28 KB - medinform_v13i1e64963_app3.docx]

Checklist 1
PRISMA (Preferred Reporting Items for Systematic Reviews and Meta-Analysis) checklist.
[PDF File, 93 KB - medinform_v13i1e64963_app4.pdf]

References

1. Vaswani A, Shazeer N, Parmar N, et al. Attention is all you need. Presented at: NIPS'17: Proceedings of the 31st International Conference on Neural Information Processing Systems; Dec 4-9, 2017; Long Beach California USA.
2. Wentao S, Ruixiao L, Tianxiang S, et al. Large language models: principles, implementation, and progress. J Comp Res Dev (2):351-361. [doi: 10.7544/issn1000-1239.202330303]
3. Guo H, Liu P, Lu R, et al. Research on a massively large artificial intelligence model and its application in medicine. Sci Sin-Vitae 2024 Jan 1;54. [doi: 10.1360/SSV-2022-0298]
4. Our stubborn quest for diagnostic certainty. N Engl J Med 1989 Nov 2;321(18):1272-1273. [doi: 10.1056/NEJM198911023211820]
5. Nour M, Senturk U, Polat K. Diagnosis and classification of Parkinson's disease using ensemble learning and 1D-PDCovNN. Comput Biol Med 2023 Jul;161:107031. [doi: 10.1016/j.compbiomed.2023.107031] [Medline: 37211002]
6. Thirunavukarasu AJ, Ting DSJ, Elangovan K, Gutierrez L, Tan TF, Ting DSW. Large language models in medicine. Nat Med 2023 Aug;29(8):1930-1940. [doi: 10.1038/s41591-023-02448-8] [Medline: 37460753]
7. McInnes MDF, Moher D, Thombs BD, et al. Preferred Reporting Items for a Systematic Review and Meta-analysis of Diagnostic Test Accuracy Studies: the PRISMA-DTA statement. JAMA 2018 Jan 23;319(4):388-396. [doi: 10.1001/jama.2017.19163] [Medline: 29362800]
8. Wolff RF, Moons KGM, Riley RD, et al. PROBAST: a tool to assess the risk of bias and applicability of prediction model studies. Ann Intern Med 2019 Jan 1;170(1):51-58. [doi: 10.7326/M18-1376] [Medline: 30596875]
9. Takita H, Kabata D, Walston SL, et al. Diagnostic performance comparison between generative AI and physicians: a systematic review and meta-analysis. medRxiv. Preprint posted online on Mar 18, 2024. [doi: 10.1101/2024.01.20.24301563]
10. Zhang J, Ma Y, Zhang R, et al. A comparative study of GPT-4o and human ophthalmologists in glaucoma diagnosis. Sci Rep 2024;14(1):30385. [doi: 10.1038/s41598-024-80917-x]

XSL•FO
RenderX

11. Makhoul M, Melkane AE, Khoury PE, Hadi CE, Matar N. A cross-sectional comparative study: ChatGPT 3.5 versus diverse levels of medical experts in the diagnosis of ENT diseases. Eur Arch Otorhinolaryngol 2024 May;281(5):2717-2721. [doi: 10.1007/s00405-024-08509-z] [Medline: 38365990]
12. Pillai J, Pillai K. Accuracy of generative artificial intelligence models in differential diagnoses of familial Mediterranean fever and deficiency of Interleukin-1 receptor antagonist. J Transl Autoimmun 2023 Dec;7:100213. [doi: 10.1016/j.jtauto.2023.100213] [Medline: 37927888]
13. Levin C, Kagan T, Rosen S, Saban M. An evaluation of the capabilities of language models and nurses in providing neonatal clinical decision support. Int J Nurs Stud 2024 Jul;155:104771. [doi: 10.1016/j.ijnurstu.2024.104771]
14. Lyons RJ, Arepalli SR, Fromal O, Choi JD, Jain N. Artificial intelligence chatbot performance in triage of ophthalmic conditions. Can J Ophthalmol 2024 Aug;59(4):e301-e308. [doi: 10.1016/j.jcjo.2023.07.016] [Medline: 37572695]
15. Sarangi PK, Narayan RK, Mohakud S, Vats A, Sahani D, Mondal H. Assessing the capability of ChatGPT, Google Bard, and Microsoft Bing in solving radiology case vignettes. Indian J Radiol Imaging 2024 Apr;34(2):276-282. [doi: 10.1055/s-0043-1777746] [Medline: 38549897]
16. Paslı S, Şahin AS, Beşer MF, Topçuoğlu H, Yadigaroğlu M, İmamoğlu M. Assessing the precision of artificial intelligence in ED triage decisions: insights from a study with ChatGPT. Am J Emerg Med 2024 Apr;78:170-175. [doi: 10.1016/j.ajem.2024.01.037] [Medline: 38295466]
17. Wang Z, Zhang Z, Traverso A, Dekker A, Qian L, Sun P. Assessing the role of GPT-4 in thyroid ultrasound diagnosis and treatment recommendations: enhancing interpretability with a chain of thought approach. Quant IMAGING Med Surg 2024 Feb 1;14(2):1602-1615. [doi: 10.21037/qims-23-1180] [Medline: 38415150]
18. Huang AS, Hirabayashi K, Barna L, Parikh D, Pasquale LR. Assessment of a large language model's responses to questions and cases about glaucoma and retina management. JAMA Ophthalmol 2024 Apr 1;142(4):371-375. [doi: 10.1001/jamaophthalmol.2023.6917] [Medline: 38386351]
19. Stoneham S, Livesey A, Cooper H, Mitchell C. ChatGPT versus clinician: challenging the diagnostic capabilities of artificial intelligence in dermatology. Clin Exp Dermatol 2024 Jun 25;49(7):707-710. [doi: 10.1093/ced/llad402] [Medline: 37979201]
20. Hirosawa T, Kawamura R, Harada Y, et al. ChatGPT-generated differential diagnosis lists for complex case-derived clinical vignettes: diagnostic accuracy evaluation. JMIR Med Inform 2023 Oct 9;11:e48808. [doi: 10.2196/48808] [Medline: 37812468]
21. Horiuchi D, Tatekawa H, Oura T, et al. ChatGPT's diagnostic performance based on textual vs. visual information compared to radiologists' diagnostic performance in musculoskeletal radiology. Eur Radiol 2025 Jan;35(1):506-516. [doi: 10.1007/s00330-024-10902-5] [Medline: 38995378]
22. Mitsuyama Y, Tatekawa H, Takita H, et al. Comparative analysis of GPT-4-based ChatGPT's diagnostic performance with radiologists using real-world radiology reports of brain tumors. Eur Radiol 2025 Apr;35(4):1938-1947. [doi: 10.1007/s00330-024-11032-8] [Medline: 39198333]
23. Hirosawa T, Mizuta K, Harada Y, Shimizu T. Comparative evaluation of diagnostic accuracy between Google Bard and physicians. Am J Med 2023 Nov;136(11):1119-1123. [doi: 10.1016/j.amjmed.2023.08.003] [Medline: 37643659]
24. Suh PS, Shim WH, Suh CH, et al. Comparing diagnostic accuracy of radiologists versus GPT-4V and Gemini Pro Vision using image inputs from Diagnosis Please cases. Radiology 2024 Jul;312(1):e240273. [doi: 10.1148/radiol.240273] [Medline: 38980179]
25. Fraser H, Crossland D, Bacher I, Ranney M, Madsen T, Hilliard R. Comparison of diagnostic and triage accuracy of Ada Health and WebMD symptom checkers, ChatGPT, and physicians for patients in an emergency department: clinical data analysis study. JMIR MHealth UHealth 2023 Oct 3;11:e49995. [doi: 10.2196/49995] [Medline: 37788063]
26. Hirosawa T, Harada Y, Yokose M, Sakamoto T, Kawamura R, Shimizu T. Diagnostic accuracy of differential-diagnosis lists generated by generative pretrained transformer 3 chatbot for clinical vignettes with common chief complaints: a pilot study. Int J Environ Res Public Health 2023 Feb 15;20(4):3378. [doi: 10.3390/ijerph20043378] [Medline: 36834073]
27. Shemer A, Cohen M, Altarescu A, et al. Diagnostic capabilities of ChatGPT in ophthalmology. GRAEFES Arch Clin Exp Ophthalmol 2024 Jul;262(7):2345-2352. [doi: 10.1007/s00417-023-06363-z] [Medline: 38183467]
28. Mohammadi M, Parviz S, Parvaz P, Pirmoradi MM, Afzalimoghaddam M, Mirfazaelian H. Diagnostic performance of ChatGPT in tibial plateau fracture in knee X-ray. Emerg Radiol 2025 Feb;32(1):59-64. [doi: 10.1007/s10140-024-02298-y] [Medline: 39613920]
29. Arslan B, Nuhoglu C, Satici MO, Altinbilek E. Evaluating LLM-based generative AI tools in emergency triage: a comparative study of ChatGPT Plus, Copilot Pro, and triage nurses. Am J Emerg Med 2025 Mar;89:174-181. [doi: 10.1016/j.ajem.2024.12.024] [Medline: 39731895]
30. Rojas-Carabali W, Cifuentes-González C, Wei X, et al. Evaluating the diagnostic accuracy and management recommendations of ChatGPT in uveitis. Ocul Immunol Inflamm 2024 Oct;32(8):1526-1531. [doi: 10.1080/09273948.2023.2253471] [Medline: 37722842]
31. Kaya K, Gietzen C, Hahnfeldt R, et al. Generative Pre-trained Transformer 4 analysis of cardiovascular magnetic resonance reports in suspected myocarditis: a multicenter study. J Cardiovasc Magn Reson 2024;26(2):101068. [doi: 10.1016/j.jocmr.2024.101068] [Medline: 39079602]

XSL•FO
RenderX

32. Delsoz M, Madadi Y, Raja H, et al. Performance of ChatGPT in diagnosis of corneal eye diseases. Cornea 2024 May 1;43(5):664-670. [doi: 10.1097/ICO.0000000000003492] [Medline: 38391243]
33. Ming S, Yao X, Guo X, et al. Performance of ChatGPT in ophthalmic registration and clinical diagnosis: cross-sectional study. J Med Internet Res 2024;26:e60226. [doi: 10.2196/60226]
34. Nakaura T, Yoshida N, Kobayashi N, et al. Preliminary assessment of automated radiology report generation with generative pre-trained transformers: comparing results to radiologist-generated reports. Jpn J Radiol 2024 Feb;42(2):190-200. [doi: 10.1007/s11604-023-01487-y] [Medline: 37713022]
35. Ito N, Kadomatsu S, Fujisawa M, et al. The accuracy and potential racial and ethnic biases of GPT-4 in the diagnosis and triage of health conditions: evaluation study. JMIR Med Educ 2023 Nov 2;9:e47532. [doi: 10.2196/47532] [Medline: 37917120]
36. Gunes YC, Cesur T. The diagnostic performance of large language models and general radiologists in thoracic radiology cases: a comparative study. J Thorac Imaging 2024 Sep 13. [doi: 10.1097/RTI.0000000000000805] [Medline: 39269227]
37. Delsoz M, Raja H, Madadi Y, et al. The use of ChatGPT to assist in diagnosing glaucoma based on clinical case reports. Ophthalmol Ther 2023 Dec;12(6):3121-3132. [doi: 10.1007/s40123-023-00805-x] [Medline: 37707707]
38. Liu X, Wu J, Shao A, et al. Uncovering language disparity of ChatGPT in healthcare: non-English clinical environment for retinal vascular disease classification. medRxiv. Preprint posted online on Jul 14, 2023. [doi: 10.1101/2023.06.28.23291931]
39. Chao LI, Youmei C, Yani D, Yaoping C, Xiuzhen C, Jie Q. Evaluation of the performance of generative artificial intelligence in generating radiology reports. Journal of New Medicine 2024;55(11):853-860. [doi: 10.3969/j.issn.0253-9802.2024.11.001]
40. Zhao P, Zhang H, Yu Q, et al. Retrieval-augmented generation for ai-generated content: a survey. arXiv. Preprint posted online on Feb 29, 2024. [doi: 10.48550/arXiv.2402.19473]
41. Meskó B. Prompt engineering as an important emerging skill for medical professionals: tutorial. J Med Internet Res 2023 Oct 4;25:e50638. [doi: 10.2196/50638] [Medline: 37792434]
42. Giray L. Prompt engineering with ChatGPT: a guide for academic writers. Ann Biomed Eng 2023 Dec;51(12):2629-2633. [doi: 10.1007/s10439-023-03272-4] [Medline: 37284994]
43. Han T, Adams LC, Bressem KK, Busch F, Nebelung S, Truhn D. Comparative analysis of multimodal large language model performance on clinical vignette questions. JAMA 2024 Apr 16;331(15):1320-1321. [doi: 10.1001/jama.2023.27861] [Medline: 38497956]
44. Horiuchi D, Tatekawa H, Oura T, et al. Comparison of the diagnostic accuracy among GPT-4 based ChatGPT, GPT-4V based ChatGPT, and radiologists in musculoskeletal radiology. medRxiv. Preprint posted online on Dec 9, 2023. [doi: 10.1101/2023.12.07.23299707]
45. Sorin V, Kapelushnik N, Hecht I, et al. Integrated visual and text-based analysis of ophthalmology clinical cases using a large language model. Sci Rep 2025 Feb 10;15(1):4999. [doi: 10.1038/s41598-025-88948-8] [Medline: 39930078]
46. He K, Mao R, Lin Q, et al. A survey of large language models for healthcare: from data, technology, and applications to accountability and ethics. Information Fusion 2025 Jun;118:102963. [doi: 10.1016/j.inffus.2025.102963]
47. Topol EJ. High-performance medicine: the convergence of human and artificial intelligence. Nat Med 2019 Jan;25(1):44-56. [doi: 10.1038/s41591-018-0300-7] [Medline: 30617339]
48. Esteva A, Robicquet A, Ramsundar B, et al. A guide to deep learning in healthcare. Nat Med 2019 Jan;25(1):24-29. [doi: 10.1038/s41591-018-0316-z] [Medline: 30617335]
49. Reddy S, Fox J, Purohit MP. Artificial intelligence-enabled healthcare delivery. J R Soc Med 2019 Jan;112(1):22-28. [doi: 10.1177/0141076818815510] [Medline: 30507284]
50. Wang C, Liu S, Yang H, Guo J, Wu Y, Liu J. Ethical considerations of using ChatGPT in health care. J Med Internet Res 2023 Aug 11;25:e48009. [doi: 10.2196/48009] [Medline: 37566454]
51. Meng X, Yan X, Zhang K, et al. The application of large language models in medicine: a scoping review. iScience 2024 May 17;27(5):109713. [doi: 10.1016/j.isci.2024.109713] [Medline: 38746668]
52. Zhang J, Sun K, Jagadeesh A, et al. The potential and pitfalls of using a large language model such as ChatGPT, GPT-4, or LLaMA as a clinical assistant. J Am Med Inform Assoc 2024 Sep 1;31(9):1884-1891. [doi: 10.1093/jamia/ocae184] [Medline: 39018498]
53. Lalmuanawma S, Hussain J, Chhakchhuak L. Applications of machine learning and artificial intelligence for Covid-19 (SARS-CoV-2) pandemic: a review. Chaos Solitons Fractals 2020 Oct;139:110059. [doi: 10.1016/j.chaos.2020.110059] [Medline: 32834612]
54. Carlà MM, Crincoli E, Rizzo S. Retinal imaging analysis performed by ChatGPT-4O and Gemini Advanced: the turning point of the revolution? Retina (Philadelphia, Pa) 2025 Apr 1;45(4):694-702. [doi: 10.1097/IAE.0000000000004351] [Medline: 39715322]
55. Ghalibafan S, Taylor Gonzalez DJ, Cai LZ, et al. Applications of multimodal generative artificial intelligence in a real-world retina clinic setting. Retina (Philadelphia, Pa) 2024 Oct 1;44(10):1732-1740. [doi: 10.1097/IAE.0000000000004204] [Medline: 39287535]

XSL•FO
RenderX

56. Raja H, Huang X, Delsoz M, et al. Diagnosing glaucoma based on the ocular hypertension treatment study dataset using chat generative pre-trained transformer as a large language model. Ophthalmol Sci 2025;5(1):100599. [doi: 10.1016/j.xops.2024.100599] [Medline: 39346574]
57. Kuzan BN, Meşe İ, Yaşar S, Kuzan TY. A retrospective evaluation of the potential of ChatGPT in the accurate diagnosis of acute stroke. Diagn Interv Radiol 2024 Sep 2. [doi: 10.4274/dir.2024.242892] [Medline: 39221691]
58. Chiang KL, Chou YC, Tung H, et al. Customized GPT model largely increases surgery decision accuracy for pharmaco-resistant epilepsy. J Clin Neurosci 2024 Dec;130:110918. [doi: 10.1016/j.jocn.2024.110918] [Medline: 39541652]
59. Ding JE, Thao PNM, Peng WC, et al. Large language multimodal models for new-onset type 2 diabetes prediction using five-year cohort electronic health records. Sci Rep 2024 Sep 6;14(1):20774. [doi: 10.1038/s41598-024-71020-2] [Medline: 39237580]
60. Maniaci A, Chiesa-Estomba CM, Lechien JR. ChatGPT-4 consistency in interpreting laryngeal clinical images of common lesions and disorders. Otolaryngol Head Neck Surg 2024 Oct;171(4):1106-1113. [doi: 10.1002/ohn.897] [Medline: 39045737]
61. Lechien JR, Naunheim MR, Maniaci A, et al. Performance and consistency of ChatGPT-4 versus otolaryngologists: a clinical case series. Otolaryngol Head Neck Surg 2024 Jun;170(6):1519-1526. [doi: 10.1002/ohn.759] [Medline: 38591726]
62. Gabashvili IS. ChatGPT in dermatology: a comprehensive systematic review. medRxiv. Preprint posted online on Jun 12, 2023. [doi: 10.1101/2023.06.11.23291252]
63. Pillai A, Joseph SP, Hardin J. Evaluating the diagnostic and treatment recommendation capabilities of GPT-4 vision in dermatology. medRxiv. Preprint posted online on Jan 26, 2024. [doi: 10.1101/2024.01.24.24301743]
64. Beam AL, Kohane IS. Big data and machine learning in health care. JAMA 2018 Apr 3;319(13):1317-1318. [doi: 10.1001/jama.2017.18391] [Medline: 29532063]
65. Rajkomar A, Oren E, Chen K, et al. Scalable and accurate deep learning with electronic health records. NPJ Digit Med 2018;1(1):18. [doi: 10.1038/s41746-018-0029-1] [Medline: 31304302]
66. Zhou J, He X, Sun L, et al. SkinGPT-4: an interactive dermatology diagnostic system with visual large language model. medRxiv. Preprint posted online on Jun 13, 2023. [doi: 10.1101/2023.06.10.23291127]
67. Betzler BK, Chen H, Cheng CY, et al. Large language models and their impact in ophthalmology. Lancet Digit Health 2023 Dec;5(12):e917-e924. [doi: 10.1016/S2589-7500(23)00201-7] [Medline: 38000875]
68. Chen X, Zhao Z, Zhang W, et al. EyeGPT: ophthalmic assistant with large language models. arXiv. Preprint posted online on Feb 29, 2024. [doi: 10.48550/arXiv.2403.00840]

Abbreviations

AI: artificial intelligence
CINAHL: Cumulative Index to Nursing and Allied Health Literature
CNKI: China National Knowledge Infrastructure
LLM: large language model
MeSH: Medical Subject Heading
PRISMA-DTA: Preferred Reporting Items for Systematic Reviews and Meta-analysis of Diagnostic Test Accuracy Studies
PROBAST: Prediction Model Risk of Bias Assessment Tool
RAG: retrieval-augmented generation

Edited by A Castonguay; submitted 31.07.24; peer-reviewed by A Jafarizadeh, S Laplante, ST Arasteh; revised version received 19.03.25; accepted 25.03.25; published 25.04.25.

Please cite as:
Shan G, Chen X, Wang C, Liu L, Gu Y, Jiang H, Shi T
Comparing Diagnostic Accuracy of Clinical Professionals and Large Language Models: Systematic Review and Meta-Analysis
JMIR Med Inform 2025;13:e64963
URL: https://medinform.jmir.org/2025/1/e64963
doi:10.2196/64963

© Guxue Shan, Xiaonan Chen, Chen Wang, Li Liu, Yuanjing Gu, Huiping Jiang, Tingqi Shi. Originally published in JMIR Medical Informatics (https://medinform.jmir.org), 25.4.2025. This is an open-access article distributed under the terms of the Creative Commons Attribution License (https://creativecommons.org/licenses/by/4.0/), which permits unrestricted use, distribution, and reproduction in any medium, provided the original work, first published in JMIR Medical Informatics, is properly cited. The complete bibliographic information, a link to the original publication on https://medinform.jmir.org/, as well as this copyright and license information must be included.

XSL•FO
RenderX

Using Large Language Models to Enhance Exercise Recommendations and Physical Activity in Clinical and Healthy Populations: Scoping Review

Xiangxun Lai[1], PhD; Jiacheng Chen[2], MD; Yue Lai[3], BSc; Shengqi Huang[2,4], MSci; Yongdong Cai[4], MSci; Zhifeng Sun[2], MSci; Xueding Wang[2], MSci; Kaijiang Pan[5], PhD; Qi Gao[1], Prof Dr; Caihua Huang[1,2], Prof Dr

[1]School of Sport Medicine and Rehabilitation, Beijing Sport University, No.48 Xinxi Road, Haidian District, Beijing, China

[2]Research and Communication Center for Exercise and Health, Xiamen University of Technology, 600 Ligong Road, Jimei District, Xiamen, China

[3]Department of Mathematics and Digital Science, Chengyi College, Jimei University, Xiamen, China

[4]School of Physical Education and Sport Science, Fujian Normal University, Fuzhou, China

[5]School of Marine Culture and Tourism, Xiamen Ocean Vocational College, Xiamen, China

Corresponding Author:
Caihua Huang, Prof Dr
School of Sport Medicine and Rehabilitation, Beijing Sport University, No.48 Xinxi Road, Haidian District, Beijing, China

Abstract

Background: Regular exercise recommendations (ERs) and physical activity (PA) are crucial for the prevention and management of chronic diseases. However, creating effective exercise programs demand substantial time and specialized expertise from both medical and sports professionals. Large language models (LLMs), such as ChatGPT, offer a promising solution by helping create personalized ERs. While LLMs show potential, their use in exercise planning remains in its early stages and requires further exploration.

Objectives: This study aims to systematically review and classify the applications of LLMs in ERs and PA. It also seeks to identify existing gaps and provide insights into future research directions for optimizing LLM integration in personalized health interventions.

Methods: A scoping review methodology was used to identify studies related to LLM applications in ERs and PA. Literature searches were conducted in Web of Science, PubMed, IEEE, and arXiv for English language papers published up to March 21, 2024. Keywords included LLMs, chatbots, ERs, PA, fitness plan, and related terms. Two independent reviewers (XL and CH) screened and selected studies based on predefined inclusion criteria. Thematic analysis was used to synthesize findings, which were presented narratively.

Results: An initial search identified 598 papers, of which 1.8% (11/598) of studies were included after screening and applying selection criteria. Of these, ChatGPT-based models were used in 55% (6/11) of the studies. In addition, 73% (8/11) of the studies used expert evaluations and user feedback to assess model usability, and 45% (5/11) of the studies used experimental designs to evaluate LLM interventions in ERs and PA. Key findings indicated that LLMs can generate tailored ERs, save time in clinical practice, and enhance safety by incorporating patient-specific data. They also increased engagement and supported behavior change. This made PA guidance more accessible, especially in remote or underserved communities.

Conclusions: This review highlights the promising applications of LLMs in ERs and PA but emphasizes that they remain a supplement to human expertise. Expert validation is essential to ensure safety and mitigate risks. Future research should prioritize pilot testing, clinician training programs, and large-scale clinical trials to enhance feasibility, transparency, and ethical integration.

(JMIR Med Inform 2025;13:e59309) doi:10.2196/59309

KEYWORDS

artificial intelligence; large language model; chatbots; exercise recommendations; physical activity; AI; LLM

Introduction

Background

Personalized, evidence-based exercise programs play a pivotal role in preventing and managing chronic conditions and reducing the risk of sports injuries. In contrast, poorly designed or inappropriate exercise practices can diminish effectiveness or even cause adverse effects [1]. Therefore, formulating scientifically sound and effective exercise recommendations (ERs) is essential to optimize the health benefits of physical activity (PA) while mitigating potential risks. This approach is instrumental in improving chronic disease conditions and

XSL•FO
RenderX

enhancing quality of life [2-4]. However, implementing these recommendations demands significant human resources and time.

Creating effective ERs requires nuanced, interdisciplinary collaboration between medical and sports professionals [5]. Medical experts, drawing on their knowledge of exercise physiology, medicine, and nutrition, consider individual health conditions, medical histories, and medication usage to ensure safety and efficacy. Simultaneously, sports professionals use their theoretical knowledge and practical experience to tailor individualized exercise plans based on skill levels and needs, working alongside medical counterparts to determine optimal recommendations.

Despite these collaborative efforts, the field of ERs has long faced a "black box" challenge, where the underlying mechanisms of exercise interventions are not fully understood, and outcomes are unpredictable [6-8]. Traditional approaches often rely on comprehensive strategies or personal intuition, introducing subjectivity and limitations. The advent of artificial intelligence (AI) in health care, however, offers promising insights into these complexities, enabling precise personalization.

AI's robust data analysis, text generation, and creative capabilities are revolutionizing ERs and PA formulation, steering it toward precision and individualization. Notably, the linguistic understanding and generation abilities of large language models (LLMs), such as those based on transformer neural network architectures, have shown potential in personalized medicine and health management across various domains [9-15].

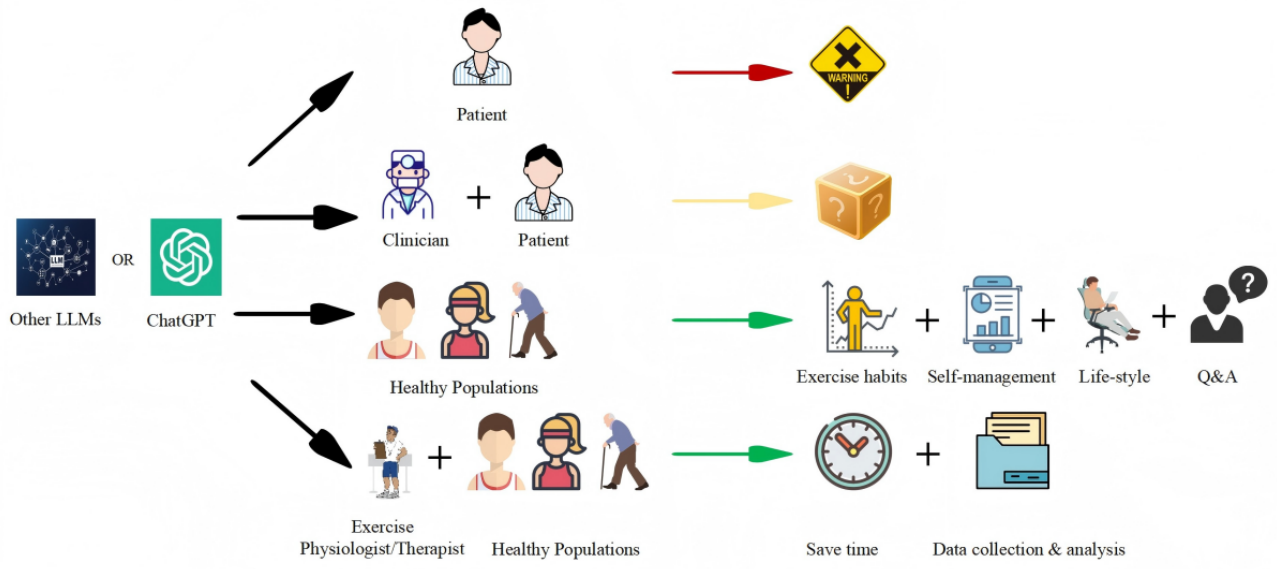
Numerous studies have successfully tailored LLMs for specific domain tasks [16,17]. Research indicates that using self-supervision or continuing pretraining on domain-specific corpora enhances model performance in downstream tasks [18-20].

Given these developments, health and wellness are poised to be vital areas for AI's future impact. By using advanced AI tools such as LLMs and chatbots, ERs and PA formulation is becoming increasingly scientific and personalized [21]. This not only has the potential to optimize exercise outcomes but may also enhance safety, ushering in a new era in chronic disease prevention and health management.

Objectives

To our knowledge, this paper represents one of the first scoping reviews of the applications of LLMs in the fields of ERs and PA, with 2 primary objectives. First, we aim to summarize and categorize the applications of LLMs used in existing ERs and PA literature to identify trends, synergies, and patterns that could guide future investigations. Second, through our comprehensive review of the literature, we seek to provide valuable insights that can inform and shape the future development of AI technologies in the field of exercise health. By highlighting gaps and opportunities, we aim to assist in directing AI advancements to better meet the needs of personalized exercise and health management. This scoping review is unique not for its focus on health outcomes of interventions but for its emphasis on applying diverse LLM methodologies within the realms of ERs and PA and for providing guidance on future advancements in this interdisciplinary field (Figure 1).

Figure 1. Potential roles and limitations of LLMs in exercise recommendations and physical activity. Direct use for patients is deemed inappropriate, while assisting clinicians requires further validation. LLMs have demonstrated benefits in promoting healthy habits and self-management among the general population. For exercise physiologists and therapists, LLMs enhance efficiency in client management, exercise suggestions, and data analysis. LLMs: large language models; Q&A: question and answer.



The search strategy was designed to address several key research questions guiding this scoping review: (1) What is the current progress in applying LLMs for ERs in the health care field, and how effectively do LLMs support health care professionals in guiding patients toward personalized, evidence-based exercise program? (2) What is the progress of LLM applications in the PA domain for healthy populations, and can these models effectively assist in promoting personalized, evidence-based

XSL•FO
RenderX

exercise program? (3) What methods have current studies used to validate the performance of LLMs, and do these models achieve the competency level of professional practitioners? (4) What challenges have been encountered in applying LLMs for ERs and PA, and what valuable insights do these challenges offer for future updates and iterations of LLM technology?

Methods

Study Design

We followed the scoping review methodology proposed by Arksey and O'Malley, which encompasses (1) identifying research questions, (2) relevant studies, (3) study selection, (4) data charting, and (5) collating, summarizing, and reporting the results. In addition, we adhered to the PRISMA-ScR (Preferred Reporting Items for Systematic Reviews and Meta-Analyses extension for Scoping Reviews) checklist to ensure comprehensive reporting.

Search Strategy Development and Study Selection

The search strategy was developed through a collaborative process involving the research team members (XL and CH), who conducted the initial design and refinement of the search terms. The terms were informed by a thorough review of existing literature, discussions among the team members, and the key research questions identified at the outset of the study. These questions focused on the application and efficacy of LLMs in ERs and PA.

To ensure the robustness of the search strategy, we targeted 4 major databases: Web of Science, PubMed, IEEE, and arXiv, using comprehensive search strings that combined terms related to AI, LLMs, and exercise science. The search strategy included combinations of keywords such as "artificial intelligence," "large language model," "exercise recommendations," and "physical activity" to capture a wide range of relevant studies.

While we did not formally consult a librarian or an information scientist, the team members leveraged their collective expertise in medical informatics and exercise science to craft a strategy that was both comprehensive and targeted. The detailed search process, including inclusion and exclusion criteria, is outlined in Table S1 in Multimedia Appendix 1.

Eligibility Criteria

Inclusion Criteria

Non–peer-reviewed and non-English publications or resources were excluded. Studies were included in this review if they met the following criteria:

1. Language: Only those papers that were published in English were considered to ensure consistency and facilitate synthesis across studies.
2. Application of LLMs/Chatbot technologies: Studies that used LLMs or chatbot technologies in the context of ERs, PA guidelines, or fitness interventions were included.
3. Medical and public health context: Papers focusing on applications within medical practice or public health settings related to ERs, PA, or fitness were deemed eligible.
4. Diverse regions and health care contexts: Studies conducted across various geographic regions and health care settings to ensure global applicability and relevance of findings were included.

In addition, studies were considered if the terms "LLMs/Chatbots" and "ERs" or "PA" appeared simultaneously in the title, abstract, or keywords.

For classification purposes, (1) if the study population consisted of patients and the research focused on disease treatment, the study was categorized under ERs; (2) if the study population comprised healthy individuals and the research aimed at enhancing health levels, the study was categorized under PA, and (3) if these specific keywords did not appear but terms such as "fitness plan" or "exercise plan" were present, the study was included after discussion among all reviewers and then appropriately categorized.

Exclusion Criteria

Studies were excluded based on the following criteria:

1. Non–peer-reviewed and non-English publications: Publications that were not peer-reviewed or not published in English were excluded.
2. Nonoriginal research content: Reviews, abstracts, letters, viewpoints, editorials, dissertations, and tutorials were excluded unless they provided original research data.
3. Lack of relevant insights: Studies that did not offer substantial insights into the utilization of LLMs or chatbot technologies in ERs or related fields were excluded.

Data-Charting Process

A data-charting form was collaboratively developed by 2 reviewers (XL and CH) to determine which variables to extract. This form comprised six sections: (1) first author and publication date, (2) study design, (3) sample size or datasets, (4) related models, (5) usability testing, and (6) outcomes or contributions. The 2 reviewers (JC and SH) independently charted the data, discussed the results, and continuously updated the data-charting form in an iterative process.

To ensure the quality and relevance of the included papers, 2 reviewers (XL and CH) independently assessed the relevance of the papers to ensure a thorough and unbiased review process. In cases of disagreement, the remaining 4 authors (JC, ZS, YC, and SH) served as arbitrators, and a final decision was made only when consensus was reached among all 6 authors. To enhance consistency among reviewers, all reviewers initially screened the same publications, discussed the results, and amended the screening and data extraction manual before commencing formal screening. Working in pairs, the reviewers sequentially evaluated the titles, keywords, and abstracts of all publications identified in our searches for potentially relevant studies. Disagreements on study selection and data extraction were resolved through consensus and, if necessary, discussion with additional reviewers. This stringent selection process strengthens the validity and reliability of our findings by ensuring that our review is based on high-quality evidence.

XSL•FO
RenderX

Data Items

We abstracted data on paper characteristics (eg, first author, publication date, and study design), engagement characteristics and contextual factors (eg, sample size or datasets, and the specific LLMs or chatbot technologies used), barriers and facilitators to engagement (eg, results from usability testing and user interaction metrics), and results of any formal assessment of engagement (eg, key outcomes, contributions, and the impact of the models on ERs or PA).

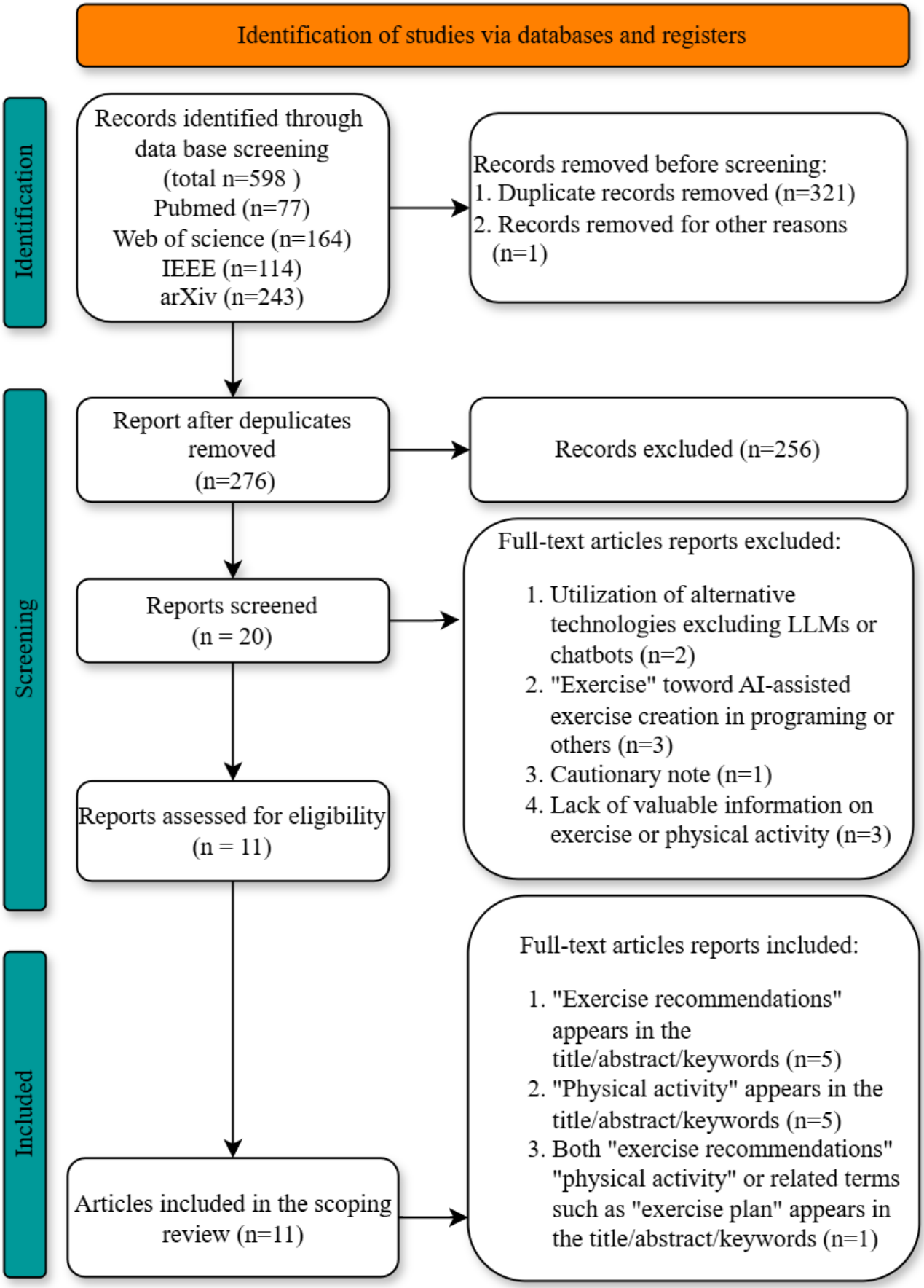
Results

Identification of Studies

An initial keyword search identified 598 papers, and after the removal of duplicates, 276 unique papers remained for screening based on their all fields. Of these, 256 papers were considered irrelevant and subsequently excluded from the review, one of the records cannot search full-text paper. After applying the study selection criteria to the remaining 20 papers, a total of 11 studies were included in the review (Figure 2).

XSL•FO
RenderX

Figure 2. PRISMA-ScR (Preferred Reporting Items for Systematic Reviews and Meta-Analyses for Scoping Review) flow diagram. AI: artificial intelligence; LLMs: large language models.



XSL•FO
RenderX

Study Characteristics

All the details regarding the study characteristics are comprehensively displayed in Tables 1 and 2.

Table . Main characteristics of 5 reports focused on exercise recommendations in this review.

Author (year)	Study designs	Sample size or datasets	Related models	Usability testing	Outcomes or contribution
Zaleski et al (2024) [22]	Mixed methods study	N/A[a]	ChatGPT (February 2023 version)	Expert evaluations	Moderate comprehensiveness (41.2%) and high accuracy (90.7%).
Dergaa et al (2024) [23]	Simulated patient case study	5 profiles	GPT-4	Expert evaluation	Lack of precision for specific conditions; AI not yet a substitute for expert prescriptions.
Haag (2024) [24]	Experimental comparison	450 JITAIs[b] decisions	GPT-4	User feedback	GPT-4-generated JITAIs rated highest in quality, effectiveness, and emotional impact, surpassing health care professionals and layperson-generated content.
Shin et al (2023) [25]	Exploratory study	18	LLM[c]-infused web interface	Expert evaluations.	AI[e]-generated exercise plans are personalized, actionable, and effective in supporting exercise routines.
Sivarajkumar et al (2023) [26]	Algorithm development and testing	13,605 patient records	Rule-based NLP[d], ChatGPT	F_1-score evaluation against gold standard dataset.	Rule-based NLP had best precision; ChatGPT had high recall and lower precision.

[a]N/A: not applicable.

[b]JITAIs: just-in-time adaptive interventions.

[c]LLM: large language model.

[d]NLP: natural language processing.

[e]AI: artificial intelligence.

XSL•FO
RenderX

Table . Main characteristics of 6 reports focused on physical activity in this review.

Author (year)	Study designs	Sample size or datasets	Related models	Usability testing	Outcomes or contribution
Willms and Liu (2024) [27]	Autoethnographic case study	N/A[a]	ChatGPT-3, Pathverse	Expert evaluations	Efficient content creation; recommended 6-step process for future mHealth[b].
Chowdhury et al (2023) [28]	System development and evaluation	1M+ recipes	Neural network (Chatbot)	Empirical validation	Effective in recommending daily fitness and diet plans; future work aims to enhance personalization and usability.
Vandelanotte et al (2023) [29]	Conceptual framework	N/A	NLP[c], ChatGPT[d]	User feedback	Developed a real-time framework for personalized interventions.
To et al (2021) [30]	Quasi-experimental study	116	Ida (Google Inc)	Self-reported	Significantly increased PA[e] among participants.
Liang et al (2021) [31]	Randomized clinical trial	107 dialogues (7808 sentences)	BERT[f]-based classifier	Expert evaluations and user interaction analysis	Personalized dialogues reduced PA barriers, provided tailored support, and improved motivation for sustained PA behaviors.
Wiratunga et al (2020) [32]	Think-aloud methodology	7 participants	Voice-based chatbot (“FitChat”)	User feedback	Enhanced PA adherence and motivation through personalized, voice-based interactions.

[a]N/A: not applicable.

[b]mHealth: mobile health.

[c]NLP: natural language processing.

[d]GPT: Generative Pre-trained Transformer.

[e]PA: physical activity.

[f]BERT: Bidirectional Encoder Representations from Transformers.

Main Findings

Five of the 11 studies reviewed used experimental designs, which constituted 45% [25,26,28,31,32]. These studies typically assessed the effectiveness of AI-driven interventions in ERs and PA, and ChatGPT-based models were used in 55% (6/11) of studies. In addition, 27% (3/11) of studies were case studies, focusing on real-world applications of chatbots and LLMs, while feasibility and development studies accounted for 27% (3/11) of studies, where prototypes and models were evaluated without full-scale trials [22,30,31].

Sample Size or Datasets

Sample-based research: 5 studies (5/11, 45%) involved direct participant testing to assess the models’ effectiveness. These studies explored how LLMs could provide personalized recommendations for various populations [22-24].

Dataset-based research: 4 studies (4/11, 36%) used large datasets to train or fine-tune models, primarily focusing on improving the models’ functionality in specific use cases such as rehabilitation [26].

Other verification methods: 2 studies (2/11, 18%) used expert-driven or simulation-based evaluations rather than using participant data.

Related Models

In the studies reviewed, ChatGPT-based models were used in 55% (6/11) of studies, with applications ranging from fitness recommendations to disease management. The remaining 45% (5/11) of studies used other LLMs or chatbot technologies, including Bidirectional Encoder Representations from Transformers–based models and specialized AI systems designed for specific interventions.

Usability Testing

Expert evaluation: 6 studies (6/11, 55%) used expert evaluation as the primary method for usability testing. These evaluations typically involved health professionals or exercise specialists assessing the generated content or ERs for accuracy, relevance, and practicality [24,31].

Other methods: In 5 studies (5/11, 45%), alternative methods were used for usability testing, which included the following:

XSL•FO
RenderX

1. User interaction metrics: Studies monitored how participants interacted with AI-generated content, measuring factors such as engagement rates, adherence to ERs, and feedback from end users [22,23].
2. Real-time adaptive feedback: Some studies used just-in-time adaptive interventions, where the usability of the model was assessed based on how well it adapted to real-time changes in participants' PA levels [24].

This mixed approach to usability testing highlights that while expert evaluations are crucial for initial validation, real-world interaction and feedback are also critical for assessing the practical application of the models in promoting ERs and PA.

Outcomes or Contributions

Exercise recommendations: In total, 45% (5/11) of studies focused on generating ERs specifically within the medical domain. These studies revealed several key contributions:

1. Tailored interventions: The use of LLMs such as ChatGPT showed promise in generating personalized ERs based on patient health data and conditions [22-24,26,27]. Studies found improvements in accuracy when addressing clinical rehabilitation needs, particularly for cardiac and orthopedic rehabilitation [22,24].
2. Time saving in clinical practice: The integration of AI-driven ERs was shown to reduce the time needed for health care providers to develop exercise plans, improving efficiency in clinical settings [23].
3. Enhanced safety: By incorporating patient-specific health data, LLMs were able to create recommendations that accounted for safety concerns, especially for populations with chronic conditions [30,31].

Physical activity: In total, 55% (6/11) of studies focused on encouraging PA in healthy or general populations. Key contributions in this area include the following:

1. Increased engagement: LLMs and chatbots were effective at increasing PA levels by providing real-time feedback, adaptive exercise plans, and motivation through interactive features. This was particularly beneficial for populations such as older adults and sedentary individuals [23,30].
2. Behavior change support: AI-driven interventions helped users establish and maintain regular PA routines through personalized just-in-time adaptive interventions, demonstrating a positive impact on long-term behavior changes [24,25,28].
3. Accessibility improvements: Chatbots and AI systems provided low-cost, scalable solutions that increased accessibility to PA recommendations, particularly in remote or underserved communities [28].

Discussion

Principal Findings

The findings suggest that LLMs, such as ChatGPT, can effectively generate customized exercise plans, save health care professionals' time, and enhance user engagement through adaptive, real-time feedback. However, it is crucial to emphasize that LLMs serve as a supplementary tool rather than a replacement for human expertise. Their outputs should always be reviewed and validated by qualified professionals, particularly in clinical settings where incorrect ERs could pose potential health risks [22-24,28]. These advantages are particularly beneficial in settings where access to personalized exercise guidance is limited. However, despite their potential, several key challenges and areas for future improvement have been identified.

Comparison With Prior Work

The rapid advancement of LLMs has significantly impacted medical systems, offering enhanced adaptability and precision compared with traditional approaches. In specialized domains such as orthopedics, spinal disorders, and psychotherapy, LLMs demonstrate greater flexibility but still require refinement to meet professional health care standards [11-15].

Unlike previous static, rule-based systems, LLMs have extended their application to complex clinical scenarios such as cardiac rehabilitation and poststroke recovery [24-26]. Their ability to offer dynamic, real-time interactions marks a significant shift. However, they still fall short of professional-level expertise, particularly in aligning with the detailed exercise prescriptions outlined by American College of Sports Medicine guidelines [22,33].

A notable limitation in existing research is the variability in sample size and dataset quality. While some studies used extensive datasets to enhance model training and generalizability, others were constrained by limited sample sizes, which can hinder the robustness of the findings [24,26,34]. This inconsistency underscores the need for standardized, large-scale datasets to better assess and refine LLMs in ERs and PA contexts.

The current landscape of LLMs also features a variety of models, with many studies predominantly relying on ChatGPT [22-24,26,27]. This model shows strong capabilities in generating personalized ERs but remains supplementary to expert input. Comparatively, other models such as Bidirectional Encoder Representations from Transformers–based systems have been explored, offering unique strengths in specific applications [30]. Future research should explore and refine these models to optimize their use in exercise science, tailoring them to address the nuanced needs of this field [30,31].

Furthermore, usability testing remains a critical component in validating LLMs. While expert evaluations have been the primary method in many studies, incorporating real-world user feedback through interaction metrics and engagement analysis offers deeper insights into the practical use of these models. This dual approach—combining expert review with user-centric testing—ensures that LLMs not only meet theoretical standards but also deliver meaningful outcomes in everyday clinical practice [35].

Building on earlier AI applications, the integration of LLMs with wearable technology holds promise for transforming ERs and PA by delivering real-time, personalized insights. However, generative AI in exercise science still requires fine-tuning and specialized data to fully realize its potential. This underscores the ongoing need for high-quality, diverse data sources and

XSL•FO
RenderX

iterative improvements to enhance the reliability and impact of LLM-driven health interventions [34].

LLMs significantly enhance patient engagement and satisfaction by delivering tailored, interactive, and context-aware health interventions. Through natural language understanding, LLMs such as ChatGPT facilitate real-time, adaptive interactions that make ERs and behavior change strategies more relatable and accessible, fostering deeper connections and prolonged participation in fitness routines [32]. Features such as just-in-time adaptive interventions ensure that guidance is provided at critical moments, reinforcing user commitment and fostering a sense of support while allowing users to dynamically adjust goals and promote sustained behavior changes [27]. Personalization is another key driver of satisfaction, as chatbots such as CHARLIE integrate fitness and diet suggestions into daily routines based on user-specific health data, schedules, and preferences, improving adherence and satisfaction [28]. However, sustaining engagement and satisfaction requires addressing challenges such as data accuracy, equitable access, and algorithmic biases. Transparent communication about data collection, robust validation mechanisms, and regulatory frameworks prioritizing inclusivity and fairness are crucial to maximize the potential of LLM-driven health interventions while ensuring scientifically grounded and emotionally supportive recommendations [29,31].

Transparency of LLM Training Data and Fine-Tuning Approaches

One critical yet underexplored aspect of LLM development in ERs and PA is the lack of transparency regarding training data and fine-tuning methodologies. Most reviewed studies did not specify whether LLMs were trained or fine-tuned on exercise- or health-specific datasets, making it difficult to assess their domain relevance and reliability [22,24]. While some studies used general purpose LLMs, their applicability to exercise science remains uncertain due to potential biases and gaps in specialized knowledge [25,30,31].

To enhance technical rigor and reproducibility, future research should focus on documenting training data sources, improving dataset specificity, and incorporating domain-relevant corpora such as clinical guidelines, sports science literature, and patient-reported exercise data. In addition, developing benchmarking frameworks to systematically evaluate LLM-generated ERs will be essential for ensuring accuracy, safety, and adaptability in health care applications. Greater transparency in dataset composition and model fine-tuning will facilitate better comparisons across studies, enabling the optimization of LLMs for evidence-based exercise prescription.

Limitations of the Study

Despite the valuable insights provided by this scoping review, several limitations should be acknowledged. First, the reviewed studies lacked transparency in data formats, training corpora, and methodologies, making it difficult to assess reproducibility and compare the effectiveness of different LLM implementations. In addition, none of the included studies evaluated the accuracy, safety, or long-term impact of LLMs on behavior change, limiting their clinical applicability. Second, small sample sizes and heterogeneous methodologies reduce the generalizability of findings [30]. Many studies focused on feasibility rather than efficacy, highlighting the need for large-scale, multicenter trials and long-term follow-up studies to validate AI-generated ERs [29]. Third, potential publication bias may have skewed the findings, as studies reporting positive outcomes are more likely to be published than those with neutral or negative results [22]. Future reviews should incorporate preprint archives and unpublished datasets for a more balanced assessment.

Finally, a lack of standardized datasets and evaluation criteria hinders direct comparisons between AI models [25]. Future research should focus on developing benchmark frameworks to ensure consistency and reliability in LLM-driven exercise prescription. Addressing these limitations will improve the transparency, safety, and clinical use of AI-assisted ERs .

Future Directions

Real-World Clinical Trials

Future research should prioritize real-world clinical trials to address the current limitations of LLMs in health care, particularly in ERs and PA. Due to the reliance on synthetic data for training, many LLMs lack the real-world data necessary for optimal performance [9-15]. These trials are crucial for collecting high-quality data, enabling better fine-tuning of LLMs and ensuring that their recommendations are accurate and applicable across diverse populations. In ERs and PA, real-world trials can validate the practical effectiveness of LLMs, assess their generalizability, and ensure that their integration into clinical practice is both feasible and scalable, ultimately enhancing personalized health interventions [35] .

Fine-Tuning Existing Models

Currently, no model matches the expertise of exercise science professionals, largely due to inadequate corpus quality and computational limitations [24,32]. The field of exercise science particularly suffers from a lack of standardized data, with many practitioners relying on personal experience or generalized approaches to develop ERs [36]. While the notion that “one set fixed all” is prevalent, it falls short of delivering truly personalized and scientifically grounded exercise guidance. Therefore, the standardization of data formats and the accumulation of a vast array of high-quality data are essential steps for advancing generative AI’s capabilities in exercise science [37-39].

Potential of Retrieval-Augmented Generation

Retrieval-augmented generation (RAG) integrates the real-time retrieval of information with the generative capabilities of LLMs, offering a significant advantage in the domain of ERs and PA [12,28]. This approach ensures that any knowledge gaps in the language model are promptly addressed, reducing the risk of misinformation and enhancing the accuracy of exercise guidance [40]. The effectiveness of RAG is, however, contingent upon the underlying model’s strength, suggesting that fine-tuning a powerful language model in conjunction with RAG could optimize performance [41]. Looking forward, the application of RAG in ERs and PA could extend into broader

XSL•FO
RenderX

health care sectors, potentially revolutionizing personalized medicine and proactive health management by providing data-driven, contextually rich, and adaptive health solutions.

Real-Time Data Collection Via Wearables and Smart Devices: Implementing a Dynamic Feedback Mechanism

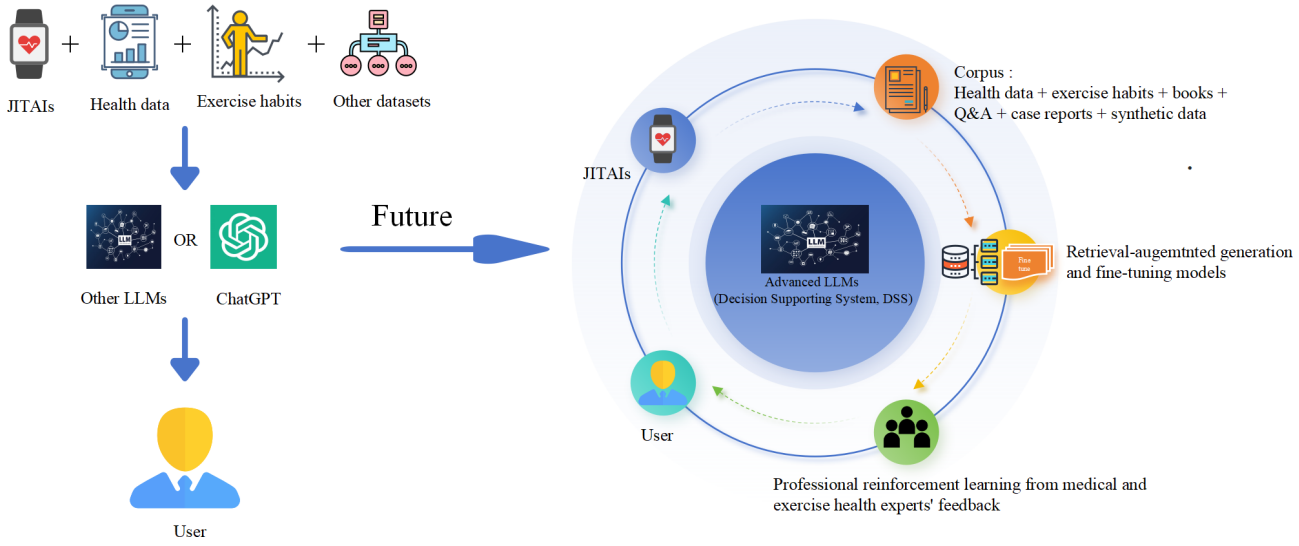
The advent of wearable technology and smart devices has opened new horizons for monitoring health and PA in real time [21,22,34]. These devices, ranging from smartwatches and fitness bands to specialized sensors, continuously track physiological and PA data, including heart rate, steps, calories burned, sleep patterns, and advanced metrics such as heart rate variability and oxygen saturation. Their integration into health care enables real-world, individualized health monitoring, offering valuable insights for ERs interventions [22,25,42].

A key feature of this future direction is the establishment of a dynamic feedback loop between users and AI systems . As users engage in prescribed exercises, performance and physiological data are continuously fed into the AI model [43]. This real-time input allows LLMs to adjust recommendations dynamically, enhancing adherence and optimizing exercise effectiveness [24,30].

However, several technical challenges remain. Data accuracy and reliability vary due to sensor inconsistencies, calibration differences, and environmental influences [28]. Standardized validation protocols and AI-driven error correction models are needed to enhance measurement consistency. In addition, device compatibility and interoperability pose integration hurdles, as wearables operate with different data formats and application programing interfaces [32]. Adopting universal data standards, such as Fast Healthcare Interoperability Resources and Open mHealth, could streamline integration across platforms.

Data privacy and security are also critical concerns, given the continuous transmission of personal health information. Compliance with health insurance portability and accountability act, general data protection regulation, and other regulatory frameworks is essential to prevent data breaches and unauthorized access [26]. End-to-end encryption, federated learning, and decentralized storage solutions can enhance security while maintaining user privacy. Addressing these challenges will be key to ensuring the safe and effective deployment of LLMs in personalized exercise interventions (Figure 3).

Figure 3. The current and future applications of LLMs in exercise recommendations. Currently, health data from JITAIs, wearable devices, exercise habits, and various datasets are processed through LLMs such as ChatGPT to provide recommendations to users. Looking forward, advanced LLMs integrated within a Decision Support System (DSS) will use retrieval-augmented generation and fine-tuning techniques based on extensive corpora including health data, exercise habits, literature, Q&A content, case reports, and synthetic data. Enhanced by real-time data collection via wearable devices and continuous professional reinforcement learning from medical and exercise health experts' feedback, this system aims to support personalized recommendations while addressing critical issues such as clinical validation, integration into health care workflows, personal privacy, artificial intelligence bias, and ethical and regulatory considerations. JITAIs: Just-in-Time Adaptive Interventions; LLMs: large language models; Q&A: question and answer.



Expanding Clinical Validation of LLMs

Despite the growing interest in LLM-driven ERs, real-world clinical validation remains limited, with most studies focusing on feasibility rather than long-term efficacy and safety [22]. To bridge this gap, emerging trials are exploring LLM-assisted exercise coaching in rehabilitation [25] and AI-driven personalized exercise plans for metabolic disorders [28].

However, large-scale, multicenter randomized controlled trials are needed to assess their impact on exercise adherence, rehabilitation outcomes, and chronic disease management across diverse populations. Future research should prioritize standardized evaluation metrics, regulatory oversight, and expert-in-the-loop models to ensure safe, effective, and evidence-based integration of LLMs into health care practice.

Integrating LLMs Into Health Care Workflows

Effective integration of LLMs into clinical practice requires interoperability with electronic health records (EHRs) and clinician training [35]. Standardizing LLM-EHR interactions through protocols such as Fast Healthcare Interoperability Resources and HL7 can enable real-time data exchange and personalized exercise prescription delivery [23]. In addition, structured clinician training programs are essential to enhance AI literacy, ensuring that health care providers can interpret,

XSL•FO
RenderX

validate, and oversee LLM-generated recommendations before clinical application [43]. Implementing expert-in-the-loop frameworks, where clinicians supervise AI outputs, will enhance trust, safety, and adoption in real-world health care settings.

Personal Privacy, AI Bias, and Ethical and Regulatory Considerations

Ensuring robust data privacy and security measures is critical in the deployment of LLMs in health care, as secure data management is essential to protect sensitive health information and safeguard users' personal privacy [28,32]. Maintaining patient confidentiality, particularly when using EHRs in precision medicine, remains a persistent challenge that requires systematic attention [25,26]. Addressing AI bias is equally crucial to prevent inequities in rehabilitation plans and ensure fair and inclusive recommendations across diverse demographic groups, especially in the context of ERs and PA. For example, general purpose LLMs may produce exercise suggestions that are overly strenuous for older adults or unsuitable for individuals with chronic conditions, thereby increasing the risk of injury or adverse health outcomes [25,28,30]. Strategies to mitigate bias include implementing advanced detection algorithms, establishing fairness metrics tailored to the exercise and health domains, and using diverse and representative datasets that encompass a wide range of ages, genders, races, and socioeconomic backgrounds. Moreover, fine-tuning LLMs with domain-specific data and incorporating expert insights from exercise physiologists can further tailor recommendations to the unique needs of these populations [22]. Incorporating feedback loops from underrepresented populations further refines model outputs, enhancing the inclusivity and effectiveness of LLM-driven interventions [16,17].

Transparency and ethical accountability play a foundational role in building user trust and fostering the successful adoption of LLMs in health care. Clear communication about data usage practices, system limitations, and decision-making processes is imperative to enhance user confidence, as a lack of transparency may discourage full engagement with AI-driven tools, ultimately reducing their effectiveness [28]. Furthermore, LLMs face significant ethical challenges, including the potential to provide inaccurate or unsafe recommendations, which could result in adverse health outcomes. Integrating expert oversight and providing explicit disclaimers about the limitations of LLM-generated advice are essential safeguards to mitigate such risks [27]. Finally, compliance with evolving regulatory standards is imperative. LLM-based systems must adhere to rigorous requirements for accuracy, reliability, and accountability to align with medical device regulations and ethical norms, ensuring their safe and effective integration into health care practices [29]. This holistic approach to privacy, bias mitigation, transparency, and regulatory compliance will not only enhance the fairness and accuracy of LLM-driven health interventions but also establish a foundation of trust necessary for their widespread acceptance and long-term success.

Conclusions

While LLMs offer promising support in creating exercise plans, they are not yet on par with expert professionals. Their role should be viewed as an adjunct to human expertise, assisting but not replacing health care and fitness professionals. Ensuring expert validation is essential to mitigate risks and optimize patient safety. Future research should prioritize pilot studies to assess the feasibility of LLM-generated ERs and clinician training programs to enhance AI literacy and integration.

Advancing LLM adoption requires large-scale trials, standardized evaluation frameworks, and regulatory oversight to improve transparency and mitigate bias. Leveraging real-time data from wearables can further refine recommendations. With these advancements, LLMs can evolve into a valuable decision support tool, enhancing accessibility and personalization in exercise science while maintaining expert oversight.

Acknowledgments

The authors would like to express their gratitude to the AI tool, ChatGPT-4 developed by OpenAI, for its assistance in refining and structuring the content during the writing process of this paper. The tool provided invaluable support in enhancing the clarity and coherence of the manuscript. This study was supported by National Intelligent Social Governance Experimental Base Project (grant 350201).

Data Availability

This study is a scoping review and does not involve the generation or analysis of new data. All data used in this review were extracted from publicly available papers indexed in Web of Science, PubMed, IEEE, and arXiv. No new datasets were created or analyzed in the course of this research. The studies included in this review can be accessed through their respective journals and databases.

Authors' Contributions

XL participated in conceptualization, literature search, data curation, and writing—original draft; CH participated in conceptualization, literature search, and writing—original draft; QG participated in conceptualization, writing—original draft, and methodology; JC and YL contributed to review and screening of literature, visualization (figures and tables), and writing—review and editing; SH contributed to review and screening of literature and writing—review and editing; YC contributed to visualization (figures and tables) and writing—review and editing; ZS contributed to writing—review and editing—and supervision; and XW and KP contributed to rereview and editing and supervision.

XSL•FO
RenderX

Conflicts of Interest

None declared.

Multimedia Appendix 1
The search strategy and detailed summary.
[DOCX File, 18 KB - medinform_v13i1e59309_app1.docx]

Checklist 1
PRISMA-ScR (Preferred Reporting Items for Systematic Reviews and Meta-Analyses extension for Scoping Reviews) checklist.
[PDF File, 134 KB - medinform_v13i1e59309_app2.pdf]

References

1. Baumgartner L, Weberruß H, Engl T, Schulz T, Oberhoffer-Fritz R. Exercise training duration and intensity are associated with thicker carotid intima-media thickness but improved arterial elasticity in active children and adolescents. Front Cardiovasc Med 2021;8:618294. [doi: 10.3389/fcvm.2021.618294] [Medline: 34307488]
2. McGee SL, Hargreaves M. Exercise adaptations: molecular mechanisms and potential targets for therapeutic benefit. Nat Rev Endocrinol 2020 Sep;16(9):495-505. [doi: 10.1038/s41574-020-0377-1] [Medline: 32632275]
3. Czosnek L, Rankin N, Zopf E, Richards J, Rosenbaum S, Cormie P. Implementing exercise in healthcare settings: the potential of implementation science. Sports Med 2020 Jan;50(1):1-14. [doi: 10.1007/s40279-019-01228-0] [Medline: 31749112]
4. Lin B, Zhang Z, Zhang W, et al. Associations of physical activity types and intensity with cardiovascular diseases by age and gender among 18,730 Chinese adults. Sci Rep 2023;13(1):14623. [doi: 10.1038/s41598-023-41768-0] [Medline: 37781995]
5. Moe MC, Özmert E, Baudouin C, et al. International Olympic Committee (IOC) consensus paper on sports-related ophthalmology issues in elite sports. BMJ Open Sport Exerc Med 2023;9(3):e001644. [doi: 10.1136/bmjsem-2023-001644] [Medline: 37485004]
6. Bonnechère B. Unlocking the black box? A comprehensive exploration of large language models in rehabilitation. Am J Phys Med Rehabil 2024 Jun 1;103(6):532-537. [doi: 10.1097/PHM.0000000000002440] [Medline: 38261757]
7. Sauceda JA, Lechuga J, Ramos ME, et al. A factorial experiment grounded in the multiphase optimization strategy to promote viral suppression among people who inject drugs on the Texas-Mexico border: a study protocol. BMC Public Health 2023;23(1):307. [doi: 10.1186/s12889-023-15172-2]
8. van der Windt M, van der Kleij RM, Snoek KM, et al. Impact of a blended periconception lifestyle care approach on lifestyle behaviors: before-and-after study. J Med Internet Res 2020 Sep 30;22(9):e19378. [doi: 10.2196/19378] [Medline: 32996885]
9. Singh B, Olds T, Brinsley J, et al. Systematic review and meta-analysis of the effectiveness of chatbots on lifestyle behaviours. NPJ Digit Med 2023 Jun 23;6(1):118. [doi: 10.1038/s41746-023-00856-1] [Medline: 37353578]
10. Capel H, Weiler R, Dijkstra M, Vleugels R, Bloem P, Feenstra KA. ProteinGLUE multi-task benchmark suite for self-supervised protein modeling. Sci Rep 2022;12(1):16047. [doi: 10.1038/s41598-022-19608-4]
11. Yi PH, Mutasa S, Fritz J. AI MSK clinical applications: orthopedic implants. Skeletal Radiol 2022 Feb;51(2):305-313. [doi: 10.1007/s00256-021-03879-5]
12. Shi W, Zhuang Y, Zhu Y, Iwinski H, Wattenbarger M, Wang MD. Retrieval-augmented large language models for adolescent idiopathic scoliosis patients in shared decision-making. : Association for Computing Machinery Presented at: BCB '23: Proceedings of the 14th ACM International Conference on Bioinformatics, Computational Biology, and Health Informatics; Sep 3-6, 2023; Houston, TX p. 1-8. [doi: 10.1145/3584371.3612956]
13. Perlis RH, Goldberg JF, Ostacher MJ, Schneck CD. Clinical decision support for bipolar depression using large language models. Neuropsychopharmacol 2024 Aug;49(9):1412-1416. [doi: 10.1038/s41386-024-01841-2]
14. De Rosario H, Pitarch-Corresa S, Pedrosa I, et al. Applications of natural language processing for the management of stroke disorders: scoping review. JMIR Med Inform 2023 Sep 6;11:e48693. [doi: 10.2196/48693] [Medline: 37672328]
15. Rojas-Carabali W, Sen A, Agarwal A, et al. Chatbots vs. human experts: evaluating diagnostic performance of chatbots in uveitis and the perspectives on AI adoption in ophthalmology. Ocul Immunol Inflamm 2024 Oct;32(8):1591-1598. [doi: 10.1080/09273948.2023.2266730] [Medline: 37831553]
16. Li Y, Li Z, Zhang K, Dan R, Jiang S, Zhang Y. ChatDoctor: a medical chat model fine-tuned on a Large Language Model Meta-AI (LLaMA) using medical domain knowledge. Cureus 2023 Jun;15(6):e40895. [doi: 10.7759/cureus.40895] [Medline: 37492832]
17. Cui J, Li Z, Yan Y, et al. ChatLaw: open-source legal large language model with integrated external knowledge bases. . Preprint posted online on 2023. [doi: 10.48550/arXiv.2306.16092]
18. Chen Z, Zhang Y, Zhang Y, et al. MEDITRON-70B: scaling medical pretraining for large language models. . Preprint posted online on 2023.

XSL•FO
RenderX

19. Parmar P, Ryu J, Pandya S, Sedoc J, Agarwal S. Health-focused conversational agents in person-centered care: a review of apps. NPJ Digit Med 2022 Feb 17;5(1):21. [doi: 10.1038/s41746-022-00560-6] [Medline: 35177772]
20. Singhal K, Tu T, Gottweis J, et al. Toward expert-level medical question answering with large language models. Nat Med 2025 Jan 8. [doi: 10.1038/s41591-024-03423-7] [Medline: 39779926]
21. Kim Y, Xui X, McDuff D. Health-LLM: large language models for health prediction via wearable sensor data. . Preprint posted online on 2024.
22. Zaleski AL, Berkowsky R, Craig KJT, Pescatello LS. Comprehensiveness, accuracy, and readability of exercise recommendations provided by an AI-based chatbot: mixed methods study. JMIR Med Educ 2024 Jan 11;10:e51308. [doi: 10.2196/51308] [Medline: 38206661]
23. Dergaa I, Ben Saad H, El Omri A, et al. Using artificial intelligence for exercise prescription in personalised health promotion: a critical evaluation of OpenAI's GPT-4 model. Biol Sport 2024;41(2):221-241. [doi: 10.5114/biolsport.2024.133661]
24. Haag D. The Last JITAI? The unreasonable effectiveness of large language models in issuing just-in-time adaptive interventions: fostering physical activity in a prospective cardiac rehabilitation setting. Hum Comput Interact 2024;39(1):123-150. [doi: 10.1080/07370024.2023.2256789]
25. Shin D, Hsieh G, Kim YH. PlanFitting: tailoring personalized exercise plans with large language models. . Preprint posted online on 2023.
26. Sivarajkumar S, Gao F, Denny P, et al. Mining clinical notes for physical rehabilitation exercise information: natural language processing algorithm development and validation study (preprint. JMIR Med Inf Preprint posted online on 2023. [doi: 10.2196/preprints.52289] [Medline: 37712352]
27. Willms A, Liu S. Exploring the feasibility of using ChatGPT to create just-in-time adaptive physical activity mHealth intervention content: case study. JMIR Med Educ 2024 Feb 29;10:e51426. [doi: 10.2196/51426] [Medline: 38421689]
28. Chowdhury D, Roy A, Ramamurthy SR, Roy N. CHARLIE: a chatbot that recommends daily fitness and diet plans. : IEEE Presented at: 2023 IEEE International Conference on Pervasive Computing and Communications Workshops and Other Affiliated Events (PerCom Workshops); Mar 13-17, 2023; Atlanta, GA p. 1-8. [doi: 10.1109/PerComWorkshops56833.2023.10150359]
29. Vandelanotte C, Trost S, Hodgetts D, et al. Increasing physical activity using an just-in-time adaptive digital assistant supported by machine learning: a novel approach for hyper-personalised mHealth interventions. J Biomed Inform 2023 Aug;144:104435. [doi: 10.1016/j.jbi.2023.104435] [Medline: 37394024]
30. To QG, Green C, Vandelanotte C. Feasibility, usability, and effectiveness of a machine learning-based physical activity chatbot: quasi-experimental study. JMIR Mhealth Uhealth 2021 Nov 26;9(11):e28577. [doi: 10.2196/28577] [Medline: 34842552]
31. Liang KH, Lange P, Oh YJ, Zhang J, Fukuoka Y, Yu Z. Evaluation of in-person counseling strategies to develop physical activity chatbot for women. . Preprint posted online on 2021.
32. Wiratunga N, Cooper K, Wijekoon A, et al. FitChat: conversational artificial intelligence interventions for encouraging physical activity in older adults. . Preprint posted online on 2020.
33. Liguori G, American College of Sports Medicine. ACSM's Guidelines for Exercise Testing and Prescription, 10th edition: Lippincott Williams & Wilkins; 2017.
34. Abedi A, Colella TJF, Pakosh M, Khan SS. Artificial intelligence-driven virtual rehabilitation for people living in the community: a scoping review. NPJ Digit Med 2024 Feb 3;7(1):25. [doi: 10.1038/s41746-024-00998-w] [Medline: 38310158]
35. Singhal K, Azizi S, Tu T, et al. Large language models encode clinical knowledge. Nature New Biol 2023 Aug;620(7972):172-180. [doi: 10.1038/s41586-023-06291-2] [Medline: 37438534]
36. Scheers H, Van Remoortel H, Lauwers K, et al. Predicting medical usage rate at mass gathering events in Belgium: development and validation of a nonlinear multivariable regression model. BMC Public Health 2022 Jan 25;22(1):173. [doi: 10.1186/s12889-022-12580-8] [Medline: 35078442]
37. Nayak N, Nan Y, Trost A, Bach S. Learning to generate instruction tuning datasets for zero-shot task adaptation. . Preprint posted online on 2024.
38. Maini P, Seto S, Bai R, Grangier D, Zhang Y, Jaitly N. Rephrasing the web: a recipe for compute and data-efficient language modeling. . Preprint posted online on 2024.
39. Sorscher B, Geirhos R, Shekhar S, et al. Beyond neural scaling laws: beating power law scaling via data pruning. . Preprint posted online on 2022.
40. Zhao P, Zhang H, Yu Q, et al. Retrieval-augmented generation for AI-generated content: a survey. . Preprint posted online on 2024.
41. Shi W, Min S, Yasunaga M, et al. REPLUG: retrieval-augmented black-box language models. . Preprint posted online on 2023.
42. Iqbal SMA, Mahgoub I, Du E, Leavitt MA, Asghar W. Advances in healthcare wearable devices. NPJ Flex Electron 2021;5(1):9. [doi: 10.1038/s41528-021-00107-x]
43. Gonzalez-Bautista E, Morsch P, Gonzalez C, Vega E. A short list of high-priority indicators of health system responsiveness for aging: an eDelphi consensus study. Rev Panam Salud Publica 2023;47:e103. [doi: 10.26633/RPSP.2023.103] [Medline: 37534053]

XSL•FO
RenderX

Abbreviations

AI: artificial intelligence
EHR: electronic health record
ER: exercise recommendation
LLM: large language model
PA: physical activity
PRISMA-ScR: Preferred Reporting Items for Systematic Reviews and Meta-Analyses extension for Scoping Reviews
RAG: retrieval-augmented generation

Edited by A Castonguay; submitted 08.04.24; peer-reviewed by AA Wani, GK Gupta, I Dergaa, S Mao, V Jouault; revised version received 09.02.25; accepted 11.02.25; published 27.05.25.

Please cite as:
Lai X, Chen J, Lai Y, Huang S, Cai Y, Sun Z, Wang X, Pan K, Gao Q, Huang C
Using Large Language Models to Enhance Exercise Recommendations and Physical Activity in Clinical and Healthy Populations: Scoping Review
JMIR Med Inform 2025;13:e59309
URL: https://medinform.jmir.org/2025/1/e59309
doi:10.2196/59309

© Xiangxun Lai, Jiacheng Chen, Yue Lai, Shengqi Huang, Yongdong Cai, Zhifeng Sun, Xueding Wang, Kaijiang Pan, Qi Gao, Caihua Huang. Originally published in JMIR Medical Informatics (https://medinform.jmir.org), 27.5.2025. This is an open-access article distributed under the terms of the Creative Commons Attribution License (https://creativecommons.org/licenses/by/4.0/), which permits unrestricted use, distribution, and reproduction in any medium, provided the original work, first published in JMIR Medical Informatics, is properly cited. The complete bibliographic information, a link to the original publication on https://medinform.jmir.org/, as well as this copyright and license information must be included.

XSL•FO
RenderX

Machine Learning and Deep Learning Techniques for Prediction and Diagnosis of Leptospirosis: Systematic Literature Review

Suhila Sawesi[1], BPharm, MPharm, PhD; Arya Jadhav[2], MS; Bushra Rashrash[3], BS

[1]Health Informatics and Bioinformatics Program, College Of Computing, Grand Valley State University, 333 Michigan St. NE, Grand Rapids, MI, United States

[2]Data Science, College Of Computing, Grand Valley State University, Allendale, MI, United States

[3]Department of Biomedical Science, College of Liberal Arts and Sciences, Grand Valley State University, Allendale, MI, United States

Corresponding Author:
Suhila Sawesi, BPharm, MPharm, PhD
Health Informatics and Bioinformatics Program, College Of Computing, Grand Valley State University, 333 Michigan St. NE, Grand Rapids, MI, United States

Abstract

Background: Leptospirosis, a zoonotic disease caused by *Leptospira* bacteria, continues to pose significant public health risks, particularly in tropical and subtropical regions.

Objective: This systematic review aimed to evaluate the application of machine learning (ML) and deep learning (DL) techniques in predicting and diagnosing leptospirosis, focusing on the most used algorithms, validation methods, data types, and performance metrics.

Methods: Using Preferred Reporting Items for Systematic Reviews and Meta-Analyses (PRISMA) guidelines, Checklist for Critical Appraisal and Data Extraction for Systematic Reviews of Prediction Modelling Studies (CHARMS), and Prediction model Risk of Bias Assessment Tool (PROBAST) tools, we conducted a comprehensive review of studies applying ML and DL models for leptospirosis detection and prediction, examining algorithm performance, data sources, and validation approaches.

Results: Out of a total of 374 articles screened, 17 studies were included in the qualitative synthesis, representing approximately 4.5% of the initial pool. The review identified frequent use of algorithms such as support vector machines, artificial neural networks, decision trees, and convolutional neural networks (CNNs). Among the included studies, 88% (15/17) used traditional ML methods, and 24% (4/17) used DL techniques. Several models demonstrated high predictive performance, with reported accuracy rates ranging from 80% to 98%, notably with the U-Net CNN achieving 98.02% accuracy. However, public datasets were underused, with only 35% (6/17) of studies incorporating publicly available data sources; the majority (65%, 11/17) relied primarily on private datasets from hospitals, clinical records, or regional surveillance systems.

Conclusions: ML and DL techniques demonstrate potential for improving leptospirosis prediction and diagnosis, but future research should focus on using larger, more diverse datasets, adopting transfer learning strategies, and integrating advanced ensemble and validation techniques to strengthen model accuracy and generalization.

(JMIR Med Inform 2025;13:e67859) doi:10.2196/67859

KEYWORDS

leptospirosis; machine learning; deep learning; prediction models; diagnosis; artificial intelligence; convolutional neural networks; support vector machines; transfer learning; zoonotic diseases

Introduction

Overview of Leptospirosis and Its Diagnosis

Leptospirosis, a zoonotic disease caused by pathogenic *Leptospira* bacteria, is a global public health concern, with an estimated 1.03 million cases and approximately 58,900 deaths annually [1]. The disease is particularly prevalent in tropical and subtropical regions, where environmental factors such as heavy rainfall, poor sanitation, and frequent flooding facilitate bacterial survival and transmission. Although less common, leptospirosis also occurs in temperate regions, including the United States, especially in areas prone to flooding or with high populations of animal carriers like rodents and livestock [1].

In the United States, the Centers for Disease Control and Prevention (CDC) reports approximately 100 - 150 cases annually, with the majority occurring in Puerto Rico and Hawaii due to their specific environmental conditions. Isolated cases in areas like New York City and California highlight the mobility of the disease and its potential for travel-related transmission [1].

Transmission primarily occurs through direct contact with the urine or reproductive fluids of infected animals or exposure to

XSL•FO
RenderX

contaminated water and soil, especially following periods of heavy rainfall [2]. High-risk activities include wading, swimming, or boating in potentially contaminated freshwater. Effective control measures include improving sanitation, controlling rodent populations, and educating at-risk populations. The disease manifests with a broad range of clinical symptoms, from mild flu-like symptoms to severe complications such as Weil's disease, characterized by jaundice, renal failure, pulmonary hemorrhage, and multi-organ dysfunction, which can lead to death if not treated promptly [1].

The diagnosis of leptospirosis is challenging due to the nonspecific nature of its early symptoms, which often overlap with other febrile illnesses. Traditional diagnostic methods include the microscopic agglutination test (MAT), considered the gold standard, and polymerase chain reaction (PCR). MAT is labor-intensive and requires specialized laboratory capabilities, making it less accessible in many endemic regions [2]. PCR, while offering early detection by identifying *Leptospira* DNA in blood or urine, also requires advanced laboratory infrastructure. Rapid diagnostic tests (RDTs) provide quicker results, but their sensitivity and specificity can vary depending on the *Leptospilora* serovars and disease stages, limiting their effectiveness in some settings [2,3].

Machine Learning and Deep Learning in Disease Detection

Machine learning (ML) and deep learning (DL) have emerged as powerful tools in the field of disease detection and management. ML involves training computers to apply past experiences to solve new problems, leveraging algorithms that enable the machine to identify patterns, make predictions, and produce insightful judgments based on data. The increasing availability of computational power and data storage has significantly boosted the application of ML across various fields, including public health. In the context of infectious diseases like leptospirosis, ML can analyze large datasets, including clinical and laboratory data, to identify patterns and relationships that might not be apparent through traditional statistical methods [4-6].

DL, a subset of ML, further enhances these capabilities by using neural networks with multiple layers to automatically extract, analyze, and understand useful information from raw data. Unlike traditional ML techniques that rely on handcrafted features, DL models are capable of automatic feature engineering, which significantly enhances classification performance. DL techniques, driven by neural networks, are known for their accuracy and performance, particularly in complex tasks such as image recognition and analysis [6-8]. For example, convolutional neural networks (CNNs) have been successfully applied to medical imaging, enabling the precise identification and classification of pathogens in microscopy images [9], which is crucial for diseases like leptospirosis.

The application of ML and DL in leptospirosis diagnosis represents a significant advancement over traditional methods. ML algorithms can analyze clinical and laboratory data, including patient symptoms, demographic information, and test results, to predict the likelihood of leptospirosis. This capability is particularly valuable in settings where access to advanced diagnostics is limited, as it allows for earlier and more accurate detection, potentially reducing the time to diagnosis and improving patient outcomes [10].

DL models, particularly CNNs, have shown great promise in analyzing blood and urine samples, medical imaging, and environmental data to predict the presence of *Leptospira* or the likelihood of an outbreak. These models can distinguish *Leptospira* bacteria in microscopy images with high accuracy, reducing the need for skilled microbiologists and improving diagnostic accessibility in low-resource settings [4].

One of the most significant advantages of using ML and DL in leptospirosis diagnosis is their ability to integrate diverse data types—such as clinical, laboratory, and environmental data—into comprehensive predictive models. These models can be used for individual patient diagnosis and public health surveillance, enabling more targeted and timely interventions. For example, predictive models that incorporate climatic and environmental factors, such as rainfall patterns and flooding data, can help identify regions at higher risk for leptospirosis outbreaks, allowing for proactive disease control measures [10].

Despite the significant potential of ML and DL to revolutionize the diagnosis and management of leptospirosis, comprehensive reviews focusing specifically on their application in this area are scarce. Most existing reviews have primarily concentrated on more prevalent conditions such as tuberculosis, malaria, and COVID-19, with minimal attention given to zoonotic diseases like leptospirosis [4,5]. Furthermore, there is a recognized gap in the literature concerning the application of advanced AI techniques in the context of neglected tropical diseases, such as leptospirosis, where the potential for these technologies to improve diagnostic accuracy remains underexplored [6,11]. This gap underscores the need for a focused review that synthesizes current research, identifies the most effective ML and DL models, and evaluates their impact on public health outcomes related to leptospirosis.

The aim of this systematic review is to comprehensively evaluate the application of ML and DL techniques in the prediction and diagnosis of leptospirosis. This review will address the following key research questions:

1. Which ML and DL algorithms are most frequently used in leptospirosis prediction and diagnosis, and how well do they perform?
2. What validation methods are most used in the evaluation of ML and DL models for leptospirosis? and how reliable are these methods?
3. What types of data are most used in ML and DL models for leptospirosis? How does the type of data influence the performance of these models?
4. What are the main challenges and limitations identified in the research studies regarding ML and DL applications in leptospirosis prediction and diagnosis?

XSL•FO
RenderX

Methods

Study Design

We conducted a systematic review following the Preferred Reporting Items for Systematic Reviews and Meta-Analyses (PRISMA) checklist [12] (Checklist 1). The Checklist for Critical Appraisal and Data Extraction for Systematic Reviews of Prediction Modelling Studies (CHARMS) was used to frame this review's objectives [13].

Search Strategy

PubMed, IEEE, ACM, and Web of Science databases were searched for articles published from inception till May 29, 2024. Hand-searching of references within included articles was conducted to shortlist other potential articles. Our search strategy used a combination of subject terms related to "machine learning" and "Leptospirosis" (see Multimedia Appendix 1).

Eligibility Criteria

We included full-text English language articles that developed or validated diagnostic or predictive ML models for human leptospirosis. Our review focused specifically on ML and DL methods, including logistic regression, Bayesian learning, and generalized additive models when these were implemented within an ML or DL framework [14].

Several categories of studies were excluded. First, we omitted case reports, case series, letters, corrigenda, editorial commentaries, literature reviews, and meta-analyses. Second, we excluded purely applied statistical methods that were not integrated with ML or DL frameworks, including traditional statistical analyses that did not incorporate ML optimization techniques. Third, non-artificial intelligence methods as well as general artificial intelligence (AI) approaches that could not be classified as either ML or DL (such as rule-based expert systems without learning components or symbolic AI methods) were excluded [14].

The distinction between included and excluded methods was based on whether the approach involved automated learning from data. For instance, while standard logistic regression was excluded, logistic regression implemented with ML techniques like automated feature selection or hyperparameter tuning was included. Similarly, simple threshold-based diagnostic rules were excluded unless they were derived through ML processes. This approach ensured our review focused specifically on applications of ML and DL technologies in leptospirosis diagnosis and prediction.

In this review, diagnostic ML models refer to models that predict the disease status of an individual, while predictive models forecast the probability of future occurrence of the disease in an individual.

Study Selection

A total of 3 independent reviewers (SS, AJ, and BR) conducted the initial search across 4 databases using predefined search terms within the title and abstract, strictly following the inclusion and exclusion criteria. Zotero bibliography software was used to manage the search results by tracking reasons for inclusion and exclusion, grouping records, importing PDFs, and exporting data to Microsoft Excel for extraction. The interrater agreement between the coauthors was evaluated using Cohen's kappa (κ>0.80) [15,16], ensuring a high level of consistency across the reviewers.

To enhance the screening process, we employed ChatGPT-4o (June 2024 version) as a fourth reviewer. This advanced large language model (LLM) was specifically selected for its proven capabilities in biomedical text analysis (OpenAI) and superior handling of technical medical terminology compared to previous versions. We opted to use only this single model to maintain consistency in evaluation criteria and avoid potential variability from multiple LLMs. During implementation, abstracts were systematically input to ChatGPT-4o with standardized prompts mirroring our inclusion and exclusion criteria, and all outputs were automatically logged for verification.

While ChatGPT-4o provided valuable preliminary classifications (achieving 88% initial alignment with human reviewers in our pilot test), we implemented a rigorous 3-stage human verification protocol: (1) initial matching of AI recommendations with human decisions, (2) consensus discussion for discrepancies (κ<0.80), and (3) final unanimous approval. For example, the model initially recommended including 12 statistical modeling studies that were properly excluded after human review. This AI-assisted process reduced initial screening time by 30% while maintaining 100% alignment with final human decisions through our verification protocol, which followed PRISMA-AI guidelines [12] to mitigate potential AI limitations.

We emphasize that ChatGPT-4o served strictly in an advisory capacity, and no studies were included solely based on its recommendation. This approach aligns with emerging best practices for LLM-assisted systematic reviews [17,18], with complete verification records available in our supplementary materials (Multimedia Appendix 2).

Quality Assessment

The articles selected for inclusion were then subjected to a quality assessment using the Prediction model Risk of Bias Assessment Tool (PROBAST) tool [13], which categorizes bias as low, medium, or high (see Multimedia Appendix 3). All authors assessed the quality of their respective parts, starting with a pilot of 5 articles to ensure consistency. The PROBAST tool evaluates risk of bias based on 4 segments—participants, predictors, outcome, and analysis. Each segment's risk of bias was rated as high, medium, low, or unclear. If any domain suggested a high risk of bias, the overall risk of bias for that study was considered high. These studies were not excluded but were analyzed to understand their limitations and impact on the overall findings. The assessment was conducted independently by all authors, ensuring a thorough evaluation process.

Data Extraction

For the extraction process, a standardized form was used to collect data relevant to the review's objectives. This form was adapted from the CHARMS [15] and the Transparent Reporting of a Multivariable Prediction Model for Individual Prognosis

XSL•FO
RenderX

or Diagnosis (TRIPOD) guidelines [19]. The extracted information included publication type, publication year, author, title, country of research, source of data, type of data (public or private), overall number of samples, and data collection methods (see Multimedia Appendix 4).

Additional details were gathered on the ML and DL algorithms used, including whether the models were pretrained or developed from scratch, as well as the use of transfer learning, data augmentation, validation methods, and evaluation metrics. The strength of leptospirosis predictions was documented using performance metrics. Tasks were categorized into segmentation, classification, and object detection, noting the type of classification and any limitations.

To ensure consistency, reviewers conducted a pilot phase where they independently extracted data from the first 5 articles and compared results, achieving a high agreement (κ=0.98). Afterward, all 17 articles were reviewed, and discrepancies were resolved through discussion. The studies were then rigorously categorized before moving to theme formation. One author (SS) defined the themes, which were reviewed and adjusted by the other authors (AJ and BR) to ensure comprehensive categorization.

Outcomes Assessed

The primary outcomes assessed in this review include the diagnostic and predictive performance of various ML and DL methods for leptospirosis detection, focusing on metrics like accuracy, area under the curve (AUC), sensitivity, and specificity. It also evaluates the applicability and generalizability of these models in health care settings, emphasizing the integration of advanced neural network architectures, transfer learning, and data augmentation to enhance performance.

Data Analysis

We grouped the collected studies into summary tables based on the type of ML and DL models used for leptospirosis detection. R (version 4.3.2; R Foundation for Statistical Computing) was used to perform both descriptive statistical analyses and create visualizations.

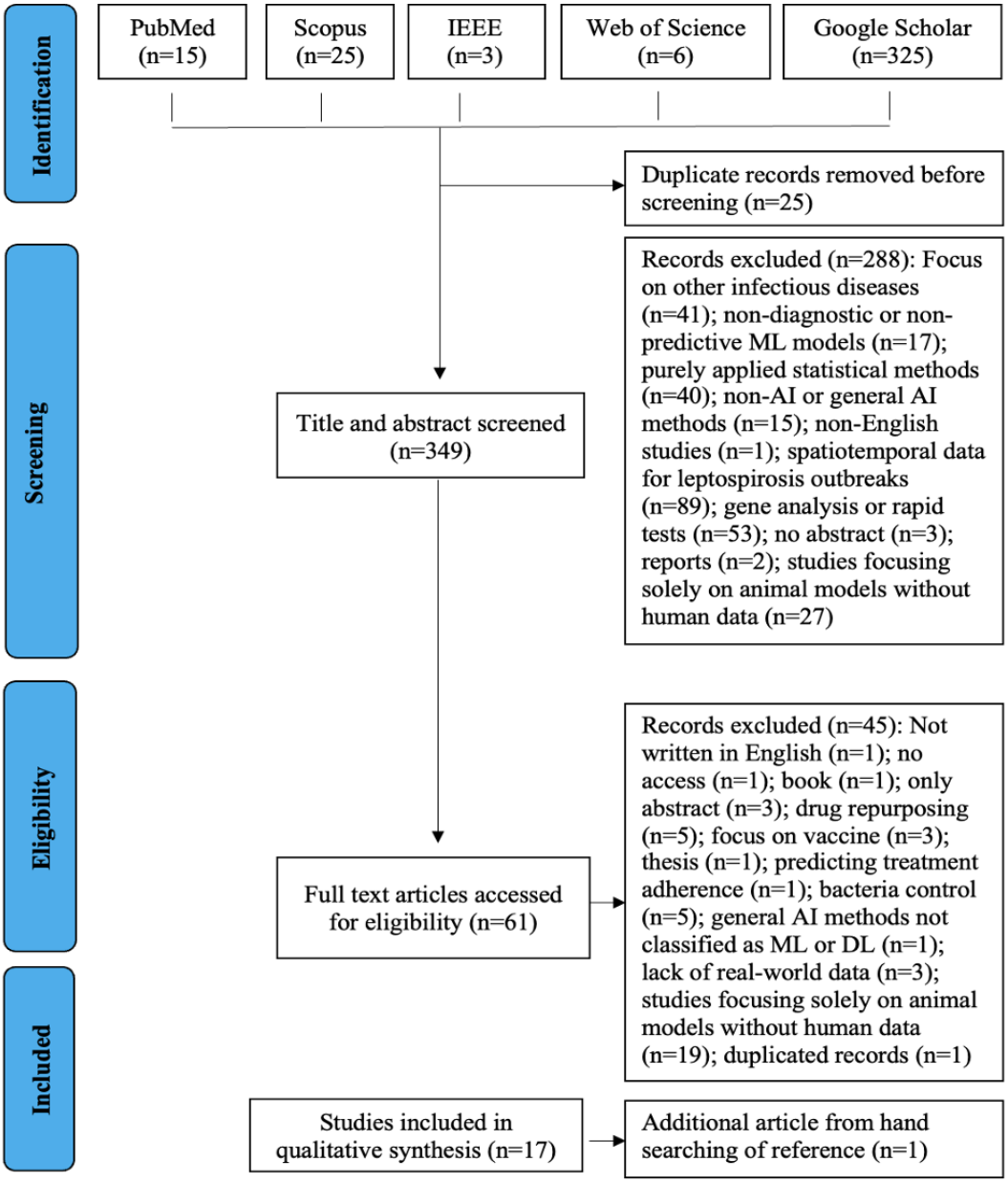
Results

Search and Selection Results

Figure 1 illustrates the process of identifying relevant literature. A comprehensive search across 5 databases yielded a total of 374 articles. After removing 25 duplicate records, 349 unique articles were screened based on their titles and abstracts. Following this initial screening, 61 articles were selected for full-text review. Of these, 45 were excluded for various reasons, including not meeting inclusion criteria or insufficient data for analysis. Ultimately, 16 studies were included in the review, with 1 additional study identified through hand-searching reference lists, bringing the total to 17 studies included in the qualitative synthesis.

XSL•FO
RenderX

Figure 1. Figure 1. PRISMA (Preferred Reporting Items for Systematic Reviews and Meta-Analyses) flow diagram illustrating the search and selection process used to identify relevant studies. AI: artificial intelligence; ML: machine learning; DL: deep learning.



Study Description

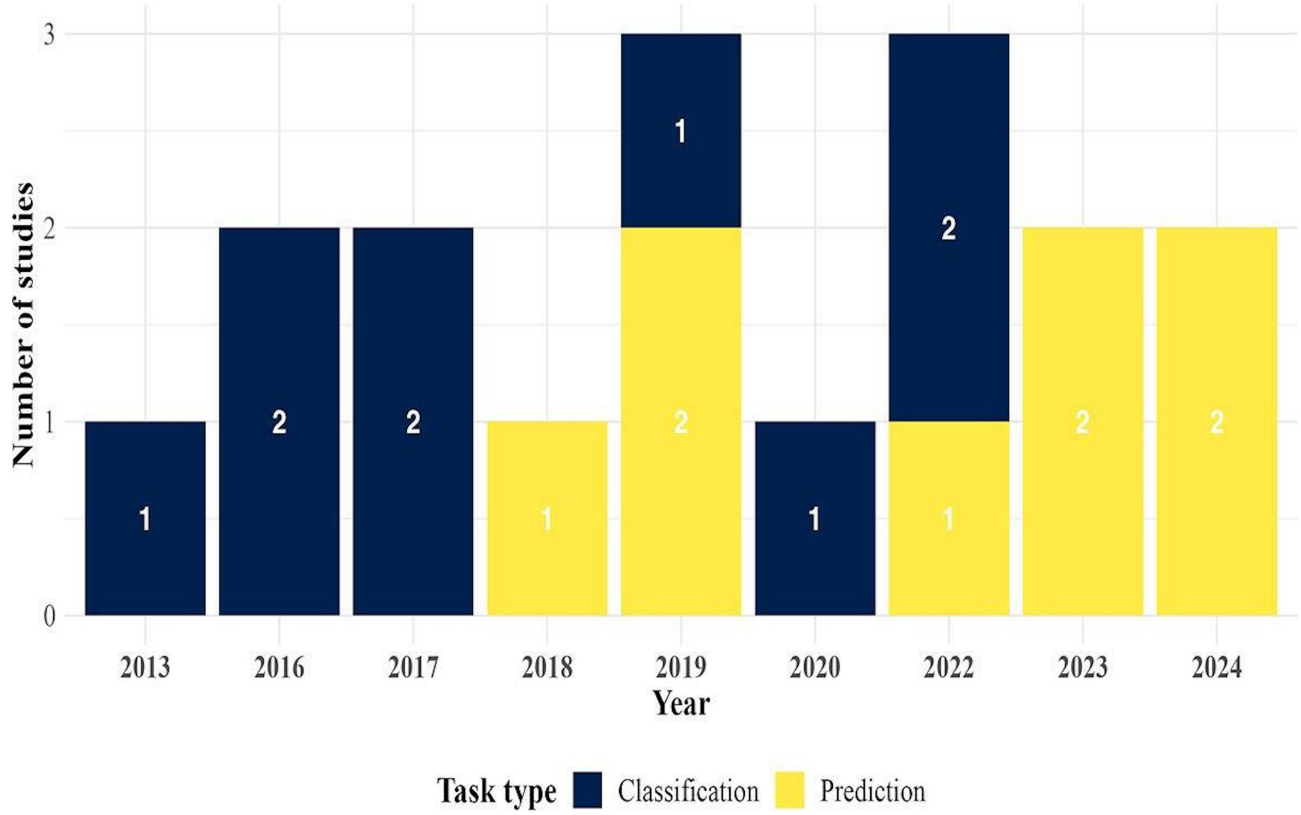
In this systematic review, we examined 17 studies (n=17) published between 2012 and 2024 that used ML and DL techniques for the prediction and diagnosis of leptospirosis (see Figure 2). Most studies were published in 2019 (n=3, 18%), 2022 (n=3, 18%), and 2023 (n=3, 18%). Brazil was the most common country of research, contributing 4 studies (24%), followed by New Caledonia with 3 studies (18%). Regarding data sources, 6 studies (35%) used health records, 6 studies (35%) used environmental data, and 5 studies (29%) used epidemiological data.

Most studies (11/17, 65%) focused on predictive modeling, while 6/17 studies (35%) concentrated on diagnosis. ML algorithms were overwhelmingly preferred, with 15/17 studies (88%) using techniques such as SVM, decision tree (DT), and random forests. DL algorithms, including CNN and multilayer perceptrons (MLPs), were used in 4/17 studies (24%), and only 1/17 study (6%) combined both ML and DL methods. All studies developed models from scratch without using transfer learning, and only 1/17 study (6%) reported the application of data augmentation techniques.

Regarding model validation, cross-validation methods were most frequently used in 11/17 studies (65%), while holdout validation methods, such as train and test splits, were used in 6/17 studies (35%).

XSL•FO
RenderX

Figure 2. Distribution of studies on machine learning and deep learning applications for leptospirosis diagnosis and prediction by year and task type.



Assessment of Risk of Bias in Machine Learning Models

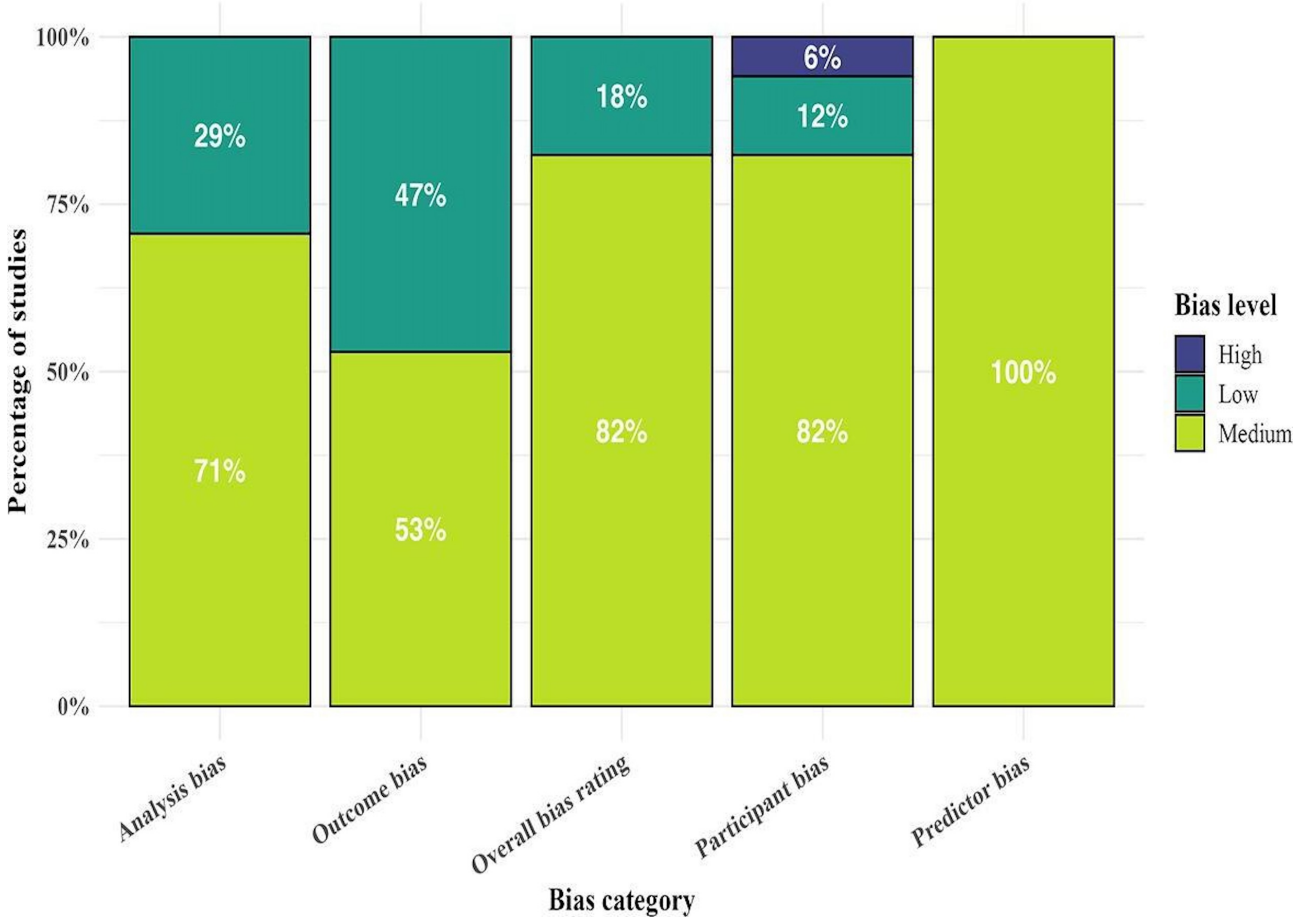
In assessing the risk of bias across the included 17 studies, most were categorized as having a medium risk across key domains (Figure 3). A total of 14 studies (82%) were rated as having a medium risk of bias related to participant selection, primarily due to the selection of specific regions or populations that may not fully represent broader leptospirosis cases. Examples include studies by [10,20-32]. In addition, 2 studies (12%) [33,34] were rated as low risk, while 1 study (6%) [35] was rated as high risk due to narrower participant selection.

Regarding predictors, 16 studies (94%) demonstrated a medium risk of bias, often because they relied heavily on environmental or clinical data without fully accounting for confounding variables. Only 1 study (6%) [34] was rated as low risk in this domain. For outcome bias, 13 studies (76%) [10,20-27,29,30,34,35] were assessed as low risk, with clear and consistent definitions applied across participants. A total of 4 studies (24%) [28,31-33] exhibited medium risk, mainly due to subjective outcome determinations or a lack of standardized measures.

In the analysis domain, 13 studies (76%) [10,22-33] demonstrated medium risk due to concerns about validation techniques, handling of missing data, and small sample sizes, while 4 studies (24%) [20,21,34,35] were rated as low risk, reflecting stronger analytical methodologies.

XSL•FO
RenderX

Figure 3. Distribution of risk of bias across domains in machine learning and deep learning studies for leptospirosis.



Frequently Used ML and DL Algorithms for Leptospirosis Prediction and Diagnosis

This systematic review considered all ML and DL techniques used in the included studies and examined their applications in either leptospirosis prediction or diagnosis (classification). Figure 4 illustrates the distribution of classifiers across the studies, highlighting the diversity of approaches and the frequency of use of certain models.

For prediction tasks, the most commonly used ML technique was support vector regression (SVR), applied in 2 studies [32,33]. In addition to SVR, several other ML techniques were prominently featured. These included the naïve networks and TAN (tree augmented naive) networks used by Mayfield et al [24] for predictive risk mapping, and the random forest classifier and M1 mixed model used by Jayaramu et al [30] for predictive risk modeling.

Models like LeptoScore and QuickLepto, applied by Galdino et al [10], further illustrate the diversity of approaches taken in predictive modeling. SVM and MLP used in predictive risk modeling by Ahangarcani et al [26], while Mohammadinia et al [27] applied geographically weighted regression, generalized linear models, artificial neural networks (ANNs), and SVM for similar tasks. In addition, feedforward neural networks were used by [31] in prediction tasks, demonstrating the growing role of neural network models in this domain.

For diagnosis (classification) tasks, ANNs were widely used, appearing in studies by [20,28]. FuzzyARTMAP and ARTMAP-IC, both variants of ANN, were also used by [20] to achieve classification. In addition, Bayesian classifiers such as Naïve Bayes were applied by [21,29], further showcasing the diversity of ML techniques in classification tasks.

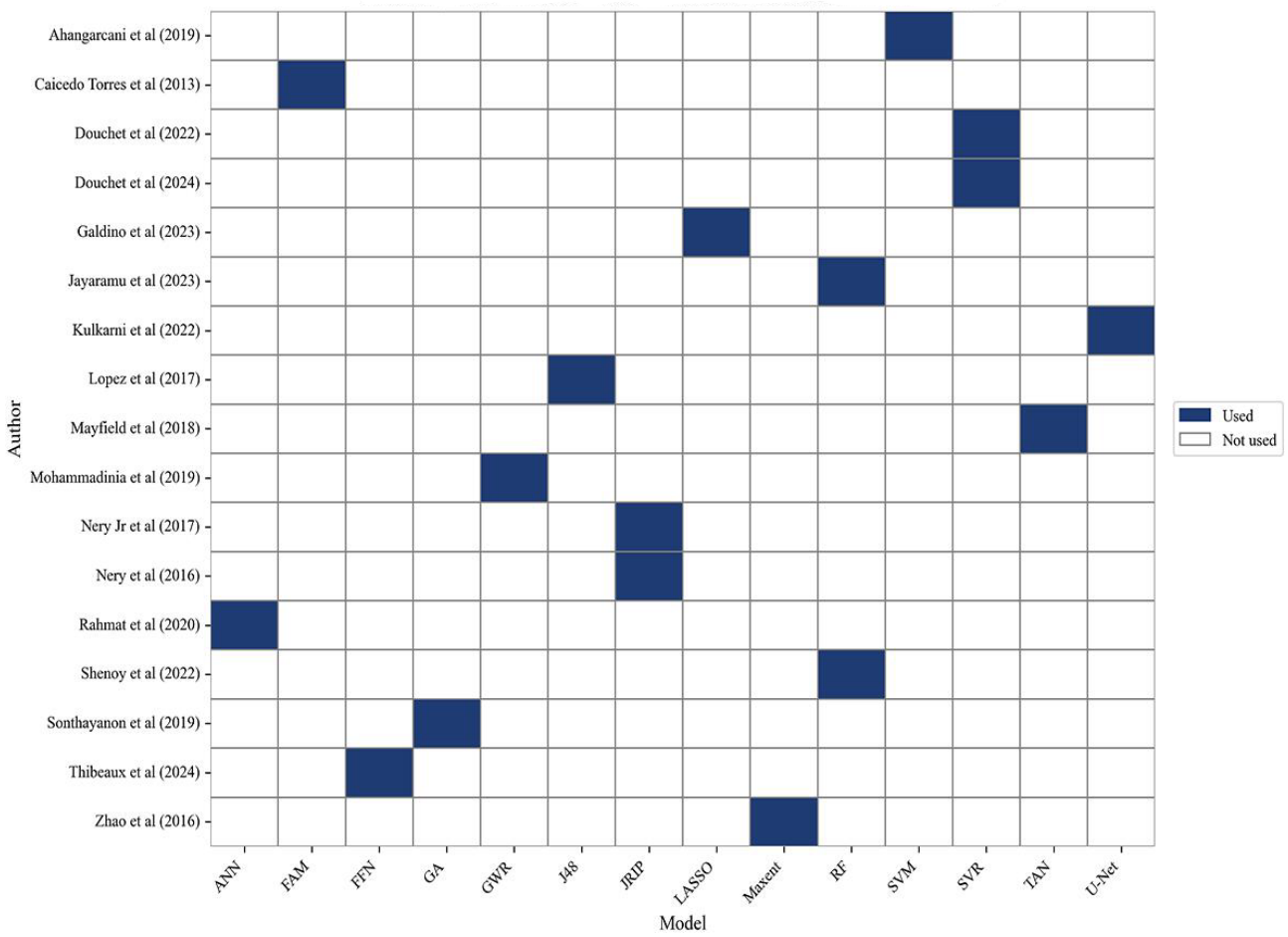
CNNs were another frequently used DL model for classification. Specifically, U-Net, a variant of CNN, was used by [34] and achieved an impressive accuracy of 98%. Other classifiers, such as k-nearest neighbors (KNNs), DTs (J48), and random forests, were used in multiple studies, with [23,29] demonstrating their efficacy in disease classification.

Performance evaluations showed that many studies combined multiple classifiers. For example [29], applied naïve Bayes, KNN, MLP, J48 decision tree, random forest, multinomial logistic regression, and Adaboost within the same study, with random forest achieving the highest performance at 87% accuracy and 91% sensitivity.

Hybrid approaches combining ML and DL were also present, such as the use of a genetic algorithm combined with both ML and DL techniques in [25], which attained an accuracy of 99%.

XSL•FO
RenderX

Figure 4. Heatmap of classifier usage across included studies [10,20-35]. ANN: artificial neural network; DL: deep learning; FAM: fuzzy adaptive resonance theory mapping; FFN: feed forward network; GA: genetic algorithm; GWR: geographically weighted regression; J48: J48 decision tree; JRIP: repeated incremental pruning to produce error reduction; LASSO: least absolute shrinkage and selection operator regression; Maxent: maximum entropy model; ML: machine learning; RF: random forest; SVM: support vector machine; SVR: support vector regression; TAN: tree augmented naïve network; U-Net: U-Net convolutional neural network.



Upon comparing prediction and diagnosis (classification) tasks, it becomes evident that ML models dominated predictive risk mapping studies, while DL models, particularly U-Net, were more frequently used in classification tasks related to disease detection. For risk modeling, techniques like decision trees (J48) and random forest classifiers were commonly applied, with high specificity rates achieved in studies such as those by [21,30].

Interestingly, 50% of the studies (n=8) used more than one algorithm to assess performance, highlighting the importance of comparative evaluations in the field. Supervised-learning algorithms were predominant throughout the studies, with no mention of unsupervised-learning methods, such as K-means, or reinforcement-learning algorithms.

In summary, the most frequent algorithms in prediction tasks were SVR and random forest, while in diagnosis, ANN and U-Net stood out as the most frequently used. Across both types of tasks, the performance metrics indicated high accuracy and sensitivity, showcasing the reliability of ML and DL techniques in leptospirosis research.

Algorithm Performance Metrics

Performance assessment is a crucial process in evaluating ML and DL models. Various metrics are used to measure model performance, including accuracy, sensitivity, specificity, precision, F_1-score, AUC, mean squared error (MSE), *R*-squared (R^2), mean absolute error (MAE), and root mean squared error (RMSE). These metrics are typically evaluated using hidden or unseen examples to assess model generalizability. In the included studies, accuracy was the most frequently reported metric, followed by sensitivity, precision, specificity, and F_1-score. For prediction tasks, MSE, MAE, RMSE, and R^2 were used to assess regression performance.

Tables 1 and 2 demonstrates the widespread use of accuracy rates across various models. The studies examined used accuracy as the primary indicator of performance, although other metrics such as sensitivity and specificity were also highlighted. For instance, the performance of the ANN in the Seremban City dataset reached 80% accuracy, 83% sensitivity, and 75% specificity, while achieving an AUC of 87%. Models such as the Fuzzy ARTMAP applied to other datasets showed lower performance, with accuracy ranging between 60% and 80%, highlighting the variability in effectiveness across different methods.

XSL•FO
RenderX

Table . Performance of best classification models from the research studies.

Study	Model	Accuracy, %	Sensitivity, %	Specificity, %	AUC[a], %	F_1-score, %
Rahmat et al [28]	ANN[b]	—[c]	86.44	79.33	89.04	—
Collins et al [19]	ANN	80	80	—	—	—
Collins et al [19]	Fuzzy ARTMAP[d]	80	80	—	—	—
Nery et al [21]	JRIP[e]	80.10	85	81	82.60	75
Shenoy et al [29]	Random forest	—	87	—	91	86
Sonthayanon et al [25]	GA[f]	98.90	—	—	—	—
Nery Jr et al [22]	JRIP	—	84	99	—	—
Kulkarni et al [34]	U-Net[g]	98.02	—	—	—	—
Lopez et al [23]	J48[h]	70.5	—	—	—	—
Zhao et al [35]	Maxent[i] model	—	—	—	96	—

[a]AUC: area under the curve.

[b]ANN: artificial neural network.

[c]Indicates metrics that were either not reported or not utilized in the original studies.

[d]ARTMAP: adaptive resonance theory mapping.

[e]JRIP: repeated incremental pruning to produce error reduction.

[f]GA: genetic algorithm.

[g]U-Net: U-Net convolutional neural network.

[h]J48: J48 decision tree.

[i]Maxent: maximum entropy.

XSL•FO
RenderX

Table . Performance of best prediction models from the research studies.

Study	Model	Accuracy, %	Sensitivity, %	Specificity, %	AUC[a], %	MSE[b]	R^2	MAE[c]	RMSE[d]
Douchet et al [32]	SVR[e]	—[f]	—	—	—	0.19	—	—	—
Sonthayanon et al [24]	TAN[g]	—	—	—	89	—	—	—	—
Jayaramu et al [30]	RFC[h]	82.60	60	96.60	—	—	—	—	—
Galdino et al [10]	LASSO[i]	78.30	81.10	57.10	—	—	—	—	—
Ahangarcani et al [26]	SVM[j]	86.55	—	—	85.48	—	—	—	—
Mohammadinia et al [27]	GWR[k]	—	—	—	—	0.05	0.85	0.01	—
Douchet et al [33]	SVR	—	—	—	—	—	0.75	0.44	—
Thibeaux et al [31]	FFN[l]	—	—	—	—	—	—	—	0.67

[a]AUC: area under the curve.

[b]MSE: mean squared error.

[c]MAE: mean absolute error.

[d]RMSE: root mean squared error.

[e]SVR: support vector regression.

[f]Indicate metrics that were not reported or used in the original studies.

[g]TAN: tree augmented naïve network.

[h]RFC: random forest classifier.

[i]LASSO: least absolute shrinkage and selection operator regression.

[j]SVM: support vector machine.

[k]GWR: geographically weighted regression.

[l]FFN: feed forward network.

However, as with all model comparisons, it is not possible to directly compare the efficiency of models trained and evaluated on dissimilar datasets. To provide a meaningful evaluation, studies that implemented multiple machine learning methods on the same datasets were carefully selected for comparison. This allows for an accurate ranking of the algorithms based on their mean scores for accuracy, sensitivity, specificity, F_1-score, and other metrics.

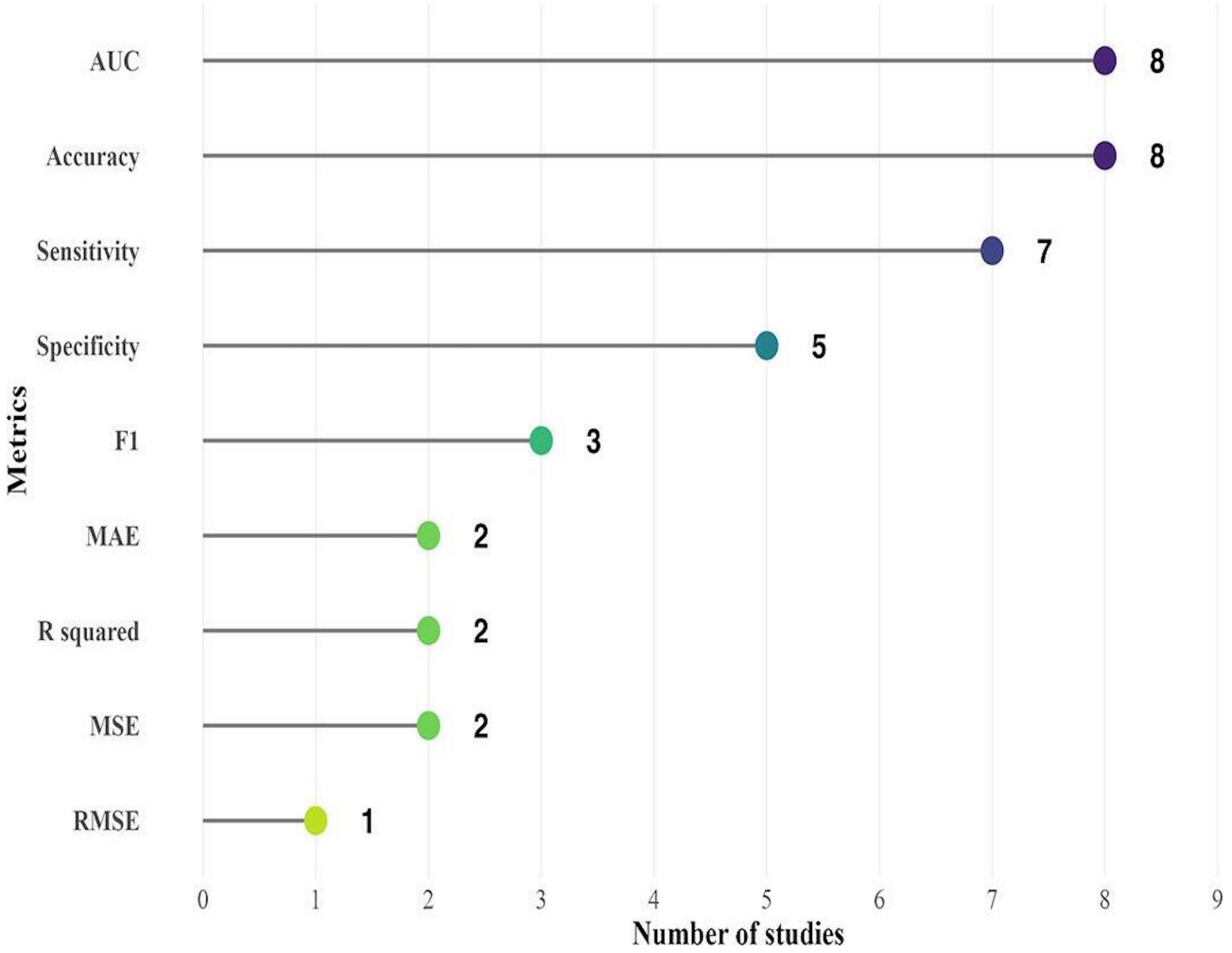
In several cases, regression models like SVR were assessed using MSE and R^2 values to gauge prediction performance. For instance, the SVR model in the Reunion Island dataset showed an MAE of 0.75 and an RMSE of 0.44, while other datasets revealed higher error rates, reflecting the challenges in prediction tasks [32].

The study also reveals that deep learning models, particularly those employing architectures like U-Net and CNN, achieved outstanding accuracy rates, with U-Net recording an accuracy of 98% [34]. Random forest models also performed consistently well, particularly in classification tasks, achieving high sensitivity and specificity.

Figure 5 shows the number of studies that reported various performance metrics, highlighting that accuracy and AUC were the most frequently used measures across the reviewed articles. This pattern reflects the widespread reliance on these metrics to evaluate classification performance in leptospirosis-related models. For instance, in one of the best-performing models, a genetic algorithm achieved an accuracy rate of 99%, significantly outperforming other models.

XSL•FO
RenderX

Figure 5. Number of algorithm performance metrics used in reviewed articles of dataset types used (public and private). AUC: area under the curve; F1: F_1-score; MAE: mean absolute error; MSE: mean squared error; RMSE: root mean squared error.



Datasets and Data Sources

ML and DL studies for leptospirosis prediction and diagnosis rely on diverse datasets with distinct characteristics (see Table 3). Public datasets, typically sourced from government agencies, provide large-scale environmental and epidemiological data ideal for transmission modeling. For instance, the Thai Surveillance System [32] offered monthly rainfall measurements (0 - 450 mm range), soil pH values (4.5 - 8.2), and 30-meter resolution elevation data across 5 Southeast Asian countries from 2003 to 2018, comprising over 15,000 data points.

XSL•FO
RenderX

Table . Comprehensive dataset characteristics of included studies.

Study	Data type (source)	Data categories	Sample size	Temporal resolution	Spatial resolution
Douchet et al [32]	Public (Thai surveillance system)	• Environmental: daily rainfall (mm)[a], soil pH • Climatic: max/min temperatures (°C) • Topographic: elevation (SRTM[b] 30m)	NS[c]	Monthly 2003 - 2018	Regional (5 countries)
Rahmat et al [28]	Public (Malaysia Meteorological Department)	• Meteorological: hourly rainfall (mm), RH[d] (%) • Clinical: PCR-confirmed[e] cases	364 weeks	Weekly 2011 - 2017	District-level (n=12)
Caicedo Torres et al [20]	Private (hospital records)	• Clinical: fever days, liver enzymes (U/L) • Demographic: age, gender, urban/rural	136 patients	Single admission	Hospital catchment
Nery et al [21]	Private (hospital records)	• Clinical: serum creatinine (mg/dL) • Epidemiological: rodent exposure index • Geospatial: residence coordinates	4675 cases	2009 - 2016	Household-level
Nery Jr et al [22]	Private (Gonçalo Moniz Institute [IGM], Federal University of Bahia [UFBA], Yale School of Public Health)	• Clinical: patient records • Epidemiological: risk factors, daily activities	4675 suspected cases (2046 confirmed, 2629 unconfirmed)	Retrospective (hospital and community cohort)	Hospital or community level (Salvador, Brazil)
Shenoy et al [29]	Private (medical records)	• Clinical: jaundice severity scale (0 - 3) • Laboratory: ELISA[f] optical densities • Comorbidities: diabetes status	800 patients	Retrospective 5y	Single tertiary center
Sonthayanon et al [25]	Private (bacterial cultures)	• Genomic: 16S rRNA[g] sequences • Proteomic: MALDI-TOF[h] peaks (2k-20k m/z)	116 isolates	2015 - 2018	Lab-level
Mayfield et al [24]	Private (serosurvey+ GIS[i])	• [j]Serological: MAT titers (1:50-1:6400) • Environmental: livestock density/km² • Village attributes: sanitation index	2152 people	Dry/wet season	GPS coordinates (82 villages)

XSL•FO
RenderX

Study	Data type (source)	Data categories	Sample size	Temporal resolution	Spatial resolution
Jayaramu et al [30]	Private (hydrological stations)	• Streamflow (m^3/s) • Water level (m) • Case reports (weekly)	517 weeks	Daily → weekly	Watershed-level
Galdino et al [10]	Private (hospital EMR[k])	• Vital signs: MAP (mmHg) • Labs: creatinine (µmol/L) • Outcomes: mortality	295 patients	2009 - 2022	3 hospitals
Ahangarcani et al [26]	Mixed (MODIS[l]+ CDC[m])	• Satellite: NDVI[n], LST (°C) • Case reports: district-level • Topography: slope (%)	1863 cases	Monthly 2009 - 2014	District-level
Kulkarni et al [34]	Public (microscopy images)	• Pixels: 256×256 RGB[o] • Annotations: spirochete masks	366 images	N/A	Pixel-level
Lopez et al [23]	Public (SINAN[p] database)	• Case reports: ICD-10[q] coded • Symptoms: 23-item checklist	890 cases	2007 - 2016	State-level
Mohammadinia et al [27]	Public (National Ministry of Health and Treatment of Iran, National Centre of Statistics of Iran, Meteorology Agency of Iran)	• Disease: positive ELISA test results	1186 positive cases (2009 - 2011)	Longitudinal (2009 - 2011)	District-level (Gilan Province, Iran)
Douchet et al [33]	Public (island surveillance)	• Climate: CHIRPS[r] rainfall (mm) • Case counts: ministry reports	Monthly NS	2010 - 2022	Island-level
Thibeaux et al [31]	Private (water monitoring)	• Hydrological: turbidity (NTU)[s] • Microbiological: qPCR[t] (copies/mL) • Weather: 5-min rainfall	226 samples	Event-based	3 km^2 watershed
Zhao et al [35]	Public (China CDC)	• Environmental: river density (km/km^2) • Socioeconomic: nightlight index • Cases: lab-confirmed	2741 cases	Annual 2004 - 2014	County-level

[a]Standard units of measurement (mm, °C, m, etc.).

[b]SRTM: Shuttle Radar Topography Mission.

[c]NS: not specified.

[d]RH: relative humidity .

[e]PCR: polymerase chain reaction.

XSL•FO
RenderX

[f]ELISA: Enzyme-Linked Immunosorbent Assay.
[g]rRNA: ribosomal ribonucleic acid.
[h]MALDI-TOF: Matrix-Assisted Laser Desorption/Ionization Time-of-Flight.
[i]GIS: Geographic Information System.
[j]MAT: microscopic agglutination test.
[k]EMR: electronic medical record.
[l]MODIS: Moderate Resolution Imaging Spectroradiometer.
[m]CDC: Centers for Disease Control and Prevention.
[n]NDVI: Normalized Difference Vegetation Index.
[o]RGB: red-green-blue color model.
[p]SINAN: Sistema de Informação de Agravos de Notificação.
[q] *ICD-10: International Classification of Diseases, Tenth Revision.*
[r]CHIRPS: Climate Hazards Group InfraRed Precipitation with Station data.
[s]NTU: Nephelometric Turbidity Unit.
[t]qPCR: quantitative polymerase chain reaction.

These datasets enabled regional risk prediction but lacked individual patient details. Similarly, Malaysia Meteorological Department records [28] provided 364 weeks of hourly rainfall data (0 - 65mm/hr) and relative humidity (45% - 100%) paired with PCR-confirmed cases across 12 districts, demonstrating how high-resolution temporal data improves ANN-based outbreak forecasting.

Private clinical datasets, while smaller in scale, delivered granular patient-level information crucial for diagnostic accuracy. The Napoleón Franco Pareja Children's Hospital dataset [20] included 136 pediatric cases with detailed clinical parameters: fever duration (1 - 21 d), liver enzyme levels (AST 15 - 980 U/L), and urban/rural residence markers. More extensive Brazilian hospital records [21] encompassed 4675 cases with serial creatinine measurements (0.2 - 9.8 mg/dL) and household GPS coordinates, though missing 12% of lab results. These datasets typically included three key data categories: (1) clinical biomarkers (serum creatinine, MAT titers 1:50-1:6400), (2) demographic information (age, gender in 89% of studies), and (3) epidemiological risk factors (rodent exposure indices).

Advanced studies combined multiple data types to overcome individual limitations. Research in China [35] integrated 2741 CDC case reports with satellite-derived nighttime light indices (0 - 63 DN values) and river density maps (0 - 5.7 km/km²), achieving exceptional predictive performance (AUC 0.95 - 0.96). Hydrological studies in New Caledonia [31] correlated 226 water samples (turbidity 0 - 1,000 NTU, qPCR 10 - 10 copies/mL) with 5-minute rainfall events, demonstrating how microenvironmental data enhances transmission understanding. These multimodal approaches compensated for individual dataset constraints through: (1) temporal complementarity (monthly climate + daily case reports), (2) spatial layering (watershed hydrology+ village coordinates), and (3) clinical-environmental linkages (serum markers + livestock density).

Discussion

Principal Findings

This systematic review of 17 studies (2012 - 2024) shows that while ML and DL techniques achieve promising accuracy (80% - 98%) in leptospirosis prediction and diagnosis, 3 critical limitations hinder clinical translation: (1) reliance on small, private clinical datasets limiting generalizability; (2) inconsistent validation methods, with only 11.8% employing temporal validation despite seasonality; and (3) underuse of advanced techniques like transfer learning (0% adoption) and data augmentation (5.9% adoption).

The most effective algorithms varied by task—SVR and Random Forest for prediction, versus U-Net CNNs for microscopy-based diagnosis—but all models faced challenges related to data quality, sample size, and geographic bias.

Textbox 1 shows the summary of the strengths and limitations identified in ML and DL studies for leptospirosis prediction and diagnosis.

XSL•FO
RenderX

Textbox 1. Summary of strengths and limitations identified in machine learning (ML) and deep learning (DL) studies for leptospirosis prediction and diagnosis.

Strengths:

- High predictive performance (80% - 98% accuracy).
- Variety of ML and DL algorithms applied (eg, random forests, support vector machines, and onvolutional neural networks).
- Integration of clinical and environmental data in some studies.
- Growing research interest and recent publications.

Limitations:

- Small, private datasets limit generalizability.
- Lack of external validation across datasets.
- Underuse of transfer learning and ensemble methods.
- Inconsistent evaluation metrics (accuracy, area under the curve, and sensitivity).

While these methods show strong performance (80% - 98% accuracy in some cases), their real-world applicability remains limited due to dataset constraints, validation inconsistencies, and underuse of advanced techniques such as transfer learning and ensemble learning. Addressing these gaps is essential to improve the robustness and clinical adoption of AI-driven leptospirosis diagnostics.

The most frequently used ML techniques for prediction tasks were SVR and Random Forest, while ANNs and CNNs, particularly U-Net, were commonly applied for diagnosis. This aligns with the increasing popularity of supervised ML methods in disease prediction.

Performance was primarily assessed using metrics such as accuracy, sensitivity, specificity, precision, and F_1-score, although AUC offers a more comprehensive measure of model performance, especially in binary classification tasks. Hybrid methods often produced better outcomes, with Random Forest and U-Net demonstrating strong accuracy and sensitivity in leptospirosis classification tasks. For instance [29], achieved 87% accuracy and 91% sensitivity using Random Forest for diagnosis, suggesting that ensemble techniques could further enhance model performance.

Despite these advancements, there are still limitations in reaching clinician-level accuracy, especially when dealing with smaller datasets or limited training data. Acceptable performance thresholds varied, with some studies using an AUC score of 0.96 or higher as a benchmark, but this was not universally applied. In addition, most studies relied on private, hospital-based datasets, limiting generalizability. The lack of external validation raises concerns about potential bias, emphasizing the need for public datasets and standardized validation protocols to improve cross-study comparability.

Cross-validation was the predominant method for evaluating the models, with k-fold or leave-one-out cross-validation being most common. However, due to the relatively small sample sizes in many studies, the conclusions drawn may not be as robust. Split validation (eg, 80:20 or 70:30 splits) was also used, but inconsistencies across studies hindered direct model comparisons. Future work should prioritize establishing standardized protocols to enhance consistency and reliability in ML and DL evaluations.

One significant finding of this review was the absence of pretrained models. Most studies developed models from scratch, limiting the generalizability and scalability of these models. Transfer learning involves using a pretrained model as a starting point and fine-tuning it for a specific task. It has proven effective in various fields, particularly in image analysis and natural language processing, by significantly improving performance on tasks with limited data.

The lack of transfer learning in these studies suggests a potential area for future research, as it could enhance the performance of DL models in leptospirosis prediction and diagnosis, especially in cases where training data is limited. Similarly, data augmentation, which helps expand training datasets through transformations (eg, rotations, translations, or noise), was only used in 1 study, highlighting a missed opportunity to improve model robustness.

Challenges and Research Gaps in ML and DL Applications for Leptospirosis Prediction and Diagnosis

While ML and DL have significant potential in leptospirosis research, this review also identified key findings that limit their broad application in clinical and public health settings.

Challenge 1: Limited Data Availability and Quality

A major challenge faced by the studies was the limited availability and quality of data. Many datasets, such as the one used in [21], had missing or incomplete data, which reduced the accuracy and generalizability of the models. Small sample sizes were a frequent issue as well, as observed in [20], where a dataset of only 136 patients resulted in high variability in model performance, especially for underrepresented cases like leptospirosis. Retrospective data collection posed further challenges, leading to biases in model training and evaluation, as noted by Shenoy et al [29].

Challenge 2: Generalizability and Regional Bias

Several studies, such as [28,33], identified biases in data collection, such as under- and over-reporting, regional

XSL•FO
RenderX

disparities, and sampling biases, which hindered the broader applicability of the models. In addition, studies like [35] noted issues with the spatial resolution of environmental data, affecting the precision of fine-scale risk mapping. Moreover, the lack of external validation across different regions and datasets, as seen in studies like [10], increased the risk of overfitting and limited the broader applicability of findings.

The review showed inconsistent performance across different ML and DL algorithms. For example, models like SVM, ANN, and CNNs performed well, with accuracy reaching up to 98% [34]. However, advanced DL architectures like ResNet, Inception, and VGG were rarely used [25,33]. Similarly, none of the studies applied transfer learning, a technique that could enhance performance, particularly when data is scarce [10,28,36]. Beyond data related challenges, there are also limitations in the ML and DL techniques currently applied to leptospirosis diagnosis, as discussed next.

Challenge 3: Underuse of Advanced Techniques

Advanced ensemble techniques, such as XGBoost and Adaboost, were notably underused [26]. While Random Forest models and U-Net architectures performed well in specific tasks [29,34], ensemble methods could provide better predictive power when combining ML and DL approaches. The review also highlighted the minimal use of data augmentation techniques, which could help address the small sample size issues observed in many studies [34].

Limitations of This Systematic Review

While this systematic review provides valuable insights, it has certain limitations. The heterogeneity of study designs, dataset sizes, and performance metrics precluded a meta-analysis, limiting our ability to provide a standardized comparison of model performances. In addition, the reliance on published studies may have introduced publication bias, as studies with less favorable results may have remained unpublished. Future systematic reviews should aim to standardize reporting metrics and ensure broader dataset accessibility to improve comparability across studies.

Recommendations for Future Research

Based on these findings, future research in ML and DL applications for leptospirosis should focus on the following areas:

- Integration of advanced DL techniques: future studies should explore the potential of advanced DL architectures, such as ResNet and Inception, which are known to improve predictive performance, especially in image-based analysis.
- Leveraging pretrained models and transfer learning: research should investigate how pretrained models can be fine-tuned for leptospirosis applications, particularly in data-limited scenarios.
- Use of ensemble and hybrid approaches: advanced ensemble techniques like XGBoost and hybrid ML-DL approaches should be explored to improve model accuracy and robustness.
- Broader geographic representation: most studies focused on regions like Southeast Asia and Brazil, with limited research in other high-risk areas like Africa and Central America. Expanding research to these regions will improve model generalizability.

The primary goal moving forward is to aggregate a comprehensive dataset from diverse sources and develop a robust data library to enhance the accuracy and reliability of leptospirosis prediction models. Given the heterogeneity of data features across different studies—ranging from clinical records to environmental data—the focus will be on standardizing and harmonizing these features for better model integration. By consolidating larger and more varied datasets, we aim to improve model generalization and tackle current challenges related to small sample sizes and overfitting. This unified dataset will serve as a foundation for applying advanced techniques, such as transfer learning and ensemble methods, to further enhance the predictive power of ML and DL models in leptospirosis detection.

Conclusion

This systematic review examined ML and DL techniques for leptospirosis prediction and diagnosis by analyzing algorithm performance, evaluation methods, and challenges. While models such as SVM, ANN, decision trees, and CNNs have shown strong predictive power, most studies have relied on private hospital-based datasets, limiting generalizability.

A key reason for the predominance of private datasets is that they often include detailed patient-level clinical information (eg, laboratory values, comorbidities, and symptoms) essential for developing diagnostic models. In contrast, available public datasets mainly provide aggregated epidemiological or environmental data, which, while valuable for outbreak prediction, lack the granular patient-specific features necessary for individual diagnosis. As a result, limited use of public datasets reflects the inherent constraints in the nature and detail of publicly available data, rather than a preference by researchers.

Furthermore, the lack of advanced techniques like transfer learning and ensemble methods remains a concern, along with small sample sizes and inconsistent validation protocols. Overall, while significant progress has been made, there is considerable potential to improve the accuracy and generalizability of leptospirosis prediction models by integrating more comprehensive datasets and adopting advanced AI methodologies in future research.

Authors' Contributions

SS led and conducted this study and contributed to the conceptualization, data extraction, analysis, and manuscript preparation and submission. AJ assisted with all steps, including data extraction, analysis, and manuscript preparation. BR contributed to data extraction, analysis, and provided critical input throughout the study.

XSL•FO
RenderX

Conflicts of Interest

None declared.

Multimedia Appendix 1
Search terms.
[DOCX File, 14 KB - medinform_v13i1e67859_app1.docx]

Multimedia Appendix 2
Agreement between human reviewers and ChatGPT-4o in study screening.
[DOCX File, 74 KB - medinform_v13i1e67859_app2.docx]

Multimedia Appendix 3
Quality assessment.
[DOCX File, 18 KB - medinform_v13i1e67859_app3.docx]

Multimedia Appendix 4
Characteristics of included studies.
[DOCX File, 35 KB - medinform_v13i1e67859_app4.docx]

Checklist 1
Preferred Reporting Items for Systematic Reviews and Meta-Analyses (PRISMA) checklist, detailing the sections, topics, checklist items, and their corresponding locations within the review.
[DOCX File, 24 KB - medinform_v13i1e67859_app5.docx]

References

1. Leptospirosis: fact sheet. World Health Organization. 2009. URL: https://www.who.int/publications/i/item/B4221 [accessed 2024-08-09]
2. About leptospirosis. Centers for Disease Control and Prevention. 2024. URL: https://www.cdc.gov/leptospirosis/about/index.html [accessed 2024-08-09]
3. Valente M, Bramugy J, Keddie SH, et al. Diagnosis of human leptospirosis: systematic review and meta-analysis of the diagnostic accuracy of the Leptospira microscopic agglutination test, PCR targeting LFB1, and IGM ELISA to Leptospira fainei serovar Hurstbridge. BMC Infect Dis 2024 Feb 7;24(1):168. [doi: 10.1186/s12879-023-08935-0] [Medline: 38326762]
4. Ching T, Himmelstein DS, Beaulieu-Jones BK, et al. Opportunities and obstacles for deep learning in biology and medicine. J R Soc Interface 2018 Apr;15(141):20170387. [doi: 10.1098/rsif.2017.0387] [Medline: 29618526]
5. Esteva A, Robicquet A, Ramsundar B, et al. A guide to deep learning in healthcare. Nat Med 2019 Jan;25(1):24-29. [doi: 10.1038/s41591-018-0316-z] [Medline: 30617335]
6. Topol EJ. High-performance medicine: the convergence of human and artificial intelligence. Nat Med 2019 Jan;25(1):44-56. [doi: 10.1038/s41591-018-0300-7] [Medline: 30617339]
7. LeCun Y, Bengio Y, Hinton G. Deep learning. Nature New Biol 2015 May 28;521(7553):436-444. [doi: 10.1038/nature14539] [Medline: 26017442]
8. Litjens G, Kooi T, Bejnordi BE, et al. A survey on deep learning in medical image analysis. Med Image Anal 2017 Dec;42:60-88. [doi: 10.1016/j.media.2017.07.005] [Medline: 28778026]
9. Sarvamangala DR, Kulkarni RV. Convolutional neural networks in medical image understanding: a survey. Evol Intell 2022;15(1):1-22. [doi: 10.1007/s12065-020-00540-3] [Medline: 33425040]
10. Galdino GS, de Sandes-Freitas TV, de Andrade LGM, et al. Development and validation of a simple machine learning tool to predict mortality in leptospirosis. Sci Rep 2023 Mar 18;13(1):4506. [doi: 10.1038/s41598-023-31707-4] [Medline: 36934135]
11. Angermueller C, Pärnamaa T, Parts L, Stegle O. Deep learning for computational biology. Mol Syst Biol 2016 Jul 29;12(7):878. [doi: 10.15252/msb.20156651] [Medline: 27474269]
12. Moher D, Liberati A, Tetzlaff J, Altman DG, PRISMA Group. Preferred reporting items for systematic reviews and meta-analyses: the PRISMA statement. PLoS Med 2009 Jul 21;6(7):e1000097. [doi: 10.1371/journal.pmed.1000097] [Medline: 19621072]
13. Moons KGM, de Groot JAH, Bouwmeester W, et al. Critical appraisal and data extraction for systematic reviews of prediction modelling studies: the CHARMS checklist. PLoS Med 2014 Oct;11(10):e1001744. [doi: 10.1371/journal.pmed.1001744] [Medline: 25314315]

XSL•FO
RenderX

14. Christodoulou E, Ma J, Collins GS, Steyerberg EW, Verbakel JY, Van Calster B. A systematic review shows no performance benefit of machine learning over logistic regression for clinical prediction models. J Clin Epidemiol 2019 Jun;110:12-22. [doi: 10.1016/j.jclinepi.2019.02.004] [Medline: 30763612]
15. Landis JR, Koch GG. The measurement of observer agreement for categorical data. Biometrics 1977 Mar;33(1):159-174. [doi: 10.2307/2529310] [Medline: 843571]
16. McHugh ML. Interrater reliability: the kappa statistic. Biochem Med (Zagreb) 2012;22(3):276-282. [doi: 10.11613/bm.2012.031] [Medline: 23092060]
17. Mu Y, He D. The potential applications and challenges of ChatGPT in the medical field. Int J Gen Med 2024;17:817-826. [doi: 10.2147/IJGM.S456659] [Medline: 38476626]
18. Miao J, Thongprayoon C, Fülöp T, Cheungpasitporn W. Enhancing clinical decision‐making: optimizing ChatGPT's performance in hypertension care. J Clinical Hypertension 2024 May;26(5):588-593. [doi: 10.1111/jch.14822]
19. Collins GS, Reitsma JB, Altman DG, Moons KGM. Transparent reporting of a multivariable prediction model for individual prognosis or diagnosis (TRIPOD): the TRIPOD statement. Ann Intern Med 2015 Jan 6;162(1):55-63. [doi: 10.7326/M14-0697] [Medline: 25560714]
20. Caicedo Torres W, Quintana M, Pinzón H. Differential diagnosis of hemorrhagic fevers using ARTMAP and an Artificial Immune System. Int J Artif Intell 2013;11(13 A):150-169 [FREE Full text]
21. Nery NRR, Claro DB, Lindow JC. Classification model analysis for the prediction of leptospirosis cases. Presented at: 2016 11th Iberian Conference on Information Systems and Technologies (CISTI); Jun 15-18, 2016; Gran Canaria, Spain p. 1-6. [doi: 10.1109/CISTI.2016.7521494]
22. Nery NRR Jr, Claro DB, Lindow JC. Prediction of leptospirosis cases using classification algorithms. IET softw 2017 Jun;11(3):93-99. [doi: 10.1049/iet-sen.2016.0193]
23. Lopez DM, de Mello FL, Giordano Dias CM, et al. Evaluating the surveillance system for spotted fever in Brazil using machine-learning techniques. Front Public Health 2017;5:323. [doi: 10.3389/fpubh.2017.00323] [Medline: 29250519]
24. Mayfield HJ, Smith CS, Lowry JH, et al. Predictive risk mapping of an environmentally-driven infectious disease using spatial Bayesian networks: a case study of leptospirosis in Fiji. PLOS Negl Trop Dis 2018 Oct;12(10):e0006857. [doi: 10.1371/journal.pntd.0006857] [Medline: 30307936]
25. Sonthayanon P, Jaresitthikunchai J, Mangmee S, et al. Whole cell matrix assisted laser desorption/ionization time-of-flight mass spectrometry (MALDI-TOF MS) for identification of Leptospira spp. in Thailand and Lao PDR. PLOS Negl Trop Dis 2019 Apr;13(4):e0007232. [doi: 10.1371/journal.pntd.0007232] [Medline: 30969958]
26. Ahangarcani M, Farnaghi M, Shirzadi MR, Pilesjö P, Mansourian A. Predictive risk mapping of human leptospirosis using support vector machine classification and multilayer perceptron neural network. Geospat Health 2019 May 14;14(1). [doi: 10.4081/gh.2019.711] [Medline: 31099515]
27. Mohammadinia A, Saeidian B, Pradhan B, Ghaemi Z. Prediction mapping of human leptospirosis using ANN, GWR, SVM and GLM approaches. BMC Infect Dis 2019 Nov 13;19(1):971. [doi: 10.1186/s12879-019-4580-4] [Medline: 31722676]
28. Rahmat F, Zulkafli Z, Juraiza Ishak A, Mohd Noor SB, Yahaya H, Masrani A. Exploratory data analysis and artificial neural network for prediction of leptospirosis occurrence in Seremban, Malaysia based on meteorological data. Front Earth Sci 2020;8. [doi: 10.3389/feart.2020.00377]
29. Shenoy S, Rajan AK, Rashid M, et al. Artificial intelligence in differentiating tropical infections: a step ahead. PLOS Negl Trop Dis 2022 Jun;16(6):e0010455. [doi: 10.1371/journal.pntd.0010455] [Medline: 35771774]
30. Jayaramu V, Zulkafli Z, De Stercke S, et al. Leptospirosis modelling using hydrometeorological indices and random forest machine learning. Int J Biometeorol 2023 Mar;67(3):423-437. [doi: 10.1007/s00484-022-02422-y] [Medline: 36719482]
31. Thibeaux R, Genthon P, Govan R, et al. Rainfall-driven resuspension of pathogenic Leptospira in a leptospirosis hotspot. Sci Total Environ 2024 Feb 10;911:168700. [doi: 10.1016/j.scitotenv.2023.168700] [Medline: 37992819]
32. Douchet L, Menkes C, Herbreteau V, et al. Climate-driven models of leptospirosis dynamics in tropical islands from three oceanic basins. PLOS Negl Trop Dis 2024 Apr;18(4):e0011717. [doi: 10.1371/journal.pntd.0011717] [Medline: 38662800]
33. Douchet L, Goarant C, Mangeas M, Menkes C, Hinjoy S, Herbreteau V. Unraveling the invisible leptospirosis in mainland Southeast Asia and its fate under climate change. Sci Total Environ 2022 Aug 1;832:155018. [doi: 10.1016/j.scitotenv.2022.155018] [Medline: 35390383]
34. Kulkarni A, Sai Dinesh Reddy P, Bassi R, Kashyap SK, Vijayalakshmi M. Spirochaeta bacteria detection using an effective semantic segmentation technique. In: Advances in Intelligent Systems and Computing 2022:355-365. [doi: 10.1007/978-981-16-9573-5_26]
35. Zhao J, Liao J, Huang X, et al. Mapping risk of leptospirosis in China using environmental and socioeconomic data. BMC Infect Dis 2016 Jul 22;16(1):343. [doi: 10.1186/s12879-016-1653-5] [Medline: 27448599]
36. Jadhav A, Sawesi S, Rashrash B. Bias and generalizability challenges in machine learning models for leptospirosis. Presented at: 2024 IEEE International Conference on Big Data (BigData); Dec 15-18, 2024; Washington, DC, USA p. 4989-4995. [doi: 10.1109/BigData62323.2024.10825588]

XSL•FO
RenderX

Abbreviation

AI: artificial intelligence
ANN: artificial neural network
AUC: area under the curve
CHARMS: Critical Appraisal and Data Extraction for Systematic Reviews of Prediction Modelling Studies
CNN: convolutional neural network
DL: deep learning
DT: decision tree
KNN: k-nearest neighbor
LLM: large language model
MAE: mean absolute error
MAT: microscopic agglutination test
ML: machine learning
MLP: multilayer perceptron
MSE: mean squared error
PCR: polymerase chain reaction
PRISMA: Preferred Reporting Items for Systematic Reviews and Meta-Analyses
PROBAST: Prediction model Risk of Bias Assessment Tool
RDT: rapid diagnostic test
RMSE: root mean squared error
SVM: support vector machine
SVR: support vector regression
TAN: tree augmented naive

Edited by A Benis; submitted 22.10.24; peer-reviewed by B Ozek, K Sutrave, M Khanna; revised version received 11.04.25; accepted 14.04.25; published 29.05.25.

Please cite as:
Sawesi S, Jadhav A, Rashrash B
Machine Learning and Deep Learning Techniques for Prediction and Diagnosis of Leptospirosis: Systematic Literature Review
JMIR Med Inform 2025;13:e67859
URL: https://medinform.jmir.org/2025/1/e67859
doi:10.2196/67859

© Suhila Sawesi, Arya Jadhav, Bushra Rashrash. Originally published in JMIR Medical Informatics (https://medinform.jmir.org), 29.5.2025. This is an open-access article distributed under the terms of the Creative Commons Attribution License (https://creativecommons.org/licenses/by/4.0/), which permits unrestricted use, distribution, and reproduction in any medium, provided the original work, first published in JMIR Medical Informatics, is properly cited. The complete bibliographic information, a link to the original publication on https://medinform.jmir.org/, as well as this copyright and license information must be included.

XSL•FO
RenderX

Preclinical Cognitive Markers of Alzheimer Disease and Early Diagnosis Using Virtual Reality and Artificial Intelligence: Literature Review

María de la Paz Scribano Parada[1,2,3], PhD; Fátima González Palau[1,4,5], PhD; Sonia Valladares Rodríguez[6,7], PhD; Mariano Rincon[7], PhD; Maria José Rico Barroeta[4], MSc; Marta García Rodriguez[4], MSc; Yolanda Bueno Aguado[4], PhD; Ana Herrero Blanco[4], MSc; Estela Díaz-López[7], PhD; Margarita Bachiller Mayoral[7], PhD; Raquel Losada Durán[4], MSc

[1]Centro de Neurorrehabilitación González Palau, Córdoba, Argentina

[2]Secretarìa de Investigación, Vicerrectorado de Investigación, Innovación y Posgrado, Universidad Siglo 21, Cordoba, Argentina

[3]Cátedras de Física BIomédica, Facultad de Ciencias Médicas, Universidad Nacional de Córdoba, Córdoba, Argentina

[4]Fundación INTRAS, Valladolid, Spain

[5]Instituto de Neurociencias y Bienestar, Insight 21, Universidad Siglo 21, Cordoba, Argentina

[6]Department of Electronics and Computing, University of Santiago de Compostela, Santiago de Compostela, Spain

[7]Department of Artificial Intelligence, National University of Distance Education, Madrid, Spain

Corresponding Author:
Fátima González Palau, PhD
Centro de Neurorrehabilitación González Palau, Córdoba, Argentina

Abstract

Background: This review explores the potential of virtual reality (VR) and artificial intelligence (AI) to identify preclinical cognitive markers of Alzheimer disease (AD). By synthesizing recent studies, it aims to advance early diagnostic methods to detect AD before significant symptoms occur.

Objective: Research emphasizes the significance of early detection in AD during the preclinical phase, which does not involve cognitive impairment but nevertheless requires reliable biomarkers. Current biomarkers face challenges, prompting the exploration of cognitive behavior indicators beyond episodic memory.

Methods: Using PRISMA (Preferred Reporting Items for Systematic Reviews and Meta-Analyses) guidelines, we searched Scopus, PubMed, and Google Scholar for studies on neuropsychiatric disorders utilizing conversational data.

Results: Following an analysis of 38 selected articles, we highlight verbal episodic memory as a sensitive preclinical AD marker, with supporting evidence from neuroimaging and genetic profiling. Executive functions precede memory decline, while processing speed is a significant correlate. The potential of VR remains underexplored, and AI algorithms offer a multidimensional approach to early neurocognitive disorder diagnosis.

Conclusions: Emerging technologies like VR and AI show promise for preclinical diagnostics, but thorough validation and regulation for clinical safety and efficacy are necessary. Continued technological advancements are expected to enhance early detection and management of AD.

(JMIR Med Inform 2025;13:e62914) doi:10.2196/62914

KEYWORDS

dementia; Alzheimer disease; mild cognitive impairment; virtual reality; artificial intelligence; early detection; qualitative review; literature review; AI

Introduction

Nowadays, widespread access to health care systems and changes in living conditions have resulted in an aging population, leading to an increase in the prevalence of neurocognitive disorders (NCD) [1,2]. This phenomenon will lead to a societal change and place an additional burden on health care systems. Therefore, the main challenge at this time lies in the development of therapeutic measures at the pharmacological level that can prevent or halt the progression of Alzheimer disease (AD). However, so far, it has not been possible to find a pharmacological product that meets the safety and efficacy criteria necessary for large-scale use [3-5].

XSL•FO
RenderX

Conversely, numerous studies have shown that factors such as access to higher education, leading a healthy lifestyle, controlling cardiovascular risk factors, and being socially active can have a preventive effect by delaying the onset of symptoms and disease progression. In this context, it is of vital importance to identify emerging markers of AD that allow a diagnosis to be made in its preclinical stage.

The definition of preclinical AD varies, marked by criteria similarities and differences. It signifies the initial stage in the AD continuum, characterized by an extended asymptomatic phase with evidence of AD pathology, yet lacking cognitive, behavioral, or activities of daily living impairment (Table 1). Duration varies (6-10 years), contingent on onset age, and progression to mild cognitive impairment (MCI) hinges on factors like age, sex, and apolipoprotein E status. The complexity arises from not all those meeting preclinical AD criteria progressing to MCI or AD dementia, adding nuances to the predictive analysis [6].

Table . The AD continuum.[a]

AD continuum	Pathological and anatomical evidence of AD	Behavioral and psychological changes and cognitive impairment	Functional deficit		
IWG-2[b]	Asymptomatic, at risk or presymptomatic	Prodromal	Mild AD dementia	Moderate AD dementia	Severe AD dementia
NIA-AA[c]	Preclinical	MCI[d] (prodromal AD)	AD with mild dementia	AD with moderate dementia	AD with severe dementia
FDA[e]	Stages 1 and 2 (up to 20 years prior to clinical AD)	Stage 3 (episodic memory, executive function, visuospatial function; disease progression to clinical AD	Stages 4-6 (all domains, in a progressive way)		

[a]AD: Alzheimer disease.

[b]IWG: International Working Group.

[c]NIA-AA: National Institute on Aging—Alzheimer's Association.

[d]MCI: mild cognitive impairment.

[e]FDA: Food and Drug Administration.

In this sense then, early biomarkers are crucial for assessing and monitoring AD. These indicators, recommended by the National Institute on Aging and the Alzheimer's Association, include the assessment of extracellular amyloid beta (Aβ) and hyperphosphorylated tau protein (p-tau) in the brain [7,8]. The latest guidelines classify neurodegeneration using biomarkers such as amyloid positron emission tomography, Aβ42 levels, tau protein, and neuroimaging techniques. Incorporating these biomarkers aids in the early detection and understanding of AD, aligning with evolving clinical practices and research efforts [9].

However, these biomarkers are expensive and not widely available in much of the world, and their results are not always consistent with the clinical manifestations of the patient, since even in the presence of positive markers, symptoms may not develop or may develop incompletely, and the time gap between the appearance of these biomarkers and the onset of symptoms has not yet been fully characterized.

Since the 1990s, there has been an increasing number of publications aiming to identify cognitive-behavioral markers of the shift from "normal" cognition (NC) to early symptoms of the disease [10-13]. In most studies, episodic memory appears as the domain that is altered in the first instance, reporting variability ranging from 20 [14] to 2 years prior to symptom onset [3,13,15-17].

More recent studies have explored other domains that could be altered earlier, especially visuospatial function and executive functions; in addition, spatial navigation tasks have appeared as a new domain with characteristics that encompasses the 2 previous ones [18-23]. Some studies have proposed to evaluate functional (such as modifications in expansive activities of daily living, changes in mobility patterns) and behavioral aspects, as well as conduct a more thorough analysis of companion reports, and even subjective memory complaints. However, there is little agreement on how to measure them and which ones exhibit true early marker behavior of the disease [24-26]. At this point, it is important to mention that the vast majority of studies are oriented to the diagnosis of NCD due to AD, with only a handful of studies exploring some characteristics of frontotemporal dementias or NCD associated with Parkinson disease, though these tend to have a much lower quality of evidence than studies for AD [27-32].

The most current approaches have incorporated artificial intelligence (AI) and machine learning (ML) tools with the purpose of developing multivariate models that take advantage of these advanced technologies to integrate neuroimaging results, neuropsychological variables, and biomarkers in the early diagnosis of AD [4,9,33-35]. In this context, the use of virtual reality (VR) environments presents a novel and yet underexplored opportunity. So far, they have mainly been used in therapeutic applications, but their potential in the field of diagnostics remains to be investigated [31,32,36-41].

This study aims to review prevalent neurocognitive markers for the preclinical stages of tauopathies, particularly AD. It also explores recent research on VR applications in this context and

XSL•FO
RenderX

aims to identify the most evidence-supported tests for assessing valuable cognitive domains.

Methods

The steps followed for article selection are based on the PRISMA (Preferred Reporting Items for Systematic Reviews and Meta-Analyses) methodology [42], as evidenced in recently published literature reviews on similar topics [43,44]. References were obtained from the search for articles in PubMed and Google Scholar. Articles from the last 10 years were included, although we also included 2 articles published more than 10 years ago because of their importance in the field. In the first instance, the terms used for the search were "pre-dementia Alzheimer's disease," "dementia early diagnosis," "dementia early diagnosis financial," "benefits of early diagnosis of Alzheimer's disease cost effectiveness," "benefits of early diagnosis of Alzheimer's disease," and "early diagnosis of Alzheimer's disease." However, the articles obtained with these operators corresponded to those with primary treatment objectives or involving exclusively biological measures in different fluids, development of new neuroimaging modalities, or developments of AI and ML algorithms without including neuropsychological parameters. We opted for the search strategy proposed by Bastin et al [12] using the following keywords: ((memory AND longitudinal AND Alzheimer's disease) AND (prodromal OR conversion OR preclinical)), ((mild cognitive impairment AND (Alzheimer's disease OR dementia) AND neuropsychology AND (prediction OR longitudinal)), and (Alzheimer's disease AND conversion AND neuropsychology).

When using these terms, none of the papers yielded results that included VR tools for diagnosis, so the pattern ((mild cognitive impairment AND (Alzheimer's disease OR dementia) AND neuropsychology AND virtual reality)) was incorporated within the search strategy, finding 13 new papers of which 11 were incorporated, including 2 review papers that are discussed towards the end. Two papers were discarded because they were rehabilitation papers. The terms were used in English for most of the search engines, except for Google Scholar where the same terms were used in Spanish. Articles in both languages were included. As inclusion criteria, we selected those papers that made a longitudinal follow-up or an extensive review either through a systematic review or meta-analysis of the proposed topic. Those papers that could show conversion from NC to MCI or from MCI to dementia were weighted.

Based on this, 58 articles were selected based on the reading of the abstract. Studies conducted in animals, those that pursued primary treatment objectives, those conducted in patients with depression or other psychiatric/psychological comorbidity, those whose primary objective was to develop an AI algorithm, those that only used markers from blood, cerebrospinal fluid, urine, saliva, or other biological markers, and research theses were excluded. After reading the full text, those papers whose primary objective was the development of diagnostic imaging methods unrelated to neurocognitive variables (mainly related to functional magnetic resonance imaging [MRI], volumetry, cortical thickness) and without development of neurocognitive assessment (the tests used were not reported, they only showed raw scores of screening tests) were eliminated, as well as those papers that did not include a control group (MCI or normal aging or healthy controls).

Moreover, the Mendeley functionalities were used for the purpose of consolidating all references drawn from the various databases consulted. Subsequently, an integrated matching tool was used to identify and eliminate duplicates. In the initial screening phase, a preliminary selection of papers was made based on their relevance to the research question. To conduct this screening, the titles and abstracts of the papers were used to ascertain whether any of the 7 exclusion criteria set out in Table 2 were met. In instances where a decision was not immediately evident, the article was designated as a potential candidate for the subsequent phase.

Table . Summary of the reasons for excluded papers.

Reason for exclusion[a]	Values (n=26+17)
Screening	
Did not report empirical data from human participants	12
Only biological markers (eg, blood, urine, cerebrospinal fluid)	4
Depression or another psychiatric comorbidity	3
Primary target: artificial intelligence algorithm development	5
Thesis	2
Eligibility	
No inclusion of MCI patients or normal aging or controls trials	5
Primary objective in development of diagnostic imaging methods	6
No neuropsychological assessment	6

[a]Reasons for excluding papers during the screening (n=26) and eligibility process (n=17).

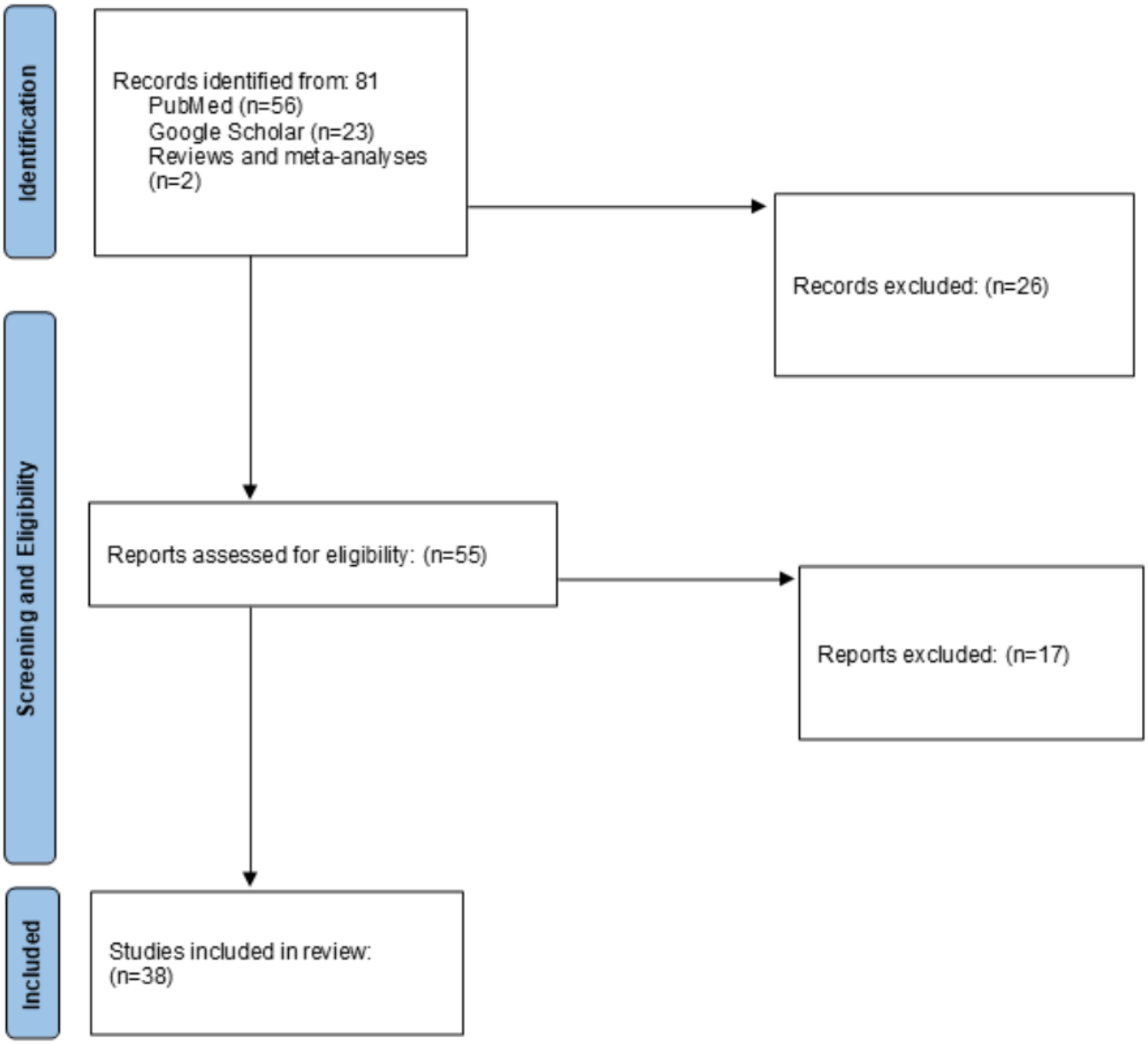
Subsequently, the full text of all papers that had been deemed eligible following the screening phase was considered. This was considered to be the most appropriate set of papers on the topic, having overcome the exclusion criteria set out in Table 2.

XSL•FO
RenderX

Results

The article selection process is outlined in Figure 1. This narrative outlines key discoveries from selected articles (Table 3 and Table 4)—studies without VR—categorizing the type of work and pinpointing the most early, sensitive, and specific neurocognitive variables according to each paper. Multiple cognitive variables, when presented, are organized by diagnostic profile. The chosen tests for variable measurements are specified. For a more detailed analysis of the reviewed articles, please consult the supplementary material (Multimedia Appendix 1). Moreover, a dedicated section and table are focused on findings related to VR and AI tools utilized for diagnosis (Table 5).

Figure 1. PRISMA (Preferred Reporting Items for Systematic Reviews and Meta-Analyses) flowchart illustrating the process of selecting eligible publications for inclusion in the literature review.



XSL•FO
RenderX

Table . Synthesis and comparison of selected studies without virtual reality.

	Reference	Neuropsychological domain	Gold standard	Validation
1	[45]	Executive functions	Cognitive markers: • Delis–Kaplan Executive Function System • Trail Making Test, Stroop, Tower Biological markers: • MRI (magnetic resonance image) • Cerebrospinal fluid p-tau/amyloid beta 42	• CH[c]-pathological amyloid beta 42/tau proteins (n=32) • CH-normal amyloid beta 42 • Tau proteins (n=33) • Mild cognitive impairment (n=39) • AD[a] (n=10)
2	[46]	Episodic memory	Cognitive markers: delayed memory testing Biological markers: atrophy of the hippocampal formation	
3	[47]	Episodic memory	Cognitive markers: • Paired-associate immediate recall (Wechsler Memory Scale) • Logical memory delayed recall (Story A) (Wechsler Memory Scale) • Boston Naming Test (Wechsler Adult Intelligence Scale) • Digit Symbol- Substitution Task (Wechsler Adult Intelligence Scale) Biological markers: • Cerebrospinal fluid p-tau/amyloid beta 42 • Magnetic resonance imaging • Blood	• Stage 0: n=102 • Stage 1: n=46 • Stage 2: n=28 • SNAP: n=46
4	[48]	Global cognition	Cognitive markers: • North American National Adult Reading Test • Vocabulary subtest of the Wechsler Adult Intelligence Scale-Revised • Years of education Biological markers: • Cerebrospinal fluid p-tau/amyloid beta 42 • Volume of the right hippocampus • Thickness of the right entorhinal cortex • Average thickness of seven cortical regions AD-related atrophy	• Low CR/[d]normal (n=108) • High CR/normal (n=126) • Low CR/progressed (n=41) • High CR/normal (n=25)

XSL•FO
RenderX

	Reference	Neuropsychological domain	Gold standard	Validation
5	[49]	Episodic memory	Cognitive markers: Free and Cued Selective Reminding Test – Free Recall and Total Recall Biological markers: PiB-PET[e]	• Aß-positive (n=71) • Aß-negative (n=5205)
6	[50]	Episodic memory	Cognitive markers: • Free and Cued Selective Reminding Test – Free Recall • Logical memory • Sequencing task Biological markers: cerebrospinal fluid p-tau/amyloid beta 42	• High p-tau/amyloid beta 42 • Low p-tau/amyloid beta 42
7	[18]	Episodic memory and spatial navigation memory	Cognitive markers: navigation time, trajectory errors, and delayed recall of a map	• Healthy control (n=20) • Mild cognitive impairment (n=18) • AD (n=20)
8	[51]	Verbal episodic memory	Cognitive markers: • Free and Cued Selective Reminding Test • Memory Binding Test • Rey-Osterreieth Complex Figure • Delayed Matched Sample test 48 items Biological markers: PiB-PET[e]	

XSL•FO
RenderX

	Reference	Neuropsychological domain	Gold standard	Validation
9	[52]	EEG changes	Cognitive markers: neuropsychological assessment Biological markers: • FDG-PET[f] • PiB-PET[e] • MRI • High-density EEG tracing with 256 channels, 1 minute resting closed eyes	
10	[34]	Global cognition	Cognitive markers: • Clinical Dementia Rating-Sum of Boxes • Alzheimer's Disease Assessment Scale - 11 score • Alzheimer's Disease Assessment Scale - 13 score • Rey Auditory verbal Learning Test Biological markers: • Magnetic resonance imaging • Demographic • APOE4[b] genetic	• Healthy control (n=184) • pMCI[g] (n=181) • sMCI[h] (n=228) • AD (n=192)
11	[35]	Episodic memory	Cognitive markers: • Forgetting Index • Logical memory • Rey Auditory Verbal Learning Test • Verbal Paired Associates Learning • Mini Mental State Examination • ADAS-Cog (Alzheimer´s Disease Assessment Scale-Cognitive) • Clinical Dementia Rating • Functional Assessment Questionnaire	• n=584 • 409 preserved the mild cognitive impairment diagnosis (4 year follow-up) • 175 mild cognitive impairment patients converted to dementia (4 year follow-up)
12	[14]	Visuospatial function and memory task (delayed recall and immediate recall)	Cognitive markers: • Complex Figure Test • Auditory Verbal Learning Test: Long-Term Memory, Selective Reminding Test, and Total Learning • Logical Delayed Recall Memory, Wechsler memory scale-Revised. • Inmediate free recall Biological markers: • APOE • Behavioral Test Score • Informants	
13	[9]	Voice		

XSL•FO
RenderX

	Reference	Neuropsychological domain	Gold standard	Validation
			• Speech or voice analysis along with analysis of emotional temperature with machine learning algorithms	
14	[30]	Hearing loss	Biological markers: • Steady-state Auditory Evoked Potentials • P300 • Pure tone audiometry	
15	[11]	Global cognition, verbal episodic memory, and attention shifting/flexibility verbal fluency	Cognitive markers: • Auditory Verbal Learning Test, Hopkins Verbal Learning Test, Rey Auditory Verbal Learning Test, Logical Memory • Mini Mental State Examination • Telephone interview for cognitive status • Trail Making Test - Part B • Semantic verbal fluency test	
16	[53]	Verbal memory task: free delayed recall	Cognitive markers: Rey Auditory Learning Verbal Test	

XSL•FO
RenderX

	Reference	Neuropsychological domain	Gold standard	Validation
17	[54]	Global cognition and health	Medical records	• AD United Kingdom=20,214 • AD France=19,458 • Healthy controls United Kingdom=20,214 • Healthy controls France=19,458
18	[17]	Sleep parameters	Cognitive markers: • Free and Cued Selective Reminding Test • Logical Memory Delayed Recall Wechsler Memory Scale - Revised • Digit Symbol-Substitution Task - Wechsler Adult Intelligence Scale • Mini Mental State Examination Biological markers: • Total sleep time, time in non-rapid eye movement sleep, time in rapid eye movement sleep, and sleep efficiency • Nonrapid eye movement slow wave activity • APOE4 • t-tau • Amyloid beta 42	n=100
19	[26]	Processing speed, community mobility, driving evaluations, AVD	Cognitive markers: • Coding subtest (WAIS-IV) • Consortium to Establish a Registry for Alzheimer's Disease - Semantic Fluency (animals) • Controlled Oral Word Association Test • Trail Making Test - Part B • Timed Instrumental Activities of Daily Living • Financial Capacity Instrument-Short Form • University of Alabama at Birmingham - Life Space Assessment • Useful Field of View • Road Sign Test • Global Driving Performance Biological markers: • MRI-s[i] • Genetic risk alleles (APOE status)	
20	[17]	Sleep disorders		

XSL•FO
RenderX

	Reference	Neuropsychological domain	Gold standard	Validation
			Cognitive markers: • Free and Cued Selective Reminding Test • Wechsler Memory Scale - Revised: Logical Memory Delayed Recall • Digit Symbol-Substitution Task - Wechsler Adult Intelligence Scale • Mini Mental State Examination Biological markers: • APOE genotype • t-tau and amyloid beta 42 in CSF • Actigraphy (Actiwatch 2, Philips Respironics) • EEG (1 channel)	
21	[19]	Visuospatial working memory, anosognosia, visuomotor control, cognition spatial		

XSL•FO
RenderX

	Reference	Neuropsychological domain	Gold standard	Validation
			Cognitive markers: • n-back task and match-to-sample tasks • Mental Rotations Test • Backward Corsi's Block-Tapping Test • Corsi's Block-Tapping Test with inhibition • Jigsaw-Puzzle Imagery Task • Delayed-Response-Activity Test • Pathway Span Task • Self-Rating Scale of Memory Functions • Memory Observation Questionnaire • Memory Complaint Questionnaire • Metamemory Questionnaire–Ability Subscale • Subjective Memory Complaint Questionnaire • Anosognosia Rating Scale • Clinical Insight Rating Scale • Experimenter Rating Scale • Tapping and Dotting Subtests (MacQuarrie's Test for Mechanical Ability) • Purdue Pegboard Test • Kas' test • Visual-Motor Speed and Precision Test • Movement Assessment Battery for Children–Second Edition • Eye-Hand Coordination Subtest (Developmental Test of Visual Perception–Third Edition) • Ego-Allo Task • Four Mountains Test Biological markers: • MRI- f • Paradigm of resting in PET	
22	[55]	Global cognition		• Low pathology • Intermediate ADNC[j] • Intermediate ADNC+ other • High ADNC • High ADNC+ other • Other pathology

XSL•FO
RenderX

Reference	Neuropsychological domain	Gold standard	Validation
		Cognitive markers: • Neuropsychiatric Inventory Questionnaire • Clinical dementia rating • Mini Mental State Examination • Dementia Rating Scale Biological markers: • Plasma amyloid beta 42, amyloid beta 40, total tau, p-tau181, p-tau231, and neurofilament light • Brain autopsy	

[a]AD: Alzheimer disease.
[b]APOE: apolipoprotein E.
[c] CH: Cognitively Healthy
[d]CR: Cognitve Reserve
[e]PiB- PET: Pittsburgh - positron emission tomography
[f]FDG- PET: Fluorodeoxyglucose - positron emission tomography
[g]pMCI: Progress Mild Congitive Impairment
[h]sMCI: Stable Mild Cognitive Impairment
[i]MRI-s: structural magnetic resonance image
[j]ADCN: AD neuropathological change

Table . Targeted neuropsychological domain without virtual reality.

Neuropsychological domain	Analytical method	Number	References
Episodic memory	Statistical: 5	5	[18,35,46,47,49]
Global cognition	Statistical: 4; artificial intelligence: 1	5	[11,34,48,54,55]
Verbal episodic memory	Statistical: 2; artificial intelligence: 1	3	[11,51,53]
Visuospatial, navigation	Statistical: 3	3	[14,19,26]
Sleep	Statistical: 2	2	[17,17]
Electroencephalogram	Statistical: 1	1	[52]
Executive functions	Statistical: 1	1	[45]
Voice	Artificial intelligence: 1	1	[9]
Audio	Statistical: 1	1	[30]

XSL•FO
RenderX

Table . A compilation of selected studies utilizing virtual reality.

	Reference	Type of study	Neuropsychological domain	Gold standard	VR[a] cognitive tasks
1	[23]	Cross-sectional	Allocentric memory, egocentric memory	VR parks and mazes	Complete neuropsychological assessment; magnetic resonance imaging with volumetry
2	[39]	Cross-sectional	Global cognition	Rivermead Behavioral Memory Test versus Montreal Cognitive Assessment; home selection task; VR versus Montreal Cognitive Assessment	Montreal Cognitive Assessment
3	[24]	Cross-sectional	Functional level in Instrumental Activities of Daily Living	Coffee cup preparation task in a virtual environment	Mini Mental State Examination, Frontal Assessment Battery, Instrumental Activities of Daily Living (Lawton and Brody)
4	[25]	Cross-sectional	Functional level with virtual reality	Tasks of daily life in a virtual environment	Complete neuropsychological battery, Magnetic Resonance Image, cognitive evoked potentials
5	[56]	Cross-sectional	Global cognition	Virtual supermarket	Complete neuropsychological battery
6	[21]	Cross-sectional	Ego/allocentric orientation	VR navigation task	Money's Road Map test to compare the paper and virtual versions
7	[20]		Ego/allocentric memory	VR navigation task	
8	[57]	Cross-sectional	Navigation task, entorhinal cortex navigation	VR navigation tasks	Digit Symbol, Free and Cued Selective Reminding Test, Mini Mental State Examination, North American National Adult Reading Test, Trail Making Test A and B, magnetic resonance imaging (entorhinal cortex)
9	[58]	Cross-sectional	Comparing traditional paper-based neurocognitive assessment with neurocognitive assessment realized with immersive VR-3D technology.	Precalibrated VR-3D tests, customized 3D-VR testing, traditional 2D digitized tests	3D tasks, 3D virtual maze, 2D tasks, T-maze
10	[59]	Cross-sectional	Prospective memory	Recall of prospective and retrospective components of 7 interventions in a virtual city	Virtual driving: left or right. Two pedals (gas and brake). Control speed.
11	[37]	Cross-sectional	Global cognition, motor performance, cognitive self-report	VR Functional Capacity Assessment Tool	Rey-Osterrieth Complex Figure, Rey Auditory Verbal Learning Test

[a]VR: virtual reality.

XSL•FO
RenderX

A large majority of articles present verbal episodic memory measured by different tests (Free and Cued Selective Reminding Test, California Verbal Learning Test, Rey Auditory Verbal Learning Test) as the earliest measure with the best sensitivity and specificity ratio for the detection of the preclinical stage of AD and the most recent works propose to support this measure with different neuroimaging formats, genetic profiling (apolipoprotein E), or markers (Aβ, tau, p-tau) in cerebrospinal fluid [11,12,46,49,50,53,60-62]. Among these papers, the one by Gagliardi's team comparing different neuropsychological tests for the measurement of episodic memory stands out [51].

Harrington and collaborators [45] focused on executive functions using the Stroop test, conducted on individuals without apparent cognitive impairment. They compared those with positive amyloid in cerebrospinal fluid to those without pathology, revealing executive failure preceding memory issues. The study emphasized the absence of standardized protocols for cognitive neural vulnerability in preclinical stages.

The works of Bastin [12] and Gainotti [46] are 2 large review papers that attempted to identify early neuropsychological markers in preclinical and conversion AD, comparing cognitively healthy subjects with and without evidence of pathology. Both papers agreed that episodic memory is the earliest marker, followed by semantic memory, although the protocols used for its assessment differed.

One of the most outstanding articles found in this search is the work of Mistridis et al [63]. The article agrees that verbal episodic memory is an early marker of cognitive impairment, detailing the sequence of decline of various cognitive functions in subjects with NC who progress to MCI. Verbal memory declines about 8 years before MCI, followed by episodic learning, visual memory, and semantic memory about 4 years before MCI. Executive functioning and processing speed declined about 2 years before MCI diagnosis. This suggests that multiple cognitive domains are valuable in assessing preclinical AD.

Another paper that attempted to establish a timeline is that of Soldan et al [47], which used a composite score to evaluate 4 study groups of cognitively unimpaired patients, with the definitions of stage 0 (high Aβ and low tau), stage 1 (low Aβ and low tau), stage 2 (low Aβ and high tau), and suspected non-AD pathology (high Aβ and high tau). The article used linear mixed-effects models to estimate longitudinal cognitive composite scores among individuals in 4 preclinical AD groups. Adjusted for baseline factors, stage 2 individuals showed greater impairment and lower baseline scores compared to others, while stage 0, stage 1, and suspected non-AD pathology groups showed no significant differences. Involving 222 NC adults over 11 years, those in stage 2 (low Aβ, high tau/p-tau) showed markedly lower baseline scores and greater cognitive impairment, suggesting that abnormal amyloid and tau levels are necessary for cognitive differences in NC individuals.

Skills related to visuospatial function, which could prove important in the development of VR environments, were addressed in depth in the work of Caselli et al [14] and Iliardi et al [19]. The first study suggested that visuospatial function deteriorates 20 years before clinical signs of AD, aligning with early pathological changes. It aims to sequence neurocognitive alterations in preclinical stages of AD. The second article addressed the importance of assessing visuospatial working memory, anosognosia, and visuomotor control in patients with MCI, who show worse performance compared to healthy controls and sometimes like patients with dementia. Assessment of visuomotor abilities may help distinguish high-risk AD patients from nonrisk AD patients.

Wadley and colleagues [26] focused on processing speed impact on patient functionality, utilizing an ecological approach integrating neurocognitive and functional variables from professional observations, informant reports, and self-reports. They correlated these with neuroimaging and genetic markers, suggesting processing speed as a stronger correlation of everyday abilities than MRI patterns consistent with AD, and more accessible for measurement. Although neuroimaging demonstrates AD-related neurodegeneration, processing speed captures combined effects, comorbidities, and cognitive reserve, serving as an early marker for functional outcomes.

Among the studies that showed other tools for assessing preclinical stages of NCD that complemented cognitive neural vulnerability, there are studies that incorporate high-resolution electroencephalography measurements [52], olfactory markers [64], auditory [30], retinal thickness measurement by optical coherence tomography [64], use of ML algorithms for speech analysis [9], and home-based sleep studies from specific devices [17]. Some of these works were intended to assess preclinical stages of dementias other than AD, and in the review done by Khan et al in 2020 [9], the proposal of voice analysis in audios and videos allowed for this analysis in several languages. These studies suggest challenges with tests in English, requiring validation for diverse languages and contexts. However, they feature smaller populations, necessitate specific devices, and occur in nonclinical settings.

Literature on the use of VR for early diagnosis of preclinical NCD was limited, unlike its extensive use in cognitive skill training. Papers related to VR for diagnosis or treatment increased from 2008 to 2017, declined until 2020, then started rising again (Table 5).

By 2011, it was confirmed that ego and allocentric memory, linked to the parietal association cortex and medial temporal cortex, could serve as early markers of cognitive decline. VR models, like park or maze navigation, facilitated assessment [23]. Moreover, a Canadian team compared NC subjects with MCI patients using the Montreal Cognitive Assessment, Rivermead Behavioral Memory Test, and a VR test where subjects choose an apartment. The VR test correlated positively with the Montreal Cognitive Assessment, unlike traditional tests, but the sample size was small [39].

The study of Allain et al [24] compares cognitively healthy controls with patients with AD (varying stages, Mini Mental State Examination 18 - 26 points) regarding functionality using a virtual coffee preparation task. Measures include completion time, achievement, and error scores compared with real-world tasks. With 24 patients with AD and 32 controls, the study demonstrates VR's feasibility in studying AD deficits in ecologically valid environments, though limited to a single task.

XSL•FO
RenderX

In 2014, Tarnanas et al [65] conducted research correlating daily living activities assessment in virtual environments with biomarkers like neuropsychological tests, event-related potentials, and MRI. Their study, robust compared to others, suggests VR performance equals biomarkers, attributed to VR's cognitive fidelity and rich behavioral data reflecting early-stage neurocognitive processes.

Zygiuris et al [56] introduced the virtual supermarket, a VR tool for rehabilitation and screening. The article extensively examined its validity with various measures and set cutoff points for a diagnostic algorithm. Several papers corroborate the apparent sensitivity of visuospatial functions in early NCD detection, evaluating ego and allocentric orientation. Morganti [21] compared a paper and VR version of Money's "Road Map" test, noting the virtual version's increased difficulty. They hypothesized that participants solve the traditional version through egocentric spatial transformations, while VR decisions are made based on on-screen interactions. This makes VR tools an interesting alternative, but one that needs to be carefully evaluated to determine what factors influence the results. Similarly, Mohammadi et al [20] used a VR navigation task to distinguish between monodomain and multidomain amnestic MCI, patients with AD, and normal controls, comparing results with traditional neuropsychological tests. They analyzed correct responses and response times in neighborhood and maze environments, establishing distinctive patterns in orientation (ego/allocentric) and visual/verbal memory.

Howett et al [57] published a study correlating entorhinal cortex volume measures, proposed as an early AD marker, with changes in immersive VR tests. They found consistent results with traditional neuropsychological tests, suggesting navigation tasks aid in early AD diagnosis [57]. Within this group, Lecouvey et al [59] utilized VR to evaluate prospective memory through tasks in a virtual city, comparing it with traditional neurocognitive measurements. Results confirmed early prospective memory alterations in AD, suggesting VR as a reliable assessment tool.

Turner's team [37] created a tablet-based tool evaluating real-world task competence in a realistic VR setting, assessing cognition, motor skills, and self-reported cognitive abilities in patients with Parkinson disease.

To conclude, 2 articles in this review elaborated VR protocols to assess neurocognitive domains, revealing the progression from NC to MCI, focusing on memory and visuospatial functions. In 1 study, an Italian team devised a protocol to detect early cognitive signs of conversion in AD, focusing on egocentric and allocentric spatial representations. Previous studies showed alterations, especially in allocentric frames, in patients with amnesia with MCI and AD. Their innovation lies in proposing an intrinsic connection between egocentric/allocentric frames and spatial relations. The results revealed deficits in allocentric coordinated judgments, implying a deviation towards AD in the representation of metric distances [22]. In the other study, Machado et al [58] highlighted the use of VR environments, in particular 3D mazes, as diagnostic tools for MCI or dementia. Their study compares traditional methods with VR environments, combining precalibrated 3D tests with validated 2D neuropsychological assessments, allowing for assessment across several cognitive domains.

Finally, these studies, when paired with advanced AI algorithms, hold promise for early diagnosis. They enable cross-referencing of various variables, enhancing diagnostic accuracy [4,33,34,57,66].

Discussion

Principal Findings

The objective of the Discussion section is to integrate the findings of this literature review and to explore their implications for advancing early diagnostic methods for AD using VR and AI. This section considers the strengths and limitations of current approaches, while also highlighting the potential role of these emerging technologies. Our findings indicate that while verbal episodic memory is a sensitive preclinical marker of AD, other cognitive domains, such as executive function and processing speed, may also serve as valuable early indicators. Furthermore, we examine the significant untapped potential of VR for the assessment of complex cognitive behaviors. VR has the capacity to simulate real-world environments, thereby enabling the evaluation of subtle deficits in cognition that would otherwise be challenging to capture in traditional assessments. AI, with its capacity to analyze multidimensional data, provides a promising approach for integrating biomarkers, cognitive data, and behavioral patterns. Nevertheless, there are considerable obstacles to the clinical implementation of these technologies, particularly in relation to the processes of validation, regulation, and ethical consideration.

The diagnosis of NCD involves advanced pathological definitions based on biomarkers but lacks changes in treatment perspectives. AD remains a paradigm, guiding NCD studies. Although pharmacological treatments are lacking, lifestyle and cardiovascular health modifications may prevent or delay onset, highlighting the importance of early diagnosis for effective intervention.

For more than 30 years, neuropsychological tests have provided the possibility of a more accurate diagnosis and of generating the basis for more specific pharmacological and nonpharmacological treatment plans. However, in recent years, with the advent of biomarkers, the scenario has become more complex [60].

Combining various diagnostic methods like amyloid and tau protein determination in cerebrospinal fluid, positron emission tomography scans with fluorodeoxyglucose or florbetapir, and brain volumetric measurements enhances diagnostic accuracy. However, controversies arise as apparently healthy individuals exhibit positive pathological markers without developing measurable symptoms over extended periods, challenging current diagnostic instruments [6,7,47,67-69].

Incorporating neuropsychological tests into composite diagnostic schemes becomes crucial for reliable conclusions in preclinical disease stages. Verbal episodic memory emerges as the earliest altered neurocognitive domain, followed by visual and semantic memory, despite measurement controversies [3,12-14].

XSL•FO
RenderX

Recent studies suggest executive functions and processing speed alterations as early markers preceding declines in episodic and semantic memory. Improving processing speed through training protocols is vital for maintaining functionality in cognitively demanding tasks like driving and managing finances for individuals with MCI [26,28,31,32,45].

Enhancing diagnostic accuracy for MCI involves indirectly estimating posteromedial parietal cortex function through simple outpatient neuropsychological tasks. Assessing visuomotor abilities in high-risk AD individuals distinguishes conversion probability. Iliardi et al [19] revealed deficits in visuospatial working memory and metamemory as conversion predictors, intricately linked to posteromedial parietal cortex neuronal activity. This innovative approach spans various domains, potentially significantly improving the care and treatment of patients with MCI.

Three recent Spanish review studies focused on identifying cognitive processes assessed via VR and determining commonly used everyday life scenarios in virtual environment design to enhance ecological validity. They noted poor correlation between traditional neuropsychological tests and activities of daily living, prompting the development of technology-based instruments like VR and serious games for evaluation [70-73]. One of these studies reported that 52.3% of works implemented immersive VR, followed by nonimmersive VR (43.2%), and finally semi-immersive VR (4.5%) [70].

VR environments are emerging as new diagnostic tools, but limitations exist. Selected studies were cross-sectional, with few patients evaluated. Gender differences, like navigation strategies in mazes, were noted. Performance in visuospatial tasks is influenced by reference points, instructions, and experimental parameters, highlighting the need for careful consideration in test design [21,24,28,32,56,58].

The translational approach merges animal models and patient evaluations, incorporating complex 3D tasks and standardized neuropsychological tests with automatic analysis, enhancing neuroscience's cognitive function investigations. A clinical module with preconfigured 2D and 3D tasks simplifies routine patient evaluations [58].

Limitations of This Literature Review

However, this literature review on preclinical cognitive markers of AD using VR and AI has several notable limitations. First, many studies were conducted with a limited number of participants, which reduces the generalizability of the findings. This small sample size makes it difficult to draw broad conclusions about the effectiveness of VR and AI for early diagnosis in different populations. Second, there is a lack of psychometric validity in some of the cognitive markers used, which raises concerns about the accuracy and reliability of these tools in assessing preclinical stages of AD. In addition, AI algorithms used in early diagnosis are often subject to bias due to the nature of the training data, potentially leading to biased decision-making that could disproportionately affect certain demographic groups. Ethical considerations also remain a challenge, particularly about privacy, consent, and transparency of AI-driven diagnostic processes. Addressing these limitations is critical to the development of robust, fair, and clinically useful AI- and VR-based tools for early detection of AD.

In conclusion, the integration of VR and AI in AD diagnosis represents a rapidly advancing and promising area in medical and neuropsychological research. Key considerations in this domain may include the following aspects:

- Diagnostic accuracy: The fusion of VR and AI provides an avenue for conducting highly accurate and objective assessments of cognitive functions in general, especially visuospatial functions. These tools can identify nuanced alterations in cognitive performance that traditional assessments frequently struggle to detect.
- Early detection: Detecting AD in its preliminary stages is crucial for early intervention and personalized support. VR and AI technologies can detect early signs of cognitive decline before symptoms manifest in daily activities, facilitating more timely and targeted interventions.
- Personalization: Through AI, VR evaluations can be personalized to match the unique capabilities and requirements of each patient. This enables tests to target specific cognitive areas of deficiency, enhancing diagnostic precision and identifying personalized areas for enhancement.
- Greater immersion: VR offers an immersive environment that replicates real-life scenarios and is ideal for evaluating patients' proficiency in everyday activities like city navigation or shopping. These tasks are challenging to replicate within traditional clinical settings, making VR assessments particularly valuable as they facilitate an ecological and nonintrusive cognitive evaluation of the person.
- Continuous data acquisition: VR and AI facilitate continuous data gathering, enabling precise monitoring of disease advancement and the efficacy of therapeutic measures over time.

Recommendations for Future Research

Further research is needed to improve the effectiveness of VR and AI practices in early diagnosis of AD, particularly by addressing personalization and diagnostic accuracy. One promising direction is to develop VR assessments that can be tailored to each patient's unique abilities and needs, ensuring that cognitive assessments are as individualized and responsive as possible. This personalization could contribute to a more accurate understanding of each patient's cognitive status, thereby improving the sensitivity of early detection. In addition, research should focus on improving diagnostic accuracy by strengthening the psychometric validity of cognitive markers used in VR environments to ensure that these assessments are both reliable and clinically meaningful. In parallel, ongoing efforts are needed to mitigate biases in AI predictions by ensuring that models are trained on diverse datasets that accurately represent the broader population, thereby reducing inequalities in diagnostic outcomes. These future research efforts are essential to refine VR and AI as effective, unbiased, and personalized tools for early detection of AD.

XSL•FO
RenderX

Conclusions

Preclinical diagnosis of NCD remains challenging, with much more exploration needed. Although VR and AI offer benefits, challenges include expensive hardware, rigorous test validation, and results interpretation by trained professionals. Ethical concerns arise from patient data collection in virtual environments, necessitating strict confidentiality measures. Despite these challenges, VR's use in AD diagnosis marks noteworthy progress in health care and NCD research. Continued technological advances will improve early detection and management. It is therefore essential to validate and regulate clinical safety and efficacy, delving into new preclinical cognitive markers. Further research is needed to improve the efficacy of VR and AI practices in the early diagnosis of AD, in particular addressing personalization and diagnostic accuracy.

Acknowledgments

This work is part of the IDENTIA project. This project is funded by PP2021-009109/MCIN/AEI/10.13039/ 501100011033, Ministry of Science and Innovation of Spain, the State Research Agency, and by the European Union "NextGeneration EU/PRTR."

Conflicts of Interest

None declared.

Multimedia Appendix 1
Tables with the full description of each item and abbreviations.
[DOCX File, 141 KB - medinform_v13i1e62914_app1.docx]

Checklist 1
PRISMA checklist.
[DOCX File, 31 KB - medinform_v13i1e62914_app2.docx]

References

1. Hugo J, Ganguli M. Dementia and cognitive impairment. Clin Geriatr Med 2014 Aug;30(3):421-442. [doi: 10.1016/j.cger.2014.04.001]
2. Prince M, Wimo A, Guerchet M, Gemma-Claire A, Wu YT, Prina M. World Alzheimer Report 2015: the global impact of dementia - an analysis of prevalence, incidence, cost and trends. Alzheimer's Disease International. 2015. [doi: 10.1111/j.0963-7214.2004.00293.x]
3. Caselli RJ, Locke DEC, Dueck AC, et al. The neuropsychology of normal aging and preclinical Alzheimer's disease. Alzheimers Dement 2014 Jan;10(1):84-92. [doi: 10.1016/j.jalz.2013.01.004] [Medline: 23541188]
4. Janghel RR, Rathore YK. Deep convolution neural network based system for early diagnosis of Alzheimer's disease. IRBM 2021 Aug;42(4):258-267. [doi: 10.1016/j.irbm.2020.06.006]
5. P DE Doctorado En Medicina Y Ciencias De La Salud, Por R, Sánchez-Juan C, Lage Martínez C, Sánchez-Juan P. Comportamiento ocular en el diagnóstico de la enfermedad de alzheimer [Report in Spanish]. URL: https://dialnet.unirioja.es/servlet/tesis?codigo=303662 [accessed 2025-01-22]
6. Porsteinsson AP, Isaacson RS, Knox S, Sabbagh MN, Rubino I. Diagnosis of early Alzheimer's disease: clinical practice in 2021. J Prev Alz Dis 2021;01:1-16. [doi: 10.14283/jpad.2021.23]
7. Janeiro MH, Ardanaz CG, Sola-Sevilla N, et al. Biomarcadores en la enfermedad de Alzheimer [Article in Spanish]. Adv Lab Med / Av en Med de Lab 2021 Mar 10;2(1):39-50. [doi: 10.1515/almed-2020-0109]
8. Bjerke M, Engelborghs S. Cerebrospinal Fluid Biomarkers for Early and Differential Alzheimer's Disease Diagnosis: IOS Press; 2018. [doi: 10.3233/JAD-170680]
9. Khan S, Barve KH, Kumar MS. Recent advancements in pathogenesis, diagnostics and treatment of Alzheimer's disease. Curr Neuropharmacol 2020;18(11):1106-1125. [doi: 10.2174/1570159X18666200528142429] [Medline: 32484110]
10. Almkvist O. Neuropsychological features of early Alzheimer's disease: preclinical and clinical stages. Acta Neurol Scand 1996 Apr;94(S165):63-71 [FREE Full text] [doi: 10.1111/j.1600-0404.1996.tb05874.x]
11. Battista P, Salvatore C, Berlingeri M, Cerasa A, Castiglioni I. Artificial intelligence and neuropsychological measures: the case of Alzheimer's disease. Neurosci & Biobehav Rev 2020 Jul;114:211-228. [doi: 10.1016/j.neubiorev.2020.04.026]
12. Bastin C, Salmon E. Early neuropsychological detection of Alzheimer's disease. Eur J Clin Nutr 2014 Nov;68(11):1192-1199. [doi: 10.1038/ejcn.2014.176] [Medline: 25182019]
13. Collie A, Maruff P. The neuropsychology of preclinical Alzheimer's disease and mild cognitive impairment. Neurosci Biobehav Rev 2000 May;24(3):365-374. [doi: 10.1016/s0149-7634(00)00012-9] [Medline: 10781696]
14. Caselli RJ, Langlais BT, Dueck AC, et al. Neuropsychological decline up to 20 years before incident mild cognitive impairment. Alzheimers Dement 2020 Mar;16(3):512-523. [doi: 10.1016/j.jalz.2019.09.085] [Medline: 31787561]

XSL•FO
RenderX

15. Buckley RF, Maruff P, Ames D, et al. Subjective memory decline predicts greater rates of clinical progression in preclinical Alzheimer's disease. Alzheimer's & Dementia 2016 Jul;12(7):796-804. [doi: 10.1016/j.jalz.2015.12.013]
16. Chételat G. Multimodal Neuroimaging in Alzheimer's Disease: Early Diagnosis, Physiopathological Mechanisms, and Impact of Lifestyle: IOS Press; 2018. [doi: 10.3233/JAD-179920]
17. Lucey BP, Wisch J, Boerwinkle AH, et al. Sleep and longitudinal cognitive performance in preclinical and early symptomatic Alzheimer's disease. Brain (Bacau) 2021 Oct 22;144(9):2852-2862. [doi: 10.1093/brain/awab272] [Medline: 34668959]
18. Cogné M, Auriacombe S, Vasa L, et al. Are visual cues helpful for virtual spatial navigation and spatial memory in patients with mild cognitive impairment or Alzheimer's disease? Neuropsychology 2018 May;32(4):385-400. [doi: 10.1037/neu0000435] [Medline: 29809030]
19. Ilardi CR, Chieffi S, Iachini T, Iavarone A. Neuropsychology of posteromedial parietal cortex and conversion factors from mild cognitive impairment to Alzheimer's disease: systematic search and state-of-the-art review. Aging Clin Exp Res 2022 Feb;34(2):289-307. [doi: 10.1007/s40520-021-01930-y] [Medline: 34232485]
20. Mohammadi A, Kargar M, Hesami E. Using virtual reality to distinguish subjects with multiple- but not single-domain amnestic mild cognitive impairment from normal elderly subjects. Psychogeriatrics 2018 Mar;18(2):132-142. [doi: 10.1111/psyg.12301] [Medline: 29409155]
21. Morganti F. Enacting space in virtual reality: a comparison between money's road map test and its virtual version. Front Psychol 2018;9:2410. [doi: 10.3389/fpsyg.2018.02410] [Medline: 30568610]
22. Ruggiero G, Ruotolo F, Iavarone A, Iachini T. Allocentric coordinate spatial representations are impaired in aMCI and Alzheimer's disease patients. Behav Brain Res 2020 Sep 1;393:112793. [doi: 10.1016/j.bbr.2020.112793] [Medline: 32619567]
23. Weniger G, Ruhleder M, Lange C, Wolf S, Irle E. Egocentric and allocentric memory as assessed by virtual reality in individuals with amnestic mild cognitive impairment. Neuropsychologia 2011 Feb;49(3):518-527. [doi: 10.1016/j.neuropsychologia.2010.12.031] [Medline: 21185847]
24. Allain P, Foloppe DA, Besnard J, et al. Detecting everyday action deficits in Alzheimer's disease using a nonimmersive virtual reality kitchen. J Int Neuropsychol Soc 2014 May;20(5):468-477. [doi: 10.1017/S1355617714000344] [Medline: 24785240]
25. Tarnanas I, Tsolaki M, Nef T, M. Müri R, Mosimann UP. Can a novel computerized cognitive screening test provide additional information for early detection of Alzheimer's disease? Alzheimers Dement 2014 Nov;10(6):790-798. [doi: 10.1016/j.jalz.2014.01.002]
26. Wadley VG, Bull TP, Zhang Y, et al. Cognitive processing speed is strongly related to driving skills, financial abilities, and other instrumental activities of daily living in persons with mild cognitive impairment and mild dementia. J Gerontol A Biol Sci Med Sci 2021 Sep 13;76(10):1829-1838. [doi: 10.1093/gerona/glaa312] [Medline: 33313639]
27. Bora E, Walterfang M, Velakoulis D. Theory of mind in behavioural-variant frontotemporal dementia and Alzheimer's disease: a meta-analysis. J Neurol Neurosurg Psychiatry 2015 Jul;86(7):714-719. [doi: 10.1136/jnnp-2014-309445] [Medline: 25595152]
28. Chicchi Giglioli IA, Pérez Gálvez B, Gil Granados A, Alcañiz Raya M. The virtual cooking task: a preliminary comparison between neuropsychological and ecological virtual reality tests to assess executive functions alterations in patients affected by alcohol use disorder. Cyberpsychol Behav Soc Netw 2021 Oct;24(10):673-682. [doi: 10.1089/cyber.2020.0560] [Medline: 33761276]
29. Fang Y, Han D, Luo H. A virtual reality application for assessment for attention deficit hyperactivity disorder in school-aged children. Neuropsychiatr Dis Treat 2019;15:1517-1523. [doi: 10.2147/NDT.S206742] [Medline: 31239686]
30. Fornaguera TJ, Zamora CM. Revisión ¿Es la pérdida de la audición una posible medida para detectar de manera precoz la enfermedad de Alzheimer y la enfermedad de Parkinson? [Website in Spanish]. 2020. URL: https://www.medigraphic.com/cgi-bin/new/resumenI.cgi?IDARTICULO=101654 [accessed 2023-07-11]
31. Nir-Hadad SY, Weiss PL, Waizman A, Schwartz N, Kizony R. A virtual shopping task for the assessment of executive functions: validity for people with stroke. Neuropsychol Rehabil 2017 Jul;27(5):808-833. [doi: 10.1080/09602011.2015.1109523] [Medline: 26558414]
32. Serino S, Baglio F, Rossetto F, et al. Picture Interpretation Test (PIT) 360°: an innovative measure of executive functions. Sci Rep 2017 Nov 22;7(1):16000. [doi: 10.1038/s41598-017-16121-x] [Medline: 29167494]
33. Fathi S, Ahmadi M, Dehnad A. Early diagnosis of Alzheimer's disease based on deep learning: a systematic review. Comput Biol Med 2022 Jul;146:105634. [doi: 10.1016/j.compbiomed.2022.105634] [Medline: 35605488]
34. Spasov S, Passamonti L, Duggento A, Liò P, Toschi N. A parameter-efficient deep learning approach to predict conversion from mild cognitive impairment to Alzheimer's disease. Neuroimage 2019 Apr 1;189:276-287. [doi: 10.1016/j.neuroimage.2019.01.031] [Medline: 30654174]
35. Pereira T, Ferreira FL, Cardoso S, et al. Neuropsychological predictors of conversion from mild cognitive impairment to Alzheimer's disease: a feature selection ensemble combining stability and predictability. BMC Med Inform Decis Mak 2018 Dec 19;18(1):137. [doi: 10.1186/s12911-018-0710-y] [Medline: 30567554]

XSL•FO
RenderX

36. Tuena C, Mancuso V, Stramba-Badiale C, et al. Egocentric and allocentric spatial memory in mild cognitive impairment with real-world and virtual navigation tasks: a systematic review. J Alzheimers Dis 2021;79(1):95-116. [doi: 10.3233/JAD-201017] [Medline: 33216034]
37. Turner TH, Atkins A, Keefe RSE. Virtual Reality Functional Capacity Assessment Tool (VRFCAT-SL) in Parkinson's disease. J Parkinsons Dis 2021;11(4):1917-1925. [doi: 10.3233/JPD-212688] [Medline: 34334421]
38. Zhu K, Lin R, Li H. Study of virtual reality for mild cognitive impairment: a bibliometric analysis using CiteSpace. Int J Nurs Sci 2022 Jan;9(1):129-136. [doi: 10.1016/j.ijnss.2021.12.007] [Medline: 35079614]
39. Nolin P, Banville F, Cloutier J, Allain P. Virtual reality as a new approach to assess cognitive decline in the elderly. AJIS 2013 Oct 1;2(8):612-616. [doi: 10.5901/ajis.2013.v2n8p612]
40. Caggianese G, Chirico A, De Pietro G, et al. Towards a virtual reality cognitive training system for mild cognitive impairment and Alzheimer's disease patients. Presented at: 2018 32nd International Conference on Advanced Information Networking and Applications Workshops (WAINA); May 16-18, 2018; Krakow p. 663-667. [doi: 10.1109/WAINA.2018.00164]
41. Mohammadi A, Hesami E, Kargar M, Shams J. Detecting allocentric and egocentric navigation deficits in patients with schizophrenia and bipolar disorder using virtual reality. Neuropsychol Rehabil 2018 Apr;28(3):398-415. [doi: 10.1080/09602011.2017.1369888] [Medline: 28880126]
42. Page MJ, McKenzie JE, Bossuyt PM, Boutron I, Hoffmann TC. Declaración PRISMA 2020: una guía actualizada para la publicación de revisiones sistemáticas [Article in Spanish]. Rev Esp Cardiol 2021;74(9):790-799. [doi: 10.1016/j.rec.2021.10.019] [Medline: 34955441]
43. Xie B, Tao C, Li J, Hilsabeck RC, Aguirre A. Artificial intelligence for caregivers of persons with Alzheimer's disease and related dementias: systematic literature review. JMIR Med Inform 2020 Aug 20;8(8):e18189. [doi: 10.2196/18189] [Medline: 32663146]
44. Choudhury A, Asan O. Role of artificial intelligence in patient safety outcomes: systematic literature review. JMIR Med Inform 2020 Jul 24;8(7):e18599. [doi: 10.2196/18599] [Medline: 32706688]
45. Harrington MG, Chiang J, Pogoda JM, et al. Executive function changes before memory in preclinical Alzheimer's pathology: a prospective, cross-sectional, case control study. PLoS ONE 2013;8(11):e79378. [doi: 10.1371/journal.pone.0079378] [Medline: 24260210]
46. Gainotti G, Quaranta D, Vita MG, Marra C. Neuropsychological Predictors of Conversion from Mild Cognitive Impairment to Alzheimer's Disease: IOS Press; 2014. [doi: 10.3233/JAD-130881]
47. Soldan A, Pettigrew C, Cai Q, et al. Hypothetical preclinical Alzheimer disease groups and longitudinal cognitive change. JAMA Neurol 2016 Jun 1;73(6):698-705. [doi: 10.1001/jamaneurol.2016.0194] [Medline: 27064267]
48. Soldan A, Pettigrew C, Cai Q, et al. Cognitive reserve and long-term change in cognition in aging and preclinical Alzheimer's disease. Neurobiol Aging 2017 Dec;60:164-172. [doi: 10.1016/j.neurobiolaging.2017.09.002] [Medline: 28968586]
49. Papp KV, Rentz DM, Mormino EC, et al. Cued memory decline in biomarker-defined preclinical Alzheimer disease. Neurol (ECronicon) 2017 Apr 11;88(15):1431-1438. [doi: 10.1212/WNL.0000000000003812] [Medline: 28283594]
50. Schindler SE, Jasielec MS, Weng H, et al. Neuropsychological measures that detect early impairment and decline in preclinical Alzheimer disease. Neurobiol Aging 2017 Aug;56:25-32. [doi: 10.1016/j.neurobiolaging.2017.04.004] [Medline: 28482211]
51. Gagliardi G, Epelbaum S, Houot M, et al. Which episodic memory performance is associated with Alzheimer's disease biomarkers in elderly cognitive complainers? Evidence from a longitudinal observational study with four episodic memory tests (Insight-PreAD). J Alzheimers Dis 2019;70(3):811-824. [doi: 10.3233/JAD-180966] [Medline: 31282413]
52. Gaubert S, Raimondo F, Houot M, et al. EEG evidence of compensatory mechanisms in preclinical Alzheimer's disease. Brain (Bacau) 2019 Jul 1;142(7):2096-2112. [doi: 10.1093/brain/awz150]
53. Ricci M, Todino V, Magarelli M, et al. Spect-neuropsychology correlations in very mild Alzheimer's disease and amnesic mild cognitive impairment. Arch Gerontol Geriatr 2020;89:104085. [doi: 10.1016/j.archger.2020.104085] [Medline: 32416463]
54. Nedelec T, Couvy-Duchesne B, Monnet F, et al. Identifying health conditions associated with Alzheimer's disease up to 15 years before diagnosis: an agnostic study of French and British health records. Lancet Digit Health 2022 Mar;4(3):e169-e178. [doi: 10.1016/S2589-7500(21)00275-2] [Medline: 35216751]
55. Smirnov DS, Ashton NJ, Blennow K, et al. Plasma biomarkers for Alzheimer's disease in relation to neuropathology and cognitive change. Acta Neuropathol 2022 Apr;143(4):487-503. [doi: 10.1007/s00401-022-02408-5] [Medline: 35195758]
56. Zygouris S, Giakoumis D, Votis K, et al. Can a virtual reality cognitive training application fulfill a dual role? Using the virtual supermarket cognitive training application as a screening tool for mild cognitive impairment. J Alzheimers Dis 2015;44(4):1333-1347. [doi: 10.3233/JAD-141260] [Medline: 25428251]
57. Howett D, Castegnaro A, Krzywicka K, et al. Differentiation of mild cognitive impairment using an entorhinal cortex-based test of virtual reality navigation. Brain (Bacau) 2019 Jun 1;142(6):1751-1766. [doi: 10.1093/brain/awz116] [Medline: 31121601]
58. Machado ML, Lefèvre N, Philoxene B, et al. New software dedicated to virtual mazes for human cognitive investigations. J Neurosci Methods 2019 Nov 1;327:108388. [doi: 10.1016/j.jneumeth.2019.108388] [Medline: 31408650]

XSL•FO
RenderX

59. Lecouvey G, Morand A, Gonneaud J, et al. An impairment of prospective memory in mild Alzheimer's disease: a ride in a virtual town. Front Psychol 2019;10:241. [doi: 10.3389/fpsyg.2019.00241] [Medline: 30809174]
60. Bondi MW, Edmonds EC, Salmon DP. Alzheimer's disease: past, present, and future. J Int Neuropsychol Soc 2017 Oct;23(9-10):818-831. [doi: 10.1017/S135561771700100X] [Medline: 29198280]
61. Frisoni GB, Boccardi M, Barkhof F, et al. Strategic roadmap for an early diagnosis of Alzheimer's disease based on biomarkers. Lancet Neurol 2017 Aug;16(8):661-676. [doi: 10.1016/S1474-4422(17)30159-X] [Medline: 28721928]
62. Mortamais M, Ash JA, Harrison J, et al. Detecting cognitive changes in preclinical Alzheimer's disease: a review of its feasibility. Alzheimer's & Dementia 2017 Apr;13(4):468-492. [doi: 10.1016/j.jalz.2016.06.2365]
63. Mistridis P, Krumm S, Monsch AU, Berres M, Taylor KI. The 12 years preceding mild cognitive impairment due to Alzheimer's disease: the temporal emergence of cognitive decline. J Alzheimers Dis 2015;48(4):1095-1107. [doi: 10.3233/JAD-150137] [Medline: 26402083]
64. An overview of new and emerging technologies for early diagnosis of Alzheimer disease. Canada's Drug Agency. URL: https://www.cda-amc.ca/overview-new-and-emerging-technologies-early-diagnosis-alzheimer-disease [accessed 2025-01-22]
65. Tarnanas I, Tsolaki M, Nef T, M Müri R, Mosimann UP. Can a novel computerized cognitive screening test provide additional information for early detection of Alzheimer's disease? Alz Dement 2014 Nov;10(6):790-798. [doi: 10.1016/j.jalz.2014.01.002] [Medline: 24656838]
66. Langbaum JB, Zissimopoulos J, Au R, et al. Recommendations to address key recruitment challenges of Alzheimer's disease clinical trials. Alzheimers Dement 2023 Feb;19(2):696-707. [doi: 10.1002/alz.12737] [Medline: 35946590]
67. Altuna-Azkargorta M, Mendioroz-Iriarte M. Blood biomarkers in Alzheimer's disease. Neurol Ed 2021;36(9):704-710. [doi: 10.1016/j.nrleng.2018.03.006] [Medline: 34752348]
68. Wei ZYD, Shetty AK. Can mild cognitive impairment and Alzheimer's disease be diagnosed by monitoring a miRNA triad in the blood? Aging Cell 2022 Jun;21(6):e13627. [doi: 10.1111/acel.13627] [Medline: 35537095]
69. Jack CR Jr, Knopman DS, Weigand SD, et al. An operational approach to National Institute on Aging-Alzheimer's Association criteria for preclinical Alzheimer disease. Ann Neurol 2012 Jun;71(6):765-775. [doi: 10.1002/ana.22628] [Medline: 22488240]
70. Delgado-Reyes AC, Sánchez Lopez JV. Escenarios virtuales para la evaluación neuropsicológica: una revisión de tema [Virtual scenarios for neuropsychological assessment: a topic review]. Panam J Neuropsychol 2021;15:2-196. [doi: 10.7714/CNPS/15.2.216]
71. Sánchez-Escudero JP, Galvis-Herrera AM, Sánchez-Trujillo D, et al. Virtual reality and serious videogame-based instruments for assessing spatial navigation in Alzheimer's disease: a systematic review of psychometric properties. Neuropsychol Rev 2024 Feb 26. [doi: 10.1007/s11065-024-09633-7] [Medline: 38403731]
72. Valladares-Rodríguez S, Fernández-Iglesias MJ, Anido-Rifón LE, Pacheco-Lorenzo M. Evaluation of the predictive ability and user acceptance of Panoramix 2.0, an AI-based e-health tool for the detection of cognitive impairment. Electronics (Basel) 2022;11(21):3424. [doi: 10.3390/electronics11213424]
73. Valladares-Rodriguez S, Perez-Rodriguez R, Facal D, Fernandez-Iglesias MJ, Anido-Rifon L, Mouriño-Garcia M. Design process and preliminary psychometric study of a video game to detect cognitive impairment in senior adults. PeerJ 2017;5:e3508. [doi: 10.7717/peerj.3508] [Medline: 28674661]

Abbreviations

AD: Alzheimer disease
AI: artificial intelligence
Aβ: amyloid beta
MCI: mild cognitive impairment
ML: machine learning
MRI: magnetic resonance imaging
NC: normal cognition
NCD: neurocognitive disorders
p-tau: hyperphosphorylated tau protein
PRISMA: Preferred Reporting Items for Systematic Reviews and Meta-Analyses
VR: virtual reality

XSL•FO
RenderX

Edited by A Benis; submitted 04.06.24; peer-reviewed by E Harriss, KK Raja; revised version received 04.11.24; accepted 03.12.24; published 28.01.25.

Please cite as:
Scribano Parada MDLP, González Palau F, Valladares Rodríguez S, Rincon M, Rico Barroeta MJ, García Rodriguez M, Bueno Aguado Y, Herrero Blanco A, Díaz-López E, Bachiller Mayoral M, Losada Durán R
Preclinical Cognitive Markers of Alzheimer Disease and Early Diagnosis Using Virtual Reality and Artificial Intelligence: Literature Review
JMIR Med Inform 2025;13:e62914
URL: https://medinform.jmir.org/2025/1/e62914
doi:10.2196/62914

© María de la Paz Scribano Parada, Fátima González Palau, Sonia Valladares Rodríguez, Mariano Rincon, Maria José Rico Barroeta, Marta García Rodriguez, Yolanda Bueno Aguado, Ana Herrero Blanco, Estela Díaz-López, Margarita Bachiller Mayoral, Raquel Losada Durán. Originally published in JMIR Medical Informatics (https://medinform.jmir.org), 28.1.2025. This is an open-access article distributed under the terms of the Creative Commons Attribution License (https://creativecommons.org/licenses/by/4.0/), which permits unrestricted use, distribution, and reproduction in any medium, provided the original work, first published in JMIR Medical Informatics, is properly cited. The complete bibliographic information, a link to the original publication on https://medinform.jmir.org/, as well as this copyright and license information must be included.

XSL•FO
RenderX

Review

Current Landscape and Future Directions for Mental Health Conversational Agents for Youth: Scoping Review

Jinkyung Katie Park[1], PhD; Vivek K Singh[2], PhD; Pamela Wisniewski[3], PhD

[1]Human-Centered Computing Division, School of Computing, Clemson University, Clemson, SC, United States

[2]Department of Library and Information, School of Communication and Information, Rutgers University, New Brunswick, NJ, United States

[3]Department of Computer Science, School of Engineering, Vanderbilt University, Nashville, TN, United States

Corresponding Author:
Jinkyung Katie Park, PhD
Human-Centered Computing Division
School of Computing
Clemson University
105 Sikes Hall
Clemson, SC
United States
Phone: 1 864 656 3444
Email: jinkyup@clemson.edu

Abstract

Background: Conversational agents (CAs; chatbots) are systems with the ability to interact with users using natural human dialogue. They are increasingly used to support interactive knowledge discovery of sensitive topics such as mental health topics. While much of the research on CAs for mental health has focused on adult populations, the insights from such research may not apply to CAs for youth.

Objective: This study aimed to comprehensively evaluate the state-of-the-art research on mental health CAs for youth.

Methods: Following PRISMA (Preferred Reporting Items for Systematic Reviews and Meta-Analyses) guidelines, we identified 39 peer-reviewed studies specific to mental health CAs designed for youth across 4 databases, including ProQuest, Scopus, Web of Science, and PubMed. We conducted a scoping review of the literature to evaluate the characteristics of research on mental health CAs designed for youth, the design and computational considerations of mental health CAs for youth, and the evaluation outcomes reported in the research on mental health CAs for youth.

Results: We found that many mental health CAs (11/39, 28%) were designed as older peers to provide therapeutic or educational content to promote youth mental well-being. All CAs were designed based on expert knowledge, with a few that incorporated inputs from youth. The technical maturity of CAs was in its infancy, focusing on building prototypes with rule-based models to deliver prewritten content, with limited safety features to respond to imminent risk. Research findings suggest that while youth appreciate the 24/7 availability of friendly or empathetic conversation on sensitive topics with CAs, they found the content provided by CAs to be limited. Finally, we found that most (35/39, 90%) of the reviewed studies did not address the ethical aspects of mental health CAs, while youth were concerned about the privacy and confidentiality of their sensitive conversation data.

Conclusions: Our study highlights the need for researchers to continue to work together to align evidence-based research on mental health CAs for youth with lessons learned on how to best deliver these technologies to youth. Our review brings to light mental health CAs needing further development and evaluation. The new trend of large language model–based CAs can make such technologies more feasible. However, the privacy and safety of the systems should be prioritized. Although preliminary evidence shows positive trends in mental health CAs, long-term evaluative research with larger sample sizes and robust research designs is needed to validate their efficacy. More importantly, collaboration between youth and clinical experts is essential from the early design stages through to the final evaluation to develop safe, effective, and youth-centered mental health chatbots. Finally, best practices for risk mitigation and ethical development of CAs with and for youth are needed to promote their mental well-being.

(JMIR Med Inform 2025;13:e62758) doi:10.2196/62758

XSL•FO
RenderX

KEYWORDS

conversational agent; chatbot; mental health; youth; adolescent; scoping review; Preferred Reporting Items for Systematic Reviews and Meta-Analyses; artificial intelligence

Introduction

Background

Conversational agents (CAs; often called chatbots) are systems with the ability to interact with users using natural human dialogue [1]. Examples of CAs range from customer service chatbots that are available on commercial websites and social media platforms to open-domain, text-based chatbots, such as OpenAI's GPT-4 and Microsoft's Bing, and voice assistants, such as Apple's Siri and Amazon's Alexa. Driven by advances in the underlying language models, CAs enable 2-way interactive communication with the user and have been applied in multiple domains, including health care [2]. Particularly, CAs are seen as an innovative digital medium to communicate information and resources with younger users, given their high digital literacy and familiarity with chat applications [3]. CAs are now increasingly used by youth for interactive knowledge discovery on sensitive topics, including mental health [4].

Youth are in a unique transitional phase between childhood and adulthood. Following the definition provided by the United Nations, in this review, we use the term *youth* to refer to adolescents and young adults aged between 15 and 24 years. Recent reports show that youth are increasingly experiencing mental health issues these days. For instance, from 2009 to 2019, the proportion of high school students reporting persistent feelings of sadness or hopelessness increased by 40%; between 2007 and 2018, suicide rates among youth aged between 10 and 24 years in the United States increased by 57% [5]. However, they are hesitant to seek professional help on mental health topics due to societal views toward the topics themselves and perceived public stigma and embarrassment associated with help seeking in those topics [6]. With the ability for humanlike interactions with the user, mental health CAs have been developed to support their unique informational, educational, and therapeutic needs related to mental health topics.

Existing systematic reviews on mental health CAs shed light on the potential of CAs to provide relevant information and resources via interactive communication. For instance, mental health CAs are used to deliver prewritten therapeutic and training content for people with depression and autism [7]. A systematic review of 13 studies on the outcome of mental health treatment delivered by mental health CAs found reductions in psychological distress after interacting with the mental health CAs [8]. However, another meta-analysis found conflicting results regarding the effect of chatbots on the severity of anxiety and positive and negative affect [9]. A more recent analysis confirmed that CA-based mental health interventions are effective in improving various mental health conditions in the short term, while substantial long-term effects were not observed [10]; artificial intelligence (AI)–based mental health CAs showed a meaningful reduction in symptoms of depression and distress, with no substantial improvement in overall psychological well-being [11]. Consequently, the trends of the clinical effectiveness of mental health CAs in the existing literature are inconclusive.

A scoping review of 37 studies focused on user perceptions toward mental health CAs showed overall positive opinions toward the CAs such as usefulness and ease of use. At the same time, they found conversations with CAs to be shallow, confusing, or brief [12]. There are some systematic reviews on mental health CAs to support people with specific mental health conditions such as substance use disorder [13], depression and anxiety [14], and serious mental illness [15]. For instance, a systematic review of 7 studies involving CAs for assessing serious mental health illness (eg, major depressive disorder and schizophrenia spectrum disorder) found generally positive outcomes regarding CAs' diagnostic quality, therapeutic efficacy, and acceptability. However, they revealed a lack of standardized measures for evaluating CAs and insufficient representation of the pediatric population [15]. As such, reviews on mental health CAs are well established and provide important insights into the benefits and pitfalls of existing research on mental health CAs. However, little work has been done to explore the trends in research on mental health CAs for younger populations such as adolescents and youth.

Recently, Balan et al [16] conducted a scoping review of 25 studies on CAs designed to improve the emotional components of mental health (eg, depression and anxiety) of the young population and found that although usability outcomes are optimistic, the clinical effectiveness of CA-based mental health interventions remains inconclusive. While trends in therapeutic CAs to improve the emotions of young populations were studied, a comprehensive trend in research on mental health CAs with various goals (eg, informational and assessment) or social, behavioral, or cognitive aspects of mental health has not been studied in previous work. In addition, trends in design aspects (eg, CA role and characteristics) and evaluation outcomes beyond efficacy (eg, strength and weaknesses of CAs and ethics) were not addressed in previous work. Therefore, to fill the gap in the literature, we conducted a scoping review of 39 studies that focused on CAs to promote the mental health of youth. In this paper, we address the following research questions (RQs):

- RQ1: What are the characteristics of empirical research on mental health CAs designed for youth?
- RQ2: What are the design and computational considerations for mental health CAs for youth?
- RQ3: What are the evaluation outcomes reported in empirical research on mental health CAs for youth?

Objectives

The objective of this study was to synthesize the current literature on mental health CAs designed for youth to understand the trends in research, the design and computational aspects of the CAs, and the strengths and weaknesses of the current mental health CAs for youth. Following the PRISMA (Preferred Reporting Items for Systematic Reviews and Meta-Analyses) 2020 statement guidelines [17], we conducted a comprehensive

XSL•FO
RenderX

review of the existing literature on mental health CAs for youth. We describe this process in the subsequent sections.

Methods

Systematic Literature Search Process

We initially searched the literature with the search string ("conversational agent" OR "chatbot") to explore synonyms of those terms used in the literature. Our initial search informed us of the various alternative terms used to describe CAs or chatbots, which allowed for a more inclusive and thorough search. Our final search string consisted of the following keywords: ("conversational agent" OR "chatbot" OR "virtual agent" OR "virtual assistant" OR "AI assistant" OR "AI bot" OR "social bot") AND (teen OR adolescent OR youth OR young) AND (mental).

Then, we identified 4 relevant and cross-disciplinary databases that included research on CAs in the health care domain, including ProQuest, Scopus, Web of Science, and PubMed. The same search string was used to retrieve articles across the 4 databases. The searches were limited to journal articles, conference papers, and book chapters written in English. The publication date was not specified. The initial search resulted in retrieving 224 articles from the 4 databases (ie, Web of Science: n=59, ProQuest: n=31, Scopus: n=85, and PubMed: n=49) in February 2024.

Inclusion and Exclusion Criteria

The purpose of this work was to review mental health CAs designed for youth. Therefore, we included full research papers that (1) were peer reviewed (journal articles and refereed conference proceedings were both included); (2) discussed CAs for providing information or resources or support on mental health topics; (3) discussed CAs designed for youth, adolescents, or young adults; (4) described CAs that permitted 2-way interactions that were fully automated (ie, without human mediation); and (5) included empirical results.

We excluded papers that (1) were nonfull or nonreviewed, such as works in progress, extended abstracts, reports, reviews, and meta-analyses; (2) did not include mental health topics (eg, physical health); (3) included forms of 1-way communication and human-mediated communication; (4) did not consider youth population; (5) did not primarily focus on the CAs (eg, explored CAs as one of the features of the mobile health apps); (6) did not focus on natural human dialogue as a primary communication mode for a 2-way interaction (eg, embodied CAs and facial recognition); and (7) were purely theoretical analyses or a review of existing studies.

Data Screening

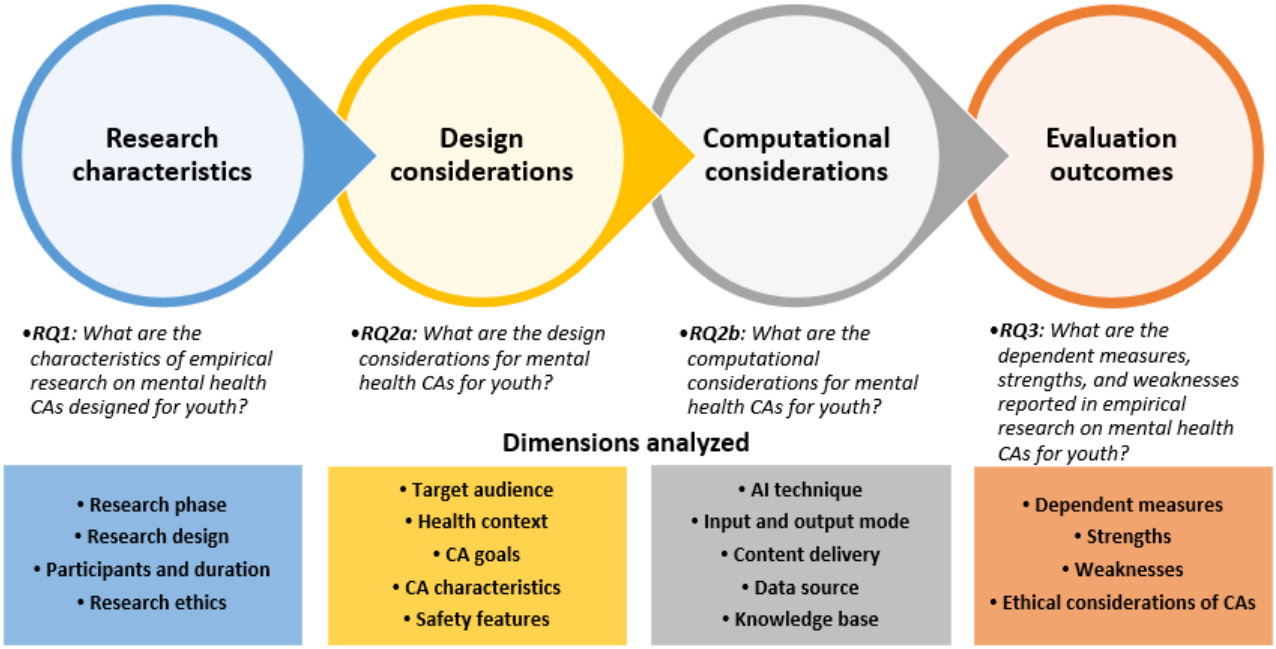
We first removed the duplicate entries from 224 articles. After removing 94 duplicates, we had 130 unique entries. Screening of articles for inclusion was performed in 2 stages. First, we screened the articles by reviewing titles, abstracts, and keywords. Next, we conducted relevancy coding by reviewing full texts based on the abovementioned criteria. The initial screening using titles and abstracts led to the removal of 54 articles. With the 76 remaining articles, we proceeded with the relevancy coding of the full texts. Through this relevancy coding process, 42 articles were removed, and a set of 34 articles were processed for cross-reference. To identify additional relevant papers that were not identified in our initial search, we cross-referenced the citations of 34 articles. Through this cross-reference process, we identified 5 relevant articles to include in our analysis. After 1 more iteration of the cross-reference process, no additional relevant papers were identified, which suggested that we reached a saturation point. The final number of articles that were included in our literature review was 39.

Data Analysis Approaches

We conducted a thematic analysis to identify major themes and trends in our dataset. We leveraged an iterative approach to our thematic analysis, which involved refining the codes as we gained a deeper understanding of the data. JKP carried out the coding, supported by frequent check-ins with PW for additional expertise on the subject matter. Furthermore, to ensure face validity, VKS quality-checked the coding during the writing of the results. For grounded thematic analysis, we analyzed the papers to identify codes for different dimensions aligning with our RQs. We familiarized ourselves with the literature identified and generated the initial codes. With the initial codes, we coded 20% (8/39) of the dataset and reviewed the codes to ensure that they were representative of our dataset. Once we finalized the codes, we coded the entire dataset. Multiple codes were sometimes assigned to the same paper where necessary. Through the grounded thematic analysis, we identified major dimensions for the characteristics of empirical research on mental health CAs for youth (ie, RQ1), design and computational considerations of mental health CAs for youth (ie, RQ2), and the evaluation outcomes of empirical research on mental health CAs for youth (ie, RQ3). Figure 1 is an overview of the framework, including RQs, dimensions, and codes that were analyzed in this review to understand the trends in research on mental health CAs for youth.

XSL•FO
RenderX

Figure 1. Overview of the analytic framework. AI: artificial intelligence; CA: conversational agent; RQ: research question.



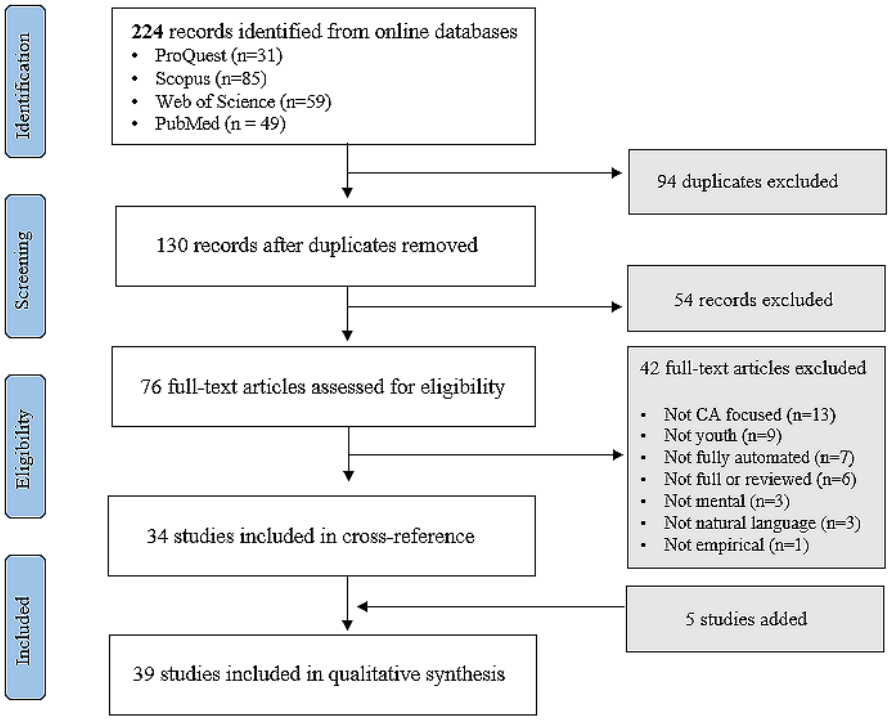
Results

Overview

Overall, we included 39 studies in this scoping review [4,18-55]. Figure 2 presents the data screening process following the PRISMA guidelines (see Multimedia Appendix 1 for the PRISMA Extension for Scoping Reviews checklist). The reviewed studies were published between 2011 and February 2024. Most of the studies (28/39, 72%) were published between 2021 and 2024, with a few published before 2021 (11/39, 28%).

The reviewed studies were conducted in various regions, including the United States (8/39, 20%); New Zealand (5/39, 13%); Australia (4/39, 10%); the United Kingdom, China, and Brazil (3/39, 8% each); Germany, Italy, and Norway (2/39, 5% each); and Argentina, Bangladesh, Belgium, Canada, the Netherlands, the Philippines, and Portugal (1/39, 3% each).

Figure 2. PRISMA (Preferred Reporting Items for Systematic Reviews and Meta-Analyses) flowchart for the study.



XSL•FO
RenderX

Characteristics of Empirical Research on Mental Health CAs for Youth

Most of the Empirical Research Involved Development and Summative Evaluation; Less Work Involved Formative Evaluation to Redesign Mental Health CAs With and for Youth

Most of the reviewed studies (36/39, 92%) included summative evaluation, followed by development (29/39, 74%), design (15/39, 38%), and formative evaluation (15/39, 38%; Table 1 and Multimedia Appendix 2 [4,18-55]). All empirical research included an evaluative phase to assess the mental health CAs for youth. Most of the studies included summative evaluation (36/39, 92%) and formative evaluation (15/39, 38%). In 31% (12/39) of the studies, both formative and summative evaluations were conducted. The term formative and summative evaluations originally referred to methodological frameworks for evaluating instructional materials [56]. In human-computer interaction research, summative evaluation is the evaluation of a design after it is nearly complete, often used during field testing. Formative evaluation is conducted during user interface development, often iteratively to achieve the desired usability level [57].

In the formative evaluation work that we reviewed, researchers interacted with youth populations to gain early feedback on the initial CA design through interviews, focus groups, and design workshops [31,32,49]. In most of the studies that included formative evaluation (12/15, 80%), summative evaluations were followed after the iterative design process. For instance, Ludin et al [33] conducted a formative user testing with school guidance counselors, clinicians, and youth to learn about the issues youth faced during the COVID-19 pandemic and lockdowns. The youth's opinions from the formative evaluations were used to inform the ongoing content iteration of the prototypes. Once the prototype was developed, the authors conducted a summative user testing to assess the usability and acceptability of the chatbot with 127 youth participants [33].

XSL•FO
RenderX

Table 1. Characteristics of the empirical research on mental health CAs[a] for youth (N=39).

Dimensions and codes	Value, n (%)	Key trends
Research phase		Most of the empirical research involved development and summative evaluation; less work involved formative evaluation to (re)design mental health CAs with youth
Design	15 (38)	
Development	29 (74)	
Formative evaluation	15 (38)	
Summative evaluation	36 (92)	
Research design		Most of the research involved user testing or experiments to evaluate mental health CAs
User testing	18 (46)	
Experiment	18 (46)	
Research participants and duration		Most commonly, the research on mental health CAs was conducted with <100 participants who are adolescents and young adults without mental health conditions for <4 wk
Participant age (y)		
Adolescents (12-18)	16 (41)	
Young adults (18-30)	14 (36)	
Youth (14-25)	9 (23)	
Participant group		
General population	21 (54)	
At-risk population	18 (46)	
Number of participants		
<100	28 (72)	
100-200	6 (15)	
>200	2 (5)	
Duration of CA interaction		
1 time	6 (15)	
<4 wk	12 (31)	
4-8 wk	5 (13)	
9-16 wk	1 (3)	
Research ethics		Research ethics such as institutional review and consent were addressed in most research; however, only a few research studies addressed data privacy and safety of youth participants
Consent	26 (67)	
Institutional review	26 (67)	
Data confidentiality	8 (20)	
Safety	4 (10)	

[a]CA: conversational agent.

Research on Mental Health CAs Was Conducted With a Small Numbers of Adolescents and Young Adults Without Mental Health Conditions for <4 Weeks

Participant Group

Most of the participants in the reviewed studies were adolescents (16/39, 41%) aged between 12 and 18 years and young adults (14/39, 36%) aged >18 years. In fewer studies, the participants were youth (9/39, 23%) aged between 14 and 25 years. Overall, in a slightly higher proportion of the empirical studies, the participants were general youth (21/39, 54%) compared to at-risk youth (18/39, 46%), such as those who are experiencing depression [51], anxiety [18], body image concerns [23], and alcohol abuse [20].

The Number of Participants

The number of youth participants ranged from a minimum of 3 young adults with autism to explore the acceptability of cognitive behavioral therapy (CBT)–based mental health CA through in-depth interviews [53] to a maximum of 798 adolescents to evaluate the effectiveness and user engagement

XSL•FO
RenderX

through a survey [48]. In most of the research, the number of participants was <100 (28/39, 72%), with few studies having participants between 100 and 200 (6/39, 15%) and >200 (2/39, 5%).

Duration of CA Interaction

Youth participants interacted with mental health CAs for a minimum of 30 minutes [20,25] to a maximum of 16 weeks [47]. In most of the reviewed studies, participants interacted with CAs for <4 weeks (12/39, 31%) or once (6/39, 15%). In fewer studies, participants interacted with CAs for 4 to 8 weeks (5/39, 13%) or 9 to 16 weeks (1/39, 3%). In general, short-term engagement with CAs was for user testing to assess user experience and acceptability. The long-term engagement with CAs was for the experiments to assess the effectiveness of CAs in reducing mental health conditions.

Most of the Research Involved User Testing or Experiments to Evaluate Mental Health CAs

User Testing

The most prevalent research design used in the empirical studies was user testing (18/39, 46%) to assess user engagement and user experience of the CAs. For instance, in a study by Beilharz et al [23], 17 adolescents and 8 parents or caregivers in Australia participated in focus group interviews to evaluate the acceptability, ease of use, and design of the *KIT* prototype, a CA designed to support people with concerns about body image and eating issues. In another study, Gabrielli et al [37] conducted a user test with 21 adolescents over 4 weeks in Italy to assess the user experience and perceived value of content delivered by mental health CAs. Surveys with Likert scale measures and open-ended questions were used to evaluate overall usefulness, ease of use, the value of the content, and suggestions for improvement [37].

Experiment

Another prevalent research design was an experiment (18/39, 46%), which was conducted to explore the effectiveness of CAs in reducing mental health conditions. With the randomized controlled trial design, for instance, young adults who completed active cancer treatment in 5 years were randomly assigned to either immediate access to mental health CA (ie, experimental group) or access to only daily emotion ratings and access to full chatbot content after 4 weeks (ie, control group). After 4 weeks, participants in the experimental group reported an average reduction in anxiety, while the control group reported an increase in anxiety [43]. With noncontrolled experiments, for instance, 105 young adults interacted with the same mental health CAs for 15 days and completed the surveys asking about their mental health conditions (ie, Patient Health Questionnaire [PHQ]) before and after the 15-day intervention period. The comparison of the average survey scores before and after the intervention confirmed that the overall scores decreased after interacting with the mental health chatbot [36].

Research Ethics Such as Institutional Review and Consent Were Addressed in the Majority of Research; However, Only a Few Research Considered Data Privacy and Safety of Youth Participants

In most of the reviewed studies, authors explicitly stated that they acquired participant consent (26/39, 67%) and that the studies were approved by their institutional review board (26/39, 67%). Beyond institutional review and participant consent, which are mandatory in many institutions, in some studies, authors addressed considerations for privacy or confidentiality of youth's digital trace data related to mental health (8/39, 20%). In only a small portion of the reviewed studies (4/39, 10%), the authors provided support to promote the safety of youth participants in empirical research in the mental health context. For instance, in the study by Nicol et al [22], there was safety monitoring provided by the study team by tracking the digital PHQ-9 assessment over 12 weeks. When the PHQ-9 assessment results indicated suicidal ideation, the principal investigator contacted the participant's primary care providers to discuss the next steps regarding the assessment of suicide risk. By the end of the 12-week study, 56% (10/18) of the participants triggered at least 1 alarm to assess for suicidal ideation [22]. In another study by Liu et al [47], participants were informed that professionals would intervene by telephone (ie, mental assistance hotline) when the participants reported that they needed emergency psychological assistance. In 10 papers, research ethics were not mentioned. None of the reviewed papers mentioned risk mitigation plans and mandated reporting or provided critical reflections on best practices for working with youth in the mental health context.

Design Considerations of Mental Health CAs for Youth

Most of the Mental Health CAs Were Designed for Older and General Youth Populations

In most of the studies, the target audience of the CAs were youth or young adults (22/39, 56%), adolescents (12/39, 31%), and college students (6/39, 15%). In most of the studies (27/39, 69%), CAs were designed for general youth populations. In a small proportion of the reviewed studies (12/39, 31%), the CAs were designed for at-risk youth populations (Table 2 and Multimedia Appendix 3 [4,18-55]).

XSL•FO
RenderX

Table 2. Design considerations of mental health CAs[a] for youth (N=39).

Dimensions and codes	Value, n (%)	Key trends
Target audience		Most of the mental health CAs were designed for older and general youth populations
Age group		
Youth or young adults	22 (56)	
Adolescent	12 (31)	
College students	6 (15)	
Health condition		
General youth	27 (69)	
At-risk youth	12 (31)	
CA goals and health context		Most mental health CAs for youth are designed to provide • Educational or informational support to promote the general mental well-being • therapeutic support to alleviate mental health conditions such as depression, anxiety, and stress
Health context		
Mental well-being	15 (38)	
Depression	12 (31)	
Anxiety	9 (23)	
Stress	8 (20)	
Substance use	3 (8)	
Body image	2 (5)	
Phone addiction	1 (3)	
CA goals		
Treatment	25 (64)	
Education or training	22 (56)	
Informational	15 (38)	
Assessment	10 (26)	
Monitoring	2 (5)	
Behavioral change	2 (5)	
CA role and characteristic		Most mental health CAs for youth were designed to be • life coaches or older peer mentors • in friendly and empathetic tones • with few options to personalize agent characters
CA role		
Coach or peer	11 (28)	
Health care professional	7 (18)	
CA characteristics		
Friendly	16 (41)	
Empathetic	11 (28)	
Culture specific	4 (10)	
Gender specific	3 (8)	
Simple and factual	2 (5)	
Personalization		
CA character	5 (13)	
App appearance	1 (3)	

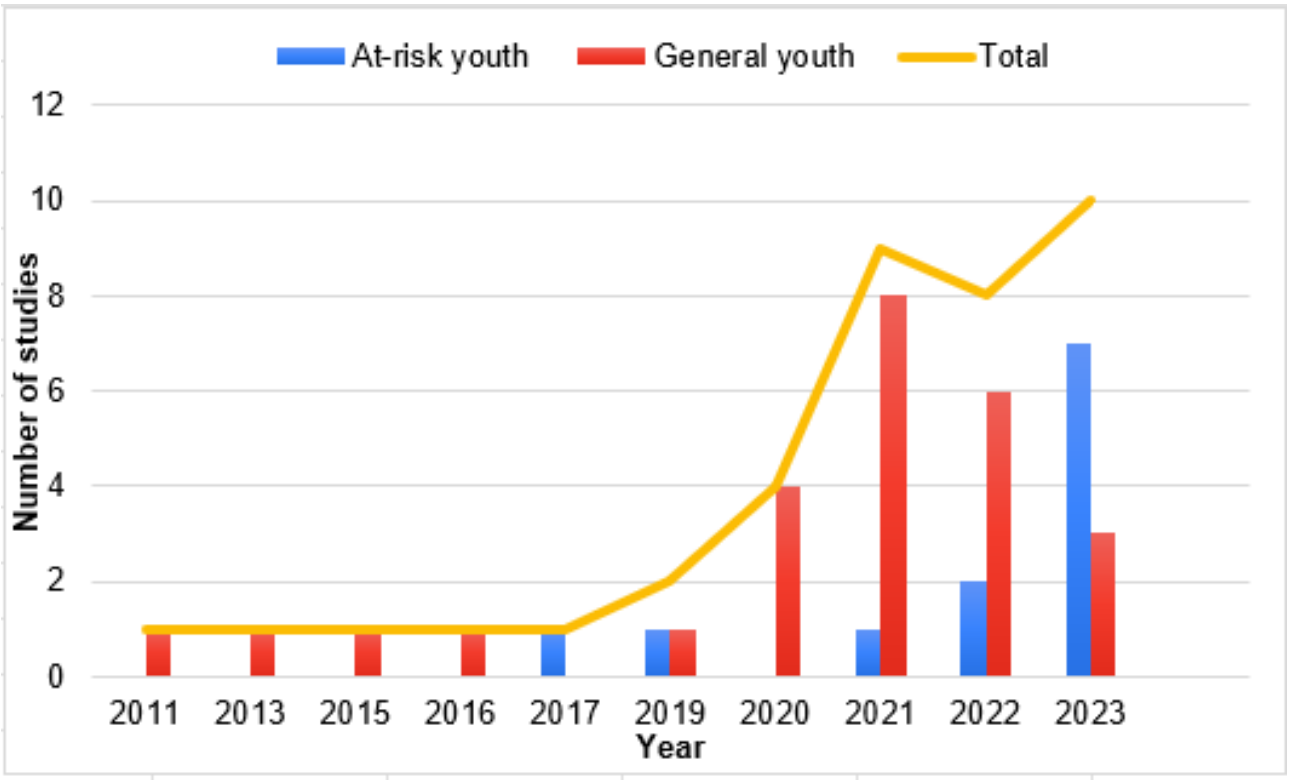
XSL•FO
RenderX

Dimensions and codes	Value, n (%)	Key trends
User avatar	1 (3)	
Safety features		Most of the mental health CAs did not have the safety features in place
Reminder	12 (31)	
Emergency contact	10 (26)	
Alert to adults or experts	2 (5)	

[a]CA: conversational agent.

Within those 12 studies, 5 (41%) studies focused on designing mental health CAs for young adults with depressive symptoms [18,19,29,51,52]. Few studies focused on CAs to promote the mental health of adolescents with type 1 diabetes [26]; adolescents with body image and eating issues [23]; young adults being treated for cancer [43]; youth at risk of HIV and sexually transmitted infections [30]; young adults from immigrant and refugee communities [49]; lesbian, gay, bisexual, transgender, queer, or questioning (LGBTQ+) youth [50]; and young adults with autism [53]. There was a trend in which the number of mental health CAs designed for at-risk youth increased, while the number of CAs for general youth decreased (Figure 3). Overall, most of the mental health CAs were designed for older (22/39, 56%) or general (27/39, 69%) youth populations, with the current trend toward designing CAs for youth who are at risk of mental health conditions.

Figure 3. Target audience of the mental health conversational agents (CAs) by year (n=38).



Mental Health CAs Are Designed to Promote the General Mental Well-Being of Youth as Well as Help Alleviate Mental Health Symptoms of Depression, Anxiety, and Stress

Health Context

Within the studies that focused on mental health CAs for youth, most of the CAs were designed to promote the general mental health or well-being of youth (15/39, 38%; eg, by promoting life skills and resilience), followed by those aimed to reduce depression (12/39, 31%), anxiety (9/39, 23%), and stress (8/39, 20%). There are a few papers that focused on mental health CAs to address the issues of substance use (3/39, 8%; ie, alcohol and drug abuse) [20,28,42], body image (2/39, 5%) [23,48], and phone addiction (1/39, 3%) [21]. Overall, nearly half (19/39, 48%) of the existing research on mental health CAs focused on supporting youth with symptoms of depression, anxiety, and stress.

CA Goals

Most CAs (25/39, 64%) for mental health were designed to help alleviate mental health symptoms such as depression and anxiety, followed by educational or training content (22/39, 56%) to promote mental health and informational support on mental health topics (15/39, 38%). Some mental health CAs were designed to assess mental health symptoms (10/39, 26%) and monitor mental health conditions (2/39, 5%). Two mental

XSL•FO
RenderX

health CAs were designed to promote behavior changes such as reduced screen time [21] and reduced alcohol consumption [41]. Overall, in most of the work, the CAs were designed to help alleviate youth's mental health symptoms or to provide educational intervention to promote youth's mental well-being, while less work has been done on CAs for informational support or the assessment or monitoring of youth's mental health condition.

Mental Health CAs Were Designed to Be Life Coaches or Older Peer Mentors With Friendly and Empathetic Tones, With Few Options to Personalize Agent Characters

CA Role

In 51% (20/39) of the studies, the CA role was mentioned. In many of those studies (11/39, 28%), the mental health CAs were designed as older peers or younger coaches to guide youth with therapeutic modules and provide youth with information to promote mental health. For instance, a mental health CA was designed to be a young person who messages the user once a day. The interaction was designed to be a brief conversation with a friend who checks in and has a helpful tip or an anecdotal story to share to help reduce stress [38]. In other studies, mental health CAs were designed to provide formal health professional–like support (7/39, 18%), for instance, that emulates therapists who encourage patients to explore their problems by asking questions to provide personalized mental health support [52].

CA Characteristics

Meanwhile, most mental health CAs were designed to provide friendly (16/39, 41%) or empathetic (11/39, 28%) responses. For instance, in response to loneliness reflected in users' input, the chatbot replied, "I'm so sorry you're feeling lonely. I guess we all feel a little lonely sometimes," or if participants showed excitement in their input, the chatbot replied, "Yay, always good to hear that!" [18]. In 10% (4/39) of the studies, mental health CAs were designed to be culture specific. For instance, in a study by Ludin et al [33], researchers collaborated with groups of Indigenous and non-Indigenous people (ie, Māori and Pākehā) in New Zealand to cocreate mental health CA called "Aroha," meaning "caring and kind" in their native language. The mental health strategies and activities were designed for and targeted Māori youth and their families [33]. A few mental health CAs were gender specific (3/39, 8%) or designed to provide short and simple answers (2/39, 5%).

CA Characters and Avatars

In most of the studies (33/39, 85%), options to personalize mental health CA characters were not addressed. In a few studies (6/39, 15%), features to support personalization of CA characters were discussed. For instance, for the CA to promote youth resilience, the avatars were designed as older peers with users' choice of gender and ethnicity representative of the target population [32]. In another study, the authors designed the body image CA with an option to choose between male and female versions of the CA avatar [48]. Some studies designed mental health CAs in which users can customize their avatars [52] and app appearance [53]. In 1 study, youth preferred to choose from 3 to 4 characters with variations of gender, avatar, age, and social role (ie, health professional vs younger coach-like) instead of personalizing each aspect separately [19].

The Majority of the Mental Health CAs Did Not Have the Safety Features in Place

Most of the studies (21/39, 54%) did not address the safety features of the designed mental health CAs. In 46% (18/39) of the studies, safety features were discussed, including a reminder that users are interacting with chatbots, not human experts, and chatbots are not replacements for health care providers or places for seeking help (12/39, 31%). There were safety features to provide emergency contact (10/39, 26%), such as crisis hotlines and those that refer to health professionals. In 2 studies, alert features were implemented to notify a trusting adult or providers when a youth was identified as a risk to themselves or others [22,31]. For instance, if trigger words such as self-harm, suicide, death, dead, kill, or die were used by youth, the alert feature to notify adults was activated. The alert recipient is a primary support contact who was identified and confirmed during the initial consent process [31]. Overall, safety features of mental health CAs were discussed in less than half of the reviewed articles (21/39, 54%).

Computational Considerations of Mental Health CAs for Youth

Most of the Mental Health CAs Were Prototypes Built Upon Existing Mobile Chat Apps

Maturity of the Device

In most studies (26/39, 67%), mental health CAs were prototypes. In 18% (7/39) of the studies, CAs were developed as fully functioning systems, and in 20% (8/39) of the studies, researchers evaluated existing systems developed in other studies. In 1 study [24], CAs were explored as concepts without having actual systems (Table 3 and Multimedia Appendix 4 [4,18-55]).

XSL•FO
RenderX

Table 3. Computational considerations of mental health CAs[a] for youth (N=39).

Dimensions and codes	Value, n (%)	Key trends
System characteristics		Most of the mental health CAs were prototypes built upon existing mobile chat apps
Maturity of device		
Prototype	26 (67)	
Fully functioning system	7 (18)	
Existing system	8 (20)	
Concept	1 (3)	
Delivery channel		
Mobile	16 (41)	
Web	11 (28)	
Desktop	6 (15)	
Communication mode		All CAs supported text-based input (free text along with quick options) with a few that supported voice input; all supported textual output, with many of them supporting visualized output such as image and video
Input mode		
Text	39 (100)	
Text+speech	2 (5)	
Free text+options	19 (49)	
Free text	13 (33)	
Quick options	5 (13)	
Output mode		
Text	39 (100)	
Image	21 (54)	
Video	12 (31)	
Audio	7 (18)	
Game	6 (15)	
AI[b] technique		Free-textual inputs were processed via NLP[c], while prewritten content was delivered via rule-based programming
NLP	19 (49)	
Rule based	15 (38)	
Content delivery		Most mental health content was delivered in flexible ways; in some cases, prewritten content was delivered in a structured manner
Flexible	25 (64)	
Structured	8 (20)	
Semistructured	3 (8)	
Knowledge base		Mental health content was built upon evidence-based expert knowledge of cognitive and behavioral therapy and positive psychology
CBT[d]	19 (49)	
Positive psychology	7 (18)	
Other therapeutic content	7 (18)	
Clinical expert knowledge	6 (15)	

[a]CA: conversational agent.

[b]AI: artificial intelligence.

[c]NLP: natural language processing.

[d]CBT: cognitive behavioral therapy.

XSL•FO
RenderX

Delivery Channel

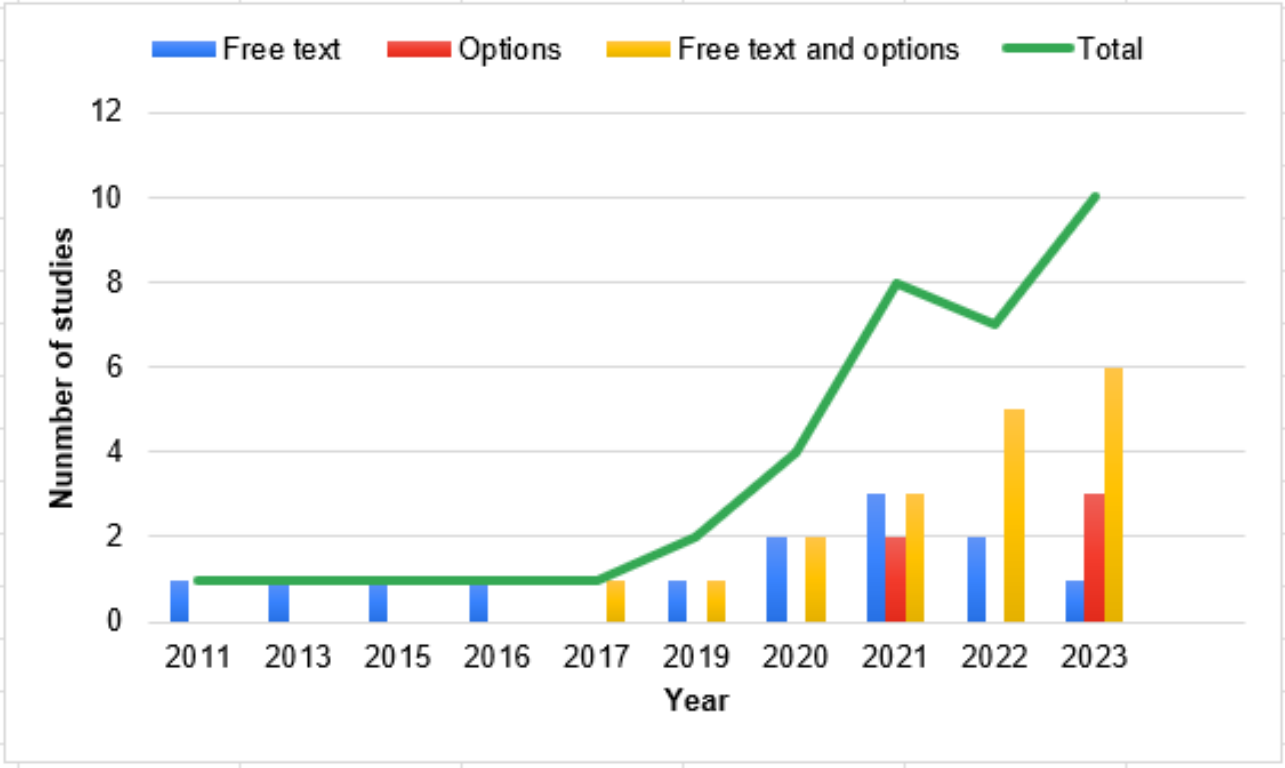
Mental health CAs were delivered via diverse channels. Most CAs were delivered through mobile apps (16/39, 41%), followed by web applications (11/39, 28%) and desktop applications (6/39, 15%). In 28% (11/39) of the studies, CAs were made available on >1 channel. In many studies (16/39, 41%), CAs were delivered using existing chat applications such as Facebook Messenger (eg, [32,33,36]), WhatsApp [51], Windows Live Messenger [42], WeChat [47], and Telegram [27].

All CAs Supported Text-Based Input; Most CAs Supported Multimedia Output

Input Modality

In all the reviewed studies (39/39, 100%), mental health CAs supported text as the primary mode of input. In 5% (2/39) of the studies, mental health CAs supported audio input along with textual input [47,51]. For text-based CAs, by extracting keywords related to mental health such as depression and anxiety from user inputs, CAs extract necessary features to develop different classification models or assess their sentiment [46,52]. For voice-based CAs, the key components include the use of automatic speech recognition and natural language understanding to comprehend users' input [47]. Text-based and voice-based chatbots are similar in their design; however, text-based CAs do not include automatic speech recognition components and instead rely on text as the primary modality of input and output. In most of the reviewed studies, CAs supported free text along with quick options (eg, "yes" or "no") as user input (19/39, 49%), rather than free text only (13/39, 33%) or quick options only (5/39, 13%). There was a trend in which the proportion of CAs that supported free text along with quick options as user input increased, while the proportion of CAs that supported free text only as user input decreased over time (Figure 4).

Figure 4. Input mode of the mental health conversational agents (CAs) by year (n=37).



Output Modality

All the CAs (39/39, 100%) supported text as the primary mode of output. In 64% (25/39) of the studies, it was indicated that CAs support multimedia outputs. In addition to textual output, most CAs (21/39, 54%) supported image output in the form of an emoji, moving images in graphics interchange format, infographics, and animated CA avatars. CAs also provided outputs in the forms of video (12/39, 31%), audio (7/39, 18%), and games (6/39, 15%). In many of the reviewed studies (12/39, 31%), CAs supported >2 types of output (eg, text, image, and video).

Many CAs Used Multiple AI Techniques: Free-Textual Inputs Were Processed via Natural Language Processing, While Prewritten Content Was Delivered via Rule-Based Programming

In many studies that we reviewed, the CAs used multiple AI-based computational methods depending on the specific section or feature. Free-textual input from users is processed using natural language processing (NLP), which processes natural language datasets, such as text and voice, using statistical and machine learning models to recognize, understand, and generate text and speech [58]. Accordingly, the AI approaches that were most frequently referred to in the reviewed papers were NLP (19/39, 49%). Meanwhile, quick options are implemented using rule-based methods. Therefore, following the NLP, the second most frequently referenced technique in the reviewed papers was rule-based approaches (15/39, 38%). Mostly, the CAs deliver prewritten conversational lessons via

XSL•FO
RenderX

rule-based programming. However, they use techniques such as NLP at certain points in the tree to determine routing to subsequent conversational nodes (eg, [18,26,38,44,54,55]). For instance, NLP is used to process users' input so that CAs can trigger prewritten therapeutic content [47] or further crises and mental health support services [26] to youth. There were a few papers in which CAs relied solely on decisions made by decision trees or rule-based programs (eg, [23,25,50,51]). With rule-based CAs, once users choose among the given options (eg, yes or no and choosing numbered options), the CAs trigger and provide the most relevant prewritten response. With the CAs that are built solely upon rule-based or decision tree techniques, there is no space for users to type free text to have conversations. None of the mental health CAs we reviewed were built upon generative AI such as large language models (LLMs).

Most Mental Health Content Was Delivered in Flexible Ways, Considering User Preferences and Autonomy

We found 3 types of CA content delivery approaches in the reviewed studies: structured, semistructured, and flexible. In most of the studies (25/39, 64%), mental health CAs implemented a flexible model. With a flexible model, CA contents are delivered depending on users' input or users have options to choose which content to navigate. For instance, CAs first detect stress levels from users' input; then, based on the stress detection result as well as the users' chatting sentence type, the CA chooses an appropriate answer from the knowledge base database [44] or users have options to choose what type of CBT-based therapy they would like to perform [53].

In 20% (8/39) of the reviewed studies, CA content was delivered in a planned and structured way. With the structured models, CA contents are prewritten and automatically delivered to users via rule-based programming for a predefined period (ie, from a few days to a few weeks). For instance, Williams et al [38] designed a mental health CA in which daily conversations and modules are prewritten for 21 days, and the CA guides them through daily activity. Particularly, in half of the papers, the structured CA content was designed to treat mental health conditions of at-risk youth, including adolescent or young adults with depressive symptoms [29,51], youth treated for cancer [43], and adolescents with type 1 diabetes [26].

In a small portion of the reviewed studies (3/39, 8%), CA content was delivered in a semistructured way [32,48,49]. For instance, the mental health CA guided the user through 10 daily sessions that introduced the psychological content modules. The same core psychological concepts (eg, psychoeducation, emotional regulation, and problem-solving) are present for all users, while users can specify their preferences for the content that they feel is most relevant to them [49]. In another study, the mental health content spanning 21 days was structurally designed for users to engage with the CA once a day with a choice of a motivational quote, joke, or an entry into a gratitude journal [32].

Mental Health Content Was Built Upon Evidence-Based Expert Knowledge of Mental Health

In all studies, primary data sources were expert knowledge (39/39, 100%). In almost half of the reviewed studies (19/39, 49%) on mental health CAs, the CA content was developed based on CBT, one of the most extensively studied evidence-based psychotherapy for a wide range of mental health issues such as depression, stress, and general mental well-being [59]. For instance, building upon the principles of CBT, He et al [29] designed 7 modules of mental health CA (ie, cognitive distortions, self-esteem, mindfulness meditation, mental energy, natural connection, self-help, and loneliness) for youth participants to complete 1 module per day during the 1-week intervention period. Besides CBT, mental health CA content was based on positive psychology (7/39, 18%) and other therapeutic content (7/39, 18%), such as interpersonal psychotherapy [19,22], acceptance commitment therapy [23], perceptual control therapy [46,52], self-compassion program [26], and microintervention to improve body image [48]. Some mental health CA content was built upon inputs from school health service experts or counselors (6/39, 15%) and positive answers collected from the web forum [44]. In some studies (4/39, 10%), the source of mental health CA content was not specified.

In summary, we found that most mental health CAs were designed as older peers to provide therapeutic and or educational content to promote youth mental well-being. Most of the CAs were built upon multiple computational methods to flexibly deliver prewritten and evidence-based mental health content. Text was the primary communication mode, with the majority supporting multimedia output. Textbox 1 presents a summary of the key trends in the design and computational aspects of mental health CAs for youth.

XSL•FO
RenderX

Textbox 1. Key trends of the design and computational aspects of mental health conversational agents (CAs) for youth.

Aspects and key trends

- Design
  - Target audience: designed for older and general youth populations
  - Health context and goals: designed to help alleviate mental health symptoms or to promote general mental well-being
  - CA role and characteristics: designed to be life coaches or older peer mentors with friendly and empathetic tones
  - Personalization: personalization of CA characters was not supported in most of the studies
  - Safety features: safety features were discussed in less than half of the studies
- Computational
  - Artificial intelligence technique: multiple computational methods (eg, natural language processing and rule based) depending on the specific features
  - Input modality: all CAs were text based, with a couple of them supporting audio input along with textual input. Most CAs supported free text along with quick options as user input
  - Output modality: all CAs supported text as the primary mode of output, with the majority supporting multimedia outputs
  - Content delivery: CA content was delivered in flexible ways, considering user preferences and autonomy. In some cases, prewritten therapeutic content was delivered in a structured manner
  - Data source: CA content was based on well-established evidence-based expert knowledge

Evaluation Outcomes Reported in Research on Mental Health CAs for Youth

Most Studies Focused on Evaluating the Effectiveness and Acceptability of CAs

Effectiveness

In most of the evaluative research (17/39, 44%), the outcome variable was the effectiveness of mental health CAs (Table 4 and Multimedia Appendix 5 [4,18-55]). In those studies, prevalidated scales such as the PHQ and Generalized Anxiety Disorder Scale were used to measure the mental health conditions of the youth before and after the use of mental health CAs. For instance, to evaluate the effectiveness of mental health CA *Tess*, Klos et al [45] conducted a randomized controlled trial with 181 Argentinian college students. The PHQ-9 [60], a questionnaire comprising 9 items that evaluate the frequency and severity of depressive symptoms, and the Generalized Anxiety Disorder-7 [61], a 7-item scale that evaluates the frequency and severity of anxious thoughts and behaviors, were used to measure the changes in participants' mental health [45].

XSL•FO
RenderX

Table 4. Evaluation outcomes of mental health CAs[a] for youth (N=39).

Dimensions and codes	Value, n (%)	Key trends
Dependent measures		Most studies focused on evaluating the effectiveness and acceptability of CAs
Effectiveness	17 (44)	
Acceptability	17 (44)	
Usability	14 (36)	
User engagement	10 (26)	
Validity or accuracy	2 (5)	
Personalization	1 (3)	
Strengths		Easy access to useful mental health information communicated through friendly, empathetic, and humanlike responses was the major strength of mental health CAs
Accessibility	14 (36)	
Useful content	14 (36)	
Interactivity or engaging	12 (31)	
Anonymity or confidentiality	7 (18)	
Empathetic or friendly responses	6 (15)	
Easy to navigate	4 (10)	
Humanlike interaction	2 (5)	
Nonjudgmental	2 (5)	
Weaknesses		Limited or repetitive content, lack of human language understanding, and robotic responses were the critical weaknesses of mental health CAs
Limited responses or content	13 (33)	
Lack of natural language understanding	8 (21)	
Lack of personalized content	7 (18)	
Non-humanlike traits	7 (18)	
Textual information with jargon	5 (13)	
Inaccurate responses	5 (13)	
Data privacy and confidentiality	5 (13)	
Ethical considerations		Ethical considerations such as privacy, confidentiality, and safety of CAs were addressed in a few studies
Privacy and confidentiality	4 (10)	
Safety	1 (3)	

[a]CA: conversational agent.

Acceptability

Another most evaluated outcome of mental health CAs was acceptability (17/39, 44%). Overall, current mental health CAs were perceived as beneficial and acceptable by not only youth but also health professionals [4]. For instance, semistructured interviews with 3 young adults with autism showed that they considered the mental health chatbot novel and they would be interested in using such systems [53]. In a study by Mariamo et al [24], yes or no questions were associated with a lower likelihood of response compared to multiple-response choice questions and a higher likelihood of response compared to open-ended questions.

Usability

Next, the usability of mental health CAs was evaluated in 36% (14/39) of the studies. For instance, Williams et al [38] engaged with 124 young adults in New Zealand to evaluate mental health CAs with 21-day stress detox modules and found that youth appreciated the interactivity, accessibility, and chatbot design, particularly due to the visualized content as it is engaging. Similarly, a week-long exploratory study with 20 rural-living LGBTQ+ youth confirmed that youth appreciated the colorful design with multimedia content of *REALbot* as well as the conversational flow to first ask users' preferred names [50].

XSL•FO
RenderX

User Engagement

User engagement was also evaluated (10/39, 26%) through analyzing log data of human-CA interaction. For instance, Matheson et al [48] evaluated user engagement with the body image chatbot *Topity*, which was designed to deliver microinterventions for adolescents. The results from randomized controlled trials with 1715 Brazilian adolescents show that 79% of the participants completed the minimum intervention dose of 1 microintervention technique. In addition, most participants chose to receive guidance from a female avatar of Topity, compared to a male avatar [48].

Accuracy and Personalization

In a few studies, the accuracy or validity of mental health assessment (2/39, 5%) as well as personalization (1/39, 3%) were also explored. For instance, a month-long user test showed that the chatbot's stress detection module achieved a precision rate of 78.34% and a recall rate of 76.12% [44]. In terms of personalization of mental health CA, while both experts and youth emphasized the need for autonomy to flexibly choose or change a module instead of a fixed schedule, experts emphasized the importance of planned therapeutic modules in a fixed sequence [19].

Easy Access to Useful Mental Health Information Communicated Through Friendly, Empathetic, and Humanlike Responses Were the Major Strengths of Mental Health CAs

In 67% (26/39) of the reviewed studies, the strengths of current mental health CAs for youth were addressed. The most frequently mentioned strengths of mental health CAs were 24/7 availability (14/39, 36%), followed by useful information and therapeutic content (14/39, 36%) and the ability to have interactive and engaging conversations with CAs (12/39, 31%). In some studies, participants pointed to the strengths of mental health CAs, such as perceived anonymity or confidentiality (7/39, 18%), empathetic and friendly responses generated by CAs (6/39, 15%), and easy to navigate (4/39, 10%). In fewer studies (4/39, 10%), participants liked nonjudgmental responses generated by CAs [23,43] delivered in multimedia output [27,54]. They also liked the sense of caring and support [34,40,41] provided by CAs. Some participants appreciated humanlike interaction with CAs[27,49], perceived CAs as smart and trustworthy friends [37], and sometimes formed connections or friendships with bots [38]. They also liked the availability of personalized support [4,29] delivered by personalized CA avatars [19].

Limited or Repetitive Content, Lack of Human Language Understanding, and Robotic Responses Were the Critical Weaknesses of Mental Health CAs

In 62% (24/39) of the reviewed studies, the weaknesses of the current mental health CAs were addressed. The most frequently addressed limitations in the reviewed studies are limited or repetitive content provided by CAs (13/39, 33%), lack of understanding of human input (8/39, 20%), and lack of personalized content (7/39, 18%). Some of the limitations of mental health CAs were related to non-humanlike traits (7/39, 18%), such as too fast responses generated by CAs [30,41], lack of empathy in their responses [37,39], lack of trust toward nonhuman agents [35], a feeling of loneliness or disconnect when interacting with a bot [38], and CAs being robotic [50,54] and not smart enough [50]. Some youth found CA content with too much textual information with jargon or inaccurate or unclear responses generated by CAs hard to understand (5/39, 13%), while some shared concerns for confidentiality and privacy of sensitive information (5/39, 13%, respectively). In some studies, participants expressed difficulties with the free-text input mode as they found it hard to express their feelings [52] and utterances [20] rather than speak naturally. In a few studies, technical limitations such as overall technical immaturity [29,41] and susceptibility to changes in platform policies and bugs [51,54] were addressed. Some of the potential safety concerns addressed in the reviewed studies were increased screen time [22], overreliance on machines over human support [4,22], risk of missing imminent risk [22,51], and age-appropriateness of CA content [25]. Table 5 shows a summary of the strengths and weaknesses of mental health CAs reported in the reviewed studies.

Table 5. Mapping of the strengths and weaknesses of mental health CAs[a] for youth by dimension.

Dimensions	Strengths	Weaknesses
CA characteristic	Empathetic and friendly responses	Too fast responses without empathy
CA content	Useful information or therapeutic content	Inaccurate or unclear responses
AI[b] technique	Interactive and engaging conversations	Limited or repetitive content and lack of understanding of human input
Input mode	Easy to start a conversation	Difficulties with terming the queries
Output mode	Multimedia output	Too much textual information with jargon
Personalization	Availability of personalized support	Lack of personalized content
Privacy and confidentiality	Perceived anonymity or confidentiality	Concerns for the privacy of sensitive information
Safety	Sense of caring and support via humanlike interaction with CAs	Potential for overreliance on CAs over human support and risk of missing imminent risk

[a]CA: conversational agent.

[b]AI: artificial intelligence.

XSL•FO
RenderX

Ethical Considerations Such as Privacy, Confidentiality, and Safety of Mental Health CAs Were Addressed in a Few Studies

Most of the reviewed studies (35/39, 90%) did not address the ethical aspects of mental health CAs. In 10% (4/39) of the included studies, ethical considerations such as privacy, confidentiality, and safety of CAs were addressed [4,22,30,35] as part of their empirical findings. For instance, safety was assessed at 2, 4, 8, and 12 weeks by parents' reports on any hospitalizations or emergency department visits made by their child for depression- or anxiety-related problems. By the end of the 12-week experiment, 1 parent from the intervention group reported that their teen was seen in an emergency department and discharged to home [22], indicating the potential safety concerns and the need for features to ensure the safety of youth. Meanwhile, in 1 study, ethical issues (eg, privacy and confidentiality, efficacy, and safety of CAs) related to mental health CAs were discussed as the primary focus of the study. Through the group discussions with youth aged between 14 and 18 years in the United Kingdom, the authors highlighted youth's concerns about mental health CAs related to their personal information. Their recommendations for designing ethical mental health CAs include (1) providing clear and transparent communication about the systems' privacy arrangement and limitations, (2) informing users of the extent to which the chatbots are evidence based and empirically tested, and (3) ensuring that automated chatbots have systems in place to prevent overreliance and encourage users to seek human support when needed [39]. Overall, more discussion on ethics standards and critical reflections on mental health CAs for the youth is needed.

Discussion

Overview

In this scoping review, we identified 39 studies that focused on CAs designed to support the mental health of youth. In the subsequent sections, we discuss the implications of our findings and outline directions for future research. Finally, we provide recommendations for designing youth-centered, effective, and safe CA systems to support the mental health of youth.

Principal Findings

Mental Health CAs That Can Support Diverse Youth With a Variety of Mental Health Issues Are Needed

In most of the reviewed studies, the target audience of mental health CAs was general youth, with a recent trend toward designing mental health CAs for at-risk youth populations. According to 2021 statistics, growing numbers of youth are at risk of poor mental health outcomes. For instance, nearly half (45%) of LGBTQ+ students seriously considered attempting suicide—far more than heterosexual students [62]. Accordingly, the US Surgeon General set an agenda to prioritize promoting the mental health of at-risk youth populations, such as racial, ethnic, sexual, and gender minority youth; individuals from lower socioeconomic backgrounds; youth with disabilities; youth involved in the juvenile justice system; and other groups [5]. Therefore, future work is needed to design and implement CAs to support the mental health of youth considered vulnerable. In addition, we found that most mental health CAs were designed to reduce symptoms of depression, anxiety, and stress, while only a few were designed to provide support for body image, phone addiction, substance use, and other mental health issues. A recent report shows that youth are increasingly experiencing diverse mental health issues, including attention-deficit/hyperactivity disorder, eating disorders, body image, suicide, and self-harm [5,62,63]. Therefore, mental health CAs that can support youth with a variety of mental health issues are needed.

Multimodal Input and Output Are Needed to Designing Mental Health CAs That Are Inclusive of Youth With Diverse Communication Needs

In terms of user input, all mental health CAs supported textual input, with very few supporting voice-based output. In most of the reviewed studies, mental health CAs supported free text along with quick options as user input, with a few supporting quick options only. Previous research showed that rule-based CAs with quick options are perceived as restricted in offering personalized advice, leading to low trust in the effectiveness of CAs in providing advice on sensitive topics [64]. Therefore, providing options to freely type queries could benefit youth to explore diverse mental health topics. At the same time, it would still be useful to have quick options to choose from or autofill features as some of the health topics are difficult to term the queries from scratch [65]. In addition, as some youth were frustrated by the need to type their utterances rather than speak naturally [20], an option for voice-based input methods could be beneficial for supporting youth with diverse communication needs. When it comes to output mode, in almost two-thirds of studies, mental health CAs provided content in the form of images, audio, video, or games along with textual information. Multimedia content provided by mental and health CAs is important, as evaluative research confirmed that some youth found lengthy texts hard to understand [37,54] and preferred interactive and engaging multimedia content [27]. Hence, along with textual information, providing health information in a multimedia format is needed for designing engaging CAs for youth.

More Advanced AI Technologies (eg, LLMs) Are Needed to Provide Interactive and Engaging Mental Health Support for Youth

Overall, mental health CAs for youth are in their infancy, as many of the systems are developed as prototypes and are being evaluated for improvement. One of the major limitations found in evaluative research was limited content or responses provided by CAs as well as a *lack of personalized content* (eg, [25,27,33,38]). This is because many of the mental health CAs were built upon a rule-based approach in which predefined sets of responses are based on domain-specific knowledge. Early evidence showed that rule-based CAs were seen as *only providing advice about mainstream*, easily accessible information that was already available on the internet [64]. The evaluative studies we reviewed also demonstrated that youth perceived mental health content provided by rule-based CAs to be *repetitive* (eg, [29,31,38,49]). However, many of the existing

XSL•FO
RenderX

research studies implemented rule-based approaches to provide mental health information for youth. Another major technical limitation found in the evaluative research was the lack of human language understanding, followed by inaccurate responses from CAs. Taken together, our findings signify the need for implementing more sophisticated language models in mental health CA development. A recent review study found that CAs enhanced by advanced AI technologies outperformed rule-based CAs in managing psychological distress [11]. Further research is warranted to explore the potential benefits of implementing advanced AI technology (eg, generative AI) in mental health CAs for youth.

Safety Should Be Prioritized When Designing and Implementing Mental Health CAs for Youth

Recent advancements in LLMs are promising in improving the technical immaturity of mental health CAs, with the ability to understand input text written in human language in prompts and generate responses [66]. Early evidence demonstrated the effectiveness of the LLMs in generating coherent and relevant answers to psychological questions [67] or detecting mental health conditions [68]. However, when applying LLMs in mental health CAs for youth, the safety aspects of the information provided by those models should be rigorously considered, given the recent documentation of age-inappropriate and inaccurate content for youth generated by LLMs [69]. Therefore, chatbot development and implementations should undergo a robust validation process to establish a reliable and expert-informed evidence base for safety, particularly with extra care when designing chatbots for youth considered vulnerable (eg, those with mental health conditions). Meanwhile, safety concerns addressed in evaluative research included increased screen time, overreliance on machines over human support, and the risk of missing imminent risk. Although research findings are conflicting, the impact of overreliance on machines and increased screen time on youth's well-being is one of the important safety concerns [70,71]. Therefore, safety features to help track screen time and nudge youth about their CA use could be considered. Safety features to alert mental health professionals for imminent risk (eg, nudges with sophisticated AI tech such as deep learning) could also be critical for mental health CAs.

Long-Term, Large-Scale, and Rigorous Evaluation Is Needed to Ensure the Efficacy and Safety of Mental Health CAs

Overall, most of the empirical research on mental health CAs was conducted with <100 older youth populations in the short term (<4 weeks). This trend was substantial as many of them involved user testing or clinical trials to assess the acceptability and feasibility of the prototypes. Although preliminary evidence shows positive trends in the effectiveness and acceptability of mental health CAs, long-term evaluative research with larger sample sizes and more robust research designs is needed to validate their efficacy before their widespread adoption and use. In addition, we noted a lack of established methods for evaluating the safety of mental health CAs for unintended adverse effects among reviewed studies. This concerning trend was consistent with the mental health CAs for general adults [72]. While empirical research showed that the age-appropriateness of mental health content was one of the weaknesses of mental health CAs [25], none of the reviewed studies evaluated whether the mental health content is developmentally appropriate for youth. Therefore, the accuracy and age-appropriateness of mental health content provided by CAs should be further explored to ensure the efficacy and safety of mental health CAs for youth.

Collaborative Efforts With Youth and Clinical Experts Are Needed to Design Safe, Effective, and Youth-Centered Mental Health CAs

The evaluation outcomes of the reviewed studies raised a few open questions in designing safe, effective, and youth-centered mental health CAs. One key issue is the humanlike traits of CAs; while youth prefer humanlike traits of CAs, existing research documented safety concerns toward the humanness of CAs. For instance, previous research shows that younger youth may lose vital human contact [73] or unintentionally share personal information with CAs [74] if they become too attached to humanlike CAs. Therefore, in some studies we reviewed, CAs were designed with non-humanlike avatars (eg, [23,25,30,34]) or there were safety features to clearly state that the CAs are not human agents (eg, [4,27,33,35,43,47,54]). Consequently, how to balance humanlike and non-humanlike traits of mental health CAs for youth is an important open question to address in collaborative research with youth and clinical experts.

Another open question is on the CA role, as evaluative research showed conflicting perceptions from youth and clinical experts; youth prefer peer- or coach-like roles, while experts were cautious about such roles for clinical purposes [19]. Therefore, careful consideration is needed when designing social roles of mental health CAs for youth taking into account specific health context, purpose, and target audience. In addition, as evaluative research showed, providing an option to choose a preferred CA avatar can help youth feel comfortable when sharing confidential issues on sensitive topics [37]. However, we found that the current empirical research on mental health CAs rarely explored how personalizing the roles and characteristics of mental health CAs impacts the effectiveness or user experience in both positive and negative ways. Therefore, further empirical research with youth and clinical experts is needed to understand how different permutations of CA roles and personalities play a role in supporting youth mental health.

In terms of personalized CA content delivery, we observed a trade-off between flexibility and structured planning in therapeutic content. Experts emphasized that planned modules could make mental health CAs more reliable and the treatment goals more visible; at the same time, they can reduce motivation and user engagement and thus lead to dropout [19]. Therefore, balancing between personalizing therapeutic content flexibly and maintaining a structured program is an open-ended question to address in future research. Finally, in most reviewed studies, the content of mental health CAs was based on well-established evidence-based expert knowledge to safely leverage CA systems. However, to understand the mental health needs of youth, it is equally critical to work with youth from the early

XSL•FO
RenderX

stages of CA design. However, very little work has been done to consider inputs from youth in content generation. Taken together, more collaborative research efforts with youth, caregivers, and domain experts need to be made to address the aforementioned open questions and build effective, safe, and youth-centered mental health CAs.

Ethics Standards and Best Practices to Design and Develop Mental Health CAs for Youth Are Needed

We found a concerning trend in the existing literature on mental health CAs for youth: most of the papers did not address the ethical aspects of mental health CAs. Many of the existing review studies pointed to the lack of ethical considerations in the development of CAs in health care [2,75,76]. While personal health data are collected and processed in mental health CAs, the majority did not provide information regarding security and privacy aspects [76]. As mental health topics are sensitive, particularly for youth [6,30], more discussion on ethics standards and critical reflections on best practices to develop mental health CAs for the youth population is needed. Another concerning trend we found was that the ethical implications and best practices of involving youth considered vulnerable in evaluative research on mental health CAs are rarely discussed. In a 12-week evaluative research study with adolescents with depression and anxiety, more than half of the participants triggered at least 1 alarm for suicidal ideation [22], which signals that safety standards and best practices are pivotal when working with populations considered vulnerable. Hence, further research is needed to establish ethical standards for working with youth, particularly youth considered vulnerable, to ensure that participating in research does not harm already populations considered vulnerable. We summarize the open questions that need to be addressed in future research in Textbox 2.

Textbox 2. Open questions related to mental health conversational agents (CAs) to be addressed in future research.

Open questions

- CA role: How do different CA roles and characteristics impact youth's interaction with mental health CAs?
- CA characteristics: How can we balance humanlike versus non-humanlike traits of mental health CAs for youth?
- CA content: What is the age-appropriate, inclusive, and accurate mental health information for youth?
- Content delivery: What are the effective and safe delivery modes (ie, structured vs flexible) of mental health CA content for youth?
- Safety: How can we design CA features to promote the safety (eg, monitoring imminent risk and screen time) of mental health CAs?
- Data privacy and confidentiality: How can we design artificial intelligence–based systems that ensure privacy and confidentiality of youth data on sensitive topics?
- Research ethics: What are the ethics standards and best practices to design and develop mental health CAs for and with youth?

Design Guidelines

On the basis of our findings and broader implications, we provide the following guidelines for designing youth-centered mental health CAs (Textbox 3).

Textbox 3. Design guidelines for mental health conversational agents (CAs) for youth.

Design guidelines

- CA role and characteristics: The CA role should be carefully designed considering the purpose and primary target audience. Regardless of roles, empathetic and friendly characteristics of mental health CAs are important.
- CA content: CA content should be age-appropriate, inclusive, and accurate. The content should be based on evidence-based expert knowledge along with inputs from youth.
- Artificial intelligence technique: More advanced language models (eg, large language models) are needed to provide diverse, context-aware, and personalized content for youth.
- Input mode: Free-textual inputs with auto-complete or quick options can help youth formulate questions that require domain knowledge. Along with textual input, an option for voice-based input can support youth with diverse communication needs.
- Output mode: Less textual content and more multimedia content can help youth understand mental health information.
- Personalization: It is important to give youth control over the personalization of CA content and avatars. Information on what is being personalized and how it is done should be clear and transparent.
- Safety: It should be clearly communicated to youth that CAs are not human, along with information on the capability and limitations of CAs. Information on confidentiality and data privacy should be clear and transparent. Safety features such as emergency contacts for imminent risk should be provided upfront and available 24/7. Additional safety features to track screen time could help reduce overreliance on CAs and prevent excessive screen time.
- Ethics: Safety standards and critical reflections on best practices to co-design CAs with the youth population are needed.

XSL•FO
RenderX

Strengths, Limitations, and Future Work

This scoping review has several strengths. First, we conducted a comprehensive literature search of multiple databases. We used holistic search terms rather than specific ones to capture the various representations of CAs used in mental health for youth. Second, we analyzed trends in empirical research on mental health CAs for youth as well as design and computational considerations of the mental health CAs studied in empirical research to provide a holistic mapping of the current landscape. Therefore, this study showcased the possible framework of mental health CAs that can be referenced by other researchers in this field.

However, our study has some limitations. First, given the novelty and multidisciplinary nature of the field, some unpublished literature presented at niche conferences and meetings may have been omitted. Second, during the data extraction process, we identified the design and computational approaches of the mental health CAs based on the descriptions reported in the reviewed studies. Hence, some of the design and computational aspects of mental health CAs that were considered yet not reported in the reviewed studies may not have been captured in this paper. As our findings suggest, the maturity of mental health CAs is still in its infancy, and further review with more in-depth analysis is needed as research in the field matures.

Conclusions

CAs are increasingly used by youth for sensitive topics such as mental health. Trends in research on mental health CAs designed for youth have been underexplored. In this review paper, we fill an important gap by synthesizing 39 studies on mental health CAs designed for youth over the last 14 years. Our scoping review highlights that research on mental health CAs is in its infancy, and early evidence shows both strengths and weaknesses in existing systems. We call attention to important open questions that researchers should address to move forward. When designing CAs for youth, a one-size-fits-all approach does not apply. With careful consideration of the health context and needs of specific target groups, mental health CAs can benefit youth. This can be only achieved when engaging with youth from the early design phases to the summative evaluation of the systems. In this regard, we call for further investigation of best practices for risk mitigation strategies and ethical development of CAs with and for youth to promote their mental well-being.

Conflicts of Interest

None declared.

Multimedia Appendix 1
PRISMA-ScR (Preferred Reporting Items for Systematic Reviews and Meta-Analyses Extension for Scoping Reviews) checklist.
[DOCX File , 85 KB - medinform_v13i1e62758_app1.docx]

Multimedia Appendix 2
Characteristics of the included studies.
[DOCX File , 33 KB - medinform_v13i1e62758_app2.docx]

Multimedia Appendix 3
Design considerations for mental health conversational agents for youth.
[DOCX File , 32 KB - medinform_v13i1e62758_app3.docx]

Multimedia Appendix 4
Computational considerations of mental health conversational agents for youth.
[DOCX File , 32 KB - medinform_v13i1e62758_app4.docx]

Multimedia Appendix 5
Evaluation outcomes of the included studies.
[DOCX File , 30 KB - medinform_v13i1e62758_app5.docx]

References

1. Rheu M, Shin JY, Peng W, Huh-Yoo J. Systematic review: trust-building factors and implications for conversational agent design. Int J Hum Comput Interact 2020 Sep 02;37(1):81-96. [doi: 10.1080/10447318.2020.1807710]
2. Tudor Car L, Dhinagaran DA, Kyaw BM, Kowatsch T, Joty S, Theng YL, et al. Conversational agents in health care: scoping review and conceptual analysis. J Med Internet Res 2020 Aug 07;22(8):e17158 [FREE Full text] [doi: 10.2196/17158] [Medline: 32763886]
3. Balaji D, He L, Giani S, Bosse T, Wiers R, de Bruijn GJ. Effectiveness and acceptability of conversational agents for sexual health promotion: a systematic review and meta-analysis. Sex Health 2022 Oct;19(5):391-405 [FREE Full text] [doi: 10.1071/SH22016] [Medline: 35863761]

XSL•FO
RenderX

4. Koulouri T, Macredie RD, Olakitan D. Chatbots to support young adults' mental health: an exploratory study of acceptability. ACM Trans Interact Intell Syst 2022 Jul 20;12(2):1-39. [doi: 10.1145/3485874]
5. Protecting youth mental health: the US surgeon general's advisory. Office of the Surgeon General (OSG). URL: https://pubmed.ncbi.nlm.nih.gov/34982518/ [accessed 2024-04-11]
6. Radez J, Reardon T, Creswell C, Lawrence PJ, Evdoka-Burton G, Waite P. Why do children and adolescents (not) seek and access professional help for their mental health problems? A systematic review of quantitative and qualitative studies. Eur Child Adolesc Psychiatry 2021 Mar 21;30(2):183-211 [FREE Full text] [doi: 10.1007/s00787-019-01469-4] [Medline: 31965309]
7. Abd-Alrazaq AA, Alajlani M, Alalwan AA, Bewick BM, Gardner P, Househ M. An overview of the features of chatbots in mental health: a scoping review. Int J Med Inform 2019 Dec;132:103978 [FREE Full text] [doi: 10.1016/j.ijmedinf.2019.103978] [Medline: 31622850]
8. Gaffney H, Mansell W, Tai S. Conversational agents in the treatment of mental health problems: mixed-method systematic review. JMIR Ment Health 2019 Oct 18;6(10):e14166 [FREE Full text] [doi: 10.2196/14166] [Medline: 31628789]
9. Abd-Alrazaq AA, Rababeh A, Alajlani M, Bewick BM, Househ M. Effectiveness and safety of using chatbots to improve mental health: systematic review and meta-analysis. J Med Internet Res 2020 Jul 13;22(7):e16021 [FREE Full text] [doi: 10.2196/16021] [Medline: 32673216]
10. He Y, Yang L, Qian C, Li T, Su Z, Zhang Q, et al. Conversational agent interventions for mental health problems: systematic review and meta-analysis of randomized controlled trials. J Med Internet Res 2023 Apr 28;25:e43862 [FREE Full text] [doi: 10.2196/43862] [Medline: 37115595]
11. Li H, Zhang R, Lee YC, Kraut RE, Mohr DC. Systematic review and meta-analysis of AI-based conversational agents for promoting mental health and well-being. NPJ Digit Med 2023 Dec 19;6(1):236 [FREE Full text] [doi: 10.1038/s41746-023-00979-5] [Medline: 38114588]
12. Abd-Alrazaq AA, Alajlani M, Ali N, Denecke K, Bewick BM, Househ M. Perceptions and opinions of patients about mental health chatbots: scoping review. J Med Internet Res 2021 Jan 13;23(1):e17828 [FREE Full text] [doi: 10.2196/17828] [Medline: 33439133]
13. Ogilvie L, Prescott J, Carson J. The use of chatbots as supportive agents for people seeking help with substance use disorder: a systematic review. Eur Addict Res 2022;28(6):405-418 [FREE Full text] [doi: 10.1159/000525959] [Medline: 36041418]
14. Lim SM, Shiau CW, Cheng LJ, Lau Y. Chatbot-delivered psychotherapy for adults with depressive and anxiety symptoms: a systematic review and meta-regression. Behav Ther 2022 Mar;53(2):334-347. [doi: 10.1016/j.beth.2021.09.007] [Medline: 35227408]
15. Vaidyam AN, Linggonegoro D, Torous J. Changes to the psychiatric chatbot landscape: a systematic review of conversational agents in serious mental illness: changements du paysage psychiatrique des chatbots: une revue systématique des agents conversationnels dans la maladie mentale sérieuse. Can J Psychiatry 2021 Apr;66(4):339-348 [FREE Full text] [doi: 10.1177/0706743720966429] [Medline: 33063526]
16. Balan R, Dobrean A, Poetar CR. Use of automated conversational agents in improving young population mental health: a scoping review. NPJ Digit Med 2024 Mar 19;7(1):75 [FREE Full text] [doi: 10.1038/s41746-024-01072-1] [Medline: 38503909]
17. Moher D, Liberati A, Tetzlaff J, Altman DG, PRISMA Group. Preferred reporting items for systematic reviews and meta-analyses: the PRISMA statement. PLoS Med 2009 Jul 21;6(7):e1000097 [FREE Full text] [doi: 10.1371/journal.pmed.1000097] [Medline: 19621072]
18. Fitzpatrick KK, Darcy A, Vierhile M. Delivering cognitive behavior therapy to young adults with symptoms of depression and anxiety using a fully automated conversational agent (Woebot): a randomized controlled trial. JMIR Ment Health 2017 Jun 06;4(2):e19 [FREE Full text] [doi: 10.2196/mental.7785] [Medline: 28588005]
19. Kuhlmeier FO, Gnewuch U, Lüttke S, Brakemeier EL, Mädche A. A personalized conversational agent to treat depression in youth and young adults – a transdisciplinary design science research project. In: Proceedings of the 17th International Conference on Design Science Research in Information Systems and Technology. 2022 Presented at: DESRIST '22; June 1–3, 2022; St Petersburg, FL p. 30-41 URL: https://dl.acm.org/doi/10.1007/978-3-031-06516-3_3 [doi: 10.1007/978-3-031-06516-3_3]
20. Elmasri D, Maeder A. A conversational agent for an online mental health intervention. In: Proceedings of the 2016 International Conference on Brain Informatics and Health. 2016 Presented at: BIH '16; October 13-16, 2016; Omaha, NE p. 243-251 URL: https://link.springer.com/chapter/10.1007/978-3-319-47103-7_24 [doi: 10.1007/978-3-319-47103-7_24]
21. Abreu C, Campos PF. Raising awareness of smartphone overuse among university students: a persuasive systems approach. Informatics 2022 Feb 23;9(1):15. [doi: 10.3390/informatics9010015]
22. Nicol G, Wang R, Graham S, Dodd S, Garbutt J. Chatbot-delivered cognitive behavioral therapy in adolescents with depression and anxiety during the COVID-19 pandemic: feasibility and acceptability study. JMIR Form Res 2022 Nov 22;6(11):e40242 [FREE Full text] [doi: 10.2196/40242] [Medline: 36413390]
23. Beilharz F, Sukunesan S, Rossell SL, Kulkarni J, Sharp G. Development of a positive body image chatbot (KIT) with young people and parents/carers: qualitative focus group study. J Med Internet Res 2021 Jun 16;23(6):e27807 [FREE Full text] [doi: 10.2196/27807] [Medline: 34132644]

XSL•FO
RenderX

24. Mariamo A, Temcheff CE, Léger PM, Senecal S, Lau MA. Emotional reactions and likelihood of response to questions designed for a mental health chatbot among adolescents: experimental study. JMIR Hum Factors 2021 Mar 18;8(1):e24343 [FREE Full text] [doi: 10.2196/24343] [Medline: 33734089]
25. Dosovitsky G, Bunge E. Development of a chatbot for depression: adolescent perceptions and recommendations. Child Adolesc Ment Health 2023 Mar;28(1):124-127. [doi: 10.1111/camh.12627] [Medline: 36507594]
26. Boggiss A, Consedine N, Hopkins S, Silvester C, Jefferies C, Hofman P, et al. Improving the well-being of adolescents with type 1 diabetes during the COVID-19 pandemic: qualitative study exploring acceptability and clinical usability of a self-compassion chatbot. JMIR Diabetes 2023 May 05;8:e40641 [FREE Full text] [doi: 10.2196/40641] [Medline: 36939680]
27. Gabrielli S, Rizzi S, Bassi G, Carbone S, Maimone R, Marchesoni M, et al. Engagement and effectiveness of a healthy-coping intervention via chatbot for university students during the COVID-19 pandemic: mixed methods proof-of-concept study. JMIR Mhealth Uhealth 2021 May 28;9(5):e27965 [FREE Full text] [doi: 10.2196/27965] [Medline: 33950849]
28. Schick A, Feine J, Morana S, Maedche A, Reininghaus U. Validity of chatbot use for mental health assessment: experimental study. JMIR Mhealth Uhealth 2022 Oct 31;10(10):e28082 [FREE Full text] [doi: 10.2196/28082] [Medline: 36315228]
29. He Y, Yang L, Zhu X, Wu B, Zhang S, Qian C, et al. Mental health chatbot for young adults with depressive symptoms during the COVID-19 pandemic: single-blind, three-arm randomized controlled trial. J Med Internet Res 2022 Nov 21;24(11):e40719 [FREE Full text] [doi: 10.2196/40719] [Medline: 36355633]
30. Sanabria G, Greene KY, Tran JT, Gilyard S, DiGiovanni L, Emmanuel PJ, et al. "A great way to start the conversation": evidence for the use of an adolescent mental health chatbot navigator for youth at risk of HIV and other STIs. J Technol Behav Sci 2023 May 11:1-10 [FREE Full text] [doi: 10.1007/s41347-023-00315-4] [Medline: 37362063]
31. Grové C. Co-developing a mental health and wellbeing chatbot with and for young people. Front Psychiatry 2020;11:606041 [FREE Full text] [doi: 10.3389/fpsyt.2020.606041] [Medline: 33597898]
32. Holt-Quick C, Warren J, Stasiak K, Williams R, Christie G, Hetrick S, et al. A chatbot architecture for promoting youth resilience. In: Bain C, Schaper LK, Merolli M, editors. Healthier Lives, Digitally Enabled. New York, NY: IOS Press; 2023:99-105.
33. Ludin N, Holt-Quick C, Hopkins S, Stasiak K, Hetrick S, Warren J, et al. A chatbot to support young people during the COVID-19 pandemic in New Zealand: evaluation of the real-world rollout of an open trial. J Med Internet Res 2022 Nov 04;24(11):e38743 [FREE Full text] [doi: 10.2196/38743] [Medline: 36219754]
34. Høiland CG, Følstad A, Karahasanovic A. Hi, can I help? Exploring how to design a mental health chatbot for youths. Human Technology 2020 Aug 31;16(2):139-169. [doi: 10.17011/ht/urn.202008245640]
35. Brandtzæg PB, Skjuve M, Kristoffer Dysthe KK, Følstad A. When the social becomes non-human: young people's perception of social support in chatbots. In: Proceedings of the 2021 CHI Conference on Human Factors in Computing Systems. 2021 Presented at: CHI '21; May 8-13, 2021; Yokohama, Japan p. 1-13 URL: https://dl.acm.org/doi/10.1145/3411764.3445318 [doi: 10.1145/3411764.3445318]
36. Oliveira AL, Matos LM, Junior M, Delabrida Z. An initial assessment of a chatbot for rumination-focused cognitive behavioral therapy (RFCBT) in college students. Lect Notes Comput Sci 2022:21. [doi: 10.1007/978-3-030-86979-3_39]
37. Gabrielli S, Rizzi S, Carbone S, Donisi V. A chatbot-based coaching intervention for adolescents to promote life skills: pilot study. JMIR Hum Factors 2020 Mar 14;7(1):e16762 [FREE Full text] [doi: 10.2196/16762] [Medline: 32130128]
38. Williams R, Hopkins S, Frampton C, Holt-Quick C, Merry SN, Stasiak K. 21-day stress detox: open trial of a universal well-being chatbot for young adults. Soc Sci 2021 Oct 30;10(11):416. [doi: 10.3390/socsci10110416]
39. Kretzschmar K, Tyroll H, Pavarini G, Manzini A, Singh I, NeurOx Young People's Advisory Group. Can your phone be your therapist? young people's ethical perspectives on the use of fully automated conversational agents (chatbots) in mental health support. Biomed Inform Insights 2019;11:1178222619829083 [FREE Full text] [doi: 10.1177/1178222619829083] [Medline: 30858710]
40. de Nieva JO, Joaquin JA, Tan CB, Marc Te RK, Ong E. Investigating students' use of a mental health chatbot to alleviate academic stress. In: Proceedings of the 6th International ACM In-Cooperation HCI and UX Conference. 2020 Presented at: CHIuXiD '20; October 21-23, 2020; Jakarta and Bandung, Indonesia p. 1-10 URL: https://dl.acm.org/doi/10.1145/3431656.3431657 [doi: 10.1145/3431656.3431657]
41. Maenhout L, Peuters C, Cardon G, Compernolle S, Crombez G, DeSmet A. Participatory development and pilot testing of an adolescent health promotion chatbot. Front Public Health 2021;9:724779 [FREE Full text] [doi: 10.3389/fpubh.2021.724779] [Medline: 34858919]
42. Crutzen R, Peters GJ, Portugal SD, Fisser EM, Grolleman JJ. An artificially intelligent chat agent that answers adolescents' questions related to sex, drugs, and alcohol: an exploratory study. J Adolesc Health 2011 May;48(5):514-519. [doi: 10.1016/j.jadohealth.2010.09.002] [Medline: 21501812]
43. Greer S, Ramo D, Chang YJ, Fu M, Moskowitz J, Haritatos J. Use of the chatbot "Vivibot" to deliver positive psychology skills and promote well-being among young people after cancer treatment: randomized controlled feasibility trial. JMIR Mhealth Uhealth 2019 Oct 31;7(10):e15018 [FREE Full text] [doi: 10.2196/15018] [Medline: 31674920]
44. Huang J, Li Q, Xue Y, Cheng T, Xu S, Jia J, et al. Teenchat: a chatterbot system for sensing and releasing adolescents' stress. In: Proceedings of the 4th International Conference on Health Information Science. 2015 Presented at: HIS '15; May

XSL•FO
RenderX

28-30, 2015; Melbourne, Australia p. 133-145 URL: https://link.springer.com/chapter/10.1007/978-3-319-19156-0_14 [doi: 10.1007/978-3-319-19156-0_14]
45. Klos MC, Escoredo M, Joerin A, Lemos VN, Rauws M, Bunge EL. Artificial intelligence-based chatbot for anxiety and depression in university students: pilot randomized controlled trial. JMIR Form Res 2021 Aug 12;5(8):e20678 [FREE Full text] [doi: 10.2196/20678] [Medline: 34092548]
46. Gaffney H, Mansell W, Edwards R, Wright J. Manage Your Life Online (MYLO): a pilot trial of a conversational computer-based intervention for problem solving in a student sample. Behav Cogn Psychother 2014 Nov;42(6):731-746. [doi: 10.1017/S135246581300060X] [Medline: 23899405]
47. Liu H, Peng H, Song X, Xu C, Zhang M. Using AI chatbots to provide self-help depression interventions for university students: a randomized trial of effectiveness. Internet Interv 2022 Mar;27:100495 [FREE Full text] [doi: 10.1016/j.invent.2022.100495] [Medline: 35059305]
48. Matheson EL, Smith HG, Amaral AC, Meireles JF, Almeida MC, Linardon J, et al. Using chatbot technology to improve Brazilian adolescents' body image and mental health at scale: randomized controlled trial. JMIR Mhealth Uhealth 2023 Jun 19;11:e39934 [FREE Full text] [doi: 10.2196/39934] [Medline: 37335604]
49. Fabian KE, Foster KT, Chwastiak L, Turner M, Wagenaar BH. Adapting a transdiagnostic digital mental health intervention for use among immigrant and refugee youth in Seattle: a human-centered design approach. Transl Behav Med 2023 Nov 05;13(11):867-875 [FREE Full text] [doi: 10.1093/tbm/ibad041] [Medline: 37418614]
50. Escobar-Viera CG, Porta G, Coulter RW, Martina J, Goldbach J, Rollman BL. A chatbot-delivered intervention for optimizing social media use and reducing perceived isolation among rural-living LGBTQ+ youth: Development, acceptability, usability, satisfaction, and utility. Internet Interv 2023 Dec;34:100668 [FREE Full text] [doi: 10.1016/j.invent.2023.100668] [Medline: 37746640]
51. Viduani A, Cosenza V, Fisher HL, Buchweitz C, Piccin J, Pereira R, et al. Assessing mood with the identifying depression early in adolescence chatbot (IDEABot): development and implementation study. JMIR Hum Factors 2023 Aug 07;10:e44388 [FREE Full text] [doi: 10.2196/44388] [Medline: 37548996]
52. Wrightson-Hester AR, Anderson G, Dunstan J, McEvoy PM, Sutton CJ, Myers B, et al. An artificial therapist (manage your life online) to support the mental health of youth: co-design and case series. JMIR Hum Factors 2023 Jul 21;10:e46849 [FREE Full text] [doi: 10.2196/46849] [Medline: 37477969]
53. Palma R, Lam HC, Shrivastava A, Karlinsey E, Nguyen K, Deol P, et al. “Monday feels like Friday!” - towards overcoming anxiety and stress of autistic young adults during times of isolation. In: Proceedings of the 18th International Conference on Information for a Better World: Normality, Virtuality, Physicality, Inclusivity. 2023 Presented at: iConference '23; March 13-17, 2023; Virtual Event p. 286-305 URL: https://link.springer.com/chapter/10.1007/978-3-031-28032-0_24 [doi: 10.1007/978-3-031-28032-0_24]
54. Kang A, Hetrick S, Cargo T, Hopkins S, Ludin N, Bodmer S, et al. Exploring young adults' views about aroha, a chatbot for stress associated with the COVID-19 pandemic: interview study among students. JMIR Form Res 2023 Oct 12;7:e44556 [FREE Full text] [doi: 10.2196/44556] [Medline: 37527545]
55. Afrin Z, Md Farid D, Al Mamun KA. A cloud-based intelligent virtual assistant for adolescents. In: Proceedings of the 1st International Conference on Intelligent Systems and Data Science. 2023 Presented at: ISDS '23; November 11-12, 2023; Virtual Event p. 110-124 URL: https://link.springer.com/chapter/10.1007/978-981-99-7649-2_9 [doi: 10.1007/978-981-99-7649-2_9]
56. Allal L. Assessment and the regulation of learning. In: Peterson P, Baker E, McGaw B, editors. International Encyclopedia of Education. New York, NY: Academic Press; 2010:348-352.
57. Hix D, Hartson HR. Formative evaluation: ensuring usability in user interfaces. Department of Computer Science, Virginia Polytechnic Institute & State University. 1992. URL: https://vtechworks.lib.vt.edu/server/api/core/bitstreams/228b4f76-bb5c-4559-b581-4491766b5a09/content [accessed 2024-04-29]
58. Chowdhary KR. Natural language processing. In: Chowdhary KR, editor. Fundamentals of Artificial Intelligence. Cham, Switzerland: Springer; 2020:603-649.
59. Butler AC, Chapman JE, Forman EM, Beck AT. The empirical status of cognitive-behavioral therapy: a review of meta-analyses. Clin Psychol Rev 2006 Jan;26(1):17-31. [doi: 10.1016/j.cpr.2005.07.003] [Medline: 16199119]
60. Kroenke K, Spitzer RL, Williams JB. The PHQ-9: validity of a brief depression severity measure. J Gen Intern Med 2001 Sep;16(9):606-613 [FREE Full text] [doi: 10.1046/j.1525-1497.2001.016009606.x] [Medline: 11556941]
61. Newman MG, Zuellig AR, Kachin KE, Constantino MJ, Przeworski A, Erickson T, et al. Preliminary reliability and validity of the generalized anxiety disorder questionnaire-IV: a revised self-report diagnostic measure of generalized anxiety disorder. Behav Ther 2002;33(2):215-233. [doi: 10.1016/S0005-7894(02)80026-0]
62. Mental health: poor mental health impacts adolescent well-being. U.S. Center for Disease Control and Prevention. URL: https://www.cdc.gov/healthyyouth/mental-health/index.htm [accessed 2024-04-11]
63. Mental health for adolescents. Office of Population Affairs. URL: https://opa.hhs.gov/adolescent-health/mental-health-adolescents [accessed 2024-04-11]

XSL•FO
RenderX

64. Nadarzynski T, Puentes V, Pawlak I, Mendes T, Montgomery I, Bayley J, et al. Barriers and facilitators to engagement with artificial intelligence (AI)-based chatbots for sexual and reproductive health advice: a qualitative analysis. Sex Health 2021 Nov;18(5):385-393. [doi: 10.1071/SH21123] [Medline: 34782055]
65. Rahman R, Rahman MR, Tripto NI, Ali ME, Apon SH, Shahriyar R. AdolescentBot: understanding opportunities for chatbots in combating adolescent sexual and reproductive health problems in Bangladesh. In: Proceedings of the 2021 CHI Conference on Human Factors in Computing Systems. 2021 Presented at: CHI '21; May 8-13, 2021; Yokohama, Japan p. 1-15 URL: https://dl.acm.org/doi/10.1145/3411764.3445694 [doi: 10.1145/3411764.3445694]
66. Jo E, Epstein DA, Jung H, Kim YH. Understanding the benefits and challenges of deploying conversational AI leveraging large language models for public health intervention. In: Proceedings of the 2023 CHI Conference on Human Factors in Computing Systems. 2023 Presented at: CHI '23; April 23-28, 2023; Hamburg, Germany p. 1-16 URL: https://dl.acm.org/doi/10.1145/3544548.3581503 [doi: 10.1145/3544548.3581503]
67. Lai T, Shi Y, Du Z, Wu J, Fu K, Dou Y, et al. Supporting the demand on mental health services with AI-based conversational large language models (LLMs). BioMedInformatics 2023 Dec 22;4(1):8-33. [doi: 10.3390/biomedinformatics4010002]
68. Xu X, Yao B, Dong Y, Gabriel S, Yu H, Hendler J, et al. Mental-llm: leveraging large language models for mental health prediction via online text data. Proc ACM Interact Mob Wearable Ubiquitous Technol 2024 Mar 06;8(1):1-32. [doi: 10.1145/3643540]
69. Kelly SM. Snapchat's new AI chatbot is already raising alarms among teens and parents. CNN. URL: https://www.cnn.com/2023/04/27/tech/snapchat-my-ai-concerns-wellness/index.html [accessed 2024-04-11]
70. Muppalla SK, Vuppalapati S, Pulliahgaru AR, Sreenivasulu H. Effects of excessive screen time on child development: an updated review and strategies for management. Cureus 2023 Jun;15(6):e40608 [FREE Full text] [doi: 10.7759/cureus.40608] [Medline: 37476119]
71. Joshi SV, Stubbe D, Li ST, Hilty DM. The use of technology by youth: implications for psychiatric educators. Acad Psychiatry 2019 Mar;43(1):101-109 [FREE Full text] [doi: 10.1007/s40596-018-1007-2] [Medline: 30446956]
72. Jabir AI, Martinengo L, Lin X, Torous J, Subramaniam M, Tudor Car L. Evaluating conversational agents for mental health: scoping review of outcomes and outcome measurement instruments. J Med Internet Res 2023 Apr 19;25:e44548 [FREE Full text] [doi: 10.2196/44548] [Medline: 37074762]
73. Law T, Chita-Tegmark M, Rabb N, Scheutz M. Examining attachment to robots: benefits, challenges, and alternatives. J Hum Robot Interact 2022 Sep 08;11(4):1-18. [doi: 10.1145/3526105]
74. Garg R, Cui H, Seligson S, Zhang B, Porcheron M, Clark L, et al. The last decade of HCI research on children and voice-based conversational agents. In: Proceedings of the 2022 CHI Conference on Human Factors in Computing Systems. 2022 Presented at: CHI '22; April 29-May 5, 2022; New Orleans, LA p. 1-19 URL: https://dl.acm.org/doi/10.1145/3491102.3502016 [doi: 10.1145/3491102.3502016]
75. Omarov B, Narynov S, Zhumanov Z. Artificial intelligence-enabled chatbots in mental health: a systematic review. Comput Mater Contin 2023;74(3):59. [doi: 10.32604/cmc.2023.034655]
76. May R, Denecke K. Security, privacy, and healthcare-related conversational agents: a scoping review. Inform Health Soc Care 2022 Apr 03;47(2):194-210. [doi: 10.1080/17538157.2021.1983578] [Medline: 34617857]

Abbreviations

AI: artificial intelligence
CA: conversational agent
CBT: cognitive behavioral therapy
LGBTQ+: lesbian, gay, bisexual, transgender, queer, or questioning
LLM: large language model
NLP: natural language processing
PHQ: Patient Health Questionnaire
PRISMA: Preferred Reporting Items for Systematic Reviews and Meta-Analyses
RQ: research question

Edited by C Lovis; submitted 30.05.24; peer-reviewed by L Magoun, B Thies; comments to author 19.10.24; revised version received 12.12.24; accepted 25.12.24; published 28.02.25.

Please cite as:
Park JK, Singh VK, Wisniewski P
Current Landscape and Future Directions for Mental Health Conversational Agents for Youth: Scoping Review
JMIR Med Inform 2025;13:e62758
URL: https://medinform.jmir.org/2025/1/e62758
doi:10.2196/62758
PMID:40053735

XSL•FO
RenderX

©Jinkyung Katie Park, Vivek K Singh, Pamela Wisniewski. Originally published in JMIR Medical Informatics (https://medinform.jmir.org), 28.02.2025. This is an open-access article distributed under the terms of the Creative Commons Attribution License (https://creativecommons.org/licenses/by/4.0/), which permits unrestricted use, distribution, and reproduction in any medium, provided the original work, first published in JMIR Medical Informatics, is properly cited. The complete bibliographic information, a link to the original publication on https://medinform.jmir.org/, as well as this copyright and license information must be included.

XSL•FO
RenderX

Review

The Use of Machine Learning for Analyzing Real-World Data in Disease Prediction and Management: Systematic Review

Norah Hamad Alhumaidi[1*], MD; Doni Dermawan[2*], MSc; Hanin Farhana Kamaruzaman[3,4], MSc; Nasser Alotaiq[5], PhD

[1]College of Medicine, Qassim University, Buraidah, Saudi Arabia

[2]Applied Biotechnology, Faculty of Chemistry, Warsaw University of Technology, Warsaw, Poland

[3]Malaysian Health Technology Assessment Section, Medical Development Division, Ministry of Health Malaysia, Wilayah Persekutuan Putrajaya, Malaysia

[4]Health Economics and Health Technology Assessment, School of Health and Wellbeing, University of Glasgow, Glasgow, United Kingdom

[5]Health Sciences Research Center, Imam Mohammad ibn Saud Islamic University (IMSIU), Riyadh, Saudi Arabia

[*]these authors contributed equally

Corresponding Author:
Nasser Alotaiq, PhD
Health Sciences Research Center
Imam Mohammad ibn Saud Islamic University (IMSIU)
Othman Bin Affan Rd. Al-Nada 13317
Riyadh
Saudi Arabia
Phone: 966 50 411 9153
Email: naalotaiq@imamu.edu.sa

Abstract

Background: Machine learning (ML) and big data analytics are rapidly transforming health care, particularly disease prediction, management, and personalized care. With the increasing availability of real-world data (RWD) from diverse sources, such as electronic health records (EHRs), patient registries, and wearable devices, ML techniques present substantial potential to enhance clinical outcomes. Despite this promise, challenges such as data quality, model transparency, generalizability, and integration into clinical practice persist.

Objective: This systematic review aims to examine the use of ML for analyzing RWD in disease prediction and management, identifying the most commonly used ML methods, prevalent disease types, study designs, and the sources of real-world evidence (RWE). It also explores the strengths and limitations of current practices, offering insights for future improvements.

Methods: A comprehensive search was conducted following the PRISMA (Preferred Reporting Items for Systematic Reviews and Meta-Analyses) guidelines to identify studies using ML techniques for analyzing RWD in disease prediction and management. The search focused on extracting data regarding the ML algorithms applied; disease categories studied; types of study designs (eg, clinical trials and cohort studies); and the sources of RWE, including EHRs, patient registries, and wearable devices. Studies published between 2014 and 2024 were included to ensure the analysis of the most recent advances in the field.

Results: This review identified 57 studies that met the inclusion criteria, with a total sample size of >150,000 patients. The most frequently applied ML methods were random forest (n=24, 42%), logistic regression (n=21, 37%), and support vector machines (n=18, 32%). These methods were predominantly used for predictive modeling across disease areas, including cardiovascular diseases (n=19, 33%), cancer (n=9, 16%), and neurological disorders (n=6, 11%). RWE was primarily sourced from EHRs, patient registries, and wearable devices. A substantial portion of studies (n=38, 67%) focused on improving clinical decision-making, patient stratification, and treatment optimization. Among these studies, 14 (25%) focused on decision-making; 12 (21%) on health care outcomes, such as quality of life, recovery rates, and adverse events; and 11 (19%) on survival prediction, particularly in oncology and chronic diseases. For example, random forest models for cardiovascular disease prediction demonstrated an area under the curve of 0.85 (95% CI 0.81-0.89), while support vector machine models for cancer prognosis achieved an accuracy of 83% (P=.04). Despite the promising outcomes, many (n=34, 60%) studies faced challenges related to data quality, model interpretability, and ensuring generalizability across diverse patient populations.

Conclusions: This systematic review highlights the significant potential of ML and big data analytics in health care, especially for improving disease prediction and management. However, to fully realize the benefits of these technologies, future research

XSL•FO
RenderX

must focus on addressing the challenges of data quality, enhancing model transparency, and ensuring the broader applicability of ML models across diverse populations and clinical settings.

(JMIR Med Inform 2025;13:e68898) doi:10.2196/68898

KEYWORDS

machine learning; big data; real-world data; disease prediction; health care management; real-world evidence; artificial intelligence; AI

Introduction

Background

Advances in big data analytics and the growing availability of real-world data (RWD) are transforming health care by enabling new applications of machine learning (ML) to improve health outcomes [1]. Real-world evidence (RWE) generated from diverse data sources, such as electronic health records (EHRs), patient registries, and wearable devices, has become central to informed decision-making in clinical practice [2,3]. When combined with ML, RWD present a promising avenue to enhance disease prediction, personalize patient management, and optimize therapeutic effectiveness. By providing a comprehensive view of patient histories and real-world health outcomes, ML applications in health care can drive actionable insights across various domains, including disease diagnosis, treatment planning, and chronic disease management [4,5]. RWD capture information about patients in naturalistic settings, revealing how health care is delivered and its outcomes. Unlike clinical trials that operate within controlled conditions, RWD offer a more representative view of patient experiences, treatment responses, and health outcomes [6]. The rise of big data technology and data management systems has facilitated the integration of vast, heterogeneous data types, allowing ML algorithms to identify complex patterns within high-dimensional datasets [7,8]. These capabilities allow health care providers to predict health outcomes, identify at-risk populations, and tailor interventions based on individual patient factors, thus making strides toward precision medicine [9].

Despite their potential, ML applications in RWD and big data contexts face several challenges. Data quality remains a primary concern, as RWD often feature inconsistencies, missing values, and a lack of standardization [10]. Unlike the structured data from controlled clinical trials, RWD demand extensive preprocessing, including advanced natural language processing (NLP) methods and imputation techniques, to address data gaps. Such efforts are critical to enhancing ML model reliability and ensuring accurate, meaningful outcomes [11,12]. Biases present another key issue. ML models trained on RWD may inherit biases from the data, often stemming from demographic imbalances or regional health care differences. If left unaddressed, these biases can lead to health care disparities, as ML-driven decisions might inaccurately represent racial and ethnic minority populations or certain patient groups [13]. Incorporating fairness-aware ML algorithms and cross validating models across multiple datasets can mitigate this challenge, although developing equitable ML models remains a high priority [14]. Another significant hurdle is the interpretability of ML models, especially deep neural network (DNN) models, which are known for their “black box” nature. While complex models deliver high accuracy, their opaque decision-making process limits the ability to verify or explain predictions. Model transparency is crucial given the high stakes in health care, where ML-based recommendations can impact lives. Advances in interpretability tools, such as Shapley Additive Explanations and Local Interpretable Model-Agnostic Explanations, have helped enhance model transparency; however, balancing interpretability with performance remains an area of active investigation [15,16].

The integration of ML with RWD poses ethical and regulatory challenges, especially regarding patient privacy, data security, and informed consent. Regulations such as the Health Insurance Portability and Accountability Act in the United States and the General Data Protection Regulation in the European Union impose strict standards for data protection. However, adapting these laws to the context of ML in health care is complex due to the scale and diversity of the data involved [17,18]. Solutions such as deidentification, secure data-sharing protocols, and clear data management strategies have become crucial to ensuring patient confidentiality while maximizing data utility [19]. Ensuring equitable treatment outcomes is another ethical imperative. ML models trained on data predominantly representing certain demographics may perform poorly on underrepresented groups; therefore, addressing these disparities is critical. By incorporating fairness-aware ML models and building representative datasets, health care practitioners can ensure that ML applications benefit all patient groups, regardless of demographics [20]. Regulatory bodies have started developing specific guidelines for the use of ML and RWD in health care. The Food and Drug Administration (FDA), for example, has issued draft guidance on using RWE for regulatory decisions, and the European Medicines Agency (EMA) has also recognized the importance of RWE in evaluating drug safety and efficacy [21]. As ML applications in health care continue to grow, a solid regulatory framework will be necessary to safeguard patient health while supporting technological innovation.

Objectives

The objective of this systematic review is to explore and critically analyze the applications, challenges, and future directions of ML in processing real-world health data and big data across various disease domains. Specifically, this review aims to identify the disease areas where ML with RWD has shown clinical utility; examine the ML algorithms and methodologies applied to big data in health care; and analyze the challenges related to data quality, bias, and model interpretability. In addition, this review addresses the ethical and regulatory frameworks pertinent to the use of ML in health

XSL•FO
RenderX

care, with an emphasis on patient privacy and fairness. Finally, it outlines future research needs and opportunities for innovation in using ML, RWD, and big data for precision medicine and public health.

Methods

Eligibility Criteria

For this systematic review, we focused exclusively on clinical trials and cohort studies that used ML techniques to analyze RWD for disease prediction and management. Studies were included if they met the following criteria: (1) they were randomized controlled trials, pragmatic clinical trials, observational clinical trials, or cohort studies; (2) they involved the application of ML methods (eg, supervised learning, unsupervised learning, and deep learning) to RWD for clinical decision-making, disease prediction, or management of common diseases, such as cardiovascular diseases, diabetes, cancer, and chronic conditions; and (3) they used real-world health data sources, such as EHRs, patient registries, or wearable health devices. Exclusion criteria included trials that did not apply ML techniques or used only data from controlled clinical trials rather than real-world settings.

Information Sources

The following information sources were used to capture the most relevant clinical trials and cohort studies: PubMed, Scopus, and the Cochrane Library. PubMed was specifically targeted for clinical trials and biomedical research, particularly studies published in leading clinical journals. Scopus and the Cochrane Library were also searched to gather clinical trial reports within the health care and ML domains. To ensure comprehensive coverage, Google Scholar was included to identify gray literature, such as theses and reports that were not indexed in traditional databases. These sources were selected to provide a broad overview of clinical trial data and their relevance to ML applications in disease management. In addition, regulatory bodies such as the US FDA and the EMA were consulted to gain insights into clinical trial guidelines and regulatory standards regarding the use of RWD in health care.

Search Strategy

A comprehensive search strategy was developed to identify clinical trials and cohort studies focused on ML applications in RWD. The search query incorporated key terms related to ML (eg, “machine learning,” “deep learning,” and “artificial intelligence”) and clinical trials (eg, “clinical trial,” “randomized controlled trial,” and “pragmatic clinical trial”) along with terms related to disease management (eg, “disease prediction,” and “healthcare outcomes”). For example, the search used the following key terms: (“machine learning” OR “deep learning”) AND (“clinical trial” OR “randomized controlled trial” OR “pragmatic trial” OR “cohort study”) AND (“real-world data” OR “electronic health records” OR “patient registries”). Boolean operators (AND and OR), truncation, and Medical Subject Headings terms were used to refine the search and ensure comprehensive coverage. The search was conducted across multiple databases, including the Cochrane Library, PubMed, and Web of Science, covering the period from January 1, 2014, to December 31, 2024, ensuring that the full range of recent literature was captured. In addition, relevant studies were identified through manual searches of reference lists from key articles and by reviewing clinical trial registries, such as ClinicalTrials.gov, to ensure comprehensive coverage of the clinical trials relevant to ML in disease management. Gray literature was identified by conducting targeted searches in Google Scholar and manually retrieving relevant documents suggested by domain experts. Only English-language publications were included. To enhance transparency and reproducibility, the full search strategy, including specific database queries and search filters, has been provided in Multimedia Appendix 1.

Study Selection

The study selection process was conducted in 2 stages: an initial screening of titles and abstracts by 2 independent reviewers, followed by a full-text review by the same 2 reviewers to ensure consistency and minimize bias. In the first stage, the titles and abstracts of all identified articles were assessed for relevance based on predefined inclusion criteria. Discrepancies between reviewers were resolved through discussion, with a third reviewer consulted when necessary. Studies that met the inclusion criteria proceeded to the second stage, where the full texts were retrieved for further evaluation (Textbox 1).

The evaluation of exclusion criteria was conducted independently by both reviewers, with disagreements resolved through discussion. To maintain transparency, the PRISMA (Preferred Reporting Items for Systematic Reviews and Meta-Analyses) flow diagram [22,23] was used to document the number of studies at each review stage, including identification, screening, eligibility, and final inclusion. The PRISMA checklist is provided in Multimedia Appendix 2.

XSL•FO
RenderX

Textbox 1. Inclusion and exclusion criteria for study selection.

Inclusion criteria

- Study type: clinical trials or cohort studies
- Data source: studies using real-world data, such as electronic health records, patient registries, claims data, or wearable device data
- Machine learning (ML) application: application of ML algorithms for disease prediction or management (eg, supervised, unsupervised, and deep learning models)
- Clinical focus: studies addressing disease prediction, management, monitoring, or outcome prediction in health care
- Outcome reporting: studies reporting ML model performance metrics (eg, accuracy, area under the curve, sensitivity, and specificity) and real-world data sources
- Language: studies published in English
- Publication type: peer-reviewed articles and indexed gray literature

Exclusion criteria

- Study type: case reports, cross-sectional studies, reviews, editorials, letters, and conference abstracts
- Data source: studies using simulated data, animal studies, or laboratory-based data
- ML application: studies using only conventional statistical models (eg, logistic regression and Cox models) or expert systems
- Clinical focus: studies unrelated to clinical decision-making, disease outcomes, or patient management
- Outcome reporting: studies lacking sufficient information on ML model performance or data sources
- Language: non–English-language publications
- Publication type: non–peer-reviewed sources (blogs and social media posts)

Data Extraction

Data extraction was performed independently by 2 reviewers using a standardized form. Key data points extracted from each clinical trial and cohort study included study characteristics (eg, authors, year of publication, and trial design), the specific ML methods used (eg, supervised learning, reinforcement learning, deep learning), disease areas targeted (eg, cardiovascular diseases, diabetes, and cancer), and the types of RWD sources used (eg, EHRs, patient registries, and wearable devices). In addition, we extracted the performance metrics of the ML models used, such as accuracy, sensitivity, specificity, and area under the receiver operating characteristic curve (AUROC), to evaluate their effectiveness in disease prediction and management. Information on the challenges and limitations of applying ML to RWD in clinical trials, such as data quality issues, biases, or model interpretability, was also collected. Any disagreements in data extraction were resolved through discussion. The extracted data were organized systematically to synthesize findings across studies.

Results

Systematic Literature Search and Study Selection Workflow

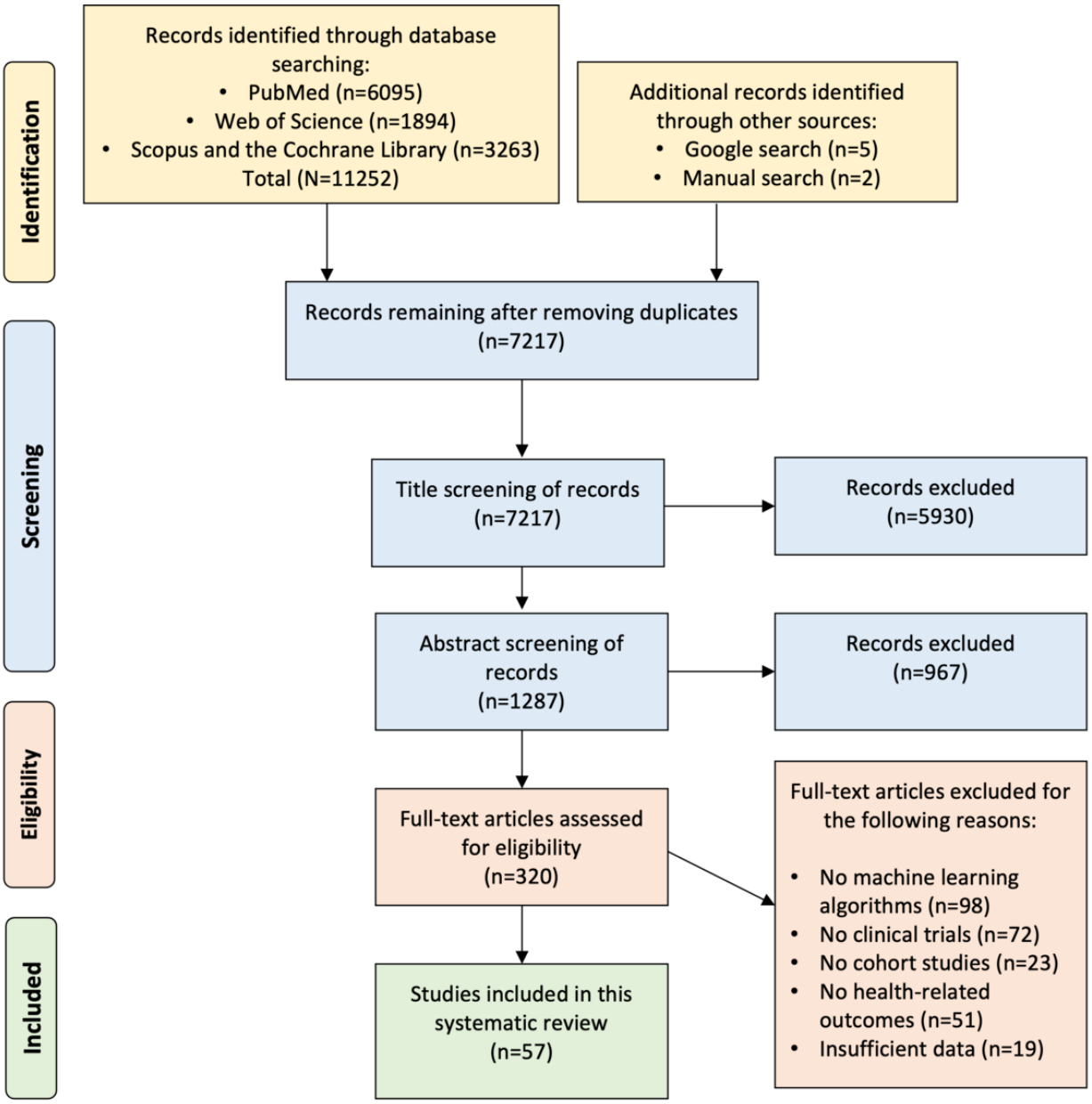
The systematic literature search was conducted to identify studies applying ML techniques to RWD in clinical trials and cohort studies, with a focus on disease prediction and management. The search covered multiple databases, including PubMed, Scopus, Web of Science, and the Cochrane Library, to capture a broad range of studies from biomedical, clinical, and health care research fields. This search yielded 11,252 records, as illustrated in the PRISMA flow diagram (Figure 1). To ensure comprehensive coverage, an additional 7 records were identified through external sources such as Google searches, manual hand searching of nonindexed journals, gray literature, and other nontraditional academic sources. After removing duplicates, 7217 (64.13%) unique studies remained for screening. The selection process followed a rigorous, multistage workflow. Title screening was first performed to assess relevance based on predefined inclusion criteria. Studies with titles not indicating the application of ML to RWD in clinical or disease management contexts were excluded, resulting in the removal of 5930 (82.17%) records and leaving 1287 (17.83%) studies for abstract screening. During the abstract screening, each abstract was carefully evaluated for inclusion criteria, including the use of ML techniques, relevant RWD sources (eg, EHRs, patient registries, or wearable device data), and relevance to disease prediction or management. This led to the exclusion of 967 (75.13%) studies that did not meet these criteria, most commonly for the following reasons: (1) a lack of ML implementation, with some studies using only conventional statistical approaches such as logistic regression (LR) or decision trees (DTs) without learning-based model development; (2) irrelevance to clinical trials or cohort study frameworks, instead focusing on simulations, animal studies, or nonhuman data sources; (3) absence of disease prediction or management applications, such as papers limited to health care policy, infrastructure, or economic modeling without patient-centered outcomes; and (4) insufficient use of RWD sources, as studies often used synthetic or trial-generated data rather than EHRs, registries, claims databases, or wearable device data. A total of 320 (24.86%) studies proceeded to the full-text review stage. At this stage, articles were assessed in detail to confirm adherence to all inclusion criteria. A total of

XSL•FO
RenderX

263 studies were excluded for specific reasons: 98 (37.3%) lacked ML algorithms (using conventional statistics instead), 72 (27.4%) were unrelated to clinical trial methodologies, 23 (8.7%) did not involve study cohorts, 51 (19.4%) were unrelated to health care outcomes, and 19 (7.2%) lacked sufficient information on ML model performance or data sources. Following this thorough, systematic, and transparent selection process, 57 studies met all eligibility criteria and were included in the final systematic review. These selected studies represented a diverse range of clinical applications, disease areas, ML methodologies, and RWD sources, offering a comprehensive overview of the current role of ML in clinical trials and cohort studies for disease prediction and management.

Table 1 summarizes these studies, while key findings and methodological details are provided in Multimedia Appendix 3 [24-80].

Figure 1. The PRISMA (Preferred Reporting Items for Systematic Reviews and Meta-Analyses) flow diagram depicting the study selection process from initial identification to final inclusion, detailing the number of records screened, excluded, and ultimately included in this systematic review.



XSL•FO
RenderX

Table 1. A summary of the studies included in this systematic review, outlining the study characteristics, diseases or medical conditions, type of study, source of real-world evidence (RWE), and machine learning (ML) methods used.

Study	Database	Diseases or medical conditions (category)	Type of study	Type of RWE	ML methods	Model performance metrics
Wissel et al [24], 2023	PubMed	Epilepsy (neurological diseases)	Evaluation of health care outcomes	EHR[a]	NLP[b]	• AUC[c]=0.79 (95% CI 0.62-0.96) • Sensitivity=0.80 (95% CI 0.29-0.99) • Specificity=0.77 (95% CI 0.64-0.88) • Positive predictive value: 0.25 (95% CI 0.07-0.52) • Negative predictive value: 0.98 (95% CI 0.87-1.00).
Ayers et al [25], 2021	PubMed	Orthotopic heart transplantation (CVD[d])	Survival prediction	Patient registries	DNN[e], RF[f], and AdaBoost[g]	• RF AUROC[h]=0.691 (95% CI 0.671-0.711) • DNN AUROC=0.691 (95% CI 0.671-0.712) • AdaBoost AUROC=0.653 (95% CI 0.632-0.674)
Nadarajah et al [26], 2023	PubMed	Atrial fibrillation (CVD)	Disease prediction	EHR	FIND-AF[i] ML algorithm	• AUROC=0.824 (95% CI 0.814-0.834)
Yadgir et al [27], 2022	PubMed	Cognitive impairment (neurological diseases)	Disease prediction	EHR	XGBoost[j]	• AUROC=0.720
Liu et al [28], 2023	PubMed	Peripheral artery disease (CVD)	Survival prediction	EHR	LR[k], GBM[l], RF, DT[m], XGBoost, neural network, Cox regression, and RSF[n]	• C-index: 0.788 (compared to 0.730 for GermanVasc Score)
Hill et al [29], 2022	PubMed	Atrial fibrillation (CVD)	Disease prediction and cost-effectiveness	EHR	PULSE-AI[o]	• Sensitivity=50% • Specificity=90%
Sheth et al [30], 2019	PubMed	Acute ischemic stroke (CVD)	Disease prediction	EHR	CNN[p]	• AUROC=0.88-0.90
Barton et al [31], 2019	PubMed	Sepsis (infectious diseases)	Disease prediction	EHR	XGBoost	• AUROC of 0.88, 0.84, and 0.83 for sepsis onset and 24 and 48 h before onset, respectively
Kao et al [32], 2023	PubMed	Atrial fibrillation (CVD)	Disease prediction	EHR	DT, SVM[q], LR, and RF	• AUROC=0.74 • Specificity=98.7%
Kim et al [33], 2022	PubMed	AHREs[r] (CVD)	Disease prediction	Wearable devices	RF, SVM, LR, and XGBoost	• RF AUROC=0.742 • SVM AUROC=0.675 • XGBoost AUROC=0.745 • LR AUROC=0.669
Park et al [34], 2023	PubMed	Coronary artery disease (CVD)	Disease prediction	Patient registries	BQR[s]	• AUC of 0.67, 0.65, 0.78, and 0.73 for per‐patient, LAD[t], LCx[u], and RCA[v], respectively
Hilbert et al [35], 2019	PubMed	Acute ischemic stroke (CVD)	Health care outcomes and decision-making	Wearable devices	ResNet[w]	• Average AUC for functional outcome was 0.71 • Average AUC for reperfusion across all folds was 0.65

XSL•FO
RenderX

Study	Database	Diseases or medical conditions (category)	Type of study	Type of RWE	ML methods	Model performance metrics
Chen et al [36], 2021	PubMed	Ewing sarcoma (tumors)	Survival prediction	Patient registries	Boosted DT, SVM, nonparametric RF, and neural network	• Sensitivity=77%-83% • Specificity=91%-94%
Koutsouleris et al [37], 2016	PubMed	Schizophrenia (neurological diseases)	Health care outcomes and decision-making	Patient registries	Nonlinear SVM	• Test-fold BAC[x]=75%
Strömblad et al [38], 2021	PubMed	Colorectal and gynecologic cancer (cancers)	Health care outcomes	EHR	GBM and LR	• —[y]
Wang et al [39], 2019	PubMed	Atrial fibrillation (CVD)	Decision-making	EHR	DT	• —
Tan et al [40], 2021	PubMed	Influenza (infectious diseases and respiratory diseases)	Health care outcomes	EHR	RF, XGBoost, and LR	• Accuracy of RF model for hospitalization=0.840, pneumonia=0.765, and sepsis or septic shock=0.857 • Accuracy of XGBoost for intensive care unit admission=0.902 • Accuracy of LR for in-hospital mortality=0.889
Goerigk et al [41], 2020	PubMed	Depression (neurological diseases)	Decision-making	Patient registries	LR, SVM, RF, tree-based stochastic gradient boosting, and XGBoost	• LR: accuracy=0.75, sensitivity=0.76, specificity=0.73, and AUC=0.792 • SVM: accuracy=0.88, sensitivity=0.85, specificity=0.91, and AUC=0.939 • RF: accuracy=0.89, sensitivity=0.88, specificity=0.91, and AUC=0.957 • XGBoost: accuracy=0.88, sensitivity=0.85, specificity=0.91, and AUC=0.954
Kijpaisalratana, et al [42], 2024	PubMed	Sepsis (infectious disease)	Decision-making	EHR	RF, XGBoost, LR, and SVM	• AUROC of ML in early sepsis identification was significantly higher than qSOFA[z], SIRS[aa], and MEWS[ab]
Sharma et al [43], 2019	PubMed	Acute coronary syndrome (CVD)	Survival prediction	Patient registries	Cox regression	• —
Singhal et al [44], 2021	PubMed	ARDS[ac] (respiratory diseases)	Disease prediction	EHR	ML algorithm called "eARDS[ad]" (neural networks, SVM, RF, LR, and XGBoost)	• AUROC=0.89 (95% CI 0.88-0.90) • Sensitivity=0.77 (95% CI 0.75-0.78) • Specificity=0.85 (95% CI 085-0.86)
Kanchanatawan et al [45], 2018	PubMed	Schizophrenia (neurological diseases)	Disease prediction	Patient registries	SVM and RF	• SVM AUROC=0.931 • RF AUROC=0.898
Huang et al [46], 2022	PubMed	Ischemic stroke (CVD)	Survival prediction	EHR	NB[ae], XGBoost, and LR	• NB AUROC=0.767 • XGBoost AUROC=0.989 • LR AUROC=0.627
She et al [47], 2023	PubMed	Sepsis (infectious disease)	Disease prediction	Patient registries	SVM and RF	• AUC=0.98
Sundar et al [48], 2022	PubMed	Gastric cancer (cancers)	Survival prediction	Patient registries	RF	• F-measure: 0.71 • AUC=0.75 (95% CI 0.50-0.99)

XSL•FO
RenderX

Study	Database	Diseases or medical conditions (category)	Type of study	Type of RWE	ML methods	Model performance metrics
Alaa et al [49], 2019	PubMed	Cardiovascular disease risk (CVD)	Disease prediction	Patient registries	Linear SVM, RF, neural networks, AdaBoost, and XGBoost	• AutoPrognosis model improved risk prediction (AUROC=0.774, 95% CI 0.768-0.780) • Framingham score (AUROC=0.724, 95% CI 0.720-0.728; *P*<.001) • Cox PH[af] model with conventional risk factors (AUROC=0.734, 95% CI 0.729-0.739; *P*<.001) • Cox PH model with all UK Biobank variables (AUROC=0.758, 95% CI 0.753-0.763; *P*<.001)
Azimi et al [50], 2017	PubMed	LSCS[ag] (spinal diseases)	Decision-making	EHR	ANN[ah] and LR	• AUC=0.89
Baxter et al [51], 2019	PubMed	Glaucoma (ocular diseases)	Decision-making	EHR	MLR[ai], RF, and ANN	• AUC=0.67
Anderson et al [52], 2015	PubMed	Type 2 diabetes (metabolic diseases)	Disease prediction	EHR	RF and SVM	• AUC=0.78
Bannister et al [53], 2018	PubMed	Stroke and myocardial infarction (CVD)	Survival prediction	Patient registries	Cox regression	• C-index was 0.59, 0.69, and 0.64 and 0.66, 0.70, and 0.70 for the GP[aj] and Cox regression models, respectively.
Scheer et al [54], 2017	Web of Science	Spinal deformity surgery (spinal diseases)	Decision-making	Patient registries	DT and ANN	• AUROC=0.89
Rau et al [55], 2016	Web of Science	Liver cancer (cancers)	Disease prediction	EHR	ANN and LR	• ANN sensitivity=0.757 • Specificity=0.755 • AUROC=0.873
Ramezankhani et al [56], 2016	Web of Science	Type 2 diabetes (metabolic diseases)	Disease prediction	Patient registries	DT	• AUC=0.78 • Sensitivity=78%
Pei et al [57], 2019	Web of Science	Type 2 diabetes (metabolic diseases)	Disease prediction	EHR	DT	• Accuracy=94.2% • Precision=94.0% • Recall=94.2% • AUC=94.8%
Oviedo et al [58], 2019	Web of Science	Postprandial hypoglycemia (metabolic diseases)	Decision-making	Wearable devices	SVM	• Specificity=79% • Sensitivity=71%
Mubeen et al [59], 2017	Web of Science	Alzheimer disease (neurological diseases)	Disease prediction	EHR	RF	• AUC=0.87 • Accuracy=80.2%
Lopez-de-Andres et al [60], 2016	Web of Science	Type 2 diabetes (metabolic diseases)	Survival prediction	Patient registries	ANN	• AUROC for Elixhauser comorbidity model=91.7% (95% CI 90.3-93.0) • AUROC for Charlson comorbidity model=88.9% (95% CI 87.5-90.2)
Kwon et al [61], 2019	Web of Science	Cardiac arrest (CVD	Survival prediction	Patient registries	DNN, LR, SVM, and RF	

XSL•FO
RenderX

Study	Database	Diseases or medical conditions (category)	Type of study	Type of RWE	ML methods	Model performance metrics
						• DNN AUROC=0.953 (95% CI 0.952-0.954) • LR AUROC=0.947 (95% CI 0.943-0.948) • RF AUROC=0.943 (95% CI 0.942-0.945) • SVM AUROC=0.930 (95% CI 0.929-0.932)
Kim et al [62], 2019	Web of Science	Breast cancer (cancers)	Decision-making	EHR	Two-class decision jungle and 2-class neural network	• AUROC was 0.917 in the high RS[ak] group and 0.744 in the low RS group in the test set
Khanji et al [63], 2019	Web of Science	Hypertension and dyslipidemia (CVD)	Health care outcomes	EHR	LR	• cvAUCs[al] of 0.73 for hypertension, 0.64 for dyslipidemia, and 0.79 for diabetes
Karhade et al [64], 2019	Web of Science	Lumbar disk herniation (spinal diseases)	Decision-making	EHR	LR, RF, XGBoost, ANN, and SVM	• AUC=0.81
Jovanovic et al [65], 2014	Web of Science	Choledocholithiasis (gastrointestinal diseases)	Decision-making	EHR	ANN	• AUROC=0.884 (95% CI 0.831-0.938); *P*<.001
Kang et al [66], 2020	Web of Science	Postinduction hypotension (anesthesia-related complications)	Health care outcomes	EHR	NB, LR, RF, and ANN	• NB AUROC=0.778 (95% CI 0.650-0.898) • LR AUROC=0.756 (95% CI 0.630-0.881) • RF AUROC=0.842 (95% CI 0.736-0.948) • ANN AUROC=0.760 (95% CI 0.640-0.880)
Isma'eel et al [67], 2018	Web of Science	Coronary artery disease (CVD)	Health care outcomes	EHR	ANN	• Sensitivity=91% (CI 81%-97%) • Specificity=65% (CI 60%-79%)
Hill et al [68], 2019	Web of Science	Atrial fibrillation (CVD)	Disease prediction	EHR	RF, SVM, and Cox regression	• RF AUROC=0.827 • SVM AUROC=0.725
Dong et al [69], 2019	Web of Science	Chinese Crohn disease (gastrointestinal diseases)	Decision-making	EHR	RF, LR, SVM, DT, and ANN	• RF AUROC=0.9864 • LR AUROC=0.9538 • SVM AUROC=0.9497 • DT AUROC=0.8809 • ANN AUROC=0.9059
Bowman et al [70], 2018	Web of Science	Carpal tunnel syndrome (musculoskeletal diseases)	Health care outcomes	EHR	LR and ANN	• AUROC=0.7
Bertsimas et al [71], 2018	Web of Science	Breast, lung, ovarian cancers (cancers)	Survival prediction	EHR	DT	• AUROC=0.83-0.86
Manz et al [72], 2020	The Cochrane Library	Cancer-related serious illness (cancers)	Decision-making	EHR	RF and SVM	• —
Tian et al [73], 2023	The Cochrane Library	Lung transplantation (respiratory diseases)	Survival prediction	EHR	RSF	• AUROC=0.879 (95% CI 0.832-0.921)
Li et al [74], 2022	The Cochrane Library	Latent profile analysis (cancers)	Decision-making	EHR	GBM	• —

XSL•FO
RenderX

Study	Database	Diseases or medical conditions (category)	Type of study	Type of RWE	ML methods	Model performance metrics
Tedeschi et al [75], 2021	The Cochrane Library	Pseudogout (rheumatic diseases)	Disease prediction	EHR	NLP	• AUC=0.86
Ambwani et al [76], 2019	The Cochrane Library	Cancer biomarkers (cancers)	Health care outcomes	EHR	LR	• Sensitivity=97.3%
Jorge et al [77], 2019	The Cochrane Library	Lupus (autoimmune disease)	Disease prediction	EHR	LR	• Specificity=97% • Sensitivity=64%
Shimabukuro et al [78], 2017	The Cochrane Library	Sepsis (infectious diseases)	Health care outcomes	EHR	LR	• AUROC=0.952 (95% CI 0.946 to –0.958) • Specificity=0.900 (95% CI 0.870 to 0.930) • Sensitivity=0.900 (95% CI 0.878 to 0.922)
Sarraju et al [79], 2021	The Cochrane Library	Atherosclerosis (CVD)	Health care outcomes	EHR	RF, GBM, XGBoost, and LR	• XGBoost AUC of 0.70 (95% CI 0.68 to –0.71) in the full CVD cohort and AUC of 0.71 (95% CI 0.69 to –0.73) in patients with ASCVD[am], with comparable performance by GBM, RF, and Lasso.
Ye et al [80], 2019	The Cochrane Library	Myopia (ocular diseases)	Health care outcomes	Wearable devices	SVM	• AUC=0.99

[a]EHR: electronic health record.
[b]NLP: natural language processing.
[c]AUC: area under the curve.
[d]CVD: cardiovascular disease.
[e]DNN: deep neural network.
[f]RF: random forest.
[g]AdaBoost: adaptive boosting.
[h]AUROC: area under the receiver operating characteristic curve.
[i]FIND-AF: Future Innovations in Novel Detection for Atrial Fibrillation.
[j]XGBoost: Extreme Gradient Boosting.
[k]LR: logistic regression.
[l]GBM: gradient boosting machine.
[m]DT: decision tree.
[n]RSF: random survival forest.
[o]PULSE-AI: Prediction of Undiagnosed Atrial Fibrillation Using a Machine Learning Algorithm.
[p]CNN: convolutional neural network.
[q]SVM: support vector machine.
[r]AHRE: atrial high-rate episode.
[s]BQR: Bayesian quantile regression.
[t]LAD: left anterior descending artery.
[u]LCx: left circumflex artery.
[v]RCA: right coronary artery.
[w]ResNet: residual neural network.
[x]BAC: balanced accuracy.
[y]Not applicable.
[z]qSOFA: quick sequential organ failure assessment.
[aa]SIRS: systemic inflammatory response syndrome.
[ab]MEWS: modified early warning score.

XSL•FO
RenderX

[ac]ARDS: acute respiratory distress syndrome.
[ad]eARDS: early onset acute respiratory distress syndrome
[ae]NB: naive Bayes.
[af]Cox PH: Cox proportional hazards.
[ag]LSCS: lumbar spinal canal stenosis.
[ah]ANN: artificial neural network.
[ai]MLR: multivariable logistic regression.
[aj]GP: genetic programming.
[ak]RS: recurrence score.
[al]cvAUC: cross-validated area under the curve.
[am]ASCVD: atherosclerotic cardiovascular disease.

Implementation of ML in RWD for Disease Prediction and Management

ML methods have become integral tools for analyzing RWD for disease prediction and management. These methods analyze complex medical data, helping clinicians make informed decisions for better patient care. Random forest (RF) is one of the most widely used ML methods, appearing in 42% (24/57) of the studies (Table 2). It is an ensemble learning technique that builds multiple DTs and combines their outputs to improve model stability and generalizability [81]. Several reviewed studies reported that RF performed well in handling large datasets with numerous variables, particularly EHRs, which are common medical data sources. Its robustness against overfitting and ability to handle missing data made it a frequently chosen method in clinical applications, where data quality could vary [82,83]. While RF has been widely applied in predictive modeling for disease outcomes, treatment responses, and patient risk assessments, further comparative studies are necessary to directly evaluate its performance against other ML models in real-world health care settings [84]. It is often applied to predict disease outcomes, assess treatment responses, and identify patient risk factors.

Table 2. The frequency of machine learning (ML) methods used in studies included in this review (N=57).

ML method	Studies, n (%)
Random forest	24 (42)
Logistic regression	21 (37)
Support vector machine	18 (32)
Extreme Gradient Boosting	12 (21)
Artificial neural network	11 (19)
Decision tree	9 (16)
Gradient boosting machine	4 (7)
Cox regression	3 (5)
Natural language processing	2 (4)
Deep neural network	2 (4)

LR was a fundamental method used for binary classification tasks and was used in 37% (21/57) of the studies. LR estimates the probability of a particular class, which is essential for predicting binary outcomes, such as the presence or absence of disease. It is a simple yet powerful tool that works well with smaller datasets and provides results that are easy to interpret, making it particularly useful in clinical settings where transparency is crucial [85,86]. LR is commonly used for disease risk prediction, helping clinicians assess the likelihood of a patient developing a condition based on their medical history and other clinical factors. Its interpretability allows for clear communication of results to health care providers, enhancing decision-making [87,88]. Support vector machine (SVM), used in 32% (18/57) of the studies, is known for its ability to handle high-dimensional data, making it suitable for complex medical datasets, including genomic and imaging data. SVM works by finding the optimal hyperplane that separates different classes in the feature space [89-91]. This method is beneficial in clinical settings where the relationship between variables is nonlinear and can be adapted for classification and regression tasks. SVM is applied in disease prediction, particularly when the dataset has many features relative to the number of observations. It is also useful for classifying patients based on genetic or demographic factors, making it a powerful tool for precision medicine [92,93]. Extreme Gradient Boosting (XGBoost) appeared in 21% (12/57) of the studies and is a highly effective method for improving predictive accuracy through boosting. XGBoost builds models sequentially to correct errors made by previous models and uses regularization to prevent overfitting. This method is effective in handling large datasets, common in clinical studies, and where computational efficiency is essential [94,95]. XGBoost is often used for survival analysis and disease outcome prediction, where it can effectively manage the complexity of large datasets and missing data. Its flexibility

XSL•FO
RenderX

allows it to be applied across various disease areas, from cancer prognosis to cardiovascular risk assessment [96,97].

Artificial neural network (ANN) models, used in 19% (11/57) of the studies, are powerful tools for modeling complex, nonlinear relationships in data. With multiple layers of interconnected neurons, an ANN can learn intricate patterns from large datasets. It is widely used in applications that involve unstructured data, such as medical imaging and genetic data, where traditional models might struggle [98,99]. ANN is frequently applied to predict disease progression and response to treatments and identify potential biomarkers. In RWD, an ANN helps identify subtle patterns in complex datasets that simpler models might not capture, such as predicting cancer progression from radiological images [100,101]. DTs, featured in 16% (9/57) of the studies, are straightforward and interpretable models that split data into subsets based on feature values. DT models are highly useful in real-world health care settings, where interpretability is essential for clinical decision-making. They are often applied in clinical decision support systems to guide treatment decisions based on patient data [102,103]. In health care, DTs predict disease outcomes, stratify patients by risk, and recommend treatment plans. Their transparency allows clinicians to understand the decision-making process, which is critical for patient trust and informed consent [104]. Gradient boosting machine (GBM) was used in 7% (4/57) of the studies and is a powerful ensemble method that focuses on correcting errors made by previous models. It is effective in producing highly accurate predictions, particularly in the presence of noisy or incomplete data. GBM is more computationally intensive than other methods, but often outperforms simpler models in accuracy. GBM is particularly useful for predicting disease progression and evaluating treatment efficacy in longitudinal studies, where multiple factors influence outcomes over time [105,106].

NLP, used in 4% (2/57) of the studies, is a subfield of artificial intelligence focused on analyzing unstructured textual data. In health care, NLP extracts relevant information from clinical notes, EHRs, and medical literature. It enables clinicians and researchers to analyze vast amounts of text data to identify trends, predict disease outcomes, and assess treatment effectiveness [107,108]. NLP is crucial in extracting insights from EHRs and other textual data sources. It can help in disease prediction by identifying patterns from patient narratives, diagnostic codes, and clinician notes that would otherwise remain hidden in unstructured formats [109]. Cox Regression, used in 5% (3/57) of the studies, is designed explicitly for survival analysis. It is widely applied in clinical research to model the time of an event, such as the onset of a disease or patient survival. This method is precious for understanding how various predictors affect the risk of an event occurring over time. In RWD, Cox regression is often used in cancer studies and other chronic diseases to predict survival times and assess the impact of different treatment regimens, making it indispensable in clinical trials and outcome-based research [110,111]. DNN models, used in 4% (2/57) of the studies, are a more complex version of ANN with multiple hidden layers. DNN models identify intricate patterns and are increasingly used in health care applications involving large and complex data types, such as medical imaging, genomics, and sensor data. DNN is particularly useful for analyzing high-dimensional data, such as medical images (eg, x-rays and magnetic resonance imaging) or genomic data, where the relationships between variables are complex and nonlinear. It helps identify disease markers and predict outcomes based on these complex datasets [112-114]. The diverse range of ML methods used in RWD for disease prediction and management demonstrates the adaptability of these techniques in clinical practice. From interpretable models such as LR and DTs to more complex methods such as DNN and XGBoost, each ML technique uniquely enhances predictive capabilities. These methods enable health care providers to make more accurate, data-driven decisions, ultimately improving patient outcomes and advancing personalized medicine.

Distribution of Diseases, Study Types, and RWE Sources in ML Applications

The distribution of disease types in studies using ML for disease prediction and management revealed a strong emphasis on cardiovascular diseases, with 19 (33%) of the 57 studies focusing on various conditions within this category (Table 3).

Table 3. Disease categories and the studies included in this review (N=57).

Diseases	Studies, n (%)
Cardiovascular diseases	19 (33)
Cancers and tumors	9 (16)
Neurological diseases	6 (11)
Infectious diseases	5 (9)
Metabolic diseases	5 (9)
Spinal diseases	3 (5)
Gastrointestinal diseases	2 (4)
Ocular diseases	2 (4)
Respiratory diseases	2 (4)
Other diseases	4 (7)

XSL•FO
RenderX

This high representation could be attributed to the multifactorial and complex nature of cardiovascular diseases, which often involve a combination of genetic, environmental, and lifestyle factors. Conditions such as atrial fibrillation, heart transplantation, and peripheral artery disease were prominent in these studies, where advanced ML models were used to enhance predictive accuracy and improve patient management. For instance, studies on heart transplantation and atrial fibrillation highlighted the potential of ML algorithms in survival prediction and early disease detection. A work demonstrated that ensemble models, combining RF, DNN, and adaptive boosting, significantly outperformed traditional LR for predicting 1-year survival rates after orthotopic heart transplantation, with an area under the receiver operating characteristic curve of 0.764 [25]. Meanwhile, another study explored the use of the Future Innovations in Novel Detection for Atrial Fibrillation ML algorithm to identify undiagnosed atrial fibrillation using data from EHRs, aiming to improve early detection and intervention. In addition, studies on peripheral artery disease and atrial fibrillation in older adults underscored the utility of ML models in survival prediction and risk assessment [26]. A study developed a predictive model for amputation-free survival after the revascularization process, with the random survival forest model achieving the highest accuracy in predicting long-term outcomes [28]. Similarly, another study used various ML methods, including DTs and RFs, to predict new-onset atrial fibrillation in older adults, achieving high specificity and performance, particularly with the RF model [32]. Furthermore, the use of ML in acute ischemic stroke, including studies by Sheth et al [30] and Hilbert et al [35], illustrated the growing role of deep learning techniques, such as convolutional neural networks and residual neural networks, in improving diagnostic accuracy and predicting patient outcomes [35]. These advancements in ML could potentially revolutionize clinical decision-making and treatment selection, especially for conditions such as stroke, where rapid and accurate assessment is critical.

A significant (9/57, 16%) portion of studies also targeted cancers and tumors, which were often characterized by their heterogeneity and the need for personalized treatment plans. ML algorithms, such as RF and SVM, enhanced early cancer detection, predicted disease recurrence, and assessed the effectiveness of different treatment protocols, demonstrating great potential in oncology settings. One key area of focus was the prediction of disease outcomes. For instance, a study developed a series of ML models to predict the 5-year survival rate for patients with Ewing sarcoma, a rare type of cancer. Using data from 2332 patients, including various algorithms such as boosted DTs, SVMs, RFs, and neural networks, the study found that the RF method performed best, with impressive sensitivity and specificity. This model is now accessible via a web-based application, providing clinicians a valuable tool for assessing survival probabilities for patients with Ewing sarcoma [36]. Another study used a predictive ML model to improve surgical scheduling in cancer surgeries, specifically for colorectal and gynecologic cancers. The research used gradient boosting and LR techniques to predict surgical durations, reducing operational inefficiencies such as patient wait times and optimizing the use of surgical resources, thereby demonstrating how ML could streamline health care operations while maintaining treatment quality [38]. Furthermore, in survival prediction, a study used an RF model to develop a gene signature that predicted the response of patients with gastric cancer to paclitaxel treatment. Their model, which identified a 19-gene signature, enabled the classification of patients into those who would benefit from the treatment, providing a novel approach to personalized cancer therapy [48].

The studies focusing on neurological diseases, including conditions such as epilepsy, cognitive impairment, and schizophrenia, highlighted the significant impact of ML in improving diagnosis, treatment prediction, and health care outcomes. These studies underscored the potential of ML to personalize patient care and optimize clinical decision-making. For instance, a study investigated the application of NLP embedded in EHR to automate alerts for pediatric patients with epilepsy. This ML-driven clinical decision support system successfully increased referrals for epilepsy surgery, with a marked improvement in presurgical evaluation rates and even higher rates of actual surgery, illustrating how NLP-based interventions could influence health care outcomes by improving referral efficiency and treatment access [24]. Similarly, another study focused on the use of XGBoost, an ML algorithm, to identify older patients in the emergency department at high risk for cognitive impairment. This predictive model, using EHR data, demonstrated high sensitivity and specificity, with the potential to reduce the need for in-person screenings and prioritize patients at high risk. By streamlining screening processes, this approach could enhance the detection of cognitive impairments in older adults, potentially leading to earlier interventions and better management of conditions such as dementia [27]. In schizophrenia, a study developed a nonlinear SVM model to predict treatment outcomes for patients with first-episode psychosis. The model was trained on pretreatment patient-reported data and successfully predicted poor versus good treatment outcomes, thus supporting clinical decision-making in terms of which treatments might be more effective for certain patients and identifying those at risk for nonadherence or poor prognosis [37]. These studies collectively demonstrated how ML methods, such as NLP, XGBoost, and RF, were revolutionizing the management of neurological diseases. By enabling early detection, better prediction of disease outcomes, and more informed decision-making, these tools offered substantial improvements in both clinical and health care settings. Infectious diseases, metabolic diseases, spinal diseases, gastrointestinal diseases, ocular diseases, and respiratory diseases each had a smaller but notable presence in the studies (n≤5). These applications generally focused on disease prediction, early diagnosis, and treatment optimization. ML models such as XGBoost and DNN were used to predict disease onset, assess risks, and improve patient management in these areas.

The data revealed that EHRs were the most frequently used form of RWE, accounting for 68% (39/57) of the studies. EHRs were a rich source of patient data, providing comprehensive records of patient health status, diagnoses, treatments, and outcomes over time. This made EHRs particularly valuable for studies that required large-scale data to identify patterns, trends,

XSL•FO
RenderX

and correlations in real-world clinical settings. The next most commonly used type of RWE was patient registries, which were used in 26% (15/57) of the studies. Patient registries typically collect data on specific patient populations with particular diseases or conditions, allowing for longitudinal tracking of disease progression and treatment outcomes. Wearable devices were the least used form of RWE, accounting for 7% (4/57) of the studies. Wearables were increasingly being used to collect real-time health data, including vital signs and activity levels, which could provide valuable insights into patients' health status outside of clinical environments. This distribution highlighted the dominance of EHR as the primary data source in these studies, reflecting its accessibility and broad applicability in health care research.

Disease prediction emerged as the most widely studied area, represented by 35% (20/57) of the studies. This suggested a strong emphasis on using ML and data analytics to predict the onset, progression, or outcomes of various diseases. The next most studied area was decision-making, with 25% (14/57) of the studies that underscored the growing interest in leveraging data-driven insights to inform clinical decisions and treatment strategies. Health care outcomes, such as quality of life, recovery rates, and adverse events, were the focus of 23% (13/57) of the studies, reflecting the importance of understanding how diseases and treatments affect patients' overall well-being. Survival prediction, accounting for 19% (11/57) of the studies, was another critical area of research, particularly in oncology and chronic diseases, where predicting patient survival and the effectiveness of interventions could guide clinical decision-making. This distribution indicated that disease prediction and decision-making were central to applying RWE in health care, with a significant focus on improving patient outcomes and guiding treatment strategies.

Discussion

Principal Findings

The findings of this study underscore the growing application of ML techniques in RWD for disease prediction and management. The results reveal that ML methods, particularly ensemble models such as RF, play a crucial role in enhancing prediction accuracy and addressing the complexities of large and high-dimensional datasets common in health care. Among the top ML methods used, RF was the most widely used, featured in 42% (24/57) of the studies, showcasing its adaptability to a variety of clinical datasets such as EHRs and patient registries. RF's ability to handle missing data, its resistance to overfitting, and its effectiveness in managing imbalanced datasets made it a powerful tool in predicting disease outcomes [115,116], such as survival rates and complications in cardiovascular diseases and cancer. Regarding disease types, cardiovascular diseases dominated the studies, with 33% (19/57) of the studies dedicated to predicting outcomes related to heart transplantation, atrial fibrillation, and peripheral artery disease. This concentration is likely attributed to the critical need for predictive tools in the early diagnosis and management of these conditions, which account for a significant burden on health care systems globally [117]. ML applications, such as DNN and random survival forests, have been shown to improve the accuracy of survival predictions, assess treatment responses, and enhance patient stratification. In addition, the study highlights the increasing application of ML in predicting conditions such as cancers, neurological disorders, and infectious diseases. These findings align with the broader trend of using RWD to bridge the gap between clinical trials and actual patient care by making predictions based on RWD sources, such as EHRs and wearable devices. As evidenced in the studies reviewed, ML techniques can process vast amounts of medical data from various sources, facilitating early detection, timely intervention, and improved management of chronic conditions. Furthermore, these advancements in ML applications are subject to increasing regulatory oversight. Agencies such as the US FDA and the EMA are actively exploring frameworks for the approval and regulation of ML-driven tools in health care. These regulations aim to ensure ML models' safety, efficacy, and transparency, especially in real-world applications where data variability and model interpretability remain key concerns. As regulatory bodies continue to define standards for using RWD and ML in clinical settings, ensuring compliance with FDA and EMA guidelines will be essential for the broader adoption and integration of these technologies into clinical practice.

Comparison With Prior Work

This systematic review aligns with and extends several recent literature reviews that have explored the application of ML to RWD in health care. Previous studies have highlighted the potential of ML models to transform health care by improving disease prediction and patient management [118,119]. However, our review emphasizes a broader scope by including a wide variety of disease types, from cardiovascular diseases and cancer to neurological and infectious diseases, reflecting the growing versatility of ML tools in clinical settings. A notable comparison can be made with a study that focused on EHRs as the primary data source for ML models, conducted by Miotto et al [120]. While their review identified the challenges associated with EHR-based studies, such as data sparsity and heterogeneity, our study similarly acknowledges these limitations but also expands the discussion to include wearable devices and patient registries as additional data sources. These emerging data sources provide a more complete picture of the patient's health status, significantly improving model performance and enabling better patient monitoring in real-world settings. Another key comparison is with a review that focused on ML's role in health care decision-making and its integration into clinical workflows [121]. While the study by Beam and Kohane [121] explored various ML algorithms in health care, our review places a stronger emphasis on the role of ensemble models, such as RF, and their applicability across diverse health care datasets. One of the key contributions of our review, which sets it apart from previous works, is the focus on regulatory challenges associated with the deployment of ML models in clinical practice. While other reviews have discussed technical aspects of ML, we specifically address the urgent need for clearer regulatory frameworks from authorities such as the FDA and EMA to ensure the safe and effective approval of ML models in health care. This is an area that has received limited attention in previous reviews but is critical as health care systems begin to

XSL•FO
RenderX

rely more heavily on automated systems for clinical decision-making. Overall, this review builds upon the foundations established by previous literature, offering an updated and comprehensive analysis that incorporates new data sources, encompasses a broader range of diseases, and addresses the challenges of regulatory approval and model interpretability in the context of ML in health care.

Limitations

This review has several limitations. First, while a comprehensive search strategy was used, it is possible that some relevant studies were missed, particularly those that did not explicitly use the selected keywords or were indexed in databases not included in this search. In addition, this review was limited to English-language publications, which may have excluded relevant studies published in other languages. Another potential limitation is the application of strict inclusion and exclusion criteria, which, while ensuring the relevance and quality of the included studies, may have led to the omission of some studies that could have provided valuable insights. For example, studies with limited methodological details or those focusing primarily on deep learning applications were often excluded due to insufficient validation or performance comparisons. Future research could consider broader inclusion criteria to capture a wider range of studies. Furthermore, the variability in study designs and data sources posed challenges in synthesizing findings across different studies. The included studies used different types of RWD, ranging from EHRs and patient registries to imaging and wearable sensor data. This heterogeneity complicates direct comparisons and generalizability. Finally, while efforts were made to minimize bias through independent study screening by 2 reviewers, inherent biases in study selection and data extraction may still exist. The reliance on published literature also introduces publication bias, as studies with negative or inconclusive results may be underrepresented. Future work could integrate unpublished data sources or conduct meta-analyses to provide a more comprehensive assessment of ML applications in RWD.

Future Work

While this systematic review aimed for comprehensive coverage by using a broad search strategy across multiple databases and gray literature sources, the large disparity between the number of initially retrieved studies and those meeting the final inclusion criteria highlights an important area for improvement in future research. A more focused, topic-specific keyword strategy, combined with the application of advanced database filters, could increase the precision of future searches by limiting the retrieval of irrelevant studies. In addition, integrating artificial intelligence–assisted search tools and NLP algorithms might further enhance the efficiency of systematic literature reviews by streamlining the identification of eligible studies based on more nuanced criteria. Future reviews may also benefit from targeting more narrowly defined subtopics within the broader field of ML applications in RWD, such as specific disease domains, ML model types, or clinical trial phases. These refinements would likely improve the overall relevance and manageability of retrieved records, ensuring a more efficient screening process and focused synthesis of findings.

Conclusions

In conclusion, this review highlights the transformative potential of integrating ML techniques with RWD in health care, specifically for disease prediction and management. The use of advanced ML models, such as ensemble methods and deep learning, has demonstrated the ability to enhance predictive accuracy, improve patient stratification, and facilitate more personalized and proactive health care. These advancements are poised to significantly impact clinical decision-making, enabling earlier diagnoses, optimized treatment strategies, and efficient resource allocation. However, despite these promising developments, several challenges remain. Issues related to data quality, generalizability across diverse populations, and the interpretability of complex ML models must be addressed to ensure their effective and widespread application. The lack of transparency in some ML algorithms, which often function as “black boxes,” remains a significant barrier to their integration into clinical workflows. Improving the explainability of these models will be crucial in gaining the trust of health care professionals and enhancing the clinical utility of ML predictions. In addition, regulatory frameworks for ML in health care are still evolving, with clear guidelines needed from regulatory bodies such as the FDA and EMA. This will help ensure that ML models meet safety standards and are deployed in clinical settings in a manner that benefits both health care providers and patients. Furthermore, as health care data becomes increasingly heterogeneous, with sources ranging from EHRs to wearable devices and patient registries, strategies for addressing data inconsistencies and ensuring data quality will be essential. Looking ahead, future research should focus on improving the robustness, transparency, and generalizability of ML models, particularly for underrepresented diseases and diverse patient populations. Establishing ethical and regulatory standards for the use of ML in clinical practice will be crucial for fostering public trust and ensuring equitable access to these innovations. Collaboration among clinicians, data scientists, and policy makers will be key to overcoming these challenges, with the ultimate goal of ensuring that ML-driven advancements in health care lead to improved health outcomes, better care delivery, and more equitable health care systems for all.

Acknowledgments

This work was supported and funded by the Deanship of Scientific Research at Imam Mohammad Ibn Saud Islamic University (IMSIU) (grant number IMSIU-DDRSP2501).

Data Availability

All data generated or analyzed during this study are included in this published article and its supplementary information files.

XSL•FO
RenderX

Authors' Contributions

NHA and DD conceptualized the study, developed the methodology, and wrote the original draft of the manuscript. HFK contributed to data collection, analysis, and interpretation. NHA, DD, and NA provided critical revisions and approved the final version of the manuscript. NA supervised the project study. All authors reviewed and approved the manuscript for publication.

Conflicts of Interest

None declared.

Multimedia Appendix 1
Full search strategy.
[DOCX File , 20 KB - medinform_v13i1e68898_app1.docx]

Multimedia Appendix 2
PRISMA (Preferred Reporting Items for Systematic Reviews and Meta-Analyses) checklist.
[PDF File (Adobe PDF File), 492 KB - medinform_v13i1e68898_app2.pdf]

Multimedia Appendix 3
A dataset of selected studies, including details such as the year of publication, authors' names, study title, database, diseases or medical conditions, disease category, study type, real-world evidence type, machine learning methods used, and key findings.
[XLSX File (Microsoft Excel File), 41 KB - medinform_v13i1e68898_app3.xlsx]

References

1. Liu F, Panagiotakos D. Real-world data: a brief review of the methods, applications, challenges and opportunities. BMC Med Res Methodol 2022 Nov 05;22(1):287 [FREE Full text] [doi: 10.1186/s12874-022-01768-6] [Medline: 36335315]
2. Dang A. Real-world evidence: a primer. Pharmaceut Med 2023 Jan;37(1):25-36 [FREE Full text] [doi: 10.1007/s40290-022-00456-6] [Medline: 36604368]
3. Klonoff DC. The expanding role of real-world evidence trials in health care decision making. J Diabetes Sci Technol 2020 Jan;14(1):174-179 [FREE Full text] [doi: 10.1177/1932296819832653] [Medline: 30841738]
4. Junaid SB, Imam AA, Balogun AO, De Silva LC, Surakat YA, Kumar G, et al. Recent advancements in emerging technologies for healthcare management systems: a survey. Healthcare (Basel) 2022 Oct 03;10(10):1940 [FREE Full text] [doi: 10.3390/healthcare10101940] [Medline: 36292387]
5. Williamson SM, Prybutok V. Balancing privacy and progress: a review of privacy challenges, systemic oversight, and patient perceptions in AI-driven healthcare. Appl Sci 2024 Jan 12;14(2):675. [doi: 10.3390/app14020675]
6. Derman BA, Belli AJ, Battiwalla M, Hamadani M, Kansagra A, Lazarus HM, et al. Reality check: real-world evidence to support therapeutic development in hematologic malignancies. Blood Rev 2022 May;53:100913 [FREE Full text] [doi: 10.1016/j.blre.2021.100913] [Medline: 35272867]
7. Rane NL, Paramesha M, Choudhary SP, Rane J. Machine learning and deep learning for big data analytics: a review of methods and applications. Partn Univers Int Res J 2024;2(3):172-197 [FREE Full text] [doi: 10.5281/zenodo.12271006]
8. Saeed S, Ahmed S, Joseph S. Machine learning in the big data age: advancements, challenges, and future prospects. ResearchGate. URL: https://www.researchgate.net/publication/377438052_Machine_Learning_in_the_Big_Data_Age_Advancements_Challenges_and_Future_Prospects [accessed 2025-05-29]
9. Javaid M, Haleem A, Pratap Singh R, Suman R, Rab S. Significance of machine learning in healthcare: features, pillars and applications. Int J Intell Netw 2022;3:58-73. [doi: 10.1016/j.ijin.2022.05.002]
10. Ogrizović M, Drašković D, Bojić D. Quality assurance strategies for machine learning applications in big data analytics: an overview. J Big Data 2024 Oct 30;11:156. [doi: 10.1186/s40537-024-01028-y]
11. Badalotti D, Agrawal A, Pensato U, Angelotti G, Marcheselli S. Development of a Natural Language Processing (NLP) model to automatically extract clinical data from electronic health records: results from an Italian comprehensive stroke center. Int J Med Inform 2024 Dec;192:105626 [FREE Full text] [doi: 10.1016/j.ijmedinf.2024.105626] [Medline: 39321491]
12. Turchin A, Florez Builes LF. Using natural language processing to measure and improve quality of diabetes care: a systematic review. J Diabetes Sci Technol 2021 May;15(3):553-560 [FREE Full text] [doi: 10.1177/19322968211000831] [Medline: 33736486]
13. Dominguez-Catena I, Paternain D, Jurio A, Galar M. Less can be more: representational vs. stereotypical gender bias in facial expression recognition. Prog Artif Intell 2024 Oct 14;14:11-31. [doi: 10.1007/s13748-024-00345-w]
14. Ferrara C, Sellitto G, Ferrucci F, Palomba F, De Lucia A. Fairness-aware machine learning engineering: how far are we? Empir Softw Eng 2024;29(1):9 [FREE Full text] [doi: 10.1007/s10664-023-10402-y] [Medline: 38027253]

XSL•FO
RenderX

15. Hassija V, Chamola V, Mahapatra A, Singal A, Goel D, Huang K, et al. Interpreting black-box models: a review on explainable artificial intelligence. Cogn Comput 2023 Aug 24;16:45-74. [doi: 10.1007/s12559-023-10179-8]
16. Ali S, Abuhmed T, El-Sappagh S, Muhammad K, Alonso-Moral JM, Confalonieri R, et al. Explainable Artificial Intelligence (XAI): what we know and what is left to attain Trustworthy Artificial Intelligence. Inf Fusion 2023 Nov;99:101805. [doi: 10.1016/j.inffus.2023.101805]
17. El Mestari SZ, Lenzini G, Demirci H. Preserving data privacy in machine learning systems. Comput Secur 2024 Feb;137:103605. [doi: 10.1016/j.cose.2023.103605]
18. Lu H, Alhaskawi A, Dong Y, Zou X, Zhou H, Ezzi SH, et al. Patient autonomy in medical education: navigating ethical challenges in the age of artificial intelligence. Inquiry 2024 Sep 18;61:469580241266364 [FREE Full text] [doi: 10.1177/00469580241266364] [Medline: 39290068]
19. Tucker K, Branson J, Dilleen M, Hollis S, Loughlin P, Nixon MJ, et al. Protecting patient privacy when sharing patient-level data from clinical trials. BMC Med Res Methodol 2016 Jul 08;16 Suppl 1(Suppl 1):77 [FREE Full text] [doi: 10.1186/s12874-016-0169-4] [Medline: 27410040]
20. Franklin G, Stephens R, Piracha M, Tiosano S, Lehouillier F, Koppel R, et al. The sociodemographic biases in machine learning algorithms: a biomedical informatics perspective. Life (Basel) 2024 May 21;14(6):652 [FREE Full text] [doi: 10.3390/life14060652] [Medline: 38929638]
21. Considerations for the use of real-world data and real-world evidence to support regulatory decision-making for drug and biological products. U.S. Food & Drug Administration. 2023 Aug. URL: https://www.fda.gov/regulatory-information/search-fda-guidance-documents/considerations-use-real-world-data-and-real-world-evidence-support-regulatory-decision-making-drug [accessed 2025-06-05]
22. Moher D, Liberati A, Tetzlaff J, Altman DG, PRISMA Group. Preferred reporting items for systematic reviews and meta-analyses: the PRISMA statement. PLoS Med 2009 Jul 21;6(7):e1000097 [FREE Full text] [doi: 10.1371/journal.pmed.1000097] [Medline: 19621072]
23. Alotaiq N, Dermawan D. Advancements in virtual bioequivalence: a systematic review of computational methods and regulatory perspectives in the pharmaceutical industry. Pharmaceutics 2024 Nov 03;16(11):1414 [FREE Full text] [doi: 10.3390/pharmaceutics16111414] [Medline: 39598538]
24. Wissel BD, Greiner HM, Glauser TA, Mangano FT, Holland-Bouley KD, Zhang N, et al. Automated, machine learning-based alerts increase epilepsy surgery referrals: a randomized controlled trial. Epilepsia 2023 Jul 27;64(7):1791-1799 [FREE Full text] [doi: 10.1111/epi.17629] [Medline: 37102995]
25. Ayers B, Sandholm T, Gosev I, Prasad S, Kilic A. Using machine learning to improve survival prediction after heart transplantation. J Card Surg 2021 Nov 19;36(11):4113-4120. [doi: 10.1111/jocs.15917] [Medline: 34414609]
26. Nadarajah R, Wahab A, Reynolds C, Raveendra K, Askham D, Dawson R, et al. Future Innovations in Novel Detection for Atrial Fibrillation (FIND-AF): pilot study of an electronic health record machine learning algorithm-guided intervention to identify undiagnosed atrial fibrillation. Open Heart 2023 Sep 30;10(2):e002447 [FREE Full text] [doi: 10.1136/openhrt-2023-002447] [Medline: 37777255]
27. Yadgir SR, Engstrom C, Jacobsohn GC, Green RK, Jones CM, Cushman JT, et al. Machine learning-assisted screening for cognitive impairment in the emergency department. J Am Geriatr Soc 2022 Mar;70(3):831-837 [FREE Full text] [doi: 10.1111/jgs.17491] [Medline: 34643944]
28. Liu Y, Xue J, Jiang J. Application of machine learning algorithms in electronic medical records to predict amputation-free survival after first revascularization in patients with peripheral artery disease. Int J Cardiol 2023 Jul 15;383:175-184. [doi: 10.1016/j.ijcard.2023.04.040] [Medline: 37119943]
29. Hill NR, Groves L, Dickerson C, Boyce R, Lawton S, Hurst M, et al. Identification of undiagnosed atrial fibrillation using a machine learning risk prediction algorithm and diagnostic testing (PULsE-AI) in primary care: cost-effectiveness of a screening strategy evaluated in a randomized controlled trial in England. J Med Econ 2022 Aug 03;25(1):974-983 [FREE Full text] [doi: 10.1080/13696998.2022.2102355] [Medline: 35834373]
30. Sheth SA, Lopez-Rivera V, Barman A, Grotta JC, Yoo AJ, Lee S, et al. Machine learning-enabled automated determination of acute ischemic core from computed tomography angiography. Stroke 2019 Nov;50(11):3093-3100. [doi: 10.1161/STROKEAHA.119.026189] [Medline: 31547796]
31. Barton C, Chettipally U, Zhou Y, Jiang Z, Lynn-Palevsky A, Le S, et al. Evaluation of a machine learning algorithm for up to 48-hour advance prediction of sepsis using six vital signs. Comput Biol Med 2019 Jun;109:79-84 [FREE Full text] [doi: 10.1016/j.compbiomed.2019.04.027] [Medline: 31035074]
32. Kao YT, Huang CY, Fang YA, Liu JC, Chang TH. Machine learning-based prediction of atrial fibrillation risk using electronic medical records in older aged patients. Am J Cardiol 2023 Jul 01;198:56-63. [doi: 10.1016/j.amjcard.2023.03.035] [Medline: 37209529]
33. Kim M, Kang Y, You SC, Park HD, Lee SS, Kim TH, et al. Artificial intelligence predicts clinically relevant atrial high-rate episodes in patients with cardiac implantable electronic devices. Sci Rep 2022 Jan 07;12(1):37 [FREE Full text] [doi: 10.1038/s41598-021-03914-4] [Medline: 34996990]

XSL•FO
RenderX

34. Park HB, Lee J, Hong Y, Byungchang S, Kim W, Lee BK, et al. Risk factors based vessel-specific prediction for stages of coronary artery disease using Bayesian quantile regression machine learning method: results from the PARADIGM registry. Clin Cardiol 2023 Mar;46(3):320-327 [FREE Full text] [doi: 10.1002/clc.23964] [Medline: 36691990]
35. Hilbert A, Ramos LA, van Os HJ, Olabarriaga SD, Tolhuisen ML, Wermer MJ, et al. Data-efficient deep learning of radiological image data for outcome prediction after endovascular treatment of patients with acute ischemic stroke. Comput Biol Med 2019 Dec;115:103516. [doi: 10.1016/j.compbiomed.2019.103516] [Medline: 31707199]
36. Chen W, Zhou C, Yan Z, Chen H, Lin K, Zheng Z, et al. Using machine learning techniques predicts prognosis of patients with Ewing sarcoma. J Orthop Res 2021 Nov 24;39(11):2519-2527 [FREE Full text] [doi: 10.1002/jor.24991] [Medline: 33458857]
37. Koutsouleris N, Kahn RS, Chekroud AM, Leucht S, Falkai P, Wobrock T, et al. Multisite prediction of 4-week and 52-week treatment outcomes in patients with first-episode psychosis: a machine learning approach. Lancet Psychiatry 2016 Oct;3(10):935-946. [doi: 10.1016/s2215-0366(16)30171-7]
38. Strömblad CT, Baxter-King RG, Meisami A, Yee SJ, Levine MR, Ostrovsky A, et al. Effect of a predictive model on planned surgical duration accuracy, patient wait time, and use of presurgical resources: a randomized clinical trial. JAMA Surg 2021 Apr 01;156(4):315-321 [FREE Full text] [doi: 10.1001/jamasurg.2020.6361] [Medline: 33502448]
39. Wang SV, Rogers JR, Jin Y, DeiCicchi D, Dejene S, Connors JM, et al. Stepped-wedge randomised trial to evaluate population health intervention designed to increase appropriate anticoagulation in patients with atrial fibrillation. BMJ Qual Saf 2019 Oct 26;28(10):835-842 [FREE Full text] [doi: 10.1136/bmjqs-2019-009367] [Medline: 31243156]
40. Tan TH, Hsu CC, Chen CJ, Hsu SL, Liu TL, Lin HJ, et al. Predicting outcomes in older ED patients with influenza in real time using a big data-driven and machine learning approach to the hospital information system. BMC Geriatr 2021 Apr 27;21(1):280 [FREE Full text] [doi: 10.1186/s12877-021-02229-3] [Medline: 33902485]
41. Goerigk S, Hilbert S, Jobst A, Falkai P, Bühner M, Stachl C, et al. Predicting instructed simulation and dissimulation when screening for depressive symptoms. Eur Arch Psychiatry Clin Neurosci 2020 Mar 12;270(2):153-168. [doi: 10.1007/s00406-018-0967-2] [Medline: 30542818]
42. Kijpaisalratana N, Saoraya J, Nhuboonkaew P, Vongkulbhisan K, Musikatavorn K. Real-time machine learning-assisted sepsis alert enhances the timeliness of antibiotic administration and diagnostic accuracy in emergency department patients with sepsis: a cluster-randomized trial. Intern Emerg Med 2024 Aug 21;19(5):1415-1424. [doi: 10.1007/s11739-024-03535-5] [Medline: 38381351]
43. Sharma A, Sun JL, Lokhnygina Y, Roe MT, Ahmad T, Desai NR, et al. Patient phenotypes, cardiovascular risk, and ezetimibe treatment in patients after acute coronary syndromes (from IMPROVE-IT). Am J Cardiol 2019 Apr 15;123(8):1193-1201. [doi: 10.1016/j.amjcard.2019.01.034] [Medline: 30739657]
44. Singhal L, Garg Y, Yang P, Tabaie A, Wong AI, Mohammed A, et al. eARDS: A multi-center validation of an interpretable machine learning algorithm of early onset Acute Respiratory Distress Syndrome (ARDS) among critically ill adults with COVID-19. PLoS One 2021 Sep 24;16(9):e0257056 [FREE Full text] [doi: 10.1371/journal.pone.0257056] [Medline: 34559819]
45. Kanchanatawan B, Tangwongchai S, Supasitthumrong T, Sriswasdi S, Maes M. Episodic memory and delayed recall are significantly more impaired in younger patients with deficit schizophrenia than in elderly patients with amnestic mild cognitive impairment. PLoS One 2018 May 15;13(5):e0197004 [FREE Full text] [doi: 10.1371/journal.pone.0197004] [Medline: 29763451]
46. Huang J, Jin W, Duan X, Liu X, Shu T, Fu L, et al. Twenty-eight-day in-hospital mortality prediction for elderly patients with ischemic stroke in the intensive care unit: interpretable machine learning models. Front Public Health 2022 Jan 12;10:1086339 [FREE Full text] [doi: 10.3389/fpubh.2022.1086339] [Medline: 36711330]
47. She H, Du Y, Du Y, Tan L, Yang S, Luo X, et al. Metabolomics and machine learning approaches for diagnostic and prognostic biomarkers screening in sepsis. BMC Anesthesiol 2023 Nov 09;23(1):367 [FREE Full text] [doi: 10.1186/s12871-023-02317-4] [Medline: 37946144]
48. Sundar R, Barr Kumarakulasinghe N, Huak Chan Y, Yoshida K, Yoshikawa T, Miyagi Y, et al. Machine-learning model derived gene signature predictive of paclitaxel survival benefit in gastric cancer: results from the randomised phase III SAMIT trial. Gut 2022 Apr 12;71(4):676-685 [FREE Full text] [doi: 10.1136/gutjnl-2021-324060] [Medline: 33980610]
49. Alaa AM, Bolton T, Di Angelantonio E, Rudd JH, van der Schaar M. Cardiovascular disease risk prediction using automated machine learning: a prospective study of 423,604 UK Biobank participants. PLoS One 2019 May 15;14(5):e0213653 [FREE Full text] [doi: 10.1371/journal.pone.0213653] [Medline: 31091238]
50. Azimi P, Mohammadi HR, Benzel EC, Shahzadi S, Azhari S. Use of artificial neural networks to decision making in patients with lumbar spinal canal stenosis. J Neurosurg Sci 2017 Dec;61(6):603-611. [doi: 10.23736/s0390-5616.16.03078-2]
51. Baxter SL, Marks C, Kuo TT, Ohno-Machado L, Weinreb RN. Machine learning-based predictive modeling of surgical intervention in glaucoma using systemic data from electronic health records. Am J Ophthalmol 2019 Dec;208:30-40 [FREE Full text] [doi: 10.1016/j.ajo.2019.07.005] [Medline: 31323204]
52. Anderson JP, Parikh JR, Shenfeld DK, Ivanov V, Marks C, Church BW, et al. Reverse engineering and evaluation of prediction models for progression to type 2 diabetes: an application of machine learning using electronic health records. J Diabetes Sci Technol 2015 Dec 20;10(1):6-18 [FREE Full text] [doi: 10.1177/1932296815620200] [Medline: 26685993]

XSL•FO
RenderX

53. Bannister CA, Halcox JP, Currie CJ, Preece A, Spasić I. A genetic programming approach to development of clinical prediction models: a case study in symptomatic cardiovascular disease. PLoS One 2018 Sep 4;13(9):e0202685 [FREE Full text] [doi: 10.1371/journal.pone.0202685] [Medline: 30180175]
54. Scheer JK, Smith JS, Schwab F, Lafage V, Shaffrey CI, Bess S, et al. Development of a preoperative predictive model for major complications following adult spinal deformity surgery. J Neurosurg Spine 2017 Jun;26(6):736-743. [doi: 10.3171/2016.10.SPINE16197] [Medline: 28338449]
55. Rau HH, Hsu CY, Lin YA, Atique S, Fuad A, Wei LM, et al. Development of a web-based liver cancer prediction model for type II diabetes patients by using an artificial neural network. Comput Methods Programs Biomed 2016 Mar;125:58-65. [doi: 10.1016/j.cmpb.2015.11.009] [Medline: 26701199]
56. Ramezankhani A, Hadavandi E, Pournik O, Shahrabi J, Azizi F, Hadaegh F. Decision tree-based modelling for identification of potential interactions between type 2 diabetes risk factors: a decade follow-up in a Middle East prospective cohort study. BMJ Open 2016 Dec 01;6(12):e013336 [FREE Full text] [doi: 10.1136/bmjopen-2016-013336] [Medline: 27909038]
57. Pei D, Zhang C, Quan Y, Guo Q. Identification of potential type II diabetes in a Chinese population with a sensitive decision tree approach. J Diabetes Res 2019 Jan 22;2019:4248218 [FREE Full text] [doi: 10.1155/2019/4248218] [Medline: 30805372]
58. Oviedo S, Contreras I, Quirós C, Giménez M, Conget I, Vehi J. Risk-based postprandial hypoglycemia forecasting using supervised learning. Int J Med Inform 2019 Jun;126:1-8. [doi: 10.1016/j.ijmedinf.2019.03.008] [Medline: 31029250]
59. Mubeen AM, Asaei A, Bachman AH, Sidtis JJ, Ardekani BA, Alzheimer's Disease Neuroimaging Initiative. A six-month longitudinal evaluation significantly improves accuracy of predicting incipient Alzheimer's disease in mild cognitive impairment. J Neuroradiol 2017 Oct;44(6):381-387. [doi: 10.1016/j.neurad.2017.05.008] [Medline: 28676345]
60. Lopez-de-Andres A, Hernandez-Barrera V, Lopez R, Martin-Junco P, Jimenez-Trujillo I, Alvaro-Meca A, et al. Predictors of in-hospital mortality following major lower extremity amputations in type 2 diabetic patients using artificial neural networks. BMC Med Res Methodol 2016 Nov 22;16(1):160 [FREE Full text] [doi: 10.1186/s12874-016-0265-5] [Medline: 27876006]
61. Kwon JM, Jeon KH, Kim HM, Kim MJ, Lim S, Kim KH, et al. Deep-learning-based out-of-hospital cardiac arrest prognostic system to predict clinical outcomes. Resuscitation 2019 Jun;139:84-91. [doi: 10.1016/j.resuscitation.2019.04.007] [Medline: 30978378]
62. Kim I, Choi HJ, Ryu JM, Lee SK, Yu JH, Kim SW, et al. A predictive model for high/low risk group according to oncotype DX recurrence score using machine learning. Eur J Surg Oncol 2019 Feb;45(2):134-140. [doi: 10.1016/j.ejso.2018.09.011] [Medline: 30348602]
63. Khanji C, Lalonde L, Bareil C, Lussier MT, Perreault S, Schnitzer ME. Lasso regression for the prediction of intermediate outcomes related to cardiovascular disease prevention using the TRANSIT quality indicators. Med Care 2019 Jan;57(1):63-72. [doi: 10.1097/MLR.0000000000001014] [Medline: 30439793]
64. Karhade AV, Ogink PT, Thio QC, Cha TD, Gormley WB, Hershman SH, et al. Development of machine learning algorithms for prediction of prolonged opioid prescription after surgery for lumbar disc herniation. Spine J 2019 Nov;19(11):1764-1771. [doi: 10.1016/j.spinee.2019.06.002] [Medline: 31185292]
65. Jovanovic P, Salkic NN, Zerem E. Artificial neural network predicts the need for therapeutic ERCP in patients with suspected choledocholithiasis. Gastrointest Endosc 2014 Aug;80(2):260-268. [doi: 10.1016/j.gie.2014.01.023] [Medline: 24593947]
66. Kang AR, Lee J, Jung W, Lee M, Park SY, Woo J, et al. Development of a prediction model for hypotension after induction of anesthesia using machine learning. PLoS One 2020 Apr 16;15(4):e0231172 [FREE Full text] [doi: 10.1371/journal.pone.0231172] [Medline: 32298292]
67. Isma'eel HA, Sakr GE, Serhan M, Lamaa N, Hakim A, Cremer PC, et al. Artificial neural network-based model enhances risk stratification and reduces non-invasive cardiac stress imaging compared to Diamond-Forrester and Morise risk assessment models: a prospective study. J Nucl Cardiol 2018 Oct;25(5):1601-1609. [doi: 10.1007/s12350-017-0823-1] [Medline: 28224450]
68. Hill NR, Ayoubkhani D, McEwan P, Sugrue DM, Farooqui U, Lister S, et al. Predicting atrial fibrillation in primary care using machine learning. PLoS One 2019 Nov 1;14(11):e0224582 [FREE Full text] [doi: 10.1371/journal.pone.0224582] [Medline: 31675367]
69. Dong Y, Xu L, Fan Y, Xiang P, Gao X, Chen Y, et al. A novel surgical predictive model for Chinese Crohn's disease patients. Medicine (Baltimore) 2019 Nov;98(46):e17510 [FREE Full text] [doi: 10.1097/MD.0000000000017510] [Medline: 31725605]
70. Bowman A, Rudolfer S, Weller P, Bland JD. A prognostic model for the patient-reported outcome of surgical treatment of carpal tunnel syndrome. Muscle Nerve 2018 Dec 15;58(6):784-789. [doi: 10.1002/mus.26297] [Medline: 29981160]
71. Bertsimas D, Dunn J, Pawlowski C, Silberholz J, Weinstein A, Zhuo YD, et al. Applied informatics decision support tool for mortality predictions in patients with cancer. JCO Clin Cancer Inform 2018 Dec;2:1-11. [doi: 10.1200/cci.18.00003]
72. Manz CR, Parikh RB, Small DS, Evans CN, Chivers C, Regli SH, et al. Effect of integrating machine learning mortality estimates with behavioral nudges to clinicians on serious illness conversations among patients with cancer: a stepped-wedge cluster randomized clinical trial. JAMA Oncol 2020 Dec 01;6(12):e204759 [FREE Full text] [doi: 10.1001/jamaoncol.2020.4759] [Medline: 33057696]

XSL•FO
RenderX

73. Tian D, Yan HJ, Huang H, Zuo YJ, Liu MZ, Zhao J, et al. Machine learning-based prognostic model for patients after lung transplantation. JAMA Netw Open 2023 May 01;6(5):e2312022 [FREE Full text] [doi: 10.1001/jamanetworkopen.2023.12022] [Medline: 37145595]
74. Li E, Manz C, Liu M, Chen J, Chivers C, Braun J, et al. Oncologist phenotypes and associations with response to a machine learning-based intervention to increase advance care planning: secondary analysis of a randomized clinical trial. PLoS One 2022 May 27;17(5):e0267012 [FREE Full text] [doi: 10.1371/journal.pone.0267012] [Medline: 35622812]
75. Tedeschi SK, Cai T, He Z, Ahuja Y, Hong C, Yates KA, et al. Classifying pseudogout using machine learning approaches with electronic health record data. Arthritis Care Res (Hoboken) 2021 Mar 25;73(3):442-448 [FREE Full text] [doi: 10.1002/acr.24132] [Medline: 31910317]
76. Ambwani G, Cohen A, Estévez M, Singh N, Adamson B, Nussbaum N, et al. PPM8 A machine learning model for cancer biomarker identification in electronic health records. Value Health 2019 May;22:S334. [doi: 10.1016/j.jval.2019.04.1631]
77. Jorge A, Castro VM, Barnado A, Gainer V, Hong C, Cai T, et al. Identifying lupus patients in electronic health records: development and validation of machine learning algorithms and application of rule-based algorithms. Semin Arthritis Rheum 2019 Aug;49(1):84-90 [FREE Full text] [doi: 10.1016/j.semarthrit.2019.01.002] [Medline: 30665626]
78. Shimabukuro DW, Barton CW, Feldman MD, Mataraso SJ, Das R. Effect of a machine learning-based severe sepsis prediction algorithm on patient survival and hospital length of stay: a randomised clinical trial. BMJ Open Respir Res 2017 Nov 09;4(1):e000234 [FREE Full text] [doi: 10.1136/bmjresp-2017-000234] [Medline: 29435343]
79. Sarraju A, Ward A, Chung S, Li J, Scheinker D, Rodríguez F. Machine learning approaches improve risk stratification for secondary cardiovascular disease prevention in multiethnic patients. Open Heart 2021 Oct 19;8(2):e001802 [FREE Full text] [doi: 10.1136/openhrt-2021-001802] [Medline: 34667093]
80. Ye B, Liu K, Cao S, Sankaridurg P, Li W, Luan M, et al. Discrimination of indoor versus outdoor environmental state with machine learning algorithms in myopia observational studies. J Transl Med 2019 Sep 18;17(1):314 [FREE Full text] [doi: 10.1186/s12967-019-2057-2] [Medline: 31533735]
81. Sun Z, Wang G, Li P, Wang H, Zhang M, Liang X. An improved random forest based on the classification accuracy and correlation measurement of decision trees. Expert Syst Appl 2024 Mar;237:121549. [doi: 10.1016/j.eswa.2023.121549]
82. Bandyopadhyay A, Albashayreh A, Zeinali N, Fan W, Gilbertson-White S. Using real-world electronic health record data to predict the development of 12 cancer-related symptoms in the context of multimorbidity. JAMIA Open 2024 Oct;7(3):ooae082. [doi: 10.1093/jamiaopen/ooae082] [Medline: 39282082]
83. Bairagade DM, Sharma K, More PR. Enhancing prediction accuracy in healthcare data using advanced DataMining techniques. J Comput Sci Eng 2024 [FREE Full text]
84. Ghosh D, Cabrera J. Enriched random forest for high dimensional genomic data. IEEE/ACM Trans Comput Biol Bioinf 2022 Sep 1;19(5):2817-2828. [doi: 10.1109/tcbb.2021.3089417]
85. Maalouf M. Logistic regression in data analysis: an overview. Int J Data Anal Tech Strateg 2011;3(3):281. [doi: 10.1504/ijdats.2011.041335]
86. Boateng EY, Abaye DA. A review of the logistic regression model with emphasis on medical research. J Data Anal Inf Process 2019 Nov;07(04):190-207. [doi: 10.4236/jdaip.2019.74012]
87. Shipe ME, Deppen SA, Farjah F, Grogan EL. Developing prediction models for clinical use using logistic regression: an overview. J Thorac Dis 2019 Mar;11(Suppl 4):S574-S584 [FREE Full text] [doi: 10.21037/jtd.2019.01.25] [Medline: 31032076]
88. Zabor EC, Reddy CA, Tendulkar RD, Patil S. Logistic regression in clinical studies. Int J Radiat Oncol Biol Phys 2022 Feb 01;112(2):271-277. [doi: 10.1016/j.ijrobp.2021.08.007] [Medline: 34416341]
89. Guido R, Ferrisi S, Lofaro D, Conforti D. An overview on the advancements of support vector machine models in healthcare applications: a review. Information 2024 Apr 19;15(4):235. [doi: 10.3390/info15040235]
90. Huang S, Cai N, Pacheco PP, Narrandes S, Wang Y, Xu W. Applications of support vector machine (SVM) learning in cancer genomics. Cancer Genomics Proteomics 2018 Jan 2;15(1):41-51 [FREE Full text] [doi: 10.21873/cgp.20063] [Medline: 29275361]
91. Pisner DA, Schnyer DM. Chapter 6 - Support vector machine. In: Mechelli A, Vieira S, editors. Machine Learning: Methods and Applications to Brain Disorders. Cambridge, MA: Academic Press; 2020.
92. Son YJ, Kim HG, Kim EH, Choi S, Lee SK. Application of support vector machine for prediction of medication adherence in heart failure patients. Healthc Inform Res 2010 Dec;16(4):253-259 [FREE Full text] [doi: 10.4258/hir.2010.16.4.253] [Medline: 21818444]
93. Manikandan G, Pragadeesh B, Manojkumar V, Karthikeyan AL, Manikandan R, Gandomi AH. Classification models combined with Boruta feature selection for heart disease prediction. Inf Med Unlock 2024;44:101442. [doi: 10.1016/j.imu.2023.101442]
94. Chen T, Guestrin C. XGBoost: a scalable tree boosting system. In: Proceedings of the 22nd ACM SIGKDD International Conference on Knowledge Discovery and Data Mining. 2016 Presented at: KDD '16; August 13-17, 2016; San Francisco, CA. [doi: 10.1145/2939672.2939785]
95. Nadkarni SB, Vijay GS, Kamath RC. Comparative study of random forest and gradient boosting algorithms to predict airfoil self-noise. Eng Proc 2023;59(1):24. [doi: 10.3390/engproc2023059024]

XSL•FO
RenderX

96. Ogunleye A, Wang QG. XGBoost model for chronic kidney disease diagnosis. IEEE/ACM Trans Comput Biol Bioinf 2020 Nov 1;17(6):2131-2140. [doi: 10.1109/tcbb.2019.2911071]
97. Chakraborty A, Tsokos CP. An AI-driven predictive model for pancreatic cancer patients using extreme gradient boosting. J Stat Theory Appl 2023 Sep 11;22(4):262-282. [doi: 10.1007/s44199-023-00063-7]
98. Zou J, Han Y, So SS. Overview of artificial neural networks. Methods Mol Biol 2008;458:15-23. [doi: 10.1007/978-1-60327-101-1_2] [Medline: 19065803]
99. Kufel J, Bargieł-Łączek K, Kocot S, Koźlik M, Bartnikowska W, Janik M, et al. What is machine learning, artificial neural networks and deep learning?-examples of practical applications in medicine. Diagnostics (Basel) 2023 Aug 03;13(15):2582 [FREE Full text] [doi: 10.3390/diagnostics13152582] [Medline: 37568945]
100. Ahmed FE. Artificial neural networks for diagnosis and survival prediction in colon cancer. Mol Cancer 2005 Aug 06;4(1):29 [FREE Full text] [doi: 10.1186/1476-4598-4-29] [Medline: 16083507]
101. Abbas S, Asif M, Rehman A, Alharbi M, Khan MA, Elmitwally N. Emerging research trends in artificial intelligence for cancer diagnostic systems: a comprehensive review. Heliyon 2024 Sep 15;10(17):e36743 [FREE Full text] [doi: 10.1016/j.heliyon.2024.e36743] [Medline: 39263113]
102. Sirocchi C, Bogliolo A, Montagna S. Medical-informed machine learning: integrating prior knowledge into medical decision systems. BMC Med Inform Decis Mak 2024 Jun 28;24(Suppl 4):186 [FREE Full text] [doi: 10.1186/s12911-024-02582-4] [Medline: 38943085]
103. Rostami M, Oussalah M. A novel explainable COVID-19 diagnosis method by integration of feature selection with random forest. Inform Med Unlocked 2022;30:100941. [doi: 10.1016/j.imu.2022.100941] [Medline: 35399333]
104. Mohsin SN, Gapizov A, Ekhator C, Ain NU, Ahmad S, Khan M, et al. The role of artificial intelligence in prediction, risk stratification, and personalized treatment planning for congenital heart diseases. Cureus 2023 Aug;15(8):e44374 [FREE Full text] [doi: 10.7759/cureus.44374] [Medline: 37664359]
105. Natekin A, Knoll A. Gradient boosting machines, a tutorial. Front Neurorobot 2013;7:21 [FREE Full text] [doi: 10.3389/fnbot.2013.00021] [Medline: 24409142]
106. Ji GW, Jiao CY, Xu ZG, Li XC, Wang K, Wang XH. Development and validation of a gradient boosting machine to predict prognosis after liver resection for intrahepatic cholangiocarcinoma. BMC Cancer 2022 Mar 11;22(1):258 [FREE Full text] [doi: 10.1186/s12885-022-09352-3] [Medline: 35277130]
107. Hossain E, Rana R, Higgins N, Soar J, Datta Barua P, Pisani AR, et al. Natural language processing in electronic health records in relation to healthcare decision-making: a systematic review. Comput Biol Med 2023 Mar;155:106649. [doi: 10.1016/j.compbiomed.2023.106649] [Medline: 36805219]
108. Rojas-Carabali W, Agrawal R, Gutierrez-Sinisterra L, Baxter SL, Cifuentes-González C, Wei YC, et al. Natural language processing in medicine and ophthalmology: a review for the 21st-century clinician. Asia Pac J Ophthalmol (Phila) 2024 Jul;13(4):100084 [FREE Full text] [doi: 10.1016/j.apjo.2024.100084] [Medline: 39059557]
109. Sheikhalishahi S, Miotto R, Dudley JT, Lavelli A, Rinaldi F, Osmani V. Natural language processing of clinical notes on chronic diseases: systematic review. JMIR Med Inform 2019 Apr 27;7(2):e12239 [FREE Full text] [doi: 10.2196/12239] [Medline: 31066697]
110. George B, Seals S, Aban I. Survival analysis and regression models. J Nucl Cardiol 2014 Aug;21(4):686-694 [FREE Full text] [doi: 10.1007/s12350-014-9908-2] [Medline: 24810431]
111. Beis G, Iliopoulos A, Papasotiriou I. An overview of introductory and advanced survival analysis methods in clinical applications: where have we come so far? Anticancer Res 2024 Feb 02;44(2):471-487. [doi: 10.21873/anticanres.16835] [Medline: 38307572]
112. Wassan S, Dongyan H, Suhail B, Jhanjhi NZ, Xiao G, Ahmed S, et al. Deep convolutional neural network and IoT technology for healthcare. Digit Health 2024 Jan 17;10:20552076231220123 [FREE Full text] [doi: 10.1177/20552076231220123] [Medline: 38250147]
113. Nazir S, Dickson DM, Akram MU. Survey of explainable artificial intelligence techniques for biomedical imaging with deep neural networks. Comput Biol Med 2023 Apr;156:106668 [FREE Full text] [doi: 10.1016/j.compbiomed.2023.106668] [Medline: 36863192]
114. Lundervold AS, Lundervold A. An overview of deep learning in medical imaging focusing on MRI. Z Med Phys 2019 May;29(2):102-127 [FREE Full text] [doi: 10.1016/j.zemedi.2018.11.002] [Medline: 30553609]
115. Genuer R, Poggi JM, Tuleau-Malot C, Villa-Vialaneix N. Random forests for big data. Big Data Res 2017 Sep;9:28-46. [doi: 10.1016/j.bdr.2017.07.003]
116. Khalilia M, Chakraborty S, Popescu M. Predicting disease risks from highly imbalanced data using random forest. BMC Med Inform Decis Mak 2011 Jul 29;11(1):51 [FREE Full text] [doi: 10.1186/1472-6947-11-51] [Medline: 21801360]
117. Kumar Y, Koul A, Singla R, Ijaz MF. Artificial intelligence in disease diagnosis: a systematic literature review, synthesizing framework and future research agenda. J Ambient Intell Humaniz Comput 2023 Jan 13;14(7):8459-8486 [FREE Full text] [doi: 10.1007/s12652-021-03612-z] [Medline: 35039756]
118. Rajkomar A, Dean J, Kohane I. Machine learning in medicine. N Engl J Med 2019 Apr 04;380(14):1347-1358. [doi: 10.1056/nejmra1814259]

XSL•FO
RenderX

119. Obermeyer Z, Powers B, Vogeli C, Mullainathan S. Dissecting racial bias in an algorithm used to manage the health of populations. Science 2019 Oct 25;366(6464):447-453 [FREE Full text] [doi: 10.1126/science.aax2342] [Medline: 31649194]
120. Miotto R, Wang F, Wang S, Jiang X, Dudley JT. Deep learning for healthcare: review, opportunities and challenges. Brief Bioinform 2018 Nov 27;19(6):1236-1246 [FREE Full text] [doi: 10.1093/bib/bbx044] [Medline: 28481991]
121. Beam AL, Kohane IS. Big data and machine learning in health care. JAMA 2018 Apr 03;319(13):1317-1318. [doi: 10.1001/jama.2017.18391] [Medline: 29532063]

Abbreviations

ANN: artificial neural network
DNN: deep neural network
DT: decision tree
EHR: electronic health record
EMA: European Medicines Agency
FDA: Food and Drug Administration
GBM: gradient boosting machine
LR: logistic regression
ML: machine learning
NLP: natural language processing
PRISMA: Preferred Reporting Items for Systematic Reviews and Meta-Analyses
RF: random forest
RWD: real-world data
RWE: real-world evidence
SVM: support vector machine
XGBoost: Extreme Gradient Boosting

Edited by A Coristine; submitted 17.11.24; peer-reviewed by A Paradise Vit, A Mavragani; comments to author 13.02.25; revised version received 27.02.25; accepted 22.04.25; published 19.06.25.

Please cite as:
Alhumaidi NH, Dermawan D, Kamaruzaman HF, Alotaiq N
The Use of Machine Learning for Analyzing Real-World Data in Disease Prediction and Management: Systematic Review
JMIR Med Inform 2025;13:e68898
URL: https://medinform.jmir.org/2025/1/e68898
doi:10.2196/68898
PMID:

©Norah Hamad Alhumaidi, Doni Dermawan, Hanin Farhana Kamaruzaman, Nasser Alotaiq. Originally published in JMIR Medical Informatics (https://medinform.jmir.org), 19.06.2025. This is an open-access article distributed under the terms of the Creative Commons Attribution License (https://creativecommons.org/licenses/by/4.0/), which permits unrestricted use, distribution, and reproduction in any medium, provided the original work, first published in JMIR Medical Informatics, is properly cited. The complete bibliographic information, a link to the original publication on https://medinform.jmir.org/, as well as this copyright and license information must be included.

XSL•FO
RenderX

Review

Current Landscape and Future Directions Regarding Generative Large Language Models in Stroke Care: Scoping Review

XingCe Zhu[1], MSc; Wei Dai[1], MSc; Richard Evans[2], PhD; Xueyu Geng[3], MMC; Aruhan Mu[4], PhD; Zhiyong Liu[1], PhD

[1]School of Medicine and Health Management, Tongji Medical College, Huazhong University of Science and Technology, Wuhan, China

[2]Faculty of Computer Science, Dalhousie University, Halifax, NS, Canada

[3]Department of Physiology and Pathophysiology, School of Basic Medical Sciences, Peking University Health Science Center, Beijing, China

[4]School of Ethnology and Sociology, Inner Mongolia University, Hohhot, China

Corresponding Author:
Zhiyong Liu, PhD
School of Medicine and Health Management
Tongji Medical College
Huazhong University of Science and Technology
No.13 Hangkong Road
Wuhan, 430030
China
Phone: 86 130 7270 6735
Email: zhiyongliu@hust.edu.cn

Abstract

Background: Stroke has a major impact on global health, causing long-term disability and straining health care resources. Generative large language models (gLLMs) have emerged as promising tools to help address these challenges, but their applications and reported performance in stroke care require comprehensive mapping and synthesis.

Objective: The aim of this scoping review was to consolidate a fragmented evidence base and examine the current landscape, shortcomings, and future directions in the design, reporting, and evaluation of gLLM-based interventions in stroke care.

Methods: In this scoping review, which adhered to the PRISMA-ScR (Preferred Reporting Items for Systematic Reviews and Meta-Analyses extension for Scoping Reviews) guidelines and the Population, Concept, and Context (PCC) framework, we searched 6 major scientific databases in December 2024 for gLLM-based interventions across the stroke care pathway, mapping their key characteristics and outcomes.

Results: A total of 25 studies met the predefined eligibility criteria and were included for analysis. Retrospective designs predominated (n=16, 64%). Key applications of gLLMs included clinical decision-making support (n=10, 40%), administrative assistance (n=9, 36%), direct patient interaction (n=5, 20%), and automated literature review (n=1, 4%). Implementations mainly used generative pretrained transformer models accessed through task-prompted chat interfaces. In total, 5 key challenges were identified from the included studies during the implementation of gLLM-based interventions: ensuring factual alignment, maintaining system robustness, enhancing interpretability, optimizing efficiency, and facilitating clinical adoption.

Conclusions: The application of gLLMs in stroke care, while promising, remains relatively new, with most interventions reflecting early-stage or relatively simple implementations. Against this backdrop, critical gaps in research and clinical translation persist. To support the development of clinically impactful and trustworthy applications, we propose an actionable framework that prioritizes real-world evidence, mandates transparent technical reporting, broadens evaluation beyond output accuracy, strengthens validation of advanced task adaptation strategies, and investigates mechanisms for safe and effective human-gLLM interaction.

(JMIR Med Inform 2025;13:e76636) doi:10.2196/76636

KEYWORDS

large language model; stroke; generative artificial intelligence; health care; artificial intelligence; AI

XSL•FO
RenderX

Introduction

Background

Stroke represents a leading cause of global morbidity and long-term disability [1], imposing a substantial burden on health care systems through its high incidence and the complex, prolonged care needs of survivors of stroke [2]. The effective management of stroke treatment and rehabilitation is limited by persistent challenges in postacute care, notably fragmented follow-up, insufficient community-based professional support, the heterogeneity of patient requirements, and frequently inadequate health literacy [3]. Despite significant progress in prevention strategies, acute treatments, and rehabilitation technologies, critical gaps persist in providing personalized, continuous, and accessible long-term support for individuals recovering from stroke [4]. These unmet needs highlight a critical opportunity for transformative technological innovation in the delivery and management of stroke care.

The analysis of clinical documentation presents an important strategic avenue for addressing stroke care challenges. Unstructured narratives within electronic health records, including clinical notes, discharge summaries, and other free-text entries, contain rich yet often underused patient information. Systematic analysis of these data can significantly support risk stratification, inform treatment planning, and improve care coordination [5]. This recognition has led to advancements in natural language processing (NLP) techniques designed to extract insights from complex clinical text. Fundamental to many clinical NLP applications are transformer-based models pretrained on extensive biomedical and general-domain corpora. Specifically, encoder-only architectures, which leverage bidirectional encoder representations from transformers and its derivatives, demonstrate proficiency in structured information extraction tasks such as named entity recognition [6] and temporal relation identification [7]. These models typically rely on domain-specific pretraining and task-specific fine-tuning. Nevertheless, they possess inherent limitations related to their generative capabilities and broader generalizability [8], with models often struggling with open-ended clinical reasoning tasks and understanding long contexts, indicating the need for architectures with enhanced generative potential.

Generative large language models (gLLMs), including decoder-only and encoder-decoder architectures (eg, the Llama [9], GPT-4 [10], and bidirectional and auto-regressive transformers [BART] [11] families), represent a significant advancement over previous NLP models. These gLLMs broaden clinical application possibilities by framing diverse tasks within a unified text generation paradigm [8,12]. Key enabling techniques include prompt-based learning, which enables task generalization without parameter updates [13], and inference-time controls (eg, decoding strategies) that modulate output characteristics, which are crucial when access to models is limited [14]. In addition, retrieval-augmented generation (RAG), often integrated with custom medical knowledge bases, enhances factual accuracy and performance for knowledge-intensive clinical applications [15,16]. Together, these advancements present important opportunities for stroke treatment and rehabilitation services [17], potentially improving efficiency through intelligent automation (eg, triage and administration); enhancing patient care through personalization and improved resource access; and accelerating research workflows, including evidence synthesis and writing. Furthermore, the introduction of multimodal functionality, as demonstrated by models such as GPT-4o [18] and the Gemini family [19], marks a pivotal shift in the development of gLLMs. By processing integrated textual, visual, and auditory inputs, these newly introduced models can augment clinical reasoning (eg, in medical image interpretation) and support more effective analysis of real-world, cross-modal patient data, better aligning digital tools with the complexities of stroke care delivery.

Objectives

While digital health technologies provide advancements for stroke care [20], the unique capabilities and rapid evolution of gLLMs require a focused investigation within this specific clinical domain. Current reviews related to digital innovations in stroke care predominantly examine technologies that predate modern gLLMs, such as mobile health platforms [21,22], early conversational agents [23], and conventional machine learning or deep learning frameworks [24-26]. Moreover, although the current literature has reviewed the general clinical utility of gLLMs [17,27-29], there remains a critical gap in systematically reviewing evidence specifically on gLLM-driven interventions applied across the stroke care pathway. To address this critical research gap, this scoping review aimed to map the current landscape of gLLM applications throughout the common stages of the stroke care pathway. Specifically, it identified their uses, implementation characteristics, and reported outcomes and outlined future research directions. The central research question guiding this review was as follows: how, for what purposes, and with what reported outcomes have gLLMs been applied in stroke care? This review used the recommended guide of the Population, Concept, and Context (PCC) framework [30], which is guided by the following subquestions:

1. What study designs are used to evaluate gLLM-driven interventions in stroke care, and what are the key characteristics of the stroke populations involved? (Population or participants)
2. What target tasks, implementation details (ie, tasks, dialogue pattern, input data, and time stamps), evaluation approaches, and outcomes are reported for gLLM-driven interventions in stroke care? (Concept)
3. What cultural settings, specific stroke care stages (ie, prevention, diagnosis, treatment, prognosis, and rehabilitation), and technology adaptation strategies are described in the evaluation of gLLM-driven interventions? (Context)
4. What challenges are reported in implementing gLLMs in stroke care, and what specific directions for future research have been proposed? (Implementation challenges and research directions)

XSL•FO
RenderX

Methods

Study Guidelines and Registration

This review aimed to capture the available knowledge concerning the intersection of stroke care and gLLM technologies. Given the observed heterogeneity and breadth of research in this field, a scoping review methodology was used to summarize the current landscape and challenges associated with gLLM-driven intervention use across the stroke care pathway (ie, prediction, diagnosis, treatment, prognosis, and rehabilitation). The main objective was to address 3 key research questions predefined according to the PCC framework and identify knowledge gaps within this interdisciplinary area. This review was conducted and reported following the PRISMA-ScR (Preferred Reporting Items for Systematic Reviews and Meta-Analyses extension for Scoping Reviews) guidelines [31] (Multimedia Appendix 1) and adhered to the methodological framework of Arksey and O'Malley [32] for scoping reviews. The review protocol was preregistered on the Open Science Framework [33].

Search Strategy

A broad search strategy was considered necessary to capture relevant citations in this relatively novel and rapidly evolving field. The terminology associated with gLLMs currently lacks consensus, requiring the use of diverse search terms. Key terms included in the search were "pretrained language model," "large language model," "natural language processing," and "generative artificial intelligence." Moreover, recognizing the important role of the generative pretrained transformer (GPT) model family in gLLM development, related terms were also incorporated into the search strategy. In addition, given the potential integration of gLLMs within conversational agents, relevant search terms for the latter were included to maximize retrieval breadth.

The search targeted peer-reviewed, full-text original research articles and was executed across 6 major scientific databases: Ovid Embase, PubMed, Scopus, CINAHL Plus with Full Text, Web of Science Core Collection, and IEEE Xplore. All database searches were completed in December 2024, with the last search performed on December 24, 2024. Search strategies were individually tailored to the syntax and indexing of each database. The complete search strategies for all databases are detailed in Multimedia Appendix 2. No restrictions regarding publication date, language, or study type were applied during the initial search phase. Potential selection bias arising from the absence of a standardized technical taxonomy or consensus definition for gLLMs was acknowledged as a limitation in this review. To mitigate this risk, snowballing techniques [34] were systematically used following the initial search. This involved both forward snowballing (ie, examining articles citing the included studies) and backward snowballing (ie, reviewing the reference lists of the included studies). However, this process did not identify any additional studies meeting this review's inclusion criteria.

Inclusion and Exclusion Criteria

To be eligible for this review, studies had to assess a gLLM-driven intervention relevant to advancing understanding or practice in stroke prediction, diagnosis, treatment, prognosis, or rehabilitation and report at least one metric or qualitative perspective related to the performance evaluation of the specified gLLM intervention. Studies were excluded if they met one or more of the following conditions: they (1) were animal trials or focused exclusively on animal models; (2) did not report any performance outcomes or evaluation pertinent to the gLLM intervention described; (3) were unrelated to the field of stroke care or its advancement; (4) focused exclusively on managing stroke risk factors (eg, diabetes mellitus, hypertension, or atrial fibrillation) without directly addressing stroke management, outcomes, or care processes; (5) had a full text that could not be accessed or obtained; or (6) did not represent original research (ie, were reflection articles, opinion pieces, editorials, letters, conference abstracts without full results, or study protocols).

Study Selection and Data Extraction

Following the literature search, all retrieved records were imported into Zotero Reference Manager (version 7.0.15; Corporation for Digital Scholarship) by one author (XZ), where duplicates were identified and removed. Independent screening of titles, abstracts, keywords, and publication types was then conducted by 2 authors (XZ and WD) to identify potentially eligible studies based on the predefined inclusion criteria. The same 2 authors subsequently reviewed the full texts of these potentially eligible studies to confirm final inclusion and conduct data extraction (Multimedia Appendix 3). Any disagreements regarding study inclusion during either screening phase were resolved through discussion involving a third reviewer (ZL) until consensus was reached. Any unresolved issues encountered during feature extraction were documented as free-text notes; clarification was sought from the original study authors via email correspondence when necessary and feasible. All reviewers possessed relevant expertise in clinical medicine or medical informatics. Data extraction and synthesis activities were conducted in Microsoft Excel (Microsoft Office Long Term Service Channel 2021). Formal interrater agreement metrics were not calculated for the screening or extraction phases. This decision was made because the primary focus of this scoping review was the synthesis of descriptive characteristics, where minor formatting or phrasing differences between reviewers could lead to low numerical agreement despite substantive consensus on the content.

Guided by the PCC framework [35] and its predefined questions, the descriptive characteristics of the included studies were organized into structured tables. To confirm the methodological landscape and current evidence base at this emerging intersection of stroke care and gLLMs, this review commenced with a summary of study features, including publication year distribution and study design types. Then, consistent with the PCC framework, the analysis focused sequentially on (1) population (ie, characteristics relevant to intervention design and implementation, such as sample size, sex and age distributions, stroke phenotypes, and reported comorbidities);

XSL•FO
RenderX

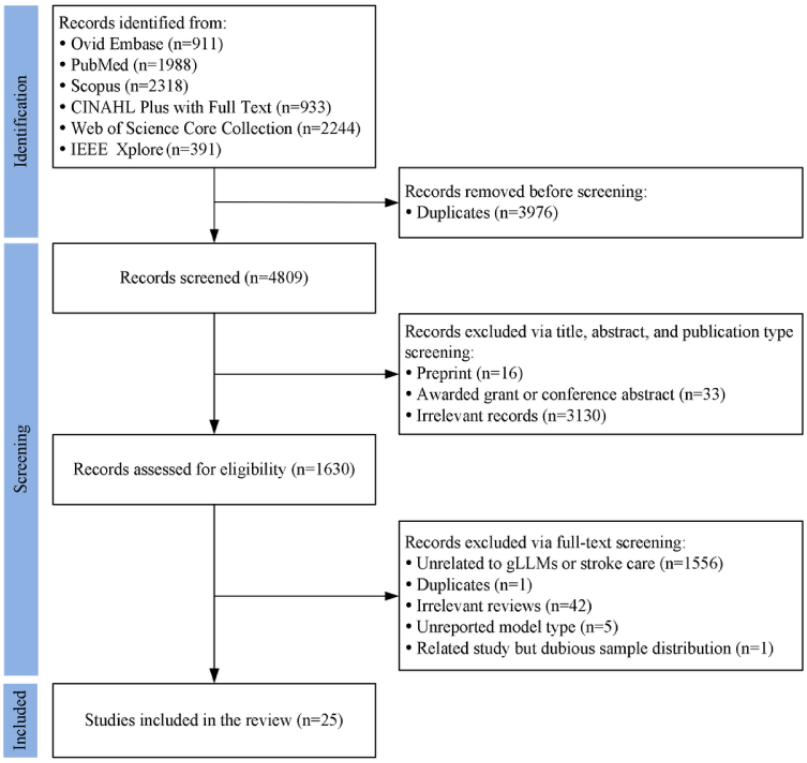
(2) concept (ie, key components describing the processes and outcomes of the gLLM-driven interventions, including the main use categories and specific tasks assigned to gLLMs; input data types used; dialogue patterns and time stamps recorded [where available]; and performance evaluation approaches based on reference standards, evaluative perspectives, and reported metrics); and (3) context, examining the broader cultural, care setting, and technical contexts surrounding the gLLM-driven interventions, including national and sociolinguistic backgrounds, the specific stage within the stroke care pathway addressed, models used, modes of gLLM access used, instruction design strategies, and other technical adaptations. Finally, key implementation challenges associated with applying gLLMs across the stroke care pathway were identified based on reported results and author discussions within the context of the included studies.

Results

Overview

The literature search identified 8785 records across all databases. Of these 8785 records, after the removal of 3976 (45.26%) duplicates, 4809 (54.74%) titles and abstracts were screened for eligibility. This initial screening led to the exclusion of 65.09% (3130/4809) of the records based on relevance and an additional 1.02% (49/4809) due to inappropriate publication types (eg, preprints, awarded grants, and conference abstracts). Consequently, 33.89% (1630/4809) of the articles underwent full-text assessment. During this stage, of the 1630 studies, 1605 (98.47%) were excluded for various reasons, including irrelevance to the application of gLLMs or stroke care context (n=1556, 96.95%), being review articles not meeting the inclusion criteria (n=42, 2.62%), insufficient evidence of gLLM use (n=5, 0.31%), being a duplicate publication identified across different formats (n=1, 0.06%), and unresolved concerns regarding stroke sample composition after author consultation (n=1, 0.06%). Ultimately, 25 studies met the inclusion criteria and were included in this scoping review. Figure 1 presents the detailed PRISMA-ScR flowchart illustrating this study selection process.

Figure 1. Flow diagram of the study selection process based on the PRISMA-ScR guidelines. gLLM: generative large language model.



General Characteristics

Table 1 summarizes the general characteristics of the 25 reviewed articles. A key characteristic was the recent publication time frame, with all included studies published in 2023 or 2024, reflecting the emerging nature of this research domain. With regard to the methodologies used, most studies (16/25, 64%) used retrospective designs analyzing existing data. A few studies (4/25, 16%) adopted prospective designs, typically involving the recruitment of healthy participants or the collection of original data from patients with stroke. There were also some observational studies (4/25, 16%), including one that used gLLMs for literature discovery during systematic review development [36], as well as a single comparative case study [37]. It should be noted that this review identified no randomized controlled trials assessing the clinical efficacy or impact of gLLM-driven interventions in populations of patients with stroke.

XSL•FO
RenderX

Table 1. Overview of study designs and stroke populations.

Study	Year	Study design	Sample size	Sex (male; %)	Age (y)	Stroke phenotype	Comorbidities	Function scoring tool
Pedro et al [38]	2025	Retrospective; pilot	163	39.3	Mean 74 (SD 18)	IS[a]	AF[b], HF[c], HTN[d], DM[e], DLP[f], CAD[g], and AC[h]	NIHSS[i]: 14.0 (9.0); ASPECTS[j]: 9.0 (2.0); mRS[k,l]
Chen et al [39]	2024	Retrospective	124 (22 simulated)	NR[m]	Median 66 (IQR NR)[n]	IS and HS[o]	HTN, HF, and ESRD[p]	NIHSS: median 12 (IQR NR)[n]; mRS: median 1 (IQR NR)[n]
Strotzer et al [40]	2024	Retrospective	Uncertain[q]	NR	NR	IS and HS	NR	NR
Kuzan et al [41]	2025	Retrospective	Uncertain[r]	NR	NR	IS	NR	NR
Fei et al [42]	2024	Prospective; cross-sectional	30[s]	60	68.03 (3.74)	Unclarified type	NR	NR
Lee et al [43]	2024	Retrospective	46	63.1	56.7 (13.9)	IS and HS	HTN, DM, DLP, AF, CAD, and other[t]	NIHSS, mRS, MRC[u] Scale for Muscle Strength, GCS[v], K-MMSE[w], FAB[x], and other[t]
Haim et al [44]	2024	Retrospective	30	NR	NR	Unclarified type	NR	NR
Chen et al [45]	2023	Experimental	20 simulated	50	65.3 (11.0)	HS	NR	GCS: 12.5 (5); ICH[y] score: 2 (2); H&H[z]: 2.5 (2)
Blacker et al [46]	2024	Observational	2 simulated	50	70.5 (4.5)	IS	AF and AC	NR
Zhang et al [37]	2023	Observational; comparative case	1 textbook case	100	62 (—[aa])	IS	DM and HTN	SIAS[ab,ac]
Sivarajkumar et al [47]	2024	Retrospective	13,605[ad]	49	75 (16)	Unclarified type	NR	NR
Guo et al [48]	2023	Retrospective	Uncertain[ae]	—	—	IS and HS	NR	NR
Lehnen et al [49]	2024	Retrospective	130 (derivation: 100; external validation: 30)	50	74.2 (13.2)	IS	NR	NIHSS: median 8 (IQR 0-24); ASPECTS: median 9 (IQR 3-10)[af]
Fiedler et al [50]	2024	Retrospective; pilot	50	62	Median 4.5 (IQR 0.75-11)	CAIS[ag], PAIS[ah], and CVST[ai]	NR	PSOM[aj]: median 0.75 (IQR 0-1.5)
Wang et al [51]	2024	Retrospective	382	54.45	72.23 (13.35)	IS	NR	NR
Goh et al [52]	2024	Retrospective	16	37.5	76.1 (11.4)	IS	AF, DM, and HTN	NR
Baro et al [53]	2025	Retrospective	Uncertain[ak]	NR	NR	Unclarified type	NR	NR
Meddeb et al [54]	2025	Retrospective	Uncertain[al]	NR	NR	IS	NR	NR
Kim et al [55]	2025	Retrospective	36,922	58.8	68.17 (12.86)	IS	HTN, AF, DM, DLP, CAD, AC, PAD[am], and HF	NIHSS: 2 (5); mRS: 2 (3)

XSL•FO
RenderX

Study	Year	Study design	Sample size	Sex (male; %)	Age (y)	Stroke phenotype	Comorbidities	Function scoring tool
Argymbay et al [56]	2024	Retrospective	4798	65.1	47.1 (23.7)	IS	HTN, DM, DLP, and obesity	NIHSS: 18.1 (11.3); mRS: 3.7 (1.9)
Neo et al [57]	2024	Prospective; mixed methods	50	NR	NR	Unclarified type	NR	NR
Wu et al [58]	2023	Observational	__[an]	—	—	—	—	—
Chen et al [59]	2025	Prospective; experimental	1[ao]	NR	NR	Unclarified type	NR	NR
Rifai et al [60]	2024	Prospective; experimental	Uncertain[ap]	NR	NR	Unclarified type	NR	NR

XSL•FO
RenderX

Study	Year	Study design	Sample size	Sex (male; %)	Age (y)	Stroke phenotype	Comorbidities	Function scoring tool
Angeles-cu et al [36]	2023	Observational	__aq	—	—	—	—	—

[a]IS: ischemic stroke.

[b]AF: atrial fibrillation.

[c]HF: heart failure.

[d]HTN: hypertension.

[e]DM: diabetes mellitus.

[f]DLP: dyslipidemia.

[g]CAD: coronary artery disease.

[h]AC: active cancer.

[i]NIHSS: National Institutes of Health Stroke Scale.

[j]ASPECTS: Alberta Stroke Program Early Computed Tomography Score.

[k]mRS: modified Rankin Scale.

[l]A total of 121 patients had an mRS score of 0 or 1, and 42 had a score of 2 or 3.

[m]NR: not reported.

[n]Description of real patients (n=102).

[o]HS: hemorrhagic stroke.

[p]ESRD: end-stage renal disease.

[q]A total of 100 magnetic resonance and computed tomography images were included, comprising 50 with lesions (25 ischemic stroke, 25 brain hemorrhage) and 50 normal controls (25 matched to each lesion group).

[r]A total of 266 radiological images from patients with acute stroke were included.

[s]A total of 90 participants were included, comprising 30 patients with stroke and 60 healthy controls.

[t]Published case report heterogeneity led to reporting barriers.

[u]MRC: Medical Research Council.

[v]GCS: Glasgow Coma Scale.

[w]K-MMSE: Korean version of the Mini-Mental State Examination.

[x]FAB: Frontal Assessment Battery.

[y]ICH: intracranial hemorrhage.

[z]H&H: Hunt and Hess scale.

[aa]Not applicable.

[ab]SIAS: Stroke Impairment Assessment Set.

[ac]A multicriteria assessment set included quantitative scores and qualitative descriptions.

[ad]In total, 50 annotated electronic health record sections were extracted from the records of 13,605 patients with stroke.

[ae]Parts from triplets, subrelations, and unlabeled text from 3 Chinese stroke-related medical datasets were included.

[af]Description of derivation (n=100).

[ag]CAIS: childhood arterial ischemic stroke.

[ah]PAIS: perinatal arterial ischemic stroke.

[ai]CVST: cerebral venous sinus thrombosis.

[aj]PSOM: Pediatric Stroke Outcome Measure.

[ak]At least 4038 stroke-related hospitalizations of insured beneficiaries were included in the study.

[al]A total of 1050 mechanical thrombectomy reports from patients with acute ischemic stroke were included.

[am]PAD: peripheral arterial disease.

[an]Two questions from the American Stroke Association website were included.

[ao]Three healthy participants were also involved in the test of the generative large language model–based hand exoskeleton controls.

[ap]Did not report whether the 12 participants were patients with stroke.

[aq]Six questions on evidence synthesis during systematic reviews were included.

Distribution of Included Stroke Populations

The first question of this review related to the *population* component of the PCC framework and asked for key characteristics of the stroke populations involved in the gLLM-driven interventions. Specifically, the review examined the characteristics of the stroke populations involved in the included studies. The analysis included sample size, sex distribution, age range, stroke phenotypes, key comorbidities, and reported functional scores as these elements can influence

XSL•FO
RenderX

intervention design and applicability. Notably, 8% (2/25) of the studies did not use patient data (real or simulated); instead, they evaluated the gLLMs using predefined question sets related to stroke care [36,57]. Among the remaining 92% (23/25) of the studies, the level of detail provided for population characteristics varied. A summary of these characteristics, including clarifications obtained via author correspondence, is presented in Table 1.

Reporting of specific population characteristics varied across the 25 studies (see Table 1 for further details). Sample sizes of involved patients were specified in most articles (17/25, 68%), demonstrating considerable range from a single case to 36,922 patients. Data on gender were available in 52% (13/25) of the studies, which indicated that male individuals comprised 56.9% of the aggregate reported sample. A total of 56% (14/25) of the studies provided age metrics (mean or median), which spanned 4.5 years (in a pediatric study) to 76.1 years. Stroke phenotype details were available in 64% (16/25) of the studies, and ischemic stroke (15/25, 60%) was found to be more commonly studied than hemorrhagic stroke (5/25, 20%). Notably, 4% (1/25) of the studies focused exclusively on pediatric patients with stroke. In total, 32% (8/25) of the studies provided information on patient comorbidities, often identified through the main text, appendices, or associated datasets. Commonly reported conditions included hypertension, diabetes mellitus, atrial fibrillation, dyslipidemia, coronary artery disease, heart failure, and active cancer. Furthermore, 36% (9/25) of the studies documented baseline severity or functional outcomes using clinical assessment tools. The most frequently used scales were the National Institutes of Health Stroke Scale and the modified Rankin Scale [38,39,43,55,56]. Other reported instruments included the Glasgow Coma Scale [43,45], Pediatric Stroke Outcome Measure [50], Stroke Impairment Assessment Set [37], intracranial hemorrhage score [45], Hunt and Hess scale [45], Medical Research Council Scale for Muscle Strength [43], Korean version of the Mini-Mental State Examination [43], and Frontal Assessment Battery [43].

Conceptual Considerations for Implementing and Evaluating gLLM-Driven Interventions in Stroke Care

In response to the second subquestion related to the *concept* component of the PCC framework, this review analyzed the target tasks, implementation details (including models, prompts, and data inputs), evaluation strategies, and reported outcomes for gLLM applications in stroke care. In total, 4 key categories of gLLM use were identified, as summarized in Table 2. The main categories focused on supporting health care professionals either through clinical decision-making assistance (10/25, 40%) or administrative workflow automation (9/25, 36%). Other identified applications included direct patient support through interactive online platforms (5/25, 20%) and enabling the discovery of evidence during systematic reviews (1/25, 4%). With regard to the implementation of gLLMs, evaluations mostly involved single-turn dialogues conducted under controlled settings (15/25, 60%), whereas the reporting of intervention time stamps was limited (5/25, 20%). Despite considerable heterogeneity across studies in terms of task objectives, input data sources, evaluation benchmarks, and assessment metrics, common themes and approaches were found within each application category.

XSL•FO
RenderX

Table 2. Summary of the implementation and evaluation of generative large language model–driven interventions in stroke care.

Study	Task objectives	Input data or sources	Dialogue patterns	Reported time stamp	Gold-standard providers or benchmarks	Evaluation perspectives	Evaluation metrics
Clinical decision-making support (n=10)							
Pedro et al [38]	Predict the mRS[a] score at 3 mo after mechanical thrombectomy	Patient H&P[b], neuroimaging, and mechanical thrombectomy procedure notes	Single turn	Yes	Stroke unit clinicians	AGS[c] for true exact and dichotomized mRS scores; bias; comparison with MT-DRAGON	Cohen κ; mean difference and 95% limits of agreement; ND[d]
Chen et al [39]	Make clinical decisions for mechanical thrombectomy	Patient H&P and neuroimaging notes	Single turn	No	Neurology specialists	AGS for mechanical thrombectomy decision; different error analysis	Counts and rate
Strotzer et al [40]	Interpret MRI[e] and CT[f] images and generate free-text reports in stroke cases	MRI and CT images	Single turn	Yes	Radiologists and nonradiologist in training	AGS for free-report items; interrun consistency; AGS for binary pathological findings; impact on nonradiologist	Agreement rate; interrun consistency rate and the Randolph free-marginal κ; accuracy, sensitivity, and specificity; rate (distribution across categories)
Kuzan et al [41]	Interpret DWI[g] and ADC[h] maps in acute stroke cases	DWI and ADC maps	Multiturn	No	Radiologists	AGS for stroke and normal or all-image interpretation	Rate; TP[i], TN[j], FP[k], FN[l], sensitivity, specificity, PPV[m], NPV[n], and accuracy
Fei et al [42]	Evaluate cognitive performance in stroke cases	Patient responses to selected RBMT-II[o], MMSE[p], and MoCA[q] items	Multiturn	No	Rehabilitation physicians	Intermodel and model-physician agreement	Intraclass correlation coefficient and *P* value
Lee et al [43]	Locate lesions based on patient H&P	Patient H&P notes	Single turn	Yes	Location description from original published case report	AGS for trial- and case-based lesion localization; different error analysis	Specificity, sensitivity, precision, and F_1-score; ND
Haim et al [44]	Calculate the NIHSS[r] score and predict the use of tissue plasminogen activator	EMR[s] periods	Single turn	No	Emergency department physicians	Intermodel and model-physician agreement; predictive validity	Cohen κ and *P* value; AUC-ROC[t]
Chen et al [45]	Calculate GCS[u], H&H[v], and ICH[w] scores	Patient neuroexamination notes without scores	Single turn	No	Scores in original neuroexamination notes	AGS for scoring; repeatability; effect of varied case complexity and prompting design	Average error rate and average error magnitude
Blacker et al [46]	Use of SNACC[x] HQRs[y] to answer questions on perioperative stroke and endovascular treatment anesthesia	Patient H&P notes	Multiturn	Yes	Anesthesiologists	HQR identification; correct reference citation; potentially harmful information	ND

XSL•FO
RenderX

Study	Task objectives	Input data or sources	Dialogue patterns	Reported time stamp	Gold-standard providers or benchmarks	Evaluation perspectives	Evaluation metrics
Zhang et al [37]	Generate rehabilitation prescriptions and ICF[z] codes in a stroke case	Patient H&P notes	Multiturn	No	Physical medicine and rehabilitation physicians	Content exhaustiveness and clinical applicability; inference logic	ND
Administrative assistance (n=9)							
Sivarajkumar et al [47]	Extract and categorize physical rehabilitation exercise information from stroke cases	EHR[aa] sections with physical therapy information	Single turn	No	Physical therapy experts	AGS for extracted items	Accuracy, precision, recall, and F_1-score
Guo et al [48]	Extract triples by fine-tuning and integrating a relation classification module	Stroke-related medical text from SEM-RC[ab], CVDEM-RC[ac], and CMeIE[ad]	—[ae]	No	Relevant items from datasets and performance of the CasCLN[af] benchmark models	AGS for total and overlapping triple extraction; performance improvements over baseline models	F_1-score; rate
Lehnen et al [49]	Extract key information for mechanical thrombectomy	Mechanical thrombectomy records	Single turn	No	Interventional neuroradiologists	AGS for extracted items; different error analysis; intermodel extraction performance comparison	Correct rate and Cohen κ; count and rate; correct rate and *P* value
Fiedler et al [50]	Extract IPSS[ag] format information and infer disease severity	Outpatient notes	Multiturn	No	Clinical investigators	AGS for extracted items	Rate
Wang et al [51]	Extract and infer key information for mechanical thrombectomy surgery	Mechanical thrombectomy records	Single turn and multiturn for correct format response	No	Interventional and junior neuroradiologists	AGS for extracted and inferred items; agreement with junior neuroradiologists; processing efficiency	Accuracy, sensitivity, specificity, AUC[ah], and mean squared error; *P* value; average case processing time
Goh et al [52]	Extract stroke audit data	Discharge summaries	Single turn	No	Relevant items from original discharge summaries	AGS for extracted items; model-clinician comparison in AGS; inference error analysis	Counts and rate; ND
Baro et al [53]	Predict stroke hospitalization by fine-tuning and integrating classification layers	Chronological health insurance data with aggregated medical events	—	No	Relevant items from original health insurance data	AGS across time windows using the general fine-tuned models; AGS comparison between general and stroke-specific fine-tuned models	F_1-score, sensitivity, specificity, and AUC
Meddeb et al [54]	Extract key information for mechanical thrombectomy items	Mechanical thrombectomy records	Single turn	No	Radiologists and clinical medical students	AGS for extracted items; efficiency improvement with EITL[ai]	Precision, recall, and F_1-score; average case time savings
Kim et al [55]	Perform data wrangling on a large dataset of patients with stroke	Metadata from the CRCS-K[aj] dataset and neurologist queries	Multiturn	No	Neurologists	Reliability and efficiency of EITL workflow and clinical knowledge alignment	ND
Direct patient interaction (n=5)							

XSL•FO
RenderX

Study	Task objectives	Input data or sources	Dialogue patterns	Reported time stamp	Gold-standard providers or benchmarks	Evaluation perspectives	Evaluation metrics
Argymbay et al [56]	Provide personalized stroke risk insights and answer medical queries based on patient data	Stroke risk values, medical literature, and patient queries	Multiturn	No	Clinicians	Stroke risk factor review, personalized health recommendation provision, and anxiety alleviation	ND
Neo et al [57]	Answer rehabilitation questions for patients with stroke and their caregivers	280 unique questions	Single turn	Yes	Clinicians	Content correctness, safety, relevance, and readability; interrater agreement; free comments for responses	3-point Likert scale; Fleiss κ and Cohen κ; ND
Wu et al [58]	Provide nonmedical professionals with stroke-related health information	2 questions about stroke prevention from the ASA[ak] website	Single turn	No	Answers available on the ASA website	Readability compared with the Google Assistant; content relevance	Word counts, GFS[al], SMOG[am] index, DCS[an], FKRT[ao], and *P* value; keyword matching counts
Chen et al [59]	Interpret commands and generate Python code for hand exoskeleton control	Recognized user voice commands	Single turn	No	Rehabilitation physicians	Executability and efficiency of tasks among models; response process in free scenarios	Success rate across trials and time; ND
Rifai et al [60]	Interpret commands and generate target coordinates for upper-limb robot control	Recognized user voice commands	Single turn	No	Predefined targets	Executability of path to targets compared with joystick control; intuitive handling; success and stable control	ND; user experience questionnaire; success rate across trials and ND
Automated literature review (n=1)							

XSL•FO
RenderX

Study	Task objectives	Input data or sources	Dialogue patterns	Reported time stamp	Gold-standard providers or benchmarks	Evaluation perspectives	Evaluation metrics
Anghelescu et al [36]	Assist in obtaining evidence on Actovegin's efficacy for ischemic stroke	6 queries on medicine, review conduction, literature exploration, and evidence synthesis	Multiturn	No	Review contributors	General and in-depth answer correctness; citation applicability; PRISMA[ap]-based evidence synthesis results	ND

[a]mRS: modified Rankin Scale.
[b]H&P: history and neurological physical examination.
[c]AGS: agreement with the gold standard.
[d]ND: narrative description.
[e]MRI: magnetic resonance imaging.
[f]CT: computed tomography.
[g]DWI: diffusion-weighted imaging.
[h]ADC: apparent diffusion coefficient.
[i]TP: true positive.
[j]TN: true negative.
[k]FP: false positive.
[l]FN: false negative.
[m]PPV: positive predictive value.
[n]NPV: negative predictive value.
[o]RBMT-II: Rivermead Behavioral Memory Test–II.
[p]MMSE: Mini-Mental State Examination.
[q]MoCA: Montreal Cognitive Assessment.
[r]NIHSS: National Institutes of Health Stroke Scale.
[s]EMR: electronic medical record.
[t]AUC-ROC: area under the receiver operating characteristic curve.
[u]GCS: Glasgow Coma Scale.
[v]H&H: Hunt and Hess scale.
[w]ICH: intracranial hemorrhage.
[x]SNACC: Society for Neuroscience in Anesthesiology and Critical Care.
[y]HQR: high-quality recommendation.
[z]ICF: International Classification of Functioning, Disability, and Health.
[aa]EHR: electronic health record.
[ab]SEMRC, stroke EMR entity and entity-related corpus.
[ac]CVDEMRC: cardiovascular EMR entity and entity relationship–labeling corpus.
[ad]CMeIE: Chinese Medical Information Extraction dataset.
[ae]Not applicable.
[af]Cas-CLN: cascade binary pointer tagging network with conditional layer normalization.
[ag]IPSS: International Pediatric Stroke Study.
[ah]AUC: area under the curve.
[ai]EITL: expert in the loop.
[aj]CRCS-K: Clinical Research Collaboration for Stroke in Korea.
[ak]ASA: American Stroke Association.
[al]GFS: Gunning fog score.
[am]SMOG: Simple Measure of Gobbledygook.
[an]DCS: Dale-Chall score.
[ao]FKRT: Flesch-Kincaid readability test.
[ap]PRISMA: Preferred Reporting Items for Systematic Reviews and Meta-Analyses.

gLLM-driven systems categorized as clinical decision-making support were mainly used to analyze clinical documentation to inform medical diagnosis, treatment planning, prognosis estimation, or rehabilitation strategies in stroke care. While textual inputs such as the medical history of patients, neurological examination results, and neuroimaging reports were common, only 8% (2/25) of the studies analyzed computed tomography or magnetic resonance imaging scans directly as

XSL•FO
RenderX

primary input [40,41]. Such gLLM-driven systems were applied across the stroke care pathway, assisting with neurological function scoring during triage (eg, the National Institutes of Health Stroke Scale [44], Glasgow Coma Scale, Hunt & Hess scale, and intracranial hemorrhage score [45]) and supporting diagnosis through direct image interpretation [40,41] or lesion mapping from textual descriptions [43]. In addition, they were used to inform acute intervention decisions, including eligibility for thrombectomy [39] or thrombolysis [44] and anesthesia planning [46]. Moreover, they facilitated rehabilitation through outcome prediction (eg, 3-month modified Rankin Scale [38]), cognitive assessment [42], or generation of personalized rehabilitation plans [37]. Performance evaluation mainly involved clinician assessment or comparison against predefined benchmarks derived from the original clinical records. Additional validation methods often included cross-comparison against the outputs of clinicians or functionally similar tools using identical inputs [38,39,42,44], as well as repeatability checks across multiple models [40,43,45]. Some studies (5/25, 20%) investigated human-computer interaction factors, examining aspects such as the impact on junior clinicians [40] or examining the reasoning processes behind model-generated conclusions [37,39,43,46]. Across these varied approaches, quantitative metrics (eg, accuracy, rate, F_1-score, k value, and P value), particularly those assessing factual accuracy and output consistency, were the primary focus of most evaluations.

gLLM-driven systems categorized as administrative support predominantly focused on alleviating clinician documentation workload and improving the management and use of clinical information. The primary functions involved extracting structured information from clinical text and generating summaries or other abstract representations to facilitate downstream use by other health care workers. These tasks used a variety of clinical data sources, including electronic health records [47], electronic medical records [48], specialized procedural records (eg, thrombectomy reports) [49,51,54], discharge summaries [52], outpatient notes [50], health insurance claim data [53], and stroke registries [55]. Evaluation methods for these administrative tasks were similar to those used for decision support tools. Most often, the alignment of gLLM outputs with gold-standard annotations was measured [47-55], or performance was compared against that of human experts or other specialized systems that were used to analyze identical data [48,49,51-53]. Quantitative metrics were used most frequently during performance assessments [47-54]. Beyond accuracy and alignment, a few studies (3/25, 12%) explicitly evaluated efficiency. For example, 4% (1/25) of the studies reported the average time required for automated data extraction from thrombectomy operative notes [51], whereas another 8% (2/25) demonstrated significant time reductions using expert-in-the-loop (EITL) workflows involving gLLMs for extracting procedural details [54] and processing large-scale registry data [55].

gLLM-driven systems involving direct patient interaction were developed primarily to support personalized out-of-hospital stroke care, reduce patient uncertainty regarding medical information, and promote adherence to preventive and rehabilitative behaviors. The main tasks performed by gLLMs in this regard included (1) answering general stroke-related queries using embedded knowledge [57,58], (2) generating individualized preventive guidance by interpreting patient profiles with relevant literature [56], and (3) translating natural language commands to control upper-limb exoskeleton robots during rehabilitation [59,60]. Consequently, study designs focused on addressing patient needs, either through simulating responses to public-facing queries [57,58] or by developing systems intended specifically for lay users [56,59,60]. Assessment strategies for these systems considered both technical output performance (eg, factual alignment [56-60] and comparative analyses against alternative methods [59,60]) and key patient-centered outcomes. The latter included metrics such as readability [57,58], safety [57], personalized support [57,58], potential for anxiety reduction [56], and overall user experience [60]. As a result, the open-ended and dialogue-driven nature of these systems required diverse evaluation methodologies. These ranged from clinician-led narrative assessments or reviews [56,57,59,60] and independent scoring protocols [57] to user feedback questionnaires [60] and standard quantitative metrics computed by the research teams [58-60].

Only 4% (1/25) of the included studies [36] investigated the application of gLLM systems to support literature review tasks. This study involved asking 6 questions to the gLLM, ranging from general medical knowledge and systematic review methodology inquiries to specific queries about evidence synthesis concerning Actovegin's efficacy for ischemic stroke. A qualitative evaluation of the gLLM-generated answers assessed their correctness and applicability for the review context. The study concluded that all responses generated by the gLLM were unreliable, resulting in their exclusion from the final systematic review conducted by the research team. Table 2 provides a summary of the target tasks, implementation characteristics, and evaluation approaches reported across the included studies.

Contextual Focus on gLLM-Driven Intervention Design in Stroke Care

In response to the third subquestion and the *context* component of the PCC framework, this review examined the settings surrounding the design and implementation of the evaluated gLLM interventions, with further information presented in Table 3. This review considered 3 primary contextual dimensions: cultural, care, and technical settings. Cultural context referred to the study location (country) and relevant national and sociolinguistic backgrounds of the participants (eg, health care professionals, patients, and caregivers). The care dimension referred to the specific phase of the stroke care pathway (ie, prevention, diagnosis, treatment, prognosis, or rehabilitation) targeted by the intervention and associated data sources. The technical dimension involved the diverse adaptation choices evident in intervention development, including approaches used in instruction design (prompt engineering), inference-time parameter configurations, and underlying model-level adaptations.

XSL•FO
RenderX

Table 3. Summary of generalized large language model–driven intervention design in stroke care.

Study	Country	Stage in the stroke care continuum	Foundation model or model series	Access	Instruction design	Other adaptation strategies
Pedro et al [38]	Portugal	Prognosis	GPT-3.5	Web-based chat interface (ChatGPT)	Zero shot	None
Chen et al [39]	United States	Treatment	GPT-4	Web-based chat interface (ChatGPT)	Zero shot, role based, context enhanced, and format constrained	None
Strotzer et al [40]	Germany	Diagnosis	GPT-4-1106-vision-preview	Official API[a] (via OpenAI platform)	Zero shot, role based, context enhanced, and format constrained	None
Kuzan et al [41]	Turkey	Diagnosis	GPT-4 Vision	Web-based chat interface (ChatGPT)	Zero shot and context enhanced	None
Fei et al [42]	China	Rehabilitation	GPT-3.5 and GPT-4	Web-based chat interface (ChatGPT)	Zero shot, role based, and context enhanced	None
Lee et al [43]	—[b]	Diagnosis	GPT-4	Unclarified	Zero shot, chain of thought, context enhanced, and format constrained	None
Haim et al [44]	Israel	Diagnosis and treatment	GPT-3.5 and GPT-4	Web-based chat interface (ChatGPT)	Zero shot and context enhanced	None
Chen et al [45]	United States	Diagnosis	GPT-4	Web-based chat interface (Bing chat)	Zero shot, role based, and context enhanced	None
Blacker et al [46]	United States	Treatment	GPT-4	Web-based chat interface (ChatGPT)	Zero shot and context enhanced	None
Zhang et al [37]	Japan	Rehabilitation	GPT-4	Web-based chat interface (ChatGPT)	Zero shot	None
Sivarajkumar et al [47]	United States	Rehabilitation	GPT-3.5-turbo	Official API (via Microsoft Azure)	Zero shot, few shot, role based, and format constrained	None
Guo et al [48]	China	Diagnosis and treatment	BART[c]-base-Chinese and BART-large-Chinese	Unclarified	—	Fine-tuning, constrained decoding, encoding representation reuse, beam search, feature fusion, and shared encoder weights
Lehnen et al [49]	Germany	Treatment	GPT-3.5 and GPT-4	Web-based chat interface (ChatGPT)	Zero shot, format constrained, and context enhanced	None
Fiedler et al [50]	United States	Diagnosis, treatment, prognosis, and rehabilitation	GPT-3.5-turbo-16k	Official API (via Microsoft Azure)	Zero shot, role based, format constrained, and context enhanced	Temperature set to 0
Wang et al [51]	China	Treatment	GPT-3.5-turbo, GPT-4, Gemini Pro, GLM-4, Spark 3, and Qwen-Max	Official APIs (via unclarified platforms)	Zero shot, format constrained, and context enhanced	None
Goh et al [52]	Australia	Diagnosis and treatment	Llama 3-70B	Local inference	Zero shot, role based, and format constrained	Temperature set to 0
Baro et al [53]	Brazil	Prevention	openCabrita 3B	Unclarified	—	Low-rank adaptation tuning

XSL•FO
RenderX

Study	Country	Stage in the stroke care continuum	Foundation model or model series	Access	Instruction design	Other adaptation strategies
Meddeb et al [54]	Germany	Treatment	Qwen-72B, Mixtral 8x7B, and BioMistral-7B	Local inference	Zero shot, format constrained, and context enhanced	None
Kim et al [55]	South Korea	Diagnosis, treatment, and prognosis	GPT-4-32k	Official API (via unclarified platform)	Few shot, format constrained, and context enhanced	Low-temperature setting
Argymbay et al [56]	Canada	Prevention	BioMistral-7B	Private API (via Hugging Face on Amazon SageMaker)	Few shot and context enhanced	Temperature set to 0.3
Neo et al [57]	Singapore	Rehabilitation	GPT-3.5-turbo and PaLM 2	Web-based chat interfaces (ChatGPT and Google Bard)	Zero shot and context enhanced	None
Wu et al [58]	United States	Prevention	GPT-3.5	Web-based chat interface (ChatGPT)	Zero shot	None
Chen et al [59]	China	Rehabilitation	GPT-4, GPT-3.5-turbo, and GLM-130B	Official APIs (via unclarified platforms)	Few shot, role based, format constrained, and context enhanced	None
Rifai et al [60]	Indonesia	Rehabilitation	GPT-4o	Official API (via unclarified platforms)	Zero shot, format constrained, and context enhanced	Temperature set to 0.5; token generation minimized
Anghelescu et al [36]	—	Treatment	Unclarified GPT[d]	Web-based chat interface (ChatGPT)	Zero shot	None

[a]API: application programming interface.

[b]Not applicable.

[c]BART: bidirectional and auto-regressive transformers.

[d]GPT: generative pretrained transformer.

Analysis of the cultural dimension identified the geographic settings for most of the included studies (23/25, 92%). The studies originated from diverse global locations, with the United States (6/25, 24%), China (4/25, 16%), and Germany (3/25, 12%) being the most represented countries. Other studies represented individual contributions from Canada, Australia, Singapore, Japan, South Korea, Turkey, Portugal, Brazil, Indonesia, and Israel. With regard to the care dimension, most gLLM interventions (11/25, 44%) focused on the treatment phase, where systems were typically used to support clinical decisions, integrate therapeutic guidelines, or extract specific treatment data (eg, surgical procedures and medication regimens) from documentation. The diagnostic phase was the second most common focus (9/25, 36%), with applications including lesion localization support, assistance with diagnostic reasoning, and extraction of pertinent diagnostic details from clinical records. Considerably fewer studies focused on stroke prevention (3/25, 12%) or prognosis (3/25, 12%). Prevention-focused interventions mainly aimed to reduce subsequent stroke-related hospitalizations or expand public access to preventive resources. Prognostic applications focused on assisting clinicians primarily by calculating prognostic scores or interpreting relevant information documented within clinical notes.

Regarding the technical dimension, adaptation strategies for the gLLM-driven systems varied across the included studies. These choices often reflected trade-offs between computational cost and task demands, aiming to align model behavior with task-specific constraints while maintaining stable output control. For relatively straightforward tasks, a *plug-and-play* strategy using standard interfaces was frequently adopted. This involved accessing closed-source models using web-based chat interfaces (12/25, 48%) or application programming interface (API) end points (8/25, 32%) without further model customization. As task complexity increased or baseline performance proved inadequate, studies often adopted multiprompt strategies to better guide model behavior. Established methods included zero-shot (20/25, 80%), few-shot (4/25, 16%), and chain-of-thought (1/25, 4%) prompting. Beyond these approaches, specific prompting techniques were used to improve control—role-based prompting assigned domain-specific personas (eg, *You are a neurologist*); format-constrained prompting enforced structured outputs (eg, JSON, CSV, standardized terminologies, and executable code); and context-enhanced prompting incorporated background knowledge, task decomposition steps, or self-reflection instructions to improve response quality.

These prompting strategies were sometimes used alongside inference-time configurations, among which temperature adjustment was the most frequently reported technique (5/25, 20%) for modulating output diversity versus coherence. In a small subset of studies requiring deeper customization (2/25, 8%), locally deployed open-source models underwent model-level adaptations. These included techniques such as

XSL•FO
RenderX

parameter-efficient fine-tuning and architectural modifications to customize the model more closely to the specific clinical application. A variety of gLLM families were used across the included studies. The GPT series (OpenAI) was mainly used in 80% (20/25) of the studies. Other models used in multiple studies included the Mixtral (and its variant, BioMistral) series (Mistral AI; 3/25, 12%), the PaLM 2 (and its successor, Gemini) series (Google DeepMind; 2/25, 8%), the Qwen series (Alibaba Cloud; 2/25, 8%), and the GLM series (Zhipu AI; 2/25, 8%). Models identified in single studies included Llama 3-70B (Meta), BART base and BART-large-Chinese (Fudan NLP Lab), Spark 3 (iFLYTEK), and openCabrita 3B (22h).

Challenges Identified During the Implementation of gLLM-Driven Interventions in Stroke Care

Through a comprehensive review of the findings of the included studies, five key challenges were identified in applying gLLMs across the stroke care pathway: (1) ensuring factual alignment, (2) maintaining system robustness, (3) enhancing model interpretability, (4) optimizing operational efficiency, and (5) facilitating adoption into clinical practice.

Factual alignment was the most frequently discussed concern [36-55,57-60], reflecting persistent difficulties in ensuring consistency among system outputs, established clinical knowledge, and input data. Documented issues included inaccurate or incomplete responses, hallucinated content, and output failures. Several studies (11/25, 44%) noted nondeterministic behavior across repeated runs [41,43,45,51], failure to retrieve pretrained knowledge [36,40,46,57], limited inclusion of up-to-date evidence [37,38], and inconsistencies between the model's reasoning steps and its final outputs [39,43]. Robustness issues were mainly associated with variability in output quality due to changes in input data or instructions. Data-related concerns included difficulty in handling rare or complex cases [38-41,43,45,50,54,55,59,60]; managing human-induced input noise such as incompleteness, ambiguity, or internal contradiction [38-40,44,45,49,51,52,54]; and adapting to distributional discrepancies between training and deployment data [40,41,43,48,57]. Instruction-level fragility was also observed as small prompt modifications led to substantial variations in output [37,40,42,43,46,47,49,50,54,58], demonstrating the sensitivity of gLLM-driven systems to prompt design.

Adoption, interpretability, and efficiency were also deemed potential concerns in applying gLLMs across the stroke care pathway. Adoption-related challenges involved the need for EITL oversight when applying gLLMs [36,37,39-41,44,45,49,50,52,58]; ongoing efforts to integrate gLLMs into clinical workflows [40,42,43,45,50,52,55,57,60]; and unresolved issues related to legal compliance, data privacy, and patient safety [43,50,57]. Interpretability challenges were associated with the opaque and uncontrollable nature of gLLM reasoning [41,43,46,55,57], the limited readability of gLLM responses [57,58], and variations in how individuals understood the same content [46,57]. Efficiency-related concerns included token processing constraints [38,39] and trade-offs between model performance and computational cost [53,59].

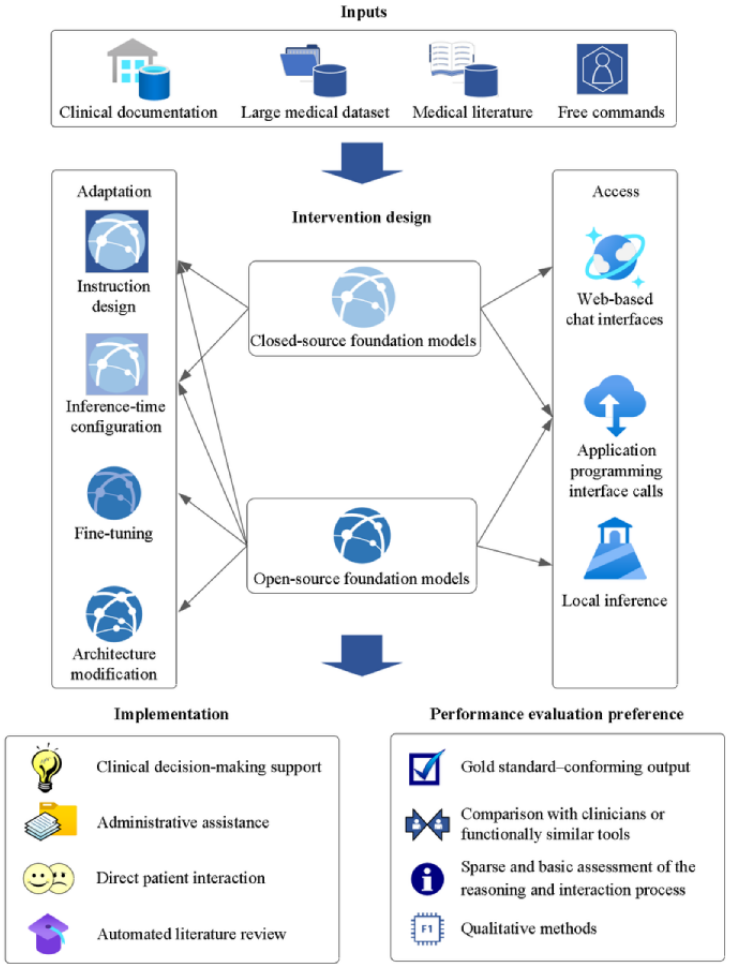
Discussion

Principal Findings

This study presented a timely scoping review mapping the intersection of stroke care and gLLMs, providing practical insights into current applications within this rapidly evolving domain. The substantial heterogeneity identified across the included studies, spanning objectives, methodologies, contexts, and outcomes, precluded meta-analysis, confirming the suitability of the chosen scoping review approach. The analysis classified gLLM-driven interventions into 4 key applications, as presented in Table 2. Examination within each category focused on the target tasks assigned to gLLMs, types of input data used, reported dialogue patterns and intervention timing, and performance evaluation methods. The findings of this review demonstrate that existing research has mainly used gLLMs with clinical document inputs for retrospective tasks such as supporting clinical decision-making or extracting data relevant to stroke diagnosis, treatment, prognosis, and rehabilitation. A smaller subset of studies (5/25, 20%) adopted a more patient-centered perspective, either by integrating gLLMs with upper-limb exoskeleton systems to potentially support motor recovery or by applying them to address open-ended patient questions regarding stroke prevention. The single study investigating gLLM use for academic writing support concluded that the outputs were unreliable for practical use, highlighting limitations in that specific application context. Given the breadth of stroke care tasks addressed, considerable diversity in the technical implementation of these gLLM interventions was observed, as shown in Table 3. Common technical approaches involved using GPT-series models, typically accessed through web-based chat interfaces or API calls and guided primarily by task-specific prompt engineering strategies. Moreover, this review identified five critical challenges pertinent to applying gLLMs effectively and safely across the stroke care pathway: (1) ensuring factual alignment, (2) maintaining system robustness, (3) enhancing model interpretability, (4) optimizing operational efficiency, and (5) facilitating adoption into clinical practice. Figure 2 illustrates the current landscape of gLLM-based interventions across the stroke care pathway.

XSL•FO
RenderX

Figure 2. Current landscape of interventions driven by generative large language models in stroke care.



Need for Rigorous Real-World Evidence to Support Clinical Translation

gLLMs represent a novel addition to digital health [14,61,62], creating new avenues for neurological care [17] and offering significant potential to improve stroke prevention and bridge gaps in care access. Despite this promise, the evidence base for gLLMs specifically in stroke care currently relies heavily on retrospective analyses of clinical documentation and experimental studies conducted in simulated settings. This cautious approach likely reflects valid concerns regarding the potential impact of these nascent technologies on patient safety and clinical decision-making [63]. Highlighting the feasibility of real-world assessment in other domains, a recent cluster-randomized trial in China demonstrated that a gLLM-driven chatbot effectively improved parental health literacy concerning human papillomavirus vaccination for adolescent girls [64]. In contrast, most of the stroke care studies included in this review (24/25, 96%) did not involve integrating gLLM-based systems into actual clinical workflows or conducting real-time interactions with patients. Consequently, the real-world effects of these systems on health care delivery efficiency, clinical outcomes, and patient health literacy within the context of stroke care remain largely unverified. This significant evidence gap highlights an urgent need within the stroke research community. Future efforts must prioritize clarifying evidence requirements and systematically generating robust real-world data on the feasibility, safety, clinical impact, and cost-effectiveness of gLLM applications to provide essential support for clinical translation.

Toward Balanced Process and Outcome Evaluation

For stroke care tasks that depend on interaction between human users (eg, health care professionals, administrative staff, or patients and their caregivers) and gLLM-based tools, evaluation needs to extend beyond outcome-oriented performance metrics. Incorporating assessments of model reasoning processes and the dynamics of human-gLLM interaction is critical for providing a complete understanding. While 8% (2/25) of the included studies focused solely on noninteractive tasks, including advanced text representation [48,53], the remaining studies (23/25, 92%) relied on human-gLLM interaction to complete stroke care tasks. Among these, more than half (12/23, 52% of the studies) assessed gLLM performance solely based on how well model outputs aligned with clinical expectations or predefined gold standards without assessing human-gLLM interaction processes or model reasoning behavior. While some of these studies (15/25, 60%) aimed to produce correct responses in single-turn dialogues, this narrow, outcome-focused evaluation perspective is insufficient for interventions that rely on gLLMs' capabilities for open-ended reasoning and interactive engagement [62]. Several studies (11/25, 44%) acknowledged simple process-related metrics in logical coherence, efficiency improvement, and user interaction experience and observed

XSL•FO
RenderX

effects. It is also important to examine how well gLLM-driven tools can identify and collect task-relevant information through multiturn interactions, especially in patient-facing contexts [62]. Fully understanding and ensuring the real-world applicability and safety of gLLM-based systems in health care settings requires broadening performance evaluation frameworks to rigorously include these dynamic processes alongside static outcomes.

Correction of Technical Reporting Deficiencies

Significant issues were raised regarding the normative reporting of gLLM intervention designs within the included studies. A common oversight appeared to be neglecting the fact that different access methods (eg, web-based chat interfaces) may use customized configurations or variants of the same underlying model. This lack of specificity was particularly evident when models were accessed using web chat interfaces. These often used restricted-access [65] or proprietary, fine-tuned, chat-optimized variants [66] (frequently branded as specific products, eg, ChatGPT) that are not directly equivalent to the base models released by developers. Despite researchers' attempts to specify the underlying models, their precise identity often remained ambiguous. As a result, conflating branded chat products with broader foundation model families (eg, ChatGPT with the GPT series) can lead to conceptual confusion and should be avoided in reporting. Furthermore, this review identified instances in which API-based access to closed-source models was inaccurately characterized, for example, as *static version use* or analogous to offline deployment [50]. In reality, such access depends on remote servers where the underlying models can be updated by the provider without explicit version notification, challenging assumptions of both offline use and version stability. Given the rapid iteration cycles common to gLLMs, consistently time-stamping the input and output stages during use could aid researchers in documenting and interpreting the specific model versions or operational states encountered. However, this practice was uncommon in the reviewed literature, with only 20% (5/25) of the studies reporting time-stamped interaction events [38,40,43,46,57]. To maintain analytical rigor amid these reporting ambiguities, this review adopted a strategy of consistently referring to general model series (eg, the GPT-4 family) when exact versions or configurations could not be definitively ascertained from the studies. The observed heterogeneities and frequent lack of precision in technical reporting highlight a critical need for the development and adoption of standardized, transparent guidelines for describing gLLM-driven intervention designs. Such standards are important for ensuring accurate interpretation, enabling reproducibility, and facilitating meaningful cross-study comparability in this advancing field.

Simple and Homogeneous Task Adaptation Strategies

The design and refinement of gLLM-driven interventions specifically for stroke care remain in their nascent stages. Current approaches mainly rely on zero- or few-shot instruction designs, enhanced using techniques such as context augmentation, role-based prompting, or format constraints to guide outputs. While prompt iteration was occasionally used to improve factual alignment [42,46,50], generated outputs still often contained inaccuracies or lacked desired nuance. Similarly, although a small subset of the included studies (2/25, 8%) investigated domain-specific fine-tuning of open-source models for better task adaptability, both prompt engineering and basic fine-tuning strategies appear insufficient for highly complex clinical settings that require integrating robust logical reasoning with precise numerical computation. Emerging architectures such as RAG [55,57] and multiagent systems [52] show promise, mirroring developments in other medical fields [67-69], but their empirical validation within stroke care is currently underexplored. Furthermore, the robustness of gLLM-based stroke care interventions against unexpected inputs or variations remains insufficiently examined. The underlying causes of potential failures were often unexplored due to a lack of proactive and systematic investigation strategies within the reviewed studies.

Underexplored Dual Gap in Human-gLLM Interaction Dynamics

Although intentionally introducing noise or adversarial inputs is a standard method for stress testing and evaluating robustness in machine learning [70], most studies (24/25, 96%) appeared to respond reactively after poor performance was observed, sometimes relying on subjective speculation regarding failure modes rather than rigorous empirical analysis. Systematically analyzing model responses to flawed, edge-case, or adversarial inputs could yield crucial insights into failure mechanisms, thereby informing the development of safer and more reliable gLLMs for stroke care [45,71]. Finally, the rapid iteration cycles and frequent updates of underlying models introduce significant uncertainties regarding the long-term performance, reliability, and transferability of the developed interventions. For example, it remains unclear how effectively interventions initially developed and validated on now deprecated models (eg, early versions of ChatGPT) will function when deployed using substantially updated successor models (such as GPT-4o) [72]. Therefore, this dynamic landscape requires ongoing evaluation, validation, and potentially continuous adaptation strategies for gLLMs intended for clinical use.

While a significant amount of research has focused on gLLM intervention design and technical optimization, how humans interact with such systems within the context of stroke care remains largely underexplored. Although concerns about the *black box* nature of gLLM reasoning processes are frequently discussed, this review suggests that the heterogeneity in users' subjective interpretations of gLLM outputs presents an equally critical yet less examined challenge. There appears to be emerging agreement on the value of EITL frameworks for deploying gLLMs in real-world settings; however, evidence from the included studies shows that clinicians can interpret the exact same generated response quite differently [46,57]. Such variability in human interpretation may significantly influence downstream trust in the system; subsequent clinical decision-making; and, ultimately, patient outcomes in stroke care.

Beyond interpretation variability, safety concerns are extended by potential user behaviors and governance gaps. For example, follow-up reprompting was reportedly used in one study to

XSL•FO
RenderX

bypass built-in safety restrictions designed to prohibit direct radiological image interpretation [40], exposing risks related to both inadequate technology governance and the potential for deliberate misuse by individuals. Moreover, actionable guidelines are urgently needed to address broader safety and ethical concerns, including the legal ambiguities surrounding artificial intelligence–driven interventions and potential conflicts between commercial deployment objectives and established clinical best practices [57].

Consequently, these underexplored dimensions point to a dual gap that limits research and the clinical translation of gLLMs in stroke care. The first gap concerns a limited understanding of optimal gLLM-driven intervention design tailored to specific stroke care tasks, including defining the operational boundaries and failure modes of such systems. The second relates to insufficient investigation into how diverse human users (eg, health care professionals, patients with stroke, and caregivers) actually interact with gLLM-based systems and how these interactions dynamically shape both user understanding and system outputs.

Future Directions

The application of gLLMs in stroke care, while promising, is relatively new, with most current interventions representing early-stage or relatively simple implementations. To enable the responsible and effective integration of such tools into health care settings, the development and adoption of formal, multidimensional frameworks that promote rigorous evaluation and informed oversight are critical. Future studies attempting to bridge the gap between potential and practice would also likely benefit from using mixed methods techniques to gain deeper, more nuanced insights into how gLLMs actually operate across diverse stroke care tasks and how they can be most effectively and safely deployed in complex clinical environments. In light of the considerations raised in this review, several priorities emerge for guiding the safe, successful, and ethical use of gLLMs across relevant stroke care domains, including clinical work, direct patient support, administrative tasks, and academic research.

First, real-world evidence should be prioritized. There is a critical need for reliable prospective strategies guided by clearly defined research questions and evidence priorities to generate robust real-world data. Such studies should focus on the clinical impact, safety, feasibility, and cost-effectiveness of specific gLLMs implemented in stroke care settings.

Second, transparent technical reporting should be mandated. The technical design and implementation details of gLLM-driven systems must be reported with greater precision and completeness. Standardized reporting should include accurate naming of models or specific product versions used, consistent time-stamping of key input and output events during evaluation, and clear descriptions of how the systems are accessed (eg, through chat interfaces, API, or local deployment).

Third, evaluation frameworks should be broadened beyond output accuracy. Existing performance evaluation for gLLMs requires expansion beyond technical metrics. Future frameworks must incorporate rigorous methods for assessing critical aspects of human-gLLM interaction dynamics, model reasoning processes, context appropriateness, usability, and overall user experience.

Fourth, validation of advanced task adaptation strategies should be strengthened. Current task adaptation strategies in stroke-focused gLLM systems remain simplistic and repetitive, relying primarily on prompt design and inference-time controls. These approaches have shown limitations in handling complex tasks. Future research should develop and evaluate emerging methods (eg, multiagent collaboration and RAG), which are being explored for their feasibility in other areas of chronic disease care.

Finally, mechanisms for safe and effective human-gLLM interaction should be investigated. There is a critical need to clarify the behavioral boundaries and failure modes of gLLM-driven interventions tailored to specific stroke care tasks. Equally important is the lack of empirical insight into how diverse users (eg, health care professionals, patients with stroke, and caregivers) interact with these systems in real-world settings. Future research should elucidate how these interactions shape user understanding and dynamically influence system outputs, supporting the development of more responsive, trustworthy, and context-aware gLLM applications in stroke care.

Limitations

This review has several limitations related to its scope and the current state of the literature. First, the decision to exclude preprints and focus solely on peer-reviewed publications, while ensuring a certain quality standard, may have omitted important nascent insights given the rapid technological iteration and common use of preprint platforms for early dissemination in the gLLM field. Second, the substantial heterogeneity identified across the included studies precluded a quantitative synthesis or meta-analysis of gLLM intervention performance. To mitigate this, supplementary details summarizing individual study findings are provided (Multimedia Appendix 4 [36-60]) to give readers further granularity where possible. Despite these limitations and the heterogeneity, most reported gLLM-driven interventions demonstrated encouraging performance on their specifically defined tasks within the study contexts. Lower comparative performance was observed in applications focused on extracting structured clinical data, which may reflect the maturity and optimization of existing methods (eg, rule-based systems, conventional machine learning, and earlier deep learning models) already well suited for these specific tasks. In studies targeting knowledge-intensive tasks (eg, lesion detection, report drafting, and evidence integration), mixed or suboptimal results were often reported, likely attributable more to the specific study design used than to an inherent limitation of gLLMs for such tasks generally. Nevertheless, these findings highlight the need for caution regarding the immediate, large-scale deployment or formal adoption of current gLLM-driven interventions in real-world stroke care settings.

Conclusions

As highlighted throughout this review, current research has yet to establish a coherent, evidence-based foundation addressing robust intervention design, comprehensive multidimensional

XSL•FO
RenderX

evaluation, and effective governance for these rapidly evolving gLLM technologies in stroke care. Consequently, this study contributes by clarifying the current complex research landscape concerning gLLM applications in stroke care, providing an updated review of the strengths and critical gaps in existing investigations, and identifying key priorities and directions for future research design and evaluation.

Acknowledgments

This research was supported by the Fundamental Research Funds for the Central Universities, Huazhong University of Science and Technology (grant 2024JYCXJJ011). The funder had no role in the study design, data collection and analysis, decision to publish, or preparation of the manuscript.

Data Availability

All data generated or analyzed during this study are included in this published article (and Multimedia Appendices 2-4).

Authors' Contributions

XZ, WD, and ZL conceptualized the scoping review and its methodology. XZ conducted the literature search and data charting, prepared the original manuscript draft, and created all figures. XZ, WD, and ZL conducted the study screening. RE, XG, and AM provided significant contributions to the refinement of the analysis and manuscript content. All authors participated in critically revising the manuscript and have read and approved the final version.

Conflicts of Interest

None declared.

Multimedia Appendix 1
PRISMA-ScR checklist.
[PDF File (Adobe PDF File), 106 KB - medinform_v13i1e76636_app1.pdf]

Multimedia Appendix 2
Search strategy.
[PDF File (Adobe PDF File), 122 KB - medinform_v13i1e76636_app2.pdf]

Multimedia Appendix 3
Data extraction variables.
[PDF File (Adobe PDF File), 100 KB - medinform_v13i1e76636_app3.pdf]

Multimedia Appendix 4
Summary of performance evaluation results for generative large language model–driven interventions in stroke care.
[PDF File (Adobe PDF File), 173 KB - medinform_v13i1e76636_app4.pdf]

References

1. Over 1 in 3 people affected by neurological conditions, the leading cause of illness and disability worldwide. World Health Organization. 2024 Mar 14. URL: https://www.who.int/news/item/14-03-2024-over-1-in-3-people-affected-by-neurological-conditions--the-leading-cause-of-illness-and-disability-worldwide [accessed 2025-02-09]
2. GBD 2019 Stroke Collaborators. Global, regional, and national burden of stroke and its risk factors, 1990-2019: a systematic analysis for the Global Burden of Disease Study 2019. Lancet Neurol 2021 Oct;20(10):795-820 [FREE Full text] [doi: 10.1016/S1474-4422(21)00252-0] [Medline: 34487721]
3. DiCarlo JA, Gheihman G, Lin DJ, 2019 Northeast Cerebrovascular Consortium Conference Stroke Recovery Workshop Participants. Reimagining stroke rehabilitation and recovery across the care continuum: results from a design-thinking workshop to identify challenges and propose solutions. Arch Phys Med Rehabil 2021 Aug;102(8):1645-1657. [doi: 10.1016/j.apmr.2021.01.074] [Medline: 33556351]
4. Duncan PW, Bushnell C, Sissine M, Coleman S, Lutz BJ, Johnson AM, et al. Comprehensive stroke care and outcomes. Stroke 2021 Jan;52(1):385-393. [doi: 10.1161/strokeaha.120.029678]
5. Sheikhalishahi S, Miotto R, Dudley JT, Lavelli A, Rinaldi F, Osmani V. Natural language processing of clinical notes on chronic diseases: systematic review. JMIR Med Inform 2019 Apr 27;7(2):e12239 [FREE Full text] [doi: 10.2196/12239] [Medline: 31066697]

XSL•FO
RenderX

6. Fraile Navarro D, Ijaz K, Rezazadegan D, Rahimi-Ardabili H, Dras M, Coiera E, et al. Clinical named entity recognition and relation extraction using natural language processing of medical free text: a systematic review. Int J Med Inform 2023 Sep;177:105122 [FREE Full text] [doi: 10.1016/j.ijmedinf.2023.105122] [Medline: 37295138]
7. Gumiel YB, Silva e Oliveira LE, Claveau V, Grabar N, Paraiso EC, Moro C, et al. Temporal relation extraction in clinical texts: a systematic review. ACM Comput. Surv 2021 Sep 17;54(7):1-36. [doi: 10.1145/3462475]
8. Xiao H, Zhou F, Liu X, Liu T, Li Z, Liu X, et al. A comprehensive survey of large language models and multimodal large language models in medicine. Inf Fusion 2025 May;117:102888. [doi: 10.1016/j.inffus.2024.102888]
9. Touvron H, Martin L, Stone K, Albert P, Almahairi A, Babaei Y, et al. Llama 2: open foundation and fine-tuned chat models. arXiv. Preprint posted online on July 19, 2023 [FREE Full text] [doi: 10.48550/arXiv.2307.09288]
10. Achiam J, Adler S, Agarwal S, Ahmad L, Akkaya I, Aleman FL, et al. GPT-4 technical report. arXiv. Preprint posted online on March 4, 2024 [FREE Full text] [doi: 10.5860/choice.189890]
11. Lewis M, Liu Y, Goyal N, Ghazvininejad M, Mohamed A, Levy O, et al. BART: denoising sequence-to-sequence pre-training for natural language generation, translation, and comprehension. arXiv. Preprint posted online on October 29, 2019 [FREE Full text] [doi: 10.18653/v1/2020.acl-main.703]
12. Peng C, Yang X, Chen A, Yu Z, Smith KE, Costa AB, et al. Generative large language models are all-purpose text analytics engines: text-to-text learning is all your need. J Am Med Inform Assoc 2024 Sep 01;31(9):1892-1903. [doi: 10.1093/jamia/ocae078] [Medline: 38630580]
13. Liu P, Yuan W, Fu J, Jiang Z, Hayashi H, Neubig G. Pre-train, prompt, and predict: a systematic survey of prompting methods in natural language processing. ACM Comput Surv 2023 Jan 16;55(9):1-35. [doi: 10.1145/3560815]
14. Lu Z, Peng Y, Cohen T, Ghassemi M, Weng C, Tian S. Large language models in biomedicine and health: current research landscape and future directions. J Am Med Inform Assoc 2024 Sep 01;31(9):1801-1811. [doi: 10.1093/jamia/ocae202] [Medline: 39169867]
15. Gilbert S, Kather JN, Hogan A. Augmented non-hallucinating large language models as medical information curators. NPJ Digit Med 2024 Apr 23;7(1):100 [FREE Full text] [doi: 10.1038/s41746-024-01081-0] [Medline: 38654142]
16. Ong CS, Obey NT, Zheng Y, Cohan A, Schneider EB. SurgeryLLM: a retrieval-augmented generation large language model framework for surgical decision support and workflow enhancement. NPJ Digit Med 2024 Dec 18;7(1):364 [FREE Full text] [doi: 10.1038/s41746-024-01391-3] [Medline: 39695316]
17. Moura L, Jones DT, Sheikh IS, Murphy S, Kalfin M, Kummer BR, et al. Implications of large language models for quality and efficiency of neurologic care: emerging issues in neurology. Neurology 2024 Jun 11;102(11):e209497. [doi: 10.1212/WNL.0000000000209497] [Medline: 38759131]
18. Hello GPT-4o. OpenAI. 2024 May 13. URL: https://openai.com/index/hello-gpt-4o/ [accessed 2025-04-03]
19. Gemini Team Google, Anil R, Borgeaud S, Alayrac JB, Yu J, Soricut R, et al. Gemini: a family of highly capable multimodal models. arXiv. Preprint posted online on May 9, 2025 . [doi: 10.5860/choice.189890]
20. Silva GS, Schwamm LH. Advances in stroke: digital health. Stroke 2021 Jan;52(1):351-355. [doi: 10.1161/strokeaha.120.033239]
21. Feigin VL, Owolabi M, Hankey GJ, Pandian J, Martins SC. Digital health in primordial and primary stroke prevention: a systematic review. Stroke 2022 Mar;53(3):1008-1019 [FREE Full text] [doi: 10.1161/STROKEAHA.121.036400] [Medline: 35109683]
22. Allan LP, Beilei L, Cameron J, Olaiya MT, Silvera-Tawil D, Adcock AK, et al. A scoping review of mHealth interventions for secondary prevention of stroke: implications for policy and practice. Stroke 2023 Nov;54(11):2935-2945. [doi: 10.1161/STROKEAHA.123.043794] [Medline: 37800373]
23. Hocking J, Oster C, Maeder A, Lange B. Design, development, and use of conversational agents in rehabilitation for adults with brain-related neurological conditions: a scoping review. JBI Evid Synth 2023 Feb 01;21(2):326-372. [doi: 10.11124/JBIES-22-00025] [Medline: 35976047]
24. Alobaida M, Joddrell M, Zheng Y, Lip GY, Rowe FJ, El-Bouri WK, et al. Systematic review and meta-analysis of prehospital machine learning scores as screening tools for early detection of large vessel occlusion in patients with suspected stroke. J Am Heart Assoc 2024 Jun 18;13(12):e033298 [FREE Full text] [doi: 10.1161/JAHA.123.033298] [Medline: 38874054]
25. Issaiy M, Zarei D, Kolahi S, Liebeskind DS. Machine learning and deep learning algorithms in stroke medicine: a systematic review of hemorrhagic transformation prediction models. J Neurol 2024 Dec 12;272(1):37 [FREE Full text] [doi: 10.1007/s00415-024-12810-6] [Medline: 39666168]
26. De Rosario H, Pitarch-Corresa S, Pedrosa I, Vidal-Pedrós M, de Otto-López B, García-Mieres H, et al. Applications of natural language processing for the management of stroke disorders: scoping review. JMIR Med Inform 2023 Sep 06;11:e48693 [FREE Full text] [doi: 10.2196/48693] [Medline: 37672328]
27. Luo X, Deng Z, Yang B, Luo MY. Pre-trained language models in medicine: a survey. Artif Intell Med 2024 Aug;154:102904. [doi: 10.1016/j.artmed.2024.102904]
28. Moor M, Banerjee O, Abad ZS, Krumholz HM, Leskovec J, Topol EJ, et al. Foundation models for generalist medical artificial intelligence. Nature 2023 Apr 12;616(7956):259-265. [doi: 10.1038/s41586-023-05881-4] [Medline: 37045921]

XSL•FO
RenderX

29. Ge W, Rice HJ, Sheikh IS, Westover MB, Weathers AL, Jones LK, et al. Improving neurology clinical care with natural language processing tools. Neurology 2023 Nov 27;101(22):1010-1018. [doi: 10.1212/WNL.0000000000207853] [Medline: 37816638]
30. Peters MD, Marnie C, Tricco AC, Pollock D, Munn Z, Alexander L, et al. Updated methodological guidance for the conduct of scoping reviews. JBI Evid Synth 2020 Oct;18(10):2119-2126. [doi: 10.11124/JBIES-20-00167] [Medline: 33038124]
31. Tricco AC, Lillie E, Zarin W, O'Brien KK, Colquhoun H, Levac D, et al. PRISMA extension for scoping reviews (PRISMA-ScR): checklist and explanation. Ann Intern Med 2018 Oct 02;169(7):467-473 [FREE Full text] [doi: 10.7326/M18-0850] [Medline: 30178033]
32. Arksey H, O'Malley L. Scoping studies: towards a methodological framework. Int J Soc Res Methodol 2005 Feb;8(1):19-32. [doi: 10.1080/1364557032000119616]
33. Zhu X, Wei D, Liu Z. Clinical use of transformer-based generative pre-trained language models in stroke: a scoping review. Open Science Framework. URL: https://osf.io/j36wv [accessed 2025-01-22]
34. Greenhalgh T, Peacock R. Effectiveness and efficiency of search methods in systematic reviews of complex evidence: audit of primary sources. BMJ 2005 Nov 05;331(7524):1064-1065 [FREE Full text] [doi: 10.1136/bmj.38636.593461.68] [Medline: 16230312]
35. The scoping review and summary of the evidence. JBI Collaboration. 2025 May 7. URL: https://jbi-global-wiki.refined.site/space/MANUAL/355862853/10.3+The+scoping+review+and+summary+of+the+evidence [accessed 2025-06-23]
36. Anghelescu A, Firan FC, Onose G, Munteanu C, Trandafir A, Ciobanu I, et al. PRISMA systematic literature review, including with meta-analysis vs. Chatbot/GPT (AI) regarding current scientific data on the main effects of the calf blood deproteinized hemoderivative medicine (Actovegin) in ischemic stroke. Biomedicines 2023 Jun 02;11(6):1623 [FREE Full text] [doi: 10.3390/biomedicines11061623] [Medline: 37371718]
37. Zhang L, Tashiro S, Mukaino M, Yamada S. Use of artificial intelligence large language models as a clinical tool in rehabilitation medicine: a comparative test case. J Rehabil Med 2023 Sep 11;55:jrm13373 [FREE Full text] [doi: 10.2340/jrm.v55.13373] [Medline: 37691497]
38. Pedro T, Sousa JM, Fonseca L, Gama MG, Moreira G, Pintalhão M, et al. Exploring the use of ChatGPT in predicting anterior circulation stroke functional outcomes after mechanical thrombectomy: a pilot study. J Neurointerv Surg 2025 Feb 14;17(3):261-265. [doi: 10.1136/jnis-2024-021556] [Medline: 38453462]
39. Chen TC, Couldwell MW, Singer J, Singer A, Koduri L, Kaminski E, et al. Assessing the clinical reasoning of ChatGPT for mechanical thrombectomy in patients with stroke. J Neurointerv Surg 2024 Feb 12;16(3):253-260. [doi: 10.1136/jnis-2023-021163] [Medline: 38184368]
40. Strotzer QD, Nieberle F, Kupke LS, Napodano G, Muertz AK, Meiler S, et al. Toward foundation models in radiology? Quantitative assessment of GPT-4V's multimodal and multianatomic region capabilities. Radiology 2024 Nov 01;313(2):e240955. [doi: 10.1148/radiol.240955] [Medline: 39589253]
41. Kuzan BN, Meşe İ, Yaşar S, Kuzan TY. A retrospective evaluation of the potential of ChatGPT in the accurate diagnosis of acute stroke. Diagn Interv Radiol 2025 Apr 28;31(3):187-195 [FREE Full text] [doi: 10.4274/dir.2024.242892] [Medline: 39221691]
42. Fei X, Tang Y, Zhang J, Zhou Z, Yamamoto I, Zhang Y. Evaluating cognitive performance: traditional methods vs. ChatGPT. Digit Health 2024 Aug 16;10:20552076241264639 [FREE Full text] [doi: 10.1177/20552076241264639] [Medline: 39156049]
43. Lee JH, Choi E, McDougal R, Lytton WW. GPT-4 performance for neurologic localization. Neurol Clin Pract 2024 Jun;14(3):e200293 [FREE Full text] [doi: 10.1212/CPJ.0000000000200293] [Medline: 38596779]
44. Haim GB, Braun A, Eden H, Burshtein L, Barash Y, Irony A, et al. AI in the ED: assessing the efficacy of GPT models vs. physicians in medical score calculation. Am J Emerg Med 2024 May;79:161-166. [doi: 10.1016/j.ajem.2024.02.016] [Medline: 38447503]
45. Chen TC, Kaminski E, Koduri L, Singer A, Singer J, Couldwell M, et al. Chat GPT as a neuro-score calculator: analysis of a large language model's performance on various neurological exam grading scales. World Neurosurg 2023 Nov;179:e342-e347. [doi: 10.1016/j.wneu.2023.08.088] [Medline: 37634667]
46. Blacker SN, Kang M, Chakraborty I, Chowdhury T, Williams J, Lewis C. Utilizing artificial intelligence and chat generative pretrained transformer to answer questions about clinical scenarios in neuroanesthesiology. J Neurosurg Anesthesiol 2024;36(4):346. [doi: 10.1097/ANA.000000d0000000949]
47. Sivarajkumar S, Gao F, Denny P, Aldhahwani B, Visweswaran S, Bove A, et al. Mining clinical notes for physical rehabilitation exercise information: natural language processing algorithm development and validation study. JMIR Med Inform 2024 Apr 03;12:e52289 [FREE Full text] [doi: 10.2196/52289] [Medline: 38568736]
48. Guo Y, Zan H, Chang H, Zhou L, Zhang K. A BART-based study of entity-relationship extraction for electronic medical records of cardiovascular diseases. In: Proceedings of the 9th China Health Information Processing Conference on Health Information Processing. 2023 Presented at: CHIP '23; October 27-29, 2023; Hangzhou, China p. 82-97 URL: https://link.springer.com/chapter/10.1007/978-981-99-9864-7_6 [doi: 10.1007/978-981-99-9864-7_6]

XSL•FO
RenderX

49. Lehnen NC, Dorn F, Wiest IC, Zimmermann H, Radbruch A, Kather JN, et al. Data extraction from free-text reports on mechanical thrombectomy in acute ischemic stroke using ChatGPT: a retrospective analysis. Radiology 2024 Apr 01;311(1):e232741. [doi: 10.1148/radiol.232741] [Medline: 38625006]
50. Fiedler AK, Zhang K, Lal TS, Jiang X, Fraser SM. Generative pre-trained transformer for pediatric stroke research: a pilot study. Pediatr Neurol 2024 Nov;160:54-59. [doi: 10.1016/j.pediatrneurol.2024.07.001] [Medline: 39191085]
51. Wang M, Wei J, Zeng Y, Dai L, Yan B, Zhu Y, et al. Precision structuring of free-text surgical record for enhanced stroke management: a comparative evaluation of large language models. J Multidiscip Healthc 2024;17:5163-5175 [FREE Full text] [doi: 10.2147/JMDH.S486449] [Medline: 39558925]
52. Goh R, Cook B, Stretton B, Booth AE, Satheakeerthy S, Howson S, et al. Large language models can effectively extract stroke and reperfusion audit data from medical free-text discharge summaries. J Clin Neurosci 2024 Nov;129:110847 [FREE Full text] [doi: 10.1016/j.jocn.2024.110847] [Medline: 39305548]
53. Baro EF, Oliveira LS, Britto AS. Predicting hospitalization with LLMs from health insurance data. Med Biol Eng Comput 2025 Apr 19;63(4):1215-1226. [doi: 10.1007/s11517-024-03251-4] [Medline: 39695069]
54. Meddeb A, Ebert P, Bressem KK, Desser D, Dell'Orco A, Bohner G, et al. Evaluating local open-source large language models for data extraction from unstructured reports on mechanical thrombectomy in patients with ischemic stroke. J Neurointerv Surg 2025 Jan 26:jnis-2024-022078. [doi: 10.1136/jnis-2024-022078] [Medline: 39095085]
55. Kim J, Lee S, Jeon H, Lee K, Bae H, Kim B, et al. PhenoFlow: a human-LLM driven visual analytics system for exploring large and complex stroke datasets. IEEE Trans Visual Comput Graphics 2025 Jan;31(1):470-480. [doi: 10.1109/tvcg.2024.3456215]
56. Argymbay M, Khan S, Ahmad N, Salih M, Mamatjan Y. A smart recommender system for stroke risk assessment with an integrated Strokebot. J Med Biol Eng 2024 Dec 09;44(6):799-808. [doi: 10.1007/S40846-024-00922-3]
57. Neo JR, Ser JS, Tay SS. Use of large language model-based chatbots in managing the rehabilitation concerns and education needs of outpatient stroke survivors and caregivers. Front Digit Health 2024 May 9;6:1395501 [FREE Full text] [doi: 10.3389/fdgth.2024.1395501] [Medline: 38784703]
58. Wu G, Krishna SS, Sakai S, Jhangiani R, Kurniawan S. Google assistant and ChatGPT: is it useful for non medical professionals looking for information about stroke or glaucoma? In: Proceedings of the 13th International Conference on the Internet of Things. 2023 Presented at: IoT '23; November 7-10, 2023; Nagoya, Japan p. 240-244 URL: https://dl.acm.org/doi/10.1145/3627050.3631579 [doi: 10.1145/3627050.3631579]
59. Chen W, Li G, Li M, Wang W, Li P, Xue X, et al. LLM-Enabled Incremental Learning Framework for Hand Exoskeleton Control. IEEE Trans Automat Sci Eng 2025;22:2617-2626. [doi: 10.1109/tase.2024.3382679]
60. Rifai Y, Ataka A, Bejo A, Badriawan YK. Upper limb rehabilitation robot control based on large language model. In: Proceedings of the 2024 International Conference on Computer, Control, Informatics and its Applications. 2024 Presented at: IC3INA '24; October 9-10, 2024; Bandung, Indonesia p. 422-427. [doi: 10.1109/ic3ina64086.2024.10732179]
61. Peng C, Yang X, Chen A, Smith KE, PourNejatian N, Costa AB, et al. A study of generative large language model for medical research and healthcare. NPJ Digit Med 2023 Nov 16;6(1):210 [FREE Full text] [doi: 10.1038/s41746-023-00958-w] [Medline: 37973919]
62. Johri S, Jeong J, Tran BA, Schlessinger DI, Wongvibulsin S, Barnes LA, et al. An evaluation framework for clinical use of large language models in patient interaction tasks. Nat Med 2025 Jan;31(1):77-86. [doi: 10.1038/s41591-024-03328-5] [Medline: 39747685]
63. WHO calls for safe and ethical AI for health. World Health Organization. URL: https://www.who.int/news/item/16-05-2023-who-calls-for-safe-and-ethical-ai-for-health [accessed 2025-03-20]
64. Hou Z, Wu Z, Qu Z, Gong L, Peng H, Jit M, et al. A vaccine chatbot intervention for parents to improve HPV vaccination uptake among middle school girls: a cluster randomized trial. Nat Med 2025 Jun 07;31(6):1855-1862. [doi: 10.1038/s41591-025-03618-6] [Medline: 40195450]
65. Get answers: find inspiration: be more productive. OpenAI. URL: https://openai.com/chatgpt/overview/ [accessed 2025-03-18]
66. Introducing ChatGPT. OpenAI. URL: https://openai.com/index/chatgpt/ [accessed 2025-03-18]
67. Kresevic S, Giuffrè M, Ajcevic M, Accardo A, Crocè LS, Shung DL. Optimization of hepatological clinical guidelines interpretation by large language models: a retrieval augmented generation-based framework. NPJ Digit Med 2024 Apr 23;7(1):102 [FREE Full text] [doi: 10.1038/s41746-024-01091-y] [Medline: 38654102]
68. Wang D, Liang J, Ye J, Li J, Li J, Zhang Q, et al. Enhancement of the performance of large language models in diabetes education through retrieval-augmented generation: comparative study. J Med Internet Res 2024 Nov 08;26:e58041 [FREE Full text] [doi: 10.2196/58041] [Medline: 39046096]
69. Goodell AJ, Chu SN, Rouholiman D, Chu LF. Large language model agents can use tools to perform clinical calculations. NPJ Digit Med 2025 Mar 17;8(1):163 [FREE Full text] [doi: 10.1038/s41746-025-01475-8] [Medline: 40097720]
70. Chen X, Ye J, Zu C, Xu N, Gui T, Zhang Q. Robustness of GPT large language models on natural language processing tasks. J Comput Res Dev 2023;61(5):1128-1142. [doi: 10.7544/issn1000-1239.202330801]
71. Zada T, Tam N, Barnard F, Van Sittert M, Bhat V, Rambhatla S. Medical misinformation in AI-Assisted self-diagnosis: development of a method (EvalPrompt) for analyzing large language models. JMIR Form Res 2025 Mar 10;9:e66207 [FREE Full text] [doi: 10.2196/66207] [Medline: 40063849]

XSL•FO
RenderX

72. Deprecations. OpenAI. URL: https://platform.openai.com/docs/deprecations [accessed 2025-02-15]

Abbreviations

API: application programming interface
BART: bidirectional and auto-regressive transformer
EITL: expert-in-the-loop
gLLM: generative large language model
GPT: generative pretrained transformer
NLP: natural language processing
PCC: Population, Concept, and Context
PRISMA-ScR: Preferred Reporting Items for Systematic Reviews and Meta-Analyses extension for Scoping Reviews
RAG: retrieval-augmented generation

Edited by C Perrin; submitted 28.04.25; peer-reviewed by T Shi, S Sung; comments to author 08.06.25; revised version received 15.06.25; accepted 23.06.25; published 07.08.25.

Please cite as:
Zhu X, Dai W, Evans R, Geng X, Mu A, Liu Z
Current Landscape and Future Directions Regarding Generative Large Language Models in Stroke Care: Scoping Review
JMIR Med Inform 2025;13:e76636
URL: https://medinform.jmir.org/2025/1/e76636
doi:10.2196/76636
PMID:

©XingCe Zhu, Wei Dai, Richard Evans, Xueyu Geng, Aruhan Mu, Zhiyong Liu. Originally published in JMIR Medical Informatics (https://medinform.jmir.org), 07.08.2025. This is an open-access article distributed under the terms of the Creative Commons Attribution License (https://creativecommons.org/licenses/by/4.0/), which permits unrestricted use, distribution, and reproduction in any medium, provided the original work, first published in JMIR Medical Informatics, is properly cited. The complete bibliographic information, a link to the original publication on https://medinform.jmir.org/, as well as this copyright and license information must be included.

XSL•FO
RenderX

Review

Evidence for the Use of Patient-Reported Outcome Measures in the Treatment of Patients With Noncommunicable Diseases: Systematic Review

Marie Villumsen[1], MScPH, PhD; Benedikte Irene von Osmanski[1,2], MD; Kirsten Elisabeth Lomborg[3,4], MSN, PhD; Kirstine Skov Benthien[4,5], MSN, PhD

[1]Center for Clinical Research and Prevention, Bispebjerg and Fredeiksberg Hospital, University Hospital Copenhagen, Frederiksberg, Denmark

[2]Signum Life Science, Copenhagen, Denmark

[3]Steno Diabetes Center Copenhagen, University Hospital Copenhagen, Herlev, Denmark

[4]Department of Clinical Medicine, University of Copenhagen, Copenhagen, Denmark

[5]Department of Pulmonary Medicine and Endocrinology, Hvidovre Hospital, University Hospital Copenhagen, Hvidovre, Denmark

Corresponding Author:
Marie Villumsen, MScPH, PhD
Center for Clinical Research and Prevention
Bispebjerg and Fredeiksberg Hospital
University Hospital Copenhagen
Nordre Fasanvej 57
Frederiksberg, 2000
Denmark
Phone: 45 38163100
Email: marie.villumsen@regionh.dk

Abstract

Background: The use of patient-reported outcome measures (PROMs) as a clinical tool for screening and decision-making has gained widespread interest, with numerous implementation activities across specialties, even though the evidence has not been clear until now.

Objective: The aim of this study was to assess the evidence for using PROMs in clinical practice for patients with diabetes, chronic obstructive pulmonary disease (COPD), heart disease, rheumatoid arthritis (RA), and inflammatory bowel disease (IBD). Additionally, we sought to determine the characteristics of the most effective PROM interventions.

Methods: We conducted a systematic review of published randomized controlled trials (RCTs) on the use of PROMs for clinical purposes, such as systematic PROM assessment alone or with a predefined PROM-based decision-making method. Eligible studies included adult patients (>18 years) with diabetes, COPD, heart disease, RA, or IBD. We excluded studies using PROMs as an outcome measure or otherwise not meeting the inclusion criteria. We searched the PubMed/MEDLINE, CINAHL, EMBASE, and Web of Science databases until February 2023. Two investigators independently screened titles, abstracts, and relevant full texts. Three investigators completed data extraction and risk-of-bias assessment using version 2 of the Cochrane risk-of-bias tool for randomized trials (RoB 2). The data were presented in a narrative synthesis and in summarized form.

Results: The search yielded 21,203 papers, 686 (3.2%) full-text papers were screened, and 56 (8.2%) original studies were included in the review. The studies included patients with heart disease (n=17, 30.4%), COPD (n=13, 23.2%), diabetes (n=10, 17.9%), IBD (n=9, 16.1%), and RA (n=6, 10.7%), as well as patients with mixed diagnoses (n=1, 1.8%). All interventions incorporated systematic PROM assessments. Some interventions additionally used a predefined method for PROM-based decision-making (n=19, 33.9%) or PROM-based dialogue (n=9, 16.1%), while 5 (8.9%) interventions aimed to substitute face-to-face consultations. The predominant mode of PROM administration was over the phone, followed by electronic devices and apps. Endpoints included disease activity, health care use, mortality, mental well-being, quality of life, self-efficacy, self-care, daily functioning, and other outcomes. Six studies with a low risk of bias demonstrated a positive effect or noninferiority of the PROM intervention.

Conclusions: The evidence base for clinical use of PROMs is sparse, with few studies evaluated to have a low or a medium risk of bias. The clinical use of PROMs does not appear superior to usual care in the five included chronic diseases on any

XSL•FO
RenderX

endpoint. To guide further research, we highlighted 6 (10.7%) studies with a low risk of bias and PROM interventions with a positive effect. These were characterized by symptom assessment with predefined cutoffs used for decision and dialogue support.

Trial Registration: PROSPERO CRD42021226896; https://www.crd.york.ac.uk/PROSPERO/view/CRD42021226896

(JMIR Med Inform 2025;13:e66160) doi:10.2196/66160

KEYWORDS

patient-reported outcome measures; chronic obstructive pulmonary disease; diabetes, heart disease; inflammatory bowel disease; rheumatoid arthritis; noncommunicable diseases; non-communicable; health care decision-making; medical informatics; systematic reviews; review

Introduction

The use of patient-reported outcome measures (PROMs) as endpoints in clinical trials is well established and recommended [1]. Furthermore, PROMs have gained interest as a tool to optimize patient-centered care and other supportive interventions that seek to include patients' preferences and values [2-4]. PROMs are often self-completed questionnaires measuring symptoms, health-related quality of life (HRQoL), personal experience of health care, and health-related behaviors. In routine practice, it has been suggested that PROMs may increase health professionals' awareness of and ability to address patients' concerns [5]. Including PROMs in the electronic health record may trigger relevant clinical actions [6,7] and allow patients and health professionals to observe important trends over time and adjust the health care accordingly [8]. Therefore, questionnaires are continuously implemented in routine health care for systematic PROM assessments, informing clinical decisions and supporting the dialogue between patients and health care professionals (HCPs) [9,10].

Despite the promising aspects of using PROMs to improve health care, efforts to put theory into practice have met several barriers. When implementing PROMs in clinical practice, it is important to know the effectiveness, and this must be evaluated in relation to the time the patient spends completing the PROMs and the resources spent by HCPs. A recent systematic review found that patients may question the relevance and validity of PROMs, lack understanding of purpose, and find the clinical use inconsistent [11]. At the same time, HCPs may be concerned with adding undue burden, cause distress, or impact health care detrimentally if the correct infrastructure is not in place [12]. Furthermore, trials may fail to include the patients most burdened by symptoms [13].

The effectiveness of PROMs in cancer has been reviewed by Graupner et al [14], who demonstrated positive effects on several outcomes, including the HRQoL and survival, but also found included studies lacking power and with a high risk of bias. Although the evidence during acute cancer treatment has been described, the evidence in other noncommunicable diseases is unclear.

To close this gap, this systematic review aimed to address the following question: What is the evidence for using PROMs to improve health care, and what characterizes the most effective interventions? Specifically, the aim of this study was to (1) assess the evidence for using PROMs to improve any endpoint in diabetes, chronic obstructive pulmonary disease (COPD), heart failure (HF), ischemic heart disease, rheumatoid arthritis (RA), and inflammatory bowel disease (IBD) and (2) identify the characteristics of effective interventions that have been evaluated and documented in publications with a low or moderate risk of bias to propose directions for future research.

Methods

Study Design

We conducted this systematic review in accordance with a predefined protocol. The review was reported in line with the PRISMA (Preferred Reporting Items for Systematic Reviews and Meta-Analyses) statement (Multimedia Appendix 1) [15,16]. The review was registered at PROSPERO (International Prospective Register of Systematic Reviews; registration number CRD42021226896; date December 18, 2020).

Eligibility Criteria

Only studies written in English were included. Studies selected for inclusion were found to meet the following PICOS (Population, Intervention, Comparison, Outcomes, and Study Design) framework (Table 1) [15]:

- Population: Eligible studies included adult patients (>18 years) with type 1 or type 2 diabetes, COPD, heart disease (HF or ischemic heart disease), RA, or IBD. These noncommunicable diseases were selected due to a high burden of disease measured by disability-adjusted life-years [17].
- Intervention: Eligible studies described any questionnaire used for assessing patient-reported health conditions in routine clinical practice, where the assessment results were forwarded to an HCP. Acceptable interventions could imply (1) systematic PROM assessment alone without a predefined plan for reacting to the responses, (2) systematic PROM assessment plus predefined PROM-based decision-making, (3) systematic PROM assessment as replacement of face-to-face visits, or (4) systematic PROM assessment implemented to support the dialogue between the HCP and the patient in a clinical health care setting.
- Comparison: Eligible studies described usual care alone or passive usage of PROMs (defined as PROM assessments where results were not forwarded to an HCP).
- Outcome measures: The studies were not restricted to specific outcomes.
- Study design: All randomized controlled trials (RCTs), including cluster RCTs and pilot studies, were included.

XSL•FO
RenderX

Table 1. Eligibility according to PICOS[a] criteria for systematic selection of studies.

PICOS framework component	Inclusion criteria	Exclusion criteria
Population	• Adult patients • Diabetes • COPD[b] • Heart disease • RA[c] • IBD[d]	• Pediatric patients • Psychiatric patients • Pregnant patients • Surgical patients
Intervention	• PROMs[e] alone • PROM-based decision-making • PROM replacement of face-to-face visits • PROM support of the dialogue	• Intervention including wearables • Multicomponent interventions
Comparison	• Usual care alone • Passive usage of PROMs	• Active usage of PROMs • Other measures
Outcomes	• Not restricted to specific outcomes	—[f]
Study design	• RCT[g] • Cluster RCT • Pilot study	• Observational study • Literature review

[a]PICOS: Population, Intervention, Comparison, Outcomes, and Study Design.

[b]COPD: chronic obstructive pulmonary disease.

[c]RA: rheumatoid arthritis.

[d]IBD: inflammatory bowel disease.

[e]PROM: patient-reported outcome measure.

[f]Not applicable.

[g]RCT: randomized controlled trial.

Search Strategy

The research team developed the search strategy. We sought advice from an information expert at the Royal Library to ensure all relevant Medical Subject Headings (MeSH) and filters were addressed. We conducted several pilot searches to capture targeted papers. The underlying principle of the search strategy is delineated in Textbox 1. The specific strategy and search strings are presented in Tables S1-S4 in Multimedia Appendix 2. We systematically searched the following electronic databases for potentially eligible papers: PubMed/MEDLINE, CINAHL, EMBASE, and Web of Science. The initial search was completed on December 18, 2020, for all databases and repeated on February 8, 2023, for PubMed/MEDLINE only (Table S5 in Multimedia Appendix 2).

Textbox 1. Principle for the search strategy.

The search strategy was constructed around three primary components: disease, intervention, and study design.

- Disease: For the disease component, we used Medical Subject Headings (MeSH) terms and conducted searches within the titles and abstracts to identify pertinent diseases.
- Intervention: We specifically searched for patient-reported outcome measures (PROMs) by directly targeting patient-reported outcomes (PROs) and PROMs, along with their synonyms. Additionally, we included synonyms for quality of life, alongside measurement terms. Our preliminary searches revealed that PROMs are frequently administered via telemedicine; thus, we incorporated telemedicine in our search to ensure comprehensiveness.
- Study design: To identify randomized trials, we used Cochrane's validated filter.

Titles and abstracts of the identified papers retrieved from electronic databases and other searches were exported to the systematic review management software Covidence, which was used solely to manage references and remove duplicates. No automated screening was performed in Covidence. Two reviewers independently screened all titles and abstracts according to the eligibility criteria. Full texts were reviewed if eligibility could not be determined by the title and abstract alone or in the case of disagreement. We made the final decision in agreement by going through all the included full texts in the group. The study selection process was reported in a flowchart.

XSL•FO
RenderX

Risk of Bias in Individual Studies

Risk of bias was assessed by one of three of the authors independently using version 2 of the Cochrane risk-of-bias tool for randomized trials (RoB 2) [18]. The assessment was hereafter reviewed by one of the other authors. In the case of discrepancies, the risk-of-bias assessment was agreed on in a joint evaluation. One author also authored one of the included studies and was not involved in the risk-of-bias assessment.

Data Synthesis

Data synthesis followed the synthesis without meta-analysis (SWiM) guidelines [19]. In short, the key characteristics of the studies were extracted and recorded in a predesigned table. If an intervention was reported in 2 or more papers, information about the first author and publication year from all papers were collapsed and reported under the primary publication. We used information from all papers to report the intervention and primary and secondary outcomes. Based on the extracted information, we created a narrative synthesis presenting the characteristics of the studies, the PROM characteristics, and the outcomes. The studies were grouped according to primary outcomes and study populations, and since the outcomes varied in content and type, data were synthesized with vote counting based on direction of effects. To ascertain the characteristics of the most effective PROM interventions, we categorized studies with a low or moderate risk of bias, reporting a positive effect if the intervention group demonstrated a statistically significant superior outcome compared to the control group or reporting noninferiority if the difference between the intervention and control groups was below the noninferiority threshold. The characteristics of these studies were synthesized separately. The PROSPERO protocol included assessment with GRADE (Grading of Recommendations Assessment, Development and Evaluation) [20]; however, this method was discarded because of intervention and outcome heterogeneity, so consistency of effects could not be assessed. More study details are described in Tables S6 and S7 in Multimedia Appendix 2.

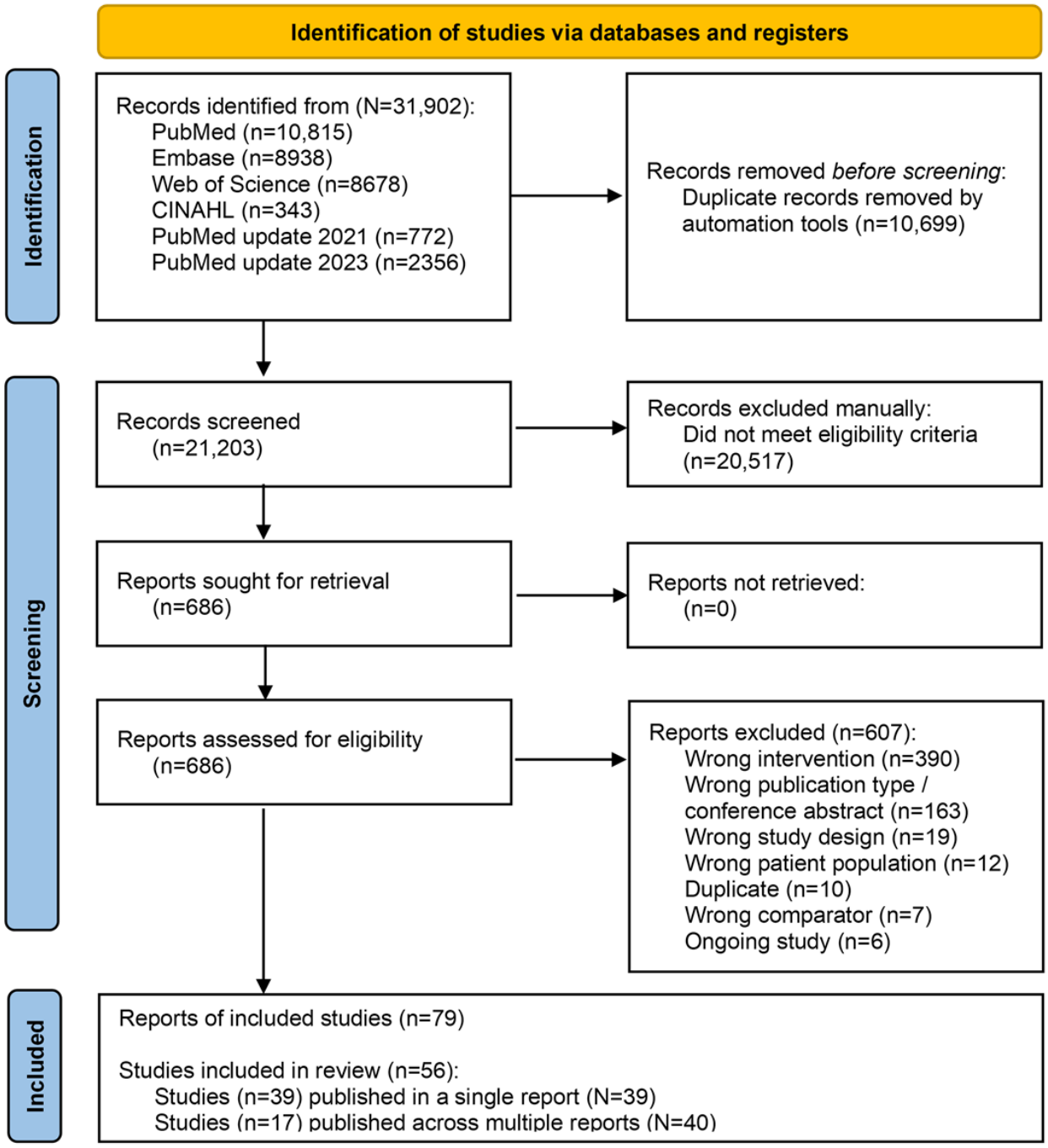
Results

Study Details

The search identified 31,902 records. After identification of duplicates, 21,203 (66.5%) papers that were screened at the title/abstract level resulted in 686 (3.2%) potentially eligible papers. Following full-text assessment, 606 (88.3%) reports were excluded, mainly due to wrong interventions and publication types, and 56 trials described in 79 (13%) papers [21-99] were included (see the flowchart in Figure 1). The number of study participants varied widely (range: 17-1653 individuals, median 212.5 individuals). Of the 56 trials, 17 (30.4%) included patients with heart disease, 13 (23.2%) included patients with COPD, 10 (17.9%) included patients with diabetes, 9 (16.1%) included patients with IBD, 6 (10.7%) included patients with RA, and, finally, 1 (1.7%) included patients with mixed diagnoses (heart disease and diabetes).

XSL•FO
RenderX

Figure 1. PRISMA flowchart for the study selection process.



PROM Characteristics

Characteristics of the selected studies and PROMs are summarized in Table 2. Telephonic PROM administration was most common, followed by devices and applications (apps). The weighted mean age among participants receiving a PROM intervention delivered over the phone was 62.9 years (63 years for phone calls and 57.9 years for SMS). The first described use of devices for collection of PROMs was published in 2008. Apps for tablets and smartphones were introduced in 2007 and 2009, respectively. The participants' weighted mean age was higher in interventions that used devices (71 years) than interventions using apps, webpages, or laptops (53.2 years).

XSL•FO
RenderX

Table 2. Overview of the characteristics of the included 56 trials reporting the results of RCTs[a] of the use of PROMs[b] in the clinic.

Study characteristics and categories	Studies (N=56), n (%)
Disease	
COPD[c]	13 (23.2)
Diabetes	10 (17.9)
Heart disease	17 (30.4)
Heart disease and diabetes	1 (1.8)
IBD[d]	9 (16.1)
RA[e]	6 (10.7)
Continent	
Asia	1 (1.8)
Europe	22 (39.3)
North America	27 (48.2)
Oceania	2 (3.6)
South America	1 (1.8)
Purpose	
Replace face-to-face visits	5 (8.9)
Systematic PROM assessment alone	24 (42.9)
Systematic PROM assessment and decision support	18 (32.1)
Systematic PROM assessment and dialogue support	9 (16.1)
Administration of PROM	
Device	10 (17.9)
Interview	3 (5.4)
Mobile app or tablet app	10 (17.9)
Paper	3 (5.4)
Telephone and SMS	16 (28.6)
Unknown	3 (5.4)
Web page or laptop	11 (19.6)
PROM intervention validation	
No, unspecified questions	15 (26.8)
No, specified questions	18 (32.1)
Yes, validated scales	23 (41.1)
Intervals between PROMs	
Daily or twice daily	20 (35.7)
Weekly or biweekly	8 (14.3)
Monthly	5 (8.9)
Bimonthly to biyearly	5 (8.9)
Before or at consultation	8 (14.3)
Optional	4 (7.1)
2-4 times	3 (5.4)
1 time	3 (5.4)
Feedback	
HCP[f]	8 (14.3)

XSL•FO
RenderX

Study characteristics and categories	Studies (N=56), n (%)
HCP by cutoff	25 (44.6)
Patient and HCP	8 (14.3)
Patient and HCP by cutoff	15 (26.8)

[a]RCT: randomized controlled trial.

[b]PROM: patient-reported outcome measure.

[a]COPD: chronic obstructive pulmonary disease.

[d]IBD: inflammatory bowel disease.

[e]RA: rheumatoid arthritis.

[f]HCP: health care professional.

All interventions included systematic PROM assessments, and some additionally included a predefined method for PROM-based decision-making (n=19, 33.9%) [21-39] or PROM-based dialogue (n=9, 16.1%) [40-48], and 5 (8.9%) interventions intended to replace face-to-face visits [49-53]. The PROM interventions used validated scales in 23 (41.1%) of the studies, while specified questions or unspecified questions were used in the remaining interventions. The content of the PROMs varied from symptoms and health status to the HRQoL, health beliefs, and self-care. All interventions included feedback to HCPs as per the inclusion criteria, while 23 (41.1%) also provided feedback to patients [22,27,28,30,32,33,36,37,39,41-43,50,51,54-62]. In 39 (69.6%) of the interventions, predefined cutoff values were used to ensure feedback to the HCPs, 18 (46.2%) of which included alerts. Intervals between PROMs were not always documented but varied widely from a single assessment to collections twice daily. In the 20 (35.7%) interventions where PROMs were collected daily or twice daily, the number of questions varied from 1 to 15. Daily collection was used for COPD (n=9, 16.1%) [28,32,34,35,43,55,63-65], heart disease (n=9, 16.1%) [36,37,57-59,61,66,67], IBD (n=1, 1.8%) [23], and RA (n=1, 1.8%) [68] treatment. The daily PROM collection continued for 3-24 months. Studies only collecting PROMs once or with long intervals between had more comprehensive questionnaires.

Characteristics of the studies and interventions are presented in Tables S6 and S7 in Multimedia Appendix 2.

Outcomes

All trials included more than one outcome. The following review of the results focuses on primary outcomes (Table S8 in Multimedia Appendix 2). Secondary outcomes are listed in Table S9 in Multimedia Appendix 2. Of the 56 trials, 12 (21.4%) had favorable results in the primary outcomes, 3 (5.4%) were noninferior, 6 (10.7%) had more than one primary outcome and mixed results, 6 (10.7%) were feasible, 1 (1.8%) was not feasible, 2 (3.6%) had no group comparison, 24 (42.9%) had no effect, and 2 (3.6%) had negative results by increasing hospital admissions with the intent of reducing them.

Of the 10 (17.9%) studies of patients with diabetes, 1 (10%) concluded noninferiority [53], 1 (10%) focused on feasibility [40], 1 (10%) demonstrated a mixed effect of PROMs [44], and the other 7 (70%) studies showed no effect [30,31,33,45,47,69,99]. For studies of patients with COPD (n=13, 23.2%), there was a positive or partially positive effect in 6 (46.2%); in addition, 2 (66.7%) of 3 feasibility studies were feasible [64,65]. In the 18 (32.1%) studies including patients with heart disease, 5 (27.8%) were positive and 1 (5.6%) intervention was feasible [59]. There was a positive effect of the intervention in 33% of the studies for patients with IBD (n=9, 16.1%), 2 (22.2%) were feasible [23,39], and 1 (11.1%) was noninferior [52]. Half of the studies including patients with RA were positive, and 1 (16.7%) intervention was noninferior [50].

Disease Activity

In 13 (23.2%) studies, disease activity or remission was reported by biomarker thresholds [30,31,44,47,53,60], Boolean remission [92], disease activity indexes [21,22,34,50-52,56], or the time to reach the final dose of medical treatment [37].

None of 5 (8.9%) studies including patients with diabetes reported an effect on glycemic control [30,44,47,60]. However, in an intervention using PROMs to decide routine visits, the hemoglobin A_{1c} (HbA_{1c}) levels were below the predefined noninferiority margin [53]. Biweekly automated telephone management was tested, with no effect on HbA_{1c} [30,31,60]. PROMs used to prioritize visits and facilitate discussion of psychological well-being [44] did not affect measures of HbA_{1c}.

A study of patients with RA receiving PROM-based telehealth with graphical overview and automated decision support was noninferior to usual care [50]. An intervention with frequent PROM monitoring using SMS did not result in Boolean remission of patients with early RA [92].

Common for 5 (8.9%) studies on patients with IBD (n=9, 16.1%), the collected PROMs triggered alerts and action plans customized for intervention patients generated based on the responses. One showed a positive effect [21], another showed noninferiority [52], whereas the others did not show a difference between the intervention group and usual care [22,51,56].

A daily telehealth approach with PROM collection and feedback reduced disease progression in patients with COPD [34]. A similar intervention for patients with HF succeeded in a faster titration of carvedilol compared to usual care [37].

Health Care Use and Mortality

Hospital admission [61], readmission [49,67,72,96,97], time to admission [32,35,54], and outpatient visits [29,84] were outcomes in 11 (19.6%) studies. In addition, 1 (1.8%) study had mortality [89] as an outcome, and 6 (10.7%) studies used a composite of admission and mortality [24,25,36,55,76,91] as

XSL•FO
RenderX

outcomes. Of 16 (28.6%) interventions evaluating the effects of PROMs on hospitalization, 3 (18.8%) reported a positive effect. A multicenter trial successfully reduced a composite endpoint of all-cause mortality and hospitalization for worsening HF in a telephone intervention using PROM to adjust treatment [25]. In contrast, no other PROM intervention studies reported effect on a composite outcome of hospital admission and death in patients with HF [24,36,76,91] or COPD [55].

An effective intervention for reducing the mean number of outpatient visits for patients with IBD included monthly reporting of PROMs into an app for tablets or smartphones with alerts prompting outpatient visits. The system intensified monitoring modules in the case of flares [84].

Two interventions used daily PROMs to generate alerts to prevent admission due to COPD exacerbations [32,35]. No difference was seen when comparing the intervention with usual care [32], whereas the time to hospitalization was shorter when comparing active feedback with passive PROMs [35]. For patients with HF, an underpowered study of daily PROMs indicated a lower mean time to the first HF-related hospitalization [54].

Two interventions using PROMs for systematic PROM assessment alone without a predefined plan for reacting to the responses did not find a reduction in hospitalization [96,97]. An intervention with daily PROMs collected via voice-activated technology had an unexpected increase in the number of hospitalizations and emergency department visits in participants with HF [61]. Two studies resulted in a higher number of readmissions using daily PROMs in patients with COPD [49] and patients with diabetes and HF [72]. A study on RA found that monitoring PROMs could reduce the number of physical visits, while maintaining tight control of disease activity [29].

Mental Well-Being

In patients with diabetes, PROMs have been used to screen for diabetes distress [40], psychological well-being [44], and depression [33,45]. In 2 (50%) studies, participants completed electronic PROMs prior to consultation, which did not show an effect on diabetes distress [40] or the depression score [33]. A favorable effect on mood was reported from an intervention using PROMs on psychological well-being as part of routine outpatient care [44]. In an intervention about self-care behavior and tailored talking points about emotional health, both control and intervention groups continued to have moderate-to-severe depression symptoms [45].

Health-Related Quality of Life

In studies aiming to improve the HRQoL using a PROM intervention (n=10, 17.7%), 2 (20%) studies showed an improvement [41,46], 1 (10%) showed noninferiority [52], 1 (10%) had mixed effects [63], 4 (40%) showed no effect [22,26,56,69], and 2 (20%) showed an unfavorable effect [49,71] compared to usual care. A multicenter trial found a significantly better health status favoring patients with COPD reporting PROMs of general well-being, symptoms, and medications. Alerts were reviewed by HCPs twice weekly, and patients were contacted either via messages or over the phone if any action was needed [63]. Automated telephone-based symptom and side effect monitoring had no effect on the quality of life (QoL) in patients with diabetic peripheral neuropathy [69].

Weekly monitoring of symptoms and medications in patients with IBD did not improve disease-specific QoL [22,56]. However, noninferiority was reported in a similar intervention with quarterly and as-needed PROM monitoring [52]. No effect was documented on quality-adjusted life-years for patients with acute coronary syndrome without a history of depression receiving systematic depression symptoms assessment with or without providing depression treatment compared to usual care [26].

Self-Efficacy, Self-Care, and Daily Functioning

Of 5 (8.9%) studies evaluating the use of PROMs to increase daily functioning [41,99], self-care [43], or self-efficacy [27,57], 4 (80%) showed positive results. In patients with HF, daily PROM collection over the phone increased self-efficacy [57]. Self-efficacy also improved among patients with RA when using PROMs prior to usual consultations with a nurse who provided patient education [27]. Self-care behavior improved in patients with COPD who answered questions on symptoms at least four times a week via a smartphone app that alerted HCPs [43]. Receiving personalized feedback on responding to somatic and psychosocial PROMs improved social participation in patients with IBD [41]. A cluster randomized trial concluded that using PROMs was inconsistent with the nurse-led detection of distress and daily functioning in routine practice [99].

Other Outcomes

Other outcomes included feasibility [23,49,59,64,65], patient satisfaction [42,62], quality of care [44,48,84], physician-patient interaction [42], and health care costs [21,28]. PROM interventions were considered feasible in 5 (8.9%) studies [23,39,59,64,65], and 1 (1.8%) intervention was considered unfeasible [49]. In 2 (22.2%) interventions for patients with IBD, the intervention was appreciated by compliers, but adherence was low [23,39], and 2 (33.3%) studies of patients with RA found that using PROMs before health care visits has no impact on patient satisfaction [42,62]. Monitoring of phycological well-being in outpatients with diabetes did not change the overall evaluation of the quality of diabetes care [44]. PROMs of psychosocial needs and priorities before routine consultations with a COPD nurse allowed shared decisions about self-management support and increased the quality of care in patients with COPD [48]. Collecting PROMs daily from patients with HF was deemed feasible by the authors, even though number of readmissions was similar in the two groups [59]. A monthly PROM-based self-management system did not enhance patient-reported quality of care [84].

Two studies evaluated cost savings [21,28]. Using daily PROMs of symptoms and medications in the treatment of COPD led to significant cost savings in a telephone intervention [28]. An intervention with proactive symptom monitoring was without a significant difference in median annual IBD-related health care charges [21].

XSL•FO
RenderX

Adverse Events

Several studies indicated adverse events [23,38,39,49,61, 65,71,72,89]. These included 2 (22.2%) studies in patients with heart disease and diabetes, which intended to reduce hospital admissions but increased the number instead [61, 72], and 1 (11.1%) study in which the subgroup analyses indicated increased mortality in women [89]. Adverse events were also observed in secondary outcomes: decreased peak performance and physical activity [65], increased hospital admissions [38], increased medical treatment [39], deterioration in symptoms [71], increased symptoms of depression [23], and higher costs [49].

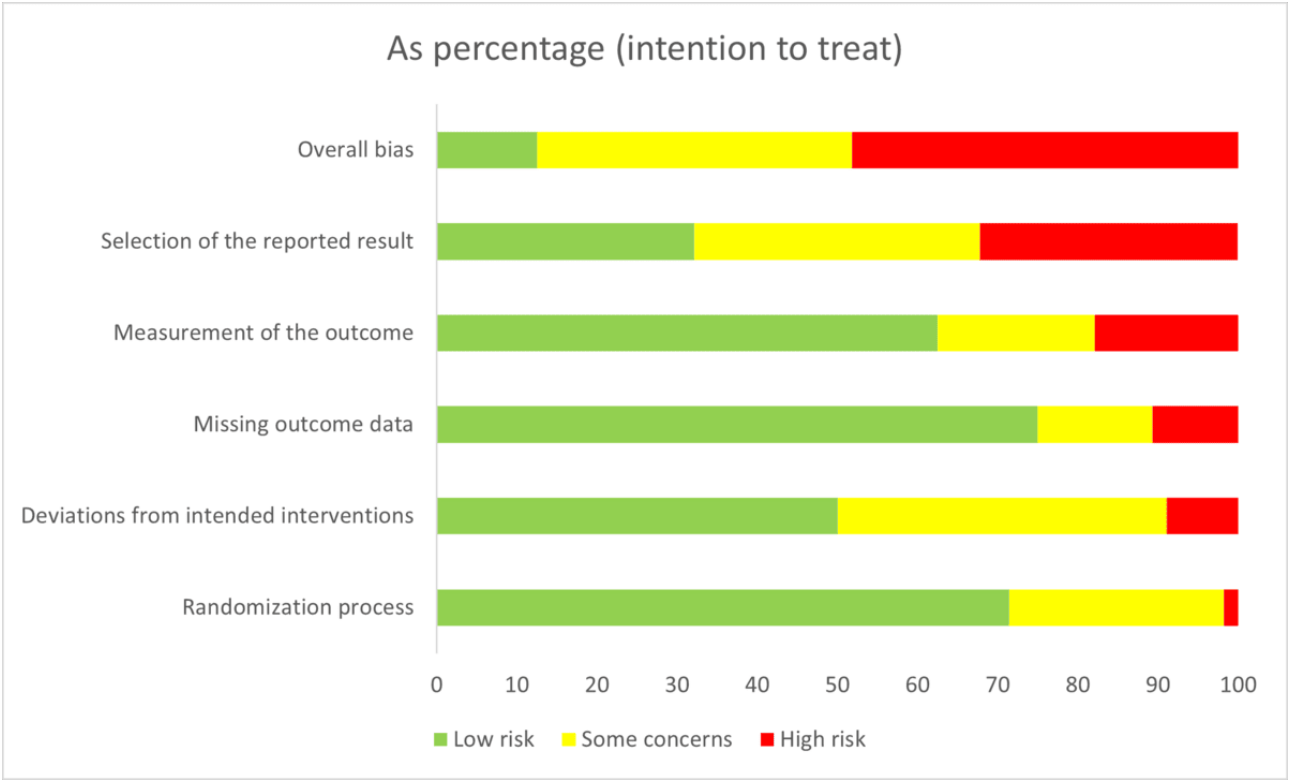
Characteristics of Effective PROMs

The predefined secondary aim of this systematic review was to describe effective PROM interventions with acceptable quality defined by a low risk of bias or some concerns. Excluding a study [24] that was later debunked by a larger study [89], 6 (10.7%) studies had positive results in the primary endpoint, had positive results in one of two primary endpoints, or were noninferior in replacing face-to-face sessions [25,42,46,50,53,57]. The PROM interventions used multiple administration forms and were focused on symptoms of disease, and 5 (83.3%) of the 6 studies included support for decisions and dialogue [25,42,46,50,53], 4 (66.7%) studies included validated PROMs [42,46,50,53], and 2 (33.3%) included specified questions [25,57]. In addition, 5 (83.3%) of the 6 had 2-week to 6-month intervals between PROM collection [25,42,46,50,53], and 4 (66.7%) of the 6 studies included feedback to patients as well as HCPs, with 3 (75%) having a graphical display of the results [42,46,50]. Furthermore, 2 (33.3%) studies included patients with heart disease [25,57], 2 (33.3%) included patients with RA [42,50], 1 (16.7%) included patients with diabetes [53], and 1 (16.7%) included patients with COPD [46]. Positive effects were achieved in the HRQoL [46], physician-reported interaction [42], self-efficacy [57], a composite endpoint with hospital admissions and death [25], and noninferior RA or diabetes activity when replacing outpatient visits with PROMs [50,53]. These 6 (10.7%) studies had little loss to follow-up, and 5 (83.3%) of the 6 studies had more study consenters than study decliners [25,42,46,50,53].

Risk of Bias

Seven studies were rated with an overall low risk of bias (Figure 2). Among the 22 (39.3%) studies with some concerns regarding risk of bias, concerns relating to the reporting of results were the most frequent (n=13, 59.1%), followed by concerns arising from deviations from the intended intervention (n=10, 45.5%), the randomization process (n=9, 40.9%), the measurement of the outcome (n=5, 22.7%), or missing outcome data (n=5, 22.7%). Nearly half of the studies had a high risk of bias (n=27, 48.2%). No studies had biases in all domains, but 2 (3.6%) studies had high risk in four of five domains [27,38]. The most frequent domain for a high risk of bias was selection of reported results (n=18, 32.1%) led by a lack of prospective descriptions of the trials in registries or protocol papers. Among studies with a low risk of bias or some concerns, 14.3% (4/28) had positive results, while among studies with a high risk of bias, 33.3% (9/27) had positive results. Risk-of-bias evaluation of the individual studies can be found in Table S8 in Multimedia Appendix 2.

Figure 2. Risk of bias across all included studies using RoB 2. RoB 2: version 2 of the Cochrane risk-of-bias tool for randomized trials.



XSL•FO
RenderX

Discussion

Principal Findings

This systematic literature review identified sparse evidence regarding the effectiveness of the clinical use of PROMs in patients with five noncommunicable diseases: diabetes, COPD, heart disease, RA, and IBD. Considering the increase in PROMs' popularity and the fact that we included five highly prevalent and burdensome diseases [100-102], it is notable that the literature search only revealed 56 trials in total, half of which had a high risk of bias. The included RCTs investigated a wide range of outcomes, thus producing a heterogeneous set of data and indicating a lack of consensus on the role of PROMs in clinical practice. Of the 56 RCTs, 12 presented positive results in the primary endpoint, 6 had mixed results in multiple primary endpoints, and 3 were noninferior. Focusing on the 28 RCTs with a low risk of bias or some concerns, 4 resulted in a better primary outcome and 2 demonstrated noninferiority. Successful interventions were characterized by using validated or specific PROMs and had little loss to follow up. They provided feedback to patients as well as HCPs, with 3 interventions incorporating a graphical display of the results.

Comparison With Prior Work

Compared to the results of this review, the results of reviews about acute cancer treatment are summarized as positive [14,103]. However, the majority of the included studies lacked power to detect group differences, and the conclusion of predominantly positive findings may be questioned [14]. The conditions of acute cancer treatment may also differ from those of long-term diseases where patients may have had more time to recognize, to learn self-management of symptoms and side effects, and to seek relevant health care.

Methodological Considerations

This review was conducted with screening by two independent researchers, and discrepancies were handled by including a third researcher in a consensus approach to ensure internal validity. The limited descriptions of interventions posed certain constraints, often lacking detail, which may have affected the external validity of this review. Adopting a more conservative approach of including only pure PROM interventions with no objective measurements at all would have reduced the number of eligible papers and the clinical relevance. Conversely, a less stringent approach, including more interventions where PROMs were one of multiple components, would have reduced focus and confidence in the results. Second, the heterogeneity of the studied PROM interventions and outcomes prevented meta-analyses and permitted only vote counting for data synthesis, which does not allow for differential weights to be allocated to each study.

The proportion of papers included in the review to the original number of studies identified in the search was less than 0.3%. The likely cause was the intervention search words that did not allow for distinction between RCTs using PROMs as endpoints and RCTs using PROMs for intervention. Attempts to reduce the number of papers for screening would have excluded relevant papers, which is why the searches were placed at a high level of sensitivity. In comparison, the systematic review by Graupner et al [14] about PROMs focusing on cancer revealed a quite similar proportion of included studies as 22 of 8341 identified studies were included.

Balancing Person-Centered Care With Evidence-Based Practice

The expectations toward PROMs are underlined by the implementation activities that have preceded robust evidence. Implementation before evaluation demonstrates the dissimilar approach toward PROM interventions to that of drug interventions that would have required robust trials before being released into the market. As demonstrated in this review, adverse effects may also occur in PROM interventions. Furthermore, PROMs require time and resources of HCPs as well as patients, and robust evaluations of PROMs are urgently needed.

PROMs are expected to support a person-centered approach. With 3 noninferiority trials, most trials evaluated superiority in a wide range of endpoints. The range of endpoints underscore the unclear expectations toward PROMs and the difficulty in operationalizing patient-centeredness. Noninferiority trials may be preferable if the purpose of PROMs is to replace face-to-face outpatient visits to compensate for the resources spent on PROM administration and implementation. However, trials to demonstrate noninferiority with a clinically acceptable margin may not be feasible to conduct [104]. Furthermore, most PROM interventions are designed as an addition to usual care, in which case only demonstrated superiority would merit spending resources on PROMs.

Future Directions

The 6 effective PROM interventions may serve as inspiration for further development. They focused on symptoms and were mostly used for systematic PROM assessment, plus a predefined PROM-based decision support method or dialogue support as opposed to systematic PROM assessment alone. This underscores the significance of the organizational structure to ensure consistent monitoring of PROMs and suitable predefined clinical actions. The effective PROM interventions had little loss to follow up and few study decliners, which is a testament to the acceptability of the interventions. A review of patients' reasons for not using digital PROMs has demonstrated the significance of patients' health (patients would forego PROMs if they were too well or too sick) and that it could be burdensome to be confronted with one's poor health and that technical problems, a lack of skills, language problems, and uncertainty about data security could all act as barriers toward the use of digital PROMs [105]. Patients with a moderate symptom burden who use PROMs could be referred to health care services at the expense of the most burdened patients who opt out of using PROMs, thereby increasing health care inequality.

Adding PROMS to usual care does not appear superior; however, replacing specific face-to-face visits with PROMS seems noninferior in patients with diabetes [53], IBD [52], and RA [50]. Noninferiority trials may be more suitable when PROMs are intended to replace face-to-face outpatient visits, thereby offsetting the resources allocated to the administration and implementation of PROMs.

XSL•FO
RenderX

Conclusion

The evidence supporting the clinical use of PROMs in the five chronic diseases included in this study is limited. In these diseases, the clinical application of PROMs does not seem to offer any advantage over standard care in terms of any endpoint. To derive insights from successful research, we highlighted 6 PROM interventions that demonstrated positive effects and exhibited a low risk of bias. These were characterized by symptom assessment with predefined cutoffs used for decision and dialogue support.

Acknowledgments

No generative artificial intelligence tools were used to create the original scientific content of the manuscript. The authors used a generative artificial intelligence tool (Paperpal) to enhance the clarity and readability of the text during manuscript revision. This work was funded by an unrestricted grant from the Capital Region, Denmark (no grant number available). The sponsor played no role in the analysis or interpretation.

Data Availability

All data generated and analyzed during this study are included in this published paper and in Multimedia Appendix 2. The databases created during the data extraction process are available from the corresponding author upon reasonable request.

Authors' Contributions

MV contributed to the protocol, screened papers, assessed the risk of bias, made the final decision to include studies, and took the lead in writing the manuscript. BIO contributed to the protocol, developed the search string, screened papers, assessed the risk of bias, and made the final decision of inclusion of studies. KSB devised the project and the main conceptual ideas, contributed to the protocol, assessed the risk of bias, made the final decision of inclusion of studies, and contributed substantially to the manuscript. KEL supervised the project. All authors provided critical feedback and helped shape the research, analysis, and manuscript. All authors have read and approved the final manuscript.

Conflicts of Interest

None declared.

Multimedia Appendix 1
PRISMA checklist.
[PDF File (Adobe PDF File), 294 KB - medinform_v13i1e66160_app1.pdf]

Multimedia Appendix 2
Search strategy, data synthesis, and additional results.
[PDF File (Adobe PDF File), 823 KB - medinform_v13i1e66160_app2.pdf]

References

1. Calvert M, Kyte D, Mercieca-Bebber R, Slade A, Chan A, King MT, the SPIRIT-PRO Group, et al. Guidelines for Inclusion of Patient-Reported Outcomes in Clinical Trial Protocols: The SPIRIT-PRO Extension. JAMA 2018 Feb 06;319(5):483-494 [FREE Full text] [doi: 10.1001/jama.2017.21903] [Medline: 29411037]
2. Almario C, Spiegel B. Employing Irritable Bowel Syndrome Patient-Reported Outcomes in the Clinical Trenches. Clin Gastroenterol Hepatol 2018 Apr;16(4):462-466.e2. [doi: 10.1016/j.cgh.2017.12.026] [Medline: 29555225]
3. Bouazza YB, Chiairi I, El Kharbouchi O, De Backer L, Vanhoutte G, Janssens A, et al. Patient-reported outcome measures (PROMs) in the management of lung cancer: a systematic review. Lung Cancer 2017 Nov;113:140-151 [FREE Full text] [doi: 10.1016/j.lungcan.2017.09.011] [Medline: 29110842]
4. Kocks JWH, Seys SF, van Duin TS, Diamant Z, Tsiligianni IG. Assessing patient-reported outcomes in asthma and COPD patients: which can be recommended in clinical practice? Curr Opin Pulm Med 2018 Jan;24(1):18-23 [FREE Full text] [doi: 10.1097/MCP.0000000000000447] [Medline: 29084018]
5. Greenhalgh J, Meadows K. The effectiveness of the use of patient-based measures of health in routine practice in improving the process and outcomes of patient care: a literature review. J Eval Clin Pract 1999 Nov;5(4):401-416 [FREE Full text] [doi: 10.1046/j.1365-2753.1999.00209.x] [Medline: 10579704]
6. Garcia SF, Wortman K, Cella D, Wagner LI, Bass M, Kircher S, et al. Implementing electronic health record-integrated screening of patient-reported symptoms and supportive care needs in a comprehensive cancer center. Cancer 2019 Nov 15;125(22):4059-4068 [FREE Full text] [doi: 10.1002/cncr.32172] [Medline: 31373682]
7. Howell D, Li M, Sutradhar R, Gu S, Iqbal J, O'Brien MA, et al. Integration of patient-reported outcomes (PROs) for personalized symptom management in "real-world" oncology practices: a population-based cohort comparison study of

XSL•FO
RenderX

impact on healthcare utilization. Support Care Cancer 2020 Oct 04;28(10):4933-4942 [FREE Full text] [doi: 10.1007/s00520-020-05313-3] [Medline: 32020357]
8. Lavallee DC, Chenok KE, Love RM, Petersen C, Holve E, Segal CD, et al. Incorporating patient-reported outcomes into health care to engage patients and enhance care. Health Aff (Millwood) 2016 Apr;35(4):575-582 [FREE Full text] [doi: 10.1377/hlthaff.2015.1362] [Medline: 27044954]
9. Marshall S, Haywood K, Fitzpatrick R. Impact of patient-reported outcome measures on routine practice: a structured review. J Eval Clin Pract 2006 Oct;12(5):559-568 [FREE Full text] [doi: 10.1111/j.1365-2753.2006.00650.x] [Medline: 16987118]
10. Black N. Patient reported outcome measures could help transform healthcare. BMJ 2013 Jan 28;346:f167 [FREE Full text] [doi: 10.1136/bmj.f167] [Medline: 23358487]
11. Carfora L, Foley CM, Hagi-Diakou P, Lesty PJ, Sandstrom ML, Ramsey I, et al. Patients' experiences and perspectives of patient-reported outcome measures in clinical care: a systematic review and qualitative meta-synthesis. PLoS One 2022 Apr 21;17(4):e0267030 [FREE Full text] [doi: 10.1371/journal.pone.0267030] [Medline: 35446885]
12. Boyce MB, Browne JP, Greenhalgh J. The experiences of professionals with using information from patient-reported outcome measures to improve the quality of healthcare: a systematic review of qualitative research. BMJ Qual Saf 2014 Jun;23(6):508-518 [FREE Full text] [doi: 10.1136/bmjqs-2013-002524] [Medline: 24505110]
13. Kjaer T, Johansen C, Andersen E, Karlsen R, Nielsen AL, Frederiksen K, et al. Do we reach the patients with the most problems? Baseline data from the WebCan study among survivors of head-and-neck cancer, Denmark. J Cancer Surviv 2016 Apr;10(2):251-260 [FREE Full text] [doi: 10.1007/s11764-015-0471-x] [Medline: 26227655]
14. Graupner C, Kimman ML, Mul S, Slok AHM, Claessens D, Kleijnen J, et al. Patient outcomes, patient experiences and process indicators associated with the routine use of patient-reported outcome measures (PROMs) in cancer care: a systematic review. Support Care Cancer 2021 Feb;29(2):573-593 [FREE Full text] [doi: 10.1007/s00520-020-05695-4] [Medline: 32875373]
15. Moher D, Liberati A, Tetzlaff J, Altman DG, PRISMA Group. Preferred reporting items for systematic reviews and meta-analyses: the PRISMA statement. BMJ 2009 Jul 21;339:b2535 [FREE Full text] [doi: 10.1136/bmj.b2535] [Medline: 19622551]
16. Page MJ, McKenzie JE, Bossuyt PM, Boutron I, Hoffmann TC, Mulrow CD, et al. The PRISMA 2020 statement: an updated guideline for reporting systematic reviews. BMJ 2021 Mar 29;372:n71 [FREE Full text] [doi: 10.1136/bmj.n71] [Medline: 33782057]
17. GBD 2019 DiseasesInjuries Collaborators. Global burden of 369 diseases and injuries in 204 countries and territories, 1990-2019: a systematic analysis for the Global Burden of Disease Study 2019. Lancet 2020 Oct 17;396(10258):1204-1222 [FREE Full text] [doi: 10.1016/S0140-6736(20)30925-9] [Medline: 33069326]
18. Higgins JPT, Altman DG, Gøtzsche PC, Jüni P, Moher D, Oxman AD, Cochrane Bias Methods Group, Cochrane Statistical Methods Group. The Cochrane Collaboration's tool for assessing risk of bias in randomised trials. BMJ 2011 Oct 18;343:d5928 [FREE Full text] [doi: 10.1136/bmj.d5928] [Medline: 22008217]
19. Campbell M, McKenzie JE, Sowden A, Katikireddi SV, Brennan SE, Ellis S, et al. Synthesis without meta-analysis (SWiM) in systematic reviews: reporting guideline. BMJ 2020 Jan 16;368:l6890 [FREE Full text] [doi: 10.1136/bmj.l6890] [Medline: 31948937]
20. Guyatt GH, Oxman AD, Vist GE, Kunz R, Falck-Ytter Y, Alonso-Coello P, GRADE Working Group. GRADE: an emerging consensus on rating quality of evidence and strength of recommendations. BMJ 2008 Apr 26;336(7650):924-926 [FREE Full text] [doi: 10.1136/bmj.39489.470347.AD] [Medline: 18436948]
21. Berinstein J, Cohen-Mekelburg S, Greenberg G, Wray D, Berry S, Saini S, et al. A care coordination intervention improves symptoms but not charges in high-risk patients with inflammatory bowel disease. Clin Gastroenterol Hepatol 2022 May;20(5):1029-1038.e9 [FREE Full text] [doi: 10.1016/j.cgh.2021.08.034] [Medline: 34461298]
22. Cross RK, Langenberg P, Regueiro M, Schwartz DA, Tracy JK, Collins JF, et al. A randomized controlled trial of telemedicine for patients with inflammatory bowel disease (TELE-IBD). Am J Gastroenterol 2019 Mar 11;114(3):472-482 [FREE Full text] [doi: 10.1038/s41395-018-0272-8] [Medline: 30410041]
23. Elkjaer M, Shuhaibar M, Burisch J, Bailey Y, Scherfig H, Laugesen B, et al. E-health empowers patients with ulcerative colitis: a randomised controlled trial of the web-guided 'constant-care' approach. Gut 2010 Dec;59(12):1652-1661 [FREE Full text] [doi: 10.1136/gut.2010.220160] [Medline: 21071584]
24. Frasure-Smith N, Prince R. The Ischemic Heart Disease Life Stress Monitoring Program: 18-month mortality results. Can J Public Health 1986;77 Suppl 1:46-50. [Medline: 3527398]
25. GESICA Investigators. Randomised trial of telephone intervention in chronic heart failure: DIAL trial. BMJ 2005 Aug 20;331(7514):425 [FREE Full text] [doi: 10.1136/bmj.38516.398067.E0] [Medline: 16061499]
26. Kronish IM, Moise N, Cheung YK, Clarke GN, Dolor RJ, Duer-Hefele J, et al. Effect of depression screening after acute coronary syndromes on quality of life: the CODIACS-QoL randomized clinical trial. JAMA Intern Med 2020 Jan 01;180(1):45-53 [FREE Full text] [doi: 10.1001/jamainternmed.2019.4518] [Medline: 31633746]

XSL•FO
RenderX

27. Ndosi M, Johnson D, Young T, Hardware B, Hill J, Hale C, et al. Effects of needs-based patient education on self-efficacy and health outcomes in people with rheumatoid arthritis: a multicentre, single blind, randomised controlled trial. Ann Rheum Dis 2016 Jun 10;75(6):1126-1132 [FREE Full text] [doi: 10.1136/annrheumdis-2014-207171] [Medline: 26162769]
28. Paré G, Poba-Nzaou P, Sicotte C, Beaupré A, Lefrançois É, Nault D, et al. Comparing the costs of home telemonitoring and usual care of chronic obstructive pulmonary disease patients: a randomized controlled trial. Eur Res Telemed 2013 Jun;2(2):35-47 [FREE Full text] [doi: 10.1016/j.eurtel.2013.05.001]
29. Pers Y, Valsecchi V, Mura T, Aouinti S, Filippi N, Marouen S, et al. A randomized prospective open-label controlled trial comparing the performance of a connected monitoring interface versus physical routine monitoring in patients with rheumatoid arthritis. Rheumatology (Oxford) 2021 Apr 06;60(4):1659-1668 [FREE Full text] [doi: 10.1093/rheumatology/keaa462] [Medline: 33020846]
30. Piette JD, Weinberger M, Kraemer FB, McPhee SJ. Impact of automated calls with nurse follow-up on diabetes treatment outcomes in a Department of Veterans Affairs health care system: a randomized controlled trial. Diabetes Care 2001 Feb;24(2):202-208 [FREE Full text] [doi: 10.2337/diacare.24.2.202] [Medline: 11213866]
31. Piette JD, Weinberger M, McPhee SJ. The effect of automated calls with telephone nurse follow-up on patient-centered outcomes of diabetes care: a randomized, controlled trial. Med Care 2000 Feb;38(2):218-230 [FREE Full text] [doi: 10.1097/00005650-200002000-00011] [Medline: 10659695]
32. Pinnock H, Hanley J, McCloughan L, Todd A, Krishan A, Lewis S, et al. Effectiveness of telemonitoring integrated into existing clinical services on hospital admission for exacerbation of chronic obstructive pulmonary disease: researcher blind, multicentre, randomised controlled trial. BMJ 2013 Oct 17;347(oct17 3):f6070 [FREE Full text] [doi: 10.1136/bmj.f6070] [Medline: 24136634]
33. Pouwer F, Tack CJ, Geelhoed-Duijvestijn PHLM, Bazelmans E, Beekman AT, Heine RJ, et al. Limited effect of screening for depression with written feedback in outpatients with diabetes mellitus: a randomised controlled trial. Diabetologia 2011 Apr;54(4):741-748 [FREE Full text] [doi: 10.1007/s00125-010-2033-0] [Medline: 21221528]
34. Rassouli F, Germann A, Baty F, Kohler M, Stolz D, Thurnheer R, et al. Telehealth mitigates COPD disease progression compared to standard of care: a randomized controlled crossover trial. J Intern Med 2021 Mar;289(3):404-410 [FREE Full text] [doi: 10.1111/joim.13230] [Medline: 33428219]
35. Sink E, Patel K, Groenendyk J, Peters R, Som A, Kim E, et al. Effectiveness of a novel, automated telephone intervention on time to hospitalisation in patients with COPD: a randomised controlled trial. J Telemed Telecare 2020 Apr;26(3):132-139 [FREE Full text] [doi: 10.1177/1357633X18800211] [Medline: 30269640]
36. Soran OZ, Piña IL, Lamas GA, Kelsey SF, Selzer F, Pilotte J, et al. A randomized clinical trial of the clinical effects of enhanced heart failure monitoring using a computer-based telephonic monitoring system in older minorities and women. J Card Fail 2008 Nov;14(9):711-717 [FREE Full text] [doi: 10.1016/j.cardfail.2008.06.448] [Medline: 18995174]
37. Spaeder J, Najjar SS, Gerstenblith G, Hefter G, Kern L, Palmer JG, et al. Rapid titration of carvedilol in patients with congestive heart failure: a randomized trial of automated telemedicine versus frequent outpatient clinic visits. Am Heart J 2006 Apr;151(4):844.e1-844.10 [FREE Full text] [doi: 10.1016/j.ahj.2005.06.044] [Medline: 16569544]
38. Subramanian U, Fihn SD, Weinberger M, Plue L, Smith FE, Udris EM, et al. A controlled trial of including symptom data in computer-based care suggestions for managing patients with chronic heart failure. Am J Med 2004 Mar 15;116(6):375-384 [FREE Full text] [doi: 10.1016/j.amjmed.2003.11.021] [Medline: 15006586]
39. Östlund I, Werner M, Karling P. Self-monitoring with home based fecal calprotectin is associated with increased medical treatment. A randomized controlled trial on patients with inflammatory bowel disease. Scand J Gastroenterol 2021 Jan;56(1):38-45 [FREE Full text] [doi: 10.1080/00365521.2020.1854342] [Medline: 33284639]
40. Hernar I, Graue M, Richards DA, Strandberg RB, Nilsen RM, Rekdal M, et al. Use of patient-reported outcome measures (PROMs) in clinical diabetes consultations: the DiaPROM randomised controlled pilot trial. BMJ Open 2021 Apr 14;11(4):e042353 [FREE Full text] [doi: 10.1136/bmjopen-2020-042353] [Medline: 33853796]
41. Hueppe A, Langbrandtner J, Raspe H. Inviting patients with inflammatory bowel disease to active involvement in their own care: a randomized controlled trial. Inflamm Bowel Dis 2014 Jun;20(6):1057-1069 [FREE Full text] [doi: 10.1097/mib.0000000000000044] [Medline: 24788217]
42. Huffstutter J, David Craig W, Schimizzi G, Harshbarger J, Lisse J, Kasle S, et al. A multicenter, randomized, open study to evaluate the impact of an electronic data capture system on the care of patients with rheumatoid arthritis. Curr Med Res Opin 2007 Jul 11;23(8):1967-1979 [FREE Full text] [doi: 10.1185/030079907x210624] [Medline: 17626700]
43. Park SK, Bang CH, Lee SH. Evaluating the effect of a smartphone app-based self-management program for people with COPD: a randomized controlled trial. Appl Nurs Res 2020 Apr;52:151231 [FREE Full text] [doi: 10.1016/j.apnr.2020.151231] [Medline: 31955942]
44. Pouwer F, Snoek F, van der Ploeg HM, Adèr HJ, Heine R. Monitoring of psychological well-being in outpatients with diabetes: effects on mood, HbA(1c), and the patient's evaluation of the quality of diabetes care: a randomized controlled trial. Diabetes Care 2001 Nov;24(11):1929-1935 [FREE Full text] [doi: 10.2337/diacare.24.11.1929] [Medline: 11679459]
45. Scollan-Koliopoulos M, Herrera I, Romano K, Gregory C, Rapp K, Bleich D. Healthcare technician delivered screening of adults with diabetes to improve primary care provider recognition of depression. J Family Med Prim Care 2012 Jul;1(2):97-102 [FREE Full text] [doi: 10.4103/2249-4863.104955] [Medline: 24479015]

XSL•FO
RenderX

46. Slok AHM, Kotz D, van Breukelen G, Chavannes NH, Rutten-van Mölken MPMH, Kerstjens HAM, et al. Effectiveness of the Assessment of Burden of COPD (ABC) tool on health-related quality of life in patients with COPD: a cluster randomised controlled trial in primary and hospital care. BMJ Open 2016 Jul 11;6(7):e011519 [FREE Full text] [doi: 10.1136/bmjopen-2016-011519] [Medline: 27401361]
47. Vo MT, Uratsu CS, Estacio KR, Altschuler A, Kim E, Alexeeff SE, et al. Prompting patients with poorly controlled diabetes to identify visit priorities before primary care visits: a pragmatic cluster randomized trial. J Gen Intern Med 2019 Jun 11;34(6):831-838 [FREE Full text] [doi: 10.1007/s11606-018-4756-4] [Medline: 30746642]
48. Zakrisson A, Arne M, Lisspers K, Lundh L, Sandelowsky H, Ställberg B, et al. Improved quality of care by using the PRISMS form to support self-management in patients with COPD: a randomised controlled trial. J Clin Nurs 2020 Jul 30;29(13-14):2410-2419 [FREE Full text] [doi: 10.1111/jocn.15253] [Medline: 32220091]
49. Bentley CL, Mountain GA, Thompson J, Fitzsimmons DA, Lowrie K, Parker SG, et al. A pilot randomised controlled trial of a telehealth intervention in patients with chronic obstructive pulmonary disease: challenges of clinician-led data collection. Trials 2014 Aug 06;15:313 [FREE Full text] [doi: 10.1186/1745-6215-15-313] [Medline: 25100550]
50. de Thurah A, Stengaard-Pedersen K, Axelsen M, Fredberg U, Schougaard LMV, Hjollund NHI, et al. Tele-health followup strategy for tight control of disease activity in rheumatoid arthritis: results of a randomized controlled trial. Arthritis Care Res (Hoboken) 2018 Mar 23;70(3):353-360 [FREE Full text] [doi: 10.1002/acr.23280] [Medline: 28511288]
51. Del Hoyo J, Nos P, Faubel R, Muñoz D, Domínguez D, Bastida G, et al. A web-based telemanagement system for improving disease activity and quality of life in patients with complex inflammatory bowel disease: pilot randomized controlled trial. J Med Internet Res 2018 Nov 27;20(11):e11602 [FREE Full text] [doi: 10.2196/11602] [Medline: 30482739]
52. McCombie A, Walmsley R, Barclay M, Ho C, Langlotz T, Regenbrecht H, et al. A noninferiority randomized clinical trial of the use of the smartphone-based health applications IBDsmart and IBDoc in the care of inflammatory bowel disease patients. Inflamm Bowel Dis 2020 Jun 18;26(7):1098-1109 [FREE Full text] [doi: 10.1093/ibd/izz252] [Medline: 31644793]
53. Laurberg T, Schougaard L, Hjollund N, Lomborg K, Hansen T, Jensen A. Randomized controlled study to evaluate the impact of flexible patient-controlled visits in people with type 1 diabetes: the DiabetesFlex trial. Diabet Med 2022 May;39(5):e14791 [FREE Full text] [doi: 10.1111/dme.14791] [Medline: 35028992]
54. Boyne JJJ, Vrijhoef HJM, Crijns HJGM, De Weerd G, Kragten J, Gorgels APM, TEHAF Investigators. Tailored telemonitoring in patients with heart failure: results of a multicentre randomized controlled trial. Eur J Heart Fail 2012 Jul;14(7):791-801 [FREE Full text] [doi: 10.1093/eurjhf/hfs058] [Medline: 22588319]
55. Cordova FC, Ciccolella D, Grabianowski C, Gaughan J, Brennan K, Goldstein F, et al. A telemedicine-based intervention reduces the frequency and severity of copd exacerbation symptoms: a randomized, controlled trial. Telemed J E Health 2016 Feb 10;22(2):114-122 [FREE Full text] [doi: 10.1089/tmj.2015.0035] [Medline: 26259074]
56. Cross RK, Cheevers N, Rustgi A, Langenberg P, Finkelstein J. Randomized, controlled trial of home telemanagement in patients with ulcerative colitis (UC HAT). Inflamm Bowel Dis 2012 Jun;18(6):1018-1025 [FREE Full text] [doi: 10.1002/ibd.21795] [Medline: 21688350]
57. Dang S, Karanam C, Gómez-Marín O. Outcomes of a mobile phone intervention for heart failure in a minority county hospital population. Telemed J E Health 2017 Jun;23(6):473-484 [FREE Full text] [doi: 10.1089/tmj.2016.0211] [Medline: 28051357]
58. Dansky K, Vasey J. Managing heart failure patients after formal homecare. Telemed J E Health 2009 Dec;15(10):983-991 [FREE Full text] [doi: 10.1089/tmj.2009.0064] [Medline: 19929234]
59. Johnson AE, Routh S, Taylor CN, Leopold M, Beatty K, McNamara DM, et al. Developing and implementing an mHealth heart failure self-care program to reduce readmissions: randomized controlled trial. JMIR Cardio 2022 Mar 21;6(1):e33286 [FREE Full text] [doi: 10.2196/33286] [Medline: 35311679]
60. Piette JD, Weinberger M, McPhee SJ, Mah CA, Kraemer FB, Crapo LM. Do automated calls with nurse follow-up improve self-care and glycemic control among vulnerable patients with diabetes? Am J Med 2000 Jan;108(1):20-27 [FREE Full text] [doi: 10.1016/s0002-9343(99)00298-3] [Medline: 11059437]
61. Shara N, Bjarnadottir MV, Falah N, Chou J, Alqutri HS, Asch FM, et al. Voice activated remote monitoring technology for heart failure patients: study design, feasibility and observations from a pilot randomized control trial. PLoS One 2022 May 6;17(5):e0267794 [FREE Full text] [doi: 10.1371/journal.pone.0267794] [Medline: 35522660]
62. Colls J, Lee Y, Xu C, Corrigan C, Lu F, Marquez-Grap G, et al. Patient adherence with a smartphone app for patient-reported outcomes in rheumatoid arthritis. Rheumatology (Oxford) 2021 Jan 05;60(1):108-112 [FREE Full text] [doi: 10.1093/rheumatology/keaa202] [Medline: 32572490]
63. Farmer A, Williams V, Velardo C, Shah SA, Yu L, Rutter H, et al. Self-management support using a digital health system compared with usual care for chronic obstructive pulmonary disease: randomized controlled trial. J Med Internet Res 2017 May 03;19(5):e144 [FREE Full text] [doi: 10.2196/jmir.7116] [Medline: 28468749]
64. Lewis KE, Annandale JA, Warm DL, Hurlin C, Lewis MJ, Lewis L. Home telemonitoring and quality of life in stable, optimised chronic obstructive pulmonary disease. J Telemed Telecare 2010;16(5):253-259 [FREE Full text] [doi: 10.1258/jtt.2009.090907] [Medline: 20483881]

XSL•FO
RenderX

65. Nguyen HQ, Gill DP, Wolpin S, Steele BG, Benditt JO. Pilot study of a cell phone-based exercise persistence intervention post-rehabilitation for COPD. Int J Chron Obstruct Pulmon Dis 2009;4:301-313 [FREE Full text] [doi: 10.2147/copd.s6643] [Medline: 19750190]
66. Boyne J, Vrijhoef H, Wit R, Gorgels A. Telemonitoring in patients with heart failure, the TEHAF study: study protocol of an ongoing prospective randomised trial. Int J Nurs Stud 2011 Jan;48(1):94-99 [FREE Full text] [doi: 10.1016/j.ijnurstu.2010.05.017] [Medline: 20615505]
67. Goldberg LR, Piette JD, Walsh MN, Frank TA, Jaski BE, Smith AL, WHARF Investigators. Randomized trial of a daily electronic home monitoring system in patients with advanced heart failure: the Weight Monitoring in Heart Failure (WHARF) trial. Am Heart J 2003 Oct;146(4):705-712 [FREE Full text] [doi: 10.1016/S0002-8703(03)00393-4] [Medline: 14564327]
68. Lee Y, Lu F, Colls J, Murray M, Suh D, Song J, et al. Effect of a mobile app to monitor patient reported outcomes in rheumatoid arthritis: a randomized controlled trial. Arthritis Rheumatol 2019;71(Suppl 10):1430-1431 [FREE Full text]
69. Adams AS, Schmittdiel JA, Altschuler A, Bayliss EA, Neugebauer R, Ma L, et al. Automated symptom and treatment side effect monitoring for improved quality of life among adults with diabetic peripheral neuropathy in primary care: a pragmatic, cluster, randomized, controlled trial. Diabet Med 2019 Jan 07;36(1):52-61 [FREE Full text] [doi: 10.1111/dme.13840] [Medline: 30343489]
70. Kargiannakis M, Fitzsimmons DA, Bentley CL, Mountain GA. Does telehealth monitoring identify exacerbations of chronic obstructive pulmonary disease and reduce hospitalisations? An analysis of system data. JMIR Med Inform 2017 Mar 22;5(1):e8 [FREE Full text] [doi: 10.2196/medinform.6359] [Medline: 28330829]
71. Berkhof FF, van den Berg JWK, Uil SM, Kerstjens HAM. Telemedicine, the effect of nurse-initiated telephone follow up, on health status and health-care utilization in COPD patients: a randomized trial. Respirology 2015 Feb;20(2):279-285 [FREE Full text] [doi: 10.1111/resp.12437] [Medline: 25400242]
72. Bowles KH, Holland DE, Horowitz DA. A comparison of in-person home care, home care with telephone contact and home care with telemonitoring for disease management. J Telemed Telecare 2009;15(7):344-350 [FREE Full text] [doi: 10.1258/jtt.2009.090118] [Medline: 19815903]
73. Boyne JJJ, Vrijhoef HJM, Spreeuwenberg M, De Weerd G, Kragten J, Gorgels APM, TEHAF investigators. Effects of tailored telemonitoring on heart failure patients' knowledge, self-care, self-efficacy and adherence: a randomized controlled trial. Eur J Cardiovasc Nurs 2014 Jun;13(3):243-252 [FREE Full text] [doi: 10.1177/1474515113487464] [Medline: 23630403]
74. Gingele AJ, Ramaekers B, Brunner-La Rocca HP, De Weerd G, Kragten J, van Empel V, et al. Effects of tailored telemonitoring on functional status and health-related quality of life in patients with heart failure. Neth Heart J 2019 Nov 14;27(11):565-574 [FREE Full text] [doi: 10.1007/s12471-019-01323-x] [Medline: 31414308]
75. Ramaekers B, Janssen-Boyne J, Gorgels A, Vrijhoef H. Adherence among telemonitored patients with heart failure to pharmacological and nonpharmacological recommendations. Telemed J E Health 2009;15(6):517-524 [FREE Full text] [doi: 10.1089/tmj.2009.0160] [Medline: 19566401]
76. Chaudhry SI, Mattera JA, Curtis JP, Spertus JA, Herrin J, Lin Z, et al. Telemonitoring in patients with heart failure. N Engl J Med 2010 Dec 09;363(24):2301-2309 [FREE Full text] [doi: 10.1056/NEJMoa1010029] [Medline: 21080835]
77. Jayaram NM, Khariton Y, Krumholz HM, Chaudhry SI, Mattera J, Tang F, et al. Impact of telemonitoring on health status. Circ Cardiovasc Qual Outcomes 2017 Dec;10(12):e004148 [FREE Full text] [doi: 10.1161/CIRCOUTCOMES.117.004148] [Medline: 29237746]
78. Bilgrami Z, Abutaleb A, Chudy-Onwugaje K, Langenberg P, Regueiro M, Schwartz DA, et al. Effect of telemedicine for inflammatory bowel disease on patient activation and self-efficacy. Dig Dis Sci 2020 Jan;65(1):96-103 [FREE Full text] [doi: 10.1007/s10620-018-5433-5] [Medline: 30604373]
79. Quinn CC, Chard S, Roth EG, Eckert JK, Russman KM, Cross RK. The telemedicine for patients with inflammatory bowel disease (TELE-IBD) clinical trial: qualitative assessment of participants' perceptions. J Med Internet Res 2019 Jun 03;21(6):e14165 [FREE Full text] [doi: 10.2196/14165] [Medline: 31162128]
80. Schliep M, Chudy-Onwugaje K, Abutaleb A, Langenberg P, Regueiro M, Schwartz D, et al. Telemedicine for patients with inflammatory bowel disease (TELE-IBD) does not improve depressive symptoms or general quality of life compared with standard care at tertiary referral centers. Crohns Colitis 360 2020 Jan;2(1):otaa002 [FREE Full text] [doi: 10.1093/crocol/otaa002] [Medline: 32201859]
81. Bilgrami Z, Abutaleb A, Chudy-Onwugaje K, Langenberg P, Regueiro M, Schwartz D, et al. Correction to: Effect of TELEmedicine for Inflammatory Bowel Disease on Patient Activation and Self-Efficacy. Dig Dis Sci 2020 Feb;65(2):668. [doi: 10.1007/s10620-019-05953-4] [Medline: 31792670]
82. Dang S, Karanam C, Gómez-Orozco C, Gómez-Marín O. Mobile phone intervention for heart failure in a minority urban county hospital population: usability and patient perspectives. Telemed J E Health 2017 Jul;23(7):544-554 [FREE Full text] [doi: 10.1089/tmj.2016.0224] [Medline: 28051761]
83. de Jong MJ, Boonen A, van der Meulen-de Jong AE, Romberg-Camps MJ, van Bodegraven AA, Mahmmod N, et al. Cost-effectiveness of telemedicine-directed specialized vs standard care for patients with inflammatory bowel diseases in a randomized trial. Clin Gastroenterol Hepatol 2020 Jul;18(8):1744-1752 [FREE Full text] [doi: 10.1016/j.cgh.2020.04.038] [Medline: 32335133]

XSL•FO
RenderX

84. de Jong MJ, van der Meulen-de Jong AE, Romberg-Camps MJ, Becx MC, Maljaars JP, Cilissen M, et al. Telemedicine for management of inflammatory bowel disease (myIBDcoach): a pragmatic, multicentre, randomised controlled trial. Lancet 2017 Sep;390(10098):959-968 [FREE Full text] [doi: 10.1016/s0140-6736(17)31327-2] [Medline: 28716313]
85. Skovsgaard C, Kruse M, Hjollund N, Maribo T, de Thurah A. Cost-effectiveness of a telehealth intervention in rheumatoid arthritis: economic evaluation of the telehealth in RA (TeRA) randomized controlled trial. Scand J Rheumatol 2023 Mar 20;52(2):118-128 [FREE Full text] [doi: 10.1080/03009742.2021.2008604] [Medline: 35048793]
86. Del Hoyo J, Nos P, Bastida G, Faubel R, Muñoz D, Garrido-Marín A, et al. Telemonitoring of Crohn's disease and ulcerative colitis (TECCU): cost-effectiveness analysis. J Med Internet Res 2019 Sep 13;21(9):e15505 [FREE Full text] [doi: 10.2196/15505] [Medline: 31538948]
87. Velardo C, Shah SA, Gibson O, Clifford G, Heneghan C, Rutter H, EDGE COPD Team. Digital health system for personalised COPD long-term management. BMC Med Inform Decis Mak 2017 Feb 20;17(1):19 [FREE Full text] [doi: 10.1186/s12911-017-0414-8] [Medline: 28219430]
88. Whelan ME, Velardo C, Rutter H, Tarassenko L, Farmer AJ. Mood monitoring over one year for people with chronic obstructive pulmonary disease using a mobile health system: retrospective analysis of a randomized controlled trial. JMIR Mhealth Uhealth 2019 Nov 22;7(11):e14946 [FREE Full text] [doi: 10.2196/14946] [Medline: 31755872]
89. Frasure-Smith N, Lespérance F, Prince RH, Verrier P, Garber RA, Juneau M, et al. Randomised trial of home-based psychosocial nursing intervention for patients recovering from myocardial infarction. Lancet 1997 Aug 16;350(9076):473-479 [FREE Full text] [doi: 10.1016/S0140-6736(97)02142-9] [Medline: 9274583]
90. Ladapo J, Davidson K, Moise N, Chen A, Clarke G, Dolor R, et al. Economic outcomes of depression screening after acute coronary syndromes: the CODIACS-QoL randomized clinical trial. Gen Hosp Psychiatry 2021;71:47-54 [FREE Full text] [doi: 10.1016/j.genhosppsych.2021.04.001] [Medline: 33933921]
91. Krum H, Forbes A, Yallop J, Driscoll A, Croucher J, Chan B, et al. Telephone support to rural and remote patients with heart failure: the chronic heart failure assessment by telephone (CHAT) study. Cardiovasc Ther 2013 Aug 18;31(4):230-237 [FREE Full text] [doi: 10.1111/1755-5922.12009] [Medline: 23061492]
92. Kuusalo L, Sokka-Isler T, Kautiainen H, Ekman P, Kauppi MJ, Pirilä L, SandRA Study Group. Automated text message-enhanced monitoring versus routine monitoring in early rheumatoid arthritis: a randomized trial. Arthritis Care Res (Hoboken) 2020 Mar 27;72(3):319-325 [FREE Full text] [doi: 10.1002/acr.23846] [Medline: 30740935]
93. Lewis KE, Annandale JA, Warm DL, Rees SE, Hurlin C, Blyth H, et al. Does home telemonitoring after pulmonary rehabilitation reduce healthcare use in optimized COPD? A pilot randomized trial. COPD 2010 Feb;7(1):44-50 [FREE Full text] [doi: 10.3109/15412550903499555] [Medline: 20214462]
94. Bernard L, Valsecchi V, Mura T, Aouinti S, Padern G, Ferreira R, et al. Management of patients with rheumatoid arthritis by telemedicine: connected monitoring. A randomized controlled trial. Joint Bone Spine 2022 Oct;89(5):105368 [FREE Full text] [doi: 10.1016/j.jbspin.2022.105368] [Medline: 35248737]
95. Stoddart A, van der Pol M, Pinnock H, Hanley J, McCloughan L, Todd A, et al. Telemonitoring for chronic obstructive pulmonary disease: a cost and cost-utility analysis of a randomised controlled trial. J Telemed Telecare 2015 Mar;21(2):108-118 [FREE Full text] [doi: 10.1177/1357633X14566574] [Medline: 25586810]
96. Schwarz KA, Mion LC, Hudock D, Litman G. Telemonitoring of heart failure patients and their caregivers: a pilot randomized controlled trial. Prog Cardiovasc Nurs 2008;23(1):18-26 [FREE Full text] [doi: 10.1111/j.1751-7117.2008.06611.x] [Medline: 18326990]
97. Sethares KA, Elliott K. The effect of a tailored message intervention on heart failure readmission rates, quality of life, and benefit and barrier beliefs in persons with heart failure. Heart Lung 2004 Jul;33(4):249-260 [FREE Full text] [doi: 10.1016/j.hrtlng.2004.03.005] [Medline: 15252415]
98. Keeffe B, Subramanian U, Tierney WM, Udris E, Willems J, McDonell M, et al. Provider response to computer-based care suggestions for chronic heart failure. Med Care 2005 May;43(5):461-465 [FREE Full text] [doi: 10.1097/01.mlr.0000160378.53326.f3] [Medline: 15838410]
99. van Dijk-de Vries A, van Bokhoven MA, Winkens B, Terluin B, Knottnerus JA, van der Weijden T, et al. Lessons learnt from a cluster-randomised trial evaluating the effectiveness of self-management support (SMS) delivered by practice nurses in routine diabetes care. BMJ Open 2015 Jun 25;5(6):e007014 [FREE Full text] [doi: 10.1136/bmjopen-2014-007014] [Medline: 26112220]
100. Noncommunicable diseases. World Health Organization. 2024 Dec 23. URL: https://tinyurl.com/ykv4rfbw [accessed 2022-07-14]
101. GBD 2017 Inflammatory Bowel Disease Collaborators. The global, regional, and national burden of inflammatory bowel disease in 195 countries and territories, 1990-2017: a systematic analysis for the Global Burden of Disease study 2017. Lancet Gastroenterol Hepatol 2020 Jan;5(1):17-30 [FREE Full text] [doi: 10.1016/S2468-1253(19)30333-4] [Medline: 31648971]
102. Safiri S, Kolahi AA, Hoy D, Smith E, Bettampadi D, Mansournia MA, et al. Global, regional and national burden of rheumatoid arthritis 1990-2017: a systematic analysis of the Global Burden of Disease study 2017. Ann Rheum Dis 2019 Nov 11;78(11):1463-1471 [FREE Full text] [doi: 10.1136/annrheumdis-2019-215920] [Medline: 31511227]

XSL•FO
RenderX

103. Kotronoulas G, Kearney N, Maguire R, Harrow A, Di Domenico D, Croy S, et al. What is the value of the routine use of patient-reported outcome measures toward improvement of patient outcomes, processes of care, and health service outcomes in cancer care? A systematic review of controlled trials. J Clin Oncol 2014 May 10;32(14):1480-1501 [FREE Full text] [doi: 10.1200/JCO.2013.53.5948] [Medline: 24711559]
104. Schumi J, Wittes JT. Through the looking glass: understanding non-inferiority. Trials 2011 May 03;12:106 [FREE Full text] [doi: 10.1186/1745-6215-12-106] [Medline: 21539749]
105. Nielsen AS, Kidholm K, Kayser L. Patients' reasons for non-use of digital patient-reported outcome concepts: a scoping review. Health Informatics J 2020 Dec 30;26(4):2811-2833 [FREE Full text] [doi: 10.1177/1460458220942649] [Medline: 32731773]

Abbreviations

COPD: chronic obstructive pulmonary disease
HbA_{1c}: hemoglobin A_{1c}
HCP: health care professional
HF: heart failure
HRQoL: health-related quality of life
IBD: inflammatory bowel disease
PICOS: Population, Intervention, Comparison, Outcomes, and Study Design
PRISMA: Preferred Reporting Items for Systematic Reviews and Meta-Analyses
PROM: patient-reported outcomes measure
PROSPERO: International Prospective Register of Systematic Reviews
QoL: quality of life
RA: rheumatoid arthritis
RCT: randomized controlled trial
RoB 2: version 2 of the Cochrane risk-of-bias tool for randomized trials

Edited by A Coristine; submitted 05.09.24; peer-reviewed by L Dennett, M Sasseville; comments to author 02.07.25; revised version received 07.08.25; accepted 02.09.25; published 16.09.25.

Please cite as:
Villumsen M, von Osmanski BI, Lomborg KE, Benthien KS
Evidence for the Use of Patient-Reported Outcome Measures in the Treatment of Patients With Noncommunicable Diseases: Systematic Review
JMIR Med Inform 2025;13:e66160
URL: https://medinform.jmir.org/2025/1/e66160
doi:10.2196/66160
PMID:

©Marie Villumsen, Benedikte Irene von Osmanski, Kirsten Elisabeth Lomborg, Kirstine Skov Benthien. Originally published in JMIR Medical Informatics (https://medinform.jmir.org), 16.09.2025. This is an open-access article distributed under the terms of the Creative Commons Attribution License (https://creativecommons.org/licenses/by/4.0/), which permits unrestricted use, distribution, and reproduction in any medium, provided the original work, first published in JMIR Medical Informatics, is properly cited. The complete bibliographic information, a link to the original publication on https://medinform.jmir.org/, as well as this copyright and license information must be included.

XSL•FO
RenderX

Review

Large Language Models in Critical Care Medicine: Scoping Review

Tongyue Shi[1,2,3,4], MS; Jun Ma[5], MD; Zihan Yu[6], MS; Haowei Xu[1,4], MS; Rongxin Yang[1,2,3,4], MS; Minqi Xiong[7], MS; Meirong Xiao[1,2,3,4], MS; Yilin Li[8], MS; Huiying Zhao[9], MD; Guilan Kong[1,2,3,4], PhD

[1]National Institute of Health Data Science, Peking University, Beijing, China
[2]Institute for Artificial Intelligence, Peking University, Beijing, China
[3]Institute of Medical Technology, Peking University Health Science Center, Beijing, China
[4]Advanced Institute of Information Technology, Peking University, Hangzhou, China
[5]Peking University Third Hospital, Beijing, China
[6]Department of Computer Science, University of Liverpool, Liverpool, United Kingdom
[7]Johns Hopkins University School of Medicine, Baltimore, MD, United States
[8]Fielding School of Public Health, University of California, Los Angeles, Los Angeles, CA, United States
[9]Department of Critical Care Medicine, Peking University People's Hospital, Beijing, China

Corresponding Author:
Guilan Kong, PhD
National Institute of Health Data Science
Peking University
Number 38 Xueyuan Road, Haidian District
Beijing, 100191
China
Phone: 86 10 82806542
Email: guilan.kong@hsc.pku.edu.cn

Abstract

Background: With the rapid development of artificial intelligence, large language models (LLMs) have shown strong capabilities in natural language understanding, reasoning, and generation, attracting much research interest in applying LLMs to health and medicine. Critical care medicine (CCM) provides diagnosis and treatment for patients with critical illness who often require intensive monitoring and interventions in intensive care units (ICUs). Whether LLMs can be applied to CCM, and whether they can operate as ICU experts in assisting clinical decision-making rather than “stochastic parrots,” remains uncertain.

Objective: This scoping review aims to provide a panoramic portrait of the application of LLMs in CCM, identifying the advantages, challenges, and future potential of LLMs in this field.

Methods: This study was conducted in accordance with the PRISMA-ScR (Preferred Reporting Items for Systematic Reviews and Meta-Analyses extension for Scoping Reviews) guidelines. Literature was searched across 7 databases, including PubMed, Embase, Scopus, Web of Science, CINAHL, IEEE Xplore, and ACM Digital Library, from the first available paper to August 22, 2025.

Results: From an initial 2342 retrieved papers, 41 were selected for final review. LLMs played an important role in CCM through the following 3 main channels: clinical decision support, medical documentation and reporting, and medical education and doctor-patient communication. Compared to traditional artificial intelligence models, LLMs have advantages in handling unstructured data and do not require manual feature engineering. Meanwhile, applying LLMs to CCM has faced challenges, including hallucinations and poor interpretability, sensitivity to prompts, bias and alignment challenges, and privacy and ethical issues.

Conclusions: Although LLMs are not yet ICU experts, they have the potential to become valuable tools in CCM, helping to improve patient outcomes and optimize health care delivery. Future research should enhance model reliability and interpretability, improve model training and deployment scalability, integrate up-to-date medical knowledge, and strengthen privacy and ethical guidelines, paving the way for LLMs to fully realize their impact in critical care.

Trial Registration: OSF Registries yn328; https://osf.io/yn328/

(JMIR Med Inform 2025;13:e76326) doi:10.2196/76326

XSL•FO
RenderX

KEYWORDS

artificial intelligence; large language model; ChatGPT; critical care; intensive care; clinical decision support; intensive care unit

Introduction

Critical care medicine (CCM), or intensive care medicine, is an essential field dedicated to managing severely ill patients, emphasizing rapid and life-critical decision-making and interventions. CCM deals with patients who have severe conditions and injuries such as acute kidney injury (AKI), sepsis, and acute respiratory distress syndrome (ARDS), potentially leading to a deteriorative state in the intensive care units (ICUs) [1-4]. The incidence of AKI in the ICU could reach over 50% worldwide [5]. Among those who received renal replacement therapy, most of whom were with critical illness in the ICU, the mortality rate was approximately 50% [6,7]. The prevalence of sepsis is around 30% during ICU stay [8]. Sepsis accounted for approximately 11 million deaths, making up about 20% of all global deaths [9]. Recent multicenter epidemiological work shows that the incidence of ARDS in the ICU was between 7.1% and 19% with hospital mortality of 32%-55% [10]. While in resource-limited settings, the ICU mortality of ARDS could be as high as 50% due to the disparities in health care services [11]. Therefore, the special environment of the ICU has imposed higher professional requirements on medical staff. Physicians and nurses in ICUs must manage large amounts of patient data while maintaining high efficiency under high pressure [11,12]. The dynamic and severe nature of critical care demands intelligent decision-support tools to help physicians improve diagnostic accuracy, optimize therapeutic strategies, and facilitate timely clinical decision-making.

Artificial intelligence (AI) technologies, especially generative artificial intelligence (GenAI) models, have developed rapidly in recent years [13,14]. The advent of large language models (LLMs), such as those based on the Transformer architecture [15] and pretrained on extensive text corpora, has marked a substantial advancement in natural language processing (NLP). With billions of parameters, these LLMs have demonstrated remarkable capabilities in understanding and generating human-like text [16]. LLMs have been implemented in various contexts, including answering questions, summarizing texts, and engaging in open-domain conversations [17]. Compared to human practitioners, LLMs have been perceived as more understanding and efficient [18]. Among these LLMs, OpenAI's ChatGPT [16] has become a focal point since its launch in November 2022. OpenAI then introduced upgraded versions of ChatGPT, offering enhanced multimodal capabilities to handle diverse inputs such as text, images, code, and table files. LLMs have revolutionized different fields, including health and medicine [13,14]. A more detailed description of the evolution and applications of LLMs in health and medicine is provided in Note S1 in Multimedia Appendix 1 [19-59].

In the field of CCM, the emergence of LLMs demonstrates its unique potential. Similar to the application of LLMs in informing patients with cancer of diagnosis, treatment methods, and side effects, LLMs in CCM can help make life-or-death decisions after fusing large volumes of patient data in a short time [60]. Physicians in CCM face enormous workloads and pressure, involving LLMs in different clinical decision-making scenarios in CCM will help reduce the workload of physicians and improve health care quality. However, LLMs face challenges when applied in CCM, such as uncertain accuracy and coherence, recency bias, hallucinations, poor interpretability, and ethical issues [61]. Among them, hallucinations are one of the biggest drawbacks of LLMs, which make them act like stochastic parrots [62].

This study aims to review the applications of LLMs in CCM, identifying the advantages, challenges, and future potential of LLMs in this field. Three key research questions were designed to be answered by this review. (1) What is the current status of LLM applications within the critical care setting? (2) What are the recognized advantages and challenges of using LLMs in CCM? (3) What research directions should be taken in the future to promote the application of LLMs in CCM? By addressing the above 3 questions, this review endeavors to provide a clear portrait of and identify the research gaps in the applications of LLMs in CCM, discerning whether they are just stochastic parrots that may mimic human responses based on probability calculation or emerging ICU experts capable of providing timely and highly personalized diagnosis and treatment recommendations. Through this comprehensive review, we aim to outline a roadmap for future research and implementation of LLMs in CCM that could enable them to transform critical care effectively.

Methods

Study Design

This scoping review followed the PRISMA-ScR (Preferred Reporting Items for Systematic Reviews and Meta-Analyses extension for Scoping Reviews) guidelines [63], and the protocol was registered in the Open Science Framework. We have included a checklist of the PRISMA-ScR guidelines in Table S1 in Multimedia Appendix 1.

Literature Search Strategy

We conducted a literature search across 7 databases, including PubMed, Embase, Scopus, Web of Science, CINAHL, IEEE Xplore, and ACM Digital Library, from the earliest available paper until August 22, 2025. Keywords related to LLMs included "large language model," "LLM," "generative pre-trained transformer," "GPT," "generative artificial intelligence," and "generative AI." For CCM, the keywords included "critical care," "intensive care units," "critical illness," "intensive care," and "ICU." All these terms were combined using the "OR" and "AND" logical operators to ensure the retrieval of literature that addresses both research areas. The detailed search terms for each database are provided in Table S2 in Multimedia Appendix 1.

Study Selection

The study selection in this scoping review was conducted to ensure comprehensive coverage and relevance of the included literature. In the first phase of the study selection, literature was

XSL•FO
RenderX

included based on the following criteria: (1) focusing on LLMs in CCM, including studies that explicitly used or commented on LLMs relevant to the field of CCM, and (2) original research papers from peer-reviewed journals and conferences, perspectives, and letters. Studies were excluded from the review if they met any of the following conditions: (1) irrelevant to LLMs or CCM, including studies that did not focus on applying LLMs within the realm of CCM; (2) conference abstracts, preprint papers, books, patents, editorials, and review papers; and (3) non-English literature. The process for selecting sources of evidence is provided in Note S2 in Multimedia Appendix 1.

Keyword Co-Occurrence Network Analysis

Keyword co-occurrence network analysis [64] is a bibliometric method to explore the relationships between keywords in academic papers. It involves constructing a network where nodes represent keywords and edges represent the co-occurrence of these keywords within the studied documents. It helps to identify the main research themes, trends, and potential research gaps by analyzing the frequency and patterns of keyword co-occurrences. This study used the VOSviewer (version 1.6.20) software to construct a bibliometric network using the visualization of similarity method [65,66]. The software automatically extracts keywords from a publication's title, abstract, or author-supplied keyword list. The frequency of co-occurrences of 2 keywords is determined by the number of publications in which both keywords appear together in the title, abstract, or keyword list. The visualization of similarity method starts by calculating the similarity between the keywords of publications based on their co-occurrence. Finally, a matrix is constructed to arrange keywords spatially according to their similarities, and it is the basis for multivariate statistical and network analysis.

Risk of Bias and Applicability Assessment

We critically appraised all included studies using the PROBAST-AI (Prediction Model Risk of Bias Assessment Tool-Artificial Intelligence) [67], rating Risk of Bias (RoB) across 4 domains (participants, predictors, outcome, and analysis) and applicability across 3 domains (participants, predictors, and outcome) on a 3-level scale (low, high, and unclear). Full evaluation criteria and rules are provided in Note S3 in Multimedia Appendix 1.

Results

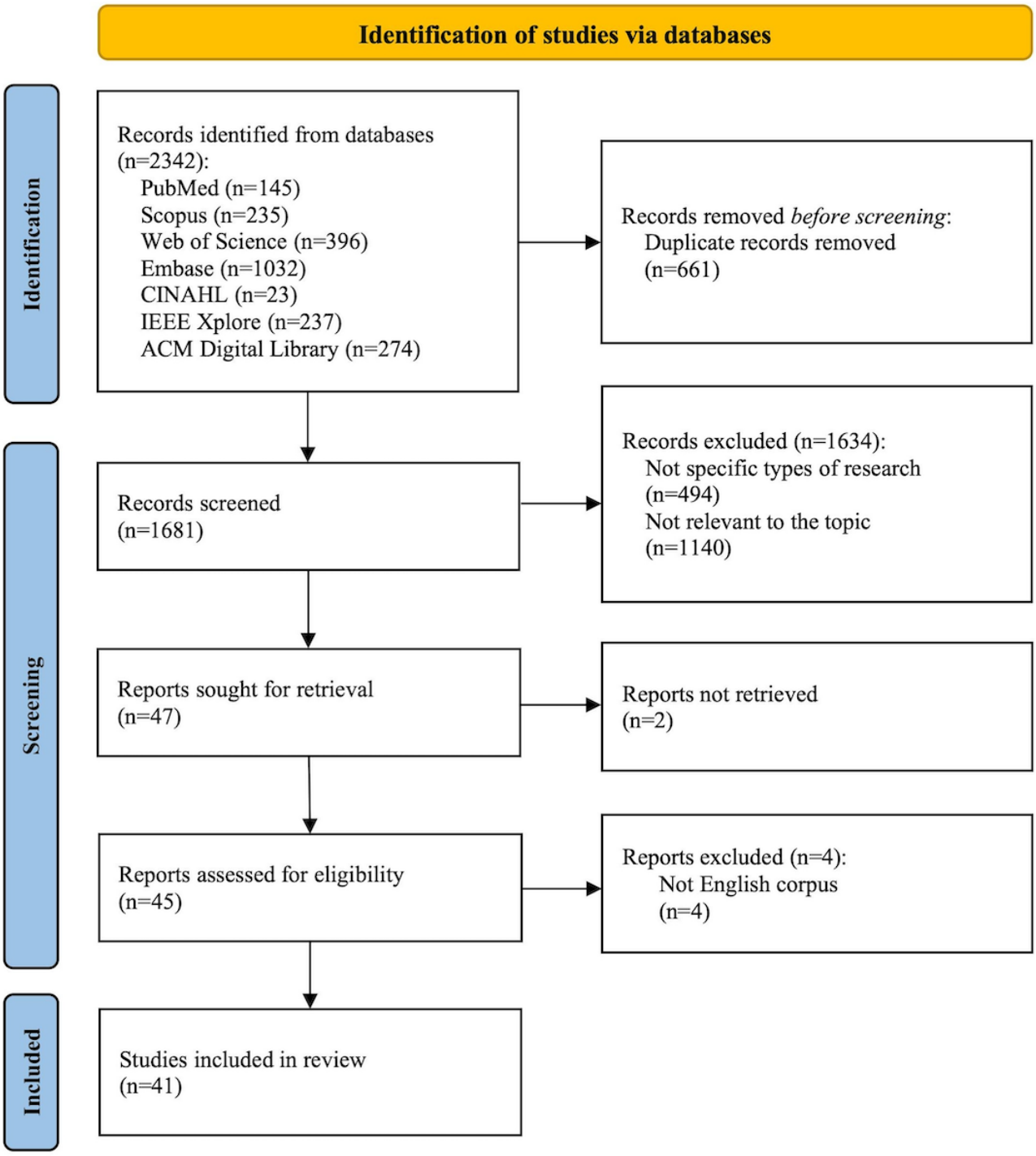
Literature Search Results

This scoping review covered publications in the 7 databases to August 22, 2025, and retrieved 2342 papers initially. The flowchart of the study selection process is presented in Figure 1.

The application of LLMs in CCM is a relatively innovative field, but research is still lacking, and the overall number of papers is relatively small. Finally, 41 papers met all the inclusion criteria and were chosen for this review. Table 1 documents the research contents and publication details of the included studies. The study design and model performance details of the included studies are in Table S3 in Multimedia Appendix 1, where metrics (such as area under the receiver operating characteristic curve and area under the precision-recall curve, and F_1-score) are described, together with the setting, implementation effect on patient outcomes, validation design, and external-validation environment.

XSL•FO
RenderX

Figure 1. The PRISMA flowchart for study selection and quality assessment. PRISMA: Preferred Reporting Items for Systematic Reviews and Meta-Analyses.



XSL•FO
RenderX

Table 1. Research contents and publication details of the included studies in this review.

Authors	Published year	Article type	Study design	Journal or conference name	Country	Model	Research contents
Savage et al [68]	2023	Original research	Retrospective	*JMIR Medical Informatics*	United States	BioMed-RoBERTa	Developed and validated a language model-based screening tool for optimizing Best Practice Alerts.
Levin et al [17]	2024	Original research	Retrospective	*International Journal of Nursing Studies*	Israel	ChatGPT-4 and Claude-2 (Anthropic PBC)	Compared LLMs[a] to neonatal nurses in clinical decision support for neonatal care.
Pham et al [69]	2024	Original research	Retrospective	*Journal of Medical Internet Research*	United States	ChatGPT-3.5 and ChatGPT-4	Evaluated LLMs in simulations for cardiac arrest and bradycardia based on the American Heart Association's Advanced Cardiovascular Life Support guidelines.
Huespe et al [70]	2023	Observational study	Retrospective	*Critical care explorations*	Argentina	ChatGPT-3.5	Evaluated the capabilities of LLMs in generating the background sections of critical care clinical research questions compared to human researchers.
Si et al [71]	2019	Original research	Retrospective	*Journal of the American Medical Informatics Association*	United States	ELMo and BERT	Applied contextual embeddings to enhance clinical concept extraction from medical texts.
Almazyad et al [72]	2023	Original research	Retrospective	*Cureus*	Saudi Arabia	ChatGPT-4	Used LLMs to enhance expert panel discussions at a medical conference, focusing on pediatric palliative care and ethical decision-making scenarios.
Chung et al [73]	2024	Original research	Retrospective	*JAMA*[b] *surgery*	United States	ChatGPT-4 Turbo	Evaluated the performance of LLMs in perioperative risk stratification and prognostication across various tasks.
Abdullahi et al [74]	2024	Original research	Retrospective	*JMIR Medical Education*	United States	Bard (Google LLC), ChatGPT-3.5, and ChatGPT-4	Assessed the effectiveness of LLMs in diagnosing rare and complex medical conditions, focusing on improving medical education and diagnostic accuracy.
Benboujja et al [75]	2024	Original research	Retrospective	*Frontiers in Public Health*	United States	ChatGPT-4	Developed and applied a multilingual, AI[c]-driven educational curriculum in pediatric care to overcome language barriers in global health care education.
Lu et al [1]	2023	Letter	Retrospective	*Annals of Biomedical Engineering*	China	ChatGPT-3.5 and ChatGPT-4	Explored potential uses of LLMs in intensive care medicine, focusing on knowledge augmentation, device management, clinical decision support, early warning systems, and ICU[d] database establishment.
Madden et al [76]	2023	Letter	Retrospective	*Intensive Care Medicine*	Ireland	ChatGPT-4	Evaluated the effectiveness of LLMs in querying and summarizing unstructured medical notes in the ICU.
Liu et al [77]	2024	Original research	Prospective	*Heliyon*	China	ChatGPT-3.5 and ChatGPT-4	Assessed LLMs in predicting the risk of endotracheal intubation after initiating high-flow oxygen therapy, highlighting potential in decision-making in critical care.
Nolan et al [78]	2024	Original research	Retrospective	*Critical Care Explorations*	United States	ChatGPT-3.5 and BERT	Investigated the use of LLMs in assisting surrogate and proxy decision-making in critical care, focusing on aligning treatment recommendations with patient values.
Shah-Mohammadi and Finkelstein [79]	2024	Original research	Retrospective	*JMIR Medical Informatics*	United States	ChatGPT-3.5	Investigated ChatGPT-3.5's application in extracting substance use information from ICU discharge summaries, highlighting improvements in accuracy with different learning scenarios.

XSL•FO
RenderX

Authors	Published year	Article type	Study design	Journal or conference name	Country	Model	Research contents
Nawab et al [80]	2024	Original research	Retrospective	*Journal of Medical Artificial Intelligence*	United States	ChatGPT-3.5 Turbo	Evaluated ChatGPT-3.5 Turbo's effectiveness in assigning *ICD-10*[e] codes to clinical notes, demonstrating improved accuracy with fine-tuning, particularly in critical care administrative tasks.
Soleimani et al [81]	2024	Original research	Retrospective	*Academic Radiology*	Iran	ChatGPT-3.5 and Claude.ai	Assessed ChatGPT's ability to generate radiology reports using MIMIC-CXR[f] data, with a 3-step prompt guiding report synthesis. Compared outputs to Bart and XLM, showing high similarity to human reports.
Oh et al [82]	2024	Original research	Prospective	*Healthcare Informatics Research*	Korea	ChatGPT-3.5 and ChatGPT-4	Analyzed ChatGPT-3.5-turbo and ChatGPT-4 in predicting sepsis mortality using data from the Korean Sepsis Alliance.
Urquhart et al [83]	2024	Original research	Retrospective	*Intensive Care Medicine Experimental*	Ireland	ChatGPT-3.5, ChatGPT-4, and Llama-2 (Meta)	Evaluated ChatGPT-4, ChatGPT, and Llama 2 for generating ICU discharge summaries, emphasizing event recall and readability.
Pabon et al [84]	2024	Original research	Retrospective	*European Journal of Heart Failure*	United States	ChatGPT-3.5	Explored in-hospital outcomes for heart failure patients with improved ejection fraction. ChatGPT-3.5 was used to extract LVEF[g] data from medical records, but incomplete data detection in some cases required manual review.
Akhondi-Asl et al [85]	2024	Original research	Retrospective	*Pediatric Critical Care Medicine*	United States	Llama-7B, Llama-65B, and BioGPT-Large	Evaluated domain-specific fine-tuned models against general LLMs for generating differential diagnoses in PICU[h] patients. Fine-tuned Llama-7B outperformed larger models, demonstrating the importance of domain-specific training.
Liu et al [86]	2025	Original research	Retrospective	*Clinical Simulation in Nursing*	China	ChatGPT-3.5	Qualitative exploration of ICU novice simulation instructors' experience with ChatGPT in case design, focusing on perceived value, potential applications, and limitations.
Berger et al [87]	2025	Original research	Retrospective	*Journal of Critical Care*	Switzerland	ChatGPT-4o	Qualitative investigation of abbreviation uses in ICU communication, focusing on risks, clinician perceptions, and patient safety implications.
Kurz et al [88]	2025	Original research	Retrospective	*NPJ Digital Medicine*	Germany	DeepSeek, InternVL, and ChatGPT-4o	Comparative benchmarking of LLMs for diagnostic accuracy using medical images plus clinical context in emergency and critical care.
Pham et al [89]	2025	Original research	Retrospective	*Cureus*	Vietnam	ChatGPT-4o	Assessment of ChatGPT-4o's ability to interpret cranial ultrasound images for PVIVH[i] diagnosis in very preterm infants, compared to pediatric radiologists.
Shi et al [90]	2025	Original research	Retrospective	*Journal of Medical Internet Research*	China	SWEDE-HEART-AI, Qwen-2, and Llama-3	Comparison of LLMs for predicting 1-year all-cause mortality post-AMI[j], using structured variables versus discharge note analysis.
Yitzhaki et al [91]	2025	Original research	Retrospective	*Journal of Paediatrics and Child Health*	Israel	ChatGPT-4o	Comparative evaluation of ChatGPT-4 versus PICU specialist in answering open-ended medical education questions sourced from a trainee WhatsApp (WhatsApp LLC) forum.

XSL•FO
RenderX

Authors	Published year	Article type	Study design	Journal or conference name	Country	Model	Research contents
Williams and Erstad [92]	2025	Original research	Retrospective	*American Journal of Health-System Pharmacy*	United States	ChatGPT-4, Copilot (Microsoft Corp), Gemini 1.5, and Meta AI	Evaluation of 4 LLMs' responses to SCCM[k] guideline–based medication questions.
Yang et al [93]	2025	Original research	Retrospective	*JMIR Medical Informatics*	China	ICU-GPT[l]	Development of an automated deployment and extraction platform to allow SQL generation and data retrieval from ICU-related databases without coding.
Workum et al [94]	2025	Original research	Retrospective	*Critical Care*	Netherlands	ChatGPT-4o, ChatGPT-4o-mini, ChatGPT-3.5-turbo, Mistral Large 2407, and Llama-3.1 70B	Benchmarking 5 LLMs using expert-level ICU MCQs[m], compared against human physicians and random guessing.
Yang et al [95]	2025	Original research	Retrospective	*Frontiers in Artificial Intelligence*	United States	ChatGPT-3.5, ChatGPT-4, Claude 2, Llama2-7B, and Llama2-13B	Comparative evaluation of 5 LLMs on multiple-choice questions in critical care pharmacotherapy education, including prompt-engineering effects and a custom GPT.
Ding et al [96]	2024	Original research	Retrospective	*Scientific Reports*	United States	BlueBERT	Developed a framework that distills LLM knowledge into structured multimodal EHR[n] predictive models for ICU health event prediction.
Walker et al [97]	2025	Original research	Retrospective	*Journal of the American Medical Informatics Association*	United States	ChatGPT-3.5	Development of CARE-SD: supervised classifiers to detect stigmatizing and doubt-marker language in ICU clinical notes using lexicon- and model-based NLP[o].
Chen et al [98]	2025	Original research	Retrospective	*BMC Medical Education*	United States	DeepL, Gemini (Google LLC), Google Translate, and Microsoft Copilot	Multimodal assessment of freely available MT[p] tools translating critical care educational content into Chinese, Spanish, and Ukrainian.
Ucdal et al [99]	2025	Original research	Retrospective	*Journal of Clinical Medicine*	Turkey	Gemini	Evaluation of Gemini's application of ACG[q] 2024 guidelines to diagnose severity and guide management in acute pancreatitis.
Balta et al [100]	2024	Original research	Retrospective	*Journal of Intensive Care Medicine*	Canada	ChatGPT-3.5 and ChatGPT-4	Comparative evaluation of ChatGPT-3.5 versus 4.0 on appropriateness, consistency, and readability of critical care recommendations.
Zhu et al [101]	2025	Original research	Retrospective	*BME Frontiers*	China	ChatGPT-4o and ChatGPT-4o mini	Evaluation of contextualized versus static word embeddings in predicting AKI[r] using ICU clinical notes and structured data, via CNN[s] models.
Pathak et al [102]	2025	Original research	Retrospective	*IEEE Journal of Biomedical and Health Informatics*	United States	RespBERT	Development and evaluation of RespBERT that identifies ARDS[t] from radiology report texts using BERT embeddings and transfer learning.
Liu et al [103]	2025	Original research	Retrospective	*IEEE Journal of Biomedical and Health Informatics*	Australia	ChatGPT-4o	Development of a note-specific hierarchical network for predicting ICU in-hospital mortality from clinical notes; compares against supervised baselines and LLMs using diverse prompting strategies.

XSL•FO
RenderX

Authors	Published year	Article type	Study design	Journal or conference name	Country	Model	Research contents
Turan et al [104]	2025	Original research	Prospective	*Journal of Clinical Anesthesia*	Turkey	ChatGPT-4	Prospective evaluation of ChatGPT-4 in interpreting ABG[u] test results compared to expert anesthesiologists.
Wang et al [105]	2025	Original research	Retrospective	*Journal of Critical Care*	China	ChatGPT-4	Evaluation of ChatGPT-4's performance on the Chinese critical care physician qualification examination covering multiple domains.
Yang et al [106]	2025	Original research	Retrospective	*Journal of Medical Internet Research*	China	ChatGPT-4, Qwen-2, and Llama-3	LLM-driven extraction of entities and relations to build a sepsis knowledge graph using multicenter clinical data.

[a]LLM: large language model.

[b]JAMA: *Journal of the American Medical Association*.

[c]AI: artificial intelligence.

[d]ICU: intensive care unit.

[e]*ICD-10: International Statistical Classification of Diseases, Tenth Revision*.

[f]MIMIC-CXR: Medical Information Mart in Intensive Care-Chest X-Ray.

[g]LVEF: left ventricular ejection fraction.

[h]PICU: pediatric intensive care unit.

[i]PV-IVH: periventricular-intraventricular hemorrhage.

[j]Post-AMI: postacute myocardial infarction.

[k]SCCM: Society of Critical Care Medicine.

[l]ICU-GPT: Intensive Care Unit-specific Generative Pre-trained Transformer.

[m]MCQ: multiple choice question.

[n]EHR: electronic health record.

[o]NLP: natural language processing.

[p]MT: machine translation.

[q]ACG: American College of Gastroenterology.

[r]AKI: acute kidney injury.

[s]CNN: convolutional neural network.

[t]ARDS: acute respiratory distress syndrome.

[u]ABG: arterial blood gas.

Bibliometric Analysis

This scoping review included a focused selection of 41 papers, providing a global perspective on LLM applications in CCM. This diverse corpus spans several countries, demonstrating widespread research interest in applying LLMs in CCM. The results of keyword co-occurrence network analysis are in Note S4 in Multimedia Appendix 1. Among the 41 papers, only 2 used prospective data, while the other 39 were retrospective studies. The distribution of the selected publications indicates substantial international collaboration and research efforts. We analyzed the countries where each selected paper's first and corresponding authors were based. The authors from the United States took the lead in most studies, followed by authors from China, Ireland, Israel, Korea, etc. It revealed that nearly half of the studies were conducted in the United States, with much fewer contributions from other countries and regions. This indicates a concentration of research activities in applying LLMs in CCM within the United States, potentially reflecting the advanced development and adoption of AI technologies in American critical care settings. Among the LLMs used, ChatGPT-4 appears most frequently, demonstrating its relevance and recent prominence in CCM applications. Other models include ChatGPT-3.5 and models such as Llama, Gemini, Claude, and DeepSeek, highlighting the breadth of generative models explored in the included studies. A minority of studies use domain-adapted or clinical NLP backbones, including BioGPT-Large, BioMed-RoBERTa, BlueBERT, and RespBERT.

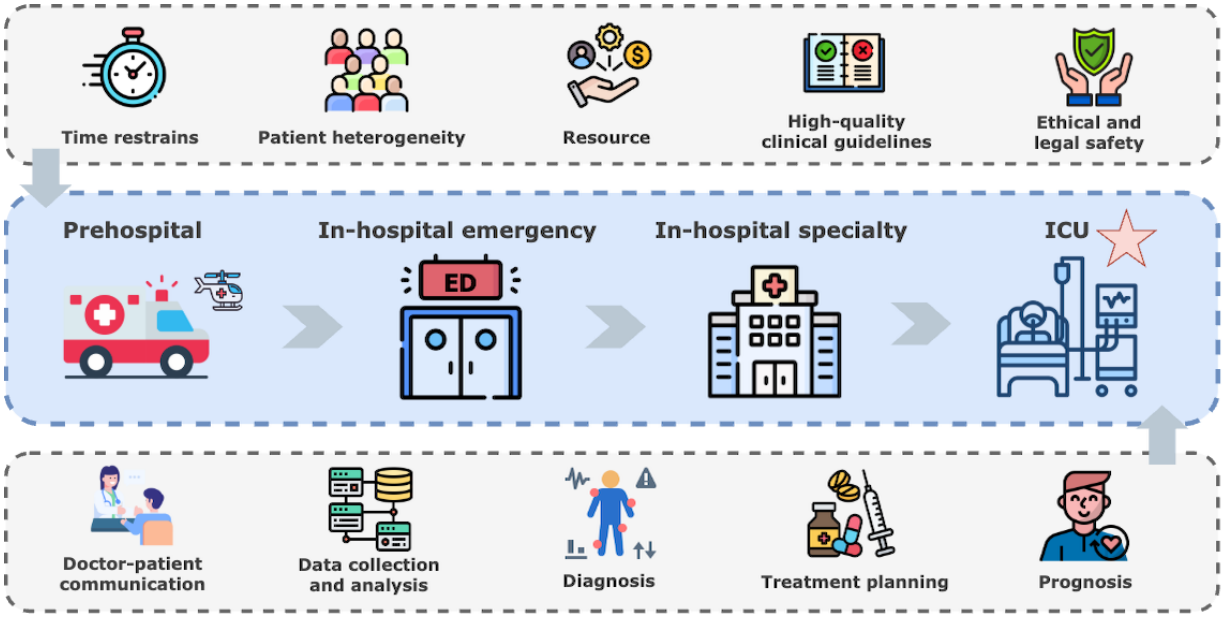
Applications of LLMs in CCM

Clinical Decision Support

As illustrated in Figure 2, the primary application of LLMs in CCM is clinical decision support. LLMs can be applied in diagnosis, treatment planning, and prognosis prediction in in-hospital critical care settings.

XSL•FO
RenderX

Figure 2. The process and characteristics of clinical decision support. ED: emergency department; ICU: intensive care unit.



In diagnosis, LLMs demonstrate the potential to aid physicians in making diagnostic decisions. Gandomi et al [107] explored the use of LLMs (Llama 70B and Mistral) in detecting ARDS from radiology reports in the MIMIC-III (Medical Information Mart for Intensive Care-III) database. The study applied LLMs to identify high-probability ARDS cases based on bilateral infiltrates. Akhondi-Asl et al [85] investigated the use of domain-specific fine-tuned models (Llama-7B and BioGPT-Large) against larger general-domain models (Llama-65B) for generating differential diagnoses in pediatric intensive care unit (PICU) patients. They found that fine-tuned Llama-7B outperformed both Llama-65B and BioGPT-Large. Kurz et al [88] benchmarked the diagnostic performance of various vision-language models on a multimodal dataset comprising medical images and associated clinical context in ICU environments. They compared several open-source vision-language models against ChatGPT-4o, finding that while open models achieved accuracy only up to 40.4%, ChatGPT-4o substantially outperformed them with an approximation of 68.1%. Pham et al [89] evaluated the diagnostic utility of ChatGPT-4o in interpreting cranial ultrasound images to detect periventricular-intraventricular hemorrhage among very preterm infants in a neonatal ICU in Vietnam. Comparing ChatGPT-4o's image-based diagnoses against pediatric radiologists, the model achieved moderate performance (area under the curve [AUC]=0.796), with 75% sensitivity and 84.2% specificity, alongside fair-to-good interrater agreement. The study highlights ChatGPT-4o's potential as a supplemental tool for early periventricular-intraventricular hemorrhage screening. Pathak et al [102] developed RespBERT, leveraging BERT-based embedding and transfer learning to automatically identify ARDS from unstructured radiology notes across multiple hospital datasets. Applying the model to notes from 2 independent institutions, RespBERT achieved F_1-scores of 74.5% and 64.2%, demonstrating robust performance across different clinical settings and indicating its potential for ARDS detection in the ICU.

In treatment planning, LLMs show considerable promise in providing personalized treatment recommendations and optimizing clinical pathways for patients with critical illness. Savage et al [68] developed and validated the LLM screening tool to selectively identify patients appropriate for Best Practice Alerts of deep vein thrombosis anticoagulation prophylaxis using the MIMIC-III database. They found that the LLM screening tool improved the precision of Best Practice Alerts, reducing the number of unnecessary alerts by 20% and increasing the applicability of alerts by 14.8%. Pham et al [69] evaluated ChatGPT's performance in treating cardiac arrest and bradycardia simulations in accordance with the American Heart Association's Advanced Cardiovascular Life Support guidelines. Using the 2020 Advanced Cardiovascular Life Support guidelines, ChatGPT's responses to 2 simulation scenarios were assessed for accuracy. They found that ChatGPT had a median accuracy of 69% for cardiac arrest and 42% for bradycardia, with significant variability in its outputs, often missing critical actions, and having incorrect medication information. Nolan et al [78] used LLMs to support critical care decision-making for incapacitated patients. The study simulated scenarios for 50 patients requiring urgent clinical decisions and incorporated patient values captured through various formats, including free-text narratives. The LLMs were tasked with extracting treatments and generating recommendations based on patient profiles. The results showed that LLMs accurately extracted treatments in 88% of cases and received high scores for providing medically plausible and value-aligned recommendations. Williams et al [92] evaluated 4 LLMs (ChatGPT-4, Copilot, Gemini version 1.5, and Meta AI) by medication-related questions based on 6 Society of Critical Care Medicine clinical practice guidelines. Copilot yielded the highest proportion of correct answers, followed by Meta AI, ChatGPT-4, and Gemini, which delivered the most incorrect responses. Despite these capabilities, none of the models consistently matched guideline recommendations, indicating that while clinically promising, AI tools require further development for

XSL•FO
RenderX

reliable use in the ICU. Ucdal et al [99] assessed the performance of Gemini in applying American College of Gastroenterology 2024 guidelines to clinical decisions in acute pancreatitis management. Using MIMIC-III data consisting of 512 patient cases, the study evaluated Gemini's accuracy in determining disease severity, recommending nutritional strategies, and antibiotic use. Gemini achieved 85% accuracy for mild cases, 82% for severe cases, and 78%-85% compliance with guideline-based nutritional and management recommendations, demonstrating solid agreement with scoring systems. This suggests that AI may support consistent, guideline-concordant decision-making in pancreatitis care. Turan et al [104] conducted a prospective observational study comparing ChatGPT-4's interpretation of arterial blood gas results with that of expert anesthesiologists using 400 ICU patient samples. The model demonstrated excellent accuracy for parameters such as pH, oxygenation, sodium, chloride, and hemoglobin, though it struggled with bilirubin. While generally reliable, it occasionally recommended unnecessary bicarbonate therapy, highlighting the promise of ChatGPT-4 as a rapid interpretive aid, but underscoring the necessity of clinician oversight. Yang et al [106] presented a pioneering study that leveraged ChatGPT-4 and a multicenter real-world sepsis dataset (10,544 patients across 3 hospitals in China) to construct a comprehensive sepsis knowledge graph. By combining clinical guidelines, public data, and advanced prompt engineering, they extracted entities and relationships, building a graph with 1894 nodes and 2021 unique connections. ChatGPT-4 achieved a high F_1-score of 76.76 on the study's sepsis-specific dataset and 65.42 under the few-shot condition, surpassing models such as Qwen-2 and Llama-3.

For prognosis prediction, Amacher et al [108] used ChatGPT-4 to predict mortality and poor neurological outcomes at hospital discharge for adult patients who had cardiac arrest. The study involved prompting ChatGPT-4 with 16 prognostic parameters from established post–cardiac arrest scores. The findings showed that ChatGPT-4 achieved an AUC of 0.85 for in-hospital mortality and 0.84 for poor neurological outcomes, comparable to traditional scoring systems. Chung et al [73] used ChatGPT-4 to perform risk stratification and predict postoperative outcomes based on procedure descriptions and preoperative clinical notes from electronic health records (EHRs). They found that ChatGPT-4 achieved F_1-scores of 0.64 for predicting hospital admission, 0.81 for ICU admission, 0.61 for unplanned admission, and 0.86 for predicting hospital mortality. Liu et al [77] conducted a prospective multicenter cohort study using ChatGPT-3.5 and ChatGPT-4 to predict the risk of endotracheal intubation within 48 hours following high-flow nasal cannula oxygen therapy in patients with critical illness. They found that ChatGPT-4 achieved an accuracy comparable to that of specialist physicians, with an AUC of 0.82, which was higher than that of non-specialist physicians (AUC=0.66). Oh et al [82] conducted a study using ChatGPT-3.5-turbo and ChatGPT-4 to predict in-hospital mortality for sepsis patients. The study used clinical data from the Korean Sepsis Alliance database, focusing on ICU admissions and using metrics such as the SOFA (Sequential Organ Failure Assessment) score and lactic acid levels. The findings demonstrated that ChatGPT-4 performed comparably to a gradient boosting machine in predicting short-term mortality, particularly for 7-day outcomes. Shi et al [90] used the MIMIC-IV (Medical Information Mart for Intensive Care-IV) database to compare the performance of 2 LLMs (Qwen-2 and Llama-3) with a specialized artificial neural network (SWEDEHEART-AI) trained on Swedish registry data, in predicting 1-year all-cause mortality among ICU patients with acute myocardial infarction. SWEDEHEART-AI outperformed both LLMs, maintained consistent area under the receiver operating characteristic curve in time-dependent analyses, and demonstrated superior clinical utility and net benefit across risk thresholds, suggesting its stronger reliability for risk stratification. Ding et al [96] proposed a novel framework, cross-modality knowledge learning and extraction, that distills knowledge from LLMs into a predictive model trained on multimodal EHR data in the ICU. By refining clinical text using LLM-generated embeddings and using a cross-modality knowledge distillation approach that combines contrastive and patient-similarity learning losses, cross-modality knowledge learning and extraction significantly improved predictive accuracy for hypertension and heart failure events, demonstrating up to a 4.48% boost over state-of-the-art models using data from the MIMIC-III database. Zhu et al [101] used clinical data from 2 Chinese hospitals and a public South Korean dataset, comprising a total of 2649 older adult patients who underwent surgery, to use LLMs (GPT-4o, ChatGPT-4o mini, Qwen2-7B-Instruct, and Llama3.1-8B-Instruct), comparing their performance against traditional ML models such as XGBoost (Extreme Gradient Boosting) and Random Forest for the task of predicting postoperative AKI. The study enhanced the LLMs' capabilities through prompt engineering techniques such as Medical Chain of Thought and instruction fine-tuning. The results demonstrated that the LLM-based frameworks achieved superior generalization on external datasets while also providing human-readable medical rationales for predictions, significantly improving interpretability and clinical utility compared to traditional ML approaches. Liu et al [103] investigated risk prediction of in-hospital mortality using routinely collected clinical notes in the ICU. It proposes a note-specific hierarchical network that adapts to different note types and benchmarks it against various supervised baselines and 34 instruction-following LLMs under zero-shot and few-shot settings, as well as chain-of-thought prompting. The hierarchical model outperformed both LLMs and supervised baselines, which consistently underperformed in this critical task, highlighting important constraints of LLMs in risk assessment of critical care patients.

Medical Documentation and Reporting

LLMs are making strides in medical documentation and reporting by automating and streamlining these processes. Shah-Mohammadi et al [79] used the ChatGPT-3.5 model to extract substance use information from ICU discharge summaries in the MIMIC-III database, focusing on tobacco, alcohol, and illicit substances. They explored both zero-shot and few-shot prompt learning settings and found that GPT's performance in identifying tobacco, alcohol, and substance use varied depending on the learning scenario. Zero-shot learning achieved high accuracy in recognizing substance use, while

XSL•FO
RenderX

few-shot learning, although lowering accuracy, improved the identification of substance use status, leading to better recall and F_1-scores but lower precision. Nawab et al [80] conducted a study using the ChatGPT-3.5 Turbo to automate the assignment of *ICD-10* codes to clinical notes in the ICU. Their findings demonstrated that fine-tuning the model with a specialized dataset improved its accuracy from 29.7% to 62.6%. Soleimani et al [81] conducted a study using ChatGPT-3.5 to evaluate the performance of radiology report generation. Using data from the MIMIC-CXR (Medical Information Mart for Intensive Care-Chest X-Ray) database, the study explored how ChatGPT, guided by a 3-step prompt, synthesized complete radiology reports. They found that ChatGPT effectively generated comprehensive reports by accurately interpreting both patient characteristics and radiological findings. Urquhart et al [83] used ChatGPT-4, ChatGPT-3.5, and Llama 2 to extract key information from ICU patient text records in an Irish population. The study evaluated the models' ability to generate concise and accurate clinical summaries from unstructured ICU admission notes. The results showed that ChatGPT-4 outperformed the other models in readability, organization, and summarization of clinically significant events, but all models struggled with completeness and narrative coherence. Pabon et al [84] used ChatGPT-3.5 for extracting left ventricular ejection fraction data from medical records in a study involving patients with heart failure with improved ejection fraction. The model achieved 100% accuracy in identifying reported left ventricular ejection fraction values but struggled with a capture completeness of 75%. Si et al [71] explored the impact of ELMo and BERT on clinical concept extraction tasks using data from the MIMIC-III and other clinical corpora. They found that contextual embeddings pretrained on a large clinical corpus outperformed traditional methods. Madden et al [76] used ChatGPT-4 to query and summarize unstructured medical notes in the ICU. They found that while the model could produce concise and useful summaries, it also had significant risks of generating hallucinations. Yang et al [93] developed a platform to facilitate the deployment and extraction of critical care-related big data using LLMs. The system leverages Docker (Docker Inc)–based automated database deployment and visualization tools, along with an ICU-fine-tuned LLM ICU-GPT to generate SQL queries and extract data from complex ICU datasets without requiring programming knowledge. This platform enables clinicians to manage, visualize, and retrieve structured insights from large critical care databases through a user-friendly web interface, reducing the technical barrier to big data research in clinical settings. Walker et al [97] developed CARE-SD, a classifier-based NLP toolkit designed to identify stigmatizing patient labels and doubt markers within ICU clinical notes. By constructing lexicons (127 stigmatizing expressions and 58 doubt markers) using literature-based stems augmented via Word2Vec and ChatGPT-3.5, and training supervised classifiers on annotated samples drawn from 18 million MIMIC-III sentences, the models achieved macro F_1-scores of 0.84 (doubt markers) and 0.79 (stigmatizing labels). This approach supports the detection of linguistic biases in critical care EHRs and could inform interventions to reduce stigmatizing language in health care.

Medical Education and Doctor-Patient Communication

LLMs are used more and more frequently in medical education now. One important area closely connected to LLMs is to generate or answer questions in medical examinations. Workum et al [94] conducted a benchmark study by evaluating 5 LLMs (GPT-4o, ChatGPT-4o-mini, ChatGPT-3.5-turbo, Mistral Large 2407, and Llama 3.1 70B) on 1181 multiple-choice questions from the European Diploma in Intensive Care examination. All models significantly outperformed human physicians, with ChatGPT-4o achieving the highest accuracy of 93.3%. Despite outstanding consistency and performance, models still produced incorrect answers and raised concerns about energy consumption, especially for ChatGPT-4o, highlighting the need for ongoing evaluation before clinical deployment. Yang et al [95] compared the performance and consistency of 5 LLMs (GPT-3.5, ChatGPT-4, Claude 2, Llama2-7B, and Llama2-13B) on a set of 219 multiple-choice questions covering critical care pharmacotherapy for Doctor of Pharmacy students. The study evaluated accuracy, response variance, and the impact of prompt engineering techniques, such as few-shot chain-of-thought prompting, and the use of a custom-trained GPT model. ChatGPT-4 emerged with the highest accuracy (71.6%), chain-of-thought prompting further improved its performance, and the variance in performance differed across models. Notably, customizing models and prompt strategies can enhance LLM reliability in pharmacy education contexts. Chen et al [98] developed and applied a multimodal evaluation framework to assess the performance of widely available machine translation (MT) tools (including DeepL, Gemini, Google Translate, and Microsoft Copilot) in translating critical care educational content from English into Mandarin Chinese, Spanish, and Ukrainian. The study used blinded bilingual clinician ratings (for fluency, adequacy, and meaning), BLEU (bilingual evaluation understudy) scores, and usability assessments to compare MT outputs against professional human translations. The results revealed no single MT tool consistently excelled across languages or metrics, human translation scored best for Chinese, Gemini performed strongest for Spanish, and Microsoft Copilot ranked highest for Ukrainian, highlighting the need for ongoing evaluation of MT tools in critical care education as they rapidly evolve. Wang et al [105] evaluated ChatGPT-4 against the Chinese Health Professional Technical Qualification Examination for Critical Care Medicine, which comprises 600 questions across fundamental knowledge, specialized knowledge, practical skills, and related medical knowledge. ChatGPT-4 achieved an overall success rate of 73.5%, surpassing the 60% passing threshold, with the highest accuracy in fundamental knowledge (81.94%). Notably, performance was significantly better on single-choice versus multiple-choice questions (76.72% vs 51.32%, P<.001), with no difference between case-based and non–case-based formats. The study underscores its potential as a clinical decision support and educational aid, while cautioning on the need for expert oversight due to potential inaccuracies.

Meanwhile, LLMs use information such as clinical guidelines to answer questions and do clinical reasoning from real-world medical scenarios. Levin et al [17] used 2 LLMs, ChatGPT-4 and Claude-2.0, to provide initial assessment and treatment

XSL•FO
RenderX

recommendations for patients in neonatal intensive care settings. The results indicated that both models demonstrated clinical reasoning abilities, with Claude-2.0 outperforming ChatGPT-4 in clinical accuracy in providing initial assessments and treatment recommendations, and response speed. Liu et al [86] conducted a qualitative study to explore how novice ICU simulation instructors experience the use of GenAI in case design. Using semistructured interviews with 13 instructors and thematic analysis, the study found that GenAI improved efficiency, provided structured and diverse scenario design, and enhanced learning engagement, especially for beginners. The findings suggest that GenAI can serve as a valuable educational tool in ICU simulation, but must be balanced with instructor-led critical thinking and validated clinical accuracy. Yitzhaki et al [91] used 100 educational questions from a PICU trainee WhatsApp forum to compare ChatGPT-4's performance against pediatric intensive care specialists. Evaluated by 10 PICU experts across multiple tertiary centers, ChatGPT-4's responses were longer and more complete for factual questions, with 60% being preferred for factual knowledge; however, specialists' responses were favored in clinical reasoning (67%), reflecting higher accuracy. Integrated answers were chosen in 37% of evaluations, emphasizing the need for expert oversight when using ChatGPT-4 in PICU education. Balta et al [100] assessed ChatGPT-3.5 versus ChatGPT-4 by having 2 independent intensivists evaluate LLM-generated recommendations to 50 curated core critical care questions from textbooks. ChatGPT-4 delivered significantly higher median appropriateness scores. The study stresses that both models can confidently produce clinically misleading or hallucinated content and thus should be used with caution in the ICU.

LLMs can also be used to overcome language barriers and enhance communication. Benboujja et al [75] developed and evaluated a multilingual, AI-driven curriculum to overcome language barriers in pediatric care. Using ChatGPT-4 for translation, the study created 45 educational video modules in English and Spanish, covering surgical procedures, perioperative care, and patient journeys. Almazyad et al [72] used ChatGPT-4 to enhance expert panel discussions in pediatric palliative care. They found that ChatGPT-4 effectively facilitated discussions on do-not-resuscitate conflicts by summarizing key themes such as communication, collaboration, patient and family-centered care, trust, and ethical considerations. Berger et al [87] conducted a study to investigate the risks associated with the use of abbreviations in critical care communication. By analyzing perspectives from ICU clinicians, the study highlighted how abbreviations, although designed to save time, often introduce ambiguity, misinterpretation, and patient safety risks in high-stakes environments. The findings emphasize that abbreviations can fall short of their intended efficiency, underscoring the importance of clear communication, standardized language, and improved training to minimize preventable errors and improve patient safety in the ICU.

RoB and Applicability Assessment

Across the literature, most studies were judged to have a high RoB in at least 1 RoB domain, most commonly analysis, including reliance on apparent performance without robust internal validation, absent calibration or uncertainty, and risks of temporal or selection leakage, followed by predictors and participants. Outcome definitions were generally aligned with ICU standards, but sometimes lacked blinded ascertainment. Applicability concerns concentrated in predictors (including dependencies on sources not readily available in real-time ICU workflows). Detailed ratings and justifications are presented in Table S4 in Multimedia Appendix 1.

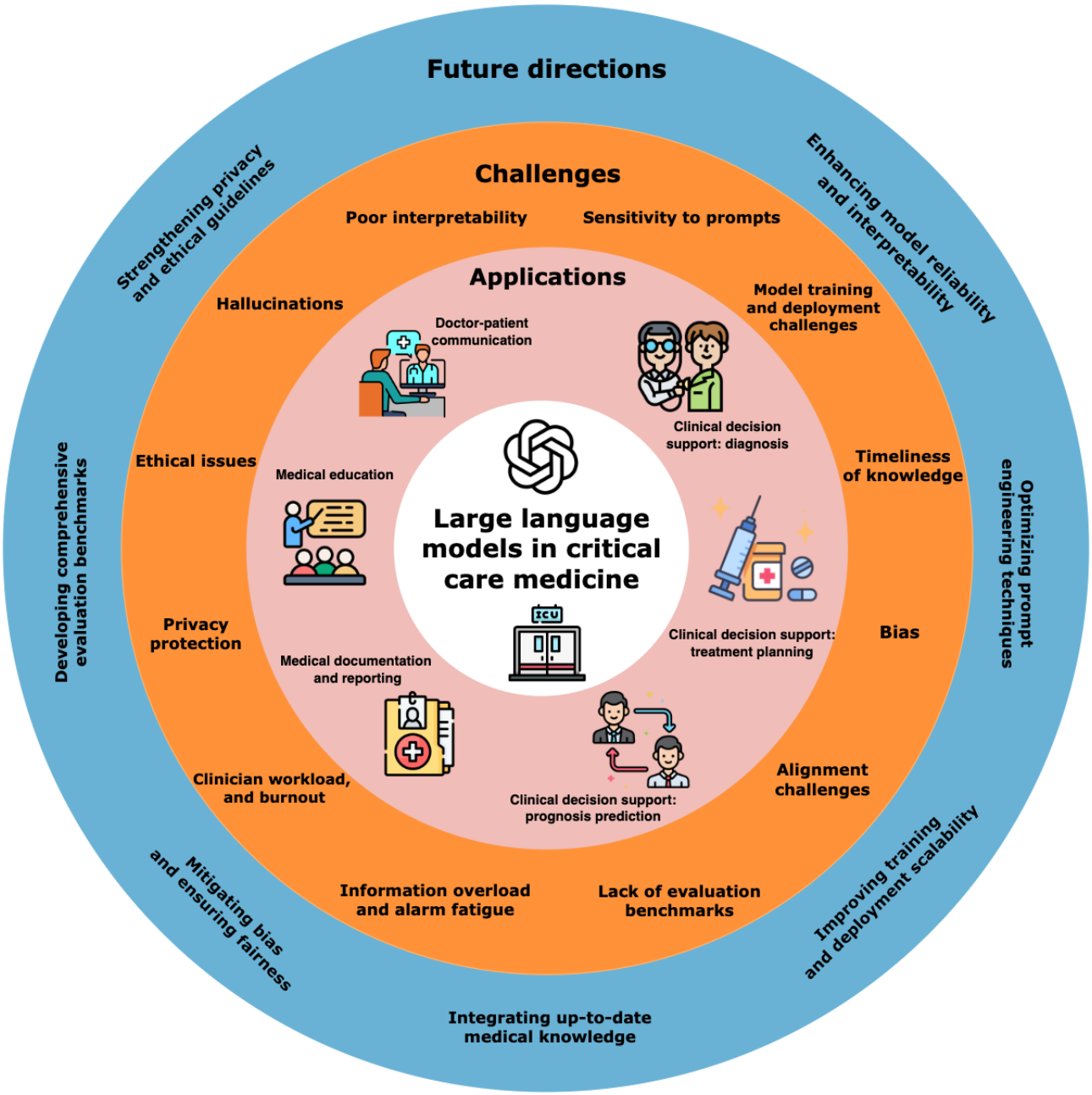
Discussion

Principal Findings

This scoping review provided a comprehensive portrait of the role of LLMs in CCM, identifying the applications, advantages, challenges, and future research directions of this area. With the recent advent of LLMs, medicine has witnessed groundbreaking developments and advancements [109]. Many review papers focus on applying LLMs in health and medicine [110,111]. Particularly, although there are some review papers on AI in CCM [112-114], few review papers focus on the application of LLMs in CCM. From the 2342 papers initially retrieved, 41 of them were selected for final review. An extensive examination of the selected literature revealed that LLMs have shown promise in some main aspects of CCM: clinical decision support, medical documentation and reporting, medical education, and doctor-patient communication. Compared with traditional AI models, LLMs have advantages in processing unstructured data and do not require manual feature engineering. At the same time, applying LLMs to CCM faces numerous challenges, including hallucinations and poor interpretability, sensitivity to prompts, bias and alignment challenges, and privacy and ethical issues. The current applications, together with the challenges and future directions of LLMs in CCM identified by this review, are shown in Figure 3. Our findings highlight the potential of LLMs in critical care practices while also underscoring the need for further research to address corresponding challenges and improve the reliability and applicability of LLMs in the critical care domain.

XSL•FO
RenderX

Figure 3. The main applications, challenges, and future directions of LLMs in CCM. CCM: critical care medicine; LLM: large language model.



The application of LLMs in CCM has demonstrated numerous advantages. Compared to traditional machine learning techniques, using LLM technology in CCM can effectively cause understanding and generate natural language, aiding clinicians in writing patient medical records and diagnostic notes [115-118]. The capabilities of LLMs extend beyond text interpretation and generation. They surpass traditional machine learning methods in handling unstructured data. LLMs can learn directly from extensive patient data without manual feature engineering. Moreover, multimodal LLMs can learn and understand medical images, such as x-rays and CT (computed tomography) scans [110]. In clinical practice, LLMs can extract critical information from a patient's historical medical records and combine it with the latest medical research, aiding physicians in identifying rare diseases or those with early symptoms that are not clearly defined [119]. For medical research, LLMs can assist researchers in summarizing data and information in literature research and providing suggestions for manuscript structure and titles, enhancing the readability and completeness of texts [118]. LLMs have a wide range of knowledge that can provide physicians with a comprehensive analysis of decision-making across different specialties [115].

Challenges

Hallucinations and Poor Interpretability

One of the most critical challenges in applying LLMs in CCM is the occurrence of hallucinations, where the model generates plausible-sounding but factually incorrect information [120,121]. These hallucinations pose risks, where incorrect recommendations can lead to inappropriate diagnoses or treatment plans, potentially endangering ICU patients' lives. Studies have documented examples where LLMs hallucinate during critical care decision-making, raising concerns about their reliability [76,81,122]. Additionally, LLM outputs often

XSL•FO
RenderX

lack transparency, making it difficult for clinicians to understand how specific decisions are reached. This opacity complicates the tracking of decision-making processes, leading to reduced trust in these systems [61,123]. The opaque nature of LLMs further complicates their application, as it becomes challenging to verify the factual basis of their outputs, particularly in the ICU, where patient safety is important. The lack of clarity regarding the sources of information makes LLMs unreliable for autonomous decision-making in CCM [76,81]. Therefore, improving the interpretability and transparency of LLMs remains a critical challenge in their integration into clinical workflows [123,124].

Sensitivity to Prompts and Inconsistent Performance

LLM-generated outputs are highly sensitive to input prompts, and different prompt strategies may affect the model's capabilities and performance [122]. In CCM, where the accuracy of information is essential, this sensitivity can lead to inconsistent results across different clinical scenarios [82,84]. The same LLM might provide different answers to slightly rephrased prompts, requiring clinicians to analyze multiple iterations to ensure accuracy. This lack of consistency raises concerns about the reliability of LLM applications in critical care, especially when time-sensitive decisions must be made. There is no universal prompt strategy that guarantees high performance across all LLMs, which means that clinicians must carefully craft prompts to suit the context of the task [75]. The absence of a one-size-fits-all approach for prompting remains a significant limitation of LLMs in critical care settings [76].

Model Training and Deployment Challenges

Training and deploying LLMs for critical care applications is a resource-intensive process, requiring vast computational power and large, diverse datasets. Public critical care databases, such as MIMIC (Medical Information Mart for Intensive Care) [125,126] and eICU [127], are commonly used for model training. Moreover, hospital regulations and privacy laws often restrict data sharing, complicating the training of models across multiple centers [107]. The deployment of LLMs in real-time ICU settings also requires substantial computational resources, which may not be feasible in all clinical environments, particularly those with constrained infrastructure [68,128,129]. Additionally, compliance with local data privacy regulations in some hospitals can limit the use of LLMs in health care settings [107]. The inability of LLMs to adapt to local computing environments due to privacy concerns further hampers their wide-scale application in critical care [68].

Timeliness of Knowledge and Model Updates

CCM is a rapidly evolving field, with frequent updates to clinical guidelines, treatments, and best practices. LLMs, however, are typically trained on static datasets, limiting their ability to remain up-to-date with the latest medical advancements [19]. This delay in knowledge poses a significant challenge, as outdated information could negatively impact patient outcomes [76,84]. To ensure their continued relevance in clinical practice, LLMs must be regularly updated with the latest medical knowledge. However, this process is computationally expensive and logistically challenging, particularly for large-scale LLMs [84,130]. Therefore, ensuring the timeliness of LLMs' knowledge base is crucial to their successful application in CCM.

Bias and Alignment Challenges

LLMs may unintentionally learn biases from the training data and reproduce them in their outputs, potentially leading to skewed or inappropriate recommendations in critical care. These biases can disproportionately affect specific patient populations, potentially leading to disparities in treatment and care [70,78,131]. In the ICU, biased outputs could result in suboptimal or even harmful decisions. Moreover, aligning LLM behavior with clinical guidelines and ethical standards is also a challenge, as models may not always adhere to best practices when generating recommendations [81,84,132]. Addressing bias and ensuring alignment with clinical guidelines and ethics are essential steps for LLMs to function as reliable tools in critical care [131,133]. Additionally, excessive reliance on AI-generated alerts can lead to "alarm fatigue," where clinicians become desensitized to frequent, nonurgent predictions, potentially missing critical care events [134].

Lack of Evaluation Benchmarks

Currently, there are no universally accepted standards for evaluating the performance of LLMs in critical care settings. Traditional model evaluation primarily focuses on the accuracy of medical question answering, which may not fully reflect the capabilities of LLMs in critical care clinical practice [135]. Across the included literature, model discrimination should not be conflated with clinical benefit. Consistent with current professional guidance and editorials, routine adoption should follow prospective evaluations that consider patient-centered outcomes rather than relying solely on technical metrics. Current benchmarks rarely include patient-relevant end points [136,137]. Without appropriate benchmarks, it is challenging to evaluate the effectiveness of LLMs in critical care or compare different models on an equal standard.

Information Overload and Alarm Fatigue in ICU Workflows

Contemporary ICUs are characterized by a proliferation of bedside devices and dense, multistream monitoring data. Qualitative and narrative evidence suggest that this technological abundance, when poorly integrated, can amplify cognitive load, desensitize clinicians to frequent alarms, and undermine situation awareness and team communication [138]. LLM-enabled systems may help by acting as context-aware filters and data-to-text summarizers that deduplicate near-identical events across monitors, ventilators, or pumps; prioritize alerts using clinical context; and attach traceable rationales for rapid verification [139,140]. However, naïve deployments could also increase burden (eg, secondary notifications and unverifiable rationales), so any use of LLMs should be aligned with human-centered monitoring principles and embedded in sociotechnical workflows rather than added as another layer.

XSL•FO
RenderX

Clinician Workload, Burnout, and Documentation Quality

While LLMs show promise for text generation and knowledge integration, clinical burden and professional burnout are often overlooked dimensions of the ICU setting [141,142]. Hallucinations and lack of interpretability shift the burden from "writing" to "reviewing and evidence verification." Inconsistent sensitivity to prompts and output leads to trial and error for frontline staff [143]. At the deployment level, the ICU's high noise level, multirole collaboration, and rigorous legal review may create new bottlenecks for editing and rework. Furthermore, language biases in generated text and paperwork bloat may compromise team communication and information retrieval efficiency. These factors collectively point to the need for systematic evaluation of clinician burden and burnout beyond model effectiveness.

Privacy and Ethical Concerns

Handling patient data responsibly is a significant concern in critical care, where vast amounts of sensitive information must be processed. Ensuring patient privacy while using LLMs presents both technical and legal challenges. Strict compliance with data protection regulations, such as the General Data Protection Regulation and HIPAA (Health Insurance Portability and Accountability Act), is necessary but can hinder the deployment of LLMs in clinical settings [68,76]. Moreover, the ethical implications of relying on LLMs for life-or-death decisions raise concerns about accountability and the potential over-reliance on AI in medical decision-making [144]. To navigate these issues, health care systems must establish clear guidelines for the responsible use of LLMs, ensuring that patient privacy is upheld and ethical standards are maintained. Addressing these privacy and ethical challenges will be essential for gaining clinician and patient trust in AI systems used in CCM [72].

Future Directions

Enhancing Model Reliability and Interpretability

Improving the reliability and interpretability of LLMs in CCM is critical for their safe integration into real-world clinical workflows. To enhance model reliability, future research should prioritize improving the quality of training data, particularly by incorporating domain-specific knowledge from critical care environments [84,107]. The accuracy and reliability of LLMs can be enhanced by improving training data quality, using ensemble learning, evidential reasoning, implementing adversarial training, and multiagent systems [145-149]. Additionally, the use of methods, such as chain-of-thought reasoning, tree-of-thoughts, and retrieval-augmented generation (RAG), can offer greater interpretability, allowing clinicians to understand how LLMs arrive at specific recommendations [150]. These interpretability techniques would provide clinicians with a clearer rationale for decision-making, thereby building trust in LLM outputs [151,152]. LLM outputs should include provenance-linked evidence and enforce concise, structured formats to curb alert or note bloat and reduce verification burden in human-centered ICU workflows [138]. Further, integrating external knowledge databases such as PubMed through plugins can improve the accuracy of LLM outputs and reduce the risk of hallucinations, particularly in critical care [108].

Optimizing Prompt Engineering Techniques

LLMs are highly sensitive to prompts, and developing robust prompt engineering techniques is essential for improving consistency and reliability in CCM. Recently, advancements such as Medprompt, which combines dynamic few-shot, self-generated chain-of-thought, and choice shuffle ensemble, have demonstrated improved performance in general LLMs, particularly in medical contexts [153]. MedGraphRAG is also a novel graph-based RAG framework designed specifically for the medical domain, enhancing the capabilities of LLMs by generating evidence-based, contextually accurate responses through a hierarchical graph structure, thereby improving transparency and reliability in handling private medical data [154]. These advancements will be particularly useful for critical care environments, where fast and reliable decision-making is essential. Future research should explore the development of prompt engineering strategies to handle complex clinical tasks [74,79].

Improving Model Training and Deployment Scalability

To address LLM training and deployment challenges, scalable model architectures, transfer learning, model pruning, and federated learning approaches can be explored to reduce computational demands and facilitate practical deployment [155]. The emergence of low-powered open-source LLMs running locally could circumvent issues related to data privacy and computational resource constraints [76]. It is crucial to convert medical datasets into easily accessible structured databases and train health care professionals in the ICUs to use LLMs in clinical practice to aid decision-making [108]. Collaboration with hospitals to develop structured medical databases will also aid in better training of LLMs for real-time decision-making in critical care environments [84,107].

Integrating Up-to-Date Medical Knowledge

Using web-based learning systems allows models to update and assimilate the latest medical research and changes in clinical practices on time. Additionally, modular update systems can swiftly integrate new medical discoveries, while expert collaboration ensures the scientific validity and timeliness of model outputs. Moreover, using RAG techniques to connect LLMs with databases in CCM can also address the knowledge timeliness issue to some extent [151,152].

Mitigating Bias and Ensuring Fairness

Bias mitigation should be approached through preprocessing, in-training, intraprocessing, and postprocessing stages [131]. Preprocessing techniques involve modifying model inputs to ensure balanced representations. In-training methods focus on adjusting model parameters to mitigate biases through gradient-based updates. Intraprocessing methods modify inference behavior without further training, while postprocessing techniques correct model outputs to ensure fair treatment across demographic groups. Developing bias detection and dataset augmentation algorithms to review and adjust model outputs regularly can help reduce model bias and ensure fairness in CCM [156].

XSL•FO
RenderX

Developing Comprehensive Evaluation Benchmarks

Recent studies demonstrated that performance varies across different medical tasks, highlighting the need for task-specific evaluations [135,157]. Future efforts should focus on developing more sophisticated evaluation frameworks that go beyond traditional metrics and consider the specific challenges of critical care [68]. For instance, the MIMIC-IV-CDM (Medical Information Mart for Intensive Care-IV-Clinical Decision Making) dataset and evaluation framework, focusing on 2400 real patient cases with acute abdominal pain, offers a new benchmark for evaluating LLMs in clinical decision-making, highlighting the need for more rigorous testing to ensure LLMs meet clinical standards, particularly guidelines [158]. We must standardize clinician-centered metrics, such as time-in-note, click or keystroke counts, handoff completion time, and note quality (accuracy, completeness, consistency, and readability), and report them alongside patient outcomes in prospective, preregistered ICU studies [159]. To establish clinical benefit and safety beyond model accuracy, future studies should use preregistered, prospective designs that prespecify outcomes such as mortality, ventilator-free days, time-to-critical interventions, and ICU length of stay, alongside calibration and uncertainty reporting [136,137]. Future work should explore comparing general LLMs against domain-adapted or fine-tuned LLMs (eg, BioGPT-Large and Llama-Med) on tasks and datasets in CCM. Additionally, collaboration between medical professionals and AI researchers will be necessary to design evaluation metrics that are meaningful, clinically applicable, and capable of guiding LLM improvements [135].

Strengthening Privacy and Ethical Guidelines

Data privacy and ethical guidelines are crucial for ensuring that LLMs are safely integrated into CCM [123,124]. As LLMs handle vast amounts of sensitive patient data, their deployment must comply with strict data protection regulations [76]. Future research should explore synthetic data generation techniques to augment training datasets while protecting patient privacy, allowing for comprehensive model training without compromising confidentiality [76,107]. Moreover, collaboration with policymakers, ethicists, and legal experts is necessary to ensure LLM applications comply with ethical and legal requirements, thus protecting patient privacy and data security [160].

This scoping review may be limited by selection bias due to the literature databases and inclusion criteria, potentially excluding relevant studies in non-English or outside the selected databases. Additionally, the rapid development of LLMs could render the findings quickly outdated, and the broad scope may have limited the depth of analysis for specific LLM applications in CCM.

Conclusions

In conclusion, although LLMs in CCM are not yet ICU experts, they act as more than stochastic parrots. Applying LLMs in CCM presents a transformative potential for enhancing critical care. LLMs are capable of reasoning beyond random generation, and they have demonstrated capabilities to improve diagnostic accuracy, plan optimal treatments, and provide valuable support in prognosis prediction. However, applying LLMs in CCM is still in its early stages, with very few large models specifically designed and fine-tuned for this domain. Future research should focus on enhancing model reliability and interpretability, optimizing prompt engineering techniques, improving training and deployment scalability, integrating up-to-date medical knowledge, mitigating bias and ensuring fairness, developing comprehensive evaluation benchmarks, and strengthening privacy and ethical guidelines. Close collaboration across multiple disciplines, such as medicine, computer science, and data science, may help catalyze the applications of LLMs in CCM. There is some way to go before making LLMs that become true ICU experts. Nevertheless, we are optimistic that LLMs in CCM will become experts in the near future, helping to improve the quality of critical care and the outcomes of patients with critical illness.

Acknowledgments

This work was supported by Grants from the National Natural Science Foundation of China (No. 82372095), the Humanities and Social Science Project of the Chinese Ministry of Education (No. 22YJA630036), the Zhejiang Provincial Natural Science Foundation of China (No. LZ22F020014), and the Beijing Natural Science Foundation of China (No. 7212201, QY23066).

Authors' Contributions

Conceptualization: TS and GK.
Data curation: TS, ZY, RY, and GK.
Formal analysis: TS, ZY, and GK.
Funding acquisition: GK.
Investigation: TS and GK.
Methodology: TS and GK.
Project administration: TS and GK.
Resources: TS, JM, HZ, and GK.
Supervision: GK.
Validation: TS, RY, and GK.
Visualization: TS.
Writing – original draft: TS, JM, ZY, HX, M Xiong, M Xiao, YL, and GK.

XSL•FO
RenderX

Writing – review & editing: TS, RY, and GK.

Conflicts of Interest

None declared.

Multimedia Appendix 1
Additional materials including Note S1 (Overview of LLMs in health and medicine), Note S2 (The process for selecting sources of evidence), Note S3 (Operational rules for PROBAST-AI ratings), Note S4 (Keyword co-occurrence network), Table S1 (PRISMA-ScR checklist), Table S2 (Search terms used across multiple databases for the scoping review), Table S3 (Design and performance summary for included studies), and Table S4 (Risk of bias and applicability assessed using the PROBAST-AI). LLM: large language model; PROBAST-AI: Prediction Model Risk of Bias Assessment Tool-Artificial Intelligence.
[PDF File (Adobe PDF File), 550 KB - medinform_v13i1e76326_app1.pdf]

References

1. Lu Y, Wu H, Qi S, Cheng K. Artificial intelligence in intensive care medicine: toward a ChatGPT/GPT-4 way? Ann Biomed Eng 2023;51(9):1898-1903 [FREE Full text] [doi: 10.1007/s10439-023-03234-w] [Medline: 37179277]
2. Shi T, Xu H, Ma J, Kong G, editors. ICU-TGNN: a Hybrid multitask transformer and graph neural network model for predicting clinical outcomes of patients in the ICU. 2024 Presented at: IEEE International Conference on Systems, Man, and Cybernetics (SMC); October 06-10, 2024; Kuching, Malaysia. [doi: 10.1109/smc54092.2024.10831750]
3. Xu H, Liu W, Shi T, Kong G. Neural granger causal discovery for derangements in icu-acquired acute kidney injury patients. AMIA Annu Symp Proc 2024;2024:1265-1274. [Medline: 40417474]
4. Liu W, Shi T, Xu H, Zhao H, Hao J, Kong G. Identifying acute kidney injury subtypes based on serum electrolyte data in ICU via K-medoids clustering. AMIA Annu Symp Proc 2024;2024:733-737. [Medline: 40417583]
5. Ostermann M, Lumlertgul N, Jeong R, See E, Joannidis M, James M. Acute kidney injury. Lancet 2025;405(10474):241-256. [doi: 10.1016/S0140-6736(24)02385-7] [Medline: 39826969]
6. Hoste EAJ, Kellum JA, Selby NM, Zarbock A, Palevsky PM, Bagshaw SM, et al. Global epidemiology and outcomes of acute kidney injury. Nat Rev Nephrol 2018;14(10):607-625. [doi: 10.1038/s41581-018-0052-0] [Medline: 30135570]
7. Lin Y, Shi T, Kong G. Acute kidney injury prognosis prediction using machine learning methods: a systematic review. Kidney Med 2025;7(1):100936 [FREE Full text] [doi: 10.1016/j.xkme.2024.100936] [Medline: 39758155]
8. Li A, Ling L, Qin H, Arabi YM, Myatra SN, Egi M, et al. Epidemiology, management, and outcomes of sepsis in ICUs among countries of differing national wealth across Asia. Am J Respir Crit Care Med 2022;206(9):1107-1116. [doi: 10.1164/rccm.202112-2743OC] [Medline: 35763381]
9. Rudd KE, Johnson SC, Agesa KM, Shackelford KA, Tsoi D, Kievlan DR, et al. Global, regional, and national sepsis incidence and mortality, 1990-2017: analysis for the global burden of disease study. Lancet 2020;395(10219):200-211 [FREE Full text] [doi: 10.1016/S0140-6736(19)32989-7] [Medline: 31954465]
10. Bardají-Carrillo M, López-Herrero R, Aguilar G, Arroyo-Hernantes I, Gómez-Sánchez E, Camporota L, et al. Epidemiological trends of mechanically ventilated acute respiratory distress syndrome in the twenty-first century: a nationwide, population-based retrospective study. J Intensive Care 2025;13(1):9 [FREE Full text] [doi: 10.1186/s40560-025-00781-3] [Medline: 39962546]
11. Crawford AM, Shiferaw AA, Ntambwe P, Milan AO, Khalid K, Rubio R, et al. Global critical care: a call to action. Crit Care 2023;27(1):28 [FREE Full text] [doi: 10.1186/s13054-022-04296-3] [Medline: 36670506]
12. Shi T, Zhang Z, Liu W, Fang J, Hao J, Jin S. Identifying subgroups of ICU patients using end-to-end multivariate time-series clustering algorithm based on real-world vital signs data. arXiv. Preprint posted online on July 11, 2023 2023. [doi: 10.48550/arXiv.2306.02121]
13. Cecconi M, Greco M, Shickel B, Vincent J, Bihorac A. Artificial intelligence in acute medicine: a call to action. Crit Care 2024;28(1):258 [FREE Full text] [doi: 10.1186/s13054-024-05034-7] [Medline: 39075468]
14. Shi T, Lin Y, Zhao H, Kong G. Artificial intelligence models for predicting acute kidney injury in the intensive care unit: a systematic review of modeling methods, data utilization, and clinical applicability. JAMIA Open 2025;8(4):ooaf065. [doi: 10.1093/jamiaopen/ooaf065] [Medline: 40620479]
15. Vaswani A, Shazeer N, Parmar N, Uszkoreit J, Jones L, Gomez A. Attention is all you need. 2017 Presented at: NIPS'17: Proceedings of the 31st International Conference on Neural Information Processing Systems; December 4-9, 2017; Long Beach California USA p. 6000-6010.
16. Zhao WX, Zhou K, Li J, Tang T, Wang X, Hou Y. A survey of large language models. arXiv. Preprint posted online November 24, 2023 2023. [doi: 10.5260/chara.21.2.8]
17. Levin C, Kagan T, Rosen S, Saban M. An evaluation of the capabilities of language models and nurses in providing neonatal clinical decision support. Int J Nurs Stud 2024;155:104771. [doi: 10.1016/j.ijnurstu.2024.104771] [Medline: 38688103]
18. Yuan M, Bao P, Yuan J, Shen Y, Chen Z, Xie Y, et al. Large language models illuminate a progressive pathway to artificial intelligent healthcare assistant. Med Plus 2024;1(2):100030. [doi: 10.1016/j.medp.2024.100030]

XSL•FO
RenderX

19. Omiye JA, Gui H, Rezaei SJ, Zou J, Daneshjou R. Large language models in medicine: the potentials and pitfalls : a narrative review. Ann Intern Med 2024;177(2):210-220. [doi: 10.7326/M23-2772] [Medline: 38285984]
20. Brown T, Mann B, Ryder N, Subbiah M, Kaplan JD, Dhariwal P, et al. Language models are few-shot learners. In: Adv Neural Inf Process Syst. 2020 Presented at: NIPS'20: Proceedings of the 34th International Conference on Neural Information Processing Systems; December 6 - 12, 2020; Vancouver BC Canada p. 1877-1901. [doi: abs/10.5555/3495724.3495883]
21. Chowdhery A, Narang S, Devlin J, Bosma M, Mishra G, Roberts A, et al. Palm: scaling language modeling with pathways. J Mach Learn Res 2023;24(240):1-113. [doi: 10.5555/3648699.3648939]
22. Han X, Zhang Z, Ding N, Gu Y, Liu X, Huo Y, et al. Pre-trained models: past, present and future. AI Open 2021;2:225-250. [doi: 10.1016/j.aiopen.2021.08.002]
23. Harshvardhan G, Gourisaria MK, Pandey M, Rautaray SS. A comprehensive survey and analysis of generative models in machine learning. Comput Sci Rev 2020;38:100285. [doi: 10.1016/j.cosrev.2020.100285]
24. Hu Z, Yang Z, Liang X, Salakhutdinov R, Xing EP. Toward controlled generation of text. 2017 Presented at: Proceedings of the 34 th International Conference on Machine Learning; March 02, 2017; Sydney, Australia p. 1587-1596. [doi: abs/10.5555/3495724.3495883]
25. Sarkar K, Liu L, Golyanik V, Theobalt C. HumanGAN: a generative model of human images. 2021 Presented at: International Conference on 3D Vision (3DV); December 01-03, 2021; London, United Kingdom p. 258-267. [doi: 10.1109/3DV53792.2021.00036]
26. Kim S, Lee SG, Song J, Kim J, Yoon S. FloWaveNet : a generative flow for raw audio. arXiv. Preprint posted online on May 20, 2019 2018. [doi: 10.48550/arXiv.1811.02155]
27. Wu J, Gan W, Chen Z, Wan S, Lin H. AI-generated content (AIGC): a survey. arXiv. Preprint posted online on Mar 26, 2023 2023. [doi: 10.48550/arXiv.2304.06632]
28. Goodfellow I, Pouget-Abadie J, Mirza M, Xu B, Warde-Farley D, Ozair S, et al. Generative adversarial networks. Commun ACM 2020;63(11):139-144. [doi: 10.1145/3422622]
29. Doersch C. Tutorial on variational autoencoders. arXiv. Preprint posted online on Jan 3, 2021 2016. [doi: 10.48550/arXiv.1606.05908]
30. Lipton ZC, Berkowitz J, Elkan C. A critical review of recurrent neural networks for sequence learning. arXiv. Preprint posted online on Oct 17, 2015 2015. [doi: 10.48550/arXiv.1506.00019]
31. Mikolov T, Karafiát M, Burget L, Cernocký J, Khudanpur S. Recurrent neural network based language model. 2010 Presented at: INTERSPEECH 2010, 11th Annual Conference of the International Speech Communication Association; September 26-30, 2010; Makuhari, Chiba, Japan p. 1045-1048. [doi: 10.1109/ICASSP.2011.5947611]
32. Hochreiter S, Schmidhuber J. Long short-term memory. Neural Comput 1997;9(8):1735-1780. [doi: 10.1162/neco.1997.9.8.1735] [Medline: 9377276]
33. Peters ME, Neumann M, Iyyer M, Gardner M, Clark C, Lee K, et al. Deep contextualized word representations. 2108 Presented at: Proceedings of the 2018 Conference of the North American Chapter of the Association for Computational Linguistics: Human Language Technologies, Volume 1 (Long Papers); June 01, 2018; New Orleans, Louisiana. [doi: 10.18653/v1/N18-1202]
34. Devlin J, Chang MW, Lee K, Toutanova K. BERT: pre-training of deep bidirectional transformers for language understanding. 2019 Presented at: Proceedings of NAACL-HLT 2019; June 02-07, 2019; Minneapolis, Minnesota p. 4171-4186. [doi: 10.18653/v1/N19-1423]
35. Radford A, Wu J, Child R, Luan D, Amodei D, Sutskever I. Language models are unsupervised multitask learners. OpenAI Blog 2019;1(8):9.
36. Lewis M, Liu Y, Goyal N, Ghazvininejad M, Mohamed A, Levy O, et al. BART: denoising sequence-to-sequence pre-training for natural language generation, translation, and comprehension. arXiv:1910.13461 2019. [doi: 10.48550/arXiv.1910.13461]
37. Kaplan J, McCandlish S, Henighan T, Brown TB, Chess B, Child R, et al. Scaling laws for neural language models. arXiv. Posted online on January 23, 2020 2020. [doi: 10.48550/arXiv.2001.08361]
38. Wei J, Bosma M, Zhao VY, Guu K, Yu AW, Lester B, et al. Finetuned language models are zero-shot learners. arXiv. Posted online on February 8, 2022 2021. [doi: 10.48550/arXiv.2109.01652]
39. Wei J, Wang X, Schuurmans D, Bosma M, Ichter B, Xia F, et al. Chain-of-thought prompting elicits reasoning in large language models. 2022 Presented at: NIPS'22: Proceedings of the 36th International Conference on Neural Information Processing Systems; November 28, 2022; Red Hook, NY, United States p. 24824-24837. [doi: 10.5555/3600270.3602070]
40. Puladi B, Gsaxner C, Kleesiek J, Hölzle F, Röhrig R, Egger J. The impact and opportunities of large language models like ChatGPT in oral and maxillofacial surgery: a narrative review. Int J Oral Maxillofac Surg 2024;53(1):78-88 [FREE Full text] [doi: 10.1016/j.ijom.2023.09.005] [Medline: 37798200]
41. Kothari AN. ChatGPT, large language models, and generative AI as future augments of surgical cancer care. Ann Surg Oncol 2023;30(6):3174-3176. [doi: 10.1245/s10434-023-13442-2] [Medline: 37052826]
42. Akinci D'Antonoli T, Stanzione A, Bluethgen C, Vernuccio F, Ugga L, Klontzas ME, et al. Large language models in radiology: fundamentals, applications, ethical considerations, risks, and future directions. Diagn Interv Radiol 2024;30(2):80-90 [FREE Full text] [doi: 10.4274/dir.2023.232417] [Medline: 37789676]

XSL•FO
RenderX

43. Shen Y, Heacock L, Elias J, Hentel KD, Reig B, Shih G, et al. ChatGPT and other large language models are double-edged swords. Radiology 2023;307(2):e230163. [doi: 10.1148/radiol.230163] [Medline: 36700838]
44. Hu X, Ran AR, Nguyen TX, Szeto S, Yam JC, Chan CKM, et al. What can GPT-4 do for diagnosing rare eye diseases? A pilot study. Ophthalmol Ther 2023;12(6):3395-3402 [FREE Full text] [doi: 10.1007/s40123-023-00789-8] [Medline: 37656399]
45. Mihalache A, Popovic MM, Muni RH. Performance of an artificial intelligence chatbot in ophthalmic knowledge assessment. JAMA Ophthalmol 2023;141(6):589-597 [FREE Full text] [doi: 10.1001/jamaophthalmol.2023.1144] [Medline: 37103928]
46. Arora A, Arora A. The promise of large language models in health care. Lancet 2023;401(10377):641. [doi: 10.1016/S0140-6736(23)00216-7] [Medline: 36841609]
47. Wu C, Zhang X, Zhang Y, Wang Y, Xie W. Towards generalist foundation model for radiology. arXiv. Posted online on November 16, 2023 2023. [doi: 10.48550/arXiv.2308.02463]
48. Hyland SL, Bannur S, Bouzid K, Castro DC, Ranjit M, Schwaighofer A, et al. MAIRA-1: a specialised large multimodal model for radiology report generation. arXiv. Posted online on April 26, 2024 2023. [doi: 10.48550/arXiv.2311.13668]
49. Yang Z, Batra SS, Stremmel J, Halperin E. Surpassing GPT-4 medical coding with a two-stage approach. arXiv. Posted online on November 22, 2023 2023. [doi: 10.48550/arXiv.2311.13735]
50. Liu J, Yang S, Peng T, Hu X, Zhu Q. ChatICD: prompt learning for few-shot ICD coding through ChatGPT. 2023 Presented at: IEEE International Conference on Bioinformatics and Biomedicine (BIBM); December 05-08, 2023; Istanbul, Turkiye p. 4360-4367. [doi: 10.1109/BIBM58861.2023.10385482]
51. Zhu L, Mou W, Chen R. Can the ChatGPT and other large language models with internet-connected database solve the questions and concerns of patient with prostate cancer and help democratize medical knowledge? J Transl Med 2023;21(1):269 [FREE Full text] [doi: 10.1186/s12967-023-04123-5] [Medline: 37076876]
52. Yoshiyasu Y, Wu F, Dhanda AK, Gorelik D, Takashima M, Ahmed OG. GPT-4 accuracy and completeness against International Consensus Statement on Allergy and Rhinology: rhinosinusitis. Int Forum Allergy Rhinol 2023;13(12):2231-2234. [doi: 10.1002/alr.23201] [Medline: 37260081]
53. Yeo YH, Samaan JS, Ng WH, Ting PS, Trivedi H, Vipani A, et al. Assessing the performance of ChatGPT in answering questions regarding cirrhosis and hepatocellular carcinoma. Clin Mol Hepatol 2023;29(3):721-732 [FREE Full text] [doi: 10.3350/cmh.2023.0089] [Medline: 36946005]
54. Lokker C, Bagheri E, Abdelkader W, Parrish R, Afzal M, Navarro T, et al. Deep learning to refine the identification of high-quality clinical research articles from the biomedical literature: Performance evaluation. J Biomed Inform 2023;142:104384 [FREE Full text] [doi: 10.1016/j.jbi.2023.104384] [Medline: 37164244]
55. Ayers JW, Poliak A, Dredze M, Leas EC, Zhu Z, Kelley JB, et al. Comparing physician and artificial intelligence chatbot responses to patient questions posted to a public social media forum. JAMA Intern Med 2023;183(6):589-596 [FREE Full text] [doi: 10.1001/jamainternmed.2023.1838] [Medline: 37115527]
56. Qureshi R, Shaughnessy D, Gill KAR, Robinson KA, Li T, Agai E. Are ChatGPT and large language models "the answer" to bringing us closer to systematic review automation? Syst Rev 2023;12(1):72 [FREE Full text] [doi: 10.1186/s13643-023-02243-z] [Medline: 37120563]
57. Atas Guvenilir H, Doğan T. How to approach machine learning-based prediction of drug/compound-target interactions. J Cheminform 2023;15(1):16 [FREE Full text] [doi: 10.1186/s13321-023-00689-w] [Medline: 36747300]
58. Li Z, Li Y, Li Q, Wang P, Guo D, Lu L, et al. LViT: Language meets vision transformer in medical image segmentation. IEEE Trans Med Imaging 2024;43(1):96-107. [doi: 10.1109/TMI.2023.3291719] [Medline: 37399157]
59. Guo Y, Qiu W, Leroy G, Wang S, Cohen T. Retrieval augmentation of large language models for lay language generation. J Biomed Inform 2024;149:104580 [FREE Full text] [doi: 10.1016/j.jbi.2023.104580] [Medline: 38163514]
60. Nadkarni GN, Sakhuja A. Clinical informatics in critical care medicine. Yale J Biol Med 2023;96(3):397-405 [FREE Full text] [doi: 10.59249/WTTU3055] [Medline: 37780994]
61. Thirunavukarasu AJ, Ting DSJ, Elangovan K, Gutierrez L, Tan TF, Ting DSW. Large language models in medicine. Nat Med 2023;29(8):1930-1940. [doi: 10.1038/s41591-023-02448-8] [Medline: 37460753]
62. Bender EM, Gebru T, McMillan-Major A, Shmitchell S. On the dangers of stochastic parrots: can language models be too big? 2021 Presented at: FAccT '21: Proceedings of the 2021 ACM Conference on Fairness, Accountability, and Transparency; March 3-10, 2021; Virtual Event Canada p. 610-623. [doi: 10.1145/3442188.3445922]
63. Tricco AC, Lillie E, Zarin W, O'Brien KK, Colquhoun H, Levac D, et al. PRISMA Extension for Scoping Reviews (PRISMA-ScR): checklist and explanation. Ann Intern Med 2018;169(7):467-473 [FREE Full text] [doi: 10.7326/M18-0850] [Medline: 30178033]
64. Chen G, Hong S, Du C, Wang P, Yang Z, Xiao L. Comparing semantic representation methods for keyword analysis in bibliometric research. J Informetrics 2024;18(3):101529. [doi: 10.1016/j.joi.2024.101529]
65. Van EN, Waltman L. Visualizing bibliometric networks. In: Measuring Scholarly Impact: Methods and Practice. Cham: Springer; 2014:285-320.
66. Van EN, Waltman L. VOS: a new method for visualizing similarities between objects. 2007 Presented at: Proceedings of the 30th Annual Conference of the Gesellschaft für Klassifikation e.V; March 8-10, 2006; Freie Universität Berlin p. 299-306. [doi: 10.1007/978-3-540-70981-7_34]

XSL•FO
RenderX

67. Moons KGM, Wolff RF, Riley RD, Whiting PF, Westwood M, Collins GS, et al. PROBAST: a tool to assess risk of bias and applicability of prediction model studies: explanation and elaboration. Ann Intern Med 2019;170(1):W1-W33 [FREE Full text] [doi: 10.7326/M18-1377] [Medline: 30596876]
68. Savage T, Wang J, Shieh L. A large language model screening tool to target patients for Best Practice Alerts: development and validation. JMIR Med Inform 2023;11:e49886 [FREE Full text] [doi: 10.2196/49886] [Medline: 38010803]
69. Pham C, Govender R, Tehami S, Chavez S, Adepoju OE, Liaw W. ChatGPT's performance in cardiac arrest and bradycardia simulations using the American heart association's advanced cardiovascular life support guidelines: exploratory study. J Med Internet Res 2024;26:e55037 [FREE Full text] [doi: 10.2196/55037] [Medline: 38648098]
70. Huespe IA, Echeverri J, Khalid A, Carboni Bisso I, Musso CG, Surani S, et al. Clinical research with large language models generated writing-clinical research with ai-assisted writing (CRAW) study. Crit Care Explor 2023;5(10):e0975 [FREE Full text] [doi: 10.1097/CCE.0000000000000975] [Medline: 37795455]
71. Si Y, Wang J, Xu H, Roberts K. Enhancing clinical concept extraction with contextual embeddings. J Am Med Inform Assoc 2019;26(11):1297-1304 [FREE Full text] [doi: 10.1093/jamia/ocz096] [Medline: 31265066]
72. Almazyad M, Aljofan F, Abouammoh NA, Muaygil R, Malki KH, Aljamaan F, et al. Enhancing expert panel discussions in pediatric palliative care: innovative scenario development and summarization with ChatGPT-4. Cureus 2023;15(4):e38249 [FREE Full text] [doi: 10.7759/cureus.38249] [Medline: 37122982]
73. Chung P, Fong CT, Walters AM, Aghaeepour N, Yetisgen M, O'Reilly-Shah VN. Large language model capabilities in perioperative risk prediction and prognostication. JAMA Surg 2024;159(8):928-937. [doi: 10.1001/jamasurg.2024.1621] [Medline: 38837145]
74. Abdullahi T, Singh R, Eickhoff C. Learning to make rare and complex diagnoses with generative ai assistance: qualitative study of popular large language models. JMIR Med Educ 2024;10:e51391 [FREE Full text] [doi: 10.2196/51391] [Medline: 38349725]
75. Benboujja F, Hartnick E, Zablah E, Hersh C, Callans K, Villamor P, et al. Overcoming language barriers in pediatric care: a multilingual, AI-driven curriculum for global healthcare education. Front Public Health 2024;12:1337395 [FREE Full text] [doi: 10.3389/fpubh.2024.1337395] [Medline: 38454985]
76. Madden MG, McNicholas BA, Laffey JG. Assessing the usefulness of a large language model to query and summarize unstructured medical notes in intensive care. Intensive Care Med 2023;49(8):1018-1020. [doi: 10.1007/s00134-023-07128-2] [Medline: 37338549]
77. Liu T, Duan Y, Li Y, Hu Y, Su L, Zhang A. ChatGPT achieves comparable accuracy to specialist physicians in predicting the efficacy of high-flow oxygen therapy. Heliyon 2024;10(11):e31750 [FREE Full text] [doi: 10.1016/j.heliyon.2024.e31750] [Medline: 38828316]
78. Nolan VJ, Balch JA, Baskaran NP, Shickel B, Efron PA, Upchurch GR, et al. Incorporating patient values in large language model recommendations for surrogate and proxy decisions. Crit Care Explor 2024;6(8):e1131 [FREE Full text] [doi: 10.1097/CCE.0000000000001131] [Medline: 39132980]
79. Shah-Mohammadi F, Finkelstein J. Extraction of substance use information from clinical notes: generative pretrained transformer-based investigation. JMIR Med Inform 2024;12:e56243 [FREE Full text] [doi: 10.2196/56243] [Medline: 39037700]
80. Nawab K, Fernbach M, Atreya S, Asfandiyar S, Khan G, Arora R, et al. Fine-tuning for accuracy: evaluation of generative pretrained transformer (GPT) for automatic assignment of international classification of disease (ICD) codes to clinical documentation. J Med Artif Intell 2024;7:8-8. [doi: 10.21037/jmai-24-60]
81. Soleimani M, Seyyedi N, Ayyoubzadeh SM, Kalhori SRN, Keshavarz H. Practical evaluation of ChatGPT performance for radiology report generation. Acad Radiol 2024;31(12):4823-4832. [doi: 10.1016/j.acra.2024.07.020] [Medline: 39142976]
82. Oh N, Cha WC, Seo JH, Choi S, Kim JM, Chung CR, et al. ChatGPT predicts in-hospital all-cause mortality for sepsis: in-context learning with the Korean Sepsis Alliance database. Healthc Inform Res 2024;30(3):266-276 [FREE Full text] [doi: 10.4258/hir.2024.30.3.266] [Medline: 39160785]
83. Urquhart E, Ryan J, Hartigan S, Nita C, Hanley C, Moran P, et al. A pilot feasibility study comparing large language models in extracting key information from ICU patient text records from an Irish population. Intensive Care Med Exp 2024;12(1):71. [doi: 10.1186/s40635-024-00656-1] [Medline: 39147878]
84. Pabon MA, Vaduganathan M, Claggett BL, Chatur S, Siqueira S, Marti-Castellote P, et al. In-hospital course of patients with heart failure with improved ejection fraction in the DELIVER trial. Eur J Heart Fail 2024;26(12):2532-2540. [doi: 10.1002/ejhf.3410] [Medline: 39300780]
85. Akhondi-Asl A, Yang Y, Luchette M, Burns JP, Mehta NM, Geva A. Comparing the quality of domain-specific versus general language models for artificial intelligence-generated differential diagnoses in PICU patients. Pediatr Crit Care Med 2024;25(6):e273-e282. [doi: 10.1097/PCC.0000000000003468] [Medline: 38329382]
86. Liu J, Wang L, He X, Xia Y, Gong X, Wu R, et al. Leveraging generative artificial intelligence to enhance ICU novice simulation instructors' case design: a qualitative study. Clin Simul Nurs 2025;105:101770. [doi: 10.1016/j.ecns.2025.101770]
87. Berger S, Grzonka P, Hunziker S, Frei AI, Sutter R. When shortcuts fall short: the hidden danger of abbreviations in critical care. J Crit Care 2025;91:155236 [FREE Full text] [doi: 10.1016/j.jcrc.2025.155236] [Medline: 40839977]

XSL•FO
RenderX

88. Kurz CF, Merzhevich T, Eskofier BM, Kather JN, Gmeiner B. Benchmarking vision-language models for diagnostics in emergency and critical care settings. npj Digit Med 2025;8(1):423 [FREE Full text] [doi: 10.1038/s41746-025-01837-2] [Medline: 40640347]
89. Pham HQT, Vo TTL, Nguyen TT, Nguyen NTK, Nguyen PMT, Tran N, et al. Validity of ChatGPT in assisting diagnosis of periventricular-intraventricular hemorrhage via cranial ultrasound imaging in very preterm infants. Cureus 2025;17(4):e82300. [doi: 10.7759/cureus.82300] [Medline: 40376373]
90. Shi B, Chen L, Pang S, Wang Y, Wang S, Li F, et al. Large language models and artificial neural networks for assessing 1-year mortality in patients with myocardial infarction: analysis from the Medical Information Mart for Intensive Care IV (MIMIC-IV) database. J Med Internet Res 2025;27:e67253 [FREE Full text] [doi: 10.2196/67253] [Medline: 40354652]
91. Yitzhaki S, Peled N, Kaplan E, Kadmon G, Nahum E, Gendler Y, et al. Comparing ChatGPT-4 and a paediatric intensive care specialist in responding to medical education questions: a multicenter evaluation. J Paediatr Child Health 2025;61(7):1084-1089. [doi: 10.1111/jpc.70080] [Medline: 40331496]
92. Williams B, Erstad BL. Analysis of responses from artificial intelligence programs to medication-related questions derived from critical care guidelines. Am J Health Syst Pharm 2025;82(19):e842-e847. [doi: 10.1093/ajhp/zxaf075] [Medline: 40119714]
93. Yang Z, Xu S, Liu X, Xu N, Chen Y, Wang S, et al. Large language model-based critical care big data deployment and extraction: descriptive analysis. JMIR Med Inform 2025;13:e63216 [FREE Full text] [doi: 10.2196/63216] [Medline: 40079079]
94. Workum JD, Volkers BWS, van de Sande D, Arora S, Goeijenbier M, Gommers D, et al. Comparative evaluation and performance of large language models on expert level critical care questions: a benchmark study. Crit Care 2025;29(1):72 [FREE Full text] [doi: 10.1186/s13054-025-05302-0] [Medline: 39930514]
95. Yang H, Hu M, Most A, Hawkins WA, Murray B, Smith SE, et al. Evaluating accuracy and reproducibility of large language model performance on critical care assessments in pharmacy education. Front Artif Intell 2025;7:1514896 [FREE Full text] [doi: 10.3389/frai.2024.1514896] [Medline: 39850846]
96. Ding S, Ye J, Hu X, Zou N. Distilling the knowledge from large-language model for health event prediction. Sci Rep 2024;14(1):30675 [FREE Full text] [doi: 10.1038/s41598-024-75331-2] [Medline: 39730390]
97. Walker A, Thorne A, Das S, Love J, Cooper HLF, Livingston M, et al. CARE-SD: classifier-based analysis for recognizing provider stigmatizing and doubt marker labels in electronic health records: model development and validation. J Am Med Inform Assoc 2025;32(2):365-374. [doi: 10.1093/jamia/ocae310] [Medline: 39724920]
98. Chen CL, Dong Y, Castillo-Zambrano C, Bencheqroun H, Barwise A, Hoffman A, et al. A systematic multimodal assessment of AI machine translation tools for enhancing access to critical care education internationally. BMC Med Educ 2025;25(1):1022 [FREE Full text] [doi: 10.1186/s12909-025-07452-9] [Medline: 40629322]
99. Ucdal M, Bakhshandehpour A, Durak MB, Balaban Y, Kekilli M, Simsek C. Evaluating the role of artificial intelligence in making clinical decisions for treating acute pancreatitis. J Clin Med 2025;14(12):4347 [FREE Full text] [doi: 10.3390/jcm14124347] [Medline: 40566092]
100. Balta KY, Javidan AP, Walser E, Arntfield R, Prager R. Evaluating the appropriateness, consistency, and readability of ChatGPT in critical care recommendations. J Intensive Care Med 2024;40(2):184-190 [FREE Full text] [doi: 10.1177/08850666241267871] [Medline: 39118320]
101. Zhu H, Wang R, Qian J, Wu Y, Jin Z, Shan X, et al. Leveraging large language models for predicting postoperative acute kidney injury in elderly patients. BME Front 2025;6:0111 [FREE Full text] [doi: 10.34133/bmef.0111] [Medline: 40071150]
102. Pathak A, Marshall C, Davis C, Yang P, Kamaleswaran R. RespBERT: a multi-site validation of a natural language processing algorithm, of radiology notes to identify acute respiratory distress syndrome (ARDS). IEEE J Biomed Health Inform 2025;29(2):1455-1463. [doi: 10.1109/JBHI.2024.3502575] [Medline: 40030382]
103. Liu J, Nguyen A, Capurro D, Verspoor K. Comparing text-based clinical risk prediction in critical care: a note-specific hierarchical network and large language models. IEEE J Biomed Health Inform 2025;29(10):7657-7667. [doi: 10.1109/JBHI.2025.3574254] [Medline: 40424107]
104. Turan E, Baydemir AE, Balıtatlı AB, Şahin AS. Assessing the accuracy of ChatGPT in interpreting blood gas analysis results ChatGPT-4 in blood gas analysis. J Clin Anesth 2025;102:111787. [doi: 10.1016/j.jclinane.2025.111787] [Medline: 39986120]
105. Wang X, Tang J, Feng Y, Tang C, Wang X. Can ChatGPT-4 perform as a competent physician based on the Chinese critical care examination? J Crit Care 2025;86:155010. [doi: 10.1016/j.jcrc.2024.155010] [Medline: 40023616]
106. Yang H, Li J, Zhang C, Sierra AP, Shen B. Large language model-driven knowledge graph construction in sepsis care using multicenter clinical databases: development and usability study. J Med Internet Res 2025;27:e65537 [FREE Full text] [doi: 10.2196/65537] [Medline: 40146985]
107. Gandomi A, Wu P, Clement DR, Xing J, Aviv R, Federbush M, et al. ARDSFlag: an NLP/machine learning algorithm to visualize and detect high-probability ARDS admissions independent of provider recognition and billing codes. BMC Med Inform Decis Mak 2024;24(1):195 [FREE Full text] [doi: 10.1186/s12911-024-02573-5] [Medline: 39014417]

XSL•FO
RenderX

108. Amacher SA, Arpagaus A, Sahmer C, Becker C, Gross S, Urben T, et al. Prediction of outcomes after cardiac arrest by a generative artificial intelligence model. Resusc Plus 2024;18:100587 [FREE Full text] [doi: 10.1016/j.resplu.2024.100587] [Medline: 38433764]
109. Hajijama S, Juneja D, Nasa P. Large language model in critical care medicine: opportunities and challenges. Indian J Crit Care Med 2024;28(6):523-525. [doi: 10.5005/jp-journals-10071-24743] [Medline: 39130386]
110. Meng X, Yan X, Zhang K, Liu D, Cui X, Yang Y, et al. The application of large language models in medicine: a scoping review. iScience 2024;27(5):109713. [doi: 10.1016/j.isci.2024.109713] [Medline: 38746668]
111. Singhal K, Azizi S, Tu T, Mahdavi SS, Wei J, Chung HW, et al. Large language models encode clinical knowledge. Nature 2023;620(7972):172-180 [FREE Full text] [doi: 10.1038/s41586-023-06291-2] [Medline: 37438534]
112. Shillan D, Sterne JAC, Champneys A, Gibbison B. Use of machine learning to analyse routinely collected intensive care unit data: a systematic review. Crit Care 2019;23(1):284 [FREE Full text] [doi: 10.1186/s13054-019-2564-9] [Medline: 31439010]
113. Moazemi S, Vahdati S, Li J, Kalkhoff S, Castano LJV, Dewitz B, et al. Artificial intelligence for clinical decision support for monitoring patients in cardiovascular ICUs: a systematic review. Front Med (Lausanne) 2023;10:1109411 [FREE Full text] [doi: 10.3389/fmed.2023.1109411] [Medline: 37064042]
114. Syed M, Syed S, Sexton K, Syeda HB, Garza M, Zozus M, et al. Application of machine learning in intensive care unit (ICU) settings using MIMIC dataset: systematic review. Informatics (MDPI) 2021;8(1):16 [FREE Full text] [doi: 10.3390/informatics8010016] [Medline: 33981592]
115. Zheng Y, Gan W, Chen Z, Qi Z, Liang Q, Yu PS. Large language models for medicine: a survey. Int J Mach Learn Cyber 2025;16(2):1015-1040. [doi: 10.1007/s13042-024-02318-w]
116. Doshi R, Amin KS, Khosla P, Bajaj S, Chheang S, Forman HP. Quantitative evaluation of large language models to streamline radiology report impressions: a multimodal retrospective analysis. Radiology 2024;310(3):e231593. [doi: 10.1148/radiol.231593] [Medline: 38530171]
117. Islam K, Nipu A, Madiraju P, Deshpandeditors. Autocompletion of chief complaints in the electronic health records using large language models. : IEEE; 2023 Presented at: IEEE International Conference on Big Data (BigData); December 15-18, 2023; Sorrento, Italy. [doi: 10.1109/bigdata59044.2023.10386778]
118. Salvagno M, Taccone FS, Gerli AG. Can artificial intelligence help for scientific writing? Crit Care 2023;27(1):75 [FREE Full text] [doi: 10.1186/s13054-023-04380-2] [Medline: 36841840]
119. Nazi Z, Peng W. Large language models in healthcare and medical domain: a review. Informatics 2024;11(3):57. [doi: 10.3390/informatics11030057]
120. Huang Q, Dong X, Zhang P, Wang B, He C, Wang J. Opera: Alleviating hallucination in multi-modal large language models via over-trust penalty and retrospection-allocation. 2024 Presented at: Proceedings of the IEEE/CVF Conference on Computer Vision and Pattern Recognition; June 17-21, 2024; Seattle, Washington. [doi: 10.1109/cvpr52733.2024.01274]
121. Azamfirei R, Kudchadkar SR, Fackler J. Large language models and the perils of their hallucinations. Crit Care 2023;27(1):120 [FREE Full text] [doi: 10.1186/s13054-023-04393-x] [Medline: 36945051]
122. Bushuven S, Bentele M, Bentele S, Gerber B, Bansbach J, Ganter J, et al. "ChatGPT, Can You Help Me Save My Child's Life?" - diagnostic accuracy and supportive capabilities to lay rescuers by chatgpt in prehospital basic life support and paediatric advanced life support cases - an in-silico analysis. J Med Syst 2023;47(1):123 [FREE Full text] [doi: 10.1007/s10916-023-02019-x] [Medline: 37987870]
123. Harrer S. Attention is not all you need: the complicated case of ethically using large language models in healthcare and medicine. EBioMedicine 2023;90:104512 [FREE Full text] [doi: 10.1016/j.ebiom.2023.104512] [Medline: 36924620]
124. Goodman RS, Patrinely JR, Stone CA, Zimmerman E, Donald RR, Chang SS, et al. Accuracy and reliability of chatbot responses to physician questions. JAMA Netw Open 2023;6(10):e2336483 [FREE Full text] [doi: 10.1001/jamanetworkopen.2023.36483] [Medline: 37782499]
125. Johnson AEW, Pollard TJ, Shen L, Lehman LH, Feng M, Ghassemi M, et al. MIMIC-III, a freely accessible critical care database. Sci Data 2016;3:160035 [FREE Full text] [doi: 10.1038/sdata.2016.35] [Medline: 27219127]
126. Johnson AEW, Bulgarelli L, Shen L, Gayles A, Shammout A, Horng S, et al. MIMIC-IV, a freely accessible electronic health record dataset. Sci Data 2023;10(1):1 [FREE Full text] [doi: 10.1038/s41597-022-01899-x] [Medline: 36596836]
127. Pollard TJ, Johnson AEW, Raffa JD, Celi LA, Mark RG, Badawi O. The eICU collaborative research database, a freely available multi-center database for critical care research. Sci Data 2018;5:180178 [FREE Full text] [doi: 10.1038/sdata.2018.178] [Medline: 30204154]
128. Das MK. Multicenter studies: relevance, design and implementation. Indian Pediatr 2022;59(7):571-579 [FREE Full text] [Medline: 34992183]
129. Wynants L, Kent DM, Timmerman D, Lundquist CM, Van Calster B. Untapped potential of multicenter studies: a review of cardiovascular risk prediction models revealed inappropriate analyses and wide variation in reporting. Diagn Progn Res 2019;3(1):6 [FREE Full text] [doi: 10.1186/s41512-019-0046-9] [Medline: 31093576]
130. Khalpey Z, Kumar U, King N, Abraham A, Khalpey AH. Large language models take on cardiothoracic surgery: a comparative analysis of the performance of four models on American board of thoracic surgery exam questions in 2023. Cureus 2024;16(7):e65083. [doi: 10.7759/cureus.65083] [Medline: 39171020]

XSL•FO
RenderX

131. Gallegos I, Rossi R, Barrow J, Tanjim M, Kim S, Dernoncourt F. Bias and fairness in large language models: a survey. Computational Linguistics 2024;50(3):1097-1179. [doi: 10.1162/coli_a_00524]
132. Suwała S, Szulc P, Guzowski C, Kamińska B, Dorobiała J, Wojciechowska K, et al. ChatGPT-3.5 passes Poland's medical final examination-Is it possible for ChatGPT to become a doctor in Poland? SAGE Open Med 2024;12:20503121241257777 [FREE Full text] [doi: 10.1177/20503121241257777] [Medline: 38895543]
133. Park Y, Pillai A, Deng J, Guo E, Gupta M, Paget M, et al. Assessing the research landscape and clinical utility of large language models: a scoping review. BMC Med Inform Decis Mak 2024;24(1):72 [FREE Full text] [doi: 10.1186/s12911-024-02459-6] [Medline: 38475802]
134. Biesheuvel LA, Dongelmans DA, Elbers PWG. Artificial intelligence to advance acute and intensive care medicine. Curr Opin Crit Care 2024;30(3):246-250 [FREE Full text] [doi: 10.1097/MCC.0000000000001150] [Medline: 38525882]
135. Wang D, Zhang S. Large language models in medical and healthcare fields: applications, advances, and challenges. Artif Intell Rev 2024;57(11):299. [doi: 10.1007/s10462-024-10921-0]
136. Armoundas AA, Narayan SM, Arnett DK, Spector-Bagdady K, Bennett DA, Celi LA, American Heart Association Institute for Precision Cardiovascular Medicine, Council on Cardiovascular Stroke Nursing, Council on Lifelong Congenital Heart Disease Heart Health in the Young, Council on Cardiovascular Radiology Intervention, Council on Hypertension, Council on the Kidney in Cardiovascular Disease, Stroke Council. Use of artificial intelligence in improving outcomes in heart disease: a scientific statement from the American heart association. Circulation 2024;149(14):e1028-e1050 [FREE Full text] [doi: 10.1161/CIR.0000000000001201] [Medline: 38415358]
137. Nagata JM, Otmar CD, Shim J, Balasubramanian P, Cheng CM, Li EJ, et al. Social media use and depressive symptoms during early adolescence. JAMA Netw Open 2025;8(5):e2511704 [FREE Full text] [doi: 10.1001/jamanetworkopen.2025.11704] [Medline: 40397441]
138. Olsen E, Novikov Z, Sakata T, Lambert MH, Lorenzo J, Bohn R, et al. More isn't always better: technology in the intensive care unit. Health Care Manage Rev 2024;49(2):127-138. [doi: 10.1097/HMR.0000000000000398] [Medline: 38393982]
139. Poncette A, Spies C, Mosch L, Schieler M, Weber-Carstens S, Krampe H, et al. Clinical requirements of future patient monitoring in the intensive care unit: qualitative study. JMIR Med Inform 2019;7(2):e13064 [FREE Full text] [doi: 10.2196/13064] [Medline: 31038467]
140. Gasciauskaite G, Lunkiewicz J, Roche TR, Spahn DR, Nöthiger CB, Tscholl DW. Human-centered visualization technologies for patient monitoring are the future: a narrative review. Crit Care 2023;27(1):254 [FREE Full text] [doi: 10.1186/s13054-023-04544-0] [Medline: 37381008]
141. Pelletier JH, Watson K, Michel J, McGregor R, Rush SZ. Effect of a generative artificial intelligence digital scribe on pediatric provider documentation time, cognitive burden, and burnout. JAMIA Open 2025;8(4):ooaf068. [doi: 10.1093/jamiaopen/ooaf068] [Medline: 40620477]
142. Williams CYK, Subramanian CR, Ali SS, Apolinario M, Askin E, Barish P, et al. Physician- and large language model-generated hospital discharge summaries. JAMA Intern Med 2025;185(7):818-825. [doi: 10.1001/jamainternmed.2025.0821] [Medline: 40323616]
143. Small WR, Austrian J, O'Donnell L, Burk-Rafel J, Hochman KA, Goodman A, et al. Evaluating hospital course summarization by an electronic health record-based large language model. JAMA Netw Open 2025;8(8):e2526339 [FREE Full text] [doi: 10.1001/jamanetworkopen.2025.26339] [Medline: 40802185]
144. The Lancet Digital Health. ChatGPT: friend or foe? Lancet Digit Health 2023;5(3):e102 [FREE Full text] [doi: 10.1016/S2589-7500(23)00023-7] [Medline: 36754723]
145. Shi T, Guo L, Shen Z, Kong G. ERTool: a python package for efficient implementation of the evidential reasoning approach for multi-source evidence fusion. Health Data Sci 2024;4:0128 [FREE Full text] [doi: 10.34133/hds.0128] [Medline: 39104599]
146. Pan S, Luo L, Wang Y, Chen C, Wang J, Wu X, et al. Unifying large language models and knowledge graphs: a roadmap. IEEE Trans Knowl Data Eng 2024;36(7):3580-3599. [doi: 10.1109/tkde.2024.3352100]
147. Fan Z, Yu Z, Yang K, Chen W, Liu X, Li G, et al. Diverse models, united goal: a comprehensive survey of ensemble learning. CAAI Trans Intel Tech 2025;10(4):959-982. [doi: 10.1049/cit2.70030]
148. Bhardwaj M, Xie T, Boots B, Jiang N. Adversarial model for offline reinforcement learning. 2023 Presented at: NIPS '23: Proceedings of the 37th International Conference on Neural Information Processing Systems; December 10-16, 2023; New Orleans, LA p. 1245-1269.
149. Gao S, Fang A, Huang Y, Giunchiglia V, Noori A, Schwarz JR, et al. Empowering biomedical discovery with AI agents. Cell 2024;187(22):6125-6151 [FREE Full text] [doi: 10.1016/j.cell.2024.09.022] [Medline: 39486399]
150. Singh C, Inala J, Galley M, Caruana R, Gao J. Rethinking interpretability in the era of large language models. arXiv. Preprint posted online on January 30, 2024 2024. [doi: 10.48550/arXiv.2402.01761]
151. Wu X, Zhao H, Zhu Y, Shi Y, Yang F, Liu T. Usable XAI: 10 strategies towards exploiting explainability in the LLM era. arXiv. Preprint posted online on May 18, 2025 2024. [doi: 10.48550/arXiv.2403.08946]
152. Zhao P, Zhang H, Yu Q, Wang Z, Geng Y, Fu F. Retrieval-augmented generation for AI-generated content: a survey. arXiv. Preprint posted online on June 21, 2024 2024. [doi: 10.48550/arXiv.2402.19473]

XSL•FO
RenderX

153. Nori H, Lee Y, Zhang S, Carignan D, Edgar R, Fusi N. Can generalist foundation models outcompete special-purpose tuning? case study in medicine. arXiv. Preprint posted online on November 28, 2023 2023. [doi: 10.48550/arXiv.2311.16452]
154. Wu J, Zhu J, Qi Y. Medical graph RAG: towards safe medical large language model via graph retrieval-augmented generation. 2024 Presented at: Proceedings of the 63rd Annual Meeting of the Association for Computational Linguistics (Volume 1: Long Papers); July 27-August 1, 2025; Vienna, Austria. [doi: 10.18653/v1/2025.acl-long.1381]
155. Li S, Miao D, Wu Q, Hong C, D'Agostino D, Li X, et al. Federated Learning in Healthcare: A Benchmark Comparison of Engineering and Statistical Approaches for Structured Data Analysis. Health Data Sci 2024;4:0196 [FREE Full text] [doi: 10.34133/hds.0196] [Medline: 39635226]
156. Mondal D, Lipizzi C. Mitigating large language model bias: automated dataset augmentation and prejudice quantification. Computers 2024;13(6):141. [doi: 10.3390/computers13060141]
157. Jahan I, Laskar MTR, Peng C, Huang JX. A comprehensive evaluation of large language models on benchmark biomedical text processing tasks. Comput Biol Med 2024;171:108189 [FREE Full text] [doi: 10.1016/j.compbiomed.2024.108189] [Medline: 38447502]
158. Hager P, Jungmann F, Holland R, Bhagat K, Hubrecht I, Knauer M, et al. Evaluation and mitigation of the limitations of large language models in clinical decision-making. Nat Med 2024;30(9):2613-2622. [doi: 10.1038/s41591-024-03097-1] [Medline: 38965432]
159. Duggan MJ, Gervase J, Schoenbaum A, Hanson W, Howell JT, Sheinberg M, et al. Clinician experiences with ambient scribe technology to assist with documentation burden and efficiency. JAMA Netw Open 2025;8(2):e2460637 [FREE Full text] [doi: 10.1001/jamanetworkopen.2024.60637] [Medline: 39969880]
160. Thirunavukarasu AJ, Mahmood S, Malem A, Foster WP, Sanghera R, Hassan R, et al. Large language models approach expert-level clinical knowledge and reasoning in ophthalmology: a head-to-head cross-sectional study. PLOS Digit Health 2024;3(4):e0000341 [FREE Full text] [doi: 10.1371/journal.pdig.0000341] [Medline: 38630683]

Abbreviations

AI: artificial intelligence
AKI: acute kidney injury
ARDS: acute respiratory distress syndrome
AUC: area under the curve
BLEU: bilingual evaluation understudy
CCM: critical care medicine
CT: computed tomography
EHR: electronic health record
GenAI: generative artificial intelligence
HIPAA: Health Insurance Portability and Accountability Act
ICU: intensive care unit
LLM: large language model
MIMIC: Medical Information Mart for Intensive Care
MIMIC-CXR: Medical Information Mart for Intensive Care-Chest X-Ray
MIMIC-III: Medical Information Mart for Intensive Care-III
MIMIC-IV: Medical Information Mart for Intensive Care-IV
MIMIC-IV-CDM: Medical Information Mart for Intensive Care-IV-Clinical Decision Making
MT: machine translation
NLP: natural language processing
PICU: pediatric intensive care unit
PRISMA-ScR: Preferred Reporting Items for Systematic Reviews and Meta-Analyses extension for Scoping Reviews
PROBAST-AI: Prediction Model Risk of Bias Assessment Tool-Artificial Intelligence
RAG: retrieval-augmented generation
RoB: Risk of Bias
SOFA: Sequential Organ Failure Assessment
XGBoost: Extreme Gradient Boosting

XSL•FO
RenderX

Edited by A Benis; submitted 23.04.25; peer-reviewed by D Yoo, JJ Beunza, VV Khanna; comments to author 09.07.25; revised version received 04.09.25; accepted 13.10.25; published 24.11.25.

Please cite as:
Shi T, Ma J, Yu Z, Xu H, Yang R, Xiong M, Xiao M, Li Y, Zhao H, Kong G
Large Language Models in Critical Care Medicine: Scoping Review
JMIR Med Inform 2025;13:e76326
URL: https://medinform.jmir.org/2025/1/e76326
doi:10.2196/76326
PMID:

©Tongyue Shi, Jun Ma, Zihan Yu, Haowei Xu, Rongxin Yang, Minqi Xiong, Meirong Xiao, Yilin Li, Huiying Zhao, Guilan Kong. Originally published in JMIR Medical Informatics (https://medinform.jmir.org), 24.11.2025. This is an open-access article distributed under the terms of the Creative Commons Attribution License (https://creativecommons.org/licenses/by/4.0/), which permits unrestricted use, distribution, and reproduction in any medium, provided the original work, first published in JMIR Medical Informatics, is properly cited. The complete bibliographic information, a link to the original publication on https://medinform.jmir.org/, as well as this copyright and license information must be included.

XSL•FO
RenderX

Original Paper

Coagulation Risk Prediction in Patients With Liver Failure: Integrated Meta-Analysis and Machine Learning Model Study

Hao Wang[1*], BS; Tao He[1*], MS; Liang Ren[1], BS; Tingjun Zhang[1], PhD

Affiliated Hospital of North Sichuan Medical College, Nanchong, China

*these authors contributed equally

Corresponding Author:
Hao Wang, BS
Affiliated Hospital of North Sichuan Medical College
No.1 Maoyuan South Road, Shunqing District
Nanchong, 637000
China
Phone: 86 15882606937
Email: 15882606937@163.com

Abstract

Background: Liver failure often results in significant coagulation dysfunction, which is a major complication. Artificial liver support systems (ALSS) have been used to ameliorate coagulation parameters, but the dynamic nature of these improvements and the development of predictive models remain insufficiently explored.

Objective: This study aimed to evaluate the effects of ALSS on coagulation function and to develop a dynamic prediction model using machine learning techniques to predict the improvement trends of coagulation parameters.

Methods: A systematic search was conducted in PubMed, Embase, and other databases to identify relevant studies, resulting in 18 studies comprising 1771 patients. A meta-analysis was performed to assess the impact of ALSS on coagulation parameters, including international normalized ratio (INR), prothrombin time (PT), activated partial thromboplastin time (APTT), and fibrinogen levels. In addition, clinical data from the Medical Information Mart for Intensive Care database were used to construct prediction models using logistic regression, extreme gradient boosting, random forest, and long short-term memory networks.

Results: Meta-analysis results showed that ALSS significantly improved INR, PT, APTT, and fibrinogen levels (all $P<.05$), with the treatment efficacy varying by modality. Among the machine learning models, the random forest model demonstrated the best performance, achieving an area under the curve of 92.12%. Dynamic INR was identified as the key predictor for coagulation abnormalities.

Conclusions: This study systematically evaluated the effects of ALSS on coagulation function in patients with liver failure, demonstrating significant improvements in key parameters such as INR, PT, and APTT, with efficacy varying across different treatment modalities. Simultaneously, a machine learning model built using intensive care unit clinical data exhibited strong predictive capability for identifying the risk of coagulation dysfunction, particularly useful in supporting early-stage clinical recognition of high-risk patients and guiding personalized coagulation management strategies. It is important to emphasize that this model is positioned as a dynamic risk alert and assessment tool, intended to assist clinical baseline evaluation and nursing interventions, rather than serving as direct validation of ALSS therapeutic efficacy.

(JMIR Med Inform 2025;13:e76348) doi:10.2196/76348

KEYWORDS

artificial liver support system; liver failure; coagulation function; meta-analysis; machine learning; predictive modeling

Introduction

Liver failure represents a critical clinical condition frequently complicated by severe coagulopathy, which significantly increases bleeding risk [1,2]. The disruption of coagulation homeostasis may lead to life-threatening complications, including gastrointestinal hemorrhage and intracranial bleeding, while potentially triggering disseminated intravascular coagulation that exacerbates multiorgan dysfunction [3,4]. As a crucial therapeutic intervention, the artificial liver support system (ALSS) demonstrates the potential for improving coagulation parameters through its detoxification, synthetic, and metabolic substitution functions [5-8]. However, the

XSL•FO
RenderX

mechanisms underlying ALSS-mediated coagulation improvement remain insufficiently investigated, particularly regarding differential effects among various modalities (eg, plasma exchange [PE] and molecular adsorbent recirculating system [MARS]). Clinical decision-making is further challenged by the lack of reliable dynamic monitoring indicators and predictive tools for optimal treatment timing and duration adjustment [9,10]. Furthermore, the highly individualized nature of coagulation dynamics in patients with liver failure cannot be adequately captured by conventional static tests (eg, prothrombin time [PT] and activated partial thromboplastin time [APTT]) [11-13]. Therefore, a comprehensive investigation of ALSS-induced dynamic coagulation changes and the development of accurate predictive models are clinically imperative for optimizing individualized treatment strategies. Addressing this scientific challenge will directly impact bleeding risk management and overall prognosis in patients with liver failure.

Although several studies have investigated the effects of ALSS on coagulation function in patients with liver failure, most suffer from limitations, such as small sample sizes and single-center designs, which compromise the reliability and generalizability of their findings [14]. More notably, the majority of these studies focus solely on short-term outcomes (eg, changes within 24 hours posttreatment), failing to capture the long-term dynamic evolution of coagulation parameters [15]. Methodologically, conventional statistical analyses (eg, *t* tests and ANOVA) are inadequate for characterizing temporal trends in coagulation indicators, limiting their utility for developing precise predictive models [16-18]. While meta-analyses can synthesize evidence from multiple studies to enhance statistical power [19], no study to date has systematically evaluated the differential effects of ALSS modalities on coagulation function. Advances in machine learning have demonstrated significant potential for medical data mining and predictive modeling [20,21]; however, their application in monitoring coagulation dysfunction in liver failure remains nascent. A critical gap persists in integrating multisource heterogeneous clinical data (eg, electronic health records, laboratory results, and vital signs), as existing studies have yet to leverage the full potential of large-scale public databases like Medical Information Mart for Intensive Care (MIMIC). These methodological limitations hinder clinicians and nurses from accurately predicting and promptly intervening in coagulation function changes among patients with liver failure.

This study uses a multidimensional and multimethod research strategy to achieve 3 key objectives. First, we conduct a systematic review and meta-analysis to comprehensively evaluate the effects of ALSS on coagulation parameters (eg, international normalized ratio [INR], PT, APTT, and fibrinogen) in patients with liver failure, while comparing the efficacy of different treatment modalities. Second, leveraging large-scale clinical data from the MIMIC database, we apply advanced machine learning algorithms to develop a dynamic, time-series predictive model for assessing coagulation function. Third, using interpretability techniques (eg, Shapley Additive Explanations [SHAP] value analysis), we identify key predictive factors influencing coagulation dynamics, providing a theoretical foundation for clinical interventions. From a scientific perspective, this study is the first to elucidate the dynamic mechanisms by which ALSS modulates coagulation function in liver failure, deepening our understanding of coagulopathy in this context and advancing precision medicine in the field. Clinically, our findings offer three major practical applications: (1) an objective, data-driven decision-support tool to optimize individualized ALSS treatment strategies; (2) early detection of coagulation abnormalities, enabling timely interventions to reduce bleeding complications; and (3) improved allocation of nursing resources, enhancing health care efficiency and ultimately patient outcomes. These innovations will significantly elevate the standard of care for patients with liver failure and serve as a methodological reference for research on other organ support therapies.

This study adopts a dual-track integrative strategy, combining meta-analysis with machine learning modeling, aiming to comprehensively elucidate the interventional value of ALSS on coagulation function in patients with liver failure and to uncover the underlying mechanisms of coagulation risk prediction across multiple levels. The meta-analysis, based on 18 clinical studies, systematically evaluated the short-term and long-term improvement effects of different ALSS modalities—including PE, MARS, and double plasma perfusion (PP)—on key coagulation indicators, such as INR, PT, APTT, and fibrinogen. The results confirmed the clinical benefits of ALSS in reducing the risk of coagulation dysfunction and provided an evidence-based foundation for subsequent predictive modeling. However, due to the limited number of patients who received ALSS treatment in the MIMIC database, the training population for the machine learning model focused on a broader cohort of patients with liver failure. The goal was to construct a generalizable and efficient dynamic coagulation risk assessment tool applicable to real-time bedside alerts and optimized resource allocation. We consider this model a “baseline tool” for risk stratification and timing judgment before ALSS initiation in clinical practice, laying a methodological foundation for the development of specialized models based on larger, ALSS-specific datasets in the future. Therefore, this study achieves an organic integration from high-level evidence synthesis to individualized risk prediction, not only enhancing the understanding of the clinical benefits of ALSS but also providing a practical path for the precise implementation of personalized interventional strategies in liver failure management.

Accordingly, the primary aim of this study is to systematically evaluate the short-term and long-term effects of ALSS on coagulation function in patients with liver failure and to further construct a clinically valuable dynamic risk prediction model for coagulation dysfunction. The specific objectives are as follows: (1) to quantify, through systematic review and meta-analysis, the improvement effects of different ALSS modalities (such as PE, MARS, and PP) on major coagulation parameters (INR, PT, APTT, and fibrinogen); (2) to use real-world clinical data from the MIMIC database and apply multiple machine learning algorithms to develop predictive models for early identification of coagulation dysfunction within the next 24 hours; and (3) to integrate model interpretability

XSL•FO
RenderX

techniques (eg, SHAP analysis) to identify key predictive variables associated with changes in coagulation function, thereby providing theoretical support for personalized treatment and nursing interventions. Through this integrated strategy, the study seeks to promote the advancement of precision ALSS therapy and offers a novel pathway for bleeding risk management and prognosis improvement in patients with liver failure.

Methods

Literature Search and Screening

This meta-analysis and systematic review were conducted in accordance with the PRISMA (Preferred Reporting Items for Systematic Reviews and Meta-Analyses) guidelines [22]. A comprehensive literature search was performed across multiple databases, including PubMed, Embase, Web of Science, and the Cochrane Library, using a combination of Medical Subject Headings terms and free-text keywords to ensure thoroughness and precision. The search strategy incorporated key terms such as liver failure, artificial liver support (ALS), blood coagulation, and hemostasis, optimized with Boolean operators (AND and OR) to balance sensitivity and specificity (refer to Table S1 in Multimedia Appendix 1 for detailed search queries). To account for variations in database syntax, the search strategy was tailored to each platform. In addition, manual screening of reference lists from included studies was performed to identify potentially eligible articles not captured by the initial database search. To confirm the novelty of this study, a search for registered systematic reviews was conducted in the PROSPERO database.

The screening process was independently carried out by 2 researchers (HW and TH) using EndNote (Clarivate) for reference management. The selection procedure consisted of two phases: (1) initial screening based on titles and abstracts to exclude clearly irrelevant studies, followed by (2) full-text review of potentially eligible articles, with documented reasons for exclusion. Any discrepancies between reviewers were resolved through discussion or adjudication by a third researcher (LR) to ensure objectivity. Interrater agreement was assessed using Cohen κ coefficient to quantify screening consistency. To enhance transparency, the study selection process was visualized using a PRISMA flow diagram, providing a clear and reproducible overview of the screening stages.

Inclusion and Exclusion Criteria

Inclusion criteria consisted of (1) study design: randomized controlled trials, cohort studies, or case-control studies; (2) participants: patients diagnosed with liver failure according to international or national guidelines (eg, Asian Pacific Association for the Study of the Liver, European Association for the Study of the Liver, and American Association for the Study of Liver Diseases); (3) intervention: use of ALSS, including but not limited to PE, double PE, MARS, or continuous blood purification, either alone or in combination with standard therapies (eg, medications or supportive care); (4) outcome reporting: studies must report coagulation parameters at multiple time points; and (5) key outcomes: at least one of the following coagulation-related indicators: PT, APTT, D-dimer, INR, or fibrinogen.

Exclusion criteria included (1) publication type: reviews, conference abstracts, book chapters, or case reports without original data suitable for meta-analysis; (2) language: non-English or non-Chinese publications; and (3) data limitations: studies that did not report changes in coagulation function before and after treatment, reported only single time-point measurements, or provided incomplete or nonextractable data.

Risk of Bias Assessment

This study used the Newcastle-Ottawa scale (NOS) to systematically evaluate the risk of bias in the included studies, ensuring the reliability and scientific validity of the meta-analysis results. The NOS assesses study quality across three domains with a maximum score of 9 points: (1) selection (maximum 4 points)—evaluates whether cases and controls were clearly defined, representative of the target population, and selected using an appropriate study design; (2) comparability (maximum 2 points)—assesses whether key confounding factors were accounted for through matching or statistical adjustment; and (3) outcome or exposure assessment (maximum 3 points)—examines the reliability of outcome or exposure measurement, adequacy of follow-up duration, and handling of attrition. Based on the NOS scores, study quality was categorized as follows: ≥7 points=high quality (low risk of bias); 5-6 points=moderate quality (moderate risk of bias); ≤4 points=low quality (high risk of bias).

Two independent reviewers (HW and TH) conducted bias assessments, with cross-verification of results. Discrepancies were resolved through discussion or adjudication by a third reviewer (LR). The risk of bias was visualized using a risk of bias graph, and a detailed summary was provided in Multimedia Appendix 1. All assessments and graphical representations were generated using Review Manager (RevMan 5.4 [Cochrane Collaboration]).

Data Extraction

The following data were extracted from each included study: (1) study characteristics: first author, publication year, study design (randomized controlled trial, cohort study, or case-control study), country, and journal; (2) participant characteristics: patient type (viral hepatitis-related liver failure), sample size, sex ratio, mean age, baseline disease severity (Child-Pugh score and model for end-stage liver disease score), and coagulation function (PT, APTT, D-dimer, INR, and fibrinogen); (3) methodological features: type of ALS therapy (PE, hemoperfusion, MARS, continuous renal replacement therapy [CRRT]) and treatment protocol (single vs multiple sessions, treatment duration); and (4) outcome measures: the primary outcomes included changes in coagulation parameters (PT, APTT, INR, and fibrinogen before and after treatment). If a study reported multiple follow-up measurements, the longest follow-up data were extracted to assess long-term effects. For missing data, the original authors were contacted for clarification. If unavailable, multiple imputations were applied. Two researchers (LR and TJ) independently extracted all data, with cross-verification to resolve discrepancies; a third researcher (HW) adjudicated unresolved disagreements. The

XSL•FO
RenderX

final dataset was entered into Microsoft Excel and double-checked to ensure accuracy and consistency.

Meta-Analysis Statistical Methods

This study used the "meta" package in R software (version 4.2; R Core Team) to conduct a meta-analysis evaluating the dynamic changes in coagulation function during ALS therapy in patients with liver failure. Heterogeneity across studies was assessed using the I^2 statistic and Q-test. A fixed-effects model was applied when I^2<50% and P>.05, indicating negligible heterogeneity. In cases of significant heterogeneity (I^2≥50% and P≤.05), a random-effects model was used, followed by an exploration of potential heterogeneity sources. The pooled effect size was calculated based on data type: standardized mean difference or mean difference with 95% CIs for continuous variables, and odds ratios or risk ratios with 95% CIs for dichotomous variables. Results were visualized using forest plots to illustrate individual and pooled effect estimates.

To further investigate the key factors influencing coagulation function, we conducted subgroup analyses based on the following variables: type of ALS (PE vs hemoperfusion vs MARS vs CRRT), liver failure classification (acute liver failure [ALF], acute-on-chronic liver failure [ACLF], and chronic liver failure), and etiology of liver failure (viral hepatitis-induced vs cirrhosis-induced liver failure).

To assess the robustness of the findings, a sensitivity analysis was performed using the leave-one-out method, in which each study was systematically excluded before rerunning the meta-analysis. This approach allowed us to evaluate whether any single study disproportionately influenced the overall results. A significant change in the pooled effect size following the exclusion of a particular study would suggest that it was a key driver of the meta-analytic findings.

Publication bias was preliminarily assessed using funnel plots and further examined through Egger linear regression test and Begg test. A statistically significant result (Egger test P<.05) was considered indicative of potential publication bias.

Data Extraction and Cleaning From Public Databases

This study used the MIMIC-IV-3.1 database, released by the Massachusetts Institute of Technology (MIT), which contains clinical data from patients admitted to the intensive care unit (ICU) at Beth Israel Deaconess Medical Center (BIDMC) between 2008 and 2019. Data extraction was performed using Navicat Premium (v15.0.12; PremiumSoft CyberTech Ltd) and structured query language. The inclusion criteria were (1) first-time ICU admission, (2) ICU stay duration exceeding 48 hours, and (3) a diagnosis of liver failure based on *International Classification of Diseases* codes (K704, K7040, K7041, K72, K720, K7200, K7201, K721, K7210, K7211, K729, K7290, K7291, and K9182).

The extracted clinical variables comprised 3 categories: demographic and admission characteristics, vital signs, and laboratory results. Demographic data included age, sex, race, admission time, ICU admission and discharge time, and hospital ID. Vital signs, such as heart rate, respiratory rate, oxygen saturation, body temperature, systolic blood pressure (BP), and diastolic BP, were recorded based on the first measurement after ICU admission. Laboratory tests covered liver and kidney function (alanine aminotransferase, aspartate aminotransferase, total bilirubin [TBIL], creatinine, urea, and albumin), complete blood count (white blood cell count, platelet count, hemoglobin, and hematocrit), inflammatory markers (C-reactive protein), and coagulation parameters, including the INR (PT), partial thromboplastin time (PTT), and functional fibrinogen. All coagulation-related measurements during the ICU stay were extracted for dynamic predictive modeling, whereas static features were derived from the first recorded value after ICU admission. Data cleaning and imputation followed established protocols [23].

The clinical data used in this study were derived from the publicly available MIMIC-IV database (version 4.0), jointly developed by MIT and BIDMC. The database has been approved by the Institutional Review Board of BIDMC and the ethics committee of MIT and is accessible to qualified researchers who have completed the required credentialing course. All authors of this study completed the Collaborative Institutional Training Initiative program data usage training and obtained PhysioNet Credentialed Access to MIMIC. This study strictly adhered to the data usage agreement and did not involve any personally identifiable patient information, thus complying with ethical standards and requiring no additional ethical approval.

Data Cleaning and Missing Value Handling

Before model construction, we conducted systematic cleaning and preprocessing of the raw clinical data from the MIMIC-IV v3.1 database. All data were merged based on the unique patient identifier (subject_id), integrating demographic information, vital signs, laboratory test results, and ICU admission and discharge times across multiple tables. The analysis window was limited to the first 24 hours following ICU admission.

To ensure the stability and interpretability of variables in the model, only candidate features with high sampling frequency and clear clinical relevance were included, and variables with a missing rate greater than 20% were excluded. For features with a missing rate between 5% and 20%, multiple imputation was performed to preserve the covariate structure as much as possible. For features with sporadic missing values, group-level median or mean imputation was applied. Categorical variables such as sex and race, which had low rates of missingness, were imputed using the mode.

For dynamic time-series variables such as INR and PTT, we applied intrasample linear interpolation or forward and backward filling methods to handle missing data. In addition, the number of missing values per variable was included as an auxiliary input feature in the model to reflect potential uncertainty in the data. To eliminate the influence of extreme outliers, we set clinically reasonable cutoff thresholds based on existing literature and expert knowledge, applying percentile truncation or direct exclusion as appropriate.

All numerical variables were standardized using z score normalization before model input to eliminate differences in measurement scale, while categorical variables were converted into dummy variables using one-hot encoding.

XSL•FO
RenderX

Sliding Window Feature Extraction

For each coagulation function record, the collection time (charttime) was treated as the current time point. We then extracted data from the preceding 24-hour window to derive statistical features for 3 key coagulation indicators: INR, PTT, and functional fibrinogen. For each indicator, 6 statistical measures were computed: mean, maximum (max), minimum (min), standard deviation (SD), the most recent value (last), and the slope of the linear regression trend (slope). This process generated a total of 18 time-series dynamic features. To ensure that the extracted features accurately reflected dynamic changes during ICU stays, only valid in-ICU records were included, thereby constructing an ICU-specific dynamic prediction dataset.

Label Construction

This study adopts a 24-hour observation window following the current time point to construct a binary label variable. The label is determined based on clinically established diagnostic thresholds for coagulopathy. A patient is classified as having a "coagulopathy event" (label=1) if any of the following abnormal indicators occur within the observation window: INR>1.5, PTT>60 seconds, or fibrinogen<150 mg/dL. Conversely, if none of these criteria are met, the case is labeled as 0. Records with insufficient laboratory data to determine abnormality are assigned a missing label (label=NaN) and excluded before modeling.

Static Model Construction

The static model incorporates patient features recorded upon ICU admission, including demographic characteristics (eg, sex, age, and race), liver and kidney function metrics, vital signs, and statistical features (mean, maximum, minimum, SD, last recorded value, and slope) of coagulation parameters (INR, PTT, and fibrinogen). The target variable is defined as the occurrence of a coagulation abnormality within 24 hours of the current time point, where an abnormality is identified if any of the following criteria are met: INR>1.5, PTT>60 seconds, or fibrinogen<150 mg/dL. Three supervised learning algorithms—logistic regression (LR), random forest (RF), and extreme gradient boosting (XGBoost)—were used for model development.

To prevent data leakage, the dataset was partitioned into training and testing sets (80:20 ratio) using a group-based hold-out split, ensuring that samples from the same patient (subject ID) were exclusively allocated to either set. During model training, stratified group k-fold cross-validation (5 folds, preserving class balance and group separation) was applied to evaluate performance metrics, including the mean area under the curve (AUC), F_1-score, accuracy, sensitivity, and specificity. Subsequently, the final models were refit on the entire training set and assessed for generalizability on the independent test set.

To prevent information leakage caused by the presence of the same patient in both the training and test sets, we adopted a group-based splitting strategy based on subject ID for static model development. Patients were randomly assigned to the training and test sets in an 80:20 ratio, resulting in 2764 patients (80% of the total 3456) in the training set and 692 patients (20%) in the test set. On the training set, we developed several static models—including LR, RF, and XGBoost—and evaluated their performance using the StratifiedGroupKFold method (5-fold cross-validation with stratification and grouping). This approach ensured robust estimation of average performance metrics, including AUC, F_1-score, accuracy, sensitivity, and specificity. Model-specific parameters are detailed in Table S2 in Multimedia Appendix 1. Based on this, final models were refitted on the entire training set and evaluated on the independent test set to assess their generalizability.

Dynamic Long Short-Term Memory Model Construction

For dynamic modeling, we used a long short-term memory (LSTM) recurrent neural network to analyze the constructed time-series data. Each sample consisted of a sequence of 5 consecutive time points, with each time point represented by sliding-window statistical features. The label indicated whether coagulation dysfunction occurred within 24 hours after the last time point in the sequence. The specific parameters are provided in Table S2 in Multimedia Appendix 1.

Model Evaluation and Visualization

The performance of each model was evaluated on the test set using the following metrics: accuracy, F_1-score, AUC, sensitivity, specificity, and precision. Visual representations included the receiver operating characteristic (ROC) curve, precision-recall (PR) curve, calibration curve, decision curve analysis, and a confusion matrix heatmap. The AUC values were computed with 95% CIs using the bootstrap method.

Robustness Validation and Model Interpretation

To enhance model robustness, the static model was further evaluated using 5-fold StratifiedGroupKFold cross-validation. This approach ensured data stratification by subject_id, maintaining label distribution while preventing data leakage. Performance metrics were reported as mean (SD).

Subsequently, model interpretability analysis was conducted using the best-performing RF model. Global feature importance rankings were derived using the Gini index, while SHAP values quantified the average contribution of each variable to model predictions. The most critical clinical predictors were identified and visualized to illustrate their impact on model outputs.

Ethical Considerations

This study does not contain any studies with human participants or animals performed by any of the authors.

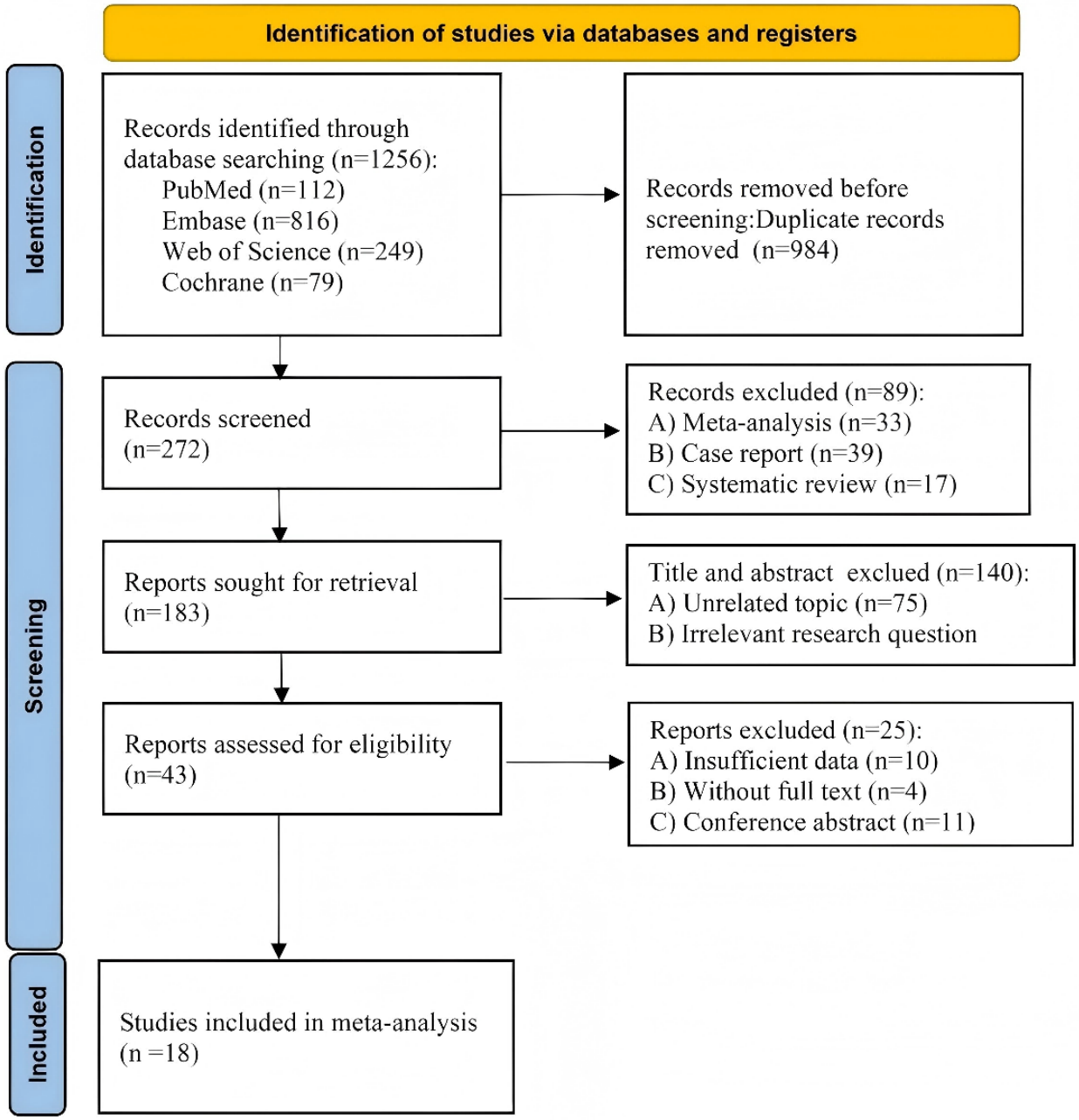
Results

Literature Search Results

As illustrated in Figure 1, a total of 1256 studies were retrieved from the database. After removing 263 duplicate records, 993 studies underwent title and abstract screening. Following initial screening, 921 studies that did not meet the inclusion criteria were excluded, leaving 72 studies for full-text evaluation. After a rigorous assessment, an additional 59 studies were excluded due to mismatches in study design, intervention methods, or outcome measures, resulting in 18 studies being included in the systematic review and meta-analysis.

XSL•FO
RenderX

Figure 1. PRISMA (Preferred Reporting Items for Systematic Reviews and Meta-Analyses) literature screening flowchart.



All 18 included studies were cohort or case-control designs, examining various ALSS (eg, PE, MARS, and PP). These studies collectively involved 1771 participants and reported changes in coagulation parameters—including INR, PT, APTT, and fibrinogen—before and after treatment. The study populations comprised patients with ALF and ACLF, with etiologies such as viral hepatitis, toxic exposure, infections, and metabolic disorders. The key characteristics of the included studies are summarized in Table 1.

XSL•FO
RenderX

Table 1. Basic features of included studies.

Study	Research design	Participant category	Etiology	Age (y)	Sex ratio (male/female), mean (SD)	Baseline disease severity	Treatment type	Indicator
Kounis et al [24]	Cohort study	ACLF[a]	Cirrhosis	21	50.6 (7.8)	MELD[b]≥30	PE[c]+CRRT[d]	a
Ninan et al [25]	Cohort study	ALF[e]	Toxication	36	31.67 (13.56)	MELD≥30	PE	bc
Yang et al [26]	Cohort study	ALF	Infection	39	7 (6.67)	Child-Pugh Grade C	PE+CRRT	a
Hu et al [27]	Cohort study	ALF	Toxication	21	1.83 (0.89)	Child-Pugh Grade C	PE	bc
Huang et al [28]	Cohort study	ACLF	HBV[f]	365	46.52 (11.38)	20≤MELD<30	PE+PP[g]	abd
Lee et al [29]	Cohort study	ACLF	Liver transplantation	15	49.7 (7.5)	—[h]	MARS[i]	a
Li et al [30]	Case-control study	ACLF	HBV	45	50.4 (10.7)	20≤MELD<30	PE	ab
Mohanka et al [31]	Cohort study	ALF	Toxication	19	32.0 (9.6)	20≤MELD<30	PE+CVVHDF[j]	a
Sorodoc et al [32]	Case-control study	ALF	Toxication	6	37.13 (18.37)	CTP[k] Grade A	MARS	b
Chen et al [33]	Cohort study	ACLF	Virus	250	—	20≤MELD<30	PE	bd
Falkensteiner et al [34]	Cohort study	ALF	Primary liver failure	49	59 (13.71)	MELD≥30	MARS	d
Colak and Ocak [35]	Cohort study	ALF	Infection	24	52 (18.25)	10≤PRISM[l]<20	PE+CVVHDF	ad
Gong et al [36]	Cohort study	ALF	—	5	60.2 (6.25)	—	SAE[m]	a
Kulkarni et al [37]	Cohort study	ALF	HBV	42	23.5 (3.625)	MELD≥30	PE	ab
Stöckert et al [38]	Cohort study	ALF	Toxication	43	52 (18.4)	MELD<20	PE	a
Pawaria et al [39]	Cohort study	ALF	Metabolic diseases	37	9 (7.41)	NWI≥11	PE	a
Hung et al [40]	Case-control study	ACLF	HBV	20	50.6 (2.86)	—	PE	c
Wan et al [41]	Cohort study	ACLF	HBV	60	50.7 (9.2)	20≤MELD<30	PE	a

[a]ACLF: acute-on-chronic liver failure.

[b]MELD: model for end-stage liver disease.

[c]PE: plasma exchange.

[d]CRRT: continuous renal replacement therapy.

[e]ALF: acute liver failure.

[f]HBV: hepatitis B virus.

[g]PP: plasma perfusion.

[h]Not available.

[i]MARS: molecular adsorbent recirculating system.

[j]CVVHDF: continuous veno-venous hemodiafiltration.

[k]CTP: Child–Turcotte–Pugh.

[l]PRISM: pediatric risk of mortality.

[m]SAE: severe adverse event.

XSL•FO
RenderX

Risk of Bias Assessment

All 18 observational studies included in this meta-analysis were evaluated for risk of bias using the NOS. Among them, 16 studies were rated as high quality (NOS score≥7), indicating robust methodological rigor in case selection, comparability between groups, and exposure assessment. The remaining 2 studies were classified as moderate quality (score=6), primarily due to incomplete follow-up data or unclear exposure assessment methods. No studies were deemed low quality (score≤5).

Overall, the included studies demonstrated high methodological quality, enhancing the reliability of our meta-analysis findings. Detailed NOS scores are presented in Table 2.

Table 2. Risk of bias assessment summary: quality evaluation for each included study using the modified Newcastle-Ottawa scale.

Study	Selection[a]				Comparability[a]	Exposure[a]			Total	Interpretation
	Q1	Q2	Q3	Q4	Q5	Q6	Q7	Q8		
Case-control studies										
Sorodoc et al [32]	1	1	1	1	2	1	1	__[b]	8	High quality
Hung et al [40]	1	1	1	1	2	1	1	1	9	High quality
Cross-sectional studies										
Kounis et al [24]	1	1	1	1	2	1	1	1	9	High quality
Ninan et al [25]	1	1	1	1	2	1	1	1	9	High quality
Yang et al [26]	1	—	1	1	2	1	1	1	8	High quality
Hu et al [27]	1	1	1	1	2	1	—	—	7	High quality
Huang et al [28]	1	—	1	1	2	1	1	1	8	High quality
Lee et al [29]	1	1	1	1	2	1	1	1	9	High quality
Mohanka et al [31]	1	—	1	1	2	1	1	1	8	High quality
Chen et al [33]	1	1	1	1	1	1	—	—	6	Moderate quality
Falkensteiner et al [34]	1	1	1	1	2	1	1	—	8	High quality
Colak and Ocak [35]	1	1	1	1	2	1	—	—	7	High quality
Gong et al [36]	1	1	1	1	1	1	—	—	6	Moderate quality
Kulkarni et al [37]	1	1	1	1	2	1	1	1	9	High quality
Stöckert et al [38]	1	—	1	1	2	1	1	1	8	High quality
Pawaria et al [39]	1	1	1	1	2	1	1	1	9	High quality
Wan et al [41]	1	—	1	1	2	1	1	1	8	High quality
Li et al [30]	1	1	1	1	1	1	—	—	6	High quality

[a]The scoring system ranges from 0 to 9 points. Higher scores indicate better methodological quality.

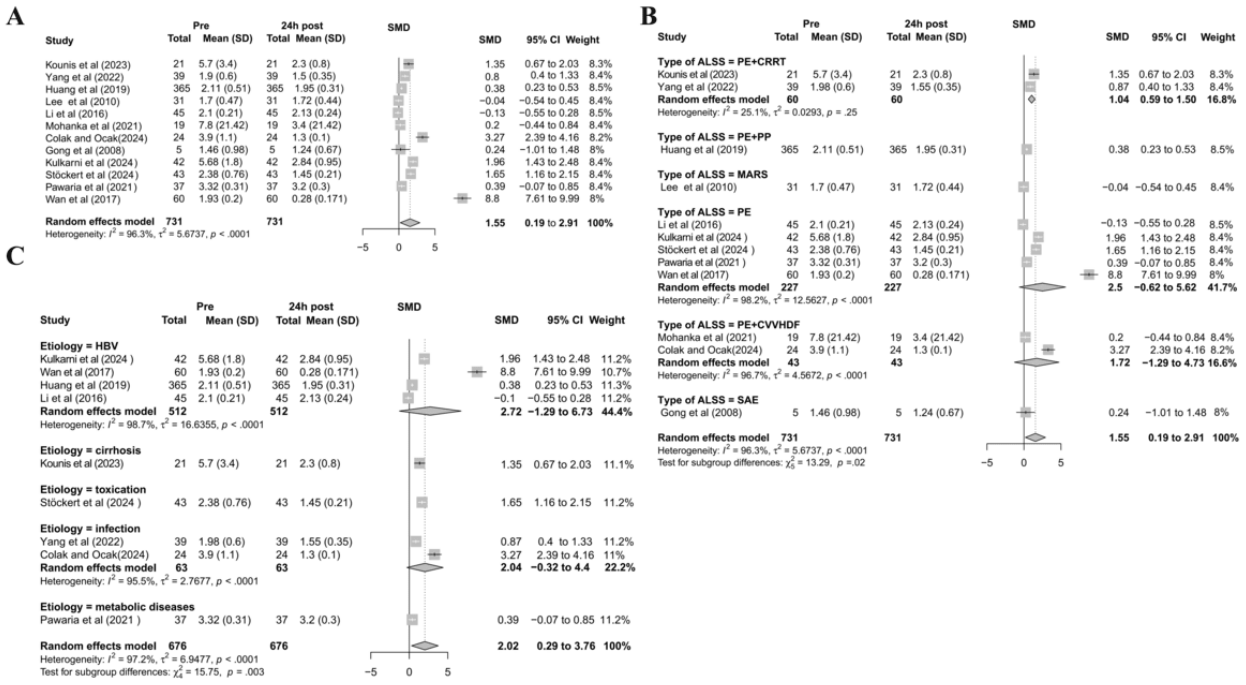
[b]Not available.

Meta-Analysis Results: INR

A total of 12 studies (encompassing 731 patients) were included to evaluate changes in INR before and 24 hours after ALS treatment. The meta-analysis revealed a significant reduction in INR posttreatment, although with considerable heterogeneity (Figure 2A).

XSL•FO
RenderX

Figure 2. Meta-analysis of the short-term effect of artificial liver support (ALS) on international normalized ratio improvement and its heterogeneity sources. (A) Forest plot comparing international normalized ratio changes within 24 hours before and after ALS treatment; (B) subgroup analysis stratified by ALS modality; (C) subgroup analysis stratified by etiology. ALSS: artificial liver support system; CRRT: continuous renal replacement therapy; CVVHDF: continuous veno-venous hemodiafiltration; HBV: Hepatitis B virus; MARS: molecular adsorbent recirculating system; PE: plasma exchange; PP: plasma perfusion; SAE: severe adverse event; SMD: standardized mean difference [33,35,37-40,44-48,50].



To investigate potential sources of heterogeneity, we conducted 3 subgroup analyses. In the ALS modality subgroup analysis, different treatment modalities exhibited significant variations in INR improvement. PE alone demonstrated the most pronounced reduction in INR, albeit with high heterogeneity. In contrast, the PE+CRRT group showed stable and significant effects alongside markedly reduced heterogeneity (Figure 2B), suggesting that treatment modality may be a key factor influencing efficacy and heterogeneity. The etiology-based subgroup analysis indicated that patients with hepatitis B virus (HBV) or infections exhibited more significant therapeutic effects, whereas those with cirrhosis or metabolic diseases showed smaller or nonsignificant effect sizes. Intergroup differences were statistically significant (Figure 2C), implying that underlying etiology may contribute to variations in INR improvement. The disease-type subgroup analysis revealed that patients with ACLF had greater INR improvement than patients with ALF, although the difference was not statistically significant (Figure S1A in Multimedia Appendix 1).

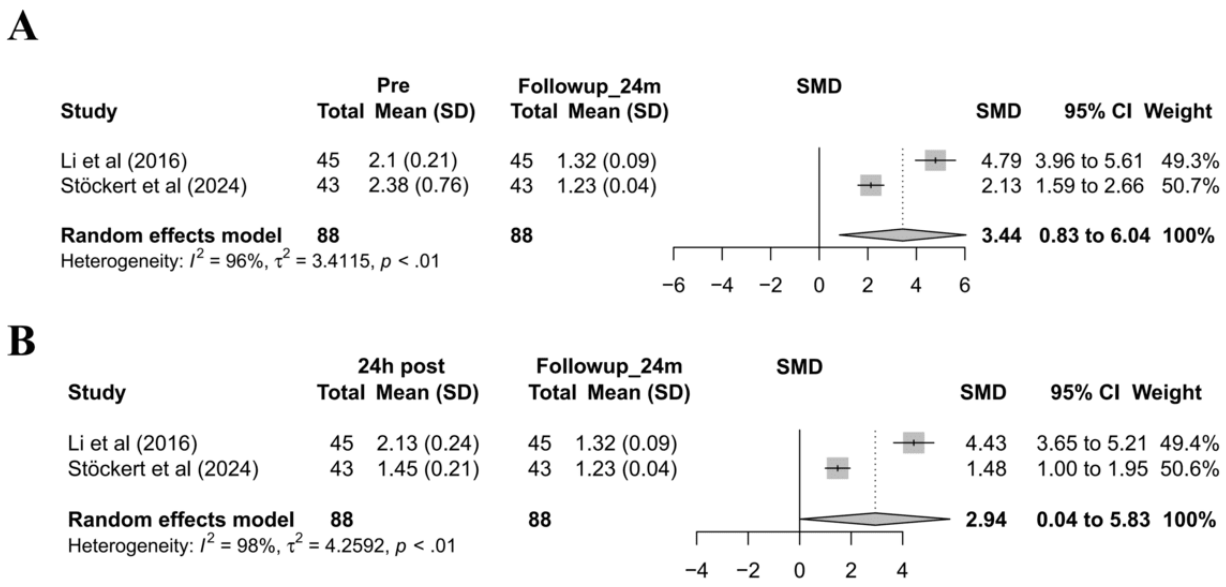
Sensitivity analysis (Figure S1B in Multimedia Appendix 1) demonstrated consistent pooled effect directions and minimal fluctuations in I^2 upon sequential exclusion of individual studies, supporting the robustness of the findings. In addition, the funnel plot exhibited approximate symmetry (Figure S1C in Multimedia Appendix 1), indicating a low likelihood of publication bias and further strengthening the reliability of the conclusions.

In summary, this study demonstrates that ALS significantly improves INR levels in patients with liver failure, with treatment efficacy potentially influenced by therapeutic modality and underlying etiology.

To evaluate long-term coagulation function changes following ALS therapy, we conducted a meta-analysis of 2 studies reporting INR values before treatment and at 24 months posttreatment. The results demonstrated a statistically significant reduction in INR at 24 months compared with baseline, although with considerable heterogeneity (Figure 3A). Furthermore, we compared INR changes between the 24-hour and 24-month time points to assess differences in short-term versus long-term efficacy. The pooled analysis, which included the same 2 studies, revealed that INR remained significantly lower at 24 months than at 24 hours, with statistical significance, suggesting that ALS therapy may have a long-term effect on improving coagulation function (Figure 3B).

XSL•FO
RenderX

Figure 3. Meta-analysis of the effects of artificial liver support (ALS) on international normalized ratio (INR) improvement at different posttreatment time points. (A) Forest plot comparing INR changes between pre-ALS and 24 months post-ALS; (B) forest plot comparing INR changes between 24 hours and 24 months post-ALS. SMD: standardized mean difference [39,47].



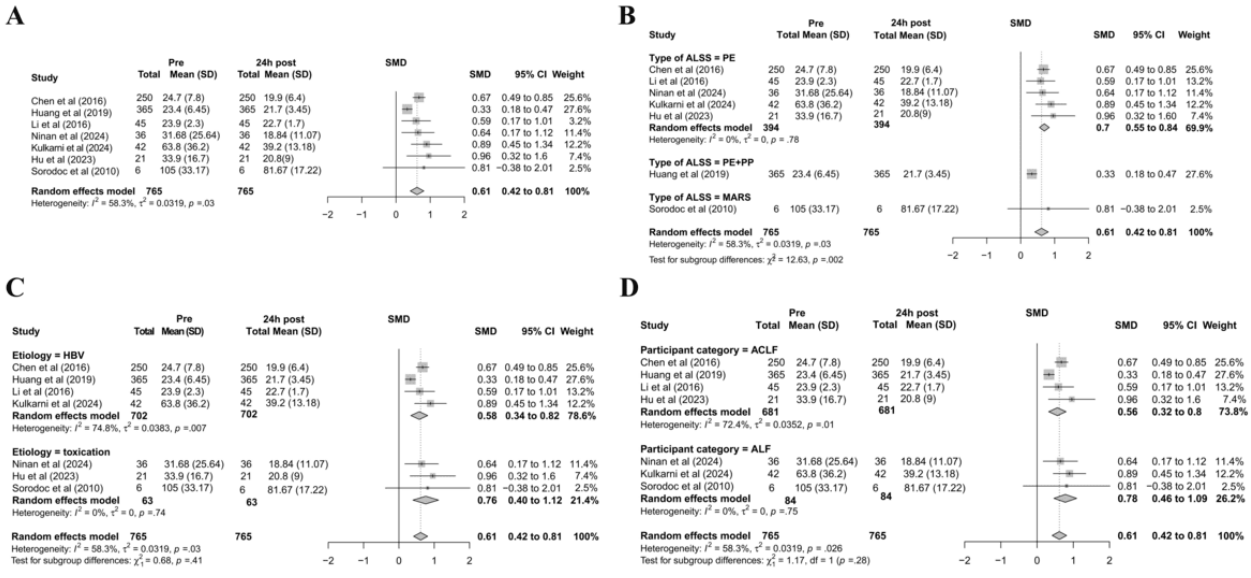
Despite moderate heterogeneity, the findings consistently indicate a progressive decline in INR over long-term follow-up, supporting the stability and durability of ALS therapy in enhancing coagulation.

In conclusion, ALS therapy significantly and persistently improves INR levels in patients with liver failure, although its efficacy may be influenced by treatment modalities and underlying etiologies.

Meta-Analysis of PT Levels Before and 24 Hours After Treatment

A total of 7 studies (combined sample size=765 patients) were included to evaluate changes in PT 24 hours before and after ALS treatment. The pooled analysis revealed a significant reduction in PT levels posttreatment, with moderate heterogeneity observed (Figure 4A).

Figure 4. Meta-analysis of PT changes before and after artificial liver support (ALS) treatment, with subgroup analyses. (A) Forest plot of PT changes within 24 hours post-ALS versus pre-ALS; (B) subgroup analysis of PT changes by ALS type; (C) subgroup analysis by etiology; (D) subgroup analysis by disease classification. ACLF: acute-on-chronic liver failure; ALF: acute liver failure; ALSS: artificial liver support system; HBV: Hepatitis B virus; MARS: molecular adsorbent recirculating system; PE: plasma exchange; PP: plasma perfusion; SMD: standardized mean difference [34,36,37,39,41,42,46].



Subgroup analysis by ALS type demonstrated statistically significant differences between groups, with the PE subgroup exhibiting no heterogeneity (I^2=0). This suggests that the type of ALS may contribute to heterogeneity and influence the degree of coagulation improvement (Figure 4B). Etiology-based subgroup analysis indicated no significant differences between HBV-related liver failure and toxic liver failure groups, with

XSL•FO
RenderX

the latter subgroup showing no heterogeneity (I^2=0). This implies that etiology may be a source of heterogeneity (Figure 4C). Disease-type subgroup analysis found no significant difference between ACLF and ALF groups (P=.28), with the ALF subgroup displaying no heterogeneity (I^2=0), suggesting disease type as a potential source of heterogeneity (Figure 4D).

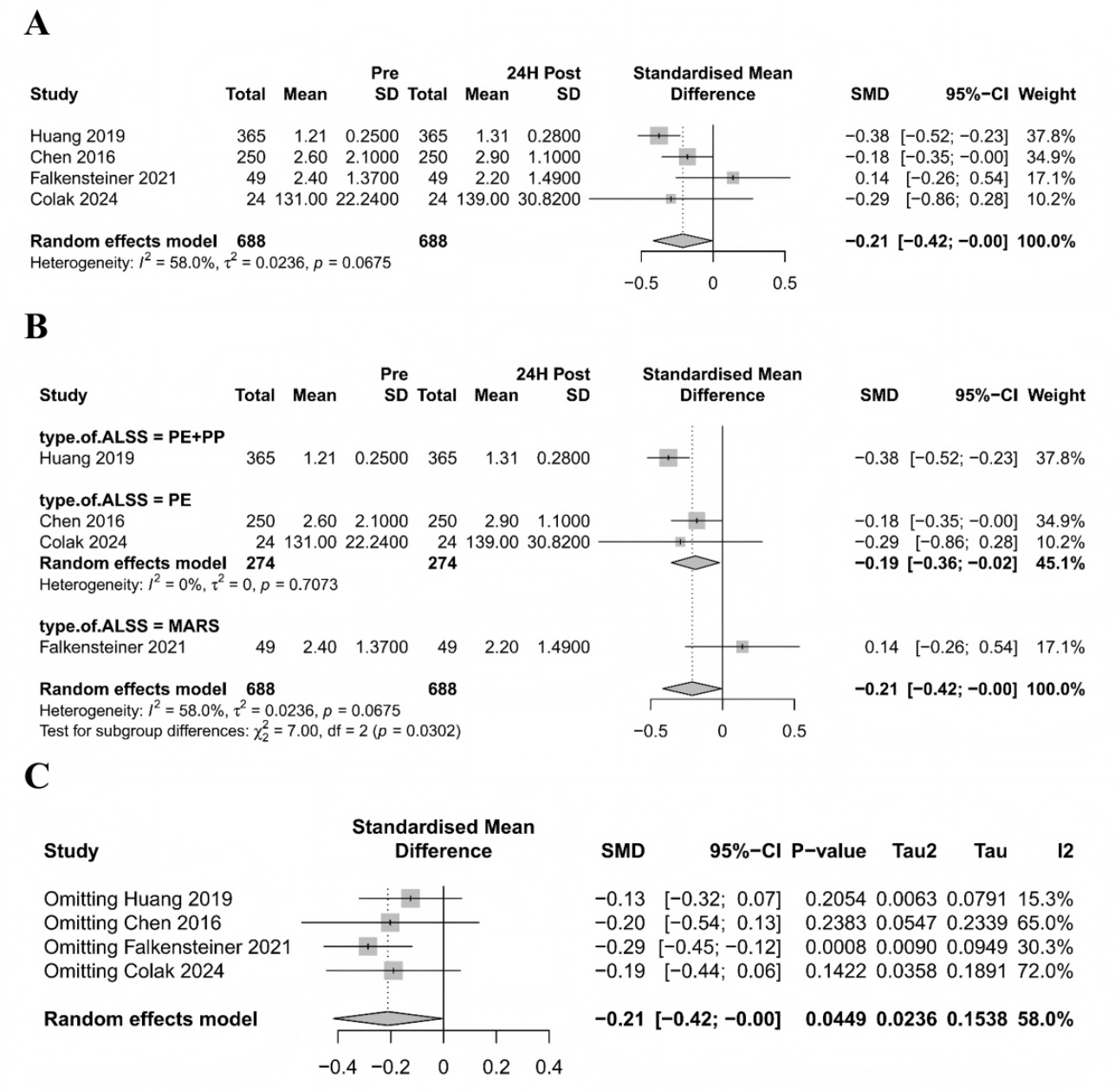
Sensitivity analysis demonstrated that the pooled effect size remained stable after the sequential exclusion of individual studies, with no substantial changes in heterogeneity, indicating robust findings (Figure S2A in Multimedia Appendix 1). Funnel plot symmetry suggested no significant publication bias (Figure S2B in Multimedia Appendix 1).

In conclusion, ALS significantly improves PT levels, with treatment type, etiology, and disease classification identified as potential key sources of heterogeneity.

Meta-Analysis of Fibrinogen Levels Before and 24 Hours After Treatment

This meta-analysis included 4 studies comprising 688 patients to evaluate changes in fibrinogen levels before and after ALS treatment. The results demonstrated a slight decrease in fibrinogen levels posttreatment, with moderate heterogeneity observed in the overall analysis (Figure 5A).

Figure 5. Meta-analysis of the effect of artificial liver support (ALS) on fibrinogen levels in patients with liver failure. (A) Forest plot of fibrinogen level changes pre- and post-ALS; (B) subgroup analysis by ALS type; (C) sensitivity analysis using the leave-one-out method. ALSS: artificial liver support system; MARS: molecular adsorbent recirculating system; PE: plasma exchange; PP: plasma perfusion; SMD: standardized mean difference [37,42-44].



Subgroup analysis by ALS therapy type revealed that the PE+PP subgroup exhibited the most significant reduction in fibrinogen levels, with statistically significant intergroup differences. Notably, the PE subgroup showed no heterogeneity (I^2=0%)

XSL•FO
RenderX

(Figure 5B), suggesting that treatment type may be a key factor influencing fibrinogen level changes and a potential source of heterogeneity. In contrast, subgroup analyses based on etiology and disease type showed no statistically significant intergroup differences, nor did they substantially alter heterogeneity (Figure S3A-B in Multimedia Appendix 1).

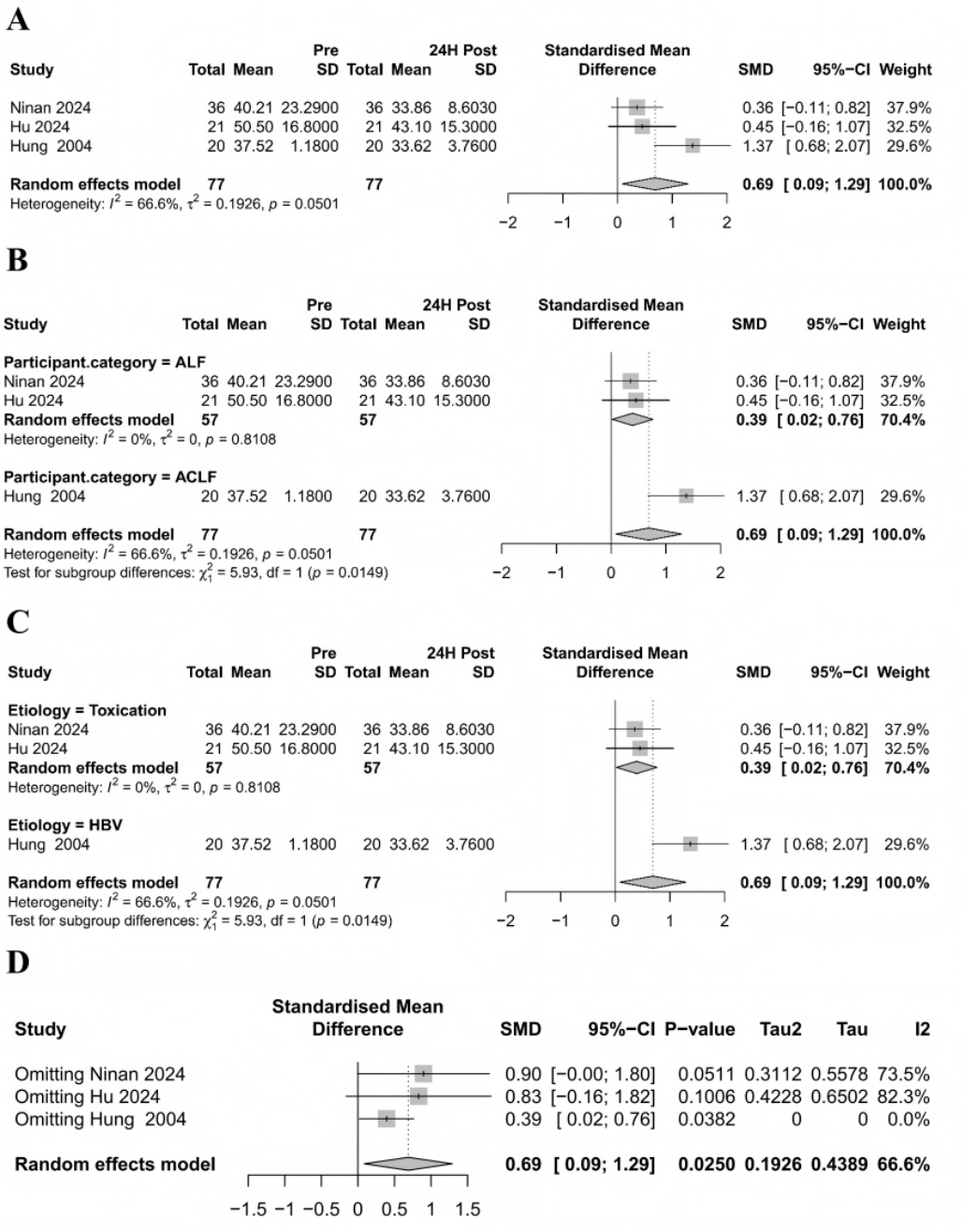
Sensitivity analysis indicated that the exclusion of individual studies only significantly reduced heterogeneity (to 15.3%) upon the removal of Huang et al [28] (Figure 5C), identifying it as a potential source of heterogeneity. Funnel plot analysis demonstrated a generally symmetrical study distribution with no evident publication bias (Figure S3C in Multimedia Appendix 1).

In conclusion, ALS therapy has a limited effect on fibrinogen levels, and the observed heterogeneity may primarily stem from differences in treatment modalities.

Meta-Analysis of APTT Levels Before and 24 Hours After Treatment

A total of 3 studies (comprising 77 patients) were included to evaluate changes in APTT before and after ALS therapy. The meta-analysis revealed a significant reduction in APTT levels posttreatment, though moderate heterogeneity was observed (Figure 6A).

Figure 6. Meta-analysis of the effect of artificial liver support on APTT in patients with liver failure. (A) Forest plot of APTT changes pre- and post–artificial liver support; (B) subgroup analysis by disease type; (C) subgroup analysis by etiology; (D) sensitivity analysis. ACLF: acute-on-chronic liver failure; ALF: acute liver failure; ALSS: artificial liver support system; HBV: Hepatitis B Virus; SMD: standardized mean difference [34,36,49].



XSL•FO
RenderX

To investigate potential sources of heterogeneity, subgroup analyses were performed based on disease type and etiology. The disease-type subgroup analysis demonstrated that patients with ACLF exhibited a greater improvement in APTT than patients with ALF, with a statistically significant intergroup difference. Notably, heterogeneity within the ALF subgroup was 0%, suggesting that disease type may contribute to heterogeneity and influence the degree of coagulation improvement (Figure 6B). The etiology-based subgroup analysis indicated that patients with HBV showed a more pronounced APTT improvement than those with toxic liver injury, with significant intergroup differences and 0% heterogeneity in the toxic etiology subgroup. This further supports etiology as a potential source of heterogeneity and a modifier of coagulation function (Figure 6C).

Sensitivity analysis confirmed the robustness of the pooled effect size after excluding Hung et al [40], with heterogeneity (I^2) decreasing to 0% (Figure 6D). Funnel plot symmetry suggested no significant publication bias (Figure S4 in Multimedia Appendix 1).

In summary, ALS therapy significantly improves APTT levels, with heterogeneity likely attributable to differences in disease type and etiology.

This study demonstrates that ALS therapy significantly enhances multiple coagulation parameters in patients with liver failure, particularly in reducing INR and PT while improving APTT. The long-term improvement in INR suggests long-term therapeutic benefits in coagulation support. Treatment efficacy varies significantly depending on the artificial liver modality (eg, PE, double PE, and MARS), etiology (eg, viral hepatitis vs toxic liver failure), and disease type (ALF vs ACLF), which are key contributors to interstudy heterogeneity. In contrast, improvements in fibrinogen levels were relatively limited, with variability primarily influenced by treatment modality. These findings underscore the importance of individualized coagulation management strategies in ALS therapy, optimizing treatment efficacy while providing evidence-based guidance for coagulation monitoring and clinical care.

Dynamic Coagulation Risk Prediction in Patients With Liver Failure

Based on previous meta-analysis findings, this study confirms that ALS therapy significantly improves coagulation function in patients with liver failure across multiple time points, demonstrating clear dynamic trends in core indicators (INR, PT, APTT, and fibrinogen). However, current clinical practice still lacks individualized predictive tools for coagulation dysfunction, hindering precise intervention and dynamic monitoring. To address this gap, we further integrated clinical data from the MIMIC database to develop a machine learning–based predictive model. By leveraging dynamic coagulation indicators as key features, this model explores predictive pathways for coagulation abnormalities, aiming to provide an intelligent decision-support tool for the early identification of high-risk patients.

A total of 3456 ICU patients with liver failure were included from the MIMIC-IV database based on strict inclusion and exclusion criteria. Patients were stratified by ID and randomly assigned to the training cohort (n=2764) and independent validation cohort (n=692). Table 3 presents the baseline demographic characteristics, vital signs, and laboratory parameters of all patients. Overall, most features were well-balanced between the training and validation sets, with no statistically significant differences. Specifically, there was no significant difference in age distribution between the 2 cohorts (P=.57), with 2262 patients (65.5%) younger than 65 years. A statistically significant difference was observed in sex distribution (P<.001), with a slightly higher proportion of males (2140/3456, 60.9%). Regarding race, White patients accounted for the largest proportion (1942/3456, 56.2%), while the proportion of Asian patients was slightly higher in the validation cohort (P=.02). For laboratory parameters—including liver function markers (alanine aminotransferase, aspartate aminotransferase, TBIL, and alkaline phosphatase), renal function (creatinine and urea), inflammatory marker (C-reactive protein), complete blood count (platelet count, hemoglobin, and hematocrit), coagulation indicators (INR_PT, PTT, and fibrinogen), and vital signs (heart rate, respiratory rate, oxygen saturation, and BP)—the overall distributions between the training and validation sets were consistent. Only hemoglobin (P=.02) and hematocrit (P=.02) showed mild differences, suggesting slight variations in hemoglobin levels among some patients.

In conclusion, the training and validation cohorts exhibited a strong balance in key clinical and laboratory characteristics, supporting their appropriateness for subsequent model development and validation.

XSL•FO
RenderX

Table 3. Baseline characteristics of patients in training and validation cohorts: demographic data, vital signs, laboratory parameters, and comparative statistics.

Group	All data	Train data	Test data	*P* value
N	3456	2764	692	nan[a]
Age (y), n (%)				
≥65	1194 (34.6)	948 (34.3)	246 (35.6)	.57
<65	2262 (65.5)	1816 (65.7)	446 (64.6)	.57
Sex, n (%)				
Female	1352 (39.1)	1124 (40.7)	228 (33)	<.001
Male	2104 (60.9)	1640 (59.3)	464 (67)	<.001
Race				
Black	274 (7.9)	210 (7.6)	64 (9.2)	.17
White	1942 (56.2)	1568 (56.7)	374 (54)	.22
Asian	100 (2.9)	70 (2.5)	30 (4.3)	.02
Other	1140 (33)	916(33.1)	224 (32.4)	.73
ALT[b], mean (SD)	446.69 (950.08)	435.07 (926.86)	493.02 (1037.01)	.20
AST[c], mean (SD)	562.95 (1031.00)	567.76 (1042.23)	543.15 (984.00)	.59
TBIL[d], mean (SD)	6.20 (8.71)	6.09 (8.62)	6.66 (9.05)	.13
ALP[e], mean (SD)	145.63 (146.90)	145.82 (152.40)	144.91 (122.78)	.87
Albumin, mean (SD)	2.92 (0.65)	2.92 (0.65)	2.91 (0.67)	.78
PLT[f], mean (SD)	154.11 (98.77)	153.59 (98.02)	156.27 (101.90)	.56
HGB[g], mean (SD)	9.99 (2.58)	9.93 (2.57)	10.20 (2.61)	.02
HCT[h], mean (SD)	30.74 (7.92)	30.57 (7.88)	31.39 (8.06)	.02
CRP[i], mean (SD)	96.36 (74.60)	96.52 (73.93)	95.77 (77.51)	.94
CRE[j], mean (SD)	1.94 (1.59)	1.92 (1.58)	1.99 (1.65)	.36
Urea, mean (SD)	37.92 (28.50)	37.97 (28.75)	37.74 (27.55)	.85
HR[k], mean (SD)	95.01 (21.89)	95.35 (22.25)	93.64 (20.36)	.05
RR[l], mean (SD)	20.98 (6.62)	20.96 (6.62)	21.07 (6.63)	.72
SpO_2[m], mean (SD)	96.65 (21.49)	96.69 (23.94)	96.49 (4.18)	.68
SBP[n], mean (SD)	115.24 (24.09)	115.37 (24.20)	114.72 (23.64)	.53
DBP[o], mean (SD)	68.65 (18.43)	68.68 (18.60)	68.54 (17.71)	.85
Fibrinogen, functional, mean (SD)	272.37 (152.93)	269.88 (149.78)	282.29 (164.66)	.11
INR_PT[p], mean (SD)	1.91 (0.66)	1.92 (0.66)	1.88 (0.64)	.13
PTT[q], mean (SD)	44.07 (12.49)	44.12 (12.42)	43.88 (12.76)	.66

[a]nan: not a number.
[b]ALT: alanine aminotransferase.
[c]AST: aspartate aminotransferase.
[d]TBIL: total bilirubin.
[e]ALP: alkaline phosphatase.
[f]PLT: platelet count.
[g]HGB: hemoglobin.
[h]HCT: hematocrit.
[i]CRP: C-reactive protein.

XSL•FO
RenderX

[j]CRE: creatinine.

[k]HR: heart rate.

[l]RR: respiratory rate.

[m]SpO_2: oxygen saturation.

[n]SBP: systolic blood pressure.

[o]DBP: diastolic blood pressure.

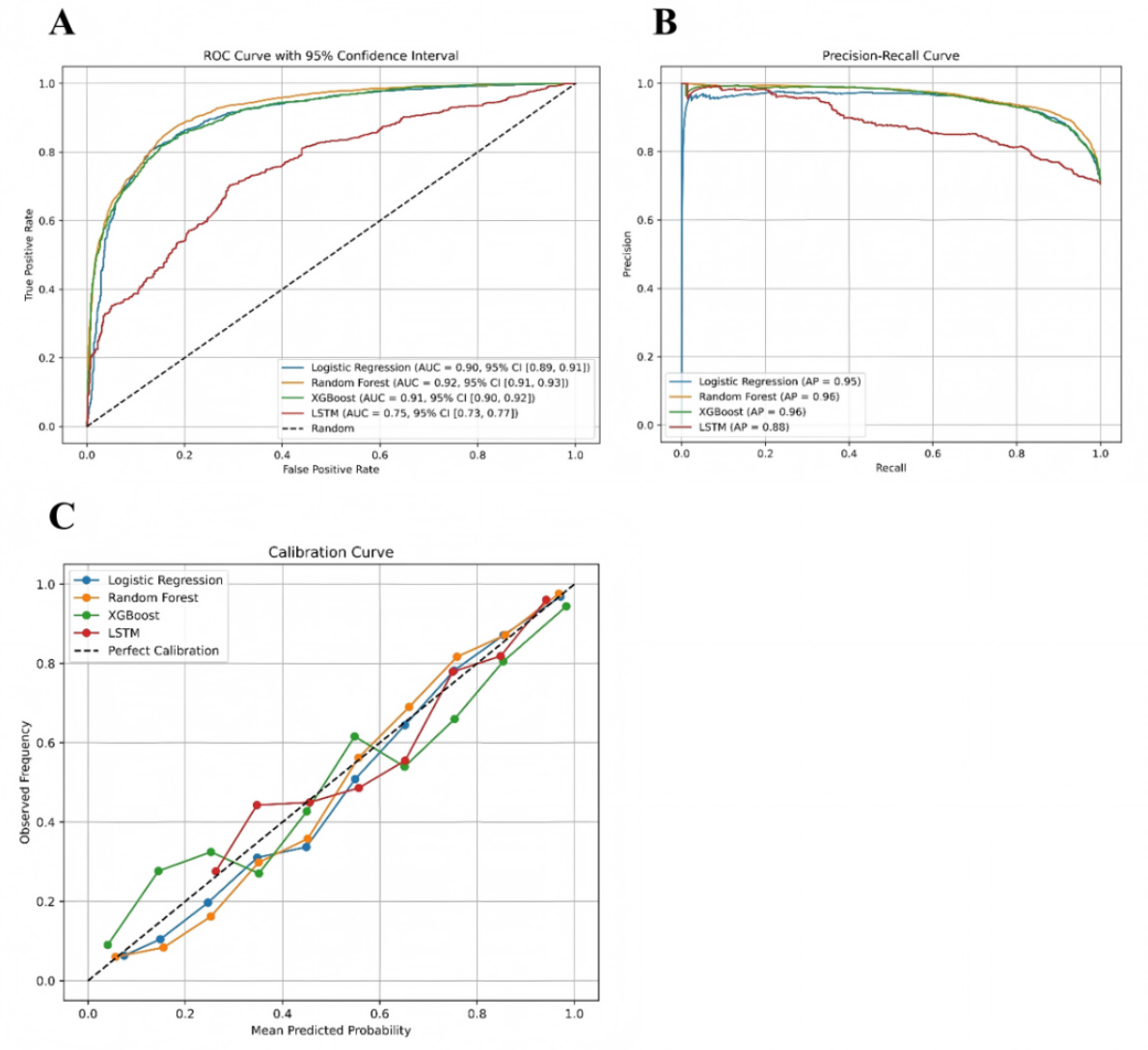
[p]INR_PT: international normalized ratio of prothrombin time.

[q]PTT: partial thromboplastin time.

Model Discriminatory Power and Performance Evaluation

A comprehensive evaluation of model performance was conducted on an independent test set, incorporating metrics such as ROC curves, PR curves, and calibration curves. The ROC curve analysis revealed that the RF model demonstrated the highest discriminatory power, with an AUC of 0.92 (95% CI 0.91-0.93). The XGBoost and LR models exhibited comparable performance, with AUC values of 0.91 (95% CI 0.90-0.92) and 0.90 (95% CI 0.89-0.91), respectively. In contrast, the LSTM dynamic model showed significantly lower discriminative ability, achieving an AUC of only 0.74 (95% CI 0.72-0.76), suggesting limited generalizability under the current data configuration (Figure 7A).

Figure 7. Performance evaluation of machine learning models in predicting coagulation dysfunction in patients with liver failure. (A) Receiver operating characteristic curves comparing the discriminative ability of logistic regression, random forest, extreme gradient boosting, and long short-term memory models in predicting coagulation abnormalities within 24 hours (test set); (B) PR curves assessing model performance in identifying positive cases under class imbalance; (C) calibration curves evaluating the agreement between predicted probabilities and observed event rates. AP: average precision; AUC: area under the curve; LSTM: long short-term memory; XGBoost: extreme gradient boosting; ROC: receiver operating characteristic.



The PR curve analysis further assessed the models' ability to identify positive cases (ie, predicting coagulation abnormalities within 24 hours). Both RF and XGBoost achieved high average precision (AP) scores of 0.96, maintaining robust precision even

XSL•FO
RenderX

at high recall levels. The LR model exhibited a slightly lower AP (0.95) but remained clinically useful. The LSTM model, however, underperformed with an AP of 0.87, reinforcing its limitations in positive predictive accuracy (Figure 7B).

Calibration curve analysis evaluated the agreement between predicted probabilities and observed outcomes. The LR and RF models demonstrated near-perfect calibration across all risk strata, indicating high reliability. The XGBoost model showed stable calibration in moderate-to-high risk ranges but minor deviations in low-risk regions. In contrast, the LSTM model exhibited substantial fluctuations in low-to-moderate risk ranges, reflecting weaker overall calibration (Figure 7C).

The confusion matrix analysis revealed distinct performance advantages among the models in the classification task. The RF model achieved the best classification performance on the test set, while LR and XGBoost exhibited comparable results, both maintaining a high true positive rate with a low misclassification rate. In contrast, although the LSTM model demonstrated superior sensitivity in identifying positive cases, it showed marked limitations in correctly classifying negative samples, resulting in lower specificity and a higher false-positive rate (Figure S5A in Multimedia Appendix 1). Overall, traditional machine learning models outperformed the LSTM in both accuracy and robustness.

To further evaluate the clinical utility of these models, we conducted decision curve analysis to assess their net benefit across different risk thresholds. The results demonstrated that LR, RF, and XGBoost models consistently outperformed the "treat all" and "treat none" strategies across most threshold ranges, indicating strong potential for clinical decision support. Notably, these models provided greater net benefit in intermediate-risk ranges, suggesting their predictive outcomes could reliably guide individualized interventions (Figure S5B in Multimedia Appendix 1).

In summary, static machine learning models—particularly RF—not only exhibited strong predictive discrimination but also demonstrated better calibration performance than the time-series–based LSTM dynamic model. These findings suggest that static models are more suitable for clinical early-warning applications in predicting coagulation dysfunction risk in patients in ICU with liver failure.

Table 4 summarizes the common performance metrics across all models. Overall, the results demonstrate that the RF model achieves the most robust performance, with an AUC of 92.1%, an F_1-score of 91%, an accuracy of 86.9%, a recall (sensitivity) of 93.3%, a precision of 88.8%, and a specificity of 71.7%.

Based on these findings, we select the RF model as our final risk prediction model.

Table 4. Performance comparison of 4 machine learning algorithms for dynamic coagulation risk prediction.

Model	F_1-score (%)	Accuracy (%)	Recall (%)	AUC[a] (%)	Sensitivity (%)	Specificity (%)
LR[b]	89.7	85.1	92.5	90.4	92.5	67.3
RF[c]	91	86.9	93.3	92.1	93.3	71.7
XGBoost[d]	89.7	85.1	92.2	90.9	92.2	68.1
LSTM[e]	82.6	72.2	93.5	75.4	93.5	21

[a]AUC: area under the curve.

[b]LR: logistic regression.

[c]RF: random forest.

[d]XGBoost: extreme gradient boosting.

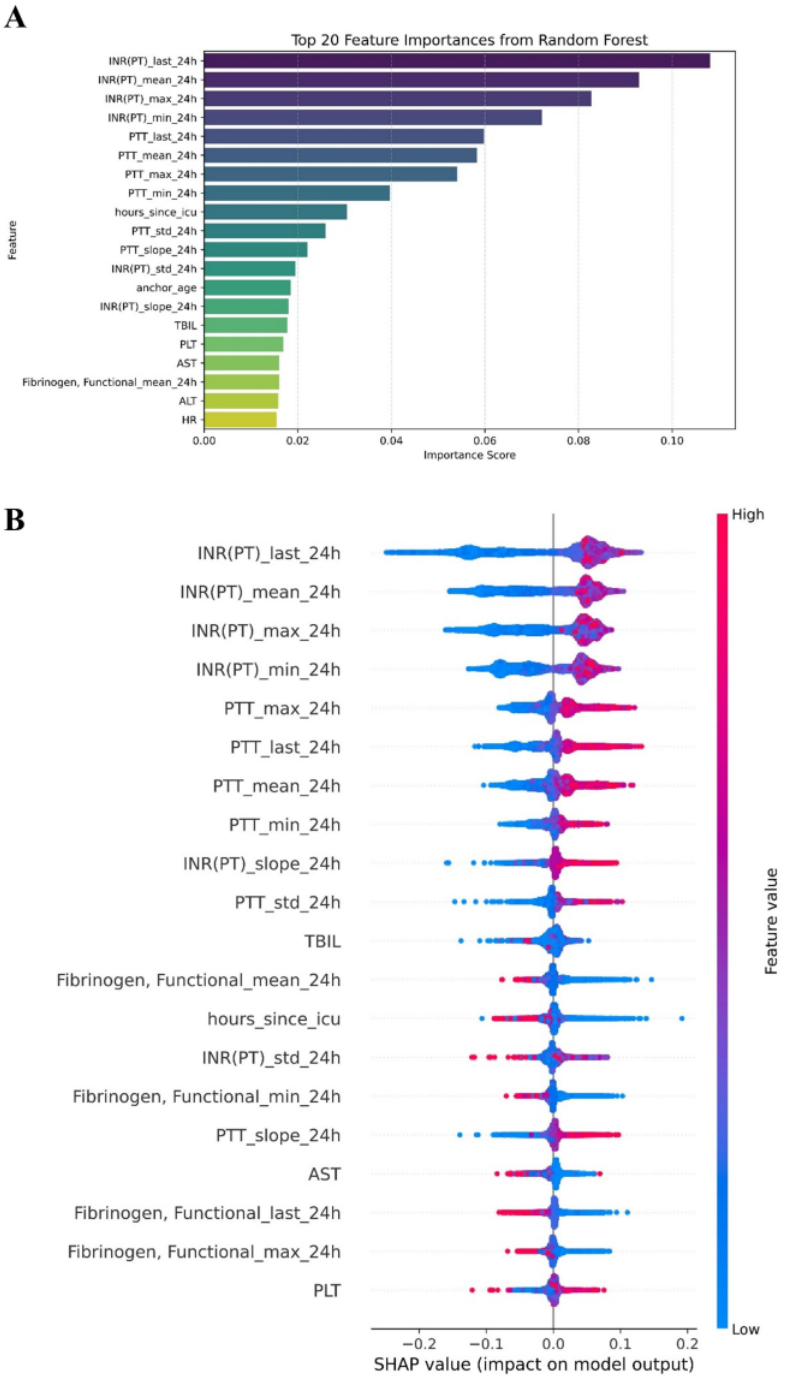
[e]LSTM: long short-term memory.

Feature Importance and Model Interpretability Analysis

To elucidate the decision-making mechanism of the predictive model, this study conducted a feature importance assessment and interpretability analysis based on the top-performing RF model. As illustrated in Figure 8A, among the dynamic features, multiple INR-related indicators—including INR(PT)_last_24h, INR(PT)_mean_24h, INR(PT)_max_24h, and INR(PT)_min_24h—exhibited the highest importance scores, indicating that INR values play a critical role in predicting coagulation abnormalities within the next 24 hours. PTT-related features (eg, PTT_last_24h, PTT_mean_24h, and PTT_max_24h) also ranked among the top 10, further underscoring the significance of dynamic coagulation time in the model's decision-making process.

XSL•FO
RenderX

Figure 8. Feature importance and interpretability analysis of the random forest model. (A) Bar plot of feature importance scores; (B) SHapley Additive exPlanations summary plot, where red and blue indicate high and low feature values, respectively, and the x-axis represents the directional impact on predictions. “INR (PT)” (labeled per MIMIC database conventions) is standardized as international normalized ratio in this study; “PTT” refers to activated partial thromboplastin time. ALT: alanine aminotransferase; AST: aspartate aminotransferase; HR: heart rate; INR: international normalized ratio; PLT: platelet count; PT: prothrombin time; PTT: partial thromboplastin time; TBIL: total bilirubin.



To enhance model interpretability, we used SHAP for visual explanation of the RF model. The results demonstrated that elevated INR(PT) and PTT values positively contributed to the prediction of coagulation abnormalities, aligning with established clinical pathophysiological mechanisms. In addition, static variables such as hours_since_icu, fibrinogen, TBIL, and anchor_age exhibited moderate predictive importance (Figure 8B).

In summary, the RF model not only demonstrates superior predictive performance but also maintains strong interpretability, effectively identifying key variables associated with coagulation dysfunction. These findings support early clinical identification of high-risk patients.

XSL•FO
RenderX

Discussion

Principal Findings

This study systematically evaluates the dynamic effects of ALS on coagulation function in patients with liver failure by integrating meta-analysis and machine learning modeling based on clinical databases. In addition, it develops an intelligent predictive model for future coagulation abnormalities. The meta-analysis results demonstrate that ALS significantly improves key coagulation parameters, including INR, PT, and APTT, highlighting its critical role in coagulation support for patients with liver failure. These findings align with previous studies [42,43], further reinforcing the evidence-based efficacy of ALS therapy in ameliorating coagulopathy. The maintained reduction in INR during long-term follow-up further underscores the stability and durability of its therapeutic efficacy. Variations in treatment modalities, etiologies, and liver failure subtypes were identified as major sources of heterogeneity in coagulation improvement.

This study adopts a dual-track strategy that integrates high-level evidence synthesis with individualized risk prediction, thereby avoiding the misconception that the meta-analysis and machine learning model are 2 parallel approaches. Specifically, the meta-analysis establishes the overall efficacy and heterogeneity of ALSS in improving coagulation parameters, which provides a rigorous evidence-based rationale for subsequent predictive modeling. Building upon these findings, the machine learning model operationalizes the most clinically relevant indicators—such as INR, PT, and APTT—into a dynamic decision-support tool for real-time risk assessment at the bedside. This methodological pathway transforms population-level evidence into patient-level prediction, thus ensuring both validity and clinical applicability.

Importantly, our results demonstrated that INR was the most significantly improved parameter in the meta-analysis and simultaneously the strongest predictive feature in the machine learning model, underscoring the translational consistency between the 2 components. This alignment exemplifies the synergistic relationship in which meta-analysis informs feature selection and validates the clinical importance of predictors, while the model extends these findings to enable individualized, real-time monitoring. Such integration reflects a broader trend in evidence-based medicine and artificial intelligence, where systematic reviews and meta-analyses provide high-level validity [44], predictive analytics enable dynamic risk assessment [45], and the convergence of these methods enhances clinical decision-making [46,47].

A related study also used MIMIC-IV v3.1 data and applied XGBoost to predict Peripherally Inserted Central Catheter–related thrombosis in patients with sepsis [48]. Compared with that work, our study differs in population (patients with liver failure undergoing ALSS vs patients with sepsis with Peripherally Inserted Central Catheter), target (coagulation abnormalities after ALSS vs catheter-related thrombosis), and methodology (integration of meta-analysis with multiple machine learning models vs single algorithm). Building upon existing literature, this study systematically compares—for the first time—the differential effects of various ALSS (eg, PE, CRRT, and MARS) on coagulation function, thereby addressing a critical research gap and providing new evidence for individualized clinical treatment strategies. These distinctions highlight the novelty and specific contribution of our approach to coagulation risk prediction in the ALSS context. Notably, ALS showed limited efficacy in improving fibrinogen levels, potentially due to differences in fibrinogen clearance efficiency across treatment methods. Subgroup analysis revealed that PE combined with CRRT yielded more consistent coagulation improvements compared with monotherapy, suggesting that hybrid ALS regimens may be more suitable for critically ill patients with severe coagulation dysfunction. In addition, disparities in APTT improvement are primarily influenced by the underlying disease type, underscoring the importance of etiological classification in guiding personalized treatment.

Unlike previous studies that primarily focused on static measurements at single time points [49], this study adopts a dynamic monitoring approach, for the first time, elucidating the evolutionary patterns and predictive value of INR, PT, APTT, and fibrinogen throughout the treatment course. Notably, the dynamic features of INR in the model—including its mean, peak, and trend—demonstrated the highest weighting, confirming its clinical significance as an early warning indicator. This dynamic modeling strategy significantly enhances predictive sensitivity and prospective utility, shifting risk assessment from post hoc evaluation to real-time intervention.

In predictive modeling, this study enhances translational potential by developing a multialgorithm model based on real-world data from MIMIC-IV. Among the tested models, the RF algorithm achieved the highest performance (AUC=92.12%, F_1-score=90.96%) in accurately predicting coagulation abnormalities within 24 hours. Unlike previous studies that primarily relied on single-algorithm approaches such as LR [50], this work systematically compared and integrated multiple machine learning models (including XGBoost and LSTM). Furthermore, SHAP interpretation was used to elucidate feature contributions, improving model transparency and clinical interpretability. The proposed model holds promise as an intelligent clinical decision–support tool in ICU settings, assisting nurses in early identification of high-risk patients for coagulation disorders. By optimizing transfusion strategies, monitoring frequency, and intervention timing, this approach may reduce bleeding-related complications while enhancing the precision and efficiency of coagulation management. Ultimately, this shift from experience-based judgment to data-driven decision-making provides a more reliable foundation for clinical workflows.

In conclusion, ALS significantly improves coagulation parameters (INR, PT, and APTT) in patients with liver failure, while the machine learning model based on dynamic indicators provides accurate risk prediction for coagulation abnormalities. These findings offer valuable support for early intervention and precision management in coagulation care. These results offer strong evidence for implementing earlier and more targeted clinical nursing interventions.

XSL•FO
RenderX

Despite the innovation and clinical utility of this study, several limitations should be acknowledged. First, although this study systematically evaluated the effects of ALSS on coagulation function in patients with liver failure through meta-analysis and developed a dynamic indicator-based coagulation risk prediction model, the constructed predictive model did not specifically target patients who received ALSS treatment. Instead, risk modeling was conducted for the broader population of patients with liver failure. This decision was primarily due to the extremely limited number of ALSS-treated cases identified in the MIMIC-IV database—only 5 patients met the strict inclusion criteria—making the sample size insufficient to meet the basic data requirements for machine learning model development or to ensure model robustness and generalizability. As a compromise, this study focused on the overall liver failure population to explore trends in coagulation function and dynamic risk prediction. This approach provides a foundational reference for future model development based on larger datasets of patients treated for ALSS.

Secondly, although LSTM networks are widely used in clinical prediction due to their temporal modeling capabilities, their predictive performance in this study was significantly inferior to that of static models. This discrepancy primarily stems from the poor temporal resolution of the MIMIC dataset. Laboratory and vital sign data are sparsely sampled, irregular, and discontinuous—particularly for variables such as INR and fibrinogen—making it difficult to construct high-quality time series inputs. In addition, the short length of ICU stays in some patients resulted in insufficient sequence data, further limiting the model's ability to learn time-dependent patterns. In contrast, the RF model, which is based on aggregated features, is less reliant on data continuity and demonstrated superior robustness and generalizability. Therefore, under the constraints of low-frequency and sparse ICU data, static models may offer greater practical value.

To address the limitations of LSTM performance, we attempted to incorporate attention mechanisms to enhance the model's ability to capture critical time points. However, due to the short feature sequences and missing key records, no significant performance improvement over LSTM was observed. In the future, we plan to further evaluate the potential of architectures, such as transformer on higher-quality, multicenter time series data to optimize temporal modeling outcomes.

Furthermore, although the RF model performed well within the MIMIC-IV database, we fully acknowledge that external validation is essential for assessing its generalizability. Given that MIMIC is derived from a single US center and exhibits gender imbalances, the model's applicability to other populations remains uncertain. The current lack of publicly available ALSS-specific, patient-level data limits the feasibility of immediate external validation. We plan to collaborate with regional multicenter hospitals, particularly in Asian populations, to conduct prospective validation studies and improve the model's cross-population adaptability.

In this study, the definition of coagulation dysfunction labels was primarily based on established clinical diagnostic criteria and expert consensus. However, due to the absence of explicitly annotated bleeding events or other coagulation-related outcomes in the MIMIC database, we were unable to validate the correlation between the threshold and actual clinical risk. We acknowledge that future work should incorporate specific clinical outcomes (eg, gastrointestinal bleeding and hemorrhagic shock) to reassess the clinical significance of the risk threshold. Furthermore, considering the complex etiology of liver failure, adopting etiology-specific or dynamically adjusted prediction thresholds may better reflect real-world clinical scenarios and improve model sensitivity and practicality. We have identified this issue as a key direction for future research.

Conclusion

In summary, this study not only provides systematic, evidence-based support for the efficacy of ALSS in improving coagulation function but also constructs a highly discriminative and interpretable risk prediction tool. The findings are of great significance for advancing individualized and intelligent coagulation support therapy and nursing interventions in patients with liver failure. Future efforts should aim to expand the model's applicability by incorporating multicenter data and nursing practice variables, thereby promoting the implementation and refinement of dynamic coagulation monitoring systems and providing data-driven decision support in critical care settings.

Although the RF model demonstrated superior performance in predicting coagulation dysfunction in patients with liver failure, it is currently well-suited for practical use due to its clear structure and transparent feature inputs. Key predictors such as dynamic INR, PTT, and fibrinogen can be visualized through a graphical user interface, allowing clinicians and nursing staff to intuitively assess individual risk and determine optimal intervention timing. In the future, we plan to deploy this model as an open-access web application or integrate it into hospital information systems, enabling rapid clinical access to short-term coagulation risk predictions. This will support intelligent optimization of ALSS treatment pathways and nursing resource allocation. We believe this translational approach will significantly enhance the model's clinical accessibility and practical value.

Funding

This study was supported by Nanchong Science and Technology Bureau City-University Cooperation Special Fund (19SXHZ0058).

Data Availability

All data generated or analyzed during this study are included in this article and/or its supplementary material files. Further enquiries can be directed to the corresponding author.

XSL•FO
RenderX

Authors' Contributions

Conceptualization: HW, TH
Data curation: HW, TH
Formal analysis: HW, TH
Funding acquisition: TH
Investigation: HW, TH, LR, TJZ
Methodology: HW, TH, LR, TJZ
Supervision: TH
Writing – original draft: HW, TH
Writing – review and editing: HW, TH, LR, TJZ
All authors read and approved the final manuscript.

Conflicts of Interest

None declared.

Multimedia Appendix 1
Machine learning for liver failure coagulation.
[DOCX File , 1366 KB - medinform_v13i1e76348_app1.docx]

References

1. Lisman T, Porte RJ. Pathogenesis, prevention, and management of bleeding and thrombosis in patients with liver diseases. Res Pract Thromb Haemost 2017;1(2):150-161 [FREE Full text] [doi: 10.1002/rth2.12028] [Medline: 30046685]
2. Islam R, Kundu S, Jha S, Rivera AP, Flores Monar GV, Islam H, et al. Cirrhosis and coagulopathy: mechanisms of hemostasis changes in liver failure and their management. Cureus 2022;14(4):e23785 [FREE Full text] [doi: 10.7759/cureus.23785] [Medline: 35518552]
3. Lagman C, Nagasawa DT, Sheppard JP, Jacky Chen CH, Nguyen T, Prashant GN, et al. End-stage liver disease in patients with intracranial hemorrhage is associated with increased mortality: a cohort study. World Neurosurg 2018;113:e320-e327. [doi: 10.1016/j.wneu.2018.02.025] [Medline: 29452322]
4. Lombardi R, Francione P, Maffi G, Sigon G, Pulixi E, Cespiati A, et al. Coagulation imbalance is associated with hepatic fibrosis and vascular complications in patients with type2 diabetes and NAFLD. Dig Liver Dis 2022;54:S38. [doi: 10.1016/j.dld.2022.01.075]
5. Pless G. Artificial and bioartificial liver support. Organogenesis 2007;3(1):20-24 [FREE Full text] [doi: 10.4161/org.3.1.3635] [Medline: 19279696]
6. Kumar A, Tripathi A, Jain S. Extracorporeal bioartificial liver for treating acute liver diseases. J Extra Corpor Technol 2011;43(4):195-206 [FREE Full text] [Medline: 22416599]
7. Larsen F. Artificial liver support in acute and acute-on-chronic liver failure. Curr Opin Crit Care 2019;25(2):187-191. [doi: 10.1097/MCC.0000000000000584] [Medline: 30672818]
8. Jasirwan COM, Muradi A, Antarianto RD. Bio-artificial liver support system: A prospective future therapy. Livers 2023;3(1):65-75. [doi: 10.3390/livers3010006]
9. Chen Y, Han T, Duan Z, Severe Liver DiseaseArtificial Liver Group, Chinese Society of Hepatology, Chinese Medical Association. Clinical application of artificial liver and blood purification: expert consensus recommendations. Hepatol Int 2023;17(1):4-17. [doi: 10.1007/s12072-022-10430-8] [Medline: 36324040]
10. Lanjuan L. Guidelines on application of artificial liver blood purification system (version 2023). Infect Microb Dis 2025;7(1):8-17. [doi: 10.1097/im9.0000000000000173]
11. Agarwal B, Wright G, Gatt A, Riddell A, Vemala V, Mallett S, et al. Evaluation of coagulation abnormalities in acute liver failure. J Hepatol 2012;57(4):780-786. [doi: 10.1016/j.jhep.2012.06.020] [Medline: 22735303]
12. Mohapatra P, Kumar A, Singh RK, Gupta R, Hussain M, Singh S, et al. The effect of sepsis and septic shock on the viscoelastic properties of clot quality and mass using thromboelastometry: a prospective observational study. Indian J Crit Care Med 2023;27(9):625-634 [FREE Full text] [doi: 10.5005/jp-journals-10071-24539] [Medline: 37719352]
13. Kleinegris MF. Coagulation testing in atherosclerosis and liver disease. Doctoral thesis.: Datawyse / Universitaire Pers Maastricht; 2016. URL: https://cris.maastrichtuniversity.nl/ws/portalfiles/portal/5919690/c5438.pdf [accessed 2025-11-20]
14. Xiang Y, Li R, Cai J, Jiang Q. Three artificial liver models of treatment of acute-on-chronic liver failure. Ther Clin Risk Manag 2024;20:731-740 [FREE Full text] [doi: 10.2147/TCRM.S485620] [Medline: 39479527]
15. Cui K, Liu C, Teng X, Chen F, Xu Y, Zhou S, et al. Association between artificial liver support system and prognosis in hepatitis B virus-related acute-on-chronic liver failure. Infect Drug Resist 2025;18:113-126 [FREE Full text] [doi: 10.2147/IDR.S500291] [Medline: 39803304]

XSL•FO
RenderX

16. Gupta J, Majumder AK, Sengupta D, Sultana M, Bhattacharya S. Investigating computational models for diagnosis and prognosis of sepsis based on clinical parameters: opportunities, challenges, and future research directions. J Intensive Med 2024;4(4):468-477 [FREE Full text] [doi: 10.1016/j.jointm.2024.04.006] [Medline: 39310065]
17. Guo K, Zhu B, Zha L, Shao Y, Liu Z, Gu N, et al. Interpretable prediction of stroke prognosis: SHAP for SVM and nomogram for logistic regression. Front Neurol 2025;16:1522868 [FREE Full text] [doi: 10.3389/fneur.2025.1522868] [Medline: 40103937]
18. Mu at F, Păduraru DN, Bolocan A, Palcău CA, Copăceanu A, Ion D, et al. Machine learning models in sepsis outcome prediction for ICU patients: integrating routine laboratory tests-a systematic review. Biomedicines 2024;12(12):2892 [FREE Full text] [doi: 10.3390/biomedicines12122892] [Medline: 39767798]
19. Ma L, Zhang X, Ma W, Ding X. Meta-analysis of the efficacy of DPMAS-based artificial liver in the treatment of ACLF. Europe PMC 2022 [FREE Full text] [doi: 10.21203/rs.3.rs-1604197/v1]
20. Yao F, Luo J, Zhou Q, Wang L, He Z. Development and validation of a machine learning-based prediction model for hepatorenal syndrome in liver cirrhosis patients using MIMIC-IV and eICU databases. Sci Rep 2025;15(1):2743 [FREE Full text] [doi: 10.1038/s41598-025-86674-9] [Medline: 39837961]
21. Wu L, Liu Z, Huang H, Pan D, Fu C, Lu Y, et al. Development and validation of an interpretable machine learning model for predicting the risk of hepatocellular carcinoma in patients with chronic hepatitis B: a case-control study. BMC Gastroenterol 2025;25(1):157 [FREE Full text] [doi: 10.1186/s12876-025-03697-2] [Medline: 40069597]
22. Moher D, Liberati A, Tetzlaff J, Altman DG, PRISMA Group. Preferred reporting items for systematic reviews and meta-analyses: the PRISMA statement. PLoS Med 2009;6(7):e1000097 [FREE Full text] [doi: 10.1371/journal.pmed.1000097] [Medline: 19621072]
23. Fan Z, Jiang J, Xiao C, Chen Y, Xia Q, Wang J, et al. Construction and validation of prognostic models in critically ill patients with sepsis-associated acute kidney injury: interpretable machine learning approach. J Transl Med 2023;21(1):406 [FREE Full text] [doi: 10.1186/s12967-023-04205-4] [Medline: 37349774]
24. Kounis I, Sacleux SC, Ordan MA, André S, Boudon M, Coilly A, et al. Efficiency and safety of total plasma exchange in critically ill cirrhotic patients with acute on chronic liver failure: a pilot study. Clin Res Hepatol Gastroenterol 2023;47(8):102206. [doi: 10.1016/j.clinre.2023.102206] [Medline: 37714512]
25. Ninan A, Mohan G, Shanbhag V, Chenna D, Shastry S, Rao S. Assessing the clinical efficacy of low-volume therapeutic plasma exchange in achieving recovery from acute liver failure induced by yellow phosphorous poisoning. J Clin Apher 2024;39(3):e22110. [doi: 10.1002/jca.22110] [Medline: 38634432]
26. Yang CF, Liu JW, Jin LM, Li YM. Association of duration and etiology with the effect of the artificial liver support system in pediatric acute liver failure. Front Pediatr 2022;10:951443 [FREE Full text] [doi: 10.3389/fped.2022.951443] [Medline: 36340721]
27. Hu J, Wang C, Bai K, Liu C. Clinical application of regional citrate anticoagulation for membrane-based therapeutic plasma exchange in children with liver failure. Front Pediatr 2023;11:1206999 [FREE Full text] [doi: 10.3389/fped.2023.1206999] [Medline: 37928357]
28. Huang K, Ji F, Xie Z, Wu D, Xu X, Gao H, et al. Artificial liver support system therapy in acute-on-chronic hepatitis B liver failure: classification and regression tree analysis. Sci Rep 2019;9(1):16462 [FREE Full text] [doi: 10.1038/s41598-019-53029-0] [Medline: 31712684]
29. Lee JY, Kim SB, Chang JW, Park SK, Kwon SW, Song KW, et al. Comparison of the molecular adsorbent recirculating system and plasmapheresis for patients with graft dysfunction after liver transplantation. Transplant Proc 2010;42(7):2625-2630. [doi: 10.1016/j.transproceed.2010.04.070] [Medline: 20832557]
30. Li YH, Xu Y, Wu HM, Yang J, Yang LH, Yue-Meng W. Umbilical cord-derived mesenchymal stem cell transplantation in hepatitis B virus related acute-on-chronic liver failure treated with plasma exchange and entecavir: a 24-month prospective study. Stem Cell Rev Rep 2016;12(6):645-653. [doi: 10.1007/s12015-016-9683-3] [Medline: 27687792]
31. Mohanka R, Rao P, Shah M, Gupte A, Nikam V, Vohra M, et al. Acute liver failure secondary to yellow phosphorus rodenticide poisoning: outcomes at a center with dedicated liver intensive care and transplant unit. J Clin Exp Hepatol 2020;11(4):424-434 [FREE Full text] [doi: 10.1016/j.jceh.2020.09.010] [Medline: 33052182]
32. Sorodoc L, Lionte C, Sorodoc V, Petris O, Jaba I. Is MARS system enough for A. phalloides-induced liver failure treatment? Hum Exp Toxicol 2010;29(10):823-832. [doi: 10.1177/0960327110363327] [Medline: 20179021]
33. Chen JJ, Huang JR, Yang Q, Xu XW, Liu XL, Hao SR, et al. Plasma exchange-centered artificial liver support system in hepatitis B virus-related acute-on-chronic liver failure: a nationwide prospective multicenter study in China. Hepatobiliary Pancreat Dis Int 2016;15(3):275-281. [doi: 10.1016/s1499-3872(16)60084-x] [Medline: 27298103]
34. Falkensteiner C, Kortgen A, Leonhardt J, Bauer M, Sponholz C. Comparison of albumin dialysis devices molecular adsorbent recirculating system and ADVanced Organ Support system in critically ill patients with liver failure-a retrospective analysis. Ther Apher Dial 2021;25(2):225-236. [doi: 10.1111/1744-9987.13533] [Medline: 32515160]
35. Colak M, Ocak I. Management of pediatric liver failure with therapeutic plasma exchange and continuous renal replacement therapy: a retrospective observational study. Medicine (Baltimore) 2024;103(19):e38093 [FREE Full text] [doi: 10.1097/MD.0000000000038093] [Medline: 38728496]

XSL•FO
RenderX

36. Gong D, Ren B, Ji D, Tao J, Xu B, Liu Z, et al. Selective albumin exchange: a novel and simple method to remove bilirubin. Int J Artif Organs 2008;31(5):425-430. [doi: 10.1177/039139880803100508] [Medline: 18609516]
37. Kulkarni AV, Venishetty S, Vora M, Naik P, Chouhan D, Iyengar S, et al. Standard-volume is as effective as high-volume plasma exchange for patients with acute liver failure. J Clin Exp Hepatol 2024;14(3):101354. [doi: 10.1016/j.jceh.2024.101354] [Medline: 38406612]
38. Stöckert P, Rusch S, Schlosser-Hupf S, Mehrl A, Zimmermann K, Pavel V, et al. Increasing incidence of mycotoxicosis in South-Eastern Germany: a comprehensive analysis of mushroom poisonings at a University Medical Center. BMC Gastroenterol 2024;24(1):450 [FREE Full text] [doi: 10.1186/s12876-024-03550-y] [Medline: 39690424]
39. Pawaria A, Sood V, Lal BB, Khanna R, Bajpai M, Alam S. Ninety days transplant free survival with high volume plasma exchange in Wilson disease presenting as acute liver failure. J Clin Apher 2021;36(1):109-117. [doi: 10.1002/jca.21848] [Medline: 33368534]
40. Hung YM, Hung GC, Hsu PI, Hung SY, Chou KJ, Chung HM. Short-term survival advantage after plasma exchange in the treatment of acute on chronic liver failure or acute liver failure. Clinical Intensive Care 2004;15(2-3):93-99. [doi: 10.1080/09563070400003714]
41. Wan YM, Li YH, Xu ZY, et al. Therapeutic plasma exchange versus double plasma molecular absorption system in hepatitis B virus-infected acute-on-chronic liver failure treated by entercavir: a prospective study. J Clin Apher 2017;32(6):453-461. [doi: 10.1002/jca.21535] [Medline: 28304106]
42. Shen Y, Wang X, Wang B, Shao JG, Liu YM, Qin Y, et al. Survival benefits with artificial liver support system for acute-on-chronic liver failure: a time series-based meta-analysis. Medicine (Baltimore) 2016;95(3):e2506 [FREE Full text] [doi: 10.1097/MD.0000000000002506] [Medline: 26817889]
43. Wu C, Peng W, Cheng D, Gu H, Liu F, Peng S, et al. Efficacy and economic evaluation of nonbiological artificial liver therapy in acute-on-chronic hepatitis B liver failure. J Clin Transl Hepatol 2023;11(2):433-440 [FREE Full text] [doi: 10.14218/JCTH.2022.00106] [Medline: 36643036]
44. Liu X, Faes L, Kale AU, Wagner SK, Fu DJ, Bruynseels A, et al. A comparison of deep learning performance against health-care professionals in detecting diseases from medical imaging: a systematic review and meta-analysis. Lancet Digit Health 2019;1(6):e271-e297 [FREE Full text] [doi: 10.1016/S2589-7500(19)30123-2] [Medline: 33323251]
45. Goldstein BA, Navar AM, Pencina MJ, Ioannidis JPA. Opportunities and challenges in developing risk prediction models with electronic health records data: a systematic review. J Am Med Inform Assoc 2017;24(1):198-208 [FREE Full text] [doi: 10.1093/jamia/ocw042] [Medline: 27189013]
46. Topol EJ. High-performance medicine: the convergence of human and artificial intelligence. Nat Med 2019;25(1):44-56. [doi: 10.1038/s41591-018-0300-7] [Medline: 30617339]
47. Rajpurkar P, Chen E, Banerjee O, Topol EJ. AI in health and medicine. Nat Med 2022;28(1):31-38. [doi: 10.1038/s41591-021-01614-0] [Medline: 35058619]
48. Hao W, She T, Yuan Z, Liu L. A predictive model for PICC-related thrombosis in sepsis patients using XGboost algorithm. Cardiovascular Disease 2025 [FREE Full text] [doi: 10.21203/rs.3.rs-6449820/v1]
49. Sahli SD, Rössler J, Tscholl DW, Studt J, Spahn DR, Kaserer A. Point-of-care diagnostics in coagulation management. Sensors (Basel) 2020;20(15):4254 [FREE Full text] [doi: 10.3390/s20154254] [Medline: 32751629]
50. Caldwell S, Carlini LE. Coagulation homeostasis in liver disease. Clin Liver Dis (Hoboken) 2020;16(4):137-141 [FREE Full text] [doi: 10.1002/cld.935] [Medline: 33163164]

Abbreviations

ACLF: acute-on-chronic liver failure
ALF: acute liver failure
ALS: artificial liver support
ALSS: artificial liver support system
AP: average precision
APTT: activated partial thromboplastin time
AUC: area under the curve
BIDMC: Beth Israel Deaconess Medical Center
BP: blood pressure
CRRT: continuous renal replacement therapy
HBV: hepatitis B virus
ICU: intensive care unit
INR: international normalized ratio
LR: logistic regression
LSTM: long short-term memory
MARS: molecular adsorbent recirculating system
MIMIC: Medical Information Mart for Intensive Care

XSL•FO
RenderX

MIT: Massachusetts Institute of Technology
NOS: Newcastle-Ottawa scale
PE: plasma exchange
PP: plasma perfusion
PR: precision-recall
PRISMA: Preferred Reporting Items for Systematic Reviews and Meta-Analyses
PT: prothrombin time
PTT: partial thromboplastin time
RF: random forest
ROC: receiver operating characteristic
SHAP: Shapley Additive Explanations
TBIL: total bilirubin
XGBoost: extreme gradient boosting

Edited by A Benis; submitted 21.04.25; peer-reviewed by H Xu, C Ma; comments to author 16.06.25; revised version received 31.07.25; accepted 05.10.25; published 08.12.25.

Please cite as:
Wang H, He T, Ren L, Zhang T
Coagulation Risk Prediction in Patients With Liver Failure: Integrated Meta-Analysis and Machine Learning Model Study
JMIR Med Inform 2025;13:e76348
URL: https://medinform.jmir.org/2025/1/e76348
doi:10.2196/76348
PMID:

©Hao Wang, Tao He, Liang Ren, Tingjun Zhang. Originally published in JMIR Medical Informatics (https://medinform.jmir.org), 08.12.2025. This is an open-access article distributed under the terms of the Creative Commons Attribution License (https://creativecommons.org/licenses/by/4.0/), which permits unrestricted use, distribution, and reproduction in any medium, provided the original work, first published in JMIR Medical Informatics, is properly cited. The complete bibliographic information, a link to the original publication on https://medinform.jmir.org/, as well as this copyright and license information must be included.

XSL•FO
RenderX

Gaps and Pathways to Success in Global Health Informatics Academic Collaborations: Reflecting on Current Practices

Elizabeth A Campbell[1*], PhD; Felix Holl[2,3*], PhD, MPH, MSc; Oliver J Bear Don't Walk IV[4], PhD; Badisa Mosesane[5], BSc; Andrew S Kanter[6], MD, MPH; Hamish Fraser[7], MBChB; Amanda L Joseph[8], MSc; Judy Wawira Gichoya[9], MD; Kabelo Leonard Mauco[10], PhD; Sansanee Craig[11], MD

[1]Johns Hopkins Center for Outbreak Response Innovation, Baltimore, MD, United States
[10]Department of Biomedical and Health Informatics, Children's Hospital of Philadelphia, Philadelphia, PA, United States
[11]Department of Biomedical Informatics, Columbia University Irving Medical Center, New York, NY, United States
[2]DigiHealth Institute, Neu-Ulm University of Applied Sciences, Wileystraße 1, Neu-Ulm, BY, Germany
[3]Leibniz ScienceCampus Digital Public Health, Bremen, Germany
[4]Department of Biomedical Informatics and Medical Education, University of Washington, Seattle, WA, United States
[5]Department of Computer Science, University of Botswana, Gaborone, Botswana
[6]Department of Biomedical Informatics, Columbia University, New York, NY, United States
[7]Brown Center for Biomedical Informatics, Brown University, Providence, RI, United States
[8]School of Health Information Science, University of Victoria, Victoria, BC, Canada
[9]Department of Learning, Informatics, Management and Ethics, Karolinska Institutet, Solna, Sweden
[*]these authors contributed equally

Corresponding Author:
Felix Holl, PhD, MPH, MSc
DigiHealth Institute, Neu-Ulm University of Applied Sciences, Wileystraße 1, Neu-Ulm, BY, Germany

Abstract

Academic global health informatics (GHI) projects are impactful collaborations between institutions in high-income and low- and middle-income countries (LMICs) and play a crucial role in enhancing health care services and access in LMICs using eHealth practices. Researchers across all involved organizations bring unique expertise to these collaborations. However, these projects often face significant obstacles, including cultural and linguistic barriers, resource limitations, and sustainability issues. The lack of representation from LMIC researchers in knowledge generation and the high costs of open-access publications further complicate efforts to ensure inclusive, accessible, and collaborative scholarship. This viewpoint describes present gaps in the literature on academic GHI collaborations and describes a path forward for future research directions and successful research community development. Key recommendations include centering community-based participatory research, developing post-growth solutions, and creating sustainable funding models. Addressing these challenges is essential for fostering effective, scalable, and equitable GHI interventions that improve global health outcomes.

(JMIR Med Inform 2025;13:e67326) doi:10.2196/67326

KEYWORDS

global health informatics; academic collaboration; global health; digital health; health equity; academic; high-income countries; low- and middle-income countries; LMIC; GHI; research community; participatory research; development; sustainability; scalability; GHI intervention; eHealth

Introduction

Global health informatics (GHI) is an interdisciplinary subfield of health informatics that aims to use eHealth practices (eg, electronic health records, mobile health [mHealth], telehealth, and technology-enabled learning), including research and innovation in enhancing provision of health care resources, services, including information access in low- and middle-income countries (LMICs). This approach has the potential to improve clinical and population health outcomes for patients in LMICs [1,2]. GHI interventions aim to empower people through context-specific technological solutions to develop innovative solutions that improve health care access and patient outcomes while being locally led and maintained [3].

Academic GHI interventions are research-driven initiatives between higher education institutions (eg, universities and medical schools) with host country governmental agencies, nongovernmental organizations, universities, and community organizations [4,5]. These projects typically have more localized

XSL•FO
RenderX

and regional scope, focusing on specific local issues within a particular community, whether in high-income or low-income settings, systems, or regions; they often address local needs without prioritizing global scalability or broad collaboration. Academic GHI collaborations can include an informatics education training component to build local capacity [6,7]. Finally, a key characteristic of academic GHI projects is that their funding typically comes from governmental agencies or foundations for institutional resources. Knowledge generation through scientific publications and obtaining maintained extramural funding are key differentiating factors between academic collaborations and other GHI interventions.

However, numerous challenges impact the long-term success of academic GHI interventions and collaborations. These include a lack of understanding of the true health care problems, goals, and workflows, "pilotitis" (ie, the lack of scale-up beyond a pilot phase), and insufficient resources or interest amongst communities to maintain interventions independently [8-10]. There is a substantial lack of representation from LMIC researchers in knowledge generation and a scarcity of literature on successful implementation and further operationalization of academic GHI interventions [11,12]. Despite the benefits of open-access publication for knowledge sharing in LMICs, there is a substantial variance in open-access article processing charges, with costs upwards of several thousand US dollars; this limits access to and dissemination of scientific knowledge from researchers in LMICs and globally [13].

While the phenomenon of "pilotitis" remains a recognized challenge in GHI, it does not universally reflect the realities on the ground. In fact, there are numerous examples of successful, long-term implementations of digital health technologies in Africa and Southeast Asia that have benefited from international collaboration while being adapted to local needs.

A leading example is OpenMRS, an open-source electronic medical record system that has been deployed and maintained across multiple countries, including Kenya, Rwanda, Uganda, and Bangladesh [14,15]. These implementations have demonstrated local ownership, strong technical communities, and policy alignment, proving that long-term sustainability is achievable when supported by appropriate governance and capacity building.

Another widely embraced platform is District Health Information Software 2, developed by the University of Oslo and implemented in over 75 countries [16]. It serves as the national health information system (HIS) in countries such as Tanzania, Nepal, and Sri Lanka, enabling robust health data management and public health decision-making at scale. District Health Information Software 2's success is rooted in its open architecture, local customization, and integration into national health strategies.

These examples highlight that international collaboration can indeed support scalable, sustainable innovation, particularly when it promotes local leadership, long-term investment, and codevelopment. Rather than suggesting that pilotitis is a universal outcome, we aim to emphasize the importance of structural enablers and collaboration models that move beyond fragmented, short-term interventions and foster enduring digital health ecosystems.

In this viewpoint, we describe current gaps in the literature on how academic GHI collaborations can be successfully implemented. Our viewpoint also explores a path forward for developing an environment that is conducive to these projects' success, and research priorities for the informatics community to expand academic GHI research. The authors would like to call attention to the use of terms such as "LMICs" throughout this piece. To foster effective global collaboration, respect for the country of origin's culture, customs, and economy is warranted. Such a perspective could place unwarranted stigma or an unequal distribution of power or influence on countries in the southern hemisphere, implying that they are unable to innovate and must remain reliant on high-income countries for solutions to local, country-specific challenges [17,18]. In the absence of alternatives, we continue to use the current nomenclature but recognize it as a limitation and a priority area for developing more inclusive terms.

Expanding the Knowledge Base for Academic GHI Project Implementation

Overview

Although academic GHI interventions are typically implemented locally, they often adopt a more expansive viewpoint by striving to contribute scientific knowledge for solutions to be applied globally. Long-term collaborations across academic institutions and other health care organizations globally are key to technological advancements and ensuring that innovations are scalable and transferable across diverse health contexts [11]. For example, interoperable systems and standards, such as Health Level Seven International, Fast Healthcare Interoperability Resources and Systematized Nomenclature of Medicine–Clinical Terms, are essential to ensuring that health information can easily be exchanged, interpreted, and used across various systems worldwide [19]. Interoperability systems and standards are essential for ensuring secure health information exchange, facilitating data analysis and secondary research use, informing organizational decision-making, and improving patient care.

Despite the critical role of GHI in advancing health care outcomes worldwide, there remains a significant gap in the literature regarding the specific challenges faced during the implementation and scale-up of such projects in LMICs. This has often led to "pilotitis," where systems are designed and implemented yet never scale or report evaluation findings beyond the initial implementation [8,12]. These challenges can be grouped into 3 categories: local context-related, resource-related, and business model-related.

Local Context–Related Challenges

Local context–related challenges encompass cultural and linguistic barriers that can lead to the development of solutions that are not suitable or compatible with the target population. For example, health data may be recorded in different languages, resulting in complicated and potentially erroneous translations, thus challenging data standardization and interoperability.

XSL•FO
RenderX

Similarly, existing medical diagnostic codes, terms, and classifications may not align with existing languages and across countries and cultures. These barriers can result in a lack of user engagement and adoption, ultimately limiting the intervention's effectiveness. These challenges can also include data privacy and security concerns, as well as divergent cultural views and perceptions of diseases and health behaviors, and trust in technology. Understanding and integrating local cultural norms, language requirements, and workflows are crucial for health informatics initiative success [20].

Resource-Related Challenges

Resource-related challenges include technological infrastructure limitations, but extend beyond those and include the availability of a skilled workforce. There is often a shortage of trained professionals (ie, technical and clinical) who can manage and maintain digital health systems, analyze health data, and ensure data security and privacy. This lack of expertise can lead to improper or inappropriate technologies, security vulnerabilities, a lack of data access and use, and unreliable data, which undermine interventions' goals [20]. To increase capacity, additional training of local staff is often necessary, a hidden cost in time and money that may not always be accounted for in grant funding or limited project timelines for academic GHI interventions. Furthermore, even in initiatives that include data science education in their activities, there is a lack of standardization in capacity-building approaches, which is needed to support global and interdisciplinary collaborations and foster strong regional partnerships [21].

Business Model–Related Challenges

Business model–related challenges involve the sustainability and scalability of health informatics projects. Projects often rely on short-term grants or donor funding and lack a long-term financial sustainability plan; this issue is further compounded by challenges faced in communicating return on investment for GHI projects to funders (eg, governments and private donors), particularly given limitations in integrating cost-recovery mechanisms into these projects due to infeasibility or ethical considerations. In addition, vague ownership models for data, systems, and technologies can limit scale-up and integration of smaller-scale informatics project products into national health systems. This issue highlights the need for robust business models that ensure continuous support, funding, and integration of digital health interventions into the broader health system framework [22,23].

In addition, there is limited analysis of how projects navigate these hurdles in real-world settings beyond the pilot stage or the effectiveness of various strategies to overcome these obstacles. While in recent years, there have been some studies on evaluating GHI projects in LMICs [14,24,25], more comprehensive evaluations and reporting on the implementation processes and intervention outcomes at scale are necessary to address these gaps. Such analyses can provide valuable insights into best practices and successful strategies for overcoming the myriad challenges faced in low-resource settings. Studies need to examine these projects' immediate impacts, along with their ability to be integrated into existing health systems, address local community needs, adaptability to changing technological landscapes and health challenges, and capacity to remain relevant and useful over time [26,27]. Centrally positioning LMIC researchers as experts in knowledge generation is imperative, as is acknowledging and mitigating harmful power dynamics between researchers from academic institutions and members of communities in which GHI projects are situated [28,29]. Addressing these gaps is essential for guiding future academic GHI collaborations toward more successful, sustainable, and impactful implementation, thereby contributing to improving global health outcomes.

Developing an Environment That Fosters Success

Global efforts to establish an enabling environment for academic GHI interventions are necessary. In such an environment, stakeholders are invested in GHI projects as a solution to address health care challenges and are prepared to engage in ethical and mutually beneficial informatics projects. As mutually beneficial collaborations, researchers in high-resource settings can benefit greatly from the expertise and interventions proven successful in low-resourced settings. For example, in response to an urgent need for COVID-19 tracking early in the pandemic, the San Francisco Department of Health partnered with Dimagi to use CommCare, an open-sourced tracking application used for 2 decades by community health workers in low-resource settings [30,31]. This partnership led to the successful expansion of the city's COVID-19 response force and scale-up of testing capabilities, forming a generalizable model for other United States jurisdictions [30].

Furthermore, successful academic GHI interventions generally require more input and control from local communities compared to typical commercial HIS seen in the US and other high-income settings. Developing interventions with community buy-in and local ownership is critical to addressing these challenges and should be incorporated into protocols and implementation efforts from a study's inception [24]. For instance, systems must function with limited power, networking, and IT support [32]. Key solutions for developing and implementing successful GHI projects in low-resource settings include flexible coding systems (eg, the Open Concept Lab for OpenMRS [33]) to represent locally important data on diseases, treatments, and social circumstances, such as transport and housing types, along with a focus on open and rigorous evaluation in clinical contexts where informatics solutions are mobilized.

Evaluating and establishing a new program needs to be driven by the equitable involvement of all relevant parties with a mutual and unified understanding of goals and pathways to be achieved. Theories and frameworks regarding technology adoption, sociocultural, user-centered design, and implementation science are important tools to help guide this process [4,34].

While our perspective highlights persistent challenges in GHI academic collaborations, we recognize and seek to build upon the substantial efforts of leading organizations and institutions. International academic partnerships around GHI have played

XSL•FO
RenderX

an important role in strengthening health systems, especially in LMICs.

The World Health Organization has played a critical role in shaping the global digital health agenda through its Global Strategy on Digital Health, the Digital Health Technical Advisory Group, and its coordination of normative frameworks and implementation support mechanisms. The Geneva University Hospitals and the Geneva Digital Health Hub have emerged as key drivers of innovation, knowledge exchange, and capacity building. As a World Health Organization Collaborating Center for eHealth and Telemedicine, Geneva University Hospitals has contributed extensively to advancing digital health solutions for global health challenges. The Geneva Digital Health Hub has further expanded this impact by convening stakeholders across sectors, translating research into policy, and facilitating collaborative digital health projects with a strong emphasis on equity and inclusion.

Other notable examples include the Academic Model Providing Access to Healthcare and the International Training and Education Center for Health at the University of Washington. These collaborations underscore the potential of cross-institutional efforts in driving sustainable health improvements through shared expertise, coleadership, and a better understanding of local contexts. One such partnership that has emerged as a promising model is the collaboration between the Children's Hospital of Philadelphia (CHOP) and the University of Botswana (UB) on GHI research efforts, which is described as a case study in detail.

Case Study: Chop-UB Partnership—a Model for Equitable Global Health Collaboration

The CHOP-UB partnership exemplifies a coleadership model built on mutual respect, shared responsibilities, and the integration of diverse expertise. CHOP brings extensive experience in pediatric health care delivery and clinical research, while UB contributes technical and contextual knowledge critical to health care delivery in Botswana. Specifically, researchers and experts at UB engage in data management and analysis through the eHealth research unit, focusing on ensuring data quality and usability. Their expertise spans digital health technologies, including electronic health records and mHealth applications, as well as compliance with ethical and regulatory frameworks governing data privacy in Botswana.

Key achievements of this collaboration include: the evaluation of health care data collection, sharing, and usage, mapping the flow of health care data, examining clinicians' perspectives on health care data management, and data science capacity development. The CHOP-UB collaboration is focused on building capacity through comprehensive training programs, which are designed and customized for local Botswana health care professionals' needs. These programs emphasized the use of health informatics tools, and the importance of data-driven decision-making in clinical settings. Key factors in this academic GHI partnership's success have been a focus on local context (eg, socioeconomic, cultural, and geographic), use of robust evaluation frameworks [35], focus on long-term outcomes, scalability, and consideration of mitigating barriers to informatics tools adoption, infrastructure deficits, and resistance to change.

A defining characteristic of the partnership has been the commitment to knowledge transfer. There has been a particular focus on knowledge transfer to empower local staff to independently manage and maintain technological advancements, thereby ensuring long-term impact and sustainability. Rather than creating dependency, the programs are designed to empower local health care workers to independently manage and adapt digital tools to meet the evolving needs of the local health system. This approach is critical for ensuring sustainability and meaningful impact. The partnership has adopted a coleadership model where leaders from both CHOP and UB bring skills and expertise ensuring local health care staff are actively involved in capacity building to achieve this knowledge transfer.

Botswana is currently making strides in implementing advanced health informatics solutions to enhance the quality of health care services across facilities. Notable efforts include electronic medical record rollouts, revitalizing primary health care systems, and the development of the health information exchange and the Botswana eHealth Enterprise Architecture. These efforts are geared toward improving patient outcomes, streamlining data management, and facilitating near-real-time clinical decision-making. The CHOP-UB academic partnership's success exemplifies the potential benefit of international collaborations in transforming health care delivery through innovative informatics solutions in low-resource settings [36].

Other stellar examples of collaborative international health informatics efforts include those led by Japan to address infectious diseases prevalent in developing nations through the Global Health Innovative Technology Fund, a public-private partnership [37], and through SATREPS (Science and Technology Research Partnership for Sustainable Development) [38]. In addition, regional partnerships among LMICs (sometimes termed "South-South") in health informatics include those among South and Southeast Asian countries, sub-Saharan African nations [39,40], and Latin American nations [7]. These efforts demonstrate the value of cross-national strengthening of HIS to promote global health outcomes. The 2022 International Medical Informatics Association Yearbook contains the most recent updates on the status of health informatics societies around the world, including Asian, Latin American, and African nations [41,42].

Lessons Learned

This case study offers several important lessons for academic GHI partnerships.

1. Contextual relevance is vital: successful collaborations require a deep understanding of local health system needs, real-life workflows during patient encounters, cultural dynamics, and HIS infrastructure realities. Tailoring solutions to these conditions has the potential to enhance adoption and sustainability.

XSL•FO
RenderX

2. Coleadership builds trust and equity: shared leadership between institutions promotes equitable partnerships and ensures both global and local stakeholders contribute meaningfully to projects and decision-making.
3. Capacity building enables sustainability: investing in local capacity through knowledge transfer and educational initiatives supports sustainable implementation. Intentionally designing knowledge transfer promotes maintenance skills and future innovation of health information technology by local experts and clinical champions.
4. Evaluation strengthens accountability: using robust evaluation frameworks not only measures impact but also guides program adaptation and scalability.
5. Infrastructure and policy alignment are key: tech solutions are more effective when aligned with national strategies and supported by strong policy environments.

Future Research Directions

GHI academic collaborations can undoubtedly draw on HIS technology intervention strengths in high-income settings; however, opportunities to truly meet the needs of diverse global health systems remain. Potential future directions include (1) centering community-based participatory research (CBPR) approaches to colead research with local experts, (2) embracing a post-growth mentality focused on quality of life and equitable distribution of technological benefits (using technology to improve quality and reach of existing health systems rather than solely focusing on growth) to develop GHI interventions, and (3) supporting frameworks for evaluation and scaling that address how to move beyond "pilotitis," and toward sustainable technology implementation and use.

CBPR approaches promote effective, long-term, and equitable collaborations between research teams and community-based organizations with community members representing underserved groups [43]. Fundamentally, the approach centers end-users from marginalized communities in all stages of research, from initial problem-statement generation to design, implementation, and evaluation of solutions. In health informatics research, CBPR applies principles borrowed from health equity and disability rights activism of "Nothing about us without us" and "Center the margins" into studies so that the final health technology product does not widen, maintain, or create novel disparities but instead meets the needs of those most affected by social drivers of health and systemic injustice [44,45].

Throughout this viewpoint, we have pointed to challenges in centering LMIC researchers as experts, power sharing, and building strong community relationships, which can all be addressed by combining CBPR and GHI. For example, incorporating the CBPR conceptual model into GHI research can help center traditional and Indigenous knowledge systems, balance action and research, and prompt colearning and coleadership [46,47]. However, by nature, CBPR has no one-size-fits-all approach and will need to be thoughtfully incorporated into GHI. Specifically, capacity building to ensure that researchers and organizations in LMICs can proactively safeguard themselves against exploitation and co-optive CBPR practices, which can foster beneficial long-term relationships and global partnerships.

One caution against leveraging HI lessons from high-income settings and applying them to LMIC contexts is that a constant search for novel and high-performing yet brittle interventions may not be suitable for lower-resource settings. IT solutions are important in all health environments, but local design input, transparency from large IT companies involved in these projects, and local control are crucial to success in diverse environments and cultures. Moving forward, GHI researchers should look to interventions that emphasize commons-based ownership (eg, of GHI interventions), voluntary simplicity, and learning from the traditional wisdom developed and preserved by many cultures globally [23,27]. Post-growth solutions might necessitate a departure from techno-solutionism, an understanding that technology can facilitate solutions, but truly addressing health inequity will require focusing on structural inequities and local innovation in health care delivery [48].

Finally, given longstanding GHI "pilotitis" issues, future research endeavors should focus on leveraging transient grant funding to develop pilots and then help local organizations sustain long-term research. This may look like assistance and support to receive grants supporting postimplementation monitoring, capacity building to ensure that local community members are well-positioned to continue deriving value from knowledge generated by GHI research (eg, entrepreneurship), as well as ensuring principles, such as commons-based ownership and voluntary simplicity. In addition, advocating for policy change is another important avenue to orient grant organizations toward the importance of long-term monitoring and support of successful GHI interventions.

Conclusions

This viewpoint identified current gaps in the literature on academic GHI implementation and underscored the need for international academic collaborations. A path forward to develop mutually beneficial partnerships and execute projects across the project life cycle phases was outlined, and to circumvent the concept of "pilotitis" was described. The authors propose a call to action to reduce facilitation barriers, strengthen implementation, and GHI knowledge dissemination and translation. This includes developing more appropriate evaluation metrics for GHI interventions outside of publications that encapsulate collaborations' impact. For example, an open register of digital health systems, such as Digital Square [49], with open data on sites, patients, technology end-users, disease coverage, longevity, etc, is an alternative or complementary metric of the scope and success of academic GHI partnerships compared to publications.

Academic institutions working on GHI interventions could collaborate to establish a global community of practice in which health informatics recommended guidelines and standards could be successfully developed, implemented, adopted, and adapted to suit individual resources (ie, human and financial). This will require more funding and support that accounts for realistic timelines given indirect costs and unique challenges to GHI

XSL•FO
RenderX

projects that differentiate them from other health informatics projects in high-income countries. It is critical to reduce barriers to care and implementation through transparent communication, knowledge transfer of lessons learned, and proven techniques to promote sustainable, mutually beneficial GHI academic collaborations. Thus, partnerships between academic institutions and industries spanning diverse countries and geographies are urgently required to address global challenges that transcend national borders without further propagating entrenched inequities [15].

Acknowledgments

The authors would like to acknowledge the members of the Global Health Informatics Working Group of the American Medical Informatics Association for their input on numerous discussions that have led to this viewpoint. Our authors bring extensive knowledge and lived experiences of global health informatics in low- and middle-income countries (LMICs), but a majority of our authors are from academic institutions based in high-income countries. Overall, 3 authors from this paper are originally from LMICs with one still based at an institution in an LMIC. The authors would like to acknowledge the use of umbrella terms, namely LMICs, in this paper. We do not believe that these terms adequately capture the diversity of culture, skills, expertise, and lived experiences of researchers from these settings. However, given the lack of another commonly used terminology, we will use these terms in our viewpoint with the hopes that this creates discourse toward the development of more representative language in the future.

Funding

This study received no external funding.

Authors' Contributions

EAC: Conceptualization, project administration, writing – original draft, and writing – review and editing
FH: Conceptualization, project administration, writing – original draft, and writing – review and editing
OJBDW: Writing – original draft and writing – review and editing
BM: Writing – original draft and writing – review and editing
ASK: Writing – original draft and writing – review and editing
HF: Writing – original draft and writing – review and editing
ALJ: Writing – original draft and writing – review and editing
JWG: Writing – original draft and writing – review and editing
KLM: Writing – original draft and writing – review and editing
SC: Writing – original draft and writing – review and editing

Conflicts of Interest

JWG receives funding from NHLBI (grant R01HL167811; R01HL177003), NIH (grant 1OT20D038065-01; 1R25OD039834-01), Clarity, Bunkerhill foundation, LUNIT. She has received conference travel support to attend the National Comprehensive Cancer Network meeting and APPOS oncology meeting. She has received honoraria for speaking fees from Cook Medical. She serves on several advisory boards including the AHA debiasing clinical care algorithms (DECCA), American College of Radiology AI advisory council and the council of medical specialty societies encoding equity initiative. She is a board member of SIIM and an associate editor for RSNA:AI journal. SC is a health equity informatics consultant to imagine pediatrics.

References

1. Eysenbach G. What is e-health? J Med Internet Res 2001;3(2):E20. [doi: 10.2196/jmir.3.2.e20] [Medline: 11720962]
2. Quintana Y, Safran C. Global health informatics—an overview. In: Global Health Informatics: Academic Press; 2017:1-13. [doi: 10.1016/B978-0-12-804591-6.00001-X]
3. Fraser HSF, Zahiri K, Kim N, Kim C, Craig S. The global health informatics landscape and JAMIA. J Am Med Inform Assoc 2023 Mar 16;30(4):775-780. [doi: 10.1093/jamia/ocad024] [Medline: 36869748]
4. Quintana Y, Cullen TA, Holmes JH, Joshi A, Novillo-Ortiz D, Liaw ST. Global health informatics: the state of research and lessons learned. J Am Med Inform Assoc 2023 Mar 16;30(4):627-633. [doi: 10.1093/jamia/ocad027] [Medline: 36924133]
5. Novillo-Ortiz D. Intergovernmental collaboration in global health informatics. In: Global Health Informatics: Academic Press; 2017:264-287. [doi: 10.1016/B978-0-12-804591-6.00013-6]
6. Jaspers MWM, Gardner RM, Gatewood LC, Haux R, Evans RS. An international summer school on health informatics: a collaborative effort of the Amsterdam medical informatics program and IPhiE--the international partnership for health informatics education. Int J Med Inform 2007 Jul;76(7):538-546. [doi: 10.1016/j.ijmedinf.2006.02.008] [Medline: 16542869]

XSL•FO
RenderX

7. Curioso WH, Fuller S, Garcia PJ, Holmes KK, Kimball AM. Ten years of international collaboration in biomedical informatics and beyond: the AMAUTA program in Peru. J Am Med Inform Assoc 2010;17(4):477-480. [doi: 10.1136/jamia.2009.002196] [Medline: 20595317]
8. Huang F, Blaschke S, Lucas H. Beyond pilotitis: taking digital health interventions to the national level in China and Uganda. Global Health 2017 Jul 31;13(1):49. [doi: 10.1186/s12992-017-0275-z] [Medline: 28756767]
9. Shuchman M. The promise and pitfalls of global mHealth. CMAJ 2014 Oct 21;186(15):1134-1135. [doi: 10.1503/cmaj.109-4861] [Medline: 25183722]
10. Waugaman A. From principle to practice: implementing the principles for digital development. : The Principles for Digital Development Working Group; 2016 URL: https://www.healthdatacollaborative.org/fileadmin/uploads/hdc/Documents/Working_Groups/RHIS/A._Standards_and_Tools/3._RHIS_management/3b._Information_and_communication_technology/3-_Digital_Principles_to_Practice.pdf [accessed 2025-11-07]
11. Luna D, Almerares A, Mayan JC III, González Bernaldo de Quirós F, Otero C. Health informatics in developing countries: going beyond pilot practices to sustainable implementations: a review of the current challenges. Healthc Inform Res 2014 Jan;20(1):3-10. [doi: 10.4258/hir.2014.20.1.3] [Medline: 24627813]
12. Faulkenberry JG, Luberti A, Craig S. Electronic health records, mobile health, and the challenge of improving global health. Curr Probl Pediatr Adolesc Health Care 2022 Jan;52(1):101111. [doi: 10.1016/j.cppeds.2021.101111] [Medline: 34969611]
13. Budzinski O, Grebel T, Wolling J, Zhang XJ. Drivers of article processing charges in open access. Scientometrics 2020 Sep;124(3):2185-2206. [doi: 10.1007/s11192-020-03578-3]
14. Verma N, Mamlin B, Flowers J, Acharya S, Labrique A, Cullen T. OpenMRS as a global good: Impact, opportunities, challenges, and lessons learned from fifteen years of implementation. Int J Med Inform 2021 May;149:104405. [doi: 10.1016/j.ijmedinf.2021.104405] [Medline: 33639327]
15. Fraser HSF, Mugisha M, Bacher I, et al. Factors influencing data quality in electronic health record systems in 50 health facilities in Rwanda and the role of clinical alerts: cross-sectional observational study. JMIR Public Health Surveill 2024 Jul 3;10(1):e49127. [doi: 10.2196/49127] [Medline: 38959048]
16. Braa J, Sahay S. The DHIS2 open source software platform: evolution over time and space. In: Global Health Informatics: Massachusetts Institute of Technology; 2017:1-12 URL: https://courses.cs.washington.edu/courses/csep590b/20sp/readings/DHIS2_2017.pdf [accessed 2025-11-07]
17. Reidpath DD, Allotey P. The problem of “trickle-down science” from the global North to the global South. BMJ Glob Health 2019;4(4):e001719. [doi: 10.1136/bmjgh-2019-001719] [Medline: 31406597]
18. Rakotonarivo OS, Andriamihaja OR. Global north-global south research partnerships are still inequitable. Nat Hum Behav 2023 Dec;7(12):2042-2043. [doi: 10.1038/s41562-023-01728-0] [Medline: 37828401]
19. de Mello BH, Rigo SJ, da Costa CA, et al. Semantic interoperability in health records standards: a systematic literature review. Health Technol (Berl) 2022;12(2):255-272. [doi: 10.1007/s12553-022-00639-w] [Medline: 35103230]
20. Mirza M, Kratz M, Medeiros D, et al. Building the foundations of an informatics agenda for global health - 2011 workshop report. Online J Public Health Inform 2012;4(1):ojphi.v4i1.4027. [doi: 10.5210/ojphi.v4i1.4027] [Medline: 23569628]
21. Kiosia A, Boylan S, Retford M, et al. Current data science capacity building initiatives for health researchers in LMICs: global & regional efforts. Front Public Health 2024;12:1418382. [doi: 10.3389/fpubh.2024.1418382] [Medline: 39664549]
22. Heavin C, University College Cork. Editor’s comments: health information systems – opportunities and challenges in a global health ecosystem. JMWAIS 2017;2017(2):1-7. [doi: 10.17705/3jmwa.00027]
23. A review of the challenges and opportunities in implementing health informatics in rural healthcare settings. Int Med Sci Res J 2024;4(5):606-631. [doi: 10.51594/imsrj.v4i5.1158]
24. Bostan S, Johnson OA, Jaspersen LJ, Randell R. Contextual barriers to implementing open-source electronic health record systems for low- and lower-middle-income countries: scoping review. J Med Internet Res 2024 Aug 1;26:e45242. [doi: 10.2196/45242] [Medline: 39088815]
25. Mohammed-Rajput NA, Smith DC, Mamlin B, Biondich P, Doebbeling BN, Open MRS Collaborative Investigators. OpenMRS, a global medical records system collaborative: factors influencing successful implementation. Presented at: AMIA Annu Symp Proc; Oct 22-26, 2011; Washington, DC p. 960-968. [Medline: 22195155]
26. Prinsloo T, Adebesin F. A synthesis of the causes of ICT4D projects’ pilotitis: prioritising the remedies for the SDG2030 agenda. Presented at: IFIP Joint Working Conference on the Future of Digital Work: The Challenge of Inequality; Dec 7-8, 2023. [doi: 10.1007/978-3-031-50154-8_7]
27. Steenhoff AP, Crouse HL, Lukolyo H, et al. Partnerships for global child health. Pediatrics 2017 Oct;140(4):e20163823. [doi: 10.1542/peds.2016-3823] [Medline: 28931576]
28. Kesande M, Jere J, McCoy SI, Walekhwa AW, Nkosi-Mjadu BE, Ndzerem-Shang E. Self-determination in global health practices - voices from the global south. Ann Glob Health 2024;90(1):16. [doi: 10.5334/aogh.4162] [Medline: 38435470]
29. McCoy D, Kapilashrami A, Kumar R, Rhule E, Khosla R. Developing an agenda for the decolonization of global health. Bull World Health Organ 2024 Feb 1;102(2):130-136. [doi: 10.2471/BLT.23.289949] [Medline: 38313156]
30. Reid M, Enanoria W, Stoltey J, et al. The SARS-CoV-2 pandemic: the race to trace: contact tracing scale-up in San Francisco-early lessons learned. J Public Health Policy 2021 Jun;42(2):211-221. [doi: 10.1057/s41271-021-00285-y] [Medline: 34088978]

XSL•FO
RenderX

31. Dayalu R, Wacksman J, Chen M, Loudon M, Lesh N. Adoption and continued use of mobile technology: an analysis of CommCare data. Procedia Eng 2015;107:247-254. [doi: 10.1016/j.proeng.2015.06.079]
32. Sharma V, Kumar N, Nardi B. Post-growth human–computer interaction. ACM Trans Comput-Hum Interact 2024 Feb 29;31(1):1-37. [doi: 10.1145/3624981]
33. Open Concept Lab. URL: https://openconceptlab.org [accessed 2025-08-01]
34. Hovenga EJ. Global health informatics education. Stud Health Technol Inform 2000;57:3-14. [Medline: 10947666]
35. Campbell JI, Aturinda I, Mwesigwa E, et al. The technology acceptance model for resource-limited settings (TAM-RLS): a novel framework for mobile health interventions targeted to low-literacy end-users in resource-limited settings. AIDS Behav 2017 Nov;21(11):3129-3140. [doi: 10.1007/s10461-017-1765-y] [Medline: 28421356]
36. Faulkenberry G, Masizana A, Mosesane B, Ndlovu K. Clinical data flow in Botswana clinics: protocol for a mixed-methods assessment. JMIR Res Protoc 2024 Oct 9;13(1):e52411. [doi: 10.2196/52411] [Medline: 39383523]
37. Slingsby BT, Kurokawa K. The global health innovative technology (GHIT) Fund: financing medical innovations for neglected populations. Lancet Glob Health 2013 Oct;1(4):e184-e185. [doi: 10.1016/S2214-109X(13)70055-X] [Medline: 25104343]
38. Adachi M, Taniguchi K, Hori H, et al. Strengthening surveillance in Ghana against public health emergencies of international concern. Trop Med Health 2022 Oct 28;50(1):81. [doi: 10.1186/s41182-022-00473-w] [Medline: 36307880]
39. Yi S, Yam ELY, Cheruvettolil K, et al. Perspectives of digital health innovations in low- and middle-income health care systems from south and southeast Asia. J Med Internet Res 2024 Nov 25;26:e57612. [doi: 10.2196/57612] [Medline: 39586089]
40. Gala B, Islam MA, Gamage R, Agarwal NK. Health information crisis during COVID-19 in the south Asian region: challenges, experiences, resilience, and collaborative efforts. Proc Assoc Inf Sci Technol 2022;59(1):570-574. [doi: 10.1002/pra2.629] [Medline: 36714424]
41. Mougin F, Hollis KF, Soualmia LF. Inclusive digital health. Yearb Med Inform 2022 Aug;31(1):2-6. [doi: 10.1055/s-0042-1742540] [Medline: 36463863]
42. Yearbook of Medical Informatics: Thieme Medical Publishers; 2022, Vol. 1. [doi: 10.1055/s-00034612]
43. Unertl KM, Schaefbauer CL, Campbell TR, et al. Integrating community-based participatory research and informatics approaches to improve the engagement and health of underserved populations. J Am Med Inform Assoc 2016 Jan;23(1):60-73. [doi: 10.1093/jamia/ocv094] [Medline: 26228766]
44. Veinot TC, Mitchell H, Ancker JS. Good intentions are not enough: how informatics interventions can worsen inequality. J Am Med Inform Assoc 2018 Aug 1;25(8):1080-1088. [doi: 10.1093/jamia/ocy052] [Medline: 29788380]
45. Rahman A, Nawaz S, Khan E, Islam S. Nothing about us, without us: is for us. Res Involv Engagem 2022 Aug 4;8(1):39. [doi: 10.1186/s40900-022-00372-8] [Medline: 35927767]
46. Wallerstein N, Duran B. Community-based participatory research contributions to intervention research: the intersection of science and practice to improve health equity. Am J Public Health 2010 Apr 1;100 Suppl 1(Suppl 1):S40-S46. [doi: 10.2105/AJPH.2009.184036] [Medline: 20147663]
47. Hall BL, Tandon R. Decolonization of knowledge, epistemicide, participatory research and higher education. Research for All 2017;1(1):6-19. [doi: 10.18546/RFA.01.1.02]
48. Benjamin R. Race After Technology: Abolitionist Tools for the New Jim Code: John Wiley & Sons; 2019.
49. Digital square. Path. 2025. URL: https://www.path.org/who-we-are/programs/digital-health/digital-square/ [accessed 2025-08-01]

Abbreviations

CBPR: community-based participatory research
CHOP: Children's Hospital of Philadelphia
GHI: global health informatics
HIS: health information system
LMIC: low- and middle-income country
mHealth: mobile health
UB: University of Botswana

XSL•FO
RenderX

Edited by A Benis; submitted 08.10.24; peer-reviewed by A Hidki, C Nguyen-Truong, Y Rivera; revised version received 01.08.25; accepted 23.10.25; published 28.11.25.

Please cite as:
Campbell EA, Holl F, Bear Don't Walk IV OJ, Mosesane B, Kanter AS, Fraser H, Joseph AL, Gichoya JW, Mauco KL, Craig S
Gaps and Pathways to Success in Global Health Informatics Academic Collaborations: Reflecting on Current Practices
JMIR Med Inform 2025;13:e67326
URL: https://medinform.jmir.org/2025/1/e67326
doi:10.2196/67326

© Elizabeth A Campbell, Felix Holl, Oliver J Bear Don't Walk IV, Badisa Mosesane, Andrew S Kanter, Hamish Fraser, Amanda L Joseph, Judy Wawira Gichoya, Kabelo Leonard Mauco, Sansanee Craig. Originally published in JMIR Medical Informatics (https://medinform.jmir.org), 28.11.2025. This is an open-access article distributed under the terms of the Creative Commons Attribution License (https://creativecommons.org/licenses/by/4.0/), which permits unrestricted use, distribution, and reproduction in any medium, provided the original work, first published in JMIR Medical Informatics, is properly cited. The complete bibliographic information, a link to the original publication on https://medinform.jmir.org/, as well as this copyright and license information must be included.

XSL•FO
RenderX

Resilience in the Face of Disruption: Viewpoint on the CrowdStrike Incident in July 2024

Christopher R Dennis, CPHIMS, BCPS, MMCi, PharmD; Christopher S Evans, MD, MPH; Kathleen Duckworth, RN NI-BC, DNP; Misty McLawhorn Skinner, RN NI-BC, MSN; John Hanna, MD; Tanya Thompson, CPHIMS, MT (ASCP), CHCIO, MMCi; Donette Herring, BSN, MBA; Richard J Medford, MD

Department of Information Services, ECU Health, 2190 Beasley Drive, Greenville, North Carolina, United States

Corresponding Author:
Christopher R Dennis, CPHIMS, BCPS, MMCi, PharmD
Department of Information Services, ECU Health, 2190 Beasley Drive, Greenville, North Carolina, United States

Abstract

In an era where health care is increasingly dependent on digital infrastructure, the resilience of health IT systems has become a cornerstone of patient safety and operational continuity. As cyber threats grow in frequency and sophistication, health care organizations have turned to advanced cybersecurity tools to safeguard their systems. Yet even the most robust defenses can falter. On July 19, 2024, a routine update from a widely used cybersecurity platform triggered a widespread IT disruption. A flawed sensor configuration led to 8647 “blue screen of death” (BSOD) events, with 729 devices requiring manual remediation. What unfolded was not just a technical crisis but a test of organizational agility, collaboration, and resilience. This viewpoint traces the response to that disruption, highlighting the pivotal role of clinical informaticists and the coordinated efforts that enabled a rapid recovery. From the formation of an incident response team to the triage and mitigation of impacted systems, the response was swift and strategic. Clinical informaticists emerged as key players, bridging the gap between technical teams and frontline care providers. They identified workflow disruptions, facilitated communication, and ensured that patient care remained as uninterrupted as possible. Despite the scale of the outage, operations continued with minimal disruption—thanks to early recognition, decisive action, and cross-disciplinary collaboration. This incident underscored the importance of a well-practiced response plan, clear communication channels, and the integration of clinical expertise in technical recovery efforts. As we reflect on this event, several lessons emerge: the need for continuous refinement of incident response strategies, the value of regular training exercises, and the critical role of clinical informatics in navigating digital crises. This paper calls for a renewed commitment to building resilient health IT ecosystems—ones that can withstand disruption and continue to support the delivery of safe, effective care.

(JMIR Med Inform 2025;13:e69958) doi:10.2196/69958

KEYWORDS

computer security; clinical informatics; health information systems; incident response; incident command system; crowdstrike health IT disruption; IT service management; system crash recovery

Introduction

Cybersecurity and the related disruptions to critical IT systems are a major concern for many organizations due to risks associated with data breaches. This is particularly true in health care organizations due to their unique risk profiles. Health care facilities are high-value targets due to their size, technological dependence, sensitive data, and vulnerability to disruptions [1]. Furthermore, there has been an increase in cyberattacks in recent years, as evidenced by a 93% increase in large breaches reported by the Office for Civil Rights under the Department of Health and Human Services between 2018 and 2022, many involving ransomware attacks [1].

The health care industry continues to deal with a barrage of attacks, with over 1400 cyberattacks globally per week [2]. The range of attack strategies used by threat actors includes social engineering, phishing, distributed denial of service, botnets, zero-day exploits, person-in-the-middle, malware, adware, and ransomware [3]. When hospitals are forced to implement downtime procedures as a result of a successful attack, the average duration is upwards of 24 days, at an average cost of US $10 million [2]. There are additional risks beyond the direct impacts to systems and the operations of the affected organizations. Cyberattacks often result in data breaches that can impact patients receiving care at the affected institutions. In 2024, over 250 million individuals were affected by health care security breaches, with 190 million of those involving a ransomware attack on the Change Healthcare network [4]. Health care entities that endure these kinds of attacks may also incur legal ramifications and reputational damage in addition to the financial impacts [3]. The legal ramifications include violations related to the Health Insurance Portability and Accountability Act (HIPAA), since the presence of any type of

XSL•FO
RenderX

malware on a covered entity's or business associate's computer is considered a security incident under the HIPAA security rule [5]. Compromised patient data can be misused for identity theft, blackmail, and even insurance fraud. Even if the threat actor does not use the information directly, it can still be disseminated on illegal forums, further increasing the risk of misuse [3].

Defense against malicious actors requires continuous vigilance and system hardening against potential attack vectors. The Center for Internet Security publishes best practices called Critical Security Controls (current version, as of this writing, is version 8.1), which detail the steps organizations can take to guard against attacks [6]. CrowdStrike is a leading cybersecurity firm that provides services to many organizations, both inside and outside of the health care sector, to achieve these goals. Among these services is the Falcon platform, which is designed to stop breaches and protect organizations from a variety of cybersecurity threats.

On July 19, 2024, at 04:09 UTC (12:09 AM local time), CrowdStrike released a sensor configuration update to Microsoft Windows systems to maintain the protection mechanisms of the Falcon platform. This update triggered a logic error, which resulted in a system crash and "blue screen of death" (BSOD) on impacted systems. This error was quickly identified by the team at CrowdStrike, and the sensor configuration update was swiftly remediated on July 19, 2024, at 05:27 UTC (1:27 AM local time). The specific machines that were impacted needed to be running the Falcon sensor for Microsoft Windows versions 7.11 and above, be online between July 19, 2024, 04:09 UTC and July 19, 2024, 05:27 UTC, and have downloaded the flawed configuration update during that interval [7].

Importantly, the system failure that occurred in this case was not the result of a cyberattack, but the impacts to critical systems and the recovery strategies used shared similarities with those that would be enacted if systems had been compromised due to a breach. While the underlying cause of the logic error was quickly identified and remediated by CrowdStrike, the downstream impacts to customers were substantial and required a coordinated strategy to mitigate.

Many health care workflows are dependent upon seamless integration of otherwise disparate systems. For example, radiology practices require coordination between imaging devices, a Picture Archiving and Communication System, and the electronic health record (EHR). Each of these components represents an independent point of failure in the event of a major health IT outage, such as the one encountered with the CrowdStrike incident [8]. Considering the time-sensitive nature of significant disruptions in health IT, it is crucial to have clear and effective communication processes, especially in large, geographically dispersed health care systems that rely on health IT infrastructure for patient care and operations.

The CrowdStrike incident highlighted the significant risks associated with workstation downtime, including medication errors, inaccessibility of images and test results, and the need to delay procedures. During the incident, many health care workflows were disrupted due to the inability to access critical patient information on affected workstations (eg, radiology images). In addition, the inability to access lab results on time further compounded the delays in diagnosing and treating patients. Although the EHR itself remained operational, the downtime of numerous workstations could have led to delays in reviewing and acting upon patient information, ultimately impacting the quality of care provided. These risks are well-documented in literature, emphasizing the importance of proactive planning for EHR downtime [9-12].

The primary objective of this viewpoint is to offer real-world insights following a major IT disruption by exploring ECU Health's response to the CrowdStrike incident. In addition, the authors share lessons learned from leveraging a multidisciplinary team across Information Services (IS), including a well-established network of embedded clinical informaticists, to navigate the response efforts. Finally, we describe opportunities for improvement that should help similar organizations address similar challenges in the future.

Background

ECU Health is a rural academic health care system that serves 29 counties in eastern North Carolina. The health care system comprises 9 hospitals spanning in size and scope from a large academic level 1 trauma center to critical access hospitals. Within this network are 185 primary care and specialty clinics in 110 locations, plus other outpatient facilities, home health, hospice, and wellness centers [13]. Together, these ambulatory practices complete over 800,000 visits annually. All ECU Health facilities are served by an enterprise-wide IS division, which oversees all aspects of health IT, including hardware, software (eg, EHR and clinical applications), networking, end-user support (EUS), and cybersecurity.

The clinical informatics team within the IS division, consisting of 19 full-time informaticists and 7 full-time informatics education specialists with diverse clinical and nonclinical expertise, serves as a critical interface between clinical teams, operational leaders, and health IT professionals. These informaticists integrate health care sciences, computer science, and information science to manage and communicate data, information, and knowledge, thereby enhancing patient care, improving health outcomes, and supporting decision-making processes [14,15].

Existing Incident Response Strategy

ECU Health's incident response strategy includes the formation of the incident response team, initial assessment and triage of the situation, and identifying key actions to mitigate impact. When an IS team member is notified of an incident affecting multiple users, the first escalation is to the IT service management team for vetting and validation. The incident is next escalated to the IS executive on call, who determines whether it should be categorized as a Priority 1 (P1)–critical outage. Incidents are categorized according to their urgency and impact, as shown in Table 1. Patient care incidents are prioritized higher than nonpatient care issues. If categorized as a P1, a major incident is created within the enterprise ticket management solution, and the operational executives on call for the impacted facilities are notified. A bridge line (ie, a

XSL•FO
RenderX

dedicated conference call line for coordinating team members) is opened, and command centers are mobilized at the impacted sites. The command center at the medical center serves as the central hub for local hospital operations and as a physical location for the systemwide command center. The systemwide command center is staffed with IS and operational leaders. Regional command centers are staffed with local operational leaders. Each command center's primary roles are to centralize communications, facilitate issue escalation, and disseminate updates as issues are corrected and functionality is restored. Additional bridge lines are opened within IS, including a technical one to problem-solve issues and determine impacted applications.

Table . Impact and urgency matrix used to categorize incidents.

Urgency	Hospital or organization-wide	Multiple users	Single user: patient care	Single user: nonpatient care
Critical	Critical (P1)[a]	Critical (P1)	High (P2)[b]	Medium (P3)[c]
High	Critical (P1)	High (P2)	Medium (P3)	Medium (P3)
Medium	High (P2)	Medium (P3)	Medium (P3)	Low (P4)[d]
Low	Medium (P3)	Low (P4)	Low (P4)	Low (P4)

[a] P1:priority 1.

[b] P2:priority 2.

[c] P3:priority 3.

[d] P4:priority 4.

During the initial assessment and triage phase, the IS command center relies on bridge line communication to determine the scope of impacted applications and incident tracking. All incidents are tracked through the ticket management system. As new incidents are reported, they are tracked as "children" of the "parent" incident if found to be related.

Finally, actions are taken to address the situation, including isolating the impacted systems, communicating with staff and patients, and initiating interventions to correct the underlying problems or implementing short-term alternatives. These measures ensure that the immediate risks are mitigated and that all stakeholders are informed about the ongoing efforts. By isolating the affected systems, further spread of the issue is prevented, while clear communication helps maintain trust and transparency. Timely initial interventions are crucial for stabilizing the situation and providing temporary solutions until a permanent fix can be implemented. This comprehensive approach helps manage the incident effectively and minimizes disruptions to operations.

Timeline of Events, Organizational Impacts, and Remediation Efforts

Following the CrowdStrike update, initial reports of devices receiving the BSOD began on July 19 at 1:30 AM. The sequence of events from the initial BSOD reports to the closure of the systemwide command center approximately 30 hours later is shown in Table 2.

XSL•FO
RenderX

Table . ECU Health event response timeline for the CrowdStrike incident.

Time	Event
Friday, July 19	
12:09 AM	CrowdStrike releases flawed sensor configuration update
1:27 AM	CrowdStrike remediates the flawed sensor configuration update
1:30 AM	Initial reports of workstations and servers receiving the BSOD[a]
1:38 AM	Initial escalation to Information Services (IS) team members
3:40 AM	Escalation to the IS executive on call and then to operational leadership
4:45 AM	Email notification sent to IS staff indicating the BSOD issue had been traced back to the CrowdStrike update
5:30 AM	The systemwide Incident Command Center was opened
6:00 AM-7:00 AM	Clinical informaticists arrive on site at hospital locations prepared for deployment
6:58 AM	Initial notification for IS personnel to report to their closest system hospital
8:20 AM	Systemwide email indicating that command centers had been activated at all system hospitals; users experiencing BSOD are encouraged to reboot their workstations twice; and for issues with ECU Health mobile devices, docking stations were to be unplugged.
10:49 AM	Staff are encouraged to submit incidents into the ticketing system for individual workstations experiencing BSOD unable to be remediated by staff directly
12:29 PM	Health care system staff informed of potential scammers posing as IT professionals attempting to gain access to computers and files
4:32 PM	Command center at the medical center converted from in-person to remote format; all community hospital command centers closed
5:00 PM	The IS meets to recap the day's events and discuss plans for the weekend
Saturday, July 20	
8:18 AM	The medical center closes its command center

[a]BSOD: blue screen of death.

Across the ECU Health enterprise, there are approximately 14,500 end point devices. There were 8647 BSOD events (approximately 60% of devices) on July 19. Most of these workstations were corrected with a reboot once the remediated sensor configuration update was available. Of those that were not corrected with a reboot, 729 devices required hands-on remediation. Approximately 150 workstation thin clients (ie, machines that rely on a central server for processing power and storage) and 100 ground control workstations (ie, centralized systems used to manage, monitor, and control devices for mobile device management) were reimaged to restore them to a functional state.

There are 3000 Windows servers used across the enterprise. Of these, 700 (23%) deliver Citrix applications, including the EHR. Approximately one-third of these devices were impacted by the flawed sensor configuration update. These servers are nonpersistent, meaning they load a golden image (ie, a preconfigured, fully functional template of a computer system and software configuration) each time they are restarted, and temporary data or changes made during the previous session are discarded. There are approximately 100 other persistent servers that provide other services related to the EHR (eg, print servers).

Users working with impacted devices could not access core applications and systems, including the EHR. However, the EHR itself remained operational throughout this incident, and not all workstations were impacted. IS leadership assessed the availability of the EHR throughout the incident to guide recovery efforts. Timing was a significant factor in keeping the EHR operational, as the incident occurred during a low-user volume period, which prevented the whole fleet of servers that deliver the EHR from being engaged and encountering the BSOD conditions.

In the months preceding this incident, the health care system deployed cell phones to clinical staff to support patient care and internal communication. Many of these were not impacted and enabled workflows such as medication administration to proceed even when nearby workstations were unavailable.

Impacted devices were first rebooted. If the issue persisted, an incident was logged to identify it for hands-on support. These devices were then physically accessed by IS personnel. The devices were booted in "Safe Mode" using a BitLocker recovery key, if necessary, and the flawed channel file (C-00000291*) was manually deleted. The device was then rebooted, which enabled the system to start without the BSOD and allowed an update to the channel file to flow across to the machine. These

XSL•FO
RenderX

steps are described in more detail on CrowdStrike's website [16]. Once CrowdStrike released the remediated sensor configuration, nonpersistent servers were corrected with a reboot. For persistent servers, these were recovered using the method described above in this paragraph, which involves booting them into "Safe Mode" and removing the flawed channel file.

Some workstations required remediation using a USB drive to boot the system with Kali Linux (Offensive Security). The IS team members ensured they had adequate privileges to perform actions on the directory that contains the CrowdStrike drivers. The files within were removed, the device was unmounted, and the machine was restarted without the USB drive so that it boots normally. If these options were unsuccessful, the devices were reimaged to restore them to a functional state.

Role of Clinical Informatics in the Recovery Efforts

As soon as clinical informatics became aware of the issue, their first course of action was to call every unit manager (or charge nurse if the unit manager was unavailable) throughout the health care system to make sure they were informed of the situation and that CIs and other IS team members would be on the units helping to troubleshoot and restore the affected devices. During those phone calls, floor staff were encouraged to self-report any machines that were known to be impacted. This was intended to expedite the discovery process, leading to a more rapid resolution. The manager of the clinical informatics team was a key contributor to the ongoing bridge line calls and kept the systemwide incident command center apprised of progress toward remediation of all devices throughout the enterprise. This enabled resources to be focused on priority areas based on the volume of workstations impacted and the propensity for delays in care if not resolved urgently.

The network of CIs was dispatched across the enterprise to their respective sites to augment remediation efforts in coordination with EUS, service desk, and other IS personnel. As a result of the collaborative relationships clinical informaticists have established with clinical operations, CIs became another contact for reporting impacted devices, particularly if there was difficulty accessing or unfamiliarity with reporting incidents. The presence of CIs also instilled a sense of calm in clinical staff, especially during the early phase of the incident. The scale of the outage, both within and outside of the organization, had the potential to create panic due to concerns that this issue was caused by a cyberattack, as expressed by some end users after perusing social media. The CIs were well-positioned to provide accurate information to staff about the nature of the incident as a faulty system update and not a cyberattack. This assuaged their fears and helped ensure staff were able to focus on completing the necessary steps to rectify the situation and bring all systems back to a functional state.

In an effort to avoid duplicate reporting, CIs used sticky notes to label impacted devices as "reported," which helped to limit confusion and focus recovery efforts. The role of CIs in the incident response varied based on diverse needs across sites and included consistent communication, incident reporting, and at-the-elbow support. At-the-elbow support was particularly beneficial because it helped clinicians identify and execute the remediation steps when necessary while ensuring patient care remained uninterrupted.

Key Lessons Learned

Health care organizations are dependent upon technologies to deliver patient care. Considering the scope of this outage, the risk of interruptions that could adversely impact patient care was high. Due to rapid problem recognition and mobilization of IS staff and resources, ECU Health continued operations as usual despite device outages. This speaks to the level of teamwork exhibited throughout the health care system. Even though ECU Health recovered most devices within 24 hours, there are still opportunities to refine its incident response.

Major incidents such as the CrowdStrike outage highlight the importance of having a well-prepared and accessible incident response plan using a framework such as the Hospital Incident Command System [17]. Incident response plans should include clear roles and responsibilities with clarity around decision-making. These plans should also include regular system audits, updates, and reviews to ensure applicability as health care systems continuously change.

Effective and consistent communication during disruptions is paramount. Device outages were first identified around 1:30 AM on July 19th. However, IS leaders were not notified until hours later, representing a missed opportunity for faster mobilization. ECU Health will refine its process for issuing broader alerts based on the event's criticality. In addition, communication challenges were observed related to reliance upon different devices and modalities for call tree escalation. Risks included issues such as battery performance, devices being out of reach, or susceptibility to outage conditions. ECU Health is exploring synchronization of contact numbers with backup redundancy, such as personal devices, to ensure communication capabilities during after-hours incidents.

Dispatching CIs who have established relationships with front-line clinicians allowed for responsive and multimodal support, including at-the-elbow support and virtual troubleshooting. This was invaluable, as it would have been impossible to manage the scale of this outage with the service desk, EUS, and IS teams alone. The effectiveness of this strategy relies on the informal cross-training of clinical informaticists across IS roles during routine operations. Our experience during this major disruption demonstrated that CIs leveraged their skill sets effectively during this crisis and showed the value of cross-training across roles.

In the months leading up to this outage, ECU Health had been deploying Microsoft Teams as the enterprise collaboration and communication platform. This tool was an effective communication method during this event when other tools were unavailable. Video meeting recordings and artificial intelligence–augmented transcription allowed for rapid summaries for team members joining multiple calls simultaneously. Further investigation will be conducted to

XSL•FO
RenderX

determine whether its availability was due to inherent fault tolerance or whether scenarios exist under which it may not be as reliable as it was during this event. More broadly, ECU Health has identified a need for an enterprise-wide alerting system to enable timely communication during emergencies. Minor challenges were encountered related to authentication processes that were required during the outage, indicating a need for better preparedness in handling such challenges in the future.

Changes Going Forward

Overview

Based on the lessons learned from this event, ECU Health is undertaking several initiatives as part of its commitment to a culture of continuous improvement. One of these initiatives involves enhancements to the IS Incident Command Structure. The key roles of the enhanced IS Incident Command Structure are shown in Figure 1, and their core responsibilities are provided in the following subheadings.

Figure 1. Key roles in the Information Services (IS) incident command system, showcasing the central role of the IS incident commander.



XSL•FO
RenderX

IS Incident Commander (Member of the Information Technology Service Management Team)

The IS incident commander will lead the incident response. This individual will coordinate all response workstreams to understand and communicate impacts to the IS executive lead. Other responsibilities include managing tasking for all IS workstreams to ensure proper prioritization of actions, managing shift planning to ensure adequate staffing throughout the incident, and developing situation reports (SITREPs) for proactive communication, which will provide a single source of truth on the impacts of actions taken. This individual will also review the outputs of workstreams and ensure objectives are met in a timely fashion.

IS Executive Lead (Member of the IS Senior Leadership Team)

The IS executive lead will work closely with the IS incident commander and serve as the primary liaison between IS and senior operational leadership. This leader will be an escalation point for any major blockers that cannot be resolved by the response team leaders. Through their interactions with IS personnel and senior operational leadership, they will maintain visibility into the recovery efforts and understand the impacts of these efforts on the wider organization.

Application Lead (IS Manager or Above)

Application leads will be assigned based on the nature of the outage and the impacted applications. Those assigned to these roles will perform an initial triage to understand the impact of the issue, ensure that people with the correct application knowledge and skill sets are engaged, and identify any relevant vendor contracts for escalation and support. As the situation evolves, they will provide updates to the IS incident commander and assist with the production of the SITREPs. They will support and guide the troubleshooting efforts, assist with tasks as necessary, and request additional resources as needs are identified. As workarounds or solutions to the problem are identified, the application lead will be responsible for specifying the testing requirements for the application to ensure successful resolution and to help anticipate potential unintended consequences.

Technical Lead (IS Manager or Above)

Technical leads will be assigned based on the nature of the outage and the impacted systems. Those assigned to these roles will perform an initial triage to understand the impact of the issue, ensure that people with the correct technical skill sets are engaged, and identify any relevant vendor contracts for escalation and support. As the situation evolves, they will provide updates to the IS incident commander and assist with the production of the SITREPs. They will support and guide the troubleshooting efforts, assist with tasks as necessary, and request additional resources as needs are identified. As workarounds or solutions to the problem are identified, the application lead will be responsible for specifying the testing requirements to ensure successful resolution and to help anticipate potential unintended consequences.

Communication Lead (Member of the IT Service Management Team)

The communication lead is responsible for controlling the messaging to staff throughout the enterprise. Examples of this messaging may include unscheduled downtime notices or IS outage communications. They will work with the operations communication team if responsibility for external communication needs to be delegated. Any requests for information will be triaged by this lead, and their response should be consistent with other messaging that is disseminated more broadly within the organization.

Logistics Lead (Supervisor, Manager, or IS Team Member)

The logistics lead is responsible for coordinating and instructing on-site resources and works closely with the application and technical leads to ensure these resources are appropriately prioritizing the work to be done. This lead is responsible for both the human resources and any equipment that is necessary to resolve the incident. This lead receives updates from on-site resources and shares this information with the application and technical leads as appropriate.

Cybersecurity Lead (Manager or Above)

The cybersecurity lead directs activities that are related to incidents stemming from cybersecurity events. This lead participates in the incident response, engages risk management and the legal team as appropriate, and ensures appropriate communication and information collection relevant to the current cybersecurity risk state. In addition to these updates to the IS incident command structure, ECU Health will conduct tabletop exercises and major incident refresher training. Tabletop exercises will involve reviewing example scenarios, and team leads will walk through the actions they would take if the scenario actually takes place. Major incident refresher training will help staff become aware of their responsibilities during these situations so they can confidently act to quickly bring these situations to a successful resolution.

A More Resilient Health Care System

This viewpoint focuses primarily on the ways ECU Health took targeted actions to mitigate an event that could have been catastrophic for the organization. It is equally important to consider opportunities to make the health care system more resilient as a whole. One such proposal would be to shift the culture toward a position of resilience that ensures clinical workflows are carefully considered and changes are thoroughly tested in simulated environments before being implemented to limit the risk of major interruptions [18]. While such a recommendation may be challenging to implement at scale, if successful, this would go a long way toward shoring up confidence and trust in these vendors and demonstrating their commitment to preventing major disruptions in the future.

Major health IT disruptions also highlight important social and economic inequalities that are pervasive in health care. As compared with smaller institutions, larger organizations often have the capital to invest more heavily in cybersecurity prevention measures and the ability to mobilize resources more

XSL•FO
RenderX

quickly when a disruption event occurs [19]. This mismatch can further exacerbate existing disparities in care by causing additional delays in delivery. A truly resilient health care system would ensure that these gaps are closed.

Conclusions

Major IT disruptions have the potential to adversely impact the delivery of patient care services. In addition, the CrowdStrike outage is estimated to have caused US $1.9 billion in losses to the health care industry [20]. This viewpoint emphasizes the critical role clinical informaticists can play in supporting health care organizations in times of crisis. By having a well-defined incident response plan, organizations can mobilize resources quickly to restore services and ensure clinicians have the tools they need to deliver care and mitigate many of the potential financial harms.

Widespread health care IT disruptions in geographically dispersed rural health care systems pose challenges for timely remediation and continuity of clinical operations while ensuring patient safety. Following the CrowdStrike outage in the summer of 2024, ECU Health relied on coordination and collaboration between multiple teams within IS, including a network of clinical informaticists integrated across practice settings. Lessons learned included the need for continuous commitment and refinement of a systemwide approach to incident response plans, clear communication channels with contingency plans if communications are disrupted, and the value of regular training, such as drills or tabletop exercises, for incident response teams. Through the diligence and collaboration of our multidisciplinary teams, IS teams, and CIs, ECU Health demonstrated resilience and adaptability to ensure we are better prepared for future challenges and remain committed to delivering uninterrupted, high-quality patient care.

Acknowledgments

The authors would like to acknowledge Joshua Smith, Wright Barbour, Brian King, and Lynette Timberlake for their contributions in ensuring that this work accurately conveys the actions taken by ECU Health to recover from this event and the plans established for mitigating future disruptions.

Data Availability

Data sharing is not applicable to this article as no datasets were generated or analyzed during the production of this viewpoint.

Authors' Contributions

CRD, CSE, and RJM conceptualized the viewpoint. CRD and CSE drafted the initial manuscript. TT validated the accuracy of the timeline and organizational strategy. KD and MMS validated the role of informaticists in the response. RJM managed the project.

Conflicts of Interest

None declared.

References

1. Healthcare sector cybersecurity. Office of the Assistant Secretary for Preparedness and Response. 2023 Dec. URL: https://aspr.hhs.gov/cyber/Documents/Health-Care-Sector-Cybersecurity-Dec2023-508.pdf [accessed 2024-08-08]
2. Gates L. Cyber attacks on interoperable electronic health records: a clear and present danger. Mo Med 2024;121(1):6-9. [Medline: 38404433]
3. Types of threat actors that threaten the healthcare sector. US Department of Health and Human Services. URL: https://www.hhs.gov/sites/default/files/types-threat-actors-threaten-healthcare.pdf [accessed 2025-05-06]
4. Alder S. The biggest healthcare data breaches of 2024. The HIPAA Journal. URL: https://www.hipaajournal.com/biggest-healthcare-data-breaches-2024/ [accessed 2025-05-06]
5. Fact sheet: ransomware and HIPAA. US Department of Health and Human Services. URL: https://www.hhs.gov/hipaa/for-professionals/security/guidance/cybersecurity/ransomware-fact-sheet/index.html [accessed 2025-05-06]
6. CIS critical security controls implementation groups. Center for Internet Security. URL: https://www.cisecurity.org/controls/implementation-groups [accessed 2024-08-22]
7. Technical details: Falcon content update for Windows hosts. CrowdStrike. URL: https://www.crowdstrike.com/blog/falcon-update-for-windows-hosts-technical-details/ [accessed 2024-08-08]
8. Gowda V, Alkasab T, Gupta R, et al. The CrowdStrike incident and practice disruption: IT concepts to address business continuity. Acad Radiol 2025 May;32(5):3092-3095. [doi: 10.1016/j.acra.2025.02.005] [Medline: 39971701]
9. Proactive planning for EHR downtime. MedPro Group. URL: https://www.medpro.com/proactive-planning-EHR-downtime [accessed 2025-07-01]
10. Larsen E, Hoffman D, Rivera C, Kleiner BM, Wernz C, Ratwani RM. Continuing patient care during electronic health record downtime. Appl Clin Inform 2019 May;10(3):495-504. [doi: 10.1055/s-0039-1692678] [Medline: 31291677]

XSL•FO
RenderX

11. Larsen E, Fong A, Wernz C, Ratwani RM. Implications of electronic health record downtime: an analysis of patient safety event reports. J Am Med Inform Assoc 2018 Feb 1;25(2):187-191. [doi: 10.1093/jamia/ocx057] [Medline: 28575417]
12. Mutair AA, Alhumaid S, Shamsan A, et al. The effective strategies to avoid medication errors and improving reporting systems. Medicines (Basel) 2021 Aug 27;8(9):46. [doi: 10.3390/medicines8090046] [Medline: 34564088]
13. System of care. ECU Health. URL: https://www.ecuhealth.org/about-us/system-of-care/ [accessed 2024-08-08]
14. About ANIA. American Nursing Informatics Association (ANIA). URL: https://www.ania.org/about-us [accessed 2024-09-17]
15. HIMSS TIGER committee informatics definitions. Healthcare Information and Management Systems Society (HIMSS). URL: https://www.himss.org/sites/hde/files/media/file/2019/12/06/tiger-initiative-informatics-definitions-v3.0-june-2018.pdf [accessed 2024-09-17]
16. Remediation and guidance hub: channel file 291 incident. CrowdStrike. URL: https://www.crowdstrike.com/falcon-content-update-remediation-and-guidance-hub/ [accessed 2024-08-16]
17. Hospital Incident Command System (HICS) Guidebook. California Emergency Medical Services Authority. 2014. URL: https://emsa.ca.gov/wp-content/uploads/sites/71/2017/09/HICS_Guidebook_2014_11.pdf [accessed 2024-08-22]
18. Kramer DB, Fu K. Promoting the resilience of health care information systems-the day hospitals stood still. JAMA Health Forum 2024 Nov 1;5(11):e243968. [doi: 10.1001/jamahealthforum.2024.3968] [Medline: 39602106]
19. Abdullah F. Social and ethical implications of the 2024 CrowdStrike vulnerability: a cybersecurity case study. : University of North Texas; 2024. [doi: 10.5281/zenodo.15468219]
20. Diaz N. CrowdStrike outage expected to cost healthcare $1.9B: report. : Beckers Hospital Review; 2024 URL: https://www.beckershospitalreview.com/healthcare-information-technology/cybersecurity/crowdstrike-outage-expected-to-cost-healthcare-1-9b-report/ [accessed 2025-06-30]

Abbreviations

BSOD: blue screen of death
EHR: electronic health record
EUS: end-user support
HIPAA: Health Insurance Portability and Accountability Act
IS: Information Services
SITREP: situation report

Edited by A Coristine; submitted 12.12.24; peer-reviewed by C Dameff, M Benhassine; revised version received 03.07.25; accepted 11.07.25; published 02.09.25.

Please cite as:
Dennis CR, Evans CS, Duckworth K, Skinner MM, Hanna J, Thompson T, Herring D, Medford RJ
Resilience in the Face of Disruption: Viewpoint on the CrowdStrike Incident in July 2024
JMIR Med Inform 2025;13:e69958
URL: https://medinform.jmir.org/2025/1/e69958
doi:10.2196/69958

© Christopher R Dennis, Christopher S Evans, Kathleen Duckworth, Misty McLawhorn Skinner, John Hanna, Tanya Thompson, Donette Herring, Richard J Medford. Originally published in JMIR Medical Informatics (https://medinform.jmir.org), 2.9.2025. This is an open-access article distributed under the terms of the Creative Commons Attribution License (https://creativecommons.org/licenses/by/4.0/), which permits unrestricted use, distribution, and reproduction in any medium, provided the original work, first published in JMIR Medical Informatics, is properly cited. The complete bibliographic information, a link to the original publication on https://medinform.jmir.org/, as well as this copyright and license information must be included.

XSL•FO
RenderX

Integration of Data and Information Systems Into the Health Data Strategy

Martin Komenda[1,2], PhD; Jakub Gregor[1,2], PhD; Daniel Klimeš[1,2], PhD; Tomáš Pavlík[1,2], PhD; Milan Blaha[1,2], PhD; Vladimíra Těšitelová[2], MSc, LLM; Ondřej Májek[1,2], PhD; Ondřej Ngo[1,2], PhD; Renata Chloupková[1,2], MSc; Karel Hejduk[1,2], MSc; Lenka Šnajdrová[1,2], PhD; Jiří Jarkovský[1,2], PhD; Jan Mužík[1,2], PhD; Petra Růžičková[1,2], MSc; Vlastimil Válek[3,4], Prof Dr; Ladislav Dušek[1,2], Prof Dr

[1]Institute of Biostatistics and Analyses, Masaryk University, Faculty of Medicine, Brno, Czech Republic

[2]Institute of Health Information and Statistics, Palackého náměstí 4, P.O.BOX 60, Prague, Czech Republic

[3]Ministry of Health of the Czech Republic, Prague, Czech Republic

[4]Department of Radiology and Nuclear Medicine, Masaryk University, Faculty of Medicine, Brno, Czech Republic

Corresponding Author:
Martin Komenda, PhD
Institute of Biostatistics and Analyses, Masaryk University, Faculty of Medicine, Brno, Czech Republic

Abstract

Integrating data and information systems into national health strategies is crucial in addressing the growing health care demands. This increase is driven by an aging population and the rising prevalence of chronic diseases. Such systems enable the collection, analysis, and publication of health data and provide critical insights based on data-driven decision-making that support policy decisions, health interventions, and service delivery. Moreover, the systems enhance the capacity for public health surveillance and enable health authorities to monitor health trends, predict disease outbreaks, and effectively manage health crises such as the recent COVID-19 pandemic. This paper highlights the key aspects and characteristics that, according to international references, a well-functioning health information system and data-driven decision-making at the national level should have. We present the outputs in the form of the National Health Data-Sharing Strategy for the Czech Republic, along with successfully implemented case studies across selected domains of its health care system. The Czech National Health Information System has been established as the backbone for centralizing health data. It is a nationwide public administration tool that collects and processes data from the essential registries of public administration bodies, ministries, health services providers, or other persons submitting data to this system. It is the foundation for shaping a health care system that is responsive to patient needs, ensures efficient resource use, and promotes a patient-centered approach. Two examples are given of the tracking of fictitious patient pathways through the health care system. The take-home message of the study is a policy-oriented endorsement of comprehensive, secure, and interoperable health information systems as the basic infrastructure for modern, patient-centered, and data-driven health care. The paper strongly advocates the National Health Information System of the Czech Republic as the primary health database for designing, implementing, and governing such a system in alignment with European and global standards.

(JMIR Med Inform 2025;13:e70066) doi:10.2196/70066

KEYWORDS

information system; health data strategy; data-driven decision support; data interoperability

Introduction

Across Europe, health systems are under increasing pressure to deliver sustainable, efficient, and patient-centered care. The integration of health data and digital infrastructure into national strategies is essential to meet these demands and deliver on European Union (EU) priorities, including the European Health Data Space (EHDS). With its National Health Information System (NHIS), the Czech Republic offers a mature, coherent, and actionable model based on interoperability, standardization, and public trust.

In the context of EU member states' efforts to modernize their health care systems, the Czech NHIS offers a transferable framework for building resilient data ecosystems that citizens trust. This ecosystem covers all segments of the Czech health care system; is structured; and, thanks to its legal alignment with EU standards, is particularly relevant for countries seeking harmonization with new EU regulations such as the General Data Protection Regulation, the Digital Services Act, and the Digital Markets Act.

Robust health information systems (HISs) such as the NHIS enable real-time data sharing, support evidence-based policy decisions, and improve public health surveillance—capabilities

XSL•FO
RenderX

that have proven critical during the COVID-19 pandemic. Furthermore, the Czech system's integration supports goals such as strengthening preventive care, reducing regional inequalities, and improving research capacities. Through the use of advanced data analytics and standardized health data exchange, the Czech NHIS is an example of how national systems can evolve toward more proactive, personalized, and efficient health care, contributing to the European Commission's overarching goal for 2019 - 2025 of creating a unified EHDS. On the basis of extensive surveys conducted in 2023, it is urgent to develop the EHDS framework in consultation with stakeholders. The use of health data scenarios to promote dialogue on technical, legal, and social aspects is crucial in this regard. Using the health data scenarios to establish a good communication channel for discussing the related technical, social, and legal aspects of the EHDS is a crucial step in this process [1].

This viewpoint highlights the Czech Republic's policy-oriented approach to health data strategy and offers practical guidance for EU member states seeking to build modern, data-driven health care systems. The Czech model emphasizes data protection, transparency, and public trust. It calls for legal alignment with EU frameworks, cooperation between different stakeholders, and long-term investment in data literacy and sustainability. Positioned as a case study, it highlights the key elements of effective national HISs—governance, methodology, and technology—while aligning with broader European and global trends. It advocates for a structured yet flexible data infrastructure as the foundation for better health outcomes and public health resilience.

State-of-the-Art Systems and Strategies

Health Information Systems

HISs vary globally in design and capability, evolving in response to technological advances and the increasing role of data in public health. Effective HIS design requires understanding user needs; ensuring data security; and building flexible, scalable systems. A notable approach is the 4-stage ontology-based method, which uses participatory design to capture user knowledge, develop and implement ontologies, and test usability to ensure system effectiveness [2]. HIS design must take into account diverse health care subdomains (eg, hospitals and primary care centers) and stakeholders, ranging from patients to laboratory technicians. National systems often operate as uncoordinated vertical programs, highlighting the need for unified standards [3]. Feature modeling helps map system functionalities, while reference architecture guides domain scoping, modeling, and design through tools such as context and layered diagrams to ensure system-wide coherence and usability across subdomains [4].

Health Data Strategies

Central health data and information system strategies offer several advantages. However, it is essential to balance these advantages with considerations regarding data privacy, security, and ethical use of health information. Making sure that patient data are handled with utmost confidentiality and security is crucial in implementing such systems. Several countries have implemented national strategies for data sharing or opening, recognizing the value of open data in driving innovation, transparency, and improved service delivery, including (but not only) the health care sector. These national strategies make nonsensitive data publicly available for transparency, encouraging innovation and allowing third parties to create value-added services. Some notable examples of organizational, methodological, and technological backgrounds in selected experienced countries are shown in Multimedia Appendix 1 [5-34]. Each mentioned country and region uses data strategies and HISs carefully designed to improve health care delivery, policymaking, and public access to information.

Governance, Methodology, and Infrastructure

Data System

Regarding health data in the Czech Republic, several bodies play a crucial role in the organizational, methodological, and technological backgrounds. These bodies form a robust system based on tangible outputs by being interconnected and sharing the fundamental idea of opening up the NHIS, which can be followed by other EU member states. The close and intensive collaboration with the Digital and Information Agency (DIA), as a leading authority responsible for the digitization of public administration, is an essential support; this agency brings a national perspective and manages the processing and publication of data. Multimedia Appendix 2 documents the current status in the Czech Republic, divided into different areas needed to coordinate the health data agenda sustainably.

Organizations and Initiatives

The Ministry of Health of the Czech Republic [35] oversees health data legislation, manages departmental agendas, and sets priorities for analytical tasks in health policy. The Institute of Health Information and Statistics [36] plays a central role in collecting, analyzing, and presenting health data, while also supporting policymaking, public information, and international cooperation. The DIA [37] supports digital services; data management; standardization; and innovation across public administration, including health care. The Czech Medical Association of Jan Evangelista Purkyně [38] contributes to physician education and acts as a domain guarantor, ensuring accurate interpretation of published NHIS data.

Methodological Frameworks

The methodological background determines the direction of the development of the data agenda in the Czech health care sector. The Strategic Analyses of Health Sector Needs [39] identify key challenges in Czech health care, such as aging populations, rising costs, and workforce shortages. They propose measures to improve access, quality, prevention, infrastructure, digitization, and legislation, while promoting patient empowerment and public health. The National Health Data-Sharing Strategy [40] outlines legal, methodological, and technical frameworks for secure and effective health data sharing across institutions, ensuring protection of personal data and supporting research and health care improvement. It defines

XSL•FO
RenderX

levels of data access, from open datasets to controlled research use.

IT Tools

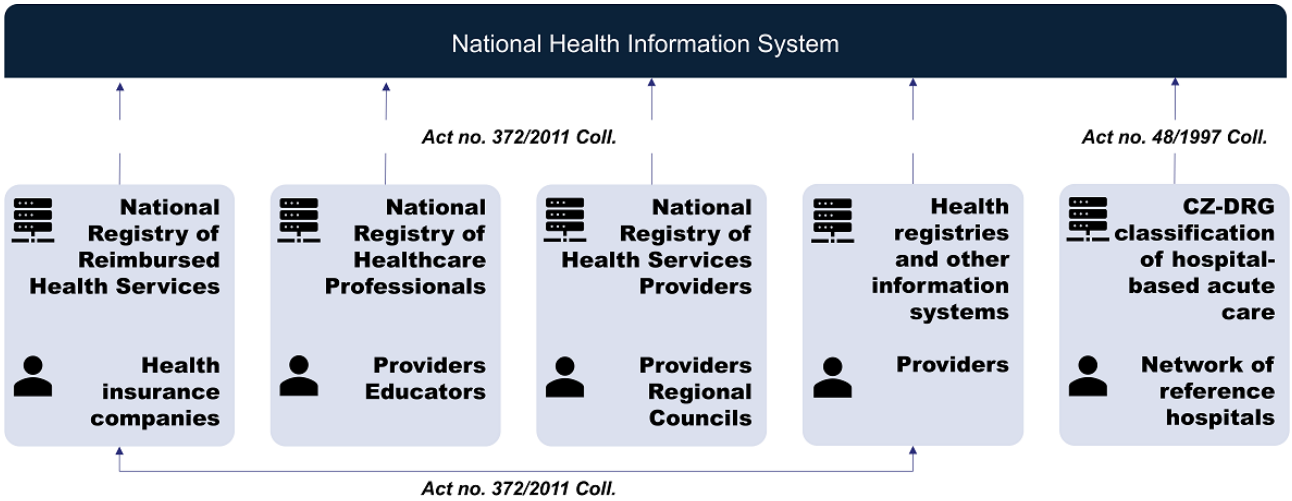
The Czech NHIS [41] is a central platform that integrates and manages health care data, which enables information sharing among stakeholders and supports health policy, service planning, and public health monitoring with reliable and timely data. NHIS has adopted the following crucial attributes based on the Czech stakeholders' and involved teams' long-term multidisciplinary experience. The National Health Information Portal (NHIP; Multimedia Appendix 3) [42] serves as a central gateway in Czech health care, offering the public, professionals, and institutions reliable, up-to-date information on health, prevention, treatments, and patients' rights. It ensures easy access to essential content and helps users navigate the health care system effectively [43].

Digital Transformation and Data Standardization in eHealth in the Czech Republic

The digital transformation of health care, with NHIS as a core component, depends on broader national developments. The health sector builds on these national structures, extending them with health care–specific attributes and services. Health care providers generate most health data during routine care, while health insurance companies centralize these data for reimbursement. Centralized data collections, especially NHIS, go beyond routine data by adding clinical, standardization, and analytical value, enabling long-term evaluation of health care effectiveness in the Czech Republic.

Primary health care data in the Czech Republic are recorded in various provider systems, which currently lack uniform standards, although all must meet basic legal requirements. Despite the coexistence of old or obsolete and modern information systems, reporting to health insurance companies follows a structured framework. Ongoing reforms, including the EHDS and the national digitization strategy, aim to introduce standardized discharge summaries, imaging, and laboratory reports. These efforts represent a shift toward more unified and quality-assured data management. Figure 1 simplistically shows the origin of the data from the perspective of the basic NHIS components and the entities responsible for entering the data, including their quality.

Figure 1. The basic components and data providers of National Health Information System (NHIS). CZ-DRG: Czech diagnosis-related group.



National Implementation in the Czech Republic

Overview

The NHIS is being developed as the backbone for centralizing health data (Multimedia Appendix 4). It is a nationwide public administration tool that collects and processes data from the essential registries of public administration bodies, ministries, health services providers, or other persons submitting data to this system. NHIS and its infrastructure could serve as an inspiration and potential model for other EU member states. The conditions of management and access to these data are governed by the legislation in force. The following components are essential to the NHIS part:

- National Health Registries (National Registry of Hospitalized Patients, National Cancer Registry, National Diabetes Registry, and others)
- National Registry of Reimbursed Health Services and the Czech diagnosis-related group classification system and its reference database
- National Registry of Health Services Providers and National Registry of Healthcare Professionals
- Data from death certificates
- Data from statistical surveys (ie, European Health Interview Survey and European Health Examination Survey)

Patient Pathway Monitoring Through the Health Care System

The following section provides a brief description of a fictitious patient's pathway [44] illustrating how the Czech health care system operates using centrally controlled data recording in the NHIS. The motivation is to describe how these patients go through the various examinations and where corresponding administrative data are recorded.

XSL•FO
RenderX

Colorectal Cancer

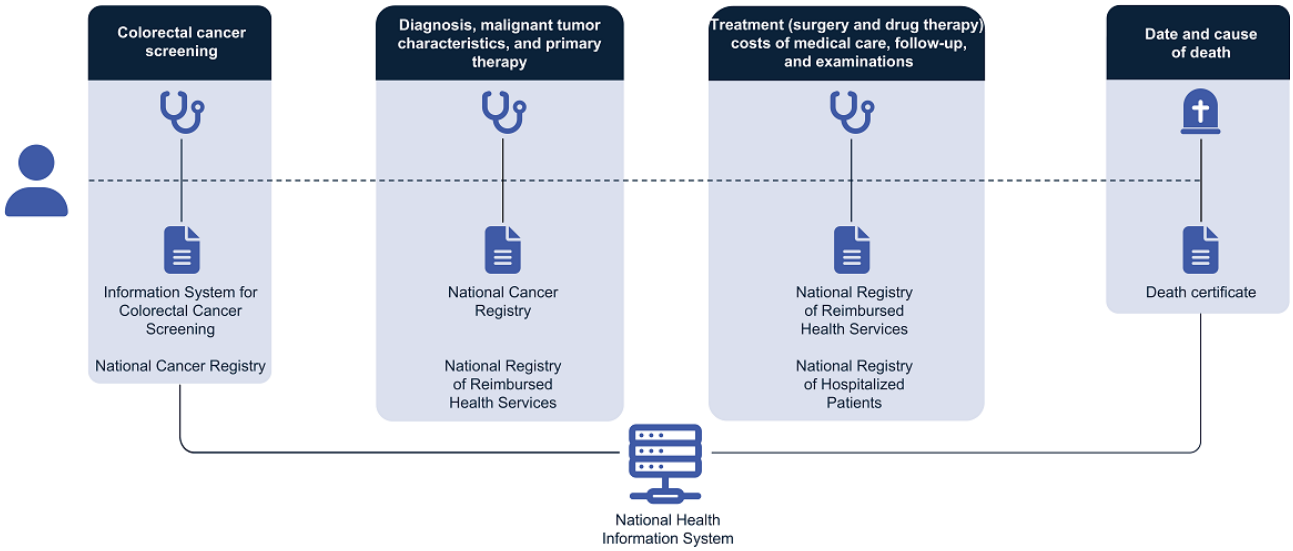
A man was diagnosed with colorectal cancer during colorectal cancer screening; more specifically, a malignant neoplasm of the rectum, that is, the C20 diagnosis according to the International Classification of Diseases, 10th Revision. The management of colorectal cancer involves a structured, multidisciplinary approach that follows established clinical pathways, which is briefly described as follows:

1. After the diagnosis of colorectal cancer was confirmed, the patient was referred to specialists (gastroenterologists, oncologists, and surgeons). They conducted further examinations to determine the stage of the disease and suggested the optimal course of treatment.
2. Treatment always depended on the stage and location of the tumor. It might involve surgery, chemotherapy, targeted therapy, immunotherapy, radiotherapy, or a combination of these. Treatment took place in accredited health care facilities specialized in cancer care.
3. Upon the completion of primary treatment, the patient attended regular checkups to detect any recurrence or complications early. This follow-up included regular checkups with specialists and additional examinations if necessary.

The recording of information related to the disease and its treatment in the NHIS (Figure 2) is as follows:

- The Information System for Colorectal Cancer Screening collects data on the screening tests performed, their results, and subsequent diagnostic and therapeutic procedures.
- The National Cancer Registry contains information on all newly diagnosed cancers and includes demographic information about each patient and details of diagnosis, treatment, and outcomes.
- The National Registry of Reimbursed Health Services records information on health care reimbursed through public health insurance (ie, information on the health services provided during the diagnostic process and treatment, medication, the cost of treatment, or data on the health services provider).
- The death certificate sets out basic information about a person's death, such as identification of the deceased, cause of death, any suspected unusual circumstances, and medical examination.

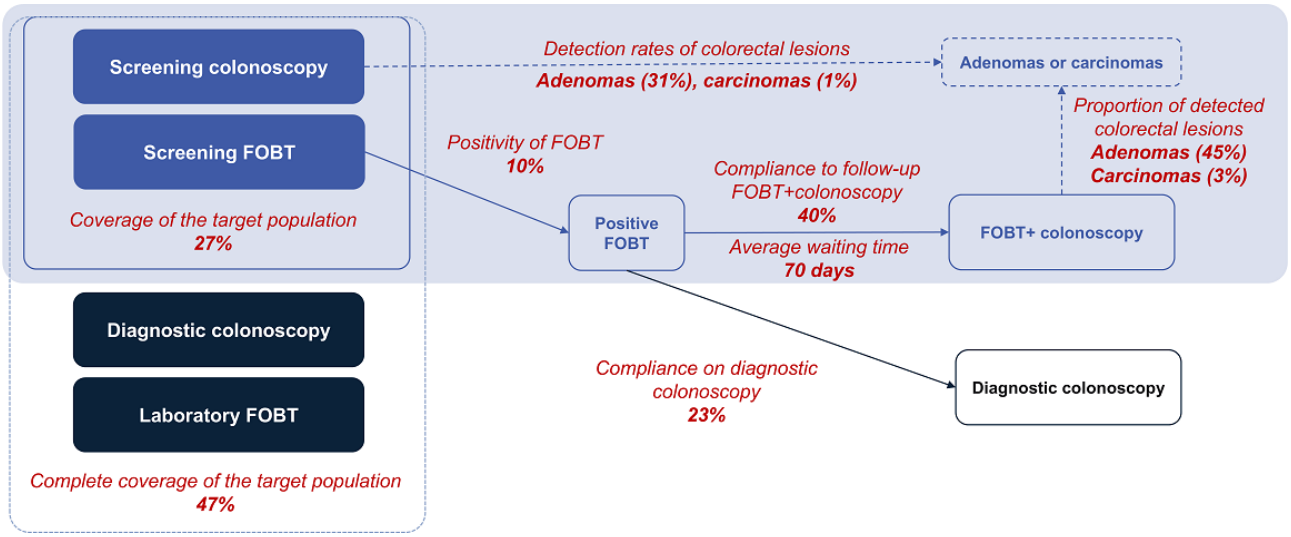
Figure 2. A pathway of a patient with cancer through the health care system.



Colorectal cancer screening, introduced in the Czech Republic in 2000, is vital in reducing the population burden [45,46]. Evaluation of the National Colorectal Cancer Screening Program, based on available NHIS data, covers patient trajectories and performance indicators. Figure 3 shows the key performance indicators of the colorectal cancer screening program in the Czech Republic for asymptomatic men and women aged ≥50 years at the population level in 2021. Performance indicators are estimated from several data sources. The target population for the program in 2021 was approximately 4.1 million people. In the same year, around 44,000 preventive colonoscopies were performed (13,000 screening colonoscopies and 31,000 FOBT+ colonoscopies). Other indicators include the positivity rate of the fecal immunochemical test (10%), the average waiting time for colonoscopy (70 d), and detection rates of adenomas (31% - 45%) and carcinomas (1% - 3%). The figure also shows that a certain proportion of the Czech population undergoes other examinations related to the early detection of colorectal lesions, with complete coverage (including both screening and diagnostic examinations) reaching 47% (4.1 million people). These performance indicators for colorectal screening demonstrate the positive impact of the screening program on the population burden. However, it is imperative to continue monitoring the program to improve its quality.

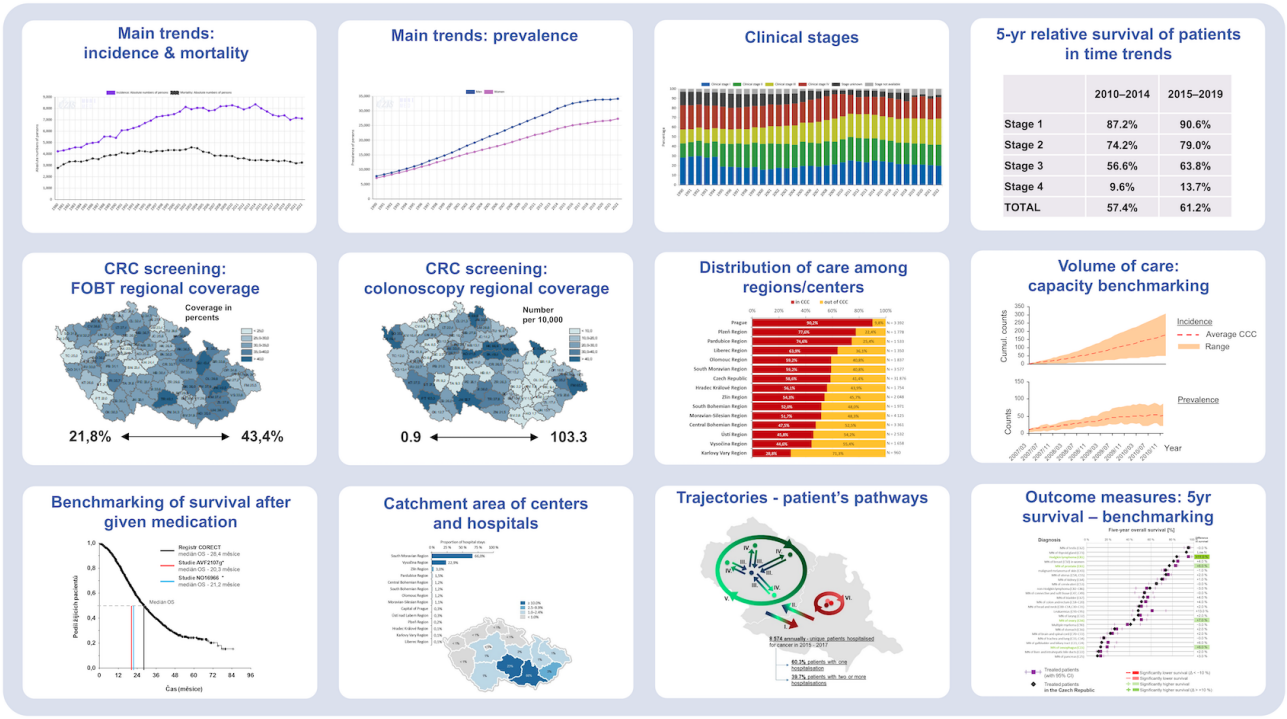
XSL•FO
RenderX

Figure 3. Results of key performance indicators (colonoscopy and fecal occult blood test [FOBT] coverage, FOBT positivity, adherence to colonoscopy recommendations, detection of findings) for colorectal cancer screening at the population level in the Czech Republic in 2021.



The monitoring and evaluation system of colorectal cancer screening is a specific part of the national cancer information system, which aims to monitor and evaluate the entire cancer control continuum (prevention, screening, treatment, survivorship, and end-of-life care) and is, therefore, an essential component of the Czech national cancer control plan. Figure 4 (the full-resolution version is in Multimedia Appendix 5) shows the indicators that enable monitoring of the health care system and benchmarking of the involved health care providers.

Figure 4. Indicators of colorectal cancer management in the Czech Republic (data source: National Cancer Registry [incidence-related parameters] and Czech Statistical Office [mortality-related parameters]). CRC: Colorectal Cancer Screening; FOBT: fecal occult blood test.



Health Data Reporting

Across the mentioned NHIS components, the NHIP team has designed and developed a new data reporting module [47]. It covers various aspects of health care, considering the target audiences for which the tailored views of health data are intended. As of July 7, 2025, a total of 364 data outputs have been published. The individual output formats with a brief description and an example are listed in Multimedia Appendix 6 [48-54]. The release of data reporting represents a significant milestone in sharing health data for the public and professionals. Different data formats are available in one place, depending on the preferences of the data users.

Strategic Framework: Legislation, Publishing Principles, and Target Groups

Overview

Various comprehensive results have been developed based on two crucial documents mentioned in the Methods section: (1)

XSL•FO
RenderX

the strategic analyses of health sector needs and (2) the National Health Data-Sharing Strategy, a guiding methodological pillar fully approved by the Ministry of Health of the Czech Republic. The most central themes included (1) general provisions and compliance with national and international standards, (2) content methodology of health data access, (3) institutionalization and author responsibilities, and (4) data publication and communication channels. The effective management of access to and distribution of centralized data involves numerous steps, including standardizing the primary data from NHIS; ensuring the data are collected, followed up on, and edited efficiently; and ensuring it is published with regular updates while considering user feedback. Centralizing data can impact the entire health care system, which includes tens of thousands of health care providers, their founders, health insurance companies, specialized institutes, and more. Thus, the system must be efficient, secure, user-friendly, and easy to manage.

Legal Background

The full implementation of the NHIS provides a database for centralized data sharing. Its components now have an explicit legislative mandate. Legislation on data collection is essential to protect patient data, ensure data security, and promote transparency in health care processes. The establishment of the NHIS is covered by a legal framework, which is essential in establishing rules for collecting, processing, and sharing health information. Sharing health data between authorized entities contributes significantly to better care coordination, improving the quality of treatment outcomes, and supporting research. Given the sensitivity of health information, compliance with legislation is essential to ensure public trust in health care systems and technology. The legal framework consists of the following list of laws:

- Act No. 372/2011 Coll., on Health Services and Conditions of Their Provision
- Act No. 325/2021 Coll., on the Digitization of Health Care
- Act No. 89/1995 Coll., on the National Statistical Service
- Act No. 285/2002 Coll., on the Donation, Procurement and Transplantations of Tissues and Organs and on Amendments to Some Acts
- Act No. 258/2000 Coll., on Protection of Public Health and Amendment to Some Related Acts.

NHIS enables a comprehensive and full-fledged analytical evaluation of health services focused on all segments of care, a long-term assessment of patient trajectories in the system, and a representative review of access to care. The already approved (although not yet published) draft regulation on the EHDS will have implications for NHIS both in primary data processing and secondary data use. In primary data management, implementing EHDS can be expected to place greater emphasis on standardizing the content of electronic documentation directly with health service providers and health insurance companies. These processes will increase the information value of data and its usability.

Data Publishing Principles

The NHIS dataset design, preparation, and publishing should respect the algorithm of dataset preparation described in a numbered list below, which always respects several principal rules: (1) individual natural persons must not be identifiable, (2) individual legal persons must not be identifiable unless expressly stated by the law, (3) secondary processing must lead to the pseudonymization of the dataset, (4) the purpose of the dataset publication must correspond to the NHIS purpose, and (5) the standardized process of approval and publishing must be adhered to. The essential requirement of a comprehensive process, which this approach meets, is to ensure the necessary completeness, validity, and overall data quality [45]. The dataset publication consists of six steps describing the critical preparation and implementation phases:

1. Proposal of a dataset concept in the form of a short description, which can be raised by any entity, usually a state institution, a health insurance company, a professional (medical) society, a research institution, or an academic institution.
2. The delivered concept is reviewed from the perspective of data availability, export feasibility, design, and personal data regulations.
3. After approval, a methodology for the dataset processing is proposed (data export from central registries, data preprocessing and cleaning, analytical adjustments, and validation mechanisms).
4. The dataset is generated in an open data standardized format according to the predefined scheme, including an obligatory description with metadata.
5. Reviewing and validating the dataset and its content is a mandatory procedure before publication (a manual approach is always needed, as well as technical control to follow open data standards and best practices).
6. Publication of the final dataset in the data reporting module under the Creative Commons Attribution 4.0 International license (CC-BY-4.0).

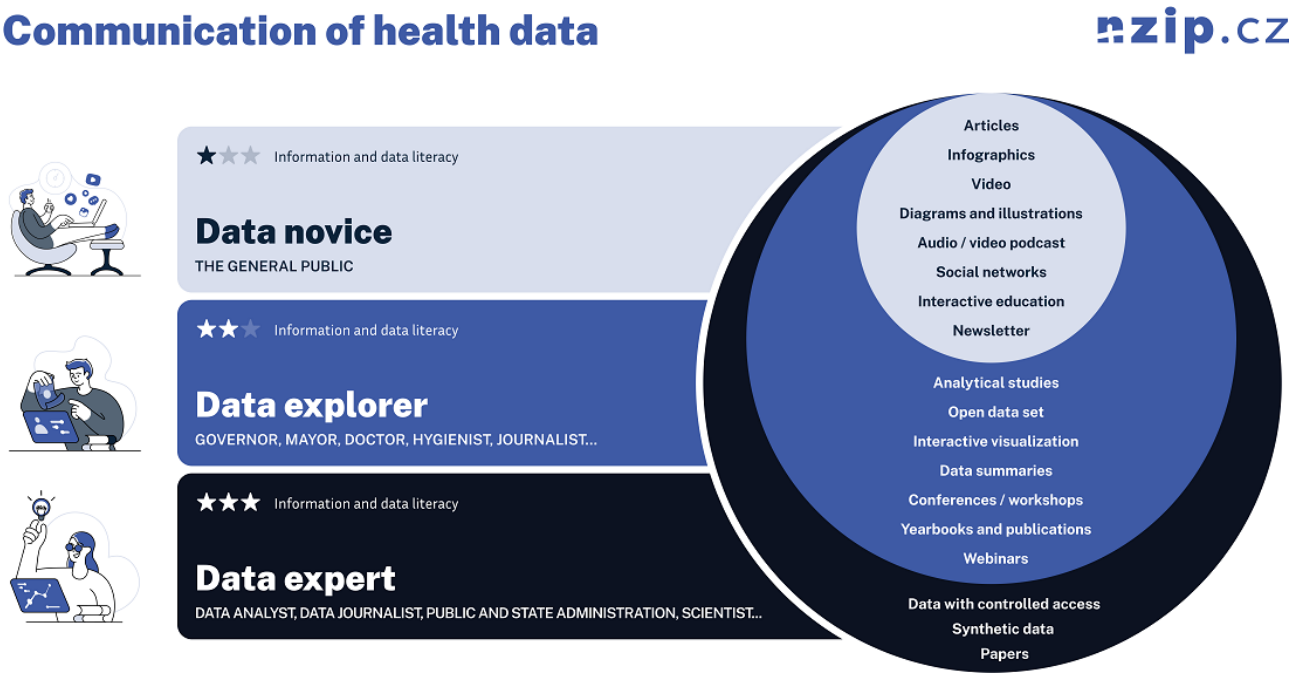
These rules allow complete control over methodological, legislative, and technical aspects significantly affecting health data preparation and sharing. At the same time, the processes set up align with the entire ministry's strategic vision, which is based on the principles of evidence-based medicine and data-based decision-making.

Target Group Focus

Effective health communication requires identifying target groups and tailoring messages to their literacy levels regarding health, information, and data. Adapting the complexity of content, language, and format not only increases understanding and engagement but also reduces the risk of misinterpretation. For instance, younger audiences may prefer digital media, while older adults may favor printed materials. Clear communication tailored to a specific audience supports informed decisions and healthier behaviors. Figure 5 illustrates the 3 main target groups according to the expected user input knowledge level, showing the different types of health data outputs.

XSL•FO
RenderX

Figure 5. Communication target group of health data.



A summary of health data use is provided in Table 1, showing the different data formats and the primary (though not exclusive) target users for each format. The motivation is to cover the largest possible group of those interested in health data and to develop health and data literacy in the Czech Republic in the long term through published data.

Table . Relationship between target user groups and published health data formats.

Output format	Data novice	Data explorer	Data expert
Open data		✓	✓
Data summaries		✓	✓
Analytic studies		✓	✓
Yearbooks and publications	✓	✓	✓
Interactive visualizations and info-graphics	✓	✓	✓
Dedicated analytical portals		✓	✓
Synthetic data			✓

Discussion

Key Lessons Learned

The Czech Republic's National Health Data-Sharing Strategy, jointly managed by the Ministry of Health, the Institute of Health Information and Statistics, and DIA, highlights several important findings. The centralization of health data through standardized national registries, electronic health records, and real-time reporting tools significantly improves health care efficiency, patient outcomes, and interoperability between health care providers, researchers, and public health authorities. The NHIP forms the backbone of data dissemination and provides interactive visualizations, open datasets, and customized data views for different users.

Privacy and security remain critical, as patient confidentiality and General Data Protection Regulation compliance directly shape data-sharing policies. To address this, the NHIS, which encompasses 61 data agendas (including national registries, prevention programs, and statistical surveys), uses advanced encryption and anonymization techniques, as well as strict access controls that enable authorized yet secure access.

The NHIS is an example of a transformative change in health care methodologies and highlights several key elements:

- Privacy and confidentiality—the protection of patient data is crucial to prevent discrimination and promote public trust and participation in health research.
- Importance for research and public health—data stratified by sex, age, education, and ethnicity are crucial for identifying inequalities and guiding targeted public health interventions (eg, World Health Organization Health Inequality Data Repository and European Cancer Information System).
- Diverse stakeholder concerns—patients, health services providers, and policymakers have different needs and expectations that must be taken into account in the design

XSL•FO
RenderX

of health data systems and the development of policy measures.
- Technological and analytical challenges—advanced technologies and sophisticated analytical methods are essential to effectively manage the complexity and volume of health data.

The digital transformation of health care in the Czech Republic, supported by the aspects mentioned in Methods (subsection: Digital Transformation and Data Standardization in eHealth in the Czech Republic), has been enhanced by new tools currently being developed and tested: a new synthetic data system (a promising innovative tool for data analysis experts to conduct sophisticated analytical studies on NHIS patient data) and artificial intelligence chatbots (which answer questions about health statistics in simple language).

Actionable Recommendations for Other European Countries

The NHIS in the Czech Republic forms the basis for designing a health care system that responds to patients' needs, uses resources efficiently, and pursues a patient-centered approach. When establishing such a robust framework for a specific area, such as health care, EU member states should focus on the following key areas:

- Compliance with regulatory and legal requirements—alignment with local, national, and international health care and legal regulations.
- Data security—protection of sensitive health data and implementation of encryption, user authentication, and access control, including a robust IT infrastructure.
- Data management and validation—ensuring the integrity and accuracy of health data, including automatic and semiautomatic control mechanisms that guarantee valid and correct data.
- Standardization—using health care standards (ie, International Classification of Diseases, 10th Revision or the Czech diagnosis-related group) and uniform lists of values among all related areas (ie, population and demography). A practical example is the shared medical record, which will enable secure access to patients' preventive care and screening data across all health care providers. Its implementation is scheduled for the end of 2025. Another example of planned standardization is the early introduction of structured and standardized discharge reports, imaging reports, and laboratory results as part of the national strategy for the digitalization of health care.
- Multidisciplinary team—appropriate composition of experts with in-depth specialist knowledge (with or without the support of subcontractors), representing all necessary professional groups (data architect, data manager, analyst, developer, web designer, communication expert, language expert, and a representative of an expert medical society) and ensuring regular internal communication.
- Support for leading institutions—all leading representatives and committees of involved stakeholders must be informed and involved in all important decisions.
- Communication and public relations—focus on the actual needs of target groups and clear presentation of data outputs, including the establishment of professional communities through conferences and workshops.
- Data outputs by target groups—provision of outputs tailored to user requirements and preferences (open data, data summaries, infographics, interactive visualizations, and synthetic data).
- User-friendliness, accessibility, and experience—the design and format of the published outputs must comply with user experience or user-friendliness rules and accessibility rules (especially for people with disabilities) and graphical and user-friendly requirements.
- Technological sustainability—minimization of technological debt and continuous development of information systems and portals based on IT trends, user behavior, and needs arising from actual use.
- Financial sustainability—efficient allocation of resources, taking into account development, maintenance, and operating costs, including process optimization, to ensure long-term cost-effectiveness.

Limitations of the Study, Especially With Regard to the Transferability of Findings

This case study examines how health data can be collected, integrated, and published at a national level. Although it is limited to one country, many of the findings are transferable to other countries, depending on the structure of the health care system, the proportion of public health insurance, and the availability of IT data. The main advantages of the Czech health care system in terms of data integration are (1) the high proportion of health services covered by public health insurance and (2) a registry in which data on these health services are centralized. This enables system-wide evaluation and analysis of diagnoses, areas of care, medications, equipment, procedures, and their reimbursement. On the other hand, there are considerable differences in the complexity of data within individual agendas and topics. Although administrative data on health services reimbursed from public health insurance cover the entire spectrum of care, procedures, and medications, clinical information is generally lacking. This is only recorded for selected care segments or diagnosis groups in specialized registries (eg, cancer care, cardiovascular surgery, and blood donation). Given the scope and nature of the data, all interpretations and conclusions drawn from NHIS data should always be made with caution and supported by sound professional knowledge and expertise, taking into account other integrated health data systems. Another significant limitation is the quality of the input data and the lack of motivation on the part of the responsible institutions to enter it correctly and completely into these systems. An example of this is the National Cancer Registry, where incomplete entry of clinical stages is often a major problem.

Conclusions

The integration of data and information systems into the Czech Republic's national health data strategy can transform health care by improving patient outcomes and optimizing resource use, for example, through improved disease surveillance, targeted prevention (eg, colorectal cancer screening), and more efficient health care planning based on integrated patient data.

XSL•FO
RenderX

To reap these benefits, policymakers have created robust interoperable infrastructures that enable real-time decision-making and evidence-based planning. Standardization across the health sector is crucial to ensure seamless communication between stakeholders and prepare for participation in EHDS, which requires legal, technical, and methodological alignment with international frameworks. The Czech Republic's NHIS is an important infrastructure for alignment with the EHDS. Successful integration into the EHDS requires the modernization of the NHIS so that it functions as a system compatible with European standards for the secure sharing and secondary use of health data. With its universal health care model and strong digital infrastructure, the Czech health care system is well positioned to take a leading role in regional efforts to transform digital health care. To fully exploit these advantages and set an example of sustainable data-driven health care governance in Europe, further progress is needed in the areas of infrastructure, harmonization of legislation, and data literacy and awareness among the population.

Acknowledgments

The authors were supported by the following grant projects: (1) systematic education and increasing health literacy through the National Health Information Portal (CZ.03.02.02/00/22_005/0001137), (2) raising awareness via the National Health Information Portal (CZ.03.4.74/0.0/0.0/15_025/0016090), (3) developing models to predict regional health care needs and related economic and personnel indicators (CZ.03.02.02/00/22_046/0002180), (4) strengthening lung cancer screening in Europe, and (5) comprehensive information facilities to improve the quality of cancer screening programs within the National Screening Center (CZ.31.8.0/0.0/0.0/23_075/0008430).

Conflicts of Interest

None declared.

Multimedia Appendix 1
Overview of organizations and initiatives.
[DOCX File, 15 KB - medinform_v13i1e70066_app1.docx]

Multimedia Appendix 2
Crucial attributes of the National Health Information System.
[DOCX File, 15 KB - medinform_v13i1e70066_app2.docx]

Multimedia Appendix 3
Screenshot of the National Health Information Portal home page.
[PNG File, 977 KB - medinform_v13i1e70066_app3.png]

Multimedia Appendix 4
Overview of all National Health Information System agendas and data sources.
[DOCX File, 16 KB - medinform_v13i1e70066_app4.docx]

Multimedia Appendix 5
Indicators of colorectal cancer management in the Czech Republic (high resolution).
[PNG File, 5232 KB - medinform_v13i1e70066_app5.png]

Multimedia Appendix 6
Overview of outputs published in the data reporting module (information valid as of July 31, 2025).
[DOCX File, 15 KB - medinform_v13i1e70066_app6.docx]

References

1. Hussein R, Scherdel L, Nicolet F, Martin-Sanchez F. Towards the European Health Data Space (EHDS) ecosystem: a survey research on future health data scenarios. Int J Med Inform 2023 Feb;170:104949. [doi: 10.1016/j.ijmedinf.2022.104949] [Medline: 36521422]
2. Kuziemsky CE, Lau F. A four stage approach for ontology-based health information system design. Artif Intell Med 2010 Nov;50(3):133-148. [doi: 10.1016/j.artmed.2010.04.012] [Medline: 20510592]
3. Braa J, Hanseth O, Heywood A, Mohammed W, Shaw V. Developing health information systems in developing countries: the flexible standards strategy. MIS Q 2007;31(2):381. [doi: 10.2307/25148796]

XSL•FO
RenderX

4. Tummers J, Tobi H, Catal C, Tekinerdogan B. Designing a reference architecture for health information systems. BMC Med Inform Decis Mak 2021 Jul 8;21(1):210. [doi: 10.1186/s12911-021-01570-2] [Medline: 34238281]
5. eHealth network. European Commission. URL: https://health.ec.europa.eu/ehealth-digital-health-and-care/eu-cooperation/ehealth-network_en [accessed 2024-10-03]
6. European Centre for Disease Prevention and Control. URL: https://www.ecdc.europa.eu/en [accessed 2024-07-07]
7. European data strategy. European Commission. URL: https://commission.europa.eu/strategy-and-policy/priorities-2019-2024/europe-fit-digital-age/european-data-strategy_en [accessed 2024-08-03]
8. European Health Data Space Regulation (EHDS). European Commission. URL: https://health.ec.europa.eu/ehealth-digital-health-and-care/european-health-data-space_en [accessed 2024-09-03]
9. European Health Information Gateway. URL: https://gateway.euro.who.int/en/ [accessed 2025-09-16]
10. Centers for Disease Control and Prevention. URL: https://www.cdc.gov/ [accessed 2024-09-16]
11. National Center for Health Statistics. Centers for Disease Control and Prevention. URL: https://www.cdc.gov/nchs/index.html [accessed 2024-07-07]
12. Assistant Secretary for Technology Policy. URL: https://www.healthit.gov/ [accessed 2025-09-16]
13. 2024-2030 federal health IT strategic plan: draft for public comment. Assistant Secretary for Technology Policy. 2024 Mar. URL: https://tinyurl.com/56yp5dz6 [accessed 2025-09-16]
14. National action plan to improve health literacy. US Department of Health and Human Services, Office of Disease Prevention and Health Promotion. 2010. URL: https://health.gov/sites/default/files/2019-09/Health_Literacy_Action_Plan.pdf [accessed 2024-10-03]
15. National Health and Nutrition Examination Survey. Centers for Disease Control and Prevention. 2005. URL: https://www.cdc.gov/nchs/nhanes/?CDC_AAref_Val=https://www.cdc.gov/nchs/nhanes/index.htm [accessed 2024-07-03]
16. The National Health Care Surveys. Centers for Disease Control and Prevention. 2024 Oct 16. URL: https://www.cdc.gov/nchs/healthcare-surveys/about/?CDC_AAref_Val=https://www.cdc.gov/nchs/dhcs/index.htm [accessed 2024-09-07]
17. National Health Service. URL: https://www.nhs.uk/ [accessed 2024-08-03]
18. General Practice Data for Planning and Research (GPDPR). NHS England. URL: https://digital.nhs.uk/data-and-information/data-collections-and-data-sets/data-collections/general-practice-data-for-planning-and-research [accessed 2024-10-03]
19. The NHS long term plan. The National Archives. 2019 Jan. URL: https://webarchive.nationalarchives.gov.uk/ukgwa/20230418155402/https:/www.longtermplan.nhs.uk/publication/nhs-long-term-plan/ [accessed 2025-09-16]
20. Digital health laws and regulations United Kingdom 2024. International Comparative Legal Guides. 2024. URL: https://iclg.com/practice-areas/digital-health-laws-and-regulations/united-kingdom [accessed 2024-07-03]
21. NHS Federated Data Platform. NHS England. URL: https://www.england.nhs.uk/digitaltechnology/nhs-federated-data-platform/ [accessed 2024-10-14]
22. Canada Health Infoway. URL: https://www.infoway-inforoute.ca/ [accessed 2024-09-03]
23. Canadian Institute for Health Information. URL: https://www.cihi.ca/en [accessed 2024-07-03]
24. Pan-Canadian health data strategy: toward a world-class health data system: expert advisory group – final report. Government of Canada. 2022 May. URL: https://tinyurl.com/5n6etdjw [accessed 2024-08-07]
25. Pan-Canadian health data content framework data content: standard version 2. Canadian Institute for Health Information. 2025 Sep. URL: https://www.cihi.ca/sites/default/files/document/pan-canadian-health-data-content-framework-data-content-standard-en.pdf [accessed 2025-09-30]
26. Open Government. Government of Canada. URL: https://open.canada.ca/en [accessed 2024-10-14]
27. Australian Digital Health Agency. URL: https://www.digitalhealth.gov.au/ [accessed 2024-09-07]
28. Australian Institute of Health and Welfare. URL: https://www.aihw.gov.au/ [accessed 2024-07-07]
29. Australian Bureau of Statistics. URL: https://www.abs.gov.au/ [accessed 2024-08-25]
30. National digital health strategy. Australian Digital Health Agency. URL: https://www.digitalhealth.gov.au/discover-the-national-digital-health-strategy-2023-2028 [accessed 2024-07-03]
31. Strategic directions 2022–2026. Australian Institute of Health and Welfare. URL: https://www.aihw.gov.au/getmedia/e1bbb306-11f1-41a4-bce9-a1582eb18cfa/aihw-strategic-directions-2022-2026.pdf
32. My Health Record. Australian Digital Health Agency. URL: https://www.digitalhealth.gov.au/initiatives-and-programs/my-health-record [accessed 2024-10-01]
33. Health professionals. Services Australia. URL: https://www.servicesaustralia.gov.au/health-professionals [accessed 2025-09-16]
34. Health data portal. Department of Health and Aged Care. URL: https://dataportal.health.gov.au [accessed 2024-07-25]
35. Ministry of Health of the Czech Republic. URL: https://mzd.gov.cz/ [accessed 2024-08-07]
36. Institute of Health Information and Statistics of the Czech Republic. URL: https://www.uzis.cz/index-en.php [accessed 2025-09-16]
37. Digital Information Agency. URL: https://www.dia.gov.cz/ [accessed 2024-09-03]
38. Czech Medical Association of Jan Evangelista Purkyně. URL: https://www.cls.cz/en [accessed 2024-07-24]

XSL•FO
RenderX

39. Válek V, Dušek L. Strategic analyses of health sector needs: a data-driven approach. Ministry of Health of the Czech Republic and Institute of Health Information and Statistics of the Czech Republic. URL: https://www.nzip.cz/koncepce2025 [accessed 2024-08-03]
40. Dušek L, Komenda M, Klimeš D, et al. National health data-sharing strategy in the Czech Republic. National Health Information Portal. 2025. URL: https://www.nzip.cz/clanek/2375-koncepce-sdileni-a-sekundarniho-vytezovani-dat-nzis [accessed 2025-05-19]
41. National health information system. Institute of Health Information and Statistics of the Czech Republic. URL: https://www.uzis.cz/index-en.php?pg=nhis [accessed 2024-10-01]
42. National health information portal. Ministry of Health of the Czech Republic and Institute of Health Information and Statistics of the Czech Republic. URL: https://www.nzip.cz/ [accessed 2024-06-03]
43. Komenda M, Jarkovský J, Klimeš D, et al. Sharing datasets of the COVID-19 epidemic in the Czech Republic. PLoS ONE 2022;17(4):e0267397. [doi: 10.1371/journal.pone.0267397] [Medline: 35446896]
44. Wind A, van der Linden C, Hartman E, Siesling S, van Harten W. Patient involvement in clinical pathway development, implementation and evaluation - a scoping review of international literature. Patient Educ Couns 2022 Jun;105(6):1441-1448. [doi: 10.1016/j.pec.2021.10.007] [Medline: 34666931]
45. Ngo O, Hejcmanová K, Suchánek Š, et al. Coverage by examinations associated with early detection of colorectal neoplasia in the Czech Republic. Eur J Public Health 2023 Jun 1;33(3):515-521. [doi: 10.1093/eurpub/ckad071] [Medline: 37141451]
46. Ngo O, Chloupková R, Štěpán S, et al. Results of the evaluation of the colorectal cancer screening programme in the Czech Republic. Gastroent Hepatol 2023;77(5):385-393. [doi: 10.48095/ccgh2023385]
47. Data reporting. Národní Zdravotnický InformačNí Portal. URL: https://www.nzip.cz/data-nzis [accessed 2024-11-22]
48. What is open data. European Union. URL: https://data.europa.eu/en/dataeuropa-academy/what-open-data [accessed 2024-09-12]
49. Soukupová J, Melicharová H, Šanca O, Bartůněk V, Jarkovský J, Komenda M. Psychiatric care: coverage of follow-up care. National Health Information Portal. 2024. URL: http://www.nzip.cz/data/2062-pokryti-navaznou-peci-psychiatrie [accessed 2025-09-14]
50. Klechová A, Jarkovský J, Drábková S, et al. Provedené kardiochirurgické operace v ČR. Národní Zdravotnický InformačNí Portál. 2024. URL: https://www.nzip.cz/data/1658-provedene-kardiochirurgicke-operace-datovy-souhrn [accessed 2024-11-14]
51. Chlíbek R, Cabrnochová H, Prymula R, et al. Vaccination in available NZIS data. National Health Information Portal. 2024. URL: https://www.nzip.cz/data/1704-ockovani-v-dostupnych-datech-nzis [accessed 2024-11-14]
52. Assisted reproduction (NRHR yearbooks). National Health Information Portal. 2024. URL: https://www.nzip.cz/data/1634-asistovana-reprodukce-rocenky-nrrz [accessed 2024-12-01]
53. Pokorná A, Štrombachová V, Mužík J, et al. Adverse events: a basic overview over time. National Health Information Portal. 2024. URL: https://www.nzip.cz/data/1957-interaktivni-vizualizace-nezadouci-udalosti [accessed 2024-12-01]
54. Krejčí D, Mužík J, Šnábl I, Gregor J. Portal of cancer epidemiology in the Czech Republic. Masaryk University. 2024. URL: https://www.svod.cz/en/ [accessed 2024-09-12]

Abbreviations

DIA: Digital and Information Agency
EHDS: European Health Data Space
EU: European Union
HIS: health information system
NHIP: National Health Information Portal
NHIS: National Health Information System

Edited by C Perrin; submitted 14.12.24; peer-reviewed by D Chrimes, S Thawillarp; revised version received 20.08.25; accepted 26.08.25; published 06.10.25.

Please cite as:
Komenda M, Gregor J, Klimeš D, Pavlík T, Blaha M, Těšitelová V, Májek O, Ngo O, Chloupková R, Hejduk K, Šnajdrová L, Jarkovský J, Mužík J, Růžičková P, Válek V, Dušek L
Integration of Data and Information Systems Into the Health Data Strategy
JMIR Med Inform 2025;13:e70066
URL: https://medinform.jmir.org/2025/1/e70066
doi:10.2196/70066

XSL•FO
RenderX

© Martin Komenda, Jakub Gregor, Daniel Klimeš, Tomáš Pavlík, Milan Blaha, Vladimíra Těšitelová, Ondřej Májek, Ondřej Ngo, Renata Chloupková, Karel Hejduk, Lenka Šnajdrová, Jiří Jarkovský, Jan Mužík, Petra Růžičková, Vlastimil Válek, Ladislav Dušek. Originally published in JMIR Medical Informatics (https://medinform.jmir.org), 6.10.2025. This is an open-access article distributed under the terms of the Creative Commons Attribution License (https://creativecommons.org/licenses/by/4.0/), which permits unrestricted use, distribution, and reproduction in any medium, provided the original work, first published in JMIR Medical Informatics, is properly cited. The complete bibliographic information, a link to the original publication on https://medinform.jmir.org/, as well as this copyright and license information must be included.

XSL•FO
RenderX

Digital Health Innovations to Catalyze the Transition to Value-Based Health Care

Lan Zhang[1], BEng, MM, PhD; Christopher Bullen[2], MBChB, MPH, PhD; Jinsong Chen[1,2,3], BHS, MPH, PhD

[1]Department of Public Administration, Law School, Hangzhou City University, Hangzhou, China

[2]National Institute for Health Innovation, University of Auckland, Auckland, New Zealand

[3]School of Public Affairs, Zhejiang University, Hangzhou, China

Corresponding Author:
Jinsong Chen, BHS, MPH, PhD
Department of Public Administration, Law School, Hangzhou City University, Hangzhou, China

Abstract

The health care industry is currently going through a transformation due to the integration of technologies and the shift toward value-based health care (VBHC). This article explores how digital health solutions play a role in advancing VBHC, highlighting both the challenges and opportunities associated with adopting these technologies. Digital health, which includes mobile health, wearable devices, telehealth, and personalized medicine, shows promise in improving diagnostic accuracy, treatment options, and overall health outcomes. The article delves into the concept of transformation in health care by emphasizing its potential to reform care delivery through data communication, patient engagement, and operational efficiency. Moreover, it examines the principles of VBHC, with a focus on patient outcomes, and emphasizes how digital platforms play a role in treatment among tertiary hospitals by using patient-reported outcome measures. The article discusses challenges that come with implementing VBHC, such as stakeholder engagement and standardization of patient-reported outcome measures. It also highlights the role played by health innovators in facilitating the transition toward VBHC models. Through real-life case examples, this article illustrates how digital platforms have had an impact on efficiencies, patient outcomes, and empowerment. In conclusion, it envisions directions for solutions in VBHC by emphasizing the need for interoperability, standardization, and collaborative efforts among stakeholders to fully realize the potential of digital transformation in health care. This research highlights the impact of digital health in creating a health care system that focuses on providing high-quality, efficient, and patient-centered care.

(JMIR Med Inform 2025;13:e57385) doi:10.2196/57385

KEYWORDS

digital health; value-based health care; VBHC; patient-reported outcome measures; PROM; digital transformation; health care innovation; patient-centric care; health technology; patient-reported outcome; PRO; outcome measure; telehealth; telemedicine; eHealth; personalized; customized; engagement; patient-centered care; standardization; implementation

Introduction

In the last few decades, the health care landscape has undergone changes due to the rapid advancement and integration of technology. This technological progress has transformed how health care is managed, both for individuals and on a scale, by providing insights into patient health and experiences through digital recording and data collection methods.

Nowadays these advancements in technology are collectively known as “digital health.” According to the Food and Drug Administration, digital health encompasses a range of technologies, including mobile health (mHealth), health information technology, wearable devices, telehealth, telemedicine, and personalized medicine [1]. The adoption of health technologies is increasingly common in the health care industry, offering prospects for improved diagnostic accuracy, treatment options, and overall health outcomes [2].

These innovations in health are driving a shift toward a value-based approach [3]. This places patients at the center of care delivery and marks a departure from health care models. However, navigating the complex digital health ecosystem poses challenges for transformations in health care.

Digital Transformation

Digital transformation refers to “a process that aims to improve an entity by triggering significant changes to its properties through combinations of information, computing, communication, and connectivity technologies” [4]. Digital transformation is reforming the modern-day health care system. Propelled by the COVID-19 pandemic, we have witnessed a surge of technology innovation to assure continuity in care delivery [5].

However, in the context of the health industry, digital transformation not only refers to managing clinical data flows

XSL•FO
RenderX

and using advanced technologies but also a wider philosophical framework of business and operation transformation via digital innovations and technologies to increase stakeholder satisfaction. Its aim goes beyond digitizing the organizational environment to facilitate the use of data and leverage the value of data insights for improving clinical governance and performance evaluation, supporting clinical decision-making and operation efficiency, as well as ensuring the highly efficient utilization of health resources [5]. Ultimately, the process of digital transformation for the health care system needs to consider how to increase the quality of care and patient satisfaction via enhancing clinical data communication and patient engagement [6].

The digital transformation of the health care industry has leveraged a range of digital solutions in each part of the patient journey, including patient assessment, treatment, and management. These digital innovations arose out of the need for treatment and patient care, but toward multidimensional well-being and multi-disciplinary health support. The digital transformation enables health care professionals and other stakeholders in the health system to accomplish value-based health care (VBHC) more efficiently and sustainably [7].

Value-Based Health Care

VBHC, defined as a health care activity that highlights value as patient-centric outcomes over the cost invested to treat patients [8,9], is one of the dominant trends in the global health industry [3,10,11]. Due to the high costs and growing inefficiency of health care in many nations, as well as the growing agreement that the existing health care paradigm is essentially unsustainable [12,13], advocating and implementing a VBHC model has become a strategic imperative for many health systems [14,15].

What is value? A definition proposed by the European Commission broadens the interpretation of "value" from a single variable based solely on monetary value in the context of cost-effectiveness to a more inclusive concept. The proposed definition of "value" includes the following four components [16]: (1) allocative "value": equitable distribution of resources across all patient groups; (2) technical "value": achievement of the best possible outcomes with available resources; (3) personal "value": appropriate care to achieve patients' personal goals; and (4) societal "value": contribution of health care to social participation and connectedness.

A system-level model and framework may be necessary to determine "value" within the many components connected by complex processes inside a health care system [17].

Under VBHC, the focus shifts from volumes (the number of physician visits, hospitalizations, procedures, and tests) to outcomes (the patients' prioritized health outcomes, such as an increase in functional independence and quality of life [18]. With a focus on the quality of patient care, the aim is to reduce the time spent in the health care sectors, avoid the development of chronic diseases, and minimize deterioration of medical conditions [18]. VBHC empowers patients and enables caregivers to provide better care at a lower cost, resulting in benefits for all stakeholders: patients, providers, payers, suppliers, and society [18].

Patient-Reported Outcome Measures

An important element of VBHC is measuring outcomes that matter to patients, including their symptoms, functionality, and their satisfaction with their health care experience. This led to the introduction and adoption of patient-centered outcomes assessments, which take into account aspects of cure and survival, as well as recovery and quality of life retained [19,20]. A patient-reported outcome (PRO) is "an outcome reported directly by patients themselves and not interpreted by an observer." PROs bring the "patient's voice" to the care journey and identify conditions or symptoms that matter the most to a patient's daily life and quality of life [21].

To measure PROs, instruments known as patient-reported outcome measures (PROMs) have been developed. These instruments are typically self-reported questionnaires that measure symptom burden, functional status, health-related quality of life, and health-related behaviors such as anxiety [22]. They are generally categorized into 2 groups: general health-related quality of life PROMs and disease-specific PROMs [22]. General PROMs focus on general well-being, mental state, and quality of life across a range of medical conditions [22], whereas disease-specific PROMs capture a combination of symptom severity and impact resulting from a specific condition or treatment [23].

PROMs are an essential part of VBHC because they measure what matters most to patients, and this drives the health care system to take a more holistic and comprehensive view of the physical, mental, and social impacts of illness. Research has found PROMs can be used in different ways to contribute to VBHC, such as enhancing patients' and clinicians' communication for identifying treatment plans; quantifying and monitoring symptoms and illness impact on life; reflecting patients' preference on treatment and care; evaluating the quality of care and improvement of health; facilitating patient adherence and satisfaction with care; and promoting informed utilization of health resources and services [24].

Traditionally, PROMs were administered and distributed on paper throughout a patient's care journey, requiring manual efforts to distribute, collect, and calculate patient scores. This can be a time-consuming and inefficient process, with additional administrative burden for clinical teams. However, web-based software, platforms, and apps are now being used for end-to-end management of PROMs, from automation of distributing, capturing, analyzing, and reporting these data. Features include automatic scoring of PROM data, interpretive dashboards and reports for clinicians, alerts to notify clinical teams of patients' acute needs for symptom management, integration with electronic health records, and notification reminders tailored for patients [25].

One example of a fully digital PROMs system is the Symptom Tracking and Reporting (STAR) system used to assess a patient's functional recovery after radical prostatectomy at Memorial Sloan-Kettering Cancer Center [26]. The web-based

XSL•FO
RenderX

system is used to collect PROMs on urinary function, sexual function, bowel function, and overall quality of life. Patients are automatically emailed a unique link with access to a web-based portal for symptom reporting. Clinicians and patients can view numerical and graphical summaries of patients' reported PROM scores, with prediction models of a patient's future functional status. Tell Us, a web-based system designed for patients with advanced cancer in palliative care, has similar functionalities to STAR, but with the additional ability to trigger real-time alerts to clinical teams when intervention is necessary. The field is growing rapidly [5,27].

Previous studies had confirmed the effect of PROMs on patients in tertiary hospitals [28,29]. A study in a tertiary care center among patients with septoplasty and functional endoscopic sinus surgery found that due to the high response rates, PROMs that use mobile digital patient engagement platforms could effectively monitor postoperative outcomes [30]. Another study in a tertiary care center specialized in skull base diseases also showed that administering digital PROMs seems appropriate for evaluating health-related quality of life in skull base disorders [31].

Research Gaps and Study Aims

In conclusion, the integration of digital transformation, VBHC, and PROMs had been discussed in the previous study [32-34]. However, few studies had ever investigated the specific role and impact of digital health solutions in driving VBHC [5], as well as specific clinical efficiency gains and resource savings from the adoption of digital health technologies [35] and the specific ways and effects of how digital health solutions could be used to personalize treatment [36,37].

Thus, this article aimed to explain the role that digital health solutions played in advancing VBHC. It examined the challenges that came with adopting these technologies and highlighted the work of health startups that were committed to assisting health care organizations in their shift toward value-based care models.

Key Challenges

Although digital transformation facilitates the transition of traditional health models toward VBHC, implementation and adaptation are also needed from the many different stakeholders [38]. A shift in the overall cultural and behavioral environment requires a transition in clinical governance, management, and policy making, which in turn needs the joint contributions of health care professionals, payers, policy makers, caregivers, and, crucially, patients.

One of the key challenges of implementing VBHC in a health system is to facilitate and incentivize stakeholders to commit to capturing and reporting PROs along with clinical outcomes. Taking insights generated from PROs into decision-making processes (eg, care plan development, selection of treatments or therapies) unleashes the power and value of PROs and other patient-generated health data (PGHD), such as objective data captured by wearable devices. However, the applications of PROs and other PGHD into routine patient care will lead to a disruption of the health care governance and clinical practice.

Despite a growing consensus on the utility of PROs in clinical care, most of their applications remain in research or academic initiatives [39]. One major barrier to integrating PROs into clinical practice is the lack of standardization of how PROs are measured [40]. Measurement of PROs can range from unstructured patient diaries to structured clinically validated questionnaires, such as PROMs. More sophisticated questions, such as when to disseminate PROMs to patients, how often to send these PROMs, and what data analysis should be done with the data, are usually raised once the appropriate PROMs are identified for a target patient group. These questions highlight the importance of standardizing the method of PROMs selection and implementation.

Even if there are incentives and standardized PROMs, leadership, resources, and support are needed to encourage current health systems and physicians to change. Introducing an additional workflow of PRO data collection and application may present significant increases in workload for health care providers. This is where a professionally developed and validated digital solution can play its role in the process of digital transformation of the health system toward VBHC. Not only can digital solutions reduce the burden of collecting and using PRO data, but they should also support health care providers in their routine workflow (eg, enabling patient screening, follow-up care, support of self-management, etc), which will further incentivize health care providers to use the platform.

Digital Health Approach

Digital health innovators are at the forefront of advocating for the adoption of VBHC, particularly in addressing the challenges of real-world implementation. Their mission is to assist health care organizations globally in transitioning to a VBHC model by providing tools that promote a patient-centered care approach.

Typically, digital solutions involve cloud-based Software as a Service digital platforms with automated and streamlined digital care pathways, reducing manual and costly processes. Digital care pathways use digital technologies to coordinate the monitoring, engagement, and support of patients throughout their care continuum, consolidating these processes into a unified system that collects, analyzes, and manages PGHD, including PROs and wearable or medical device data. They also deliver educational information to patients and providers.

Moving beyond traditional electronic data capture systems and generic customer relationship management platforms, digital platforms can seamlessly combine clinical and non-clinical data through integration with electronic medical records and clinical workflows. Thus, with a fully configurable, disease and device-agnostic platform, health professionals are equipped with a single, patient-centric system for managing communication, data collection, and analysis, providing real-time actionable information and insights to inform and improve patient care and management. The digital care pathway enhanced access to patient information and accelerated the provision of early specialist care [41]. Previous study had confirmed that digital transmural care pathway was feasible and

XSL•FO
RenderX

beneficial in daily clinical care for patients with lung cancer [42].

For each medical condition and treatment, there are four broad phases in developing value-based digital care pathways: (1) defining schedules, (2) content creation, (3) automated patient engagement, and (4) insight generation. In developing new digital care pathways, they assist health care organizations in identifying areas of digitization that best benefit individual organizations and align with best practice recommendations, such as the frameworks set up by the International Consortium for Health Outcomes Measurement (ICHOM). Every touchpoint within a patient's care journey is digitally transformed and automated from their admission to discharge, including communication sent out to patients, the type and frequency of health data collected, the educational material delivered, and reports to be generated. For each digital interaction, a patient's health data is automatically captured and presented with actionable insights, ensuring providers have access to the right information for delivering high-quality care.

All 4 key components of value (allocative, technical, personal, and societal) can be enhanced through adopting digital health platforms [18]. The digital platform helps in the following ways.

The first is by improving data collection. Digital innovations transform the way data is collected, shared, and analyzed, significantly enhancing clinical decision-making, improving quality of care, and reducing health care costs [43]. The digital platform enables efficient collection of patient-generated data (eg, PROMs) through automation, thus overcoming barriers like time constraints and resource limitations. This leads to a broader scope of data collection beyond clinical data, reducing the time spent administering assessments. A systematic review found that electronic platforms simplified the implementation of PROMs in the lung cancer daily clinic [44].

The second is by enhancing clinical outcomes. To improve clinical health outcomes, both health care providers and patients need access to specific tools for the collection and analysis of patient data: assessment forms, wearables, or medical devices. These specialized tools are being used more and more to identify health risks and support diagnosis, treatment, and monitoring of both health and disease [45]. In this way, health care providers gain a holistic understanding of each patient's unique health status and needs, leading to better-informed diagnosis and treatment decisions.

The third is by improving the performance and standardization of PROMs. Addressing the challenge of standardization in value-based care is crucial. The digital platform aids in implementing a structured and standardized approach to collecting and processing PROMs. A digital platform can allow for detailed measurement of recovery by regularly collecting PROMs, which can be used clinically to support recovery. Using a digital platform makes it possible to automate PROM data collection and characterize recovery across multiple domains, and this approach is likely to be implementable in clinical settings [29]. By adopting digital and automated condition-specific care pathways, health care providers can obtain high-quality data that drive personalization of patient diagnostic and treatment plans and achieve cross-organizational benchmarking for performance and quality of care improvement.

Case Example: Implementation of Digital Platform for PROMs

Patients with lung cancer undergoing chemotherapy commonly experience a range of symptoms that vary in severity, with some indicative of critical oncological emergencies. To monitor patients' symptoms and progress, traditional care processes can take up to 30 minutes, which includes having a nurse practitioner call patients for a weekly check-in, manually noting and transferring this information to an electronic medical record, and then working through required interventions. However, this is a time- and resource-intensive process, inefficient for the management of increasing workloads and patients.

Based on the following reasons, a hospital in Brisbane was selected to work with. First, a tertiary hospital in Brisbane, Australia, was selected as the case study site based on the actual needs and achievements of the hospital in the application of digital health platforms. There was a high demand for the management of postchemotherapy side effects in patients with lung cancer at this hospital, and it was already practically applying the digital platform for monitoring and intervention, which provides a realistic basis for the study. Second, the hospital's challenges in managing postchemotherapy side effects, such as inefficiencies in traditional methods that result in high time and resource costs, make the hospital's real-world problem consistent with the study's goals on how to improve health care efficiencies and patient outcomes through digital health innovations based on PROMs. Working with the hospital, the authors used a digital health platform to monitor and address postchemotherapy side effects in patients with lung cancer. The platform was used to configure a digital care pathway that enabled the automation of the collection and analysis of 12 key posttreatment chemotherapy-related symptoms using PROMs, with real-time alerts when oncological emergencies were reported. This initiative has had positive impacts for both clinical teams and patients: improved clinical efficiencies, patient outcomes, and patient empowerment.

Capturing patient responses allowed clinical teams to effectively analyze patient outcomes, contributing to improved and personalized treatment decisions. Clinical teams have noted significant time and cost savings, with an average reduction of 10 posttreatment phone calls, spanning 20 minutes per call, to identify patients requiring clinical interventions [46]. Improved operational efficiency has allowed the oncology team to handle an increasing workload while maximizing patient outcomes.

Additionally, real-time data on patient conditions improve clinical decision-making and reduce unnecessary hospitalization and travel costs for patients. Clinical teams have noted that employment of the digital health platform has allowed the effective identification of patients suitable for treatments without hospital consultations compared to those requiring a doctor's review. By including patients' voices in the decision-making process, it empowers patients to actively engage in their

XSL•FO
RenderX

treatment plans and feel confident in reporting their outcomes using the digital service.

To conclude, at the hospital in Brisbane, the digital platform enabled clinical process optimization by automating the monitoring and handling of chemotherapy side effects. The use of this digital platform demonstrated that patient care could be significantly more efficient and effective by collecting and analyzing patient data in real time. The digital platform not only reduced the reliance on traditional phone checks but also provided a real-time alert system that quickly identified patients in need of urgent care. This approach highlighted the practical application of digital health solutions in VBHC and their contribution to improving patient outcomes. Meanwhile, the case hospital reduced phone check-in time per patient through the digital platform, reducing the number of calls to be handled from an average of 10 to 0. In addition, the clinical team was able to more efficiently identify and prioritize patients requiring urgent intervention. These improvements not only increased efficiency but also saved significant time and resources, allowing the hospital to handle a larger patient load. This illustrated how digital health tools could help hospitals improve clinical efficiency despite limited resources. Furthermore, the digital platform enabled the hospital's oncology team to provide more personalized care through real-time data analytics that allowed them to adjust treatment plans based on each patient's specific symptoms. This customized approach to treatment helped optimize outcomes for each patient and improve overall quality of care. It illustrated how digital platforms could support VBHC through a personalized approach, enhancing the precision and effectiveness of patient care.

Contribution

This paper could make several important contributions to the field of VBHC and the knowledge base of digital transformation in health care. First, it enhanced understanding of digital health solutions by analyzing the roles of various digital health technologies, including mHealth, wearable devices, telehealth, and personalized medicine. This study clarified how these innovations contributed to the goals of VBHC. It provided a nuanced discussion on how these technologies could improve diagnostic accuracy, expand treatment options, and enhance overall health outcomes. Second, this research identified key challenges in the implementation of VBHC, such as the need for stakeholder engagement and the standardization of PROMs. It provided a detailed discussion of these challenges and proposed potential solutions, thereby offering practical guidance for overcoming barriers to VBHC adoption. Third, this study provided empirical evidence of digital platforms through real-life case studies. This study demonstrated the tangible impacts of digital platforms on health care efficiencies, patient outcomes, and patient empowerment, and the case example offered concrete evidence of how digital health solutions could facilitate the transition to VBHC models and improved care delivery.

Overall, this paper contributed valuable insights into how digital transformation and VBHC could be effectively integrated to create a health care system that prioritizes high-quality, efficient, and patient-centered care.

Future Directions

Digital solutions have played a growing role in the accomplishment of VBHC. In the near future, digital solutions with strong interoperability and accreditation from academic or standardization development bodies (eg, ICHOM) will have their competitive advantages. With the increasing number of digital solutions and systems to be used by a health system, interoperability plays a vital role in determining how easily a digital solution can work across different systems. Working closely with academic or standardization development bodies will ensure digital solutions are more usable and adaptable by health care providers, with measures developed or codeveloped by providers and validated in real-world settings. Due to the lack of standardized regulatory and coding standards with the provision of PROMs, revision and development of policies to support standards for PROMs usage and interoperability need to be better developed for the successful adoption of value-based models. With better regulation and policies in place, this would encourage more funding opportunities for value-based initiatives. While it has been a complex health care process, we have seen the accelerated growth and adaptation enabled by the COVID-19 pandemic [47], with many more untapped needs to be addressed.

Conclusions

The paradigm shift toward VBHC represents not merely a shift in health care delivery metrics but also a fundamental transformation in how health care value is perceived and measured. Central to this transformation is the role of digital technology, which has become a cornerstone in the global pursuit of VBHC.

Digital transformation in health care involves far more than just the adoption of new technologies. It encompasses the standardization of measures to ensure consistency and comparability across different systems and regions. This standardization is crucial for accurately assessing and comparing health care outcomes, which is a fundamental aspect of VBHC. Additionally, innovation in data applications plays a pivotal role. The ability to effectively collect, analyze, and use vast amounts of health data can drive improvements in patient care, enhance operational efficiency, and inform policy decisions.

Engagement with stakeholders is another critical element in this transition. VBHC requires the active participation of all parties involved in health care, including providers, patients, payers, policy makers, and technology developers. Each stakeholder brings unique insights and expertise, contributing to a more holistic approach to health care reform. Collaborative efforts are essential in addressing the challenges and leveraging the opportunities presented by digital transformation.

The execution of digital transformation in health care offers numerous opportunities for stakeholders to work together toward a common goal. This collaboration can lead to the development of innovative solutions, the optimization of resource allocation, and the delivery of care that truly meets the needs and expectations of patients. Moreover, it can ensure that the benefits

XSL•FO
RenderX

of VBHC are realized broadly, leading to tangible improvements in health care outcomes, patient satisfaction, and system sustainability.

In conclusion, the journey toward VBHC is complex and challenging, yet it is filled with immense potential. By embracing digital transformation and fostering collaboration among all stakeholders, the health care sector can achieve a system that not only values quality over quantity but also delivers care that is equitable, efficient, and truly patient-centered. The future of health care lies in harnessing the power of digital innovation to create a system where value and quality are at the forefront of every decision and action.

Acknowledgments

The writing of this viewpoint was fully supported by Hangzhou City University. We extend our gratitude to Miss Natasha Tang, the business development manager at The Clinician Ltd., for participating in our interview and sharing valuable insights for the case example discussed in the manuscript.

Authors' Contributions

LZ contributed to the article writing and article review. CB contributed to the concept development and article reviewing. JC provided cultural insights for article writing and article reviewing.

Conflicts of Interest

None declared.

References

1. What is digital health? U.S. Food & Drug Administration. 2020. URL: https://www.fda.gov/medical-devices/digital-health-center-excellence/what-digital-health [accessed 2025-01-14]
2. McGinnis JM, Fineberg HV, Dzau VJ. Advancing the learning health system. N Engl J Med 2021 Jul 1;385(1):1-5. [doi: 10.1056/NEJMp2103872] [Medline: 34192452]
3. Kokshagina O, Keränen J. Institutionalizing value-based healthcare in a service system: a policy and document analysis over three decades. J Bus Ind Market 2022 Jun 21;37(8):1607-1622. [doi: 10.1108/JBIM-08-2020-0380]
4. Vial G. Understanding digital transformation: a review and a research agenda. J Strateg Inf Syst 2019 Jun;28(2):118-144. [doi: 10.1016/j.jsis.2019.01.003]
5. Rosalia RA, Wahba K, Milevska-Kostova N. How digital transformation can help achieve value-based healthcare: Balkans as a case in point. Lancet Reg Health Eur 2021 May;4:100100. [doi: 10.1016/j.lanepe.2021.100100] [Medline: 34557815]
6. Will tech save healthcare? About Digital Health. 2021. URL: https://aboutdigitalhealth.com/2021/02/10/will-tech-save-healthcare [accessed 2025-01-14]
7. Rani R, Kumar R, Mishra R, Sharma SK. Digital health: a panacea in COVID-19 crisis. J Family Med Prim Care 2021 Jan;10(1):62-65. [doi: 10.4103/jfmpc.jfmpc_1494_20] [Medline: 34017704]
8. Herzlinger RE. How to solve the cost crisis in health care. Harv Bus Rev 2011 Nov;89(11):22, discussion 23. [Medline: 22111427]
9. Blackstone EA, Fuhr JP. Redefining health care: creating value-based competition on results. Atl Econ J 2007 Dec;35(4):491-501. [doi: 10.1007/s11293-007-9091-9]
10. Moliner MA. Loyalty, perceived value and relationship quality in healthcare services. J Serv Manag 2009 Mar 13;20(1):76-97. [doi: 10.1108/09564230910936869]
11. Lee SJ, Venkataraman S, Heim GR, Roth AV, Chilingerian J. Impact of the value‐based purchasing program on hospital operations outcomes: an econometric analysis. J of Ops Management 2020 Jan;66(1-2):151-175. [doi: 10.1002/joom.1057]
12. Broerse JEW, Grin J. The future of healthcare systems: beyond the persistence of contemporary challenges. In: Toward Sustainable Transitions in Healthcare Systems: Routledge; 2017. [doi: 10.4324/9781315232133]
13. Porter ME, Kaplan RS. How to pay for health care. Harvard Business Review. 2016. URL: https://hbr.org/2016/07/how-to-pay-for-health-care [accessed 2025-01-14]
14. Berry LL. Service innovation is urgent in healthcare. AMS Rev 2019 Jun;9(1-2):78-92. [doi: 10.1007/s13162-019-00135-x]
15. Zeigler B, Traoré M, Zacharewicz G, Duboz R. Value-Based Learning Healthcare Systems: Integrative Modeling and Simulation: The Institution of Engineering and Technology; 2018.
16. Teisberg E, Wallace S, O'Hara S. Defining and implementing value-based health care: a strategic framework. Acad Med 2020 May;95(5):682-685. [doi: 10.1097/ACM.0000000000003122] [Medline: 31833857]
17. Lehtonen L, Wild C, Ricciardi W, et al. Defining Value in "Value-Based Healthcare": Report of the Expert Panel on Effective Ways of Investing in Health (EXPH): European Union; 2019.
18. Fendrick AM, Chernew ME, Levi GW. Value-based insurance design: embracing value over cost alone. Am J Manag Care 2009 Dec;15(10 Suppl):S277-S283. [Medline: 20088631]

XSL•FO
RenderX

19. Enthoven AC, Crosson FJ, Shortell SM. “Redefining health care”: medical homes or archipelagos to navigate? Health Aff (Millwood) 2007;26(5):1366-1372. [doi: 10.1377/hlthaff.26.5.1366] [Medline: 17848447]
20. Warsame R, D’Souza A. Patient reported outcomes have arrived: a practical overview for clinicians in using patient reported outcomes in oncology. Mayo Clin Proc 2019 Nov;94(11):2291-2301. [doi: 10.1016/j.mayocp.2019.04.005] [Medline: 31563425]
21. Black N. Patient reported outcome measures could help transform healthcare. BMJ 2013 Jan 28;346:f167. [doi: 10.1136/bmj.f167] [Medline: 23358487]
22. Cleeland CS. Symptom burden: multiple symptoms and their impact as patient-reported outcomes. J Natl Cancer Inst Monogr 2007;2007(37):16-21. [doi: 10.1093/jncimonographs/lgm005] [Medline: 17951226]
23. Gibbons C, Porter I, Gonçalves-Bradley DC, et al. Routine provision of feedback from patient-reported outcome measurements to healthcare providers and patients in clinical practice. Cochrane Database Syst Rev 2021 Oct 12;10(10):CD011589. [doi: 10.1002/14651858.CD011589.pub2] [Medline: 34637526]
24. Bennett AV, Jensen RE, Basch E. Electronic patient-reported outcome systems in oncology clinical practice. CA Cancer J Clin 2012;62(5):337-347. [doi: 10.3322/caac.21150] [Medline: 22811342]
25. Vickers AJ, Savage CJ, Shouery M, Eastham JA, Scardino PT, Basch EM. Validation study of a web-based assessment of functional recovery after radical prostatectomy. Health Qual Life Outcomes 2010 Aug 5;8:82. [doi: 10.1186/1477-7525-8-82] [Medline: 20687938]
26. Cox CE, Wysham NG, Kamal AH, et al. Usability testing of an electronic patient-reported outcome system for survivors of critical illness. Am J Crit Care 2016 Jul;25(4):340-349. [doi: 10.4037/ajcc2016952] [Medline: 27369033]
27. Perry LM, Morken V, Peipert JD, et al. Patient-reported outcome dashboards within the electronic health record to support shared decision-making: protocol for co-design and clinical evaluation with patients with advanced cancer and chronic kidney disease. JMIR Res Protoc 2022 Sep 21;11(9):e38461. [doi: 10.2196/38461] [Medline: 36129747]
28. Orman ES, Ghabril MS, Desai AP, et al. Patient-reported outcome measures modestly enhance prediction of readmission in patients with cirrhosis. Clin Gastroenterol Hepatol 2022 Jun;20(6):e1426-e1437. [doi: 10.1016/j.cgh.2021.07.032] [Medline: 34311111]
29. Mori M, Dhruva SS, Geirsson A, Krumholz HM. Characterization of multi-domain postoperative recovery trajectories after cardiac surgery using a digital platform. NPJ Digit Med 2022 Dec 24;5(1):192. [doi: 10.1038/s41746-022-00736-0] [Medline: 36564550]
30. Khanwalkar AR, Shen J, Kern RC, et al. Utilization of a novel interactive mobile health platform to evaluate functional outcomes and pain following septoplasty and functional endoscopic sinus surgery. Int Forum Allergy Rhinol 2019 Apr;9(4):345-351. [doi: 10.1002/alr.22273] [Medline: 30586227]
31. Steiert C, Lambeck J, Grauvogel TD, Beck J, Grauvogel J. Digital patient-reported outcome measures assessing health-related quality of life in skull base diseases-analysis of feasibility and pitfalls two years after implementation. Healthcare (Basel) 2023 Feb 6;11(4):472. [doi: 10.3390/healthcare11040472] [Medline: 36833006]
32. Fuchs B, Schelling G, Elyes M, et al. Unlocking the power of benchmarking: real-world-time data analysis for enhanced sarcoma patient outcomes. Cancers (Basel) 2023 Sep 2;15(17):4395. [doi: 10.3390/cancers15174395] [Medline: 37686671]
33. Walshe J, Akbari A, Hawthorne AB, Laing H. Data linkage can reduce the burden and increase the opportunities in the implementation of Value-Based Health Care policy: a study in patients with ulcerative colitis (PROUD-UC Study). Int J Popul Data Sci 2021;6(3):1705. [doi: 10.23889/ijpds.v6i3.1705] [Medline: 37649471]
34. Silveira Bianchim M, Crane E, Jones A, et al. The implementation, use and impact of patient reported outcome measures in value-based healthcare programmes: a scoping review. PLoS One 2023;18(12):e0290976. [doi: 10.1371/journal.pone.0290976] [Medline: 38055759]
35. Carini E, Villani L, Pezzullo AM, et al. The impact of digital patient portals on health outcomes, system efficiency, and patient attitudes: updated systematic literature review. J Med Internet Res 2021 Sep 8;23(9):e26189. [doi: 10.2196/26189] [Medline: 34494966]
36. Cancela J, Charlafti I, Colloud S, Wu C. Chapter 2 - digital health in the era of personalized healthcare: opportunities and challenges for bringing research and patient care to a new level. In: Syed-Abdul S, Zhu X, Fernandez-Luque L, editors. Digital Health: Mobile and Wearable Devices for Participatory Health Applications: Elsevier; 2021:7-31. [doi: 10.1016/B978-0-12-820077-3.00002-X]
37. Johnson KB, Wei WQ, Weeraratne D, et al. Precision medicine, AI, and the future of personalized health care. Clin Transl Sci 2021 Jan;14(1):86-93. [doi: 10.1111/cts.12884] [Medline: 32961010]
38. Snyder CF, Aaronson NK, Choucair AK, et al. Implementing patient-reported outcomes assessment in clinical practice: a review of the options and considerations. Qual Life Res 2012 Oct;21(8):1305-1314. [doi: 10.1007/s11136-011-0054-x] [Medline: 22048932]
39. Basch E. Patient-reported outcomes - harnessing patients’ voices to improve clinical care. N Engl J Med 2017 Jan 12;376(2):105-108. [doi: 10.1056/NEJMp1611252] [Medline: 28076708]
40. Monitoring and evaluating digital health interventions. World Health Organization. 2016. URL: https://www.who.int/publications/i/item/9789241511766 [accessed 2025-01-14]

XSL•FO
RenderX

41. Connell A, Black G, Montgomery H, et al. Implementation of a digitally enabled care pathway (part 2): qualitative analysis of experiences of health care professionals. J Med Internet Res 2019 Jul 15;21(7):e13143. [doi: 10.2196/13143] [Medline: 31368443]
42. Demedts I, Himpe U, Bossuyt J, et al. Clinical implementation of value based healthcare: Impact on outcomes for lung cancer patients. Lung Cancer (Auckl) 2021 Dec;162:90-95. [doi: 10.1016/j.lungcan.2021.10.010] [Medline: 34763159]
43. Nguyen H, Butow P, Dhillon H, Sundaresan P. A review of the barriers to using patient-reported outcomes (PROs) and patient-reported outcome measures (PROMs) in routine cancer care. J Med Radiat Sci 2021 Jun;68(2):186-195. [doi: 10.1002/jmrs.421] [Medline: 32815314]
44. Bouazza YB, Chiairi I, El Kharbouchi O, et al. Patient-reported outcome measures (PROMs) in the management of lung cancer: a systematic review. Lung Cancer (Auckl) 2017 Nov;113:140-151. [doi: 10.1016/j.lungcan.2017.09.011] [Medline: 29110842]
45. Bombard Y, Ginsburg GS, Sturm AC, Zhou AY, Lemke AA. Digital health-enabled genomics: opportunities and challenges. Am J Hum Genet 2022 Jul 7;109(7):1190-1198. [doi: 10.1016/j.ajhg.2022.05.001] [Medline: 35803232]
46. The clinician case study. Amazon Web Services. 2021. URL: https://aws.amazon.com/solutions/case-studies/the-clinician-case-study [accessed 2025-01-14]
47. Nimako K, Kruk ME. Seizing the moment to rethink health systems. Lancet Glob Health 2021 Dec;9(12):e1758-e1762. [doi: 10.1016/S2214-109X(21)00356-9] [Medline: 34506770]

Abbreviations

ICHOM: International Consortium for Health Outcomes Measurement
mHealth: mobile health
PGHD: patient-generated health data
PRO: patient-report outcome
PROM: patient-reported outcome measure
STAR: Symptom Tracking and Reporting
VBHC: value-based health care

Edited by C Lovis; submitted 15.02.24; peer-reviewed by A George; revised version received 23.09.24; accepted 15.11.24; published 20.01.25.

Please cite as:
Zhang L, Bullen C, Chen J
Digital Health Innovations to Catalyze the Transition to Value-Based Health Care
JMIR Med Inform 2025;13:e57385
URL: https://medinform.jmir.org/2025/1/e57385
doi:10.2196/57385

© Lan Zhang, Christopher Bullen, Jinsong Chen. Originally published in JMIR Medical Informatics (https://medinform.jmir.org), 20.1.2025. This is an open-access article distributed under the terms of the Creative Commons Attribution License (https://creativecommons.org/licenses/by/4.0/), which permits unrestricted use, distribution, and reproduction in any medium, provided the original work, first published in JMIR Medical Informatics, is properly cited. The complete bibliographic information, a link to the original publication on https://medinform.jmir.org/, as well as this copyright and license information must be included.

XSL•FO
RenderX

Digital Representation of Patients as Medical Digital Twins: Data-Centric Viewpoint

Stanislas Demuth[1,2], MD, MSc; Jérôme De Sèze[2,3], MD, PhD; Gilles Edan[4], MD, PhD; Tjalf Ziemssen[5], MD, PhD; Françoise Simon[6,7], PhD; Pierre-Antoine Gourraud[1,8], MPH, PhD

[1]INSERM U1064, CR2TI - Center for Research in Transplantation and Translational Immunology, Nantes University, 30 Bd Jean Monnet, Nantes, France

[2]INSERM CIC 1434 Clinical Investigation Center, University Hospital of Strasbourg, Strasbourg, France

[3]Department of Neurology, University Hospital of Strasbourg, Strasbourg, France

[4]Department of Neurology, University Hospital of Rennes, Rennes, France

[5]Center of Clinical Neuroscience, University Hospital Carl Gustav Carus, Dresden, Germany

[6]Department of Health Policy & Management, Columbia University, New York, NY, United States

[7]Mount Sinai School of Medicine, New York, NY, United States

[8]Pôle Hospitalo-Universitaire 11: Santé Publique, Clinique des données, INSERM, CIC 1413, Nantes University Hospital, Nantes, France

Corresponding Author:
Pierre-Antoine Gourraud, MPH, PhD
INSERM U1064, CR2TI - Center for Research in Transplantation and Translational Immunology, Nantes University, 30 Bd Jean Monnet, Nantes, France

Abstract

Precision medicine involves a paradigm shift toward personalized data-driven clinical decisions. The concept of a medical “digital twin” has recently become popular to designate digital representations of patients as a support for a wide range of data science applications. However, the concept is ambiguous when it comes to practical implementations. Here, we propose a medical digital twin framework with a data-centric approach. We argue that a single digital representation of patients cannot support all the data uses of digital twins for technical and regulatory reasons. Instead, we propose a data architecture leveraging three main families of digital representations: (1) multimodal dashboards integrating various raw health records at points of care to assist with perception and documentation, (2) virtual patients, which provide nonsensitive data for collective secondary uses, and (3) individual predictions that support clinical decisions. For a given patient, multiple digital representations may be generated according to the different clinical pathways the patient goes through, each tailored to balance the trade-offs associated with the respective intended uses. Therefore, our proposed framework conceives the medical digital twin as a data architecture leveraging several digital representations of patients along clinical pathways.

(JMIR Med Inform 2025;13:e53542) doi:10.2196/53542

KEYWORDS

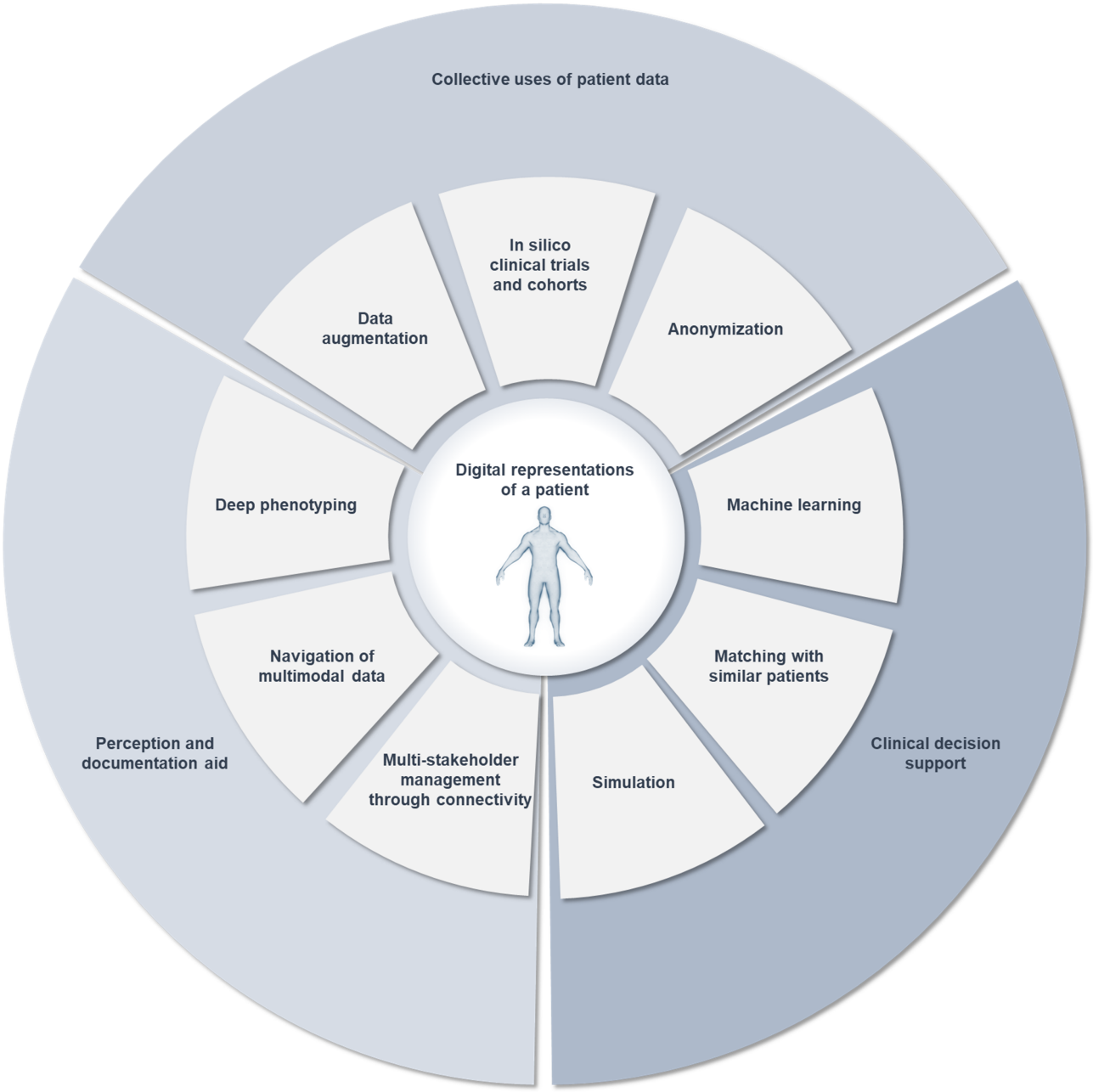
digital twin; artificial intelligence; data architecture; synthetic data; computational modeling; precision medicine; conceptual clarification; conceptual; patient; medicine; health record; digital records; synthetic patient

Introduction

Much has been published about digital twins as a landmark of the digital transition of medicine and as a technology to address the uniqueness of patients in a precision medicine framework [1]. The digital twin concept combines engineering technologies attempting to represent objects digitally while maintaining a continuous connection with the physical object in the real world [2]. The manufacturing industry uses digital twins to model physical assets computationally to optimize procedures along their life cycles such as in silico prototyping, production of regulatory evidence, and predictive maintenance [3]. However, in health care, the term “digital twin” may refer to 2 distinct frameworks. One is industrial and aims at representing medical devices digitally and their physiological environments [4]. The other is medical and aims at representing patients digitally in the context of a medical procedure [5]. As such, medical digital twins embody a paradigm shift in the intentionality of health data, from health records to actionable digital representations of patients supporting various data science applications in health (Figure 1).

XSL•FO
RenderX

Figure 1. Intended data uses related to digital twins in precision medicine. They rely on various ways of representing patients digitally. Each one may be designated as a "digital twin" in the literature, yielding ambiguity.



Representing patients digitally involves 2 major challenges compared to engineering: the complexity of the represented system and the sensitivity of patients' data. As the term "digital twin" gains popularity, confusion arises from its use to designate a wide range of data usage in health [6], summarized in Figure 1. As mentioned, from an industrial viewpoint, it may designate models of medical devices along their product life cycle [7] or patients in a virtual cohort to run in silico trials [8]. From a management viewpoint, it may designate software agents for care coordination during trauma management [9]. In a patient-centric view, it may designate a multi-stakeholder documentation system, enabling health care providers (HCPs) and patients to visualize multimodal data comprehensively [10]. In data management, it may designate the most similar record to a patient found by a matching algorithm in a reference database [11,12]. In modeling, it may designate a biomechanistic model of a body part, such as circulatory systems [13,14] or digital hearts [15]. Such broad usage of the term led to ambiguity about the nature of a medical digital twin in practice.

Here, we propose a framework for the implementation of medical digital twins from a data-centric perspective. We explain why digital representations of patients are limited due to technical and regulatory constraints. We propose three main families of digital representations (Table 1 and Figure 2) and outline their purposes and limitations: (1) multimodal dashboards integrating raw health records at the points of care to assist with perception and documentation; (2) virtual patients, which provide nonsensitive data for collective secondary uses; and (3) individual predictions that support clinical decisions along clinical pathways and medical procedures. We conclude that a single digital representation of patients cannot support a medical digital twin. Instead, we recommend designing data

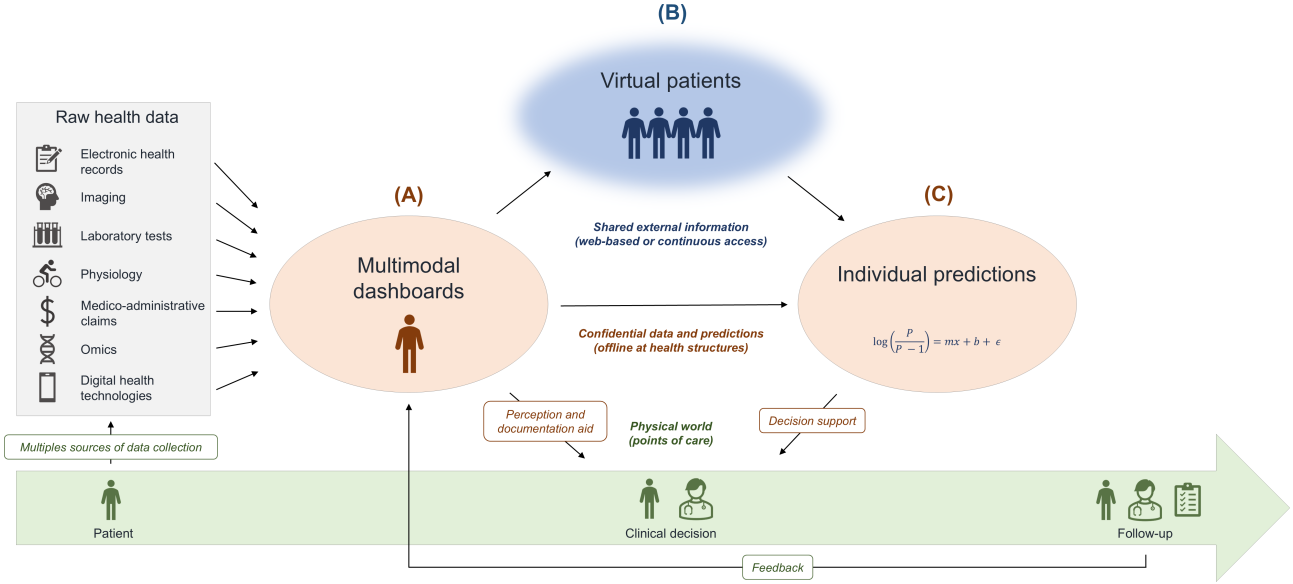
XSL•FO
RenderX

architectures, leveraging multiple digital representations of the same patient, whose characteristics would be determined by predefined data uses.

Table . Definition of the 3 types of digital representations.

Digital representation	Definition	Purpose	Limits
Multimodal dashboard	Comprehensive visualization of multimodal data	Perception and documentation aid	• Only retrospective • Regulatory obstacles to data sharing
Virtual patient	Computer-generated observations	Collective value	• On-purpose generation • Loss of the connection to the original patient
Individual prediction	Results of predictive analytics and the input preprocessed data	Clinical decision support	• Need of data preprocessing • Typically instantiated once

Figure 2. The proposed medical digital twin framework is a data architecture leveraging 3 main families of digital representations of patients. Patients are encountered at points of care (green timeline). Their data are collected in different records from multiple stakeholders (physicians, nurses, patients, etc) and modalities of investigation. These data are raw materials to be refined into different digital representations with different values. (A) The comprehensive visualization of patient data into multimodal dashboards may provide perception and documentation aid. Such data are strictly personal and confidential (orange). (B) Virtual patients may be generated as proxies of sensitive datasets to share their information content as anonymous data (blue). Careful trade-offs about utility and privacy make them useful for collective secondary uses such as the development of predictive analytics. (C) Individual predictions enrich multimodal dashboards with external information provided by predictive analytics. This data architecture also enhances follow-up by structuring the collection of data during the procedures of the corresponding clinical pathways.



Multimodal Dashboards to Provide Perception and Documentation Aids

Definition and Purpose

The first family of digital representations is the multimodal dashboard. It fetches the raw health records of a patient at the point of care from various data modalities and disparate sources across an institution's information system or a national health system. These sources may be electronic health records (EHRs), imaging, laboratory tests, physiological tests, medico-administrative claims, and more recently, telemedicine through digital health technologies. The latter may include wearable medical devices and web platforms to collect patient-reported outcome measures. The comprehensive collection of these modalities of data into multimodal dashboards aims to provide HCPs with actionable visualizations to aid their perception of a patient's health status and history (Figure 2A).

Capture of Deep Phenotypes

The state-of-the-art digital representation of patients is a set of documents. Typically, general-purpose EHRs (also called "documentation systems") only capture medico-administrative, treatments, or diagnosis codes in a structured fashion. The history and phenotypic details of the patients are captured as text data from documents and clinical notes, despite efforts to encode them into interoperable concepts [16,17]. This limits dashboards to medico-administrative timelines. Specialized EHRs encourage comprehensive structured data collection, also known as deep phenotyping [18]. Their dashboards can thus provide individual timelines relevant to particular diseases, showing trajectories of specialized concepts (eg, a disability rating scale or a specific biomarker) and histories of

XSL•FO
RenderX

disease-modifying treatments. For patients with multiple sclerosis (MS), this is featured by the European Database for Multiple Sclerosis (EDMUS) and Multiple Sclerosis Documentation System 3D (MSDS 3D) [19,20]. The structured data collection about key features of MS diagnosis and follow-up enables them to provide neurologists with summary timelines. The collected data also feed the French and German national MS registries, respectively. Disease registries are currently an invaluable tool for clinical research as they enable retrospective cohort studies to be performed on high-volume databases with specialized concepts that could not be extracted from general-purpose EHRs [21-23]. A limit of the "registry era" is that patients are typically represented only in tabular data. It is a loss of granularity because it requires HCPs to extract the features from raw imaging and signal data. It may also aggregate the information such as representing a clinical phenotype as a 1D disability scale rating. The active data collection yields a problematic amount of missing data, especially during outpatient follow-ups. As such, completion and data quality management by research assistants is usually required.

Navigation of Raw Multimodal Data

Multimodal dashboards aim at fetching data passively and provide innovative interfaces. The MS BioScreen is an iPad (Apple Inc)-based dashboard illustrating the passive integration of the clinical, biological, and raw imaging data relevant to the assessment of patients with MS [24]. This academic software fetched data collected for the EPIC cohort at the University of California, San Francisco. In addition to the specialized individual timeline, neurologists could navigate the different modalities of raw data (imaging, functional tests, genetics, etc) through the touchscreen to obtain a comprehensive view of the patient's status. Likewise, the navigation of 3D reconstructions of imaging data (sometimes called "digital clones" [25]) may support surgery planning through augmented reality [26] or robot-assisted procedures [27]. Current limits of secondary data collection include the lack of interoperability at the scale of national health systems [28]. There are efforts to develop "EHR-agnostic" platforms such as BRIDGE (University of California, San Francisco) [29]. It relies on interoperable standards to first fetch data from multiple sources and then provide customizable clinic-specific dashboards implemented as Substitutable Medical Applications and Reusable Technologies (SMART) on Fast Healthcare Interoperability Resources apps. Efficient and reliable data linkage between the various sources is critical to synchronize the records [30].

Management by Multiple Stakeholders Through Connectivity

Interoperable web-based records promise to enable multiple stakeholders to access dashboards and to contribute to the data collection along with patient follow-up. In a participative approach, patients themselves may visualize their data to support their self-management, as proposed by the open version of the MS BioScreen project [31]. Medical procedures may be continuously monitored by collecting data streams, either during a surgery procedure to give real-time feedback to the operator or along so-called "integrative digital clinical pathways" for outpatients [32]. For instance, data integration from multiple devices has been developed as an agent-based care coordination framework along a clinical pathway of severe trauma management [9]. Process-"digital twins" were developed as web microservices collecting data from the prehospital and in-hospital phases and making it accessible to the different stakeholders through their respective software agents in a multi-agent system environment. In a quality management approach, the data collection about medical procedures through MSDS 3D integrates the concept of digital clinical pathways. Its interface generates dynamically a quality matrix according to the patient's diagnosis and prescriptions [10]. Quality matrices are visual summaries derived from a set of checklists completed by all relevant stakeholders. They later support the optimization of the clinical pathways.

Summary and Limits

Therefore multimodal dashboards would be the perceptive side of the medical digital twin framework and would support the connectivity between the twin and the patient. One patient's data could be displayed by multiple dashboards, each one adapted to the role of each HCP in the relevant clinical pathway. The first limit would be their retrospective nature as external information is needed to give prospective insights and support decisions [33]. The second limit is the regulatory obstacles to sharing patient data, especially for other purposes than the care of the respective patients. Concerns about privacy and consent-restricted secondary uses of patient data have led to regulatory frameworks such as the general data protection regulation in Europe [34]. Patient data are personal, sensitive, and parsimoniously collected from and for the patient. Their collection remains centered on their primary use (ie, personal care), disregarding other secondary uses in research or clinical decision support for other patients. As a consequence, the primary personal and secondary collective uses of data are split (Table 2). The first may be done individually and confidentially. The second relies on the transfer of pseudonymized data between health care and research structures. However, medical practice in a medical digital twin framework would require continuous access to external information through reference data and predictive analytics (Table 2). Data sharing is still underdeveloped in health care because of the loss of usage control and because pseudonymized data only prevents direct reidentification [35].

XSL•FO
RenderX

Table . Key distinctions made by the proposed data architecture.

	Concept 1	Concept 2
Data processing	Data collection (full granularity)	Data preprocessing for a predictive analytic (formatted for specific analytics)
Data exchange and access	Data transfer (restricted exchange between 2 organizations)	Data sharing (continuously accessible data)
Data usage (and values)	Primary (personal care)	Secondary (research and care of others)
Data privacy	Pseudonymized (deidentified)	Anonymized (unlinked to the source patient)
Purpose	Epidemiology (optimize decisions at the populational-level)	Precision medicine (optimize decisions at the individual-level)

Virtual Patients for Collective Uses of Health Data

Definition and Purpose

The second family of digital representations is the virtual patient. It is an individual observation in a set of computer-generated observations called "synthetic data" [36]. The generation of synthetic datasets might be arbitrary, random, rule-based, or simulated from statistical or machine-learning models. Synthetic data have recently gained popularity as a technology that could facilitate secondary data uses (Figure 2B) [36,37]. An example of external information supporting medical practices is the use of normative datasets to define reference ranges for quantitative biomarkers or to standardize biomarker values according to a population distribution [38,39]. They may also help interpret qualitative biomarkers such as the pathologic significance of genetic variations. However, precision medicine requires access to data of lower granularity to personalize the assessment of patients. At the scale of a single institution, the MS BioScreen illustrates the personalization of various MS biomarkers' reference ranges according to subgroups of patients with similar profiles [24]. Reference data with individual granularity are also required to develop data-driven predictive analytics. The utility of synthetic datasets stems from (1) the structural similarity (ie, the same level of granularity), (2) the veracity of the information content (ie, the comparison with real data yields the same aggregated results), and (3) indiscernibility (ie, neither experts nor artificial intelligence can distinguish synthetic data from original data).

Potential to Develop Predictive Analytics Through Data Augmentation

Data-driven predictive analytics are developed through machine learning. In cases where high-volume datasets are not available, synthetic data may augment datasets as a workaround for laborious data collection and expert-demanding data labeling [40]. Data augmentation increases the amount of training data either by generating additional slightly modified data points [41] or by using generative artificial intelligence models, such as generative adversarial networks, variational autoencoders, or large language models [42]. For instance, synthetic magnetic resonance imaging (MRI) images with pathologic features of Alzheimer disease may be generated with a variational autoencoder, yielding increased predictive performances of an analytic predicting the diagnosis from the MRI images [43]. The augmentation may also be restricted to data from specific prediction classes to mitigate class imbalance. Synthetic Minority Over-Sampling Technique (SMOTE) is a common technique to do so [44]. In these cases, the utility of synthetic data comes from the gain of predictive performance on an external validation dataset [40,45].

Potential to Produce Evidence Through In Silico Clinical Trials and Cohorts

Synthetic data may accelerate the production of scientific or regulatory evidence through in silico studies, which rely on fully synthetic study populations. The VICTRE (Virtual Imaging Clinical Trials for Regulatory Evaluation) trial illustrates the case when real datasets would be too expensive to create [46]. This in silico cross-sectional study compared the performances of a computational reader to detect breast cancer on 31,055 synthetic full-field mammography versus 27,960 synthetic breast tomosynthesis images. Synthetic cohorts may also be generated with longer follow-ups than what could be available in real datasets. In MS, a study generated a longitudinal synthetic cohort with a discrete event simulation model of MS activity and forecast its evolution with a lifetime horizon, although the treatment of interest (ofatumumab) had only been approved in 2021 [47]. The goal was to simulate its prescription as a first-line therapy against a second-line therapy with various delays. The simulation predicted better long-term benefits of ofatumumab when prescribed as a first-line therapy. Such a synthetic dataset makes statistical inference more interpretable. Instead of analyzing the "black box" of the model itself, it uses the model in a generative fashion to represent the information it captured as a cohort of virtual patients, which can be analyzed classically.

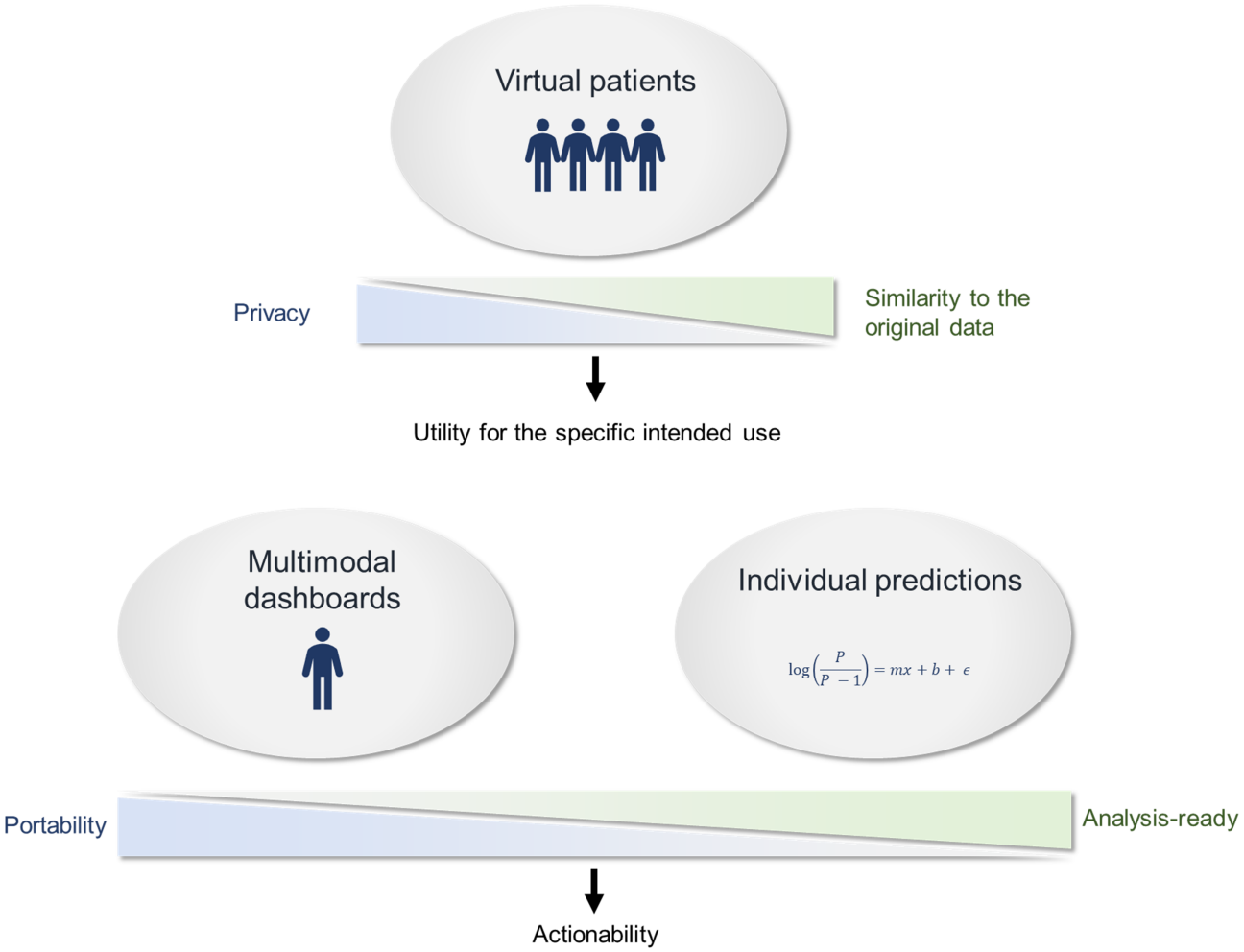
Potential to Share Information Through Anonymization

Since synthetic data are computer-generated, they are not linkable to a person and are thus assumed to be truly anonymous, as opposed to pseudonymized data. Anonymous data are shareable outside the constraints of regulatory frameworks applied to potentially identifying data. However, synthetic data generators typically do not take privacy protection into account. The generative model is indeed a link between the synthetic and the real data as the information content of the sensitive dataset is represented as a new set of individual observations. Concerns are rising about the risk of linkage between a virtual patient and a real patient (ie, membership inference attacks) [48-50]. Some synthetic data generators are first designed as

XSL•FO
RenderX

anonymization techniques, such as the avatars [51]. The avatars take real data as input to generate virtual patients with a probabilistic local model based on the nearest neighbors. The novelty of the method is that it provides privacy metrics to assess that the avatars are no longer identifiable records, even in the case of distance-based membership inference attacks. This privacy-by-design approach to synthetic data generation brings a trade-off [52]. The generation must be destructive enough to protect patients from reidentification while keeping utility for the specific intended use (Figure 3) [37].

Figure 3. The main trade-offs are addressed by the 3 families of digital representation. Real sensitive patient data may be formatted according to interoperable data models to favor data portability for multimodal dashboards or preprocessed for a specific predictive analytic. Virtual patients must balance privacy and similarity to the original data to be valuable proxies of real identifying records.



Summary and Limits

In our medical digital twin framework, we argue that virtual patients could be proxies of sensitive patient data to create collective value by sharing the information contained in sensitive datasets. The generation of synthetic data has to be on purpose to prioritize the variables to be represented in the virtual patients and to set the right trade-off between similarity to the original data and privacy. Specific utility for a given use would imply different generation settings (Table 2 and Figure 3). It could be (1) closed-loop software benchmarking with low-similarity synthetic data, (2) medical education [53] or addressing population-level questions in epidemiology (eg, performing a retrospective cohort study) with an intermediate similarity, or (3) supporting individual decisions in precision medicine with high-similarity synthetic data. Therefore, multiple virtual patients could be generated from the data of a given patient. Yet, the connection to the original patient that would be expected from a medical digital twin would be destroyed in all of them. This prevents virtual patients from supporting personal health care and to support individual predictions.

Individual Predictions to Support Clinical Decisions

Definition and Purpose

The third family of digital representations is individual prediction. Individual predictions are the results of predictive analytics that may use knowledge-based, data visualization, or model-based algorithms [54]. They enable HCPs to assess alternative scenarios to support clinical decisions such as treatment selection, risk factor prevention, or surgery planning (Figure 2C). The individual predictions of most prognosis scores in medicine use population models [55,56], meaning that decisions are optimized on average at the scale of a population. Medical digital twins aim to optimize decisions at the individual level with personalized analyses.

XSL•FO
RenderX

Personalization of the Context of Usage of Predictive Analytics

Prognosis scores and predictive analytics in general are validated in restricted contexts of usage [57]. In a chronic disease such as MS, these contexts may be diagnosis, initial prognosis, treatment selection, assessment of therapeutic response, or assessment of the transition to a secondary progressive phase [54]. Therefore management of 1 patient would require the integration of multiple predictive analytics to support different clinical decisions at different points of care along its clinical pathway. Such an approach is conveyed by the digital twin quality management framework of the MSDS 3D [10]. The structuration of health care into digital clinical pathways eases the description of the tree structure of clinical contexts along the management of chronic diseases. As such, different treatment-specific prognosis scores could be used to assess the probability of a patient to respond to each option. This could be further personalized according to the stage or subtype of the disease.

Personalization of the Analytics to Run Mechanistic Simulations

The most personalized analytics are those modeling the individual. This is the case of organ-level biomechanistic models, such as digital hearts. Their first layer is classically an anatomical mesh of an organ extracted from raw imaging data. The coupling of other modeling layers such as cell and tissue behavior yields an “embodiment” of a generic organ model in each patient’s specific anatomy [5]. Atrial fibrillation (AF) is a case where such modeling is in an early stage of clinical translation [58]. The Optimal Target Identification via the Modeling of Arrhythmogenesis procedure involves a computational model of the left atrium [58,59]. Geometric, fiber orientation, and electrophysiological tissue property layers are simulated to detect the topography of AF re-entrant drivers, including latent ones that electrocardiographic imaging would not detect. It also predicts de novo re-entrant drivers that may later perpetuate arrhythmia according to alternative scenarios of virtual ablation patterns. Thus, the Optimal Target Identification via the Modeling of Arrhythmogenesis procedure integrates the outputs of these simulations to tailor the intervention plan by performing preventive adjuvant ablations of the predicted re-emergent targets [15]. The close-loop of the disease is approached as a multi-scale system and the model enables to simulate emergence phenomena (eg, reentrant drivers) that would not be measurable, or that would occur under various therapeutic scenarios.

Personalization of the Data Use Based on the Matching With Similar Patients

In cases of statistical modeling, predictive analytics may be personalized by fitting the model at query time only on similar patients recorded in a reference database. The model decision boundaries would thus be optimized in the subset of similar patients matching the patient. The selection of similar patients may be distance-based according to a patient-similarity metric. This may imply a digital representation of patients as data points in a latent reduced multidimensional space, using linear or nonlinear dimension-reduction algorithms [60,61]. On the other hand, the selection of similar patients may be filter-based. The MS-VISTA (Nantes University) prototype of the Projections in Multiple Sclerosis project illustrates the querying of groups of similar patients in an MS randomized clinical trial dataset and the computation of a personalized prognosis to support treatment selection [62]. As such, these analytics personalize the use of continuously accessible reference data.

Summary and Limits

Individual predictions in our medical digital twin framework would therefore enrich patient data with external information provided by predictive analytics. Unlike one-size-fits-all population models, the analytic would be personalized according to the patient’s characteristics to yield a patient-specific embodiment of the model. One limit is that each model is typically instantiated once at the point of care corresponding to the respective context of usage. Even organ-level models are typically not maintained in the long run, which would be expected from medical digital twins to remain connected to the patient and support further data collection. Another limit is the need to preprocess patient data to run analytics such as the extraction of an anatomical mesh from a stack of raw images. This may involve feature extraction, feature selection, and feature engineering (eg, longitudinal aggregation, criteria fulfilments, events definition from biomarker trajectories, etc). The preprocessed digital representation of a patient therefore loses portability for other data uses (Figure 3). It may require significant computation costs and be subject to an analytic variability that would make it unfit to support personal care outside the context of usage of the analytic. Therefore, even if the analytics are personalized, a medical digital twin would have to leverage multiple shared predictive analytics, each one informing a limited number of decisions or procedures along a given clinical pathway.

Recommendations

We covered the main digital-twin applications for precision medicine and argued that they cannot all be supported by a single digital representation of a patient due to technical and regulatory constraints. We believe that the clarification of the different digital representations of patients is a foundation for an effective data strategy leveraging various concepts that are currently commonly confounded under the term “digital twins.” We highlighted three main families of digital representations (Figure 2): (1) multimodal dashboards to assist with perception and documentation; (2) virtual patients to facilitate secondary data uses; and (3) individual predictions supporting clinical decisions. For a given patient, multiple digital representations may be generated according to the different clinical pathways the patient goes through, each tailored to balance the trade-offs associated with the respective intended uses (Figure 3).

Therefore the proposed framework conceptualizes the medical digital twin as a data architecture leveraging a multitude of digital representations. It clarifies several distinctions between the characteristics of data usages (Table 2): between data collection and data preprocessing for a predictive analytic, between data transfer and data sharing, between primary personal and secondary collective usages of health data, between

XSL•FO
RenderX

pseudonymized and anonymous data, and between population models and personalized analytics. Raw health records are therefore raw material to be refined into various digital representations of patients to fuel precision medicine. Based on this clarification, we propose 3 strategic recommendations, that would ease data architecture efforts to overcome the limitations of the different families of digital representations (Textbox 1).

Textbox 1. Three recommendations to address the trade-offs of medical digital twin data architectures.

- Medical digital twin data architectures should relate several digital representations of patients, instead of a single all-encompassing representation.
- Intended data uses should be clearly defined to identify the right family of digital representation to use and to set the right trade-off when generating it.
- For collective usages, real sensitive data should be substituted by synthetic data whenever possible.

Discussion

This paper proposes a data-centric approach to clarify the practical digital representations at play in a medical digital twin framework from the intended data uses. It does not cover ethical, property, and usage control issues. Clarification efforts about medical digital twins have already been made from other perspectives. Ethical clarification has been proposed about the benefits and risks of medical digital twins [1], as well as about the conditions for medical digital twins to take on ethically justifiable forms of representation [63]. The scope of digital twin applications in the whole health care sector has been reviewed and led to advocate a global collaboration between stakeholders [6]. Clarifications of the means and objectives of the development of “supermodels” have also been postulated [64]. Efforts are made to develop the concept of medical digital twins in the form of computational modeling platforms [65]. In cardiology, a model-centric framework has been formulated, seeking the synergy between deductive and inductive reasoning, respectively conveyed by mechanistic and statistical models [5]. In MS, the clarification has been proposed in a quality management framework [10].

To highlight the perspectives of our framework, we propose road maps for 3 fictional medical digital twin projects (Table 3). Taking the management of AF as an example [58], the multimodal dashboard would collect and integrate all health data relevant to the patient within the clinical pathway of AF management. Second, synthetic heart MRIs would be used to benchmark generic AF heart models. Third, the patient-specific embodiment of an AF heart model would be used to plan an AF ablation procedure [59]. In epilepsy, the patient history and phenotype could be navigated through an epilepsy-specific dashboard. Synthetic electroencephalogram signals could help develop a seizure forecast model [66] or fit a virtual brain model [67] to the patient to support the planning of the ablation of the epileptogenic zone [68]. In MS, patients could complete symptom diaries on patient portals between the visits. They would be integrated with their imaging and therapeutic history in an MS-specific, ophthalmologist-specific, or rehabilitation-specific dashboard depending on the point of care [69]. Virtual patients generated with the avatars [51] could enable the development of a statistical model detecting transitional states to secondary progressive MS [70]. The subset of virtual patients matching the patient characteristics and planned therapeutic scenario could also be analyzed to support treatment selection [62].

XSL•FO
RenderX

Table . Road maps for fictional medical digital twin projects.

Projects	Multimodal dashboards	Virtual patients	Input and output of predictive analytics
AF[a]	• Patient-centric dashboard with anticoagulant treatment plan • AF-specific dashboard for the cardiologist	Synthetic heart MRI[b] for medical education and to benchmark mechanistic organ-level models	• Virtual heart model for AF ablation planning.
Epilepsy	• Patient-centric dashboard with antiseizure and disease-modifying treatment plans • Epilepsy-specific dashboard tailored to the epileptic disease for the neurologist	Synthetic electroencephalogram signals generated with the virtual brain to train deep learning models	• Seizure prediction model • Virtual brain to plan for the ablation of the epileptic zone
MS[c]	• Patient-centric dashboard with treatment plans and symptoms diaries • Ophtalmologist-specific dashboard tailored to optic neuritis • MS-specific dashboard for the neurologist • MS-specific dashboard for rehabilitation	Synthetic cohort of tabular individual patient data generated with the avatars to fit statistical models	• Statistical model for detection of transitional state to secondary progressive MS • Matching with similar patients to support treatment selection

[a]AF: atrial fibrillation.

[b]MRI: magnetic resonance imaging.

[c]MS: multiple sclerosis.

Conclusion

We propose a medical digital twin framework as a data architecture leveraging several digital representations of patients, instead of a single all-encompassing representation. The generations of digital representations would be determined by the technical and regulatory constraints of the intended data uses as well as their positioning along clinical pathways.

Acknowledgments

We thank Mike Hess, MSc, and Nathalie Virag, PhD, at Medtronic, a medical device company, and Shibeshih Mitiku Belachew, MD, PhD, at Biogen, a biopharmaceutical company, for their interviews, feedback, and proposals that helped conceptualize this viewpoint.

Conflicts of Interest

PAG is the founder of Methodomics (2008) and the cofounder of Big Data Santé (2018). He consults for major pharmaceutical companies, all of which are handled through academic pipelines (AstraZeneca, Biogen, Boston Scientific, Cook, Edimark, Ellipses, Elsevier, Methodomics, Merck, Mérieux, Sanofi-Genzyme, and Octopize). PAG is a volunteer board member at AXA not-for-profit mutual insurance company (2021). He has no prescription activity with either drugs or devices. JDS declares an honorarium and travel grant from Biogen and Merck. SD, GE, TZ, and FS have nothing to disclose.

References

1. Popa EO, van Hilten M, Oosterkamp E, Bogaardt MJ. The use of digital twins in healthcare: socio-ethical benefits and socio-ethical risks. Life Sci Soc Policy 2021 Jul 5;17(1):6. [doi: 10.1186/s40504-021-00113-x] [Medline: 34218818]
2. Grieves M, Vickers J. Digital twin: mitigating unpredictable, undesirable emergent behavior in complex systems. In: Kahlen FJ, Flumerfelt S, Alves A, editors. Transdisciplinary Perspectives on Complex Systems: Springer International Publishing; 2017:85-113. [doi: 10.1007/978-3-319-38756-7_4]
3. Tao F, Cheng J, Qi Q, Zhang M, Zhang H, Sui F. Digital twin-driven product design, manufacturing and service with big data. Int J Adv Manuf Technol 2018 Feb;94(9-12):3563-3576. [doi: 10.1007/s00170-017-0233-1]
4. Morrison TM, Pathmanathan P, Adwan M, Margerrison E. Advancing regulatory science with computational modeling for medical devices at the FDA's office of science and engineering laboratories. Front Med (Lausanne) 2018;5:241. [doi: 10.3389/fmed.2018.00241] [Medline: 30356350]
5. Corral-Acero J, Margara F, Marciniak M, et al. The "Digital Twin" to enable the vision of precision cardiology. Eur Heart J 2020 Dec 21;41(48):4556-4564. [doi: 10.1093/eurheartj/ehaa159] [Medline: 32128588]

XSL•FO
RenderX

6. Katsoulakis E, Wang Q, Wu H, et al. Digital twins for health: a scoping review. NPJ Digit Med 2024 Mar 22;7(1):77. [doi: 10.1038/s41746-024-01073-0] [Medline: 38519626]
7. Hirschvogel M, Jagschies L, Maier A, Wildhirt SM, Gee MW. An in silico twin for epicardial augmentation of the failing heart. Numer Methods Biomed Eng 2019 Oct;35(10):e3233. [doi: 10.1002/cnm.3233]
8. Björnsson B, Borrebaeck C, Elander N, et al. Digital twins to personalize medicine. Genome Med 2019 Dec 31;12(1):4. [doi: 10.1186/s13073-019-0701-3] [Medline: 31892363]
9. Croatti A, Gabellini M, Montagna S, Ricci A. On the integration of agents and digital twins in healthcare. J Med Syst 2020 Aug 4;44(9):161. [doi: 10.1007/s10916-020-01623-5] [Medline: 32748066]
10. Voigt I, Inojosa H, Dillenseger A, Haase R, Akgün K, Ziemssen T. Digital twins for multiple sclerosis. Front Immunol 2021;12:669811. [doi: 10.3389/fimmu.2021.669811] [Medline: 34012452]
11. Fagherazzi G. Deep digital phenotyping and digital twins for precision health: time to dig deeper. J Med Internet Res 2020 Mar 3;22(3):e16770. [doi: 10.2196/16770] [Medline: 32130138]
12. Acosta JN, Falcone GJ, Rajpurkar P, Topol EJ. Multimodal biomedical AI. N Med 2022 Sep;28(9):1773-1784. [doi: 10.1038/s41591-022-01981-2] [Medline: 36109635]
13. Chakshu NK, Carson J, Sazonov I, Nithiarasu P. A semi‐active human digital twin model for detecting severity of carotid stenoses from head vibration—a coupled computational mechanics and computer vision method. Int J Numer Method Biomed Eng 2019 May;35(5):e3180. [doi: 10.1002/cnm.3180] [Medline: 30648344]
14. Chakshu NK, Sazonov I, Nithiarasu P. Towards enabling a cardiovascular digital twin for human systemic circulation using inverse analysis. Biomech Model Mechanobiol 2021 Apr;20(2):449-465. [doi: 10.1007/s10237-020-01393-6] [Medline: 33064221]
15. Boyle PM, Zghaib T, Zahid S, et al. Computationally guided personalized targeted ablation of persistent atrial fibrillation. Nat Biomed Eng 2019 Nov;3(11):870-879. [doi: 10.1038/s41551-019-0437-9] [Medline: 31427780]
16. Athena. URL: https://athena.ohdsi.org/search-terms/start [accessed 2025-01-24]
17. Chang E, Mostafa J. The use of SNOMED CT, 2013-2020: a literature review. J Am Med Inform Assoc 2021 Aug 13;28(9):2017-2026. [doi: 10.1093/jamia/ocab084]
18. Delude CM. Deep phenotyping: the details of disease. Nat New Biol 2015 Nov 5;527(7576):S14-S15. [doi: 10.1038/527S14a] [Medline: 26536218]
19. Confavreux C, Compston DA, Hommes OR, McDonald WI, Thompson AJ. EDMUS, a European database for multiple sclerosis. J Neurol Neurosurg Psychiatry 1992 Aug;55(8):671-676. [doi: 10.1136/jnnp.55.8.671] [Medline: 1527537]
20. Eisele J, Kern R, Alexander S, Großmann L, Schultheiss T, Ziemssen T. Multiple Sclerosis Documentation System MSDS3D - innovative management of patients with multiple sclerosis (I8-1.003). Neurol (ECronicon) 2014 Apr 8;82(10_supplement):I8-1.003. [doi: 10.1212/WNL.82.10_supplement.I8-1.003] [Medline: 24343307]
21. Demuth S, Collongues N, Audoin B, et al. Rituximab de-escalation in patients with neuromyelitis optica spectrum disorder. Neurol (ECronicon) 2023 Jul 25;101(4):e438-e450. [doi: 10.1212/WNL.0000000000207443] [Medline: 37290967]
22. Jouvenot G, Courbon G, Lefort M, et al. High-efficacy therapy discontinuation vs continuation in patients 50 years and older with nonactive MS. JAMA Neurol 2024 May 1;81(5):490-498. [doi: 10.1001/jamaneurol.2024.0395] [Medline: 38526462]
23. Gavoille A, Rollot F, Casey R, et al. Acute clinical events identified as relapses with stable magnetic resonance imaging in multiple sclerosis. JAMA Neurol 2024 Aug 1;81(8):814-823. [doi: 10.1001/jamaneurol.2024.1961] [Medline: 38949816]
24. Gourraud PA, Henry RG, Cree BAC, et al. Precision medicine in chronic disease management: the multiple sclerosis BioScreen. Ann Neurol 2014 Nov;76(5):633-642. [doi: 10.1002/ana.24282] [Medline: 25263997]
25. Conejo J, Dayo AF, Syed AZ, Mupparapu M. The digital clone: intraoral scanning, face scans and cone beam computed tomography integration for diagnosis and treatment planning. Dent Clin North Am 2021 Jul;65(3):529-553. [doi: 10.1016/j.cden.2021.02.011] [Medline: 34051929]
26. Molina CA, Theodore N, Ahmed AK, et al. Augmented reality–assisted pedicle screw insertion: a cadaveric proof-of-concept study. J Neurosurg Spine 2019;31(1):139-146. [doi: 10.3171/2018.12.SPINE181142]
27. Kim HJ, Jung WI, Chang BS, Lee CK, Kang KT, Yeom JS. A prospective, randomized, controlled trial of robot-assisted vs freehand pedicle screw fixation in spine surgery. Int J Med Robot 2017 Sep;13(3):e1779. [doi: 10.1002/rcs.1779] [Medline: 27672000]
28. Lehne M, Sass J, Essenwanger A, Schepers J, Thun S. Why digital medicine depends on interoperability. NPJ Digit Med 2019;2:79. [doi: 10.1038/s41746-019-0158-1] [Medline: 31453374]
29. Bove R, Schleimer E, Sukhanov P, et al. Building a precision medicine delivery platform for clinics: the University of California, San Francisco, BRIDGE experience. J Med Internet Res 2022 Feb 15;24(2):e34560. [doi: 10.2196/34560] [Medline: 35166689]
30. Guardiolle V, Bazoge A, Morin E, et al. Linking biomedical data warehouse records with the national mortality database in France: large-scale matching algorithm. JMIR Med Inform 2022 Nov 1;10(11):e36711. [doi: 10.2196/36711] [Medline: 36318244]

XSL•FO
RenderX

31. Schleimer E, Pearce J, Barnecut A, et al. A precision medicine tool for patients with multiple sclerosis (the Open MS BioScreen): human-centered design and development. J Med Internet Res 2020 Jul 6;22(7):e15605. [doi: 10.2196/15605] [Medline: 32628124]
32. Voigt I, Benedict M, Susky M, et al. A digital patient portal for patients with multiple sclerosis. Front Neurol 2020;11:400. [doi: 10.3389/fneur.2020.00400] [Medline: 32670174]
33. Sutton RT, Pincock D, Baumgart DC, Sadowski DC, Fedorak RN, Kroeker KI. An overview of clinical decision support systems: benefits, risks, and strategies for success. NPJ Digit Med 2020;3:17. [doi: 10.1038/s41746-020-0221-y] [Medline: 32047862]
34. Chico V. The impact of the General Data Protection Regulation on health research. Br Med Bull 2018 Dec 1;128(1):109-118. [doi: 10.1093/bmb/ldy038] [Medline: 30445448]
35. Rocher L, Hendrickx JM, de Montjoye YA. Estimating the success of re-identifications in incomplete datasets using generative models. Nat Commun 2019 Jul 23;10(1):3069. [doi: 10.1038/s41467-019-10933-3] [Medline: 31337762]
36. Gonzales A, Guruswamy G, Smith SR. Synthetic data in health care: a narrative review. PLOS Dig Health 2023 Jan;2(1):e0000082. [doi: 10.1371/journal.pdig.0000082] [Medline: 36812604]
37. El Emam K. Seven ways to evaluate the utility of synthetic data. IEEE Secur Priv 2020;18(4):56-59. [doi: 10.1109/MSEC.2020.2992821]
38. Benkert P, Meier S, Schaedelin S, et al. Serum neurofilament light chain for individual prognostication of disease activity in people with multiple sclerosis: a retrospective modelling and validation study. Lancet Neurol 2022 Mar;21(3):246-257. [doi: 10.1016/S1474-4422(22)00009-6] [Medline: 35182510]
39. Su Q, Zhang S, Hu M, et al. Reference range and sociodemographic characteristics of TSH among reproductive age women in rural China. Biol Trace Elem Res 2019 Jun;189(2):336-343. [doi: 10.1007/s12011-018-1480-1] [Medline: 30143915]
40. Chen RJ, Lu MY, Chen TY, Williamson DFK, Mahmood F. Synthetic data in machine learning for medicine and healthcare. Nat Biomed Eng 2021 Jun;5(6):493-497. [doi: 10.1038/s41551-021-00751-8] [Medline: 34131324]
41. Chlap P, Min H, Vandenberg N, Dowling J, Holloway L, Haworth A. A review of medical image data augmentation techniques for deep learning applications. J Med Imaging Radiat Oncol 2021 Aug;65(5):545-563. [doi: 10.1111/1754-9485.13261] [Medline: 34145766]
42. Demuth S, Paris J, Faddeenkov I, De Sèze J, Gourraud PA. Clinical applications of deep learning in neuroinflammatory diseases: a scoping review. Rev Neurol (Paris) 2024 May 20:S0035-3787(24)00522-8. [doi: 10.1016/j.neurol.2024.04.004] [Medline: 38772806]
43. Chadebec C, Thibeau-Sutre E, Burgos N, Allassonnière S. Data augmentation in high dimensional low sample size setting using a geometry-based variational autoencoder. IEEE Trans Pattern Anal Mach Intell 2022;45(3):2879-2896. [doi: 10.1109/TPAMI.2022.3185773]
44. Chawla NV, Bowyer KW, Hall LO, Kegelmeyer WP. SMOTE: Synthetic Minority Over-Sampling Technique. JAIR 2002;16:321-357. [doi: 10.1613/jair.953]
45. Tran NT, Tran VH, Nguyen NB, Nguyen TK, Cheung NM. On data augmentation for GAN training. IEEE Trans Image Process 2021;30:1882-1897. [doi: 10.1109/TIP.2021.3049346] [Medline: 33428571]
46. Badano A, Graff CG, Badal A, et al. Evaluation of digital breast tomosynthesis as replacement of full-field digital mammography using an in silico imaging trial. JAMA Netw Open 2018 Nov 2;1(7):e185474. [doi: 10.1001/jamanetworkopen.2018.5474] [Medline: 30646401]
47. Montgomery SM, Green L, Karoui H, Nicholas R, Loh J. To wait, or too late? Modeling the effects of delayed ofatumumab treatment in relapsing-remitting multiple sclerosis. J Med Econ 2023 Dec 31;26(1):139-148. [doi: 10.1080/13696998.2022.2161746] [Medline: 35575251]
48. Chen Y, Esmaeilzadeh P. Generative AI in medical practice: in-depth exploration of privacy and security challenges. J Med Internet Res 2024 Mar 8;26:e53008. [doi: 10.2196/53008] [Medline: 38457208]
49. Roundtable of G7 data protection and privacy authorities statement on generative AI. CNIL. 2023. URL: https://www.cnil.fr/sites/cnil/files/2023-06/g7roundtable_202306_statement.pdf [accessed 2025-01-24]
50. Sun H, Zhu T, Zhang Z, Jin D, Xiong P, Zhou W. Adversarial attacks against deep generative models on data: a survey. IEEE Trans Knowl Data Eng 2023;35(4):3367-3388. [doi: 10.1109/TKDE.2021.3130903]
51. Guillaudeux M, Rousseau O, Petot J, et al. Patient-centric synthetic data generation, no reason to risk re-identification in biomedical data analysis. NPJ Digit Med 2023 Mar 10;6(1):37. [doi: 10.1038/s41746-023-00771-5] [Medline: 36899082]
52. Demuth S, Rousseau O, Faddeenkov I, et al. Privacy-by-design generation of two virtual clinical trials in multiple sclerosis and their release as open datasets. In Review. Preprint posted online on Sep 20, 2024 URL: https://www.researchsquare.com/article/rs-4958414/v2 [accessed 2025-01-03] [doi: 10.21203/rs.3.rs-4958414/v1]
53. Boisaubert H, Vincent L, Lejus-Bourdeau C, Sinoquet C. Simulation of the evolution of a virtual patient's physiological status in the operating room: application to computer-assisted anaesthesia training. Presented at: 15th International Conference on Health Informatics; Feb 9-11, 2022. [doi: 10.5220/0010981000003123]
54. Demuth S, Ed-Driouch C, Dumas C, et al. Scoping review of clinical decision support systems for multiple sclerosis management: leveraging information technology and massive health data. Eur J Neurol 2025 Jan;32(1):e16363. [doi: 10.1111/ene.16363] [Medline: 38860844]

XSL•FO
RenderX

55. Pocock SJ, McCormack V, Gueyffier F, Boutitie F, Fagard RH, Boissel JP. A score for predicting risk of death from cardiovascular disease in adults with raised blood pressure, based on individual patient data from randomised controlled trials. BMJ 2001 Jul 14;323(7304):75-81. [doi: 10.1136/bmj.323.7304.75] [Medline: 11451781]
56. van den Ham HA, Klungel OH, Singer DE, Leufkens HGM, van Staa TP. Comparative performance of ATRIA, CHADS2, and CHA2DS2-VASc risk scores predicting stroke in patients with atrial fibrillation: results from a national primary care database. J Am Coll Cardiol 2015 Oct 27;66(17):1851-1859. [doi: 10.1016/j.jacc.2015.08.033] [Medline: 26493655]
57. Assessing the credibility of computational modeling and simulation in medical device submissions. U.S. Food & Drug Administration. 2022. URL: https://www.fda.gov/regulatory-information/search-fda-guidance-documents/assessing-credibility-computational-modeling-and-simulation-medical-device-submissions [accessed 2025-01-24]
58. Heijman J, Sutanto H, Crijns H, Nattel S, Trayanova NA. Computational models of atrial fibrillation: achievements, challenges, and perspectives for improving clinical care. Cardiovasc Res 2021 Jun 16;117(7):1682-1699. [doi: 10.1093/cvr/cvab138] [Medline: 33890620]
59. McDowell KS, Zahid S, Vadakkumpadan F, Blauer J, MacLeod RS, Trayanova NA. Virtual electrophysiological study of atrial fibrillation in fibrotic remodeling. PLOS ONE 2015;10(2):e0117110. [doi: 10.1371/journal.pone.0117110] [Medline: 25692857]
60. Wang Z, Wang Y. Extracting a biologically latent space of lung cancer epigenetics with variational autoencoders. BMC Bioinformatics 2019 Nov 25;20(Suppl 18):568. [doi: 10.1186/s12859-019-3130-9] [Medline: 31760935]
61. Attyé A, Renard F, Anglade V, et al. Data-driven normative values based on generative manifold learning for quantitative MRI. Sci Rep 2024 Mar 30;14(1):7563. [doi: 10.1038/s41598-024-58141-4] [Medline: 38555415]
62. Ed-Driouch C, Chéneau F, Simon F, et al. Multiple sclerosis clinical decision support system based on projection to reference datasets. Ann Clin Transl Neurol 2022 Dec;9(12):1863-1873. [doi: 10.1002/acn3.51649] [Medline: 36412095]
63. Braun M. Represent me: please! Towards an ethics of digital twins in medicine. J Med Ethics 2021 Mar 15;47:394-400. [doi: 10.1136/medethics-2020-106134] [Medline: 33722986]
64. Brown SA. Principles for developing patient avatars in precision and systems medicine. Front Genet 2015;6:365. [doi: 10.3389/fgene.2015.00365] [Medline: 26779255]
65. Laubenbacher R, Adler F, An G, et al. Toward mechanistic medical digital twins: some use cases in immunology. Front Digit Health 2024;6:1349595. [doi: 10.3389/fdgth.2024.1349595] [Medline: 38515550]
66. Kuhlmann L, Lehnertz K, Richardson MP, Schelter B, Zaveri HP. Seizure prediction - ready for a new era. Nat Rev Neurol 2018 Oct;14(10):618-630. [doi: 10.1038/s41582-018-0055-2] [Medline: 30131521]
67. Sanz-Leon P, Knock SA, Spiegler A, Jirsa VK. Mathematical framework for large-scale brain network modeling in The Virtual Brain. Neuroimage 2015 May 1;111:385-430. [doi: 10.1016/j.neuroimage.2015.01.002] [Medline: 25592995]
68. Makhalova J, Villalon SM, Wang H, et al. Virtual epileptic patient brain modeling: relationships with seizure onset and surgical outcome. Epilepsia 2022 Aug;63(8):1942-1955. [doi: 10.1111/epi.17310] [Medline: 35604575]
69. Wenk J, Voigt I, Inojosa H, Schlieter H, Ziemssen T. Building digital patient pathways for the management and treatment of multiple sclerosis. Front Immunol 2024;15:1356436. [doi: 10.3389/fimmu.2024.1356436] [Medline: 38433832]
70. Ziemssen T, Vandercappellen J, Jordan Mondragon V, Giovannoni G. MSProDiscuss™ clinical decision support tool for identifying multiple sclerosis progression. J Clin Med 2022 Jul 28;11(15):4401. [doi: 10.3390/jcm11154401] [Medline: 35956018]

Abbreviations

AF: atrial fibrillation
EDMUS: European Database for Multiple Sclerosis
EHR: electronic health record
HCP: health care provider
MRI: magnetic resonance imaging
MS: multiple sclerosis
MSDS 3D: Multiple Sclerosis Documentation System 3D
SMART: Substitutable Medical Applications and Reusable Technologies
SMOTE: Synthetic Minority Over-Sampling Technique
VICTRE: Virtual Imaging Clinical Trials for Regulatory Evaluation

XSL•FO
RenderX

Edited by C Lovis; submitted 10.10.23; peer-reviewed by M Vesinurm, O Halminen; revised version received 20.09.24; accepted 13.10.24; published 28.01.25.

Please cite as:
Demuth S, De Sèze J, Edan G, Ziemssen T, Simon F, Gourraud PA
Digital Representation of Patients as Medical Digital Twins: Data-Centric Viewpoint
JMIR Med Inform 2025;13:e53542
URL: https://medinform.jmir.org/2025/1/e53542
doi:10.2196/53542

© Stanislas Demuth, Jérôme De Sèze, Gilles Edan, Tjalf Ziemssen, Françoise Simon, Pierre-Antoine Gourraud. Originally published in JMIR Medical Informatics (https://medinform.jmir.org), 28.1.2025. This is an open-access article distributed under the terms of the Creative Commons Attribution License (https://creativecommons.org/licenses/by/4.0/), which permits unrestricted use, distribution, and reproduction in any medium, provided the original work, first published in JMIR Medical Informatics, is properly cited. The complete bibliographic information, a link to the original publication on https://medinform.jmir.org/, as well as this copyright and license information must be included.

XSL•FO
RenderX

Developing an Intelligent Mobile Clinic—A Medical Vehicle for Improve Access to Healthcare in Remote Areas: Evidence From China

Xinlei Chen[1*], BSc, MSc; Xufang Huang[2*], BSc; Yimiao Xu[1*], BSc, MSc; Jiabin Xu[3], BSc; Yanan Wang[3], BSc; Xinyue Ren[3], BSc; Xuebo Zhu[4], MMgt, PhD; Xiaoge Xie[4], MMed; Yeqin Yang[1], MMed, PhD

[1]School of Nursing, Zhejiang Chinese Medical University, No. 548, Binwen Road, Binjiang District, Hangzhou, Zhejiang Province, China

[2]Department of Nursing, Lishui Central Hospital, Lishui, China

[3]School of Nursing, Wenzhou Medical University, Wenzhou, China

[4]School of Medical and Humanities Management, Wenzhou Medical University, Wenzhou, China

[*]these authors contributed equally

Corresponding Author:
Yeqin Yang, MMed, PhD
School of Nursing, Zhejiang Chinese Medical University, No. 548, Binwen Road, Binjiang District, Hangzhou, Zhejiang Province, China

Abstract

Lishui, a mountainous city in Zhejiang Province, China, is characterized by extensive mountainous terrain and a dispersed population. To address this issue, Lishui has introduced the intelligent mobile clinic service. This model leverages 5G technology and integrates the benefits of mobile clinics and telehealth, tailored to the region's geography and demographic characteristics. The intelligent mobile clinic uses real-time data analysis to deliver medical services effectively to remote mountainous areas. Medical personnel from the intelligent mobile clinic visit villages to provide in-person professional health services and facilitate residents' access to higher-level hospital resources through telehealth. This model has received widespread praise and recognition from residents and has yielded significant outcomes. During 2018-2023, a total of 25,000 visits have been made, benefiting 648,000 individuals. The intelligent mobile clinic provides a valuable reference for enhancing health care access in similar regions.

(JMIR Med Inform 2025;13:e59103) doi:10.2196/59103

KEYWORDS

primary health care; medical resource; telehealth; intelligent mobile clinic; China; remote area

Introduction

The unequal distribution of medical resources is a global issue, particularly in remote areas where access to health care is severely limited.

Telehealth presents an effective solution to address this disparity in health care resources. Its primary aim is to enhance health care access by providing services to individuals who face barriers to obtaining care [1]. Initially, telehealth was employed to treat acute conditions, such as trauma or stroke [2]. As health care demands have risen, telehealth has expanded to include care for military personnel, prisoners, and rural populations [3]. While telehealth has significant potential, its development depends on conditions such as network infrastructure and coverage. Mobile clinics provide an additional solution to the unequal distribution of health care resources. Mobile clinics are mobile health care units, typically modified ambulances, designed to deliver services to both urban and rural communities [4]. This flexible health care model overcomes both time and geographical challenges, bringing medical services directly to remote areas. However, the limited space in the mobile clinic restricts the number of staff and equipment available, making it difficult to meet the diverse health care needs of residents [5].

In Lishui City, Zhejiang Province, China, an innovative integration of telehealth and mobile clinics has resulted in the creation of the intelligent mobile clinic. This model effectively combines the strengths of both telehealth and mobile clinics to address the health care needs of those in mountainous regions.

In this study, we introduce an innovative medical model for improving medical services in remote mountainous areas in Lishui City, Zhejiang Province, China. We will use the application, effectiveness and difficulties of the intelligent mobile clinic model in remote mountainous areas of Lishui City to provide reference experience for other remote areas to improve the uneven medical resources and provide high-quality medical services.

XSL•FO
RenderX

Health Care Inequities and Telehealth Innovations in Rural China

China is a predominantly agricultural country with a large rural population. As of 2022, the rural population in China reached 491.04 million, accounting for 34.78% of the total population [6]. Residents in remote areas face difficulties accessing health care due to factors such as economic constraints, distance, and time limitations [7-9]. For example, they have to spend a whole day seeking medical treatment, and some people may not even know that they are sick until their condition is very serious or has reached an advanced stage [10].

In response, the development of rural health care and medical systems has been the core of the new health care reform launched by China since 2009, which aimed at narrowing the urban-rural and regional disparities [11]. However, despite government efforts to implement medical reforms, there are still issues such as disparity distribution of health resources, a shortage of medical personnel, and inefficiencies in medical services [11,12]. Recognizing these challenges, the Chinese government has introduced various methods. One such method is the use of telehealth. Previous research has confirmed that telehealth can save residents time and costs in seeking medical treatment and promote the management of chronic diseases [13,14]. However, telehealth has not fully filled the health gap in rural areas, mainly due to young people flocking to urban centeres in search of better opportunities. This migration has left rural areas with a population dominated by older persons who face significant challenges in accessing and using e-health resources [15]. Consequently, these barriers prevent elderly residents from fully benefiting from telehealth services, exacerbating the health care disparities between rural and urban areas.

To address these challenges, China has been exploring innovative telehealth models that better suit the country's unique circumstances in recent years.

Intelligent Mobile Clinic in Lishui, China

A notable example is Lishui City, where a new solution has been introduced to address the specific health care needs of its rural population.

Lishui City is located in the mountainous region of southwest Zhejiang Province, where rugged mountains and hills dominate, with mountainous areas covering around 90% of the total land area. The region is home to more than 250 mountain villages, most of which are situated over 80 kilometers from the town center. Despite the local government's efforts to improve health care services, the spread-out population and small village sizes make it difficult for health care to reach every village, failing to meet the basic health care needs of the residents. As a result, residents often face long journeys, taking an entire day to reach a health care facility.

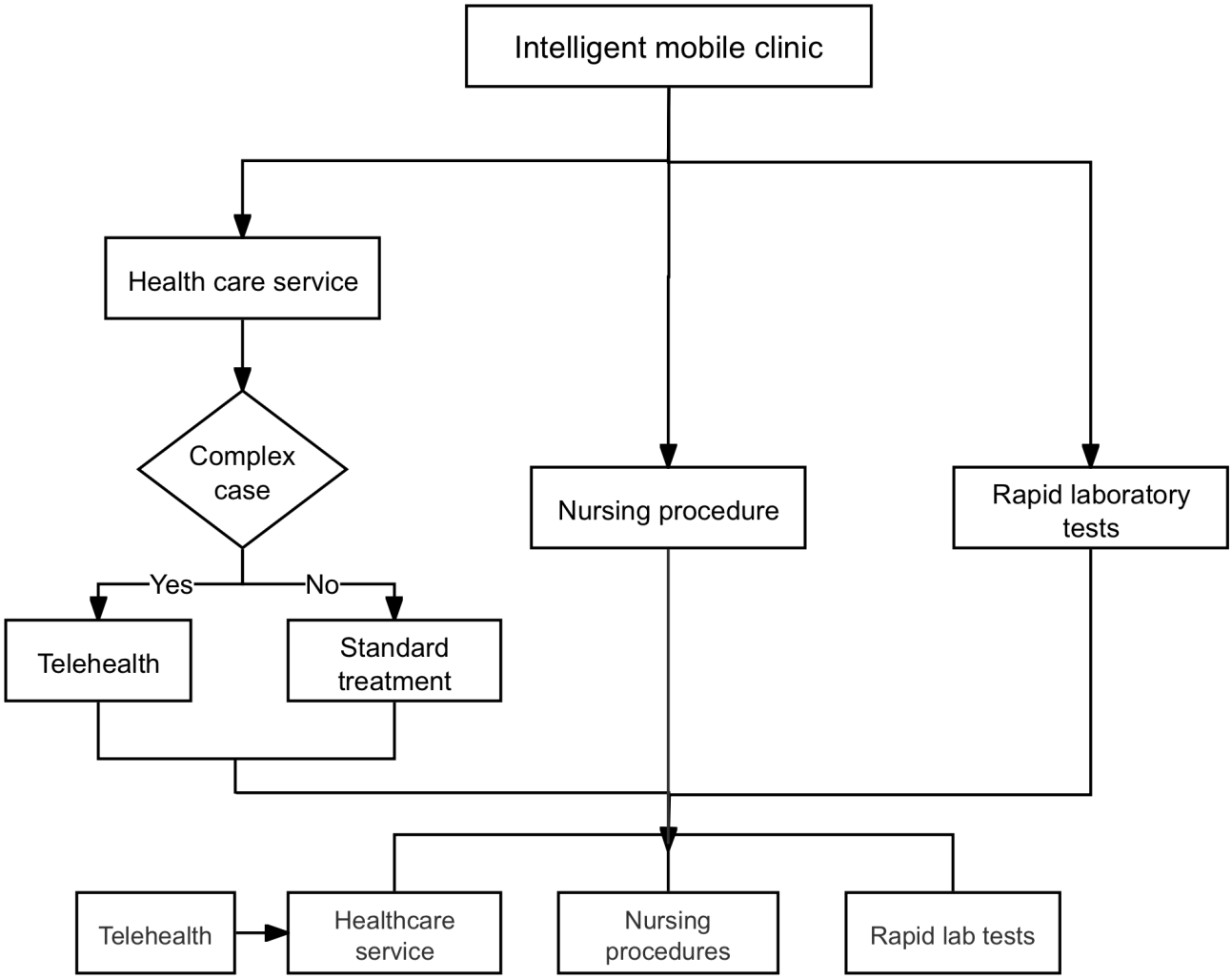
In Lishui's mountainous areas, as is the case in many rural parts of China, the population is largely elderly. These individuals often face additional challenges such as illiteracy, difficulty speaking Mandarin, and an inability to use smartphones or other smart devices. Although telehealth has significant potential to improve health care access, it struggles to address these issues in Lishui's rural context. As a solution, the government of Lishui City has developed the intelligent mobile clinic, which delivers more accessible and effective health care services to the rural population. The intelligent mobile clinic represents an innovative response to the distinct needs of Lishui's residents. The next section will provide a detailed introduction to the intelligent mobile clinic.

The Intelligent Mobile Clinic: An Innovation Solution for Remote Area Health Care

The intelligent mobile clinic offers an innovative solution by combining mobile clinics, telehealth, 5G technology, and big data to tackle the unequal distribution of medical resources in remote areas. This model integrates several advanced technologies to provide high-quality and accessible health care services to people in remote regions (Figure 1).

XSL•FO
RenderX

Figure 1. Flowchart of the intelligent mobile clinic health care service for residents.



The intelligent mobile clinic utilizes modified medical vehicles, equipped with essential diagnostic tools, to deliver health care services to even the most remote mountainous areas. These vehicles provide services such as routine health check-ups and rapid laboratory tests. When the doctor encounters cases that surpass their expertise, the telehealth system connects them with specialists at higher-level hospitals. This real-time consultation enables more accurate diagnoses and effective treatments, even in distant locations.

The roles of 5G and big data are pivotal in supporting the intelligent mobile clinic. 5G technology ensures smooth communication and the real-time transfer of medical data, while big data helps gather and analyze health information to refine services, monitor regional health trends, and improve the distribution of medical resources.

Mobile Clinic Services in the Intelligent Mobile Clinic

The intelligent mobile clinic provides medical services to residents in remote areas. The mobile medical vehicles of the intelligent mobile clinic arrive at mountain villages at fixed times every month to provide medical services to residents.

Doctors provide direct consultations, perform routine tests, diagnose common diseases, and prescribe medication when needed. If a resident's medical needs exceed the available services, doctors can consult experts at senior hospitals through telemedicine systems to ensure that residents receive specialized care. The nurse administers injections and performs dressing changes. Medical technicians perform rapid laboratory tests such as blood pressure monitoring, blood sugar tests, and electrocardiograms to assist in diagnosis. To improve communication with elderly people who are not fluent in Mandarin, the intelligent mobile clinic recruited local volunteers who are fluent in Mandarin and regional dialects. These volunteers play a vital role in maintaining order and helping elderly patients onto medical vehicles. It is worth noting that in order to ensure that patients who are bedridden at home can also enjoy medical care services, doctors provide medical services for patients at home, replace drainage tubes, urine bags, etc.

Telehealth in the Intelligent Mobile Clinic

When medical vehicles are unable to fully meet the health care needs of residents, the intelligent mobile clinic doctors use telemedicine to consult experts in senior hospitals. Through telemedicine devices, doctors can transmit real-time health data to specialists, which ensures that residents have access to vital health care services and receive timely medical attention.

In addition, the 5G network improves the efficiency of telemedicine within the intelligent mobile clinic. It provides a reliable, stable link for online consultations, overcomes

XSL•FO
RenderX

geographical barriers, and gives mountain residents access to the same medical services and resources as urban residents. As a result, the intelligent mobile clinic has significantly improved the accessibility and quality of health care services in remote areas.

Big Data Support in the Intelligent Mobile Clinic

Big data technology is the key technology for the intelligent mobile clinic to achieve precision medicine. Relying on 5G network technology, the intelligent mobile clinic transmits the relevant data of 50 medical vehicles in real time, including GPS positioning information, diagnosis and treatment records, and disease conditions of patients in various regions to the Lishui Health Information Platform and terminal personnel can form regional health information self-portraits according to the information transmitted by all medical vehicles through big data. It is worth noting that the medical staff on board each medical diagnosis and treatment vehicle can only view the relevant diagnosis and treatment information in their own area of responsibility to protect the privacy of patients.

Extra Functions of the Intelligent Mobile Clinic

The intelligent mobile clinic has taken into account the varied medical needs of villagers, including the delivery of medications to mountainous areas. Due to certain restrictions, the intelligent mobile clinic is not able to carry all types of medicine. When specific medications are needed, the doctor will write a prescription and request confirmation from higher-level doctors via the network. Upon approval, the medication is prepared by the higher-level hospital and sent to the villagers free of charge through express delivery.

Furthermore, to better meet the medical needs of the villagers, the intelligent mobile clinic also functions as a first-line emergency responder. In emergency situations in remote villages, such as bleeding injuries or drowning incidents, villagers can contact the emergency hotline. The dispatcher will then assign the nearest medical vehicle from the local health center to respond based on the villager's location.

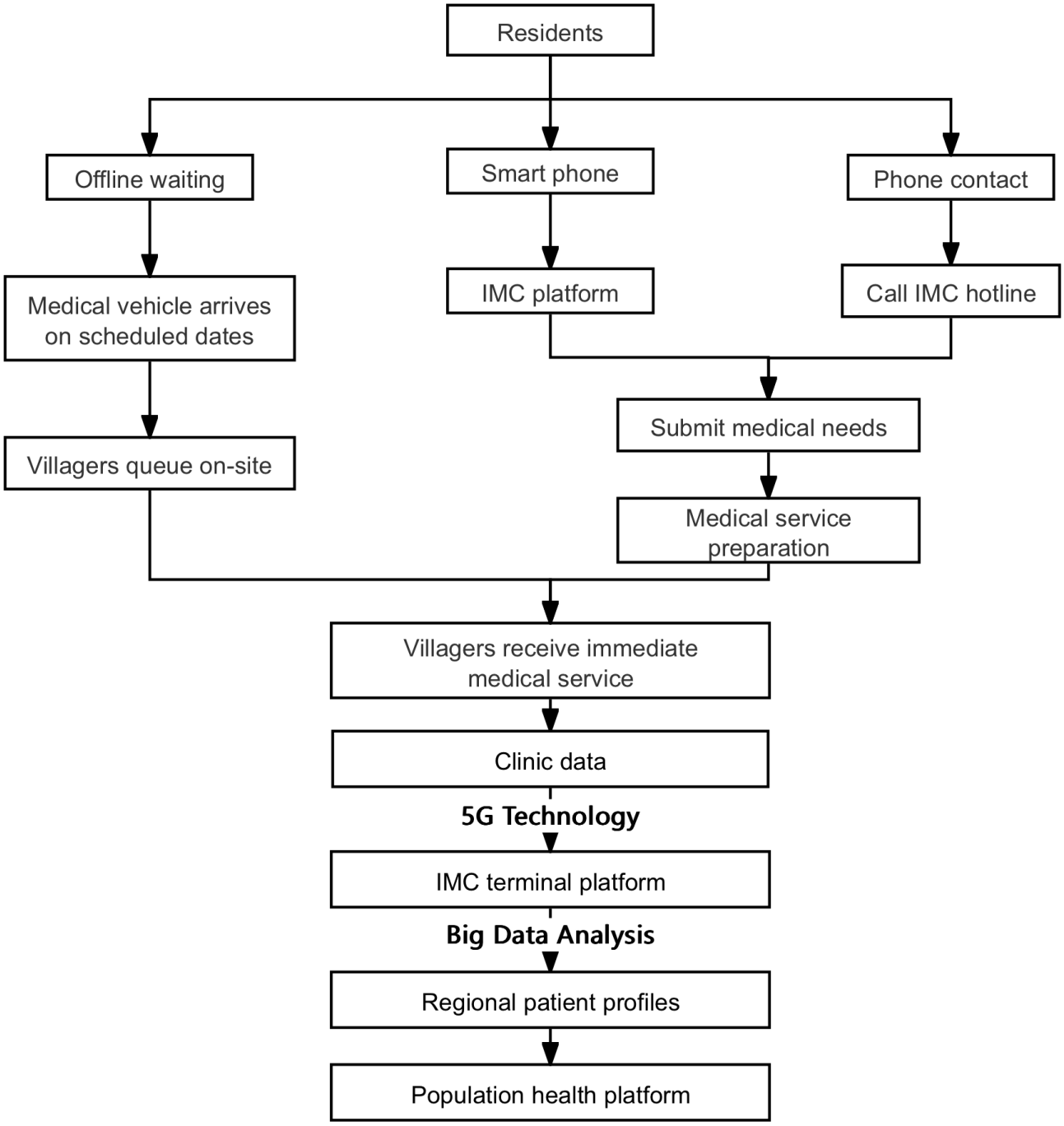
Routine Operation and Management

The intelligent mobile clinic collects and addresses the medical needs of the villagers through multiple channels: most villagers line up at the medical site on a fixed date each month. Villagers who have the ability to use mobile phones can access the feedback module by logging into the interface to submit medical requests, while those who do not have access to phones can make requests through the hotline, and the information is entered into the system by staff. Local community hospitals or health centers flexibly adjust the allocation of medical staff and drug supplies based on these real-time data.

In order to achieve efficient service management, the intelligent mobile clinic has created a comprehensive database by integrating vehicle information, medical personnel files, service data, GPS coordinates, and digital maps. The management platform transmits diagnostic records, treatment processes, and vehicle operating status in the diagnosis and treatment vehicle to the terminal platform in real time through 5G technology; and generates regional health information portraits through big data analysis. As regulators, the government and health departments can remotely verify the number of medical personnel, vehicle positioning, and diagnosis and treatment process with the help of monitoring cameras in the diagnosis and treatment vehicle to ensure the quality of service. In the design of the system, the information security mechanism is especially strengthened, and regional data rights management is implemented, that is, doctors in each region can only access the patient information in their jurisdiction, and the privacy security of villagers is protected from the technical level (Figure 2).

XSL•FO
RenderX

Figure 2. Flowchart of the intelligent mobile clinic (IMC) routine operation and management.



Comparing the Intelligent Mobile Clinic With the Mobile Clinic and Internet Hospitals

Overview

Several models currently exist to provide primary health care services to residents in remote areas. Mobile clinics represent an innovative health care service model that delivers flexible medical services to targeted populations through a customized motor vehicle [16]. Internet hospitals are platforms where registered doctors provide consultations and treatments via the internet, primarily addressing common or chronic health conditions [17]. The rapid development of internet hospitals in China is expected to improve the availability of medical resources and reduce the cost of telehealth services [18].

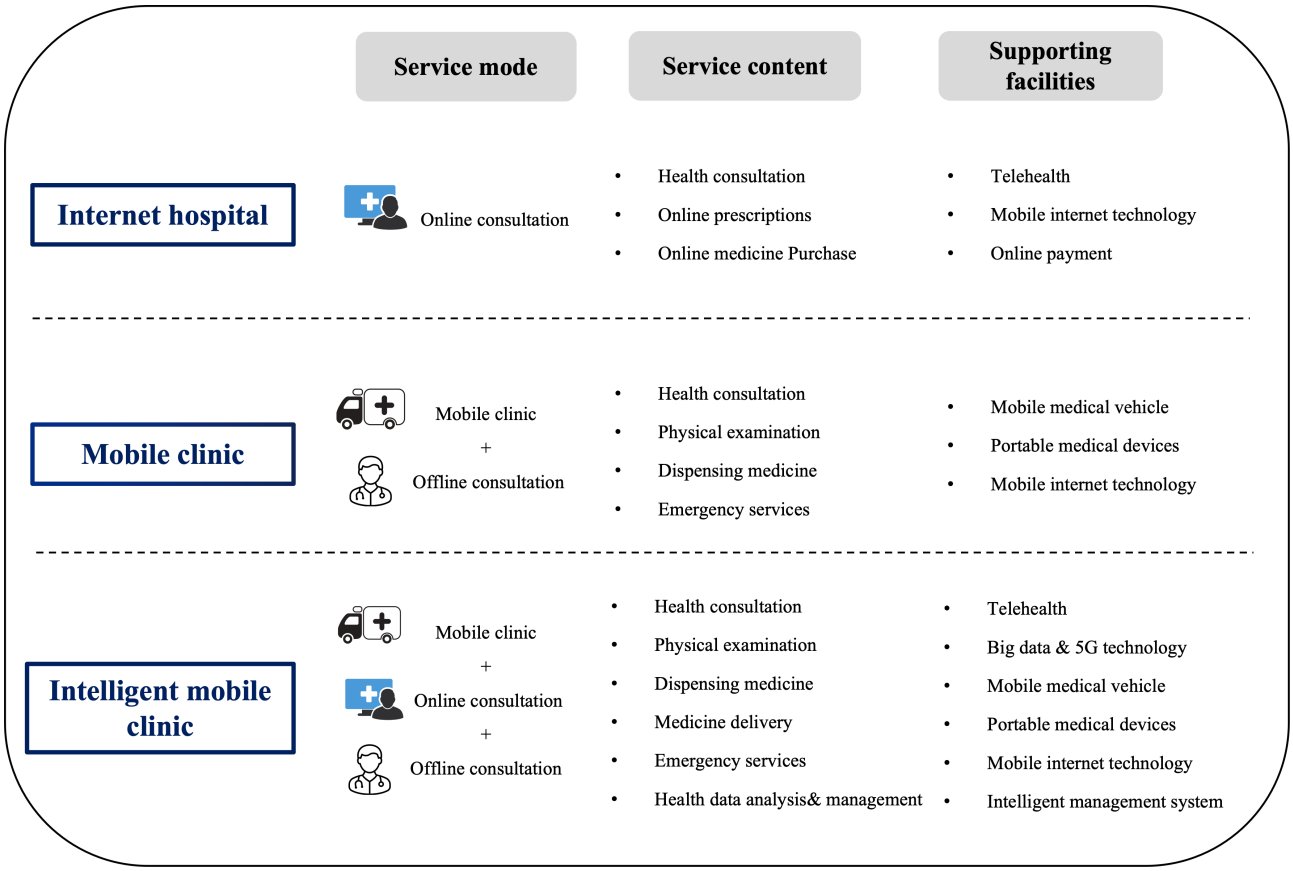
Despite their benefits, both models have certain limitations. Mobile clinics are restricted by the limited space in medical vehicles, which limits the amount of equipment, medicines, and medical personnel that can be carried on each visit [19]. As a result, in unexpected situations, the medical needs of residents may not be fully met. Internet hospitals services are faced with multiple practical challenges when used for primary medical coverage. First, internet hospitals have high requirements for mobile devices and lack communication equipment in remote mountainous areas [20,21], which makes it difficult for people to effectively enjoy telehealth services [22,23]. Second, the physical isolation between doctors and patients in the remote

XSL•FO
RenderX

diagnosis and treatment mode makes it impossible for doctors to perform basic physical examinations for patients, which may affect the completeness and accuracy of the clinical diagnosis. Third, after using intelligent terminals to complete online consultation, elderly patients also need to go through the drug logistics and distribution link, which increases the time cost compared with traditional medical treatment [24].

In contrast to mobile clinics and internet hospitals, the intelligent mobile clinic integrates the benefits of both online and offline services. Local doctors provide in-person consultations and treatments. When additional expertise is needed, the telehealth system connects them with specialists from higher-level hospitals, offering effective support and guidance. Additionally, the convenience of these services results in high patient satisfaction. This combined approach allows the intelligent mobile clinic to address the limitations of both mobile clinics and internet hospitals, delivering a more comprehensive and accessible health care solution for remote populations (Figure 3).

Figure 3. Comparison of 3 medical models.



To evaluate the real user experience of the intelligent mobile clinic, a telephone follow-up was conducted with residents in January 2024. The research team focused on villagers from Bihu Town, Lishui City, conducting qualitative interviews with them (Table 1). The interviews collected data on basic user characteristics, home addresses, and their evaluations of the intelligent mobile clinic services. The findings reveal that the respondents gave high ratings to the intelligent mobile clinic, highlighting that it significantly meets their health care needs.

XSL•FO
RenderX

Table . Qualitative interviews of the user experience of the intelligent mobile clinic (IMC).

Interviewee #	Age, y	Gender	Disease	Job	Interview content
1	50	Female	Diabetes	Run a grocery store	I have diabetes and need to take my medication regularly. The medical vehicle visits our village, which makes it very convenient for me to get my medication. I can receive it immediately without needing to go to the hospital.
2	52	Male	Disability, hypertension	Farmer	I am disabled and have high blood pressure, so I must take medication every day. Given my condition, I cannot travel to an external hospital by myself. The medical vehicle visits our village once a week, which is very helpful.
3	57	Female	Hypertension, hypothyroidism	Farmer	The IMC is a great help. We live in a rural area with no public transportation, and the medical vehicle comes every week, mainly to visit patients with chronic diseases. For more serious cases, the doctor will refer patients to a higher-level hospital for treatment.
4	56	Female	Hypertension	Farmer	The IMC is well-received by the villagers. They come once a week and bring fresh medicines. Since we do not have a clinic in our village, we have to travel to nearby towns or urban areas for medical care. This has led many people in the village to wait in line for the mobile vehicle to arrive.
5	50	Female	Hyperlipidemia	Farmer	It is far more convenient to see a doctor and get medication, as there is no need to wait in long lines as in traditional hospitals. The outpatient fee at the mobile clinic in the village is just 5 RMB (US $0.7).

Ethical Considerations

This work adheres to ethical guidelines for scholarly commentary. All referenced studies comply with institutional ethics standards. The original research cited in this article was approved by the Zhejiang Chinese Medical University Institutional Review Board (IRB#20250220-1). All the patients

XSL•FO
RenderX

provided informed consent for use of their data; all the data were de-identified.

Results

From 2018 to the end of 2023, the intelligent mobile clinic had a total of 50 mobile medical vehicles, a total of 18,000 visits, 100 years of travel within the area of 10,000 kilometers, a total of 25,000 village medical services, 33,000 medical personnel, a total of 657,000 services, covering 758 remote villages without medical facilities (Table 2). In addition, the average emergency response time in mountainous areas reduced from 34 minutes to 14 minutes. According to data from the Lishui government, the goal of mountainous residents to have "shorter medical treatment times and the ability to address minor illnesses within the village" has increasingly become a reality.

Table . Characteristics of patients who used the intelligent mobile clinic from 2021 to 2023.

Characteristics, n (%)	2021	2022	2023	Total
Total users	91,287 (10.38)	130,445 (14.84)	656,998 (74.78)	878,730
Number of medical vehicle rounds	2113 (11.60)	5550 (30.47)	10,549 (57.93)	18,212
Number of village visits	4942 (19.11)	5426 (20.98)	15,492 (59.91)	25,860
Number of medical staff	3043 (9.01)	9486 (28.08)	21,257 (62.91)	33,786
Type of medical service				
Diagnosis and treatment	9646 (3.54)	46,465 (17.05)	21,6471 (79.41)	272,582
Traditional Chinese medicine	4765 (4.76)	19,222 (19.20)	76,115 (76.04)	100,102
Prescription	700 (0.35)	36,553 (18.17)	164,591 (81.48)	201,144
Laboratory testing	386 (1.30)	1821 (6.15)	27,386 (92.55)	29,593
Chronic disease follow-up	68,790 (25.71)	26,384 (9.86)	172,435 (64.43)	267,609

Discussion

The emergence of the intelligent mobile clinic has effectively alleviated the unequal distribution of medical resources in remote mountainous areas of Lishui City, and increasing numbers of villagers can get timely treatment. As noted earlier, the population in the remote areas of Lishui is spread across the mountains, making it difficult for residents to access medical resources from urban areas. Building hospitals in these regions would serve only a small portion of the population, potentially resulting in a waste of resources. Additionally, many residents in these mountainous areas are elderly and face challenges such as illiteracy, an inability to speak Mandarin, or limited access to the internet. These factors mean that internet hospitals and mobile clinics may not fully meet their needs. Each region has its own unique circumstances, and local governments must carefully assess these conditions and implement appropriate measures to provide suitable services for residents, such as capsule clinics in Ningbo or internet hospitals in Guangzhou. The intelligent mobile clinic is a new health care service model that integrates the advantages of telehealth and mobile clinics, developed by the local government to address the specific conditions of the area. With the guidance of big data, the intelligent mobile clinic is able to deliver accurate health care services to residents in remote mountainous regions. Medical staff from the intelligent mobile clinic also help elderly residents communicate with specialists through the internet.

Conclusion and Limitations

The intelligent mobile clinic presents an innovative and effective solution for promoting the equal distribution of medical resources in remote areas. By combining the benefits of telehealth and mobile clinics, the intelligent mobile clinic tackles the health care challenges in the mountainous regions of Lishui. The success of the intelligent mobile clinic in Lishui offers a valuable example for addressing similar issues in other remote areas of China and even in countries facing comparable challenges.

Nonetheless, each region must carefully evaluate its specific circumstances and develop suitable approaches to meet the health care needs of its residents, ensuring a balanced distribution of medical resources across various areas.

Acknowledgments

We would like to thank the Lishui Central Hospital for their support of this research. This study was sponsored by National Social Science Foundation of China: "Constructing a Family Medicine Education System with Chinese Characteristics in the Context of Major Public Health Emergencies" (BIA200197).

This research data are provided by the Lishui City Government, Zhejiang Province, China. Due to the confidentiality agreement signed, part of the original data and core steps cannot be shared. All the data in this paper have passed official verification.

XSL•FO
RenderX

Authors' Contributions

YY and XC conceived and designed the study. XH, YX, JX, YW, and XR participated in field research. YY, XC, XH, and YX wrote the original draft. YY, XC, XZ, and XX substantively revised the manuscript. All authors have read and approved the final manuscript.

Conflicts of Interest

None declared.

References

1. Ryu S. History of telemedicine: evolution, context, and transformation. Healthc Inform Res 2010;16(1):65. [doi: 10.4258/hir.2010.16.1.65] [Medline: 21818439]
2. Levine SR, Gorman M. "Telestroke": the application of telemedicine for stroke. Stroke 1999 Feb;30(2):464-469. [doi: 10.1161/01.str.30.2.464] [Medline: 9933289]
3. Brown EM. The Ontario telemedicine network: a case report. Telemed J E Health 2013 May;19(5):373-376. [doi: 10.1089/tmj.2012.0299] [Medline: 23301768]
4. Hill CF, Powers BW, Jain SH, Bennet J, Vavasis A, Oriol NE. Mobile health clinics in the era of reform. Am J Manag Care 2014 Mar;20(3):261-264. [Medline: 24884754]
5. Guruge S, Hunter J, Barker K, McNally MJ, Magalhães L. Immigrant women's experiences of receiving care in a mobile health clinic. J Adv Nurs 2010 Feb;66(2):350-359. [doi: 10.1111/j.1365-2648.2009.05182.x] [Medline: 20423418]
6. Main data of the seventh national population census. National Bureau of Statistics of China. 2021. URL: https://www.stats.gov.cn/english/PressRelease/202105/t20210510_1817185.html [accessed 2024-11-01]
7. Arcury TA, Preisser JS, Gesler WM, Powers JM. Access to transportation and health care utilization in a rural region. J Rural Health 2005;21(1):31-38. [doi: 10.1111/j.1748-0361.2005.tb00059.x] [Medline: 15667007]
8. Begashaw B, Tessema F, Gesesew HA. Health care seeking behavior in Southwest Ethiopia. PLOS ONE 2016;11(9):e0161014. [doi: 10.1371/journal.pone.0161014] [Medline: 27626804]
9. Bhan N, Madhira P, Muralidharan A, et al. Health needs, access to healthcare, and perceptions of ageing in an urbanizing community in India: a qualitative study. BMC Geriatr 2017 Jul 19;17(1):156. [doi: 10.1186/s12877-017-0544-y] [Medline: 28724399]
10. He C, Zhou Q, Chen W, et al. Using an Internet-based hospital to address maldistribution of health care resources in rural areas of Guangdong province, China: retrospective and descriptive study. JMIR Med Inform 2018 Dec 21;6(4):e51. [doi: 10.2196/medinform.9495] [Medline: 30578195]
11. Zheng D, Gong J, Zhang C. Efficiency of medical service systems in the rural areas of Mainland China: a comparative study from 2013 to 2017. Public Health (Fairfax) 2019 Jun;171:139-147. [doi: 10.1016/j.puhe.2019.04.003]
12. Zhou K, Zhang X, Ding Y, Wang D, Lu Z, Yu M. Inequality trends of health workforce in different stages of medical system reform (1985-2011) in China. Hum Resour Health 2015 Dec 8;13:94. [doi: 10.1186/s12960-015-0089-0] [Medline: 26645960]
13. Marcin JP, Shaikh U, Steinhorn RH. Addressing health disparities in rural communities using telehealth. Pediatr Res 2016 Jan;79(1-2):169-176. [doi: 10.1038/pr.2015.192] [Medline: 26466080]
14. Jaglal SB, Haroun VA, Salbach NM, et al. Increasing access to chronic disease self-management programs in rural and remote communities using telehealth. Telemed J E Health 2013 Jun;19(6):467-473. [doi: 10.1089/tmj.2012.0197] [Medline: 23570277]
15. Paige SR, Miller MD, Krieger JL, Stellefson M, Cheong J. Electronic health literacy across the lifespan: measurement invariance study. J Med Internet Res 2018 Jul 9;20(7):e10434. [doi: 10.2196/10434] [Medline: 29986848]
16. Malone NC, Williams MM, Smith Fawzi MC, et al. Mobile health clinics in the United States. Int J Equity Health 2020 Mar 20;19(1):40. [doi: 10.1186/s12939-020-1135-7] [Medline: 32197637]
17. Zhi L, Yin P, Ren J, et al. Running an internet hospital in China: perspective based on a case study. J Med Internet Res 2021 Sep 16;23(9):e18307. [doi: 10.2196/18307] [Medline: 34342267]
18. Tu J, Wang C, Wu S. The internet hospital: an emerging innovation in China. Lancet Glob Health 2015 Aug;3(8):e445-e446. [doi: 10.1016/S2214-109X(15)00042-X] [Medline: 26187488]
19. Yu SWY, Hill C, Ricks ML, Bennet J, Oriol NE. The scope and impact of mobile health clinics in the United States: a literature review. Int J Equity Health 2017 Oct 5;16(1):178. [doi: 10.1186/s12939-017-0671-2] [Medline: 28982362]
20. Maassen O, Fritsch S, Gantner J, et al. Future mobile device usage, requirements, and expectations of physicians in German university hospitals: web-based survey. J Med Internet Res 2020 Dec 21;22(12):e23955. [doi: 10.2196/23955] [Medline: 33346735]
21. Al-Turjman F, Nawaz MH, Ulusar UD. Intelligence in the internet of medical things era: a systematic review of current and future trends. Comput Commun 2020 Jan;150:644-660. [doi: 10.1016/j.comcom.2019.12.030]
22. Cortelyou-Ward K, Atkins DN, Noblin A, Rotarius T, White P, Carey C. Navigating the digital divide: barriers to telehealth in rural areas. J Health Care Poor Underserved 2020;31(4):1546-1556. [doi: 10.1353/hpu.2020.0116] [Medline: 33416736]

XSL•FO
RenderX

23. Almathami HKY, Win KT, Vlahu-Gjorgievska E. Barriers and facilitators that influence telemedicine-based, real-time, online consultation at patients' homes: systematic literature review. J Med Internet Res 2020 Feb 20;22(2):e16407. [doi: 10.2196/16407] [Medline: 32130131]
24. Ge Y, Zhang G, Meqdad MN, Chen S. A systematic and comprehensive review and investigation of intelligent IoT-based healthcare systems in rural societies and governments. Artif Intell Med 2023 Dec;146:102702. [doi: 10.1016/j.artmed.2023.102702] [Medline: 38042611]

Abbreviations

Edited by A Benis; submitted 02.04.24; peer-reviewed by F Zhou, H Sritart; revised version received 23.04.25; accepted 26.04.25; published 02.06.25.

Please cite as:
Chen X, Huang X, Xu Y, Xu J, Wang Y, Ren X, Zhu X, Xie X, Yang Y
Developing an Intelligent Mobile Clinic—A Medical Vehicle for Improve Access to Healthcare in Remote Areas: Evidence From China
JMIR Med Inform 2025;13:e59103
URL: https://medinform.jmir.org/2025/1/e59103
doi:10.2196/59103

© Xinlei Chen, Xufang Huang, Yimiao Xu, Jiabin Xu, Yanan Wang, Xinyue Ren, Xuebo Zhu, Xiaoge Xie, Yeqin Yang. Originally published in JMIR Medical Informatics (https://medinform.jmir.org), 2.6.2025. This is an open-access article distributed under the terms of the Creative Commons Attribution License (https://creativecommons.org/licenses/by/4.0/), which permits unrestricted use, distribution, and reproduction in any medium, provided the original work, first published in JMIR Medical Informatics, is properly cited. The complete bibliographic information, a link to the original publication on https://medinform.jmir.org/, as well as this copyright and license information must be included.

XSL•FO
RenderX

Artificial Intelligence (AI) and Emergency Medicine: Balancing Opportunities and Challenges

Félix Amiot, MD; Benoit Potier, MD

Emergency Department, Service d'Aide Médicale Urgente (SAMU50), Service Mobile d'Urgence et de Réanimation (SMUR), Saint-Lô Memorial Hospital, 715 rue Henri Dunant, Saint-Lô, France

Corresponding Author:
Félix Amiot, MD
Emergency Department, Service d'Aide Médicale Urgente (SAMU50), Service Mobile d'Urgence et de Réanimation (SMUR), Saint-Lô Memorial Hospital, 715 rue Henri Dunant, Saint-Lô, France

Abstract

Artificial intelligence (AI), particularly large language models (LLMs) such as ChatGPT, has rapidly evolved and is reshaping various fields, including clinical medicine. Emergency medicine stands to benefit from AI's capacity for high-volume data processing, workflow optimization, and clinical decision support. However, important challenges exist, ranging from model "hallucinations" and data bias to questions of interpretability, liability, and ethical use in high-stake environments. This updated viewpoint provides a structured overview of AI's current capabilities in emergency medicine, highlights real-world applications, and explores concerns regarding regulatory requirements, safety standards, and transparency (explainable AI). We discuss the potential risks and limitations of LLMs, including their performance in rare or atypical presentations common in the emergency department and potential biases that could disproportionately affect vulnerable populations. We also address the regulatory landscape, particularly the liability for AI-driven decisions, and emphasize the need for clear guidelines and human oversight. Ultimately, AI holds enormous promise for improving patient care and resource management in emergency medicine; however, ensuring safety, fairness, and accountability remains vital.

(JMIR Med Inform 2025;13:e70903) doi:10.2196/70903

KEYWORDS

artificial intelligence; artificial general intelligence; large language model; emergency medicine; explainable artificial intelligence; bias; liability; regulation; AI; AGI; LLM; XAI; health data

Introduction

Artificial intelligence (AI), particularly large language models (LLMs) such as OpenAI's ChatGPT, is experiencing rapid growth in adoption, with a user base of tens of millions on a monthly basis [1]. While the United States and China are making significant advancements in AI technology, Europe is experiencing a lag due to challenges in investment and regulatory frameworks [2,3]. This disparity limits the European public's comprehension of AI's potential applications and implications.

In medicine, AI demonstrates exceptional capabilities in processing complex health data [4], advanced medical imaging [5,6], anatomopathology [5], and electrocardiogram interpretation [6]. Furthermore, AI exhibits proficiency in "internship competitions" [7] and has the potential to surpass practitioners in medical diagnoses [8]. AI significantly contributes to medical research by aiding the creation of scientific articles [9] and advancing new therapeutic areas, especially in infectiology [10].

Nevertheless, it is posited that there is an underestimation of the substantial impact of this technology on contemporary and future medicine. Recent advancements in AI, propelled by extensive computational power rather than conceptual innovations, demonstrate that the potential of these systems depends primarily on the accumulation of data, duration of training, and financial resources [11]. This observation suggests that the improvement of AI systems necessitates an increase in high-quality data, extended training periods, and financial investment, rather than relying solely on the ingenuity of researchers.

Emergency medicine is a high-stakes field in which rapid and accurate decision-making is crucial. Overcrowded departments, resource constraints, and time pressure create significant challenges that advanced AI can mitigate. However, the complexity and unpredictability of emergency medicine highlight the importance of safety, liability, and ethical considerations. This paper presents the current applications of AI in emergency medicine, emphasizing both real-world implementations and critical challenges, such as hallucination, bias, and interpretability.

XSL•FO
RenderX

Current AI Capabilities in Emergency Medicine

AI systems, particularly deep learning networks, can be used to identify patterns in large, complex datasets, significantly contributing to medical science by analyzing variables to reliably predict outcomes [12,13]. In emergency departments (EDs), this enables improved triage, patient flow management, and resource allocation in overcrowded settings where resources are limited and time is critical [14-19]. Hospitals are also investigating AI's potential to optimize resource allocation by forecasting bed availability and scheduling staff [20,21]. In one study, an AI tool analyzing historical admission patterns, vital signs, and laboratory data enhanced ED throughput by identifying high-risk patients for earlier admission [22].

Moreover, AI has demonstrated high accuracy in clinical tasks such as the recognition of acute coronary syndromes, recognition of acute appendicitis, and rapid interpretation of imaging for fractures or head injuries [23-30]. These tasks involve pattern recognition in large data streams—vital signs, laboratory results, or imaging scans—and can reduce diagnostic delays. Some EDs have tested AI models for specific conditions, such as early sepsis detection, by monitoring the vital signs and laboratory results [31]. This approach has shown promise in reducing the time to antibiotic administration, although the results vary across different populations.

Conventional clinical decision support systems (CDSSs) have been widely used in health care settings to assist medical professionals in making informed decisions. These systems typically operate on the basis of predefined rules, scoring systems, or algorithms developed by experts in the field. Although effective in many scenarios, these traditional CDSSs have limitations in their ability to adapt to new information or complex, multifaceted clinical situations [32]. In contrast, AI models, particularly LLMs, represent a paradigm shift in clinical decision support. These models leverage vast amounts of data to learn patterns and associations without the need for explicit rule-coding [33,34]. This data-driven approach allows AI models to potentially identify subtle or complex relationships within medical data that may be overlooked by traditional CDSSs or even by human experts [35]. However, it introduces challenges in interpretability as the "reasoning" behind AI outputs may be opaque.

Although these early successes are encouraging, robust prospective trials remain limited. Further evidence from large-scale, peer-reviewed studies is necessary to confirm whether AI-driven solutions consistently improve patient outcomes in emergency care settings.

Challenges and Limitations

A widely documented phenomenon in LLMs is "hallucination," where the model confidently generates inaccurate or fabricated information [36-38]. While all diagnostic tools are susceptible to errors, AI hallucinations can be especially problematic because they are delivered convincingly, making them difficult to spot. In emergency settings, where time constraints are acute, misleading AI outputs can significantly affect patient care. The current research highlights the need for rigorous validation of LLM outputs, particularly when used for direct patient management. Because AI models are trained on large datasets, their performance is strongest for common presentations. Infrequent conditions such as rare genetic disorders or atypical manifestations of common pathologies are prone to misclassification. Moreover, LLMs struggle with rare and atypical cases that are common in emergency medicine, making them less effective in unconventional clinical situations. This limitation arises because LLMs rely on statistical correlations, favoring common cases over unique ones [39]. Additionally, LLMs are not programmed to indicate uncertainty, which increases the risk of misleading information in critical situations [40,41].

Data-driven models of emergency care can significantly improve patient outcomes and operational efficiency. However, their reliance on historical data can perpetuate the existing biases, leading to unequal treatment across diverse patient populations. This is concerning in emergency settings, where rapid decision-making is crucial and biased algorithms can be life-threatening. An AI system trained predominantly on data from one ethnic group might misinterpret the symptoms presented by patients from other backgrounds, resulting in delayed or inappropriate care. A study using an AI-powered dermatological algorithm clearly demonstrated this problem. When applied to Fitzpatrick skin type 6 (dark skin) dermatological conditions, the AI system achieved only 17% diagnostic accuracy compared to 69.9% for Caucasian skin types [42]. Interestingly, AI systems can also be designed to detect limitations when faced with unfamiliar data. Conformal prediction techniques have been shown to flag unreliable predictions when an AI system encounters new data from different laboratories, scanners, or pathology assessments [43]. This approach could help mitigate risks associated with AI systems, such as incorrect diagnoses for patients from underrepresented groups. Diversifying training datasets is critical to ensure that AI models are exposed to a wide range of patient demographics and clinical presentations. Implementing fairness-aware algorithms that consider and adjust for potential biases during decision-making is equally important. Continuous monitoring and auditing of AI system performance across demographic subgroups is essential for identifying and rectifying emerging disparities. This vigilance, combined with regular updates to models and training data, can help ensure that AI-driven emergency care systems serve all patients equally, regardless of their background or socioeconomic status.

Model Interpretability and Explainable AI (XAI)

AI-based triage systems in emergency medicine are powerful and complex tools for optimizing patient care. The "black-box" nature of these algorithms raises ethical concerns in high-stakes emergency settings, where rapid and accurate decision-making is crucial [44]. When an opaque AI system designates a patient as "low priority" without clear justification, it may lead to

XSL•FO
RenderX

prolonged wait times or reduced attention, potentially compromising patient outcomes.

Explainable artificial intelligence (XAI) is important in emergency medicine. Transparent and interpretable AI models are essential to maintain trust, accountability, and safety in emergency care [45]. XAI techniques such as Shapley Additive Explanations or Local Interpretable Model-Agnostic Explanations can provide insights into which variables most influence a model's output, making AI-based recommendations more transparent to health care professionals [46]. This interpretability is crucial in emergency settings, where clinicians must quickly understand and validate AI recommendations.

In the fast-paced environment of emergency medicine, the balance between model performance and explainability is critical. Although complex models may offer superior predictive power, their opacity can hinder clinical trust and integration [47]. Developing AI systems that maintain high accuracy while providing clear explanations for their decisions is an active research area, particularly relevant to emergency care, where trust and clarity are paramount [48].

To address these challenges, transparent and XAI triage mechanisms tailored to emergency medicine are crucial. These systems should provide immediate insights into the decision-making process, allowing health care professionals to quickly understand and validate AI recommendations in time-sensitive situations. Structured override processes must be established to enable rapid human intervention, when necessary, ensuring that algorithmic decisions can be reviewed and adjusted based on clinical judgment and contextual factors.

By prioritizing transparency, explainability, and human oversight in AI-based triage systems for emergency medicine, health care institutions can harness AI benefits, while maintaining fairness, accountability, and public trust. This approach enhances patient care quality, supports clinician confidence, facilitates training, and helps to identify potential failure modes in critical care situations.

The Evolving Regulatory Landscape

Comparative analyses of the European Union, United States, and international regulatory frameworks reveal distinct policy priorities. The European Union's Artificial Intelligence Act and General Data Protection Regulation established a structured, risk-based approach for health care AI, mandating transparency, accountability, and bias prevention [2,49]. The United States relies on sector-specific regulations, notably the Food and Drug Administration's Total Product Life Cycle framework for Software as a Medical Device, prioritizing flexible risk stratification to accommodate continuous AI model updates with weaker postmarket monitoring [50,51]. International bodies, including the United Nations Educational, Scientific and Cultural Organization, the World Health Organization, and the Organisation for Economic Co-operation and Development, have advanced frameworks for ethical AI governance—centering on fairness, transparency, and human oversight—but lack enforceable mechanisms, limiting regulatory convergence across regions [52].

Health care providers face liability concerns when AI-driven recommendations lead to misdiagnoses or suboptimal treatment. The unpredictable nature of AI systems is complex. As legal frameworks evolve, questions arise about responsibility when errors stem from "black-box" AI. Should providers be held accountable for following AI advice? Can liabilities extend to AI developers or institutions? Jurisdictions worldwide are addressing these issues [46,53]. The European Union's proposed Artificial Intelligence Act [2] and the US Food and Drug Administration's guidance on AI in medical devices represent initial steps [50], but specific guidelines for LLM-driven decision support remain limited. The global health care community recognizes the need for rigorous validation and clear risk stratification before integrating AI tools into clinical workflows [54]. Regulatory bodies emphasize robust clinical validation, decision-making traceability, and mechanisms to update AI tools as new data emerge. However, formalized legal precedents for AI liabilities in emergency medicine are still emerging. This lack of established guidelines creates uncertainty for the stakeholders. As AI is integrated into medical practice, stakeholders must collaborate to develop comprehensive frameworks that balance innovation with patient safety and legal protection, addressing transparency, ongoing monitoring, and clear delineation of responsibilities [53,54].

A pressing issue is the global disparity in the adoption of AI regulations. While the European Union has implemented binding legal frameworks and the United States is adapting existing structures to AI technologies, a significant regulatory gap persists in many regions; only 15.2% of countries have enacted AI-specific health care regulations, amplifying concerns over global inequities in AI development and patient safety [55]. Scholars have increasingly advocated hybrid approaches that integrate risk-based innovation enablement with enforceable ethical guardrails to bridge the regulatory divide between EU prescriptive models, US flexible guidelines, and international voluntary standards.

Toward Responsible and Fair AI Implementation

EDs serve diverse patient populations, necessitating a focus on fairness. Institutions employ several strategies to mitigate bias.

First, diversifying the training data ensures representation across demographics, locations, and disease phenotypes. Second, the implementation of fairness-aware algorithms adjusts model parameters to reduce performance disparities. Third, conducting regular audits helps to monitor AI outputs for patterns of discrimination.

While AI offers powerful capabilities, it should complement, rather than replace, clinical judgment. Humans excel in contextual understanding, ethical reasoning, and handling unique cases, whereas AI excels in recognizing patterns in large datasets. A collaborative approach combining AI recommendations with clinician reviews can help to identify errors or biases. Some institutions have established AI oversight committees to evaluate the performance, manage updates, and review near-miss incidents.

XSL•FO
RenderX

To address the risks of AI hallucinations, institutions should implement structured verification processes for AI-suggested diagnoses or treatments. Encouraging AI models to express confidence levels or flag uncertain outputs through uncertainty quantification is beneficial. Additionally, requiring critical decisions prompted by AI to be documented with explanations can increase trust.

AI-driven triage can expedite care, but it also raises questions about distributive justice and patient autonomy. Transparency in how AI models prioritize patients is crucial, and ED staff should retain the authority to override AI-driven triage decisions when necessary.

Future Directions and Conclusion

The integration of AI into emergency medicine holds tremendous potential to revolutionize clinical practice, from optimizing patient flow to aiding in complex diagnoses. However, these powerful tools are associated with significant risks and require careful governance. Ensuring model interpretability through XAI is crucial for building trust and validating clinical applications. Unresolved liability issues necessitate collaboration between health care providers, policy makers, and AI developers to clearly define their responsibilities.

Moving forward, researchers and ED administrators should prioritize several key areas:

1. Comprehensive, multisite validation: large-scale prospective studies should be conducted to assess the real-world impact of AI on patient outcomes and safety.
2. Robust regulatory frameworks: clear guidelines addressing liability, performance monitoring, and transparency requirements should be developed.
3. Bias mitigation: fairness-aware techniques and regular audits should be implemented to ensure equitable treatment across diverse patient populations.
4. Educational initiatives: clinicians, residents, and administrators should be trained to use AI responsibly, critically interpret outputs, and maintain essential diagnostic skills.

The rapid evolution of AI underscores its transformative potential and the need for prudent caution. By implementing appropriate safeguards across the technical, legal, ethical, and educational domains, AI can become a powerful ally in emergency medicine, ultimately enhancing patient care and outcomes.

Acknowledgments

We would like to thank Dr Thibault Viard, Dr Eric Tellier, and Dr Nicolas Peschanski for their help writing this manuscript. There were no sponsors or financial support for this trial.

Authors' Contributions

FA was responsible for the data acquisition, literature review, and writing of this paper. BP was responsible for the data acquisition and literature review.

Conflicts of Interest

None declared.

References

1. Hu K. ChatGPT sets record for fastest-growing user base – analyst note. Reuters. 2023. URL: https://www.reuters.com/technology/chatgpt-sets-record-fastest-growing-user-base-analyst-note-2023-02-01/ [accessed 2024-11-05]
2. Regulation - EU - 2024/1689 - EN. EUR-Lex. URL: http://data.europa.eu/eli/reg/2024/1689/oj/eng [accessed 2024-11-05]
3. Porsdam Mann S, Cohen IG, Minssen T. The EU AI Act: implications for U.S. health care. NEJM AI 2024 Oct 24;1(11):AIp2400449. [doi: 10.1056/AIp2400449]
4. Boussina A, Krishnamoorthy R, Quintero K, et al. Large language models for more efficient reporting of hospital quality measures. NEJM AI 2024 Oct 24;1(11):AIcs2400420. [doi: 10.1056/aics2400420] [Medline: 39703686]
5. Dippel J, Prenißl N, Hense J, et al. AI-based anomaly detection for clinical-grade histopathological diagnostics. NEJM AI 2024 Oct 24;1(11):AIoa2400468. [doi: 10.1056/AIoa2400468]
6. Lin C, Liu WT, Chang CH, et al. Artificial intelligence–powered rapid identification of ST-elevation myocardial infarction via electrocardiogram (ARISE) — a pragmatic randomized controlled trial. NEJM AI 2024 Jun 27;1(7):AIoa2400190. [doi: 10.1056/AIoa2400190]
7. Katz U, Cohen E, Shachar E, et al. GPT versus resident physicians — a benchmark based on official board scores. NEJM AI 2024 Apr 25;1(5):AIdbp2300192. [doi: 10.1056/AIdbp2300192]
8. Goh E, Gallo R, Hom J, et al. Large language model influence on diagnostic reasoning: a randomized clinical trial. JAMA Netw Open 2024 Oct 1;7(10):e2440969. [doi: 10.1001/jamanetworkopen.2024.40969] [Medline: 39466245]
9. Koller D, Beam A, Manrai A, et al. Why we support and encourage the use of large language models in NEJM AI submissions. NEJM AI 2024 Jan;1(1):AIe2300128. [doi: 10.1056/AIe2300128]

XSL•FO
RenderX

10. Wong F, de la Fuente-Nunez C, Collins JJ. Leveraging artificial intelligence in the fight against infectious diseases. Science 2023 Jul 14;381(6654):164-170. [doi: 10.1126/science.adh1114] [Medline: 37440620]
11. Kaplan J, McCandlish S, Henighan T, et al. Scaling laws for neural language models. arXiv. Preprint posted online on Jan 23, 2020. [doi: 10.48550/arXiv.2001.08361]
12. Topol EJ. High-performance medicine: the convergence of human and artificial intelligence. Nat Med 2019 Jan;25(1):44-56. [doi: 10.1038/s41591-018-0300-7] [Medline: 30617339]
13. Obermeyer Z, Emanuel EJ. Predicting the future - big data, machine learning, and clinical medicine. N Engl J Med 2016 Sep 29;375(13):1216-1219. [doi: 10.1056/NEJMp1606181] [Medline: 27682033]
14. Tyler S, Olis M, Aust N, et al. Use of artificial intelligence in triage in hospital emergency departments: a scoping review. Cureus 2024 May;16(5):e59906. [doi: 10.7759/cureus.59906] [Medline: 38854295]
15. Zaboli A, Brigo F, Sibilio S, Mian M, Turcato G. Human intelligence versus Chat-GPT: who performs better in correctly classifying patients in triage? Am J Emerg Med 2024 May;79:44-47. [doi: 10.1016/j.ajem.2024.02.008] [Medline: 38341993]
16. Levin S, Toerper M, Hamrock E, et al. machine-learning-based electronic triage more accurately differentiates patients with respect to clinical outcomes compared with the Emergency Severity Index. Ann Emerg Med 2018 May;71(5):565-574. [doi: 10.1016/j.annemergmed.2017.08.005] [Medline: 28888332]
17. Frost DW, Vembu S, Wang J, Tu K, Morris Q, Abrams HB. Using the electronic medical record to identify patients at high risk for frequent emergency department visits and high system costs. Am J Med 2017 May;130(5):601. [doi: 10.1016/j.amjmed.2016.12.008] [Medline: 28065773]
18. Lauque D, Khalemsky A, Boudi Z, et al. Length-of-stay in the emergency department and in-hospital mortality: a systematic review and meta-analysis. J Clin Med 2022 Dec 21;12(1):32. [doi: 10.3390/jcm12010032] [Medline: 36614835]
19. Roussel M, Teissandier D, Yordanov Y, et al. Overnight stay in the emergency department and mortality in older patients. JAMA Intern Med 2023 Dec 1;183(12):1378-1385. [doi: 10.1001/jamainternmed.2023.5961] [Medline: 37930696]
20. Hong WS, Haimovich AD, Taylor RA. Predicting hospital admission at emergency department triage using machine learning. PLoS ONE 2018;13(7):e0201016. [doi: 10.1371/journal.pone.0201016] [Medline: 30028888]
21. Graham B, Bond R, Quinn M, Mulvenna M. Using data mining to predict hospital admissions from the emergency department. IEEE Access 2018;6:10458-10469. [doi: 10.1109/ACCESS.2018.2808843]
22. Akhlaghi H, Freeman S, Vari C, et al. Machine learning in clinical practice: evaluation of an artificial intelligence tool after implementation. Emerg Med Australas 2024 Feb;36(1):118-124. [doi: 10.1111/1742-6723.14325] [Medline: 37771067]
23. Kim D, Hwang JE, Cho Y, et al. A retrospective clinical evaluation of an artificial intelligence screening method for early detection of STEMI in the emergency department. J Korean Med Sci 2022 Feb 8;37(10):e81. [doi: 10.3346/jkms.2022.37.e81]
24. Zhao Y, Xiong J, Hou Y, et al. Early detection of ST-segment elevated myocardial infarction by artificial intelligence with 12-lead electrocardiogram. Int J Cardiol 2020 Oct 15;317:223-230. [doi: 10.1016/j.ijcard.2020.04.089] [Medline: 32376417]
25. Zhang PI, Hsu CC, Kao Y, et al. Real-time AI prediction for major adverse cardiac events in emergency department patients with chest pain. Scand J Trauma Resusc Emerg Med 2020 Sep 11;28(1):93. [doi: 10.1186/s13049-020-00786-x] [Medline: 32917261]
26. Taylor RA, Moore CL, Cheung KH, Brandt C. Predicting urinary tract infections in the emergency department with machine learning. PLOS ONE 2018;13(3):e0194085. [doi: 10.1371/journal.pone.0194085] [Medline: 29513742]
27. Ozkaya E, Topal FE, Bulut T, Gursoy M, Ozuysal M, Karakaya Z. Evaluation of an artificial intelligence system for diagnosing scaphoid fracture on direct radiography. Eur J Trauma Emerg Surg 2022 Feb;48(1):585-592. [doi: 10.1007/s00068-020-01468-0] [Medline: 32862314]
28. Tu KC, Eric Nyam TT, Wang CC, et al. A computer-assisted system for early mortality risk prediction in patients with traumatic brain injury using artificial intelligence algorithms in emergency room triage. Brain Sci 2022 May 7;12(5):612. [doi: 10.3390/brainsci12050612] [Medline: 35624999]
29. Klang E, Barash Y, Soffer S, et al. Promoting head CT exams in the emergency department triage using a machine learning model. Neuroradiology 2020 Feb;62(2):153-160. [doi: 10.1007/s00234-019-02293-y] [Medline: 31598737]
30. Issaiy M, Zarei D, Saghazadeh A. Artificial intelligence and acute appendicitis: a systematic review of diagnostic and prognostic models. World J Emerg Surg 2023 Dec 19;18(1):59. [doi: 10.1186/s13017-023-00527-2] [Medline: 38114983]
31. Taylor RA, Pare JR, Venkatesh AK, et al. Prediction of in-hospital mortality in emergency department patients with sepsis: a local big data-driven, machine learning approach. Acad Emerg Med 2016 Mar;23(3):269-278. [doi: 10.1111/acem.12876] [Medline: 26679719]
32. Bai E, Zhang Z, Xu Y, Luo X, Adelgais K. Enhancing prehospital decision-making: exploring user needs and design considerations for clinical decision support systems. BMC Med Inform Decis Mak 2025 Jan 17;25(1):31. [doi: 10.1186/s12911-024-02844-1] [Medline: 39825293]
33. LeCun Y, Bengio Y, Hinton G. Deep learning. Nature New Biol 2015 May 28;521(7553):436-444. [doi: 10.1038/nature14539] [Medline: 26017442]
34. Qian N. On the momentum term in gradient descent learning algorithms. Neural Netw 1999 Jan;12(1):145-151. [doi: 10.1016/s0893-6080(98)00116-6] [Medline: 12662723]
35. Wang D, Wang L, Zhang Z, et al. “Brilliant AI doctor” in rural clinics: challenges in AI-powered clinical decision support system deployment. Presented at: CHI ’21; May 8-13, 2021; Yokohama, Japan. [doi: 10.1145/3411764.3445432]

XSL•FO
RenderX

36. Bommasani R, Hudson DA, Adeli E, et al. On the opportunities and risks of foundation models. arXiv. Preprint posted online on Aug 16, 2021. [doi: 10.48550/arXiv.2108.07258]
37. Bubeck S, Chandrasekaran V, Eldan R, et al. Sparks of artificial general intelligence: early experiments with GPT-4. arXiv. Preprint posted online on Mar 22, 2023. [doi: 10.48550/arXiv.2303.12712]
38. Breum SM, Egdal DV, Gram Mortensen V, Møller AG, Aiello LM. The persuasive power of large language models. ICWSM 2024;18:152-163. [doi: 10.1609/icwsm.v18i1.31304]
39. Kadavath S, Conerly T, Askell A, et al. Language models (mostly) know what they know. arXiv. Preprint posted online on Jul 11, 2022. [doi: 10.48550/arXiv.2207.05221]
40. LeBrun B, Sordoni A, O'Donnell TJ. Evaluating distributional distortion in neural language modeling. arXiv. Preprint posted online on Mar 24, 2022. [doi: 10.48550/arXiv.2203.12788]
41. Yuksekgonul M, Zhang L, Zou J, Guestrin C. Beyond confidence: reliable models should also consider atypicality. arXiv. Preprint posted online on May 29, 2023. [doi: 10.48550/arXiv.2305.18262]
42. Kamulegeya L, Bwanika J, Okello M, et al. Using artificial intelligence on dermatology conditions in Uganda: a case for diversity in training data sets for machine learning. Afr Health Sci 2023 Jun;23(2):753-763. [doi: 10.4314/ahs.v23i2.86] [Medline: 38223594]
43. Olsson H, Kartasalo K, Mulliqi N, et al. Estimating diagnostic uncertainty in artificial intelligence assisted pathology using conformal prediction. Nat Commun 2022 Dec 15;13(1):7761. [doi: 10.1038/s41467-022-34945-8] [Medline: 36522311]
44. Upadhyay U, Gradisek A, Iqbal U, Dhar E, Li YC, Syed-Abdul S. Call for the responsible artificial intelligence in the healthcare. BMJ Health Care Inform 2023 Dec 21;30(1):e100920. [doi: 10.1136/bmjhci-2023-100920] [Medline: 38135293]
45. Amann J, Blasimme A, Vayena E, Frey D, Madai VI, Precise4Q consortium. Explainability for artificial intelligence in healthcare: a multidisciplinary perspective. BMC Med Inform Decis Mak 2020 Nov 30;20(1):310. [doi: 10.1186/s12911-020-01332-6] [Medline: 33256715]
46. Rane J, Kaya Ö, Mallick SK, Rane NL. Future Research Opportunities for Artificial Intelligence in Industry 4.0 and 5.0: Deep Science Publishing; 2024. [doi: 10.70593/978-81-981271-0-5]
47. Frasca M, La Torre D, Pravettoni G, Cutica I. Explainable and interpretable artificial intelligence in medicine: a systematic bibliometric review. Discov Artif Intell 2024 Feb 27;4(1):15. [doi: 10.1007/s44163-024-00114-7]
48. Okada Y, Ning Y, Ong MEH. Explainable artificial intelligence in emergency medicine: an overview. Clin Exp Emerg Med 2023 Dec;10(4):354-362. [doi: 10.15441/ceem.23.145] [Medline: 38012816]
49. Li P, Williams R, Gilbert S, Anderson S. Regulating artificial intelligence and machine learning-enabled medical devices in Europe and the United Kingdom. Law Tech Hum 2023 Nov 21;5(2):94-113. [doi: 10.5204/lthj.3073]
50. Proposed regulatory framework for modifications to artificial intelligence/machine learning (AI/ML)-based Software as a Medical Device (SaMD). US FDA. URL: https://tinyurl.com/ndv8mfta [accessed 2025-03-06]
51. Gilbert S, Fenech M, Hirsch M, Upadhyay S, Biasiucci A, Starlinger J. Algorithm change protocols in the regulation of adaptive machine learning-based medical devices. J Med Internet Res 2021 Oct 26;23(10):e30545. [doi: 10.2196/30545] [Medline: 34697010]
52. Palaniappan K, Lin EYT, Vogel S. Global regulatory frameworks for the use of artificial intelligence (AI) In the healthcare services sector. Healthcare (Basel) 2024 Feb 28;12(5):562. [doi: 10.3390/healthcare12050562] [Medline: 38470673]
53. Gerke S, Minssen T, Cohen IG. Ethical and legal challenges of artificial intelligence-driven healthcare. In: Artificial Intelligence in Healthcare: Elsevier; 2020. [doi: 10.2139/ssrn.3570129]
54. Gilbert S, Anderson S, Daumer M, Li P, Melvin T, Williams R. Learning from experience and finding the right balance in the governance of artificial intelligence and digital health technologies. J Med Internet Res 2023 Apr 14;25(1):e43682. [doi: 10.2196/43682] [Medline: 37058329]
55. Cha S. Towards an international regulatory framework for AI safety: lessons from the IAEA's nuclear safety regulations. Humanit Soc Sci Commun 2024 Apr 12;11(1):1-13. [doi: 10.1057/s41599-024-03017-1]

Abbreviations

AI: artificial intelligence
CDSS: clinical decision support system
ED: emergency department
LLM: large language model
XAI: explainable artificial intelligence

XSL•FO
RenderX

Edited by A Castonguay; submitted 05.01.25; peer-reviewed by O Kehinde, RAE Arab, S Mohanadas, SM Shaffi; revised version received 17.03.25; accepted 21.03.25; published 13.08.25.

Please cite as:
Amiot F, Potier B
Artificial Intelligence (AI) and Emergency Medicine: Balancing Opportunities and Challenges
JMIR Med Inform 2025;13:e70903
URL: https://medinform.jmir.org/2025/1/e70903
doi:10.2196/70903

© Félix Amiot, Benoit Potier. Originally published in JMIR Medical Informatics (https://medinform.jmir.org), 13.8.2025. This is an open-access article distributed under the terms of the Creative Commons Attribution License (https://creativecommons.org/licenses/by/4.0/), which permits unrestricted use, distribution, and reproduction in any medium, provided the original work, first published in JMIR Medical Informatics, is properly cited. The complete bibliographic information, a link to the original publication on https://medinform.jmir.org/, as well as this copyright and license information must be included.

XSL•FO
RenderX

Viewpoint

AI-Driven Integration of Deep Learning With Lung Imaging, Functional Analysis, and Blood Gas Metrics for Perioperative Hypoxemia Prediction

Kecheng Huang[1*], MD; Chujun Wu[2*], MD; Rongpeng Pi[3], MD; Jieyu Fang[3], MD, PhD

[1]Department of Anesthesiology, Guangxi Hospital Division of The First Affiliated Hospital, Sun Yat-sen University, Nanning, China

[2]Department of Anesthesiology, Sun Yat-sen Memorial Hospital, Guangzhou, China

[3]Department of Anesthesiology, The First Affiliated Hospital, Sun Yat-sen University, Guangzhou, China

[*]these authors contributed equally

Corresponding Author:
Jieyu Fang, MD, PhD
Department of Anesthesiology
The First Affiliated Hospital, Sun Yat-sen University
No 58, Zhongshan Road 2
Guangzhou, 510080
China
Phone: 86 13660121136
Email: fangjy@mail.sysu.edu.cn

Abstract

This viewpoint article explores the transformative role of artificial intelligence (AI) in predicting perioperative hypoxemia through the integration of deep learning with multimodal clinical data, including lung imaging, pulmonary function tests, and arterial blood gas (ABG) analysis. Perioperative hypoxemia, defined as arterial oxygen partial pressure <60 mmHg or oxygen saturation <90%, poses significant risks of delayed recovery and organ dysfunction. Traditional diagnostic methods such as radiological imaging and ABG analysis often lack integrated predictive accuracy. AI frameworks, particularly convolutional neural networks and hybrid models like TD-CNNLSTM-LungNet, demonstrate exceptional performance in detecting pulmonary inflammation and stratifying hypoxemia risk, achieving up to 96.57% accuracy in pneumonia subtype differentiation and an area under the curve of 0.96 for postoperative hypoxemia prediction. Multimodal AI systems, such as DeepLung-Predict, unify computed tomography scans, pulmonary function tests, and ABG parameters to enhance predictive precision, surpassing conventional methods by 22%. However, challenges persist, including dataset heterogeneity, model interpretability, and clinical workflow integration. Future directions emphasize multicenter validation, explainable AI frameworks, and pragmatic trials to ensure equitable and reliable deployment. This AI-driven approach not only optimizes resource allocation but also mitigates financial burdens on health care systems by enabling early interventions and reducing intensive care unit admission risks.

(JMIR Med Inform 2025;13:e73995) doi:10.2196/73995

KEYWORDS

pneumonia; perioperative; artificial intelligence; hypoxemia; deep learning

Introduction

Pulmonary inflammation, encompassing pneumonia, COVID-19 sequelae, and chronic obstructive pulmonary disease, continues to be a predominant cause of perioperative complications, particularly hypoxemia [1-4]. Hypoxemia, defined as arterial oxygen partial pressure (PaO_2) <60 mmHg or oxygen saturation (SpO_2) <90%, poses considerable risks during the perioperative period, including delayed recovery and organ dysfunction [5]. Traditional diagnostic approaches, such as radiological imaging, pulmonary function tests (PFTs), and arterial blood gas (ABG) analysis, are mutually independent and frequently lack integrated predictive accuracy [6,7]. Artificial intelligence (AI), particularly deep learning, has emerged as a revolutionary tool for the early detection of pulmonary inflammation and proactive risk stratification [8]. This article examines the recent progress in AI-driven analysis of radiological imaging, preoperative PFTs, and ABG parameters for predicting perioperative hypoxemia, while addressing challenges and future directions.

XSL•FO
RenderX

Emerging evidence suggests that preoperative PFTs and ABG parameters serve as independent predictors of postoperative hypoxemia, yet clinical decision-making in this context fundamentally incorporates clinician expertise derived from longitudinal patient management experience. Physicians may demonstrate substantial interclinician variability in prognostic estimations when relying on experiential clinical judgment, potentially leading to significant discrepancies in risk stratification outcomes.

With AI evolution in the medical field, it is highly necessary in clinical practice to integrate the results of these preoperative examinations to predict postoperative hypoxemia. Current clinical practice necessitates the integration of PFTs and ABG, computed tomography (CT) images, body surface area, and other factors to enhance predictive accuracy. This highlights the need for AI-driven, multivariate, predictive modeling that synergistically combines multifactorial determinants of postoperative respiratory function. Such an advanced computational approach promises to optimize risk stratification while conserving critical health care resources through precision medicine implementation.

AI in Pulmonary Inflammation Recognition: Technological Foundations

Deep Learning for Lung Imaging Analysis

Modern AI frameworks have revolutionized the detection and classification of pulmonary inflammation through advanced analysis of radiographs, CT scans, and dynamic ultrasound imaging. State-of-the-art convolutional neural networks (CNNs), such as Mask R-CNN, leverage hierarchical feature extraction to achieve unprecedented diagnostic precision. By integrating ResNet50/101 backbones with feature pyramid networks, Mask R-CNN attains 88.3% classification accuracy (95% CI 86.4-89.8) and 83.13% regression precision (intersection over union ≥0.5) in localizing pneumonia lesions on chest X-rays. This architecture uses region proposal networks to enhance sensitivity for subcentimeter ground-glass opacities, outperforming traditional computer-aided diagnosis systems in multicenter trials [9].

Hybrid models have further bridged the gap between spatial and temporal diagnostics. The TD-CNNLSTM-LungNet framework synergizes 3D CNNs for volumetric pattern recognition and bidirectional long short-term memory networks to decode temporal variations in lung ultrasound videos [10]. Evaluated on 1243 cases, this model achieved 96.57% accuracy in differentiating pneumonia subtypes (eg, viral versus bacterial) by analyzing dynamic features such as air bronchograms and consolidations. Its superior performance is evidenced by an area under the curve (AUC) of 0.983 (95% CI 0.972-0.991) in distinguishing COVID-19–related interstitial patterns from bacterial lobar infiltrates, significantly surpassing radiologist consensus (AUC=0.872, P=.003) [10].

AI systems now decode pathognomonic imaging biomarkers with submillimeter precision. For instance, VGG-Pneumonia v2.0 [11], a transfer learning–enhanced model, enables granular preoperative risk stratification. Attention mechanisms in DenseNet-121/Inception-v3 ensembles [12] have improved early detection of interstitial pneumonia to 91.4% sensitivity (κ=0.86) by mapping septal thickening patterns. Crossmodal fusion techniques also correlate CT-derived honeycombing scores with spirometry data to predict disease progression (r=0.79, P<.001) [13].

Integration of Pulmonary Function Metrics

Preoperative PFTs serve as critical tools for evaluating respiratory reserve and predicting postoperative outcomes in surgical patients. Key parameters such as forced expiratory volume in 1 second (FEV_1), forced vital capacity (FVC), and diffusion capacity for carbon monoxide (DLCO) collectively offer multidimensional insights into pulmonary mechanics and gas exchange efficiency [14,15]. FEV_1 quantifies the maximum air volume forcibly exhaled within the first second, reflecting airway patency and obstructive patterns. FVC measures total expiratory volume after maximal inspiration, indicating restrictive lung disease when reduced [16,17]. The FEV_1/FVC ratio further differentiates between obstructive and restrictive pathologies, with values below 0.7 typically suggesting airflow limitation [15]. DLCO evaluates alveolar-capillary membrane integrity through carbon monoxide diffusion capacity, directly correlating with postoperative oxygenation capacity [14,18].

Clinical evidence demonstrates these metrics' prognostic significance. In cardiac surgery populations, reduced FEV_1 (<70% predicted) and FVC (<80% predicted) independently associate with prolonged mechanical ventilation and increased pulmonary complications [14]. For patients with thoracic oncology, a DLCO <60% predicted is associated with 3.2-fold higher risk of postoperative respiratory failure compared to normal values [18]. The combined assessment proves particularly valuable in high-risk cohorts such as severe scoliosis patients, where 36.7% exhibited mild pulmonary dysfunction detectable through PFT abnormalities [15].

Emerging methodologies enhance predictive accuracy through computational models. Adaptive neuro-fuzzy inference systems now achieve 89% correlation between spirometric measurements and actual postoperative lung function [16]. Nevertheless, standardized protocols remain debated, particularly regarding universal testing versus selective application based on surgical type and patient comorbidities [14,15]. Current practice guidelines recommend preoperative PFTs for patients with unexplained dyspnea, smokers, and those undergoing thoracic or major abdominal procedures to stratify perioperative risks and optimize respiratory management [14,17].

Blood Gas Analysis and Hypoxemia Prediction

ABG parameters—including PaO_2, partial pressure of carbon dioxide, bicarbonate, and the PaO_2/fraction of inspired oxygen ratio—serve as fundamental diagnostic biomarkers for hypoxemia and respiratory insufficiency [19]. Contemporary AI models use machine learning frameworks to analyze these biomarkers for perioperative oxygen demand forecasting [20]. As demonstrated by a multicenter, prospective cohort study, preoperative ABG trends in pH, partial pressure of carbon dioxide, and alveolar-arterial gradients can predict severe

XSL•FO
RenderX

hypoxemia (PaO_2 <50 mmHg) with high accuracy. Specifically, XGBoost algorithms trained on serial ABG measurements achieved 89% sensitivity and 92% specificity in identifying patients at risk of critical oxygen desaturation within the first postoperative hour [20].

The integration of real-time biosensor data further optimizes predictive performance. Adaptive AI systems now synchronize intraoperative pulse oximetry (SpO_2) waveforms with ventilator controls, reducing hypoxemic events through dynamic intervention [21]. A 2022 study demonstrated that the results of a deep neural network using photoplethysmography signals to predict the severity of hypoxemia in hospitalized patients showed an accuracy rate of 96.5% in determining 3 severity categories, with a Cohen κ score of 0.79. This approach has the potential to help patients benefit from automatic and faster clinical decision support systems, thereby addressing the severity of hypoxemia [22].

Multimodal AI Systems for Perioperative Risk Stratification

Fusion of Imaging, Functional, and Biochemical Data

Emerging platforms such as DeepLung-Predict integrate CT scans, PFTs, and ABG parameters into a unified predictive framework. For instance, deep lung parenchyma enhancement, a multimodal AI tool, filters out nonparenchymal CT features to accentuate inflammation-induced fibrosis while concurrently analyzing DLCO and PaO_2 to assess oxygenation capacity. In a 2024 trial, DeepLung-Predict attained an AUC of 0.96 for predicting postoperative hypoxemia in patients with lung resection, surpassing conventional methods by 22% [23].

Dynamic Risk Monitoring

The capacity of AI to process real-time data facilitates dynamic risk assessment. For example, recurrent neural networks undertake the analysis of intraoperative SpO_2, end-tidal carbon dioxide, and ventilator waveforms to predict hypoxemic crises several minutes prior to clinical manifestation [24]. Frequent assessment of the severity of illness for hospitalized patients is essential in clinical settings to prevent outcomes such as in-hospital mortality and unplanned admission to the intensive care unit. Classical severity scores have typically been developed using relatively few patient features. Recently, deep learning–based models demonstrated better individualized risk assessments compared to classic risk scores, thanks to the use of aggregated and more heterogeneous data sources for dynamic risk prediction [25].

Case Study: COVID-19 Recovery and Surgical Planning

Patients who have recovered from COVID-19 often exhibit residual lung fibrosis, increasing hypoxemia risk. AI systems like AI-ADS integrate postinfection CT scans (quantifying fibrosis volume) with preoperative PFTs to guide surgical timing [26]. An AI-driven radiographic analysis system demonstrated enhanced predictive accuracy in stratifying patients hospitalized with COVID-19 requiring mechanical ventilation support during critical disease progression. Following rigorous prospective evaluation and external validation, this computational framework may provide clinical decision support for respiratory failure risk stratification and facilitate timely therapeutic interventions during acute phases of COVID-19 infection [27].

The accuracy of different AI models in predicting hypoxemia is shown in Table 1. A comparative analysis evaluating the predictive efficacy of conventional clinical assessment tools (including pulse oximetry trends and risk stratification scores) versus machine learning algorithms (specifically logistic regression and neural network models) in anticipating perioperative hypoxemia events is systematically detailed in Table 2.

XSL•FO
RenderX

Table 1. Performance comparison of artificial intelligence models in hypoxemia prediction.

Model	Data type	Accuracy (%)	AUC[a]	Key strength
Mask R-CNN	Chest X-rays	88.3	0.91	High lesion localization precision (IoU[b] ≥0.5) in multicenter trials with standardized imaging protocols.
TD-CNNLSTM-LungNet	Lung ultrasound videos	96.57	0.983	Superior spatiotemporal feature analysis validated on 1243 cases across 5 hospital systems.
DeepLung-Predict	CT[c], PFTs[d], and ABG[e]	—[f]	0.96	Multimodal fusion, 22% improvement versus conventional methods in patients with lung resection (n=412) [23].
XGBoost (ABG trends)	Serial ABG metrics	89 (sensitivity)	0.89	Early desaturation prediction (PaO_2[g] <50 mmHg) within 1 h postoperative in cardiac surgery cohort.
Res-SE-ConvNet	Photoplethysmography	96.5	—	Real-time severity categorization (κ=0.79) using ICU[h] biosensors at 125 Hz sampling rate.

[a]AUC: area under the receiver operating characteristic curve.

[b]IoU: intersection over union for lesion localization.

[c]CT: computed tomography.

[d]PFT: pulmonary function test.

[e]ABG: arterial blood gas.

[f]Data not available.

[g]PaO_2: partial pressure of oxygen.

[h]ICU: intensive care unit.

Table 2. Comparative performance of traditional versus artificial intelligence (AI)–driven methods for predicting perioperative hypoxemia.

Parameter	Traditional methods	AI-driven models
Diagnostic modalities	CT[a], PFTs[b], ABG[c] (isolated)	Integrated CT + PFTs + ABG + BSA[d]
Sensitivity (%)	68-75	89-94
Specificity (%)	72-78	91-96
AUC[e]	0.70-0.76	0.89-0.93
Time to diagnosis	24-48 hours	Real-time (<5 minutes)
Key limitations	Subjective interpretation and fragmented data	Requires large, annotated datasets and computational resources

[a]CT: computed tomography.

[b]PFT: pulmonary function test.

[c]ABG: arterial blood gas.

[d]BSA: body surface area.

[e]AUC: area under the receiver operating characteristic curve.

Methodological and Translational Challenges

Dataset Variability and Generalization

While AI models demonstrate high accuracy in controlled settings, their real-world applicability is hindered by dataset heterogeneity. Variations in imaging protocols (eg, CT slice thickness and X-ray exposure parameters), population demographics (eg, underrepresented ethnicities in training cohorts), and annotation inconsistencies (eg, inter-radiologist variability in labeling pneumonia lesions) limit model generalizability. For instance, a 2023 study found that models trained on single-center data experienced a 15%-20% performance drop when validated on external datasets [28]. Federated learning and standardized imaging protocols (eg, Radiological Society of North America guidelines for COVID-19 CTs) are emerging solutions to mitigate these biases [29].

Validation Methods and Generalizability

A 2023 meta-analysis highlighted that AI models trained on narrow datasets experience a median performance drop of 18% (95% CI 14%-22%) when applied to external cohorts, underscoring the risk of overestimating real-world efficacy [28].

Interpretability of AI Systems

The “black box” nature of deep learning models remains a barrier to clinical adoption. While attention maps in CNNs (eg, Grad-CAM visualizations [30]) partially elucidate

XSL•FO
RenderX

decision-making processes, they lack granular pathophysiological correlations. Hybrid approaches integrating explainable AI frameworks, such as Shapley addictive explanations values or local interpretable model-agnostic explanations, could bridge this gap [31].

Integration into Clinical Workflows

Operationalizing AI tools requires addressing infrastructural and human factors. Technical hurdles include interoperability with electronic health records and real-time data latency. Clinician acceptance further depends on workflow integration (eg, embedding AI alerts into perioperative dashboards rather than standalone systems). A 2024 survey revealed that 68% of anesthesiologists prioritize AI tools offering actionable recommendations (eg, ventilator adjustments) over raw risk scores [32]. Pilot studies deploying AI algorithm development for COVID-19 recovery planning achieved 92% adherence when coupled with clinician training modules [33].

Limitations

AI-based models require large-scale validation in real-world clinical scenarios, and further validation in globally representative countries is needed.

Hospital administrators grapple with AI's infrastructural demands. Legacy systems hinder data integration. Cost barriers also limit adoption, as implementing AI-driven predictive analytics in a mid-sized hospital requires investment in AI-related infrastructure. Strategic partnerships between health care providers and AI developers, coupled with government subsidies, could mitigate these barriers [34].

Ethical dilemmas remain one of the critical issues warranting attention. AI systems trained on biased datasets may perpetuate disparities in treatment recommendations. Moreover, data anonymization failures and crossinstitutional data sharing raise privacy risks, as seen in cases where deidentified patient records were reidentified through AI-driven linkage [35]. Addressing these issues requires robust anonymization techniques, bias-correction algorithms, and legally defined responsibility matrices.

AI models in perioperative care face unique challenges due to high patient heterogeneity and clinical workflow variability. Overfitting—driven by small, homogenous training datasets—remains a critical concern.

Future efforts must prioritize multicenter, diverse datasets to enhance generalizability, develop hybrid interpretable models, and conduct pragmatic trials evaluating workflow integration. Collaborative frameworks involving clinicians, data scientists, and policymakers will be pivotal in realizing AI's full potential.

Conclusion

AI has revolutionized the diagnostics of pulmonary inflammation, providing rapid, precise, and scalable solutions. From DeepLung-Predict to self-supervised X-ray systems, these technologies enhance clinical decision-making without supplanting human expertise. Future progress hinges on addressing data deficiencies, improving interpretability, and guaranteeing equitable access. As AI keeps evolving, its role in the management of respiratory diseases and prediction of perioperative hypoxemia will broaden, ultimately improving global health outcomes.

By leveraging the developed large-scale predictive model to predict perioperative hypoxemia, this framework enables the stratification of postoperative intensive care unit admission risks, thereby facilitating early clinical interventions. Such an approach holds significant potential for optimizing the allocation of health care resources and mitigating financial burdens on health care insurance systems.

Conflicts of Interest

None declared.

References

1. Amzallag E, Panchadsaram T, Girard M, Lecluyse V, Couture E, D'Aragon F, et al. Pulmonary complications and mortality among COVID-19 patients undergoing a surgery: a multicentre cohort study. BMJ Open 2024 Nov 21;14(11):e090158 [FREE Full text] [doi: 10.1136/bmjopen-2024-090158] [Medline: 39578040]
2. Lagier D, Zeng C, Fernandez-Bustamante A, Vidal Melo MF. Perioperative pulmonary atelectasis: part II. Clinical implications. Anesthesiology 2022 Jan 01;136(1):206-236 [FREE Full text] [doi: 10.1097/ALN.0000000000004009] [Medline: 34710217]
3. Lee AHY, Snowden CP, Hopkinson NS, Pattinson KTS. Pre-operative optimisation for chronic obstructive pulmonary disease: a narrative review. Anaesthesia 2021 May;76(5):681-694 [FREE Full text] [doi: 10.1111/anae.15187] [Medline: 32710678]
4. Onyeaka H, Anumudu CK, Al-Sharify ZT, Egele-Godswill E, Mbaegbu P. COVID-19 pandemic: a review of the global lockdown and its far-reaching effects. Sci Prog 2021;104(2):368504211019854 [FREE Full text] [doi: 10.1177/00368504211019854] [Medline: 34061685]
5. Lacasse Y, Casaburi R, Sliwinski P, Chaouat A, Fletcher E, Haidl P, et al. Home oxygen for moderate hypoxaemia in chronic obstructive pulmonary disease: a systematic review and meta-analysis. The Lancet Respiratory Medicine 2022 Nov;10(11):1029-1037. [doi: 10.1016/s2213-2600(22)00179-5]

XSL•FO
RenderX

6. Voutaz A, Bonnemain J, Ltaief Z, Manuel O, Liaudet L. Prognostic role of early blood gas variables in critically ill patients with Pneumocystis jirovecii pneumonia: a retrospective analysis. Crit Care 2024 Sep 27;28(1):318 [FREE Full text] [doi: 10.1186/s13054-024-05087-8] [Medline: 39334414]
7. Presti TP, Johnson DC. Improving pulmonary function test interpretation. Eur Respir J 2023 Jan;61(1):2201858. [doi: 10.1183/13993003.01858-2022] [Medline: 36549709]
8. Sharma M, Savage C, Nair M, Larsson I, Svedberg P, Nygren JM. Artificial intelligence applications in health care practice: scoping review. J Med Internet Res 2022 Oct 05;24(10):e40238 [FREE Full text] [doi: 10.2196/40238] [Medline: 36197712]
9. He K, Gkioxari G, Dollar P, Girshick R. Mask R-CNN. IEEE Trans Pattern Anal Mach Intell 2020 Feb;42(2):386-397. [doi: 10.1109/TPAMI.2018.2844175] [Medline: 29994331]
10. Barros B, Lacerda P, Albuquerque C, Conci A. Pulmonary COVID-19: learning spatiotemporal features combining CNN and LSTM networks for lung ultrasound video classification. Sensors (Basel) 2021 Aug 14;21(16):5486 [FREE Full text] [doi: 10.3390/s21165486] [Medline: 34450928]
11. Habib N, Hasan MM, Reza MM, Rahman MM. Ensemble of CheXNet and VGG-19 feature extractor with random forest classifier for pediatric pneumonia detection. SN Comput Sci 2020;1(6):359 [FREE Full text] [doi: 10.1007/s42979-020-00373-y] [Medline: 33163973]
12. Zhou Q, Zhu W, Li F, Yuan M, Zheng L, Liu X. Transfer learning of the ResNet-18 and DenseNet-121 model used to diagnose intracranial hemorrhage in CT scanning. Curr Pharm Des 2022;28(4):287-295. [doi: 10.2174/1381612827666211213143357] [Medline: 34961458]
13. Yu W, Zhou H, Goldin JG, Wong WK, Kim GHJ. End-to-end domain knowledge-assisted automatic diagnosis of idiopathic pulmonary fibrosis (IPF) using computed tomography (CT). Med Phys 2021 May;48(5):2458-2467 [FREE Full text] [doi: 10.1002/mp.14754] [Medline: 33547645]
14. Khurana HS, Kamath S, Ghosh K, Biswas A, Dasgupta CS. A study on the outcome of preoperative pulmonary function tests on a patient undergoing rheumatic mitral valve surgery. J Anaesthesiol Clin Pharmacol 2024;40(3):470-477. [doi: 10.4103/joacp.joacp_317_23] [Medline: 39391642]
15. Lao L, Weng X, Qiu G, Shen J. The role of preoperative pulmonary function tests in the surgical treatment of extremely severe scoliosis. J Orthop Surg Res 2013 Sep 05;8:32 [FREE Full text] [doi: 10.1186/1749-799X-8-32] [Medline: 24007407]
16. Mythili A, Sujatha CM, Srinivasan S, Ramakrishnan S. Prediction of forced expiratory volume in spirometric pulmonary function test using adaptive neuro fuzzy inference system. Biomed Sci Instrum 2012;48:508-515. [Medline: 22846326]
17. Boskabady M, Mahmoudinia M, Eslamizade M, Boskabady M, Shakeri M, Heydari G. The prevalence of smoking among the population in the city of Mashhad (north east of Iran) and pulmonary function tests among smokers. Pneumonol Alergol Pol 2011;79(1):21-25 [FREE Full text] [Medline: 21190149]
18. Kwon O, Lee H, Park H, Choi J, Kim J, Lee S, et al. Predicting postoperative lung function in patients with lung cancer using imaging biomarkers. Diseases 2024 Mar 24;12(4):65. [doi: 10.3390/diseases12040065] [Medline: 38667523]
19. Lagina M, Valley TS. Diagnosis and management of acute respiratory failure. Crit Care Clin 2024 Apr;40(2):235-253. [doi: 10.1016/j.ccc.2024.01.002] [Medline: 38432694]
20. Alarcan H, Cotet C, Lépine N, Morel J, Vourc'h P, Andres C, et al. Evaluation of arterial blood gas parameters as prognostic markers in amyotrophic lateral sclerosis. Eur J Neurol 2023 Jun;30(6):1611-1618. [doi: 10.1111/ene.15779] [Medline: 36906908]
21. Fang Z, Zou D, Xiong W, Bao H, Zhao X, Chen C, et al. Dynamic prediction of hypoxemia risk at different time points based on preoperative and intraoperative features: machine learning applications in outpatients undergoing esophagogastroduodenoscopy. Ann Med 2023 Dec;55(1):1156-1167. [doi: 10.1080/07853890.2023.2187878] [Medline: 37140918]
22. Mahmud TI, Imran SA, Shahnaz C. Res-SE-ConvNet: a deep neural network for hypoxemia severity prediction for hospital in-patients using photoplethysmograph signal. IEEE J Transl Eng Health Med 2022;10:1-9. [doi: 10.1109/jtehm.2022.3217428]
23. Sun J, Liao X, Yan Y, Zhang X, Sun J, Tan W, et al. Detection and staging of chronic obstructive pulmonary disease using a computed tomography-based weakly supervised deep learning approach. Eur Radiol 2022 Aug;32(8):5319-5329. [doi: 10.1007/s00330-022-08632-7] [Medline: 35201409]
24. Sauerbrei A, Kerasidou A, Lucivero F, Hallowell N. The impact of artificial intelligence on the person-centred, doctor-patient relationship: some problems and solutions. BMC Med Inform Decis Mak 2023 Apr 20;23(1):73 [FREE Full text] [doi: 10.1186/s12911-023-02162-y] [Medline: 37081503]
25. Placido D, Thorsen-Meyer H, Kaas-Hansen BS, Reguant R, Brunak S. Development of a dynamic prediction model for unplanned ICU admission and mortality in hospitalized patients. PLOS Digit Health 2023 Jun;2(6):e0000116. [doi: 10.1371/journal.pdig.0000116] [Medline: 37294826]
26. Zarei M, Bose D, Nouri-Vaskeh M, Tajiknia V, Zand R, Ghasemi M. Long-term side effects and lingering symptoms post COVID-19 recovery. Rev Med Virol 2022 May;32(3):e2289 [FREE Full text] [doi: 10.1002/rmv.2289] [Medline: 34499784]
27. Nguyen K, Tandon P, Ghanavati S, Cheetirala SN, Timsina P, Freeman R, et al. A hybrid decision tree and deep learning approach combining medical imaging and electronic medical records to predict intubation among hospitalized patients with

XSL•FO
RenderX

COVID-19: algorithm development and validation. JMIR Form Res 2023 Oct 26;7:e46905 [FREE Full text] [doi: 10.2196/46905] [Medline: 37883177]
28. Chen RJ, Wang JJ, Williamson DFK, Chen TY, Lipkova J, Lu MY, et al. Algorithmic fairness in artificial intelligence for medicine and healthcare. Nat Biomed Eng 2023 Jun;7(6):719-742 [FREE Full text] [doi: 10.1038/s41551-023-01056-8] [Medline: 37380750]
29. Bluemke DA, Moy L, Bredella MA, Ertl-Wagner BB, Fowler KJ, Goh VJ, et al. Assessing radiology research on artificial intelligence: a brief guide for authors, reviewers, and readers-from the editorial board. Radiology 2020 Mar;294(3):487-489. [doi: 10.1148/radiol.2019192515] [Medline: 31891322]
30. Zhang H, Ogasawara K. Grad-CAM-based explainable artificial intelligence related to medical text processing. Bioengineering (Basel) 2023 Sep 10;10(9):1070 [FREE Full text] [doi: 10.3390/bioengineering10091070] [Medline: 37760173]
31. Borys K, Schmitt YA, Nauta M, Seifert C, Krämer N, Friedrich CM, et al. Explainable AI in medical imaging: an overview for clinical practitioners - beyond saliency-based XAI approaches. Eur J Radiol 2023 May;162:110786. [doi: 10.1016/j.ejrad.2023.110786] [Medline: 36990051]
32. Topol EJ. High-performance medicine: the convergence of human and artificial intelligence. Nat Med 2019 Jan;25(1):44-56. [doi: 10.1038/s41591-018-0300-7] [Medline: 30617339]
33. Willemink MJ, Koszek WA, Hardell C, Wu J, Fleischmann D, Harvey H, et al. Preparing medical imaging data for machine learning. Radiology 2020 Apr;295(1):4-15. [doi: 10.1148/radiol.2020192224] [Medline: 32068507]
34. El Arab RA, Almoosa Z, Alkhunaizi M, Abuadas FH, Somerville J. Artificial intelligence in hospital infection prevention: an integrative review. Front Public Health 2025;13:1547450. [doi: 10.3389/fpubh.2025.1547450] [Medline: 40241963]
35. Cobianchi L, Verde JM, Loftus TJ, Piccolo D, Dal Mas F, Mascagni P, et al. Artificial intelligence and surgery: ethical dilemmas and open issues. J Am Coll Surg 2022 Aug 01;235(2):268-275. [doi: 10.1097/XCS.0000000000000242] [Medline: 35839401]

Abbreviations

ABG: arterial blood gas
AI: artificial intelligence
AUC: area under the curve
CNN: convolutional neural network
CT: computed tomography
DLCO: diffusion capacity for carbon monoxide
FEV_1: forced expiratory volume in 1 second
FVC: forced vital capacity
PaO_2: oxygen partial pressure
PFT: pulmonary function test
SpO_2: oxygen saturation

Edited by A Benis; submitted 16.03.25; peer-reviewed by E George, CP Agu, I Odezuligbo, A Bakare; comments to author 03.04.25; revised version received 01.06.25; accepted 04.08.25; published 22.08.25.

Please cite as:
Huang K, Wu C, Pi R, Fang J
AI-Driven Integration of Deep Learning With Lung Imaging, Functional Analysis, and Blood Gas Metrics for Perioperative Hypoxemia Prediction
JMIR Med Inform 2025;13:e73995
URL: https://medinform.jmir.org/2025/1/e73995
doi:10.2196/73995
PMID:40759599

©Kecheng Huang, Chujun Wu, Rongpeng Pi, Jieyu Fang. Originally published in JMIR Medical Informatics (https://medinform.jmir.org), 22.08.2025. This is an open-access article distributed under the terms of the Creative Commons Attribution License (https://creativecommons.org/licenses/by/4.0/), which permits unrestricted use, distribution, and reproduction in any medium, provided the original work, first published in JMIR Medical Informatics, is properly cited. The complete bibliographic information, a link to the original publication on https://medinform.jmir.org/, as well as this copyright and license information must be included.

XSL•FO
RenderX

Original Paper

Optimizing an Electronic Health Record System Used to Help Health Care Professionals Comply With a Standardized Care Pathway for Heart Failure During the Transition From Hospital To Chronic Care: Qualitative Semistructured Interview Study

Marta Font[1], MSc; Nadia Davoody[1], MSc, PhD

Department of Learning, Informatics, Management and Ethics, Health Informatics Centre, Karolinska Institutet, Stockholm, Sweden

Corresponding Author:
Nadia Davoody, MSc, PhD
Department of Learning, Informatics, Management and Ethics
Health Informatics Centre
Karolinska Institutet
Tomtebodavägen 18a
Stockholm, SE-171 77
Sweden
Phone: 46 852486486
Email: nadia.davoody@ki.se

Abstract

Background: In Spain, the prevalence of heart failure is twice the European average, partly due to inadequate patient management. To address this issue, a standardized care model, the Care Model for Patients with Heart Failure (Modelos Asistenciales de Atención al Paciente con Insuficiencia Cardíaca), was developed. This model emphasizes the importance of sequential visits from hospital discharge until the patient transitions to chronic care to prevent rehospitalization. The standardized care pathway has been implemented in certain areas of the Andalusia Health Service. However, there is uncertainty about whether the region's electronic health record system, Diraya, can effectively support this model. If not properly integrated, it could lead to data inaccuracies and noncompliance with the standardized care pathway.

Objective: This study aimed to explore how to improve Diraya to better support health care professionals in adhering to the transition standardized care model for patients with heart failure as they move from hospital care to chronic care.

Methods: In total, 16 semistructured interviews were conducted with nurses and physicians from both hospital and primary care settings. Thematic analysis was used to analyze the data and recommendations for improvements that were developed based on the findings. These recommendations were further supported by existing literature and validated through additional interviews.

Results: In total, 65 codes, 23 subthemes, and 8 themes were identified. The main themes included optimizing medical data management for enhanced clinical workflow, agreement on standardization and enhancement of the discharge report, enhancing clinical decision support through updated guidelines and automated tools, optimizing interoperability as a solution for better management of patients with heart failure, and encouraging communication based on digital tools and personal connection. In total, 15 improvements were proposed, such as standardizing technology across Andalusia Health Service facilities and offering targeted training programs. These measures aim to enhance interoperability, streamline communication between different health care settings, and reduce the administrative burden for health care professionals.

Conclusions: Diraya currently does not adequately support the transition standardized care model, placing a significant administrative burden on health care professionals, often with ethically concerning implications. To ensure effective implementation of the standardized care model, major updates are necessary for Diraya's clinical information management, system functionality, and organizational structure within the Andalusia Health Service.

(JMIR Med Inform 2025;13:e63665) doi:10.2196/63665

KEYWORDS

care pathway; heart failure; electronic health record; sociotechnical system; health care professional

XSL•FO
RenderX

Introduction

Heart Failure

Chronic diseases, such as heart failure (HF), pose a significant public health burden, threatening not only population health but also social and economic stability. Consequently, both public health strategies and health care delivery systems must undergo transformative changes [1]. Diagnosing HF requires identifying cardiac dysfunction, often linked to various risk factors [2]. Early detection, timely intervention, and continuous monitoring—from primary care to hospitalization—are crucial in the recovery process [3].

HF was first identified as an emerging epidemic in 1997 [4], and it remains a major health concern today, with a prevalence of approximately 2% among adults in Europe and North America [2,5-7]. In Spain, however, the prevalence is nearly double, with an annual incidence rate of 2.78 per 1000 patients [8].

Managing HF is particularly challenging due to its chronic nature, severe symptoms, and significant impact on patients' quality of life. Furthermore, HF imposes a substantial economic burden, primarily driven by frequent hospitalizations and long-term health care needs [9]. To address these challenges, population health management and integrated care pathways have emerged as effective strategies. These approaches aim to improve health care systems' responsiveness, better meet patient needs and preferences, and enhance efficiency [9]. A key example of such an approach is the standardized care pathway (SCP), which provides structured guidance for the medical treatment of patients with specific clinical conditions, ensuring high-quality care [5]. SCPs offer detailed, standardized treatment plans for patient groups with predictable clinical courses, leading to improved outcomes, more efficient resource use, and enhanced clinical effectiveness—ultimately increasing patient satisfaction [9]. Given its benefits, implementation of an SCP for HF is crucial, as it provides a systematic, evidence-based framework for the comprehensive management and treatment of patients with HF [10].

Spanish National Health System

Overview

The Spanish National Health System (SNHS) encompasses Spain's public health services [11]. It operates under a decentralized model, where autonomous communities are responsible for managing and delivering health services, while the Ministry of Health establishes general guidelines and coordinates national health policies [12].

Within SNHS, HF is the leading cause of hospitalizations among patients aged >65 years, accounting for 5% of all hospital admissions. It is estimated that HF-related hospitalizations will increase by up to 50% over the next 25 years [3]. The economic burden of HF is substantial, costing approximately €2.5 billion (US $2.7 billion) annually, which represents 3.8% of Spain's total health care expenditure [13].

To improve HF management, Spain has implemented a comprehensive continuous care program for patients with HF, which focuses on patient and family education, comprehensive assessment, and continuity of care [14]. Despite these efforts, cardiovascular diseases remain the leading cause of hospitalization and mortality in Spain and effectively managing patients with HF continues to be a challenge [15]. To address this issue, Spain developed a standardized care model known as the Care Model for Patients with HF, (Modelos Asistenciales de Atención al Paciente con Insuficiencia Cardíaca [MAIC]), aimed at improving the quality and coordination of HF care across health care settings [16].

Spanish Care Model for Patients With HF

The Care Model for Patients with HF project is led by several key medical societies in Spain, including the Spanish Society of Cardiology, the Spanish Society of Internal Medicine, the Spanish Society of Primary Care Physicians, the Spanish Society of Family and Community Medicine, the Spanish Society of Healthcare Executives, and the Spanish Society of Hospital Pharmacy, with Antares Consulting and Boehringer Ingelheim as investors [16]. To address challenges in pathology and optimize patient care, these organizations developed a comprehensive document in 2020, synthesizing current literature and interviews with health care professionals (HCPs). This document includes implementation tools, key considerations for HF care as a SCP, and a flowchart detailing the entire patient journey—from hospitalization to chronic treatment and follow-up (Multimedia Appendix 1 [16]).

The transition from hospital discharge to outpatient follow-up is a critical phase for ensuring continuity of care, as it significantly impacts patient prognosis, the risk of decompensation, and the likelihood of hospital readmissions. Figure 1 highlights the main transition SCP (TSCP), which focuses on patient discharge from the hospital to primary care.

After hospital discharge, a hospital nurse (HN) and a cardiologist or internal medicine (C/IM) specialist oversee the patient transition. Within the first 48 to 72 hours, a primary care nurse (PCN) contacts the patient by phone to check their condition. Shortly after, the patient has an in-person visit with both a PCN and a primary care physician (PCP) for further assessment. Finally, 2 to 3 weeks later, the C/IM specialist conducts a follow-up visit, ensuring the patient's transitions to chronic HF care. The standardized care model, MAIC [16]. was implemented during the first semester of 2024 in 5 hospitals and their respective primary care centers in Spain, with 29 additional hospitals in the process of adopting this standardized care model. The implementation follows a 6-8–month timeline during which health care centers are evaluated and monitored for adherence to the care model. The progress tracking covers a year, using process and outcome indicators from health care data to assess improvements.

Andalusia Health Service

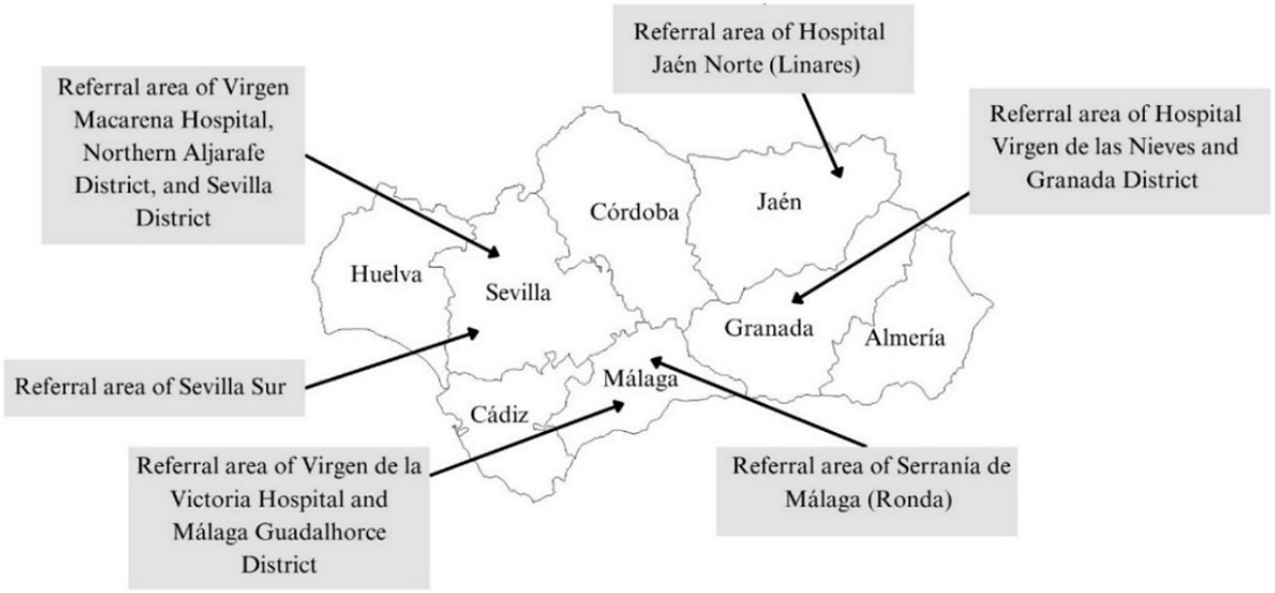
The TSCP is currently in operation across several autonomous communities in Spain, including Andalusia. Located in the southern part of the country, Andalusia is the most populous and the second largest autonomous community. The Andalusia Health Service (AHS) is committed to providing accessible, equitable, and high-quality public health care services to its

XSL•FO
RenderX

citizens [17]. The AHS consists of a network of health care services, organized into 15 health areas, which include 5 regional hospitals, 10 specialized hospitals, 19 district hospitals, and 16 high-resolution hospitals [18]. Each health area is structured around a reference hospital and its associated primary care centers, ensuring comprehensive coverage for the population. In terms of HF, approximately 140,000 individuals have been diagnosed with the condition in Andalusia [19].

In December 2023, the AHS initiated the implementation of the SCP in 6 hospitals and their corresponding primary care settings, collectively designated as referral areas, across Andalusia (Figure 1). The goal is to expand this implementation throughout the autonomous community.

Figure 1. Map of Andalusia highlighting each referral area where the standardized care pathway has been implemented. Courtesy of Antares Consulting Company.



The TSCP involves 4 key actors, each playing a crucial role in the process. These actors come from 2 health care settings, hospital and primary care, and represent 2 professions: physicians and nurses. Each participant has distinct responsibilities, performs specific tasks, and receives different training (Table 1). However, their collaboration is crucial to achieving better outcomes for patients with HF.

Table 1. Description of the health care professionals' roles involved in the care of patients with heart failure.

Role	TSCP[a] role description
Cardiologist or internal medicine specialist	• Performs the discharge assessment and a visit after 2-3 wk of the discharge. The main tasks are as follows: manage and assess the discharge report; medication management; communication with primary care, that is, reviewing hospital reports
Hospital nurse	• Performs the nurse assessment for the patient discharge. The main task that is performed is to manage and assess the discharge report.
PCN[b]	• Does the first evaluation after the discharge, via phone call. Then they perform a face-to-face visit. The main tasks that are performed are as follows: educate, check warning signs, and titrate medication (blood test and writing the report, among other); manage upcoming and follow-up visits in the unit; communicate with the hospital, that is, review hospital reports.
PCP[c]	• First medical evaluation after the discharge. This visit must be completed in less than a week. The main tasks are as follows: conduct the initial face-to-face and subsequent follow-up visits after discharge (assessment and medical history among writing the report, among others); manage medication; communicate with the hospital, that is, review hospital reports

[a]TSCP: transition standardized care pathway.

[b]PCN: primary care nurse.

[c]PCP: primary care physician.

XSL•FO
RenderX

Electronic Health Records for HF Practice

To successfully implement an SCP, electronic support, particularly an electronic health record (EHR) system, is essential [20]. The EHR needs to align with the different steps of the SCP and meet the specific needs of HCPs [21]. Diraya, the EHR system used by the AHS, was implemented in 2005 and has undergone multiple updates to adapt to the evolving demands of the health care sector [22].

Diraya consists of various modules that share information across different health care environments and among professionals. These interconnected components ensure that each piece of data are recorded uniquely and can be accessed when needed [22]. For the care of a patient with HF, Diraya uses the following modules in both hospital and primary care settings [23]: (1) the Primary Care Clinical History module allows for the visualization and editing of data, including personal information, health programs, care processes, medical history, allergies, prescriptions, medication orders, medication, work disabilities, and follow-up records by the family doctors; (2) Hospital Clinical History module in hospitals, excluding emergencies, manages care processes associated with clinical profiles from the perspective of hospital care, generating basic and specialized reports; (3) Hospital Clinical Care handles nursing records related to patient care and organizes them into structures reports; (4) Mailbox manages automated notifications to professionals in primary and hospital care, serving as a key communication channel, for example, when a patient with HF is discharged, their PCP receives a notification; and (5) Single Navigator provides access to all reports, regardless of their origin.

The implementation of EHR systems like Diraya enhances health care services by streamlining medical information management. However, a key challenge remains: does Diraya effectively support HCPs in managing care for patients with HF within the SCP?

Aim of the Study

In Spain, patients with HF who are discharged without specific measures face a high risk of readmission within the first month. Optimizing Diraya is imperative to improving care for patients with HF and ensuring better adherence to the SCP. Achieving this requires a comprehensive understanding of the needs of HCPs involved in the transition from hospital to primary care. To our knowledge, no studies have explored the optimization of an EHR system for patients with HF transitions based on HCPs' needs in adhering to an SCP—either within the AHS or in other Spanish regions.

This study aimed to identify ways to improve Diraya to better support HCPs in following the TSCP for patients with HF during the transition from hospital to chronic care. The research focuses on the clinical content, human-computer interaction, technical aspects, and organizational and communication needs in HF care within the EHR and TSCP. In addition, it seeks to provide a list of recommended improvements for Diraya.

Methods

Study Design

The study used a qualitative approach to gain an in-depth understanding of HCPs' needs. Semistructured interviews with open-ended questions were chosen as the data collection method. The sociotechnical system (STS) model [24] served as both the framework and the interview guide for this study. The interviews were analyzed using thematic analysis, combining both deductive and inductive reasoning to thoroughly explore the data. Following the analysis, drafts summarizing the results and highlighting relevant improvements to meet HCPs' needs were created. These results were then verified and validated with a representative from each health care setting. This validation process adhered to the principles of qualitative research methodology, ensuring the reliability and credibility of the data collected.

Study Setting and Participants

The study was conducted across 6 health care areas of AHS where the SCP was in the process of being implemented. The areas were as follows: (1) referral area of Virgen Macarena Hospital, Northern Aljarafe District, and Sevilla District; (2) referral area of Hospital Jaén Norte; (3) referral area of South Sevilla; (4) referral area of Virgen de la Victoria Hospital and Málaga Guadalhorce District; (5) referral area of Serranía de Málaga; and (6) referral area of Hospital Virgen de las Nieves and Granada District.

To ensure the participation of relevant HCPs involved in the TSCP across both health care settings and during the discharge transition, 4 key roles were included: PCPs, PCNs, HNs, and C/IM specialists. Participants were selected using purposive sampling [25], and to expand the participant pool, snowball sampling was also applied [26]. Sampling continued until data saturation was achieved.

Initial contact with potential participants was made via email, with follow-up phone calls or WhatsApp (Meta Platforms) messages when necessary. During these interactions, a concise overview of the study, including its aims and objectives, was provided. Interested participants received an informed consent document, which they were required to sign and return before the interview. Recruitment was facilitated through Antares Consulting [27].

The inclusion criteria required participants to be actively engaged in the care of patient with HF, employed within the AHS, and working in either hospitals or primary care settings as nurses or physicians. The study excluded participants with <3 years of experience and those currently on sick leave. The limited number of participants and the focus on specific areas in Andalusia may limit the generalizability of our study. Future research should include a larger and more diverse participant base. This limitation is discussed further in the Discussion section.

Data Collection

To address the research question, data were collected through interviews guided by the STS model. In addition, the identified

XSL•FO
RenderX

needs and corresponding improvements were verified through follow-up interviews.

Interviews

The interviews were conducted individually, using a semistructured format, with open-ended questions. The process was carried out in 2 phases: the first phase explored the needs of HCPs, while the second phase verified the proposed improvements. For the second phase, 2 participants with different roles were selected from each health care setting.

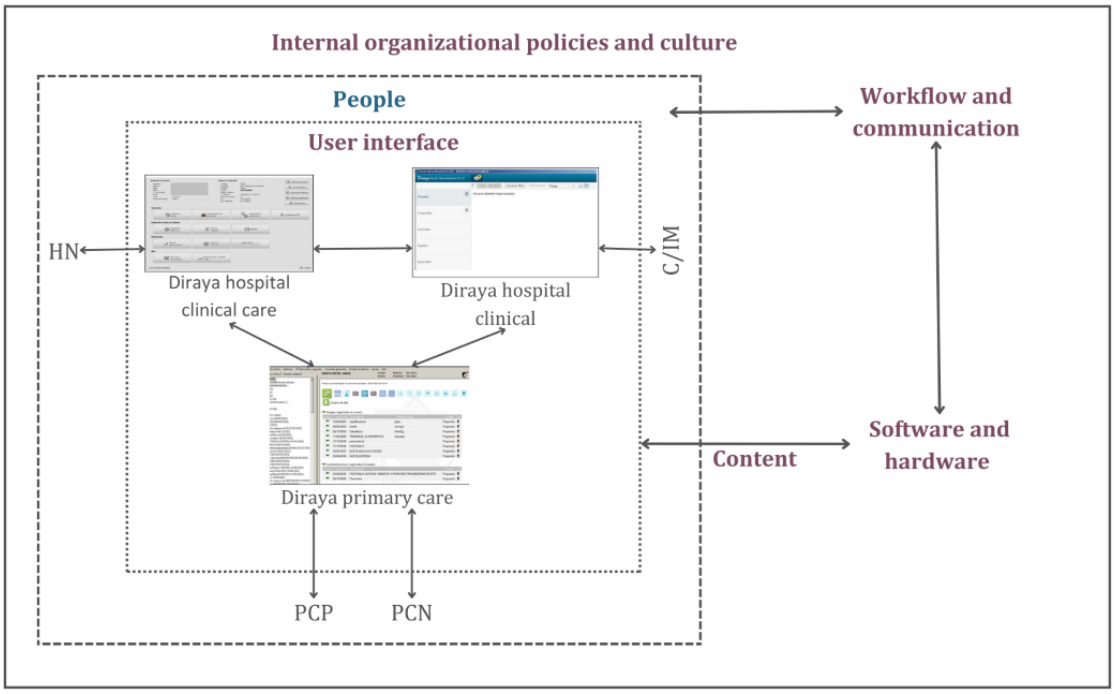
All interviews were conducted via Microsoft Teams, recorded, and transcribed verbatim using the platform's transcription feature. They were conducted in Spanish, the native language of both the participants and the study's first author (MF). The interviews lasted an average of 30 to 45 minutes.

The STS Model

In the study, the STS model was primarily used to develop the interview guide and analyze the data. It also provided a comprehensive understanding of the TSCP by addressing both its technical and organizational aspects. The STS framework integrates technical components, such as hardware and software, with social needs to ensure an effective human-computer interaction [28]. Within this framework, an STS aligns closely with an EHR, as its effectiveness depends not only on the technological infrastructure but also on how well it integrates with workflows, user needs, and the behaviors of individuals and organizations [28,29]. This perspective is supported by Coiera [30], who highlights that those systems that are reliant on complex human organizational structures, such as health care systems, are particularly well-suited to the STS approach. Moreover, Sittig and Singh [24] argue that models used for explaining technological systems are insufficient in capturing the full range of factors necessary for designing and implementing health care systems.

The STS model defines 8 dimensions [24], 5 of which were used in this study: clinical content, human-computer interface, hardware and software, workflow and communication, and internal organizational policies, procedures, and culture (Figure 2). The dimensions of external rules and regulations, as well as measurement and monitoring, were excluded, as they were less relevant to the 4 key actors in the study, given that clinicians are not directly familiar with these dimensions. The people dimension was also excluded because the direct interactions of HCPs with the system had already been analyzed before the interviews.

Figure 2. Interrelationships among the 6 dimensions of the sociotechnical model. C/IM: cardiologist or internal medicine; HN: hospital nurse; PCN: primary care nurse; PCP: primary care physician.



Data Analysis

The data were analyzed using thematic analysis. After each interview, a preliminary analysis was conducted, followed by a comprehensive analysis at the end of the data collection. Initially, a deductive approach was used to identify the codes based on the 5 dimensions of the STS model. This was then followed by an inductive analysis to explore subthemes and themes in greater depth. As the interviews were conducted in Spanish, all quotes were translated into English. The data were organized in a Microsoft Excel spreadsheet, where the authors (MF and ND) familiarized themselves with the collected data, developed codes, and generated themes based on these codes [31,32]. On the basis of the data analysis, a list of improvements and recommendations was developed.

Ethical Considerations

Although data collection was conducted across 6 health care areas within AHS, the Karolinska Institutet was the principal research institution. The study was carried out in accordance

XSL•FO
RenderX

with the Swedish Ethical Review Act (SFS 2003:460) [33,34]. Since the research did not involve the handling of sensitive personal information as understood by the European General Data Protection Regulation, Regulation (EU) 2016/679 [35], ethics approval was not required. However, ethical requirements still apply. Candidates who expressed interest in participating received an informed consent form before the interview. In addition, participants recruited for the second phase signed an additional consent form. The informed consent form explained the study's objectives, detailed how data would be handled to maintain anonymity, and clarified that the interview would be recorded and immediately transcribed. All participants were informed that their participation was voluntary and that they had the right to withdraw from the study at any time without any consequences. Additionally, no financial compensation was provided to any participants. Participants were given the opportunity to ask questions, and their understanding of the study was confirmed before proceeding. In addition, at the start of each Teams interview, participants provided oral consent before the recording began.

To ensure confidentiality and anonymity, only the study authors (MF and ND) had access to the data. A participant randomization document was created, listing names, demographic data, and participant codes. This document was stored in a password-protected Microsoft Excel database accessible only to the authors (MF and ND). The coded interview data were not linked to participants' names. Antares Consulting, which is collaborating on the SCP implementation with Boehringer Ingelheim, shared nonsensitive and relevant data for the study, including participant contact information. In addition, during the interviews, 2 participants shared their screens to provide a clearer visualization of clinical history. Both participants used a fictitious profile, ensuring that the clinical history data did not belong to a real patient.

Generative Artificial Intelligence Disclosure

In this study, generative artificial intelligence (AI) technologies, such as Grammarly (Grammarly Inc) and OpenAI's ChatGPT (GPT-3.5; OpenAI), were used to help the authors (MF and ND) translate the quotes and documents from Spanish to English. These tools were not used to modify or influence qualitative data or the thematic analysis. The data collected were analyzed in their original form to ensure they accurately reflected participants' responses. The tools were used in the preparation of the manuscript to enhance grammatical accuracy and clarity of the text. After using these tools, the authors (MF and ND) reviewed and edited all AI-generated content to ensure it aligned with the study's objectives and maintained the integrity of the content. The authors (MF and ND) thoroughly reviewed and edited all aspects of grammatical accuracy and textual clarity to ensure alignment with the study's objectives and preserve the integrity of the content, taking full responsibility for the publication's content.

Results

Participants' Demographic Data

Between January 15, 2024, and April 15, 2024, 30 HCPs were contacted, and 53% (n=16) agreed to participate in the study. While the goal was to recruit a balanced representation from each area, half (8/16, 50%) of the participants came from areas 3 and 4, resulting in lower representation from the remaining areas. Regarding professional roles, nurses made up 50% (8/16) of the participants, family doctors accounted for 25% (4/16), and nearly 20% (3/16) were cardiologists. As effective communication between different health care settings is essential for improving the transition of patients with HF to chronic care, an equal number of participants were selected from both primary care and hospital care. The detailed characteristics of the participants are presented in Table 2.

XSL•FO
RenderX

Table 2. Characteristics of study participants, including ID, age, clinical specialty, health care setting, and years of experience.

Participant ID	Age (y)	Clinical specialty	Health care setting	Experience (y)
PCP[a] 1	30-40	Family and community medicine	Primary care	5-10
PCP 2	>60	Family and community medicine	Primary care	21-25
PCP 3	41-50	Family and community medicine	Primary care	21-25
PCP 4	51-60	Family and community medicine	Primary care	26-30
PCN[b] 1	51-60	Nursing	Primary care	36-40
PCN 2[c]	41-50	Nursing	Primary care	26-30
PCN 3	30-40	Nursing	Primary care	11-15
PCN 4	30-40	Nursing	Primary care	11-15
HN[d] 1	51-60	Nursing	Hospital care	36-40
HN 2[c]	30-40	Nursing	Hospital care	16-20
HN 3	30-40	Nursing	Hospital care	5-10
HN 4	41-50	Nursing	Hospital care	21-25
C/IM[e] 1	51-60	Cardiologist	Hospital care	26-30
C/IM 2	51-60	Cardiologist	Hospital care	26-30
C/IM 3	51-60	Internal medicine	Hospital care	26-30
C/IM 4	30-40	Cardiologist	Hospital care	11-15

[a]PCP: primary care physician.

[b]PCN: primary care nurse.

[c]Participants corroborated the interviews after the analysis and proposed improvements.

[d]HN: hospital nurse.

[e]C/IM: cardiologist or internal medicine.

Thematic Analysis

Overview

The results of the thematic analysis are presented in Table 3. The first column identifies the dimension of the STS, and the second and third columns list the subthemes and themes. In total, 65 codes, 23 subthemes, and 8 themes were identified. In addition, a matrix was developed to integrate the results with the actors.

XSL•FO
RenderX

Table 3. An overview of sociotechnical dimensions, subthemes, and themes.

Sociotechnical dimensions and themes	Subthemes
Clinical content	
Optimizing medical data management for enhanced clinical workflow	• Implementation of standardized clinical reports • Reporting management challenges
Agreement on standardization and enhancement of the discharge report	• Enhancement of the discharge nursing report • Summarization of the medical discharge report
Enhancing clinical decision support through updated guidelines and automated tools	• Nursing support to achieve better educational care • Possibility of a medical decision support
Human-computer interaction	
Improving UX[a] and usability for enhanced clinical efficiency and less time-consuming experience	• Need for learnability • Need to improve the visual design • Noneffective iconography • Nonefficiency interaction
Hardware and software computing infrastructure	
Enhancing technical infrastructure to improve HCP[b] efficiency	• Hardware infrastructure limitations • Network connectivity • Technical apparatus issues • Software infrastructure challenges
Optimizing interoperability as a solution for better management of patients with heart failure	• Unification of the EHR[c] modules • Streamlining processes with shared scales
Workflow and communication	
Encourage communication based on digital tools and personal connection	• Inclusion of mailbox as a communication tool in workflow • TSCP[d] implementation workflow on EHR practices • Fostering of effective internal communication • Enhancement of external communication
Internal organizational policies, procedures, and culture	
Cultivating a culture in nursing practice and professional organizational integration	• Willingness to improve the nursing care between primary care and hospital • Training upon joining • Cultivating culture

[a]UX: user experience.

[b]HCP: health care professional.

[c]EHR: electronic health record.

[d]TSCP: transition standardized care pathway.

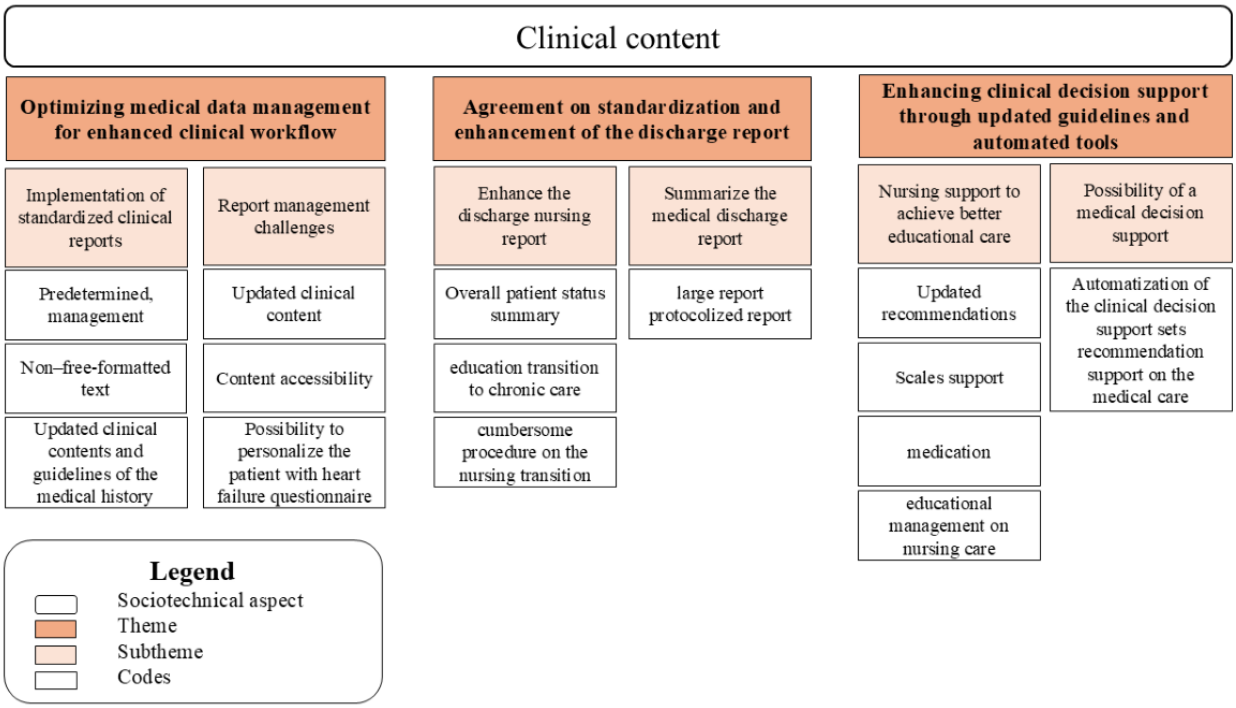
Clinical Content

Overview

Figure 3 illustrates the relationship between the sociotechnical dimension of clinical content, the codes, and subthemes related to the themes—optimizing medical management for enhanced clinical workflow, agreement on standardization and enhancement of the discharge report, and enhancing clinical decision support (CDS) through updated guidelines and automated tools.

XSL•FO
RenderX

Figure 3. A hierarchical structure displaying the sociotechnical dimension, the codes, and the subtheme for themes 1, 2, and 3. CDS: clinical decision support; HF: heart failure.



Theme 1: Optimizing Medical Data Management for Enhanced Clinical Workflow

Primary care professionals, both in nursing and medical roles, are required to report each visit with a document that includes the patient's medical history and relevant examination information. In AHS, after consultations with patients with HF, both PCPs and PCNs must complete the aforementioned report using 1 of the 2 available formats: either a regular clinical report or a report manager. Efficient management of the medical data collected during visits is crucial. Thus, this is facilitated by a protocol-based strategy designed to enhance clinical workflow. This theme explores the outcomes of both formats, addressing their clinical content as well as structural and technical usability aspects, especially in the context of HF practice.

One method of documenting involves using the clinical report, in which the medical history appears at the beginning of the report, followed by details of the physical examination. Nonetheless, variability exists in this format, as participants expressed the need for a standardized version. This approach would ensure consistency in both medical data and clinical content within the reports, particularly during the first visit after discharge. It would also minimize redundant data entry, saving time, and reducing the risks of confusion, misinformation, and errors. However, keeping the medical history up to date remains a challenge, as only physicians are authorized to make updates, and this task depends on their workload and willingness:

> *The medical history data is only updated when completed by the practitioner, leading to occasional information gaps...Sometimes, when a patient visits without a prior diagnosis of HF, I have to review the entire medical history to understand their condition.* [PCN3]

The alternative documentation format is through a report manager, which uses a questionnaire-style format detailing the actions required during a general HF visit. However, participant engagement with this tool is low, only 13% (1/8) of the participants had used it, while 63% (n=5) were unaware of its existence. Aside from increasing awareness of the report manager, the interviews identified several other needs and shortcomings. For example, participants recommended that both data entries and questions remain up to date and relevant, while also being user-friendly and requiring minimal effort to complete:

> *The content sometimes contains inaccuracies or is not aligned with the requirements of the visit...I need the content to be current...some scales that are included are not typically performed in primary care and should only be conducted in the hospital.* [PCP1]

Thus, it was also suggested that each questionnaire's content be specifically tailored to the professional's roles and the type of care they provide. Finally, all clinical content is currently saved as plain text, which limits navigation. Therefore, professionals expressed a preference for a more structured format:

> *When the Report Manager is filled out, the information is directly transferred to the clinical record, where it appears overly condensed and difficult to read. I would prefer the information to be displayed in bullet points, following the same sections as the Report Manager.* [PCP1]

Theme 2: Agreement on Standardization and Enhancement of the Discharge Report

To identify the needs and areas for improvement in the nursing discharge report (NDR), both HN and PCN were asked specific

XSL•FO
RenderX

questions. As HCPs from both settings, their collaboration helped pinpoint which parameters could be optimized.

Focusing first on PCN, they revealed that they never review the NDR because the information appears "copied and pasted" and lacks patient-specific details. Therefore, PCNs used to read the medical discharge report (MDR) instead:

> *Well, I'll tell you that when they discharge a patient, the nurse fills out a form that nobody really reads. Are these responses to a questionnaire about what has happened to the patient? How does he sleep? Does he have any risks? How is his ulcer treated? How is he catheterized? .... I have too many questions that are not provided and others that are unnecessary. If the patient is not catheterized, I don't need to know that he doesn't have a catheter; it's only relevant if he does...* [PCN 3]

Following up with HNs, professionals confirmed that the information received from PCNs is often incomplete. HNs often do not have time to complete the NDR, and if they do, it tends to be very broad and not personalized. They would like to have parameters, such as social risk, patient polypharmacy, fall risk, Barthel scale, edema, weight at discharge, oxygen therapy, dyspnea, and feeding, among other options. This would provide PCNs with a summarized and relevant report of the status of patient with HF. Moreover, it would enhance communication between both health settings:

> *Patient education and management of medication and alarm signs are essential information that must be worked on in both settings. But knowing how these are being addressed and what the patient's status is from PC and in HC is essential so [that] it can be agreed upon and worked on together.* [PCN 3]

In contrast, PCPs commented that the MDR is overly extensive and tedious, requiring a significant amount of time to thoroughly review the details. They suggested that a more concise report, with specific parameters, would be beneficial. This should include key information, such as the confirmation of the initial diagnosis, etiology of the condition, left ventricular ejection fraction data, potassium levels, creatinine levels, and the treatment plan of the patient, including therapies and doses.

Theme 3: Enhancing CDS Through Updated Guidelines and Automated Tools

Although CDS features exist in the current Diraya system, they are limited to nursing professionals. In the Diraya primary care recommendations based on the responses are provided upon completing a questionnaire. Nonetheless, PCNs have expressed concerns regarding the clinical content and functionality of the CDS:

> *It will be nice to have recommendations together with the scale result, the associated risks, and how to manage the patient. I usually remember from experience, but it's harder to recall after some days off.* [PCN3]

In addition, managing medication for patients with HF is crucial for ensuring adherence to treatment and reducing readmissions. PCNs would find it beneficial if medication information included its purpose and use instructions:

> *Sometimes, the treatment involving medication reconciliation causes certain confusions: medications are added without educating the patient. Occasionally, medication is duplicated, and the primary care physician suggests resolving it with the hospital's internal medicine department.* [PCN1]

A key component of the TSCP is patient education after hospital discharge through telephone or on-site visits. In addition to providing medication information, it also involves informing patients about their illness, warning signs, and associated risks according to HN and PCNs having a checklist including this information would be helpful:

> *Having a checklist with all the necessary information would ensure nothing is overlooked.* [HN2]

Regarding the report manager, the CDS provides prompts based on questionnaire results. However, these prompts are in free text and do not link directly to actions in the EHR. Automating the CDS to enhance patient management and streamline administrative tasks would be beneficial. In contrast, PCPs do not receive any system-generated recommendations during their visits. Addressing this gap is essential to improving their experience, so feedback and needs were collected:

> *It would be incredible if the system could guide me based on protocols and guidelines for HF patients, such as in scales and patient examinations. This would enable me to make more informed decisions.* [PCP 2]

Finally, it is also important to mention the integration of CDS during the TSCP while the patient is hospitalized. An HN suggested that including recommendations for assessing scales used at the time of discharge would be helpful. Similarly, C/IM specialists mentioned that CDS could provide valuable guidelines and recommendations for patient evaluations during follow-up visits, potentially improving overall care practices.

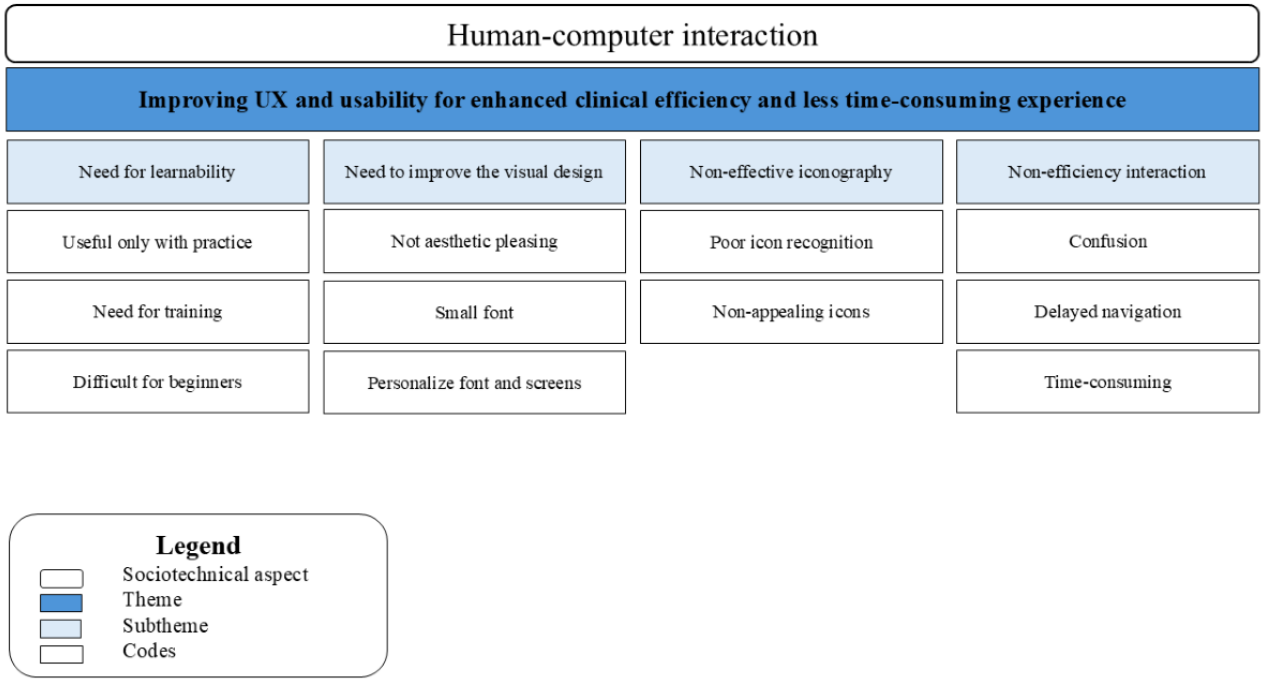
Human-Computer Interaction

Overview

The interaction among the 4 groups of interface users varied depending on the health care setting and the professional role. PCPs used one module of the interface, while hospital users used 2 different modules, and primary care HCPs only had access to one module. Although these 3 modules differed, participants shared similar needs and insights. Figure 4 illustrates the relationship between the sociotechnical dimension of human-computer interaction, the codes, and subthemes related to the theme—improving user experience (UX) and usability for enhanced clinical efficiency and time-consuming experience.

XSL•FO
RenderX

Figure 4. A hierarchical structure displaying the sociotechnical dimension, the codes, and the subtheme for theme 4. UX: user experience.



Theme 4: Improving UX and Usability for Enhanced Clinical Efficiency and Time-Consuming Experiences

All HCPs agreed that they gradually became proficient in using the EHR for HF care through practice, indicating that the interface is not intuitive. Some found it challenging at first, though 1 PCN mentioned that it became manageable after gaining experience:

> *For me, once learned, its [the EHR] operation was straightforward.* [PCN4]

Professionals also emphasized the need for adjustable font sizes to meet various needs. They suggested that visual enhancements could streamline information retrieval, ultimately improving attention and efficiency.

Moreover, HN explained completing the NDR involves navigating numerous pages, making system interaction cumbersome and the design unappealing. Notably, C/IM specialists reported greater satisfaction with the interface compared to PCPs.

All PCPs commented that the interface icons, particularly those used for medical history, were unclear:

> *For patients with COPD, a lung icon appears; for cervical cancer, there is a figure of a woman; and for HF, a heart icon is used. However, it is not immediately clear whether the icon represents HF. I would use a clearer icon, or better yet, the diagnosis in text form.* [PCP2]

Some (5/8, 63%) participants noted that the icons used throughout the questionnaire were difficult to understand:

> *You need to recognize that one icon represents nursing and another medicine; others stand for medication, vaccine, diagnosis, video call, and more. But with no text in line with the icons, their meanings are unclear.* [PCN 3]

Regarding access to EHRs across different health care settings, hospital participants reported rarely having time to consult the primary care EHR. Conversely, primary care participants often find time, express interest in learning more about hospital data, or value the patient, which motivates them to review the hospital EHR. However, they emphasized the difficulty of doing this regularly or systematically due to time constraints:

> *There is no time and accessing the hospital EHR is time-consuming; it can take up to five minutes to find specific information, which wastes quality time with the patient.* [PCN2]

Therefore, many HCPs choose not to access the data regularly, disrupting communication between professionals.

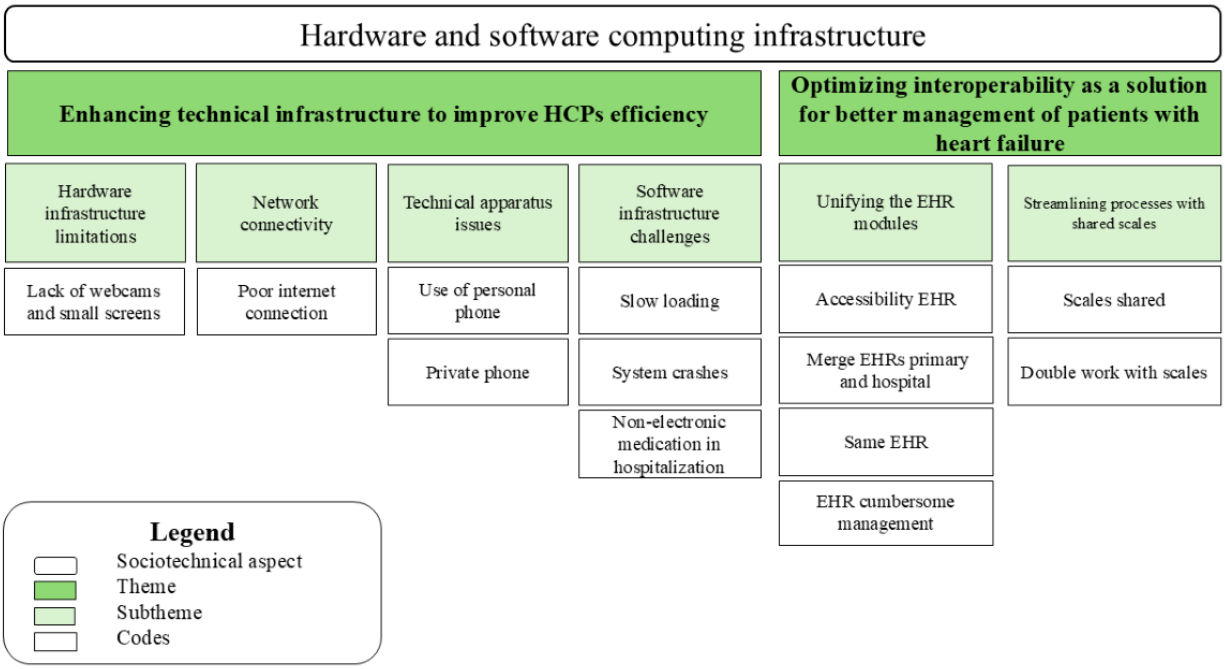
Hardware and Software Infrastructure

Overview

In this dimension, the findings indicated that the technology used in primary care centers and hospitals was of low quality, resulting in significant delays and extended waiting times. Moreover, interoperability played a vital role in connecting both settings, which was crucial for the effective management of patient care during the discharge transition. Figure 5 illustrates the relationship between the sociotechnical dimension of hardware and software computing infrastructure, the codes, and subthemes related to the themes—improving technical aspects reduces unnecessary task time, thereby enhancing the quality of work; and optimizing interoperability as a solution for better management of patients with HF.

XSL•FO
RenderX

Figure 5. A hierarchical structure displaying the sociotechnical dimension, the codes, and the subtheme for themes 5 and 6. EHR: electronic health record; HCP: health care professional; HF: heart failure.



Theme 5: Improving Technical Aspects Reduces Unnecessary Task Time, Thereby Enhancing the Quality of Work

Most of the participants highlighted the inefficiency of current technology, including hardware, software, and internet connectivity—used in their health care settings. They reported frequent internet outages, especially during rainfall, along with system crashes and slow loading times when using the Diraya system. Participants working in hospitals also faced malfunctioning computers, which caused significant delays in accessing necessary documentation tools:

> *The internet goes down at least three times a week. [C/IM 3])*

Another issue was the use of corporate phones with long and unrecognizable numbers, which affected the availability of PCNs for patient follow-ups within 48 hours to 72 hours after discharge as patients often ignored these numbers:

> *Patients frequently disregard calls from unknown, lengthy numbers, leading to missed follow-up opportunities.... Providing patients with recognizable extension numbers would greatly enhance communication. [PCN 2])*

In addition, some HCPs do not have access to corporate phones, forcing them to use their personal devices for work-related communication. This raises several concerns, such as the traceability of patient interactions and data privacy:

> *I have a friend who works in the cardiology department of another hospital. When I know a patient is from her area, I use WhatsApp to inform her...which means I take work home and there's no traceability for these patient interactions.* [HN 4]

This issue extends even to professionals within the same health care center. Some PCNs mentioned that informal communication methods, such as WhatsApp messages or post-it notes, are used to arrange extra notes for patients with HF after discharge. These practices highlight the need for a more structured and reliable communication system to ensure patient care effectively.

Theme 6: Optimizing Interoperability as a Solution for Better Management of Patients With HF

To provide appropriate care for patients with HF during hospital discharge, it is essential that medical reports are saved and accessible across different health care settings. The single health record allows HCPs to view comprehensive patient reports across facilities. However, many professionals expressed dissatisfaction with its interoperability.

PCPs often struggle to access important clinical discharge reports or test results because they are either not uploaded or incomplete:

> *From the Single Health Record, I often cannot access the discharge report from medicine or nursing...it is either not uploaded, or there are tests that are not included in the report, so I have to review the hospital EHR, which takes a lot of time.* [PCP 2]

This might be due to a lack of awareness among HCPs regarding the correct process for adding information:

> *For the nursing report to be uploaded correctly, you need to click on an icon, and many times professionals are not aware of this.* [HN2]

Some PCPs mentioned that they access the hospital's single health record only when necessary due to the cumbersome and time-consuming process. Ideally, this should be regular practice to ensure continuity of care. Within hospital settings, C/IM

XSL•FO
RenderX

professionals also echoed this concern, emphasizing the importance of seamless integration between primary care and hospital systems to facilitate smoother patient care transitions:

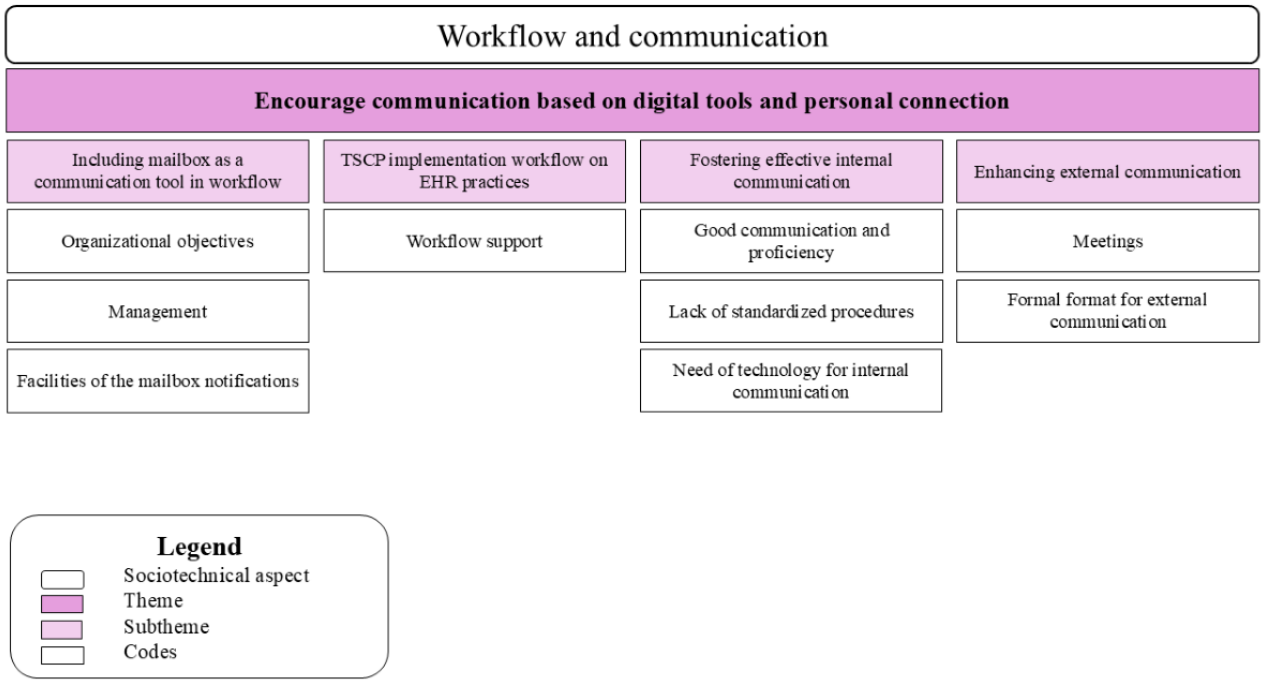
> *At the time of hospital discharge for heart failure patients, having all the information from primary care is crucial during the initial visit.* [C/IM 4]

Workflow and Communication

Overview

As previously stated, during the interviews, the importance of communication between different settings and professionals was clear, emphasizing its crucial role in ensuring a smooth transition from acute to chronic care. Data analysis showed that communication through EHR can take various forms—internal, external, and both direct and indirect. Internal communication occurs among HCPs within the same health care setting and can be either direct (eg, face-to-face conversations and meetings) or indirect (eg, through the EHR and messages). In contrast, external communication occurs between HCPs from different health care settings and can also be either direct (eg, seminars) or indirect (eg, via the Diraya mailbox or interconsultations). Consequently, participants identified several needs and suggested improvements for these different forms of communication. Figure 6 illustrates the relationship between the sociotechnical dimension of workflow and communication, the codes, and subthemes for the theme—encourage communication based on digital tools.

Figure 6. A hierarchical structure displaying the sociotechnical dimension, the codes, and the subtheme for theme 7. EHR: electronic health record; TSCP: transition standardized care pathway.



Theme 7: Encourage Communication Based on Digital Tools

Regarding internal communication, participants mentioned that it is usually informal yet effective and efficient in most cases. Some centers explained that to communicate with a colleague, they often leave a note, send a WhatsApp message, or speak directly to them. Nonetheless, other participants explained that storing sensitive information in a written note or spoken conversation is not the safest approach for medical care. Moreover, using personal phones to store confidential information is a concern:

> *I usually knock on the door or I leave the information on a post-it.... It would be useful to have an integrated communication and chat system, as currently, we communicate informally.... It would be beneficial if the information were automatically transmitted through the system.* [PCN4]

In contrast, some participants emphasized that certain primary care centers are quite familiar with their current process and feel no technological innovation is necessary. They rely on notes in clinical history for another professional to view, and this approach usually works well:

> *In my opinion, within our field, I would not recommend any technological aid because it could lead to a loss of personalization. As I have the nurse next door, I would not like to have a chat.* [PCP4]

Some PCPs mentioned that they share schedules with PCNs to discuss patients, but these schedules are rarely used.

Within the hospital system, 50% (2/4) HNs indicated that communication with the medical department during hospital discharge needs improvement. A major issue is that, often, when a patient is discharged, the nurse is not informed by the physician, which sometimes causes delays in completing the discharge report for patients with HF:

> *Sometimes, when the patient is discharged, I am not informed. Although communication with colleagues*

XSL•FO
RenderX

> *is good, sometimes the workload causes a noneffective communication.* [HN2]

Regarding communications between HCPs from different medical settings, known as external communications, participants noted that direct communication between physicians from both settings is more established and standardized than communication between nurses across these contexts. However, one participant pointed out:

> *In my center, we maintain a very fluid relationship because I know the head of the cardiology department at the hospital; however, it is informal communication. In other centers or specialties, this type of one-way communication does not exist.* [PCP 3]

Nevertheless, the same participant added:

> *The idea of conducting clinical sessions is excellent and useful, but it requires time and resources that are unavailable.* [PCP 3]

In addition, from the primary care perspective, there is a recognized need to establish a bidirectional communication channel with cardiologists, as information is sometimes lost. From the hospital's medical site, C/IM departments commented that communication is sufficient, with improvements mainly needed in document interoperability. They also pointed out that in some centers, teleconsultations between PCPs and C/IM staff are very successful and efficient.

In contrast, nursing professionals all agreed on the need to enhance direct communication between nursing professionals from both settings. They emphasized the importance of workshops or sessions to standardize patient care and better understand nursing practices across settings:

> *I would like to hold sessions with PCNs to learn about what they do and how I can better emphasize patient care. Sometimes I send them information, but I think they do not consider it important. I would like to meet the PCNs to become more efficient in managing the patient during the transition. For example, educating the patient about medication for HF is very important, and I would like to know how they do it so I can determine what information I need to provide at the time of discharge.* [HN3]

One communication method in place is the mailbox module, which sends notifications to primary care professionals when a patient's status changes, such as when a patient is discharged from the hospital. For patients with HF following the TSCP, when the patient is discharged, both the PCP and PCN receive a notification that includes the patient's name, medical history, and the reason for the previous hospitalization. If no follow-up appointment has been scheduled, the nurse must call the patient within 48 hours to 72 hours and visit them at the primary care center. Even though the protocol was clear, several shortcomings and needs in this communication method were identified during the interviews.

Several PCPs expressed that upon receiving this alert, they need access to more comprehensive patient information:

> *When I receive an alert and the reason for admission is not heart failure but another condition that refers to heart failure, ... I do not call the patient or review the medical history. As a result, this patient is overlooked.... If I had more time and better organizational support, I could handle it more effectively.* [PCN 4]

In contrast, the hospital lacks a Diraya mailbox module, thus discontinuing the communication from primary care. Among professionals, interconsultations through Diraya between physicians at primary care and hospitals are commonly used, which are generally effective according to the participants. However, for nursing staff, such interconsultations are not available. Consequently, nurses have expressed the desire to implement such interconsultations between both settings, when necessary, to enhance the management of patients with HF at discharge.

In primary care, HCPs are accustomed to managing visits for patients with HF. However, when using Diraya, the purpose of each visit often remains unclear. To improve care during the transition to discharge, professionals need to have a clear guide that outlines the specific tasks for each visit. Implementing an HF guide or protocol within the system would streamline these visits, enabling HCPs to effectively adhere to the SCP:

> *I would appreciate having instructions to understand the patient's status and which post-discharge visit they're attending.... All this information is protocolized, but we don't see it; we have to know it by heart.* [PCN2]

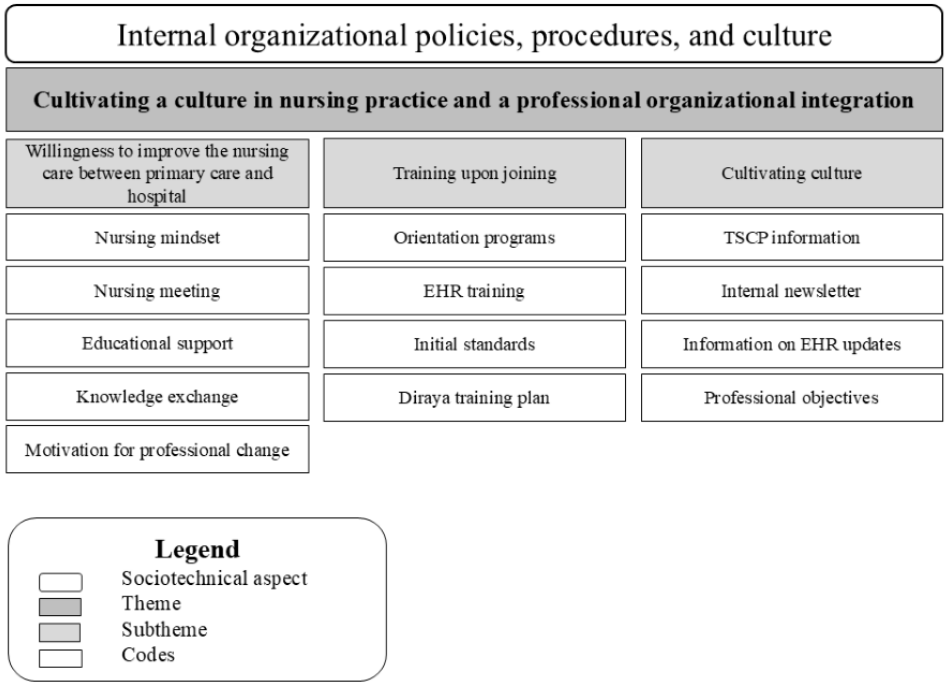
Internal Organizational Policies, Procedures, and Culture

Overview

Figure 7 illustrates the relationship among the sociotechnical dimensions of internal organizational policies, procedures, and culture; the codes; and the subthemes for the theme—cultivating a culture in nursing practice and professional organizational integration.

XSL•FO
RenderX

Figure 7. A hierarchical structure displaying the sociotechnical dimension, the codes, and the subtheme for theme 8. EHR: electronic health record; TSCP: transition standardized care pathway.



Theme 8: Cultivating a Culture in Nursing Practice and a Professional Organizational Integration

Nurses were interested in taking on a more empowered role and increasing their involvement in decision-making during the patient transition to a higher level of care:

> *I would like the cardiology specialist nurses to provide us with training, so we can gain more knowledge.* [PCN2]

Indirectly, all of them suggested the importance of collaboration to facilitate cultural change between hospitals and primary care settings:

> *I am very eager to undertake projects to improve patient education for those with HF.... I look forward to meeting the primary care nurses who treat these patients to understand what they do.* [HN4]

Participants reported no organizational dissatisfaction regarding the implementation of the TSCP. However, they identified a potential incentive for HCPs: incorporating TSCP-related tasks into primary care employment objectives. This approach would encourage staff participation and enable verification of each HCP's work.

Some participants expressed the need for structured training on Diraya when starting a new job, recognizing it as crucial for onboarding. However, they noted that HCPs often join on short notice, leaving no time for formal training. Others believed formal training was unnecessary, stating:

> *It's not necessary; you learn on the job. If it's an optional course, no one will take it. What is needed is support during your initial days.* [C/IM2]

In addition, some professionals mentioned that at AHS, Diraya training sessions are available and can be completed in their free time:

> *At AHS, there are straightforward and accessible Diraya courses, but we have to complete them at home. Ideally, these should be part of work hours or count towards points in the employment pool.* [HN2]

Finally, 3 participants noted that they receive little information about organizational updates, which they consider crucial.

They expressed a desire for managers to keep them better informed about improvements.

Suggestions for Improvements Based on the Results

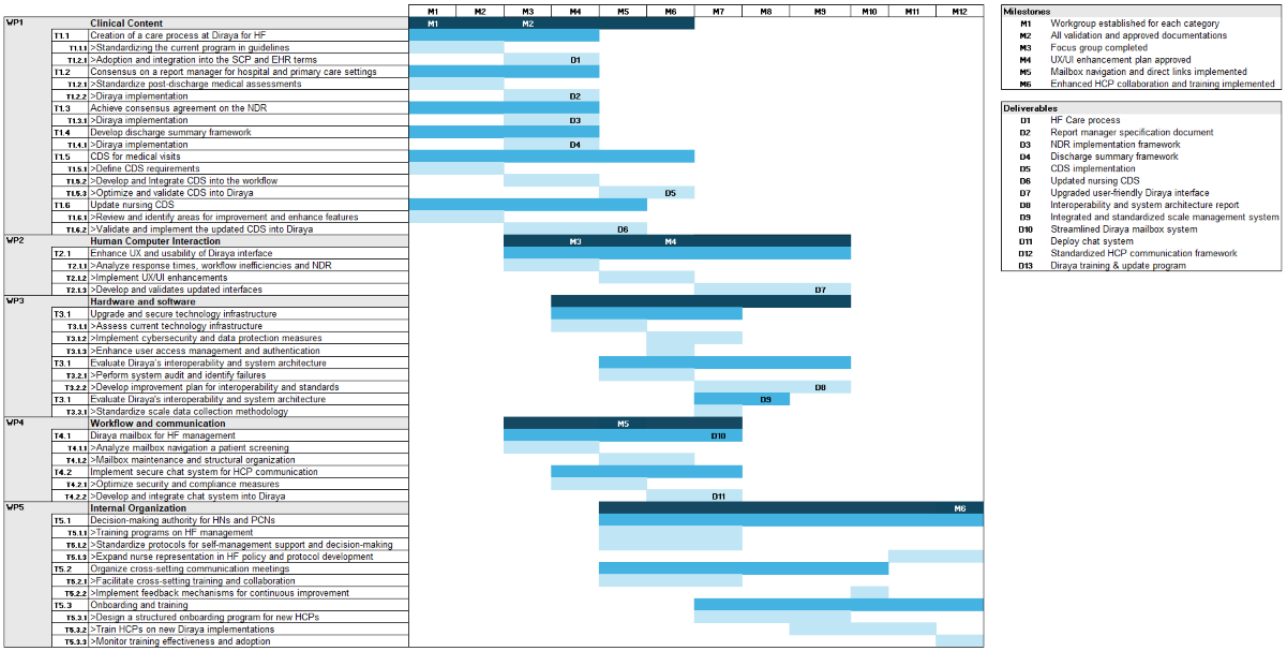
On the basis of the needs identified in the interviews, several improvements and recommendations have been proposed. These were validated by additional interviews with 2 participants, HN2 and PCP2. A summary of the proposed improvements and suggested actions, linking them to the corresponding key findings in each theme and the HCPs involved in the TSCP, can be found in Multimedia Appendix 2. In addition, each improvement was assigned to a priority scale, which was corroborated by HN2 and PCP2. The priority levels were (1) not important—enhances HCP performance but is not critical for managing patients with HF within the TSCP; (2) important—optimizes HCP workflow and is important for managing patients with HF within the TSCP, though not crucial for its implementation; and (3) urgent—crucial for optimizing HCP workflow and urgently needed for managing patients with HF within the TSCP, as its absence prevents the correct implementation of the TSCP.

XSL•FO
RenderX

Proposed Implementation Plan

Engaging diverse stakeholders, including IT teams, policy makers, and patients, is crucial for the successful optimization and implementation of EHRs and it is also an aspect of the implementation process of the MAIC toolkit. Strategies such as structured communication channels, collaborative platforms, advisory committees, training sessions, and feedback systems can facilitate this engagement. Establishing consistent communication with different stakeholders can identify and address potential barriers during the implementation. In addition, forming committees with representatives from each stakeholder group ensures diverse perspectives are considered. To optimize and implement improvements, incorporating a Gantt chart into the implementation process is recommended. In Figure 8, each work package represents a dimension of the STS, with tasks correlated to the improvements in Multimedia Appendix 2. A 1-year implementation plan is suggested, based on the progression of tasks and subtasks, and should be tailored to the available resources of the health care system. The proposal includes conducting training sessions and regular meetings to align expectations and identify needs. Specific working groups will be established to enhance communication and task execution. In addition, focus groups with end users are proposed to gather feedback and adjust the implementation according to their needs.

Figure 8. Suggestion for a detailed implementation plan. CDS: clinical decision support; EHR: electronic health record; HCP: health care professionals; HF: heart failure; HN: hospital nurse; NDR: nursing discharge report; PCN: primary care nurse; SCP: standardized care pathway; UX/UI: user experience/user interface.



Discussion

Principal Results and Comparison With Previous Work

This study identified the needs of HCPs when implementing the transition standardized care model, MAIC [16], for HF practice within the Diraya system. In addition, it provided recommendations for optimizing the EHR within this context. Notably, the HCPs involved in this study include PCPs, PCNs, HN, and C/IM specialists.

The results showed that the Diraya system does not adequately support the implementation of the TSCP. HCPs are required to complete many unnecessary tasks, ultimately increasing their workload. In addition, these tasks are often ethically inappropriate and add to the administrative burden. The findings also suggested that to implement the TSCP more efficiently, changes and improvements are needed in clinical information within Diraya, the computer system, and the AHS organization.

The first theme, *optimizing medical data management to enhance clinical workflow*, primarily addressed in primary care settings during the initial visits after discharge, suggested the creation of a specific care process for HF in Diraya, as well as achieving a committee consensus on a report manager. The findings highlighted that, as part of the EHR optimization, it is crucial to ensure smooth clinical workflow and personalized data exploration [36]. These 2 improvements, considered high priority, aligned with studies emphasizing the optimization of data management as a key initial requirement [37]. In addition, other studies showed that customizing report managers and care processes for each EHR helps with accurate patient evaluation and effective data analysis. This underscores the need for HCPs to collect and analyze health indicators to better understand the disease state [38,39]. Moreover, customizing the EHR through consensus among various HCPs is consistent with current literature, which underscores the importance of incorporating quality standards in the EHR development through HCP collaboration [21].

As discussed, in the second theme, *agreement on standardization and enhancement of the discharge report* is recommended to create a consensus document for both the NDR and a discharge summary for the MDR. This would improve

XSL•FO
RenderX

communication between health care settings and ensure compliance with the proposed TSCP. The findings highlighted 2 key aspects. First, they identify technological barriers to implementing an automation tool in the EHR system—an essential feature for managing HCPs' workload but also a challenge for the software [40]. Therefore, it is crucial to ensure that the tool is intuitive and user-friendly for HCPs before implementation. Second, the results aligned with studies emphasizing the importance of a nursing care plan during the discharge process to enhance patient care [39].

Regarding the third theme, *enhancing clinical decision support through updated guidelines and automated tools*, it was proposed to implement CDS tools for both medical visits and to update the nursing CDS, including the NDR and the PCN report manager. This would ensure proper compliance with the TSCP during patient visits and provide essential support to HCPs across different health care settings. This recommendation aligns with studies suggesting that effectively integrating CDS tools reduces the cognitive burden on HCPs, enhances clinical decision-making, and leads to better patient outcomes [41]. In addition, research on HF has shown that comprehensive CDS tools significantly reduce hospital readmissions and improve adherence to treatment protocols, such as TSCP [42,43]. Therefore, updating the nursing CDS and implementing CDS tools in medical visits is crucial.

Regarding the fourth theme, *improving UX and usability for enhanced clinical efficiency*, the study highlights how the interface design subtly influences daily procedures and, over time, impacts the workflow of HCPs managing HF practices. To address interface limitations, 2 key recommendations are proposed. The first and most urgent step is to improve the iconography of specific HF-related symbols and the text size. Once this is achieved, the focus should shift to broader improvements across the entire interface to enhance overall usability. These changes are essential, as studies show that complex or poorly designed EHR systems can create stress and pressure on HCPs, negatively affecting their daily work. Enhancing these aspects would directly support HCPs in efficiently performing TSCP-related tasks [44].

The findings from theme 5, *enhancing technical infrastructure to improve HCPs* efficiency, highlighted several critical needs and shortcomings that must be addressed to efficiently implement the TSCP. These include improvements in both hardware and software, network connectivity, and technical equipment. In addition, evaluating the cybersecurity infrastructure is essential, as the system stores sensitive data, and HCPs often resort to using private resources due to issues, such as low connectivity. These findings align with previous research indicating that inadequate technical infrastructure is a major barrier to implementing an SCP in specific health care settings [45].

Regarding theme 6, *optimizing interoperability as a solution for better management of patients with HF*, the need for improved interoperability emerged consistently throughout all interviews. To address this, it is recommended to evaluate the system's current standards and protocols and integrate common assessment scales across health care settings. This would enable better patient monitoring and communication between hospitals and primary care. These findings align with studies emphasizing the importance of sharing documents across different health care settings to improve communication [39].

The interoperability challenges, usability concerns, and workflow inefficiencies in the current EHR system in general are global challenges. The World Health Organization (WHO) emphasizes the need for standardized data exchange and interoperability to ensure seamless health information flow across different systems and regions [46]. They also highlight the importance of user-friendly digital health solutions and the necessity of optimizing digital health tools to support efficient workflow. Several best practices have been established to address these issues. WHO emphasized that digital interventions for health systems should leverage standardized health data exchange formats [47]. For achieving interoperability among systems, standards, such as HL7 Fast Healthcare Interoperability Resources, and terminologies like International Classification of Disease, Systematized Nomenclature of Medicine Clinical Terms, and Logical Observation Identifiers, Names, and Codes are crucial for the seamless integration of EHR systems [48-50]. The WHO Digital Health Guidelines emphasize human-centered design principles to improve EHR usability, ensuring intuitive interfaces and role-specific workflows [47].

Regarding theme 7, *encouraging communication based on digital tools and personal activities*, effective communication is the cornerstone of this study. In an SCP dedicated to discharge and the transition to primary care, clear and efficient communication is essential [51]. Many of the other identified challenges within Diraya are also linked to communication barriers. Research confirms that poor communication is a common issue, and overcoming it requires stronger relationships between HCPs to facilitate referral processes [52]. In addition, studies have shown that electronic communication between primary care and other health care settings is both feasible and beneficial, as it enhances accuracy in information sharing [53]. However, it is crucial to address the privacy concerns surrounding the use of informal communication tools, such as WhatsApp and handwritten notes, particularly regarding data security and compliance with local privacy regulations. Informal communication tools may not provide the necessary safeguards to protect patient information, potentially leading to violation of confidentiality and noncompliance with regulations like the General Data Protection Regulation and the Health Insurance Portability and Accountability Act [54,55]. Ensuring that all communication methods adhere to stringent data security standards is vital to maintaining patient trust and safeguarding sensitive health information. On the basis of the results of this study, the authors (MF and ND) suggested implementing a chat system for internal and external communication among HCPs, ensuring timely mailbox updates, and organizing meetings and training sessions to improve external communication between both settings.

Finally, theme 9, *cultivating a culture in nursing practice and a professional organizational integration*, emphasized the need to strengthen HF care by empowering nurses in their daily work. Suggested strategies include providing seminars, educational programs, and decision-making assessments within the TSCP

XSL•FO
RenderX

tasks. These improvements directly relate to the importance of designing an EHR system that serves both nurses and physicians equally. Current literature supports the idea that nurses must have a significant role in shaping digital tools like EHRs to ensure their smooth integration into patient care workflows. Several studies have demonstrated the positive impact of nurse-led interventions in transitional HF care. Nurse-coordinated transitioning of care significantly reduces readmission rates for patients with HF. Nurse-led transitional care interventions decrease health care use, including all-cause and HF-specific readmissions. These interventions also reduce mortality and improve psychosocial outcomes, such as health-related quality of life and self-care behaviors. In addition, nurse-led transitional care programs improve readmission rates, self-efficacy, functional status, and quality of life among patients with heart disease [56-59].

Nurses bring valuable clinical insights, which are critical for developing technologies that support decision-making and improve care delivery. However, challenges, such as excessive documentation, inefficient workflows, and poor system interoperability, can contribute to nurse burnout and affect care quality. To address these issues, the National Academy of Medicine recommended improvements to EHRs and related technologies to better support nurses and ultimately enhance patient care outcomes [60].

The findings of this study could be applicable to other regions in Spain for managing HF or other chronic conditions requiring coordination between primary care and hospital services. This is particularly relevant as the transition from hospital discharge to primary care in Spain faces significant challenges due to poor interoperability among EHR systems. This fragmentation hinders effective communication and continuity of care across different levels of the health care system. A study [61] highlights that one of the main issues in the SNHS is the lack of interoperability in the EHR systems, which negatively impacts communication between primary and specialized care. For example, in the principality of Asturias, a digital tool has been introduced to assess adherence to HF clinical practice guidelines within internal medicine departments. Hospitals also have a clinical protocol for managing and following up on HF. In addition, the comprehensive continuous care program for patients with HF has been implemented in 5 out of 62 nationwide units. The systems in use include Selene, Millennium, Catalonia primary clinical station, and others, causing a nonunified EHR system [62].

Our findings align with existing research emphasizing the critical role of sociotechnical factors in the successful implementation of EHR systems. By examining both social and technical factors, potential barriers and adoption, the risk of nonadoption or abandonment, and the impact of stakeholders, including patients and HCPs, can be identified [63]. Adhistya et al [64] highlight the critical role of a sociotechnical framework in the implementation of electronic medical records to enhance patient safety. Their research identifies those factors such as user behavior, system design, and the availability of supporting infrastructure influence patient safety outcomes [64].

Limitations of the Study

While the qualitative approach using semistructured interviews and thematic analysis is appropriate, the sample size of 16 participants and the focus on specific areas within Andalusia may limit the generalizability of our findings.

To improve the generalizability of the results, future research should include a more extensive and diverse participant base. This could involve expanding the sample size and including HCPs from various regions and settings, such as rural and urban areas, and different hospital levels. In addition, incorporating perspectives from other stakeholders, such as IT professionals, patients with HF, administrative staff, and pharmacists, would provide a more comprehensive understanding of the challenges and opportunities for EHR optimization. In addition, a dedicated study group on case manager nurses is needed to explore their specific roles within the TSCP in greater detail. Exploring the impact of different socioeconomic and cultural aspects on EHR adoption and use would further enhance the applicability of the findings. Another limitation of this study was time constraints, which allowed for corroboration and validation of findings with only 2 participants, which was insufficient given the initial sample size. Future research addressing this limitation is necessary.

Conclusions

Effective communication is essential for managing patients with HF, as it involves coordination across multiple health care settings, various HCPs, and electronic systems. This requires both technological advancements and improved interpersonal strategies to facilitate efficient document sharing and follow-up calls. Improving the Diraya system's infrastructure, usability, and support tools—along with establishing seminars and an asynchronous chat system—significantly improves the care of patients with HF and adherence to protocols.

Overall, Diraya does not adequately support the TSCP, placing an excessive administrative burden on HCPs. The proposed improvements aim to enhance patient care, reduce hospital readmission rates, and improve overall patient well-being. Achieving these goals will require both technological improvements and the promotion of a collaborative health care culture that strengthens nursing practices and streamlines care transitions between settings.

Acknowledgments

The authors would like to thank Antares Consulting Company for helping recruit the participants. In addition, they would like to thank all participants who participated in this study for their time and valuable insights. The author ND received no specific funding for this work. MF received Erasmus+ Traineeship funding from Karolinska Institutet for this work.

XSL•FO
RenderX

Authors' Contributions

All authors (MF and ND) were involved in the design of the study. Data collection and initial data analysis were performed by MF. The analysis was then reviewed and refined by ND. Both authors (MF and ND) contributed to the subsequent writing and reviewing of the manuscript.

Conflicts of Interest

During this study, MF was employed by Antares Consulting Company.

Multimedia Appendix 1
Flowchart illustration of the visits and decision-making processes within the standardized care pathway for patients with heart failure. Adapted from Comin-Colet et al [16]. CR: cardiac rehabilitation; HC: home care; HD: hospital day; HF: heart failure; HFP: heart failure program; HFpEF: heart failure with preserved Ejection Fraction; HFU: heart failure unit; IM: internal medicine; LVEF: left ventricular ejection; PC: primary care; SCP: standardized care pathway. [PDF file (Adobe Acrobat), 211 kB].
[PDF File (Adobe PDF File), 211 KB - medinform_v13i1e63665_app1.pdf]

Multimedia Appendix 2
Proposed improvements, key findings, involved key actors, and priority scale based on the thematic analysis and feedback from health care professionals. [PDF file (Adobe Acrobat), 201 kB].
[PDF File (Adobe PDF File), 202 KB - medinform_v13i1e63665_app2.pdf]

References

1. Hacker K. The burden of chronic disease. Mayo Clin Proc Innov Qual Outcomes 2024 Mar;8(1):112-119 [FREE Full text] [doi: 10.1016/j.mayocpiqo.2023.08.005] [Medline: 38304166]
2. Schwinger RH. Pathophysiology of heart failure. Cardiovasc Diagn Ther 2021 Mar;11(1):263-276 [FREE Full text] [doi: 10.21037/cdt-20-302] [Medline: 33708498]
3. Taylor RS, Dalal HM, McDonagh ST. The role of cardiac rehabilitation in improving cardiovascular outcomes. Nat Rev Cardiol 2022 Mar;19(3):180-194 [FREE Full text] [doi: 10.1038/s41569-021-00611-7] [Medline: 34531576]
4. Visseren FL, Mach F, Smulders YM, Carballo D, Koskinas KC, Bäck M, ESC Scientific Document Group. 2021 ESC Guidelines on cardiovascular disease prevention in clinical practice. Eur J Prev Cardiol 2022 Mar 19;29(1):5-115. [doi: 10.1093/eurjpc/zwab154] [Medline: 34558602]
5. Cowie MR, Anker SD, Cleland JG, Felker GM, Filippatos G, Jaarsma T, et al. Improving care for patients with acute heart failure: before, during and after hospitalization. ESC Heart Fail 2014 Dec 21;1(2):110-145 [FREE Full text] [doi: 10.1002/ehf2.12021] [Medline: 28834628]
6. Delgado JF, Oliva J, Llano M, Pascual-Figal D, Grillo JJ, Comín-Colet J, et al. Health care and nonhealth care costs in the treatment of patients with symptomatic chronic heart failure in Spain. Rev Esp Cardiol (Engl Ed) 2014 Aug;67(8):643-650. [doi: 10.1016/j.rec.2013.12.014] [Medline: 25037543]
7. Delgado JF, Bueno H. Can we improve care for heart failure in Spain? Med Clin (Barc) 2022 Jul 22;159(2):90-91. [doi: 10.1016/j.medcli.2022.03.010] [Medline: 35644626]
8. Sayago-Silva I, García-López F, Segovia-Cubero J. Epidemiology of heart failure in Spain over the last 20 years. Rev Esp Cardiol (Engl Ed) 2013 Aug;66(8):649-656. [doi: 10.1016/j.rec.2013.03.012] [Medline: 24776334]
9. Savarese G, Becher P, Lund L, Seferovic P, Rosano G, Coats A. Global burden of heart failure: a comprehensive and updated review of epidemiology. Cardiovasc Res 2023 Jan 18;118(17):3272-3287. [doi: 10.1093/cvr/cvac013] [Medline: 35150240]
10. Barton C, Gordon S, Safa A, Plymen CM. Heart failure care pathways: the power of collaboration and marginal gains. Br J Cardiol 2022;29(1):5 [FREE Full text] [doi: 10.5837/bjc.2022.005] [Medline: 35747308]
11. Annual report on the National Health System of Spain 2022. Spanish Ministry of Health. URL: https://www.sanidad.gob.es/estadEstudios/estadisticas/sisInfSanSNS/tablasEstadisticas/InfAnualSNS2022/ExecutiveSummary_2022.pdf [accessed 2024-04-29]
12. Home page. Ministerio de Sanidad, Consumo y Bienestar. URL: https://www.sanidad.gob.es/en/home.htm [accessed 2024-04-29]
13. Bueno H, Bernal JL, Jiménez-Jiménez V, Martín-Sánchez FJ, Rossello X, Moreno G, ICA-SEMES ad hoc COHERENT study group. The Clinical outcomes, healthcare resource utilization, and related costs (COHERENT) model. Application in heart failure patients. Rev Esp Cardiol (Engl Ed) 2022 Jul;75(7):585-594. [doi: 10.1016/j.rec.2021.08.009] [Medline: 34688580]
14. Programa UMIPIC. Sociedad Española de medicina interna. URL: https://www.fesemi.org/grupos/cardiaca/umipic/programa [accessed 2024-04-29]
15. Comín-Colet J, Alcober L, Calero-Molina E, Cobo M, Corbella X, Cruzado C. Factores clave para modelos de atención a la insuficiencia cardiaca. CardioClinics 2022;57(1):24-38 [FREE Full text] [doi: 10.1016/j.rccl.2021.05.006]

XSL•FO
RenderX

16. Comín-Colet J, Cobo M, García-Pinilla J, Núñez J, Corbella X, González-Franco Á, et al. Modelos Asistenciales de Atención al Paciente con Insuficiencia Cardíaca. MAIC. URL: https://www.cronicidadhoy.es/arxius/imatgesbutlleti/Informe-Proyecto-MAIC.pdf [accessed 2024-04-29]
17. Noticias. Servicio Andaluz de Salud, Junta de Andalucia. URL: https://www.sspa.juntadeandalucia.es/servicioandaluzdesalud/pagina-inicial [accessed 2024-04-29]
18. El Servicio Andaluz de Salud. Servicio Andaluz de Salud. URL: https://www.sspa.juntadeandalucia.es/servicioandaluzdesalud/el-sas/el-servicio-andaluz-de-salud [accessed 2024-04-29]
19. ¿En qué podemos ayudarte? Junta de Andalucia. URL: https://www.juntadeandalucia.es [accessed 2024-04-29]
20. Sangal RB, Liu RB, Cole KO, Rothenberg C, Ulrich A, Rhodes D, et al. Implementation of an electronic health record integrated clinical pathway improves adherence to COVID-19 hospital care guidelines. Am J Med Qual 2022;37(4):335-341 [FREE Full text] [doi: 10.1097/JMQ.0000000000000036] [Medline: 35026785]
21. Busse TS, Jux C, Laser J, Rasche P, Vollmar HC, Ehlers JP, et al. Involving health care professionals in the development of electronic health records: scoping review. JMIR Hum Factors 2023 Jul 10;10:e45598 [FREE Full text] [doi: 10.2196/45598] [Medline: 37428524]
22. Diraya. Servicio Andaluz de Salud. URL: https://www.sspa.juntadeandalucia.es/servicioandaluzdesalud/profesionales/sistemas-de-informacion/diraya [accessed 2024-04-29]
23. Asistenciales. Servicio Andaluz de Salud. URL: https://www.sspa.juntadeandalucia.es/servicioandaluzdesalud/ayudadigital/aplicaciones/categoria/asistenciales [accessed 2024-04-29]
24. Sittig DF, Singh H. A new sociotechnical model for studying health information technology in complex adaptive healthcare systems. Qual Saf Health Care 2010 Oct;19 Suppl 3(Suppl 3):i68-i74 [FREE Full text] [doi: 10.1136/qshc.2010.042085] [Medline: 20959322]
25. Campbell S, Greenwood M, Prior S, Shearer T, Walkem K, Young S, et al. Purposive sampling: complex or simple? Research case examples. J Res Nurs 2020 Dec 18;25(8):652-661 [FREE Full text] [doi: 10.1177/1744987120927206] [Medline: 34394687]
26. Naderifar M, Goli H, Ghaljaie F. Snowball sampling: a purposeful method of sampling in qualitative research. Strides Dev Med Educ 2017 Sep 30;14(3):33. [doi: 10.5812/sdme.67670]
27. Over 25 years of commitment to transforming health. Antares Consulting. URL: https://www.antares-consulting.com/en/home-en/ [accessed 2024-04-29]
28. Chisholm RF, Ziegenfuss JT. A review of applications of the sociotechnical systems approach to health care organizations. J Appl Behav Sci 1986 Jul 26;22(3):315-326. [doi: 10.1177/002188638602200310] [Medline: 10301200]
29. Irizarry T, Barton AJ. A sociotechnical approach to successful electronic health record implementation: five best practices for clinical nurse specialists. Clin Nurse Spec 2013;27(6):283-285 [FREE Full text] [doi: 10.1097/NUR.0b013e3182a872e3] [Medline: 24107749]
30. Coiera E. Putting the technical back into socio-technical systems research. Int J Med Inform 2007 Jul;76 Suppl 1:S98-103. [doi: 10.1016/j.ijmedinf.2006.05.026] [Medline: 16807084]
31. Alhojailan MI. Thematic analysis: a critical review of its process and evaluation. West East J Soc Sci 2012;1(1):39-47 [FREE Full text]
32. Nowell LS, Norris JM, White DE, Moules NJ. Thematic analysis: striving to meet the trustworthiness criteria. Int J Qual Methods 2017 Oct 02;16(1):1-13 [FREE Full text] [doi: 10.1177/1609406917733847]
33. Lag (2003:460) om etikprövning av forskning som avser människor. Sveriges riksdag. URL: https://www.riksdagen.se/sv/dokument-och-lagar/dokument/svensk-forfattningssamling/lag-2003460-om-etikprovning-av-forskning-som_sfs-2003-460/ [accessed 2024-04-29]
34. What the act says. Swedish Ethical Review Authority. URL: https://etikprovningsmyndigheten.se/en/what-the-act-says/#fl-main-content [accessed 2025-04-03]
35. Regulation (EU) 2016/679 of the European Parliament and of the Council of 27 April 2016 on the protection of natural persons with regard to the processing of personal data and on the free movement of such data, and repealing Directive 95/46/EC (General Data Protection Regulation) (Text with EEA relevance). European Commission. URL: https://eur-lex.europa.eu/eli/reg/2016/679/oj/eng [accessed 2024-04-29]
36. Zayas-Cabán T, Okubo TH, Posnack S. Priorities to accelerate workflow automation in health care. J Am Med Inform Assoc 2022 Dec 13;30(1):195-201 [FREE Full text] [doi: 10.1093/jamia/ocac197] [Medline: 36259967]
37. Yip M, Ackery A, Jamieson T, Mehta S. The priorities of end users of emergency department electronic health records: modified Delphi study. JMIR Hum Factors 2023 Mar 10;10:e43103 [FREE Full text] [doi: 10.2196/43103] [Medline: 36897633]
38. Vuori MA, Kiiskinen T, Pitkänen N, Kurki S, Laivuori H, Laitinen T, FinnGen, et al. Use of electronic health record data mining for heart failure subtyping. BMC Res Notes 2023 Oct 11;16(1):208 [FREE Full text] [doi: 10.1186/s13104-023-06469-x] [Medline: 37697398]
39. Zilahi G, O'Connor E. Information sharing between intensive care and primary care after an episode of critical illness; a mixed methods analysis. PLoS One 2019 Feb 28;14(2):e0212438 [FREE Full text] [doi: 10.1371/journal.pone.0212438] [Medline: 30818372]

XSL•FO
RenderX

40. Prusch AE, Suess TM, Paoletti RD, Olin ST, Watts SD. Integrating technology to improve medication administration. Am J Health Syst Pharm 2011 May 01;68(9):835-842. [doi: 10.2146/ajhp100211] [Medline: 21515868]
41. Lu Y, Melnick ER, Krumholz HM. Clinical decision support in cardiovascular medicine. BMJ 2022 May 25;377:e059818. [doi: 10.1136/bmj-2020-059818] [Medline: 35613721]
42. Giscombe SR, Baptiste DL, Koirala B, Asano R, Commodore-Mensah Y. The use of clinical decision support in reducing readmissions for patients with heart failure: a quasi-experimental study. Contemp Nurse 2021 May 05;57(1-2):39-50. [doi: 10.1080/10376178.2021.1919161] [Medline: 33863268]
43. Njie GJ, Proia KK, Thota AB, Finnie RK, Hopkins DP, Banks SM, Community Preventive Services Task Force. Clinical decision support systems and prevention: a community guide cardiovascular disease systematic review. Am J Prev Med 2015 Dec;49(5):784-795 [FREE Full text] [doi: 10.1016/j.amepre.2015.04.006] [Medline: 26477805]
44. Vainiomäki S, Heponiemi T, Vänskä J, Hyppönen H. Tailoring EHRs for specific working environments improves work well-being of physicians. Int J Environ Res Public Health 2020 Jul 30;17(13):4715 [FREE Full text] [doi: 10.3390/ijerph17134715] [Medline: 32630043]
45. Evans-Lacko S, Jarrett M, McCrone P, Thornicroft G. Facilitators and barriers to implementing clinical care pathways. BMC Health Serv Res 2010 Jul 28;10(1):182 [FREE Full text] [doi: 10.1186/1472-6963-10-182] [Medline: 20584273]
46. Global strategy on digital health 2020-2025. World Health Organization. URL: https://iris.who.int/bitstream/handle/10665/344249/9789240020924-eng.pdf?sequence=1 [accessed 2024-04-29]
47. WHO guideline: recommendations on digital interventions for health system strengthening. World Health Organization. 2019. URL: https://iris.who.int/bitstream/handle/10665/311941/9789241550505-eng.pdf?sequence=31 [accessed 2024-04-29]
48. Rossander A, Lindsköld L, Ranerup A, Karlsson D. A state-of-the art review of SNOMED CT terminology binding and recommendations for practice and research. Methods Inf Med 2021 Dec 28;60(S 02):e76-e88 [FREE Full text] [doi: 10.1055/s-0041-1735167] [Medline: 34583415]
49. Bathelt F, Lorenz S, Weidner J, Sedlmayr M, Reinecke I. Application of modular architectures in the medical domain - a scoping review. J Med Syst 2025 Mar 18;49(1):27. [doi: 10.1007/s10916-025-02158-3] [Medline: 39964566]
50. Tabari P, Costagliola G, De Rosa M, Boeker M. State-of-the-Art Fast Healthcare Interoperability Resources (FHIR)-based data model and structure implementations: systematic scoping review. JMIR Med Inform 2024 Oct 24;12:e58445 [FREE Full text] [doi: 10.2196/58445] [Medline: 39316433]
51. Saluja S, Hochman M, Bourgoin A, Maxwell J. Primary care: the new frontier for reducing readmissions. J Gen Intern Med 2019 Dec 16;34(12):2894-2897 [FREE Full text] [doi: 10.1007/s11606-019-05428-2] [Medline: 31621049]
52. Zuchowski JL, Rose DE, Hamilton AB, Stockdale SE, Meredith LS, Yano EM, et al. Challenges in referral communication between VHA primary care and specialty care. J Gen Intern Med 2015 Mar 20;30(3):305-311 [FREE Full text] [doi: 10.1007/s11606-014-3100-x] [Medline: 25410884]
53. Branger PJ, van der Wouden JC, Schudel BR, Verboog E, Duisterhout JS, van der Lei J, et al. Electronic communication between providers of primary and secondary care. BMJ 1992 Oct 31;305(6861):1068-1070 [FREE Full text] [doi: 10.1136/bmj.305.6861.1068] [Medline: 1467688]
54. Data protection under GDPR. European Commission. URL: https://europa.eu/youreurope/business/dealing-with-customers/data-protection/data-protection-gdpr/index_en.htm [accessed 2024-04-29]
55. HIPAA for professionals: laws and regulations. U.S. Department of Health & Human Services. URL: http://hhs.gov/hipaa/for-professionals/security/laws-regulations/index.html [accessed 2024-04-29]
56. Slyer JT, Concert CM, Eusebio AM, Rogers ME, Singleton J. A systematic review of the effectiveness of nurse coordinated transitioning of care on readmission rates for patients with heart failure. JBI Libr Syst Rev 2011;9(15):464-490. [doi: 10.11124/jbisrir-2011-130]
57. Li M, Li Y, Meng Q, Li Y, Tian X, Liu R, et al. Effects of nurse-led transitional care interventions for patients with heart failure on healthcare utilization: a meta-analysis of randomized controlled trials. PLoS One 2021 Dec 16;16(12):e0261300 [FREE Full text] [doi: 10.1371/journal.pone.0261300] [Medline: 34914810]
58. Li Y, Fang J, Li M, Luo B. Effect of nurse-led hospital-to-home transitional care interventions on mortality and psychosocial outcomes in adults with heart failure: a meta-analysis. Eur J Cardiovasc Nurs 2022 Jul 02;21(4):307-317. [doi: 10.1093/eurjcn/zvab105] [Medline: 34792110]
59. Zhang P, Xing FM, Li CZ, Wang FL, Zhang XL. Effects of a nurse-led transitional care programme on readmission, self-efficacy to implement health-promoting behaviours, functional status and life quality among Chinese patients with coronary artery disease: a randomised controlled trial. J Clin Nurs 2018 Mar 08;27(5-6):969-979. [doi: 10.1111/jocn.14064] [Medline: 28880419]
60. Gartley CE. Identify opportunities to improve the EHR experience. American Nurse. URL: https://www.myamericannurse.com/identify-opportunities-to-improve-the-ehr-experience/ [accessed 2024-04-29]
61. Wangberg SC, Sørensen T, Andreassen HK. Using the internet to support exercise and diet: a stratified Norwegian survey. Med 2 0 2015 Aug 26;4(2):e3 [FREE Full text] [doi: 10.2196/med20.4116] [Medline: 26310277]
62. Welcome to the public sector contracting platform. Contratación del Sector Público. URL: https://tinyurl.com/eddejjzs [accessed 2024-04-29]

XSL•FO
RenderX

63. Moll J, Scandurra I, Bärkås A, Blease C, Hägglund M, Hörhammer I, et al. Sociotechnical cross-country analysis of contextual factors that impact patients' access to electronic health records in 4 European countries: framework evaluation study. J Med Internet Res 2024 Aug 26;26:e55752 [FREE Full text] [doi: 10.2196/55752] [Medline: 39186760]
64. Adhistya M, Kekenusa JS, Sinolungan JS. Socio-technical aspects of electronic medical record use related to patient safety at prof Dr. R. D. Kandou Manado Hospital. Neo J Econ Soc Humanit 2023 Jun 15;2(2):59-70. [doi: 10.56403/nejesh.v2i2.106]

Abbreviations

AHS: Andalusia Health Service
AI: artificial intelligence
C/IM: cardiologist or internal medicine
CDS: clinical decision support
EHR: electronic health record
HCP: health care professional
HF: heart failure
HN: hospital nurse
MAIC: modelos Asistenciales de Atención al Paciente con Insuficiencia Cardíaca
MDR: medical discharge report
NDR: nursing discharge report
PCN: primary care nurse
PCP: primary care physician
SCP: standardized care pathway
SNHS: Spanish National Health System
STS: sociotechnical system
TSCP: transition standardized care pathway
UX: user experience
WHO: World Health Organization

Edited by C Lovis; submitted 26.06.24; peer-reviewed by M Popovic, J Walsh; comments to author 06.02.25; revised version received 26.02.25; accepted 18.03.25; published 15.04.25.

Please cite as:
Font M, Davoody N
Optimizing an Electronic Health Record System Used to Help Health Care Professionals Comply With a Standardized Care Pathway for Heart Failure During the Transition From Hospital To Chronic Care: Qualitative Semistructured Interview Study
JMIR Med Inform 2025;13:e63665
URL: https://medinform.jmir.org/2025/1/e63665
doi:10.2196/63665
PMID:

©Marta Font, Nadia Davoody. Originally published in JMIR Medical Informatics (https://medinform.jmir.org), 15.04.2025. This is an open-access article distributed under the terms of the Creative Commons Attribution License (https://creativecommons.org/licenses/by/4.0/), which permits unrestricted use, distribution, and reproduction in any medium, provided the original work, first published in JMIR Medical Informatics, is properly cited. The complete bibliographic information, a link to the original publication on https://medinform.jmir.org/, as well as this copyright and license information must be included.

XSL•FO
RenderX

Original Paper

Interpretable Artificial Intelligence Analysis of Functional Magnetic Resonance Imaging for Migraine Classification: Quantitative Study

Guohao Li[1], MEng; Hao Yang[1], DEng; Li He[1], MD; Guojun Zeng[2], MD

[1]West China Hospital, Sichuan University, Chengdu, China

[2]Division of Vascular Surgery, Department of General Surgery, West China Hospital, Sichuan University, Chengdu, China

Corresponding Author:
Guojun Zeng, MD
Division of Vascular Surgery
Department of General Surgery
West China Hospital, Sichuan University
No. 37 Guoxue Lane, Chengdu, Sichuan Province
Chengdu
China
Phone: 86 13550337171
Email: zengguojun@wchscu.cn

Abstract

Background: Deep learning has demonstrated significant potential in advancing computer-aided diagnosis for neuropsychiatric disorders, such as migraine, enabling patient-specific diagnosis at an individual level. However, despite the superior accuracy of deep learning models, the interpretability of image classification models remains limited. Their *black-box* nature continues to pose a major obstacle in clinical applications, hindering biomarker discovery and personalized treatment.

Objective: This study aims to investigate explainable artificial intelligence (XAI) techniques combined with multiple functional magnetic resonance imaging (fMRI) indicators to (1) compare their efficacy in migraine classification, (2) identify optimal model-indicator pairings, and (3) evaluate XAI's potential in clinical diagnostics by localizing discriminative brain regions.

Methods: We analyzed resting-state fMRI data from 64 participants, including 21 (33%) patients with migraine without aura, 15 (23%) patients with migraine with aura, and 28 (44%) healthy controls. Three fMRI metrics—amplitude of low-frequency fluctuation, regional homogeneity, and regional functional connectivity strength (RFCS)—were extracted and classified using GoogleNet, ResNet18, and Vision Transformer. For comprehensive model comparison, conventional machine learning methods, including support vector machine and random forest, were also used as benchmarks. Model performance was evaluated through accuracy and area under the curve metrics, while activation heat maps were generated via gradient-weighted class activation mapping for convolutional neural networks and self-attention mechanisms for Vision Transformer.

Results: The GoogleNet model combined with RFCS indicators achieved the best classification performance, with an accuracy of >98.44% and an area under the receiver operating characteristic curve of 0.99 for the test set. In addition, among the 3 indicators, the RFCS indicator improved accuracy by approximately 8% compared with the amplitude of low-frequency fluctuation. Brain activation heat maps generated by XAI technology revealed that the precuneus and cuneus were the most discriminative brain regions, with slight activation also observed in the frontal gyrus.

Conclusions: The use of XAI technology combined with brain region features provides visual explanations for the progression of migraine in patients. Understanding the decision-making process of the network has significant potential for clinical diagnosis of migraines, offering promising applications in enhancing diagnostic accuracy and aiding in the development of new diagnostic techniques.

(JMIR Med Inform 2025;13:e72155) doi:10.2196/72155

KEYWORDS

migraine; personalized diagnosis; convolutional neural networks; explainable artificial intelligence; XAI; gradient-weighted class activation mapping

XSL•FO
RenderX

Introduction

Background

Migraines are a common, incapacitating neurovascular disorder characterized by attacks of severe headaches and autonomic nervous system dysfunction [1,2]. Diagnosing migraines, in general, is a complex task due to the subjective nature of the condition [3]. The symptoms of patients vary greatly, often overlapping with those of other neurological or medical diseases, and the lack of distinct biomarkers or image characteristics also increases diagnostic challenges. Furthermore, migraine with aura (MWA) and migraine without aura (MWoA) are the 2 primary types of migraines [4]. The main challenge in distinguishing between these categories lies in the fact that the warning signs of MWA do not always manifest and vary considerably in duration and severity from person to person [5,6].

In recent years, the study of magnetic resonance imaging (MRI) has greatly advanced our understanding of the neural mechanisms underlying migraines [7], using blood oxygenation level–dependent (BOLD) signals to measure neural activity [8]. Most related findings were obtained by applying mass-univariate analysis techniques to detect group differences and probe the pathogenesis of migraines [9]. Three commonly used indicators—amplitude of low-frequency fluctuation (ALFF), regional homogeneity (ReHo), and regional functional connectivity strength (RFCS)—can effectively help us analyze functional magnetic resonance imaging (fMRI) data because they reflect brain activity characteristics from different perspectives. As a result, these metrics have been widely applied in neuropsychiatric research and have proven valuable in uncovering the neural mechanisms of diseases [10-12]. For example, compared with healthy controls (HCs), patients with migraines have been shown to exhibit significant ALFF variations in the bilateral middle occipital cortex or cuneus and ReHo changes in the prefrontal cortex, orbitofrontal cortex [13], insula [14], and cuneus [15]. Altered functional connectivity (FC) has also been identified between the dorsolateral prefrontal cortex and the dorsal anterior cingulate cortex [16]. However, this analysis lacks a personalized diagnosis for patients in a clinic setting.

Recent studies have highlighted the potential of machine learning in migraine classification; however, challenges such as inconsistent study design and lack of methodological transparency underscore the need for robust frameworks such as deep learning to improve generalization and clinical applicability [17]. Deep learning has been applied to medical data across a variety of fields, allowing for inferences at the level of individual participants and thus solving this problem. Furthermore, it is sensitive to subtle and spatially distributed differences in the brain; excels in automatically extracting intermediate and high-level feature representations from raw data; and identifies the crucial features necessary for accurate classification, which might be undetectable in group comparisons. Ashina et al [18] further emphasized that even though deep learning models demonstrate superior accuracy, their “black box” nature remains a critical barrier to achieving biomarker discovery and personalized treatment. Therefore, developing deep learning frameworks that integrate both high accuracy and interpretability is essential for deciphering the heterogeneous mechanisms of migraine and advancing precision medicine [18].

Objectives

We hypothesize that deep learning models can classify patients with migraine versus HCs using resting-state fMRI (rs-fMRI) data with higher accuracy than traditional methods, while explainable techniques will reveal distinct neurofunctional patterns that align with known migraine-related pathophysiology, thereby bridging the “black box” gap. In this research, we used an array of deep learning architectures, including GoogleNet [19] and ResNet [20], and integrated the self-attention mechanism of the Vision Transformer (ViT) [21] model, alongside various modalities of MRI data for classification purposes. These deep learning architectures each have their own advantages and can extract features from rs-fMRI data from different perspectives. Moreover, these models have been widely applied in medical image analysis and proven effective [22]. We implemented the gradient-weighted class activation mapping (Grad-CAM) [23] technique for convolutional neural networks (CNNs). This method significantly enhances the interpretability of the classification results, thereby increasing the model’s credibility in the context of migraine diagnosis. For the ViT model, we leveraged the attention mechanism to improve interpretability by visualizing attention weights. This allows us to visually identify the regions of the image that the model focuses on when making classification decisions. By using these explainable artificial intelligence (XAI) [24] techniques and visualizing attention maps, we can delineate the approximate locations of the regions of interest via a heat map, thus facilitating the interpretation of the classification results generated by the deep learning models.

Methods

Participants

This study enrolled 64 individuals, categorized into 3 groups: 21 (33%) patients with MWoA, 15 (23%) patients with MWA, and 28 (44%) HC. The patients were recruited from the internal medicine–neurology department of West China Hospital, Sichuan University, and diagnoses were confirmed by neurologists specializing in headache disorders based on the International Classification of Headache Disorders criteria.

Participants were right-handed adults aged 18 to 50 years. They discontinued analgesic medications for ≥2 weeks and other medications for ≥1 month before the study, with no ongoing prophylactic treatment. All patients remained migraine free for at least 72 hours before the brain scan and throughout the 48-hour follow-up period after scanning. Exclusion criteria included for the HCs, and inclusion criteria required no personal or family history of migraine or other headache disorders and no history of neuropsychiatric disorders or neurological impairments. Controls were age matched (±7 y) and sex matched to patients. Exclusion criteria for all groups included MRI contraindications, substance abuse history, and neurodevelopmental disorders. HCs underwent additional

XSL•FO
RenderX

screening via structured clinical interviews to exclude headache disorders.

It is important to note that while the presence of a clinical diagnosis of neuropsychiatric disorders was an exclusion criterion, subclinical levels of depression and anxiety were not. The inclusion of participants with varying degrees of depression and anxiety allowed us to investigate the natural variability of these conditions within the migraine population and HCs. Exclusion criteria for both patient and control groups included the presence of chronic migraines, concurrent pain conditions, history of neuropsychiatric disorders, or any other neurological impairments that could affect the imaging results.

Demographic data (age, sex, and education) and psychometric scores (Hamilton Depression Scale and Hamilton Anxiety Scale) were collected during initial screening using standardized report forms. Psychometric evaluations revealed varied levels of depression and anxiety among the groups, quantified by the Hamilton Depression Scale and Hamilton Anxiety Scale.

Ethical Considerations

The research was approved by the institutional review board of West China Hospital, Sichuan University (2020-666; Figure S1 in Multimedia Appendix 1). All participants provided written informed consent, including explicit permission for secondary data analysis. Participants were informed about the study's purpose, data use, and privacy protections. The consent forms allowed future reuse of anonymized data. All data were deidentified before analysis, with Digital Imaging and Communications in Medicine header information removed using specialized tools. No identifiable facial features or personal metadata were present in any of the presented images.

Statistical Analysis

This study used the Kruskal-Wallis *H* test from the *scipy.stats* package of Python (Python Software Foundation) to analyze the experimental data. This is a nonparametric test used to determine whether there are statistically significant differences in medians among ≥3 independent samples [25].

The specific method involves combining all data from the 3 sample types used in this study and ranking them by value, assigning each data point a corresponding rank. If values are tied, the average rank is calculated. Next, the rank sums (R1, R2, and R3) for each sample group are computed separately. The *H* statistic is then calculated using the Kruskal-Wallis *H* test formula:



where N represents the total sample size across all groups, k represents the number of groups (in this case, k=3), n_i represents the sample size of the i-th group, and R_i represents the rank sum of the i-th group.

Finally, the calculated *H* value is compared with the chi-square distribution with 2 *df*sto obtain the corresponding *P* value. If $P \leq .05$, it indicates that at least 1 of the 3 sample groups has a median significantly different from the others. If $P > .05$, there is insufficient evidence to conclude a significant difference in medians among the 3 sample groups.

Neuroimaging Data Acquisition and Preprocessing

Data acquisition was performed using a 3.0 Tesla MRI system (Trio Tim, Siemens). Participants were instructed to rest with their eyes closed, remain awake, and avoid active thinking. Structural imaging was conducted using a transverse echoplanar imaging sequence with the following parameters: the ratio of repetition time to echo time (TR/TE)=2000/30 ms, flip angle=90°, slice thickness/gap=5/0 mm, field of view =240×240 mm^2, matrix=64×64, and voxel size=3.75×3.75×5 mm^3. The scanning duration for all participants was 6 minutes (360 s), corresponding to 180 time points.

We preprocessed the data using the Graph Theoretical Network Analysis toolbox and Statistical Parametric Mapping. The preprocessing steps included the following:

- The first 10 time points were removed from each functional dataset to account for initial signal instability and participant adaptation, leaving 170 time points (340 s) for subsequent processing
- Slice timing correction and realignment were performed to minimize motion artifacts. Participants with head motion exceeding 2-mm displacement or 2° rotation were excluded. All participants in this study met these motion criteria.
- Spatial normalization was conducted to standard Montreal Neurological Institute space with 3-mm isotropic voxels
- Bandpass filtering (0.01-0.08 Hz) was applied to each voxel's time series to reduce low-frequency drift and high-frequency physiological noise [26]
- Spatial smoothing was conducted using a 4-mm full width at half maximum Gaussian kernel.
- Regression of nuisance covariates was performed to mitigate the influence of nonneuronal signals.

Finally, the ALFF, ReHo, and RFCS were calculated. ALFF serves as a reliable metric of regional intrinsic neuronal activity [27]. Time series from each voxel were converted to the frequency domain via fast Fourier transform to derive the power spectrum. The square root of the power spectrum was then averaged over a predefined frequency range. Within the 0.01 to 0.08 Hz frequency band, ALFF was calculated per voxel using the rs-fMRI Data Analysis Toolkit (REST, Provided by the REST team led by Professor ZANG Yu-Feng, ORCID: 0000-0003-1833-8010) software. To control for interparticipant variability, the ALFF values of individual voxels were normalized by dividing them by the global mean ALFF. ReHo, quantified using the Kendall coefficient of concordance, measures the temporal similarity between a voxel and its immediate neighbors, yielding consistent outcomes in rs-fMRI analyses. In our study, a cubic cluster of 27 voxels was defined for each normalized and resliced image, with the ReHo value of each cluster attributed to the central voxel. Higher ReHo values indicate greater local synchronization of rs-fMRI signals among adjacent voxels. Similar to ALFF normalization, each voxel's ReHo value was divided by the global mean ReHo value per participant. These procedures were carried out using REST software.

XSL•FO
RenderX

The rs-fMRI enables the evaluation of brain function through the measurement of FC among distinct brain regions. To mitigate the impact of regions of interest selection on FC outcomes, we adopted the RFCS approach, which evaluates the average correlation between a given brain region and all others [28]. To calculate resting-state FC, we controlled for the spurious effects of nuisance covariates [29]. The rs-fMRI data were parcellated into 116 regions of interest based on the automated anatomical labeling (AAL) template, yielding 116 FC results for each participant. The RFCS values were subsequently determined using a methodology detailed in a previous study by Jiang et al [30]. The RFCS was defined as follows:



The preprocessed neuroimaging data were managed using the NiBabel library, converting 4D data into 2D matrices suitable for CNNs. Throughout the data conversion process, MRI scans from all 64 participants were processed. Each scan initially produced 33 slices; the first 3 slices were discarded due to potential quality issues, leaving 30 valid slices per participant. Each slice then underwent 3 feature mappings, resulting in a total of 5760 images: 1890 from patients with MWoA, 1350 from patients with MWA, and 2520 from HCs. We ensured that no slices from the same patient appeared in both the training and testing sets to avoid data leakage. To mitigate overfitting, data augmentation techniques, such as cropping, rotating, and flipping of input images, were implemented [31,32]. Further data augmentation, involving random shuffling and resizing to 224×224 pixels, increased the diversity of the dataset. The entire training phase was conducted on a high-performance GPU (Nvidia 4070 Ti with CUDA support), using the PyTorch framework for the implementation of the deep learning model.

Model Validation

For the machine learning applications, we first performed a 5-fold cross-validation to split the participants' data into training and testing sets. Specifically, the entire dataset is first randomly divided into 5 roughly equal parts, a step commonly referred to as folding. Next, 5 iterations are performed. In each iteration, 1 fold is selected as the test set, while the remaining 4 folds are combined to form the training set. The model is trained on the training set and evaluated on the test set, with the evaluation results recorded. After all 5 iterations are completed, the results of the 5 evaluations are averaged to obtain the final model performance assessment. This averaged value provides a more stable and reliable reflection of the model's performance on the data.

In addition, we also used leave-one-out cross-validation (LOOCV) methodology for comparative validation purposes.

Deep Learning Architecture

CNN architectures include several CNN layers that transform an input image step by step, ultimately yielding a class prediction. This study examines some of the most popular CNN architectures used for image recognition tasks, including GoogleNet and ResNet18. In contrast, the ViT is a transformer-based architecture that divides an image into multiple small patches, treating these patches as elements in a sequence, and processes them through the Transformer model. This approach leverages self-attention mechanisms to capture global contextual information within the image. Compared with traditional CNNs, ViT offers greater flexibility and scalability in image processing. The introduction of ViT has brought a new perspective to the field of image recognition, achieving remarkable performance on various benchmark tests. These different models were included to test the impact of network architecture on visualization performance. Results derived from each model were compared, and the best-performing algorithm was used as the basis for visualization.

In addition, to provide a more comprehensive performance comparison, we included 2 widely used traditional machine learning methods—support vector machine and random forest—as baseline models, performing 3-class classification directly using features extracted from RFCS.

Transfer Learning

Currently, optimization algorithms such as Stochastic Gradient Descent [33] have significantly improved our training efficiency. To further enhance model performance and reduce training time, we also used transfer learning. Transfer learning increases a model's robustness and accuracy when performing new classification tasks by leveraging knowledge acquired from related tasks, which is particularly beneficial for small training datasets [34]. Initialization weights that have been trained to recognize various items in different images are easier to train than initial random weights, as image recognition primarily involves detecting combinations of edges. The initial weights used in our model included transfer learning weights from the ImageNet competition, derived from images with similar features. In addition, all weights throughout the network were frozen and did not participate in backpropagation, except for those in the last convolutional layer and the fully connected layer. These layers were replaced with new layers exhibiting random weights. By training only the updated layers, we reduced runtime by limiting the number of calculations required in each forward pass iteration. This approach also improved classification performance by simplifying the model and reducing the number of parameters.

XAI Methods

XAI methods are designed to enhance the transparency of machine learning models, enabling a clear understanding of the models' decision-making processes. XAI is particularly well suited for applications that demand a high level of trust and safety. Among the commonly used interpretability techniques are Grad-CAM and the visualization of self-attention mechanisms.

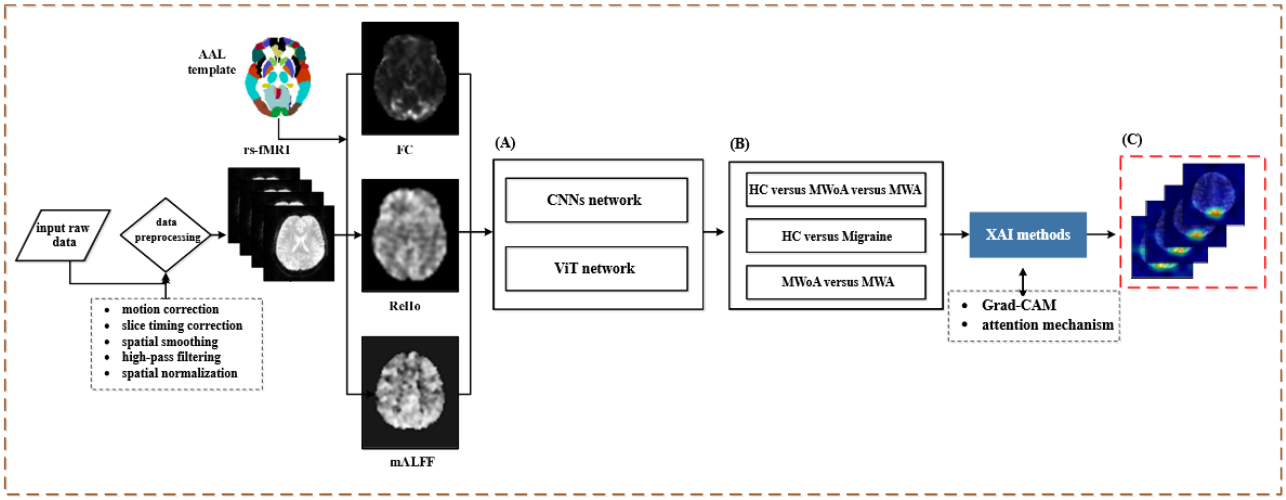
Grad-CAM merges the gradients of target concepts with the final convolutional layer to produce a coarse localization map, highlighting the important regions in an image for the purpose of predicting feature concepts. A previous study by Hao et al [35] has asserted that deeper representations of models allow for the capture of higher-level visual constructs. In addition, convolutional features naturally retain spatial information, which is lost in fully connected layers. As such, we can expect the last

XSL•FO
RenderX

convolutional layer to exhibit the best compromise between high-level semantics and detailed spatial information. Grad-CAM can also be used to represent so-called counterfactual explanations, regions that (if removed) could change the classification results. Neurons in the latter layers of a CNN are mostly used to identify semantic class-specific information in an image (ie, specific structures). In contrast, Grad-CAM uses gradient information passed to the last convolutional layer of the CNN to understand the importance of each neuron for a decision of interest.

The ViT model enhances its ability to capture image features by dividing the image into multiple patches and using the self-attention mechanism [36] in the Transformer architecture. This approach captures the relationships and global contextual information between different regions of the image. By visualizing the attention weights, we can intuitively see which areas of the image the model focuses on when making classification decisions. This visualization of attention maps provides a clear method for understanding the model's decision-making process, thereby improving its interpretability. This enhanced understanding of how the model identifies and distinguishes different categories of images is crucial for increasing the model's transparency and credibility. A flowchart for this process is shown in Figure 1.

Figure 1. A schematic illustration of the proposed classification process. (A) Deep learning models; (B) Output layer; (C) Activation map. AAL: Automated Anatomical Labeling; CNN: convolutional neural network; FC: functional connectivity; Grad-CAM: gradient-weighted class activation mapping; HC: healthy control; mALFF: mean amplitude of low-frequency fluctuation; MWA: migraine with aura; MWoA: migraine without aura; ReHo: regional homogeneity; rs-fMRI: resting-state function magnetic resonance imaging; ViT: Vision Transformer; XAI: explainable artificial intelligence.



Evaluation Criteria

Receiver Operating Characteristic Curve

Prediction model performance was evaluated for the test sets using a receiver operating characteristic (ROC) curve [37]. The area under the curve (AUC) is a quantitative metric assessing the overall performance of a binary classifier without setting a specific threshold. AUC ranges from 0 to 1, where an AUC of 1 indicates perfect classification, and an AUC of 0.5 suggests the model performs no better than random guessing. Values <0.5 are uncommon in practice, as reversing the classification would improve results. Higher AUC values (>0.5) indicate better class separation.

To comprehensively evaluate the classification performance, both AUC and the F_1-score were used as key performance indicators. AUC measures the model's ability to distinguish between classes across all thresholds, making it robust to class imbalance and useful when misclassification costs vary between classes. The F_1-score, defined as the harmonic mean of precision and recall, provides a balanced measure especially suitable for imbalanced datasets where both false positives and false negatives are of concern [38]. The relevant metrics are defined as follows:

where *TP*, *FP*, *TN*, and *FN* represent true positive, false positive, true negative, and false negative, respectively.

Confusion Matrix

An analysis table can be used to summarize prediction results for a classification model and is particularly beneficial for multiclass objects (ie, distinguishing MWoA, MWA, and HC). In this process, decisions for specific data are summarized in a matrix form, using the real category and classification judgments made by the model. A confusion matrix was applied in this study to quantify the consistency between predicted and actual results.

Results

Classification Performance

Table 1 presents the research data, demonstrating that the observed differences in psychometric assessments were not confounded by demographic variables, such as sex, age, or education level.

XSL•FO
RenderX

Table 1. Baseline characteristics of patients with migraine[a].

Variables	MWoA[b]	MWA[c]	HC[d]	*P* value
Sex, n (%)				.40
Male	7 (11%)	4 (6%)	13 (20%)	
Female	14 (22%)	11 (17%)	15 (24%)	
Age (y), median (IQR)	29.00 (26.00-31.00)	29.00 (27.00-35.00)	29.00 (27.00-34.25)	.47
Education (y), median (IQR)	19.00 (16.00-19.00)	16.00 (15.00-16.00)	16.00 (16.00-19.00)	.002
24-HAMD[e], median (IQR)	4.00 (1.00-9.00)	10.00 (6.00-15.00)	1.00 (0.00-3.00)	<.001
14-HAMA[f], median (IQR)	3.00 (1.00-6.00)	6.00 (5.00-9.50)	0.00 (0.00-3.00)	<.001

[a]Statistical differences between groups were calculated using the Kruskal-Wallis test.

[b]MWoA: migraine without aura.

[c]MWA: migraine with aura.

[d]HC: healthy control.

[e]HAMD: Hamilton Depression Scale.

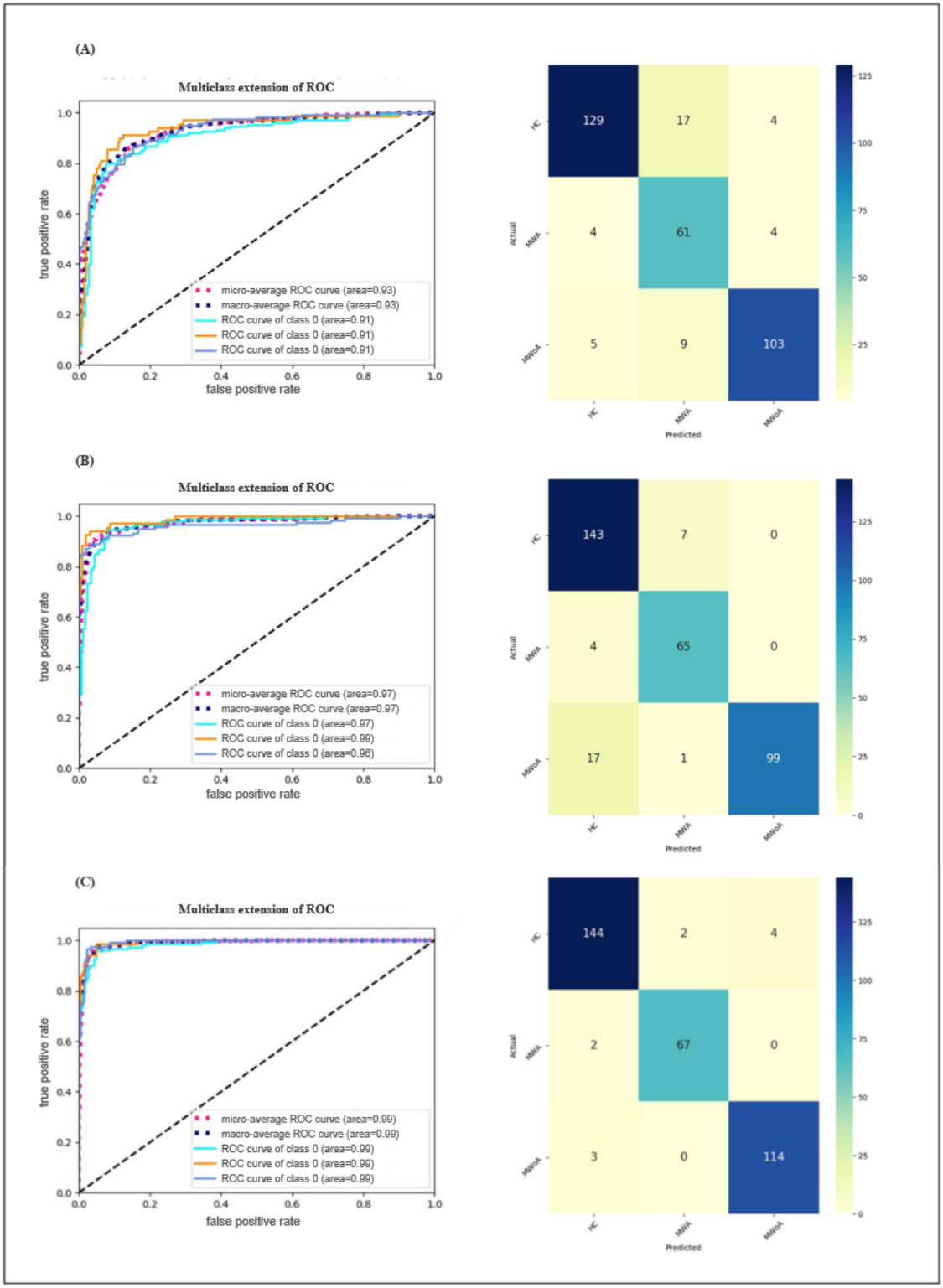
[f]HAMA: Hamilton Anxiety Scale.

Classification performance was tested using deep learning models with different rs-fMRI indicators (ALFF, ReHo, and RFCS). The data were divided into 2 groups before being input to the model: migraine versus HC and MWA versus MWoA. The loss of training and testing data were measured during the training phase. All models exhibited an improved classification accuracy (>84%) when compared with conventional machine learning methods applied to the same data. Our group previously used the LOOCV technique to obtain higher ranking features from the square of a weight vector coefficient, used as a ranking criterion to determine features for training a multicore support vector machine classifier [39].

Confusion matrices and ROC curves were also calculated for each model and used to display the classification results. We found that GoogleNet produced the highest classification accuracy for a given set of indicators, as shown in Figure 2.

XSL•FO
RenderX

Figure 2. Performance classification as determined by various indicators. (A) The ALFF indicator as input to GoogleNet; (B) The ReHp indicator as input to GoogleNet; (C) The RFCS indicator as input to GoogleNet. ALFF: amplitude of low-frequency fluctuation; HC: healthy control; MWA: migraine with aura; MWoA: migraine without aura; ReHo: regional homogeneity; RFCS: regional functional connectivity strength; ROC: receiver operating characteristic curve.



In addition, RFCS achieved the best performance for each classifier among the tested indicators. Therefore, GoogleNet combined with RFCS provided the highest average precision for identifying patients with migraine. In the results, we observed that the use of the ViT-B/16 model did not yield an improvement in accuracy. In fact, compared with the straightforward CNN architecture, the classification outcomes of the ViT model showed a decrease in performance across various MRI modalities. The ultimate accuracy of the models was then determined by averaging the accuracies from 4 distinct trials, as illustrated in Table 2. In addition, we performed LOOCV using the GoogleNet model that achieved the best classification performance, with results available in Table S1 in Multimedia Appendix 1.

XSL•FO
RenderX

Table 2. Results of 5-fold cross-validation based on 3 metrics across different deep learning models.

Model, indicator, and data group	Accuracy (%), mean (SD)	F_1-score (%), mean (SD)
ResNet18		
ALFF[a]		
HC[b] versus migraine	87.20 (0.64)	87.13 (0.62)
HC versus MWoA[c] versus MWA[d]	86.83 (1.84)	86.70 (1.85)
ReHo[e]		
HC versus migraine	92.56 (0.94)	92.50 (0.90)
HC versus MWoA versus MWA	91.07 (0.37)	90.95 (0.35)
RFCS[f]		
HC versus migraine	97.81 (0.39)	97.7 (0.40)
HC versus MWoA versus MWA	96.75 (1.93)	96.55 (1.95)
GoogleNet		
ALFF		
HC versus migraine	90.69 (1.12)	90.50 (1.10)
HC versus MWoA versus MWA	89.95 (0.65)	89.8 (0.65)
ReHo		
HC versus migraine	94.79 (1.29)	94.6 (1.30)
HC versus MWoA versus MWA	93.52 (0.51)	93.4 (0.50)
RFCS		
HC versus migraine	98.71 (0.14)	98.65 (0.15)
HC versus MWoA versus MWA	98.44 (0.29)	98.3 (0.30)
ViT-B/16[g]		
ALFF		
HC versus migraine	84.58 (1.83)	84.03 (0.67)
HC versus MWoA versus MWA	84.51 (0.56)	83.95 (0.60)
ReHo		
HC versus migraine	87.78 (0.61)	87.3 (0.65)
HC versus MWoA versus MWA	86.7 (1.27)	86.1 (1.30)
RFCS		
HC versus migraine	93.04 (0.50)	92.8 (0.50)
HC versus MWoA versus MWA	92.93 (1.25)	92.6 (1.30)

[a]ALFF: amplitude of low-frequency fluctuation.

[b]HC: healthy control.

[c]MWoA: migraine without aura.

[d]MWA: migraine with aura.

[e]ReHo: regional homogeneity.

[f]RFCS: regional functional connectivity strength.

[g]ViT: Vision Transformer.

The ROC curves are shown in Figure 3, and the classification results are presented in Table 3.

XSL•FO
RenderX

Figure 3. The regional functional connectivity strength (RFCS) indicator as input to support vector machine (SVM) and random forest. AUC: area under the curve; ROC: receiver operating characteristic curve.

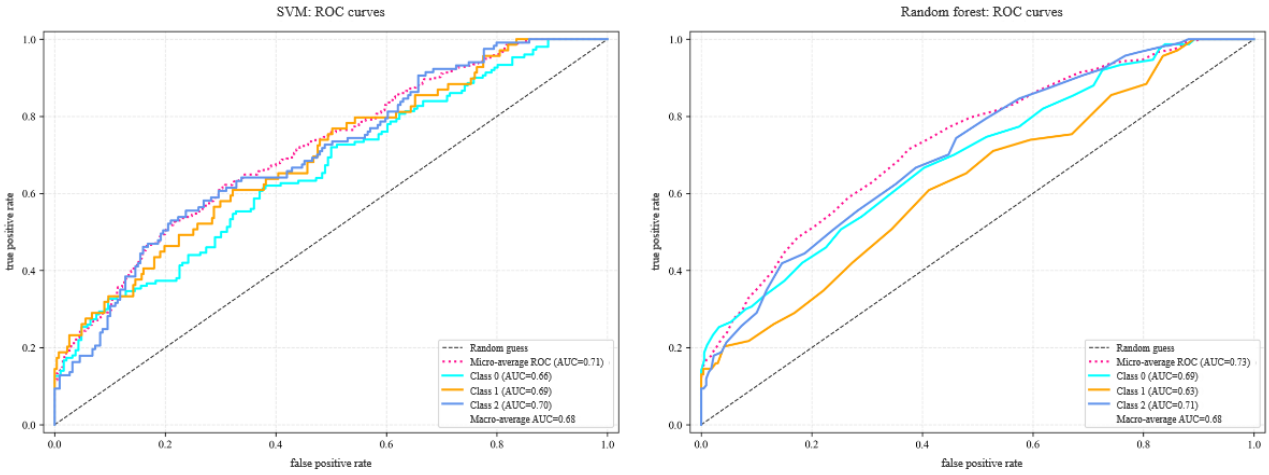


Table 3. Three-class classification performance of support vector machine (SVM), random forest (RF), and deep learning models using regional functional connectivity strength (RFCS) features.

Metric: HC[a] versus MWoA[b] versus MWA[c]	SVM: accuracy (%), mean (SD)	RF: accuracy (%), mean (SD)	GoogleNet: accuracy (%), mean (SD)
Accuracy	50.71 (1.65)	53.45 (1.12)	98.44 (0.29)
Precision	47.7 (2.08)	60.48 (2.96)	86.44 (0.26)
Recall	46.74 (1.89)	45.27 (1.19)	84.1 (0.32)
F_1-score	46.91 (2.00)	44.08 (1.50)	98.3 (0.30)
AUC[d]	66.29 (1.47)	66.9 (0.57)	98.63 (0.19)

[a]HC: healthy control.

[b]MWoA: migraine without aura.

[c]MWA: migraine with aura.

[d]AUC: area under the curve.

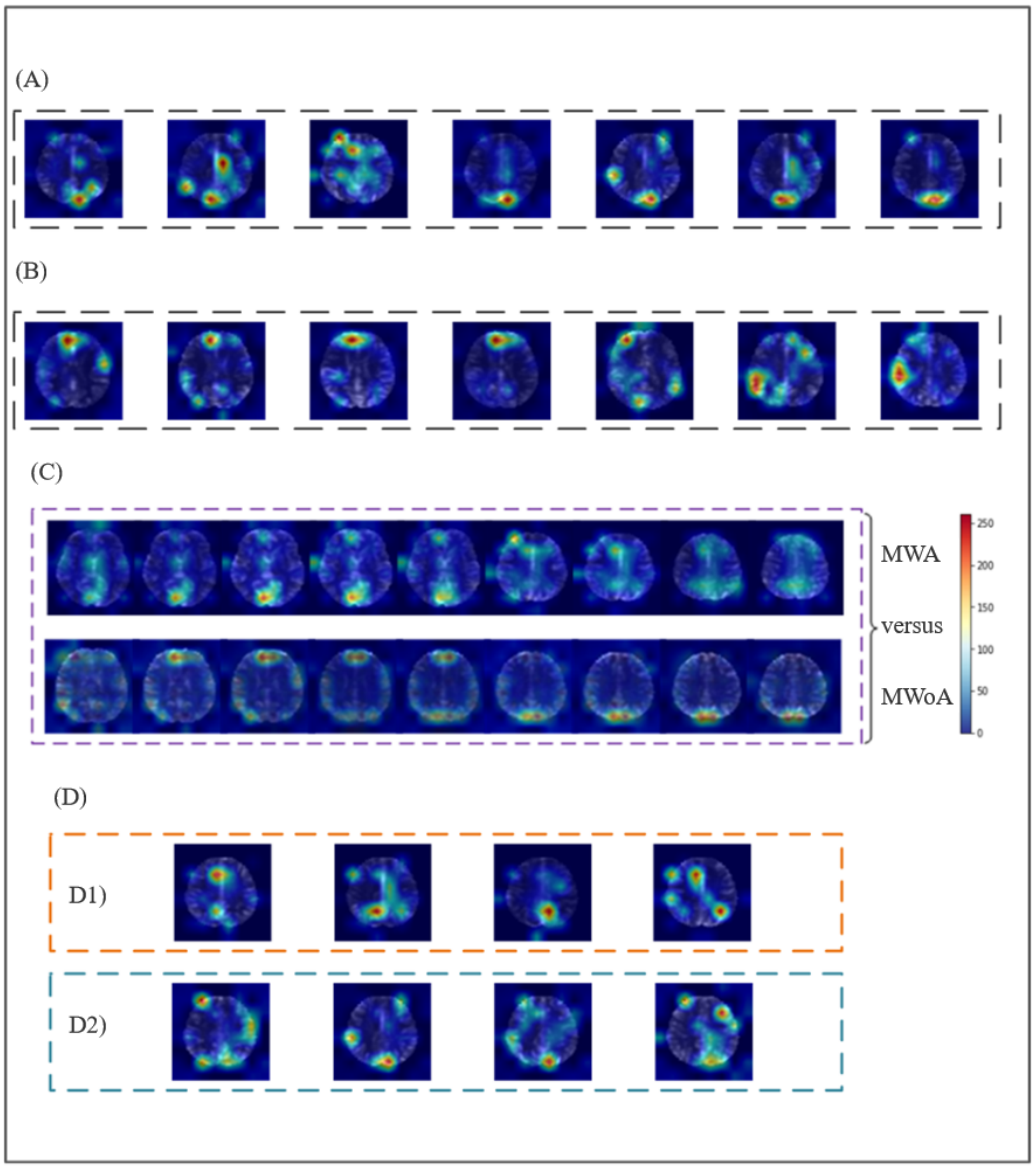
Model Visualization

Grad-CAM was used to visualize the GoogleNet model that achieved the best classification performance across various tasks. This process, representing the first time that CNN visualization of migraine classification results has been conducted using different MRI indicators, can be described in several steps. First, backpropagation was performed from the correctly classified images of patients with migraine. The mean gradient in each channel was then determined and multiplied by postactivated values in the feature map. Second, the absolute values of the gradient-weighted feature maps were summed to produce a coarse localization map, which was then thresholded and resized to the original image resolution. This localization map was converted into a heat map by applying a color scale to identify specific brain regions involved in classification tasks.

In this study, 3 MRI indicators—ALFF, ReHo, and RFCS—were registered and spatially mapped onto the AAL template to ensure accurate localization. Using these indicators, we generated heat maps to determine the areas of the brain that contributed most significantly to the classification performance. For example, the ALFFs that produced the most prominent heat maps are shown in Figure 4. Heat maps produced with ReHo and RFCS are shown in Figures 5A and 5B. In addition, we generated heat map results for the ViT model based on its self-attention mechanism. In the self-attention layers, the model calculates the relationship weights between each patch and all other patches in the sequence. By aggregating the attention weight matrices of each patch with others, we obtain the attention distribution of each patch within the image, thus creating the model's heat map (Figure S2B in Multimedia Appendix 1). However, the heat map lacks distinct hot spots, which may be due to the similar attention weights across patches, leading to a uniform attention distribution. This uniformity in the heat map could also explain the reduced classification performance of the model.

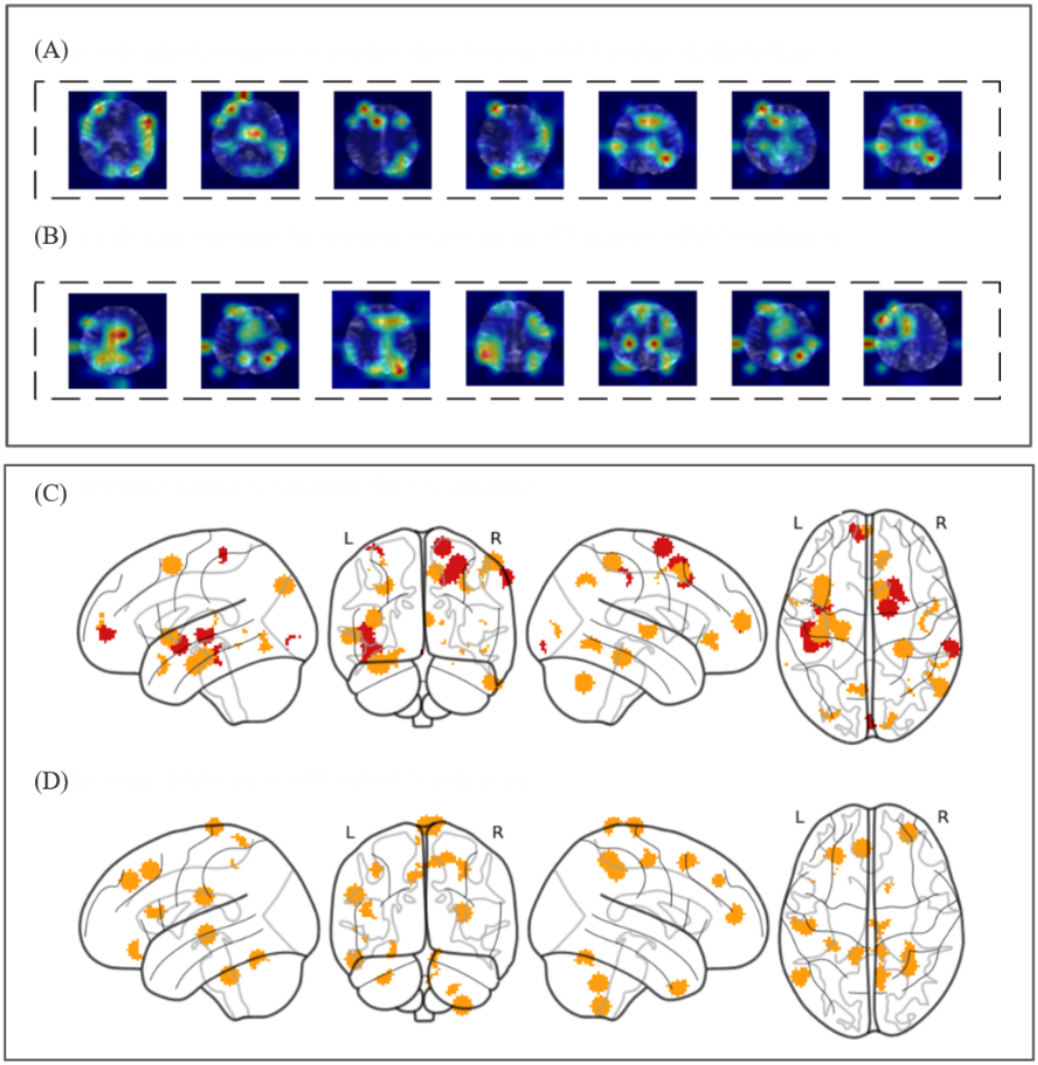
XSL•FO
RenderX

Figure 4. Activation heat maps derived from amplitude of low-frequency fluctuation (ALFF) features. (A) Activation heatmaps for multiple slices from a patient with MWA. (B) Activation heatmaps for multiple slices from a patient with MWoA. (C) Mean activation heatmaps for MWA versus MWoA. (D) Activation heatmaps for incorrectly classified images; (D1) HC samples incorrectly classified as patient with migraine; (D2) MWA samples incorrectly classified as MWoA. HC: healthy control; MWA: migraine with aura; MWoA: migraine without aura.



XSL•FO
RenderX

Figure 5. Activation heat maps derived from regional homogeneity (ReHo) and regional functional connectivity strength (RFCS) metrics, along with high-resolution activation heat maps based on RFCS, demonstrating the activation patterns across multiple brain regions. (A)Activation heatmaps for multiple slices from an MWA patient (ReHo indicator); (B) Activation heatmaps for multiple slices from an MWA patient (RFCS indicator). (C) Group 1: health control versus migraine (RFCS indicator); (D) Group 2: MWoA versus MWA (RFCS indicator). MWA: migraine with aura; MWoA: migraine without aura.



In addition, to obtain clearer and more intuitive activation maps, we additionally visualized the RFCS indicator activation area on another enlarged and high-definition brain template to achieve more precise localization of brain activity, as shown in Figures 5C and 5D. In Figure 5, group 1 displays the most discriminative activations between HCs and patients with migraine, with red intensity indicating stronger activation, and group 2 highlights the most discriminative activation regions between MWA and MWoA.

Discussion

Principal Findings

This study used the XAI methods to interpret deep learning models' decision-making processes and produce activation heat maps for class-discriminative regions in MRI slices. Various fMRI indicators were included as input data for the classification of migraines by a deep learning model. Results were compared for various MRI indicators (ALFF, ReHo, and RFCS) and different network architectures (GoogleNet, ResNet18, and ViT-B/16). The GoogleNet model combined with RFCS indicators produced the best classification performance (>98.44%). Heat maps confirmed Grad-CAM to be a promising visualization technique for the clinical diagnosis of migraines.

We compared 3 deep learning models based on different fMRI indicators. GoogleNet achieved the best results among the 3 models, producing a performance increase of 2% to 3% (AUC) for each indicator (Table 1). The inception module in GoogleNet could merge receptive fields of different sizes simultaneously with a concatenation filter, which improved classification performance [40]. It was evident in this study that the selection of indicators had a significant effect on classification results, with the RFCS indicator improving accuracy by approximately 8% compared with ALFF. RFCS measures the average correlation between a given brain region and other regions. This was often based on the AAL template-116 brain region [41], which contained important information about the whole brain to enhance accuracy rates. In contrast, ALFF was used to calculate the intensity of brain activity in a single voxel and included far fewer features than RFCS. This result suggested that the improvements in classification were partly the result of

XSL•FO
RenderX

model selection and primarily a consequence of indicator preference. In reviewing the literature, we found that education level was not always directly associated with migraines [42]. Therefore, its ultimate impact on classification performance might be small.

Comparison With Prior Work

A comparison of average localization maps with the AAL template suggested the most discriminative brain regions, for differentiating the migraine and HC groups, to be the cuneus and precuneus. There was also some slight activation present in the frontal gyrus. The most significant areas for distinguishing MWoA from MWA were the frontal gyrus and bilateral cuneus. These findings are in agreement with similar results from other studies. For example, Li et al [43] reported a significant decrease in ALFF in the bilateral middle occipital cortex and cuneus, when compared with HC. In addition, regions exhibiting decreased ALFF in patients with migraine included the bilateral cerebellum posterior lobe, left cerebellum anterior lobe, bilateral orbital cortex, middle frontal gyrus, bilateral occipital lobe, right fusiform gyrus, and bilateral postcentral gyrus [44]. There was no obvious pattern in the HC group, which suggests that pain is somewhat randomly distributed in normal cases.

Similarly, Farago et al [45] studied the low-frequency components of a BOLD signal (0.01-0.08 Hz) in MWoA and MWA groups [45]. Results showed the resting-state amplitude of BOLD fluctuations in the bilateral frontal regions to be higher in patients with MWA than in those with MWoA. This is in agreement with this study, as the cuneus is part of the visual cortex area of the brain [46].

Our study demonstrated the feasibility and clinical relevance of interpretable deep learning techniques in distinguishing between HCs and patients with migraine based on neuroimaging biomarkers. The identified patterns aligned with existing clinical knowledge: the cuneus, involved in visual processing, was associated with migraine as patients often exhibited light sensitivity and photophobia during attacks; the role of the precuneus in self-referential processing and pain modulation might explain the altered FC observed in patients with migraine; and dysregulation in the frontal cortex could be contributed to impaired pain inhibition and cognitive symptoms in chronic migraine [47].

Grad-CAM propagated gradients from the final convolutional layer to the input space, highlighting regions critical for category-specific predictions. The self-attention mechanism was particularly suitable for processing sequential data or data with complex dependencies. In migraine rs-fMRI data analysis, the self-attention mechanism helped the model identify key patterns of FC between different brain regions. In summary, our discovery of abnormal brain regions was supported by abundant literature. By leveraging interpretable models, we not only validated these biologically plausible findings but also provided clinicians with actionable insights. Our method might enhance the convenience of personalized diagnosis or targeted neural regulation therapy in certain scenarios. Therefore, in clinical translation, both methods alleviate the *black box* problem by providing visual explanations (heat maps), enabling clinicians to validate findings against established neurobiological knowledge, thereby increasing trust in model outputs for discovering potential biomarkers.

Limitations

While deep learning–based diagnostic tools have advantages, incorrect decisions can adversely affect patients, leading to misdiagnoses or missed diagnoses. Inaccuracies in our model could result in patients with migraine not receiving timely and appropriate treatment or subject normal participants to unnecessary medical interventions. Therefore, we emphasize the importance of thorough validation before clinical application and suggest using this model as an adjunct rather than the sole diagnostic tool.

Certain limitations existed in this study that should be noted. First, the sample size was relatively small. During the training of the ViT model, overfitting occurred (Figure S2A in Multimedia Appendix 1). For some specific clinical scenarios, a more complex and deeper network does not necessarily yield the best results; instead, it is crucial to select an appropriate model based on the characteristics and scale of the dataset. This was addressed in the study by using data augmentation techniques (ie, rotation, reflection, and cropping in PyTorch) and adding a dropout layer before the fully connected layer to mitigate overfitting. Second, the heat maps exhibited relatively limited resolution, due to a size limit imposed by feature maps in the last convolutional layer. The architecture and class activation map algorithm could be optimized using higher-resolution medical images to produce larger-scale feature maps.

Future Directions

Future research should aim to enhance the model's resolution capabilities, consider other imaging modalities or biological markers, and explore the adversarial attack approach to enrich the data and improve the robustness of the results [48]. In addition, we are also seeking collaborations with similar studies to share datasets, though this process may take time due to the high costs of such data collection. Meanwhile, we are making efforts to acquire data from other hospitals, despite current challenges in obtaining external data. We plan to incorporate multicenter data to evaluate the model's generalizability across different populations and MRI scanners. In addition, we will conduct more in-depth comparisons with neurologists' diagnostic consistency to assess the model's value in assisting clinical diagnosis. As for sex differences, our preliminary analysis did not reveal a significant impact on the model's performance. Nonetheless, given the known variations in migraine prevalence and manifestation between sexes, further research is warranted to explore this aspect in greater detail.

Conclusions

This study has demonstrated that XAI techniques, combined with fMRI-derived FC metrics, can achieve high classification accuracy in distinguishing patients with migraine from HCs while providing interpretable biomarkers. The GoogleNet model paired with RFCS emerged as the optimal framework, achieving exceptional performance (accuracy >98.44%; AUC=0.99) and outperforming conventional machine learning benchmarks. Generating heat maps by identifying the most discriminative

XSL•FO
RenderX

brain regions also confirms that XAI using Grad-CAM is a promising visualization technique.

Acknowledgments

This research was funded by the Sichuan University West China Hospital's horizontal project for the development of a proactive prediction and early warning management system and equipment for venous thromboembolism based on big data and artificial intelligence (project). It was also funded by West China Hospital, Sichuan University's "Development and Application of an Intelligent Decision Support System for Comprehensive VTE Risk Assessment and Prevention-Control Strategies Based on Large Language Models" 135 Project (project).

Data Availability

The datasets generated or analyzed during this study are not publicly available due to hospital institutional review board regulations but are available from the corresponding author on reasonable request. The implementation details and source code are publicly accessible at our GitHub repository [49].

Authors' Contributions

GL conceptualized and designed the study, conducted the research, performed the magnetic resonance imaging analysis, analyzed the data, and wrote the manuscript. LH and HY performed the magnetic resonance imaging analysis and approved the data. GZ conceptualized and designed the study. All authors contributed to editorial revisions, read and approved the final manuscript, participated sufficiently in the work, and agreed to be accountable for all aspects of the study.

Conflicts of Interest

None declared.

Multimedia Appendix 1
Ethical review supporting documentation and comparative experimental results.
[DOC File , 1083 KB - medinform_v13i1e72155_app1.doc]

References

1. Lance JW, Goadsby PJ. Mechanism and Management of Headache. New York, NY: Butterworth-Heinemann; 1998.
2. Agostoni E, Aliprandi A. The complications of migraine with aura. Neurol Sci 2006 May;27 Suppl 2(S2):S91-S95. [doi: 10.1007/s10072-006-0578-y] [Medline: 16688637]
3. Calandre EP, Bembibre J, Arnedo ML, Becerra D. Cognitive disturbances and regional cerebral blood flow abnormalities in migraine patients: their relationship with the clinical manifestations of the illness. Cephalalgia 2002 May 01;22(4):291-302. [doi: 10.1046/j.1468-2982.2002.00370.x] [Medline: 12100092]
4. Le Pira F, Zappalà G, Giuffrida S, Lo Bartolo ML, Reggio E, Morana R, et al. Memory disturbances in migraine with and without aura: a strategy problem? Cephalalgia 2000 Jun 01;20(5):475-478. [doi: 10.1046/j.1468-2982.2000.00074.x] [Medline: 11037744]
5. Breslau N, Lipton RB, Stewart WF, Schultz LR, Welch KM. Comorbidity of migraine and depression: investigating potential etiology and prognosis. Neurology 2003 Apr 22;60(8):1308-1312. [doi: 10.1212/01.wnl.0000058907.41080.54] [Medline: 12707434]
6. Arnold M. Headache classification committee of the International Headache Society (IHS) the international classification of headache disorders, 3rd edition. Cephalalgia 2018 Jan 25;38(1):1-211. [doi: 10.1177/0333102417738202] [Medline: 29368949]
7. Lauterbur PC. Image formation by induced local interactions: examples employing nuclear magnetic resonance. Nature 1973 Mar;242(5394):190-191 [FREE Full text] [doi: 10.1038/242190a0]
8. Ogawa S, Lee TM, Kay AR, Tank DW. Brain magnetic resonance imaging with contrast dependent on blood oxygenation. Proc Natl Acad Sci U S A 1990 Dec;87(24):9868-9872 [FREE Full text] [doi: 10.1073/pnas.87.24.9868] [Medline: 2124706]
9. Davatzikos C. Why voxel-based morphometric analysis should be used with great caution when characterizing group differences. Neuroimage 2004 Sep;23(1):17-20. [doi: 10.1016/j.neuroimage.2004.05.010] [Medline: 15325347]
10. Li J, Zhao P. Deep learning applications in fMRI – a review work. In: Proceedings of the 12th International Conference on Bioscience, Biochemistry and Bioinformatics. 2023 Presented at: ICBBB '23; January 13-16, 2023; Tokyo, Japan p. 5 URL: https://dl.acm.org/doi/fullHtml/10.1145/3586139.3586150 [doi: 10.1145/3586139.3586150]
11. Li G, Song Y, Liang H, Sun X, Yu J, Zhai R, et al. Deep learning based diagnosis of mild cognitive impairment using resting-state functional MRI. J. Med. Biol. Eng 2024 Oct 30;44(6):809-820 [FREE Full text] [doi: 10.1007/s40846-024-00912-5]

XSL•FO
RenderX

12. Zeng Y, Ye Z, Zheng W, Wang J. Efficacy of cerebellar transcranial magnetic stimulation for post-stroke balance and limb motor function impairments: meta-analyses of random controlled trials and resting-state fMRI studies. Cerebellum 2024 Aug 27;23(4):1678-1696 [FREE Full text] [doi: 10.1007/s12311-024-01660-7] [Medline: 38280142]
13. Hadjikhani N, Ward N, Boshyan J, Napadow V, Maeda Y, Truini A, et al. The missing link: enhanced functional connectivity between amygdala and visceroceptive cortex in migraine. Cephalalgia 2013 Nov 29;33(15):1264-1268 [FREE Full text] [doi: 10.1177/0333102413490344] [Medline: 23720503]
14. Zhao L, Liu J, Dong X, Peng Y, Yuan K, Wu F, et al. Alterations in regional homogeneity assessed by fMRI in patients with migraine without aura stratified by disease duration. J Headache Pain 2013 Oct 17;14(1):85 [FREE Full text] [doi: 10.1186/1129-2377-14-85] [Medline: 24134520]
15. Yu D, Yuan K, Zhao L, Liang F, Qin W. Regional homogeneity abnormalities affected by depressive symptoms in migraine patients without aura: a resting state study. PLoS One 2013 Oct 16;8(10):e77933 [FREE Full text] [doi: 10.1371/journal.pone.0077933] [Medline: 24147100]
16. Xue T, Yuan K, Cheng P, Zhao L, Zhao L, Yu D, et al. Alterations of regional spontaneous neuronal activity and corresponding brain circuit changes during resting state in migraine without aura. NMR Biomed 2013 Sep 24;26(9):1051-1058. [doi: 10.1002/nbm.2917] [Medline: 23348909]
17. Petrušić I, Savić A, Mitrović K, Bačanin N, Sebastianelli G, Secci D, et al. Machine learning classification meets migraine: recommendations for study evaluation. J Headache Pain 2024 Dec 05;25(1):215 [FREE Full text] [doi: 10.1186/s10194-024-01924-x] [Medline: 39639193]
18. Ashina M, Terwindt GM, Al-Karagholi MA, de Boer I, Lee MJ, Hay DL, et al. Migraine: disease characterisation, biomarkers, and precision medicine. Lancet 2021 Apr 17;397(10283):1496-1504. [doi: 10.1016/S0140-6736(20)32162-0] [Medline: 33773610]
19. Szegedy C, Liu W, Jia Y, Sermanet P, Reed S, Anguelov D, et al. Going deeper with convolutions. In: Proceedings of the 2015 IEEE Conference on Computer Vision and Pattern Recognition. 2015 Presented at: CVPR '15; June 7-12, 2015; Boston, MA p. 1-9 URL: https://www.computer.org/csdl/proceedings-article/cvpr/2015/07298594/12OmNyOq4YE [doi: 10.1109/cvpr.2015.7298594]
20. He K, Zhang X, Ren S, Sun J. Deep residual learning for image recognition. In: Proceedings of the 2016 IEEE Conference on Computer Vision and Pattern Recognition. 2016 Presented at: CVPR '16; June 27-30, 2016; Las Vegas, NV p. 770-778 URL: https://ieeexplore.ieee.org/document/7780459 [doi: 10.1109/cvpr.2016.90]
21. Dosovitskiy A, Beyer L, Kolesnikov A, Weissenborn D, Zhai X, Unterthiner T, et al. An image is worth 16x16 words: transformers for image recognition at scale. arXiv. Preprint posted online on October 22, 2020 2020 [FREE Full text]
22. van der Velden BH, Kuijf HJ, Gilhuijs KG, Viergever MA. Explainable artificial intelligence (XAI) in deep learning-based medical image analysis. Med Image Anal 2022 Jul;79:102470 [FREE Full text] [doi: 10.1016/j.media.2022.102470] [Medline: 35576821]
23. Selvaraju RR, Cogswell M, Das A, Vedantam R, Parikh D, Batra D. Grad-CAM: visual explanations from deep networks via gradient-based localization. In: Proceedings of the 2017 IEEE International Conference on Computer Vision. 2017 Presented at: ICCV '17; October 22-29, 2017; Venice, Italy p. 618-626 URL: https://ieeexplore.ieee.org/document/8237336 [doi: 10.1109/iccv.2017.74]
24. Arrieta AB, Díaz-Rodríguez N, Del Ser J, Bennetot A, Tabik S, Barbado A, et al. Explainable Artificial Intelligence (XAI): concepts, taxonomies, opportunities and challenges toward responsible AI. Inf Fusion 2020 Jun;58:82-115. [doi: 10.1016/j.inffus.2019.12.012]
25. Sawilowsky S, Fahoome G. Kruskal-Wallis test: basic. In: Balakrishnan N, Colton T, Everitt B, Piegorsch WW, Ruggeri F, Teugels JL, editors. Wiley StatsRef: Statistics Reference Online. Hoboken, NJ: John Wiley & Sons; 2014.
26. Lowe MJ, Mock BJ, Sorenson JA. Functional connectivity in single and multislice echoplanar imaging using resting-state fluctuations. Neuroimage 1998 Feb;7(2):119-132. [doi: 10.1006/nimg.1997.0315] [Medline: 9558644]
27. Yu-Feng Z, He Y, Zhu CZ, Cao QJ, Sui MQ, Liang M, et al. Altered baseline brain activity in children with ADHD revealed by resting-state functional MRI. Brain Dev 2007 Mar;29(2):83-91 [FREE Full text] [doi: 10.1016/j.braindev.2006.07.002] [Medline: 16919409]
28. Dai Z, Yan C, Wang Z, Wang J, Xia M, Li K, et al. Discriminative analysis of early Alzheimer's disease using multi-modal imaging and multi-level characterization with multi-classifier (M3). Neuroimage 2012 Feb 01;59(3):2187-2195 [FREE Full text] [doi: 10.1016/j.neuroimage.2011.10.003] [Medline: 22008370]
29. Fox MD, Snyder AZ, Vincent JL, Corbetta M, Van Essen DC, Raichle ME. The human brain is intrinsically organized into dynamic, anticorrelated functional networks. Proc Natl Acad Sci U S A 2005 Jul 05;102(27):9673-9678 [FREE Full text] [doi: 10.1073/pnas.0504136102] [Medline: 15976020]
30. Jiang T, He Y, Zang Y, Weng X. Modulation of functional connectivity during the resting state and the motor task. Hum Brain Mapp 2004 May;22(1):63-71 [FREE Full text] [doi: 10.1002/hbm.20012] [Medline: 15083527]
31. Liu (, Karagoz G, Meratnia N. Analyzing the impact of data augmentation on the explainability of deep learning-based medical image classification. Mach Learn Knowl Extr 2024 Dec 25;7(1):1 [FREE Full text] [doi: 10.3390/make7010001]

XSL•FO
RenderX

32. Chlap P, Min H, Vandenberg N, Dowling J, Holloway L, Haworth A. A review of medical image data augmentation techniques for deep learning applications. J Med Imaging Radiat Oncol 2021 Aug;65(5):545-563 [FREE Full text] [doi: 10.1111/1754-9485.13261] [Medline: 34145766]
33. Simonyan K, Zisserman A. Very deep convolutional networks for large-scale image recognition. arXiv. Preprint posted online on September 4, 2014 2014 [FREE Full text]
34. Bottou L. Stochastic gradient descent tricks. In: Montavon G, Orr GB, Müller KR, editors. Neural Networks: Tricks of the Trade. Berlin, Germany: Springer; 2012.
35. Hao Y, Dong L, Wei F, Xu K. Self-attention attribution: interpreting information interactions inside transformer. Proc AAAI Conf Artif Intell 2021 May 18;35(14):12963-12971. [doi: 10.1609/aaai.v35i14.17533]
36. Du C, Wang Y, Wang C, Shi C, Xiao B. Selective feature connection mechanism: concatenating multi-layer CNN features with a feature selector. Pattern Recognit Lett 2020 Jan;129:108-114. [doi: 10.1016/j.patrec.2019.11.015]
37. Bradley AP. The use of the area under the ROC curve in the evaluation of machine learning algorithms. Pattern Recognit 1997 Jul;30(7):1145-1159. [doi: 10.1016/s0031-3203(96)00142-2]
38. Kim B, Mathai TS, Helm K, Pinto PA, Summers RM. Classification of multi-parametric body MRI series using deep learning. IEEE J Biomed Health Inform 2024 Nov;28(11):6791-6802 [FREE Full text] [doi: 10.1109/jbhi.2024.3448373]
39. Zhang Q, Wu Q, Zhang J, He L, Huang J, Zhang J, et al. Discriminative analysis of migraine without aura: using functional and structural MRI with a multi-feature classification approach. PLoS One 2016 Sep 30;11(9):e0163875 [FREE Full text] [doi: 10.1371/journal.pone.0163875] [Medline: 27690138]
40. Luo W, Li Y, Urtasun R, Zemel R. Understanding the effective receptive field in deep convolutional neural networks. arXiv. Preprint posted online on January 15, 2017 2017 [FREE Full text]
41. Tzourio-Mazoyer N, Landeau B, Papathanassiou D, Crivello F, Etard O, Delcroix N, et al. Automated anatomical labeling of activations in SPM using a macroscopic anatomical parcellation of the MNI MRI single-subject brain. Neuroimage 2002 Jan;15(1):273-289. [doi: 10.1006/nimg.2001.0978] [Medline: 11771995]
42. Winter AC, Berger K, Buring JE, Kurth T. Associations of socioeconomic status with migraine and non-migraine headache. Cephalalgia 2012 Jan;32(2):159-170 [FREE Full text] [doi: 10.1177/0333102411430854] [Medline: 22174348]
43. Li Z, Zeng F, Yin T, Lan L, Makris N, Jorgenson K, et al. Acupuncture modulates the abnormal brainstem activity in migraine without aura patients. Neuroimage Clin 2017;15:367-375 [FREE Full text] [doi: 10.1016/j.nicl.2017.05.013] [Medline: 28580293]
44. Wang JJ, Chen X, Sah SK, Zeng C, Li YM, Li N, et al. Amplitude of low-frequency fluctuation (ALFF) and fractional ALFF in migraine patients: a resting-state functional MRI study. Clin Radiol 2016 Jun;71(6):558-564. [doi: 10.1016/j.crad.2016.03.004] [Medline: 27055741]
45. Faragó P, Tuka B, Tóth E, Szabó N, Király A, Csete G, et al. Interictal brain activity differs in migraine with and without aura: resting state fMRI study. J Headache Pain 2017 Dec 25;18(1):8 [FREE Full text] [doi: 10.1186/s10194-016-0716-8] [Medline: 28124204]
46. Boccia M, Sulpizio V, Teghil A, Palermo L, Piccardi L, Galati G, et al. The dynamic contribution of the high-level visual cortex to imagery and perception. Hum Brain Mapp 2019 Jun 01;40(8):2449-2463 [FREE Full text] [doi: 10.1002/hbm.24535] [Medline: 30702203]
47. Dumkrieger G, Chong CD, Ross K, Berisha V, Schwedt TJ. Static and dynamic functional connectivity differences between migraine and persistent post-traumatic headache: a resting-state magnetic resonance imaging study. Cephalalgia 2019 Oct 01;39(11):1366-1381. [doi: 10.1177/0333102419847728] [Medline: 31042064]
48. Bohning DE, Pecheny AP, Epstein CM, Speer AM, Vincent DJ, Dannels W, et al. Mapping transcranial magnetic stimulation (TMS) fields in vivo with MRI. Neuroreport 1997 Jul 28;8(11):2535-2538. [doi: 10.1097/00001756-199707280-00023] [Medline: 9261822]
49. Migraine_XAI. GitHub. URL: https://github.com/yanghaoljx/Migraine_XAI [accessed 2025-05-29]

Abbreviations

AAL: automated anatomical labeling
ALFF: amplitude of low-frequency fluctuation
AUC: area under the curve
BOLD: blood oxygenation level–dependent
CNN: convolutional neural network
FC: functional connectivity
fMRI: functional magnetic resonance imaging
Grad-CAM: gradient-weighted class activation mapping
HC: healthy control
LOOCV: leave-one-out cross-validation
MRI: magnetic resonance imaging
MWA: migraine with aura

XSL•FO
RenderX

MWoA: migraine without aura
ReHo: regional homogeneity
RFCS: regional functional connectivity strength
ROC: receiver operating characteristic curve
rs-fMRI: resting-state functional magnetic resonance imaging
ViT: Vision Transformer
XAI: explainable artificial intelligence

Edited by A Coristine; submitted 04.02.25; peer-reviewed by J Lei, C Zhang, I Odezuligbo, G Ma; comments to author 24.03.25; revised version received 26.05.25; accepted 30.07.25; published 03.09.25.

Please cite as:
Li G, Yang H, He L, Zeng G
Interpretable Artificial Intelligence Analysis of Functional Magnetic Resonance Imaging for Migraine Classification: Quantitative Study
JMIR Med Inform 2025;13:e72155
URL: https://medinform.jmir.org/2025/1/e72155
doi:10.2196/72155
PMID:

©Guohao Li, Hao Yang, Li He, Guojun Zeng. Originally published in JMIR Medical Informatics (https://medinform.jmir.org), 03.09.2025. This is an open-access article distributed under the terms of the Creative Commons Attribution License (https://creativecommons.org/licenses/by/4.0/), which permits unrestricted use, distribution, and reproduction in any medium, provided the original work, first published in JMIR Medical Informatics, is properly cited. The complete bibliographic information, a link to the original publication on https://medinform.jmir.org/, as well as this copyright and license information must be included.

XSL•FO
RenderX

Development of a New Electronic Death Certificate and Death Management Module Integrated Into the Health Information System of a Tertiary Hospital in Mali: Implementation Report

Mahmoud Cissé[1,2], MD, MPH; Mahamoudane Niang[1,3], MD, MPH; Abdrahamane Anne[1,2]; Mariam Sidibé[1]; Dramane Traoré[1], MD; Abdoulaye Traoré[1]; Idrissa Traoré[1]; Cheick Oumar Bagayoko[1,2], MD, PhD

[1]Center for Expertise and Research in Telemedicine and E-Health - CERTES, Bamako, Mali

[2]Department of Study and Research in Public Health (DERSP), Faculty of Medicine and Odontostomatology (FMOS), University of Sciences, Techniques and Technologies of Bamako, Bamako, Mali

[3]Mother and Child Hospital, Bamako, Mali

Corresponding Author:
Mahmoud Cissé, MD, MPH
Center for Expertise and Research in Telemedicine and E-Health - CERTES, Bamako, Mali

Abstract

Background: Death certification provides reliable epidemiological data that are essential for public health decision-making. Implementing an electronic death certificate improves data quality, accuracy, and timeliness. Recognizing its importance, we developed and integrated a mortality management module into the hospital "Le Luxembourg," enhancing mortality data collection and utilization.

Objective: This implementation aimed to improve the completeness and accuracy of mortality data, accelerate the timeliness of death reporting, and facilitate the downstream use of data to inform public health planning and research.

Methods: We began by analyzing the existing infrastructure and organizational setup within the hospital. Through a series of interviews, we identified the needs of all users, enabling the design of a module suited to all levels of operation. We implemented a module comprising multiple functionalities, including certificate editing, validation, storage, mortality statistics generation. It also integrates *ICD-10* coding and follows the World Health Organization (WHO) model, while remaining adapted to the hospital's specific context. To ensure optimal usability, we assembled a project team that included a mortality audit committee. After implementation, all users received training and continuous direct technical support was provided.

Results: We developed a new death certificate model in line with WHO recommendations. Access to the certificate is secured by a unique username and password. To improve data quality, the certification process involves several validation steps: initial recording, which can be modified when the medical section is not completed by a senior physician; pre-validation by the senior physician and final validation by the mortality audit committee. The chain of morbid events is documented using *ICD-10* diagnoses. Beyond the certificate itself, the system also allows for civil registration of the death. Moreover, the module can generate statistics based on multiple criteria. This process takes place with the involvement and active engagement of all stakeholders.

Conclusions: We established a unique, secure, WHO-compliant death certificate model that ensures high-quality, easily exploitable, and well-archived data. The experience of this hospital may serve as a foundation for scaling up this model to other healthcare facilities within the country.

(JMIR Med Inform 2025;13:e62949) doi:10.2196/62949

KEYWORDS

death certificate; hospital Information Systems; international classification of diseases; vital statistics; digital health

Introduction

Background

Knowledge of the causes of mortality is an integral part of the foundation of public health policies, strategies and programs [1]. Death certification plays a central role in the collection of demographic and epidemiological data worldwide. Not only does it identify the causes of mortality, it is also a fundamental tool for guiding public health policies.

For several years now, high-income countries, notably in Europe and North America, have been deploying electronic death certification systems to improve the efficiency, accuracy and speed of the information collected [2,3]. For example, France introduced such a system in 2007 with the CertDc project to gradually replace traditional paper forms [3]. In Portugal, a

XSL•FO
RenderX

similar system has been in place since 2013, having made a 100% successful transition from paper to electronic certification after 2 years.

The advantages of such a system are multiple. Firstly, digitizing the process eliminates manual transcription errors, but also speeds up data processing, as shown by a French study on the contribution of electronic certification [4].

In Africa, where the civil registry system is still largely dominated by traditional methods, the need for modernization is pressing. The United Nations Economic Commission for Africa (UNECA) report on death registration highlights that of the 46 World Health Organization (WHO) member states in the African region, only 1 can provide high-quality cause-of-death data (Mauritius), and 3 others can provide low- or medium-quality data (ie, South Africa, Seychelles and Zimbabwe) [5]. Nevertheless, we noted a few rare initiatives, such as Burkina Faso's implementation of an electronic death certificate at Bobo University Hospital [6].

On the other hand, Mali like many other African countries, faces similar challenges, notably insufficient coverage of the civil registry system, delays in the transmission of paper death certificates and frequent errors in data collection.

These aspects reduce the quality of national and international mortality statistics and limits their value for health planning and health policy development [7]. Mali is no exception, despite its high maternal, infant, child, infant-child and neonatal mortality rates [8]

In Mali, death certificates vary across health facilities and even within the same hospital. Some services lack a standard form, relying on handwritten notes. This inconsistency limits mortality data availability and accuracy, with records often incomplete, containing only basic details like name, sex, date of death, and a vague diagnosis (eg, cardio-respiratory arrest). Archiving is neither systematic nor organized, and copies are not always retained. Deaths are often tracked by marking "Deceased" or "DCD" in patient registers.

To overcome these problems, we need adapted and harmonized methods and tools that comply with certain norms and standards, and the advantage of using digital tools in our context is no longer in doubt [8-10].

The hospital "Le Luxembourg" in Bamako initiated a system to digitize and integrate the death certificate into its Health Information System (HIS) to improve mortality data management. Despite its technical capacity and nationwide patient intake, it faced challenges similar to other health facilities in collecting and using mortality data. Recording 556 deaths annually, the hospital wants to develop an electronic death certificate for better archiving and data use, as detailed in this implementation report.

Objectives

The implementation aimed to improve the completeness and accuracy of mortality data, accelerate the timeliness of death reporting, and facilitate the downstream use of data to inform public health planning and research.

Methods

Conception and Development

This project was part of a thesis internship, led by a student with support from the Center for Expertise and Research in Telemedicine and E-Health (CERTES), which maintains the HIS. Implemented at the hospital "Le Luxembourg," it involved system analysis, requirement collection, and specifications drafting. Development took three months, carried out by two CERTES developers and the student.

For the successful implementation of the project, a team was established, composed of the head of the public health and medical informatics department of "Le Luxembourg" Hospital, the trainee, the developers of the Cinz@n (HIS), the users represented by doctors (ie, residents, general practitioners, and specialists), nurses from various departments, and the hospital registrar.

All users were involved from the design phase through interviews aimed at understanding their needs. Physicians participated in the validation of the medical component, while administrative staff contributed to the design of the printable certificate. Their involvement facilitated acceptance of the new process.

Analysis of the ongoing certification process and HIS

When a death occurs or is confirmed on arrival, a doctor or resident issues a death certificate in duplicate. One copy is provided to the family for administrative use, while the other serves as proof for body deposit and burial. The deceased's name is recorded in consultation registers or a dedicated logbook, but no cause of death is documented.

At the end of each month, hospital staff manually count the number of deaths and submit a monthly activity report to the HIS officer, who enters the data into DHIS2, a national HIS. However, this report lacks patient demographics and cause-of-death details.

The hospital operates Cinz@n, a PHP/MySQL-based HIS that integrates patient records, consultations, hospitalization, pharmacy, and related data. However, it does not track death records.

New electronic certification process implemented

A new digital death certification system has been introduced to improve record accuracy and medical data storage. This system ensures that both administrative and medical information are electronically archived in Cinz@n for statistical purposes. The key actors in the certification process are: doctors and residents, nurses, civil registrar and death audit committee.

The module includes the following key functionalities:

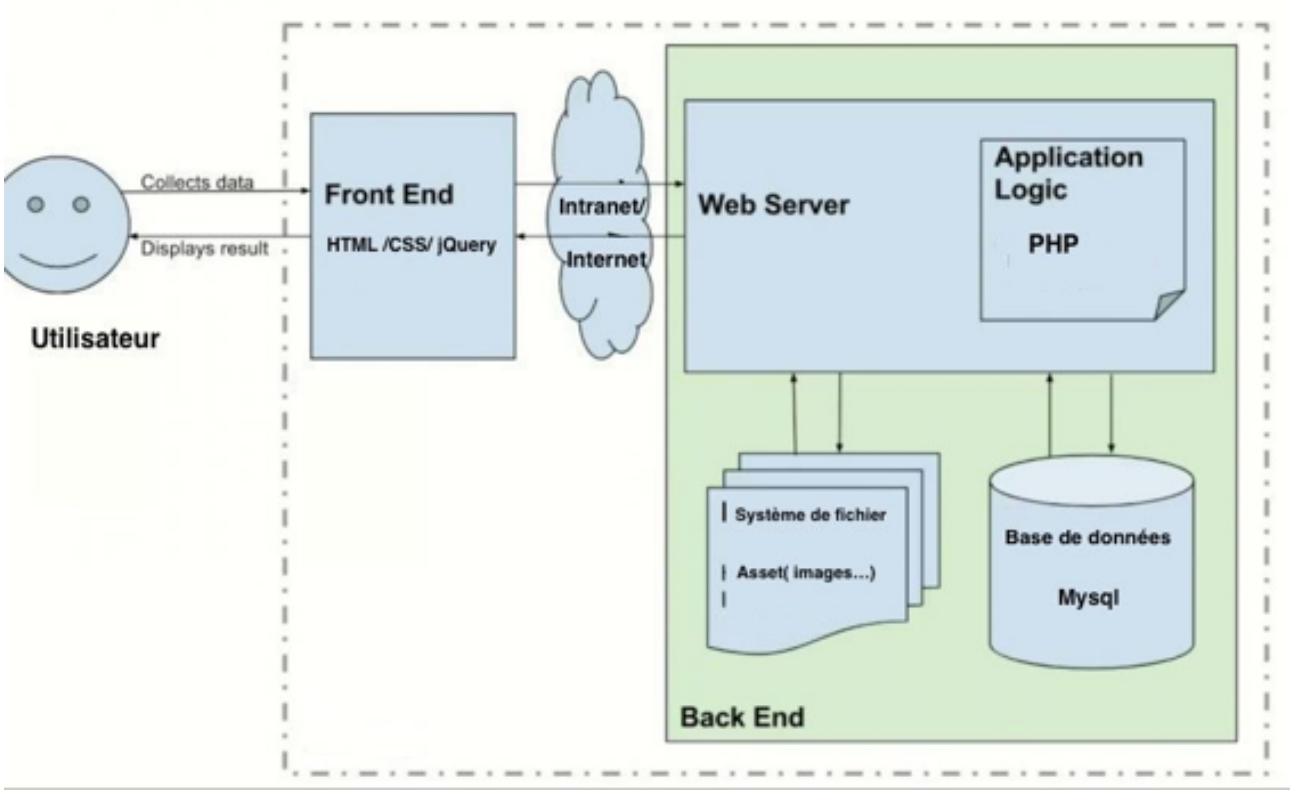
- Generation of death certificates: This feature is composed of two main sections:
- An administrative section that records patient identity, hospital details, time of death, and burial information
- A medical section that digitally captures cause-of-death details, comorbidities, and relevant external factors

XSL•FO
RenderX

- Deceased patients list: a searchable registry of all recorded deaths within the facility
- Certificates pending preliminary validation: death certificates awaiting review and approval by a senior physician
- Certificates pending final validation: certificates that have not yet been approved by the audit committee
- Archived certificates: a secure and structured repository of validated death certificates
- Statistical dashboard: aggregated data on mortality trends by sex, age, hospital unit, causes of death, and more
- Configuration panel: allows customization of fields, labels, access rights, and other module parameters

The module architecture is based on that of the HIS "*Cinz@n*" (Figure 1).

Figure 1. Architecture of the HIS "Cinz@n". HIS: Health information system; PHP: Hypertext preprocessor.



In terms of security, the server ensures security by recognizing devices using encrypted authentication, tracking access logs, and deactivating accounts after three failed attempts. A dedicated backup server ensures regular and secure data replication to prevent loss. User access is profile-based, ensuring that each stakeholder (ie, physicians, administrators, civil registry officers) can only access the information relevant to their responsibilities.

The module integrates International Classification of Diseases, Tenth Revision (*ICD-10)* for causes of death, consultations, and comorbidities, while Cinz@n uses the same patient ID and HL7 (Health Level Seven) standards, to facilitate the integration of this module into other systems.

A total of 66 users including 33 doctors, 26 resident doctors, 6 nurses, and 1 midwife, were trained to use the death module and code causes of death. The training consisted of lectures, practical tutorials, and WHO-provided exercises to enhance proficiency.

Budget Report

The project required no additional budget as the hospital already had the necessary infrastructure. The module is maintained internally by the hospital's medical informatics department, with updates managed by a trained technical focal point. With maintenance limited to software support, the solution is sustainable without external funding. Its design also allows for easy deployment in other hospitals using the same HIS.

Ethical Considerations

This project, integrated into routine hospital activities, aimed only to digitalize the death certificate and enable the secure storage and structured use of mortality data. No sensitive or identifiable patient information was used, and no direct interaction with patients or their relatives occurred. In accordance with local guidelines, no ethical approval was required. Data confidentiality and security were strictly maintained.

This manuscript complies with the implementation reporting guidelines [11].

Implementation (Results)

Coverage and Stage

After the design and development phases, we implemented a new model of death certificate at the hospital "Le Luxembourg," which included an administrative (Multimedia Appendix 1) and medical (Multimedia Appendix 2) component. This

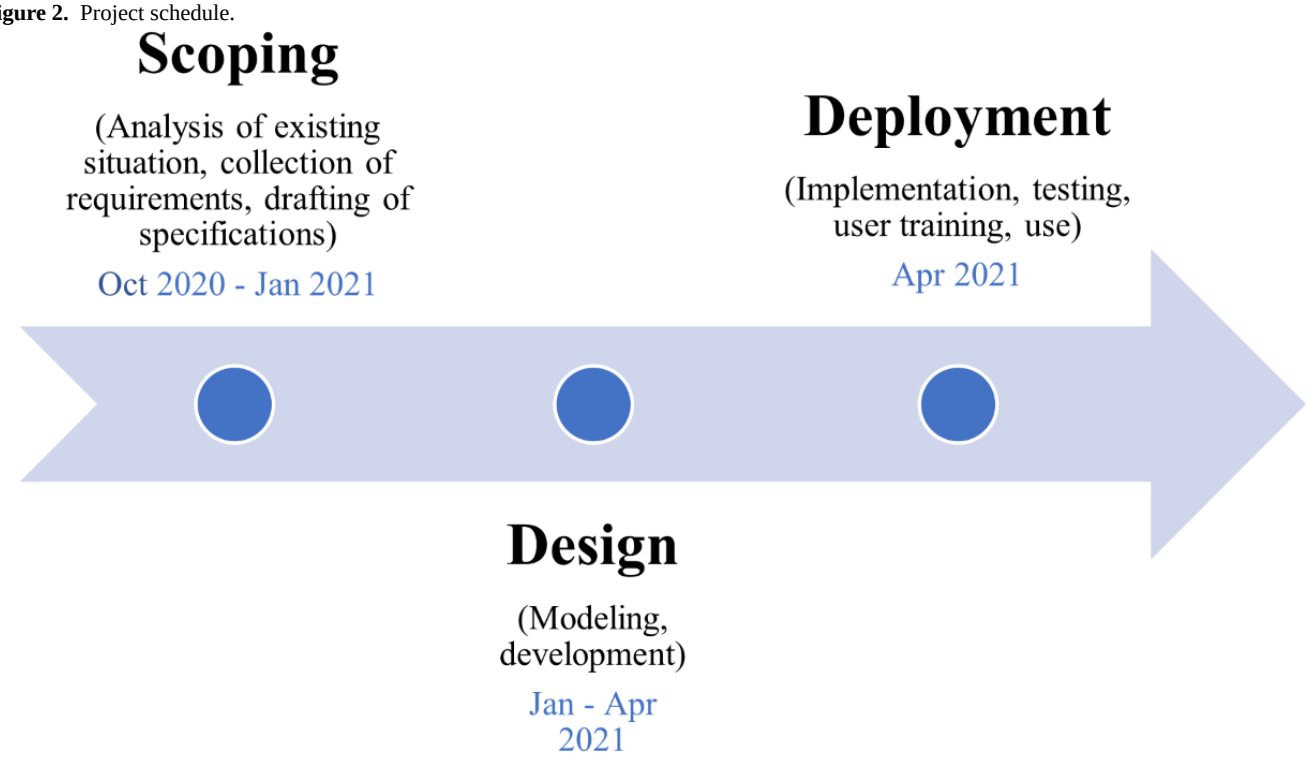
XSL•FO
RenderX

multifunctional death management module (Multimedia Appendix 3) is now integrated into the HIS. Before implementation, from a methodological standpoint, we adopted an iterative approach, starting with an initial prototype tested in one hospital department, which was then improved through several short cycles, incorporating user feedback at each stage.

User feedback at the end of each training session and two months postimplementation indicated a high level of satisfaction. This was especially attributed to the ease of access to patient information and the automatic generation of certificates.

The project timeline is presented in Figure 2.

Figure 2. Project schedule.



To access the death management module, users require a username and password. Key features include creating death certificates, listing deceased patients, viewing certificates awaiting prevalidation and validation, accessing archived certificates, statistics, and settings.

Users can search for a patient using an ID number, name, or phone number before issuing a death certificate.

The "Establish a Death Certificate" menu integrates both administrative and medical components. Administrative data (Multimedia Appendix 4) are automatically retrieved from the patient's record. The medical section (Multimedia Appendix 5) also pulls relevant information, including reason for admission and comorbidities, with *ICD-10* used for cause-of-death coding.

The validation process follows a structured approach. Automatic alerts remind doctors to correct pending certificates, and pop-ups confirm actions before validation. This validation process ensures data quality, with data being easily obtained and managed from the dedicated menu. Users can filter data and export reports in the Microsoft Excel format for further analysis.

A dedicated interface allows the civil registrar to access the administrative section of the certificate and process official death declarations. By searching the deceased's ID number, the registrar records details of the declarant (ie, relative) before confirming the declaration. Once completed, the entry becomes inactive and validated.

Within three months of implementation, a total of 62 death certificates were recorded. Although the volume appears modest, the key value of the system lies in the structured storage and availability of comprehensive mortality data.

Lessons Learned, Key Success Factors, and Failure

The success of the project was driven by strong leadership, particularly the involvement of key institutional figures such as the heads of the medical informatics department and the medical board. Integrating the module directly into the existing HIS, rather than creating a parallel system, greatly facilitated adoption. Initial resistance from users was overcome through training and support. The inclusion of *ICD-10* coding improved data quality and encouraged broader use of the system. Academic clinicians engaged early, motivated by access to structured data for research. The availability of IT infrastructure also played a critical role. However, limited staff numbers in departments hindered real-time data entry, underscoring the need to consider workforce constraints in future implementations.

Discussion

Principal Findings

Our results emphasize the need to standardize mortality data collection. We developed Mali's first electronic death certificate, aligning with WHO recommendations.

XSL•FO
RenderX

This improvement in data quantity and quality was found by Lefeuvre D et al [12] in a study on the quality of electronic and paper death certificates in France in 2010. Our results highlight challenges such as inconsistent certificates, missing forms, incomplete data, and confidentiality concerns.

The implementation of ICD-10 for coding causes of death improves data reliability and allows international comparability [13].

Reliable mortality data support effective health policies. Accurate coding aids in reducing maternal and child mortality, while the new database improves data archiving and accessibility.

Electronic data storage is undeniably better than traditional storage, optimizing record search and use [14,15]. Our structured approach incorporating an alert system and a multilevel correction and validation process, serves not only to secure data confidentiality but also to elevate the overall data quality, enabling greater precision and accuracy, all of which are part of data quality criteria [16].

Our work introduced many doctors to *ICD-10*, which is not currently part of medical education or patient records in Mali. For civil registrars, digital certificates and automatic searches improved death declarations. The statistics module in Cinz@n enables multicriteria searches and better data analysis.

From an implementation perspective, this work confirmed that successful digital health integration relies on strong institutional leadership, alignment with existing systems, and user engagement. Embedding the module within the current HIS facilitated adoption and minimized resistance, especially when paired with targeted training and ongoing support. The integration of *ICD-10* coding improved data quality and encouraged broader use of the medical record. The involvement of academic clinicians, driven by their need for structured data, further enhanced project ownership. However, limited staffing constrained timely data entry, highlighting the need to consider workforce capacity in similar initiatives. Overall, the project illustrates that a user-centered, standards-based, and system-integrated approach can enhance the adoption and sustainability of digital health tools.

Limitations of Study

One limitation of the project is the absence of a formal long-term evaluation of its impact on the quality of mortality data

Bests Practices and Recommendations

The lessons we have learned are

- The importance of carrying out an analysis of existing user needs as the basis for the success of such a project;
- The advantage of having pre-existing IT infrastructure;
- The academic incentives can strengthen adoption;
- The need for a clear description and definition of the role of each player in the process;
- Setting up a monitoring and steering committee, in our case the death audit committee;
- Training and support for users throughout the implementation process.

Following our work, we recommend:

- Ensuring early involvement of institutional leaders and stakeholders to build trust and alignment
- Prioritizing integration with existing systems to streamline workflows and reduce change management efforts
- Anticipating and addressing workforce constraints by exploring strategies such as task redistribution or automation.
- Investing in tailored user training and post-deployment support to facilitate adoption
- Engaging academic staff by linking system outputs with research and publication opportunities

Acknowledgments

We extend our sincere thanks to everyone who contributed to the success of this project, with special appreciation to the Center for Expertise and Research in Telemedicine and E-Health (CERTES) team for their technical support. We also thank the hospital staff and administration for their valuable assistance. A special acknowledgment goes to Jacky and Michèle Borghini, Janine Guex, Pierre Marie Leibzig, Johan Roelant, and Dr. Sophie Delaigue for proofreading the document and for their generous support throughout the process. We are also deeply grateful to the Journal of Medical Internet Research (JMIR) for granting us a full waiver of the Article Processing Fee, thereby making the publication of this work possible.

All authors declared that they had insufficient funding to support open access publication of this manuscript, including from affiliated organizations or institutions, funding agencies, or other organizations. JMIR Publications provided article processing fee (APF) support for the publication of this article.

Conflicts of Interest

None declared.

Multimedia Appendix 1
Administrative component of the new model of death certificate.
[PNG File, 988 KB - medinform_v13i1e62949_app1.png]

XSL•FO
RenderX

Multimedia Appendix 2
Medical component of the new model of death certificate.
[PNG File, 153 KB - medinform_v13i1e62949_app2.png]

Multimedia Appendix 3
Interface to the Death Module in the Cinzan HIS.
[PNG File, 105 KB - medinform_v13i1e62949_app3.png]

Multimedia Appendix 4
Completing the administrative section of the death certificate.
[PNG File, 369 KB - medinform_v13i1e62949_app4.png]

Multimedia Appendix 5
Completing the medical section of the death certificate.
[PNG File, 1258 KB - medinform_v13i1e62949_app5.png]

Checklist 1
iCHECK-DH checklist
[DOCX File, 29 KB - medinform_v13i1e62949_app6.docx]

References

1. Rampatige R, Mikkelsen L, Hernandez B, Riley I, Lopez AD. Systematic review of statistics on causes of deaths in hospitals: strengthening the evidence for policy-makers. Bull World Health Organ 2014 Nov 1;92(11):807-816. [doi: 10.2471/BLT.14.137935] [Medline: 25378742]
2. CDC/NCHS, National Center for Health Statistics. National vital statistics system improvements. 2021.
3. Rey G. Les données des certificats de décès en France: processus de production et principaux types d'analyse. La Revue de Médecine Interne 2016 Oct;37(10):685-693. [doi: 10.1016/j.revmed.2016.01.011]
4. Seriot PE. L'usage du certificat de décès électronique par les médecins exerçants en structure impliquée dans la permanence des soins ambulatoires: etat des lieux des pratiques et ressenti sur l'application mobile certdc au sein de l'association SOS médecins amiens. Thèse de médecine Université de Picardie Jules Verne / Unité De Formation et de Recherche de médecine d'Amiens. 2022. URL: https://dumas.ccsd.cnrs.fr/dumas-04084761v1/document [accessed 2024-04-07]
5. United Nations Economic Commission for Africa. Décennie du repositionnement de l'enregistrement des faits d'état civil et des statistiques de l'état civil en Afrique. : Enregistrement des décès. Éthiopie: United Nations Economic Commission for Africa; 2016 URL: https://archive.uneca.org/sites/default/files/uploaded-documents/ACS/4th-CoM-on-CRVS/report-on-the-status-of-civil-registration-and-vital-statistics-in-africa_fr.pdf [accessed 2025-05-01]
6. Barro GS, Staccini P. Certification Des Causes de Décès En Afrique: « Analyse de Modèle Au CHU Souro Sanou de Bobo Dioulasso, Burkina Faso: Aix Marseille Université; 2014. [doi: 10.3233/978-1-61499-432-9-1110]
7. Naghavi M, Richards N, Chowdhury H, et al. Improving the quality of cause of death data for public health policy: are all "garbage" codes equally problematic? BMC Med 2020 Mar 9;18(1):55. [doi: 10.1186/s12916-020-01525-w] [Medline: 32146899]
8. Mikkelsen L, Moesgaard K, Hegnauer M, Lopez AD. ANACONDA: a new tool to improve mortality and cause of death data. BMC Med 2020 Mar 9;18(1):61. [doi: 10.1186/s12916-020-01521-0] [Medline: 32146907]
9. Brooks EG, Reed KD. Principles and pitfalls: a guide to death certification. Clin Med Res 2015 Jun;13(2):74-82. [doi: 10.3121/cmr.2015.1276] [Medline: 26185270]
10. Barro GS, Dufour JC, Traoré IA, Staccini P. Évaluation de la qualité du dispositif de codage automatisé des causes de décès dans un hôpital d'Afrique Bobo Dioulasso, Burkina Faso. Revue D'Épidémiologie et de Santé Publique 2014 Sep;62:S197-S198. [doi: 10.1016/j.respe.2014.06.086]
11. Perrin Franck C, Babington-Ashaye A, Dietrich D, et al. iCHECK-DH: guidelines and checklist for the reporting on digital health implementations. J Med Internet Res 2023;25:e46694. [doi: 10.2196/46694]
12. Lefeuvre D, Pavillon G, Aouba A, et al. Quality comparison of electronic versus paper death certificates in France, 2010. Popul Health Metr 2014 Feb 17;12(1):3. [doi: 10.1186/1478-7954-12-3] [Medline: 24533639]
13. Mremi IR, Rumisha SF, Chiduo MG, et al. Hospital mortality statistics in Tanzania: availability, accessibility, and quality 2006-2015. Popul Health Metr 2018 Nov 20;16(1):16. [doi: 10.1186/s12963-018-0175-3] [Medline: 30458804]
14. Wang B, Lai J, Liu M, Jin F, Peng Y, Yao C. Electronic source data transcription for electronic case report forms in China: validation of the electronic source record tool in a real-world ophthalmology study. JMIR Form Res 2022 Dec 16;6(12):e43229. [doi: 10.2196/43229] [Medline: 36525285]
15. Olsen IC, Haavardsholm EA, Moholt E, Kvien TK, Lie E. NOR-DMARD data management: implementation of data capture from electronic health records. Clin Exp Rheumatol 2014;32(5 Suppl 85):S-158. [Medline: 25365108]

XSL•FO
RenderX

16. Ehsani-Moghaddam B, Martin K, Queenan JA. Data quality in healthcare: a report of practical experience with the Canadian Primary Care Sentinel Surveillance Network data. HIM J 2021 Jan;50(1-2):88-92. [doi: 10.1177/1833358319887743]

Abbreviations

HIS: Health Information System
ICD-10: International Classification of Diseases, Tenth Revision
WHO: World Health Organization

Edited by C Perrin; submitted 05.06.24; peer-reviewed by G Rey, PP Pastor, SP Akhade; revised version received 30.07.25; accepted 30.07.25; published 18.09.25.

Please cite as:
Cissé M, Niang M, Anne A, Sidibé M, Traoré D, Traoré A, Traoré I, Bagayoko CO
Development of a New Electronic Death Certificate and Death Management Module Integrated Into the Health Information System of a Tertiary Hospital in Mali: Implementation Report
JMIR Med Inform 2025;13:e62949
URL: https://medinform.jmir.org/2025/1/e62949
doi:10.2196/62949

© Mahmoud Cissé, Mahamoudane Niang, Abdrahamane Anne, Mariam Sidibé, Dramane Traoré, Abdoulaye Traoré, Idrissa Traoré, Cheick Oumar Bagayoko. Originally published in JMIR Medical Informatics (https://medinform.jmir.org), 18.9.2025. This is an open-access article distributed under the terms of the Creative Commons Attribution License (https://creativecommons.org/licenses/by/4.0/), which permits unrestricted use, distribution, and reproduction in any medium, provided the original work, first published in JMIR Medical Informatics, is properly cited. The complete bibliographic information, a link to the original publication on https://medinform.jmir.org/, as well as this copyright and license information must be included.

XSL•FO
RenderX

Lessons Learned From Building a Data Platform for Longitudinal, Analytical Use Cases and Scaling to 77 German Hospitals: Implementation Report

Markus Bockhacker[1], Dr med, MSc; Peter Martens[2], MSc; Clara von Münchow[1], MSc; Sarah Löser[2], MSc; Rosita Günther[1], Ass iur; Ralf Kuhlen[3], Prof Dr med; Olaf Kannt[1], Prof Dr med, MBA; Sebastian Ortleb[1], MSc

[1]Helios Kliniken, Friedrichstraße 136, Berlin, Germany

[2]Helios IT Service GmbH, Berlin, Germany

[3]Helios Health Institute, Berlin, Germany

Corresponding Author:
Sebastian Ortleb, MSc
Helios Kliniken, Friedrichstraße 136, Berlin, Germany

Abstract

Background: Increasing adoption of electronic health records (EHRs) enables research on real-world data. In Germany, this has been limited to university hospitals, and data from acute care hospitals below the university level are lacking. To address this, we used established design patterns to build a data platform that aggregates and standardizes pseudonymized EHR data with patients' consent.

Objective: We report on the design and implementation of the research platform, as well as patient participation and lessons learned during the scaling of the platform, to incorporate real-world data (with participant consent) from 77 hospitals into a unified data lake.

Methods: Due to variations in EHR adoption, IT infrastructure, software vendors, interface availability, and regulatory requirements, we used an agile development cycle that involves constant, incremental standardization of data. We implemented a layered lambda infrastructure built on Apache Hadoop. Decentralized connectors ensured data minimization and pseudonymization.

Implementation (Results): We successfully scaled our data model both vertically and horizontally in 77 hospitals. However, we encountered issues during the scaling of real-time data pipelines and IHE (Integrating the Healthcare Enterprise) interfaces. During the first 2 years, patients were asked to consent to secondary data use 1,475,244 times during inpatient admission. We registered 1,023,633 broad instances of consent (consent rate 70.2%).

Conclusions: Patients are generally willing to provide consent for secondary use of their data, but obtaining consent requires considerable effort. Building a research data platform is not an end goal, but rather a necessary step in collecting and standardizing longitudinal data to enable research on real-world data. Through the combination of agile development, phased rollouts, and very high levels of automation, we have been able to achieve fast turnaround times for incorporating user feedback and are constantly improving data quality and standardization.

(JMIR Med Inform 2025;13:e69853) doi:10.2196/69853

KEYWORDS

research platform; secondary data use; data science; Hadoop; broad consent; medical informatics

Introduction

Adoption of electronic health record (EHR) systems has continuously increased in Germany over the past 20 years [1], mainly driven by billing requirements and mandatory digital reporting for quality management. EHR data hold promise for medical quality assurance as well as clinical and health services research [2-4], referred to as secondary data use. However, data silos limit accessibility and hinder cross-institutional analyses.

In 2018, the German Ministry of Health initiated a national health data platform for research on real-world data collected from university hospitals. As part of the German Medical Informatics Initiative, several consortia received funding to develop Health Level Seven (HL7) Fast Healthcare Interoperability Resources (FHIR) models [5], governance processes [6-8], and a broad consent standard for secondary data use [9]. Although European Union and national laws regulate secondary use, consent is typically required to use such data for medical research in Germany [10]. The Helios Hospital

XSL•FO
RenderX

group, operating more than 89 acute care hospitals and 230 outpatient care centers in Germany as of December 2024, has championed voluntary data collection and reporting for quality management, enabling cross-institutional research and peer review [11-14]. Secondary analysis of claims data across our hospital network has already generated insights into admission rates and mortality during the COVID-19 pandemic [15-17]. Existing data centers, network infrastructure, and a unified IT department enable us to build a data platform for secondary data analysis of EHR, quality assurance, and claims datasets in-house.

Methods

Aims and Objective

We describe the design and implementation of a cross-institutional, multidomain data and analytics platform with a modular data model across our organization. While similar platforms have been described for one or a few institutions [18-24], integrating multiple hospitals with differing EHR systems presents unique, yet undocumented challenges [25]. We emphasize highlighting these challenges and presenting our lessons learned for scaling a data platform across diverse software systems, regions, and data domains. Specific research projects are beyond this paper's scope. We used iCHECK-DH (Guidelines and Checklist for the Reporting on Digital Health Implementations) [26] to structure this report.

Requirements Engineering

Upon project initiation, we assembled a cross-functional team comprising research, compliance, project management, and engineering members to ascertain requirements. We considered both data and user perspectives in the design. We conducted an initial high-level data discovery process and interviews with medical, technical, and regulatory subject matter experts. Though unstructured, the interviews helped define key requirements and agile personas (Table 1) to guide development.

Table . Agile personas to guide developing the data platform.

	Persona "Heather"	Persona "Mere"	Persona "Dave"
Function	Health services researcher	Medical researcher	Data engineer/scientist
Background	Epidemiologist with strong statistical background	Physician-scientist with advanced statistical knowledge	Computer scientist
Reasoning	Ensure and improve quality of treatment of patients nationally	Perform and publish peer-reviewed medical research	Advise business users and monitor data quality
Objectives	Facilitate change in processes or standard operating procedures and guidelines	Perform retrospective cohort studies or decide on feasibility of prospective clinical trials	Provide data to users
Example problem	Are antibiotics dosed correctly and routinely monitored during therapy?	Do courses of therapy differ between urban and rural regions?	Does the amount of data correlate to the number of patients who consented to secondary data use?

Infrastructure and Software

Because of regulatory requirements, we implemented an on-premise data platform instead of a cloud-based "platform-as-a-service" solution. Our requirements mandated integration of multiple data types, from tabular data to binary blobs. We selected a lambda architecture based on the Apache Hadoop stack, as discussed by McPadden et al [18], enhanced by Python and R notebooks for rapid analytics [27]. To reduce operational complexity, we used a Hadoop distribution offering cluster configuration, monitoring tools, and vendor support. Our setup operates in fully kerberized mode, requiring authentication for each data operation and generating auditable logs.

We provide three tools to interact with the data lake:

1. Apache Hue with access to Impala-SQL, Hive-SQL, H-Base, and the Hadoop Distributed File System
2. A hosted data science environment with containerized runtimes for Python, R, and custom data applications
3. Hosted BI-Tools for self-service analytics using dashboards

Consent Management

Participation is opt in and requires written consent. This consent is modular, covering broad consent for research on real-world data and contact for clinical trial recruitment. While similar to the Medical Informatics Initiative broad consent, our version excludes modules like biobanking or genetic data, as these domains are rarely available in our hospitals.

We developed a consent management system from scratch to handle modular consent with validity periods. Two interfaces (HL7v2 and REST-API via HTTPS) connect the back end to EHR-integrated front ends, minimizing clicks and avoiding disruptions. Consent information is stored in a multitenant database linked to case number and a validity period. Authorized staff can trigger withdrawals; stored procedures remove expired or withdrawn consent daily to maintain an up-to-date list.

Extract, Transform, Load

Extract, transform, load processes for EHR systems have been described previously [28-30]. This paper details our approach to integrating individual hospitals into a unified data lake. We also outline our data modeling and standardization processes. Figure 1 summarizes the data flow.

EHR adoption levels vary across German hospitals, including within our group, as measured by the electronic medical record adoption model level [31]. For historical reasons, Helios uses EHR systems from different vendors with different subsystems.

XSL•FO
RenderX

Hence, we developed an ingest layer supporting diverse formats and delivery methods.

The connector is a containerized Linux system configurable for single- or multitenant use. Java and Python runtimes filter, minimize, and pseudonymize the data before pushing it to the Hadoop cluster.

XSL•FO
RenderX

Figure 1. Data flows from EHR systems through the CONNECTOR into a data lake. Spark pipelines transform data through a layered structure. Users access data in horizontally and vertically sliced data marts. AES: advanced encryption standard; API: application programming interface; CBC: cipher block chaining; EHR: electronic health record; FHIR: Fast Healthcare Interoperability Resources; HeSaMeDa: Helios Safe Medical Data (Platform); ODBC: open database connectivity; RFC: remote function call; SFTP: secure file transfer protocol.

XSL•FO
RenderX

Data Minimization and Pseudonymization

Regulatory requirements mandate that data be minimized to research-relevant information and pseudonymized once they leave the regulatory hospital domain [32].

Preferably, source systems would filter for patient consent, pseudonymize records, and push these to the platform. Some EHR systems allow custom business logic via remote function calls to meet these requirements. FHIR application programming interfaces (APIs) often support minimization through custom profiles that exclude personally identifiable attributes (eg, MedicationAdministration.performer). Systems without API access require vendor support for custom interfaces or queries. Additional minimization and pseudonymization are typically applied within the connector for compliance.

Helios treats patients across inpatient and outpatient settings and across multiple hospitals. To ensure correct longitudinal mapping, we implemented a unique pseudonymous identifier using a dedicated master patient index (MPI). The MPI, based on validated probabilistic criteria [33], consolidates records via the IHE (Integrating the Healthcare Enterprise) protocol (Patient Identifier Cross-referencing [34]) into a unique pseudonymous patient entry. This identifier is transmitted back to the connector to replace the original patient ID. Before granting data access to researchers, we add a second layer of pseudonymization to further reduce reidentification risk across projects [32].

Data Modeling and Transformation

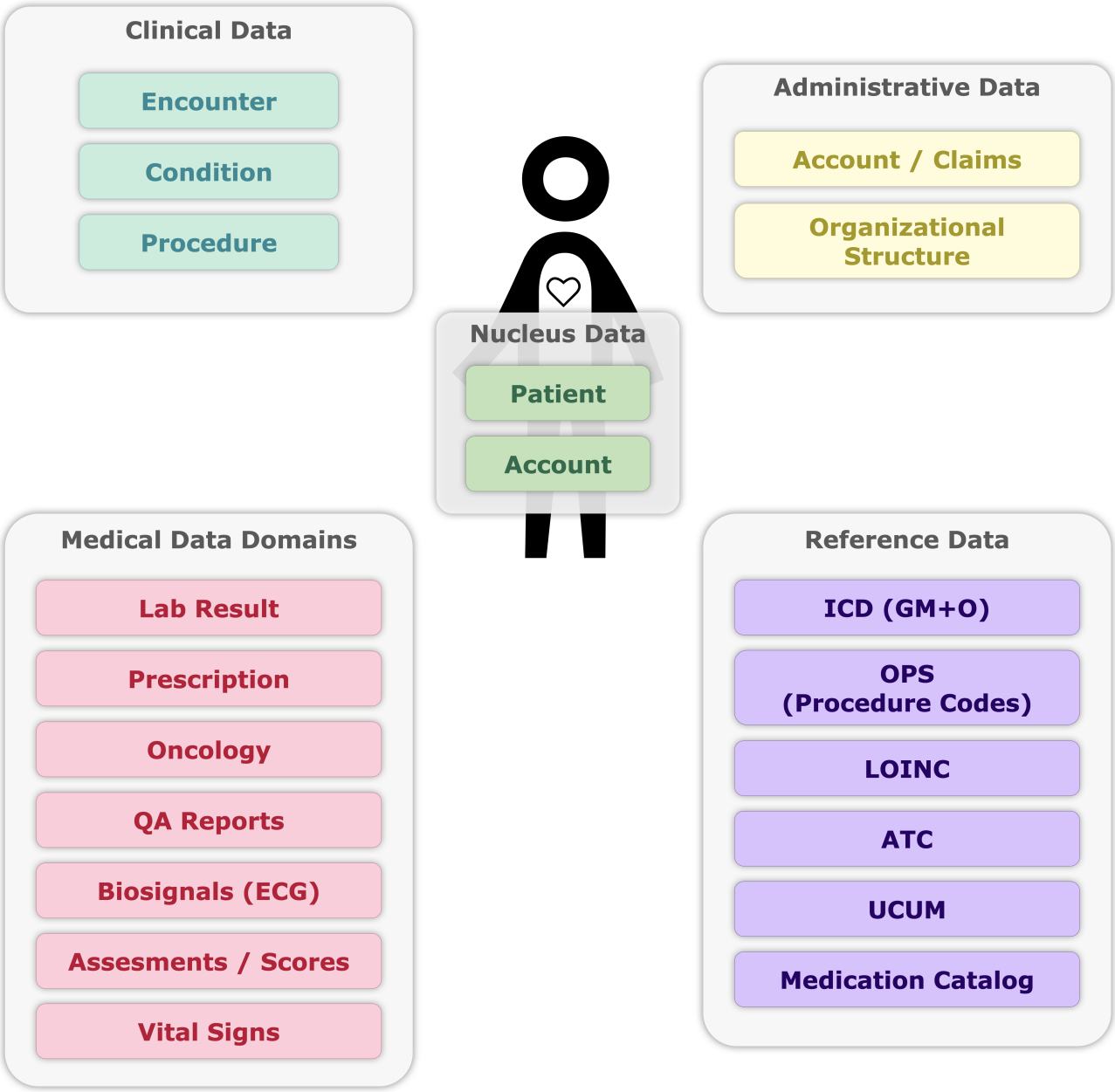
We designed a simple core data model and a four-layer transformation architecture:

1. A raw layer keeps ingested data in append-only store, without relational schema constraints.
2. A transformation layer uses Apache Spark to process raw data in pipelines grouped by source system. Code is continuously deployed via a continuous integration and continuous deployment (CI/CD) pipeline and transforms data into our data model. Transformations run in batches by data source similarity, not by hospital, reducing pipeline complexity.
3. The consumption layer unifies data from different EHR systems into a single EHR core domain, enriches it with semantic information like readable text for codes, and performs data quality and plausibility checks.
4. The data mart layer offers researchers sliced subsets of the consumption layer. Data marts can be stored as checksummed archives to ensure reproducible analyses.

The data model centers on structured data compatible with the HL7 FHIR resources for patients and accounts (Figure 2), enabling representation of inpatient and outpatient visits linked to constant patient objects. Our model closely follows the core dataset of the German Medical Informatics Initiative [35] with deviations for data privacy reasons (eg, reducing birth date to birth year) and data availability (eg, excluding employee data like *requester and performer* in *MedicationRequest* or missing *device* attribute of the *observation*). Two design principles were used: preserving raw data and prioritizing speed over complete standardization. Because most users are experienced in statistics and data analysis, we iteratively refined standardization based on insights from analytical projects. Examples include calculating patient age at admission and converting lab results to international standards like the Unified Code for Units of Measure. Raw values are provided alongside transformed data to maintain trust, though an interactive data lineage is not available.

XSL•FO
RenderX

Figure 2. Data domains. Reference data are used to enrich and standardize data in other data domains and are used mainly for transformation processes. Other data domains contain pseudonymized data from patients who gave consent for secondary data use. ATC: Anatomic Therapeutic Chemical (classification); ECG: electrocardiogram; *ICD*: *International Classification of Diseases*; *ICD GM*: *ICD German Modification*; *ICD O*: *ICD Oncology*; LOINC: Logical Observation Identifiers Names and Codes; OPS: operation and procedure codes (in Germany); QA: quality assurance; UCUM: Unified Code for Units and Measurements.

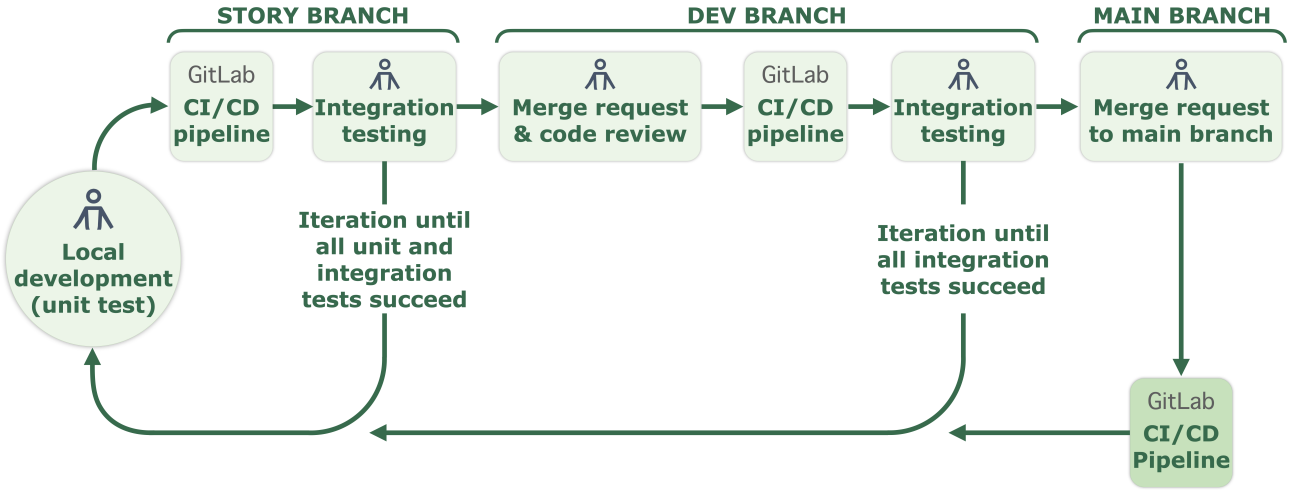


Development Workflow and Process Scheduling

All transformation code is stored in a versioned repository (git), with each feature developed in its own branch, per agile practices. A CI/CD pipeline runs unit and integration tests on each commit using reproducible Docker builds, with a focus on conditional branching. Code is deployed to production only via the CI/CD pipeline (Figure 3) after tests and manual review. Execution and scheduling, including dependencies, are managed via directed acyclic graphs in Apache Airflow. After a successful run, the story owner conducts a user acceptance test before sign-off and archiving of the feature branch.

XSL•FO
RenderX

Figure 3. Agile development workflow using continuous integration and continuous deployment (CI/CD). PySpark code from story branches is tested and evaluated multiple times before it can be merged into production. With each iteration the level of scrutiny increases, from unit tests to integration into tests and manual code review.



Governance

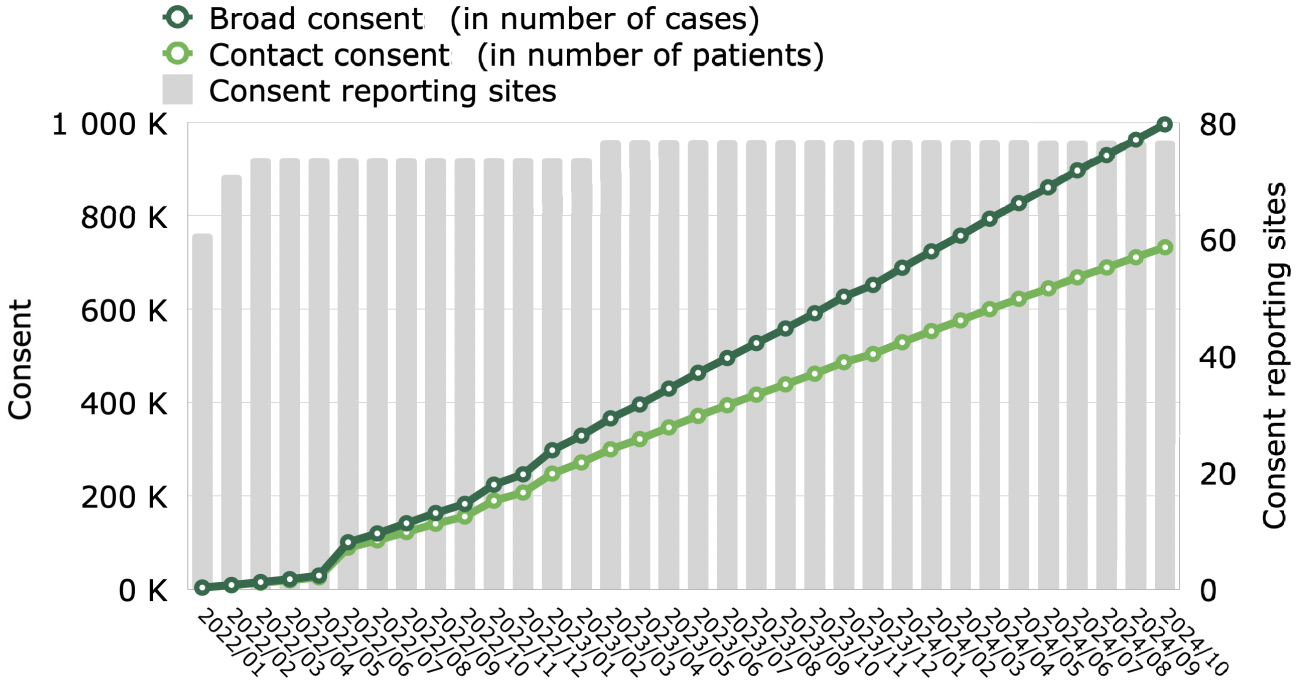
Data governance follows German guidelines for secondary data analysis [36]. The multidisciplinary Usage and Access Committee (UAC) grants data access per use case, enforced at column and row level by user- or group-based policies in Apache Atlas. Reidentification of patients requires approval from researchers, the ethics committee, and the UAC, typically for clinical trial inclusion, and is performed only at the data-providing hospital, to preserve data sovereignty.

Implementation (Results)

Consent Management

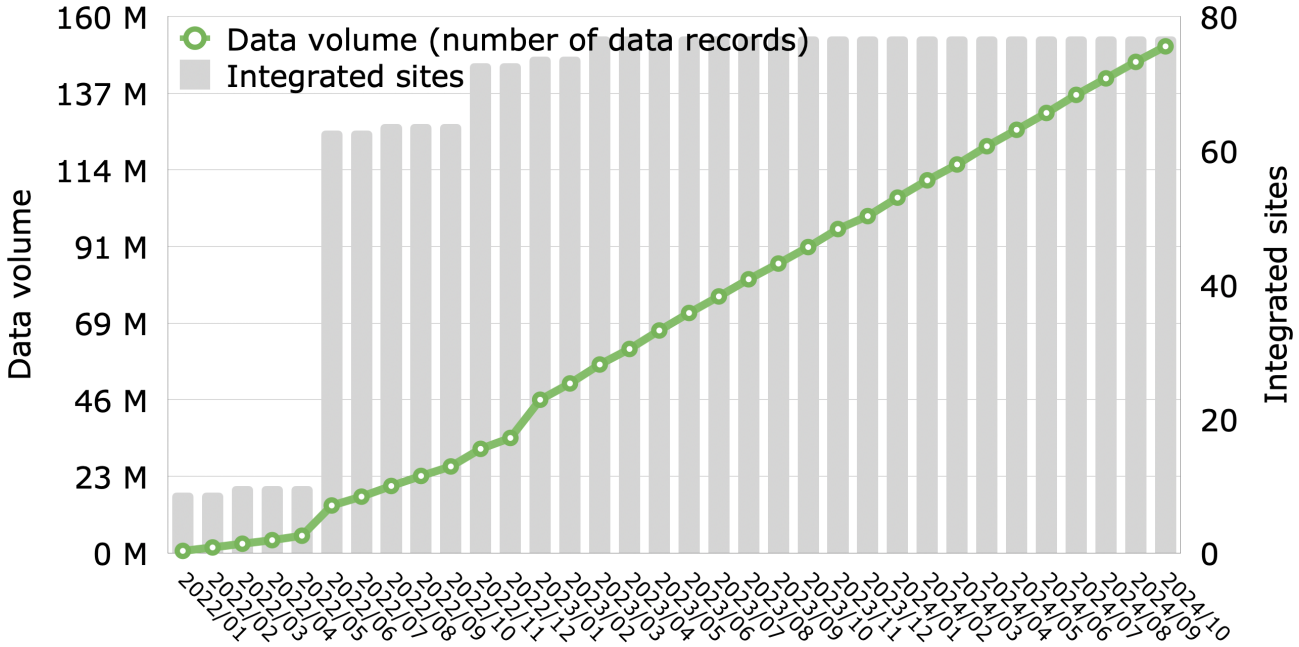
From January 2022 to July 2023, the consent management system was implemented in 77 hospitals (Figure 4 and Figure 5). Ten hospitals were excluded due to their specialization (psychiatric) or incomplete network integration.

Figure 4. Broad consent and contact consent since project launch. Consent infrastructure, as measured by the number of hospitals (sites) reporting consent, was rolled out faster than data infrastructure (see also Figure 5).



XSL•FO
RenderX

Figure 5. Data volume over time, as measured by record counts in the consumption layer in relation to the integrated sites (hospitals), which illustrates a staged rollout and scaling of data infrastructure.



In general, EHR updates occur in cycles within our hospital network. Consent management, which is integrated into the administrative user interface, requires thorough testing before deployment, as updates have to wait until the next cycle. Scaling was rapid: 61 facilities were integrated within the first month and 10 more within the second, and there were a total of 74 within 3 months. Staff received training during the rollout, yet in the initial 6 months, only 40% of patients were asked for consent, with a variation of plus or minus 24% across hospitals. Additional training boosted the rate to 63% by the end of 2023.

Rapid consent integration caused a significant load on the MPI during peak patient admission in the morning. To avoid time-outs, the Patient Identifier Cross-referencing interface was wrapped in an HTTPS API behind a high-availability load balancer.

Over a 24-month period, 1,475,244 patients were asked for consent during admission. In total, we received 1,023,633 instances of broad consent (consent rate: 70.2%), and 732,485 (71.6%) of these also included agreement to be contacted by researchers.

Notably, consent was not uniformly distributed: 714521 (69.8%) of instances stemmed from planned admissions, 217583 (21.3%) from unplanned admissions through the emergency department (ED), and 91529 (8.9%) from outpatient cases in the ED.

Data Volume

After 24 months, the consumption layer held approximately 15.1 billion records (averaging 102 unique medical data points per case), as shown in Figure 5. This amounted to approximately 14.1 terabytes of data as of October 2024. The ingest layer managed on average 1.9 million HL7 messages and 45,378 FHIR bundles per year, per hospital.

Data Modeling and Transformation

An iterative development approach results in frequent, additive changes to the data model, which are difficult to communicate to users. Therefore, we developed an interactive data catalog as a web application that displays the current state of all tables in the Hive Metastore.

We implemented an automated data quality framework to ensure data model conformity, assess data relationships, and detect outliers. This helped identify point-of-care devices reporting lab results in nonstandard units during LOINC (Logical Observation Identifiers Names and Codes) mapping [37].

Since transformations evolve, we implemented data version control [38] to store versioned code and data for reproducibility. It worked very well, but required familiarity with git and command line interfaces.

Lessons Learned

Infrastructure Scaling

The Hadoop ecosystem handles structured, semistructured, and unstructured data. Due to data minimization, data volumes grow more slowly than the compute demand, driven mainly by standardization and data quality checks. Therefore, we added another physical host to the cluster in the first year.

The consent rollout required addressing regulatory compliance, seamless technical integration into patient management systems, and an organizational transition to embed consent into the admission process, which presented unexpected challenges. A stable consent rate of 70% showed strong patient willingness to support research.

Strategies for Scaling the Data Lake

In summary, a 2-phase data integration strategy, starting with a few hospitals, has proven effective. The initial phase facilitates

XSL•FO
RenderX

refinement of interfaces, data modeling, and transformation processes, laying the foundation for seamless integration with a larger number of hospitals during subsequent scaling. Scaling the consent management system prior to data integration also proved beneficial, ensuring a consistent backlog of data for integration into the data lake.

Notably, as our data ingestion interfaces matured, technical integration of new data domains like ICU or cancer registries accelerated. However, full data model integration still requires substantial input from subject matter experts.

Batched Data Scales More Easily Than Streaming Data

Scaling adversely affected our MPI and HL7v2/IHE data ingestion, as these systems rely on an existing communication infrastructure that is not readily scalable. Future real-time data integration will likely shift toward local clinical data repositories for preprocessing, rather than introducing new streaming pipelines with technologies like Apache Kafka.

Interoperability and Standardization

Standardization, even for basic resources, presents difficulties, as transformations impact semantics and may lead to permanent information loss, despite agreement on rules by involved parties (ie, subject matter experts and data engineers).

Divergence in target values across different EHR installations poses risks to information integrity, notably during initial HL7 message processing due to profile limitations excluding certain HL7 "Z-segment" permutations. Consequently, a "raw-data first" policy was implemented to mitigate future data loss, albeit at the expense of increased bandwidth and storage capacity needs. Standardization can also result in decreased precision, particularly when transforming observations that were recorded without adhering to standards like LOINC [37].

Automation

Automation is essential to enhance efficiency, accuracy, and productivity. Versioned code and reproducible builds from the CI/CD pipeline helped to quickly revert changes that turned out to be suboptimal prior to production deployment. We also had substantially more success in onboarding new personnel onto automated, rather than manual, processes. We argue this learning is especially valuable for research institutions, which experience frequent personnel changes among graduate students and postdoctoral researchers.

Unintended Consequences

With 70% of cases in our dataset stemming from planned admissions, ED cases were underrepresented, introducing a selection bias. This disparity compromises the validity of results extrapolated to the ED setting and may distort the performance metrics of predictive models and risk stratification algorithms, possibly resulting in suboptimal outcomes. Thus, meticulous methodological scrutiny, starting in the design phase of each project, is required to mitigate these biases when using this dataset for translational research.

To enhance unbiased subsampling and improve generalizability, we categorized admission criteria for accounts and encounters. Nevertheless, our aim is to seek consent from every patient, irrespective of admission type, ensuring dataset balance. Obviously, in urgent medical situations, obtaining consent may not be feasible for patients who are distressed or have an altered mental state. A potential solution is to separate consent from administrative admission, seeking it during the inpatient stay instead, although this approach would demand extra resources. Unfortunately, vulnerable patient groups (eg, homeless or uninsured patients) will also be underrepresented in our dataset, since most of their interaction with the medical system is through the ED. Ethical implications extend beyond consent collection. The potential for algorithmic bias in medical research based on our dataset must be carefully considered. Researchers using our platform are required to report on the demographic composition of their study populations and explicitly address potential biases in their analyses.

Discussion

We hope to inspire other private hospital networks to build data lakes. Adhering to best practices as defined by national and international research consortia is key to ensure compatibility and to allow for integration with other research consortia in the future. Combining data from academic and nonacademic institutions and health care providers could enable longitudinal analysis of patients across multiple health care sectors, and the German Medical Informatics Initiative has begun branching out into nonacademic health care providers via progress hubs [39].

Our approach centralizes data from all participating hospitals after integration, whereas the German Medical Informatics Initiative operates local data integration centers at every participating hospital or within smaller hospital clusters. Decentralized data repositories provide local autonomy and resilience against system failures but demand infrastructure and personnel investment at every site. A decentralized approach seems ideal for academic institutions because local data expertise can be used for local research projects and education of computer science students as well as physician scientists receiving specialization training. For hospital networks below the level of university medical centers, centralization might be preferable, especially if there are already shared IT resources (infrastructure and personnel) within the network. We acknowledge, however, that our decision to use open source software and implement the platform from scratch was only feasible because our IT organization already runs its own data centers and has developer as well as development operations experience. Nevertheless, the global trend toward platform-as-a-service providers (hyperscalers) for storage and compute tasks poses challenges in recruiting experienced staff for on-premise installations. This presents a pain point for hospital networks: regulatory requirements require on-premise data storage, while most other sectors move to the cloud.

High levels of automation and agile development, characterized by short feature cycles and consistent data quality improvements, are necessary for user satisfaction. However, achieving swift project rollout and overall success necessitates continuous organizational investment and subject matter expert support.

Future developments will involve the extraction of knowledge from unstructured text, and we have collected preliminary

XSL•FO
RenderX

findings on document pseudonymization [40]. Building research data platforms is not a purpose in itself. Meaningful research conducted on these platforms is needed to justify the collection of EHR data, even with patient consent. We are looking forward to research reports beyond the technical level on projects realized with our implementation.

Conflicts of Interest

None declared.

Checklist 1
iCHECK-DH checklist.
[DOCX File, 27 KB - medinform_v13i1e69853_app1.docx]

References

1. Stüer T, Juhra C. Usability of electronic health records in Germany - an overview of satisfaction of university hospital physicians. Stud Health Technol Inform 2022 Aug 17;296:90-97. [doi: 10.3233/SHTI220808] [Medline: 36073493]
2. Safran C, Bloomrosen M, Hammond WE, et al. Toward a national framework for the secondary use of health data: an American Medical Informatics Association white paper. J Am Med Inform Assoc 2007;14(1):1-9. [doi: 10.1197/jamia.M2273] [Medline: 17077452]
3. Luo J, Wu M, Gopukumar D, Zhao Y. Big data application in biomedical research and health care: a literature review. Biomed Inform Insights 2016;8:1-10. [doi: 10.4137/BII.S31559] [Medline: 26843812]
4. Prokosch HU, Ganslandt T. Perspectives for medical informatics. Reusing the electronic medical record for clinical research. Methods Inf Med 2009;48(1):38-44. [Medline: 19151882]
5. The Medical Informatics Initiative's core data set. Medical Informatics Initiative. URL: https://www.medizininformatik-initiative.de/en/medical-informatics-initiatives-core-data-set [accessed 2023-06-28]
6. Wulff A, Haarbrandt B, Marschollek M. Clinical knowledge governance framework for nationwide data infrastructure projects. Stud Health Technol Inform 2018;248:196-203. [Medline: 29726437]
7. Haarbrandt B, Schreiweis B, Rey S, et al. HiGHmed - an open platform approach to enhance care and research across institutional boundaries. Methods Inf Med 2018 Jul;57(S 01):e66-e81. [doi: 10.3414/ME18-02-0002] [Medline: 30016813]
8. Löbe M, Kamdje-Wabo G, Sinza AC, Spengler H, Strobel M, Tute E. Towards harmonized data quality in the medical informatics initiative - current state and future directions. Stud Health Technol Inform 2022 Jan 14;289:240-243. [doi: 10.3233/SHTI210904] [Medline: 35062137]
9. Zenker S, Strech D, Ihrig K, et al. Data protection-compliant broad consent for secondary use of health care data and human biosamples for (bio)medical research: towards a new German national standard. J Biomed Inform 2022 Jul;131:104096. [doi: 10.1016/j.jbi.2022.104096] [Medline: 35643273]
10. Faden RR, Kass NE, Goodman SN, Pronovost P, Tunis S, Beauchamp TL. An ethics framework for a learning health care system: a departure from traditional research ethics and clinical ethics. Hastings Cent Rep 2013;Spec No:S16-S27. [doi: 10.1002/hast.134] [Medline: 23315888]
11. Schmitt J, Roessler M, Scriba P, et al. Effect of clinical peer review on mortality in patients ventilated for more than 24 hours: a cluster randomised controlled trial. BMJ Qual Saf 2023 Jan;32(1):17-25. [doi: 10.1136/bmjqs-2021-013864] [Medline: 35383128]
12. Schwarzkopf D, Nimptsch U, Graf R, Schmitt J, Zacher J, Kuhlen R. Opportunities and limitations of risk adjustment of quality indicators based on inpatient administrative health data - a workshop report. Z Evid Fortbild Qual Gesundhwes 2021 Jun;163:1-12. [doi: 10.1016/j.zefq.2021.04.003] [Medline: 34023246]
13. Bollmann A, Ueberham L, Schuler E, et al. Cardiac tamponade in catheter ablation of atrial fibrillation: German-wide analysis of 21 141 procedures in the Helios atrial fibrillation ablation registry (SAFER). Europace 2018 Dec 1;20(12):1944-1951. [doi: 10.1093/europace/euy131] [Medline: 29982554]
14. Buda S, Tolksdorf K, Schuler E, Kuhlen R, Haas W. Establishing an ICD-10 code based SARI-surveillance in Germany - description of the system and first results from five recent influenza seasons. BMC Public Health 2017 Jun 30;17(1):612. [doi: 10.1186/s12889-017-4515-1] [Medline: 28666433]
15. Bollmann A, Hohenstein S, König S, Meier-Hellmann A, Kuhlen R, Hindricks G. In-hospital mortality in heart failure in Germany during the Covid-19 pandemic. ESC Heart Fail 2020 Dec;7(6):4416-4419. [doi: 10.1002/ehf2.13011] [Medline: 32915516]
16. Bollmann A, Hohenstein S, Meier-Hellmann A, Kuhlen R, Hindricks G. Emergency hospital admissions and interventional treatments for heart failure and cardiac arrhythmias in Germany during the Covid-19 outbreak: insights from the German-wide Helios hospital network. Eur Heart J Qual Care Clin Outcomes 2020 Jul 1;6(3):221-222. [doi: 10.1093/ehjqcco/qcaa049] [Medline: 32502261]

XSL•FO
RenderX

17. Reichardt P, Bollmann A, Hohenstein S, et al. Decreased incidence of oncology admissions in 75 Helios hospitals in Germany during the COVID-19 pandemic. Oncol Res Treat 2021;44(3):71-75. [doi: 10.1159/000512935] [Medline: 33333506]
18. McPadden J, Durant TJ, Bunch DR, et al. Health care and precision medicine research: analysis of a scalable data science platform. J Med Internet Res 2019 Apr 9;21(4):e13043. [doi: 10.2196/13043] [Medline: 30964441]
19. Yao Q, Tian Y, Li PF, Tian LL, Qian YM, Li JS. Design and development of a medical big data processing system based on Hadoop. J Med Syst 2015 Mar;39(3):1-11. [doi: 10.1007/s10916-015-0220-8] [Medline: 25666927]
20. Rinner C, Gezgin D, Wendl C, Gall W. A clinical data warehouse based on OMOP and i2b2 for Austrian health claims data. Stud Health Technol Inform 2018;248:94-99. [doi: 10.3233/978-1-61499-858-7-94] [Medline: 29726424]
21. Gagalova KK, Leon Elizalde MA, Portales-Casamar E, Görges M. What you need to know before implementing a clinical research data warehouse: comparative review of integrated data repositories in health care institutions. JMIR Form Res 2020 Aug 27;4(8):e17687. [doi: 10.2196/17687] [Medline: 32852280]
22. Unberath P, Prokosch HU, Gründner J, Erpenbeck M, Maier C, Christoph J. EHR-independent predictive decision support architecture based on OMOP. Appl Clin Inform 2020 May;11(3):399-404. [doi: 10.1055/s-0040-1710393] [Medline: 32492716]
23. Ozaydin B, Zengul F, Oner N, Feldman SS. Healthcare research and analytics data infrastructure solution: a data warehouse for health services research. J Med Internet Res 2020 Jun 4;22(6):e18579. [doi: 10.2196/18579] [Medline: 32496199]
24. Visweswaran S, McLay B, Cappella N, et al. An atomic approach to the design and implementation of a research data warehouse. J Am Med Inform Assoc 2022 Mar 15;29(4):601-608. [doi: 10.1093/jamia/ocab204] [Medline: 34613409]
25. Bernstam EV, Warner JL, Krauss JC, et al. Quantitating and assessing interoperability between electronic health records. J Am Med Inform Assoc 2022 Apr 13;29(5):753-760. [doi: 10.1093/jamia/ocab289] [Medline: 35015861]
26. Perrin Franck C, Babington-Ashaye A, Dietrich D, et al. iCHECK-DH: guidelines and checklist for the reporting on digital health implementations. J Med Internet Res 2023 May 10;25(1):e46694. [doi: 10.2196/46694] [Medline: 37163336]
27. Wheeler NR, Benchek P, Kunkle BW, et al. Hadoop and PySpark for reproducibility and scalability of genomic sequencing studies. Pac Symp Biocomput 2020;25:523-534. [Medline: 31797624]
28. Ong TC, Kahn MG, Kwan BM, et al. Dynamic-ETL: a hybrid approach for health data extraction, transformation and loading. BMC Med Inform Decis Mak 2017 Sep 13;17(1):134. [doi: 10.1186/s12911-017-0532-3] [Medline: 28903729]
29. Tute E, Steiner J. Modeling of ETL-processes and processed information in clinical data warehousing. Stud Health Technol Inform 2018;248:204-211. [Medline: 29726438]
30. Yüksekogul N, Meyer N, Aguduri LS, Merzweiler A, Heinze O. Implementing ETL-processes for a medical data integration center - first experiences from the Heidelberg University Hospital. In: Deutsche Gesellschaft Für Medizinische Informatik, Biometrie Und Epidemiologie 64 Jahrestagung Der Deutschen Gesellschaft Für Medizinische Informatik, Biometrie Und Epidemiologie eV (GMDS): German Medical Science GMS Publishing House; 2019. [doi: 10.3205/19gmds169]
31. Amelung V, Angelkorte M, Augurzky B, et al. Ergebnisse & Berichte. DigitalRadar. 2021 Jun 30. URL: https://www.digitalradar-krankenhaus.de/reifegradmessung/ergebnisse/ [accessed 2023-07-09]
32. Gött R, Stäubert S, Strübing A, et al. 3LGM2IHE: requirements for data-protection-compliant research infrastructures-a systematic comparison of theory and practice-oriented implementation. Methods Inf Med 2022 Dec;61(S 02):e134-e148. [doi: 10.1055/a-1950-2791] [Medline: 36150711]
33. Brandner R, Ihls A. Herausforderung identifikation: pflege eines master patient index. In: Kongress Medizin und Gesellschaft 2007: German Medical Science GMS Publishing House; 2007.
34. Patient Identifier Cross-referencing (PIX). IHE International. 2022. URL: https://profiles.ihe.net/ITI/TF/Volume1/ch-5.html [accessed 2025-07-23]
35. Ammon D, Kurscheidt M, Buckow K, et al. Interoperability Working Group: core dataset and information systems for data integration and data exchange in the Medical Informatics Initiative. Bundesgesundheitsblatt Gesundheitsforschung Gesundheitsschutz 2024 Jun;67(6):656-667. [doi: 10.1007/s00103-024-03888-4] [Medline: 38753022]
36. Swart E, Gothe H, Geyer S, et al. Good practice of secondary data analysis (GPS): guidelines and recommendations. Gesundheitswesen 2015 Feb;77(2):120-126. [doi: 10.1055/s-0034-1396815] [Medline: 25622207]
37. Belov V, Münchow-Pohl C, Kittner M, et al. Multicentric outlier detection algorithm for healthcare laboratory data. : German Medical Science GMS Publishing House; 2024 Presented at: Gesundheit – Gemeinsam Kooperationstagung Der Deutschen Gesellschaft Für Medizinische Informatik, Biometrie Und Epidemiologie (GMDS), Deutschen Gesellschaft Für Sozialmedizin Und Prävention (DGSMP), Deutschen Gesellschaft Für Epidemiologie (DGEpi), Deutschen Gesellschaft Für Medizinische Soziologie (DGMS) Und Der Deutschen Gesellschaft Für Public Health (DGPH). [doi: 10.3205/24gmds158]
38. Data Version Control. 2025. URL: https://dvc.org/ [accessed 2025-03-30]
39. Krefting D, Bavendiek U, Fischer J, et al. Digital health progress hubs-data integration beyond university hospitals. Bundesgesundheitsblatt Gesundheitsforschung Gesundheitsschutz 2024 Jun;67(6):701-709. [doi: 10.1007/s00103-024-03883-9] [Medline: 38753021]
40. Bockhacker M, Schruhl D, Münchow C, Martens P, Ortleb S, Kittner M. Using named entity recognition and large language models to enhance de-identification of semi-structured EMR data – preliminary results and lessons learned. In: GMDS Proceedings: German Medical Science GMS Publishing House. [doi: 10.3205/23gmds114]

XSL•FO
RenderX

Abbreviations

API: application programming interface
CI/CD: continuous integration and continuous deployment
ED: emergency department
EHR: electronic health record
FHIR: Fast Healthcare Interoperability Resources
GDPR: general data privacy regulation
HDFS: Hadoop File System
HL7: Health Level Seven
ICU: intensive care unit
IHE: Integrating the Healthcare Enterprise
LOINC: Logical Observation Identifiers Names and Codes
MPI: master patient index
UAC: Usage and Access Committee

Edited by M Focsa; submitted 10.12.24; peer-reviewed by S Hume, S Meister; revised version received 22.07.25; accepted 29.07.25; published 12.09.25.

Please cite as:
Bockhacker M, Martens P, von Münchow C, Löser S, Günther R, Kuhlen R, Kannt O, Ortleb S
Lessons Learned From Building a Data Platform for Longitudinal, Analytical Use Cases and Scaling to 77 German Hospitals: Implementation Report
JMIR Med Inform 2025;13:e69853
URL: https://medinform.jmir.org/2025/1/e69853
doi:10.2196/69853

© Markus Bockhacker, Peter Martens, Clara von Münchow, Sarah Löser, Rosita Günther, Ralf Kuhlen, Olaf Kannt, Sebastian Ortleb. Originally published in JMIR Medical Informatics (https://medinform.jmir.org), 12.9.2025. This is an open-access article distributed under the terms of the Creative Commons Attribution License (https://creativecommons.org/licenses/by/4.0/), which permits unrestricted use, distribution, and reproduction in any medium, provided the original work, first published in JMIR Medical Informatics, is properly cited. The complete bibliographic information, a link to the original publication on https://medinform.jmir.org/, as well as this copyright and license information must be included.

XSL•FO
RenderX

Real-World Evaluation of AI-Driven Diabetic Retinopathy Screening in Public Health Settings: Validation and Implementation Study

Mona Duggal[1,2*], MD; Anshul Chauhan[2*], PhD; Vishali Gupta[2], MS; Ankita Kankaria[3], MD; Deepmala Budhija[2], MCA; Priyanka Verma[2], MPH; Vaibhav Miglani[2], MSc; Preeti Syal[4], MS; Gagandeep Kaur[2], BOptom; Lakshay Kumar[2], BOptom; Naveen Mutyala[2], MSc; Rishabh Bezbaruah[4], MSc; Nayanshi Sood[5], MS; Ashleigh Kernohan[6], PhD; Geeta Menon[7], MS; Luke Vale[6], PhD

[1]ICMR-National Institute for Research in Digital Health and Data Science (NIRDHDS), Ansari Nagar East, New Delhi, India

[2]Advanced Eye Centre, Post Graduate Institute of Medical Education and Research, Chandigarh, India

[3]Department of Community Medicine and School of Public Health, Post Graduate Institute of Medical Education and Research, Chandigarh, India

[4]National Institute of Transforming India (NITI) Aayog, Delhi, India

[5]Department of Ophthalmology, Department of Health and Family Welfare, Mohali, Punjab, India

[6]Global Health Economics Centre, Public Health and Policy, London School of Hygiene and Tropical Medicine, London, United Kingdom

[7]Frimley Health NHS Foundation Trust, Frimley, United Kingdom

[*]these authors contributed equally

Corresponding Author:
Mona Duggal, MD
ICMR-National Institute for Research in Digital Health and Data Science (NIRDHDS), Ansari Nagar East, New Delhi, India

Abstract

Background: Artificial intelligence (AI) algorithms offer an effective solution to alleviate the burden of diabetic retinopathy (DR) screening in public health settings. However, there are challenges in translating diagnostic performance and its application when deployed in real-world conditions.

Objective: This study aimed to assess the technical feasibility of integration and diagnostic performance of validated DR screening (DRS) AI algorithms in real-world outpatient public health settings.

Methods: Prior to integrating an AI algorithm for DR screening, the study involved several steps: (1) Five AI companies, including four from India and one international company, were invited to evaluate their diagnostic performance using low-cost nonmydriatic fundus cameras in public health settings; (2) The AI algorithms were prospectively validated on fundus images from 250 people with diabetes mellitus, captured by a trained optometrist in public health settings in Chandigarh Tricity in North India. The performance evaluation used diagnostic metrics, including sensitivity, specificity, and accuracy, compared to human grader assessments; (3) The AI algorithm with better diagnostic performance was integrated into a low-cost screening camera deployed at a community health center (CHC) in the Moga district of Punjab, India. For AI algorithm analysis, a trained health system optometrist captured nonmydriatic images of 343 patients.

Results: Three web-based AI screening companies agreed to participate, while one declined and one chose to withdraw due to low specificity identified during the interim analysis. The three AI algorithms demonstrated variable diagnostic performance, with sensitivity (60%-80%) and specificity (14%-96%). Upon integration, the better-performing algorithm AI-3 (sensitivity: 68%, specificity: 96, and accuracy: 88·43%) demonstrated high sensitivity of image gradability (99.5%), DR detection (99.6%), and referral DR (79%) at the CHC.

Conclusions: This study highlights the importance of systematic AI validation for responsible clinical integration, demonstrating the potential of DRS to improve health care access in resource-limited public health settings.

(JMIR Med Inform 2025;13:e67529) doi:10.2196/67529

KEYWORDS

diabetic retinopathy; artificial intelligence; validation, implementation, integration; Screening, public health settings; screening

XSL•FO
RenderX

Introduction

The global prevalence of diabetes is growing [1], leading to increased vision loss and blindness associated with it [2]. There is an urgent need for diabetic retinopathy (DR) screening programs to identify vision-threatening DR to enable timely treatment [3,4]. However, this rising prevalence is straining health care systems already struggling to improve care and manage health care costs [4].

Despite its critical role, DR screening (DRS) remains limited in many low-resource settings. Conventional screening with trained human graders is often costly, time-consuming, and challenging to scale [5,6]. The gap between eye care needs and ophthalmologist availability exacerbates public health challenges [7]. In India, DR management faces challenges due to limited screening programs, low public awareness, and poor understanding of routine retinal exams [8]. Artificial intelligence-driven DRS enables faster, more affordable, and efficient screening, especially in underserved areas [9,10]. It allows noneye health professionals to conduct screenings and refer without specialists [11].

AI algorithms have demonstrated performance comparable to or exceeding human experts in DR classification [12,13]. However, concerns exist about their suboptimal performance in real-world settings and across diverse populations [14]. Real-world validation is critical to ensure AI algorithms perform accurately in diverse settings, as disease prevalence, image quality, and patient-related factors may differ from the training dataset [15-17]. Prospective studies are essential for evaluating AI systems in the contexts where they will be deployed [18]. Hence, integrating AI into clinical practice requires alignment with clinical workflows and stronger evidence on its real-world accuracy and user experiences [11,14].

This is the first Indian study to validate multiple commercial AI algorithms for DRS and to assess the feasibility of implementing a validated AI system in public health settings.

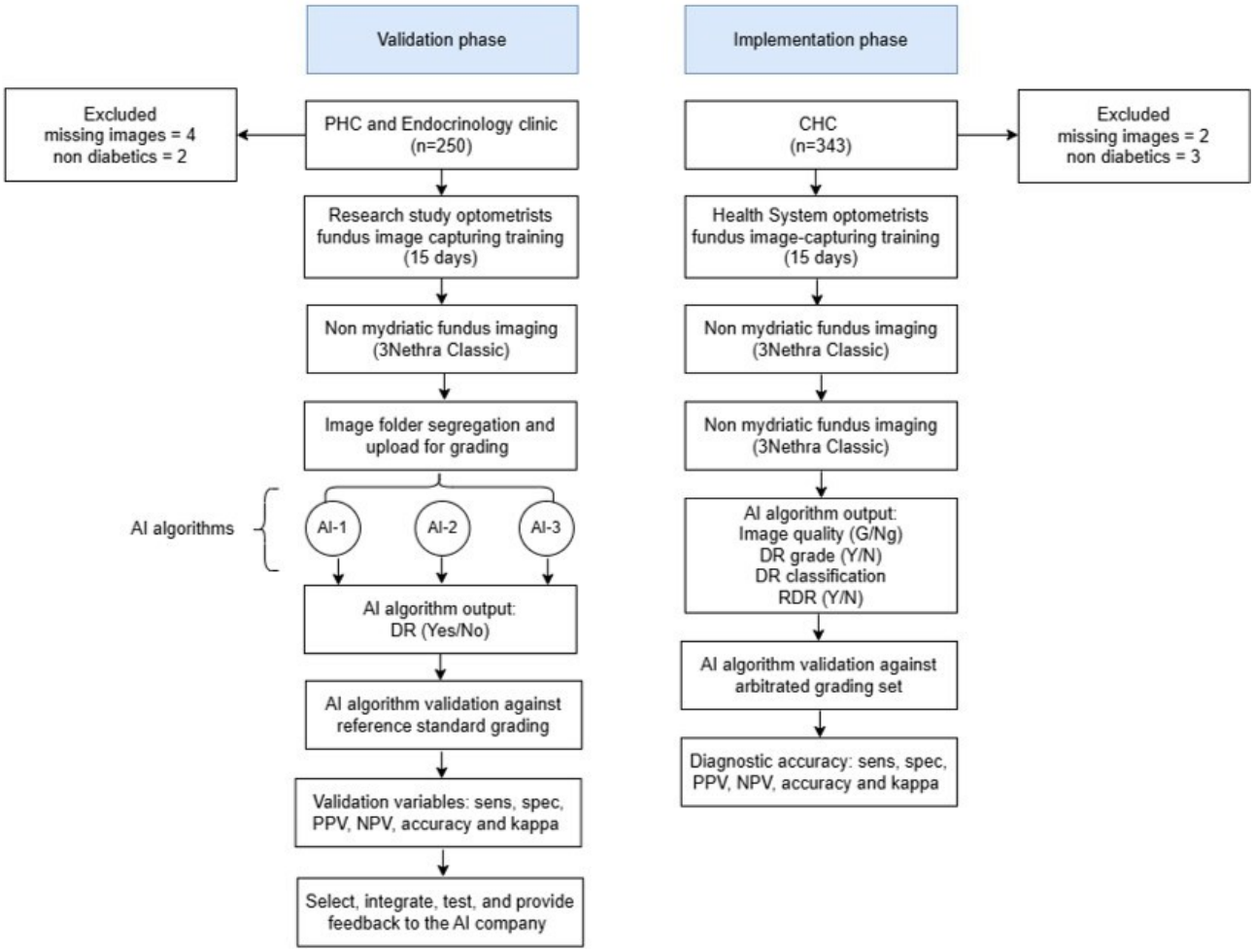
Methods

Study Design

The study prospectively validated three DR detection AI algorithms (validation phase) and assessed the technical feasibility of implementing a validated AI algorithm in public health settings (implementation phase). The STARD (Standards for Reporting of Diagnostic Accuracy Studies) checklist [19] was used to report the completeness and transparency of the diagnostic accuracy study and the iCHECK-DH framework to enhance the completeness and transparency of reporting related to the digital health implementation components [20]. Figure 1 summarizes the study design.

XSL•FO
RenderX

Figure 1. Study flow chart. Implementation phase occurred after the completion of the validation phase (ie, not simultaneously). AI: artificial intelligence; CHC: community health center; DR: diabetic retinopathy; PHC: primary health center; PPV: positive predictive value; NPV: negative predictive value; RDR: referable diabetic retinopathy.



Ethical Considerations

The study received approval from the Postgraduate Institute of Medical Education and Research (PGIMER) Institutional Ethics Committee (PGI/IEC/2020/001342) and followed the recommendations of the Declaration of Helsinki. The study was prospectively registered with the Clinical Trials Registry India (CTRI/2022/10/046185). Individuals aged > 30 years with a history of diabetes mellitus were screened for DR, following the National Program for Prevention and Control of Non-Communicable Diseases [21]. Informed consent was obtained, and their routine care remained unchanged. All data used in this study were anonymized prior to analysis, with no personal identifiers retained.

Study Site (Real-World Settings)

Validation was conducted from March to June 2021 at the Department of Endocrinology, PGIMER, Chandigarh, and a Primary Health Center (PHC) in Khizrabad, District Mohali, Punjab. The AI-enabled DRS was implemented between February 2022 and June 2022 at a community health center (CHC) in Badhani Kalan, Moga District, Punjab, India.

Sample Size

Sample sizes (validation=256; implementation=348) were calculated assuming DR prevalence of 17%, nongradable image rates of 18.4% in validation and 30.3% during implementation, 70% sensitivity, 86% specificity, 95% CI, and nonresponse rates of 10% and 15% in validation and implementation, respectively [3,22-25].

AI Algorithms

Based on a scoping review, five AI companies that used cloud-based AI (four Indian, one international) were invited. Before validation, they received the study objectives and camera or image specifications.

Fundus Image Acquisition

Training of Optometrists

Two experienced optometrists were trained for 15 days at the Advanced Eye Centre (AEC) and PHC settings before validation (Table S1 in Multimedia Appendix 1) [26]; two distinct optometrists received similar training for implementation in Moga district. Training covered identifying good-quality images [27] and capturing additional images when needed. They were supervised until proficient in independent data collection and imaging.

XSL•FO
RenderX

Camera

All participants underwent nonmydriatic, two-field (macula and disc-centered), 45° FOV fundus photography using a 3Netra Classic Portable Benchtop Fundus Camera (Forus Health) [26].

Recruitment Process

During validation, participants were recruited through Accredited Social Health Activist (ASHA) workers at PHCs and by research staff in the endocrinology department . The study did not alter patients' routine care during the recruitment process. During implementation, recruitment at the CHC was assisted by a nurse from the medicine clinic.

Darkroom

[To minimize ungradable images from nonmydriatic cameras that are a key challenge for real-world DRS programs, [28]dark rooms with sealed windows and ventilators were set up at PHC Khijrabad and at CHC Badhani Kalan (Figure S1 in Multimedia Appendix 1), with participants seated in the dark for ≥2 minutes to achieve physiological mydriasis before imaging.

Image Grading

Image identifiers were removed, and images remained unprocessed before AI analysis. The research optometrist sorted and uploaded them by eye laterality (ie, right and left eye). AI companies had no direct access; only the uploading optometrist handled the images per the agreement with the companies. A separate, role-based account was created for image upload and grading, accessible only to the optometrist. Audit logs tracked access, and secure file transfer protocols protected the transmission of images and the human grader had similar restricted access. Validation images were not used for training or testing the AI.

AI Grading Protocol

The AI algorithms' screening outcomes were inconsistent in providing DR stages (mild nonproliferative diabetic retinopathy (NPDR)), moderate NPDR, severe NPDR, and proliferative diabetic retinopathy (PDR)), diabetic macular edeme (DME) (yes/no), and referable DR (RDR) (Figure S2 in Multimedia Appendix 1). Hence, the DR grade (yes/no) was chosen to validate the AI algorithms discussed elsewhere [29].

Reference Standard Grading

All AI screening outputs were manually graded by human graders using the International Classification for Diabetic Retinopathy (ICDR) classification system [30]. Images were labeled as "gradable" or "non-gradable," and DR as "present" or "absent." DR was classified as mild, moderate, or severe NPDR and PDR [30]. Microaneurysms that are early signs of DR, indicate mild NPDR [31]. Any DR mentioned above, including moderate NPDR were considered referable DR (RDR) [30]. DME was defined as hard exudates with or without foveal involvement [3]. Images with ≥80% visibility and clear view up to the third vascular branch were considered gradable and assessed for DR [27].

- Validation phase*:* Two masked human graders (HG1 and HG2), a trained optometrist with three years of grading experience, and a retina-trained ophthalmologist with seven years of grading experience, with different institutional affiliations, independently graded all the fundus images. A senior vitreoretinal expert with 25 years of grading experience re-evaluated 224 images from 56 participants (75%) where HG1 and HG2 disagreed on DR presence. A strong level of agreement [32] (κ=0.85) was observed between HG2 and the senior retina specialist; hence, HG2 grading was considered the reference standard (RS) for AI validation.
- Implementation phase*:* All images were independently graded by two masked human graders (HG1 and HG2), who were different from those involved in the validation phase. In cases of disagreement, the grades were reviewed and adjudicated by a senior vitreoretinal specialist with over eight years of experience in grading. The final consensus-based, arbitrated dataset served as the RS and was used for all statistical analyses.

AI Integration and Implementation

The better-performing AI algorithm was integrated into the 3Netra Classic and pilot-tested for two weeks at AEC and District Hospital (DH), Mohali. This phase ensured hardware-software compatibility, assessed internet connectivity, and included dummy tests to validate outputs before implementation. The two-week testing at PGIMER and DH Mohali validated the full AI workflow, identified technical issues, assessed reliability in clinical settings, and highlighted data and reporting bottlenecks.

This feedback led to key refinements, including better internet connectivity, mandatory clinical variables, faster result turnaround, and local data storage on the National Institute of Transforming India (NITI) server for compliance. Final adjustments were implemented at Moga and Mohali sites (Figure S3 in Multimedia Appendix 1). The AI algorithm did not undergo additional training during the implementation period. Testing was conducted by optometrists, supported by a research optometrist, and supervised by the data scientist and principal investigator. The research team coordinated with the AI company to address feedback, and the machine learning scientist assisted with preimplementation adjustments.

Poststudy, a follow-up mechanism was established to ensure continued service delivery (6 mo), with the optometrist monitored for adherence to screening protocols. Notably, the retinal camera and adjustable stand were retained at the CHC rather than being reclaimed as study assets, reinforcing sustainability through local ownership and continuity of service.

Referral Recommendation and Telephonic Follow-Up

Referral were based on cases diagnosed as moderate or more severe, as well as those with DME [30]. Participants requiring follow-up were contacted by phone one month after their DRS appointment to assess compliance, with up to three contact attempts made to gather this information.

Data Analysis

The study data was collected using Research Electronic Data Capture (REDCap) [33]. Deidentified data were downloaded

XSL•FO
RenderX

from REDCap and imported into Stata/IC (version 15.1; StataCorp) [34] for analysis.

The AI platform's sensitivity, specificity, positive predictive value (PPV), and negative predictive value (NPV) were estimated with 95% exact binomial CIs. A *P* value of <·05 was considered significant for all statistical tests. A κ value was calculated monthly during the implementation phase to assess the optometrists learning in image acquisition and the AI algorithm's performance in image quality and DR diagnosis. This measured the agreement between AI and RSs for image quality and DR diagnosis. The folders with missing bilateral or macula-centered images and people without diabetes mellitus were excluded from the analysis. All analyses were conducted on an eye-wise basis.

Results (Implementation)

Three AI algorithm companies Leben Care Health Services, Retinal AI Diagnostic Software, and SigTuple Technologies. Each AI platform was masked from the others and randomly assigned labels such as AI 1, AI 2, and AI 3. One Indian AI algorithm declined participation, and an Food and Drug Administration (FDA)-approved algorithm was excluded due to low specificity in interim analysis. Two Indian AI companies approached during the implementation phase but were not included.

Sociodemographic Details of the Study Participants

Among the 250 participants in the validation phase, 182 were recruited at the PHC Khijrabad and 68 from the endocrinology clinic. The mean age of the participants was 53.5 (SD 7) years in the PHC and 47.2 (SD 4) years in the Endocrinology clinic, respectively. Overall, 87/250 (48.3%) participants in the PHC group were men and 95 (51.7%) were women, and those in the Endocrinology group included 38 (55.8%) men and 30 (44.1%) women. In the implementation phase, 343 participants were recruited. The participants' mean age was 58.48 (SD 10.41) years, with 202/343 (59%) women and 140 (41%) men (Table 1).

Table . Study participants demographic characteristics.

Characteristics	Validation phase (n=250)	Implementation phase (n=343)
Gender n (%)		
Men	121(48.4%)	141 (41)
Women	129(51.6%)	202 (59)
Age (years), mean (SD)	54.4 (13.8)	58.4 (10.4)
Duration of diabetes (years), mean (SD)	7.1 (6.1)	6.2 (5.9)
Education, n (%)		
Illiterate	72(28.8)	135(39.4)
Primary	79(31.6)	125(36.4)
Matriculation	70(28)	63(18.4)
Secondary	14(6.8)	8(2.3)
Graduation and above	15(6)	12(3.5)

Validation Phase

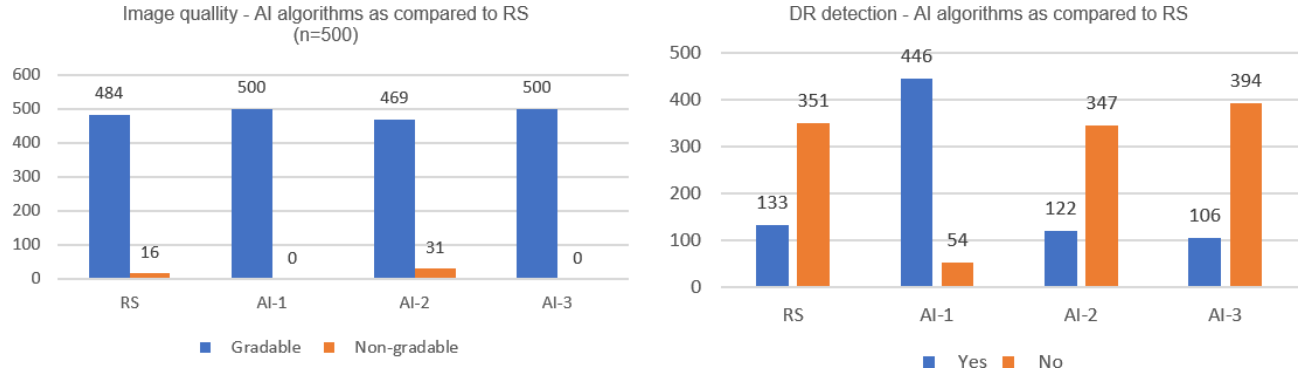
The analysis included 1099 fundus images of 500 eyes from 250 participants. According to the RS, 484 (96·8%) of eyes were gradable, with 16 (3·2%) being ungradable. AI 1, AI 2, and AI 3 achieved excellent gradability (100%, 93.8%, and 100%, respectively). The RS detected DR in 133 (27.48%) of the eyes; AI 1 detected notably more cases of DR in 446 (89.2%) eyes compared with AI 2, 122 (26.22%), and AI 3, 106 (21.2%) (Figure 2).

AI 3 showed the best performance with specificity of detecting DR, 96.01% (93·24 - 97·72); sensitivity, 68.42% (59·71 - 76.05); PPV, 86.67% (78.31 - 92.26); accuracy, 88.43%; and agreement with the RS (κ=0·65) and was selected for implementation (Table S2 in Multimedia Appendix 1). The validation results have been presented elsewhere [29].

Based on our study findings and recommendations from the project technical oversight committee which comprised ophthalmologists, public health experts, academicians, technologists, and research scientists providing technical expertise and strategic direction to evaluate, guide, and strengthen the project's scientific rigor. The AI company was recommended to train its algorithm for DR stages, DME grading, and referral guidelines, incorporating inputs on camera integration, connectivity, and platform functionality. Changes were completed within four months, and implementation began at CHC, with testing images excluded from the final set (Table S3 in Multimedia Appendix 1). Changes were incorporated within four months and implemented at CHC.

XSL•FO
RenderX

Figure 2. Image quality of artificial intelligence (AI) algorithms as compared to the reference standard (RS). DR: diabetic retinopathy.

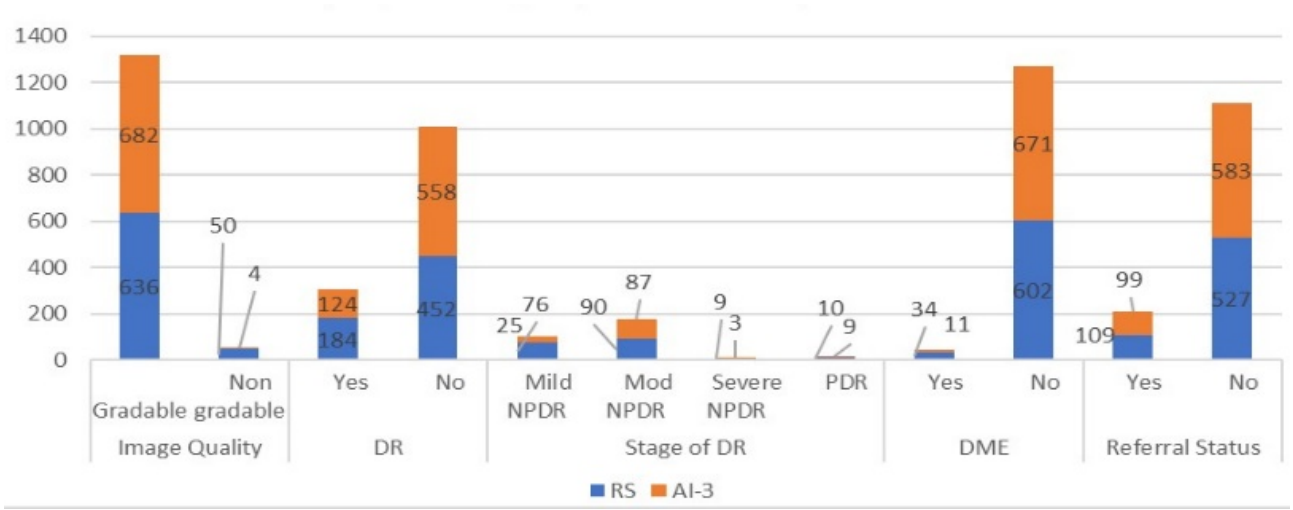


Implementation Phase

During the implementation phase, 1372 fundus images were captured from 686 eyes of 343 participants. AI-3 exhibited slightly higher image gradability (682, 99.5%) than the RS (336, 92.71%). AI-3 identified 124 (18.2%) of participants with DR, while the RS detected 189 (28.9%). Moderate NPDR was most common (AI-3 at 87 (12.8%) and RS at 90 (14.1%). DME detection was lower for AI-3, 11 (1.6%) than the RS, 34 (5.3%). Referral rates were almost similar, (AI-3: 99; 14.5%) and RS (109, 17.1%) (Figure 3).

Among the 50/686 (7.3%) ungradable eyes graded by HG, 21 (42%) had cataracts, while none labeled as ungradable by AI had cataract. The sensitivity, specificity, PPV, and NPV of AI-3 algorithm for DR detection were 99.6%, 64.7%, 87.4%, and 98.3%, respectively. For DME, specificity, PPV, and NPV were 99.7%, 81.8%, and 96%, respectively. However, sensitivity is relatively low (26.5%); for detecting RDR, sensitivity and specificity were 78.9% and 98.1%. For image gradability, the AI's sensitivity was excellent at 100%, but specificity was low (8%) (Table 2).

Figure 3. Diabetic retinopathy screening outputs of AI as compared to the reference standard at Community Health Center Moga. AI: artificial intelligence; DME: diabetic macular edeme; DR: diabetic retinopathy; PDR: proliferative diabetic retinopathy; NPDR: nonproliferative diabetic retinopathy.



XSL•FO
RenderX

Table . Sensitivity, specificity, PPV[a], NPV[b] of the AI[c] algorithm for various outcome variables with a reference standard.

Outcome variables	Image gradability	DR[d] grade	DME[e] grade	RDR[f]
Sensitivity (%)	100	99·6	26·5	78·9
Specificity (%)	8	64·7	99·7	98·1
PPV (%)	93·2	87·4	81·8	89·6
NPV (%)	100	98·3	96	95·7
κ value	0.69	0.72	0.38	0.81

[a]PPV: Positive predictive value.

[b]NPV: Negative predictive.

[c]AI: artificial intelligence.

[d]DR: Diabetic retinopathy.

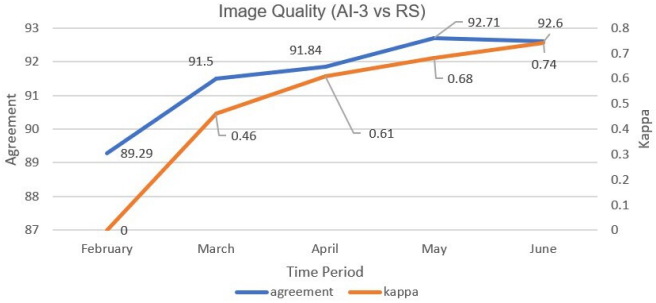
[e]DME: Diabetic macular edeme.

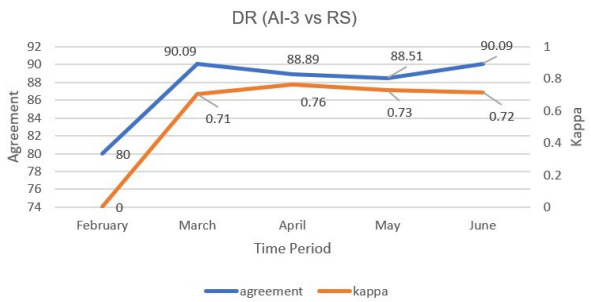
[f]RDR: referable diabetic retinopathy.

κ Statistic Variation Across the Study Period

Figure 4 shows κ variations for image quality and DR grades over 4.5 months when the health system optometrist captured the images. κ values of image quality increased from 0 in February to 0.74 in June, and for DR grade from 0 to 0.71 in June. This steady improvement could be attributed to the enhanced image quality captured by the optometrist over the study period and higher; in DR, this increase can be linked to better image quality and higher detection, with slight dips due to variation in DR severity or case complexity.

Figure 4. Agreement and kappa statistics for image quality and DR grade between AI and reference standard. AI: artificial intelligence; DR: diabetic retinopathy; RS: reference standard.





Participant Referral and Follow-Up

Of 64 referred participants, 28 (43.8%) were contacted; only 9 (14%) adhered to referral advice and visited an ophthalmologist for a review. Of these, 1 received an Optical Coherence Tomography referral, 5 went to facilities without eye care services, 1 received eye drops, 1 was advised antivascular endothelial growth factor injection, 1 left after receiving laser treatment, and 1 had a follow-up visit.

Reasons for nonadherence included harvesting season (n=11), lack of family support (n=2), time constraints (n=2), extended absence from home (n=1), financial dependence on family (n=2), and comorbidities (n=1).

Discussion

Principal Findings

This study is among the first in India to validate multiple AI algorithms for DRS, critically assessing their technical feasibility for integration into real-world public health settings. We evaluated the best-performing AI algorithm using images captured by a skilled research optometrist. This study outlines the Government of India's efforts to foster an ecosystem that ensures the integration of responsible AI technologies before application to end users [35].

In our study, AI system performance during validation varied significantly: sensitivity (59.7%97.74%), specificity (14.25%96.01%), PPV (30.16%86.67%), NPV (85%94.34%), and accuracy (37.19%88.43%). A multicenter study by Lee et al systematically compared seven AI-based DRS algorithms, revealing high NPVs (82.72%93.69%) but widely varying sensitivities (50.98%85.90%) in real-world performance [36]. In pivotal clinical trials for the IDX AI algorithm, the FDA's benchmark for superiority was set at 85% sensitivity and 82.5% specificity [13]. Although AI-3 sensitivity (68.3%) was below the FDA's >85% threshold, it outperformed other AIs in other diagnostic metrics: specificity (96.01%), PPV (86.67%), NPV (88.92%), and accuracy (88.43%). Prospective validation of a DRS algorithm at two Indian tertiary eye care hospitals demonstrated 89% sensitivity and 92% specificity on nonmydriatic images [37].

However, there are challenges in comparing algorithms using published results due to the variations in study methodologies [38]. One challenge is the dependence of an AI algorithm's accuracy on the quality of the retinal images obtained [27]. Our

XSL•FO
RenderX

study included ungradable images in validation, contrasting with many studies that preprocess or exclude lower-quality images in their training data sets [12,13,39-41] (Figure S6 in Multimedia Appendix 1). Excluding these images fails to reflect real-world settings, potentially lowering the algorithm's performance [13,41]. To date, validation studies demonstrate that most AI algorithms using mydriatic fundus images achieve high diagnostic accuracy [42]. In the validation phase, the dark room environment facilitated nonmydriatic conditions, yielding 0% ungradability for AI-1 and AI-3, 6.2% for AI-2, and 3.2% by human grader, contrasting with 1830% in LMIC settings per a systematic review [38,42].

Cataracts are a leading cause of ungradable images [28]. However, no images with cataract or other media opacities were classified as ungradable during implementation, potentially affecting AI-3 specificity (Table 2). Notably, the AI-3 algorithm failed to detect 21 (42%) eyes with cataracts, categorized as gradable. The AI-3 algorithm's sensitivity increased significantly from 68.4% to 99.6%, while specificity decreased from 96% to 64.7% between the validation and implementation phases. The sensitivity likely improved post validation due to algorithm training (Table S2 in Multimedia Appendix 1). The presence of cataracts, affecting media opacity and gradability, likely could have decreased specificity by increasing false positives [43]. After algorithmic training, AI-3 detected DME (Table 2) and sensitivity (26.5%), highlighting the need for improved training to enhance DME sensitivity and subsequently achieve higher RDR sensitivity (78.9%).

Optometrists serve as frontline eye care providers globally and are ideally positioned for task-sharing in DRS. Their integration into DRS and care pathways is well-established in diverse models worldwide, supporting sustainable and scalable eye care delivery [44-46]. In this study, a health system optometrist was trained and engaged in DRS at the CHC, with oversight from the research team. Over the study period, image quality and DR detection improved, reflecting a positive learning curve (Figure 3). These findings highlight the potential of optometrist-led AI-assisted screening in strengthening task-shifting models and expanding access to DR care in resource-limited settings [47-49]. Implementing an opportunistic AI-enabled DRS model holds promise for enhancing detection rates [47]. However, our study's adherence to referral recommendations remains suboptimal, with approximately 14% of participants attending recommended follow-up visits at an eye care facility. Key barriers to referral adherence include awareness gaps, logistical challenges (ie, travel, DR related cost), and persisting health system limitations, including weak referral pathways and poor patient tracking [48]. Personalized approaches, such as phone calls, voicemails, and detailed result letters, are shown to be effective in improving referral adherence [49]. Low referral adherence underscores the need for effective, coordinated referral pathways before introducing new screening models, while recognizing the vital role of teleophthalmology in such systems [47,50].

A notable strength of this study is its real-time implementation, conducted during regular clinics by a health system optometrist within a public health care setting. This marks a significant milestone that is likely to substantially enhance DRS services. The study showed that training and monitoring fundus image quality could significantly improve the effectiveness of the AI-enabled DRS program.

However, several limitations should be considered when interpreting the results. Using a single fundus camera may limit generalizability, as AI performance may vary across camera models and imaging conditions. Additionally, the study relied on a specific AI algorithm, which may not account for variations in other models or evolving AI systems. Setting-specific constraints such as workflow integration and infrastructure availability could also impact scalability. Furthermore, potential biases in real-world data, such as variations in patient demographics, image quality, and disease prevalence, may influence AI performance and limit broader applicability. Integrating DRS was feasible; however, we could monitor the optometrist only for three months poststudy. Regular monitoring is crucial for program sustainability and healthcare provider motivation.

Lessons Learnt

Operational challenges in DRS included limited patient access due to long travel distances, poor transport, and low awareness; inadequate infrastructure; and ergonomic barriers affecting both patients and screeners. Uncontrolled lighting and power issues led to 26% ungradable images. Adaptive measures, such as transport support, ergonomic adjustments, darkroom setups, and equipment reinforcements, raised image gradeability to 95.6% and improved efficiency. Addressing these barriers through infrastructure upgrades, controlled environments, and community facilitation is essential for sustainable DRS in primary health care systems.

In conclusion, this study highlights the essential role of systematic AI validation in integrating technology responsibly into clinical workflows. By demonstrating AI's feasibility for DRS in Indian public health settings, our findings support scalable solutions to improve health care accessibility in resource-constrained contexts across the Global South. However, long-term sustainability and large-scale implementation will require ongoing funding, a robust workforce, and effective policy integration. Further research is needed to evaluate the large-scale deployment of AI-driven screening strategies, examining their clinical effectiveness, cost-effectiveness, and the challenges of implementing them in real-world settings.

Acknowledgments

We extend our gratitude to the Punjab Health Department, Civil Surgeons of Mohali and Moga, Senior Medical Officers of Boothgarh and Badhani Kalan, and the Deputy Commissioner of Moga for their support in conducting this study. The study was funded by the National Institution for Transforming India (NITI) Aayog, the Government of India.

XSL•FO
RenderX

Parts of this study were presented in abstract form at the Global Partnership on Artificial Intelligence (GPAI) Summit, New Delhi, India, 12–14 December 2023 [29].

Authors' Contributions

Conceptualization: AC, A Kankaria, GM, MD, VG
Data curation: DB, GK, LK, NM, PV
Formal analysis: AC, VM
Methodology: AC, A Kankaria, GM, MD, VG
Validation: AC, MD, VM
Writing – original draft: AC, A Kankaria, MD
Writing – review & editing: A Kernohan, GM, LV, NS

Conflicts of Interest

None declared.

Multimedia Appendix 1
Supplementary materials.
[DOCX File, 792 KB - medinform_v13i1e67529_app1.docx]

Checklist 1
iCHECK-DH: Guidelines and Checklist for the Reporting on Digital Health Implementations.
[PDF File, 160 KB - medinform_v13i1e67529_app2.pdf]

References

1. Cho NH, Shaw JE, Karuranga S, et al. IDF Diabetes Atlas: global estimates of diabetes prevalence for 2017 and projections for 2045. Diabetes Res Clin Pract 2018 Apr;138:271-281. [doi: 10.1016/j.diabres.2018.02.023] [Medline: 29496507]
2. International Diabetes Federation. IDF Diabetes Atlas, 7th edition: International Diabetes Federation; 2015.
3. Scanlon PH. The English National Screening Programme for diabetic retinopathy 2003-2016. Acta Diabetol 2017 Jun;54(6):515-525. [doi: 10.1007/s00592-017-0974-1] [Medline: 28224275]
4. Alowais SA, Alghamdi SS, Alsuhebany N, et al. Revolutionizing healthcare: the role of artificial intelligence in clinical practice. BMC Med Educ 2023 Sep 22;23(1):689. [doi: 10.1186/s12909-023-04698-z] [Medline: 37740191]
5. Padhy SK, Takkar B, Chawla R, Kumar A. Artificial intelligence in diabetic retinopathy: a natural step to the future. Indian J Ophthalmol 2019 Jul;67(7):1004-1009. [doi: 10.4103/ijo.IJO_1989_18] [Medline: 31238395]
6. Grzybowski A, Brona P, Lim G, et al. Artificial intelligence for diabetic retinopathy screening: a review. Eye (Lond) 2020 Mar;34(3):451-460. [doi: 10.1038/s41433-019-0566-0] [Medline: 31488886]
7. Bali J, Bali O, Sahu A, Boramani J, Senthil T, Deori N. State of the nation survey on cataract surgery in India. Indian J Ophthalmol 2022 Nov;70(11):3812-3817. [doi: 10.4103/ijo.IJO_1151_22] [Medline: 36308101]
8. Ramasamy K, Raman R, Tandon M. Current state of care for diabetic retinopathy in India. Curr Diab Rep 2013 Aug;13(4):460-468. [doi: 10.1007/s11892-013-0388-6] [Medline: 23657764]
9. Beede E, Baylor E, Hersch F, et al. A human-centered evaluation of a deep learning system deployed in clinics for the detection of diabetic retinopathy. 2020 Apr 21 Presented at: Conference on Human Factors in Computing Systems - Proceedings; Apr 21, 2020; Honolulu HI USA. [doi: 10.1145/3313831.3376718]
10. Chassagnon G, Vakalopoulou M, Paragios N, Revel MP. Artificial intelligence applications for thoracic imaging. Eur J Radiol 2020 Feb;123:108774. [doi: 10.1016/j.ejrad.2019.108774] [Medline: 31841881]
11. Keel S, Lee PY, Scheetz J, et al. Feasibility and patient acceptability of a novel artificial intelligence-based screening model for diabetic retinopathy at endocrinology outpatient services: a pilot study. Sci Rep 2018 Mar 12;8(1):4330. [doi: 10.1038/s41598-018-22612-2] [Medline: 29531299]
12. Gulshan V, Peng L, Coram M, et al. Development and validation of a deep learning algorithm for detection of diabetic retinopathy in retinal fundus photographs. JAMA 2016 Dec 13;316(22):2402-2410. [doi: 10.1001/jama.2016.17216] [Medline: 27898976]
13. Abràmoff MD, Lavin PT, Birch M, Shah N, Folk JC. Pivotal trial of an autonomous AI-based diagnostic system for detection of diabetic retinopathy in primary care offices. NPJ Digit Med 2018;1(1):39. [doi: 10.1038/s41746-018-0040-6] [Medline: 31304320]
14. Romero-Brufau S, Wyatt KD, Boyum P, Mickelson M, Moore M, Cognetta-Rieke C. A lesson in implementation: a pre-post study of providers' experience with artificial intelligence-based clinical decision support. Int J Med Inform 2020 May;137:104072. [doi: 10.1016/j.ijmedinf.2019.104072] [Medline: 32200295]

XSL•FO
RenderX

15. Kohner EM, Aldington SJ, Stratton IM, et al. United Kingdom Prospective Diabetes Study, 30: diabetic retinopathy at diagnosis of non-insulin-dependent diabetes mellitus and associated risk factors. Arch Ophthalmol 1998 Mar;116(3):297-303. [doi: 10.1001/archopht.116.3.297] [Medline: 9514482]
16. Topol EJ. High-performance medicine: the convergence of human and artificial intelligence. Nat Med 2019 Jan;25(1):44-56. [doi: 10.1038/s41591-018-0300-7] [Medline: 30617339]
17. Kanagasingam Y, Xiao D, Vignarajan J, Preetham A, Tay-Kearney ML, Mehrotra A. Evaluation of artificial intelligence-based grading of diabetic retinopathy in primary care. JAMA Netw Open 2018 Sep 7;1(5):e182665. [doi: 10.1001/jamanetworkopen.2018.2665] [Medline: 30646178]
18. Kelly CJ, Karthikesalingam A, Suleyman M, Corrado G, King D. Key challenges for delivering clinical impact with artificial intelligence. BMC Med 2019 Oct 29;17(1):195. [doi: 10.1186/s12916-019-1426-2] [Medline: 31665002]
19. Cohen JF, Korevaar DA, Altman DG, et al. STARD 2015 guidelines for reporting diagnostic accuracy studies: explanation and elaboration. BMJ Open 2016 Nov 14;6(11):e012799. [doi: 10.1136/bmjopen-2016-012799] [Medline: 28137831]
20. Perrin Franck C, Babington-Ashaye A, Dietrich D, et al. iCHECK-DH: Guidelines and Checklist for the Reporting on Digital Health Implementations. J Med Internet Res 2023;25:e46694. [doi: 10.2196/46694]
21. National program for prevention and control of cancer, diabetes, cardiovascular diseases and stroke (NPCDCS)—handbook for counselors reducing risk factors for noncommunicable diseases risk factors for NCDs. Directorate General of Health Services Ministry of Health and Family Welfare Government of India. URL: https://nhm.gov.in/index1.php?lang=1&level=2&sublinkid=1048&lid=604 [accessed 2023-10-11]
22. Arenas-Cavalli JT, Abarca I, Rojas-Contreras M, Bernuy F, Donoso R. Clinical validation of an artificial intelligence-based diabetic retinopathy screening tool for a national health system. Eye (Lond) 2022 Jan;36(1):78-85. [doi: 10.1038/s41433-020-01366-0] [Medline: 33432168]
23. Rêgo S, Dutra-Medeiros M, Soares F, Monteiro-Soares M. Screening for diabetic retinopathy using an automated diagnostic system based on deep learning: diagnostic accuracy assessment. Ophthalmologica 2021;244(3):250-257. [doi: 10.1159/000512638] [Medline: 33120397]
24. Sivaprasad S, Netuveli G, Wittenberg R, et al. Complex interventions to implement a diabetic retinopathy care pathway in the public health system in Kerala: the Nayanamritham study protocol. BMJ Open 2021 Jun 28;11(6):e040577. [doi: 10.1136/bmjopen-2020-040577] [Medline: 34183333]
25. Sivaprasad S, Raman R, Conroy D, et al. The ORNATE India Project: United Kingdom-India Research Collaboration to tackle visual impairment due to diabetic retinopathy. Eye (Lond) 2020 Jul;34(7):1279-1286. [doi: 10.1038/s41433-020-0854-8] [Medline: 32398841]
26. Darwish DY, Patel SN, Gao Y, et al. Diagnostic accuracy and reliability of retinal pathology using the Forus 3Nethra fundus camera compared to ultra wide-field imaging. Eye (Lond) 2019 May;33(5):856-857. [doi: 10.1038/s41433-019-0339-9] [Medline: 30679873]
27. Shi C, Lee J, Wang G, Dou X, Yuan F, Zee B. Assessment of image quality on color fundus retinal images using the automatic retinal image analysis. Sci Rep 2022 Jun;12(1):10455. [doi: 10.1038/s41598-022-13919-2]
28. Yip MYT, Lim G, Lim ZW, et al. Technical and imaging factors influencing performance of deep learning systems for diabetic retinopathy. NPJ Digit Med 2020;3:40. [doi: 10.1038/s41746-020-0247-1] [Medline: 32219181]
29. Duggal M, Chauhan A, Kankaria A, et al. Responsible adoption of cloud-based artificial intelligence in health care: a validation case study of multiple artificial intelligence algorithms for diabetic retinopathy screening in public health settings. In: Advancing Responsible AI in Public Sector Application: Taylor and Francis; 2024.
30. Wong TY, Sun J, Kawasaki R, et al. Guidelines on Diabetic Eye Care: The International Council of Ophthalmology Recommendations for Screening, Follow-up, Referral, and Treatment Based on Resource Settings. Ophthalmology 2018 Oct;125(10):1608-1622. [doi: 10.1016/j.ophtha.2018.04.007] [Medline: 29776671]
31. Wang Z, Li X, Yao M, Li J, Jiang Q, Yan B. A new detection model of microaneurysms based on improved FC-DenseNet. Sci Rep 2022 Dec;12(1):1. [doi: 10.1038/s41598-021-04750-2]
32. McHugh ML. Interrater reliability: the kappa statistic. Biochem Med 2012:276-282. [doi: 10.11613/BM.2012.031]
33. Harris PA, Taylor R, Thielke R, Payne J, Gonzalez N, Conde JG. Research electronic data capture (REDCap)--a metadata-driven methodology and workflow process for providing translational research informatics support. J Biomed Inform 2009 Apr;42(2):377-381. [doi: 10.1016/j.jbi.2008.08.010] [Medline: 18929686]
34. Stata statistical software: release 17. StataCorp. 2021. URL: https://www.stata.com/ [accessed 2025-08-20]
35. AI & emerging technologies group promoting the adoption of cutting-edge technologies to create significant economic and societal impact. Government of India, Ministry of Electronics and Information Technology. URL: https://tinyurl.com/5f4a3kr7 [accessed 2024-06-10]
36. Lee AY, Yanagihara RT, Lee CS, et al. Multicenter, head-to-head, real-world validation study of seven automated artificial intelligence diabetic retinopathy screening systems. Diabetes Care 2021 May;44(5):1168-1175. [doi: 10.2337/dc20-1877] [Medline: 33402366]
37. Gulshan V, Rajan RP, Widner K, et al. Performance of a deep-learning algorithm vs manual grading for detecting diabetic retinopathy in India. JAMA Ophthalmol 2019 Sep 1;137(9):987-993. [doi: 10.1001/jamaophthalmol.2019.2004] [Medline: 31194246]

XSL•FO
RenderX

38. Sosale B, Sosale AR, Murthy H, Sengupta S, Naveenam M. Medios- An offline, smartphone-based artificial intelligence algorithm for the diagnosis of diabetic retinopathy. Indian J Ophthalmol 2020 Feb;68(2):391-395. [doi: 10.4103/ijo.IJO_1203_19] [Medline: 31957735]
39. Abràmoff MD, Lou Y, Erginay A, et al. Improved automated detection of diabetic retinopathy on a publicly available dataset through integration of deep learning. Invest Ophthalmol Vis Sci 2016 Oct 1;57(13):5200-5206. [doi: 10.1167/iovs.16-19964] [Medline: 27701631]
40. Gargeya R, Leng T. Automated identification of diabetic retinopathy using deep learning. Ophthalmology 2017 Jul;124(7):962-969. [doi: 10.1016/j.ophtha.2017.02.008] [Medline: 28359545]
41. Bhaskaranand M, Ramachandra C, Bhat S, et al. The value of automated diabetic retinopathy screening with the eyeart system: a study of more than 100,000 consecutive encounters from people with diabetes. Diabetes Technol Ther 2019 Nov;21(11):635-643. [doi: 10.1089/dia.2019.0164] [Medline: 31335200]
42. Piyasena M, Murthy GVS, Yip JLY, et al. Systematic review and meta-analysis of diagnostic accuracy of detection of any level of diabetic retinopathy using digital retinal imaging. Syst Rev 2018 Nov 7;7(1):182. [doi: 10.1186/s13643-018-0846-y] [Medline: 30404665]
43. Scanlon PH, Foy C, Malhotra R, Aldington SJ. The influence of age, duration of diabetes, cataract, and pupil size on image quality in digital photographic retinal screening. Diabetes Care 2005 Oct;28(10):2448-2453. [doi: 10.2337/diacare.28.10.2448] [Medline: 16186278]
44. Melles RB, Conell C, Siegner SW, Tarasewicz D. Diabetic retinopathy screening using a virtual reading center. Acta Diabetol 2020 Feb;57(2):183-188. [doi: 10.1007/s00592-019-01392-9] [Medline: 31377925]
45. George PP, Yun OCS, Siow K, et al. Is there scope for expanding the optometrist's scope of practice in Singapore? - a survey of optometrists, opticians in Singapore. Cont Lens Anterior Eye 2019 Jun;42(3):258-264. [doi: 10.1016/j.clae.2019.02.008] [Medline: 30819628]
46. Baker H, Ratnarajan G, Harper RA, Edgar DF, Lawrenson JG. Effectiveness of UK optometric enhanced eye care services: a realist review of the literature. Ophthalmic Physiol Opt 2016 Sep;36(5):545-557. [doi: 10.1111/opo.12312] [Medline: 27580754]
47. Scheetz J, Koca D, McGuinness M, et al. Real-world artificial intelligence-based opportunistic screening for diabetic retinopathy in endocrinology and indigenous healthcare settings in Australia. Sci Rep 2021 Aug 4;11(1):15808. [doi: 10.1038/s41598-021-94178-5] [Medline: 34349130]
48. Padhy D, Marmamula S, Mettla AL, et al. Changing trends in barriers to accessing eye care services in rural South India: results from the longitudinal Andhra Pradesh Eye Disease Study III (APEDS III) cohort. Eye (Lond) 2024 Aug;38(11):2209-2215. [doi: 10.1038/s41433-024-03155-5] [Medline: 38844584]
49. Bonilla-Escobar FJ, Eibel MR, Le L, Gallagher DS, Waxman EL. Follow-up in a point-of-care diabetic retinopathy program in Pittsburgh: a non-concurrent retrospective cohort study. BMC Ophthalmol 2024 Aug 20;24(1):356. [doi: 10.1186/s12886-024-03581-9] [Medline: 39164678]
50. Xie Y, Nguyen QD, Hamzah H, et al. Artificial intelligence for teleophthalmology-based diabetic retinopathy screening in a national programme: an economic analysis modelling study. Lancet Digit Health 2020 May;2(5):e240-e249. [doi: 10.1016/S2589-7500(20)30060-1] [Medline: 33328056]

Abbreviations

AI: artificial intelligence
CHC: community health center
DME: diabetic macular edeme
DR: diabetic retinopathy
DRS: diabetic retinopathy screening
NPDR: nonproliferative diabetic retinopathy
NPV: negative predictive value
PDR: proliferative diabetic retinopathy
PHC: primary health center
PPV: positive predictive value
RDR: referable diabetic retinopathy
RS: reference standard
STARD: Standards for Reporting of Diagnostic Accuracy Studies

XSL•FO
RenderX

Edited by C Perrin; submitted 14.10.24; peer-reviewed by G Lim, JJ Drinkwater, S Vipparthi; revised version received 08.06.25; accepted 08.06.25; published 09.09.25.

Please cite as:
Duggal M, Chauhan A, Gupta V, Kankaria A, Budhija D, Verma P, Miglani V, Syal P, Kaur G, Kumar L, Mutyala N, Bezbaruah R, Sood N, Kernohan A, Menon G, Vale L
Real-World Evaluation of AI-Driven Diabetic Retinopathy Screening in Public Health Settings: Validation and Implementation Study
JMIR Med Inform 2025;13:e67529
URL: https://medinform.jmir.org/2025/1/e67529
doi:10.2196/67529

© Mona Duggal, Anshul Chauhan, Vishali Gupta, Ankita Kankaria, Deepmala Budhija, Priyanka Verma, Vaibhav Miglani, Preeti Syal, Gagandeep Kaur, Lakshay Kumar, Naveen Mutyala, Rishabh Bezbaruah, Nayanshi Sood, Ashleigh Kernohan, Geeta Menon, Luke Vale. Originally published in JMIR Medical Informatics (https://medinform.jmir.org), 9.9.2025. This is an open-access article distributed under the terms of the Creative Commons Attribution License (https://creativecommons.org/licenses/by/4.0/), which permits unrestricted use, distribution, and reproduction in any medium, provided the original work, first published in JMIR Medical Informatics, is properly cited. The complete bibliographic information, a link to the original publication on https://medinform.jmir.org/, as well as this copyright and license information must be included.

XSL•FO
RenderX

Enhancing Efficiency and User Experience of Digital Community Health Worker Payments in Zanzibar: Implementation Report

Lee Pyne-Mercier[1,2], MA, MPH; Krishna Jafa[2], MBBS, MPH; Susan Maigua[2], BA; Jennifer Muli[2], BSC, MPH; Elijah Gichinga[2], BS; Antony Khaemba[2], BScN; Nitusima Kataraia[3], BSc; Aisha Mohammed[3], BA, MA; Frank Kamangadazi Tembo[3], BA, CA; Imran Esmail[3], BSc, MSc; Giulia V R Besana[3], BA, DLSHTM, MSc; Heiko Hornung[3], PhD; Ali Makame Zubeir[4], BS, MA

[1]University of Washington, 3980 15th Ave NE, Seattle, WA, United States

[2]Medic, San Francisco, CA, United States

[3]D-tree, Norwell, MA, United States

[4]Ministry of Health, Zanzibar, United Republic of Tanzania

Corresponding Author:
Lee Pyne-Mercier, MA, MPH
University of Washington, 3980 15th Ave NE, Seattle, WA, United States

Abstract

Background: Community health workers (CHWs) are essential for achieving universal health coverage and reaching the Sustainable Development Goals. Paying CHWs for their work increases their motivation and effectiveness, and is recommended by the World Health Organization and advocacy organizations such as the Community Health Impact Coalition. Many implementing organizations currently pay CHWs using mobile money or other digital means. However, most payment systems are designed without the involvement of CHWs.

Objective: In this implementation report, we describe efforts to improve efficiency, accuracy, and user experience of the CHW payment process of the Jamii ni Afya project in Zanzibar.

Methods: We applied Medic's design process to develop new functionality for the open-source Community Health Toolkit. We reviewed documentation and engaged with users to understand their needs and experiences with the current payment system. This information formed the basis of technical specifications, which were developed into a revised workflow. The workflow was iteratively tested and refined. Several steps that were managed offline, such as resolving payment discrepancies, were formalized and incorporated into the workflow. We conducted user acceptance testing to assess functionality and user experience.

Implementation (Results): The workflow was able to accurately translate programmatic data into payment information for each CHW and securely transmitted this information to a payment service provider. User acceptance testing revealed that CHWs felt the revised payment system provided them with more information and gave them a greater sense of control. Program staff felt the workflow would increase the efficiency and accuracy of the payment process, while simplifying the resolution of payment discrepancies.

Conclusions: Engaging users in the design and optimization of digital payment systems has the potential to improve the efficiency and accuracy of digital payment systems while enhancing satisfaction among all users, contributing to improved sustainability and impact of CHW programs. Definitive conclusions will depend on evaluation of the system after implementation.

(JMIR Med Inform 2025;13:e65325) doi:10.2196/65325

KEYWORDS

digital payment; mobile health; digital health; mobile payments; mobile money; user experience; Zanzibar; Africa; implementation report; community health worker

Introduction

Context

In 2015, countries worldwide committed to the Sustainable Development Goals (SDGs). The SDGs set ambitious targets for the health workforce [1]. Most countries are not on track to meet the 2030 targets without additional investments [2]. The World Health Organization (WHO) has projected a shortage of 18 million health workers by 2030 if current trends continue [3].

Community health workers (CHWs) provide health promotion and preventive and curative care for people at their doorstep. CHWs can effectively deliver various interventions, including maternal and child health services, family planning, and

XSL•FO
RenderX

prevention and management of infectious and noncommunicable diseases [4]. For example, in Rwanda and Liberia, CHWs treat half of malaria cases, and in many countries, they were essential in maintaining health services during the COVID-19 pandemic [5]. In Brazil, CHWs reached two-thirds of the population and have helped reduce child mortality by 75% [6]. CHWs are estimated to provide a return on investment of US $10 for every US $1 invested [7].

Most CHWs in low- and middle-income countries (LMICs) remain unpaid despite evidence that CHWs save lives and are highly cost-effective [4,8-10]. In Africa, 86% of CHWs are volunteers with little or no compensation [11]. The WHO's 2018 CHW guidelines recommend remuneration commensurate with job demands, complexity, hours worked, and training [9]. Satisfaction with incentives is shown to improve performance while reducing attrition [12,13]. In contrast, inadequate, partial, or delayed payments reduce motivation and intervention coverage [13].

Significant challenges have been documented with cash payments for CHWs. The logistics needed to safely transport and accurately disburse cash become increasingly difficult with scale. This can result in delayed and incomplete payments, corruption, high administrative costs, and security risks [13-18]. Digital payments have been championed as a solution. According to researchers at Makerere University, "digital payments can create a transparent record that can improve management and reduce payment delays and leakage of funds. Digitizing payments can increase the likelihood of health workers receiving complete, on-time, and convenient payment, increase transparency, reduce resource leakage, and improve service delivery's cost-effectiveness" (Makerere University, 2022; website changed and material no longer available).

Digital CHW Payments

D-tree was among the first organizations working in an LMIC to adopt digital payments. In 2011, D-tree piloted mobile money payments for CHWs, supervisors, and emergency transportation services [19,20]. In the next decade, organizations introduced digital payments for CHWs, such as malaria spray teams in Zambia, CHWs in Bangladesh and Kenya, tuberculosis screeners in Pakistan, and many others [19,21-24].

Donors accelerated the digital transition. In 2014, the US Agency for International Development mandated digital payments as the default payment mode, including those for CHWs [25]. The Global Polio Eradication Initiative began scaling up digital payments for vaccination campaign workers in 2020, reaching >250,000 recipients within a year [13,26]. The uptake of digital payments for health workers has been rapid compared to an average of 14 years for drug and/or technology innovations to reach scale [27].

Because most reports on digital payments appear in the gray literature, they tend to present positive perspectives, overlooking challenges and limitations. Regardless, several challenges have been identified. Health worker registries are often poorly maintained [13]. Resolving payment discrepancies can be time-consuming [28,29]. There are gaps in phone ownership, cellular networks, and mobile money agents [13,15,19,28]. Some CHWs have low literacy, are unfamiliar with technology, or distrust mobile money [19,28]. Requirements for a national identity document can be a barrier [19]. Financial management capacity may be insufficient [13]. Finally, transaction fees can significantly reduce the take-home pay of recipients [13,30].

Despite the rapid increase in digital payments for CHWs, there is limited evidence on the topic. There is a need for more research on the effect of digital payments on health workers' morale, performance, quality of care, intervention coverage, and health outcomes [14,17,18]. Thankfully, there are new initiatives aiming to fill the gap, notably the Digital Health Payment Initiative at Makerere University [14,31].

Participating Entities

Medic serves as the steward of the Community Health Toolkit (CHT), an open-source digital public good that supports health workers as they deliver care [32]. The CHT is a collection of technologies and resources that enable implementers to support various features and health issues. As of December 2023, in total, 75,241 CHWs and their supervisors in 18 countries used CHT-based tools to deliver care during 117.5 million home visits [33].

Medic has embraced human-centered design, engaging individuals who will use the tools in the environments where they are deployed. The CHT is intended to empower health workers to care for members of their community, and Medic's design process considers the interests of the person overall [34]. Medic has intentionally situated its staff in the communities where our tools are deployed, including Kenya, Nepal, Senegal, and Uganda.

D-tree is a global health organization working to improve access to quality health care. In Zanzibar, D-tree works with the Ministry of Health (MOH) to support Jamii ni Afya (JnA), one of the world's first nationally scaled, digitally enabled community health programs. JnA includes about 2300 CHWs and 220 CHW supervisors serving a population of nearly 2 million. The JnA smartphone app (built on CHT) guides CHWs to provide services for maternal and child health, nutrition, water, sanitation, hygiene, and early childhood development.

To support, incentivize, and monitor CHWs, a pay-for-performance scheme is used to calculate monthly remuneration. The current maximum monthly payment is approximately US $21 for CHWs and US $13 for supervisors (who are generally facility-based MOH staff). The program is included in Zanzibar's digital and community health strategies [35,36]. Higher rates of facility deliveries and reduced child stunting have been documented in the 5 years following JnA's scale-up [35].

Problem Statement

While JnA already made mobile money payments to CHWs, the process had several drawbacks. Multiple steps were needed to collect performance data, review them, and translate them into digital payments. The CHT and digital payment systems were not integrated. Users felt that they did not always have the information they needed, and several routine tasks were managed offline. In addition, financial data were not yet

XSL•FO
RenderX

included in CHT. We are not aware of peer-reviewed literature documenting how to proactively involve CHWs in designing digital payment systems. This implementation report documents our experiences working on CHW digital payments in Zanzibar and follows the i-CHECK-DH (Guidelines and Checklist for the Reporting on Digital Health Implementations) guidelines (Checklist 1) for reporting on digital health implementations [37].

Aims and Objectives

The goal of this initiative was to improve the efficiency, accuracy, and user experience of the CHW payment process. Specific objectives included reducing effort to make payments, increasing accuracy, providing real-time information to all users, and streamlining discrepancy resolution. This implementation report describes the process to design the digital tool in the preimplementation phase through the lens of user acceptance testing (UAT). UAT evaluated the product's user experience, functionality, and interoperability with a small number of users. It is outside of the scope of this report to measure more distal outcomes, such as coverage, accuracy, or impact. Once the digital payments solution is implemented, we will be positioned to report on these outcomes.

Methods

Blueprint Summary

Medic designers started by gathering information on current processes and systems via reviewing existing documentation and calls with JnA project staff. In March 2023, a team of 3 Medic staff with design and software development expertise traveled to Zanzibar for a design visit. In addition to gathering information about the current payment system, we aimed to understand users' experience with the system. We conducted interviews and focus groups with program staff and CHWs. Participants' age ranged 20-50 years. We were also able to shadow supervisors and attend monthly meetings that were an important step in the payment process.

D-tree's existing payment process is shown in Figure 1. The entire process takes approximately 2 weeks once data are synced. CHWs have 5 days at the end of each month to sync their data. Supervisors ensure that data are synced for all CHWs. Program officers subsequently review data using a custom-built dashboard. Data are exported to Microsoft Excel to calculate payments. Once approved by the project director, the finance team reformats data per payment service provider requirements, and this is uploaded using a web-based portal. Payment discrepancies are handled case-by-case by program staff.

Challenges identified by users were one input for the design. Poor connectivity and depleted mobile data often prevented CHWs from syncing, leading to payment discrepancies. CHWs felt uncertain when to expect payments or how calculations were made. Resolving payment discrepancies was time-consuming, and CHWs would sometimes incur out-of-pocket costs to follow up on payments. Some supervisors adopted improvised solutions such as the use of screenshots from CHWs' phones to verify data accuracy.

Finance staff explained that manual steps sometimes led to errors. The existing payment service provider did not offer an easy, robust, and customizable way to integrate with CHT. D-tree is transitioning management for JnA to the Zanzibar MOH by 2026, and the payment scheme needs to integrate with government administrative systems. The workflow needed to be sustainable by the program without external inputs and feasible within CHT's parameters while creating value for users.

We validated findings with stakeholders via videoconference. Part of our process entailed creating personas who interacted with the software. For each persona, we considered their job responsibilities, needs, context, and motivations. Personas were based on information collected from the design visit and included CHWs, supervisors, monitoring and evaluation officers, finance officers, directors, and district health staff.

We developed a draft workflow and refined it during several remote coworking sessions. Mostly, the steps in the workflow did not change from the existing process. However, several steps that used text message or phone communication were formalized and incorporated into the workflow. We identified 7 candidate Payment Service Providers (PSPs) through web searches and consultation with local informants. Selection criteria were adapted from global best practice [38]. The PSP was selected because of their presence in Zanzibar, available digital payment modalities (mobile networks and banks), data security, existing application programming interfaces (APIs), and reputation.

We tested the workflow in several stages using a structured test plan and we incorporated feedback iteratively. By October 2023, we had finalized integration with the PSP and returned to Zanzibar for 4 days of user acceptance testing (Figure 2). Our goals with UAT were to assess functionality of the software and to gather user feedback. Medic's designers observed users interacting with the system and interviewed them about their experiences. Participants included 23 CHWs, 8 supervisors, 8 MOH staff, and 10 D-tree staff. Participants were selected through a purposive random sample and included CHWs from both urban and rural settings because we hypothesized they might have different challenges. Examples of the user interface are shown in Figures 3 and 4. Screenshots show the English translations, but the UAT was conducted in Kiswahili. Personally identifiable information in the screenshots have been replaced by test data. Results from the UAT will inform changes to the software before finalization.

XSL•FO
RenderX

Figure 1. Existing payment process map. CHW: community health worker.

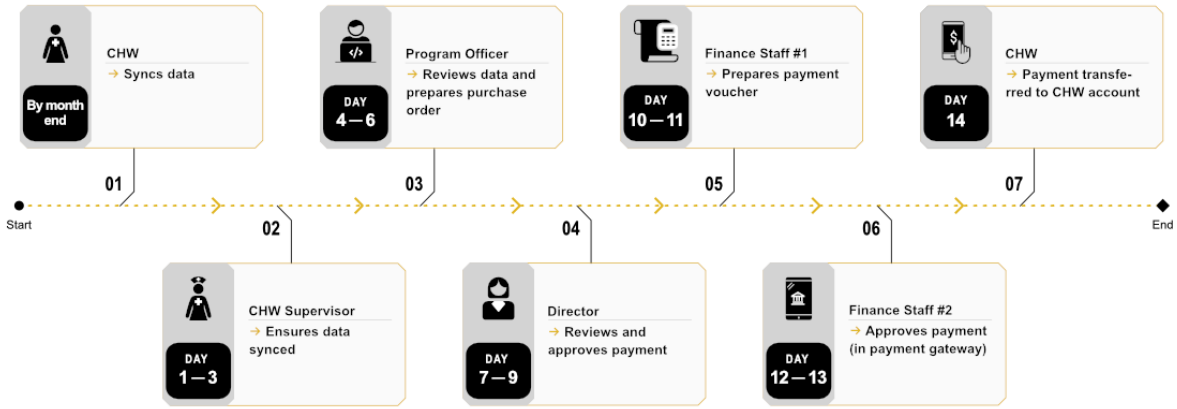
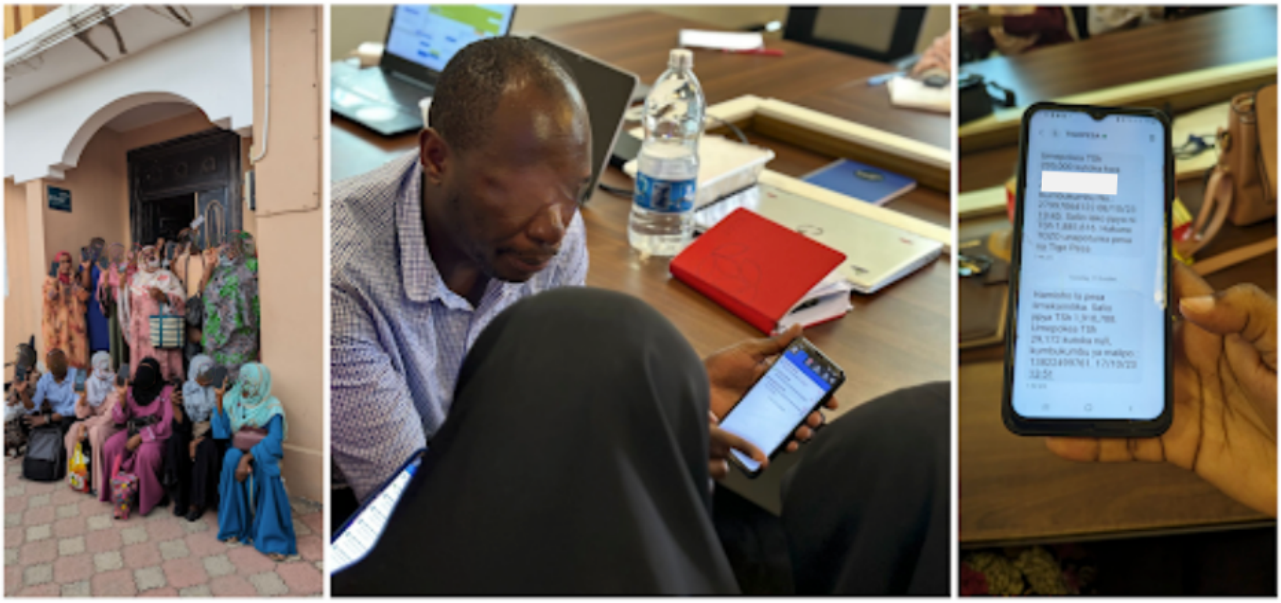
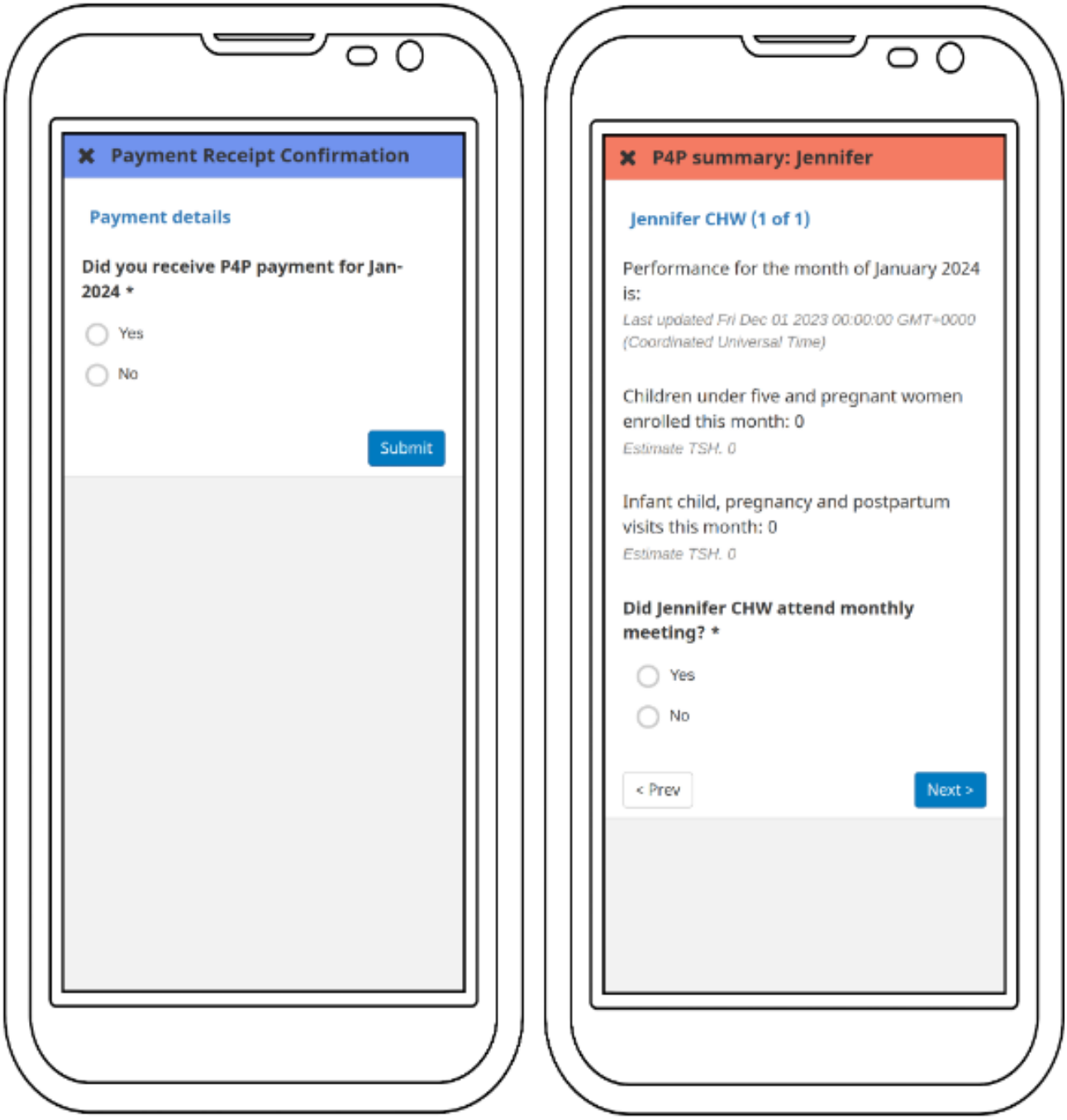


Figure 2. User acceptance testing conducted in Zanzibar.



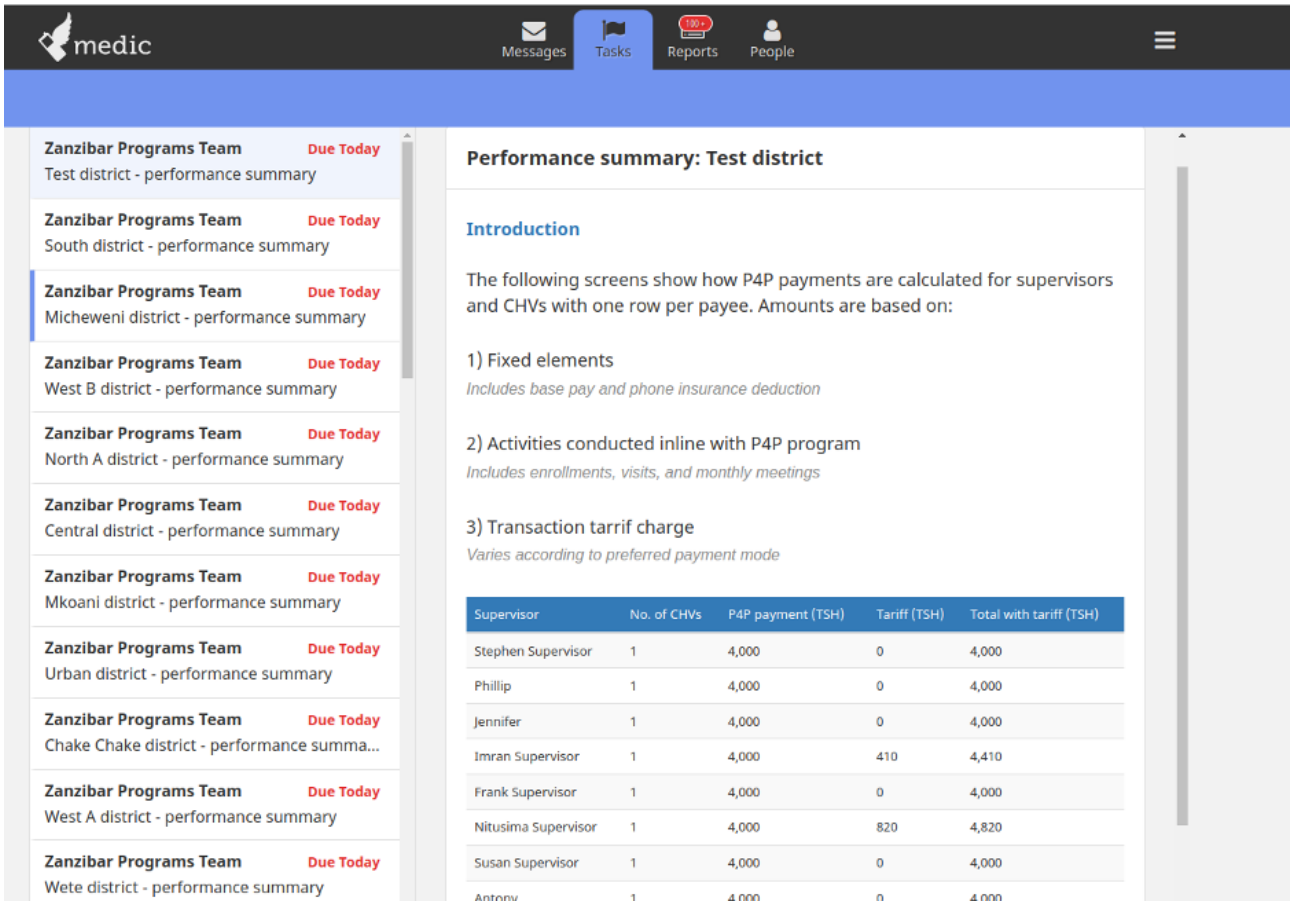
XSL•FO
RenderX

Figure 3. Screenshots of 2 example forms in the CHT (Community Health Toolkit) digital payments workflow. CHW: community health worker.



XSL•FO
RenderX

Figure 4. Screenshot of an example digital payments summary. CHV: community health volunteer.



Technical Design

The workflow was built using the CHT, which serves as the backbone of the JnA app [39]. CHT was selected by the government of Zanzibar because it is open-source, has a growing support community, can be hosted locally, and the expertise to manage the software is readily available [35]. The software was designed to function in low-bandwidth environments using affordable Android smartphones. CHWs and supervisors generally access JnA using smartphones, while office staff access JnA using a web browser.

Target Audience

The target audience consisted of all JnA stakeholders who were involved in the payment process, including CHWs, supervisors, and staff at the MOH and D-tree. The broader CHT community is a secondary audience. As an open-source tool, CHT features can be widely adapted and used by community members.

Data

The workflow we developed uses existing data, including personal identifiers for CHWs, process data, and mobile banking details. Data are collected during enrollment and while CHWs and supervisors conduct their routine activities. The workflow hierarchy was designed to protect sensitive information and is governed by a data privacy policy, which users consent to during enrollment [40]. Financial data are managed in compliance with government regulations [41]. We plan to conduct penetration testing to ensure data security at a later stage of development.

Interoperability and Integration

CHT can exchange data with other components of national health information systems based on standards including Fast Healthcare Interoperability Resources, Open Health Information Exchange, and the Open Health Information Mediator [39]. We built a custom mediator to calculate performance-based payments and to disburse them via the payment service provider's API. Available standards for financial service interoperability do not include health use cases [42]. There is a need for interoperability standards in health-related financial services.

Budget Planning and Sustainability

The Community Health Toolkit is free to use but requires funding for adaptation, hardware, and hosting. These costs are included in the Zanzibar Community Health Strategy, in addition to CHW stipends, commodities, training, and logistics costs [35]. JnA's annual operating cost is estimated at US $2.73 million per year or US $1.70 per capita. The government is currently paying the salaries of CHW supervisors and has committed to fully fund the program by 2026 with the vision of absorbing CHW as part of the health workforce. A financing strategy is currently under development. Payment service provider fees were between US $0.30 and US $0.50 per transaction during testing, representing a significant percentage of the total payments. However, fees are negotiable, and our experience was based on a very small transaction volume during the test phase.

XSL•FO
RenderX

Implementation (Results)

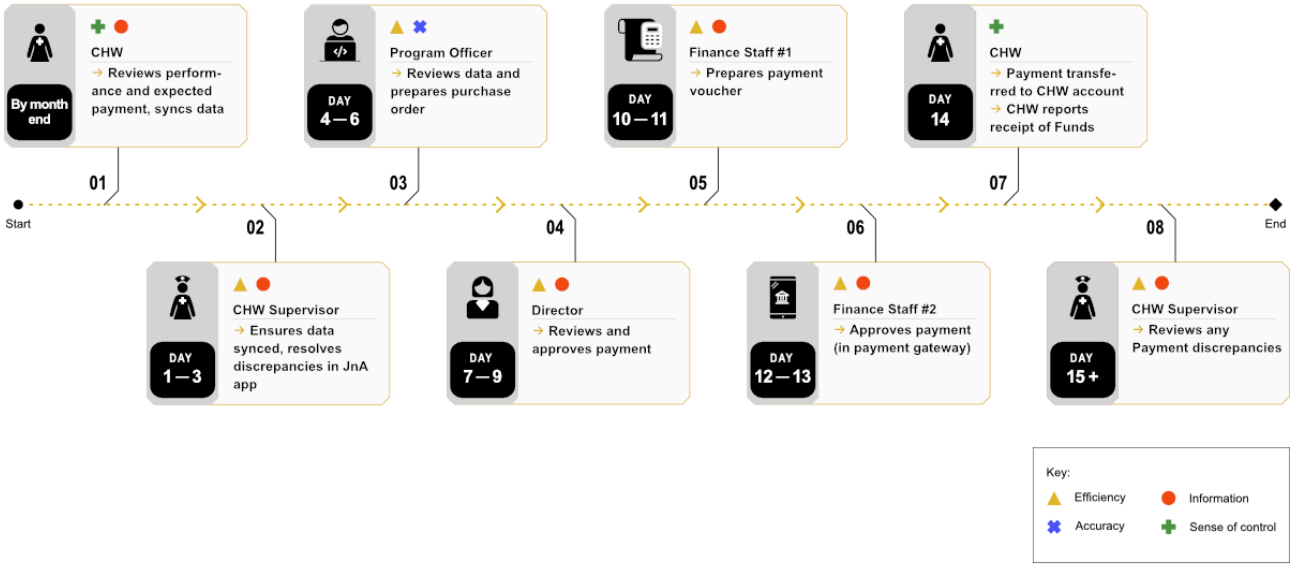
We assessed the product's functionality, user experience, and interoperability with 49 users. The workflow functioned as designed and was positively received by staff and CHWs. Most steps felt familiar, since additional functions were generally incorporated into existing forms. Participants recommended several improvements that would simplify data entry, remove unnecessary information, enable detailed or summary views, and highlight outlier data. They also recommended a process for escalating approvals to avoid delays if approvers were not available.

CHWs reported feeling a greater sense of control because they confirm their data at the beginning of the payment cycle and report payment receipt at the end. They appreciated seeing how their stipends are calculated in the app. While increased transparency is thought to increase motivation and trust, there could be other consequences such as task prioritization based on reimbursement levels. It will be important to monitor changes over time.

Supervisors felt that the workflow would facilitate performance management by providing accurate, timely data. Program staff felt that the software reduced their workload, particularly less enjoyable tasks such as reformatting data to meet PSP requirements. They thought that automated calculations would increase accuracy and believed that the workflow's ability to document approvals was easier than existing processes. Several user groups felt that the process for tracking and resolving payment discrepancies would increase responsiveness.

CHT has been primarily used for clinical and programmatic data, and its ability to manage financial information was unproven. The software reliably used performance data to calculate payments and securely communicated this information with the PSP. Some of the developed functionality, such as display of tabular information, is based on the XForm standard and can be deployed on any XForm-compatible platform like OpenDataKit to empower effective decision-making. A simplified visual of the steps in the workflow and the perceived benefits at each stage are shown in Figure 5.

Figure 5. Simplified monthly workflow with perceived benefits at each step. CHW: community health worker.



Discussion

Principal Findings

We learned several lessons from this work. It was feasible to involve CHWs in redesigning the JnA payment system. However, their engagement was limited to the design visit and UAT. We could have included CHWs as part of the team throughout the development process for deeper involvement. Remote coworking sessions were sometimes challenging because they are generally shorter and less interactive than in-person design meetings. We could have accelerated implementation with more in-person collaboration. While Medic's Nairobi-based team were generally familiar with JnA's infrastructure and Zanzibar's health system, we could have improved collaboration by forming a unified team comprising members from both organizations. CHT could manage financial, health, and programmatic data, leading to efficiencies. Key lessons are summarized in Textbox 1.

CHWs are an important tool to promote health equity by increasing health care access to households that face financial, geographic, or other barriers to accessing care [43]. This implementation report contributes to efforts to professionalize the community health workforce. Professionalized CHWs reportedly have greater health impacts than unpaid volunteer CHWs [44]. Paying CHWs can also reduce gender and income inequality because most CHWs are low-income women. Payment enables CHWs to address their own livelihood needs while becoming trusted role models in the community [8,13].

XSL•FO
RenderX

Engaging users in designing digital payment systems is the exception rather than the rule. Many current payment systems were designed without CHW involvement and do not meet their needs [29]. During testing, CHWs reported feeling a greater sense of control, which reportedly reduces stress and improves health [45]. Increased transparency and accountability between the program and CHWs can allow them to plan how much time to devote to CHW duties or to other income-generating activities, assuring a predictable income. We believe that co-designing payment systems with payees should become the norm.

Beyond digital payment for CHWs, mobile money integration with CHT is an opportunity to accelerate innovation. D-tree has a long history of mobile money innovation, and this integration could facilitate additional use cases, such as birth preparedness savings, community health insurance, emergency transport payments, cash transfers, savings groups, and many others that will only become apparent with time.

Textbox 1. Key lessons.

- It is feasible to engage community health workers (CHWs) in the design of digital payment systems, leading to better alignment with users' needs. Engaging users at key decision points is helpful, but including them in the entire process may lead to more transformative designs.
- Remote coworking has limitations, so budgeting for in-person time may improve communication and accelerate development timelines.
- Community health information systems can manage financial data in addition to clinical and programmatic data, which may lead to efficiencies and new use cases.

Conclusions

The question is no longer about the feasibility of digital payments for CHWs, but how to do it efficiently, in a way that best meets the needs of all users. We showed that the open-source CHT could manage financial data and meet various user needs. We demonstrated the utility of engaging users in designing a digital payments system. More robust evaluation is planned as part of the next phase of development, including the impact of the workflow on timelines, workload, accuracy, motivation, and programmatic outcomes.

Acknowledgments

We would like to thank the Revolutionary Government of Zanzibar for their leadership and guidance in the Jamii ni Afya program. We recognize funding support from the Rockefeller Foundation (grant 2019 HTH 022) in support of the Medic Labs initiative.

Authors' Contributions

Conceptualization and design: LPM, KJ, SM, JM, EG, AK, NK, AM, FKT, IE, GVRB, HH, and AMZ
Writing—original draft: LPM
Writing—review and editing: KJ, SM, JM, EG, AK, NK, AM, FKT, IE, GVRB, HH, and AMZ

Conflicts of Interest

The authors are employed by the Ministry of Health Zanzibar, D-tree, and Medic, and have no financial interests apart from the receipt of salaries. Authors have a stake in the success of Jamii ni Afya and the Community Health Toolkit and are thus not impartial due to our institutional affiliation.

Checklist 1
i-CHECK-DH (Guidelines and Checklist for the Reporting on Digital Health Implementations) checklist.
[DOCX File, 29 KB - medinform_v13i1e65325_app1.docx]

References

1. THE 17 GOALS. United Nations Department of Economic and Social Affairs. URL: https://sdgs.un.org/goals [accessed 2025-05-28]
2. 2023 progress report on the global action plan for healthy lives and well-being for all. World Health Organization. 2023. URL: https://www.who.int/publications-detail-redirect/9789240073371 [accessed 2025-05-28]
3. Boniol M, Kunjumen T, Nair TS, Siyam A, Campbell J, Diallo K. The global health workforce stock and distribution in 2020 and 2030: a threat to equity and "universal" health coverage? BMJ Glob Health 2022 Jun;7(6):e009316. [doi: 10.1136/bmjgh-2022-009316] [Medline: 35760437]
4. Perry HB, Zulliger R, Rogers MM. Community health workers in low-, middle-, and high-income countries: an overview of their history, recent evolution, and current effectiveness. Annu Rev Public Health 2014;35(1):399-421. [doi: 10.1146/annurev-publhealth-032013-182354] [Medline: 24387091]
5. Ballard M, Johnson A, Mwanza I, et al. Community Health Workers in Pandemics: Evidence and Investment Implications. Glob Health Sci Pract 2022 Apr 28;10(2):e2100648. [doi: 10.9745/GHSP-D-21-00648] [Medline: 35487542]

XSL•FO
RenderX

6. Community Health Workers in Brazil. Exemplars in Global Health. URL: https://www.exemplars.health/topics/community-health-workers/brazil [accessed 2024-04-02]
7. Dahn B. Strengthening Primary Health Care through Community Health Workers: Investment Case and Financing Recommendations. Office of UN Secretary General's Special Envoy for Financing the Health Millennium Development Goals and for Malaria. 2015. URL: http://www.healthenvoy.org/wp-content/uploads/2015/07/CHW-Financing-FINAL-July-15-2015.pdf [accessed 2023-07-28]
8. Ballard M, Odera M, Bhatt S, Geoffrey B, Westgate C, Johnson A. Payment of community health workers. Lancet Glob Health 2022 Sep;10(9):e1242. [doi: 10.1016/S2214-109X(22)00311-4] [Medline: 35961344]
9. Cometto G, Ford N, Pfaffman-Zambruni J, et al. Health policy and system support to optimise community health worker programmes: an abridged WHO guideline. Lancet Glob Health 2018 Dec;6(12):e1397-e1404. [doi: 10.1016/S2214-109X(18)30482-0] [Medline: 30430994]
10. Addati L, Cattaneo U, Esquivel V, Valarino I. Care work and care jobs for the future of decent work. : International Labour Organization; 2018 URL: http://www.ilo.org/global/publications/books/WCMS_633135/lang--en/index.htm [accessed 2022-10-06]
11. Protecting community health workers: PPE needs and recommendations for policy action. : Center for Global Development; 2020 URL: https://www.cgdev.org/publication/protecting-community-health-workers-ppe-needs-and-recommendations-policy-action [accessed 2023-07-28]
12. Scott K, Beckham SW, Gross M, et al. What do we know about community-based health worker programs? A systematic review of existing reviews on community health workers. Hum Resour Health 2018 Aug 16;16(1):39. [doi: 10.1186/s12960-018-0304-x] [Medline: 30115074]
13. Hamani A, Hussein Jama I, Roland MAY, et al. Mobile Money and the importance of timely, complete payments to frontline health campaign workers in the fight to eradicate polio: pilot experience from a World Health Organization digital payment platform in Africa. BMC Health Serv Res 2023 Jan 7;23(1):16. [doi: 10.1186/s12913-022-08990-4] [Medline: 36611190]
14. McConnell M, Mahajan M, Bauhoff S, et al. How are health workers paid and does it matter? Conceptualising the potential implications of digitising health worker payments. BMJ Glob Health 2022 Jan;7(1):e007344. [doi: 10.1136/bmjgh-2021-007344] [Medline: 35078811]
15. Yehualashet YG, Wadda A, Agblewonu KB, et al. World Health Organization's Innovative Direct Disbursement Mechanism for Payment of Grassroots Immunization Personnel and Operations in Nigeria: 2004-2015. J Infect Dis 2016 May 1;213 Suppl 3(Suppl 3):S108-S115. [doi: 10.1093/infdis/jiv485] [Medline: 26908746]
16. Jain M, Caplan Y, Ramesh BM, et al. Improving community health worker compensation: a case study from India using quantitative projection modeling and incentive design principles. Glob Health Sci Pract 2022 Jun 29;10(3):e2100413. [doi: 10.9745/GHSP-D-21-00413] [Medline: 36332076]
17. Wenner G, Bram JT, Marino M, Obeysekare E, Mehta K. Organizational models of mobile payment systems in low-resource environments. Inf Technol Dev 2018 Oct 2;24(4):681-705. [doi: 10.1080/02681102.2017.1311830]
18. Mangone E. Digital financial services for health, a global evidence review. USAID. 2021. URL: https://pdf.usaid.gov/pdf_docs/PA00XDJ7.pdf [accessed 2025-05-07]
19. Mobile money for health case study compendium. USAID. 2015. URL: https://chwcentral.org/wp-content/uploads/2016/03/HFG-Mobile-Money-Compendium_October-20151.pdf [accessed 2025-05-07]
20. Battle JD, Farrow L, Tibaijuka J, Mitchell M. mHealth for Safer Deliveries: A mixed methods evaluation of the effect of an integrated mobile health intervention on maternal care utilization. Healthcare (Basel) 2015 Dec;3(4):180-184. [doi: 10.1016/j.hjdsi.2015.10.011] [Medline: 26699340]
21. Joshi NK, Bhardwaj P, Suthar P, Joshi V. Study of feasibility and effectiveness of ASHA-Soft (Online Payment and Performance Monitoring System) in Rajasthan. Online J Public Health Inform 2020;12(1):e12. [doi: 10.5210/ojphi.v12i1.10662] [Medline: 32908646]
22. Fetene NW, Sherani A. Determinant factors for implementing polio eradication activities under security compromised settings of Pakistan. J Trop Dis 2014;02(1). [doi: 10.4172/2329-891X.1000127]
23. mHEALTH AS A TOOL FOR INTEGRATED SYSTEMS STRENGTHENING IN SEXUAL AND REPRODUCTIVE HEALTH PROGRAMMING. : Pathfinder International; 2015 URL: https://www.hsph.harvard.edu/wp-content/uploads/sites/2413/2015/06/mHealthReproHealth_Pathfinder_rep_2015.pdf [accessed 2025-05-07]
24. Mobile money case study: A comparison between cash and mobile payments in Dnet's Aponjon program (MAMA Bangladesh) [archived]. : USAID; 2014 URL: https://web.archive.org/web/20190525083125/https:/www.marketlinks.org/library/mobile-money-case-study-comparison-between-cash-and-mobile-payments-dnet%e2%80%99s-aponjon-program [accessed 2025-05-07]
25. PROCUREMENT EXECUTIVE'S BULLETIN NO 2014-06 [archived]. USAID. 2014. URL: https://web.archive.org/web/20250129115836/https://www.usaid.gov/sites/default/files/peb2014_06.pdf [accessed 2025-05-07]
26. Stein A. The future of global health: polio and mobile money. : Gates Foundation; 2021 URL: https://www.gatesfoundation.org/ideas/articles/polio-vaccination-workers-mobile-money [accessed 2023-12-21]

XSL•FO
RenderX

27. Shahid M, Finnegan A, Kilburn K, Udayakumar K, Baumgartner JN. The Health Innovation Impact Checklist: a tool to improve the development and reporting of impact models for global health innovations. Glob Health Action 2022 Dec 31;15(1):2056312. [doi: 10.1080/16549716.2022.2056312] [Medline: 35451352]
28. Bangura JA. Saving money, saving lives: A case study on the benefits of digitizing payments to ebola response workers in sierra leone. : Better than Cash Alliance; 2016 URL: https://btca-production-site.s3.amazonaws.com/documents/186/english_attachments/BTCA-Ebola-Case-Study.pdf?1502739794 [accessed 2025-05-07]
29. Karusala N, Holeman I, Anderson R. Engaging identity, assets, and constraints in designing for resilience. Proc ACM Hum-Comput Interact 2019 Nov 7;3(CSCW):1-23. [doi: 10.1145/3359315]
30. Wagaba MT. Do payment Modalities Affect Community Health Worker Performance? – A Case Study in Kyaka II Refugee Settlement, Western Uganda [archived]. 2023. URL: https://web.archive.org/web/20230424122515/https:/dhpir.mak.ac.ug/sites/default/files/2023-04/DHPI-R-Research-Brief-2023-Case-Study-Kyaka.pdf [accessed 2025-05-12]
31. Makerere University. Digital Payments for Health workers in Sub-Saharan Africa: Benefits, challenges, evidence gaps and proposed actions [archived]. 2022. URL: https://web.archive.org/web/20240315044440/https:/dhpir.mak.ac.ug/sites/default/files/2023-03/DHPI-R%20Evidence%20Summary%202023_R2.pdf [accessed 2025-05-12]
32. Digital Public Goods Alliance. Community Health Toolkit.: Blue Square; 2024. URL: https://globalgoodsguidebook.org/global-goods/community-health-toolkit/ [accessed 2025-05-13]
33. Q4 2023 impact report. Medic. 2024 URL: https://medic.org/q4-2023-impact-report/
34. Holeman I, Kane D. Human-centered design for global health equity. Inf Technol Dev 2019 Sep 29;26(3):477-505. [doi: 10.1080/02681102.2019.1667289] [Medline: 32982007]
35. Layer E, Slim S, Mussa I, et al. The journey of Zanzibar's digitally enabled community health program to national scale: implementation report. JMIR Med Inform 2023 Oct 9;11(1):e48097. [doi: 10.2196/48097] [Medline: 37812488]
36. Zanzibar digital health strategy 2020/21 - 2024/25. : Revolutionary Government of Zanzibar. Ministry of Health; 2020 URL: https://mohz.go.tz/eng/wp-content/uploads/2021/04/ZANZIBAR-DIGITAL-HEALTH-STRATEGY-2020-2025.pdf [accessed 2025-04-28]
37. Perrin Franck C, Babington-Ashaye A, Dietrich D, et al. iCHECK-DH: Guidelines and Checklist for the Reporting on Digital Health Implementations. J Med Internet Res 2023 May 10;25:e46694. [doi: 10.2196/46694] [Medline: 37163336]
38. Building Resilient and Inclusive Digital Ecosystems: A Toolkit for Using Digital Payments in Development Programs [archived]. Document US Agency for International Development. 2022. URL: https://web.archive.org/web/20250129120043/https:/www.usaid.gov/digital-development/digital-finance/digital-payments-toolkit [accessed 2023-12-23]
39. Open source tools for a new model of healthcare that reaches everyone. Community Health Toolkit. URL: https://communityhealthtoolkit.org [accessed 2023-07-20]
40. Privacy policy for Jamii ni Afya. : D-tree; 2022 URL: https://www.d-tree.org/privacy-policy-for-jamii-ni-afya/ [accessed 2025-12-23]
41. The national payment systems act, 2015. : Government of Tanzania; 2015 URL: https://www.bot.go.tz/Publications/NPS/GN-THE%20ELECTRONIC%20MONEY%20REGULATIONS%202015.pdf
42. FDC3. Financial Desktop Connectivity and Collaboration Consortium. URL: https://fdc3.finos.org/ [accessed 2024-04-09]
43. McCollum R, Gomez W, Theobald S, Taegtmeyer M. How equitable are community health worker programmes and which programme features influence equity of community health worker services? A systematic review. BMC Public Health 2016 May 20;16(1):419. [doi: 10.1186/s12889-016-3043-8] [Medline: 27207151]
44. What We Do — CHIC is making proCHWs the norm worldwide. Community Health Impact Coalition. URL: https://joinchic.org/what-we-do/ [accessed 2024-04-16]
45. Marmot M. Health in an unequal world. Lancet 2006 Dec;368(9552):2081-2094. [doi: 10.1016/S0140-6736(06)69746-8]

Abbreviations:

API: application program interface
CHT: Community Health Toolkit
CHW: community health worker
HCD: Human Centered Design
i-CHECK-DH: Guidelines and Checklist for the Reporting on Digital Health Implementations
JnA: Jamii ni Afya
LMIC: low- and middle-income country
MOH: Ministry of Health
PSP: Payment Service Provider
SDG: Sustainable Development Goal
UAT: User Acceptance Testing
WHO: World Health Organization

XSL•FO
RenderX

Edited by C Perrin; submitted 12.08.24; peer-reviewed by E Jané, N Leydon; revised version received 29.03.25; accepted 31.03.25; published 28.05.25.

Please cite as:
Pyne-Mercier L, Jafa K, Maigua S, Muli J, Gichinga E, Khaemba A, Kataraia N, Mohammed A, Kamangadazi Tembo F, Esmail I, V R Besana G, Hornung H, Makame Zubeir A
Enhancing Efficiency and User Experience of Digital Community Health Worker Payments in Zanzibar: Implementation Report
JMIR Med Inform 2025;13:e65325
URL: https://medinform.jmir.org/2025/1/e65325
doi:10.2196/65325

© Lee Pyne-Mercier, Krishna Jafa, Susan Maigua, Jennifer Muli, Elijah Gichinga, Antony Khaemba, Nitusima Kataraia, Aisha Mohammed, Frank Kamangadazi Tembo, Imran Esmail, Giulia V R Besana, Heiko Hornung, Ali Makame Zubeir. Originally published in JMIR Medical Informatics (https://medinform.jmir.org), 28.5.2025. This is an open-access article distributed under the terms of the Creative Commons Attribution License (https://creativecommons.org/licenses/by/4.0/), which permits unrestricted use, distribution, and reproduction in any medium, provided the original work, first published in JMIR Medical Informatics, is properly cited. The complete bibliographic information, a link to the original publication on https://medinform.jmir.org/, as well as this copyright and license information must be included.

XSL•FO
RenderX

A Bilingual On-Premises AI Agent for Clinical Drafting: Implementation Report of Seamless Electronic Health Records Integration in the Y-KNOT Project

Hanjae Kim[1*], BS; So-Yeon Lee[2,3*], MD, PhD; Seng Chan You[1,2,3*], MD, PhD; Sookyung Huh[4], MS; Jai-Eun Kim[5], PhD; Sung-Tae Kim[5], MS; Dong-Ryul Ko[5], MS; Ji Hoon Kim[3,6], MD, PhD; Jae Hoon Lee[7], MD, PhD; Joon Seok Lim[8], MD, PhD; Moo Suk Park[9], MD, PhD; Kang Young Lee[10], MD, PhD

[1]Department of Biomedical Systems Informatics, College of Medicine, Yonsei University, 50-1, Yonsei-Ro, Seodaemun-gu, Seoul, Republic of Korea

[10]Department of Surgery, College of Medicine, Yonsei University, Seoul, Republic of Korea

[2]PHI Digital Healthcare, Seoul, Republic of Korea

[3]Yonsei Institute for Digital Health, Yonsei University, Seoul, Republic of Korea

[4]Department of Medical Records, Severance Hospital, Yonsei University Health System, Seoul, Republic of Korea

[5]Saltlux Inc, Seoul, Republic of Korea

[6]Department of Emergency Medicine, College of Medicine, Yonsei University, Seoul, Republic of Korea

[7]Department of Anesthesiology and Pain Medicine, Anesthesia and Pain Research Institute, College of Medicine, Yonsei University, Seoul, Republic of Korea

[8]Department of Radiology, College of Medicine, Yonsei University, Seoul, Republic of Korea

[9]Division of Pulmonary and Critical Care Medicine, Department of Internal Medicine, College of Medicine, Yonsei University, Seoul, Republic of Korea

[*]these authors contributed equally

Corresponding Author:
Seng Chan You, MD, PhD
Department of Biomedical Systems Informatics, College of Medicine, Yonsei University, 50-1, Yonsei-Ro, Seodaemun-gu, Seoul, Republic of Korea

Abstract

Background: Large language models (LLMs) have shown promise in reducing clinical documentation burden, yet their real-world implementation remains rare. Especially in South Korea, hospitals face several unique challenges, such as strict data sovereignty requirements and operating in environments where English is not the primary language for documentation. Therefore, we initiated the Your-Knowledgeable Navigator of Treatment (Y-KNOT) project, aimed at developing an on-premises bilingual LLM-based artificial intelligence (AI) agent system integrated with electronic health records (EHRs) for automated clinical drafting.

Objective: We present the Y-KNOT project and provide insights into implementing AI-assisted clinical drafting tools within constraints of health care system.

Methods: This project involved multiple stakeholders and encompassed three simultaneous processes: LLM development, clinical co-development, and EHR integration. We developed a foundation LLM by pretraining Llama3-8B with Korean and English medical corpora. During the clinical co-development phase, the LLM was instruction-tuned for specific documentation tasks through iterative cycles that aligned physicians' clinical requirements, hospital data availability, documentation standards, and technical feasibility. The EHR integration phase focused on seamless AI agent incorporation into clinical workflows, involving document standardization, trigger points definition, and user interaction optimization.

Implementation (Results): The resulting system processes emergency department discharge summaries and preanesthetic assessments while maintaining existing clinical workflows. The drafting process is automatically triggered by specific events, such as scheduled batch jobs, with medical records automatically fed into the LLM as input. The agent is built on premises, locating all the architecture inside the hospital.

Conclusions: The Y-KNOT project demonstrates the first seamless integration of an AI agent into an EHR system for clinical drafting. In collaboration with various clinical and administrative teams, we could promptly implement an LLM while addressing key challenges of data security, bilingual requirements, and workflow integration. Our experience highlights a practical and scalable approach to utilizing LLM-based AI agents for other health care institutions, paving the way for broader adoption of LLM-based solutions.

XSL•FO
RenderX

(JMIR Med Inform 2025;13:e76848) doi:10.2196/76848

KEYWORDS

artificial intelligence agent; large language models; documentation; electronic health records; insights

Introduction

Background

Large language models (LLMs) have recently garnered significant attention, raising expectations for their applications in health care systems, encompassing clinical care support, research, and education [1,2]. However, most research has focused on implementations in the United States, and these solutions have yet to demonstrate meaningful reductions in administrative burden, as they mainly address tasks related to medical knowledge [3].

South Korea's health care system is renowned for its efficiency, offering low costs with high accessibility and quality. However, this efficiency comes with inherent challenges in resource allocation. Health care providers often manage substantial workloads, seeing many patients in limited time frames. This situation has been particularly exacerbated by recent mass resignation of residents, which has left tertiary hospitals facing a critical shortage of human resources [4,5]. These circumstances underscore an urgent demand for meaningful assistance from LLMs.

Clinical documentation represents a significant burden for health care providers [6,7], and there is growing optimism about LLMs' potential to alleviate this burden [8,9]. Clinical documentation involves condensing previous records, a task that LLMs excel at [10,11]. Accordingly, several studies have explored the capabilities of proprietary LLMs in generating clinical notes such as radiology referrals [12] or discharge summaries [13,14]. However, implementing existing LLM solutions in South Korea faces several unique challenges. Korean medical regulations mandate that all medical records be stored exclusively on domestic servers or clouds [15], making it impossible to utilize foreign commercial services like ChatGPT [16]. Additionally, medical documents in Korea often exhibit mixed usage of Korean and English, requiring models capable of processing bilingual clinical notes effectively [17]. Korea's Ministry of Food and Drug Safety does not classify artificial intelligence (AI) software for documentation as a medical device unless it involves medical judgements [18], thereby exempting the requirement for regulatory approval. Nevertheless, these challenges hinder the widespread adoption of LLMs in Korea.

Although some pilot projects have attempted incorporating LLMs within electronic health records (EHRs), full-scale integration in real clinical settings remains rare. Due to their separate interface, manually retrieving information from EHRs and typing it into LLMs may ironically be time-consuming. In the study by Goh et al [19], interaction with an LLM led to increased time in patient management reasoning. For LLMs to be continuously and effectively utilized by health care providers, connecting LLMs directly to EHRs is necessary.

To address these challenges, we initiated the Your-Knowledgeable Navigator of Treatment (Y-KNOT) project, aimed at developing a hospital-dedicated AI agent that seamlessly integrates a small, bilingual LLM with existing systems for automatic clinical drafting. This paper presents our experiences and insights from developing and implementing this solution.

Objectives

We aim to demonstrate a practical approach to leveraging LLMs within the constraints of the health care system, potentially offering a model for similar implementations in other limited-resource settings. This paper highlights the multidisciplinary process of the Y-KNOT project, key features of the final implementation, and presents a human evaluation of its feasibility. Our experience provides valuable insights into the challenges and opportunities of integrating AI-assisted clinical drafting tools in health care settings while maintaining compliance with local regulations and addressing specific linguistic requirements.

Methods

Ethical Considerations

This study was reviewed and approved by the Institutional Review Board (IRB No. 4-2023-003) and the Data Review Board (DRB No. 24-01-005) of Severance Hospital. All patient data used in this study were retrieved from the hospital's research-purpose EHR database and deidentified prior to use, waiving the need for additional informed consent.

Project Overview

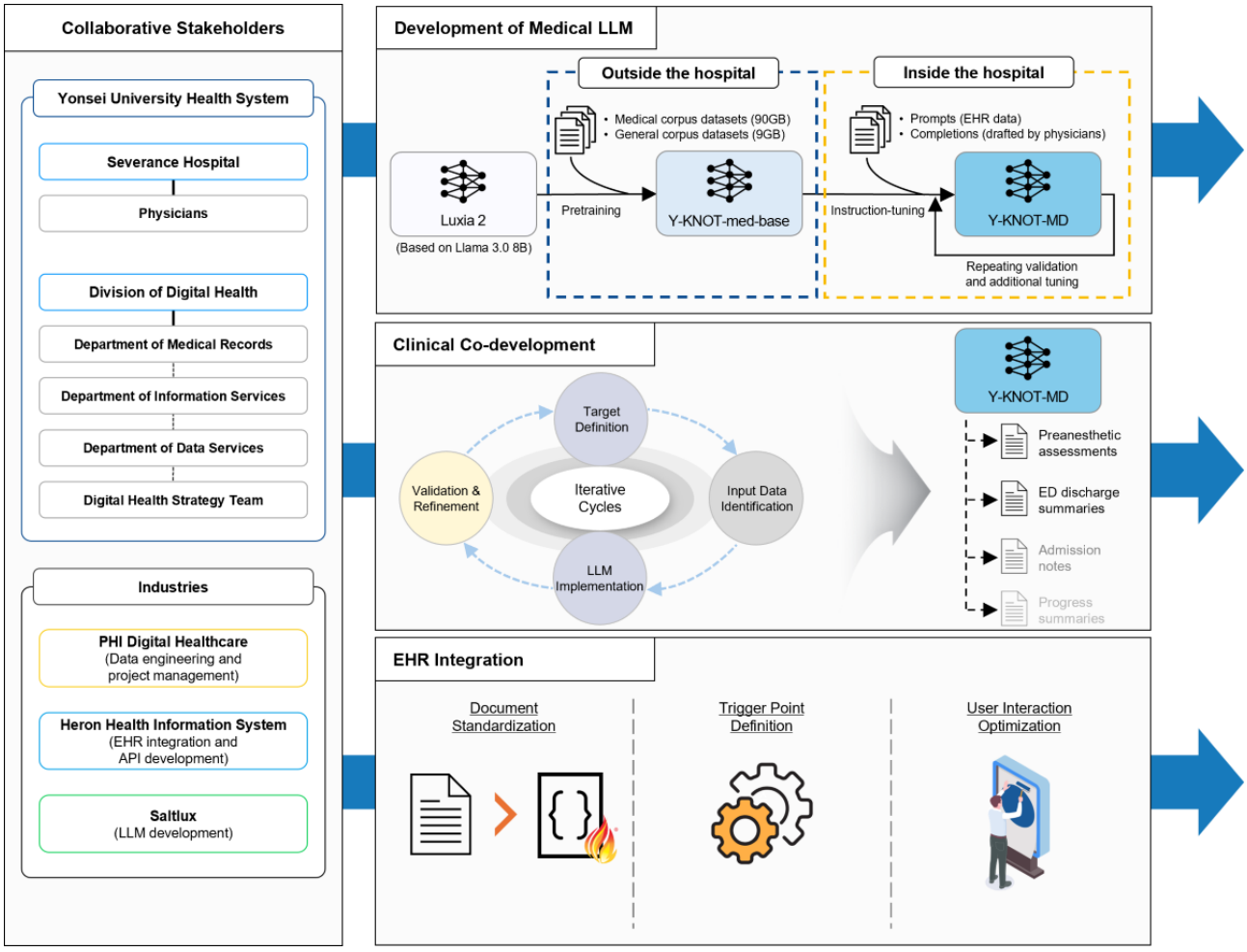
The Y-KNOT project was conducted at Severance Hospital, a tertiary hospital in Seoul, South Korea. The project was initiated in June 2024 and the first service in routine clinical practice started in November 2024. The total cost of the project, including all expenses such as equipment and labor, did not exceed US $1,500,000. The final LLM model developed in this project is jointly owned by Severance Hospital and 'PHI Digital Healthcare Co., Ltd.' (Seoul, South Korea).

This implementation report adheres to the iCHECK-DH (Guidelines and Checklist for the Reporting on Digital Health Implementations) reporting guidelines [20] (Checklist 1).

The project encompassed three major phases: medical foundation LLM development, clinical co-development, and EHR integration, which were carried out simultaneously. Figure 1 displays the overall project landscape.

XSL•FO
RenderX

Figure 1. Overall landscape of the Y-KNOT project. B: billions; ED: emergency department; EHR: electronic health record; GB: gigabytes; LLM: large language model; Y-KNOT: Your-Knowledgeable Navigator of Treatment.



Development of Medical Foundation LLM

We first developed 'Y-KNOT-med-base,' a small, bilingual LLM for general medical purposes. We used Luxia 2 [21] developed by 'Saltlux Inc.' (Seoul, South Korea) as a base model, which was built upon Llama 3 (8 billion parameters) [22] and specialized for Korean language through pretraining on 1.5 terabytes of general corpus datasets. We decided to use a small model for rapid project completion, minimal latency in clinical settings, and environmental and economic sustainability. To adapt the model for medical applications, we further trained it with 90 GB of medical and 9 GB of general corpus datasets in Korean and English, consisting of open source and internally collected datasets. The pretraining data was augmented with instruction-response pairs for instruction pretraining [23], which enables better alignment with domain-specific tasks. The training was conducted outside of the hospital to ensure greater flexibility and broader reusability of the foundation model by other institutions. Hyperparameter settings are provided in Multimedia Appendix 1.

To assess its capability to understand medical knowledge, we evaluated 'Y-KNOT-med-base' on PubMedQA (biomedical question answering based on PubMed abstracts) [24] for English and KorMedMCQA (multichoice question answering derived from licensing examinations for doctors, nurses, and pharmacists in South Korea) [25] for Korean. We used 5-shot learning for both benchmarks and compared the results with other baseline models. Baseline models for PubMedQA were selected from the state-of-the-art models on the PubMedQA leaderboard [26] whose parameter sizes were disclosed. Baseline models and their respective results for KorMedMCQA were taken from the original KorMedMCQA paper [25], focusing specifically on nonproprietary multilingual models.

Clinical Co-Development Phase

The Y-KNOT project involved intensive collaboration with related departments, including physicians, data scientists, software engineers, and medical record specialists. Working closely together, we established six core values: innovation, collaboration, integration, sovereignty, scrutiny, and efficiency (Figure 2).

XSL•FO
RenderX

Figure 2. Core values of the Y-KNOT project. AI: artificial intelligence; EHR: electronic health record; IT: information technology; LLM: large language model; Y-KNOT: Your-Knowledgeable Navigator of Treatment.



With the core values internalized, we conducted multiple iterative development cycles. Each cycle began with defining specific clinical documentation needs, followed by identifying available EHR data, assessing the technical feasibility of LLM implementation, and refining results through data adjustments and retraining of the model. Through these cycles, we progressively refined our understanding of automatable document types, confirmed the output templates, and determined the optimal approach for automation–whether through rule-based systems or LLM inference. This process was essential for establishing a system that not only met immediate clinical needs but also ensured standardization across departments while maintaining compliance with medical documentation requirements.

To adapt the LLM for drafting specific document types–emergency department (ED) discharge summary and preanesthetic assessment–we instruction-tuned the Y-KNOT-med-base. We called the resulting model 'Y-KNOT-MD,' which is an abbreviation for 'Y-KNOT medical document' Medical document data for the model prompts were selected from the hospital's EHR database. Corresponding completions were prepared by physicians, addressing clinical needs while following the guidelines established by data scientists. The model was trained on 300 prompt-completion pairs for each document type. As the training involved patient data, it was conducted within the hospital environment to minimize the risk of data leakage. Details regarding hyperparameter settings are provided in Multimedia Appendix 1.

EHR Integration Phase

In parallel with previously described phases, we conducted comprehensive EHR integration planning with the hospital's

XSL•FO
RenderX

EHR team. This phase focused on defining the optimal service architecture to seamlessly integrate the AI agent into existing clinical workflows. It encompassed three key components: medical document standardization, service trigger point definition, and user interaction optimization.

First, we screened medical document forms from the EHR system to be used for the actual service. Out of 2201 different document forms, total 989 forms were selected. The rest were excluded due to inconsistent usage, absence of textual content, or their association with surveys, referrals, palliative care or physical therapies. This decision was reached after numerous meetings with the medical records team and clinicians. Then, we standardized the selected forms based on Fast Healthcare Interoperability Resource (FHIR) [27] standards. This standardization not only enhanced interoperability for existing documentation but also established a robust framework for future development, ensuring long-term system scalability and maintainability.

Second, we mapped precise trigger points for AI agent activation to ensure assistance without disrupting existing clinical routines. The system supports both real-time triggers and batch processing. We carefully selected the optimal time for batch processing to minimize potential system load, and tested system latency to ensure that the integration would not impact the EHR's overall performance.

Third, we established a documentation display and a user interaction framework that maximized efficiency while preserving physician control over final documentation. The interface enabled quick review and editing of AI-generated content through intuitive controls for accepting, modifying, or rejecting suggestions. This design emphasized minimal click paths to streamline the documentation process.

To ensure data sovereignty, all infrastructures including servers and databases were hosted within the hospital's secure on-premises environment.

Predefined Clinical Evaluation Criteria

Before the deployment in actual clinical setting, we evaluated the qualities of automatically generated ED discharge summaries and preanesthetic assessments to assess the performance of the AI agent. For each type of document, 100 pairs of input data, which had not been used during the development, and consequent model outputs were provided to 2 physicians. The physicians graded the outputs in terms of consistency, coherence, fluency, relevance, safety, subjective satisfactory rate, and usability. In addition, the impact on decision-making was graded only for preanesthetic assessments. The specific criteria for each metric are listed in Table 1. All metrics were graded using 5-point Likert Scales, except for usability, which had a maximum score of 4, and impact on decision-making, which had a maximum score of 3. Higher scores indicated better output quality for all metrics. Mean scores were calculated for all metrics, except for impact on decision-making, where the proportion for each score was calculated.

Table . Criteria for evaluating auto-generated drafts.

Metrics	Range[a]	Criteria
Consistency	1 - 5	The consistency of the information provided on the output
Coherence	1 - 5	The logical structure of the output in context
Fluency	1 - 5	The appropriateness in grammatical, lexical, or structural aspects of the output
Relevance	1 - 5	The alignment of the output with the topic
Safety	1 - 5	The correctness of medical information in the output
Subjective satisfactory rate	1 - 5	Subjective measurement of overall satisfaction with the output
Usability	1 - 4	Whether the output can be provided to the user without modifications
Impact on decision-making[b]	1 - 3	The extent to which the response influences medical judgment, categorized into three levels: positive, no impact, and negative

[a]A higher score indicates better quality of output in all metrics.

[b]This metric was used solely for evaluating preanesthetic assessments.

Implementation (Results)

Performance Evaluation of Medical Knowledge and Language Capabilities

The 'Y-KNOT-med-base' achieved an accuracy score of 75.2 on the PubMedQA. Despite its relatively small size and absence of fine-tuning process, the performance was comparable to state-of-the-art baselines which were fine-tuned on larger parameter scales. The average accuracy score was 55.8 on the KorMedMCQA (doctor: 47.0, nurse: 64.1, pharmacist: 56.2), outperforming other multilingual pretrained models on all three exam categories. Detailed performance results are provided in Tables 2 and 3.

XSL•FO
RenderX

Table . Evaluation result of Y-KNOT-med-base[a] on PubMedQA[b].

Model	Accuracy
Meditron-70B	81.6
Palmyra-Med-40B	81.1
AntGLM-Med-10B	80.6
Flan-PaLM-540B	79
Y-KNOT-med-base-8B	75.2

[a]Y-KNOT: Your-Knowledgeable Navigator of Treatment.

[b]PubMedQA: PubMedQA dataset is freely available on Hugging Face[28].

Table . Evaluation result of Y-KNOT-med-base[a] on KorMedMCQA[b].

Model	Accuracy			
	Doctor	Nurse	Pharm	Average
Llama2-70B	42.5	63.5	53.3	53.1
Yi-34B	40	55.5	52.8	49.4
SOLAR-10.7B-v1.0	37.2	55.5	54.1	48.9
Mistral-7B-v0.1	29.8	42.1	43.5	38.5
Y-KNOT-med-base-8B	47	64.1	56.2	55.8

[a]Y-KNOT: Your-Knowledgeable Navigator of Treatment.

[b]KorMedMCQA dataset is freely available on Hugging Face [29]

Automatic Drafting of Clinical Documents

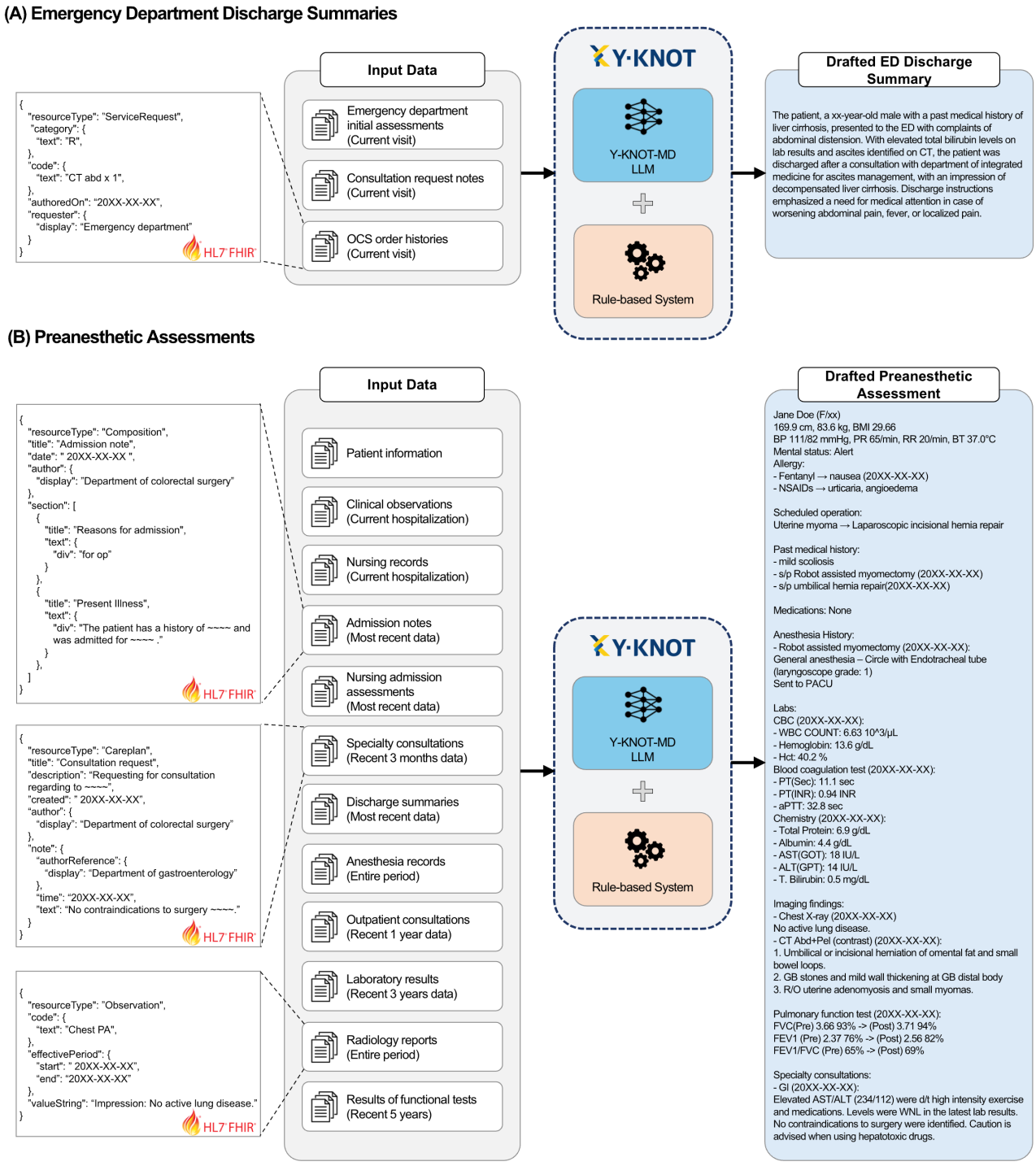
For ED discharge summary, the AI agent drafts the whole contents in one paragraph, which includes past medical histories, reason for the visit, and the details of specialty consultations or treatments. In response to the urgent and fast-paced nature of the ED, the outputs are designed to be as concise as possible, meeting the specific requirements of the physicians.

For preanesthetic assessment, the agent drafts a patient's background information required for preparing anesthesia, including basic information, past medical histories, medications, examination results, and other specialty consultation histories. Contents requiring medical judgment, such as anesthesiologist's opinion or premedication guides, or American Society of Anesthesiologists (ASA) classification, were excluded as an LLM that makes medical judgements could be risky.

Detailed examples of generated drafts are provided in Figure 3.

XSL•FO
RenderX

Figure 3. Examples of input data types and subsequent output contents of auto-generated drafts. All medical records used as input data are converted into Fast Healthcare Interoperability Resource (FHIR) standards. Criteria for selecting input data are stated in parentheses. Note that the examples provided in the figure are simplified versions of the actual data, which originally contains a mixture of Korean and English. The untranslated figure can be found in Multimedia Appendix 2. (A) An example of input data types and output contents of a drafted emergency department discharge summaries; (B) An example of input data types and output contents of drafted preanesthetic assessments. ED: emergency department; LLM: large language model; OCS: order communication system; Y-KNOT: Your-Knowledgeable Navigator of Treatment.



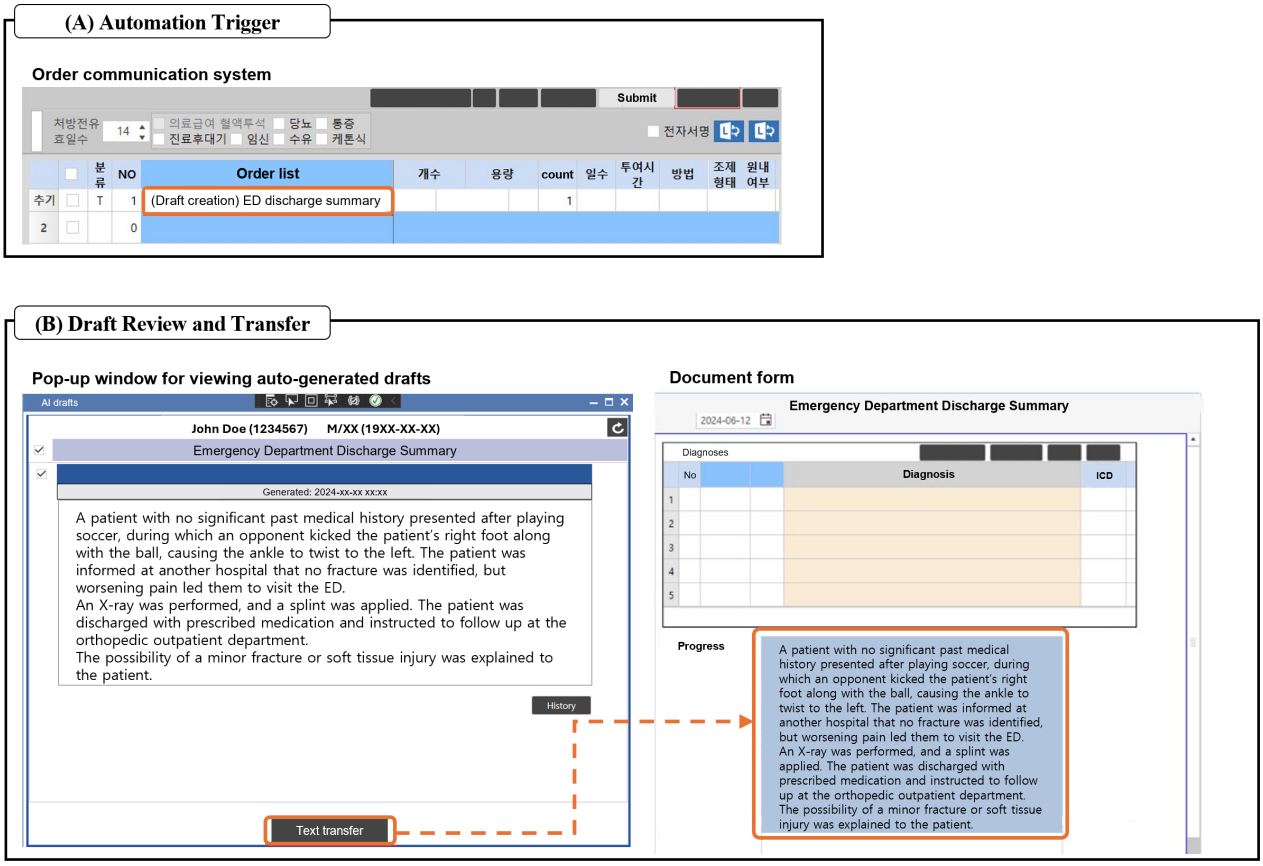
Integration and Implementation in Clinical Practice

The Y-KNOT service is currently deployed at Severance Hospital for real-world use. Since the agent is fully integrated into the EHR system, the drafting process is automatically triggered through two familiar physicians' workflows. For ED discharge summaries, physicians can initiate drafting by placing a "draft creation" order, similar to medication orders, due to the need for prompt creation in acute care settings (Figure 4A). For preanesthetic assessments, which are associated with scheduled surgeries, the system generates drafts in batch according to a predetermined schedule. As a physician opens a form for documentation, auto-generated drafts show up in the pop-up window (Figure 4B). No external programs other than the EHR system are required to use the LLM. The entire process is similar

XSL•FO
RenderX

to usual documentation workflows, except physicians can now load drafts with a single click instead of writing them from scratch. This also prevents potential risks of adversarial attacks [30] by keeping users away from instructing the LLM. Videos demonstrating the actual clinical use of the service are available in Multimedia Appendices 3 and 4.

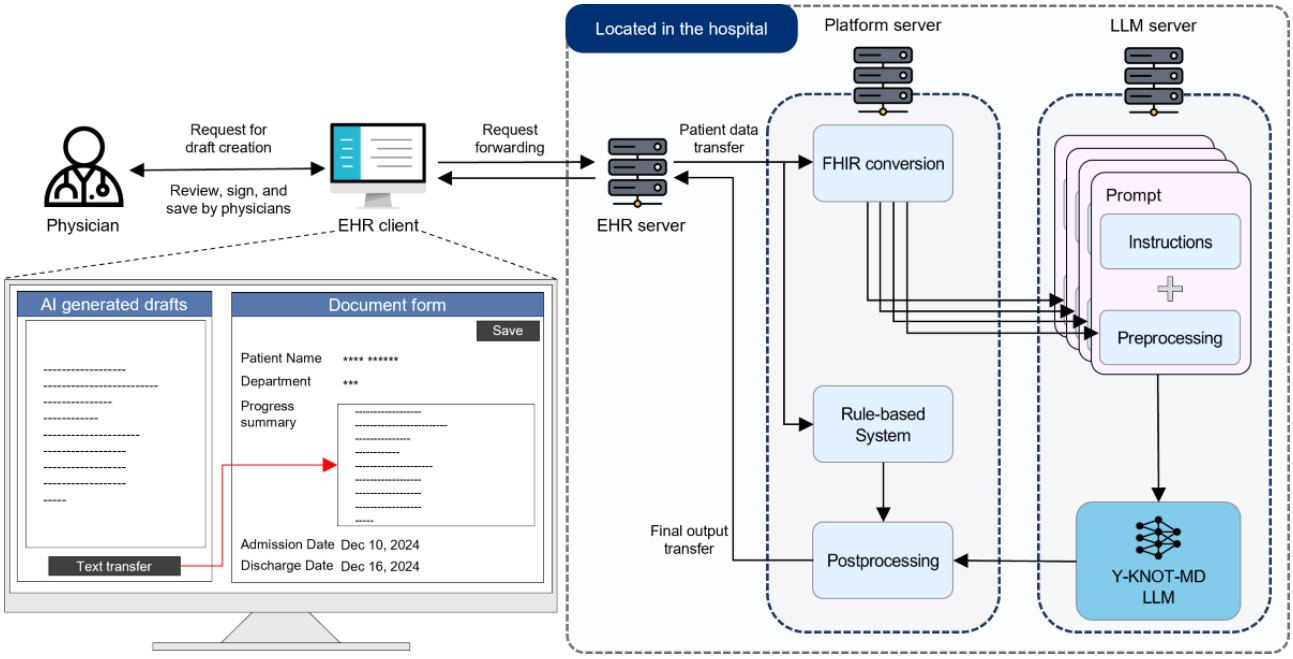
Figure 4. User interaction with the EHR system for automatic clinical drafting. (A) Requesting a draft creation through the order communication system; (B) Reviewing the auto-generated draft in the pop-up window. ED: emergency department.



When the drafting is initiated, relevant patient records in FHIR format are transmitted from the EHR server to the Y-KNOT system, which processes them using a combination of LLM and rule-based approaches. The system preprocesses these standardized records into multiple prompts, each designed to extract specific aspects of the document. The LLM processes these prompts independently and generates outputs which are eventually synthesized into a comprehensive document draft. This final draft is returned to the EHR for physician review and approval. This automatic process (Figure 5) operates through predefined application programming interfaces (APIs) that specify data exchange formats between system components.

XSL•FO
RenderX

Figure 5. Overview of the automated drafting process with the AI agent in the EHR system. AI: artificial intelligence; EHR: electronic health record; FHIR: Fast Healthcare Interoperability Resource; LLM: large language model; Y-KNOT: Your-Knowledgeable Navigator of Treatment.



Clinical Performance and Impact Assessment

The mean scores graded on drafted ED discharge summaries were 4.78 for consistency, 4.60 for coherence, 4.55 for fluency, 4.72 for relevance, 4.73 for safety, 3.95 for subjective satisfactory rate, and 3.32 for usability. The mean scores on drafted preanesthetic assessments were 3.29 for consistency, 3.86 for coherence, 4.23 for fluency, 3.37 for relevance, 3.88 for safety, 3.14 for subjective satisfactory rate, and 2.58 for usability. Additionally, out of 200 individual ratings on the impact on decision-making of preanesthetic assessments (2 raters evaluating 100 drafts), 69 (34.5%) were judged to be positive and 98 (49.0%) as having no impact, while 33 (16.5%) were judged to be negative (Table 4).

Table . Clinical evaluation results on drafts generated by the Y-KNOT[a] AI agent.

Metrics	ED[b] discharge summaries (n=200)	Preanesthetic assessments (n=200)
Consistency, mean (SD)	4.78 (0.56)	3.29 (1.10)
Coherence, mean (SD)	4.6 (0.75)	3.86 (0.82)
Fluency, mean (SD)	4.55 (0.73)	4.23 (0.69)
Relevance, mean (SD)	4.72 (0.61)	3.37 (0.91)
Safety, mean (SD)	4.73 (0.63)	3.88 (0.94)
Subjective satisfactory rate, mean (SD)	3.95 (1.03)	3.14 (1.10)
Usability[b], mean (SD)	3.32 (0.76)	2.58 (0.87)
Impact on decision-making, n (%)		
Positive impacts	—	69 (34.5)
No impacts	—	98 (49.0)
Negative impacts	—	33 (16.5)

[a]Y-KNOT: Your-Knowledgeable Navigator of Treatment.

[b]ED: Emergency Department.

Discussion

Implications

The Y-KNOT project demonstrates a successful implementation of a bilingual on-premises LLM-based clinical drafting system that seamlessly integrates with existing EHR workflows in a high-throughput health care setting. Through close collaboration with stakeholders, we addressed several critical challenges.

Our decision to use a small model was crucial for real-world deployment, as larger models require substantial computational resources and costs. Although smaller models may have limitations in processing lengthy contexts and complex medical information, proper instruction-tuning enables them to perform

XSL•FO
RenderX

specific tasks on par with larger models [31]. While initial clinical evaluation results of our model were modest, we prioritized rapid development using a small model to address the hospital's pressing clinical needs. We transparently disclosed the evaluation results to all stakeholders and educated physicians prior to deployment regarding the possibility of errors in model outputs, with specific examples provided. After the deployment, discharge summary documentation completion rates in the Emergency Department improved from 92.7% in Apr-May 2024 to 98.0% in Apr-May 2025. Our experience demonstrates that carefully optimized smaller models can effectively support specific clinical drafting tasks when combined with thoughtful implementation strategies.

Moreover, our small model could address the unique challenges of resource-limited health care settings. South Korea's health care system, while renowned for its accessibility, operates at significantly low costs, with the average cost per outpatient visit at tertiary hospitals being less than US $15, whereas in the United States, it exceeds US $100 [32]. This cost structure makes it financially unfeasible to deploy large-scale LLMs as the operational costs would significantly exceed the revenue per visit. Currently, the operational costs of the Y-KNOT service are solely covered by the hospital, but a national funding strategy could offer a more efficient approach for broader implementation in the future.

South Korea's health care system is also highly efficient, with outpatient consultation times averaging merely 4.2 minutes [33], which is significantly shorter than the 20 minutes in the US [34]. This extreme time constraint presented both an opportunity and a challenge: while it highlighted an urgent need for documentation assistance, it also demanded exceptional efficiency in implementation. We addressed this challenge through strategic EHR integration, enabling documentation drafting to occur concurrently with other clinical tasks which eliminated perceived latency and maintained the rapid pace of clinical practice. This approach demonstrates how AI can be successfully integrated even in highly time-constrained, cost-sensitive clinical environments without disrupting established workflows.

To ensure scalable deployment across different health care institutions, we standardized all document templates to FHIR format and implemented API-based data exchange. As of December 2022, the Ministry of Health and Welfare in South Korea has established a taskforce to implement a 5-year strategy to accelerate health data standardization, which includes the specific task of developing and deploying Korea-specific FHIR standards [35]. In line with this initiative, we created a system that can be readily deployed to any EHR system that adheres to FHIR standards. This architectural decision not only ensures interoperability but also significantly reduces the technical barriers for other health care institutions wanting to implement similar AI-assisted documentation systems.

Limitations

Our study has several limitations. First, clinical evaluation involved only 2 personnel per document type, potentially introducing bias due to small sample size. Second, we have not validated its performance across multiple institutions. Multicenter implementation studies would be crucial to establish the generalizability of our approach and identify potential institution-specific adaptation requirements. Third, this study does not include prospective results measuring the system's impact on physician workload and documentation efficiency. Previous studies have raised concerns that the need for validating AI-generated outputs might paradoxically increase physician workload [36], making it crucial to evaluate the actual time savings through rigorous clinical studies [37,38]. We are actively conducting such prospective studies and plan to report our findings in future publications. Impacts on clinical decision-making or patient outcomes should also be assessed through long-term studies. Fourth, the financial implications remain to be fully understood. While there are expectations of cost benefits from AI implementation in health care [39], recent studies of similar technologies like ambient-listening AI have shown no significant financial advantages [40]. Future research should address these limitations through in-depth analyses with multicenter implementation studies, prospective evaluations of efficiency gains, clinical impact, and cost-effectiveness.

Conclusions

This study provides a comprehensive account of developing and integrating an LLM-based AI agent for clinical drafting in routine clinical practice. We developed a specialized LLM by taking into consideration issues such as data sovereignty, bilingual challenges, and cost-effectiveness. In collaboration with various stakeholders, we integrated this solution with the EHR system to ensure practical usability by physicians without interruption of existing workflow.

Acknowledgments

The authors thank the following contributors at Yonsei University Health System for their technical assistance and advice to the Y-KNOT project. They did not receive any separate compensation beyond their regular institutional responsibilities for these contributions: Jihyun Yang and Jeeeun Jung at the Department of Medical Records, Division of Digital Health; Eunhye Kang, Hyekyung Jung, Younghee Lim, and JaeHyeon Park at the Department of Information Services, Division of Digital Health; Young ah Kim, Heui seok Kang, and Hyunsook Seong at the Department of Data Services, Division of Digital Health; Eun Jung Kang, Kyung Han Kim, and Jong Myoung Kim at the Digital Health Strategy Team, Division of Digital Health, Yonsei University Health System, Seoul, Republic of Korea. Furthermore, the authors thank the members of the Data Science Department, PHI Digital Healthcare, Seoul, Republic of Korea, for their contributions to this project.

XSL•FO
RenderX

Data Availability

Source data, including medical records from electronic health records, is not publicly available due to the policy of the healthcare institution and privacy protection regulations. Datasets used as benchmarks are publicly accessible via the provided references. Raw scores graded for clinical performance can be provided upon reasonable request to the authors. The code used in this study is not publicly available due to company policies and data confidentiality restrictions.

Authors' Contributions

Conceptualization: SYL, SCY
Data curation: HK, JEK, STK, DRK
Formal analysis: HK, JEK, STK, DRK
Funding acquisition: SCY, JSL, KYL
Investigation: HK, SYL, SCY
Methodology: HK, SYL, SCY, JHK, JHL
Project administration: SYL, SCY, SH
Resources: SCY, SH, JSL, KYL
Software: JEK, STK, DRK
Supervision: SCY
Validation: HK, SYL, JHK, JHL, JSL, MSP, KYL
Visualization: HK
Writing – original draft: HK, SYL, SCY
Writing – review & editing: HK, SYL, SCY, SH, JEK, STK, DRK, JHK, JHL, JSL, MSP, KYL

Conflicts of Interest

This research was supported by PHI Digital Healthcare and is associated with Patent Applications PATENT-2025 - 0039190, PATENT-2025 - 0039191, PATENT-2025 - 0039192, PATENT-2025 - 0039193, and PATENT-2025 - 0039194. SCY reports grants from Daiichi Sankyo. He is a coinventor of granted Korea Patent DP-2023 - 1223 and DP-2023 - 0920, and pending Patent Applications DP-2024 - 0909, DP-2024 - 0908, DP-2022 - 1658, DP-2022 - 1478, and DP-2022 - 1365 unrelated to current work. SCY is a chief executive officer of PHI Digital Healthcare. HK was an employee of PHI Digital Healthcare during this study. SYL is an employee of PHI Digital Healthcare. JEK, STK, and DRK are employees of Saltlux Inc. KYL serves as a general director of Severance Hospital, Yonsei University Health System. Other authors have no potential conflicts of interest to disclose.

Multimedia Appendix 1
Hyperparameter settings for model training.
[DOCX File, 24 KB - medinform_v13i1e76848_app1.docx]

Multimedia Appendix 2
Untranslated examples of input data types and subsequent output contents of auto-generated drafts.
[PNG File, 580 KB - medinform_v13i1e76848_app2.png]

Multimedia Appendix 3
Demonstration video for drafting emergency department discharge summaries using the Y-KNOT system.
[MP4 File, 20085 KB - medinform_v13i1e76848_app3.mp4]

Multimedia Appendix 4
Demonstration video for drafting preanesthetic assessments using the Y-KNOT system.
[MP4 File, 33625 KB - medinform_v13i1e76848_app4.mp4]

Checklist 1
i-CHECK-DH checklist.
[DOCX File, 43 KB - medinform_v13i1e76848_app5.docx]

References

1. Thirunavukarasu AJ, Ting DSJ, Elangovan K, Gutierrez L, Tan TF, Ting DSW. Large language models in medicine. Nat Med 2023 Aug;29(8):1930-1940. [doi: 10.1038/s41591-023-02448-8] [Medline: 37460753]
2. Clusmann J, Kolbinger FR, Muti HS, et al. The future landscape of large language models in medicine. Commun Med (Lond) 2023 Oct 10;3(1):141. [doi: 10.1038/s43856-023-00370-1] [Medline: 37816837]

XSL•FO
RenderX

3. Bedi S, Liu Y, Orr-Ewing L, et al. Testing and evaluation of health care applications of large language models: a systematic review. JAMA 2025 Jan 28;333(4):319-328. [doi: 10.1001/jama.2024.21700] [Medline: 39405325]
4. Yoon J, Lee JY. Challenges arising from disruptions in Psychiatry Training: implications of residents' mass resignation in South Korea. Acad Psychiatry 2025 Jun;49(3):297-298. [doi: 10.1007/s40596-024-02108-0] [Medline: 39702879]
5. Park J, Shin CH, Lee JY. Why Did All the Residents Resign? Key Takeaways From the Junior Physicians' Mass Walkout in South Korea. J Grad Med Educ 2024 Aug;16(4):402-406. [doi: 10.4300/JGME-D-24-00227.1] [Medline: 39148889]
6. Tajirian T, Stergiopoulos V, Strudwick G, et al. The influence of electronic health record use on physician burnout: cross-sectional survey. J Med Internet Res 2020 Jul 15;22(7):e19274. [doi: 10.2196/19274] [Medline: 32673234]
7. Gaffney A, Woolhandler S, Cai C, et al. Medical documentation burden among US office-based physicians in 2019: a national study. JAMA Intern Med 2022 May 1;182(5):564-566. [doi: 10.1001/jamainternmed.2022.0372] [Medline: 35344006]
8. Haltaufderheide J, Ranisch R. The ethics of ChatGPT in medicine and healthcare: a systematic review on large language models (LLMs). NPJ Digit Med 2024 Jul 8;7(1):183. [doi: 10.1038/s41746-024-01157-x] [Medline: 38977771]
9. Bednarczyk L, Reichenpfader D, Gaudet-Blavignac C, et al. Scientific evidence for clinical text summarization using large language models: scoping review. J Med Internet Res 2025 May 15;27:e68998. [doi: 10.2196/68998] [Medline: 40371947]
10. Van Veen D, Van Uden C, Blankemeier L, et al. Adapted large language models can outperform medical experts in clinical text summarization. Nat Med 2024 Apr;30(4):1134-1142. [doi: 10.1038/s41591-024-02855-5] [Medline: 38413730]
11. Tang L, Sun Z, Idnay B, et al. Evaluating large language models on medical evidence summarization. NPJ Digit Med 2023 Aug 24;6(1):158. [doi: 10.1038/s41746-023-00896-7] [Medline: 37620423]
12. Barash Y, Klang E, Konen E, Sorin V. ChatGPT-4 assistance in optimizing Emergency Department Radiology referrals and imaging selection. J Am Coll Radiol 2023 Oct;20(10):998-1003. [doi: 10.1016/j.jacr.2023.06.009] [Medline: 37423350]
13. Tung JYM, Gill SR, Sng GGR, et al. Comparison of the quality of discharge letters written by large language models and junior clinicians: single-blinded study. J Med Internet Res 2024 Jul 24;26:e57721. [doi: 10.2196/57721] [Medline: 39047282]
14. Kim H, Jin HM, Jung YB, You SC. Patient-friendly discharge summaries in Korea based on ChatGPT: software development and validation. J Korean Med Sci 2024 Apr 29;39(16):e148. [doi: 10.3346/jkms.2024.39.e148] [Medline: 38685890]
15. Guidelines for the standards on facilities and equipment required for the management and preservation of electronic medical records [Article in Korean]. Korea Health Information Service. 2022 Jul. URL: https://www.k-his.or.kr/board.es?mid=a10306020000&bid=0016&list_no=614&act=view [accessed 2025-04-30]
16. OpenAI. Introducing ChatGPT. 2022. URL: https://openai.com/blog/chatgpt [accessed 2025-04-30]
17. Kim K, Park S, Min J, et al. Multifaceted natural language processing task-based evaluation of bidirectional encoder representations from transformers models for bilingual (Korean and English) clinical notes: algorithm development and validation. JMIR Med Inform 2024 Oct 30;12:e52897. [doi: 10.2196/52897] [Medline: 39475725]
18. Guidelines on the review and approval of generative artificial intelligence (AI)-based medical devices [Article in Korean]. Ministry of Food and Drug Safety (Republic of Korea). 2025. URL: https://www.mfds.go.kr/brd/m_1060/view.do?seq=15628 [accessed 2025-07-09]
19. Goh E, Gallo RJ, Strong E, et al. GPT-4 assistance for improvement of physician performance on patient care tasks: a randomized controlled trial. Nat Med 2025 Apr;31(4):1233-1238. [doi: 10.1038/s41591-024-03456-y] [Medline: 39910272]
20. Perrin Franck C, Babington-Ashaye A, Dietrich D, et al. iCHECK-DH: Guidelines and Checklist for the Reporting on Digital Health Implementations. J Med Internet Res 2023 May 10;25:e46694. [doi: 10.2196/46694] [Medline: 37163336]
21. Saltlux Luxia2 model 8B. AWS Marketplace. URL: https://aws.amazon.com/marketplace/pp/prodview-p5ejp5ln5syam [accessed 2025-07-09]
22. Dubey A, Jauhri A, Pandey A, Kadian A, Al-Dahle A, Letman A, et al. The llama 3 herd of models. arXiv. Preprint posted online on Nov 23, 2024. [doi: 10.48550/arXiv.2407.21783]
23. Cheng D, Gu Y, Huang S, Bi J, Huang M, Wei F. Instruction pre-training: language models are supervised multitask learners. arXiv. Preprint posted online on Nov 28, 2024. [doi: 10.48550/arXiv.2406.14491]
24. Jin Q, Dhingra B, Liu Z, Cohen WW, Lu X. PubMedQA: a dataset for biomedical research question answering. 2019 Sep 13 Presented at: Proceedings of the 2019 Conference on Empirical Methods in Natural Language Processing and the 9th International Joint Conference on Natural Language Processing (EMNLP-IJCNLP. [doi: 10.18653/v1/D19-1259]
25. Kweon S, Choi B, Kim M, Park RW, Choi E. KorMedMCQA: multi-choice question answering benchmark for Korean healthcare professional licensing examinations. arXiv. Preprint posted online on Mar 5, 2024. [doi: 10.48550/arXiv.2403.01469]
26. Jin Q. PubMedQA. URL: https://pubmedqa.github.io/ [accessed 2025-04-30]
27. HL7 FHIR release 4. URL: https://hl7.org/fhir/R4/index.html [accessed 2025-04-30]
28. Qiaojin/pubmedqa. Hugging Face. URL: https://huggingface.co/datasets/qiaojin/PubMedQA/ [accessed 2025-07-09]
29. Sean0042/kormedmcqa. Hugging Face. URL: https://huggingface.co/datasets/sean0042/KorMedMCQA/ [accessed 2025-07-09]
30. Kim M, Kim Y, Kang HJ, et al. Fine-tuning LLMs with medical data: can safety be ensured? NEJM AI 2025 Jan;2(1):AIcs2400390. [doi: 10.1056/AIcs2400390]

XSL•FO
RenderX

31. Zhang T, Ladhak F, Durmus E, Liang P, McKeown K, Hashimoto TB. Benchmarking large language models for news summarization. Trans Assoc Comput Linguist 2024 Jan 31;12:39-57. [doi: 10.1162/tacl_a_00632]
32. Lee J, Son K, Kang T. A review of outpatient visit trends in korea and other countries [Article in Korean]. : Research Institute for Healthcare Policy, Korean Medical Association; 2019 URL: https://rihp.re.kr/bbs/board.php?bo_table=research_report&wr_id=293&sst=wr_hit&sod=asc&sop=and&page=17 [accessed 2025-10-22]
33. Lee CH, Lim H, Kim Y, Park AH, Park EC, Kang JG. Analysis of appropriate outpatient consultation time for clinical departments. HPM 2014 Sep 30;24(3):254-260. [doi: 10.4332/KJHPA.2014.24.3.254]
34. Irving G, Neves AL, Dambha-Miller H, et al. International variations in primary care physician consultation time: a systematic review of 67 countries. BMJ Open 2017 Nov 8;7(10):e017902. [doi: 10.1136/bmjopen-2017-017902] [Medline: 29118053]
35. Kwon A, Lee HY, Shin SY, et al. Current health data standardization project and future directions to ensure interoperability in Korea. Healthc Inform Res 2024 Apr;30(2):93-102. [doi: 10.4258/hir.2024.30.2.93] [Medline: 38755100]
36. Preiksaitis C, Sinsky CA, Rose C. ChatGPT is not the solution to physicians' documentation burden. Nat Med 2023 Jun;29(6):1296-1297. [doi: 10.1038/s41591-023-02341-4] [Medline: 37169865]
37. Roberts K. Large language models for reducing clinicians' documentation burden. Nat Med 2024 Apr;30(4):942-943. [doi: 10.1038/s41591-024-02888-w] [Medline: 38561439]
38. Landman AB, Tilak SS, Walker GA. Artificial intelligence-generated emergency department summaries and hospital handoffs. JAMA Netw Open 2024 Dec 2;7(12):e2448729. [doi: 10.1001/jamanetworkopen.2024.48729] [Medline: 39625728]
39. Sahni N, Stein G, Zemmel R, Cutler DM. The potential impact of artificial intelligence on healthcare spending.: National Bureau of Economic Research Working Paper Series; 2023. URL: http://www.nber.org/papers/w30857 [accessed 2025-04-30]
40. Liu TL, Hetherington TC, Dharod A, et al. Does AI-Powered clinical documentation enhance clinician efficiency? A longitudinal study. NEJM AI 2024 Nov 27;1(12):AIoa2400659. [doi: 10.1056/AIoa2400659]

Abbreviations

AI: artificial intelligence
API: application programming interfaces
EHR: electronic health record
FHIR: Fast Healthcare Interoperability Resource
LLM: large language model
Y-KNOT: Your-Knowledgeable Navigator of Treatment

Edited by C Perrin; submitted 02.05.25; peer-reviewed by P Hong, Y Zhao; revised version received 26.08.25; accepted 10.09.25; published 24.11.25.

Please cite as:
Kim H, Lee SY, You SC, Huh S, Kim JE, Kim ST, Ko DR, Kim JH, Lee JH, Lim JS, Park MS, Lee KY
A Bilingual On-Premises AI Agent for Clinical Drafting: Implementation Report of Seamless Electronic Health Records Integration in the Y-KNOT Project
JMIR Med Inform 2025;13:e76848
URL: https://medinform.jmir.org/2025/1/e76848
doi:10.2196/76848

© Hanjae Kim, So-Yeon Lee, Seng Chan You, Sookyung Huh, Jai-Eun Kim, Sung-Tae Kim, Dong-Ryul Ko, Ji Hoon Kim, Jae Hoon Lee, Joon Seok Lim, Moo Suk Park, Kang Young Lee. Originally published in JMIR Medical Informatics (https://medinform.jmir.org), 24.11.2025. This is an open-access article distributed under the terms of the Creative Commons Attribution License (https://creativecommons.org/licenses/by/4.0/), which permits unrestricted use, distribution, and reproduction in any medium, provided the original work, first published in JMIR Medical Informatics, is properly cited. The complete bibliographic information, a link to the original publication on https://medinform.jmir.org/, as well as this copyright and license information must be included.

XSL•FO
RenderX

Cost-Benefit Analysis of Preventing Acute Care Use in Oncology Patients Following Systemic Therapy Using Medicare Claims Data: Retrospective Cohort Study

Sara Alessandra Keller[1,2], MSc; Maximilian Schuessler[3], MSc, MPP; Behzad Naderalvojoud[1], PhD; Tina Seto[4], MS; Lu Tian[1,3], ScD; Mohana Roy[5,6], MD; Tina Hernandez-Boussard[1,3], MS, MPH, PhD

[1]Division of Computational Medicine, Stanford University, 1265 Welch Rd, Stanford, CA, United States

[2]Department of Health Sciences and Technology, ETH Zurich, Zurich, Switzerland

[3]Department of Biomedical Data Science, Stanford University, Stanford, CA, United States

[4]Department of Technology & Digital Solutions, Stanford Health Care, Stanford, CA, United States

[5]Department of Medicine, Stanford University School of Medicine and Stanford Cancer Institute, Stanford, CA, United States

[6]Department of Medicine, Med/Oncology, Stanford University, Stanford, CA, United States

Corresponding Author:
Tina Hernandez-Boussard, MS, MPH, PhD
Division of Computational Medicine, Stanford University, 1265 Welch Rd, Stanford, CA, United States

Abstract

Background: Acute care use (ACU) represents a major economic burden in oncology, which can ideally be prevented. Existing models effectively predict such events.

Objective: We aimed to quantify the cost savings achieved by implementing a model to predict ACU in oncology patients undergoing systemic therapy.

Methods: This retrospective cohort study analyzed patients with cancer at an academic medical center from 2010 to 2022. We included patients who received systemic therapy and identified ACU events occurring after treatment initiation, excluding those with known death dates within the study period. Data on ACU-related expenses were gathered from Medicare claims and mapped to service codes in electronic health records, yielding average daily costs for each patient over 180 days following the start of therapy. The exposure was an ACU event.

Results: The main outcome was the average daily cost per patient at the end of the first 180 days of systemic therapy. We observed that expense accumulation flattened earlier and more rapidly among non-ACU patients. This study included 20,556 patients, of whom 3820 (18.58%) experienced at least 1 ACU. The average daily cost per patient for those with and without ACU was US $94.62 (SD US $72.54; 95% CI US $92.32-$96.92) and US $53.28 (SD US $59.92; 95% CI US $52.37-$54.19), respectively. The average total cost per ACU and non-ACU patient was US $17,031.92 (SD US $13,056.63; 95% CI US $16,616.74-$17,445.09) and US $9591.06 (SD US $10,785.83; 95% CI US $9427.64-$9754.48), respectively. To estimate the long-term financial impact of deploying the predictive model, we conducted a cost-benefit analysis based on an annual cohort size of 2177 patients. In the first year alone, the model yielded projected savings of US $910,000. By year 6, projected savings grew to US $9.46 million annually. The cumulative avoided costs over a 6-year deployment period totaled approximately US $31.11 million. These estimates compared the baseline cost model to the intervention model assuming a prevention rate of 35% for preventable ACU events and an average ACU cost of US $17,031.92 (SD US $13,037).

Conclusions: Predictive analytics can significantly reduce costs associated with ACU events, enhancing economic efficiency in cancer care. Further research is needed to explore potential health benefits.

(JMIR Med Inform 2025;13:e77891) doi:10.2196/77891

KEYWORDS

patient care; evidence-based emergency medicine; machine learning; electronic health records; cost-benefit analysis; cost savings; emergency service; oncology service; preventive services; Medicare

XSL•FO
RenderX

Introduction

Acute Care Use Burden in Oncology

Systemic therapy, such as chemotherapy, while essential for treating cancer, can be highly toxic, often leading to complications that result in patients requiring acute care use (ACU), including unplanned hospitalizations and emergency department visits [1]. These events can be classified as avoidable or unavoidable based on clinical context, with avoidable ACU events being potentially preventable through prompt interventions. ACU events are linked to higher rates of repeat visits and mortality [2], and there is evidence suggesting that up to 35% of ACU events are preventable within 180 days of therapy start [3], whereas other sources even discuss possible prevention from 40% to 67% [4-6]. For that reason, these events not only are detrimental to patient health but also significantly contribute to health care costs. Therefore, the Centers for Medicare and Medicaid Services (CMS) has named certain ACU events as preventable and has begun using them as quality metrics, as seen with the Outpatient Quality Reporting Program and the OP-35 measure [7]. The potential to reduce preventable ACU events presents an important opportunity to improve patient outcomes and lower costs for both hospitals and patients.

Predictive Advancements

Recent advancements in machine learning (ML) have greatly improved the identification of patients at elevated risk of ACU events [1]. Innovations in deep learning and natural language processing now enable more accurate and reliable predictive models, supporting precise risk stratification while remaining robust across diverse populations and periods [8-10]. This capacity creates a paradigm-shifting opportunity; by predicting ACU events before they occur, these models empower health care systems to shift from reactive to proactive care. These electronic health record (EHR)–derived risk scores allow clinicians to deliver targeted interventions for patients at high risk of ACU and potentially prevent costly ACU events.

However, realizing this potential requires navigating significant challenges [11]. This includes the need for dedicated staffing, regulatory compliance, and integration with existing systems, all of which incur significant costs that must be considered in return-on-investment (ROI) assessments. Moreover, successful implementation depends on both technical execution and clinical adoption [11]. Literature on model deployment challenges, clinical integration, and operational cost considerations shows that algorithms fail in practice due to workflow misalignment, lack of interpretability, and the hidden resource burden of sustained use [11-13]. Model transparency and reporting frameworks are increasingly critical for building clinician trust as they document intended use cases, performance characteristics across subpopulations, and potential biases, which are all essential considerations when deploying predictive models in health care settings [10]. The deployment of ML models in health care incurs significant costs related to data preparation, regulatory compliance, integration with existing systems, and ongoing maintenance and monitoring [12,14]. Additionally, deploying these models requires an investment in workforce training and infrastructure, making it a costly endeavor [13]. Therefore, despite the promise of ML in health care, the cost of its deployment must be weighed against the savings it generates, which is a complex and often overlooked aspect of deployment in health care. The deployment of ML models in clinical settings presents challenges beyond technical performance [11]. Equally critical for clinical adoption are workflow optimization, staff training, and clinician trust [13]. This trust must be built through transparent tools such as model cards [10,15] that document performance and potential biases across diverse patient populations. Accounting for these demands is essential as their cumulative cost can undermine the financial viability of even the most promising models.

Bridging the Gap

To address this gap, we developed a cost analysis to assess the expenses associated with deploying an ML model and the potential savings from preventing ACU events among patients with cancer starting treatment at a comprehensive cancer center (CCC). Our hypothesis was that implementing an ML model would lead to cost savings by preventing ACU events and reducing hospital costs. This study aimed to fill a critical gap in the literature [13,16-18] about the ROI for ML deployment in health care, particularly in oncology. This work paves the way for future studies to explore the broader health benefits, potentially driving the adoption of ML in various areas of patient care. Unlike previous studies focused primarily on model performance, this analysis evaluated real-world financial return, offering critical insights for health care systems considering predictive model deployment.

Methods

Study Design

This retrospective cohort study used structured EHR data from routine care from a CCC that includes an academic hospital, a community hospital, and a health care alliance. This study provides a cost analysis comparing daily patient costs with and without a prediction model for preventing ACU admissions. A cost-benefit analysis was conducted from the Medicare payer perspective comparing usual care to an intervention involving predictive model deployment. Costs, including staffing and IT infrastructure, were estimated using institutional records and published benchmarks [13,16,19]. We modeled the deployment of a prediction system using standard cost estimates for artificial intelligence tools (see Multimedia Appendix 1). Savings were derived by applying the preventable ACU proportion to the total cohort and the associated cost differential. Claims data mapped to EHR service codes were used to estimate care costs over the 180-day posttherapy window.

Ethical Considerations

This retrospective analysis was approved by the Stanford University Institutional Review Board (protocol 47644), with a waiver of informed consent due to secondary use of existing records. This research also used publicly available Medicare claims data. All procedures complied with institutional policies, the Declaration of Helsinki, and applicable privacy regulations. In addition, our study adheres to the Minimum Information for Medical Artificial Intelligence Reporting guidelines [15].

XSL•FO
RenderX

Data Preparation

We calculated costs using a combination of Medicare Physician Fee Schedule (MPFS) [19,20] and average sales price (ASP) [21] data following the CMS methodology and previous published research [16,22,23] (see Table S1 and equations 1-7 in Multimedia Appendix 1). MPFS values were determined based on 3 components: relative value units assigned to each service, a geographic practice cost index to account for regional cost variations, and a conversion factor that translates relative value units into dollar amounts. ASP values were calculated as 106% of the ASP, reflecting the CMS payment limit for drugs and biologicals. For each Healthcare Common Procedure Coding System (HCPCS) code each year and quarter, we summed the MPFS and ASP values to produce a combined fee for a given service at a specific point in time (equation 3 in Multimedia Appendix 1) [23].

Operational Implementation

The rationale behind the algorithm is that patients predicted to be at high risk of ACU events will be flagged using pop-up notifications (as shown in Figure S1 in Multimedia Appendix 1). To estimate deployment costs within our cost model, we incorporated key operational needs for a predictive model in outpatient oncology care. These included infrastructure setup, model validation, workflow integration, maintenance, and staffing needs. Deployment costs were the largest contributor and encompassed data infrastructure, integration with the Epic EHR system, and real-time workflow design [12,13,24]. Annual maintenance costs comprised technical audits, software updates, and training. We assumed an initial onboarding session per health care provider to cover alert interpretation, risk stratification logic, and escalation protocols. Although the system is not yet deployed, this assumption reflects institutional norms and previous implementations. Ongoing training for new staff and protocol updates were included in maintenance costs. To operationalize the intervention, we included staffing of 0.25 full-time equivalent (FTE) for a registered nurse, who triages alerts and provides patient education. Published data on remote symptom alert triage in oncology indicate that time per alert ranges from under 5 to 10 minutes, with 52% resolved in under 5 minutes and 36% resolved in 5 to 10 minutes [25]. In addition, 0.5 FTE were estimated for an advanced practice provider (APP), who coordinates clinical follow-up with primary oncology teams [3,23]. All operational assumptions were informed by published oncology implementation studies [13,24,26], internal clinical workflows, and expert discussions. A detailed visualization of the modeled deployment workflow is provided in Figure S2 in Multimedia Appendix 1.

Estimating Costs

To quantify the cost of care for a patient, we mapped MPFS and ASP values to each patient's services using HCPCS codes [23], including level 1 codes corresponding to Current Procedural Terminology (CPT) codes from the American Medical Association. Service codes and dates were linked to these combined fees to compute the total cost incurred by each patient on each day of the observation period. These daily costs were then aggregated over the therapy period to calculate the total cost per patient per period (TCPP), representing the full cost of services and drugs received by an individual during the entire treatment window. To standardize this measure and enable comparisons across patients with different observation lengths, we derived the cost of care per patient per day (CCPD) by dividing each patient's TCPP by the number of days in their observation period. Thus, the CCPD represents an average daily cost across the full treatment window, distinct from the raw daily totals. Variable definitions are provided in Table S4 in the Multimedia Appendix 1, with patient-level CCPD values summarized in Table S4 in Multimedia Appendix 1. To estimate the annual cost of ACU before deploying (without) a predictive model, we multiplied the total patient population by the baseline ACU prevalence to obtain the expected number of ACU events ($N_{acu,0}$). This value was then multiplied by the average cost per ACU case (C_{acu}), resulting in an overall cost estimate in the absence of intervention. We developed the following formula for the total cost estimation without a prediction model (C_0; equation 1; Multimedia Appendix 1):

$$(1) C0(X) = Cacu \cdot Nacu,0 \cdot X$$

To assess the cost with a deployed predictive model, we included the model's implementation cost (C_{deploy}); ongoing annual maintenance (C_{annual}); residual ACU costs after prevention efforts ($C_{acu,1}$); and additional staffing required for proactive care, including cost of nurses (C_{nurse}) and APPs (C_{app}) [16,17]. We estimated the number of preventable ACU events and calculated the proportion of those correctly identified by the model. We also accounted for false positives, patients incorrectly flagged as high risk, and their implications. The false positives were obtained by first calculating how many patients were not at risk of an ACU event and, among these, identifying how many were incorrectly predicted as being at risk. Accordingly, we developed the following formula for the total cost calculation with a prediction model (C_1; equation 21 in Multimedia Appendix 1):

$$(2) C1(x) = Cdeploy + Cannual \cdot (x-1) + Cacu,1 \cdot x + Cnurse \cdot x + Capp \cdot x$$

Service costs were derived as described previously [23] by mapping MPFS and ASP values to each patient's clinical activity using HCPCS and CPT codes. They were then linked by date and aggregated to compute the TCPP and CCPD as outlined previously. HCPCS and CPT codes were grouped into service categories using CMS classification files. We included professional fees via MPFS and ASP values for drug-related codes. Facility fees, patient cost sharing, and contractual adjustments were excluded. The cost models in the detail section in Multimedia Appendix 1 provide more details of the cost models generated with and without a predictive model. Codes were mapped to the cost on CMS-allowed amounts for professional services and drugs. Facility and patient-specific fees were excluded. Figure S6 in Multimedia Appendix 1 shows the most common and most expensive services observed in the cohort.

Data Analysis

A cost-benefit analysis was conducted to compare the total costs of ACU admissions with and without the use of a prediction model based on the estimated number of preventable events reported in the literature [27]. The total cost without the model

XSL•FO
RenderX

was calculated by multiplying the prevalence of ACU cases by the total number of patients and the cost per ACU case. The cost associated with the model includes deployment costs, annual maintenance, and the additional personnel required to interpret predictions and conduct patient outreach (eg, nurses and APPs). The model's impact on cost reduction was evaluated by estimating the number of preventable ACU cases and extrapolating the potential savings from excluding these cases. We assumed a conservative lower-bound prevention rate of 35% based on an estimate of the proportion of ACU events deemed preventable in the published literature [3,4], which aligns with the minimal threshold observed across multiple oncology care studies. We then applied this rate to the number of high-risk patients identified by the model. Data analyses were conducted using Python (Python Software Foundation) and libraries such as Seaborn and Matplotlib for visualization and SciPy for statistical testing. A Mann-Whitney *U* test was used for nonnormal data distributions with an α level of .05. Chi-square tests were conducted to assess differences in features within the cohort, and 2-tailed *t* tests were applied to evaluate cost differences at various time points (30, 90, and 180 days; Table S1 in Multimedia Appendix 1). A paired *t* test was used to analyze the monetary reduction between the C_0 cost model without and the C_1 cost model with deployment over the first 6 years of implementation comparing the means of the paired samples.

Sensitivity Analysis

To evaluate the robustness of our cost-benefit analysis, we conducted a deterministic break-even sensitivity analysis of the ML model and the cost model. Full formulae and constants can be found in Multimedia Appendix 1. For the ML model, the analysis identified threshold values of key model parameters, namely, the sensitivity of the prediction model (R_{sens}), the prevalence of ACU events (p_{prev}), and the total patient volume (N_{total}) that would result in an ROI of ≥0. Each parameter was varied independently while holding the others constant. We defined the cost without a prediction model (C) as the product of the average ACU cost and the expected number of patients with ACU events. The cost with a prediction model (C_1) included fixed deployment costs, annual maintenance costs, reduced ACU burden due to model sensitivity and prevention rate (p_{pred}), and additional costs. We defined p_{pred} as the proportion of preventable ACU events. For the cost model sensitivity, we conducted a one-way sensitivity test on p_{pred} keeping the other variables constant.

Results

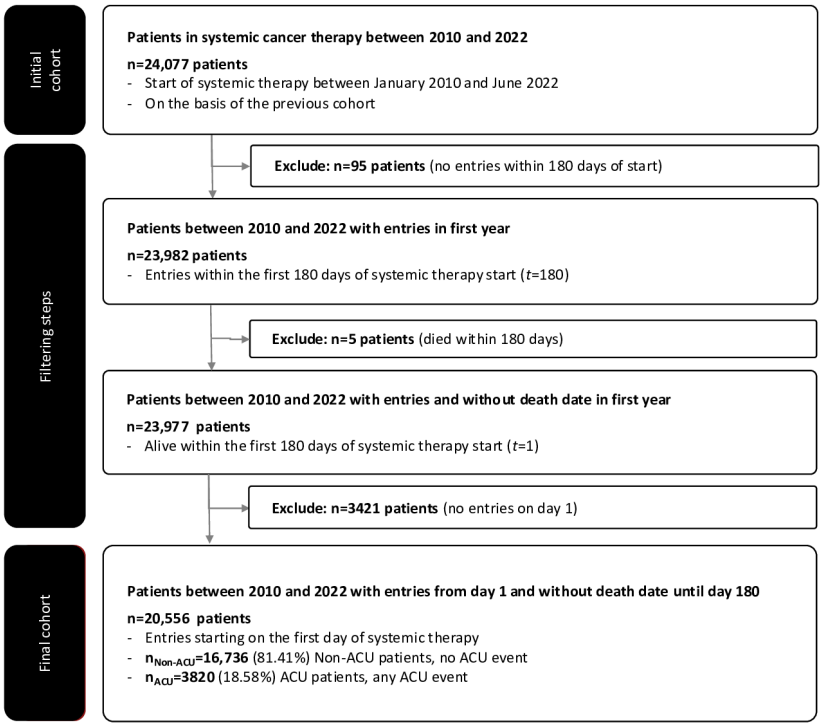
Study Cohort

The cohort comprised oncology patients at the CCC who received systemic therapy from 2010 to 2022. Data from the first day of therapy until 180 days after therapy initiation were included, with features such as patient demographics, clinical information, and health services received. Patients without entries within the first year of therapy, those who died within this period, and those without data on the first day of therapy were excluded (Figure 1). Patients were categorized into 2 groups: those with and without ACU admissions, labeled using a binary classification to show whether an ACU admission occurred [10].

The cohort included 20,556 patients, of whom 16,736 (81.42%) had no ACU events and 3820 (18.58%) had at least 1 ACU event, which we defined as the ACU prevalence (Figure 1). Characteristics by ACU status are presented in Table S3 in Multimedia Appendix 1. Differences across demographic and clinical factors were observed in this cohort, including gender, ethnicity, race, insurance type, tumor stage, and tumor type (all $P<.05$; see Table S3 in Multimedia Appendix 1). While several comparisons were statistically significant, we also considered their clinical relevance, as disparities in ACU incidence across demographic groups may reflect differences in acces to care, quality of treatment, or underlying health status. For example, the ACU rate in genitourinary cancer was 42% higher than in breast cancer (23.1% vs 16.2%). Higher ACU proportions were observed for Medicaid coverage (29%; $P<.001$), advanced tumor stage (stage 4: 30%; $P<.001$; stage 3: 22%; $P=.002$), and tumor types including genitourinary (35%; $P<.001$), pancreas (33%; $P<.001$), sarcoma (33%; $P<.001$), and lymph (28%; $P<.001$), whereas breast cancer showed a lower ACU proportion (10%; $P<.001$). Differences in race were also observed between Asian (20%; $P=.001$), Black (23%; $P=.009$), and Hawaiian or Pacific Islander patients (27%, $P=.002$). These findings are descriptive and indicate associations within this cohort rather than causal effects. Patients with ACU events incurred significantly higher costs ($P<.001$), including a TCPP of US $17,031.92 within the first 180 days (approximately 6 months) compared to US $9591.06 for those without ACU events. Daily costs were double for ACU patients (US $94.62 vs US $53.28, respectively; Table S4 in Multimedia Appendix 1).

XSL•FO
RenderX

Figure 1. Cohort selection process for cost analysis: flowchart outlining the cohort selection and filtering process for patients undergoing systemic cancer therapy from 2010 to 2022. The initial cohort of 24,077 patients [16] was narrowed down to 20,556 (85.38%) after exclusions based on entry timing, survival within 180 days (approximately 6 months), and missing day 1 records. The final cohort of 20,556 patients included 16,736 (81.42%) non–acute care use (ACU) patients and 3820 (18.58%) ACU patients.



Cost per Day

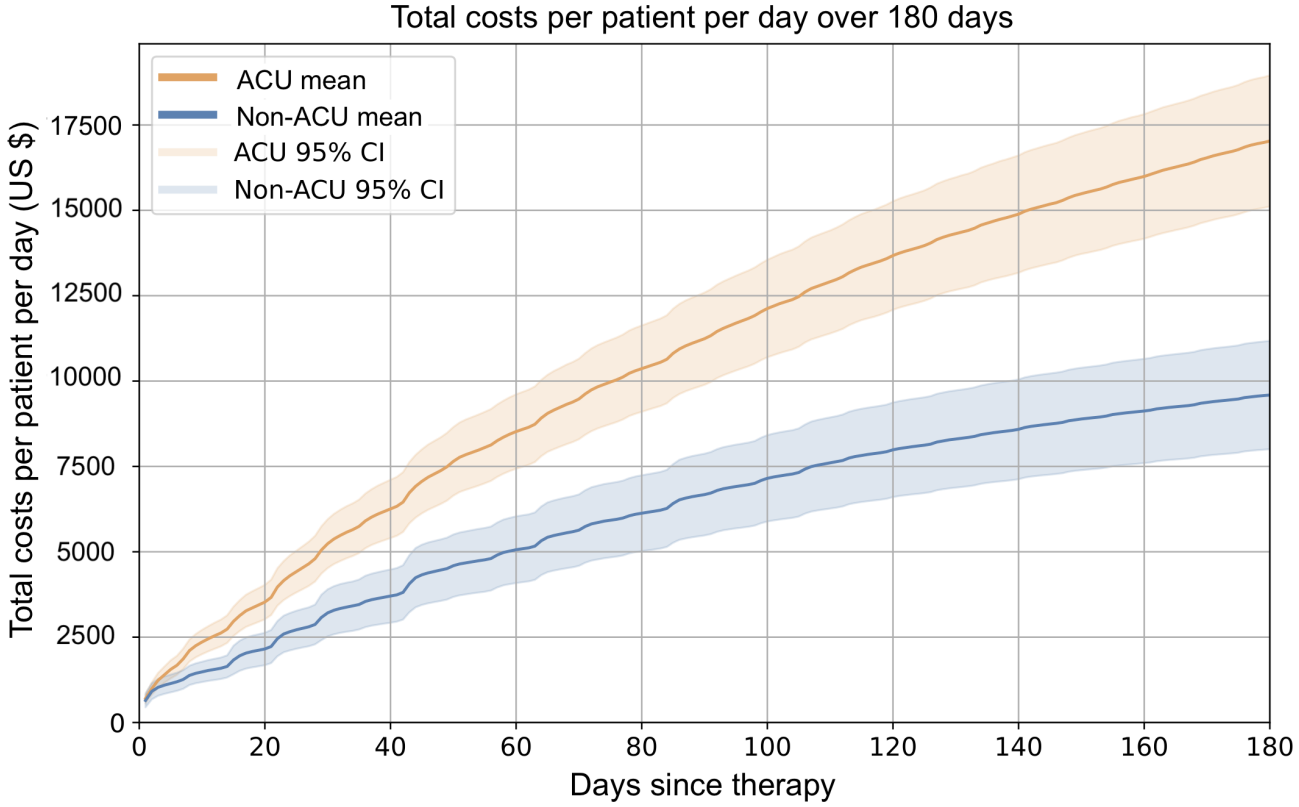
Cost analysis revealed that CCPD and TCPP differed significantly between ACU and non-ACU patients (P<.001), with CCPD decreasing over time for all patients but total expenses rising for those with ACU events. At 180 days, the average CCPD in the ACU group was nearly double that of non-ACU patients (US $94.62, SD US $72.54 vs US $53.28, SD US $59.92), respectively; P<.001; Table S4 in Multimedia Appendix 1). The higher costs in ACU patients were driven by greater frequency of pathology, laboratory, and medicine-related procedures (Figure S8 and S9 in Multimedia Appendix 1). The cost differences between groups were both statistically and clinically significant (P<.001), with ACU patients incurring approximately 78% higher total and daily costs over 180 days than non-ACU patients (US $17,031.92, SD US $13,056.63) vs US $9591.06, SD US $10,785.83, respectively; US $94.62, SD US $72.54 per day vs US $53.28, SD US $ 59.92 per day, respectively).

TCPP Results

The average TCPP for patients with ACU within the first 180 days was US $17,031.92 (SD US $13,056.63) compared to US $9591.06 (SD US $10,785.83) for those without such events (Figure 2and Figure S5 in Multimedia Appendix 1). We observed that expense accumulation flattened earlier and more rapidly for non-ACU patients (P<.001). The shaded areas illustrate the variation of the total costs from the mean. On day 180, the average daily cost for those with ACU was US $94.62 (SD US $72.54) compared to US $53.28 (SD US $59.92) for those without ACU, which means that patients with ACU events incurred twice the daily costs (P<.001) (Figure 2 and Figure S6 in Multimedia Appendix 1).

XSL•FO
RenderX

Figure 2. Total costs per patient over 180 days with and without acute care use (ACU) events. The mean total costs per patient per day (US $) over 180 days are presented for patients with ACU events (n=3820; orange line) and those without ACU events (n=16,736; blue line). The shaded areas represent the 95% CIs. Patients experiencing ACU events incurred consistently higher costs throughout the 180-day period.



Cost Model Results

Operational requirements for implementing the predictive model included supplementary staffing of 0.25 FTE nurses and 0.5 FTE APPs, with combined annual staffing costs of US $112,765. Additional fixed costs of model deployment included software integration, staff training, and compliance with health care IT standards, totaling US $1 million in year 1, with US $200,000 in annual maintenance thereafter. The model showed a positive ROI starting in year 1 (US $910,000) and cumulative savings of US $9.46 million by year 6 (Figure 3). If higher prevention rates of up to 64% are achieved, as suggested in the literature, cost savings could increase further. ROI was calculated as net savings divided by total implementation cost, with break-even achieved within the first year. We used a least absolute shrinkage and selection operator model with a sensitivity of 0.84 and specificity of 0.51 to predict ACU events (Figure S7 in Multimedia Appendix 1), identifying 1.65% (339/20,556) of the patients in the cohort as high risk, enabling targeted intervention planning. As mentioned previously, we assumed that 35% of ACU events were preventable as this value represents a conservative lower bound supported by published literature [3,4]. Using this number in our model, we obtained 119 yearly prevented events and projected cost savings of US $31.11 million over 6 years in our cohort. We expected a cost saving of approximately US $1 million in the year of deployment. There is potential for greater impact as we used a prevention rate of 35% and different prevention rates have been observed in different studies (between 35% and 67%) [4-6]. In contrast to the annualized economic analysis, we estimate with the ACU rate of 18.58% (3820/20,556) in a similar sized cohort, that the number of patients experiencing ACU events over 6 years would be reduced from 8484 to 5985, resulting in 2499 fewer ACU-affected patients. This reduction in avoidable acute care episodes underscores the clinical benefit of early triage and intervention.

XSL•FO
RenderX

Figure 3. Projected cost comparison with and without the prediction model. Cumulative costs (US $) of patient management are shown over 6 years for a cohort of 2177 patients. Costs with the prediction model (C_1; green line) showed large savings compared to costs without the model (C_0; red line), with cumulative savings of US $31.11 million after accounting for the implementation and operational costs of the predictive model. The prediction model showed a clear economic advantage in managing long-term expenses.



Sensitivity Analysis

The model reached break-even within 6 years if the prevention rate was higher than 27%. Prevention rates of 35% or higher [4-6] consistently led to early cost savings within the first year of deployment. Lower-effectiveness scenarios did not achieve break even within the evaluation window (see the sensitivity analysis section in Multimedia Appendix 1 and Figure S10 in Multimedia Appendix 1).

Discussion

Principal Findings

Overview

In this retrospective study, we explored the economic impact of ACU in oncology patients starting chemotherapy and the cost benefits of implementing a predictive model to identify and intervene on high-risk patients. Our analysis of over 20,000 patients initiating chemotherapy revealed that ACU events nearly double daily costs, significantly burdening both patients and the health care system. By implementing an ML model to identify patients at high risk of ACU, we observed substantial cost reductions and a favorable ROI for the health care system. These findings underscore the importance of proactive interventions in oncology, demonstrating that predictive analytics and digital tools can enhance patient management, improve outcomes, and address health care inequities.

Economic Burden of ACU Events

The cost implications of ACU events within our cohort were significant, with patients experiencing ACU incurring an average total cost per patient of US $17,031.92 in the first 180 days of treatment compared to just US $9591.06 for those without ACU events (P<.001). The 77.5% higher total costs for ACU patients were not just statistically significant but also clinically meaningful, directly impacting both health care budgets and patient quality of life. This stark contrast in costs between patient groups reinforces previous research that underscores the considerable financial burden that ACU places on both patients and health care systems [16]. Furthermore, we observed that the cumulative financial impact of ACU events increased over time, further straining health care resources, as noted by Iqbal [27] and Oluwagbade and Covenant [28]. The notable differences in CCPD between the 2 groups emphasize the critical importance of early identification of high-risk patients to mitigate unnecessary health care expenditures. This notion aligns with existing literature that advocates for early risk identification and preventive interventions, which can lead to more efficient health care resource allocation [29].

Cost Savings From Preventive Intervention

This study highlights that deploying a predictive model is an effective strategy for reducing preventable ACU events. Our ML model successfully identified high-risk patients, enabling proactive interventions that have the potential to decrease unplanned care. In the literature, the proportion of such preventable events is reported to range from 35% to 67% [3-6]. Our cost analysis indicated that preventing events could result in savings of approximately US $31 million over 6 years (assuming 2177 patients per year), with a positive ROI observed in the first year of implementation. Our sensitivity analyses demonstrated that the intervention achieved cost savings from prevention rates at 27%, with higher-performance scenarios yielding immediate returns. These findings underscore that even moderately effective clinical decision support tools can result in substantial cost savings when targeted to high-risk populations. Future implementations should include continuous

XSL•FO
RenderX

performance monitoring to ensure that projected prevention rates are achieved. The estimated reduction in ACU events can translate to a meaningful decrease in hospital days and patient morbidity beyond financial savings. Our study targeted earlier cancer treatment stages, particularly chemotherapy, emphasizing the prevention of avoidable hospital admissions and emergency department visits. This approach not only enhances cost efficiency but also underscores the value of integrating predictive models into health care operations to improve patient outcomes. Over a 6-year period, the predictive model reduced projected costs by approximately US $31.11 million compared to the baseline. In the first year alone, the model yielded estimated savings of approximately US $910,000, increasing to US $9.46 million in year 6. The US $31.11 million figure represents the total avoided expenditure over 6 years when comparing the prediction model to standard care. These projections are based on an annual cohort of 2177 patients and an average ACU cost of US $17,031.92.

Precision Oncology

Traditional approaches to ACU risk often rely on reactive care, addressing complications only after they occur. In contrast, our model supports a preventative approach by identifying high-risk patients before chemotherapy begins. This enables clinicians to proactively adjust treatment plans, such as dose modifications or enhanced supportive care, aligning interventions with patient-specific vulnerabilities. Model projections suggest that proactive triage informed by our risk scores could prevent ACU events in approximately 2499 patients over 6 years. As oncology shifts toward value-based care, tools that enable early, risk-based intervention while preserving operational efficiency are critical for sustainable implementation [1,2].

Implementation Considerations

Successful implementation of predictive models requires careful attention to both clinical integration and operational feasibility. The economic viability of implementing ML algorithms in clinical workflows depends on seamless clinical integration, recommendation-action pairing, clinical oversight, and effective prioritization [30,31]. These costs include data preparation, model validation, integration into existing systems, staff training, and ongoing maintenance [13,24]. Our analysis includes the need for added staffing, including nurses and practice providers, to pair model recommendations with clinical actions. Upon deployment, patients flagged as high risk could be routed to case managers or nursing staff for follow-up via calls or assessments, with workflows integrated into existing care management protocols. While this requires training and coordination, it aligns with current practices in outpatient oncology. Even accounting for these resources, the model delivers a strong ROI. Furthermore, if higher prevention rates up to 67% are realized, as suggested by other studies [6], the resulting cost savings could be even more substantial. Overall, predictive models represent a strategic approach to reducing ACU events while improving both financial and clinical outcomes.

Cost Model Limitations

Our study has several important limitations regarding cost estimation. First, while Medicare fee schedules (MPFS and ASP) provide standardized benchmarks, they cannot capture real-world billing complexities such as payer-specific contractual adjustments below Medicare levels (typically 15%-40% below Medicare rates) [32] or variable patient cost sharing [33]. Second, the single-center design misses undocumented out-of-network ACU events. This may underestimate ACU rates and the associated cost savings. In addition, while this CCC reflects the environment of many other cancer centers, the generalizability of our findings to other health care systems may be limited. Third, unmodeled implementation costs (eg, workforce training and workflow changes) may reduce net savings. While our ROI estimates remained positive in sensitivity analyses, real-world returns could be modestly lower. These trade-offs were necessary to enable standardized cross-center comparisons, but future work should incorporate multipayer claims data to improve precision. Fourth, specific medical costs were not available for this study; therefore, we extrapolated expenses using MPFS and ASP values from the CMS, primarily relying on Medicare fees. Fifth, ROI estimates, as shown in the one-way sensitivity analysis, are sensitive to the assumed prevention rate. If the true prevention rate is lower than modeled, the ROI may be overestimated, highlighting the importance of validation in real-world settings. Finally, we did not explicitly model all potential operational challenges, such as hiring, training, and compliance-related overhead. These unaccounted-for costs may reduce net savings in practice and should be evaluated in future implementation studies.

Conclusions

In conclusion, this study reinforces the substantial financial burden associated with ACU in oncology patients, with marked cost differences between those who experience ACU and those who do not. By identifying high-risk patients, our model supports timely interventions that lower avoidable ACU costs and improve outcomes. These findings support the integration of predictive analytics into clinical workflows to optimize resource use, reduce preventable ACU events, and improve patient outcomes. As health care systems evolve, data-driven strategies such as ours may play a pivotal role in enhancing the efficiency and quality of cancer care.Use of Generative AI

Acknowledgments

The generative artificial intelligence (AI) tool ChatGPT (version 4; OpenAI) was used in grammatical editing. AI-generated content was reviewed, fact-checked, and integrated into the manuscript with full author and study group oversight.

XSL•FO
RenderX

Data Availability

The data used for this paper contain patient identifiers and, therefore, are not publicly available. Access is only granted through institutional review board approval.

Authors' Contributions

TH-B designed the study. SAK and TH-B developed the methods. SAK and TS extracted the data. SAK and LT conducted the analyses. SAK wrote the first draft of the manuscript. All authors interpreted the results and reviewed the manuscript. TH-B provided support, guidance, and leadership for the project and oversaw the research process.

Conflicts of Interest

None declared.

Multimedia Appendix 1
Additional methods, cohort characteristics, and extended cost and model performance results.
[DOC File, 3314 KB - medinform_v13i1e77891_app1.doc]

References

1. Alsuhebany N, Brown J, Echave J, McBride A. Evaluation of emergency department visits by oncology patients: a running comparison to admissions and ED visits under the CMS OP-35 ruling. J Adv Pract Oncol 2022 May;13(4):367-378. [doi: 10.6004/jadpro.2022.13.4.2] [Medline: 35755896]
2. Griffin JL, Yersin M, Baggio S, et al. Characteristics and predictors of mortality among frequent users of an emergency department in Switzerland. Eur J Emerg Med 2018 Apr;25(2):140-146. [doi: 10.1097/MEJ.0000000000000425] [Medline: 27749377]
3. Peterson DJ, Ostberg NP, Blayney DW, Brooks JD, Hernandez-Boussard T. Machine learning applied to electronic health records: identification of chemotherapy patients at high risk for preventable emergency department visits and hospital admissions. JCO Clin Cancer Inform 2021 Oct;5:1106-1126. [doi: 10.1200/CCI.21.00116] [Medline: 34752139]
4. Alishahi Tabriz A, Turner K, Hong YR, Gheytasvand S, Powers BD, Elston Lafata J. Trends and characteristics of potentially preventable emergency department visits among patients with cancer in the US. JAMA Netw Open 2023 Jan 3;6(1):e2250423. [doi: 10.1001/jamanetworkopen.2022.50423] [Medline: 36656584]
5. Lash RS, Hong AS, Bell JF, Reed SC, Pettit N. Recognizing the emergency department's role in oncologic care: a review of the literature on unplanned acute care. Emerg Cancer Care 2022;1(1):6. [doi: 10.1186/s44201-022-00007-4] [Medline: 35844666]
6. Kajdacsy-Balla Amaral AC, Hill AD, Pinto R, et al. The effects of acute care hospitalization on health and cost trajectories for nursing home residents: a matched cohort study. Medicine (Baltimore) 2022 Oct 14;101(41):e31021. [doi: 10.1097/MD.0000000000031021] [Medline: 36254032]
7. Hospital outpatient quality reporting program. Centers for Medicare & Medicaid Services. URL: https://www.cms.gov/medicare/quality/initiatives/hospital-quality-initiative/hospital-outpatient-quality-reporting-program [accessed 2025-02-19]
8. Fanconi C, van Buchem M, Hernandez-Boussard T. Natural language processing methods to identify oncology patients at high risk for acute care with clinical notes. AMIA Jt Summits Transl Sci Proc 2023;2023:138-147. [Medline: 37350895]
9. Tran KA, Kondrashova O, Bradley A, Williams ED, Pearson JV, Waddell N. Deep learning in cancer diagnosis, prognosis and treatment selection. Genome Med 2021 Sep 27;13(1):152. [doi: 10.1186/s13073-021-00968-x] [Medline: 34579788]
10. Schuessler M, Fleming S, Meyer S, Seto T, Hernandez-Boussard T. Diagnostic framework to validate clinical machine learning models locally on temporally stamped data. Commun Med (Lond) 2025 Jul 1;5(1):261. [doi: 10.1038/s43856-025-00965-w] [Medline: 40596645]
11. Zhang A, Xing L, Zou J, Wu JC. Shifting machine learning for healthcare from development to deployment and from models to data. Nat Biomed Eng 2022 Dec;6(12):1330-1345. [doi: 10.1038/s41551-022-00898-y] [Medline: 35788685]
12. Rajagopal A, Ayanian S, Ryu AJ, et al. Machine learning operations in health care: a scoping review. Mayo Clin Proc Digit Health 2024 Sep;2(3):421-437. [doi: 10.1016/j.mcpdig.2024.06.009] [Medline: 40206123]
13. Morse KE, Bagley SC, Shah NH. Estimate the hidden deployment cost of predictive models to improve patient care. Nat Med 2020 Jan;26(1):18-19. [doi: 10.1038/s41591-019-0651-8] [Medline: 31932778]
14. Sendak MP, Ratliff W, Sarro D, et al. Real-world integration of a sepsis deep learning technology into routine clinical care: implementation study. JMIR Med Inform 2020 Jul 15;8(7):e15182. [doi: 10.2196/15182] [Medline: 32673244]
15. Hernandez-Boussard T, Bozkurt S, Ioannidis JP, Shah NH. MINIMAR (MINimum information for medical AI reporting): developing reporting standards for artificial intelligence in health care. J Am Med Inform Assoc 2020 Dec 9;27(12):2011-2015. [doi: 10.1093/jamia/ocaa088] [Medline: 32594179]

XSL•FO
RenderX

16. Blayney DW, Seto T, Hoang N, Lindquist C, Kurian AW. Benchmark method for cost computations across health care systems: cost of care per patient per day in breast cancer care. JCO Oncol Pract 2021 Oct;17(10):e1403-e1412. [doi: 10.1200/OP.20.00462] [Medline: 33646822]
17. Wang Y, Liu C, Hu W, et al. Economic evaluation for medical artificial intelligence: accuracy vs. cost-effectiveness in a diabetic retinopathy screening case. npj Digit Med 2024;7(1):43. [doi: 10.1038/s41746-024-01032-9]
18. Areia M, Mori Y, Correale L, et al. Cost-effectiveness of artificial intelligence for screening colonoscopy: a modelling study. Lancet Digit Health 2022 Jun;4(6):e436-e444. [doi: 10.1016/S2589-7500(22)00042-5] [Medline: 35430151]
19. Magnani CJ, Bievre N, Baker LC, Brooks JD, Blayney DW, Hernandez-Boussard T. Real-world evidence to estimate prostate cancer costs for first-line treatment or active surveillance. Eur Urol Open Sci 2021 Jan;23:20-29. [doi: 10.1016/j.euros.2020.11.004] [Medline: 33367287]
20. Physician fee schedule. Centers for Medicare & Medicaid Services. 2024 Jul 12. URL: https://www.cms.gov/medicare/payment/fee-schedules/physician [accessed 2024-08-02]
21. Average sales price (ASP) reporting. Centers for Medicare & Medicaid Services. 2024 Jul 23. URL: https://www.cms.gov/medicare/payment/part-b-drugs/asp-reporting [accessed 2024-08-02]
22. Healthcare Common Procedure Coding System (HCPCS). Centers for Medicare & Medicaid Services. 2024 Jul 9. URL: https://www.cms.gov/medicare/coding-billing/healthcare-common-procedure-system [accessed 2024-08-02]
23. Caston NE, Franks JA, Balas N, et al. Evaluating nurses' time to response by severity and cancer stage in a remote symptom monitoring program for patients with breast cancer. JCO Clinical Cancer Informatics 2023 Jun;7(7):e2300015. [doi: 10.1200/CCI.23.00015] [Medline: 37279409]
24. Singer SJ, Kellogg KC, Galper AB, Viola D. Enhancing the value to users of machine learning-based clinical decision support tools: A framework for iterative, collaborative development and implementation. Health Care Manage Rev, 2nd edition. 2022 p. E21-E31. [doi: 10.1097/HMR.0000000000000324]
25. Patel TA, Heintz J, Chen J, et al. Spending analysis of machine learning-based communication nudges in oncology. NEJM AI 2024 Jun;1(6):AIoa2300228. [doi: 10.1056/aioa2300228] [Medline: 39036423]
26. Bayati M, Braverman M, Gillam M, et al. Data-driven decisions for reducing readmissions for heart failure: general methodology and case study. PLOS ONE 2014;9(10):e109264. [doi: 10.1371/journal.pone.0109264] [Medline: 25295524]
27. Iqbal K. Resource optimization and cost reduction for healthcare using big data analytics. IJSA 2023;8(1):13-26 [FREE Full text]
28. Oluwagbade E, Covenant L. How AI can help healthcare providers identify high-risk patients for early intervention. : Scientific Research; 2024 Nov 17 URL: https://www.researchgate.net/publication/386177260_How_AI_Can_Help_Healthcare_Providers_Identify_High-Risk_Patients_for_Early_Intervention [accessed 2025-11-27]
29. Hernandez-Boussard T, Lee AY, Stoyanovich J, Biven L. Promoting transparency in AI for biomedical and behavioral research. Nat Med 2025 Jun;31(6):1733-1734. [doi: 10.1038/s41591-025-03680-0]
30. Wang Y, Liu C, Hu W, et al. Economic evaluation for medical artificial intelligence: accuracy vs. cost-effectiveness in a diabetic retinopathy screening case. npj Digit Med ;7(1). [doi: 10.1038/s41746-024-01032-9]
31. Bardhan IR, Thouin MF. Health information technology and its impact on the quality and cost of healthcare delivery. Decis Support Syst 2013 May;55(2):438-449. [doi: 10.1016/j.dss.2012.10.003]
32. Health care price transparency: meaningful price information is difficult for consumers to obtain prior to receiving care. US Government Accountability Office. 2011 Jul 28. URL: https://www.gao.gov/products/gao-11-791 [accessed 2024-08-04]
33. Wikén I, Andersson TML, Radkiewicz C. Seasonal effects on cancer incidence and prognosis. Acta Oncol 2023 Feb;62(2):103-109. [doi: 10.1080/0284186X.2023.2178325] [Medline: 36790070]

Abbreviations

ACU: acute care use
APP: advanced practice provider
ASP: average sales price
CCC: comprehensive cancer center
CCPD: cost of care per patient per day
CMS: Centers for Medicare and Medicaid Services
CPT: Current Procedural Terminology
EHR: electronic health record
FTE: full-time equivalent
HCPCS: Healthcare Common Procedure Coding System
ML: machine learning
MPFS: Medicare Physician Fee Schedule
ROI: return-on-investment
TCPP: total cost per patient per period

XSL•FO
RenderX

Edited by C Perrin; submitted 21.05.25; peer-reviewed by M Gasmi, M Beltrão, S Aluvaka; revised version received 24.09.25; accepted 13.10.25; published 11.12.25.

Please cite as:
Keller SA, Schuessler M, Naderalvojoud B, Seto T, Tian L, Roy M, Hernandez-Boussard T
Cost-Benefit Analysis of Preventing Acute Care Use in Oncology Patients Following Systemic Therapy Using Medicare Claims Data: Retrospective Cohort Study
JMIR Med Inform 2025;13:e77891
URL: https://medinform.jmir.org/2025/1/e77891
doi:10.2196/77891

© Sara Alessandra Keller, Maximilian Schuessler, Behzad Naderalvojoud, Tina Seto, Lu Tian, Mohana Roy, Tina Hernandez-Boussard. Originally published in JMIR Medical Informatics (https://medinform.jmir.org), 11.12.2025. This is an open-access article distributed under the terms of the Creative Commons Attribution License (https://creativecommons.org/licenses/by/4.0/), which permits unrestricted use, distribution, and reproduction in any medium, provided the original work, first published in JMIR Medical Informatics, is properly cited. The complete bibliographic information, a link to the original publication on https://medinform.jmir.org/, as well as this copyright and license information must be included.

XSL•FO
RenderX

Creation and Implementation of an Electronic Sexual Assault Record at the Geneva University Hospital

Sara Cottler-Casanova[1*], MSc, PhD; Laurène Rimondi[2*], MSc; Monique Lamuela Naulin[1], MSc; Tony Fracasso[3], MD; Jasmine Abdulcadir[1], MD

[1]Division of Gynecology, Department of Woman, Child and Adolescent, Geneva University Hospitals, Bd de la Cluse 30, Geneva, Switzerland

[2]Faculty of Medicine, University of Geneva, Geneva, Switzerland

[3]Centre universitaire romand de médecine légale, Geneva, Lausanne, Switzerland

[*]these authors contributed equally

Corresponding Author:
Jasmine Abdulcadir, MD
Division of Gynecology, Department of Woman, Child and Adolescent, Geneva University Hospitals, Bd de la Cluse 30, Geneva, Switzerland

Abstract

Background: In Switzerland, sexual assault reports have historically been documented on paper, which limited standardization, completeness, and challenges to produce reliable statistics.

Objective: This study describes the development and implementation of an Electronic Sexual Assault Record (eSAR) within Geneva University Hospitals' Electronic Medical Record (EMR) system, with the aim of improving data quality, documentation, and multidisciplinary coordination.

Methods: The eSAR was developed by a multidisciplinary team including forensic doctors, gynecologists, nurses (clinical and informatics), epidemiologists, and IT specialists. Its structure was based on existing hospital protocols and international recommendations. Variables were defined as "essential" or "highly recommended," with structured fields to ensure completeness and comparability. Confidentiality was safeguarded through restricted access and regular audits.

Results: The eSAR was launched in June 2022 and revised in 2023 after user feedback and training. Since implementation, 382 reports have been completed. Data quality improved substantially, with major reductions in missing information. The system also streamlined workflows and strengthened collaboration across specialties.

Conclusions: The eSAR improved documentation and data reliability, providing a replicable model for standardized sexual assault reporting in Switzerland.

(JMIR Med Inform 2025;13:e66764) doi:10.2196/66764

KEYWORDS

Geneva; sexual assault; data collection; dataset; electronic health records; registry; administrative hospital data; computerized medical records; medical records; EHR; health records; records; hospital data; Europe; European; Obstetrics; Gynecology; EMR; efficiency; clinical workflow; Swiss; Switzerland; implementation; administrative

Introduction

The Burden of Sexual Violence in Switzerland

Sexual violence is a serious public health concern in Switzerland. According to a 2019 population-based survey involving 4500 women, 22% of women and girls aged 16 and older reported having experienced nonconsensual sexual acts, and 12% had sex against their will [1]. In 2023, police and victim assistance centers (LAVI/Opferhilfe) reported a total of 1647 cases of sexual violence against women to the Swiss Federal Statistical Office, including 822 cases of rape (Art. 190) and 549 cases of sexual assault (Art. 189) [2].

Switzerland ratified the Istanbul Convention in 2017. Since then, monitoring efforts by the Council of Europe's Group of Experts on Action against Violence against Women and Domestic Violence (GREVIO) have highlighted several gaps and issued specific recommendations. These include strengthening standardized postrape care pathways, such as screening, treatment, injury documentation, and referral to specialized services; improving health care professional training across disciplines, and establishing harmonized standards for forensic data collection throughout the country [3].

To support implementation of these recommendations, the Swiss National Action Plan (PAN CI) [4] for 2022 - 2026 was adopted. It prioritized three urgent measures: (1) scaling up post-rape care services across cantons (2) developing

XSL•FO
RenderX

harmonized healthcare protocols, and (3) improving national statistics to support evidence-based policymaking.

In Romandie, the French-speaking part of Switzerland, several cantons, including Geneva, Vaud and Valais have established specialized sexual assault support centers that reflect GREVIO's standards. These cantons offer joint forensic and gynecological examinations within emergency settings, conducted by medical professionals trained in trauma-informed care. Importantly, access to these services is not contingent on filing a police report, reinforcing a survivor-centered approach to care. Treatment includes postexposure prophylaxis for HIV and sexually transmitted infections (STIs), emergency contraception, crisis mental health support, and referrals for medium- and long-term follow-up [5]. Patients may be directed to a range of specialties within the hospital network, including infectious diseases, psychiatry, the Interdisciplinary Unit for Medicine and Prevention of Violence (UIMPV), addiction medicine, and surgical specialties when needed [5,6].

In parallel to providing clinical care, medico-legal exams serve the function of collecting and documenting forensic evidence. Accurate and thorough documents can improve judicial outcomes by increasing the likelihood of successful prosecution [7]. However, because there is not unified national protocol for the medico-legal exam, data collection practices vary across institutions. The development of harmonized cantonal and national guidelines depends on the availability of high-quality, systematically collected data.

Limitations of Manual Documentation

Until 2021, medico-legal sexual assault reports (SARs) at the Valais, Vaud and Geneva centers were completed by hand. While this method supported a detailed narrative documentation, it posed several challenges. A retrospective study conducted between 2018 and 2021 on 740 sexual assault reports from Geneva and Lausanne University Hospitals revealed areas for improvement, particularly regarding the consistency and comprehensiveness of forensic documentation [8]. Accurate and thorough documentation is crucial not only for optimal patient care but also for judicial decision-making, including whether cases proceed to trial [9].

Despite the HUG's (Geneva University Hospital) reputation as a standard for trauma-informed care, the manual completion of sexual assault reports across multiple departments contributed to administrative delays and occasional data gaps. This variability in documentation impacted the ability to systematically capture essential information such as assault context, risk factors, and sociodemographic characteristics of both victims and perpetrators. Whether or not the patient had previously experienced sexual violence was not documented in 64% of sexual assault records. Between 34% and 50% of all sexual assault reports were missing information on treatments that were prescribed (eg, emergency contraception, gonorrhea, chlamydia, HIV prophylaxis).

The Need for a Digital Standardized Report

The absence of a standardized and harmonized approach to data collection posed challenges in evaluating service utilization and identifying unmet needs. Consequently, the ability to generate evidence-based recommendations for strengthening postrape care services, in line with public health strategies at a national and international level such as those from the Istanbul Convention and GREVIO, were limited.

Aims and Objectives

Recognizing these opportunities for improvement, HUG initiated the development of an Electronic Sexual Assault Record (eSAR) within its Electronic Medical Record (EMR) system. This innovation aimed to maintain HUG's standard of care while enhancing data quality, streamlining clinical workflows, and supporting multidisciplinary collaboration. Our primary aim is to describe the eSAR and its creation and implementation into the HUG's existing EMR System. The report is structured following the iCHECK-DH (Guidelines and Checklist for the Reporting on Digital Health Implementations) guidelines [10].

Methods

Technical Design

The integration of the eSAR into the EMR system was strategically planned from the outset, following the findings of the 2022 retrospective report as the optimal solution for reducing inconsistencies, improving data completeness, and providing high-quality evidence to inform policy-making and the development of best-practice guidelines. The Chiefs of Forensic Medicine and the Gynecology and Obstetrics Emergency Department proactively engaged with the hospital's medical leadership and the information systems directorate to initiate the creation of the eSAR. A nurse specialized in informatics was allocated to the project to help with the development of the digital form within the EMR system. The design of the eSAR involved a multidisciplinary team, including nurse specialized in informatics, a nurse from the Gynecology and Obstetrics Emergency Department, an epidemiologist, a statistician, the Chief of the Gynecology and Obstetrics Emergency Department, and the Chief of the Forensic Medicine unit.

The eSAR was also multidisciplinary in its design. Given that gynecologists and forensic doctors from two separate departments needed access to create, modify, and sign the same record, the informatics directorate developed a specialized protocol granting multiple units access to the shared form. The eSAR workflow is fully integrated across both units, and for traceability, all user interactions, including who accessed the form and what modifications were made, are systematically recorded.

Target

The eSAR was developed to be used by forensic doctors, gynecologists and nurses for all sexual assault reports made in the Gynecology and Obstetrics Emergency Department at the HUG. The eSAR needed to be valid for any patient seen in this emergency unit including cisgender women, nonbinary, queer, transgender men with a vulva and vagina and transgender women- regardless of age. While the patients under 16 are treated in the pediatric department, the gynecological exam is conducted in the Gynecology and Obstetrics Emergency Department. The eSAR may also be used in the gynecology

XSL•FO
RenderX

outpatient clinic, where sexual assault reports are conducted if more than 7 days has elapsed since the sexual assault. Past seven days, evidence on the patient's body will most likely have disappeared and the intervention of a forensic doctor is no longer necessary. The eSAR is also used, regardless of whether the medico-legal exam was mandated by the police or the public prosecutor.

The multidisciplinary team synthesized input from clinical practice guidelines, expert clinical knowledge, and relevant classifications, international recommendations, and guidelines. The starting point was HUG's annually revised clinical practice guidelines for documenting sexual assault, known as "attitude sheets" [11]. Additional sources included international recommendations and clinical scales, such as World Health Organization's guidelines [12-14], the International Classification of Diseases, the Tanner Score, European AIDS Clinical Society recommendations [15], and ethical considerations on gender from the Inclusion Group of Geneva University [16]. This comprehensive approach ensured that the eSAR was evidence-based, aligned with best practices, and tailored to meet the needs of both healthcare providers and patients.

The preliminary sexual assault report form framework included socio-demographic and clinical characteristics, risk factors, complaint status, relationship to the perpetrator, description of events, genital, anal and bodily injuries, pictures, and a description of samples collected. Once the overall structure was outlined, the team designed the individual variables using binary options, multiple-choice selections, and drop-down lists. Most fields are structured to ensure the desired information is captured, in a neutral and unbiased way. Free-text fields were retained as additional fields, as requested by the forensic doctors to ensure that all information could be documented. However, the structured fields ensure consistency, comparability and ease of analysis for research purposes.

3 key performance indicators were envisaged to evaluate the eSAR:

- Descriptive statistics of the number of eSARs in progress and finalized
- Proportion of eSARs with no missing data
- Access to the eSARs by authorized health care professionals only and verifiable

Blueprint Summary

The sexual assault report framework is composed of eight sections (Table 1).

Table . The 8 sections composing the sexual assault report framework.

Section	Description
Sexual assault characteristics	Details on sexual assault, including: (1) patient characteristics, (2) assault characteristics, including (3) perpetrator characteristics, and (4) violence characteristics
Post-Assault Characteristics	Details on post-assault medical and forensic evaluations, including: (1) forensic exam and evidence, (2) gynecological exam, and (3) service referrals and treatment
Forensic Laboratory Kit	Comprehensive list of samples collected, including swabs, smears, slides, blood, urine, and saliva. It documents the date, time, and signature of the forensic doctor
Infectious Diseases Consultation Request Form	Completed when Post-Exposure Prophylaxis (PEP) for HIV prevention is administered and a consultation with the infectious disease department is requested
Confidentiality/Release of Information Form	Signed by the patient to authorize the release of information to police and magistrates if a complaint is filed; a hand-signed copy is scanned for the record
Employment Leave Certificate	Assesses work capacity and the possibility of filing an accident report for health or accident insurance, in compliance with Swiss law
Provisional Medical Certificate	Printed for the patient and scanned for the record. It provides initial findings, a summary of the medical consultation, additional remarks, and signatures of the gynecologist and forensic physician
Full eSAR[a] Patient Information Document	Completed by the gynecologist and forensic physician, handed to the patient. It includes a summary of medical examinations, test results, treatments administered (eg, emergency contraception, antibiotics, HIV prophylaxis), follow-up appointments, and documents provided to the patient

[a]e-SAR: electronic sexual assault records.

Data

The variables were divided in two categories: "essential" variables that are required to sign the file, and "highly recommended" variables, to provide more details depending on medico-legal situation. A pop-up window indicates whether any data is missing; both essential and highly recommended. To ensure harmonized data entry, the users can consult definitions and detailed descriptions of lesion types and diagrams of anatomical sites. The exact anatomical location

XSL•FO
RenderX

and terminology for genital injuries are provided in a diagram of the vulva. An automatic data quality check was built into the system to identify any data entry errors, such as extreme outliers.

The results of the laboratory tests for pregnancy and STIs, as blood chemistry, complete blood count and vaginal bacteriology, are available in the patient's EMR. The monthly list of health professionals accessing the eSAR are reviewed by the CURML (Centre Universitaire Romand de Médecine Légale, University Center for Legal Medicine in French-speaking Switzerland) to verify the access of only authorized health professionals. The triage nurse collects blood and urine samples for toxicological analysis, and ensures their dispatch to the laboratory or Medico-Legal Institute. During the medical examination, the nurse also coordinates follow-up appointments and administers necessary prophylactic treatments. Employment leave and medical certificates are printed and an alert is sent to the laboratory to warn about the arrival of the samples for STIs, improving traceability.

Confidentiality

To open the eSAR, the user must be authorized and provide justification. Access rights are restricted to gynecologists, forensic doctors and nurses directly involved in the medical care of the patient's sexual assault, together with the infectious disease specialists, the psychologists and medical team of the UIMPV and other medical staff (eg, proctologist, psychiatrist, pediatrician, otorhinolaryngologist). Strict confidentiality measures are required to prevent unauthorized access, with any breach punishable by law. To reinforce oversight, a monthly audit report listing all healthcare professionals who accessed the eSAR is reviewed by the CURML. Data security is managed by the IT department of HUG, with all records securely stored on proprietary servers. For research purposes, deidentified data extracts can be obtained through the Magellan informatics module. However, the use of eSAR data for research requires both patient consent and approval from the Swiss ethics committee, ensuring compliance with ethical and legal standards.

Implementation (Results)

Content Validation

The content validation process for the eSAR was multi-phased and collaborative. Initially, structured meetings and iterative refinements were conducted by a multidisciplinary team composed of forensic doctors, gynecologists, a nurse from the gynecology and obstetrics emergency department, a nurse specialized in informatics and an epidemiologist. During these early stages, the team reviewed anonymized sexual assault files and implemented several key changes, including standardized terminology (eg, shifting from "victim" to "patient") (Multimedia Appendix 1), revising question phrasing for clarity, and introducing new variables to better capture details on assault characteristics, injuries, and treatments. Response formats were adjusted, for example by replacing ambiguous free-text responses with binary or multiple-choice options to improve data quality and comparability. The sequence of form sections was also reorganized for greater usability and workflow integration.

The draft eSAR was then presented to clinicians from the Obstetrics and Gynecology Emergency Department for further feedback. Because gynecologists and nurses were already familiar with the hospital's electronic medical record system, dedicated training sessions were organized specifically for forensic doctors to ensure smooth adoption. The eSAR was officially launched in June 2022 (Table 2).

Table . The eSAR timeline.

eSAR timeline	Content
2018 - 2021	Retrospective study reveals documentation gaps (paper SAR)[a]
Q3/4 2021	Project planning, leadership engagement
Q1 2022	Multidisciplinary team formed, prototype design
Q2 2022	Structured meetings, iterative development, early validation
Q2–Q3 2022	Focus groups, pilot testing, refinement
June 2022	eSAR version 1 launched (Gynecology/ObGyn ED)[b]
Q4 2022	Ongoing user feedback, additional training
Sep 2023	Major revision (version 2; expert feedback, improved flow, new response options)
2023 - 2024	Expansion, routine use, continuous updates
2024	Full integration, data extraction or reporting

[a]SAR: sexual assault report.

[b]ObGyn ED: Obstetrics and Gynecology Emergency Department.

After implementation of the first eSAR version, expert focus groups were convened to assess usability, clarify clinical workflow, and refine the eSAR structure based on real patient cases. These focus groups comprised 12 participants: 4 forensic doctors, 3 gynecologists, 2 nurses, 2 informatics specialists, and 1 epidemiologist. Discussions in these focus groups mapped out the patient journey during sexual assault consultations, defined clear roles and responsibilities at each care stage, and identified opportunities to streamline data entry while minimizing patient burden.

XSL•FO
RenderX

The most significant set of revisions followed these focus groups and expert feedback, culminating in the release of eSAR version 2 in September 2023. This update included improved question phrasing and form flow, a shift to more neutral terminology, and the addition of a "+" button for documenting multiple injuries with automatic body region classification. New response options such as "does not remember" (for cases of amnesia) and "does not know" (for patients unable to answer) were also introduced, ensuring greater accuracy and completeness.

Workflow

The focus groups played a key role in clarifying the workflow, particularly in determining how the eSAR is filled out and by whom. These discussions helped refine the division of tasks, ensuring a structured and efficient process. The nurse selects a triage motive according to the Swiss Triage Scale, with the reason for the encounter recorded in the DPI (Dossier Patient Intégré or Integrated Patient File) system and displayed on department screens.

Further, the focus groups provided valuable insights into the data entry process, particularly regarding computer use. Physicians noted that they take turns entering information to maintain patient engagement. For example, the gynecologist switches to the computer while the forensic doctor conducts the medico-legal history, documents bodily traumatic lesions, and collects forensic samples. During the consultation, the gynecologist conducts the exam and administers prophylactic treatments, while the forensic doctor simultaneously completes the electronic record. This streamlined approach minimizes consultation time while ensuring double verification of data, enhancing accuracy and completeness in medical and forensic reporting.

Results

The digitalization of the sexual assault report has significantly improved data reliability and accessibility, enabling the extraction of accurate statistics with ease. With a single click, data can be retrieved based on the number of eSARs per year, month, or type (legal mandate) providing a clearer picture of trends and service utilization (Tables 3 and 4). Since the eSAR was introduced in June 2022, a total of 382 reports have been recorded, with 134 in 2023 and 162 in 2024, reflecting an increase in the number of sexual assaults reported. Most eSARs (84/134, 63%; 102/162, 63%) were completed without a legal mandate, while 37% (50/134 in 2023 and 60/162 in 2024) were mandated cases. The monthly distribution of eSARs varied, with the highest numbers recorded in July of both 2023 and 2024 (15/134, 12% in 2023 and 19/162, 12% in 2024). The peaks in reported cases in July 2023 and 2024 may be explained by increased summer festivals, holidays, and public awareness campaigns, which together create more risk situations and encourage more survivors to seek care [8].

Table . Number of eSARs[a] per year.

eSAR	eSARs (N=382), n	With legal mandate, n (%)	Without legal mandate n, (%)
2022 (01.06.22 - 31.12.22)	86	N/A[b]	N/A
2023	134	50 (37)	60 (37)
2024	162	84 (63)	102 (63)

[a]eSAR: electronic sexual assault records.

[b]Not applicable.

Table . Distribution by month of eSARs[a] (2023).

Month of the eSAR	2023 (n=134), n (%)	2024 (n=162), n (%)
January	5 (4)	16 (10)
February	12 (9)	17 (11)
March	15 (11)	13 (8)
April	12 (9)	11 (7)
May	13 (10)	14 (9)
June	14 (10)	14 (9)
July	15 (12)	19 (12)
August	9 (7)	14 (9)
September	14 (10)	9 (6)
October	10 (7)	17 (11)
November	8 (6)	7 (4)
December	7 (5)	11 (7)

[a]e-SAR: electronic sexual assault records.

XSL•FO
RenderX

The eSAR is comprised of approximately 500 data points, with 44 “essential variables” covering victim, assault, and violence characteristics, as well as postassault details, forensic evidence, gynecological exams, and service referrals, ensuring that all fundamental aspects of every case are recorded. Additionally, 108 highly recommended data points provide more detailed insights depending on the medico-legal context, including documentation of ano-genital injuries, bodily injuries, and ejaculation. Reliable informatic data extraction is now feasible for clinical purposes and annual reports. Moreover, eSAR data is being used to populate the electronic case report form for a prospective study on sexual assault conducted at HUG, which began in November 2022.

Since its implementation, the eSAR has significantly improved the completeness of essential data documentation compared to the previous paper-based SAR, where missing information posed major challenges. In the earlier system, 64% (n=467) of records lacked information on prior sexual assault history, 75% omitted details about decisions to press charges, and 34% to 50% were missing data on prescribed treatments. With the eSAR, these gaps have been substantially reduced: missing data now account for only 8.5% (n=13, see Table 5 below) regarding prior assault history, 0% (n=0) for whether charges were filed, 32% (n=52) for whether future charges will be filed, and just 3.7% (n=6) for postexposure prophylaxis (PEP).

Table . Improvements in missing data.

Variables	No, n (%)	Yes, n (%)	Unknown/Missing, n (%)	Not applicable, n
Retrospective study (Before eSAR), n=727	121 (17)	139 (19)	467 (64)	13
2024 (After eSAR implementation), n=162	50 (32.7)	90 (58.8)	13 (8.5)	9

The eSAR also facilitates the medical follow-up of the patient. Patient appointments can be made at the time of the medico-legal consultation with the click of a button. Previously, a fax system was used to send patient appointment information between the ObGyn (Obstetrics and Gynecology) emergency unit and the infectious diseases unit. The eSAR also helps with multidisciplinary medical follow-by infectious disease specialists, as well as the staff of the UIMPV and gynecology outpatient clinic, allowing the doctors and psychologists to read the patient’s sexual assault file and better prepare, without the patient having to repeat details from their assault.

Efficiency

A crucial outcome for patients is the time needed to finalize the medico-legal report with all the necessary information. The development and the implementation of the eSAR facilitates and streamlines the entire workflow. The administrative burden has been considerably lightened since paper documents are not physically transported anymore through medical departments. The electronic traceability also allows to monitor the administrative process of filling, finalizing and signing the eSAR. The training of new doctors confirmed the implementation of the eSAR facilitates the continuity of the medical care and clinical practice with less experienced doctors.

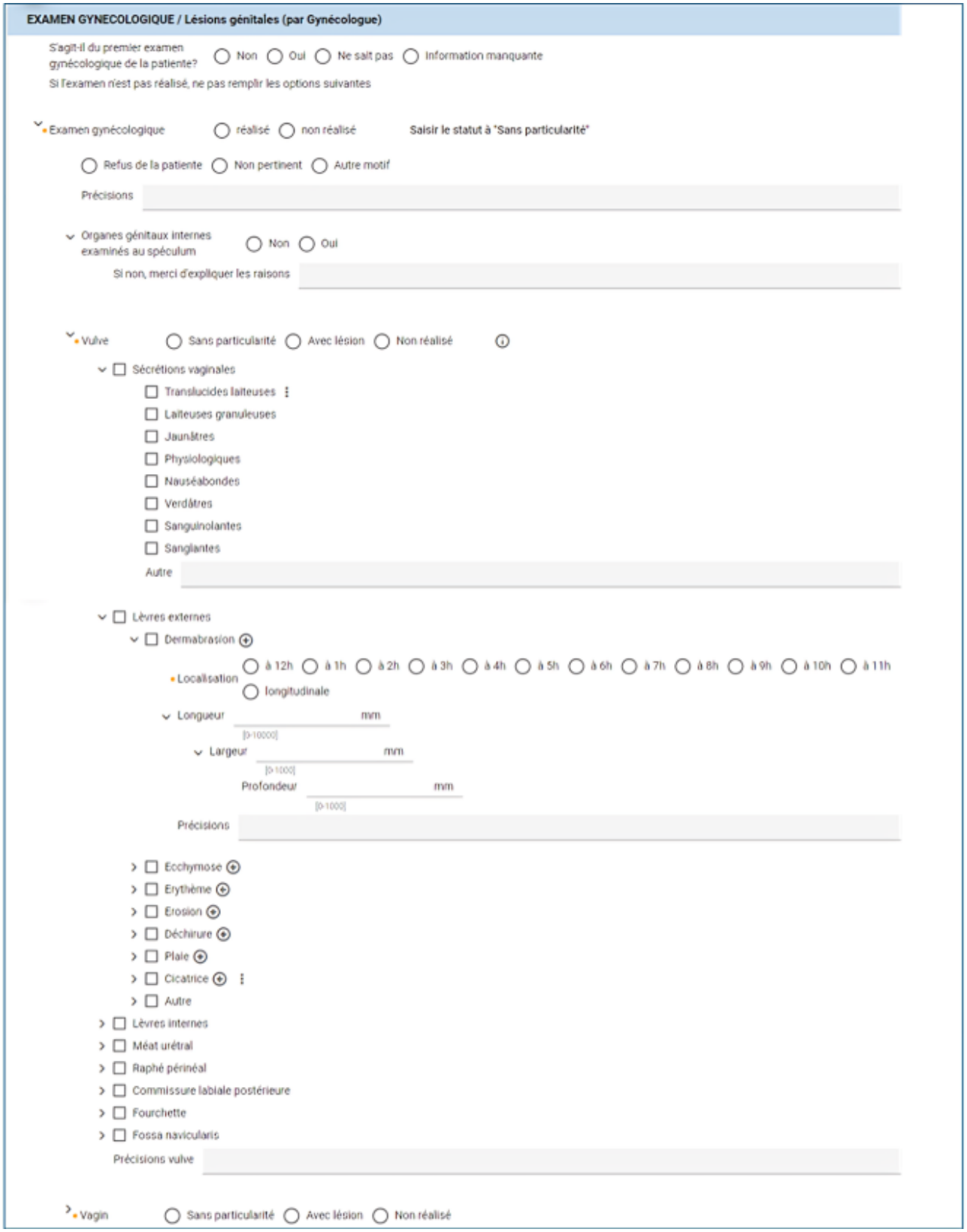
A list of eSARs in draft mode (unsigned) as well as some basic patient information can be accessed by authorized personnel (Textbox 1). Doctors receive a notification on their task list when an update or modification is required. This list will help to manage the workflow and help doctors meet their deadlines, (eSARs should be finalized within 30 d). Beyond this deadline, the color of the task in their workflow changes from blue to red and they start to receive reminder notifications. The user interface also allows doctors to click on dedicated buttons to validate sections or complete the report, and simultaneously, a PDF version is automatically generated, ensuring a seamless and efficient way to produce a finalized output (Figures 1 and 2).

Textbox 1. List of eSARs (electronic sexual assault records) in Draft Mode (unsigned)

- Finalization of the file (signatures)
- Date of signatures
- Creation of eSAR (date and hour)
- Number of this medical event
- Identification number assigned to the patient
- Name, First name, date of birth (necessary information to identify the file)
- Date of the consultation
- Date de the sexual assault
- Names of the gynecologist and the forensic physician

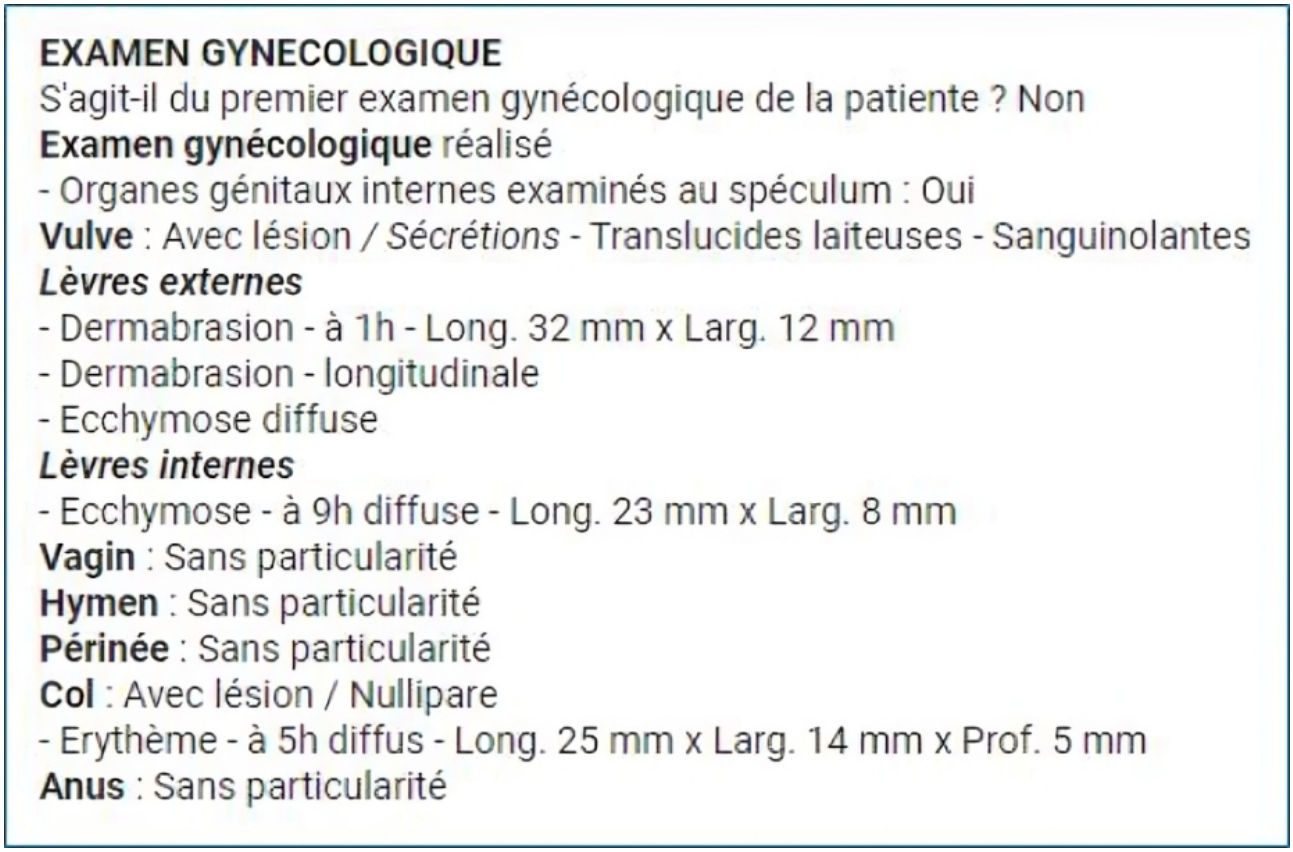
XSL•FO
RenderX

Figure 1. User interface of eSAR (electronic sexual assault records).



XSL•FO
RenderX

Figure 2. PDF output of eSAR (electronic sexual assault records).



Interoperability

This electronic sexual assault report form is reproducible in other Swiss cantons or other countries. The eSAR is available in French and translations of all variables are available in English and German. The eSAR is integrated into the EMR platform known as DPI, which has been in use at HUG since 2000. A license is required for the use of DPI, which was acquired by the Valais Hospital in 2023. The informatic languages used are HTML-5 and LOINC. For the use with any other information system other than DPI, the eSAR framework can be exported in CSV file, by contacting the corresponding author of this paper. The eSAR is currently being adapted for patients with penises, both children and adults, in collaboration with the pediatric and adult ED.

Participating Entities and Budget Planning

The eSAR is a part of a multicentric research project, funded by a grant of 684,029.80 CHF (US $ 752,433) from the Swiss Federal Office for Gender Equality (FOGE) in Switzerland and HUG. The project includes a retrospective study, built on a cohort studied between 2018 - 2021 in Geneva and Lausanne. It also includes a prospective study, elaborated to analyze the data collected from eSAR since implementation and a long-term follow-up questionnaire. The FOGE played no role in the design and conduct of the study. FOGE did not fund the development of the eSAR but only the working time of the epidemiologist. The remaining costs were covered by HUG (70,510 CHF; equivalent to US $ 77,561), including creation of the forms (23,000 CHF; 25,300), informatic development (38,400 CHF, equivalent to US $ 42,240), tablets for schemas and signature from patients and physicians (3,360 CHF, equivalent to US $ 3696), methodical support for data analysis (5,750 CHF, equivalent to US $ 6325). Other costs for the human resources were covered by their routine salaries. The ongoing study results will be published in peer-reviewed journals. There are no conflicts of interests to declare.

Sustainability

Twice a year, training for the care and treatment of patients of sexual assault and the eSAR is organized by the ObGyn ED. It includes theoretical presentations, use of the eSAR and a simulation of triage, history taking, and treatment of a fictitious patient where gender inclusivity and interpersonal skills must be put to practice. These trainings target forensic doctors, nurses, midwives, and gynecologists, some of whom rotate every 6 months. In total, there are 7 forensic doctors and 11 gynecologists (9 residents and 2 chief residents), 10 midwives and 19 nurses.

Discussion

Strengths

The eSAR is the first electronic sexual assault record implemented in Switzerland, representing a major advance in standardized documentation and data collection for sexual assault cases. Developed through a multidisciplinary collaboration and continuously refined for both clinical and research purposes, the eSAR provides a robust, real-time dataset through its integration into the EMR. This integration not only enhances patient care and facilitates research, quality improvement, and monitoring of service utilization, but also

XSL•FO
RenderX

supports the development of institutional protocols and serves as a foundation for evidence-based policymaking and national best-practice guidelines in sexual assault care.

Interest in this standardized form from various health departments and hospitals continues to enrich ongoing discussions and contributes to the advancement of best practices. Furthermore, the eSAR enables the creation of a regional sexual assault patient cohort, allows tracking of patient loss to follow-up, and provides opportunities to develop performance indicators and improve clinical governance through real-time surveillance and benchmarking. Despite representing only 1.16% of total gynecology emergency consultations, sexual assault cases involve a significant administrative workload, as records must be reviewed and validated by supervisors. By analyzing each step in the care process, eSAR data can help identify opportunities to improve workflow efficiency. Furthermore, the continuous revisions and improvements led by HUG experts strengthen its role as a comprehensive medicolegal tool for both clinical application and research.

Lessons Learned

Forensic doctors were initially hesitant about the digitalization of the SAR, as they were accustomed to writing paper reports in a free-form manner, which they viewed as an integral part of their medical practice. Concerns were also raised about the time required to complete the eSAR, which was initially estimated to take about an hour. However, once implemented, the eSAR was eventually positively received, as its design effectively aligned with medical practice needs, demonstrating its adaptability and usefulness. As the Chief Forensic doctor was involved in its development, resident and intern forensic doctors, despite any initial reluctance, were required to use the eSAR for all sexual assault reports. Over time, they began to appreciate its advantages, particularly the time saved and the standardization of key variables, which improved both the consistency and quality of documentation.

Unintended Consequences

The implementation of the eSAR has further strengthened collaboration between departments bringing together professionals from different fields to exchange expertise, align practices, and enhance coordination across specialties. This interdisciplinary dialogue has helped further optimize the HUG's overall response to sexual assault cases.

Similar Intervention

Australia [17] and Finland [18] have demonstrated that a national, standardized and centralized approach to sexual assault support centers, increases access to quality and holistic care, as well as collaboration among different institutional actors. The number of police-reported offenses has increased, as have the criminal procedures in addition to patient satisfaction. Systematically collected data and official statistics support the development of targeted government strategies, something we strive to achieve.

Limitations

A key limitation of the eSAR is that it exclusively includes patients who present to public hospitals and consent to a joint medico-legal examination, as defined by the HUG protocol. This excludes individuals who do not report the assault, who decline medico-legal procedures, or who seek care outside of the hospital system. As a result, the cohort is not representative of all survivors of sexual assault. Future efforts must address how to identify and include these underrepresented populations to ensure a more comprehensive understanding of postassault care needs.

At present, the eSAR is not yet available for patients with penises (ie, children and adults), but its use will become mandatory in the pediatric and adult emergency departments once the adapted version is implemented, as is already the case in gynecology and obstetrics.

Conclusion

The implementation of eSAR at HUG marks a significant advancement in improving data collection, care processes, and the development of patient-centered services. Establishing a regional or national standard and ultimately, a sexual violence observatory, as recommended by the Istanbul Convention is an achievable goal, requiring collaboration between cantons and coordination at the national level. The eSAR is a replicable model for both adult and minor individuals of all genders. It is a powerful tool in advancing the objectives outlined by GREVIO, particularly the implementation of standardized care pathways and the development of national standards for forensic data collection.

Data Availability

For the use with any other information system other than DPI, the eSAR framework can be exported in CSV file, by contacting the corresponding author of this paper.

Conflicts of Interest

None declared.

Multimedia Appendix 1
Swiss Sexual Violence Standardized Data Set - Gynecological and Obstetric Emergencies Unit - HUG.
[DOCX File, 556 KB - medinform_v13i1e66764_app1.docx]

XSL•FO
RenderX

Checklist 1
i-CHECK-DH checklist
[PDF File, 242 KB - medinform_v13i1e66764_app2.pdf]

References

1. Le harcèlement sexuel et les violences sexuelles faites aux femmes sont répandus en suisse. GFS.Bern. 2019. URL: https://cockpit.gfsbern.ch/fr/cockpit/violence-sexuelles-en-suisse/ [accessed 2023-01-23]
2. Office fédéral de la statistique violence sexualisée: infractions et personnes lésées. Office fédéral de la statistique. URL: https://www.bfs.admin.ch/bfs/fr/home/statistiques/criminalite-droit-penal/police/violence-sexualisee.assetdetail.30887608.html [accessed 2025-01-06]
3. Group of Experts on Action against Violence against Women and Domestic Violence (GREVIO). GREVIO's (baseline) evaluation report (switzerland) on legislative and other measures giving effect to the provisions of the council of europe convention on preventing and combating violence against women and domestic violence (istanbul convention). : Strasbourg: Secretariat of the monitoring mechanism of the Council of Europe Convention on Preventing and Combating Violence against Women and Domestic Violence; 2022 URL: https://rm.coe.int/grevio-inf-2022-27-eng-final-draft-report-on-switzerland-publication/1680a8fc73 [accessed 2025-01-10]
4. Plan d'action national de la suisse en vue de la mise en œuvre la convention d'Istanbul de 2022 à 2026. Bureau fédéral de l'égalité entre femmes et hommes (BFEG). 2022. URL: https://www.ebg.admin.ch/ebg/fr/home/themes/droit/droit-international/conseil-de-l-europe/convention-d-istanbul.html [accessed 2024-07-01]
5. Unité interdisciplinaire de médecine et prévention de la violence (UIMPV). Hôpitaux universitaires genève. 2024. URL: https://www.hug.ch/medecine-premier-recours/uimpv [accessed 2025-01-07]
6. Maladies infectieuses. Hôpitaux Universitaires Genève. 2024. URL: https://www.hug.ch/maladies-infectieuses [accessed 2025-01-07]
7. La Harpe R, Burkhardt S, Ricard-Gauthier D, Poncet A, Yaron M, Fracasso T. Factors influencing the filing of complaints, their investigation, and subsequent legal judgment in cases of sexual assault. J Forensic Sci 2019 Jul;64(4):1119-1124. [doi: 10.1111/1556-4029.13971] [Medline: 30556905]
8. Cottler-Casanova S, Lourenço V, Guillot C, et al. Sexual assault reporting: study to improve prevention, information, and care of victims in emergency care settings. : Geneva: Geneva and Lausanne University Hospitals; 2023 Nov URL: https://www.hug.ch/sites/interhug/files/structures/GR-Journaliste/documents/constat-agression-sexuelle-en.pdf [accessed 2025-01-07]
9. Kjærulff M, Bonde U, Astrup BS. The significance of the forensic clinical examination on the judicial assessment of rape complaints - developments and trends. Forensic Sci Int 2019 Apr;297:90-99. [doi: 10.1016/j.forsciint.2019.01.031] [Medline: 30797159]
10. Perrin Franck C, Babington-Ashaye A, Dietrich D, et al. iCHECK-DH: Guidelines and Checklist for the Reporting on Digital Health Implementations. J Med Internet Res 2023 May 10;25:e46694. [doi: 10.2196/46694] [Medline: 37163336]
11. Protocole complet de prise en charge au departement de gynecologie et d'Obstetrique des Hopitaux Universitaires de Geneve des personnes victime d'Agression sexuelle. Hôpitaux Universitaires de Genève. 2022 Jul. URL: https://www.hug.ch/sites/interhug/files/structures/medecine_de_premier_recours/Strategies/cas-protocole.pdf [accessed 2025-01-07]
12. Strengthening the medico-legal response to sexual violence. : World Health Organization; 2016 Aug Report No.: WHO/RHR/15.24 URL: https://iris.who.int/bitstream/handle/10665/197498/WHO_RHR_15.24_eng.pdf?sequence=1 [accessed 2024-12-01]
13. Guidelines for medico-legal care of victims of sexual violence. World Health Organization. 2003. URL: https://iris.who.int/handle/10665/42788 [accessed 2025-09-15]
14. United Nations Entity for Gender Equality and the Empowerment of Women (UN Women) and World Health Organization (WHO) Global. Technical guidance: improving the collection and use of administrative data on violence against women. : New York: UN Women; 2022.
15. Post-exposure prophylaxis (PEP): recommendations for PEP. European AIDS Clinical Society (EACS). URL: https://eacs.sanfordguide.com/en/eacs-hiv/art/eacs-post-exposure-prophylaxis [accessed 2025-01-07]
16. Bioscope de l'Université de genève en collaboration avec RTS découverte. Sexesss: Mon corps sous la loupe. 2024. URL: https://www.unige.ch/ssi/files/9317/0737/7214/Brochure_SEXESSS_FR_2024_WEB.pdf [accessed 2025-01-07]
17. Outcomes framework 2023–2032: Under the national plan to end violence against women and children 2022–2032. Department of Social Services, Commonwealth of Australia. 2023. URL: https://www.dss.gov.au/system/files/resources/np-outcomes-framework.pdf [accessed 2025-01-07]
18. Korjamo R. The background of the clients in seri support centers, their use of support services and the progress of the criminal procedure: an interim report (article in swedish). Valtioneuvosto Statsradet. 2021 Nov. URL: http://urn.fi/URN:ISBN:978-952-383-350-0 [accessed 2025-01-07]

XSL•FO
RenderX

Abbreviations

CURML: Centre Universitaire Romand de Médecine Légale
DPI: Dossier Patient Intégré
EMR: Electronic Medical Record
eSAR: electronic sexual assault record
FOGE: Federal Office for Gender Equality
GREVIO: Group of Experts on Action against Violence against Women and Domestic Violence
HUG: Geneva University Hospital
ObGyn: Obstetrics and Gynecology
ObGyn ED: Obstetrics and Gynecology Emergency Department
PEP: post-exposure prophylaxis
SAR: sexual assault reports
STI: sexually transmitted infections
UIMPV: Interdisciplinary Unit for Medicine and Prevention of Violence

Edited by C Perrin; submitted 22.09.24; peer-reviewed by A Amadasi, A Babington-Ashaye, S Delaigue; revised version received 20.08.25; accepted 26.08.25; published 20.11.25.

Please cite as:
Cottler-Casanova S, Rimondi L, Lamuela Naulin M, Fracasso T, Abdulcadir J
Creation and Implementation of an Electronic Sexual Assault Record at the Geneva University Hospital
JMIR Med Inform 2025;13:e66764
URL: https://medinform.jmir.org/2025/1/e66764
doi:10.2196/66764

© Sara Cottler-Casanova, Laurène Rimondi, Monique Lamuela Naulin, Tony Fracasso, Jasmine Abdulcadir. Originally published in JMIR Medical Informatics (https://medinform.jmir.org), 20.11.2025. This is an open-access article distributed under the terms of the Creative Commons Attribution License (https://creativecommons.org/licenses/by/4.0/), which permits unrestricted use, distribution, and reproduction in any medium, provided the original work, first published in JMIR Medical Informatics, is properly cited. The complete bibliographic information, a link to the original publication on https://medinform.jmir.org/, as well as this copyright and license information must be included.

XSL•FO
RenderX

Implementation of WHO SMART Guidelines-Digital Adaptation Kits in Pathfinder Countries in Africa: Processes and Early Lessons Learned

Rosemary K Muliokela[1], MPIA; Kuwani Banda[2], BSN; Abdulaziz Mohammed Hussen[3,4,5], MPH; Sarai Bvulani Malumo[6], MBChB; Andrew Kashoka[7], MBA; Angel Mwiche[8], MBChB; Innocent Chiboma[7], MBA; Maria Barreix[1], MPH; Muyereka Nyirenda[9], MMed; Zvanaka Sithole[10], MPH; Natschja Ratanaprayul[11], MS; Berhanu Fikadie Endehabtu[4,12], MPH; Hanna Abayneh Telake[3,4], MD; Adane Weldeab[3,13,14], PhD; William J M Probert[15], PhD; zge Tunçalp[1], MD, PhD; Ernest Maya[16], MD; Mulatu Woldetsadik[6], MD; Binyam Tilahun[12], PhD; Chris Guure[16], PhD; Kafui Senya[17], MD; Lale Say[1], MD; Tigest Tamrat[1], MPH

[1]Department of Sexual Reproductive Health and Research, World Health Organization, Avenue Appia 20, 1211, Geneva, Switzerland

[10]Reproductive, Maternal, Newborn Child and Adolescent Health, World Health Organization, Country Office, Harare, Zimbabwe

[11]Department of Digital Health and Innovations, World Health Organization, Geneva, Switzerland

[12]Department of Health Informatics, Institute of Public Health, College of Medicine and Health Science, University of Gondar, Gondar, Ethiopia

[13]Health Research Development Directorate, Amhara Public Health Institute, Amhara, Ethiopia

[14]Department of Health Promotion and Health Behavior, University of Gondar, Gondar, Ethiopia

[15]Department of Global HIV, Hepatitis, and STIs Programmes, World Health Organization, Geneva, Switzerland

[16]School of Public Health, University of Ghana, Accra, Ghana

[17]HIV, TB and Hepatitis (HTH) unit, World Health Organization, Country Office, Accra, Ghana

[2]IHM Southern Africa, Lusaka, Zambia

[3]College of Medicine and Health Sciences, University of Gondar, Gondar, Ethiopia

[4]Center for Digital Health Implementation Science, University of Gondar, Addis Abba, Ethiopia

[5]Julius Global Health, Julius Centre for Health Sciences and Primary Care, University Medical Centre Utrecht, Utrecht University, Utrecht, Netherlands

[6]Immunization Maternal Newborn Child Health Cluster, World Health Organization, Country Office, Addis Ababa, Ethiopia

[7]Department of Information Communication Technology (ICT), Ministry of Health, Lusaka, Zambia

[8]Department of Public Health, Ministry of Health, Lusaka, Zambia

[9]Universal Health Coverage and Lifecourse Cluster, World Health Organization, Country Office, Lusaka, Zambia

Corresponding Author:
Rosemary K Muliokela, MPIA
Department of Sexual Reproductive Health and Research, World Health Organization, Avenue Appia 20, 1211, Geneva, Switzerland

Abstract

Background: The adoption of digital systems requires processes for quality assurance and uptake of standards to achieve universal health coverage. The World Health Organization developed the Digital Adaptation Kits (DAKs) within the SMART (Standards-based, Machine-readable, Adaptive, Requirements-based, and Testable) guidelines framework to support the uptake of standards and recommendations through digital systems. DAKs are a software-neutral mechanism for translating narrative guidelines to support the design of digital systems. However, a systematic process is needed to implement and ensure the impact of DAKs in country contexts.

Objective: This paper details the structured process and stepwise approach to customize the DAKs to the national program and digital context in 5 countries in Africa with diverse program guideline uptake and significant digital health investments: Ethiopia, Ghana, Malawi, Zambia, and Zimbabwe. All these countries have existing digital systems, which have the potential to be updated with the DAKs.

Methods: A DAK assessment tool was developed and used to assess guideline digitization readiness and opportunities for system uptake in each country. Multistakeholder teams were established to conduct the content review and alignment of the generic DAK to national guidelines and protocols through a series of stakeholder consultations, including stakeholder orientation, content review and alignment, content validation, and software update meetings.

Implementation (Results): Country adaptation processes identified requirements for national-level contextualization and highlighted opportunities for refinement of DAKs. Quality assurance of the content during the content review and validation

XSL•FO
RenderX

processes ensured alignment with national protocols. Adaptation processes also facilitated the adoption of the DAKs approach into national guidelines and strategic documents for sexual and reproductive health.

Conclusions: Country experiences offered early insights into the opportunities and benefits of a structured approach to digitalizing primary health care services. They also highlighted how this process can be continuously refined and sustained to enhance country-level impact.

(JMIR Med Inform 2025;13:e58858) doi:10.2196/58858

KEYWORDS

guidelines; reproductive health; maternal health; antenatal care; clinical decision support; clinical decision support systems; digital health; HIV/AIDS; family planning; electronic medical records; electronic health record; standards; interoperability; system uptake; digital health governance

Introduction

Background

Globally, many countries are transitioning from paper-based to digital health systems to achieve universal health coverage [1]. However, this process has not been without challenges. Digital ecosystems, in low- and middle-income countries, continue to be flooded with a multiplicity of digital tools [2]. It is also often difficult to ascertain the design process of these tools [3] and whether the underlying content is developed in accordance with the evolving clinical evidence base, protocols, and guidelines. This is largely due to the existing process of translating narrative guidelines into digital systems, which is often laborious, prone to error, and lacks accompanying technical documentation appropriate for digital use [4]. This results in disjointed digital health ecosystems with inadequate standards that hinder the quality of care, exchange of data, and reporting and hamper continuity of care [5]. To deliver sustainable digital health solutions for country impact, digital system development needs to be based on principles of transparency, accessibility, scalability, and interoperability [6]; be adherent to clinical guidelines [7] and data use and sharing standards; and be guided by national digital strategies.

To ensure an accurate reflection of guidance within digital systems, the World Health Organization (WHO) developed the SMART (Standards-based, Machine-readable, Adaptive, Requirements-based, and Testable) guideline approach, which includes Digital Adaptation Kits (DAKs) [6]. DAKs translate narrative guidelines into a format that informs the design of digital systems. They have been developed for health service areas such as antenatal care (ANC) [8], HIV [9], and family planning (FP) [10], with more health domains in the pipeline. DAKs are packaged as an operational guidance document (PDF) with four web annexes (Excel files): (1) core data elements/data dictionary, (2) decision support tables, (3) program indicator definitions, and (4) functional and nonfunctional requirements. They are structured into components, such as personas, workflows, data dictionaries, and decision-support logic [5], that are intended to be customized and adapted across diverse country digital and program landscapes and contexts. These include settings that already have established digital systems, as well as those that are preparing to transition from paper to digital systems.

Considering that SMART guidelines and DAKs are new concepts, it is important to establish defined processes to introduce, adapt, and integrate DAK content within countries' existing digital ecosystems and programmatic landscapes. Drawing on experiences from 5 African countries (Ethiopia, Ghana, Malawi, Zambia, and Zimbabwe), we aim to develop and refine a replicable process for the country adaptation and implementation of DAKs. This will contribute to the creation of a framework that can be adapted by other countries, ensuring a consistent approach to digitalizing primary health care services. This article details the processes and lessons learned in developing a framework for the systematic implementation of DAKs within different country contexts.

Objectives

The paper highlights the processes and lessons learned toward the development of a framework for the systematic implementation of DAKs within a country. The structured approach used to contextualize DAKs to national settings was conducted across 5 diverse programs and digital landscapes: Ethiopia, Ghana, Malawi, Zambia, and Zimbabwe.

Methods

Implementation Setting and Criteria

The selected countries were part of a broader United Nations interagency initiative [11] to strengthen sexual and reproductive health and rights (SRHR) (Malawi, Zambia, and Zimbabwe), while Ethiopia and Ghana were positioned for implementation research leveraging this established process. Selected countries had prior significant digital investments, and the DAK country adaptation was conducted with the aim to enhance the following national digital systems: Bahmni (Ethiopia), eTracker (Ghana), Malawi Health Information System (Malawi), SmartCare (Zambia), and Impilo (Zimbabwe) in the respective countries.

Implementation Approach

Overview

This implementation report was guided by and adheres to the Implementation Science Research Reporting Guidelines for Digital Health Interventions (iCHECK-DH) checklist, which provides a structured approach for documenting digital health implementations [12].

A stepwise approach was developed to introduce the DAKs. Multistakeholder DAK adaptation teams consisting of program

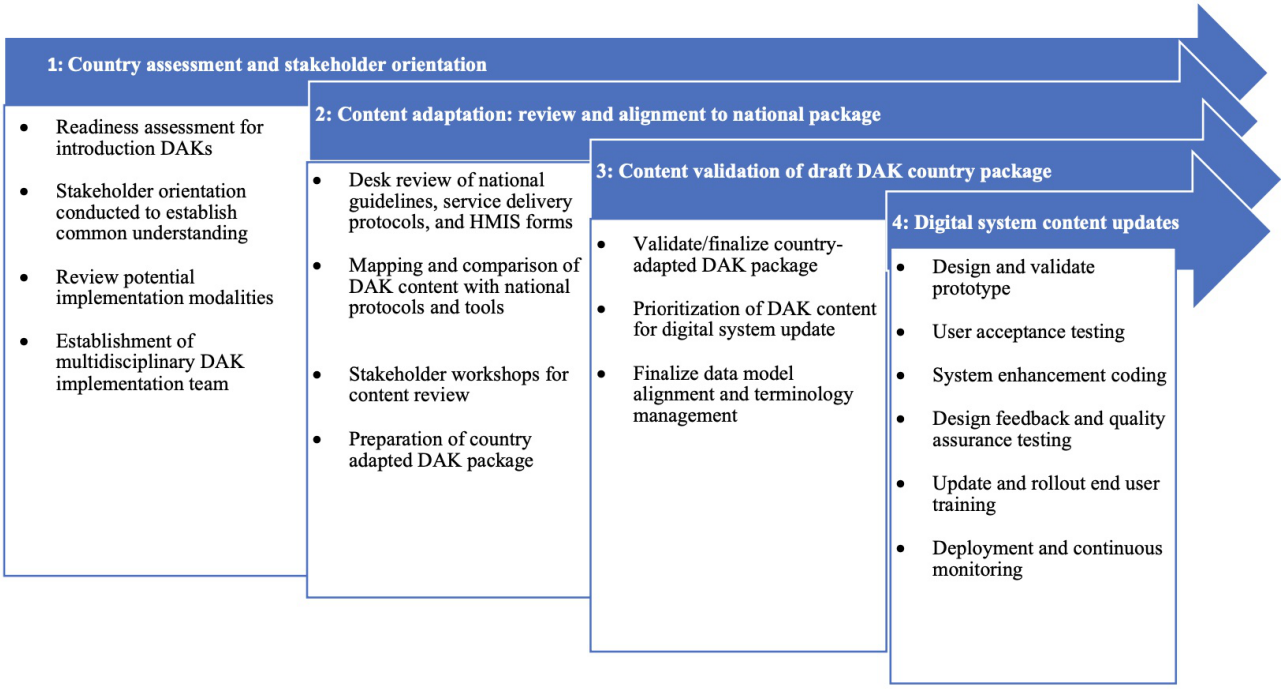
XSL•FO
RenderX

and digital health Ministry of Health (MOH) focal points, implementing partners, and health care providers were assembled and engaged throughout the adaptation processes. The ANC and FP DAKs were used as the initial set of content areas to inform a standard methodology and process for DAK country customization and integration into respective country digital health systems. This method builds on processes for customizing the WHO ANC digital module [13] using the ANC DAK in Zambia and Rwanda [14] and a broader methodology for applying the DAKs to the existing digital systems in a country. Challenges included inadequate narrative guideline uptake [15]; lack of requirements documentation; delays in guideline uptake and adoption; and the evolving digital landscape, including transitions between systems and inadequate clarity regarding which system to enhance.

Localization and Adaptation Processes

The approach included the following steps: (1) country assessment and stakeholder orientation; (2) content adaptation: review and alignment to national package; (3) content validation of the draft DAK country package; and (4) digital system and content updates and monitoring (Figure 1). Subsequent steps, such as the design of the system prototype (Step 4), will be expanded on through standard software development processes, including quality assurance assessments and user acceptance tests to facilitate further iterations and enhance the readiness for deployment. Related deployment activities, including system monitoring, training, and continuous support and feedback, are acknowledged as part of the overall process inherent for all digital implementations and not detailed in the framework. To guide and document this process for future replication, we developed operational tools (Table 1).

Figure 1. DAK adaptation process steps and phases. DAK: Digital Adaptation Kit; HMIS: health management information system.



XSL•FO
RenderX

Table . Tools used in Digital Adaptation Kit (DAK) country adaptation.

Step number	Tool	Purpose and description	DAK adaptation steps	Point of use/when used	DAK component reviewed
1	Guideline extraction	Provides a high-level comparison between country and WHO[a] narrative guidelines.	Country assessment and stakeholder orientation	• Prestakeholder orientation workshop • Precontent review and alignment workshop	• Health interventions and recommendations
2	Country assessment	The assessment tool evaluates a country's digital health landscape, governance, and workforce capacity [13]. It examines existing digital systems, guidelines, leadership structures, strategic priorities, and services. It seeks to identify relevant governance frameworks, and investment plans to guide the selection and sustainability of the digital system to be used for DAK content updates.	Country assessment and stakeholder orientation	• Pre/during stakeholder orientation workshop	• Health interventions and recommendations Personas
3	Premapping tool	This is adapted from the generic DAK data dictionary for specific health domain areas and includes questions to determine whether the DAK data element already exists in the country's protocols/guidelines/registers; whether it should be added to the country-adapted DAK, and if any modifications are required. It also considers data elements that exist in the country protocols but not in the DAKs, with a provision to include a description of the new data element and indicates any removals, notes, or justifications.	Content adaptation: review and alignment with national protocols/guidelines	• Content review and alignment with national protocols/guidelines workshop	• Health interventions and recommendations • Personas • Business processes and workflows • Core data elements • Decision support logic • Indicators and performance metrics
4	Monitoring, evaluation, and reporting alignment	The tool is used to systematically review and align DAK elements added to the country-adapted DAK to existing reporting tools (eg, paper registers).	Content adaptation: review and alignment with national protocols/guidelines	• Content review and national protocols/guidelines workshop	• Core data elements • Decision support logic • Indicators and performance metrics

XSL•FO
RenderX

Step number	Tool	Purpose and description	DAK adaptation steps	Point of use/when used	DAK component reviewed
5	Country adaptation log	The log provides a comprehensive overview of changes (additions, removals, and modifications) made to the data dictionary and decision support logic for the adaptation of the DAK in an existing system.	Content validation of the draft country package	• Post content review and alignment workshop	• Core data elements • Decision support logic • Indicators and performance metrics

[a]WHO: World Health Organization.

Country Assessment and Stakeholder Orientation

As an initial step to the introduction of DAKs, we developed a country assessment tool to assess the digital and health program context to determine country adaptation requirements. Considerations in this tool were derived from the WHO/International Telecommunications Union eHealth Strategy building blocks, which include leadership and governance, services, and applications; strategy and investment; service and applications, standards, and interoperability; and workforce [16]. In addition, to ascertain the status of the guideline dissemination and existing content within existing systems, we included a pillar on public health content and the health domain. Selected countries were introduced to the concept and initiative at a web-based orientation. The country assessment tool was used to initiate discussions with MOH stakeholders and decisions around the health programs and digital system for prioritization. This was followed by an in-person orientation workshop to review the results from the assessment tool, establish a common understanding among the country's SRH and digital stakeholders, and consolidate plans for implementation. A high-level overview of the DAK components, including the user personas, workflows, and data dictionaries was provided to illustrate what a DAK entails and preview potential modifications that may be needed. Further, multistakeholder DAK implementation teams were established in each country to lead the content review and alignment of the generic WHO DAK to national guidelines and protocols [14], including a subgroup to initiate the desk reviews and guideline comparisons for informing the areas for country adaptation.

Content Adaptation: Review and Alignment to National Package

To guide the content review process, a guideline extraction tool was developed to facilitate a high-level comparison between national guidelines or protocols and WHO guidelines. This tool aimed to identify deviations and adaptation requirements and facilitated an understanding of customizing user personas and workflows. A premapping tool was developed using editable versions of the DAK data dictionaries and decision support logic in Excel spreadsheets, which included additional columns for detailed documentation of the adaptations. A subset of the implementation team systematically reviewed the data elements and decision support tables and documented the alignment between the DAK content in relation to what may be available in national documentation. Adaptations were categorized into 3 types: modifications (taken from the generic WHO DAK but with wording changes), adoptions (taken as is from the DAK), and removals (not incorporated in the country DAK). A country adaptation log was also completed alongside the changes being documented in the spreadsheets in order to summarize and track the updates. Additionally, content that existed in a country's protocol or documentation but not in the generic WHO DAK was also highlighted. The outputs of the premapping were subsequently reviewed in stakeholder consultations for feedback and resulted in a draft adapted country package to undergo further validation.

Validation of DAK Country Package

The validation of the draft DAK country package was conducted as the final step before integration. Stakeholder meetings were convened to review the adapted content, verifying that it was accurately localized and aligned with national clinical and digital health guidelines and standards. This process involved reviewing the adaptation logs to establish a common understanding of the DAK components that were localized based on the criteria outlined in the content adaptation section above (ie, modifications, adoptions, additions, and removals). Additionally, content was prioritized for integration based on the digital platform's capacity and available resources, as well as the alignment needed for the data models of the intended digital systems. The draft packages were then cleaned, approved, and certified by national authorities as "ready" for system integration.

Digital System Content Update

The preparation for the digital system content update was initiated once the DAK software package had been validated by system developers and digital experts. It began with a thorough review of the identified existing system digital system's architecture and design; particularly the code structure, functionalities, and its capacity to support DAK content and functionalities as part of a software planning meeting. Furthermore, an extensive evaluation of the existing systems' components, underlying technology, and business processes was carried out in order to ascertain how each DAK may improve current workflows and interface with the respective electronic health records components. The next step was to create an integration plan that included the technical specifications, schedules, and required resources (including digital vendors) for the DAK system enhancements.

XSL•FO
RenderX

Ethical Considerations

For Malawi, Zambia, and Zimbabwe, this was part of WHO technical support, and there was no engagement with human subjects; therefore, ethics review was not required. Ghana and Ethiopia were part of an implementation research study that was approved by the WHO/Human Reproduction Program Research Project Review Panel, the WHO Ethical Review Committee (A66031), and the National Ethics Committee of the 2 countries (University of Gondar, Ethiopia Institutional Review Board [VP/RTT/05/752/2024] and Ghana Health Service Ethics Review Committee [GHS-ERC: 025/07/22]).

Implementation (Results)

Stakeholder Orientation and Country Assessment

When first presenting the concept of SMART guidelines and DAKs, they were initially perceived as abstract materials, and stakeholders in the countries often requested an understanding of what the "end product" would look like. Stakeholders often expected a tangible digital tool and required extensive communication on how SMART guidelines-DAKs work to inform their existing digital systems as software-neutral resources. Furthermore, a reference software app reflecting DAK content was often demonstrated during the orientation to provide clarity on how the DAKs would eventually appear in a digital interface. Demonstrating this linkage between the data elements and decision support logic in the DAK (in spreadsheet form) and how they would appear on a digital platform/system can also help distinguish the DAKs from the software app (Table 2).

Table . Summary of challenges, recommendations/best practices, and lessons learned.

Challenges	Recommendations/best practice	Lessons learned
• Inadequate uptake and adoption of guidelines at the point of care or a lack of updated guidelines during the introduction of DAKs[a].	• Assess the guideline status within the country, including conducting site visits to ascertain gaps and areas in which DAKs can strengthen prior to adaptation.	• As a guideline derivative product, DAKs can be used to accelerate guideline update processes by highlighting differences in global and national protocols.
• Limited existing system documentation. • Limited knowledge of existing systems by clinicians.	• DAKs will serve as a starting point for requirements gathering. • Showcase the system during content adaptation sessions.	• Engaging system users in content adaptation processes is critical for both system adoption and quality assurance of the content.
• Continuous evolution of digital ecosystems and varying maturity stages.	• Align with existing national digital system strategies.	• Integration of the DAKs within broader digital and health strategic documents is key for system adoption and sustainability.
• The initial content adaptation process might require more time due to the volume of DAK elements.	• Conduct preparatory steps, such as guideline extraction and premapping to assess/select initial areas for adaptation, prior to stakeholder validation.	• The content adaptation process is not linear, and multiple iterations and layers might be required for alignment with other components of the digital ecosystem, including the health management information systems for reporting.

[a]DAK: Digital Adaptation Kit.

In addition, this orientation and socialization of the DAKs identified additional scenarios to support countries' digital health journeys, such as informing assessments of existing digital systems and enabling a common reference standard, particularly in settings where there may be several electronic medical records systems, like Malawi. The DAKs were found to be clearly structured, with some MOHs proposing to adopt the DAK approach to document business processes. For example, in Zambia, this approach has been adopted and is currently being leveraged for other health domains. Additionally, engaging the system users in the adaptation processes will be essential to ensuring the adoption of the system (Table 2).

Validation of the DAK Country Package

The overall content adaptation and validation process provided an opportunity for countries to collectively review their business requirements processes for standardizing content within their digital system. This was a new process for stakeholders, especially as some health program managers were not familiar with digital system design or requirements gathering. The review and validation process, which included respective DAK domain service providers, provided an opportunity for both digital and health literacy capacity building. Clinicians not only saw themselves providing service to clients through the review processes but also actively participated in the process of developing a digital module that they themselves would be using.

Digital System Content Updates

In preparing for the digital system content update, DAKs were found to be clearly structured, with some MOHs proposing to adopt the DAK approach to document business processes for other health domains and include it as part of their broader strategy to digitalizing SRH services at the primary health care level. Examples include Malawi and Zambia [17] where the ANC and FP DAKs have been integrated into the respective

XSL•FO
RenderX

health domain guidelines and strategies. Decision support functionalities were found to be a valuable addition due to their potential to guide or remind clinicians of key clinical recommendations during the provision of care. This is especially important since most digital systems they were accustomed to focused heavily on data collection rather than person-centered care.

Discussion

Principal Findings

These initial experiences of introducing and implementing DAKs across 5 countries provide a foundation for developing a replicable, software-neutral integration process. Additionally, the findings will be important for informing not only the development of global DAKs but also how WHO and implementing agencies can support countries with their integration. The country assessment was critical across all sites for initiating conversations around digital systems, as well as for bringing stakeholders such as program managers on board. Additionally, the set-up of multistakeholder teams including the program, digital health leads, clinical informatics specialists, and clinicians was critical for driving the adaptation process forward. The structured format of DAKs facilitated a transparent process for content review and validation. Moreover, the collaboration across sectors, with the program and health domain experts leading ensured that the process was centered around the user—a critical component for system adoption [18,19].

The DAKs were initially viewed as "abstract" by stakeholders, and as software rather than health content due to limited engagement in the design of digital systems. The stakeholder consultations also provided opportunities for users to review existing systems and also appreciate existing gaps and propose how these could be enhanced with DAK content. The adaptation process revealed several layers of adaptation, and that multiple iterations would be required, including considerations around linkages with other components such as health management information systems. Some challenges included the large volume of DAK elements, which was initially overwhelming and time-consuming at the beginning of the review and content adaptation process. However, we learned that conducting preparatory steps, including guideline extraction and premapping, can help to optimize time and resources by first highlighting expected adaptations for stakeholder review (Table 2). Last, it is important to consider the different stages of digital maturity of a system; and the current strategic direction and priorities of the government during the introduction of DAKs at the country level (Table 2).

Aligning With Health System Strategic Policies and Guidelines

To integrate the DAKs within a country's national health system, it is vital to align them with the broader national health strategic priorities and frameworks [20]. The examples highlighted above from Zambia and Malawi represent a great starting point for harmonization and integration into broader health strategic documents and plans. This ensures that DAKs are embedded as critical elements of the national strategy rather than being viewed as isolated initiatives—which can negatively affect their adoption at different levels of the health system (Table 2). It is, therefore, imperative that government stakeholders, particularly MOH program managers and health domain and digital health experts, actively advocate for and ensure the inclusion of these guidelines into national policies, during annual and midterm policy and health strategic reviews and planning. This will require strong leadership and coordination across relevant sectors.

Leveraging DAKs to Accelerate Narrative Guideline Updates and Other Paper Tools

As a guideline derivative product, DAKs can be used to accelerate guideline update processes by highlighting differences in global and national protocols (including reporting tools), particularly in settings where the narrative guidelines are not up-to-date (Table 2). The adaptation process can be useful for informing the updates for narrative guidelines and aligning to the latest WHO guidelines. However, the DAK itself cannot be a substitute for undergoing the formal process of updating national health program guidelines [12]. However, it will be important to also consider the current status of guideline uptake at the facility level. Conducting a site visit to a health facility, as part of the content review process, will not only enhance the DAK adaptation process by highlighting areas within the guideline content that require reinforcement but can also improve the uptake of the guidelines (Table 2).

Determining the Approach for DAK Implementation

When introducing DAKs within a country's digital and program ecosystem, it is important to consider the modality for DAK implementation. This can be particularly challenging in settings where there have been prior digital investments that are disease-specific. Where the identified digital system might be used for certain health areas (eg, HIV), clinicians would already be used to these systems, leading to the underuse of other modules. Enhancing the "other" modules with the DAKs within such platforms would require adequate awareness and training to improve uptake and use. The localized DAK could act as the benchmark that all other digital systems adhere to if there are many digital systems with varying degrees of coverage and maturity. Moreover, showcasing the system during content adaptation sessions could be a helpful approach to increase understanding of the various digital modules within a point-of-care system. Additionally, implementation modalities should also consider engagement with private sector partners and subnational adaptations based on the program and digital landscape of the countries.

Strengths and Limitations

The strength of this paper is that it represents replicable processes that have been developed through firsthand learning from countries and offers a foundation that can undergo further refinement as new countries embark on the implementation of SMART guidelines, specifically DAKs. These learnings will be complemented through implementation research [21] and communities of practice, and culminate in the development of a living technical guidance to facilitate the effective uptake of DAKs. Some of the limitations and challenges, such as the

XSL•FO
RenderX

intensive resources initially required, were due to the novelty of the approach and having limited prior reference in the implementation of SMART guidelines. Additionally, another limitation is the absence of detailed cost estimates for the DAK adaptation and implementation processes, as a systematic evaluation of costs was not included. Given the focus on methodological processes and the variability in country contexts, providing a comprehensive budget was not feasible at this stage. Furthermore, it is important to note that countries' digital systems are dynamic and constantly changing. Despite DAKs being software agnostic, critical reflections are also needed on transitioning a package adapted for a legacy system to newer versions, while also introducing interoperability standards, such as Fast Healthcare Interoperability Resources (FHIR) [22].

Conclusions

Leveraging existing digital investments to reinforce evidence-based recommendations offers a sustainable pathway for institutionalizing WHO SMART guidelines-DAKs within health systems. However, to achieve this, a multifaceted approach will be necessary: strong digital health leadership and governance [23], along with coordination and strategic direction for digital investments, will be critical [21], particularly in countries where systems are still disease-specific [24]. Moreover, the collaboration between program leads, policy makers, and digital teams will also be vital, including engaging program managers and policy makers in system update training, continuous system monitoring and identification of "system champions" at the facility level. Further, plans for interoperability and data use standards will also need to be incorporated. These initial sets of country experiences offer insights into the requirements and opportunities to optimize the use of WHO SMART guidelines-DAKs as a tool for strengthening countries' digital investments in a structured manner. This approach sets the foundation for a systematic approach to implementing DAKs and will be further refined through research to evaluate the resulting impact on service delivery outcomes and data flows [9]. Overall, standardizing a common approach to DAK implementation will be important to facilitate peer-to-peer exchange among countries, foster regional and global cooperation required for standards-based digital transformation, and ultimately optimize the impact of digital health systems for universal health coverage.

Acknowledgments

The authors would like to thank the following from the World Health Organization (WHO) Africa Regional Office for their support in facilitating country stakeholder engagement and consultations: Dr Hillary Kipruto, Dr Ayotunede Adegboyega, and Dr Adeniyi Aderoba. The authors would also like to thank the following from the WHO country offices of Zambia, Malawi, Zimbabwe, Ethiopia, Kenya, and Ghana: Dr Azmach Gebregiorgis, Mr Peter Chalusa, Dr Solome Nampewo, Dr Stanely Midzi, and Ms Batani Moyo; Dr Kassu Gurma and Dr Haimanot Workineh; and Mr Eric Maira, Dr Martin Owusu, and Mr Dominic Atweam. The authors also thank the following individuals from the Ministries of Health of Zambia, Malawi, Zimbabwe, Ethiopia, and Ghana Health Service respectively: Ms Dynes Kaluba, Ms Ruth Bweupe, Ms Winne Bbwantu, Mr Muya Mwansa, Mr Shem Kabesa, Mr Oovst Chooye, and Mr Andrew Chanshika; Ms Christina Muchoma, Mr Kennedy Kanyimbo, and Mr Innocent Yowa; Dr Simukai Zizhou and Dr Robert Gongora; Mr Gemechis Melkamu, Mr Abinet Seife, Mr Gezahegn Feyssa, Dr Zerihun Bogale, Dr Abebe Ketema, Mrs Yirgalem Negash, and Mr Sheleme Humnessa; and Dr Kofi Issah, Dr Chris Fofie, Mr Geegee Kwame Adu, and Mr Oswald Kanyirbee Dachaga. The authors also thank Mrs Addiszemen Chanie from the Amhara Regional Health Office and Dr Dawit Kassahun and Dr Solomon Berhe from the University of Gondar, Ethiopia. The authors also acknowledge Dr Sam Dery, Dr Frances B da Costa Vroom, and Mr Seth Kwaku Afagbedzi from the University of Ghana. This work was funded through the UNDP-UNFPA-UNICEF-WHO-World Bank Special Programme of Research, Development and Research Training in Human Reproduction, a cosponsored program executed by the WHO. The named authors alone are responsible for the views expressed in this publication and do not necessarily represent the decisions or the policies of the WHO nor the UNDP-UNFPA-UNICEF-WHO-World Bank Special Programme of Research, Development and Research Training in Human Reproduction.

Authors' Contributions

RKM wrote the first draft in collaboration with TT. KB, SBM, and IC provided input on the initial adaptation experience from Zambia that informed adaptation processes for other countries. Additionally, CG, SD, EM, BT, AN, AM, HAT, and BFE from Ghana and Ethiopia also contributed to the methodologies. All authors reviewed and provided input into the manuscript based on their country's implementation and technical experience.

Conflicts of Interest

KB is a clinical informatics specialist who works for IHM Southern Africa—a technology/health informatics company that supports the implementation of the digital system in Zambia.

Checklist 1
Checklist of iCHECK-DH guidelines. iCHECK-DH: Guidelines and Checklist for the Reporting on Digital Health Implementations.
[DOCX File, 33 KB - medinform_v13i1e58858_app1.docx]

XSL•FO
RenderX

References

1. Seventy-first World Health Assembly: Geneva, 21–26 May. Resolutions and decisions annexes. World Health Organization. 2018. URL: https://iris.who.int/handle/10665/326571 [accessed 2023-04-15]
2. Holl F, Kircher J, Hertelendy AJ, Sukums F, Swoboda W. Tanzania's and Germany's digital health strategies and their consistency with the World Health Organization's global strategy on digital health 2020-2025: comparative policy analysis. J Med Internet Res 2024 Mar 18;26:e52150. [doi: 10.2196/52150] [Medline: 38498021]
3. Duffy A, Christie GJ, Moreno S. The challenges toward real-world implementation of digital health design approaches: narrative review. JMIR Hum Factors 2022 Sep 9;9(3):e35693. [doi: 10.2196/35693] [Medline: 36083628]
4. SMART guidelines. World Health Organization. 2021. URL: https://www.who.int/teams/digital-health-and-innovation/smart-guidelines [accessed 2023-04-15]
5. Tamrat T, Ratanaprayul N, Barreix M, et al. Transitioning to digital systems: the role of World Health Organization's digital adaptation kits in operationalizing recommendations and interoperability standards. Glob Health Sci Pract 2022 Feb 28;10(1):e2100320. [doi: 10.9745/GHSP-D-21-00320] [Medline: 35294382]
6. Mehl G, Tunçalp Ö, Ratanaprayul N, et al. WHO SMART guidelines: optimising country-level use of guideline recommendations in the digital age. Lancet Digit Health 2021 Apr;3(4):e213-e216. [doi: 10.1016/S2589-7500(21)00038-8] [Medline: 33610488]
7. Meybohm P, Ghanem A, von Dincklage F, Kranke P, Börm P. Digital guidelines of the twenty-first century : requirements for the structured development, application and evaluation of medical knowledge. Anaesthesiologie 2023 Aug;72(8):584-589. [doi: 10.1007/s00101-023-01310-3] [Medline: 37326637]
8. Digital adaptation kit for antenatal care: operational requirements for implementing WHO recommendations in digital systems. World Health Organization. 2021. URL: https://www.who.int/publications/i/item/9789240020306 [accessed 2023-04-15]
9. Digital adaptation kit for HIV: operational requirements for implementing WHO recommendations in digital systems. World Health Organization. 2022. URL: https://www.who.int/publications/i/item/9789240054424 [accessed 2023-04-15]
10. Digital adaptation kit for family planning: operational requirements for implementing WHO recommendations in digital systems. World Health Organization. 2021. URL: https://www.who.int/publications/i/item/9789240029743 [accessed 2023-04-15]
11. Government of Sweden and four UN agencies announce new joint programme to boost efforts to achieve universal access to sexual and reproductive health and to end AIDS. World Health Organization Regional Office for Africa. URL: https://www.afro.who.int/media-centre/statements-commentaries/government-sweden-and-four-un-agencies-announce-new-joint [accessed 2023-03-15]
12. Perrin Franck C, Babington-Ashaye A, Dietrich D, et al. iCHECK-DH: guidelines and checklist for the reporting on digital health implementations. J Med Internet Res 2023 May 10;25:e46694. [doi: 10.2196/46694] [Medline: 37163336]
13. Haddad SM, Souza RT, Cecatti JG, et al. Building a digital tool for the adoption of the World Health Organization's antenatal care recommendations: methodological intersection of evidence, clinical logic, and digital technology. J Med Internet Res 2020 Oct 1;22(10):e16355. [doi: 10.2196/16355] [Medline: 33001032]
14. Muliokela R, Uwayezu G, Tran Ngoc C, et al. Integration of new digital antenatal care tools using the WHO SMART guideline approach: experiences from Rwanda and Zambia. Digit Health 2022;8:20552076221076256. [doi: 10.1177/20552076221076256] [Medline: 35127117]
15. Peters S, Sukumar K, Blanchard S, et al. Trends in guideline implementation: an updated scoping review. Implement Sci 2022 Jul 23;17(1):50. [doi: 10.1186/s13012-022-01223-6] [Medline: 35870974]
16. National eHealth strategy toolkit. World Health Organization. 2012. URL: https://www.who.int/publications/i/item/national-ehealth-strategy-toolkit [accessed 2024-04-16]
17. Zambia family planning guidelines and protocols. Republic of Zambia Ministry of Health. URL: https://www.moh.gov.zm/?wpfb_dl=267 [accessed 2024-10-02]
18. Akwaowo CD, Sabi HM, Ekpenyong N, et al. Adoption of electronic medical records in developing countries-a multi-state study of the Nigerian healthcare system. Front Digit Health 2022;4:1017231. [doi: 10.3389/fdgth.2022.1017231] [Medline: 36479191]
19. Berihun B, Atnafu DD, Sitotaw G. Willingness to use electronic medical record (EMR) system in healthcare facilities of Bahir Dar City, Northwest Ethiopia. Biomed Res Int 2020;2020:3827328. [doi: 10.1155/2020/3827328] [Medline: 32908886]
20. Labrique AB, Wadhwani C, Williams KA, et al. Best practices in scaling digital health in low and middle income countries. Global Health 2018 Dec;14(1). [doi: 10.1186/s12992-018-0424-z]
21. Kouanda S, Ouedraogo AM, Sogo AE, et al. New Antenatal Model in Africa and India (NAMAI) study: implementation research to improve antenatal care using WHO recommendations. Health Res Policy Sys 2023;21(1). [doi: 10.1186/s12961-023-01014-5]
22. Chukwu E, Garg L, Obande-Ogbuinya N, Chattu VK. Standardizing primary health care referral data sets in Nigeria: practitioners' survey, form reviews, and profiling of fast healthcare interoperability resources (FHIR). JMIR Form Res 2022 Jul 7;6(7):e28510. [doi: 10.2196/28510] [Medline: 35797096]

XSL•FO
RenderX

23. Layer E, Slim S, Mussa I, et al. The journey of Zanzibar's digitally enabled community health program to national scale: implementation report. JMIR Med Inform 2023 Oct 9;11:e48097. [doi: 10.2196/48097] [Medline: 37812488]
24. Were MC, Savai S, Mokaya B, et al. mUzima mobile electronic health record (EHR) system: development and implementation at scale. J Med Internet Res 2021 Dec 14;23(12):e26381. [doi: 10.2196/26381] [Medline: 34904952]

Abbreviations

ANC: antenatal care
DAK: Digital Adaptation Kit
FHIR: Fast Healthcare Interoperability Resources
FP: family planning
MOH: Ministry of Health
SMART: Standards-based, Machine-readable, Adaptive, Requirements-based, and Testable
SRH: sexual and reproductive health
SRHR: sexual and reproductive health and rights
WHO: World Health Organization

Edited by C Perrin; submitted 22.04.24; peer-reviewed by H Lin, M Randriambelonoro, S Delaigue, U Sinha; revised version received 09.11.24; accepted 11.11.24; published 07.02.25.

Please cite as:
Muliokela RK, Banda K, Hussen AM, Malumo SB, Kashoka A, Mwiche A, Chiboma I, Barreix M, Nyirenda M, Sithole Z, Ratanaprayul N, Endehabtu BF, Telake HA, Weldeab A, Probert WJM, Tunçalp , Maya E, Woldetsadik M, Tilahun B, Guure C, Senya K, Say L, Tamrat T
Implementation of WHO SMART Guidelines-Digital Adaptation Kits in Pathfinder Countries in Africa: Processes and Early Lessons Learned
JMIR Med Inform 2025;13:e58858
URL: https://medinform.jmir.org/2025/1/e58858
doi:10.2196/58858

© Rosemary K Muliokela, Kuwani Banda, Abdulaziz Mohammed Hussen, Sarai Bvulani Malumo, Andrew Kashoka, Angel Mwiche, Innocent Chiboma, Maria Barreix, Muyereka Nyirenda, Zvanaka Sithole, Natschja Ratanaprayul, Berhanu Fikadie Endehabtu, Hanna Abayneh Telake, Adane Weldeab, William J M Probert, zge Tunçalp, Ernest Maya, Mulatu Woldetsadik, Binyam Tilahun, Chris Guure, Kafui Senya, Lale Say, Tigest Tamrat. Originally published in JMIR Medical Informatics (https://medinform.jmir.org), 7.2.2025. This is an open-access article distributed under the terms of the Creative Commons Attribution License (https://creativecommons.org/licenses/by/4.0/), which permits unrestricted use, distribution, and reproduction in any medium, provided the original work, first published in JMIR Medical Informatics, is properly cited. The complete bibliographic information, a link to the original publication on https://medinform.jmir.org/, as well as this copyright and license information must be included.

XSL•FO
RenderX

Dolodoc, an App to Leverage Self-Management of Chronic Pain: Design, Development, and Implementation Report

Frederic Ehrler[1], PhD; Julie Guebey[1], MSc; Jessica Rochat[1], MSc; Laetitia Gosetto[1], MSc; Benno Rehberg[2,3], MD; Christian Lovis[1,3], PhD; Aude Molinard-Chenu[1], PhD

[1]Division of medical information science, Diagnostic department, University Hospital of Geneva, Gabrielle Perret Gentil 4, Geneva, Switzerland

[2]Anesthesiology, University Hospital of Geneva, Geneva, Switzerland

[3]Medicine Faculty, University of Geneva, Geneva, Switzerland

Corresponding Author:
Frederic Ehrler, PhD
Division of medical information science, Diagnostic department, University Hospital of Geneva, Gabrielle Perret Gentil 4, Geneva, Switzerland

Abstract

Background: Chronic pain affects approximately 19% of the European population and presents major challenges, both in terms of individual impact and the economic burden on health care systems. While clinical expertise remains essential, patient empowerment through self-management tools has become a key component in the long-term management of chronic pain.

Objective: This report describes the development and implementation of Dolodoc, a mobile app designed to support patients with chronic pain in monitoring and managing their condition.

Methods: Developed by a research and development team at the University Hospitals of Geneva, Dolodoc enables users to track their pain across 7 dimensions of daily life. A digital coach provides personalized guidance, drawing from a corpus of over 80 evidence-based recommendations elaborated by clinical experts. The project was conducted over 4 years with the early involvement of stakeholders, including pain specialists and end users, to ensure alignment with user needs. Emphasis was placed on both the scientific validity and accessibility of the recommendations.

Results: The project was completed on time and within budget. The app was made freely available to patients identified as likely to benefit. However, a notable limitation is the absence of predefined key performance indicators to assess the impact of the intervention quantitatively.

Conclusions: This implementation report illustrates how mobile technology can be leveraged in a university hospital context to address the needs of patients with chronic pain and promote self-management. Early and sustained collaboration with stakeholders was instrumental in aligning the solution with both clinical evidence and user expectations.

(JMIR Med Inform 2025;13:e71597) doi:10.2196/71597

KEYWORDS

implementation; chronic pain; mHealth; self-management; health behavior change; user-centered design

Introduction

Context

Chronic pain is defined by the International Association for the Study of Pain as “an unpleasant sensory and emotional experience associated with, or resembling that associated with, actual or potential tissue damage, that persists over a period of at least three months” [1]. It is a ubiquitous issue affecting about 19% of the European population [2], associated with considerable burden and high health care costs globally [3,4]. Follow-up studies of patients with chronic pain report a persistence rate of approximately 50% - 71% after 1 year [5,6], with high interindividual variability depending on biopsychosocial factors, functional limitations, and comorbidities [7,8]. Over the years, chronic pain treatment has evolved into a multimodal arsenal, including lifestyle changes [9], physical therapy [10], psychotherapy [11], interventional treatments [12], and medications [13]. In addition to pain reduction, integrated follow-up in a multidisciplinary pain center can improve disability and quality of life [14].

Alongside expert health care support, patient-directed strategies have become crucial in addressing long-term pain conditions effectively [15]. With the widespread adoption of mobile devices, smartphone-delivered interventions for pain management have gained prominence in the field of chronic pain care [16].

Problem Statement

The availability of professional multidisciplinary follow-up is limited and costly. Moreover, the longitudinal evolution of pain

XSL•FO
RenderX

and quality of life indicators is not easily gathered by patients and health care professionals. Patient engagement in pain management strategies between appointments is also difficult. [17].

These issues could be addressed by a digital intervention that transmits targeted health information, including behavior change communication such as multimodal chronic pain self-management strategies. It should also allow users to track and share long-term data on pain levels and quality of life. To improve user engagement, this mobile app must be user-centered, intuitive, and inviting.

Similar Interventions

Dolodoc's development was inspired by existing mobile apps for chronic pain management [18], which typically focus on one or more of the following objectives: education, monitoring, and management [19]. Unlike these, Dolodoc integrates all 3 objectives into a cohesive, patient-centered system, adding significant value by fostering active patient engagement and collaboration with health care professionals [20]. Key differentiators include an emphasis on quality-of-life reporting and a digital coach that offers personalized activity recommendations and feedback. This helps users identify effective pain management strategies and supports adherence to these strategies through motivational interactions. Furthermore, Dolodoc is specifically tailored for French-speaking users, addressing a linguistic gap in the availability of such tools.

Following the iCHECK-DH (Checklist for the Reporting on Digital Health Implementations; Checklist 1) guidelines for reporting on digital health implementations [21], we describe "Dolodoc," a mobile app co-designed with patients with chronic pain and health care professionals to monitor pain and quality of life, and provide multimodal self-management strategies that can be experienced and assessed within the mobile app.

Methods

Aim and Objectives

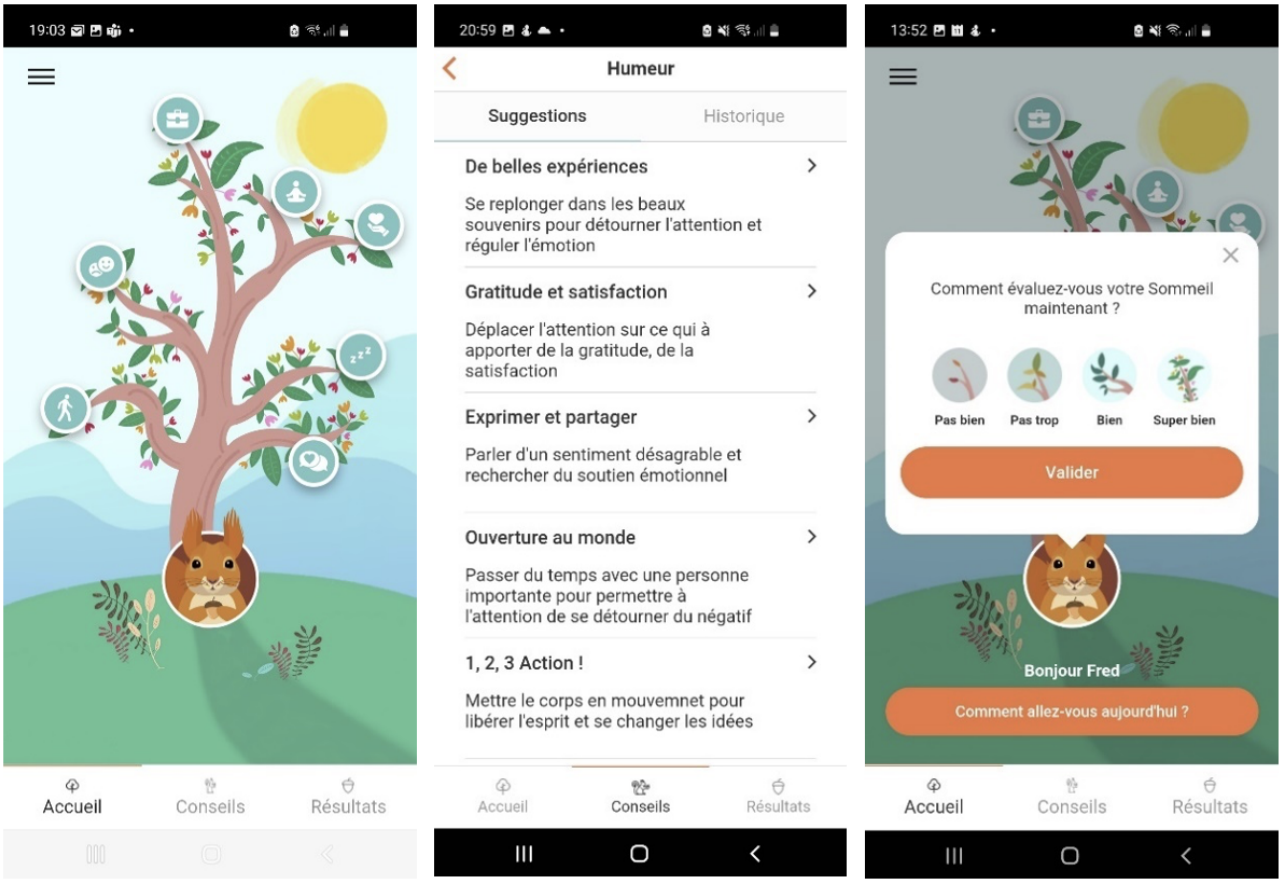
Our goal was to develop a system that assists patients with chronic pain in actively managing their condition, providing continuous support, and empowering patients to engage in a personalized approach to improving their well-being.

Blueprint and Summary

Dolodoc is a mobile app, in French, that enables users to report their perceptions of pain and the impact of pain on various aspects of their quality of life [22]. The system includes advice as well as activities that patients can plan and assess to identify effective pain management strategies. Dolodoc engages patients through a digital coach that reacts to the planification of activities, based on the strategies included in the app. Additionally, the coach prompts users to regularly report their perceptions of pain and their daily functioning. Furthermore, the app provides an option to share progress with health care professionals, fostering a collaborative approach to managing chronic pain. A gamified metaphorical universe—represented by a tree that flourishes or withers based on the user's evaluations—aiming to enhance engagement and motivation (Figure 1). Overall, Dolodoc combines elements addressing the 3 objectives that are usually found in digital interventions for chronic pain [19]: education, monitoring, and management.

XSL•FO
RenderX

Figure 1. Screenshots of the Dolodoc app.



The development of Dolodoc included 3 primary phases: conception, content creation and validation, and technical implementation. The original concept was fostered in a research and development department combining medical clinical expertise and psychology skills. To ensure user-centered design and relevance, all phases of the app development were elaborated in a user-centered manner, including critical stakeholders such as patients and health care professionals involved in the Geneva Pain Network. A focus group of 10 patients with chronic pain was interviewed about the dimensions of their quality of life that they would relate to chronic pain. Seven dimensions emerged from open discussions in the group: daily activities, mood, work, relaxation, social support, sleep, and intimacy. Based on scientific evidence, a psychologist wrote a first version of multiple advice per dimension. Then, an experienced pain clinician and a member of the hospital communication team revised the advice. The current version of the app contains a database of 84 expert-recommended strategies related to patient-centered dimensions of quality of life. Patients with chronic pain also participated in the conception of the app by providing regular feedback on the prototyped screen as well as on the proposed graphical design of the app. Finally, the app has been reviewed by a user experience designer in order to identify usability problems.

The technical implementation included the development of a mobile app, incorporating gamification and privacy features. The graphic environment of the app was built according to the feedback of the focus group. Indeed, to facilitate engagement, Dolodoc uses a gamified metaphor: a digital tree that flourishes or withers according to the patient's self-assessment in the 7 dimensions of quality of life.

After a development phase, the app was released on Android and Apple app stores in March 2023. Minor bugs were addressed in several updates until the last release in June 2024.

For deployment, a communication campaign was conducted in January 2024, including printed flyers that were arranged at the pain center as well as billboards that were placed within the hospital and in neighboring high-traffic areas, and targeted social media advertisements, to raise awareness of the app among potential users. These efforts aimed to maximize outreach and ensure adoption among the chronic pain community.

Technical Design

The Dolodoc app was developed internally to align with the hospital's strategic goal of creating a cohesive ecosystem of apps tailored to patient needs. The internal development approach ensured seamless integration of hospital-curated advice and positioned the app for future connectivity with the clinical information system, enhancing follow-up for chronic disease patients.

From a technological perspective, coach interactions are currently driven by a predefined rule-based system, meaning that all the coach's interactions are statically coded. While its current state relies on predefined interactions, there is potential to incorporate large language models to improve personalization and adaptability in the future. The app is free to download and fully owned by the University Hospitals of Geneva (HUG),

XSL•FO
RenderX

aligning with their patient-first, noncommercial ethos. This ownership guarantees control over intellectual property and the ability to integrate evolving technologies and data security measures. The app's open architecture supports long-term alignment with the hospital's digital health investment roadmap, emphasizing interconnected and user-centric solutions.

Target

Dolodoc was developed to primarily target French-speaking patients enduring chronic pain. However, since the app is free and available for download by a large population, we foresee that the content of the app (eg, the advice) could also be used by other members of the health system around a chronic pain situation, such as health care professionals and caregivers.

Data

The app ensures data privacy and security in line with health care data management standards. Dolodoc uses a device-based data governance approach, where all personal data collected by the app is stored locally on the user's device. Data goes through a lifecycle that includes collection, processing, and storage on the device itself, without being transferred to external servers or cloud-based storage. As such, data ownership remains entirely with the patient, who has full access and control over their information. Data regarding the use of the app is collected anonymously through the Piwik web analytics tool installed on-premises on our infrastructure. Consent for data collection is obtained when the user accepts the disclaimer presented at the initial setup of the app, clearly outlining data handling practices and user responsibilities.

Patients have the option to share their personal data with clinicians in a secure, confidential manner by generating a PDF report directly from the app. Sharing the report is initiated solely at the user's discretion and responsibility. Given that the data remains on the user's device, data protection measures are focused on device security, recommending that users follow best practices in device security (eg, password protection and regular software updates).

Interoperability

The current version of the app is not connected to another system.

Participating Entities

The Dolodoc app was developed at the HUG, one of Switzerland's largest university hospitals. This project was carried out within the SIMED (Medical Information Science Department), a research and development service dedicated to research projects and specializing in human-machine interaction. The SIMED leveraged the multidisciplinary competencies of the team, such as ergonomics, psychology, clinical expertise, and technical ones to cover all aspects of the project. Cooperation with pain experts from the Geneva pain network, as well as patients, ensured adequacy of the tool with targeted user needs, as well as compliance with the latest medical evidence. Funding was provided by the Fondation Privée des HUG, a foundation focused on supporting projects enhancing the quality of care at the hospital through private donations. The funds covered expenses related to the app's conception, development, and design. The project involved pain management specialists and patient-partners to ensure the app's relevance and efficacy. This funding was sufficient to fully support the implementation phase. The final product and intellectual property will remain under the ownership of HUG after implementation.

Budget

The development of Dolodoc required an estimated budget of approximately CHF 250,000 (US $250,000). A substantial portion of the budget was allocated to content creation and validation. The budget covers the complete lifecycle of Dolodoc creation and deployment, ensuring a robust foundation for ongoing use and impact.

Sustainability

Dolodoc operates as an institutional project focused on enhancing patient support for chronic pain management, rather than generating financial profit. The primary goal of the app is to provide long-term value to patients by offering a self-management tool that empowers users and improves quality of life. Sustainability is ensured through institutional backing, where ongoing costs are centered on maintaining the app within the technical framework. This includes updates to ensure compatibility with evolving device operating systems, security enhancements, and periodic content revisions to maintain relevance and accuracy.

Ethical Considerations

This study did not require approval from an ethics review board, as it did not involve the collection or analysis of identifiable personal health data, nor any clinical experimentation. The development and implementation of Dolodoc were conducted as part of a quality improvement and service design initiative at the HUG, in accordance with Swiss federal guidelines under the Human Research Act (2014), Article 2(1), which exempts projects not involving health-related personal data from ethics approval requirements. During the co-design process, patients participated voluntarily in interviews and usability testing sessions focused on app functionality and content design. No health or sensitive data were recorded, and all feedback was anonymized at the point of collection. Users of the final version of the app consent to anonymous usage data collection through an internal instance of the Piwik analytics platform, as clearly outlined in the initial disclaimer presented upon first use of the app. No participants received any form of compensation. As such, the project complies with institutional and national standards for service-level digital health development outside the scope of research involving human participants.

Results

Coverage

The coverage of the implementation is international since it is available on several app stores. Indeed, use analysis showed that Dolodoc was used in 23 different countries. However, Dolodoc is designed in French, and French-speaking countries (Switzerland and France) account for >90% of the users. In

XSL•FO
RenderX

Switzerland, for example, 22.8% of the population speaks French as a main language [23].

Outcome

Since it is publicly available until November 2024, Dolodoc was downloaded 2284 times in total, including Android and Apple stores. The promotional strategy was efficient since it boosted downloads, reaching a maximum of 206/week during the first month of the campaign.

At the pain center, Dolodoc has been included in the multimodal therapeutic strategy that is discussed between patients and pain specialists. It is mentioned in our medical reports, and it is also used in psychotherapy sessions.

Clinical indicators about self-efficacy and quality of life were not systematically collected in our implementation process since the budget did not include a clinical impact study. Hence, a dedicated study should be planned to address the clinical added value of this implementation.

Qualitative feedback was obtained from open discussions with Dolodoc users in the context of a digital navigation [24] follow-up at the pain center. The role of a digital navigator is to help users navigate digital technologies efficiently by guiding, answering questions, exposing all the digital possibilities according to each patient, and fixing technical problems.

Participants reported that they appreciated the variety of recommendations and the way they were presented, which sometimes alleviated helplessness. While the number of strategies was at times overwhelming, users appreciated having alternatives. Considering whether the strategy is “achievable” helped to relieve the guilt of not doing everything without losing motivation. In fact, patients spontaneously reported that the strategies are delivered in a nonjudgmental and informative way, and the variety of strategies was also greatly appreciated, as emphasized in the following quote: “It makes you realize that there are many ways to take care of yourself”. Self-management strategies were considered the app’s main value, even as reminders. The strategies, which were given as a resource, are also applicable outside of painful crises and have general health benefits, which were appreciated. Some weaknesses in the navigability within the app were also reported by participants: the fact that users must actively browse and choose a suitable strategy within the app was perceived as an obstacle to action. The lack of a reminder feature was also noticed as a barrier to use. Indeed, users commented on the importance of motivational aspects in chronic pain self-management that were not entirely fulfilled by Dolodoc.

Lessons Learned

The involvement of patients and specialists, such as psychologists and pain experts, from the initial stages of conception proved to be a critical success factor in ensuring the app aligned with the needs of its target users. Engaging these stakeholders helped to identify meaningful pain management strategies and ensured that the app addressed real-world challenges faced by individuals with chronic pain. The adoption of a user-centered user interface/user experience design approach further strengthened the solution, incorporating steps like user requirement identification, prototyping, and iterative testing. This ensured that the app was intuitive and functional before technical implementation began. Additionally, trust in the app was bolstered by its development under the sponsorship of a nonprofit health care institution, reassuring users of its credibility and noncommercial intent.

However, generating personalized and relevant advice for patients posed a significant challenge. This required extensive evidence assessment, interviews with end users, and iterative reviews by experts and communication specialists to ensure the advice was both scientifically grounded and comprehensible to users. Budget constraints added another layer of difficulty, as the project was bound by a predefined budget set before finalizing the full specifications. Some features, initially thought to be straightforward, proved much more complex and resource-intensive to implement, underscoring the importance of thorough feasibility assessments during the planning phase. Moreover, the lack of budget for a clinical impact study prevents us from anchoring our implementation on specific evidence about Dolodoc, although global evidence supports the effectiveness of self-management apps for chronic pain [16].

Unintended Consequences

Although pain specialists at the pain center were informed about and convinced of the utility of adding Dolodoc to their therapeutic arsenal, it took time for them to integrate this novel tool into their regular clinical practice. The engagement of patients in using the app also turned out to be a limitation. Indeed, we noticed that even when the pain specialist provided information about Dolodoc during a medical visit, most patients did not use the app until the following visit. These 2 pitfalls are part of a well-described phenomenon regarding the implementation of digital health interventions [25]. It could perhaps be addressed by integrating digital navigators into our clinical practice.

Discussion

Dolodoc’s implementation demonstrates the transformative potential of mobile health apps in addressing chronic pain management challenges. By equipping patients with self-monitoring tools and personalized strategies, Dolodoc addresses key barriers like limited access to multidisciplinary care and low patient engagement between visits.

User-centered design and stakeholder engagement were critical to the app’s success. Ongoing collaboration with patients with chronic pain, clinicians, and psychologists ensured usability and relevance. Gamification and a strong privacy framework also boosted trust and engagement.

Users reported benefits such as reduced feelings of inadequacy and better access to new strategies. However, they also emphasized the difficulty of finding suitable strategies during episodes of intense pain, highlighting the need to improve accessibility and navigation during pain crises, consistent with previous findings [26]. The lack of predefined key performance indicators and budgetary provisions for a clinical impact study highlights a significant limitation, underscoring the need for future implementations to include robust evaluation frameworks.

XSL•FO
RenderX

These would validate the clinical efficacy of digital tools and provide insights for iterative improvements.

Looking ahead, Dolodoc presents opportunities to advance chronic pain management on multiple fronts. Integration with hospital information systems could enhance the app's utility in clinical settings, supporting coordinated care. Additionally, leveraging technologies such as large language models could enable more dynamic and personalized patient interactions. However, overcoming challenges in adoption—both among clinicians and patients—remains essential. Strategies like integrating digital health navigators and expanding awareness campaigns could boost utilization rates and long-term engagement.

Ultimately, Dolodoc exemplifies how mobile health tools can improve self-management and quality of life for patients with chronic pain. Broader use and integration of evaluation frameworks could lead to significant improvements in pain care and serve as a model for future digital health innovations.

Acknowledgments

We thank Pre Anne-Françoise Allaz, Pr Jules Desmeules, Dre Valérie Piguet, and Pre Christine Cedraschi for sharing their expertise on the topic, Myriam Perrier for the development, as well as the fondation privée des University Hospitals of Geneva for the funding of the project.

Authors' Contributions

FE and AMC supervised the project and contributed to the development of the app and to the writing of this publication (original draft, revising, and editing). JR contributed to the development of the app, collected user experience data, and contributed to the writing of this publication (revising and editing). JG collected user experience data and contributed to the writing of this publication (revising and editing). LG contributed to the writing of this publication (revising and editing) and supervised JG. CL supervised FE, JR, LG, JG, and AMC and contributed to the development of the app and to the writing of this publication (revising and editing). BR contributed to the development of the app and to the writing of this publication (revising and editing).

Conflicts of Interest

None declared.

Checklist 1
iCHECK-DH (Checklist for the Reporting on Digital Health Implementations) checklist.
[PDF File, 157 KB - medinform_v13i1e71597_app1.pdf]

References

1. Raja SN, Carr DB, Cohen M, et al. The revised international association for the study of pain definition of pain: concepts, challenges, and compromises. Pain 2020 Sep 1;161(9):1976-1982. [doi: 10.1097/j.pain.0000000000001939] [Medline: 32694387]
2. Breivik H, Collett B, Ventafridda V, Cohen R, Gallacher D. Survey of chronic pain in Europe: prevalence, impact on daily life, and treatment. Eur J Pain 2006 May;10(4):287-333. [doi: 10.1016/j.ejpain.2005.06.009] [Medline: 16095934]
3. Rice ASC, Smith BH, Blyth FM. Pain and the global burden of disease. Pain 2016;157(4):791-796. [doi: 10.1097/j.pain.0000000000000454]
4. Barsky AJ, Orav EJ, Bates DW. Somatization increases medical utilization and costs independent of psychiatric and medical comorbidity. Arch Gen Psychiatry 2005 Aug;62(8):903-910. [doi: 10.1001/archpsyc.62.8.903] [Medline: 16061768]
5. Gureje O, Simon GE, Von Korff M. A cross-national study of the course of persistent pain in primary care. Pain 2001 May;92(1-2):195-200. [doi: 10.1016/s0304-3959(00)00483-8] [Medline: 11323140]
6. Itz CJ, Geurts JW, van Kleef M, Nelemans P. Clinical course of non-specific low back pain: a systematic review of prospective cohort studies set in primary care. Eur J Pain 2013 Jan;17(1):5-15. [doi: 10.1002/j.1532-2149.2012.00170.x] [Medline: 22641374]
7. Gaynor SM, Bortsov A, Bair E, et al. Phenotypic profile clustering pragmatically identifies diagnostically and mechanistically informative subgroups of chronic pain patients. Pain 2021 May 1;162(5):1528-1538. [doi: 10.1097/j.pain.0000000000002153] [Medline: 33259458]
8. Dunn KM, Jordan K, Croft PR. Characterizing the course of low back pain: a latent class analysis. Am J Epidemiol 2006 Apr 15;163(8):754-761. [doi: 10.1093/aje/kwj100] [Medline: 16495468]
9. Nijs J, Malfliet A, Roose E, et al. Personalized multimodal lifestyle intervention as the best-evidenced treatment for chronic pain: state-of-the-art clinical perspective. J Clin Med 2024 Jan 23;13(3):644. [doi: 10.3390/jcm13030644] [Medline: 38337338]
10. Geneen LJ, Moore RA, Clarke C, Martin D, Colvin LA, Smith BH. Physical activity and exercise for chronic pain in adults: an overview of Cochrane reviews. Cochrane Database Syst Rev 2017 Jan 14;1(1):CD011279. [doi: 10.1002/14651858.CD011279.pub2] [Medline: 28087891]

XSL•FO
RenderX

11. Williams ADC, Fisher E, Hearn L, Eccleston C. Psychological therapies for the management of chronic pain (excluding headache) in adults. Cochrane Database Syst Rev 2020 Aug 12;8(8):CD007407. [doi: 10.1002/14651858.CD007407.pub4] [Medline: 32794606]
12. Sayed D, Grider J, Strand N, et al. The American Society of Pain and Neuroscience (ASPN) evidence-based clinical guideline of interventional treatments for low back pain. J Pain Res 2022;15:3729-3832. [doi: 10.2147/JPR.S386879] [Medline: 36510616]
13. Roe M, Sehgal A. Pharmacology in the management of chronic pain. Anaesthesia & Intensive Care Medicine 2016 Nov;17(11):548-551. [doi: 10.1016/j.mpaic.2016.08.010]
14. Breugelmans L, Smeets R, Köke AJA, Winkens B, Oosterwijk RFA, Beckers L. Outpatient interdisciplinary multimodal pain treatment programme for patients with chronic musculoskeletal pain: a longitudinal cohort study. Disabil Rehabil 2025 Mar;47(5):1114-1125. [doi: 10.1080/09638288.2024.2364822] [Medline: 38910313]
15. Nicholas MK, Blyth FM. Are self-management strategies effective in chronic pain treatment? Pain Manag 2016;6(1):75-88. [doi: 10.2217/pmt.15.57] [Medline: 26678703]
16. Pfeifer AC, Uddin R, Schröder-Pfeifer P, Holl F, Swoboda W, Schiltenwolf M. Mobile application-based interventions for chronic pain patients: a systematic review and meta-analysis of effectiveness. J Clin Med 2020 Nov 5;9(11):3557. [doi: 10.3390/jcm9113557] [Medline: 33167300]
17. Mirzaei M, Aspin C, Essue B, et al. A patient-centred approach to health service delivery: improving health outcomes for people with chronic illness. BMC Health Serv Res 2013 Jul 3;13(1):251. [doi: 10.1186/1472-6963-13-251] [Medline: 23819721]
18. Lalloo C, Jibb LA, Rivera J, Agarwal A, Stinson JN. "There's a Pain App for That": review of patient-targeted smartphone applications for pain management. Clin J Pain 2015 Jun;31(6):557-563. [doi: 10.1097/AJP.0000000000000171] [Medline: 25370138]
19. Moreno-Ligero M, Moral-Munoz JA, Salazar A, Failde I. mHealth intervention for improving pain, quality of life, and functional disability in patients with chronic pain: systematic review. JMIR Mhealth Uhealth 2023 Feb 2;11(1):e40844. [doi: 10.2196/40844] [Medline: 36729570]
20. Piguet V, Mazouri S, Rochat J, Ehrler F, Cedraschi C, Luthy C. Applications mobiles et autogestion des douleurs chroniques [mobile applications and self-management of chronic pain]. Revue Médicale Suisse 2020;16(700):1367-1371. [doi: 10.53738/REVMED.2020.16.700.1367]
21. Perrin Franck C, Babington-Ashaye A, Dietrich D, et al. iCHECK-DH: guidelines and checklist for the reporting on digital health implementations. J Med Internet Res 2023 May 10;25:e46694. [doi: 10.2196/46694] [Medline: 37163336]
22. Dolodoc. University Hospitals of Geneva. URL: https://www.hug.ch/application-mobile/dolodoc [accessed 2024-02-20]
23. Main languages, languages spoken at home and at work. Federal Statistical Office. 2024. URL: https://www.bfs.admin.ch/bfs/fr/home/statistiques/population/langues-religions/langues.html [accessed 2024-02-10]
24. Wisniewski H, Torous J. Digital navigators to implement smartphone and digital tools in care. Acta Psychiatr Scand 2020 Apr;141(4):350-355. [doi: 10.1111/acps.13149] [Medline: 31930477]
25. Chaudoir SR, Dugan AG, Barr CHI. Measuring factors affecting implementation of health innovations: a systematic review of structural, organizational, provider, patient, and innovation level measures. Implement Sci 2013 Feb 17;8(1):22. [doi: 10.1186/1748-5908-8-22] [Medline: 23414420]
26. Ledel Solem IK, Varsi C, Eide H, et al. Patients' needs and requirements for ehealth pain management interventions: qualitative study. J Med Internet Res 2019 Apr 1;21(4):e13205. [doi: 10.2196/13205] [Medline: 30877780]

Abbreviations

HUG: University Hospitals of Geneva
iCHECK-DH: Checklist for the Reporting on Digital Health Implementations
SIMED: Medical Information Science Department

Edited by C Perrin; submitted 22.01.25; peer-reviewed by H Witteman, Y Lee; revised version received 03.04.25; accepted 27.04.25; published 08.08.25.

Please cite as:
Ehrler F, Guebey J, Rochat J, Gosetto L, Rehberg B, Lovis C, Molinard-Chenu A
Dolodoc, an App to Leverage Self-Management of Chronic Pain: Design, Development, and Implementation Report
JMIR Med Inform 2025;13:e71597
URL: https://medinform.jmir.org/2025/1/e71597
doi:10.2196/71597

XSL•FO
RenderX

© Frederic Ehrler, Julie Guebey, Jessica Rochat, Laetitia Gosetto, Benno Rehberg, Christian Lovis, Aude Molinard-Chenu. Originally published in JMIR Medical Informatics (https://medinform.jmir.org), 8.8.2025. This is an open-access article distributed under the terms of the Creative Commons Attribution License (https://creativecommons.org/licenses/by/4.0/), which permits unrestricted use, distribution, and reproduction in any medium, provided the original work, first published in JMIR Medical Informatics, is properly cited. The complete bibliographic information, a link to the original publication on https://medinform.jmir.org/, as well as this copyright and license information must be included.

XSL•FO
RenderX

Leveraging Interoperable Electronic Health Record (EHR) Data for Distributed Analyses in Clinical Research: Technical Implementation Report of the HELP Study

Julia Palm[1*]; Kutaiba Saleh[2*]; André Scherag[1]; Danny Ammon[2]

[1]Institute of Medical Statistics, Computer and Data Sciences, Jena University Hospital, Bachstraße 18, Jena, Germany

[2]Data Integration Center, Jena University Hospital, Jena, Germany

[*]these authors contributed equally

Corresponding Author:
Julia Palm
Institute of Medical Statistics, Computer and Data Sciences, Jena University Hospital, Bachstraße 18, Jena, Germany

Abstract

Background: The Medical Informatics Initiative (MII) Germany established 38 data integration centers (DIC) in university hospitals to improve health care and biomedical research through the use of electronic health record (EHR) data. To showcase the value of these DIC, the HELP (Hospital-wide Electronic Medical Record Evaluated Computerized Decision Support System to Improve Outcomes of Patients with Staphylococcal Bloodstream Infection) study was initiated as a use case. This study is a clinical trial designed to assess the impact of a computerized decision support system for managing staphylococcal bacteremia.

Objective: In this paper, we present the lessons learned during the use case from a technical perspective. This paper outlines the challenges encountered and solutions developed during our initial implementation of this infrastructure, providing insights applicable to other research platforms using EHR data. These insights are organized into 3 key areas: study-specific data definition and modeling, interoperable data integration and transformation, and distributed data extraction and analysis.

Methods: An interdisciplinary team of clinicians, computer scientists, and statisticians created a catalog of items to identify data elements necessary for the study's evaluation and developed a domain-specific information model. DIC developed extract-transform-load pipelines to collect the disparate, site-specific EHR data and to transform it into a common data format. Health Level Seven International (HL7) Fast Healthcare Interoperability Resources (FHIR) and the MII's core dataset profiles were adopted for consistent data representation across sites. Additionally, data not present in EHRs was gathered using structured electronic case report forms. Analysis scripts were then distributed to the sites to preprocess the data locally, followed by a central analysis of the preprocessed data to generate the final overall results.

Implementation (Results): Our analysis revealed significant heterogeneity in data quality and implementation of interoperability standards, requiring substantial harmonization efforts. The development of analysis scripts and data extraction processes demanded multiple iterative cycles and close collaboration with local data experts. Despite these challenges, the successful implementation demonstrated the feasibility of distributed EHR analyses while highlighting the importance of thorough data quality assessment, realistic timeline planning, and multidisciplinary expertise.

Conclusions: The HELP study highlights challenges and opportunities in leveraging EHR data for clinical research, particularly in the absence of mandatory data standards and resource-intensive data harmonization efforts. Despite limitations in data availability and quality, progress in digitization and interoperability frameworks offers hope for future improvements. Lessons learned from this study can inform the development of standardized methodologies and infrastructures for sustainable EHR data integration in research.

(JMIR Med Inform 2025;13:e68171) doi:10.2196/68171

KEYWORDS

clinical decision support system; data collection methods; electronic health records; health information interoperability; software design

XSL•FO
RenderX

Introduction

Context

The digitization of the health sector has significantly increased interest in using electronic health record (EHR) data for biomedical research, leading to the development of new infrastructures for data integration and sharing. In line with this trend, the Medical Informatics Initiative (MII) Germany established 38 data integration centers (DIC) in university hospitals to improve health care and biomedical research based on EHR data [1,2]. To demonstrate the usefulness of these DIC, several use cases were designed, encompassing various studies that leveraged the DIC infrastructure. One notable use case was the HELP (Hospital-wide Electronic Medical Record Evaluated Computerized Decision Support System to Improve Outcomes of Patients with Staphylococcal Bloodstream Infection) [3] study, which aimed to enhance the clinical management of *Staphylococcus* bacteremia. This condition requires prompt and guideline-compliant treatment. While involving an infectious disease specialist can improve patient outcomes, immediate access to these specialists is not always available. From June 2020 to October 2022, the HELP trial explored whether a computerized decision support system (CDSS) could safely enhance the standard of care for these patients. Conducted as a multicenter, noninferiority, interventional stepped-wedge cluster randomized controlled trial at 5 German university hospitals, the CDSS assisted physicians in managing bacteremia until an infectious disease specialist became available. It was deployed as a website with an interactive decision tree, accessible via smartphones, desktops, or laptops. An archived version of the CDSS is available online [4].

Problem Statement

Clinical evaluation of interventions such as the HELP CDSS through traditional randomized controlled trials is resource-intensive, particularly due to extensive data collection and management requirements. However, much of this necessary data already exists within EHR but remains largely inaccessible due to proprietary data formats and fragmented storage across multiple systems. The MII addresses this challenge by collecting, harmonizing, and transforming this data into interoperable standards, making it readily available for studies like HELP. By using EHR data for the evaluation of interventions in clinical trials, we can blend the characteristics of traditional randomized controlled trials with the practicality of being embedded within the clinical routine. While this setup imposes some restrictions on data availability and quality, it may more closely mirror real-world clinical scenarios, potentially contributing to an improved ecological validity of the trial [5]. Mc Cord et al [6] recently showed that randomized trials using routinely collected data show lower, but likely more realistic, effect estimates than traditional trials. Since this effect persists even when controlling for data quality, the authors suggest that trials using routinely collected data are less prone to overoptimistic treatment adherence and related biases. Even if one may not agree to use EHR data for the most important outcomes, secondary use of EHR data has the potential to reduce the documentation burden associated with traditional trials, offering a more pragmatic study design [7].

While the clinical results of the trial are published elsewhere [8], this manuscript details the lessons learned from the technical perspective.

Methods

Aims and Objectives

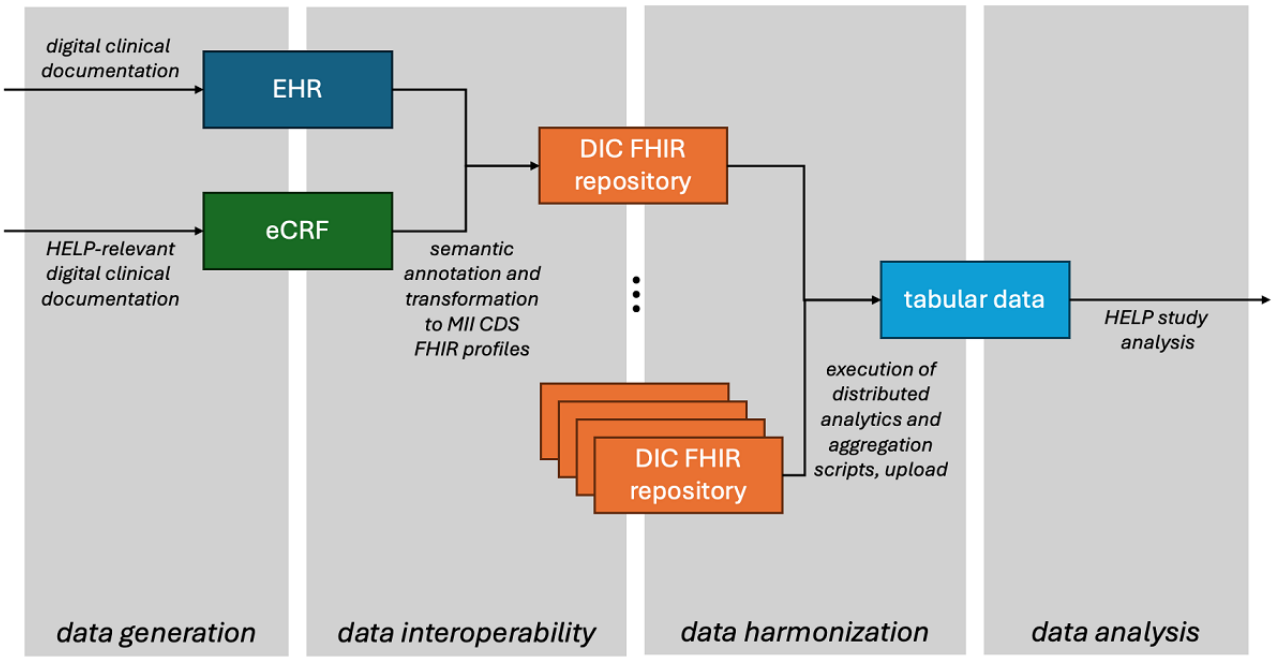
Our study was designed as a proof of concept of a distributed analysis approach combining EHR data with structured electronic case report form (eCRF) data to evaluate outcomes of a randomized clinical trial. This implementation aimed to illustrate how the secondary use of EHR data can streamline clinical trial processes.

Blueprint Summary

To gather data for analysis, the trial used a hybrid data collection approach and relied on the DIC structures for data extraction, transformation, and harmonization (Figure 1). Data available from EHRs were collected directly, while additional data were gathered via eCRFs. All data, regardless of source, were collected in the DIC and transformed into an interoperable, standardized format.

XSL•FO
RenderX

Figure 1. Overall data flow in the HELP (Hospital-wide Electronic Medical Record Evaluated Computerized Decision Support System to Improve Outcomes of Patients with Staphylococcal Bloodstream Infection) study, based on interoperable formats created in data integration centers (DIC). EHR: electronic health record; eCRF: electronic case report form; FHIR: Fast Healthcare Interoperability Resources; MII CDS: core dataset of the Medical Informatics Initiative.



Technical Design

Study-Specific Data Definition and Modeling

At the outset of the study, a comprehensive, study-specific data dictionary, a catalog of items (COI) was developed to serve as a reference for each DIC, detailing the specific data that needed to be extracted from the EHR. The initial version of the COI was developed in several modeling sessions involving at least 2 infectious disease specialists, at least 1 statistician, and at least 2 medical informaticians from the DIC. In these sessions, under the guidance of DIC staff, the following results were achieved:

1. Clinical definition of evidence-based treatment procedures for suspected staphylococcal bloodstream infections (prepared with relevant studies by medical staff from different disciplines).
2. Development of a visualized algorithm for the treatment steps in BPMN format (based on modeling expertise of DIC staff).
3. Identification of critical data and time points that are essential for the evaluation of the patient's status as well as the study results (prepared based on treatment and analysis expertise of medical and statistical staff with different hierarchy levels).
4. Mapping of these data and time points to a COI (prepared using COI development templates by DIC staff).

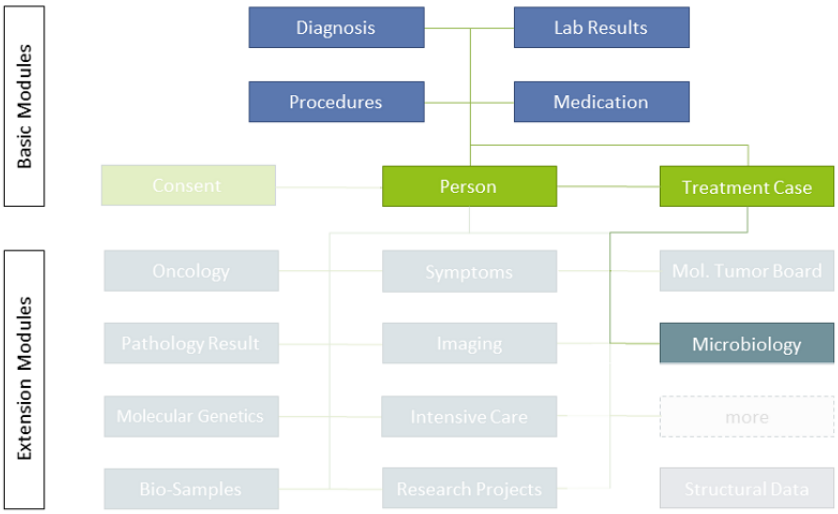
The interdisciplinary collaboration allowed infectious disease specialists and experts in medical microbiology to contribute their expertise and ensure comprehensive requirements gathering, while DIC staff coordinated the collection and specification of the COI to ensure consistency, completeness, and suitability for further technical specification. Initially, an extensive spreadsheet was created, containing all identified items. This spreadsheet included detailed information on each item, such as its name, data source, and categorization. For illustrative purposes, this tabular COI has been published [9]. In the next step, the items needed to be further specified. Precise names, properties, and relationships between items can be documented and visualized by developing a domain-specific information model [10]—a process also used in the MII [11]. Given the complexity of clinical data, information models ensure clarity, relationships, and visualization between required items, allowing for semantic enrichment of information that can be useful in later analysis. Various notations can be used for information modeling; in the HELP study, the ART-DECOR tool (version 2.2), developed for the standardization of health data, was used [12]. This approach ensured that details such as the dosage of relevant antibiotics for patients were represented correctly [13]. Thus, domain-specific modeling is the first step toward creating an interoperable data basis across multiple locations.

Interoperable Data Integration and Transformation

To facilitate multicenter biomedical research projects based on secondary use of EHR data with the newly established DIC [14], the contents of the EHR in the German university hospitals had to be made accessible gradually. Beginning in 2017, the MII Interoperability Working Group therefore started to define the MII core dataset (CDS; see Figure 2), which separates basic, consistently required data elements of EHR from discipline-specific elements through modularization [11]. Implementing the CDS, the DIC started by providing access to data from the basic modules across all locations and then successively included the extension modules based on current research projects at each location. The HELP study was part of these efforts, using data from both basic and extension modules of the CDS.

XSL•FO
RenderX

Figure 2. Illustration of modules of the Medical Informatics Initiative (MII) core dataset. The HELP (Hospital-wide Electronic Medical Record Evaluated Computerized Decision Support System to Improve Outcomes of Patients with Staphylococcal Bloodstream Infection) study used the basic modules "person," "treatment case," "diagnosis," "procedures," "lab results," "medication" [15], and the extension module "microbiology" [16].



The step-by-step implementation of the CDS is due to the wide variety of primary documentation systems (hospital information systems, intensive care systems, laboratory information systems, etc) from different vendors operating in German hospitals, whose data together comprise the contents of an EHR. DIC have been designed to eliminate the need for data scientists to collect and merge proprietary formats from different systems and locations repeatedly for every project.

Within the MII, a consensus was reached to use Health Level Seven International (HL7) Fast Healthcare Interoperability Resources (FHIR) for the technical representation and exchange of CDS data across DIC [11]. Despite some limitations for secondary data use, this standard was chosen based on its ability to support a wide variety of research questions and based on its relevance as a common standard for EHR in the German and European health care system in the future [17]. Adopting a health care interoperability standard enables site- and vendor-independent EHR data representation, explicating data properties through a variety of metadata [17-19]. To address specifics of the German health care system (eg, national terminologies), secondary use requirements (eg, custom search parameters), and FHIR usage guidelines, the MII CDS modules were developed as FHIR profiles derived from the international standard. These profiles were balloted and published in the form of implementation guides for application in the DIC [11]. For the HELP study, the relevant modules of the MII CDS could be identified based on the established COI (Figure 2).

The subsequent phase thus involved integrating the data elements required for the HELP study from the various primary documentation systems in all participating locations and transforming them to the FHIR format of the MII CDS modules in the DIC. At the time of the HELP study, the majority of hospitals in Germany did not yet have FHIR interfaces for their EHR systems and thus hardly any interoperable access to the data required for use. The most important task for the DIC in the process of being established was therefore the identification and connection of data source systems. The relevant EHR data are captured in different IT systems, which also had to be connected in different ways: the hospital information system for patient master data, patient movement data, diagnoses, and procedures; the laboratory information system for laboratory tests and microbiology results; and the clinical workplace system or the e-medication system for medication administrations. These connections were established by implementing ETL (extract-transform-load) pipelines for data integrations either directly from the persistence layers or database systems of the source systems or by processing already exchanged message formats for communication between the clinical IT systems—in particular HL7v2, which is often used in Germany, with many proprietary extensions. The selection of the specific connection method is highly location- and vendor-dependent. Due to the hybrid data collection approach of the study, which included the use of eCRFs for data not accessible in the EHR, the data collected via eCRFs also had to be transformed into the FHIR format, for which a separate eCRF2FHIR transformation tool was developed.

Distributed Data Extraction and Analysis

The FHIR standard's use of JSON or XML as notation, its alignment with contemporary web API (Application Programming Interface) practices, and its resource-based data modeling approach are optimized for modern implementation as well as for the precise representation of health care information. The nested JSON data structure is particularly useful to accommodate a number of the FAIR (Findable,

XSL•FO
RenderX

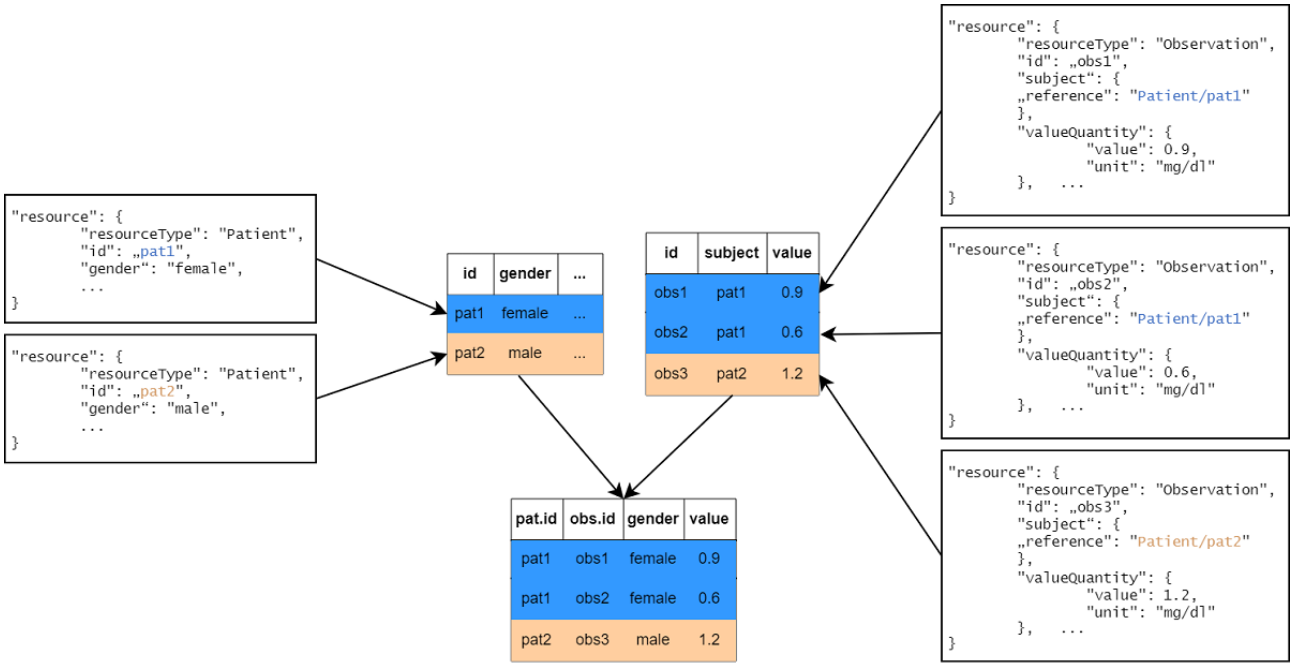
Accessible, Interoperable, Reusable) principles [20], especially that data should be enhanced with "rich metadata" and be "richly described with a plurality of accurate and relevant attributes." Even beyond the use of FHIR in health care settings, JSON and similar nested data formats have been gaining popularity for big data and open data repositories [21,22]. In the health care context, FHIR benefits significantly from the flexibility of nested structures. This is because the dynamic nature of health care data, with its varying elements and data types, is more accurately represented in nested structures than in traditional tabular data formats.

The statistical analysis in our study, however, required tabular data, as most common data analysis techniques do. To make the FHIR data available for this statistical analysis, we therefore transformed the FHIR data into tables using the *fhircrackr* package (version 2.1) [23] within the R statistical computing environment (version 4.1) [24]. Despite all harmonization efforts, both the primary data from the EHR and their FHIR implementation were expected to be at least partly different across the 5 study sites. Consequently, we developed individual data extraction and tabularization scripts for each DIC, taking into account the local characteristics of the data. The scripts, versioned and distributed via a GitLab repository, queried the required data from the respective FHIR server, tabularized it, and performed local aggregation and anonymization steps.

A crucial step in the data analysis was the classification of patients into intervention versus control conditions, followed by the identification and extraction of all study-relevant data items for those patients. In the stepped-wedge design, clinical wards are assigned to the intervention and control conditions, instead of individual patients [25]. Thus, the classification of a patient into either the control or intervention group was based on the ward where the patient was treated when they received their first blood culture result indicating a possible Staphylococcus infection. This required querying data from different data sources represented at each DIC and was implemented by the following overall workflow: (1) process questionnaire data from the eCRFs to identify all patients participating in the trial; (2) analyze encounter data to track patient movement through wards; (3) review medical microbiology reports to identify the first blood culture positive for *Staphylococcus*; (4) link the medical microbiology report dates with the encounter data to determine whether the patient was on a control or intervention ward at the time of the positive blood culture result; and (5) download and tabularize all data for the primary or secondary endpoint analysis as well as for the clinical description of the patient cohort.

FHIR resources containing the relevant data were processed by type, with a separate table created for each resource type during the initial tabularization step. The information from different resources was then connected by joining these tables based on the references linking the original FHIR resources (see Figure 3).

Figure 3. One table was created per resource type; afterwards, tables were joined based on references.



The statistical analysis of the trial data was divided into 2 parts. The first analysis step was conducted locally at each DIC to remove patient-identifying information and aggregate the data where possible, thereby minimizing the risk of re-identification. The data was processed based on its importance for the trial evaluation. Data for the primary and secondary endpoints were maintained at the patient level to maximize statistical power in the central analysis. These data were reduced to the minimal set of variables necessary for statistical analysis and sent to Jena for central analysis using generalized linear mixed models [26]. Conversely, data needed for the clinical description of the study population were aggregated at each site (eg, to mean and SD or counts) and then centrally combined using meta-analytic methods. All data were transferred to the central analysis site manually via a securely provided cloud, since the central MII infrastructure for data sharing was not established yet [27].

XSL•FO
RenderX

Implementation (Results)

Outcomes

Study-Specific Data Definition and Modeling

Identification and explicit description of the data to be used in the study constituted the first step, but creating a finalized, binding version of the COI proved to be an iterative and complex process. A major challenge was the varying status of available data and its assessment regarding clinical priorities, which required a continuous refinement of the COI even during the data integration and transformation phase. Throughout the data extraction process, we encountered numerous occasions where the data found in the EHR did not match the items from the COI exactly, requiring repeated consultations with infectious disease specialists and DIC employees to clarify specific datasets.

We initially planned to use project-specific FHIR profiles for the HELP use case and started with their development. However, both the amount of work involved in generating profiles derived from the CDS and tailored to the project and the unclear benefits—as compliance with the stricter requirements of project-specific profiles at the sites could not be verified—made it questionable whether the time saved in the analysis by project-specific FHIR implementation guides justified these efforts. Consequently, we did not complete the profiling work, but the results and experiences were incorporated into the further development of the CDS extension modules. The reliance on interoperability standards for data analysis must be investigated further in future projects [28].

Interoperable Data Integration and Transformation

Both the transformation of proprietary, vendor- and location-specific health care data into interoperability standards and the processing of such interoperable data for analysis in a research study required the development of software tools: ETL pipelines, semantic annotation and mapping programs, structure conversions for data analysis, and data analysis scripts. Project-specific software development, however, inadvertently causes errors and bugs, most of which can only be found when the software is used practically in the intended context. Consequently, software development required significant time during the study, which is unsurprising given that many of the tasks the software addressed were novel to this project. However, this time investment is only justifiable if the software can be reused in future projects; otherwise, it is not sustainable.

The main obstacle during data extraction and transformation was the varying quality of the EHR data, which we encountered in 3 distinct forms:

1. In cases where data are entered manually into the EHR, the person documenting it may be rushed or may not consider it important to ensure accuracy. As a result, manual data entries can contain errors, which may be corrected later or remain, leading to inconsistencies or contradictions in the extracted data.
2. Many entries in EHR are only given in free text form and do not provide semantically annotated information. This prevented the processing of the contained information in the HELP study and led to the described approach of hybrid documentation.
3. Even structured data are not always unconditionally machine-readable. An example is the coding of measurement units in laboratory data. In communication between clinicians, variations in how a measurement unit is presented, how a formula is formatted, or even minor errors in notation are typically understood in context due to the clinician's background knowledge. Figure 4, for example, represents 4 different notations of alanine aminotransferase (ALT) and aspartate aminotransferase (AST) measurement units encountered in an EHR. While any clinician can easily see that the unit described is µmol/(l * s), computers are unable to interpret these discrepancies without explicit standardization.

XSL•FO
RenderX

Figure 4. Examples for units of measurement for alanine aminotransferase (ALT) and aspartate aminotransferase (AST) in German laboratory results, captured from a PDF.

Furthermore, relevant data were captured at different locations and by different individuals using different software, which can also change over time [29]. One possible countermeasure to those differences would have been a stricter specification of uniform data, which can be achieved through project-specific FHIR profiling with more extensive constraints than those provided by the MII CDS. However, this was not feasible within the HELP study (cf previous paragraph).

Distributed Data Extraction and Analysis

As a result of the heterogeneity of the primary data described earlier, the data provided by the 5 DIC showed substantial heterogeneity as well. Although all DIC theoretically follow a comparable IT and service architecture [11], their practical implementations vary significantly, often due to local requirements. Differences emerged even at the initial access stage: some DIC required analysis scripts to be delivered in Docker containers, while others only accepted plain R scripts to be executed by DIC employees. Additionally, some DIC had installed a FHIR repository dedicated solely to the HELP use case, containing data only for study participants, whereas other DIC used a single, comprehensive FHIR repository with all available data. This necessitated individualized querying routines that were developed in a highly iterative workflow and close collaboration with each DIC.

On the next level, the implementation of the FHIR resources differed significantly (see Figure 5). Although all resources were supposed to conform to the same profiles defined in the CDS, we identified two major sources of variation. First, the DIC differed in the primary data sources connected at the time of the study. For example, diagnoses originated from data exports for subsequent billing by the hospitals at some DIC and from clinical documentation during patient treatment at others. This resulted in varying FHIR resources, as specific data elements were not available in some sources (eg, the diagnosis date in billing data) and led to different interpretations (eg, diagnoses optimized for billing purposes after treatment versus purposes during treatment). Second, the implementation of profile-conformant FHIR resources was at different stages. For instance, the CDS provides a multilevel model for representing encounter data that aligns with the administrative structure of a German hospital. However, at the time of the study, only 1 of the 5 DIC had fully implemented this complex model, while the other 4 used more rudimentary, simplified representations.

XSL•FO
RenderX

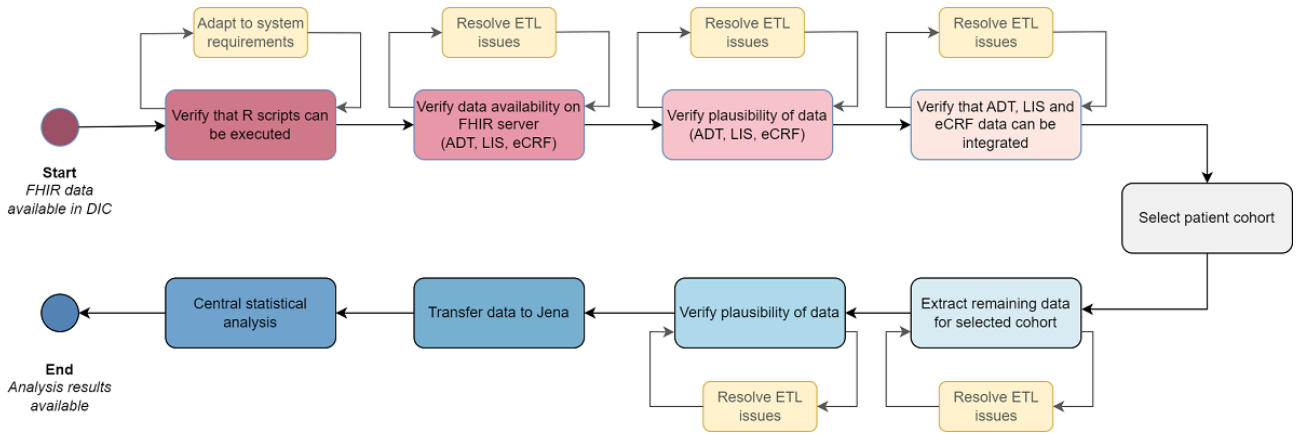
Figure 5. Two exemplary FHIR (Fast Healthcare Interoperability Resources) resources, illustrating potential differences despite adhering to the same FHIR profile. Elements that exist in both resources but contain different codes are highlighted in yellow, while elements present in only 1 resource are marked in red. The resources have been shortened and anonymized.


```
{
    "resourceType": "Observation",
    "status": "final",
    "category": [{
            "coding": [{
                    "system": "
                    http://terminology.hl7.org/CodeSystem/observation-category"
                    "code": "laboratory",
                    "display": "Laboratory"
                },{
                    "system": "http://loinc.org",
                    "code": "26436-6",
                    "display": "Laboratory studies (set)"
                }
            ]
        }
    ],
    "code": {
        "coding": [{
                "system": "https://uk2.de/LAB/Nexus/Swisslab/Observation/Code",
                "version": "1.0.0",
                "code": "zBILI",
                "display": "Bilirubin (gesamt)"
            }, {
                "system": "http://loinc.org",
                "code": "1975-2"
            }
        ]
    },
    "subject": {
        "reference": "Patient/d34bsdtn658q32werfdvfxfgu8j8345"
    },
    "effectiveDateTime": "2021-01-30T01:01:00+01:00",
    "issued": "2021-01-30T01:01:00+01:00",
    "valueQuantity": {
        "value": 0.6,
        "unit": "mg/dl"
        "system": "http://unitsofmeasure.org",
        "code": "mg/dL"
    }
}
```

```
{
    "resourceType": "Observation",
    "status": "final",
    "category": [{
            "coding": [{
                    "system": "
                    http://terminology.hl7.org/CodeSystem/observation-category",
                    "code": "laboratory",
                    "display": "Laboratory"
                }, {
                    "system": "http://loinc.org",
                    "code": "26436-6",
                    "display": "Laboratory studies (set)"
                }
            ]
        }
    ],
    "code": {
        "coding": [{
                "system": "http://loinc.org",
                "code": "14631-6",
                "display": "Bilirubin.total [Moles/volume] in Serum or Plasma"
            }, {
                "system": "http://www.ukl.de/CodeSystem/ILM/analyt",
                "code": "BILI_S",
                "display": "BILI_S"
            }
        ]
    },
    "subject": {
        "reference":
        "Patient/deb5d5f1e5fbdddb1e80adfa6231e1f9e1c0a2720a6aedd72fb18ec6c0cd60c2"
    },
    "encounter": {
        "reference":
        "Encounter/cb5077b7c795955f8b4692ffe38cd0b971031524759443 7b0484547e1cbd3543"
    },
    "effectiveDateTime": "2020-10-13T08:22:48+01:00",
    "valueQuantity": {
        "value": 6.1,
        "unit": "µmol/l",
        "system": "http://unitsofmeasure.org",
        "code": "umol/L"
    }
}
```


These sources of data heterogeneity, which persisted even after being transformed to an interoperable format, had to be addressed through harmonization during data extraction and analysis. According to Nguyen [30], interoperability involves the transactional sharing of health care data, while data harmonization integrates data from multiple sources to preserve context and normalize meanings across datasets. FHIR, as an interoperability standard, allows for unified data representation from different sources but does not address data harmonization, which requires understanding the context and meaning of the data. While FHIR resources can provide context in the form of metadata (eg, indicating whether a diagnosis originated from billing or clinical information), managing these different contexts in the analysis is a task of harmonization. In multicenter projects like HELP, it is crucial to recognize that no single person can anticipate the heterogeneous data across all study sites. This is because understanding such data requires site-specific information about the clinical routines and the distinct features of the individual information systems used at each location. In our case, the harmonization therefore required numerous iterations of communication and script adaptation with the respective data providers. To ensure feasibility, we broke the extraction process down into manageable subtasks as depicted in Figure 6. Each subtask was iterated with each DIC until it produced plausible results.

Figure 6. Iterative data extraction and analysis process in the HELP (Hospital-wide Electronic Medical Record Evaluated Computerized Decision Support System to Improve Outcomes of Patients with Staphylococcal Bloodstream Infection) study. FHIR: Fast Healthcare Interoperability Resources; DIC: data integration center; ADT: admission, discharge, and transfer data; LIS: laboratory information system; eCRF: electronic case report form; ETL: extract-transform-load.



The infrastructure for our distributed analysis needed to be straightforward to implement, flexible, and compliant with strict privacy regulations for health data. The requirement for stringent data protection precluded the use of any cloud computation services. Additionally, the need for simplicity ruled out established privacy-preserving solutions like DataSHIELD [31], as setting up a dedicated OPAL server at each DIC was not feasible for this study. Instead, we opted for a straightforward infrastructure by distributing plain R scripts via GitLab and Docker images through Docker Hub. Overall, the script

XSL•FO
RenderX

development process was extremely time-consuming, partly because the technical infrastructure and FHIR mapping were still under construction during the analysis. While this helped identify problems in DIC development early on, it required more iterations than anticipated.

Lessons Learned

Overview

The lessons learned presented in this paper emerged from systematic observations and collaborative discussions throughout our study's implementation phase. Our experience demonstrates that distributed analyses using EHR data are feasible but require careful planning and consideration of key challenges. While these insights were primarily derived from our experiences within the MII, they extend beyond this framework and offer valuable guidance for researchers planning clinical trials that incorporate EHR data. Based on our experience implementing distributed analyses, we identified 3 fundamental considerations that warrant careful attention during the project-planning phase. These insights are particularly relevant for study coordinators and researchers who aim to leverage EHR data in clinical research, regardless of their institutional context.

The Precise Definition and Quality Assessment of Required Data Elements are Paramount

While interoperable EHR formats facilitate data exchange, they do not inherently resolve underlying data quality issues. Rather, standardization tends to illuminate existing quality challenges, making thorough preliminary data quality assessment essential. Researchers must realistically evaluate whether available EHR data meets the quality thresholds necessary for their specific research objectives.

Project Timelines Should Accommodate Iterative Development and Refinement Cycles

The notion of plug-and-play solutions for analyzing EHR data across different institutions proves unrealistic in practice. Scientific research inherently involves trial and error, particularly when working with heterogeneous EHR data sources. Successfully navigating these iterations requires sufficient time allocation in project planning.

Team Composition Significantly Influences Project Success

Effective distributed EHR analysis demands a multidisciplinary approach, combining team members with complementary expertise. Essential roles include local data stewards with intimate knowledge of institutional data structures, alongside specialists who understand various aspects of EHR data utilization. This diversity of perspectives enables comprehensive problem-solving and robust methodology development.

Discussion

Principal Results

The HELP study was designed as a use case for the secondary use of EHR data, limited to 5 university hospitals participating in the MII in Germany. Therefore, the lessons learned in this paper apply specifically to this context. The study commenced in the early phases of DIC development, which introduced challenges that may be resolved over time. A key issue was the absence of mandatory data standards in Germany's health care, which complicated our efforts. However, the implementation of national standards is anticipated in the future [32], and such standards are essential for efficient multicenter secondary EHR data usage. In this regard, the DIC were pioneers in applying HL7 FHIR in German university hospitals. Nonetheless, the processing of FHIR remains subject to optimization, as we were unable to develop and apply project-specific information models and FHIR profiles for the HELP study as intended. This was largely due to the extensive workload required for profiling as well as data integration and transformation, which fell on small teams. In particular, not every EHR data use project can be expected to have the resources and expertise in FHIR profiling to be able to technically express project-specific data requirements.

For some phases of the study, other methods of data harmonization could also have been considered. For example, a Common Data Model can be used to harmonize cross-site datasets, with Observational Medical Outcomes Partnership (OMOP) [33] playing a particularly important role in the area of health data. However, due to the mandatory use of international terminologies and the incompatibility of national specifications or site-specific data properties, various relevant data items could not be represented in OMOP for the German HELP study either, as has already been shown for the MII CDS [34,35]. Examples include the vital status within 90 days, blood culture results, or hospital readmission after discharge, which would have required additional logic or custom extensions in OMOP, while FHIR offered more flexible options through resources like Observation and Encounter. Common Data Models, in turn, remain highly relevant for use in internationally conducted observational studies.

It is evident that the scalability of any comparable cross-facility research project is impaired by the divergent clinical documentation in facilities and their specialist departments, which can vary greatly in details due to different manufacturers, different billing forms, and individual decisions, especially complicating distributed analyses. The enhancement of secondary use can only be achieved through the implementation of billing-independent ontologies such as SNOMED CT for the semantic annotation of clinical data [17], as is envisaged for the European Health Data Space (EHDS [36]), for instance.

In the HELP study, data availability posed a significant challenge, particularly regarding patient movement between wards as well as medication records. These data types were often difficult to use due to their manual documentation and their frequent updates in many settings. A broader issue was the lack of standardized formats for certain data, with some not being available digitally at all. To address these limitations, we supplemented the existing data collection with additional eCRF. However, during the course of the study, digitization of clinical documentation increased, offering hope that such challenges may be mitigated in future research.

In addition to data availability challenges, we encountered significant data quality issues during both data transformation

XSL•FO
RenderX

to interoperable standards and subsequent analysis. While several formal frameworks exist for assessing and improving EHR data quality—notably the framework proposed by Kahn et al [37], which has gained traction in the MII [38,39]—these were not yet robustly established for FHIR-based data at the time of our study. Our experience underscores the critical need for standardized data quality assessment methodologies, and future research in the field should systematically explore and implement comprehensive frameworks like that proposed by Kahn et al.

While a distributed analysis approach, as used in our study, is not statistically ideal—centralized, patient-level analyses provide greater flexibility and statistical power—it was the only feasible method given the ethical and data protection constraints induced by not being able to obtain informed consent from every participant. In the future, our manual approach to distributed analysis will likely be replaced by more formal frameworks for distributed analysis of EHR data, incorporating FHIR-based APIs. Examples include the Personal Health Train [40] and the Federated Learning and Analysis in Medicine platform [41]. These platforms, however, were not available at the time of the HELP study [42].

Comparison to Other EHR Data Applications

Since the start of the HELP use case, several other use cases have emerged within the MII. Zoch et al [43] highlight lessons learned from studies on rare diseases conducted in the MII context, many of which align with our findings. For instance, they also emphasize the importance of multidisciplinary teams in successful data use projects and the need for a solid understanding of EHR data sources. Building on their insights, we took a broader view of secondary data use, abstracting beyond the specific MII structures. Additionally, we place greater emphasis on the iterative nature required for projects of this kind.

Extending the scope beyond Germany, many countries have undertaken initiatives similar to the MII to develop infrastructures for the secondary use of EHR data. Notable examples include the Dutch Health-RI initiative, the Swiss Personalized Health Network, and the US National Patient-Centered Clinical Research Network. These initiatives share a common goal: to collect and standardize EHR data for research purposes. In Europe, these efforts will soon be consolidated under the EHDS [36], which aims to create a unified infrastructure for the secondary use of EHR data across the continent. It is our hope to share the lessons learned from this project and use them to shape the integration efforts of the various approaches.

Conclusions

In this paper, we have shared key insights from conducting a clinical trial that leveraged EHR data. By applying these lessons and fostering cross-institutional collaboration, we can advance toward more sophisticated and efficient use of interoperable EHR systems in clinical research. This approach, while challenging, has the potential to enhance our understanding of patient care and clinical outcomes, providing valuable insights that can inform both clinical practice and future research endeavors. As the field continues to evolve, the lessons learned from current implementations will serve as important guideposts for developing robust and sustainable approaches to EHR data integration in clinical research.

Acknowledgments

This work was supported by the German Federal Ministry of Education and Research (grant numbers for the 5 study centers are Jena University Hospital: 01ZZ1803C, Halle University Hospital: 01ZZ1803N, Leipzig University Hospital: 01ZZ1803D, Aachen University Hospital: 01ZZ1803B, and Essen University Hospital: 01ZZ1803P). The German Federal Ministry of Education and Research also funded part of the project as part of the funding program “quantum technologies – from basic research to market”; contract number: 13N15711.

Data Availability

The tabular catalog of items and HELP (Hospital-wide Electronic Medical Record Evaluated Computerized Decision Support System to Improve Outcomes of Patients with Staphylococcal Bloodstream Infection) dataset in ART-DECOR are openly available as cited in the manuscript. The *fhircrackr* package is also openly accessible and actively developed on GitHub [44].

Conflicts of Interest

None declared.

Checklist 1
i-CHECK-DH checklist. i-CHECK-DH: Guidelines and Checklist for the Reporting on Digital Health Implementations.
[DOCX File, 15 KB - medinform_v13i1e68171_app1.docx]

References

1. Albashiti F, Thasler R, Wendt T, Bathelt F, Reinecke I, Schreiweis B. Data integration centers-from a concept in the Medical Informatics Initiative to its local implementation in the Network of University Medicine. Bundesgesundheitsblatt Gesundheitsforschung Gesundheitsschutz 2024 Jun;67(6):629-636. [doi: 10.1007/s00103-024-03879-5] [Medline: 38662020]

XSL•FO
RenderX

2. Gehring S, Eulenfeld R. German Medical Informatics Initiative: unlocking data for research and health care. Methods Inf Med 2018 Jul;57(S 01):e46-e49. [doi: 10.3414/ME18-13-0001] [Medline: 30016817]
3. Hagel S, Gantner J, Spreckelsen C, et al. Hospital-wide ELectronic medical record evaluated computerised decision support system to improve outcomes of Patients with staphylococcal bloodstream infection (HELP): study protocol for a multicentre stepped-wedge cluster randomised trial. BMJ Open 2020 Feb 10;10(2):e033391. [doi: 10.1136/bmjopen-2019-033391] [Medline: 32047014]
4. Pletz M, Hagel S, Kimmig A, et al. HELP CDSS v. 1.0.SMITH - smart medical information technology for healthcare. : Zenodo; 2024 URL: https://zenodo.org/records/10704513 [doi: 10.5281/zenodo.10704513]
5. van Berkel N, Clarkson MJ, Xiao G, et al. Dimensions of ecological validity for usability evaluations in clinical settings. J Biomed Inform 2020 Oct;110:103553. [doi: 10.1016/j.jbi.2020.103553] [Medline: 32891762]
6. Mc Cord KA, Ewald H, Agarwal A, et al. Treatment effects in randomised trials using routinely collected data for outcome assessment versus traditional trials: meta-research study. Br Med J 2021 Mar 3;372:n450. [doi: 10.1136/bmj.n450] [Medline: 33658187]
7. Mc Cord KA, Al-Shahi Salman R, Treweek S, et al. Routinely collected data for randomized trials: promises, barriers, and implications. Trials 2018 Jan 11;19(1):29. [doi: 10.1186/s13063-017-2394-5] [Medline: 29325575]
8. Palm J, Alaid S, Ammon D, et al. Leveraging electronic medical records to evaluate a computerized decision support system for Staphylococcus bacteremia. NPJ Digit Med 2025 Mar 28;8(1):180. [doi: 10.1038/s41746-025-01569-3] [Medline: 40148479]
9. HELP study group. HELP Study Data Dictionary/Catalog of Items: Zenodo; 2024. [doi: 10.5281/zenodo.13739833]
10. Schulz S, Stegwee R, Chronaki C. Standards in healthcare data. In: Kubben P, Dumontier M, Dekker A, editors. Fundamentals of Clinical Data Science: Springer; 2019:19-36. [doi: 10.1007/978-3-319-99713-1_3]
11. Ammon D, Kurscheidt M, Buckow K, et al. Interoperability Working Group: core dataset and information systems for data integration and data exchange in the Medical Informatics Initiative. Bundesgesundheitsblatt Gesundheitsforschung Gesundheitsschutz 2024 Jun;67(6):656-667. [doi: 10.1007/s00103-024-03888-4] [Medline: 38753022]
12. Heitmann K. ART-DECOR: an open-source tool bridging the chasm between clinicians and health IT. Health Level Seven International. 2014. URL: http://www.hl7.org/documentcenter/public/newsletters/HL7_NEWS_20140908.pdf [accessed 2025-07-21]
13. HELP study group. HELP dataset. ART-DECOR. 2018. URL: https://art-decor.org/ad/#/help-/datasets/dataset/2.16.840.1.113883.3.1937.777.22.1.1/2018-05-07T19:20:17 [accessed 2025-07-21]
14. Lehne M, Sass J, Essenwanger A, Schepers J, Thun S. Why digital medicine depends on interoperability. NPJ Digit Med 2019;2:79. [doi: 10.1038/s41746-019-0158-1] [Medline: 31453374]
15. Sass J, Zabka S, Essenwanger A, Schepers J, Boeker M, Thun S. Fast Healthcare Interoperability Resources (FHIR®) representation of medication data derived from German Procedure Classification Codes (OPS) using identification of medicinal products (IDMP) compliant terminology. Stud Health Technol Inform 2021 May 24;278:231-236. [doi: 10.3233/SHTI210074] [Medline: 34042899]
16. Rinaldi E, Drenkhahn C, Gebel B, et al. Towards interoperability in infection control: a standard data model for microbiology. Sci Data 2023 Sep 23;10(1):654. [doi: 10.1038/s41597-023-02560-x] [Medline: 37741862]
17. Vorisek CN, Lehne M, Klopfenstein SAI, et al. Fast Healthcare Interoperability Resources (FHIR) for interoperability in health research: systematic review. JMIR Med Inform 2022 Jul 19;10(7):e35724. [doi: 10.2196/35724] [Medline: 35852842]
18. Menzel F, Waltemath D, Henkel R. Exploring new possibilities for research data exploration using the example of the German Core Data Set. Stud Health Technol Inform 2023 May 18;302:749-750. [doi: 10.3233/SHTI230255] [Medline: 37203485]
19. Ulrich H, Behrend P, Wiedekopf J, Drenkhahn C, Kock-Schoppenhauer AK, Ingenerf J. Hands on the Medical Informatics Initiative Core Data Set - lessons learned from converting the MIMIC-IV. Stud Health Technol Inform 2021 Sep 21;283:119-126. [doi: 10.3233/SHTI210549] [Medline: 34545827]
20. Wilkinson MD, Dumontier M, Aalbersberg IJJ, et al. The FAIR Guiding Principles for scientific data management and stewardship. Sci Data 2016 Mar 15;3:160018. [doi: 10.1038/sdata.2016.18] [Medline: 26978244]
21. Möller M, Scharlau N, Klettke M. An empirical study of open data JSON files. Presented at: 23rd International Workshop on Design, Optimization, Languages and Analytical Processing of Big Data; Mar 23, 2021; Nicosia, Cyprus URL: https://ceur-ws.org/Vol-2840/#short9 [accessed 2025-07-21]
22. Yusof MK. Efficiency of JSON for data retrieval in Big Data. Indonesian J Elect Eng Comput Sci 2017;7(1):250. [doi: 10.11591/ijeecs.v7.i1.pp250-262]
23. Palm J, Meineke FA, Przybilla J, Peschel T. "fhircrackr": An R Package Unlocking Fast Healthcare Interoperability Resources for Statistical Analysis. Appl Clin Inform 2023 Jan;14(1):54-64. [doi: 10.1055/s-0042-1760436] [Medline: 36696915]
24. The R project for statistical computing. URL: https://www.r-project.org/ [accessed 2025-07-21]
25. Hemming K, Haines TP, Chilton PJ, Girling AJ, Lilford RJ. The stepped wedge cluster randomised trial: rationale, design, analysis, and reporting. Br Med J 2015 Feb 6;350:h391. [doi: 10.1136/bmj.h391] [Medline: 25662947]
26. McCullagh P, Nelder JA. Generalized Linear Models, 2nd edition: London, Chapman and Hall; 1989.

XSL•FO
RenderX

27. Hund H, Wettstein R, Kurscheidt M, Schweizer ST, Zilske C, Fegeler C. Interoperability is a process - the data sharing framework. Stud Health Technol Inform 2024 Jan 25;310:28-32. [doi: 10.3233/SHTI230921] [Medline: 38269759]
28. Rosenau L, Behrend P, Wiedekopf J, Gruendner J, Ingenerf J. Uncovering harmonization potential in health care data through iterative refinement of fast healthcare interoperability resources profiles based on retrospective discrepancy analysis: case study. JMIR Med Inform 2024 Jul 23;12:e57005. [doi: 10.2196/57005] [Medline: 39042420]
29. Shah SM, Khan RA. Secondary use of electronic health record: opportunities and challenges. IEEE Access 2020;8:136947-136965. [doi: 10.1109/ACCESS.2020.3011099]
30. Nguyen A. Hands-On Healthcare Data: Taming the Complexity of Real-World, 1st edition: O'Reilly Media; 2022.
31. Marcon Y, Bishop T, Avraam D, et al. Orchestrating privacy-protected big data analyses of data from different resources with R and DataSHIELD. PLoS Comput Biol 2021 Mar;17(3):e1008880. [doi: 10.1371/journal.pcbi.1008880] [Medline: 33784300]
32. Fuhrmann F, Adjei B, Hartge F. Interop roadmap 2024-2025. INA. 2024. URL: https://www.ina.gematik.de/en/technical-topics-and-roadmap [accessed 2024-10-07]
33. Stang PE, Ryan PB, Racoosin JA, et al. Advancing the science for active surveillance: rationale and design for the Observational Medical Outcomes Partnership. Ann Intern Med 2010 Nov 2;153(9):600-606. [doi: 10.7326/0003-4819-153-9-201011020-00010] [Medline: 21041580]
34. Maier C, Lang L, Storf H, et al. Towards implementation of OMOP in a German University Hospital Consortium. Appl Clin Inform 2018 Jan;9(1):54-61. [doi: 10.1055/s-0037-1617452] [Medline: 29365340]
35. Peng Y, Henke E, Reinecke I, Zoch M, Sedlmayr M, Bathelt F. An ETL-process design for data harmonization to participate in international research with German real-world data based on FHIR and OMOP CDM. Int J Med Inform 2023 Jan;169:104925. [doi: 10.1016/j.ijmedinf.2022.104925] [Medline: 36395615]
36. Directorate-General for Health and Food Safety. Proposal for a regulation on the European health data space. EUR-Lex. 2022. URL: https://eur-lex.europa.eu/legal-content/EN/TXT/HTML/?uri=CELEX:52022PC0197 [accessed 2025-07-21]
37. Kahn MG, Callahan TJ, Barnard J, et al. A harmonized data quality assessment terminology and framework for the secondary use of electronic health record data. EGEMS (Wash DC) 2016;4(1):1244. [doi: 10.13063/2327-9214.1244] [Medline: 27713905]
38. Draeger C, Tute E, Schmidt CO, et al. Identifying relevant FHIR elements for data quality assessment in the German Core Data Set. Stud Health Technol Inform 2023 May 18;302:272-276. [doi: 10.3233/SHTI230117] [Medline: 37203661]
39. Löbe M, Kamdje-Wabo G, Sinza AC, Spengler H, Strobel M, Tute E. Towards harmonized data quality in the medical informatics initiative - current state and future directions. Stud Health Technol Inform 2022 Jan 14;289:240-243. [doi: 10.3233/SHTI210904] [Medline: 35062137]
40. Mou Y, Li F, Weber S, et al. Distributed privacy-preserving data analysis in NFDI4Health with the personal health train. Proc Conf Res Data Infrastr 2023;1:1. [doi: 10.52825/cordi.v1i.282]
41. PrivateAIM. URL: https://privateaim.de/ [accessed 2024-10-08]
42. Wirth FN, Meurers T, Johns M, Prasser F. Privacy-preserving data sharing infrastructures for medical research: systematization and comparison. BMC Med Inform Decis Mak 2021 Aug 12;21(1):242. [doi: 10.1186/s12911-021-01602-x] [Medline: 34384406]
43. Zoch M, Gierschner C, Andreeff AK, et al. Secondary use of patient data within decentralized studies using the example of rare diseases in Germany: a data scientist's exploration of process and lessons learned. Digit Health 2024;10:20552076241265219. [doi: 10.1177/20552076241265219] [Medline: 39130526]
44. POLAR-fhir/fhircrackr. GitHub. URL: https://github.com/polar-fhir/fhircrackr [accessed 2025-07-21]

Abbreviations

CDS: core dataset
CDSS: computerized decision support system
COI: catalog of items
DIC: data integration center
eCRF: electronic case report form
EHR: electronic health record
ETL: extract-transform-load
FHIR: Fast Healthcare Interoperability Resources
HELP: Hospital-wide Electronic Medical Record Evaluated Computerized Decision Support System to Improve Outcomes of Patients with Staphylococcal Bloodstream Infection
HL7: Health Level Seven International
MII: Medical Informatics Initiative
OMOP: Observational Medical Outcomes Partnership

XSL•FO
RenderX

Edited by J Klann; submitted 30.10.24; peer-reviewed by M Wolfien, M Boeker, S Oworah; revised version received 06.05.25; accepted 15.05.25; published 30.07.25.

Please cite as:
Palm J, Saleh K, Scherag A, Ammon D
Leveraging Interoperable Electronic Health Record (EHR) Data for Distributed Analyses in Clinical Research: Technical Implementation Report of the HELP Study
JMIR Med Inform 2025;13:e68171
URL: https://medinform.jmir.org/2025/1/e68171
doi:10.2196/68171

© Julia Palm, Kutaiba Saleh, André Scherag, Danny Ammon. Originally published in JMIR Medical Informatics (https://medinform.jmir.org), 30.7.2025. This is an open-access article distributed under the terms of the Creative Commons Attribution License (https://creativecommons.org/licenses/by/4.0/), which permits unrestricted use, distribution, and reproduction in any medium, provided the original work, first published in JMIR Medical Informatics, is properly cited. The complete bibliographic information, a link to the original publication on https://medinform.jmir.org/, as well as this copyright and license information must be included.

XSL•FO
RenderX

Implementing Electronic Health Records in Philippine Primary Care Settings: Mixed-Methods Pilot Study

Anton Elepaño[1], MD, MSc; Carol Stephanie Tan-Lim[2,3], MD, MSc; Mark Anthony Javelosa[3], MSc; Regine Ynez De Mesa[2], MHS; Mia Rey[2,4], PhD; Josephine Sanchez[2]; Leonila Dans[2,3], MD MSc; Antonio Miguel Dans[2], MD, MSc

[1]Nuffield Department of Primary Care Health Sciences, Medical Sciences Division, University of Oxford, Radcliffe Observatory Quarter, 43 Woodstock Road, Oxford, United Kingdom

[2]Program on Health Systems Development, Center for Integrative and Development Studies, University of the Philippines Diliman, Quezon City, Philippines

[3]Department of Clinical Epidemiology, College of Medicine, University of the Philippines Manila, Manila, Philippines

[4]Department of Accounting and Finance, Cesar E.A. Virata School of Business, University of the Philippines Diliman, Quezon City, Philippines

Corresponding Author:
Anton Elepaño, MD, MSc
Nuffield Department of Primary Care Health Sciences, Medical Sciences Division, University of Oxford, Radcliffe Observatory Quarter, 43 Woodstock Road, Oxford, United Kingdom

Abstract

Background: Between 2020 and 2022, the Philippine Primary Care Studies program, a government-funded initiative supporting universal health care implementation, piloted two electronic health records (EHR) systems across urban, rural, and remote primary care sites.

Objective: The study aimed to evaluate the implementation of two EHR systems in diverse primary care settings in the Philippines over a three-year period.

Methods: This implementation study used an explanatory mixed methods design. Two EHR systems were deployed: an Open Medical Records System (OpenMRS)-based platform in 2016, and a Microsoft-based system in 2021. Both systems integrated clinical documentation, pharmacy, laboratory, and reporting modules. Implementation strategies included training workshops and materials, iterative user feedback loops, and infrastructure cofinancing with local governments. Surveys were administered yearly to all end users. The primary outcome was behavioral intention to use the system. Quantitative data were supplemented by inductive content analysis of qualitative responses to explain observed trends.

Results: A total of 351 survey responses were collected from 2020 to 2022. In 2020, the intention to use the OpenMRS-based EHR was high across all sites. By 2022, following the launch of the Microsoft-based EHR, acceptability declined significantly among doctors and administrative staff, particularly at the urban site. In contrast, the remote site which retained the OpenMRS-based system maintained high acceptability levels. Qualitative findings revealed that while the new EHR system provided a more privacy-focused design, users preferred a cross-platform EHR to allow more flexible access to patient data. At the rural site where the EHR was used to facilitate task-shifting among nurses involved in clinical management, users were less impacted by this shift.

Conclusions: The disparities in EHR acceptability across urban, rural, and remote sites were influenced by contextual, technical, and demographic factors. The decline in acceptability following the EHR system transition highlights the importance of implementation strategies that reflect the specific needs and capacities of each setting. These findings offer practical insights for adapting EHR systems to diverse primary care contexts.

(JMIR Med Inform 2025;13:e63036) doi:10.2196/63036

KEYWORDS

electronic health records; medical informatics; digital health; implementation report; electronic health records system

Introduction

Following the enactment of the Philippine Universal Health Care Law, which mandated the national implementation of electronic health records (EHR) for primary care providers [1], the adoption of EHR systems has faced multifaceted challenges encompassing sociotechnical, organizational, and environmental barriers [2,3].

EHRs are considered digital health interventions intended to address multiple health system challenges [4]. These challenges include poor data quality, underutilization of health care, and operational inefficiencies related to paper-based clinical

XSL•FO
RenderX

documentation and insurance claims processing [5,6]. EHRs also aim to address transportation and communication barriers, human resource shortages, and referral inefficiencies, particularly by facilitating task-shifting models in which nonphysician providers such as nurses and midwives assume expanded clinical roles in remote areas [7].

Despite the development of many EHR systems tailored for rural primary care facilities in the Philippines, adoption remains limited [2] and implementation reports or user-centered evaluations are scarce [8]. However, when successfully implemented, EHRs can enhance the collection, storage, and retrieval of health information across clinical, paramedical, and administrative domains [4].

To provide recommendations for the widespread implementation of EHR systems, the Philippine Primary Care Studies (PPCS) initiated a digitalization program in three pilot sites that reflect the country's primary care contexts: urban (Quezon City, National Capital Region), rural (Samal, Bataan), and remote (Bulusan, Sorsogon). This initiative aligned with the national digital health strategy, which designated EHR adoption as a foundational step in building an integrated health information system to support evidence-based policy and health financing decisions [1].

Initial surveys during the first year of program implementation revealed high EHR acceptability across a diverse range of users and settings [5]. Since then, both the contextual landscape and system features have evolved. Some rural facilities have reverted to or continued using paper-based systems [8]. This study provided a comprehensive reassessment of how various factors have shaped the EHR implementation over time.

Methods

Study outcomes

The overall aim of the implementation was to assess how EHR systems could be effectively used across various primary care contexts. The primary outcome was user acceptability, operationalized as continued intention to use the system [9]. Distal outcomes such as sustainability and clinical outcomes were beyond the scope of this study. The secondary objective was to explain variations in acceptability by delving into contextual factors influencing system adoption. This study adhered to the iCHECK-DH (Checklist for the Reporting on Digital Health Implementations) guidelines [10] and the GRAMMS (Good Reporting of A Mixed Methods Study) reporting standards [11].

Blueprint Summary

The digital health interventions integrated several components including electronic medical records, health management information systems, laboratory and diagnostics information, and pharmacy information [4]. Two EHRs were implemented across PPCS pilot sites, one in 2016 and another in 2021. Training was delivered through workshops and asynchronous instructional materials. Broader implementation strategies included internet infrastructure deployment (in collaboration with the local government units), and continuous feedback loops between system developers and users. Prescribing and laboratory data were integrated into the EHR to monitor costs and support the development of a primary care benefits package [12].

Technical Design

The first EHR system, built on the open-source Open Medical Records System (OpenMRS) platform was introduced in 2016 at an urban site, and subsequently in 2019 at the rural and remote sites. Developed in-house by the PPCS team, this system connected primary care services, laboratory units, and pharmacies. Main features included triage and queueing modules, clinical notes accessible only to authorized providers, laboratory request and result interfaces, pharmacy dispensing modules, and administrative reporting tools.

The second EHR system, launched in April 2021 for the urban and rural sites, used a Microsoft-based desktop and cloud infrastructure. This Microsoft-based EHR was not implemented at the remote site due to the lack of high-speed broadband internet. Developed by a government-owned digital solutions subsidiary, this system introduced role-based access for nonphysician providers to draft clinical notes and propose management plans for physician approval. Additional functionalities included real-time referral notifications and a redesigned user interface. Core features remained consistent with the OpenMRS-based EHR platform.

Target

The three primary care settings of the PPCS program were selected to represent urban, rural, and remote contexts. Rural sites are defined by the National Statistics Office as municipalities with a population density of fewer than 1000 people per square kilometer [13], while remote sites are designated by the Department of Health as geographically isolated and disadvantaged areas [14]. The urban site, located within a public university in a high-income municipality in Quezon City, provided primary care services to approximately 15,051 faculty members, employees, and their dependents. The rural site, situated in a low-income municipality in Bataan, served 35,298 residents with a population density of 627 inhabitants/km^2 [15,16]. The remote site, located in a low-income geographically isolated mountainous area in Sorsogon, catered to 22,884 residents (238 inhabitants/km^2) [16,17].

End users included administrative personnel, community health workers, nurses, midwives, physicians, dentists, nutritionists, pharmacists, and laboratory technicians. These users were responsible for data entry, service provision, and generating reports for local and national reporting.

Data

Patient data were entered through password-protected accounts and stored on secure servers managed by the system providers. Data sharing was restricted to health professionals managing the same patients. Data privacy protocols conformed to the Data Privacy Act of 2012, which grants patients the right to be informed, access, and modify their data [18]. Third-party use of data for research required clearance under the National Ethics Guidelines for Health and Health-Related Research (2017) [19].

XSL•FO
RenderX

Interoperability

Both systems adhered to national data standards issued by the Department of Health [1]. The OpenMRS-based EHR supported Fast Healthcare Interoperability Resources, while the Microsoft-based version did not. Clinical notes were primarily composed of sectioned free-text fields (eg, chief complaint, history of present illness). Diagnoses were entered using *ICD-10* codes via auto-populated dropdown menus. Similarly, prescriptions were entered using dropdown lists based on the national drug formulary.

Participating Entities

The program was implemented by PPCS under the Program on Health Systems Development, University of the Philippines Center of Integrative and Development Studies. Funding was provided by the Department of Health, the Philippine Health Insurance Corporation, the Emerging Interdisciplinary Research Program, and the Philippine Council on Health Research and Development. The Microsoft-based EHR was developed through the Technology Transfer and Business Development Office of the University of the Philippines Diliman. This EHR was subsequently co-owned by the system provider and the university.

Budget Planning

The total cost of the project was estimated at Php 6,000,000 (USD 104,572). Capital costs were cofinanced by local government units and the implementing agency. This covered internet infrastructure (ten internet towers amounting to Php 800,000 (USD 13,943)), network equipment (routers and cables worth Php 40,000 (USD 697)), EHR development (developers' salaries over Php 1,000,000 (USD 17,429)), and workstations (desktops, laptops, and printers worth Php 2,000,000 (USD 34,857)). Recurring costs for IT support personnel were approximately Php 800,000 (USD 13,943) annually. Licensing costs were not incurred as both systems were developed in-house.

Sustainability

Postpilot funding for both systems varied, depending on the discretion of local government units. Although this evaluation focused on acceptability rather than sustainability, the latter was implicitly linked to user endorsement. EHR users, who also served on local health boards, played advocacy roles in securing funding.

Evaluation

A sequential mixed-methods design was used to assess user acceptability. Surveys were conducted annually from 2020 to 2022. An interpretivist approach underpinned the analysis, acknowledging the co-construction of meaning between researchers and participants. Survey design was guided by the Unified Theory of Acceptance and Use of Technology (UTAUT) [20].

Mixed methods allowed the team to capture the evolving nature of the intervention [21]. Quantitative data identified patterns in acceptability, whereas qualitative data provided context to these observations. Although data collection was concurrent, analysis occurred sequentially, with priority given to quantitative data. This sequential approach facilitated identification of relevant questions to guide the content analysis of qualitative data. Integrating datasets enabled corroboration and elaboration of findings.

All EHR users were invited to participate and provided written informed consent. The survey instruments featured a combination of Likert-scale questions and free-text fields. Survey validation and Unified Theory of Acceptance and Use of Technology model testing are detailed elsewhere [5]. Free-text responses were analyzed using semantic, inductive content analysis. Due to brevity of responses, coding was kept descriptive to highlight user experiences [22]. The final synthesis was reviewed by the core research team and the PPCS steering committee.

Ethical Considerations

This study received ethics approval from the University of the Philippines Manila Research Ethics Board (2015-489-0) and the Department of Health Single Joint Research Ethics Board (2029 - 55). Written informed consent was obtained from all participants. They were free to decline participation or withdraw from the study at any time. No financial or material compensation was provided for completing the questionnaire. Identifying information was removed during analysis to ensure participant anonymity.

Results

Coverage

Surveys were carried out at sites where the EHRs were implemented, covering 21 barangay health stations (14 in Samal and seven in Bulusan), two rural health units (one in Samal and one in Bulusan), and one university-affiliated clinic in Quezon City. The surveys achieved response rates of 53% (135/255) in 2020, 48% (127/263) in 2021, and 68% (89/131) in 2022. Respondents were predominantly female and were within the 31-60 age group (Table 1). Nurses and midwives accounted for the majority of respondents across all three sites, comprising 175 (50%) of the total sample. A total of 165 respondents (47%) reported having less than five years of service, while 221 (63%) reported more than 48 weeks of experience using the EHRs.

XSL•FO
RenderX

Table . Demographic characteristics of survey respondents.

Characteristics	Year 2020 (n=135), n (%)	Year 2021 (n=127), n (%)	Year 2022 (n=89), n (%)
Location			
Remote	45 (33)	43 (34)	24 (27)
Rural	48 (36)	39 (31)	42 (47)
Urban	42 (31)	45 (35)	23 (26)
Age (years)			
≤30	22 (16)	26 (21)	16 (18)
31 - 60	101 (75)	93 (73)	66 (74)
>60	12 (9)	8 (6)	7 (8)
Sex			
Female	114 (84)	108 (85)	73 (82)
Male	21 (16)	19 (15)	16 (18)
Role			
Administrative staff	24 (18)	17 (13)	8 (9)
Doctor	16 (12)	16 (13)	24 (27)
Midwife/nurse	70 (52)	63 (50)	42 (47)
Paramedical staff	25 (19)	31 (24)	15 (17)
EHR[a] use (months)			
≤12	76 (56)	20 (16)	40 (45)
13 - 24	59 (44)	27 (22)	14 (16)
25 - 36	0 (0)	1 (1)	5 (6)
>36	0 (0)	77 (62)	30 (34)

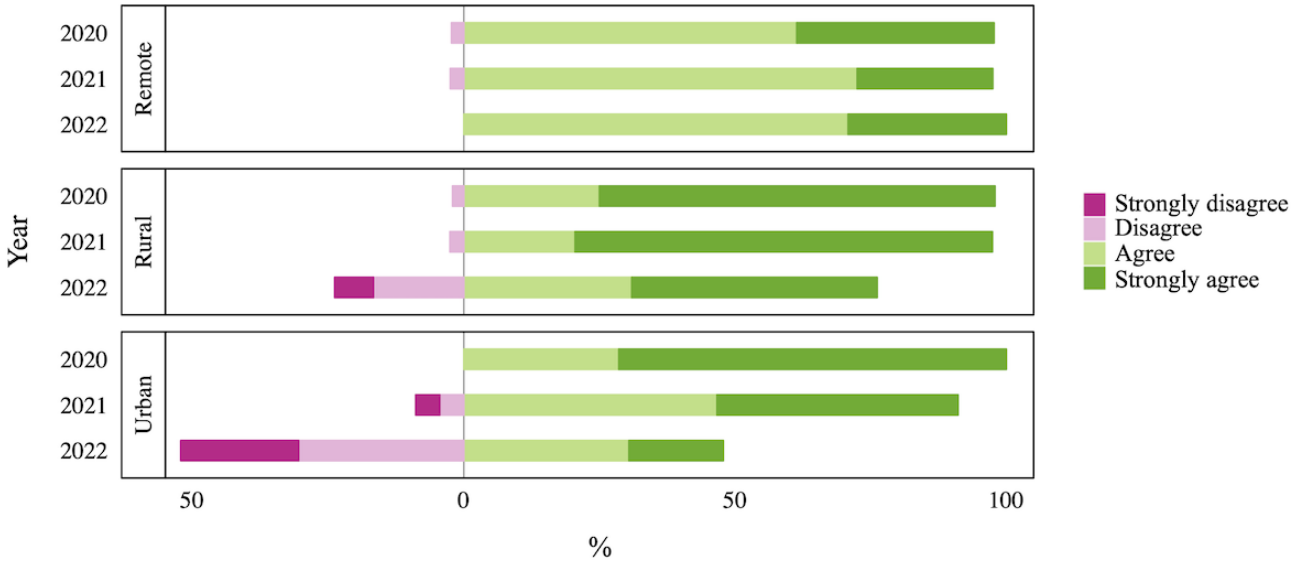
[a]EHR: electronic health record.

Acceptability Surveys

The acceptability of the EHR system showed distinct patterns over the three-year study period (Figure 1). In 2020, respondents generally expressed positive intention to use the OpenMRS-based EHR across the three sites. However, by 2021, with the transition to the new EHR system in the urban and rural sites, a noticeable shift in acceptability occurred, especially in the urban site, where some users expressed disagreement with the continued use of the EHR. By 2022, more than half of the urban site respondents disagreed with the continued use of the EHR. This trend was mirrored, though to a lesser extent, among rural users. The remote site users, who continued using the OpenMRS-based EHR, maintained consistent acceptability levels towards the EHR throughout the three years.

XSL•FO
RenderX

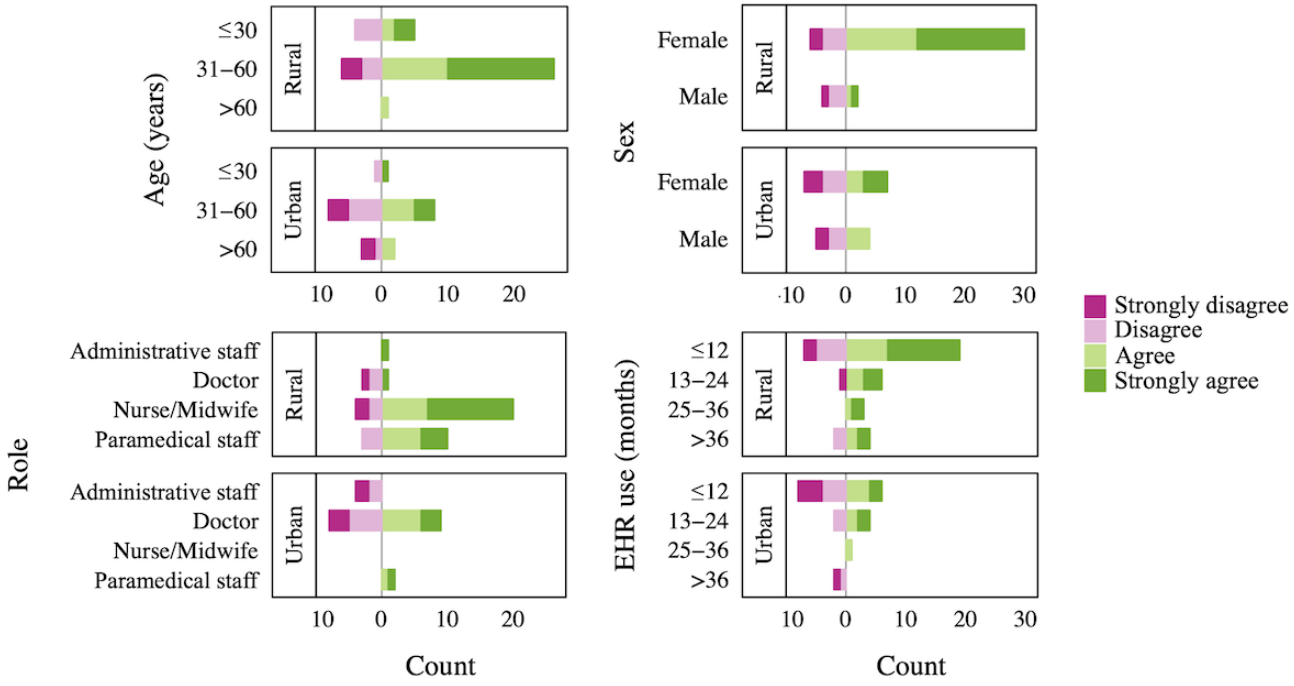
Figure 1. Percentage responses to the item "I intend to use the EHR in the next 12 months" revealing shifts in behavioral intention from 2020 to 2022 across pilot sites.



Of the 64 respondents (72%) in the 2022 endline survey who also participated in the 2020 baseline survey, 28 (43%) reported a decreased intention to use EHR, 9 (14%) showed an increased intention, and another 27 (43%) maintained the same opinion.

Subgroup analyses (Figure 2) of users from urban and rural sites, both of which transitioned to the Microsoft-based EHR by April 2021, revealed high levels of disagreement with continued EHR use among administrative staff and doctors in the urban setting. At the rural site, more doctors expressed disagreement compared to other roles. Urban site responses were symmetrically distributed with both positive and negative sentiments across age groups and sex. Conversely, in the rural setting, women and younger users expressed higher intent-to-use the EHR compared to men and older respondents. Acceptability was lowest among users with less than 12 months of EHR use.

Figure 2. Total counts of responses to the question "I intend to use the EHR in the next 12 months" across different subgroups in 2022.



Content Analysis of User Feedback

The preliminary analysis of quantitative data raised the following questions for content analysis: (1) Why was acceptability different in the urban and rural sites despite using the same EHR system?; (2) Why was acceptability lower among doctors in urban and rural settings compared to other professions?; (3) Why was acceptability higher at the remote site despite similar, if not more, resource constraints compared to the rural site?; (4) Why was acceptability lower among less experienced users?

Content Analysis of User Feedback

Common feedback included positive sentiments toward fundamental features such as record input (from administrative staff, pharmacists, and midwives), access to patient information

XSL•FO
RenderX

(noted by midwives, nurses, and doctors), and data integration within the hospital system (mentioned by nutritionists and doctors). However, pervasive concerns about unresponsive interfaces were reported across all sites, attributed to slow laptop performance at the urban site and slow internet connectivity at rural and remote sites. Users also expressed frustration with system bugs and freezes, indicating a perceived lack of readiness for the Microsoft-based EHR implementation. Additionally, physicians in urban and rural sites, who used the Microsoft-based EHR, specifically commented on the interface complexity for having an excess of on-screen buttons (Table 2).

Table . Content analysis of unstructured responses from the acceptability surveys.

Categories	Data extracts
Useful core features, but repetitive and cumbersome interface	"Easy to find information of the patient" (rural, laboratory technician)
	"Slow opening of application and too many save buttons to click when closing the chart" (urban, physician)
Need for multidevice support and workflow integration	"Not cross-compatible with other devices (computer/mobile phone)" (rural, administrative staff)
	"I wish it was integrated with Appointlet or my email. I wish I could just click on a button to contact a patient through text or Viber or Zoom" (urban, physician)
Dependence on unreliable internet connectivity	"Slow when the internet is weak" (remote, midwife)
Lack of time and opportunity for system (re)training	"There was a change or an upgrade of the platform at one point and I just did not have the time to relearn" (urban, physician)

Integrating Quantitative and Qualitative Findings

Disparities observed in acceptability were linked to both the demographic composition of survey respondents and the specific EHR system used. The urban setting had a higher concentration of physicians, while the rural site featured a mix of midwives and physicians, and the remote site had fewer physician respondents. Integrating quantitative and qualitative datasets yielded the following interpretations.

Despite using the same Microsoft-based EHR system, lower acceptability in the urban setting compared to the rural site can be attributed to several factors. Although urban respondents did not identify internet connection issues unlike their rural counterparts, demographic differences played a role. Urban site respondents were predominantly doctors, who displayed a more critical stance compared to other healthcare professionals.

Higher acceptability at the remote site, despite experiencing more resource constraints than the rural site, was influenced by the continued use of the OpenMRS-based EHR. Dissatisfaction at the rural site, particularly among doctors, was due to the lack of multidevice support of the Microsoft-based EHR. Common concerns across rural and remote sites included internet dependency and interface issues, although the remote site reported fewer problems with bugs and freezes with the OpenMRS-based EHR.

Investigating why acceptability was lower among physicians in both the urban and rural settings compared to other health care professionals revealed several insights. Flexibility was a success factor, with physicians emphasizing the need for a cross-platform EHR system that enabled easier access to patient information and integration with their workflow and other productivity tools. The Microsoft-based EHR's restrictions led to additional workflow disruptions, including reliance on low-performance computers and intermediary note-taking methods (eg, pen and paper, personal computers)—an unintended consequence which arose from efforts to implement a desktop-based, privacy-focused design.

Beyond technical implementation barriers, social factors also influenced adoption. Exploring the lower acceptability among less experienced users highlighted the learning curve associated with new platforms and the need for periodic technical support. New users appreciated the transition from paper to electronic records but identified system navigation complexity as a concern, especially for those with limited technological literacy. Recommendations included a self-explanatory interface and a help window for direct support.

Lessons Learned

Successful implementation of the EHR systems was facilitated by the active involvement of users, developers, and site managers. This collaboration allowed timely feedback cycles, leading to iterative improvements and the adoption of an integrated EHR used not only by physicians but also by nurses and midwives. The Microsoft-based EHR was intentionally designed to enable task-shifting: nurses would document and prescribe treatment plans for asynchronous physician review. In practice, this worked well in the rural site. However, the same approach proved less relevant in the urban site, where nurses typically worked alongside physicians. Acceptability declined in this setting after the EHR transition, as the initial system was locally installed. To address this, the Microsoft-based EHR was later migrated to a web-based platform that supported access from laptops and mobile devices.

The implementation also benefited from favorable policy timing. The COVID-19 pandemic in 2020 accelerated digital adoption out of necessity [8], while the Universal Healthcare Law (enacted in 2019) created legal incentives to adopt EHRs that complied with national reporting and claims processing standards [1]. These contextual enablers were not originally anticipated in the project's planning phase, but enhanced uptake.

XSL•FO
RenderX

However, structural challenges persisted, particularly with internet connectivity. Although limited access was acknowledged during planning, the actual impact was more severe than expected. For example, the Microsoft-based EHR, which was reliant on stable broadband, could not be launched in to remote site. Internet service providers and EHR vendors did not have strong financial incentives to serve low-density areas. The PPCS experience showed that reframing paramedical staff as core users, not secondary ones, can strengthen the business case for scaling EHRs in underserved areas [7]. Nonetheless, government support remains essential to overcome the limited commercial viability.

Budget allocation was further complicated by the decentralized governance structure in the Philippines [23]. While some infrastructure costs were cofinanced by local government units, the actual continuity of support varied. One site discontinued EHR use following a change in local leadership, despite the original plan for sustainability beyond the pilot phase. With local elections occurring every three years, digital health programs remain susceptible to political turnover [24]. This introduces unpredictability that can deter significant upfront investments in infrastructure and innovation.

Discussion

This study described the implementation strategy, intervention components, and the evolving acceptability of two EHR systems over a three-year period across three primary care settings. Acceptability declined notably in both urban and rural sites following the transition to a Microsoft-based EHR. Conversely, the remote site, which continued using a OpenMRS-based EHR, consistently reported high levels of acceptability. User feedback highlighted doctors' preference for a more flexible EHR that could operate across various devices. Paramedical staff pointed out recurrent bugs in the Microsoft-based EHR, suggesting premature implementation. The transition between EHR systems posed challenges, necessitating users to adapt to new interfaces, with inadequate support identified as a significant barrier.

The study's outcome measurement approach had several limitations. First, the absence of in-depth interviews and direct observation limited the ability to capture richer insights, particularly from users who may have opted out of system use. Second, is the low response rate from 2020 to 2022, likely influenced by the online format of the survey. This may have introduced selection bias and skewed the results toward participants with higher technological capacity.[25] While the rates in our study were higher than those from similar surveys [26-28], the views of nonrespondents could differ meaningfully [26-28]. Additionally, the COVID-19 pandemic in 2020 drastically altered the health care landscape and may have influenced respondents' sentiments towards the EHR systems.

Efforts to scale up EHRs in primary care should recognize the complex interplay between system design, user needs, and contextual factors. A user-centered model designed for a rural context may not seamlessly apply to an urban setting. Consequently, adopting a single system nationwide risks replicating the misalignments observed in this program. Future national strategies should balance standardization with flexibility, allowing for context-sensitive adaptations to maximize EHR use across varied health system settings.

Acknowledgments

The authors wish to acknowledge research assistants who delivered and processed the survey forms. Gratitude is also extended to healthcare workers and staff in each pilot site for their time and support for the program. This study was funded by the Philippine Department of Health, the Philippine Health Insurance Corporation, the Emerging Interdisciplinary Research Program, the University of the Philippines Center for Integrative and Development Studies, and the Philippine Council on Health Research and Development.

Conflicts of Interest

None declared.

Checklist 1
iCHECK-DH (Checklist for the Reporting on Digital Health Implementations) guidelines.
[DOCX File, 21 KB - medinform_v13i1e63036_app1.docx]

Checklist 2
Good Reporting of A Mixed Methods Study reporting standards.
[DOCX File, 15 KB - medinform_v13i1e63036_app2.docx]

References

1. Villaverde M, Espiritu II N, Adora J. Universal Health Care in the Philippines: From Policy to Practice: Manila, Philippines: Department of Health - Health Policy and Systems Development Team; 2022.
2. Macabasag RLA, Mallari EU, Pascual PJC, Fernandez-Marcelo PGH. Normalisation of electronic medical records in routine healthcare work amidst ongoing digitalisation of the Philippine health system. Soc Sci Med 2022 Aug;307:115182. [doi: 10.1016/j.socscimed.2022.115182] [Medline: 35797835]

XSL•FO
RenderX

3. Ebardo RA, Celis NJ. Barriers to the adoption of electronic medical records in select Philippine hospitals. 2019 Apr 19 Presented at: ICCAI '19: Proceedings of the 2019 5th International Conference on Computing and Artificial Intelligence; Apr 19-22, 2019; Bali Indonesia. [doi: 10.1145/3330482.3330503]
4. Melh G, Tamrat T. Classification of digital health interventions v 10.: Geneva, Switzerland: World Health Organization; 2018. URL: https://www.who.int/publications/i/item/WHO-RHR-18.06 [accessed 2024-12-18]
5. De Mesa RYH, Galingana CLT, Tan-Lim CSC, et al. Facing the digital frontier: exploring user acceptance of electronic health records in an urban, rural and remote setting in the Philippines. BMJ Open Qual 2024 Apr 18;13(2):e002621. [doi: 10.1136/bmjoq-2023-002621] [Medline: 38637020]
6. Lagrada-Rombaua L, Encluna J, Gloria E. Consolidating primary health care financing in a devolved setting: case study from the Philippines. The Lancet Global Health Commission on Financing Primary Health Care. 2022. URL: https://www.lshtm.ac.uk/media/59836 [accessed 2025-05-03]
7. Galingana CLT, De Mesa RYH, Marfori JRA, et al. Setting core competencies of health workers towards quality primary care: proceedings of a national consultative workshop. Acta Med Philipp 2020 Oct 5;54. [doi: 10.47895/amp.v54i0.2068]
8. Acacio-Claro PJ, Estuar M, Villamor DAR, Bautista MCG, Pulmano CE, Sugon QM Jr. Understanding adoption of electronic medical records (EMRs) during a health emergency: an analysis of EMR usage logs from rural health facilities in the Philippines. Acta Med Philipp 2024;58(22):7-13. [doi: 10.47895/amp.vi0.8911] [Medline: 39817114]
9. Lemonnier A, Adelé S, Dionisio C. The determinants of acceptability and behavioural intention of automated vehicles – a review. Trav Hum 2020 Nov 26;Vol. 83(4):297-342. [doi: 10.3917/th.834.0297]
10. Perrin Franck C, Babington-Ashaye A, Dietrich D, et al. iCHECK-DH: Guidelines and Checklist for the Reporting on Digital Health Implementations. J Med Internet Res 2023 May 10;25:e46694. [doi: 10.2196/46694] [Medline: 37163336]
11. O'Cathain A, Murphy E, Nicholl J. The quality of mixed methods studies in health services research. J Health Serv Res Policy 2008 Apr;13(2):92-98. [doi: 10.1258/jhsrp.2007.007074] [Medline: 18416914]
12. Rey MP, De Mesa RYH, Marfori JRA, et al. The cost of primary care: an experience analysis in an urban setting. Acta Med Philipp 2024;58(23):7-18. [doi: 10.47895/amp.vi0.6589] [Medline: 39830417]
13. 1990 census of population and housing. National Statistics Office. 1992. URL: https://psa.gov.ph/system/files/main-publication/1990%2520CPH%2520Rpt.%2520No%25204%2520-%2520Ilocos%2520Norte.pdf [accessed 2024-12-18]
14. Guidelines on identifying geographically-isolated and disadvantaged areas and strengthening their health systems. Republic of the Philippines, Department of Health, Office of the Secretary. 2023. URL: https://law.upd.edu.ph/wp-content/uploads/2020/06/DOH-AO-No-2020-0023.pdf [accessed 2023-12-18]
15. Municipality of Samal. Philippine Statistics Authority. 2020. URL: https://psa.gov.ph/classification/psgc/barangays/0300812000 [accessed 2024-04-03]
16. Population, land area, population density, and percent change in population density of the philippines by region, province/highly urbanized city, and city/municipality: 2010, 2015, and 2020. Philippine Statistics Authority. 2020. URL: https://psa.gov.ph/content/highlights-population-density-philippines-2020-census-population-and-housing-2020-cph [accessed 2024-12-18]
17. Municipality of Bulusan. Philippine Statistics Authority. 2020. URL: https://psa.gov.ph/classification/psgc/barangays/0506204000 [accessed 2024-04-03]
18. Republic Act 10173 Data Privacy Act of 2012. National Privacy Commission. 2012. URL: https://privacy.gov.ph/data-privacy-act/ [accessed 2025-02-18]
19. Data privacy guidelines on the processing of health information–administrative order no. 2020-0030. Department of Health-Office of the Secretary. 2020. URL: https://law.upd.edu.ph/wp-content/uploads/2020/07/DOH-AO-No-2020-0030.pdf [accessed 2025-02-18]
20. Venkatesh V, Morris MG, Davis GB, Davis FD. User acceptance of information technology: toward a unified view. MIS Q 2003;27(3):425. [doi: 10.2307/30036540]
21. Moore GF, Audrey S, Barker M, et al. Process evaluation of complex interventions: Medical Research Council guidance. BMJ 2015 Mar 19;350:h1258. [doi: 10.1136/bmj.h1258] [Medline: 25791983]
22. Maxwell JA, Mittapalli K. Realism as a stance for mixed methods research. In: SAGE Handbook of Mixed Methods in Social &Amp; Behavioral Research, 2nd edition 2010:145-168. [doi: 10.4135/9781506335193.n6]
23. Liwanag HJ, Wyss K. What conditions enable decentralization to improve the health system? Qualitative analysis of perspectives on decision space after 25 years of devolution in the Philippines. PLoS ONE 2018;13(11):e0206809. [doi: 10.1371/journal.pone.0206809] [Medline: 30395625]
24. Yu VG, Lasco G, David CC, Baysic IS. 'Kontra-partido': untangling oppositional local politics and healthcare devolution in the Philippines. Health Policy and Plan 2023 Aug 2;38(7):840-850. [doi: 10.1093/heapol/czad039]
25. Marinescu I, Chamberlain A, Smart M, Klein N. Incentives can reduce bias in online employer reviews. J Exp Psychol Appl 2021 Jun;27(2):393-407. [doi: 10.1037/xap0000342] [Medline: 33764122]
26. Cheung CS, Tong EL, Cheung NT, et al. Factors associated with adoption of the electronic health record system among primary care physicians. JMIR Med Inform 2013 Aug 26;1(1):e1. [doi: 10.2196/medinform.2766] [Medline: 25599989]
27. Luyten J, Marneffe W. Examining the acceptance of an integrated electronic health records system: insights from a repeated cross-sectional design. Int J Med Inform 2021 Jun;150:104450. [doi: 10.1016/j.ijmedinf.2021.104450] [Medline: 33848941]

XSL•FO
RenderX

28. Bloom BM, Pott J, Thomas S, Gaunt DR, Hughes TC. Usability of electronic health record systems in UK EDs. Emerg Med J 2021 Jun;38(6):410-415. [doi: 10.1136/emermed-2020-210401] [Medline: 33658268]

Abbreviations

EHR: electronic health record
OpenMRS: Open Medical Record System
PPCS: Philippine Primary Care Studies

Edited by C Perrin; submitted 07.06.24; peer-reviewed by B Senst, IT Isip-Tan; revised version received 15.05.25; accepted 26.05.25; published 15.07.25.

Please cite as:
Elepaño A, Tan-Lim CS, Javelosa MA, De Mesa RY, Rey M, Sanchez J, Dans L, Dans AM
Implementing Electronic Health Records in Philippine Primary Care Settings: Mixed-Methods Pilot Study
JMIR Med Inform 2025;13:e63036
URL: https://medinform.jmir.org/2025/1/e63036
doi:10.2196/63036

© Anton Elepaño, Carol Stephanie Tan-Lim, Mark Anthony Javelosa, Regine Ynez De Mesa, Mia Rey, Josephine Sanchez, Leonila Dans, Antonio Miguel Dans. Originally published in JMIR Medical Informatics (https://medinform.jmir.org), 15.7.2025. This is an open-access article distributed under the terms of the Creative Commons Attribution License (https://creativecommons.org/licenses/by/4.0/), which permits unrestricted use, distribution, and reproduction in any medium, provided the original work, first published in JMIR Medical Informatics, is properly cited. The complete bibliographic information, a link to the original publication on https://medinform.jmir.org/, as well as this copyright and license information must be included.

XSL•FO
RenderX

Patient-Centered Outpatient Process Optimization System Based on Intelligent Guidance in a Large Tertiary Hospital in China: Implementation Report

Xiaoyi Wang[1*], BPA; Rujia Zhang[1*], BPA; Zhihong Gao[2], MSE; Mengxuan Xia[2], PhD; Songjia Zhang[1], BPA; Lizheng Ge[1], BPA; Yuyang Zhu[3], BPA; Haojie Jin[1], BPA; Shenglian Pan[4], MM; Manman Zheng[5*], BPA; Chun Chen[1*], PhD; Xiangyang Zhang[6*], BPA

[1]School of Medical Humanities and Management, Wenzhou Medical University Tea Mountain Campus, Tongren Building 7B304, Ou Hai District, Wenzhou, China

[2]Information Technology Section, The First Hospital of Wenzhou Medical University, Wenzhou, China

[3]Cixi Biomedical Research Institute, Wenzhou Medical University, Wenzhou, China

[4]Acupuncture and Tuina Department, Wenzhou Hospital of Traditional Chinese Medicine, Wenzhou, China

[5]Graduate School of Wenzhou Medical University, Wenzhou, China

[6]Medical Affairs Department, First Affiliated Hospital of Wenzhou Medical University, Shangcai Village, Nanbaixiang Street, Ouhai District, Wenzhou, Zhejiang, China

[*]these authors contributed equally

Corresponding Author:
Xiangyang Zhang, BPA
Medical Affairs Department, First Affiliated Hospital of Wenzhou Medical University, Shangcai Village, Nanbaixiang Street, Ouhai District, Wenzhou, Zhejiang, China

Abstract

Background: In large tertiary hospitals across China, outpatient patients often encounter the “three longs and one short” (long registration time, long waiting time, long time for medicine collection, and short time for medical treatment) phenomenon. This scenario contributes to suboptimal patient experiences and declining satisfaction with health care services. To address the issue of long waiting times, many hospitals in China have implemented a range of measures. However, these measures have only improved individual aspects of the patient experience, with limited overall impact. Currently, there is a lack of comprehensive, intelligent reform for the entire patient service process in the medical system. Therefore, there is an urgent need to integrate and optimize the entire patient service process, providing real-time intelligent guidance within hospitals. This would help reduce waiting times for patients and enhance their satisfaction.

Objective: This study aims to introduce a patient-centered intelligent guidance system and report on the impact of its implementation on outpatient waiting times and patient satisfaction in hospitals.

Methods: The intelligent guidance system was designed with a patient-centered approach, leveraging internet and big data technologies. The system seamlessly connects various steps of the outpatient medical process, facilitating functions including automated check-in and comprehensive intelligent guidance for patients’ medical visits, thus enhancing the efficiency and quality of health care delivery. This system has been implemented in a tertiary hospital in China. To assess the system’s effectiveness, we compared outpatient visit data, waiting time data, and patient satisfaction levels between the preimplementation and postimplementation periods from 2019 to 2022. We analyzed the changes in patients’ average waiting times and satisfaction levels after the system was implemented.

Results: One year after the introduction of the intelligent guidance system, the number of outpatient visits increased from 5,067,958 to 5,456,151. The waiting time for outpatient patients was significantly reduced. The waiting time for consultation decreased by 2.84 minutes (mean 41.14, SD 2.31 min vs mean 38.30, SD 1.89 min; P<.001). The waiting time for examination decreased by 3.35 minutes (mean 47.83, SD 1.10 min vs mean 44.48, SD 1.67 min; P<.001). Consultation time increased to 3.43 minutes (mean 2.85, SD 0.03 min vs mean 3.43, SD 0.26 min; P<.001). After the system was launched, patient satisfaction increased from 89.99% (SD 2.78%) in 2021 to 92.72% (SD 0.18%) in 2022 (P=.005).

Conclusions: The patient-centered intelligent guidance system reported in this study proved beneficial for tertiary medical institutions striving to alleviate the outpatient burden caused by prolonged waiting times. Through continuous transformation and upgrading of the outpatient service process centered on patients, the efficiency of outpatient services and patient satisfaction

XSL•FO
RenderX

improved. Therefore, the patient-centered principle method and process integration concepts for the system can be further promoted and implemented.

(JMIR Med Inform 2025;13:e60219) doi:10.2196/60219

KEYWORDS

patient-centered; intelligent system; outpatient service; waiting time; patient satisfaction

Introduction

Context

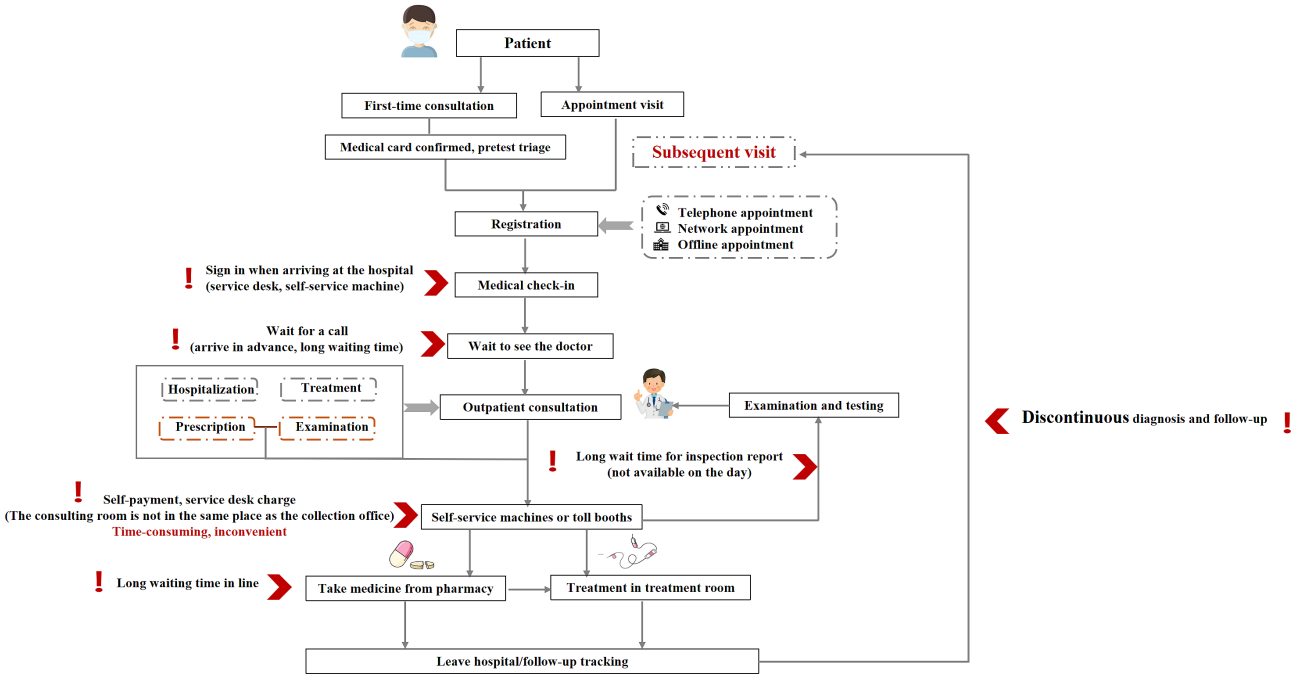
With the continuous global development of the economy and society, people have developed higher expectations of their health systems. The World Health Organization (WHO) has proposed that the current health system is a physician-driven system overly focused on disease, neglecting the patient experience, such that nearly half of patients are dissatisfied with the system [1]. Therefore, the WHO proposed the principle of people-centeredness, which aims to create a patient-centered health system. Many countries have actively responded to this principle, including Peru [2], Canada [3], and Germany [4]. Several scholars have conducted research on integrating patient-centered principles into the nursing field [5,6]. Researchers have experimentally compared inpatient care experiences between systems implementing and not implementing patient-centered principles, demonstrating improved service quality and optimized patient experiences [7].

Problem Statement

Patient-centered principles remain limited in China due to its vast population and relatively scarce high-quality medical resources. Additionally, China's medical process differs from other nations where strict family doctor first-visit systems manage common illnesses locally and refer complex cases to hospitals [8]. China's hospitals are graded by the government (Levels I, II, and III) [9]. Level I and II hospitals manage common illnesses, while Level III (tertiary) hospitals, equipped with the best resources, handle critical cases [10,11]. Chinese patients choose their hospitals by themselves [12]. Consequently, many Chinese patients seek care for common ailments like colds at large tertiary hospitals, compelling these institutions to handle both minor and serious conditions [13]. This leads to persistent overcrowding and queues.

During observation of a traditional hospital consultation process, most first-time patients exhibited confusion upon arrival (Figure 1). They struggled to locate key departments like consultation rooms or pharmacies, leading to repeated queuing at information desks for staff guidance. This manual consultation dependency significantly prolongs waiting times and wastes patient time. Doctors' consultation times for each patient receiving medical services are shortened accordingly. This leads to a situation in which patients need a long time to register, queue for long periods, take a long time for examinations, and see a doctor for a short amount of time [14]. Excessive waiting times also degrade the patient's experience of care, resulting in decreased satisfaction [15-17].

Figure 1. Traditional outpatient procedures and existing problems.



XSL•FO
RenderX

Similar Interventions

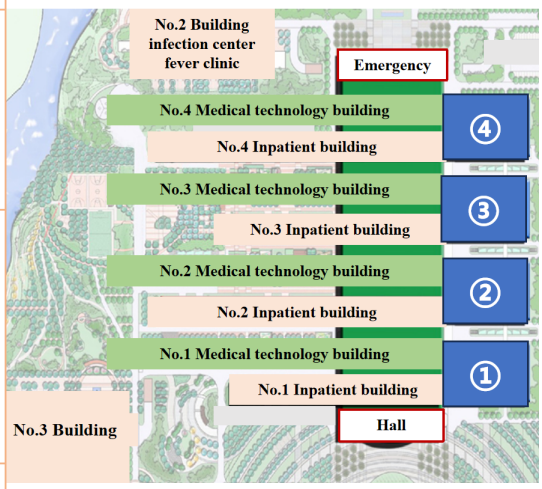
Prolonged outpatient waiting times have been found to lower patient satisfaction across multiple countries, including China, Canada, Malaysia, and the United States [18-20]. Studies have examined patient-centered care principles in China. Surveys assessed patients' perceptions and satisfaction [21], while research explored the application of patient-centered care principles to health care challenges [22]. Analysis of the 2015 China National Patient Survey found these principles improve care quality, efficiency, and satisfaction [23]. Many public tertiary hospitals in China have made numerous attempts at improvement [13]. For example, a public tertiary hospital in Southern China balanced supply-demand interventions by simplifying appointments, regulating doctor attendance, and implementing app-based visit reminders [14]. Postintervention, this hospital reduced patient waiting time by 28.3 minutes (from 179.7 to 151.4 min), while satisfaction scores rose from 89.10 to 90.26 [14]. Other hospitals have optimized outpatient processes by introducing current technologies, such as web-based approaches to health care delivery [24]. Other researchers have designed smart navigation systems to shorten queues [25].

Previous health care reforms typically addressed fragmentary treatment aspects while neglecting overall care pathways and patient habits. For example, underutilized artificial intelligence guidance systems and app-based solutions often exclude older adult patients due to poor accessibility [26]. These fragmented initiatives fail to address the widespread issue of "three long and one short" (long registration, waiting, and payment times, coupled with short consultation times). Although long-term solutions such as equalizing access to high-quality medical resources and implementing a first-visit system are essential, they lack immediate impact. In the short term, optimizing outpatient processes in tertiary hospitals offers a practical approach to reducing wait times and enhancing patient experience.

This report examines the implementation of a patient-centered intelligent guidance system at a large Chinese tertiary hospital (Figure 2 shows its outpatient building and department layout). The report adheres to the iCHECK-DH (Guidelines and Checklist for the Reporting on Digital Health Implementations) (Checklist 1) [27].

Figure 2. Hospital map and department distribution.

Outpatient	
No.1 Outpatient building	**First floor:** otolaryngology **Second floor:** obstetrics and gynecology, gastroenterology **Third floor**: ophthalmology, stomatology **Fourth floor**: administrative office area
No.2 Outpatient building	**First floor:** orthopedics, traditional Chinese medicine, massage physiotherapy **Second floor:** dermatology, medical cosmetology, plastic surgery **Third floor**: cardiovascular medicine, cardiothoracic surgery, cardiac assistance examination **Fourth floor**: nephrology, urology (male), transplantation
No.3 Outpatient building	**First floor:** surgical oncology, interventional therapy, radiotherapy, burn, gastroenterology, hepatobiliary, endoscopic, vascular, anorectal **Second floor:** respiratory, endocrinology, cadre health **Third floor**: mental health, sleep medicine, neurosurgery, rehabilitation **Fourth floor**: neurology, neuroimmunization, electromyography room, evoked potential room, electroencephalogram room, transcranial Doppler room
No.4 Outpatient building	**First floor:** emergency ward, emergency observation room, emergency intensive care area **Second floor:** emergency ward, emergency observation room, emergency intensive care area **Third floor**: distinguished physicians' clinic



Methods

Aims and Objectives

This study evaluated the intelligent guidance system's efficacy in reducing treatment waiting times and improving patient satisfaction. Herein, we discuss the system's development and implementation, then compare waiting time and satisfaction data preimplementation and postimplementation.

Blueprint Summary

The intelligent guidance system, grounded in patient-centered principles, integrates multisource data and smart sensing technologies to streamline the entire treatment process. It features an automatic check-in module and indoor navigation system linked to hospital databases and installed at entrance gates (Figure 3). Using identity recognition for contactless check-in and hybrid Wi-Fi/Bluetooth positioning for real-time tracking, the system analyzes treatment data to deliver personalized navigation routes via SMS text messaging

XSL•FO
RenderX

notifications. It dynamically adjusts guidance based on real-time positioning and treatment progress, ensuring seamless transitions across consultations, examinations, pharmacy visits, and follow-ups until patient departure. The intelligent medical guidance system avoids mandatory app downloads, using SMS text messaging for inclusive notifications [25]. Unlike traditional systems requiring manual input [26,28], it integrates registration, check-in, and examinations, providing real-time updates and automatic route planning (Table 1). It acts as a personal medical assistant, guiding patients throughout their visit.

Figure 3. Upgraded intelligent guidance system.

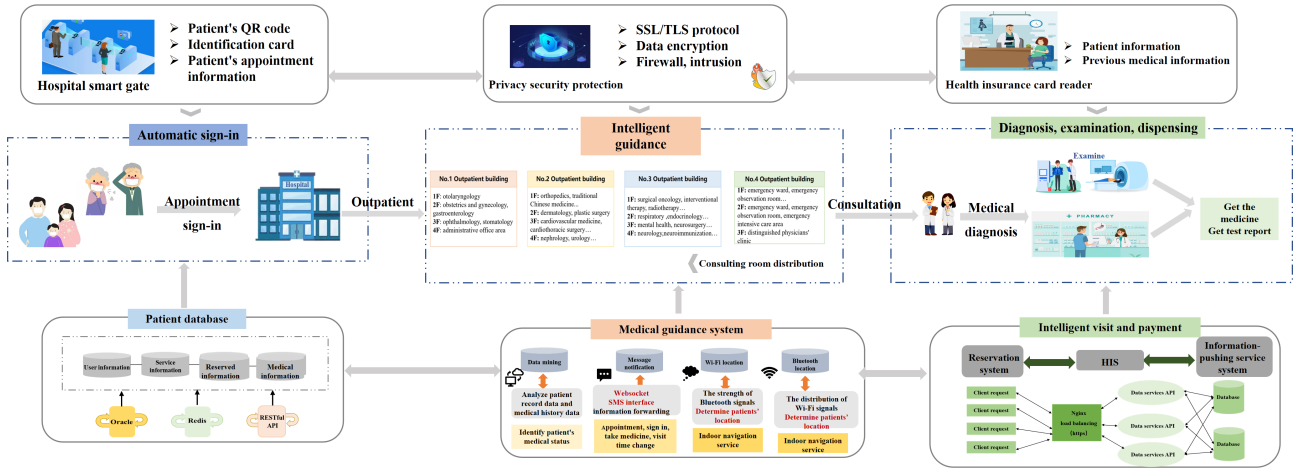


Table . Comparison between traditional guidance systems and intelligent guidance systems.

Category	Traditional guidance systems	Intelligent guidance system
Service acquisition	Download the hospital app or use a specialized device	A phone that can receive text messages
Main function	Simplified functionality: dedicated exclusively to hospital navigation services	Diverse functionalities: assist patients with automatic check-in, link medication pickup, examinations, and treatments, dynamically update patients' medical information in real time, and automatically plan routes to guide them
Features	Noncontinuous service	Continuous service
Principle	Non–patient-centered	Patient-centered

Technical Support for the Intelligent Guidance System

The upgraded system uses a cloud-native microservice system architecture that is convenient for deployment in different environments. Each system is independent and provides better isolation, scalability, ease of maintenance, and other characteristics. The main technology stacks used by the software are Spring Cloud, VUE, Rabbit MQ message queuing, Redis caching, distributed scheduling tasks, Docker, Kubernetes, and DevOps. The cloud-native technology architecture can be used to quickly expand service resources and perform peak business data processing in hospitals. The daily throughput can reach tens of millions, the response time for most requests is in milliseconds, and the data processing capacity can rapidly expand with the amount of data.

Target

The intelligent guidance system was launched in October 2020 at a large tertiary hospital in China and aimed to reduce excessive outpatient waiting times and enhance patient satisfaction. The system provides services to all outpatient patients annually at the hospital. After two years of operation, it has demonstrated initial effectiveness, with subsequent adoption by other tertiary hospitals across China.

Ethical Considerations

This retrospective analysis of fully anonymized hospital operational data received ethical approval from the Ethics Committee of Wenzhou Medical University (approval number 2020 - 075), which explicitly authorized reuse of existing system data without additional consent. Patients retained an opt-out mechanism by rejecting the system's terms through the initial pop-up notification. We are committed to strict confidentiality regarding the personal information and privacy of all research participants, and we have implemented multiple measures to ensure data privacy and security. The collected health and personal data will be stored using industry-standard encryption techniques, and only authorized researchers will have access to these data. All data usage and storage processes will follow strict data management policies to prevent unauthorized access and data breaches. No compensation was provided due to the noninterventional nature of this research using anonymized data.

Data

The intelligent guidance system retrieves real-time patient data, including appointments and Wi-Fi– and Bluetooth-based locations, via the health information system (HIS) interface,

XSL•FO
RenderX

excluding sensitive information. It analyzes patient locations and schedules, generating optimized navigation routes and updating queuing systems upon check-in. Data are securely stored in encrypted local servers and synchronized with the HIS every 10 seconds; anonymized trajectory data are retained for system optimization, while original logs are purged quarterly. Patients access medical records via the hospital portal after ethical approval and informed consent, with security ensured through localized storage, role-based access control, 2-factor authentication, and intranet-restricted analysis. The system interfaces with the HIS, electronic medical record platform, and Internet of Things devices via application programming interface synchronization, enabling real-time updates and anonymized navigation logs for optimization, complying with China's Personal Information Protection Law (Article 28). Patients authorize data usage through electronic agreements, with privacy-by-design principles, encrypted transmission, and strict adherence to data localization (Cybersecurity Law, Article 37) and classified protection (Data Security Law, Article 21).

Interoperability

The intelligent guidance system achieves real-time integration with the hospital's HIS system, synchronizing patient registration and medical information while automatically aligning diagnostic data with optimal treatment pathways. The system supports cross-brand communication devices and navigation terminals, ensuring interoperability across various patient devices within the hospital, thereby enhancing the convenience and accuracy of navigation routes.

Participating Entities

The intelligent guidance system was developed by the IT department of a public hospital. Guided by government policies emphasizing patient service optimization, the hospital's IT center manages HIS integration, enabling secure real-time data exchange across registration, testing, and pharmacy services, along with system maintenance. The outpatient department contributes to route planning and status updates, while the logistics department handles device deployment. Clinical staff provide practical feedback for system improvement, with funding primarily from hospital resources.

Budget Planning

The intelligent guidance system underwent a 12-month development and 3-month pilot deployment. Budget allocation prioritized software and algorithm optimization (50%), covering navigation engine development, HIS integration, and patient interface design. Hardware integration, including Bluetooth beacons and signage, accounted for 20%. Cross-department collaboration received 15%, change management for process updates 10%, and the remaining 5% supported stress testing and patient flow optimization during the pilot phase.

Sustainability

The intelligent guidance system achieves routine operation through integration with the HIS. Financially, initial development was funded by the hospital's IT budget, with sustainable revenue growth realized through enhanced efficiency and increased patient volume. Operationally, the system reduces the need for manual guidance staff, saving human resources while optimizing patient flow and reducing in-hospital stay duration.

Implementation (Results)

Coverage

We used 2019 as the baseline to evaluate waiting times before the system's October 2020 launch, excluding 2020 due to COVID-19 impacts and system buffer time. Data from 2019, 2021, and 2022 were analyzed for waiting time improvements, while 2021 - 2022 data tracked satisfaction trends. Patient satisfaction was measured using structured questionnaires with 5-point Likert scales. Respondents were patients who received treatment at the hospital. After completing all medical consultation procedures, satisfaction questionnaires were automatically pushed by the system. Consultation and examination waiting times for patients aged ≥60 were analyzed separately, though satisfaction data, collected anonymously, lacked age stratification.

The changes in the basic situation of outpatients before and after system optimization and upgrade are summarized in Table 2, which includes the total number of outpatients in 2019, 2020, 2021, and 2022, the sex distribution of outpatients, the age distribution, and the number of examination bills issued in recent years. From 2019 to 2022, the total number of outpatient visits fluctuated. The number of visits increased from 5,067,958 in 2019 to 5,456,151 in 2022. The growth rate during this period was 7.66%. We categorized the patients into the following groups: younger individuals aged 18 years and under, adults aged 19 - 40 years, adults aged 41 - 59 years, and older adults aged ≥60 years. From 2019 to 2022, the number of outpatients in different age groups steadily increased. Patients aged 41 - 59 years accounted for the highest proportion of all outpatients across all study years: 38.6% in 2019, 39.5% in 2020, 40.0% in 2021, 39.5% in 2022. Patients aged 18 accounted for the lowest proportion. The proportion of female outpatients in recent years was generally greater than that of male outpatients. Except for 2020, the proportion of male patients (56%) was higher than the proportion of female patients (44%). The number of invoices also showed an increasing trend from 3,555,896 in 2019 to 3,778,609 in 2022, with a growth rate of 6.26%.

XSL•FO
RenderX

Table . Characteristics of hospital outpatients from 2019 to 2022.

Characteristics	2019	2020	2021	2022
Total patients	5,067,958	4,327,575	5,160,841	5,456,151
Number of invoices	3,555,896	3,075,948	3,665,579	3,778,609
Age group (years), n (%)				
≤18	302,925 (6)	220,846 (5.1)	264,557 (5.1)	277,774 (5.4)
19 - 40	1,563,163 (30.8)	1,283,780 (29.7)	1,538,196 (29.8)	1,542,894 (30)
41 - 59	1,956,001 (38.6)	1,710,187 (39.5)	2,062,394 (40)	2,029,534 (39.5)
≥60	1,245,869 (24.6)	1,112,762 (25.7)	1,295,694 (25.1)	1,292,841 (25.1)
Gender, n (%)				
Male	2,238,480 (44.2)	3,075,948 (56)	2,254,364 (43.7)	2,218,642 (43.9)
Female	2,829,478 (55.8)	2,415,691 (44)	2,906,477 (56.3)	2,829,622 (56.1)

Outcomes

Patient waiting time includes consultation and examination waits. Consultation time is the interval between check-in and doctor login; examination time is the interval between prescription and formal check-in. From 2019 to 2021, overall waiting times decreased: consultation wait times dropped by 3.39 minutes (41.14 to 38.30 min) and examination wait times dropped by 3.35 minutes (47.83 to 44.48 min), while consultation duration increased from 2.85 to 3.43 minutes (Table 3). For patients aged ≥60 years, wait times decreased by 1.82 minutes (42.37 to 40.55 min) and examination wait times decreased by 4.41 minutes (52.04 to 47.63 min), with consultation duration rising from 3.14 to 3.40 minutes (Table 4). Figures 4 and 5 visualize these trends. After optimization and upgrading of the system, patients' satisfaction with the outpatient process continued to improve, and overall satisfaction increased from 89.99 in 2021 to 92.72 in 2022 (P=.005). Figure 4 more clearly visualizes the change in waiting time and the change in satisfaction.

Table . Total patient wait times and satisfaction from 2019 to 2022.

Study phase	2019, mean (SD)	2020, mean (SD)	2021, mean (SD)	2022, mean (SD)	F test (df)	P value
Waiting time for consultation (minutes)	41.14 (2.31)	36.03 (2.78)	38.30 (1.89)	42.42 (2.31)	17.974 (3)	<.001
Waiting time for examination (minutes)	47.83 (1.10)	56.14 (13.34)	45.63 (1.67)	44.48 (1.56)	7.219 (3)	<.001
Consultation time	2.85 (0.03)	3.12 (0.31)	3.04 (0.96)	3.43 (0.26)	16.198 (3)	<.001
Degree of satisfaction (total)	—[a]	—	89.99 (2.78)	92.72 (0.18)	9.981 (11.09)[b]	.005

[a]Not applicable.

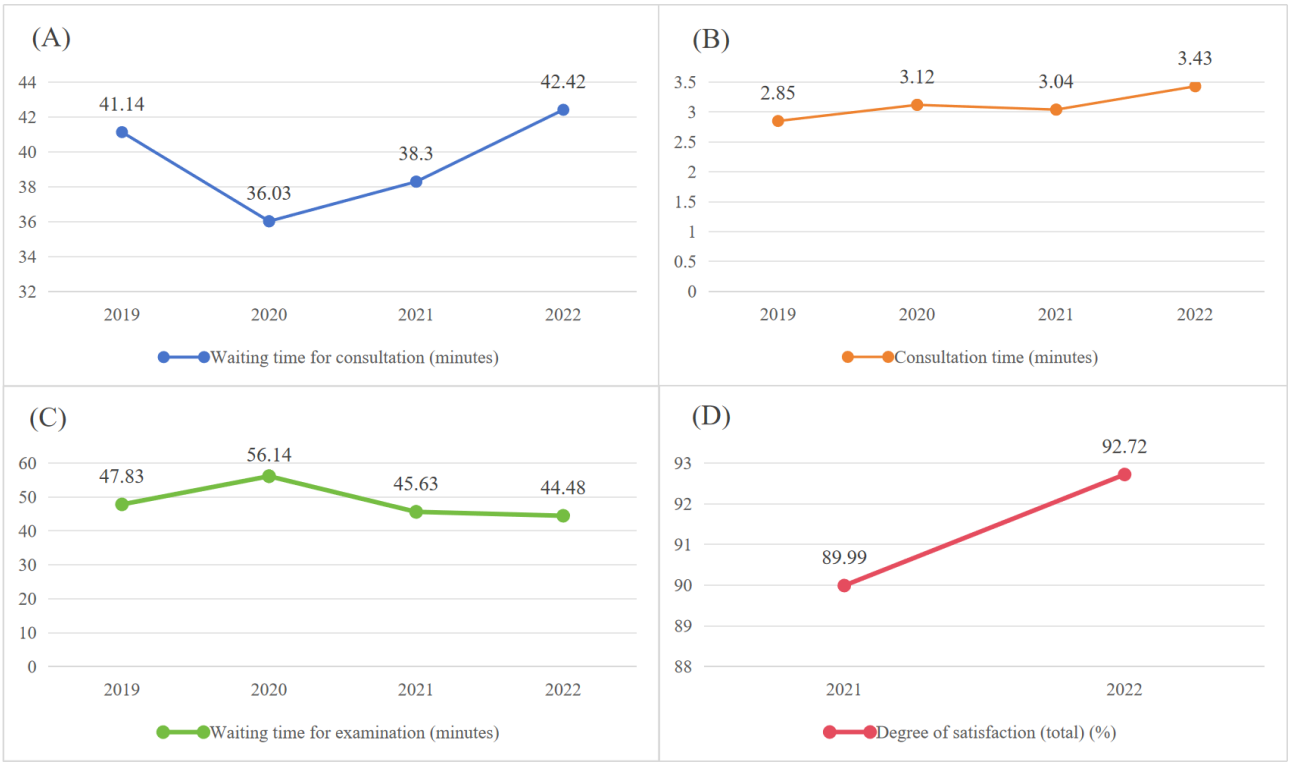
[b]Degrees of freedom are presented as decimals due to the use of Welch ANOVA correction for violation of the homogeneity of variances assumption (Levene test, P<.05). Standard ANOVA results are reported when assumptions were met.

Table . Waiting times for patients aged ≥60 years from 2019 to 2022.

Study phase	2019, mean (SD)	2020, mean (SD)	2021, mean (SD)	2022, mean (SD)	F test (df)	P value
Waiting time for consultation (minutes)	42.37 (2.62)	37.61 (4.02)	40.55 (1.80)	43.68 (2.54)	10.16 (3)	<.001
Waiting time for examination (minutes)	52.04 (1.52)	65.30 (21.25)	47.63 (1.60)	46.58 (1.54)	7.75 (3)	<.001
Consultation time	3.14 (0.04)	3.47 (0.33)	3.40 (0.10)	3.72 (0.22)	16.35 (3)	<.001

XSL•FO
RenderX

Figure 4. Changes in total patient wait times and satisfaction from 2019 to 2022. (A) Waiting time for consultation. (B) Consultation time. (C) Waiting time for examination. (D) Degree of satisfaction (total).



XSL•FO
RenderX

Figure 5. Changes in older patient wait times and satisfaction from 2019 to 2022. (A) Waiting time for consultation. (B) Consultation time. (C) Waiting time for examination.

XSL•FO
RenderX

Discussion

Principal Findings

Applying patient-centered principles, our study transformed a tertiary hospital's medical service process through an intelligent guidance system. This mobile-guided system integrates admission, waiting, and examinations, significantly reducing queues and exam waits while extending consultation times and improving outpatient satisfaction.

Reduced patient waiting times, this reform's primary outcome, align with multiple intervention studies. South Korean physicians used queuing theory to achieve a 30% reduction in outpatient waiting times [20]. A New York pediatric clinic reduced waiting times by 3.2-8.8 minutes through targeted interventions [29]. In China, a tertiary hospital streamlined nonemergency registrations, cutting waiting times from 25.05 to 1.00 minutes [13]. Another redesigned its outpatient pharmacy, halving prescription pickup times from 1 hour to 30 minutes [30]. Similarly, a hospital implementing artificial intelligence–assisted consultations reduced median waiting times from 1.97 to 0.38 hours [31]. However, the waiting time for visits in 2022 increased by 1.28 minutes compared to 2019. The system initially went live in 2020, and the time was reduced in 2021. Considering the huge demand for high-quality medical resources and support for system optimization, the hospital opened more appointments in the same time frame. In the future, after further improvement of the system, it is hoped that the number of tertiary hospitals included will continue to expand in stages to meet the medical needs of more patients.

Another significant benefit of implementing the intelligent guidance system was the increase in the duration of patient consultation time. Consultation time is a crucial factor as it influences the quality of care and patient satisfaction [32-34]. Notably, extending consultation time may enhance satisfaction more substantially than reducing waiting time [9]. Consultation time in Sweden is 10 - 20 minutes [35]. Research conducted in the United States indicated that the average consultation time ranges from 10 to 15 minutes [36]. At a tertiary hospital in China, the average consultation time in 2017 was 6.52 minutes. Globally, consultation durations remain consistently shorter than patient waiting times despite cross-country variations. One hospital even reported reduced consultation times postreform, decreasing from 6.52 to 3.12 minutes [14]. Our smart guidance system progressively extended consultation time. This improvement stemmed from streamlined registration and navigation processes, which reduced missed appointments and clinic crowding, freeing physicians to concentrate on clinical consultations rather than on maintaining order.

Patient satisfaction serves as a crucial gauge of health care quality [37]. A study conducted in Canada demonstrated a significant association between waiting time and patient satisfaction, reporting an odds ratio of 0.92 (95% CI 0.86 - 0.98; *P*=.01) [38]. Nonphysician tasks like registration and pharmacy services prolong wait times, thus reducing patient satisfaction given the inverse wait time/satisfaction relationship [17,39,40]. Our research findings are consistent with this. Tertiary hospitals tend to occupy large areas and have many campuses and buildings. Even when landmarks and walls indicate their locations, patients often get lost in hospitals [41]. The intelligent navigation system addresses this by guiding patients to their appointments, embodying patient-centered care. It significantly boosts satisfaction.

This study demonstrates the significant effectiveness of applying an intelligent guidance system to optimize patient flow in a tertiary hospital, with this experience holding clear generalizability for other tertiary hospitals facing similar challenges such as high patient volume, complex spatial layouts, and prolonged waiting times. The system's core logic—integrating admission check-in, treatment waiting, and examination scheduling with precise mobile guidance—combined with its modular design, can be directly implemented in other large tertiary hospitals to efficiently optimize patient visit processes. Sustainability relies on routine maintenance rather than continuous technical investment, while reduced waiting times increase throughput, allowing more appointments within existing time frames to boost revenue. For successful adoption, hospitals must preserve traditional channels for older adult patients, implement phased pilots starting with high-volume departments, and thoroughly evaluate local contexts including digital capabilities, regional disparities, and patient demographics before staged adaptation.

Limitations and Lessons Learned

The implementation phase consistently presented the greatest challenges, aligning with common industry observations. First, indoor positioning inaccuracies occasionally caused patient navigation errors, requiring supplementary staff guidance that diminished expected efficiency gains. Second, challenges in reaching all patient groups remained, particularly older adults. Despite including features like SMS text message reminders to help bridge the gap, a significant "digital divide"persisted. Most older adult patients preferred traditional methods like physical queuing or in-person assistance. This lower adoption rate among older adults meant the system could not deliver its intended benefits equally to everyone. Future work will tailor research and designs specifically for older adult patient adoption. Finally, deep integration with complex hospital systems caused intermittent interface instability and data synchronization delays, impacting workflow accuracy. During high patient volumes, peak-hour response delays exposed deficiencies in initial stress testing and capacity planning.

Nevertheless, methodological limitations warrant caution. Unadjusted confounders such as departmental variations may partially explain outcomes. For example, the Obstetrics, Surgery, and Cardiology departments face longer waits due to complex workflows. Visit type differences also exist, where initial consultations require more time than follow-ups. Temporal factors like peak-hour or weekday clinics with higher volumes further complicate analysis. Satisfaction surveys incurred self-selection bias as anonymously distributed mobile questionnaires prevented response rate tracking, restricting analysis to voluntary respondents who systematically differ from nonrespondents. Although age, sex data, and wait times for those aged ≥60 years were documented, key potential confounders including education level, digital literacy, and visit

XSL•FO
RenderX

type lacked statistical control. Consequently, outcome associations may be confounded despite standardized HIS metrics, hindering the exploration of variables influencing system usage. Future studies need stratified randomization, multivariable adjustment, and enhanced response strategies to isolate intervention effects.

Conclusions

The WHO advocates patient-centered care to improve medical experiences. Implementing intelligent guidance systems alleviates outpatient issues like prolonged queuing, excessive waits, and low satisfaction through continuous service. This model offers global reference value, particularly for China and similar settings, by upgrading processes with intelligent technologies to reduce waits and increase satisfaction.

Acknowledgments

Drs. Chun Chen and Xiangyang Zhang contributed equally as corresponding authors to the supervision, coordination, and correspondence of this study. We would like to thank the First Affiliated Hospital of Wenzhou Medical University for their assistance and support with the field research. This study was sponsored by the Science and Technology Department of Zhejiang Province China (2023C03165), National Natural Science Foundation of China (72274141), and Wenzhou Science and Technology Bureau Fund Project (Y2023800). The sponsors were not involved in the design and conduct of the study; the collection, management, analysis, and interpretation of data; or the preparation, review, and approval of the manuscript.

Authors' Contributions

Conceptualization: CC (lead), ZG (equal), XW (equal), RZ (equal), MX (equal).
Data curation: XW (lead), RZ (equal), MX (equal), SZ (supporting), LG (supporting), YZ (supporting), HJ (supporting), SP (supporting), MZ (supporting).
Formal analysis: XW (lead), RZ (supporting), MX (supporting).
Funding acquisition: CC (lead), XZ (equal), ZG (equal).
Investigation: XW (lead), RZ (supporting), SZ (supporting), LG (supporting), YZ (supporting), HJ (supporting).
Methodology: XW (lead), RZ (equal), MX (equal).
Resources: ZG (lead), XZ (equal).
Supervision: CC (lead), ZG (equal), XZ (equal).
Validation: XW (lead), SZ (supporting), LG (supporting), YZ (supporting), HJ (supporting), MZ (supporting), SP (supporting).
Visualization: RZ.
Writing – original draft: CC (lead), XW (equal), RZ (equal).
Writing – review & editing: CC (lead), XZ (equal), XW (equal), RZ (equal).

Conflicts of Interest

None declared.

Checklist 1
iCHECK-DH checklist.
[DOCX File, 22 KB - medinform_v13i1e60219_app1.docx]

References

1. People-centred health care: a policy framework. World Health Organization. 2007. URL: https://www.who.int/publications/i/item/9789290613176 [accessed 2025-08-22]
2. Alarcón-Yaquetto DE, de Ferrari A, Málaga G. The road to patient-centred care in Peru: the difficulties and opportunities to achieve participatory health care. Z Evid Fortbild Qual Gesundhwes 2022 Jun;171:113-116. [doi: 10.1016/j.zefq.2022.04.027] [Medline: 35610135]
3. Montague T, Gogovor A, Aylen J, et al. Patient-centred care in Canada: key components and the path forward. Healthc Q 2017;20(1):50-56. [doi: 10.12927/hcq.2017.25136] [Medline: 28550701]
4. Achstetter K, Köppen J, Hengel P, Blümel M, Busse R. Drivers of patient perceptions of health system responsiveness in Germany. Int J Health Plann Manage 2022 Dec;37 Suppl 1:166-186. [doi: 10.1002/hpm.3570] [Medline: 36184993]
5. Ekman I, Swedberg K, Taft C, et al. Person-centered care--ready for prime time. Eur J Cardiovasc Nurs 2011 Dec;10(4):248-251. [doi: 10.1016/j.ejcnurse.2011.06.008] [Medline: 21764386]
6. Gluyas H. Patient-centred care: improving healthcare outcomes. Nurs Stand 2015 Sep 23;30(4):50-57. [doi: 10.7748/ns.30.4.50.e10186] [Medline: 26394978]
7. Jakobsson S, Ringström G, Andersson E, et al. Patient safety before and after implementing person-centred inpatient care - a quasi-experimental study. J Clin Nurs 2020 Feb;29(3-4):602-612. [doi: 10.1111/jocn.15120] [Medline: 31769572]

XSL•FO
RenderX

8. Hann M, Reeves D, Sibbald B. Relationships between job satisfaction, intentions to leave family practice and actually leaving among family physicians in England. Eur J Public Health 2011 Aug;21(4):499-503. [doi: 10.1093/eurpub/ckq005] [Medline: 20142402]
9. Sun J, Lin Q, Zhao P, et al. Reducing waiting time and raising outpatient satisfaction in a Chinese public tertiary general hospital-an interrupted time series study. BMC Public Health 2017 Aug 22;17(1):668. [doi: 10.1186/s12889-017-4667-z] [Medline: 28830400]
10. Yan M, Zhi M, Xu Y, Hu L, Liu Y. Inpatient satisfaction with nursing care and its impact factors in Chinese tertiary hospitals: a cross-sectional study. Int J Environ Res Public Health 2022 Dec 9;19(24):16523. [doi: 10.3390/ijerph192416523] [Medline: 36554403]
11. Liu Y, Zhang F, Guan C, et al. Patient satisfaction with humanistic nursing in Chinese secondary and tertiary public hospitals: a cross-sectional survey. Front Public Health 2023;11:1163351. [doi: 10.3389/fpubh.2023.1163351]
12. Zhao X, Jiang L, Zhao K. 3D differential equation model for patients' choice of hospital in China. Front Public Health 2022;10:760143. [doi: 10.3389/fpubh.2022.760143]
13. Xie W, Yang X, Cao X, Liu P. Effects of a comprehensive reservation service for non-emergency registration on appointment registration rate, patient waiting time, patient satisfaction and outpatient volume in a tertiary hospital in China. BMC Health Serv Res 2019 Nov 1;19(1):782. [doi: 10.1186/s12913-019-4652-6] [Medline: 31675973]
14. Shen J, Zhang J, He Q, et al. "Without the need for a second visit" initiative improves patient satisfaction with updated services of outpatient clinics in China. BMC Health Serv Res 2021 Mar 23;21(1):267. [doi: 10.1186/s12913-021-06260-3] [Medline: 33757490]
15. Cheung YY, Goodman EM, Osunkoya TO. No more waits and delays: streamlining workflow to decrease patient time of stay for image-guided musculoskeletal procedures. Radiographics 2016;36(3):856-871. [doi: 10.1148/rg.2016150174] [Medline: 27163595]
16. Luo JYN, Liu PP, Wong MCM. Patients' satisfaction with dental care: a qualitative study to develop a satisfaction instrument. BMC Oral Health 2018 Jan 30;18(1):15. [doi: 10.1186/s12903-018-0477-7] [Medline: 29382318]
17. Bleustein C, Rothschild DB, Valen A, Valatis E, Schweitzer L, Jones R. Wait times, patient satisfaction scores, and the perception of care. Am J Manag Care 2014 May;20(5):393-400. [Medline: 25181568]
18. Kalan L, Chahine RA, Lasfer C. The effectiveness and relevance of the Canadian triage system at times of overcrowding in the emergency department of a private tertiary hospital: a United Arab Emirates (UAE) study. Cureus 2024 Jan;16(1):e52921. [doi: 10.7759/cureus.52921] [Medline: 38406095]
19. Almomani I, AlSarheed A. Enhancing outpatient clinics management software by reducing patients' waiting time. J Infect Public Health 2016;9(6):734-743. [doi: 10.1016/j.jiph.2016.09.005] [Medline: 27663518]
20. Lee H, Choi EK, Min KA, Bae E, Lee H, Lee J. Physician-customized strategies for reducing outpatient waiting time in South Korea using queueing theory and probabilistic metamodels. IJERPH 2022;19(4):2073. [doi: 10.3390/ijerph19042073]
21. Zhou LM, Xu RH, Xu YH, Chang JH, Wang D. Inpatients' perception of patient-centered care in Guangdong Province, China: a cross-sectional study. Inquiry 2021;58:469580211059482. [doi: 10.1177/00469580211059482] [Medline: 34872361]
22. Xiong X, Luo L. Patient-centred method to evaluate the spatial accessibility of primary health care in a case study in Shanghai. Aust J Prim Health 2020 Aug;26(4):344-350. [doi: 10.1071/PY19233] [Medline: 32669196]
23. Sun J, Hu G, Ma J, et al. Consumer satisfaction with tertiary healthcare in China: findings from the 2015 China National Patient Survey. Int J Qual Health Care 2017 Apr 1;29(2):213-221. [doi: 10.1093/intqhc/mzw160] [Medline: 28096280]
24. Liu HY, Lee WC, Sun YC, et al. Hospital-owned apps in Taiwan: nationwide survey. JMIR mHealth uHealth 2018 Jan 16;6(1):e22. [doi: 10.2196/mhealth.8636] [Medline: 29339347]
25. Teramoto K, Kuwata S. Design and evaluation of a smartphone medical guidance app for outpatients of large-scale medical institutions: retrospective observational study. JMIR Form Res 2022 Apr 21;6(4):e32990. [doi: 10.2196/32990] [Medline: 34818208]
26. Xie X, Zhou W, Lin L, et al. Internet hospitals in China: cross-sectional survey. J Med Internet Res 2017 Jul 4;19(7):e239. [doi: 10.2196/jmir.7854] [Medline: 28676472]
27. Perrin Franck C, Babington-Ashaye A, Dietrich D, et al. iCHECK-DH: Guidelines and Checklist for the Reporting on Digital Health Implementations. J Med Internet Res 2023 May 10;25:e46694. [doi: 10.2196/46694] [Medline: 37163336]
28. Taha J, Czaja SJ, Sharit J, Morrow DG. Factors affecting usage of a personal health record (PHR) to manage health. Psychol Aging 2013 Dec;28(4):1124-1139. [doi: 10.1037/a0033911] [Medline: 24364414]
29. Racine AD, Davidson AG. Use of a time-flow study to improve patient waiting times at an inner-city academic pediatric practice. Arch Pediatr Adolesc Med 2002 Dec;156(12):1203-1209. [doi: 10.1001/archpedi.156.12.1203] [Medline: 12444831]
30. Pierce II RA, Rogers EM, Sharp MH, Musulin M. Outpatient pharmacy redesign to improve work flow, waiting time, and patient satisfaction. Am J Health Syst Pharm 1990 Feb 1;47(2):351-356. [doi: 10.1093/ajhp/47.2.351]
31. Li X, Tian D, Li W, et al. Artificial intelligence-assisted reduction in patients' waiting time for outpatient process: a retrospective cohort study. BMC Health Serv Res 2021 Mar 17;21(1):237. [doi: 10.1186/s12913-021-06248-z] [Medline: 33731096]

XSL•FO
RenderX

32. Deveugele M, Derese A, van den Brink-Muinen A, Bensing J, De Maeseneer J. Consultation length in general practice: cross sectional study in six European countries. BMJ 2002 Aug 31;325(7362):472. [doi: 10.1136/bmj.325.7362.472] [Medline: 12202329]
33. Cape J. Consultation length, patient-estimated consultation length, and satisfaction with the consultation. Br J Gen Pract 2002 Dec;52(485):1004-1006. [Medline: 12528588]
34. Jabour AM. The impact of electronic health records on the duration of patients' visits: time and motion study. JMIR Med Inform 2020 Feb 7;8(2):e16502. [doi: 10.2196/16502] [Medline: 32031539]
35. Andersson SO, Mattsson B. Length of consultations in general practice in Sweden: views of doctors and patients. Fam Pract 1989 Jun;6(2):130-134. [doi: 10.1093/fampra/6.2.130] [Medline: 2744297]
36. al-Faris EA, al-Dayel MA, Ashton C. The effect of patients' attendance rate on the consultation in a health centre in Saudi Arabia. Fam Pract 1994 Dec;11(4):446-452. [doi: 10.1093/fampra/11.4.446] [Medline: 7895975]
37. Boudreaux ED, Mandry CV, Wood K. Patient satisfaction data as a quality indicator: a tale of two emergency departments. Acad Emerg Med 2003 Mar;10(3):261-268. [doi: 10.1111/j.1553-2712.2003.tb02000.x] [Medline: 12615592]
38. Chan BJ, Barbosa J, Moinul P, et al. Patient satisfaction with wait times at an emergency ophthalmology on-call service. Can J Ophthalmol 2018 Apr;53(2):110-116. [doi: 10.1016/j.jcjo.2017.08.002] [Medline: 29631820]
39. Mehra P. Outpatient clinic waiting time, provider communication styles and satisfaction with healthcare in India. Int J Health Care Qual Assur 2016 Aug 8;29(7):759-777. [doi: 10.1108/IJHCQA-02-2016-0017] [Medline: 27477932]
40. Ham HS, Peck EH, Moon HS, Yeom HA. Predictors of patient satisfaction with tertiary hospitals in Korea. Nurs Res Pract 2015;2015:749754. [doi: 10.1155/2015/749754] [Medline: 25722886]
41. Devlin AS. Wayfinding in healthcare facilities: contributions from environmental psychology. Behav Sci (Basel) 2014 Oct 31;4(4):423-436. [doi: 10.3390/bs4040423] [Medline: 25431446]

Abbreviations

HIS: health information system
iCHECK-DH: Guidelines and Checklist for the Reporting on Digital Health Implementations
WHO: World Health Organization

Edited by C Perrin; submitted 05.05.24; peer-reviewed by H Guo, J Kaswija, T Yang; revised version received 07.07.25; accepted 17.07.25; published 29.08.25.

Please cite as:
Wang X, Zhang R, Gao Z, Xia M, Zhang S, Ge L, Zhu Y, Jin H, Pan S, Zheng M, Chen C, Zhang X
Patient-Centered Outpatient Process Optimization System Based on Intelligent Guidance in a Large Tertiary Hospital in China: Implementation Report
JMIR Med Inform 2025;13:e60219
URL: https://medinform.jmir.org/2025/1/e60219
doi:10.2196/60219

© Xiaoyi Wang, Rujia Zhang, Zhihong Gao, Mengxuan Xia, Songjia Zhang, Lizheng Ge, Yuyang Zhu, Haojie Jin, Shenglian Pan, Manman Zheng, Chun Chen, Xiangyang Zhang. Originally published in JMIR Medical Informatics (https://medinform.jmir.org), 29.8.2025. This is an open-access article distributed under the terms of the Creative Commons Attribution License (https://creativecommons.org/licenses/by/4.0/), which permits unrestricted use, distribution, and reproduction in any medium, provided the original work, first published in JMIR Medical Informatics, is properly cited. The complete bibliographic information, a link to the original publication on https://medinform.jmir.org/, as well as this copyright and license information must be included.

XSL•FO
RenderX

Artificial Intelligence–Based Computerized Digit Vigilance Test in Community-Dwelling Older Adults: Development and Validation Study

Gong-Hong Lin[1], PhD; Dorothy Bai[2], PhD; Yi-Jing Huang[3,4], PhD; Shih-Chieh Lee[3,5], PhD; Mai Thi Thuy Vu[1,6], MS; Tsu-Hsien Chiu[7], MS

[1]International Ph.D. Program in Gerontology and Long-Term Care, College of Nursing, Taipei Medical University, Taipei, Taiwan

[2]School of Gerontology and Long-Term Care, College of Nursing, Taipei Medical University, 250 Wuxing Street, Xinyi District, Taipei, Taiwan

[3]School of Occupational Therapy, College of Medicine, National Taiwan University, Taipei, Taiwan

[4]Department of Physical Medicine and Rehabilitation, National Taiwan University Hospital, Taipei, Taiwan

[5]Department of Psychiatry, National Taiwan University Hospital, Taipei, Taiwan

[6]Nam Dinh University of Nursing, Nam Dinh, Nam Đ nh Province, Vietnam

[7]Department of Civil Engineering, National Taiwan University, Taipei, Taiwan

Corresponding Author:
Dorothy Bai, PhD
School of Gerontology and Long-Term Care, College of Nursing, Taipei Medical University, 250 Wuxing Street, Xinyi District, Taipei, Taiwan

Abstract

Background: The Computerized Digit Vigilance Test (CDVT) is a well-established measure of sustained attention. However, the CDVT only measures the total reaction time and response accuracy and fails to capture other crucial attentional features such as the eye blink rate, yawns, head movements, and eye movements. Omitting such features might provide an incomplete representative picture of sustained attention.

Objective: This study aimed to develop an artificial intelligence (AI)–based Computerized Digit Vigilance Test (AI-CDVT) for older adults.

Methods: Participants were assessed by the CDVT with video recordings capturing their head and face. The Montreal Cognitive Assessment (MoCA), Stroop Color Word Test (SCW), and Color Trails Test (CTT) were also administered. The AI-CDVT was developed in three steps: (1) retrieving attentional features using OpenFace AI software (CMU MultiComp Lab), (2) establishing an AI-based scoring model with the Extreme Gradient Boosting regressor, and (3) assessing the AI-CDVT's validity by Pearson *r* values and test-retest reliability by intraclass correlation coefficients (ICCs).

Results: In total, 153 participants were included. Pearson *r* values of the AI-CDVT with the MoCA were −0.42, −0.31 with the SCW, and 0.46–0.61 with the CTT. The ICC of the AI-CDVT was 0.78.

Conclusions: We developed an AI-CDVT, which leveraged AI to extract attentional features from video recordings and integrated them to generate a comprehensive attention score. Our findings demonstrated good validity and test-retest reliability for the AI-CDVT, suggesting its potential as a reliable and valid tool for assessing sustained attention in older adults.

(JMIR Med Inform 2025;13:e73038) doi:10.2196/73038

KEYWORDS

artificial intelligence; assessment; cognition; age-friendly; attention

Introduction

Sustained attention can be defined as a state of readiness to detect and respond to certain changes in the environment that occur at random intervals over extended periods of time [1,2]. The effects of aging on sustained attention are complex; while some aspects of attention may decline, some studies suggested that older adults can maintain more stable performance on certain vigilance tasks than their younger counterparts [3,4]. This phenomenon is not thought to reflect general superiority but rather several factors, including that older adults report fewer task-unrelated thoughts (ie, less mind-wandering) [5,6] and adopt a more cautious, top-down response strategy that prioritizes accuracy over speed. Research indicated that the performance and variability of sustained attention in older adults are related to frailty and fall risks [7,8]. Consequently, monitoring sustained attention in older adults could be an effective way to manage the health of older adults.

XSL•FO
RenderX

The Computerized Digit Vigilance Test (CDVT) is a widely used measure of sustained attention with established reliability and validity [9,10]. However, like many traditional cognitive tests, it relies on a single modality of data, performance metrics (ie, reaction time and accuracy). This unimodal approach overlooks a rich stream of behavioral data that contains valuable information about a person's attentional state. For instance, subtle increases in the blink duration, downward gaze shifts, and slight head drooping are all well-documented physical manifestations of waning vigilance and attentional lapses [11-14]. By failing to capture these overt behaviors, the test's reliability is constrained, as fluctuations in reaction time alone might not fully or consistently reflect an individual's true attentional state.

The concept of using automated, vision-based systems to infer cognitive states from behavioral cues is well-established in other fields. For instance, in transportation safety, extensive research has focused on developing systems that monitor driver vigilance by analyzing features like the blink rate, gaze direction, and head pose to detect drowsiness and prevent accidents [15,16]. Similarly, in educational technology and human-computer interactions, computer vision techniques are used to assess student engagement and cognitive load by tracking similar behavioral markers [17,18]. These applications demonstrate the value of using objective, observable behaviors as proxies for internal attentional states. However, despite success in these domains, this multimodal approach has seen limited application in enhancing standardized clinical neuropsychological assessments, particularly for older adults.

Artificial intelligence (AI) offers a promising approach to analyze facial features [19,20], potentially providing valuable supplementary data for attention assessments [11]. AI-powered software can directly extract attentional features, such as the eye blink rate, yawn frequency, head rotation, and eye movements, from images or videos of faces [19,20]. Traditionally, collecting these features required specialized equipment such as eye trackers or virtual reality headsets [11]. AI-based software offers a more cost-effective and feasible alternative for collecting attentional data [19,20], particularly in clinical settings and for older adult populations.

In this study, we attempted to bridge this gap by leveraging AI to integrate these disparate data streams. AI, particularly machine learning models, is exceptionally well-suited for this task because it can learn complex, nonlinear patterns from multimodal data, automatically determining the optimal weight to assign each feature—from reaction time to eyelid distance—to produce a single, comprehensive score. Therefore, in this study, we attempted to enhance the psychometric properties of the CDVT by integrating an additional modality of data. We developed an artificial intelligence–based Computerized Digit Vigilance Test (AI-CDVT) that uses machine learning to combine traditional performance metrics with facial and behavioral features captured on video. The primary hypothesis was that by creating a more comprehensive, multimodal assessment, we could improve the test-retest reliability of the measure while maintaining its convergent validity.

Methods

Participants

Participants were recruited via convenience sampling from community care centers in Taiwan. A member of the research team visited these centers, provided an oral presentation to groups of older adults explaining the study's purpose and procedures, and invited interested individuals to enroll. Participants were eligible if they met the following criteria: (1) aged 65 years or older, (2) having had no hospitalization in the past 6 months, and (3) willing to participate in the study. Exclusion criteria were a doctor-diagnosed disability or an unwillingness to record videos during the CDVT assessment.

Procedures

This study consisted of 2 waves of data collection. In the first wave, participants were assessed once to gather cross-sectional data. Assessments included the CDVT and Montreal Cognitive Assessment (MoCA) [21]. In the second wave, participants were assessed twice, with a 2-week interval between assessments, to collect test-retest data. Both assessments involved the CDVT and MoCA. Additionally, in the first assessment, the Stroop Color Word Test (SCW) [22] and both parts of the Color Trails Test (CTT) [23] were assessed. At the start of the first assessment session for each participant, a trained assessor administered a brief questionnaire to collect demographic information, including age, sex, and educational attainment (Multimedia Appendix 1). Each participant was individually assessed by a trained assessor in a quiet, one-on-one setting at a community care center. All assessments were conducted on a laptop computer with a 15.6-inch screen, an Intel i5 processor, 8 GB of DDR4 RAM, and a GTX 950 graphics card. Participants were seated approximately 50 cm from the screen. Video recordings capturing participants' heads and faces were obtained using the laptop's built-in HD webcam (1.3 megapixels) during CDVT assessments.

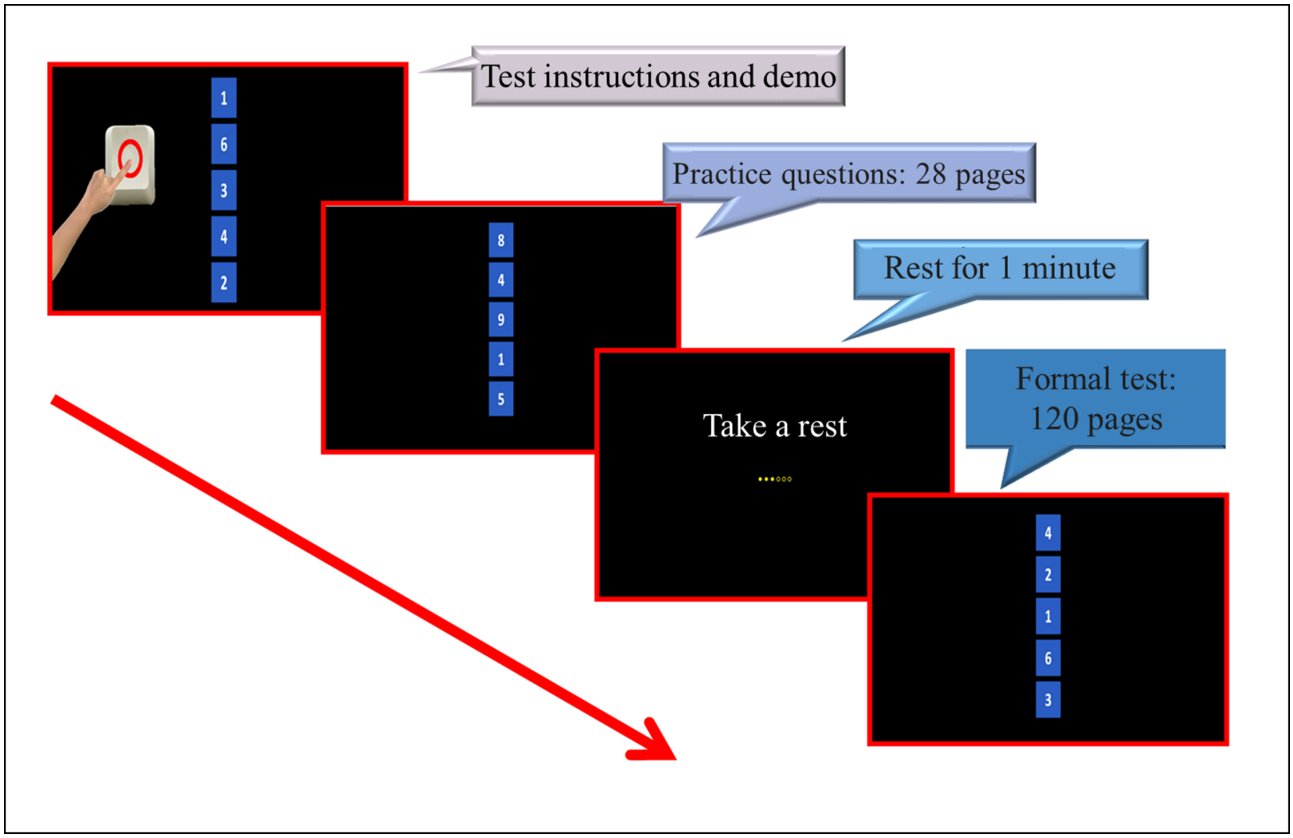
Measures

Computerized Digit Vigilance Test (CDVT)

The CDVT is a computer-based test designed to assess sustained attention. Participants use 2 buttons (a circle and an X) to respond to the presence of the numeral "6" on the screen (Figure 1). The test records response times and errors to evaluate sustained attention, with shorter times indicating better focus. Studies showed good validity and reliability of the CDVT in patients with stroke and schizophrenia [9,10].

XSL•FO
RenderX

Figure 1. Computerized Digit Vigilance Test process and items.



Montreal Cognitive Assessment (MoCA)

The MoCA is a cognitive screening tool used to assess various cognitive domains in older adults. The MoCA evaluates short-term memory, visuospatial abilities, executive functions, attention, concentration, working memory, language, and orientation. The total score on the MoCA is 30, with a higher score indicating better cognitive performance. The MoCA demonstrated good validity and reliability in older adults [24,25]. Further details on the instrument and its authorized use are provided in Multimedia Appendix 1.

Stroop Color Word Test (SCW)

The SCW is a neuropsychological assessment tool used to evaluate cognitive function, particularly attention and executive functioning. During the SCW, participants are presented with a list of color words printed in incongruent font colors (eg, “RED” printed in blue). Participants are asked to verbally name the color of the font, inhibiting the prepotent response of reading the word itself. Faster completion times on the SCW are indicative of better attention and executive functioning. Good reliability and validity of the SCW were reported in older adults [26]. The specific version used in this study is cited in Multimedia Appendix 1.

Color Trails Test (CTT)

The CTT is a language-free version of the Trail Making Test, designed to measure sustained attention and divided attention in adults. The CTT involves connecting circles in an ascending numbered sequence (from 1 to 25) in the CTT1 and alternating between pink and yellow colors while connecting numbers in ascending order in the CTT2. Numbers are presented twice, once in pink and once in yellow, requiring the client to consecutively follow the sequence while avoiding the same color in a row. The time taken to complete each part of the CTT is recorded in seconds. Good reliability of the CTT was determined in older adults [27]. The specific version used in this study is cited in Multimedia Appendix 1.

Data Analysis

To determine whether the AI-CDVT can evaluate participants’ attention according to their facial videos and CDVT output, we developed the AI-CDVT in 3 steps, retrieving attentional features, establishing an AI-based scoring model, and validating the AI-CDVT. In the first step, we adopted OpenFace (CMU MultiComp Lab) [28] to retrieve attentional features from a participant’s face in videos. Attentional features were extracted from each video frame. The eight primary features included: (1-2) the distance between the eyelids for each eye, serving as a continuous measure of eye openness (a smaller distance indicates greater closure, as a proxy for blinks); (3) the distance between the lips, indicating mouth opening or yawning; (4 - 6) head rotation angles across 3 axes, corresponding to pitch (nodding), yaw (side-to-side rotation), and roll (ear-to-shoulder tilt); and (7-8) the X-Y coordinates of the estimated gaze point. For each of the 120 trials in the CDVT, we aggregated the frame-by-frame data by calculating the mean value for each of these 8 features. Within any given trial, video frames where OpenFace failed to successfully track facial features were excluded from this calculation; the mean was computed only from the successfully captured frames. Furthermore, because the CDVT is a computerized test that requires a response before proceeding to the next item, there were no missing test items. This process yielded a single value per feature for each trial.

XSL•FO
RenderX

Finally, we calculated the overall mean and SD of these 120 trial-level values for each feature. These 16 summary statistics (8 features×2 statistics), along with the mean and SD of the reaction time and response accuracy from the original CDVT, constituted the final set of 20 input features for the AI model. All input features were normalized to a common scale before being used in the model.

In the second step, we adopted an AI algorithm, the Extreme Gradient Boosting (XGBoost) regressor [29], to receive inputs of attentional features and estimate scores of the CDVT as scores of the AI-CDVT. The XGBoost regressor leverages the aggregation of random forest regressors to improve the predictive accuracy and has been successfully used in medication situations [29]. In addition, the XGBoost regressor offers an importance ranking of attentional features to generate AI-CDVT scores.

In the third step, we validated the AI-CDVT using a 3-fold cross-validation procedure [30]. In this procedure, we randomly separated our data into 3 subdatasets. Then, we validated the AI-CDVT 3 times. For each validation instance, we used 2 subdatasets to train the XGBoost regressor and used the remaining subdataset to validate the convergent validity and test-retest reliability. Notably, a different subdataset was used each time for validation.

Then, we calculated the mean and SD of the indices of validity across the 3 validation times. The convergent validity was examined using Pearson *r* values to evaluate associations between AI-CDVT scores and those of the MoCA, CTT, and SCW. In addition, we also calculated Pearson *r* values between CDVT scores and those of the MoCA, CTT, and SCW. If Pearson *r* values of the AI-CDVT were similar to those of the CDVT, the convergent validity of the AI-CDV was considered good [31].

The test-retest reliability was examined using an intraclass correlation coefficient (ICC) to evaluate the agreement of scores in the test and retest assessment sections. An ICC value of > 0.75 indicates good test-retest reliability [32].

Finally, to provide a more rigorous evaluation of the AI-CDVT's clinical utility beyond correlational metrics, we conducted a supplementary classification analysis. The goal was to determine whether the multimodal features captured by the AI-CDVT offered incremental value in predicting a clinically relevant outcome. We used the MoCA score as a proxy for the cognitive status, dichotomizing participants into 2 groups based on the common clinical cutoff for potential cognitive impairment "at risk" (MoCA score ≤25) and "not at risk" (MoCA score >25). We then compared the performance of the 2 XGBoost classification models in predicting this binary outcome. The first model ("CDVT-Only") used only the mean reaction time and mean accuracy from the CDVT as input features. The second model ("AI-CDVT Top 5") used the 5 most important features identified in our initial regression model (see Table 1), which included a mix of performance and facial metrics. Specifically, these top 5 features were the mean reaction time, the mean distance between the right eyelids, the mean Y coordinate of the gaze point, the mean accuracy, and the mean angle of head rotation in the Y axis (yaw). Model performance was evaluated using the accuracy and F_1-score across the same 3-fold cross-validation procedure.

XSL•FO
RenderX

Table . Rank of importance of attentional features in the artificial intelligence–based Computerized Digit Vigilance Test.

Rank	Attentional feature
1	Mean of the reaction time
2	Mean of the distance between the right eyelids
3	Mean of the Y coordinate of the gaze point
4	Mean of the accuracy
5	Mean of the angle of head rotation in the Y axis (yaw)
6	SD of the Y coordinate of the gaze point
7	SD of the distance between the right eyelids
8	Mean of the distance between the left eyelids
9	SD of the angle of head rotation in the Z-axis (roll)
10	SD of the X coordinate of the gaze point
11	Mean of the angle of head rotation in the Z-axis (roll)
12	Mean of the distance between the lips
13	Mean of the angle of head rotation in the X-axis (pitch)
14	SD of the accuracy
15	SD of the distance between the lips
16	SD of the angle of head rotation in the X-axis (pitch)
17	SD of the distance between the left eyelids
18	Mean of the X coordinate of the gaze point
19	SD of the angle of head rotation in the Y-axis (yaw)
20	SD of the reaction time

Ethical Considerations

This study was approved by an institutional review board (Taipei Medical University, approval number: N202010008), and all participants provided written informed consent. Participants received a small honorarium of a gift voucher equivalent to US $3 for their time and participation. The informed consent process explicitly detailed the nature of the video recording and its purpose. To ensure data privacy and confidentiality, all video data were stored on an encrypted, offline hard drive. The raw video files were permanently deleted immediately after the deidentified facial features were extracted by OpenFace software, and only these numerical, nonidentifiable data points were retained for analysis.

Results

In total, 153 participants were used for the cross-sectional data (n=87) and test-retest data (n=66). In the cross-sectional data, the average age of participants was 70.8 years, and most of them were female (64/87, 73.6%). In general, they had no cognitive impairment according to the average MoCA score (25.5, SD 2.8). Characteristics of the test-retest data were similar to those of cross-sectional data, as there were no significant differences between them. Table 2 shows further information on these characteristics.

XSL•FO
RenderX

Table . Demographic and baseline cognitive characteristics of study participants.

Variable	Cross-sectional data (n=87)	Test-retest data (n=66)	*t* test or chi-square (*df*)	*P* value
Age (years), mean (SD)	70.8 (5.9)	72.4 (5.9)	1.66 (151)	.10
Sex (male), n (%)	64 (73.6)	49 (74.2)	.009 (1)	.92
Educational level, n (%)			6.06 (4)	.19
Graduate school	6 (6.9)	5 (7.6)		
University	37 (42.5)	17 (25.8)		
High school	32 (36.8)	36 (54.5)		
Junior high school	6 (6.9)	3 (4.5)		
Elementary school	6 (6.9)	5 (7.6)		
MoCA[a], mean (SD)	25.5 (2.8)	25 (3.3)	1.01 (151)	.31
CDVT[b], mean (SD)	239.6 (25.2)	247.3 (26.8)	1.82 (151)	.07
AI-CDVT[c], mean (SD)	239.2 (24.6)	247.3 (27)	1.93 (151)	.06

[a]MoCA: Montreal Cognitive Assessment.

[b]CDVT: Computerized Digit Vigilance Test.

[c]AI-CDVT: artificial intelligence–based Computerized Digit Vigilance Test.

Pearson *r* values of AI-CDVT scores with external criteria were −0.42 (SD 0.19) with the MoCA score, −0.31 (SD 0.16) with the SCW score, 0.46 (SD 0.17) with CTT1 score, and 0.61 with CTT2 scores, and. Pearson *r* values of the AI-CDVT were similar to those of the CDVT. Specifically, Pearson *r* values between the CDVT score and external criteria scores were −0.41 (SD 0.17), −0.29 (SD 0.10), 0.44 (SD 0.21), and 0.55 (SD 0.15), respectively.

The average ICC of the AI-CDVT was 0.78 with a range of 0.68 - 0.84 according to 3-fold cross-validation (Table 3). Similar results were found for the CDVT, for which the average ICC was 0.71 with a range of 0.64 - 0.76.

Table . Test-retest reliability of the artificial intelligence–based Computerized Digit Vigilance Test (AI-CDVT) and original Computerized Digit Vigilance Test (CDVT) over a 2-week interval.

Performance metric	CDVT	AI-CDVT
Cross-validation: Fold 1, ICC[a] (95% CI)	0.72 (0.44 - 0.87)	0.84 (0.67 - 0.93)
Cross validation: Fold 2, ICC[a] (95% CI)	0.76 (0.5 - 0.89)	0.81 (0.61 - 0.92)
Cross validation: Fold 3, ICC[a] (95% CI)	0.64 (0.32 - 0.83)	0.68 (0.27 - 0.87)
Average across 3-fold cross validation, mean (SD)	0.71 (0.06)	0.78 (0.09)

[a]ICC: intraclass correlation coefficient.

In the supplementary classification analysis, the model using the top 5 AI-CDVT features demonstrated improved performance in predicting the cognitive status (MoCA ≤25) compared to the model using only traditional CDVT metrics. Specifically, the AI-CDVT Top 5 model achieved an average accuracy of 58.9% and an F_1-score of 50.6% across the 3 folds. This represents a modest improvement over the CDVT-only model, which scored an accuracy of 57.5% and an F_1-score of 48.6%.

Importance values of attentional features of the AI-CDVT are listed in Table 1. The top 5 most important attentional features were the mean of the reaction time, the distance between the right eyelids, the Y coordinate of the gaze point, mean of the accuracy, and the horizontal rotation angle of the head (Table 1).

Discussion

Principal Findings

The primary rationale for developing the AI-CDVT was to determine if integrating multiple, objective behavioral data streams could enhance the psychometric robustness of a standard sustained-attention test. While the AI-CDVT did not shorten the test's administration time nor demonstrate superior correlations with external cognitive measures, our findings support the study's main hypothesis: the AI-CDVT achieved a notable improvement in the test-retest reliability while maintaining convergent validity comparable to the original CDVT. This suggests that by capturing a richer, multimodal snapshot of an individual's attentional state, the AI-CDVT offers a more stable and reliable assessment tool.

XSL•FO
RenderX

Compared to the CDVT, the AI-CDVT demonstrated equivalent validity and improved test-retest reliability. This enhanced reliability might be attributed to the incorporation of additional attentional features in the AI-CDVT [33,34]. By incorporating a broader range of attentional features, AI-CDVT scores likely benefited from greater stability and robustness. The AI-CDVT score may be less vulnerable to fluctuations solely due to response speed or accuracy. The findings suggest that incorporating a wider range of attentional features during assessments can lead to more reliable scores.

While the AI-CDVT's convergent validity correlations were similar to those of the original CDVT, its primary clinical and functional value lies not in superior predictive accuracy but in its enhanced psychometric robustness and the potential for a more nuanced interpretation of attentional performance. The improved test-retest reliability, for example, is a direct clinical benefit, as it provides a more stable and trustworthy score for longitudinal monitoring or evaluating intervention effects [32]. Furthermore, by capturing a wider array of behaviors like gaze shifts and eyelid closure, the AI-CDVT provides a richer dataset. This could allow clinicians to move beyond a single performance score to understand the underlying nature of an individual's attentional difficulties, distinguishing, for instance, between general cognitive slowing and specific lapses in vigilance [33]. This multimodal approach offers a more holistic view of sustained attention [34], paving the way for future research into distinct behavioral phenotypes of attentional decline that are invisible to traditional, response-time-based measures.

The results of our supplementary classification analysis warrant careful interpretation. The modest improvements (1.4% in accuracy and 2.0% in F_1-score), while not dramatic, provide a crucial proof-of-concept. They suggest that the multimodal features captured by the AI-CDVT contain a small but detectable signal that is relevant to clinical outcomes (ie, potential cognitive impairment as flagged by the MoCA). This finding lends support to our central hypothesis that integrating objective behavioral markers, even if their individual predictive power is small, can incrementally enhance the clinical utility of a traditional cognitive test. While the immediate clinical impact of this gain is limited, it establishes a methodological foundation for future work. It is plausible that this incremental value could be magnified in larger, more clinically diverse samples or by using more advanced machine learning architectures, highlighting a promising avenue for subsequent research.

It is important to appropriately position the contribution of this study. We did not develop a new AI algorithm from the ground up; rather, our innovation lies in the practical application and integration of established, open-source tools (OpenFace and XGBoost) to enhance a standard clinical assessment. The novelty of this work is therefore not in a deep methodological invention but in demonstrating the feasibility and clinical utility of creating a multimodal assessment of sustained attention. By showing that combining behavioral response data with easily captured facial metrics can improve psychometric properties like reliability, this study provides a proof-of-concept and a methodological template for other researchers aiming to enrich traditional neuropsychological tests with objective, behavioral data streams.

Comparison to Prior Work

By leveraging the flexibility of AI models, such as XGBoost regressors, the AI-CDVT can potentially address the challenge of interpreting individual attentional features in isolation [35]. For instance, directly comparing attention between individuals with high accuracy but slow response times and those with lower accuracy but faster responses can be difficult [36]. The AI-CDVT illustrates a viable method for integrating and interpreting various attentional features into a unified score for future studies and attentional tests.

A related methodological consideration is the selection of the 20 input features. This set was not chosen arbitrarily. Each feature was included because it had been identified in the existing scientific literature as a physiological or behavioral marker related to attention and vigilance [11,12,37]. Our approach was to build a comprehensive model based on these established, theory-driven features. While this could introduce redundancy between some inputs (eg, left and right eyelid distance), the chosen XGBoost algorithm is robust to such multicollinearity, as it inherently performs feature selection during its training process [38]. The final feature importance rankings in Table 1 are a direct result of this process, demonstrating how the model itself identified the most valuable contributors from the initial set of theory-driven features.

An examination of the feature importance rankings (Table 1) provides insights into how the AI-CDVT achieves its robust performance. While traditional metrics like reaction time and accuracy are unsurprisingly the most critical predictors, the model also heavily weighs physiological and behavioral markers. For example, the "distance between the eyelids" emerged as a top feature. This is consistent with literature linking decreased eyelid aperture and blink rate dynamics to drowsiness and lapses in vigilance [39]. Similarly, the "Y coordinate of the gaze point" was highly predictive, likely because a downward shift in gaze is a well-established behavioral marker of task disengagement and mind-wandering [40,41]. The inclusion of these features allows the AI-CDVT to capture subtle, moment-to-moment fluctuations in attentional states that are not reflected in response times alone, thereby providing a more comprehensive and ecologically valid assessment.

A final consideration is the interpretability of the AI model, which is a critical factor for its clinical adoption [42,43]. Complex models like XGBoost are often termed "black boxes" because they do not produce a simple, transparent formula in the way a linear regression model can [44]. There is an inherent tradeoff between the high predictive accuracy of such models and their direct interpretability [45]. In this study, our primary tool for interpretation is the feature importance table (Table 1). While it does not explain how the features are combined for any single individual, it provides clinicians with a clear and valuable understanding of what the model is paying attention to [46]. It confirms that the AI-CDVT's score is driven by a combination of performance metrics and behavioral patterns (eg, eye closure and gaze aversion) that are clinically consistent

XSL•FO
RenderX

with inattention. This allows clinicians to trust that the model's logic aligns with established knowledge, even if the precise weighting algorithm remains complex [47,48].

Limitations

This study has several notable limitations. First, the generalizability of our findings is constrained by the characteristics of our sample. The study included cognitively healthy older adults with MoCA scores in a narrow range, limiting the applicability of the results to clinical populations with cognitive impairments. Furthermore, the sample was predominantly female (64/87, 73.6%), raising concerns about potential gender bias in the AI model's performance [49]. The test-retest reliability analysis was also based on a relatively small subset (n=66), which warrants caution in the interpretation of ICC values until replicated with a larger sample.

Second, the scope of our validation methodology was limited. The model's performance was evaluated using internal cross-validation; the lack of an external validation with an independent dataset means that the model's generalizability remains to be confirmed. Our psychometric evaluation also focused primarily on correlational and reliability metrics. Other key psychometric properties, such as responsiveness to change, were also not assessed.

Finally, it is important to acknowledge a conceptual limitation regarding what is being measured. The facial and behavioral metrics captured by the AI-CDVT, such as eye closure, are well-established proxies for vigilance. However, they are not direct measures of underlying cognitive processes. Therefore, the observed correlations with cognitive tests should be interpreted as a relationship between observable behaviors and cognitive performance, not as evidence that the AI-CDVT measures cognition in the same way as traditional tests.

Future Directions

Building on these findings, future research should prioritize several key areas. First, the AI-CDVT must be validated in a larger, more diverse cohort, specifically including a more balanced gender representation and a wider range of cognitive abilities, to address the limitations of our current sample. Second, external validation on an independent dataset is essential to confirm the model's generalizability. Third, its utility in clinical populations, such as individuals with mild cognitive impairment or dementia, should be explored to determine its diagnostic and monitoring potential. Finally, longitudinal studies are needed to assess other key psychometric properties, such as responsiveness to change over time or in response to an intervention.

Conclusions

The objective of this study was to address a key psychometric weakness in a standard test of sustained attention by transforming it from a unimodal to a multimodal assessment. We demonstrated that using accessible AI tools to integrate objective behavioral data with traditional performance metrics, and we developed an AI-CDVT with superior test-retest reliability compared to the original version, while maintaining its convergent validity. The primary contribution of this work is not the development of a novel algorithm, but the demonstration that the psychometric robustness of established clinical tools can significantly be enhanced through this multimodal approach. The resulting AI-CDVT represents a more stable and reliable instrument for assessing sustained attention in older adults.

Funding

This work was supported by the National Science and Technology Council, Taiwan (112 - 2314-B-038 - 056). The funder had no role in the design, data collection, data analysis, or reporting of the study.

Disclaimer

During the preparation of this manuscript, the authors used a large language model (LLM) to assist with initial language polishing. Subsequently, the manuscript was professionally reviewed by an English-language editor to improve clarity and readability. The LLM was not used for data analysis, data interpretation, or for generating the core scientific arguments of the paper. All content was reviewed and edited by the authors, who take full responsibility for the final version of the manuscript.

Data Availability

The deidentified numerical dataset generated and analyzed during the current study is available from the corresponding author on reasonable request.

Authors' Contributions

GHL was responsible for conceptualization, methodology, data curation, supervision, formal analysis, and writing – original draft. DB assisted with conceptualization, data curation, and writing – review & editing. YJH, SCL, MTTV, and THC were responsible for writing – review & editing.

Conflicts of Interest

None declared.

Multimedia Appendix 1

XSL•FO
RenderX

Participant demographic questionnaire and assessment version citations.
[DOCX File, 17 KB - medinform_v13i1e73038_app1.docx]

References

1. Wickens CD, Huey BM. Workload Transition: Implications for Individual and Team Performance: National Academies Press; 1993.
2. Warm JS. Sustained Attention in Human Performance: John Wiley and Sons; 1984.
3. Vallesi A, Tronelli V, Lomi F, Pezzetta R. Age differences in sustained attention tasks: a meta-analysis. Psychon Bull Rev 2021 Dec;28(6):1755-1775. [doi: 10.3758/s13423-021-01908-x] [Medline: 33772477]
4. Robison MK, Diede NT, Nicosia J, Ball BH, Bugg JM. A multimodal analysis of sustained attention in younger and older adults. Psychol Aging 2022 May;37(3):307-325. [doi: 10.1037/pag0000687] [Medline: 35446084]
5. Welhaf MS, Banks JB, Bugg JM. Age-related differences in mind wandering: the role of emotional valence. J Gerontol B Psychol Sci Soc Sci 2024 Jan 1;79(1):gbad151. [doi: 10.1093/geronb/gbad151] [Medline: 37813376]
6. Diede NT, Gyurkovics M, Nicosia J, Diede A, Bugg JM. The effect of context on mind-wandering in younger and older adults. Conscious Cogn 2022 Jan;97:103256. [doi: 10.1016/j.concog.2021.103256] [Medline: 34902670]
7. O'Halloran AM, Finucane C, Savva GM, Robertson IH, Kenny RA. Sustained attention and frailty in the older adult population. J Gerontol B Psychol Sci Soc Sci 2014 Mar;69(2):147-156. [doi: 10.1093/geronb/gbt009] [Medline: 23525545]
8. O'Halloran AM, Pénard N, Galli A, Fan CW, Robertson IH, Kenny RA. Falls and falls efficacy: the role of sustained attention in older adults. BMC Geriatr 2011 Dec 19;11:1-10. [doi: 10.1186/1471-2318-11-85] [Medline: 22182487]
9. Yang CM, Lin GH, Chen MH, Hsueh IP, Hsieh CL. Development of a computerized Digit Vigilance Test and validation in patients with stroke. J Rehabil Med 2015 Apr;47(4):311-317. [doi: 10.2340/16501977-1945] [Medline: 25728353]
10. Lin GH, Wu CT, Huang YJ, et al. A reliable and valid assessment of sustained attention for patients with schizophrenia: the computerized digit vigilance test. Arch Clin Neuropsychol 2018 Mar 1;33(2):227-237. [doi: 10.1093/arclin/acx064] [Medline: 28981615]
11. Armstrong T, Olatunji BO. Eye tracking of attention in the affective disorders: a meta-analytic review and synthesis. Clin Psychol Rev 2012 Dec;32(8):704-723. [doi: 10.1016/j.cpr.2012.09.004] [Medline: 23059623]
12. McIntire LK, McKinley RA, Goodyear C, McIntire JP. Detection of vigilance performance using eye blinks. Appl Ergon 2014 Mar;45(2):354-362. [doi: 10.1016/j.apergo.2013.04.020] [Medline: 23722006]
13. Abe T. PERCLOS-based technologies for detecting drowsiness: current evidence and future directions. Sleep Adv 2023;4(1):zpad006. [doi: 10.1093/sleepadvances/zpad006] [Medline: 37193281]
14. Cori JM, Anderson C, Shekari Soleimanloo S, Jackson ML, Howard ME. Narrative review: do spontaneous eye blink parameters provide a useful assessment of state drowsiness? Sleep Med Rev 2019 Jun;45:95-104. [doi: 10.1016/j.smrv.2019.03.004] [Medline: 30986615]
15. Bergasa LM, Nuevo J, Sotelo MA, Barea R, Lopez ME. Real-time system for monitoring driver vigilance. IEEE Trans Intell Transport Syst 2006 Mar;7(1):63-77. [doi: 10.1109/TITS.2006.869598]
16. Ji Q, Yang X. Real-time eye, gaze, and face pose tracking for monitoring driver vigilance. Real-Time Imaging 2002 Oct;8(5):357-377. [doi: 10.1006/rtim.2002.0279]
17. D'mello SK, Kory J. A review and meta-analysis of multimodal affect detection systems. ACM Comput Surv 2015 Apr 16;47(3):1-36. [doi: 10.1145/2682899]
18. Zaletelj J, Košir A. Predicting students' attention in the classroom from Kinect facial and body features. J Image Video Proc 2017 Dec;2017(1):80. [doi: 10.1186/s13640-017-0228-8]
19. Canedo D, Neves AJR. Facial expression recognition using computer vision: a systematic review. Appl Sci (Basel) 2019;9(21):4678. [doi: 10.3390/app9214678]
20. Oloyede MO, Hancke GP, Myburgh HC. A review on face recognition systems: recent approaches and challenges. Multimed Tools Appl 2020 Oct;79(37-38):27891-27922. [doi: 10.1007/s11042-020-09261-2]
21. Nasreddine ZS, Phillips NA, Bédirian V, et al. The Montreal Cognitive Assessment, MoCA: a brief screening tool for mild cognitive impairment. J Am Geriatr Soc 2005 Apr;53(4):695-699. [doi: 10.1111/j.1532-5415.2005.53221.x] [Medline: 15817019]
22. Scarpina F, Tagini S. The Stroop Color and Word Test. Front Psychol 2017;8:557. [doi: 10.3389/fpsyg.2017.00557] [Medline: 28446889]
23. Dugbartey AT, Townes BD, Mahurin RK. Equivalence of the Color Trails Test and Trail Making Test in nonnative English-speakers. Arch Clin Neuropsychol 2000 Jul;15(5):425-431. [Medline: 14590218]
24. Delgado C, Araneda A, Behrens MI. Validation of the Spanish-language version of the Montreal Cognitive Assessment test in adults older than 60 years. Neurología (English Edition) 2019 Jul;34(6):376-385. [doi: 10.1016/j.nrleng.2018.12.008]
25. Feeney J, Savva GM, O'Regan C, King-Kallimanis B, Cronin H, Kenny RA. Measurement error, reliability, and minimum detectable change in the Mini-Mental State Examination, Montreal Cognitive Assessment, and Color Trails Test among community living middle-aged and older adults. J Alzheimers Dis 2016 May 31;53(3):1107-1114. [doi: 10.3233/JAD-160248] [Medline: 27258421]

XSL•FO
RenderX

26. Kang C, Lee GJ, Yi D, et al. Normative data for healthy older adults and an abbreviated version of the Stroop test. Clin Neuropsychol 2013;27(2):276-289. [doi: 10.1080/13854046.2012.742930] [Medline: 23259830]
27. Cheng SC, Hua MS, Liao YC, Chang HT. Psychometric properties and norms of the trail making test and the Color Trails Test for Taiwan's elderly population: a preliminary study. CJP 2024;66(2):215-246. [doi: 10.6129/CJP.202406_66(2).0002]
28. Baltrusaitis T, Robinson P, Morency LP. OpenFace: an open source facial behavior analysis toolkit. Presented at: 2016 IEEE Winter Conference on Applications of Computer Vision (WACV); Mar 7-10, 2016. [doi: 10.1109/WACV.2016.7477553]
29. Chen T, Guestrin C. XGBoost: a scalable tree boosting system. Presented at: KDD '16: The 22nd ACM SIGKDD International Conference on Knowledge Discovery and Data Mining; Aug 13-17, 2016. [doi: 10.1145/2939672.2939785]
30. Zollanvari A. Model evaluation and selection. In: Machine Learning with Python: Theory and Implementation: Springer; 2023:237-281. [doi: 10.1007/978-3-031-33342-2_9]
31. De Vet HC, Terwee CB. Measurement in Medicine: A Practical Guide: Cambridge University Press; 2011.
32. Koo TK, Li MY. A guideline of selecting and reporting intraclass correlation coefficients for reliability research. J Chiropr Med 2016 Jun;15(2):155-163. [doi: 10.1016/j.jcm.2016.02.012] [Medline: 27330520]
33. Stuss DT, Murphy KJ, Binns MA, Alexander MP. Staying on the job: the frontal lobes control individual performance variability. Brain (Bacau) 2003 Nov;126(Pt 11):2363-2380. [doi: 10.1093/brain/awg237] [Medline: 12876148]
34. Ettenhofer ML, Hershaw JN, Barry DM. Multimodal assessment of visual attention using the Bethesda Eye & Attention Measure (BEAM). J Clin Exp Neuropsychol 2016;38(1):96-110. [doi: 10.1080/13803395.2015.1089978] [Medline: 26595351]
35. Ngiam KY, Khor IW. Big data and machine learning algorithms for health-care delivery. Lancet Oncol 2019 May;20(5):e262-e273. [doi: 10.1016/S1470-2045(19)30149-4] [Medline: 31044724]
36. Draheim C, Mashburn CA, Martin JD, Engle RW. Reaction time in differential and developmental research: a review and commentary on the problems and alternatives. Psychol Bull 2019 May;145(5):508-535. [doi: 10.1037/bul0000192] [Medline: 30896187]
37. St John M, Risser MR, Kobus DA. Toward a usable closed-loop attention management system: predicting vigilance from minimal contact head, eye, and EEG measures. Presented at: 2nd Annual Augmented Cognition; Oct 15-17, 2006.
38. Cichosz P. Data Mining Algorithms: Explained Using R: John Wiley and Sons; 2014. [doi: 10.1002/9781118950951]
39. Maffei A, Angrilli A. Spontaneous blink rate as an index of attention and emotion during film clips viewing. Physiol Behav 2019 May 15;204:256-263. [doi: 10.1016/j.physbeh.2019.02.037] [Medline: 30822434]
40. Bixler R, D'Mello S. Automatic gaze-based user-independent detection of mind wandering during computerized reading. User Model User-Adap Inter 2016 Mar;26(1):33-68. [doi: 10.1007/s11257-015-9167-1]
41. Smilek D, Carriere JSA, Cheyne JA. Out of mind, out of sight: eye blinking as indicator and embodiment of mind wandering. Psychol Sci 2010 Jun;21(6):786-789. [doi: 10.1177/0956797610368063] [Medline: 20554601]
42. Ribeiro MT, Singh S, Guestrin C. Why should i trust you?": explaining the predictions of any classifier. Presented at: 22nd ACM SIGKDD International Conference on Knowledge Discovery and Data Mining; Aug 13-17, 2016.
43. Doshi-Velez F, Kim B. Towards a rigorous science of interpretable machine learning. arXiv. Preprint posted online on Feb 28, 2017. [doi: 10.48550/arXiv.1702.08608]
44. Lundberg SM, Lee SI. A unified approach to interpreting model predictions. arXiv. Preprint posted online on May 22, 2017. [doi: 10.48550/arXiv.1705.07874]
45. Murdoch WJ, Singh C, Kumbier K, Abbasi-Asl R, Yu B. Definitions, methods, and applications in interpretable machine learning. Proc Natl Acad Sci USA 2019 Oct 29;116(44):22071-22080. [doi: 10.1073/pnas.1900654116]
46. Molnar C. Interpretable Machine Learning: LuluCom: Lulu Press; 2020.
47. Amann J, Blasimme A, Vayena E, Frey D, Madai VI, Precise4Q consortium. Explainability for artificial intelligence in healthcare: a multidisciplinary perspective. BMC Med Inform Decis Mak 2020 Nov 30;20(1):310. [doi: 10.1186/s12911-020-01332-6] [Medline: 33256715]
48. Rudin C. Stop explaining black box machine learning models for high stakes decisions and use interpretable models instead. Nat Mach Intell 2019 May;1(5):206-215. [doi: 10.1038/s42256-019-0048-x] [Medline: 35603010]
49. Ho JQH, Hartanto A, Koh A, Majeed NM. Gender biases within artificial intelligence and ChatGPT: evidence, sources of biases and solutions. Comput Hum Behav Artif Hum 2025 May;4:100145. [doi: 10.1016/j.chbah.2025.100145]

Abbreviations

AI: artificial intelligence
AI-CDVT: artificial intelligence–based Computerized Digit Vigilance Test
CDVT: Computerized Digit Vigilance Test
CTT: Color Trails Test
ICC: intraclass correlation coefficient
MoCA: Montreal Cognitive Assessment
SCW: Stroop Color Word Test

XSL•FO
RenderX

XGBoost: Extreme Gradient Boosting

Edited by A Coristine; submitted 24.02.25; peer-reviewed by A Hartanto, HW Liang, P Sharan; revised version received 06.11.25; accepted 07.11.25; published 26.11.25.

Please cite as:
Lin GH, Bai D, Huang YJ, Lee SC, Vu MTT, Chiu TH
Artificial Intelligence–Based Computerized Digit Vigilance Test in Community-Dwelling Older Adults: Development and Validation Study
JMIR Med Inform 2025;13:e73038
URL: https://medinform.jmir.org/2025/1/e73038
doi:10.2196/73038

© Gong-Hong Lin, Dorothy Bai, Yi-Jing Huang, Shih-Chieh Lee, Mai Thi Thuy Vu, Tsu-Hsien Chiu. Originally published in JMIR Medical Informatics (https://medinform.jmir.org), 26.11.2025. This is an open-access article distributed under the terms of the Creative Commons Attribution License (https://creativecommons.org/licenses/by/4.0/), which permits unrestricted use, distribution, and reproduction in any medium, provided the original work, first published in JMIR Medical Informatics, is properly cited. The complete bibliographic information, a link to the original publication on https://medinform.jmir.org/, as well as this copyright and license information must be included.

XSL•FO
RenderX

Estimating 10-Year Cardiovascular Disease Risk in Primary Prevention Using UK Electronic Health Records and a Hybrid Multitask BERT Model: Retrospective Cohort Study

Tianyi Liu[1*], BSc, MSc; Lei Lu[1*], PhD; Yanzhong Wang[1], Prof Dr; Andrew J Krentz[1,2], ChB, MD, Prof Dr; Vasa Curcin[1], Prof Dr

[1]Department of Population Health Sciences, School of Life Course & Population Sciences, King's College London, Addison House, Guy's Campus, London, United Kingdom

[2]Metadvice, London, United Kingdom

[*]these authors contributed equally

Corresponding Author:
Tianyi Liu, BSc, MSc
Department of Population Health Sciences, School of Life Course & Population Sciences, King's College London, Addison House, Guy's Campus, London, United Kingdom

Abstract

Background: Cardiovascular disease (CVD) remains a leading cause of preventable morbidity and mortality, highlighting the need for early risk stratification in primary prevention. Traditional Cox models assume proportional hazards and linear effects, limiting flexibility. While machine learning offers greater expressiveness, many models rely solely on structured data and overlook time-to-event (TTE) information. Integrating structured and textual representations may enhance prediction and support equitable assessment across clinical subgroups.

Objective: This study aims to develop a hybrid multitask deep learning model (MT-BERT [multitask Bidirectional Encoder Representations from Transformers]) integrating structured and textual features from electronic health records (EHRs) to predict 10-year CVD risk, enhancing individualized stratification and supporting equitable assessment across diverse demographic groups.

Methods: We used data from Clinical Practice Research Datalink (CPRD) Aurum comprising 469,496 patients aged 40 - 85 years to develop MT-BERT for 10-year CVD risk prediction. Structured EHR variables and their corresponding textual representations were jointly encoded using a multilayer perceptron and a distilled version of the BERT model (DistilBERT), respectively. A fusion layer and stacked multihead attention modules enabled cross-modal interaction modeling. The model generated both binary classification outputs and TTE risk scores, optimized using a custom FocalCoxLoss function with uncertainty-based weighting. Prediction targets encompassed composite and individual CVD outcomes. Model performance was evaluated using the area under the receiver operating characteristic curve (AUROC), concordance index, and Brier score, with subgroup analyses by ethnicity and deprivation, and heterogeneity assessed using Higgins I^2 and Cochran Q statistics. Generalizability was assessed via external validation in a held-out London cohort.

Results: The MT-BERT model yielded AUROC values of 0.744 (95% CI 0.738 - 0.749) in males and 0.782 (95% CI 0.768 - 0.796) in females on the test set (n=711,052), and 0.736 (95% CI 0.729 - 0.741) and 0.775 (95% CI 0.768 - 0.780), respectively in "spatial external" validation (n=144,370). Brier scores were 0.130 in males and 0.091 in females. Individuals classified as high-risk (≥40% risk in males and ≥34% in females) demonstrated significantly reduced 10-year event-free survival relative to lower-risk individuals (log-rank P<.001). Model performance was consistently higher in females across all metrics. Subgroup analyses revealed substantial heterogeneity across ethnicity and deprivation (I^2>70%), especially among males, with lower AUROC in South Asian and Black ethnic groups. These findings reflect variation in model performance across demographic groups while supporting its applicability to large-scale CVD risk stratification.

Conclusions: The proposed hybrid MT-BERT model predicts 10-year CVD risk for primary prevention by integrating structured variables and unstructured clinical text from EHRs. Its multitask design facilitates both individualized risk stratification and TTE estimation. While performance was modestly reduced in deprived and minority ethnic subgroups, these findings provide preliminary support for advancing equity-aware, data-driven prevention strategies in increasingly diverse health care settings.

(JMIR Med Inform 2025;13:e76659) doi:10.2196/76659

XSL•FO
RenderX

KEYWORDS

cardiovascular diseases; risk prediction; deep learning; electronic health records; health equity; survival analysis

Introduction

Background

Cardiovascular disease (CVD) is a major public health challenge, accounting for 1 in 4 deaths in the United Kingdom and affecting 7.6 million individuals. In 2022, over 1,00,000 hospital admissions were attributed to acute coronary syndromes [1]. Beyond morbidity and mortality, CVD imposes US $15 billion in annual health care costs and US $35 billion in economic losses. Additionally, 6‐8 million individuals have undiagnosed or uncontrolled hypertension, further increasing preventable CVD-related complications [1,2].

To address this, the United Kingdom has implemented national prevention strategies, with the UK's National Institute for Health and Care Excellence (NICE) guidelines [3] recommending CVD risk assessments for individuals aged ≥40 years every 5 years via general practitioners (GPs). These assessments rely on structured clinical data and established 10-year risk prediction models such as QRISK3 [4] (developed and validated in UK populations) and Pooled Cohort Equations [5] (developed in US cohorts). Despite their widespread use, these conventional models rely on Cox regression, whose linear and proportional assumptions hinder their ability to model complex risk interactions, thereby limiting predictive performance in clinical practice [6,7].

Significant disparities in CVD burden persist. For instance, South Asians in the United Kingdom have nearly twice the coronary heart disease (CHD) incidence of White Europeans, with South Asian females experiencing rates similar to White European males [8]. Black African and Caribbean individuals do not show an elevated risk but receive fewer preventive treatments despite clinical indications [9]. Socioeconomic deprivation further exacerbates disparities, with higher CVD risk factor prevalence, hospital admissions, lower treatment uptake, and twice the mortality rate for individuals younger than 75 years in the most deprived areas [10]. Although conventional models can incorporate subgroup characteristics, they often lack the flexibility to model the complex, interdependent factors contributing to these disparities [11].

Machine learning (ML) approaches have emerged as promising alternatives to traditional CVD risk estimation models. A range of ML methods, from logistic regression and decision trees to ensemble techniques such as boosting, bagging, and stacking, have been explored for CVD risk prediction [6]. However, particularly in the context of primary prevention, many existing ML-based algorithms are limited by relatively small sample sizes, heterogeneous data quality, and a lack of consistent external validation, which may restrict their clinical applicability. Moreover, while some recent ML-based survival models, such as DeepSurv (Deep Neural Network–based Cox Model) [12], incorporate time-to-event (TTE) information, many CVD risk prediction algorithms continue to treat outcomes as binary events, without explicitly addressing censoring or time-dependent risk [7]. In addition, most models primarily use structured clinical variables and often overlook unstructured sources, such as physician notes and patient-reported symptoms, that could provide important contextual information for risk stratification [13].

Natural language processing (NLP), particularly Transformer-based models such as BERT [14] (Bidirectional Encoder Representations from Transformers), presents a novel approach to integrating unstructured clinical text into CVD risk prediction. Transformers use self-attention mechanisms to model long-range dependencies and complex relationships between variables. As an encoder-based Transformer model, BERT generates dense, context-rich embeddings by capturing bidirectional contextual information. Pretrained on large-scale corpora through transfer learning, BERT can effectively extract meaningful features from clinical text. Given that patient comorbidities, lifestyle factors, and social determinants are often recorded in unstructured formats, NLP models such as BERT can bridge critical gaps in cardiovascular risk assessment.

With increasing digital health adoption, NLP-driven models offer a scalable and cost-effective approach to CVD risk stratification. In particular, pretrained Transformer-based architectures such as BERT enable efficient fine-tuning on domain-specific datasets without the need for extensive retraining, reducing resource demands for clinical implementation. By integrating structured electronic health record (EHR) data with unstructured text sources such as patient interactions, chatbots, and clinical notes, future models could further enhance risk prediction and address limitations of conventional approaches. In this study, we emulate such integration by transforming structured variables into textual representations, providing an initial step toward leveraging both data modalities. Transformer-based models can better capture complex risk patterns across diverse populations, supporting more timely and equitable cardiovascular risk assessment for primary prevention.

Rationale and Objectives

This study aims to develop a hybrid Multitask BERT model (MT-BERT) for prognostic CVD risk assessment, integrating structured and textual representations derived from UK EHR data using phenotyping techniques. The model is designed to support primary care decision-making by predicting 10-year CVD risk to guide early intervention, statin initiation, and lifestyle modification, potentially enhancing or replacing conventional statistical approaches.

While traditional survival models rely primarily on structured clinical variables, the proposed MT-BERT approach incorporates unstructured information (eg, physician notes and comorbidity narratives) to improve predictive performance, particularly among underrepresented high-risk populations.

To achieve this, we develop a model for both CVD outcome classification and TTE hazard ranking, enhancing individualized risk stratification and addressing biases in structured datasets. We also introduce a novel FocalCoxLoss function, enabling

XSL•FO
RenderX

uncertainty-weighted joint optimization of classification and survival objectives. The study emphasizes model development, feature engineering, and optimization and includes external validation using data from a distinct London region to assess spatial generalizability. Additionally, we leverage longitudinal EHR data to better support practical implementation in primary care.

The specific objectives of this study were as follows:

1. Extract structured and unstructured predictors, CVD outcomes (binary classification and TTE data) from Clinical Practice Research Datalink (CPRD) Aurum [15] via phenotyping.
2. Develop the MT-BERT model integrating textual and structured variables for CVD risk prediction, incorporating the novel FocalCoxLoss for multitask learning.
3. Evaluate model performance across individual and composite CVD outcomes, with subgroup analyses by ethnicity and socioeconomic deprivation, focusing on discrimination, calibration, and fairness metrics.
4. Ensure transparent reporting according to the TRIPOD+AI (Transparent Reporting of a multivariable prediction model for Individual Prognosis Or Diagnosis + artificial intelligence) [16], including detailed documentation of feature engineering, data harmonization, and hyperparameter optimization.

The aim of this study was to evaluate the effectiveness of multimodal deep learning for long-term CVD risk prediction and to advance personalized health care through the integration of NLP and structured data from UK EHR.

Methods

Overview

This study follows the guidelines outlined in the TRIPOD+AI [16] statement (Checklist 1); an extension of the TRIPOD statement specifically designed for AI (including ML) prediction models.

Study Design and Patient Records Inclusion

This study uses a retrospective EHR-based design, leveraging CPRD Aurum [15] (study registration protocol no.: 21_000346) to develop NLP-driven CVD risk prediction models using longitudinal patient records. CPRD Aurum is a routinely updated UK primary care database integrating deidentified patient records from 1359 GP practices (primary care sites), covering 16.6% of UK GPs and representing one-fifth of the UK population. It includes demographic data, diagnoses, symptoms, prescriptions, and dosages, standardized via MedCode ID to ensure interoperability with Read Code and SNOMED CT. As of January 2022 (version 2.7), it comprises over 40 million research-eligible patients with a median follow-up of 8.74 years (IQR 3.22-19.87).

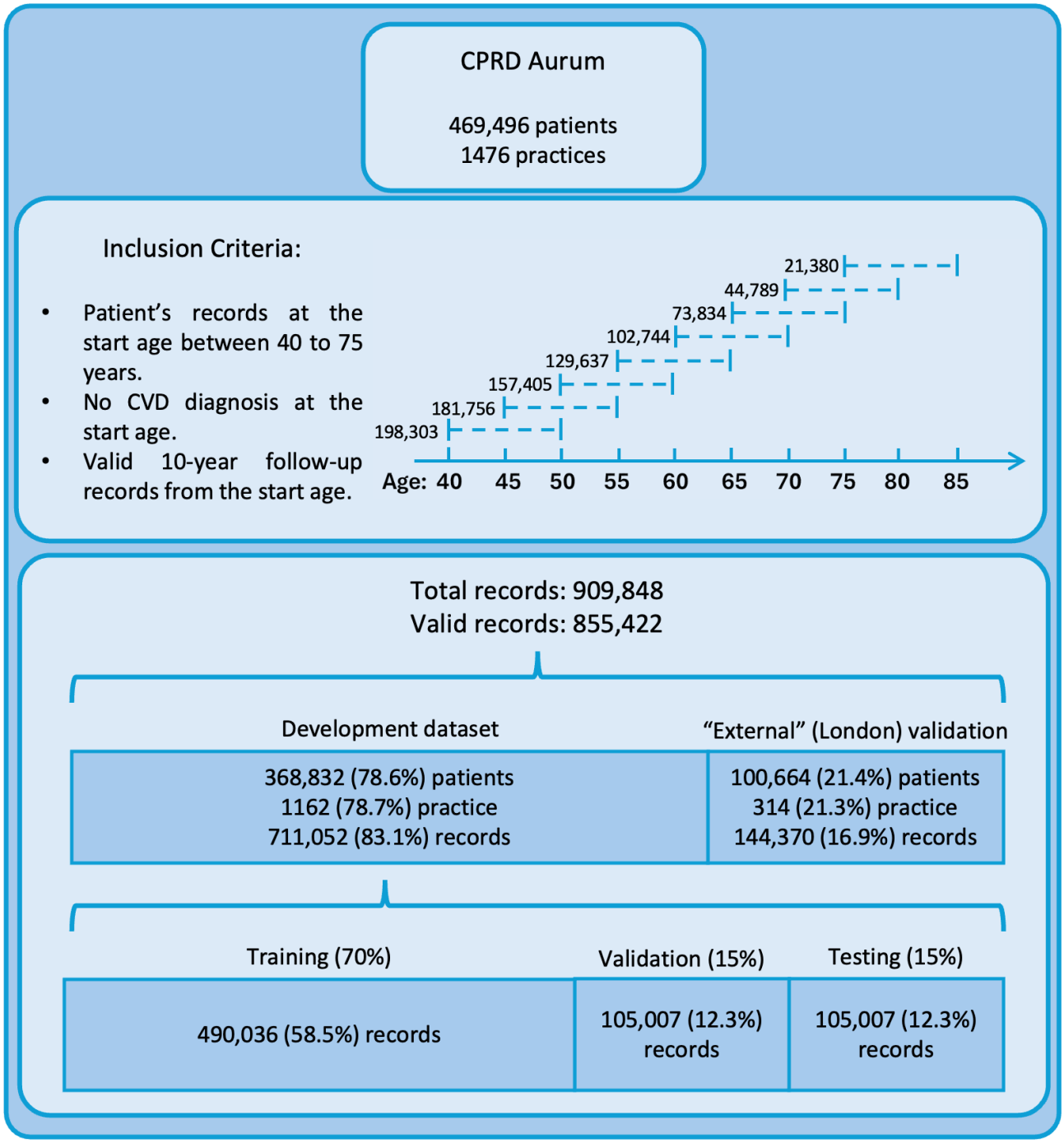
The “External” (London) validation set represents a “spatial” external cohort from CPRD practices located in Greater London, selected to ensure demographic diversity, particularly higher proportions of ethnic minority patients.

The data preprocessing workflow followed our prior work [17]. As shown in Figure 1, we selected a stratified random sample of 469,496 patients aged 40 to 85 years who were registered between 2011 and 2021. Unique CPRD identifiers were used to link records and reconstruct longitudinal health trajectories, ensuring a representative UK primary care cohort. Patients with at least one 10-year follow-up period were included to verify consistency in registration and clinical event timestamps. Follow-up intervals began at ages 40 to 75 years in 5-year increments, allowing individuals to contribute multiple independent 10-year records if they were CVD-free at entry. To emulate clinical practice, we extracted multiple fixed-horizon prediction episodes for each patient, reflecting periodic risk assessments recommended in the UK NICE guidelines [3] for adults aged 40 to 85 years. Consistent with our prior ML-based survival study, all baseline models were trained in exactly the same pipeline with identical predictors, censoring rules, preprocessing, and the same development and validation splits. This setup enables like-for-like comparisons and effectively represents structure-only, single-objective ablation settings against which MT-BERT is evaluated. While the guidelines do not specify data extraction procedures, this design strategy ensures alignment with real-world primary prevention workflows and enhances model relevance for general practice.

Given the scale and representativeness of CPRD Aurum, sample size adequacy was evaluated according to the framework proposed by Riley et al [17] for clinical prediction model development. The cohort substantially exceeded recommended thresholds for minimum events per predictor, enabling robust model development, rare event estimation, and stratified subgroup analyses.

XSL•FO
RenderX

Figure 1. Workflow for study population and records extraction. CPRD: Clinical Practice Research Datalink; CVD: cardiovascular disease.



Extraction and Textual Transformation of Predictors

We extracted all predictor variables at the cohort entry year, primarily based on QRISK3 definitions, with minor adaptations where appropriate (Table 1). Phenotypes were defined using the HDRUK Phenotype Library [18], while comorbidities were identified through CArdiovascular disease research using LInked BEspoke studies and Electronic health Records (CALIBER, developed by the University College London Institute of Health Informatics [CALIBER research team]) [19], with corresponding *ICD-10* (*International Classification of Diseases, Tenth Revision*) codes detailed in Table S1 (Multimedia Appendix 1). MedCode IDs were documented and mapped to controlled terminologies to ensure consistency, facilitate updates, and enhance transparency (Multimedia Appendix 2).

Static variables (eg, gender, ethnicity, and deprivation) were assigned based on the most recent record available. Time-dependent variables (eg, smoking status and medication use) were determined within a 6-month window around the entry year; in the absence of recent records, smoking status was inferred from prior history, and medication use was classified based on any previous prescription. Comorbidities were considered present if recorded before cohort entry within the same time frame. Absence of records was interpreted as no occurrence rather than missing data.

XSL•FO
RenderX

For continuous variables (eg, BMI, systolic blood pressure, and total cholesterol/high-Ddensity lipoprotein ratio), if no values were available within the acceptable window, missing data were imputed using linear regression, provided that at least 3 prior measurements existed within a 2-year span.

To integrate established risk assessment into ML models, we derived an additional predictor based on the QRISK score calculated by an R package [20], represented in categorical form, aligned with UK clinical thresholds for statin treatment initiation.

Unlike traditional models based on structured data, this study transforms structured predictors into text representations for NLP-based modeling. To implement this approach, categorical variables including risk groups, ethnicity, smoking status, and comorbidities were converted into textual descriptions reflecting patient status at cohort entry, avoiding numerical encoding. Age and BMI were also expressed in textual form. Continuous variables were otherwise retained in their original form. The textual transformation template is provided in Table 1.

XSL•FO
RenderX

Table . Overview of predictors, outcome definitions, and preprocessing approaches.

Variable	Textual transformation/Preprocessing description
Continuous predictors	
Age	*"The patient is a {age_category}"*, where age < 45=young adult, 45 - 59=middle-aged adult, 60 - 74=young-old adult, and age ≥ 75=older adult
BMI (kg/m²)	Appended as: *"with a BMI classified as {bmi_category}"*, where BMI <18.5=underweight, 18.5 - 24.9=normal weight, 25.0 - 29.9=overweight (preobesity), 30.0 - 34.9=Class 1 obesity, 35.0 - 39.9=Class 2 obesity, BMI ≥40.0=Class 3 obesity (severe obesity)
Systolic blood pressure (mmHg)	Normalized to [0, 1] range using min-max scaling
SD of systolic blood pressure	Normalized to [0, 1] range using min-max scaling
Diastolic blood pressure (mmHg)	Normalized to [0, 1] range using min-max scaling
Total/High-density lipoprotein ratio	Normalized to [0, 1] range using min-max scaling
Townsend score	Normalized to [0, 1] range using min-max scaling
Categorical predictors	
Ethnicity (9 categories)	Appended as: *"and is of {ethnicity_group} ethnicity"*
Smoking status (5 categories)	Appended as: *"The patient is a {smoking_status}"*
Prestratified risk group (4 categories)	Appended as: *"Pre-stratified risk indicating a {risk_group}"*, where 0% - 4.9%%=low risk, 5.0% - 9.9%%=moderate risk, 10.0% - 19.9%%=high risk, and ≥20.0%=extreme high risk
Binary comorbidity predictors	
Type 1/2 diabetes mellitus	Appended as: *"The patient has a history of {condition_1, condition_2,.}"*
Chronic kidney disease stage 3, 4, or 5	Appended as: *"The patient has a history of {condition_1, condition_2, .}"*
Family history of coronary heart disease	Appended as: *"The patient has a history of {condition_1, condition_2, .}"*
Atrial fibrillation	Appended as: *"The patient has a history of {condition_1, condition_2, .}"*
Erectile dysfunction	Appended as: *"The patient has a history of {condition_1, condition_2, .}"*
HIV/AIDS	Appended as: *"The patient has a history of {condition_1, condition_2, .}"*
Migraine	Appended as: *"The patient has a history of {condition_1, condition_2, .}"*
Rheumatoid arthritis	Appended as: *"The patient has a history of {condition_1, condition_2, .}"*
Systemic lupus erythematosus	Appended as: *"The patient has a history of {condition_1, condition_2, .}"*
Severe mental illness	Appended as: *"The patient has a history of {condition_1, condition_2, .}"*
Antipsychotic	Appended as: *"The patient has a history of {condition_1, condition_2, .}"*
Corticosteroid	Appended as: *"The patient has a history of {condition_1, condition_2, .}"*
Treated hypertension	Appended as: *"The patient has a history of {condition_1, condition_2, .}"*
Cardiovascular disease outcomes	
Coronary heart disease	Used as binary outcome labels indicating disease presence (1=event occurred, 0=no event). Corresponding time-to-event (TTE) values were recorded in days, with a maximum follow-up of 3650 days for censored cases
Myocardial infarction	Used as binary outcome labels indicating disease presence (1=event occurred, 0=no event). Corresponding TTE values were recorded in days, with a maximum follow-up of 3650 days for censored cases
Ischemic stroke	Used as binary outcome labels indicating disease presence (1=event occurred, 0=no event). Corresponding TTE values were recorded in days, with a maximum follow-up of 3650 days for censored cases
Heart failure	Used as binary outcome labels indicating disease presence (1=event occurred, 0=no event). Corresponding TTE values were recorded in days, with a maximum follow-up of 3650 days for censored cases

XSL•FO
RenderX

Variable	Textual transformation/Preprocessing description
Angina	Used as binary outcome labels indicating disease presence (1=event occurred, 0=no event). Corresponding TTE values were recorded in days, with a maximum follow-up of 3650 days for censored cases
Cardiovascular disease (QRISK)	A composite outcome including coronary heart disease (CHD), stroke, and transient ischemic attack (TIA). TTE was defined as the time to the earliest occurring event, in days
Cardiovascular disease (Composite)	A composite outcome including the above cardiovascular conditions, plus abdominal aortic aneurysm (AAA), and peripheral artery disease (PAD). TTE was defined as the time to the earliest occurring event, in days
Vascular dementia	Used as a binary outcome label indicating disease presence (1=event occurred, 0=no event). TTE was recorded in days, with a maximum follow-up of 3650 days for censored cases

CVD Outcome and TTE Specification

Each CVD outcome (Table 1) was defined using phenotype-based criteria and assessed individually with its corresponding TTE, including CHD (*ICD-10*: I20-I25), stroke (I63-I66, I69), transient ischemic attack (G45-G46), heart failure (I50), abdominal aortic aneurysm (I71), and peripheral arterial disease (I73-I74). Additionally, 2 composite CVD outcomes, one aligned with QRISK and one containing all of the above, were defined based on the earliest occurrence of any included CVD event. Although not a classical CVD outcome, vascular dementia (F01) was included as an exploratory end point due to its close association with cerebrovascular disease. CVD events were recorded if they occurred within the 10-year follow-up or up to 6 months thereafter. Absence of records was interpreted as no event rather than missing data. The definition and mapping of CVD outcomes are detailed in Table S2 in Multimedia Appendix 1 and in Multimedia Appendix 2.

Model Architecture and Training Strategy

As shown in Figure 2, we developed an MT-BERT framework for the prediction of CVD outcomes, which integrates a distilled version of the BERT model (DistilBERT) [21] for textual features and a multilayer perceptron (MLP) for structured clinical predictors, incorporating multihead attention and residual connections to refine feature interactions. DistilBERT retains representational power while reducing computational complexity by removing token-type embeddings and the pooler layer. Unlike conventional concatenation-based approaches, our model applies a transformation layer for feature alignment before passing the fused representation through stacked attention layers, enabling dynamic cross-modal refinement. The MLP module, implemented in PyTorch, consists of fully connected layers with Rectified Linear Unit activations and dropout, ensuring structured feature regularization. For prediction, the model simultaneously outputs binary classification logits (CVD presence) and a log hazard score (TTE) for survival analysis, with temperature scaling improving classification stability. Full implementation details are provided in Table S3 (Multimedia Appendix 1).

Structured features were MinMax scaled, and text data were tokenized using the DistilBERT tokenizer. The dataset was split in a 7:2:1 ratio into training, validation, and testing sets (Figure 1) using stratified sampling to maintain class balance. Labels and TTE values were converted into tensors for model compatibility. Class imbalance was addressed with a dynamically adjusted weighting scheme, scaling standard balanced class weights based on the observed event rate. The processed data were structured into TensorDatasets and loaded for training.

Our model uses a customized FocalCoxLoss, a multitask loss function that combines Focal Loss, a class imbalance-aware variant of cross-entropy loss, for event classification, which optimizes decision boundaries, and Cox Loss, as used in DeepSurv [12], for survival analysis, which optimizes risk ranking. The 2 components are balanced using learnable uncertainty-based weighting [22] as follows:

$$L = (12\sigma_{focal2})L_{focal} + (12\sigma_{cox2})L_{cox} + \log \sigma_{focal} + \log \sigma_{cox}$$

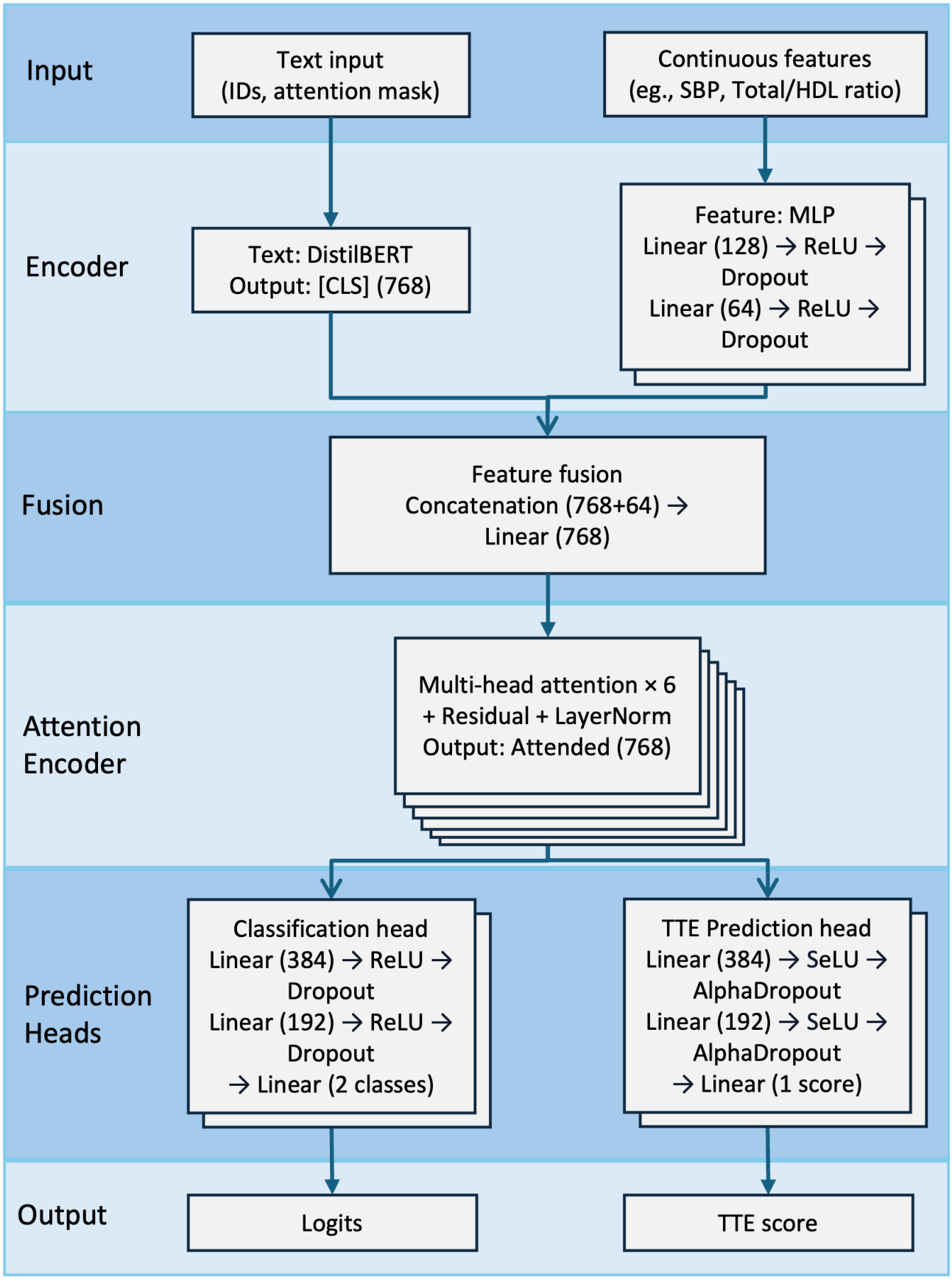
where σ_{focal} and σ_{cox} are learnable task-specific variance parameters. Unlike fixed-weight loss functions, this approach enables dynamic adjustment of task contributions by assigning higher effective weights to tasks with lower predicted uncertainty, thereby optimizing the trade-off between binary CVD event prediction and TTE risk estimation during training.

To ensure stability, we adopted a 2-stage training strategy. Initially, was frozen, maintaining a fixed loss ratio to prevent early instability. After 10 epochs, it was unfrozen, allowing adaptive loss scaling. DistilBERT remained trainable throughout, enabling concurrent optimization of textual and structured representations.

Training used AdamW with cosine annealing, gradient clipping, and early stopping for stable convergence. Dropout rates were optimized via Optuna hyperparameter tuning, while learning rate (initially 3e-4) and weight decay (1e-4) were manually set. During training, the learning rate was dynamically adjusted using a cosine annealing schedule with warm restarts. Model selection was based on the area under the curve and C-statistic maximization.

XSL•FO
RenderX

Figure 2. Architecture of the Multitask Bidirectional Encoder Representations from Transformers model for cardiovascular disease risk prediction. HDL: high-density lipoprotein; MLP: multilayer perceptron; SBP: systolic blood pressure; TTE: time-to-event.



XSL•FO
RenderX

Performance Evaluation, Generalizability, and Fairness

Model performance was assessed on the held-out test set using the optimal hyperparameters identified during training (Figure 1). Calibration was performed via isotonic regression and assessed using Brier scores and calibration plots across risk deciles. Discrimination was quantified by the AUROC and the C-statistic, with 95% CIs estimated via 1000 bootstrap resamples. Internal validity was assessed through 10-fold cross-validation. Classification metrics, including accuracy, recall, and specificity, were reported at the optimized threshold. Kaplan-Meier (KM) survival curves stratified by predicted risk groups were used to evaluate risk separation and clinical utility.

To evaluate generalizability and fairness, we performed "spatial external" validation using a London held-out cohort (Figure 1), selected for its higher proportion of ethnic minority patients. AUROC with 95% CIs was computed across all 9 ethnicity categories and Townsend deprivation deciles. In parallel, we reported aggregated subgroup results for broader ethnicity groupings including White, South Asian (Indian, Pakistani, and Bangladeshi), and Black (African and Caribbean). We further evaluated performance variation across individual Townsend quintiles. To quantify heterogeneity in model performance, Higgins I^2 statistic and Cochran Q values [23] were computed across ethnicity and deprivation groups, where the Higgins I^2 statistic quantifies the percentage of total variation across studies due to heterogeneity rather than chance, and the Q value tests whether the observed differences in study results are due to chance or true heterogeneity.

Ethical Considerations

This study uses CPRD Aurum data under protocol number 21_000346, which was reviewed and approved by the Independent Scientific Advisory Committee (ISAC) on behalf of the Medicines and Healthcare Products Regulatory Agency. The study relies on anonymized patient records and follows ethical guidelines for research using deidentified health care data. No patient or public consent was required, as the research was conducted using fully anonymized data. There was no direct patient or public involvement in the study's design, execution, analysis, or dissemination. No financial compensation was provided.

Results

Baseline Characteristics of Study Population

We extracted 909,848 records from 469,496 patients across 1476 practices in England (Figure 1). After quality control to remove records with extreme values for continuous features, 855,422 valid records were retained. Of these, 144,370 records (16.9%) from practices located in London were held out as the spatial external validation set. The remaining 711,052 records (83.1%) constituted the development dataset, which was randomly split into training, validation, and testing sets using a 70:15:15 ratio.

Table 2 summarizes the background characteristics of both the development dataset and the spatial validation set, disaggregated by gender. The statistics show that most comorbidities and CVD outcomes are significantly more common among males, which makes gender-specific modeling indispensable for this task. In addition, a substantially higher proportion, approximately one-third of individuals from minority ethnic backgrounds, is observed in the spatial validation set, whereas over 90% of the development dataset is White. This demographic contrast supports the use of the London practice cohort as a spatially distinct external validation set, particularly for assessing model generalizability and fairness in managing CVD risk among ethnic minority populations.

XSL•FO
RenderX

Table . Baseline characteristics of the study population by gender.

Characteristics	Male (n=403,545, 47.17%)		Female (n=451,877, 52.82%)	
	Development (n=335,891)	Spatial validation (n=67,654)	Development (n=375,161)	Spatial validation (n=76,716)
Continuous features, mean (SD)				
Age	50.62 (9.16)	50.51 (9.10)	51.29 (9.51)	51.13 (9.43)
BMI	27.45 (4.42)	27.25 (4.31)	27.18 (5.47)	26.54 (5.30)
Systolic blood pressure	135.17 (12.30)	134.79 (12.02)	131.32 (14.83)	129.63 (14.88)
SD of systolic blood pressure	9.05 (4.83)	8.93 (4.88)	9.87 (4.88)	9.50 (4.79)
Diastolic blood pressure	81.82 (7.42)	81.75 (7.33)	79.18 (7.93)	78.47 (7.93)
Total/High-density lipoprotein ratio	4.08 (0.83)	4.20 (0.84)	4.11 (0.84)	4.19 (0.85)
Categorical features, %				
Ethnicity				
White	93.44	64.82	93.92	65.65
Indian	1.50	8.33	1.46	8.32
Pakistani	1.02	2.05	0.91	1.62
Bangladeshi	0.26	1.35	0.22	1.18
Chinese	0.23	0.96	0.28	1.04
Other Asian	0.50	4.40	0.47	4.28
Black Caribbean	0.50	5.32	0.58	6.57
Black African	0.35	6.73	0.30	6.10
Other ethnic group	2.20	6.04	1.84	5.24
Smoking status				
Nonsmoker	45.73	47.10	58.42	59.71
Ex-smoker	51.73	50.71	39.40	38.50
Light smoker	0.61	0.47	0.75	0.63
Moderate smoker	1.17	1.04	0.99	0.80
Heavy smoker	0.76	0.67	0.44	0.35
Risk group				
Low risk	41.97	44.54	57.11	61.42
Moderate risk	26.67	26.74	22.59	21.51
High risk	21.63	20.53	14.98	13.07
Extreme high risk	9.73	8.18	5.32	3.99
Binary comorbidity, %				
Type 1 and 2 diabetes mellitus	4.75	3.82	3.61	2.82
Chronic kidney disease stage 3, 4, or 5	0.89	0.89	1.31	1.52
Family history of coronary heart disease	3.72	2.72	4.80	3.23
Atrial fibrillation	0.80	0.92	0.45	0.46
Erectile dysfunction	4.12	4.25	NA	NA
HIV/AIDS	0.12	0.05	0.03	0.03
Migraine	2.36	2.91	6.40	7.17

XSL•FO
RenderX

Characteristics	Male (n=403,545, 47.17%)		Female (n=451,877, 52.82%)	
	Development (n=335,891)	Spatial validation (n=67,654)	Development (n=375,161)	Spatial validation (n=76,716)
Rheumatoid arthritis	0.37	0.35	0.89	0.79
Systemic lupus erythematosus	0.05	0.05	0.21	0.22
Severe mental illness	0.96	0.68	0.96	0.84
Antipsychotic	0.42	0.34	0.42	0.37
Corticosteroid	3.22	2.53	4.68	3.87
Treated hypertension	13.83	12.72	14.43	13.01
Cardiovascular disease outcomes, %				
Cardiovascular disease (QRISK)	8.19	6.84	4.91	3.57
Cardiovascular disease (Composite)	10.87	9.04	6.59	4.97
Coronary heart disease	4.80	3.65	2.47	1.52
Myocardial infarction	2.60	2.13	0.98	0.76
Stroke	2.26	1.97	1.73	1.34
Transient ischemic attack	1.38	1.31	1.14	0.92
Abdominal aortic aneurysm	0.46	0.37	0.08	0.09
Peripheral artery disease	1.27	0.85	0.62	0.49
Heart failure	1.28	1.02	0.97	0.65
Angina	3.78	3.37	2.26	1.61
Vascular dementia	0.75	0.63	0.91	0.77

Model Predictive Performance and Risk Stratification

We developed the MT-BERT model for multiple CVD outcomes, and all performance metrics were derived from the held-out test set unless otherwise stated (Table 3), including discrimination, calibration, and classification results for both composite and individual outcomes.

For both genders, the model trained to predict the composite CVD outcome achieved the highest discrimination. In males, the AUROC was 0.744 (95% CI 0.738 - 0.749), and in females, 0.782 (95% CI 0.768 - 0.796), higher than models trained on QRISK-defined CVD outcomes (males: 0.723, 95% CI 0.717 - 0.732; females: 0.767, 95% CI 0.760 - 0.777). The corresponding concordance index (C-index) values were 0.713 (95% CI 0.710 - 0.716) in males and 0.732 (95% CI 0.725 - 0.742) in females for composite CVD.

Among individual outcomes, ischemic stroke (males: 0.738, females: 0.769) and CHD (males: 0.732, females: 0.769) demonstrated relatively strong discriminatory performance. Angina also showed acceptable discrimination (males: 0.713, females: 0.741). In contrast, myocardial infarction exhibited lower discrimination (males: 0.679, females: 0.717), particularly in males, where recall was high but overall accuracy was reduced. Vascular dementia was additionally explored on an experimental basis and showed overall limited performance across evaluation metrics, similar to the pattern observed for myocardial infarction.

Continuous variables are presented as mean values with 2 decimal places for consistency. Individual clinical measurements (eg, blood pressure) are typically recorded as integers, but decimal values arise when reporting cohort-level averages.

“Cardiovascular disease (QRISK)” is a composite outcome including CHD, stroke, and transient ischemic attack. “Cardiovascular disease (Composite)” includes the above conditions plus abdominal aortic aneurysm and peripheral artery disease. Benchmark model results were adapted from our prior work [24], where models were trained and evaluated using the same CPRD Aurum cohort and standardized preprocessing for consistent comparability. RSF (Random Survival Forest), GBSA (Gradient Boosted Survival Analysis), XGBS (Extreme Gradient Boosted Survival Model), DeepSurv, and DeepHit (Deep Neural Network for Competing Risks).

KM curves are plotted with a full 0 - 1 *y*-axis; shaded bands denote 95% CIs. Insets provide a zoomed view of the upper survival range for readability. Segments after time points with <10 individuals at risk are suppressed. High- versus low-risk groups use sex-specific thresholds (men≥40%, women≥34%). *P* values are from log-rank tests.

XSL•FO
RenderX

Table . Performance metrics of the Multi-Task Bidirectional Encoder Representations from Transformers model across cardiovascular disease outcomes by gender (test set).

Predicted outcome	AUROC[a] (95% CI)	C-index[b] (95% CI)	Brier score	Accuracy	Specificity	Recall	Baseline threshold (%)
Male							
CVD[c] (Composite)	0.744 (0.738-0.749)	0.713 (0.710-0.716)	0.130	0.823	0.874	0.405	0.40
CVD (QRISK)	0.723 (0.717-0.732)	0.699 (0.696-0.702)	0.119	0.733	0.750	0.548	0.34
CHD[d]	0.732 (0.726-0.739)	0.707 (0.704-0.709)	0.107	0.782	0.795	0.518	0.34
Stroke	0.738 (0.702-0.764)	0.688 (0.684-0.692)	0.065	0.676	0.676	0.656	0.33
MI[e]	0.679 (0.670-0.694)	0.667 (0.663-0.674)	0.133	0.125	0.102	0.958	0.35
Angina	0.713 (0.702-0.723)	0.701 (0.695-0.706)	0.104	0.765	0.775	0.517	0.33
Female							
CVD (Composite)	0.782 (0.768-0.796)	0.732 (0.725-0.742)	0.091	0.861	0.887	0.487	0.34
CVD (QRISK)	0.767 (0.760-0.777)	0.752 (0.749-0.757)	0.077	0.914	0.9456	0.2950	0.31
CHD	0.769 (0.750-0.785)	0.732 (0.725-0.742)	0.059	0.872	0.883	0.427	0.28
Stroke	0.769 (0.717-0.852)	0.737 (0.732-0.745)	0.018	0.934	0.936	0.256	0.23
MI	0.717 (0.680-0.761)	0.687 (0.682-0.696)	0.078	0.408	0.403	0.900	0.27
Angina	0.741 (0.731-0.754)	0.721 (0.718-0.724)	0.070	0.878	0.887	0.387	0.29

[a]AUROC: area under the receiver operating characteristic curve.

[b]C-index: concordance index.

[c]Cardiovascular disease (QRISK)" is a composite outcome including coronary heart disease (CHD), stroke, and transient ischemic attack (TIA). "Cardiovascular disease (Composite)" includes the above conditions plus abdominal aortic aneurysm (AAA) and peripheral artery disease (PAD).

[d]CHD: coronary heart disease.

[e]MI: myocardial infarction.

The left panel of Figure 3 visualizes the AUROC values with 95% CIs across all CVD outcomes by gender, aligning with the summary in Table 3. The model showed the clearest advantage for composite CVD, with a higher AUROC than both QRISK-defined and individual outcome-specific models.

Across all outcomes, C-index values were consistently 0.01‐0.05 lower than AUROC. Model performance was generally higher in females across AUROC, C-index, and accuracy. The thresholds used to classify positive cases ranged from 0.23% to 0.40% in males and 0.23% to 0.34% in females, with higher thresholds observed in males, consistent with their event distribution and calibration characteristics.

In the right panel of Figure 3, the MT-BERT model is compared against benchmark models, including conventional approaches (QRISK3 [4] and CoxPH [25]), ensemble-based methods (RSF, GBSA, and XGBS), and deep learning models (DeepSurv [12] and DeepHit [26]). These benchmark models were implemented based on our previous work [24]. In this evaluation, the hybrid model consistently outperformed all comparators, with the greatest AUROC gains observed for composite CVD, especially in females.

XSL•FO
RenderX

Figure 3. Discrimination performance of the Multitask Bidirectional Encoder Representations from Transformers model across cardiovascular disease outcomes, in comparison with benchmark conventional and machine learning models. AUROC: area under the receiver operating characteristic curve; CHD: coronary heart disease; CVD: cardiovascular disease; DeepSurv: Deep Neural Network–based Cox Model; DeepHit: Deep Neural Network for Competing Risks; GBSA: Gradient Boosted Survival Analysis; RSF: Random Survival Forest; XGBS: Extreme Gradient Boosted Survival Model.

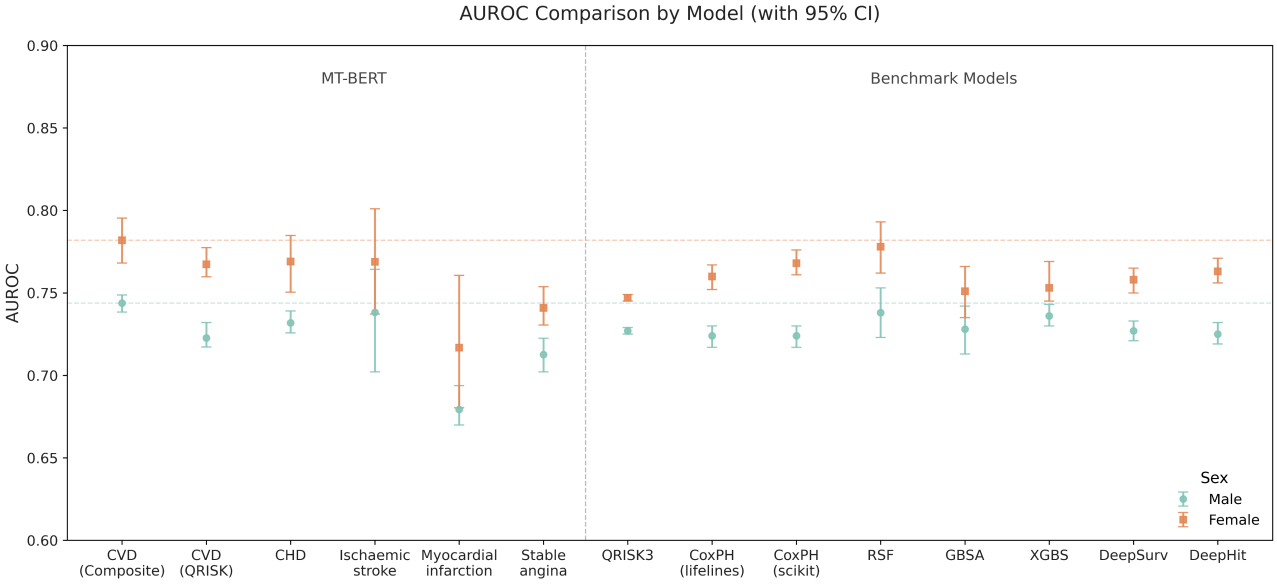
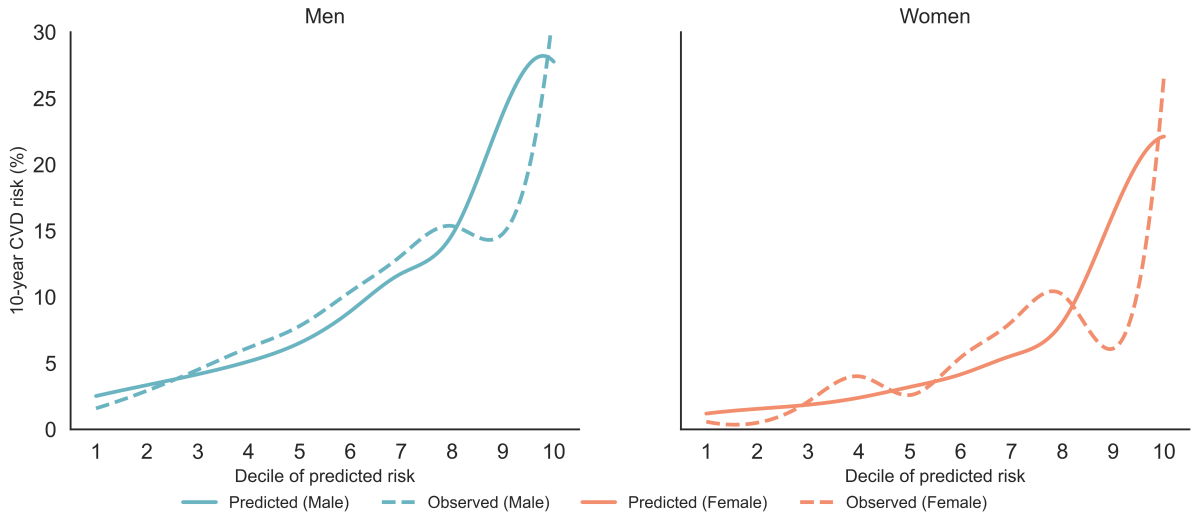


Figure 4 presents the calibration plot for the predicted 10-year composite CVD risk using the MT-BERT model, stratified by gender. Predicted risks and observed event rates were plotted across deciles of predicted risk. In both genders, predicted risks increased monotonically across deciles, indicating good overall calibration. However, risk overestimation was evident in the upper deciles, particularly among males, suggesting inflation at the highest predicted risk levels. In females, predicted and observed risks were closely aligned in lower-risk and midrisk ranges, though moderate overprediction was also observed at the top deciles, where event rates were more variable. In particular, a dip in the observed rates was seen in the ninth decile, which we attribute to event sparsity and statistical variability in the highest risk groups. These findings are consistent with the Brier scores in Table 3, where males had a score of 0.130 and females had 0.091, reflecting slightly better overall calibration in women. Taken together, the hybrid model provided reasonably calibrated risk estimates for composite CVD, with modest overprediction at higher predicted risk levels, especially in males.

Figure 4. Calibration plots for 10-year cardiovascular disease risk by gender. CVD: cardiovascular disease.

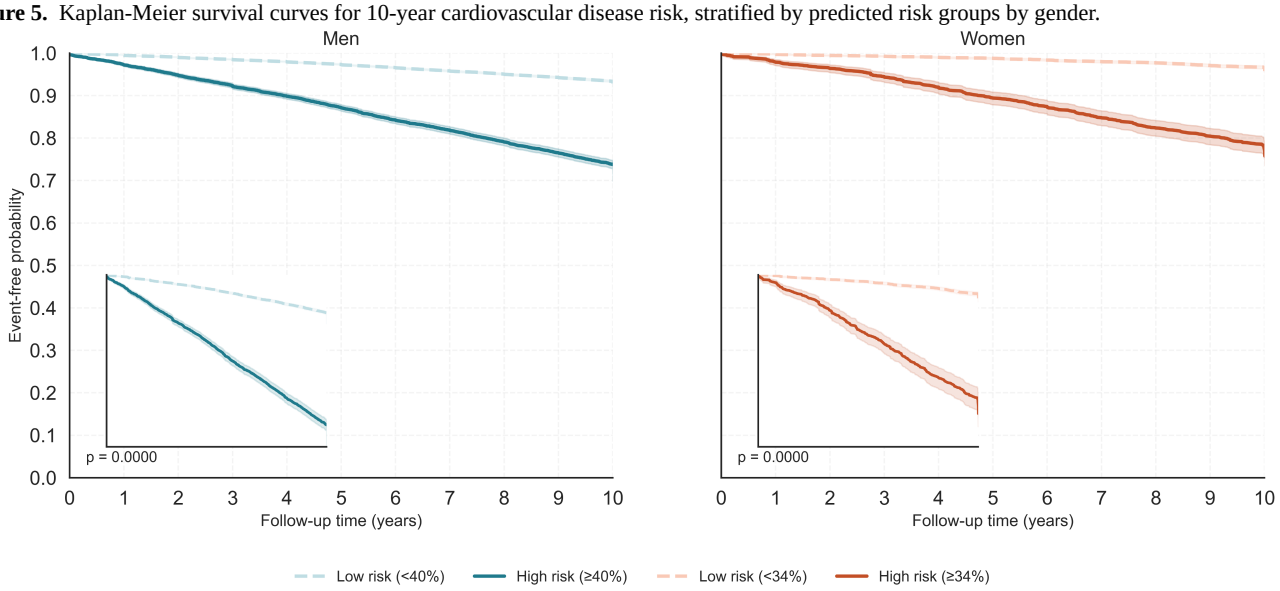


KM survival curves for 10-year composite CVD risks are presented in Figure 5, stratified by predicted risk groups in both genders. Participants were classified into high- and low-risk categories using gender-specific thresholds: 40% or greater for men and 34% or greater for women. In both genders, individuals in the high-risk group exhibited significantly lower event-free survival over time, confirming the model's ability to stratify patients according to long-term risk. Among males, the 10-year event-free probability declined to approximately 74% in the high-risk group, compared to over 93% in the low-risk group. A similar pattern was observed in females, with high-risk individuals showing notably steeper declines in survival probability. Log-rank tests yielded P values <.001 in both genders, indicating statistically significant separation between

XSL•FO
RenderX

risk groups. These results support the prognostic utility of the model's predicted risk scores, demonstrating effective stratification for composite CVD outcomes over a 10-year follow-up period.

Figure 5. Kaplan-Meier survival curves for 10-year cardiovascular disease risk, stratified by predicted risk groups by gender.



Ethnicity (n=9) subgroups include White, Indian, Pakistani, Bangladeshi, Chinese, Other Asian, Black Caribbean, Black African, and Other ethnic groups. Ethnicity (n=3) aggregates broader categories into White, Asian (including Indian, Pakistani, Bangladeshi, Chinese, and Other Asian), and Black (Caribbean and African). Deprivation (n=5) refers to Townsend quintiles, while deprivation (n=10) refers to Townsend deciles.

Model Fairness and Generalizability Across Demographics

We assessed the performance of the MT-BERT model on the composite CVD outcome across ethnic and deprivation subgroups in the spatial validation set, separately by gender. Figure 6 shows AUROC values with 95% CIs for major ethnic and deprivation categories. Table 4 presents I^2 and Q statistics based on both broad and more granular subgroup definitions. All results pertain to the composite CVD outcome.

Among all patients, the AUROC for composite CVD was 0.736 (95% CI 0.729 - 0.741) in males and 0.775 (95% CI 0.768 - 0.780) in females. These represent a moderate decline compared to the internal test set, though overall generalizability remained acceptable. Other performance metrics are provided in Table S4 in Multimedia Appendix 1, where similar trends were observed—slight reductions compared to internal validation, but performance remained within a reasonable range. Across all subgroups, model discrimination was consistently higher in females than in males (Figure 6), with an average AUROC difference of approximately 0.04 - 0.05 between genders. This pattern was consistent with results from the training, validation, and test sets (Table S4 in Multimedia Appendix 1; Table 3).

In males, model performance in the White ethnic group was marginally higher than in the overall male cohort, though the difference was not statistically significant. AUROC in the Black ethnic group was slightly lower, but the CIs overlapped with the overall population, indicating broadly comparable performance. The lowest AUROC was observed in the South Asian group, where a more pronounced decline was seen, and the CIs did not overlap with those of the White or overall male population, suggesting reduced discriminative ability in this subgroup. In females, similar patterns were observed. AUROC remained relatively consistent across the 3 main ethnic groups, though a modest decline was again noted in South Asian females, and a more notable drop was observed in Black females. When aggregated into 3 ethnic groups, I^2 values were 93.03% in males and 91.41% in females, indicating substantial heterogeneity (Table 4). Even with finer stratification into 9 ethnic groups, I^2 remained elevated (71.51% in males and 77.06% in females), suggesting that differences in model discrimination were not solely driven by broad grouping.

For deprivation, Figure 6 shows a decreasing trend in AUROC from the least to the most deprived groups. In females, AUROC declined steadily across the most deprived 40%. In males, performance dropped notably in the 60% - 80% deprivation quantile but showed partial recovery in the most deprived group. Correspondingly, heterogeneity in deprivation-based analyses remained high, with I^2 values of 83.34% (quintile-based) and 74.91% (decile-based) in males, and 82.73% and 81.55%, respectively, in females (Table 4).

Overall, heterogeneity across both ethnicity and deprivation subgroups was notable, with I^2 consistently above 70% and all Q-tests statistically significant (P<.001), except for the 9-category ethnicity analysis in males. These findings suggest that while the model maintained acceptable generalizability, subgroup-level variability in performance exists and may warrant further investigation in future work.

XSL•FO
RenderX

Figure 6. Assessment of model fairness across ethnic and deprivation subgroups ("spatial" validation set). AUROC: area under the receiver operating characteristic curve.

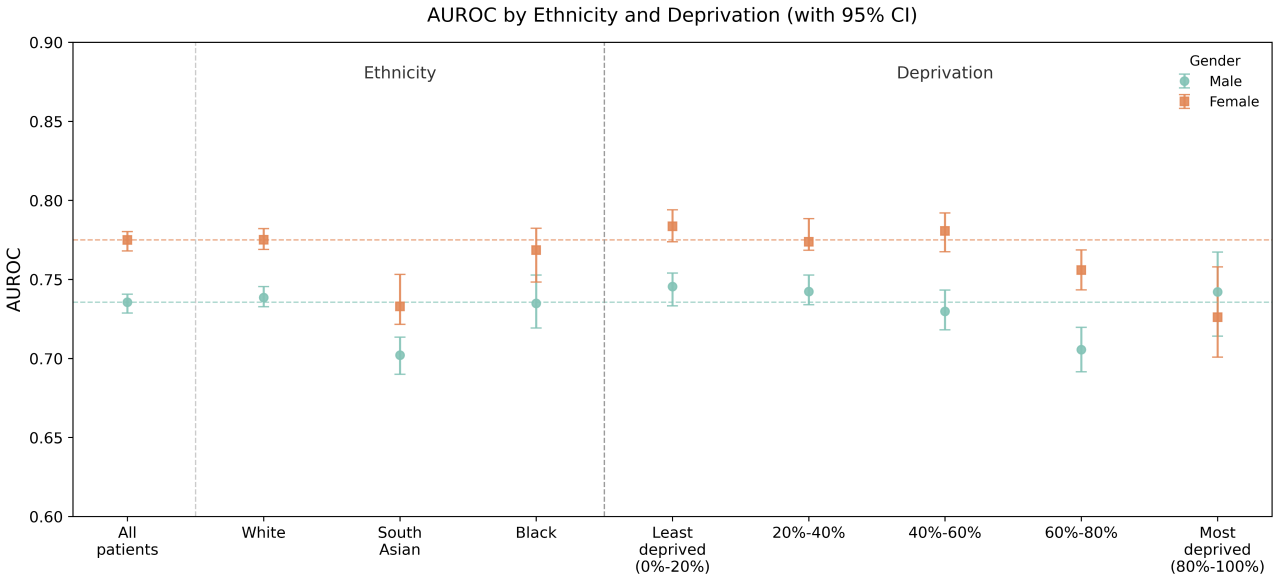


Table . Heterogeneity (I^2 and Q Statistics) by ethnicity and deprivation subgroups in the "spatial" validation set.

Subgroup (n)	Male		Female	
	I^2 (%)	Q (*P* value)	I^2 (%)	Q (*P* value)
Ethnicity (3)	93.03	28.70 (*P*<.001)	91.41	23.28 (*P*<.001)
Ethnicity (9)	71.51	28.08 (*P*<.001)	77.06	34.87 (*P*<.001)
Deprivation (5)	83.34	24.01 (*P*<.001)	82.73	23.16 (*P*<.001)
Deprivation (10)	74.91	35.87 (*P*<.001)	81.55	48.78 (*P*<.001)

Discussion

Principal Findings

The proposed hybrid MT-BERT model demonstrated strong performance in predicting 10-year CVD risk by integrating structured variables and free-text clinical notes from EHRs. While previous studies have explored the use of clinical text for risk prediction [27,28], few have focused on long-term CVD outcomes or used integrated multitask modeling. In this study, the model achieved high discrimination, demonstrated good calibration across predicted risk groups, and enabled effective survival stratification based on KM curves. Compared to conventional and ML-based survival models, the inclusion of unstructured text improved performance, particularly in females. These findings were consistent across both the internal test set and a demographically distinct "spatial external" validation cohort from London, supporting the model's generalizability and potential clinical utility.

A key methodological contribution of this study is the integration of structured and unstructured EHR data within a BERT-MLP architecture, optimized through a unified multitask learning framework. Compared to categorical or binary representations, textual input can provide richer information about disease severity, temporal context, or interactions between conditions that structured variables may not explicitly encode. Moreover, transforming structured features into natural language text reduces data sparsity and produces denser, more learnable representations [29]. This transformation is particularly suited for BERT, which is optimized for NLP and benefits from pretrained language representations that enhance its ability to model semantic relationships, even in low-resource settings or when encountering rare comorbidities [30]. Thus, our approach allows for both increased model expressiveness and improved generalization to underrepresented patient profiles.

Building on prior work in deep survival modeling, such as DeepSurv [12] and DeepHit [26], the model incorporates a classification objective to support threshold-based clinical decision-making. By jointly minimizing a combined Focal and Cox-based loss, it enables simultaneous optimization of binary classification (AUROC) and survival risk ranking (C-index). This dual-objective design allows the model to capture both event occurrence and timing, enhancing its applicability in real-world risk stratification.

To ensure comparability, data extraction followed the protocol from our previous work [24] on ML-based survival models for CVD, maintaining consistency in preprocessing and enabling direct performance comparisons. Under this aligned experimental setup, the hybrid model outperformed earlier conventional and ML-based models, demonstrating the effectiveness of combining representation learning with multiobjective optimization. Importantly, these comparators already realize the principal ablation settings within an identical

XSL•FO
RenderX

pipeline, namely, structure-only survival modeling with a single Cox objective (CoxPH, RSF, and DeepSurv). They therefore provide a pragmatic assessment of modality and loss without reimplementing stripped-down variants of MT-BERT.

Furthermore, compared to training separate models for classification and survival analysis, our multitask learning framework offers several advantages. First, by sharing representations between tasks, the model captures both static risk factors and temporal dynamics more efficiently, leveraging complementary information to enhance overall predictive performance [31,32]. Binary classification and survival modeling address distinct but related goals [12]: classification focuses on identifying individuals at high immediate risk, while survival modeling captures the time-dependent risk trajectory. Learning these jointly allows the model to optimize decision thresholds and risk ranking simultaneously. Additionally, shared representations act as a form of regularization, improving generalization especially in underrepresented subgroups [31]. Although we did not run a full factorial ablation, the existing comparators already realize the principal ablation settings within the same pipeline, namely, structure-only survival modeling with a single Cox objective. The consistent gains in both discrimination and calibration indicate a benefit from multitask integration, and we will conduct targeted ablations in future work to quantify incremental contributions beyond these baselines.

Despite these overall gains, subgroup analyses revealed reduced discrimination in certain populations, particularly males from deprived and ethnic minority groups. Similar disparities have been observed in other clinical ML applications [33], underscoring the importance of fairness-aware evaluation and algorithm refinement. Substantial heterogeneity (I^2>70%) across ethnicity and deprivation strata further highlights the need for subgroup-specific performance auditing. These findings emphasize the necessity of addressing demographic variability to support equitable deployment of predictive models in diverse populations.

Limitations

This study has several limitations that merit consideration. While the hybrid MT-BERT architecture offers enhanced representational capacity by integrating free-text and structured data, it also introduces considerable complexity [13,29]. BERT-based models are computationally intensive, requiring substantially more memory and processing time than MLPs trained solely on structured inputs. The need to process long token sequences increases both training and inference latency, which may limit scalability in resource-constrained environments. Additionally, textual representations derived from BERT may suffer from noise due to variability in clinical phrasing and tokenization. For instance, expressions such as “No history of diabetes” and “Diabetes: none” may yield inconsistent embeddings, introducing ambiguity in comorbidity interpretation. This variability in tokenization can further propagate semantic drift, where slight differences in phrasing result in divergent embeddings despite similar clinical meaning. These factors suggest that although BERT provides valuable semantic richness, its use must be balanced against concerns around efficiency, representational stability, and semantic fidelity in EHR settings.

Another methodological challenge lies in the joint optimization of binary classification (AUROC) and survival ranking (C-index) within a multitask framework. Although this design captures complementary dimensions of CVD risk, the 2 objectives are not always easily harmonized. In our results, C-index scores were consistently lower than AUROC, indicating difficulty in modeling TTE information with the same fidelity as event discrimination. In addition, evaluating a true 10-year TTE objective with censoring and aligning predictors with outcome timing typically yields a more conservative AUROC than shorter or time-gated tasks, which helps explain why our discrimination is lower than some reports. Future work may benefit from refined training strategies or alternative loss functions to better align these targets.

Model comparisons were conducted under a shared experimental framework established in our prior work [24], with consistent data extraction and preprocessing across all models. This enabled fair benchmarking but does not eliminate concerns about potential biases from repeated records or unobserved confounding. Given that the same CPRD dataset, variable and outcome definitions, cohort construction strategies, and censoring handling were applied, these models serve as appropriate comparators for evaluating the added value of MT-BERT. Within this like-for-like design, MT-BERT exceeded the conventional and ML baselines from our previous benchmark, with gains that were modest in absolute terms yet consistent across outcomes, and with clearer KM separation and better calibration. Independent replication in other settings will nonetheless be critical to validate generalizability.

The model also showed differential performance across outcomes. Prediction was most effective for composite CVD events, likely due to broader definitions and higher case counts [34]. In contrast, individual outcomes such as MI and vascular dementia were more difficult to model, reflecting data sparsity and noisier labels. MI is commonly harder because many events are precipitated by acute triggers that are not present in baseline features, which limits discriminability over a 10-year horizon. These findings highlight the practical value of composite endpoints in primary care, where follow-up is long and individual outcomes are rare. Future work will incorporate richer short-term and time-varying signals, for example, recent trajectories of vitals and laboratory results, medication changes, secondary-care encounters, and uncertainty-aware learning, to strengthen outcome-specific prediction.

Although generalizability was demonstrated between the development and spatial external validation sets, the model has not yet been evaluated across other health care systems or geographic regions. The London cohort provided important demographic diversity, especially in ethnicity and deprivation, but broader validation is required. Notably, performance declined in South Asian and socioeconomically deprived males, potentially due to lower case numbers and greater uncertainty. This highlights the need for targeted data enrichment and uncertainty-aware learning in underrepresented subgroups. Fairness-related issues also remain. While subgroup audits were

XSL•FO
RenderX

conducted, mitigation strategies such as sample reweighting or recalibration were not applied, and systematic subgroup-specific auditing will be required before equitable clinical deployment can be ensured.

From an implementation perspective, the present work relied on DistilBERT, a relatively lightweight model pretrained on general rather than medical corpora. This choice reduced computational cost, allowing training within hours on high-performance computing environments and inference within seconds on standard CPUs, demonstrating feasibility for near real-time use in primary care dashboards, such as flagging high-risk patients for recall or displaying updated risk estimates during consultations. However, the absence of domain-specific pretraining remains a limitation, and larger biomedical language models trained on richer corpora are likely to achieve superior performance in the future. While deployment at scale is unlikely to pose major challenges, training requirements will ultimately depend on the size and complexity of the pretrained models used, and these aspects will need to be formally evaluated.

Interpretability also remains a key barrier to adoption. Deep learning models are often considered "black boxes," in contrast to conventional statistical methods [6]. For structured variables, attribution methods such as SHapley Additive exPlanations (SHAP) can provide ranked contributions, enabling clinicians to see which risk factors (eg, blood pressure and diabetes status) were most influential. For clinical text, attention mechanisms can highlight salient tokens or phrases (eg, "chest pain" and "family history of stroke") that received higher model weights, offering a complementary perspective. These cross-modal explanations require distinct visualization strategies, and we did not implement a systematic framework for presenting them to clinicians in this study. While such tools may improve explainability, the trade-off between predictive performance and interpretability must be carefully considered [35]. In contexts where textual data add limited value, simpler approaches such as RSF may provide comparable results with greater transparency. For long-term CVD prediction, robust risk stratification may ultimately be more clinically relevant than token-level explanations, yet future research should examine how to deliver outputs in formats that are both faithful to the model and usable in practice.

Importantly, this model is not intended to replace established risk tools such as QRISK4 [36], which have undergone extensive validation. Rather, it illustrates the potential of combining structured and unstructured EHR data within a multitask learning framework to support multioutcome prediction. Prospective validation in external health systems, integration into clinical care pathways, development of clinician-facing interpretability tools, and incorporation of fairness-aware strategies will be essential to translate these preliminary findings into real-world practice.

Conclusion

This study presents a multitask deep learning model for 10-year CVD risk prediction using real-world EHR data, integrating structured variables and unstructured clinical text through an MT-BERT architecture. By jointly optimizing classification and survival objectives, the model achieves strong discrimination, robust calibration, and meaningful risk stratification over a 10-year follow-up. Performance remained consistent in a demographically diverse London subgroup, supporting its generalizability. Although improvements over previously tested ML-based models were modest, these findings provide preliminary evidence that combining representation learning and multiobjective optimization is a promising direction for risk prediction in primary care. However, subgroup differences across ethnicity and deprivation highlight persistent fairness concerns. Future work should focus on improving interpretability, validating in external populations, and evaluating clinical impact to support real-world implementation.

Acknowledgments

VC is supported by the Engineering and Physical Sciences Research Council (EPSRC)-funded King's Health Partners Digital Health Hub (EP/X030628/1). TL is a PhD student at KCL's DRIVE-Health CDT supported by Metadvice Ltd. and the National Institute for Health Research (NIHR) Biomedical Research Centre based at Guy's and St Thomas' NHS Foundation Trust and King's College London (IS-BRC-1215-20006). The views expressed are those of the author(s) and not necessarily those of the NHS, the NIHR, or the Department of Health.

Data Availability

The CPRD Aurum EHR dataset used in this study is accessible through a formal application [37]. The model implementation, algorithm details, and technical components are openly available within the article and on GitHub [38].

Authors' Contributions

TL developed the deep learning model, performed the statistical analyses, generated the results figures and tables, and prepared the initial manuscript draft under the guidance of VC and LL. YW, AK, and LL contributed to manuscript revisions and provided valuable insights. All authors critically reviewed the manuscript and approved the final version for publication.

Conflicts of Interest

AK serves as the Chief Medical Officer at Metadvice, a company specializing in precision medicine technologies.

XSL•FO
RenderX

Multimedia Appendix 1
Supplementary tables providing detailed information on model features, disease definitions, software packages, and extended performance metrics of the multitask BERT model across cardiovascular disease outcomes by gender and dataset split.
[DOCX File, 48 KB - medinform_v13i1e76659_app1.docx]

Multimedia Appendix 2
Supplementary file containing phenotype definitions used in this study, including cardiovascular disease outcomes, comorbidities, and related risk factors, provided as individual CSV files.
[ZIP File, 77 KB - medinform_v13i1e76659_app2.zip]

Checklist 1
Transparent Reporting of a multivariable prediction model for Individual Prognosis Or Diagnosis checklist.
[PDF File, 13389 KB - medinform_v13i1e76659_app3.pdf]

References

1. UK cardiovascular disease factsheet. British Heart Foundation. 2024 Jan. URL: https://www.bhf.org.uk/-/media/files/for-professionals/research/heart-statistics/bhf-cvd-statistics-uk-factsheet.pdf?rev=5503842f012d416994618f73f5e76667&hash=B25531514E2326EBAD737D565D969EEA [accessed 2025-10-28]
2. Number of people living with diabetes in the UK tops 5 million for the first time. Diabetes UK. 2023. URL: https://www.diabetes.org.uk/about-us/news-and-views/number-people-living-diabetes-uk-tops-5-million-first-time [accessed 2025-10-28]
3. Cardiovascular disease: risk assessment and reduction, including lipid modification report no: NG238. National Institute for Health and Care Excellence (NICE). 2023 Dec. URL: https://www.nice.org.uk/guidance/ng238 [accessed 2024-07-15]
4. Hippisley-Cox J, Coupland C, Brindle P. Development and validation of QRISK3 risk prediction algorithms to estimate future risk of cardiovascular disease: prospective cohort study. BMJ 2017 May 23;357:j2099. [doi: 10.1136/bmj.j2099] [Medline: 28536104]
5. Virani SS, Newby LK, Arnold SV, et al. 2023 AHA/ACC/ACCP/ASPC/NLA/PCNA Guideline for the management of patients with chronic coronary disease: a report of the American Heart Association/American College of Cardiology Joint Committee on Clinical Practice Guidelines. Circulation 2023 Aug 29;148(9):e9-e119. [doi: 10.1161/CIR.0000000000001168] [Medline: 37471501]
6. Liu T, Krentz A, Lu L, Curcin V. Machine learning based prediction models for cardiovascular disease risk using electronic health records data: systematic review and meta-analysis. Eur Heart J Digit Health 2025 Jan;6(1):7-22. [doi: 10.1093/ehjdh/ztae080] [Medline: 39846062]
7. Liu T, Krentz AJ, Huo Z, Ćurčin V. Opportunities and challenges of cardiovascular disease risk prediction for primary prevention using machine learning and electronic health records: a systematic review. Rev Cardiovasc Med 2025 Apr;26(4):37443. [doi: 10.31083/RCM37443] [Medline: 40351688]
8. Razieh C, Zaccardi F, Miksza J, et al. Differences in the risk of cardiovascular disease across ethnic groups: UK Biobank observational study. Nutr Metab Cardiovasc Dis 2022 Nov;32(11):2594-2602. [doi: 10.1016/j.numecd.2022.08.002] [Medline: 36064688]
9. Eastwood SV, Mathur R, Sattar N, Smeeth L, Bhaskaran K, Chaturvedi N. Ethnic differences in guideline-indicated statin initiation for people with type 2 diabetes in UK primary care, 2006-2019: a cohort study. PLoS Med 2021 Jun;18(6):e1003672. [doi: 10.1371/journal.pmed.1003672] [Medline: 34185782]
10. Socioeconomic inequalities in heart and circulatory diseases in england: an analysis. British Heart Foundation. 2025 Jan. URL: https://www.bhf.org.uk/what-we-do/our-research/heart-statistics/health-inequalities-research/inequalities-in-heart-and-circulatory-diseases-in-england [accessed 2025-10-28]
11. Rajkomar A, Dean J, Kohane I. Machine learning in medicine. N Engl J Med 2019 Apr 4;380(14):1347-1358. [doi: 10.1056/NEJMra1814259] [Medline: 30943338]
12. Katzman JL, Shaham U, Cloninger A, Bates J, Jiang T, Kluger Y. DeepSurv: personalized treatment recommender system using a Cox proportional hazards deep neural network. BMC Med Res Methodol 2018 Feb 26;18(1):24. [doi: 10.1186/s12874-018-0482-1] [Medline: 29482517]
13. Shickel B, Tighe PJ, Bihorac A, Rashidi P. Deep EHR: a survey of recent advances in deep learning techniques for electronic health record (EHR) analysis. IEEE J Biomed Health Inform 2018 Sep;22(5):1589-1604. [doi: 10.1109/JBHI.2017.2767063] [Medline: 29989977]
14. Devlin J, Chang MW, Lee K, Toutanova K. BERT: pre-training of deep bidirectional transformers for language understanding. arXiv. Preprint posted online on May 24, 2019. [doi: 10.48550/arXiv.1810.04805]
15. CPRD Aurum January 2022. : Clinical Practice Research Datalink; 2022. [doi: 10.48329/DB7T-AY41]
16. Collins GS, Moons KGM, Dhiman P, et al. TRIPOD+AI statement: updated guidance for reporting clinical prediction models that use regression or machine learning methods. BMJ 2024 Apr 16;385:e078378. [doi: 10.1136/bmj-2023-078378] [Medline: 38626948]

XSL•FO
RenderX

17. Riley RD, Snell KI, Ensor J, et al. Minimum sample size for developing a multivariable prediction model: PART II - binary and time - to - event outcomes. Stat Med 2019 Mar 30;38(7):1276-1296. [doi: 10.1002/sim.7992]
18. Thayer DS, Mumtaz S, Elmessary MA, et al. Creating a next-generation phenotype library: the health data research UK Phenotype Library. JAMIA Open 2024 Jul;7(2):ooae049. [doi: 10.1093/jamiaopen/ooae049] [Medline: 38895652]
19. Denaxas S, Gonzalez-Izquierdo A, Direk K, et al. UK phenomics platform for developing and validating electronic health record phenotypes: CALIBER. J Am Med Inform Assoc 2019 Dec 1;26(12):1545-1559. [doi: 10.1093/jamia/ocz105] [Medline: 31329239]
20. Yan L. QRISK3: 10-year cardiovascular disease risk calculator (QRISK3 2017). ClinRisk Ltd. 2019. URL: https://10.32614/CRAN.package.QRISK3 [accessed 2025-10-28]
21. Sanh V, Debut L, Chaumond J, Wolf T. DistilBERT, a distilled version of BERT: smaller, faster, cheaper and lighter. arXiv. Preprint posted online on Mar 1, 2020. [doi: 10.48550/arXiv.1910.01108]
22. Kendall A, Gal Y, Cipolla R. Multi-task learning using uncertainty to weigh losses for scene geometry and semantics. arXiv. Preprint posted online on Apr 24, 2018. [doi: 10.48550/arXiv.1705.07115]
23. Higgins JPT, Thompson SG, Deeks JJ, Altman DG. Measuring inconsistency in meta-analyses. BMJ 2003 Sep 6;327(7414):557-560. [doi: 10.1136/bmj.327.7414.557] [Medline: 12958120]
24. Liu T, Krentz AJ, Lu L, Wang Y, Curcin V. Benchmarking survival machine learning models for 10-year cardiovascular disease risk prediction using large-scale electronic health records. Digit Health 2025 Apr 30 [FREE Full text]
25. Davidson-Pilon C. Lifelines: survival analysis in Python. J Open Source Softw 2019 Aug 4;4(40):1317. [doi: 10.21105/joss.01317]
26. Lee C, Zame W, Yoon J, Van der Schaar M. DeepHit: a deep learning approach to survival analysis with competing risks. Presented at: Proceedigs of the AAAI Conference on Artificial Intelligence; Feb 2-7, 2018. [doi: 10.1609/aaai.v32i1.11842]
27. Weng SF, Reps J, Kai J, Garibaldi JM, Qureshi N. Can machine-learning improve cardiovascular risk prediction using routine clinical data? PLoS ONE 2017;12(4):e0174944. [doi: 10.1371/journal.pone.0174944] [Medline: 28376093]
28. Yang X, Chen A, PourNejatian N, et al. A large language model for electronic health records. npj Digit Med ;5(1):194. [doi: 10.1038/s41746-022-00742-2]
29. Yang Z, Mitra A, Liu W, Berlowitz D, Yu H. TransformEHR: transformer-based encoder-decoder generative model to enhance prediction of disease outcomes using electronic health records. Nat Commun 2023 Nov 29;14(1):7857. [doi: 10.1038/s41467-023-43715-z]
30. Alsentzer E, Murphy JR. Publicly available clinical BERT embeddings. arXiv. Preprint posted online on Jun 20, 2019. [doi: 10.48550/arXiv.1904.03323]
31. Ruder S. An overview of multi-task learning in deep neural networks. arXiv. Preprint posted online on Jun 15, 2017. [doi: 10.48550/ARXIV.1706.05098]
32. Harutyunyan H, Khachatrian H, Kale DC, Ver Steeg G, Galstyan A. Multitask learning and benchmarking with clinical time series data. Sci Data 2019 Jun 17;6(1):96. [doi: 10.1038/s41597-019-0103-9] [Medline: 31209213]
33. Colacci M, Huang YQ, Postill G, et al. Sociodemographic bias in clinical machine learning models: a scoping review of algorithmic bias instances and mechanisms. J Clin Epidemiol 2025 Feb;178:111606. [doi: 10.1016/j.jclinepi.2024.111606] [Medline: 39532254]
34. Rajkomar A, Oren E, Chen K, et al. Scalable and accurate deep learning with electronic health records. NPJ Digit Med 2018 May 8;1(1):18. [doi: 10.1038/s41746-018-0029-1]
35. Lundberg S, Lee SI. A unified approach to interpreting model predictions. arXiv. Preprint posted online on Nov 25, 2017. [doi: 10.48550/arXiv.1705.07874]
36. Hippisley-Cox J, Coupland CAC, Bafadhel M, et al. Development and validation of a new algorithm for improved cardiovascular risk prediction. Nat Med 2024 May;30(5):1440-1447. [doi: 10.1038/s41591-024-02905-y]
37. Access to data. CPRD. URL: https://www.cprd.com/access-data [accessed 2025-10-30]
38. TLiuBB/bert_paper. GitHub. URL: https://github.com/TLiuBB/BERT_paper [accessed 2025-10-28]

Abbreviations

AI: artificial intelligence
AUROC: area under the receiver operating characteristic curve
BERT: Bidirectional Encoder Representations from Transformers
C-index: concordance index
CALIBER: Clinical research using Linked Bespoke studies and Electronic health Records
CALIBER: CArdiovascular disease research using LInked BEspoke studies and Electronic health Records
CHD: coronary heart disease
CPRD: Clinical Practice Research Datalink
CT: Systematized Nomenclature of Medicine – Clinical Terms
CVD: cardiovascular disease
DeepHit: Deep Neural Network for Competing Risks

XSL•FO
RenderX

DeepSurv: Deep Neural Network-based Cox Model
EHR: electronic health record
GBSA: Gradient Boosted Survival Analysis
GP: general practitioner
***ICD-10*:** *International Classification of Diseases, Tenth Revision*
ISAC: Independent Scientific Advisory Committee
KM : Kaplan-Meier
ML: machine learning
MLP: multilayer perceptron
NICE: National Institute for Health and Care Excellence
NLP: natural language processing
RSF: Random Survival Forest
SBP: systolic blood pressure
SHAP: SHapley Additive exPlanations
TRIPOD: Transparent Reporting of a multivariable prediction model for Individual Prognosis Or Diagnosis
TTE: time-to-event
XGBS: Extreme Gradient Boosting Survival
XGBS: Extreme Gradient Boosted Survival Model

Edited by A Benis; submitted 28.04.25; peer-reviewed by C Manlhiot, J Dong; revised version received 14.10.25; accepted 16.10.25; published 13.11.25.

Please cite as:
Liu T, Lu L, Wang Y, Krentz AJ, Curcin V
Estimating 10-Year Cardiovascular Disease Risk in Primary Prevention Using UK Electronic Health Records and a Hybrid Multitask BERT Model: Retrospective Cohort Study
JMIR Med Inform 2025;13:e76659
URL: https://medinform.jmir.org/2025/1/e76659
doi:10.2196/76659

© Tianyi Liu, Lei Lu, Yanzhong Wang, Andrew J Krentz, Vasa Curcin. Originally published in JMIR Medical Informatics (https://medinform.jmir.org), 13.11.2025. This is an open-access article distributed under the terms of the Creative Commons Attribution License (https://creativecommons.org/licenses/by/4.0/), which permits unrestricted use, distribution, and reproduction in any medium, provided the original work, first published in JMIR Medical Informatics, is properly cited. The complete bibliographic information, a link to the original publication on https://medinform.jmir.org/, as well as this copyright and license information must be included.

XSL•FO
RenderX

Automated Chronic Obstructive Pulmonary Disease Phenotyping and Control Assessment in Primary Care: Retrospective Multicenter Study Using the Seleida Model

José David Maya Viejo[1*], MD; Fernando M Navarro Ros[2*], MD

[1]Centro de Salud de Camas, Santa María de Gracia 54, Seville, Spain

[2]Centro de Salud Plaza Segovia, Valencia, Spain

[*]all authors contributed equally

Corresponding Author:
José David Maya Viejo, MD
Centro de Salud de Camas, Santa María de Gracia 54, Seville, Spain

Abstract

Background: Chronic obstructive pulmonary disease (COPD) remains a leading global health burden. In primary care, the inconsistent availability of spirometry and symptom scores limits the detection of patients with poor disease control. There is a pressing need for scalable, data-driven tools that leverage routinely collected clinical information to support timely, equitable, and guideline-concordant interventions.

Objective: This study aims to validate the performance of Seleida—a fully automated, deterministic, and bijective model for COPD control assessment and phenotyping—using real-world primary care data and to evaluate its feasibility for integration into electronic health record (EHR)–based informatics systems.

Methods: Seleida estimates the probability of poor control (*Pr*) using two objective EHR variables: (1) annual dispensations of short-acting bronchodilators—specifically short-acting β2-agonists (SABA), short-acting muscarinic antagonists (SAMA), or both, and (2) number of dispensed antibiotic courses for bronchitis or COPD exacerbations. Its bijective structure supports both forward risk estimation and reverse phenotype inference. In a retrospective cohort of 106 patients, agreement was assessed between 2 phenotyping systems (a 126-combination model and a streamlined 21-combination version) and with clinician-assigned classifications. Due to sample size limitations, a provisional risk threshold of *Pr*>.50 was adopted for internal stratification.

Results: Seleida showed perfect agreement between phenotyping systems (Cohen κ=1.00; *P*<.001) and substantial concordance with clinician-assigned profiles (Cohen κ=0.70; *P*<.001). The model operates transparently, without machine learning, and can be embedded into EHR platforms or applied manually using a visual framework. It enables individualized risk estimation, phenotype-driven treatment planning, and population-level case identification—particularly in settings with limited access to traditional diagnostic tools.

Conclusions: Seleida provides a reproducible and interpretable framework for COPD control monitoring using high-frequency prescribing data. Its transparent logic, low data burden, and interoperability enable integration across diverse digital infrastructures, including resource-limited settings. By supporting both individualized care and population-level risk stratification, Seleida bridges predictive analytics with real-world clinical decision-making. Ongoing multicenter validation will determine its generalizability, clinical impact, and cost-effectiveness at scale.

(JMIR Med Inform 2025;13:e74932) doi:10.2196/74932

KEYWORDS

COPD; phenotyping; predictive model; poor control; primary care; exacerbations; risk estimation; electronic health record; health care utilization; precision medicine; chronic obstructive pulmonary disease

Introduction

Chronic obstructive pulmonary disease (COPD) remains a major global health challenge, with more than 3.2 million deaths annually and more than 390 million people affected worldwide [1,2]. In Europe, direct health care costs exceed $56.5 billion per year (the cost that was originally reported in euros [€] was converted to US dollars using the exchange rate of €1=$1.18 as of September 15, 2025, based on the European Central Bank reference rates) [3], with the burden concentrated in primary care, where early interventions are most feasible [4].

Yet in real-world settings, early identification of patients at risk of exacerbation or poor control remains limited. Nearly 50% of individuals with COPD experience at least 1 moderate to severe

XSL•FO
RenderX

exacerbation annually, often without prior clinical detection [5-8]. These events are not only indicators of disease instability but also independent risk factors for cardiovascular morbidity and mortality. Large-scale studies have shown sharply increased risks of death and cardiovascular events—such as myocardial infarction, heart failure, stroke, and arrhythmias—within 30 days of an exacerbation, with elevated risk persisting for up to a year [9-12].

The underlying pathophysiology—driven by systemic inflammation, hypoxia, and prothrombotic states—may explain this sustained vulnerability [10,11]. The effect is cumulative: each subsequent exacerbation further increases cardiopulmonary risk [9]. These episodes also drive disproportionate health care use and cost, particularly via emergency and hospital care [11,13].

In this context, it is essential to develop tools that not only predict a patient's level of COPD control but also accurately phenotype them, since therapeutic optimization depends heavily on phenotype-specific characteristics. Personalized inhaled treatment, guided by phenotype, has the potential to reduce exacerbations and mitigate their associated systemic and economic consequences.

While current frameworks—such as Global Initiative for Chronic Obstructive Lung Disease (GOLD) 2025 and GesEPOC 2021—guide treatment decisions, they rely on clinical data often unavailable in primary care, including spirometry and symptom scales [14-17]. Moreover, they underutilize objective, high-frequency prescribing data—such as rescue bronchodilator or antibiotic use—despite their predictive value for clinical instability [12].

To address this gap, we developed Seleida: a fully automated classification system that is deterministic, meaning it produces the same output for any given input without randomness, and bijective, meaning each patient profile corresponds to a unique, reversible clinical category. The model is based solely on 2 universally available variables in structured electronic health records (EHRs): the annual number of short-acting β2-agonists (SABA) and short-acting muscarinic antagonists (SAMA) dispensations, or both, and the annual number of antibiotic dispensations for respiratory events, specifically bronchitis and COPD exacerbations [18-20]. These variables serve as robust proxies for symptom burden and exacerbation frequency, facilitating seamless integration into routine clinical workflows [21-23].

By intentionally excluding low-access metrics (eg, forced expiratory volume in the first second of expiration, patient-reported outcomes), Seleida prioritizes scalability and feasibility without sacrificing predictive accuracy. Prior work suggests minimal added value from incorporating such variables into risk models [18,20].

This study aimed to validate the Seleida model using real-world data from 2 Spanish primary care centers. We hypothesized that a deterministic, fully automated system based solely on prescribing data—specifically, annual SABA or SAMA and antibiotic dispensations—could reliably stratify patients with COPD by control status and phenotype, without relying on spirometry or symptom scales. To this end, the study pursued 3 interrelated goals: validating the model's bijective structure, comparing model-derived phenotypes against the 2025 GOLD ABE classification and between the 126- and 21-combination configurations, and evaluating Seleida's clinical use for early risk identification and digital deployment in routine care.

Methods

Study Design, Setting, and Population

This retrospective, multicenter pilot cohort validation study was nested within the Seleida project—an initiative to develop scalable models, based on EHRs, for identifying poor control in chronic respiratory diseases. The Seleida model had been previously developed and internally validated using two consistently recorded variables in structured EHRs: (1) annual dispensations of rescue inhalers (SABA, SAMA, or both) and (2) respiratory antibiotics [24,25]. These variables were chosen for their clinical relevance, high traceability, and interoperability with primary care informatics systems [21-23].

For this validation study, anonymized patient-level EHR data were extracted from 2 urban primary care centers in Seville and Valencia, both integrated within the Spanish National Health System [21,26]. These centers serve demographically diverse populations and represent real-world contexts for Seleida deployment.

From a reference population of 82,631 adults, a stratified random sample of 110 individuals aged 40 - 80 years was drawn. Selection was based on the presence of a COPD diagnosis (*International Classification of Diseases, Tenth Revision* [*ICD-10*]), on compatible pharmacological treatment for at least 3 months per year over the previous 2 years, or on both criteria [6,8]. Predefined exclusion criteria were active malignancy, palliative care, systemic corticosteroids or biologics for nonrespiratory indications, pregnancy, severe disability, enrollment in clinical trials, asthma-COPD overlap syndrome, and absence of recorded pharmacological activity during the 12-month observation period.

All dispensing records were cross-validated with linked pharmacy databases to minimize misclassification bias from unfilled or partially filled prescriptions [27,28]. Variables with more than 50% missing data were excluded, following standard epidemiological guidance [28,29]. Operational definitions, measurement units, and coding conventions are described in section S2 in Multimedia Appendix 1.

Four patients (4/6, 3.6%) met exclusion criteria, leaving a final analytical cohort of 106 patients (60/106, 56.6%) from Seville and from Valencia (46/106, 43.4%), with a mean age of 68.8 (SD 8.2) years; most were male (77/106, 72.6%).

To ensure data integrity, automated quality checks were performed to detect missing fields and inconsistencies. Data processing and storage followed international health informatics standards [27,30]. The methodological infrastructure was designed to support interoperability with HL7 FHIR (Health Level Seven Fast Healthcare Interoperability Resources; see

XSL•FO
RenderX

section S7 in Multimedia Appendix 1), enabling future integration into clinical decision support tools [21,22,31-33].

Objective and Methodology

The primary aim of this study was to validate the predictive performance and mathematical structure of the Seleida model—a deterministic and bijective algorithm designed for real-time COPD control assessment—using structured, real-world EHR data from primary care. The secondary aim was to evaluate its feasibility for integration into digital health infrastructures and its ability to support automated phenotyping in routine clinical workflows.

To address the primary aim, the study pursued 3 interrelated objectives:

1. To validate Seleida's bijective structure, which ensures a one-to-one correspondence between clinical inputs and predicted risk estimates. It guarantees that each unique combination of rescue inhaler use and exacerbation frequency produces a distinct, reproducible phenotypic classification [20,34].

2. To compare Seleida's model–derived phenotypes with established clinical classifications based on the 2025 GOLD guidelines. This included:

- Comparing the 126-combination high-resolution phenotyping system to the guideline-defined 2025 GOLD ABE classification [27,35],
- Comparing the 21-combination streamlined system to the 2025 GOLD ABE classification [4], and
- Assessing the agreement between the 126- and 21-combination structures.

Both systems support two phenotyping methods: (1) basic phenotyping (closely aligned with the ABE classification in GOLD 2025) and (2) expanded phenotyping (combines the ABE classification with stratification based on SABA use levels—low or high: L or H), offering a nuanced characterization aligned with Seleida's risk profiles.

3. To assess the model's clinical use for early risk detection and phenotype-driven decision support. The goal is to enable proactive, data-driven interventions for poorly controlled patients in EHR-integrated environments [20,36].

By combining mathematical determinism with real-world clinical traceability, Seleida offers a scalable and interpretable alternative to conventional risk classification systems. Its design supports automated control monitoring, granular patient segmentation, and guideline-concordant decision-making in both high- and low-resource care settings [34,37,38].

Outcome Definition and Model Application

The operational definition of poor control in COPD was adapted to align with Seleida's data-driven thresholds: ≥1 moderate exacerbation (requiring antibiotics or systemic corticosteroids without hospitalization), ≥1 severe exacerbations (requiring hospitalization or emergency room visit), or annual use of at least 3 SABA or SAMA canisters or both [14,17,25]. This definition enables continuous risk stratification and phenotype inference without the need for spirometry or symptom scales, improving scalability in digital health environments. By these criteria, 55.7% (59/106) of the cohort was classified as poorly controlled. Control status was evenly distributed across sites (χ^2_1=1.055; *P*=.304), and baseline demographic and clinical characteristics were compared for balance [39-41].

Model Development, Validation, and Performance Evaluation

The analytical cohort comprised 106 patients, selected pragmatically based on feasibility and validated against formal criteria for clinical prediction modeling. With a binary outcome (poor vs good control) and a 55.7% (59/106) prevalence of poor control, the training subset (85/106, 80% of the cohort) included approximately 47 events. This yielded an events-per-variable ratio of 23.5 for the 2 selected predictors—annual rescue inhaler canisters and respiratory antibiotic courses dispensed—well above the recommended ≥10 events-per-variable threshold for stable logistic regression estimates [29,41,42].

Additional clinical and demographic variables—age, sex, geographic origin, exacerbation history, daily inhalation frequency, and emergency visits—were collected for descriptive purposes and evaluated for potential inclusion. An exploratory multivariable logistic regression including age group, sex, SABA or SAMA use, or both, and antibiotic prescriptions confirmed the independent predictive strength of the 2 primary variables (*P*=.001 and *P*<.001, respectively). In contrast, age and sex were not statistically significant (*P*=.65 and *P*=.65), and their inclusion caused numerical instability due to sparse subgroup representation (eg, patients aged 80 years without exacerbations or females with high SABA or SAMA use or both). This led to quasi-complete separation and convergence failures, manifested as inflated standard errors, infinite odds ratios [Exp(β) >10], and singularities in the Hessian matrix—classic indicators of model overspecification in small samples. Full diagnostics and regression results are detailed in section S5 in Multimedia Appendix 1. Following best practices for parsimonious and deployable models [4,6], age and sex were excluded from the final Seleida model to reduce overfitting, preserve statistical stability, and maintain generalizability in small or imbalanced datasets.

The final Seleida model, including only the 2 primary predictors, achieved strong predictive performance in the initial validation: area under the receiver operating characteristic curve of 0.978, sensitivity of 92.86%, specificity of 87.50%, κ coefficient of 0.80, and positive likelihood ratio (LR+) of 7.43. Bootstrap resampling (1000 iterations) confirmed metric stability, supporting both clinical use and statistical robustness [24,25].

Internal validity was also assessed with bootstrap resampling (1000 iterations), following Steyerberg's framework for early-phase models [25,29]. The α level was set at .05, and the minimum detectable effect size was estimated from the observed event distribution and prior literature [24,25]. In addition, 10,000 Monte Carlo simulations using real-world covariate distributions indicated a model-level statistical power (1–β) of 92.4% (95% CI 91.85 - 92.87), supporting high reliability for detecting clinically relevant effects in this sample and predictor configuration. Bootstrap-derived CIs quantified uncertainty in coefficient estimates and performance metrics.

XSL•FO
RenderX

All analyses were conducted using R (version 4.3.4.2; R Core Team), following established best practices for early-phase predictive modeling. Model development used logistic regression with Least Absolute Shrinkage and Selection Operator (LASSO) regularization to enhance parsimony and reduce overfitting in a small to moderate sample context (section S4 in Multimedia Appendix 1) [33]. Predictors were modeled without scaling to preserve clinical interpretability.

Building on this validated model, this study evaluates 2 deterministic phenotyping frameworks derived from its final equation: a 126-combination system and a simplified 21-combination version. Both were assessed using classification-based performance metrics—sensitivity, specificity, predictive values, LRs, and Cohen κ—against real-world clinical phenotypes. Internal concordance between systems was evaluated using κ statistics. Additionally, the 126-combination system was also benchmarked against the 2025 GOLD ABE classification to assess alignment with guideline-based stratification [22,31,43,44].

Furthermore, the simplified phenotyping system was evaluated for computational efficiency and its potential integration into HL7 FHIR–compliant health information systems (section S7 in Multimedia Appendix 1) [22,31,32]. All procedures followed TRIPOD guidelines and contemporary standards for internal validation of clinical prediction models [45,46].

Reverse Model Definition

A defining feature of the Seleida model is its deterministic and bijective architecture, establishing a one-to-one correspondence between 2 routinely collected clinical variables and the predicted probability of poor COPD control (sections S1 and S2 in Multimedia Appendix 1). Specifically:

- ***a*** represents the annual number of SABA or SAMA canisters or both dispensed per patient, serving as a proxy for symptom burden and short-acting bronchodilator dependence [18,47].
- ***b*** denotes the annual number of antibiotic dispensations for bronchitis or COPD exacerbations, reflecting exacerbation frequency and infection-driven instability [48,49].

Both variables were chosen for their objectivity, universal availability in structured EHRs, and strong predictive value in prior studies [25,50]. The predicted probability of poor control (*Pr*) is calculated with a logistic regression model:

$$\text{logit}(Pr)=\alpha+\beta 1\cdot a+\beta 2\cdot b,$$

where α is the intercept, and β_1 and β_2 are positive coefficients estimated using LASSO regularization, ensuring parsimony and coefficient stability (section S4 in Multimedia Appendix 1).

This structure supports two complementary functions: (1) forward inference: estimating *Pr* from any (*a*, *b*) combination, and (2) reverse inference: retrieving the (*a*, *b*) pairs matching a target risk level. The latter enables real-time, automated phenotyping and individualized decision-making in EHR-integrated workflows.

Although Seleida can estimate risk directly from observed data, it is explicitly designed for bidirectional operation. This means that it can both predict risk from clinical inputs and perform inverse mapping to retrieve all (*a*, *b*) pairs that match a given probability. This reverse functionality is critical for dynamic alert systems, phenotype-driven decision pathways, and real-time decision support tools.

This bidirectional capability has practical implications. For example, a patient with 3 annual SABA or SAMA inhalers or both (*a*=3) and 1 antibiotic course (*b*=1) maps to a unique cell (3,1) in the 126-combination system, with a predicted poor control risk of 95.53%. In the simplified 21-combination version, the same profile is classified as *a*=3 (midrange inhaler use) and *b*=1 (moderate exacerbation frequency), preserving its phenotypic identity—GOLD A1/B1 with high rescue inhaler use (H)—within a reduced but clinically actionable framework. This structured mapping supports therapeutic reassessment and integration into EHR-based alert systems, where predefined thresholds (eg, *Pr*>.50) can trigger guideline-aligned interventions.

In contrast to black box machine learning models, often criticized for limited interpretability, Seleida's transparent structure ensures full traceability from risk estimate to actionable clinical profile. This enhances clinical confidence and facilitates deployment across diverse health care settings, including resource-constrained environments [20,34,37,38]. A detailed mathematical demonstration of these bijective properties, with exhaustive verification of all input-output mappings, appears in the following section and in section S3 in Multimedia Appendix 1.

Mathematical Proof of Bijectivity

Bijectivity is not merely a theoretical refinement but a functional cornerstone of the Seleida model. As detailed in section S1, its formal proof guarantees three essential capabilities: (1) each predicted probability is uniquely traceable to a specific clinical phenotype, ensuring transparency and auditability; (2) every clinically relevant risk threshold corresponds to at least 1 valid input combination, providing full operational coverage; and (3) no ambiguity or discontinuity occurs in model behavior, maintaining consistency in decision support and regulatory contexts. Without this formal validation, the model's dual interpretability and reproducibility would remain unverified.

To confirm these properties, we validated that each (*a*, *b*) input pair yields a unique predicted probability (*injectivity*), and that the entire risk spectrum (0<*Pr*<1) is covered by the input domain (*surjectivity*). These conditions are defined as follows:

- Injectivity: Each unique (*a*, *b*) pair—representing the annual number of dispensed SABA or SAMA canisters or both and respiratory antibiotics—must map to a single, distinct predicted probability of poor COPD control (*Pr*).
- Surjectivity: Every probability value within the model's codomain must be attainable from at least 1 clinically plausible (*a*, *b*) combination, ensuring that there are no gaps in the risk scale.

We followed a rigorous, multistep validation process to formally demonstrate the bijective nature of the Seleida model:

XSL•FO
RenderX

- Bounding inputs: The variables—annual SABA or SAMA canisters or both (*a*) and annual antibiotic regimens (*b*)—were explicitly restricted to integers: a=0 - 20 and b=0 - 5 (inclusive). These ensured a finite, fully enumerable input space.
- Analytical proof of injectivity: We demonstrated that no 2 distinct input pairs (a_1 , b_1) and (a_2 , b_2) produce the same output probability. The logistic model's coefficients structure confirmed unique mappings for all valid pairs.
- Computational proof of surjectivity: Using a custom Python algorithm, we calculated all 126 possible output probabilities to 14 decimal places. Every value was checked for uniqueness, confirming that the entire codomain is covered.
- Conclusion: Independent confirmation of both injectivity and surjectivity verified that Seleida is bijective, enabling forward risk estimation and reverse phenotype reconstruction with mathematical certainty.

No repeated or missing outputs were found, confirming a perfect alignment between input and output spaces. This property ensures robust reverse inference and reproducible phenotype classification across real-world COPD datasets. All source code, verification tables, and derivations are provided in section S3 in Multimedia Appendix 1 [45,51].

Ethical Considerations

The study was approved by the ethics committee of Hospital Universitario Doctor Peset of Valencia (protocol code CEIm 132.22, approval date March 6, 2023). The project was registered in the *Portal de Ética de la Investigación Biomédica de Andalucía* through the *Sistema de Información de los Comités de Ética de la Investigación* (protocol code 1140-N-23, approval date September 12, 2023). The SEMERGEN research department gave its endorsement to the project (2023-00035, approval date June 6, 2023) [27,28]. For the purpose of this study, only patient data recorded in EHRs were collected. All data were fully anonymized in compliance with the General Data Protection Regulation (2016/679). No procedures were performed on participants and, to ensure confidentiality, each patient was assigned a unique study identifier. Informed consent was formally waived due to the retrospective design and the absence of patient contact. Due to the nature of the study, compensation to patients was not applicable.

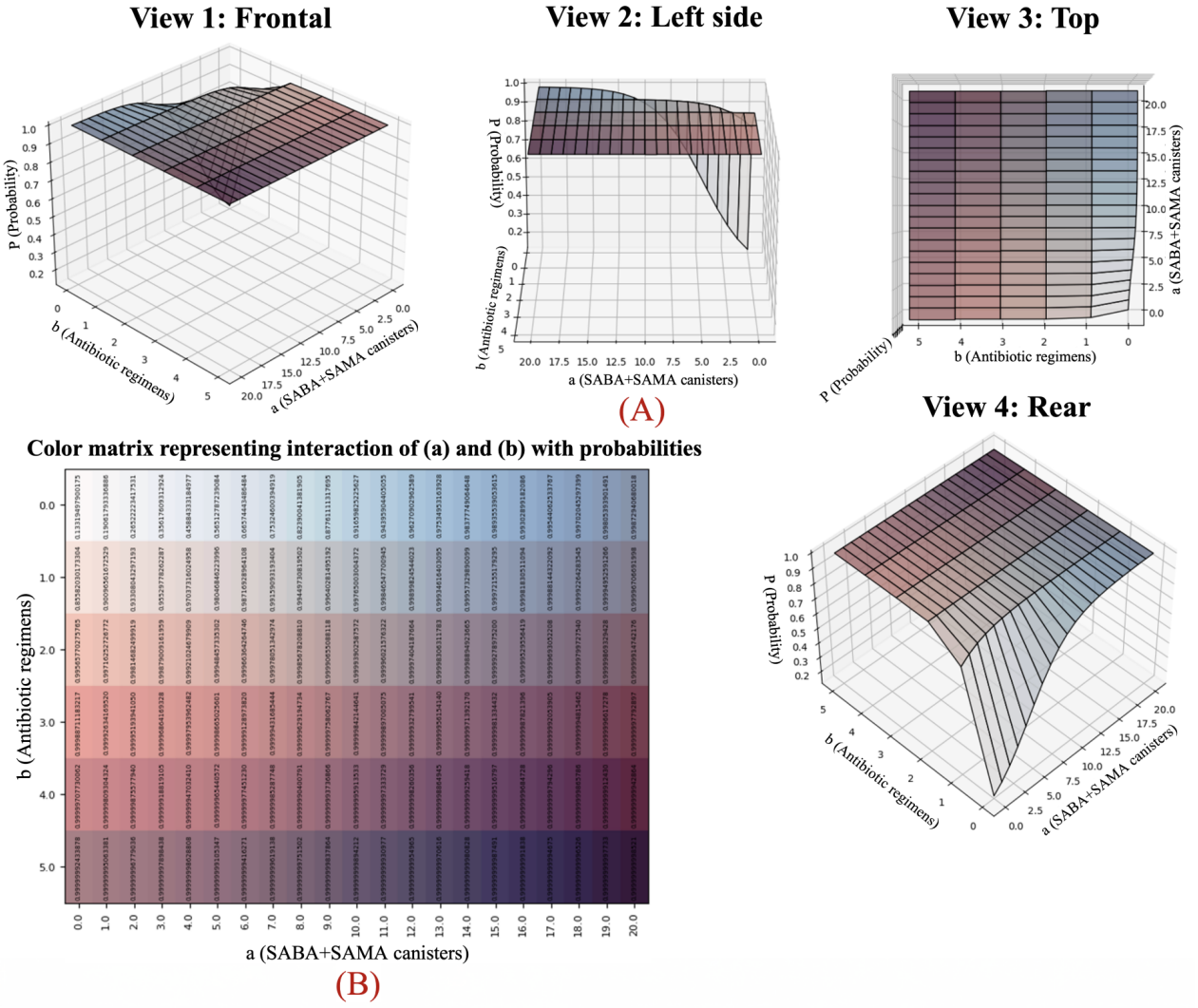
Results

Expanded Phenotyping: Analysis of the 126-Combination System

The 126-combination phenotyping framework systematically integrates 2 structured prescribing variables—annual dispensations of rescue inhalers (*a*) and respiratory antibiotic regimens (*b*)—to generate a continuous, 3D map of predicted COPD control probabilities (Figure 1A and B). Blue gradients reflect increasing use of SABA or SAMA canisters or both (*a*), red gradients indicate the frequency of antibiotic courses (*b*), and purple regions highlight zones of sharply elevated clinical risk [35]. Each unique (*a*, *b*) pair yields a distinct probability estimate, delineating a mathematically robust and clinically interpretable risk surface with actionable thresholds [20,34].

XSL•FO
RenderX

Figure 1. Visual mapping of the Seleida model's 126-combination system. The 4 images in panel (A) show 3D perspectives of how annual rescue inhaler use (*a*) and antibiotic prescriptions (*b*) combine to yield the probability of poor chronic obstructive pulmonary disease control (*Pr*). Panel (B) provides a color matrix of exact *Pr* values across all combinations. Darker red indicates higher predicted risk. Clinically, higher values of *b* (≥2 antibiotics per year) are stronger drivers of poor control than *a*, highlighting infection burden as a key modifiable factor. SABA: short-acting β2-agonists; SAMA: short-acting muscarinic antagonists.



To guarantee bijectivity, the input domain was discretized to include integer values from 0 to 20 for *a* and from 0 to 5 for *b* (both inclusive). Any observed values exceeding these bounds are computationally capped at *a*=20 and *b*=5, preserving full injectivity and surjectivity across the model's codomain. This bounded structure ensures reversibility and enables exhaustive phenotype enumeration while maintaining operational realism.

Model outputs demonstrate that antibiotic burden (*b*) exerts a greater marginal influence on the predicted probability of poor control than rescue bronchodilator use (*a*), particularly within intermediate strata. For example, the phenotype (*a*=3, *b*=1) is associated with substantially elevated risk, whereas combinations with $a \geq 15$ and $b \geq 4$ approach probability ceilings exceeding 99% [36,52]. These gradients reflect the compounding effects of symptom burden and exacerbation frequency, underscoring the need for integrated monitoring of both variables in routine care.

By translating complex statistical interactions into visually intuitive gradients, the 126-combination system provides clinicians with a practical, high-resolution tool for individualized COPD phenotyping—enabling phenotype-driven interventions, anticipatory care strategies, and optimized treatment planning (section S6 in Multimedia Appendix 1) [4,34,38].

Expanded Phenotyping: Analysis of the 21-Combination System

To enhance feasibility in real-world clinical settings, the original 126-combination system was streamlined into a 21-combination framework by constraining the antibiotic regimen variable (*b*) to a range of 0 - 2 and the SABA or SAMA canisters or both variable (*a*) to 0 - 6. These thresholds were empirically defined to preserve the model's bijective architecture while concentrating on clinically meaningful stratification intervals [4,20,24].

Despite its reduced dimensionality, the simplified system maintains robust predictive performance (Figure 2) and offers improved technical and operational feasibility for integration into health information systems and routine care workflows [20-22,43,50,53]. Its lower computational complexity supports

XSL•FO
RenderX

real-time patient stratification and personalized COPD management in both primary care and resource-constrained environments (section S6 in Multimedia Appendix 1) [34,38,44].

Figure 2. Chronic obstructive pulmonary disease phenotyping using the simplified 21-combination Seleida system. Each cell reflects the predicted risk level based on rescue inhaler use (*a*) and antibiotic courses (*b*), capped at clinically relevant thresholds ($a \leq 6$; $b \leq 2$). Color intensity indicates increasing probability of poor control. This tool enables rapid identification of high-risk patients using prescribing data alone, without spirometry or symptom scores, supporting scalable risk stratification in primary care. This visual framework enables clinicians to stratify patients using only prescribing data, even without algorithmic integration. H: high; L: low; SABA: short-acting β2-agonists; SAMA: short-acting muscarinic antagonists.



Expanded Phenotyping: Comparing Real and Combination Systems

Seleida's expanded phenotyping system refines the 2025 GOLD ABE classification by incorporating the annual use of SABA or SAMA or both as a stratification axis. Each GOLD category—E (≥2 moderate or ≥1 severe exacerbation), A1/B1 (1 moderate exacerbation), and A0/B0 (no exacerbations)—is subdivided into high SABA users (H; ≥3 canisters per year) and low users (L; <3 canisters per year). This additional layer of segmentation enhances sensitivity for detecting early manifestations of disease instability and symptom burden, yielding a more granular and actionable classification of COPD phenotypes (Table 1).

XSL•FO
RenderX

Table . Performance metrics of the 126-combination system for each chronic obstructive pulmonary disease phenotype[a].

	Accuracy, %	Se[b], %	Sp[c], %	PPV[d], %	NPV[e], %	LR+[f]	LR−	κ value	Significance of κ[g]
A0/B0 H[h]	95.3	100	94.8	66.7	100	19.2	0.00	0.774	<.001[i]
A0/B0 L[j]	96.2	97.7	95.2	93.3	98.4	20.5	0.02	0.922	<.001[i]
A1/B1 H	85.8	50	90.4	40	93.4	5.2	0.55	0.365	.002[k]
A1/B1 L	93.4	81.3	95.6	76.5	96.6	18.3	0.20	0.749	<.001[i]
E H	86.8	38.9	96.6	70	88.5	11.4	0.63	0.431	<.001[i]
E L	97.2	57.1	100	100	97.1		0.43	0.714	<.001[i]

[a]Sensitivity, specificity, PPV, NPV, and LR+/LR− for each phenotype identified by the 126-combination system. These metrics evaluate the model's ability to replicate real phenotyping and highlight its strengths in common phenotypes (eg, A0/B0 H and A0/B0 L) as well as areas requiring refinement for less frequent phenotypes (eg, E H and A1/B1 H).

[b]Se: sensitivity.

[c]Sp: specificity.

[d]PPV: positive predictive value.

[e]NPV: negative predictive value.

[f]LR: likelihood ratio.

[g]Significance (*P* value) of Cohen κ coefficient.

[h]H: high.

[i]Hypothesis tests applied to assess the statistical significance of the coefficient: Fisher exact test.

[j]L: low.

[k]Hypothesis tests applied to assess the statistical significance of the coefficient: χ^2 test.

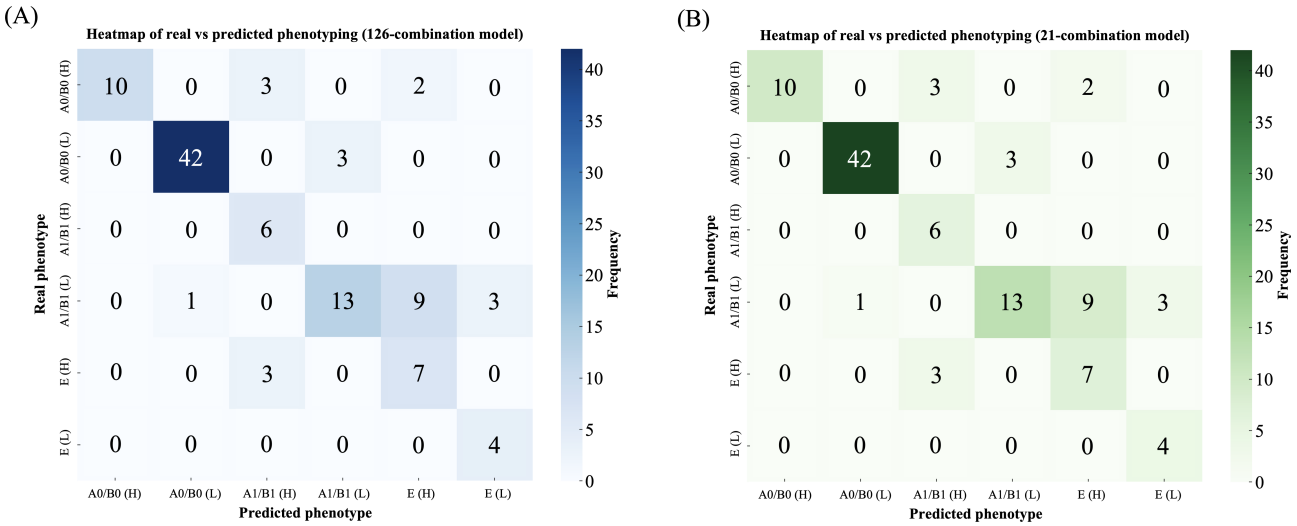
Two phenotyping strategies were evaluated: (1) The 126-combination system, designed for high-resolution stratification, is ideally suited to research settings and complex clinical scenarios [27,35]. (2) The simplified 21-combination system, optimized for routine clinical application, offers a favorable balance between predictive performance and computational efficiency [4,39]. Its lower complexity makes it especially appropriate for primary care and resource-limited environments, where operational simplicity and rapid decision-making are essential [43,44].

Both systems exhibited strong concordance with clinician-assigned phenotypes based on real-world data (Cohen κ=0.70, SE=0.050; *P*<.001). Sensitivity and specificity were notably high for the most prevalent phenotypes, with specificity exceeding 90% and sensitivity reaching or surpassing 97% for categories such as A0/B0-H, A0/B0-L, and E-L. In contrast, sensitivity was lower for less frequent phenotypes, underscoring the importance of clinical judgment in borderline cases and reinforcing the complementary role of Seleida alongside expert assessment.

Internal agreement between the 126- and 21-combination models was perfect (Cohen κ=1.00, *P*<.001) (Figure 3A and B). Despite its reduced granularity, the simplified system preserved high specificity, minimizing false positives and confirming its suitability for real-time clinical implementation. These features make it particularly advantageous for integration into EHR systems and point-of-care workflows, especially in settings with constrained health care infrastructure [22,31,43,44,53].

XSL•FO
RenderX

Figure 3. (A) Heatmap of real versus predicted phenotyping by 126-combination system. (B) Heatmap of real versus predicted phenotyping by 21-combination system.



Overall, the expanded phenotyping approach implemented in Seleida offers a scalable, automated solution for enhancing risk stratification and supporting targeted therapeutic interventions in COPD management [20,24,25,38]. By identifying high-risk individuals early, Seleida facilitates more personalized care, prioritizing interventions for those most likely to benefit while reducing overtreatment in stable cases [4,24,25,36]. This paradigm not only improves clinical outcomes but also promotes more efficient use of health care resources—aligning with the growing imperative for data-driven decision-making in contemporary health care systems [21,33,38].

Basic Phenotyping: Evaluating the 126-Combination System for GOLD 2025 Phenotypes

The performance of Seleida's 126-combination system was assessed in replicating GOLD 2025 phenotypes [14]—A0/B0 (no exacerbations), A1/B1 (1 moderate exacerbation), and E (≥2 moderate or ≥1 severe exacerbation)—using the annual number of respiratory antibiotic regimens (variable *b*) as the sole predictor (Table 2) [48,49]. The model's discriminatory capacity across these clinical categories was demonstrated by the following results:

- A0/B0 (no exacerbations): sensitivity=98.1%, specificity=84.9%, and accuracy=97.5%, with near-perfect agreement (κ=0.83; *P*<.001). These findings confirm the model's high reliability in identifying well-controlled patients.
- A1/B1 (1 moderate exacerbation): sensitivity=67.9%, specificity=83.3%, and accuracy=79.3%, with moderate agreement (κ=0.49; *P*<.001). This level of performance reflects a balanced capacity to detect patients at intermediate risk, despite the inherent clinical heterogeneity of this group.
- E (≥2 moderate or ≥1 severe exacerbation): specificity=96.3%, sensitivity=44%, accuracy=84%, and a high positive LR+=11.9. These metrics indicate robust identification of high-risk patients with minimal false positives, supporting timely and targeted interventions.

Table . Performance metrics of the 126-combination system for Global Initiative for Chronic Obstructive Lung Disease 2025 chronic obstructive pulmonary disease phenotypes[a].

	Accuracy, %	Se[b], %	Sp[c], %	PPV[d], %	NPV[e], %	LR+[f]	LR−	κ value	Significance of κ[g]
A0/B0	97.5	98.1	84.9	86.7	97.8	6.5	0.02	0.830	<.001[h]
A1/B1	79.3	67.9	83.3	59.4	87.8	4.1	0.39	0.489	<.001[i]
E	84	44	96.3	78.6	84.8	11.9	0.58	0.475	<.001[h]

[a]Sensitivity, specificity, PPV, NPV, LR+ /LR−, accuracy, and κ for each phenotype identified by the reverse Seleida model. The metrics reflect the model's ability to replicate real-world phenotyping and its strengths in classifying Global Initiative for Chronic Obstructive Lung Disease 2025 phenotypes.

[b]Se: sensitivity.

[c]Sp: specificity.

[d]PPV: positive predictive value.

[e]NPV: negative predictive value.

[f]LR: likelihood ratios.

[g]Statistical significance (*P* value) of Cohen κ coefficient.

[h]Hypothesis tests applied to assess the statistical significance of the κ coefficient: Fisher exact test.

[i]Hypothesis tests applied to assess the statistical significance of the κ coefficient: χ^2 test.

XSL•FO
RenderX

Collectively, these results underscore the robustness of Seleida's basic phenotyping system in stratifying patients based solely on antibiotic prescribing data. However, the model's ability to discriminate between A and B categories—particularly within the intermediate-risk stratum—may benefit from the incorporation of symptom-based measures, such as the modified Medical Research Council dyspnea scale and the COPD Assessment Test, both of which are widely used in routine practice [16,17,54,55]. Future iterations integrating these variables could enhance phenotypic granularity and improve the model's adaptability across diverse health care settings.

Despite these acknowledged limitations, Seleida demonstrates strong performance when classifying COPD phenotypes using a single, objective, and consistently recorded variable: annual antibiotic use. The system reliably identifies patients with stable disease (A0/B0), achieves moderate accuracy for those at intermediate risk (A1/B1), and exhibits high specificity for detecting individuals with frequent or severe exacerbations (E). These findings reinforce Seleida's potential as a pragmatic, evidence-based tool for real-world clinical decision-making, offering scalable, reproducible, and personalized support for COPD management across a wide range of practice environments [29,33,34,38].

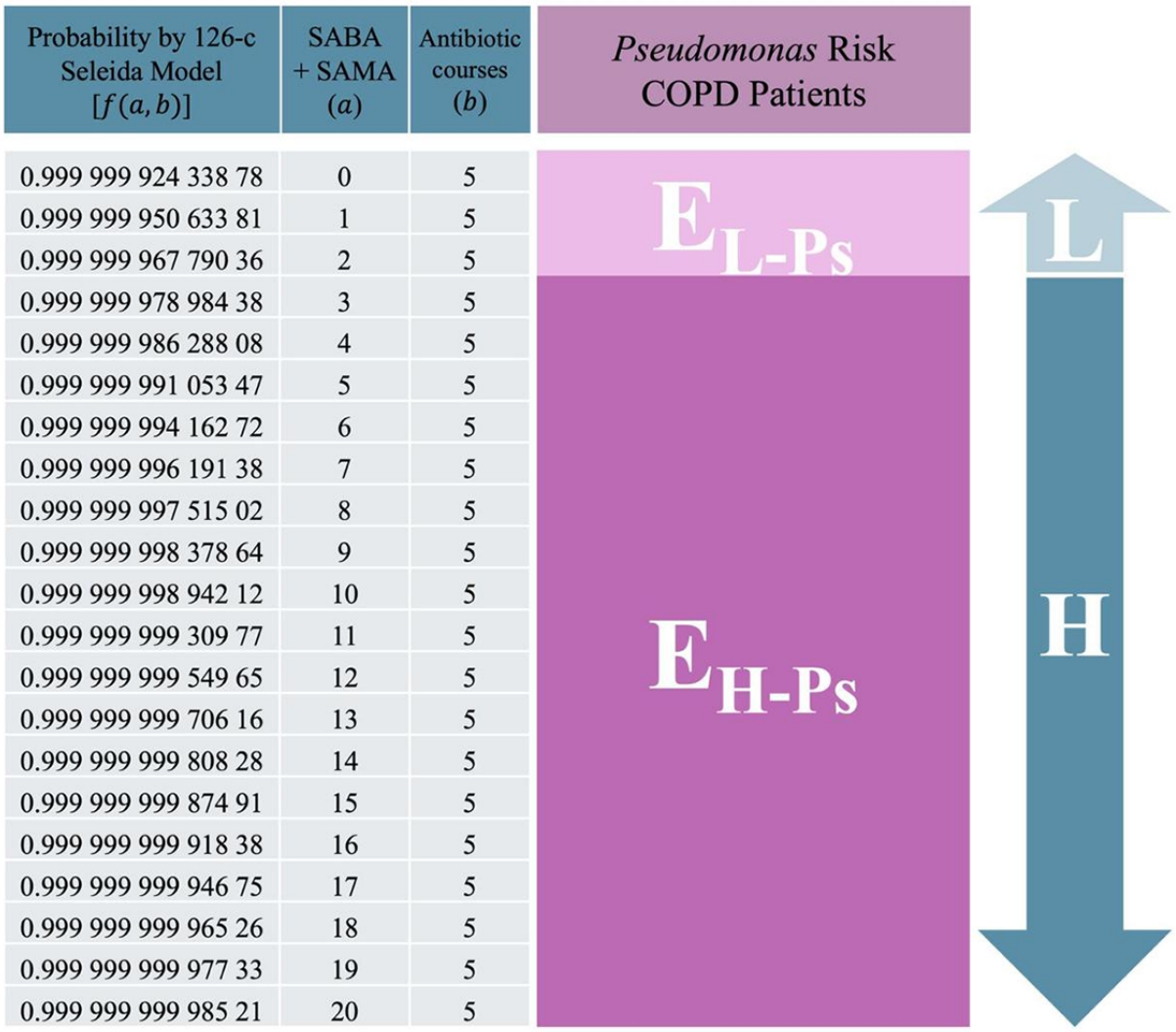
Expanded Phenotyping: Integration of *Pseudomonas* Risk in the 126-Combination System

The 126-combination phenotyping system was further evaluated for its capacity to identify patients with COPD at an increased risk of *Pseudomonas aeruginosa* colonization or infection. Evidence indicates that individuals receiving more than 4 respiratory antibiotic regimens annually exhibit a markedly elevated risk of frequent exacerbations and poor disease control [48,56-58]. By incorporating this threshold into the Seleida model, the system enhances its ability to detect high-risk phenotypic profiles—facilitating targeted interventions such as antimicrobial stewardship and intensified clinical monitoring [48,59].

In contrast, the 21-combination system—by design—limits the antibiotic variable (*b*) to a maximum of 2 prescriptions per year, potentially reducing its sensitivity for identifying this severe phenotype. The expanded resolution of the 126-combination system, which accommodates values of *b* up to 5, enables more accurate detection of complex clinical cases. As illustrated in Figure 4, profiles with $b \geq 5$ are consistently associated with very high predicted risk, capturing severe phenotypes that may otherwise be underrepresented in streamlined models.

XSL•FO
RenderX

Figure 4. Identification of patients with chronic obstructive pulmonary disease at high risk of *Pseudomonas aeruginosa* colonization using the 126-combination Seleida model. The shaded area highlights phenotypes with high predicted risk (*Pr*≥0.99), ≥5 antibiotics per year (*b*), and high or low rescue inhaler use (H or L). These patients should be prioritized for sputum culture screening and potential referral to pulmonology. This supports targeted infection surveillance based on real-world prescribing data. COPD: chronic obstructive pulmonary disease; H: high; L: low; SABA: short-acting β2-agonists; SAMA: short-acting muscarinic antagonists.



Integrating *Pseudomonas*-related risk factors into the high-resolution framework strengthens Seleida's use for proactive therapeutic planning. This refinement supports the early identification of patients requiring microbiological surveillance, targeted antimicrobial strategies, or referral to hospital-based specialist care—ultimately contributing to the mitigation of antibiotic resistance and the improvement of long-term clinical outcomes (section S6 in Multimedia Appendix 1) [49,60,61].

By capturing a broader spectrum of disease severity, this extension reinforces the adaptability of the Seleida model and underscores its value as a precision tool for guiding personalized interventions in the management of complex COPD phenotypes across a range of clinical environments.

Impact of Rescue Medication Use on Health Care Utilization in Patients With COPD

High rescue medication use (H) among patients with COPD is a well-established indicator of increased health care resource utilization. In the present cohort (n=106), 71.4% (15/21) of high-use patients required at least 1 respiratory-related clinical consultation annually, compared with 40% (34/85) of low-use patients (χ^2=6.691; *P*=.010). A moderate yet statistically significant correlation was observed between rescue medication consumption and health care consultations (Pearson *r*=0.251; *P*=.009), as illustrated in Multimedia Appendix 2.

These findings highlight the use of rescue medication as a reliable and actionable marker for patient stratification within the Seleida phenotyping system [25]. Early identification of high-use individuals facilitates the deployment of targeted interventions, including optimization of maintenance therapy, structured education to reduce inhaler overreliance, and scheduling of more frequent clinical follow-ups [15,62,63].

XSL•FO
RenderX

The ≥1 consultation per year threshold serves as a pragmatic and clinically interpretable metric to prioritize high-risk patients in care workflows and inform strategic health care resource allocation. Future analyses incorporating additional parameters—such as disease severity, multimorbidity profiles, and treatment adherence—will be essential to refine predictive accuracy and enhance the model's capacity to support resource optimization in diverse clinical settings [48,64-66].

Exacerbations in the Last Year and Rescue Medication Use

In this cohort of 106 patients with COPD, a significant association was observed between exacerbation history and increased use of SABA. Among patients with no exacerbations in the preceding 12 months, 88.7% (47/53) used fewer than 3 rescue canisters annually. In contrast, 28.3% (15/53) of those with ≥1 exacerbation required ≥3 canisters (χ^2_1=4.810, P=.028; Pearson r=0.213, P=.028), as depicted in Multimedia Appendix 3.

This correlation underscores the heightened reliance on rescue therapy among patients with recent exacerbations—often reflecting suboptimal maintenance treatment or inadequate symptom control [47,67,68]. These findings support the implementation of targeted clinical strategies, such as optimizing long-term inhaled therapy and reinforcing adherence interventions, to reduce SABA dependence and enhance overall disease management.

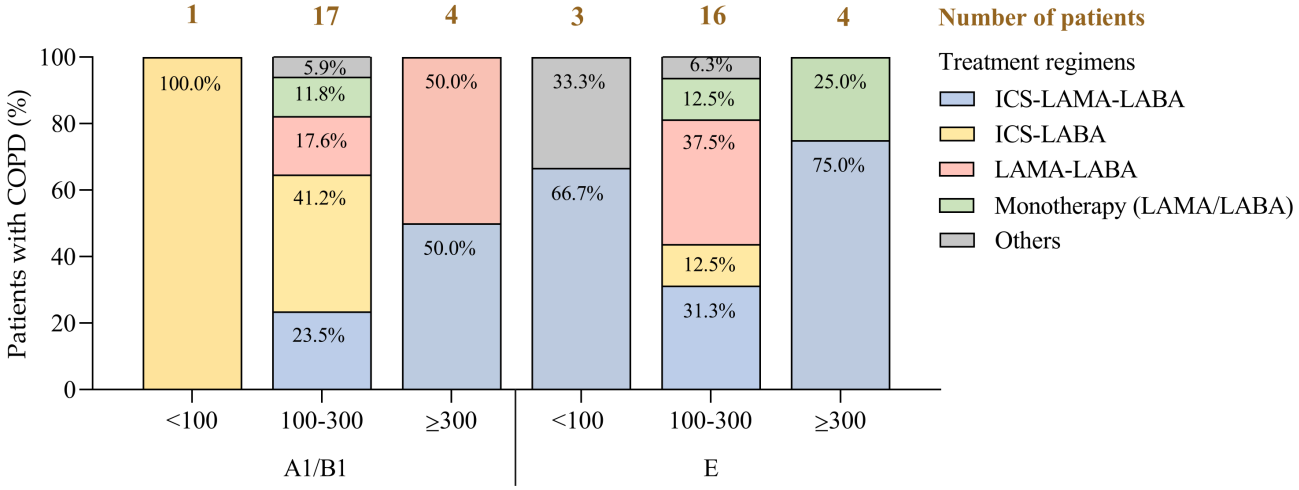
Incorporating this association into predictive modeling frameworks can improve risk stratification and enable more personalized treatment planning [69,70]. Future analyses should account for potential confounding factors—such as comorbid conditions, medication adherence, and variability in EHR completeness—to further refine the model's predictive performance and clinical applicability across heterogeneous patient populations [27,46].

Treatment Patterns in Patients With Exacerbated COPD

This analysis examined treatment patterns among 53 patients with COPD who experienced at least 1 moderate exacerbation in the past year. After excluding 8 individuals due to missing eosinophil count data, the final sample comprised 45 patients. The Seleida model was applied to assess deviations from current therapeutic recommendations as outlined in established clinical practice guidelines [25].

Among patients with blood eosinophil counts of <100 cells/µL (4/45, 8.89%)—where the use of inhaled corticosteroids (ICS) is generally not recommended [14]—66.7% (2/3) of those classified as phenotype E, along with 1 patient in the A1/B1 category, were nonetheless prescribed ICS-containing regimens. Exceptions to this pattern were documented in cases where eosinophil counts of ≥100 cells/µL had been recorded previously, justifying continued ICS use (Figure 5). In addition, 11.1% (5/45) of patients were receiving bronchodilator monotherapy, and 22.2% (10/45) were treated with ICS–long-acting β2-agonist combinations, despite GOLD 2025 guidelines recommending dual bronchodilation (long-acting muscarinic antagonist–long-acting β2-agonists) in these clinical scenarios [14].

Figure 5. Treatment regimen by annual mean eosinophilia and exacerbation phenotype. COPD: chronic obstructive pulmonary disease; ICS: inhaled corticosteroids; LABA: long-acting β2-agonists; LAMA: long-acting muscarinic antagonists.



Conversely, ICS underutilization was observed in patients who met criteria for triple therapy—particularly those with eosinophil counts of ≥100 cells/µL—suggesting that nonclinical factors (eg, logistical or prescriber-related) may contribute to deviations from phenotype-aligned treatment pathways [71].

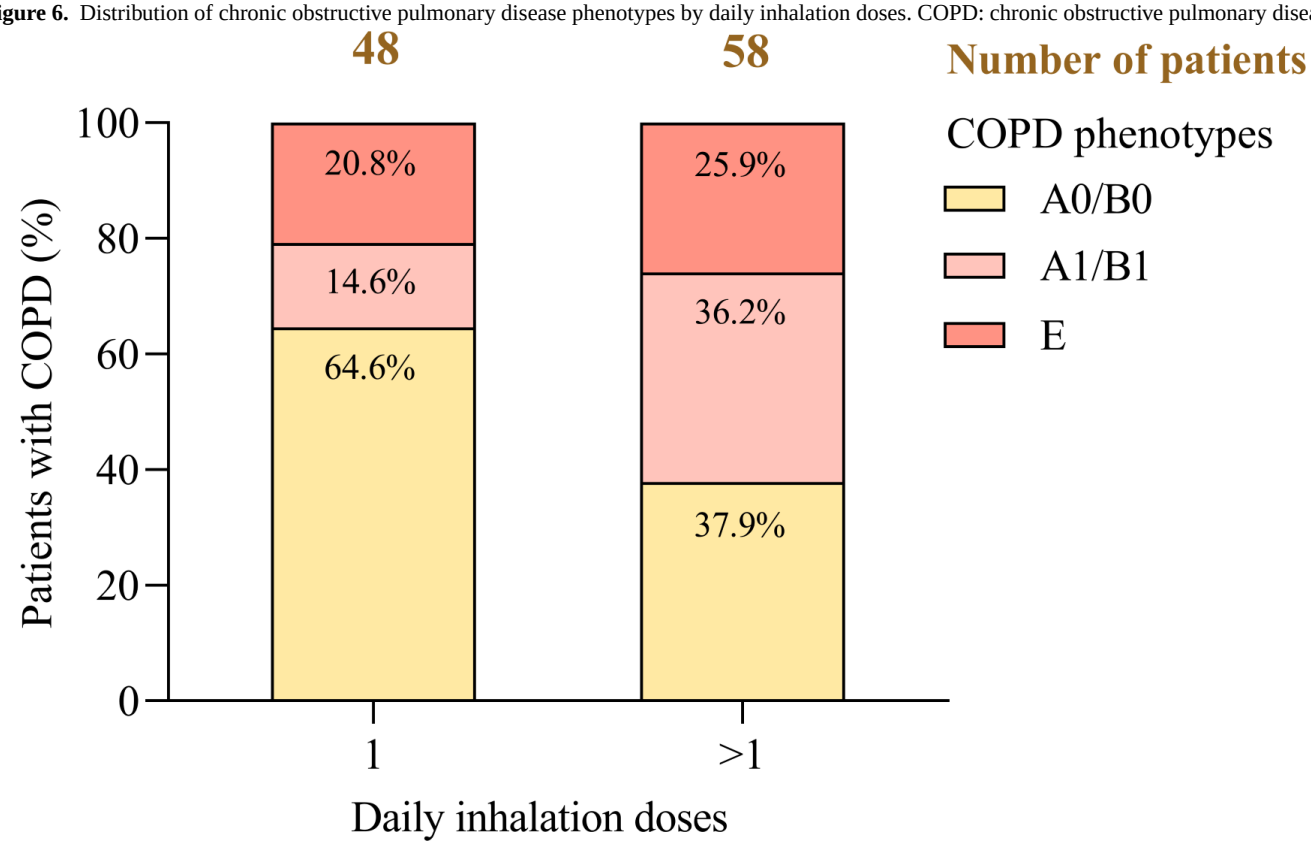
By automating phenotypic classification based on exacerbation history, the Seleida combination systems—when integrated with eosinophil count and treatment data—allow for the systematic identification of discrepancies between recommended and actual therapy [31,70]. This functionality supports improved alignment with evidence-based guidelines, promoting optimal ICS use, minimizing unnecessary adverse effects, and enhancing overall COPD management outcomes [20,34].

Real-World COPD Phenotypes Across Daily Inhalation Patterns

This analysis evaluated the relationship between daily inhalation regimens and COPD phenotypes—A0/B0, A1/B1, and E—in a cohort of 106 patients, examining treatment intensity in relation to clinical severity and exacerbation history (Figure 6).

XSL•FO
RenderX

Figure 6. Distribution of chronic obstructive pulmonary disease phenotypes by daily inhalation doses. COPD: chronic obstructive pulmonary disease.



Among A0/B0 patients (n=53), 58.5% (51/53) required a single inhalation per day, whereas 41.5% (22/53) used 2 or more. In the A1/B1 group (n=28), 75% (21/28) required at least 2 daily inhalations, reflecting higher therapeutic demands. Phenotype E patients (n=25), defined by ≥2 moderate or ≥1 severe exacerbations, exhibited greater variability: 60% (15/25) used 2 or more inhalations daily, while 40% (10/25) managed with a single dose.

Statistical testing revealed a significant association between inhalation frequency and clinical phenotype (χ^2_2=8.662; *P*=.013). A linear trend (*P*=.048), alongside weak but statistically significant correlations (Pearson *r*=0.193, *P*=.047; Spearman *r*=0.215, *P*=.027), suggests that patients with higher-risk phenotypes tend to receive more intensive inhalation regimens.

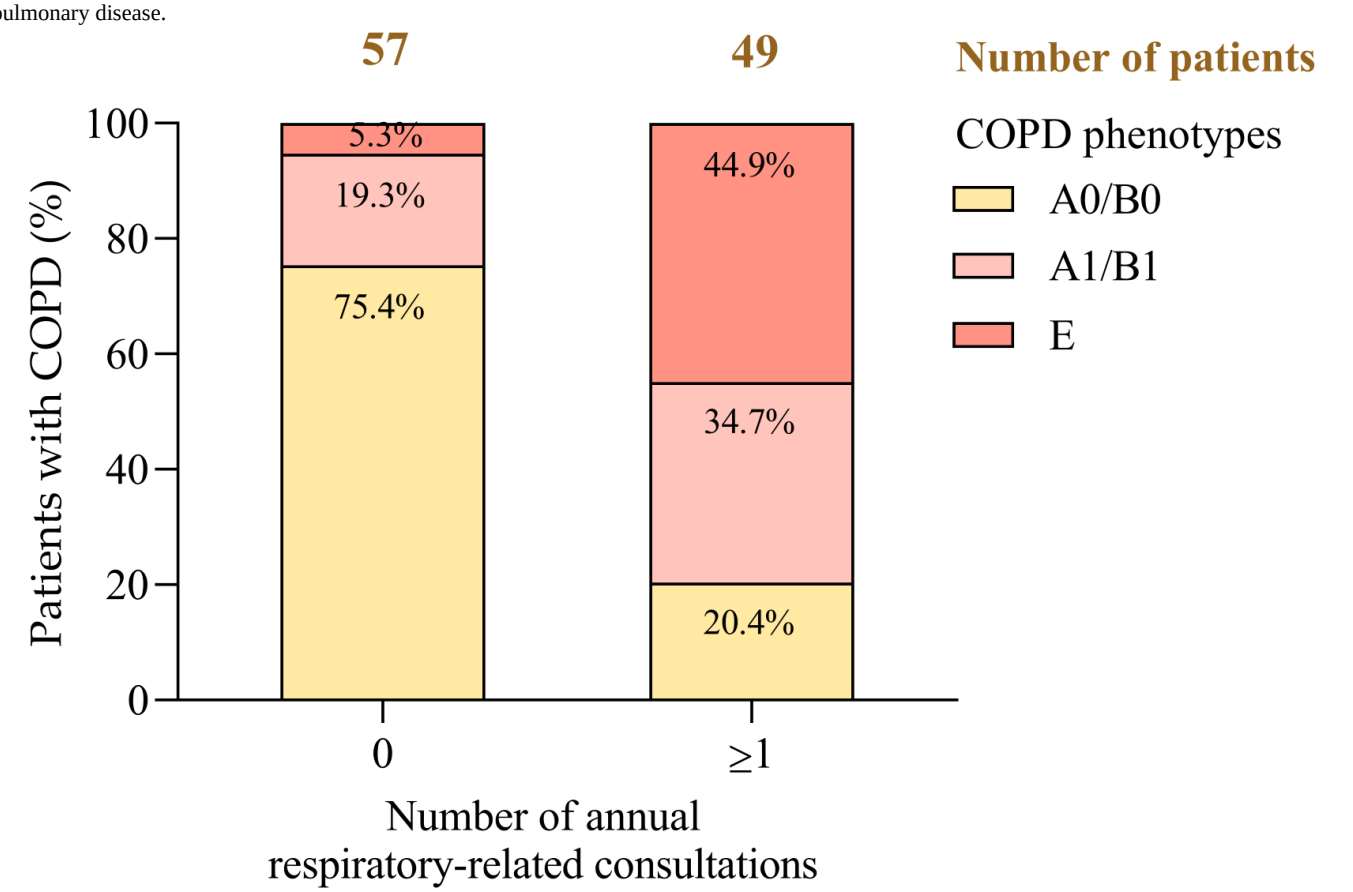
These findings underscore the relevance of phenotype-guided treatment strategies: while low-intensity regimens may suffice for A0/B0 patients, individuals classified as A1/B1 or E typically require escalation of therapy. Incorporating daily inhalation patterns into predictive models enhances clinical personalization, supports adherence to guideline-based care, and contributes to improved patient outcomes—advancing the principles of precision medicine in COPD management [70].

Real-World COPD Phenotypes and Health Care Utilization

This analysis examined the association between COPD phenotypes—A0/B0, A1/B1, and E—and respiratory-related health care utilization in a cohort of 106 patients, with a focus on the need for at least 1 annual clinical consultation (Figure 7).

XSL•FO
RenderX

Figure 7. Proportion of chronic obstructive pulmonary disease phenotypes by number of annual health care consultations. COPD: chronic obstructive pulmonary disease.



- A0/B0 phenotype (n=53): 81.1% (43/53) of patients required no respiratory-related consultations, while 18.9% (10/53) needed at least 1, reflecting stable disease and low health care demand.
- A1/B1 phenotype (n=28): 60.7% (17/28) required at least 1 consultation, indicating increased follow-up needs linked to a history of moderate exacerbations.
- E phenotype (n=25): 88% (22/25) required at least 1 consultation, representing the highest level of health care utilization, consistent with more severe disease and frequent exacerbations.

Statistical analysis confirmed a robust association between phenotype and health care utilization (χ^2_2=35.873; P<.001), with strong, statistically significant correlations observed (Pearson r=0.578; Spearman r=0.582; both P<.001).

These findings demonstrate that health care resource demand increases in parallel with disease severity—ranging from minimal utilization in patients with stable phenotypes (A0/B0) to substantially elevated needs in those classified as phenotype E. Integrating phenotype-based stratification into clinical workflows can support more efficient resource allocation, ensuring timely intervention for high-risk patients while minimizing unnecessary consultations among those with controlled disease.

Discussion

Principal Findings

This study presents and internally validates Seleida—a fully automated, deterministic, and bijective model designed to assess COPD control and generate clinically interpretable phenotypes using structured EHR data. By relying exclusively on routinely recorded prescribing information—specifically, the annual number of dispensed SABA or SAMA canisters or both and respiratory antibiotics—Seleida offers a scalable and transparent alternative to conventional classification frameworks such as GOLD 2025 and GesEPOC 2021. These frameworks often depend on intermittently documented spirometry results and symptom scores, limiting their feasibility and consistency in real-world, especially primary care, settings [14,17,18,47,52,72].

The decision to implement LASSO over Ridge or Elastic Net in the Seleida model was based on a comparative analysis of regularization techniques. While all 3 approaches demonstrated acceptable discrimination, LASSO provided the best balance between predictive accuracy, parsimony, and clinical interpretability. Ridge regression tended to overshrink coefficients, whereas Elastic Net offered no additional benefit in a low-dimensional, low-collinearity setting (section S4 in Multimedia Appendix 1). This methodological choice reinforces Seleida's role as a computationally efficient and clinically actionable tool for phenotype-guided COPD management.

The model demonstrated perfect agreement between its 126- and 21-combination phenotyping schemas (Cohen κ=1.00;

XSL•FO
RenderX

$P<.001$) and substantial concordance with clinician-assigned phenotypes based on GOLD 2025 criteria ($\kappa=0.70$; $P<.001$), confirming its internal robustness and interpretive reliability [42,73]. By leveraging high-frequency, objective EHR variables, Seleida enables dynamic risk stratification even in the absence of structured clinical assessments—particularly relevant in settings where such data may be unavailable or inconsistently applied.

Given that nearly half of individuals with COPD experience at least 1 moderate to severe exacerbation annually—often without being flagged as uncontrolled by current tools—Seleida addresses a critical gap by providing continuous, data-driven risk stratification embedded within routine care pathways [4,5].

To date, no automated or EHR-integrated phenotyping model has been formally established for COPD in real-world clinical settings. Unlike existing unidirectional risk scores or machine learning classifiers focused on exacerbation or mortality risk, Seleida was explicitly designed as a bidirectional and bijective system tailored to primary care populations. This architecture enables both forward prediction from observed data and reverse inference of phenotypic profiles from computed probabilities—features essential for transparency, auditability, and integration into decision support environments.

Crucially, the model relies solely on structured variables that are universally available across health systems, ensuring interoperability and scalability. As such, benchmark comparisons against nonbijective models were deemed conceptually misaligned and methodologically uninformative. Instead, internal comparisons were performed (section S4 in Multimedia Appendix 1), and the final implementation was selected based on predictive accuracy, sparsity, and operational interpretability.

To the best of the authors' knowledge—based on an exhaustive PubMed search using combinations of terms such as COPD, automatic phenotyping, clinical decision support systems, electronic health records, predictive modeling, algorithmic classification, bijective model, and rule-based phenotyping—no published model currently exists that is specifically designed for the automatic phenotyping of patients with COPD and suitable for direct integration into health care information systems. Future studies may explore head-to-head evaluations once externally validated phenotyping frameworks become available.

Implications for Digital Health Integration

Seleida was designed to overcome long-standing barriers to the adoption of clinical decision support tools, including limited data availability, platform heterogeneity, and clinician disengagement driven by system opacity or poor integration. Its deterministic and parsimonious architecture ensures full traceability and facilitates seamless integration across heterogeneous digital infrastructures. The model's implementation potential can be articulated across 3 core domains:

- EHR integration and technical feasibility: Seleida requires only 2 structured input variables—annual dispensations of SABA or SAMA canisters or both and respiratory antibiotics—which are consistently recorded in most EHRs. Its architecture adheres to HL7 FHIR standards, as detailed in section S7 in Multimedia Appendix 1, where all model outputs were successfully validated using the official HL7 FHIR validator (v6.5.28) without structural or semantic errors across 440 resources. These outputs were generated through an automated simulation of valid (*a, b*) input combinations—not from real patient data—and were used to demonstrate the model's technical interoperability under HL7 FHIR specifications. The structured Fast Healthcare Interoperability Resources (FHIR) bundles include *RiskAssessment* (risk and rationale), *DetectedIssue* (clinical recommendations), *Condition* (disease state), and *Provenance* (model metadata), ensuring syntactic integrity, semantic traceability, and compatibility with clinical decision support platforms.
- Clinical decision support integration: The generated FHIR bundles enable real-time deployment within EHR-based dashboards and alert systems via standard Application Programming Interfaces. For instance, exceeding predefined thresholds (eg, >3 inhalers per year or ≥2 antibiotic courses) can trigger automated clinical recommendations through the *DetectedIssue* resource, which remains fully auditable via associated *Provenance* metadata. This architecture supports reproducible and scalable implementation in both open-source platforms (eg, OpenMRS) and commercial systems compliant with HL7 R5.
- Scalability and global interoperability: The model's minimal data requirements and exclusive reliance on universally structured prescribing variables make it well suited for adoption in low- and middle-income countries. Its lightweight, FHIR-compliant design allows integration into national health information infrastructures aligned with the World Health Organization's Digital Health Strategy. The use of international terminologies (SNOMED CT and LOINC) and standardized value sets further enables longitudinal data integration, federated learning, and interoperability across certified clinical environments worldwide.

Advancing Precision COPD Management

Seleida contributes to the advancement of precision medicine in COPD by enabling automated, phenotype-driven decision pathways tailored to real-world primary care data. Its deterministic architecture supports individualized care planning through multiple mechanisms. First, the model's integration of 2025 GOLD ABE classification with SABA dependency stratification facilitates personalized pharmacologic strategies—informing step-up or step-down adjustments based on quantified risk levels. Beyond pharmacologic guidance, Seleida helps identify patients who may benefit from nonpharmacologic interventions such as structured pulmonary rehabilitation or smoking cessation support, reinforcing a holistic, patient-centered approach to disease control [74,75]. Moreover, the ability to isolate phenotypes associated with frequent exacerbations or suggestive of *P aeruginosa* colonization offers additional value for microbiological surveillance and early antimicrobial stewardship [76].

XSL•FO
RenderX

Seleida's modular structure permits future expansion. Variables such as comorbidity profiles, vaccination status, or inflammatory biomarkers (eg, eosinophil count and C-reactive protein) can be incorporated without compromising interpretability—enhancing predictive precision and adaptability to diverse clinical settings.

Health System Optimization and Economic Potential

Beyond individual risk estimation, Seleida generates population-level insights that can inform health system optimization and performance monitoring. Its probabilistic outputs enable benchmarking of COPD control across institutions and regions, helping identify care gaps and guiding policy interventions to reduce diagnostic inertia, undertreatment, and geographic disparities in disease management.

At the public health level, the model supports strategic planning by quantifying the projected impact of interventions—such as seasonal vaccination campaigns, air quality alerts, or therapeutic adjustments—on exacerbation rates and control metrics at scale. Its forecasting capacity also informs resource allocation, enabling estimates of emergency visits, hospitalization demands, and inhaler supply needs—particularly critical in overstretched systems or during seasonal peak periods.

From an economic perspective, COPD exacerbations—especially those requiring hospitalization—account for more than 70% of direct disease-related health care expenditures [77]. By identifying high-risk patients early, Seleida may help reduce exacerbation incidence by approximately 15% - 25%, consistent with reductions observed in phenotype-guided management programs [74,75]. Preventing a single severe exacerbation may yield direct savings of $1700 to $4720 (the cost that was originally reported in euros [€] was converted to US dollars using the exchange rate of €1=$1.18 as of September 15, 2025, based on the European Central Bank reference rates per patient annually) [21]. While these projections remain hypothetical within Seleida's current context, they underscore its potential contribution to value-based care. Confirmatory evidence from prospective cost-effectiveness evaluations in multicenter implementation studies will be essential to fully quantify this impact.

As health care systems face mounting pressure to improve outcomes while managing resource constraints, tools such as Seleida—anchored in objective, high-frequency data and deployable across diverse infrastructures—offer a pragmatic path toward more efficient, equitable, and data-driven respiratory care.

Interpretability and Clinical Use in Real-World Practice

Seleida was designed for seamless integration into EHR systems, where structured clinical inputs—specifically rescue inhaler use and antibiotic prescriptions—can be continuously analyzed to generate real-time risk estimates and automated alerts. The model can also be applied manually in settings without digital integration, allowing clinicians to interpret the probability of poor control as a continuous indicator of exacerbation risk, with higher values reflecting proportionally greater clinical vulnerability. This dual deployment capacity is particularly valuable in resource-constrained environments where decision support infrastructures are limited.

For exploratory implementation, a provisional risk threshold was established. Because the sample size of this pilot study precluded formal statistical derivation, a reference point of $Pr>.50$ was selected based on the internal distribution of predicted probabilities. This should be interpreted not as a strict clinical cutoff but as an operational inflection point to guide prioritization. The model supports graded stratification across the risk spectrum, enabling providers to flag higher-risk profiles (eg, $Pr>.70$) for proactive evaluation, treatment adjustment, or closer follow-up.

Beyond individual patient care, Seleida enables population-level case finding using prescribing data alone, without requiring recent consultations or the patient's physical presence. This capability allows the generation of risk-stratified reports for entire patient panels, facilitating earlier identification of those likely to be poorly controlled. The transition from reactive recognition during encounters to anticipatory detection at the database level supports a scalable, equitable, and resource-efficient approach to COPD management. By combining point-of-care guidance with population surveillance, Seleida offers a flexible solution adaptable to diverse health care settings.

From a clinical perspective, fully automated and bijective phenotyping enables early detection of unstable COPD without the need for spirometry or symptom scores. By generating actionable, guideline-aligned classifications from routine EHR data, Seleida supports timely treatment selection, targeted microbiological assessment, and precise referral. Prioritizing follow-up for poorly controlled patients has the potential to reduce primary care and emergency visits, exacerbations, hospitalizations, and even mortality, while improving disease control and optimizing health care resource use.

Seleida's deterministic and bijective framework delivers precise, phenotype-driven COPD management using only routinely collected prescribing data. By translating high-frequency medication patterns into actionable risk profiles, it facilitates earlier therapeutic escalation, targeted treatment stratification, and proactive follow-up scheduling—particularly in patients who might otherwise remain undetected by conventional spirometry-based or symptom-based approaches.

The model's simplicity, transparency, and full EHR interoperability enable smooth integration into clinical workflows, supporting earlier detection of instability, automated triage, and efficient resource allocation. At the system level, Seleida empowers population-wide surveillance, equitable access to timely interventions, and optimization of health care resources—priorities central to contemporary primary care and health system planning.

At the health system level, proactive, database-driven detection enables earlier triage and strategic resource allocation across the care continuum. Identifying high-risk patients before clinical deterioration allows services to intensify follow-up, focus preventive interventions, and streamline emergency response.

XSL•FO
RenderX

This anticipatory approach promotes equitable access to timely care, reduces unnecessary utilization, and decreases the likelihood of preventable hospitalizations—enhancing the efficiency, scalability, and sustainability of COPD management while maximizing the effectiveness of interventions in primary care.

Limitations and Validation Needs

Despite its strengths, several limitations warrant consideration:

- Sample size and scope: The model was validated retrospectively in a single-country cohort of 106 patients from 2 Spanish primary care centers. While the results support internal consistency, the generalizability to other health systems, demographic groups, and care models remains to be established through multicenter external validation [45]. To address this, future validation studies are planned with larger and more heterogeneous cohorts drawn from multiple Spanish regions, aiming to evaluate the model's performance across broader demographic, geographic, and clinical contexts. Given its reliance on universally recorded prescribing data, Seleida also has strong potential for applicability in diverse international settings, and validation efforts will extend to health care systems in both European and non-European countries.
- Variable parsimony: Seleida was intentionally designed for simplicity and scalability, relying on 2 objective, high-frequency prescribing variables. However, this design may limit sensitivity in clinically complex or multimorbid phenotypes. In particular, the model may underperform in identifying atypical exacerbation profiles, discordant symptom patterns, or overlapping syndromes such as asthma-COPD overlap syndrome, eosinophilic COPD, or symptom-dominant cases with low exacerbation burden [78].
- Fixed thresholds and model rigidity: The deterministic and bijective architecture of Seleida requires predefined integer inputs (a, b), which enhances reproducibility and transparency but may reduce flexibility. This could limit performance in borderline or transitional cases, especially in patients with fluctuating clinical trajectories near decision thresholds. Future iterations may incorporate hybrid models with continuous or adaptive inputs, leveraging machine learning–based adjustments to enhance model responsiveness and flexibility [79].
- Omission of conventional clinical metrics: The exclusion of spirometry (eg, forced expiratory volume in the first second of expiration), symptom scores (eg, COPD Assessment Test, modified medical research council, and patient-reported outcomes enhances operational feasibility but may reduce clinical acceptability in settings where such metrics are routinely used for monitoring, reimbursement, or treatment authorization. Furthermore, Seleida may not fully capture disease burden in patients whose impact is driven more by symptoms than by exacerbation frequency—highlighting the need for future multimodal extensions.

Future Directions

To support broader adoption, equity, and scientific transparency, several development paths are under consideration:

1. Multinational validation: Future collaborations with international partners—such as the WHO Digital Health Programme—may enable cross-context evaluation of Seleida using open-source EHR infrastructures such as OpenMRS. This would facilitate assessment in diverse health care systems, including low- and middle-income settings.
2. Artificial intelligence–enhanced predictive modeling: Planned extensions include the incorporation of machine learning components to enable dynamic thresholds, time series forecasting, and the integration of social and environmental determinants of health. These enhancements aim to improve contextual relevance, longitudinal accuracy, and model adaptability in complex clinical scenarios.
3. Open-science reproducibility: A complete technical framework—including public, detailed model documentation, and executable pseudocode—could be released to support independent replication, collaborative development, and global dissemination. This approach would follow successful precedents in predictive modeling platforms, such as QRISK [80].

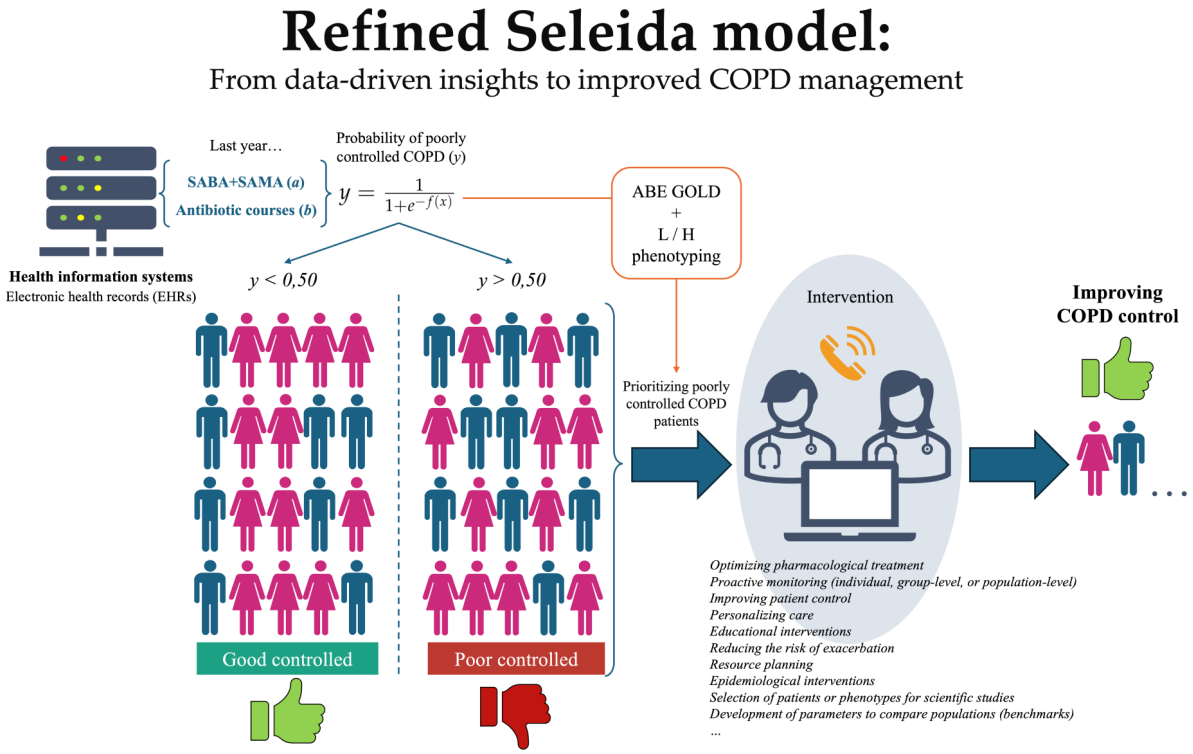
Ethical Considerations and Equity

Future iterations will incorporate algorithmic fairness audits to detect and mitigate potential biases in risk estimation—particularly among historically underrepresented or underserved populations. Equity by design is a foundational principle of the Seleida framework. By relying exclusively on structured prescribing data—universally recorded across health systems—and remaining independent of costly diagnostic tools or patient-reported inputs, Seleida is inherently scalable and adaptable to low-resource settings. Its compatibility with open-source EHR infrastructures, such as OpenMRS, facilitates national-scale deployment in both high- and middle-income countries. Partnerships with public health authorities and patient advocacy groups are envisioned to ensure that Seleida promotes access and actively reduces—rather than reinforces—structural disparities in COPD management [81-84].

By bridging predictive analytics with frontline clinical decision-making, Seleida supports equitable, individualized care (Figure 8). Its automated, interoperable, and fully transparent architecture enables the early identification of poorly controlled patients and the delivery of actionable, risk-aligned interventions. Through the transformation of routine prescribing data into clinically interpretable phenotypes, Seleida contributes not only to personalized medicine but also to system-level optimization and population risk mitigation.

XSL•FO
RenderX

Figure 8. Applications of the refined Seleida model. The model uses EHR data to identify patients with poorly controlled chronic obstructive pulmonary disease, enabling phenotyping and targeted interventions to improve disease management. COPD: chronic obstructive pulmonary disease; EHR: electronic health care record; GOLD: Global Initiative for Chronic Obstructive Lung Disease; H: high; L: low; SABA: short-acting β2-agonists; SAMA: combined with short-acting muscarinic antagonists.



Planned multicenter validation and open-science dissemination are expected to further reinforce Seleida's role as a cornerstone in the emerging field of data-driven respiratory precision medicine—advancing a vision grounded in accessibility, transparency, and global equity.

Conclusions

This study presents Seleida as the first model for assessing COPD control that is fully automated, mathematically bijective, and clinically validated using structured data routinely captured in primary care. By leveraging 2 objective, high-frequency prescribing variables—namely, the number of dispensed rescue inhaler canisters and respiratory antibiotic courses—Seleida enables scalable, reproducible, and clinically interpretable phenotyping aligned with real-world care workflows.

The model demonstrated strong internal validity, with perfect concordance between its high-resolution and streamlined phenotyping systems (κ=1.00; P<.001), and substantial agreement with clinician-assigned phenotypes based on GOLD 2025 criteria (κ=0.70; P<.001), supporting both its discriminative capacity and interpretive reliability. Its deterministic structure supports real-time risk estimation and reverse phenotype mapping, enabling individualized treatment planning within EHR-integrated environments.

Designed for seamless digital integration, Seleida's low data burden and full compatibility with HL7 FHIR standards facilitate implementation across a broad range of informatics platforms—including dashboards, telehealth systems, and registry-based surveillance tools. These features, along with its transparency and interoperability, make the model particularly applicable to resource-limited settings.

While the present validation was limited to a retrospective cohort from 2 Spanish primary care centers, prospective multicenter studies are underway to evaluate Seleida's generalizability, economic impact, and performance across diverse health systems. Future model iterations aim to enhance flexibility and contextual precision through adaptive thresholds, multimodal inputs, and algorithmic fairness auditing.

By transforming routinely collected prescribing data into actionable, risk-aligned insights, Seleida offers a reproducible and ethically grounded approach to phenotype-guided COPD care. It provides a concrete, scalable contribution toward operationalizing precision medicine principles in everyday respiratory practice.

Acknowledgments

Medical writing assistance was provided by EP Health Marketing SL, Spain. A heartfelt acknowledgment goes to Mrs Filipa Lopes-Coelho for her outstanding dedication and professionalism.

XSL•FO
RenderX

Authors' Contributions

Both authors contributed equally to the conceptualization, methodology, and draft preparation through their scientific and medical expertise. All authors have read and agreed to the published version of the manuscript.

This research was funded by EP Health Marketing SL.

Conflicts of Interest

JDMV has received research grants from AMGEN, AstraZeneca, Boehringer Ingelheim, Chiesi, GSK, Menarini and Novartis. He is a member of the SEMERGEN and SEMG and he belongs to the SEMERGEN respiratory work group. FMNR has received research grants from AstraZeneca, Boehringer Ingelheim, Chiesi, Esteve, Ferrer, GSK, Kern Parma, Lundbeck, MSD, Novartis, Novo Nordisk, Pfizer, Sanofi and Viatris. He is a member of the SEMERGEN and he belongs to the SEMERGEN respiratory work group.

Multimedia Appendix 1
Supplementary methods and results (sections S1-S7).
[DOCX File, 1562 KB - medinform_v13i1e74932_app1.docx]

Multimedia Appendix 2
Health care consultations by rescue medication use (L/H). COPD: chronic obstructive pulmonary disease; H: high; L: low.
[PNG File, 359 KB - medinform_v13i1e74932_app2.png]

Multimedia Appendix 3
Exacerbations in the last year by rescue medication use (L/H). COPD: chronic obstructive pulmonary disease; H: high; L: low.
[PNG File, 322 KB - medinform_v13i1e74932_app3.png]

References

1. Boers E, Barrett M, Su JG, et al. Global burden of chronic obstructive pulmonary disease through 2050. JAMA Netw Open 2023 Dec 1;6(12):e2346598. [doi: 10.1001/jamanetworkopen.2023.46598] [Medline: 38060225]
2. GBD 2019 Chronic Respiratory Diseases Collaborators. Global burden of chronic respiratory diseases and risk factors, 1990-2019: an update from the Global Burden of Disease Study 2019. EClinicalMedicine 2023 May;59:101936. [doi: 10.1016/j.eclinm.2023.101936] [Medline: 37229504]
3. Harries TH, White P. Spotlight on primary care management of COPD: electronic health records. Chron Respir Dis 2021;18:1479973120985594. [doi: 10.1177/1479973120985594] [Medline: 33455426]
4. Sandelowsky H, Weinreich UM, Aarli BB, et al. COPD—do the right thing. BMC Fam Pract 2021 Dec 11;22(1):244. [doi: 10.1186/s12875-021-01583-w] [Medline: 34895164]
5. Jones RCM, Price D, Ryan D, et al. Opportunities to diagnose chronic obstructive pulmonary disease in routine care in the UK: a retrospective study of a clinical cohort. Lancet Respir Med 2014 Apr;2(4):267-276. [doi: 10.1016/S2213-2600(14)70008-6] [Medline: 24717623]
6. Joo MJ, Au DH, Fitzgibbon ML, McKell J, Lee TA. Determinants of spirometry use and accuracy of COPD diagnosis in primary care. J Gen Intern Med 2011 Nov;26(11):1272-1277. [doi: 10.1007/s11606-011-1770-1] [Medline: 21713542]
7. Joo MJ, Sharp LK, Au DH, Lee TA, Fitzgibbon ML. Use of spirometry in the diagnosis of COPD: a qualitative study in primary care. COPD 2013 Aug;10(4):444-449. [doi: 10.3109/15412555.2013.766683] [Medline: 23537230]
8. Price DB, Yawn BP, Jones RCM. Improving the differential diagnosis of chronic obstructive pulmonary disease in primary care. Mayo Clin Proc 2010 Dec;85(12):1122-1129. [doi: 10.4065/mcp.2010.0389] [Medline: 21123639]
9. Daniels K, Lanes S, Tave A, et al. Risk of death and cardiovascular events following an exacerbation of COPD: the EXACOS-CV US Study. Int J Chron Obstruct Pulmon Dis 2024;19:225-241. [doi: 10.2147/COPD.S438893] [Medline: 38259591]
10. Hawkins NM, Nordon C, Rhodes K, et al. Heightened long-term cardiovascular risks after exacerbation of chronic obstructive pulmonary disease. Heart 2024 Apr 25;110(10):702-709. [doi: 10.1136/heartjnl-2023-323487] [Medline: 38182279]
11. Zysman M, Nordon C, Fabry-Vendrand C, et al. Risk of cardiovascular events according to the severity of an exacerbation of chronic obstructive pulmonary disease. Eur J Prev Cardiol 2025 Feb 20:1-9. [doi: 10.1093/eurjpc/zwaf086] [Medline: 39977232]
12. Nordon C, Simons SO, Marshall J, et al. The sustained increase of cardiovascular risk following COPD exacerbations: meta-analyses of the EXACOS-CV studies. ERJ Open Res 2025 May;11(3):01091-02024. [doi: 10.1183/23120541.01091-2024] [Medline: 40524923]
13. Singh H, Schiff GD, Graber ML, Onakpoya I, Thompson MJ. The global burden of diagnostic errors in primary care. BMJ Qual Saf 2017 Jun;26(6):484-494. [doi: 10.1136/bmjqs-2016-005401] [Medline: 27530239]

XSL•FO
RenderX

14. Global strategy for the diagnosis, management, and prevention of chronic obstructive pulmonary disease. : Global Initiative for Chronic Obstructive Lung Disease Inc; 2025 URL: https://goldcopd.org/wp-content/uploads/2024/11/GOLD-2025-Report-v1.0-15Nov2024_WMV.pdf [accessed 2025-09-14]
15. Miravitlles M, Calle M, Molina J, et al. Spanish COPD Guidelines (GesEPOC) 2021: updated pharmacological treatment of stable COPD. Arch Bronconeumol 2022 Jan;58(1):69-81. [doi: 10.1016/j.arbres.2021.03.005] [Medline: 33840553]
16. Miravitlles M, Soler-Cataluña JJ, Calle M, et al. Spanish COPD Guidelines (GesEPOC) 2017. Pharmacological treatment of stable chronic obstructive pulmonary disease. Arch Bronconeumol 2017 Jun;53(6):324-335. [doi: 10.1016/j.arbr.2017.03.017] [Medline: 28477954]
17. Cosío BG, Hernández C, Chiner E, et al. [Translated article] Spanish COPD Guidelines (GesEPOC 2021): non-pharmacological treatment update. Arch Bronconeumol 2022 Apr;58(4):345-351. [doi: 10.1016/j.arbres.2021.08.024]
18. Gondalia R, Bender BG, Theye B, Stempel DA. Higher short-acting beta-agonist use is associated with greater COPD burden. Respir Med 2019;158:110-113. [doi: 10.1016/j.rmed.2019.10.007] [Medline: 31655317]
19. Rockenschaub P, Jhass A, Freemantle N, et al. Opportunities to reduce antibiotic prescribing for patients with COPD in primary care: a cohort study using electronic health records from the Clinical Practice Research Datalink (CPRD). J Antimicrob Chemother 2020 Jan 1;75(1):243-251. [doi: 10.1093/jac/dkz411] [Medline: 31598669]
20. Zeng S, Arjomandi M, Tong Y, Liao ZC, Luo G. Developing a machine learning model to predict severe chronic obstructive pulmonary disease exacerbations: retrospective cohort study. J Med Internet Res 2022 Jan 6;24(1):e28953. [doi: 10.2196/28953] [Medline: 34989686]
21. Braa J, Hanseth O, Heywood A, Mohammed W, Shaw V. Developing health information systems in developing countries: the flexible standards strategy. MIS Q 2007;31(2):381. [doi: 10.2307/25148796]
22. Shull JG. Digital health and the state of interoperable electronic health records. JMIR Med Inform 2019 Nov 1;7(4):e12712. [doi: 10.2196/12712] [Medline: 31682583]
23. Booth HP, Gallagher AM, Mullett D, et al. Quality improvement of prescribing safety: a pilot study in primary care using UK electronic health records. Br J Gen Pract 2019 Sep;69(686):e605-e611. [doi: 10.3399/bjgp19X704597] [Medline: 31262845]
24. Navarro Ros FM, Maya Viejo JD. Preclinical evaluation of electronic health records (EHRs) to predict poor control of chronic respiratory diseases in primary care: a novel approach to focus our efforts. J Clin Med 2024 Sep 21;13(18):5609. [doi: 10.3390/jcm13185609] [Medline: 39337095]
25. Maya Viejo JD, Navarro Ros FM. Preclinical identification of poorly controlled COPD: patients with a single moderate exacerbation matter too. J Clin Med 2025;14(1):22. [doi: 10.3390/jcm14010022] [Medline: 40725735]
26. Marovic B, Curcin V. Impact of the European General Data Protection Regulation (GDPR) on health data management in a European Union candidate country: a case study of Serbia. JMIR Med Inform 2020 Apr 17;8(4):e14604. [doi: 10.2196/14604] [Medline: 32301736]
27. Weiskopf NG, Weng C. Methods and dimensions of electronic health record data quality assessment: enabling reuse for clinical research. J Am Med Inform Assoc 2013 Jan 1;20(1):144-151. [doi: 10.1136/amiajnl-2011-000681] [Medline: 22733976]
28. Sterne JAC, White IR, Carlin JB, et al. Multiple imputation for missing data in epidemiological and clinical research: potential and pitfalls. BMJ 2009 Jun 29;338:b2393. [doi: 10.1136/bmj.b2393] [Medline: 19564179]
29. Peduzzi P, Concato J, Kemper E, Holford TR, Feinstein AR. A simulation study of the number of events per variable in logistic regression analysis. J Clin Epidemiol 1996 Dec;49(12):1373-1379. [doi: 10.1016/s0895-4356(96)00236-3] [Medline: 8970487]
30. Palojoki S, Saranto K, Reponen E, Skants N, Vakkuri A, Vuokko R. Classification of electronic health record-related patient safety incidents: development and validation study. JMIR Med Inform 2021 Aug 31;9(8):e30470. [doi: 10.2196/30470] [Medline: 34245558]
31. Mandel JC, Kreda DA, Mandl KD, Kohane IS, Ramoni RB. SMART on FHIR: a standards-based, interoperable apps platform for electronic health records. J Am Med Inform Assoc 2016 Sep;23(5):899-908. [doi: 10.1093/jamia/ocv189] [Medline: 26911829]
32. FHIR overview. HL7 FHIR Release 5. URL: https://www.hl7.org/fhir/overview.html [accessed 2025-09-14]
33. Canova-Barrios C, Machuca-Contreras F. Interoperability standards in Health Information Systems. Semin Med Writ Educ 2022;1(7):1-13. [doi: 10.56294/mw20227]
34. Trinkley KE, Kroehl ME, Kahn MG, et al. Applying clinical decision support design best practices with the practical robust implementation and sustainability model versus reliance on commercially available clinical decision support tools: randomized controlled trial. JMIR Med Inform 2021 Mar 22;9(3):e24359. [doi: 10.2196/24359] [Medline: 33749610]
35. Pikoula M, Quint JK, Nissen F, Hemingway H, Smeeth L, Denaxas S. Identifying clinically important COPD sub-types using data-driven approaches in primary care population based electronic health records. BMC Med Inform Decis Mak 2019 Apr 18;19(1):86. [doi: 10.1186/s12911-019-0805-0] [Medline: 30999919]
36. Halpin DMG, Miravitlles M, Metzdorf N, Celli B. Impact and prevention of severe exacerbations of COPD: a review of the evidence. Int J Chron Obstruct Pulmon Dis 2017;12:2891-2908. [doi: 10.2147/COPD.S139470] [Medline: 29062228]

XSL•FO
RenderX

37. Saini V, Technical S, Manager P, et al. Data quality assurance strategies in interoperable health systems. J Artif Intell Res 2022;2(2):322-358.
38. Sutton RT, Pincock D, Baumgart DC, Sadowski DC, Fedorak RN, Kroeker KI. An overview of clinical decision support systems: benefits, risks, and strategies for success. NPJ Digit Med 2020;3(1):17. [doi: 10.1038/s41746-020-0221-y] [Medline: 32047862]
39. Collins GS, de Groot JA, Dutton S, et al. External validation of multivariable prediction models: a systematic review of methodological conduct and reporting. BMC Med Res Methodol 2014 Mar 19;14(1):40. [doi: 10.1186/1471-2288-14-40] [Medline: 24645774]
40. Collins GS, Ogundimu EO, Altman DG. Sample size considerations for the external validation of a multivariable prognostic model: a resampling study. Stat Med 2016 Jan 30;35(2):214-226. [doi: 10.1002/sim.6787] [Medline: 26553135]
41. Riley RD, Ensor J, Snell KIE, et al. Calculating the sample size required for developing a clinical prediction model. BMJ 2020 Mar 18;368:m441. [doi: 10.1136/bmj.m441] [Medline: 32188600]
42. Riley RD, Snell KI, Ensor J, et al. Minimum sample size for developing a multivariable prediction model: PART II —binary and time-to-event outcomes. Stat Med 2019 Mar 30;38(7):1276-1296. [doi: 10.1002/sim.7992] [Medline: 30357870]
43. Labrique AB, Wadhwani C, Williams KA, et al. Best practices in scaling digital health in low and middle income countries. Global Health 2018 Nov 3;14(1):103. [doi: 10.1186/s12992-018-0424-z] [Medline: 30390686]
44. Ma Y, Zhao C, Zhao Y, et al. Telemedicine application in patients with chronic disease: a systematic review and meta-analysis. BMC Med Inform Decis Mak 2022 Apr 19;22(1):105. [doi: 10.1186/s12911-022-01845-2] [Medline: 35440082]
45. Moons KGM, Altman DG, Reitsma JB, et al. Transparent Reporting of a multivariable prediction model for Individual Prognosis or Diagnosis (TRIPOD): explanation and elaboration. Ann Intern Med 2015 Jan 6;162(1):W1-W73. [doi: 10.7326/M14-0698] [Medline: 25560730]
46. Snell KIE, Archer L, Ensor J, et al. External validation of clinical prediction models: simulation-based sample size calculations were more reliable than rules-of-thumb. J Clin Epidemiol 2021 Jul;135:79-89. [doi: 10.1016/j.jclinepi.2021.02.011] [Medline: 33596458]
47. Janson C, Wiklund F, Telg G, Stratelis G, Sandelowsky H. High use of short-acting β2-agonists in COPD is associated with an increased risk of exacerbations and mortality. ERJ Open Res 2023 May;9(3):00722-02022. [doi: 10.1183/23120541.00722-2022] [Medline: 37342089]
48. Rockenschaub P, Hayward A, Shallcross L. Antibiotic prescribing before and after the diagnosis of comorbidity: a cohort study using primary care electronic health records. Clin Infect Dis 2020 Oct 23;71(7):e50-e57. [doi: 10.1093/cid/ciz1016] [Medline: 31631225]
49. Vollenweider DJ, Frei A, Steurer-Stey CA, Garcia-Aymerich J, Puhan MA. Antibiotics for exacerbations of chronic obstructive pulmonary disease. Cochrane Database Syst Rev 2018 Oct 29;10(10):CD010257. [doi: 10.1002/14651858.CD010257.pub2] [Medline: 30371937]
50. Benchimol EI, Smeeth L, Guttmann A, et al. The Reporting of studies Conducted using Observational Routinely-collected health Data (RECORD) statement. PLoS Med 2015 Oct;12(10):e1001885. [doi: 10.1371/journal.pmed.1001885] [Medline: 26440803]
51. Collins GS, Reitsma JB, Altman DG, Moons KGM. Transparent reporting of a multivariable prediction model for individual prognosis or diagnosis (TRIPOD): the TRIPOD statement. BMJ 2015 Jan 7;350:g7594. [doi: 10.1136/bmj.g7594] [Medline: 25569120]
52. Whittaker H, Rubino A, Müllerová H, et al. Frequency and severity of exacerbations of COPD associated with future risk of exacerbations and mortality: a UK routine health care data study. Int J Chron Obstruct Pulmon Dis 2022;17:427-437. [doi: 10.2147/COPD.S346591] [Medline: 35264849]
53. Bender D, Sartipi K. HL7 FHIR: an agile and RESTful approach to healthcare information exchange. 2013 Presented at: Proceedings of the 26th IEEE International Symposium on Computer-Based Medical Systems; Jun 20-22, 2013; Porto, Portugal p. 381-385. [doi: 10.1109/CBMS.2013.6627810]
54. Jones PW, Harding G, Berry P, Wiklund I, Chen WH, Kline Leidy N. Development and first validation of the COPD Assessment Test. Eur Respir J 2009 Sep;34(3):648-654. [doi: 10.1183/09031936.00102509] [Medline: 19720809]
55. Miravitlles M, Soler-Cataluña JJ, Calle M, et al. A new approach to grading and treating COPD based on clinical phenotypes: summary of the Spanish COPD guidelines (GesEPOC). Prim Care Respir J 2013 Mar;22(1):117-121. [doi: 10.4104/pcrj.2013.00016] [Medline: 23443227]
56. Eklöf J, Sørensen R, Ingebrigtsen TS, et al. Pseudomonas aeruginosa and risk of death and exacerbations in patients with chronic obstructive pulmonary disease: an observational cohort study of 22 053 patients. Clin Microbiol Infect 2020 Feb;26(2):227-234. [doi: 10.1016/j.cmi.2019.06.011] [Medline: 31238116]
57. Eklöf J, Alispahic IA, Armbruster K, et al. Systemic antibiotics for Pseudomonas aeruginosa infection in outpatients with non-hospitalised exacerbations of pre-existing lung diseases: a randomised clinical trial. Respir Res 2024 Jun 6;25(1):236. [doi: 10.1186/s12931-024-02860-9] [Medline: 38844921]
58. Garcia-Vidal C, Almagro P, Romaní V, et al. Pseudomonas aeruginosa in patients hospitalised for COPD exacerbation: a prospective study. Eur Respir J 2009 Nov;34(5):1072-1078. [doi: 10.1183/09031936.00003309] [Medline: 19386694]

XSL•FO
RenderX

59. Butler CC, Gillespie D, White P, et al. C-reactive protein testing to guide antibiotic prescribing for COPD exacerbations. N Engl J Med 2019 Jul 11;381(2):111-120. [doi: 10.1056/NEJMoa1803185] [Medline: 31291514]
60. Martinez-Garcia MA, Miravitlles M. The impact of chronic bronchial infection in COPD: a proposal for management. Int J Chron Obstruct Pulmon Dis 2022;17:621-630. [doi: 10.2147/COPD.S357491] [Medline: 35355582]
61. Miravitlles M, Anzueto A. Chronic respiratory infection in patients with chronic obstructive pulmonary disease: what is the role of antibiotics? Int J Mol Sci 2017 Jun 23;18(7):1344. [doi: 10.3390/ijms18071344] [Medline: 28644389]
62. Federman AD, O'Conor R, Nnemnbeng J, et al. Feasibility trial of a comprehensive, highly patient-centered COPD self-management support program. Chronic Obstr Pulm Dis 2024 Jan 25;11(1):13-25. [doi: 10.15326/jcopdf.2023.0419] [Medline: 37813826]
63. Poot CC, Meijer E, Kruis AL, Smidt N, Chavannes NH, Honkoop PJ. Integrated disease management interventions for patients with chronic obstructive pulmonary disease. Cochrane Database Syst Rev 2021 Sep 8;9(9):CD009437. [doi: 10.1002/14651858.CD009437.pub3] [Medline: 34495549]
64. Bates DW, Saria S, Ohno-Machado L, Shah A, Escobar G. Big data in health care: using analytics to identify and manage high-risk and high-cost patients. Health Aff (Millwood) 2014 Jul;33(7):1123-1131. [doi: 10.1377/hlthaff.2014.0041] [Medline: 25006137]
65. Brandsma CA, Van den Berge M, Hackett TL, Brusselle G, Timens W. Recent advances in chronic obstructive pulmonary disease pathogenesis: from disease mechanisms to precision medicine. J Pathol 2020 Apr;250(5):624-635. [doi: 10.1002/path.5364] [Medline: 31691283]
66. Steyerberg EW, Vergouwe Y. Towards better clinical prediction models: seven steps for development and an ABCD for validation. Eur Heart J 2014 Aug 1;35(29):1925-1931. [doi: 10.1093/eurheartj/ehu207] [Medline: 24898551]
67. Maltais F, Naya IP, Vogelmeier CF, et al. Salbutamol use in relation to maintenance bronchodilator efficacy in COPD: a prospective subgroup analysis of the EMAX trial. Respir Res 2020 Oct 22;21(1):280. [doi: 10.1186/s12931-020-01451-8] [Medline: 33092591]
68. Fan VS, Gylys-Colwell I, Locke E, et al. Overuse of short-acting beta-agonist bronchodilators in COPD during periods of clinical stability. Respir Med 2016 Jul;116:100-106. [doi: 10.1016/j.rmed.2016.05.011] [Medline: 27296828]
69. Michaux KD, Metcalfe RK, Burns P, et al. Implementing Predictive Analytics towards efficient COPD Treatments (IMPACT): protocol for a stepped-wedge cluster randomized IMPACT study. Diagn Progn Res 2023 Feb 14;7(1):3. [doi: 10.1186/s41512-023-00140-6] [Medline: 36782301]
70. Chen Z, Hao J, Sun H, Li M, Zhang Y, Qian Q. Applications of digital health technologies and artificial intelligence algorithms in COPD: systematic review. BMC Med Inform Decis Mak 2025 Feb 13;25(1):77. [doi: 10.1186/s12911-025-02870-7] [Medline: 39948530]
71. Price D, West D, Brusselle G, et al. Management of COPD in the UK primary-care setting: an analysis of real-life prescribing patterns. Int J Chron Obstruct Pulmon Dis 2014;9:889-904. [doi: 10.2147/COPD.S62750] [Medline: 25210450]
72. Marott JL, Çolak Y, Ingebrigtsen TS, Vestbo J, Nordestgaard BG, Lange P. Exacerbation history, severity of dyspnoea and maintenance treatment predicts risk of future exacerbations in patients with COPD in the general population. Respir Med 2022 Feb;192:106725. [doi: 10.1016/j.rmed.2021.106725] [Medline: 34972025]
73. Wynants L, Van Calster B, Collins GS, et al. Prediction models for diagnosis and prognosis of covid-19: systematic review and critical appraisal. BMJ 2020 Apr 7;369:m1328. [doi: 10.1136/bmj.m1328] [Medline: 32265220]
74. Calverley PMA, Anzueto AR, Carter K, et al. Tiotropium and olodaterol in the prevention of chronic obstructive pulmonary disease exacerbations (DYNAGITO): a double-blind, randomised, parallel-group, active-controlled trial. Lancet Respir Med 2018 May;6(5):337-344. [doi: 10.1016/S2213-2600(18)30102-4] [Medline: 29605624]
75. Hurst JR, Vestbo J, Anzueto A, et al. Susceptibility to exacerbation in chronic obstructive pulmonary disease. N Engl J Med 2010 Sep 16;363(12):1128-1138. [doi: 10.1056/NEJMoa0909883] [Medline: 20843247]
76. Løkke A, Hilberg O, Lange P, Ibsen R, Bakke P, Ørts LM. The impact on future risk of one moderate COPD exacerbation in GOLD a patients—a cohort study. Eur Respir J 2022;60(suppl 66):4520. [doi: 10.1183/13993003.congress-2022.4520]
77. Miravitlles M, Murio C, Guerrero T, Gisbert R. Costs of chronic bronchitis and COPD: a 1-year follow-up study. Chest 2003 Mar;123(3):784-791. [doi: 10.1378/chest.123.3.784] [Medline: 12628879]
78. Viegi G, Pistelli F, Sherrill DL, Maio S, Baldacci S, Carrozzi L. Definition, epidemiology and natural history of COPD. Eur Respir J 2007 Nov;30(5):993-1013. [doi: 10.1183/09031936.00082507] [Medline: 17978157]
79. Rajkomar A, Dean J, Kohane I. Machine learning in medicine. N Engl J Med 2019 Apr 4;380(14):1347-1358. [doi: 10.1056/NEJMra1814259] [Medline: 30943338]
80. Hippisley-Cox J, Coupland C, Vinogradova Y, et al. Predicting cardiovascular risk in England and Wales: prospective derivation and validation of QRISK2. BMJ 2008 Jun 28;336(7659):1475-1482. [doi: 10.1136/bmj.39609.449676.25] [Medline: 18573856]
81. Vayena E, Blasimme A, Cohen IG. Machine learning in medicine: addressing ethical challenges. PLoS Med 2018 Nov;15(11):e1002689. [doi: 10.1371/journal.pmed.1002689] [Medline: 30399149]
82. Obermeyer Z, Powers B, Vogeli C, Mullainathan S. Dissecting racial bias in an algorithm used to manage the health of populations. Science 2019 Oct 25;366(6464):447-453. [doi: 10.1126/science.aax2342] [Medline: 31649194]

XSL•FO
RenderX

83. Ethics and governance of artificial intelligence for health: WHO guidance. World Health Organization. 2021. URL: https://iris.who.int/bitstream/handle/10665/341996/9789240029200-eng.pdf?sequence=1 [accessed 2025-02-20]
84. Vogelmeier CF, Román-Rodríguez M, Singh D, Han MK, Rodríguez-Roisin R, Ferguson GT. Goals of COPD treatment: focus on symptoms and exacerbations. Respir Med 2020 May;166:105938. [doi: 10.1016/j.rmed.2020.105938] [Medline: 32250871]

Abbreviations

COPD: chronic obstructive pulmonary disease
EHR: electronic health record
FHIR: Fast Healthcare Interoperability Resources
GOLD: Global Initiative for Chronic Obstructive Lung Disease
H: high
HL7 FHIR: Health Level Seven Fast Healthcare Interoperability Resources
ICD-10: International Classification of Diseases, Tenth Revision
ICS: inhaled corticosteroid
L: low
LABA: Long-acting β2-agonists
LAMA: Long-acting muscarinic antagonists
LASSO: Least Absolute Shrinkage and Selection Operator
LR: likelihood ratio
ML: machine learning
NPV: Negative predictive value
PPV: Positive predictive value
Pr: Probability of poor control
SABA: short-acting β2-agonists
SAMA: short-acting muscarinic antagonists
Se: Sensitivity
Sp: Specificity

Edited by J Klann; submitted 25.03.25; peer-reviewed by CY Chen, T Yusuff, Y Wang; revised version received 26.08.25; accepted 27.08.25; published 13.10.25.

Please cite as:
Maya Viejo JD, Navarro Ros FM
Automated Chronic Obstructive Pulmonary Disease Phenotyping and Control Assessment in Primary Care: Retrospective Multicenter Study Using the Seleida Model
JMIR Med Inform 2025;13:e74932
URL: https://medinform.jmir.org/2025/1/e74932
doi:10.2196/74932

© José David Maya Viejo, Fernando M Navarro Ros. Originally published in JMIR Medical Informatics (https://medinform.jmir.org), 13.10.2025. This is an open-access article distributed under the terms of the Creative Commons Attribution License (https://creativecommons.org/licenses/by/4.0/), which permits unrestricted use, distribution, and reproduction in any medium, provided the original work, first published in JMIR Medical Informatics, is properly cited. The complete bibliographic information, a link to the original publication on https://medinform.jmir.org/, as well as this copyright and license information must be included.

XSL•FO
RenderX

Scalable Big Data Platform With End-to-End Traceability for Health Data Monitoring in Older Adults: Development and Performance Evaluation

Ander Cejudo[1,2], MSc; Yone Tellechea[1], MSc; Amaia Calvo[1], MSc; Aitor Almeida[2], PhD; Cristina Martín[1,2,3], PhD; Andoni Beristain[1,3,4], PhD

[1]Vicomtech Foundation, Basque Research and Technology Alliance (BRTA), Mikeletegi 57, Donostia-San Sebastián, Basque Country, Spain

[2]Faculty of Engineering, University of Duesto, Bilbao, Spain

[3]e-Health Department, Biodonostia Health Research Institute, San Sebastián, Spain

[4]Computer Science and Artificial Intelligence Department, University of the Basque Country UPV/EHU, Donostia-San Sebastián, Spain

Corresponding Author:
Ander Cejudo, MSc
Vicomtech Foundation, Basque Research and Technology Alliance (BRTA), Mikeletegi 57, Donostia-San Sebastián, Basque Country, Spain

Abstract

Background: The increasing use of real-time health data from wearable devices and self-reported questionnaires offers significant opportunities for preventive care in aging populations. However, current health data platforms often lack built-in mechanisms for data and model traceability, version control, and coordinated management of heterogeneous data streams, which are essential for clinical accountability, regulatory compliance, and reproducibility. The absence of these features limits the reuse of health data and the reproducibility of analytical workflows across research and clinical environments.

Objective: This work presents DeltaTrace, a unified big data health platform designed with traceability as a key architectural feature. The platform integrates end-to-end tracking of data and model versions with real-time and batch processing capabilities. Built entirely on open source technologies, DeltaTrace combines components for data management, model management, orchestration, and visualization. The main objective is to demonstrate that embedding traceability within the architecture enables scalable, auditable, and version-controlled processing of health data, thereby facilitating reproducible analytics and long-term maintenance of health monitoring systems.

Methods: DeltaTrace adopts a medallion architecture implemented with Delta Lake to ensure atomic and version-controlled data transformations. Apache Spark is used for distributed computation, Apache Kafka for continuous data ingestion, and Apache Airflow for orchestration of batch and streaming workflows. MLflow manages the lifecycle and versioning of machine learning models, while Grafana provides visualization dashboards for real-time and aggregated data inspection. The platform is evaluated using continuous physiological signals from wearable devices and batch-ingested questionnaire data, combining synthetic and real data from the LifeSnaps dataset. Performance tests are conducted on central processing unit–only servers with 8-core and 24-core configurations to assess ingestion, aggregation, visualization, and anomaly detection latency.

Results: DeltaTrace supports continuous processing for approximately 1500 users with end-to-end delays below 10 minutes. Ingestion and visualization tasks operate between mean 4.9 (SD 0.12) and 7.5 (SD 0.28) minutes, while aggregation and anomaly detection required less than mean 5.6 (SD 0.04) and 10.5 (SD 1.70) minutes, respectively. Increasing from 8 to 24 cores improved ingestion and cleaning latency by up to 25% and anomaly detection performance by up to 50%. The system maintains consistent performance across different data types, processing modes, and loads.

Conclusions: DeltaTrace provides a scalable and modular architecture that incorporates traceability as a core component together with functions for model management, orchestration, and visualization. The platform enables complete version control across data and models and maintains performance under limited hardware conditions. These characteristics support reproducible and auditable health data processing and make DeltaTrace suitable for continuous monitoring and preventive health care in aging populations.

(JMIR Med Inform 2025;13:e81701) doi:10.2196/81701

KEYWORDS

older adults; data management; telemonitoring; early detection; wearable; big data

XSL•FO
RenderX

Introduction

Background

According to the World Health Organization, the number of individuals aged 60 years and older is expected to reach 2.1 billion by 2050, nearly doubling from 1.1 billion in 2020 [1]. This demographic shift is particularly pronounced in Europe, where persons aged 60 years or older are projected to account for 36% of the total population by 2050 [2]. Aging is associated with a higher prevalence of chronic and degenerative diseases, including cardiovascular conditions, diabetes, neurodegenerative disorders, and frailty syndromes. These often coexist, resulting in multimorbidity, which leads to increased health care demands, hospital admissions, and long-term care requirements [3,4].

Preventive care has become essential to address the growing health care burden in aging populations. Evidence suggests that interventions focusing on early detection, continuous monitoring, and timely management of health risks can significantly reduce complications, improve outcomes, and delay institutionalization [5,6]. Enabling older adults to remain at home with autonomy requires technical solutions that support preventive action through continuous observation and timely data-driven decisions.

Big data platforms have emerged as a relevant approach to support these goals. By integrating diverse data sources such as physiological signals from wearable devices [7] and electronic health records [8], these platforms can enable large-scale remote monitoring, predictive analytics, and personalized health care delivery [9]. Real-time processing, interoperability, and scalability are commonly addressed in many recent frameworks [10,11]. However, other critical features such as model traceability and data version control are often omitted [12-14]. These capabilities enable the tracking of each model inference and its underlying data, thereby supporting reproducibility and accountability.

Traceability is essential in health care applications, serving as an important process for recording data origins and the history of data generation and processing [15]. Within this domain, clinical decisions, audits, and regulatory compliance critically depend on knowing precisely which data, model, and processing logic were used at each stage of the data pipeline. This transparency ensures accountability and supports compliance requirements. However, despite this vital need, current solutions often prioritize data integrity during sharing but frequently lack transparency, traceability, and comprehensive integrity audits for cloud-stored medical data [16]. This absence of clear visibility can undermine patient trust and pose challenges related to computational power consumption and latency when sharing sensitive data across institutions [16].

Related Work

Several studies have used big data technologies to analyze data for specific health conditions. The approach proposed by Ismail et al [12] developed a novel stream extract, transform, load (ETL) framework for real-time Twitter-based sentiment analysis using Kafka, Spark, Hadoop Distributed File System (HDFS), Hive, HBase, and Cassandra. Their experiments assessed performance across trigger intervals, dataset sizes, and storage technologies, ultimately finding HDFS to be the most effective storage solution. The authors reported increased ETL execution time when sentiment classification was integrated, highlighting trade-offs between system parameters and resource allocation. Similarly, Saeed and Saeed [13] used Apache Spark and Spark Streaming to analyze real-time hospital health care data for diabetes prediction. Their experiments found the gradient boosted tree classifier to be the most accurate, achieving 90.14% accuracy. The system was scalable and suitable for timely diagnosis, with future work aiming to incorporate additional data sources. Saleh et al [14] proposed TransformerFusionNet, a novel artificial intelligence (AI) model for real-time intensive care unit heart failure mortality prediction, achieving 91.72% accuracy. The model used Apache Spark and Kafka to stream and process structured and clinical note data, enabling scalable, real-time clinical decision support.

Beyond specific health conditions, other studies have proposed big data platforms designed for broader or more general applications. The Personal Health Dashboard introduced by Bahmani et al [10] used Kubernetes, Secure File Transfer Protocol, and serverless architectures to deliver scalable and secure health management using wearable, clinical, and omics data. Their experiments demonstrated dynamic scaling and presymptomatic COVID-19 detection, although further research was needed on omics data privacy. Similarly, Liu [17] developed a health data platform that calculated BMI from user-inputted height and weight, applied Chinese health standards, and provided personalized advice. While the core functionality was realized, the system remained preliminary, with ongoing work required to improve data integration and data quality.

A growing line of research has focused on data provenance, model management, and the reproducibility of machine learning (ML) pipelines in health care. According to Ahmed et al [15], data provenance frameworks play a crucial role in documenting data lineage and ensuring accountability in clinical decision systems; yet, they are often limited to metadata capture and do not scale effectively to large, heterogeneous health care datasets. The study by Belbasis and Panagiotou [18] highlighted that reproducibility and transparency remain major challenges for ML prediction models in health services research, emphasizing the need for comprehensive documentation of data, code, and analyses rather than focusing solely on large-scale processing. Xie et al [16] demonstrated the potential of MLflow for tracking model experiments in medical imaging tasks, but their work concentrated on model-level traceability rather than managing the entire data lifecycle. Finally, Mora-Cantallops et al [19] reviewed practices and data models for traceability in the context of building AI systems and observed that, despite the availability of many reproducibility tools, a common integrated approach for provenance and version control is currently lacking.

In summary, big data technology stacks have proven effective in delivering real-time, scalable health care solutions through advanced analytics and AI. However, existing solutions often lack a comprehensive approach that incorporates data traceability, including version control and lineage, critical requirements for health care applications. As summarized in Table 1 (see complete table in Multimedia Appendix 1), current

XSL•FO
RenderX

systems also tend to treat key features such as model management, resource monitoring, data visualization, and distributed processing in a fragmented manner.

Table . Overview of recent studies using big data capabilities in health-related applications[a].

Reference	Big data capabilities								
	Versioning	Scalability	Model management	Monitoring	Scheduling	Storage	Processing	Real time	Visualization
Ismail et al [12]					✓	✓	✓	✓	✓
Saeed and Saeed [13]							✓	✓	✓
Saleh et al [14]							✓	✓	
Ed-daoudy et al [20]		✓				✓	✓	✓	✓
Yıldırım et al [21]							✓	✓	✓
Ismail Ebada et al [22]							✓	✓	
Bahmani et al [10]		✓	✓	✓		✓	✓	✓	✓
Rashid et al [23]						✓	✓	✓	
Zheng and Ding [24]						✓	✓	✓	
Yongqiu et al [25]						✓	✓	✓	
DeltaTrace (ours)	✓	✓	✓	✓	✓	✓	✓	✓	✓

[a]Capabilities include versioning (data version control), scalability (scalability testing and handling large-scale data), model management (machine learning model management), monitoring (system or resource monitoring), scheduling (event or workflow scheduling), storage (distributed data storage), processing (distributed data processing), real time (real-time analytics support), and visualization (built-in data visualization tools). The final columns denote the primary task performed (eg, classification and anomaly detection) and the purpose or target condition addressed (eg, diabetes and general monitoring).

Objective

This study addresses the lack of integrated data and model traceability in existing health data platforms, where version control and auditability are often treated as secondary features. The main objective is to design and develop a unified health data platform in which traceability is established as a central architectural principle, implemented together with essential components for scalability, model management, orchestration, and visualization, ensuring complete reproducibility and accountability throughout the data lifecycle.

The design of DeltaTrace is guided by research objectives that align with key big data capabilities identified in the literature and analyzed in the state-of-the-art review (Table 1). Specifically, the platform aims (1) to integrate versioning and traceability mechanisms to ensure full data and model lineage across the processing pipeline; (2) to support scalable storage and processing to handle continuous and batch data streams under variable system loads; and (3) to provide coordinated model management, scheduling, monitoring, and visualization within a single architecture to enable consistent and auditable workflows.

These objectives determined the overall architectural design, which is implemented using open source technologies chosen for their robustness, transparency, accessibility, and long-term sustainability. This approach ensures that the proposed platform not only addresses the limitations identified in existing solutions but also establishes traceability as a verifiable and reproducible property of the system architecture.

The paper is structured as follows. The Methods section describes the design of the DeltaTrace platform, detailing its key components, technologies, and evaluation setup. The Results section presents the main findings, including system performance, scalability, and visualization outcomes. The Discussion section summarizes the principal findings, interprets their clinical relevance, compares DeltaTrace with prior work, and outlines limitations and directions for future research. Finally, the Conclusions section highlights the main contributions and implications of DeltaTrace for reproducible and accountable health data management.

XSL•FO
RenderX

Methods

Design

DeltaTrace is designed to ingest, curate, transform, and store data from multiple heterogeneous sources, such as wearables and self-reported questionnaires, which differ in collection frequency, formats, and quality. The diversity of these sources requires a structured approach, motivating the use of an extract, load, transform (ELT) strategy and a medallion architecture to preserve raw data, enable flexible transformations, and maintain traceability throughout all processing stages.

The ETL approach often leads to irreversible transformations and potential loss of raw data. DeltaTrace adopts an ELT strategy, that is, raw data are first ingested and stored without alteration, ensuring full traceability and the ability to apply different transformation pipelines tailored to diverse processing or model input needs. This approach not only preserves original data but also supports reproducibility, facilitates auditing, and enhances compliance with the General Data Protection Regulation, which governs the processing of personal data in Europe, by supporting controlled and purposeful data transformations.

A key feature of the platform is end-to-end traceability. Every data transformation, model-related operation, such as training, evaluation, or inference, or change in the system is recorded, ensuring that the origin of each prediction or decision can be audited. This requirement is especially relevant for health care, where transparency is critical.

To address these needs, DeltaTrace is built upon the medallion architecture, a multilayered data structure that provides increasing levels of data quality, as recommended by Databricks. Each layer adheres to principles of atomicity, consistency, isolation, and durability (ACID), ensuring data reliability and recoverability. Data availability is ensured through the use of distributed and fault-tolerant components, such as Apache Spark and HDFS, which replicate data and store periodic checkpoints to enable recovery in case of system failure. Data accuracy is maintained by performing schema validation at ingestion, running automated data quality checks, and leveraging ACID transactions in Delta Lake to prevent corruption and guarantee consistency. Data usability is achieved through clear metadata definitions, versioned storage, and a configuration layer that enables data lineage tracking and reproducibility. By leveraging this architecture, DeltaTrace supports data governance, including availability, accuracy, and usability, across the entire data lifecycle. The quality of the data in each layer is described by the terms bronze (raw, ingested data), silver (cleaned datasets), and gold (enriched and aggregated data, ready for analytics and visualization). The medallion architecture does not replace other dimensional modeling techniques, and the schemas and tables within each layer can vary.

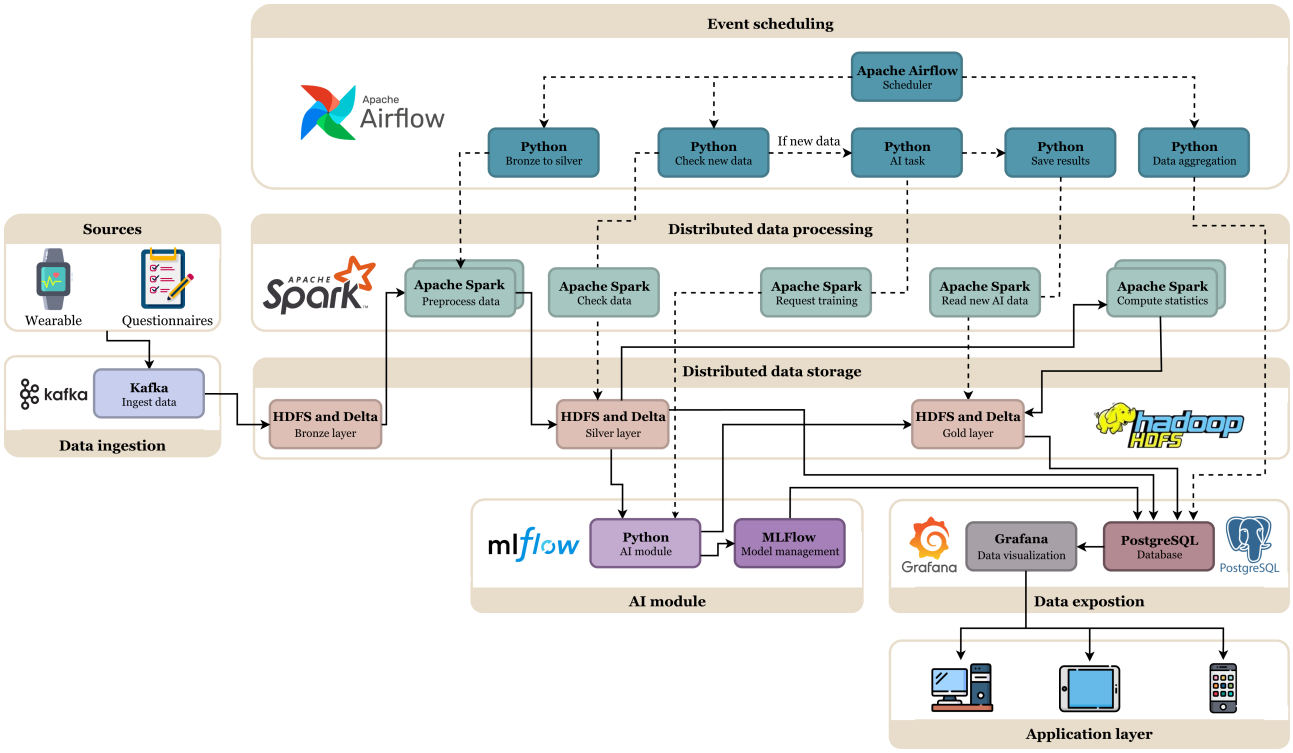
In addition to data engineering, DeltaTrace includes AI model lifecycle management. The platform supports all major steps in the model pipeline: data preparation, training, testing, and deployment. To enable full traceability of model versions, training data, and results, the system integrates MLflow [26], an open source MLOps platform. MLflow provides experiment tracking, pipeline versioning, and model serving. With MLflow, each model run is logged with detailed metadata, parameters, and outputs, enabling reproducible analysis and facilitating explainability by linking predictions to input features and model versions. Fairness auditing is supported through logging of model performance, while model metrics stored in MLflow enable continuous monitoring for potential data drift, alerting users to deviations in performance over time. These features allow the system to audit AI-driven decisions and evaluate the evolution of models over time, ensuring both transparency and reproducibility.

The automatic orchestration of data processing pipelines is essential to maintain the consistency and up-to-date status of the data lake. In the context of big data, 2 primary processing paradigms are used: batch processing and stream processing. The selection between these modes is driven by the nature and frequency of data collection. For instance, data collected at longer intervals, such as daily self-reports or weekly summaries, are typically handled through batch processing [27], which is well-suited for executing complex ELT tasks and periodic aggregations on larger volumes of data. Conversely, high-frequency data, such as minute-level readings from wearable sensors, are managed through stream processing. This model, implemented via Apache Kafka, enables real-time ingestion and processing by feeding data continuously into analytics components.

All data-related workflows, including batch and real-time, are orchestrated using Apache Airflow [28], enabling flexible and robust task scheduling. Airflow manages the ELT pipeline across the different data layers, triggers model training when new data become available, and coordinates visualization updates and aggregation tasks. The high-level architecture of the DeltaTrace platform is presented in Figure 1. To support end-to-end data lifecycle management, from ingestion to visualization, the platform incorporates a comprehensive suite of open source technologies. The core components with the specific used software versions are described in Multimedia Appendix 2.

XSL•FO
RenderX

Figure 1. Schema of the DeltaTrace data platform. The continuous arrows indicate the direction of information flow, whereas the dashed arrows trigger the execution of a process. AI: artificial intelligence; HDFS: Hadoop Distributed File System.



DeltaTrace has not only been built upon a carefully selected combination of open source technologies that support advanced analytics, real-time processing, and a high degree of traceability, but it has also been implemented alongside a dedicated configuration layer that enables full control of the data flow through simple configuration files. This layer abstracts operational complexity by allowing all core aspects, such as data source definitions, scheduling intervals, model parameters, and storage destinations, to be specified and modified without altering the underlying code. As a result, the platform is highly adaptable and maintainable, enabling rapid deployment and reconfiguration across different use cases or environments. More information about the configuration of DeltaTrace is provided in Multimedia Appendix 3.

All components in DeltaTrace are orchestrated to generate detailed logs to facilitate continuous monitoring and troubleshooting across the entire data processing pipeline. These logs record key operational events and system metrics, allowing users to verify the correct functioning of each component and trace the execution of data flows in real time. In addition, several of the integrated open source technologies inherently support data versioning and metadata management. For instance, intermediate results and model outputs are stored along with version identifiers and temporal metadata, enabling users to reconstruct historical states of the system or reproduce specific analyses. Checkpoints are also periodically generated to ensure fault tolerance and provide recovery capabilities, contributing to the overall transparency and reliability of platform operations.

Data Ingestion

DeltaTrace has been designed to accommodate heterogeneous data sources, integrating both continuous sensor streams and periodic user-reported inputs. In the current implementation, 2 primary data sources are supported:

- Wearable devices: Data are streamed through 10 dedicated Apache Kafka topics, each corresponding to a specific measured variable (eg, heart rate, physical activity, or sleep). These topics receive both daily summaries and high-frequency time-series measurements, such as minute-level heart rate and detailed sleep stages.
- Self-reported questionnaires: Each questionnaire is made available to older adults through a dedicated web interface. Once completed, the responses are transmitted via a Representational State Transfer (REST) application programming interface (API) for further processing. These instruments are designed to assess various domains, including emotional well-being, motivation, and behavioral readiness. Specifically, the collected questionnaires include the State-Trait Anxiety Inventory (STAI), Positive and Negative Affect Schedule, Transtheoretical Model, and Behavioral Regulation in Exercise Questionnaire. These questionnaires are used to gather structured data and do not include unstructured text input, enabling consistent analysis across participants.

All the incoming data are continuously processed, providing real-time capabilities for data ingestion. Upon ingestion, the data are stored in the bronze layer of the Delta Lake storage system. This layer acts as an immutable repository of raw data, preserving the original structure and enabling flexible, reproducible processing at later stages. By maintaining the data in the original form, the system supports multiple downstream analyses and transformation strategies without imposing a fixed processing logic at the point of ingestion.

XSL•FO
RenderX

Data Storage

Overview

DeltaTrace adopts a medallion architecture to organize and manage data across multiple layers (bronze, silver, and gold), each representing a progressively refined stage of data processing. This layered structure is implemented using Delta Lake, an open-source storage framework that brings ACID transaction support and scalable metadata handling to big data workloads. Delta Lake enables reliable data versioning, time travel, and schema enforcement. This architecture is further enhanced by AI-driven processes that operate on the curated data. AI models are trained using historical records and then deployed to perform real-time inference. Through this process, the AI layer transforms clean data into actionable insights, enriching the data pipeline and supporting decision-making. Each of the data layers is described below.

Bronze Layer: Raw Data

The bronze layer serves as the foundation, containing raw data ingested from multiple sources. These sources include wearable device data streamed through Kafka topics and questionnaire data collected via the REST API. For each source, a dedicated table is created to store the information in the original format, without structural modifications. This design preserves the integrity of the incoming data and supports traceability by ensuring that the unaltered raw inputs remain accessible for future processing or validation. Both wearable and questionnaire datasets follow a common structure that includes a user identifier and a date column, which enables seamless integration and cross-referencing between data types. This uniform schema allows data from heterogeneous sources to be combined efficiently for downstream analysis, as illustrated in Figure 1, where information from both wearables and questionnaires is jointly represented.

Silver Layer: Clean Data

The silver layer comprises data that have undergone refined cleaning operations aimed at improving consistency and usability. Typical tasks at this stage include the removal of duplicate records or the elimination of empty or irrelevant columns. These data support longitudinal and cross-sectional analyses, making them suitable for intermediate analytical workflows and for training ML models.

Gold Layer: Data Aggregations

The gold layer contains refined, domain-specific outputs tailored for end-user consumption. These include aggregated statistics, anomaly detection, and metrics intended to guide decisions made by clinicians, caregivers, or the older adults themselves. The gold layer is also the primary source for dynamic visualizations and alerts.

In parallel with this layered storage structure, a PostgreSQL (PSQL) [29] database is used to manage structured data essential for the proper functioning of the platform. This includes user registry information, authentication credentials, authorization roles, and other metadata required to support access control and administrative operations.

Data Processing

Data processing is conducted in a distributed and scalable manner using Apache Spark, a widely adopted framework for large-scale data computation [30]. Spark enables parallel execution across multiple compute and storage nodes (Spark Workers), thereby facilitating the efficient transformation of high-volume datasets and ensuring that the system can scale horizontally by incorporating additional resources.

Each processing job operates independently and includes the necessary Delta Lake dependencies to support ACID transactions, schema enforcement, and versioning. Data are read from the appropriate Delta Lake table, transformed according to defined logic, and subsequently written to the next layer, maintaining full traceability throughout the process.

For each dataset stored in the bronze layer, a dedicated Spark job is defined and scheduled by Apache Airflow. These jobs are responsible for continuously reading newly ingested data, applying cleaning and normalization procedures, and writing the results to the corresponding silver table. To avoid redundant processing, Spark checkpoints are used to ensure that only new records are handled during each execution cycle. In addition to avoiding duplicate computation, checkpoints store essential metadata, including application configuration, the sequence of streaming transformations applied to the data, and information about incomplete batches, into fault-tolerant storage, enabling the system to recover easily from failures and maintain uninterrupted data processing.

The transition from silver to gold is also managed through Spark jobs. These processes may involve aggregations (eg, computation of means, counts, or other statistical metrics) or the preparation of data for ML inference. In cases where predictive analytics is required, the silver data are forwarded to the AI module, and the resulting outputs, such as model predictions or recommendations, are stored in the gold layer for downstream visualization and user interaction.

Event Scheduling

DeltaTrace supports both batch and streaming modes for executing data processing tasks. In either case, data are ingested, transformed, and written to the appropriate storage layer (bronze, silver, or gold) according to the specific processing pipeline.

In the batch model, predefined tasks are executed at regular intervals, such as daily or weekly. This mode is suited for operations that do not require immediate responsiveness and benefit from scheduled, periodic processing. In contrast, the streaming model enables continuous ingestion and transformation of data as new records become available. Streaming pipelines are designed to operate persistently and are equipped with mechanisms to prevent duplication and handle errors, thereby ensuring data integrity.

All pipeline executions, both batch and streaming, are managed by the orchestrator of the platform, implemented using Apache Airflow. The orchestrator is responsible for scheduling task executions, monitoring resource use, logging events, sending error notifications, and automatically restarting pipelines in the event of failure. Streaming tasks are configured to run

XSL•FO
RenderX

continuously and are automatically relaunched if they terminate unexpectedly.

Apache Airflow structures workflow execution using directed acyclic graphs (DAGs), where tasks are defined as nodes and dependencies as edges. DAGs provide a declarative mechanism to specify the execution order and relationships among tasks. Each task may consist of a discrete operation, such as an HTTP request or a Python script, or more complex jobs like Spark batch transformations or Kafka-based streaming listeners. The Airflow user interface enables visual monitoring and editing of these DAGs, facilitating clear and maintainable pipeline management.

AI Module

The AI module is implemented as an independent component within the platform architecture, located between the silver and gold data layers. Designed as an optional step in the pipeline, it enables the transformation of clean silver-layer data into aggregated outputs, such as clustering or classification, for storage in the gold layer. This integration allows for the deployment of advanced analytics while preserving traceability and modularity. Although the MLlib library, built-in Apache Spark, provides capabilities for training models directly on DataFrames, a separate Python 3–based module has been adopted in DeltaTrace. This approach offers higher flexibility, allowing for seamless integration with MLflow for experiment tracking, support for a wide variety of models, and more comprehensive comparison and evaluation workflows.

The AI module is designed to support 1 or multiple AI pipelines capable of processing and inferring from the structured datasets available in the silver layer. To facilitate ease of use, the module exposes its functionality through a REST API developed using FastAPI. Two endpoints are provided:

- Train models: This endpoint orchestrates the data loading, preprocessing, and training procedures for all configured AI pipelines. Training metrics, model parameters and hyperparameters, and experiment metadata are logged to the MLflow tracking server. If a previous model exists for the same data source, its performance is compared to the newly trained model. If the new model achieves superior performance, this is registered as the latest version and made available for production.
- Predict: This end point initiates data loading, preprocessing, model retrieval, and inference stages. The system checks the model repository for a trained model corresponding to the input data source. If no model is available, an error is returned; otherwise, predictions are computed and returned as output.

Exposing the AI module as a REST service enables flexible integration with AI pipelines implemented in different programming languages. The AI models are stored in a centralized object repository, MinIO. In this case, a deep learning model based on recurrent neural networks has been selected for anomaly detection in wearable data [31]. Anomalies are defined as values that deviate from expected behavior, potentially triggering alerts to support preventive actions by health care providers. The chosen AI model is capable of learning temporal patterns in the data [32] to predict future values. These predicted values are then compared with the actual observations, and the resulting differences are modeled using a normal distribution. This approach enables the use of *z* scores to quantify deviations [33]. Depending on the magnitude of the deviation and predefined thresholds, anomalies are categorized into 3 levels: green (minor), yellow (moderate), and red (critical).

Model training and prediction tasks are orchestrated using Apache Airflow, which defines a pipeline composed of three primary stages: (1) checking for the availability of new data, (2) training or retraining the model, and (3) storing the resulting outputs. In the first stage, the orchestrator queries the Delta Lake silver layer to determine whether the volume of new data exceeds a predefined threshold for each data source. If this condition is met, an HTTP request is sent to the AI module containing identifiers such as the user_id, the variable to predict, and the relevant time range, serving primarily as a trigger for the AI module. Within the AI module, the corresponding data are loaded directly from Delta Lake based on these identifiers and processed to detect anomalies, and the results are then written to the gold table.

The anomaly detection component of DeltaTrace is based on predictive modeling using time-series data from wearable devices. The validation of these models included baseline, ML, and deep learning approaches for next-value prediction tasks, evaluated through user-based 3-fold cross-validation. The performance metrics included mean absolute error and root mean squared error. The selected model is required to achieve the lowest score among all evaluated models across these metrics and to demonstrate a clear improvement over the baseline approach. Based on these criteria, the attention-based long short-term memory (AttentionLSTM) model is selected for deployment due to its superior predictive performance. Details on the experimental setup, hyperparameter optimization, and model comparison are provided in Multimedia Appendix 4. Although the convolutional long short-term memory achieves a lower average mean absolute error for step prediction, the difference compared with AttentionLSTM is not statistically significant (P=.16, paired 2-tailed t test). Therefore, using the AttentionLSTM across all prediction tasks ensures consistency in the performance evaluation of DeltaTrace without compromising predictive accuracy. Anomalies are categorized using z score thresholds derived from the variability of the LifeSnaps dataset. To balance the 3 categories, we use $z \geq 1.04$ for green (minor), $z \geq 1.29$ for yellow (moderate), and $z \geq 1.65$ for red (critical). These thresholds also ensure that most anomalies remain minor, with fewer moderate and critical cases.

Data Exposition

To support effective data visualization, selected outputs from the processing and inference stages are written in real time to a PSQL database. This database serves as a structured, query-efficient layer specifically designed to support time-series visualization tools such as Grafana.

Separate tables are created within the PSQL database to organize information by data type (eg, sleep, physical activity, and heart rate). Each table includes timestamp fields and primary keys,

XSL•FO
RenderX

which facilitate time-series indexing, efficient joints, and fast query execution.

This architectural choice enables seamless integration with Grafana, allowing the platform to generate dynamic dashboards that display both real-time and historical data. Dashboards are configured to support multiple levels of analysis, including individualized monitoring for clinical care and aggregated views for population-level analytics. These visual interfaces enhance the interpretability of the system, supporting use cases such as anomaly detection, longitudinal health tracking, and cohort-based evaluations.

Evaluation Design

To evaluate the performance and robustness of DeltaTrace, 2 complementary datasets are used: one synthetic dataset specifically generated for this study and one real-world dataset, LifeSnaps, selected for the richness and representativeness of multimodal health data. The combination of both datasets allows for a comprehensive evaluation, covering both controlled data generation scenarios and real-life variability, noise, and complexity.

- The synthetic dataset is created to simulate realistic health-related signals such as steps, heart rate, and sleep duration. To do so, first, the key variables to be simulated are identified and then established physiologically plausible value ranges for each of them, based on publicly available health guidelines and literature [34,35]. Data points are then generated with coherent temporal structure (eg, steps per day and heart rate per minute) using random sampling within the specified ranges. Finally, the simulated data stream is sent to Kafka, which ingests the information into the bronze layer of DeltaTrace for further processing. Performance results are reported in terms of requests per second, where a request is defined as the ingestion of a single record for a given topic (eg, 1 temperature value per second or 1 heart rate measurement per second). Each simulated user includes multiple wearable-derived data sources, with up to 10 variables (topics) captured concurrently, assuming a frequency of 1 record per second. This dataset enables the generation of all necessary records in a controlled manner, allowing scalability tests to be conducted without constraints on data volume.
- The second dataset is LifeSnaps [36], a publicly available, multimodal, longitudinal dataset collected over approximately 4 months from 71 participants across Europe. It integrates high-resolution wearable data, ecological momentary assessments, and validated surveys, resulting in over 35 distinct types of measurements captured at temporal granularities ranging from seconds to days. The wearable device used for data capture is a Fitbit Sense, which includes readings from vital signals such as heart rate, sleep patterns, steps, blood oxygen saturation, temperature, and stress-related metrics. Additionally, ecological momentary assessment data encompass contextual and mood surveys, while traditional survey instruments cover personality, motivation, and emotional states. Altogether, the dataset comprises over 71 million rows, allowing comprehensive evaluation across physiological, behavioral, and psychological health dimensions.

For each experiment, performance is evaluated in terms of computational time as the number of requests per second increases. This process, known as a stress test, is conducted using the simulated dataset, while visualizations are produced with the LifeSnaps dataset.

The performance testing server for DeltaTrace is a Linux-based Ubuntu system with a 5.15 kernel, powered by dual Intel Xeon Gold 5218 central processing units (CPUs; 24 cores total at 2.30 GHz). It has 64 GB error-correcting code RAM, 8 GB swap, and a multilevel cache (L1: 256 KB and L2 and L3: 32 MB each). The server runs in a kernel-based virtual machine virtualized environment. Storage includes a 500 GB primary disk, a 60 GB secondary disk, and several small loop devices.

Ethical Considerations

This study did not involve any direct physical or mental intervention with participants. All data used were either synthetic, generated based on reference values reported in the literature, or obtained from LifeSnap, a publicly available dataset. Thus, this study did not require ethics approval, as it did not involve human participants or personal identifiable information.

Results

Silver Layer: Clean Data

In this set of experiments, the stress test is run and assessed until the clean data are available for visualization and consultation. The objective is to assess whether DeltaTrace is capable of handling high-throughput scenarios as demand scales. In addition, real data are visualized to show the system output. The results of the stress test are presented in Figure 2, where the x-axis represents the number of requests per second, each request corresponding to a single record of wearable data, such as a heart rate measurement, and the y-axis shows the processing time in minutes.

XSL•FO
RenderX

Figure 2. Time needed to process raw data from generation to the silver layer and make it available for visualization. (**A**) Time from data generation to silver layer and (**B**) time required for each data topic to be processed and available in the silver layer.

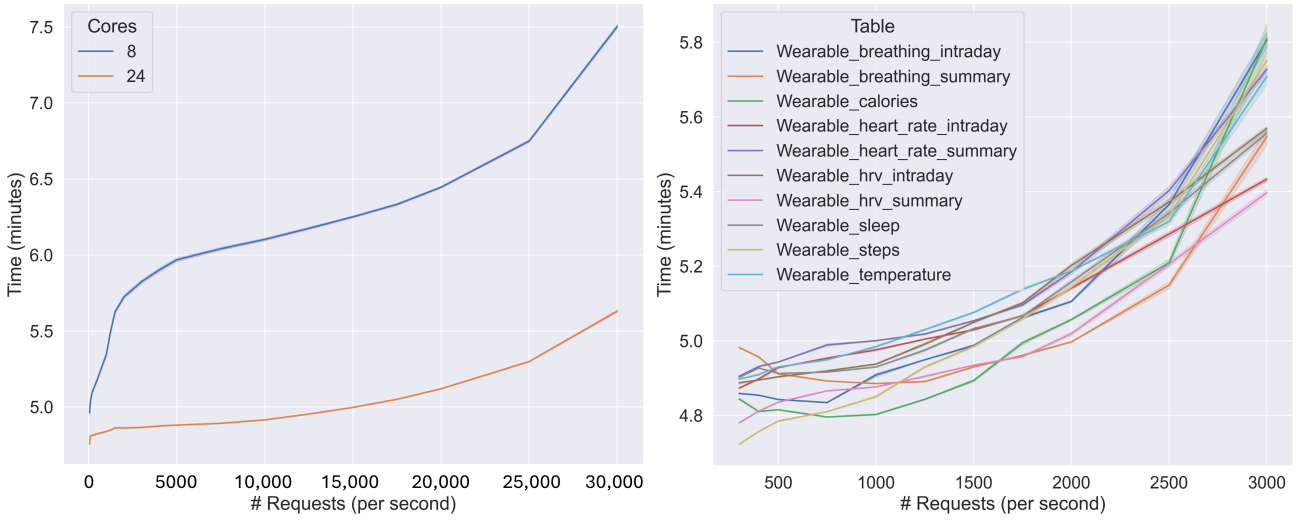


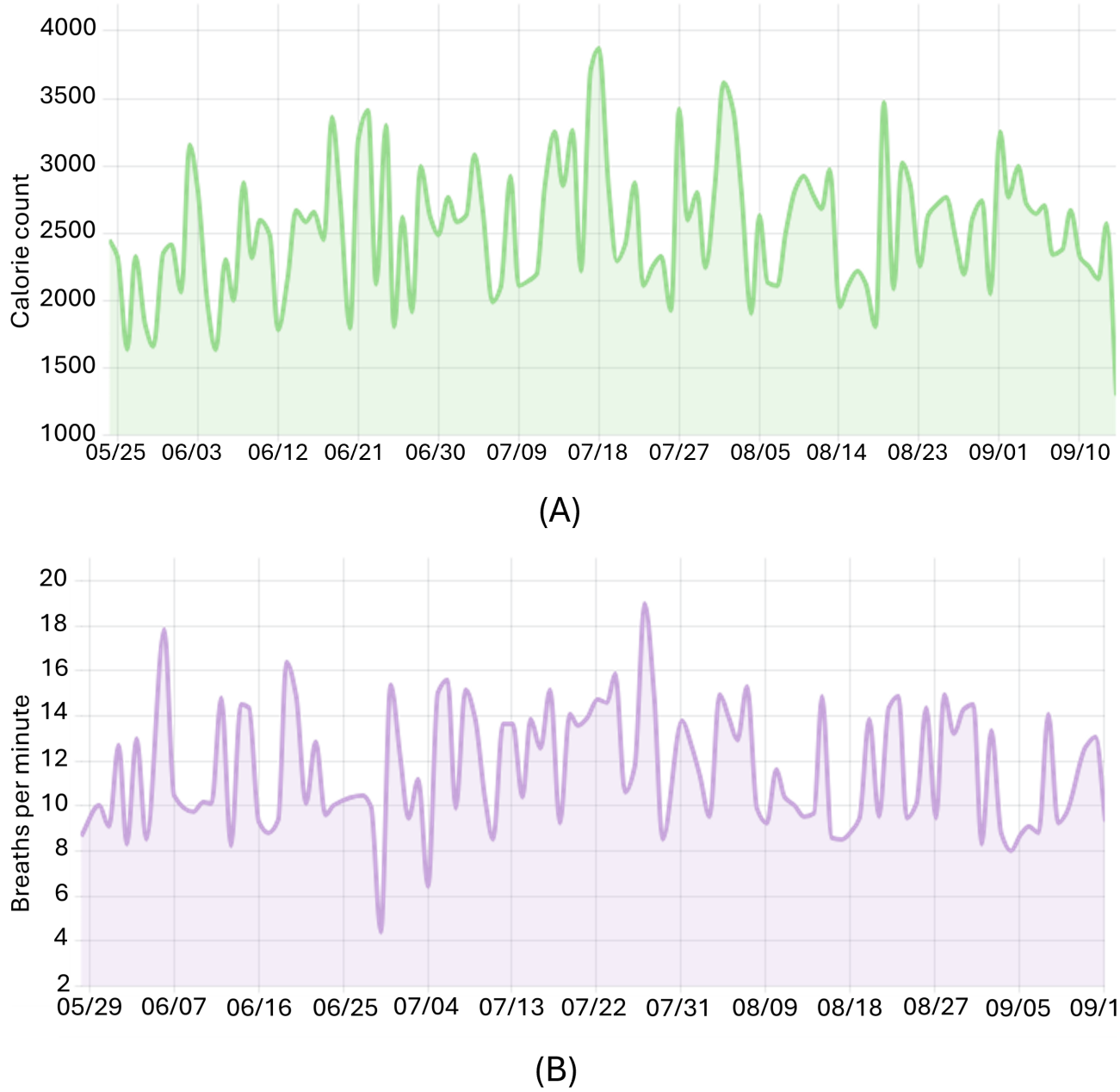
Figure 2A shows the time required to process data from the moment they are sent until they become available in the silver layer (y-axis), for different CPU configurations (8 and 24 cores) and increasing request rates (x-axis). At 50 requests per second, the 8-core setup requires a mean of 5.1 (SD 0.2) minutes, while the 24-core setup requires a mean of 4.9 (SD 0.12) minutes (a difference of 0.2 minutes). At 15,000 requests per second, the mean time increases to 6.3 (SD 0.14) minutes (8 cores) and 5 (SD 0.06) minutes (24 cores), with a difference of 1.3 minutes. At 30,000 requests per second, the mean values reach 7.5 (SD 0.28) and 5.6 (SD 0.19) minutes, respectively, with a difference of 1.9 minutes. These values correspond to an improvement of 4.15%, 20.05%, and 24.95%, respectively, when using 24 cores compared to the 8-core configuration.

Figure 2B provides a more detailed view by showing the processing time per data topic sent by the wearable device using the 24-core setup. When 500 requests per second are received, the time ranges between 4.7 and 4.9 minutes depending on the data topic. At 1500 requests per second, the range increases slightly (4.9 to 5.1 minutes). At 3000 requests per second, the time ranges from 5.4 to 5.8 minutes. This indicates a maximum difference of 25 seconds between the fastest and slowest topics (processed simultaneously), which reflects consistent behavior across data streams.

In Figure 3, actual data from the LifeSnaps dataset are shown using Grafana. In Figure 3A, the x-axis represents the date of the record, and the y-axis shows the calorie count, while in Figure 3B, the y-axis represents the number of breaths per minute. The data are plotted in real time, with an observed delay of approximately 4.6 minutes when 71 users are monitored. Two data sources are shown for illustration purposes: Figure 3A presents the number of calories burnt throughout the day, and Figure 3B shows the number of breaths per minute, both collected over several days.

XSL•FO
RenderX

Figure 3. Data received from wearable devices, ingested into the platform, and cleaned in the silver layer. (A) Daily calorie consumption and (B) number of breaths per minute.



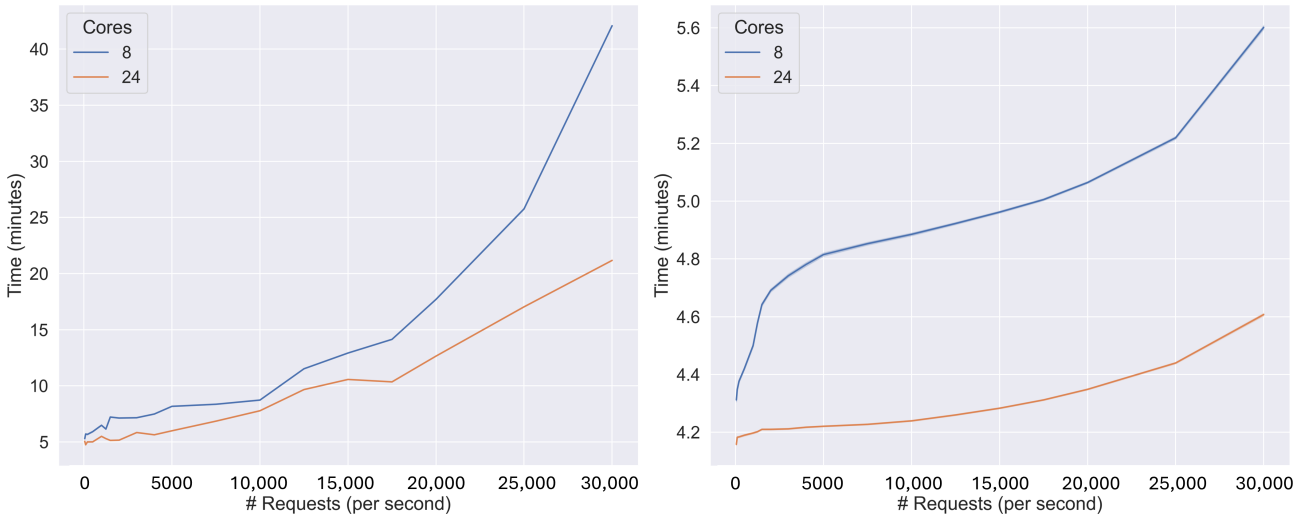
In summary, the computational cost as the platform load increases is evaluated, with the 24-core configuration being up to 24.95% more efficient than the 8-core configuration. The time measurements include the full processing pipeline (from data ingestion to visualization at the silver layer). Additionally, the time difference between data topics remains within 25 seconds under all tested loads, indicating uniform performance across heterogeneous sources. These results confirm that DeltaTrace maintains consistent latency and scales proportionally with the number of requests for data to be available for visualization and consultation.

Gold Layer: Data Aggregations

In this second set of experiments, the efficiency of DeltaTrace in performing aggregations over clean data under increasing loads is evaluated. The goal is to assess system performance when a real-time AI model and statistical aggregation processes continuously read data from the silver layer and write results to the gold layer. Computational time is measured under 8- and 24-core CPU configurations, as the request rate increases. In Figure 4, the x-axis represents the number of requests per second, while the y-axis indicates the processing time in minutes. The performance of the AI model is detailed in Multimedia Appendix 4.

XSL•FO
RenderX

Figure 4. Time required to process raw data from generation to plotting in the gold layer for both anomaly detection and statistical analysis, comparing 8- and 24-core configurations under increasing request rates. (A) Time from data generation to anomaly detection (gold) and (B) time from data generation to statistical analysis (gold).



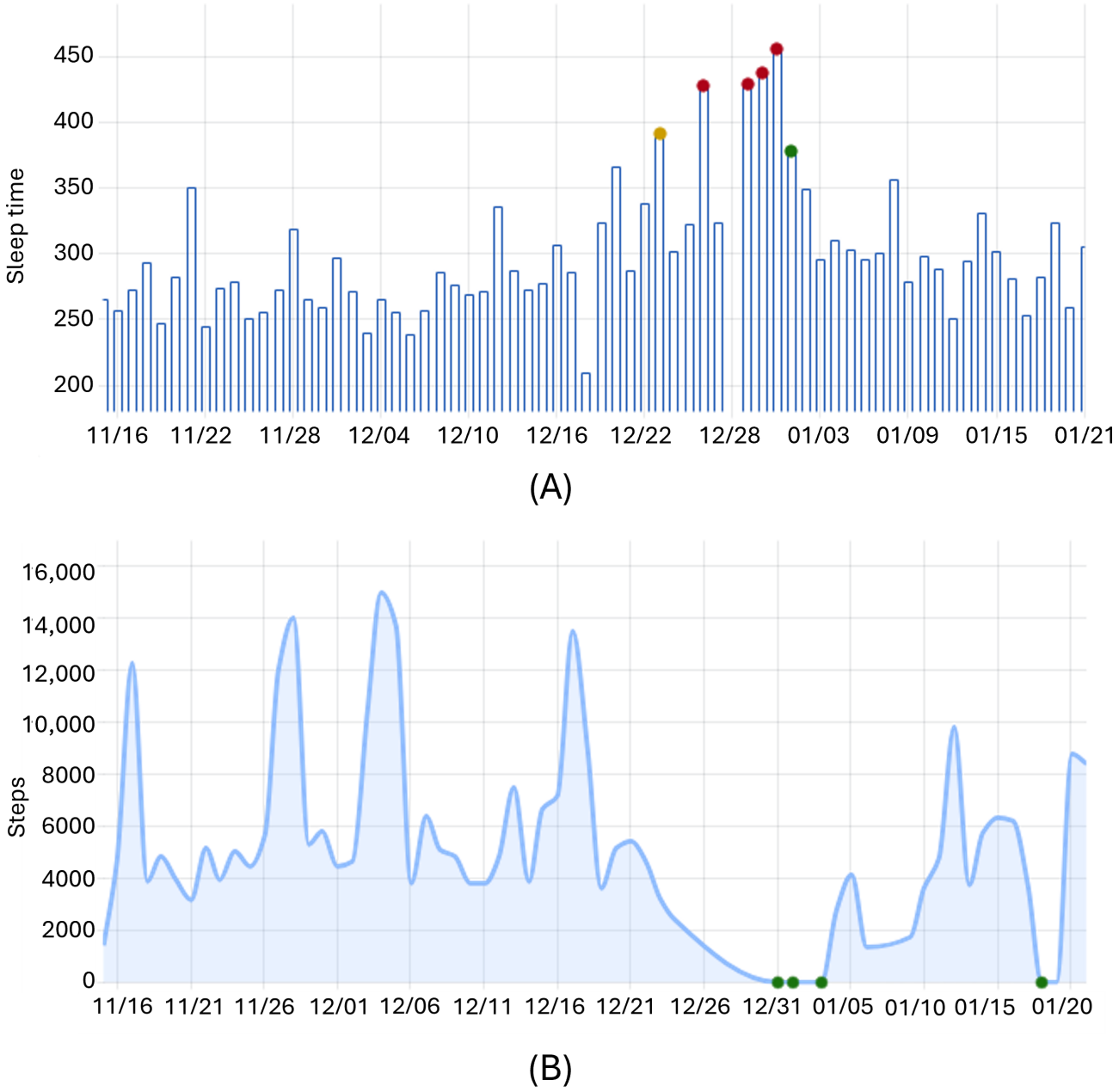
As shown in Figure 4A, the time required from the moment the data are sent until anomalies are generated and made available for visualization is represented on the y-axis, with the request rate shown on the x-axis. At 50 requests per second, the difference between the 8- and 24-core settings is 0.2 minutes. This difference increases to 2.1 minutes at 1500 requests per second and to 2.4 minutes at 15,000 requests per second. At 30,000 requests per second, the difference reaches 20.9 minutes. These results correspond to improvements of 3.78% at 50 requests per second, 18.58% at 15,000 requests per second, and 49.67% at 30,000 requests per second when using 24 cores compared to the 8-core setup. The 24-core configuration also consistently exhibits lower SDs, indicating more stable performance under all tested loads.

In Figure 4B, the processing time required to compute and visualize statistical aggregations (such as mean values) is shown. At 50 requests per second, the 24-core configuration processes data 0.1 minutes faster than the 8-core setup. This difference increases to 0.4 minutes at 1500 requests per second and to 0.7 minutes at 15,000 requests per second. At 30,000 requests per second, the difference reaches 1 minute. These values represent improvements of 8.62%, 14.11%, and 17.86%, respectively, when using the 24-core configuration.

The anomalies detected in the LifeSnaps dataset are presented in Figure 5. Figure 6A displays sleep duration (in minutes) for a single user, with anomalies marked in color based on the level of deviation from learned user patterns. In this case, consecutive anomalies appear between December 23, 2021, and January 1, 2022, with 1 yellow anomaly followed by 4 red and 1 green anomaly, all corresponding to unusually long sleep durations. In Figure 5B, step count data show 4 green anomalies identified as potential inactivity events, which could also be attributed to not wearing the wearable device during those days.

XSL•FO
RenderX

Figure 5. Visualization of behavioral anomalies in wearable data based on sleep and step patterns. Anomalies are marked in color: red (critical), yellow (moderate), and green (minor), indicating deviations from the typical pattern. (A) Sleep duration over time, measured in minutes with the detected anomalies and (B) step count per day with the detected anomalies.



In addition, a web application for health care professionals has been developed, as shown in Figure 6, being part of the application layer in Figure 1. Grafana panels are embedded for visual analysis and are continuously updated as new data arrive, with delays indicated in Figure 4. The left panel displays anomalies detected in daily step counts, while the right panel shows scores for the STAI anxiety trait. Unlike sensor data, STAI questionnaires are received at irregular intervals and processed in batches through tasks scheduled in Apache Airflow, which optimizes resource use for low-frequency sources. This configuration enables visual comparison between anomalies in activity data and self-reported questionnaire results.

XSL•FO
RenderX

Figure 6. Web application for health care professionals enabling user selection, visualization grouping, and date filtering. The left panel displays daily step count for the selected user, highlighting anomalies by deviation severity: red (critical), yellow (moderate), and green (minor). The right panel shows the reported score for the anxiety trait from the State-Trait Anxiety Inventory scale.



In summary, this set of experiments presents the computational time required to aggregate real-time data and make it available to health care professionals. When the request rate is 15,000 per second, statistical aggregations are available in approximately 4.3 minutes, whereas the anomaly detection model requires 10.5 minutes, times that are sufficient for several clinical use cases [37-45] and consistent with those reported in previous studies of similar big data platforms [10,46]. At lower request rates (below 15,000 per second), anomalies are computed in 5 to 10 minutes after the data are sent. However, at 30,000 requests per second, anomaly detection latency exceeds 40 minutes in the 8-core configuration, compared to 20 minutes in the 24-core setup. This nonlinear increase suggests saturation in the lower-resource configuration, with the latency line showing a marked nonlinearity (saturation) starting around 20,000 requests per second. This relationship is fitted by a quadratic model (polynomial regression, adjusted of 0.98 for 8 cores and 0.99 for 24 cores), confirming a significant nonlinear relationship (P<.0001 for the quadratic term). In contrast, statistical aggregations remain under 5.6 minutes across all loads, indicating more stable and scalable performance. These results highlight the need to allocate sufficient computational resources depending on the expected load and latency requirements for data to be available for visualization and consultation.

Discussion

Principal Findings

The experimental results demonstrate the performance of DeltaTrace across different data processing layers and system loads. In the first set of experiments, which focuses on the processing time from data generation to the silver layer, the platform can maintain mean processing times between 4.9 (SD 0.12) and 7.5 (SD 0.28) minutes depending on the request rate and data topic. The 24-core configuration shows improvements of up to 24.95% compared to the 8-core configuration. While perfect scaling would yield an improvement of 66%, this is unrealistic since part of the workload is not parallelizable. According to Amdahl's law [37], an efficiency of 80% - 85% would typically produce 25% - 40% improvement, consistent with our observation. In all cases, the delay between different data sources remains approximately 25 seconds, which confirms the consistency of the system across heterogeneous input streams.

In the second set of experiments, which evaluates the processing time to deliver statistical aggregations and anomaly detection in the gold layer, the computational demand of anomaly detection is higher than that of simple aggregations. With 15,000 requests per second, the time required for statistical output is approximately 4.3 minutes, whereas the time for anomaly detection reaches 10.5 minutes. At 30,000 requests per second, the 8-core configuration exceeds 40 minutes for anomaly detection, while the 24-core setup remains under 20 minutes. Statistical aggregations, in contrast, remain under 5.6 minutes in all configurations and scenarios, showing predictable and stable behavior.

These results demonstrate that DeltaTrace maintains stable performance and predictable latency under increasing data loads, confirming the scalability of the proposed architecture when limited computing resources are available. Beyond performance,

XSL•FO
RenderX

the experimental evaluation confirms that the platform design successfully fulfills the defined research objectives. The implemented mechanisms ensure versioning and traceability across all data processing layers, stable scalability under varying loads, and consistent operation of model management, scheduling, and monitoring components. These results demonstrate that DeltaTrace does not only integrate well-known technologies but also applies them within a coherent architecture that operationalizes traceability as a core and verifiable property of a health data platform. The real-time monitoring capabilities and traceability features evaluated in these experiments have direct implications for clinical applications, which are further elaborated in the following subsection.

Clinical Implications

DeltaTrace provides a transparent and reproducible foundation for clinical applications where accountability and data integrity are essential. By allowing clinicians to trace each alert or output back to its source data, processing pipeline, and model version, the platform builds trust in automated decision support. This is especially important when clinical actions depend on system-generated insights. The ability to monitor trends in sleep, mobility, or heart rate in near real time can support early identification of health deterioration, enabling more proactive care for older adults. These features make DeltaTrace a strong candidate for integration into remote patient monitoring programs and digital health strategies focused on prevention and early intervention.

In this work, the platform has been intentionally evaluated using a minimal hardware configuration to establish a lower bound on the resources required to provide near real-time processing. Under these conditions, DeltaTrace can detect and process anomalies for approximately 1500 users in under 10 minutes. This response time is suitable for a wide range of clinical and health monitoring applications where reactions within this time frame are beneficial. These include chronic conditions such as sleep apnea [38], hormonal cycle irregularities [39], or psychiatric events that evolve over time [40-42]. In contrast, other conditions, such as stroke, anaphylaxis, or cardiac arrest [43-45], require faster interventions, often within minutes. In such cases, additional resources (eg, graphics processing units [GPUs] for inference and multiple server nodes) can be deployed to reduce latency. Similar processing delays (5 to 10 minutes) have been reported in previous studies [10,46].

Comparison With Prior Work

Previous work has reported enhanced efficiency with Apache Spark and HDFS if more hardware resources are provided [47,48]. As reported by Sewal and Singh [49], the execution time can decrease from 1019 to 382 seconds if 5 nodes are provided, which implied an improvement of 73.51%. Similarly, evaluations reported by Buber and Diri [50] have shown that GPU-based processing can accelerate execution by a factor of 4 to 5 compared to CPU-only configurations. These enhancements can be achieved without requiring modifications to the software architecture, thereby maintaining consistency, traceability, and scalability across different deployment environments.

In this paper, a separate AI module with API-based communication is proposed for detecting anomalies in wearable data. This is a general design that provides a significant benefit, as the AI process is decoupled, and any AI task can be included in the pipeline without modifying the architecture, such as classification and clustering tasks. The MLflow framework allows the logging of any type of model, including ML and deep learning, and also state-of-the-art models such as large language models and transformer-based models. The software layer implemented on top of this architecture allows the evaluation of the performance when the load increases, being able to identify if the hardware allocation is proper for the specified AI task and use case. This design contributes to open challenges [51] and current trends [52] identified by previous reviews, especially with deep learning models such as recurrent neural networks, regarding model scaling, distributed computing, and high-scale data processing, all of these while keeping traceability features.

DeltaTrace also contributes to ongoing initiatives such as the European Health Data Space (EHDS) Regulation, which aims to establish a common framework for the secure use and exchange of health data within the European Union. Traceability and data governance are among the core pillars of this regulation [53-55]. The platform provides full traceability, including version control for data, models, and code, as well as detailed tracking of all transformations applied after data ingestion. These capabilities directly support EHDS requirements for auditability and transparency in both primary and secondary uses of health data [56,57]. In addition, the system integrates model management, resource monitoring, and real-time analytics under a unified architecture based on open source components, aligning with the EHDS objective of promoting trusted and scalable health data infrastructures [58]. These characteristics position DeltaTrace as a suitable technical foundation for future EHDS-compliant deployments.

This alignment with EHDS is particularly valuable when comparing DeltaTrace with previous work, as most existing platforms focus primarily on large-scale data processing, real-time analytics, or specific task performance but provide limited support for traceability, versioning, model management, and comprehensive orchestration. As shown in Table 1, many prior studies omit key mechanisms for tracking data and model transformations, monitoring system resources, and ensuring reproducibility across the pipeline. In contrast, DeltaTrace integrates end-to-end versioning of datasets and models through MLflow, robust orchestration and workflow scheduling via Apache Airflow, scalable processing of batch and streaming data with Apache Spark, and fault-tolerant storage and metadata management with Delta Lake. By combining these capabilities, DeltaTrace ensures traceability, auditability, and reproducibility, providing a more comprehensive and transparent framework for health data management and a stronger technical foundation for EHDS-compliant deployments.

Limitations

The evaluation of DeltaTrace was first conducted in a single-server environment to establish a controlled baseline and analyze system performance under stable and reproducible

XSL•FO
RenderX

conditions. Within this setup, experiments were executed using constant data input rates and a fixed anomaly detection model, which simplified testing and allowed for consistent performance assessment. This configuration may not fully reflect the variability and operational challenges present in multinode or real-world deployments. In the current implementation, the AI inference module operates as a standalone Python service, which may limit scalability compared to the distributed data processing components. However, the modular architecture based on containerized services allows future extensions toward distributed or parallel inference using orchestration frameworks such as Kubernetes. This design intentionally separates the AI inference module from the distributed data layer to enable flexible integration of custom deep learning pipelines. For the present implementation, these distributed capabilities have not been tested, and this represents a limitation of the current proposal. Moreover, the anomaly detection model cannot, in its current form, distinguish between true behavioral anomalies (eg, inactivity) and data quality issues (eg, sensor nonadherence or device-off). Additionally, aspects such as human interaction and workflow integration were not examined. Despite these constraints, the obtained results provide a solid foundation for understanding DeltaTrace behavior under controlled conditions and for guiding future evaluations in larger and more dynamic environments.

Strengths and Future Work

All technologies composing the platform are open source, offering transparency, adaptability, and long-term sustainability. This choice also supports future work focused on enhancing the security and interoperability mechanisms of the proposed big data platform [59]. Core components such as Kafka, Delta Lake, MLflow, and Airflow include built-in features such as encrypted data transmission (Transport Layer Security), encrypted storage (Advanced Encryption Standard), role-based access control, and execution logging, which are integrated into the platform. Data processed throughout the system are consistently associated with anonymized identifiers, used to securely match heterogeneous sources such as questionnaire responses and physiological signals. These identifiers are also used by the AI module to construct temporal sequences and apply sliding window techniques across unified data streams. Although accountability, data integrity, and traceability are demonstrated through system mechanisms and workflow examples (Figure 1 and Multimedia Appendix 3), their empirical validation under real deployment conditions remains part of future work.

Future work will include testing the platform in distributed and GPU-accelerated environments to further assess performance and responsiveness under higher data volumes. Further evaluations will also involve human-in-the-loop scenarios to examine usability and workflow integration in operational health settings. In addition, new developments will focus on implementing advanced access control mechanisms and extending support to other data modalities, including imaging, audio, and unstructured text. These developments aim to enhance interoperability and clinical applicability while maintaining the architectural principles that ensure full traceability.

Conclusions

This study set aimed to design and evaluate a health data platform where traceability is implemented as a central architectural feature integrated with model management, orchestration, and visualization components. DeltaTrace supports both real-time and batch processing of health-related data with built-in traceability features. In this evaluation, continuous monitoring from wearable devices has been used to assess real-time processing, while questionnaire data have been included as a representative case of batch ingestion. The evaluation demonstrated that the platform can sustain near real-time performance, processing data for approximately 1500 users with end-to-end delays below 10 minutes on a single CPU-based server. These findings confirm that the platform achieves scalable and reproducible processing under constrained computational resources.

By embedding traceability within the data lifecycle and integrating complementary components for monitoring and management, DeltaTrace addresses key requirements for auditability, reproducibility, and accountability in digital health infrastructures. The platform aligns with the objectives of the EHDS by providing a technical foundation that supports secure, version-controlled, and verifiable health data processing. The evaluation confirms that the proposed design effectively meets the defined research objectives, demonstrating that traceability, scalability, and coordinated management can be achieved within a unified and reproducible platform architecture. Future work will focus on extending DeltaTrace to strengthen privacy, interoperability, and the inclusion of additional data modalities, further aligning the platform with the long-term goals of the EHDS.

Acknowledgments

The authors would like to acknowledge the work done by researchers Markel Arrojo, Naroa Mendez, and Daniel R Torres from Vicomtech. ChatGPT 5 (OpenAI) was used only for language editing. All scientific content was generated and verified by the authors.

Funding

This research was funded by the government of the Basque Country (grant ZE-2021/00003).

XSL•FO
RenderX

Data Availability

The data sets and source code generated and analyzed during this study are available from the corresponding author on reasonable request. The LifeSnaps dataset analyzed during this study is available in Kaggle [36].

Authors' Contributions

Conceptualization: A Cejudo, AB
Methodology: A Cejudo, AB, YT, A Calvo
Software: A Cejudo, YT, A Calvo
Validation: AB, CM, AA
Data curation: A Cejudo, YT, A Calvo
Writing—original draft preparation: A Cejudo, YT
Writing—review and editing: A Cejudo, AB, CM, AA
Supervision: AB, CM, AA
Project administration: AB
Funding acquisition: AB

Conflicts of Interest

None declared.

Multimedia Appendix 1
Overview of recent studies using big data capabilities in health-related applications.
[DOCX File, 32 KB - medinform_v13i1e81701_app1.docx]

Multimedia Appendix 2
Software components of the DeltaTrace platform, including Airflow, Hadoop Distributed File System, Kafka, Spark, Delta Lake, Docker, Grafana, MLflow, and PostgreSQL.
[DOCX File, 24 KB - medinform_v13i1e81701_app2.docx]

Multimedia Appendix 3
DeltaTrace platform configuration and workflow, with MLflow screenshots, Airflow directed acyclic graphs, and example configuration files for data ingestion and processing.
[DOCX File, 970 KB - medinform_v13i1e81701_app3.docx]

Multimedia Appendix 4
Results of artificial intelligence–based time-series modeling for anomaly detection in wearable data, comparing baseline, machine learning, and deep learning models with mean absolute error and root mean squared error metrics.
[DOCX File, 33 KB - medinform_v13i1e81701_app4.docx]

References

1. Decade of healthy ageing: baseline report. : World Health Organization; 2021 URL: https://www.who.int/publications/i/item/9789240017900 [accessed 2025-12-05]
2. Department of Economic and Social Affairs. World population ageing 2023: challenges and opportunities of population ageing in the least developed countries. : United Nations Research Institute for Social Development; 2024.
3. Tomita A, Leyna GH, Kim HY, et al. Patterns of multimorbidity and their association with hospitalisation: a population-based study of older adults in urban Tanzania. Age Ageing 2021 Jun 28;50(4):1349-1360. [doi: 10.1093/ageing/afab046]
4. Guo J, Huang X, Dou L, et al. Aging and aging-related diseases: from molecular mechanisms to interventions and treatments. Signal Transduct Target Ther 2022 Dec 16;7(1):391. [doi: 10.1038/s41392-022-01251-0] [Medline: 36522308]
5. Mbata AO, Soyege OS, Nwokedi CN, et al. Preventative medicine and chronic disease management: reducing healthcare costs and improving long-term public health. Int J Multidisc Res Growth Eval 2024;5(6):1584-1600. [doi: 10.54660/.IJMRGE.2024.5.6.1584-1600]
6. Rina S, Aldiana A, Putri UT, Saputra A, Muhammad HD. The importance of early detection in disease management. J World Future Med Health Nurs 2024;2:51-63. [doi: 10.55849/health.v2i1.692]
7. Kanakaprabha S, Ganesh KG, Peddi RB, Ravi RY, Mohan RPC. Wearable devices and health monitoring: big data and AI for remote patient care. In: Intelligent Data Analytics for Bioinformatics and Biomedical Systems: Wiley; 2024:291-311. [doi: 10.1002/9781394270910]

XSL•FO
RenderX

8. Qiao S, Li X, Olatosi B, Young SD. Utilizing Big Data analytics and electronic health record data in HIV prevention, treatment, and care research: a literature review. AIDS Care 2024 May 3;36(5):583-603. [doi: 10.1080/09540121.2021.1948499]
9. Al-Quraishi T, Al-Quraishi N, AlNabulsi H, AL-Qarishey H, Ali AH. Big data predictive analytics for personalized medicine: perspectives and challenges. Appl Data Sci Anal 2024;2024:32-38. [doi: 10.58496/ADSA/2024/004]
10. Bahmani A, Alavi A, Buergel T, et al. A scalable, secure, and interoperable platform for deep data-driven health management. Nat Commun 2021;12(1):5757. [doi: 10.1038/s41467-021-26040-1]
11. Cruz R, Guimarães T, Peixoto H, Santos MF. Architecture for intensive care data processing and visualization in real-time. Procedia Comput Sci 2021;184:923-928. [doi: 10.1016/j.procs.2021.03.115]
12. Ismail A, Sazali FH, Agos Jawaddi SN, Mutalib S. Stream ETL framework for Twitter-based sentiment analysis: leveraging big data technologies. Expert Syst Appl 2025 Feb;261:125523. [doi: 10.1016/j.eswa.2024.125523]
13. Saeed MA, Saeed MA. Real-time diabetes detection using machine learning and Apache Spark. Presented at: 2024 4th International Conference on Emerging Smart Technologies and Applications (eSmarTA); Aug 6-7, 2024. [doi: 10.1109/eSmarTA62850.2024.10638853]
14. Saleh H, McCann M, El-Sappagh S, Breslin JG. TransformerFusionNet: a real-time multimodal framework for ICU heart failure mortality prediction using big data streaming. Presented at: 2024 International Conference on Computer and Applications (ICCA); Dec 2, 2024. [doi: 10.1109/ICCA62237.2024.10927742]
15. Ahmed M, Dar AR, Helfert M, Khan A, Kim J. Data provenance in healthcare: approaches, challenges, and future directions. Sensors (Basel) 2023 Jul 18;23(14):6495. [doi: 10.3390/s23146495] [Medline: 37514788]
16. Xie M, Zhang Z, Hong H, Zhang G, Qin Y. Secure medical data sharing featuring traceable data usage and automatic audit mechanism. IEEE Internet Things J 2025;12(13):25587-25600. [doi: 10.1109/JIOT.2025.3559926]
17. Liu H. Research on health management system based on big data technology. Presented at: ICBDR 2022: The 6th International Conference on Big Data Research; Aug 10-12, 2022. [doi: 10.1145/3564665.3564677]
18. Belbasis L, Panagiotou OA. Reproducibility of prediction models in health services research. BMC Res Notes 2022 Jun 11;15(1):204. [doi: 10.1186/s13104-022-06082-4] [Medline: 35690767]
19. Mora-Cantallops M, Sánchez-Alonso S, García-Barriocanal E, Sicilia MA. Traceability for trustworthy AI: a review of models and tools. Big Data Cogn Comput 2021;5(2):20. [doi: 10.3390/bdcc5020020]
20. Ed-daoudy A, Maalmi K, El Ouaazizi A. A scalable and real-time system for disease prediction using big data processing. Multimed Tools Appl 2023 Aug;82(20):30405-30434. [doi: 10.1007/s11042-023-14562-3]
21. Yıldırım E, Çalhan A, Cicioğlu M. Performance analysis of disease diagnostic system using IoMT and real‐time data analytics. Concurr Comput 2022 Jun 10;34(13):e6916. [doi: 10.1002/cpe.6916]
22. Ismail Ebada A, Elhenawy I, Jeong CW, Nam Y, Elbakry H, Abdelrazek S. Applying Apache Spark on streaming big data for health status prediction. Comput Mater Contin 2022;70(2):3511-3527. [doi: 10.32604/cmc.2022.019458]
23. Rashid M, Singh H, Goyal V, Parah SA, Wani AR. Big data based hybrid machine learning model for improving performance of medical internet of things data in healthcare systems. In: Healthcare Paradigms in the Internet of Things Ecosystem: Academic Press; 2021:47-62. [doi: 10.1016/B978-0-12-819664-9.00003-X]
24. Zheng X, Ding X. Research on medical big data of health management platform based on Hadoop. Presented at: 2022 21st International Symposium on Distributed Computing and Applications for Business Engineering and Science (DCABES); Oct 14-18, 2022. [doi: 10.1109/DCABES57229.2022.00062]
25. Tu Y, Lu Y, Chen G, Zhao J, Yi F. Architecture design of distributed medical big data platform based on Spark. Presented at: 2019 IEEE 8th Joint International Information Technology and Artificial Intelligence Conference (ITAIC); May 24-26, 2019. [doi: 10.1109/ITAIC.2019.8785620]
26. Usha MG, Shreya MS, Supreeth S, Shruthi G, Pruthviraja D, Chavan P. Kidney tumor detection using MLflow, DVC and deep learning. Presented at: 2024 Second International Conference on Advances in Information Technology (ICAIT); Jul 24-27, 2024. [doi: 10.1109/ICAIT61638.2024.10690537]
27. Benjelloun S, Aissi MEME, Loukili Y, et al. Big data processing: batch-based processing and stream-based processing. Presented at: 2020 Fourth International Conference on Intelligent Computing in Data Sciences (ICDS); Oct 21-23, 2020. [doi: 10.1109/ICDS50568.2020.9268684]
28. Harenslak Bas P, De Ruiter J. Data Pipelines with Apache Airflow: Simon and Schuster; 2021.
29. Salahaldin J, Achim V, Andrey V. Learning PostgreSQL: Packt Publishing Ltd; 2015.
30. Zaharia M, Xin RS, Wendell P, et al. Apache Spark. Commun ACM 2016 Oct 28;59(11):56-65. [doi: 10.1145/2934664]
31. Cejudo A, Beristain A, Almeida A, Rebescher K, Martín C, Macía I. Smart home-assisted anomaly detection system for older adults: a deep learning approach with a comprehensive set of daily activities. Med Biol Eng Comput 2025 Jun;63(6):1821-1835. [doi: 10.1007/s11517-025-03308-y]
32. Medsker LR, Jain LC. Recurrent Neural Networks: Design and Applications: CRC Press; 2001.
33. Su Y, Zhao Y, Niu C, Liu R, Sun W, Pei D. Robust anomaly detection for multivariate time series through stochastic recurrent neural network. Presented at: Proceedings of the 25th ACM SIGKDD International Conference on Knowledge Discovery & Data Mining; Aug 4-8, 2019. [doi: 10.1145/3292500.3330672]
34. Patel Aakash K, Vamsi R, Shumway Karlie R, Physiology AJF. Sleep Stages: StatPearls Publishing; 2025.

XSL•FO
RenderX

35. Del Bene Victor E. Temperature, 3rd edition: Butterworths; 1990.
36. Yfantidou S, Karagianni C, Efstathiou S, et al. LifeSnaps, a 4-month multi-modal dataset capturing unobtrusive snapshots of our lives in the wild. Sci Data 2022;9(1):663. [doi: 10.1038/s41597-022-01764-x]
37. Gebremichael L. Scalability and efficiency in multi-core and many-core advanced computing systems. J Adv Comput Syst 2024;4(9):45-53. [doi: 10.69987/JACS.2024.40905]
38. Marin-Oto M, Vicente EE, Marin JM. Long term management of obstructive sleep apnea and its comorbidities. Multidisc Respir Med 2019;14:21. [doi: 10.1186/s40248-019-0186-3] [Medline: 31312448]
39. Masuda H, Okada S, Shiozawa N, et al. Machine learning model for menstrual cycle phase classification and ovulation day detection based on sleeping heart rate under free-living conditions. Comput Biol Med 2025 Mar;187:109705. [doi: 10.1016/j.compbiomed.2025.109705]
40. Tazarv A, Labbaf S, Reich SM, Dutt N, Rahmani AM, Levorato M. Personalized stress monitoring using wearable sensors in everyday settings. Presented at: 2021 43rd Annual International Conference of the IEEE Engineering in Medicine & Biology Society (EMBC); Nov 1-5, 2021. [doi: 10.1109/EMBC46164.2021.9630224]
41. Dalmeida KM, Masala GL. HRV features as viable physiological markers for stress detection using wearable devices. Sensors (Basel) 2021 Apr 19;21(8):2873. [doi: 10.3390/s21082873] [Medline: 33921884]
42. Banerjee JS, Mahmud M, Brown D. Heart rate variability-based mental stress detection: an explainable machine learning approach. SN Comput Sci 2023;4(2). [doi: 10.1007/s42979-022-01605-z]
43. Rao G, Savage DW, Erickson G, Kyryluk N, Lingras P, Mago V. Enhancing cardiopulmonary resuscitation quality using a smartwatch: neural network approach for algorithm development and validation. JMIR Mhealth Uhealth 2025 May 5;13:e57469. [doi: 10.2196/57469] [Medline: 40324161]
44. Emergency treatment of anaphylaxis guidelines for healthcare providers. : Resuscitation Council UK; 2021 URL: https://www.resus.org.uk/sites/default/files/2021-05/Emergency%20Treatment%20of%20Anaphylaxis%20May%202021_0.pdf [accessed 2025-12-05]
45. Zhang Z, Wu X, Zou Z, et al. Heat stroke: pathogenesis, diagnosis, and current treatment. Ageing Res Rev 2024;100:102409. [doi: 10.1016/j.arr.2024.102409] [Medline: 38986844]
46. Dhinakaran D, Edwin Raja S, Ramesh T, Thevahi B, Prabaharan G. SI-CL-SDEO algorithm for improving HDFS performance and data reliability. Results Eng 2025 Jun;26:104773. [doi: 10.1016/j.rineng.2025.104773]
47. Khotimah H, Wilda Al Aluf B, Ari Rifqi M, Hernawan A, Satya Nugraha G. Performance analysis of the distributed support vector machine algorithm using Spark for predicting flight delays. E3S Web Conf 2023;465:02037. [doi: 10.1051/e3sconf/202346502037]
48. Cahya Indirman MD, Wiriasto GW, Irfan Akbar LAS. Distributed machine learning using HDFS and Apache Spark for big data challenges. E3S Web Conf 2023;465:02058. [doi: 10.1051/e3sconf/202346502058] [Medline: 37703057]
49. Sewal P, Singh H. Performance comparison of Apache Spark and Hadoop for machine learning based iterative GBTR on HIGGS and Covid-19 datasets. Scalable Comput Pract Exp 2024;25(3):1373-1386. [doi: 10.12694/scpe.v25i3.2687]
50. Buber E, Diri B. Performance analysis and CPU vs GPU comparison for deep learning. Presented at: 2018 6th International Conference on Control Engineering & Information Technology (CEIT); Oct 5-27, 2018. [doi: 10.1109/CEIT.2018.8751930]
51. Selmy HA, Mohamed HK, Medhat W. Big data analytics deep learning techniques and applications: a survey. Inf Syst 2024 Feb;120:102318. [doi: 10.1016/j.is.2023.102318]
52. Alam MA, Sajib M, Rahman F, et al. Implications of big data analytics, AI, machine learning, and deep learning in the health care system of Bangladesh: scoping review. J Med Internet Res 2024 Oct 28;26:e54710. [doi: 10.2196/54710] [Medline: 39466315]
53. Terzis P, Santamaria Echeverria OE. Interoperability and governance in the European Health Data Space regulation. Med Law Int 2023 Dec;23(4):368-376. [doi: 10.1177/09685332231165692]
54. Raab R, Küderle A, Zakreuskaya A, et al. Federated electronic health records for the European Health Data Space. Lancet Digit Health 2023 Nov;5(11):e840-e847. [doi: 10.1016/S2589-7500(23)00156-5] [Medline: 37741765]
55. Evroux C, Heflich A, Saulnier JL. Towards EU leadership in the space sector through open strategic autonomy—cost of non-Europe. European Parliamentary Research Service. 2023. URL: https://www.europarl.europa.eu/thinktank/en/document/EPRS_STU(2023)734691 [accessed 2025-12-06]
56. Li W, Quinn P. The European Health Data Space: an expanded right to data portability? Comput Law Secur Rev 2024 Apr;52:105913. [doi: 10.1016/j.clsr.2023.105913]
57. van Drumpt S, Chawla K, Barbereau T, Spagnuelo D, van de Burgwal L. Secondary use under the European Health Data Space: setting the scene and towards a research agenda on privacy-enhancing technologies. Front Digit Health 2025;7:1602101. [doi: 10.3389/fdgth.2025.1602101]
58. Implementing the European Health Data Space. : EIT Health Think Tank; 2024 URL: https://eithealth.eu/think-tank-topic/implementing-the-european-health-data-space/ [accessed 2025-12-06]
59. Kapitan D, Heddema F, Dekker A, Sieswerda M, Verhoeff BJ, Berg M. Data interoperability in context: the importance of open-source implementations when choosing open standards. J Med Internet Res 2025 Apr 15;27:e66616. [doi: 10.2196/66616] [Medline: 40232773]

XSL•FO
RenderX

Abbreviations

ACID: atomicity, consistency, isolation, and durability
AI: artificial intelligence
API: application programming interface
AttentionLSTM: attention-based long short-term memory
CPU: central processing unit
DAG: directed acyclic graph
EHDS: European Health Data Space
ELT: extract, load, transform
ETL: extract, transform, load
GPU: graphics processing unit
HDFS: Hadoop Distributed File System
ML: machine learning
PSQL: PostgreSQL
REST: Representational State Transfer
STAI: State-Trait Anxiety Inventory

Edited by A Coristine; submitted 02.08.25; peer-reviewed by CFR Geyer, MRU Zaman Sajib; revised version received 24.11.25; accepted 24.11.25; published 22.12.25.

Please cite as:
Cejudo A, Tellechea Y, Calvo A, Almeida A, Martín C, Beristain A
Scalable Big Data Platform With End-to-End Traceability for Health Data Monitoring in Older Adults: Development and Performance Evaluation
JMIR Med Inform 2025;13:e81701
URL: https://medinform.jmir.org/2025/1/e81701
doi:10.2196/81701

© Ander Cejudo, Yone Tellechea, Amaia Calvo, Aitor Almeida, Cristina Martín, Andoni Beristain. Originally published in JMIR Medical Informatics (https://medinform.jmir.org), 22.12.2025. This is an open-access article distributed under the terms of the Creative Commons Attribution License (https://creativecommons.org/licenses/by/4.0/), which permits unrestricted use, distribution, and reproduction in any medium, provided the original work, first published in JMIR Medical Informatics, is properly cited. The complete bibliographic information, a link to the original publication on https://medinform.jmir.org/, as well as this copyright and license information must be included.

XSL•FO
RenderX

A Weighted Voting Approach for Traditional Chinese Medicine Formula Classification Using Large Language Models: Algorithm Development and Validation Study

Zhe Wang[1,2], MSc; Keqian Li[3], MM; Suyuan Peng[4], MD, PhD; Lihong Liu[4], MM; Xiaolin Yang[1], PhD; Keyu Yao[4], PhD; Heinrich Herre[2,5], Prof Dr; Yan Zhu[4], PhD

[1]Institute of Basic Medical Sciences, Chinese Academy of Medical Sciences; School of Basic Medicine, Peking Union Medical College, Beijing, China

[2]Institute for Medical Informatics, Statistics and Epidemiology, University of Leipzig, Leipzig, Germany

[3]School of Medical Information, Changchun University of Chinese Medicine, Changchun, China

[4]Institute of Information on Traditional Chinese Medicine, China Academy of Chinese Medical Sciences, No 16, Nanxiao Street, Dongzhimen, Beijing, China

[5]Institute for Computer Science, University of Leipzig, Leipzig, Germany

Corresponding Author:
Yan Zhu, PhD
Institute of Information on Traditional Chinese Medicine, China Academy of Chinese Medical Sciences, No 16, Nanxiao Street, Dongzhimen, Beijing, China

Abstract

Background: Several clinical cases and experiments have demonstrated the effectiveness of traditional Chinese medicine (TCM) formulas in treating and preventing diseases. These formulas contain critical information about their ingredients, efficacy, and indications. Classifying TCM formulas based on this information can effectively standardize TCM formulas management, support clinical and research applications, and promote the modernization and scientific use of TCM. To further advance this task, TCM formulas can be classified using various approaches, including manual classification, machine learning, and deep learning. Additionally, large language models (LLMs) are gaining prominence in the biomedical field. Integrating LLMs into TCM research could significantly enhance and accelerate the discovery of TCM knowledge by leveraging their advanced linguistic understanding and contextual reasoning capabilities.

Objective: The objective of this study is to evaluate the performance of different LLMs in the TCM formula classification task. Additionally, by employing ensemble learning with multiple fine-tuned LLMs, this study aims to enhance classification accuracy.

Methods: The data for the TCM formula were manually refined and cleaned. We selected 10 LLMs that support Chinese for fine-tuning. We then employed an ensemble learning approach that combined the predictions of multiple models using both hard and weighted voting, with weights determined by the average accuracy of each model. Finally, we selected the top 5 most effective models from each series of LLMs for weighted voting (top 5) and the top 3 most accurate models of 10 for weighted voting (top 3).

Results: A total of 2441 TCM formulas were curated manually from multiple sources, including the Coding Rules for Chinese Medicinal Formulas and Their Codes, the Chinese National Medical Insurance Catalog for proprietary Chinese medicines, textbooks of TCM formulas, and TCM literature. The dataset was divided into a training set of 1999 TCM formulas and test set of 442 TCM formulas. The testing results showed that Qwen-14B achieved the highest accuracy of 75.32% among the single models. The accuracy rates for hard voting, weighted voting, weighted voting (top 5), and weighted voting (top 3) were 75.79%, 76.47%, 75.57%, and 77.15%, respectively.

Conclusions: This study aims to explore the effectiveness of LLMs in the TCM formula classification task. To this end, we propose an ensemble learning method that integrates multiple fine-tuned LLMs through a voting mechanism. This method not only improves classification accuracy but also enhances the existing classification system for classifying the efficacy of TCM formula.

(JMIR Med Inform 2025;13:e69286) doi:10.2196/69286

KEYWORDS

traditional Chinese medicine; TCM formula classification; large language models; ensemble learning; algorithm development

XSL•FO
RenderX

Introduction

Background

Traditional Chinese medicine (TCM) formulas are combinations of medicinal substances developed through clinical experience and guided by TCM theory. They are developed through a systematic process involving syndrome differentiation, etiological analysis, determination of therapeutic principles, selection of appropriate herbs, dosage adjustment, formulation considerations, and specification of use, all in accordance with fundamental compositional structures [1]. Several studies have shown that TCM formulas have significant efficacy in the treatment and prevention of disease in both clinical and experimental studies [2-4]. A randomized clinical trial demonstrated that the TCM compound Tongxinluo significantly improved clinical outcomes in patients diagnosed with ST-segment elevation myocardial infarction [5]; the traditional medicine Pien Tze Huang prevents colorectal cancer by influencing the gut microbiota, enhancing beneficial metabolites, and suppressing oncogenic and proinflammatory factors [6].

Classical TCM formulas represent exemplary applications of TCM prescriptions. The selection and cataloging system for classical formulas streamlines the approval process for Chinese herbal compound preparations by exempting them from pharmacological studies and clinical trial data submissions. These formulas are defined as “those derived from ancient classical prescriptions that remain widely used today, demonstrate proven efficacy, exhibit distinctive characteristics and advantages, and were documented in medical texts prior to or during the Qing Dynasty.” However, after thousands of years of clinical practice, TCM has accumulated an immense number of formulas by the late Qing period, incomplete statistics indicate that over 100,000 had been recorded [7]. Current TCM formula textbooks and national standards still follow the efficacy-oriented classification system established in Wang Ang’s Qing Dynasty work *Yi Fang Ji Jie* (Compilation of Medical Formulas, 医方集解) [8]. Prior to the introduction of this system, many formulas lacked clear categorization, making manual classification both labor-intensive and susceptible to inconsistencies.

As the foundation of TCM syndrome differentiation and treatment, systematic classification of TCM formulas based on efficacy enables a comprehensive exploration of their latent information and reveals herb-disease relationship patterns. Previous research primarily relied on expert experience to develop classification systems organized by therapeutic methods (efficacy) [9,10]. With advances in artificial intelligence, new methodological pathways have emerged for automated formula classification. Gu [11] used the k-nearest neighbor algorithm in machine learning to calculate and classify the similarity of TCM formulas. However, the complex relationships between herbs and diseases in TCM formulas complicate the classification process. Cheng et al [12] present an improved deep learning model: S-TextBLCNN for the TCM formula classification task; it has an accuracy of 0.858 and an F_1-score of 0.762. To further explore the optimal deep learning models in the TCM formula classification task, Ren et al [13] combined several deep learning models to classify TCM formulas and found that bidirectional encoder representation from transformers-convolutional neural network was the most effective, achieving an accuracy of 77.87%, as well as weighted precision, weighted recall, and weighted F_1-score of 79.46%, 77.87%, and 77.44%, respectively. In 2022, OpenAI released applications such as ChatGPT [14], have demonstrated strong performance in tasks like question answering and translation. Moreover, large language models (LLMs) have achieved remarkable results in the biomedical domain. For instance, Google’s Med-PaLM2, which was fine-tuned from PaLM2 using data from the medical domain, achieved 86.5% accuracy on the MedQA dataset [15], which is close to the response level of clinical doctors [16]. Nijkamp et al [17] have trained the ProGen2 model on many different sequence datasets and demonstrated state-of-the-art performance both in generating novel viable protein sequences and in predicting protein fitness tasks. Some scholars tried to use LLMs to classify the text [18,19], therefore, to verify the classification ability of LLMs. In our previous study [20], we used the prompt templates and LLMs, such as ChatGLM-6B [21], ChatGLM2-6B [22], InternLM-20B [23], ChatGLM-130B [24], and ChatGPT, to classify TCM formula and validate the potential of LLMs in the field of TCM.

Based on our previous study [20], this study further explores the classification of TCM formulas by fine-tuning 10 distinct LLMs. It introduces an ensemble voting method based on multiple fine-tuned LLMs. This approach emphasizes the integration of predictions from each model through voting mechanisms, including both hard voting and weighted voting. The adoption of multiple LLMs for TCM formula classification offers a novel perspective on the application of LLMs in the field of TCM.

Research Question

In our previous work [20], we used LLMs to investigate TCM formula classification. We used prompt templates and both fine-tuned and original LLMs. The experimental results demonstrated that fine-tuned LLMs can enhance classification task accuracy. Therefore, in this study, we aim to explore the potential of LLMs in TCM formula classification tasks and rationality by posing the following research questions (RQs):

- RQ1: What is the performance of different LLMs for TCM formula classification?
- RQ2: How to improve the performance of TCM formula classification by multiple LLMs?
- RQ3: What is the rationality of TCM formula classification using LLMs?

To explore RQ1, we used 10 LLMs and fine-tuned them on a manually curated TCM formula dataset, followed by a comparative analysis of the results. To address RQ2, we used an ensemble learning approach. Using the average accuracy derived from the fine-tuned LLMs as model weights, we performed both hard and weighted voting on the results. In addition, we explored the effectiveness of different strategies, including selecting the best-performing model within each category and weighted voting based on the 3 best-performing models, to determine the approach that yields optimal results.

XSL•FO
RenderX

To investigate RQ3, TCM experts manually reviewed the predicted results generated by the fine-tuned LLMs. This process involved analyzing discrepancies between the voting results of the LLMs and the reference answer, thereby exploring the rationality behind the classification by the LLMs in the TCM formula classification task.

Methods

Data Preparation

We used 2441 TCM formulas manually curated from the Coding Rules for Chinese Medicinal Formulas and Their Codes [25], the Chinese National Medical Insurance Catalog for proprietary Chinese medicines (2023) [26], and textbooks of formulas of Chinese medicine [10]. After manual review [13], each formula consists of the formula name, ingredients, efficacy, and indications. The data processing procedure is as follows: only efficacy-related classifications are retained, while non-efficacy classifications, such as ethnic minority medicine, are removed; formulas under identical or similar classifications are consolidated (with classification names standardized according to national guidelines), while unique formula classifications are preserved; finally, the resulting data are subjected to deduplication.

In the Qing Dynasty, Wang Ang, in his work *Yifang Jijie*, proposed an integrated classification method that prioritized the efficacy of the TCM formula. This method was not only used in the textbooks of Chinese medicine formulas throughout various dynasties [27] and the secondary classification of the Chinese National Medical Insurance Catalog for proprietary Chinese medicines [28] but also served as the method used in the national standard, the Coding Rules for Chinese Medicinal Formulas and Their Codes. Therefore, this study established a harmonized efficacy classification system based on national standards, integrating multisource TCM formula data through structural realignment and category consolidation (the data remain intact with only standardized nomenclature adjustments made to classification categories exhibiting terminological variations, following national regulatory requirements), resulting in 22 standardized categories. However, The emetic formulations category contained insufficient samples and was therefore excluded; based on this categorization, a total of 2441 formulations were identified across 21 categories, as detailed in Table 1.

Table . Statistical information of traditional Chinese medicine formula data.

Standard efficacy	Abbreviation	Chinese name	Formulations (N=2441), n (%)
Supplementing and boosting formula	SBF	补益剂	417 (17.08)
Heat-clearing formula	HCF	清热剂	411 (16.84)
Blood-regulating formula	BRF	理血剂	372 (15.24)
Desiccating formula	DF	祛湿剂	246 (10.08)
Superficies relieving formula	SF	解表剂	160 (6.55)
Resolving phlegm relieving cough and relieving wheezing formula	RPRCRWF	化痰-止咳-平喘剂	160 (6.55)
Qi regulated formula	QRF	理气剂	134 (5.49)
Formula for wind disorder	FWD	治风剂	119 (4.86)
Warming interior formula	WIF	温里剂	73 (2.99)
Formula for purgation	FP	泻下剂	60 (2.46)
Reconciling formula	RF	和解剂	43 (1.76)
Tranquillization formula	TF	安神剂	39 (1.60)
Digestive formula	DIF	消食剂	38 (1.56)
Astringent formula	AF	固涩剂	32 (1.31)
Softening hard lumps and dispelling nodes formula	SHLDNF	消肿散结剂	27 (1.11)
Formula for treating carbuncle and ulcer	FTCU	痈疡剂	25 (1.02)
Summer-heat-expelling formula	SHEF	祛暑剂	22 (0.90)
Formula for resuscitation	FR	开窍剂	21 (0.86)
Antidryness formula	ADF	治燥剂	16 (0.66)
Resolving turbidity and lowering lipids formula	RTLLF	化浊降脂剂	16 (0.66)
Antihelminthic formula	AHF	驱虫剂	10 (0.41)

XSL•FO
RenderX

Selected LLMs

Since TCM formulas are documented in Chinese or ancient Chinese, in this study, the LLMs that have exceptional performance in Chinese or support multilingualism were selected to facilitate the model's understanding of this information [29].

ChatGLM

ChatGLM-6B, ChatGLM2-6B, and ChatGLM3 are a series of open bilingual language models developed by the Knowledge Engineering Group and Data Mining of Tsinghua University. These models can be easily deployed and fine-tuned on standard consumer-grade graphics processing units, enabling users to perform personalized tasks [21,22,29]. The official script was used to fine-tune these LLMs in this study.

InternLM

The Shanghai Artificial Intelligence Laboratory, SenseTime Technology, the Chinese University of Hong Kong, and Fudan University jointly introduced InternLM-20B and InternLM-7B, which showed exceptional performance in areas such as mathematics, code, dialogue, and creative writing [23]. In this study, Xtuner [30] was used to fine-tune InternLM-20B for TCM formula classification. This tool helps users to fine-tune LLMs with limited hardware resources.

Baichuan2

Baichuan2 is a multilanguage LLM developed by Baichuan-AI. It has been trained on 2.6 trillion tokens and performs well in medical and legal areas. Currently, Baichuan2 has released 7B and 13B to users [31]. We fine-tuned Baichuan2-7B and Baichuan2-13B for our task using Xtuner.

Qwen

Qwen is a series of language models introduced by AliCloud, including Qwen-1.8B, Qwen-7B, Qwen-14B, and Qwen-72B [32]. The official script was used to fine-tune these models in this study. It is worth noting that we fine-tuned Qwen-1.8B with full parameters to improve the performance of the task.

BLOOM

BigScience [33] has launched a series of models of different sizes, known as the BigScience Large Open-Science Open-Access Multilingual Language Model (BLOOM), including 1B, 7B, 13B, and 176B. BLOOM's LLM generates text in multiple languages and codes. In this study, we fine-tuned the BLOOM-1.7B with full parameters using the LLMTuner tool [34].

Ensemble Voting Algorithms for TCM Formula Classification

In our prior work, we used methods with prompt templates and fine-tuned LLMs to classify TCM formulas. The fine-tuned ChatGLM2-6B demonstrated optimal performance, achieving an accuracy rate of 71% in the classification task. However, other models did not surpass the 70% accuracy rate. Its performance failed to surpass that of the deep learning model trained on a single task. In a different study, Chatterjee et al [35] proposed that an ensemble voting method outperforms traditional single classifiers in accurately diagnosing Alzheimer disease. To improve the accuracy of the fine-tuned LLMs in the TCM formula classification task, we adopted an ensemble learning approach, this methodology involved using several fine-tuned LLMs and developing a voting mechanism specifically tailored to their outputs. The goal of this methodology is to combine the predictions of multiple models thereby increasing the accuracy of the TCM formula classification task.

(1)yhard=arg maxc∑i=0N1(Ci=c)

In equation 1, we have N fine-tuned LLMs, where the predicted value for LLM_i is denoted by Ci , N=10, and c represents all classes of the TCM formula. 1(Ci=c) is the indicator function, equal to 1 if Ci=c, and 0 otherwise. The final prediction result yhard is determined by selecting the class with the highest number of votes.

(2)yweighted=arg maxc∑i=0Nαi1(Ci=c)

In equation 2, αi represents the average accuracy of each LLM, the votes for each LLM are multiplied by the corresponding weights, and the resulting weighted votes are summed. Finally, the TCM formula class with the highest weighted sum is finally selected as the final prediction.

Evaluation Metrics

To evaluate the performance of the fine-tuned LLMs on text classification tasks, we used the accuracy, precision, recall, and F_1-score, as defined in equation 3-6, based on true positives (TP), true negatives (TN), false positives (FP), and false negatives (FN).

(3)Accuracy=TP+TNTP+TN+FP+FN

(4)Precision=TPTP+FP

(5)Recall=TPTP+FN

(6)F1-score=2·recall·precisionrecall+precision

Due to the unbalanced distribution of the TCM formula in our test set, we calculated the weighted precision, the weighted recall, and the weighted F_1-score to comprehensively evaluate the performance of the models in multiclassification tasks in equation 7-9.

(7)Precisionweighted-avg=∑i=1L(Precisioni·ωi)

(8)Recallweighted-avg=∑i=1L(Recalli·ωi)

(9)F1-scoreweighted-avg=∑i=1L(F1-scorei·ωi)

With the weighted approach, the performance in detecting classes with a larger number of samples can be adequately represented by assigning weights based on the percentage of sample numbers. In our current investigation, we are dealing with a dataset containing 21 classes of TCM formulas. In equation 7-9, L=21, where ωi is the proportion of each TCM formula in the total dataset.

Experiment

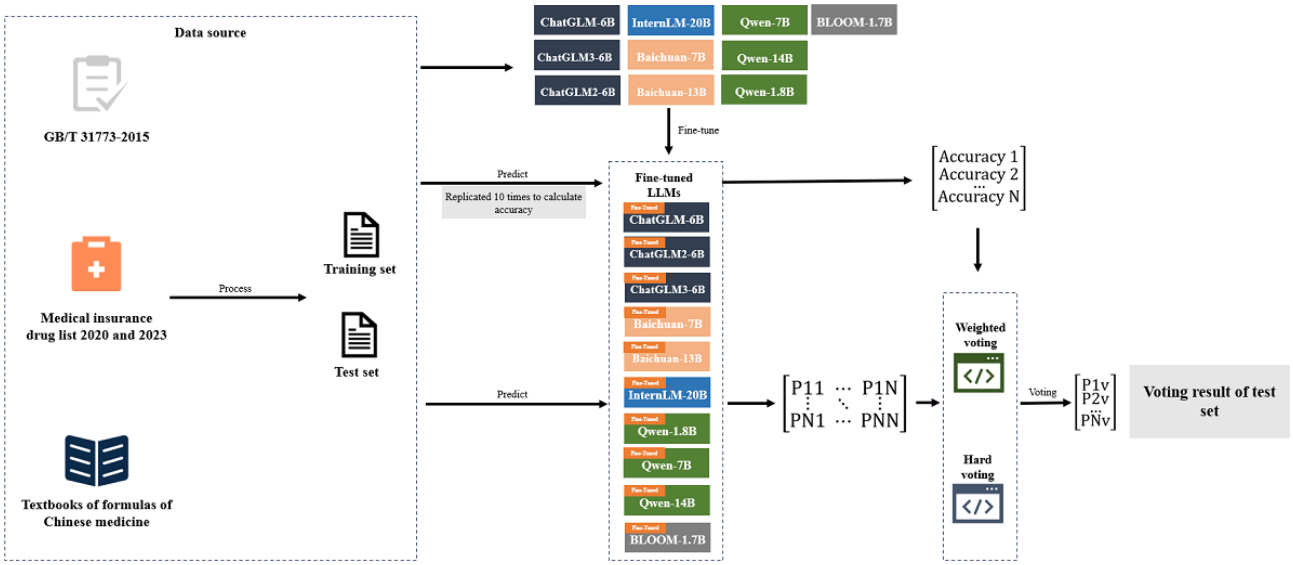
Experimental Design and Verification

Overview

We designed the following experiment to explore the RQ1, RQ2, and RQ3, as shown in Figure 1.

XSL•FO
RenderX

Figure 1. Workflow of traditional Chinese medicine formula classification using large language models. BLOOM: BigScience Large Open-Science Open-Access Multilingual Language Model.



Experiment 1

To address RQ1, a prompt dataset was formulated from the curated TCM formula data. The processed prompt dataset was then divided into a training set and a test set containing 1999 and 442 formulas, respectively. The selected LLMs were fine-tuned using the training set, and their performance was evaluated using the test set. This process was iterated 10 times to obtain the average accuracy.

Experiment 2

To validate RQ2, we used a multistage validation process. First, we implemented a hard voting approach to aggregate model predictions and derive a consolidated result. We then calculated the accuracy of this method. In the next step, we assigned weights to each model based on its average accuracy. Using a weighted voting strategy, we then calculated the accuracy of the weighted voting method. In the third step, we selected the model with the highest accuracy from each category and used these selections for weighted voting. Finally, we identified the top 3 models among the fine-tuned LLMs and conducted a weighted vote to determine the most effective voting method.

Experiment 3

To validate RQ3, we extracted a subset of data from the voting results that met the following two conditions:(1) All model predictions were identical but different from the reference answer, or (2) more than 80% of the model predictions were the same but different from the reference answer. TCM experts subsequently reviewed this subset to evaluate the rationality of the LLMs' classification results.

Experimental Configuration Parameter and Platform

To ensure robust performance, we fine-tuned LLMs using the common configurations and selected the model that achieved the most stable and optimal results. The details of the configurations for the fine-tuned LLMs are shown in Multimedia Appendix 1. The fine-tuning and verification were done by running and validating the LLMs on graphics processing unit computer servers.

Ethical Considerations

We confirm that this study did not involve human or animal subjects. It used publicly available, deidentified text data and sourced from the web. Therefore, no ethics approval was required in accordance with relevant institutional guidelines and the JMIR editorial policy on ethics review requirements.

Results

The Experimental Results of Each Fine-Tuned LLM

In experiment 1, we performed a 10-iteration validation for each model using the test set. Figure 2 shows the mean accuracy for each model. Notably, Qwen-14B (mean 75.32%, SD 0.48%) and Qwen-7B (mean 74.32%, SD 0.37%) showed the highest performance. Close behind were Qwen-1.8B (mean 72.96%, SD 0.53%), InternLM-20B (mean 72.40%, SD 0.47%), Baichuan2-7B (mean 70.86%, SD 0.32%), Baichuan2-13B (mean 71.63%, SD 0.38%), ChatGLM-6B (mean 70.09%, SD 0.30%), ChatGLM2-6B (mean 71.09%, SD 0.80%), and BLOOM-1.7B (mean 70.45%, SD 0.44%), all with accuracies above 70%. However, ChatGLM3-6B (mean 66.70%, SD 0.44%) did not exceed 70% accuracy (Table 2). The fine-tuning of individual LLMs does not lead to remarkable results for the TCM formula classification task in this study. It is noteworthy that the Qwen series of LLMs showed promising performance in the TCM classification task, and Qwen-1.8B and BLOOM-1.7B achieved significant accuracy after full-parameter fine-tuning.

XSL•FO
RenderX

Figure 2. The average accuracy of each large language model in experiment 1. BLOOM: BigScience Large Open-Science Open-Access Multilingual Language Model.

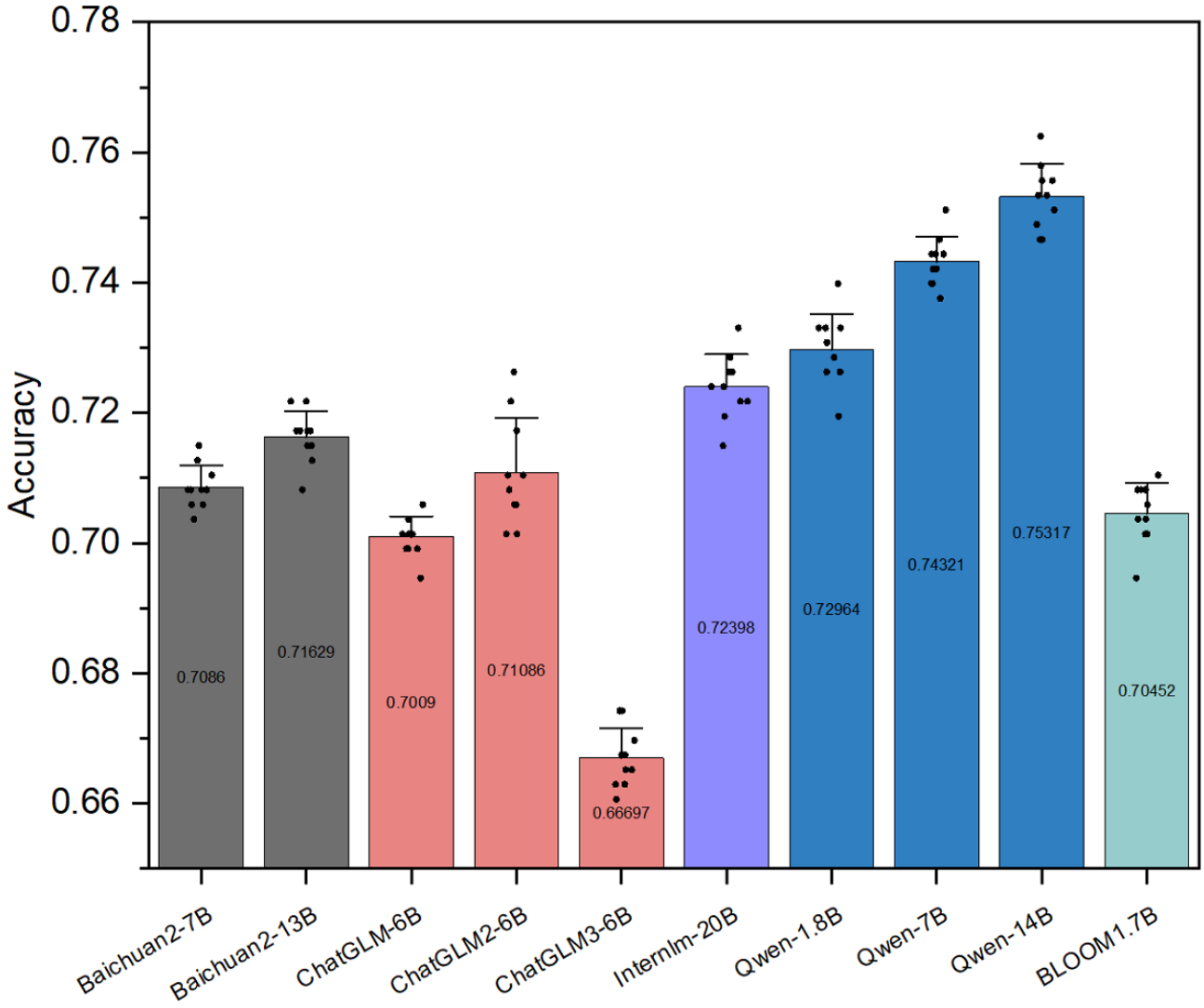


Table . The experimental results of each fine-tuned large language model (LLM).

LLMs	Accuracy (%), mean (SD)
Qwen-14B	75.32 (0.48)
Qwen-7B	74.32 (0.37)
Qwen-1.8B	72.96 (0.53)
InternLM-20B	72.40 (0.47)
Baichuan2-7B	70.86 (0.32)
Baichuan2-13B	71.63 (0.38)
ChatGLM-6B	70.09 (0.30)
ChatGLM2-6B	71.09 (0.80)
ChatGLM3-6B	66.70 (0.44)
BLOOM-1.7B	70.45 (0.44)

TCM Formula Classification Using Ensemble Learning

In experiment 2, to improve the accuracy of the classification task for validating RQ2, we used an ensemble learning approach by integrating fine-tuned LLMs for collective voting predictions. Given the clear result type of our fine-tuned model results (Table 3), we first applied hard voting, which resulted in an accuracy of 75.79%. The weighted precision, weighted recall, and weighted F_1-scores were calculated as 76.10%, 75.79%, and 75.31%, respectively. The confusion matrix is shown in Figure 3B. These results outperformed those of the single models;

XSL•FO
RenderX

however, due to the generally low accuracy of our fine-tuned models, the single model results could potentially influence the final results. We therefore developed a weighted voting method using the average accuracy of each model as the weight. This approach resulted in an accuracy of 76.47%, with weighted precision, weighted recall, and weighted F_1-scores of 76.57%, 76.47%, and 75.98%, respectively. The weighted voting results not only outperformed direct hard voting but also showed superior performance on the 21 classifications within the test set, as shown in Figure 3C.

Figure 3. Accuracy, weighted precision, weighted recall, and weighted F_1-score and their confusion matrices in experiment 2. (A) Accuracy, weighted precision, weighted recall, and weighted F_1-score of different ensemble voting methods. (B) Confusion matrix of the hard voting method. (C) Confusion matrix of the weighted voting method. ADF: antidryness formula; AF: astringent formula; AHF: antihelminthic formula; BRF: blood-regulating formula; DF: desiccating formula; DIF: digestive formula; FP: formula for purgation; FR: formula for resuscitation; FTCU: formula for treating carbuncle and ulcer; FWD: formula for wind disorder; HCF: heat-clearing formula; QRF: Qi regulated formula; RF: reconciling formula; RPRCRWF: resolving phle-m relieving cough and relieving wheezing formula; RTLLF: resolving turbidity and lowering lipids formula; SBF: supplementing and boosting formula; SF: superficies relieving formula; SHEF: summer-heat-expelling formula; SHLDNF: softening hard lumps and dispelling nodes formula; TF: tranquilization formula; WIF: warming interior formula.

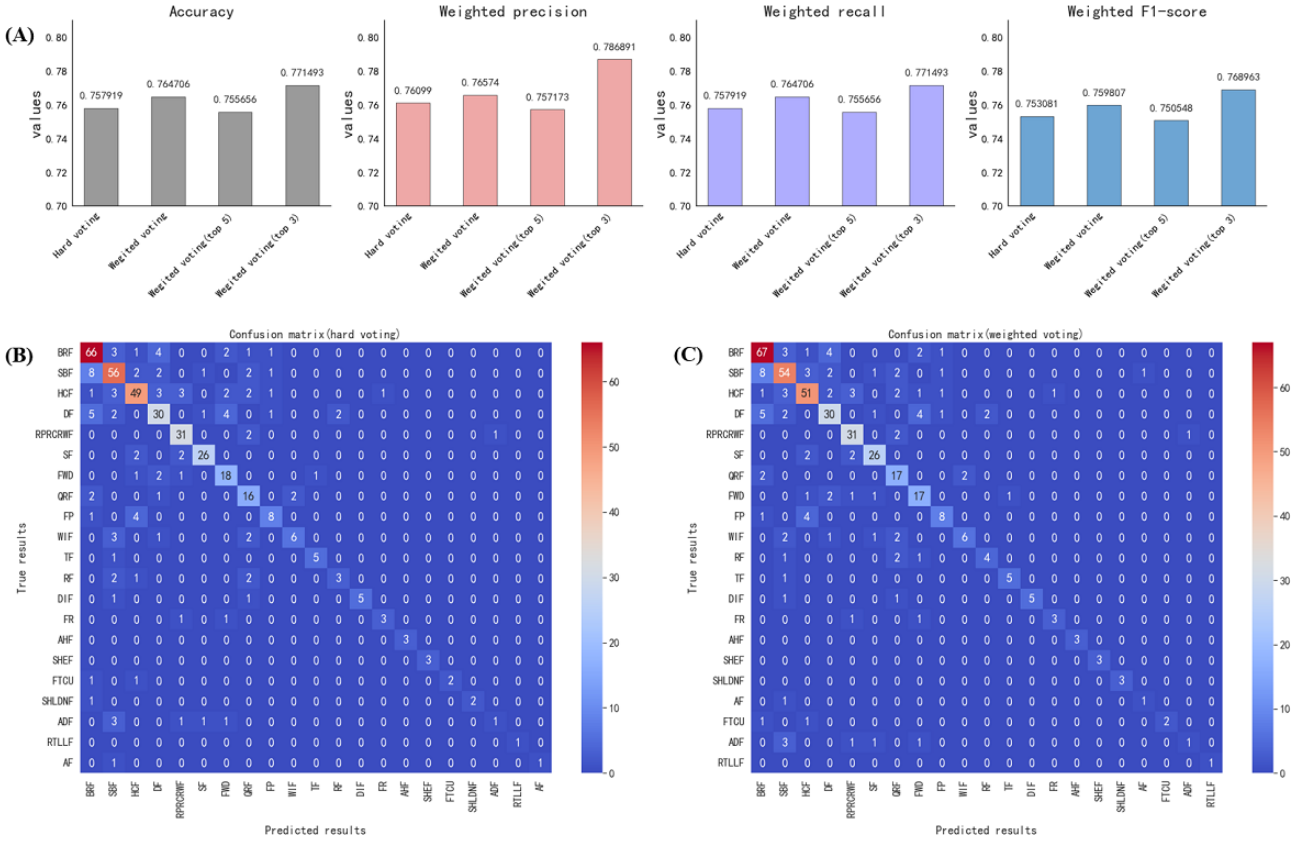


Table . Findings of experiment 2.

Method	Accuracy (%)	Weighted precision (%)	Weighted recall (%)	Weighted F_1- score (%)
Hard voting	75.79	76.10	75.79	75.31
Weighted voting	76.47	76.57	76.47	75.98
Weighted voting (top 5)	75.57	75.72	75.57	75.05
Weighted voting (top 3)	77.15	78.69	77.15	76.90

To further investigate the impact of multiple LLMs on the voting results, we selected the best-performing model within each category (top 5) and performed weighted voting, such as Baichuan-13B, ChatGLM2-6B, InternLM-20B, Qwen-14B, and BLOOM-1.7B. The statistical results showed an accuracy of 75.57%, a weighted precision of 75.72%, a weighted recall of 75.57%, and a weighted F_1-score of 75.05%, as shown in Figure 3A. The confusion matrix is shown in Multimedia Appendix 2.

We selected the 3 models with the highest accuracy, such as Qwen-14B, Qwen-7B, and Qwen-1.8B, to subject their prediction results to weighted voting. The resulting accuracy was 77.15%, the weighted precision was 78.69%, the weighted recall was 77.15%, and the weighted F_1-score was 76.90%, as shown in Figure 3A. The confusion matrix is shown in Multimedia Appendix 3. As can be seen in Figure 3A, the accuracy obtained by weighted voting (top 3) was the highest, surpassing the accuracy obtained by hard voting. Hard voting

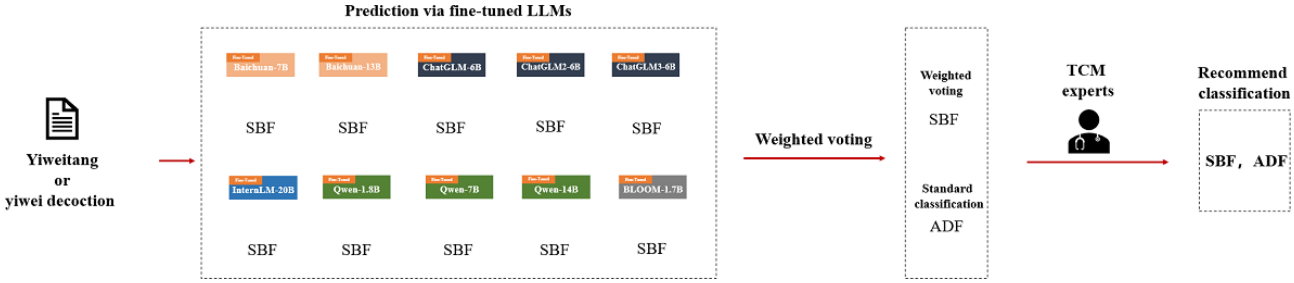
XSL•FO
RenderX

and weighted voting (top 5) were similar, with no significant differences.

Results Analysis of Test Set

During the analysis of LLM voting results on the test set, through TCM expert discussions on the classification results, we observed that in some cases, all LLMs voted the same way, but the results did not match the standard answers. Experts judged that the voting results of the LLMs had a certain degree of rationality. In such cases, it is necessary to discuss why the models reached the same voting results that deviate from the original answers and the rationality of these voting results. We illustrate this with a typical example (Figure 4).

Figure 4. Results analysis of TCM experts. ADF: antidryness formula; LLM: large language model; SBF: supplementing and boosting formula; TCM: traditional Chinese medicine.



TCM formula "Yiweitang or Yiwei decoction (YWD)" consists of Chinese herbs: Bei Sha Shen, Mai Dong, Bing Tang, Di Huang, and Yu Zhu. The indications for treatment are stomach yin injury syndrome. Symptoms include a burning and dull pain in the stomach, lack of appetite despite hunger, dry mouth and throat, dry and hard stool, dry retching, and hiccups. The existing classification of YWD is antidryness formula. However, current scholars have researched Yiwei decoction for the treatment of premature ovarian insufficiency [36,37] and the prevention of osteoporosis related to it [38], proving its efficacy through methods such as network pharmacology and molecular research. Zhang and Zhu [39] have also used the spectrum-effect relationship and network pharmacology to screen for the antioxidant components of Yiwei decoction, demonstrating its function in nourishing stomach yin. Both the treatment or prevention of premature ovarian insufficiency and its related diseases, as well as the nourishing stomach yin function of YWD, fall under the category of supplementing and boosting formula.

In summary, through these discussion points and specific examples, we can gain a deeper understanding of the performance of LLMs in the classification of TCM formula. This can serve as a basis for exploring and reflecting on the existing classification system of formula efficacy. It provides reference and insights for future research on formula efficacy classification.

Discussion

Principal Findings

TCM formulas contain valuable information on ingredients, efficacy, and indications. They serve as important reference for researchers in both clinical and experimental contexts. In this study, we used fine-tuned LLMs in combination with an ensemble learning approach to classify TCM formulas and identify potential information, thereby improved the accuracy of TCM formula classification. Our approach provides a new method for studying formulaic information in TCM.

In this study, we posed 3 RQs and designed corresponding experiments to explore the potential and rationality of fine-tuned LLMs in the TCM formula classification task. The results showed that the fine-tuned Qwen-14B performed remarkably well in the task, achieving an average accuracy of 75.32% (SD 0.48%). However, the accuracy of a single model did not exceed that of deep learning models trained for a single task. To enhance accuracy, we used 2 ensemble methods: hard voting and weighted voting. These methods integrate the 10 fine-tuned LLMs. The accuracy of hard voting and weighted voting reached 75.79% and 76.47%, respectively. The results demonstrate that both hard voting and weighted voting outperform the individual LLMs. Notably, weighted voting (top 3) achieved the highest accuracy, reaching an 77.15%. To evaluate the rationality of the LLMs in the task, we analyzed their prediction errors. In the selected example, all models produced the same prediction, which differed from the reference answer based on YWD. After being analyzed by TCM experts, some of the results predicted by the LLMs were deemed reasonable and can be used as a reference to improve the existing efficacy classification of TCM formulas.

For RQ3, compared to traditional rule-based or deep learning approaches, LLMs demonstrate superior capabilities in automatically identifying latent relationships between herbal formulas. By integrating multidimensional information, such as herbal composition, therapeutic effects, clinical indications, and modern medical research, they build more comprehensive classification systems to uncover potential information. Experimental results show that LLMs can detect potential categories that are not recognized in existing expert classification frameworks. In typical examples, LLM-predicted classifications were validated as clinically plausible by expert panel reviews and literature evidence, suggesting their potential to provide novel scientific foundations for updating and optimizing expert-based classification systems.

Therefore, from both theoretical and technical perspectives, we posit that LLMs can generate more meaningful outcomes for TCM formula classification. This serves as a basis for exploring and reflecting on the existing classification system of formula

XSL•FO
RenderX

efficacy, providing references and insights for the subsequent screening of classic formulas.

Limitations

However, despite numerous studies on the effectiveness of LLMs in classification tasks [40-42], there is a lack of research on text classification in the field of TCM. Our study confirmed that LLMs can achieve a certain effect in the TCM formula classification task. Due to the complexity of TCM knowledge, achieving high accuracy with simple fine-tuning and prompt engineering is difficult. In future research, the composition of herbs in formulas can be encoded through vectors to better explore potential relationships in TCM formula. LLMs in the Qwen series are trained on large-scale, high-quality, and diverse Chinese and English corpora, and have performance across various tasks, in our study, we fully fine-tuned Qwen-1.8B to enhance its capability in classifying TCM formulas and achieved significant accuracy. In the future, we plan to fully fine-tune more LLMs, such as internLM-1.8B [43], and use a weighted voting approach to improve classification accuracy.

Several limitations may have influenced the predicted results. The predictive performance of the LLMs was affected by the relatively small and unevenly distributed dataset of TCM formula in our study. In the future, we plan to collect and curate a large, high-quality TCM formula dataset and integrate it with knowledge graphs to enhance the prediction accuracy of a single LLM. Additionally, we also aim to further improve the performance of the TCM formula classification task by refining our weighted voting methodology.

Conclusions

This study explored the performance of various fine-tuned LLMs in the TCM formula classification task. To improve classification accuracy, both hard voting and weighted voting methods were employed. In conclusion, we also examined the rationality of using LLMs for TCM formula classification and discussed the potential of improving existing classification standards of TCM formulas through the application of LLMs.

Acknowledgments

This work was supported by Beijing Natural Science Foundation (7254504 and 7252253), CAMS Innovation Fund for Medical Sciences (2021-I2M-1-057), National Natural Science Foundation of China (82174534), Noncommunicable Chronic Diseases-National Science and Technology Major Project (2024ZD0532900), and the Fundamental Research Funds for the Central Public Welfare Research Institutes (ZZ160311). The authors acknowledge the use of graphics processing unit and high-performance computing platform at the Center for Bioinformatics, Institute of Basic Medical Sciences, Chinese Academy of Medical Sciences; School of Basic Medicine, Peking Union Medical College.

Conflicts of Interest

None declared.

Multimedia Appendix 1
Configuration parameters for each fine-tuned large language model.
[DOCX File, 19 KB - medinform_v13i1e69286_app1.docx]

Multimedia Appendix 2
Confusion matrix of the weighted voting method with the top 5 models.
[PNG File, 68 KB - medinform_v13i1e69286_app2.png]

Multimedia Appendix 3
Confusion matrix of the weighted voting method with the top 3 models.
[PNG File, 66 KB - medinform_v13i1e69286_app3.png]

References

1. Deng Z. Formulary Version 1: China Press of Chinese Medicine; 2017.
2. Kong Q, Wu Y, Gu Y, et al. Analysis of the molecular mechanism of Pudilan (PDL) treatment for COVID-19 by network pharmacology tools. Biomed Pharmacother 2020 Aug;128:110316. [doi: 10.1016/j.biopha.2020.110316] [Medline: 32505821]
3. Huang L, Xie D, Yu Y, et al. TCMID 2.0: a comprehensive resource for TCM. Nucleic Acids Res 2018 Jan 4;46(D1):D1117-D1120. [doi: 10.1093/nar/gkx1028] [Medline: 29106634]
4. Zhang L, Zheng X, Bai X, et al. Association between use of Qingfei Paidu Tang and mortality in hospitalized patients with COVID-19: a national retrospective registry study. Phytomedicine 2021 May;85:153531. [doi: 10.1016/j.phymed.2021.153531]
5. Yang Y, Li X, Chen G, et al. Traditional Chinese medicine compound (Tongxinluo) and clinical outcomes of patients with acute myocardial infarction: the CTS-AMI randomized clinical trial. JAMA 2023 Oct 24;330(16):1534-1545. [doi: 10.1001/jama.2023.19524] [Medline: 37874574]

XSL•FO
RenderX

6. Gou H, Su H, Liu D, et al. Traditional medicine Pien Tze Huang suppresses colorectal tumorigenesis through restoring gut microbiota and metabolites. Gastroenterology 2023 Dec;165(6):1404-1419. [doi: 10.1053/j.gastro.2023.08.052] [Medline: 37704113]
7. Zhu Y, Zhu L, Wang J, Cui M. An efficient approach of acquiring knowledge from ancient prescriptions and medicines based on information extraction. J Tradit Chin Med Pharm 2015;30(5):5.
8. Chen Q, Lin Y. An analysis of the academic thought of “Collected Exegesis of Recipe”. Trad Chin Med J 2019;18(5):9-11.
9. Jiang H, Jia B. Shallow discussion about classification of prescriptions. Henan Tradit Chin Med 2018;38(11):4.
10. Xie M. Formulaology Version 3: People’s Medical Publishing House; 2016.
11. Gu Z. Research on prescription classification using text classification technology. J Liaoning Univ Tradit Chin Med 2010;2:45-46.
12. Cheng N, Chen Y, Gao W, et al. An improved deep learning model: S-TextBLCNN for traditional Chinese medicine formula classification. Front Genet 2021;12:807825. [doi: 10.3389/fgene.2021.807825] [Medline: 35003231]
13. Ren Q, et al. TCM function multi-classification approach using deep learning models. Presented at: Web Information Systems and Applications: 20th International Conference, WISA 2023; Sep 15-17, 2023; Chengdu, China p. 246-258. [doi: 10.1007/978-981-99-6222-8_21]
14. Introducing ChatGPT. OpenAI. URL: https://openai.com/blog/chatgpt [accessed 2025-06-17]
15. Jin D, Pan E, Oufattole N, Weng WH, Fang H, Szolovits P. What disease does this patient have? A large-scale open domain question answering dataset from medical exams. Appl Sci (Basel) 2021;11(14):6421. [doi: 10.3390/app11146421]
16. Singhal K, Tu T, Gottweis J, et al. Toward expert-level medical question answering with large language models. Nat Med 2025 Mar;31(3):943-950. [doi: 10.1038/s41591-024-03423-7] [Medline: 39779926]
17. Nijkamp E, Ruffolo JA, Weinstein EN, Naik N, Madani A. ProGen2: Exploring the boundaries of protein language models. Cell Syst 2023 Nov 15;14(11):968-978. [doi: 10.1016/j.cels.2023.10.002] [Medline: 37909046]
18. Kant N, Puri R, Yakovenko N, Catanzaro B. Practical text classification with large pre-trained language models. arXiv. Preprint posted online on Dec 4, 2018. [doi: 10.48550/arXiv.1812.01207]
19. Sun X, Li X, Li J, et al. Text classification via large language models. 2023 Presented at: Findings of the Association for Computational Linguistics; Dec 6-10, 2023; Singapore. [doi: 10.18653/v1/2023.findings-emnlp.603]
20. Wang Z, Li K, Ren Q, Yao K, Zhu Y. Traditional Chinese medicine formula classification using large language models. Presented at: 2023 IEEE International Conference on Bioinformatics and Biomedicine (BIBM); Dec 5-8, 2023; Istanbul, Turkiye. [doi: 10.1109/BIBM58861.2023.10385776]
21. ChatGLM-6B. GitHub. URL: https://github.com/THUDM/ChatGLM-6B [accessed 2025-06-17]
22. ChatGLM2-6B. GitHub. URL: https://github.com/THUDM/ChatGLM2-6B [accessed 2025-06-17]
23. InternLM. GitHub. URL: https://github.com/InternLM/InternLM [accessed 2025-06-17]
24. Du Z, Qian Y, Liu X, et al. GLM: general language model pretraining with autoregressive blank infilling. Presented at: Proceedings of the 60th Annual Meeting of the Association for Computational Linguistics (Volume 1: Long Papers); May 22-27, 2022; Dublin, Ireland. [doi: 10.18653/v1/2022.acl-long.26]
25. Coding rules for Chinese medicinal for mulae and their codes (GB/T 31773-2015). State Administration for Market Regulation. 2015. URL: https://openstd.samr.gov.cn/bzgk/gb/newGbInfo?hcno=A67D217316F6BCC4535E30586570D16F [accessed 2025-06-17]
26. Drug catalogue of national basic medical insurance, work related injury insurance and maternity insurance. Administration NHS, CM. 2023. URL: https://www.gov.cn/zhengce/zhengceku/2023-01/18/content_5737840.htm [accessed 2025-06-17]
27. Zhao Z, Li C, Yang J, et al. Discussion on classification of Chinese herbal formulas. J Guangzhou Univ Tradit Chin Med 2019;36(5):746-751.
28. Zhao W, Zhan R, Yang Y, et al. Category exploration to Chinese patent medicine on clinic application. Modern Tradit Chin Med Mater Medica-World Sci Technol 2012;14(2):1357-1362.
29. ChatGLM3. GitHub. URL: https://github.com/THUDM/ChatGLM3 [accessed 2025-06-17]
30. XTuner. GitHub. URL: https://github.com/InternLM/xtuner [accessed 2025-07-07]
31. Yang A, Xiao B, Wang B, et al. Baichuan 2: open large-scale language models. arXiv. Preprint posted online on Apr 17, 2023. [doi: 10.48550/arXiv.2309.10305]
32. Bai J, Bai S, Chu Y, et al. Qwen technical report. arXiv 2023 Sep 28. [doi: 10.48550/arXiv.2309.16609]
33. A one-year long research workshop on large multilingual models and datasets. BigScience. URL: https://bigscience.huggingface.co [accessed 2025-07-23]
34. LLMTuner: large language model instruction tuning tools. GitHub. 2023. URL: https://github.com/zejunwang1/LLMTuner [accessed 2025-07-07]
35. Chatterjee S, Byun YC. Voting ensemble approach for enhancing Alzheimer’s disease classification. Sensors (Basel) 2022 Oct 9;22(19):19. [doi: 10.3390/s22197661] [Medline: 36236757]
36. Fan W, Lei H, Li X, Zhao Y, Zhang Y, Li Y. Exploring the mechanism of Yiwei decoction in the intervention of a premature ovarian insufficiency rat based on network pharmacology and the miRNA-mRNA regulatory network. ACS Omega 2024 Apr 30;9(17):19009-19019. [doi: 10.1021/.3c09551] [Medline: 38708213]

XSL•FO
RenderX

37. Fan W, Zhang Y, Wang D, Wang C, Yang J. The impact of Yiwei decoction on the LncRNA and CircRNA regulatory networks in premature ovarian insufficiency. Heliyon 2023 Sep;9(9):e20022. [doi: 10.1016/j.heliyon.2023.e20022]
38. Fan W, Meng Y, Zhang J, et al. To investigate the mechanism of Yiwei decoction in the treatment of premature ovarian insufficiency-related osteoporosis using transcriptomics, network pharmacology and molecular docking techniques. Sci Rep 2023 Nov 3;13(1):19016. [doi: 10.1038/s41598-023-45699-8] [Medline: 37923747]
39. Zhang L, Zhu W. Screening antioxidant components in Yiwei decoction using spectrum-effect relationship and network pharmacology. J Anal Methods Chem 2024;2024(1):5514265. [doi: 10.1155/2024/5514265] [Medline: 39445127]
40. Gretz S, Halfon A, Shnayderman I, et al. Zero-shot topical text classification with LLMs—an experimental study. 2023 Presented at: Findings of the Association for Computational Linguistics; Dec 6-10, 2023; Singapore. [doi: 10.18653/v1/2023.findings-emnlp.647]
41. Abburi H, Suesserman M, Pudota N, et al. Generative AI text classification using ensemble LLM approaches. arXiv. Preprint posted online on Sep 14, 2023. [doi: 10.48550/arXiv.2309.07755]
42. Chen S, Li Y, Lu S, et al. Evaluating the ChatGPT family of models for biomedical reasoning and classification. J Am Med Inform Assoc 2024 Apr 3;31(4):940-948. [doi: 10.1093/jamia/ocad256] [Medline: 38261400]
43. Internlm2-1_8b. Hugging Face. URL: https://huggingface.co/internlm/internlm2-1_8b [accessed 2025-07-07]

Abbreviations

BLOOM: BigScience Large Open-Science Open-Access Multilingual Language Model
FN: false negative
FP: false positive
TN: true negative
TP: true positive
GPUs: Graphics Processing Units
LLM: large language model
RQ: research question
TCM: traditional Chinese medicine
YWD: Yiweitang or Yiwei decoction

Edited by A Castonguay; submitted 26.11.24; peer-reviewed by M Wang, X Li, Y Liu; revised version received 30.04.25; accepted 23.05.25; published 24.07.25.

Please cite as:
Wang Z, Li K, Peng S, Liu L, Yang X, Yao K, Herre H, Zhu Y
A Weighted Voting Approach for Traditional Chinese Medicine Formula Classification Using Large Language Models: Algorithm Development and Validation Study
JMIR Med Inform 2025;13:e69286
URL: https://medinform.jmir.org/2025/1/e69286
doi:10.2196/69286

© Zhe Wang, Keqian Li, Suyuan Peng, Lihong Liu, Xiaolin Yang, Keyu Yao, Heinrich Herre, Yan Zhu. Originally published in JMIR Medical Informatics (https://medinform.jmir.org), 24.7.2025. This is an open-access article distributed under the terms of the Creative Commons Attribution License (https://creativecommons.org/licenses/by/4.0/), which permits unrestricted use, distribution, and reproduction in any medium, provided the original work, first published in JMIR Medical Informatics, is properly cited. The complete bibliographic information, a link to the original publication on https://medinform.jmir.org/, as well as this copyright and license information must be included.

XSL•FO
RenderX

Federated Analysis With Differential Privacy in Oncology Research: Longitudinal Observational Study Across Hospital Data Warehouses

Théo Ryffel[1], PhD; Perrine Créquit[2], MD; Maëlle Baillet[1], MD; Jason Paumier[1], MSc; Yasmine Marfoq[1], MSc; Olivier Girardot[1], MSc; Thierry Chanet[1], MSc; Ronan Sy[1], MSc; Louise Bayssat[1], MSc; Julien Mazières[3,4,5], MD, PhD; Vincent Vuiblet[6], MD; Julien Ancel[4,6], MD; Maxime Dewolf[6], MD; François Margraff[7], MSc; Camille Bachot[7], MSc; Jacek Chmiel[7], MSc

[1]Arkhn, 9, rue d'Alexandrie, Paris, France

[2]Hôpital Foch, Suresnes, France

[3]Centre Hospitalier Universitaire de Toulouse, Service de Pneumologie, Toulouse, France

[4]INSERM, Paris, France

[5]Centre de Recherches en Cancérologie Oncopole, Toulouse, France

[6]Centre Hospitalier Universitaire de Reims, Service de Pneumologie, Reims, France

[7]Roche SAS, Boulogne, France

Corresponding Author:
Théo Ryffel, PhD
Arkhn, 9, rue d'Alexandrie, Paris, France

Abstract

Background: Federated analytics in health care allows researchers to perform statistical queries on remote datasets without access to the raw data. This method arose from the need to perform statistical analysis on larger datasets collected at multiple health care centers while avoiding regulatory, governance, and privacy issues that might arise if raw data were collected at a central location outside the health care centers. Despite some pioneering work, federated analytics is still not widely used on real-world data, and to our knowledge, no real-world study has yet combined it with other privacy-enhancing techniques such as differential privacy (DP).

Objective: The first objective of this study was to deploy a federated architecture in a real-world setting. The oncology study used for this deployment compared the medical health care management of patients with metastatic non–small cell lung cancer before and after the first wave of COVID-19 pandemic. The second goal was to test DP in this real-world scenario to assess its practicality and use as a privacy-enhancing technology.

Methods: A federated architecture platform was set up in the Toulouse, Reims, and Foch centers. After harmonization of the data in each center, statistical analyses were performed using DataSHIELD (Data aggregation through anonymous summary-statistics from harmonized individual-level databases), a federated analysis R library, and a new open-source DP DataSHIELD package was implemented (dsPrivacy).

Results: A total of 50 patients were enrolled in the Toulouse and Reims centers and 49 in the Foch center. We have shown that DataSHIELD is a practical tool to efficiently conduct our study across all 3 centers without exposing data on a central node, once a sufficient setup has been established to configure a secure network between hospitals. All planned aggregated results were successfully generated. We also observed that DP can be implemented in practice with promising trade-offs between privacy and accuracy, and we built a library that will prove useful for future work.

Conclusions: The federated architecture platform made it possible to run a multicenter study on real-world oncology data while ensuring strong privacy guarantees using differential privacy.

(JMIR Med Inform 2025;13:e59685) doi:10.2196/59685

KEYWORDS

federated analysis; differential privacy; real-world oncology study; non-small cell lung cancer; COVID-19; lung cancer; cancer; privacy; oncology; oncology study; cell lung cancer; oncology data

XSL•FO
RenderX

Introduction

Federated analytics (FA) [1] allow researchers to perform statistical queries on remote datasets without accessing raw data. This method has emerged from the need of conducting statistical analyses on larger datasets originating from multiple health care centers, while avoiding regulation, governance, and privacy related issues that could occur if the raw data were gathered in a central location external to the health care centers.

DataSHIELD (Data aggregation through anonymous summary-statistics from harmonized individual-level databases) [2] is one of the pioneering open-source software solutions for bioscience collaboration using federated analysis. It has been used in several projects including the EU Child Cohort Network [3] and German MIRACUM consortium [4]. However, even if it has been identified as a next step in some oncology studies [5], to the best of our knowledge it has not been used on real-world oncology data. One possible reason for this can be that data harmonization is actually the sticking point, since it proves to be challenging on real-world data when not already done ahead of time.

While FA ensures that sensitive data are never directly exposed, results from statistical queries can still leak some information from individuals. Indeed, several privacy attacks [6,7] have been proposed to exploit common statistical analysis results and disclose private information. To mitigate these attacks, differential privacy (DP) can be used in combination with FA to provide stronger privacy guarantees. DP [8,9] is a method for computing statistical analyses on a sensitive dataset in such a way that the results do not compromise the privacy of the initial raw data. It proves particularly appropriate for studies on patient health data which are highly sensitive, but as far as we know, no real-world data study have already combined FA and privacy-enhancing techniques such as DP. Our study focuses on a scenario with 3 hospital nodes, consistent with typical real-world deployments in health care, where the number of participating centers is usually small (on the order of a few nodes). Scalability and performance metrics (eg, query response times and network latency) were therefore not the primary focus of this pilot.

The goal of this study, called Distributed Analytics for Research in Hospitals (DARAH), is to evaluate the operational deployment of a federated architecture in the context of a real-world oncology study. Another objective is to analyze the impact of DP in a federated analysis on the meaningfulness of the study results.

Methods

Use of DataSHIELD

At the time of starting the project, we evaluated multiple FA frameworks and chose DataSHIELD due to its comprehensive privacy controls, stable community support, and mature set of statistical functions. DataSHIELD's unique strength lies in its local, decentralized authorization mechanism and built-in privacy disclosure checks, which prevent analysts from executing arbitrary code on remote servers. The "default privacy disclosure mode" enforces a baseline set of privacy checks (eg, thresholds on minimum cell counts) that align with real-world clinical data governance needs. While other tools like NVidia FLARE or custom Python/R frameworks exist, they often lack these out-of-the-box privacy safeguards, making DataSHIELD a practical choice for our use case. We maintained the default privacy settings throughout the study to ensure a fair demonstration of DataSHIELD's capabilities without additional configuration.

Use of Differential Privacy

DP provides a measurement of the privacy risk associated with publishing each particular result on a sensitive dataset, by measuring the maximum leakage that each result can cause about the individuals' data. In practice, it often works through the addition of a controlled amount of statistical noise to obscure the contributions to the result from each individual in the dataset.

Several open-source libraries exist that implement DP, most of which are written in Python or expose a Python interface. Popular ones include Google's DP library [10], PyDP [11] from the OpenMined community and OpenDP [12]. In R, the main open-source library is the diffpriv library [13] that implements some DP mechanisms but not a real suite of functions ready to use, and which is not actively supported with last contributions going back to 2017. Furthermore, none of these tools were directly compatible with the DataSHIELD framework, which requires a specific interface in R. As a result, a new open-source a DP R package (R Core Team) for DataSHIELD has been implemented: dsPrivacy. It is available in the Arkhn GitHub repository.

dsPrivacy implements common statistical operations such as mean (SD) with DP and can be directly integrated into DataSHIELD. More specifically, pure DP has been implemented, which means that the statistical noise added to the result is drawn from a Laplacian distribution. Privacy is therefore defined with a single parameter "ε" (which corresponds to the inverse of the noise variance) and it is called the privacy budget. The privacy budget ε controls the amount of noise injected in the computation and hence the privacy of the analysis, smaller the privacy budget ε, higher the noise, which means better privacy guarantees since the private information is better covered by the noise.

DP induces a trade-off between privacy and accuracy of the analysis [14] as privacy is ensured with noise, better privacy means a lower signal-to-noise ratio and less meaningful results. Conversely, when ε is high, the noise is reduced and privacy degrades. Choosing the right value for ε from a privacy standpoint is quite controversial [15] and is highly dependent on the context and the study considered.

dsPrivacy in the context of FA works by adding Laplacian noise locally at each center on the results computed on the local datasets before results are aggregated on a central node. This is referred to as local DP, as opposed to central DP, where the noise is added after the aggregation part on the central node. This paradigm is detailed in the Discussion section.

XSL•FO
RenderX

Use Case: Differences in the Patient Drug Exposure of Patients With Non–Small Cell Lung Cancer Before and After the First Wave of the COVID-19 Pandemic

Context

In order to test the implementation of a federated platform with DP, a study was conducted using real-world oncology data, with the aim of analyzing the differences in the patient drug exposure of patients with non–small cell lung cancer before and after the first wave of the COVID-19 pandemic. Specifically, the analyses were based on the first line of treatment, including its duration and disease progression at 24 months. The study was carried out in 3 hospitals: Foch Hospital, Toulouse University Hospital Center, and Reims University Hospital Center.

Patient Selection

The inclusion criteria were adult patients with metastatic non–small cell lung cancer treated with chemotherapy, immunotherapy, antiangiogenic therapy, or any combination of these treatments at Foch, Toulouse, and Reims centers between March 2019 and March 2021. The list of considered treatments is available in Multimedia Appendix 1.

The exclusion criteria included patients objecting to the reuse of their data, protected adult patients (patients under curatorship, tutorship, or advisership), patients undergoing a clinical trial, patients whose follow-up did not start in one of these centers, patients who are not immediately metastatic, and patients with an epidermal growth factor receptor mutation, anaplastic lymphoma kinase translocation, or ROS proto-oncogene 1 mutation.

For this study, the objective was to have 25 patients per period and per site (ie, 50 patients per center). Initially, patients were preselected using the inclusion criteria present in the chemotherapy prescription software CHIMIO, namely the date and type of treatment. Since the other criteria for inclusion and exclusion were not available in CHIMIO, physicians in each center manually assessed whether the patients could be included in the study.

Variables

In this study, the variables of interest were the duration of the first line of treatment and the disease progression at 24 months following or during the first line of treatment. The start of a second line of treatment or death following (before the start of a second line) or during the first line of treatment were the proxies used for disease progression at 24 months. These events had to have occurred during the observation period, which was 2 years after the patient's inclusion in the study. The explanatory variable was the patient's inclusion period, before the first wave of COVID-19 (March 1, 2019, to March 1, 2020) or after the first wave of COVID-19 (March 2, 2020, to March 31, 2021). Some potential confounders were also studied, such as age, gender, BMI, blood creatinine level, and type of treatment. All these variables were extracted from the CHIMIO software and are listed in Multimedia Appendix 2.

Data Harmonization

In this study, a physician visited each participating site to ensure consistent variable definitions, coding standards, and data formats. We chose Fast Healthcare Interoperability Resources (FHIR) as the initial data standard [16,17], due to its maturity and support in oncology, and the data model is available in Multimedia Appendix 3. Harmonization involved reviewing data dictionaries at each hospital, resolving semantic ambiguities (eg, different coding for treatments), and ensuring uniform data types and units. This manual process, though time-consuming, proved crucial for producing a common dataset compatible with federated queries. In future implementations, automated or semiautomated harmonization workflows, potentially protected by DP to further safeguard patient privacy during preprocessing, could streamline this step. To facilitate the analyses, a tabularized version of the FHIR standard has been produced and the correspondence between the variables of interest used in the datasets and the FHIR attributes are presented in Multimedia Appendix 2.

Statistical Definition Without Differential Privacy

First, univariate and bivariate descriptive statistics were performed for the variables of interest, the explanatory variables and the confounding factors. For the qualitative variables, percentages per category were calculated. For the quantitative variables, the mean but also the 5th, 25th, 50th, 75th, and 95th percentiles were computed. The minimums and maximums were not computed because these values are considered disclosive (eg, the presence of an outlier) in DataSHIELD standard configuration.

Then, to ensure the absence of confounding factors, covariates for which there was a difference between the 2 groups (before and after the first COVID-19 wave) in bivariate analysis with a P value of <.20 were included in the multivariate models. A Student t test was used for quantitative variables. A chi-square test was used for qualitative variables with at least 5 elements in each class. Otherwise, a Fisher test was used.

Finally, to investigate a difference in management between patients in the first and second waves, a linear regression was performed. The variable of interest was the duration of first-line treatment at the metastatic stage and the explanatory variable was the period (before or after the first wave). The duration of treatment was defined as the period from day 1 to the last day of the first line. A multivariate survival analysis (Cox model) was also performed in which the event of interest was the disease progression at 24 months. The explanatory variable was also the period (before or after the first wave). Potential confounders identified in the previous step were included in both multivariate analyses. A difference was considered significant if the CI did not contain 1 for linear regression and survival analysis.

Statistical Definition With Differential Privacy

The univariate and bivariate statistical analyses presented in above were also performed with DP. The global strategy used to implement DP has been discussed in "Use of Differential Privacy" section and some details for each part of the study are detailed here.

XSL•FO
RenderX

All the univariate analyses run code from PyDP [11] that we wrapped in dsPrivacy. As adding DP preserves privacy, the minimum and maximum values could be computed instead of 5th and 95th percentiles. Then bivariate analyses were carried out. For quantitative variables, an implementation of the Student *t* test is used and from the result of this test, a *P* value is inferred. For qualitative variables, occurrence tables are computed (under the hood, the function tableDP from DPPack [18] is used in each center and all the tables are summed) and then a chi-square or Fisher test is performed with the R functions "chisq.test" and "fisher.test." Linear regression and Cox models were not implemented with DP.

Determining appropriate ε values is challenging and context-dependent. In this study, our priority was to maintain analytical use. After testing lower ε values (closer to 1) that yielded excessive noise and unusable results, we selected ε=5.0 for univariate analyses and ε=60.0 for complex operations like the Student *t* tests. While ε=60.0 is higher than common DP standards in theoretical literature, this choice reflects our small sample size (~50 patients/center) and the need to ensure meaningful statistical inference. In scenarios with more patients or improved aggregation techniques (eg, secure aggregation enabling central DP), lower ε values could be achieved. As this was a feasibility study, we highlight that future work should explore more advanced DP mechanisms, larger sample sizes, and improved cryptographic methods to reduce the required privacy budget.

Ethical Considerations

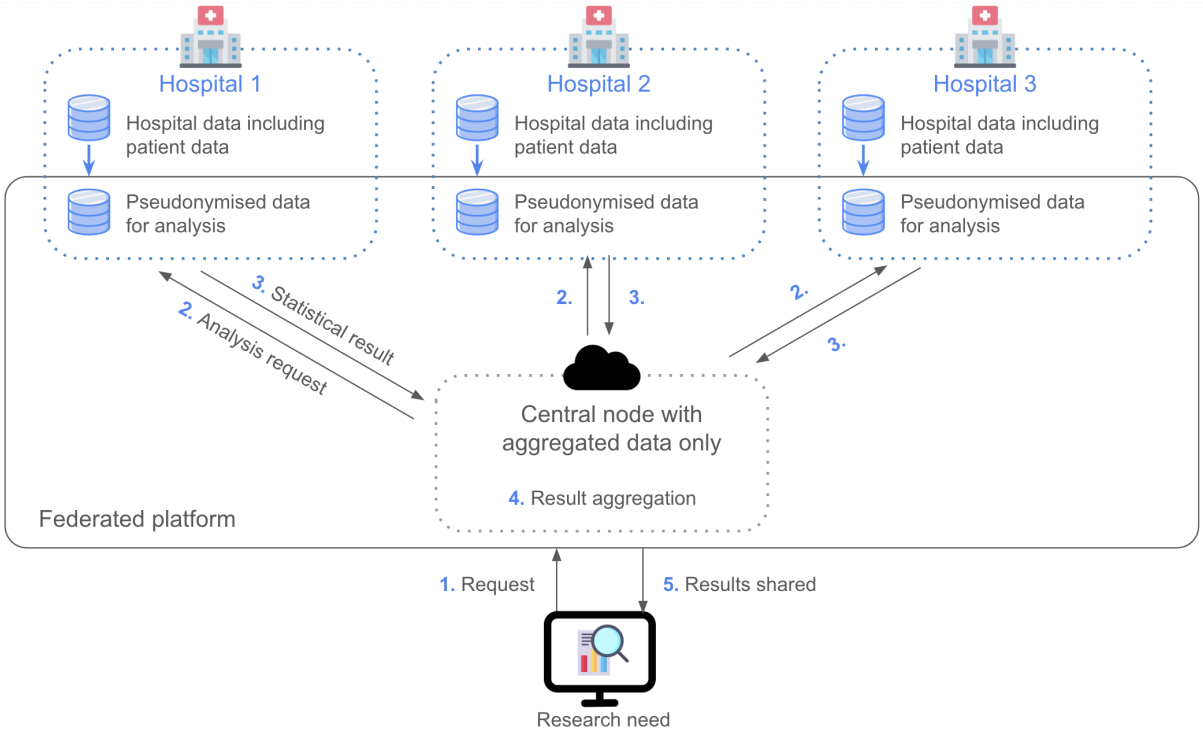
From an ethical and regulatory standpoint, this study complied with the MR-004 reference methodology and adhered to GDPR requirements since DP alone does not classify data as anonymized under current regulatory frameworks. However, the use of DP strengthens data protection, and aligns with emerging privacy regulations by minimizing data exposure risks. These regulatory environments emphasize data sovereignty, patient consent, and robust security, all of which are supported by our federated, privacy-enhancing architecture. All patients enrolled in this study were informed individually, and those who exercised their right to opt out were removed from the study. This is an observational study and the research ethics committees of all three centers in Toulouse, Reims, and Foch have confirmed that no ethical approval is required and have authorized this project on their patient data.

Results

Deployment of Federated Architecture in the Three Centers

The schema of our federated architecture is given in Figure 1. Researchers connect through a VPN to a central node hosted on a cloud provider–certified ISO (International Organization for Standardization) 27001 standard. This central node coordinates the execution of the queries on the remote data assets hosted in the different hospitals and aggregate all the responses received. Each hospital exposes through the private network pseudonymized datasets, which originate from their local harmonized data architecture, but which are completely isolated on a dedicated infrastructure for security purposes. Each hospital receives and executes remote requests from the central node that match local permissions set in DataSHIELD regarding data assets, authorized functions, and legitimate users. This ensures that hospitals keep full sovereignty on how their data are exploited.

Figure 1. Federated architecture diagram.



One key element is deploying a secure private network between all stakeholders, ensuring that each hospital only exposes pseudonymized data within a controlled environment. Although these pseudonymized datasets were not themselves protected

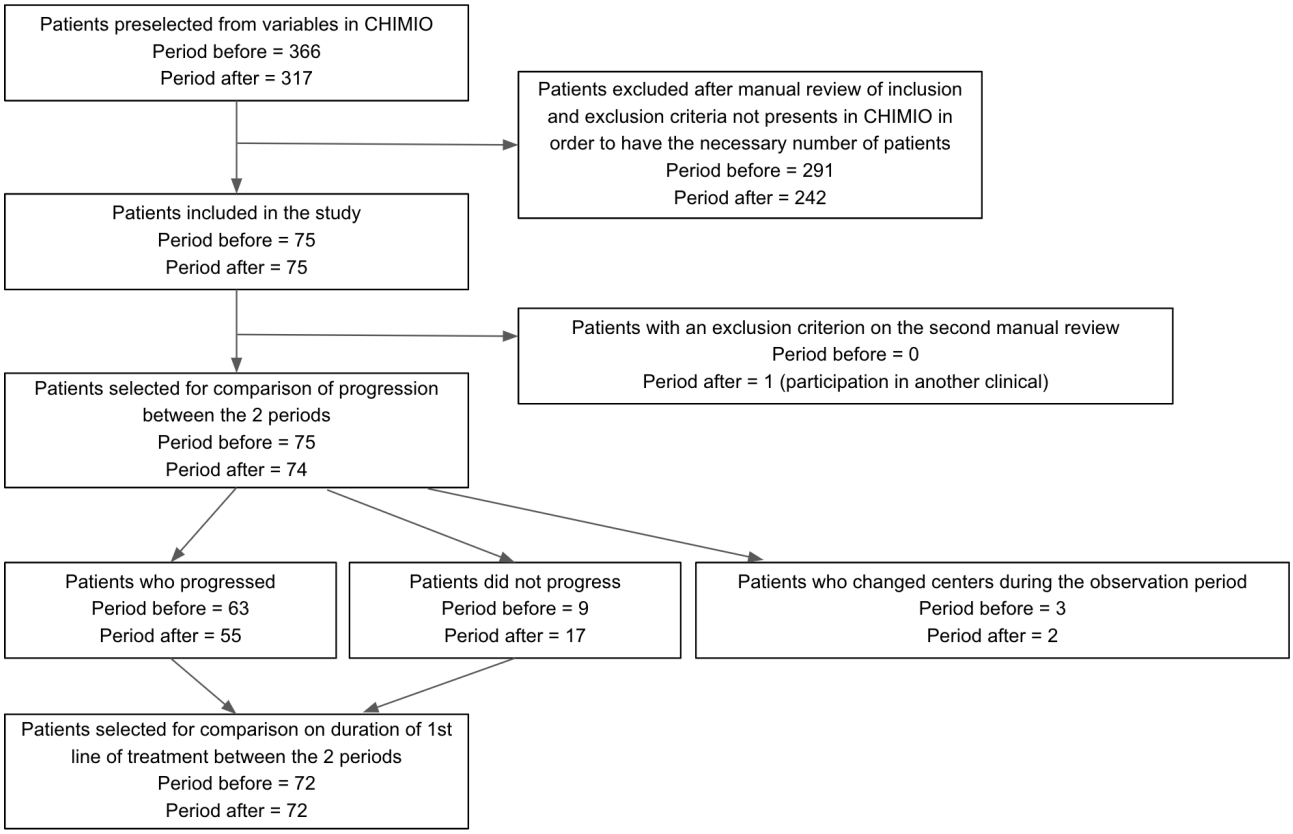
XSL•FO
RenderX

by DP before analysis (since DP is applied at query-time), the secure network, encryption (TLS), and isolation measures minimize risks. We did not use "Let's Encrypt" for certificates due to internal security policies favoring certificates from recognized authorities and the controlled VPN environment lacking public domain validation. Instead, a custom approach using a trusted certificate authority provided both strong authentication and encryption tailored to our network configuration.

Flowchart

The flowchart is presented in Figure 2. In total, 75 and 74 patients from respectively before and after the first wave were included in the analysis comparing disease progression. Of the patients in the period before, 63 had progressed, 9 were progression-free, and 3 had changed groups during the observation period and were therefore censored at the time of transfer. Of the patients in the period after, 55 had progressed, 17 were progression-free and 2 had changed groups during the observation period and were therefore censored at the time of transfer. Thus, after exclusion of patients who changed centers, 72 patients from each period were included in the analysis of the duration of the first line of treatment.

Figure 2. Patient selection and exclusion process between two periods: before and after the first wave (BW and AW).



Bivariate Analysis and Selection of Potential Confounders

Combined univariate analyses without and those with DP are presented in Multimedia Appendix 4. Combined bivariate analyses without and with DP are presented in Tables 1 and 2, respectively. Direct comparison between DP and no-DP analyses across all periods is available in Table 3. In analysis without and with DP, the covariates selected for multivariate analyses were the treatment type (<.001) only.

XSL•FO
RenderX

Table . Bivariate analyses without differential privacy.

Variables	Patients (period before; n=75)	Patients (period after; n=74)	*P* value
Variables of interest			
Disease progression, n (%)			.21
No	12 (16)	19 (25.7)	
Yes	63 (84)	55 (74.3)	
Missing	0 (0)	0 (0)	
First line duration (days)			.09
Mean (SD)	179.7 (267.1)	255.2 (274.6)	
Median (IQR)	75.7 (14.7 - 190)	141.8 (45.1 - 420.8)	
5th and 95th percentiles	0 - 592.4	15 - 792.8	
Missing, n (%)	(0)	(0)	
Covariables			
Organization, n (%)			.99
Toulouse University Hospital	25 (33.3)	25 (33.8)	
Reims University Hospital	25 (33.3)	25 (33.8)	
Foch Hospital	25 (33.3)	24 (32.4)	
Missing	0 (0)	0 (0)	
Gender, n (%)			.79
Female	33 (44)	30 (40.5)	
Male	42 (56)	44 (59.5)	
Missing	0 (0)	0 (0)	
Age (years), n (%)			.38
<55	12 (16)	10 (13.5)	
55 - 65	30 (40)	23 (31.1)	
>65	33 (44)	41 (55.4)	
Missing	0 (0)	0 (0)	
BMI (kg/m²), n (%)			.39
<18.5	13 (17.3)	19 (25.7)	
18.5 - 25	34 (45.3)	27 (36.5)	
>25	28 (37.3)	28 (37.8)	
Missing	0 (0)	0 (0)	
Treatment category, n (%)			<.001
Chemotherapy	46 (61.3)	30 (40.5)	
Chemotherapy+angiogenesis inhibitor	6 (8)	0 (0)	
Chemotherapy+immunotherapy	7 (9.3)	33 (44.6)	
Immunotherapy	16 (21.3)	11 (14.9)	
Missing	0 (0)	0 (0)	
Creatinemia (µmol/l)			.47
Mean (SD)	66.7 (20.3)	64.3 (18.9)	
Median (IQR)	60.0 (54.7 - 73.3)	63.7 (55.1 - 73.1)	
5th and 95th percentiles	46.7 - 98.8	41.1 - 82.8	
Missing, n (%)	0 (0)	1 (1.4)	

XSL•FO
RenderX

Table . Bivariate analyses with differential privacy.

Variables	Patients (period before)	Patients (period after)	*P* value
Variables of interest			
Disease progression (ε[a]=5.0), n (%)			.27
No	12 (16)	18 (24.7)	
Yes	63 (84)	55 (75.3)	
Firstline duration (days ; ε=5.0, except *P* value: ε=60.0)			.051
Mean (SD)	189.5 (231.1)	287.4 (286.3)	
Median	81.8	132.6	
Range	0.3 - 1359.5	8.5 - 827.1	
Covariables			
Gender (ε=5.0), n (%)			.92
Female	32 (43.2)	30 (41.1)	
Male	42 (56.6)	43 (58.9)	
Age (years; ε=5.0), n (%)			.37
<55	12 (16.2)	10 (13.7)	
55 - 65	29 (39.2)	22 (30.1)	
>65	33 (44.6)	41 (56.2)	
BMI (kg/m²; ε=5.0), n (%)			.38
<18.5	13 (17.1)	19 (25.7)	
18.5 - 25	34 (44.7)	27 (36.5)	
>25	29 (38.2)	28 (37.8)	
Treatment category (ε=5.0), n (%)			.001
Chemotherapy	46 (61.3)	31 (39.7)	
Chemotherapy+angiogenesis inhibitor	6 (8)	0 (0)	
Chemotherapy+immunotherapy	7 (9.3)	35 (44.9)	
Immunotherapy	16 (21.3)	12 (15.4)	
Creatinemia (µmol/L) (ε=5.0 except for *P* value: ε=60.0)			.53
Mean (SD)	65.4 (18.9)	61.9 (17.1)	
Median	64.4	65.4	
Range	48.8 - 88.9	37.4 - 86.1	

[a]ε: privacy budget.

XSL•FO
RenderX

Table . Comparison of bivariate analyses across all periods (before and after), with and without differential privacy.

Variables	Global results (before and after combined) without DP[a]	Global results (before and after combined) with DP (ε^b=5.0)
Variables of interest		
Disease progression, n		
No	31	31
Yes	118	118
First-line duration (days)		
Mean (SD)	217.2 (269.4)	198.9 (286)
Median	113.5	126.4
Range	0.5 - 785.6	0.1 - 524.8
Covariables		
Gender, n (%)		
Female	63	63
Male	86	87
Age (years), n		
<55	22	21
55 - 65	53	52
>65	74	75
BMI (kg/m²), n		
<18.5	32	32
18.5 - 25	61	61
>25	56	56
Treatment category, n		
Chemotherapy	76	76
Chemotherapy+ angiogenesis inhibitor	6	6
Chemotherapy+ immunotherapy	40	41
Immunotherapy	27	27
Creatinemia (µmol/L)		
Mean (SD)	65.5 (19.6)	64.6 (15.15)
Median	62.3	64.3
Range	43.9 - 92.8	45.6 - 83.7

[a] DP: differential privacy.

[b] ε: privacy budget.

Comparison of the Progression Between Two Periods (Cox Model)

In the analysis without DP, the hazard ratio of the cox model for the period before compared with the period after the first wave was 0.98 (95% CI 0.65-1.46). As the 95% CI includes 1, the two periods were not considered significantly different in terms of disease progression at 24 months after adjustment for a significant covariate (treatment type).

Comparison of the Duration of the First Line of Treatment Between the Two Periods (Linear Regression)

In the analysis without DP, the coefficient of linear regression for the first period compared with the second one was –13.84 (95% CI –103.82 to 76.14). As the CI includes 1, the two periods were not considered significantly different in terms of first line duration after adjustment for significant covariate (treatment type).

XSL•FO
RenderX

Discussion

Principal Findings

In this study, a federated analysis with and without DP was performed on a real-world study in oncology. The real-world study showed consistent results in both settings. In particular, identical conclusions were drawn regarding the lack of difference in first-line treatment duration and disease progression at 24 months in non–small cell lung cancer patients treated before or after the first wave of COVID-19 pandemic.

Real-world deployment in 3 centers has shed light on some key aspects in terms of security. Regarding tools, DataSHIELD offers a lot of flexibility as it allows the use of custom libraries such as dsPrivacy implemented as part of this study. The downside is that community libraries are not always well maintained and bugs can be encountered (eg, dsStats had to be fixed manually). DataSHIELD builds upon Opal [19], a convenient data management application which comes with straightforward but very satisfactory user management and makes it easy to configure access to specific data to specific users. Opal is also secured by design and enforces many good security practices like CSRF (Cross-Site Request Forgery) and HTTPS usage. However, available docker images to deploy it have several major known security vulnerabilities and do not seem regularly updated. Regarding network configuration, setting up strong security standards across all sites has proved challenging. An IpSec bridge was set up to enable secure communication between the central node and the hospitals. Communication among all stakeholders was a key factor for this step and formal processes (network schema, requirements formalization, debugging methods, and so on) proved decisive in order to facilitate discussions. Regarding certificates to secure communications inside the private network, the primary intention was to use certificates signed by hospitals internal certificate authority because it would not match our security requirements so certificates signed by public certificate authority have been claimed. Some hospitals provided a Sertigo certificate but it was not natively recognized by the central node server. Another hospital used instead a public certificate generated by the central node manager (Arkhn). This last solution has proven to be the best solution in terms of efficiency and security, even if the domain names covered by these certificates are not representing the actual ownership of hosts.

Regarding data standards, we chose FHIR, since it appeared to be the most mature health standard in oncology at the beginning of this project [16,17]. However, Observational Medical Outcomes Partnership (OMOP) is developing extensions for oncology and is rapidly closing the gap [20,21]. As the FHIR standard corresponds to json files that are not very suitable for analytical purposes, we anticipate that moving to OMOP will be more convenient for future analyses.

Overall, our experience suggests that the most time and work intensive parts are building harmonized data models locally and setting up the network infrastructure. As both these steps are agnostic of the study considered, we anticipate that they can be easily leveraged to scale the number of studies carried out on this infrastructure.

On the DP side, it has been decided not to perform linear regression and Cox models with DP because implementing it with a moderate privacy budget was deemed too complex. Privacy budgets used in this study (especially for computing the *P* values) are quite high compared with the literature [15,22], in order to achieve reasonable accuracy on differentially private results but we have shown that we are able to derive similar results compared with plain FA. As underlined above, the appropriate level of privacy is highly dependent on the context considered. Here, given that this study was already compliant to the French MR-004 methodology without DP, DP was used by prioritizing usefulness over privacy. In other contexts, especially if DP becomes recognized as a legitimate and safe technology to process personal data, and hence benefits from a dedicated regulatory status, lower privacy budgets will probably be required (alongside privacy-focused pen tests). We have identified 3 directions to achieve this. The first direction is to increase the number of patients per center. This is the most straightforward option to improve the privacy vs accuracy trade-off, since the amount of noise to add to reach a certain privacy budget ε directly depends on the number of individuals. We have included close to 50 patients per center, which is quite low especially for some budget intensive operations for which we estimate that a thousand patients would be adapted. Second, by using central DP. If the noise is added on the central node, it is computed considering the sum of the patients across all the centers and enables lower noise for the same privacy budget. This is especially powerful if many centers are participating in the federated analysis. However, this means that by default the central node can see the contribution of each center without any noise which is a privacy breach if it cannot be trusted. A common solution is to implement secure aggregation [23], meaning that all contributions are hidden and are only disclosed after the aggregation operation, using cryptographic mechanisms such as secure multiparty computation [24], homomorphic encryption [25], or functional encryption [26]. Secure aggregation is not yet implemented in dsPrivacy and is left as future work. Finally, it can be achieved by improving the DP mechanism. We have used pure or ε-DP, which is a simple mechanism and which makes composition very simple, since the privacy budget of a sequence of operations is the sum of the budget of each operation. More complex mechanisms such as (ε, δ)-DP [6] or Rényi DP [27] provide more optimized composition properties [28] that allow for a tighter privacy budget management.

Conclusions

The DARAH project illustrates FA are a practical method to conduct scientific projects while improving data privacy, by keeping patient data stored in the hospitals and leveraging their already existing data architecture. It highlights some key challenges to be anticipated and possible answers to ensure the success of this type of projects. It also shows that DP can be used in addition to FA to improve privacy guarantees, but more experimentation is needed to develop guidelines and best practices, especially around the trade-off between accuracy and privacy. Finally, in an emerging ecosystem where tools for FA and DP are not yet well integrated, the dsPrivacy library will

XSL•FO
RenderX

prove useful for researchers who want to explore privacy-friendly analysis methods.

Acknowledgments

This work was supported by private funding from Roche. Apart from this, the authors declare that no funds, grants, or other support were received during the preparation of this manuscript.

Data Availability

All generic source code has been made available as open source in the dsPrivacy and is available on Arkhn GitHub organization. Specific code to reproduce the study will be made available upon reasonable request to the corresponding author. The data underlying this article cannot be made publicly available due to the privacy of the patients involved in this study.

Conflicts of Interest

None declared.

Multimedia Appendix 1
List of treatments of interest and their category.
[DOCX File, 15 KB - medinform_v13i1e59685_app1.docx]

Multimedia Appendix 2
Correspondence between the variables of interest used in the dataset and the FHIR (Fast Healthcare Interoperability Resources) attributes.
[DOCX File, 16 KB - medinform_v13i1e59685_app2.docx]

Multimedia Appendix 3
Data model to standardize data from centers in tabularized FHIR (Fast Healthcare Interoperability Resources) standard.
[DOCX File, 85 KB - medinform_v13i1e59685_app3.docx]

Multimedia Appendix 4
Combined univariate analyses across all centers without and with differential privacy.
[DOCX File, 20 KB - medinform_v13i1e59685_app4.docx]

References

1. Rieke N, Hancox J, Li W, et al. The future of digital health with federated learning. NPJ Digit Med 2020;3:119. [doi: 10.1038/s41746-020-00323-1] [Medline: 33015372]
2. Gaye A, Marcon Y, Isaeva J, et al. DataSHIELD: taking the analysis to the data, not the data to the analysis. Int J Epidemiol 2014 Dec;43(6):1929-1944. [doi: 10.1093/ije/dyu188] [Medline: 25261970]
3. Jaddoe VWV, Felix JF, Andersen AMN, et al. The LifeCycle Project-EU Child Cohort Network: a federated analysis infrastructure and harmonized data of more than 250,000 children and parents. Eur J Epidemiol 2020 Jul;35(7):709-724. [doi: 10.1007/s10654-020-00662-z] [Medline: 32705500]
4. Prokosch HU, Acker T, Bernarding J, et al. MIRACUM: Medical Informatics in Research and Care in University Medicine. Methods Inf Med 2018 Jul;57(S 01):e82-e91. [doi: 10.3414/ME17-02-0025] [Medline: 30016814]
5. Gruendner J, Wolf N, Tögel L, Haller F, Prokosch HU, Christoph J. Integrating Genomics and Clinical Data for Statistical Analysis by Using GEnome MINIng (GEMINI) and Fast Healthcare Interoperability Resources (FHIR): system design and implementation. J Med Internet Res 2020 Oct 7;22(10):e19879. [doi: 10.2196/19879] [Medline: 33026356]
6. Shokri R, Stronati M, Song C, Shmatikov V. Membership inference attacks against machine learning models. Presented at: 2017 IEEE Symposium on Security and Privacy (SP); May 22-24, 2017; San Jose, CA, USA p. 3-18. [doi: 10.1109/SP.2017.41]
7. Melis L, Song C, De Cristofaro E, Shmatikov V. Exploiting unintended feature leakage in collaborative learning. : IEEE Presented at: 2019 IEEE Symposium on Security and Privacy (SP); May 19-23, 2019; San Francisco, CA, USA p. 691-706. [doi: 10.1109/SP.2019.00029]
8. Dwork C, et al. Our data, ourselves: privacy via distributed noise generation. Presented at: Advances in Cryptology-EUROCRYPT 2006: 24th Annual International Conference on the Theory and Applications of Cryptographic Techniques 2006; May 28, 2006. [doi: 10.1007/11761679_29]
9. Dwork C, Roth A. The algorithmic foundations of differential privacy. FNT in Theoretical Computer Science 2014;9(3-4):211-407. [doi: 10.1561/0400000042]

XSL•FO
RenderX

10. Google/differential-privacy. GitHub. URL: https://github.com/google/differential-privacy [accessed 2023-11-29]
11. OpenMined/pydp. GitHub. URL: https://github.com/OpenMined/PyDP [accessed 2023-11-29]
12. Opendp/opendp. GitHub. URL: https://github.com/opendp/opendp [accessed 2023-11-29]
13. Brubinstein/diffpriv. GitHub. URL: https://github.com/brubinstein/diffpriv [accessed 2023-11-29]
14. Alvim MS, Andrés ME, Chatzikokolakis K, et al. Differential privacy: on the trade-off between utility and information leakage. Presented at: Formal Aspects of Security and Trust; Aug 25, 2011 p. 39-54. [doi: 10.1007/978-3-642-29420-4_3]
15. Hsu J, Gaboardi M, Haeberlen A, et al. Differential privacy: an economic method for choosing epsilon. Presented at: 2014 IEEE 27th Computer Security Foundations Symposium (CSF); Jul 19-22, 2014; Vienna. [doi: 10.1109/CSF.2014.35]
16. Welcome to FHIR. HL7 FHIR. URL: https://build.fhir.org/ig/InstitutNationalduCancer/ImplementationGuide_OsirisFHIR/branches/ [accessed 2023-11-29]
17. Minimal common oncology data elements (mcode) implementation guide. HL7 FHIR. URL: https://build.fhir.org/ig/HL7/fhir-mCODE-ig/ [accessed 2023-11-29]
18. Differentially private contingency table. R Documentation. URL: https://search.r-project.org/CRAN/refmans/DPpack/html/tableDP.html [accessed 2023-11-29]
19. Opalr: “Opal” data repository client and “datashield” utils. CRAN: Package opalr. 2024. URL: https://cran.r-project.org/web/packages/opalr/index.html [accessed 2025-06-09]
20. Belenkaya R, Gurley MJ, Golozar A, et al. Extending the OMOP common data model and standardized vocabularies to support observational cancer research. JCO Clin Cancer Inform 2021 Jan;5:12-20. [doi: 10.1200/CCI.20.00079] [Medline: 33411620]
21. OHDSI/oncologywg. GitHub. URL: https://github.com/OHDSI/OncologyWG/wiki [accessed 2023-11-29]
22. Lee J, Clifton C. How much is enough? choosing ε for differential privacy. Presented at: Information Security: 14th International Conference, ISC 2011:325–40; Oct 26-29, 2011. [doi: 10.1007/978-3-642-24861-0_22]
23. Bonawitz K, Ivanov V, Kreuter B, et al. Practical secure aggregation for federated learning on user-held data. arXiv. Preprint posted online on 2016.
24. Beaver D. Efficient multiparty protocols using circuit randomization. Presented at: Advances in Cryptology — CRYPTO ’91; Aug 11-15, 1991 p. 420-432. [doi: 10.1007/3-540-46766-1_34]
25. Paillier P. Public-key cryptosystems based on composite degree residuosity classes. Presented at: Advances in Cryptology — EUROCRYPT ’99; May 2-6, 1999 p. 223-238. [doi: 10.1007/3-540-48910-X_16]
26. Boneh D, Sahai A, Waters B. Functional encryption: definitions and challenges. Presented at: Theory of Cryptography; Mar 28-30, 2011 p. 253-273. [doi: 10.1007/978-3-642-19571-6_16]
27. Mironov I. Rényi differential privacy. Presented at: 2017 IEEE 30th Computer Security Foundations Symposium (CSF); Aug 21-25, 2017; Santa Barbara, CA. [doi: 10.1109/CSF.2017.11]
28. Kairouz P, Oh S, Viswanath P. 2015 Presented at: International conference on machine learning; Jul 13-19, 2015. [doi: 10.1109/TIT.2017.2685505]

Abbreviations

CSRF: Cross-Site Request Forgery
DARAH: Distributed Analytics for Research in Hospitals
DataSHIELD: Data aggregation through anonymous summary-statistics from harmonized individual-level databases
DP: differential privacy
FA: federated analytics
FHIR: Fast Healthcare Interoperability Resources
ISO: International Organization for Standardization
OMOP: Observational Medical Outcomes Partnership

Edited by C Lovis; submitted 19.04.24; peer-reviewed by A Imine, J Passerat-Palmbach; revised version received 09.12.24; accepted 30.01.25; published 31.07.25.

Please cite as:
Ryffel T, Créquit P, Baillet M, Paumier J, Marfoq Y, Girardot O, Chanet T, Sy R, Bayssat L, Mazières J, Vuiblet V, Ancel J, Dewolf M, Margraff F, Bachot C, Chmiel J
Federated Analysis With Differential Privacy in Oncology Research: Longitudinal Observational Study Across Hospital Data Warehouses
JMIR Med Inform 2025;13:e59685
URL: https://medinform.jmir.org/2025/1/e59685
doi:10.2196/59685

XSL•FO
RenderX

© Théo Ryffel, Perrine Créquit, Maëlle Baillet, Jason Paumier, Yasmine Marfoq, Olivier Girardot, Thierry Chanet, Ronan Sy, Louise Bayssat, Julien Mazières, Vincent Vuiblet, Julien Ancel, Maxime Dewolf, François Margraff, Camille Bachot, Jacek Chmiel. Originally published in JMIR Medical Informatics (https://medinform.jmir.org), 31.7.2025. This is an open-access article distributed under the terms of the Creative Commons Attribution License (https://creativecommons.org/licenses/by/4.0/), which permits unrestricted use, distribution, and reproduction in any medium, provided the original work, first published in JMIR Medical Informatics, is properly cited. The complete bibliographic information, a link to the original publication on https://medinform.jmir.org/, as well as this copyright and license information must be included.

XSL•FO
RenderX

Estimating Nurse Workload Using a Predictive Model From Routine Hospital Data: Algorithm Development and Validation

Paul Meredith[1,2], PhD; Christina Saville[1,2], PhD; Chiara Dall'Ora[1,2], RN, PhD; Tom Weeks[3,4]; Sue Wierzbicki[3,4], MSc, RN; Peter Griffiths[1,2,3], RN, PhD

[1]School of Health Sciences, Faculty of Environmental and Life Sciences, University of Southampton, Building 67, University Road, Southampton, United Kingdom

[2]Workforce & Health Systems, National Institute for Health Research Applied Research Collaboration (Wessex), Southampton, United Kingdom

[3]Portsmouth Hospitals NHS Trust, Portsmouth, United Kingdom

[4]Isle of Wight NHS Trust, Newport, United Kingdom

Corresponding Author:
Paul Meredith, PhD
School of Health Sciences, Faculty of Environmental and Life Sciences, University of Southampton, Building 67, University Road, Southampton, United Kingdom

Abstract

Background: Managing nurse staffing is complex due to fluctuating demand based on ward occupancy, patient acuity, and dependency. Monitoring staffing adequacy in real time has the potential to inform safe and efficient deployment of staff. Patient classification systems (PCSs) are being used for per shift workload measurement, but they add a frequent administrative task for ward nursing staff.

Objective: The objective of this study is to explore whether an algorithm could estimate ward workload using existing routinely recorded data.

Methods: Anonymized admission records and assessments from a PCS supporting the safer nursing care tool were used to determine nursing care demand in medical and surgical wards in a single UK hospital between February 2017 and February 2020. Records were linked by ward and time. The data were split into a training set (75%) and a test set (25%). We built a predictive model of ward workload (as measured by the PCS) using routinely recorded administrative data and admission National Early Warning Score. The outcome variable was ward workload derived from the patient classifications, measured as the number of whole-time equivalent (WTE) nursing staff per patient.

Results: In a test set of 11,592 ward assessments from 42 wards with a mean WTE per patient of 1.64, the model's mean absolute error was 0.078, with a mean percentage error of 4.9%. A Bland-Altman plot of the differences between the predicted values and the assessment values showed 95% of them within 0.21 WTE per patient.

Conclusions: Predictions of nursing workload from a relatively small number of routinely collected variables showed moderate accuracy for general wards in 1 English hospital. This demonstrates the potential for automating assessments of nurse staffing requirements from routine data, reducing time spent on this nonclinical overhead, and improving monitoring of real-time staffing pressures.

(JMIR Med Inform 2025;13:e71666) doi:10.2196/71666

KEYWORDS

workload; staffing; nursing staff; safer nursing care tool; predictive model

Introduction

Nursing workload management is complex and involves the processes of forecasting, scheduling, staffing, and monitoring [1]. Monitoring a ward's nursing workload in real time or near time is difficult because of patient movements and because of changes in patient acuity and care needs. This is important because there is a body of evidence that shows nurse understaffing is associated with adverse outcomes for patients and for staff [2,3]. Monitoring supports the identification of staffing deficiencies and informs decisions concerning the deployment or redeployment of resources to address them.

Common structured methods of monitoring staffing requirements make use of patient classification systems (PCSs). Through these systems, care intensity is determined for each patient and is then summed to calculate the total care demand for the ward. Examples are the acuity or dependency assessments in the safer nursing care tool (SNCT) [4], the Oulu Patient Classification qualisan (OPCq) used in RAFAELA [5] and the Perroca Patient Classification System [6]. Assessing

XSL•FO
RenderX

and documenting the nursing intensity for every patient on the ward is an additional task for ward nurses, often repeated every shift. Automating the nursing intensity and workload monitoring using data already recorded has the potential to free up valuable staff time in the provision of patient care.

There is little published work on automating PCSs used to measure nursing intensity and workload. However, a model was developed to determine each patient's workload category as defined by the Perroca Patient Classification Instrument (PPCI) from routine electronic health record data in a Brazilian hospital [7]. A random forest classification model used electronic variables chosen as indicators for each of the 9 care areas in the tool. The classifier was 72% accurate when categorizing the patients overall with a c-statistic of 0.82. An individual patient misclassification may not have much effect on the ward workload estimation as a whole, but there were no details of how to translate the patient workload categories into nurse staffing requirements for wards.

Our aim was to build a predictive model using routine electronic data from 1 hospital, which might be known in real time to estimate nurse staffing requirements for wards. Our objective was to match the recorded values determined by using the patient classification instrument from the SNCT, the most widely used tool in England for determining staffing requirements based on patient need [8]. The SNCT originated as a way of estimating nurse staffing establishment requirements (whole-time equivalent (WTE) posts) by means of twice-a-year audits of ward workload. It included a PCS, which is now in use once, twice, or thrice a day in many hospitals in England to monitor ward workload.

Methods

Ethical Considerations

This research was a secondary analysis of data collected for a study that considered the costs and consequences of different nursing staff configurations (Trial Registration: ClinicalTrials.gov NCT04374812) [9]. That study had a waiver for informed consent after assessment via the Health Research Authority integrated research application service (IRAS ref 273185). The ethical review undertaken by the faculty research ethics committee at the University of Southampton (ERGO 52957) for that study was extended for this secondary analysis on the basis that its objectives were aligned with the purpose for which the data had been obtained. The dataset had previously been anonymized with no linkages back to individuals so privacy and confidentiality were respected. The hospital trusts that provided the data gave approvals for this secondary analysis. Dataset construction and all analyses were performed using R (version 4.4.0; R Core Team); further details of the software and packages used can be found in Multimedia Appendix 1.

Data Sources and Linkage

We analyzed data from adult inpatient wards in 1 hospital trust for admissions from February 2017 to February 2020. The data consisted of anonymized admission records and patient classification assessments made using the SNCT acuity instrument. SNCT acuity assessments had been undertaken in admission units, general wards, and high-care wards but not in intensive care units. The admission units in this hospital were the medical emergency and surgical emergency assessment units, which assess patients before transferring them to a general or high-care ward as required. In the UK, a general ward is an inpatient adult ward not specializing in maternity or psychiatric care. A high-care ward has some high-care beds which are defined as providing level 2 care according to the UK intensive care society, deemed as needing 0.5 WTE of nursing care per bed. A UK intensive care unit, on the other hand, provides the highest level of care, level 3, and this requires one-to-one nursing care. The SNCT acuity assessments data provided counts of patients in a ward for each acuity and dependency category at a point in time. The admission records included each patient's first NEWS (National Early Warning Score) [10]. NEWS is a patient assessment method in routine use in UK hospitals based on vital signs observations, which nurses use regularly to identify patients at risk of deterioration.

The patient categorization instrument used for ward workload assessments in SNCT involves matching patients to 1 of 5 ordinal categories according to descriptions of acuity and dependency needs. Level 0 is for stable patients with needs met in general wards, level 1a patients are acutely ill patients requiring intervention or those with a greater potential to deteriorate, level 1b patients are stable but are more dependent on nursing care, and level 2 patients are unstable, at risk of deteriorating, and require specialized care. Level 3 patients, who require multiple organ support, did not exist in our dataset of assessments. Each category has a value (called a multiplier) corresponding to a staffing WTE needed to provide 24-hour care after considering annual leave and sickness absence. Multipliers were developed from ward observational studies [11]. One set of multipliers is used for general wards and another for admission units to take into account the extra workload associated with the higher throughput of patients. The multiplier values for the patients in a ward are summed to produce a point-in-time WTE estimate for the ward [4].

All admission records that could be linked by ward and by assessment date and time were included for wards that were routinely carrying out the assessments. Since the assessment records did not record any patient identifiers, linkage to patient records was by ward and time. Linked records were analyzed where the number of patients in the ward assessment matched the number of occupants in the ward according to the patient administration system at the time of the assessment. A comparison of linked and unlinked assessments was conducted to check for bias resulting from this selection process.

Study Variables

The dependent variable for the prediction model was the WTE calculated by the assessment tool divided by the number of assessed patients. Patients' data for the assessed patients, as determined by the linkage described earlier, were aggregated to ward level by taking means for continuous variables and proportions for binary variables, as shown in the table. The choice of candidate predictors (Table 1) was made according to data availability, published nurse workload models, and clinical protocols regarding nurse assessments for new ward

XSL•FO
RenderX

arrivals. Multi-variable models using all the candidate predictors were built since there was evidence or conceptual reasons for including them, and the objective of the modeling was predictive accuracy rather than quantifying effects of individual predictors. Univariable regressions were performed on the candidate predictors out of interest. The predictors include the use of 2 derived variables: the Charlson comorbidity index [12] and the summary hospital mortality indicator (SHMI) risk [13]. The diagnostic predictors were proportions of patients with a recorded diagnosis belonging to a particular diagnostic group: respiratory conditions, cardiac conditions, renal conditions, cancer, frailty syndromes [14], a self-harm diagnosis, and a history of poisoning. The details of the diagnostic groups are provided in Multimedia Appendix 1. Lastly, an indicator was added for admission units to reflect the alternate set of patient category multipliers used for assessments in them.

XSL•FO
RenderX

Table . Model predictors.

Category and predictor		Ward aggregation
Demographic		
	Age (mid-point of 5 year age group)	Mean
	Male gender	Proportion
Clinical		
	Admission NEWS[a]	Mean
Pathway		
	Elective admission	Proportion
	Prior length of stay	Median
	Number of ward transfers	Mean
	Number of consultant transfers	Mean
	From admission unit (same day transfer)	Proportion
	From theaters (same day transfer)	Proportion
	From high or intensive care (same day transfer)	Proportion
	New hospital admission (same day, no prior ward)	Proportion
Diagnostic		
	Renal condition	Proportion
	Cardiac condition	Proportion
	Cancer condition	Proportion
	Frailty syndrome: dementia or delirium	Proportion
	Frailty syndrome: dependence or care	Proportion
	Frailty syndrome: incontinence	Proportion
	Frailty syndrome: falls or fractures	Proportion
	Frailty syndrome: pressure ulcers or weight loss	Proportion
	Frailty syndrome: anxiety or depression	Proportion
	Frailty syndrome: mobility problems	Proportion
	Respiratory condition	Proportion
	History of poisoning	Proportion
	Self-harm diagnosis	Proportion
Organizational		
	Admission unit	Binary
Derived		
	SHMI[b] mortality risk	Mean
	Charlson Comorbidity Index	Mean

[a]NEWS: National Early Warning Score.

[b]SHMI: summary hospital mortality indicator.

Analysis

A generalized additive regression model (GAM) [15] with an identity link function was chosen for the modelling since this could handle nonlinear relationships between the individual predictors and the WTE per patient response variable.

The data were randomly split into training and test sets (75% vs 25%), and a regression model was created on the training set. All the predetermined candidate predictors were used after checking for high pairwise correlations. Removal of any predictor was found to worsen model fit judging by the Akaike information criterion, so all were retained. A calibration was computed to optimize the predictions by means of a smoothing

XSL•FO
RenderX

of the model estimates on the assessed ones [16]. The model and the calibration were applied to the test set.

A Bland-Altman plot [17] was constructed and used to look at the agreement between the model prediction and the assessed WTE per patient. When examining this plot by ward subset, 2 wards had more than a third of their predictions outside the limits of agreement. This was a markedly higher proportion of assessments than for the other wards, so these wards were excluded from the datasets, and the GAM model was rebuilt.

Results

The distribution of WTE per patient for all assessments (median 1.63, IQR 1.48-1.72) shows a distinct peak near the value of the multiplier for level 1b (Figure 1).

The data came from 44 wards, including 8 admission units and 4 high-care wards, covering 1,481,801 patient categorizations by care level from 71,027 ward-level assessments relating to 125,595 admissions. Most patient assessments in general wards (n=809,296, 59.3%) were recorded as level 1b (Table 2).

Figure 1. Distribution of whole-time equivalent (WTE) per patient values from safer nursing care tool ward assessments.

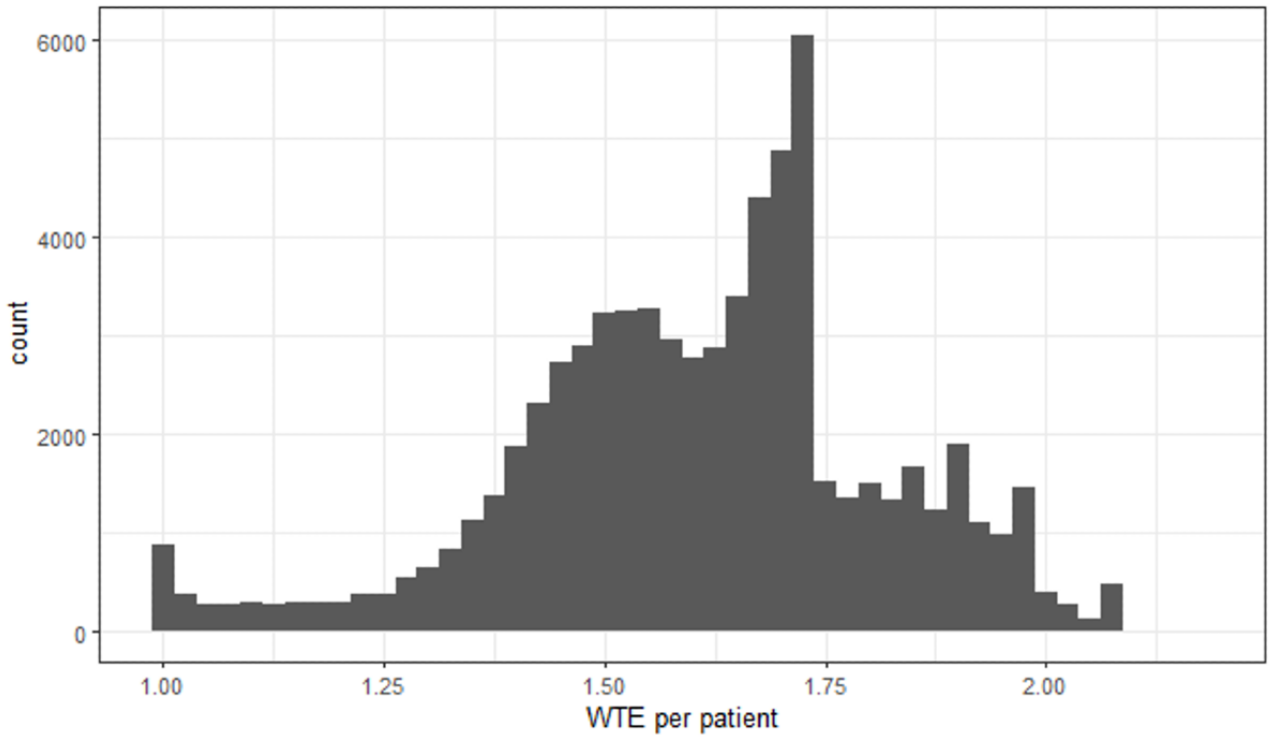


Table . Percentage of assessed patient categorizations by care level.

	Patient categorizations, n	Level 0, n (%)	Level 1a, n (%)	Level 1b, n (%)	Level 2, n (%)
General or high-care ward	1,364,690	232,620 (17.0)	220,621 (16.2)	809,296 (59.3)	102,153 (7.5)
Admission unit	117,111	29,324 (25.0)	44,505 (38.0)	42,717 (36.5)	565 (0.5)

Requiring the number of ward occupancy records to match the number of patients assessed reduced the dataset by 32% to 48,493 assessments relating to 108,558 admissions; however, the WTE per patient distribution was little changed (median 1.65, IQR 1.51-1.73), suggesting no systematic bias. The ward occupancy and therefore the number of patients per assessment in the matched dataset had a median of 20 with an IQR of 11-29.

A patient might be assessed on a number of occasions in a number of wards during their admission. The cohort of assessed patients consisted of 85.5% (n=92,766) emergency admissions and 46.9% (n=50,877) men, with most coming from the 80 - 84 age bracket (Table 3). Long-term conditions were common, with 53.1% (n=57,635) having a Charlson Comorbidity Index of more than 5. The median length of stay was 4.4 (IQR 2.0-10.5) days, and 4.9% (n=5332) died in the hospital.

XSL•FO
RenderX

Table . Admission descriptives for modeled dataset.

		Value (n=108,558)
Sex (male), n (%)		50,877 (46.9)
Emergency admission, n (%)		92,766 (85.5)
Age group (years), n (%)		
	10 - 14	1 (0.0)
	15 - 19	1105 (1.0)
	20 - 24	2765 (2.5)
	25 - 29	2946 (2.7)
	30 - 34	3274 (3.0)
	35 - 39	3275 (3.0)
	40 - 44	3212 (3.0)
	45 - 49	4525 (4.2)
	50 - 54	5775 (5.3)
	55 - 59	7031 (6.5)
	60 - 64	7405 (6.8)
	65 - 69	8663 (8.0)
	70 - 74	11,997 (11.1)
	75 - 79	11,830 (10.9)
	80 - 84	12,886 (11.9)
	85 - 89	11,973 (11.0)
	90 - 120	9895 (9.1)
Charlson Index, n (%)		
	0	32,933 (30.3)
	1-5	17,734 (16.3)
	>5	57,635 (53.1)
	Missing	256 (0.2)
SHMI risk[a] (%), mean (SD)		7.0 (10.0)
NEWS2[b], n (%)		
	Zero, 0	60,179 (55.4)
	Low, 1 - 4	36,789 (33.9)
	Med, 5 - 6	6708 (6.2)
	High, 7 - 20	3343 (3.1)
	(Missing)	1539 (1.4)
Length of stay (days), median (IQR)		4.4 (2.0-10.5)
Hospital death, n (%)		5332 (4.9)

[a]Summary Hospital Mortality Indicator.

[b]National Early Warning Score (version 2).

We fitted a GAM to the training set to model the nursing workload measured in WTE per patient associated with the set of patients in each manual ward assessment. When applied to the test set of 11,592 ward assessments from 42 wards and a calibration applied, the mean absolute error of the predictions was 0.078 WTE per patient (a mean absolute percentage error of 4.9% with a 95th centile of 13.9%). The root mean square error was 0.106 WTE per patient, and the percentage of variance explained by the model was 65%. The predictors that contributed most to explaining the workload (Figure 2) were the admission unit indicator, mean patient age, mean Charlson comorbidity index, the proportion of men, the mean NEWS, and the proportion of patients with a diagnosed renal condition. The relative contribution of each predictor was computed by

XSL•FO
RenderX

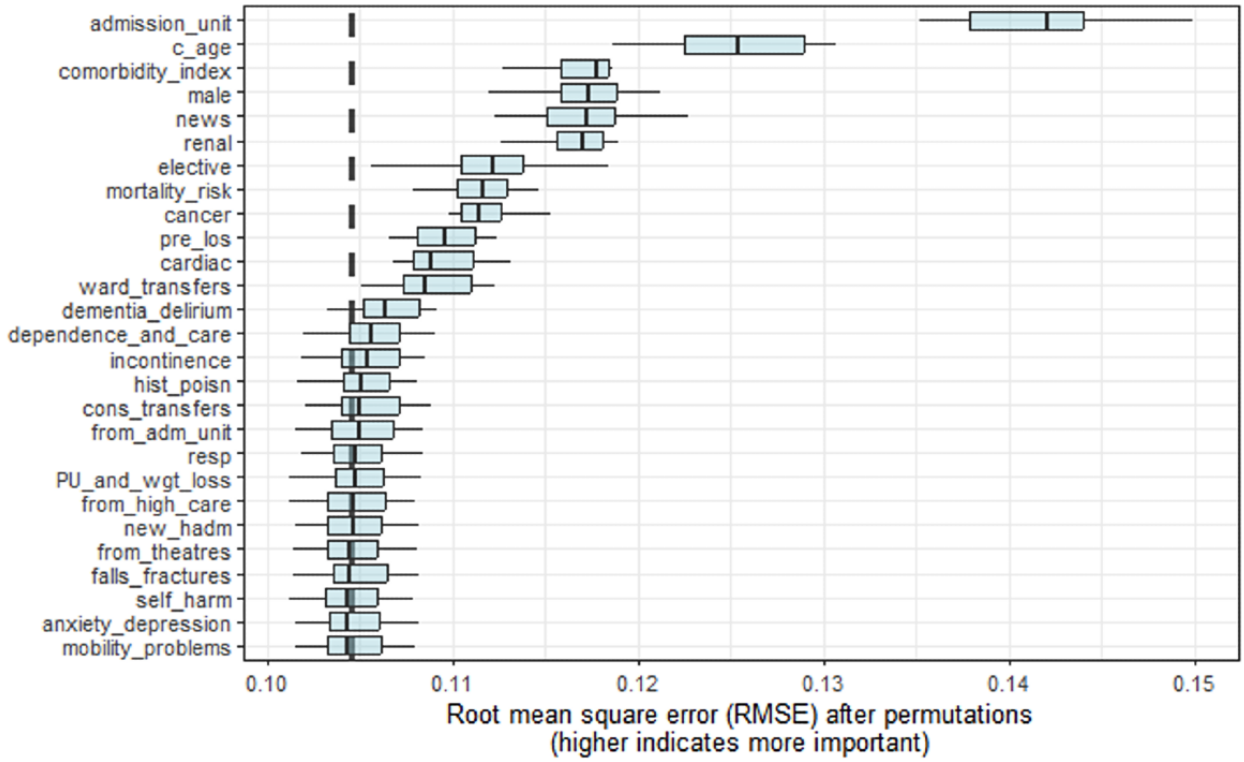
calculating the root mean square error if removed from the model.

Univariable regressions of each of the predictors showed them all to be significant, apart from transfer from an admission unit on the day of assessment (Table S4 in Multimedia Appendix 1). All predictors were retained in the GAM model.

A calibration plot of predictions in the test set against the recorded WTE per patient with the addition of a loess smoothing line forming a calibration curve [18] shows that there was some underestimation of workload at high values (Figure 3).

A Bland-Altman plot of differences between the recorded WTE per patient and model predictions in the test set (Figure 4) had a mean difference of 0.002 WTE per patient. The limits of agreement are at ±0.21 WTE per patient, meaning 95% of assessments fall in this range.

Figure 2. Relative contribution each predictor makes to the model fit.



XSL•FO
RenderX

Figure 3. Calibration of predictions in the test set. WTE: whole-time equivalent.

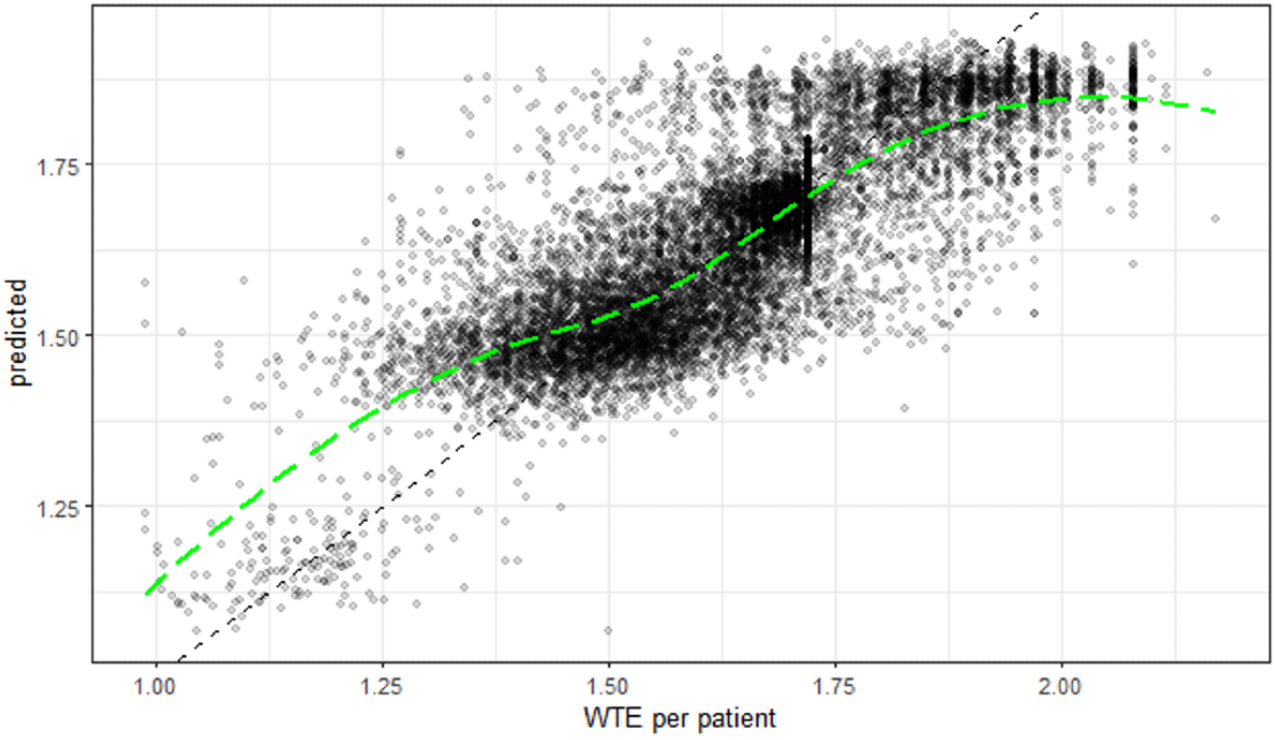
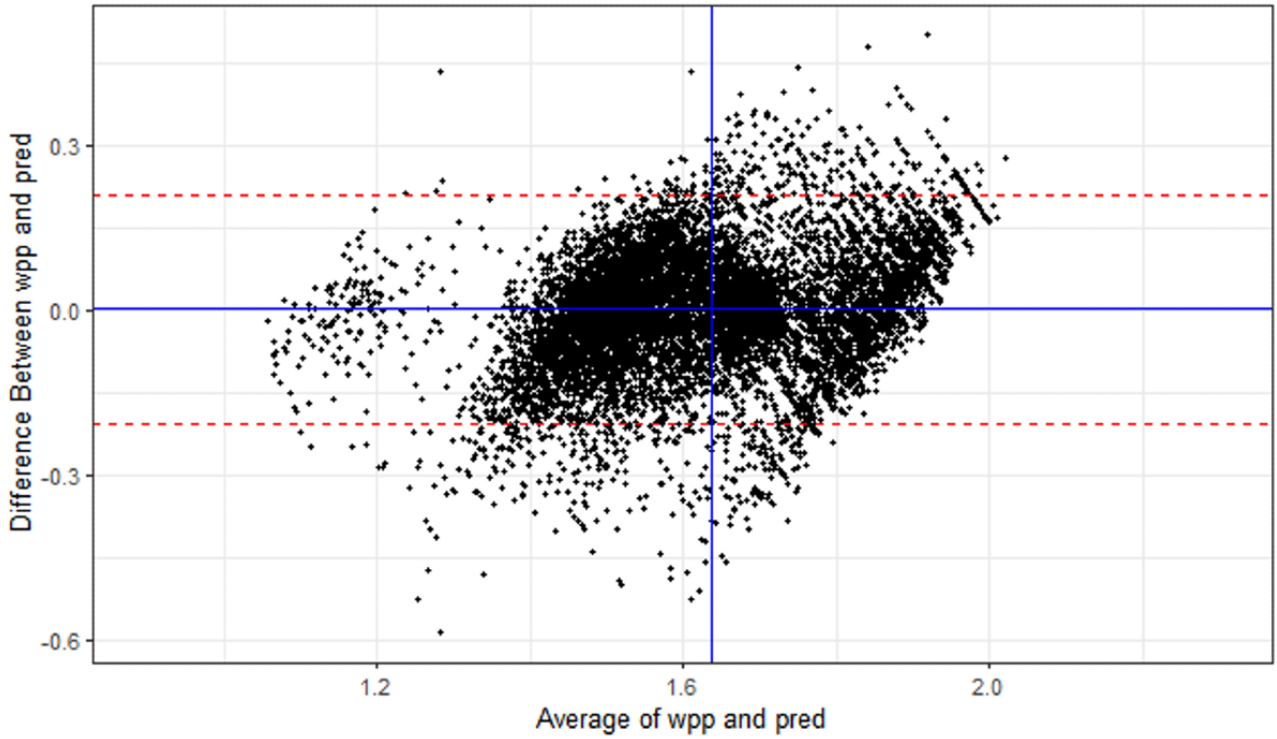


Figure 4. Bland-Altman plot of test model assessments and predictions. pred: model prediction; wpp: whole-time equivalent per patient.



Discussion

Main Findings

In this study, we used a limited set of routine patient data to estimate the demand for nursing staff on general and high-care hospital wards and admission units. We found that data on patient demographics, routes of admission, ward transfers, diagnoses, and admission NEWS, which are available in hospital systems, could be used to estimate the results of assessments made using a PCS with a moderate degree of precision. The predictions of WTE per patient were on average within 5% of the recorded estimates when applied to a test set. Calibration "in the large" was good in the test set, with the mean prediction being only 0.002 WTE per patient less than the recorded mean [18]. However, a calibration curve showed that the model tended to underestimate at higher workloads. This would be the case

XSL•FO
RenderX

if some dimensions of patients' care needs in more acute wards were not being adequately represented in the dataset. A "by ward" sub-analysis of the model estimates showed that the surgical high care unit and the renal transplant unit were the 2 wards where the model underestimated the most (as proportions of predictions). This might indicate the model is lacking variables that adequately capture the acuity and dependency of patients after major surgery. If the model were to be used as it is, a professional judgment framework, such as that published by Saville et al [19], should be used, which might recommend considering adjustment of the estimates where they exceeded 1.75 WTE or where there were high-care beds in the ward.

The predictors were not chosen to be orthogonal; they clearly have correlations when considering their potential effect on nurse workload. That means Figure 2 explaining their contribution to estimating workload needs to be interpreted with care. It is not surprising that the admission unit indicator makes the largest contribution since an approximately 10% uplift in nurse staffing for admission units is baked into the PCS, which determines the target WTE per patient. It is perhaps expected that the age, comorbidity index, and admission NEWS case mix variables of ward occupancy influence estimates of workload. However, the marked contribution of gender invites comment. It may reflect staffing in single-sex wards dealing with gynecological or urological conditions.

While overall fit was good, the Bland-Altman plot shown in Figure 4 revealed a distinct artifact of 45-degree downward-sloping lines, which arises from ranges of continuous prediction values estimating a given workload derived from the discrete set of multiplier values in the PCS and the numbers of patients in wards. There is a degree of subjectivity in categorizing patients in the PCS into one of the 4 levels, and there is a possibility that there was some up-coding of assessments in which patients were put into a higher category, for example, level 1b rather than level zero, which might boost a ward's chances of getting more resources [20]. The high proportion of patient assessments in the level 1b category shown in Table 2 possibly suggests some of these were erroneous, although patients with dependent care needs may have longer than average stays with opportunity for more categorizations at that level.

In conversations, safe staffing managers and leads at a number of hospitals have expressed concerns regarding the accuracy and reliability of manual patient categorizations by ward staff. An automated workload prediction system would be objective and eliminate or reduce a source of bias. It would also remove the need for training staff in carrying out the assessments and retraining them when assessment methods are revised.

The OPCq and Perroca patient classification instruments for assessing patient care needs are more structured than the SNCT instrument, as they require scoring a patient across several domains before determining an overall category. The drawback to this rigor is that the assessments take longer. One nurse quoted in the publication by Ayan et al (2024) [21] concerning the Perroca instrument said: "Since we have been using it continuously, it does not take me much time now. It only takes five minutes to assess a patient; it couldn't be easier."

Our observational data (unpublished) from another study [22] suggests that assessing all patients on a 30-bedded ward 3 times per day with SNCT categorizations could occupy a senior nurse for up to 30 minutes per day, plus extra time for data entry.

The identification of 2 wards with outlier predictions is of interest. In the private patient unit, the model tended to predict higher staffing requirements than those identified in the assessments. This could arise because of a selection effect, whereby the occurrence of more elective procedures on more medically fit patients was not reflected in the variables used for this population. In contrast, the predicted workload estimates for the surgical high care unit tended to be too low, and this might mean the model is not adjusting adequately for these acutely ill patients. Additional predictors to adjust for operational severity might improve the predictions.

The surprising accuracy of the predictions on limited data opens up the possibility of automated near-time assessments and consequently freeing up some nursing time. The feasibility of implementing the prediction algorithm in real-time or near-time is dependent on the data items being recorded and accessible in a timely manner. In the United Kingdom, basic patient admission data is usually recorded in near-time in a patient administration system with electronic interfacing, though the clinical coding of diagnoses in the same system is often much later. However, the diagnoses the algorithm uses are largely for long-term conditions or conditions known on presentation, in which case they may already be present in the electronic clinical history or recorded in nursing or clinical handover documentation. A National Health Service (NHS) England-sponsored digital maturity assessment of UK hospital trusts reports that 32 of 132 acute trusts have electronic nursing and physician documentation [23], and that number is rising, so real-time electronic provision of patient conditions is becoming more widespread.

Comparison With Prior Work

The approach taken in this study differs from previous studies that built models or made estimates of actual historic staffing levels [24-26]. In contrast, our approach was to build a model of estimated staffing requirements trained on the records of an existing staffing estimation tool [27]. Unlike the classifier model built by Rosa [7], which was trained on values from the PPCI to make patient categorizations, ours was a prediction model of ward staffing requirements. While the prediction of PPCI values was only moderately accurate (72% correct classification), in our study, the magnitude of errors for estimating ward staffing requirements was, on average, small, with a mean average percentage error of less than 5% and 95% of estimates within 14% of the assessed value. The required precision is an open question, but staffing within ±15% of measured demand is used as a criterion to define acceptable variation in one widely used system [28].

The method we have used to build a model that is trained on the ward workload is flexible and would work for other patient acuity and dependency scoring instruments that assign an ordinal value for the patient's care needs.

XSL•FO
RenderX

Limitations

The dataset was limited in terms of longitudinal clinical data regarding patient conditions. While it contained the NEWS on admission, it did not have subsequent scores or individual vital signs. Without time-varying variables such as NEWS and other assessments that reflect a patient's evolving acuity, the model is relying on the ward case mix not varying from the average in terms of proportions of patients medically fit for discharge or proportions deteriorating. These 2 cases work in opposite directions in terms of workload, those patients who are medically fit probably requiring less nursing care, while those who deteriorate probably requiring more nursing care. A systematic bias in the model performance is not easy to determine without further information. Also, as noted earlier in the main findings, the poor performance of the model in the private patient unit and in surgical high care might result from the model lacking information on surgical procedures and operation severity. This limits the settings in which the current model might be used.

Another limitation that might have impacted the accuracy of the predictions was the reliability of the recorded patient classifications. The use of the acuity categorization tool for estimating staffing requirements in the dataset was new to the hospital at the time; hence, the reliability of the assessment may have depended for a period on the effectiveness of training given to ward assessors and monitoring of the use of the tool.

The robustness and generalizability of the model need to be checked by assessing its performance using data from other hospitals. It is possible that variation in patient case mix and in how hospitals apply SNCT patient acuity categorizations could affect model performance. It should also be noted that while the aim of this study was to estimate workload that matched the existing SNCT-based assessments, the tool in use did not refine workload requirements by skill mix, for example, advising how many registered nurses and how many nurse support staff might meet the requirements, nor about requirements for specialist skills. This would be a useful step in matching requirements to available resources and might be the subject of further work.

Conclusions

This research demonstrated a way of building a moderately accurate prediction model of nurse staffing requirements from a limited dataset of routine data by training the model on records of an established patient acuity and dependency patient classification tool. The results demonstrate the potential for automating assessments of nurse staffing requirements from routine data, reducing time spent on this nonclinical overhead, and improving monitoring of real-time staffing pressures.

Acknowledgments

This study was funded by the National Institute of Health Research (NIHR) Applied Research Collaboration Wessex. For the purpose of open access, the author has applied a CC BY public copyright license to any author accepted manuscript version arising from this submission.

Data Availability

The datasets generated or analyzed during this study are not publicly available due to the nature of the data (individual patient data) and the data-sharing agreements with the data providers.

Conflicts of Interest

None declared.

Multimedia Appendix 1
Diagnosis groupings, results, and software.
[DOCX File, 37 KB - medinform_v13i1e71666_app1.docx]

References

1. Workforce management, PCAS, and the RFP process. Nursing World. 2017. URL: https://www.nursingworld.org/practice-policy/nurse-staffing/workforce-management-pcas-and-the-rfp-process/ [accessed 2024-09-03]
2. Shin S, Park JH, Bae SH. Nurse staffing and nurse outcomes: a systematic review and meta-analysis. Nurs Outlook 2018;66(3):273-282. [doi: 10.1016/j.outlook.2017.12.002] [Medline: 29685321]
3. Dall'Ora C, Saville C, Rubbo B, Turner L, Jones J, Griffiths P. Nurse staffing levels and patient outcomes: a systematic review of longitudinal studies. Int J Nurs Stud 2022 Oct;134:104311. [doi: 10.1016/j.ijnurstu.2022.104311] [Medline: 35780608]
4. Safer nursing care tool. NHS England. 2013. URL: https://www.england.nhs.uk/nursingmidwifery/safer-staffing-nursing-and-midwifery/safer-nursing-care-tool/ [accessed 2025-07-25]
5. Fagerström L, Lønning K, Andersen MH. The RAFAELA system: a workforce planning tool for nurse staffing and human resource management. Nurs Manag (Harrow) 2014 May;21(2):30-36. [doi: 10.7748/nm2014.04.21.2.30.e1199] [Medline: 24779764]

XSL•FO
RenderX

6. Perroca MG. The new version of a patient classification instrument: assessment of psychometric properties. J Adv Nurs 2013 Aug;69(8):1862-1868. [doi: 10.1111/jan.12038] [Medline: 23157307]
7. Rosa NGD, Vaz TA, Lucena AF. Nursing workload: use of artificial intelligence to develop a classifier model. Rev Lat Am Enfermagem 2024;32:e4239. [doi: 10.1590/1518-8345.7131.4239] [Medline: 38985046]
8. Griffiths P, Saville C, Ball JE, et al. The Safer Nursing Care Tool as a guide to nurse staffing requirements on hospital wards: observational and modelling study. Health Serv Deliv Res 2020;8(16):1-162. [doi: 10.3310/hsdr08160]
9. Consequences, costs and cost-effectiveness of different workforce configurations in English acute hospitals: a longitudinal retrospective study using routinely collected data. NIHR Funding and Awards. 2020. URL: https://www.fundingawards.nihr.ac.uk/award/NIHR128056 [accessed 2024-09-13]
10. National Early Warning Score (NEWS) 2. Royal College of Physicians. 2022. URL: https://www.rcplondon.ac.uk/projects/outputs/national-early-warning-score-news-2 [accessed 2023-08-17]
11. Smith S, Casey A, Hurst K, Fenton K, Scholefield H. Developing, testing and applying instruments for measuring rising dependency-acuity's impact on ward staffing and quality. Int J Health Care Qual Assur 2009;22(1):30-39. [doi: 10.1108/09526860910927934] [Medline: 19284169]
12. Sundararajan V, Henderson T, Perry C, Muggivan A, Quan H, Ghali WA. New ICD-10 version of the Charlson comorbidity index predicted in-hospital mortality. J Clin Epidemiol 2004 Dec;57(12):1288-1294. [doi: 10.1016/j.jclinepi.2004.03.012] [Medline: 15617955]
13. Campbell MJ, Jacques RM, Fotheringham J, Maheswaran R, Nicholl J. Developing a summary hospital mortality index: retrospective analysis in English hospitals over five years. BMJ 2012 Mar 1;344(7848):e1001. [doi: 10.1136/bmj.e1001] [Medline: 22381521]
14. Soong JTY, Kaubryte J, Liew D, et al. Dr Foster global frailty score: an international retrospective observational study developing and validating a risk prediction model for hospitalised older persons from administrative data sets. BMJ Open 2019 Jun 22;9(6):e026759. [doi: 10.1136/bmjopen-2018-026759] [Medline: 31230009]
15. Wood SN, Pya N, Säfken B. Smoothing parameter and model selection for general smooth models. J Am Stat Assoc 2016 Oct 1;111(516):1548-1563 [FREE Full text] [doi: 10.1080/01621459.2016.1180986]
16. Ojeda FM, Jansen ML, Thiéry A, et al. Calibrating machine learning approaches for probability estimation: a comprehensive comparison. Stat Med 2023 Dec 20;42(29):5451-5478. [doi: 10.1002/sim.9921] [Medline: 37849356]
17. Martin Bland J, Altman D. Statistical methods for assessing agreement between two methods of clinical measurement. Lancet 1986 Feb;327(8476):307-310. [doi: 10.1016/S0140-6736(86)90837-8]
18. Van Calster B, McLernon DJ, van Smeden M, Wynants L, Steyerberg EW, Topic Group 'Evaluating diagnostic tests and prediction models' of the STRATOS initiative. Calibration: the Achilles heel of predictive analytics. BMC Med 2019 Dec 16;17(1):230. [doi: 10.1186/s12916-019-1466-7] [Medline: 31842878]
19. Saville C, Griffiths P, Casey A, et al. Professional judgement framework: a guide to applying professional judgement in nurse staffing reviews.: ePrints Soton; 2022. URL: https://eprints.soton.ac.uk/478317/ [accessed 2025-06-03]
20. Hurst K. Gaming and up-coding. Nurs Manag (Harrow) 2009 Feb;15(9):19-23. [doi: 10.7748/nm2009.02.15.9.19.c6880] [Medline: 19248324]
21. Ayan G, Türkmen E, Uğur E, et al. Determination of nursing care times based on the perroca patient classification instrument in the inpatient oncology unit: a mixed method study. Semin Oncol Nurs 2024 Apr;40(2):151608. [doi: 10.1016/j.soncn.2024.151608] [Medline: 38402019]
22. Griffiths P, Saville C, Ball J, Culliford D, Pattison N, Monks T. Performance of the Safer Nursing Care Tool to measure nurse staffing requirements in acute hospitals: a multicentre observational study. BMJ Open 2020 May 15;10(5):e035828. [doi: 10.1136/bmjopen-2019-035828] [Medline: 32414828]
23. Future Health Intelligence. URL: https://digitalhealthintelligence.net/digital-maturity-acute-nhs-snapshot-report/ [accessed 2024-11-10]
24. Meyer KR, Fraser PB, Emeny RT. Development of a nursing assignment tool using workload acuity scores. J Nurs Adm 2020 Jun;50(6):322-327. [doi: 10.1097/NNA.0000000000000892] [Medline: 32427663]
25. Musy SN, Endrich O, Leichtle AB, Griffiths P, Nakas CT, Simon M. The association between nurse staffing and inpatient mortality: a shift-level retrospective longitudinal study. Int J Nurs Stud 2021 Aug;120:103950 [FREE Full text] [doi: 10.1016/j.ijnurstu.2021.103950] [Medline: 34087527]
26. Ostberg N, Ling J, Winter SG, et al. Quantifying paediatric intensive care unit staffing levels at a paediatric academic medical centre: a mixed-methods approach. J Nurs Manag 2021 Oct;29(7):2278-2287. [doi: 10.1111/jonm.13346] [Medline: 33894027]
27. Smith J, Forde V, Goodman M, Cannaby AM, Radford M. How to keep score of acuity and dependency. Nurs Manag (Harrow) 2009 Nov 26;16(8):14-19. [doi: 10.7748/nm2009.12.16.8.14.c7392]
28. Rauhala A, Fagerström L. Determining optimal nursing intensity: the RAFAELA method. J Adv Nurs 2004 Feb;45(4):351-359. [doi: 10.1046/j.1365-2648.2003.02918.x] [Medline: 14756829]

XSL•FO
RenderX

Abbreviations

GAM: generalized additive regression model
NEWS: National Early Warning Score
OPCq: Oulu Patient Classification qualisan
PCS: patient classification system
PPCI: Perroca Patient Classification Instrument
SHMI: summary hospital mortality indicator
SNCT: safer nursing care tool
WTE: whole-time equivalent

Edited by A Castonguay; submitted 24.01.25; peer-reviewed by A Leichtle, J Choi; revised version received 11.06.25; accepted 17.06.25; published 31.07.25.

Please cite as:
Meredith P, Saville C, Dall'Ora C, Weeks T, Wierzbicki S, Griffiths P
Estimating Nurse Workload Using a Predictive Model From Routine Hospital Data: Algorithm Development and Validation
JMIR Med Inform 2025;13:e71666
URL: https://medinform.jmir.org/2025/1/e71666
doi:10.2196/71666

© Paul Meredith, Christina Saville, Chiara Dall'Ora, Tom Weeks, Sue Wierzbicki, Peter Griffiths. Originally published in JMIR Medical Informatics (https://medinform.jmir.org), 31.7.2025. This is an open-access article distributed under the terms of the Creative Commons Attribution License (https://creativecommons.org/licenses/by/4.0/), which permits unrestricted use, distribution, and reproduction in any medium, provided the original work, first published in JMIR Medical Informatics, is properly cited. The complete bibliographic information, a link to the original publication on https://medinform.jmir.org/, as well as this copyright and license information must be included.

XSL•FO
RenderX

Original Paper

Retracted: A Dynamic Adaptive Ensemble Learning Framework for Noninvasive Mild Cognitive Impairment Detection: Development and Validation Study

Aoyu Li[1], PhD; Jingwen Li[2], BD; Yishan Hu[3], PhD; Yan Geng[4], MD; Yan Qiang[5], PhD; Juanjuan Zhao[1,3], PhD

[1]School of Software, Taiyuan University of Technology, Jingzhong, China

[2]School of Computer Science, Xijing University, Xian, China

[3]College of Computer Science and Technology, Taiyuan University of Technology, Jinzhong, China

[4]Clinical Laboratory and Geriatric, Shanxi Provincial People's Hospital, Taiyuan, China

[5]School of Software, North University of China, Taiyuan, China

Corresponding Author:
Juanjuan Zhao, PhD
School of Software
Taiyuan University of Technology
No. 319, University Street, Yuji District
Jingzhong, 030600
China
Phone: 86 18636664123
Email: zhaojuanjuan@tyut.edu.cn

Related Articles:

Companion article: https://medinform.jmir.org/2025/1/e75352/

Do not cite this article - this article has been retracted.Retraction notice: https://medinform.jmir.org/2025/1/e77635

Abstract

Background: The prompt and accurate identification of mild cognitive impairment (MCI) is crucial for preventing its progression into more severe neurodegenerative diseases. However, current diagnostic solutions, such as biomarkers and cognitive screening tests, prove costly, time-consuming, and invasive, hindering patient compliance and the accessibility of these tests. Therefore, exploring a more cost-effective, efficient, and noninvasive method to aid clinicians in detecting MCI is necessary.

Objective: This study aims to develop an ensemble learning framework that adaptively integrates multimodal physiological data collected from wearable wristbands and digital cognitive metrics recorded on tablets, thereby improving the accuracy and practicality of MCI detection.

Methods: We recruited 843 participants aged 60 years and older from the geriatrics and neurology departments of our collaborating hospitals, who were randomly divided into a development dataset (674/843 participants) and an internal test dataset (169/843 participants) at a 4:1 ratio. In addition, 226 older adults were recruited from 3 external centers to form an external test dataset. We measured their physiological signals (eg, electrodermal activity and photoplethysmography) and digital cognitive parameters (eg, reaction time and test scores) using the clinically certified Empatica 4 wristband and a tablet cognitive screening tool. The collected data underwent rigorous preprocessing, during which features in the time, frequency, and nonlinear domains were extracted from individual physiological signals. To address the challenges (eg, the curse of dimensionality and increased model complexity) posed by high-dimensional features, we developed a dynamic adaptive feature selection optimization algorithm to identify the most impactful subset of features for classification performance. Finally, the accuracy and efficiency of the classification model were improved by optimizing the combination of base learners.

Results: The experimental results indicate that the proposed MCI detection framework achieved classification accuracies of 88.4%, 85.5%, and 84.5% on the development, internal test, and external test datasets, respectively. The area under the curve for the binary classification task was 0.945 (95% CI 0.903-0.986), 0.912 (95% CI 0.859-0.965), and 0.904 (95% CI 0.846-0.962) on these datasets. Furthermore, a statistical analysis of feature subsets during the iterative modeling process revealed that the decay

XSL•FO
RenderX

time of skin conductance response, the percentage of continuous normal-to-normal intervals exceeding 50 milliseconds, the ratio of low-frequency to high-frequency (LF/HF) components in heart rate variability, and cognitive time features emerged as the most prevalent and effective indicators. Specifically, compared with healthy individuals, patients with MCI exhibited a longer skin conductance response decay time during cognitive testing (P<.001), a lower percentage of continuous normal-to-normal intervals exceeding 50 milliseconds (P<.001), and higher LF/HF (P<.001), accompanied by greater variability. Similarly, patients with MCI took longer to complete cognitive tests than healthy individuals (P<.001).

Conclusions: The developed MCI detection framework has demonstrated exemplary performance and stability in large-scale validations. It establishes a new benchmark for noninvasive, effective early MCI detection that can be integrated into routine wearable and tablet-based assessments. Furthermore, the framework enables continuous and convenient self-screening within home or nonspecialized settings, effectively mitigating underresourced health care and geographic location constraints, making it an essential tool in the current fight against neurodegenerative diseases.

(JMIR Med Inform 2025;13:e60250) doi:10.2196/60250

KEYWORDS

mild cognitive impairment; ensemble learning; harmony search; combination optimization; digital cognitive assessment; physiological signal; cognitive impairment; detection; machine learning; cognitive metrics; photoplethysmography; neurodegenerative; Alzheimer; cognitive decline

Introduction

Background

Neurodegenerative conditions such as Alzheimer disease (AD) and related dementias precipitate accelerated cognitive deterioration, markedly impacting patients' daily lives and social engagement [1]. Current estimates suggest that approximately 50 million individuals worldwide suffer from dementia, with this number expected to soar to 152 million by 2050 [2]. Generally, patients diagnosed with mild cognitive impairment (MCI) are at a much higher risk of developing dementia [3]. MCI serves as an intermediate stage between normal cognitive aging and the severe pathological decline of dementia, influencing individuals' cognitive functions, social abilities, and mental health, and may lead to emotional disorders that disrupt daily life [4]. Epidemiological data reveal that the incidence of MCI is 6.7% among those aged 60-64 years, 8.4% for 65- to 69-year-olds, 10.1% for 70- to 74-year-olds, 14.8% for 75- to 79-year-olds, and 25.2% for 80- to 84-year-olds [5]. The annual transition rate from MCI to dementia or AD is about 10%-15% [6], significantly higher than the 1%-2% annual incidence of dementia in the general population. Despite various potential treatments for AD, including enzymes that inhibit the production of amyloid-β and antibodies that clear amyloid-β from the brain [7], no current medications can fully cure dementia or significantly alter its clinical course. Moreover, studies indicate that early intervention is effective, necessitating precise and sensitive diagnostic measures for MCI [8]. Thus, early identification of MCI is crucial as it enables timely interventions to slow cognitive decline and alleviate the burden of dementia [9].

Wearable devices provide a near-continuous, passive data collection method, offering a convenient and minimally invasive approach for the ongoing monitoring and tracking of cognitive decline in patients with MCI. Existing studies have demonstrated that various physiological indicators, such as heart rate variability [10], electrodermal activity [11], gait variability [12], skin temperature [13], respiratory rate [14], electroencephalography [15], eye movement [16], and electromyography [17], can be effectively used to assess cognitive function changes, providing an objective basis for the auxiliary diagnosis of early cognitive impairment. However, despite the availability of diverse physiological data from patients with MCI, challenges remain in the effective utilization of these data due to the complexity of high-dimensional information (eg, feature redundancy, strong interfeature correlations, and noise interference) and the technical difficulties in multimodal data integration (eg, insufficient feature extraction and dimensionality reduction methods, challenges in aligning heterogeneous modalities, and limitations in handling noise and missing data).

In recent years, machine learning techniques have been increasingly applied to analyzing and processing complex, high-dimensional physiological data to facilitate the early detection of cognitive disorders, including MCI. Traditional algorithms such as naive Bayes [18], k-nearest neighbors (KNN) [19], support vector machines (SVM) [20], and logistic regression (LR) [21] have demonstrated a certain degree of effectiveness in identifying high-risk MCI populations. However, due to the limitations of single algorithms in modeling high-dimensional and multimodal data, such as insufficient representational capacity and unstable generalization performance, researchers have gradually shifted toward exploring ensemble methods, including bagging [22], boosting [23], and stacking [24]. These ensemble learning techniques integrate predictions from multiple models, effectively mitigating the limitations of single models and significantly improving overall predictive accuracy and robustness.

In addition, various swarm intelligence algorithms have been introduced for critical tasks such as feature selection and hyperparameter optimization to enhance the performance of machine learning models in high-dimensional data analysis. Swarm intelligence algorithms, including Harmony Search (HS) [25], Particle Swarm Optimization [26], and Genetic Algorithms [27], simulate cooperative behaviors observed in nature and have demonstrated outstanding potential in solving global optimization problems. The HS algorithm has gained attention as a metaheuristic optimization technique due to its simplicity,

XSL•FO
RenderX

ease of implementation, and low-parameter adjustment requirements. Inspired by musical harmony improvisation, the HS algorithm iteratively adjusts the pitch of each instrument (analogous to high-dimensional features) to find the optimal feature combination. This approach offers an effective solution for feature selection involving physiological data and cognitive parameters of MCI patients, showing promising prospects in improving model prediction accuracy and computational efficiency.

Objective

We propose a Dynamic Adaptive Ensemble Learning Framework based on an Improved Harmony Search (DAELF-HSI), designed to enhance MCI detection by addressing issues of feature redundancy and the inefficiency of multimodal data fusion. In contrast to previous studies, this research integrates multimodal physiological data collected through wearable wristbands (eg, heart rate variability and electrodermal activity) with cognitive assessment metrics recorded on tablet devices (eg, reaction time and test scores), aiming to exploit the potential value of multisource data comprehensively, thereby improving the accuracy and clinical utility of MCI detection. We hypothesize that the DAELF-HSI framework will not only effectively distinguish between patients with MCI and healthy individuals but also uncover critical discriminative information pertinent to MCI.

Methods

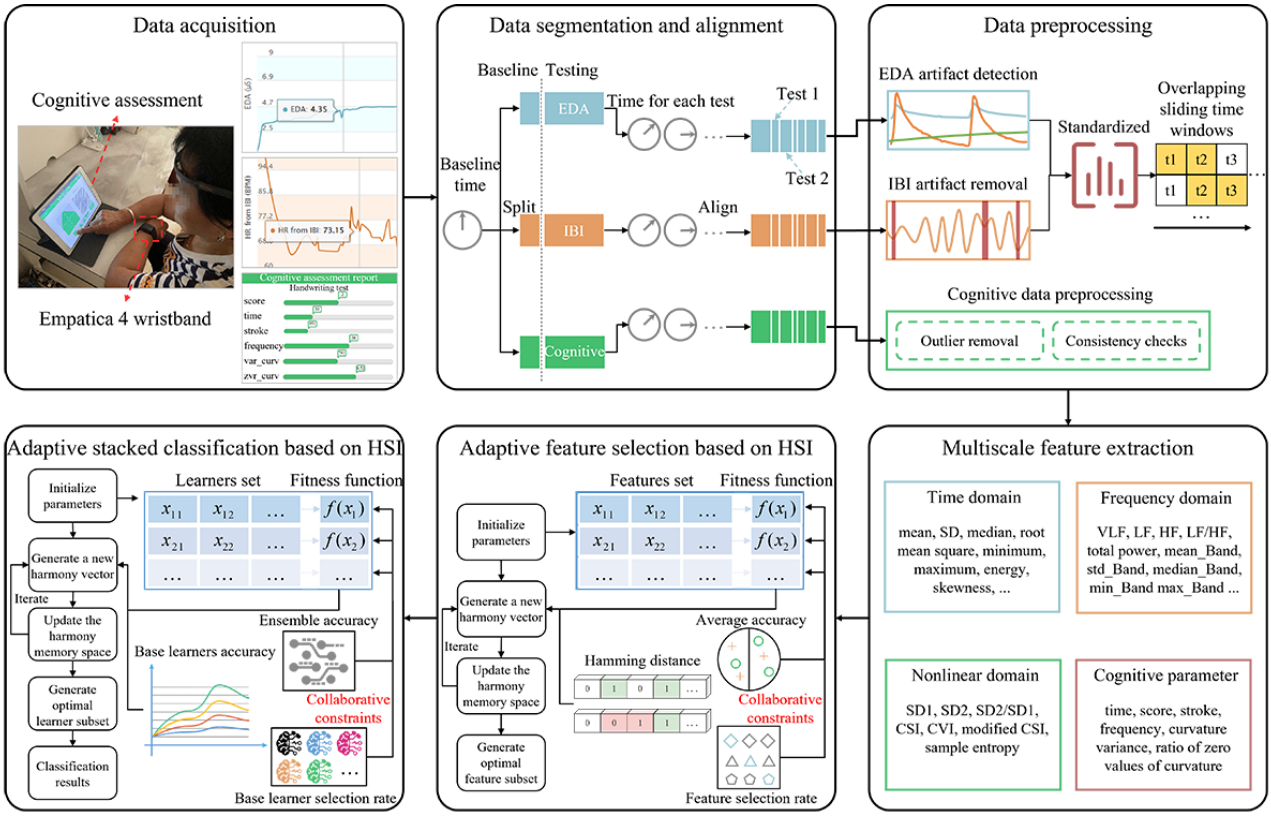
Ethical Considerations

The research was reviewed and approved by the Biomedical Ethics Review Committee of Taiyuan University of Technology (20240124). All methods were performed following relevant guidelines and regulations. Written informed consent was obtained from eligible participants under the principles of the Declaration of Helsinki. All participants signed an informed consent form. We provided US $10 to eligible older adults as compensation for participation.

Overview of the Proposed Detection Framework

Figure 1 illustrates a Dynamic Adaptive Ensemble Learning Framework for MCI detection, integrating multimodal data that integrates individual physiological signals with cognitive tasks derived from serious games. The framework begins with data collection, followed by time series segmentation, alignment, and preprocessing. It then progresses to feature extraction and selection, culminating in constructing a classification model. Notably, the modules within the framework are interconnected and sequentially executed, forming a cohesive unit. The following sections will detail the stages, demonstrating the adaptability and effectiveness of the proposed MCI detection framework.

Figure 1. A dynamic adaptive ensemble learning framework for mild cognitive impairment detection. CSI: cardiac sympathetic index; CVI: cardiovascular index; EDA: electrodermal activity, HF: high frequency; HSI: harmony search improved; IBI: interbeat interval; LF: low frequency; VLF: very low frequency.



Experimental Participants and Procedures

The dataset used for machine learning modeling involves 843 participants aged 60 and older recruited from partner hospitals. The participants were randomly divided into a development dataset (674/843), and an independent testing dataset (169/843) in a ratio of 4:1. In addition, 226 older adults were recruited from 3 external centers to constitute an external testing dataset.

XSL•FO
RenderX

Participants were identified using a purposive sampling method [28], with the process being meticulously overseen by experienced neurologists. The inclusion criteria for participants were (1) age ≥60 years; (2) normal hearing and vision, or corrected to normal; (3) completion of the Mini-Mental State Examination (MMSE) test; (4) completion of the Montreal Cognitive Assessment (MoCA) test; (5) capability to engage in moderate activity without physical disabilities; (6) absence of severe depressive symptoms or other neurological disorders such as stroke or Parkinson disease; (7) ability to effectively use smart devices such as smartphones and tablets; and (8) informed consent signed by the participants or their guardians.

Neurologists contacted potential participants during their clinic visits, explaining the study's purpose, related procedures, and the possible impact of the research findings. Once potential participants expressed interest, neurologists conducted comprehensive medical evaluations, including detailed medical history collection, physical examinations, brain imaging (magnetic resonance imaging or computed tomography scans), and cognitive function assessments (using the MMSE and MoCA scales). The MCI group comprised 514 (48.1%) participants who scored below 26 on the MoCA, while the healthy control (HC) group included 555 (51.9%) healthy individuals without symptoms of cognitive decline. Brain imaging scans revealed no structural abnormalities causing cognitive impairment. Furthermore, all patients with MCI met the criteria proposed by the National Institute of Neurological and Communicative Disorders and Stroke and the Alzheimer's Disease and Related Disorders Association [29]. We also administered the habitual hand questionnaire [30], which consisted of 13 items, to all participants. The MCI and HC groups were matched for age, gender, hand preference, education, average sleep duration (in general), and years of smart device use. All participants completed cognitive tasks with the assistance of researchers, and there were no dropouts during the testing process. Table 1 summarizes the clinical and demographic characteristics of the 1069 participants enrolled across the development, internal, and external datasets.

Table 1. Characteristics of the 1069 participants enrolled across the development, internal, and external datasets.

	Training (n=674)		Testing (n=169)		External (n=226)		*P* value[c]
	MCI[a] (n=328)	HC[b] (n=346)	MCI (n=78)	HC (n=91)	MCI (n=108)	HC (n=118)	
Age (years), mean (SD)	70.39 (6.330)	69.64 (5.919)	69.85 (6.004)	69.46 (5.763)	74.29 (8.477)	73.9 (8.613)	.11[d]; .67[e]; .73[f]
Gender, n (%)							.22[d]; .81[e]; .64[f]
Women	181 (55.2)	207 (59.8)	44 (56.4)	53 (58.2)	61 (56.5)	63 (53.4)	—
Men	147 (44.8)	139 (40.2)	34 (43.6)	38 (41.8)	47 (43.5)	55 (46.6)	—
Hand preference, n (%)							.60[d]; .80[e]; .88[f]
Left	41 (12.5)	48 (13.9)	6 (7.7)	8 (7.5)	13 (12.0)	15 (12.7)	—
Right	287 (87.5)	298 (86.1)	72 (92.3)	83 (91.2)	95 (88.0)	103 (87.3)	—
Education years, mean (SD)	5.81 (3.781)	6.32 (3.744)	6.22 (4.012)	6.48 (3.903)	5.34 (3.421)	5.22 (3.457)	.08[d]; .66[e]; .79[f]
Hours of sleep, mean (SD)	7.53 (1.165)	7.40 (1.115)	7.51 (1.066)	7.82 (1.060)	7.13 (1.421)	7.01 (1.362)	.14[d]; .06[e]; .51[f]
Smart device use (years), mean (SD)	4.97 (2.060)	5.07 (1.918)	4.32 (2.665)	4.79 (2.563)	4.71 (2.336)	4.90 (2.326)	.53[d]; .24[e]; .55[f]

[a]MCI: mild cognitive impairment.

[b]HC: health control.

[c]*P* value: 2-tailed *t* tests (for continuous variables) and chi-square tests (for categorical variables).

[d]*P* value: statistical comparisons were performed between the MCI and HC groups within the training dataset.

[e]*P* value: statistical comparisons were performed between the MCI and HC groups within the testing dataset.

[f]*P* value: statistical comparisons were performed between the MCI and HC groups within the external dataset.

In the experimental setting, a well-trained experimenter instructed participants to sit on a comfortable chair and wear the Empatica 4 on their nondominant wrist. The Empatica 4 is a watch-like multisensor device that measures physiological data such as electrodermal activity (EDA), photoplethysmography, skin temperature, and accelerometer readings. It is compact, lightweight, and comfortable to wear, making it suitable for unobtrusive continuous monitoring during cognitive screening of older adults. The participants performed cognitive tasks on a 2019 iPad using the Brain Nursing mobile app developed by our team (Multimedia Appendix 1) [31], completing drawing-related tasks with an Apple Pencil. The system includes 11 single tasks and 3 dual tasks, each taking only 1-3 minutes, designed to assess attention; short-term memory; working memory; scene recall and situational reconstruction; visual-conceptual and visual-motor tracking; orientation; executive function; language comprehension and expression; logical thinking; and fine motor control. To minimize interference from the nondominant hand during the painting tasks, the experimenter provided appropriate assistance,

XSL•FO
RenderX

such as stabilizing the tablet. Upon completion of the testing, the Empatica 4 wristband was removed from the participant's wrist, physiological data were retrieved and downloaded through the Empatica 4 Connect portal, and cognitive data were exported from the cloud.

Data Segmentation and Alignment

Overview

For the collected multisource data, such as EDA, interbeat interval (IBI) for describing heart rate variability (HRV), and cognitive data, ensuring the integrity, continuity, and temporal alignment of the data is crucial. As participants perform cognitive tasks, the tablet automatically records timestamps for each test, providing a reference for aligning physiological data. Thus, we align the EDA and IBI data using the start and end times of each test, as described in the procedures listed below.

EDA Time Series Processing

Considering that the EDA.csv file downloaded from the cloud only contains information about the start time of the session and the sampling rate, it lacks the timestamps corresponding to each second of the signal. To address this deficiency, we generate a timestamp every 4 data points based on the session start time and the sensor sampling rate (4 Hz). Subsequently, we align the timestamps of the cognitive tests with the EDA series timestamps, thereby extracting the EDA signal segments corresponding to the specific cognitive tests.

IBI Time Series Processing

Due to the automatic discarding of unidentifiable heartbeats by the Empatica 4 wristband during measurement, the IBI.csv file contains discontinuities that do not match the actual measuring intervals. It is crucial to accurately identify and fill these measurement gaps to ensure data integrity in the analysis of IBI time series for various test tasks. Following the suggestions of Rafi et al [32], this study limits the physiologically feasible range for IBI to within 2 seconds, and any data beyond the threshold was automatically labeled as a measurement gap. Subsequently, cubic spline interpolation [33] is used to estimate the missing values within these gaps. The overall continuity of the IBI dataset in the temporal dimension is optimized by using a curve-fitting method based on available data points. Finally, new timestamps are added to the IBI data, aligning the timestamps of cognitive tests with those of the IBI series.

Data Preprocessing

Overview

Commercial wearable devices are prone to artifacts, measurement gaps, or deviations from the measurement regime during data recording [34,35]. To ensure reliable information is extracted from field-collected data, rigorous preprocessing is required to filter noise and artifacts and restore the original signal. Considering the differences among EDA, IBI, and digital parameters, we will detail the preprocessing methods for these metrics.

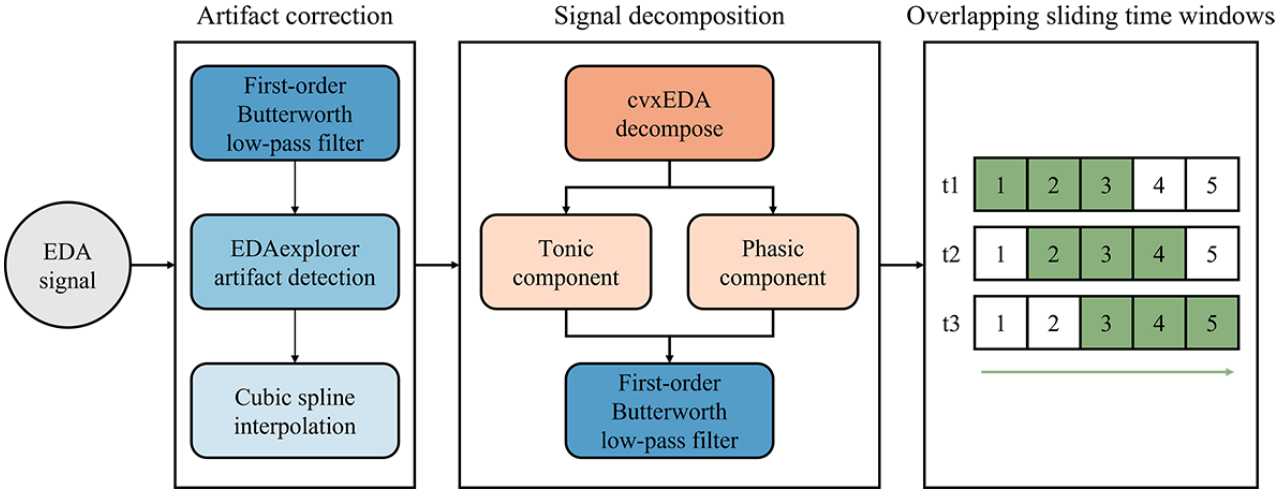
EDA Signal Preprocessing

EDA serves as a biosignal, mirroring the individual physiological and emotional states, and consists mainly of slowly varying tonic and rapidly fluctuating phasic activities. Tonic activity, also known as skin conductance level (SCL), primarily reflects the physiological activity level of an individual at rest, indicating the continuous regulation of the autonomic nervous system. In contrast, phasic activity, or SCR, is a rapid and transient physiological response to specific stimuli, revealing an individual's adaptability and reactivity to sudden events. To enhance EDA signal quality, we propose a multistage automatic artifact removal method, including artifact correction, signal decomposition, and overlapping sliding time windows, as shown in Figure 2. The specific steps involved are:

1. Low-pass filtering: EDA signal is filtered using a first-order Butterworth low-pass filter with a cutoff frequency of 0.6 Hz [36], which preserves its low-frequency components and eliminates high-frequency noise.
2. Artifact detection: EDAexplorer [37] is used to detect artifacts in the filtered signal, identifying and marking anomalies within the signal to provide a basis for data repair.
3. Cubic spline interpolation: apply cubic spline interpolation to the identified artifact segments, using segmented cubic polynomials to approximate missing data points while ensuring continuity in function values and their first and second derivatives, thereby smoothly completing the missing data.
4. Signal decomposition: by solving the convex optimization approach, cvxEDA [38] separates the signal into tonic and phasic components, enabling enhanced analysis and interpretation of the underlying physiological mechanisms within the EDA signal.
5. Component filtering: refilter the decomposed tonic and phasic components using a low-pass Butterworth filter to eliminate negative SCR and SCL values, enhancing the signal quality.
6. Time window segmentation: segment the processed tonic and phasic components into overlapping time windows of 60 seconds with a step size of 1 second to facilitate subsequent feature extraction.

XSL•FO
RenderX

Figure 2. Electrodermal activity signal preprocessing flow.



IBI Signal Preprocessing

Wearable devices commonly use photoplethysmography sensors to monitor the continuous variations in interbeat or R-R intervals. However, obtaining raw photoplethysmography data from the Empatica 4 wristband presents challenges, so we shifted to analyzing IBI data, which is more readily accessible. Analyzing IBI data allows for calculating HRV, reflecting the variations in time between consecutive heartbeats. Although Empatica 4 offers convenience and noninvasiveness for recording HRV, it still faces issues such as artifacts or measurement gaps [39,40]. Therefore, we initially adopted 4 artifact detection rules to identify artifacts, as shown in Textbox 1. Subsequently, detected artifacts were interpolated using cubic spline interpolation to fill in missing values. Finally, the cleaned IBI data was segmented into overlapping time windows of 60 seconds with a 1-second step size, creating datasets for subsequent feature extraction.

Textbox 1. List of interbeat interval artifact detection rules.

Study and rule description

Rafi et al [32]

- Discard any interbeat intervals that do not fall within the physiological range of 250-2000 milliseconds (equivalent to a heart rate of 30-240 beats per minute).

Malik et al [41]

- Each interbeat interval should be at most 20% from the previous one.

Acar et al [42]

- Calculate the average of the 9 interbeat intervals preceding the current interbeat interval. It should be removed if the current interbeat interval differs from this average by more than 20%.

Karlsson et al [43]

- Remove any interbeat interval that differs by more than 20% from the average of its immediate preceding and succeeding interbeat intervals.

Cognitive Data Preprocessing

Outlier removal and data consistency checks were performed manually to preprocess digital cognitive parameters. The specific steps include (1) format validation: ensuring that all data entries adhere to the required format specifications (eg, the time recorded in seconds and scores in numerical format) and correcting any inconsistencies; (2) range validation: checking that all data values fall within predefined acceptable ranges, such as ensuring reaction times are within a reasonable range of seconds; (3) continuity validation: assessing the continuity of the data, including verifying that the timestamps for each test are in sequential order and checking for any missing data points. Through these steps, we aim to identify and eliminate extreme outliers caused by user errors or external interference while ensuring the logical consistency of data format, range, and time series, thereby improving the overall quality and reliability of the data.

Multiscale Feature Extraction

In this study, we comprehensively analyzed data collected from the Empatica 4 wristband and tablet devices to explore participants' physiological and cognitive responses to various cognitive tasks. Specifically, we used the FLIRT toolkit [44] and NeuroKit2 [45] to extract 39 EDA-related features (including 17 SCL features and 22 SCR features) from the EDA signals and 23 features (including HR and HRV) from the IBI data. Furthermore, we collected several cognitive parameters,

XSL•FO
RenderX

including time, score, stroke, frequency, and curvature (variance and the ratio of 0 values) during each test. Detailed information regarding all these features is available in Multimedia Appendix 1.

Dynamic Adaptive Feature Selection Based on Improved Harmony Search

Feature selection plays a critical role in handling high-dimensional datasets, as not all features impact the outcome. An excessive number of features can result in the curse of dimensionality and increased model complexity. Therefore, this study proposes a feature selection algorithm based on HSI to sift through extracted physiological and cognitive features. Analogous to musical notes, each feature represents a note that may or may not be selected into a subset. Musicians repeatedly adjust the notes to achieve the best harmony effect until reaching a satisfactory harmony. Similarly, the feature selection algorithm based on HSI continuously tunes parameters and modifies the generated feature subset to ensure diversity and avoid convergence to local optima. In particular, we integrate Hamming distance into the HSI algorithm to gauge the disparity between the newly generated harmony vector and the optimal vector in the harmony memory. The Hamming distance is used to assess the similarity between these vectors to fine-tune the search probability. A high Hamming distance leads to a moderate reduction in the search probability to promote exploratory efforts, while a low Hamming distance results in a moderate increase in leveraging known information. Finally, to evaluate the quality of the harmony effect, we minimize the average classification error rate of all base learners and the feature selection rate as optimization objectives. The detailed algorithm is provided in Multimedia Appendix 2.

Dynamic Adaptive Stacking Classification Based on Improved Harmony Search

An essential goal of this study is to distinguish between healthy individuals and patients with MCI effectively. As mentioned, we opt for a subset of features demonstrating balanced performance across all base learners during the feature selection phase. Nevertheless, certain learners continue to demonstrate suboptimal performance, and merely stacking multiple base learners increases algorithmic complexity and computational demands. In essence, the selection of learners, akin to feature selection, constitutes a combinatorial optimization problem focused on enhancing classification performance. Thus, this study proposes using HSI to optimize the stacking of base learners. Unlike feature selection algorithms that use HSI, it leverages the accuracy of the current base learners and their quantity to guide hyperparameter adjustments. The strategy aims to mitigate the adverse effects of underperforming learners on the overall model while simultaneously enhancing model efficiency and minimizing computational costs. Furthermore, we selected the KNN, decision tree (DT), random forest (RF), Gaussian naive Bayes, SVM, multilayer perceptron, LR, gradient boosting DT, and XGBoost as base learners, with LR serving as the meta-learner. The detailed algorithm is provided in Multimedia Appendix 2.

Statistical Analysis and Machine Learning Model

This study analyzed demographic characteristics, cognitive parameters, and physiological features using the Statistical Package for the Social Sciences (SPSS, version 22.0 for Windows, IBM). Initially, the Kolmogorov-Smirnov test was used to assess whether continuous variables such as age, years of education, hours of sleep, years of smart device usage, and cognitive data conformed to a normal distribution. Descriptive statistics were described using means (SD) for normally distributed variables. Subsequently, the *t* test was used for between-group comparisons to determine if there were significant differences between the HC group and the MCI group. In contrast, we used the nonparametric Mann-Whitney U test for nonnormally distributed variables to assess intergroup differences. For categorical variables such as gender and hand preference, data were described in terms of counts (percentages), and the chi-square test was used for group comparisons. The significance level for all statistical analyses was set at $P<.05$. Furthermore, to validate the performance of the proposed detection framework, experiments were conducted using a 5-fold cross-validation approach, using 4 evaluation metrics (accuracy, precision, recall, and F_1-score) to assess the classification outcomes. All learners used the HSI for feature selection, and the average values were used as the final classification results.

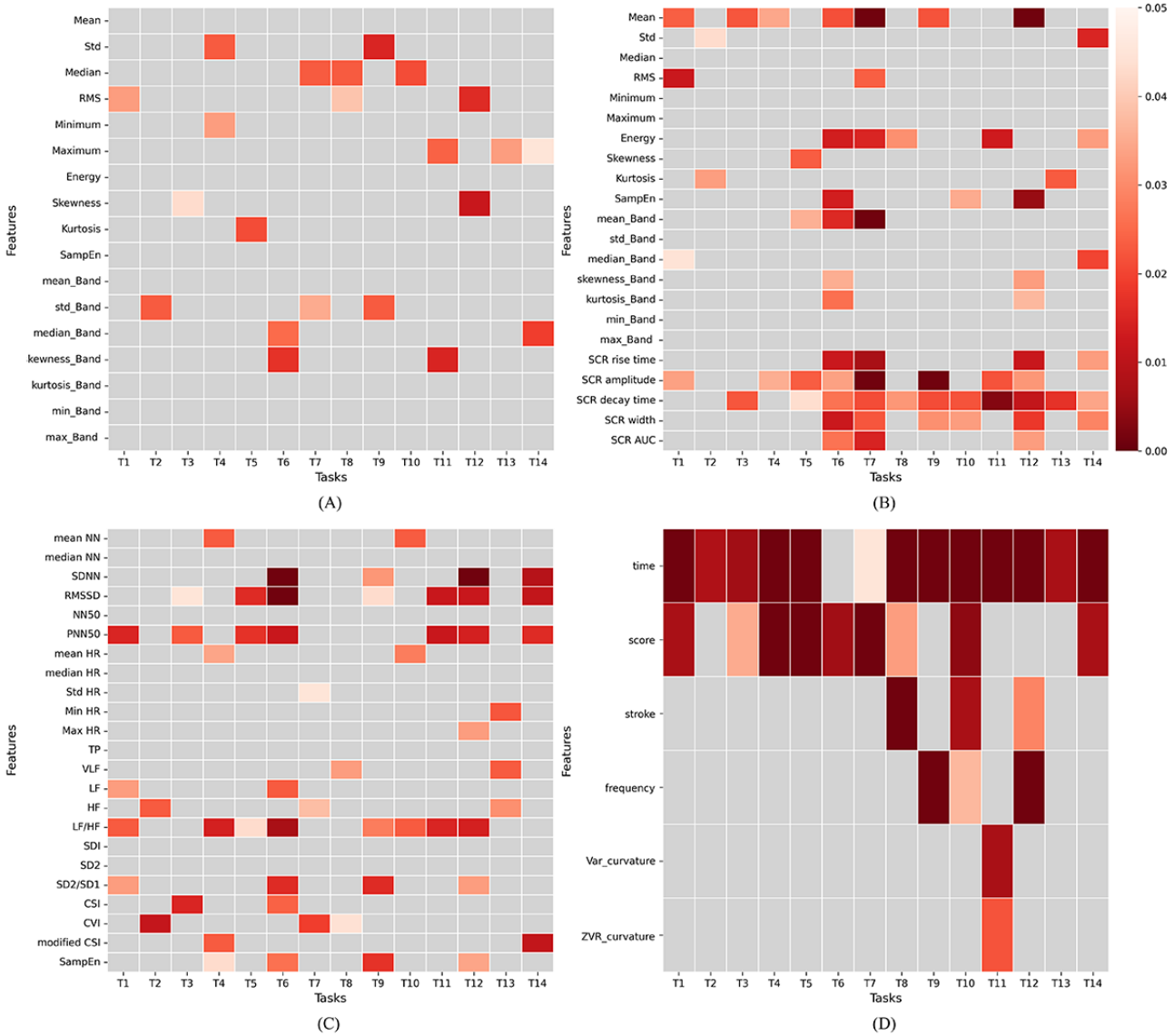
Results

Statistical Comparison of EDA, HRV, and Cognitive Features Between Groups

We conducted statistical analyses on features extracted from EDA, HRV, and cognitive tasks to identify the key features distinguishing between healthy individuals and patients with MCI. As shown in Figure 3, red squares indicate significant differences ($P<.05$) between the 2 groups on specific features during certain cognitive tasks, and the depth of the color reflects the degree of significance of these differences.

XSL•FO
RenderX

Figure 3. Results of the t tests performed on features extracted from electrodermal activity, heart rate variability, and cognitive tasks between groups. HRV: heart rate variability; SCL: skin conductance level; SCR: skin conductance response.



Based on observations from Figure 3A, relatively few SCL features distinguish between patients with MCI and healthy individuals, including the SD, median, root mean square, and SD of spectral power. Conversely, Figure 3B reveals more significant differences in SCR features, including mean, energy, amplitude, rise time, delay time, and width in the time domain and mean in the frequency domain. These findings highlight several key points: (1) the SD and root mean square of SCL indicate variability and instability in physiological responses, with differences between patients with MCI and healthy individuals reflecting disparate levels of physiological variability; (2) statistical differences in the SD of SCL spectral power between the groups indicate that patients with MCI exhibit significantly different physiological responses within specific frequency ranges, possibly related to impaired cognition associated with MCI; (3) statistical differences in SCR time domain features between groups indicate that patients with MCI exhibit variations in the intensity and timing of physiological responses, suggesting impaired regulatory capabilities of their nervous systems; and (4) variations in the mean values in the SCR frequency domain indicate that patients with MCI have different physiological response frequency distributions when processing stimuli compared with healthy individuals.

Figure 3C depicts the statistical analysis results applied to features extracted from HRV between patients with MCI and healthy controls. The analysis indicates statistically significant distinctions in HRV indices such as SDNN (SD of N-N intervals), RMSSD (root mean square of successive differences), PNN50 (percentage of successive R-R intervals > 50 ms), LF/HF (low-frequency to high-frequency ratio) ratio, SD2/SD1 (ratio of the SD2 and SD1 of Poincaré plot), and SampEn (sample entropy). These results highlight several key aspects which are (1) SDNN, RMSSD, and PNN50, which quantify overall and short-term heart rate variations, reveal disparities in autonomic nervous system functioning between the groups; (2) the LF/HF ratio reflects imbalances between sympathetic and parasympathetic nervous activities, indicating autonomic dysregulation in patients with MCI relative to controls; and (3) SD2/SD1 and SampEn focus on balance between long-term and short-term variability, as well as the complexity and irregularity

XSL•FO
RenderX

of HRV, illustrating differences in autonomic nervous system adaptability and complexity between groups. Finally, observations from Figure 3D reveal that (1) multiple cognitive tests using time and scores as indicators can significantly distinguish between healthy individuals and patients with MCI, and (2) features such as handwriting, frequency, and curvature show varying degrees of significant differences across different drawing tasks.

Performance of the DAELF-HSI in Mild Cognitive Impairment Detection

Table 2 lists the classification outcomes of the DAELF-HSI compared with 6 machine learning models and the application of HSI for feature selection in these models. Following a thorough assessment involving 100 iterations of 5-fold cross-validation, the DAELF-HSI demonstrated an average accuracy of 88.5%, surpassing the performance of other algorithms significantly. Moreover, it exhibited superior precision, recall, and F_1-score metrics, achieving 89.1%, 88.7%, and 88.9%, respectively, all at notably high levels. When HSI-based feature selection was not employed, the SVM model outperformed other machine learning algorithms with an accuracy of 79.6%. However, after integrating HSI feature selection, models like KNN-HSI and multilayer perceptron-HSI displayed improved performance, surpassing that of SVM-HSI. Noteworthy is the consistent enhancement in performance observed across all machine learning models upon the introduction of HSI feature selection, with accuracy improvements ranging from 3% to 5%, resulting in all models achieving accuracy levels exceeding 81%. It highlights the efficacy of the feature selection algorithm based on HSI in identifying crucial features that enhance the predictive capabilities of the machine learning models under investigation.

Table 2. Performance comparison of Dynamic Adaptive Ensemble Learning Framework based on an Improved Harmony Search with 6 machine learning models and applying Improved Harmony Search to model feature selection.

Methods	Accuracy, mean (SD)	Precision, mean (SD)	Recall, mean (SD)	F_1-score, mean (SD)
KNN[a]	0.792 (0.018)	0.775 (0.023)	0.806 (0.029)	0.790 (0.019)
SVM[b]	0.796 (0.024)	0.788 (0.025)	0.800 (0.020)	0.794 (0.027)
GNB[c]	0.771 (0.022)	0.787 (0.019)	0.796 (0.022)	0.791 (0.025)
DT[d]	0.786 (0.025)	0.791 (0.033)	0.783 (0.025)	0.787 (0.033)
MLP[e]	0.790 (0.017)	0.807 (0.025)	0.794 (0.026)	0.800 (0.019)
LR[f]	0.784 (0.020)	0.789 (0.034)	0.791 (0.028)	0.790 (0.038)
KNN-HSI[g]	0.842 (0.017)	0.848 (0.018)	0.830 (0.027)	0.839 (0.024)
SVM-HSI	0.831 (0.022)	0.833 (0.023)	0.839 (0.030)	0.825 (0.027)
GNB-HSI	0.815 (0.023)	0.815 (0.030)	0.800 (0.025)	0.807 (0.027)
DT-HSI	0.827 (0.019)	0.833 (0.022)	0.809 (0.028)	0.821 (0.031)
MLP-HSI	0.836 (0.022)	0.839 (0.024)	0.842 (0.025)	0.840 (0.018)
LR-HSI	0.817 (0.025)	0.815 (0.027)	0.823 (0.031)	0.819 (0.035)
DAELF-HSI[h] (ours)	0.885 (0.020)	0.891 (0.021)	0.887 (0.024)	0.889 (0.025)

[a]KNN: k-nearest neighbors.

[b]SVM: support vector machines.

[c]GNB: Gaussian naive Bayes.

[d]DT: decision tree.

[e]MLP: multilayer perceptron.

[f]LR: logistic regression.

[g]HSI: Improved Harmony Search.

[h]DAELF-HSI: Dynamic Adaptive Ensemble Learning Framework based on an Improved Harmony Search.

Similarly, Table 3 presents the effectiveness of DAELF-HSI in classification compared with 5 ensemble learning models, augmented by HSI feature selection. In line with the findings in Table 2, DAELF-HSI maintains its superior performance. Noteworthy is that the ensemble learning techniques outperform the individual machine learning models discussed earlier, with XGBoost achieving a commendable average accuracy of 81.9%. The Bagging model, which uses KNN as a base learner, demonstrates improved performance compared with the stand-alone KNN model. However, the bagging model using ensemble SVM as a base learner falls short of expectations, slightly underperforming compared with the stand-alone SVM model, possibly due to the inherent instability advantages associated with SVM.

XSL•FO
RenderX

Table 3. Performance comparison of Dynamic Adaptive Ensemble Learning Framework based on an Improved Harmony Search with 5 ensemble learning models and applying HSI to model feature selection.

Methods	Accuracy, mean (SD)	Precision, mean (SD)	Recall, mean (SD)	F_1-score, mean (SD)
Bag (KNN[a])	0.794 (0.022)	0.791 (0.031)	0.794 (0.026)	0.792 (0.027)
Bag (SVM[b])	0.779 (0.011)	0.788 (0.021)	0.780 (0.017)	0.784 (0.021)
RF[c]	0.804 (0.015)	0.802 (0.037)	0.816 (0.027)	0.809 (0.025)
GBDT[d]	0.813 (0.019)	0.816 (0.028)	0.813 (0.027)	0.814 (0.019)
XGBoost	0.819 (0.015)	0.825 (0.024)	0.810 (0.026)	0.817 (0.024)
Bag (KNN)-HSI[e]	0.833 (0.024)	0.842 (0.029)	0.821 (0.034)	0.831 (0.036)
Bag (SVM)-HSI	0.811 (0.016)	0.812 (0.024)	0.819 (0.027)	0.815 (0.024)
RF-HSI	0.854 (0.017)	0.858 (0.018)	0.847 (0.021)	0.852 (0.024)
GBDT-HSI	0.848 (0.027)	0.839 (0.025)	0.852 (0.023)	0.845 (0.016)
XGBoost-HSI	0.854 (0.022)	0.860 (0.020)	0.849 (0.028)	0.854 (0.029)
DAELF-HSI[f] (ours)	0.885 (0.020)	0.891 (0.021)	0.887 (0.024)	0.889 (0.025)

[a]KNN: k-nearest neighbors.

[b]SVM: support vector machines.

[c]RF: random forest.

[d]GBDT: gradient boosting decision tree.

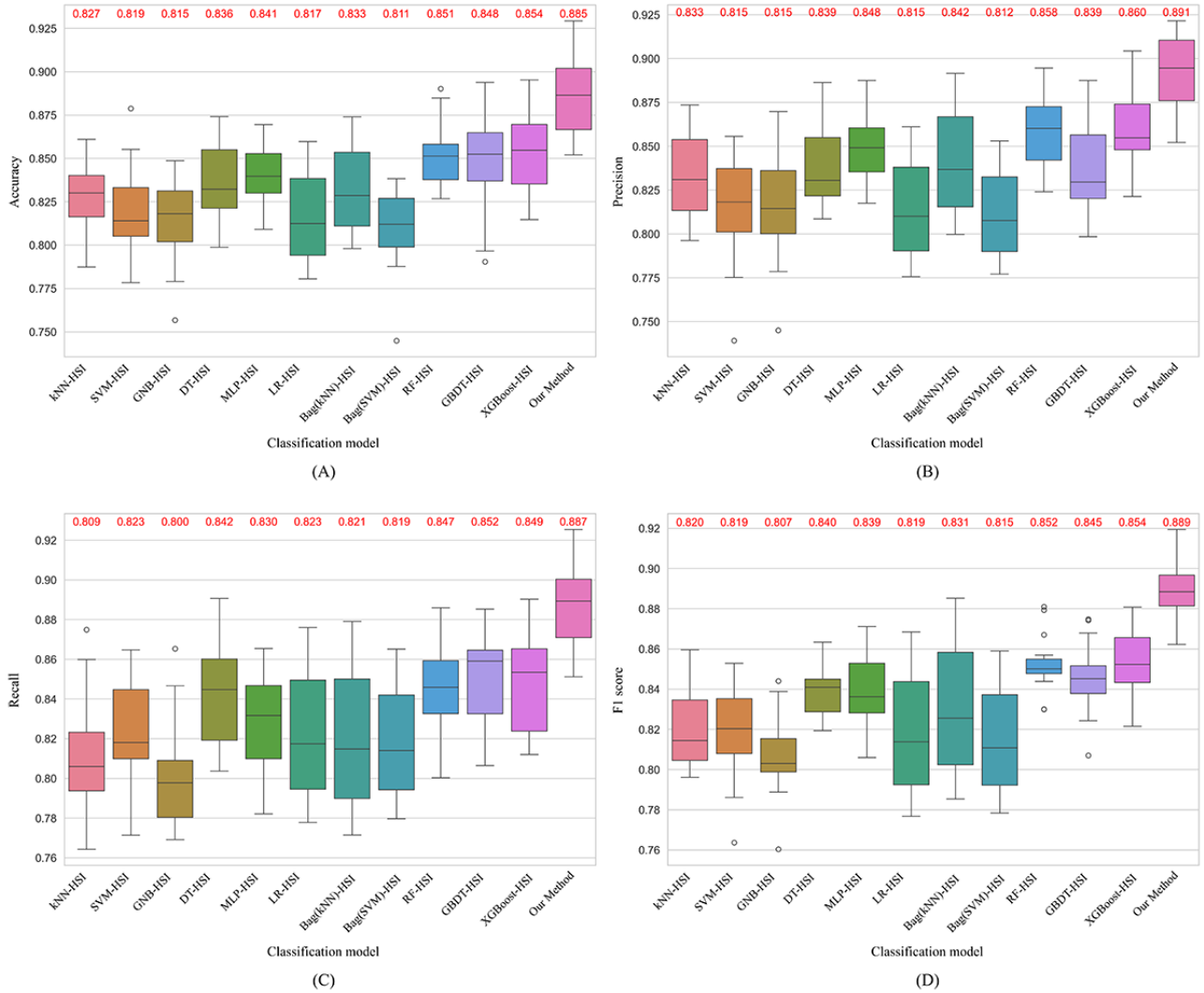
[e]HSI: Improved Harmony Search.

[f]DAELF-HSI: Dynamic Adaptive Ensemble Learning Framework based on an Improved Harmony Search.

Figure 4 illustrates the box plots of 12 algorithms after 100 independent experiments across 4 evaluation metrics. The quartiles within each box plot depict algorithmic performance, while the red numbers above each box plot represent the mean values for the respective metrics. DAELF-HSI outstrips competing models across all metrics, demonstrating superior stability and an absence of significant outliers. Conversely, SVM-HSI and GNB-HSI exhibit more outliers, indicating challenges in achieving precise model fits for specific data distributions, leading to notable performance fluctuations. Although LR-HSI and Bag (KNN)-HSI do not display outliers, their wide IQR suggests instability across diverse feature distributions. Notably, RF-HSI demonstrates significant outliers in the F_1-score, highlighting the model's vulnerability to certain data distributions or feature sets.

XSL•FO
RenderX

Figure 4. Comparison of evaluation metrics between Dynamic Adaptive Ensemble Learning Framework based on an Improved Harmony Search and various machine learning models applying harmony search improved feature selection. DT: decision tree; GBDT-HSI: gradient boosting decision tree-harmony search improved; GNB: Gaussian naïve Bayes; LR: logistic regression; KNN: k-nearest neighbors; RF-HSI: random forest-harmony search improved; SVM: support vector machines.

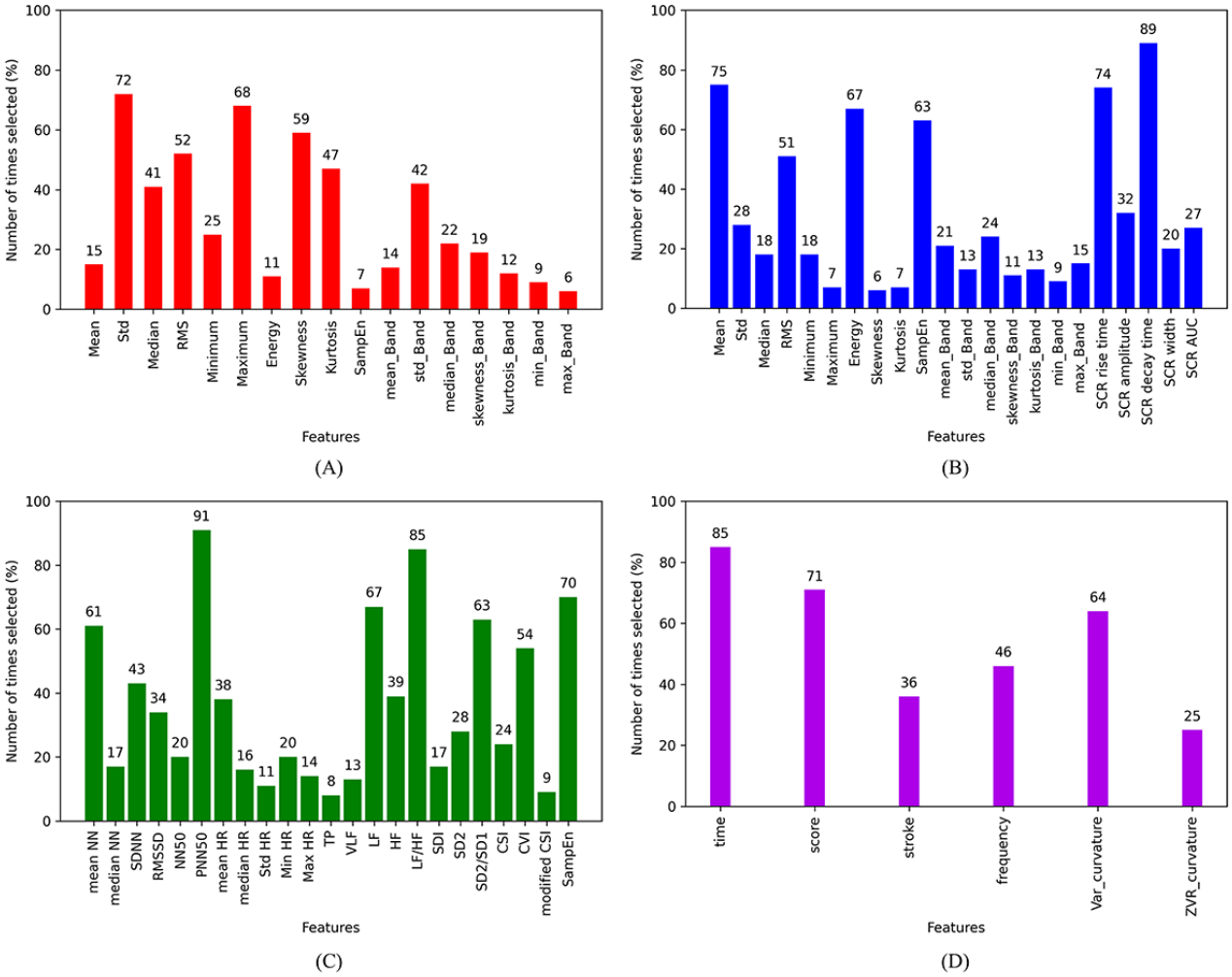


Analysis of the Optimization Module of the DAELF-HSI

Figure 5 presents the frequency analysis of physiological features (including SCL, SCR, and HRV) and digital cognitive parameters during 100 iterations of the DAELF-HSI model. Notably, SCR decay time (SCR feature set), PNN50, LF/HF (HRV feature set), and time (cognitive feature set) are highlighted for their importance in distinguishing between the 2 groups, appearing in over 80% of the selections. However, certain SCR features (eg, SCR amplitude, SCR width, and mean band) and HRV features (eg, SDNN, RMSSD, and mean HR), despite showing statistically significant differences (P<.05; Figure 3) in group differentiation, were infrequently chosen. This infrequency suggests that these parameters are highly correlated with features previously selected, leading the HSI feature selection algorithm to deem them redundant. Overall, the proposed HSI feature selection optimization algorithm can identify critical features, address redundancy, and accurately detect patients with MCI with limited features.

XSL•FO
RenderX

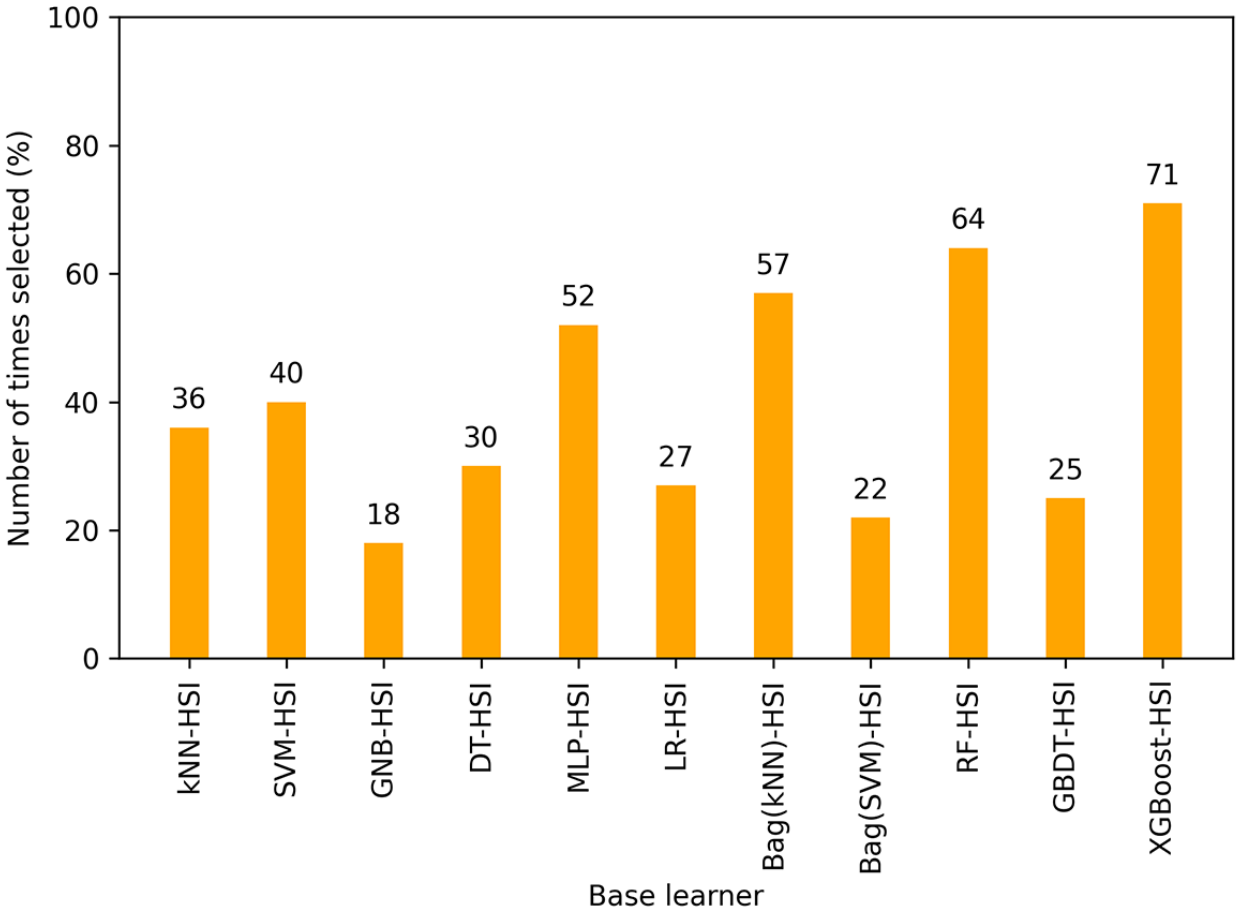
Figure 5. The number of times each skin conductance level, skin conductance response, heart rate variability, and cognitive feature was selected for mild cognitive impairment detection.



In addition, Figure 6 illustrates the frequency distribution of various base learners across 100 iterations within the DAELF-HSI model. Specifically, RF-HSI and XGBoost-HSI are the predominant selections, highlighting their substantial contributions to model efficacy and demonstrating the model's proficiency in selecting optimal learners. Conversely, GNB-HSI, Bag (SVM)-HSI, and GBDT-HSI are chosen less frequently. This bias in selection can be primarily attributed to 2 factors: first, these base learners inherently exhibit lower accuracy, leading the adaptive hyperparameter strategy of the DAELF-HSI to assign them reduced weights; second, a high level of correlation exists between these learners and other high-performing ensemble members, making their inclusion less impactful due to redundant error distributions and similarities in learner characteristics with more effective alternatives.

XSL•FO
RenderX

Figure 6. The number of times each base learner was selected for mild cognitive impairment detection. DT: decision tree; GBDT-HSI: gradient boosting decision tree-harmony search improved; GNB: Gaussian naïve Bayes; LR: logistic regression; KNN: k-nearest neighbors; RF-HSI: random forest-harmony search improved; SVM: support vector machines.



Finally, we substantiate the importance of feature selection and stacking optimization stages within the DAELF-HSI through ablation experiments. As delineated in Table 4, a total of 3 experimental models were structured to assess the impact of omitting 1 or both optimization stages, where "✓" denotes the inclusion of that stage. The models are configured as follows:

1. Model A uses 11 machine learning models as base learners and LR as the meta-learner, incorporating all features.
2. Model B uses 11 machine learning models as base learners with LR as the meta-learner, but only includes features selected through the HSI algorithm.
3. Model C integrates the HSI for stacking with 11 machine learning models, incorporating all features.

Table 4. Performance comparison of different ablation modules applied to the DAELF-HSI[a].

Methods	HSI[b] features selection	HSI learners stacking	Accuracy, mean (SD)	Precision, mean (SD)	Recall, mean (SD)	F_1-score, mean (SD)
Model A			0.826 (0.023)	0.819 (0.026)	0.831 (0.024)	0.825 (0.029)
Model B	✓		0.837 (0.027)	0.831 (0.028)	0.839 (0.030)	0.835 (0.035)
Model C		✓	0.854 (0.025)	0.858 (0.019)	0.849 (0.022)	0.853 (0.025)
DAELF-HSI	✓	✓	0.885 (0.020)	0.891 (0.021)	0.887 (0.024)	0.889 (0.025)

[a]DAELF-HSI: Dynamic Adaptive Ensemble Learning Framework based on an Improved Harmony Search.

[b]HSI: Improved Harmony Search.

According to the results in Table 4, model A shows lackluster classification performance in the absence of the 2 optimization stages, primarily due to the poor performance of certain base learners and the inclusion of numerous redundant features during training. Model B, which incorporates HSI-selected features, demonstrates a slight performance improvement of around 1%, suggesting that merely reducing feature redundancy is insufficient to enhance the output of underperforming base learners significantly. Furthermore, Model C, which solely incorporates the base learner stacking optimization stage, improves performance by nearly 3%, underscoring the importance of high-quality base learners in stacking algorithms.

XSL•FO
RenderX

Notably, the simultaneous implementation of both optimization stages substantially enhances the model's performance, highlighting the essential contribution of each stage to the overall efficacy of the algorithm.

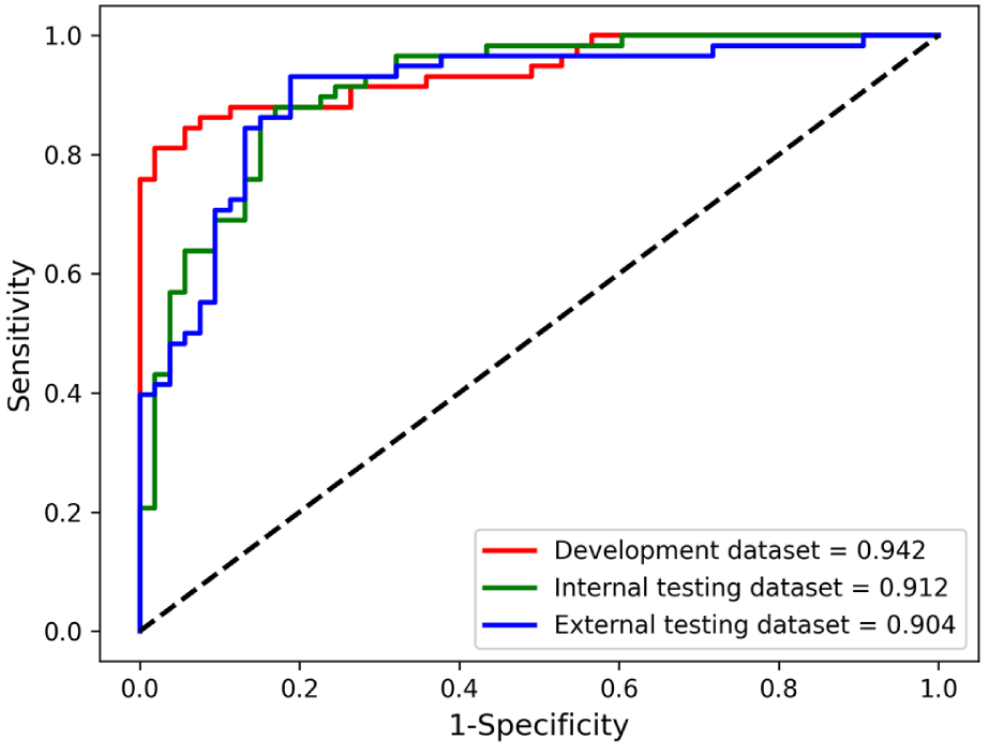
Performance Evaluation of DAELF-HSI Across Different Datasets

As shown in Table 5, we also used 4 metrics (including accuracy, sensitivity, specificity, and area under the curve [AUC]) to evaluate the binary classification performance of the classification model for patients with MCI versus healthy individuals in internal and external test datasets. Specifically, the model demonstrated excellent performance in the development dataset, with accuracy, sensitivity, and specificity at 88.4%, 86.1%, and 90.9%, respectively. In the internal test dataset, the model's accuracy slightly decreased to 85.5%, while sensitivity remained unchanged at 86.1%, and specificity dropped to 84.9%, suggesting that a small number of healthy individuals were misclassified as patients with MCI, but overall performance remained satisfactory. However, in the external test dataset, the model's accuracy, sensitivity, and specificity decreased by 3.9%, 0.4%, and 8.1%, respectively. Nevertheless, these results demonstrate the model's effectiveness, especially when evaluated on new and diverse samples. Furthermore, the AUC, which serves as an indicator of the model's validity, was recorded at 0.945 (95% CI 0.903-0.986), 0.912 (95% CI 0.859-0.965), and 0.904 (95% CI 0.846-0.962) across the 3 datasets, as illustrated in Figure 7. The AUC value reflects the classification performance of the model on different datasets. The DAELF-HSI model has an AUC value above the threshold of 0.9 on these datasets, demonstrating excellent sensitivity and specificity in detecting patients with MCI. In other words, the model cannot only effectively identify patients with MCI but also reduce the probability of misjudgment, enhancing reliability in clinical applications.

Table 5. The diagnostic value of the classification model in differentiating between healthy older adults and patients with mild cognitive impairment was assessed using internal and external testing datasets.

Dataset	Accuracy	Sensitivity	Specificity	Area under the curve (95% CI)	*P* value
Development dataset	0.884	0.861	0.909	0.945 (0.903-0.986)	<.001
Internal testing dataset	0.855	0.861	0.848	0.912 (0.859-0.965)	<.001
External testing dataset	0.845	0.857	0.828	0.904 (0.846-0.962)	<.001

Figure 7. The receiver operating characteristic curve of our model across different datasets.



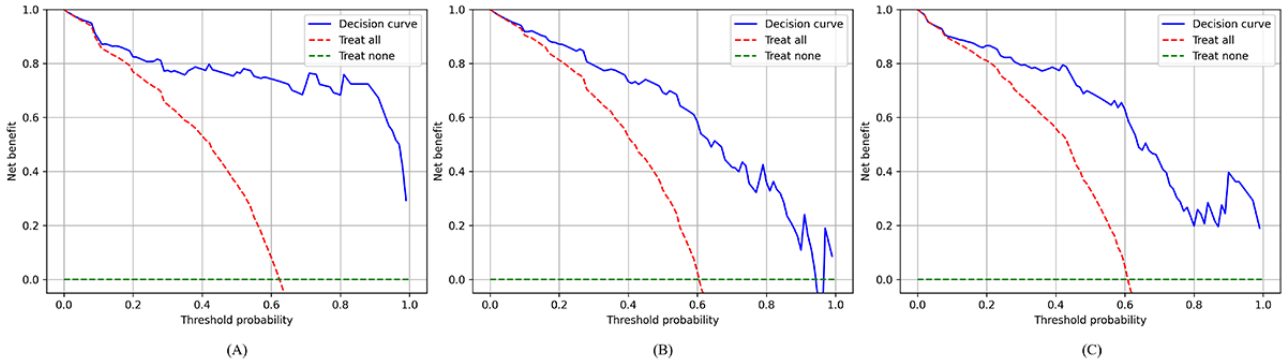
Clinical Utility Analysis

To assess the practical clinical value of the proposed model, we performed decision curve analysis (DCA) on the development, internal testing, and external testing sets, presenting the model's decision curve along with the "Treat all" and "Treat none" strategies, as shown in Figure 8. Specifically, the model's decision curve demonstrated clear clinical benefits in the development set, with its net benefit consistently exceeding that of the "Treat all" and "Treat none" strategies. Notably, in the 0 to 0.85 threshold range, the model's net benefit declined from 1 to 0.75 and further decreased to 0.3 in the higher threshold

XSL•FO
RenderX

range, indicating that the model effectively avoids overtreatment in low-risk patient groups. In the internal testing set, the decision curve remained stable, with a gradual decline in net benefit that aligned with expectations, suggesting that as the threshold increased, the model opted for fewer treatment decisions, and validated the model's effectiveness in high-risk patient populations and its alignment with the clinical need to reduce unnecessary treatments. However, the model's decision curve showed slight variations in the external testing set compared with the other sets. The net benefit decreased from 1 to 0.2 in the 0-0.8 threshold range, indicating reduced efficacy in this range. However, in the 0.8-0.9 range, the net benefit rose from 0 to 0.4, suggesting that adjusting the threshold appropriately enhanced the model's predictive accuracy. In the 0.9-1 threshold range, the net benefit dropped again to 0.2, which may indicate cautious predictions in the high-risk zone, thus limiting its clinical utility. In conclusion, the model demonstrated a net benefit consistently higher than both the "Treat all" and "Treat none" strategies across the 3 sets, particularly in the mid-to-low threshold ranges, highlighting that the model can effectively guide clinical decision-making, reduce unnecessary treatments, and improve early disease detection and intervention efficiency.

Figure 8. Decision curve analysis on different datasets, showing the model's decision curves for the binary classification task, along with the "Treat all" and "Treat none" strategies. (A) Development set, (B) internal testing set, and (C) external testing set.



Discussion

Interpretability of Physiological Features

Previous studies demonstrate that HRV is an essential physiological assessment indicator that could differentiate physiological responses between patients with MCI and HCs under diverse stressors and conditions [46,47]. In this study, compared with healthy counterparts, patients with MCI exhibited decreased HR, prolonged N-N intervals, and an increased ratio of low to high-frequency components, consistent with trends observed in past research [10,48]. Moreover, higher levels of HRV have been associated with improved cognitive function, whereas lower HRV correlates with cognitive impairment [49]. During cognitive tasks, abnormal responses in the autonomic nervous system of patients with MCI were observed through monitoring HRV, highlighting the efficacy of HRV as a sensitive physiological indicator during cognitive engagement.

On the other hand, this research assessed the applicability of EDA features for identifying MCI, advancing upon sparse existing research in this field. Specifically, the EDA signal was segregated into tonic and phasic components, from which 39 features encompassing time, frequency, and SCR time domains were derived. Comparative statistical analysis revealed that, during cognitive tasks, patients with MCI exhibited significantly enhanced SCR amplitudes, elongated SCR widths, and protracted SCR decay time relative to healthy counterparts, indicating a more intense or unexpectedly elevated physiological response to stimuli. These pronounced variations in SCR parameters effectively discriminate between patients with MCI and healthy individuals, highlighting the sensitivity of EDA features in detecting autonomic nervous system dysfunctions, a common correlate of cognitive impairments [50].

Predictive Accuracy of the Proposed Model

A challenge in enhancing the classification accuracy for discriminating patients with MCI involves identifying the most discriminative feature set. Thus, we proposed a feature selection algorithm based on HSI to mitigate the presence of redundant features and alleviate the adverse effects of high-dimensional data on classification learning, as high dimensionality can impede effective target classification [11]. Furthermore, we explored how to balance the diversity of base learners and classification quality in stacking for a specific dataset, treating the selection of appropriate base learners as a combinatorial optimization problem and solving it using heuristic algorithms. The superior performance of the DAELF-HSI model has been validated on development, internal testing, and external testing datasets, achieving accuracy of 88.4%, 85.5%, and 84.5%. Furthermore, the model demonstrated excellent sensitivity and specificity in detecting patients with MCI, with corresponding AUC of 0.945 (95% CI 0.903-0.986), 0.912 (95% CI 0.859-0.965), and 0.904 (95% CI 0.846-0.962) for these datasets.

Clinical Implications

The proposed framework offers significant clinical potential for the early detection of MCI through a noninvasive and cost-effective approach, providing a viable solution for widespread screening, particularly in home settings. Heart rate variability, a sensitive marker of autonomic nervous system dysfunction, can serve as a reliable indicator of cognitive impairment, helping clinicians identify at-risk individuals early in the progression of MCI. Similarly, electrodermal activity features, such as skin conductance responses, effectively differentiate patients with MCI from healthy individuals, further highlighting the potential of autonomic measures in cognitive health assessments. Furthermore, the framework enables more

XSL•FO
RenderX

convenient and personalized MCI screening, especially in remote or underserved areas with limited access to specialized medical expertise. Its adaptability allows seamless integration into various health care environments without significant infrastructural changes, reducing the cost and logistical barriers typically associated with traditional diagnostic methods. Moreover, the model's high sensitivity and specificity, as demonstrated by its AUC performance, indicate its reliability in identifying patients with MCI, which is critical for timely intervention and monitoring the progression of dementia to more severe stages. In conclusion, it provides clinicians with a powerful tool for early detection, improving patient outcomes and ultimately alleviating the burden of cognitive disorders on health care systems.

Limitations and Future Work

For our study, it is important to acknowledge several potential limitations and proposed solutions. First, the developed detection model relies on data from electrodermal activity, photoplethysmography, and cognitive parameters and untested generalizability across different datasets, such as electroencephalogram and eye-tracking data. Future research plans to expand the dataset under laboratory conditions through electroencephalogram and eye-tracking tests to enhance the algorithm's adaptability to various data modalities. In addition, the clinical applicability of the Empatica 4 wristband is limited by its high cost, which may impede its widespread adoption for household use. Subsequent studies will explore the potential and accuracy of more cost-effective commercial wearables (such as Xiaomi Mi Bands, Huawei Bands, and Garmin Smart 5) in screening for MCI.

Conclusion

In this study, we proposed a Dynamic Adaptive Ensemble Learning Framework based on Improved Harmony Search, designed to consolidate data collected from wearable wristbands and tablet devices to establish a comprehensive and reliable method for auxiliary diagnosis of MCI. The framework uses the Empatica 4 wristband to collect EDA and photoplethysmography from participants, optimizing these physiological signals through a designed multistage automatic artifact removal algorithm. In addition, based on Improved Harmony Search, a dynamic adaptive feature selection algorithm deepens the analysis of the time, frequency, and nonlinear domain features, enhancing the model's predictive performance. An experimental study involving 1069 participants aged 60 and above demonstrated that DAELF-HSI achieved classification accuracies of 88.4%, 85.5%, and 84.5% on development, internal testing, and external testing datasets, respectively, proving its effectiveness in identifying discriminative information related to MCI. In summary, this study combines an iPad-based cognitive assessment tool with wearable devices, providing an innovative solution for developing a portable, home-friendly early detection and screening system for MCI, offering vital support to clinicians in early detection, improving patient outcomes, and alleviating the burden of cognitive impairments on health care systems.

Acknowledgments

This research received funding from the National Natural Science Foundation of China (grants 62476190, 62376183, and U21A20469), the Central Government-Guided Science and Technology Development Program (grant YDZJSX2022C004), and Shanxi Provincial Administration of Traditional Chinese Medicine Scientific Research Project Plan (grant 2024ZYY2A033). We sincerely thank the volunteers whose invaluable participation made the successful completion of this study possible.

Conflicts of Interest

None declared.

Multimedia Appendix 1
Detailed description of physiological features and cognitive parameters.
[PDF File (Adobe PDF File), 621 KB - medinform_v13i1e60250_app1.pdf]

Multimedia Appendix 2
Detailed description of feature selection and stacked classification algorithms.
[PDF File (Adobe PDF File), 215 KB - medinform_v13i1e60250_app2.pdf]

References

1. Murman DL. The impact of age on cognition. Semin Hear 2015;36(3):111-121 [FREE Full text] [doi: 10.1055/s-0035-1555115] [Medline: 27516712]
2. Zeisel J, Bennett K, Fleming R. World Alzheimer Report 2020: Design, dignity, dementia: dementia-related design and the built environment. London, UK: Alzheimer's Disease International; 2020.
3. Prince M, Wimo A, Guerchet M, Ali GC, Wu YT, Prina M. The Global Impact of Dementia: An Analysis of Prevalence, Incidence, Cost and Trends. In: World Alzheimer Report 2015. London, UK: Alzheimer's Disease International; 2015.

XSL•FO
RenderX

4. Yates JA, Clare L, Woods RT, Wales Cognitive Function Ageing Study. What is the relationship between health, mood, and mild cognitive impairment? J Alzheimers Dis 2017;55(3):1183-1193 [FREE Full text] [doi: 10.3233/JAD-160611] [Medline: 27792011]
5. Petersen RC, Lopez O, Armstrong MJ, Getchius TSD, Ganguli M, Gloss D, et al. Practice guideline update summary: mild cognitive impairment: report of the guideline development, dissemination, and implementation subcommittee of the American Academy of Neurology. Neurology 2018;90(3):126-135 [FREE Full text] [doi: 10.1212/WNL.0000000000004826] [Medline: 29282327]
6. Petersen RC, Roberts RO, Knopman DS, Boeve BF, Geda YE, Ivnik RJ, et al. Mild cognitive impairment: ten years later. Arch Neurol 2009;66(12):1447-1455 [FREE Full text] [doi: 10.1001/archneurol.2009.266] [Medline: 20008648]
7. Karran E, De Strooper B. The amyloid hypothesis in Alzheimer disease: new insights from new therapeutics. Nat Rev Drug Discov 2022;21(4):306-318. [doi: 10.1038/s41573-022-00391-w] [Medline: 35177833]
8. Liss JL, Seleri Assunção S, Cummings J, Atri A, Geldmacher DS, Candela SF, et al. Practical recommendations for timely, accurate diagnosis of symptomatic Alzheimer's disease (MCI and dementia) in primary care: a review and synthesis. J Intern Med 2021;290(2):310-334 [FREE Full text] [doi: 10.1111/joim.13244] [Medline: 33458891]
9. Tong T, Thokala P, McMillan B, Ghosh R, Brazier J. Cost effectiveness of using cognitive screening tests for detecting dementia and mild cognitive impairment in primary care. Int J Geriatr Psychiatry 2017;32(12):1392-1400 [FREE Full text] [doi: 10.1002/gps.4626] [Medline: 27874210]
10. Alharbi EA, Jones JM, Alomainy A. Non-invasive solutions to identify distinctions between healthy and mild cognitive impairments participants. IEEE J Transl Eng Health Med 2022;10:2700206 [FREE Full text] [doi: 10.1109/JTEHM.2022.3175361] [Medline: 35711336]
11. Rasmussen KW, Salgado S, Daustrand M, Berntsen D. Using nostalgia films to stimulate spontaneous autobiographical remembering in Alzheimer's disease. J Appl Res Mem Cogn 2021;10(3):400-411. [doi: 10.1016/j.jarmac.2020.11.001]
12. Montero-Odasso M, Muir SW, Speechley M. Dual-task complexity affects gait in people with mild cognitive impairment: the interplay between gait variability, dual tasking, and risk of falls. Arch Phys Med Rehabil 2012;93(2):293-299. [doi: 10.1016/j.apmr.2011.08.026] [Medline: 22289240]
13. Eggenberger P, Bürgisser M, Rossi RM, Annaheim S. Body temperature is associated with cognitive performance in older adults with and without mild cognitive impairment: a cross-sectional analysis. Front Aging Neurosci 2021;13:585904 [FREE Full text] [doi: 10.3389/fnagi.2021.585904] [Medline: 33643019]
14. Yaffe K, Laffan AM, Harrison SL, Redline S, Spira AP, Ensrud KE, et al. Sleep-disordered breathing, hypoxia, and risk of mild cognitive impairment and dementia in older women. JAMA 2011;306(6):613-619 [FREE Full text] [doi: 10.1001/jama.2011.1115] [Medline: 21828324]
15. Xue C, Li A, Wu R, Chai J, Qiang Y, Zhao J, et al. VRNPT: a neuropsychological test tool for diagnosing mild cognitive impairment using virtual reality and EEG signals. Int J Hum-Comput Int 2023;40(20):6268-6286. [doi: 10.1080/10447318.2023.2250605]
16. Cheng S, Wang J, Sheng D, Chen Y. Identification with your mind: a hybrid bci-based authentication approach for anti-shoulder-surfing attacks using EEG and eye movement data. IEEE Trans Instrum Meas 2023;72:1-14. [doi: 10.1109/tim.2023.3241081]
17. Marinelli L, Trompetto C, Puce L, Monacelli F, Mori L, Serrati C, et al. Electromyographic patterns of paratonia in normal subjects and in patients with mild cognitive impairment or Alzheimer's disease. J Alzheimers Dis 2022;87(3):1065-1077. [doi: 10.3233/JAD-215526] [Medline: 35431243]
18. Bhagya Shree SR, Sheshadri HS. Diagnosis of Alzheimer's disease using naive Bayesian classifier. Neural Comput Applic 2016;29(1):123-132. [doi: 10.1007/s00521-016-2416-3]
19. Elgammal YM, Zahran MA, Abdelsalam MM. A new strategy for the early detection of Alzheimer disease stages using multifractal geometry analysis based on k-nearest neighbor algorithm. Sci Rep 2022;12(1):22381 [FREE Full text] [doi: 10.1038/s41598-022-26958-6] [Medline: 36572791]
20. Syaifullah AH, Shiino A, Kitahara H, Ito R, Ishida M, Tanigaki K. Machine learning for diagnosis of AD and prediction of MCI progression from brain MRI using brain anatomical analysis using diffeomorphic deformation. Front Neurol 2020;11:576029 [FREE Full text] [doi: 10.3389/fneur.2020.576029] [Medline: 33613411]
21. Kato S, Homma A, Sakuma T, Nakamura M. Detection of mild Alzheimer's disease and mild cognitive impairment from elderly speech: binary discrimination using logistic regression. Annu Int Conf IEEE Eng Med Biol Soc 2015;2015:5569-5572. [doi: 10.1109/EMBC.2015.7319654] [Medline: 26737554]
22. Dai P, Gwadry-Sridhar F, Bauer M, Borrie M. Bagging ensembles for the diagnosis and prognostication of Alzheimer's disease. 2016 Presented at: AAAI'16: Proceedings of the Thirtieth AAAI Conference on Artificial Intelligence; 2016; Phoenix, AZ. [doi: 10.1609/aaai.v30i1.9915]
23. Ianculescu M, Paraschiv E, Alexandru A. Addressing mild cognitive impairment and boosting wellness for the elderly through personalized remote monitoring. Healthcare (Basel) 2022;10(7):1214 [FREE Full text] [doi: 10.3390/healthcare10071214] [Medline: 35885741]
24. Khan A, Zubair S. Development of a three tiered cognitive hybrid machine learning algorithm for effective diagnosis of Alzheimer's disease. J King Saud Univ Comput Inf Sci 2022;34(10):8000-8018. [doi: 10.1016/j.jksuci.2022.07.016]

XSL•FO
RenderX

25. Moayedikia A, Ong K, Boo YL, Yeoh WG, Jensen R. Feature selection for high dimensional imbalanced class data using harmony search. Eng Appl Artif Intell 2017;57:38-49. [doi: 10.1016/j.engappai.2016.10.008]
26. Esmin AAA, Coelho RA, Matwin S. A review on particle swarm optimization algorithm and its variants to clustering high-dimensional data. Artif Intell Rev 2013;44(1):23-45. [doi: 10.1007/s10462-013-9400-4]
27. da S. Bohrer J, Dorn M. Enhancing classification with hybrid feature selection: a multi-objective genetic algorithm for high-dimensional data. Expert Syst Appl 2024;255:124518. [doi: 10.1016/j.eswa.2024.124518]
28. Polit DF, Beck CT. Nursing Research: Generating and Assessing Evidence for Nursing Practice. United States: Lippincott Williams & Wilkins; 2016.
29. McKhann GM, Knopman DS, Chertkow H, Hyman BT, Jack CR, Kawas CH, et al. The diagnosis of dementia due to Alzheimer's disease: recommendations from the National Institute on Aging-Alzheimer's Association workgroups on diagnostic guidelines for alzheimer's disease. Alzheimers Dement 2011;7(3):263-269 [FREE Full text] [doi: 10.1016/j.jalz.2011.03.005] [Medline: 21514250]
30. Chapman LJ, Chapman JP. The measurement of handedness. Brain Cogn 1987;6(2):175-183. [doi: 10.1016/0278-2626(87)90118-7] [Medline: 3593557]
31. Li A, Xue C, Wu R, Wu W, Zhao J, Qiang Y. Unearthing subtle cognitive variations: a digital screening tool for detecting and monitoring mild cognitive impairment. Int J Hum-Comput Interact 2024:1-21. [doi: 10.1080/10447318.2024.2327179]
32. Rafi H, Benezeth Y, Reynaud P, Arnoux E, Song FY, Demonceaux C. Personalization of AI models based on federated learning for driver stress monitoring. 2022 Presented at: Computer Vision – ECCV 2022 Workshops; October 23-27, 2022; Tel Aviv, Israel p. 575-585.
33. McKinley S, Levine M. Cubic spline interpolation. College of the Redwoods 1998;45(1):1049-1060.
34. Smital L, Haider CR, Vitek M, Leinveber P, Jurak P, Nemcova A, et al. Real-time quality assessment of long-term ECG signals recorded by wearables in free-living conditions. IEEE Trans Biomed Eng 2020;67(10):2721-2734. [doi: 10.1109/TBME.2020.2969719] [Medline: 31995473]
35. Larradet F, Niewiadomski R, Barresi G, Caldwell DG, Mattos LS. Toward emotion recognition from physiological signals in the wild: approaching the methodological issues in real-life data collection. Front Psychol 2020;11:1111 [FREE Full text] [doi: 10.3389/fpsyg.2020.01111] [Medline: 32760305]
36. Kalimeri K, Saitis C. Exploring multimodal biosignal features for stress detection during indoor mobility. 2016 Presented at: Proceedings of the 18th ACM International Conference on Multimodal Interaction; 2016 October 31; Tokyo, Japan p. 53-60.
37. Taylor S, Jaques N, Chen W, Fedor S, Sano A, Picard R. Automatic identification of artifacts in electrodermal activity data. Annu Int Conf IEEE Eng Med Biol Soc 2015;2015:1934-1937 [FREE Full text] [doi: 10.1109/EMBC.2015.7318762] [Medline: 26736662]
38. Greco A, Valenza G, Lanata A, Scilingo E, Citi L. cvxEDA: a convex optimization approach to electrodermal activity processing. IEEE Trans Biomed Eng 2016;63(4):797-804. [doi: 10.1109/TBME.2015.2474131] [Medline: 26336110]
39. Bent B, Goldstein BA, Kibbe WA, Dunn JP. Investigating sources of inaccuracy in wearable optical heart rate sensors. NPJ Digit Med 2020;3:18 [FREE Full text] [doi: 10.1038/s41746-020-0226-6] [Medline: 32047863]
40. Nelson BW, Low CA, Jacobson N, Areán P, Torous J, Allen NB. Guidelines for wrist-worn consumer wearable assessment of heart rate in biobehavioral research. NPJ Digit Med 2020;3:90 [FREE Full text] [doi: 10.1038/s41746-020-0297-4] [Medline: 32613085]
41. Malik M, Bigger JT, Camm AJ, Kleiger RE, Malliani A, Moss AJ, et al. Heart rate variability. Standards of measurement, physiological interpretation, and clinical use. Task force of the European Society of Cardiology and the North American Society of Pacing and Electrophysiology. Eur Heart J 1996;17(3):354-381. [Medline: 8737210]
42. Acar B, Savelieva I, Hemingway H, Malik M. Automatic ectopic beat elimination in short-term heart rate variability measurement. Comput Methods Programs Biomed 2000;63(2):123-131. [doi: 10.1016/s0169-2607(00)00081-x] [Medline: 10960745]
43. Karlsson M, Hörnsten R, Rydberg A, Wiklund U. Automatic filtering of outliers in RR intervals before analysis of heart rate variability in Holter recordings: a comparison with carefully edited data. Biomed Eng Online 2012;11:2 [FREE Full text] [doi: 10.1186/1475-925X-11-2] [Medline: 22236441]
44. Föll S, Maritsch M, Spinola F, Mishra V, Barata F, Kowatsch T, et al. FLIRT: a feature generation toolkit for wearable data. Comput Methods Programs Biomed 2021;212:106461 [FREE Full text] [doi: 10.1016/j.cmpb.2021.106461] [Medline: 34736174]
45. Makowski D, Pham T, Lau ZJ, Brammer JC, Lespinasse F, Pham H, et al. NeuroKit2: a Python toolbox for neurophysiological signal processing. Behav Res Methods 2021;53(4):1689-1696. [doi: 10.3758/s13428-020-01516-y] [Medline: 33528817]
46. Arsalan A, Majid M. Human stress classification during public speaking using physiological signals. Comput Biol Med 2021;133:104377. [doi: 10.1016/j.compbiomed.2021.104377] [Medline: 33866254]
47. Tanev G, Saadi DB, Hoppe K, Sorensen HBD. Classification of acute stress using linear and non-linear heart rate variability analysis derived from sternal ECG. Annu Int Conf IEEE Eng Med Biol Soc 2014;2014:3386-3389. [doi: 10.1109/EMBC.2014.6944349] [Medline: 25570717]

XSL•FO
RenderX

48. Saif N, Yan P, Niotis K, Scheyer O, Rahman A, Berkowitz M, et al. Feasibility of using a wearable biosensor device in patients at risk for Alzheimer's disease dementia. J Prev Alzheimers Dis 2020;7(2):104-111 [FREE Full text] [doi: 10.14283/jpad.2019.39] [Medline: 32236399]
49. Forte G, Favieri F, Casagrande M. Heart rate variability and cognitive function: a systematic review. Front Neurosci 2019;13:710 [FREE Full text] [doi: 10.3389/fnins.2019.00710] [Medline: 31354419]
50. Rasmussen KW, Salgado S, Daustrand M, Berntsen D. Using nostalgia films to stimulate spontaneous autobiographical remembering in Alzheimer's disease. J Appl Res Mem Cogn 2021;10(3):400-411. [doi: 10.1016/j.jarmac.2020.11.001]

Abbreviations

AD: Alzheimer disease
AUC: area under the curve
DAELF-HSI: Dynamic Adaptive Ensemble Learning Framework based on an Improved Harmony Search
DCA: decision curve analysis
DT: decision tree
EDA: electrodermal activity
HC: healthy control
HRV: heart rate variability
IBI: interbeat interval
KNN: k-nearest neighbors
LF/HF: low-frequency to high-frequency ratio
LR: logistic regression
MCI: mild cognitive impairment
MLP: multilayer perceptron
MoCA: Montreal Cognitive Assessment
PNN50: percentage of successive R-R intervals > 50 ms
RF: random forest
RMSSD: root mean square of successive differences
SampEn: sample entropy
SCL: skin conductance level
SCR: skin conductance response
SD2/SD1: ratio of the SD2 and SD1 of Poincaré plot
SDNN: SD of N-N intervals
SVM: support vector machine

Edited by C Lovis; submitted 06.05.24; peer-reviewed by L Yao, N Xiao, Y Huusi, T Ramsey; comments to author 25.07.24; revised version received 12.08.24; accepted 15.11.24; published 20.01.25.

Please cite as:
Li A, Li J, Hu Y, Geng Y, Qiang Y, Zhao J
Retracted: A Dynamic Adaptive Ensemble Learning Framework for Noninvasive Mild Cognitive Impairment Detection: Development and Validation Study
JMIR Med Inform 2025;13:e60250
URL: https://medinform.jmir.org/2025/1/e60250
doi:10.2196/60250
PMID:

©Aoyu Li, Jingwen Li, Yishan Hu, Yan Geng, Yan Qiang, Juanjuan Zhao. Originally published in JMIR Medical Informatics (https://medinform.jmir.org), 20.01.2025. This is an open-access article distributed under the terms of the Creative Commons Attribution License (https://creativecommons.org/licenses/by/4.0/), which permits unrestricted use, distribution, and reproduction in any medium, provided the original work, first published in JMIR Medical Informatics, is properly cited. The complete bibliographic information, a link to the original publication on https://medinform.jmir.org/, as well as this copyright and license information must be included.

XSL•FO
RenderX

Original Paper

Applying Robotic Process Automation to Monitor Business Processes in Hospital Information Systems: Mixed Method Approach

Adam Park[1*], BE; Se Young Jung[1,2*], MD, MPH, PhD; Ilha Yune[1], BS; Ho-Young Lee[1,3], MD, PhD

[1]Office of eHealth Research and Business, Seoul National University Bundang Hospital, Seongnam-si, Republic of Korea

[2]Department of Family Medicine, College of Medicine, Seoul National University, Seoul, Republic of Korea

[3]Department of Nuclear Medicine, College of Medicine, Seoul National University, Seoul, Republic of Korea

[*]these authors contributed equally

Corresponding Author:
Ho-Young Lee, MD, PhD
Office of eHealth Research and Business
Seoul National University Bundang Hospital
Dolmar-ro 182
Seongnam-si, 13605
Republic of Korea
Phone: 82 31 787 0114
Email: debobkr@gmail.com

Abstract

Background: Electronic medical records (EMRs) have undergone significant changes due to advancements in technology, including artificial intelligence, the Internet of Things, and cloud services. The increasing complexity within health care systems necessitates enhanced process reengineering and system monitoring approaches. Robotic process automation (RPA) provides a user-centric approach to monitoring system complexity by mimicking end user interactions, thus presenting potential improvements in system performance and monitoring.

Objective: This study aimed to explore the application of RPA in monitoring the complexities of EMR systems within a hospital environment, focusing on RPA's ability to perform end-to-end performance monitoring that closely reflects real-time user experiences.

Methods: The research was conducted at Seoul National University Bundang Hospital using a mixed methods approach. It included the iterative development and integration of RPA bots programmed to simulate and monitor typical user interactions with the hospital's EMR system. Quantitative data from RPA process outputs and qualitative insights from interviews with system engineers and managers were used to evaluate the effectiveness of RPA in system monitoring.

Results: RPA bots effectively identified and reported system inefficiencies and failures, providing a bridge between end user experiences and engineering assessments. The bots were particularly useful in detecting delays and errors immediately following system updates or interactions with external services. Over 3 years, RPA monitoring highlighted discrepancies between user-reported experiences and traditional engineering metrics, with the bots frequently identifying critical system issues that were not evident from standard component-level monitoring.

Conclusions: RPA enhances system monitoring by providing insights that reflect true end user experiences, which are often overlooked by traditional monitoring methods. The study confirms the potential of RPA to act as a comprehensive monitoring tool within complex health care systems, suggesting that RPA can significantly contribute to the maintenance and improvement of EMR systems by providing a more accurate and timely reflection of system performance and user satisfaction.

(JMIR Med Inform 2025;13:e59801) doi:10.2196/59801

KEYWORDS

robotic process automation; RPA; electronic medical records; EMR; system monitoring; health care information systems; user-centric monitoring; performance evaluation; business process management; BPM; healthcare technology; mixed methods research; process automation in health care

XSL•FO
RenderX

Introduction

The cutting-edge technologies in health care demand intense transformations in electronic medical records (EMRs) by adopting new services, including artificial intelligence (AI)–driven predictions, Internet of Things (IoT) supports, telemedicine interfaces, and cloud-based open services [1-5]. These transformations imply a rapid growth in complexity and necessitate process re-engineering in EMR systems. Complexity management in dynamic health care environments has been studied by researchers who perceived the uncertainty and unpredictability inherent to electronic health record (EHR) systems [6-8].

One significant limitation is that the actual end user experience is gradually neglected as the performance metric "improves." The focus is predominantly on component-level analyses, allowing engineers to divide labor and concentrate efforts. This approach can create gaps between the perceptions of end users and engineers in measuring system performance.

The crux of the problem lies in revealing the "interrelatedness of components" in EHRs, meaning that the mutual influences among services, modules, and business processes should be measured and tracked [9]. No single standardized model has yet emerged, leaving various complex approaches for identifying interacting components [10]. One contribution to identifying the degree of interrelatedness is end-to-end performance monitoring, which suggests measuring system complexity from an external, comprehensive, and user-centric perspective. Application performance monitoring (APM), for example, measures transaction latency from user applications, hence complementing the efforts of engineers focused on small, manageable, and self-contained components [11]. However, such approaches, sensitive to data interoperability and dynamically changing environments [12], have been too costly to be widely adopted in health care where the focus is on business re-engineering rather than system maintenance and monitoring [13].

Robotic process automation (RPA) shows potential competitiveness in external monitoring with functions focusing on human-mimicking features. A robot, in this sense, is an automated assistant residing in a computing environment, performing tasks that imitate those of people controlling other applications, usually upon an operating system [14]. The robotic metaphor thus includes 3 internal features corresponding to the human abilities of perceiving, deciding, and inputting, which have all been revolutionized by AI-based cognitive computing [15] and the three internal features are (1) an RPA bot interprets symbols on the graphical user interface (GUI); (2) an RPA bot determines actions to comply with predefined business rules; and (3) an RPA bot inputs signals into applications, mimicking those from peripheral devices used by end users.

These abilities allow the automated agents to perform manual and labor-intensive tasks, automating administrative tasks in back offices [16], including dashboard monitoring, low-judgment auditing tasks, and accounting process automation in finance, banking, and IT services [14,17-19]. Therefore, the implication of RPA in complexity management is end-to-end performance monitoring that reflects the experiences of end users by simulating their activities and freeing engineers from excessive feedback [20]. A "robot" can fulfill external monitoring with an outside-in approach that witnesses the same glitches end users perceive [21].

RPA, with its "build above system" features, has the potential to combine with business process management (BPM) and overcome the intrinsic limitation that systems should be re-engineered. BPM has succeeded in establishing patterns for business process integrations in health care but has not been effective at guiding process monitoring for risk management [22,23]. Continuous reforms in health care organizations have been mandated for their operational success and patient-focused process improvements [24,25]. Thus, the expected synergy between the 2 methodologies is that RPA enhances costly process automation, while BPM provides the holistic perspective of detecting, auditing, and optimizing business processes [26].

This study explored the potential of RPA in complex EMR systems with its role as "a canary in a coal mine" [11], presenting generalizable findings from a 3-year project at Seoul National University Bundang Hospital (SNUBH).

The paper posits RPA as a means to bridge the gap between the limitations of both component-level system monitoring and application-level monitoring. The former, with its engineering-centric approach, often fails to align with the end users' experiences, as system monitoring reports may not accurately reflect what end users actually encounter. The latter, while focused on the application level, cannot offer a universal solution due to its lack of scalability and the high costs associated with performance analyses. RPA, in contrast, facilitates a user-centric perspective by designing bots that act as representative users within the hospital, performing the most essential and shared activities. Consequently, any failures or performance degradations observed by the RPA bots are indicative of significant issues within the system, potentially leading to a systemic collapse in the worst case.

The analysis revealed significantly enhanced capabilities of RPA bots beyond initial expectations. Much like a meticulous human tester, RPA bots frequently identified errors immediately following software deployments and detected failures in external services outside the expertise of in-house developers. However, certain challenges hindered RPA from becoming a universal solution for monitoring services. This conclusion is supported by both quantitative data from RPA process outputs and qualitative insights obtained from interviews with hospital practitioners.

Methods

Ethical Considerations

Human Subject Ethics Review Approvals or Exemptions

This study was conducted in accordance with the ethical guidelines of the institutional review board (IRB) of SNUBH (approval number SNUBH-IRB-2021-004). The research involved secondary analysis of anonymized patient data extracted from hospital information systems. In addition, our

XSL•FO
RenderX

study included user interviews, for which individual approvals were obtained in accordance with the IRB guidelines. Due to the anonymization of patient data, the IRB granted an exemption from requiring individual informed consent for the secondary data analysis, as per institutional policies and national regulations.

Informed Consent

As the study used pre-existing anonymized data, informed consent was waived by the IRB. The original data collection process ensured that all participants consented to the use of their data for research purposes, which was documented in the hospital's consent forms. For the user interviews conducted as part of the study, individual informed consent was obtained from all participants, aligning with the guidance provided by the IRB. The scope of the consent for both the secondary data and interviews included future secondary analyses, adhering to institutional policies.

Privacy and Confidentiality

All patient data were anonymized before analysis, with direct identifiers removed and indirect identifiers encrypted. Access to the data was restricted to authorized personnel only, and secure servers were used to store and process the information. Data-sharing protocols adhered to the guidelines stipulated by the Health Insurance Portability and Accountability Act (HIPAA).

Compensation Details

No compensation was provided to participants, as this study exclusively involved the analysis of pre-existing, anonymized data and user interviews. The nature of the research did not require any direct monetary engagement with participants.

Project Background

SNUBH management expressed strong interest in integrating monitoring services to identify continuous performance degradations from the end user's perspective. The Healthcare Information and Management Systems Society in the United States has mandated health care organizations, especially those that have achieved Stage 7 certification, to detect and prepare for unexpected system downtime [21,27]. Furthermore, internal reports from users regarding performance degradations were often overlooked by engineers due to the absence of appropriate analysis tools. Application-level monitoring frameworks, such as APM [28], were not favored by the management mainly, primarily due to high reengineering costs associated with re-engineering [12].

In the meantime, hospital managers found themselves redundantly checking the performance of business processes in unsystematic ways. The requirement to manually perform these tasks led to intermittent execution and a lack of precision. Consequently, hospital management anticipated that RPA's mechanism could supplant the labor wasted on manual testing to monitor performance regression [29].

Robotic Process Automation Integration

Iterative Development Process

A task force team engaged in an iterative process to implement system-monitoring RPA bots. The objectives were to reliably simulate business workflows on the hospital's production systems and to establish an organizational protocol for responding to detected performance anomalies.

The proof of Concept process, spanning from January to July 2020, involved repeating cycles from developing requirements to implementing prototypes. This approach was adopted because of the belief that establishing business requirements for a novel methodology should be carried out with meticulous attention to detail. To broaden their understanding of the field, the administration contracted with different RPA third-party vendors at each iteration. Alongside the software prototype development, managers also put in place organizational protocols to react to alerts, with responses tailored to the severity level of the incident.

The development of RPA bots followed an iterative process to address challenges specific to monitoring EMR systems. Frequent user interface (UI) updates initially made it difficult for bots to recognize dynamic elements, but this was resolved by implementing advanced pattern recognition algorithms and adaptive learning techniques to enable automatic adjustments to UI changes. Early versions of the bots also relied on timer-based execution, which caused inefficiencies when dealing with variable system latencies. To address this, event-driven configurations were introduced, allowing the bots to respond dynamically to system triggers.

Ensuring stable performance across diverse environments was another challenge. Extensive pilot testing and iterative adjustments refined the bots' logic, enabling them to operate reliably in varied setups. Incorporating feedback from multiple departments presented additional complexity, but this was streamlined by centralizing feedback and conducting regular cross-functional meetings to align bot functionality with operational needs.

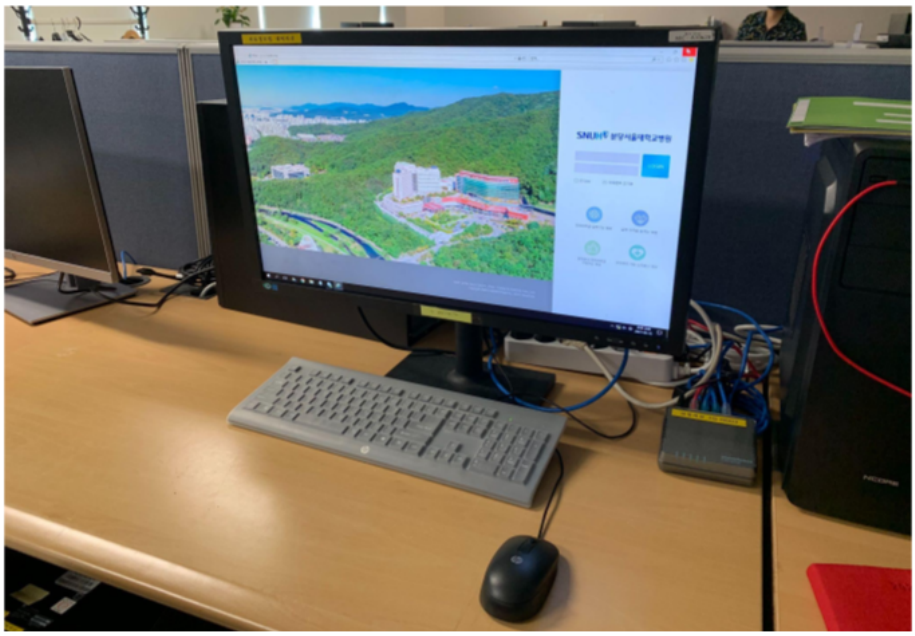
This iterative approach significantly improved bot performance and adaptability for broader health care applications.

Technical Environment

The RPA bot environment is set up to mirror that of a worker performing the target tasks. This setup includes a dedicated personal computer in an IT office, equipped with the RPA program, one virtual private network program, and 3 hospital system applications. To enable manual oversight, a monitor, keyboard, and mouse are also provided, allowing a manager to take control of the machine if necessary. A notable feature in security configuration is that RPA bots can use the same virtual private network program that workers use to access external networks. This capability distinguishes RPA from other automation technologies and thus necessitates additional security channels. Figure 1 shows the personal computer dedicated to RPA usage in the hospital office.

XSL•FO
RenderX

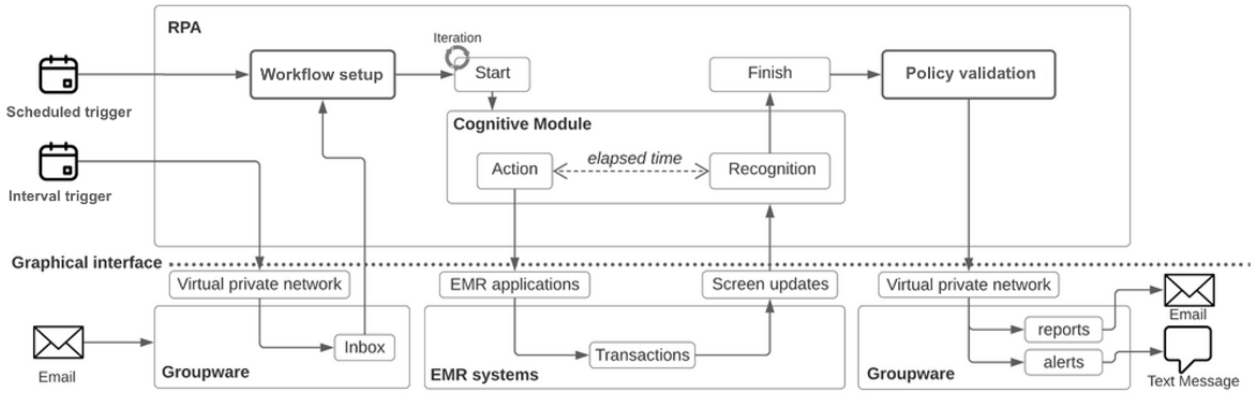
Figure 1. Monitoring unit with robotic process automation in Seoul National University Bundang Hospital. EMR: electronic medical record.



Robotic Process Automation Reports and Governance

RPA reporting processes and reactive governance were refined over several iterations. RPA bots could be activated either through a periodic scheduling system or upon receiving an email order from a supervisor. A single bot was responsible for executing dozens of business processes, estimating and reporting application performance while interacting with 18 modules within the systems. Each RPA business process was designed to mirror a critical business process within the hospital, affecting numerous other processes or significant clinical practices. The methodology for performance measurement was aligned with use perception. For instance, a request initiated by clicking a button on the interface was considered complete once a change was detected on a specific part of the screen. The performance metrics captured during this process were then recorded and documented in an Excel file. Based on the severity and abnormality of the data found, the RPA bot was also programmed to decide the recipients of email and SMS text message notifications, ensuring timely communication of potential issues. Figure 2 illustrates the process of system monitoring fulfilled by RPA agents.

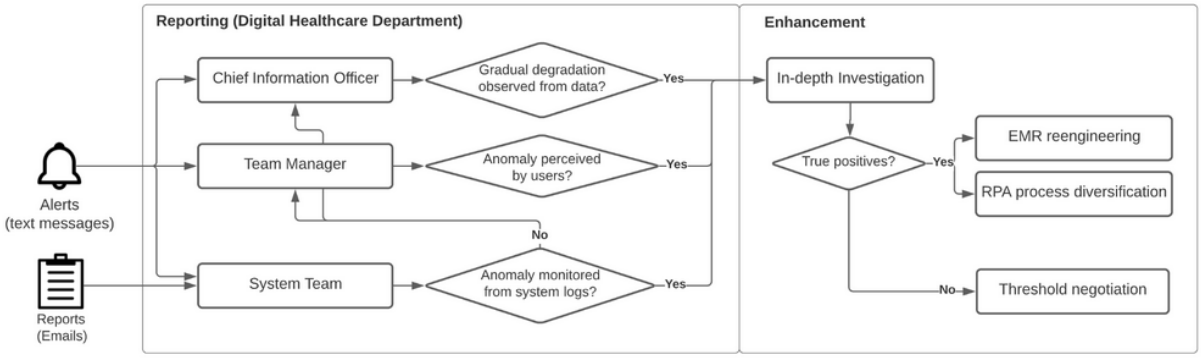
Figure 2. Process monitoring with robotic process automation.



There was a strong consensus within the organization that the governance should capitalize on the RPA alerts by establishing a feedback loop to prevent the IT department from disregarding the findings due to excess false positives. This governance mechanism was designed to align with the hospital's reporting structure. Mobile text messages were used to alert stakeholders about serious anomalies detected, while email served as the primary channel for routine reporting. To ensure oversight and prompt action, all alerts, if overlooked by middle managers and engineers, were escalated to the hospital's Chief Information Officer. Figure 3 depicts the governance structure for reporting anomalies detected by RPA agents.

XSL•FO
RenderX

Figure 3. Organization's reporting structure chart. EMR: electronic medical record; RPA: robotic process automation.



Robotic Process Automation Monitoring Analysis

Overview

The goal of this study was to investigate the functionalities and advantages derived from implementing RPA in end-to-end monitoring within the health care sector. Given the innovative nature of this methodology in health care and the absence of quantitative benchmarks, a mixed methods approach was adopted. This approach aimed to assess the multifaceted value of RPA attributes, facilitating an understanding of how findings from quantitative and qualitative data converge [30].

Task-Oriented Robotic Process Automation Process Selection

The selection of RPA processes was deemed a critical aspect of the project to optimize the benefits of automation. Initially, 10 standardized processes at SNUBH, frequently used by clinicians, were identified. These encompassed 3 types of patient visits (inpatient, outpatient, emergency), as well as subsequent processes such as physician orders, common laboratory examinations, pharmacy visits, etc. These processes, while central to clinical practice, were noted for their significant latencies. RPA managers adopted a task-oriented approach in selecting the processes, aiming to ensure that the improvements or any degradations in performance would have a substantial effect on user experiences. As a result, functionalities across 56 pages in the main hospital application, which represent core interactions between the hospital's main system application and its end users, were selected for automation.

Monitoring Data

The monitoring data comprised request-response duration data, alert records, and resolutions provided by the engineering team. For the selected functionalities, RPA agents performed the defined processes by navigating through 17 large service modules of the hospital information systems. During each interaction, primarily initiated by mouse clicks, the RPA agent awaited a detectable change on the screen and verified whether the expected execution had taken place. A screen change was deemed "adequate" if the image match rate exceeded 90% upon comparison with the standard screen where fetched data were expected to appear. After each execution, thresholds were consulted to decide if an alert should be issued.

RPA agents were scheduled 4 times daily from January 2021 to December 2024. A report was generated and sent to managers whenever the response time exceeded the set threshold. Over 3 years, more than 700 such events were reported to the management. Engineers worked alongside managers to pinpoint root causes and resolve the cases whenever feasible.

The data produced by RPA bots effectively highlighted the long-standing discrepancies between end users' and engineers' perceptions. Many recorded latencies showed unexpectedly large variances, underscoring the challenge of replicating the slowdowns experienced by end users. To quantify this issue, the gradual increase in latencies over several years was calculated, with processes showing significantly high variations subject to in-depth analysis. Indeed, most services were showing meaningful high fluctuations. In some complex cases, it was discovered that a module required a fundamental overhaul of its information structure, indicating that extensive refactoring was unavoidable.

Robotic Process Automation Manager Interview

The qualitative study targeted managers and system engineers within the IT department of SNUBH who had experience in developing or managing the RPA program. The objective was to uncover the core experiences to shed light on the role and effectiveness of RPA in the organization [31].

The sample size was directed by the research question [32], consisting of 8 managers and 7 engineers, each with at least 3 years of experience at the hospital. Purposeful samples were collected using snowball sampling until data redundancy or saturation was achieved, this point was identified when no new information emerged and was added to the findings extracted from previous interviews [33].

The analysis of participants' experiences was primarily reductive as responses were broken down into smaller categories and later assembled to evaluate the measurement metrics. Initially, researchers thoroughly read the transcripts to immerse themselves in the texts. Subsequently, they coded the transcripts by identifying passages and meaning units that highlighted participants' fundamental experiences of RPA. Of the 15 transcripts, a total of 392 significant meaning units were extracted. Finally, researchers revisited the transcripts alongside

XSL•FO
RenderX

the measurement metrics to identify themes emerging from the meaning units.

Results

Overview

The results presented herein were derived from a dual approach that incorporates both quantitative and qualitative methods, combining the data generated by RPA robots with interviews conducted with RPA managers. The RPA bots, which have operated on predefined processes for over 3 years as introduced in the Methods section, have accumulated reports revealing significant insights. These insights, combined with the engineering team's reactions to the reports, particularly highlight gaps in the user-perspective analysis that engineers have struggled to bridge. Multimedia Appendix 1 outlines the business processes monitored by RPA, including the domain, category, specific process steps, screen names, and threshold values (in seconds) for triggering alerts. Sample monitoring results are provided in Tables S1 and S2 in Multimedia Appendix 2.

The quantitative analyses in the sections mentioned below, "Uncovering User-Level Performance Fluctuations: RPA Bridges the Analysis Gap Between Users and Engineers," "Holistic Incident Reporting: RPA Broadly Captures Diverse Causes of Issues," and "RPA Manager Interviews: Best Practices are Calibrated Through Iterative Discussions," focus on a comprehensive analysis akin to traditional end-to-end system monitoring. That is, the modern trend in software system monitoring emphasizes identifying core components and concentrating expertise in individual areas. However, the complexity of hospital information systems precludes a universally applicable strategy of compartmentalizing the structure. Unseen dimensions gradually undermine user experiences. The role of RPA agents has proven extremely effective in supplementing the existing monitoring governance, by performing important clinical processes "by hand." The most unexpected result is the extensive coverage of RPA processes, which ensured system stability by identifying hidden errors after regular system deployments. This indicates a broader variety of reasons for the RPA agent to report incidents, offering a more accurate reflection of realistic user experiences.

These insights uncover long-standing challenges that users have implicitly faced for years. Sections mentioned below, "Quantifying 'Real' User Experience: RPA Detects Gradual Degradation in End-to-End Service Latencies" and "Uncovering User-Level Performance Fluctuations: RPA Bridges the Analysis Gap Between Users and Engineers," detail how gradual performance degradation and inconsistencies have historically created disparities between user experiences and engineers' performance metrics. Furthermore, the section "Holistic Incident Reporting: RPA Broadly Captures Diverse Causes of Issues" extends the discussion beyond mere performance tracking to include external influences and errors invoked by a deployment. While these issues should not happen theoretically, they become apparent only when combined with substantial real-world data, which sometimes contradicts the consistency assumed by engineers.

Finally, interviews with 20 managers, as discussed in the section "RPA Manager Interviews: Best Practices are Calibrated Through Iterative Discussions," have further clarified the desired direction for RPA-driven monitoring systems. These interviews aimed to gather insights on both the perspective and progress of managers regarding RPA agents. The ability of RPA tools to provide a high-level system overview has quickly grown confidence in managerial support for RPA technology leading to more precise calibration of RPA tool usage. However, initial reservations about trust and data sensitivity persisted, highlighting areas where RPA agents are not effectively adaptable. This reveals practical limits that may vary depending on culturally diverse work ethics.

Quantifying End-to-End Level User Experience: Robotic Process Automation Detects Gradual Degradation in End-to-End Service Latencies

Table 1 summarizes the latency of service calls, sampled from the interaction reports of RPA processes, which exhibited performance degradation accumulated over 3 years. The sampled service calls belong to 3 categories: infrastructure check, outpatient process, and inpatient process. This summary presents the first comprehensive evidence of end user experience, concretely demonstrating the long-term latency increase.

XSL•FO
RenderX

Table 1. Service latency analysis over years.

Robotic process automation process	Mean of latencies (seconds)			
Theme and service call	Year 2021	Year 2022	Year 2023	Increase
Infrastructure				
Run the main client	4.9	5.1	6.5	1.6
Login to the main client	4.8	5.2	5.9	1.1
Run picture archiving and communication system	2	2	2.2	0.2
Login to picture archiving and communication system	9.2	9.5	12.2	3.0
Run groupware	3.5	3.6	3.8	0.3
Run virtual desktop infrastructure	12.9	13.4	13.2	0.3
Outpatient				
Outpatient listing	17.8	23.9	25	7.2
Outpatient selection	15	20.4	20.2	+5.2
Outpatient navigation	3.6	4.4	5	+1.4
Inpatient				
Inpatient listing	1.5	1.6	1.6	+0.1
Inpatient selection	2.3	2.8	3.2	+0.9
Inpatient navigation	2.5	2.3	2.5	+0
Nursing list	2.8	2.8	3	+0.2
Nursing list2	4	4.1	4.7	+0.7

The table above lists three representative cases of processes and their selected functions executed by the RPA agent on various time frames on a daily basis. The changes in end-to-end latencies are recorded over 3 years. Among the most distinct cases, the outpatient process emerges as the most challenging to manage, displaying a clearly increasing trend in latency.

This straightforward result serves as critical evidence for the user experiences of many end users of the hospital systems who frequently complain about the system “feeling like” it is slowing them down. Engineering teams typically focus their monitoring efforts on the system’s principal components, such as database queries, server API calls, and network latencies. These measures are particularly effective in the early stages of the health care organization because improvements in these components typically lead to noticeable enhancements in user experiences. However, as the complexity of the hospital information system increases and services mature, hidden factors increasingly contribute to its performance degradation.

Uncovering User-Level Performance Fluctuations: Robotic Process Automation Bridges the Analysis Gap Between Users and Engineers

Table 2 samples service calls that were highly ranked for showing significant variations. “Event Count” refers to the number of incidents reported by RPA agents over 3 years (2021-2023) due to exceeding their corresponding thresholds.

Table 2. Latency fluctuations.

Service call	Mean (SD)	Event count	Threshold
Nurse inpatient list	3.03 (0.55)	4	5
Nurse injection reservation	15.9 (1.6)	11	18
Health screening reservation	3.05 (0.52)	4	5
Examination results	6.94 (0.98)	19	8
Nutrition manage registration	2.66 (0.55)	7	5
Patient record viewer	4.24 (0.58)	112	5

One of the most significant contributions made by the RPA agent is the quantification of fluctuations in user experience. A significant number of the latencies recorded by the RPA agent demonstrated high SD, indicating that multiple incidents were detected and finally reported to hospital managers. For instance, the examination results function, which involves retrieving examination results for daily outpatients, exhibited notable instability, with an SD of almost 1 second against its usual

XSL•FO
RenderX

latencies of 7 seconds. This function encompasses multiple sub-fetching calls, updated weekly, making it difficult for individual performance testing to ensure stability from a holistic perspective, despite latencies generally falling within acceptable thresholds according to engineers' environments.

This evidence of a broad spectrum of latencies is particularly valuable in debates between users and engineers struggling with the lack of reproducibility of the delayed system response users experience. Even small bugs are difficult to pinpoint from a user's perspective, which is not their primary role in the organization. Expanding the scope to performance, many diagnoses suggested by users were considered insufficient as engineering reports were consistently indicating component-level monitoring within 0.01-second intervals. However, such evidence collected by engineers has failed to capture the true user experience.

Indeed, the complex nature of these systems, with their interdependencies and the frequent updates of components, can obscure the root causes of performance fluctuations. As systems evolve and expand over decades, new features introduced outside the existing framework often inadvertently introduce inefficiencies. Moreover, even if all individual factors are efficiently manageable, the dynamic nature of hospital operations, including variable patient loads and the unpredictable demand for different functions, exacerbates these challenges.

Holistic Incident Reporting: Robotic Process Automation Broadly Captures Diverse Causes of Issues

Table 3 groups events reported by RPA agents based on the cause of the occurrence and the response to each event. Initially, the focus was solely on detecting query degradation events. However, as monitoring progressed, the scope of categories expanded. Identifying erroneous deployment events proved particularly effective in preventing significant operational disruptions in the hospital. Query degradation is focused on specific query inefficiencies, while performance inconsistency encompasses broader, variable performance fluctuations across the system. Erroneous deployment: errors detected immediately after deployment due to misconfigurations or incomplete processes. Bad deployment: performance degradation observed postdeployment caused by insufficient planning or testing.

Table 3. Incident cases.

Event type	Cases	Reasons	Resolutions
Erroneous deployment	9	An error was detected immediately following a software deployment.	Resolve the identified error.
External program issues	5	External programs caused issues (network, authority, error, etc)	Resolve the identified issue.
Bad deployment	3	Performance deteriorated noticeably right after software deployment.	Optimize performance post-deployment.
Query degradation	3	Inefficiencies in query execution became evident with increasing data volume.	Enhance query efficiency and performance.
Performance inconsistency	660	Query response times fluctuate with daily data volume changes.	Develop a strategy for structural improvements.

One of the unexpected yet invaluable contributions of the RPA agent has been its holistic approach to testing. Originally aimed at measuring system performance from the users' perspective and quantifying their experiences, the scope of the RPA agent's coverage extended far beyond these initial objectives. For example, in the case of erroneous deployment, the RPA agent identified errors immediately following regular software deployments, with all 9 reported cases attributable to the intricate complexities of the hospital information systems. Often, modifications in one module inadvertently trigger errors in another, through the information flow of real data. These are the types of issues typically addressed by application-level testing, yet designing a comprehensive experiment often eludes the grasp of individual engineers.

Furthermore, the RPA's goal cannot solely be the exhaustive identification of errors, which is extremely difficult to achieve. Instead, the true value of the automated agent's reports lies in ensuring that common processes (daily tasks performed by thousands of employees for tens of thousands of patients) remain unaffected. This precaution helps prevent incidents from escalating into broader performance issues that could impact the entirety of hospital operations.

Second, the second row in the table illustrates that, while the RPA processes operate in the same environment as users, they are susceptible to the influence of external, peripheral, and temporary system components. Notably, one incident was reported due to a memory leak from an embedded external program. The integration of third-party applications or web-based services is sometimes overlooked due to their perceived minimal impact on the overall system. However, the trend toward incorporating a diverse array of software products has transformed the system into a complex assembly of heterogeneous components that interact with one another, potentially affecting major processes through their services.

Finally, as detailed in this section, the identification of 660 cases of performance inconsistencies has prompted the engineering team to strategize toward stabilizing the end-to-end latencies of major practices, including the outpatient management process. This initiative underscores the RPA agent's crucial role in addressing diverse issues; it not only detects immediate issues following regular deployments but also facilitates long-term improvements to enhance system reliability and user satisfaction.

XSL•FO
RenderX

Robotic Process Automation Manager Interviews: Best Practices Are Calibrated Through Iterative Discussions

The qualitative data collected through interviews illuminated how the adoption of RPA impacted the system and the organization. A central point of discussion was "Which processes should be monitored?" leading to a more explicit understanding of the pros and cons of adopting RPA bots.

Key phrases extracted from the interviews were then categorized into 5 clusters aligned with core themes: understanding of RPA, prediction capability, trust in robots, downsides of cognitive agents, governance facilitator, and the RPA epiphany. These encodings provide concrete descriptions of the abstract themes, underpinned by sampled phrases.

Table 4 categorizes the primary advantages of implementing RPA as identified by managers, with specific themes and corresponding coding. Sample phrases from interviews illustrate the practical impact of these benefits on process efficiency, cross-departmental cooperation, and governance within the organization.

Table 4. Summary of robotic process automation benefits based on managerial feedback.

Themes (pros) and coding	Sample phrases
Ease of understanding	
• Simplicity of processes • Repetition of processes • Well-defined processes	"The simplicity is that the task does not require human judgment and is defined by a clear business rule"
Cooperation invoking	
• Cross-departmental collaboration • Joint software update tests	"...Moreover, we can impose an RPA[a] bot on all tasks that were covered by 16 managers from different departments"
• Responsive governance	"...However, the bot now delivers an SMS or email to each manager responsible for each process. Speed has always been an issue, and now it is working...."
Governance facilitation	
• Evolving thresholds • Engineer-user negotiation	"...I argued that the right way is to focus more on whether it hampers the process for the user. Thresholds were set in such a conservative manner. "
• Enhancing business interoperability	"...And then another email can re-trigger RPA bots to confirm the resolution of the issue."

[a]RPA: robotic process automation.

A majority of managers highlighted the benefits of adopting this new technology as a reliable system monitoring and comprehensive testing service. First, the ease of understanding RPA was seen as a significant advantage, offering managers user-friendly methods to interpret processes focused primarily on clinical practices. Managers appreciated the intuitive and understandable process definitions, clearly outlined on the system's GUI.

Second, RPA to foster departmental cooperation was seen as ideal for addressing the challenges posed by hospital information systems, which are often divided into disjointed components. From the UI perspective, with which the RPA agent interacts to simulate human behaviors without assuming any engineering team affiliation, one RPA process can interact with up to a dozen components, identifying cross-departmental issues arising from information inconsistencies. Addressing one issue typically requires collaboration among engineers from multiple departments to determine its root cause.

Third, the RPA agent acts as a governance facilitator, enabling more realistic and evidence-based negotiations between engineers and users. The previously dominant engineer-driven metrics proved inadequate for sustaining effective discussions on system performance management. However, as indicated in the sections above, the focus could be shifted toward quantifying user experiences, thereby identifying how efforts should be allocated for process improvements.

Table 5 summarizes managerial feedback on the drawbacks of RPA, including trust issues, cognitive limitations, and insightful epiphanies from its application.

XSL•FO
RenderX

Table 5. Managerial insights on robotic process automation challenges.

Themes (cons) and coding	Sample phrases
Trust issues with the robots	
• Recognition accuracy • Handling of sensitive clinical tasks	"...The system suddenly alerts me of OCR failures which was the case until yesterday. We cannot allow its applications to patient-related tasks if it isn'*t* 100% consistently guaranteed."
Downsides of cognitive agents	
• Ambiguous state definition	"...The current configuration checks whether the hospital logo is floating to decide if the website has loaded. However, the image server often fails while the other functions are completely working."
• Unexpected maintenance costs	"...Yes, robotic process automation recognizes a shape as people do, but that depends on the context. The bot can find a red button after being relocated but it won't find the button when color or text changes."
Deriving robotic process automation epiphanies	
• Persuasive demonstration • Generation of personalized ideas	"...and I felt 'Oh, that's what this is doing'. After that, the application seemed to be limitless..."

However, the accumulated experiences have not repositioned RPA bots as a universal solution applicable to all clinical processes. First, the most sensitive issue relates to the scope of information that RPA agents handle. Many major processes involving complex and critical clinical information require RPA agents to manipulate information states. Although all state-modifying operations are designed to work with dummy data generated exclusively for the RPA agent, unpredictable incidents can arise from misinterpreting commands, affecting data on the production server. Ironically, as AI-based decisions become more complex and human-like, the likelihood of errors increases, mirroring those made by inexperienced workers. This risk has deterred managers from extending the monitoring scopes to clinically sensitive services, which are deemed crucial areas for robotic coverage.

Second, contrary to expectations, RPA agents, as cognitive agents, lack flexibility in varying situations. OCR-based recognitions depend on hints from managers, which may become outdated due to system maintenance. Since RPA processes involve complex commands based on OCR recognition logic (eg, detecting some pop-ups) there is a greater chance of encountering unadaptable modifications. For example, an unrelated pop-up appearing during a process, easily dismissed by a human tester, poses a challenge for an RPA agent interpreting it as an incorrect message response. These scenarios have led to unexpected maintenance costs and increased frustration due to inconsistencies, making the unambiguous definition of UI interactions a significant challenge for managing the vast number of RPA agents.

Third, the "RPA epiphany" has not been universally shared. Developing a productive RPA process requires the cooperation of clinicians and other hospital staff, yet reactions to the same approach can vary. Some employees fear job loss to highly efficient robots, while others see it as creating a burdensome new task, compelling them to manage the tedious robot postinitialization. Both perspectives hold some validity, necessitating extensive discussions to expand use cases.

Discussion

Study Summary

The effectiveness of RPA in monitoring EMR systems was measured through latency data and interviews. In response to the demand of end users who have sought a new indicator reflecting the quantification of their experiences, RPA processes were carefully chosen to monitor the essential clinical processes containing information-heavy user tasks. The latency data collected through the monitoring process proved that indeed the comprehensive perspective of RPA bots serves as the bridge valuing the cross-disciplinary efforts of users and engineers. Finally, the qualitative interview revealed notable characteristics of RPA that affected the EMR management organization to reform the governance, and highlighted RPA bots, as a new cognitive agent resembling humans, having pros and cons.

Which process should be selected for the monitoring tasks? This simple question has been an important topic ever since the first emergence of BPM [34] because most automation project lifecycles started from process identifications. With a prevalent top-down approach, the start of a project was focused on business goals [35] and then spread to subordinate departments and users. However, such an approach was often attributed to the failure of recent RPA implementations, motivating studies to standardize and quantify process selections in RPA projects [36,37]. The strategy used by managers in the SNUBH project involved iteratively identifying the most common components impacting real-world practices, with a focus on using RPA agents to simulate the tedious testing tasks performed by end users. This approach, though simple, proved to be exceptionally effective. The collected reports provided insights into end user experiences that were among the closest to any similar efforts done to gather data for the same purpose.

Previous studies in APM have been challenged by significant fluctuations due to user-level performance measurements, requiring extensive expert analysis [11,12]. However, the integration of RPA bots, aimed at mirroring the "real" user experience as closely as possible, transforms the apparent downside of APM into an advantage. The delays observed in

XSL•FO
RenderX

Table 1, although mostly under 5 seconds, may not significantly impact end user experience on an individual basis. However, the cumulative effect of these small delays over extended working hours could influence overall productivity. Furthermore, understanding the root cause of such delays is crucial. Delays resulting from natural database growth might be considered acceptable, while those stemming from other factors should prompt further investigation. RPA plays a pivotal role in identifying and quantifying these delays, enabling management to assess whether they fall within acceptable performance thresholds and take corrective actions when necessary. The RPA project team prioritized ensuring the usability of the most critical hospital processes to enhance end user experiences. This approach is entirely user-centric, lacking any scientific purpose or methodology, stemming from the recognition that the system's complexity prevents engineers from maintaining a comprehensive view of the services. User-driven process monitoring accurately reflects true priorities, preventing engineers from becoming overly fixated on component-level details.

The observed increase in task completion times, as shown in Table 1, aligns with the natural growth of the database over time, which can contribute to delays in end-to-end service. In addition, the system management (SM) team at the study hospital develops and implements approximately 700 new programs annually to enhance EMR operational efficiency. These frequent updates can also impact service performance. The integration of RPA proved beneficial in detecting such delays, enabling targeted analyses of their root causes. This facilitated database tuning by database administrators and prompted the SM team to review and optimize newly implemented program code, ultimately improving system performance and ensuring operational continuity.

Moreover, the monitoring process can still be initiated by engineers, serving as a starting point for identifying key areas for improvement. Performance degradation data collected by RPA agents involve multiple factors, necessitating cross-departmental collaboration, which can lead to inefficient practices in identifying root causes. Indeed, most cases required several hours to days to identify potential engineering factors. However, there is a consensus that these factors are of the highest priority for affecting the real-time practices of end users, and the performance standards to be maintained can be relatively easily negotiated. On the other hand, the consistent increase in system complexity has made component-centric analysis and improvements less impactful, as they no longer directly enhance user experiences. RPA agents act as proxy users, emphasizing the most critical information flows that the system must maintain smoothly. The low standard deviation observed in Table 2 indicates minimal fluctuation in delay times, suggesting stability. However, this stability also reveals that delays are consistently recurring rather than sporadic. Such persistent delays, even if small, can accumulate over time and impact overall system efficiency. This underscores the importance of addressing not just large fluctuations but also ongoing, minor delays. RPA's capability to monitor and report these patterns enables targeted optimization efforts, helping to mitigate their long-term effects on system performance and user experience.

Interview themes unveiled the complex ways in which the organization leverages new technology. RPA, acting as a cognitive agent, introduced a novel approach to automation integration. RPA bots remained "lightweight," effortlessly accessing functions by overlaying the interface of target EHR applications [38]. These features made technical barriers minimal, allowing RPA managers to implement RPA logic with their extensive knowledge of application-level practices without frequently consulting EHR engineers during the project. The speed of integration was accelerated by the straightforward development process and the flexible recognition capabilities supported by RPA.

However, as mentioned in the Method section, unforeseen drawbacks of RPA emerged due to its reliance on UI-based interactions. These included a vast number of screen change recognitions, and although RPA was adaptable enough to approximate detections, such as locating a button with a specific phrase, modifications to the UI itself exceeded the scope of its flexibility. Consequently, UI elements, being primarily graphical and perceived as less critical to service logic, now require a shift in perception and further study for extended and reliable RPA use.

An incident where an engineer identified the hospital logo as a weak point of the configuration, which defined the loaded groupware web page, illustrates this challenge. The logo's reliance on a content delivery network service, which frequently failed, underscored a common misunderstanding of UI behaviors. In previous studies, this issue has been explored in ontology-oriented UIs, which advocate for the declaration of high-level models and their translation into program UIs [39]. An ontology, in this context, is defined as "a logical theory comprising a formal vocabulary" [40] that supports UIs, ensuring precise and consistent conceptual organization of the UI [41]. Therefore, developing an intermediate ontological model of the UI to support RPA projects could be a crucial preliminary step.

Observation of the RPA adoption led to an evaluation of the organizational-level contribution of RPA to the complexity management of EHR systems. Meaningful subjects included threshold evolution, responsive governance, and business interoperability facilitation. Threshold evolution was the unanticipated practice where engineers and supervisors negotiated thresholds of alerting performances to cut off false positives while preserving enough predictive qualities.

Beyond performance monitoring, SNUBH supervisors emphasized that the RPA project significantly enhanced responsive governance. RPA acted as a conduit between users and machines, transforming subjective empirical experiences into objective, meaningful data. From this perspective, RPA emerged as an ideal evidence collector, silently tracking fluctuations in system performance without the burden of its repetitive, tedious tasks.

In terms of business interoperability, organizational responsiveness was notably improved through the use of RPA bots, which served as digital messengers at the application level. Users could send requests to and receive reports from RPA bots via email, mirroring the function of chatbots—computer

XSL•FO
RenderX

programs designed to simulate human conversation. Gradually, RPA bots became part of the workforce team, communicating through standard messaging channels and enhancing end user satisfaction [42].

Core Implications

This study's outcomes will enlighten decision-makers about the capabilities of RPA in evaluating business process performance, with a specific focus on simulating user activities on complex EHR systems. Initially, the adoption of RPA for monitoring EHR systems was anticipated to surge rapidly due to its direct and intuitive development procedures. However, the revealed end user experience was remarkably poor: the study uncovered significant variations in the latencies of crucial common service calls. Such monitoring data can be regarded as the definitive "ground truth" of end user experiences, fostering constructive discussions between users and engineers.

Nonetheless, challenges like UI-driven maintenance issues and the complexity of interpreting results complicate ongoing quality control efforts. To mitigate these issues, there should be the establishment of standardized, iterative practices aimed at judiciously identifying areas deserving daily attention from RPA agents. Furthermore, psychological resistance could decelerate RPA adoption in health care settings. This reluctance stems from the cognitive capabilities of RPA bots, which closely mimic tasks traditionally performed by human employees, raising concerns about their potential impact on the job market in the industry.

Future Directions

RPA naturally overcame the shortcomings by providing event-driven configurations based on cognitive analysis of the screen changes. However, some questions recognized in this study should be answered to aid in the success of future RPA projects.

Could RPA bots entirely replace traditional GUI-based testing frameworks? After stabilizing RPA bots to detect process performance degradations, the EMR management team found that RPA bots are eventually fulfilling an advanced GUI-based testing role by resolving the following challenges. Most GUI tests showed target application-dependent performance measurements [43] and object recognition techniques [44] that limited their usage across a large system. Also, GUI testing automation suffered a "temporal synchronization problem" arising from timer-based process execution, limiting flexibility for any latencies [45,46]. Recent studies seem to recognize the potential benefits of RPA in the field [47,48].

How can system complexity be managed after RPA adoptions? This question is directly connected to the practice in the project but, as a goal of this study, also applies to future RPA implementation projects. Since RPA sits upon the other systems, it creates another layer of complexity in the automation. It is anticipated that most RPA projects will devise a monitoring protocol as part of the automation to maintain performance. Furthermore, RPA is considered slow by certain companies because its front-end level execution is inferior to that of back-end systems [49], and performance measurement is difficult, so overall system complexity after integration has to be considered in the decision to adopt RPA.

How can RPA build trust among users of EHR systems? A common misunderstanding about RPA is that the automation is accurate simply because the implementation is easy and intuitive for users. However, as revealed in this study, users were skeptical in at least 2 cases. First, the mismatch between GUI and user intent remained unresolved. Ontological models were suggested to match the domain behind GUI. The growing importance of such models is due to their practical usage, which allows workers and automation engineers to seamlessly accept the domain that supports the GUI. Second, contrary to this pragmatic view, user trust in cognitive recognition was not sufficient even though failure rates were low. User trust issues in automation are not new and require time because EHR users tend to be more conservative about this.

How can RPA harmonize with organizations and their governance? It has been acknowledged that a common mistake in treating RPA is to limit its role as a simple piece of software rather than as a foundation for leading digital transformations [50]. Therefore, RPA governance should be an integral aspect of the implementation of RPA so that scalable cross-departmental use is realized. The components of RPA governance may include process identification and prioritization, distribution of RPA bot responsibility, RPA knowledge management, and reward systems [51].

Study Limitations

The limitations of this study lie in the practical constraints of the SNUBH project. First, this study only applied RPA to a single testbed. Significant considerations were required to make the business process performance monitoring model generalizable. However, the project results and other references imply that expanding and transferring RPA implementation is relatively straightforward once demonstrated to work for one scenario, unlike frameworks relying on specific technology stacks. This low degree of system dependency allows RPA modules to be adapted to similar systems.

A second limitation is that RPA was not configured to cover the diverse infrastructural environments and actual end user experiences. End users working in SNUBH have divergent computer environments and application usage patterns. This has raised criticism as to whether RPA bots properly contribute to complexity management when they operate in such a controlled environment. A compromise had to be made by setting the computer running RPA bots to mirror the computers used by general end users as closely as possible. This decision was also influenced by the fact that the initial goal of this project was not to measure the user experience comprehensively but to identify performance outliers where there was a noticeable change in business processes.

Third, the level of understanding of RPA among the interview participants was inconsistent, which was eventually accepted as part of their characteristics. The study intended to measure the differences from existing methodologies, but the perception of RPA was more varied than expected. For example, some engineers focused on RPA's effects as an automation tool rather

XSL•FO
RenderX

than understanding it as a source of modifying the governance structure of the organization. Furthermore, some supervisors lacked a clear understanding of the technical definition of RPA.

Fourth, implementing RPA in diverse health care settings presents additional challenges not addressed in this study. Variations in organizational structures, technological systems, and regulatory environments can significantly influence the success of RPA adoption. For instance, RPA integration may face difficulties in environments with legacy systems or fragmented workflows. In addition, scaling RPA across larger institutions often requires substantial resource allocation and staff training, which may limit its applicability. Compliance with data protection and privacy regulations adds another layer of complexity, demanding meticulous planning to ensure alignment with legal standards. Future research should investigate these challenges to provide a more comprehensive understanding of RPA's role in diverse health care contexts.

Acknowledgments

The authors thank the staff and management of SNUBH for their support and cooperation. Special thanks to Se-jin Nam, PhD, AI Team Leader at ezCareTech, for providing the essential technology for this research. This research is supported by the SNUBH Research Fund (grant number 14-2021-0041).

Conflicts of Interest

None declared.

Multimedia Appendix 1
Target business processes and example data.
[DOCX File , 22 KB - medinform_v13i1e59801_app1.docx]

Multimedia Appendix 2
Target business processes and example data and sample results of system monitoring.
[DOCX File , 43 KB - medinform_v13i1e59801_app2.docx]

References

1. Davenport T, Kalakota R. The potential for artificial intelligence in healthcare. Future Healthc J 2019;6(2):94-98 [FREE Full text] [doi: 10.7861/futurehosp.6-2-94] [Medline: 31363513]
2. Wang F, Preininger A. AI in health: state of the art, challenges, and future directions. Yearb Med Inform 2019;28(1):16-26 [FREE Full text] [doi: 10.1055/s-0039-1677908] [Medline: 31419814]
3. Zeadally S, Siddiqui F, Baig ZA, Ibrahim AM. Smart healthcare. PRR 2019;4(2):149-168. [doi: 10.1108/prr-08-2019-0027]
4. Alamri A. Ontology middleware for integration of IoT healthcare information systems in EHR systems. Computers 2018;7(4):51. [doi: 10.3390/computers7040051]
5. Zhang R, Liu L. Security models and requirements for healthcare application clouds. : IEEE; 2010 Presented at: IEEE 3rd International Conference on Cloud Computing; 2010 July 05-10; Miami, FL, USA p. 268-275. [doi: 10.1109/cloud.2010.62]
6. Plsek PE, Greenhalgh T. Complexity science: the challenge of complexity in health care. BMJ 2001;323(7313):625-628 [FREE Full text] [doi: 10.1136/bmj.323.7313.625] [Medline: 11557716]
7. Tutty MA, Carlasare LE, Lloyd S, Sinsky CA. The complex case of EHRs: examining the factors impacting the EHR user experience. J Am Med Inform Assoc 2019;26(7):673-677 [FREE Full text] [doi: 10.1093/jamia/ocz021] [Medline: 30938754]
8. Greenhalgh T, Papoutsi C. Studying complexity in health services research: desperately seeking an overdue paradigm shift. BMC Med 2018;16(1):95 [FREE Full text] [doi: 10.1186/s12916-018-1089-4] [Medline: 29921272]
9. Kannampallil TG, Schauer GF, Cohen T, Patel VL. Considering complexity in healthcare systems. J Biomed Inform 2011;44(6):943-947 [FREE Full text] [doi: 10.1016/j.jbi.2011.06.006] [Medline: 21763459]
10. Abbott PA, Foster J, Marin HDF, Dykes PC. Complexity and the science of implementation in health IT--knowledge gaps and future visions. Int J Med Inform 2014;83(7):e12-e22. [doi: 10.1016/j.ijmedinf.2013.10.009] [Medline: 24444700]
11. Molyneaux I. The Art of Application Performance Testing: From Strategy to Tools. Sebastopol, California: O'Reilly Media Inc; 2014.
12. Heger C, van Hoorn A, Mann M. Application performance management: state of the art and challenges for the future. 2017. URL: https://dl.acm.org/doi/abs/10.1145/3030207.3053674 [accessed 2025-01-16]
13. Bate P, Robert G. Bringing User Experience to Healthcare Improvement: The Concepts, Methods and Practices of Experience-based Design. United Kingdom: Radcliffe Publishing; 2007.
14. Taulli T. The robotic process automation handbook. In: A Guide to Implementing RPA Systems. Berkeley: Apress; 2020.
15. Primer A. Institute for Robotic Process Automation. 2015. URL: https://www.irpaai.com/wp-content/uploads/2015/05/Robotic-Process-Automation-June2015.pdf [accessed 2025-01-16]

XSL•FO
RenderX

16. Aguirre S, Rodriguez A. Automation of a business process using robotic process automation (RPA): a case study. : Springer International Publishing; 2017 Presented at: Applied Computer Sciences in Engineering; 2017 September 27-29; Cartagena, Colombia p. 65-71. [doi: 10.1007/978-3-319-66963-2_7]
17. Huang F, Vasarhelyi MA. Applying robotic process automation (RPA) in auditing: a framework. International Journal of Accounting Information Systems 2019;35:100433. [doi: 10.1016/j.accinf.2019.100433]
18. Kaya CT, Turkyilmaz M, Birol B. Impact of RPA technologies on accounting systems. Muhasebe ve Finansman Dergisi. 2019. URL: https://tinyurl.com/4fk8a9r2 [accessed 2025-01-16]
19. Moffitt KC, Rozario A, Vasarhelyi MA. Robotic process automation for auditing. Journal of Emerging Technologies in Accounting 2018;15(1):1-10. [doi: 10.2308/jeta-10589]
20. Belden JL, Grayson R, Barnes J. Defining and testing EMR usability: principles and proposed methods of EMR usability evaluation and rating. Information Experience Laboratory Publications (MU). 2009. URL: https://mospace.umsystem.edu/xmlui/handle/10355/3719 [accessed 2025-01-16]
21. van der Aalst WMP, Bichler M, Heinzl A. Robotic process automation. Bus Inf Syst Eng 2018;60(4):269-272. [doi: 10.1007/s12599-018-0542-4]
22. Muehlen MZ, Ho DTY. Risk management in the BPM lifecycle. Berlin Heidelberg: Springer; 2006 Presented at: Business Process Management Workshops; 2005 September 05; Nancy, France p. 454-466. [doi: 10.1007/11678564_42]
23. Lenz R, Reichert M. IT support for healthcare processes – premises, challenges, perspectives. Data & Knowledge Engineering 2007;61(1):39-58. [doi: 10.1016/j.datak.2006.04.007]
24. Musa MA, Othman MS. Business process reengineering in healthcare: literature review on the methodologies and approaches. RES 2016;8(1):20. [doi: 10.5539/res.v8n1p20]
25. Buttigieg S, Dey PK, Gauci D. Business process management in health care: current challenges and future prospects. IEH 2016:1 [FREE Full text] [doi: 10.2147/IEH.S68183]
26. Flechsig C, Lohmer J, Lasch R. Realizing the full potential of robotic process automation through a combination with BPM. In: Logistics Management. Cham: Springer; 2019:104-119.
27. Dumas M, La RM, Mendling J, Reijers HA. Fundamentals of Business Process Management. Berlin, Heidelberg: Springer; 2013.
28. Kowall J, Cappelli W. Magic quadrant for application performance monitoring. Gartner Research ID G. 2012. URL: https://sci-hub.do/https://dsimg.ubm-us.net/envelope/79303/309612/1346278314_streamReprintPDF.pdf [accessed 2025-01-16]
29. Ahmed T, Bezemer C, Chen T, Hassan A, Shang W. Studying the effectiveness of application performance management (APM) tools for detecting performance regressions for web applications: an experience report. : ACM; 2016 Presented at: MSR '16: Proceedings of the 13th International Conference on Mining Software Repositories; 2016 May 14-22; Austin Texas p. 1-12. [doi: 10.1145/2901739.2901774]
30. Venkatesh V, Brown SA, Bala H. Bridging the qualitative-quantitative divide: guidelines for conducting mixed methods research in information systems. MISQ 2013;37(1):21-54. [doi: 10.25300/misq/2013/37.1.02]
31. Neubauer BE, Witkop CT, Varpio L. How phenomenology can help us learn from the experiences of others. Perspect Med Educ 2019;8(2):90-97 [FREE Full text] [doi: 10.1007/s40037-019-0509-2] [Medline: 30953335]
32. Pope C, Ziebland S, Mays N. Qualitative research in health care. Analysing qualitative data. BMJ 2000 Jan 08;320(7227):114-116 [FREE Full text] [doi: 10.1136/bmj.320.7227.114] [Medline: 10625273]
33. Marshall MN. Sampling for qualitative research. Fam Pract 1996;13(6):522-525. [doi: 10.1093/fampra/13.6.522] [Medline: 9023528]
34. Lee RG, Dale BG. Business process management: a review and evaluation. Business Process Management Journal 1998;4(3):214-225. [doi: 10.1108/14637159810224322]
35. Cho C, Lee S. A study on process evaluation and selection model for business process management. Expert Systems with Applications 2011;38(5):6339-6350. [doi: 10.1016/j.eswa.2010.11.105]
36. Wanner J, Hofmann A, Fischer M, Imgrund F. Process selection in RPA projects-towards a quantifiable method of decision making. 2019. URL: https://tinyurl.com/ye2ybx5z [accessed 2021-12-31]
37. Soybir S, Schmidt C. Project management and RPA. In: Liermann V, Stegmann C, editors. The Digital Journey of Banking and Insurance, Volume I: Disruption and DNA. Cham: Springer International Publishing; 2021:289-305.
38. Willcocks LP, Lacity M, Craig A. The IT function and robotic process automation. 2015. URL: http://eprints.lse.ac.uk/64519/1/OUWRPS_15_05_published.pdf [accessed 2025-01-16]
39. Kleshchev A, Gribova V. From an ontology-oriented approach conception to user interface development. 2003. URL: http://sci-gems.math.bas.bg:8080/jspui/handle/10525/918 [accessed 2021-12-30]
40. Guarino N. Formal ontologies and information systems. : IOS Press; 1998 Presented at: Proceedings of the First International Conference (FOIS'98); 1998 June 6-8; Trento, Italy.
41. Shahzad S, Granitzer M, Helic D. Ontological model driven GUI development: user interface ontology approach. : IEEE; 2011 Presented at: 6th International Conference on Computer Sciences and Convergence Information Technology (ICCIT); 2011 November 29; Seogwipo, Korea (South) p. 214-218.
42. Anagnoste S. Robotic automation process - the operating system for the digital enterprise. Proc Int Conf Bus Excell 2018;12(1):54-69. [doi: 10.2478/picbe-2018-0007]

XSL•FO
RenderX

43. Adamoli A, Zaparanuks D, Jovic M, Hauswirth M. Automated GUI performance testing. Software Qual J 2011;19(4):801-839. [doi: 10.1007/s11219-011-9135-x]
44. Alégroth E, Feldt R, Ryrholm L. Visual GUI testing in practice: challenges, problemsand limitations. Empir Software Eng 2014;20(3):694-744. [doi: 10.1007/s10664-013-9293-5]
45. Borjesson E, Feldt R. Automated system testing using visual GUI testing tools: a comparative study in industry. : IEEE; 2012 Presented at: 2012 IEEE Fifth International Conference on Software Testing, Verification and Validation; 2012 April 17-21; Montreal, QC, Canada p. 350-359. [doi: 10.1109/icst.2012.115]
46. Yuan X, Cohen MB, Memon AM. Towards dynamic adaptive automated test generation for graphical user interfaces. 2009 Presented at: 2009 International Conference on Software Testing, Verification, and Validation Workshops; 2009 April 01-04; Denver, CO, USA p. 2009. [doi: 10.1109/icstw.2009.26]
47. Cernat M, Staicu A, Stefanescu A. Improving UI test automation using robotic process automation. 2020 Presented at: 15th International Conference on Software Technologies; 2020 July 7-9; Lieusaint, Paris, France p. 260-267. [doi: 10.5220/0009911202600267]
48. Heiskanen A. Robotic process automation in automated GUI testing of web applications. 2021. URL: https://www.diva-portal.org/smash/record.jsf?pid=diva2:1609800 [accessed 2022-03-28]
49. Osman CC. Robotic process automation: lessons learned from case studies. IE 2019;23(4/2019):66-71. [doi: 10.12948/issn14531305/23.4.2019.06]
50. Willcocks L, Hindle J, Lacity M. Executive Res Rep, Knowl Capital Partners, USA, Tech Rep. Keys to RPA success. URL: https://www.blueprism.com/uploads/resources/white-papers/KCP_Summary-Executive_Research_Report_Final.pdf [accessed 2025-01-16]
51. Smeets M, Erhard R, Kaußler T. Introduction of RPA governance. In: Robotic Process Automation (RPA) in the Financial Sector: Technology - Implementation - Success For Decision Makers and Users. Wiesbaden: Springer Fachmedien Wiesbaden; 2021:99-117.

Abbreviations

AI: artificial intelligence
APM: application performance monitoring
BPM: business process management
EHR: electronic health record
EMR: electronic medical record
GUI: graphical user interface
HIPAA: Health Insurance Portability and Accountability Act
IoT: Internet of Things
IRB: institutional review board
RPA: robotic process automation
SM: system management
SNUBH: Seoul National University Bundang Hospital
UI: user interface

Edited by C Lovis; submitted 22.04.24; peer-reviewed by D Etinger, L Agrawal; comments to author 25.12.24; revised version received 05.01.25; accepted 12.01.25; published 07.03.25.

Please cite as:
Park A, Jung SY, Yune I, Lee HY
Applying Robotic Process Automation to Monitor Business Processes in Hospital Information Systems: Mixed Method Approach
JMIR Med Inform 2025;13:e59801
URL: https://medinform.jmir.org/2025/1/e59801
doi:10.2196/59801
PMID:40053771

©Adam Park, Se Young Jung, Ilha Yune, Ho-Young Lee. Originally published in JMIR Medical Informatics (https://medinform.jmir.org), 07.03.2025. This is an open-access article distributed under the terms of the Creative Commons Attribution License (https://creativecommons.org/licenses/by/4.0/), which permits unrestricted use, distribution, and reproduction in any medium, provided the original work, first published in JMIR Medical Informatics, is properly cited. The complete bibliographic information, a link to the original publication on https://medinform.jmir.org/, as well as this copyright and license information must be included.

XSL•FO
RenderX

Original Paper

Extracting Multifaceted Characteristics of Patients With Chronic Disease Comorbidity: Framework Development Using Large Language Models

Junyan Zhang[1], MEng; Junchen Zhou[2], MPA; Liqin Zhou[2], PhD; Zhichao Ba[3], PhD

[1]Base of the State Key Laboratory of Urban Environmental Process and Digital Modelling, Capital Normal University, Beijing, China

[2]School of Medicine and Health Management, Huazhong University of Science and Technology, Wuhan, China

[3]Research Institute for Data Management & Innovation, Nanjing University, Suzhou, China

Corresponding Author:
Liqin Zhou, PhD
School of Medicine and Health Management
Huazhong University of Science and Technology
13 Hangkong Road
Wuhan, 430030
China
Phone: 86 15927686325
Email: zhoulq92@163.com

Abstract

Background: Research on chronic multimorbidity has increasingly become a focal point with the aging of the population. Many studies in this area require detailed patient characteristic information. However, the current methods for extracting such information are complex, time-consuming, and prone to errors. The challenge of quickly and accurately extracting patient characteristics has become a common issue in the study of chronic disease comorbidities.

Objective: Our objective was to establish a comprehensive framework for extracting demographic and disease characteristics of patients with multimorbidity. This framework leverages large language models (LLMs) to extract feature information from unstructured and semistructured electronic health records pertaining to these patients. We investigated the model's proficiency in extracting feature information across 7 dimensions: basic information, disease details, lifestyle habits, family medical history, symptom history, medication recommendations, and dietary advice. In addition, we demonstrated the strengths and limitations of this framework.

Methods: We used data sourced from a grassroots community health service center in China. We developed a multifaceted feature extraction framework tailored for patients with multimorbidity, which consists of several integral components: feasibility testing, preprocessing, the determination of feature extraction, prompt modeling based on LLMs, postprocessing, and midterm evaluation. Within this framework, 7 types of feature information were extracted as straightforward features, and three types of features were identified as intricate features. On the basis of the straightforward features, we calculated patients' age, BMI, and 12 disease risk factors. Rigorous manual verification experiments were conducted 100 times for straightforward features and 200 times for intricate features, followed by comprehensive quantitative and qualitative assessments of the experimental outcomes.

Results: The framework achieved an overall F_1-score of 99.6% for the 7 straightforward feature extractions, with the highest F_1-score of 100% for basic information. In addition, the framework demonstrated an overall F_1-score of 94.4% for the 3 intricate feature extractions. Our analysis of the results revealed that accurate information content extraction is a substantially advantage of this framework, whereas ensuring consistency in the format of extracted information remains one of its challenges.

Conclusions: The framework incorporates electronic health record information from 1225 patients with multimorbidity, covering a diverse range of 41 chronic diseases, and can seamlessly accommodate the inclusion of additional diseases. This underscores its scalability and adaptability as a method for extracting patient-specific characteristics, effectively addressing the challenges associated with information extraction in the context of multidisease research. Research and medical policy personnel can extract feature information by setting corresponding goals based on the research objectives and directly using the LLM for zero-sample target feature extraction. This approach greatly improves research efficiency and reduces labor requirements; moreover, due to the framework's high accuracy, it can increase study reliability.

XSL•FO
RenderX

(JMIR Med Inform 2025;13:e70096) doi:10.2196/70096

KEYWORDS

large language model; zero-shot prompting; information extraction; chronic disease; multimorbidity; natural language processing

Introduction

Overview

Research on chronic multimorbidity has increasingly become a focal point with the aging of the population [1]. Major research directions include exploring multimorbidity patterns [2,3], investigating multimorbidity development and prediction [4,5], and examining the mutual interplay between multimorbidity and patient characteristics [6]. Amid ongoing research on frequently occurring diseases, extracting patient characteristics holds paramount importance. However, traditional machine learning–based feature extraction methods often rely heavily on extensive sample sizes for model training, and in some cases, even necessitate manual annotation. This renders the task of extracting patient features, albeit just 1 aspect of the research, not only laborious and time-consuming but also susceptible to errors [7]. To address this, we developed a framework specifically tailored for extracting features related to patients with multimorbidity. Leveraging the powerful capabilities of natural language understanding and the automation features of large language models (LLMs), this framework aims to expedite the feature extraction process, minimize extraction errors, and efficiently handle vast amounts of electronic health records (EHRs). Consequently, it significantly reduces the time and human resources required for subsequent research on comorbidities, enabling more efficient and accurate insights into this complex field.

In the task of feature extraction for patients with multimorbidity, natural language processing (NLP) technologies hold significant advantages, effectively addressing challenges such as participant scarcity and the intricacies of information extraction. Recently, LLMs have garnered significant attention across various domains, including NLP, biomedical sciences [8], and clinical practice, particularly after the emergence of ChatGPT with GPT-4. Through fine-tuning LLMs [9] and designing prompt modeling [10,11], researchers have successfully tackled diverse NLP tasks; for instance, Hu et al [10] developed prompt modeling specifically for radiology reports, enabling the extraction of pertinent disease information from these reports. In addition, Datta et al [11] designed a system based on LLMs using prompt modeling to automatically identify medical eligibility criteria. Inspired by these advancements, we propose using LLMs that have undergone medical information training and fine-tuning to extract features of patients with multimorbidity from EHRs.

We developed a comprehensive framework designed to extract pertinent feature information from patients with multimorbidity. This framework is rooted in ZuoyiGPT, a powerful architecture that builds upon the transformer model and has undergone extensive training and fine-tuning using extensive medical literature, clinical records, both online and offline patient visit data, and expert annotations. Compared to ChatGPT with GPT-4, ZuoyiGPT boasts more specialized medical information and clinical experience. Furthermore, unlike the Taiyi LLM [12], ZuoyiGPT has undergone more extensive training on clinical information and incorporates a user interaction platform, which enhances its utility and accessibility. The framework established in this study is highly adaptable and knowledge driven, ensuring its flexibility and relevance in various scenarios. Feasibility tests have confirmed the viability of ZuoyiGPT in extracting patient characteristics from EHRs. Moreover, the postprocessing module has enhanced the consistency and accuracy of the extracted feature information. To assess the framework's performance in a zero-shot scenario, we evaluated the results of extracting both straightforward and intricate features from 300 EHRs. In a zero-shot setting, LLMs evaluated are able to extract patient characteristics solely based on the content and format requirements specified in the prompts, without relying on any additional demonstrations or training.

The study conducted patient characteristic extraction on a vast array of EHRs to ensure consistency, scalability, and interoperability. The capability to facilely extract multidimensional patient characteristics through prompt content holds significant value for analyzing a wide range of comorbidities. This framework allows for the aggregation of diverse combinations of multimorbidity, symptoms, and semistructured and unstructured mixed treatment recommendations from EHRs as objects for feature information extraction. We have delved into the strengths and weaknesses of the framework presented in the evaluation framework, identified potential future optimization suggestions, conducted a concise analysis, and provided research recommendations tailored to the demands of multidisease research. The main contributions of this study are outlined as follows:

1. A comprehensive framework based on zero-shot LLMs has been established for extracting demographic and disease-related characteristics of patients with multimorbidity, without the need for manual annotation. This framework categorizes the extraction of feature information from semistructured and unstructured EHRs into straightforward and intricate tasks.
2. The prompt modeling of the framework is adaptable to various tasks aimed at extracting different characteristics, offering flexibility and the ability to span across different disease domains. It can seamlessly be extended to accommodate extraction tasks pertaining to patient EHRs with diverse formats and structures.

Background and Significance

An EHR contains a diverse array of patient information, including demographic statistics, disease profiles, and examination details. This comprehensive dataset serves as a cornerstone for numerous disease studies, facilitating clinical decision support and translational research endeavors; for example, Naimark et al [13] leveraged an EHR patient portal to help patients formulate their health care goals. Given the

XSL•FO
RenderX

widespread embrace of EHRs [14], extracting pertinent information from these records has emerged as a pivotal focus of research [15]. Most information extraction efforts have primarily focused on 3 key subtasks: entity recognition, relation extraction, and event extraction [16-18]. By contrast, our study directly addresses the exigencies of chronic disease and multimorbidity research by concentrating on the extraction of multiple patient characteristics.

Numerous studies on multimorbidity [19-21] require the necessity of incorporating patient-specific and disease-specific features as inputs for predictive modeling, serving as the foundation for disease prediction modeling. Specifically, in the research on predicting cardiovascular disease risk in patients with type 2 diabetes [19], the initial step involves extracting patient age, gender, and disease codes as crucial inputs for the prediction model. Furthermore, when anticipating the future disease progression of patients with 0, 1, or 2 major chronic diseases [20], it becomes imperative to screen patients with 1 or 2 major chronic diseases, as well as those without any major chronic diseases, as inputs for the prediction. In addition, Lu and Uddin [21] highlight the importance of considering factors such as patient age, gender, disease codes, and smoking history in predicting chronic diseases. Consequently, the use of scientific and efficient methods for extracting disease and personal information features holds paramount importance in the study of multimorbidity.

A substantial amount of work [22-24] involves methods for extracting feature information. Kumar et al [22] used classical machine learning and deep learning approaches, using word embeddings and bag-of-words representations combined with feature selection techniques to extract features from clinical records and identify incidence rates. Kamp et al [23] adopted manual annotation to extract data from a large corpus of literature regarding the definitions, measurement methods, included conditions, and characteristics of patients investigated in studies on multiple diseases. Hu et al [24] achieved entity recognition and relationship extraction of symptoms and details within EHRs through an end-to-end overlapping joint extraction approach.

LLMs exhibit emergent behavior due to their transformer-based architecture [25]. Since the release of ChatGPT, LLMs have garnered significant attention and are currently being applied across various fields, including NLP, data analysis, medicine, and artificial intelligence. In clinical practice, LLMs can generate diagnostic lists and aid in clinical decision-making by leveraging their intelligent question-answering capabilities [26]. In the field of medical research, LLMs are able to abstract complex social determinants of health from original and unidentified medical notes [27], which can also assess the likelihood of epidemics based on the content of tweets [28]. In addition, in the realm of medical texts, these models are capable of generating patient clinical information and medical records [29]. It is anticipated that LLMs may one day facilitate real-time monitoring and predictive analysis [30].

In the medical field, numerous studies have explored the use of LLMs for NLP. A significant proportion of these studies have emphasized the fine-tuning of these models to simulate physician-patient communication, ultimately aiming to provide patients with electronic physician services [12,31,32]. Specifically, Yang et al [31] introduced the first Chinese-based medical LLaMA–based LLM, which progressed through a comprehensive process ranging from continuous pretraining (supervised fine-tuning) to human feedback reinforcement learning. Luo et al [12] focused on bilingual fine-tuning of LLMs for various biomedical NLP tasks. Furthermore, Chen et al [32] are concentrated on psychological counseling, enhancing the empathy capabilities of LLMs through immersive multiturn dialogue contexts.

In the realm of information extraction, LLMs are primarily used to extract radiology reports [10] and meta-information from scientific literature [33]. In recent research, an LLM was used to develop an eligibility criteria extraction system [11], successfully extracting eligibility criteria from clinical trial data; however, this system is designed for 9 specific diseases and extracts information from a limited number of dimensions. Current research on chronic diseases and multimorbidity is patient oriented, requiring a broader range of dimensions. Notably, there is a dearth of studies exploring the use of LLMs for extracting patient characteristic information, which constitutes the focal point of our investigation.

Although both Hu et al [10] and Datta et al [11] alluded to suboptimal extraction results arising from the use of generic LLMs, few studies have capitalized on LLMs specifically fine-tuned with medical and clinical insights, apart from those exclusively dedicated to fine-tuning or creating such models. Consequently, drawing on previous research and anticipating future prospects, this study embraced ZuoyiGPT, an LLM that has undergone extensive training and fine-tuning, incorporating literature, clinical data, and expert physician insights. ZuoyiGPT offers an interactive, web-based platform tailored for patient feature extraction. Through a feasibility testing system, we assessed ZuoyiGPT's proficiency in extracting patient features and subsequently used it to successfully extract a comprehensive set of 84 patient features. Notably, our feature extraction framework holds the potential to significantly reduce or even eliminate the reliance on manual annotation, thereby expanding its applicability to a broader range of feature extraction tasks.

Methods

Data

We conducted a systematic random sampling from the EHRs of 19,000 patients with chronic diseases at the Wanping Community Health Service Center in Beijing, China, and manually extracted desensitized EHRs for 1225 (6.45%) patients. All participants were aged >40 years and had multiple chronic diseases. These EHRs included details of 41 chronic diseases, 235 symptoms, and 312 drug recommendations. Notably, 986 (80.49%) of these 1225 EHRs contained preliminary consultation information, including personal details, medical histories, family backgrounds, lifestyle habits, self-reported symptoms, drug recommendations, and nonmedication advice. Conversely, the remaining EHRs (239/1225, 19.51%) lacked initial consultation data and solely contained personal information, medical histories, family

XSL•FO
RenderX

backgrounds, and lifestyle habits. We selected a combination of longitudinal and cross-sectional EHR information for our experiments. The EHRs include both semistructured and unstructured information. The semistructured information mainly comprises basic personal details of patients, such as gender and date of birth, as well as medical history; family history; and lifestyle information related to smoking, drinking, and physical activity. The unstructured information consists of 2 parts: the patient's presenting complaints, which contain symptom information, and the physician's diagnostic results, which include dietary and medication recommendations. Consequently, we categorized the extraction of semistructured information as straightforward feature extraction and the extraction of unstructured data as complex feature extraction.

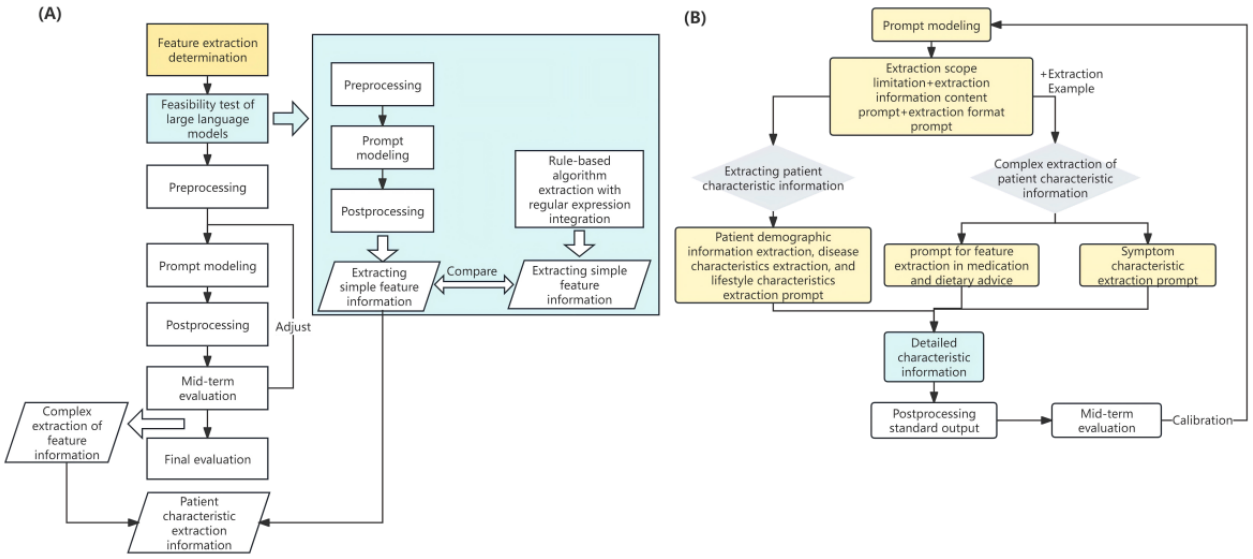
We used two methodologies to extract straightforward features from the 1225 EHRs: (1) a rule-based algorithm integrated with symbolic NLP and (2) ZuoyiGPT. Specifically, 10 features were used for prompt design, while 5 were designated for rapid prompt calibration. Furthermore, we manually annotated straightforward extraction information from 50 (4.08%) of the 1225 EHRs—those with preliminary diagnosis records as well as those without—to evaluate the capability of the LLM to extract simple features, thereby validating the feasibility of the ZuoyiGPT. Subsequently, ZuoyiGPT was used to extract intricate features from 986 (80.49%) of the 1225 EHRs, using 10 features for prompt design and 5 for rapid prompt calibration. Of these 986 EHRs, 200 (20.3%) were manually annotated to evaluate the LLM framework's performance in extracting patient features. Our manual annotations were completed by medical experts, and the prompt design was also guided by their expertise.

Framework for Extracting Characteristics of Patients With Multimorbidity

Overview

We developed a framework for extracting multifaceted characteristics of patients with multimorbidity. Leveraging the extensive language capabilities of ZuoyiGPT, this framework automatically retrieves demographic and disease-related information from EHRs. The following subsections introduce the various components of this framework, as illustrated in Figure 1.

Figure 1. System overview.

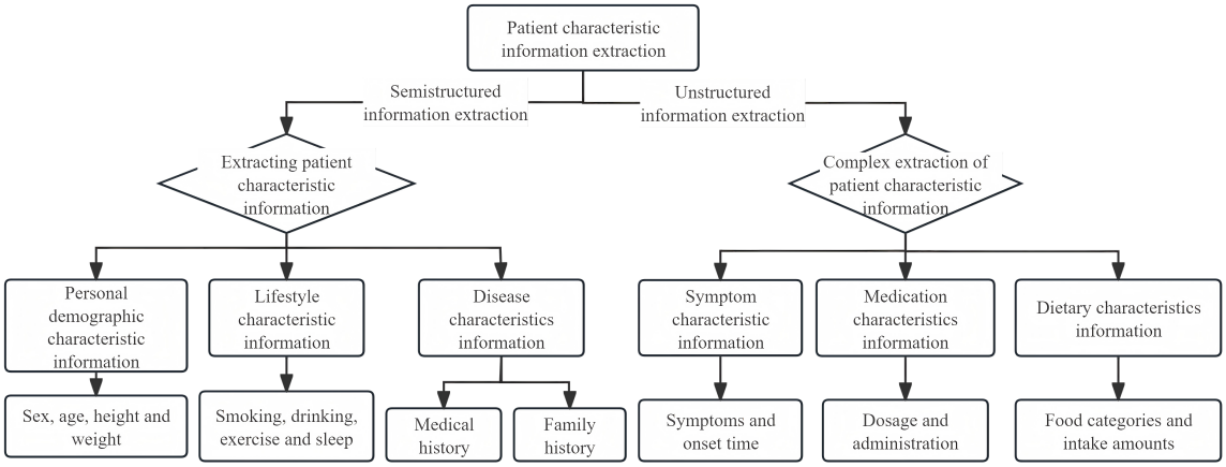


Feature Extraction Determination

Drawing upon insights from clinical experts and medical experts and extensive research literature on comorbidities associated with chronic and frequently occurring diseases, we arrived at a comprehensive set of extracted patient characteristic information. As outlined in the study by Cezard et al [4], research on chronic diseases typically falls into 2 categories: cross-sectional studies and longitudinal studies. Cross-sectional studies primarily focus on exploring symptoms and states as well as common risk factors, including age, unhealthy behaviors, and socioeconomic status. Conversely, longitudinal studies delve deeper into the exploration of diseases and their sequelae, tracing the trajectory of the illness over time. Dong et al [5] predicted multimorbidity through a graph convolutional network that integrated population phenotypes (including diet, physical activity, sleep, and smoking) and disease networks. Feng et al [6] investigated the effects of age and gender differences on multimorbidity. Ultimately, we opted to adopt a combined longitudinal and cross-sectional approach to studying chronic diseases. This holistic method integrates information extracted from electronic medical records, encompassing demographic characteristics, disease characteristics, lifestyle habits, symptomatic manifestations, medication profiles, and dietary patterns. This comprehensive approach aims to cater to the evolving needs of extracting patient characteristic information in future research endeavors on chronic diseases, as illustrated in Figure 2.

XSL•FO
RenderX

Figure 2. Extraction of patient characteristics.



Demographic information comprises patient ID, gender, date of birth, age, height, weight, and BMI. Among these, patient ID, gender, date of birth, height, and weight can be directly extracted from EHRs. Nevertheless, to facilitate subsequent research endeavors, we calculated the patients' age and BMI based on the extracted birth date, height, and weight.

Disease-related information consists of medical history and family history. The medical history includes 41 prevalent chronic diseases such as hypertension, type 2 diabetes, coronary heart disease, and stroke, along with the duration of each disease. The family history delves into 12 aspects, including whether the father or mother has coronary heart disease, diabetes, hypertension, hyperlipidemia, cerebrovascular disease, or stroke.

Lifestyle characteristic information includes smoking status, smoking duration, alcohol consumption, exercise patterns, sleep quality, and sleep disorders. Smoking status is categorized as follows: 1 signifies current smoking, 0 indicates nonsmoking, and –1 represents smoking cessation. For individuals who do not smoke or have quit smoking, smoking duration is recorded as 0. Similarly, alcohol consumption is classified as 1 for current drinking, 0 for nondrinking, and –1 for abstinence. Exercise status is differentiated into 5 categories: 3 represents daily exercise, 2 signifies exercising >3 times weekly, 1 indicates exercising 1 to 2 times weekly, 0 stands for no exercise, and –1 denotes irregular exercise. Sleep states are categorized into 3 levels: 3 for sleeping >10 hours daily, 2 for sleeping between 6 and 10 hours daily, and 1 for sleeping ≤6 hours daily. Finally, sleep disorders are dichotomized into 0 for the absence of sleep disorders and 1 for the presence of sleep disorders.

Symptom characteristic information includes a diverse range of manifestations, including dizziness, nausea, elevated blood pressure, dry mouth, headache, and 230 other symptoms. Our framework meticulously extracts the specific symptoms experienced by each patient, along with the corresponding time of symptom occurrence.

The drug characteristic information is equally extensive, encompassing enteric-coated aspirin tablets, acarbose tablets, controlled-release nifedipine tablets, atorvastatin calcium tablets, and a further 308 medications. Our framework accurately captures the medication information and dosage recommendations provided by physicians during the initial consultation for each patient. Dietary characteristic information covers 74 distinct types of food. Our framework diligently extracts the dietary categories and corresponding intake recommendations tailored by physicians during the initial consultation for each patient.

Furthermore, our framework demonstrates remarkable scalability and generalization ability by leveraging LLMs to expand its repertoire of diseases, symptoms, drug recommendations, and dietary suggestions. This enables it to continuously adapt and enhance its coverage, reflecting its sophisticated capabilities.

Feasibility Testing of LLMs

We used a rule-based algorithm integrated with symbolic NLP regular expressions to extract patient characteristics. These extracted results served as a benchmark for assessing the feasibility of leveraging LLMs for feature information extraction. Specifically, we used regular expressions such as "\d+\\.\d*" to identify patients' height characteristics and "\d+\.\d*|\d{2}|\d{3}" to identify and recognize their weight characteristics, enabling us to extract pertinent demographic and disease-related information. Our algorithm initially scanned through all EHRs of patients, pinpointing and cataloging all disease descriptions mentioned. Subsequently, based on the recommendations of medical experts, we consolidated various disease descriptions; for instance, "rheumatoid arthritis" was merged with "arthropathy" and "arthritis" into "rheumatoid arthritis," while "delusion" was merged with "mental illness" into "mental illness." Ultimately, we identified 41 chronic diseases, some of which encompass multiple disease characteristics, as detailed in Textbox 1.

XSL•FO
RenderX

Textbox 1. Characteristics of chronic diseases and comorbid conditions.

Disease categories and descriptions of the included diseases

- Cancer: cancer and malignant tumor
- Cerebrovascular diseases: cerebral infarction, cerebral ischemia, brain infarction, transient ischemic attack, cerebral thrombosis, cerebral arteriosclerosis, and atherosclerosis
- Mental illness: delusions and other psychiatric disorders
- Rheumatoid arthritis: osteoarthritis, arthritis, osteomyelitis
- Cardiovascular diseases (excluding coronary heart disease): heart failure, myocardial ischemia, valvular heart disease, and premature cardiac contractions
- Chronic ophthalmic diseases: bilateral retinitis pigmentosa and fundus atrophy

Subsequently, we selected 41 diseases as our benchmark and developed algorithms leveraging regular expressions to extract patient demographic characteristics, lifestyle information, disease details, and family histories from the semistructured text format.

We categorized EHRs into semistructured and unstructured information and implemented patient feature extraction and applied LLM-based extraction methods tailored to each type. Semistructured information incorporates explicit format identifiers, such as colons, carriage returns, and labels such as “personal information,” whereas unstructured information consists of patient-reported symptoms, physician-provided guidance based on patient descriptions and medical histories, as well as nonpharmacological guidance. We used the extraction of semistructured information as a feasibility test for assessing the information extraction capabilities of ZuoyiGPT. To facilitate processing by the LLM, we eliminated redundant spaces and carriage returns, simplifying the information extraction process.

On the basis of the specific information content required for extraction, we iteratively developed, tested, and calibrated a comprehensive prompt tailored as the input for ZuoyiGPT’s interactive platform. For the extraction of semistructured information, our prompt comprised 4 integral components: scope definition, extraction content prompt, extraction format prompt, and prompt query for the original text. The scope definition instructs the LLM to focus solely on extracting information from the provided text. The extraction content specification outlines the precise details that the model needs to capture. The extraction format guidance mandates the model to present the extracted information in a predefined format. The prompt query referencing the original text pertains to the segment of the EHR serving as the source material. Given the immense volume of original text involved in this information extraction task, we opted not to include an extraction example prompt. The actual prompt text and its output are illustrated in Textbox 2.

XSL•FO
RenderX

Textbox 2. Characteristics of chronic diseases and comorbid conditions.

Prompt composition

1. Please extract the following information based on the provided content:

2. height, weight, medical history, family history, smoking status, smoking duration, alcohol consumption, exercise habits, sleep duration, and sleep disorders.

3. Output the extracted results in the following format:

Height: XXX cm;

Weight: XX kg;

Medical History:

① Diagnosed with XXX disease in XXXX;

② ...;

Family History (1 if the parent has the respective disease, otherwise 0):

Father with coronary heart disease: 1/0

Father with diabetes: 1/0

Father with hypertension: 1/0

Father with hyperlipidemia: 1/0

Father with cerebrovascular disease: 1/0

Father with stroke: 1/0

Mother with coronary heart disease: 1/0

Mother with diabetes: 1/0

Mother with hypertension: 1/0

Mother with hyperlipidemia: 1/0

Mother with cerebrovascular disease: 1/0

Mother with stroke: 1/0

Smoking Status: Smoker/Non-smoker/Ex-smoker;

Smoking Duration (current year is 2024): XX years (0 if non-smoker);

Alcohol Consumption: Drinker/Non-drinker/Ex-drinker/Other;

Exercise Habits: Sedentary/Irregular exercise/Exercise 1-2 times per week/Exercise 3 times per week/Exercise more than 3 times per week;

Sleep Duration: XX hours;

Sleep Disorders: Present/Absent.

4. Original Text: 【Demographic Characteristics Information + Medical History + Family History + Lifestyle Habits

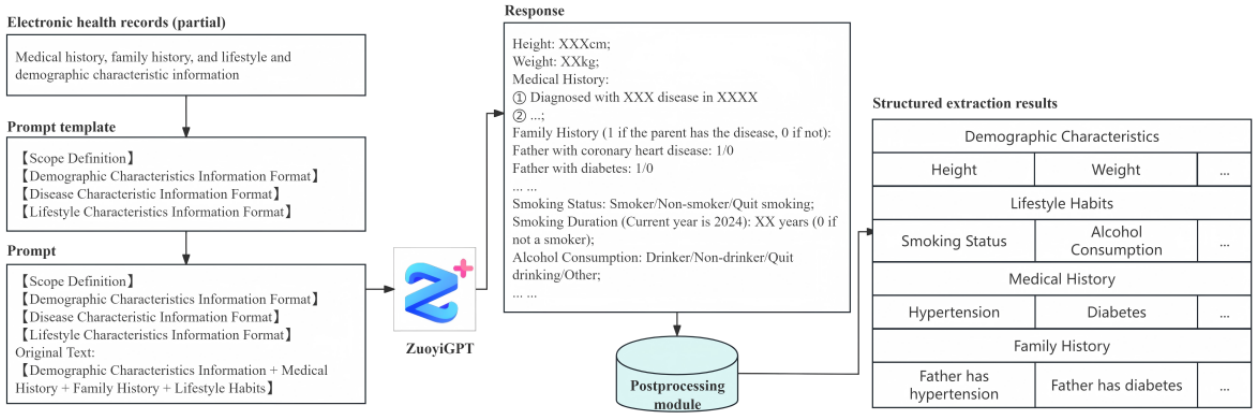
Sample output

- Height: 168.0 cm; Weight: 65.0 kg; Medical History: ① Diagnosed with coronary heart disease in August 2013; ② Diagnosed with hyperlipidemia in May 2013; Family History: Father - Coronary heart disease: Yes; Father - Diabetes: No; Father - Hypertension: No; Father - Hyperlipidemia: Yes; Father - Cerebrovascular disease: No; Father - Stroke: No; Mother - Coronary heart disease: No; Mother - Diabetes: No; Mother - Hypertension: No; Mother - Hyperlipidemia: No; Mother - Cerebrovascular disease: No; Mother - Stroke: No; Smoking Status: Non-smoker; Smoking Duration (current year is 2024): 0 years; Alcohol Consumption: Drinks alcohol; Exercise Frequency: 1-2 times per week; Sleep Duration: 6 hours; Sleep Disturbances: Present.

After using ZuoyiGPT for batch information extraction from semistructured data, we resolved formatting issues in the actual extracted results using a straightforward rule-based algorithm; for instance, we corrected instances where the LLM merged 2 lines of output into a single line by adding line breaks and eliminating redundant line breaks. Subsequently, we used a rule-based algorithm to extract keywords and numerical values from the LLM's output, along with performing numerical substitutions. As an example, we extracted "coronary heart disease" and "2013" from "coronary heart disease in 2013," and converted "Smoking Status: Smoking" to "Smoking Status: 1." These extracted keywords and numerical values were then assigned to their corresponding labels, effectively transforming them into a structured tabular format. Figure 3 illustrates the entire process of extracting simple patient feature information from an EHR.

XSL•FO
RenderX

Figure 3. Overview of the process of simple extraction of feature information using a large language model (ZuoyiGPT).



Finally, from the 1225 EHRS, we randomly selected 100 (8.16%) and manually annotated their semistructured data sections, including past medical history, family history, lifestyle, and specific objective examinations. Subsequently, we conducted a comparative analysis of the extraction results obtained through a rule-based algorithm and those achieved by using the LLM on these 100 EHRs. The comprehensive final results, showing the F_1-score values for both the rule-based algorithm and LLM extraction methods, are presented in Table 1.

Table 1. F_1-score values for simple extraction of feature information using a rule-based algorithm and a large language model (LLM).

Extraction method	Basic information (%)	Lifestyle (%)	Medical history (%)	Family history (%)	Overall (%)	SD value (%)
Rule-based algorithm	98	95	99.66	99.67	98.08	1.9049
LLM	100	99	99.7	99.67	99.59	0.3656

Clearly, the results extracted by the LLM outperformed those extracted by the rule-based algorithm, with F_1-score values consistently exceeding 95%, thus confirming the feasibility of using an LLM for patient feature information extraction.

Preprocessing

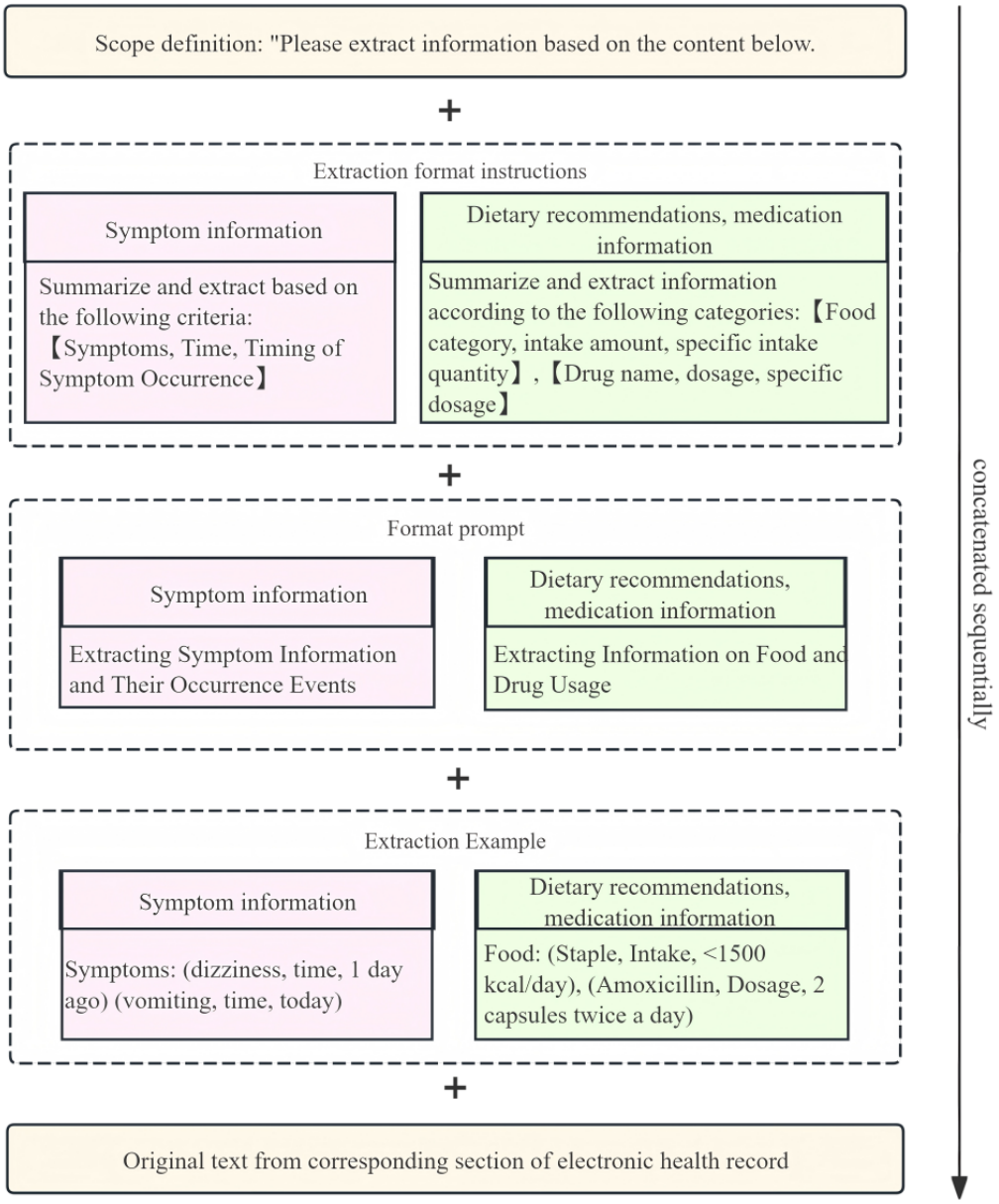
We began by considering the composition of unstructured text in EHRs and dividing each EHR into 2 sections: current illness history and medication guidance. The current illness history includes the patient's initial self-reported information, while the medication guidance consists of 4 parts: Western medicine prescription guidance, traditional Chinese medicine prescription guidance, nondrug guidance, and physician advice. Using prompt modeling, we guided the LLM to extract pertinent symptom information from the current illness history, including symptom names and their respective occurrence times. We also extracted medication guidance and dietary advice from the medication section, including drug names, dosages, food categories, and recommended intake quantities. We used the rule-based algorithm to extract the text related to the patients' chief complaints, as well as the sections on medication and nonmedication guidance, from the patients' EHRs. Unnecessary formatting elements, such as extraneous whitespace and line breaks, were removed.

Prompt Modeling

Compared to complex feature extraction, the original text content for simple feature extraction is considerably more limited in scope. To guarantee accurate information extraction by an LLM, we crafted a more comprehensive prompt and fed it into the ZuoyiGPT, which excels in identifying all facets of complex feature extraction. This model underwent rigorous iterative experiments, testing, and prompt calibration. Ultimately, we developed 2 stand-alone comprehensive prompts: one dedicated to extracting symptom information and the other to extracting drug recommendations and dietary advice. Each prompt consisted of five integral components: (1) scope definition, (2) extraction format prompt, (3) extraction content prompt, (4) extraction example, and (5) prompt query text. Figure 4 illustrates the formation of the comprehensive prompt; Textbox 3 showcases example prompt templates for symptom information, along with the corresponding output; and Textbox 4 presents medication recommendation and dietary advice information, along with the corresponding output.

XSL•FO
RenderX

Figure 4. Components of complex extraction feature information prompt modeling.



Textbox 3. Example of symptom information prompt, along with the corresponding output.

Prompt composition

1. Please translate the following content.
2. Summarize and extract the food and drug information from the text in the format of: 【Food Category, Intake Amount, Specific Intake Quantity】, 【Drug Name, Dosage, Specific Dosage】
3. Example: (Main Food, Intake Amount, <1500 kcal/day), (Metformin Hydrochloride Tablets, Dosage, 0.5mg / 4 times/day)

Original Text

【Drug Guidance + Non-Drug Guidance】

Sample output

【Diet】

Triples: (Low-sodium, low-fat diabetes diet, intake, no specific amount); (Sodium salt, intake, less than 6g/day); (Cooking oil, intake, less than 25g/day); (vegetables, intake, no specific amount); (Foods rich in vitamin C, intake, no specific amount)

【Medication】

Triples: (L-type amlodipine besylate tablets, dosage, 5mg once daily); (Simvastatin dispersible tablets, dosage, 20mg once daily)

XSL•FO
RenderX

Textbox 4. Examples of drug suggestion information and dietary advice prompts, along with the corresponding output.

Prompt composition

1. Please summarize and extract the temporal information of symptoms based on the following content.
2. Organize the information in the format of 【Symptom Name, Time, Symptom Occurrence Time】.
3. For example:【Symptom: (Dizziness, Time, 2022), (Vomiting, Time, 1990)】
4. The original text includes 【Present Illness History, Chief Complaint】

Sample output

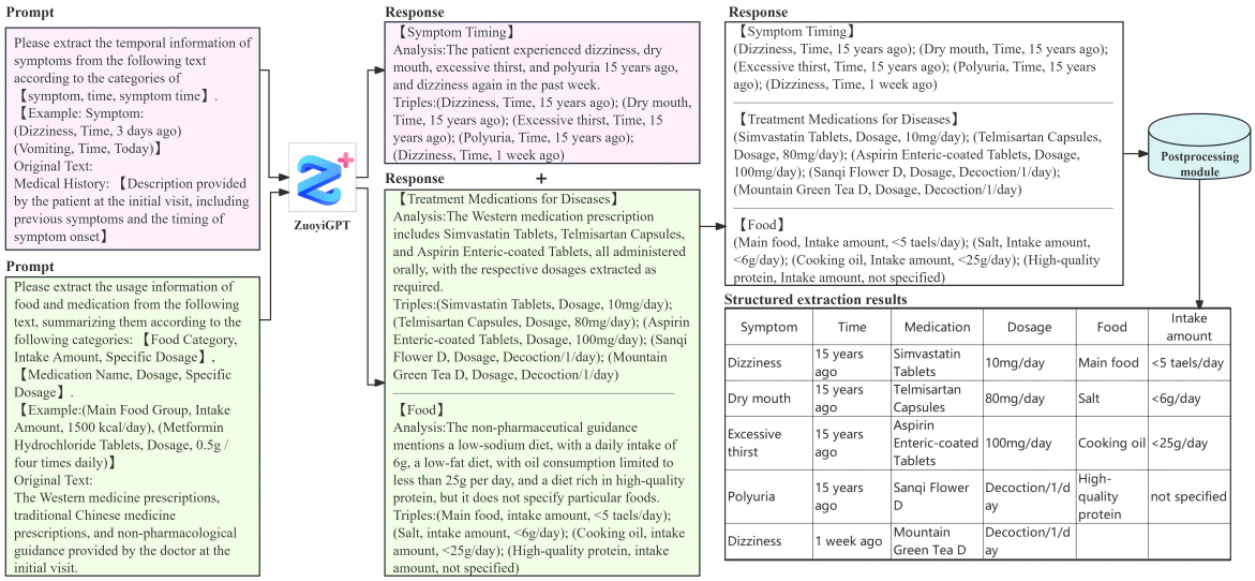
- Symptoms Triplet: (Dizziness, Time, 1985) (Weakness in Lower Extremities, Time, 1990) (Palpitations, Time, 1990)
- (Sweating, Time, 1990)

Using a prompt template, we developed a web automation program that leverages an LLM to efficiently extract information from EHRs in batches and obtain their corresponding responses. For each EHR, we initiated a new conversation to prevent the extraction results from being influenced by previous dialogues. Given the potential challenge of the LLM not recognizing the output format, we opted for the ZuoyiGPT, which is trained to generate triples. Although the training format of the Left-Hand Doctor model does not exactly match our required format, it includes the format and content we need. Therefore, we decided to save the output of each EHR into separate documents and subsequently process the extraction results in a sequential manner.

Postprocessing

Although we provided structured output requirements, the primary purpose of LLMs is to simulate human communication. The LLMs we used have been trained in formats different from our requirements. Therefore, the results extracted by the LLM are not always in line with our expectations. To address this issue, we developed a rule-based postprocessing module with regular expressions to convert the chaotic semistructured answers into structured answers that are conducive to generating tables. Specifically, we identified the positions of all triples related to symptoms, medication characteristics, and dietary recommendations and used regular expressions to recognize the 3 parts of the triples, outputting a unified format. Each EHR involves 3 parts of triples, which are separated by specific formats and subsequently exported to individual documents for each record. Ultimately, we converted all triples into electronic medical record formats into a tabular format, ensuring consistency in the output content throughout this process; for example, terms such as “oil type,” “oil,” and “cooking oil” were unified as “cooking oil,” while “heart and brain unblocking” and “heart and brain unblocking tablets” were unified as “heart and brain unblocking tablets.” In addition, when the LLM expressed the meaning of “not mentioned,” the results could appear as “not mentioned,” “not found,” or “not mentioned.” We unified these expressions as “not mentioned” in this module and removed any “not mentioned” entries from food categories, symptom names, and medication names. Figure 5 provides a comprehensive overview of the process of extracting complex feature information from a patient’s EHRs.

Figure 5. Overview of the process of extracting complex patient feature information using a large language model. The pink areas represent the extraction of symptom information, while the green areas represent the extraction of medication and dietary recommendations.



XSL•FO
RenderX

Evaluation

As part of the midterm evaluation of the patient feature extraction framework, we manually assessed the prompts and iteratively refined them based on feedback provided by medical experts. For the final framework evaluation, we conducted both quantitative and qualitative assessments. In terms of quantitative evaluation, we used 200 trial documents, manually annotated by medical experts. We reported the framework's precision, recall, and F_1-score values in identifying symptoms, symptom timing, medications, medication dosages, foods, and intake amounts. Furthermore, we calculated the framework's accuracy in extracting complex information across 3 categories. Specifically, we reported accuracy metrics for 3 combinations: symptom+symptom duration, medication+dosage, and food category+food intake, where each label had to match precisely with manually annotated information. In addition, we initiated a new dialogue for extracting EHRs for each patient to generate more accurate responses from LLMs. The data is split into 2 sets of 100, with each set being manually annotated by a different group, and the groups then cross-validate each other's annotations. For qualitative evaluation, we conducted a thematic analysis of missing and incorrect standard entities in 200 trials to explain the strengths and weaknesses of the patient feature extraction framework specifically tailored for patients with chronic disease.

Ethical Considerations

This study was approved by the Ethics Committee of Tongji Medical College, Huazhong University of Science and Technology (approval number:2024 IEC (A177), as part of the project "Research on Risk Situation Awareness and Response Strategies for Chronic Disease Comorbidity Based on Knowledge Association". This study used a desensitized dataset obtained from community health service centers in Beijing, China. The collection of this dataset complied with the "ethical review measures for biomedical research involving humans".

Results

Framework Performance

The framework's performance in terms of precision, recall, and F_1-score performance across symptoms, symptom duration, medications, medication dosage, food, and intake quantity is shown in Table 2.

Table 2. Performance measurements of 6 complex extraction features.

Features	Precision (%)	Recall (%)	F_1-score (%)
Symptoms	100	97.05	98.5
Symptom duration	99.85	96.89	98.35
Medication	99.86	98.07	98.96
Dosage	77.2	94.6	84.98
Food	87.83	97.91	92.6
Intake	89.36	96.49	92.79
Overall	92.35	96.84	94.36
SD value	8.466	1.144	4.963

Table 3 demonstrates the framework's performance in extracting intricate patient information features, particularly from unstructured textual data. Notably, the framework performed well in identifying these 6 complex feature types, with the highest accuracy for medication extraction (98.96%) and the lowest for medication dosage extraction (84.98%). The framework achieved a high overall F_1-score of 94.36% across all labels. Table 3 presents the accuracy measurements for 3 combinations, revealing overall F_1-score values of 98.42%, 92.64%, and 88.05%, respectively.

Table 3. Accuracy measurements of 3 combinations.

Feature combination	Precision (%)	Recall (%)	F_1-score (%)
Symptom+symptom duration	99.92	96.97	98.42
Medication+dosage	88.99	96.6	92.64
Food category+food intake	80.38	97.35	88.05

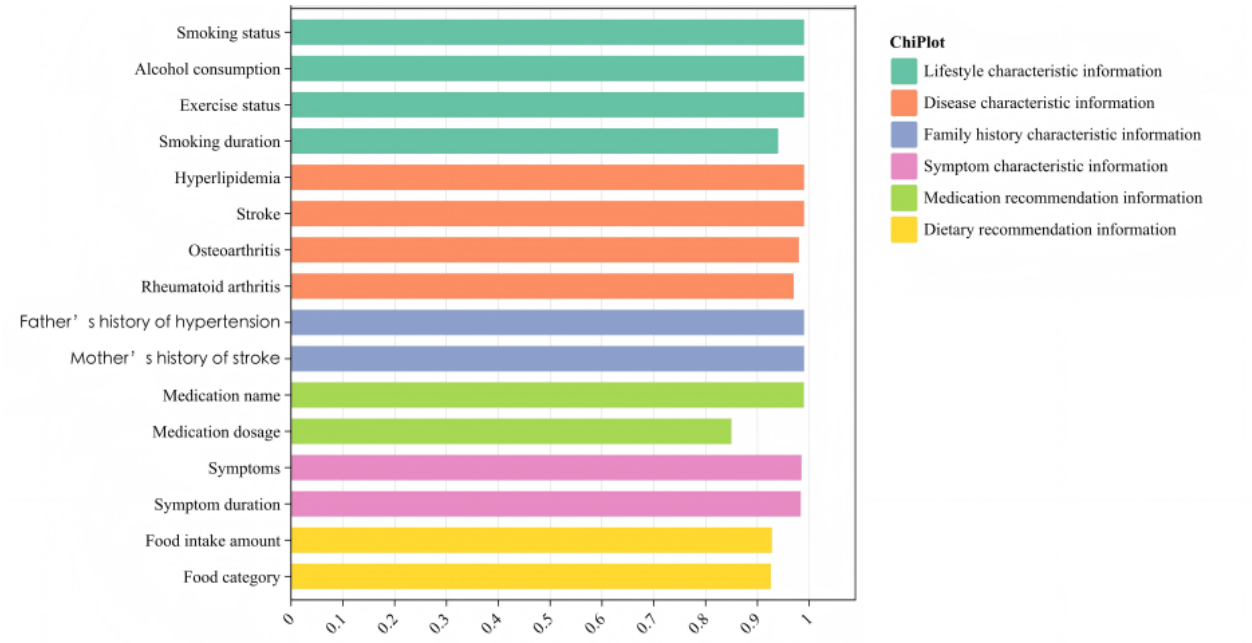
Extraction Accuracy

By integrating the results of both simple and complex feature extraction, we visualized the F_1-score values of all features with extraction accuracy not reaching 100%, as shown in Figure 6. Of the 67 feature labels, 61 (91%) pertained to simple extraction, while the remaining 6 (9%) concerned complex extraction. Notably, the extraction results of simple features significantly outperformed those of complex features. Of the 61 simple extraction features, 10 (16%) exhibited errors during the extraction process. These errors were observed in lifestyle-related features, including "smoking status," "smoking duration," "drinking status," and "exercise status," with F_1-score values of 99%, 94%, 99%, and 99%, respectively. In the disease feature information, errors occurred in the extraction of "hyperlipidemia," "rheumatoid arthritis," "stroke," and

XSL•FO
RenderX

"osteoarthritis," with F_1-score values of 99%, 97%, 99%, and 98%, respectively. In addition, errors were encountered in the extraction of family history features, specifically "father with hypertension" and "mother with stroke," both achieving an F_1-score of 99%. Notably, all 6 complex features exhibited errors in their extraction.

Figure 6. Overview of F_1-score values for feature extraction.



Discussion

Feature Extraction Error Analysis

We developed a framework based on LLMs for extracting features of patients with multimorbidity. After completing performance measurements, we conducted an error analysis to elucidate the system's shortcomings in each category. The F_1-score values for all extracted features are visualized in Figure 6. Notably, the extraction of simple features involving unstructured text, such as "smoking status," "drinking status," and "exercise status," resulted in extraction errors. Our investigation revealed that the LLM incorrectly characterized smoking status as "Smoking status: Frequent (≥5 cigarettes/day)," whereas accurate descriptions typically followed the format "Smoking status: Started in 1982, Frequent (≥5 cigarettes/day)." The absence of smoking commencement years in patient health records hindered the model's ability to accurately infer smoking status based solely on the "smoking status: frequent" descriptor. Similarly, errors in "drinking status" stemmed from the omission of the prefix "drinking status:" in the text description, leading to misclassification and extraction by the model. The challenge with "exercise status" mirrored that of "drinking status" because it lacked the explicit textual segmentation "exercise status:"—this compromised the model's ability to accurately extract data from partially structured texts lacking proper segmentation. When errors occurred in the semantic segmentation of the text and the semantic understanding of general knowledge, we enhanced semantic segmentation by inserting line breaks before the "smoking status," "drinking status," and "exercise status" during the preprocessing of medical records. A better extraction method is to use general-purpose LLMs, such as Kimi and DeepSeek, for feature extraction tasks that do not heavily involve medical background knowledge. These models are superior in their training and understanding of everyday common knowledge compared to general-purpose LLMs that are trained extensively on medical terminology at a later stage.

In disease condition recognition, LLMs exhibit a lower probability of making errors in associating disease occurrence practices with disease names; for example, in the electronic medical record of a patient where the disease is described as "2013-06, hyperlipidemia; 2008-06, stroke," the LLM might incorrectly interpret it as indicating that the patient had hyperlipidemia in 2008 and stroke in 2013. The triggering factor for such recognition errors is unrelated to the names or categories of the diseases. Such errors can often be addressed by enhancing text preprocessing, for example, by inserting formatting separators such as a newline character or other delimiters after each disease.

In the recognition of family history, LLMs may erroneously attribute the disease status of siblings to that of the father or mother. Therefore, if a sibling has a certain disease, and this situation is described in the family history, it could lead to incorrect identification and extraction by the LLM. This issue can be addressed by incorporating the prompt "Please note the distinction between sibling illness and parental illness" into the prompt modeling or by using rule-based methods to eliminate cases of sibling illness during text preprocessing. Experiments show that adding the clarification prompt yields better results than deleting portions of the text during preprocessing.

The error rate of complex feature extraction is relatively higher than that of simple feature extraction. We categorized these errors into 6 distinct types: *incorrect extraction*, *nonrecordable*, *formatting error*, *incomplete extraction task*, *recognition error*, and *missed extraction*. *Incorrect extraction* refers to the situation

XSL•FO
RenderX

where the LLM includes information that does not belong to the intended label, such as extracting “exercise regularly” into the “symptoms” label. *Nonrecordable* occurs when the LLM includes information that, while fitting the category of the label, exceeds the required range, such as extracting “clear mind” into the “symptoms” label. A *formatting error* happens when the LLM fails to output the extraction results according to the specified format, leading to missing or incorrect information in the structured table, for example, extracting “dizziness a year ago” as “(dizziness; a year ago).” An *incomplete extraction task* refers to instances where the model fails to fully extract the required content for a given label, resulting in blank entries for this label in the corresponding medical records. A *recognition error* occurs when the extraction result fits both the label category and range but does not match the actual description in the medical record, such as extracting “dizziness a year ago” as (dizziness, symptom time, a week ago). *Missed extraction* happens when the LLM completes the extraction task for the corresponding label but fails to capture all relevant information described in the medical record, for instance, only extracting (dizziness, symptom time, a year ago) from a record that also mentions “dry mouth.” The distribution of the 6 types of errors is shown in Table 4. A total of 430 (11.03%) errors were identified among the 3898 valid information entries from 200 patients, resulting in an accuracy rate of 88.97% for valid information extraction. Among the 6 types of errors, formatting errors, incomplete extraction task, and incorrect extraction were the most prevalent.

Table 4. Incidence of 6 types of errors in complex feature extraction.

Error types	Incorrect extraction	Nonrecordable	Formatting error	Incomplete extraction task	Recognition error	Missed extraction
Symptoms	12	10	0	0	0	0
Symptom onset	2	19	0	0	1	0
Drug	14	0	5	0	6	13
Drug dosage	18	0	119	0	4	50
Food category	9	0	23	4	10	35
Food intake	9	0	27	4	6	33

Formatting errors and incomplete extraction task are most likely to occur in drug dosages. Our error analysis revealed that the causes of these errors often related to the LLM’s poor understanding of formatting, which aligned with our previous error analysis on simple feature extraction. When outputting drug triplet information, the LLM may produce results such as (Aspirin Enteric-Coated Tablets, drug, Aspirin Enteric-Coated Tablets), as well as expressions such as (Aspirin Enteric-Coated Tablets, dosage, 100mg once daily) or (Aspirin Enteric-Coated Tablets, dosage, 100mg daily). During postprocessing, it is challenging to uniformly handle such random and varied results using rule-based algorithms. If the LLM only provides extraction results such as (Aspirin Enteric-Coated Tablets, drug, Aspirin Enteric-Coated Tablets), it becomes even more difficult during postprocessing to obtain information on drug dosages without reviewing the original electronic medical record, increasing the risk of missing or inaccurate dosage entries in the structured output table. Format output errors can be resolved using a second feature extraction method with a general-purpose language model. Specifically, after the medical LLM performs the first feature extraction, we can concatenate the formatting requirements with the first extraction results and input them into a general-purpose language model (such as Kimi, DeepSeek, ERNIE Bot, etc) to obtain feature extraction results that meet our requirements through secondary extraction from these LLMs; for example, we inputted the information presented in Textbox 5 into ZuoyiGPT.

The extraction results obtained are presented in Textbox 6.

XSL•FO
RenderX

Textbox 5. Example of prompt content for simple extraction of patient characteristic information, along with the corresponding output.

- Please summarize and extract the symptom time information in the format of 【symptom name, time, symptom occurrence time】 【Example: Symptom: (dizziness, time, 2022) (vomiting, time, 1990)】. At the same time, summarize and extract food and drug information in the non-drug guidance according to the format of 【food category, intake amount, specific intake amount】, 【drug name, dosage, specific dosage】. Example: (staple food, intake amount, <1500 kcal/day), (metformin hydrochloride tablets, dosage, 0.5mg/4/day)】. Original text: Medical history: The patient experienced paroxysmal dizziness with nausea 15 years ago without obvious inducements, no vomiting, no significant activity impairment, no speech difficulties, no facial drooping, and no consciousness impairment. Blood pressure was recorded at a maximum of 160/100 mmHg, and the patient was subsequently referred to another hospital, where they were diagnosed with grade 2 hypertension. After treatment with 'amlodipine besylate tablets, orally / 1/day, 10.0000mg each', the blood pressure was controlled around 130-140 / 80-90 mmHg, and the dizziness symptoms significantly alleviated. Since the onset of the disease, the patient has been clear-minded, mentally stable, with normal diet and sleep, and normal bowel and bladder function.

Medication treatment

- Western Medicine Prescription: Clopidogrel Bisulfate Tablets, orally once daily, 1.0000 tablet per dose; Amlodipine Besylate Tablets, orally once daily, 10.0000 mg per dose; Simvastatin Tablets, orally once daily, 1.0000 tablet per dose.
- Traditional Chinese Medicine Prescription: None.
- Non-Drug Guidance: 1. Follow a low-salt, low-fat diet, controlling daily salt intake to less than 6 grams. 2. For abdominal obesity and overweight, maintain a reasonable diet, engage in moderate exercise, increase muscle mass, and enhance physical fitness. 3. Ensure a balanced diet with adequate nutrition, consume more vegetables and fruits, eat foods rich in vitamin C, reduce oil consumption to less than 25 grams per day, and limit staple food intake to less than half a kilogram per day. 4. Maintain a positive mood and reduce stress from work and life. 5. Reduce waist circumference and weight; prevent osteoporosis, falls, and accidental injuries; provide self-rescue guidance; regulate emotions, maintain psychological balance, avoid extreme emotions, maintain a balanced lifestyle, and cultivate a tranquil mind.
- Doctor's Advice: 1. Consistently adhere to prescribed antihypertensive medication and monitor blood pressure (self-monitor weekly and keep a record; measure clinic blood pressure at least once a month), and seek medical attention for any changes in condition. 2. Regularly conduct blood tests, urine tests, stool tests, chest X-rays (anteroposterior view), electrocardiograms, liver and kidney function tests, and fundus examinations. 3. Engage in appropriate gentle outdoor activities in sunny environments, and avoid exercising in windy, cold, or snowy conditions.

Textbox 6. Extraction results.

Symptoms

- (dizziness, time, 15 years ago)
- (nausea, time, 15 years ago)

Food

- (salt, intake, <6 grams/day)
- (cooking oil, intake, <25 grams/day)
- (staple food, intake, <250 grams/day)

Medication

- (Clopidogrel hydrogen sulfate tablets, dosage, 1/day, specific dosage, 1.0000 tablet)
- (Amlodipine besylate tablets, dosage, 1/day, specific dosage, 10.0000 mg)
- (Simvastatin tablets, dosage, 1/day, specific dosage, 1.0000 tablet)

We summarized the time information for the symptoms extracted according to the format "[symptom name, time, symptom occurrence time]". 【Example: Symptoms: (dizziness, time, 2022) (vomiting, time, 1990)】. At the same time, we summarized the nonmedication guidance for food and medication information according to the format "[food category, intake, specific intake amount], [medication name, dosage, specific dosage]". 【Example: (staple food, intake, <1500 kcal/day), (Metformin hydrochloride tablets, dosage, 0.5 mg/4/day)】. By concatenating the results extracted by ZuoyiGPT with the input to Kimi, a more standardized result that is conducive to postprocessing can be obtained (Textbox 7).

XSL•FO
RenderX

Textbox 7. Example of standardized extraction results after concatenating ZuoyiGPT outputs with Kimi input.

- Symptom Timeline Information
- (Dizziness, time, 15 years ago)
- (Nausea, time, 15 years ago)
- Food Information
- (Salt, intake, <6 grams/day)
- (Oil, intake, <25 grams/day)
- (Staple food, intake, <250 grams/day)
- Medication Information
- (Clopidogrel bisulfate tablets, dosage, 1 tablet/day)
- (Amlodipine besylate tablets, dosage, 10 mg/day)
- (Simvastatin tablets, dosage, 1 tablet/day)

The experimental results showed that Kimi exhibited the best sensitivity to formatting.

First, the error rates and quantities for various food categories and food intake amounts exhibited remarkable similarity. Second, there were significant instances of erroneous extractions without labels; yet, these errors were distributed almost uniformly across all complex feature extractions, excluding symptom timing. We conducted separate analyses for these 2 phenomena.

Incorrect extraction of food categories can lead to erroneous extraction of food intake. Our observations revealed that, among the 4 types of feature information pertaining to drug and food information, errors in time and dosage features were as frequent as—or more frequent than—those in content features. This is because, within the same feature type, errors in content often indicate that the corresponding descriptive information is also incorrect. Therefore, if an incorrect food category is extracted, such as misidentifying smoking and drinking as food, the subsequent extraction of food intake amounts often results in extracting information about quitting smoking and drinking. Similarly, the failure to extract food categories also leads to the failure to extract food intake amounts, and the omission of food categories results in the omission of food intake amounts. LLMs have relatively chaotic definitions of "food categories" and sometimes interpret the task of extracting food recommendations as tasks unrelated to drug guidance. This has led to incorrect extraction, omission, and even incomplete extraction. However, based on input from medical experts and observations of the extraction results, we identified a consistent pattern in physicians' dietary recommendations for patients with chronic and multiple diseases. These recommendations are typically focused on categories such as salt, cooking oil, vegetables, foods rich in vitamin C, staple foods, and foods high in dietary fiber. Moreover, the corresponding intake amounts remain almost unchanged. In other words, the description of food recommendation information is fixed, with fewer categories. Therefore, it is possible to first perform a rough extraction using an LLM and then summarize the results to provide a combination of food recommendations as a reference during prompt modeling, allowing the LLM to complete the secondary feature information extraction of food recommendations.

The issue of erroneous extraction remains consistently prevalent across 3 feature extraction categories: symptoms, medication characteristic information, and food recommendations. LLMs occasionally misclassify information into incorrect labels during the output process. Common errors include misclassifying diseases as symptoms, dietary recommendations as medication characteristic information, and lifestyle recommendations as dietary recommendations. This problem can be somewhat mitigated by incorporating error examples in the prompts.

Comparative Experimental Study of Multiple LLMs

To further validate the ability of LLMs to extract patient features, we performed complex feature extraction experiments on data from 100 patients using 8 general-purpose or domain-specific LLMs—Kimi, DeepSeek, Tiangong, ERNIE Bot, Qwen, ChatGPT with GPT-4, ChatGLM, and Taiyi—and 1 biomedical domain model, BioBERT. For consistency and fair comparison, we applied the same prompt framework used with the ZuoyiGPT model. As shown in Table 5, the F_1-score values of 8 LLMs on complex feature extraction tasks indicated that each model had its own advantage in different feature extraction scenarios. Due to extensive training on medical clinical data, ZuoyiGPT performed well and consistently in symptom and drug extraction tasks. Kimi specializes in providing extraction results that better meet user formatting requirements; however, due to inadequate training in medical data, it occasionally misdiagnosed diseases as symptoms and even produced hallucinations in drug and food extraction tasks, adding features that were not present in the text. DeepSeek showed the best overall performance, but it showed misidentification problems in the symptom recognition task and unstable performance. Tiangong and ChatGPT with GPT-4 were prone to combining multiple symptoms and tended to misclassify "aerobic exercise" as food during the food extraction task. This problem also occurred with ChatGLM when extracting food but to a greater extent: in addition to misidentifying "aerobic exercise," ChatGLM extracted "fall prevention," "multiple diabetes diet," and other items as food categories. This resulted in the poor performance of ChatGLM on the food

XSL•FO
RenderX

extraction task. In addition to the 8 LLMs discussed, we tested Taiyi and BioBERT. However, these 2 models lack training on targeted feature extraction and extraction format, and the extraction performance is relatively poor. Therefore, we excluded them from the results table as the performance reference for evaluating large model performance on the feature extraction task.

Table 5. F_1-score values for complex extraction features using 8 large language models (LLMs).

LLMs	Symptoms (%)	Symptom duration (%)	Medication (%)	Dosage (%)	Food (%)	Intake (%)	Overall (%)	SD value (%)
Kimi	100	100	88.89	88.89	88.89	88.89	90.93	5.5
DeepSeek	93.61	93.61	100	100	94.74	94.74	96.12	2.58
ZuoyiGPT	98.5	98.35	98.96	84.98	92.6	92.79	94.36	4.96
Tiangong	80.6	80.6	97.44	97.44	88.89	88.89	88.98	6.88
ERNIE Bot	91.89	91.89	91.89	91.89	100	100	94.59	3.82
Qwen	90.41	90.41	100	100	92.86	92.86	94.42	4.09
ChatGPT with GPT-4	80.6	80.6	97.44	97.44	88.89	88.89	88.98	6.88
ChatGLM	96.1	96.1	100	100	46.15	46.15	97.43	29.66

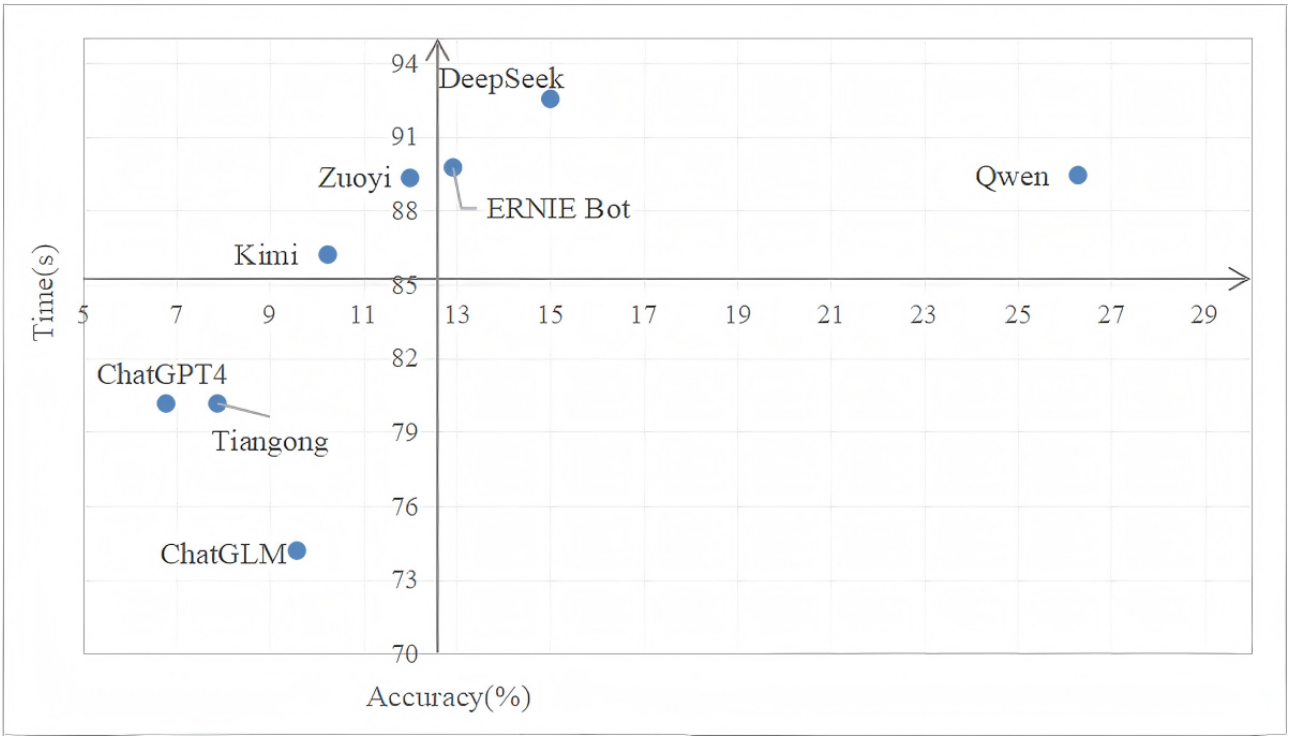
Finally, we compiled the average time and accuracy of all complex feature extractions from the EHRs of individual patients for extracting features from 8 LLMs, as shown in Table 6. To understand their respective advantages, we integrated these tables into a chart, as illustrated in Figure 7. The performances of ZuoyiGPT and ERNIE Bot were more comprehensive, ChatGPT with GPT-4 required the least amount of time, and DeepSeek achieved the highest accuracy.

Table 6. The extraction time and overall accuracy of 8 large language models (LLMs).

LLMs	Time (s)	Accuracy (%)	SD value (%)
Kimi	10.24	86.2	4.32
DeepSeek	15.00	92.53	3.55
ZuoyiGPT	12.00	89.32	7.72
Tiangong	7.88	80.15	5.83
ERNIE Bot	12.92	89.74	4.23
Qwen	26.29	89.43	3.96
ChatGPT with GPT-4	6.78	80.15	7.23
ChatGLM	9.58	74.17	30.22

XSL•FO
RenderX

Figure 7. The extraction time and overall accuracy of 7 large language models.



A Practical Survey of Clinical and Research Applications

To validate the practicality of LLMs in extracting patient features for clinical practice, health policy, and medical research, we designed a survey and invited 2 clinical medicine experts, 2 health care policy managers, and 2 medical researchers to respond. All participants had >5 years of experience in health care–related work. The survey included questions about the application of LLMs in EHRs, the advantages and challenges of extracting patient features using these models, and the practicality of these methods in clinical practice, medical research, and the implementation and formulation of health care policies. It also solicited opinions on the accuracy of extracting patient features using LLMs and requested suggestions for method improvement. Statistical analysis indicated that, although the older medical experts and health care policy managers were not very familiar with the use of LLMs and the methods for extracting patient features, all 6 participants recognized the high practicality of these methods in clinical medicine, health care policy formulation, and medical research after using them. At the same time, all participants indicated that they would use and promote the use of LLMs to extract patient characteristic information in future work. The average κ statistic for this method was 83.41, with an average Cohen κ coefficient of 0.98 for the 2 clinical medicine experts, 0.95 for the 2 medical researchers, and 0.89 for the 2 health care policy managers. The Kendall W coefficient for the survey was 0.87, and the Cronbach α coefficient was 0.97. In summary, this method of extracting patient characteristics using LLMs is clinically valuable, and the survey demonstrated high reliability.

Conclusions

We developed a scalable framework for extracting the characteristics of patients with multimorbidity based on LLMs capable of extracting patient characteristic information from unstructured and semistructured EHRs. This framework has the potential to be extended to new disease domains and patient populations without the need for manual data labeling, thereby facilitating large-scale analysis. In medical research, researchers can quickly extract the necessary patient characteristic information using this method without extensive training or manual involvement, streamlining the research process for multimorbidity and other disease areas, significantly enhancing research efficiency and reliability, and aiding in the construction of knowledge bases and knowledge graphs. In clinical practice, clinicians can rapidly access information about patients through this method, greatly assisting their work and treatment decisions. In addition, health care policy makers can similarly use this approach to quickly understand the characteristics of patient clusters, providing a strong foundation for the formulation and implementation of health care policies.

Acknowledgments

This research was funded by the National Natural Science Foundation of China (72004071 and 72474074) and the Humanities and Social Science Foundation of the Ministry of Education (20YJC870016).

XSL•FO
RenderX

Data Availability

This dataset was specifically created for this research and has not been publicly disclosed.

Conflicts of Interest

None declared.

References

1. Skou ST, Mair FS, Fortin M, Guthrie B, Nunes BP, Miranda JJ, et al. Multimorbidity. Nat Rev Dis Primers 2022 Jul 14;8(1):48 [FREE Full text] [doi: 10.1038/s41572-022-00376-4] [Medline: 35835758]
2. Fan J, Sun Z, Yu C, Guo Y, Pei P, Yang L, China Kadoorie Biobank Collaborative Group. Multimorbidity patterns and association with mortality in 0.5 million Chinese adults. Chin Med J (Engl) 2022 Mar 20;135(6):648-657 [FREE Full text] [doi: 10.1097/CM9.0000000000001985] [Medline: 35191418]
3. Geng Y, Jie W, He Y, Zhou X, Zhang S, Dong W, et al. Prevalence and patterns of multimorbidity among adults aged 18 years and older - China, 2018. China CDC Wkly 2023 Jan 13;5(2):35-39 [FREE Full text] [doi: 10.46234/ccdcw2023.007] [Medline: 36776686]
4. Cezard G, McHale CT, Sullivan F, Bowles JK, Keenan K. Studying trajectories of multimorbidity: a systematic scoping review of longitudinal approaches and evidence. BMJ Open 2021 Nov 22;11(11):e048485 [FREE Full text] [doi: 10.1136/bmjopen-2020-048485] [Medline: 34810182]
5. Dong G, Zhang Z, Feng J, Zhao XM. MorbidGCN: prediction of multimorbidity with a graph convolutional network based on integration of population phenotypes and disease network. Brief Bioinform 2022 Jul 18;23(4):bbac255. [doi: 10.1093/bib/bbac255] [Medline: 35780382]
6. Feng X, Sarma H, Seubsman SA, Sleigh A, Kelly M. Impact of age and gender differences in the prevalence and patterns of multimorbidity in the Thai Cohort Study. Int Health 2024 Jul 02;16(4):454-462 [FREE Full text] [doi: 10.1093/inthealth/ihae018] [Medline: 38520373]
7. Ford E, Carroll JA, Smith HE, Scott D, Cassell JA. Extracting information from the text of electronic medical records to improve case detection: a systematic review. J Am Med Inform Assoc 2016 Sep 05;23(5):1007-1015 [FREE Full text] [doi: 10.1093/jamia/ocv180] [Medline: 26911811]
8. Chen A, Yu Z, Yang X, Guo Y, Bian J, Wu Y. Contextualized medication information extraction using transformer-based deep learning architectures. J Biomed Inform 2023 Jun;142:104370 [FREE Full text] [doi: 10.1016/j.jbi.2023.104370] [Medline: 37100106]
9. Dagdelen J, Dunn A, Lee S, Walker N, Rosen AS, Ceder G, et al. Structured information extraction from scientific text with large language models. Nat Commun 2024 Feb 15;15(1):1418 [FREE Full text] [doi: 10.1038/s41467-024-45563-x] [Medline: 38360817]
10. Hu D, Liu B, Zhu X, Lu X, Wu N. Zero-shot information extraction from radiological reports using ChatGPT. Int J Med Inform 2024 Mar;183:105321. [doi: 10.1016/j.ijmedinf.2023.105321] [Medline: 38157785]
11. Datta S, Lee K, Paek H, Manion FJ, Ofoegbu N, Du J, et al. AutoCriteria: a generalizable clinical trial eligibility criteria extraction system powered by large language models. J Am Med Inform Assoc 2024 Jan 18;31(2):375-385 [FREE Full text] [doi: 10.1093/jamia/ocad218] [Medline: 37952206]
12. Luo L, Ning J, Zhao Y, Wang Z, Ding Z, Chen P, et al. Taiyi: a bilingual fine-tuned large language model for diverse biomedical tasks. J Am Med Inform Assoc 2024 Sep 01;31(9):1865-1874. [doi: 10.1093/jamia/ocae037] [Medline: 38422367]
13. Naimark J, Tinetti ME, Delbanco T, Dong Z, Harcourt K, Esterson J, et al. Leveraging an electronic health record patient portal to help patients formulate their health care goals: mixed methods evaluation of pilot interventions. JMIR Form Res 2024 Aug 29;8:e56332 [FREE Full text] [doi: 10.2196/56332] [Medline: 39207829]
14. Blumenthal D. Launching HITECH. N Engl J Med 2010 Feb 04;362(5):382-385. [doi: 10.1056/NEJMp0912825] [Medline: 20042745]
15. Wang Y, Wang L, Rastegar-Mojarad M, Moon S, Shen F, Afzal N, et al. Clinical information extraction applications: a literature review. J Biomed Inform 2018 Jan;77:34-49 [FREE Full text] [doi: 10.1016/j.jbi.2017.11.011] [Medline: 29162496]
16. Pletscher-Frankild S, Pallejà A, Tsafou K, Binder JX, Jensen LJ. DISEASES: text mining and data integration of disease-gene associations. Methods 2015 Mar;74:83-89 [FREE Full text] [doi: 10.1016/j.ymeth.2014.11.020] [Medline: 25484339]
17. Bekoulis G, Deleu J, Demeester T, Develder C. Joint entity recognition and relation extraction as a multi-head selection problem. Expert Syst Appl 2018 Dec;114:34-45. [doi: 10.1016/j.eswa.2018.07.032]
18. Derczynski L, Maynard D, Rizzo G, van Erp M, Gorrell G, Troncy R, et al. Analysis of named entity recognition and linking for tweets. Inf Process Manag 2015 Mar;51(2):32-49. [doi: 10.1016/j.ipm.2014.10.006]
19. Hossain ME, Uddin S, Khan A. Network analytics and machine learning for predictive risk modelling of cardiovascular disease in patients with type 2 diabetes. Expert Syst Appl 2021 Feb;164:113918. [doi: 10.1016/j.eswa.2020.113918]
20. Uddin S, Wang S, Lu H, Khan A, Hajati F, Khushi M. Comorbidity and multimorbidity prediction of major chronic diseases using machine learning and network analytics. Expert Syst Appl 2022 Nov;205:117761. [doi: 10.1016/j.eswa.2022.117761]

XSL•FO
RenderX

21. Lu H, Uddin S. A weighted patient network-based framework for predicting chronic diseases using graph neural networks. Sci Rep 2021 Nov 19;11(1):22607. [doi: 10.1038/s41598-021-01964-2] [Medline: 34799627]
22. Kumar V, Recupero DR, Riboni D, Helaoui R. Ensembling classical machine learning and deep learning approaches for morbidity identification from clinical notes. IEEE Access 2021;9:7107-7126. [doi: 10.1109/access.2020.3043221]
23. Kamp M, Achilonu O, Kisiangani I, Nderitu DM, Mpangase PT, Tadesse GA, as members of the MADIVA Research Hubthe DS-I Africa Consortium. Multimorbidity in African ancestry populations: a scoping review. BMJ Glob Health 2023 Dec 07;8(12):e013509 [FREE Full text] [doi: 10.1136/bmjgh-2023-013509] [Medline: 38084495]
24. Hu Q, Liu N, Wang J, Wu Z, Zhang X, Liu Q, et al. An overlapping sequence tagging mechanism for symptoms and details extraction on Chinese medical records. Comput Electr Eng 2021 May;91:107019-107014 [FREE Full text] [doi: 10.1016/j.compeleceng.2021.107019]
25. Vaswani A, Shazeer N, Parmar N, Uszkoreit J, Jones J, Jones L, et al. Attention is all you need. Neural information processing systems, neural information processing systems. In: Proceedings of the 31st International Conference on Neural Information Processing Systems. 2017 Presented at: NIPS '17; December 4-9, 2017; Long Beach, CA p. 6000-6010 URL: https://dl.acm.org/doi/10.5555/3295222.3295349
26. Fraser H, Crossland D, Bacher I, Ranney M, Madsen T, Hilliard R. Comparison of diagnostic and triage accuracy of Ada Health and WebMD symptom checkers, ChatGPT, and physicians for patients in an emergency department: clinical data analysis study. JMIR Mhealth Uhealth 2023 Oct 03;11:e49995 [FREE Full text] [doi: 10.2196/49995] [Medline: 37788063]
27. Ralevski A, Taiyab N, Nossal M, Mico L, Piekos S, Hadlock J. Using large language models to abstract complex social determinants of health from original and deidentified medical notes: development and validation study. J Med Internet Res 2024 Nov 19;26:e63445 [FREE Full text] [doi: 10.2196/63445] [Medline: 39561354]
28. Deiner MS, Deiner NA, Hristidis V, McLeod SD, Doan T, Lietman TM, et al. Use of large language models to assess the likelihood of epidemics from the content of tweets: infodemiology study. J Med Internet Res 2024 Mar 01;26:e49139 [FREE Full text] [doi: 10.2196/49139] [Medline: 38427404]
29. Chintagunta B, Katariya N, Amatriain X. Medically aware GPT-3 as a data generator for medical dialogue summarization. In: Proceedings of the 2nd Workshop on Natural Language Processing for Medical Conversations. 2021 Presented at: NLPMC '21; July 6, 2021; Virtual Event p. 66-76 URL: https://aclanthology.org/2021.nlpmc-1.9.pdf [doi: 10.18653/v1/2021.nlpmc-1.9]
30. Liu J, Wang C, Liu S. Utility of ChatGPT in clinical practice. J Med Internet Res 2023 Jun 28;25:e48568 [FREE Full text] [doi: 10.2196/48568] [Medline: 37379067]
31. Yang S, Zhao H, Zhu S, Zhou G, Xu H, Jia Y, et al. Zhongjing: enhancing the Chinese medical capabilities of large language model through expert feedback and real-world multi-turn dialogue. In: Proceedings of the 38th AAAI Conference on Artificial Intelligence and 36th Conference on Innovative Applications of Artificial Intelligence and Fourteenth Symposium on Educational Advances in Artificial Intelligence. 2024 Mar 24 Presented at: AAAI '24/IAAI '24/EAAI '24; February 20-27, 2024; Virtual Event p. 19368-19376 URL: https://dl.acm.org/doi/10.1609/aaai.v38i17.29907 [doi: 10.1609/aaai.v38i17.29907]
32. Chen Y, Xing X, Lin J, Zheng H, Wang Z, Liu Q, et al. SoulChat: improving LLMs' empathy, listening, and comfort abilities through fine-tuning with multi-turn empathy conversations. In: Proceedings of the 2023 International Conference on Computational Linguistics. 2023 Presented at: EMNLP '23; December 6-10, 2023; Singapore, Singapore p. 1170-1183 URL: https://aclanthology.org/2023.findings-emnlp.83.pdf [doi: 10.18653/v1/2023.findings-emnlp.83]
33. Guo M, Wu F, Jiang J, Yan X, Chen G, Li W. Investigations on scientific literature meta information extraction using large language models. In: Proceedings of the 2023 IEEE International Conference on Knowledge Graph. 2023 Presented at: ICKG '23; December 1-2, 2023; Shanghai, China p. 249-254 URL: https://ieeexplore.ieee.org/document/10412837 [doi: 10.1109/ickg59574.2023.00036]

Abbreviations

EHR: electronic health record
LLM: large language model
NLP: natural language processing

XSL•FO
RenderX

Edited by A Castonguay; submitted 17.12.24; peer-reviewed by X Huang, K Adegoke; comments to author 28.02.25; revised version received 20.03.25; accepted 17.04.25; published 15.05.25.

Please cite as:
Zhang J, Zhou J, Zhou L, Ba Z
Extracting Multifaceted Characteristics of Patients With Chronic Disease Comorbidity: Framework Development Using Large Language Models
JMIR Med Inform 2025;13:e70096
URL: https://medinform.jmir.org/2025/1/e70096
doi:10.2196/70096
PMID:

©Junyan Zhang, Junchen Zhou, Liqin Zhou, Zhichao Ba. Originally published in JMIR Medical Informatics (https://medinform.jmir.org), 15.05.2025. This is an open-access article distributed under the terms of the Creative Commons Attribution License (https://creativecommons.org/licenses/by/4.0/), which permits unrestricted use, distribution, and reproduction in any medium, provided the original work, first published in JMIR Medical Informatics, is properly cited. The complete bibliographic information, a link to the original publication on https://medinform.jmir.org/, as well as this copyright and license information must be included.

XSL•FO
RenderX

Original Paper

Automated Literature Screening for Hepatocellular Carcinoma Treatment Through Integration of 3 Large Language Models: Methodological Study

Chen Pan[1], BMed; Wei Lu[1], BMed; Bingliang Chen[1], BMed; Gang Zhang[1], MD; Zhiming Yang[1], MD; Jingcheng Hao[1], MD

Department of Hepatobiliary and Vascular Surgery, First Affiliated Hospital of Chengdu Medical College, Chengdu, China

Corresponding Author:
Jingcheng Hao, MD
Department of Hepatobiliary and Vascular Surgery
First Affiliated Hospital of Chengdu Medical College
Baoguang Avenue 278, Xindu District
Chengdu, 610599
China
Phone: 86 18908011416
Email: jingcheng.hao@cmc.edu.cn

Abstract

Background: Primary liver cancer, particularly hepatocellular carcinoma (HCC), poses significant clinical challenges due to late-stage diagnosis, tumor heterogeneity, and rapidly evolving therapeutic strategies. While systematic reviews and meta-analyses are essential for updating clinical guidelines, their labor-intensive nature limits timely evidence synthesis.

Objective: This study proposes an automated literature screening workflow powered by large language models (LLMs) to accelerate evidence synthesis for HCC treatment guidelines.

Methods: We developed a tripartite LLM framework integrating Doubao-1.5-pro-32k, Deepseek-v3, and DeepSeek-R1-Distill-Qwen-7B to simulate collaborative decision-making for study inclusion and exclusion. The system was evaluated across 9 reconstructed datasets derived from published HCC meta-analyses, with performance assessed using accuracy, agreement metrics (κ and prevalence-adjusted bias-adjusted κ), recall, precision, F_1-scores, and computational efficiency parameters (processing time and cost).

Results: The framework demonstrated good performance, with a weighted accuracy of 0.96 and substantial agreement (prevalence-adjusted bias-adjusted κ=0.91), achieving high weighted recall (0.90) but modest weighted precision (0.15) and F_1-scores (0.22). Computational efficiency varied across datasets (processing time: 248-5850 s; cost: US $0.14-$3.68 per dataset).

Conclusions: This LLM-driven approach shows promise for accelerating evidence synthesis in HCC care by reducing screening time while maintaining methodological rigor. Key limitations related to clinical context sensitivity and error propagation highlight the need for reinforcement learning integration and domain-specific fine-tuning. LLM agent architectures with reinforcement learning offer a practical path for streamlining guideline updates, though further optimization is needed to improve specialization and reliability in complex clinical settings.

(JMIR Med Inform 2025;13:e76252) doi:10.2196/76252

KEYWORDS

methodology; large language model; hepatocellular carcinoma; treatment; literature screening

Introduction

Background

Primary liver cancer (PLC) is the sixth most commonly diagnosed cancer and the third leading cause of cancer-related deaths worldwide [1]. Among PLCs, hepatocellular carcinoma (HCC) is the most common, accounting for approximately 80% to 90% of liver cancer cases worldwide [2,3]. HCC has a poor prognosis. In general, the overall 5-year survival rate for patients diagnosed with HCC is typically <20%, which is similar to that for lung cancer but notably lower than for colon cancer [4-6]. In addition, the treatment of HCC is highly individualized and

XSL•FO
RenderX

complex [7]. In general, for patients with early-stage HCC, surgical intervention is a viable option, and they often have a relatively good prognosis [8]. However, patients with HCC frequently present at an intermediate or advanced stage, and surgery alone may not be beneficial. Conversion therapies, guided by systemic and local therapy approaches, have demonstrated efficacy in downstaging and potentially resecting intermediate and advanced HCC, as well as enhancing outcomes [9,10]. It is evident that HCC is notably more complex to treat than many other medical conditions, requiring a nuanced decision-making process guided by evidence-based research and clinical guidelines.

However, there is often a delay between research publication and its incorporation into academic discourse, especially with guidelines based on systematic reviews and meta-analyses. An example of this lag can be observed in the 2021 guidelines disseminated by the Society for Immunotherapy of Cancer, which did not incorporate the outcomes of the HIMALAYA trial that same year [11,12]. This randomized controlled trial (RCT) demonstrated that the single tremelimumab regular interval durvalumab regimen, a combination of a single high dose of tremelimumab given as a first-line treatment followed by maintenance treatment with durvalumab, significantly improved overall survival and constitutes a new treatment option [12]. As such, the timely updating of information is of paramount importance, as it facilitates the refinement of guidelines and the evolution of treatment plans. Systematic reviews and meta-analyses represent the highest levels of evidence in the hierarchy of evidence [13]. They play an important role in updating the guidelines. However, meta-analysis and systematic reviews are time-consuming processes, especially the process of collecting and screening literature records [14]. To keep guidelines up to date, faster methods for conducting meta-analyses are essential. Given the standardized PRISMA (Preferred Reporting Items for Systematic Reviews and Meta-Analyses) framework, integrating artificial intelligence (AI) can help automate and improve this process.

AI is a discipline that allows computers to simulate intelligent human behavior, enabling machines to emulate human intelligence and problem-solving abilities [15]. Large language models (LLMs), built on transformer architectures, have become a central focus in AI research. By predicting the next word in a sequence, LLMs learn statistical patterns in text. Leveraging the transformer's self-attention mechanism, they effectively capture long-range dependencies and contextual meaning [16]. Therefore, LLM can be used to extract structured data from unstructured texts [17,18]. Previous studies have explored the automation of the literature screening process in systematic reviews and meta-analyses using a single LLM with good results [19,20]. However, previous studies often used a single LLM without simulating collaboration among models in different roles [19,20]. Meanwhile, newer models with more parameters or reinforcement learning have shown better performance than earlier approaches.

Objectives

In this study, we propose a literature screening workflow that leverages 3 distinct language models to automatically analyze titles and abstracts from multiple databases, aiming to support systematic reviews and meta-analyses. We evaluate its effectiveness in simulating real-world screening procedures and conflict resolution, using datasets from published studies. Furthermore, we investigate the types and causes of model errors across different datasets and explore the integration of reinforcement learning to enhance decision-making.

Methods

Overview

The overall process of this study is divided into 3 stages: application design, validation, and statistical analysis. In the application design section, a multimodule system was developed to parse literature entries, interface with the LLM service provided by the cloud computing platform, and perform literature entry analysis. Verification involved conducting simulations and constructing datasets based on meta-analyses published in high-impact journals, followed by comprehensive validation through analytic procedures implemented in our previously developed system. The final phase involved a comparative and analytic examination of the results generated by the system and the definitive inclusion outcomes of the aforementioned meta-analyses. All programmatic flows were implemented in Python (version 3.12.3; Python Software Foundation) and R (version 4.4.1; R Foundation for Statistical Computing).

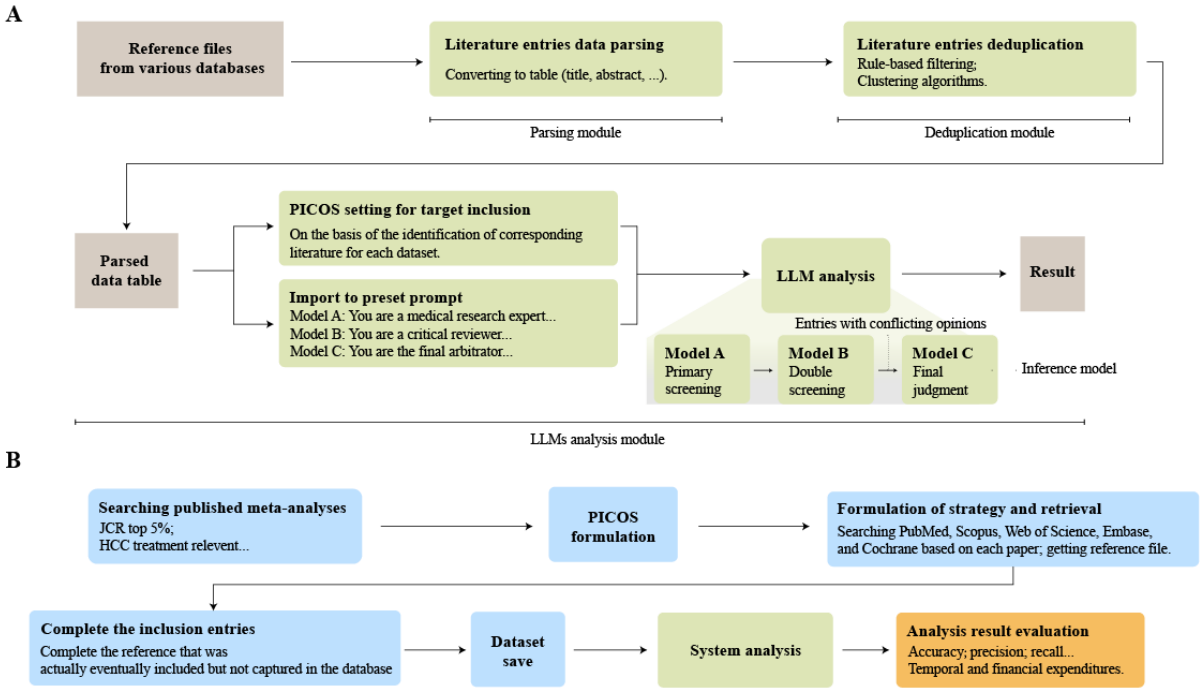
Application Design

This study constructed a multimodule system consisting of 3 major parts: literature entry data parsing, duplicate item removal, and LLMs analysis. The workflow of the developed system is shown in Figure 1A. In the literature record parsing part, automated programs were used to process search results saved in RIS and NBIB formats, extracting key fields such as titles, author information, and abstracts into structured data tables. The deduplication part deployed a process based on certain fields of the literature entries to remove highly duplicated entries, as detailed in Multimedia Appendix 1. In the analysis of LLMs part, the program preset roles and inserted the population, intervention, comparison, outcome, and study design (PICOS) guidelines for 3 different large models and embedded the literature entries that needed to be analyzed into prompts in batches. Any analysis task performed by the system must contain at least 1 nonempty element from PICOS. Tasks lacking specific PICOS elements were flagged by the program as unspecified and triggered an expanded search scope. Specifically, this process was divided into 3 parts. The program first assigned model A as the initial reviewer, which made preliminary inclusion or exclusion judgments on the inputted literature entries based on the predefined PICOS criteria, along with the corresponding reasoning. Subsequently, model B was designated as the critic, reviewing the same literature entries and evaluating model A's decisions based on the same PICOS criteria, providing its own judgments and reasoning. Finally, model C was assigned the role of arbitrator, reanalyzing those entries for which models A and B had provided conflicting decisions and making the final determination along with the supporting reasoning. The role prompts and the hyperparameters used for

XSL•FO
RenderX

these 3 models are provided in Multimedia Appendix 1. In addition, a detailed explanation of this system is provided in Multimedia Appendix 1.

Figure 1. Schematic workflow of the study. (A) Workflow of the developed system. The system first parsed the fields in the referenced documents, then used the deduplication function to remove duplicates and parsed a data table. Subsequently, after setting the PICOS objectives of the studies to be included, it was sequentially submitted to three large language models for processing in combination with the prompts. (B) Workflow of the validation process performed for the system. The verification step first relied on existing meta-analyses in highly cited journals, manually identified their PICOS, and reproduced them according to the methods described in the articles to construct a dataset. Subsequently, the analysis process was carried out using the system we had developed. HCC: hepatocellular carcinoma; JCR: Journal Citation Reports; LLM: large language model; PICOS: Population, Intervention, Comparison, Outcome and Study Design.



Validation

The validation section includes the preparation of the verification datasets, system analysis, and data statistics, as shown in Figure 1B. To construct multiple validation datasets, we searched for meta-analyses related to the treatment strategies for PLC. The following inclusion criteria were used: (1) studies published within the past 5 years, (2) meta-analyses of treatment strategies for PLC, (3) studies that reported the search platforms used and described the basic search strategy in the text, and (4) studies published in the top 5% of journals indexed in the Science Citation Index Expanded and compliant with the PRISMA guidelines. The exclusion criteria included studies with search strategies that could not be replicated based on the description in the text, non-English studies, studies without accessible full texts, and studies that overlapped with or duplicated other publications.

After determining the meta-analyses to be included, each meta-analysis was manually reviewed, and the following tasks were undertaken: (1) identifying the PICOS elements by human (leave blank if PICOS components cannot be identified), (2) implementing search strategy to retrieve records according to the method part of each meta-analysis, (3) downloading NBIB or RIS files from various databases, and (4) deduplicating and converting NBIB or RIS files into data tables using the analysis system to construct the datasets. The initial number of candidate records in the data tables was aligned as closely as possible with the corresponding numbers in the PRISMA flow diagrams of the respective meta-analyses. To ensure minimal human intervention in the simulation, any studies that were ultimately included in the original meta-analyses but were missing from the search results were not added back to the datasets.

After constructing all the datasets, 3 major language models were selected based on considerations of research cost and model performance. These models were Doubao-1.5-pro-32k from ByteDance (model A), DeepSeek-v3 (model B), and DeepSeek-R1-Distill-Qwen-7B (model C), with model C distinguished as a reasoning-optimized LLM. The technical specifications for these models are outlined in Table 1. All datasets were analyzed using the previously described analytic workflow of our system, using default hyperparameters as detailed in Multimedia Appendix 1, and the results were exported in tabular format.

XSL•FO
RenderX

Table 1. Large language models used in the validation process of the review screening workflow.

Model designation	Model name	Model type	Strengths	Limitations
Model A	Doubao-1.5-pro-32k	Closed; general purpose; MoE[a]	High performance and multimodal capability	Closed source model with low transparency
Model B	DeepSeek-V3	Open; general purpose; MoE	Open source, efficient training model	Signs of distillation may lead to identity inconsistency or output bias
Model C	DeepSeek-R1-Distill-Qwen-7B	Open; reasoning optimized	Open source, reasoning, small and efficient for local deployment	Relatively weak in long-context or multimodal tasks

[a]MoE: mixture of experts.

Statistical Analysis

The result tables from each validation set analyzed by the system were compared with the actual final results (excluding entries with missing or empty abstracts from the simulated search) included in their corresponding papers. The accuracy, precision, recall, F_1-score, κ, and prevalence-adjusted bias-adjusted κ (PABAK) of the analysis results for all datasets were calculated, where precision and recall were calculated separately based on exclusion and inclusion as the final goal. To improve comparability in imbalanced scenarios, F-β (a weight harmonic mean of precision and recall), balanced accuracy, and Matthews correlation coefficient (MCC) were also evaluated. The statistical indicators of the average were reported using the mean and, where applicable, the standard deviation (SD). The calculation formulas for the statistical metrics are presented in Multimedia Appendix 1. To further evaluate the effect of class imbalance on agreement measures, paired statistical significance tests were conducted to compare κ and PABAK to determine whether κ was systematically depressed under imbalanced class distributions. Depending on the distribution of the paired differences, either a paired 2-tailed *t* test or a Wilcoxon signed rank test was used at a significance level of $P<.05$. In addition, we evaluated the time and economic costs for the analysis of each dataset. The time cost was determined by recording the start and end time stamps from the analysis logs for each dataset. Due to billing latency in cloud computing platforms, the economic cost was estimated through a simulation program based on platform pricing and then validated against actual billing statements. The detailed design of the simulation program is described in Multimedia Appendix 1.

Results

Overview of Datasets

On the basis of the simulation process in the validation, 9 meta-analyses were ultimately included and used to construct the simulated datasets [21-29]. These studies were published in various prestigious journals, including the *British Journal of Surgery*, *Liver Cancer*, *Journal of Hepatology*, *JAMA Oncology*, and *Annals of Surgery*. Published between 2020 and 2025, these meta-analyses formed the foundation of the dataset and addressed a diverse range of topics related to PLC treatments, such as systemic therapies, radiation-based approaches, and posttransplant outcomes. These studies, conducted across multiple regions, including the United States, Europe, and Asia, involved single-center and multicenter collaborations. In addition, they used diverse data sources (RCTs, observational cohorts, and individual patient-level data) and applied meta-analytic methods, including pairwise comparisons, network meta-analyses, single-arm analyses, and individual patient data assessments.

In each of the meta-analyses included, 9 datasets were created to represent the initial records identified during their search process, as shown in Table 2. The number of initially identified records in these simulated datasets ranged from 309 to 8733. These datasets encompassed multiple perspectives on the treatment of PLC, including a diverse range of candidate study types, such as RCTs; observational studies (eg, cohort and case-control designs); systematic reviews; meta-analyses; and other evidence-based reports sourced from databases such as PubMed, Cochrane Library, and clinical trial registries. These datasets also featured various types of meta-analyses and varying numbers of initially identified records, reflective of real-world meta-analysis scenarios where data availability and completeness can differ widely. Information on these datasets, including the PICOS criteria corresponding to each meta-analysis and the search strategies used to construct the respective datasets, is provided in Multimedia Appendix 1.

XSL•FO
RenderX

Table 2. Characteristics of meta-analysis studies included in the validation stage.

Dataset name	Study title	Included records (n/N, %)[a]	Published journal	Study type
LORC-CH[b]	Laparoscopic versus open resection of hepatocellular carcinoma in patients with cirrhosis: meta-analysis [21]	11/770 (1.4%)	*British Journal of Surgery*	Meta-analysis of 2 interventions based on RCTs[c] and PSM[d] studies
FLSTN-AH[e]	First-line systemic therapies for advanced hepatocellular carcinoma: a systematic review and patient-level network meta-analysis [22]	11/5417 (0.20%)	*Liver Cancer*	Network meta-analysis based on RCTs
TLP-AH[f]	Efficacy and safety of transarterial chemoembolization combined with lenvatinib and PD-1 inhibitor in the treatment of advanced hepatocellular carcinoma: a meta-analysis [23]	12/309 (3.9%)	*Pharmacology & Therapeutics*	Single-intervention, multiple-control meta-analysis based on cohort studies
NCN-UH[g]	Comparative efficacy of novel combination strategies for unresectable hepatocellular carcinoma: a network metanalysis of phase III trials [24]	9/1698 (0.54%)	*European Journal of Cancer*	Network meta-analysis based on RCTs
FSTN-AH[h]	Efficacy and safety of frontline systemic therapy for advanced HCC: a network meta-analysis of landmark phase III trials [25]	15/8733 (0.17%)	*JHEP Reports*	Network meta-analysis based on RCTs
PTICI-PTHO[i]	Impact of pre-transplant immune checkpoint inhibitor use on post-transplant outcomes in HCC: a systematic review and individual patient data meta-analysis [26]	21/558 (3.8%)	*Journal of Hepatology*	Individual patient data meta-analysis
SBRT-HMG[j]	Stereotactic body radiation therapy for hepatocellular carcinoma: meta-analysis and international stereotactic radiosurgery society practice guidelines [27]	13/897 (1.4%)	*International Journal of Radiation Oncology - Biology - Physics*	Single-arm meta-analysis based on observational studies
STSN-AH[k]	Systemic therapy and sequencing options in advanced hepatocellular carcinoma: a systematic review and network meta-analysis [28]	13/3522 (0.37%)	*JAMA Oncology*	Network meta-analysis based on RCTs
LRAMC[l]	Liver resection versus local ablation therapies for hepatocellular carcinoma within the Milan criteria: a systematic review and meta-analysis [29]	24/6078 (0.39%)	*Annals of Surgery*	Meta-analysis of 2 interventions based on RCTs and NRTs[m]

[a]N represents the sample size of the corresponding dataset by simulating the retrieval strategy from the corresponding study, followed by system parsing, deduplication, and removal of entries with blank abstracts in our research; n indicates the actual number of final included literature records after excluding those not retrieved by our simulated search strategy and entries with missing abstracts, based on the final inclusion results from the corresponding study.

[b]LORC-CH: laparoscopic versus open resection in cirrhotic hepatocellular carcinoma

[c]RCT: randomized controlled trial.

[d]PSM: propensity score matching.

[e]FLSTN-AH: first-line systemic therapy network meta-analysis for advanced hepatocellular carcinoma.

[f]TLP-AH: transarterial chemoembolization plus lenvatinib plus programmed death receptor 1 inhibitor in advanced hepatocellular carcinoma.

[g]NCN-UH: novel combination network meta-analysis for unresectable hepatocellular carcinoma.

[h]FSTN-AH: frontline systemic therapy network meta-analysis for advanced hepatocellular carcinoma.

[i]PTICI-PTHO: pre-transplant immune checkpoint inhibitors impact on post-transplant hepatocellular carcinoma outcomes.

[j]SBRT-HMG: stereotactic body radiation therapy in hepatocellular carcinoma meta-analysis and guidelines.

[k]STSN-AH: systemic treatment sequencing network meta-analysis for advanced hepatocellular carcinoma.

[l]LRAMC: liver resection versus ablation within Milan criteria.

[m]NRT: nonrandomized trial.

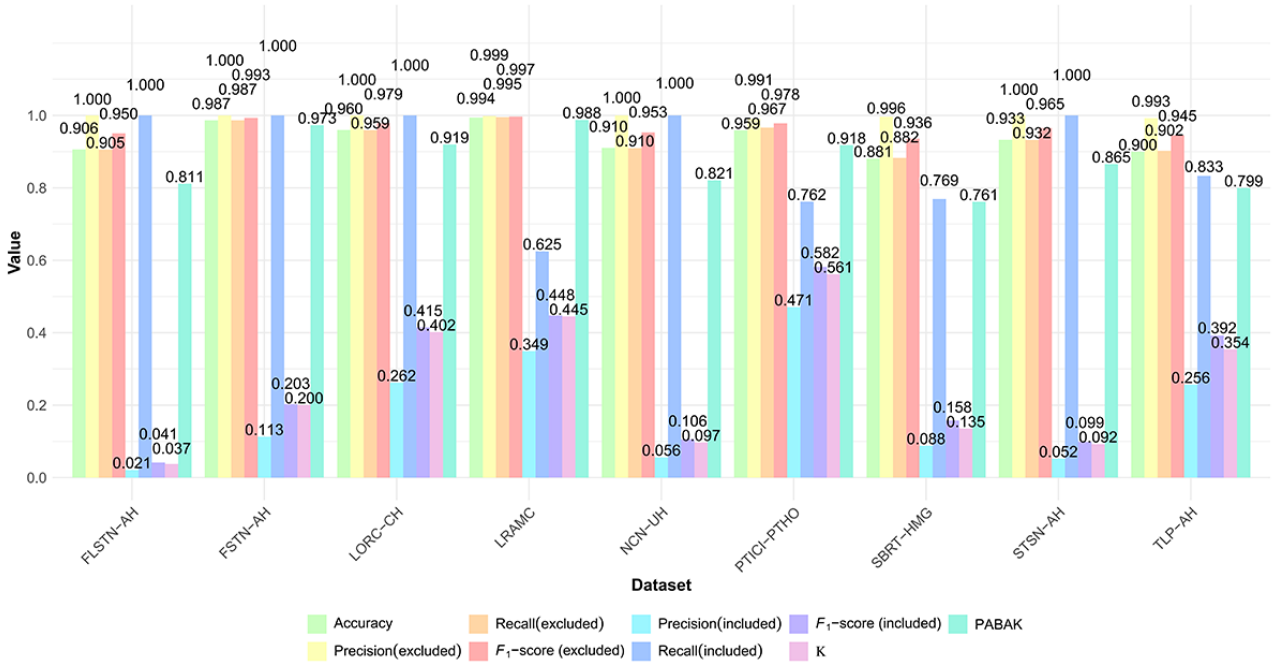
Performance

The system performed well in both inclusion and exclusion tasks, as shown in Figure 2. Overall, the system correctly classified 26,735 (95.54%) of 27,982 records across the 9 datasets. When targeting exclusion, the weighted average precision and recall reached approximately 1.00 (SD < 0.01; range 0.99-1.00) and 0.96 (SD 0.04; range 0.90-1.00), respectively. In contrast, when targeting inclusion, the weighted average precision was 0.15 (SD 0.13; range 0.05-0.47), while the weighted recall was 0.90 (SD 0.16; range 0.62-1.00). F_1-scores for included articles were modest, with a weighted average of 0.22 (SD 0.16; range 0.04-0.58). Detailed inclusion and exclusion status and more detailed performance metrics are presented in Tables S1 and S2 in Multimedia Appendix 1. Furthermore, the paired *t* test comparing the mean κ (0.258) and the mean PABAK (0.873) revealed a statistically significant

XSL•FO
RenderX

difference (t_8=−11.740; P<.001), confirming that class imbalance biased κ downward and justifying the use of PABAK for a more accurate assessment of consistency. The weighted mean PABAK value across all datasets was high at 0.91 (range 0.76-0.99), indicating excellent overall consistency of the model predictions. The calculation results of the significance test of the difference between κ and PABAK are provided in Multimedia Appendix 1. In addition, the 3 metrics for imbalanced datasets, F-β, balanced accuracy, and MCC, demonstrated moderate performance levels. When β was set to 2, the weighted average of F-β was 0.45 (range 0.09-0.68). The weighted average of balanced accuracy was 0.93 (range 0.81-0.99). The weighted average of MCC was 0.27 (range 0.14-0.58). More detailed information about imbalance metrics is provided in Table S3 in Multimedia Appendix 1.

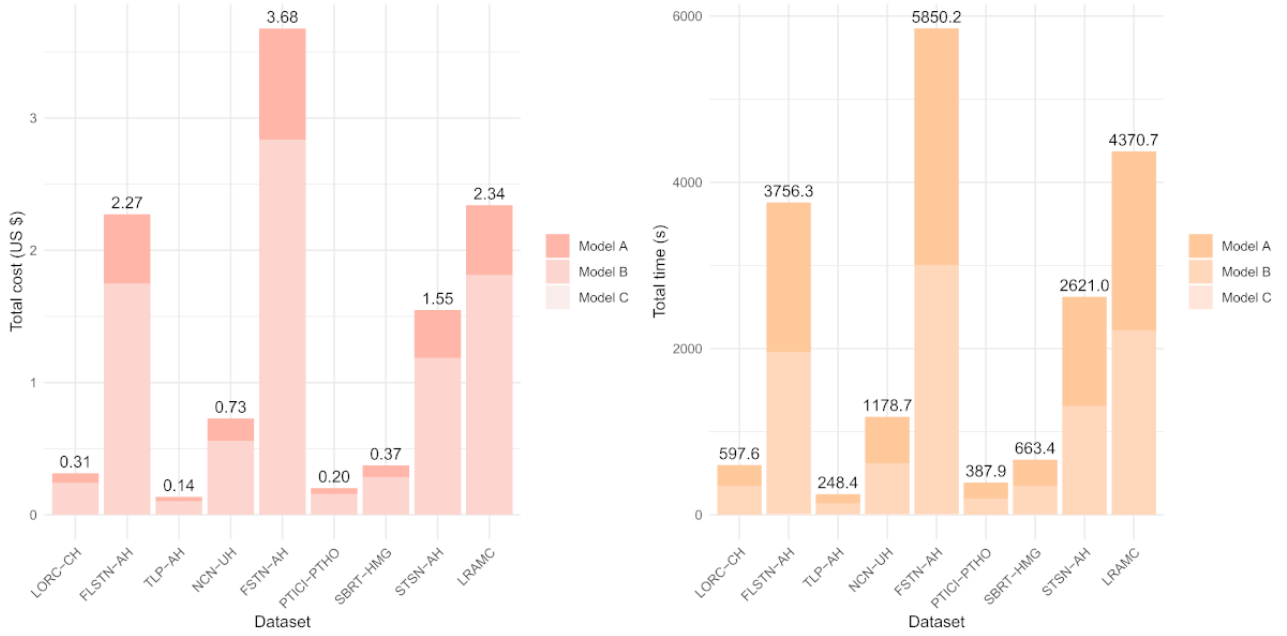
Figure 2. Comparative performance of 3 large language model–based analytic systems across 9 benchmark datasets. The metrics include accuracy, precision, recall, F1-score, κ, and prevalence-adjusted bias-adjusted kappa (PABAK). Precision, recall, and F1-score were calculated twice, once with "included" as the positive class (targeting the correct identification of articles to include) and once with "excluded" as the positive class (targeting the correct identification of articles to exclude). The system achieved high accuracy across all datasets, with recall and PABAK consistently displaying relatively high values, especially when focusing on inclusion. FLSTN-AH: first-line systemic therapy network meta-analysis for advanced hepatocellular carcinoma; FSTN-AH: frontline systemic therapy network meta-analysis for advanced hepatocellular carcinoma; LORC-CH: laparoscopic versus open resection in cirrhotic hepatocellular carcinoma; LRAMC: liver resection versus ablation within Milan criteria; NCN-UH: novel combination network meta-analysis for unresectable hepatocellular carcinoma; PTICI-PTHO: pre-transplant immune checkpoint inhibitors impact on post-transplant hepatocellular carcinoma outcomes; SBRT-HMG: stereotactic body radiation therapy in hepatocellular carcinoma meta-analysis and guidelines; STSN-AH: systemic treatment sequencing network meta-analysis for advanced hepatocellular carcinoma; TLP-AH: transarterial chemoembolization plus lenvatinib plus programmed death receptor 1 inhibitor in advanced hepatocellular carcinoma.



In terms of time and economic costs, as this system used cloud-based LLM calls and processing, most of the time and monetary costs depended on the processing time and pricing of the cloud computing platform. On the basis of the processing capacity and quotation of Volcano Engine (a cloud computing platform in mainland China), under the default hyperparameter settings, the system's expenditure could be considered low, as shown in Figure 3. Regarding time costs, 19,674.2 seconds (approximately 5 h and 28 min) were spent analyzing the 9 datasets, with an average of 2186.0 seconds (approximately 36 min; SD 2052.4 seconds) per dataset. In addition, the time required to analyze each 1000 entries was approximately 703.1 seconds (approximately 12 min). Among these datasets, the processing time ranged from 248.4 seconds (approximately 4 min [the shortest] observed for transarterial chemoembolization plus lenvatinib plus programmed death receptor 1 inhibitor in advanced hepatocellular carcinoma [TLP-AH];12/309, 3.9%) to 5850.2 seconds (approximately 1 h and 37 min [the longest] observed for the frontline systemic therapy network meta-analysis for advanced hepatocellular carcinoma [FSTN-AH]; 15/8733, 0.17%). Furthermore, the economic costs were modest, with the analysis of all datasets totaling US $11.59, an average of US $1.29 (SD US $1.25) per dataset, and approximately US $0.41 per 1000 entries. Among the individual datasets, the smallest (TLP-AH) incurred a cost of US $0.14, whereas the largest (FSTN-AH) incurred a cost of US $3.68. These fluctuations in time and economic costs underscore the computational resource implications associated with disparate dataset characteristics, as further elucidated in Tables S4 and S5 in Multimedia Appendix 1.

XSL•FO
RenderX

Figure 3. Comparative analysis of financial and time costs for the system across 9 datasets. (A) Financial costs (in US $) associated with analyzing each validation dataset using 3 large language models (LLMs): model A (Doubao-1.5-pro-32k), model B (DeepSeek-v3), and model C (DeepSeek-R1-Distill-Qwen-7B). Each stacked bar represents the total cost per dataset, with segments corresponding to the expenditure for each individual model. (B) Time costs (in seconds) required by the same 3 LLMs to process each dataset. Stacked segments similarly represent the time consumed by each model. This figure provides a direct visual comparison of the distribution and overall scale of economic and temporal resources consumed by each model during the literature screening process across different validation datasets. FLSTN-AH: first-line systemic therapy network meta-analysis for advanced hepatocellular carcinoma; FSTN-AH: frontline systemic therapy network meta-analysis for advanced hepatocellular carcinoma; LORC-CH: laparoscopic versus open resection in cirrhotic hepatocellular carcinoma; LRAMC: liver resection versus ablation within Milan criteria; NCN-UH: novel combination network meta-analysis for unresectable hepatocellular carcinoma; PTICI-PTHO: pre-transplant immune checkpoint inhibitors impact on post-transplant hepatocellular carcinoma outcomes; SBRT-HMG: stereotactic body radiation therapy in hepatocellular carcinoma meta-analysis and guidelines; STSN-AH: systemic treatment sequencing network meta-analysis for advanced hepatocellular carcinoma; TLP-AH: transarterial chemoembolization plus lenvatinib plus programmed death receptor 1 inhibitor in advanced hepatocellular carcinoma.



Discussion

Principal Findings

Automation in the literature screening process during meta-analysis can save scholars significant time and effort. Targeting inclusion, our system achieved a weighted average accuracy of 0.96 and a weighted average PABAK value of 0.91. In addition, the system achieved a weighted average recall of 0.90, with evaluations across multiple datasets showing a recall value of 1.00. This suggests that our system and approach may have potential practical use. Furthermore, our system leverages a program that sends local requests to the LLM's cloud computing service, resulting in minimal requirements for user-side devices. It does not necessitate high-performance GPUs, and only terminal devices capable of multithreading are required, which greatly facilitates user deployment. Through the multithreaded design combined with certain cloud computing services, the processing duration ranged from approximately 4.1 minutes for the quickest run to approximately 1.6 hours for the most extensive one, thereby saving users' time. Simultaneously, owing to our selection of LLMs that are not mainstream top-tier ones, the costs remain low. On specific platforms, the analysis of our most complex dataset incurred <US $4, substantially expanding practical accessibility for researchers with limited budgets. Regarding scalability considerations, the system's multithreaded architecture can be enhanced by increasing the number of threads to achieve greater parallelism, thereby reducing processing times for larger datasets. In addition, expanding batch processing sizes would optimize LLM invocations, allowing more efficient handling of high-volume data. Finally, adopting more optimized models with faster inference could further improve performance and adaptability, ensuring viability for extensive real-world meta-analyses while maintaining modest resource demands.

A cornerstone of our system is the collaborative integration of multiple LLMs, drawing inspiration from the tripartite collaborative framework in cognitive science [30]. This design enables decision sharing among language models through the transmission of information, allowing subsequent models to optimize their judgments based on the results of preceding models. Such an iterative approach not only improves analytic accuracy but also enhances interpretability, partially mirroring the collaborative nature of manual meta-analysis. A previous study [19] has used a single GPT-4o model for similar classification tasks, achieving an accuracy of 0.91, whereas our system achieved a weighted average accuracy of 0.96, outperforming this prior work. Unlike prior studies reliant on a single model, such as ChatGPT, our system uses 3 distinct LLMs, which offer performance comparable to GPT-4o at reduced costs, and an advanced open-source reasoning model that further lowers deployment expenses [19,20,31].

Presently, there are already several tools that use AI in a comparable manner. These include Scispace, Elicit, Consensus, and Scite, which use literature titles and abstract information

XSL•FO
RenderX

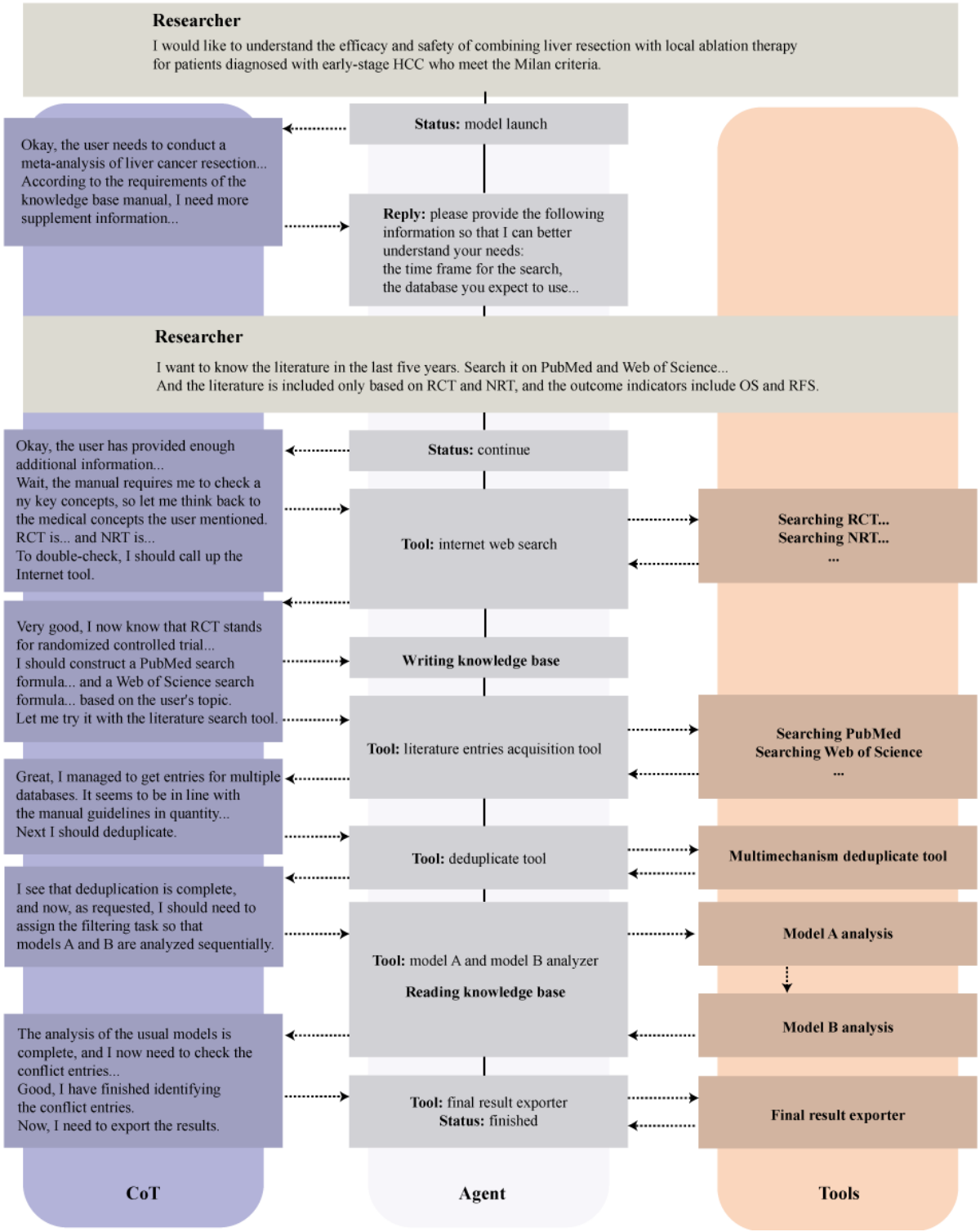
to leverage LLMs to extract key insights from literature and integrate them. However, most of these platforms are primarily designed for conducting literature reviews, and these supporting systematic review analyses often come with high economic costs and lack transparency. In addition, platforms such as DistillerSR and RobotAnalyst have automated the systematic review process [32,33]. However, these tools are not currently strongly integrated with LLMs. In contrast, our system combines the strengths of LLMs and programmatic pipelines within its workflow to support the updating of systematic reviews and meta-analyses.

Our system has certain limitations. Although our datasets encompass multiple topics with substantial numbers of records initially identified, the Sankey diagram, as shown in Table S6 and Figure S1 in Multimedia Appendix 1, revealed that data flow across datasets exhibits remarkable consistency, indicating limited divergent perspectives generated by the secondary model. Refinements to model temperature and prompt engineering may prove beneficial in addressing this limitation [34,35]. Crucially, it should not be ignored that our overall precision and F_1-scores are relatively low, as shown in Figure 2. We conducted an in-depth analysis of the cases where misidentification occurred. First, nonspecialized models and potentially insufficient training corpora may be responsible for the initial misclassification of literature entries, as they fail to accurately grasp the key conceptual features within the texts, leading to incorrect categorization. For example, we found that cost-effectiveness analyses derived from RCTs published by other researchers were incorrectly identified as RCTs themselves. Providing a detailed description of key concepts in the prompt or collaboratively using a chain of knowledge approach may be a potential solution to improve this aspect [36]. In addition, the degradation in contextual understanding under long prompt contexts may limit model performance, which could be attributed to attention dilution [37]. Reducing batch size may mitigate this issue. Our selected model, DeepSeek-V3, being a distilled version, exhibits limitations in conceptual transformation and performance [38]. This phenomenon can be ascribed, at least in part, to the model collapse problem inherent to LLM [39,40]. Model collapse is a systematic degradation phenomenon that occurs in generative models during recursive training, which manifests itself as loss of output diversity, reduced semantic coherence, and even logical confusion [40]. This problem can be optimized in subsequent training of LLMs, such as through the use of data specific to the treatment of liver cancer to train or fine-tune, thereby reducing the risk of overgeneralization or improvements at the architectural level [41,42]. Moreover, our dataset is currently focused on HCC treatment. Although we selected HCC treatment as a complex test case to rigorously evaluate our system, and the workflow is theoretically generalizable, its performance on broader oncology topics or other disease domains remains to be validated.

Architecture construction based on LLM agents and reinforcement learning (RL) may be a more practical approach to address potential issues, such as the low recall observed in this study. Despite the lack of a unified definition, the LLM agent is driven by a core LLM that acts as the brain, completing the logical chain through collaboration [43-46]. As illustrated in Figure 4, our proposed system uses a reasoning model as the core foundation, leveraging its complete chain of thought capabilities. For ambiguous tasks, such as analyzing the “liver resection versus ablation within Milan criteria” dataset’s objectives (comparing efficacy and safety of liver resection combined with local ablation in early-stage HCC meeting Milan criteria), the model accepts the request, references the knowledge base for guidelines, and queries the researcher on parameters such as publication time range and search platforms. Upon receiving sufficient input, the core model initiates planning: it invokes internet tools to iteratively search key concepts (eg, Milan criteria metrics and local ablation therapies) until a reward threshold is met, storing results in the knowledge base. It then constructs platform-specific search queries, directing a literature acquisition tool to retrieve entries (including titles and abstracts) until the threshold is reached. Subsequently, a deduplication tool processes multiplatform entries to yield unique results. The core model then assigns 2 distinct regular models for primary and secondary screening, referencing the knowledge base, and resolves conflicts to finalize outcomes. This integration of RL and model specialization creates an advanced system, akin to OpenAI’s deep research feature, which eases the step of reviews. Nevertheless, it is important to note that hallucinations in LLMs are difficult to avoid, and appropriate human intervention remains crucial [47]. Key challenges include automating document retrieval across platforms and embedding RL throughout, warranting further empirical validation.

XSL•FO
RenderX

Figure 4. Integrated framework for systematic literature screening using a large language model (LLM) agent and reinforcement learning (RL) optimization. This diagram illustrates the workflow of a systematic literature screening process driven by an integrated LLM agent. The central agent uses a chain of thought (CoT) approach as its core reasoning mechanism, supported by automated tools and optimized throughout by RL. The process starts when the researcher initiates a request, prompting the agent to clarify the analysis scope, including publication timeframe, selected databases, and key outcome indicators. Following this, the central agent uses internet-based searches to verify essential medical concepts. Subsequently, automated tools conduct structured literature searches across databases, retrieving and deduplicating entries for a refined set. The central agent directs models for sequential initial and secondary screenings, then synthesizes results, resolves conflicts, and generates an optimized final output. HCC: hepatocellular carcinoma; RCT: randomized controlled trial; NRT: nonrandomized trial.



Conclusions

The results of this study showed that an automated screening process for systematic reviews and meta-analyses based on LLM was feasible in the context of treatment interventions for HCC. Our findings demonstrated the feasibility and effectiveness of an automated literature screening approach leveraging LLMs for systematic reviews and meta-analyses

XSL•FO
RenderX

related to treatment interventions in HCC. The proposed methodology exhibited high recall rates and promising accuracy metrics, highlighting its capability to reliably identify relevant literature while reducing both the time and financial resources required for manual screening. The tripartite collaborative integration of general-purpose LLMs with a reasoning-optimized model further enhanced transparency and interpretability throughout the analysis process. We propose refining the current framework by integrating an agent-based workflow augmented with RL, which could further enhance analytic precision and clinical relevance. Subsequent studies are warranted to empirically validate the effectiveness and feasibility of these proposed enhancements.

Acknowledgments

This study was supported by the research project fund of Chengdu Medical College (grant CYYZZ24-07). The authors gratefully acknowledge the technical support and service assistance provided by the Volcano Engine Computing Platform of ByteDance for the large language model used in this study.

Data Availability

The datasets generated or analyzed during this study are available from the corresponding author on reasonable request. A free demo is hosted on Hugging Face [48]. The source code is openly available on GitHub [49].

Authors' Contributions

CP contributed to the application development, testing, validation, statistical analysis, and manuscript drafting of this project. WL checked the original papers and corresponding datasets used for validation. BC ensured data integrity by verifying the accuracy of statistical results. GZ and ZY provided professional guidance on the medical academic practical use and core medical concepts of the application. JH played a key role in project management, provided medical expertise guidance, conducted code reviews, and participated in manuscript revision.

Conflicts of Interest

None declared.

Multimedia Appendix 1
Supplementary information.
[DOCX File , 366 KB - medinform_v13i1e76252_app1.docx]

References

1. Sung H, Ferlay J, Siegel RL, Laversanne M, Soerjomataram I, Jemal A, et al. Global Cancer Statistics 2020: GLOBOCAN estimates of incidence and mortality worldwide for 36 cancers in 185 countries. CA Cancer J Clin 2021 May;71(3):209-249 [FREE Full text] [doi: 10.3322/caac.21660] [Medline: 33538338]
2. Rumgay H, Ferlay J, de Martel C, Georges D, Ibrahim AS, Zheng R, et al. Global, regional and national burden of primary liver cancer by subtype. Eur J Cancer 2022 Jan;161:108-118. [doi: 10.1016/j.ejca.2021.11.023] [Medline: 34942552]
3. Desjonqueres E, Campani C, Marra F, Zucman-Rossi J, Nault J. Preneoplastic lesions in the liver: molecular insights and relevance for clinical practice. Liver Int 2022 Mar 17;42(3):492-506. [doi: 10.1111/liv.15152] [Medline: 34982503]
4. Lee YT, Wang JJ, Luu M, Noureddin M, Kosari K, Agopian VG, et al. The mortality and overall survival trends of primary liver cancer in the United States. J Natl Cancer Inst 2021 Nov 02;113(11):1531-1541 [FREE Full text] [doi: 10.1093/jnci/djab079] [Medline: 34010422]
5. Falette Puisieux M, Pellat A, Assaf A, Ginestet C, Brezault C, Dhooge M, et al. Therapeutic management of advanced hepatocellular carcinoma: an updated review. Cancers (Basel) 2022 May 10;14(10):2357 [FREE Full text] [doi: 10.3390/cancers14102357] [Medline: 35625962]
6. Tran S, Zou B, Kam L, Lee K, Huang DQ, Henry L, et al. Updates in characteristics and survival rates of hepatocellular carcinoma in a nationwide cohort of real-world US patients, 2003-2021. J Hepatocell Carcinoma 2023;10:2147-2158 [FREE Full text] [doi: 10.2147/JHC.S420603] [Medline: 38076642]
7. Rizzo A, Brandi G. Radiofrequency ablation, radiation therapy, transarterial chemoembolization, and yttrium 90: no differences for local treatment of liver cancer? Acta Oncologica 2022 Mar 07;61(6):730. [doi: 10.1080/0284186x.2022.2046849]
8. Hu L, Lin J, Wang A, Shi X, Qiao Y. Comparison of liver resection and radiofrequency ablation in long-term survival among patients with early-stage hepatocellular carcinoma: a meta-analysis of randomized trials and high-quality propensity score-matched studies. World J Surg Oncol 2024 Feb 19;22(1):56 [FREE Full text] [doi: 10.1186/s12957-024-03330-8] [Medline: 38369480]

XSL•FO
RenderX

9. Tomonari T, Tani J, Sato Y, Tanaka H, Tanaka T, Taniguchi T, et al. Clinical features and outcomes of conversion therapy in patients with unresectable hepatocellular carcinoma. Cancers (Basel) 2023 Oct 30;15(21):5221 [FREE Full text] [doi: 10.3390/cancers15215221] [Medline: 37958395]
10. Xu H, Zhang H, Li B, Chen K, Wei Y. Systemic conversion therapies for initially unresectable hepatocellular carcinoma: a systematic review and meta-analysis. BMC Cancer 2024 Aug 14;24(1):1008 [FREE Full text] [doi: 10.1186/s12885-024-12772-y] [Medline: 39143584]
11. Kudo M. The society for immunotherapy of cancer clinical practice guideline on immunotherapy for hepatocellular carcinoma. Hepatobiliary Surg Nutr 2023 Apr 10;12(2):256-260 [FREE Full text] [doi: 10.21037/hbsn-23-122] [Medline: 37124680]
12. Abou-Alfa GK, Lau G, Kudo M, Chan SL, Kelley RK, Furuse J, et al. Tremelimumab plus durvalumab in unresectable hepatocellular carcinoma. NEJM Evid 2022 Aug;1(8):EVIDoa2100070. [doi: 10.1056/EVIDoa2100070] [Medline: 38319892]
13. Hessami K, Qaderi S, Shamshirsaz AA. Obstetrical journal requirements for publication of systematic review and meta-analysis. Am J Obstet Gynecol MFM 2022 Sep;4(5):100644. [doi: 10.1016/j.ajogmf.2022.100644] [Medline: 35413471]
14. Borah R, Brown AW, Capers PL, Kaiser KA. Analysis of the time and workers needed to conduct systematic reviews of medical interventions using data from the PROSPERO registry. BMJ Open 2017 Feb 27;7(2):e012545 [FREE Full text] [doi: 10.1136/bmjopen-2016-012545] [Medline: 28242767]
15. Shrivastava DA. Artificial Intelligence (AI): evolution, methodologies, and applications. Int J Res Appl Sci Eng Technol 2024 Apr 30;12(4):5501-5505. [doi: 10.22214/ijraset.2024.61241]
16. Singh S, Mahmood A. The NLP cookbook: modern recipes for transformer based deep learning architectures. IEEE Access 2021;9:68675-68702. [doi: 10.1109/access.2021.3077350]
17. Telenti A, Auli M, Hie BL, Maher C, Saria S, Ioannidis JPA. Large language models for science and medicine. Eur J Clin Invest 2024 Jun 21;54(6):e14183. [doi: 10.1111/eci.14183] [Medline: 38381530]
18. Schilling-Wilhelmi M, Ríos-García M, Shabih S, Gil MV, Miret S, Koch CT, et al. From text to insight: large language models for chemical data extraction. Chem Soc Rev 2025 Feb 03;54(3):1125-1150. [doi: 10.1039/d4cs00913d] [Medline: 39703015]
19. Guo E, Gupta M, Deng J, Park YJ, Paget M, Naugler C. Automated paper screening for clinical reviews using large language models: data analysis study. J Med Internet Res 2024 Jan 12;26:e48996 [FREE Full text] [doi: 10.2196/48996] [Medline: 38214966]
20. Issaiy M, Ghanaati H, Kolahi S, Shakiba M, Jalali AH, Zarei D, et al. Methodological insights into ChatGPT's screening performance in systematic reviews. BMC Med Res Methodol 2024 Mar 27;24(1):78 [FREE Full text] [doi: 10.1186/s12874-024-02203-8] [Medline: 38539117]
21. Kabir T, Tan ZZ, Syn NL, Wu E, Lin JD, Zhao JJ, et al. Laparoscopic versus open resection of hepatocellular carcinoma in patients with cirrhosis: meta-analysis. Br J Surg 2021 Dec 17;109(1):21-29. [doi: 10.1093/bjs/znab376] [Medline: 34757385]
22. Fong KY, Zhao JJ, Sultana R, Lee JJ, Lee SY, Chan SL, et al. First-line systemic therapies for advanced hepatocellular carcinoma: a systematic review and patient-level network meta-analysis. Liver Cancer 2023 Feb 23;12(1):7-18 [FREE Full text] [doi: 10.1159/000526639] [Medline: 36872922]
23. Wang L, Lin L, Zhou W. Efficacy and safety of transarterial chemoembolization combined with lenvatinib and PD-1 inhibitor in the treatment of advanced hepatocellular carcinoma: a meta-analysis. Pharmacol Ther 2024 May;257:108634. [doi: 10.1016/j.pharmthera.2024.108634] [Medline: 38499069]
24. Fulgenzi CA, D'Alessio A, Airoldi C, Scotti L, Demirtas CO, Gennari A, et al. Comparative efficacy of novel combination strategies for unresectable hepatocellular carcinoma: a network metanalysis of phase III trials. Eur J Cancer 2022 Oct;174:57-67 [FREE Full text] [doi: 10.1016/j.ejca.2022.06.058] [Medline: 35970037]
25. Fulgenzi CA, Scheiner B, Korolewicz J, Stikas C, Gennari A, Vincenzi B, et al. Efficacy and safety of frontline systemic therapy for advanced HCC: a network meta-analysis of landmark phase III trials. JHEP Rep 2023 May;5(5):100702 [FREE Full text] [doi: 10.1016/j.jhepr.2023.100702] [Medline: 37025943]
26. Rezaee-Zavareh MS, Yeo YH, Wang T, Guo Z, Tabrizian P, Ward SC, et al. Impact of pre-transplant immune checkpoint inhibitor use on post-transplant outcomes in HCC: a systematic review and individual patient data meta-analysis. J Hepatol 2025 Jan;82(1):107-119 [FREE Full text] [doi: 10.1016/j.jhep.2024.06.042] [Medline: 38996924]
27. Bae SH, Chun SJ, Chung J, Kim E, Kang J, Jang WI, et al. Stereotactic body radiation therapy for hepatocellular carcinoma: meta-analysis and international stereotactic radiosurgery society practice guidelines. Int J Radiat Oncol Biol Phys 2024 Feb 01;118(2):337-351 [FREE Full text] [doi: 10.1016/j.ijrobp.2023.08.015] [Medline: 37597757]
28. Sonbol MB, Riaz IB, Naqvi SA, Almquist DR, Mina S, Almasri J, et al. Systemic therapy and sequencing options in advanced hepatocellular carcinoma: a systematic review and network meta-analysis. JAMA Oncol 2020 Dec 01;6(12):e204930 [FREE Full text] [doi: 10.1001/jamaoncol.2020.4930] [Medline: 33090186]
29. Shin SW, Ahn KS, Kim SW, Kim T, Kim YH, Kang KJ. Liver resection versus local ablation therapies for hepatocellular carcinoma within the Milan criteria: a systematic review and meta-analysis. Ann Surg 2021 Apr 01;273(4):656-666. [doi: 10.1097/SLA.0000000000004350] [Medline: 33074898]

XSL•FO
RenderX

30. Jensen MS, Wiley J. When three heads are better than two. Proc Annu Meet Cogn Sci Soc 2023;28(1):2375-2380 [FREE Full text]
31. Chen H, Lv K, Hu C, Li Y, Yuan Y, He Y, et al. ChineseEcomQA: a scalable e-commerce concept evaluation benchmark for large language models. arXiv Preprint posted online on February 27, 2025 [FREE Full text] [doi: 10.1145/3711896.3737374]
32. Hamel C, Kelly SE, Thavorn K, Rice DB, Wells GA, Hutton B. An evaluation of DistillerSR's machine learning-based prioritization tool for title/abstract screening - impact on reviewer-relevant outcomes. BMC Med Res Methodol 2020 Oct 15;20(1):256 [FREE Full text] [doi: 10.1186/s12874-020-01129-1] [Medline: 33059590]
33. Marshall I, Kuiper J, Banner E, Wallace BC. Automating biomedical evidence synthesis: RobotReviewer. Proc Conf Assoc Comput Linguist Meet 2017 Jul;2017:7-12 [FREE Full text] [doi: 10.18653/v1/P17-4002] [Medline: 29093610]
34. Peeperkorn M, Kouwenhoven T, Brown D, Jordanous A. Is temperature the creativity parameter of large language models? arXiv Preprint posted online on May 1, 2024 [FREE Full text] [doi: 10.48550/arXiv.2405.00492]
35. Sahoo P, Singh AK, Saha S, Jain V, Mondal S, Chadha A. A systematic survey of prompt engineering in large language models: techniques and applications. arXiv Preprint posted online on February 5, 2024 [FREE Full text] [doi: 10.48550/arXiv.2402.07927]
36. Vatsal S, Dubey H. A survey of prompt engineering methods in large language models for different NLP tasks. arXiv Preprint posted online on July 7, 2024 [FREE Full text] [doi: 10.48550/arXiv.2407.12994]
37. Liu NF, Lin K, Hewitt J, Paranjape A, Bevilacqua M, Petroni F. Lost in the middle: how language models use long contexts. arXiv Preprint posted online on July 6, 2023 [FREE Full text] [doi: 10.48550/arXiv.2307.03172]
38. Lee S, Zhou J, Ao C, Li K, Du X, He S, et al. Quantification of large language model distillation. arXiv Preprint posted online on January 22, 2025 [FREE Full text] [doi: 10.18653/v1/2025.acl-long.248]
39. Garry M, Chan WM, Foster J, Henkel LA. Large language models (LLMs) and the institutionalization of misinformation. Trends Cogn Sci 2024 Dec;28(12):1078-1088. [doi: 10.1016/j.tics.2024.08.007] [Medline: 39393958]
40. Shumailov I, Shumaylov Z, Zhao Y, Papernot N, Anderson R, Gal Y. AI models collapse when trained on recursively generated data. Nature 2024 Jul 24;631(8022):755-759. [doi: 10.1038/s41586-024-07566-y] [Medline: 39048682]
41. Feng Y, Dohmatob E, Yang P, Charton F, Kempe J. Beyond model collapse: scaling up with synthesized data requires verification. arXiv Preprint posted online on June 11, 2024 [FREE Full text] [doi: 10.48550/ARXIV.2406.07515]
42. Gong X, Liu M, Chen X. Large language models with knowledge domain partitioning for specialized domain knowledge concentration. OSF Preprint posted online on June 6, 2024 [FREE Full text] [doi: 10.31219/osf.io/srgpx]
43. Zhang Q, Hu Y, Yan J, Zhang H, Xie X, Zhu J, et al. Large-language-model-based AI agent for organic semiconductor device research. Adv Mater 2024 Aug 06;36(32):e2405163. [doi: 10.1002/adma.202405163] [Medline: 38816034]
44. Xu L, Mohaddes D, Wang Y. LLM agent for fire dynamics simulations. arXiv Preprint posted online on December 22, 2024. [doi: 10.5260/chara.21.2.8]
45. Sakurai T, Shiramatsu S, Kinoshita R. LLM-based agent for recommending information related to web discussions at appropriate timing. In: Proceedings of the 2024 IEEE International Conference on Agents. 2024 Presented at: ICA '24; December 4-6, 2024; Wollongong, Australia p. 120-123 URL: https://ieeexplore.ieee.org/document/10807435 [doi: 10.1109/ica63002.2024.00033]
46. Hassouna AB, Chaari H, Belhaj I. LLM-agent-UMF: LLM-based agent unified modeling framework for seamless integration of multi active/passive core-agents. arXiv Preprint posted online on September 17, 2024 [FREE Full text] [doi: 10.48550/ARXIV.2409.11393]
47. Xu Z, Jain S, Kankanhalli M. Hallucination is inevitable: an innate limitation of large language models. arXiv Preprint posted online on January 22, 2024 [FREE Full text] [doi: 10.5860/choice.189890]
48. review-screening-analyzer. huggingface. URL: https://huggingface.co/spaces/chitsanfei/review-screening-analyzer [accessed 2025-05-29]
49. chitsanfei / review-screening-analyzer. GitHub. URL: https://github.com/chitsanfei/review-screening-analyzer [accessed 2025-05-29]

Abbreviations

AI: artificial intelligence
HCC: hepatocellular carcinoma
LLM: large language model
MCC: Matthews correlation coefficient
PABAK: prevalence-adjusted bias-adjusted κ
PICOS: population, intervention, comparison, outcome, and study design
PLC: primary liver cancer
PRISMA: Preferred Reporting Items for Systematic Reviews and Meta-Analyses
RCT: randomized controlled trial
RL: reinforcement learning

XSL•FO
RenderX

Edited by A Benis; submitted 19.04.25; peer-reviewed by X Jiang, JCL Chow, S Matsuda; comments to author 24.06.25; revised version received 05.08.25; accepted 15.08.25; published 08.09.25.

Please cite as:
Pan C, Lu W, Chen B, Zhang G, Yang Z, Hao J
Automated Literature Screening for Hepatocellular Carcinoma Treatment Through Integration of 3 Large Language Models: Methodological Study
JMIR Med Inform 2025;13:e76252
URL: https://medinform.jmir.org/2025/1/e76252
doi:10.2196/76252
PMID:

©Chen Pan, Wei Lu, Bingliang Chen, Gang Zhang, Zhiming Yang, Jingcheng Hao. Originally published in JMIR Medical Informatics (https://medinform.jmir.org), 08.09.2025. This is an open-access article distributed under the terms of the Creative Commons Attribution License (https://creativecommons.org/licenses/by/4.0/), which permits unrestricted use, distribution, and reproduction in any medium, provided the original work, first published in JMIR Medical Informatics, is properly cited. The complete bibliographic information, a link to the original publication on https://medinform.jmir.org/, as well as this copyright and license information must be included.

XSL•FO
RenderX

Understanding Health Information Systems Utilization Across Public Health Centers in Indonesia: Cross-Sectional Study

Dewi Nur Aisyah[1,2,3], PhD; Agus Heri Setiawan[2], MPH; Chyntia Aryanti Mayadewi[2], MSc; Alfiano Fawwaz Lokopessy[2], BSc; Zisis Kozlakidis[4], PhD; Logan Manikam[1,5], PhD

[1]Department of Epidemiology and Public Health, Institue of Epidemiology and Health Care, University College London, 1-19 Torrington Place, London, United Kingdom

[2]Digital Transformation Office, Ministry of Health Republic of Indonesia, Jakarta, Indonesia

[3]Department of Public Health, Monash University Indonesia, Tangerang, Indonesia

[4]International Agency for Research on Cancer World Health Organization, Lyon, France

[5]Aceso Global Health Consultants Pte Limited, Singapore, Singapore

Corresponding Author:
Logan Manikam, PhD
Department of Epidemiology and Public Health, Institue of Epidemiology and Health Care, University College London, 1-19 Torrington Place, London, United Kingdom

Abstract

Background: The primary health care service in Indonesia consists of 10,260 public health centers (Puskesmas), which play a major role in providing health care in the community, recording and reporting health data using digital health information systems (HIS) or manual reports. The utilization of HIS across Puskesmas is crucial to capture the dynamic evolution of health problems and monitor interventions, thus providing effective primary health care services for the community.

Objective: This paper provides a national-level baseline mapping of HIS utilization in Indonesian Puskesmas. It evaluates the number of HIS used, associated challenges, and contextual factors influencing system adoption.

Methods: A cross-sectional survey was carried out covering all Puskesmas across 34 Indonesian provinces between January and February 2022. The questionnaire covered a list of HIS used by Puskesmas, which developed the HIS, and the utilization and challenges during HIS implementation. Descriptive statistical analysis and bivariate analysis were applied.

Results: A total of 2606 (25.5%) public health centers across 34 provinces participated in this study. On average, Puskesmas reported using 30 different HIS platforms, with notable variation across provinces and islands. Most systems (n=62,060, 72.94%) were developed by national ministries, though local governments and third parties also contributed. Despite 91.5% of respondents reporting that HIS aligned with their needs and 90% claiming data use for decision-making, many centers faced operational barriers: 49% (n=132,300) of systems required excessive data entry, 33% (n=89,100) experienced frequent downtime, and 29% (n=78,300) lacked automated analysis features. In terms of the infrastructure supporting HIS implementation, 9.45% (n=138) of Puskesmas have no access to the internet, while only 28.9% (n=422) have access to robust and efficient internet connections. As for the human resources, the study reveals that each health personnel manages up to six different HIS for data reporting tasks, 74.30% (n=1133) of Puskesmas only received training at the initial system's implementation stage, and 80.51% (n=1225) of respondents report the existence of an informal knowledge transfer process among the staff. The bivariate analysis shows that Puskesmas with the characteristics of being located in Java island and urban areas possessed higher accreditation levels, had more training and knowledge transfer, and had a greater chance to use >30 HIS.

Conclusions: This descriptive study highlights substantial fragmentation in Indonesia's HIS environment and reveals critical disparities in system infrastructure, usability, and workforce capacity. Recommendations should be tailored to different contexts: offline-compatible systems and basic digital literacy training are needed in rural areas, while urban Puskesmas may benefit from advanced integration and analytics tools. Future research should address HIS interoperability, impact assessment, cost-effectiveness, and qualitative user experience through longitudinal and mixed methods studies to guide Indonesia's digital health transformation.

(JMIR Med Inform 2025;13:e68613) doi:10.2196/68613

KEYWORDS

public health centers; Puskesmas; health information system; infrastructure; primary health care

XSL•FO
RenderX

Introduction

Health information systems (HIS) are defined as a set of structures—including data, information, indicators, procedures, devices, technology, and human resources—that are interrelated and managed in an integrated manner; they provide information support for the decision-making process, health program planning, implementation monitoring, and evaluation at every level of health administration [1,2]. Globally, HIS have been used in primary health care facilities to record, analyze, report, and transfer patients' data, in which the data will be highly important to improve the health system's management [3]. The World Health Organization (WHO) report in 2010 highlighted the importance of HIS as a contributing factor to overall health management improvement [4]. Studies from low- and middle-income countries show that HIS implementation has been carried out, despite challenges and barriers to successful implementation [5].

Indonesia is the world's fourth most populous country with over 270 million people residing across more than 17,000 islands [6,7]. The country has adopted a decentralized administrative system since 1999, which granted provincial governors and district leaders the authority to govern their own areas, including health care service governance [8,9]. At the national level, the Ministry of Health plays a vital role in formulating health policies, regulations, and strategies that guide the entire health care system, setting standards, coordinating resources, and implementing national health programs. This responsibility extends to the provincial level, where each of the provinces has its own health office (provincial health office) responsible for implementing region-specific health care policies and programs. Additionally, at the district level, the 514 district health offices (DHOs) play a crucial role in managing and monitoring the provision of health care services [8,9].

The smallest unit of public health care service at the subdistrict level is called Puskesmas (Pusat Kesehatan Masyarakat or public health center), which stands for the primary health care service for the local community. The number of Puskesmas increased by 9.3% over the past decade, from 9510 in 2012 to 10,260 in 2021 [10,11]. The Puskesmas are spread across all areas of Indonesia, with the ratio of Puskesmas per subdistrict currently at 1.04, which means that in each subdistrict, there is at least one Puskesmas [7]. Puskesmas serve as the first point of contact for individuals seeking health care, providing preventive, curative, and rehabilitative services in the area of general medicine, maternal and child health, family planning, immunization, and more [12,13]. At the same time, each Puskesmas has the obligation to record and report all health program activities or health data within its working area, using digital HIS or manual reports, and submit it regularly to the DHO [14].

It is crucial for Puskesmas to ensure that robust HIS can accommodate the dynamic monitoring of health problems and interventions, supporting the provision of effective primary health care services for the community. HIS facilitate the collection, storage, analysis, and retrieval of health-related data, empowering Puskesmas and the DHO in making informed decisions within their working area [15]. Thus, Puskesmas can better manage patient records, track disease outbreaks, plan resource allocation, and contribute to the overall improvement of health care services in Indonesia [16,17]. Maintaining a timely and accurate data collection infrastructure, policy makers can then better allocate resources, plan health care services, and implement targeted interventions that address the health care challenges faced by the growing population [18-20].

To date, the use of HIS continues to grow across Indonesia, including in Puskesmas. However, only limited publications are available that discuss the national-scale HIS implementation in Indonesia. A study reported on the implementation of 12 selected HIS in Puskesmas at the national level [21]. Most studies discussed the HIS utilization only for specific programs, such as tuberculosis [22], immunization [23], malaria [24], and electronic medical record system [25,26]. Many studies only focus on HIS implementation in specific areas such as provinces [27,28]. A literature review highlights the utility of HIS but is limited to the Puskesmas scale and only focuses on Puskesmas' management information systems [27,29]. A narrative study in 2015 reveals the barriers and challenges of HIS implementation in a low- and middle-income country (LMIC) on a general basis [3].

This paper aims to provide, for the first time, a comprehensive national overview of the utilization of HIS across Puskesmas in Indonesia. It presents a descriptive mapping of the types and number of HIS in use, the institutional and infrastructural conditions that may be associated with their implementation, and the common challenges encountered at the facility level. The analysis includes aspects such as internet availability, accreditation status of Puskesmas, system usability, and the availability of training. Additionally, the study explores key workforce characteristics, including staff education background and reported HIS-related workloads. While the study does not assess system interoperability, causality, or performance impact, it offers a foundational evidence base to inform future digital health strategies and more targeted research.

Methods

Data Collection

A cross-sectional approach was chosen, using a survey carried out between January 28 and February 28, 2022. The population study covered 10,260 Puskesmas across 34 provinces in Indonesia. Slovin calculator [30] was used to count the sample size based on 5% margin of error. The Slovin formula was used in this study as it is widely used in public health and social science research, where the total population size is known but the population's variance or SD information is limited. The Slovin formula offers a practical and transparent means of estimating a representative sample size. Although it does not explicitly account for CI or statistical power, this limitation was addressed by selecting a conservative margin of error of 5%, in line with the accepted research standard. Accordingly, an expected sample was 385 participants out of 10,260 Puskesmas. To account for potential data incompleteness, an additional 10% was added, resulting in a final minimum sample size of 424 Puskesmas.

XSL•FO
RenderX

A questionnaire was used to obtain the data from the participants. The questionnaire was developed referring to the PRISM (Performance of Routine Information Systems Management) framework [31] to assess routine HIS in LMICs. We used and adopted the routine health information tools overview tool to list the information systems that exist in the country and the type of data they collect. A pilot survey test was conducted to ensure questionnaire validity and reliability with a total of 20 participants, resulting in a satisfactory Cronbach α value (0·76). The questionnaire consisted of two sections: (1) a list of HIS used by Puskesmas, which developed the HIS, and the utilization and challenges during HIS implementation; and (2) an exploration of factors that influence the utilization of HIS in Puskesmas, including human resources, supporting facilities, and infrastructure. The identities of participants were also captured as representatives from Puskesmas. As the survey relied on self-reporting from designated Puskesmas personnel, responses may reflect individual perceptions or institutional biases rather than objective system evaluations. To reduce response bias, the questionnaire was anonymized, and standardized definitions were provided throughout.

Data Analysis

Univariate analysis was conducted using SPSS (IBM Corp) software to examine the HIS utilization in Puskesmas across Indonesia. The major islands in Indonesia were divided into six categories: (1) Java Island, covering provinces such as Banten, DKI Jakarta (special capital region of Jakarta), West Java, Central Java, Yogyakarta Special Region, and East Java; (2) Bali and Nusa Tenggara, including Bali, East Nusa Tenggara, and West Nusa Tenggara provinces; (3) Sumatera, covering Aceh, North Sumatra, West Sumatra, Riau, Riau Islands, Jambi, South Sumatra, Bengkulu, Bangka Belitung, and Lampung provinces; (4) Kalimantan, including West Kalimantan, Central Kalimantan, South Kalimantan, East Kalimantan, and North Kalimantan provinces; (5) Sulawesi, including South Sulawesi, North Sulawesi, Central Sulawesi, Gorontalo, Southeast Sulawesi, and West Sulawesi; and (6) Maluku and Papua, consisting of Maluku, North Maluku, Papua, and West Papua provinces.

Puskesmas are systematically distributed across various regions, ensuring accessible health care services are available to all communities. Based on Article 21 of the Ministry of Health Decree Number 75 Year 2014 [12], Puskesmas are divided into three characteristic regions, which are urban, rural, and remote areas. To explore factors associated with HIS implementation in Indonesia, we used the average number of HIS [30] to calculate the degree of association of some risk factors. As the study uses a cross-sectional design, it captures association at a single point in time and cannot establish causality between factors such as training frequency, accreditation, or geographic location and HIS use.

Box plots were used as data visualization tools to depict the average number of HIS used in Puskesmas, along with the minimum and maximum numbers across 34 provinces. Cross-tab analysis was used to examine the frequency of HIS utilization based on the type of Puskesmas' geographic characteristics (urban, rural, and remote) and accreditation level. Puskesmas accreditation level in Indonesia is categorized as follows: (1) not accredited, (2) basic accreditation (dasar), (3) medium accreditation (madya), (4) major accreditation (utama), and (5) comprehensive accreditation (paripurna).

Ethical Considerations

We declare that the data collected for this paper do not require ethical approval as no individual data are presented and informed consents were collected during the survey implementation. As such, this research qualifies for exemption from full ethical review in accordance with the provisions outlined in the 2021 Pedoman dan Standar Etik Penelitian dan Pengembangan Kesehatan Nasional (2021 National Health Research and Development Ethical Guidelines and Standards), issued by the Komite Etik Penelitian dan Pengembangan Kesehatan Nasional (KEPPKN)—National Health Research and Development Ethics Committee—under the Indonesian Ministry of Health [32]. Specifically, the exemption applies to studies that involve no personal identifiers, pose minimal to no risk, and focus on evaluating or monitoring public programs, as outlined in the guideline's section on research exemption criteria. These provisions are consistent with the earlier 2017 guideline and remain the current ethical standard [33]. In accordance with these criteria, all survey responses were anonymized upon collection, and no individual or facility-level identifiers were retained in the analytical dataset. Informed consent was embedded at the beginning of the survey, which provided thorough information about the study and what to expect from the participants. It also states that participation was entirely voluntary and no compensation was given in any form. Data were securely stored on encrypted servers with restricted access, ensuring the confidentiality and integrity of the dataset. The exemption status of this study was reviewed and confirmed by the Digital Transformation Office of the Indonesian Ministry of Health.

Results

Number of HIS Used in Puskesmas

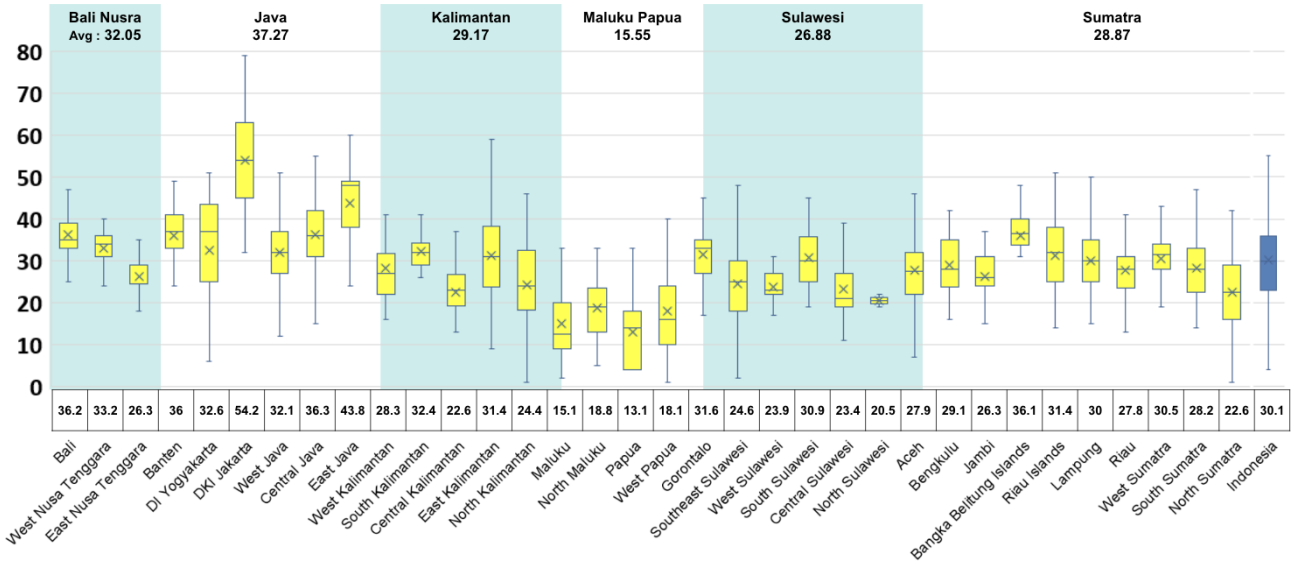
A total of 2616 public health centers (25.5% of the total 10,260 public health centers in Indonesia) spread across 320 districts or cities from 34 provinces participated in the survey. Provinces with the highest number of participating health centers were Central Java (326), Lampung (227), and Aceh (214). Among the health centers, 779 of 2700 (28.85%) were located in urban areas; 1143 of 2700 (42.33%) in rural areas; and 475 of 2700 (17.59%) in remote areas.

Based on the study results, the average number of HIS used in public health centers nationwide was 30 (SD 11.2). However, this number varied across provinces. The province with the highest average number of HIS was DKI Jakarta, with 54 (SD 12.6) systems deployed and used for recording and reporting various health services, followed by East Java (43, SD 8.0), Central Java (SD 9.7), Bali (SD 8.7), Bangka Belitung Islands (SD 6.5), and Banten (SD 7.6), which were all around 36 systems in average, while Papua had the lowest average of 13 (SD 9.1) systems. The variation of the number of HIS used by Puskesmas can also be observed based on the distribution of

XSL•FO
RenderX

major islands, with Java having the highest average of 37 (SD 11.3) systems, followed by Bali Nusra (32, SD 7.8), Kalimantan (29, SD 10.3), Sumatra (28, SD 8.8), Sulawesi (26, SD 8.5), and the lowest being 15 (SD 9.5) in Maluku Papua (Figure 1).

Figure 1. Average number of health information systems used by public health centers based on provinces and major islands.



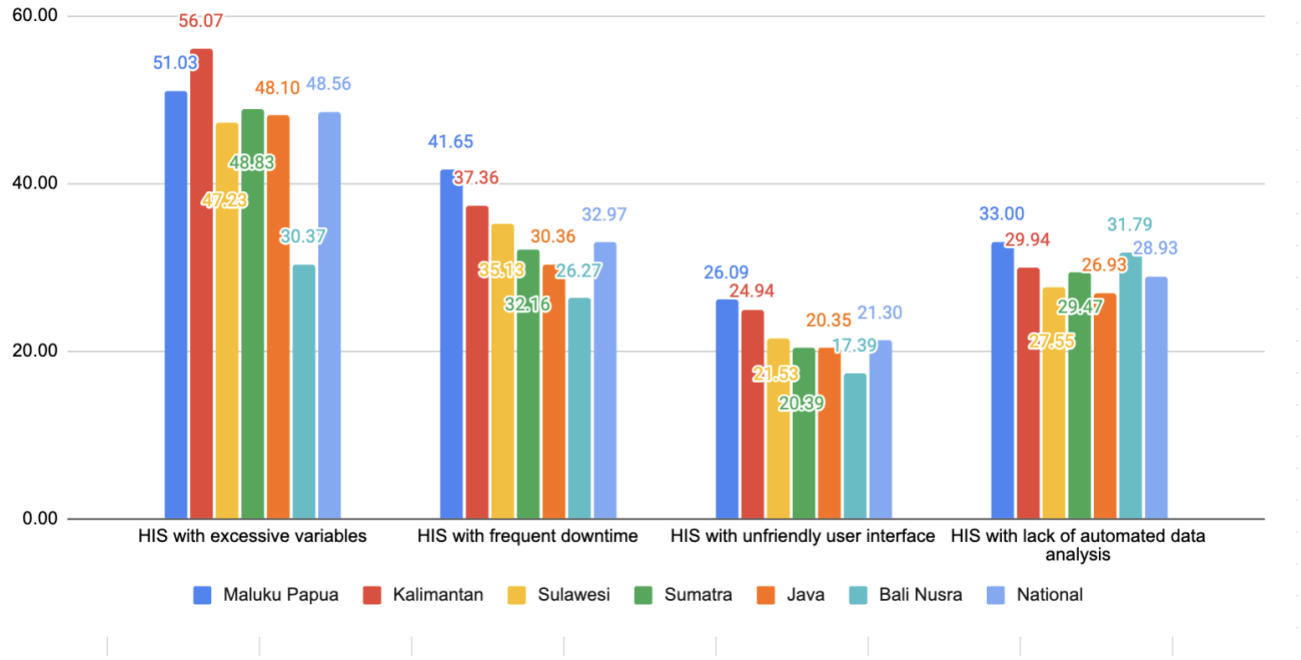
On average, 72.94% (n=62,060) of the HIS used were provided or developed by the Indonesian Ministries (National Government), making the central government the primary contributor to the abundant number of different HIS available. City or district governments also play a significant role, contributing to 17.45% (n=14,844) of the HIS development, while the provincial government accounts for 5.27% (n=4485). Moreover, third-party organizations and other stakeholders contributed 4.33% (n=3685) and Puskesmas 0.01% (n=12) to the overall HIS deployment. A total of 75.07% (n=63,872) of the HIS were from health-related government offices, while 24.93% (n=21,214) were from non–health-related (eg, the Ministry of Internal Affairs, Ministry of Communication and Informatics, Ministry of Finance, Local and Provincial Governments).

Based on the study, the HIS used by public health centers was 91.54%, which aligned with their needs, and 90% of the data collected has been used as a reference for decision-making, health policy formulation, or program development. However, there exist challenges in using the existing HIS as depicted in the following graph.

The findings depicted in Figure 2 revealed major challenges of the existing HIS used by Puskesmas across Indonesia. Approximately, 49% (n=132,300) of all HIS in the country had excessive data input variables, leading to prolonged form-filling, extended patient registration queue times, and increased screen time for health care personnel. In addition, 33% (n=89,100) of the systems experience frequent downtime, posing challenges in health care service delivery and data management, 21% (n=56,700) of HIS were not user-friendly, and 29% (n=78,300) of HIS did not have the ability to generate automated data analysis.

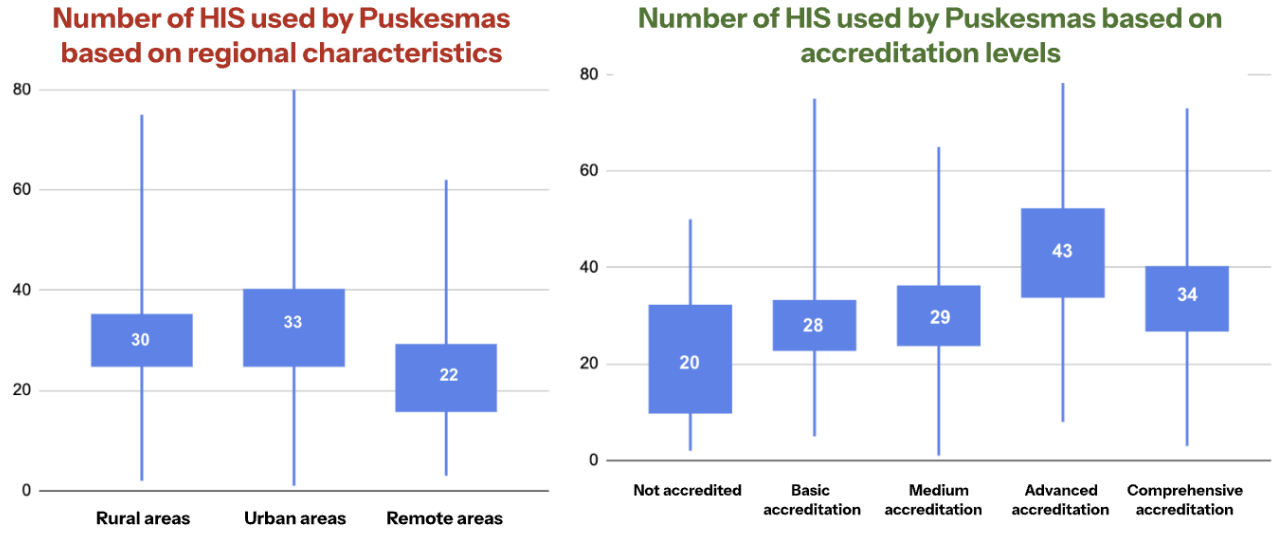
XSL•FO
RenderX

Figure 2. Several limitations of existing HIS based on major islands. HIS: health information systems.



Public health centers in rural areas used an average of 30 different HIS, while urban areas used 33 systems, and remote areas used 22 systems (Figure 3). Furthermore, based on the accreditation level, public health centers with no accreditation used an average of 20 different HIS, while Puskesmas with basic (*dasar*), medium (*madya*), accreditation (*utama*), and comprehensive accreditation (*paripurna*) levels used 28, 29, 43, and 34 systems, respectively.

Figure 3. Number of HIS used by Puskesmas based on geographic characteristics and accreditation levels. HIS: health information systems.



Factors Influencing HIS Utilization Across Public Health Centers

Internet Availability

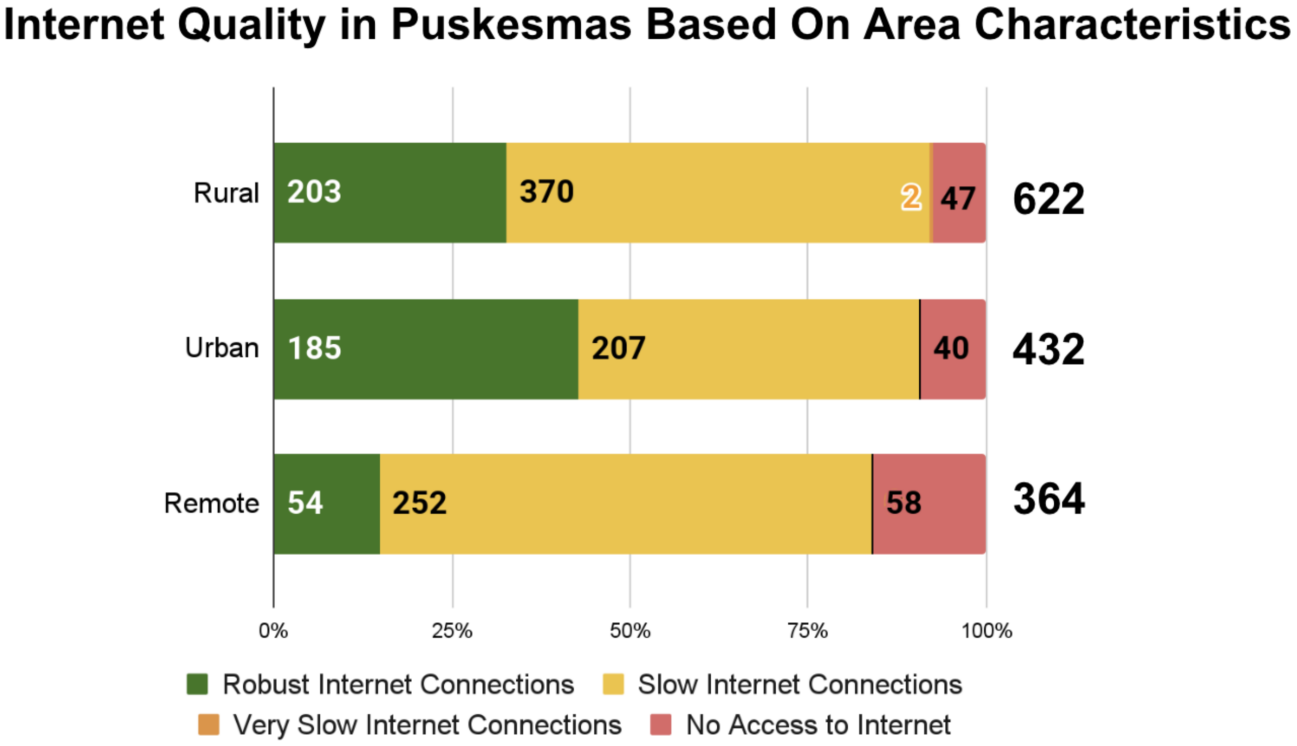
A separate analysis was carried out to explore factors influencing HIS utilization. Based on the survey, 9.45% (138/1460) of Puskesmas had no access to the internet. Specifically, the majority of Puskesmas have internet access, but only 28.9% (422/1460) have access to robust and efficient internet connections; meanwhile, 51.1% (746/1460) reported slow internet connections, and 10.55% (154/1460) reported very slow internet connections (Figure 4A).

Figure 4B shows the types of internet facilities mostly used by health care personnel to access HIS in Puskesmas. Among the surveyed Puskesmas (n=1309), 417 (31.88%) relied solely on Puskesmas Wi-Fi for their internet access to input the health data reports; 280 (21.40%) used Puskesmas Wi-Fi and private home internet; and a large portion reported using a combination of Wi-Fi, private home internet, and internet credit fund paid by Puskesmas (422/1309, 32.27%). Figure 4C depicts that in urban areas, 42.8% (185/432) of Puskesmas have robust internet connections, while 47.9% (207/432) experience slow internet, and only 9.3% (40/432) have no access to the internet. In contrast, in remote areas, only 14.84% (54/364) of Puskesmas

XSL•FO
RenderX

have robust connections, whereas 69.2% (252/364) experience slow internet, and 15.93% (58/364) have no access.

Figure 4. (A) Internet quality in public health centers and (B) types of internet facilities used by health care personnel to access HIS in Puskesmas. (C) Internet quality in public health centers based on area characteristics. HIS: health information systems.



Human Resources

Human resources are pivotal in affecting the utilization and adoption of HIS. Table 1 depicts the background education of HIS managers in Puskesmas. Out of the total surveyed individuals (n=1330), 344 (25.86%) of HIS managers were from other health care professions such as nutritionists and pharmacists, followed by nurses (327/1330, 24.59%), public health staff (255/1330, 19.17%), non–health care professionals such as informaticians and computer technicians (241/1330, 18.10%), and midwives (147/1330, 11.05%).

Table . Educational background of HIS[a] managers in public health centers (n=1330).

Educational background of HIS managers	HIS personnel, n (%)
Other health care personnel	344 (28.86)
Nurse	327 (24.59)
Public health personnel	255 (19.17)
Nonhealth care personnel	241 (18.12)
Midwife	147 (11.05)
Doctor	14 (1.05)
Pharmacist	2 (0.15)

[a]HIS: health information systems.

Table 2 provides insights into the number of HIS or programs input by Puskesmas personnel. Among the surveyed Puskesmas (n= 850), the data showed that 22.71% (193/850) of Puskesmas required each health personnel to input data into one to two different HIS. Additionally, 188 (22.12%) of the Puskesmas personnel managed and input data into more than six different HIS or programs, while 159 (18.71%) of them handled one to three programs.

XSL•FO
RenderX

Table . Number of HIS[a] programs input by public health centers personnel (n=850).

HIS programs input by public health center personnel	Puskesmas, n (%)
More than 6 programs	188 (22.1)
1 - 6 programs	79 (9.3)
1 - 5 programs	91 (10.7)
1 - 4 programs	87 (10.2)
1 - 3 programs	159 (18.7)
1 - 2 programs	193 (22.7)
1 program	53 (6.2)

[a]HIS: health information systems.

Further analysis shows that 74.30% (1133/1525) of personnel in Puskesmas only received training at the initial system's installation, 13.64% (157/1525) indicate that the training only occurs once a year, and 10.30% (157/1525) report that there was no training available for data input and management. Furthermore, 80.51% (1225/1521) of respondents report the existence of a knowledge transfer process, highlighting the significance of sharing expertise and information among the staff.

Table 3 presents a bivariate analysis of various characteristics influencing the adoption of information systems in public health centers. We categorized the below and above average number of HIS (30 HIS as a cutoff) and conducted binary logistic regression analysis on SPSS. Key variables include geographic factors (main islands and geographic characteristics), accreditation levels, training frequency, knowledge transfer, number of HIS programs input by personnel, and internet quality. Among geographic factors, health centers in Java show the highest likelihood of having >30 information systems (odds ratio [OR] 32.85, 95% CI 14.9-72·41) compared to Maluku Papua. Urban areas have a greater likelihood of higher system adoption compared to rural and remote areas (OR 4.73, 95% CI 3.43-6·50). Accreditation levels are strongly associated with system adoption, with comprehensively accredited centers being the most likely to use >30 systems (OR 10.20, 95% CI 3.41-30.51). Training frequency also plays a role, where biannual training is significantly associated with higher adoption (OR 1.77, 95% CI 1.01-3.08). Knowledge transfer presence slightly increases the likelihood of greater system use (OR 1.33, 95% CI 0.97-1.81). The number of HIS programs input by personnel does not show a strong pattern. Internet quality does not exhibit a substantial impact, as OR values remain close to 1.

XSL•FO
RenderX

Table . Factors influencing HIS[a] utilization.

Characteristics	Total Puskesmas (n)	Below average (≤30 HIS), n (%)	Above average (>30 HIS), n (%)	Univariable, OR[b] (95% CI)
Main island				
Maluku Papua	175	162 (92.6)	13 (7.4)	1 (reference)
Kalimantan	231	163 (70.6)	68 (29.4)	6.18 (2.82 - 13.52)
Bali Nusra	315	187 (59.4)	128 (40.6)	5.53 (2.05 - 14.89)
Sulawesi	956	567 (59.3)	389 (40.7)	3.54 (1.56 - 7.98)
Sumatra	106	33 (31.1)	73 (68.9)	6.25 (2.94 - 13.28)
Java	645	149 (23.1)	496 (76.9)	32.85 (14.9 - 72.41)
Geographic characteristics				
Remote areas	595	458 (77)	137 (23)	1 (reference)
Rural areas	1077	505 (46.9)	572 (53.1)	3.41 (2.54 - 4.59)
Urban areas	748	294 (39.3)	454 (60.7)	4.73 (3.43 - 6.50)
Accreditation levels				
Not accredited	154	114 (74)	40 (26)	1 (reference)
Basic accreditation	513	291 (56.7)	222 (43.3)	2.26 (1.22 - 4.21)
Medium accreditation	1273	695 (54.6)	578 (45.4)	1.54 (0.86 - 2.7)
Advanced accreditation	400	146 (36.5)	254 (63.5)	2.82 (1.47 - 5.41)
Comprehensive accreditation	88	15 (17)	73 (83)	10.2 (3.41 - 30.51)
Training frequency				
No training	158	105 (66.5)	53 (33.5)	1 (reference)
Occurs at the beginning of system socialization	3	2 (66.7)	1 (33.3)	0.24 (0.01 - 3.23)
Once a year	1067	528 (49.5)	539 (50.5)	1.4 (0.86 - 2.27)
Twice a year	209	114 (54.5)	95 (45.5)	1.77 (1.01 - 3.08)
Knowledge transfer				
No knowledge transfer process	282	178 (63.1)	104 (36.9)	1 (reference)
Knowledge transfer processexistst	1140	558 (48.9)	582 (51.1)	1.33 (0.97 - 1.81)
Number of HIS or programs input by public health center personnel				
1	61	34 (55.7)	27 (44.3)	1 (reference)
1 - 2	197	111 (56.3)	86 (43.7)	1.38 (0.74 - 2.54)
1 - 3	161	72 (44.7)	89 (55.3)	0.82 (0.57 - 1.2)
1 - 4	91	44 (48.4)	47 (51.6)	1.1 (0.72 - 1.66)
1 - 5	94	49 (52.1)	45 (47.9)	1.08 (0.64 - 1.81)
1 - 6	77	43 (55.8)	34 (44.2)	0.72 (0.41 - 1.25)
≥6	670	336 (50.1)	334 (49.9)	1.06 (0.58 - 1.93)
Internet quality				
No access to internet	121	63 (52.1)	58 (47.9)	1 (reference)
Very slow internet connections	120	54 (45)	66 (55)	1.27 (0.74 - 2.16)
Slow internet connections	711	362 (50.9)	349 (49.1)	1.04 (0.69 - 1.56)
Robust internet connections	367	194 (52.9)	173 (47.1)	1.03 (0.67 - 1.59)

XSL•FO
RenderX

[a]HIS: health information systems.

[b]OR: odds ratio.

Discussion

Principal Findings

HIS are foundational to modern health care delivery and serve as critical tools for supporting evidence-based decision-making and policy development [34]. Well-functioning HIS should not only collect health data but also enable the analysis, synthesis, and timely dissemination of information across all components of the health system [35]. Previous studies have demonstrated that effective HIS use can contribute to improved care coordination, more efficient facility management, and enhanced patient safety outcomes [34-36]. While most existing research has focused on hospital-level or disease-specific HIS implementations, this study offers the first national-level descriptive mapping of HIS utilization across Indonesia's public primary health care centers (Puskesmas). It identifies the number and types of systems in use and highlights contextual factors that may influence HIS adoption and implementation at the facility level.

Various innovations in resource-limited areas are also making significant investments in national HIS. These initiatives are anticipated to enhance access to quality health care and contribute to the reduction of overall costs in the health care sector) [37-41]. This study reveals that there was a massive, recent development of multiple HIS or digital apps within Indonesia, driven by government initiatives (at all levels of government, from central, provincial, to district). In particular, massive development of HIS in Indonesia is caused by different needs of a key performance indicator for each division or directorate of the central government in Indonesia. Thus, there have been increased numbers of projects to develop different digital apps and HIS that focus on specific diseases, such as SITB (Sistem Informasi Tuberkulosis), for tuberculosis information system; SIHA (Sistem Informasi HIV-AIDS), for HIV-AIDS information system; SIHEPI (Sistem Informasi Hepatitis), or Hepatitis Information System; SIPTM (Sistem Informasi Penyakit Tidak Menular), or NonCommunicable Disease Information SysteM; SIPD3I (Sistem Informasi Penyakit yang Dapat Dicegah dan Diobati dengan Imunisasi), or Vaccine Preventable Diseases Information System; ESISMAL (Electronic System of Malaria), or Malaria Information System.

Digital app development initiatives were also increased due to a new specific program introduced by the central government to monitor specific programs, such as PISPK (Program Indonesia Sehat Pendekatan Keluarga), or the Healthy Family Program; SISTBM (Sistem Informasi Sanitasi Total Berbasis Masyarakat), or Health Sanitation Population-Based; e-PPGBM (Electronic Pencatatan dan Pelaporan Gizi Berbasis Masyarakat), or Nutrition Information System; SKDR (Sistem Kewaspadaan Dini dan Respon), or Early Warning of Epidemic Diseases; ASPAK (Aplikasi Sarana Prasarana dan Alat Kesehatan), or Health Facilities and Supplies Application; P-Care (Primary care), a medical record for health insurance; HFIS (Health Financing Information System), for financing of health insurance, and many more introduced by each provincial or district level due to decentralization health system regulation [21,37]. This greatly magnifies the fragmentation, disparities, burden for health care workers, fragmented data, lack of data integration and interoperability, and low level of system standardization [37-40]. Another common HIS in Puskesmas is also called SIMPUS (Sistem Informasi Manajemen Puskesmas), or Puskesmas Management Information System, which manages both patient electronic medical record management and administrative matters ranging from human resources, finance and planning, pharmaceuticals and medical devices, and reporting [42].

Based on Articles 3 and 6 of the Ministry of Health Decree Number 31 Year 2019 [15], SIMPUS is part of the district information system. In order to simplify all the different existing apps or information systems used by health care facilities, including Puskesmas, a national HIS (Sistem Informasi Kesehatan Nasional) is currently being developed by the Ministry of Health of Indonesia [43]. The systemic goal is to allow the deployment of Fast Healthcare Interoperability Resources-based standardization to be used by health care facilities' HIS developers to connect all health care institutions' services at all levels in the whole country [43]. In the context of primary health care, each Puskesmas and DHO has the opportunity to customize and enhance its SIMPUS framework as long as it complies with the Sistem Informasi Kesehatan Nasional standard, to better address its unique priorities, ensuring that the system effectively meets the diverse needs of its community. This initiative enables each district to confidently engage a diverse array of information technology developers.

The large number of HIS used is a major challenge. At the simplest level, the amount of different HIS affects the responsibility burden of each health worker, from data recording to reporting [44]. The reporting obligation of Puskesmas is centrally mandated; however, using different numbers of HIS adds to the medical staff workload. The study shows an average number of 30 different HIS used for various health data reporting functions, indicating a high burden for health care personnel to input data into different systems that are not integrated. Inevitably, this landscape of multiple siloed systems leads to duplication in data entry. It impacts the allocation of adequate time for health workers to deliver health care services due to data recording and reporting tasks [45].

In addition, the results suggest different numbers of HIS used for data reporting across provinces and major islands in Indonesia. This would create a technical challenge to future data integration attempts at a central government level. Java and Sumatra Island tend to use more HIS compared to Bali, Nusra, and other islands. This reflects the relative population distribution (much higher population density in Java and Sumatra in the western region of Indonesia) and is thus influenced by several factors such as the availability of human resources, infrastructure, organizational support, aid funding, and program priorities [45-47].

XSL•FO
RenderX

Considering the experiences of other countries, it seems that one of the root causes of the failure of HIS is the absence of adequate information and communication technology infrastructure [48]. A previous study shows that adequate access to the internet, computer availability, and availability of electricity play roles in the success rate of HIS utilization [49]. Findings in Haiti also show that the important factor for long-term implementation success of complex information systems is balancing investments in hardware and software infrastructure upkeep [50], and many other studies suggested that HIS utilization will be optimal, effective, and efficient when they are supported by adequate facilities and infrastructure [46-49]. In spite of the potential and opportunities that lie in HIS to transform the health care sector, including helping to foster the development of evidence-based policy, many challenges are evident and imminent. These challenges range from issues related to the technology infrastructure, human resources, system users, and financial constraints [49,51].

Based on the study results, health care workers felt that the variables of data that need to be recorded and reported in the HIS are too many, with complicated user interfaces. Data input with long required variables for reporting caused data duplication and poor usability of HIS [45,52]. Poor usability has been linked to a reduced acceptance of digital systems in the long term, increased errors, and reduced user efficiency and can even adversely affect patient safety [52,53]. The International Standard Organization has defined the usability of systems with three features of effectiveness, efficiency, and satisfaction, and user interface problems can be associated with all of these features [54]. Previous studies have shown that usability problems, such as overcrowded pages and many steps to perform a task, entail reduced user productivity [55,56]. Another study in Iran showed that HIS “flexibility and efficiency of use” and “consistency and standard” are problematic [3,5]. Furthermore, diversity in the presentation and visualization of data variables can result in ineffective communication and data reporting. For Indonesia, where universal health care coverage was introduced only recently in 2014, it is critical to use common standards and observe the consistency of data variables across the whole system [57]. Moreover, presented information in any format should be self-explanatory, so that the users can initiate actions at any time without recalling their experience from the previous use of the system [58].

Health care organizations are expected to increasingly depend on business intelligence tools, including “dashboards,” to capture, analyze, and present data on performance metrics [59]. For example, dashboards allow users to quickly visualize actionable data to inform and optimize clinical and organizational performance [60]. However, the multiplicity of HIS, and as such, the multiplicity of produced dashboards, is likely to impede the utilization of collected data. Thus, the data management problem is one of the important findings in this study, especially the lack of automated data analysis generation through the dashboard of the existing HIS. In reality, dashboards are typically embedded in complex health care organizations with massive data streams, servicing end users with distinct needs. Thus, designing effective dashboards is a challenging task, and the theoretical underpinnings of health care dashboards are poorly characterized; even the concept of the dashboard remains ill-defined [55]. Several LMICs face the same problem of insufficient quality of data produced by the systems that limit their usefulness with regard to decision-making [61-63].

The continuity of using HIS during routine operations depends on the information technology infrastructure. The discrepancies in communication technology infrastructure availability across the 34 provinces in Indonesia remain one of the obstacles when it comes to the need for a stable internet connection, even in urban areas that already have communication infrastructure with 5G networks [64]. The limitations of the internet coverage and limited network capacity impact HIS operability, since it may limit the network coverage area to only the registration counter [49]. Frequent downtime of HIS was found in this study, showing the need for further improvements in infrastructure and facilities. This lack of and instability of information technology infrastructure, such as the limitation of internet access, electricity supply, and availability of computers, was similar to that found previously in Brazil, Sub-Saharan Africa, and Tanzania [65-67].

Finally, human resources play a pivotal role in implementing the HIS in Puskesmas. However, the IT personnel remain one of the challenges to date, as the procurement of IT personnel in a primary health care center is not a mandatory requirement yet in Indonesia. This absence of highly trained IT personnel could be mitigated by well-trained health care staff; however, this is not the case, as most staff have reported inadequate amounts of training. According to this study, the amount of HIS managed by each staff ranges from one to six, combining the possibility of suboptimal handling of HIS with existing high workloads [49]. This is similar to studies in Saudi Arabia, Malaysia, and other LMICs [68,69].

Further analysis identified factors associated with the utilization of HIS. However, due to its cross-sectional nature, the study does not allow us to determine the direction or causality of observed relationships between institutional characteristics and HIS adoption. For example, while higher accreditation levels or urban status are associated with higher HIS use, these findings should be interpreted as correlational, not causal. Table 3 indicates that Java Island has a significantly higher number of HIS utilization (>30 information systems) compared to Sumatera, Kalimantan, Sulawesi (central part), and Maluku and Papua (eastern part). This pattern is common in LMICs where the numbers of HIS utilization are strongly influenced by several factors such as human resources, institutional funding, foreign aid, transparency, and prioritization issues [49]. Table 3 also shows the disparities in the numbers and percentages of HIS utilization based on geographical characteristics. In general, urban and rural areas had more HIS utilization than remote areas. The existence of information technology infrastructure remains the main challenge in LMICs, especially in rural and remote areas. These areas often have limited or no internet access, computer availability, and electricity supply [49]. The lack of stable and affordable internet connectivity can be an obstacle in using the HIS for sending and receiving health data effectively [33]. The findings indicate that Puskesmas with slower internet connectivity are making considerable efforts to effectively use the existing HIS. Interestingly, their performance

XSL•FO
RenderX

appears slightly better than that of Puskesmas with more robust internet connectivity. However, it should be noted that the majority of data input in areas with limited internet access is primarily conducted by the DHO.

This study has also evaluated the effectiveness of health care organization accreditation [38]. A previous study shows that accreditation leads to improved quality of care, better strategic planning, enhanced human resource management, stronger leadership, improved archiving, and increased patient satisfaction [38]. Based on our findings, the top level of accreditation status uses more numbers of HIS than the other levels of accreditation (medium and basic).

The human resource and capacity factor plays a vital role in the effectiveness of information systems implementation. This study demonstrates that when Puskesmas provides regular training and facilitates knowledge transfer among staff regarding the HIS, there is a marked increase in the system's utilization. This emphasizes the significance of ongoing education and support in optimizing the advantages of information systems. Like other studies conducted in Ethiopia [38,39], the study findings indicate that the odds of using HIS were significantly higher among primary health care that engaged in regular training and knowledge transfer. This might be due to the fact that health professionals who were trained on HIS had the potential to compile, analyze, and use information generated in the routine day-to-day activities.

Out of the variables that showed no significant difference between the numbers of HIS program input by the Puskesmas staff (1 - 5 staff and ≥6 staff) and the numbers of HIS utilization. This might be due to several factors, such as staff awareness, commitment, and motivation [50]. A study conducted in India underlined that, although the utilization of HIS is contingent upon data analysis skills, organizational factors play a crucial role in the effective application of these skills [40]. Reports also showed that strengthening HIS, focusing not only on technical but also behavioral and organizational structures, is one essential component for improving the quality and use of data for decision-making at all levels of the health system [68].

Strengths and Limitations

The research exhibits several strengths that contribute to its significance in the field. First, it represents the first-ever study of its kind, involving public health centers on a national scale to portray the utilization of HIS. This wide-scale view provides a comprehensive understanding of the current state of HIS implementation in Puskesmas throughout Indonesia. Additionally, beyond the mapping of HIS use, the research highlighted the key challenges faced by field personnel in effectively using HIS, offering insights into potential areas for improvement.

However, certain limitations should be acknowledged. First, while the overall sample size exceeded the national threshold, some provinces (eg, South Sulawesi, East Nusa Tenggara, and Jambi) were significantly underrepresented, limiting generalizability at the provincial level. Second, the cross-sectional nature of the study restricts causal interpretation; relationships observed between institutional characteristics and HIS use should be treated as associative rather than explanatory. Third, as the study relied on self-reported data, it is subject to recall and reporting bias, even though measures were taken to ensure anonymity and standardization. Fourth, the study did not capture qualitative insights from HIS users, which could have provided valuable context around user behavior, system workarounds, and local adaptations. Fifth, while fragmentation of systems was reported, no technical assessment of interoperability, data exchange mechanisms, or governance structures was conducted. Sixth, while basic human resource data were collected (eg, education, training, and HIS load), we were unable to assess the impact of digital workload on staff well-being, task performance, or gender-specific roles. Seventh, although 90% of respondents reported that HIS data supported decision-making, we did not explore how the data were used, by whom, or with what outcomes. Finally, we did not assess the cost-effectiveness or financial sustainability of managing multiple HIS platforms—an area that is especially important for integration planning and national budgeting.

To address these gaps, we recommend that future studies adopt stratified or purposive sampling strategies to ensure adequate representation of undersampled provinces. Longitudinal and mixed method research will be critical to explore causal mechanisms and contextual dynamics of HIS adoption and adaptation. System audits and process evaluations can help validate reported use and assess HIS quality, reliability, and integration performance. Additionally, qualitative interviews with HIS users and implementers—particularly in remote and low-resource settings—can shed light on the lived realities of system implementation and usability. Research on human resource burden, digital competency gaps, and gendered work distribution is also needed to inform equitable capacity building. Finally, economic evaluations and costing studies should be embedded into HIS consolidation efforts to assess long-term sustainability and ensure efficient resource allocation.

Despite these limitations, this baseline study provides critical insights into the HIS landscape in Indonesia and serves as a foundation for evidence-informed policy-making and more effective digital health planning.

Conclusions

HIS play a significant role in supporting policy-making at public health centers, districts or cities, provinces, and the national level. This study, the first of its kind to assess HIS utilization across more than 2600 Puskesmas nationwide, reveals a highly fragmented digital environment, with health centers operating an average of 30 different HIS platforms—many of which are redundant, nonintegrated, and burdensome to manage. The findings highlight challenges in internet connectivity, system usability, workforce digital readiness, and alignment with service delivery needs. Further analysis in this study suggests that geographic location, accreditation level, and training frequency are among the most influential factors in the adoption of information systems.

Policy interventions must consider the diverse operating environments of Puskesmas to avoid one-size-fits-all approaches. Urban Puskesmas, often with stronger infrastructure and digital capacity, are well-positioned to adopt interoperable

XSL•FO
RenderX

dashboards, advanced analytics tools, and integrated HIS platforms aligned with national systems like SATUSEHAT. These centers may also benefit from certification-based training in data analytics and the recruitment of dedicated digital health personnel to enhance system management and interoperability. In contrast, rural and remote Puskesmas operate with limited internet access, power supply, and IT support. For these settings, policy makers should prioritize offline-compatible, simplified HIS that minimizes data entry burdens and operates on low-resource devices, such as mobile phones. Training efforts should focus on basic digital literacy, with peer-to-peer cascading models to enhance local knowledge transfer and sustainability. Infrastructure support, such as solar-powered equipment or network boosters, may also be critical enablers in these areas.

Governance reforms should promote regional coordination, enabling DHOs to provide HIS oversight and technical support, particularly for underserved areas. National initiatives to consolidate and standardize HIS should be complemented with financial and operational feasibility studies to ensure sustainability, especially where overfragmentation currently burdens frontline services.

This baseline study provides a foundational understanding of HIS use and challenges in Indonesia and calls for differentiated, evidence-informed strategies tailored to each health center's digital maturity and contextual needs. Future research should explore HIS interoperability, real-world data use, user experience, and economic impact to guide Indonesia's journey toward a more integrated and equitable digital health ecosystem.

Acknowledgments

The authors would like to thank the Digital Transformation Office Ministry of Health Republic of Indonesia for supporting the study implementation; the Public Health Centers, Districts, and Provincial Health Offices across Indonesia who have participated in the study; and MoH Data and Information Center (Pusdatin), Directorate General of Public Health, Directorate General of Health Care Services who have supported the study implementation.

Data Availability

The datasets generated during or analyzed during this study are available from the corresponding author on reasonable request.

Authors' Contributions

DNA led the study design, built the paper concept, main structure, and methodology. AHS, CAM, and AFL carried out the study and accessed and analyzed the data. DNA, AHS, CAM, and AFL wrote the first draft of the paper. ZK and LM validated the study and critically revised the manuscript content. DNA and AHS had primary responsibility for the final content. All authors read and contributed to reviewing the study data, the manuscript design, and the approval of the final manuscript.

Conflicts of Interest

The authors declare no potential conflicts of interest with respect to the research, authorship, and publication of this paper. While the author is affiliated with Aceso Global Health Consultants Pte Limited, which is a private company, we declare that this research project does not receive funding from Aceso Global Health Consultants. The company does not have a role in the study design, data collection and analysis, decision to publish, or preparation of the manuscript. LM is the director of the company and contributed to this paper on a pro-bono basis. Where authors are identified as personnel of the International Agency for Research on Cancer/WHO, the authors alone are responsible for the views expressed in this article, and they do not necessarily represent the decisions, policy, or views of the International Agency for Research on Cancer/WHO.

References

1. Health information systems and rehabilitation. WHO. 2017. URL: https://tinyurl.com/25nvu34t [accessed 2025-08-20]
2. Kirch W, editor. Encyclopedia of Public Health, 1st edition: Springer Netherlands; 2008.
3. Yazdi-Feyzabadi V, Emami M, Mehrolhassani MH. Health information system in primary health care: the challenges and barriers from local providers' perspective of an area in Iran. Int J Prev Med 2015;6:57. [doi: 10.4103/2008-7802.160056] [Medline: 26236444]
4. World Health Statistics 2010: World Health Organization; 2010. URL: https://www.who.int/docs/default-source/gho-documents/world-health-statistic-reports/en-whs10-full.pdf [accessed 2025-08-25]
5. Bagherian H, Sattari M. Health information system in developing countries: a review on the challenges and causes of success and failure. Med J Islam Repub Iran 2022;36:111. [doi: 10.47176/mjiri.36.111] [Medline: 36447547]
6. Martha S. The analysis of geospatial information for validating some numbers of islands in Indonesia. IJG 2017 Dec 27;49(2):204. [doi: 10.22146/ijg.12792]
7. Population, total. World Bank Group. 2022. URL: https://data.worldbank.org/indicator/SP.POP.TOTL [accessed 2023-08-07]
8. Yodi M, Laksono T, Shita L, Prastuti S, Tiara M, Pandu H, et al. The Republic of Indonesia Health System Review: World Health Organization; 2017, Vol. 7.

XSL•FO
RenderX

9. Ministry of health decree number 46 year 2016: technical guidelines for organizing provincial and district/city health offices. : Indonesia Ministry of Health; 2016. URL: https://peraturan.bpk.go.id/Details/139228/permenkes-no-46-tahun-2015
10. Jumlah Rumah Sakit Umum, Rumah Sakit Khusus, dan Puskesmas (Unit), 2015 [Article in Indonesian]. Central Bureau of Statistics. 2013. URL: https://www.bps.go.id/id/statistics-table/2/MjMyIzI=/jumlah-rumah-sakit-umum-rumah-sakit-khusus-dan-puskesmas.html [accessed 2023-08-02]
11. Jumlah Puskesmas Mencapai 10.260 Unit pada 2021. Data Indonesia. 2022. URL: https://dataindonesia.id/kesehatan/detail/jumlah-puskesmas-mencapai-10260-unit-pada-2021 [accessed 2023-08-02]
12. Indonesia ministry of health decree number 75 year 2014—about the community center health care (puskesmas). : Indonesia Ministry of Health; 2014. URL: https://peraturan.bpk.go.id/details/139202/permenkes-no-75-tahun-2014
13. Operating procedure an health promotion in puskesmas. : Indonesia Ministry of Health; 2013. URL: https://ayosehat.kemkes.go.id/permenkes-no65-tahun-2013-tentang-pedoman-pelaksanaan-dan-pembinaan-pemberdayaan-masyara
14. Indonesia ministry of health decree number 43 year 2019—about the community health centre. : Indonesia Ministry of Health; 2019. URL: https://peraturan.bpk.go.id/Details/138635/permenkes-no-43-tahun-2019
15. Indonesia ministry of health decree number 31 year 2019 about the puskesmas information system. : Indonesia Ministry of Health; 2019. URL: https://peraturan.bpk.go.id/Details/138622/permenkes-no-31-tahun-2019
16. Berutu LK, Nst MAE. Sistem Informasi Pelayanan Kesehatan di Puskesmas Belawan Menggunakan Metode Service Quality Berbasis Web [Article in Indonesian]. Inf Syst J 2020;4(2):158. [doi: 10.22303/infosys.4.2.2020.158-168]
17. Rahmawati MD, Nugroho E. Faktor-faktor yang mempengaruhi keberhasilan implementasi simpus di puskesmas kabupaten sragen [Article in Indonesian]. J Inf Syst Public Health 2020 Nov 16;2(3):1. [doi: 10.22146/jisph.33146]
18. Juddoo S, George C, Duquenoy P, Windridge D. Data governance in the health industry: investigating data quality dimensions within a big data context. ASI 2018 Nov 1;1(4):43. [doi: 10.3390/asi1040043]
19. Wang J, Liu Y, Li P, Lin Z, Sindakis S, Aggarwal S. Overview of data quality: examining the dimensions, antecedents, and impacts of data quality. J Knowl Econ 2023 Feb 10:1-20. [doi: 10.1007/s13132-022-01096-6] [Medline: 40479478]
20. Hassenstein MJ, Vanella P. Data quality—concepts and problems. Encyclopedia 2022 Feb 14;2(1):498-510. [doi: 10.3390/encyclopedia2010032]
21. Idaiani S, Hendarwan H, Herawati MH. Disparities of health program information systems in Indonesia: a cross-sectional Indonesian health facility research 2019. Int J Environ Res Public Health 2023 Mar 1;20(5):4384. [doi: 10.3390/ijerph20054384] [Medline: 36901393]
22. Pertiwi F, Masudin I, Zulfikarijah F, Restuputri DP, Setiawan M. Technology acceptance model of tuberculosis integrated information system in Indonesian primary healthcare. Cogent Public Health 2022 Dec 31;9(1). [doi: 10.1080/27707571.2022.2151929]
23. Aisyah DN, Utami A, Rahman FM, et al. Using an electronic immunization registry (Aplikasi Sehat IndonesiaKu) in Indonesia: cross-sectional study. Interact J Med Res 2025 Mar 27;14:e53849. [doi: 10.2196/53849] [Medline: 40146988]
24. Hasyim H, Firdaus F, Prabawa A, et al. Potential for a web-based management information system to improve malaria control: an exploratory study in the Lahat District, South Sumatra Province, Indonesia. PLOS One 2020;15(6):e0229838. [doi: 10.1371/journal.pone.0229838] [Medline: 32516344]
25. Juliansyah R, Aqid BM, Salsabila AP, Nurfiyani K. Implementation of EMR system in indonesian health facilities: benefits and constraints. arXiv. Preprint posted online on Oct 16, 2024. [doi: 10.48550/arXiv.2410.12226]
26. Nathan DS, Rostiaty E. An analysis study on the effect of the use of electronic medical records on the effectiveness and efficiency of services at public health centers (Puskesmas) in Indonesia: a systematic review. Int J Med Sci Health 2024;5(7):20-34. [doi: 10.70070/zphqxk59]
27. Amalia N, Rustam MZA, Rosarini A, Wijayanti DR, Riestiyowati MA. The implementation of electronic medical record (EMR) in the development health care system in Indonesia. IJALSR 2021 Jul 21;4(3):8-12. [doi: 10.31632/ijalsr.2021.v04i03.002]
28. Erwina W. Iber kasehatan in sukamiskin: utilisation of the plural health information & communication system in the sunda region of west java, indonesia [iber kasehatan in sukamiskin: utilisation of the plural health information & communication system in the sunda region of west java, indonesia]. : Universiteit Leiden; 2019 URL: https://scholarlypublications.universiteitleiden.nl/access/item%3A2909431/view [accessed 2024-01-04]
29. Hanafi ST, Panjaitan WU, Ramadhan AR, Purba SH. Penerapan sistem informasi kesehatan di puskesmas di Indonesia [Article in Indonesian]. Sagita Acad J 2025;3(1):19-23. [doi: 10.61579/sagita.v3i1.333]
30. Slovin calculator. Globalstatistik Academic. URL: https://www.globalstatistik.com/kalkulator-statistik/ [accessed 2022-01-10]
31. Aqil A, Lippeveld T, Hozumi D. PRISM framework: a paradigm shift for designing, strengthening and evaluating routine health information systems. Health Policy Plan 2009 May;24(3):217-228. [doi: 10.1093/heapol/czp010] [Medline: 19304786]
32. Pedoman dan standar etik penelitian dan pengembangan kesehatan nasional 2021 [guidelines and ethical standards for national health research and development 2021]. Indonesia Ministry of Health. URL: https://tinyurl.com/2vuef4zh [accessed 2025-08-20]
33. Pedoman dan standar etik penelitian dan pengembangan kesehatan nasional [Ethical guidelines and standards for national health research and development]. Indonesia Ministry of Health. URL: https://kepk.poltekkestasikmalaya.ac.id/wp-content/uploads/2018/05/2017-KEPPKN-Standar-dan-Pedoman-.pdf [accessed 2025-08-20]

XSL•FO
RenderX

34. Chanyalew MA, Yitayal M, Atnafu A, Tilahun B. Routine health information system utilization for evidence-based decision making in Amhara national regional state, northwest Ethiopia: a multi-level analysis. BMC Med Inform Decis Mak 2021 Jan 26;21(1):28. [doi: 10.1186/s12911-021-01400-5] [Medline: 33499838]
35. Mutale W, Chintu N, Amoroso C, et al. Improving health information systems for decision making across five sub-Saharan African countries: implementation strategies from the African Health Initiative. BMC Health Serv Res 2013;13 Suppl 2(Suppl 2):S9. [doi: 10.1186/1472-6963-13-S2-S9] [Medline: 23819699]
36. Johnson III RJ. A comprehensive review of an electronic health record system soon to assume market ascendancy: EPIC®. J Healthcare Commun 2016;01(4). [doi: 10.4172/2472-1654.100036]
37. Irmawati S, Rosdianah R, Mahendika D, Bakri AA. The role of health information systems to enhance health services in remote and underserved areas: challenges and solutions. Jurnal eduhealth 2023 Jun 3;14(2808-4608):713-719 [FREE Full text]
38. El-Jardali F, Hemadeh R, Jaafar M, et al. The impact of accreditation of primary healthcare centers: successes, challenges and policy implications as perceived by healthcare providers and directors in Lebanon. BMC Health Serv Res 2014 Feb 25;14:86. [doi: 10.1186/1472-6963-14-86] [Medline: 24568632]
39. Shiferaw AM, Zegeye DT, Assefa S, Yenit MK. Routine health information system utilization and factors associated thereof among health workers at government health institutions in East Gojjam Zone, Northwest Ethiopia. BMC Med Inform Decis Mak 2017 Aug 7;17(1):116. [doi: 10.1186/s12911-017-0509-2] [Medline: 28784115]
40. Mesfin A. Health policy and the extent of health information use in the Woreda health care system of Arsi zone, Oromia region, Ethiopia. : Addis Ababa University; 2011.
41. Krishnan A, Nongkynrih B, Yadav K, Singh S, Gupta V. Evaluation of computerized health management information system for primary health care in rural India. BMC Health Serv Res 2010 Nov 16;10(1):310. [doi: 10.1186/1472-6963-10-310] [Medline: 21078203]
42. Strengthening health information systems in low- and middle-income countries: a model to frame what we know and what we need to learn. : USAID, Measure evaluation; 2017. URL: https://www.measureevaluation.org/resources/publications/tr-17-156/at_download/document
43. Blue Print of Digital Health Transformation Strategy: Ministry of Health; 2024.
44. Wahid F, Dirgahayu RT, Hamzah A, Setiaji H. When more is less: the case of disconnected information systems in Indonesian public health facilities. IOP Conf Ser: Mater Sci Eng 2018 Mar 1;325:012017. [doi: 10.1088/1757-899X/325/1/012017]
45. Siyam A, Ir P, York D, et al. The burden of recording and reporting health data in primary health care facilities in five low- and lower-middle income countries. BMC Health Serv Res 2021 Sep 13;21(Suppl 1):691. [doi: 10.1186/s12913-021-06652-5] [Medline: 34511083]
46. Tooranloo HS, SS AAS. Evaluation of failure causes in employing hospital information systems. J Syst Manage 2021;6(3):31-76. [doi: 10.30495/jsm.2021.678894]
47. Thomas JC. Contextual factors affecting health information system strengthening. Global Public Health 2017 Dec;12(12):1568-1578. [doi: 10.1080/17441692.2016.1256419] [Medline: 27841079]
48. Ebnehoseini Z, Tabesh H, Deldar K, Mostafavi SM, Tara M. Determining the hospital information system (HIS) success rate: development of a new instrument and case study. Open Access Maced J Med Sci 2019 May 15;7(9):1407-1414. [doi: 10.3889/oamjms.2019.294] [Medline: 31198444]
49. Afrizal SH, Handayani PW, Hidayanto AN, Eryando T, Budiharsana M, Martha E. Barriers and challenges to primary health care information system (PHCIS) adoption from health management perspective: a qualitative study. Inf Med Unlocked 2019;17:100198. [doi: 10.1016/j.imu.2019.100198]
50. deRiel E, Puttkammer N, Hyppolite N, et al. Success factors for implementing and sustaining a mature electronic medical record in a low-resource setting: a case study of iSanté in Haiti. Health Policy Plan 2018 Mar 1;33(2):237-246. [doi: 10.1093/heapol/czx171]
51. A Study of the Impact of Health Information Quality on Care Delivery Quality and Satisfaction from the Care Provider's Perspective: University of Texas; 2017.
52. Middleton B, Bloomrosen M, Dente MA, et al. Enhancing patient safety and quality of care by improving the usability of electronic health record systems: recommendations from AMIA. J Am Med Inform Assoc 2013 Jun;20(e1):e2-e8. [doi: 10.1136/amiajnl-2012-001458] [Medline: 23355463]
53. Lowry SZ, Ramaiah M, Taylor S, Patterson ES, Spickard Prettyman S, Simmons D, et al. Technical Evaluation, Testing, and Validation of the Usability of Electronic Health Records: Empirically Based Use Cases for Validating Safety-Enhanced Usability and Guidelines for Standardization: National Institute of Standards and Technology; 2015.
54. Bevan N. International standards for usability should be more widely used. J Usability Stud 2009;4(3):106-113 [FREE Full text]
55. Kuqi K, Eveleigh T, Holzer T, Sarkani S, Levin JE, Crowley RS. Design of electronic medical record user interfaces: a matrix-based method for improving usability. J Healthcare Eng 2013;4(3):427-452. [doi: 10.1260/2040-2295.4.3.427] [Medline: 23965597]
56. Angela N, Adisasmito WBB. CPOE in reducing medication error: a narrative review. Jurnal ARSI 2019;5:137-146 [FREE Full text]

XSL•FO
RenderX

57. Agustina R, Dartanto T, Sitompul R, et al. Universal health coverage in Indonesia: concept, progress, and challenges. Lancet 2019 Jan;393(10166):75-102. [doi: 10.1016/S0140-6736(18)31647-7]
58. Atashi A, Khajouei R, Azizi A, Dadashi A. User interface problems of a nationwide inpatient information system: a heuristic evaluation. Appl Clin Inform 2016;7(1):89-100. [doi: 10.4338/ACI-2015-07-RA-0086] [Medline: 27081409]
59. Al Knawy B, McKillop MM, Abduljawad J, et al. Successfully implementing digital health to ensure future global health security during pandemics: a consensus statement. JAMA Netw Open 2022 Feb 1;5(2):e220214. [doi: 10.1001/jamanetworkopen.2022.0214] [Medline: 35195701]
60. Helminski D, Kurlander JE, Renji AD, et al. Dashboards in health care settings: protocol for a scoping review. JMIR Res Protoc 2022 Mar 2;11(3):e34894. [doi: 10.2196/34894] [Medline: 35234650]
61. Ahanhanzo YG, Ouedraogo LT, Kpozèhouen A, Coppieters Y, Makoutodé M, Wilmet-Dramaix M. Factors associated with data quality in the routine health information system of Benin. Arch Public Health 2014;72(1):25. [doi: 10.1186/2049-3258-72-25] [Medline: 25114792]
62. Nutley T, Reynolds HW. Improving the use of health data for health system strengthening. Global Health Action 2013 Feb 13;6(1):20001. [doi: 10.3402/gha.v6i0.20001] [Medline: 23406921]
63. Health analytical profile 2016 cameroon. : Ministry of Public Health (MOPH); 2016. URL: https://www.afro.who.int/publications/health-analytical-profile-cameroon-2016
64. Gemiharto I, Priyadarshani HEN. The challenges of the digital divide in the online learning process during the COVID-19 pandemic in Indonesia. Ilomata Int J Manage 2022 Feb;3(1):343-356. [doi: 10.52728/ijjm.v3i1.426]
65. Yoshiura VT, de Azevedo-Marques JM, Rzewuska M, et al. A web-based information system for a regional public mental healthcare service network in Brazil. Int J Ment Health Syst 2017;11(1):1. [doi: 10.1186/s13033-016-0117-z] [Medline: 28053659]
66. Odekunle FF, Odekunle RO, Shankar S. Why sub-Saharan Africa lags in electronic health record adoption and possible strategies to increase its adoption in this region. Int J Health Sci (Qassim) 2017;11(4):59-64. [Medline: 29085270]
67. Sukums F, Mensah N, Mpembeni R, et al. Promising adoption of an electronic clinical decision support system for antenatal and intrapartum care in rural primary healthcare facilities in sub-Saharan Africa: the QUALMAT experience. Int J Med Inform 2015 Sep;84(9):647-657. [doi: 10.1016/j.ijmedinf.2015.05.002] [Medline: 26073076]
68. Alqahtani A. Barriers to the adoption of EHR systems in the Kingdom of Saudi Arabia: an exploratory study using a systematic literature review. Health Informatics J 2017 Jul;11(2) [FREE Full text]
69. ChePa N, Jasin NM, Bakar NAA. How change management can prevent the failure of information systems implementation among malaysian government hospitals? Presented at: The 2nd International Conference on Applied Science and Technology 2017 (ICAST'17); Oct 3, 2017; Kedah, Malaysia p. 020037. [doi: 10.1063/1.5005370]

Abbreviations

DHO: district health office
HIS: health information systems
LMIC: low- and middle-income country
OR: odds ratio
PRISM: Performance of Routine Information Systems Management
WHO: World Health Organization

Edited by C Perrin; submitted 11.11.24; peer-reviewed by N Kamonroek, N Scphub, S Sujarwoto; revised version received 16.07.25; accepted 17.07.25; published 03.09.25.

Please cite as:
Aisyah DN, Setiawan AH, Mayadewi CA, Lokopessy AF, Kozlakidis Z, Manikam L
Understanding Health Information Systems Utilization Across Public Health Centers in Indonesia: Cross-Sectional Study
JMIR Med Inform 2025;13:e68613
URL: https://medinform.jmir.org/2025/1/e68613
doi:10.2196/68613

© Dewi Nur Aisyah, Agus Heri Setiawan, Chyntia Aryanti Mayadewi, Alfiano Fawwaz Lokopessy, Zisis Kozlakidis, Logan Manikam. Originally published in JMIR Medical Informatics (https://medinform.jmir.org), 3.9.2025. This is an open-access article distributed under the terms of the Creative Commons Attribution License (https://creativecommons.org/licenses/by/4.0/), which permits unrestricted use, distribution, and reproduction in any medium, provided the original work, first published in JMIR Medical Informatics, is properly cited. The complete bibliographic information, a link to the original publication on https://medinform.jmir.org/, as well as this copyright and license information must be included.

XSL•FO
RenderX

Nurses' Experience Regarding Barriers to Providing Internet Plus Continuous Nursing: Mixed Methods Study

Huanhuan Huang[1,2], PhD; Zhiyu Chen[3], PhD; Lijuan Chen[1,2], BSN; Xingyao Du[1,2], BSN; Qi Huang[4], BSc; Wenbi Jia[2], BSN; Qinghua Zhao[1,2], BSN

[1]Department of Nursing, The First Affiliated Hospital of Chongqing Medical University, 1st Youyi Road, Chongqing, China

[2]Nursing Research Centre, The First Affiliated Hospital of Chongqing Medical University, Chongqing, China

[3]Department of Orthopedics, The First Affiliated Hospital of Chongqing Medical University, Chongqing, China

[4]School of Public Health, Chongqing Medical University, Chongqing, China

Corresponding Author:
Qinghua Zhao, BSN
Department of Nursing, The First Affiliated Hospital of Chongqing Medical University, 1st Youyi Road, Chongqing, China

Abstract

Background: The novel medical model of "Internet Plus continuous nursing" has received much attention under the dual background of aging and digitalization in China. However, there is a scarcity of studies that report on the potential barriers and challenges associated with the implementation of this practice.

Objective: This study aimed to investigate and understand nurses' experience regarding barriers to providing Internet Plus continuous nursing.

Methods: A sequential mixed methods design was adopted. In the first phase, a self-made questionnaire was used to quantify the barriers and challenges into 3 domains: management, relational, and information continuity. In the second phase, nurses who participated in the Internet Plus continuous nursing program were invited to attend semistructured interviews to further explore, explain, and understand the complexities behind these data, obtaining more detailed information on participants' experiences, perspectives, and meanings.

Results: A total of 4638 participants from 312 hospitals were selected for the final analysis; the adjusted mean score of the survey was 3.49 (SD 0.83). Among the 3 domains, management continuity had the lowest score (mean 3.32, SD 0.97), followed by relational continuity (mean 3.44, SD 0.9) and information continuity (mean 3.62, SD 0.92). The results of the multivariable analysis showed that age, education level, and a greater number of working years were predictors of continuity for Internet Plus continuous nursing (P<.001). Following the qualitive study, 8 subthemes emerged from 72 initial codes and were grouped into 3 themes: organizational changes, practice changes, and future directions.

Conclusions: This mixed methods study revealed that Chinese nurses may have differential challenges when providing Internet Plus continuous nursing, particularly in management continuity. To better benefit patients and improve health care delivery, health care organizations and policymakers should implement strategies to improve interdisciplinary relationships, establish and perfect organizational management, and enhance communication.

(JMIR Med Inform 2025;13:e65445) doi:10.2196/65445

KEYWORDS

transitional care; digital governance; influencing factors; barrier; nursing; mixed methods study; internet; digitalization; China; digital health; self-made questionnaire; interview; Chinese nurses; health care delivery; policymakers; communication; care quality; patient satisfaction

Introduction

Continuous nursing refers to a comprehensive approach to providing uninterrupted care and attention to patients in health care settings [1], combining the continuation of nursing services and time and health services [2]. As a part of overall care and as a core element of high-quality primary care, continuous nursing has been shown to reduce mortality rates and health costs, improve patient satisfaction, and enhance overall health care outcomes [3-5]. However, the traditional continuous nursing model still suffers from some drawbacks and does not comprehensively satisfy the complicated care needs of patients.

With the rapid development of mobile technology and the widespread use of mobile phones and the internet, the traditional continuous nursing model has slowly shifted to what is termed "Internet Plus continuous nursing," which has gained significant attention. Particularly, the outbreak of the COVID-19 pandemic has reminded the health care system of the importance of

XSL•FO
RenderX

creating new strategies, using traditional approaches alongside information technologies [6]. Internet Plus continuous nursing represents a paradigm shift in health care delivery [7], referring to the integration of internet technology with continuous nursing care or monitoring [8]. This approach aims to build a connection between health care providers and patients by leveraging the power of the internet to facilitate real-time monitoring, communication, and data sharing. Health care professionals can thus remotely monitor patients' vital signs, provide guidance, offer medication reminders, and deliver personalized care plans [9,10]. In addition, the novel model could also streamline clinical workflows [11], enhance patient engagement [12], and facilitate knowledge sharing [13]. The Chinese government and industry attach great importance to the development of this work and have introduced multiple policies to provide further guidance, such as the National Nursing Development Plan (2021 - 2025) [14] and the Action Plan for Further Improvement of Care Services (2023 - 2025) [15]. Driven by strong policy support, the initiative has garnered widespread attention from health care institutions and the public.

However, Internet Plus continuous nursing is still in the pilot stage in China and primarily targets key populations such as discharged patients, maternal and infant groups, and patients with chronic diseases [15]. For example, data from one Chinese province revealed that 85.45% of hospitals have yet to adopt "Internet Plus nursing services," despite 97.87% of nurses expressing a willingness to participate [16]. Only 14.55% of nurses are currently engaged in such services within their hospitals. Even among hospitals that have implemented these programs, gaps persist between service offerings (eg, scope, scheduling, continuity) and actual market demand [17].

Although prior research has examined the factors influencing nursing care continuity [18,19], few have specifically examined Internet Plus continuous nursing. Existing research has investigated nurse willingness and program effectiveness [20,21], yet there is a critical gap in understanding the implementation barriers and challenges, particularly in primary hospitals, where logistical and resource constraints may amplify these issues. Identifying these barriers from the perspective of participating nurses is essential not only for preparedness but also for improving service quality.

Therefore, the aim of this mixed methods study is to investigate the factors influencing the implementation of Internet Plus continuous nursing across primary, secondary, and tertiary hospitals, with a specific focus on barriers. The findings of this study will provide valuable insights for policymakers, health care administrators, and nursing practitioners, enabling them to develop strategies and interventions that can strengthen the continuity of care in the digital era.

Methods

Ethical Considerations

Ethics approval was obtained from the First Affiliated Hospital of Chongqing Medical University's research ethics committee (2023-34). All procedures complied with the Declaration of Helsinki.

Written informed consent was obtained from all participants prior to their involvement in the study. For online interviewees, verbal consent was obtained and documented. Participants were explicitly informed of their right to withdraw from the study at any time without penalty. No secondary data analysis was conducted in this study.

All collected data were deidentified prior to analysis. Personal identifiers were removed and replaced with coded numbers to protect participant confidentiality. Electronic data were stored on password-protected servers with access restricted to the research team.

Participants did not receive financial compensation for their involvement in this study. However, they were provided with the study results upon request and had access to any potential benefits emerging from the research findings.

Quantitative Study

Participants

Participants were convenience sampled from January 2021 to March 2021 in Chongqing, China. The inclusion criteria were: (1) nurses directly involved in Internet Plus continuous nursing services, (2) who had over 1 year of experience and (3) provided informed consent and were willing to participate. The exclusion criteria were: (1) visiting nurses who were not affiliated to the hospital and (2) nurses who were on vacation during data collection.

Measurement Tools

A 14-item questionnaire specifically tailored to health care professionals was developed based on the Continuity of Care model [22], with reference to patient-reported measures [23,24]. The questionnaire was constructed using the Delphi method (Multimedia Appendix 1), demonstrating strong expert consensus with authoritative coefficients (Cr) of 0.85 and 0.91 for the 2 rounds, respectively. The instrument comprises 3 domains, namely relational (5 items; Cronbach coefficient=0.832), information (3 items; Cronbach coefficient=0.865), and management (6 items; Cronbach coefficient=0.840) continuity, with a good content validity index (0.96) and an overall Cronbach coefficient of 0.871. Each item was scored from 1 ("Rarely") to 5 ("Always") on a 5-point Likert scale; higher scores reflect higher quality and efficiency of implementation of Internet Plus continuous nursing.

Data Collection

The questionnaire was distributed to hospitals through an online survey tool, Wenjuanxing [25], by the Chongqing Hospital Association. The hospital manager then sent the link to Internet Plus continuous nursing–related health care providers. On the first page of the questionnaire, the objective, process, and anonymization of data were introduced in detail. Individuals who received the link were also requested to provide informed consent. In addition, only those who clicked "accept" had access to the full questionnaire.

Statistical Analysis

The software SPSS version 26.0 (IBM Corporation) was used for analysis, the measurement of normal distribution data were

XSL•FO
RenderX

described by means and SDs, and 2-tailed independent sample *t* tests were used for comparison between groups. The count data were represented by the use case (%), and a chi-square test was used for the comparison between groups. The test level was bilateral (α=.05).

Qualitative Study

Participants

Participants (referred to as as P1, P2, and so on, up to P15) were selected using purposive and snowball sampling methods. The inclusion and exclusion criteria were the same as those for the quantitative study. To meet the maximum variation, the level, setting, and Internet Plus continuous nursing experience of the hospital were taken into account. Recruitment ceased once theoretical saturation was reached (ie, when no new codes and themes emerged from the data) [26]. Finally, a total of 15 participants were recruited (Table 1).

Table . Demographic information of participants in the qualitative study.

	Level of hospital	Age (years), n	Professional title	Working years, n
P1	Tertiary	49	Vice-senior	27
P2	Tertiary	32	Senior	31
P3	Tertiary	46	Vice-senior	27
P4	Secondary	48	Vice-senior	30
P5	Secondary	55	Vice-senior	32
P6	Secondary	47	Vice-senior	29
P7	Secondary	52	Middle	29
P8	Secondary	49	Middle	27
P9	Secondary	48	Middle	26
P10	Primary	47	Vice-senior	27
P11	Primary	50	Middle	29
P12	Primary	53	Middle	31
P13	Primary	48	Primary	28
P14	Primary	56	Vice-senior	36
P15	Primary	52	Middle	32

Interview Outline

The intention of holding interviews was to further explore, explain, and understand the complexities behind these data, obtaining more detailed information on participants' experiences, perspectives, and meanings. An interview outline containing 4 questions was used to structure the interview (Table 2). The outline was formed through literature review [27,28] and the quantitative study results, and pilot-tested with 4 participants to ensure the quality and feasibility.

Table . Interview outline.

Interview guideline	Detailed inquiry
Please provide a brief introduction to the current development of Internet Plus continuous nursing services at your esteemed institution.	1. What was the driving force behind the initiation of this endeavor? 2. Why was it not implemented? What challenges were faced?
As an implementer, what obstacles do you think have been encountered during the process?	1. Could you share your views on "information continuity"? 2. Could you share your views on "organizational continuity"? 3. Could you share your views on "management continuity"?
As an implementer, what factors do you think have facilitated the process?	1. In your opinion, how should these facilitating factors be implemented?
What advice would you give to organizations that have not yet implemented Internet Plus continuous nursing services?	—[a]

[a]Not applicable.

Data Collection

Descriptive qualitative research methods were applied and data were collected through semistructured interviews. Each interview was conducted by the first and second authors, who have both received qualitative research training and have experience interviewing. Due to the impact of the pandemic, interviews were conducted using a combination of online (n=5)

XSL•FO
RenderX

and offline (n=10) approaches. Prior to the interviews, the purpose, content, and methods of the study were communicated to the participants. For all interviewees, informed consent was obtained from before the interviews commenced. A quiet and independent space was chosen and sufficient time was provided for the interviews. Similarly, online interviews were scheduled based on a mutually agreed upon time, and participants were advised to select a quiet environment in an independent space and were provided with ample time. The online interviews were conducted via WeChat video calls, and video recordings were taken after obtaining informed consent from the interviewees. Throughout the interviews, a neutral stance was maintained by the interviewers, encouraging the participants to express themselves fully. When necessary, their viewpoints were clarified and confirmed. Note-taking and audio recording were performed during all interviews.

Statistical Analysis

A qualitative content analysis was used [29], comprising several rigorous steps:

1. Data processing: 2 researchers independently transcribed the raw data and generated initial codes. A third researcher verified the coding consistency and accuracy. The team discussed discrepancies until a full consensus was reached.
2. Thematic development: a researcher conducted higher-level analysis by synthesizing codes into meaningful categories and identifying emerging themes through iterative comparison [30]. Data collection continued until theoretical saturation was achieved (ie, no new codes emerged after 3 consecutive interviews and established themes demonstrated sufficient depth and variation) [26].
3. Validation procedures: all research team members participated in regular peer debriefings to compare interpretations of themes and subthemes and resolve any analytical disagreements through discussion. Member checking was implemented by sharing interview summaries with participants and incorporating their feedback to ensure the accurate representation of experiences [31].

Results

Quantitative Study

Overall, a total of 4911 health care providers from 312 institutions received the questionnaire, while only 4638 were selected for the final analysis (response rate=94.44%); 98 were excluded according to the inclusion and exclusion criteria, 135 were excluded for incomplete answers, and, to control quality, 40 were excluded for response times outside the 5th-95th percentile range.

As shown in Table 3, respondents were predominantly from tertiary hospitals (n=2630, 56.71%) or secondary hospitals (n=1883, 40.60%), and most were female (n=4505, 97.13%). The largest age group was 26 - 35 years (n=2750, 59.29%). Notably, older participants (≥46 years) accounted for 6.81% (n=316) but had the highest continuity scores (mean 91.0, SD 10.9). Most held an undergraduate degree (n=3386, 73.01%), while only 0.52% (n=24) had received graduate-level education. Job titles were primarily primary-level (n=2768, 59.68%), and the majority had 5 - 9 years of work experience (n=2679, 57.76%). Those with ≥10 years of experience (n=1039, 22.40%) reported significantly higher continuity scores (mean 84.1, SD 11.5).

XSL•FO
RenderX

Table . Demographic characteristics and multivariable analysis.

Variables	Participants, n (%)	Continuity score, mean (SD)	Coefficient (multivariable)	
			β (95% CI)	*P* value
Hospital level				
Primary	125 (2.70)	74.8 (10.7)	Reference	—[a]
Secondary	1883 (40.60)	76.1 (11.2)	0.76 (–1.21 to 2.73)	.45
Tertiary	2630 (56.71)	77.6 (12.3)	1.73 (–0.22 to 3.69)	.08
Sex				
Male	133 (2.87)	76.5 (11.9)	Reference	—
Female	4505 (97.13)	76.9 (11.9)	–1.70 (–3.59 to 0.19)	.08
Age (years)				
<25	670 (14.45)	91.0 (10.9)	Reference	—
26 - 35	2750 (59.29)	72.5 (10.6)	16.39 (14.05 to 18.74)	<.001
36 - 45	902 (19.45)	75.0 (11.1)	–14.81 (–16.78 to –12.84)	<.001
≥46	316 (6.81)	81.4 (10.5)	–9.47 (–11.09 to –7.85)	<.001
Education level				
College and below	1228 (26.48)	76.3 (12.5)	Reference	—
Undergraduate	3386 (73.01)	77.2 (11.6)	–1.12 (–1.96 to –0.29)	.008
Graduate	24 (0.52)	72.8 (11.4)	–6.38 (–10.81 to –1.94)	.005
Job title				
Primary	2768 (59.68)	74.8 (11.4)	Reference	—
Middle	1497 (32.28)	78.6 (11.5)	–0.36 (–1.20 to 0.47)	.40
Advanced	373 (8.04)	86.0 (11.6)	–1.64 (–3.32 to 0.05)	.05
Working years				
≤2	365 (7.87)	72.6 (10.7)	Reference	—
2~4	555 (11.97)	72.8 (11.3)	–0.15 (–1.65 to 1.35)	.85
5~9	2679 (57.76)	75.6 (11.1)	1.94 (0.30 to 3.59)	.02
≥10	1039 (22.40)	84.1 (11.5)	3.94 (1.88 to 6.00)	<.001

[a]Not applicable.

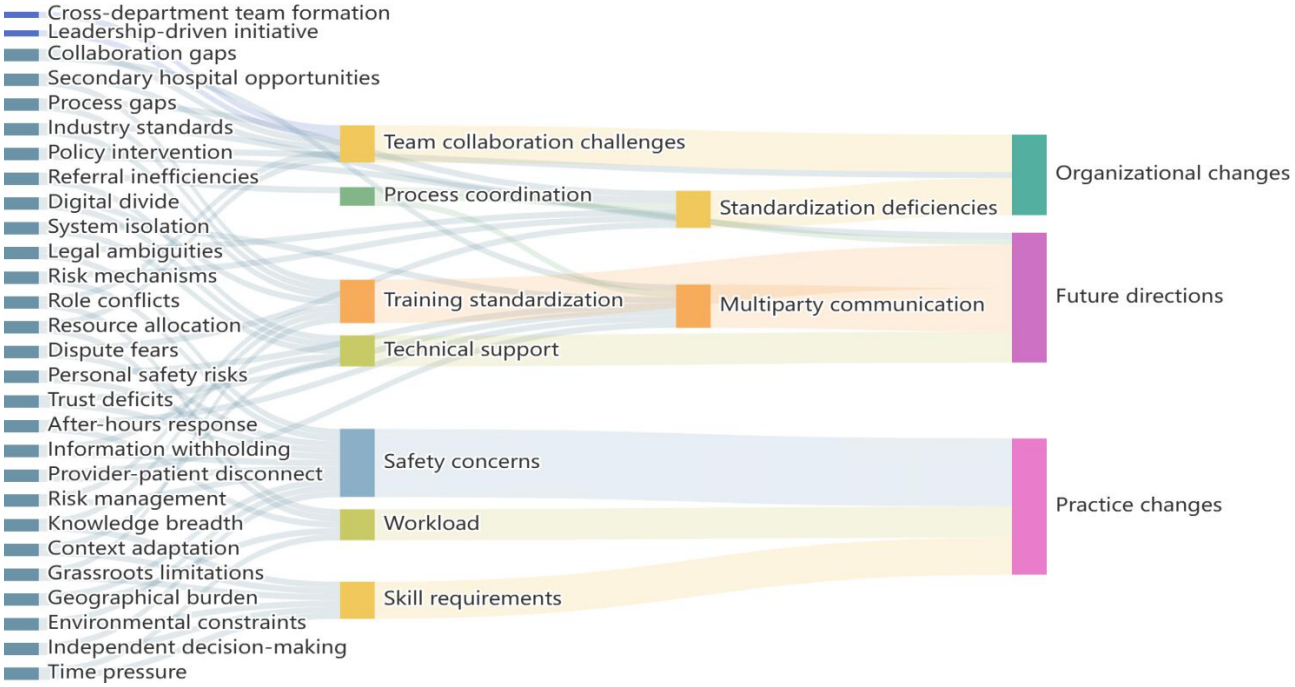
Among the continuity domains, the information domain scored highest (mean 3.62, SD 0.92), followed by the relational domain (mean 3.44, SD 0.90) and management domain (mean 3.32, SD 0.97). The overall mean continuity score was 3.49 (SD 0.83), indicating moderate-to-high levels of perceived continuity. The results of multivariable analysis showed that age, education level, and a greater number of working years were predictors of continuity for Internet Plus continuous nursing (P<.05).

Qualitative Study

The initial open coding identified 72 initial codes (eg, “Process gaps,” “Legal ambiguities”), which were then clustered into 8 subthemes (eg, “Team collaboration challenges,” “Safety concerns”). After verification by team members, these were consolidated into 3 final themes, as illustrated in Figure 1.

XSL•FO
RenderX

Figure 1. Three-level coding framework for Internet Plus continuity care. Data were derived from the qualitative analysis of 15 health care providers.



Theme 1: Organizational Changes

Team Collaboration Challenges

Participants reported significant difficulties in establishing and sustaining interdisciplinary teams for Internet Plus continuity care, citing role ambiguity, resource disparities, and institutional resistance. P11 described the lack of structured team development: “We assembled staff from different departments overnight without clear role assignments. This meant starting everything from scratch.” The absence of transitional frameworks exacerbated role confusion, particularly in lower-resource settings. P13 emphasized disparities in institutional capacity: “How can we match tertiary hospitals? Our IT team consists of only 1.5 full-time staff maintaining basic systems.” Functional teamwork remained elusive even when teams were formally established. P4 noted systemic neglect: “The IT department never attends our meetings. When systems fail, we are told, ‘This is not a priority.’”

Standardization Deficiencies

Participants across all hospital tiers identified critical gaps in clinical protocols, legal safeguards, and financial sustainability, which collectively hindered Internet Plus continuity care implementation. Tertiary hospitals developed internal protocols, but these were rarely adopted by primary or secondary institutions. P3 stated, “We created our own post-discharge monitoring checklist, but it is ineffective if community clinics do not use it.” P2 raised critical questions about accountability: “If a patient deteriorates after a virtual consultation, who is responsible—the platform, the nurse, or the hospital? Without clear liability frameworks, many nurses as well as patients hesitate to engage fully.” Variability in care quality was another challenge, particularly in resource-limited settings. P12 noted, “Our rural patients expect hospital-level care at home, but with no training protocols, outcomes vary wildly.” Financial sustainability emerged as a major barrier too. Over 80% (12/15) of participants reported providing Internet Plus continuity care as an uncompensated service due to unclear reimbursement policies. P15 contrasted this with privatized models: “Affluent urban hospitals charge fees through third-party apps, but our rural patients cannot afford to pay. Shouldn’t the government subsidize this essential service?”

Theme 2: Practice Changes

Workload

The expansion of Internet Plus continuous nursing extends the reach of nursing services, enhancing patient care accessibility. However, in settings with existing nursing shortages, clinical staff face increased workloads due to additional responsibilities, training demands, and after-hours patient interactions. Nurses must balance traditional duties with Internet Plus continuous nursing tasks, leading to role overload. Most institutions lack specialized roles for this project, forcing existing nurses to absorb extra tasks. P1 stated, “After joining the team, I not only need to deal with the previous affairs, but also need to spend extra personal time to study and attend training, which increases the workload virtually.” Patients often seek support outside standard working hours, contributing to burnout. “The frequency of overtime work is higher, because some patients may contact you after work hours” (P15). Home visits for remote patients also add physical and logistical strain. “Some patients live in a faraway address, travel a long way, one after another cause people are also very tired” (P4).

Safety Concerns

In interviews, participants reported a wide range of worries and insecurities. First and foremost was the safety of medical staff. P7 stated, “At the beginning, I was very worried about going to a strange family to provide services, afraid of accidents,” and P9 added, “I prefer to interact with discharged patients who I manage, and we know each other better. For strange orders, I will have some concerns, so before the service is carried out, I

XSL•FO
RenderX

will generally communicate well in advance." Secondly, some respondents reported their own practice safety: "Some family environments have restrictions, lack of necessary space, equipment or drugs, and sometimes I even have no suitable place to carry out operations" (P10) and "I am very worried that some patients and their families do not take the initiative to report the history of allergy and infection because of their own reasons, which is very dangerous for patients and myself" (P14). Finally, some respondents cited concerns about medical disputes: "Although it hasn't happened yet, I hope it never will... What should I do in the event of a patient's death or medical malpractice?" (P6).

Skill Requirements

Implementing Internet Plus continuity services requires a higher level of competence from health care professionals, but in practice, most providers still report having their own challenges. Nurses often face questions or requests outside their specialization, requiring ad hoc problem-solving without immediate support. "This is not an individual case, when you provide a specialized service, the patient or family may 'politely' ask you some other questions, which may be beyond your expertise," stated P3. Unlike hospital settings, Internet Plus continuous nursing sometimes requires solo decision-making with a few colleagues or specialists for consultation. "This is very different from the hospital scene, you know that your teammates are around you, but at this time, you may be alone" (P11). Older or rural patients struggle with technology, forcing nurses to double as tech support. P13 noted, "Half my visit time is spent teaching older patients how to use the app. They forget by the next week, and we start over."

Theme 3: Future Directions

Multiparty Communication

Participants observed in their clinical practice that Internet Plus continuous nursing involves multiple stakeholders, and that there is a need to strengthen communication to ensure the smooth implementation of services. Patients often distrust community hospitals' capabilities, viewing them as limited to basic services (eg, health education), while overestimating tertiary hospitals' roles in continuous care. P3 suggested that "If community clinics adopt our monitoring tools, patients would see them as equal partners in care." Nurses reported inefficiencies when transferring patients between tertiary, secondary, and primary care due to unfamiliarity with the community teams. P8 stated, "Let patients meet 'their' community nurse before discharge—it humanizes the transition." Additionally, participants also admitted that while the model expands care accessibility, it also depersonalizes care, eroding rapport and leading to miscommunication. P5 provided the following insight: "We need to learn how to make 'digital warmth'—emojis aren't enough."

Technical Support

Although the current level of informatization varies significantly across health care institutions in China, interviewees expressed optimism about the potential for technical support to enhance the implementation of Internet Plus continuous care in the future. Participants emphasized that addressing existing disparities and investing in robust digital infrastructure could pave the way for the seamless integration of services. Several participants highlighted the need for a centralized patient record system as a cornerstone of future technical advancements. P13 suggested that "A centralized patient record system would eliminate duplicate tests and lost information." This sentiment was echoed by P4, who added, "In the future, we should aim for region-level interoperability so that patient data flows seamlessly across different levels of care." Additionally, participants expressed excitement about the potential of emerging technologies, such as artificial intelligence, big data analytics, and wearable devices, to transform continuous care. P7 offered a forward-looking view: "These innovations will require substantial investment and collaboration, but they hold immense promise for improving outcomes and reducing costs."

Training Standardization

Skill gaps, particularly in primary and secondary care settings, were a major concern. P3 noted, "Personnel are unprepared for new challenges, including risk prediction and process adaptation." P7 suggested targeted training in areas like data literacy and digital tools to bridge these gaps. Managing risks such as data breaches and miscommunication was seen as critical. P14 recommended training in risk prediction and mitigation. P9 added, "Predictive analytics tools can help nurses identify high-risk patients and intervene proactively." To ensure practical application, experiential learning and peer networks were suggested. P4 advocated for simulations, while P15 highlighted the value of collaborative platforms for sharing best practices.

Discussion

Principal Findings

In the context of aging populations and rapid digitalization, Internet Plus continuity care has garnered significant attention in China from both scholars and clinicians. To our knowledge, this is the first mixed methods study exploring nurses' experiences with Internet Plus continuity care services in China. Our research not only identified the most challenging aspects of implementation through objective measurements but also delved into the underlying reasons via semistructured interviews.

Consistent with prior studies [32], our results show that information continuity scored highest among the 3 dimensions of the Continuity of Care model. This aligns with the consensus that seamless information flow is critical for care continuity, with technology platforms serving as its backbone [33]. However, our qualitative data reveal persistent gaps: participants highlighted poor interoperability between institutional systems and emphasized the need for remote assistance. These findings are further supported by evaluations of 17 Internet Plus nursing service applications in China, where most platforms were rated "average" or "poor" in credibility (82%) and demand fulfillment (94%) [34]. To address these issues, future platform development should adopt a co-design approach, ensuring that the needs of both health care providers and recipients are prioritized [35].

XSL•FO
RenderX

Furthermore, our research demonstrates that relational continuity scores exhibit average performance. While continuity of care relies on stable, trusting relationships between patients and providers [36], it also depends on effective interdisciplinary collaboration [37]. Nurses play a pivotal role in sustaining continuity, even in physician-driven services [38], yet hierarchical nursing teams often struggle with complex supervision and authorization processes. This leads to diminished confidence among nurses [39,40], as reflected in our interviews. To mitigate this, preservice training, ongoing education, and structured support are essential to empower nurses in multidisciplinary teamwork and task delegation.

The most significant barrier identified was management continuity, mirroring the findings of Roy et al [41], who cited administrative burdens as a primary obstacle. In the Internet Plus context, these challenges appear amplified. Nurses in our study prioritized safety, income security, and collaboration with patients and their family—concerns echoed in prior research [8,42]. Safety risks, in particular, stem from perceived inadequacies in personal competency, lack of prescription authority, insufficient emergency equipment, and limited team support [43,44]. Notably, while shared nurses demonstrated moderate emergency response capabilities, their recovery capacity scored lowest [45]. Cross-sectional studies suggest that successful implementation hinges on insurance coverage, hospital-affiliated licensing, clear contractual terms, real-time location tracking, and emergency alert systems [46].

Our work clearly has some limitations. First, the questionnaire was self-developed and lacks external validation, though qualitative insights help counterbalance this concern. Future research should employ validated tools, such as the scale by Tian et al [47], for comparative analysis. Second, while all interviewees had experience with Internet Plus continuity care, the perspectives of nonparticipating nurses remain unexplored and warrant investigation. Despite these limitations, our findings provide actionable insights for improving the quality and scalability of Internet Plus continuous nursing services in China.

Conclusion

This study addresses a significant gap in the literature by investigating the barriers and challenges faced by nurses in providing Internet Plus continuous nursing, a novel medical model that has gained considerable attention under the dual background of aging and digitalization in China. Our findings revealed that Chinese nurses may have differential challenges when providing Internet Plus continuous nursing, particularly in management continuity. We recommend that, to better benefit patients and improve health care delivery, health care organizations and policymakers implement strategies to improve interdisciplinary relationships, establish and perfect organizational management, and enhance communication.

Acknowledgments

The authors would like to thank all the participants who contributed their time to the study. This research was funded by the Doctoral Project of Chongqing Social Science Planning Project (grant 2024BS055) .

Authors' Contributions

HH and QZ designed the study and participated in writing and revising the manuscript. WJ and QH contributed to interpreting the data and participated in writing and revising the manuscript. LC, XD, ZC collected the data, performed the statistical analysis, and contributed to interpreting the data. All authors have read and approved the manuscript.

Conflicts of Interest

None declared.

Multimedia Appendix 1
Basic information of experts collected via the Delphi survey.
[DOCX File, 21 KB - medinform_v13i1e65445_app1.docx]

References

1. Bahr SJ, Weiss ME. Clarifying model for continuity of care: a concept analysis. Int J Nurs Pract 2019 Apr;25(2):e12704. [doi: 10.1111/ijn.12704] [Medline: 30393894]
2. Teng Y, Liu T, Li X, et al. The Ottawa Decision-Making Supportive Framework-based nursing care in the outcome of patients with chronic heart failure. Contrast Media Mol Imaging 2022;2022:6000160. [doi: 10.1155/2022/6000160] [Medline: 36237578]
3. Harris E. Review finds benefits of primary care continuity. JAMA 2023 Jun 27;329(24):2119. [doi: 10.1001/jama.2023.9930]
4. Baker R, Freeman GK, Haggerty JL, Bankart MJ, Nockels KH. Primary medical care continuity and patient mortality: a systematic review. Br J Gen Pract 2020 Sep;70(698):e600-e611. [doi: 10.3399/bjgp20X712289] [Medline: 32784220]
5. Mahase E. Mortality rates are lower with higher continuity of care, review finds. BMJ 2020 Aug 11;370:m3184. [doi: 10.1136/bmj.m3184]

XSL•FO
RenderX

6. Sumikawa Y, Yamamoto-Mitani N. Transitional care during COVID-19 pandemic in Japan: calls for new strategies to integrate traditional approaches with information and communication technologies. Biosci Trends 2021 Mar 15;15(1):55-57. [doi: 10.5582/bst.2021.01056] [Medline: 33627572]
7. Yang Q, Ju M, Li Y, Zheng S, Li L. On intelligent nursing construction based on the Internet plus strategy. Journal of Nursing Science 2017;32(11):8-10. [doi: 10.7748/ns.32.10.11.s11]
8. Yang J, Ma B, Chen S, et al. Nurses' preferences for working in Uber-style "Internet plus" nursing services: a discrete choice experiment. Int J Nurs Stud 2025 Jan;161:104920. [doi: 10.1016/j.ijnurstu.2024.104920]
9. Shi H, Zhang Y, Wang X, et al. An analysis of the current situation of China's model of combining medical care with nursing care under the background of the internet plus. Minerva Med 2023 Jul 18. [doi: 10.23736/S0026-4806.23.08793-1] [Medline: 37462475]
10. Yao J, He W, Chen H, Qi Y. Nursing effect of continuous nursing intervention based on "Internet Plus" on patients with severe adrenal tumor. Medicine (Baltimore) 2023 Mar 10;102(10):e33187. [doi: 10.1097/MD.0000000000033187] [Medline: 36897676]
11. Kirkland-Kyhn H, Howell M, Senestraro J, Walsh S. Leveraging technology to improve wound care delivery and care transitions. Nurs Manage 2021 Nov 1;52(11):24-28. [doi: 10.1097/01.NUMA.0000795592.38063.7c] [Medline: 34723882]
12. Diehl TM, Barrett JR, Van Doorn R, et al. Promoting patient engagement during care transitions after surgery using mobile technology: lessons learned from the MobiMD pilot study. Surgery 2022 Jul;172(1):219-225. [doi: 10.1016/j.surg.2021.12.018] [Medline: 35086727]
13. Ritchie CS, Houston TK, Richman JS, et al. The E-Coach technology-assisted care transition system: a pragmatic randomized trial. Transl Behav Med 2016 Sep;6(3):428-437. [doi: 10.1007/s13142-016-0422-8] [Medline: 27339715]
14. Notice of the National Health Commission on issuing the National Nursing Development Plan (2021-2025) [Web page in Chinese]. The State Council of the People's Republic of China. 2021. URL: https://www.gov.cn/zhengce/zhengceku/2022-05/09/content_5689354.htm [accessed 2023-08-07]
15. Notice on issuing the Action Plan for Further Improvement of Care Services (2023-2025) [Web page in Chinese]. The State Council of the People's Republic of China. 2023. URL: https://www.gov.cn/zhengce/zhengceku/202306/content_6887303.htm [accessed 2023-08-07]
16. Li Y, Li L, Deng R. Internet + nursing service perception among nursing staff: a cross-sectional study at Guizhou Province, China. Risk Manag Healthc Policy 2024;17(2929–2935):2929-2935. [doi: 10.2147/RMHP.S487878] [Medline: 39619626]
17. Zhao B, Zhang X, Huang R, Yi M, Dong X, Li Z. Barriers to accessing internet-based home care for older patients: a qualitative study. BMC Geriatr 2021 Oct 18;21(1):565. [doi: 10.1186/s12877-021-02474-6] [Medline: 34663218]
18. Fakha A, Groenvynck L, de Boer B, van Achterberg T, Hamers J, Verbeek H. A myriad of factors influencing the implementation of transitional care innovations: a scoping review. Implement Sci 2021 Feb 26;16(1):21. [doi: 10.1186/s13012-021-01087-2] [Medline: 33637097]
19. McGilton KS, Vellani S, Krassikova A, et al. Understanding transitional care programs for older adults who experience delayed discharge: a scoping review. BMC Geriatr 2021 Mar 29;21(1):210. [doi: 10.1186/s12877-021-02099-9] [Medline: 33781222]
20. Tian F, Xi Z, Ai L, et al. Investigation on nurses' willingness to "Internet + Nursing Service" and analysis of influencing factors. J Multidiscip Healthc 2023;16:251-260. [doi: 10.2147/JMDH.S396826] [Medline: 36726482]
21. Xu X, Li N, Gao F, et al. Residents' willingness and awareness to participate in internet+nursing service in China: a meta-analysis. Medicine (Baltimore) 2025 Jan 10;104(2):e41219. [doi: 10.1097/MD.0000000000041219] [Medline: 39792730]
22. Haggerty JL, Reid RJ, Freeman GK, Starfield BH, Adair CE, McKendry R. Continuity of care: a multidisciplinary review. BMJ 2003 Nov 22;327(7425):1219-1221. [doi: 10.1136/bmj.327.7425.1219] [Medline: 14630762]
23. Uijen AA, Schellevis FG, van den Bosch W, Mokkink HGA, van Weel C, Schers HJ. Nijmegen Continuity Questionnaire: development and testing of a questionnaire that measures continuity of care. J Clin Epidemiol 2011 Dec;64(12):1391-1399. [doi: 10.1016/j.jclinepi.2011.03.006] [Medline: 21689904]
24. Chen HM, Chen CM. A Chinese version of the Patient Continuity of Care Questionnaire: reliability and validity assessment. J Clin Nurs 2017 May;26(9-10):1338-1350. [doi: 10.1111/jocn.13679] [Medline: 27906485]
25. Wenjuanxing [Website in Chinese]. URL: https://www.wjx.cn [accessed 2025-06-10]
26. Sandelowski M. Sample size in qualitative research. Res Nurs Health 1995 Apr;18(2):179-183. [doi: 10.1002/nur.4770180211] [Medline: 7899572]
27. Yu HY, Xu SH, Chen YL, Li YX, Yang QH. Nurses' perceptions regarding barriers to implementing the Internet Plus Nursing Service programme: a qualitative study. J Nurs Manag 2022 Mar;30(2):511-520. [doi: 10.1111/jonm.13533] [Medline: 34890482]
28. Amiri-Farahani L, Gharacheh M, Sadeghzadeh N, Peyravi H, Pezaro S. Iranian midwives' lived experiences of providing continuous midwife-led intrapartum care: a qualitative study. BMC Pregnancy Childbirth 2022 Sep 23;22(1):724. [doi: 10.1186/s12884-022-05040-z] [Medline: 36151533]
29. Braun V, Clarke V. Using thematic analysis in psychology. Qual Res Psychol 2006 Jan;3(2):77-101. [doi: 10.1191/1478088706qp063oa]

XSL•FO
RenderX

30. Bailey KM, Marshall C, Rossman GB. Designing Qualitative Research. Mod Lang J 1996;80(3):403. [doi: 10.2307/329453]
31. Lincoln YS, Guba EG. But is it rigorous? Trustworthiness and authenticity in naturalistic evaluation. New Directions for Program Evaluation 1986 Jun;1986(30):73-84. [doi: 10.1002/ev.1427]
32. Wei Q, Yuan B, Xu J, He P, Xu H, Meng Q. Continuity of health care: measurement and application in two rural counties of Guangxi Province, China. BMC Health Serv Res 2023 Aug 29;23(1):917. [doi: 10.1186/s12913-023-09916-4] [Medline: 37644426]
33. Hsieh PJ, Lai HM, Ma CC, Alexander JW, Lin MY. An extended expectation-confirmation model for mobile nursing information system continuance. Res Theory Nurs Pract 2016 Nov 1;30(4):282-301. [doi: 10.1891/1541-6577.30.4.282] [Medline: 28304259]
34. Yuan S, Liu M, Peng Y, et al. “Internet+Nursing Service” mobile apps in China app stores: functionality and quality assessment study. JMIR Mhealth Uhealth 2024 Feb 16;12:e52169. [doi: 10.2196/52169] [Medline: 38409754]
35. Juel A, Berring LL, Erlangsen A, Larsen ER, Buus N. Sense of psychological ownership in co-design processes: a case study. Health Expect 2024 Feb;27(1):e13886. [doi: 10.1111/hex.13886] [Medline: 37890859]
36. Byrne AL, Baldwin A, Harvey C, et al. Understanding the impact and causes of “failure to attend” on continuity of care for patients with chronic conditions. PLoS ONE 2021;16(3):e0247914. [doi: 10.1371/journal.pone.0247914] [Medline: 33651826]
37. Chen CC, Chiang YC, Lin YC, Cheng SH. Continuity of care and coordination of care: can they be differentiated? Int J Integr Care 2023;23(1):10. [doi: 10.5334/ijic.6467] [Medline: 36819617]
38. Walker FA, Ball M, Cleary S, Pisani H. Transparent teamwork: the practice of supervision and delegation within the multi-tiered nursing team. Nurs Inq 2021 Dec;28(4):e12413. [doi: 10.1111/nin.12413] [Medline: 33886166]
39. Prussing E, Browne G, Dowse E, Hartz D, Cummins A. Implementing midwifery continuity of care models in regional Australia: a constructivist grounded theory study. Women Birth 2023 Feb;36(1):99-107. [doi: 10.1016/j.wombi.2022.03.006] [Medline: 35410848]
40. Crevacore C, Jacob E, Coventry LL, Duffield C. Integrative review: factors impacting effective delegation practices by registered nurses to assistants in nursing. J Adv Nurs 2023 Mar;79(3):885-895. [doi: 10.1111/jan.15430] [Medline: 36062891]
41. Roy A, Breton M, Loslier J. Providing continuity of care to a specific population: attracting new family physicians. Can Fam Physician 2016 May;62(5):e256-e262. [Medline: 27255634]
42. He Y, Feng G, Wang C, et al. Nurses’ job preferences on the internet plus nursing service program: a discrete choice experiment. BMC Nurs 2024 Feb 15;23(1):120. [doi: 10.1186/s12912-023-01692-0] [Medline: 38360597]
43. Johannessen T, Ree E, Aase I, Bal R, Wiig S. Exploring challenges in quality and safety work in nursing homes and home care - a case study as basis for theory development. BMC Health Serv Res 2020 Apr 3;20(1):277. [doi: 10.1186/s12913-020-05149-x] [Medline: 32245450]
44. Craven C, Byrne K, Sims-Gould J, Martin-Matthews A. Types and patterns of safety concerns in home care: staff perspectives. Int J Qual Health Care 2012 Oct;24(5):525-531. [doi: 10.1093/intqhc/mzs047] [Medline: 22864107]
45. Huang N, Che Y, Hu X, Liu J, He C. Current status and factors influencing emergency response capability of shared nurses in the Internet + Nursing Service model: a descriptive cross-sectional study. Risk Manag Healthc Policy 2024;17(803–814):803-814. [doi: 10.2147/RMHP.S452053] [Medline: 38606346]
46. Huang R, Xu M, Li X, Wang Y, Wang B, Cui N. Internet-based sharing nurse program and nurses’ perceptions in China: cross-sectional survey. J Med Internet Res 2020 Jul 22;22(7):e16644. [doi: 10.2196/16644] [Medline: 32706711]
47. Tian F, Peng Z, Mi Y, et al. Development and validation of a rating scale for barriers to and facilitators of nurses’ participation intentions in “Internet + Nursing Service”. BMC Nurs 2024 Aug 13;23(1):559. [doi: 10.1186/s12912-024-02215-1] [Medline: 39135197]

Edited by A Castonguay; submitted 15.08.24; peer-reviewed by L Bacalhau, R Kr; revised version received 22.04.25; accepted 23.05.25; published 02.07.25.

Please cite as:
Huang H, Chen Z, Chen L, Du X, Huang Q, Jia W, Zhao Q
Nurses’ Experience Regarding Barriers to Providing Internet Plus Continuous Nursing: Mixed Methods Study
JMIR Med Inform 2025;13:e65445
URL: https://medinform.jmir.org/2025/1/e65445
doi:10.2196/65445

©Huanhuan Huang, Zhiyu Chen, Lijuan Chen, Xingyao Du, Qi Huang, Wenbi Jia, Qinghua Zhao. Originally published in JMIR Medical Informatics (https://medinform.jmir.org), 2.7.2025. This is an open-access article distributed under the terms of the Creative Commons Attribution License (https://creativecommons.org/licenses/by/4.0/), which permits unrestricted use, distribution, and reproduction in any medium, provided the original work, first published in JMIR Medical Informatics, is properly cited. The

XSL•FO
RenderX

complete bibliographic information, a link to the original publication on https://medinform.jmir.org/, as well as this copyright and license information must be included.

XSL•FO
RenderX

Health Information Systems' Support for Management and Changing Work: Survey Study Among Physicians

Tarja Heponiemi[1], PhD; Lotta Virtanen[1], MSSc; Emma Kainiemi[1], RM, MNSc; Petra Saukkonen[1], MSc; Jarmo Reponen[2,3], MD, PhD; Tinja Lääveri[4,5], MD, PhD

[1]Department of Healthcare and Social Welfare, Finnish Institute for Health and Welfare, P.O. Box 30, Helsinki, Finland

[2]Research Unit of Health Sciences and Technology, University of Oulu, Oulu, Finland

[3]Medical Research Centre Oulu, Wellbeing Services County of North Ostrobothnia and the University of Oulu, Oulu, Finland

[4]Department of Computer Science, School of Science, Aalto University, Espoo, Finland

[5]Infectious Diseases, Inflammation Center, University of Helsinki and Helsinki University Hospital, Helsinki, Finland

Corresponding Author:
Tarja Heponiemi, PhD
Department of Healthcare and Social Welfare, Finnish Institute for Health and Welfare, P.O. Box 30, Helsinki, Finland

Abstract

Background: The digitalization of health care has advanced significantly in recent years. Consequently, physicians have needed to increasingly adopt new digital health technologies such as electronic health record systems and other health information systems. Digitalization has changed physicians' clinical work, work environment, management work, and use of tools for leadership. Many physician leaders have been critical of the capabilities of health information systems (HISs) to support leadership, management, and knowledge management.

Objective: We aimed to examine the association between leadership position and perceived changes in clinical work due to digitalization among a nationally representative sample of Finnish physicians and physician leaders. In addition, we examined physician leaders' perceptions of HISs as a support for management and whether their opinions differed based on their perceptions on changes in clinical work due to digitalization.

Methods: Altogether 4630 Finnish physicians (2960/4586, 64% women) responded to a cross-sectional nation-wide web-based survey conducted in spring 2021. Perceptions of improved preventive work, facilitated access to patient information, progressed interprofessional collaboration, and accelerated clinical encounters were used as measures of changes due to digitalization. First, we examined with multivariable logistic regression analyses whether being in a leadership position was associated with perceived changes in work due to digitalization (improved preventive work, facilitated access to patient information, progressed interprofessional collaboration, and accelerated clinical encounters in separate analyses) in the total sample. Second, we examined with analyses of covariance whether the variables related to perceived changes in work due to digitalization were associated with perceived management support from HISs among those who had administrative or management responsibilities (n=817). All analyses were adjusted for gender, age, and sector.

Results: Physician leaders had greater odds of agreeing that digitalization had improved preventive work (odds ratio [OR] 1.62, 95% CI 1.33 - 1.98), facilitated access to patient information (OR 1.28, 95% CI 1.09 - 1.51), progressed interprofessional collaboration (OR 1.81, 95% CI 1.53 - 2.14), and accelerated clinical encounters (OR 1.31, 95% CI 1.01 - 1.70) than those in nonleadership positions. Furthermore, leaders who perceived these changes in work due to digitalization positively also considered that health information systems supported their management work.

Conclusions: Physician leaders appeared to view the changes in work due to digitalization more positively than other physicians. In addition, those leaders who perceived these changes positively also perceived that HISs supported their management work. Thus, leaders should thoroughly evaluate and address physicians' perceptions of their routine clinical work and its evolving nature. Doing so ensures access to up-to-date and accurate insights, enabling more effective planning of staffing, training programs, and future implementations. Furthermore, our results show that to guarantee positive views about digitalization among physician leaders, information systems should also support managerial work. This highlights the need to focus on the quality, utility, and usability of information systems.

(JMIR Med Inform 2025;13:e65913) doi:10.2196/65913

KEYWORDS

health care digitalization; leadership position; work change; digitalization; health information systems; support; management; leadership; Finland; cross sectional; online survey; survey; patient information; physician leaders; monitoring; information system

XSL•FO
RenderX

Introduction

Digitalization of health care has progressed during the past 20 years. Consequently, physicians have needed to increasingly adopt new digital health technologies (DHTs), such as electronic health record systems (EHRs) and other health information systems (HISs), remote monitoring, artificial intelligence, and robotics [1,2]. The clinical goals of healthcare digitalization include, for example, enhancing the possibilities for preventive work, facilitating access to patient data, progressing with interprofessional collaboration, and improving the efficiency of clinical encounters [3,4].

Digitalization has changed physicians' clinical work and work environment [5,6], and use of tools for leadership [7]. For example, clinical decision support systems may help physicians by acting as diagnostic support, assisting in administrative functions, helping clinical management, and improving patient safety [8]. Furthermore, physicians have described that the digitalization may support collaboration, decision making, continuous learning, and staying informed [6]. Indeed, health care professionals have stated that increased digitalization has accelerated their work and strengthened multidisciplinary collaboration, due to lower threshold for contacting colleagues of different professional groups [5]. Common data archives and databases facilitate the transfer of information between different units and service providers, and digitization of referrals has expedited the handling of patient matters [5]. Furthermore, previous studies show that HISs can facilitate in filtering, integrating, and interpreting information from diverse sources through better information sharing, improved communication, and timely access to data [9,10].

Despite the identified benefits, digitalization may also lead to pitfalls such as fragmented workflow, alert fatigue, and interoperability [8]. In addition, increasing number of studies report HISs-related stress among physicians [11,12]. Consequently, only a few physicians have perceived that the changes in clinical work due to digitalization were in line with the strategic goals [13], instead, they feel burdened by the undesired changes [14]. A qualitative study suggested that frontline health and social care professionals may perceive more adverse changes associated with digitalization in their work than their leaders [5]. These negative ramifications of digitalization present a challenge, as the reactions of employees play a pivotal role in determining the likelihood of the success or failure of such changes [15,16].

Many physician leaders have yet been critical of the capabilities of HIS support for leadership, management, and knowledge management [17]. They experience a need to put a lot of effort to gathering and updating necessary information from many different sources, and the information may be unreliable [17-19]. Physician leaders working in hospitals have reported that HISs supported decision-making and improved the ease of access to information, but did not improve the speed of access to information [20]. Furthermore, they had to use several systems to support their decision-making and wished for one HIS offering all the necessary information to support their decision-making [20]. Middle management has expressed difficulties in collection, mining, and systematic use of information due to different ways of producing and reporting information of the HISs [19]. Nevertheless, data collection for these findings occurred before the COVID-19 pandemic, during which information assets for knowledge management in healthcare may have evolved.

This study focused on examining the association between leadership position and perceived changes in clinical work due to digitalization (improved preventive work, facilitated access to patient information, progressed interprofessional collaboration, and accelerated clinical encounters) among a nationally representative sample of Finnish physicians and physician leaders. In addition, we examined physician leaders' perceptions of HISs as a support for management and whether their opinions differed based on their perceptions on changes in clinical work due to digitalization.

Methods

Sample

The data were collected with a web-based survey between January and March 2021 as a part of the "EHR systems as a tool for physicians 2021" study [21]. An invitation to participate was sent by email to all working-age (aged 65 y and younger) physicians from the Finnish Medical Association's register. A detailed description of the data collection, measures used in the questionnaire and the evolution of the questionnaire can be found elsewhere [21]. Altogether 4683 physicians (estimated response rate 24.5%) responded to the survey. We excluded 53 respondents who indicated that they did not use EHRs at all. Thus, the final sample included 4630 physicians. The sample was representative of the target population, with a slightly more older physicians, specialists, and hospital physicians compared to the eligible population [22].

Ethical Considerations

The study was conducted according to national laws, regulations, and the Declaration of Helsinki. The survey did not require a statement from the ethics committee, given that the Finnish National Board on Research Integrity [23] has defined that the administration of surveys to gather respondents' opinions, which are not anticipated to result in harm, does not necessitate a statement from the ethics committee. All respondents provided informed consent to participate, participated voluntarily, and received written information about the study. All responses were anonymous and the research data did not include any personally identifiable information. No compensation was provided to participants.

Measures

The variables used in this study can be found in Multimedia Appendix 1.

Perceived changes in clinical work due to digitalization were measured by respondents' opinions on the following statements on how the digitalization of health care had changed their work in the past 3 years:

1. Possibilities for preventive work have improved (improved possibilities for preventive work).

XSL•FO
RenderX

2. It has become easier to obtain information on patients (facilitated access to patient information).
3. Interprofessional collaboration has progressed (progressed interprofessional collaboration).
4. Consultations with patients have become faster (accelerated clinical encounters).

The statements were rated: 1=fully agree, 2=somewhat agree, 3=neither agree nor disagree, 4=somewhat disagree, and 5=fully disagree, which were then recoded as 0=disagree or neutral (response options 3 - 5) and 1=agree (1-2). These statements were developed by clinicians and healthcare digitalization experts according to the strategic goals of digitalization of health care [4] and pilot tested with physicians. The statements have been associated, for example, with work-related time pressure and stress related to information systems [14].

Perceived management support from HISs was assessed with 3 items (Cronbach α=0.81) measuring the supportiveness of information systems for knowledge management. The respondents were directed to this section if their professional title indicated that they might have a leading or managerial position. Furthermore, the respondents were advised that if they do not have administrative or management responsibilities, they should not grade these statements (817 responded to these statements). They were asked how, in all, do the information systems used in their organization work as tools for leadership and management The items were: “I use information systems daily for activity monitoring,” “information systems facilitate monitoring the quality of activities,” and “information systems help me to monitor the targets set by my unit (eg, numbers of patients, periods of treatment, and types of operations).” The response options with 5-point Likert scale ranged from 1=fully disagree to 5=fully agree. A mean of these three items was calculated, higher scores indicating better support for management. Respondents were advised not to answer this question if they do not have administrative or management responsibilities; thus, those who answered this question were considered as being in leadership position.

Furthermore, the survey asked respondents’ age (which was categorized as under 35, 35 - 44, 45 - 54, and 55 - 64 years) and employment sector (hospitals, primary care, private, and other such as universities). Respondents’ gender was received from registers.

Statistical Analyses

First, we examined whether being in a leadership position was associated with perceived changes in work due to digitalization in the total sample. Multivariable logistic regression analyses were conducted with the perceived changes in clinical work due to digitalization (improved preventive work, facilitated access to patient information, progressed interprofessional collaboration, and accelerated clinical encounters in separate analyses) as dependent variables and leadership position (yes or no), gender, age, and sector as independent variables.

Second, we examined whether the variables related to perceived changes in work due to digitalization were associated with perceived management support from HISs among those who had administrative or management responsibilities (n=817). Analyses of covariance were conducted, with perceived management support from HIS as the dependent variable and the four statements regarding perceived changes in clinical work due to digitalization as independent variables (in the same analysis), adjusted for gender, age, and sector. All analyses were conducted using IBM SPSS Statistics software (version 28).

Results

Characteristics of the study sample can be seen in Table 1. Almost 2 in 3 of the respondents were women. More than half of the respondents worked in specialized care. Approximately 1 in 6 worked in a leadership position. In addition, 1 in 5 agreed that digitalization had improved preventive work and more than 2 in 5 agreed that it had facilitated access to patient information. In total, 30% agreed that digitalization had progressed interprofessional collaboration, whereas only 1 in 10 agreed that it had accelerated clinical encounters. Among physician leaders, the mean score for perceiving HISs as supporting management was 2.70 (SD 0.99).

XSL•FO
RenderX

Table . Characteristics of the study sample.

Characteristics	Value, n (%)
Gender	
Man	1626 (35.5)
Woman	2960 (64.5)
Age (years)	
<35	948 (20.6)
35 - 44	1211 (26.4)
45 - 54	1148 (25.0)
55 - 64	1284 (28.0)
Sector	
Hospital	2759 (59.6)
Primary care	1037 (22.4)
Private	610 (13.2)
Other	221 (4.8)
Leadership position	
No	3813 (82.4)
Yes	817 (17.6)
Improved preventive work	
Disagree or neutral	3622 (80.4)
Agree	884 (19.6)
Facilitated access to patient information	
Disagree or neutral	2565 (56.4)
Agree	1986 (43.6)
Progressed interprofessional collaboration	
Disagree or neutral	2948 (65.0)
Agree	1586 (35.0)
Accelerated clinical encounters	
Disagree or neutral	4084 (90.2)
Agree	445 (9.8)
Information systems as support for management (range 1 - 5), mean (SD)	2.70 (0.99)

Table 2 shows the results of the logistic regression analysis for changes in clinical work due to digitalization in the total sample. Women had lower odds of agreeing that digitalization had accelerated clinical encounters than men. Older respondents had lower odds of agreeing that digitalization had improved preventive work and greater odds of agreeing that digitalization had facilitated access to information than younger respondents. Compared to respondents working in public specialized care, those working in public primary care and private care had greater odds of agreeing that digitalization had improved preventive work and facilitated access to information. Furthermore, respondents working in public primary care had greater odds of agreeing that digitalization had progressed interprofessional collaboration, and respondents working in private sector had greater odds of agreeing that digitalization had accelerated clinical encounters than those working in public specialized care. Respondents in leadership positions had greater odds of agreeing with all the statements concerning clinical work change due to digitalization than others. The clearest difference was observed regarding progressed interprofessional collaboration and improved preventive work.

XSL•FO
RenderX

Table . The results of the logistic regression analysis for changes in work due to digitalization, shown in odds ratios (ORs) and their 95% CIs (n=4630).

	Preventive work		Access to information		Interprof[a] collaboration		Accelerated encounters	
	OR (95% CI)	*P* value	OR (95% CI)	*P* value	OR (95% CI)	*P* value	OR (95% CI)	*P* value
Gender		.05		.06		.25		<.001
Man	1[b]		1		1		1	
Woman	0.86 (0.73-1.00)		0.88 (0.78-1.00)		0.93 (0.81 - 1.06)		0.65 (0.53-.79)	
Age		.006		.047		.22		.46
<35	1		1		1		1	
35 - 44	0.72 (0.57 - 0.90)		1.01 (0.84 - 1.21)		0.83 (0.69 - 1.00)		0.99 (0.72 - 1.36)	
45 - 54	0.79 (0.63 - 1.00)		1.06 (0.88 - 1.28)		0.87 (0.71 - 1.05)		1.20 (0.87 - 1.66)	
55 - 64	0.68 (0.54 - 0.86)		1.24 (1.03 - 1.50)		0.92 (0.76 - 1.11)		1.17 (0.85 - 1.61)	
Sector		<.001		<.001		<.001		<.001
Hospital	1		1		1		1	
Primary care	1.70 (1.41 - 2.05)		1.52 (1.31 - 1.77)		1.53 (1.31 - 1.78)		1.17 (0.90 - 1.52)	
Private	2.88 (2.32 - 3.57)		2.06 (1.71 - 2.49)		1.17 (0.96 - 1.43)		2.19 (1.68 - 2.87)	
Other	2.00 (1.43 - 2.80)		1.75 (1.32 - 2.32)		1.38 (1.03 - 1.85)		1.34 (0.85 - 2.13)	
Leadership position		<.001		.003		<.001		.04
No	1		1		1		1	
Yes	1.62 (1.33 - .98)		1.28 (1.09 - .51)		1.81 (1.53-2.14)	<.001	1.31 (1.01 - .70)	

[a]Interprof: interprofessional.

[b]Reference category.

Table 3 shows the results of the analyses of variance for perceived management support from HISs among those who were in leadership positions. HISs were least experienced as supporting management in public primary care. Multimedia Appendix 2 shows that those who agreed that digitalization had improved preventive work, facilitated access to patient information, progressed interprofessional collaboration, or accelerated clinical encounters perceived HISs as more supportive compared to those who disagreed or were neutral about these statements.

XSL•FO
RenderX

Table . Results of the analyses of variance for information systems as support for management and its estimated marginal means according to independent variables (n=817).

Variable	*F* test (*df*)	*P* value	Mean[a] (SE)
Gender	0.93 (1)	.34	
Man			3.02 (0.08)
Woman			2.95 (0.07)
Age (years)	0.54 (2)	.58	
<45			2.94 (0.10)
45 - 54			3.03 (0.08)
55 - 64			2.99 (0.08)
Sector	9.95 (3)	<.001	
Hospital			2.94 (0.06)
Primary care			2.61 (0.09)
Private			3.40 (0.13)
Other			2.99 (0.16)
Improved preventive work	6.07 (1)	.01	
Disagree or neutral			2.89 (0.07)
Agree			3.09 (0.09)
Facilitated access to patient information	19.01 (1)	<.001	
Disagree or neutral			2.84 (0.08)
Agree			3.14 (0.08)
Progressed interprofessional collaboration	23.74 (1)	<.001	
Disagree or neutral			2.81 (0.08)
Agree			3.16 (0.07)
Accelerated clinical encounters	13.31 (1)	<.001	
Disagree or neutral			2.80 (0.06)
Agree			3.18 (0.11)

[a]Estimated marginal mean adjusted for all variables in the table.

Discussion

Principal Findings and Comparison With Previous Work

This study found that physician leaders agreed more often that digitalization had improved preventive work, facilitated access to patient information, progressed interprofessional collaboration, and accelerated clinical encounters compared to those without leadership positions. This suggests that leaders have a more positive view related to ramifications of digitalization than physicians without leadership positions. However, physician leaders did not experience that HISs support their management work, given that their average rating for support was 2.7 on a scale of 1 to 5. Nevertheless, although physician leaders considered HISs support for leadership and management insufficient, those who agreed with these statements also gave more positive responses about the impacts of digitalization.

Our finding that physician leaders had a more positive view related to digitalization than other physicians is congruent with a previous study [5]. A qualitative study among health and social care professionals suggests that leaders may overlook the new digital skills needs and problems caused by combining continuous learning with busy work schedules [5]. A possible reason why health care leaders may have a more positive attitude toward digitalization is that they play an active role in leading these initiatives by striving to demonstrate a visible commitment towards new DHTs [24]; they also try to convince reluctant users to envision digitalization in a more favorable manner [25]. It has been suggested that the successful implementation of DHTs among health care professionals is contingent upon managers being convinced of its positive effects [26].

Our study found that those leaders who agreed with the positive statements related to the changes in clinical work due to digitalization also perceived more often that HISs supported management work compared to those who disagreed or were

XSL•FO
RenderX

neutral. Due to the cross-sectional nature of our study, we cannot identify the causality of this association; that is, we cannot definitely identify whether effective support from HISs leads to improved efficiency in management work for leaders and contributes to a positive view toward digitalization. Alternatively, it could be that those who have noticed that digitalization has improved preventive work, facilitated access to patient information, promoted collaboration, and accelerated clinical encounters are therefore also more inclined to rate that HISs support their management work. It is possible that the general satisfaction with the benefits of digitalization for leaders in health care is reflected in their responses. Thus, it seems important to ensure that leaders keep themselves well-informed about the realities of clinical work and thereby avoid having excessively positive view related to digitalization [26]. Many physician leaders participate also to clinical work which makes it easier to stay up to date about the situation in clinical care. However, physicians working in nonleadership positions need to communicate work-related issues and digital challenges to management, providing nuanced insights for decision-making [26].

Our results suggest sector-specific variations, with physicians working in specialized care perceiving less improvement in preventive work and facilitated access to information compared to physicians working elsewhere. Whereas primary care focuses on preventive measures and health promotion, specialized care physicians mainly treat the diseases in their own specialty [27]. A previous study among specialized care physicians showed that day-to-day operations management HISs supported decision-making to some extent but did not improve access to information [18]. Hospital physicians have also reported that they need to use a number of information systems to support decision making instead of one HIS which they would prefer [18]. Hospital physicians have also reported that they were more able to monitor the use of personnel, equipment, or room resources through HISs compared to primary care physicians [17]. Furthermore, physicians in specialized care settings have previously stated fragmentation of information and data overload resulting from difficult-to-use EHRs [28]. In addition, the implementation of HISs has led to changes in professionals' workflow, potentially causing cognitive burden [29]. Notably, high levels of stress related to HISs have been reported, particularly among physicians working in specialized care [12]. These challenges may contribute to the perception of less improvement in access to information among physicians in specialized care. Furthermore, contextual factors such as workload, resource allocation and availability, and on-call work may have affected these sector-specific differences.

Physician leaders in primary care perceived that HISs supported less their management work than leaders from other sectors. This is congruent with previous results in Finland which showed that, of different working sectors, leaders from primary care were most dissatisfied with HISs in guiding daily activity, facilitating measurement of functional quality, and monitoring the achieving of the set targets [17]. Primary care leaders have been found to use less managerial HISs compared to physicians in specialized care and private sector [17]. Compared to other sectors, primary care differs in aspects such as care processes, outcome goals, and the validity of summative quality scorecards [30]; thus, needs for managerial HISs also vary. For example, patient-centered reporting and outcomes (eg, reduction in days of avoidable disability) have been suggested as priorities for quality management in primary care [30].

In our study, older physicians were less likely to perceive that digitalization has improved preventive work or facilitated access to information than younger physicians. This corresponds with previous findings that, compared to younger physicians, older physicians are less likely to perceive that HISs will improve data and care coordination [31]. Older physicians have also been found to perceive less affinity toward digitalization, as well as use and trust mobile apps less in their professional lives than younger physicians [32]. Our finding that older physicians did not consider digitalization as having facilitated preventive work, may influence their likelihood to recommend preventive DHTs to patients. Consequently, this may impact the extent of digital preventive work, as patients' unawareness of the potential DHTs or their benefits has been mentioned amongst the barriers of digital prevention [33].

Our study did not find many gender differences. However, we found that women were less likely to perceive that digitalization had accelerated clinical encounters compared to men. A previous study among physician students did not find gender differences related to fear of digital challenges, but women rated their knowledge in different fields of digital medicine as worse than men, whereas men frequently reported keeping themselves informed about digital medicine outside of their studies [34]. It has been found that women physicians tend to perceive digitalization-related differences in working conditions as more stress-reducing than men physicians [35].

Limitations

There are some limitations to this study. A major limitation of our study is the use of cross-sectional survey data, thus we cannot draw any causal inferences. Therefore, according to our data it is not possible to say whether efficient support from HISs to management work leads to more positive views toward digitalization or vice versa. Thus, future studies with longitudinal design should examine more thoroughly the causal associations between HISs support for management and perceptions of digitalization. Furthermore, a question related to problems associated with an inflation of the strengths of relationships and with common method variance always arise when using self-rated measures. Self-reported data are subject to many biases such as recall, desirability, and response biases along with problems in accuracy and generalizability [36]. The reliability of the variable measuring how HISs support management was .81; thus, it can be considered reliable.

In addition, even though we adjusted our analyses for age, gender, and employment sector, we cannot put aside the possibility of residual confounding. Some variables that were not adjusted for, such as competence in knowledge management, may have influenced the associations we examined and, thus, cause bias to our results. Furthermore, usability of HISs and experience as an HIS users are among factors that might have affected our findings, for example, by influencing the overall attitude toward HISs. We excluded 53 respondents who did not

XSL•FO
RenderX

use EHRs at all; thus, their opinion was not considered here. This was done because we reasoned that their work did not involve such tasks that they could accurately answer our questions related to digitalization and the supportiveness of information systems for knowledge management.

Our results can be considered generalizable to other countries with universal access to health care and long history of HISs [37]. Furthermore, generalizability of our findings is compromised by rather low response rate of our study, which indicates likelihood of nonresponse bias. However, our sample was rather large and it has been shown to be representative of the target population [22]. The response rates have been found similarly low also in other physician studies [38]. Unfortunately, it seems that response rates among health and social care professionals especially in Finland seem to have decreased. A potential factor contributing to the declining response rates may be survey fatigue, given the high volume of various surveys conducted in this sector in Finland. Another reason for low response rate in our survey may be that the survey was conducted via email, which may have caused problems in message deliveries and email addresses might have changed.

Conclusions

This study found that physician leaders were more optimistic related to the changes in clinical work due to digitalization compared to other physicians. Furthermore, those leaders who perceived these changes positively also perceived that HISs supported their management work. Leaders should comprehensively assess and address the perceptions of physicians in routine clinical work concerning work and its changes. This approach ensures that leaders possess current and accurate information to optimize planning for personnel resources, training initiatives, and future DHT implementations.

Furthermore, to ensure that leaders have a positive view related to digitalization, it is important that HISs support their management work. Thus, it is important to focus on the quality and usability of information systems. For example, it has been suggested that HISs designed for leaders should be flexible and consider the needs of different users to support a shared situational awareness and operational intelligence in the management [39]. It is important that the success of HIS development would be regularly monitored and that future studies would address HISs' effect to clinical and management work. Especially, because our study was cross-sectional, future studies with longitudinal study design are needed.

Acknowledgments

We would like to thank the Finnish Medical Association for collection of this data. We are also deeply grateful to all the physicians who took the time to respond to this survey. The study was funded by the Strategic Research Council at the Academy of Finland (grant 352501 for the DigiIN Project) and Finnish Work Environment Fund (grant 240074). The authors attest that there was no use of generative artificial intelligence (AI) in the generation of text, figures, or other informational content of this manuscript.

Data Availability

The datasets generated or analyzed during this study are available from the corresponding author on reasonable request

Authors' Contributions

All authors have made contributions to the conception of the work, such as the formulation and evolution of overarching research goals and aims. TH, LV, JR, and TL contributed to the design of the study. TH drafted the original manuscript. TH, LV, EK, and PS contributed to the development and design of methodology, statistical analyses, tables, and visualization. JR and TL contributed to the supervision of the study. All the writers participated in the writing of the study, including critical review, commentary, and revision. All authors reviewed and approved the final version of the manuscript.

Conflicts of Interest

TL has previously been employed by a publicly owned health information system (HIS) software provider, but the employer did not provide any support, financial or otherwise, to the study. The employer also was not involved in the design of the study or the collection, analysis, and interpretation of the data.

Multimedia Appendix 1
The items of the variables used in this study.
[DOCX File, 18 KB - medinform_v13i1e65913_app1.docx]

Multimedia Appendix 2
The estimated marginal means of information systems' support for management according to perceived changes in work due to digitalization (adjusted for age, gender, employment sector, and all perceived changes in work due to digitalization variables).
[PNG File, 51 KB - medinform_v13i1e65913_app2.png]

References

XSL•FO
RenderX

1. Demeke HB, Pao LZ, Clark H, et al. Telehealth practice among health centers during the COVID-19 pandemic - United States, July 11-17, 2020. MMWR Morb Mortal Wkly Rep 2020 Dec 18;69(50):1902-1905. [doi: 10.15585/mmwr.mm6950a4] [Medline: 33332297]
2. Golinelli D, Boetto E, Carullo G, Landini MP, Fantini MP. How the COVID-19 pandemic is favoring the adoption of digital technologies in healthcare: a rapid literature review. medRxiv. Preprint posted online on 2020. [doi: 10.1101/2020.04.26.20080341]
3. Global strategy on digital health 2020-2025. : World Health Organization; 2021 URL: https://www.who.int/publications/i/item/9789240020924 [accessed 2025-01-14]
4. Information to support well-being and service renewal: eHealth and eSocial Strategy 2020. : Ministry of Social Affairs and Health; 2015 URL: http://urn.fi/URN:ISBN:978-952-00-3575-4 [accessed 2025-01-16]
5. Kaihlanen AM, Laukka E, Nadav J, et al. The effects of digitalisation on health and social care work: a qualitative descriptive study of the perceptions of professionals and managers. BMC Health Serv Res 2023 Jun 30;23(1):714. [doi: 10.1186/s12913-023-09730-y] [Medline: 37386423]
6. Vallo Hult H, Hansson A, Svensson L, Gellerstedt M. Flipped healthcare for better or worse. Health Informatics J 2019 Sep;25(3):587-597. [doi: 10.1177/1460458219833099] [Medline: 30887867]
7. Avolio BJ, Kahai S, Dodge GE. E-leadership: implications for theory, research, and practice. Leadersh Q 2000;11(4):615-668. [doi: 10.1016/S1048-9843(00)00062-X]
8. Sutton RT, Pincock D, Baumgart DC, Sadowski DC, Fedorak RN, Kroeker KI. An overview of clinical decision support systems: benefits, risks, and strategies for success. NPJ Digit Med 2020;3(1):17. [doi: 10.1038/s41746-020-0221-y] [Medline: 32047862]
9. Graber ML, Byrne C, Johnston D. The impact of electronic health records on diagnosis. Diagnosis (Berl) 2017 Nov 27;4(4):211-223. [doi: 10.1515/dx-2017-0012] [Medline: 29536944]
10. Shojaei P, Vlahu-Gjorgievska E, Chow YW. Security and privacy of technologies in health information systems: a systematic literature review. Computers 2024;13(2):41. [doi: 10.3390/computers13020041]
11. Heponiemi T, Hyppönen H, Kujala S, et al. Predictors of physicians' stress related to information systems: a nine-year follow-up survey study. BMC Health Serv Res 2018 Apr 13;18(1):284. [doi: 10.1186/s12913-018-3094-x] [Medline: 29653530]
12. Heponiemi T, Hyppönen H, Vehko T, et al. Finnish physicians' stress related to information systems keeps increasing: a longitudinal three-wave survey study. BMC Med Inform Decis Mak 2017 Oct 17;17(1):147. [doi: 10.1186/s12911-017-0545-y] [Medline: 29041971]
13. Saukkonen P, Elovainio M, Virtanen L, et al. The interplay of work, digital health usage, and the perceived effects of digitalization on physicians' work: network analysis approach. J Med Internet Res 2022 Aug 17;24(8):e38714. [doi: 10.2196/38714] [Medline: 35976692]
14. Virtanen L, Kaihlanen AM, Saukkonen P, et al. Associations of perceived changes in work due to digitalization and the amount of digital work with job strain among physicians: a national representative sample. BMC Med Inform Decis Mak 2023 Nov 8;23(1):252. [doi: 10.1186/s12911-023-02351-9] [Medline: 37940995]
15. Nilsen P, Seing I, Ericsson C, Birken SA, Schildmeijer K. Characteristics of successful changes in health care organizations: an interview study with physicians, registered nurses and assistant nurses. BMC Health Serv Res 2020 Feb 27;20(1):147. [doi: 10.1186/s12913-020-4999-8] [Medline: 32106847]
16. Greenhalgh T, Robert G, Macfarlane F, Bate P, Kyriakidou O. Diffusion of innovations in service organizations: systematic review and recommendations. Milbank Q 2004;82(4):581-629. [doi: 10.1111/j.0887-378X.2004.00325.x] [Medline: 15595944]
17. Lääveri T, Reponen J, Vänskä J, Kaila M, Vainiomäki S, Metsäniemi P. Tiedollako johdetaan? tietojärjestelmät johtamisen tukena 2014 ja 2017 lääkärikyselyjen mukaan [Article in Finnish]. Finn Med J 2020;49(2693):9 [FREE Full text]
18. Peltonen LM, Junttila K, Salanterä S. Front-line physicians' satisfaction with information systems in hospitals. Stud Health Technol Inform 2018;247:865-869. [Medline: 29678084]
19. Kontio E, Lundgren-Laine H, Kontio J, Korvenranta H, Salanterä S. Information utilization in tactical decision making of middle management health managers. Comput Inform Nurs 2013 Jan;31(1):9-16. [doi: 10.1097/NXN.0b013e318261f192] [Medline: 22872042]
20. Peltonen LM, Lundgrén-Laine H, Siirala E, Löyttyniemi E, Aantaa R, Salanterä S. Assessing managerial information needs: modification and evaluation of the hospital shift leaders' information needs questionnaire. J Nurs Manag 2018 Mar;26(2):108-119. [doi: 10.1111/jonm.12515] [Medline: 29380914]
21. Saastamoinen P. Physicians' experiences of electronic health records systems. In: Vehko T, editor. E-Health and E-Welfare of Finland - Check Point 2022: Finnish Institute for Health and Welfare; 2022.
22. Potilastietojärjestelmät lääkärin työvälineenä 2021 [Web page in Finnish]. Lääkäriliitto. 2019. URL: https://www.laakariliitto.fi/wp-content/uploads/2024/10/Potilastietojarjestelmat-laakarin-tyovalineena-2021.pdf [accessed 2025-01-05]
23. The ethical principles of research with human participants and ethical review in the human sciences in Finland: Finnish national board on research integrity TENK guidelines 2019 [Report in Finnish]. : Finnish National Board on Research

XSL•FO
RenderX

Integrity; 2019 URL: https://www.tenk.fi/sites/tenk.fi/files/Ihmistieteiden_eettisen_ennakkoarvioinnin_ohje_2019.pdf [accessed 2025-01-16]
24. Poon EG, Blumenthal D, Jaggi T, Honour MM, Bates DW, Kaushal R. Overcoming barriers to adopting and implementing computerized physician order entry systems in U.S. hospitals. Health Aff (Millwood) 2004;23(4):184-190. [doi: 10.1377/hlthaff.23.4.184] [Medline: 15318579]
25. Dugstad J, Eide T, Nilsen ER, Eide H. Towards successful digital transformation through co-creation: a longitudinal study of a four-year implementation of digital monitoring technology in residential care for persons with dementia. BMC Health Serv Res 2019 Jun 10;19(1):366. [doi: 10.1186/s12913-019-4191-1] [Medline: 31182093]
26. Gjellebæk C, Svensson A, Bjørkquist C, Fladeby N, Grundén K. Management challenges for future digitalization of healthcare services. Futures 2020 Dec;124:102636. [doi: 10.1016/j.futures.2020.102636]
27. Health services. Ministry of Social Affairs and Health. 2024. URL: https://stm.fi/en/health-services [accessed 2025-01-16]
28. Quinn M, Forman J, Harrod M, et al. Electronic health records, communication, and data sharing: challenges and opportunities for improving the diagnostic process. Diagnosis (Berl) 2019 Aug 27;6(3):241-248. [doi: 10.1515/dx-2018-0036] [Medline: 30485175]
29. Moy AJ, Hobensack M, Marshall K, et al. Understanding the perceived role of electronic health records and workflow fragmentation on clinician documentation burden in emergency departments. J Am Med Inform Assoc 2023 Apr 19;30(5):797-808. [doi: 10.1093/jamia/ocad038] [Medline: 36905604]
30. Young RA, Roberts RG, Holden RJ. The challenges of measuring, improving, and reporting quality in primary care. Ann Fam Med 2017 Mar;15(2):175-182. [doi: 10.1370/afm.2014] [Medline: 28289120]
31. Anderson J. Older physicians leery of info technology. Caring for the Ages 2012 Mar;13(3):21 [FREE Full text]
32. Burmann A, Tischler M, Faßbach M, Schneitler S, Meister S. The role of physicians in digitalizing health care provision: web-based survey study. JMIR Med Inform 2021 Nov 11;9(11):e31527. [doi: 10.2196/31527] [Medline: 34545813]
33. Kampmeijer R, Pavlova M, Tambor M, Golinowska S, Groot W. The use of e-health and m-health tools in health promotion and primary prevention among older adults: a systematic literature review. BMC Health Serv Res 2016 Sep 5;16 Suppl 5(Suppl 5):290. [doi: 10.1186/s12913-016-1522-3] [Medline: 27608677]
34. Faihs V, Figalist C, Bossert E, Weimann K, Berberat PO, Wijnen-Meijer M. Medical students and their perceptions of digital medicine: a question of gender? Med Sci Educ 2022 Oct;32(5):941-946. [doi: 10.1007/s40670-022-01594-x] [Medline: 36276758]
35. Wekenborg MK, Förster K, Schweden F, et al. Differences in physicians' ratings of work stressors and resources associated with digital transformation: cross-sectional study. J Med Internet Res 2024 Jun 17;26:e49581. [doi: 10.2196/49581] [Medline: 38885014]
36. Gorber SC, Tremblay MS. The objective monitoring of physical activity: contributions of accelerometry to epidemiology, exercise science and rehabilitation. In: Shephard RJ, Tudor-Locke C, editors. Self-Report and Direct Measures of Health: Bias and Implications: Springer International Publishing; 2016:369-376. [doi: 10.1007/978-3-319-29577-0_14]
37. Keskimäki I, Tynkkynen LK, Reissell E, et al. Finland: health system review. In: Health Systems in Transition: European Observatory on Health Systems and Policies; 2019, Vol. 21:1-166.
38. Cunningham CT, Quan H, Hemmelgarn B, et al. Exploring physician specialist response rates to web-based surveys. BMC Med Res Methodol 2015 Apr 9;15:32. [doi: 10.1186/s12874-015-0016-z] [Medline: 25888346]
39. Peltonen LM, Siirala E, Junttila K, et al. Information needs in day-to-day operations management in hospital units: A cross-sectional national survey. J Nurs Manag 2019 Mar;27(2):233-244. [doi: 10.1111/jonm.12700] [Medline: 30298534]

Abbreviations

DHT: digital health technology
EHR: electronic health record
HIS: health information system
OR: odds ratio

Edited by A Coristine; submitted 30.08.24; peer-reviewed by FA Dhabbari, J Walsh; revised version received 26.05.25; accepted 26.05.25; published 26.06.25.

Please cite as:
Heponiemi T, Virtanen L, Kainiemi E, Saukkonen P, Reponen J, Lääveri T
Health Information Systems' Support for Management and Changing Work: Survey Study Among Physicians
JMIR Med Inform 2025;13:e65913
URL: https://medinform.jmir.org/2025/1/e65913
doi:10.2196/65913

XSL•FO
RenderX

© Tarja Heponiemi, Lotta Virtanen, Emma Kainiemi, Petra Saukkonen, Jarmo Reponen, Tinja Lääveri. Originally published in JMIR Medical Informatics (https://medinform.jmir.org), 26.6.2025. This is an open-access article distributed under the terms of the Creative Commons Attribution License (https://creativecommons.org/licenses/by/4.0/), which permits unrestricted use, distribution, and reproduction in any medium, provided the original work, first published in JMIR Medical Informatics, is properly cited. The complete bibliographic information, a link to the original publication on https://medinform.jmir.org/, as well as this copyright and license information must be included.

XSL•FO
RenderX

Construction and Application of an Information Closed-Loop Management System for Maternal and Neonatal Access and Exit Rooms: Non Randomized Controlled Trial

Shafeng Jia[1], BD; Naifeng Zhu[2], BD; Jia Liu[3], BD; Niankai Cheng[3], BD; Ling Jiang[3], BD; Jing Yang[1], BD

[1]Department of Obstetrics, The Affiliated Suzhou Hospital of Nanjing Medical University, No. 26 Daoqian Street, Gusu District, Suzhou, Jiangsu, China

[2]Department of Obstetrics and Neonatology, The Affiliated Suzhou Hospital of Nanjing Medical University, Suzhou, Jiangsu, China

[3]Department of Nursing, The Affiliated Suzhou Hospital of Nanjing Medical University, Suzhou, Jiangsu, China

Corresponding Author:
Jing Yang, BD
Department of Obstetrics, The Affiliated Suzhou Hospital of Nanjing Medical University, No. 26 Daoqian Street, Gusu District, Suzhou, Jiangsu, China

Abstract

Background: Traditional management methods can no longer meet the demand for efficient and accurate neonatal care. There is a need for an information-based and intelligent management system.

Objective: This study aimed to construct an information closed-loop management system to improve the accuracy of identification in mother-infant rooming-in care units and enhance the efficiency of infant admission and discharge management.

Methods: Mothers who delivered between January 2023 and June 2023 were assigned to the control group (n=200), while those who delivered between July 2023 and May 2024 were assigned to the research group (n=200). The control group adopted traditional management methods, whereas the research group implemented closed-loop management. Barcode technology, a wireless network, mobile terminals, and other information technology equipments were used to complete the closed loop of newborn exit and entry management. Data on the satisfaction of mothers and their families, the monthly average qualification rate of infant identity verification, and the qualification rate of infant consultation time were collected and statistically analyzed before and after the closed-loop process was implemented.

Results: After the closed-loop process was implemented, the monthly average qualification rate of infant identity verification increased to 99.45 (SD 1.34), significantly higher than the control group before implementation 83.58 (SD 1.92) (*P*=.02). The satisfaction of mothers and their families was 96.45 (SD 3.32), higher than that of the control group before the closed-loop process was implemented 92.82 (SD 4.73) (*P*=.01). Additionally, the separation time between infants and mothers was restricted to under 1 hour.

Conclusion: The construction and application of the information closed-loop management system significantly improved the accuracy and efficiency of maternal and infant identity verification, enhancing the safety of newborns.

(JMIR Med Inform 2025;13:e66451) doi:10.2196/66451

KEYWORDS

mother-infant same-room management; information-based identity verification; closed-loop management system; newborn safety management

Introduction

In the modern medical environment, ensuring the safe movement of newborns and mothers and effectively managing room exits and entry is an important part of obstetric care and newborn health management. In the 2022 Safety Goals for Patients and the Action Plan to Improve Maternal and Infant Safety, the China Hospital Association clearly emphasized the importance of strengthening maternal and newborn safety. Strategies include improving neonatal access management systems, implementing continuous quality improvement measures, and enhancing safety protocols [1-3]. However, studies have shown that patient identification error rates in medical settings remain as high as 20% despite strict reconciliation procedures [4]. Intelligent systems play an important role in the treatment and care of diseases [5,6]. As the scale of the hospital and the number of beds increases, the traditional manual records and management methods can no longer meet the demands for efficient and accurate management; an information-based and intelligent management system is urgently needed to optimize this process [7]. Although information technology has been widely used in patient identity verification, there are limited reports on its

XSL•FO
RenderX

application in identity verification and door access time monitoring in the neonatal ward. The infant room entry and exit information management system for mother-infant co-care uses modern information technology and 'Internet of things' devices to achieve full process monitoring and management of an infant's movement from the rooms [8]. It uses radio-frequency identification tags, two-dimensional code scanning, and biometric identification technologies to automatically record and track an infant's entry and exit information and achieve closed-loop management. Implementing a full-process closed-loop management system is a core strategy of modern nursing quality management that can improve the intelligent neonatal care. Starting from July 2023, our hospital implemented identity verification and door access–time monitoring for the infant entry and exit rooms based on the mobile nursing platform and implemented closed-loop information management. This study expanded the application of information technology in the field of newborn identity verification and explored the effectiveness of closed-loop management in newborn care, which was an important supplement to the field of intelligent neonatal care. This study aimed to construct an information closed-loop management system to improve the accuracy of identification in mother-infant rooming-in care units and enhance the efficiency of infant admission and discharge management.

Methods

Study Setting

In July 2023, the information closed-loop management system for barrier-free neonatal wards was officially launched in the Obstetrics and Gynecology ward of the hospital. The study included 400 mothers (n=200 per group) admitted to the hospital between January 2023 and May 2024. The exclusion criteria were as follows: the mothers needed to be transferred to another hospital after admission, the medical records were incomplete, or the newborns needed to be isolated from the mother due to illness. The parturients admitted to the hospital between January 2023 and June 2023 were assigned to the control group, while those admitted between July 2023 and May 2024 were assigned to the research group. Data on metrics such as the workload and work efficiency of nurses, the satisfaction of mothers and their families, the standard rate of newborn identity verification, and newborn visit time qualification rate were collected and statistically analyzed.

Information Closed-Loop Management System for Mother and Infant Newborns

Manual inspection methods are used in the traditional newborn admission and discharge management process. These methods rely on nursing staff to visually compare the wristband and foot information of the mother and the newborn and to conduct oral checks on the following main content: (1) room information verification, (2) oral confirmation, and (3) postadmission information verification. This method mainly relies on nursing staff or inquiries from the mother and her family, where the human factor has a large impact. Reports show that 40 - 60% of mothers experience postpartum fatigue, which manifests as decreased attention during medical examinations and communication, thereby increasing the risk of verification errors and medical accidents [9-11].

Design of a Closed-Loop Management System for the Neonatal Access Room

The closed-loop management system includes three functional modules: (1) the medical order module, which includes the medical order system and the electronic nursing system; (2) the label barcode printing module, which prints maternal wristbands and newborn 'A and B' wristbands; and (3) the statistical function module, which manages the statistical room time pass rates.

The management system includes a database management system (DBMS), handheld personal digital assistant (PDA) devices, and QR barcode recognition technology. PDAs equipped with a barcode scanner can print and scan the QR codes, which serve as identifiers, to read and transmit data to the central database server through a wireless network. The DBMS is responsible for processing data requests from the PDA device. During the management of newborn entry and exit, the PDA device is used to verify whether the QR code matches the DBMS records. If the match is successful, the server sends the confirmation information back to the PDA device and displays the correct identification details along with a voice prompt on the PDA device, indicating successful authentication. Simultaneously, the interface records the job number of the nursing staff and the time of entering and leaving the room for process management. It is worth noting that only authorized caregivers can use the PDA device for identification, ensuring the security of the system and avoiding mistrust. This management system provides a fast, accurate, and safe method for confirming the identity of the mother and child, thereby improving the efficiency of hospital work and ensuring the safety of the newborn.

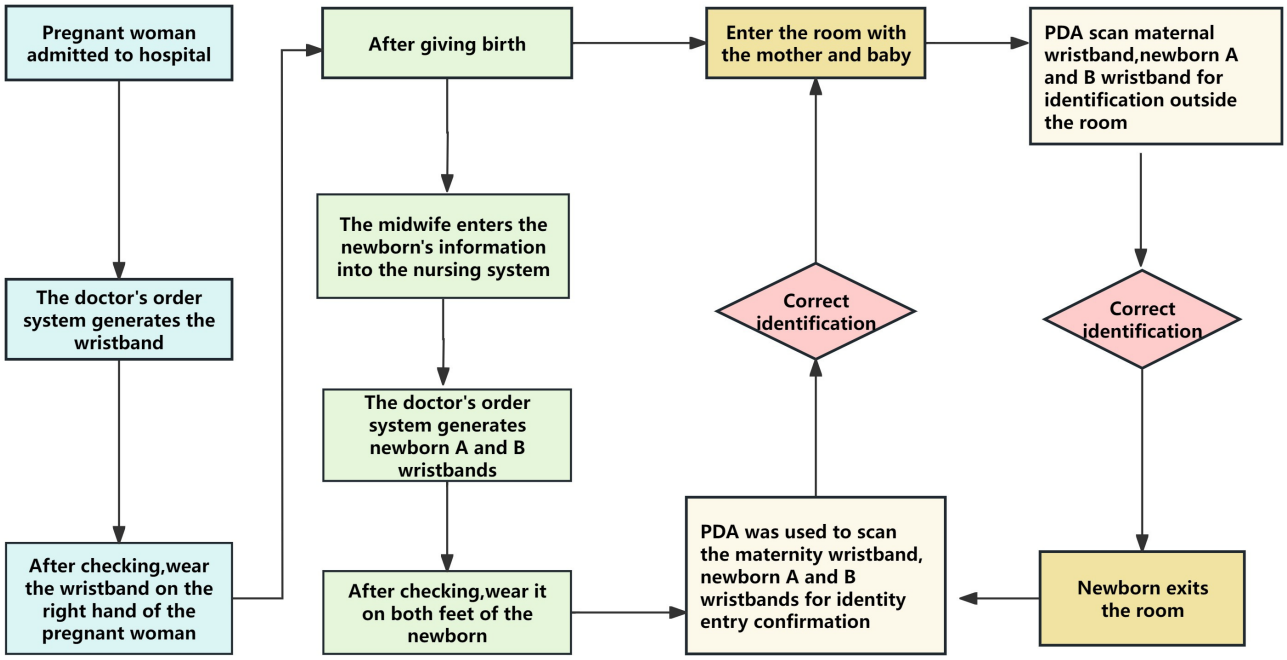
Management Plan for Building a Closed-Loop Information System for Newborn Admission and Discharge

The management team comprised five members, including one leader, with the deputy director of the nursing department responsible for leading the entire closed-loop management work. The team members organized the neonatal exit and entry operation through multiple surveys and consulted relevant literature [12-17]. In conjunction with the Information Department, they designed the closed-loop management system for neonatal exit and entry with the objective of monitoring and controlling the entire process, to ensure the safety of children. The process uses barcode technology, a wireless network, mobile terminals, and other information technology equipment to facilitate closed-loop management of newborn exit and entry. Furthermore, the team secured a computer software copyright (certificate number: 11934939). The specific operational process is shown in Figure 1. This flowchart describes the closed-loop information management process from the time the newborn is separated from the mother to the time of returned to the mother, covering admission, through delivery, and the mother's discharge. The process is divided into the following steps:

XSL•FO
RenderX

1. Pregnant women complete admission registration in the outpatient system, generating accurate personal information based on their identity card or medical insurance card, including name, age, and unique hospitalization number.
2. Pregnant women enter the ward and use the ward system to generate wristbands, which are verified by two staff members before being worn on the right hand, include details such as name, hospitalization number, age and a QR code.
3. After the baby is delivered, the system imports delivery information and generates neonatal A and B wristbands with QR codes, which are verified by two staff members, and worn on the wrists and feet of the newborn.
4. When the mother and newborn leave the delivery room, a PDA device is used to scan the QR code on the wristbands of the mother and newborn for identification.
5. When the mother and infant enter the room, a ward nurse uses a PDA device to scan the QR code on the wristband of the mother and newborn again for identification to form a closed loop of admission and exit.
6. When the newborn leaves the mother for examination, vaccination, or treatment, a PDA device is used to scan the QR code on the mother and the newborn's wristband for identification in the exit room.
7. When returning to the mother, a PDA device is used to scan the wristbands of the mother and newborn again to check the QR codes at the admission identification site to form a closed loop of access. The entire process emphasizes closed-loop management, ensuring the safety and correct identification of mothers and infants during hospitalization and improving the quality and efficiency of medical services.

Figure 1. Identification process for neonatal admission and discharge. PDA: personal digital assistant.



Identity Verification of Pregnant Women's Admission Information

After the pregnant woman is admitted to the hospital, the identity verification process follows three steps: (1) completion of hospitalization registration: the system automatically assigns a unique hospitalization number as the pregnant woman's identifier within the hospital; (2) wristband printing: after the pregnant woman is transferred to the ward, the nursing staff initiates the wristband printing function through the medical order system. The wristband is printed with the name, gender, time of admission, age, the hospital number of the pregnant woman, and a unique information QR code; (3) review: before wearing the wristband, the nursing staff strictly review the printed information and the actual details of the pregnant women to ensure the consistency of information.

Newborn Identity Verification After Delivery

After delivery, the newborn identity verification process is as follows: (1) information entry: the midwife records the basic information of the newborn on the mobile nursing platform in the delivery room or operating room, including birth time, gender, and weight; (2) newborn wristband generation: the maternal personal medical consultation system generates the corresponding newborn A and B wristbands comprising the newborn's information. The wristband is printed by a barcode printer with information including the name of the pregnant woman, sex of the newborn, weight, hospital number, and QR code; (3) information check: the midwife performs a double-check to ensure that the wristband details match those of the newborn and the mother; (4) wristband wearing: after examination, the midwife attaches A and B wristbands to the newborn's ankles and informs the mother and family of their significance, emphasizing that they should not be removed to ensure the safety of the newborn; (5) identity matching: before the mother is transferred to the mother-baby room, the midwife scans the mother's and the newborn's A and B wristbands. If the PDA device shows a match, the identification is confirmed, and both are safely transferred to the room.

XSL•FO
RenderX

Verification of Maternal Identity in the Mother-and-Baby

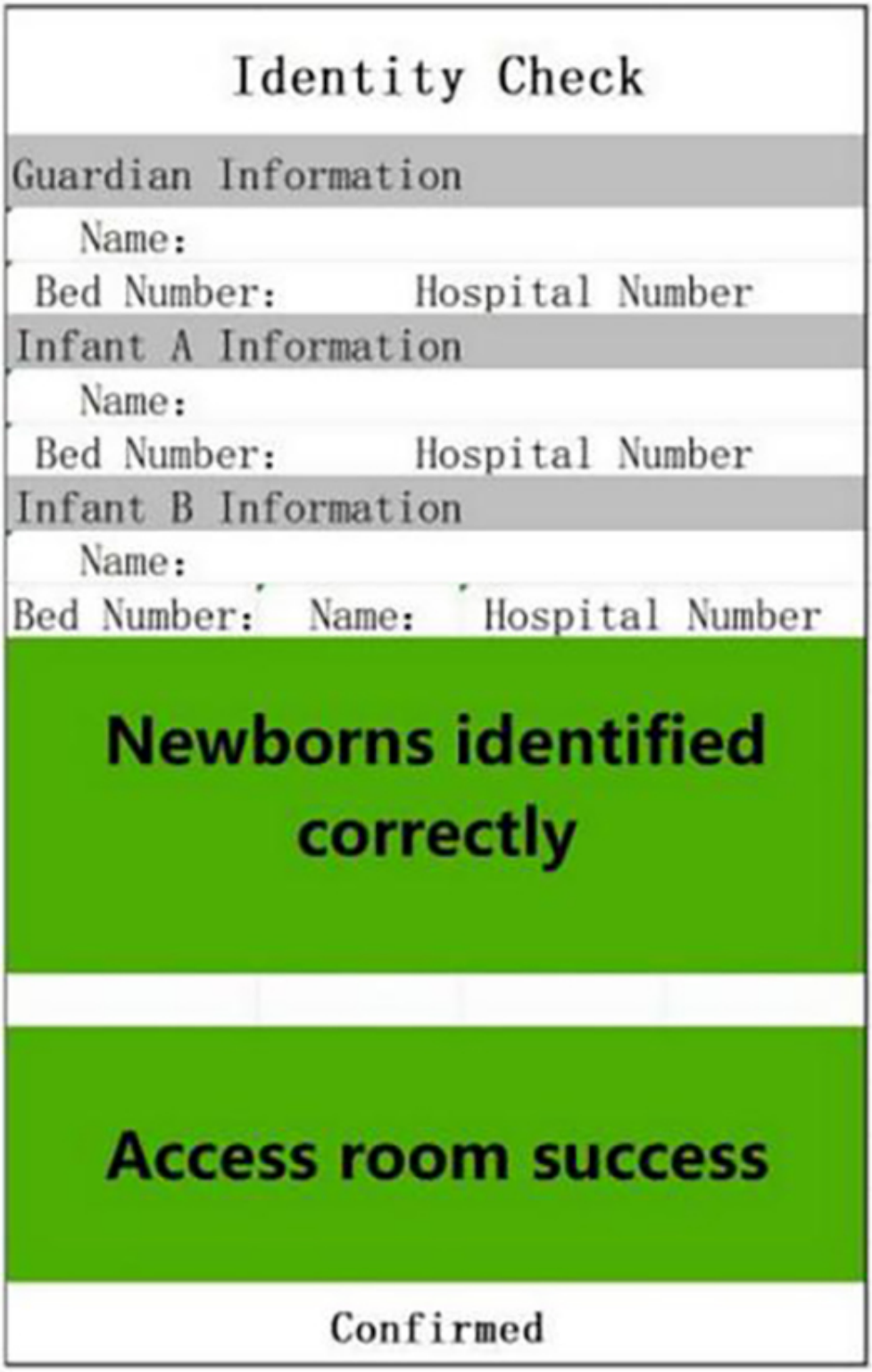
To ensure the safety of the mother and child within the same room, the following strict identity verification process is implemented: (1) handover and information check: the midwife and nursing staff conduct a detailed handover according to the protocol, verifying the basic information of the mother and newborn and record them; (2) PDA scan to verify identity: the mother and child use the PDA device in the same room to scan the mother's wristband and the two-dimensional QR codes of the A and B newborn wristbands, ensuring identity consistency; (3) authentication completion: if the PDA indicates a successful match, the authentication process is considered complete.

Identity Verification During Newborn Entry and Exit from the Mother-and-Baby Room

Newborns often need to be temporarily separated from their mothers for routine nursing activities such as morning baths, examinations, and vaccinations. In this context, the safety risks are increased as multiple newborns may be under the custody of the nursing staff at the same time [18]. Accurate identity verification plays a vital role in ensuring the safety of newborns and avoiding identity confusion. The following identity verification process is executed: (1) identification before leaving the room: nursing staff use PDA equipment to scan the A and B wristbands of mothers and newborns to confirm the identity information. The PDA device confirms the identity-matching with the green module and voice prompt, and displays the job number of the executor and the time of the newborn's exit (Figure 2); the nurse confirms the information with the mother and family members to ensure accuracy; (2) post-entry verification: when the newborn is returned to the ward after completing the relevant project activities, the nursing staff scan the QR code of the mother and newborn again. Similarly, the PDA device verifies the identity and records the job number and the entry time of the executor to complete the entry verification.

XSL•FO
RenderX

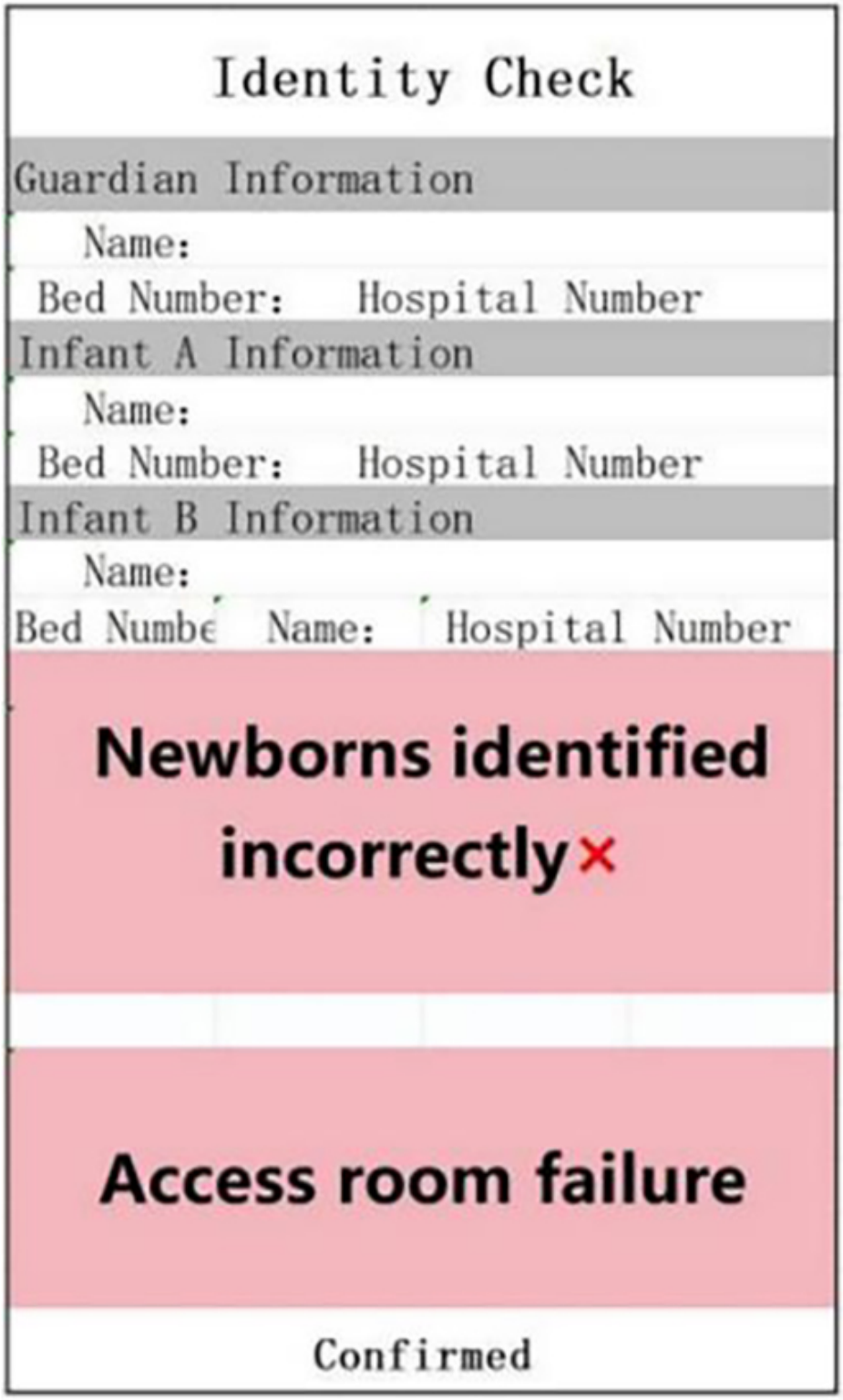
Figure 2. The system successfully identifies and confirms the mother-infant identity match.



Throughout the process, any error or unsuccessful verification is immediately indicated by the red module and the voice prompt "recognition error" (Figure 3), allowing for timely correction. The PDA green module and voice prompt confirm the accuracy of identity verification. This process not only improves the efficiency of identity verification but also enhances caregivers' alertness through color coding and voice prompts [19]. Additionally, new mothers and their families can actively participate in nursing safety management, increasing the sense of trust in the operation of nursing staff and ensuring the safety of both mother and child.

XSL•FO
RenderX

Figure 3. Identification failures due to identity mismatch or other issues.



Time Management of Newborns During Mother-Baby Separation

The evaluation criteria of baby-friendly hospitals require that—except for the separation of mother and child with medical indications—the mother and newborn should remain together for 24 hours, with separation not exceeding 1 hour per day. Therefore, to support this requirement, time statistics and alarm functions relating to the newborn access room were added to the closed-loop management system (Figure 4). When the separation time exceeds the set threshold (ie, 45 min), the PDA immediately issues an alarm, to remind the nursing staff to send the newborn back to the room promptly.

XSL•FO
RenderX

Figure 4. Key information on the management of neonatal admission and exit rooms.

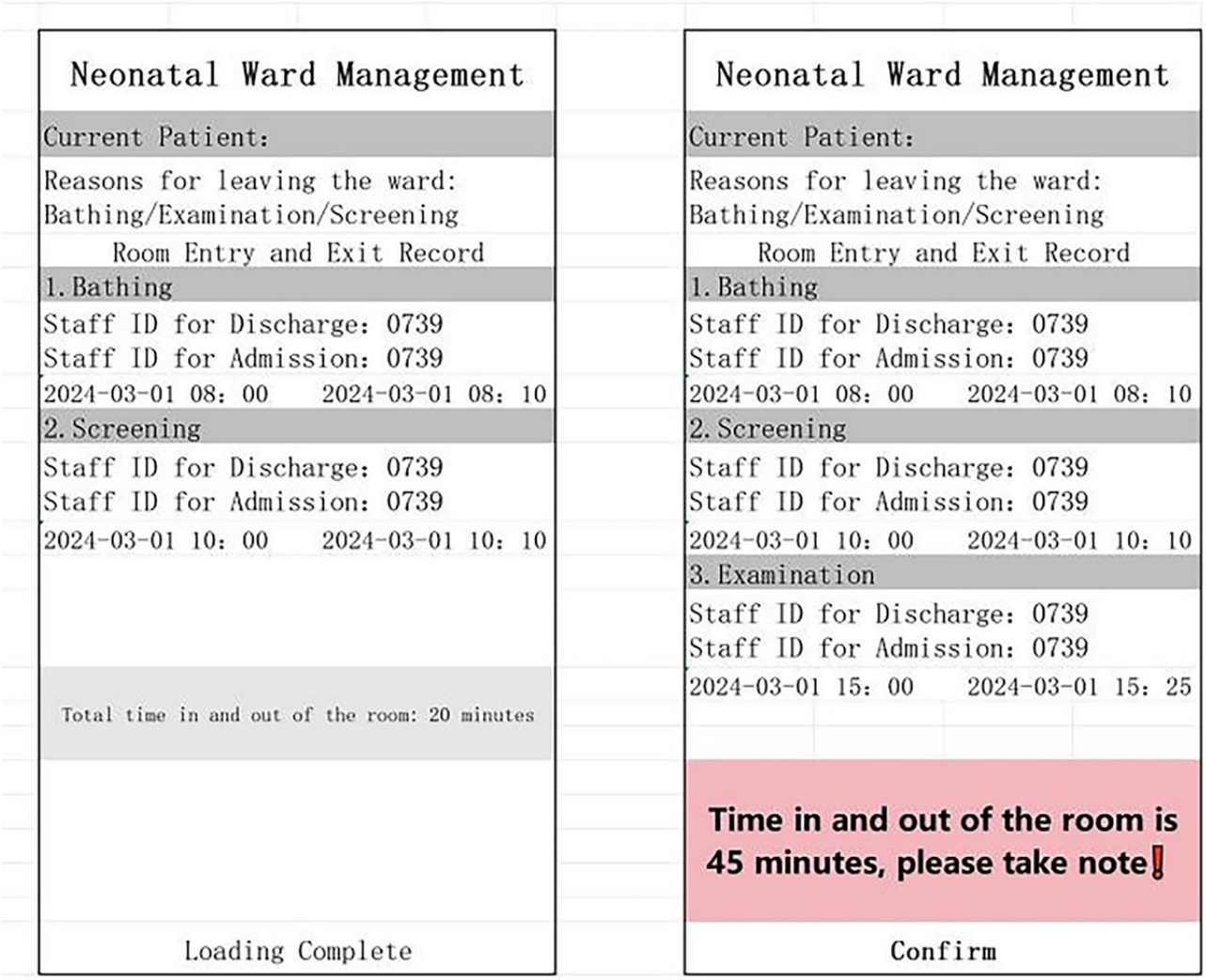


Figure 4 provides key information on the management of neonatal admission and exit rooms, specifically including the following aspects:

1. Patient information display: the interface displays information about the current neonatal patient.
2. Reasons for leaving the ward: the system lists reasons for the newborn leaving the ward, including bathing, examination, or disease screening.
3. Time record: the exact time at which the newborn leaves and returns to the mother is recorded.
4. Staff identification: the identification number of the responsible staff member for the admission and exit of the newborn is recorded to facilitate tracking of the person.
5. Entry and exit time limit prompt: the interface particularly emphasizes that the time limit for newborns to enter and exit the room is 45 minutes and reminds the staff to pay attention to the time, so as not to exceed the specified time (ie, 1 h).
6. Warning tone function: if the mother-infant separation time exceeds 45 minutes, the system issues a warning tone, which helps the staff track the newborns and ensures the safety and standardization of the process.

Statistical Analysis

The SPSS software (version 26.0; IBM Corp) was used for statistical processing. A paired design *t* test (two-tailed) was used for the comparison between the two groups. Categorical data were expressed as frequency (n) or percentage (%), and a *P* value of <.05 was considered statistically significant.

Ethical Considerations

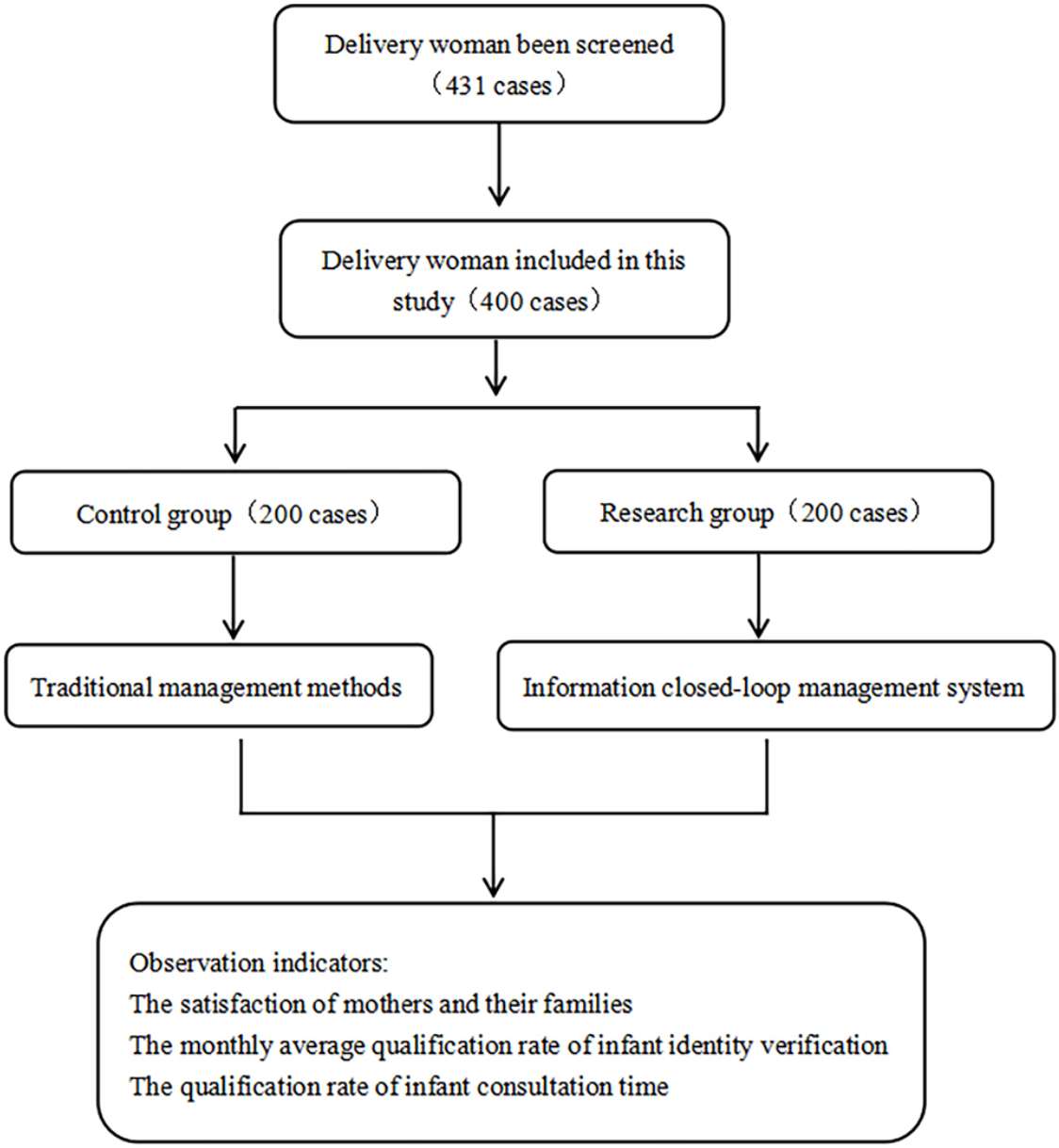
This study was conducted in accordance with the Declaration of Helsinki. This study was conducted with approval from the Ethics Committee of The Affiliated Suzhou Hospital of Nanjing Medical University (ID: KL901515). All family members of newborns gave their informed consent to this study. All data collected during this study were anonymized to protect the privacy and confidentiality of the participants. No personally identifiable information was retained in the dataset. The data were stored securely, with access restricted to the research team members who had undergone appropriate training in data handling and confidentiality. No financial compensation was provided to the participants for their involvement in this study. Participation was voluntary, and no incentives were offered. No images or supplementary materials containing identifiable features of the participants were included in the manuscript.

XSL•FO
RenderX

Results

The participant screening process is shown in (Figure 5).

Figure 5. The participant screening process.



Effect Evaluation

There were no significant differences in age, time of delivery, mode of delivery, economic status, educational level, or general characteristics between the study groups (*P*=.14).

Identity Verification Pass Rate

Identity verification was performed at each entry, with the first verification result used as the assessment index for the identity verification pass rate. After implementation of the closed-loop process between July 2023 and May 2024, the average monthly pass rate of neonatal identity verification was 99.45 (SD 1.34), which was higher than that of the control group, 83.58 (SD 1.92) before the operation process (*P*=.02) (Table 1).

Table . Comparison of identity verification pass rate and satisfaction level between groups.

Variables	Control group (n=200), mean (SD)	Research group (n=200), mean (SD)	*P* value
Average monthly pass rate of neonatal identity verification	83.58 (1.92)	99.45 (1.34)	.02
Satisfaction level	92.82 (4.73)	96.45 (3.32)	.01

XSL•FO
RenderX

Satisfaction Level

After the closed-loop process, the satisfaction among the pregnant women and their families was 96.45 (SD 3.32), which is higher than that of the control group, 92.82 (SD 4.73) before the closed-loop process (P=.01) (Table 1).

Efficiency of the Entry and Exit Process

The efficiency of the traditional neonatal entry and exit process is low; for 80 newborns, a nurse must verify 240 labels daily, requiring approximately 80 minutes for copying and checking the labels. Compared to the traditional process, the closed-loop management system significantly reduced the execution time, decreasing the total verification time for 80 identity verifications to 15 minutes, with daily quality control verification requiring only 2 minutes. This improvement enhances the efficiency of neonatal nursing work and significantly improves the accuracy and efficiency of the verification work; thus, the process not only reduces the workload of nurses but also improves the quality of nursing services and ensures the safety of newborns. Before the implementation of the system, the exit and entry process could not effectively monitor the separation time between newborns and their mothers. After the implementation, the statistics of the background system showed that the real-time tracking and management of the newborn access times were achieved, with all newborns separations remaining below the 1-hour limit. These findings show that the newborn entry and exit times were effectively controlled to ensure their safety and timely nursing.

Discussion

Principal Findings

In this study, the monthly average qualification rate of infant identity verification after the implementation of the closed-loop process was higher than that of the control group. After the closed-loop process was implemented, the satisfaction of mothers and their families was higher than before the closed-loop process was implemented, and the separation time between infants and mothers was controlled within 1 hour.

Innovation and Implementation Effect

The primary aim of closed-loop management is to ensure the safety of mother and child and improve the quality of care. In the existing literature, research on information closed-loop management systems for neonatal access rooms is relatively rare, particularly regarding changes in the implementation rate of identity verification standards before and after the implementation of the system, as well as statistical analyses of time monitoring within the access room. The closed-loop information management system developed in this study demonstrates significant innovation. Through the close collaboration between the interdisciplinary team, this system not only simplifies the traditional manual verification process but also ensures the accuracy and real-time performance of information.

Research has shown that intelligent systems can help practitioners make decisions, reduce their workload, and increase their efficiency and accuracy by incorporating artificial intelligence systems into their daily practice [20,21]. Regarding implementation effectiveness, a comparative analysis of the data before and after implementation, we found that the implementation rate of the newborn identity verification standards was significantly improved. The average monthly pass rate of neonatal identity verification in the study group was higher than that in the control group before the operational process, with a statistically significant difference. With precise time management, we ensured that newborns received timely and continuous care and improved the efficiency and response speed of care work. After the implementation of the system, 24-hour neonatal access room time supervision was achieved, and the qualification rate reached 100%, demonstrating high efficiency and systematic improvement in time management. Detailed statistical analyses of different ventricular event durations provided valuable data support. These data provided the basis for both the evaluation and improvement of current care processes and a scientific temporal database for future process optimization and the development of time management strategies. By analyzing these data, potential bottlenecks can be identified, the allocation of resources can be optimized, and the overall quality and efficiency of nursing services can be improved.

Closed-loop management methods have been explored in blood transfusion, breastfeeding, and care of premature newborns, yielding promising results [22-25]. Compared to traditional neonatal access management approaches, the closed-loop management system can not only reduce human interference factors but also trace the source of the whole process, strengthen supervision, further reduce risks, enhance doctor-patient relationships, and enhance trust, facilitate postpartum recovery, and reduce the risk of postpartum anxiety [26-28]. This closed-loop management system can also be extended to continuous blood glucose monitoring in critically ill newborns and pharmaceutical management for newborns, further enhancing full-process management and advancing precision medical digitalization [29,30].

Improvements in Maternal and Infant Safety and Nursing Quality

The implementation of closed-loop management not only improves the safety of mothers and neonates but also significantly improves the quality of care. Through the data analyzed in this study, we found that after the implementation of closed-loop information management, the integrity of newborn access room records was significantly improved, and the traceability of nursing quality was enhanced. The completeness and traceability of data increased the safety of the mother and baby. Additionally, the intelligent system reduced the time burden on the nursing staff and provided convenient management of mother and baby information, which improved the quality of nursing and patient satisfaction. After the implementation of the system, caregivers' time spent on identity verification decreased by 84.55%, which enabled them to devote more time and energy to direct nursing work, thus improving the overall quality of nursing services. Specifically, in the patient satisfaction survey, maternal and family satisfaction was significantly higher after the implementation of the closed-loop process than before, with a statistically significant difference.

XSL•FO
RenderX

System Optimization and Prospects

Despite the system's positive outcomes, there are still areas for improvement. For example, real-time monitoring, security alerts, and authentication need to be enhanced. In the future, we will continue to optimize information use to further refine nursing processes and improve the humanization and intelligence level of the system, to achieve more accurate and efficient nursing services. Additionally, we will also focus on how to achieve better closed-loop management and security measures through upgrading technology.

Conclusion

The construction and application of an information-based closed-loop management system have enabled both real-time monitoring of newborns and comprehensive management of the entire nursing process. This system has significantly improved the safety of newborn care.

Data Availability

All data generated or analyzed during this study are included in this published article.

Authors' Contributions

Conceptualization: SJ
Data curation: JY, SJ
Formal analysis: JY, NZ
Methodology: SJ
Project administration: LJ, NC, SJ, NZ
Resources: LJ, NZ
Writing – original draft: JL, JY, LJ, NC, SJ, NZ
Writing – review & editing: JL, JY, LJ, NC, SJ, NZ

Conflicts of Interest

None declared.

References

1. Stephansson O, Sandström A. Can short- and long-term maternal and infant risks linked to hypertension and diabetes during pregnancy be reduced by therapy? J Intern Med 2024 Sep;296(3):216-233. [doi: 10.1111/joim.13823] [Medline: 39045893]
2. Hu JMY, Arbuckle TE, Janssen PA, et al. Gestational exposure to organochlorine compounds and metals and infant birth weight: effect modification by maternal hardships. Environ Health 2024 Jul 1;23(1):60. [doi: 10.1186/s12940-024-01095-x] [Medline: 38951908]
3. Zeng B, Liu X, Yang Q, Wang J, Ren Q, Sun F. Efficacy and safety of vaccines to prevent respiratory syncytial virus infection in infants and older adults: a systematic review and meta-analysis. Int J Infect Dis 2024 Sep;146:107118. [doi: 10.1016/j.ijid.2024.107118] [Medline: 38878994]
4. Wang S, Zhao Y, Yang Z, et al. 919 granules improve postpartum depression through the regulation of abnormal peripheral blood IL-1β. Biomedicine & Pharmacotherapy 2024 May;174:116623. [doi: 10.1016/j.biopha.2024.116623]
5. Shin J, Kim S, Lee J, et al. Efficacy of mobile app-based cognitive behavioral therapy for insomnia: multicenter, single-blind randomized clinical trial. J Med Internet Res 2024 Jul 26;26:e50555. [doi: 10.2196/50555] [Medline: 39058549]
6. Bold KW, Garrison KA, DeLucia A, et al. Smartphone apps for smoking cessation: systematic framework for app review and analysis. J Med Internet Res 2023 Jul 13;25:e45183. [doi: 10.2196/45183] [Medline: 37440305]
7. Li X, Zhang P, Zhang Y, Cui G, Du H. Effect of midwives' application of intelligent delivery room management system on delivery outcome. Comput Math Methods Med 2022:4912053. [doi: 10.1155/2022/4912053] [Medline: 35669374]
8. Wang Y, Fu W, Gu Y, et al. Comparative survey among paediatricians, nurses and health information technicians on ethics implementation knowledge of and attitude towards social experiments based on medical artificial intelligence at children's hospitals in Shanghai: a cross-sectional study. BMJ Open 2023 Nov;13(11):e071288. [doi: 10.1136/bmjopen-2022-071288]
9. Han H, Yuan B. Analysis and countermeasures of the causes of patient identification defect [Chinese]. Pharmaceutical economics of China 2013;04:392-393 [FREE Full text] [doi: 10.3969/j.issn.1673-5846.2013.04.228]
10. Ling K, Hong M, Jin L, Wang J. Blood metabolomic and postpartum depression: a Mendelian randomization study. BMC Pregnancy Childbirth 2024 Jun 14;24(1):429. [doi: 10.1186/s12884-024-06628-3] [Medline: 38877415]
11. Baattaiah BA, Alharbi MD, Aldhahi MI, Khan F. Factors associated with postpartum fatigue: an exploration of the moderating role of resilience. Front Public Health 2024;12:1394380. [doi: 10.3389/fpubh.2024.1394380] [Medline: 38947349]
12. Yu C, Zheng S. Used HFMEA to improve the newborn identification process [Chinese]. Contemporary Nurses 2020;27(8):186-189 [FREE Full text] [doi: 10.19792/j.cnki.1006-6411.2020.23.079]
13. Tian A, Shi M. Analysis of safety nursing key points for neonatal identification [Chinese]. Clin Med Res 2017;2(28):182-183 [FREE Full text] [doi: 10.19347/j.cnki.2096-1413.201728090]

XSL•FO
RenderX

14. Xu R, Wang H, Yang W, et al. Evidence summary of patient identification [Chinese]. Chinese Nursing Journal 2021;56(6):921-928. [doi: 10.3761/j.issn.0254-1769.2021.06.021]
15. Wang L, Wang H, Xu R, et al. Summary of the best evidence for patient identification tools/techniques [Chinese]. Journal of Nursing 2021;36(4):97-100 [FREE Full text] [doi: 10.3870/j.issn.1001-4152.2021.04.097]
16. Xiaoqian H, Kong C. The effect of ISBAR communication mode on nurse shift handover in obstetrics and gynecology wards. Int J Nurs (N Y) 2019;38(13):1927-1930 [FREE Full text] [doi: 10.3760/cma.j.issn.1673-4351.2019.13.003]
17. Jiang J. The application effect of mobile nursing quality control management information platform in nursing quality control. Evidence-based care 2023;9(12):2259-2261 [FREE Full text] [doi: 10.12102/j.issn.2095-8668.2023.12.032]
18. Tonismae TR, Tucker Edmonds B, Bhamidipalli SS, et al. Intention to treat: obstetrical management at the threshold of viability. Am J Obstet Gynecol MFM 2020 May;2(2):100096. [doi: 10.1016/j.ajogmf.2020.100096] [Medline: 33345962]
19. Yan Y, Man Y, Sun X, Yan S, Zuo J. On the use of color elements in nursing management [Chinese]. J Clin Nurs 2013;12(5):73-74 [FREE Full text] [doi: 10.3969/j.issn.1671-8933.2013.05.036]
20. Desai GS. Artificial intelligence: the future of obstetrics and gynecology. J Obstet Gynaecol India 2018 Aug;68(4):326-327. [doi: 10.1007/s13224-018-1118-4] [Medline: 30065551]
21. Iftikhar P, Kuijpers MV, Khayyat A, Iftikhar A, DeGouvia De Sa M. Artificial intelligence: a new paradigm in obstetrics and gynecology research and clinical practice. Cureus 2020 Feb 28;12(2):e7124. [doi: 10.7759/cureus.7124] [Medline: 32257670]
22. Hu X, Lu J, Zhang J, et al. Survey on human milk feeding and enteral feeding practices for very-low-birth-weight infants in NICUs in China Neonatal Network. BMC Pediatr 2023 Feb 11;23(1):75. [doi: 10.1186/s12887-023-03862-0] [Medline: 36765301]
23. Low CS, Ho JJ, Nallusamy R. Impact of a new aggressive nutrition policy incorporating early introduction of parenteral nutrition and mother's own milk on growth of preterm infants. World J Pediatr 2016 Nov;12(4):450-454. [doi: 10.1007/s12519-016-0037-7] [Medline: 27286688]
24. Olusanya BO, Ogunlesi TA, Kumar P, et al. Management of late-preterm and term infants with hyperbilirubinaemia in resource-constrained settings. BMC Pediatr 2015 Apr 12;15:39. [doi: 10.1186/s12887-015-0358-z] [Medline: 25884679]
25. Alfirevic Z, Milan SJ, Livio S. Caesarean section versus vaginal delivery for preterm birth in singletons. Cochrane Database Syst Rev 2013 Sep 12;2013(9):CD000078. [doi: 10.1002/14651858.CD000078.pub3] [Medline: 24030708]
26. Munda A, Kovacic C, Pongrac Barlovic D. Real-world data on the Minimed 780G advanced hybrid closed-loop system use during type 1 diabetes pregnancy: One centre observational study. J Diabetes Complications 2024 Aug;38(8):108795. [doi: 10.1016/j.jdiacomp.2024.108795] [Medline: 38878423]
27. Giannoulaki P, Kotzakioulafi E, Nakas A, Kontoninas Z, Evripidou P, Didangelos T. Use of advanced hybrid closed-loop system during pregnancy: strengths and limitations of achieving a tight glycemic control. J Clin Med 2024 Mar 1;13(5):1441. [doi: 10.3390/jcm13051441] [Medline: 38592281]
28. Stafford IG, Lai NM, Tan K. Automated oxygen delivery for preterm infants with respiratory dysfunction. Cochrane Database Syst Rev 2023 Nov 30;11(11):CD013294. [doi: 10.1002/14651858.CD013294.pub2] [Medline: 38032241]
29. Guibert C, Amoura L, Rakotoarisoa L, et al. MiniMedTM 780G advanced hybrid closed-loop system study in pregnant women with type 1 diabetes. Diabetes Technol Ther 2023 Dec;25(12):893-901. [doi: 10.1089/dia.2023.0267] [Medline: 37956265]
30. Schouten TMR, Abu-Hanna A, van Kaam AH, et al. Prolonged use of closed-loop inspired oxygen support in preterm infants: a randomised controlled trial. Arch Dis Child Fetal Neonatal Ed 2024 Feb 19;109(2):221-226. [doi: 10.1136/archdischild-2023-325831] [Medline: 37827816]

Abbreviations

DBMS: database management system
PDA: personal digital assistant

Edited by C Lovis; submitted 13.09.24; peer-reviewed by J Zhang, Y Yuan; revised version received 11.02.25; accepted 19.02.25; published 07.04.25.

Please cite as:
Jia S, Zhu N, Liu J, Cheng N, Jiang L, Yang J
Construction and Application of an Information Closed-Loop Management System for Maternal and Neonatal Access and Exit Rooms: Non Randomized Controlled Trial
JMIR Med Inform 2025;13:e66451
URL: https://medinform.jmir.org/2025/1/e66451
doi:10.2196/66451

XSL•FO
RenderX

© Shafeng Jia, Naifeng Zhu, Jia Liu, Niankai Cheng, Ling Jiang, Jing Yang. Originally published in JMIR Medical Informatics (https://medinform.jmir.org), 7.4.2025. This is an open-access article distributed under the terms of the Creative Commons Attribution License (https://creativecommons.org/licenses/by/4.0/), which permits unrestricted use, distribution, and reproduction in any medium, provided the original work, first published in JMIR Medical Informatics, is properly cited. The complete bibliographic information, a link to the original publication on https://medinform.jmir.org/, as well as this copyright and license information must be included.

XSL•FO
RenderX

Correlation Between Diagnosis-Related Group Weights and Nursing Time in the Cardiology Department: Cross-Sectional Study

Chen Lv[1], MD; Yi-Hong Gong[2], MD; Xiu-Hua Wang[3], BD; Jun An[4], BD; Qian Wang[5], BD; Jing Han[6], BD; Xiao-Feng Chen[7], MD

[1]Department of Nursing, Beijing Chest Hospital, Capital Medical University, Beijing, China

[2]Department of Performance and Reform, Beijing Chest Hospital, Capital Medical University, Beijing, China

[3]Department of Nursing, Beijing Chest Hospital, Capital Medical University, Beijing, China

[4]Department of Information Center, Beijing Chest Hospital, Capital Medical University, Beijing, China

[5]Department of Orthopaedics, Beijing Chest Hospital, Capital Medical University, Beijing, China

[6]Department of Cardiology, Beijing Chest Hospital, Capital Medical University, Beijing, China

[7]Department of Intensive Care Unit, Beijing Chest Hospital, Capital Medical University, No.9 Beiguan Street, Area 1, Tongzhou District, Beijing, China

Corresponding Author:
Xiao-Feng Chen, MD
Department of Intensive Care Unit, Beijing Chest Hospital, Capital Medical University, No.9 Beiguan Street, Area 1, Tongzhou District, Beijing, China

Abstract

Background: Diagnosis-related group (DRG) payment has become the main form of medical expense settlements, and its application is becoming increasingly extensive.

Objective: This study aimed to explore the correlation between DRG weights and nursing time and to develop a predictive model for nursing time in the cardiology department based on DRG weights and other factors.

Methods: A convenience sampling method was used to select patients who were hospitalized in the cardiology ward of Beijing Chest Hospital between April 2023 and April 2024. Nursing time was measured by direct and indirect nursing time. To determine the distributions of nursing time based on different demographics, a Pearson correlation was used to analyze the relationship between DRG weight and nursing time, and a multiple linear regression was used to determine the influencing factors of total nursing time.

Results: A total of 103 subjects were included in this study. The DRG weights were positively correlated with direct nursing time (r=0.480; P<.001), indirect nursing time (r=0.394; P<.001), and total nursing time (r=0.448; P<.001). Moreover, age was positively correlated with the 3 nursing times (direct: r=0.235; indirect: r=0.192; total: r=0.235; all P<.001). The activities of daily living (ADL) score on admission was negatively correlated with the 3 nursing times (direct: r=−0.316; indirect: r=−0.252; total: r=−0.301; all P<.001). In addition, the nursing level on the first day of admission was positively correlated with the 3 nursing times (direct: r=0.333; indirect: r=0.332; total: r=0.352; all P<.001). Furthermore, the multivariate analysis found that the nursing level on the first day of admission, complications or comorbidities, DRG weight, and ADL score on admission were the influencing factors of nursing time (R^2=0.328; $F_{5,97}$=69.58; P<.001).

Conclusions: DRG weight showed a strong correlation with nursing time and could be used to predict nursing time, which may assist in nursing resource allocation in cardiology departments.

(JMIR Med Inform 2025;13:e65549) doi:10.2196/65549

KEYWORDS

diagnosis-related groups; nursing time; workload; human resources; nursing

Introduction

Measuring nursing time is beneficial to effectively avoid excess nursing labor costs from unreasonable time allocations. Nursing time is closely associated with the disease severity of patients [1], which is currently assessed through quantitative scoring systems, such as the Acute Physiology and Chronic Health Evaluation II scores and the Nursing Activity Scale [2]. However, these assessment methods are only suitable for assessing critically ill patients and have limitations [3]. The Patient Classification System (PCS) involves activities such as categorizing and quantifying the nursing level required by a

XSL•FO
RenderX

patient at a given time, assigning work using scales, and calculating personnel requirements [4]. The PCS-based scientific management of nursing personnel is of great significance [5]. The diagnosis-related group (DRG) system is a diagnosis and treatment classification system that can effectively evaluate the severity of a disease classification and can combine cases based on the discharge diagnosis and careful consideration of complex disease-related factors, such as patient complications, different treatment methods, and other patient-specific differences [6]. The basic principles of DRGs are as follows: they are patient-centered; grouping is performed according to factors such as disease diagnosis, treatment methods and individual characteristics; prepaid systems are used to control costs; they encourage hospitals to improve service efficiency and quality; and they ensure reasonable costs through supervision. At the same time, grouping and payment standards are continuously optimized with the development of medical technologies to improve the quality of medical services and patient satisfaction.

DRG classification is globally recognized as an effective tool for hospital management and health care quality evaluation, and there has been research on the application of DRG systems in China since the 1980s. The DRG system divides patients into different diagnostic groups for management according to factors such as disease diagnosis, treatment methods, age, comorbidities, complications, disease severity, and disease progression [7]. In 1983, Medicare (a US federal health care insurance program) used DRG systems for the first time as a health care payment method amid health care reform. The DRG system's prepaid model has highlighted certain advantages for controlling unreasonable medical expenses, standardizing diagnosis and treatment behaviors, enhancing patients' experience with medical treatment, and incentivizing hospitals to strengthen their internal management. Subsequently, it has been rapidly popularized, applied worldwide, and has become one of the most dominant medical payment methods for hospitals internationally [8]. Additionally, some research has been conducted internationally on the effects of the DRG payment model on nursing, mainly including the quality of nursing [9], career development of nurses [9], nursing costs [10], and nursing time. In the meantime, studies in China have also shown that DRG systems can be used as an evaluation index for the quality of medical services, work efficiency, operating costs, and performance [11]. In recent years, a meta-analysis showed that the DRG payment model can significantly reduce the length of hospital stays and medical costs for patients, help to comprehensively and effectively control medical costs, improve the quality of medical services, and help incentivize hospitals to improve their operation and management. Furthermore, it effectively reduces the management and medical expenditures of the medical insurance department, which facilitates the formation of a standardized model for medical resource expenditures [12]. Studying the relationship between DRG weight and nursing time is important for optimizing the allocation of nursing resources, improving the quality of nursing services, promoting the implementation of the DRG payment system, and promoting the development of the nursing discipline. As an advanced medical classification and payment system, DRGs have been used worldwide, but nursing management still needs to progress simultaneously. Through in-depth research, we can accurately predict the demand for nursing resources for different DRGs, avoid the wasting of resources, and improve nursing efficiency. At the same time, GRCs help nursing staff to better identify patient needs, provide personalized services, ensure patient safety, reduce adverse events, and provide a strong support for DRG payment system reform and nursing discipline innovation.

In August 2011, the General Office of the Ministry of Health of China issued the Notice on Promoting the Application of Diagnosis-Related Groups for Hospital Evaluation, which began using DRGs for related evaluations, such as hospital service performance [13]. In 2016, the National Health and Family Planning Commission stated that the DRG system is one of the critical tools for medical quality management [14]. In 2017, the Opinions of the General Office of the State Council on Further Deepening the Guidance Reform for the Payment of Basic Medical Insurance pointed out that it is necessary to carry out pilot programs for DRGs, actively explore the framework of DRG-based payment, and promote the reform of medical insurance payment mode in China. Since nursing is a part of medical treatment, the application and implementation of the DRG system not only promotes the reform of medical treatments but also exhibits a great impact on the profession of nursing. Therefore, this study explores the correlation between DRG weight and nursing time and establishes a nursing time prediction model based on DRG weight and other factors. The model can make up for DRG-related gaps in nursing time evaluation and provide a reference for the application of DRG weight and related indicators in nursing performance appraisal and staffing.

Methods

Ethical Considerations

This study was conducted in accordance with the Declaration of Helsinki and approved by the Ethics Committee of Beijing Chest Hospital, Capital Medical University (LW-2024-032). This study obtained the informed consent of the patient or their family member and mainly carried out observational research and data analysis after obtaining patients' informed consent, which clearly indicated that this study will not have any negative impact on the rights and interests of the subjects and informed the patients that they do not need to give additional consent for secondary analysis of the existing data in the study. The research project adopts a method for data analysis that did not involve individual identification. For patients, this study only analyzed the costs incurred during the hospitalization of patients, without any additional time commitments of the patients. Thus, financial compensation was not given to patients.

General Data

This was a cross-sectional study on the relationship between DRG weight and nursing time. The convenience sampling method was used to select study participants who were hospitalized in the cardiology ward of Beijing Chest Hospital between April 2023 and April 2024. The inclusion criteria were as follows: (1) patients diagnosed with angina pectoris, hypertension, sudden death, arrhythmia, heart failure, premature beat, myocardial infarction, cardiomyopathy, myocarditis, or

XSL•FO
RenderX

other cardiovascular diseases and (2) patients who purchased employee medical insurance, urban and rural residents medical insurance, or commercial insurance. The exclusion criteria were as follows: (1) patients with aortic surgery, heart valve surgery, coronary artery surgery, acute myocardial infarction, major organ transplantation, haematopoietic stem cell transplantation, or severe primary pulmonary hypertension and (2) patients with multiple organ failure.

A total of 103 patients who were hospitalized aged 15 - 89 (mean 58.85, SD 15.17) years were included in this study, including 67 women with a mean age of 66.2 years and 36 men with a mean age of 58.1 years. The disease diagnoses were as follows: coronary atherosclerotic heart disease (n=28), paroxysmal supraventricular tachycardia (n=1), atrial fibrillation (n=5), unstable angina pectoris (n=44), and other cardiovascular diseases (n=25). These diseases were diagnosed by coronary angiography (n=74) or interventional cardiology procedures (n=29). Patients were assessed for clear consciousness (n=102) or somnolence (n=1). Furthermore, the activities of daily living (ADL) scores on admission were between 20-100 (mean 87.41, SD 18.61) points, including scores of 100 points (n=37), 41 - 99 points (n=51), and <40 points (n=15). Some patients had complications or comorbidities (n=77), including hypertension (n=47), diabetes (n=10), and others (n=30). The research was carried out in strict compliance with the Strengthening the Reporting of Observational Studies in Epidemiology (STROBE) cross-sectional checklist [15].

Workload Measurements

Identification of Nursing Items

The in-hospital nursing program for patients consisted of 2 parts: direct nursing and indirect nursing. Following the Technical Operating Procedures and Quality Management Standards for Nursing [16] and the Guidelines for Clinical Nursing Practice [17], nursing staff (1 nurse, 2 senior nurses, 4 supervisor nurses and 1 chief superintendent nurse) with different nursing experiences and professional titles in the cardiology department were organized by the research team to participate in the discussion of nursing items 3 times. Ultimately, 10 direct and 12 indirect nursing items were included for the calculation (Multimedia Appendix 1).

Preparation

First was the selection of observers. Nurses in the department with less than 3 years of service were selected as observers and received training over the course of 3 sessions in the following: use of timers, operation timing, precautions for frequency records of direct nursing operations, requirements for indirect nursing timing, and other techniques. Digital timers were purchased and calibrated by the logistics department. The Frequency Statistics Sheet for Cardiology Patients Receiving Direct Nursing was formulated, which included the date and direct nursing items and their frequency. The statistics sheet was distributed to the nursing group of the cardiology department, and nurses were informed of the requirements for completion.

Calculation of Nursing Hours

After training, the observers selected 6 members of the nursing staff (2 nurses, 2 senior nurses and 2 supervisor nurses) from the cardiology department by lottery to complete each direct nursing operation. The observers calculated the average duration for each direct nursing operation from the time the nurse prepared the supplies until the completion of the operation, rounding down to the nearest second with a timer. Each nursing operation was timed by the same observer. Finally, the average duration for each direct nursing operation was calculated. Meanwhile, the nurse responsible for the patient's nursing recorded the frequency of the direct nursing items during the hospitalization using the Frequency Statistics Sheet for Cardiology Patients Receiving Direct Nursing. Specifically, direct nursing time during hospitalization for each patient was calculated (direct nursing time = ∑average time consumption per direct nursing item × frequency of that item during hospitalization). Moreover, the indirect nursing time for patients during hospitalization was collected based on the observations from each nurse. The total nursing time per patient was equal to the sum of the direct nursing time and indirect nursing time during hospitalization.

Acquisition of Patients' DRG Weights

The DRG weight refers to the average cost or total cost of a DRG case divided by the average cost or total cost of all cases in the region, respectively [18], with other external influencing factors also taken into account according to regional differences [5]. In addition to the cost of the diagnosis and treatment of diseases, calculations for DRG weights also account for the proportion of first-level nursing, the average length of hospital stays, and mortality. To a certain extent, DRG weights reflect the consumption of nursing resources. In this study, case statisticians uploaded the data to the inpatient medical service performance evaluation platform after a quality audit of the data on the first page of the discharge paperwork. Then, they obtained the corresponding DRG weights through the DRG grouping device on the platform, which were then divided into DRG weights of ≤1, >1 to ≤2, and >2, in unit intervals. The number of patients with different DRG weights reflected the distribution of disease severity.

Activities of Daily Living Scale

The ADL scale included 10 items of examination, with each item having a total scoring criteria between 0 and 15 points, and the maximum total score was 100 points [19]. An ADL score of 0 points indicated that the patient was completely dependent on others for daily living, while a score of 100 indicated that the patient was completely self-sufficient in their daily living. Patients with a score of <40 points had a severe impairment in their ADL, while those with 41 - 60 points had a moderate impairment in their ADL, and those with >61 points had a mild impairment in their ADL. For each patient, the first assessment was performed 2 days after the stability of their vital signs or when they entered the study, and the second assessment was performed 6 months into the course of the disease.

XSL•FO
RenderX

Statistical Analysis

The SPSS version 26.0 software package (IBM Corp) was used for the statistical analysis, and the normality test was conducted using the Kolmogorov-Smirnov method. Measurement data that were normal were expressed as mean and SD, and a 2-tailed sample *t* test was used to compare the nursing times based on the patient's sex, complications, angiography, and surgery. The nursing time, nursing level, and DRG weight on the first day of admission were compared using a 1-way ANOVA. The Student-Newman-Keuls method was used for pairwise comparisons. Count data were expressed as frequency or rate, and the χ^2 test was used for intergroup comparisons. Pearson correlation analysis or Spearman rank correlation analysis was used for the correlation analyses, and the multivariate analysis was performed through multiple linear regression. A bilateral *P* value of <.05 was considered statistically significant.

Results

Nursing Time and DRG Weights for Included Patients

The screening process of the research is shown in Figure 1. A total of 103 subjects were included in this study. During hospitalization, the direct nursing time for patients was between 70.65 - 1228.71 minutes, with a median of 335.33 (IQR 277.44-452.09) minutes. The indirect nursing time was between 30.86 - 1024.30 minutes, with a median of 362.46 (IQR 229.97-584.15) minutes, and the total nursing time was between 116.48 - 2169.05 minutes, with a median of 702.76 (IQR 518.55-1019.64) minutes. The average daily nursing time per patient was 134.58 minutes, and the average daily direct and indirect nursing times were 70.34 minutes and 64.24 minutes, respectively. Additionally, the DRG weights for the included patients were between 0.52 - 2.57 (mean 1.51, SD 0.42; Table 1).

Figure 1. Research screening process. DRG: diagnosis-related group.

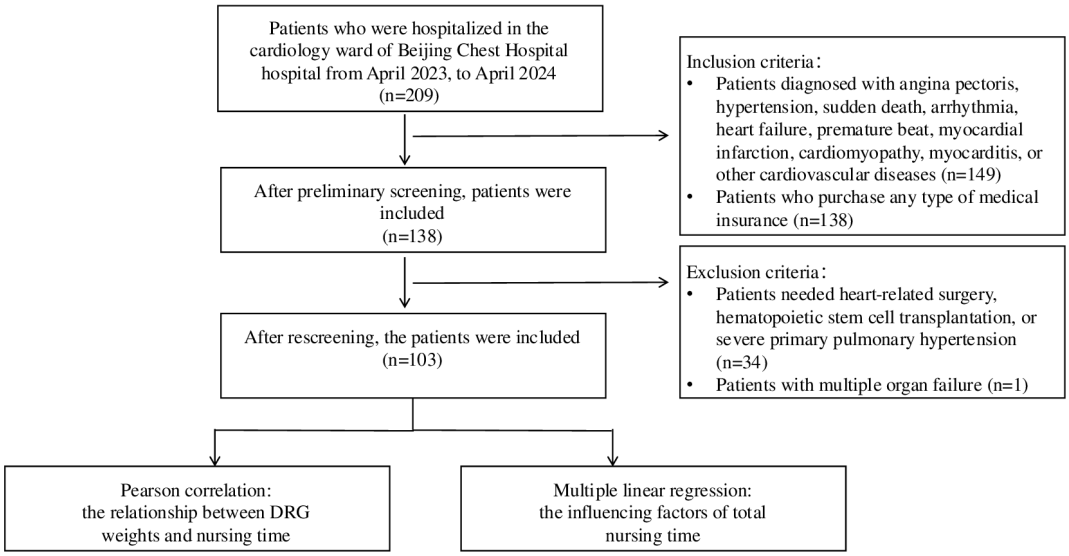


Table . Overall nursing time.

Variables	Values	Range
Direct nursing time (min), median (IQR)	335.33 (277.44 - 452.09)	70.65 - 1228.71
Indirect nursing time (min), median (IQR)	362.46 (229.97 - 584.15)	30.86 - 1024.30
Total nursing time (min), median (IQR)	702.76 (518.55 - 1019.64)	116.48 - 2169.05
DRG[a] weights, mean (SD)	1.51 (0.42)	0.52 - 2.57

[a]DRG: diagnosis-related group.

Correlation Analysis of Patient Nursing Time

The results suggested that DRG weights were positively correlated with direct nursing time, indirect nursing time, and total nursing time (direct: *r*=0.480; indirect: *r*=0.394; total: *r*=0.448; all *P*<.001). Furthermore, age was positively correlated with the 3 nursing times (direct: *r*=0.235; indirect: *r*=0.192; total: *r*=0.235; all *P*<.001). The ADL score on admission was negatively correlated with the 3 nursing times (direct: *r*=−0.316; indirect: *r*=−0.252; total *r*=−0.301; all *P*<.001), and nursing levels on the first day of admission were positively correlated

XSL•FO
RenderX

with the 3 nursing times (direct: r=0.333; indirect: r=0.332; total r=0.352; all P<.001), as shown in Table 2 .

Table . Correlation analysis of patient nursing time.

Item	Direct nursing time		Indirect nursing time		Total nursing time	
	Correlation coefficient	*P* value	Correlation coefficient	*P* value	Correlation coefficient	*P* value
DRG[a] weight	0.480	<.001	0.394	<.001	0.448	<.001
Age	0.235	<.001	0.192	<.001	0.235	<.001
ADL[b] score on admission	−0.316	<.001	−0.252	<.001	−0.301	<.001
Nursing level on the first day of admission	0.333	<.001	0.332	<.001	0.352	<.001

[a]DRG: diagnosis-related group.

[b]ADL: activities of daily living.

Univariate Analysis of Patient Nursing Time

The results showed significant differences in the logarithmic values for direct nursing time (t_{101}=2.230; P=.03), indirect nursing time (t_{101}=2.449; P=.02), and total nursing time (t_{101}=2.445; P=.02) between patients with or without complications. There were also significant differences between patients with or without surgeries (direct: t_{101}=5.324; indirect: t_{101}=4.584; total: t_{101}=5.199; all P<.001), patients with different nursing levels on the first day of admission (direct: $F_{2,100}$=45.421; indirect: $F_{2,100}$=25.435; total: $F_{2,100}$=35.495; all P<.001), and patients with different DRG weights (direct: $F_{2,100}$=32.455, indirect: $F_{2,100}$=28.581, total: $F_{2,100}$=29.435, all P<.001). However, no significant differences were observed for the natural logarithmic values for direct nursing time, indirect nursing time, or total nursing time between patients with different sexes or for patients with or without an angiography, as shown in Table 3.

XSL•FO
RenderX

Table . Comparison of nursing time of cardiology patients with different characteristics.

Item	Direct nursing time			Indirect nursing time			Total nursing time		
	Time (ln[min]), mean (SD)	*t* test or *F* test (*df*)	*P* value	Time (ln[min]), mean (SD)	*t* test or *F* test (*df*)	*P* value	Time (ln[min]), mean (SD)	*t* test or *F* test (*df*)	*P* value
Sex		0.613[a] (101)	.06		0.735[a] (101)	.46		0.723[a] (101)	.43
Male (n=36)	5.83 (0.42)			5.90 (0.67)			6.62 (0.48)		
Female (n=67)	5.85 (0.41)			5.83 (0.74)			6.55 (0.57)		
Complications		2.230[a] (101)	.03		2.449[a] (101)	.02		2.445[a] (101)	.02
Yes (n=26)	5.64 (0.40)			5.64 (0.61)			6.43 (0.50)		
No (n=77)	5.94 (0.43)			5.96 (0.61)			6.66 (0.52)		
Angiography		1.682[a] (101)	.12		1.882[a] (101)	.06		1.911[a] (101)	.06
No (n=29)	5.91 (0.46)			5.95 (0.71)			6.64 (0.54)		
Yes (n=74)	5.84 (0.37)			5.76 (0.70)			6.55 (0.50)		
Surgery		5.324[a] (101)	<.001		4.584[a] (101)	<.001		5.199[a] (101)	<.001
No (n=70)	5.63 (0.45)			5.54 (0.73)			6.31 (0.55)		
Yes (n=33)	5.95 (0.38)			6.00 (0.61)			6.70 (0.49)		
Nursing level on the first day of admission		45.421[b] (2, 100)	<.001		25.435[b] (2, 100)	<.001		35.495[b] (2, 100)	<.001
Level 2 (n=61)	5.80 (0.29)			5.73 (0.55)			6.51 (0.38)		
Level 1 (n=20)	5.67 (0.42)			5.60 (0.71)			6.40 (0.53)		
Premium level (n=22)	6.30 (0.54)			6.38 (0.90)			7.16 (0.65)		
DRG[c] weight		32.455[b] (2, 100)	<.001		28.581[b] (2, 100)	<.001		29.435[b] (2, 100)	<.001
≤1 (n=47)	5.61 (0.43)			5.44 (0.73)			6.30 (0.55)		
>1 to ≤2 (n=54)	5.91 (0.35)			5.90 (0.60)			6.60 (0.45)		
>2 (n=2)	6.27 (0.40)			6.36 (0.55)			7.09 (0.41)		

[a]*t* test.

[b]*F* test.

[c]DRG: diagnosis-related group.

Multivariate Analysis of Patient Nursing Time

Stepwise regression analysis was performed with the participant's nursing time as the dependent variable and the collected information as independent variables. Categorical variables were grouped and coded, as shown in Table 4. The results showed that when 4 variables (nursing level on the first day of admission, complications or comorbidities, DRG weight, and ADL score on admission) were included and other variables were excluded, the model R^2 was 0.328, indicating that these 4 variables could explain 32.8% of the factors affecting the patients' nursing time. In addition, the $F_{5,97}$ test result of 69.58 (P<.001) indicated that the dependent variable fit well with these 4 variables. The Debin-Watson index was 1.842, suggesting no correlation between the independent variables of this model, and the significance test for all 4 independent variables indicated that they were statistically significant in the model and should be retained. Additionally, due to a variance inflation factor value of <10 for all 4 independent variables, there was no covariance between the respective variables, and the multiple linear regression equation was as follows:

$$Y=6.423+0.482X1+0.091X2-0.005X3+0.167X4$$

According to the standardized partial regression coefficients in the model, it can be concluded that the effect of the 4 independent variables on patient nursing time was ranked as

XSL•FO
RenderX

follows (from strongest to weakest): DRG weight>nursing level on the first day of admission>ADL score on admission>complications or comorbidities (Table 5).

Table . Assigned values for variables.

Item and group	Assigned value
Nursing level on the first day of admission	
Level 1 nursing	1
Level 2 nursing	2
Premium-level nursing	3
Complications or comorbidities	
Yes	1
No	2
Surgery	
Yes	1
No	2
DRG[a] weight	Original value
ADL[b] score on admission	Original value
Age	Original value

[a]DRG: diagnosis-related group.

[b]ADL: activities of daily living.

Table . Multiple linear regression analysis of total nursing time. R=0.573, R^2=0.328, adjusted R^2=0.289; $F_{5,97}$=69.58.

Variable	Partial regression coefficient	Standardized partial regression coefficient (SE)	*t* test (*df*)	*P* value	VIF[a]
Constant	6.423	—[b]	8.395 (101)	<.001	—[b]
DRG[c] weight	0.482	0.446 (0.104)	8.352 (101)	<.001	2.194
Nursing level on the first day of admission	0.091	0.273 (0.110)	8.332 (101)	<.001	1.422
ADL[d] score on admission	−0.005	−0.191 (0.004)	9.535 (101)	<.001	1.310
Complications or comorbidities	0.167	0.161 (0.089)	6.582 (101)	<.001	2.140

[a]VIF: variance inflation factor.

[b]The standardized partial regression coefficient was not calculated for the constant value.

[c]DRG: diagnosis-related group.

[d]ADL: activities of daily living.

Discussion

By analyzing the correlation between DRG weight and nursing time, this study established a nursing time prediction model based on DRG weight and other factors. The results showed that DRG weight was positively correlated with direct nursing time, indirect nursing time, and total nursing time. The influencing factors affecting the patient's nursing time include DRG weight, the nursing level on the first day of admission, ADL score on admission, and complications or comorbidities.

Scholars in China have learned from more advanced nursing time measurement tools that are used globally, such as the Severity of Illness Index for Pediatric Patients, Comprehensive Nursing Intervention Score, and Patient Illness Severity Nursing Index, and they have conducted weighted evaluations of factors such as project difficulty and risk, without considering factors such as the complexity of disease and treatment methods for patients. Currently, the most commonly used metric for nursing time in China is the measurement of work hours [20]; however, this is time-consuming and labor-intensive with many influencing factors, making it difficult to implement in clinical practice. Kang et al [21] performed nursing time statistics based on the hospital information platform, and despite the slightly improved efficiency, the statistical workload was still a lot due to the extraction of data from multiple systems. Meanwhile,

XSL•FO
RenderX

Zhang et al [22] calculated nursing time using the load weighting method. The assignment of load weights mainly depended on the subjective assessment of experts, with a large influence from human factors. In contrast, DRG weights comprehensively considered factors such as the severity and complexity of the disease, different treatment methods, individual patient differences, and discharge outcomes [23]. These included many patient factors related to nursing time, such as the disease itself and individual characteristics, which could objectively reflect the nursing time, and the acquisition of parameters was relatively simple and easy to implement.

This study found that the average daily nursing time per patient during hospitalization in the cardiology department was 134.58 minutes. This was close to the average daily nursing time per patient (113.59 minutes) in a study by Yang et al [24] but less than the average daily total nursing time (171.02 minutes) calculated by Cai et al [25] for neurosurgery patients. This discrepancy was mainly due to the different types of diseases treated in the cardiology and neurosurgery departments, where the nursing times for neurosurgical operations were greater than that for internal medicine operations. In this study, the average daily direct nursing time per patient was 70.34 minutes, which was less than the average daily direct nursing time per patient (75 minutes) measured by Wang et al [26] for neurology patients. This was mainly due to the overall self-care ability of the cardiology patients included in this study, with 35.9% (37/103) having an ADL score of 100 on admission and 49.5% (51/103) having a score between 40 - 99, while neurology patients experienced more severe functional impairments and greater dependence on care, thus increasing the burden on nursing staff. Moreover, the average daily indirect nursing time per cardiology patient in this study was 64.24 minutes, which was longer than the average daily indirect nursing time per patient (45.34 minutes) measured by Zhang et al [27]. This was directly due to the different clinical support systems of the hospitals [28], in which a well-developed clinical support system helped to reduce indirect nursing time while increasing direct nursing time.

Specifically, DRG weights regard the treatment cost of the disease as the main factor while comprehensively considering factors such as primary nursing care, average length of the hospital stay, and mortality. This was followed by obtaining the DRG weight value through data modelling, with the corresponding DRG weight value for a disease type calculated through the DRG Grouper tool. In the univariate analysis, despite the correlation between complications or comorbidities, surgery, nursing level on the first day of admission, and age, the correlation between DRG weight and nursing time was more prominent and evident. This is because DRG weights have incorporated factors related to nursing labor costs, thereby making them more valuable for implementation in the management of nursing personnel. Furthermore, the results showed that DRG weights had the greatest impact on nursing time, and although evaluating nursing time with nursing levels alone is not desirable [29], nursing levels, to some extent, reflect the severity of the disease. Moreover, the time required for some direct nursing operations was different, such as bed-making and admission assessment, which corresponded to different ADL scores. The higher the ADL score was, the less the time was required for these items, indicating a negative correlation, thereby affecting the total nursing time [29]. Furthermore, the comorbidities of cardiovascular diseases were mainly hypertension and diabetes, with 45.6% (47/103) of the patients experiencing hypertension and 9.7% (10/103) experiencing diabetes, requiring an increased monitoring of blood pressure and blood glucose, respectively, which increased nursing time. Therefore, the above factors were all related to the nursing time in the multivariate regression analysis. At the same time, the prediction of workload using a multivariate regression equation with DRG weight as the main factor can be helpful for nursing managers to measure and adjust future staffing needs based on the current staffing situation in combination with other departmental needs.

DRGs have many contributions to nursing management. They promote the standardization of the nursing process, optimize the allocation of resources, improve the efficiency of nursing work, and make nursing services more efficient and stable [24]. At the same time, DRGs promote the transformation of hospital management from extensive to refined, provide data support for nursing management departments, and enable them to make more scientific, data-based decisions [21]. In addition, DRGs help to reduce nursing risks, improve patient satisfaction, and provide more personalized nursing services for patients. Through DRG systems, hospitals can more accurately meet the nursing needs of patients and ensure patient safety. Finally, the application of DRGs puts forward higher requirements for the professional skills of nursing staff, promotes the professional development of nursing staff, and promotes the innovation of nursing research. In short, the application of DRGs has brought many positive effects to nursing management, which helps improve the quality of nursing services and promotes the modernization and scientific process of the nursing speciality.

However, this study also has some limitations. First, due to the limitation of data accessibility, this study only used the data of one hospital, and the number of cases was small. This could lead to a deviation in data selection, and there may have been some bias in the extrapolation of results. Therefore, in future studies, multicenter longitudinal studies with a larger sample size can be used for further verification. In addition, due to an untimely update of hospital disease diagnosis and surgical coding, as well as operational errors by medical staff, the data quality of the first page of medical records was low, which affected the case registration rate. The training and practical operation of medical staff on DRG-related knowledge should be strengthened before future research.

In summary, DRG weight has a strong correlation with nursing time, which can be used to predict nursing time and contribute to the allocation of nursing resources in cardiology departments. This study can improve the satisfaction of patients and their families with hospital nursing work and reduce the pain of patients. In addition, this study can also make up for the DRG-related gap in the evaluation of nursing time in cardiology departments and provide a reference for the application of DRG weight and related indicators in nursing performance evaluations and staffing.

XSL•FO
RenderX

Acknowledgments

We would like to express our gratitude to all those who helped us during the writing of this manuscript. This work was supported by Digital Intelligence Nursing Basic Clinical Collaborative Research Specialization (SZHL23Q07. FY2023).

Data Availability

All data generated or analyzed during this study are included in this published article.

Authors' Contributions

CL and YHG conceived of the study. JA, QW, and XFC participated in the study design and coordination. JH, QW, and XHW helped to draft the manuscript. All authors read and approved the final manuscript. All authors made a significant scientific contribution to the research in the manuscript, approved its claims and agreed to be an author.

Conflicts of Interest

None declared.

Multimedia Appendix 1
List of direct and indirect nursing items.
[XLSX File, 10 KB - medinform_v13i1e65549_app1.xlsx]

Checklist 1
Strengthening the Reporting of Observational Studies in Epidemiology (STROBE) Checklist.
[DOCX File, 27 KB - medinform_v13i1e65549_app2.docx]

References

1. Jia L, Rong L. Correlation between bedside arterial blood lactic acid level and nursing workload in critically ill patients. Guizhou Med J 2024;48(5):827-829. [doi: 10.3969/j.issn.1000-744X.2024.05.057]
2. Laczynski DJ, Gallop J, Sicard GA, et al. Benchmarking a center of excellence in vascular surgery: using acute physiology and chronic health evaluation II to validate outcomes in a tertiary care institute. Vasc Endovasc Surg 2023 Nov;57(8):856-862. [doi: 10.1177/15385744231183744] [Medline: 37295071]
3. Joya RM, Cottrell L, Kiefer A, Polak MJ. Diagnosis-related group weight and derived case mix index to assess the complexity among twins. Am J Perinatol 2022 Aug;39(11):1223-1228. [doi: 10.1055/s-0040-1721847] [Medline: 33378771]
4. Bogdanov C, Hohenstein S, Brederlau J, Groesdonk HV, Bollmann A, Kuhlen R. A Comparison of different intensive care unit definitions derived from the German administrative data set: a methodological, real-world data analysis from 86 Helios Hospitals. J Clin Med 2024 Jun 10;13(12):3393. [doi: 10.3390/jcm13123393] [Medline: 38929923]
5. Chen YJ, Zhang XY, Yan JQ, Qian MC, Ying XH. Impact of diagnosis-related groups on inpatient quality of health care: a systematic review and meta-analysis. Inquiry 2023;60:469580231167011. [doi: 10.1177/00469580231167011] [Medline: 37083281]
6. Liu Y, Wang G, Qin TG, Kobayashi S, Karako T, Song P. Comparison of diagnosis-related groups (DRG)-based hospital payment system design and implementation strategies in different countries: the case of ischemic stroke. Biosci Trends 2024 Mar 19;18(1):1-10. [doi: 10.5582/bst.2023.01027] [Medline: 38403739]
7. Berry JG, Hall M, Cohen E, et al. Hospitals' diversity of diagnosis groups and associated costs of care. Pediatrics 2021 Mar;147(3):e2020018101. [doi: 10.1542/peds.2020-018101] [Medline: 33627373]
8. Ma Y, Wang W. The impact of diagnosis related group payment on the performance of public hospitals. Am J Transl Res 2021;13(6):6796-6801. [Medline: 34306429]
9. Fabrizi D, Bernasconi DP, Locatelli G, et al. How are diagnosis-related groups and staffing allocation systems associated with the complexity of nursing care? An observational study. Healthcare (Basel) -> Healthc (Basel) 2024 Oct 5;12(19):1988. [doi: 10.3390/healthcare12191988] [Medline: 39408168]
10. Gluckman TJ, Spinelli KJ, Wang M, et al. Trends in diagnosis related groups for inpatient admissions and associated changes in payment from 2012 to 2016. JAMA Netw Open 2020 Dec 1;3(12):e2028470. [doi: 10.1001/jamanetworkopen.2020.28470] [Medline: 33284340]
11. Shi LY, Xu XW. Research on the cost control path of public hospitals in DRGs payment methods. China's Nat 2024;32(20):118-121. [doi: 10.19621/j.cnki.11-3555/r.2024.2031]
12. Zou K, Li HY, Zhou D, Liao ZJ. The effects of diagnosis-related groups payment on hospital healthcare in China: a systematic review. BMC Health Serv Res 2020 Feb 12;20(1):112. [doi: 10.1186/s12913-020-4957-5] [Medline: 32050962]

XSL•FO
RenderX

13. Notice of the General Office of the Ministry of Health on promoting the application of diagnosis related groups (drgs) in hospital evaluation. National Health Commission of the People's Republic of China. 2011. URL: http://www.nhc.gov.cn/cms-search/xxgk/getManuscriptXxgk.htm?id=52531 [accessed 2024-12-24]
14. Weiwei O. Research on the implementation of DRG payment method policy in guangxi L[D]. : Guangxi University; 2023 URL: https://med.wanfangdata.com.cn/Paper/Detailid=DegreePaper_D03231878&dbid=WF_XW [accessed 2025-02-20]
15. von Elm E, Altman DG, Egger M, et al. The strengthening the reporting of observational studies in epidemiology (STROBE) statement: guidelines for reporting observational studies. J Clin Epidemiol 2008 Apr;61(4):344-349. [doi: 10.1016/j.jclinepi.2007.11.008] [Medline: 18313558]
16. Ministry of Health of the People's Republic of China Guidelines for Clinical Nursing Practice (2011 Edition): People's Military Medical Press; 2011:1-152.
17. Yushan G, Sihan W, Jiehong L. Construction of nursing low-value item list based on clinical nursing practice guidelines in China. J Nurs Sci 2023;38(4):66-71. [doi: 10.3870/j.issn.1001-4152.2023.04.066]
18. Gao J, Gao Q, Huo L, Yang J. Impaired activity of daily living status of the older adults and its influencing factors: a cross-sectional study. Int J Environ Res Public Health 2022 Nov 24;19(23):15607. [doi: 10.3390/ijerph192315607] [Medline: 36497680]
19. Liu H, Ma Y, Lin L, Sun Z, Li Z, Jiang X. Association between activities of daily living and depressive symptoms among older adults in China: evidence from the CHARLS. Front Public Health 2023;11:1249208. [doi: 10.3389/fpubh.2023.1249208] [Medline: 38035294]
20. Wang F, Wu L, Wang D. Study on the allocation of nursing human resources in tumor day ward based on direct time study-intensive sampling method. H Med Voc Educ Mod ;7(5):412-415. [doi: 10.3969/j.issn.2096-501X.2024.05.009]
21. Kang F, Liu T, Mao Y, Li L, Li Y. Performance evaluation study on the workload of nursing units. Chin Nurs Res 2018;32(5):753-759 [FREE Full text]
22. Zhang Y, Li Y, Peng L, He A, Yang T, Long Y, et al. Application of load weighting method in calculating nursing workload in wards. J Nurs Sci 2013;28(21):51-54. [doi: 10.3870/hlxzz.2013.21.051]
23. Hu L, Zhu J. Application of DRGs in the performance evaluation of medical services in clinical departments. Hosp Manag Forum 2019;36(10):10-14 [FREE Full text]
24. Yang L, Liu J. Measurement and classification of nursing hours in different departments of one hospital. Chin Nurs Manag 2012;12(9):58-61. [doi: 10.3969/j.issn.1672-1756.2012.09.017]
25. Cai W, Yin Z, Liang J, Li J, Jia J, Tian C. Discussion on reasonable allocation of human resources for neurosurgical nursing care based on working hours measurement. J Nurs Sci 2016;31(12):61-64. [doi: 10.3870/j.issn.1001-4152.2016.12.061]
26. Wang Y, Huang H, Yan K. The effect of working hours measurement for mobile nursing systems on nurses' work. Int J Nurs (N Y) 2018;37(12):1699-1702. [doi: 10.3760/cma.j.issn.1673-4351.2018.12.036]
27. Zhang J, Ma Y, Ln H. Nursing hours measurement and analysis of its influencing factors in general hospitals. Chin Nurs Res 2013;27(9):3039-3041. [doi: 10.3969/j.issn.1009-6493.2013.27.050]
28. Marco-Benedí V, Jarauta Simón E, Laclaustra Gimeno M, Civeira Murillo F. Nursing workload. Calculation of cardiovascular risk and therapeutic objectives. Clin Investig Arterioscler 2021 May;33 Suppl 1:10-17. [doi: 10.1016/j.arteri.2020.12.006] [Medline: 33966807]
29. Chang R, Cheng Y, Zhou J. Analysis of nursing difficulty of inpatients in general surgery based on disease diagnosis related groups. Chin Nurs Manag 2024;24(5):731-736. [doi: 10.3969/j.issn.1672-1756.2024.05.017]

Abbreviations

ADL: activities of daily living
DRG: diagnosis-related group
PCS: Patient Classification System
STROBE: Strengthening the Reporting of Observational Studies in Epidemiology

Submitted 19.08.24; this is a non–peer-reviewed article;accepted 20.11.24; published 04.03.25.

Please cite as:
Lv C, Gong YH, Wang XH, An J, Wang Q, Han J, Chen XF
Correlation Between Diagnosis-Related Group Weights and Nursing Time in the Cardiology Department: Cross-Sectional Study
JMIR Med Inform 2025;13:e65549
URL: https://medinform.jmir.org/2025/1/e65549
doi:10.2196/65549

XSL•FO
RenderX

© Chen Lv, Yi-Hong Gong, Xiu-Hua Wang, Jun An, Qian Wang, Jing Han, Xiao-Feng Chen. Originally published in JMIR Medical Informatics (https://medinform.jmir.org), 4.3.2025. This is an open-access article distributed under the terms of the Creative Commons Attribution License (https://creativecommons.org/licenses/by/4.0/), which permits unrestricted use, distribution, and reproduction in any medium, provided the original work, first published in JMIR Medical Informatics, is properly cited. The complete bibliographic information, a link to the original publication on https://medinform.jmir.org/, as well as this copyright and license information must be included.

XSL•FO
RenderX

The Perceptions of Potential Prerequisites for Artificial Intelligence in Danish General Practice: Vignette-Based Interview Study Among General Practitioners

Natasha Lee Jørgensen[1], MSc; Camilla Hoffmann Merrild[1], MSc, PhD; Martin Bach Jensen[1], MD, PhD; Thomas B Moeslund[2], MSc, PhD; Kristian Kidholm[3], MSc, PhD; Janus Laust Thomsen[1], MD, PhD

[1]Center for General Practice at Aalborg University, Department of Clinical Medicine, Aalborg University, Selma Lagerløfs vej 249, Aalborg, Denmark
[2]Visual Analysis and Perception Lab, Department of Architecture, Design, and Media Technology, Aalborg University, Aalborg, Denmark
[3]Centre for Innovative Medical Technology, Odense University Hospital, Odense, Denmark

Corresponding Author:
Natasha Lee Jørgensen, MSc
Center for General Practice at Aalborg University, Department of Clinical Medicine, Aalborg University, Selma Lagerløfs vej 249, Aalborg, Denmark

Abstract

Background: Artificial intelligence (AI) has been deemed revolutionary in medicine; however, no AI tools have been implemented or validated in Danish general practice. General practice in Denmark has an excellent digitization system for developing and using AI. Nevertheless, there is a lack of involvement of general practitioners (GPs) in developing AI. The perspectives of GPs as end users are essential for facilitating the next stage of AI development in general practice.

Objective: This study aimed to identify the essential prerequisites that GPs perceive as necessary to realize the potential of AI in Danish general practice.

Methods: This study used semistructured interviews and vignettes among GPs to gain perspectives on the potential of AI in general practice. A total of 12 GPs interested in the potential of AI in general practice were interviewed in 2019 and 2021. The interviews were transcribed verbatim and thematic analysis was conducted to identify the dominant themes throughout the data.

Results: In the data analysis, four main themes were identified as essential prerequisites for GPs when considering the potential of AI in general practice: (1) AI must begin with the low-hanging fruit, (2) AI must be meaningful in the GP's work, (3) the GP-patient relationship must be maintained despite AI, and (4) AI must be a free, active, and integrated option in the electronic health record (EHR). These 4 themes suggest that the development of AI should initially focus on low-complexity tasks that do not influence patient interactions but facilitate GPs' work in a meaningful manner as an integrated part of the EHR. Examples of this include routine and administrative tasks.

Conclusions: The research findings outline the participating GPs' perceptions of the essential prerequisites to consider when exploring the potential applications of AI in primary care settings. We believe that these perceptions of potential prerequisites can support the initial stages of future development and assess the suitability of existing AI tools for general practice.

(JMIR Med Inform 2025;13:e63895) doi:10.2196/63895

KEYWORDS

general practice; general practitioners; GPs; artificial intelligence; AI; prerequisites; interviews; vignettes; qualitative study; thematic analysis

Introduction

The research and development of artificial intelligence (AI) has progressed rapidly in recent years and has been deemed revolutionary in medicine. However, AI is still in its early phases of validation and implementation in all health care fields [1,2]. AI tools have predominantly been developed for hospital settings but are also believed to hold transformative potential in general practice, despite fewer AI tools being developed in this setting [3,4].

Denmark is a leading country in the digitization of health care systems [5]. Today, all Danish general practices use digital technology to handle electronic health records (EHRs), send prescriptions to pharmacies and referrals to hospitals, and receive laboratory analysis results and hospital discharge letters. Furthermore, emails and video consultations have become available [6,7]. Owing to this advanced digitization and the collection and management of data in Danish general practice, it is reasonable to believe that AI can be used at some level. In a review of 2023, identifying digital solutions for decision

XSL•FO
RenderX

support in Danish general practice, only 1 study dealt with AI [8]. This study described an AI tool for the identification of liver disease [9]. Since the publication of the abovementioned review, an additional study has reported an AI model that predicts cancer risk in patients referred from general practice based on routine blood tests [10]. None of the 2 AI tools reported in the identified studies are currently implemented in general practice. Thus, based on the identified evidence, research in this area is limited, with no validation, implementation, or application of AI tools currently available in Danish general practice.

When developing new technology, including potential end users and other stakeholders is essential [11]. This is defined as the exploration phase, an important step in the implementation process, creating awareness of the existing issues that need attention and potential improvement [12]. Contradictorily, the involvement of general practitioners (GPs) in developing concrete AI tools for general practice is limited [13,14]. In addition, limited research has been conducted to clarify the qualitative perspectives of GPs and other stakeholders regarding AI in general practice [15-20]. A closer examination of the same research reveals that only 3 studies have exclusively addressed the perspectives of GPs [18-20]. The research shows that GPs and other stakeholders generally have a positive attitude toward AI [15-18,20], but the practical and ethical implications of applying AI in general practice need clarification. This includes privacy, liability, and financial considerations [15]. Multiple uses of AI are envisioned in general practice, particularly within tasks of an administrative character [16,17]. This is due to concerns about replacing human competencies with AI [15,18,19]. Finally, it is essential to consider co-creation and collaboration with end users to ensure optimal adoption of AI in general practice [16,17,20].

Thus, when considering the development of AI in Danish general practice, it is necessary to understand the contexts and perspectives of the end users. Therefore, this study aimed to explore and define the prerequisites for applying AI in general practice from the GPs' perspective. GPs can provide insights into the essential conditions that must be met to realize the potential of AI in this setting. Establishing these foundational requirements will support the next steps toward advancing AI development in Danish general practice.

Methods

Qualitative Approach

This study applied an inductive approach using semistructured interviews and vignettes to iteratively explore and provide detailed insights into the GPs' perspectives on the prerequisites for AI in general practice. The vignette method was chosen to exemplify hypothetical scenarios of AI in general practice and create meaningful engagement with the participating GPs, as no AI tool has been implemented and validated in Danish general practice. Vignettes are typically used in qualitative research as sociological tools to study beliefs, attitudes, values, and perceptions [21-23]. The authors followed the Standards for Reporting Qualitative Research (SRQR) [24].

Researcher Characteristics and Reflexivity

The first author is a PhD student studying user perspectives on AI in general practice. The second author, an associate professor of anthropology, specializes in qualitative methods and perspectives of patients and GPs. The third author is a professor and a GP focused on integrating new technology as a support tool in general practice. The fourth author is a professor who specializes in responsible and value-driven AI. The fifth author, a professor of health economics, concentrates on health care innovations in medical technology. The final author is a professor and a GP studying the potential of new technology in general practice. All the authors believe that ethically applied and legally compliant AI can benefit general practice.

Context

Denmark is a welfare state with universal health care that ensures free and direct access to primary health care for all residents. The health care system is organized into 5 administrative regions, with general practice serving as a gatekeeper and the first point of contact [6]. The study was conducted in the North Denmark Region.

Sampling Strategy

Purposive sampling [25] was applied to recruit participants who were characterized as "first adopters" [26]. Therefore, the GP network was used to recruit GPs associated with the Center for General Practice at Aalborg University (CAM AAU) and consultants affiliated with the Quality Unit for General Practice in the North Denmark Region (Nord-KAP). We categorized GPs associated with these organizations as "first adopters" within their profession, as they typically demonstrate a distinctive interest in research in new medicine and technology. Thus, by sampling these specific GPs, we ensured satisfactory AI literacy for the interviews when discussing viewpoints on AI in general practice.

The study's first author, who also served as the only interviewer, had no personal or professional relationship with the participants, which might have influenced the results. Although the third and last authors were acquainted with several respondents, they did not know who provided specific statements. This ensured that any possible casual acquaintances had minimal influence on the analysis or conclusions of the study.

Ethical Considerations

Owing to the nature of the study, ethical approval was deemed unnecessary under Danish law (Section 14, Subsection 2 of of the Danish Act on Committees) [27]. This decision was based on legal provisions and confirmed through consultation with the institutional guidelines. According to Danish law, ethical approval is not required for qualitative interview studies that do not involve human biological materials or sensitive personal health data. However, written informed consent was obtained from all participants. To ensure privacy and confidentiality, all data were pseudonymized. Participants received no compensation for their participation in the interviews.

XSL•FO
RenderX

Data Collection Methods and Instruments

Interviews were conducted in Danish and face-to-face at the general practice clinics. The interviews lasted 35 to 95 minutes and were recorded using a dictaphone. Each interview began with introducing the respondents to the study and its purpose. The respondents were then presented with 5 individual vignettes, followed by questions from a semistructured interview guide. All vignettes depicted scenarios concerning a female patient presenting in general practice where different forms of AI are applied. The first vignette aimed to initiate a discussion on the understanding of data and AI to create a common frame of reference between the interviewer and the respondent. The following vignettes (numbers 2 - 5) aimed to clarify the GPs' point of view on AI in general practice, first on AI used in tasks concerning automation and then on AI applied to tasks related to decision support. The GPs were presented with a generic case and a more specific example for each type of AI task. The interview guide consisted of open-ended questions and prompted the exploration of GPs' perspectives on their experiences with new technology and AI in general practice, challenges and benefits, and their overall attitudes toward technology and AI in health care. The vignettes applied in this study are found in (Multimedia Appendix 1).

Units of Study

A total of 12 GPs participated in this study. In total, 9 semistructured interviews were conducted in 2019, and the remaining 3 were conducted in 2021. In addition, 6 men and 6 women participated in the study. At the time of the interviews, participants' ages ranged from 36 to 66 years, with a mean age of 47.7 years. Their professional experience as GPs varied from 2 to 30 years, with an average of 11 years. This diversity in age and experience closely reflects the general Danish GP population [28].

Data Processing and Analysis

For data processing, all collected interview data were stored safely on a file share server administered by Aalborg University in line with the obligations of the European Union's General Data Protection Regulation (GDPR). All the data were pseudonymized when uploaded to the secure file share with a key for safe reference storage.

In addition, 2 student assistants were assigned to transcribe all interview data verbatim for subsequent analysis. The student assistants were verbally instructed and provided written guidelines for the assigned tasks.

NVivo 14 (QSR International) coding software was used for all data analysis. Thematic analysis guided by this study's research question was conducted on the collected interview data [29]. The analysis commenced with familiarization with the data by reading and rereading the transcripts and listening to the interview audio recordings. Initial insights and analytical ideas were noted while reading and listening to the data. Data coding was then initiated, which involved systematically coding the interview transcripts and identifying themes through an iterative process that prioritized transparency and rigor. All coded data were then re-read to collate the data relevant to each code. The initial themes were generated based on the developed codes. Each theme was then reviewed and refined to align with the study objective, resulting in a final set of themes. The authors have translated the quotes stated in this paper from Danish to English.

Techniques to Enhance Trustworthiness

A pilot test was conducted with 2 GPs before the primary data collection to enhance the validity and reliability of the vignettes and the interview guide. The pilot test evaluated the clarity, relevance, and comprehensibility of the vignettes and the appropriateness of the interview questions. Feedback provided by the GPs during this process was systematically incorporated to refine and improve the vignettes and interview guide, ensuring that they effectively addressed the study objectives and were suitable for target participants.

Although purposive sampling was used to ensure that participants were selected based on their relevance to the research objectives, efforts were made to achieve diversity among participants. This included considering variations in age, gender, and years of professional experience. Striving for diversity enhances the robustness of the findings by ensuring a broader range of perspectives.

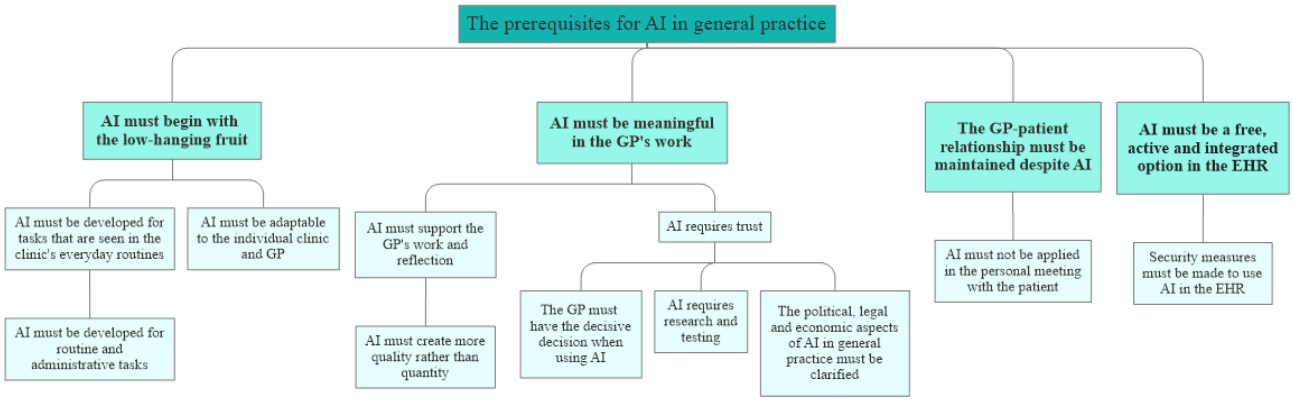
The iterative process of dialogue and consensus building among all the authors validated the findings, strengthened the credibility of the results, and ensured that the final manuscript reflected the collective agreement of the authors.

Results

The analysis of data resulted in four themes: (1) AI must begin with the low-hanging fruit, (2) AI must be meaningful in the GP's work, (3) the GP-patient relationship must be maintained despite AI, and (4) AI must be a free, active, and integrated option in the EHR. All 4 themes contain codes that support the results of the analysis. Figure 1 shows the hierarchy of themes and codes.

XSL•FO
RenderX

Figure 1. Illustration of the four themes and connected codes defined in the analysis of the interview data. AI: artificial intelligence; GP: general practitioner; EHR: electronic health record.



AI Must Begin With the Low-Hanging Fruit

When GPs were asked to identify the most relevant tasks in general practice with the potential to develop AI, their response was to address "the low-hanging fruit," which was the first theme of the analysis. GPs defined "the low-hanging fruit" as low-complexity tasks with the necessary data available to develop AI that can facilitate GPs' work at a practical level, with minimal impact on the GP-patient relationship. The GPs highlighted the importance of developing AI for everyday clinical tasks rather than for rare or highly specialized diagnostic processes that might have limited use. They emphasized that AI should enhance tasks and tools that already perform well in general practice but have the potential for further optimization. A significant opportunity lies in applying AI to routine administrative tasks such as managing medications and processing test results, which are time-consuming but cognitively straightforward. In addition, the GPs suggested exploring the possibility of developing AI for tasks typically handled by practice staff, such as organizing test responses and scheduling annual check-ups, where systematic and repetitive processes dominate. Furthermore, the GPs emphasized that AI would be received constructively if initially introduced for tasks considered "low-hanging fruit," as this approach would allow them to build confidence in the technology through early practical successes.

The GPs also emphasized that AI must be grounded in tasks embodied in the practices and workflows of individual GPs and clinics. Owing to the individual general practice clinics varying in organization with different workflows and ways of approaching and handling tasks, it is necessary that AI can be adapted to a specific setting.

> *... but then again, I just think it is important that you get the opportunity to tailor it to the individual practice, that it does not just become a system that has to fit all clinics because we do it very differently. Some only do an annual check, some don't do annual checks at all, and some, as we do here, for example, have split it up and made an individual plan for people. It is not certain that you need to come for an annual check once a year; there may well be a large check every two years, but then you come to a smaller check. It has to be something where you can put your own prerequisites on it (AI), but it could be something like when the patient walks out the door, that you say send a message to the patient that they should contact us for the purpose of blood tests or something in six months.* [Participant No. 7]

AI Must Be Meaningful in GP's Work

The second theme is "AI must be meaningful in the GP's work." The GPs state that any AI with the potential for application in general practice must be relevant and sensible. Irrelevant information in the EHR becomes an annoyance rather than an aid in the GP's information-intensive work life.

> *There is a lack of reflection like this to say, well, when is this pop-up relevant, and when do we have to be confronted with it? Well, if you had set aside an hour to do a review of automated responses or what do I know, you could perhaps achieve a lot more health in that hour than on the four patients you see in an hour. So, it is a question of where you put your resources.* [Participant No. 4]

To be meaningful, the GPs emphasize that AI must function as a supportive tool in their work, leveraging its strengths, such as data analysis and processing, to enhance their practice. The GPs also proposed using AI as a sparring partner to support and challenge their professional judgment and create reflection in their practice. Furthermore, Participant No. 3 accentuated that AI should contribute to more quality than quantity in general practice to achieve "less useless work and more useful work." The GPs anticipate that introducing AI into general practice will likely lead to a redistribution of tasks. Consequently, more health-promoting activities will be prioritized, but the overall workload will remain high.

> *I think it's an illusion that we'll get to the point where robots and AI take over our work so that we don't have to work in the future - because it always brings other things along, but it's a good idea, as it can give me less useless work and more useful work. That's fine. But I think that the sum of work, it probably will for my part - and here in the clinic - it will probably be constant regardless of what you do. But it is also because we will probably just admit more patients and more tasks. That is what I imagine.* [Participant No. 3]

XSL•FO
RenderX

Trust is a critical prerequisite for GPs to find AI meaningful. The GPs emphasized that AI must not function independently but should assist the GP's work. It is also stated that authority should remain with the GP, as fear of AI taking control could lead to mistrust. Consequently, GPs suggest that the data generated by AI should be crosschecked with the GPs' observations and intuition to ensure that the tasks are performed correctly. In addition, AI must be flawless to benefit GP. The GPs prefer a challenging daily workload, valuing their ability to perform their tasks well rather than on AI for suboptimal results.

> …*What you can fear about AI is that it gets its own authority in a way—that the authority goes away—or that the decision goes from being the doctor's to being the system's. It is a slippery slope. It's not either or, it's on the way to something … Then, it has to be compared with the processes I go through when I sit across from a person who has all kinds of stories and compare them with the data I look at and perhaps all the ones I do not look at, which could be a weakness in my situation, but which can be the strength in the AI's situation. So this AI will have its strengths, but can also in some ways trump and perhaps blind us to some things we would otherwise have seen if we had sat and talked to the patient instead.* [Participant No. 4]

Several GPs stated the importance of making conclusive decisions and maintaining awareness of their responsibility rather than unquestioningly trusting AI. Consequently, questions were raised regarding the role of AI if GPs must always oversee and approve the decision-making process. Double-checking multiple outcomes is time-consuming if the GPs have to modify or override the AI-generated results.

Knowledge and familiarity with the AI algorithm were highlighted among the GPs as necessary. Thus, AI requires further research and testing to ensure the trust of GPs. Any AI tool developed for general practice is expected to undergo comprehensive evaluation in research studies to assess both the advantages and disadvantages of the technology. It is also essential to explore the impact of AI on external factors, such as work structures and the organization of general practice, as well as to consider patients' perspectives on AI tools.

In addition to the research-related and external outcomes of AI in general practice, the GPs emphasize the need to address political, legal, and economic aspects to build trust in the technology. Politically, the GPs stress that the use of AI should be initiated by the GPs themselves, ensuring that AI does not become a tool for political management. AI must be developed and used primarily for the benefit of general practice. and most importantly, for the benefit of patients. The legal implications of AI must be clarified, particularly regarding the distribution of liability in the event of errors. Finally, the GPs expect an investigation into the economic impact of AI in general practice at a societal level.

The GP-Patient Relationship Must Be Maintained Despite AI

Preserving the GP-patient relationship despite the integration of AI in general practice is the third essential prerequisite. The GPs consider a significant part of their work to occur at the human level, particularly during personal interactions with patients. While GPs see technological tools as beneficial for more standardized procedures such as administrative tasks, they view them as a distancing factor during patient consultations. Patients must not feel that they are interacting with a computer, as personal contact between the GP and the patient remains central to the practice. The GPs clarify that most health-promoting outcomes arise from the time spent with patients, and they would prefer to dedicate time to patient care rather than to computers and other technological aids.

> *So, what I am skeptical about is whether the patient feels they have a doctor or whether they feel they have a computer. So, the thing about whether you trust that the doctor knows that something has to be done and all that - I can fear that both I as a doctor will lose that, but also that patients will feel that they are losing it. Thus, the doctor-patient relationship could suffer slightly in such a scenario. However, it could also be that it does not suffer because they're just smart up there in that hospital, right ... So in that way, I am not so opposed to it, but I have some skepticism about whether you will achieve what you want with it.* [Participant No. 5]

To preserve the personal relationship between the GP and the patient, the GPs strongly prefer that AI is not present during consultations. Given that consultations typically last only 10 minutes, GPs must carefully manage their time to achieve all objectives, making it challenging to envision how AI can support personal connections with patients. Consequently, they did not foresee the use of AI during consultations. Instead, they suggested using AI to analyze historical data related to the reason for inquiry.

AI Must Be a Free, Active, and Integrated Option in the EHR

The fourth prerequisite highlighted by the GPs is the seamless integration of AI into existing clinical EHR systems. This integration should allow the AI to function as an optional tool that can be activated and accessed on demand. This ensures that GPs can use AI tools to seek assistance and support for specific tasks. The GPs express strong opposition to any interruptions in the EHR workflow, such as pop-ups, and emphasize the need for complete control over the AI functionality, including the ability to turn it on and off as needed, regardless of the tool's type or purpose.

A high level of security is another prerequisite for the GPs to adopt AI into EHR systems. The GPs emphasize that information must not be lost as it moves from human oversight to AI processes, nor should it accumulate unnecessarily within the EHR. Robust safety measures are essential to ensure that tasks handled by AI are appropriately followed by GPs or other practice staff, even if the information is not immediately

XSL•FO
RenderX

necessary. In addition, a "backstop" mechanism should be integrated into the EHR to collect and safeguard any AI-handled information that has not been acknowledged by a GP or other practice staff, ensuring no data is overlooked or mishandled.

> *No, then I wouldn't like it, because there are many of the test answers, we get here in the house, that are normal, but normal answers can also give rise to some form of action. So, if you imagine that you had a machine that sent normal responses to the patient, something would go wrong. Then we must have a stumbling block in relation to follow-up.* [Participant No. 6]

Discussion

Statement of Principal Findings

This study identified 4 main themes as prerequisites that GPs consider essential for realizing the perceived potential of AI in general practice: (1) AI must begin with the low-hanging fruit, (2) AI must be meaningful in the GP's work, (3) the GP-patient relationship must be maintained despite AI, and (4) AI must be a free, active, and integrated option in the EHR.

Strengths and Weaknesses of the Study

In this study, we applied vignettes as a stimulus for reflecting on hypothetical scenarios, given that AI has not yet been implemented or validated in Danish general practice. The vignettes served as a tool to facilitate discussions on topics in which the included GPs generally had limited experience. However, because vignettes are traditionally designed to simulate real-world scenarios, the absence of AI in current practice may reduce their perceived credibility [30].

A key reason for including first adopters associated with CAM AAU and Nord-KAP was to ensure satisfactory AI literacy among participants, addressing the low AI literacy observed in similar studies [15,20,31]. At the outset of the interviews, the participants were asked about their knowledge of AI, and we determined that their AI literacy was sufficient for the study. However, this study has limitations due to purposive sampling and recruitment from a limited geographical area (the North Denmark Region). This may have affected the transferability of the study to other contexts. Despite these limitations, the age and professional experience of the participating GPs provided a reasonable range of diversity, closely resembling that of the general Danish GP population [28]. Therefore, the results of this study should be interpreted in the specific context of data collection and as reflective of the participants' perceptions [29].

The interview data were collected in 2019 and 2021, and with the rapid technological advancements in AI in recent years, the evidence presented in this study may be outdated. However, because AI has not yet been widely implemented in general practice, the overall development of AI remains less directly relevant to the daily work of GPs. In addition, the core values of general practice have remained unchanged since the time of the interviews [32]. This argument is underlined in the paper by Nassehi and Ramvi [33], which states the continuous importance of care in general practice despite the prevalence of digital technologies. Thus, the insights from this study remain relevant in the context of the ongoing development of AI in general practice.

Comparison With Previous Work

Several views and attitudes similar to those identified in this study on the prerequisites for AI in general practice can, upon closer examination, be found in previous research [15-20]. Regarding what this study defined as "low-hanging fruit," referring to starting AI development for low-complexity tasks, other studies have shown comparable preferences, for example, introducing AI to reduce administrative burdens [17,19,20]. For instance, it has been suggested that the daily workload of GPs can be alleviated through preselection and patient prioritization [20].

In addition, the potential of AI to support administrative tasks such as clinical documentation, practice operations, and triage is seen to enhance efficiency. This allows GPs more time and cognitive freedom to focus on the medical and social complexities of patient care [17]. These findings highlight a discrepancy between the needs of GPs and the current dominant research trends in AI, such as diagnostic decision support tools [13]. This further emphasizes the importance of defining the prerequisites for AI, as outlined in this study, to ensure that the core values of general practice are preserved.

This study found that the included GPs are open to the potential of AI to alleviate specific routine tasks without diminishing their primary responsibilities. Other studies also support this view, emphasizing that AI will never fully replace GPs, especially in clinical decision-making [17]. It has been established that AI should act as a support tool, complementing the GP's clinical judgment while remaining sensitive to the patient's specific concerns and context [15,20]. Furthermore, 1 study demonstrated that technology could negatively influence GPs' decision-making, potentially impacting treatment outcomes [20]. Thus, our study findings reinforce that GPs should retain authority to make decisive decisions when working with AI.

Similarly, trust appears to be a crucial factor in AI acceptance of the included GPs. Our findings align with those of other studies that emphasize trust as a key driver of AI adoption and usage by GPs [34]. GPs must be open to AI and confident in the information it provides [15]. However, trust extends beyond GPs; patients' trust in AI depends on their GP's trust and acceptance [35]. Therefore, successful integration of AI into general practice depends on the trust of both GPs and patients, ensuring that a human-centric approach is at the core of AI adoption.

Furthermore, the GPs in our study underscored that AI should not detract time from patients. Comparably, previous research indicates that GPs fear that AI may compromise the quality of patient care and undermine the GP-patient relationship [15]. It has also been suggested by previous research that GPs believe that AI lacks the essential human competencies required for patient care [19]. AI is seen as unable to account for the social and economic factors that influence patient care, as the ability to maintain a holistic view of care develops through long-term relationships between individuals and communities [17,19,20]. Therefore, preserving the GP-patient relationship must be a key

XSL•FO
RenderX

consideration when developing AI for general practice, underscoring the importance of protecting this relationship in the AI integration process.

Finally, similar to our findings, previous studies have noted that the minimum requirements for AI in EHRs are essential for ensuring optimal use. For example, AI systems should be designed to preserve autonomy, health data privacy, and security within the EHR system [15,20]. GPs must be able to use AI intuitively and issues such as software interoperability, usability, and workflow integration must be addressed to ensure that AI has a meaningful impact on general practice [15,17]. This underscores the importance of minimizing the effort required by GPs to effectively use AI, making it a critical prerequisite for designing AI tools for general practice.

Possible Mechanisms and Implications of the Study

The GPs included in this study believe that meaningful use of AI in general practice begins with low-complexity tasks, aligning with the earlier definition of "low-hanging fruit." In this study, we understand "meaningful" as a quality in human-computer interaction [36]. Thus, by realizing AI for administrative and supporting tasks already embedded in everyday clinical routines, AI can support GPs' actual work and reflections at a practical level.

The results of this study further demonstrate that the GP-patient relationship can be preserved if AI is designed to handle routine and administrative tasks. The included GPs underline their central role in patient interactions, and their suggestion to assign AI to more peripheral tasks further underpins the narrative of GPs as family doctors [37]. However, today's general practice has evolved significantly from traditional family medicine, particularly regarding patient independence and symptom interpretation [38]. The time and space available to patients are becoming more restrained in modern general practice, yet patient involvement and autonomy are reaching unprecedented significance. Therefore, it is essential to clarify how AI can support the modernization of general practice while preserving the essence of GP-patient relationships.

It has previously been determined that patients trust the use of AI if their GPs trust it [35]. The trust of GPs in this study hinges on understanding the underlying algorithm and making conclusive decisions based on AI outputs. However, this raises the question of whether GPs can trust AI, particularly its current "black box" form. This challenge underscores the importance of exploring the possibility of explainable AI (XAI) [39]. XAI is an emerging research area that should be considered to realize the potential of transparent and trustworthy AI in general practice.

Furthermore, ensuring that AI is an optional and customizable feature within the EHR is critical. Allowing individual clinics to adjust AI tools according to their preferences and routines can improve their adaptability. This will enable GPs to determine the extent to which AI assists in health care work. Thus, modernizing the EHR system is essential for using the AI capacity. This ensures that the GP's use of AI remains an active and deliberate choice, reinforcing their autonomy and trust in the technology.

To further enhance trust and meaningful AI in general practice, it is essential to establish close collaboration among GPs, EHR suppliers, and other information technology stakeholders when developing and potentially implementing AI. This collaborative synergy would ensure that potential AI tools meet general practice needs while aligning with the upcoming regulatory framework introduced by the European Union, such as the GDPR and AI Act. These frameworks enhance transparency, accountability, and trust in AI systems, thereby supporting their integration into general practice [40,41].

Unanswered Questions and Future Research

When examining the study's defined prerequisites for AI in general practice, it becomes evident that the included GPs recognize the transformative potential of AI. Nevertheless, further research is imperative to identify relevant low-complexity tasks of a routine and administrative nature before commencing the development of suitable AI tools. Classifying suitable low-complexity tasks for AI in general practice will require comprehensive effort, but such classification is critical for aligning development with implementation. By identifying tasks suitable for AI in general practice, groundwork can be laid for a seamless transition from design to deployment.

While this study only addressed the exploration phase of implementation [12], it is essential to consider the remaining implementation phases before initiating development [42,43]. Furthermore, it could be favorable to incorporate the study's prerequisites into early implementation strategies, which could ensure the alignment of new AI tools with GPs' expectations and perceptions of how AI should function in general practice.

While the study results highlight the importance of addressing political, legal, and economic aspects to build trust in AI, it does not delve into concerns regarding privacy, liability, and financial considerations stated in previous research [15]. Future research exploring these areas within the context of AI in Danish general practice would be highly valuable.

As no AI tool has been implemented or validated in Danish general practice, we believe that the defined prerequisites of the study can guide the initial phases of the future development of AI. It will also be valuable to consider these prerequisites when evaluating new AI tools to determine whether they are suitable for general practice.

Acknowledgments

We extend our gratitude to the study participants for sharing their time, experiences, and insights.

XSL•FO
RenderX

Authors' Contributions

NLJ was the primary researcher in this study and was responsible for designing the study, conducting all interviews, analyzing the data, and serving as the primary author of this paper. CHM and JLT assisted in the study design, vignettes, and interview guide, and contributed to the data analysis. To enhance the trustworthiness of the findings, all authors participated in collaborative discussions to review and refine the themes. These discussions involved thoroughly examining the raw data, including excerpts from the transcripts to ensure that the themes accurately represented the participants' perspectives. MBJ, TBM, and KK provided feedback and assistance throughout the study. All authors have read and approved the final manuscript.

Conflicts of Interest

None declared.

Multimedia Appendix 1
Vignettes applied in the study.
[DOCX File, 17 KB - medinform_v13i1e63895_app1.docx]

References

1. Alowais SA, Alghamdi SS, Alsuhebany N, et al. Revolutionizing healthcare: the role of artificial intelligence in clinical practice. BMC Med Educ 2023 Sep 22;23(1):689. [doi: 10.1186/s12909-023-04698-z] [Medline: 37740191]
2. Rajpurkar P, Chen E, Banerjee O, Topol EJ. AI in health and medicine. Nat Med 2022 Jan;28(1):31-38. [doi: 10.1038/s41591-021-01614-0] [Medline: 35058619]
3. Lin S. A clinician's guide to artificial intelligence (AI): why and how primary care should lead the health care AI revolution. J Am Board Fam Med 2022;35(1):175-184. [doi: 10.3122/jabfm.2022.01.210226] [Medline: 35039425]
4. Lin SY, Mahoney MR, Sinsky CA. Ten ways artificial intelligence will transform primary care. J Gen Intern Med 2019 Aug;34(8):1626-1630. [doi: 10.1007/s11606-019-05035-1] [Medline: 31090027]
5. Health at a glance: Europe 2016: state of health in the EU cycle. : OECD/European Union; 2016. [doi: 10.1787/health_glance_eur-2016-62-en]
6. Pedersen KM, Andersen JS, Søndergaard J. General practice and primary health care in Denmark. J Am Board Fam Med 2012 Mar;25 Suppl 1:S34-S38. [doi: 10.3122/jabfm.2012.02.110216] [Medline: 22403249]
7. Lüchau EC, Atherton H, Olesen F, Søndergaard J, Assing Hvidt E. Interpreting technology: use and non-use of doctor-patient video consultations in Danish general practice. Soc Sci Med 2023 Oct;334:116215. [doi: 10.1016/j.socscimed.2023.116215] [Medline: 37690154]
8. Clausen A, Christensen ER, Jakobsen PR, Søndergaard J, Abrahamsen B, Rubin KH. Digital solutions for decision support in general practice - a rapid review focused on systems developed for the universal healthcare setting in Denmark. BMC Prim Care 2023 Dec 14;24(1):276. [doi: 10.1186/s12875-023-02234-y] [Medline: 38097998]
9. Blanes-Vidal V, Lindvig KP, Thiele M, Nadimi ES, Krag A. Artificial intelligence outperforms standard blood-based scores in identifying liver fibrosis patients in primary care. Sci Rep 2022 Feb 21;12(1):2914. [doi: 10.1038/s41598-022-06998-8] [Medline: 35190650]
10. Soerensen PD, Christensen H, Gray Worsoe Laursen S, Hardahl C, Brandslund I, Madsen JS. Using artificial intelligence in a primary care setting to identify patients at risk for cancer: a risk prediction model based on routine laboratory tests. Clin Chem Lab Med 2022 Nov 25;60(12):2005-2016. [doi: 10.1515/cclm-2021-1015] [Medline: 34714986]
11. Handley MA, Gorukanti A, Cattamanchi A. Strategies for implementing implementation science: a methodological overview. Emerg Med J 2016 Sep;33(9):660-664. [doi: 10.1136/emermed-2015-205053] [Medline: 26893401]
12. Aarons GA, Hurlburt M, Horwitz SM. Advancing a conceptual model of evidence-based practice implementation in public service sectors. Adm Policy Ment Health 2011 Jan;38(1):4-23. [doi: 10.1007/s10488-010-0327-7] [Medline: 21197565]
13. Kueper JK, Terry AL, Zwarenstein M, Lizotte DJ. Artificial intelligence and primary care research: a scoping review. Ann Fam Med 2020 May;18(3):250-258. [doi: 10.1370/afm.2518] [Medline: 32393561]
14. Sørensen NL, Bemman B, Jensen MB, Moeslund TB, Thomsen JL. Machine learning in general practice: scoping review of administrative task support and automation. BMC Prim Care 2023 Jan 14;24(1):14. [doi: 10.1186/s12875-023-01969-y] [Medline: 36641467]
15. Nash DM, Thorpe C, Brown JB, et al. Perceptions of artificial intelligence use in primary care: a qualitative study with providers and staff of Ontario Community Health Centres. J Am Board Fam Med 2023 Apr 3;36(2):221-228. [doi: 10.3122/jabfm.2022.220177R2] [Medline: 36948536]
16. Terry AL, Kueper JK, Beleno R, et al. Is primary health care ready for artificial intelligence? What do primary health care stakeholders say? BMC Med Inform Decis Mak 2022 Sep 9;22(1):237. [doi: 10.1186/s12911-022-01984-6] [Medline: 36085203]
17. Upshaw TL, Craig-Neil A, Macklin J, et al. Priorities for artificial intelligence applications in primary care: A Canadian deliberative dialogue with patients, providers, and health system leaders. J Am Board Fam Med 2023 Apr 3;36(2):210-220. [doi: 10.3122/jabfm.2022.220171R1] [Medline: 36948537]

XSL•FO
RenderX

18. Allen MR, Webb S, Mandvi A, Frieden M, Tai-Seale M, Kallenberg G. Navigating the doctor-patient-AI relationship - a mixed-methods study of physician attitudes toward artificial intelligence in primary care. BMC Prim Care 2024 Jan 27;25(1):42. [doi: 10.1186/s12875-024-02282-y] [Medline: 38281026]
19. Blease C, Kaptchuk TJ, Bernstein MH, Mandl KD, Halamka JD, DesRoches CM. Artificial intelligence and the future of primary care: exploratory qualitative study of UK general practitioners' views. J Med Internet Res 2019 Mar 20;21(3):e12802. [doi: 10.2196/12802] [Medline: 30892270]
20. Buck C, Doctor E, Hennrich J, Jöhnk J, Eymann T. General practitioners' attitudes toward artificial intelligence-enabled systems: interview study. J Med Internet Res 2022 Jan 27;24(1):e28916. [doi: 10.2196/28916] [Medline: 35084342]
21. Hughes R, Huby M. The construction and interpretation of vignettes in social research. SWSSR 2004 Jan 1;11(1):36-51. [doi: 10.1921/swssr.v11i1.428]
22. Jenkins N, Bloor M, Fischer J, Berney L, Neale J. Putting it in context: the use of vignettes in qualitative interviewing. Qual Res 2010 Apr;10(2):175-198. [doi: 10.1177/1468794109356737]
23. Barter C, Renold E. The use of vignettes in qualitative research. Social research update. 1999. URL: https://sru.soc.surrey.ac.uk/SRU25.html
24. O'Brien BC, Harris IB, Beckman TJ, Reed DA, Cook DA. Standards for reporting qualitative research: A synthesis of recommendations. Acad Med 2014 Sep;89(9):1245-1251. [doi: 10.1097/ACM.0000000000000388] [Medline: 24979285]
25. Etikan I, Musa SA, Alkassim RS. Comparison of convenience sampling and purposive sampling. AJTAS 2016;5(1):1. [doi: 10.11648/j.ajtas.20160501.11]
26. Rogers EM, Singhal A, Quinlan MM. Diffusion of Innovations: Routledge 2014.
27. Overview of mandatory reporting. The Danish National Center for Ethics. URL: https://researchethics.dk/information-for-researchers/overview-of-mandatory-reporting [accessed 2025-02-27]
28. Organisation of General Practitioners in Denmark (PLO), PLO fact sheet 2024. URL: https://laeger.dk/media/qaelslew/plo-faktaark-2024.pdf [accessed 2025-02-03]
29. Braun V, Clarke V. Conceptual and design thinking for thematic analysis. Qualitative Psychology 2022;9(1):3-26. [doi: 10.1037/qup0000196]
30. Wilson J, While AE. Methodological issues surrounding the use of vignettes in qualitative research. J Interprof Care 1998 Jan;12(1):79-86. [doi: 10.3109/13561829809014090]
31. Long D, Magerko B. What is AI literacy? competencies and design considerations. : Association for Computing Machinery Presented at: CHI '20: Proceedings of the 2020 CHI Conference on Human Factors in Computing Systems; Apr 23-30, 2020 URL: https://dl.acm.org/doi/proceedings/10.1145/3313831 [doi: 10.1145/3313831.3376727]
32. Nordic Federation of General Practice (NFGP). Core values and principles of Nordic general practice/family medicine. Scand J Prim Health Care 2020 Dec;38(4):367-368. [doi: 10.1080/02813432.2020.1842674] [Medline: 33284030]
33. Nassehi D, Ramvi E. Care in the era of digital health: experiences from Norwegian general practitioners. Scand J Prim Health Care 2024:1-9. [doi: 10.1080/02813432.2024.2437417] [Medline: 39639473]
34. Asan O, Bayrak AE, Choudhury A. Artificial intelligence and human trust in healthcare: focus on clinicians. J Med Internet Res 2020 Jun 19;22(6):e15154. [doi: 10.2196/15154] [Medline: 32558657]
35. Mikkelsen JG, Sørensen NL, Merrild CH, Jensen MB, Thomsen JL. Patient perspectives on data sharing regarding implementing and using artificial intelligence in general practice - a qualitative study. BMC Health Serv Res 2023 Apr 4;23(1):335. [doi: 10.1186/s12913-023-09324-8] [Medline: 37016412]
36. Mekler ED, Hornbæk K. A framework for the experience of meaning in human-computer interaction. : Association for Computing Machinery Presented at: CHI '19: Proceedings of the 2019 CHI Conference on Human Factors in Computing Systems; May 4-9, 2019 URL: https://dl.acm.org/doi/proceedings/10.1145/3290605 [doi: 10.1145/3290605.3300455]
37. Wonca Europe. The European definition of general practice/family medicine. URL: https://www.woncaeurope.org/page/definition-of-general-practice-family-medicine [accessed 2024-07-04]
38. Andersen RS, Høybye MT, Risør MB. Expanding medical semiotics. Med Anthropol 2024 Feb 17;43(2):91-101. [doi: 10.1080/01459740.2024.2324892] [Medline: 38437012]
39. Muddamsetty SM, Jahromi MNS, Moeslund TB. Expert level evaluations for explainable AI (XAI) methods in the medical domain. : Springer, Cham Presented at: Pattern Recognition ICPR International Workshops and Challenges ICPR 2021 Lecture Notes in Computer Science. [doi: 10.1007/978-3-030-68796-0_3]
40. Al Meslamani AZ. Why are digital health policies crucial? J Med Econ 2024;27(1):167-169. [doi: 10.1080/13696998.2024.2302254] [Medline: 38174851]
41. European Parliament. EU AI Act: first regulation on artificial intelligence. URL: https://www.europarl.europa.eu/topics/en/article/20230601STO93804/eu-ai-act-first-regulation-on-artificial-intelligence [accessed 2024-07-04]
42. Damschroder LJ, Reardon CM, Widerquist MAO, Lowery J. The updated Consolidated Framework for Implementation Research based on user feedback. Implement Sci 2022 Oct 29;17(1):75. [doi: 10.1186/s13012-022-01245-0] [Medline: 36309746]
43. Damschroder LJ, Aron DC, Keith RE, Kirsh SR, Alexander JA, Lowery JC. Fostering implementation of health services research findings into practice: a consolidated framework for advancing implementation science. Implement Sci 2009 Aug 7;4:50. [doi: 10.1186/1748-5908-4-50] [Medline: 19664226]

XSL•FO
RenderX

Abbreviations

AI: artificial intelligence
CAM AAU: Center for General Practice at Aalborg University
EHR : electronic health record
GDPR : General Data Protection Regulation
GP : general practitioner
Nord-KAP : Quality Unit for General Practice in the North Denmark Region
SRQR: Standards for Reporting Qualitative Research
XAI: explainable artificial intelligence

Edited by C Lovis; submitted 04.07.24; peer-reviewed by B Senst, M Neher, S Pesälä; revised version received 03.02.25; accepted 06.02.25; published 12.03.25.

Please cite as:
Jørgensen NL, Merrild CH, Jensen MB, Moeslund TB, Kidholm K, Thomsen JL
The Perceptions of Potential Prerequisites for Artificial Intelligence in Danish General Practice: Vignette-Based Interview Study Among General Practitioners
JMIR Med Inform 2025;13:e63895
URL: https://medinform.jmir.org/2025/1/e63895
doi:10.2196/63895

© Natasha Lee Jørgensen, Camilla Hoffmann Merrild, Martin Bach Jensen, Thomas B Moeslund, Kristian Kidholm, Janus Laust Thomsen. Originally published in JMIR Medical Informatics (https://medinform.jmir.org), 12.3.2025. This is an open-access article distributed under the terms of the Creative Commons Attribution License (https://creativecommons.org/licenses/by/4.0/), which permits unrestricted use, distribution, and reproduction in any medium, provided the original work, first published in JMIR Medical Informatics, is properly cited. The complete bibliographic information, a link to the original publication on https://medinform.jmir.org/, as well as this copyright and license information must be included.

XSL•FO
RenderX

Original Paper

Identifying and Optimizing Factors Influencing the Implementation of a Fast Healthcare Interoperability Resources Accelerator: Qualitative Study Using the Consolidated Framework for Implementation Research–Expert Recommendations for Implementing Change Approach

Jane Li[1], MBBS, PhD; Emma Maddock[1], BSc; Michael Hosking[1], BOT; Kate Ebrill[1], BHSc, MPH; Jeremy Sullivan[2]; Kylynn Loi[1], BPharm; Danielle Tavares-Rixon[1], BIT; Rajiv Jayasena[1], PhD; Grahame Grieve[3], PhD; Alana Delaforce[1], BN, MN, PhD

[1]Australian e-Health Research Centre, CSIRO, Brisbane, Australia

[2]Australian Government Department of Health, Disability and Ageing, Canberra, Australia

[3]Health Intersections Pty Ltd, Melbourne, Australia

Corresponding Author:
Alana Delaforce, BN, MN, PhD
Australian e-Health Research Centre
CSIRO
Level 7, Surgical Treatment and Rehabilitation Service
296 Herston Road, Herston
Brisbane, 4029
Australia
Phone: 61 07 3253 3647
Email: alana.delaforce@csiro.au

Abstract

Background: Fragmented sharing of health information is known to negatively impact patient care and outcomes. To support the sharing of health information between systems, Fast Healthcare Interoperability Resources (FHIR) has emerged as the global interoperability standard for health information exchange. To speed up the process of adoption, various FHIR accelerator groups have been formed. FHIR accelerators such as the Sparked program in Australia enable communities and collaborative groups to develop high-quality FHIR standards for health care information exchange and encourage widespread uptake. However, limited research exists on the development, delivery, and implementation of FHIR accelerator programs.

Objective: This study used qualitative methods to identify the key components of the Sparked FHIR accelerator, what factors influence implementation, and which strategies may help enhance its delivery.

Methods: Semistructured interviews were conducted with Sparked stakeholders in the early stage of the program. The Sparked FHIR accelerator intervention components were described using a standardized reporting checklist (Template for Intervention Description and Replication). The Consolidated Framework for Implementation Research (CFIR) 2.0 was used to analyze factors influencing implementation. On the basis of a cumulative majority analysis, the most mentioned factors influencing implementation were identified. These factors were then mapped to the Expert Recommendations for Implementing Change (ERIC) tool to identify strategies for enhancing the implementation of the Sparked program.

Results: A total of 17 participants were interviewed, including program leads, cochairs, representatives of software industry implementers, clinicians, and consumers. In total, 8 key CFIR influencing factors were identified: engaging, innovation design, assessing needs, local conditions, access to knowledge and information, partnerships and connections, capability, and work infrastructure. After mapping the top CFIR influencing factors to the ERIC tool, 5 strategy clusters were identified: adapt and tailor to context, develop stakeholder interrelations, support participants, train and educate stakeholders, and use evaluative and iterative strategies.

Conclusions: This study enabled the core components of the Sparked FHIR accelerator to be defined and identified the factors that have the strongest influence on program implementation. Using the CFIR-ERIC approach facilitated the generation of

XSL•FO
RenderX

expert-informed recommendations for improving the implementation of Sparked, but researcher recommendations were needed to supplement the tool. This research offers valuable insights for decision makers and implementers.

(JMIR Med Inform 2025;13:e66421) doi:10.2196/66421

KEYWORDS

Fast Healthcare Interoperability Resources accelerator; FHIR accelerator; Sparked; Consolidated Framework for Implementation Research; Expert Recommendations for Implementing Change; implementation enhancement plan; digital health; interoperability standards

Introduction

Background

The adoption of digital health information systems and interventions is on the rise. However, the data informing these systems, such as requests for pathology tests and medical imaging, are often fragmented and represented using inconsistent terminologies and measurement units across various platforms. This phenomenon is known as the absence of interoperability. A lack of interoperability between digital health information systems and interventions can lead to adverse health outcomes and higher costs to the health system (eg, redundant laboratory testing, higher health care expenditure, and medication errors) [1-3]. To address fragmentation and promote interoperability, it is necessary to establish standardized measurements and terminologies that can be embedded into various health information systems. The Fast Healthcare Interoperability Resources (FHIR) [4] has rapidly emerged as one of the most favored standards for health information sharing and continues to show promise in developing an application-based approach to interoperability and health information exchange [5,6].

Health Level Seven (HL7) International, the global accredited standard development organization, has suggested 5 aspects of a rigorous standard development process that emphasizes consensus, fitness for purpose, implementability, community engagement, and ongoing maintenance [7]. During standard development, working groups adhere to a structured decision-making process to achieve consensus, openness, and fair representation of interests. In addition, all proposed standards undergo a formal balloting process to collect and reconcile feedback on specifications before they are published as normative standards. Despite the known benefits of implementing FHIR, work is needed to increase their uptake, adoption, and implementation [8,9].

Worldwide, numerous FHIR accelerators have been established to facilitate the development and adoption of agreed-upon core datasets, including Argonaut, CodeX, Gravity, and Da Vinci, as listed by HL7 [10]. These accelerators aim to develop local standards that expedite the adaptation and development of health information systems in an interoperable manner, enabling clinical information systems and health data applications to seamlessly and consistently share information regardless of the application source.

The Sparked accelerator program commenced in Australia in July 2023 [11]. This was part of the federal budget to implement new initiatives that improve digital health information sharing. It is facilitated by the Commonwealth Scientific and Industrial Research Organisation (CSIRO) Australian e-Health Research Centre and serves as a collaborative consortium to bring together government entities, technology vendors, health care organizations, peak bodies, practitioners, and domain experts to accelerate the creation, use, and adoption of national FHIR standards for health care information exchange [11,12]. By fostering community collaboration, Sparked aims to enable the community to develop robust, nationally agreed-upon, Australian context–specific HL7 FHIR standards, clinical information models, and terminology value sets. Technical and clinical design groups have been formed to bring a holistic perspective when defining requirements and specifications, as well as validating and implementing critical health care data and FHIR standards.

Although FHIR accelerators, including Sparked, have been carried out in various countries over the last few years, there is currently limited research available in peer-reviewed literature that reports on the development, delivery, implementation, and evaluation of accelerator programs. Furthermore, there is a lack of evidence concerning the key attributes and factors influencing the implementation of successful community practices in accelerator programs. A lack of formal intervention or program descriptions is not uncommon in the literature, and related work has focused on the technical development of FHIR implementation guides and pilot-testing of the FHIR standards to support a specialized domain, such as genomics, oncology, and health research [8,9,13-16]. Lessons learned from these smaller-scale individual developments have highlighted the importance of engagement from clinical work groups in addition to communication and coordination between the standard developers and the implementation team. These pilots have pointed out future directions in supporting community-driven HL7 FHIR accelerators, including the critical need for collaboration among the communities in developing consensus to accelerate interoperable data modeling and applications [9,13,14,16]. These lessons learned are often published on informal websites, and there is a lack of peer-reviewed evidence that operationalizes theory to help synthesize these learnings into generic recommendations. Standardized analysis and reporting of success can be achieved using implementation science.

Implementation science offers theories, models, and frameworks that help explain the conditions needed to optimize the uptake of evidence-based practice. In this context, there is evidence of the need to implement interoperable systems to promote health outcomes. In our study, the Consolidated Framework for Implementation Research (CFIR), a conceptual framework designed to systematically assess implementation using multiple

XSL•FO
RenderX

lenses (called domains), was used to identify factors influencing intervention implementation [17,18]. The CFIR, resulting from a systematic review of available implementation frameworks, integrates factors associated with effective implementation from various theoretical and empirical studies into a set of domains and constructs. The CFIR comprises 5 major domains: intervention characteristics, inner setting, outer setting, characteristics of the individuals involved, and implementation process. Among these domains are 48 constructs and 19 subconstructs. It has been widely cited since its publication in 2009 and recently updated as the CFIR 2.0 [17-20]. The study authors developed a virtual care *expansion pack* to the CFIR 2.0 that includes extended constructs related to the uptake of virtual care innovations, and it used in this study [21]. On its own, the CFIR is highly useful for gathering insights into implementation, but to truly maximize the output data, it should be used in conjunction with an implementation strategy selection tool.

The Expert Recommendations for Implementing Change (ERIC) tool was first developed to create a refined taxonomy of implementation strategies that can be used to improve the uptake of evidence [22]. In 2019, the strategies were mapped to the CFIR framework to identify which strategies are best suited to addressing factors influencing implementation [23]. The mapping process occurred through consensus among implementation experts and resulted in the development of the CFIR-ERIC Matching Tool [24]. Despite known heterogeneity in agreement among experts as to what strategies best address CFIR constructs, approaches using the combined CFIR-ERIC tool have been demonstrated to improve the uptake of interventions, including one study that showed a 10-fold improvement in compliance with clinical recommendations related to the optimization of patients' blood preoperatively [22,24-26]. The CFIR-ERIC approach can be flexibly applied and is particularly useful for guiding the evaluation of complex digital health care interventions, enabling the systematic identification of factors influencing the implementation of interventions across different contexts [27-30].

Implementation science promotes standardized reporting of interventions, and the Template for Intervention Description and Replication (TIDieR) checklist has been used to support clear articulation of intervention components [31]. Even when the optimal conditions for implementation are known, efforts to replicate these can be hampered by variations in the interventions for which the conditions are relevant. While we may understand the optimal conditions for implementing an FHIR accelerator, without knowing all the program elements that are necessary for success, key activities may be missed in future implementation attempts. For example, one FHIR accelerator may heavily rely on a mix of face-to-face and hybrid participation, and if this is not sufficiently articulated, other FHIR accelerators that instead rely on delivering the program entirely on the web may fail without realizing why despite having optimized the conditions for implementation. In this study, the TIDieR checklist was completed to enable replication of the Sparked program at the intervention level.

In this paper, we describe the core components of the Sparked FHIR accelerator and demonstrate how the CFIR-ERIC approach facilitated an understanding of factors influencing the implementation of the Sparked program. Our research provides actionable findings for decision makers and program implementers.

Objectives

This study had three key objectives: (1) to define the core components of the Sparked accelerator program and understand how those components interact with each other, (2) to identify factors influencing the implementation of the Sparked accelerator program as perceived by relevant stakeholders, and (3) to leverage implementation science theory to develop an implementation enhancement plan to improve the adoption of FHIR standards by optimizing the Sparked FHIR accelerator program.

Methods

Semistructured interviews were conducted with stakeholders of the Sparked program. Interview questions were developed based on CFIR constructs and focused on stakeholders' perspectives on the program's components, engagement experience, perceptions of the FHIR development process, and factors influencing its success.

Participants and Recruitment

Participants included those involved in the conceptualization, coordination, and delivery of the Sparked program and its target population, such as program leaders, cochairs, members of the clinical and technical work groups, and consumer representatives. We aimed to recruit a minimum of 2 to 3 individuals from all relevant stakeholder groups to ensure adequate representation.

A Sparked program manager sent invitation emails to potential participants. A purposive, snowball sampling approach was used for recruitment, where additional stakeholders may be revealed as the research progresses [32]. Participants were provided with an electronic invitation (a recruitment flyer) that contained a link to complete a digital information and consent form through a secure REDCap (Research Electronic Data Capture; Vanderbilt University) server hosted by the CSIRO.

Data Collection

Interview sessions were conducted over a 3-month period, with the first interview taking place 4 months after the program commenced. Each session was conducted via videoconferencing (Microsoft Teams; Microsoft Corp) and lasted 45 to 60 minutes. Audiovisual recordings of the interviews were professionally transcribed. In total, 4 authors conducted the interviews as available (JL, AD, EM, and RJ).

Data Analysis

The transcribed data were exported into Microsoft Excel (Microsoft Corp) for cleaning and preparation for coding. Once complete, 3 researchers (JL, AD, and EM) carried out the coding process using the CFIR. A directed content analysis approach was adopted, enabling results to be aligned with CFIR 2.0 constructs. Additional constructs relevant to virtual care generated from a previous systematic review and designed as

XSL•FO
RenderX

an extension to the CFIR, which are available as a preprint, were also used [21].

The initial coding was conducted independently by 2 researchers (JL and EM), and results were discussed and refined. Following this, a codebook was developed by 2 researchers (AD and JL) to define the CFIR constructs in the Sparked context (Multimedia Appendix 1). On the basis of the codebook, 2 researchers (AD and JL) independently evaluated and revised the initial results in a second-round coding and consistency-checking process. After finalizing the coding, a prioritization exercise was undertaken to identify the most mentioned influencing factors (barriers and enablers) based on the cumulative majority, similarly to other studies using the CFIR [27,28]. A list of brief statements for each of these factors was generated by the 2 researchers. Mapping of the barriers and enablers to the ERIC tool was conducted to select theory-informed strategies that could enhance the running of the Sparked program.

We reviewed information published on the Sparked website [9] and analyzed participants' descriptions of Sparked components using the TIDieR checklist. We focused on the statements from program leaders and cochairs as they had an overall understanding of the program. The TIDieR items were further validated through author consensus (KE, JS, MH, KL, DT-R, and GG). The checklist enabled standardized reporting of Sparked components from an intervention perspective. Understanding the processes and contextual factors surrounding the Sparked program supported the development of the codebook during the analysis of CFIR influencing factors.

Ethical Considerations

Ethics approval was obtained from the CSIRO Health and Medical Human Research Ethics Committee (project ID 2023_057_LR). All participants provided digital informed consent through the secure REDCap server hosted by the CSIRO before participation. Interview transcripts were deidentified before analysis, and the results were reported in an aggregated format to ensure participant anonymity. Participants did not receive compensation for taking part.

Results

Demographics of the Participants

A total of 17 participants were interviewed, including 5 (29%) program leads from the CSIRO, 4 (24%) cochairs, 3 (18%) technical design group members from software vendors, 4 (24%) clinical design group members, and 1 (6%) consumer representative. The demographics of the participants are summarized in Table 1. Participants' digital health experience ranged from 2 to >25 years. Regarding HL7 and FHIR standards, their individual experiences varied from 1 to >25 years.

Table 1. Demographics of the participants (N=17).

Characteristic	Participants, n (%)
Role	
CSIRO[a] program lead or manager	5 (29)
Cochair and lead	4 (24)
Software vendor	3 (18)
Clinician	4 (24)
Consumer representative	1 (6)
Sex	
Female	5 (29)
Male	12 (71)
Experience with digital health (years)	
>25	4 (24)
15-25	7 (41)
5-15	5 (29)
<5	1 (6)
Experience with standards (years)	
>25	3 (18)
15-25	4 (24)
5-15	4 (24)
<5	6 (35)

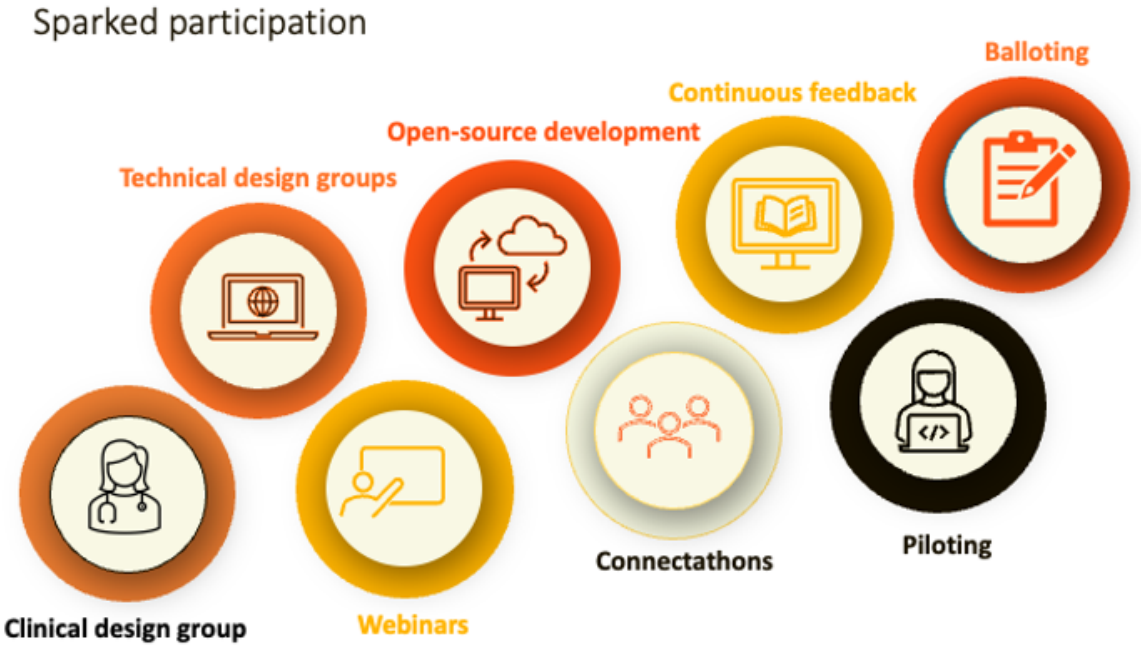
[a]CSIRO: Commonwealth Scientific and Industrial Research Organisation.

XSL•FO
RenderX

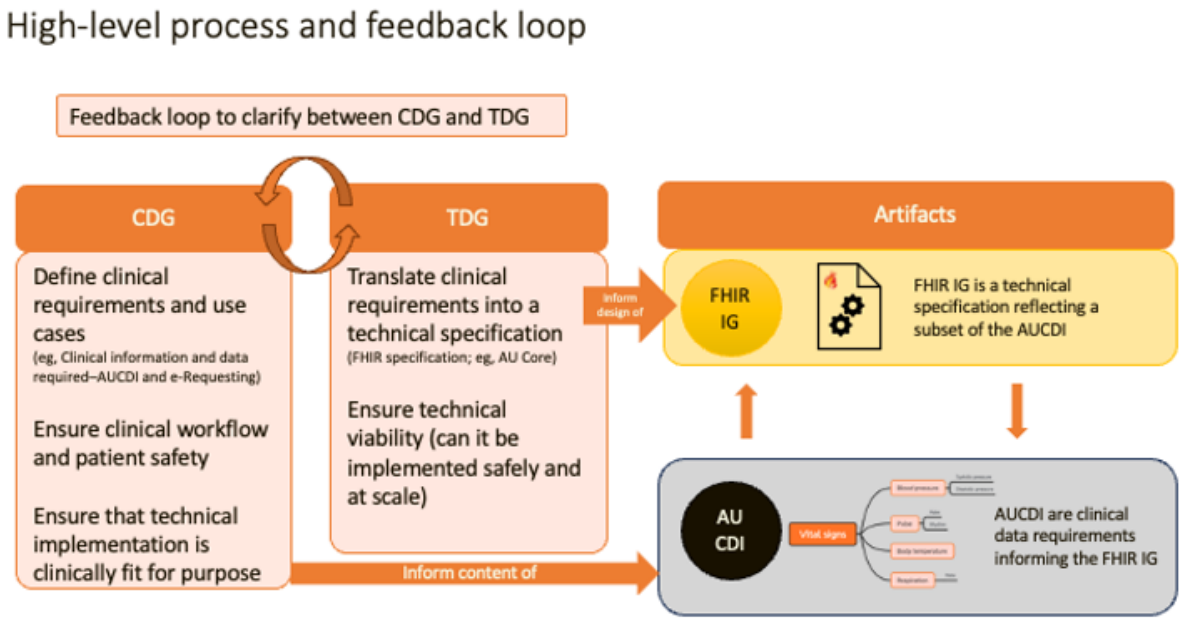
Sparked Components in the TIDieR Checklist

A detailed description of the Sparked intervention components is presented using the TIDieR checklist in Multimedia Appendix 2, including items and explanations related to the rationale, procedures, and materials; who was involved; and how the program is tailored, modified, and delivered. Figure 1 illustrates the components related to participation of design groups and their procedures and interactions with knowledge and artifacts.

Figure 1. Sparked participation (A) and process of interaction and feedback loop (B). AU: Australian; AUCDI: Australian Core Data for Interoperability; CDG: clinical design group; FHIR: Fast Healthcare Interoperability Resources; IG: implementation guide; TDG: technical design group.



A



B

Top CFIR Influencing Factors

Using a cumulative majority (frequency of mention on a per-participant basis), our results identified factors that positively or negatively influenced the participants' experience in the Sparked program and their perceptions of Sparked delivery.

A total of 65% (44/68) of the CFIR constructs were identified as factors influencing implementation. In addition, 44% (4/9)

XSL•FO
RenderX

of the newly proposed virtual care CFIR constructs [21] were identified as being relevant. We then identified the top 25% most mentioned barriers and enablers and combined them to create a final list of 8 influencing factors to be addressed, as summarized and highlighted in Table 2. These 8 constructs were considered as key influencing factors and were selected for prioritization and ERIC mapping. These constructs were engaging, innovation design, assessing needs, local conditions, access to knowledge and information, partnerships and connections, capability, and work infrastructure.

Table 2. Top Consolidated Framework for Implementation Research influencing factors (N=17).

Construct	Participants, n (%)
Engaging	17 (100)
Innovation design	17 (100)
Assessing needs	16 (94)
Local conditions	16 (94)
Access to knowledge and information	15 (88)
Partnerships and connections	15 (88)
Capability	13 (76)
Work infrastructure	11 (65)

Detailed Findings on the Top Factors Influencing Implementation

Overview

In the following sections, we present findings related to the 8 influencing factors organized by their CFIR domains. Their associated key (most mentioned) implementation condition statements in the Sparked context and exemplar quotes related to these statements are presented below. A full list of statements associated with each of these constructs is provided in Multimedia Appendix 3.

Innovation

Innovation design is related to how Sparked is designed and packaged, including how it is assembled, bundled, and presented. The key implementation condition statements for this influencing factor are presented in Textbox 1. Participants agreed that successful FHIR accelerators would require consensus-driven approaches, concurrent technical and clinical development, and effective coordination to ensure scalability and sustainability, supported by engagement that would encourage user interests and participation. Establishing a diverse community comprising the government, technology vendors, health care provider organizations, and experts was considered essential, and a centralized knowledge management system would be vital for information sharing among stakeholders.

Textbox 1. Innovation design—implementation condition statements.

A community comprising different stakeholders accelerates the creation and use of national Fast Healthcare Interoperability Resources standards

- "The aim for Sparked is actually to build community...and build a really active community that together will actually localize and profile the FHIR Foundation, SNOMED etc for use within Australia. So it's about coming together as a community together we go faster and actually fast tracking the adoption of these standards." [P5]

A facility to allow for concurrent technical and clinical development with opportunities to collaborate is needed

- "The trouble part is the connection between the clinical and the technical, we all come from different camps and we all have different...agendas or approaches, what we technically think we are capable of doing against what they clinically really want...so there can be a lot of tension between the two and I would highlight...we just sort of don't easily gravitate, integrate with each other." [P11]

A consensus-driven approach is a foundational component

- "I think keeping a genuine focus on community and consensus like genuine open consensus, so not sort of closing anyone out and focusing on an approach that does enable sort of an open market and really using this to sort of set foundations for Australia and I think key to success is...trying to see this as a bipartisan, multi-year initiative." [P15]

A centralized knowledge management system is integral for information sharing

- "They're the two elements, sort of the technical artifacts and the specifications and then the sort of the community process and making sure that that's inclusive, open and transparent and traceable...I think the biggest challenge...is making sure that people understand what they are, what the scope of them are, how they should be used, who should be governing them, how they should be maintained." [P4]

XSL•FO
RenderX

Outer Setting

Local conditions is related to the economic, environmental, political, and technological conditions that enable the outer setting to support the implementation and delivery of Sparked. The key implementation condition statements for this influencing factor are presented in Textbox 2. Australia has a mature digital ecosystem that recognizes interoperability as a key priority. However, participants also felt that some sectors of health care lagged in understanding the importance and implications of interoperability. The program's success may be influenced by uncertain political landscapes, and there was a perceived need for stronger support from educational and training institutions to enable a larger workforce to deliver program outputs.

Partnership and connections is related to how well the Sparked program and its members are networked with external entities. The key implementation condition statements for this influencing factor are presented in Textbox 3. Participants pointed out that Sparked had drawn individuals and organizations into participating, and the ongoing commitment of these stakeholders is vital for the program's sustainability. These partnerships not only strengthen the credibility and global recognition of the program but also facilitate the sharing of valuable lessons learned. However, there was a perceived gap between the technical and clinical realms, and this could pose a challenge to the program's output viability.

Textbox 2. Local conditions—implementation condition statements.

The digital ecosystem (at the macrolevel) in Australia has reached a requisite level of maturity

- "I think we're at a juncture in time in Australia where many in the industry, particularly the leaders that really are looking to see initiatives like FHIR really move forward, because of the efficiencies that it does bring the vendor, there's at least for the time being there's a window of opportunity for us to really bring them on board and use principles of good faith to work collaboratively together." [P14]

Some areas of health care (at the meso level) lack awareness of interoperability and its impact

- "There's different levels of maturity or organizations in terms of their understanding and awareness of what this is and what this means and specifically what this means for them. Like the aged care sector is quite a bit behind in terms of understanding how this works and how it can enable improved care delivery and information sharing." [P4]

The Sparked program's viability hinges on potentially turbulent political changes

- "I feel confident that the program can deliver, where it is today. It's probably other forces that are political of nature that are always probably the bigger risk points of budget changes and all that sort of stuff change...Hopefully that won't happen." [P15]

Greater engagement and support from educational and training institutions

- "The biggest pain point that we've got, I mean general lack of resources in the country...There's a finite set of FHIR experts, so how do we do this in the most efficient way possible...there's a longer term around how do we encourage across, like across universities...it's not shortage of people doing IT, it's shortage of people doing IT that want to go into healthcare." [P5]

Textbox 3. Partnership and connections—implementation condition statements.

The partnerships with important stakeholders support the sharing of lessons learned

- "There's many FHIR accelerators that are hosted by HL7 international...and a lot of those have been actually running a very long time...so we have been in communication with those folks for at least three years, sort of seeing what they're doing, learning how they've done things, what are their lessons learned." [P2]

The partnerships with important stakeholders strengthen the credibility and visibility of Sparked to be recognized as a world-class Fast Healthcare Interoperability Resources accelerator

- "Looking at the role of HL 7 International in supporting, particularly if you're wanting to use Sparked as an exemplar...the Sparked program could go international with the blessing and support and potentially additional resources from the international community." [P14]

There is a perceived disconnect between the technical and clinical worlds impeding the viability of the program outputs

- "You've got the clinicians providing the desirability and then you have the technologists or the TDG group providing the viability aspect, but it seems like there's a disconnect there, like they need to be working together more, those two teams need to be collaborating somehow and provide decision-making in tandem as opposed to like one to the other." [P10]

Inner Setting

Work infrastructure is related to the organization of tasks and responsibilities within and between individuals and teams and general staffing levels to support functional performance in Sparked. The key implementation condition statements for this influencing factor are presented in Textbox 4. Participants stated that balancing the need for progress with participants' time and energy constraints was challenging, especially in extensive consensus building and in an accelerated environment. To ensure smooth operations and effective event management, comprehensive administrative and logistical preparation was

XSL•FO
RenderX

required. Some participants pointed out that enhanced visibility of key participating organizations such as HL7 International would be essential for increasing community engagement, and the program would also require tools provided by software developers for delivering the test service and reference implementation.

Access to knowledge and information is related to how stakeholders in Sparked can access guidance and training to support their participation in the program. The key implementation condition statements for this influencing factor are presented in Textbox 5. Participants agreed that the Sparked program had ensured open access to program information and encouraged active use of its Confluence page. The program could benefit from a basic education package for individuals such as clinicians seeking to enhance their FHIR skills and from providing more detailed and user-friendly prereading materials.

Textbox 4. Work infrastructure—implementation condition statements.

Difficulty of balancing the need for progress with the demands on participants' time and energy

- "There's a lot of community good dialogue needed...There's not one way to solve the challenge...So consensus building takes time...and we're working in an accelerated environment...It's a lot of demand on their energy and time...I would say one of our challenges going forward will be sustaining the energy of our community to see it through." [P2]

Comprehensive administrative and logistical preparation is key for ensuring a smooth and productive event

- "Throwing more resources at the problem isn't necessarily going to solve the problem, but I do think in the case of the events coordination that would be something that would be beneficial and even a design team, a dedicated design team to help build much more digestible resources." [P4]

Enhanced visibility of each participating organization would enhance engagement

- "The role of HL 7...needs to be more visible. I know that they're a volunteer organization, so I think that's a change that could be very helpful and they should be more independent anyway. So they are the standards organization here, so I think their role needs to be a bit more, just a bit more forward in this...that as an optical suggestion is I think really important." [P15]

Need for software developers to provide tools to support delivering the test service and the reference implementation

- "Resourcing...for delivering the test service and the reference implementation and for our support of the standards we need tooling, software, tooling, so we need software developers to provide tools." [P1]

Textbox 5. Access to knowledge and information—implementation condition statements.

A basic education package or resources for consumers or people wanting upskilling would be helpful

- "There's been certainly attempts to explain the FHIR, but I do feel like we need to say go a little bit...it is a technical topic, so there's no avoiding it, but how do you make that a little bit more accessible for some of the, particularly some of the clinicians involved." [P15]

Anyone can access information about the Sparked program

- "We have a confluence page that CSIRO hosts that that information is available on—like our road map, our plans, the clinical group actually sets off that and for the technical groups they actually set off the HL7 pages. So all that is public, so anyone can make a judgment and share that communication." [P2]

Prereading materials could be more detailed or easier to understand

- "Just noting that...a good amount of the audience aren't technical FHIR experts. So a little bit more concise direction in this is what we're asking you to consider for this part of the workshop, these are the things that we'd like you to think about and discuss. I think just a little bit more clarity with those could've been helpful on the day." [P17]

Individuals

Capability is related to stakeholders' interpersonal competence, knowledge, and skills to fulfill their roles to participate in and deliver the Sparked program. The key implementation condition statements for this influencing factor are presented in Textbox 6. Enhancing training and education across various skill levels using practical examples was highlighted as a way to facilitate broader understanding and more meaningful engagement. There is a need to support technical and clinical knowledge development and address the challenge of enabling equal participation among stakeholders with varying backgrounds and knowledge levels. In addition to leveraging previous experience in FHIR activities to enhance capability, scaling existing formal academic training partnerships was identified as a potential solution.

XSL•FO
RenderX

Textbox 6. Capability—implementation condition statements.

Previous experience, knowledge, and involvement in other Fast Healthcare Interoperability Resources activities improve capability

- "I'm lucky in that I had some maybe it's tangential experience with FHIR...so I have some benefit of several years of that being developed and production...whereas most the people on those phone calls they are not from vendors who have had that US experience and so it's going to take them a longer time to understand what is going on?" [P6]

Formal academic training partnerships exist—they need to be scaled

- "In the short term, what we are trying to do is how do we build as much capacity as possible. So there's a training program which the digital health agency funds HL7, CSIRO and Uni of Melbourne to pull together to actually train as many people around FHIR. The shortest-term fix that we've got is actually to ramp up the training." [P5]

Implementation Process

Assessing needs is related to how well the Sparked program assesses the priorities, preferences, and needs of stakeholders participating to guide the delivery of the program. The key implementation condition statements for this influencing factor are presented in Textbox 7. Engaging diverse stakeholder perspectives was considered as important for understanding participant requirements, and tangible examples are necessary to assess community and clinician needs effectively. Participants pointed out that achieving consensus among stakeholders with diverse backgrounds can be challenging. Providing discussion options in documents before meetings could help facilitate decision-making, and active participation has been encouraged in Sparked consensus processes, such as contributing ideas on Confluence pages. Insufficient representation from specific stakeholder groups (eg, consumers and individuals from rural areas) could risk excluding their voices. Ensuring adequate representation of special interest groups could enhance efficiency and relevance of input.

Engaging is related to how Sparked attracts and encourages participation. The key implementation condition statements for this influencing factor are presented in Textbox 8. Engaging all relevant stakeholders to enable meaningful co-design and stakeholder integration was seen as crucial to the accelerator's success. Study participants believed that running events had played an important role in attracting participants and generating excitement and that the Sparked team had created an environment that supported and championed the engagement culture. Participants argued that ensuring an inclusive environment that accommodates diverse participant backgrounds and knowledge levels remained a significant challenge, whereas communicating the purpose and benefits of FHIR accelerators in accessible ways would be key to building interest. Creating a cohesive media and communication strategy was also considered as important despite challenges due to administrative and resource constraints.

Textbox 7. Assessing needs—implementation condition statements.

Community engagement that prioritizes listening to and recording of diverse stakeholder perspectives

- "There's been a real mix of like the people who've been in Digital Health for a long time but...a lot of new clinicians coming and joining...lots of people from different areas. So we've got a bunch of like immunologists who've joined, ED clinicians—all of these new digitally health young clinicians—I think that's really exciting to have new people to help carry that energy forward." [P3]

Achieving consensus among different stakeholders can be challenging at times

- "It's too hard, we can't do it or the technical people go and design this perfect solution and then the clinicians are like but that doesn't work for me. So for us it's really important that we remain in lockstep and make sure like yes we may be a little bit asynchronous, but we need to always be aware of where each other are going and not go too far ahead or in two different directions." [P3]

Ensuring adequate stakeholder representation and expertise of special interest groups ensures valuable input

- "As an example, we look at the Royal College of Australasian Pathologists. They are in the category of clinical and so we funnel them into the clinical design group for input and they are also very key to the E-requesting. So we make sure that there are also on the technical and functional input for the E-requesting FHIR engine, not necessarily the core though, because that one doesn't apply to them." [P1]

XSL•FO
RenderX

Textbox 8. Engaging—implementation condition statements.

Engaging all relevant stakeholders is seen as crucial

- "Overall the accelerator program has done a really good job of bringing communities together with a very diverse range of stakeholders and clinicians...so I think they're doing the best they can and really trying to be a very inclusive environment, very open...there's a genuine attempt by Sparked to gain consensus on decisions." [P7]

Communicating the purpose and benefits of Fast Healthcare Interoperability Resources accelerators in a way anyone can understand builds interest in participation

- "It needs to be technically based, that's what it's about, but to get clinician engagement you need them to understand what the potential benefits are and that's that marrying of the technical...you know this has been done I think very well by the CSIRO in the past and...to get clinicians involved." [P8]

Ensuring meaningful co-design and integration of stakeholder input

- "It's probably, it's the best I've seen, an approach, of having a community approach, where everyone's genuinely involved, rather than being told this is what we're doing, we'll have your feedback, but this is where we're going and I do think it's got a very good, so far, co-design culture about it and approach." [P15]

A dedicated effort to create cohesive media and communication strategies among partner organizations

- "I understand it can be a nightmare managing so many people and so many things at the same time, but it's just we're getting a lot of emails...So far it's been good...but sooner or later I'll reach a stage where I'll lag behind on all of these things...so how do we ensure we're not spamming everyone with comms...it has to be very relevant to the point and ensuring engagement." [P4]

ERIC Strategy Mapping

The top 8 influencing factors were mapped to the ERIC tool to guide implementation strategy selection. We used the updated CFIR-ERIC Matching Tool [33] for this purpose. Strategies were subsequently categorized into clusters to make application easier [25]. Strategies that had the highest percentage of agreement (eg, highest expert consensus regarding being effective to address barriers or amplify enablers) were selected and generated into high-level recommendations. However, not all CFIR 2.0 constructs currently have recommendations. Where recommendations were absent, the research team reviewed the strategy list in conjunction with evidence to recommend strategies for use.

These strategies were collated into an implementation enhancement plan for action. The recommended ERIC strategy clusters include adapt and tailor to context, develop stakeholder interrelations, support participants, train and educate stakeholders, and use evaluative and iterative strategies, as outlined in Multimedia Appendix 4.

Discussion

Principal Findings: Identification of Influencing Factors for the Implementation of the Sparked FHIR Accelerator and Strategies for Enhancement

Overview

This study enabled the identification of the core components of the Sparked FHIR accelerator and the factors that positively and negatively influence program implementation. The CFIR supported the identification of key factors influencing the implementation of the Sparked program. Subsequent mapping to the ERIC framework enabled the development of tailored strategies for enhancing the implementation of FHIR accelerator programs. However, researcher recommendations accounted for >50% of the strategies due to a lack of consensus in the ERIC tool, suggesting that future work is needed to improve the reliability and comprehensiveness of the tool.

In this section, we examine the top influencing factors and associated recommendations generated through ERIC and researcher recommendations in the context of the current body of evidence.

Innovation Design

Innovation design was identified as a key enabler for Sparked in this study. Our results highlighted the core components required for a successful FHIR accelerator, including a consensus-driven approach, concurrent technical and clinical development, effective coordination for scalability and sustainability, and engagement that encourages user interests and participation. The collaborative consortium aspect of the FHIR program can be conceptualized as a community of practice. Challenges faced by communities of practice have been reported in studies of health care programs that involve diverse groups working together toward a common goal to address specific problems [34-36]. Similarly to insights reported from FHIR standard developments [9,34], our participants noted that achieving consensus among stakeholders with diverse backgrounds and needs could be difficult at times during standard development. In the context of large-scale digital health initiatives such as the United Kingdom's delivery of digital health and well-being programs, tensions between communities of practice and the need for delivery at pace and scale were reported [37,38].

In digital health, co-design methods are used in the process of ideation, validation, and deployment involving both digital and health experts with different needs [39]. In the context of domain-specific FHIR standard development, community-driven connectathons, balloting, and centralized knowledge management systems for accessing program information have been pivotal in supporting the process [9,15]. Open dialogue

XSL•FO
RenderX

between the clinical and technical work groups helps in confirming comprehension, resolving discrepancies, and providing feedback on standard specifications [9]. The ERIC tool suggests adapting and tailoring approaches to context, such as identifying the ways in which Sparked can be tailored to meet local needs while retaining core elements of the program to preserve its integrity (eg, generating tailored educational materials to ensure wide engagement), creating a use case–focused group structure to help bring clarity.

Local Conditions

Studies on large-scale digital health implementation have shown various levels of factors influencing readiness, including macro (eg, market, infrastructure, and policy), meso (eg, organizational), and micro (eg, professional or public) levels [37,38,40]. In Australia, the digital ecosystem involving the government, vendors, professional organizations, and clinicians has attained a requisite level of maturity to support interoperability [11,12]. However, our study found that certain health care sectors at the meso level still lack a full understanding of the significance of interoperability. Concerns were also raised about the potential effects of an unpredictable political climate on the program and challenges associated with enhanced data sharing, such as liability and cost.

A longitudinal evaluation of a national digital health initiative highlighted the need for greater investment in infrastructure, guidelines for safe and transparent use, incentives for interoperability, and upskilling for professionals and the public [38]. These recommendations are consistent with the researcher-selected ERIC strategies, which include securing commitments from key partners (eg, governments, professional colleges, and vendors who provide support or incentive to participate), involving existing Sparked governance structures (eg, boards of directors, HL7, and medical boards) to address quality management needs, and enhancing support from educational and training institutions to build a larger workforce to deliver program outputs.

Partnership and Connections

Sparked has attracted a diverse range of individuals and organizations, with their continued involvement playing a key role in ensuring the program's long-term sustainability [11]. Partnerships with HL7 International will enhance the program's international visibility and foster the exchange of valuable lessons learned [10]. However, the perceived disconnect between the technical and clinical domains in Sparked was raised as one of the challenges.

Research on developing genomics data FHIR standards highlights the importance of involving potential adopters (eg, pathology testing laboratories) alongside technical developers during standard development and pilot-testing [9]. Evaluations of digital health innovations in the Australian context have also emphasized the need for ongoing partnerships between innovation implementers and a diverse range of innovation recipients (eg, health care professionals and consumers) [30,41]. In addition to these insights, the ERIC tool suggests strategies for building a coalition, such as continuing activities that attract stakeholders, as well as promoting network weaving, such as building on existing high-quality working relationships and networks to promote a shared vision.

Work Infrastructure

One of the most frequently reported barriers to collaboration in health care innovations is that community members such as clinicians often lack the time to participate and prioritize other commitments, such as service provision [34,35]. Our study found that this challenge was compounded by the difficulty of progressing while balancing the time and energy constraints of participants, especially in extensive consensus building among work group members. From an infrastructure and resource perspective, the program also required software developers for test service delivery and reference implementation, as well as a coordination team for comprehensive administration and logistical tasks.

Recent research on communities of practice in health care settings suggests that nonhierarchical collaborations between participating organizations, shared ownership of outputs, and a centralized leadership structure with rotating leaders can be effective [42,43]. Similarly, the need for an enhanced visibility of key participating organizations such as HL7 International to increase community engagement was identified in our study. These suggestions align with the researcher-selected ERIC strategies, which include developing partnerships with organizations that have the necessary resources to implement the program, shifting and revising roles among professionals managing the program, and redesigning job characteristics if needed.

Access to Knowledge and Information

Effective knowledge management and information sharing are crucial for innovations involving communities of practice [36,42,43]. The Sparked program uses knowledge management systems such as the online collaboration workspace Confluence as a central resource for program information and hosts community events to support ongoing knowledge development. Our study participants were positive about the open access to program information and the promotion of active engagement with Confluence and events. They also suggested that individuals such as clinicians seeking to enhance their FHIR skills would benefit from additional educational resources.

Research on communities of practice has reported similar effective methods for creating shared information spaces, such as learning hub platforms with website resources and asynchronous online discussion forums and periodic email updates with news and forum notifications [42,43]. Using live transcripts for groups with diverse skills and sharing meeting recordings to accommodate varying schedules also help members catch up [42]. The ERIC tool also suggests several strategies for training and educating stakeholders, including conducting educational meetings tailored to different groups; developing manuals and toolkits in ways that make it easier to learn about the program; providing supporting materials for clinicians to facilitate understanding of Sparked program products; and distributing educational materials through various channels, such as in-person sessions, mail, and email.

XSL•FO
RenderX

Capability

Stakeholders' requisite capabilities to participate in and deliver the Sparked program, such as health domain knowledge for technical work group members and FHIR knowledge for clinical work group members, were identified as an area for improvement in our study. Previous FHIR development efforts have also shown the need to support technical and clinical knowledge development and address the challenge of enabling equal participation among stakeholders with varying backgrounds and expertise levels [9].

While studies of digital health implementation have identified health care professionals' digital technology skills, abilities, and experience as one of the barriers [30,44,45], research on communities of practice has shown that community members can continuously advance their knowledge through ongoing learning and active engagement [36]. Enhancing cross-training and education for technical and clinical work groups and across various skill levels, along with practical real-world examples, will help facilitate broader understanding and more meaningful engagement, as suggested by the ERIC tool. In addition to leveraging previous experience in FHIR activities to enhance capability, scaling existing formal academic training partnerships was identified by the ERIC tool as a potential solution.

Assessing Needs

Community engagement that prioritizes listening to and recording diverse stakeholder perspectives (eg, clinical, consumer, and technical levels) emerged as an enabler in understanding stakeholder needs related to program operation and delivery. Encouraging active participation in consensus processes and collecting feedback during the ballot process has enabled stakeholders to voice their thoughts and raise issues freely. However, limited representation from certain groups, such as consumers or individuals from rural areas, might result in their perspectives being overlooked.

Studies on FHIR development have shown the importance of adequate representation and expertise within special interest groups to drive efficiency and ensure that stakeholders' needs are collected [9,13,14]. In addition to Sparked's current practices of ongoing monitoring of participation and engagement, researcher-selected ERIC strategies identified ways to enhance needs assessment activities. These include using evaluative and iterative methods (eg, surveys) to gather and analyze information on stakeholder needs for their participation in the program and developing an audit schedule to check that agreed-upon processes (eg, data sharing) are consistently followed.

Engaging

Engaging all relevant stakeholders to enable meaningful co-design and integration was considered as both an enabler and a barrier by our study participants. The Sparked program has engaged stakeholders through various activities with a focus on enhancing participation through both in-person and online events. However, the size and pace of some events make it difficult for participants with less experience in standards to contribute effectively. A stronger effort is needed to gather insights from clinicians and nonexperts.

Our study has shown that, to engage a wider range of organizations and clinicians in the program, the concept of standards needs to be communicated in a way that aligns with their interests. As observed in other community-based health care consortiums, effectively communicating the purpose and benefits of a program in accessible ways is one of the approaches to build interest [34,42]. Participants in our study suggested a dedicated effort to enhance the media and communication strategy, such as more targeted and coherent emails and media content. A study on a large-scale national digital health program also highlighted the importance of clear communication and branding in a multi-agent, heterogenous partnership model [37,38]. It also emphasized the need to engage smaller business partners, who often show less interest in co-design compared to large multinational companies. Echoing the recommendations from digital health implementations [30,37,38,46], the ERIC tool suggested strategies related to further development of stakeholder interrelations, such as identifying champions who dedicate themselves to supporting, marketing, and driving the implementation; involving consumers and other currently underrepresented sectors; and offering more flexibility and opportunities to facilitate their active engagement.

Implementation Science Approaches for Future Evaluations of FHIR Accelerators

Implementation science theory and approaches have been increasingly used in developing an improved understanding of how digital health services and innovations can be designed, developed, and delivered [27-30,47]. To our knowledge, no studies have reported the use of a systematic approach in evaluating FHIR accelerator implementation, thereby limiting the understanding of influencing factors and systematic investigation of the program implementation process. Our study illuminates the applicability and benefit of using the CFIR to identify factors influencing implementation and generate a structured, evidence-based plan to enhance it further. The findings of this study have informed an actionable implementation enhancement plan that has been developed by the Sparked team and will be evaluated later in the year.

We believe that the approach outlined in this study holds broad applicability and encourages others to adopt the CFIR with the ERIC tool to enhance the efficient delivery of accelerator programs. As FHIR and similar accelerator initiatives continue to expand [10], using research approaches and implementation evaluations guided by the CFIR and ERIC frameworks can facilitate more effective translation of the aims and objectives of FHIR accelerators and provide meaningful comparisons across them. These implementation science frameworks provide a common language and systematic approach for researchers to comprehensively study the implementation of multicomponent interventions. This approach enables synthesis of findings across different settings, interventions, and studies, contributing to an evidence base for understanding implementation processes and developing strategies to support successful collaborative FHIR standard development.

Limitations and Future Work

While this study identified factors influencing the FHIR accelerator program and theoretically informed enhancement

XSL•FO
RenderX

plan, several limitations should be acknowledged. First, this study was conducted within an accelerator program based in Australia; the results should be interpreted within the context, such as government support and Australian health care settings. Second, this study was conducted during the first quarter of the 2-year program, whereas ongoing efforts to improve the program by the Sparked management team have continued since then. Third, it is worth noting that the theoretically informed strategies will need to be discussed and co-designed with key stakeholders of the accelerator program for the Sparked team to develop actionable enhancement plans. Finally, this research forms part of a broader evaluation of the Sparked program, where we will incorporate a mixed methods design and additional evaluation data, such as surveys at multiple time points, to enrich the insights and contributions of the findings.

Conclusions

This paper demonstrated how we identified the factors influencing collaborative practices and engagement within a complex accelerator program tasked with developing FHIR standards. It outlines recommendations to address the factors influencing the implementation of the program. Our methodology involved using the TIDieR guidelines to understand the activities of the Sparked accelerator program, the CFIR to develop interpretive statements (assessing the key influencing factors), and the CFIR-ERIC Matching Tool in conjunction with researcher recommendations (informed by evidence) to derive an implementation enhancement plan relevant to activities within the Sparked program. These insights facilitated the identification of strategic improvements that program leaders can use to adapt and refine activities to better engage technical, clinical, and other stakeholders, thereby supporting the delivery and outcomes of the accelerator program.

Acknowledgments

The authors would like to thank the interview participants for their support of this study.

Conflicts of Interest

None declared.

Multimedia Appendix 1
Codebook for the data analysis.
[PDF File (Adobe PDF File), 41 KB - medinform_v13i1e66421_app1.pdf]

Multimedia Appendix 2
Sparked descriptions based on the Template for Intervention Description and Replication checklist.
[PDF File (Adobe PDF File), 39 KB - medinform_v13i1e66421_app2.pdf]

Multimedia Appendix 3
Key influencing factors and associated statements.
[PDF File (Adobe PDF File), 88 KB - medinform_v13i1e66421_app3.pdf]

Multimedia Appendix 4
Implementation enhancement plan.
[PDF File (Adobe PDF File), 80 KB - medinform_v13i1e66421_app4.pdf]

References

1. Everson J, Adler-Milstein J. Gaps in health information exchange between hospitals that treat many shared patients. J Am Med Inform Assoc 2018 Sep 01;25(9):1114-1121 [FREE Full text] [doi: 10.1093/jamia/ocy089] [Medline: 30010887]
2. Thompson MP, Graetz I. Hospital adoption of interoperability functions. Healthc (Amst) 2019 Sep;7(3):100347. [doi: 10.1016/j.hjdsi.2018.12.001] [Medline: 30595558]
3. Warren LR, Clarke J, Arora S, Darzi A. Improving data sharing between acute hospitals in England: an overview of health record system distribution and retrospective observational analysis of inter-hospital transitions of care. BMJ Open 2019 Dec 05;9(12):e031637 [FREE Full text] [doi: 10.1136/bmjopen-2019-031637] [Medline: 31806611]
4. FHIR overview. HL7 International. URL: https://build.fhir.org/overview.html [accessed 2025-02-12]
5. Benson T, Grieve G. Principles of Health Interoperability: SNOMED CT, HL7 and FHIR. Cham, Switzerland: Springer; 2016.
6. Ayaz M, Pasha MF, Alzahrani MY, Budiarto R, Stiawan D. The Fast Health Interoperability Resources (FHIR) standard: systematic literature review of implementations, applications, challenges and opportunities. JMIR Med Inform 2021 Jul 30;9(7):e21929 [FREE Full text] [doi: 10.2196/21929] [Medline: 34328424]

XSL•FO
RenderX

7. Understanding the standards process. HL7 International. URL: https://confluence.hl7.org/display/HL7/Understanding+the+Standards+Process [accessed 2025-02-12]
8. Vorisek CN, Lehne M, Klopfenstein SA, Mayer PJ, Bartschke A, Haese T, et al. Fast healthcare interoperability resources (FHIR) for interoperability in health research: systematic review. JMIR Med Inform 2022 Jul 19;10(7):e35724 [FREE Full text] [doi: 10.2196/35724] [Medline: 35852842]
9. Freimuth RR, Milius RP, Murugan M, Terry M. Clinical genomic data on FHIR®: case studies in the development and adoption of the genomics reporting implementation guide. In: Mccormick J, Pathak J, editors. Genomic Data Sharing: Case Studies, Challenges, and Opportunities for Precision Medicine. New York, NY: Academic Press; 2023:91-110.
10. HL7 FHIR ACCELERATOR™ program. HL7 International. URL: https://www.hl7.org/about/fhir-accelerator/ [accessed 2025-02-12]
11. CSIRO. Sparked. URL: https://sparked.csiro.au/ [accessed 2025-02-12]
12. Sparked FHIR accelerator. HL7 Australia. URL: https://confluence.hl7.org/display/HA/Sparked+FHIR+Accelerator [accessed 2025-02-12]
13. Murugan M, Babb LJ, Taylor CO, Rasmussen LV, Freimuth RR, Venner E, et al. Genomic considerations for FHIR®; eMERGE implementation lessons. J Biomed Inform 2021 Jun;118:103795 [FREE Full text] [doi: 10.1016/j.jbi.2021.103795] [Medline: 33930535]
14. Dolin RH, Heale BS, Alterovitz G, Gupta R, Aronson J, Boxwala A, et al. Introducing HL7 FHIR Genomics Operations: a developer-friendly approach to genomics-EHR integration. J Am Med Inform Assoc 2023 Feb 16;30(3):485-493 [FREE Full text] [doi: 10.1093/jamia/ocac246] [Medline: 36548217]
15. Osterman TJ, Terry M, Miller RS. Improving cancer data interoperability: the promise of the minimal common oncology data elements (mCODE) initiative. JCO Clin Cancer Inform 2020 Nov(4):993-1001. [doi: 10.1200/cci.20.00059]
16. Richesson RL, Lynch CO, Hammond WE. Developing and promoting data standards for clinical research. In: Richesson RL, Andrews JE, Hollis KF, editors. Clinical Research Informatics. Cham, Switzerland: Springer; 2023:389-412.
17. Damschroder LJ, Aron DC, Keith RE, Kirsh SR, Alexander JA, Lowery JC. Fostering implementation of health services research findings into practice: a consolidated framework for advancing implementation science. Implement Sci 2009 Aug 07;4:50 [FREE Full text] [doi: 10.1186/1748-5908-4-50] [Medline: 19664226]
18. Damschroder LJ, Reardon CM, Widerquist MA, Lowery J. The updated consolidated framework for implementation research based on user feedback. Implement Sci 2022 Oct 29;17(1):75 [FREE Full text] [doi: 10.1186/s13012-022-01245-0] [Medline: 36309746]
19. Rouleau G, Wu K, Ramamoorthi K, Boxall C, Liu RH, Maloney S, et al. Mapping theories, models, and frameworks to evaluate digital health interventions: scoping review. J Med Internet Res 2024 Feb 05;26:e51098 [FREE Full text] [doi: 10.2196/51098] [Medline: 38315515]
20. Rangachari P, Mushiana SS, Herbert K. A scoping review of applications of the Consolidated Framework for Implementation Research (CFIR) to telehealth service implementation initiatives. BMC Health Serv Res 2022 Nov 30;22(1):1450 [FREE Full text] [doi: 10.1186/s12913-022-08871-w] [Medline: 36447279]
21. Delaforce A, Maddock E, Wheeler P, Jayasena R, Parkinson J. Factors that influence the uptake of virtual care solutions in Australian primary care practice: a systematic scoping review. JBI Evid Implement (Forthcoming) 2024 Oct 22. [doi: 10.1097/XEB.0000000000000475] [Medline: 39431485]
22. Powell BJ, McMillen JC, Proctor EK, Carpenter CR, Griffey RT, Bunger AC, et al. A compilation of strategies for implementing clinical innovations in health and mental health. Med Care Res Rev 2012 Apr;69(2):123-157 [FREE Full text] [doi: 10.1177/1077558711430690] [Medline: 22203646]
23. Waltz TJ, Powell BJ, Fernández ME, Abadie B, Damschroder LJ. Choosing implementation strategies to address contextual barriers: diversity in recommendations and future directions. Implement Sci 2019 Apr 29;14(1):42 [FREE Full text] [doi: 10.1186/s13012-019-0892-4] [Medline: 31036028]
24. Powell BJ, Waltz TJ, Chinman MJ, Damschroder LJ, Smith JL, Matthieu MM, et al. A refined compilation of implementation strategies: results from the Expert Recommendations for Implementing Change (ERIC) project. Implement Sci 2015 Feb 12;10:21 [FREE Full text] [doi: 10.1186/s13012-015-0209-1] [Medline: 25889199]
25. Waltz TJ, Powell BJ, Matthieu MM, Damschroder LJ, Chinman MJ, Smith JL, et al. Use of concept mapping to characterize relationships among implementation strategies and assess their feasibility and importance: results from the Expert Recommendations for Implementing Change (ERIC) study. Implement Sci 2015 Aug 07;10:109 [FREE Full text] [doi: 10.1186/s13012-015-0295-0] [Medline: 26249843]
26. Perry CK, Damschroder LJ, Hemler JR, Woodson TT, Ono SS, Cohen DJ. Specifying and comparing implementation strategies across seven large implementation interventions: a practical application of theory. Implement Sci 2019 Mar 21;14(1):32 [FREE Full text] [doi: 10.1186/s13012-019-0876-4] [Medline: 30898133]
27. Paulsen MM, Varsi C, Paur I, Tangvik RJ, Andersen LF. Barriers and facilitators for implementing a decision support system to prevent and treat disease-related malnutrition in a hospital setting: qualitative study. JMIR Form Res 2019 May 09;3(2):e11890 [FREE Full text] [doi: 10.2196/11890] [Medline: 31094333]

XSL•FO
RenderX

28. Ardito V, Golubev G, Ciani O, Tarricone R. Evaluating barriers and facilitators to the uptake of mHealth apps in cancer care using the consolidated framework for implementation research: scoping literature review. JMIR Cancer 2023 Mar 30;9:e42092 [FREE Full text] [doi: 10.2196/42092] [Medline: 36995750]
29. Delaforce A, Duff J, Munday J, Hardy J. Preoperative anemia and iron deficiency screening, evaluation and management: barrier identification and implementation strategy mapping. J Multidiscip Healthc 2020;13:1759-1770 [FREE Full text] [doi: 10.2147/JMDH.S282308] [Medline: 33293819]
30. Delaforce A, Li J, Grujovski M, Parkinson J, Richards P, Fahy M, et al. Creating an implementation enhancement plan for a digital patient fall prevention platform using the CFIR-ERIC approach: a qualitative study. Int J Environ Res Public Health 2023 Feb 21;20(5):3794 [FREE Full text] [doi: 10.3390/ijerph20053794] [Medline: 36900804]
31. Hoffmann TC, Glasziou PP, Boutron I, Milne R, Perera R, Moher D, et al. Better reporting of interventions: template for intervention description and replication (TIDieR) checklist and guide. BMJ 2014 Mar 07;348:g1687 [FREE Full text] [doi: 10.1136/bmj.g1687] [Medline: 24609605]
32. Palinkas LA, Horwitz SM, Green CA, Wisdom JP, Duan N, Hoagwood K. Purposeful sampling for qualitative data collection and analysis in mixed method implementation research. Adm Policy Ment Health 2015 Sep 6;42(5):533-544 [FREE Full text] [doi: 10.1007/s10488-013-0528-y] [Medline: 24193818]
33. Strategy design. Center for Clinical Management Research. URL: https://cfirguide.org/choosing-strategies [accessed 2025-02-12]
34. Pivik JR, Goelman H. Evaluation of a community-based participatory research consortium from the perspective of academics and community service providers focused on child health and well-being. Health Educ Behav 2011 Jun;38(3):271-281. [doi: 10.1177/1090198110372876] [Medline: 21364234]
35. Barnes C, Sutherland R, Jones G, Kingon N, NCOIS Research Collaborative, Wolfenden L. Development and piloting of a community of practice to support learning and improvement in health promotion practice within NSW local health district. Public Health Res Pract 2023 Sep 13;33(3):3332326 [FREE Full text] [doi: 10.17061/phrpp3332326] [Medline: 37699767]
36. Choi HJ, Ahn JC, Jung SH, Kim JH. Communities of practice and knowledge management systems: effects on knowledge management activities and innovation performance. Knowl Manag Res Pract 2019 Apr 18;18(1):53-68. [doi: 10.1080/14778238.2019.1598578]
37. Devlin AM, McGee-Lennon M, O'Donnell CA, Bouamrane MM, Agbakoba R, O'Connor S, et al. Delivering digital health and well-being at scale: lessons learned during the implementation of the dallas program in the United Kingdom. J Am Med Inform Assoc 2016 Jan;23(1):48-59 [FREE Full text] [doi: 10.1093/jamia/ocv097] [Medline: 26254480]
38. Lennon MR, Bouamrane MM, Devlin AM, O'Connor S, O'Donnell C, Chetty U, et al. Readiness for delivering digital health at scale: lessons from a longitudinal qualitative evaluation of a national digital health innovation program in the United Kingdom. J Med Internet Res 2017 Feb 16;19(2):e42 [FREE Full text] [doi: 10.2196/jmir.6900] [Medline: 28209558]
39. Duffy A, Christie GJ, Moreno S. The challenges toward real-world implementation of digital health design approaches: narrative review. JMIR Hum Factors 2022 Sep 09;9(3):e35693 [FREE Full text] [doi: 10.2196/35693] [Medline: 36083628]
40. Sheikh A, Cornford T, Barber N, Avery A, Takian A, Lichtner V, et al. Implementation and adoption of nationwide electronic health records in secondary care in England: final qualitative results from prospective national evaluation in "early adopter" hospitals. BMJ 2011 Oct 17;343:d6054 [FREE Full text] [doi: 10.1136/bmj.d6054] [Medline: 22006942]
41. Bourke JA, Jerram KA, Arora M, Craig A, Middleton JW. Using the consolidated framework for implementation research to integrate innovation recipients' perspectives into the implementation of a digital version of the spinal cord injury health maintenance tool: a qualitative analysis. BMC Health Serv Res 2024 Mar 28;24(1):390 [FREE Full text] [doi: 10.1186/s12913-024-10847-x] [Medline: 38549148]
42. Fruchtman CS, Khalid MB, Keakabetse T, Bonito A, Saulnier DD, Mupara LM, et al. Digital communities of practice: one step towards decolonising global health partnerships. BMJ Glob Health 2022 Feb;7(2):e008174 [FREE Full text] [doi: 10.1136/bmjgh-2021-008174] [Medline: 35110274]
43. Shaw L, Jazayeri D, Kiegaldie D, Morris ME. Implementation of virtual communities of practice in healthcare to improve capability and capacity: a 10-year scoping review. Int J Environ Res Public Health 2022 Jun 29;19(13):7994 [FREE Full text] [doi: 10.3390/ijerph19137994] [Medline: 35805649]
44. Ross J, Stevenson F, Lau R, Murray E. Factors that influence the implementation of e-health: a systematic review of systematic reviews (an update). Implement Sci 2016 Oct 26;11(1):146 [FREE Full text] [doi: 10.1186/s13012-016-0510-7] [Medline: 27782832]
45. Gesulga JM, Berjame A, Moquiala KS, Galido A. Barriers to electronic health record system implementation and information systems resources: a structured review. Procedia Comput Sci 2017;124:544-551. [doi: 10.1016/j.procs.2017.12.188]
46. Njoku C, Green Hofer S, Sathyamoorthy G, Patel N, Potts H. The role of accelerator programmes in supporting the adoption of digital health technologies: a qualitative study of the perspectives of small- and medium-sized enterprises. Digit Health 2023;9:20552076231173303 [FREE Full text] [doi: 10.1177/20552076231173303] [Medline: 37256012]
47. Nilsen P. Making sense of implementation theories, models and frameworks. Implement Sci 2015 Apr 21;10:53 [FREE Full text] [doi: 10.1186/s13012-015-0242-0] [Medline: 25895742]

XSL•FO
RenderX

Abbreviations

CFIR: Consolidated Framework for Implementation Research
CSIRO: Commonwealth Scientific and Industrial Research Organisation
ERIC: Expert Recommendations for Implementing Change
FHIR: Fast Healthcare Interoperability Resources
HL7: Health Level Seven
REDCap: Research Electronic Data Capture
TIDieR: Template for Intervention Description and Replication

Edited by A Coristine; submitted 12.09.24; peer-reviewed by Y He, M Nakayama; comments to author 25.12.24; revised version received 14.02.25; accepted 17.03.25; published 27.05.25.

Please cite as:
Li J, Maddock E, Hosking M, Ebrill K, Sullivan J, Loi K, Tavares-Rixon D, Jayasena R, Grieve G, Delaforce A
Identifying and Optimizing Factors Influencing the Implementation of a Fast Healthcare Interoperability Resources Accelerator: Qualitative Study Using the Consolidated Framework for Implementation Research–Expert Recommendations for Implementing Change Approach
JMIR Med Inform 2025;13:e66421
URL: https://medinform.jmir.org/2025/1/e66421
doi:10.2196/66421
PMID:

©Jane Li, Emma Maddock, Michael Hosking, Kate Ebrill, Jeremy Sullivan, Kylynn Loi, Danielle Tavares-Rixon, Rajiv Jayasena, Grahame Grieve, Alana Delaforce. Originally published in JMIR Medical Informatics (https://medinform.jmir.org), 27.05.2025. This is an open-access article distributed under the terms of the Creative Commons Attribution License (https://creativecommons.org/licenses/by/4.0/), which permits unrestricted use, distribution, and reproduction in any medium, provided the original work, first published in JMIR Medical Informatics, is properly cited. The complete bibliographic information, a link to the original publication on https://medinform.jmir.org/, as well as this copyright and license information must be included.

XSL•FO
RenderX

Original Paper

Health Care Professionals' Perspectives on Implementing Patient-Accessible Electronic Health Records in Primary Care: Qualitative Study

Irene Muli[1], PhD; Åsa Cajander[2], PhD; Isabella Scandurra[3†], PhD; Maria Hägglund[1], PhD

[1]Participatory eHealth and Health Data Research Group, Department of Women's and Children's Health, Uppsala University, Uppsala, Sweden

[2]Department of Information Technology, Uppsala University, Uppsala, Sweden

[3]Centre of Empirical Research in Information Systems, School of Business, Örebro University, Örebro, Sweden

[†]deceased

Corresponding Author:
Irene Muli, PhD
Participatory eHealth and Health Data Research Group
Department of Women's and Children's Health
Uppsala University
Dag Hammarskjölds väg 14B
Uppsala, 75185
Sweden
Phone: 46 0734697473
Email: irene.muli@uu.se

Abstract

Background: Patients are increasingly being offered online record access (ORA) through patient-accessible electronic health records (PAEHRs), but implementation is often met with resistance from health care professionals (HCPs). Experiences from previous implementations may provide important insights into potential barriers and facilitators.

Objective: This study aimed to investigate the factors influencing the implementation of the Swedish PAEHR system in primary care from the perspectives of HCPs.

Methods: We conducted 14 semistructured interviews with a diverse group of HCPs shortly after the implementation of the Swedish PAEHR system. The interviews were analyzed using the Consolidated Framework for Implementation Research (CFIR) and content analysis, identifying key themes related to PAEHR implementation.

Results: The analysis identified several potential factors influencing the implementation of the Swedish PAEHR system. According to the HCPs, the PAEHR system was *flawed* but also *flexible*. The HCPs described working in *a complex and imperfect organization*, which nonetheless had an *existing structure, support, and established communication* with patients. They also described *nondocumentation-related use of the electronic health record system*. Moreover, they reported dealing with a *complicated patient group* with varying needs and high expectations. The HCPs expressed that they worked in a patient-centered way and with *patient engagement*. The HCPs could see both the *advantages and disadvantages* of the PAEHR system and had some concerns. There were *mixed views of the extent of the change*, where some felt patient ORA would not affect their work at all and others expected a substantial impact. Some HCPs had experience using the PAEHR system themselves, while some *lacked knowledge and interest*. Furthermore, the implementation process was perceived as *long and uneventful*, with *fragmented communication*, where *existing communication activities were used*. The HCPs also reported receiving some information and education about PAEHRs outside the organization. The HCPs had limited awareness of how patients were introduced to the PAEHR system.

Conclusions: This study underscores the importance of having a usable electronic health record system and addressing organizational issues, such as issues with the work environment, for optimal implementation of eHealth services such as the PAEHR system. It also highlights the importance of HCPs' views and experiences with their patients, and their perceptions and attitudes toward the intervention. Additionally, this study stresses the importance of effective implementation processes and communication strategies for both HCPs and patients.

(JMIR Med Inform 2025;13:e64982) doi:10.2196/64982

XSL•FO
RenderX

KEYWORDS

patient accessible electronic health record; implementation; consolidated framework for implementation research; primary care

Introduction

Background

In the present health care landscape, patient-accessible electronic health records (PAEHRs) have been implemented in several countries worldwide [1-4]. With the European Health Data Space proposal, this transformation is set to accelerate further [5]. Yet, despite the reported benefits of patient online record access (ORA), including improved patient-provider relationships, improved medication adherence, and reduced anxiety [6], implementation has proven challenging in many contexts, not the least due to concerns and resistance from health care professionals (HCPs) [7-10].

HCPs have expressed several concerns regarding patient ORA [11-15]. For example, although they acknowledge some potential benefits of PAEHRs, they also believe that the records might be incomprehensible or that patients might misunderstand them due to the presence of medical language and potentially complex content. Concerns are that patients may become unnecessarily worried or make decisions based on misunderstanding that could cause harm. HCPs have also reported changing documentation practices to reduce the risk of confusion by writing notes more comprehensively and by omitting hypotheses [12,16], which may make the documentation less clinically useful [17]. In addition, HCPs have been concerned about the potential increase in their workload due to the implementation of ORA [8]. After implementation, HCPs have reported some increase in their workload [12,16] related to, for example, helping patients access PAEHRs and understand their content. In contrast, for some professional groups, there have been reports of a decrease in workload related to administering paper copies of electronic health records (EHRs) to patients [16].

Furthermore, HCPs have expressed concerns that the record's content might worry patients [14,15]. After implementation, patients have reported experiencing distress from reading their records online [12,18]. In Sweden, according to a national survey study, 26% of participants worried about something they had read, and they usually searched for answers online, called the hospital, or raised their concerns at their next visit [18]. Another concern among HCPs is the safeguarding of vulnerable patient groups (eg, domestic abuse victims and at-risk children) [13,19]. Patients are, however, not as concerned about security and privacy and have not experienced many breaches [20-22].

While several studies have focused on attitudes and experiences of PAEHRs, few have investigated their implementation and how the implementation process could affect the concerns of HCPs. According to the Consolidated Framework for Implementation Research (CFIR), 5 domains are important to consider when studying the implementation of interventions: intervention characteristics, inner setting, outer setting, characteristics of the individuals involved, and the implementation process itself [23]. The framework can be used to both plan implementation projects and study successful and failed implementations. Considering the challenges and delays described in the implementation of patient ORA, it is important to deepen our understanding of the factors that may affect the introduction in different contexts, including HCP concerns. In this study, we used the CFIR to structure our analysis and help explain HCPs' concerns and attitudes toward patient ORA and their experiences of the implementation in a Swedish primary care context.

In Sweden, the first patient ORA trial took place in a primary care center (PCC) in 1997 and had promising results [24], but implementation soon faced legal roadblocks, which took years to resolve [25]. In 2008, the new Patient Data Act allowed health care providers to give patients ORA, and implementation could resume. Scale-up was step-wise, and eventually, all patients in Region Uppsala gained access to PAEHRs in 2012. The local PAEHR system was integrated with the National Health Information Exchange infrastructure in 2015, and in 2016, 17 of the 21 Swedish regions were providing patients with access to their EHRs [25]. By 2018, all Swedish regions were providing patients with ORA.

Aspects, such as what health record information is accessible to patients, who can access it, and when is it made available, can vary from region to region and between health care providers [1-4,26,27]. Sweden has a national regulatory framework for patient ORA, first established in 2012 with mandatory and elective paragraphs [28]. Due to the legal framework's flexibility, the 21 autonomous Swedish regions made different decisions on what information can be accessed, when it can be accessed, and who can access it. An updated national regulatory framework from 2016 promises more unification [29], but it is yet to be fully adopted. Individual HCPs have little control over the system and can, for example, not delay access to certain information. Health care providers can, however, opt to make specific keywords used in the EHR inaccessible to patients in PAEHRs to safeguard patients (eg, early hypotheses or concerns for domestic abuse) [30].

Swedish regions adopted different implementation strategies and faced various barriers [31]. In Uppsala, the first region to implement PAEHRs, HCPs were not involved, leading to resistance and negative impacts on implementation. Recognizing this, other regions engaged HCPs, influencing decisions such as restriction of patient access to EHR entries made after implementation [31]. Stakeholders globally emphasized that HCP and patient involvement and education, and institutional change strategies are key to successful implementation [7,32].

As HCPs play a critical role in the adoption of patient ORA, it is essential to further deepen our understanding of what factors, from their perspectives, influence successful implementation. This study, therefore, explores the implementation of the Swedish PAEHR system in primary care from the HCP perspective. Investigation of the factors influencing implementation might increase our understanding of important barriers and facilitators, offering valuable insights into the challenges and potential areas of improvement in PAEHR implementation.

XSL•FO
RenderX

To analyze the factors influencing the implementation of PAEHRs, we used the CFIR. The CFIR was chosen because it is a well-established and widely used framework in implementation science, providing a structured approach to identifying both barriers and facilitators across multiple levels of the health care system. Compared to other implementation frameworks, such as the Normalization Process Theory and the Theoretical Domains Framework, the CFIR offers a broader scope by incorporating individual, organizational, and contextual factors, making it particularly suitable for studying the adoption of digital health interventions in complex health care settings. The CFIR has previously been applied in research on eHealth implementation, including patient portals and EHRs, further supporting its relevance for this study [33].

Aim

We aimed to investigate the factors influencing the implementation of the Swedish PAEHR system in primary care from HCPs' perspectives.

Methods

Study Setting

The study was part of an investigation into the implementation of a PAEHR system in primary care and its usability and implications for HCPs. Swedish health care is mainly tax-funded, and most hospitals and PCCs are managed by regional councils [34]. Since the regions are autonomous, primary care can vary between regions. Both publicly and privately owned PCCs exist, and they are generally publicly funded. Most PCCs are team-based with a mix of different HCPs (eg, general practitioners [GPs], nurses, physiotherapists, and dietitians). The average national primary care visit count was 4.3 per person in 2009 [34]. Compared to the health care systems in other countries, the Swedish health care system struggles with waiting times, continuity of care, and support for chronically ill patients [35]. The PCC included in this study is located in the largest Swedish region, Region Stockholm, and has a mixed patient population with varying socioeconomic backgrounds. While it may not be representative of all PCCs in Sweden, it is an interesting center with a fairly large and diverse patient population and a common mix of health care and administrative staff.

The Swedish PAEHR system, also known as 1177 Journal, is accessible through the national patient portal [36]. Citizens in Region Stockholm had access to medical notes, lab results, diagnoses, and information about visits when the PAEHR system was launched (2016/2017). In 2023, they were provided access to maternity care, vaccination, and referral records, as well as log reports [37].

In Stockholm, over 73% of the population had good self-reported health, and the life expectancy was 82 years in 2014 [38].

Recruitment of Study Participants

Study participants were recruited from an academic PCC, which has a special focus on education and research. Information about the study was distributed via email through the PCC manager as well as orally during workplace meetings. HCPs were eligible to participate in the study if they were involved in the clinical documentation process by writing clinical notes themselves in the EHRs (eg, nurses), dictating clinical notes (eg, physicians), or being involved in the transcription of clinical notes (eg, medical secretaries). A convenience sampling approach was used, and it was voluntary to participate. Nonparticipation was not analyzed.

Data Collection

Data were collected through individual interviews. The interviews were conducted face-to-face at the PCC by the last author (MH) 6 months after the launch of the PAEHR system in Region Stockholm (2017). MH is a female researcher/lecturer with a PhD degree, who, at the time of the interviews, had extensive experience in qualitative research. The interviews were conducted using a semistructured interview guide developed by MH and the third author (IS). The interview guide was pilot-tested with 1 primary care physician, and minor changes were made to the order of questions and the terminology used. The interview guide is presented in Multimedia Appendix 1. The HCPs were interviewed about their experiences of the implementation process, which was the focus of this analysis, as well as the impact of the PAEHR system on the work environment [16] and what they would like to improve to increase the usability and usefulness of the PAEHR system [39]. The interviews were conducted in Swedish and lasted for 30 to 45 minutes. The interviews were audio recorded.

Data saturation was not fully achieved due to challenges in recruiting study participants.

Data Analysis Using the CFIR

The recorded interviews were transcribed and analyzed by the first author (IM) in discussion with the rest of the authors. The transcribed interviews were read and reread. The analysis was conducted in 2 steps using an abductive approach, that is, a combination of inductive and deductive analysis [40]. First, the analysis was conducted deductively using the CFIR, and the information was coded using the CFIR domains (intervention characteristics, inner setting, outer setting, characteristics of individuals, and implementation process) [23]. In this study, the CFIR was a fitting choice owing to its comprehensive nature and ability to capture the multifaceted implementation aspects in health care settings. By employing the CFIR, the analysis systematically examined various factors influencing the implementation of the PAEHR system, providing a holistic understanding of implementation. The information under the different domains was thereafter inductively analyzed using content analysis according to Graneheim and Lundman [41]. The information was coded, and the codes were grouped into categories under the theme of each CFIR domain. Feedback from participants was not collected. The analysis was conducted using NVivo 1.4 (Lumivero).

According to the CFIR, the following five domains are essential for the implementation of interventions in health care: (1) characteristics of the intervention (eg, adaptability and complexity), (2) inner setting (eg, structural characteristics and culture), (3) outer setting (eg, patient needs and resources;

XSL•FO
RenderX

cosmopolitanism), (4) characteristics of the individuals involved (eg, knowledge and beliefs), and (5) implementation process (eg, engagement, evaluation, and reflection).

The CFIR combines different theories and provides a comprehensive framework for implementation research. The different domains are further described below in the results section.

Consolidated Criteria for Reporting Qualitative Research (COREQ) guided the reporting of this study [42].

Ethical Considerations

The study received ethical approval from the Stockholm Ethical Review Board (2017/1028-31). All study participants provided written informed consent before participating in the study. In accordance with the requirements of the Swedish Ethical Review Authorities, participants were informed that their participation was voluntary and that they could choose to revoke their participation at any time. Transcribed interviews were deidentified to protect the participants' privacy, and confidentiality was preserved when reporting the results. No compensation was given for study participation.

Results

Fourteen interviews were conducted with a mix of HCPs, including a counsellor, dietitians, physicians, physiotherapists, medical secretaries, registered nurses, and an occupational therapist (Table 1). The ages of the participants ranged from 27 to 67 years, and their work experiences ranged from 5 to 36 years.

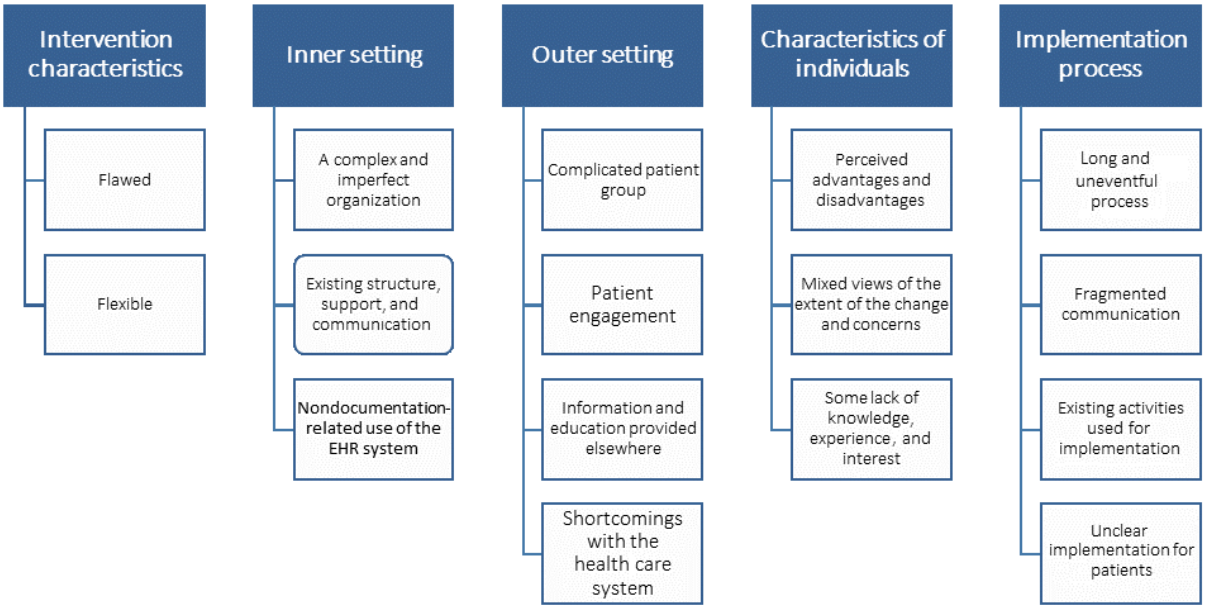
The analysis of the 14 interviews resulted in 15 categories under themes that were equivalent to the 5 CFIR domains (Figure 1). The categories have been further described below, with any subcategories italicized.

Table 1. Participant characteristics.

Characteristic	Value (N=14), n (%)
Profession	
Counsellor	1 (7)
Dietician	2 (14)
Medical secretary	3 (21)
Nurse	2 (14)
Occupational therapist	1 (7)
Physician	3 (21)
Physiotherapist	2 (14)
Age (years)	
<39	1 (7)
40-49	5 (36)
50-59	3 (21)
≥60	5 (36)
Experience (years)	
5-9	3 (21)
10-19	6 (43)
20-39	5 (36)

XSL•FO
RenderX

Figure 1. Themes that emerged under the Consolidated Framework for Implementation Research dimensions. EHR: electronic health record.



Intervention Characteristics

In the CFIR, intervention characteristics refer to the attributes of the intervention itself, including intervention source, features, complexity, and adaptability. In our case, the intervention was the PAEHR system that made EHRs accessible to patients. Our study uncovered two categories: (1) flawed and (2) flexible. These are mainly related to the concepts of complexity and adaptability in the CFIR domain.

Flawed

The HCPs voiced concerns regarding various shortcomings within the system, pointing to complexities in usage, challenges with terminology, and limitations in safeguarding sensitive patient information. The EHR system, from which information is shown to the patient through the PAEHR system, was perceived as complicated. Templates used to structure the documentation were perceived as challenging; hence, *writing the records was difficult*. Moreover, patient ORA caused uncertainties regarding medical terminology use.

> *It would have been good for patients if the record's templates looked the same, and for us too. I mean, the record's templates are difficult to follow sometimes. It's a lot to fill in and a lot to klick to fill in and sometimes it is forgotten.* [Dietician]

Additionally, the HCPs expressed that the PAEHR system *lacked flexibility* and *safeguarding features*, particularly for mental health patients. Some HCPs were worried that patients could still see if information was hidden, and 1 HCP felt reluctant to document suspicions or early hypotheses as a consequence.

In contrast, some HCPs would have liked more information from the EHRs to be accessible to patients and to be able to monitor patient activities in the PAEHR system.

Flexible

The HCPs highlighted features that would enable discreet communication between HCPs, options for some information blocking, and allowances for incomplete records not to be shown to patients for up to 14 days.

> *[…] we talked about the existence of the hidden part, where one could write where they [the patients] could not see.* [Dietician]

The HCPs also reported being aware of previous implementations of the PAEHR system, with favorable outcomes.

> *We were informed that Uppsala {another region} had also used it and that they were happy.* [Physician]

Moreover, the PAEHR system was perceived to be *more confidential* than paper copies. For example, for patients experiencing domestic violence, it reduced the risk of paper copies being accessible to others.

Inner Setting

According to the CFIR, inner setting refers to the organization's internal environment where implementation takes place. It encompasses the organization's structural, cultural, and political aspects [23]. In our case, it refers to the PCC where the HCPs worked. Three categories emerged under this domain: (1) a complex and imperfect organization, (2) existing structure, support, and communication, and (3) nondocumentation-related use of the EHR system.

A Complex and Imperfect Organization

The HCPs described a *challenging work environment*, with varying tasks and a high workload, where they constantly discuss priorities. They mentioned that reflection, education, and documentation are not prioritized.

> *We must increase the number of visits, we can't go to education since it takes time. There is a desire to be better and produce more simultaneously. There is no*

XSL•FO
RenderX

> *common sense and no regard for the staff, it should just move faster and faster and people can't keep up.* [Physician]

According to the HCPs, they cannot *adequately prepare* for visits, which can upset some patients. They deal with *unpredictable visits*, *unclear/unsolvable conditions*, and *complicated treatments*. Assessments can be complex, affecting the clarity of notes. Moreover, the visits are short, and there is a lot of knowledge and information transfer, requiring confirmation of the understanding of patients. In cases related to children, they may be required to rely on information from parents. Misunderstandings can thus occur.

In addition, *communication with patients was restricted*. Certain information (eg, test results) was supposed to be communicated by the responsible physician, which hindered other HCPs (eg, medical secretaries and nurses) from answering patient questions. Moreover, requests to make changes to the record must pass through the manager.

Further, some HCPs had *dealt with threatening, aggressive, and rude patients* and were fearful. Moreover, the HCPs were repeatedly questioned about the records by their manager and patients. Patients could question slightly irregular but otherwise typical test results, and explanations could be time-consuming. Additionally, the HCPs avoided documenting suspicion and were uncertain of how safeguarding functions, such as hidden keywords and hiding unsigned records, work.

> *Sometimes you get aggressive patients that yell and act badly […] we are exposed to a lot. If for example there is only 30 slots today but there is a lot of people calling.* [Registered nurse]

Furthermore, the HCPs *had encountered several issues* when caring for patients, and these were related to the systems they use in general. Serious diagnoses had mistakenly been revealed to patients, referrals and reports had disappeared, and lab orders had remained active despite completion. Their IT systems were described as ineffective, difficult to use, and annoying.

The HCPs also reported a *lack of unification in documentation practices*. Physicians dictate and others transcribe the notes, while other HCPs write their notes themselves. Some respondents wrote on notepads first. The length of the notes varied, often with more junior HCPs writing more comprehensive notes.

The HCPs also described issues with the *record's quality*. Errors and gaps could occur during transcription due to the transcriber's lack of experience. Substandard language could also be used. Moreover, patients have reported errors in their records, and the HCPs were uncertain if the errors were corrected. According to 1 respondent, corrections are seldom made.

Further, *documenting and transcribing on time were challenging*. Some HCPs reported documenting after every patient or on the next day, and some dictated their notes with patients in the room. Additionally, *unsigned records were problematic* for the management. Transcribed notes are not always reviewed due to time constraints, and unsigned notes may contain blanks and errors. According to 1 HCP, some HCPs simply refuse to sign.

> *That's something that is constantly being pointed out, that we have to sign the records. [Counsellor]*

Existing Structure, Support, and Communication

The HCPs reported *some documentation structure*. They have always been conscious of their writing but might be more restrictive now. The transcribing medical secretaries have always strived to write comprehensively, and this is something they learned during their education.

Moreover, some HCPs have always *strived to document and sign records promptly*. Some HCPs had received directives to document quickly to ensure nothing lingers. Further, according to 1 HCP, HCPs have time allocated for administration, which should enable them to complete the tasks. Certain registrations were also required for financial reasons.

> *I usually sign them immediately because I know they will linger on a list which will be difficult to sign afterwards.* [Registered nurse]

Additional structures include functionality for tracking the people accessing the records. Sometimes, HCPs must have the patient's consent to view the records. There are also routines for providing patients with paper copies and dealing with upset patients, as well as channels for communication between nurses and physicians related to patient requests.

Furthermore, in relation to the implementation of new services, there is an organizational desire to change and improve, and the HCPs had previously participated in pilot projects.

Moreover, *support for documenting is provided* in different stages. HCPs might point out significant errors to each other. Transcribers, who are often medical secretaries, point out or alert physicians to errors or missing information in the records. At times, they may correct the errors and inform the physician. Moreover, medical secretaries assist physicians with insurance-related documentation. Furthermore, unsigned records are tracked by managers, who remind HCPs to sign.

> *I try to reconstruct what the physicians have dictated, I try to reconstruct it into a more understandable language for patients.* [Medical secretary]

Further, a *structure for communication with patients about their health care exists*, but it varies among HCPs**.** Moreover, there is *established internal communication* among HCPs through regular discussions, seminars, and education about eHealth, which are led by HCPs at the PCC.

Nondocumentation-Related Use of the EHR System

Additionally, a few HCPs reported using the EHR system as an alternative communication channel among HCPs. HCPs could send internal letters to each other.

Outer Setting

In the CFIR, outer setting refers to the external context surrounding the organization where the implementation occurs. It includes patient needs and resources, external policies and regulations, and the broader sociocultural and economic environment. We have therefore included categories related to patients' needs and resources in this theme: (1) complicated

XSL•FO
RenderX

patient group, (2) patient engagement, (3) information and education are provided elsewhere, and (4) shortcomings with the health care system.

Complicated Patient Group

According to the HCPs, their *patients are heterogeneous* with varying levels of knowledge and engagement in their care. While some patients are *good at scheduling appointments and understanding*, are *curious*, and *show interest* in their health records, HCPs also encounter patients who do not cooperate and who misinterpret, overanalyze, and get stuck. Parents who come in without their children and patients who are worried, confused, or forgetful (losing papers and copies) can be unreachable. The HCPs reported having a mix of new patients and patients they meet often and know well. Many of their patients are old, and some are immigrants with difficulties with the Swedish language. These groups were perceived by our respondents to be less likely to read their records online. Moreover, 1 HCP believed that only a few people read their PAEHRs, with readers being those engaged in their care. The PAEHR system was described as inaccessible for some and thus was described as excluding. Moreover, the HCPs thought that patients would only be interested in reviewing their records in special cases. In addition, while there were many requests for printed copies, few were collected.

Further, according to the HCPs, the PCC's patient population has *substantial health care needs*, which the available care cannot meet. Patients were described as frustrated over the lack of accessibility. Some HCPs acknowledged the difficulty for patients, both in reaching the health care center and managing the information provided during the visit.

> *We have patients waiting for an appointment who haven't gotten to meet a physician. 'But you were here the day before yesterday…' and they say 'But now it is about this issue…* [Registered nurse]

Moreover, according to the HCPs, patients have *high expectations* and are often unsatisfied. The HCPs stated that there was an expectation to remember everything, have answers to all questions, and read the records before a meeting, or they may be perceived as unprofessional. Unpreparedness can upset patients. The HCPs also described unsatisfied patients who perceive HCPs as incompetent and may want to change or include notes in the record and request a second opinion, with some wanting to change health care centers. Some patients were described as being controlling.

Furthermore, according to the HCPs, some patients lack necessary technical equipment like a printer, a telephone, and personal electronic identification (eID), as well as knowledge about the use of the internet.

Patient Engagement

The HCPs reported working in a patient-centered way and *engaging patients in their care*. They aimed to engage patients in shared decision-making and encouraged patients to, for example, follow-up and prepare questions before their meetings. The HCPs also reported engaging patients during the meetings by showing them their records and encouraging them to use the PAEHR system when copies are requested. The HCPs also described how they engage patients in the documentation by confirming their notes with the patients and mentioned that they may read and explain part of the records to the patients. In addition, HCPs could meet with patients for a follow-up earlier if requested.

> *I have done it for many years, asked patients to write down things they are wondering about and they can also bring up things they have read.* [Counsellor]

Information and Education Provided Elsewhere

Some HCPs reported learning about documenting PAEHRs at their previous work or during their education. One HCP also recognized similarities to another implemented initiative called SVF (standardized care process), where HCPs must document findings quickly.

Shortcomings With the Health Care System

A few HCPs expressed *perceived shortcomings with the health care system*, including a lack of reimbursement, misprioritization, and unnecessary care processes.

Characteristics of Individuals

In the context of the CFIR, characteristics of individuals refer to the personal attributes, attitudes, and behaviors of individuals directly involved in the implementation. This domain considers their knowledge, skills, beliefs, and motivations related to the implemented intervention. In our case, the individuals are the HCPs, and we have included their more general opinions on patient ORA and the use of PAEHRs in health care. Three categories emerged under this theme: (1) perceived advantages and disadvantages, (2) mixed views of the extent of the change and concerns, and (3) some lack of experiences, knowledge, and interest.

Perceived Advantages and Disadvantages

The HCPs stated both the advantages and disadvantages of the PAEHR system. While some HCPs thought it was essential, others were ambivalent. Some had become more positive over time, while some remained negative. Some HCPs explicitly expressed that they were against ORA, while others were described as angry by their colleagues.

The HCPs perceived that the implementation of the PAEHR system was *patient-driven* and that it was at the request of patients. There was also the perception that the records are the patient's property and that the PAEHR system is the patient's right and beyond the control of HCPs. The HCPs also thought that it was part of a general trend toward more transparency in health care. One HCP reflected that the lack of understanding of the need for patients to read their records may be due to their old-fashioned views. Moreover, the PAEHR system was believed to increase access to records and participation and to engage patients. Further, the HCPs thought that patients accessed the records for many reasons: they were interested or curious, they wanted to follow-up, they wanted to remind themselves about the findings, they wanted to improve their understanding, and they desired to participate in decision-making. Some HCPs thought that some patients read their records because they were worried or because they were suspicious and wanted to see what was not said at the visit.

XSL•FO
RenderX

> *I think it is good for openness that it isn't a closed document, that they should be able to read {the record} without asking for it.* [Dietician]

In health care in general, the HCPs thought that the PAEHR system *increased health care quality*. It made them more reflective, clearer, more precise, and more direct with their assessments. The PAEHR system was also described as a reminder to write the notes on time, and patient understanding was thought to be more critical than using medical terms. Moreover, the PAEHR system was considered environmentally sustainable since it reduces the number of paper copies and letters sent. The HCPs perceived the PAEHR system to be beneficial for transparency. According to some HCPs, reading the records is important since it concerns the individual's health and is essential for patients to follow their care. They also perceived it as time-saving for patients and a way of making the information more accessible, especially for patients experiencing difficulties due to disability. Moreover, the PAEHR system was seen as a control function, where patients can see that the most important information is included and can make sure agreed-upon actions are being taken, such as sending referrals. The quality of documentation and the quality of care could potentially be improved if patients could point out errors. The HCPs also hypothesized that increased accessibility of the records would increase the likelihood of use among patients.

> *In terms of gains I don't know but the advantages in terms of me thinking a little extra of what I am doing in relation to patients. That I think about it so that it is clearer maybe in general.* [Counsellor]

For themselves, the HCPs saw a *potential to lighten the workload* of writing summaries and reduce calls from patients. The HCPs could refer to the PAEHR system if paper copies of the records were requested. Moreover, once patients read the reports online, they might not see the need to book a face-to-face visit, reducing unnecessary visits. They also saw the potential of using the PAEHR system as a treatment tool to clarify treatment plans and goals.

For patients, the HCPs saw the potential for the PAEHR system to *support participation and collaboration* through increased availability and accessibility. With the PAEHR system, patients could have information from a visit in writing, which could support understanding. This was especially important since the visits could be emotionally charged for some patients, making it hard to retain information and resulting in misunderstandings. According to 1 HCP, it is also a way for patients to see that something comes from the visit. The HCPs noted an opportunity for making treatment plans clearer for patients and potentially increasing compliance, and they wished that patients would read the reports in preparation for a visit. This could potentially reduce patients' worry and increase their confidence in health care.

> *I think a positive effect can be that patients may get a little control over their record and can look. We write what we have done and they follow the test results.* [Physician]

Additionally, the HCPs saw potential for increasing patients' involvement in their care by, for example, tracking medication changes and test results, and for facilitating patients' understanding of how their behaviors may influence their health. Further, the PAEHR system was perceived to be beneficial for families of older patients and patients with different health care providers as it gathers all information in one place. In addition, ORA was perceived to be time-saving and cost-saving, improving patients' response times when issues arise. According to some HCPs, the service was also easy to use. However, the PAEHR system was not purely positive according to some HCPs.

> *I think there are both pros and cons. If you are hypochondriac it can also be a risk. If you get more information than you need.* [Medical secretary]

According to the HCPs, *records have other sometimes contradictory purposes*. On the one hand, the HCPs perceived patients as the owners of their records, while on the other hand, the records were considered a professional tool and thus must be detailed. The records could include information that patients might not want on record and assessments that patients might disagree with.

Moreover, the HCPs argued that the records could contain confidential and sensitive information and that not all information is meant for the patient. Documentation is a way to reduce the cost of, for example, test duplication, and to be able to protect other patients from, for example, infections. Moreover, documentation is needed since patients may not be entirely honest about their previous health care contacts.

Further, some HCPs saw *limited benefit* with the PAEHR system or even considered it an *unnecessary* service. A few HCPs were uncertain of or did not see the importance of patient ORA. They thought that better solutions are present to engage patients in their care and argued that they keep the documentation in the best interest of patients, making it unnecessary for patients to access it. They could not see the benefits of the PAEHR system, as they believed that notes from the PCC might be basic, stressing that patients could already request copies of their records on paper if needed. They believed that health outcomes and personal contact between the HCP and patient were more important and that too much focus was being placed on EHRs. Moreover, they believed that the PAEHR system was unnecessary as their previously experienced issues with unsent referrals, which PAEHRs might have resolved, had already been addressed.

> *I don't think benefit from reading what the physician has written or what that test results show. If they are very interested they can ask.* [Physician]

Moreover, according to the HCPs, the PAEHR system was *not optimal*. They believed that the records contained little information, which might not be visually optimal. The information provided might also not be essential or summarized for patients. In addition, documentation was not standardized. Further, the HCPs thought that the service should be restricted to signed records and access should be delayed. Moreover, they thought that the platform was difficult to navigate.

Additionally, the HCPs believed that the PAEHR system was *unavailable or inaccessible to some patients*. They believed

XSL•FO
RenderX

that most users would be younger, while elderly people, people with dementia, and migrants with language difficulties would be excluded, creating a double system. They also believed that patients with low health or digital literacy would be excluded and that the use of the system would depend on the patient's illness.

> *I think the day I myself get dementia and sitting there struggling with all the passwords, It would be horrible and you cannot keep that organized.* [Physiotherapist]

Further, some HCPs believed that the PAEHR system would be a *disservice to patients.* It would give a false sense of control, increase worry, and be misinterpreted, increasing HCP workload with additional calls and questions. One HCP speculated that patients might read their records to find things to get sick over. Additionally, it might be unpleasant for patients to read serious diagnoses by themselves. According to 1 HCP, it might also be *difficult for patients to understand* the content without a medical education, and additional visits would be needed regardless. According to these HCPs, an oral explanation would be ideal, addressing additional uncertainties during a visit. One HCP did not think patients should read their records at all and stated that patients with severe mental health issues might be negatively affected. According to 1 HCP, the risk depends on the person.

Mixed Views of the Extent of the Change and Concerns

According to some HCPs, the implementation of the PAEHR system meant *little to no change*, potentially since the introduction was so recent that any impact was yet to be seen. Some HCPs were *unmoved* by the implementation. They did not believe the PAEHR system was meant to change care delivery or affect documentation due to, for example, fear of repercussions from patients. According to them, everyone knew it was coming long in advance and they were prepared.

Moreover, *few documentation requirements were new, and the HCPs therefore made little to no changes* to their practice. The HCPs reported that they have always been reflective when writing and tried to be careful and precise. They wrote in a way that the records would be readable for patients. Some HCPs reported that they always wrote and signed the records quickly. Moreover, the HCPs always discussed the notes with patients. The difference now was that the records were online.

> *What I have thought a little more about is writing the notes on time but that is something that should be done anyway so it is not really new. But it is a reminder to write more understandably which also is not something new, just a little extra.* [Occupational therapist]

In contrast, some HCPs thought that *the PAEHR system would require a change* for those HCPs who had not previously been educated about patient documentation. This could be especially true for more senior HCPs who often use medical terms and abbreviations. Some HCPs thought that it would take time to get accustomed to it and would be time-consuming since it was unfamiliar. One HCP reported that they now try to avoid Latin words, which requires effort.

Concerns

Many of the previously mentioned issues concerned HCPs, worrying them and making them skeptical. Some HCPs were skeptical as a patient as well. Although much had not turned out as they feared, there were still concerns that effects might come later. One HCP expressed that the novelty of the PAEHR system was scary.

The HCPs worried about *potential consequences*. They feared potential increases in criticism, questioning, and being reprimanded. They believed that their workload would increase, especially for physicians, due to patient calls and questions. Furthermore, they believed that the system could affect the health care center's reimbursement. In addition, the HCPs had *many thoughts and questions about implementation* and the related practicalities. The increased demands for clarity and timeliness of documentation were causes for stress due to the existing time pressures in their work. Furthermore, the HCPs were concerned that the documentation changes would make the notes less understandable. One HCP felt unprepared.

> *It was more of how it going to happen. What would happen if patients read, are they going to scold us …will they get mad over the information they have gotten.* [Registered nurse]

Further, the HCPs *worried that patients might be negatively affected.* They were worried that the records would upset their patients and that the patients would not like or agree with the contents and would shop around for care. This was particularly concerning in regard to children (eg, social service reports could potentially influence children's confidence in their providers). They were also worried that reading the records could affect patients' confidence or trust in their providers or the treatment. Moreover, the HCPs were concerned about patients who were unable to ask questions or get support from a provider. They believed that the system could cause unnecessary worry. They thought that the records might be especially difficult to understand or interpret for patients not working in health care, which might lead patients to search for information on Google. One HCP suspected that some patients had concealed an appointment upon reading the records, which was concerning. Patients also felt anxious because they did not know what was being written about them.

Moreover, the HCPs were *concerned about the security* and integrity of patients, the preservation of doctor-patient confidentiality, and unauthorized access to records.

However, the HCPs also expressed that things *did not turn out as they had thought or feared.* Patients were not reading their records before being contacted, calls to the PCC did not increase, and they were not reprimanded by the management. They had not made any of the changes that they thought they would need to make. According to 1 HCP, everything had solved itself.

Some Lack of Knowledge, Experience, and Interest

There was *little to no knowledge about the functions of the PAEHR system* among the HCPs. Some HCPs were unaware or unsure of what patients could view. One HCP wished that they had insights into implementation experiences from other regions.

XSL•FO
RenderX

> *I know they can see the notes, test results and referrals I think, but not for example biopsies and such, I don't think they can see that, and not Xrays.* [Physician]

Furthermore, the HCPs had *little to no knowledge about the service's benefits and effects on patients*. Patients' experiences and the number of patients accessing their records were unknown. A few HCPs had second-hand information about patients' experiences. According to some HCPs, patients appeared not to be reading their records and should be reading more. According to 1 HCP, few patients seemed to use online services in general, with 1 HCP speculating that patients in specialist care might be more interested.

Some HCPs did *have personal experiences* reading their own records or a family member's records online or on paper. Those with some ORA experience had just tried it once, and some of their records were empty. A few of them had read their records at the doctor's office out of interest, whereas some had requested paper copies of their hospital records. One HCP had experience with other services on the patient portal, and a few HCPs explicitly expressed disinterest in the service and in reading their records.

> *I have been in mine and apparently I have nothing there. But I have looked with my husband at his and then everything was actually correct.* [Registered nurse]

Implementation Process

According to the CFIR, implementation process refers to the methods, strategies, and activities used to facilitate the adoption and integration of an intervention into a particular setting or organization. This domain examines how the intervention is introduced, implemented, monitored, and evaluated over time. Four categories emerged under this theme: (1) long and uneventful process, (2) fragmented communication, (3) use of existing activities for implementation, and (4) unclear implementation for patients.

Long and Uneventful Process

According to the HCPs, information was provided, but the time until the service was available appeared *outdrawn* for some. It had been ongoing for years, and some HCPs had to be reminded that it was ongoing. According to 1 HCP, many had grown tired of nothing happening. Making the services available was, however, quick and smooth, and suddenly, it was there overnight. The long implementation process reportedly led to some loss of motivation to act.

> *The negative is that it had been talked about for so long but it never got started.* [Physiotherapist]

Fragmented Communication

HCPs were *partially informed*, discussions occurred, and some participated in educational activities. According to 1 HCP, they had a seminar about 1 year before the implementation of the PAEHR system. Some HCPs recollected an education day for some professions, where they learned about and looked at the service. They, however, received no information about when and how the PAEHR system would be launched. According to the HCPs, they did not discuss the technical aspects of the service. One HCP reflected that maybe they did not need more information, while another thought that a user video would have been beneficial.

> *I have no idea how it was done […] we just got information that it going to be online. Nothing more.* [Physician]

Additionally, the scope of information about different aspects of the implementation varied. According to the HCPs, there were discussions about work processes, safeguarding functionalities, how to write, and flexibility aspects, and the importance of completing the records on time was also emphasized. According to 1 HCP, they were told to "do as they do." Furthermore, the HCPs reported receiving information about experiences from other implementations and having some follow-ups at their usual meetings, according to individual accounts.

Existing Activities Used for Implementation

According to the HCPs, information related to the implementation of ORA was provided during their existing meetings related to eHealth. Information was also provided by the usual leader of these meetings, who was one of the HCPs at the center.

Unclear Implementation for Patients

The HCPs were uncertain about how patients were informed, and according to some HCPs, *patients were uninformed*. The HCPs had not noticed any major information campaign targeting patients. Some thought that HCPs were supposed to inform patients, and some occasionally did so. Those informing patients mainly did so with patients who showed an interest. One HCP reported now informing patients more frequently (6 months after implementation). Moreover, there were reports of some brochures in the waiting rooms. There were attempts to encourage physicians to inform patients.

> *[…] if they got something in their mailbox, I do not know but I don't think so.* [Medical secretary]

Discussion

Principal Findings

Although patients in Sweden have had ORA since 2018 (the first implementation began as early as 2012), few studies have focused specifically on implementation in primary care from the perspective of HCPs. To our knowledge, this is the first comprehensive study of the implementation of PAEHRs in Swedish primary care from the perspective of a diverse group of HCPs. Our study identified several potential barriers and facilitators related to PAEHRs, the primary care setting, and patients' and HCPs' characteristics, as well as barriers and facilitators related to the implementation process (Table 2). We will discuss the identified barriers and facilitators in relation to previous research.

XSL•FO
RenderX

Table 2. Potential barriers and facilitators related to patient-accessible electronic health record implementation.

Domain	Barriers	Facilitators
Intervention characteristics	• Shortcomings of PAEHRs[a]	• Flexibility of PAEHRs
Inner setting	• A complex and imperfect organization • Nondocumentation-related use of the EHR[b] system	• Existing structure, support, and communication
Outer setting	• Complicated patient group • Shortcomings with the health care system	• Patient engagement • Information and education provided elsewhere
Characteristics of individuals	• Perceived disadvantages of PAEHRs • Mixed views of the extent of the change and concerns • Some lack of experience, knowledge, and interest	• Perceived advantages of PAEHRs • Mixed views of the extent of the change
Implementation process	• Long and uneventful process • Fragmented communication • Unclear implementation for patients	• Use of existing activities for implementation

[a]PAEHRs: patient-accessible electronic health records.

[b]EHR: electronic health record.

Barriers for the Implementation of PAEHRs

The HCPs reported several shortcomings with the PAEHR system. Complexities in usage, challenges with terminology, and a lack of safeguarding features could be potential implementation barriers. Complexities in EHR system usage might explain the reported lack of unification in documentation practices, the poor quality, and the difficulties with accomplishing and signing the records, further explaining the related concerns. Challenges using EHR systems have previously been described [43,44], and documentation for patients is an additional challenge where support is needed. This reflects complexity, which is one of the intervention characteristics that influence implementation according to the CFIR [23]. Additionally, adaptability influences implementation according to the CFIR, and the PAEHR 1177 journal lacked flexibility regarding sensitive information according to the HCPs. However, the definition of sensitive information by the HCPs might need to be considered together with that by patients, as the limitation of information in the PAEHR system has previously been considered problematic by patients [45]. The improvement suggestions by HCPs have been related to these described issues [39]. Many related improvement suggestions have aligned with patients' experiences, but suggestions related to the restriction of information have not aligned, and patients want access to more information [46]. Enhancing the usability of the PAEHR system and providing support and education are potential solutions to these barriers.

The complexity of the health care organization and its imperfections are other potential barriers. The strained working environment has been raised as a cause for concern by HCPs in both specialized and primary care [14,47,48]. Further, the HCPs described several potential barriers related to documentation practices, that is, a lack of unification in documentation practices, poor quality, and difficulties documenting on time and signing the records. In a recent survey of GPs in the United Kingdom, the majority believed patients would find errors in their GP records [8]. Swedish patients have also reported finding errors in their records [49]. Addressing system-level issues within the primary care system by, for example, increasing resources and training HCPs might reduce these barriers.

HCPs' descriptions of their patient groups as challenging might explain their concerns about the negative impacts on patients. It has previously been reported that patients potentially do not understand their records [12-14], and patients have had similar concerns [50] and have reported difficulties understanding their records [51]. However, some research suggests that most patients understand most of the information available in their PAEHRs [20,52].

The potential exclusion of some patient groups has also previously been described [19,20] and needs to be addressed. Experts have recommended education or support for patients in using PAEHRs as a core part of the implementation of the PAEHR system [32].

According to the CFIR, beliefs and attitudes toward the intervention impact implementation [23]. Resistance among HCPs has been previously highlighted as the main barrier to PAEHR implementation [19]. According to the HCPs in this study, one of the perceived disadvantages was that the purpose of an EHR might not align with the purpose of a PAEHR, which has previously been highlighted [13,14]. As previously mentioned, the HCPs were unsure what needed to be changed. When ORA was first introduced in Sweden, the assumption was that this would not require substantial changes to HCPs' work processes [31], yet this is not the experience of all HCPs. Addressing this ambivalence with guidelines on how ORA will impact HCPs' documentation practices could overcome some of the experienced resistance.

Another disadvantage was that the HCPs perceived that there was little to no benefit of the PAEHR system. This could reflect a lack of existing research at the time of interviews or simply a lack of communication of existing evidence to HCPs. Current

XSL•FO
RenderX

research shows several benefits for patients [6], with minorities and elderly people reporting more significant benefits from ORA [20]. Whether the benefits are sufficient to motivate the introduction of ORA also seems to be questioned by HCPs.

The mixed views on the extent of the changes ORA entails highlight the previously mentioned ambiguity regarding the service. These mixed views might explain the perceived disadvantages expressed by some respondents, and as previously mentioned, the purpose of PAEHRs needs to be clarified. Regarding documentation, there have been several reports of it changing due to the implementation of ORA [12,16,17,53-55]. However, HCPs have also previously reported not experiencing all they feared [13,16,55].

Furthermore, HCPs and other stakeholders have previously expressed several of the concerns raised [13,31]. Studies have shown some negative impacts on HCPs' work environments in terms of increased demand and loss of control, as well as some positive impacts in terms of increased support [12,16]. Moreover, patients have expressed a fear of being worried [50]. According to a Swedish national patient survey, 26% of patients had been worried by information on their record, and they commonly called or raised their concerns at subsequent visits with their providers [18]. Furthermore, concerns regarding privacy and security have previously been raised [13]. Patients also have these security and privacy concerns, but to a smaller extent, and have not experienced many breaches [20,21,49]. Additionally, patients have mainly reported improvements in patient-provider relations due to ORA and have not reported worsening of the relations [21].

A lack of experience with the service among some HCPs could be another potential barrier, as previous research has found that HCPs with experience in using PAEHRs are more positive toward the service [56]. Exposing HCPs to the PAEHR system could thus potentially have a positive impact on its implementation.

The long and uneventful implementation process and the fragmented communication are potential barriers and might explain the lack of knowledge, experience, and interest among our respondents. In a study about PAEHR communication reach, HCPs (eg, nurses and physicians) received information from different sources, and despite several efforts, 7% of the HCPs had not received information at all [57,58]. A method for evaluating information reach might be a potential solution to this issue.

A more effective process for communication about delays could also have been beneficial. HCPs in other settings have requested more detailed information and more involvement in implementation [57]. More and timelier information about the service is thus a potential solution that could have mitigated some of the concerns.

Follow-up also seems to have been limited, which could have contributed to the concerns. According to the CFIR, reflection and evaluation are essential implementation activities [23]. More continuous discussions about the implementation of PAEHRs could have supported the implementation.

How the PAEHR system was introduced to patients was also unclear and could be related to the fragmented communication. There are reports of patient involvement in the development of the PAEHR system, but these efforts were minimal during regional implementation [7]. Better implementation activities for patients in terms of support and education in a more structured manner might mitigate HCPs' concerns about the potential negative effects on patients. There is also an indication that education might support patient use [59], and it has been recommended by experts [32]. The involvement of both HCPs and patients has been identified as an essential factor for successfully implementing PAEHRs [7]. A clearer and comprehensive implementation process for both HCPs and patients is a potential solution to these barriers.

Facilitators for the Implementation of PAEHRs

The HCPs acknowledged some system flexibility related to communication between HCPs, information blocking, and access to incomplete records, which could be potential facilitators. Flexibility is an influential intervention characteristic according to the CFIR, and further development of flexible software solutions enabling HCPs to closely monitor and control ORA could further facilitate acceptance and implementation.

The HCPs did report some existing structures and support for documentation, potentially facilitating implementation. The fact that there was some structure for communication with patients about their health care and some structure for documentation could have facilitated the implementation of ORA. By further strengthening these existing structures, perceived issues could potentially be mitigated and implementation could be facilitated. Outlining them could also be part of a readiness assessment of the inner setting.

Prior patient engagement could have fostered the perceived advantage of PAEHRs in supporting collaboration and patient engagement. The additional information channel provided by the PAEHR system might have been a facilitator since conventional channels have been proven inadequate [57].

The PAEHR system might also be a potential solution to some of the issues HCPs experience with patients. As highlighted by some HCPs, ORA can increase understanding and trust, and reduce workload. Moreover, HCPs have reported increased support in their working environment in patient interactions due to PAEHRs [16]. The HCPs did describe the PAEHR system as helpful for patients, and they mentioned that it could possibly improve health care quality, which is a potential facilitator. These views are supported by patient-reported benefits of PAEHRs, such as improved patient-doctor relationships, medication adherence, and reduced anxiety [6,12]. The reasons for reading, according to HCPs, also align with patient-reported reasons for reading [18]. These perceived advantages could be used to inform HCPs and change attitudes toward the service.

The use of existing activities might have been a potential facilitator. However, complementary activities are warranted as research demonstrates the lack of reach of existing communication channels [57,58].

We found substantial ambiguity and high variation in the opinions and experiences of HCPs regarding the implementation

XSL•FO
RenderX

of ORA. HCPs' views on the ability and readiness of patients to engage with ORA and their views on the purpose and usefulness of EHRs appear to affect their perceptions of the impact (positive or negative) ORA will have on their work. This can become a barrier or facilitator to implementation, depending on what narrative dominates a specific context. Understanding this relationship is essential to adapt implementation activities and communication strategies to HCPs' experiences.

Strengths and Limitations

The recruitment of HCPs from a single PCC, which can cause center-related bias, was a limitation. The inclusion of HCPs with different professions, which can provide multiple perspectives, was a strength that reduced the risk of profession-related bias. Medical secretaries might not have the same accountability as other HCPs regarding the records, which might have influenced their views. However, since they play an essential role in the documentation process, their inclusion was a strength. While data saturation was not fully achieved, the information provided by the HCPs was rich, providing many valuable insights.

Conducting the interviews at the center might have influenced the findings from the interviews. Yet, this influence appears to be minimal, as the interviews generated a diverse set of views and opinions. Based on the qualitative nature of the study, it was not possible to determine the prevalence of the identified barriers and facilitators for ORA implementation. Further research with a quantitative study design is therefore needed.

On one hand, the use of an interviewer without an HCP background can be considered a strength since it mitigates bias toward the views of HCPs. On the other hand, there might be a loss of information and understanding due to a lack of experience in the health care setting.

Since the analysis was conducted several years after the interviews, new experiences and information might have influenced the analysis and interpretation. The analyzing author attempted to keep the analysis close to the interviews and was mindful of alternative interpretations, all while discussing uncertainties and emerging themes with the other authors, which can be considered a strength. Additionally, using the CFIR in the analysis might have mitigated some risk of bias but might have influenced the generated themes.

Implications

Health care systems can better support HCPs adopting PAEHRs, particularly in settings with limited resources and high patient loads, by addressing the barriers highlighted in this study. They could enhance EHR systems, address the challenges with the primary care setting, support patients, address HCPs' concerns and knowledge gaps, and adopt clearer and comprehensive implementation strategies. Integrating patient experiences is also essential for improving PAEHR usability and its impact on care. Future research should examine systematic approaches, such as surveys, focus groups, and co-design methods, to ensure patient voices inform ongoing development and optimization. Exploring how PAEHRs can be integrated with emerging technologies to enhance coordination, personalization, and decision support presents another important avenue for future research and policy development.

While long-term engagement strategies were not the focus of our study, our findings suggest that ongoing support is crucial. Participants emphasized the need for open dialogue, shared experiences, and organizational backing to navigate the challenges of PAEHRs. These insights point to the potential value of sustained training, peer-support mechanisms, and clear communication from leadership as part of long-term implementation efforts.

While this study focused on Sweden, its findings may be relevant to other countries implementing PAEHRs. Many of the identified challenges, such as HCP engagement, documentation practices, and patient comprehension, are common across health care systems, regardless of national policies. However, variations in regulatory frameworks, EHR infrastructure, and patient access policies may influence how these findings translate to other settings. Future research could explore how similar challenges manifest in different health care models to further understand the global applicability of PAEHR implementation strategies.

Our study also revealed that some HCPs may alter or omit certain details in their documentation due to concerns about how patients might react, potentially affecting completeness. For example, the participants mentioned avoiding sensitive terms or adjusting wording to prevent misunderstandings. While we did not specifically evaluate the impact on clinical decision-making, these changes may have implications for the accuracy and utility of records. These issues have been explored in a recent scoping review [60], which also identified this as an area that warrants further investigation to understand the potential effects on care quality.

Conclusions

This study underscores the importance of having a usable EHR system to support developments such as the implementation of ORA. It also emphasizes the importance of addressing organizational issues, such as the work environment in primary care, for optimal implementation of eHealth services such as the PAEHR system. This study also highlights the importance of HCPs' views and experiences with their patients and their perceptions and attitudes toward the intervention in the implementation of services such as patient ORA. Additionally, this study stresses the importance of effective implementation processes and communication strategies for both HCPs and patients.

In summary, issues with the EHR system and organizational shortcomings need to be addressed for optimal implementation of ORA, where both patients and HCPs benefit and risks are mitigated. Furthermore, improved information and education for patients and HCPs are potential solutions to address many of the concerns and perceived disadvantages of implementing PAEHRs.

XSL•FO
RenderX

Acknowledgments

This study was funded by FORTE – the Swedish Research Council for Health, Working Life and Welfare through the research projects “PACESS” (2016-00623) and Beyond Implementation of eHealth (2020-01229), and AFA Insurance through the “ePrIm” project (190210). FORTE funded the data collection, and AFA funded the analysis. We used generative artificial intelligence technology (Grammarly, Grammarly Inc) to enhance the grammatical accuracy and vocabulary richness of the manuscript.

Data Availability

The datasets generated and analyzed during this study are not publicly available due to the qualitative nature of the materials and the terms of the ethical approval, but are available from the corresponding author upon reasonable request.

Authors' Contributions

Conceptualization: MH, IS
Data curation: MH, IM
Formal analysis: IM, MH, IS, ÅC
Funding acquisition: MH, IS
Investigation: MH
Methodology: MH, IS
Project administration: MH
Supervision: MH, ÅC, IS
Visualization: IM
Writing – original draft: IM
Writing – review and editing: IM, MH, ÅC

Conflicts of Interest

None declared.

Multimedia Appendix 1
Interview guide for health care professionals.
[DOCX File , 25 KB - medinform_v13i1e64982_app1.docx]

References

1. Essén A, Scandurra I, Gerrits R, Humphrey G, Johansen MA, Kierkegaard P, et al. Patient access to electronic health records: Differences across ten countries. Health Policy and Technology 2018 Mar;7(1):44-56. [doi: 10.1016/j.hlpt.2017.11.003]
2. Nohr C, Wong MC, Turner P, Almond H, Parv L, Gilstad H, et al. Citizens' access to their digital health data in eleven countries - a comparative study. Stud Health Technol Inform 2016;228:685-689. [Medline: 27577472]
3. Kharko A, Blease C, Johansen M, Moen A, Scandurra I, McMillan B, et al. cover Mapping Patients’ Online Record Access Worldwide: Preliminary Results from an International Survey of Healthcare Experts. In: Bichel-Findlay J, Otero P, Scott P, Huesing E, editors. MEDINFO 2023 - The Future Is Accessible. Amsterdam, Netherlands: IOS Press; 2024:114-118.
4. Eriksen J, Monkman H, Adler-Milstein J, Eriksen KT, Nøhr C. cover Citizens’ Access to Online Health Information - An International Survey of IMIA Member Countries. In: Bichel-Findlay J, Otero P, Scott P, Huesing E, editors. MEDINFO 2023 - The Future Is Accessible. Amsterdam, Netherlands: IOS Press; 2024:1297-1301.
5. European Health Union: A European Health Data Space for people and science. European Commission. 2022. URL: https://ec.europa.eu/commission/presscorner/detail/en/ip_22_2711 [accessed 2024-03-15]
6. Tapuria A, Porat T, Kalra D, Dsouza G, Xiaohui S, Curcin V. Impact of patient access to their electronic health record: systematic review. Inform Health Soc Care 2021 Jun 02;46(2):192-204 [FREE Full text] [doi: 10.1080/17538157.2021.1879810] [Medline: 33840342]
7. Cijvat CD, Cornet R, Hägglund M. Factors influencing development and implementation of patients' access to electronic health records-a comparative study of Sweden and the Netherlands. Front Public Health 2021;9:621210 [FREE Full text] [doi: 10.3389/fpubh.2021.621210] [Medline: 34169054]
8. Blease CR, Kharko A, Dong Z, Jones RB, Davidge G, Hagglund M, et al. Experiences and opinions of general practitioners with patient online record access: an online survey in England. BMJ Open 2024 Feb 01;14(1):e078158. [doi: 10.1136/bmjopen-2023-078158] [Medline: 38302414]
9. de Lusignan S, Mold F, Sheikh A, Majeed A, Wyatt JC, Quinn T, et al. Patients' online access to their electronic health records and linked online services: a systematic interpretative review. BMJ Open 2014 Sep 08;4(9):e006021 [FREE Full text] [doi: 10.1136/bmjopen-2014-006021] [Medline: 25200561]

XSL•FO
RenderX

10. Hägglund M, McMillan B, Whittaker R, Blease C. Patient empowerment through online access to health records. BMJ 2022 Sep 29;378:e071531 [FREE Full text] [doi: 10.1136/bmj-2022-071531] [Medline: 36175012]
11. Grünloh C, Myreteg G, Cajander Å, Rexhepi H. "Why do they need to check me?" Patient participation through eHealth and the doctor-patient relationship: qualitative study. J Med Internet Res 2018 Jan 15;20(1):e11 [FREE Full text] [doi: 10.2196/jmir.8444] [Medline: 29335237]
12. Turner A, Morris R, McDonagh L, Hamilton F, Blake S, Farr M, et al. Unintended consequences of patient online access to health records: a qualitative study in UK primary care. Br J Gen Pract 2023 Jan;73(726):e67-e74 [FREE Full text] [doi: 10.3399/BJGP.2021.0720] [Medline: 36316163]
13. Davidge G, Brown L, Lyons M, Blease C, French D, van Staa T, et al. Primary care staff's views and experience of patients' online access to their electronic health record: a qualitative exploration. Br J Gen Pract 2023 Jun;73(731):e418-e426 [FREE Full text] [doi: 10.3399/BJGP.2022.0436] [Medline: 37068967]
14. Grünloh C, Cajander Å, Myreteg G. "The record is our work tool!"-Physicians' framing of a patient portal in Sweden. J Med Internet Res 2016 Jun 27;18(6):e167 [FREE Full text] [doi: 10.2196/jmir.5705] [Medline: 27349531]
15. Cajander Å, Moll J, Englund S, Hansman A. Medical records online for patients and effects on the work environment of nurses. Stud Health Technol Inform 2018;247:271-275. [Medline: 29677965]
16. Muli I, Scandurra I, Cajander Å, Hägglund M. Healthcare professionals' experiences of the work environment after patients' access to their electronic health records - a qualitative study in primary care. Stud Health Technol Inform 2022 May 25;294:530-534. [doi: 10.3233/SHTI220515] [Medline: 35612136]
17. Blease C, Torous J, Hägglund M. Does patient access to clinical notes change documentation? Front Public Health 2020;8:577896 [FREE Full text] [doi: 10.3389/fpubh.2020.577896] [Medline: 33330320]
18. Moll J, Rexhepi H, Cajander Å, Grünloh C, Huvila I, Hägglund M, et al. Patients' experiences of accessing their electronic health records: national patient survey in Sweden. J Med Internet Res 2018 Nov 01;20(11):e278 [FREE Full text] [doi: 10.2196/jmir.9492] [Medline: 30389647]
19. Niazkhani Z, Toni E, Cheshmekaboodi M, Georgiou A, Pirnejad H. Barriers to patient, provider, and caregiver adoption and use of electronic personal health records in chronic care: a systematic review. BMC Med Inform Decis Mak 2020 Jul 08;20(1):153 [FREE Full text] [doi: 10.1186/s12911-020-01159-1] [Medline: 32641128]
20. Walker J, Leveille S, Bell S, Chimowitz H, Dong Z, Elmore JG, et al. OpenNotes after 7 years: patient experiences with ongoing access to their clinicians' outpatient visit notes. J Med Internet Res 2019 May 06;21(5):e13876 [FREE Full text] [doi: 10.2196/13876] [Medline: 31066717]
21. Hagström J, Åhlfeldt RM, Blease C, Cajander Å, Rexhepi H, Moll J, et al. Security and privacy of online record access: a survey of adolescents' views and experiences in Sweden. J Adolesc Health 2024 Nov;75(5):730-736 [FREE Full text] [doi: 10.1016/j.jadohealth.2023.12.027] [Medline: 38349307]
22. Bärkås A, Kharko A, Åhlfeldt RM, Hägglund M. Patients' experiences of unwanted access to their online health records. Stud Health Technol Inform 2023 May 18;302:356-357. [doi: 10.3233/SHTI230138] [Medline: 37203682]
23. Damschroder LJ, Aron DC, Keith RE, Kirsh SR, Alexander JA, Lowery JC. Fostering implementation of health services research findings into practice: a consolidated framework for advancing implementation science. Implement Sci 2009 Aug 07;4:50 [FREE Full text] [doi: 10.1186/1748-5908-4-50] [Medline: 19664226]
24. Eklund B, Joustra-Enquist I. Sustains--direct access for the patient to the medical record over the Internet. Stud Health Technol Inform 2004;100:182-189. [Medline: 15718578]
25. Hägglund M, Scandurra I. Patients' online access to electronic health records: current status and experiences from the implementation in Sweden. Stud Health Technol Inform 2017;245:723-727. [Medline: 29295193]
26. Hagström J, Scandurra I, Moll J, Blease C, Haage B, Hörhammer I, et al. Minor and parental access to electronic health records: differences across four countries. Stud Health Technol Inform 2022 May 25;294:495-499. [doi: 10.3233/SHTI220508] [Medline: 35612129]
27. Bärkås A, Scandurra I, Rexhepi H, Blease C, Cajander Å, Hägglund M. Patients' access to their psychiatric notes: current policies and practices in Sweden. Int J Environ Res Public Health 2021 Aug 30;18(17):9140 [FREE Full text] [doi: 10.3390/ijerph18179140] [Medline: 34501730]
28. Scandurra I, Lyttkens L, Eklund B. Implications of Swedish National Regulatory Framework of the Patient Accessible Electronic Health Record. In: Hoerbst A, Hackl WO, de Keizer N, Prokosch HU, Hercigonja-Szekeres M, de Lusignan S, editors. Exploring Complexity in Health: An Interdisciplinary Systems Approach. Amsterdam, Netherlands: IOS Press; 2016:695-699.
29. Scandurra I, Pettersson M, Eklund B, Lyttkens L. Analysis of the Updated Swedish Regulatory Framework of the Patient Accessible Electronic Health Record in Relation to Usage Experience. In: Gundlapalli AV, Jaulent MC, Zhao D, editors. MEDINFO 2017: Precision Healthcare through Informatics. Amsterdam, Netherlands: IOS Press; 2017:798-802.
30. Åldersgränser i 1177- tjänster: Utredningsrapport och barnkonsekvensanalys. Inera. 2022. URL: https://www.inera.se/contentassets/522d66f534a7475baabb638ed1b0655d/utredningsrapport_inera_aldersgranser1177.pdf [accessed 2025-05-22]
31. Erlingsdottir G, Petersson L. Employees' work environment and patients' rights, conflicting responsibilities when implementing patient online access to their EHR. Lund University. 2016. URL: https://lup.lub.lu.se/search/publication/623726ac-ab4d-4625-b758-88ecae6fb475 [accessed 2025-05-22]

XSL•FO
RenderX

32. Wiljer D, Urowitz S, Apatu E, DeLenardo C, Eysenbach G, Harth T, Canadian Committee for Patient Accessible Health Records. Patient accessible electronic health records: exploring recommendations for successful implementation strategies. J Med Internet Res 2008 Oct 31;10(4):e34 [FREE Full text] [doi: 10.2196/jmir.1061] [Medline: 18974036]
33. Rangachari P, Mushiana SS, Herbert K. A scoping review of applications of the Consolidated Framework for Implementation Research (CFIR) to telehealth service implementation initiatives. BMC Health Serv Res 2022 Nov 30;22(1):1450 [FREE Full text] [doi: 10.1186/s12913-022-08871-w] [Medline: 36447279]
34. Sweden: health system review. World Health Organization. 2012. URL: https://iris.who.int/handle/10665/330318 [accessed 2025-05-22]
35. International Health Policy Survey 2021. Vardanalys. URL: https://www.vardanalys.se/in-english/reports/international-health-policy-survey-2021 [accessed 2022-10-26]
36. 1177. URL: https://www.1177.se/ [accessed 2025-05-28]
37. 1177 journal. Inera. URL: https://www.inera.se/tjanster/alla-tjanster-a-o/1177-journal/ [accessed 2023-11-22]
38. Folkhälsokollen. URL: https://www.folkhalsokollen.se/ [accessed 2024-04-26]
39. Muli I, Scandurra I, Hägglund M. Primary healthcare professionals' improvement suggestions for the patient accessible health record. Stud Health Technol Inform 2024 Jan 25;310:489-493. [doi: 10.3233/SHTI231013] [Medline: 38269857]
40. Graneheim UH, Lindgren B, Lundman B. Methodological challenges in qualitative content analysis: A discussion paper. Nurse Educ Today 2017 Sep;56:29-34. [doi: 10.1016/j.nedt.2017.06.002] [Medline: 28651100]
41. Graneheim UH, Lundman B. Qualitative content analysis in nursing research: concepts, procedures and measures to achieve trustworthiness. Nurse Educ Today 2004 Feb;24(2):105-112. [doi: 10.1016/j.nedt.2003.10.001] [Medline: 14769454]
42. Tong A, Sainsbury P, Craig J. Consolidated criteria for reporting qualitative research (COREQ): a 32-item checklist for interviews and focus groups. Int J Qual Health Care 2007 Dec;19(6):349-357. [doi: 10.1093/intqhc/mzm042] [Medline: 17872937]
43. Vehko T, Hyppönen H, Puttonen S, Kujala S, Ketola E, Tuukkanen J, et al. Experienced time pressure and stress: electronic health records usability and information technology competence play a role. BMC Med Inform Decis Mak 2019 Aug 14;19(1):160 [FREE Full text] [doi: 10.1186/s12911-019-0891-z] [Medline: 31412859]
44. Hertzum M, Ellingsen G, Cajander Å. Implementing Large-Scale Electronic Health Records: Experiences from implementations of Epic in Denmark and Finland. Int J Med Inform 2022 Nov;167:104868. [doi: 10.1016/j.ijmedinf.2022.104868] [Medline: 36194994]
45. Hägglund M, Scandurra I. Usability of the Swedish accessible electronic health record: qualitative survey study. JMIR Hum Factors 2022 Jun 23;9(2):e37192 [FREE Full text] [doi: 10.2196/37192] [Medline: 35737444]
46. Kujala S, Simola S, Wang B, Soone H, Hagström J, Bärkås A, et al. Benchmarking usability of patient portals in Estonia, Finland, Norway, and Sweden. Int J Med Inform 2024 Jan;181:105302 [FREE Full text] [doi: 10.1016/j.ijmedinf.2023.105302] [Medline: 38011806]
47. Golay D, Salminen Karlsson M, Cajander Å. Negative emotions induced by work-related information technology use in hospital nursing. Comput Inform Nurs 2021 Aug 04;40(2):113-120 [FREE Full text] [doi: 10.1097/CIN.0000000000000800] [Medline: 34347645]
48. Wändell P, Carlsson AC, Wettermark B, Lord G, Cars T, Ljunggren G. Most common diseases diagnosed in primary care in Stockholm, Sweden, in 2011. Fam Pract 2013 Oct;30(5):506-513. [doi: 10.1093/fampra/cmt033] [Medline: 23825186]
49. Bärkås A, Kharko A, Blease C, Cajander Å, Johansen Fagerlund A, Huvila I, et al. Errors, omissions, and offenses in the health record of mental health care patients: results from a nationwide survey in Sweden. J Med Internet Res 2023 Nov 03;25:e47841 [FREE Full text] [doi: 10.2196/47841] [Medline: 37921861]
50. Valeur HS, Lie AK, Moen K. Patient rationales against the use of patient-accessible electronic health records: qualitative study. J Med Internet Res 2021 May 28;23(5):e24090 [FREE Full text] [doi: 10.2196/24090] [Medline: 34047711]
51. Kujala S, Hörhammer I, Väyrynen A, Holmroos M, Nättiaho-Rönnholm M, Hägglund M, et al. Patients' experiences of web-based access to electronic health records in Finland: cross-sectional survey. J Med Internet Res 2022 Jun 06;24(6):e37438 [FREE Full text] [doi: 10.2196/37438] [Medline: 35666563]
52. Zanaboni P, Kummervold PE, Sørensen T, Johansen MA. Patient use and experience with online access to electronic health records in Norway: results from an online survey. J Med Internet Res 2020 Feb 07;22(2):e16144 [FREE Full text] [doi: 10.2196/16144] [Medline: 32031538]
53. Zanaboni P, Kristiansen E, Lintvedt O, Wynn R, Johansen MA, Sørensen T, et al. Impact on patient-provider relationship and documentation practices when mental health patients access their electronic health records online: a qualitative study among health professionals in an outpatient setting. BMC Psychiatry 2022 Jul 28;22(1):508 [FREE Full text] [doi: 10.1186/s12888-022-04123-7] [Medline: 35902841]
54. Moll J, Cajander Å. On patient accessible electronic health records and the experienced effect on the work environment of nurses. Stud Health Technol Inform 2020 Jun 16;270:1021-1025. [doi: 10.3233/SHTI200316] [Medline: 32570536]
55. Kristiansen E, Johansen M, Zanaboni P. Healthcare personnels' experience with patients' online access to electronic health records. 2019 Presented at: 17th Scandinavian Conference on Health Informatics; November 12-13, 2019; Oslo, Norway URL: https://ep.liu.se/ecp/161/016/ecp19161016.pdf

XSL•FO
RenderX

56. Scandurra I, Jansson A, Forsberg-Fransson M, Ålander T. Is ‘patient's online access to health records’ a good reform? – Opinions from Swedish healthcare professionals differ. Procedia Computer Science 2015;64:964-968. [doi: 10.1016/j.procs.2015.08.614]
57. Jonnergård K, Petersson L, Erlingsdóttir G. Communicating the implementation of open notes to health care professionals: mixed methods study. JMIR Med Inform 2021 Aug 16;9(8):e22391 [FREE Full text] [doi: 10.2196/22391] [Medline: 34398794]
58. Petersson L, Erlingsdottir G. Communicating to employees the implementation of patient online access to their EHR. The case of adult psychiatry in Southern Sweden. 2016 Presented at: 14th Scandinavian Conference on Health Informatics; April 6-7, 2016; Gothenburg, Sweden URL: https://ep.liu.se/ecp/122/002/ecp16122002.pdf
59. Denneson LM, Pisciotta M, Hooker ER, Trevino A, Dobscha SK. Impacts of a web-based educational program for veterans who read their mental health notes online. J Am Med Inform Assoc 2019 Jan 01;26(1):3-8 [FREE Full text] [doi: 10.1093/jamia/ocy134] [Medline: 30445648]
60. Meier-Diedrich E, Lyckblad C, Davidge G, Hägglund M, Kharko A, McMillan B, et al. Impact of patient online record access on documentation: scoping review. J Med Internet Res 2025 Feb 20;27:e64762 [FREE Full text] [doi: 10.2196/64762] [Medline: 39977853]

Abbreviations

CFIR: Consolidated Framework for Implementation Research
EHR: electronic health record
GP: general practitioner
HCP: health care professional
ORA: online record access
PAEHR: patient-accessible electronic health record
PCC: primary care center

Edited by A Benis; submitted 01.08.24; peer-reviewed by H Shah, Y Chu; comments to author 29.11.24; revised version received 28.02.25; accepted 18.05.25; published 06.06.25.

Please cite as:
Muli I, Cajander Å, Scandurra I, Hägglund M
Health Care Professionals' Perspectives on Implementing Patient-Accessible Electronic Health Records in Primary Care: Qualitative Study
JMIR Med Inform 2025;13:e64982
URL: https://medinform.jmir.org/2025/1/e64982
doi:10.2196/64982
PMID:40478617

©Irene Muli, Åsa Cajander, Isabella Scandurra, Maria Hägglund. Originally published in JMIR Medical Informatics (https://medinform.jmir.org), 06.06.2025. This is an open-access article distributed under the terms of the Creative Commons Attribution License (https://creativecommons.org/licenses/by/4.0/), which permits unrestricted use, distribution, and reproduction in any medium, provided the original work, first published in JMIR Medical Informatics, is properly cited. The complete bibliographic information, a link to the original publication on https://medinform.jmir.org/, as well as this copyright and license information must be included.

XSL•FO
RenderX

Ensuring General Data Protection Regulation Compliance and Security in a Clinical Data Warehouse From a University Hospital: Implementation Study

Christine Riou[1], MD; Mohamed El Azzouzi[2], ME; Anne Hespel[1], PhD; Emeric Guillou[1], MEng; Gouenou Coatrieux[3], PhD; Marc Cuggia[2], MD, PhD

[1]University Hospital of Rennes, 2 rue Henri Le Guilloux, Rennes, France

[2]DOMASIA, LTSI, UMR INSERM, University of Rennes, Rennes, France

[3]IMT Atlantique Bretagne Pays de Loire, Brest, France

Corresponding Author:
Christine Riou, MD
University Hospital of Rennes, 2 rue Henri Le Guilloux, Rennes, France

Abstract

Background: The European Union's General Data Protection Regulation (GDPR) has profoundly influenced health data management, with significant implications for clinical data warehouses (CDWs). In 2021, France pioneered a national framework for GDPR-compliant CDW implementation, established by its data protection authority (Commission Nationale de l'Informatique et des Libertés). This framework provides detailed guidelines for health care institutions, offering a unique opportunity to assess practical GDPR implementation in health data management.

Objective: This study evaluates the real-world applicability of France's CDW framework through its implementation at a major university hospital. It identifies practical challenges for its implementation by health institutions and proposes adaptations relevant to regulatory authorities in order to facilitate research in secondary use data domains.

Methods: A systematic assessment was conducted in May 2023 at the University Hospital of Rennes, which manages data for over 2 million patients through the eHOP CDW system. The evaluation examined 116 criteria across 13 categories using a dual-assessment approach validated by information security and data protection officers. Compliance was rated as met, unmet, or not applicable, with criteria classified as software-related (n=25) or institution-related (n=91).

Results: Software-related criteria showed 60% (n=15) compliance, with 28% (n=7) noncompliant or partially compliant and 12% (n=3) not applicable. Institution-related criteria achieved 72% (n=28) compliance for security requirements. Key challenges included managing genetic data, implementing automated archiving, and controlling data exports. The findings revealed effective privacy protection measures but also highlighted areas requiring regulatory adjustments to better support research.

Conclusions: This first empirical assessment of a national CDW compliance framework offers valuable insights for health care institutions implementing GDPR requirements. While the framework establishes robust privacy protections, certain provisions may overly constrain research activities. The study identifies opportunities for framework evolution, balancing data protection with research imperatives.

(JMIR Med Inform 2025;13:e63754) doi:10.2196/63754

KEYWORDS

clinical data warehouse; privacy; personal data protection; legislation; security; compliance; personal data; applicability; experiential analysis; university hospitals; French; France; data hub; operational challenge

Introduction

Health data, once primarily recorded on paper, are now predominantly digital worldwide. The rise of artificial intelligence (AI) methods has amplified the value of these digital data across academic and industrial sectors globally. Countries around the world, including France, the United Kingdom, Germany, and the United States, are implementing strategies to structure, secure, and ethically process these data. For instance, the United Kingdom's NHS Digital and Germany's medical data initiatives are designed to centralize and facilitate data sharing, thereby stimulating research and innovation, particularly in AI algorithm development [1-3].

In the European Union, the European Health Data Space (EHDS) initiative aims to create a unified framework for health data access and exchange across member states. The EHDS will empower individuals by giving them greater control over their electronic personal health data and will support the reuse of

XSL•FO
RenderX

these data for research, innovation, and policy-making, fostering a genuine single market for electronic health record systems and AI-based health technologies [4,5].

Similarly, France's Health Data Hub centralizes health data to promote research and innovation, emphasizing the critical role played by clinical data warehouses (CDWs), particularly those within hospitals. These CDWs compile data generated during care for reuse, which is essential for achieving the ambitious goals set by these data strategies [6,7]. This approach is encouraged by public authorities, as evidenced by specific calls for projects in 2022 and 2023 [8]. The national ambition is to have large datasets to support extensive research projects. The University Hospital of Rennes, with its eHOP CDW [9], is a pioneer and has extended its use to other institutions [10].

However, these data, as personally identifiable information (PII), are subject to strict regulations, including the General Data Protection Regulation (GDPR) [11] and the French Data Protection Act (Loi Informatique et Libertés) [12]. Additionally, in 2021, the French data protection authority (Commission Nationale de l'Informatique et des Libertés; CNIL) published a specific framework for the processing of PII in the creation of CDWs [13], referred to as the CDW framework in this paper. While this regulatory framework ensures data security, it is also cumbersome to implement. Compliance with these stringent regulations is both a prerequisite and a necessity, but it poses significant challenges in practical application.

The aim of the GDPR is to protect citizens' privacy in the context of widespread digitization while facilitating the circulation of data. It emphasizes transparency in processing health data and enhances patients' control over their use, which are widely regarded as positive steps. However, the recent literature underscores several challenges in applying GDPR to the reuse of health data for research. It is often perceived as a barrier to data sharing due to burdensome administrative procedures [14-16] and strict requirements for preventing reidentification of individuals [15]. Moreover, discrepancies in interpretation among European Union member states lead to inconsistencies between national regulations, particularly in balancing privacy and solidarity [14,17]. Such disparities complicate the coordination of international research projects [14-18]. A survey conducted across 28 European countries found a slight preference among patients for direct control over their data rather than delegation to a scientific authority [18].

Proposals for implementing CDWs with privacy and security measures by design have been advanced in Ireland [19]. These include deidentification processes, stringent access controls, safeguards against cyberattacks, regulatory compliance, and governance structures defining authorized users and use parameters. However, these proposals remain theoretical and lack national-level recommendations. In France, the implementation of CDWs must align with the CNIL CDW framework, which sets rigorous standards to ensure GDPR compliance while enabling the seamless reuse of health data in a competitive environment.

To date, no other country has established comprehensive guidelines for CDW implementation, nor has any published an evaluation of the practical application of such measures. This paper addresses this gap by sharing insights from the deployment of the eHOP CDW in university hospitals (Centre Hospitalier Universitaire) across Western France.

The objective of this study is to assess the applicability of this pioneering framework. The evaluation criterion is the level of compliance of the eHOP CDW with the CNIL CDW framework. For requirements where compliance proves challenging, we propose adjustments for consideration by national authorities. This paper first outlines the defining features of CDWs and the regulatory requirements stemming from GDPR and the French Data Protection Act. It then introduces the CNIL CDW framework and the methodology for compliance assessment. Finally, we discuss the applicability of certain requirements in light of research challenges and propose alternative measures to facilitate the implementation of CDWs in health care institutions.

Methods

Ethical Considerations

The research reported in the paper was not a study on human participants, and no treatment of personal data was carried out during the research. The European GDPR does not apply to this research. The eHOP data warehouse was authorized by the French data protection authority (CNIL). Deliberation 2020-028 of February 27, 2020, authorized the University Hospital of Rennes to implement personal data processing for the purpose of a health data warehouse called "eHOP Rennes," ensuring respect of patients' information and rights.

Clinical Data Warehouses

A CDW is a repository of large health data already collected elsewhere, consolidated into a single database for reuse in various treatments whose purposes are not known in advance and differ from the initial purpose of collection. These data are stored for a long period.

The hospital CDW centralizes all health data from patients who visited the institution by extracting information from the hospital information system. The CDW is based on a robust technical architecture and an adapted data model, ensuring the reliability and relevance of the stored information. Before any use, the data undergo integration steps including pseudonymization, standardization, and validation.

To exploit the CDW, it is equipped with secure tools for targeting study populations, multicriteria queries, and data visualization. For each study, specific datasets called datamarts are generated.

Each CDW operates under a robust governance structure and strict access policies to ensure the security and ethical use of health data. In this study, we examine the eHOP CDW as a representative example. The development and implementation of eHOP CDW are the results of a collaborative effort between the University Hospital of Rennes, Institut National de la Santé et de la Recherche Médicale UMR 1099, and Enovacom, a subsidiary of the company Orange Healthcare, which specializes in digital health care solutions.

XSL•FO
RenderX

The deployment and maintenance of the eHOP CDW are managed by a dedicated team within each hospital. This multidisciplinary team comprises medical IT specialists, IT engineers, data scientists, and a data protection officer (DPO), ensuring compliance with data protection regulations and operational effectiveness. As of December 2024, the eHOP CDW at the University Hospital of Rennes holds health information on 2 million patients, represented across 167 million documents and including 1.3 billion data elements.

Current Regulations

The GDPR governs the processing of personal data belonging to European citizens. Adopted in 2016, it replaced European Directive 95/46/EC [20] to address the challenges posed by emerging digital technologies. While directly applicable in all European Union member states, the regulation allows some flexibility for the introduction of supplementary national provisions. Citizens' rights have been strengthened, particularly in terms of information and transparency regarding the processing of their personal data. New rights have also been introduced, such as the right to be forgotten (also referred to as the right to erasure).

The GDPR introduces key concepts such as "accountability" and "privacy by design," aimed at increasing the accountability of stakeholders and ensuring that privacy is considered from the earliest stages of data processing operations. It also requires data controllers to conduct a Data Protection Impact Assessment for high-risk processing operations. The regulation is built on 6 fundamental principles: lawfulness and transparency, explicit and legitimate purposes, data minimization (proportionality), storage period limitation, accuracy, and security—particularly confidentiality and integrity during data processing.

The French Data Protection Act (Loi Informatique et Libertés) has been amended to align with the GDPR and introduces specific provisions for processing health data, particularly in the context of research, study, or evaluation in the health field [21]. To simplify procedures, it includes reference methodologies such as MR004, which applies to studies not involving human participants [22]. It also provides reference frameworks for data controllers, offering them legal certainty in their operations. Additionally, the French National Commission for Data Protection and Liberties (CNIL) has issued guidelines for the creation and management of health data warehouses.

These guidelines define the legal and technical framework applicable to CDWs, establishing a trusted environment for the reuse of health data. They specify authorized purposes, governance principles, data categories to be processed, required security measures, and conditions for the use of CDW data in health-related research [23].

In 2022, the CNIL enhanced its recommendations by publishing a compliance checklist [24], which includes 116 criteria addressing 108 requirements. These criteria are grouped into 13 categories, with a particular focus on security and patient rights. Specifically, 56 (48.3%) criteria, representing nearly half, pertain to security measures, while 23 (19.8%) criteria focus on patient information and rights.

Evaluation Process

Once the CDW framework was published, an exchange was initiated between institutions and the CNIL to clarify the measures required for compliance with the framework's specifications. This process aimed to minimize the risk of misinterpretation.

In May 2023, we conducted an evaluation of the CDC's compliance at the University Hospital of Rennes with the CNIL framework. The framework's requirements were categorized into 2 groups: those related to the eHOP software and those pertaining to the health institution's implementation processes. Each criterion in the compliance checklist was assessed using 1 of 3 possible values: true, false, or not applicable. A criterion was deemed not applicable if the functionality addressed by the criterion was not present in the eHOP software (eg, manual CDW feeding). A criterion was marked true if appropriate measures were implemented to meet the requirement; otherwise, it was marked false.

The value assigned to each criterion was determined by consensus between 2 assessors. For criteria where consensus could not be reached, the information security officer (ISO) and the DPO of the University Hospital of Rennes reviewed the assessment. Their input provided the definitive evaluation for those criteria. Once all criteria were assessed, final validation was conducted by both the ISO and the DPO.

This approach enabled the identification of discrepancies with the CDW framework and the determination of the overall compliance level of the CDW. Results were presented by category and expressed as the number and percentage of criteria that were not applicable, met, or not met. The overall compliance level was calculated based on all applicable criteria.

Results

Evaluation of Criteria Relevant to the eHOP Software

Overview

Of the 116 criteria in the CDW framework, 25 were identified as relevant to the eHOP software (Tables 1 and 2), representing 22% (n=25) of the criteria. Compliance with the framework was 68% (n=15).

The results are presented in Table 2. In total, 3 of these 25 (12%) criteria were deemed not applicable to our implementation context. A total of 15 (60%) criteria were judged compliant, such as those concerning the storage of directly identifiable data in a separate space and those concerning user profiles, and 7 (28%) criteria were considered noncompliant or partially compliant and were subject to an action plan.

XSL•FO
RenderX

Table . Criteria from the clinical data warehouse framework.

Category	Criteria, n	Application eHOP, n	Institution, n
1. Target audience	1	0	1
2. Purpose	3	0	3
3. Governance	4	0	4
4. Legal basis for processing	1	0	1
5. Personal data included	12	1	11
6. Access to information	4	1	3
7. Retention period	4	4	0
8. Information for individuals—Patients	15	0	15
9.1. Information for individuals—Professionals	2	0	2
9.2. Rights of individuals	6	2	4
10. Security	56	17	39
11. Subcontractor	5	0	5
12. Transfer outside the European Union	1	0	1
13. Privacy impact assessment	2	0	2
Total	116	25	91

XSL•FO
RenderX

Table . Compliance of criteria relevant to eHOP software on May 5, 2023.

Number	Criterion	Compliance
5.2.1.1	Directly identifiable data mentioned in 5.2.1.1 are stored separately from other data	Yes
6.2	Access and use of identifiable data restricted to authorized persons for patient recontact and rights exercise	Yes
7.1 to 7.3	Data retention periods	No
7.4	Deletion or anonymization of data beyond the retention period	No
9.6	Rights of individuals: mechanism when there are no identifiable data or correspondence tables	N/A[a]
9.7	Exercise of the right to object possible permanently	Yes
10. Security		
SEC-LOG-5	Separation of profiles for access to identifiable and pseudonymized data	Yes
SEC-LOG-6.1	Separate encryption for genetic data and location data from other data	No
SEC-LOG-6.2	Encryption key for genetic data and location data accessible only by a data manager profile	No
SEC-ALI-2	Strong authentication for manual feeding of the clinical data warehouse from data entry software	N/A
SEC-PSE-1.1 to SEC-PSE-1.4	Pseudonymization of patients' personal data	Yes
SEC-PSE-2	New pseudonymization of already pseudonymized data	Yes
SEC-PSE-3	Pseudonymization of personal data collected from health care professionals	N/A
SEC-PSE-4	Deidentification of unstructured documents	Partially
SEC-HAB-1	Different authorization profiles are provided to manage access to data as needed and exclusively	Yes
SEC-HAB-2	Granularity of access (aggregated data, pseudonymized data, directly identifiable data)	Yes
SEC-ESP-2.1	Data minimization in study datamarts	Yes
SEC-ESP-2.2	Random generation of pseudonyms for each study	Yes
SEC-ESP-3	For cohort follow-up, the same unique pseudonym can be reused across multiple workspaces	Yes
SC-JOU-1	User action logging	Yes

[a]N/A: not applicable.

Nonapplicable Criteria

The nonapplicable criteria were as follows:

- Criterion 9.6: Linkage tables enabling patient reidentification eliminate the need for additional mechanisms to respect rights. In the absence of these tables, the warehouse could be queried based on information provided by a patient to respond to their rights requests.
- Criterion 10 SEC-ALI-2: The absence of a manual feeding modality for the CDW means that no specific authentication mechanism is implemented.
- Criterion SEC-PSE-3: No PII concerning health care professionals is collected in a structured form.

Compliant Criteria

The eHOP CDW database is divided into multiple segregated databases, ensuring that identifying data are stored separately from medical data, in compliance with requirement 5.2.1.1 of the framework

Access rights management is based on several predefined profiles, categorized as manager and user profiles, in alignment with SEC-HAB-1 and SEC-HAB-2 requirements. The data

XSL•FO
RenderX

manager profile is responsible for managing data flows from the hospital information system's source software to the CDW, integrating data, and ensuring database quality. The study manager profile allows for the creation of datamarts for specific studies without initially including any data and manages access rights. This profile has no direct access to the CDW data. The datamart manager profile enables querying the entire CDW, except for identifying data. This user populates the datamart with query results and ensures compliance with the SEC-ESP-2.1 minimization principle by selecting only the categories of documents and information strictly necessary for the study.

User profiles are divided into 3 levels with varying access permissions. They access only data of the study datamart. Level 1 users are limited to accessing aggregated statistics; they can query the database and retrieve aggregated results but cannot view individual patient information. Level 2 users inherit level 1 permissions and can access pseudonymized documents and individual data. Level 3 users are granted access to identifying data only under exceptional circumstances, such as for pharmacovigilance professionals performing regulatory tasks. A specialized recontact manager profile has been created to meet requirements 6.2 and SEC-LOG-5. This profile allows access to a datamart's patient list for recontact purposes. Authorized individuals with this profile cannot directly access identifying data but can activate the patient list generation function for specific studies.

The exercise of data participants' rights is governed by institutional procedures and facilitated by a dedicated module within the eHOP CDW for managing opposition. The Medical Information Department centrally collects opposition data, which is recorded in the patient-identifying database. Rather than maintaining a "blacklist," the system automatically excludes data from patients who have expressed opposition during the creation of datamarts, in compliance with paragraph 9.6 of the CDW framework.

Pseudonymization is performed during data integration into the CDW using a collision-free function that generates 20-byte random identifiers for patients, hospital stays, and documents. Correspondence with hospital information system identifiers is securely stored in a protected area. For each study, new pseudonyms are generated, and their correspondence with CDW identifiers is stored separately from the datamarts. All datamarts within a study share the same pseudonyms, ensuring compliance with SEC-PSE-1, SEC-PSE-2, SEC-ESP-2, and SEC-ESP-3 requirements.

Deidentification of unstructured documents is an area of ongoing improvement. Patient data deidentification has been effective since the warehouse's inception, while health care professionals' data are deidentified using external public databases. However, current processing times are incompatible with real-time integration of medical documents. As a result, health care professionals' data are deidentified only in datamarts. A new algorithm, developed using machine learning methods, shows promising performance, with *F* scores ranging from 0.96 to 0.99 in initial evaluations. Its integration into the CDW would enable full compliance with the SEC-PSE-4 requirement. Access traceability is ensured through a robust logging system, with all access logs securely maintained.

Partially Compliant Criterion

The partially compliant criterion was as follows:

- Criterion SEC-PSE-4: The pseudonymization of health care professionals' data in unstructured documents was not fully deployed due to incompatible processing times with real-time data integration into the CDW. However, this procedure is applied to study datamarts before making them available to users. A solution has been provided since May 2023.

Noncompliant Criteria

The noncompliant criteria were as follows:

- Criteria 7.1 to 7.3: Data retention periods are not yet managed in the eHOP software.
- Criteria SEC-LOG-6.1 and SEC-LOG-6.2: Implementing the functionality for encrypting and decrypting genetic data proves complex during analysis, as it requires a specific technical procedure and adapted organizational measures.

Evaluation of Criteria Relevant to Institutions

Overview

Among the 116 criteria outlined in the CDW framework, 91 (78%) are under the direct responsibility of health care institutions. These criteria encompass a range of domains, including governance, patient information, individuals' rights, and data security.

CDW Governance

Each institution is responsible for implementing the governance of its CDW. For instance, the University Hospital of Rennes has established governance structures such as the steering committee (comité de pilotage) and the scientific and ethical council (conseil scientifique et éthique [CSE]). The comité de pilotage determines scientific and ethical orientations and connects with other institutional bodies. The CSE provides opinions on projects requiring the use of CDW data.

Patient Information

The University Hospital of Rennes provides general, individual, and collective information regarding the reuse of care data for research and the implementation of the CDW through systematic notes given to patients upon their visit, posters, the welcome booklet, and the institution's website. Additionally, the University Hospital of Rennes has collectively informed the public through press releases and awareness campaigns.

For each study based on the CDW, a note complying with Article 14 of the GDPR is posted on the institution's website. For patients not informed about the reuse of their data and who have not revisited the institution since the CDW activation, a request for derogation from individual information was submitted to the CNIL. This derogation is required for studies involving large volumes of data where individual information is too complex and resource-intensive to implement.

XSL•FO
RenderX

Patient Rights

A procedure is in place to allow patients to exercise their rights. The health institution responsible for processing provides the patient with a contact point mentioned in the information note, usually the DPO. Existing procedures adopted by the institution to allow patients to exercise their rights of access and rectification of their health data are applied.

The exercise of the right to erasure (right to be forgotten) and the right to object is managed by a specific software module for managing oppositions. Once the opposition is registered, the data are flagged in the system, ensuring that they are not used in future studies. The right to erasure is treated similarly to the right to object. Patients can exercise these rights at any time.

For studies using the CDW, correspondence tables have been created to link patients' identity data with respective studies. Thus, any unexercised right to opposition can still be applied, provided it does not compromise the study's objectives under Article 21 of the GDPR. These guidelines regarding patient information and rights have been communicated to other institutions.

Security

Security requirements account for nearly half of the criteria outlined in the CDW framework. Of these, only 17 criteria are directly related to the eHOP software. For the remaining criteria, the responsibility for implementing the necessary measures to ensure compliance lies with the institution. As of May 5, 2023, 28 (72%) security criteria were deemed compliant, 3 (8%) were considered nonapplicable, and 8 (20%) were found to be noncompliant (Table 3). The overall compliance rate for security requirements stands at 77%.

Table . Criteria relevant to the institution's information system evaluated as nonapplicable or noncompliant on May 5, 2023.

Number	Criterion	Compliance
SEC-EXP-4	Anonymous reporting of management indicators according to G29 criteria; otherwise, a reidentification risk analysis.	N/A[a]
SEC-EXP-5	Monitoring of indicator exports.	N/A
SEC-SEN-3.2	Agreement established if workstations are not under the responsibility of the controller.	N/A
SEC-ESP-1	Warehouse data are handled by researchers only in internal workspaces dedicated to each research project, isolated from the warehouse database and each other.	Partially
SEC-AUT-1.1	Access to personal data requires strong multifactor authentication.	No
SEC-AUT-2	Strong authentication for internal and external access.	No
SEC-EXP-1	Data exports outside the CDW or workspaces only if anonymized according to G29 criteria. This conformity must be documented. Otherwise, a reidentification risk analysis must be conducted and documented.	No
SEC-EXP-3.1	Exports are monitored automatically or manually by a specialized operator to verify anonymity.	No
SEC-EXP-3.2	If monitoring is automatic, noncompliant exports are flagged, quarantined, and manually verified by a trained and authorized individual.	No
SEC-JOU-2	System and network administrator access requires strong authentication and detailed access traceability, for example, using an admin bastion.	No
SEC-JOU-3	Regular control of logs, at least bimonthly, and at the end of each authorization period by an automatic monitoring solution with alert processing by an authorized operator or semiautomatic control with a manual review of abnormal logs.	No

[a]N/A: not applicable.

Nonapplicable Criteria

The nonapplicable criteria were as follows:

- Criteria SEC-EXP-4 and SEC-EXP-5: As of now, there are no dashboards for monitoring accessible from the CDW implemented at the University Hospital of Rennes.

XSL•FO
RenderX

- Criterion SEC-SEN-3.2: Workstations allowing access to the CDW at the University Hospital of Rennes are under the institution's responsibility.

Partially Compliant Criterion

The partially compliant criterion was as follows:

- Criterion SEC-ESP-1: Considered partially compliant, this criterion is verified for data exploitation via the eHOP interface. Each datamart is isolated, and analyses are conducted on a secure server with controlled access. To fully comply, digital workspaces specific to each study with necessary processing and analysis tools need to be implemented for datamart exploitation.

Noncompliant Criteria

The noncompliant criteria were as follows:

- Criteria SEC-AUT-1.1 and SEC-AUT-2: Strong authentication was implemented in October 2023 after evaluation. This authentication concerns internal access within the institution. No external access is planned.
- Criterion SEC-EXP-1: Most studies result in publication; thus, users commit to publishing only anonymized data. They must verify the anonymity of exported results. The action plan includes revising the CDW use charter to specify this point and drafting a best practice guide for ensuring anonymity. The CSE will also verify that study protocols detail the content of the results.
- Criteria SEC-EXP-3.1 and SEC-EXP-3.2: Individual data exports are performed by CDW experts. Currently, only CDW experts conduct analyses within the CDW environment. Users commit to exporting only anonymized data.
- Criterion SEC-JOU-2: Compliance is planned.
- Criterion SEC-JOU-3: Specific alerts for the CDW have been configured since May 2023. Tools implemented by the institution, in accordance with its security policy, cover the CDW environment.

Discussion

Principal Findings

The framework, which is aligned with the GDPR, necessitates substantial technological and organizational adaptations to ensure compliance. Our findings highlight both the benefits and challenges associated with its implementation, offering a comprehensive perspective on its impact on CDWs.

In this discussion, we explore the study's contributions and limitations along with the areas for improvement identified within the CDW framework. Finally, we propose measures to facilitate research projects using CDW data. These recommendations could guide regulatory authorities in future framework developments.

Contributions and Limitations of the Study

This study is the first to evaluate the application of the CDW framework in a real-world setting within French university hospitals. The results were obtained through a rigorous evaluation process, involving dual assessments and consensus-building for all criteria. The findings were further validated by the ISO and the DPO of the University Hospital of Rennes. The proposed adjustments are grounded in practical and actionable solutions.

Our findings provide institutions with concrete insights into the challenges they face, the steps they can take to address these challenges, and potential regulatory adjustments. National authorities gain valuable field-based feedback and specific recommendations for refining the framework. Moreover, the compliance checklist proves to be an effective tool for monitoring privacy measures and could support future labeling or certification processes for CDWs.

However, the study has certain limitations. It focuses on a single institution in the French Great Western region and a single CDW technology. To generalize these findings, further studies involving diverse institutions and CDW solutions are necessary. Such studies would help uncover additional enablers and barriers to the application of the framework's criteria.

In terms of methodology, we initially considered using a validated evaluation grid to assess the applicability of the CNIL framework. However, this approach was not adopted due to its potential for introducing bias. The CNIL framework was published after the CDW's implementation, and a prior consultation phase with the CNIL had already defined the necessary compliance measures. Consequently, applying a retrospective evaluation grid would have been inconsistent with the timeline of the framework's release. Instead, we opted for a descriptive approach, which effectively highlights barriers to compliance and enables the proposal of tailored, practical alternatives.

Weaknesses of the Framework and Proposed Adjustments

Using CDW data for research requires balancing the advancement of scientific knowledge to improve patient care with the imperative to protect patient privacy. The framework imposes stringent data protection requirements, which, while essential, can hinder research efforts due to their complexity and associated costs. Our study has identified several key obstacles to the optimal use of CDW data for research purposes.

To address these challenges, regulatory adaptations could help streamline the implementation of research projects. We propose adjustments to the framework that aim to facilitate the efficient and compliant conduct of research studies and projects.

Regarding Data Categories

Vital Status and Date of Death

The framework permits the collection of this information solely from medical records, which limits the CDW to recording only hospital deaths. However, the French National Institute of Statistics and Economic Studies provides a comprehensive database of deceased individuals. Several matching algorithms have been developed to use these data effectively [25-28]. Integrating French National Institute of Statistics and Economic Studies data into the CDW could address this limitation, particularly as these data are publicly available and the matching algorithms have demonstrated satisfactory performance.

XSL•FO
RenderX

Genetic Data

According to the CNIL, variants and mutations are classified as genetic data. The CDW framework mandates their specific encryption, which complicates their reuse despite their critical importance for personalized medicine. These data often appear in diverse document types, such as genetic reports or hospitalization records, making them challenging to isolate. We recommend limiting this encryption requirement to sequencing data exclusively, as this would simplify their management and reuse while maintaining compliance with the framework.

Regarding Security Requirements

Some of the framework's security requirements are already part of hospitals' cybersecurity plans (eg, network flow segmentation, user awareness, alert setup, incident handling, and access review) [29,30]. Thus, the increasing investment of institutions in their cybersecurity should allow compliance, provided that substantial financial support is provided.

Pseudonymization is a major framework measure ensuring data confidentiality. However, this procedure does not ease regulatory steps, as pseudonymized data cannot be considered anonymous according to the European Data Protection Board [31]. Some authors argue that medical data anonymization is almost impossible [32,33], and the recommended anonymization methods are complex to implement [33]. Moreover, anonymity leads to information loss, potentially making an AI model less relevant. Greene et al [34] propose evaluating anonymity case-by-case, considering contextual factors, especially other data sources available to the user that may link back to the patient's identity. A reidentification risk analysis, as proposed by the Health Data Hub [35], could be conducted for CDW studies by the implementation manager. If the reidentification risk is deemed minimal for a study, individual patient information could be considered nonmandatory.

The framework stipulates that only anonymized data exports are permitted. However, in research using multisource data, pseudonymized individual data exports to secure data processing platforms should be possible. The crucial point is that this environment meets security requirements. We recommend explicitly stating this possibility in the framework.

Verifying study results exported from the CDW or its workspace in aggregate form by a specialized operator seems excessive for a health care institution. Researchers' commitment to ensuring anonymity should suffice for compliance. However, they should be supported with a best practice guide on result anonymization.

Trace control by institutions can be performed through automated control systems implemented as part of their cybersecurity plans. Integrating CDW traces into such systems is feasible, but exploiting these traces by a dedicated human operator capable of handling alerts requires additional resources that most institutions currently lack.

Architecture Schematics

Sample architecture diagrams of the "information system" for the CDW, including workspaces, should be included in the framework. These examples would help institutions build their CDWs in line with CNIL expectations.

Patient Information and Rights Exercise

MR004 refers to a French reference methodology for health data research that does not involve human participants. The MR004 facilitated research project implementation by waiving new individual information for each study when initial information on data reuse for research was provided to the patient, provided a transparency portal is implemented by the institution. However, initial information on CDW implementation can be challenging to deliver in practice within hospitals. One communication means to consider is the "Mon Espace Santé" platform [36], available to all citizens since February 2022. "Mon Espace Santé" is a French digital health platform where individuals can access their health data and manage their health information. Patient information could leverage this platform, similar to how organ donation opposition is integrated into the personal health record (dossier médical partagé) [37]. However, a survey by France Assos Santé, a French patient association, found that less than 50% of the population has activated their health space [38].

Public information campaigns at national, regional, and local levels would reach most of the population [39]. Collective information through a transparency portal could then replace individual study information [39].

Exercise of Rights in CDW Studies

Current procedures allow patients to exercise their rights over integrated CDW data. However, the right to opposition and erasure for CDW studies raises questions. Once data are being analyzed, removing them seems challenging without compromising the project.

Dynamic consent and meta-consent mechanisms should be considered. Dynamic consent [40], based on transparency, allows patients to consent to each study via a dedicated platform. However, this may lead to digital divide risk and frequent patient solicitations, which could harm system acceptance, leading to default responses (consent or refusal) unrelated to the study [41].

Meta-consent [41,42] could be a more interesting solution. It involves giving prior consent to study categories based on the data nature (medical records, genomic data, etc) and research context (public or private, commercial or noncommercial, and national or international). A study by Cumyn et al [42] on meta-consent acceptability shows that the public and national nature of the processing entity, nonidentifying data, and the absence of genetic data use are factors favoring patient acceptance.

Conclusions

This study represents the first effort to evaluate the application of the CNIL CDW framework within a real-world operational context, emphasizing its alignment with GDPR requirements. While the framework significantly enhances data security and compliance, its implementation poses practical challenges and requires substantial resources. Despite the study being limited to a single institution in France, the findings are broadly

XSL•FO
RenderX

relevant, given the GDPR's overarching influence in Europe and beyond.

The insights gained from this study are particularly pertinent, as they offer valuable lessons for other European countries and international bodies aiming to implement similar frameworks. The EHDS initiative, which seeks to create a unified framework for health data access and exchange across the European Union, can benefit from the findings of this study. The challenges and proposed adjustments highlighted here can inform the development of more efficient and scalable data governance frameworks that balance the need for rigorous data protection with the imperatives of research and innovation.

Future research should focus on expanding the scope to include multiple institutions and various CDW technologies to generalize the results and identify further facilitators or barriers to the framework's application. Additionally, international collaborations could provide a broader perspective on best practices and innovative solutions for managing health data securely and effectively.

The importance of harmonizing data protection standards and facilitating secure data sharing cannot be overstated, especially in the context of global health crises like the COVID-19 pandemic. Effective data governance frameworks, such as the CDW framework evaluated in this study, are crucial for enabling the rapid and secure exchange of health data, which is essential for timely public health responses and ongoing medical research.

In summary, while the CDW framework provides a robust foundation for data security and compliance, its practical implementation requires careful consideration of the challenges identified in this study. By addressing these issues and fostering international cooperation, we can enhance the utility of health data warehouses, thereby supporting advancements in health care research and ultimately improving patient outcomes across the globe.

Acknowledgments

The authors thank the jurists and the technical experts of the French Data Protection Authority (Commission Nationale de l'Informatique et des Libertés) for their advice. The authors remain solely responsible for the results of the conformity assessment to clinical data warehouse framework and the proposals for development. This research was funded by Agence Nationale de la Recherche (grant ANR-22PESN-0006). The funding body had no role in the design of the study, the collection, analysis, and interpretation of data, or in writing the manuscript. The sponsors were not involved in the study design, data collection, analysis, and interpretation, manuscript preparation, or the decision to submit the manuscript for publication.

Authors' Contributions

CR conceptualized the study, developed the methodology, and wrote the original draft of the manuscript. MEA contributed to the data collection, analysis, and interpretation. GC, AH, and EG provided critical revisions and approved the final version of the manuscript. MC supervised the project study. All authors reviewed and approved the manuscript for publication.

Conflicts of Interest

None declared.

References

1. Cuggia M, Combes S. The French Health Data Hub and the German Medical Informatics Initiatives: two national projects to promote data sharing in healthcare. Yearb Med Inform 2019 Aug;28(1):195-202. [doi: 10.1055/s-0039-1677917] [Medline: 31419832]
2. Sheikh A, Anderson M, Albala S, et al. Health information technology and digital innovation for national learning health and care systems. Lancet Digit Health 2021 Jun;3(6):e383-e396. [doi: 10.1016/S2589-7500(21)00005-4] [Medline: 33967002]
3. National Academy of Medicine, The Learning Health System Series. In: Carman KL, Grossmann C, Zirkle M, Adams I, Siddiqi S, Ahmed M, editors. Health Data Sharing to Support Better Outcomes: Building a Foundation of Stakeholder Trust: National Academies Press (US); 2021.
4. Arrêté du 29 novembre 2019 portant approbation d'un avenant à la convention constitutive du groupement d'intérêt public "Institut national des données de santé" portant création du groupement d'intérêt public "Plateforme des données de santé" [Web page in French]. Légifrance. URL: https://www.legifrance.gouv.fr/jorf/id/JORFTEXT000039433105/ [accessed 2023-06-19]
5. Décret n° 2021-848 du 29 juin 2021 relatif au traitement de données à caractère personnel Dénommé "système national des données de santé" [Web page in French]. Légifrance. URL: https://www.legifrance.gouv.fr/jorf/id/JORFTEXT000043715694 [accessed 2023-06-19]
6. Bocquet F, Campone M, Cuggia M. The challenges of implementing comprehensive clinical data warehouses in hospitals. Int J Environ Res Public Health 2022 Jun 16;19(12):7379. [doi: 10.3390/ijerph19127379] [Medline: 35742627]
7. Entrepôts de données de santé hospitaliers en France [Web page in French]. Haute Autorité de Santé. URL: https://www.has-sante.fr/jcms/p_3386123/fr/ [accessed 2023-06-19]

XSL•FO
RenderX

8. France2030-entrepôts de données [Web page in French]. Health Data Hub. URL: https://www.health-data-hub.fr/sites/default/files/2022-03/France2030_entrep%C3%B4t%20de%20donn%C3%A9es_VF.pdf [accessed 2025-04-10]
9. Cuggia M, Garcelon N, Campillo-Gimenez B, et al. Roogle: an information retrieval engine for clinical data warehouse. Stud Health Technol Inform 2011;169:584-588. [Medline: 21893816]
10. Karakachoff M, Goronflot T, Coudol S, et al. Implementing a biomedical data warehouse from blueprint to bedside in a regional French university hospital setting: unveiling processes, overcoming challenges, and extracting clinical insight. JMIR Med Inform 2024 Jun 24;12:e50194. [doi: 10.2196/50194] [Medline: 38915177]
11. Règlement (UE) 2016/679 du parlement européen et du conseil du 27 avril 2016 relatif à la protection des personnes physiques à l'égard du traitement des données à caractère personnel et à la libre circulation de ces données, et abrogeant la directive 95/46/CE (Règlement général sur la protection des données) [Web page in French]. EUR-LEX. URL: https://eur-lex.europa.eu/legal-content/FR/TXT/PDF/?uri=CELEX:32016R0679 [accessed 2023-06-19]
12. Loi n° 78-17 du 6 janvier 1978 relative à l'informatique, aux fichiers et aux libertés modifiée [Web page in French]. Légifrance. URL: https://www.legifrance.gouv.fr/loda/id/JORFTEXT000000886460 [accessed 2023-06-19]
13. Délibération no 2021-118 du 7 octobre 2021 portant adoption D'un référentiel relatif aux traitements de données à caractère personnel mis en œuvre à des fins de création D'entrepôts de données dans le domaine de la santé [Web page in French]. CNIL (Commission nationale de l'informatique et des libertés). URL: https://www.legifrance.gouv.fr/cnil/id/CNILTEXT000044243098?init=true&page=1&query=%2A&searchField=ALL&tab_selection=cnil [accessed 2023-06-19]
14. Bak MAR, Ploem MC, Tan HL, Blom MT, Willems DL. Towards trust-based governance of health data research. Med Health Care Philos 2023 Jun;26(2):185-200. [doi: 10.1007/s11019-022-10134-8] [Medline: 36633724]
15. Vukovic J, Ivankovic D, Habl C, Dimnjakovic J. Enablers and barriers to the secondary use of health data in Europe: General Data Protection Regulation perspective. Arch Public Health 2022 Apr 9;80(1):115. [doi: 10.1186/s13690-022-00866-7] [Medline: 35397557]
16. Bernier A, Molnár-Gábor F, Knoppers BM, et al. Reconciling the biomedical data commons and the GDPR: three lessons from the EUCAN ELSI collaboratory. Eur J Hum Genet 2024 Jan;32(1):69-76. [doi: 10.1038/s41431-023-01403-y] [Medline: 37322132]
17. Gehrmann J, Herczog E, Decker S, Beyan O. What prevents us from reusing medical real-world data in research. Sci Data 2023 Jul 13;10(1):459. [doi: 10.1038/s41597-023-02361-2] [Medline: 37443164]
18. Lalova-Spinks T, Saesen R, Silva M, et al. Patients' knowledge, preferences, and perspectives about data protection and data control: an exploratory survey. Front Pharmacol 2023;14:1280173. [doi: 10.3389/fphar.2023.1280173] [Medline: 38445168]
19. Thantilage RD, Le-Khac NA, Kechadi MT. Healthcare data security and privacy in data warehouse architectures. Inform Med Unlocked 2023;39:101270. [doi: 10.1016/j.imu.2023.101270]
20. Directive 95/46/EC of the European Parliament and of the Council of 24 October 1995 on the protection of individuals with regard to the processing of personal data and on the free movement of such data. EUR-Lex. URL: https://eur-lex.europa.eu/legal-content/EN/TXT/HTML/?uri=CELEX:31995L0046 [accessed 2024-04-12]
21. Lesaulnier F. Recherche en santé et protection des données personnelles à l'heure du Règlement général relatif à la protection des données [Article in French]. Médecine Droit 2019 Oct;2019(158):103-111. [doi: 10.1016/j.meddro.2018.10.001]
22. Délibération n° 2018-155 du 3 mai 2018 portant homologation de la méthodologie de référence relative aux traitements de données à caractère personnel mis en œuvre dans le cadre des recherches n'impliquant pas la personne humaine, des études et évaluations dans le domaine de la santé (MR-004) [Web page in French]. Légifrance. URL: https://www.legifrance.gouv.fr/jorf/id/JORFTEXT000037187498#:~:text=de%20donn%C3%A9es%20...-,D%C3%A9lib%C3%A9ration%20n%C2%B0%202018%2D155%20du%203%20mai%202018%20portant,la%20sant%C3%A9%20(MR%2D004) [accessed 2023-06-19]
23. Bocquet F, Raimbourg J, Bigot F, Simmet V, Campone M, Frenel JS. Opportunities and obstacles to the development of health data warehouses in hospitals in France: the recent experience of comprehensive cancer centers. Int J Environ Res Public Health 2023 Jan 16;20(2):1645. [doi: 10.3390/ijerph20021645] [Medline: 36674399]
24. Entrepôt de données de santé: la CNIL publie une "check list" de conformité [Web page in French]. CNIL. URL: https://www.cnil.fr/fr/entrepots-de-donnees-de-sante-la-cnil-publie-une-check-list-de-conformite-son-referentiel [accessed 2023-06-19]
25. Guardiolle V, Bazoge A, Morin E, et al. Linking biomedical data warehouse records with the national mortality database in France: large-scale matching algorithm. JMIR Med Inform 2022 Nov 1;10(11):e36711. [doi: 10.2196/36711] [Medline: 36318244]
26. Lauzanne O, Frenel JS, Baziz M, Campone M, Raimbourg J, Bocquet F. Optimizing the retrieval of the vital status of cancer patients for health data warehouses by using open government data in France. Int J Environ Res Public Health 2022 Apr 2;19(7):4272. [doi: 10.3390/ijerph19074272] [Medline: 35409956]
27. Cossin S, Diouf S, Griffier R, Le Barrois d'Orgeval P, Diallo G, Jouhet V. Linkage of hospital records and death certificates by a search engine and machine learning. JAMIA Open 2021 Jan;4(1):ooab005. [doi: 10.1093/jamiaopen/ooab005] [Medline: 33709061]

XSL•FO
RenderX

28. Appariement de masse au fichier des décès [Web page in French]. Data.gouv.fr. URL: https://www.data.gouv.fr/fr/reuses/appariement-de-masse-au-fichier-des-deces [accessed 2023-06-19]
29. La cybersécurité: un enjeu majeur pour les établissements de santé [Web page in French]. Ministère de la Santé et de la Prévention. URL: https://sante.gouv.fr/systeme-de-sante/e-sante/sih/dossier-cybersecurite/article/la-cybersecurite-un-enjeu-majeur-pour-les-etablissements-de-sante [accessed 2023-06-19]
30. Les mesures prioritaires de sécurisation des systèmes d'information: référentiels à destination des établissements de santé [Web page in French]. Ministère de la Santé et de la Prévention. URL: https://sante.gouv.fr/IMG/pdf/cybersecurite_referentiel_des_mesures_prioritaires.pdf [accessed 2023-06-28]
31. Groupe de travail "Article 29" sur la protection des données avis 05/2014 sur les techniques d'anonymisation [Web page in French]. Commission Européenne. URL: https://ec.europa.eu/justice/article-29/documentation/opinion-recommendation/files/2014/wp216_fr.pdf [accessed 2023-06-19]
32. Dossier intelligence artificielle nicolas papernot il faut capturer de façon globale les enjeux de performance et de sécurité et de vie privée et d'équité [Web page in French]. CNIL. URL: https://linc.cnil.fr/nicolas-papernot-il-faut-capturer-de-facon-globale-les-enjeux-de-performance-et-de-securite-et-de [accessed 2025-04-10]
33. Artificial intelligence and privacy. Norvegian Data Protection Authority (Datatilsynet). URL: https://www.datatilsynet.no/globalassets/global/english/ai-and-privacy.pdf [accessed 2023-06-27]
34. Greene T, Shmueli G, Ray S, Fell J. Adjusting to the GDPR: the impact on data scientists and behavioral researchers. Big Data 2019 Sep;7(3):140-162. [doi: 10.1089/big.2018.0176] [Medline: 31033336]
35. Guide d'évaluation du caractère anonyme d'un jeu de données dans le cadre d'un projet de recherche [Web page in French]. Health Data Hub. URL: https://www.health-data-hub.fr/sites/default/files/2022-09/Guide%20d%E2%80%99%C3%A9valuation%20du%20caract%C3%A8re%20anonyme%20d%E2%80%99un%20jeu%20de%20donn%C3%A9es%20v2%20%281%29.pdf [accessed 2025-04-10]
36. Pour un patient maître de ses données de santé [Web page in French]. Com'Publics. URL: http://www.compublics.com/sites/default/files/u3/livre_blanc_sante_2.pdf [accessed 2023-06-19]
37. Article R1111-42—code de la santé publique [Web page in French]. Légifance. URL: https://www.legifrance.gouv.fr/codes/article_lc/LEGIARTI000043923231 [accessed 2025-04-09]
38. Etat des lieux: mon espace santé [Web page in French]. France Assos Santé. URL: https://www.france-assos-sante.org/wp-content/uploads/2022/12/CSA-pour-France-Assos-Sante-Mon-espace-sante-Rapport.pdf [accessed 2023-06-19]
39. Cumyn A, Ménard JF, Barton A, Dault R, Lévesque F, Ethier JF. Patients' and members of the public's wishes regarding transparency in the context of secondary use of health data: scoping review. J Med Internet Res 2023;25:e45002. [doi: 10.2196/45002]
40. Goncharov L, Suominen H, Cook M. Dynamic consent and personalised medicine. Med J Aust 2022 Jun 20;216(11):547-549. [doi: 10.5694/mja2.51555] [Medline: 35611469]
41. Ploug T, Holm S. Meta consent—a flexible solution to the problem of secondary use of health data. Bioethics 2016 Nov;30(9):721-732. [doi: 10.1111/bioe.12286] [Medline: 27628305]
42. Cumyn A, Barton A, Dault R, Safa N, Cloutier AM, Ethier JF. Meta-consent for the secondary use of health data within a learning health system: a qualitative study of the public's perspective. BMC Med Ethics 2021 Jun 29;22(1):81. [doi: 10.1186/s12910-021-00647-x] [Medline: 34187453]

Abbreviations

AI: artificial intelligence
CDW : clinical data warehouse
CNIL : Commission Nationale de l'Informatique et des Libertés
CSE : conseil scientifique et éthique
DPO: data protection officer
EHDS : European Health Data Space
GDPR : General Data Protection Regulation
ISO: information security officer
PII : personally identifiable information

XSL•FO
RenderX

Edited by C Lovis; submitted 01.07.24; peer-reviewed by B Bhushan, M Mahmudul Hasan; revised version received 10.12.24; accepted 25.12.24; published 17.04.25.

Please cite as:
Riou C, El Azzouzi M, Hespel A, Guillou E, Coatrieux G, Cuggia M
Ensuring General Data Protection Regulation Compliance and Security in a Clinical Data Warehouse From a University Hospital: Implementation Study
JMIR Med Inform 2025;13:e63754
URL: https://medinform.jmir.org/2025/1/e63754
doi:10.2196/63754

© Christine Riou, Mohamed El Azzouzi, Anne Hespel, Emeric Guillou, Gouenou Coatrieux, Marc Cuggia. Originally published in JMIR Medical Informatics (https://medinform.jmir.org), 17.4.2025. This is an open-access article distributed under the terms of the Creative Commons Attribution License (https://creativecommons.org/licenses/by/4.0/), which permits unrestricted use, distribution, and reproduction in any medium, provided the original work, first published in JMIR Medical Informatics, is properly cited. The complete bibliographic information, a link to the original publication on https://medinform.jmir.org/, as well as this copyright and license information must be included.

XSL•FO
RenderX

Analyzing Sleep Behavior Using BERT-BiLSTM and Fine-Tuned GPT-2 Sentiment Classification: Comparison Study

Yihan Deng[1,2], MS; Julia van der Meer[3], PhD; Athina Tzovara[1,4], PhD; Markus Schmidt[3], MD, PhD; Claudio Bassetti[3], MD, PhD; Kerstin Denecke[2], PhD

[1]Institute of Computer Science, University of Bern, Neubrückstrasse 10, Bern, Switzerland

[2]Institute Patient-centred Digital Health, School of Engineering and Computer Science, Bern University of Applied Sciences, Biel/Bienne, Switzerland

[3]Department of Neurology, University Hospital of Bern, Bern, Switzerland

[4]Center for Experimental Neurology - Sleep Wake Epilepsy Center - NeuroTec, Department of Neurology, Inselspital Bern, University Hospital, University of Bern, Bern, Switzerland

Corresponding Author:
Yihan Deng, MS
Institute of Computer Science, University of Bern, Neubrückstrasse 10, Bern, Switzerland

Abstract

Background: The diagnosis of sleep disorders presents a challenging landscape, characterized by the complex nature of their assessment and the often divergent views between objective clinical assessment and subjective patient experience. This study explores the interplay between these perspectives, focusing on the variability of individual perceptions of sleep quality and latency.

Objective: Our primary goal was to investigate the alignment, or lack thereof, between subjective experiences and objective measures in the assessment of sleep disorders.

Methods: To study this, we developed an aspect-based sentiment analysis method for clinical narratives: using large language models (Falcon 40B and Mixtral 8X7B), we are identifying entity groups of 3 aspects related to sleep behavior (day sleepiness, sleep quality, and fatigue). To phrases referring to these aspects, we are assigning sentiment values between 0 and 1 using a BERT-BiLSTM–based approach (accuracy 78%) and a fine-tuned GPT-2 sentiment classifier (accuracy 87%).

Results: In a cohort of 100 patients with complete subjective (Karolinska Sleepiness Scale [KSS]) and objective (Multiple Sleep Latency Test [MSLT]) assessments, approximately 15% exhibited notable discrepancies between perceived and measured levels of daytime sleepiness. A paired-sample *t* test comparing KSS scores to MSLT latencies approached statistical significance (t_{99}=2.456; *P*=.06), suggesting a potential misalignment between subjective reports and physiological markers. In contrast, the comparison using text-derived sentiment scores revealed a statistically significant divergence (t_{99}=2.324; *P*=.047), indicating that clinical narratives may more reliably capture discrepancies in sleepiness perception. These results underscore the importance of integrating multiple subjective sources, with an emphasis on narrative free text, in the assessment of domains such as fatigue and daytime sleepiness—where standardized measures may not fully reflect the patient's lived experience.

Conclusions: Our method has potential in uncovering critical insights into patient self-perception versus clinical evaluations, which enables clinicians to identify patients requiring objective verification of self-reported symptoms.

(JMIR Med Inform 2025;13:e70753) doi:10.2196/70753

KEYWORDS

sleep disorder; clinical documentation; free text; sentiment analysis; opinion discrepancy; LLM; prompting; supervised fine-tuning; large language model

Introduction

Overview

The interplay between sleep quality, daytime fatigue, and daytime sleepiness is critical for understanding and diagnosing sleep disorders. Sleep quality—a multifaceted concept encompassing depth, continuity, and restorative nature of sleep [1]—is commonly assessed through polysomnography (PSG) or questionnaires [2]. Daytime fatigue significantly impacts quality of life [3], while daytime sleepiness reflects the propensity for unintended sleep episodes.

Past studies have shown inconsistencies between subjective experiences and objective measures. For example, Zavecz et al [4] linked self-reported sleep quality to cognitive performance, while O'Donnell et al [5] reported poor alignment between PSG outcomes and patient-reported sleep quality. Similarly, Aurora et al [6] analyzed how well Epworth Sleepiness Scale (ESS)

XSL•FO
RenderX

scores correspond to Multiple Sleep Latency Test (MSLT) values. In psychiatric populations, similar dissociations have been reported between perceived and physiologically measured fatigue, as demonstrated by Stanyte et al [7] who found that individuals with anxiety and mood disorders often exhibit mismatched subjective fatigue ratings and objective sleep parameters.

Critically, objective metrics such as sleep onset latency (SOL) and total sleep time (TST) require disorder-contextual interpretation. Valko et al [8] demonstrate that shortened SOL indicates pathological sleep-wake fragmentation in narcolepsy but signifies health in normal sleepers, while subjectively prolonged SOL in insomnia reflects hyperarousal despite normal PSG. Similarly, fatigue—though quantifiable via scales such as the Fatigue Severity Scale (FSS)—lacks consistent PSG correlates across disorders, complicating objectification[9].

Despite these assessments being routinely documented clinically, no study has leveraged real-world clinical records to analyze subjective-objective alignment across disorders.

To address this gap, we propose a novel natural language processing (NLP) framework for modeling subjective-objective alignment through aspect-based sentiment analysis. Our system extracts (1) patient-reported experiences, (2) objective test results (eg, MSLT and PSG), and (3) clinician commentary on alignment or mismatch between the two. This triadic analysis allows for identifying patterns of misperception—for instance, patients who perceive severe sleep onset problems despite normal PSG values.

Unlike prior work that focused on isolated biomarkers such as Apnea-Hypopnea Index (AHI) or ESS scores, our approach uses language models to extract detailed clinical reasoning from documentation. This allows identification of emerging “sleep-wake discrepancy” phenotypes, such as patients with objectively normal sleep but persistently poor subjective reports.

Sentiment Analysis in Clinical Text

Sentiment analysis in medical and clinical text has received increasing attention over the past decade [10,11]. Clinical documents often contain detailed descriptions of a patient’s health status, including observations, diagnostic findings, and treatment plans. Analyzing this information is important for determining whether patient outcomes are improving or deteriorating, and for assessing the overall impact of a condition on the patient’s well-being. In addition to objective clinical data, patients’ self-reported experiences may also offer useful indicators that complement medical assessments.

Recent developments in pretrained language models, such as those introduced by Devlin et al [12], have enabled the use of BERT-based architectures for sentiment analysis across multiple languages and granularities. In our work, we define sentiment across 5 discrete levels, which facilitates scaling into a normalized range between 0 and 1. Behera et al [13] presented a model combining Word2Vec embeddings with convolutional and recurrent layers (convolutional neural network and long short-term memory), achieving 91.2% accuracy. Their method also includes polarity normalization to improve classification performance. Other established techniques for sentiment and aspect identification in English-language texts include BiLSTM [12,14], TextCNN [15], TextRNN [16], TextRCNN [17,18], and DPCNN [19].

With the emergence of transformer-based models, research has increasingly focused on controlling language model behavior during fine-tuning, inference, and output postprocessing [20]. For example, Ziegler et al [21] applied reinforcement learning (RL) with human feedback to improve output coherence, while Schulman et al [22] proposed the Proximal Policy Optimization (PPO) algorithm for stable policy updates. Pascual et al [23] introduced Keyword2Text, a framework that guides text generation based on semantic similarity and topic constraints. These control strategies can enhance performance in tasks such as sequence labeling and sentiment classification.

Despite these advances, the use of large language models (LLMs) for aspect recognition in German clinical text remains limited. In addition, data privacy regulations restrict the use of commercial cloud-based models in health care environments. To address these challenges, our study investigates the deployment of open-source language models in secure, on-premises settings. We evaluate their performance in aspect recognition using manually annotated German clinical data. Subsequently, we apply sentiment analysis using a fine-tuned BERT model and compare its performance to a German GPT-2 model, which we adapt through supervised learning and reinforcement-based posttraining techniques.

As can be seen in Table 1, prior work has explored sentiment in clinical text [10,11], or compared ESS to MSLT [6], but none have jointly modeled aspect-level sentiment, LLM-based extraction, and alignment between subjective and objective sleep data. Our contributions include:

1. First application of aspect-based sentiment analysis to German clinical sleep data for sleep disorders.
2. Integration of LLM-based aspect extraction (Falcon 40B and Mixtral 8x7B).
3. Five-level sentiment scoring with normalization.
4. Quantified misalignment modeling between patient-reported and physiological sleep data.
5. Identification of misperception profiles at a large scale using real-world clinical records.

XSL•FO
RenderX

Table . Comparison of related work and contribution of this study.

Study and Method	Domain	Model type	Aspect extraction	Sentiment analysis	Subjective-objective alignment	Sleep focused	Contribution notes
Denecke and Deng [24]	Clinical (general)	Rule-based+ML[a]	Limited	✓	✓	✓	Early sentiment methods in clinical text
Aurora et al [6]	Sleep disorders	Statistical correlation	✓	✓	✓ (sleepiness)	✓	Compared subjective and objective sleepiness (ESS[b] vs MSLT)[c]
Hermans et al [10]	Sleep misperception	EEG[d] analysis	✓	✓	✓	✓	Focus on objective EEG markers of misperception
Denecke and Reichenpfader [14]	Clinical NLP[e]	Transformer (RoBERTa)	✓ (limited)	✓	✓	✓	Survey of clinical sentiment tools
Ziegler et al [21]	General NLP	GPT-2+RLHF	✓	✓ (general)	✓	✓	Introduce RL-based[f] alignment for subjective text
Our study	Sleep disorder	BiLSTM+RoBERTa/GPT-2+RL	✓ (LLM-extracted)[g]	✓ (5-stage scale)	✓ (quantified misalignment)	✓	Joint subjective-objective modeling, LLM-aspect extraction, scoring, feedback mining

[a]ML: machine learning.

[b]ESS: Epworth Sleepiness Scale.

[c]MSLT: Multiple Sleep Latency Test.

[d]EEG: electroencephalogram.

[e]NLP: natural language processing.

[f]RL: reinforcement learning.

[g]LLM: large language model.

Methods

Overview

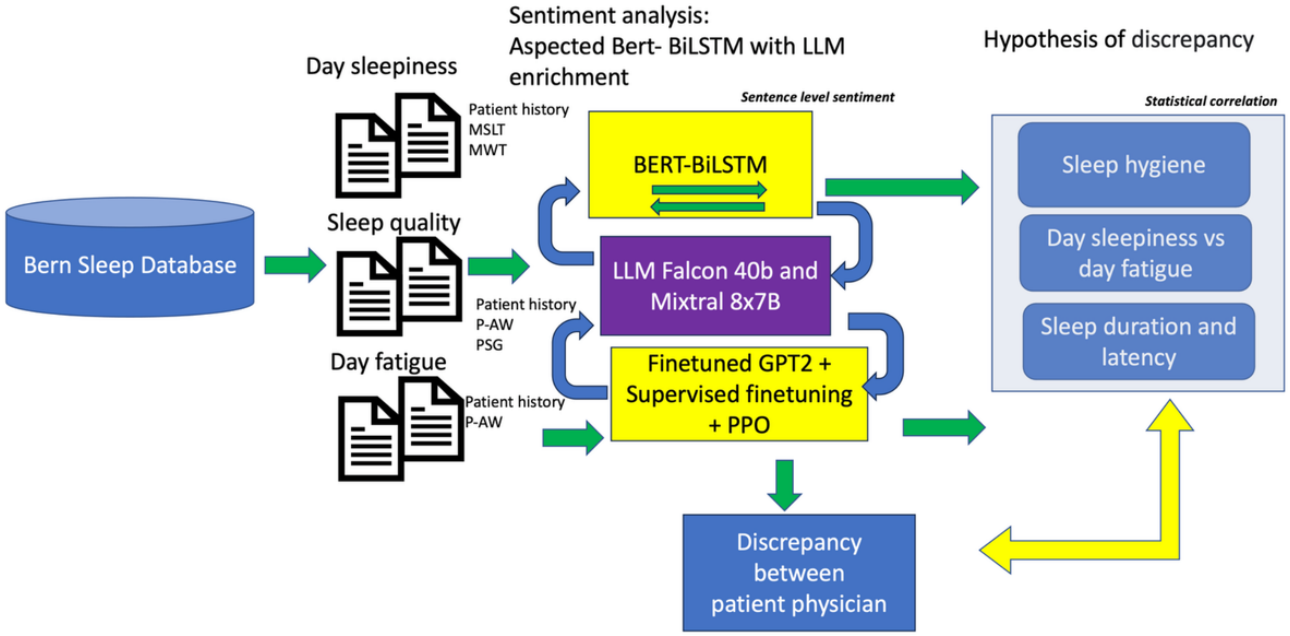
The developed pipeline for aspect-oriented sentiment analysis is shown in Figure 1. The single steps are described together with the dataset in the following. Our approach involves extracting subjective perceptions of sleep quality, daytime sleepiness, and daily fatigue from the clinical documentation. Specifically, we consider the documented patient history descriptions and the reports related to the PSG examination.

Concurrently, objective benchmarks will be gathered from numerical results in objective sources, including MSLT, MWT (Maintenance of Wakefulness Test), P-AW (Actigraphy Wrist), and parts of the PSG report.

In a first step, entities and phrases referring to our 3 aspects of interest (day sleepiness, sleep quality, and fatigue) are extracted. Once these aspects are identified, we classify them according to the sentiment expressed for each aspect separately. The next step involves calibrating the objective numerical assessments to match the subjective sentiment scores, allowing for a direct comparison between subjective and objective data. Finally, by evaluating these 2 sets of sentiment values, we statistically analyze the extent of discrepancies in the diagnosis of sleep disorders, providing insights into how patient perceptions align with clinical assessments.

XSL•FO
RenderX

Figure 1. Workflow of sentiment analysis in sleep disorders. LLM: large language model; MSLT: Multiple Sleep Latency Test; MWT: Maintenance of Wakefulness Test; P-AW: Actigraphy Wrist; PPO: Proximal Policy Optimization; PSG: polysomnography.



Dataset

Our dataset originates from inpatient records created at the sleep laboratory of the University Hospital Bern, covering treatments between 2000 and 2021. This collection is part of the Bern Sleep Registry [25]. Its secondary use received approval from the Cantonal Ethics Committee (KEK-Nr. 2022 - 00415: "Bern Sleep Registry: the sleep disorder patient cohort of the Inselspital, University Hospital Bern").

The database comprises German-language coded clinical records of patients diagnosed with sleep disorders. Over 10,000 of these records have been retrospectively and meticulously categorized by physicians specialized in sleep disorders based on the *International Classification of Sleep Disorders, Third Edition* (*ICSD-III*). Table 2 shows the types of text documents that are considered from this database for this paper.

XSL•FO
RenderX

Table . The sentiment analysis mainly focuses on the subjective text (second column), while the objective value extractions are related to test results. Sample sizes reflect prevalence in clinical notes; fatigue records are rarer than sleep quality.

Aspect	Subjective data sources	Information sources and documents	Objective data sources	Statistics
Daytime sleepiness (129 records)	History: Daytime sleepiness, Epworth Sleepiness Scale, MSLT[a] /MWT[b] KSS[c]	History, Multiple Sleep Latency Test, Maintenance of Wakefulness Test	MSLT and MWT: eg, "In summary, a mild daytime sleepiness can be objectified," vigilance test results	• 36 (28%) of records show SOL-KSS[d] discrepancy • ESS[e] >10 correlates with MSLT latency <8 minutes (r=–0.72) • "Mild daytime sleepiness" documented in 58 (63%) of 92 cases with MSLT 5-8 min
Fatigue exhaustion depressive symptoms (450 records)	History: Fatigue, Fatigue Severity Scale, BDI-II[f]	Hist[g], P-AW[h]	Increased inactivity component	• FSS[i] >5 correlates with BDI-II >14 (r=0.68) • 189 (42%) show activity reduction • "Increased inactivity" noted in 112 (89%) of 126 severe fatigue cases
Sleep quality (3815 records)	Hist: Sleep quality, Insomnia PSG[j] Report: Estimated sleep onset Latency and sleep duration	Hist, PSG, P-AW	PSG Report: Objective sleep onset Latency and sleep duration, sleep efficiency (¡ 80%: reduced). Actigraphy Report: Actimetric sleep efficiency	• 2557 (67%) underestimate TST[k] (mean diff: –73 min) • SE <80% in 82%[l] of insomnia diagnosis • "Reduced efficiency" documented in 94%[m] of SE<75% cases

[a]MSLT: Multiple Sleep Latency Test.

[b]MWT: Maintenance of Wakefulness Test.

[c]KSS: Karolinska Sleepiness Scale.

[d]SOL-KSS: Sleep Onset Latency Karolinska Sleepiness Scale

[e]ESS: Epworth Sleepiness Scale.

[f]BDI-II: Beck Depression Inventory II.

[g]Hist: patient history.

[h] P-AW: Actigraphy Wrist.

[i]FSS: Fatigue Severity Scale.

[j]PSG: polysomnography.

[k]TST: total sleep time.

[l]Absolute number not available; based on weighted insomnia subset

[m]Absolute counts unavailable due to conditional subgroup definitions.

For various validations, we have prepared the following manually annotated datasets to validate and fine-tune the pretrained model:

1. Aspect extraction benchmark: 150 sentences manually labeled to validate entity and aspect extraction performance.
2. Sentiment analysis corpus: 2000 sentences annotated on a 5-point sentiment scale using on-premises LLMs (Falcon 40B [26,27] and Mixtral 8x7B [28]), with human-in-the-loop correction.

The 2000 sentences were sampled from clinical documents belonging to 100 unique patients, spanning multiple sleep disorder categories. These sentences were drawn proportionally from patient histories, diagnostic summaries, and follow-up reports to ensure a representative mix across conditions and report types. Stratified sampling was used to balance diagnoses, age groups, and sentiment distribution. To avoid patient-level bias, no more than 10 sentences per patient were included in the annotated set.

To ensure robust analysis of subjective-objective alignment in daytime sleepiness, we included only those patients who had complete paired data for the following instruments: Karolinska Sleepiness Scale (KSS)—subjective measure, MSLT—objective physiological measure, and MWT—behavioral sleepiness measure. This resulted in a final cohort of 100 patients with complete records across all 3 modalities, allowing for valid

XSL•FO
RenderX

computation of discrepancy and misperception scores. For other dimensions, such as fatigue and sleep quality, which currently lack standardized objective clinical benchmarks, we retained a broader set of records (eg, 3815 entries for sleep quality) to support exploratory sentiment-based analysis.

Aspect and Sentiment Distribution

To analyze sentiment by aspect, we annotated 50 representative sentences per aspect totaling 150 sentences. Table 3 summarizes the frequency of extracted entity groups by category, while Table 4 presents the sentiment annotations and related statistics.

Table . Aspect benchmark statistics regarding sleep quality, daytime sleepiness, fatigue, and the entire corpus.

Aspects	List of entity groups	Entity count
Sleep quality (50 sentences)	Sleep quality, Latency, Duration, Estimation	75
Daytime sleepiness (50 sentences)	Day sleepiness, Latency, PVT (Vigilance test), ESS[a]/KSS[b]	35
Fatigue (50 sentences)	Fatigue Severity Scale, Measurements BDI-II[c]	77
Entire benchmark (150 sentences)	Symptoms, Diseases, Complaints, Feedback, Measurements	119

[a]ESS: Epworth Sleepiness Scale.

[b]KSS: Karolinska Sleepiness Scale.

[c]BDI-II: Beck Depression Inventory II.

XSL•FO
RenderX

Table . Sentiment statistics regarding sleep quality, daytime sleepiness, fatigue, and the entire corpus.

Sentiment class	Count	Percentage	Average sentence length	Lexical characteristics
Very Negative	180	9%	22.4 (5.8) words	Sleep quality: "severe insomnia," "non-restorative sleep," "fragmented sleep all night" Fatigue: "debilitating exhaustion," "unable to function" Sleepiness: "dangerous sleep attacks," "uncontrollable drowsiness"
Negative	680	34%	18.6 (4.2) words	Sleep quality: "frequent awakenings," "prolonged sleep latency," "restless sleep" Fatigue: "persistent tiredness," "low energy throughout day" Sleepiness: "excessive daytime sleepiness," "struggling to stay awake"
Neutral	920	46%	14.2 (3.1) words	Sleep quality: "TST 6.2 hours," "sleep efficiency 82%," "PSG: 4 REM cycles" Fatigue: "reports moderate fatigue," "FSS score: 4.2" Sleepiness: "ESS: 12," "MSLT mean latency: 8.3 min"
Positive	180	9%	16.8 (3.9) words	Sleep quality: "improved sleep continuity," "satisfactory sleep duration" Fatigue: "reduced fatigue levels," "manageable tiredness" Sleepiness: "mild daytime sleepiness," "occasional drowsiness"
Very Positive	40	2%	19.3 (4.7) words	Sleep quality: "excellent sleep quality," "fully restorative sleep" Fatigue: "complete resolution of fatigue," "sustained energy" Sleepiness: "full alertness," "no daytime sleepiness"
Total	2000	100%	16.8 (4.6) words	—

[a]TST: total sleep time.

[b]PSG: polysomnography

[c]REM: rapid eye movement.

Mathematical Description of Aspect-Based Sentiment Analysis for Sleep Disorder

In the following, we define the dataset and tasks considered in this paper.

Dataset Definition

Let the dataset be defined as:

$D=\{(x_i, A_i, y_i)|=1,...,N$

Where:

- x_i is the tokenized and embedded representation of sentence i, obtained via BERT or RoBERTa (shape: $T\times d$, where T=tokens, d=embedding dimension).
- A_i is the set of extracted aspect terms from x_i using LLMs (eg, Falcon 40B and Mixtral 8x7B).
- y_i is the discrete sentiment label $\in$ {0, 1, 2, 3, 4} representing 5-stage sentiment levels.
- The normalized score is:

XSL•FO
RenderX

si=yi4So $S_i \in [0,1]$

Aspect Extraction via LLMs

For each input sentence x_i and aspect category, for example, $c \in$ C_Categories, we define a prompt P_c and extract:

$a_i^{(c)=LLM\,(P_c,x_i)}$ for each aspect category c

The union of these yields the aspect set:

$A_i=U_c a_i^{(c)}$

To align with canonical medical terms, compute cosine similarity:

sim(e, c) = cosine(embedding(e), embedding(c))

Accept the match if sim≥threshold

Sentiment Classification (BiLSTM+Self-Attention)

1. Input embeddings
   Each x_iR is passed to a bidirectional LSTM:
   $h_i = BiLSTM\,(x_i) \in R^{T \times h}$
2. Sequential feature aggregation (concatenation or pooling):
   $f_i = Self - Attention\,(h_i) \in R^{h'}$
3. Classification layer (with softmax over 5 sentiment classes):
   Using a linear layer with parameters *W*, *b*:
   pi=softmax(W×fi+b) with y^i=argmax(pi)
   Where:

- $W \in R^{5 \times h'}$, $b \in R^5$are learnable parameters,
- $p_i \in R^5$ is the predicted class distribution.

Training Objective (Supervised Fine-Tuning: L1)

Use categorical cross-entropy for supervision:

LCE=−1N∑i=1N∑k=151yi=k·log(pi,k)

Sentiment Control via GPT-2 (L2: Reinforcement Learning)[29]

After initial fine-tuning, a GPT-2 model is trained to modify or generate text while controlling for sentiment class y_i

Logit Biasing /Reward Shaping: to

LRL=Exi^πθ[r(xi^,yi)]

Where r(xi^,yi) is a reward signal based on:

- Keyword inclusion (aspect control),
- Matching predicted sentiment from a fixed classifier with y_i

The full objective (SFT+RL) becomes:

$L_{total}=L_{CE}+\lambda \cdot L_{RL}$

where $\lambda \in [0,1]$ is a hyperparameter controlling the influence of reinforcement-based alignment.

Normalization of Subjective and Objective Measures

Min-max normalization for raw clinical scores *r* over scale [S_{min}, S_{max}]:

s=Smax−rSmax−Smin

Examples:

- Epworth Sleepiness Scale (0 - 24):
  s=24−r24
- Fatigue Severity Scale (1-7):s=7−r6
- Beck Depression Inventory II (0 - 63)
  s=63−r63
- Karolinska Sleepiness Scale (KSS) (1-9):
  s=9−KSS9−1

Aspect Extraction From Diagnostic Text

For aspect extraction, we define 4 distinct groups of clinical entities based on their frequency and contextual relevance, with the aim of analyzing discrepancies between subjective reports and objective clinical findings (see Table 2). While aggregating sentiment scores can offer a general view of polarity across different textual spans (eg, sentences or paragraphs), they are insufficient for capturing detailed sentiment variations related to specific medical aspects such as symptoms, complaints, diagnoses, or co-occurring conditions. To address this limitation, we implemented a fine-grained entity extraction approach that combines open-source LLMs with standard clinical entity recognition techniques.

Specifically, we use 2 self-hosted models: Falcon 40B [27] and Mixtral 8x7B [30]. Falcon 40B is a dense, decoder-only language model designed for a broad range of NLP tasks. Mixtral 8x7B, by contrast, follows a sparse mixture-of-experts architecture, activating 2 expert modules per token, thereby achieving a favorable balance between performance and computational efficiency. Despite having 46.7 billion parameters in total, only a subset is used at each step, making it suitable for resource-constrained environments. We evaluated Falcon 40B as a baseline but used Mixtral 8x7B for all final extractions reported here.

Aspect-level sentiment scoring is achieved by linking the extracted entities to their corresponding sentiment values within a given sentence. This allows us to compute sentiment scores that are specific to individual clinical aspects. The entity extraction process is carried out in 2 stages: (Stage 1) Aspect identification using prompt-based querying with the locally hosted Mixtral 8x7B model. Separate prompts are constructed for each category—symptoms, complaints, diagnoses, and patient feedback—to ensure focused and interpretable extraction.

To extract patient feedback entities, we design targeted natural language prompts structured to guide the model toward recognizing relevant subjective expressions. Below is a representative prompt used with the Falcon 40B model:

Prompt

You are a helpful clinical entity extractor. Given the following medical note, please extract any patient feedback or evaluative statements related to their condition, treatment experience, or overall well-being.

Text: “[Insert clinical sentence here]”

Output format: [feedback_1, feedback_2, ...]

The given prompt for entity extraction from clinical patient data can be efficiently reused by systematically substituting the target

XSL•FO
RenderX

category in the text. By iteratively inserting each category (eg, “symptoms,” “diseases,” “complaints,” and “feedback”) into the prompt, the same prompt structure can be applied multiple times to extract entities for one category at a time. This approach allows looping over the list of aspect categories and generating a valid JSON object for each without needing multiple distinct prompts. It ensures structured and repeatable extraction across all defined aspects.

To improve the identification of measurement-related entities in German clinical texts, which are often missed by LLMs due to domain-specific phrasing in German clinical texts, we apply a semantic similarity approach based on sentence embeddings. This method is more robust to morphological variation, word order, and paraphrasing than traditional string metrics such as Levenshtein distance.

We used German-specific sentence embeddings generated by the sentence-transformers library with the multilingual model distiluse-base-multilingual-cased-v1, which supports high-quality semantic representations of German phrases.

Matching Procedure

To identify and align relevant sleep-related entities from clinical narratives, we implemented a multistep matching procedure combining lexical, semantic, and synonym-based techniques, as detailed below:

1. Entity candidate generation: Candidate phrases were extracted from clinical documents using regex-based pattern matching and contextual heuristics (eg, token windows around sleep-related terms).
2. Embedding computation: Sentence embeddings were computed for each candidate phrase and compared to embeddings of canonical terms from our curated sleep measurement lexicon.
3. Similarity scoring: Cosine similarity was used to measure semantic closeness between candidate and canonical embeddings. A similarity threshold of 0.83 was used to determine a valid match based on manual validation (see Table 5).
4. Synonym expansion: A manually defined dictionary of common medical synonyms (eg, “Schlafqualität” ≈ “Qualität des Schlafes”) was integrated into the matching logic to further boost recall.

Table . Embedding-based semantic matching for German sleep disorder terms.

Canonical term	Variant detected in text	Cosine similarity	Matched?	English translation
Schlafqualität	Qualität des Schlafes	0.86	True	Sleep quality
Schlaflatenz	Zeit bis zum Einschlafen	0.85	True	Time to fall asleep
REM-Schlafanteil[a]	REM Schlafphasen Dauer	0.81	False	Duration of REM sleep phases

[a]REM: rapid eye movement.

Objective Measure Calibration

To enable comparability across heterogeneous clinical measurements and support sentiment interpretation, we apply min-max normalization to both objective and subjective metrics. This ensures all scores lie within the interval [0, 1], where 0 indicates maximal symptom burden and 1 indicates no impairment. This transformation provides a unified scale for downstream sentiment mapping.

For objective physiological measures such as PSG-recorded sleep latency, we applied the following normalization: Normalized Latency Score=1–(Raw Value/Max Latency) where the clinically derived maximum latency was set to 120 minutes, in accordance with standard clinical PSG protocols. This formulation ensures shorter latency (indicative of better sleep initiation) corresponds to higher normalized scores.

Subjective scale normalization

For subjective clinical questionnaires (see Table 6), we used min-max normalization based on each scale’s full range. The transformation ensures that higher symptom burden maps to lower normalized values:

Normalized Score=(Max Score – Raw Score) /(Max Score – Min Score)

Table . Normalization mappings between the objective score.

Instrument	Score range	Normalization formula
Karolinska Sleepiness Scale (KSS)	1 - 9	(9 – Raw Score) / (9 – 1)
Epworth Sleepiness Scale (ESS)	0 - 24	(24 – Raw Score) / (24 – 0)
Fatigue Severity Scale (FSS)	1 - 7	(7 – Raw Score) / (7 – 1)
Beck Depression Inventory II (BDI-II)	0 - 63	(63 – Raw Score) / (63 – 0)

This ensures that 0 corresponds to the maximum raw score (most negative sentiment), and 1 corresponds to the minimum raw score (most positive sentiment).

Architecture for Clinical Sentiment Analysis

We deploy a BERT-based BiLSTM architecture to perform sentence-level sentiment classification across 5 polarity levels (see Figure 2). The model ingests token sequences up to 250

XSL•FO
RenderX

tokens, with BERT embeddings (768 dimensions) [31] providing context-aware representations.

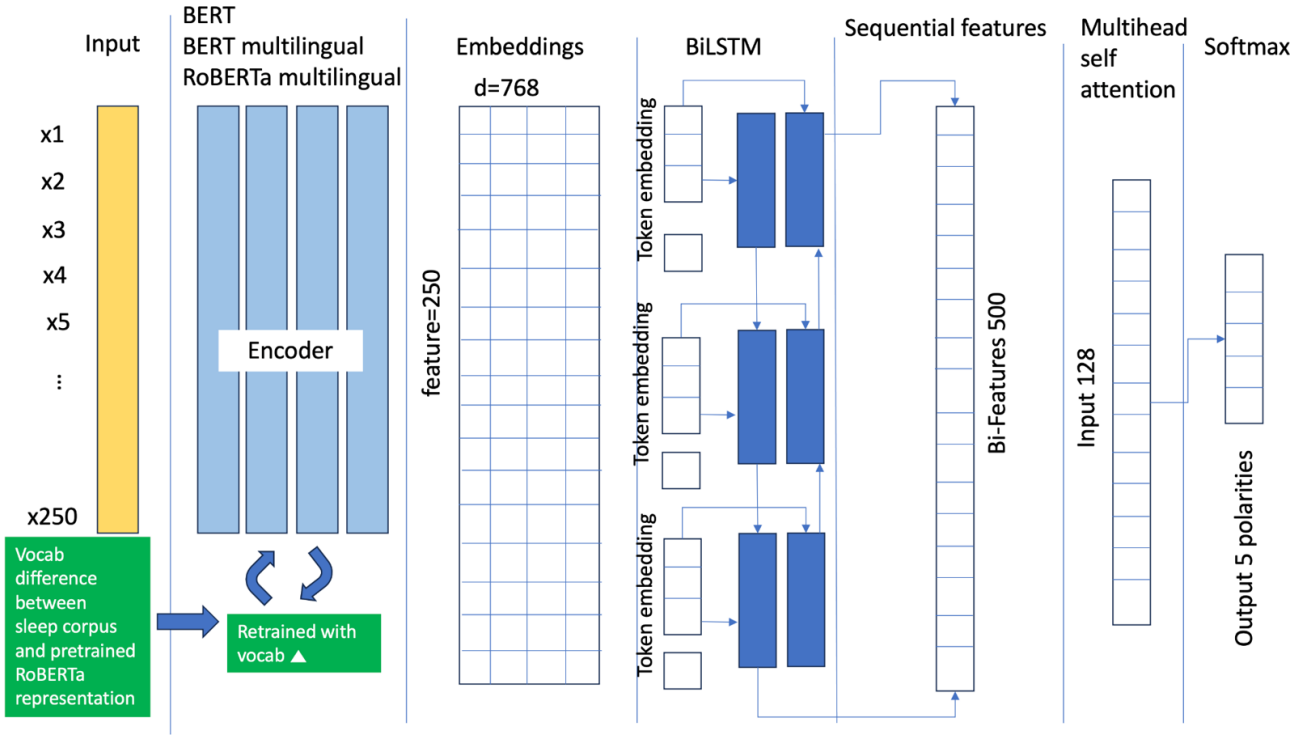
We fine-tune both multilingual BERT and XLM-RoBERTa [32] on a corpus of 1200 German clinical sentences annotated with 5-stage sentiment labels, derived from Mixtral 8X7B prompting and manual correction (interannotator agreement >89%).

Negated expressions in German are normalized into unified tokens prior to BERT encoding to stabilize polarity signals. The resulting embeddings are processed by a BiLSTM layer followed by sequential feature aggregation. The output logits are mapped to 5 sentiment classes, which are rescaled to a [0, 1] range:

0 (very negative), 1 (negative), 2 (neutral), 3 (positive), 4 (very positive)

The model is trained using a 60/20/20 split across training (1200), validation (400), and test (400) sets.

Figure 2. BiLSTM based on BERT language modeling for clinical sentiment analysis.



Feature Fusion and Context Learning

The architecture incorporates multiple contextual sources:

F_{Mask}: local contextual features via dynamic masking

$F_{weighting}$: Dynamically weighted local embeddings

$F_{disorder}$: global BiLSTM features

The 5 stages of sentiment resulting from with or without BERT alignment and fine-tuning will be evaluated on these benchmarks.

Feature Ensemble and Context Learning for BERT BiLSTM

During the unified contextual feature assembling process for sleep disorder topics, both local and global contextual features derived from the contextual feature dynamic mask technique, the dynamic weighting mechanism, and the BiLSTM layers are integrated. In addition, features enriched by LLMs are incorporated. Specifically, the learned local and global contextual features are concatenated to produce a unified contextual feature output. This procedure is mathematically represented as follows:

Fensemble=Fmaskl Fweightingl Fdisorderaspectg

In this equation, FmaskL represents the set of local contextual embedding vectors computed by the dynamic mask technique, while FweightingL denotes the set of local contextual embedding vectors examined through the dynamic weighting mechanism. $F_{disorder}$ aspect refers to the set of global contextual embedding vectors captured via BiLSTM layers. The operator indicates the concatenation of these feature sets. These fused features are further processed through BiLSTM to capture sequential dependencies and then transmitted into Feedforward Network with Softmax to perform fine-grained aspect-based sentiment classification.

Network Configuration and Hyperparameters for BERT BiLSTM

The hyperparameter Table 7 outlines the configuration of the network, which operates in 2 main stages. In the first stage, aspect recognition is performed using the initial set of network parameters. The recognized aspects are then incorporated into the second stage through feature fusion, where they are linearly combined and pooled together with position features. This fused feature set is subsequently applied and jointly optimized within the fine-tuned RoBERTa model's loss function. The optimization is carried out using a 5-stage polarity classification,

XSL•FO
RenderX

ensuring that both aspect-level insights and positional information are effectively used for enhanced performance.

Table . Model hyperparameters for fine-tuning of BERT and RoBERTa BiLSTM multilingual.

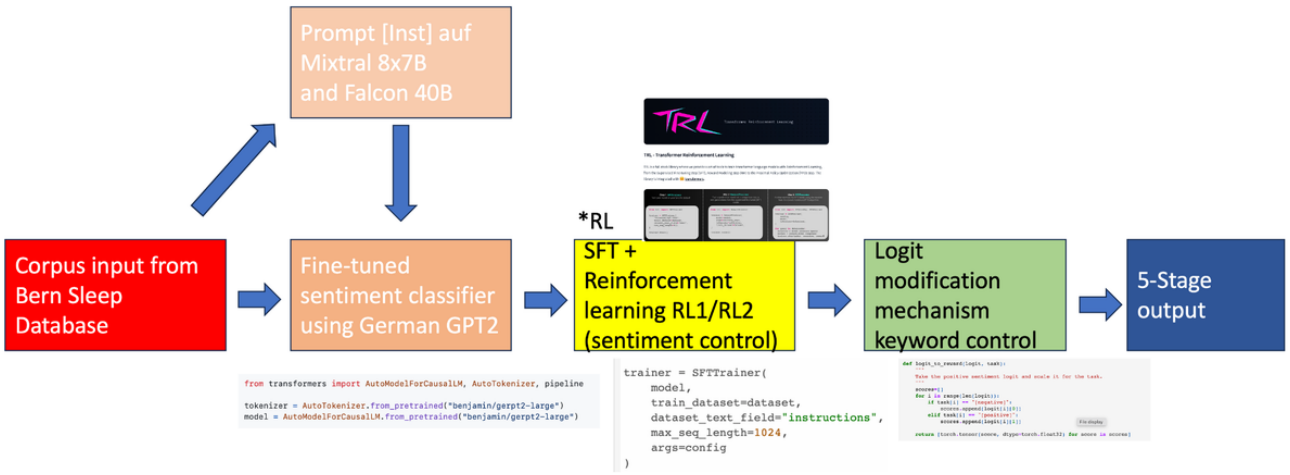
Parameter	Value
Embedding dimension	768
Transformer encoder	12
Attention head	12
Optimizer	Adam[a]
Learning rate	5e-5
Epoch	50
Dropout rate	0.2
Batch size	32

[a]Adam: adaptive moment estimation is a stochastic optimization algorithm.

Finetuned German GPT-2 With Supervised Fine-Tuning and Logit Modification

In addition to our BERT-BiLSTM sentiment classification baseline, we fine-tune a German GPT-2 model [26,33,34] to generate text reflecting 5 clinically relevant stages of sentiment in sleep disorder narratives. As illustrated in Figure 3, our 2-stage fine-tuning approach involves both supervised learning (L1) and reinforcement learning (L2) to align the model's generations with targeted sentiment levels. In the first stage (L1), we perform supervised fine-tuning (SFT) using the Hugging Face Transformer Reinforcement Learning (TRL) framework [28] on a corpus of 1200 annotated German clinical texts (Table 8), each labeled with 1 of 5 sentiment classes: strong negative, minor negative, neutral, minor positive, and strong positive. The SFT phase runs for 3 epochs with a learning rate of 5e-5, a batch size of 16, and a maximum sequence length of 1024 tokens, using standard language modeling loss to adapt the pretrained GPT-2 model to the clinical sleep domain and sentiment-specific instruction format. Further details regarding the implementation are available in the GitHub repository [35].

Figure 3. Fine-tuned German GPT-2 followed by supervised fine-tuning, reinforcement learning, and logit modification. *RL indicates the steps of reinforcement learning RL1 and RL2. RL: reinforcement learning; SFT: supervised fine-tuning.



XSL•FO
RenderX

Table . Model hyperparameters for GPT-2 supervised fine-tuning.

Parameter	Value
GPT-2 sentiment classifier learning rate	2e-5
GPT-2 sentiment classifier batch size	16
SFT trainer learning rate	5e-5
SFT training epochs	3
SFT maximum sequence length	1024
RL[a] generation kwargs top-k	3
RL generation kwargs top-p	0.5
Maximum new tokens	100
RL PPO[b] mini-batch size	16
RL PPO configuration steps	41,000

[a]RL: reinforcement learning.

[b]PPO: Proximal Policy Optimization.

The second stage (L2) consists of RL via PPO [33], using the sentiment classifier as a reward model. Here, the model generates responses conditioned on prompts and randomly sampled target sentiment tokens. The classifier evaluates each generation and assigns a reward signal based on the logit of the target sentiment class, encouraging the model to reinforce sentiment-accurate responses. This process is iteratively optimized over 41,000 PPO steps, using a PPO mini-batch size of 16, and generation hyperparameters including top-k=3, top-p=0.5, and a maximum of 100 new tokens per sample.

We designate these PPO training phases as RL1 and RL2, which are now clearly labeled in Figures 1 and 3 *RL. Each RL phase refines the generator's ability to follow sentiment conditioning with increasing precision. This logit-based reward shaping strategy ensures granular control over sentiment realization in the output. Our evaluation metric during PPO optimization is the accuracy of generated sentiment, as classified by the same frozen classifier used for reward computation. The combination of supervised preadaptation and reward-driven fine-tuning allows our GPT-2 model to generate sentiment-aligned narratives that preserve clinical plausibility while reflecting emotional tone variations essential for downstream affective or patient-centered NLP tasks.

Derived Subjective Sleepiness Scoring and Comparison to Objective Measures

Subjective Sleepiness Approach

To robustly assess subjective sleepiness, we combined inputs from the KSS and clinician-documented descriptions to produce a harmonized subjective score. KSS ratings were first converted to a 5-stage ordinal scale (0‐4), with thresholds mapped as follows: 1‐2=4 (very severe sleepiness),

3‐4=3, 5‐6=2, 7‐8=1, 9=0 (no sleepiness).

This reverse scoring reflects the interpretation that lower KSS values indicate greater momentary sleepiness.

In parallel, clinical text segments were processed using a sentiment analysis pipeline based on a fine-tuned GPT-2 model trained with RL to optimize accuracy across 5 sentiment stages. This model provided a text-derived sleepiness score on the same 0‐4 scale, where 0 indicated no subjective complaints and 4 indicated severe functional impairment due to sleepiness.

Objective Sleepiness Derivation

The MSLT was used to obtain an objective index of daytime sleepiness. Since shorter latencies reflect greater sleepiness, raw MSLT values were inverted and scaled onto a 0‐4 range: objective score = ((20 – MSLT latency) / 20)×4. This allowed direct comparison of subjective and objective sleepiness on the same scale.

Paired Comparison and Findings

To evaluate the degree of alignment between subjective and objective sleepiness, we performed a paired-sample *t* test. For each patient, we computed the difference between the harmonized KSS sleepiness stage and GPT-2-RL–derived text score and the corresponding objective sleepiness score derived from MSLT latency.

The paired-sample *t* test evaluates whether the mean difference between the subjective and objective scores across all patients significantly differs from zero. The test statistic is calculated using:

$$t=\bar{d}Sd/n$$

where d is the mean of the differences between paired observations:

$$\bar{d}=1n\sum i=1n(xi-yi)$$

S_d is the standard deviation of the differences:

$$Sd=1n-1\sum i=1n(di-\bar{d})2$$

n is the number of paired samples, x_i is the subjective score for patient i, and y_i is the objective score for patient i.

Ethical Considerations

Ethical approval for this study was obtained from the Kantonale Ethik Kommission Bern (Cantonal Ethics Committee Bern) for multiple project components: Project part 1: SNS Project

XSL•FO
RenderX

(2000-2016), BASEC-ID 2016-00409 and Project part 2: Bern Sleep Registry ("The sleep disorder patient cohort of the Inselspital, University Hospital Bern"), KEK-Nr. 2022-00415.

The secondary use of data from the Bern Sleep Registry was also approved by the Cantonal Ethics Committee. All data were handled in accordance with institutional and Swiss data protection regulations. Informed consent was obtained as required for each project component, and all participants were informed of their ability to opt out of data use. All data were fully de-identified prior to analysis to protect participant privacy and ensure compliance with applicable data protection standards.

Results

Overview

This section presents the results of our aspect-based sentiment analysis pipeline, including [1] 5-stage sentiment classification using transformer-based models, and [2] LLM-based extraction of clinical entity aspects. The analyses were applied to a dataset of sleep-related medical texts and further supported by clinical insights into subjective-objective misperception.

Evaluation of the Aspect-Based Sentiment Analysis

Table 9 summarizes the performance of several models for 5-stage sentiment classification, evaluated using standard multiclass metrics. Initial models such as BERT and RoBERTa achieved moderate performance (accuracy 61% and 69%, respectively). Incorporating a BiLSTM layer improved performance to 78%. Further gains were achieved with a fine-tuned GPT-2 model. SFT alone yielded 81% accuracy, and RL with logit-space modulation increased it to 87%. These results demonstrate the effectiveness of multistage alignment in modeling sentiment nuances. Metrics reported in Table 9 are macro-averaged across 5 sentiment classes, based on an 80/20 stratified test split.

Table . Performance of sentiment classification of semiautomatically annotated 5-stage sentiment. Training: 1200 sentences (60%), Validation: 400 (20%), Test: 400 (20%) for hyperparameter optimization.

Sentiment task	Accuracy	AUC-ROC[a]	Precision (macro)	Recall (macro)	F_1-score (macro)
BERT 5-stage	0.61	0.76	0.62	0.60	0.61
RoBERTa 5-stage	0.69	0.84	0.70	0.68	0.69
RoBERTa+BiLSTM	0.78	0.90	0.79	0.77	0.78
GPT-2+SFT[b]	0.81	0.93	0.82	0.81	0.81
GPT-2+SFT+RL1[c]+ logit mod	0.85	0.95	0.86	0.85	0.85
GPT-2+SFT+RL2+logit mod	0.87	0.96	0.88	0.87	0.87

[a]AUC-ROC: area under the receiver operating characteristic curve.

[b]SFT: supervised fine-tuning.

[c]RL: reinforcement learning.

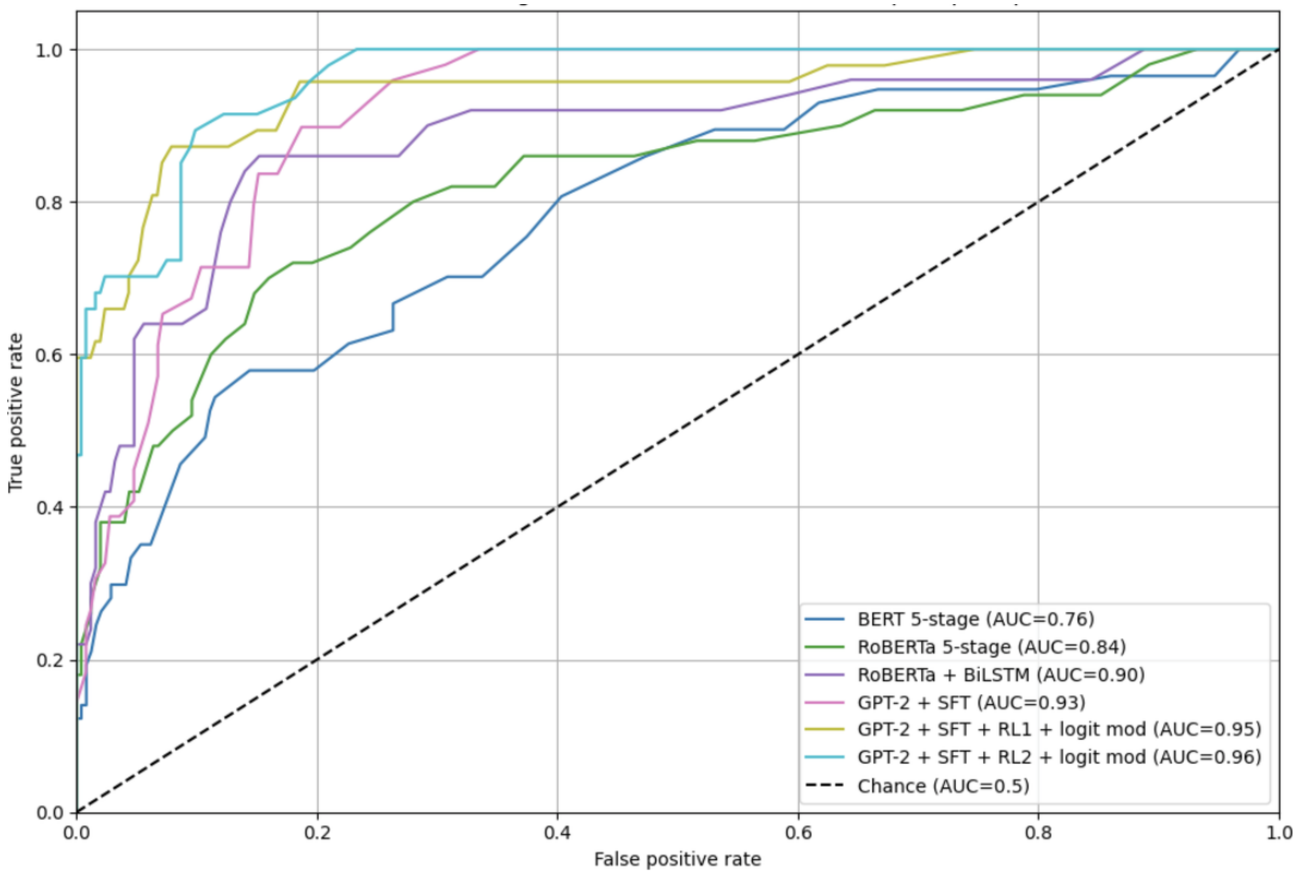
All metrics were computed using macro-averaging, giving equal weight to all sentiment classes. The AUC-ROC (area under the receiver operating characteristic curve) values were obtained using a one-vs-rest strategy, macro-averaged across 5 classes. These approaches ensure that both frequent and rare sentiment classes are equally represented in performance assessment.

Figure 4 visualizes the ROC curves of the models. GPT-2 variants with SFT+RL training consistently outperformed the baselines, reflecting enhanced class separability through reinforcement learning and logit regularization.

The ROC-AUC curves illustrate the one-vs-rest performance of 6 models on the 5-stage sentiment classification task using clinical text from sleep disorder records. All models perform substantially above the chance level (AUC=0.5), with performance steadily improving from BERT (AUC=0.76) to RoBERTa (AUC=0.84), and further to RoBERTa+BiLSTM (AUC=0.90). Fine-tuned GPT-2 (SFT) achieves strong performance (AUC=0.93), which is further enhanced by reinforcement learning (RL1 and RL2) and logit modification, reaching up to AUC=0.96. The stair-step shapes reflect the small test set (400 samples), but the consistent trend shows that reinforcement learning significantly boosts the model's ability to distinguish fine-grained sentiment levels, supporting its potential for clinical decision support in contexts such as misperception of sleepiness.

XSL•FO
RenderX

Figure 4. AUC-ROC (area under the receiver operating characteristic curves) for 5-class sentiment classification across transformer-based models. SFT: supervised fine-tuning.



Aspect Extraction Through LLM Falcon 40B and Mixtral 8X7B

Clinical entity extraction was performed using prompting strategies applied to Falcon 40B and Mixtral 8X7B models. Table 10 compares their performance on 4 annotated categories: Symptoms, Diseases, Complaints, and Feedback. Mixtral 8X7B showed strong performance with macro F_1 of 0.8490, outperforming Falcon 40B (macro F_1 of 0.7265).

Table . Performance of the aspect extraction and benchmarks: 150 manually labeled sentiment aspects.

Performance of aspect extraction	Precision	Recall	Micro F_1	AUC-ROC[a]
Falcon 40B instruct entity extraction				
Symptoms	0.8157	0.7963	0.8054	0.903
Diseases	0.8321	0.8485	0.8397	0.920
Complaints	0.7829	0.7134	0.7466	0.873
Feedback	0.5416	0.4896	0.5142	0.757
Marco F_1	—[b]	—	0.7265	—
Mixtral 8X7B Instruct v0.1 entity extraction				
Symptoms	0.9175	0.9114	0.9054	0.953
Diseases	0.8812	0.8804	0.8797	0.940
Complaints	0.8411	0.8338	0.8266	0.913
Feedback	0.8616	0.8028	0.8312	0.903
Marco F_1	—	—	0.8490	—

[a]AUC-ROC: area under the receiver operating characteristic curves.

[b]Not available.

XSL•FO
RenderX

Since Mixtral 8X7B consistently outperformed Falcon 40B across all evaluated categories, we applied Mixtral 8X7B for all entity extraction tasks in our sentiment analysis pipeline. Beyond the benchmark evaluation, the model extracted a total of 873 unique symptom terms, along with 59 distinct diseases, 432 complaints, and 224 feedback-related entities across the full clinical corpus.

Sentiment Distribution Patterns

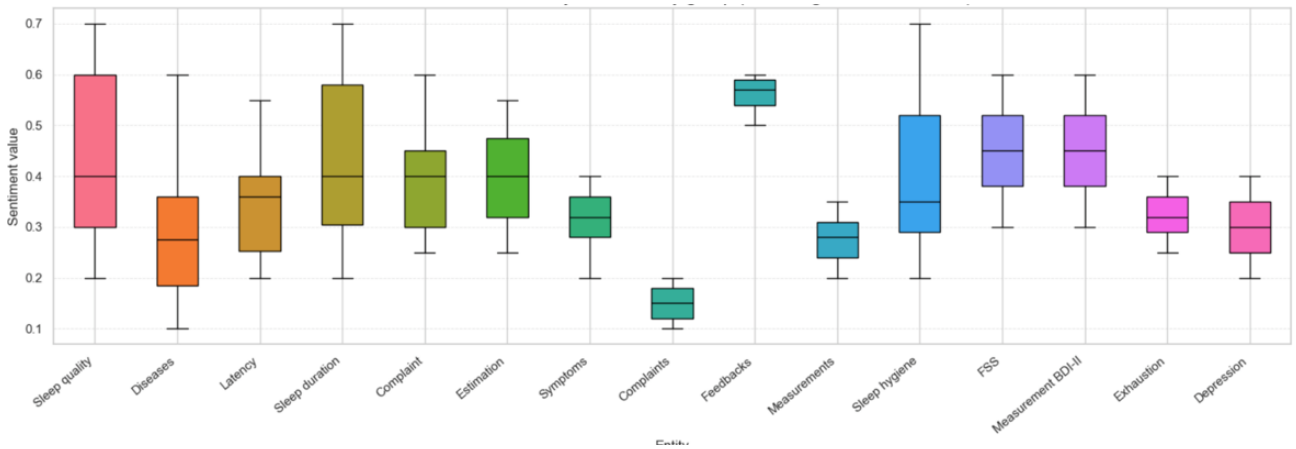
Currently, there are no established objective ground truth standards for evaluating misperception in insomnia, and for disorders such as hypersomnia or sleep-disordered breathing, further clinical validation is required. Thus, our focus was placed on daytime sleepiness, where both subjective (KSS) and objective (MSLT and MWT) data were consistently available.

The KSS and the ESS both assess subjective sleepiness but differ in temporal focus: KSS captures momentary state-level sleepiness, while ESS reflects trait-level sleepiness across habitual situations. Because KSS is time-specific, it aligns more directly with objective measures such as MSLT latency.

In this study, we focus exclusively on KSS—with or without clinical text—to assess momentary misperception in daytime sleepiness. This approach avoids confounding from chronic perception scales such as ESS and enables precise modeling of state-dependent discrepancies.

Figures 5-7 visualize the distribution of sentiment values across different clinical contexts. Figure 5 presents sentiment grouped by clinical entity (eg, Sleep quality, Symptoms, and Feedback). Positive sentiment distributions were observed for Feedback and Sleep Hygiene, while negative sentiment dominated in entities such as Complaints and Diseases. Figure 6 shows sentiment variation across document types: patient-generated narratives (P) and Actigraphy Wrist (P-AW) reports tended to be more emotionally expressive than historical records (Hist). Figure 7 aggregates sentiment by clinical aspect groupings, showing that Sleep quality included more variability in sentiment, whereas Fatigue and Day sleepiness showed predominantly negative sentiment patterns—suggesting a greater emotional burden associated with these complaints.

Figure 5. Sentiment distribution by clinical entity group. FSS: Fatigue Severity Scale; MSLT: Multiple Sleep Latency Test; MWT: Maintenance of Wakefulness Test.



XSL•FO
RenderX

Figure 6. Sentiment distribution by document type (Hist:History, P:Polysomnography, P-AW:Actigraphy Wrist), 5-stage sentiment score normalized into value between 0 and 1.

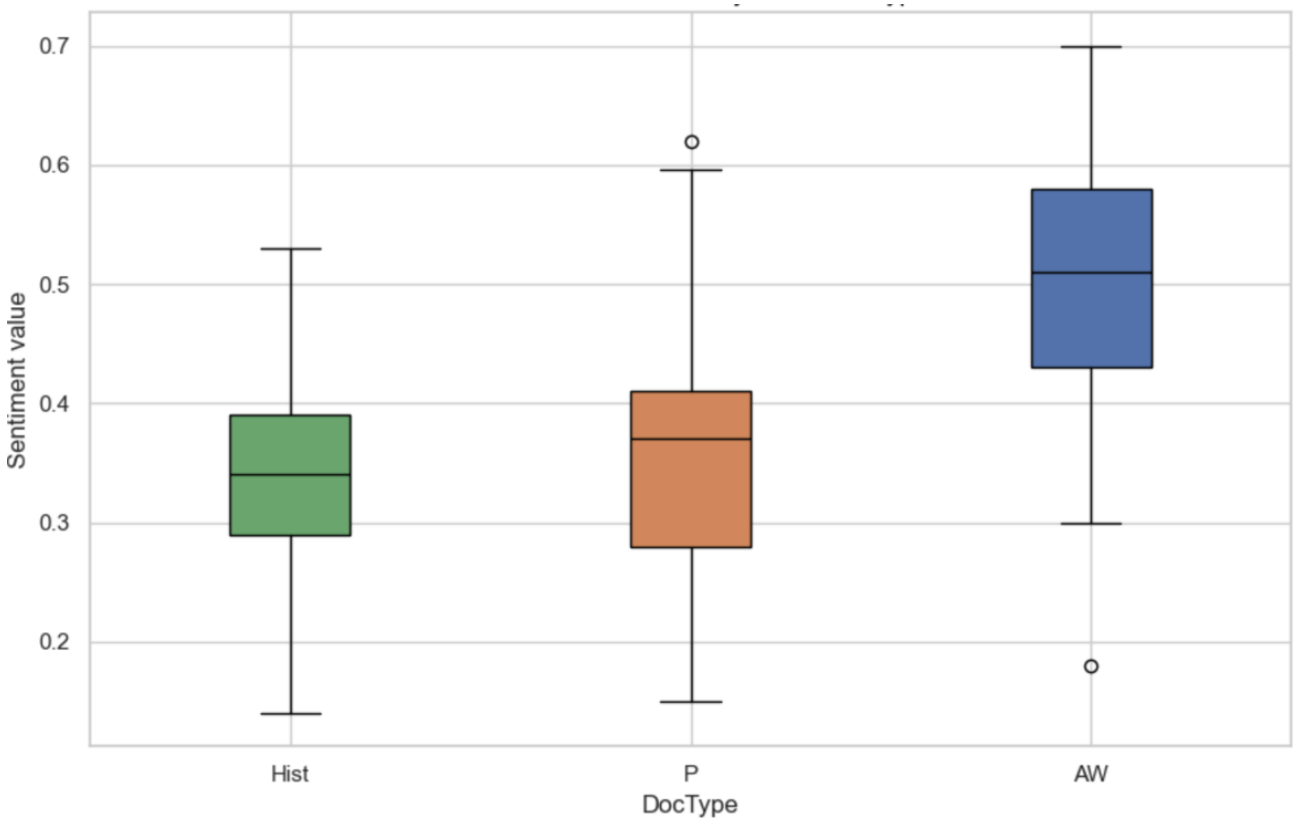
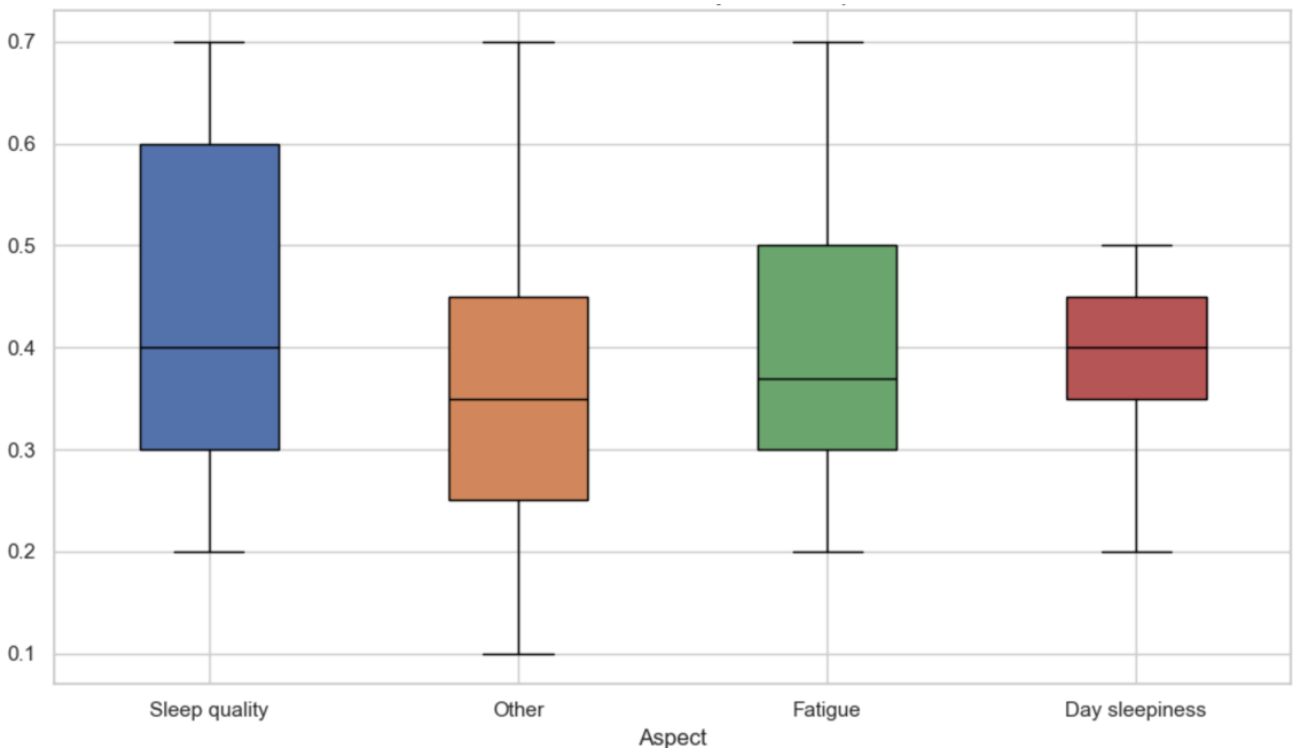


Figure 7. Sentiment distribution by sleep disorder aspect (quality, fatigue, and sleepiness).



Subjective-Objective Mismatch in Sleepiness Reporting

To examine potential misperceptions in day sleepiness, we compared subjective KSS reports with objective latency data from MSLT and MWT protocols. KSS values were normalized to a 0 - 1 range using the formula: KSS_normalized=(9–Raw Score)/(9–1) This transformation enables alignment with the inverse latency scale.

Figure 8 presents the misperception score distribution across 3 test conditions: 10 minutes pair: mslt_kssdur_10 versus latency_10, 12 minutes pair: mslt_kssdur_12 versus latency_12,

XSL•FO
RenderX

and mwt_kssdur versus latency. Misperception was defined as the deviation between normalized KSS and expected sleep latency levels. Across all pairings, positive misperception scores indicate that patients tend to report higher subjective sleepiness than measured objectively. The largest variability appeared in the mslt_kssdur_12 condition, while MWT tests showed narrower error bands.

Table 11 presents a representative subset of 10 patients illustrating questionnaire-expert-validated, text-predicted, and measured sleepiness scores. Although individual patterns vary, a general trend of overestimated sleepiness is observable.

Figure 8. Mismatch between subjective sleepiness (Karolinska Sleepiness Scale) and objective sleep latency (Multiple Sleep Latency Test and Maintenance of Wakefulness Test) in day sleepiness documents with a threshold of 10 and 12 minutes of latency. KSS: Karolinska Sleepiness Scale; MSLT: Multiple Sleep Latency Test; MWT: Maintenance of Wakefulness Test.

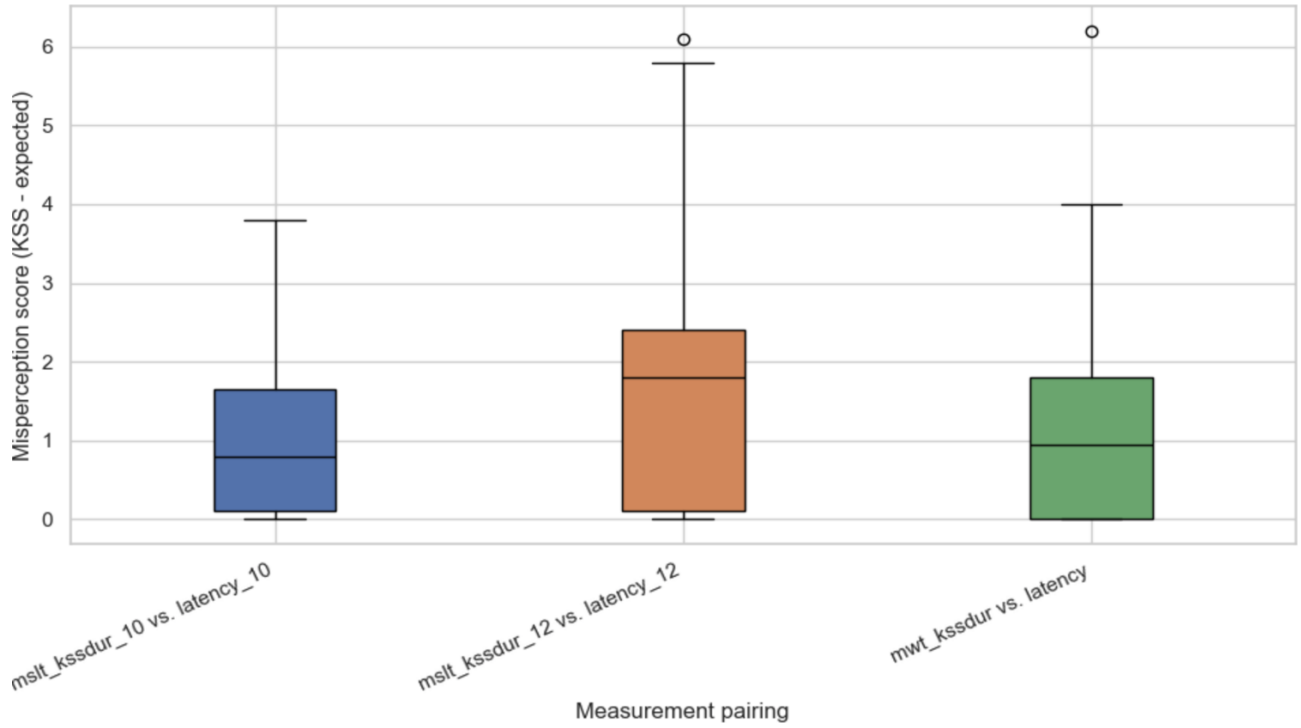


Table . A snapshot and working example with 10 patients from the selected cohort of 100 patients for day sleepiness, illustrating normalized Karolinska Sleepiness Scale (momentary) and text-derived score, expert-labeled and predicted subjective scores, along with corresponding Multiple Sleep Latency Test latencies and normalized objective scores.

Patient ID	KSS[a] stage	Text sentiment stage	MSLT[b] latency (min)	Objective score (0 - 4)	Differences KSS MSLT	Differences text MSLT
P001	2	2	5.04	2.992	−0.992	−0.992
P002	2	1	1.12	3.78	−1.78	−2.78
P003	3	2	7.76	2.45	0.55	−0.45
P004	0	1	1.13	3.77	−3.77	−2.77
P005	3	1	0.14	3.97	−0.97	−2.97
P006	2	1	15.99	0.80	1.20	0.20
P007	0	1	9.9	2.02	−2.02	−1.02
P008	3	1	10.54	1.89	1.11	−0.89
P009	3	3	8.83	2.23	0.77	0.77
P010	4	2	9.93	2.01	1.99	−0.01

[a]KSS: Karolinska Sleepiness Scale.

[b]MSLT: Multiple Sleep Latency Test.

A paired-sample *t* test conducted across the full cohort (n=100) revealed distinct patterns in the alignment between subjective and objective sleepiness assessments. While KSS scores showed a borderline nonsignificant divergence from MSLT-derived latencies (t_{99}=2.456, *P*=.06), text-derived sentiment scores demonstrated a statistically significant misalignment (t_{99}=2.324, *P*=.05). These findings suggest that free-text clinical narratives

XSL•FO
RenderX

more consistently diverge from physiological measures of sleepiness than structured scales such as the KSS. This may reflect the emotionally nuanced and context-rich nature of patient-reported symptoms embedded in narrative records. Importantly, although both subjective measures showed overestimation of sleepiness, only the text-derived sentiment reached statistical significance (P=.05), indicating a consistent, though not necessarily larger, misalignment with physiological data. More details can be found in Multimedia Appendix 1.

Discussion

Principal Findings

This study introduced a sentiment analysis framework for clinical sleep narratives, revealing key insights into both method performance and clinical relevance. The BERT-BiLSTM architecture improved sentiment accuracy by addressing negations and drift, while the Mixtral 8X7B model outperformed Falcon 40B in aspect extraction due to better handling of complex German syntax. A fine-tuned GPT-2 model with reinforcement learning achieved high sentiment classification accuracy (87%) and offered a resource-efficient alternative to LLMs. Clinically, sentiment-derived scores revealed consistent misperception patterns—such as underestimated sleep latency and overestimated duration—highlighting the importance of aligning subjective and objective measures. These findings support the integration of sentiment-informed misperception analysis into sleep medicine workflows to improve diagnosis, treatment selection, and patient safety.

Method Evaluation

In this study, we introduced and evaluated an aspect-based sentiment analysis approach tailored to clinical narratives in sleep medicine. Several key observations emerged from our findings. First, when mapping sentiment model outputs to scalar indicators of sleep disorders, it became necessary to adjust for negations and drifted sentiment—especially in baseline BERT models. Phrases that negated the presence of symptoms or diagnoses were frequently misinterpreted as negative sentiment. This issue was mitigated using a BERT-BiLSTM architecture, which improved performance through representation adaptation and fine-tuning.

For aspect (entity) extraction using prompted LLMs, recall was generally low, particularly for feedback-related content. In contrast, precision was high for identifying symptoms, diseases, and complaints. The poor recall is primarily attributed to the token limit and the generation style of Falcon 40B under one-shot prompting. Interestingly, few-shot prompting increased precision but further reduced recall and F_1-score. This reveals a trade-off that may be addressed either by increasing computational capacity (current setup: 128 GB Nvidia DGX server) or optimizing prompting strategies.

The Mixtral 8X7B model significantly outperformed Falcon 40B, delivering higher precision and recall for aspect recognition, even under single-shot settings. Its ability to handle longer input contexts and complex linguistic structures—such as German postnegation—proved particularly advantageous in the clinical domain. These results support the use of Mixtral 8x7B for German-language medical NLP tasks where nuanced comprehension is critical.

Compared to BERT-BiLSTM, a fine-tuned GPT-2 model trained on 1200 sleep-related clinical sentences achieved comparable performance (accuracy: 81%). Incorporating keyword-guided SFT and 2 RL epochs with logit modification raised accuracy to 87%. This dual-phase tuning strategy enhanced the model's flexibility and control. It also outperformed sequential prompting approaches commonly used with larger LLMs—offering higher precision with lower resource requirements, particularly important in privacy-sensitive clinical settings.

Clinical Outcomes

The interpretation of sentiment-derived misperception patterns must consider both the nature of subjective reporting and the inherent limitations of objective measurement in clinical sleep data. Misperception—defined as a mismatch between how patients feel and how their physiological state is measured—varies across dimensions of sleep disorders, with important diagnostic and therapeutic implications.

A key finding in our study was the divergence in sentiment-derived scores for similar clinical constructs. For instance, patients frequently underestimated their sleep latency (eg, reporting quick sleep onset) yet simultaneously overestimated their sleep duration, contrary to PSG and MSLT results. This subjective-objective mismatch—commonly referred to as sleep misperception—was particularly evident across latency, duration, and fatigue indicators. While traditional statistical tests may not fully capture the nuances of sentiment-informed scores, the consistent directionality and magnitude of these mismatches highlight their clinical importance.

However, the objectification of sleep quality and fatigue is inherently complex. Short sleep latency, often seen as a marker of healthy sleep, can paradoxically indicate pathological hypersomnolence in conditions such as narcolepsy. Similarly, fatigue—unlike sleepiness—lacks a gold-standard physiological test and is primarily self-reported, making its objectification more elusive. These nuances emphasize the need to interpret subjective scores considering disorder-specific clinical contexts.

In contrast, daytime sleepiness offers a more quantifiable target for misperception analysis. Here, subjective ratings such as the KSS and text-derived sentiment scores can be directly compared with objective markers such as MSLT latency. The KSS is particularly useful in this context, as it captures state-based, momentary sleepiness, allowing for meaningful trial-by-trial comparisons. For example, KSS values close to 0 (indicating "extremely sleepy") should theoretically align with MSLT latencies under 8 minutes. In our analysis framework, misperception magnitude increases when a patient reports low KSS (ie, "did not fall asleep") while objective data confirm they did—for example, falling asleep within 10 - 20 minutes in MSLT trials. This alignment enables fine-grained modeling of momentary misperception and supports targeted subanalysis of repeated MSLT and KSS pairs (eg, mslt_kssdur_10 vs mslt_sleeplatency_10).

XSL•FO
RenderX

From a clinical perspective, understanding the type and direction of misperception has actionable relevance.

For instance, in insomnia, patients often report exaggerated sleep difficulties (eg, longer sleep latency than measured). These cases may benefit more from cognitive behavioral therapy for insomnia rather than pharmacotherapy. Discussing the misperception with the patient is often therapeutic. However, because objective tests such as PSG are rarely used in routine insomnia management, wearable technologies (eg, smartwatches) could serve as surrogate tools to estimate sleep latency, duration, and fragmentation—offering scalable insight into real-world misperception.

In hypersomnia or sleep-disordered breathing, the opposite trend may occur—patients feel they slept well but exhibit abnormal sleep architecture or excessive daytime sleepiness in tests. In such cases, unrecognized sleepiness can elevate safety risks, such as motor vehicle or occupational accidents. Early identification of these cases using sentiment-objective comparison could trigger earlier clinical intervention or patient education.

Altogether, our sentiment analysis framework, enriched with structured objective metrics, offers a promising route for personalized assessment of sleep misperception. By comparing KSS, ESS, and text-derived sentiment scores against MSLT latency across multiple configurations, we can determine which input combination best captures the true subjective state. This multipronged analysis will inform future iterations of our clinical decision-support tools and help stratify patients for tailored treatment approaches.

Clinical Applications

Integrating sentiment analysis and misperception scoring into clinical workflows opens up new avenues for personalized, perception-aware sleep medicine:

1. Flag discrepancies in sleep latency and duration for targeted discussion or reassessment.
2. Stratify patients by degree of misperception to inform whether cognitive behavioral therapy for insomnia or pharmacotherapy is appropriate.
3. Highlight the underestimation of sleepiness in MSLT and MWT contexts for workplace or safety interventions.
4. Incorporate wearable data to validate or challenge patient self-reporting in follow-up care.

By aligning sentiment-derived patterns with objective sleep markers, clinicians can better understand not only what the patient reports but how they perceive their condition—a critical step toward improving diagnostic accuracy, treatment matching, and long-term outcomes.

Conclusion and Future Work

This study demonstrates that sentiment analysis applied to structured clinical narratives can uncover meaningful patterns in how patients perceive and report sleep disorders—especially in identifying discrepancies between subjective self-reports and objective assessments. Among the models evaluated, the BERT-BiLSTM architecture showed strong performance in domain-specific sentiment detection. However, the fine-tuned German GPT-2 model, enhanced with supervised and reinforcement learning (PPO), achieved the highest accuracy for 5-stage sentiment classification, offering an effective balance between adaptability and computational efficiency.

Our findings highlight the clinical value of sentiment-based misperception modeling. For example, patients with insomnia often overestimate wakefulness, while those with hypersomnia or sleep apnea tend to underreport daytime sleepiness. The use of reinforcement learning techniques proved especially effective for capturing emotionally nuanced language in clinical narratives while maintaining sensitivity to domain-specific clinical distinctions.

However, this study is not without limitations. All data were drawn from a single clinical registry, which may limit the generalizability of findings across institutions or populations. Furthermore, the annotated training set for sentiment and entity extraction was relatively small, potentially constraining model robustness and the diversity of learned patterns.

In future work, we aim to expand the dataset by incorporating records from additional clinical centers and to enrich the annotation set to enable more nuanced model training and validation. Sentiment modeling will be extended to cover additional clinical entities such as pain and cognitive symptoms, while correlations between sentiment-derived misperception scores and treatment outcomes or resistance will be further explored. We also plan to integrate physiological features—such as microarousals and sleep stage transitions—to improve subtype classification and to leverage wearable sensor data to validate and calibrate sentiment-based misperception metrics. Ultimately, our goal is to develop a precision sleep medicine framework that integrates objective physiological markers with patients' emotional and cognitive interpretations of their symptoms, captured through advanced sentiment and entity modeling of clinical narratives.

Acknowledgments

The secondary usage of Bern Sleep Data Base (BSDB) from Inselspital, University Hospital Bern, was approved by the local ethics committee (KEK-Nr. 2022 - 00415).

Data Availability

The datasets analyzed in this study are not publicly available due to data privacy considerations [31], but they may be obtained from the institutional review board of Inselspital upon reasonable application.

XSL•FO
RenderX

Authors' Contributions

YD and KD contributed to the conceptualization, methodology, validation, and original draft preparation. MS, CLAB, and JVDM were responsible for data curation. YD conducted the investigation. YD, KD, JVDM, AT, MS, and CLAB reviewed and edited the manuscript. AT also contributed to conceptualization.

Conflicts of Interest

None declared.

Multimedia Appendix 1
Mismatch between subjective sleepiness (Karolinska Sleepiness Scale) and objective sleep latency (Multiple Sleep Latency Test) with a threshold of 10 and 12 minutes among 100 patients.
[PNG File, 133 KB - medinform_v13i1e70753_app1.png]

References

1. Michal M, Wiltink J, Kirschner Y, et al. Complaints of sleep disturbances are associated with cardiovascular disease: results from the Gutenberg Health Study. PLoS One 2014;9(8):e104324. [doi: 10.1371/journal.pone.0104324] [Medline: 25093413]
2. Kotterba S, Neusser T, Norenberg C, et al. Sleep quality, daytime sleepiness, fatigue, and quality of life in patients with multiple sclerosis treated with interferon beta-1b: results from a prospective observational cohort study. BMC Neurol 2018 Aug 24;18(1):123. [doi: 10.1186/s12883-018-1113-5] [Medline: 30143019]
3. Mendonca F, Mostafa SS, Morgado-Dias F, Ravelo-Garcia AG, Penzel T. A review of approaches for sleep quality analysis. IEEE Access 2019;7:24527-24546. [doi: 10.1109/ACCESS.2019.2900345]
4. Zavecz Z, Nagy T, Galkó A, Nemeth D, Janacsek K. The relationship between subjective sleep quality and cognitive performance in healthy young adults: evidence from three empirical studies. Sci Rep 2020 Mar 17;10(1):4855. [doi: 10.1038/s41598-020-61627-6] [Medline: 32184462]
5. O'Donnell D, Silva EJ, Münch M, Ronda JM, Wang W, Duffy JF. Comparison of subjective and objective assessments of sleep in healthy older subjects without sleep complaints. J Sleep Res 2009 Jun;18(2):254-263. [doi: 10.1111/j.1365-2869.2008.00719.x] [Medline: 19645969]
6. Aurora RN, Caffo B, Crainiceanu C, Punjabi NM. Correlating subjective and objective sleepiness: revisiting the association using survival analysis. Sleep 2011 Dec 1;34(12):1707-1714. [doi: 10.5665/sleep.1442] [Medline: 22131609]
7. Stanyte A, Podlipskyte A, Alonderis A, Macijauskiene J, Burkauskas J, Steibliene V. Relationship between subjective and objective fatigue and sleep characteristics in individuals with anxiety and mood disorders: an exploratory study. Physiol Behav 2024 Feb 1;274:114429. [doi: 10.1016/j.physbeh.2023.114429] [Medline: 38065423]
8. Valko PO, Hunziker S, Graf K, Werth E, Baumann CR. Sleep-wake misperception. A comprehensive analysis of a large sleep lab cohort. Sleep Med 2021 Dec;88:96-103. [doi: 10.1016/j.sleep.2021.10.023] [Medline: 34742039]
9. Abbey SE, Garfinkel PE. Chronic fatigue syndrome and depression: cause, effect, or covariate. Rev Infect Dis 1991;13 Suppl 1:S73-S83. [doi: 10.1093/clinids/13.supplement_1.s73] [Medline: 2020805]
10. Hermans LWA, Leufkens TR, van Gilst MM, et al. Sleep EEG characteristics associated with sleep onset misperception. Sleep Med 2019 May;57:70-79. [doi: 10.1016/j.sleep.2019.01.031] [Medline: 30897458]
11. Herzog R, Crosbie F, Aloulou A, et al. A continuous approach to explain insomnia and subjective-objective sleep discrepancy. Commun Biol 2025 Mar 12;8(1):423. [doi: 10.1038/s42003-025-07794-6] [Medline: 40075150]
12. Devlin J, Chang MW, Lee K, Toutanova K. BERT: pre-training of deep bidirectional transformers for language understanding. Presented at: Proceedings of the 2019 Conference of the North; Jun 2-9, 2019; Minneapolis, Minnesota p. 4171-4186 URL: http://aclweb.org/anthology/N19-1 [doi: 10.18653/v1/N19-1423]
13. Behera RK, Jena M, Rath SK, Misra S. Co-LSTM: Convolutional LSTM model for sentiment analysis in social big data. Inf Process Manag 2021;58(1):102435. [doi: 10.1016/j.ipm.2020.102435]
14. Denecke K, Reichenpfader D. Sentiment analysis of clinical narratives: a scoping review. J Biomed Inform 2023 Apr;140:104336. [doi: 10.1016/j.jbi.2023.104336] [Medline: 36958461]
15. Kim Y. Convolutional neural networks for sentence classification. 2014 Presented at: Proceedings of the 2014 Conference on Empirical Methods in Natural Language Processing (EMNLP); Oct 25-29, 2014. [doi: 10.3115/v1/D14-1181]
16. Rehman AU, Malik AK, Raza B, Ali W. A hybrid CNN-LSTM model for improving accuracy of movie reviews sentiment analysis. Multimed Tools Appl 2019 Sep;78(18):26597-26613. [doi: 10.1007/s11042-019-07788-7]
17. Wang Z, Yang B. Attention-based bidirectional long short-term memory networks for relation classification using knowledge distillation from BERT. Presented at: 2020 IEEE Intl Conf on Dependable, Autonomic and Secure Computing, Intl Conf on Pervasive Intelligence and Computing, Intl Conf on Cloud and Big Data Computing, Intl Conf on Cyber Science and Technology Congress (DASC/PiCom/CBDCom/CyberSciTech); Aug 17-22, 2020. [doi: 10.1109/DASC-PICom-CBDCom-CyberSciTech49142.2020.00100]
18. Yang X, Li Y, Li Q, Liu D, Li T. Temporal-spatial three-way granular computing for dynamic text sentiment classification. Inf Sci (Ny) 2022 Jun;596:551-566. [doi: 10.1016/j.ins.2022.03.036] [Medline: 35693835]

XSL•FO
RenderX

19. Yu L, Dong J, Chen L, et al. PBCNN: packet bytes-based convolutional neural network for network intrusion detection. Comput Netw 2021 Jul;194:108117. [doi: 10.1016/j.comnet.2021.108117]
20. Liu P, Qiu X, Huang X. Recurrent neural network for text classification with multi-task learning. Presented at: IJCAI'16: Proceedings of the Twenty-Fifth International Joint Conference on Artificial Intelligence; Jul 19-15, 2016; New York USA p. 2873-2879.
21. Ziegler DM, Stiennon N, Wu J, et al. FineTuning language models from human preferences. arXiv. Preprint posted online on 2020. [doi: 10.48550/arXiv.1909.08593]
22. Schulman J, Wolski F, Dhariwal P, Radford A, Klimov O. Proximal policy optimization algorithms. arXiv. Preprint posted online on 2017. [doi: 10.48550/arXiv.1707.06347]
23. Pascual D, Egressy B, Meister C, Cotterell R, Wattenhofer R. A plug-and-play method for controlled text generation. Presented at: Findings of the Association for Computational Linguistics; Nov 7-11, 2021. [doi: 10.18653/v1/2021.findings-emnlp.334]
24. Denecke K, Deng Y. Sentiment analysis in medical settings: new opportunities and challenges. Artif Intell Med 2015 May;64(1):17-27. [doi: 10.1016/j.artmed.2015.03.006] [Medline: 25982909]
25. Aellen F, Van der Meer J, Dietmann A, Schmidt M, Bassetti CLA, Tzovara A. The Bern Sleep Database: clustering of patients with sleep disorders. Sleep Med 2022 Dec;100:S106. [doi: 10.1016/j.sleep.2022.05.295]
26. Werra L. Tune GPT-2 to generate controlled sentiment reviews. preprint, under review. Google Collab. URL: https://colab.research.google.com/drive/19CWnz8xhuV026nBuDEEUEMflTK9ENMIj?usp=sharing [accessed 2025-10-15]
27. Falcon 40B LLM repository. Hugging Face. URL: https://huggingface.co/tiiuae/falcon-40b-instruct [accessed 2025-10-14]
28. Werra L, Belkada Y, Tunstall L, et al. TRL: transformer reinforcement learning. GitHub. URL: https://github.com/huggingface/trl
29. Zhang H, Song H, Li S, Zhou M, Song D. A survey of controllable text generation using transformer-based pre-trained language models. ACM Comput Surv 2024 Mar 31;56(3):1-37. [doi: 10.1145/3617680]
30. Mixtral 8x7b repository. Hugging Face. URL: https://huggingface.co/mistralai/Mixtral-8x7B-Instruct-v0.1 [accessed 2025-10-14]
31. BERT base multilingual cased. Hugging Face. URL: https://huggingface.co/google-bert/bert-base-multilingual-cased [accessed 2025-10-14]
32. XLM-roberta base. Hugging Face. URL: https://huggingface.co/FacebookAI/xlm-roberta-base [accessed 2025-10-14]
33. Werra L. Tune GPT-2 to generate positive reviews. Hugging Face. URL: https://huggingface.co/tiiuae/falcon-40b-instruct [accessed 2025-10-14]
34. German GPT-2. URL: https://huggingface.co/benjamin/gerpt2model [accessed 2025-10-15]
35. Code repository. GitHub. URL: https://github.com/dyhpf/sleepmisperception [accessed 2025-10-15]

Abbreviations

AHI: Apnea-Hypopnea Index
ESS: Epworth Sleepiness Scale
FSS: Fatigue Severity Scale
***ICSD-III*:** *International Classification of Sleep Disorders, Third Edition*
KSS: Karolinska Sleepiness Scale
LLM: large language model
MSLT: Multiple Sleep Latency Test
MWT: Maintenance of Wakefulness Test
NLP: natural language processing
P-AW: Actigraphy Wrist
PPO: Proximal Policy Optimization
PSG: polysomnography
RL: reinforcement learning
SFT: supervised fine-tuning
SOL: sleep onset latency
TRL: Transformer Reinforcement Learning
TST: total sleep time

XSL•FO
RenderX

Edited by J Klann; submitted 31.12.24; peer-reviewed by D Teodoro, JM Immanuvel Arockiasamy, M Chatzimina, M Gandhi, PK Jain, Y Chen; revised version received 30.09.25; accepted 30.09.25; published 10.11.25.

Please cite as:
Deng Y, van der Meer J, Tzovara A, Schmidt M, Bassetti C, Denecke K
Analyzing Sleep Behavior Using BERT-BiLSTM and Fine-Tuned GPT-2 Sentiment Classification: Comparison Study
JMIR Med Inform 2025;13:e70753
URL: https://medinform.jmir.org/2025/1/e70753
doi:10.2196/70753

© Yihan Deng, Julia van der Meer, Athina Tzovara, Markus Schmidt, Claudio Bassetti, Kerstin Denecke. Originally published in JMIR Medical Informatics (https://medinform.jmir.org), 10.11.2025. This is an open-access article distributed under the terms of the Creative Commons Attribution License (https://creativecommons.org/licenses/by/4.0/), which permits unrestricted use, distribution, and reproduction in any medium, provided the original work, first published in JMIR Medical Informatics, is properly cited. The complete bibliographic information, a link to the original publication on https://medinform.jmir.org/, as well as this copyright and license information must be included.

XSL•FO
RenderX

Large Language Model Versus Manual Review for Clinical Data Curation in Breast Cancer: Retrospective Comparative Study

Young-Joon Kang[1], MD, PhD; Hocheol Lee[2], PhD; Jae Pak Yi[1], MD; Hyobin Kim[1], MD; Chang Ik Yoon[3], MD, PhD; Jong Min Baek[4], MD, PhD; Yong-seok Kim[5], MD, PhD; Ye Won Jeon[6], MD, PhD; Jiyoung Rhu[7], MD; Su Hyun Lim[1], MD; Hoon Choi[1], MD; Se Jeong Oh[1], MD, PhD

[1]Department of Surgery, College of Medicine, The Catholic University of Korea, Incheon St Mary's Hospital, 56, Dongsu-ro, Bupyeong-gu, Incheon, Republic of Korea

[2]Department of AI Health Information Management, Yonsei University (Mirae), Wonju, Republic of Korea

[3]Department of Surgery, College of Medicine, The Catholic University of Korea, Seoul St Mary's Hospital, Seoul, Republic of Korea

[4]Department of Surgery, College of Medicine, The Catholic University of Korea, Yeouido St Mary's Hospital, Seoul, Republic of Korea

[5]Department of Surgery, College of Medicine, The Catholic University of Korea, Uijeongbu St Mary's Hospital, Uijeongbu, Republic of Korea

[6]Department of Surgery, College of Medicine, The Catholic University of Korea, St Vincent's Hospital, Suwon, Republic of Korea

[7]Department of Surgery, College of Medicine, The Catholic University of Korea, Bucheon St Mary's Hospital, Bucheon, Republic of Korea

Corresponding Author:
Young-Joon Kang, MD, PhD
Department of Surgery, College of Medicine, The Catholic University of Korea, Incheon St Mary's Hospital, 56, Dongsu-ro, Bupyeong-gu, Incheon, Republic of Korea

Abstract

Background: Manual review of electronic health records for clinical research is labor-intensive and prone to reviewer-dependent variations. Large language models (LLMs) offer potential for automated clinical data extraction; however, their feasibility in surgical oncology remains underexplored.

Objective: This study aimed to evaluate the feasibility and accuracy of LLM-based processing compared with manual physician review for extracting clinical data from breast cancer records.

Methods: We conducted a retrospective comparative study analyzing breast cancer records from 5 academic hospitals (January 2019-December 2019). Two data extraction pathways were compared: (1) manual physician review with direct electronic health record access (group 1: 1366/3100, 44.06%) and (2) LLM-based processing using Claude 3.5 Sonnet (Anthropic) on deidentified data automatically extracted through a clinical data warehouse platform (group 2: 1734/3100, 55.94%). The automated extraction system provided prestructured, deidentified data sheets organized by clinical domains, which were then processed by the LLM. The LLM prompt was developed through a 3-phase iterative process over 2 days. Primary outcomes included missing value rates, extraction accuracy, and concordance between groups. Secondary outcomes included comparison with the Korean Breast Cancer Society national registry data, processing time, and resource use. Validation involved 50 stratified random samples per group (900 data points each), assessed by 4 breast surgical oncologists. Statistical analysis included chi-square tests, 2-tailed *t* tests, Cohen κ, and intraclass correlation coefficients. The accuracy threshold was set at 90%.

Results: The LLM achieved 90.8% (817) accuracy in validation analysis. Missing data patterns differed between groups: group 2 showed better lymph node documentation (missing: 152/1734, 8.76% vs 294/1366, 21.52%) but higher missing rates for cancer staging (211/1734, 12.17% vs 43/1366, 3.15%). Both groups demonstrated similar breast-conserving surgery rates (1107/1734, 63.84% vs 868/1366, 63.54%). Processing efficiency differed substantially: LLM processing required 12 days with 2 physicians versus 7 months with 5 physicians for manual review, representing a 91% reduction in physician hours (96 h vs 1025 h). The LLM group captured significantly more survival events (41 vs 11; *P*=.002). Stage distribution in the LLM group aligned better with national registry data (Cramér V=0.03 vs 0.07). Application programming interface costs totaled US $260 for 1734 cases (US $0.15 per case).

Conclusions: LLM-based curation of automatically extracted, deidentified clinical data demonstrated comparable effectiveness to manual physician review while reducing processing time by 95% and physician hours by 91%. This 2-step approach—automated data extraction followed by LLM curation—addresses both privacy concerns and efficiency needs. Despite limitations in integrating multiple clinical events, this methodology offers a scalable solution for clinical data extraction in oncology research. The 90.8% accuracy rate and superior capture of survival events suggest that combining automated data extraction systems with LLM processing can accelerate retrospective clinical research while maintaining data quality and patient privacy.

XSL•FO
RenderX

(JMIR Med Inform 2025;13:e73605) doi:10.2196/73605

KEYWORDS

natural language processing; breast neoplasms; data mining; clinical oncology; large language model; artificial intelligence

Introduction

Background

Recent advances in artificial intelligence, particularly in large language models (LLMs), have demonstrated remarkable capabilities of automated data extraction and organization from complex clinical documents [1-3]. These artificial intelligence–driven approaches can be used to process large volumes of clinical data with a consistent methodology, potentially reducing human bias and improving the collection efficiency of research data. Although LLMs show promise in health care applications, few studies on their practical efficacy compared with that of traditional, manual processing by physicians have been published, particularly in complex areas such as the extraction of surgical oncology data [4].

Clinical Challenges in Cancer Data Curation

In the field of breast cancer surgery, retrospective data analysis presents unique challenges owing to the complexity of unstructured clinical data. Electronic health records (EHRs) contain diverse information across clinical charts, operation records, and pathology reports, often in a free-text format. The complexity is compounded by breast cancer–specific characteristics, including the bilateral nature of the organs, concurrent malignant and benign lesions, and multiple radiological features. This complicates automated data curation and has traditionally necessitated manual review by physicians for accurate data interpretation and collection.

However, this manual approach has several limitations. As the volume of clinical data increases, consistency in physician reviews becomes increasingly difficult to maintain, potentially leading to discrepancies in data interpretation [5,6]. The time-intensive nature of manual review and the risk of errors in the processing of large volumes of clinical data present considerable challenges in retrospective research [7-10]. In addition, direct EHR access for manual data extraction raises privacy concerns when sensitive patient information is handled [11-13]. Although LLM-based automation of information extraction from anonymized EHR data may address these challenges, its effectiveness compared with that of traditional physician reviews remains to be evaluated.

Study Objectives

Although LLMs have been validated for the extraction of specific medical data, their potential for the curation of comprehensive data of patients with cancer remains largely unexplored [14]. In this study, we compared traditional physician reviews with LLM-based processing of anonymized clinical data in the field of breast cancer, focusing on the development of a practical approach for surgical oncologists. We hypothesized that LLM-based analysis would yield comparable results to manual review in handling large volumes of clinical data while reducing processing time and resource use.

Methods

Study Design and Data Collection

This retrospective comparative study included patients with breast cancer who underwent surgery at 5 academic hospitals from January 1, 2019, to December 31, 2019. This study was designed to compare 2 practical data curation pathways available in real-world clinical research settings. The manual review pathway represents the traditional method of direct EHR access. The LLM processing pathway uses preextracted, deidentified data. This study adheres to the Transparent Reporting of a Multivariable Prediction Model for Individual Prognosis or Diagnosis–Large Language Model (TRIPOD-LLM) reporting guidelines (Checklist 1).

We compared 2 data extraction methods: manual physician review (group 1) and LLM-based processing (group 2). In group 1, 1 dedicated breast-surgical oncologist from each hospital reviewed data spanning 2 years (2019 - 2020) over 7 months (May 2021–November 2021) using a standardized data collection form (Multimedia Appendix 1). The data encompassed 89 clinical variables across 3 domains: patient demographics (basic information, medical history, and family history), treatment information (surgical details, neoadjuvant or adjuvant therapy, complications, and follow-up treatment), and pathological information (tumor characteristics, tumor stage, biomarker status, and margin status). Follow-up observations regarding recurrence and mortality were updated until January 2024.

Patients in group 2 were initially identified using the clinical data warehouse (CDW) of Catholic Medical Center, an integrated data platform of 8 affiliated academic hospitals in Korea [15,16]. The CDW supports this research by providing anonymous clinical data to investigators following institutional review board approval [15]. The LLM structured 31 clinical factors from the raw data, including patient demographics (basic information, survival data, and diagnostic data), treatment information (surgery types and neoadjuvant or adjuvant therapy), pathological information (tumor characteristics, tumor stage, biomarker status, and nodal status), and imaging features. Data extraction and curation were performed from October 20, 2024, to November 1, 2024.

The CDW query identified 17,317 patients diagnosed with invasive breast cancer or ductal carcinoma in situ between July 2018 and July 2021. From this cohort, we selected patients diagnosed during the study period (January 2019-December 2019) who underwent breast cancer surgery. CDW extraction included unstructured EHR reports containing clinical information, operation records, and pathology reports (Multimedia Appendices 2-4). Follow-up data through October 31, 2023, were used.

XSL•FO
RenderX

Data Curation in LLM-Processing Group

Unstructured data extracted from the CDW were processed using Claude 3.5 Sonnet (Anthropic) to extract and structure the required factors into predefined categories.

LLM Implementation and Application Programming Interface (API) Access

We accessed Claude 3.5 Sonnet through the Anthropic web interface (claude.ai) using a professional subscription account. The implementation specifications are as follows:

1. Access method: web-based interface with manual copy-paste of clinical documents.
2. Processing approach: sequential processing of individual patient records.
3. Input size limitations: documents exceeding 100,000 characters were split into logical sections (diagnosis, surgery, and pathology) and processed sequentially.
4. Output format: structured CSV format directly generated by the LLM.
5. Session management: new conversation initiated for each batch of 50 patients to prevent context contamination.
6. Quality control: real-time review of outputs with immediate reprocessing for any parsing errors.

No API programming or authentication keys were required, as we used the standard web interface. This approach, while manual, ensured direct oversight of the extraction process and immediate error detection.

Prompt Development Process

Overview

The LLM prompt was developed through a 3-phase iterative process over 2 days (from October 20, 2024, to October 21, 2024). Rather than manually crafting the extraction rules, we used an interactive dialogue approach with the LLM itself to develop the prompt. We provided the LLM with sample data and target output requirements, and then iteratively refined the extraction protocol through conversational feedback.

The iterative refinement process consists of 3 phases.

Phase 1

This was the initial framework development phase and we included 10 cases. We presented the LLM with representative raw data and developed extraction rules through dialogue. The LLM proposed initial patterns for data extraction, which were tested using sample cases.

Phase 2

This was the rule refinement phase, and we included 20 cases. On the basis of the phase 1 outputs, we organized errors through manual review and engaged LLM to analyze the errors and modify them. Key refinements included diagnosis deduplication using International Classification of Diseases, 10th Revision code comparison, surgical procedure hierarchy establishment, pathology section prioritization, and biomarker interpretation standardization (particularly for human epidermal growth factor receptor 2 [HER2] status requiring in situ hybridization confirmation for 2+ cases).

Phase 3

This was the edge case handling phase, and we included 30 cases. The refined prompt was tested in diverse clinical scenarios. Additional instructions were added for handling bilateral cases (processing each breast separately), multiple surgical procedures (capturing all relevant operations), ambiguous staging information (requiring explicit notation rather than inference), and complex biomarker patterns (particularly HER2 equivocal cases).

The final prompt is available in the Multimedia Appendix 5. Due to its length, we provide a condensed version highlighting the key extraction rules, while the complete prompt with all edge cases and examples can be obtained from the corresponding author.

Prompt Structure and Components

The final prompt focused on accurate extraction from 4 distinct data categories: diagnostic information, clinical measurements, surgical procedures, and pathological findings.

Global Processing Rules Module

This module established standardized data formats and processing conventions. Key specifications included patient ID formatting (R[9-digit number]), laterality coding (right or left or bilateral), date standardization (YYYY-MM-DD), missing data coding (999,999), and CSV output structure. Each case was processed by laterality to handle bilateral breast cancers as separate entities, maintaining distinct Case_IDs formatted as “Patient_ID_Laterality” (eg, R000000001_RT).

Clinical Data Processing Module

This module handled diagnosis information, surgical procedures, and mortality data with specific extraction hierarchies. For diagnosis processing, the system prioritized primary diagnosis information, extracted English text only while removing Korean text, and implemented deduplication logic by comparing International Classification of Diseases, 10th Revision codes (first three characters) to identify identical diagnoses while preserving distinct diagnoses. For surgical information, we established clear precedence rules where therapeutic operations took priority over diagnostic procedures, with specific terminology mapping for breast procedures (eg, “wide excision,” “modified radical mastectomy,” and “lumpectomy”) and axillary procedures (sentinel lymph node biopsy [SLNB] and axillary lymph node dissection [ALND]).

Pathology Data Extraction Module

Given the variability in pathology report formats, we defined a section priority hierarchy: (1) microscopic description, (2) diagnosis, (3) immunohistochemistry, and (4) gross description. Specific extraction patterns were defined within each section. For tumor size determination, the search sequence was: “tumor size (size of largest invasive carcinoma)," “greatest dimension of largest invasive focus,” “size of largest invasive focus,” and “estimated size (extent) of DCIS.” For lymph node assessment, we standardized various reporting formats (eg, “X/Y [positive/total]," “metastatic carcinoma [n/total]," “lymph node metastasis; present or absent [n/total]") and classified metastasis

XSL•FO
RenderX

by size (macrometastasis >2 mm, micrometastasis 0.2 - 2 mm, and isolated tumor cell ≤0.2 mm).

Quality Control Module

this module implemented validation rules and error prevention strategies. The prompt excluded error-prone extractions, such as gross specimen sizes, surgical margin measurements, and lymph node sizes. It required explicit documentation of missing data rather than inference, implemented range validation for biomarkers (estrogen receptor or progesterone receptor or Allred score 0 - 8, Ki-67 0% - 100%), and cross-reference verification between different report sections.

Task Sequence and Processing Flow

Prompt execution of tasks in a specific sequence to ensure data integrity:

1. Initial parsing: identify patient ID and laterality from diagnostic records
2. Temporal alignment: establish diagnosis date as a reference point for all subsequent data
3. Hierarchical extraction: process data in order of clinical importance: diagnosis → surgery → pathology → imaging
4. Integration check: validate consistency across different data sources
5. Output generation: structure extracted data into a predefined .CSV format with quality flags

The prompt instructed the LLM to generate outputs directly in .CSV format with predefined column structures, automated date formatting (YYYY-MM-DD), and standardized missing data codes (999,999), eliminating the need for extensive after processing. The structured output was validated through the methodology described in the Data Quality Assessment and Validation section.

Objectives and Statistical Analysis

This study aimed to assess the feasibility of replacing manual physician reviews with LLM-based processing of breast cancer–related clinical data. We compared the demographic characteristics, clinical parameters, treatment patterns, disease characteristics, and survival outcomes between the 2 groups.

Categorical variables were compared using chi-square or Fisher exact tests, with agreement assessed using Cohen κ coefficient (κ<0.20=poor, 0.21 - 0.40=fair, 0.41 - 0.60=moderate, 0.61 - 0.80=good, >0.80=very good). Continuous variables were analyzed using the Student *t* test and the intraclass correlation coefficient. Effect sizes were calculated using Cohen *d* (continuous) and Cramér V (categorical).

Overall survival was analyzed using the Kaplan-Meier method and compared using the log-rank test. Both approaches were validated using the Korean Breast Cancer Society (KBCS) 2019 national registry data by comparing age, tumor stage, surgical procedures, molecular subtypes, and survival trends [17].

Data Quality Assessment and Validation

For validation, 50 cases from each group were selected using proportionate stratified random sampling. Stratification was based on the cancer stage (0-IV) and type of surgical intervention (breast-conserving surgery vs mastectomy) to ensure representative sampling across key clinical categories. Random selection was performed using Python (version 3.8; Python Software Foundation) with the *NumPy* (v.1.21.0) and *pandas* (v.1.3.0) libraries and a fixed random seed of 2,02,41,201 for reproducibility. Four breast-surgical oncologists (SJO, JPY, HK, and SL) independently evaluated 18 predefined clinical factors in each case (900 data points per group). Accuracy rates were calculated as the percentage of correctly extracted factors relative to the total number of factors. A dual-reference validation approach was implemented: group 1 was validated against the EHR, whereas group 2 was compared to the CDW raw data. The evaluation included both present and missing values. The accuracy threshold was set at 90% based on previous validation studies of clinical data extraction systems [18].

Ethical Considerations

This study was approved by the institutional review board of the Catholic Medical Center (approval: OC24WIDI0138). As this was a retrospective analysis of existing clinical data, the requirement for informed consent was waived by the institutional review board. All patient data were deidentified prior to analysis, with personal identifiers replaced by anonymized codes. The CDW platform ensures privacy protection through automated deidentification. No compensation was provided to participants, as this study involved retrospective data analysis only.

Results

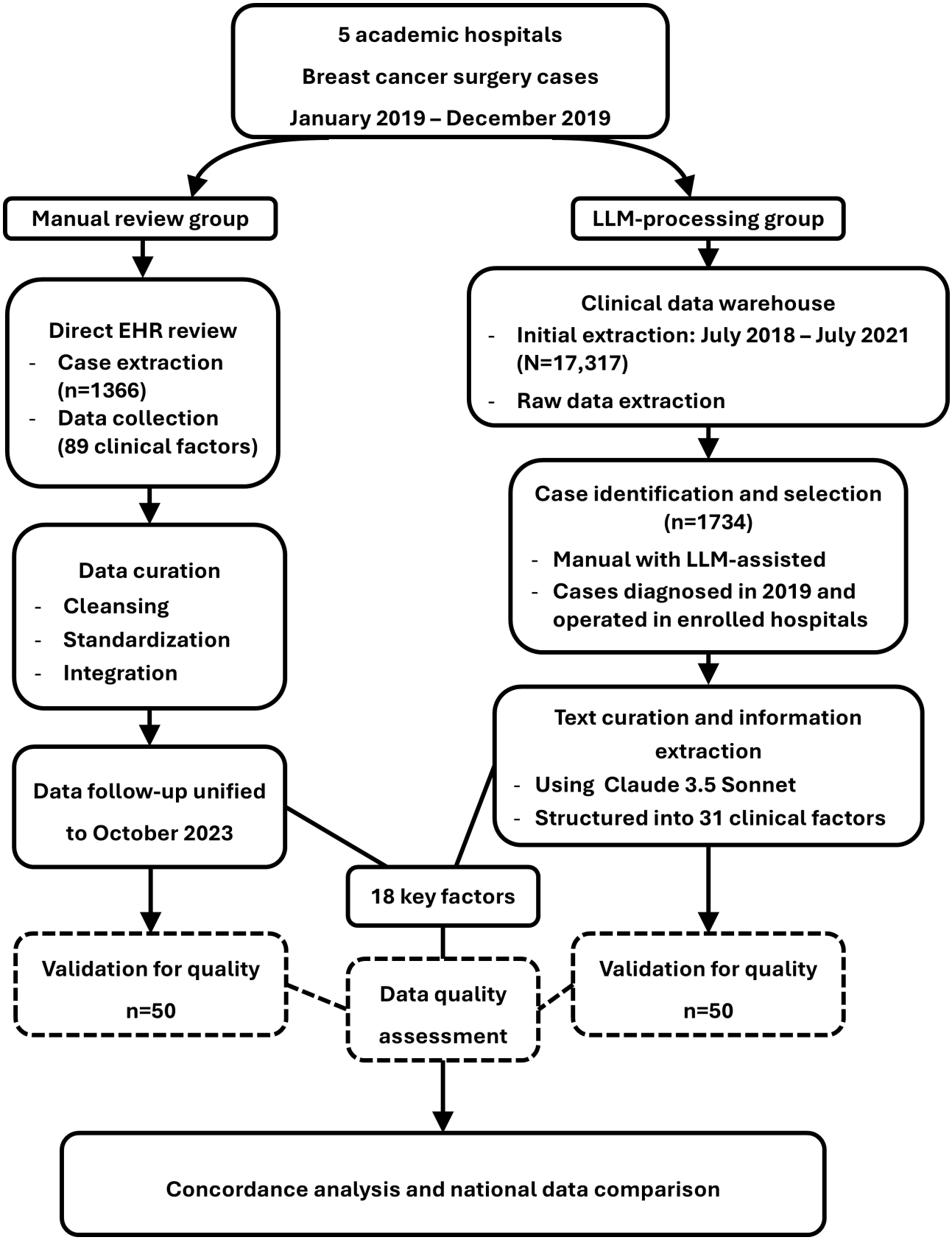
Outcomes

For comparative analysis, 18 key clinical factors were selected from both groups (Figure 1). The manual review (group 1) and LLM processing (group 2) groups comprised 1366 and 1734 cases, respectively. Although both groups completely captured age data, they exhibited different patterns of missing data for the other parameters. Group 2 had higher missing rates in terms of cancer stage (12.2% vs 3.1%) and HER2 status (15.1% vs 11.0%), whereas group 1 had more missing data for lesion size (20.5% vs 5.9%) and lymph node assessment (21.5% vs 8.8%). Both groups maintained high documentation rates (>90%) for hormone receptor status (Figure 2).

The validation analysis encompassed 1800 data points (900 per group) across clinical factors. Group 1 demonstrated perfect accuracy with no discrepancies. Group 2 exhibited 83 discordant factors out of 900 data points with an accuracy rate of (817/900, 90.8%). Among 1734 patients in group 2, 260 (15%) underwent multiple surgical procedures. The LLM successfully integrated data from sequential operations in 53% (138/260) of these cases, while missing data integration in 47% (122/260).

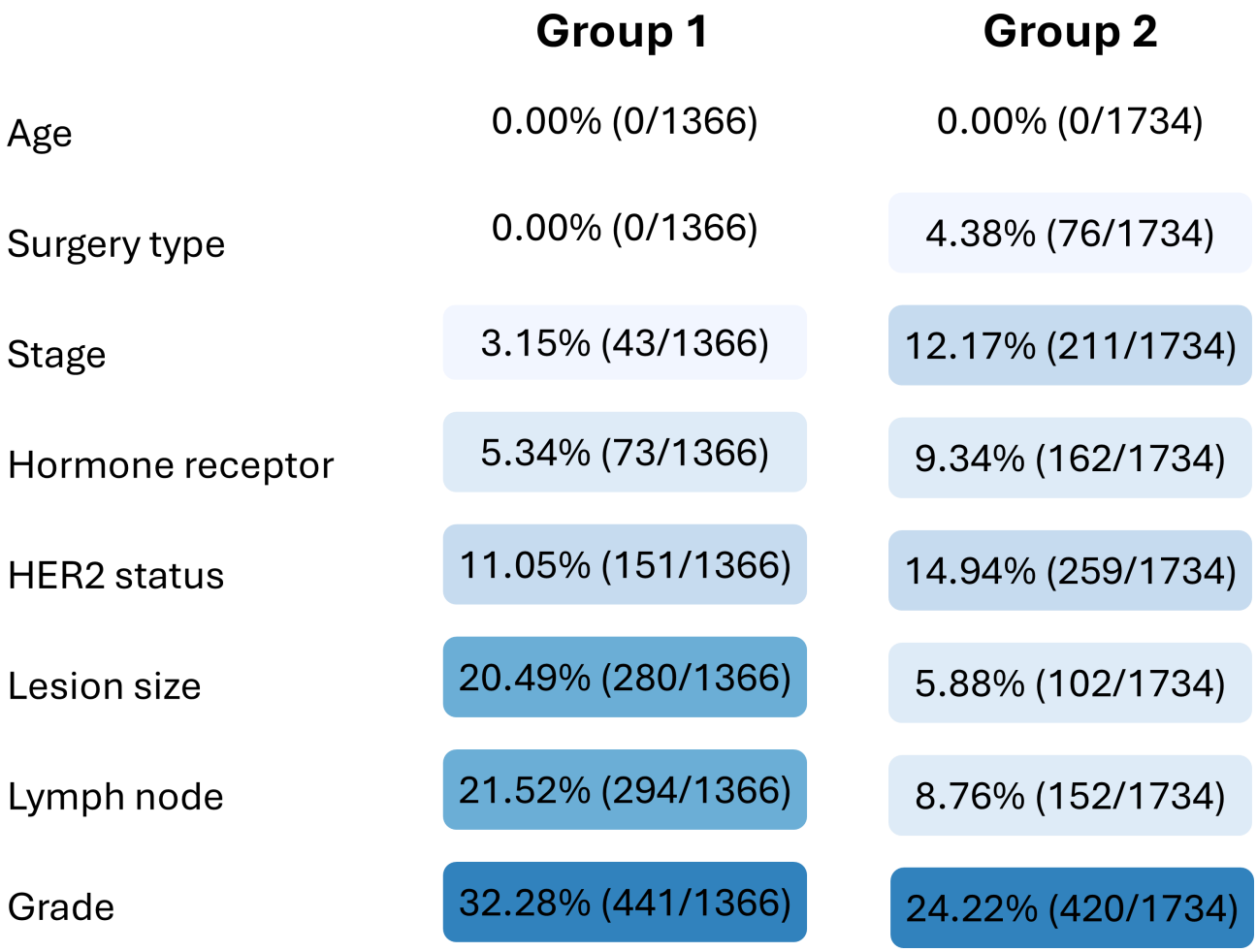
XSL•FO
RenderX

Figure 1. Study design chart showing the comparison between the manual review and large language model (LLM)-processing groups. EHR: electronic health record.



XSL•FO
RenderX

Figure 2. Comparison of missing data rates (%) between manual review (group 1) and large language model (LLM) processing (group 2). Color intensity represents the magnitude of missing data, with darker shades indicating higher missing rates. HER2: human epidermal growth factor receptor 2.



Processing Time and Resource Use

LLM-based processing demonstrated efficiency gains compared to manual review (Table 1). Group 1 required 7 months (May 2021-November 2021) with 5 dedicated breast surgical oncologists. In contrast, group 2 processing was completed in 12 days (from October 20, 2024, to November 1, 2024) by 2 physicians, with data extraction taking 10 days and validation requiring 2 additional days.

Table . Comparison of processing efficiency.

Parameter	Manual review (group 1)	LLM[a] processing (group 2)	Difference
Total cases	1336	1734	+368
Processing period	7 months	12 days	−95%
Number of physicians	5	2	−60%
Total physician hours	Approximately 1025	Approximately 96	−91%
Direct EHR[b] access required	Yes	No	N/A[d]
API[c] cost	N/A[d]	Approximately $260	N/A

[a]LLM: large language model.

[b]EHR: electronic health record.

[c]API: application programming interface.

[d]N/A: not applicable.

Manual review required approximately 1025 physician hours total across 7 months. LLM processing required approximately 96 physician hours in total over 12 days, a 91% reduction in time investment.

Resource use differed substantially between the methods. The manual review required 5 breast surgical oncologists with a direct EHR access infrastructure and dedicated data entry personnel. LLM processing required 2 physicians using a

XSL•FO
RenderX

standard workstation without EHR access. The API cost for LLM processing was approximately $0.15 per case, totaling $260 for 1734 cases. Although direct personnel costs were not calculated due to institutional variations in physician compensation, the 91% reduction in physician hours represents substantial resource savings.

Demographics and Clinical Characteristics

The baseline characteristics of both groups are summarized in Table 2. The mean age differed slightly between groups 1 and 2 (55, SD 11.5 vs 53.5, SD 11.4 y; $P<.001$; Cohen $d=0.13$). For breast surgery, total mastectomy was performed in 19.2% of cases in group 1 and 26.5% in group 2, while nipple (skin)-sparing mastectomy rates were 15.7% and 9.6%, respectively ($\chi^{2}_{3}=164.3$; $P<.001$; Cramér V=0.29). When these procedures were combined, groups 1 and 2 exhibited similar proportions of breast-conserving surgery (63.5% vs 63.9%) and mastectomy (34.8% vs 36%), with a small effect size (Cramér V=0.10).

XSL•FO
RenderX

Table . Baseline characteristics of study groups. Statistical significance set at $P<.05$. Analyses were performed using chi-square test for categorical variables and *t* test for continuous variables[a].

Characteristics	Manual review (n=1366)	LLM[b] processing (n=1734)	*P* value
Demographics, mean (SD)			
Age (y)	55.0 (11.5)	53.5 (11.4)	<.001
Surgical procedures, n			
Breast operation			<.001
Breast-conserving surgery	63.53 (868/1366)	63.90 (949/1485)	
Total mastectomy	19.18 (262/1366)	26.46 (393/1485)	
N(S)SM[c]	15.67 (214/1366)	9.56 (142/1485)	
Other procedures	1.61 (22/1366)	0.07 (1/1485)	
Combined mastectomy[d]	34.85 (476/1366)	36.03 (535/1485)	
Axillary surgery			<.001
No surgery	11.20 (153/1366)	19.37 (321/1657)	
SLNB[e]	68.30 (933/1366)	59.75 (990/1657)	
ALND[f]	20.50 (280/1366)	20.88 (346/1657)	
Pathological results, mean (SD)			
Tumor size (mm)	20.5 (16.4)	21.5 (16.9)	.156
Lymph node status, mean (SD)			
Harvested nodes	7.79 (7.0)	7.11 (7.2)	.016
Metastatic nodes	0.95 (3.0)	0.98 (3.2)	.802
Stage distribution, n (%)			<.001
0	17.91 (237/1323)	15.56 (237/1523)	
IA	35.68 (472/1323)	43.27 (659/1523)	
IB	0.60 (8/1323)	1.31 (20/1523)	
IIA	22.22 (294/1323)	20.75 (316/1523)	
IIB	11.11 (147/1323)	10.83 (165/1523)	
IIIA	7.48 (99/1323)	5.65 (86/1523)	
IIIB	0.83 (11/1323)	0.07 (1/1523)	
IIIC	3.70 (49/1323)	2.56 (39/1523)	
IV	0.45 (6/1323)	0.00 (0/1523)	
Biomarker status			
ER[g] positive, % (n/N)	78.28 (1012/1293)	76.21 (1198/1572)	.172
PR[h] positive, % (n/N)	68.68 (886/1290)	67.50 (1059/1569)	.525
HER2[i] positive, % (n/N)	20.49 (249/1215)	20.20 (298/1475)	.003
Ki-67, mean (SD)	25.4 (23.0)	26.6 (22.6)	.204
Histologic grade, % (n/N)			.764
Grade 1	22.81 (211/925)	21.54 (283/1314)	
Grade 2	44.65 (413/925)	46.35 (609/1314)	
Grade 3	32.54 (301/925)	32.12 (422/1314)	
Nuclear grade, % (n/N)			<.001

XSL•FO
RenderX

Characteristics	Manual review (n=1366)	LLM[b] processing (n=1734)	*P* value
Grade 1	16.75 (171/1021)	12.90 (199/1543)	
Grade 2	42.51 (434/1021)	51.52 (795/1543)	
Grade 3	40.78 (416/1021)	35.58 (549/1543)	
Survival outcomes, % (n/N)			
Death	0.81 (11/1366)	2.42 (42/1734)	.001

[a]Percentages calculated based on cases with available data for each variable

[b]LLM: large language model.

[c]N(S)SM: nipple or skin-sparing mastectomy.

[d]Combined mastectomy includes total mastectomy and N(S)SM.

[e]SLNB: sentinel lymph node biopsy.

[f]ALND: axillary lymph node dissection.

[g]ER: estrogen receptor.

[h]PR: progesterone receptor.

[i]HER2: human epidermal growth factor receptor 2.

In terms of axillary surgery, group 1 had a higher rate of SLNB than group 2 (68.4% vs 59.7%), whereas the rates of ALND were similar (χ^2_2=47.2; *P*<.001; Cramér V=0.13). The mean (SD) value of the harvested lymph nodes was similar between the groups (7.79, SD 7.03 vs 7.11, SD 7.20; *P*=.016).

The stage distribution differed between groups (χ^2_8=68.9; *P*<.001), but only slightly (Cramér V=0.16), with group 1 identifying more cancers as advanced. Hormone receptor status was similar between the groups (estrogen receptor: 78.3% vs 76.2%, *P*=.172; progesterone receptor: 68.7% vs 67.5%, *P*=.525). HER2 status differed negligibly, and Ki67 expression was similar between the groups (HER2: *P*=.003, Cramér V=0.003; Ki67: *P*=.391, Cramér V was approximately 0.00). Histological grade distributions were similar between the groups (*P*=.764).

Interrater Agreement Analysis

ICC analysis of continuous variables demonstrated a consistently low agreement: age (ICC 0.013, 95% CI –0.035 to 0.060), tumor size (ICC 0.029, 95% CI –0.021 to 0.078), number of metastatic lymph nodes (ICC 0.031, 95% CI –0.019 to 0.081), number of harvested lymph nodes (ICC 0.025, 95% CI –0.025 to 0.075), and Ki67 expression (ICC 0.027, 95% CI –0.023 to 0.077). All ICC values were negligible, and all CIs included zero.

Survival Outcomes

Survival analysis revealed significant differences between the groups (hazard ratio 2.917, 95% CI 1.496 to 5.688; *P*=.002). Group 2 captured more events (11 vs 41). The proportional hazards assumption was met (χ^2_1 =2.37; *P*=.120), and the log-rank test confirmed a difference in survival distributions (χ^2_1 =10.9; *P*=.001).

Comparison With National Registry Data

Comparison with the KBCS 2019 registry data (N=9447) revealed small differences in breast surgery patterns for both groups (Cramér V=0.03 - 0.04; *P*≤.018; Table 3). For axillary surgery, both groups had lower SLNB rates (group 1: 68.30% and group 2: 59.75% vs KBCS: 73.18%) and similar ALND rates (20.50% vs 20.88% vs 18.60%). Group 2 had a higher rate of no axillary surgery than group 1 (19.37% vs 11.20%).

Stage distribution analysis revealed significant but small differences from the national data (group 1: Cramér V=0.076, *P*<.001; group 2: Cramér V=0.038, *P*=.003). Regarding biomarker subtypes, both groups had slightly higher proportions of hormone receptor–positive with HER2-negative (group 1: 67.02% and group 2: 66.57% vs KBCS: 63.14%) and triple-negative cases (12.70% and 13.59% vs 11.98%) with minimal effect sizes (Cramér V=0.03 - 0.04).

XSL•FO
RenderX

Table . Comparison of clinical characteristics with Korean Breast Cancer Society (KBCS) 2019 national registry data[a].

Characteristic	Group 1 (n=1366)	Group 2 (n=1734)	KBCS 2019 (N=9447)	Effect size (Cramér's V)	P value[b]
Breast surgery type, n (%)				• 0.03-0.04	• <.001
Breast-conserving surgery	868 (63.53)	949 (63.90)	6067 (64.26)		
Total mastectomy	476 (34.85)	535 (36.03)	3380 (35.78)		
Others	22 (1.61)	1 (0.07)	0 (0.00)		
Axillary surgery type, n (%)				• Group 1: 0.13 • Group 2: 0.15	• <.001
SLNB[d]	933 (68.30)	990 (59.75)	6913 (73.18)		
ALND[e]	280 (20.50)	346 (20.88)	1757 (18.60)		
No surgery	153 (11.20)	321 (19.37)	777 (8.22)		
Cancer stage distribution, n (%)				• Group 1: 0.07 • Group 2: 0.03	• <.001 • 0.003
Stage 0	237 (17.91)	237 (15.56)	1588 (16.81)		
Stage I	480 (36.28)	679 (44.58)	4015 (42.50)		
Stage II	441 (33.33)	481 (31.58)	2948 (31.20)		
Stage III	159 (12.02)	126 (8.27)	896 (9.48)		
Biomarker status,[f] n (%)				• 0.03-0.04	• 0.003
ER[k] positive	1012 (78.28)	1198 (76.21)	7163 (75.82)		
PR[h] positive	886 (68.68)	1059 (67.50)	6254 (66.20)		
HER2[i] positive	249 (20.49)	298 (20.20)	1748 (18.50)		

[a]Percentages calculated based on cases with available data for each variable

[b]Statistical significance set at $P<.05$. Chi-square tests were used for categorical comparisons.

[c]KBCS: Korean Breast Cancer Society

[d]SLNB: sentinel lymph node biopsy.

[e]ALND: axillary lymph node dissection.

[f]Molecular subtypes were determined based on combined estrogen receptor (ER), progesterone receptor (PR), and HER2 status. HR+ defined as ER+ or PR+.

[g]ER: estrogen receptor.

[h]PR: progesterone receptor.

[i]HER2: human epidermal growth factor receptor 2.

Discussion

Principal Findings

This comparative study demonstrated that LLM-based processing achieved 90.8% accuracy in extracting clinical data from breast cancer records, with significant reductions in processing time (12 d vs 7 mo) and resource requirements (2 vs 5 physicians). The LLM approach captured substantially more survival events (41 vs 11; $P=.002$) and showed better documentation of lymph node assessment (91.2% vs 78.5%), although it had higher missing rates for integrated assessments such as cancer staging (12.2% vs 3.1%). Both methods yielded similar patterns in key clinical parameters, including breast-conserving surgery rates (63.5% vs 63.9%) and biomarker distributions.

A particular finding was the substantial difference in captured survival events between LLM processing (41 events) and manual review (11 events). This discrepancy may reflect fundamental differences in how humans and LLMs approach large-scale data extraction. Manual reviewers processing many charts may inadvertently adopt a mechanical approach, focusing on the most obvious data fields, while potentially overlooking mortality information scattered across multiple sections of the medical record. In contrast, LLM maintained consistent thoroughness throughout the extraction process, systematically examining all available data sources for each case without the cognitive fatigue that affects human reviewers during repetitive tasks.

XSL•FO
RenderX

This finding challenges the assumption that manual review is the gold standard for all types of clinical data extraction. While human expertise remains essential for complex clinical interpretation, our results suggest that LLM processing may provide a more complete capture of certain objective outcomes, particularly those requiring synthesis across multiple data fields. However, this interpretation requires further research to confirm whether the additional events captured by the LLM represent true positives or extraction errors.

Comparison With Prior Work

Although LLMs have shown favorable results in extracting specific medical data from radiology and pathology reports [19-22], our study represents the first comprehensive evaluation of surgical oncology data curation. Previous studies have focused on the extraction of single data points or specific types of reports. For instance, Park et al [20] demonstrated the effectiveness of LLM in extracting pulmonary disease information from radiology reports, whereas Cheng [22] reviewed its applications in pathology. Our study extends these findings by demonstrating that LLMs can handle the complex integration required for comprehensive oncological data including surgical procedures, pathological findings, and survival outcomes.

The observed statistical differences between groups, while significant, were mostly clinically negligible (Cramér V<0.30 for all comparisons), suggesting that LLM processing maintains clinical validity. The observed accuracy of 90.8% is comparable to recent studies, where LLMs achieved similar performance in extracting structured information from clinical notes, including the social determinants of health [23]. Although comprehensive systematic reviews of LLM applications in healthcare are still emerging [3], individual studies have consistently demonstrated their potential for automated clinical data extraction. However, unlike previous studies that focused on extracting discrete clinical variables or single-domain information [19-23], surgical oncology data require integration of multiple interconnected factors, presenting unique challenges in automated extraction.

Strengths and Limitations

Our study had several strengths. The large sample size provided robust statistical power. The use of real-world clinical data from multiple institutions enhanced the generalizability of the results. The head-to-head comparison with a manual physician review rather than against a reference standard alone provides practical insights for clinical research applications. Additionally, the demonstrated efficiency gains (12 d vs 7 mo) highlight the potential for scaling oncological research.

However, several limitations of this study must be acknowledged.

First, LLMs showed limitations in integrating multiple clinical events. Although the model performed well in extracting explicit data points, it struggled to synthesize information across sequential surgical procedures. This was evidenced by the higher rate of missing surgical data (12.2% vs 3.1%) in patients who underwent multiple operations. Manual reviewers could identify and integrate multiple surgical steps, such as lymph node assessment after initial diagnostic excision, while the LLM typically captured data from a single representative operation.

Second, the validation sample size of 50 cases per group represented only 2.9% and 2.6% of the respective cohorts. While this sample was stratified to ensure representation across cancer stages and surgical types and achieved adequate power for detecting clinically meaningful differences, a larger validation set would strengthen confidence in the accuracy estimates.

Third, differences in data sources between the groups may have affected direct comparability. The manual review group accessed complete EHRs directly, whereas the LLM group processed CDW-extracted data. This methodological design was unavoidable; manual reviewers needed direct EHR access for a comprehensive review, while the LLM required deidentified extracted data for processing. However, this means we cannot isolate whether performance differences stemmed from the extraction approach itself or from the inherent differences in available data. Future studies comparing both methods using identical raw data would overcome this limitation.

Fourth, generalizability to other LLM models requires evaluation. We used Claude 3.5 Sonnet, but the performance may vary across models, versions, and prompting strategies. The rapid evolution of LLM capabilities suggests that our findings represent a snapshot of current technology rather than definitive limits.

Future Directions

Future research should address several key issues. The first is the development of improved prompting strategies to handle complex clinical scenarios that require integrated assessment, particularly for sequential surgical procedures and temporal relationships. Second, LLM processing is compared with manual review using identical raw data sources to isolate the actual performance differences between the methods. Third, feasibility studies of integrated data curation across multiple clinical events are needed to overcome the current limitations in synthesizing longitudinal patient data. Fourth, a systematic examination of the performance characteristics of different LLM models is required to identify optimal models for specific clinical data types.

Conclusions

LLM-based processing demonstrated comparable effectiveness to manual review by physicians for breast cancer clinical data extraction, while significantly reducing processing time and resource utilization. Despite the limitations of integrated assessments requiring synthesis across multiple clinical events, this approach offers a solution for efficient clinical data extraction in oncology research. The ability to process large volumes of data consistently and rapidly while maintaining an accuracy above 90% suggests that LLM-based methods can accelerate retrospective clinical research.

XSL•FO
RenderX

Acknowledgments

This work was supported by the National Research Foundation of Korea grant funded by the Korea government (Ministry of Science and ICT; RS-2025-19643006). This study used the Claude 3.5 Sonnet (Anthropic) web interface (claude.ai) for large language model (LLM)-based data extraction, which did not require programming code. The extraction was performed through manual copy-paste operations with the structured prompt provided in Multimedia Appendix 5. Statistical analyses were performed using Python (version 3.8; Python Software Foundation) with NumPy (v.1.21.0) and pandas (v.1.3.0) libraries.

Authors' Contributions

Conceptualization: YJK
Data curation: YJK, JPY, HK, CIY, JMB, YSK, YWJ, JR
Formal analysis: YJK, HL
Funding acquisition:
Investigation: JPY, HK, SHL, SJO
Methodology: YJK, HL
Project administration: YJK
Resources: CIY, JMB, YSK, YWJ, JR
Software: YJK
Supervision: HC, SJO
Validation: HL, JPY, HK, SHL
Writing – original draft: YJK
Writing – review & editing: YJK, HL, HC, SJO
All authors have read and approved the final manuscript.

Conflicts of Interest

None declared.

Multimedia Appendix 1
Standardized data collection form used for manual physician review
[PNG File, 492 KB - medinform_v13i1e73605_app1.png]

Multimedia Appendix 2
Example of grouped data sheets extracted from the clinical data warehouse.
[PNG File, 328 KB - medinform_v13i1e73605_app2.png]

Multimedia Appendix 3
Pathology reports extracted from the clinical data warehouse
[PNG File, 23585 KB - medinform_v13i1e73605_app3.png]

Multimedia Appendix 4
Radiology reports extracted from the clinical data warehouse.
[PNG File, 496 KB - medinform_v13i1e73605_app4.png]

Multimedia Appendix 5
The condensed prompt.
[DOCX File, 24 KB - medinform_v13i1e73605_app5.docx]

Checklist 1
TRIPOD-LLM checklist.
[PDF File, 70 KB - medinform_v13i1e73605_app6.pdf]

References

1. Baclic O, Tunis M, Young K, Doan C, Swerdfeger H, Schonfeld J. Challenges and opportunities for public health made possible by advances in natural language processing. Can Commun Dis Rep 2020 Jun 4;46(6):161-168. [doi: 10.14745/ccdr.v46i06a02] [Medline: 32673380]
2. Minaee S, Mikolov T, Nikzad N, Chenaghlu M, Socher R, Amatriain X, et al. Large language models: a survey. arXiv. Preprint posted online on Feb 9, 2024. [doi: 10.48550/arXiv.2402.06196]

XSL•FO
RenderX

3. Bedi S, Liu Y, Orr-Ewing L, et al. Testing and evaluation of health care applications of large language models: a systematic review. JAMA 2025 Jan 28;333(4):319-328. [doi: 10.1001/jama.2024.21700] [Medline: 39405325]
4. Stroganov O, Schedlbauer A, Lorenzen E, et al. Unpacking unstructured data: A pilot study on extracting insights from neuropathological reports of Parkinson's disease patients using large language models. Biol Methods Protoc 2024;9(1):bpae072. [doi: 10.1093/biomethods/bpae072] [Medline: 39464853]
5. Guo C, Chen J. Big data analytics in healthcare. In: Nakamori Y, editor. Knowledge Technology and Systems: Toward Establishing Knowledge Systems Science: Springer Nature Singapore; 2023:27-70. [doi: 10.1007/978-981-99-1075-5_2]
6. Wani MA, Jabin S. Big data: issues, challenges, and techniques in business intelligence. In: Aggarwal V, Bhatnagar V, Mishra D, editors. Big Data Analytics Advances in Intelligent Systems and Computing: Springer Singapore; 2018. [doi: 10.1007/978-981-10-6620-7_59]
7. Garza MY, Williams T, Ounpraseuth S, et al. Error rates of data processing methods in clinical research: a systematic review and meta-analysis of manuscripts identified through PubMed. Int J Med Inform 2025 Mar;195(105749):105749. [doi: 10.1016/j.ijmedinf.2024.105749] [Medline: 39647291]
8. Wang W, Krishnan E. Big data and clinicians: a review on the state of the science. JMIR Med Inform 2014 Jan 17;2(1):e1. [doi: 10.2196/medinform.2913] [Medline: 25600256]
9. Hoffman S. Big data analytics: What can go wrong. Ind Health L Rev 2018;15:227. [doi: 10.18060/3911.0048]
10. Fan J, Han F, Liu H. Challenges of big data analysis. Natl Sci Rev 2014 Jun;1(2):293-314. [doi: 10.1093/nsr/nwt032] [Medline: 25419469]
11. Kim M, Kim Y, Kang HJ, et al. Fine-tuning LLMs with medical data: can safety be ensured? NEJM AI 2025 Jan;2(1):AIcs2400390. [doi: 10.1056/AIcs2400390]
12. Rengers TA, Thiels CA, Salehinejad H. Academic surgery in the era of large language models: a review. JAMA Surg 2024 Apr 1;159(4):445-450. [doi: 10.1001/jamasurg.2023.6496] [Medline: 38353991]
13. Jeyaraman M, Balaji S, Jeyaraman N, Yadav S. Unraveling the ethical enigma: artificial intelligence in healthcare. Cureus 2023 Aug;15(8):e43262. [doi: 10.7759/cureus.43262] [Medline: 37692617]
14. Wulcan JM, Jacques KL, Lee MA, et al. Classification performance and reproducibility of GPT-4 omni for information extraction from veterinary electronic health records. Front Vet Sci 2024;11:1490030. [doi: 10.3389/fvets.2024.1490030] [Medline: 39885843]
15. Choi IY, Park S, Park B, et al. Development of prostate cancer research database with the clinical data warehouse technology for direct linkage with electronic medical record system. Prostate Int 2013;1(2):59-64. [doi: 10.12954/PI.12015] [Medline: 24223403]
16. Park SJ, Lee SJ, Kim H, et al. Machine learning prediction of dropping out of outpatients with alcohol use disorders. PLoS One 2021;16(8):e0255626. [doi: 10.1371/journal.pone.0255626] [Medline: 34339461]
17. Choi JE, Kim Z, Park CS, et al. Breast cancer statistics in Korea, 2019. J Breast Cancer 2023 Jun;26(3):207-220. [doi: 10.4048/jbc.2023.26.e27] [Medline: 37387348]
18. Woodfield R, Grant I, UK Biobank Stroke Outcomes Group, UK Biobank Follow-Up and Outcomes Working Group, Sudlow CLM. Accuracy of electronic health record data for identifying stroke cases in large-scale epidemiological studies: a systematic review from the UK Biobank Stroke Outcomes Group. PLoS ONE 2015;10(10):e0140533. [doi: 10.1371/journal.pone.0140533] [Medline: 26496350]
19. López-Úbeda P, Martín-Noguerol T, Juluru K, Luna A. Natural language processing in radiology: update on clinical applications. J Am Coll Radiol 2022 Nov;19(11):1271-1285. [doi: 10.1016/j.jacr.2022.06.016] [Medline: 36029890]
20. Park HJ, Huh JY, Chae G, Choi MG. Extraction of clinical data on major pulmonary diseases from unstructured radiologic reports using a large language model. PLoS ONE 2024;19(11):e0314136. [doi: 10.1371/journal.pone.0314136]
21. Soni N, Ora M, Agarwal A, Yang T, Bathla G. A review of the opportunities and challenges with large language models in radiology: the road ahead. AJNR Am J Neuroradiol 2024 Nov 21:ajnr. [doi: 10.3174/ajnr.A8589]
22. Cheng J. Applications of large language models in pathology. Bioengineering (Basel) 2024 Mar 31;11(4):342. [doi: 10.3390/bioengineering11040342] [Medline: 38671764]
23. Gu B, Shao V, Liao Z, et al. Scalable information extraction from free text electronic health records using large language models. BMC Med Res Methodol 2025 Jan 28;25(1):23. [doi: 10.1186/s12874-025-02470-z] [Medline: 39871166]

Abbreviations

ALND: axillary lymph node dissection
API: application programming interface
CDW: clinical data warehouse
EHR: electronic health record
HER2: human epidermal growth factor receptor 2
ICC: intraclass correlation coefficient
KBCS: Korean Breast Cancer Society
LLM: large language model

XSL•FO
RenderX

SLNB: sentinel lymph node biopsy
TRIPOD-LLM: Transparent Reporting of a Multivariable Prediction Model for Individual Prognosis or Diagnosis–Large Language Model

Edited by A Benis; submitted 07.03.25; peer-reviewed by A Khanteymoori, Á García-Barragán; revised version received 06.10.25; accepted 07.10.25; published 06.11.25.

Please cite as:
Kang YJ, Lee H, Yi JP, Kim H, Yoon CI, Baek JM, Kim YS, Jeon YW, Rhu J, Lim SH, Choi H, Oh SJ
Large Language Model Versus Manual Review for Clinical Data Curation in Breast Cancer: Retrospective Comparative Study
JMIR Med Inform 2025;13:e73605
URL: https://medinform.jmir.org/2025/1/e73605
doi:10.2196/73605

© Young-Joon Kang, Hocheol Lee, Jae Pak Yi, Hyobin Kim, Chang Ik Yoon, Jong Min Baek, Yong-seok Kim, Ye Won Jeon, Jiyoung Rhu, Su Hyun Lim, Hoon Choi, Se Jeong Oh. Originally published in JMIR Medical Informatics (https://medinform.jmir.org), 6.11.2025. This is an open-access article distributed under the terms of the Creative Commons Attribution License (https://creativecommons.org/licenses/by/4.0/), which permits unrestricted use, distribution, and reproduction in any medium, provided the original work, first published in JMIR Medical Informatics, is properly cited. The complete bibliographic information, a link to the original publication on https://medinform.jmir.org/, as well as this copyright and license information must be included.

XSL•FO
RenderX

An Extraction Tool for Venous Thromboembolism Symptom Identification in Primary Care Notes to Facilitate Electronic Clinical Quality Measure Reporting: Algorithm Development and Validation Study

John Novoa-Laurentiev[1], MS; Mica Bowen[1], BA; Avery Pullman[1], BS; Wenyu Song[1,2], PhD; Ania Syrowatka[1,2], PhD; Jin Chen[3], PhD; Michael Sainlaire[1], MS; Frank Chang[1], MSE; Krissy Gray[4], AAS; Purushottam Panta[4], MS; Luwei Liu[1], MS; Khalid Nawab[5,6], MD; Shadi Hijjawi[5,6], MBA, MD; Richard Schreiber[5,7], MD; Li Zhou[1,2], MD, PhD; Patricia C Dykes[1,2], RN, PhD

[1]Department of Medicine, Brigham & Women's Hospital, 75 Francis Street, Boston, MA, United States

[2]Department of Medicine, Harvard Medical School, Boston, MA, United States

[3]Department of Medicine, University of Alabama at Birmingham, Birmingham, AL, United States

[4]Department of Biomedical Informatics, University of Kentucky, Lexington, KY, United States

[5]Department of Information Services, Penn State Health, Hershey, PA, United States

[6]Department of Medicine, Penn State College of Medicine, Hershey, PA, United States

[7]Department of Biomedical Informatics and Data Science, Johns Hopkins School of Medicine, Baltimore, MD, United States

Corresponding Author:
John Novoa-Laurentiev, MS
Department of Medicine, Brigham & Women's Hospital, 75 Francis Street, Boston, MA, United States

Abstract

Background: Diagnosis of venous thromboembolism (VTE) is often delayed, and facilitating earlier diagnosis may improve associated morbidity and mortality. Clinical notes contain information not found elsewhere in the medical record that could facilitate timely VTE diagnosis and accurate quality measurement. However, extracting relevant information from unstructured clinical notes is complex. Today, there are relatively few electronic clinical quality measures (eCQMs) in our national payment program and none that use natural language processing (NLP) techniques for data extraction. NLP holds great promise for making quality measurement more accurate and more efficient. Given the potential of NLP-based applications to facilitate more accurate VTE detection, primary care is one clinical setting in urgent need of this type of tool.

Objective: This study aimed to develop a tool that extracts VTE symptoms from clinical notes for use within an eCQM to quantify the rate of delayed diagnosis of VTE in primary care settings.

Methods: We iteratively developed an NLP-based data extraction tool, venous thromboembolism symptom extractor (VTExt), on an internal dataset using a rule-based approach to extract VTE symptoms from primary care clinical note text. The VTE symptoms lexicon was derived and optimized with physician guidance and externally validated using datasets from 2 independent health care organizations. We performed 26 rounds of performance evaluation of notes sampled from the case cohort (17,585 patient progress note sentences from 279 patient notes), and 5 rounds of evaluation of the control cohort (2838 patient progress note sentences from 50 patient notes). VTExt's performance was evaluated using evaluation metrics, including area under the curve, positive predictive value, negative predictive value, sensitivity, and specificity.

Results: VTExt achieved near-perfect performance in extracting VTE symptoms from primary care notes sampled from records of patients diagnosed with or without VTE. In external validation, VTExt achieved promising performance in 2 additional geographically distant organizations using different electronic health record systems. When compared against a deep learning model and 4 machine learning models, VTExt exhibited similar or even improved performance across all metrics.

Conclusions: This study demonstrates a data-driven NLP-based approach to clinical note information extraction that can be generalized to different electronic health record systems across different institutions. Due to the robust performance of this tool, VTExt is the first NLP application to be used in a nationally endorsed eCQM.

(JMIR Med Inform 2025;13:e63720) doi:10.2196/63720

XSL•FO
RenderX

KEYWORDS

natural language processing; venous thromboembolism; electronic clinical quality measure; timely diagnosis; primary care; NLP; thromboembolism; clinical quality; algorithm development; algorithm validation; VTE; diagnosis; primary care; extraction tool; tool; clinical note; extraction; AI; artificial intelligence

Introduction

Venous thromboembolism (VTE) is an often undetected condition that includes both deep vein thrombosis (clots in the deep veins of the body [1]), and pulmonary embolism (PE; clot breaking free and entering the pulmonary arteries [1,2]). VTE is associated with increased morbidity and mortality [3] with a 1-year VTE case-fatality rate estimated at 23% [4] and associated with increased health care costs [5].

The incidence of VTE in the United States is unknown as there is currently no national VTE surveillance system in place [1]. Cases are often missed since they are asymptomatic or associated with symptoms similar to those of other chronic conditions, leading to substantial undercounting. In a 2015 literature review, Heit [6] identified the incidence of VTE as ranging from 104 to 183 cases per 100,000 person-years. This rate is based largely on Caucasian populations [4,7-16] and differs by race where African American individuals face higher rates of VTE [17-19], and Asian [20], Asian American [21,22], and Native American individuals [23] see a lower VTE incidence. Higher levels of education, income, and employment status have also been shown to be associated with decreased risk of VTE [24]. Risk factors for VTE include a history of VTE [25] (rates of recurrent VTE range from 20% - 36% within 10 years of the initial VTE event [26,27]), older age [1], recent immobility or surgery, cancer, smoking, thrombophilia [28], and obesity [6].

Delayed diagnosis of VTE is common due to its nonspecific symptoms [29]. VTE can also be difficult to identify in the electronic health record (EHR) due to variability in how VTE is documented and coded [30]. Due to these challenges and the lack of national surveillance, the incidence of VTE is likely underestimated [31,32]. Tools to facilitate measurement and earlier diagnoses of VTE may help in better understanding VTE risk factors, reduce associated morbidity and mortality [33,34], and improve patient safety.

The widespread adoption of interoperable EHR systems after the 2009 Health Information Technology for Economic and Clinical Health Act [35,36] has led to a significant increase in unstructured text data, such as radiology reports, progress notes, and discharge summaries [37]. These unstructured data are estimated to constitute over 80% of health and biomedical information [37]. Free-text clinical notes in EHRs hold valuable insights for population-level quality improvement, but efficient strategies leveraging AI, machine learning, and natural language processing (NLP) are essential to harness this potential.

NLP is useful for analyzing unstructured EHR data in areas like radiology [38], oncology [39,40], endocrinology [41], substance misuse [42], PE identification [43], and postoperative VTE [44]. By extracting information from text, NLP creates structured data, reducing manual review and enabling large-scale automated processing [45]. High-throughput phenotyping algorithms using NLP-derived and structured data show promise for developing standardizing labeling [46] particularly for managing complex diseases in large-scale patient populations. NLP can also uncover critical information overlooked using structured variables [47,48]. While large language models (LLMs) are popular for NLP tasks, they are often more resource-intensive and costly than traditional machine learning or rule-based methods [49]. Though machine learning methods tend to have improved performance, a rule-based approach has advantages, such as traceability of results and speed of development [50].

NLP tools can detect VTE events, but more sensitive tools are needed to identify VTE events specifically in primary care EHR progress notes [44,51]. The objective of this study was to develop a simple, accessible NLP tool for identifying VTE symptoms in primary care EHRs, suitable for both high- and low-resource settings and aligned with the national quality payment program. The tool was tested on external datasets to evaluate its performance compared with deep learning and machine learning models. This main aim is to use narrative EHR data for clinical quality reporting to identify missed or delayed diagnoses of VTE after a primary care visit. A delayed diagnosis is defined as one that occurs >24 hours after the primary care visit when the VTE symptoms were documented.

Methods

Data Sources, Cohort Development, and Feature Selection Strategy

The study was conducted at Mass General Brigham (MGB), an integrated health care delivery system in Greater Boston, Massachusetts, using data from the MGB Enterprise Data Warehouse (EDW), an MGB central clinical data warehouse.

We used 2 internal datasets to develop and evaluate our NLP application for symptom extraction, and 2 independent external datasets to test how well it works in other settings. The first internal dataset, the case cohort, was used for development and evaluation. Inclusion criteria for this cohort are described below. The second internal dataset, the control cohort, included patients who did not meet case cohort inclusion criteria and was used for further evaluation. The external validation datasets came from 2 university health systems: the University of Kentucky and Penn State Health. These datasets were used to test if our symptom extractor works well with notes from different EHR vendors and health care systems.

We developed a multifactor phenotyping algorithm to identify VTE patients in the MGB cohort [52]. This included patients diagnosed with VTE from 2016 through 2021 who had a primary care visit in the 30 days before the date of diagnosis. We started by using *ICD-10* (*International Statistical Classification of Diseases, Tenth Revision*) codes to identify an initial VTE patient cohort. Then we combined data from imaging records

XSL•FO
RenderX

(eg, current procedural terminology [CPT] codes) and anticoagulant orders (RxNorm codes) to further refine the initial cohort and develop the final VTE case cohort. The diagnosis date and time of VTE diagnosis was defined as when the radiologist signed off on the scan report [52,53].

We used a rule-based approach to identify terms from a lexicon derived from a set of VTE signs and symptoms. The lexicon was divided into 3 parts: one with relevant symptoms dependent on the part of the body (eg, swelling), another with the relevant symptom locations (eg, leg), and the last containing location-independent symptoms (eg, cough). Location-dependent symptoms required identification of both the symptom and a relevant location to be considered a symptom match. The lexicon was reviewed and revised over the course of the study in accordance with physician expert guidance.

Clinician-Guided VTE Lexicon Development and Optimization

We identified VTE-related signs and symptoms by combining a literature review with interviews of physicians with experience in treating VTE patients. Multiple optimization steps were conducted: first, we conducted a comprehensive literature review to create an initial list of signs and symptoms. Then, we held 1-hour semistructured interviews with 5 experienced physicians to provide additional insight into signs and symptoms based on clinical experience. Signs and symptoms were also reviewed by a technical expert panel over the course of development, and their feedback was used to finalize the lexicon. In total, we included 29 distinct symptoms in the lexicon, consisting of 7 location-independent symptoms, 7 location-dependent symptoms, and 4 relevant locations. The final VTE symptom 3-part lexicon can be found in Multimedia Appendix 1. Inclusion criteria *ICD-10*, CPT, and RxNorm codes are provided in Multimedia Appendix 2. The prevalence of each symptom in each dataset is provided in Multimedia Appendix 3.

Extractor Development and Optimization

The Medical Text Extraction, Reasoning and Mapping System (MTERMS) [54] venous thromboembolism symptom extractor (VTExt) was developed using the Python programming language. We chose a rule-based approach to identify symptoms in order to facilitate transferability of the tool and to ensure transparency of its workings, which can be challenging when using more complex machine learning or LLM-based approaches [55]. Using a rule-based approach also suited the need for VTExt to identify VTE symptoms within specific contexts, for example, at specific body locations.

The development cycle used in the creation of VTExt entailed initial analysis of symptom extractor requirements, design and implementation of the extractor, iterative testing on samples of patient notes, and adjusting VTExt based on error analyses. The overall study design and development process is provided in Figure 1.

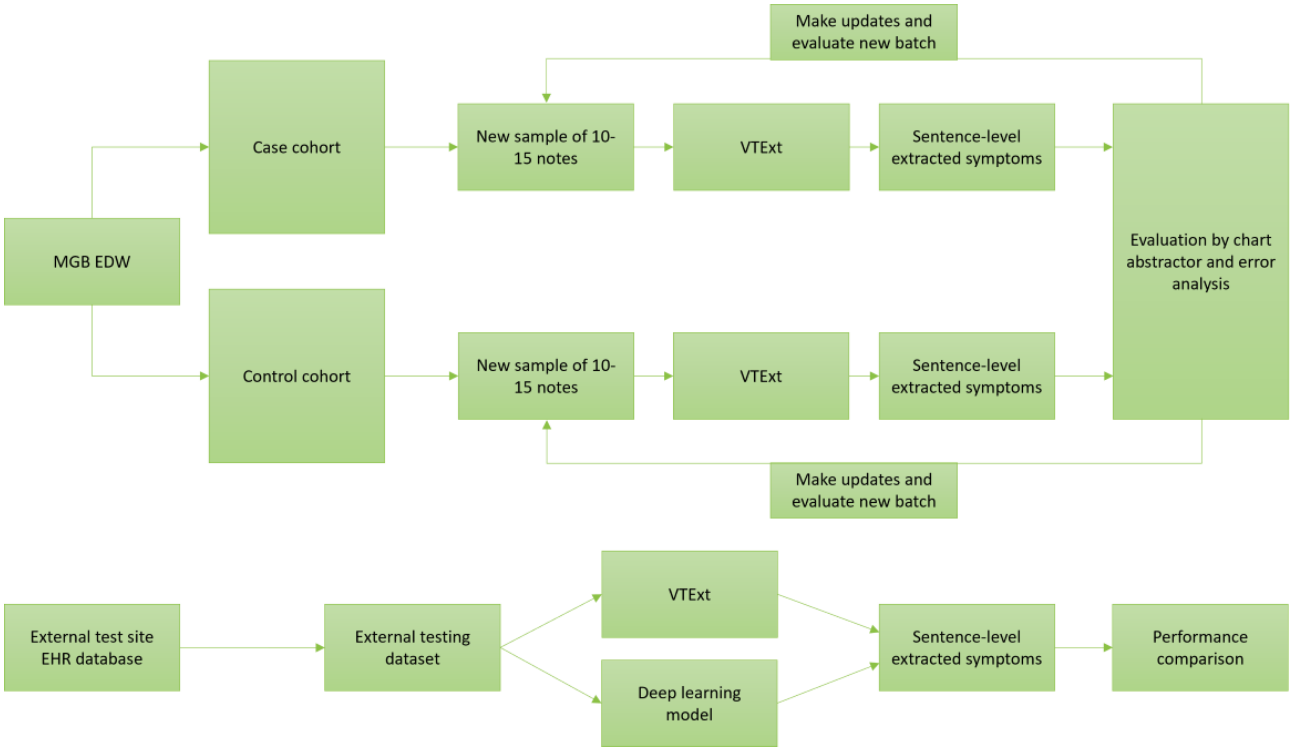
We first reviewed a small sample of cases from the dataset described above to understand how VTE symptoms appear in primary care progress notes, for example, how providers document VTE symptoms. The initial version of VTExt was then used to extract symptoms from a batch of sampled primary care progress notes. A trained chart abstractor reviewed each sentence analyzed by VTExt and determined whether the structured output was accurate, marking each case as a true positive, true negative, false positive, or false negative. Whenever an error occurred, the reason was identified, and adjustments were made to the extractor to avoid the error in the processing of future batches. We repeated this optimization process of running the extractor on a new sample of 10 - 15 notes, reviewing output, and refining the pattern-matching to iteratively improve the performance of the symptom extractor until we achieved a precision (positive predictive value [PPV]) of at least 0.95.

For each round, one progress note from each patient visit was extracted and combined into a single file. Patient notes were split into sentences using the MTERMS NLP system [54]. The symptom extractor then used regular expression-based rules to identify signs and symptoms of VTE in the curated lexicon and wrote output to a structured query language database to allow for integration of extractor output into other pipelines, including mapping symptoms to standardized terminologies. The NLP output table contains one column for each VTE symptom in the lexicon. Each row in the table corresponds to 1 patient note, and a binary output value for each symptom field indicates whether a given symptom was detected in the note by VTExt—if yes, presence was indicated with a value of “1,” and if not, a value of “0.”

To facilitate the clinical implementation of our tool, we developed a streamlined version of VTExt with simplified output for use with the electronic clinical quality measure (eCQM). Instead of producing output values for presence of individual signs and symptoms, this version produced a single “0” or “1” value for each patient note to indicate whether at least 1 VTE symptom was identified. This streamlined version of VTExt was used in the external evaluation of the tool. Pseudocode for the tool can be found on our project GitHub page [56].

XSL•FO
RenderX

Figure 1. Venous thromboembolism symptom extractor development and evaluation process. EDW; enterprise data warehouse; EHR; electronic health record; MGB; Mass General Brigham; VTExt: venous thromboembolism symptom extractor.



Note Processing and Evaluation

We evaluated the VTExt symptom extractor using both internal and external datasets. For internal evaluation, we used both a case cohort and a control cohort. The case cohort included patients who met our inclusion criteria for incident VTE based on the presence of 3 codes; *ICD-10* VTE codes, CPT imaging codes, and RxNorm anticoagulation codes [53]. The control cohort included patients who did not meet these criteria.

Internal evaluation of the VTExt symptom extractor was an iterative process, illustrated in Figure 1. From all patients who met the case cohort inclusion criteria, we randomly selected batches of 10 to 15 patient visits for each round of testing. We used a similar method to sample control notes to evaluate how well the symptom extractor generalized to patients that did not meet the case cohort inclusion criteria (eg, patients who did not have a VTE diagnosis).

External Evaluation

We worked with collaborators at both the University of Kentucky and Penn State Health (PSH) to test VTExt on patient notes. These sites used different EHR systems which also differed from MGB and had different textual data structures. In Epic (used at MGB), patient notes exist in tables, which include note-related information including metadata and the note content itself. Veradigm (formerly Allscripts; used by University of Kentucky) and Oracle Cerner (used by PSH) similarly store patient note data in document tables. For free text notes in Veradigm and Oracle Cerner, note contents of many documents are stored in “Character Large Objects” or “Binary Large Objects” fields. Notes in these areas of the database require special querying techniques to extract unstructured text, usually requiring certified analysts. Despite these differences, once note text data are available, the NLP tool functions properly irrespective of the EHR as it is not dependent on the EHR itself.

In addition, each system served a different population: MGB serving mostly urban and metro, University of Kentucky serving more rural, and PSH serving a mixed population of urban, metro, and rural. The diversity of sites included served as a good preliminary test for generalizability of VTExt.

During external evaluation, we compared the performance of the rule-based extractor against a pretrained sequence classification deep learning model derived from Bio+Clinical BERT (bidirectional encoder representations from transformers; using the HuggingFace transformers Python package), a contextualized word representation model based on BioBERT and trained further on Medical Information Mart for Intensive Care (MIMIC) data [57-60]. We also compared performance against 4 classical machine learning models: logistic regression, support vector machine (SVM), and random forest, implemented using the Python Scikit-learn module, and gradient boosting, implemented using the Python XGBoost module [61-63]. MGB data used during the development of VTExt were preprocessed using the Bio+Clinical BERT tokenizer for further training of the deep learning model. For training the four classical models, the MGB data were instead represented as unigrams transformed using term frequency—inverse document frequency (TF-IDF) [64]. For all models, data were divided into training and validation sets for training and tuning of model parameters, respectively. Final parameters for deep learning and machine learning models are provided in Multimedia Appendix 4. Each external site manually labeled a testing set of 500 note sentences for evaluation, 250 containing at least one VTE symptom and 250 with no VTE symptoms.

XSL•FO
RenderX

Ethical Considerations

This project was reviewed and approved by the Mass General Brigham institutional review board (protocol #2020P003979). In this protocol, a waiver of informed consent and a waiver of HIPAA (Health Insurance Portability and Accountability Act) authorization was requested because this quality improvement research involves no more than minimal risk to the participants and the research could not practicably be carried out without the waiver given the large number of patients who had a VTE diagnosis in a primary care setting. In addition, this research could not practicably be conducted without access to and use of the protected health information. The following procedures were followed to prevent breach in confidentiality: (1) data were accessed only behind MGB firewall using password-protected, secure devices by Collaborative Institutional Training Initiative–certified study staff, and (2) we will destroy all patient identifiers at the end of the study, once analysis and publications are finalized. In accordance with the approved institutional review board protocol, all electronic data were kept in password-protected files on a secure server behind the MGB firewall. Only study personnel were given a unique identifier—no participant identifiers are linked to the data. No compensation was provided for participation.

Results

We performed 26 rounds of evaluation of VTExt performance on notes sampled from the case cohort. This included 17,585 patient progress note sentences from 279 notes from distinct patients, 171 of which were found to contain 1 or more VTE symptoms. Evaluation of the control cohort included 2838 note sentences from 50 patient notes over the course of five rounds of evaluation, of which 21 notes contained at least 1 relevant symptom.

Performance was evaluated at the sentence level. We measured precision (PPV), recall (sensitivity), specificity, and negative predictive value (NPV; Table 1). Of these metrics, achieving a high precision score proved to be the greatest challenge. Many false positives initially arose due to 3 kinds of errors, shown in Table 2. Some errors were due to word misspellings in the notes (which we refer to as type A errors). For example, misspelling of the word “denies” caused VTExt to miss negation of subsequent VTE symptoms. In other cases, an error occurred because a symptom was identified but was attributed to the incorrect body part (a type B error). Many false positives arose in early stages of evaluation from failure to detect negation or context, as in the Type C error examples in Table 2.

Table . Venous thromboembolism symptom extractor validation performance on notes of case cohort (patients with venous thromboembolism diagnosis).

Validation round	Patients, n	Precision (positive predictive value)	Recall (sensitivity)	Specificity	Negative predictive value
Round 1	673	0.500	0.863	0.929	0.988
Round 9	692	0.851	0.966	0.984	0.997
Round 17	489	0.750	1.000	0.998	1.000
Round 26	938	1.000	1.000	1.000	1.000

Table . Examples of common sources of symptom extractor false positive errors.

Error type	Examples
Type A: misspelling	She “deneis” shortness of breath or pleuritic chest pain
Type B: symptom attributed to wrong body part	Worsening R hip “pain” as well as recent development of R “leg,” ankle, and foot erythema
Type C: negation or context	“Resolution” of hypoxia and chest pain. Nitroglycerin 0.4 MG SL tablet place 1 tablet (0.4 mg total) under the tongue every 5 (five) minutes “as needed” for chest pain

For the first example, VTExt captured the symptom hypoxia without identifying the negating phrase “resolution of.” In the second example, though chest pain is mentioned, it appears in the context of a medication to be taken as needed, which we deemed not to be strong enough evidence of the presence of a symptom. Repeated validation allowed us to learn what contexts and negating phrases appeared in clinical text, and this knowledge was used to improve VTExt’s ability to locate them.

Through this process, precision improved from 0.5 in the first round of testing to near-perfect in the final round. Near-perfect performance was also achieved for recall, specificity, and NPV in the final round of validation. In addition, we tested the extractor on several random samples of primary care clinical notes of patients in the cohort, that is, those not diagnosed with VTE (Table 3, in batches of 10 - 15 notes, with precision ultimately reaching 0.85).

XSL•FO
RenderX

Table . Venous thromboembolism symptom extractor validation performance on notes of the control cohort (patients with no venous thromboembolism diagnosis).

Validation round	N	Precision (positive predictive value)	Recall (sensitivity)	Specificity	Negative predictive value
Round 1	281	0.533	1.000	0.974	1.000
Round 2	471	0.556	1.000	0.991	1.000
Round 3	613	0.750	1.000	0.998	1.000
Round 4	559	0.806	1.000	0.989	1.000
Round 5	912	0.850	0.895	0.997	0.998

As seen in the external evaluation results in Table 4, performance metrics for the rule-based extractor were similar or better than those for the deep learning and machine learning models at both external testing sites. While VTExt's precision and specificity scored high, sensitivity showed room for improvement (0.61 and 0.66 at PSH and University of Kentucky, respectively).

Error analysis of external testing results showed many deep learning model false negatives falling into 2 categories. Some errors can be attributed to overrepresentation of negated instances of certain VTE symptoms in the training dataset. This then makes the model more inclined to mark note sentences containing said symptoms as negative, even when the symptom is not negated. For the second category, less common terms used to describe relevant symptoms appear in testing data, for example, "malleoli" used in describing swelling of ankle. If such terms are not present in the training data, the model has no way of knowing they are relevant.

The rule-based model also produced false negatives, many belonging to one of two types. First, some errors can be attributed to double negation, which VTExt is not currently able to handle. For example, "SOB not resolved"—here, we see a VTE symptom, shortness of breath (SOB), followed by negating term "resolved." However, "resolved" itself has been negated, and so this represents a positive instance. The second error type pertains to synonymous terms of phrases of VTE symptoms that are not currently included in the lexicon, for example, "black and blue area" as another way to phrase bruising. Since the phrase "black and blue area" is not part of the symptom lexicon, the rule-based model did not detect the symptom.

The results for the eCQM have been reported elsewhere [53]. The calculated rate of delayed VTE diagnosis was over 70% at both MGB and University of Kentucky, suggesting a clinically and practically meaningful measure for understanding delayed diagnosis rates across diverse health care sites.

XSL•FO
RenderX

Table . Performance of venous thromboembolism symptom extractor, deep learning, and machine learning models at University of Kentucky and Penn State Health sites.

Metric (95% CI)	PPV[a]	NPV[b]	Sensitivity	Specificity	Accuracy	AUROC[c]	AUPRC[d]
University of Kentucky							
VTExt[e]	1.00	0.75	0.66	1.00	0.83	—[f]	—
Deep learning	1.00 (1.00 - 1.00)	0.63 (0.58 - 0.68)	0.42 (0.35 - 0.48)	1.00 (1.00 - 1.00)	0.71 (0.67 - 0.75)	0.71 (0.68 - 0.74)	0.85 (0.83 - 0.87)
XGBoost	0.98 (0.96 - 1.00)	0.71 (0.66 - 0.76)	0.60 (0.53 - 0.66)	0.99 (0.97 - 1.00)	0.79 (0.76 - 0.83)	0.79 (0.76 - 0.82)	0.89 (0.87 - 0.91)
Logistic regression	0.95 (0.87 - 1.00)	0.54 (0.49 - 0.58)	0.16 (0.11 - 0.20)	0.99 (0.98 - 1.00)	0.57 (0.53 - 0.62)	0.57 (0.55 - 0.60)	0.76 (0.71 - 0.80)
Random forest	1.00 (1.00 - 1.00)	0.52 (0.48 - 0.57)	0.08 (0.05 - 0.12)	1.00 (1.00 - 1.00)	0.54 (0.50 - 0.58)	0.54 (0.52 - 0.56)	0.77 (0.75 - 0.79)
SVM[g]	0.98 (0.94 - 1.00)	0.56 (0.51 - 0.61)	0.22 (0.16 - 0.27)	1.00 (0.99 - 1.00)	0.61 (0.56 - 0.65)	0.61 (0.58 - 0.63)	0.79 (0.76 - 0.82)
PSH							
VTExt	0.98	0.84	0.61	0.99	0.87	—	—
Deep learning	0.90 (0.85 - 0.94)	0.82 (0.79 - 0.84)	0.55 (0.49 - 0.60)	0.97 (0.96 - 0.98)	0.83 (0.81 - 0.86)	0.76 (0.73 - 0.79)	0.80 (0.77 - 0.83)
XGBoost	0.87 (0.82 - 0.91)	0.82 (0.80 - 0.85)	0.58 (0.53 - 0.63)	0.96 (0.94 - 0.97)	0.83 (0.81 - 0.86)	0.77 (0.74 - 0.80)	0.79 (0.76 - 0.83)
Logistic regression	0.86 (0.80 - 0.91)	0.76 (0.73 - 0.79)	0.37 (0.32 - 0.43)	0.97 (0.96 - 0.98)	0.77 (0.75 - 0.8)	0.67 (0.65 - 0.70)	0.72 (0.68 - 0.76)
Random forest	0.95 (0.88 - 1.00)	0.70 (0.67 - 0.73)	0.12 (0.08 - 0.15)	1.00 (0.99 - 1.00)	0.71 (0.68 - 0.74)	0.56 (0.54 - 0.58)	0.68 (0.64 - 0.71)
SVM	0.87 (0.82 - 0.92)	0.77 (0.74 - 0.80)	0.40 (0.35 - 0.45)	0.97 (0.96 - 0.98)	0.78 (0.76 - 0.81)	0.69 (0.66 - 0.71)	0.73 (0.70 - 0.77)

[a]PPV: positive predictive value.

[b]NPV: negative predictive value.

[c]AUROC: area under the receiver operating characteristic curve.

[d]AUPRC: area under the precision-recall curve.

[e]VTExt: venous thromboembolism symptom extractor.

[f]Not available.

[g]SVM: support vector machine.

Discussion

Principal Findings

Much of the data not captured in structured EHR fields, like patient symptoms, are found in clinical notes [48]. In this study, we developed and validated a simple and generalizable NLP tool to identify and extract signs and symptoms of VTE from primary care notes through an iterative optimization process. VTExt is novel as the first NLP application linked to a nationally endorsed eCQM [65], helping to quantify the rate of delayed diagnosis of VTE in primary care. Through multiple rounds of optimization, VTExt showed robust performance and speed. Testing at two external sites demonstrated its ability to work well with different datasets and system configurations and its potential for optimizing quality measurement. We suggest that analysts familiar with their EHR and its local configurations could readily apply this NLP tool to their patient notes.

We learned several important lessons during optimization. Reducing the prevalence of false positives was crucial for improving extractor performance. In early rounds of validation, type B and type C errors often arose in long sentences due to a lack of constraint on the allowed search distance between a VTE symptom and a body part, or between a negating or contextual phrase and a symptom. We experimented with search distances of various lengths and found a distance of 150 characters struck a good balance of incorporating context without introducing too much noise, improving precision while maintaining high sensitivity.

We focused on primary care progress notes for developing and testing VTExt. Our external evaluation indicated that differences in note styles and hospital policies can affect performance. However, consistent performance observed between the 2 external sites highlighted VTExt's strong generalizability. VTExt's rule-based approach offers advantages including easier implementation, faster processing, and easier interpretation of

XSL•FO
RenderX

results when compared with the tested machine learning and deep learning models. Error analysis also revealed further improvement opportunities for the symptom extractor. Working with collaborators at external sites to further refine VTExt to reduce false negatives would prove beneficial in improving sensitivity and NPV.

Comparison With Previous Work

Shi et al [44] developed an NLP tool to detect postoperative VTE from free-text EHR notes. Internal validation demonstrated a sensitivity of 0.71 and specificity of 0.99. In the 2 health care systems tested, this NLP approach demonstrated superior performance in DVT surveillance than existing tools, and similar performance in PE surveillance compared with existing tools. Chapman et al [51] developed an NLP-based application to classify pulmonary angiography reports for document-level identification of PE, with test set performance resulting in sensitivity of 0.98 and PPV of 0.83. Sabra et al [66] incorporated Unified Medical Language System concept mapping into an NLP tool to generate feature vectors. These were then used to train and test an SVM machine learning model that achieved a PPV and sensitivity of 0.55 and 0.86, respectively. Work done by Jin et al [67] to identify VTE in inpatient notes using rule-based NLP methods highlights an approach that achieved similar performance to VTExt (0.90 sensitivity, 1.0 specificity), splitting notes into sentences, and then aggregating sentence-level information to make VTE inference at the sentence, document, and patient level. Although many of their tools would not be sufficient for our study's goal of VTE symptom identification for quantifying delayed diagnosis, these studies show that NLP tools can effectively identify VTE events, and there is a need for more sensitive tools to identify VTE events using EHR progress notes in the primary care setting.

Limitations

Our study has a number of limitations. First, VTExt is currently unable to handle misspellings in note text. Revising VTExt to handle misspellings would result in improved performance. Second, MGB was unable to view clinical note data used by external sites in the testing of VTExt in order to maintain patient data privacy. This reduced our ability to improve the tool's generalizability, as MGB was unable to directly review output from the University of Kentucky and PSH other than performance metrics. Third, development and refinement of VTExt was based on 279 patient notes. While high performance was achieved, a wider dataset would provide additional context and understanding of the ways VTE symptoms are documented in clinical note text, allowing for further improvement of the tool.

Future Directions

While a rule-based approach was simpler to implement, future improvements in accessible, high-performance LLMs could make them useful and feasible for quality measurement. These tools have already shown good results in extracting information from radiology reports [68], and could also be used to extract signs and symptoms from other types of clinical notes. Since LLMs are trained on large volumes of data, such an approach may generalize better across different health care systems and differently formatted notes when compared with a rule-based method. An LLM approach may more easily generalize to extracting symptoms from types of notes other than primary care progress notes, a logical future direction for research in this area. An immediate LLM-based approach was not pursued because we began this project in 2020 before there was mass public access to LLMs. While LLMs prove a promising direction for future work, the cost, time, and knowledge required to test such an approach at the collaborating sites were real limiting factors. In addition to an LLM approach, future work to improve model performance could include expanding the lexicon of symptom synonyms, as well as more robust handling of context and negation.

In addition to an LLM approach, future work to improve model performance could include expanding the lexicon of symptom synonyms, as well as more robust handling of context and negation.

Conclusions

We developed a robust and efficient NLP-based tool, VTExt, to extract VTE-associated symptoms from primary care notes. VTExt achieved high sensitivity and specificity, performance that matches or exceeds that of deep learning models and demonstrates its reliability for clinical use. High sensitivity ensures that most patients with VTE symptoms are correctly identified, reducing the risk of missed or delayed diagnoses, which can have serious or fatal consequences. High specificity minimizes false positives, helping avoid unnecessary tests, anxiety, and resource use. Together, these metrics underscore VTExt's clinical value in supporting timely, accurate identification of potential VTE cases from unstructured data.

VTExt's generalizability across health care systems further supports its real-world applicability, enabling scalable deployment in diverse EHR environments. Its rule-based design facilitates transparency and ease of implementation, particularly for quality measurement initiatives such as tracking delayed diagnosis. Furthermore, the clinician-guided optimization process developed alongside VTExt provides a replicable framework for future NLP tool development and integration into clinical workflows, helping bridge the gap between EHR data and actionable insights for patient safety and care improvement.

Acknowledgments

This study was supported by the Gordon and Betty Moore Foundation Diagnostic Delay Of VTE (DOVE) grant, and by the Penn State Clinical and Translational Research Institute, Penn State University Clinical and Translational Science Award, National Institutes of Health/National Center for Advancing Translational Sciences (grant number UL1 TR000127). The contents are

XSL•FO
RenderX

solely the responsibility of the authors and do not necessarily represent the official views of the National Institutes of Health or National Center for Advancing Translational Sciences.

Data Availability

The datasets generated and analyzed during this study are not publicly available as they contain protected health information from patient health records.

Authors' Contributions

JN was responsible for formal analysis, investigation, methodology, software, validation, visualization, writing the original draft, and reviewing and editing the draft. MB contributed to project administration and writing the original draft. AP handled formal analysis and project administration. WS managed conceptualization, methodology, supervision, and reviewing and editing the manuscript draft. AS contributed to conceptualization, formal analysis, methodology, supervision, and reviewing and editing the manuscript draft. JC conducted investigation, methodology, resources, and supervision. MS managed data curation, investigation, and software. FC handled data curation and software. KG was responsible for data curation, investigation, and software. PP handled data curation, formal analysis, software, and validation. LL conducted formal analysis. KN contributed to data curation, funding acquisition, investigation, software, and validation. SH handled supervision, reviewing, and editing. RS managed funding acquisition, investigation, methodology, resources, supervision, writing the original draft, and reviewing and editing the manuscript draft. LZ was responsible for investigation, resources, supervision, and reviewing and editing the manuscript. PCD contributed to conceptualization, funding acquisition, investigation, methodology, resources, supervision, and review and editing the manuscript.

Conflicts of Interest

None declared.

Multimedia Appendix 1
Venous thromboembolism symptom lexicon.
[DOCX File, 13 KB - medinform_v13i1e63720_app1.docx]

Multimedia Appendix 2
Inclusion criteria *ICD-10* (*International Statistical Classification of Diseases, Tenth Revision*) and RxNorm codes.
[DOCX File, 17 KB - medinform_v13i1e63720_app2.docx]

Multimedia Appendix 3
Symptom prevalence, patient note level.
[DOCX File, 14 KB - medinform_v13i1e63720_app3.docx]

Multimedia Appendix 4
Deep learning and machine learning model parameters.
[DOCX File, 14 KB - medinform_v13i1e63720_app4.docx]

References

1. Beckman MG, Hooper WC, Critchley SE, Ortel TL. Venous thromboembolism: a public health concern. Am J Prev Med 2010 Apr;38(4 Suppl):S495-S501. [doi: 10.1016/j.amepre.2009.12.017] [Medline: 20331949]
2. Bruni-Fitzgerald KR. Venous thromboembolism: An overview. J Vasc Nurs 2015 Sep;33(3):95-99. [doi: 10.1016/j.jvn.2015.02.001]
3. Kahn SR, Ginsberg JS. Relationship between deep venous thrombosis and the postthrombotic syndrome. Arch Intern Med 2004 Jan 12;164(1):17-26. [doi: 10.1001/archinte.164.1.17] [Medline: 14718318]
4. Tagalakis V, Patenaude V, Kahn SR, Suissa S. Incidence of and mortality from venous thromboembolism in a real-world population: the Q-VTE study cohort. Am J Med 2013 Sep;126(9):832. [doi: 10.1016/j.amjmed.2013.02.024] [Medline: 23830539]
5. Ruppert A, Steinle T, Lees M. Economic burden of venous thromboembolism: a systematic review. J Med Econ 2011;14(1):65-74. [doi: 10.3111/13696998.2010.546465] [Medline: 21222564]
6. Heit JA. Epidemiology of venous thromboembolism. Nat Rev Cardiol 2015 Aug;12(8):464-474. [doi: 10.1038/nrcardio.2015.83] [Medline: 26076949]
7. Anderson FA Jr, Wheeler HB, Goldberg RJ, et al. A population-based perspective of the hospital incidence and case-fatality rates of deep vein thrombosis and pulmonary embolism. The Worcester DVT Study. Arch Intern Med 1991 May;151(5):933-938. [Medline: 2025141]

XSL•FO
RenderX

8. Hansson PO, Welin L, Tibblin G, Eriksson H. Deep vein thrombosis and pulmonary embolism in the general population. "The Study of Men Born in 1913". Arch Intern Med 1997;157(15):1665-1670. [Medline: 9250227]
9. Silverstein MD, Heit JA, Mohr DN, Petterson TM, O'Fallon WM, Melton LJ 3rd. Trends in the incidence of deep vein thrombosis and pulmonary embolism: a 25-year population-based study. Arch Intern Med 1998 Mar 23;158(6):585-593. [doi: 10.1001/archinte.158.6.585] [Medline: 9521222]
10. Oger E, the EPI-GETBO Study Group. Incidence of venous thromboembolism: a community-based study in western France. Thromb Haemost 2000;83(5):657-660. [doi: 10.1055/s-0037-1613887]
11. Cushman M, Tsai AW, White RH, et al. Deep vein thrombosis and pulmonary embolism in two cohorts: the longitudinal investigation of thromboembolism etiology. Am J Med 2004 Jul 1;117(1):19-25. [doi: 10.1016/j.amjmed.2004.01.018] [Medline: 15210384]
12. Heit JA. Venous thromboembolism: disease burden, outcomes and risk factors. J Thromb Haemost 2005 Aug;3(8):1611-1617. [doi: 10.1111/j.1538-7836.2005.01415.x]
13. Spencer FA, Emery C, Lessard D, et al. The Worcester Venous Thromboembolism study: a population-based study of the clinical epidemiology of venous thromboembolism. J Gen Intern Med 2006 Jul;21(7):722-727. [doi: 10.1111/j.1525-1497.2006.00458.x] [Medline: 16808773]
14. Næss IA, Christiansen SC, Romundstad P, Cannegieter SC, Rosendaal FR, Hammerstrøm J. Incidence and mortality of venous thrombosis: a population ‐ based study. J Thromb Haemost 2007 Apr;5(4):692-699. [doi: 10.1111/j.1538-7836.2007.02450.x]
15. Spencer FA, Emery C, Joffe SW, et al. Incidence rates, clinical profile, and outcomes of patients with venous thromboembolism. The Worcester VTE study. J Thromb Thrombolysis 2009 Nov;28(4):401-409. [doi: 10.1007/s11239-009-0378-3] [Medline: 19629642]
16. Huang W, Goldberg RJ, Anderson FA, Kiefe CI, Spencer FA. Secular trends in occurrence of acute venous thromboembolism: the Worcester VTE study (1985-2009). Am J Med 2014 Sep;127(9):829-839. [doi: 10.1016/j.amjmed.2014.03.041] [Medline: 24813864]
17. White RH, Zhou H, Romano PS. Incidence of idiopathic deep venous thrombosis and secondary thromboembolism among ethnic groups in California. Ann Intern Med 1998 May 1;128(9):737-740. [doi: 10.7326/0003-4819-128-9-199805010-00006] [Medline: 9556467]
18. Schneider D, Lilienfeld DE, Im W. The epidemiology of pulmonary embolism: racial contrasts in incidence and in-hospital case fatality. J Natl Med Assoc 2006 Dec;98(12):1967-1972. [Medline: 17225843]
19. Zakai NA, McClure LA, Judd SE, et al. Racial and regional differences in venous thromboembolism in the United States in 3 cohorts. Circulation 2014 Apr 8;129(14):1502-1509. [doi: 10.1161/CIRCULATIONAHA.113.006472] [Medline: 24508826]
20. Cheuk BLY, Cheung GCY, Cheng SWK. Epidemiology of venous thromboembolism in a Chinese population. Br J Surg 2004 Apr;91(4):424-428. [doi: 10.1002/bjs.4454] [Medline: 15048741]
21. Klatsky AL, Armstrong MA, Poggi J. Risk of pulmonary embolism and/or deep venous thrombosis in Asian-Americans. Am J Cardiol 2000 Jun 1;85(11):1334-1337. [doi: 10.1016/s0002-9149(00)00766-9] [Medline: 10831950]
22. White RH, Zhou H, Murin S, Harvey D. Effect of ethnicity and gender on the incidence of venous thromboembolism in a diverse population in California in 1996. Thromb Haemost 2005 Feb;93(2):298-305. [doi: 10.1160/TH04-08-0506] [Medline: 15711746]
23. Hooper WC, Holman RC, Heit JA, Cobb N. Venous thromboembolism hospitalizations among American Indians and Alaska Natives. Thromb Res 2002 Dec 15;108(5-6):273-278. [doi: 10.1016/s0049-3848(03)00058-6] [Medline: 12676185]
24. Jørgensen H, Horváth-Puhó E, Laugesen K, Braekkan S, Hansen JB, Sørensen HT. Socioeconomic status and risk of incident venous thromboembolism. J Thromb Haemost 2021 Dec;19(12):3051-3061. [doi: 10.1111/jth.15523] [Medline: 34498381]
25. Alikhan R, Cohen AT, Combe S, et al. Risk factors for venous thromboembolism in hospitalized patients with acute medical illness: analysis of the MEDENOX Study. Arch Intern Med 2004 May 10;164(9):963-968. [doi: 10.1001/archinte.164.9.963] [Medline: 15136304]
26. Khan F, Rahman A, Carrier M, et al. Long term risk of symptomatic recurrent venous thromboembolism after discontinuation of anticoagulant treatment for first unprovoked venous thromboembolism event: systematic review and meta-analysis. BMJ 2019 Jul 24;366:l4363. [doi: 10.1136/bmj.l4363] [Medline: 31340984]
27. Albertsen IE, Nielsen PB, Søgaard M, et al. Risk of recurrent venous thromboembolism: a Danish nationwide cohort study. Am J Med 2018 Sep;131(9):1067-1074. [doi: 10.1016/j.amjmed.2018.04.042] [Medline: 30266273]
28. Campello E, Prandoni P. Evolving knowledge on primary and secondary prevention of venous thromboembolism in carriers of hereditary thrombophilia: a narrative review. Semin Thromb Hemost 2022 Nov;48(8):937-948. [doi: 10.1055/s-0042-1753527] [Medline: 36055262]
29. Ageno W, Agnelli G, Imberti D, et al. Factors associated with the timing of diagnosis of venous thromboembolism: results from the MASTER registry. Thromb Res 2008;121(6):751-756. [doi: 10.1016/j.thromres.2007.08.009] [Medline: 17920107]
30. Pellathy T, Saul M, Clermont G, Dubrawski AW, Pinsky MR, Hravnak M. Accuracy of identifying hospital acquired venous thromboembolism by administrative coding: implications for big data and machine learning research. J Clin Monit Comput 2022 Apr;36(2):397-405. [doi: 10.1007/s10877-021-00664-6] [Medline: 33558981]

XSL•FO
RenderX

31. Office of the Surgeon General (US), National Heart, Lung, and Blood Institute (US). The Surgeon General's Call to Action to Prevent Deep Vein Thrombosis and Pulmonary Embolism: Office of the Surgeon General (US); 2008. URL: https://www.ncbi.nlm.nih.gov/books/NBK44178/ [accessed 2022-10-11]
32. Raskob GE, Silverstein R, Bratzler DW, Heit JA, White RH. Surveillance for deep vein thrombosis and pulmonary embolism: recommendations from a national workshop. Am J Prev Med 2010 Apr;38(4 Suppl):S502-S509. [doi: 10.1016/j.amepre.2010.01.010] [Medline: 20331950]
33. Dalen JE. Pulmonary embolism: what have we learned since Virchow? Natural history, pathophysiology, and diagnosis. Chest 2002 Oct;122(4):1440-1456. [doi: 10.1378/chest.122.4.1440] [Medline: 12377877]
34. Ozsu S, Oztuna F, Bulbul Y, et al. The role of risk factors in delayed diagnosis of pulmonary embolism. Am J Emerg Med 2011 Jan;29(1):26-32. [doi: 10.1016/j.ajem.2009.07.005] [Medline: 20825770]
35. Burde H. Health Law the hitech act-an overview. Virtual Mentor 2011 Mar 1;13(3):172-175. [doi: 10.1001/virtualmentor.2011.13.3.hlaw1-1103] [Medline: 23127320]
36. Charles D, Gabriel M, Searcy T. Adoption of electronic health record systems among U.S. non-federal acute care hospitals: 2008-2014. 2015 URL: https://www.healthit.gov/sites/default/files/data-brief/2014HospitalAdoptionDataBrief.pdf [accessed 2025-08-06]
37. Martin-Sanchez F, Verspoor K. Big data in medicine is driving big changes. Yearb Med Inform 2014 Aug 15;9(1):14-20. [doi: 10.15265/IY-2014-0020] [Medline: 25123716]
38. Steinkamp J, Cook TS. Basic artificial intelligence techniques: natural language processing of radiology reports. Radiol Clin North Am 2021 Nov;59(6):919-931. [doi: 10.1016/j.rcl.2021.06.003] [Medline: 34689877]
39. Zeng J, Banerjee I, Henry AS, et al. Natural language processing to identify cancer treatments with electronic medical records. JCO Clin Cancer Inform 2021 Apr;5:379-393. [doi: 10.1200/CCI.20.00173] [Medline: 33822653]
40. Savova GK, Danciu I, Alamudun F, et al. Use of natural language processing to extract clinical cancer phenotypes from electronic medical records. Cancer Res 2019 Nov 1;79(21):5463-5470. [doi: 10.1158/0008-5472.CAN-19-0579] [Medline: 31395609]
41. Egleston BL, Bai T, Bleicher RJ, Taylor SJ, Lutz MH, Vucetic S. Statistical inference for natural language processing algorithms with a demonstration using type 2 diabetes prediction from electronic health record notes. Biometrics 2021 Sep;77(3):1089-1100. [doi: 10.1111/biom.13338] [Medline: 32700317]
42. Riddick TA, Choo EK. Natural language processing to identify substance misuse in the electronic health record. Lancet Digit Health 2022 Jun;4(6):e401-e402. [doi: 10.1016/S2589-7500(22)00096-6] [Medline: 35623795]
43. Johnson SA, Signor EA, Lappe KL, et al. A comparison of natural language processing to ICD-10 codes for identification and characterization of pulmonary embolism. Thromb Res 2021 Jul;203:190-195. [doi: 10.1016/j.thromres.2021.04.020] [Medline: 34044246]
44. Shi J, Hurdle JF, Johnson SA, et al. Natural language processing for the surveillance of postoperative venous thromboembolism. Surgery 2021 Oct;170(4):1175-1182. [doi: 10.1016/j.surg.2021.04.027] [Medline: 34090671]
45. Kreimeyer K, Foster M, Pandey A, et al. Natural language processing systems for capturing and standardizing unstructured clinical information: a systematic review. J Biomed Inform 2017 Sep;73:14-29. [doi: 10.1016/j.jbi.2017.07.012] [Medline: 28729030]
46. Yu S, Chakrabortty A, Liao KP, et al. Surrogate-assisted feature extraction for high-throughput phenotyping. J Am Med Inform Assoc 2017 Apr 1;24(e1):e143-e149. [doi: 10.1093/jamia/ocw135] [Medline: 27632993]
47. Yu S, Ma Y, Gronsbell J, et al. Enabling phenotypic big data with PheNorm. J Am Med Inform Assoc 2018 Jan 1;25(1):54-60. [doi: 10.1093/jamia/ocx111] [Medline: 29126253]
48. Koleck TA, Dreisbach C, Bourne PE, Bakken S. Natural language processing of symptoms documented in free-text narratives of electronic health records: a systematic review. J Am Med Inform Assoc 2019 Apr 1;26(4):364-379. [doi: 10.1093/jamia/ocy173] [Medline: 30726935]
49. Chen L, Zaharia M, Zou J. FrugalGPT: how to use large language models while reducing cost and improving performance. arXiv. Preprint posted online on May 9, 2023. [doi: 10.48550/arXiv.2305.05176]
50. Kluegl P, Toepfer M, Beck PD, Fette G, Puppe F. UIMA Ruta: Rapid development of rule-based information extraction applications. Nat Lang Eng 2016 Jan;22(1):1-40. [doi: 10.1017/S1351324914000114]
51. Chapman BE, Lee S, Kang HP, Chapman WW. Document-level classification of CT pulmonary angiography reports based on an extension of the ConText algorithm. J Biomed Inform 2011 Oct;44(5):728-737. [doi: 10.1016/j.jbi.2011.03.011] [Medline: 21459155]
52. Syrowatka A, Pullman A, Pajares E, et al. Accurately identifying incident cases of venous thromboembolism in the electronic health record: Performance of a novel phenotyping algorithm. Thromb Res 2024 Nov;243:109143. [doi: 10.1016/j.thromres.2024.109143] [Medline: 39303403]
53. Dykes PC, Bowen M, Chang F, et al. Testing of an electronic clinical quality measure for diagnostic delay of venous thromboembolism (DOVE) in primary care. AMIA Annu Symp Proc 2023;2023:339-348. [Medline: 38222335]
54. Zhou L, Plasek JM, Mahoney LM, et al. Using medical text extraction, reasoning and mapping system (MTERMS) to process medication information in outpatient clinical notes. AMIA Annu Symp Proc 2011;2011:1639-1648. [Medline: 22195230]

XSL•FO
RenderX

55. Le Glaz A, Haralambous Y, Kim-Dufor DH, et al. Machine learning and natural language processing in mental health: systematic review. J Med Internet Res 2021 May 4;23(5):e15708. [doi: 10.2196/15708] [Medline: 33944788]
56. Dove_vtext. GitHub. URL: https://github.com/jnlaurentiev/dove_vtext [accessed 2025-08-06]
57. Alsentzer E, Murphy JR, Boag W. Publicly available clinical BERT embeddings. arXiv. Preprint posted online on Jun 20, 2019. [doi: 10.48550/arXiv.1904.03323]
58. Lee J, Yoon W, Kim S, et al. BioBERT: a pre-trained biomedical language representation model for biomedical text mining. Bioinformatics 2020 Feb 15;36(4):1234-1240. [doi: 10.1093/bioinformatics/btz682] [Medline: 31501885]
59. Johnson AEW, Pollard TJ, Shen L, et al. MIMIC-III, a freely accessible critical care database. Sci Data 2016 May 24;3(1):160035. [doi: 10.1038/sdata.2016.35] [Medline: 27219127]
60. Wolf T, Debut L, Sanh V, et al. HuggingFace's transformers: state-of-the-art natural language processing. . Preprint posted online on Jul 13, 2020. [doi: 10.48550/arXiv.1910.03771]
61. Breiman L. Random forests. Mach Learn 2001;45(1):5-32. [doi: 10.1023/A:1010933404324]
62. Pedregosa F, Varoquaux G, Gramfort A, et al. Scikit-learn: machine learning in python. J Mach Learn Res 2011;12(85):2825-2830. [doi: 10.5555/1953048.2078195]
63. Chen T, Guestrin C. XGBoost: a scalable tree boosting system. : ACM; 2016 Presented at: 22nd ACM SIGKDD International Conference on Knowledge Discovery and Data Mining; Aug 13-17, 2016; San Francisco, CA p. 785-794. [doi: 10.1145/2939672.2939785]
64. Tf-idf weighting. URL: https://nlp.stanford.edu/IR-book/html/htmledition/tf-idf-weighting-1.html [accessed 2022-09-21]
65. Diagnostic delay of venous thromboembolism (DOVE) in primary care. Partnership for Quality Measurement. URL: https://p4qm.org/measures/3749e [accessed 2024-01-01]
66. Sabra S, Mahmood Malik K, Alobaidi M. Prediction of venous thromboembolism using semantic and sentiment analyses of clinical narratives. Comput Biol Med 2018 Mar 1;94:1-10. [doi: 10.1016/j.compbiomed.2017.12.026] [Medline: 29353160]
67. Jin ZG, Zhang H, Tai MH, Yang Y, Yao Y, Guo YT. Natural language processing in a clinical decision support system for the identification of venous thromboembolism: algorithm development and validation. J Med Internet Res 2023 Apr 24;25(1):e43153. [doi: 10.2196/43153] [Medline: 37093636]
68. Le Guellec B, Lefèvre A, Geay C, et al. Performance of an open-source large language model in extracting information from free-text radiology reports. Radiol Artif Intell 2024 Jul;6(4):e230364. [doi: 10.1148/ryai.230364] [Medline: 38717292]

Abbreviations

AUPRC: area under the precision-recall curve
AUROC: area under the receiver operating characteristic curve
BERT: bidirectional encoder representations from transformers
DVT: deep vein thrombosis
eCQM: electronic clinical quality measure
EDW: enterprise data warehouse
EHR: electronic health record
HIPAA: Health Insurance Portability and Accountability Act
***ICD-10*:** *International Statistical Classification of Diseases, Tenth Revision*
LLM: large language model
MGB: Mass General Brigham
MIMIC: Medical Information Mart for Intensive Care
MTERMS: Medical Text Extraction, Reasoning and Mapping System
NLP: natural language processing
NPV: negative predictive value
PE: pulmonary embolism
PPV: positive predictive value
PSH: Penn State Health
SOB: shortness of breath
SVM: support vector machine
TF-IDF: term frequency—inverse document frequency
VTE: venous thromboembolism
VTExt: venous thromboembolism symptom extractor

XSL•FO
RenderX

Edited by A Coristine; submitted 28.06.24; peer-reviewed by GK Gupta, ST Arasteh; revised version received 05.06.25; accepted 05.06.25; published 26.08.25.

Please cite as:
Novoa-Laurentiev J, Bowen M, Pullman A, Song W, Syrowatka A, Chen J, Sainlaire M, Chang F, Gray K, Panta P, Liu L, Nawab K, Hijjawi S, Schreiber R, Zhou L, Dykes PC
An Extraction Tool for Venous Thromboembolism Symptom Identification in Primary Care Notes to Facilitate Electronic Clinical Quality Measure Reporting: Algorithm Development and Validation Study
JMIR Med Inform 2025;13:e63720
URL: https://medinform.jmir.org/2025/1/e63720
doi:10.2196/63720

© John Novoa-Laurentiev, Mica Bowen, Avery Pullman, Wenyu Song, Ania Syrowatka, Jin Chen, Michael Sainlaire, Frank Chang, Krissy Gray, Purushottam Panta, Luwei Liu, Khalid Nawab, Shadi Hijjawi, Richard Schreiber, Li Zhou, Patricia C Dykes. Originally published in JMIR Medical Informatics (https://medinform.jmir.org), 26.8.2025. This is an open-access article distributed under the terms of the Creative Commons Attribution License (https://creativecommons.org/licenses/by/4.0/), which permits unrestricted use, distribution, and reproduction in any medium, provided the original work, first published in JMIR Medical Informatics, is properly cited. The complete bibliographic information, a link to the original publication on https://medinform.jmir.org/, as well as this copyright and license information must be included.

XSL•FO
RenderX

Natural Language Processing and ICD-10 Coding for Detecting Bleeding Events in Discharge Summaries: Comparative Cross-Sectional Study

Frederic Gaspar[1,2*], PhD; Mehdi Zayene[3], MSc; Claire Coumau[1,2,4], MSc; Elliott Bertrand[3], MSc; Marie Bettex[5], MD; Marie Annick Le Pogam[5*], MD, PhD; Chantal Csajka[2,4*], PhD

[1]Center for Research and Innovation in Clinical Pharmaceutical Sciences, Rue du Bugnon 19, Lausanne, Switzerland

[2]School of Pharmaceutical Sciences, University of Geneva, Geneva, Switzerland

[3]Effixis SA, Lausanne, Switzerland

[4]Institute of Pharmaceutical Sciences of Western Switzerland, University of Geneva, Geneva and Lausanne, Switzerland

[5]Department of Epidemiology and Health Systems, Center for Primary Care and Public Health (Unisanté), University of Lausanne, Lausanne, Switzerland

[*]these authors contributed equally

Corresponding Author:
Frederic Gaspar, PhD
Center for Research and Innovation in Clinical Pharmaceutical Sciences, Rue du Bugnon 19, Lausanne, Switzerland

Abstract

Background: Bleeding adverse drug events (ADEs), particularly among older inpatients receiving antithrombotic therapy, represent a major safety concern in hospitals. These events are often underdetected by conventional rule-based systems relying on structured electronic medical record data, such as the *ICD-10 (International Statistical Classification of Diseases and Related Health Problems 10th Revision*) codes, which lack the granularity to capture nuanced clinical narratives.

Objective: This study aimed to develop and evaluate a natural language processing (NLP) model to detect and categorize bleeding ADEs in discharge summaries of older adults. Specifically, the model was designed to distinguish between "clinically significant bleeding," "severe bleeding," "history of bleeding," and "no bleeding," and was compared with a rule-based algorithm using *ICD-10* codes.

Methods: Clinicians manually annotated 400 discharge summaries, comprising 65,706 sentences, into four categories: "no bleeding," "clinically significant bleeding," "severe bleeding," and "history of bleeding." The dataset was divided into a training set (70%, 47,100 sentences) and a test set (30%, 18,606 sentences). Two detection approaches were developed and evaluated: (1) an NLP model using binary logistic regression and support vector machine classifiers, and (2) a traditional rule-based algorithm relying exclusively on predefined *ICD-10* codes. To address class imbalance, with most sentences categorized as irrelevant ("no bleeding"), a class-weighting strategy was applied in the NLP model. Model performance was assessed using accuracy, precision, recall, F_1-score, and receiver operating characteristic (ROC) curve analyses, with manual annotations as the gold standard.

Results: The NLP model significantly outperformed the rule-based approach across all evaluation metrics. At the document level, the NLP model achieved macro-average scores of 0.81 for accuracy and 0.80 for F_1-score. Precision was particularly high for detecting severe (0.92) and clinically significant bleeding events (0.87), demonstrating strong classification capability despite class imbalance. ROC analyses confirmed the model's robust diagnostic performance, yielding an area under the curve (AUC) of 0.91 when distinguishing irrelevant sentences from potential bleeding events, 0.88 for identifying historical mentions of bleeding, and notably, 0.94 for differentiating clinically significant from severe bleeding. In contrast, the rule-based *ICD-10* model demonstrated high precision (0.94) for clinically significant bleeding but poor recall (0.03) for severe bleeding events, reflecting frequent missed detections. This limitation arose due to its reliance on commonly used *ICD-10* codes (eg, gastrointestinal hemorrhage) and inadequate capture of rare severe bleeding conditions such as shock due to hemorrhage.

Conclusions: This study highlights the considerable advantage of NLP over traditional *ICD-10*–based methods for detecting bleeding ADEs within electronic medical records. The NLP model effectively captured nuanced clinical narratives, including severity, negations, and historical bleeding events, demonstrating substantial promise for improving patient safety surveillance and clinical decision-making. Future research should extend validation across multiple institutions, diversify annotated datasets, and further refine temporal reasoning capabilities within NLP algorithms.

International Registered Report Identifier (IRRID): RR2-10.2196/40456

(JMIR Med Inform 2025;13:e67837) doi:10.2196/67837

XSL•FO
RenderX

KEYWORDS

decision support systems; deep learning; hemorrhage; international classification of diseases; machine learning; ML; natural language processing; NLP; cross-sectional; logistic regression; bleeding; discharge summaries; adverse drug events; older adults; elderly; electronic medical records; medical records; artificial intelligence; AI; healthcare; decision-making

Introduction

Adverse drug events (ADEs) are a significant patient safety issue, particularly among older adult inpatients. Globally, ADEs are estimated to affect 10%-40% of hospitalized patients, contributing to increased morbidity, mortality, and health care costs [1-3]. Among older adult patients, who are often treated using complex medication regimens, the risk of ADEs is even higher due to age-related physiological changes and a higher prevalence of polypharmacy [4,5]. Data on the incidence and impact of ADEs in Switzerland's hospitals are sparse, however, making it difficult to fully assess the scope of the problem [6].

Antithrombotic therapy, commonly prescribed to prevent thrombotic events, significantly increases the risk of bleeding by inhibiting normal clotting mechanisms. Studies have shown that approximately 36% of older adult inpatients on antithrombotic therapy experience bleeding complications, which can lead to extended hospital stays and increased morbidity and mortality [5]. The widespread use of polypharmacy in this population further compounds the risk of drug interactions, contributing to ADEs [7]. In Swiss hospitals, the timely and accurate detection of bleeding events is considered crucial to improve patient outcomes and ensure safer care [8].

Electronic medical records (EMRs) provide an opportunity to automate the detection of ADEs such as bleeding. Bleeding events are commonly identified through structured data, particularly via the diagnostic codes in the (*ICD*) *International Classification of Diseases*, which are frequently used for billing purposes. However, *ICD* codes often lack the specificity required to capture the complexity and nuances of bleeding ADEs [9-11]. Research has shown that *ICD* codes frequently underreport ADEs, with sensitivities below 50% in many cases, leading to an incomplete picture of patient safety [12]. In addition, coding algorithms for detecting ADEs usually exhibit low sensitivity and precision, and there is no universally accepted set of *ICD-10* (*International Classification of Diseases, 10th Revision*) codes or algorithms that ensures the consistent identification of bleeding ADEs in administrative data [13]. Although a manual review of medical records can be more accurate, it is labor-intensive and impractical for widespread use [10].

Natural language processing (NLP), a branch of artificial intelligence, provides a scalable solution to the automated extraction and classification of information on bleeding ADEs from unstructured text, such as inpatient discharge summaries and clinical notes [14,15]. These notes often contain detailed narrative descriptions of clinical events, such as "nonglomerular microhematuria" or "no visible bleeding at the anamnesis," which billing codes might miss [16]. NLP models can detect key clinical information buried within these narrative notes, providing more accurate insights into patients' conditions than frequently used methods such as *ICD* coding. Previous studies have demonstrated that NLP can detect ADEs from clinical notes with accuracies as high as 85%-90%, significantly outperforming standard methods [17-20]. By leveraging NLP and integrating it into hospital workflows, health care professionals can improve the surveillance of ADEs, make more timely interventions, and provide more responsive, personalized patient care [21].

In this study, conducted within the framework of the Swiss Monitoring of Adverse Drug Events (SwissMADE) project [8], we hypothesized that an NLP-based approach would be more effective than *ICD* code–based algorithms for detecting and categorizing bleeding ADEs among older adult inpatients receiving antithrombotic therapy at Lausanne University Hospital. The primary objective was to develop an NLP model capable of identifying bleeding ADEs from the discharge summaries of older adult inpatients hospitalized in 2015 and 2016 and to categorize these events based on their timing (ie, before admission or during the hospital stay) and severity (clinically significant bleeding or severe bleeding). The secondary objective was to compare the NLP model's performance against standard *ICD-10*–based algorithms and identify the most effective automated method for detecting bleeding ADEs in Switzerland's health care context.

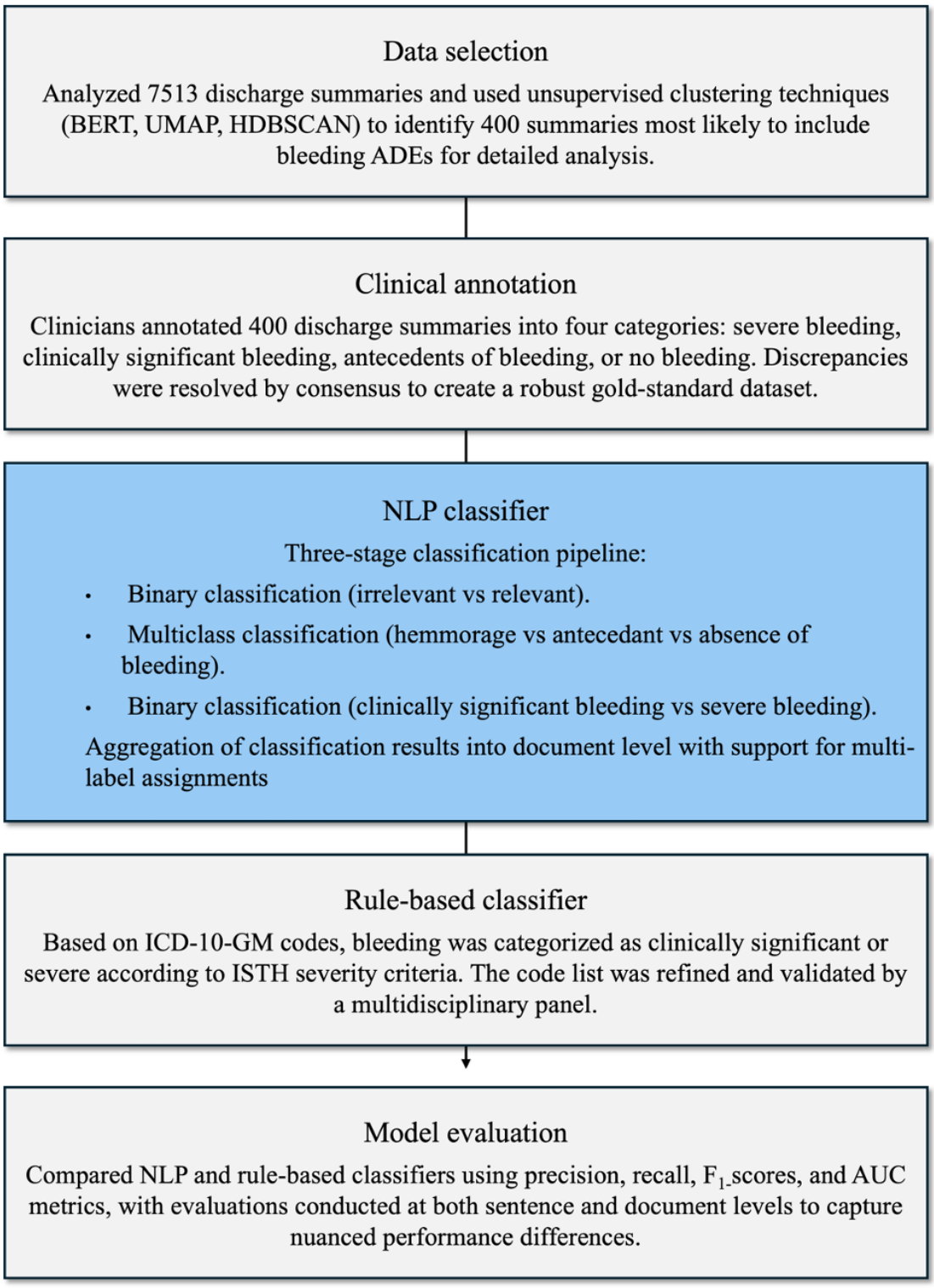
Methods

Study Design

We conducted a secondary analysis of unstructured data in the EMRs investigated by the SwissMADE study, a multicenter, cross-sectional study that used retrospective medical data from 4 large Swiss hospitals [8]. Figure 1 provides an overview of the methodological framework used in this study.

XSL•FO
RenderX

Figure 1. Overview of the methodological framework used in this study. ADE: adverse drug event; AUC: area under the curve; BERT: Bidirectional Encoder Representations from Transformers; HDBSCAN: hierarchical density-based spatial clustering of applications with noise; *ICD-10-GM*: *German Modification of the International Statistical Classification of Diseases and Related Health Problems, 10th Revision*; ISTH: International Society on Thrombosis and Haemostasis; NLP: natural language processing; UMAP: uniform manifold approximation and projection.



Study Population and Dataset Selection

The dataset comprised the discharge summaries of patients aged 65 or older who were hospitalized for more than 24 hours in 2015 and 2016 and received at least one antithrombotic medication during their stay. These summaries also included administrative data, such as *ICD-10-GM* (*International Classification of Diseases, 10th Revision, German Modification*)

XSL•FO
RenderX

diagnostic codes. A detailed description of the SwissMADE study's methods has been published previously [8].

Of the 7513 discharge summaries examined, an unsupervised machine learning approach identified 400 as likely to contain bleeding ADEs (Figure S1 in Multimedia Appendix 1). This approach involved text scanning, thematic aggregation, and data extraction. The study generated unique sentence embeddings by integrating Bidirectional Encoder Representations from Transformers (BERT) into the Sentence Transformer library [22]. Techniques such as Uniform Manifold Approximation and Projection (UMAP) [23] and Hierarchical Density-Based Spatial Clustering of Applications with Noise (HDBSCAN) [24] were applied to organize these embeddings into "clusters" of bleeding ADEs. This methodology was instrumental in selecting the 400 discharge summaries most relevant to the study.

Annotation of Clinical Documents

The 400 discharge summaries were first annotated by clinicians and then divided into a training set (n=280) and a test set (n=120). The distribution of summaries was randomized to ensure the sample remained representative of the overall population of hospitalized patients.

Three clinicians independently annotated each discharge summary using four predefined labels:

1. Presence of severe bleeding: this label was used when a discharge summary explicitly identified severe bleeding, either by using the term "severe" or by describing conditions that meet the criteria for severe bleeding, such as fatal bleeding, bleeding at critical sites (eg, intracranial and intraspinal), a drop in hemoglobin of ≥20 g/L, or transfusion of ≥2 units of blood, as defined by the International Society on Thrombosis and Haemostasis (ISTH) [25].
2. Presence of clinically significant bleeding: this label was used when bleeding was mentioned in the clinical documentation but did not meet the criteria for severe bleeding.
3. History of bleeding: this label was applied when a discharge summary mentioned bleeding in the patient's medical history before their hospital admission.
4. Absence of bleeding: this label was used when a discharge summary did not mention bleeding.

A fourth clinician resolved any disagreements, and this classification was used as the gold standard for training the machine learning model. Fleiss kappa coefficient, calculated from 30 summaries, showed 96% agreement among clinicians, allowing a shift to a single-reviewer approach. Only discharge summaries signed by an attending physician were included to ensure data credibility.

Development of the NLP-Based Classifier

The development method comprised three phases: segmenting discharge summaries into sentences, classifying those sentences, and aggregating them at the document level.

Phase 1: Segmentation

Sentences were segmented from the discharge summaries using the pretrained French spaCy model (Explosion AI) [19], chosen for its efficiency, robustness, and widespread adoption in NLP pipelines [26]. Given that sentence segmentation is a standard preprocessing step with minimal differences among comparable models [27], no additional comparative analyses were performed. To reduce noise, sentences with fewer than three characters were excluded, a decision supported by pilot tests demonstrating minimal loss of meaningful content.

Phase 2: Classification Process

The classification process addressed the challenge of class imbalance, particularly at the sentence level, where the majority of sentences were labeled as "Irrelevant," indicating no bleeding-related information.

To mitigate this imbalance during training, a class-weighting strategy was applied in the logistic regression model used for the initial binary classification [28]. This approach adjusted the contribution of each class to the loss function by assigning higher weights to minority classes, such as "severe bleeding," and lower weights to the majority class, "Irrelevant." This adjustment improved the model's ability to identify rare but clinically critical cases. Additional details on the dataset preparation and the class-weighting strategy are provided in the supplementary materials.

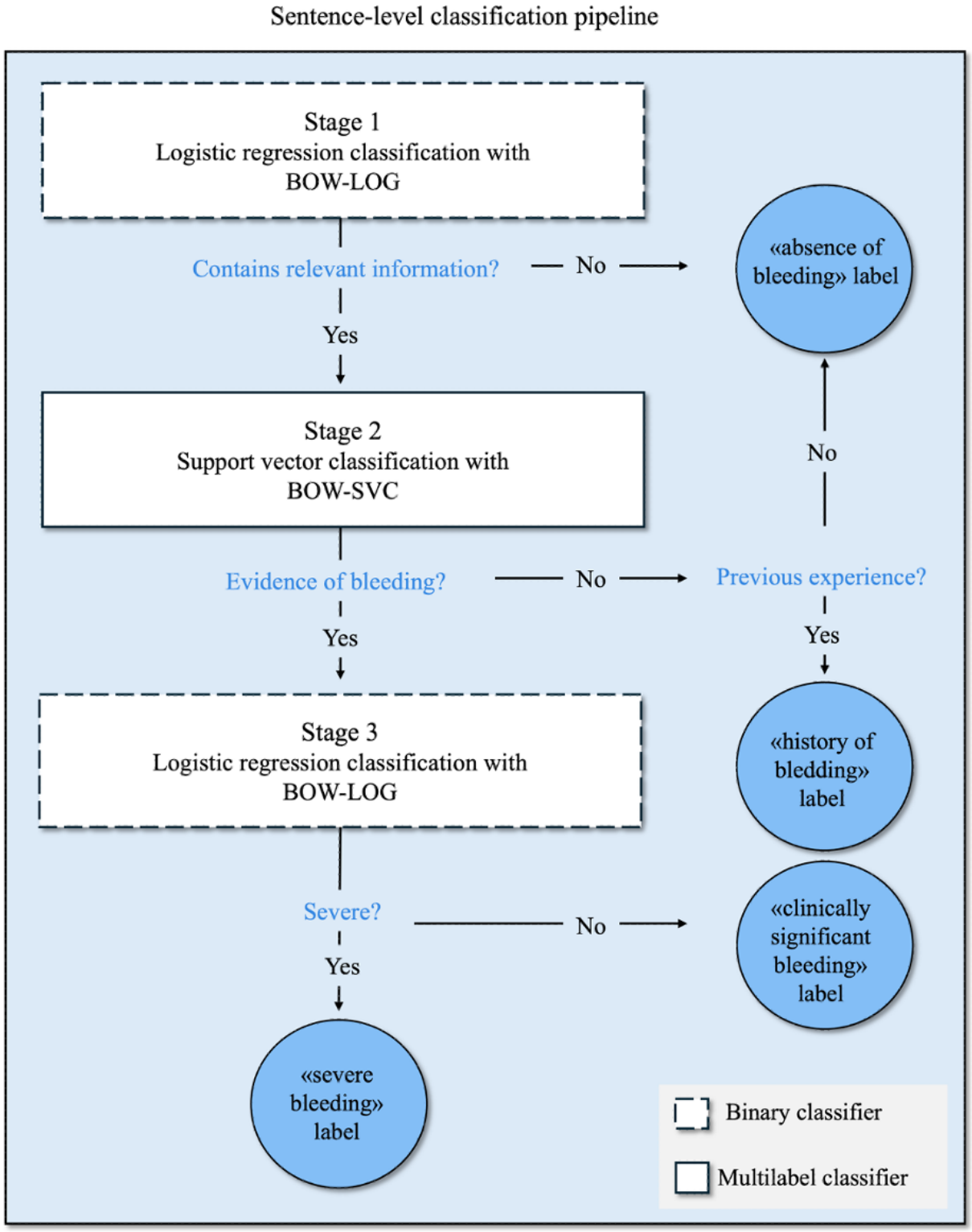
Figure 2 illustrates the multistage classification process for identifying bleeding ADEs in clinical narratives. Stage 1 used a binary logistic regression model to classify sentences as either containing bleeding-related information (labeled "relevant;" value=1) or not ("irrelevant;" value=0), reducing the number of nonrelevant sentences. Stage 2 used a support vector machine (SVM) classifier to further divide the relevant sentences into three categories: "irrelevant," "antecedent," or "bleeding-related." Stage 3 applied a second binary classification to "bleeding-related" sentences, categorizing them as either "clinically significant" (value=0) or "severe" (value= 1).

Logistic regression and a bag-of-words–based SVM were selected due to their simplicity, interpretability, and effectiveness on smaller datasets, minimizing the risk of overfitting compared to more complex deep learning methods. Preliminary experiments using deep learning models yielded poor performance, likely due to the limited size of the dataset; therefore, these methods were not pursued further in this study.

The entire process used bag-of-words encoding to convert the text into a format suitable for machine learning algorithms. Robustness was ensured through 5-fold cross-validation [29], regularization techniques (eg, L2 regularization for logistic regression and optimization of the penalty parameter [C] in SVM), and hyperparameter tuning via grid search [30,31]. These methodological choices optimized performance while preventing overfitting.

XSL•FO
RenderX

Figure 2. Sentence-level classification pipeline for detecting bleeding events. In this pipeline: BOW-LOG: logistic regression classification using a bag-of-words (BOW) model to determine whether the sentence contains bleeding-relevant information; BOW-SVM: support vector machine (SVM) classification using a BOW model to assess whether there is evidence of bleeding in the sentence; BOW-LOG: a second logistic regression classification using a BOW model to evaluate the severity of the bleeding event (ie, whether it is severe or clinically significant).



Phase 3: Document Aggregation

Sentence-level classification results were aggregated at the discharge summary level by grouping sentences under their corresponding document ID and combining the predictions using a union-like operation. If all sentences in a document were labeled “irrelevant,” the entire document was classified the same. Otherwise, the document was assigned one or more of the following labels: “antecedent,” “clinically significant

XSL•FO
RenderX

bleeding," or "severe bleeding." Unlike sentences, documents could receive multiple labels.

Rule-Based Classifier Development

In parallel with the NLP approach, we developed a rule-based classifier using *ICD-10-GM* codes to detect bleeding ADEs. This classifier enabled us to compare the analysis with the NLP methods. We began by compiling a comprehensive list of *ICD-10* diagnostic codes related to bleeding, drawing on subdivisions defined by the ISTH and codes identified in previous studies [32-34].

We thoroughly explored *ICD-10* ontologies to identify additional codes for terms such as "bleeding" and "hemorrhage." A multidisciplinary panel of physicians, pharmacologists, pharmacists, and statisticians reviewed and expanded this list, adding codes for conditions such as hemodynamic instability, drug-induced bleeding, and contusions. We then categorized these codes into two mutually exclusive groups based on the ISTH's severity criteria: "clinically significant bleeding" and "severe bleeding." The classification considered factors such as the site of bleeding.

The complete list of codes used appears in Tables S1 and S2 in Multimedia Appendix 1. However, unlike the NLP approach, the rule-based method was limited to just 2 labels due to the absence of specific *ICD-10* codes for identifying a patient's history of bleeding. Moreover, the rule-based approach did not account for timing, making it difficult to determine whether bleeding occurred before or during the hospital stay.

Model Evaluation and Comparison

We conducted a comparative analysis of the rule-based classifier and the NLP method to assess their effectiveness and accuracy in identifying hemorrhagic events from discharge summaries. Using the independent test dataset to ensure unbiased assessments, we applied standardized evaluation metrics, namely precision, recall, specificity, and F_1-score, focusing on each method's ability to detect clinically significant and severe bleeding. We used a receiver operating characteristic (ROC) curve to evaluate the NLP model's diagnostic capacity, measuring its overall performance through its area under the curve (AUC) [35]. We also calculated Cohen kappa to facilitate a comparative analysis of the methods' detection accuracies [36].

All statistical analyses were performed using Python software (version 3.9, Python Software Foundation), ensuring a robust computational environment. We calculated both micro- and macro-averages to provide a comprehensive evaluation of the classifiers' performances. Micro-averages were computed at the sentence level, measuring overall performance across all sentences, while macro-averages were calculated at the document level, giving equal weight to each document regardless of the number of sentences it contained.

Ethical Considerations

This study involved secondary analysis of pre-existing clinical data from discharge summaries collected within the SwissMADE project, a multicenter, retrospective, cross-sectional study approved by the Swiss Ethics Committees (CER-VD, No. 2016 - 02008). This analysis used retrospective data from EMRs collected within the SwissMADE study. The original study protocol, approved by the ethics committee, included a waiver of informed consent. Due to the narrative nature of the clinical data, complete anonymization was not feasible. Strict confidentiality measures were implemented, including restricted data access, secure data handling, and reporting of results in aggregate form only, in compliance with Swiss federal and institutional data protection standards. No patient compensation was provided, as the study involved secondary analysis of pre-existing clinical data. No identifiable images or other materials from individual patients were included in this paper or its supplementary materials. Consequently, there was no requirement for obtaining consent from individuals for use of identifiable images.

Results

Overview

A total of 400 discharge summaries were analyzed, comprising 65,706 annotated sentences. Of these, 47,100 sentences were allocated to the training set and 18,606 to the test set. Detailed demographic and clinical characteristics of the hospital stays associated with each dataset are presented in Table 1.

The distribution of sentence lengths in Figure 3 reveals a right-skewed pattern, with most sentences under 100 characters. To reduce noise, sentences shorter than 3 characters were excluded, accounting for 2.72% of the dataset, ensuring more meaningful content for robust model training and evaluation.

Sentence-level analysis revealed a predominance of "irrelevant" annotations, reflecting the large amount of information in discharge summaries unrelated to bleeding. However, class distribution was more balanced at the document level, demonstrating the complexity of clinical documentation, where multiple annotations often coexist within a single summary. Table 2 provides the detailed distribution of these categories.

The NLP model demonstrated strong classification capabilities, achieving over 85% accuracy across all categories at the document level. It also showed robust performance, with a precision exceeding 72% across categories and a recall of 98% for "irrelevant" instances. F_1-scores indicated balanced performance despite class imbalances, highlighting the model's ability to manage diverse data distributions. A detailed summary of the performance metrics for our multilabel classification model is provided in Table 3.

As shown in Figure 4, ROC curve analysis further highlighted the model's diagnostic accuracy. In stage one, the model achieved an AUC of 0.91 for classifying sentences as either "irrelevant" or "potentially bleeding-related," effectively filtering out irrelevant data. In stage 2, it refined these classifications into the "irrelevant" and "antecedent" categories, with AUCs of 0.88 and 0.83, respectively. Stage 3 focused on distinguishing "clinically significant bleeding" from "severe bleeding," achieving an AUC of 0.94. Overall, the ROC curves demonstrated the model's consistently high performance across all stages, with elevated AUC values reflecting its strong ability to distinguish between classes.

XSL•FO
RenderX

The rule-based classifier, while simpler than the multilabel NLP model, showed high precision in identifying clinically significant bleeding events. Table 4 provides a detailed comparison of the algorithm's metrics and those of the NLP model.

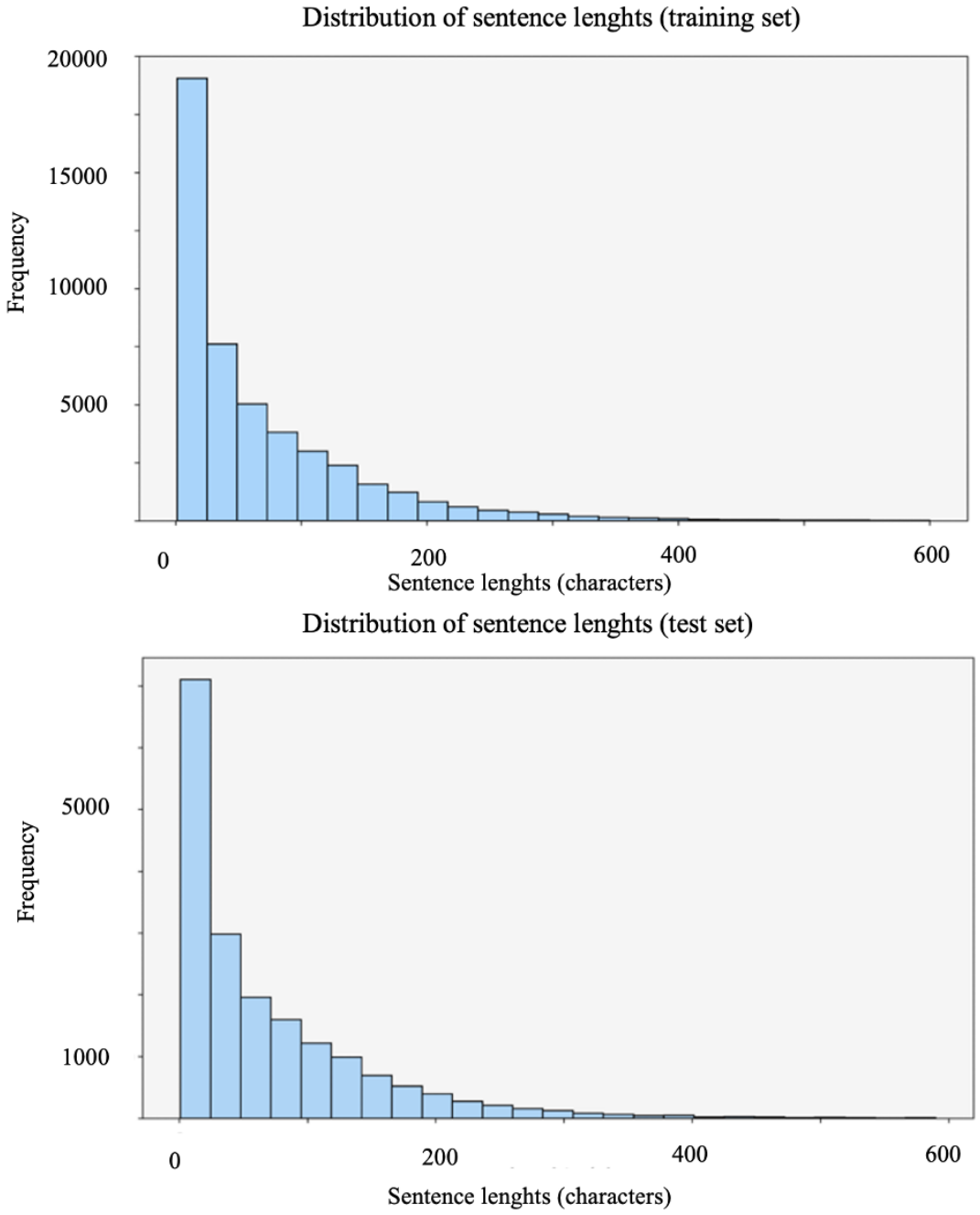
Table . Training and testing set patients' characteristics.

Variable	Training set	Test set
Discharge summaries, n (%)	280 (70)	120 (30)
Sentences, n (%)	47100 (72)	18606 (28)
Unique patients, n (%)	270 (96)	120 (100)
Length of stay (days), median (IQR)	15 (8–28)	13 (7-22)
Female, n (%)	111 (40)	89 (74)
Age (years), median (IQR)	81 (74-87)	79 (72-85)
ICU[a] admissions, n (%)	17 (6)	4 (3)
Modes of admission, n (%)		
Emergency	214 (76)	89 (74)
Planned,	49 (18)	20 (17)
Internal transfer	15 (5)	6 (5)
Transfer within 24 hours	2 (1)	5 (4)

[a]ICU: intensive care unit.

XSL•FO
RenderX

Figure 3. Distribution of sentence lengths in training and test sets.



XSL•FO
RenderX

Table . Class distribution in the training and test sets at the sentence and document levels.

Classification label	Sentence level[a]		Document level[b]	
	Training set, n (%)	Test set, n (%)	Training set, n (%)	Test set, n (%)
Irrelevant (absence of bleeding)	45897 (97.45)	18118 (97.38)	103 (36.79)	44 (36.67)
History of bleeding	154 (0.33)	58 (0.31)	67 (23.93)	22 (18.33)
Clinically significant bleeding	900 (1.91)	373 (2.00)	141 (50.36)	60 (50.00)
Severe bleeding	149 (0.32)	57 (0.31)	77 (27.50)	31 (25.83)

[a]Sentence level: frequency and proportion of each classification label per individual sentence.

[b]Document level: frequency and proportion of documents containing at least one instance of the respective classification label.

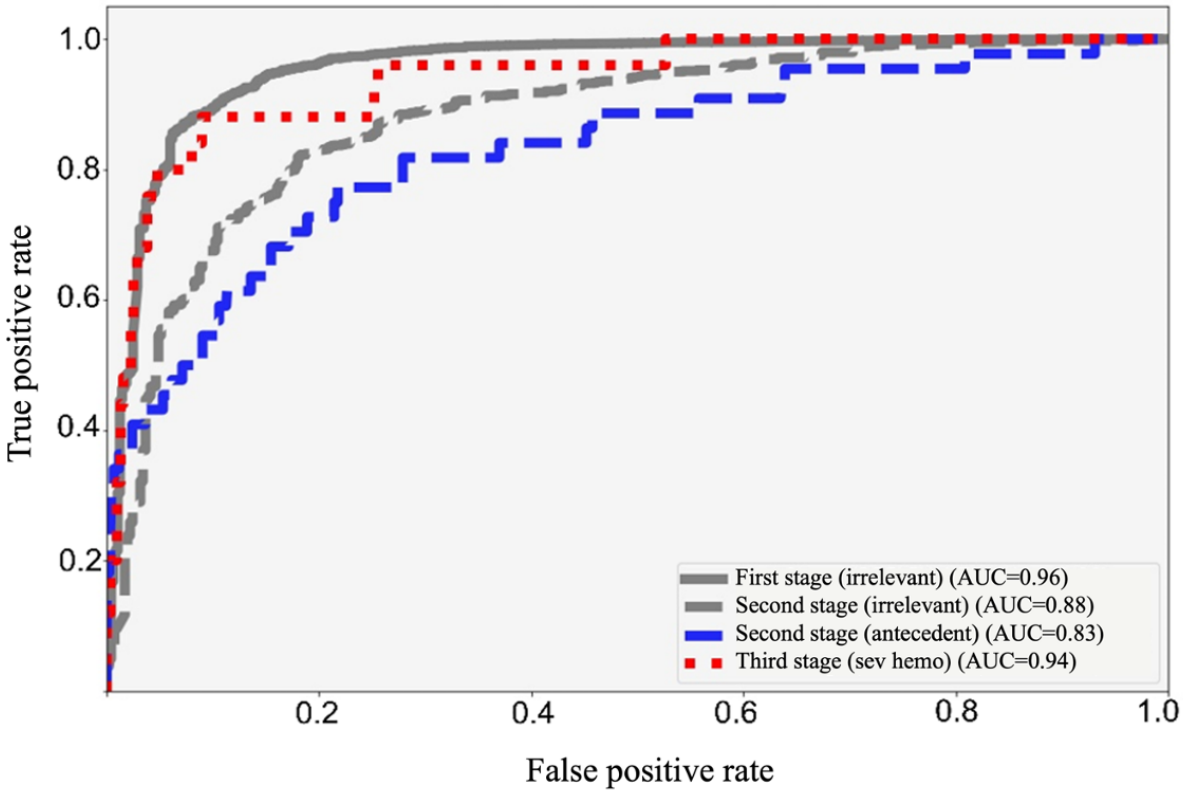
Table . Detailed performance metrics of the multilabel classification model.

Metric	Irrelevant	History of bleeding	Clinically significant bleeding	Severe bleeding	Macro-average[a]	Micro-average[b]
Accuracy	0.83	0.68	0.86	0.89	0.81	0.84
Precision	0.81	0.72	0.87	0.92	0.83	0.85
Recall	0.98	0.88	0.59	0.31	0.69	0.71
F_1-score	0.89	0.65	0.88	0.70	0.78	0.80

[a]Macro-average: average performance across document-level classifications.

[b]Micro-average: average performance across sentence-level classifications.

Figure 4. Receiver operating characteristic (ROC) curves showing the diagnostic performance of the multistage classification model at various thresholds, illustrating the trade-off between the true positive rate (sensitivity) and the false positive rate (1 - specificity).



XSL•FO
RenderX

Table . Detailed performance metrics of the rule-based classification model.

Metric	Irrelevant	Antecedent[a]	Clinically significant bleeding	Severe bleeding	Macro-average	Micro-average[b]
Accuracy	0.81	—[c]	0.86	0.74	0.80	—
Precision	0.80	—	0.94	0.50	0.75	—
Recall	0.95	—	0.77	0.03	0.58	—
F_1-score	0.87	—	0.84	0.06	0.59	—

[a]Metrics for the "Antecedent" category are not provided due to the absence of corresponding *International Statistical Classification of Diseases and Related Health Problems, 10th Revision* codes.

[b]"Micro-average" was not calculated as the rule-based model uses *International Statistical Classification of Diseases and Related Health Problems, 10th Revision* codes linked to hospital stays.

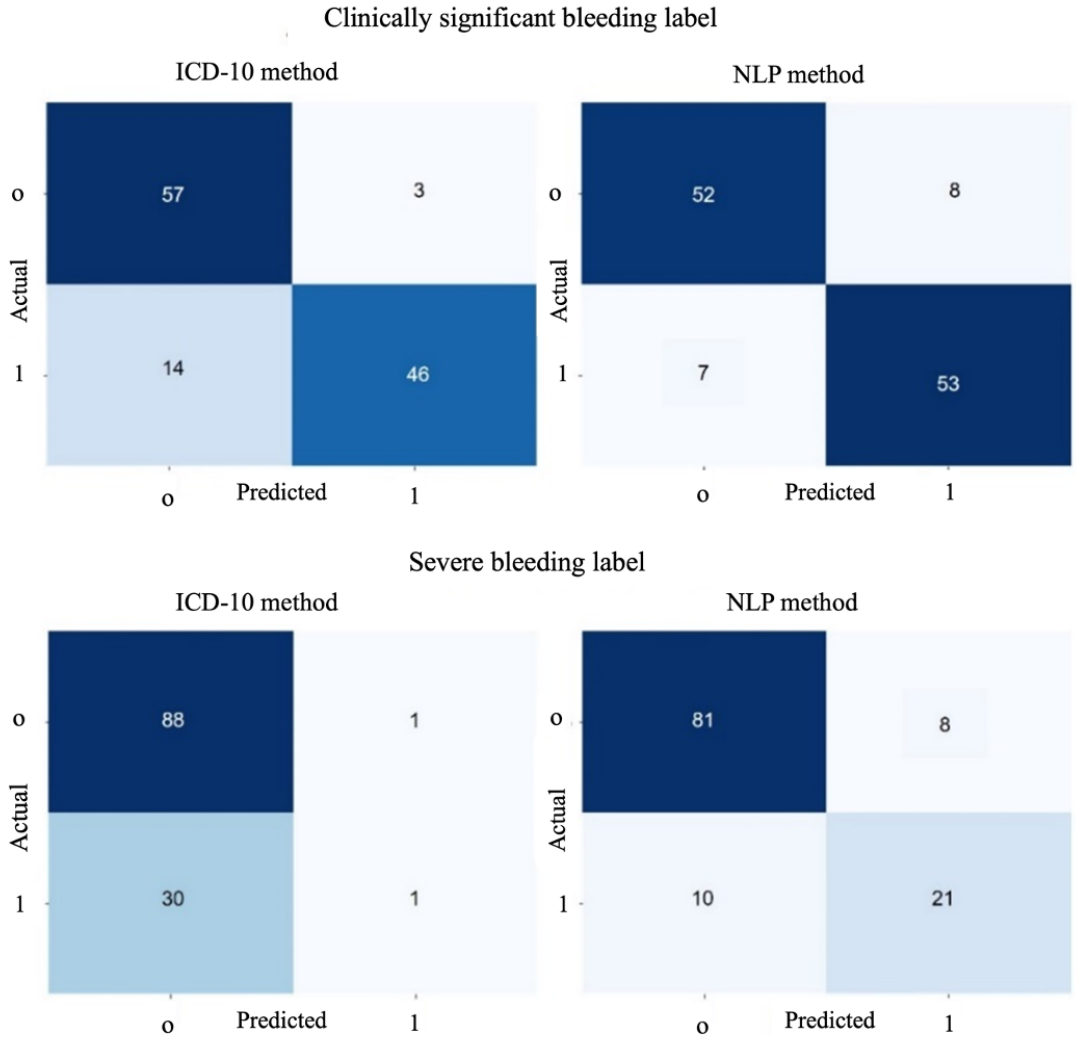
[c]Not available.

The rule-based classifier achieved a precision score of 0.94 for "clinically significant bleeding," highlighting its accuracy in detecting these events. However, its performance in identifying "severe bleeding" was significantly weaker, with a recall of only 0.03. This low recall indicates that while the model could detect severe bleeding when present, it also frequently missed such events.

For "clinically significant bleeding," the classifier relied heavily on frequently used *ICD-10* codes, such as K92.2 (gastrointestinal hemorrhage, unspecified), R31 (hematuria, unspecified), and K26.4 (gastric ulcer, acute with hemorrhage), which contributed to its high precision. In contrast, codes associated with "severe bleeding," including R57.1 (shock due to hemorrhage) and I85.3 (esophageal varices with bleeding), were less common in the dataset, resulting in poorer performance for this category. The rule-based model achieved an F_1-score of 0.84 for "clinically significant bleeding" but only 0.06 for "severe bleeding," underscoring the disparity in its ability to handle these 2 categories. Figure 5 highlights the comparative performance of the NLP and rule-based models in detecting clinically significant and severe bleeding. The NLP model consistently demonstrated higher recall and balanced classification across both categories, effectively addressing limitations observed in the rule-based approach.

XSL•FO
RenderX

Figure 5. Comparative analysis of confusion matrices for bleeding detection using natural language processing (NLP) and *ICD* (*International Classification of Diseases*) coding methods. This figure contrasts the performance of the NLP model and the *ICD* coding approach, displaying the counts of true positives, true negatives, false positives, and false negatives, thus providing a comparative evaluation of both methods. *ICD-10*: *International Statistical Classification of Diseases and Related Health Problems, 10th Revision*.



Discussion

Principal Findings

This study developed and validated an NLP-based model for detecting bleeding events from clinical narratives, achieving a high level of accuracy. The model demonstrated 91% sentence-level accuracy and 88% document-level accuracy. Compared to traditional *ICD-10* code–based methods, the NLP model provided more nuanced and precise detection of bleeding events, effectively capturing details that *ICD-10* codes often miss, particularly in cases involving secondary conditions or multiple types of bleeding ADEs. These findings underscored NLP's potential to improve the detection and management of adverse events.

One of the model's primary strengths lies in its high precision and recall, even in the presence of class imbalance, particularly when differentiating between "clinically significant" and "severe bleeding." It performed well in interpreting complex clinical data, including negations (eg, "no evidence of bleeding") and secondary conditions, which are typically challenging for rule-based *ICD-10* approaches [9]. By integrating these nuances, the NLP model provided a more comprehensive understanding of patients' clinical status. Its ability to analyze unstructured clinical narratives highlights its potential for real-time decision-making, enabling clinicians to identify bleeding events more accurately and promptly, ultimately improving patient outcomes in hospital settings [10,11,37].

Comparison With Prior Work

The model's accuracy, precision, recall, and F_1-scores compare favorably with those reported in the literature, including models based on deep learning architectures such as biLSTM-CRF or transformers such as BERT [38]. However, most of these studies use larger English-language datasets and cover a broader range of clinical events. Differences in language (French vs English),

XSL•FO
RenderX

dataset size, annotation schemes, and outcome definitions make direct comparisons difficult. While transformer-based models have shown excellent performance in clinical NLP [39,40], their computational demands and limited interpretability may hinder real-world implementation [41]. In this study, we prioritized interpretable and efficient models, such as logistic regression and SVM, offering a favorable trade-off between performance and usability. Future efforts may explore hybrid frameworks that combine advanced performance with interpretability [42].

A distinctive advantage of our approach is the use of multilabel classification, which allows the model to detect co-occurring conditions, such as clinically significant and severe bleeding, or current and historical bleeding, within a single document. This contrasts with most previous studies that rely on single-label classifiers and enhance adaptability to real-world clinical scenarios. However, the model still faced challenges with temporal reasoning, particularly in distinguishing recent events from past ones, underscoring the need for more advanced temporal analysis techniques [43-45].

The limitations of *ICD-10* coding, particularly its inability to reflect clinical nuances, are well documented in the literature. As previously observed by Johnson et al [46], reliance on a small number of broad codes, such as K92.2 (gastrointestinal bleeding, unspecified) and R57.1 (shock due to bleeding), likely contributed to low recall for severe bleeding. *ICD-10* lacks the granularity to differentiate historical versus active bleeding, mild versus severe presentations, or to correctly interpret negations. Furthermore, *ICD* codes are primarily designed for billing and administrative purposes, contributing to underreporting or misclassification of bleeding ADEs [9-11,17]. These limitations further support the relevance of NLP approaches, which offer greater flexibility and contextual understanding.

Negation handling was a particular strength of our model. Where many previous approaches have struggled, our model correctly interpreted expressions such as “no source of bleeding” [47], substantially reducing false positives and enhancing clinical utility [48]. In hospital settings, accurate interpretation of negation is essential to avoid unnecessary investigations or treatments [49].

Limitations

This study had several limitations that should be acknowledged. First, the dataset consisted solely of discharge summaries from Lausanne University Hospital, which may limit its generalizability. Data from a single large tertiary care institution might not represent the variety of clinical settings and regions in which the model could be deployed. In addition, the over-representation of certain *ICD-10* codes, such as K92.2, likely contributed to the model’s high precision for detecting clinically significant bleeding. Expanding the baseline dataset could help improve the model’s robustness and ability to generalize across different hospital environments [50]. Future work should therefore focus on expanding the dataset with discharge summaries from multiple hospitals, enabling broader validation and assessment of the model’s temporal robustness and applicability in diverse health care environments.

Second, class imbalance in the dataset, particularly the limited number of “severe bleeding” cases, posed a challenge. While the model performed well overall, its detection of rare events was enhanced by applying class weighting during training, adjusting the contribution of each class to the loss function. This strategy improved detection of underrepresented but clinically important categories without compromising overall performance. Further improvements could involve oversampling techniques, synthetic data generation, or advanced loss functions such as the segmented harmonic loss [51,52]. Domain-specific keyword-enhanced classification may also refine the model’s ability to identify severe bleeding [53]. Despite these possible improvements, the current class-weighting strategy and multistage framework offered a robust and interpretable solution suited for deployment in resource-constrained health care settings.

Third, despite satisfactory overall performance, the model’s accuracy for detecting severe bleeding dropped to around 70%. This decrease was largely due to the model’s tendency to overinterpret numerical data (eg, hemoglobin and hematocrit values) as indicative of severe bleeding, particularly when such values appeared near bleeding-related terms. These misclassifications led to false positives and suggest a need for improved contextual differentiation between clinically relevant data and incidental numeric values. The model also struggled to capture the timing of bleeding events, a critical limitation in clinical decision-making, where understanding whether a condition is active or historical can influence diagnosis and treatment [54]. Future research should aim to enhance contextual differentiation and temporal reasoning capacities within NLP models.

Finally, the study was restricted to data from 2015 to 2016 due to the reliance on high-quality, manually annotated data from the SwissMADE project, making our analysis primarily a proof-of-concept. Future studies should integrate more recent clinical discharge summaries to validate temporal robustness further and ensure the model remains applicable in evolving health care environments [55].

Future Directions

NLP models, particularly those using deep learning or transformer-based architectures, require significant computational resources for training and deployment. Although our model was relatively efficient, scalability remains challenging, particularly for real-time clinical applications requiring continuous updates and large datasets. Furthermore, although integrating large language models such as GPT-3 (OpenAI) or BERT holds the promise of improved performance, it also introduces concerns around computational cost and the secure handling of sensitive patient data [50,56-59]. These practical challenges will have to be addressed before the widespread adoption of NLP models in clinical settings [54,60].

Conclusions

Despite some limitations, this study adds to the growing evidence supporting the use of NLP for detecting ADEs such as bleeding. The model outperformed standard *ICD-10*–based approaches by capturing nuanced clinical information often

XSL•FO
RenderX

missed in structured data, including negations and secondary conditions. The use of multilabel classification improved its flexibility, allowing it to handle overlapping bleeding events in complex clinical scenarios. These features position NLP as a promising tool for enhancing real-time clinical decision-making and patient safety. Future work should focus on expanding the dataset to include records from multiple hospitals and care settings, improving generalizability. Integrating additional data sources, such as laboratory results, imaging, and progress notes, and exploring advanced NLP techniques such as BERT or GPT could further improve accuracy and temporal reasoning. Validating the model across diverse clinical environments and combining structured with unstructured data will be essential to build robust tools for bleeding ADE detection and support broader clinical implementation.

Acknowledgments

The authors would like to acknowledge all members of the SwissMADE study group for their contributions to the overall project. We particularly thank the IT team at Lausanne University Hospital, notably Nathalie Casati, for their invaluable support and efforts in extracting the clinical narratives used in this study. This study was supported by the Swiss National Science Foundation (grant no 407440_167381).

Data Availability

In compliance with patient confidentiality requirements and institutional agreements, the dataset used in this study is not publicly accessible. Researchers interested in collaborative projects may contact the corresponding author.

Authors' Contributions

FG, MZ, CCO, ZS, MB, EB, MALP, and CCS wrote the manuscript. FG, MZ, MALP, and CCS designed the research. FG, MZ, CCO, ZS, MB, EB, MALP, and CCS conducted the research. FG, MZ, CCO, ZS, MB, EB, MALP, and CCS analyzed the data. FG, MZ, CCO, EB, MALP, and CCS managed the project and acquired the necessary resources.

Conflicts of Interest

None declared.

Multimedia Appendix 1
A comparative cross-sectional study of natural language processing and *ICD-10* (*International Classification of Diseases, 10th Revision*) coding for detecting bleeding events in discharge summaries.
[DOCX File, 321 KB - medinform_v13i1e67837_app1.docx]

References

1. Cook DJ, Griffith LE, Walter SD, et al. The attributable mortality and length of intensive care unit stay of clinically important gastrointestinal bleeding in critically ill patients. Crit Care 2001 Dec;5(6):368-375. [doi: 10.1186/cc1071] [Medline: 11737927]
2. Krähenbühl-Melcher A, Schlienger R, Lampert M, Haschke M, Drewe J, Krähenbühl S. Drug-related problems in hospitals: a review of the recent literature. Drug Saf 2007;30(5):379-407. [doi: 10.2165/00002018-200730050-00003] [Medline: 17472418]
3. Berger JS, Bhatt DL, Steg PG, et al. Bleeding, mortality, and antiplatelet therapy: results from the Clopidogrel for High Atherothrombotic Risk and Ischemic Stabilization, Management, and Avoidance (CHARISMA) trial. Am Heart J 2011 Jul;162(1):98-105. [doi: 10.1016/j.ahj.2011.04.015] [Medline: 21742095]
4. Classen DC, Pestotnik SL, Evans RS, Burke JP. Computerized surveillance of adverse drug events in hospital patients. JAMA 1991 Nov 27;266(20):2847-2851. [Medline: 1942452]
5. Kanagaratnam L, Abou Taam M, Heng M, De Boissieu P, Roux MP, Trenque T. Serious adverse drug reaction and their preventability in the elderly over 65 years. Therapie 2015;70(5):477-484. [doi: 10.2515/therapie/2015029] [Medline: 26223243]
6. Beeler PE, Stammschulte T, Dressel H. Hospitalisations related to adverse drug reactions in Switzerland in 2012-2019: characteristics, in-hospital mortality, and spontaneous reporting rate. Drug Saf 2023 Aug;46(8):753-763. [doi: 10.1007/s40264-023-01319-y] [Medline: 37335465]
7. Long SJ, Brown KF, Ames D, Vincent C. What is known about adverse events in older medical hospital inpatients? A systematic review of the literature. Int J Qual Health Care 2013 Oct;25(5):542-554. [doi: 10.1093/intqhc/mzt056] [Medline: 23925507]
8. Gaspar F, Lutters M, Beeler PE, et al. Automatic detection of adverse drug events in geriatric care: study proposal. JMIR Res Protoc 2022 Nov 15;11(11):e40456. [doi: 10.2196/40456] [Medline: 36378522]

XSL•FO
RenderX

9. Wilchesky M, Tamblyn RM, Huang A. Validation of diagnostic codes within medical services claims. J Clin Epidemiol 2004 Feb;57(2):131-141. [doi: 10.1016/S0895-4356(03)00246-4] [Medline: 15125622]
10. Bates DW, Evans RS, Murff H, Stetson PD, Pizziferri L, Hripcsak G. Detecting adverse events using information technology. J Am Med Inform Assoc 2003;10(2):115-128. [doi: 10.1197/jamia.m1074] [Medline: 12595401]
11. Hohl CM, Karpov A, Reddekopp L, Doyle-Waters M, Stausberg J. ICD-10 codes used to identify adverse drug events in administrative data: a systematic review. J Am Med Inform Assoc 2014;21(3):547-557. [doi: 10.1136/amiajnl-2013-002116] [Medline: 24222671]
12. Hazlehurst B, Mullooly J, Naleway A, Crane B. Detecting possible vaccination reactions in clinical notes. AMIA Annu Symp Proc 2005;2005:306-310. [Medline: 16779051]
13. Shehab N, Ziemba R, Campbell KN, et al. Assessment of ICD-10-CM code assignment validity for case finding of outpatient anticoagulant-related bleeding among Medicare beneficiaries. Pharmacoepidemiol Drug Saf 2019 Jul;28(7):951-964. [doi: 10.1002/pds.4783] [Medline: 31144403]
14. Nadkarni PM, Ohno-Machado L, Chapman WW. Natural language processing: an introduction. J Am Med Inform Assoc 2011;18(5):544-551. [doi: 10.1136/amiajnl-2011-000464] [Medline: 21846786]
15. Yim WW, Yetisgen M, Harris WP, Kwan SW. Natural language processing in oncology: a review. JAMA Oncol 2016 Jun 1;2(6):797-804. [doi: 10.1001/jamaoncol.2016.0213] [Medline: 27124593]
16. Mehta N, Pandit A. Concurrence of big data analytics and healthcare: A systematic review. Int J Med Inform 2018 Jun;114:57-65. [doi: 10.1016/j.ijmedinf.2018.03.013] [Medline: 29673604]
17. Li R, Hu B, Liu F, et al. Detection of bleeding events in electronic health record notes using convolutional neural network models enhanced with recurrent neural network autoencoders: deep learning approach. JMIR Med Inform 2019 Feb 8;7(1):e10788. [doi: 10.2196/10788] [Medline: 30735140]
18. Tang B, Cao H, Wu Y, Jiang M, Xu H. Clinical entity recognition using structural support vector machines with rich features. 2012 Oct 29 Presented at: CIKM'12; Oct 29, 2012; Maui, HI URL: https://dl.acm.org/doi/proceedings/10.1145/2390068 [doi: 10.1145/2390068.2390073]
19. Hao T, Huang Z, Liang L, Weng H, Tang B. Health natural language processing: methodology development and applications. JMIR Med Inform 2021 Oct 21;9(10):e23898. [doi: 10.2196/23898] [Medline: 34673533]
20. Hossain E, Rana R, Higgins N, et al. Natural language processing in electronic health records in relation to healthcare decision-making: a systematic review. Comput Biol Med 2023 Mar;155:106649. [doi: 10.1016/j.compbiomed.2023.106649] [Medline: 36805219]
21. Locke S, Bashall A, Al-Adely S, Moore J, Wilson A, Kitchen GB. Natural language processing in medicine: a review. Trends in Anaesthesia and Critical Care 2021 Jun;38:4-9. [doi: 10.1016/j.tacc.2021.02.007]
22. Grootendorst M. BERTopic: neural topic modeling with a class-based TF-IDF procedure. arXiv. Preprint posted online on Mar 11, 2022 URL: https://arxiv.org/pdf/2203.05794
23. McInnes L, Healy J, Melville J. Umap: uniform manifold approximation and projection for dimension reduction. arXiv. Preprint posted online on Feb 9, 2018 URL: https://arxiv.org/abs/1802.03426
24. Birant D, Kut A. ST-DBSCAN: An algorithm for clustering spatial–temporal data. Data Knowl Eng 2007 Jan;60(1):208-221. [doi: 10.1016/j.datak.2006.01.013]
25. Schulman S, Kearon C, Subcommittee on Control of Anticoagulation of the Scientific and Standardization Committee of the International Society on Thrombosis and Haemostasis. Definition of major bleeding in clinical investigations of antihemostatic medicinal products in non-surgical patients. J Thromb Haemost 2005 Apr;3(4):692-694. [doi: 10.1111/j.1538-7836.2005.01204.x] [Medline: 15842354]
26. Honnibal M, Montani I. spaCy 2: Natural language understanding with Bloom embeddings, convolutional neural networks and incremental parsing. Sentometrics Research (forthcoming) 2017;7(1):411-420 [FREE Full text]
27. Kiss T, Strunk J. Unsupervised multilingual sentence boundary setection. Computational Linguistics 2006 Dec;32(4):485-525. [doi: 10.1162/coli.2006.32.4.485]
28. He J, Cheng MX. Weighting methods for rare event identification from imbalanced datasets. Front Big Data 2021;4:715320. [doi: 10.3389/fdata.2021.715320] [Medline: 35005617]
29. Moss HB, Leslie DS, Rayson P. Using JK fold cross validation to reduce variance when tuning NLP models. arXiv. Preprint posted online on Jun 19, 2018 URL: https://arxiv.org/abs/1806.07139
30. Liu Y, Lian J, Bartolacci MR, Zeng QA. Density‐based penalty parameter optimization on C‐SVM. ScientificWorldJournal 2014;2014(1):851814. [doi: 10.1155/2014/851814] [Medline: 25114978]
31. Radzi SFM, Karim MKA, Saripan MI, Rahman MAA, Isa INC, Ibahim MJ. Hyperparameter tuning and pipeline optimization via grid search method and tree-based AutoML in breast cancer prediction. J Pers Med 2021 Sep 29;11(10):978. [doi: 10.3390/jpm11100978] [Medline: 34683118]
32. Walther D, Halfon P, Tanzer R, et al. Hospital discharge data is not accurate enough to monitor the incidence of postpartum hemorrhage. PLoS One 2021;16(2):e0246119. [doi: 10.1371/journal.pone.0246119] [Medline: 33534862]
33. Hartenstein A, Abdelgawwad K, Kleinjung F, Privitera S, Viethen T, Vaitsiakhovich T. Identification of International Society on Thrombosis and Haemostasis major and clinically relevant non-major bleed events from electronic health records:

XSL•FO
RenderX

a novel algorithm to enhance data utilisation from real-world sources. Int J Popul Data Sci 2023;8(1):2144. [doi: 10.23889/ijpds.v8i1.2144] [Medline: 38414540]
34. Joos C, Lawrence K, Jones AE, Johnson SA, Witt DM. Accuracy of ICD-10 codes for identifying hospitalizations for acute anticoagulation therapy-related bleeding events. Thromb Res 2019 Sep;181:71-76. [doi: 10.1016/j.thromres.2019.07.021] [Medline: 31357146]
35. Metz CE. Basic principles of ROC analysis. Semin Nucl Med 1978 Oct;8(4):283-298. [doi: 10.1016/s0001-2998(78)80014-2] [Medline: 112681]
36. Sim J, Wright CC. The kappa statistic in reliability studies: use, interpretation, and sample size requirements. Phys Ther 2005 Mar;85(3):257-268. [Medline: 15733050]
37. Sun W, Cai Z, Li Y, Liu F, Fang S, Wang G. Data processing and text mining technologies on electronic medical records: a review. J Healthc Eng 2018;2018:4302425. [doi: 10.1155/2018/4302425] [Medline: 29849998]
38. Mitra A, Rawat BPS, McManus D, Kapoor A, Yu H. Bleeding entity recognition in electronic health records: a comprehensive analysis of end-to-end systems. AMIA Annu Symp Proc 2020;2020:860-869. [Medline: 33936461]
39. Alsentzer E, Murphy JR, Boag W, et al. Publicly available clinical BERT embeddings. arXiv 2019 Jun 20 [FREE Full text]
40. Li Y, Dong W, Ru B, Black A, Zhang X, Guan Y. Generic medical concept embedding and time decay for diverse patient outcome prediction tasks. iScience 2022 Sep;25(9):104880. [doi: 10.1016/j.isci.2022.104880]
41. Lewis P, Ott M, Du J, Stoyanov V. Pretrained language models for biomedical and clinical tasks: understanding and extending the state-of-the-art. Presented at: Proceedings of the 3rd Clinical Natural Language Processing Workshop; Oct 19, 2020; Online. [doi: 10.18653/v1/2020.clinicalnlp-1.17]
42. Wu S, Roberts K, Datta S, et al. Deep learning in clinical natural language processing: a methodical review. J Am Med Inform Assoc 2020 Mar 1;27(3):457-470. [doi: 10.1093/jamia/ocz200] [Medline: 31794016]
43. Zhou L, Hripcsak G. Temporal reasoning with medical data--a review with emphasis on medical natural language processing. J Biomed Inform 2007 Apr;40(2):183-202. [doi: 10.1016/j.jbi.2006.12.009] [Medline: 17317332]
44. Zhou L, Melton GB, Parsons S, Hripcsak G. A temporal constraint structure for extracting temporal information from clinical narrative. J Biomed Inform 2006 Aug;39(4):424-439. [doi: 10.1016/j.jbi.2005.07.002] [Medline: 16169282]
45. Jagannatha A, Liu F, Liu W, Yu H. Overview of the first natural language processing challenge for extracting medication, indication, and adverse drug events from electronic health record notes (MADE 1.0). Drug Saf 2019 Jan;42(1):99-111. [doi: 10.1007/s40264-018-0762-z] [Medline: 30649735]
46. Johnson SA, Signor EA, Lappe KL, et al. A comparison of natural language processing to ICD-10 codes for identification and characterization of pulmonary embolism. Thromb Res 2021 Jul;203:190-195. [doi: 10.1016/j.thromres.2021.04.020] [Medline: 34044246]
47. Pedersen JS, Laursen MS, Rajeeth Savarimuthu T, et al. Deep learning detects and visualizes bleeding events in electronic health records. Res Pract Thromb Haemost 2021 May;5(4):e12505. [doi: 10.1002/rth2.12505] [Medline: 34013150]
48. Taggart M, Chapman WW, Steinberg BA, et al. Comparison of 2 natural language processing methods for identification of bleeding among critically ill patients. JAMA Netw Open 2018 Oct 5;1(6):e183451. [doi: 10.1001/jamanetworkopen.2018.3451] [Medline: 30646240]
49. Zeng Z, Deng Y, Li X, Naumann T, Luo Y. Natural language processing for EHR-based computational phenotyping. IEEE/ACM Trans Comput Biol Bioinform 2019;16(1):139-153. [doi: 10.1109/TCBB.2018.2849968] [Medline: 29994486]
50. Dave T, Athaluri SA, Singh S. ChatGPT in medicine: an overview of its applications, advantages, limitations, future prospects, and ethical considerations. Front Artif Intell 2023;6:1169595. [doi: 10.3389/frai.2023.1169595] [Medline: 37215063]
51. Ray S, et al. Segmented harmonic loss: handling class-imbalanced multi-label clinical data for medical coding with large language models. arXiv. Preprint posted online on 2023 URL: https://doi.org/10.48550/arXiv.2310.04595
52. Henning S, Beluch W, Fraser A, Friedrich A. A survey of methods for addressing class imbalance in deep-learning based natural language processing. 2022 Feb 22 Presented at: Proceedings of the 17th Conference of the European Chapter of the Association for Computational Linguistics; Dubrovnik, Croatia URL: https://aclanthology.org/2023.eacl-main [doi: 10.18653/v1/2023.eacl-main.38]
53. Blanchard AE, Gao S, Yoon HJ, et al. A keyword-enhanced approach to handle class imbalance in clinical text classification. IEEE J Biomed Health Inform 2022 Jun;26(6):2796-2803. [doi: 10.1109/JBHI.2022.3141976] [Medline: 35020599]
54. Deng J, Zubair A, Park YJ. Limitations of large language models in medical applications. Postgrad Med J 2023 Nov 20;99(1178):1298-1299. [doi: 10.1093/postmj/qgad069] [Medline: 37624143]
55. Sallam M, Salim NA, Barakat M, Al-Tammemi AB. ChatGPT applications in medical, dental, pharmacy, and public health education: A descriptive study highlighting the advantages and limitations. Narra J 2023 Apr;3(1):e103. [doi: 10.52225/narra.v3i1.103] [Medline: 38450035]
56. Chen Z, Cano AH, Romanou A, et al. MEDITRON-70B: Scaling medical pretraining for large language models. arXiv 2023 Nov 27 [FREE Full text]
57. Yang X, PourNejatian N, Shin HC, et al. GatorTron: a large language model for clinical natural language processing. medRxiv. Preprint posted online on 2022. [doi: 10.1101/2022.02.27.22271257]

XSL•FO
RenderX

58. Nori H, King N, McKinney SM, et al. Capabilities of GPT-4 on medical challenge problems. arXiv 2023 Apr 12 [FREE Full text]
59. Haupt CE, Marks M. AI-Generated medical advice-GPT and beyond. JAMA 2023 Apr 25;329(16):1349-1350. [doi: 10.1001/jama.2023.5321] [Medline: 36972070]
60. Head CB, Jasper P, McConnachie M, Raftree L, Higdon G. Large language model applications for evaluation: Opportunities and ethical implications. New Drctns Evaluation 2023 Jun;2023(178-179):33-46. [doi: 10.1002/ev.20556]

Abbreviations

ADE: adverse drug event
AUC: area under the curve
BERT: Bidirectional Encoder Representations from Transformers
EMR: electronic medical record
HDBSCAN: Hierarchical Density-Based Spatial Clustering of Applications with Noise
***ICD*:** *International Classification of Diseases*
***ICD-10*:** *International Statistical Classification of Diseases and Related Health Problems 10th Revision*
***ICD-10-GM*:** *German Modification of the International Statistical Classification of Diseases and Related Health Problems, 10th Revision*
ISTH: International Society on Thrombosis and Haemostasis
NLP: natural language processing
ROC: receiver operating characteristic
SVM: support vector machine
SwissMADE: Swiss Monitoring of Adverse Drug Events
UMAP: Uniform Manifold Approximation and Projection

Edited by A Coristine; submitted 22.10.24; peer-reviewed by LH Yao, PH Liao, S Laplante; revised version received 06.05.25; accepted 07.05.25; published 29.08.25.

Please cite as:
Gaspar F, Zayene M, Coumau C, Bertrand E, Bettex M, Le Pogam MA, Csajka C
Natural Language Processing and ICD-10 Coding for Detecting Bleeding Events in Discharge Summaries: Comparative Cross-Sectional Study
JMIR Med Inform 2025;13:e67837
URL: https://medinform.jmir.org/2025/1/e67837
doi:10.2196/67837

© Frederic Gaspar, Mehdi Zayene, Claire Coumau, Elliott Bertrand, Marie Bettex, Marie Annick Le Pogam, Chantal Csajka. Originally published in JMIR Medical Informatics (https://medinform.jmir.org), 29.8.2025. This is an open-access article distributed under the terms of the Creative Commons Attribution License (https://creativecommons.org/licenses/by/4.0/), which permits unrestricted use, distribution, and reproduction in any medium, provided the original work, first published in JMIR Medical Informatics, is properly cited. The complete bibliographic information, a link to the original publication on https://medinform.jmir.org/, as well as this copyright and license information must be included.

XSL•FO
RenderX

A Machine Learning Approach for Identifying People With Neuroinfectious Diseases in Electronic Health Records: Algorithm Development and Validation

Arjun Singh[1,2*], MBBS; Shadi Sartipi[1,2*], PhD; Haoqi Sun[2], PhD; Rebecca Milde[3], BSc; Niels Turley[3], BSc; Carson Quinn[1,4], MD; G Kyle Harrold[1,2,4], MD; Rebecca L Gillani[1], MD, PhD; Sarah E Turbett[5,6], MD; Sudeshna Das[1,2], PhD; Sahar Zafar[1,2], MD; Marta Fernandes[1,2*], PhD; M Brandon Westover[1,2,3], MD, PhD; Shibani S Mukerji[1,2*], MD, PhD

[1]Department of Neurology, Massachusetts General Hospital, 55 Fruit St, Wang ACC 835, Boston, MA, United States

[2]Harvard Medical School, Boston, MA, United States

[3]Department of Neurology, Beth Israel Deaconess Medical Center, Boston, MA, United States

[4]Department of Neurology, Brigham and Women's Hospital, Boston, MA, United States

[5]Department of Pathology, Massachusetts General Hospital, Boston, MA, United States

[6]Department of Medicine, Massachusetts General Hospital, Boston, MA, United States

[*]these authors contributed equally

Corresponding Author:
Shibani S Mukerji, MD, PhD
Department of Neurology, Massachusetts General Hospital, 55 Fruit St, Wang ACC 835, Boston, MA, United States

Abstract

Background: Identifying neuroinfectious disease (NID) cases using International Classification of Diseases billing codes is often imprecise, while manual chart reviews are labor-intensive. Machine learning models can leverage unstructured electronic health records to detect subtle NID indicators, process large data volumes efficiently, and reduce misclassification. While accurate NID classification is needed for research and clinical decision support, using unstructured notes for this purpose remains underexplored.

Objective: The objective of this study is to develop and validate a machine learning model to identify NIDs from unstructured patient notes.

Methods: Clinical notes from patients who had undergone lumbar puncture were obtained using the electronic health record of an academic hospital network (Mass General Brigham [MGB]), with half associated with NID-related diagnostic codes. Ground truth was established by chart review with 6 NID-expert physicians. NID keywords were generated with regular expressions, and extracted texts were converted into bag-of-words representations using n-grams (n=1, 2, 3). Notes were randomly split into training (80%), 2400 notes out of 3000, and hold-out testing (20%), 600 notes out of 3000, sets. Feature selection was performed using logistic regression with L1 regularization. An extreme gradient boosting (XGBoost) model classified NID cases, and performance was evaluated using the area under the receiver operating curve (AUROC) and the precision-recall curve (AUPRC). The performance of the natural language processing (NLP) model was contrasted with the Llama 3.2 auto-regressive model on the MGB test set. The NLP model was additionally validated on external data from an independent hospital (Beth Israel Deaconess Medical Center [BIDMC]).

Results: This study included 3000 patient notes from MGB from January 22, 2010, to September 21, 2023. Of 1284 initial n-gram features, 342 were selected, with the most significant features being "meningitis," "ventriculitis," and "meningoencephalitis." The XGBoost model achieved an AUROC of 0.98 (95% CI 0.96 - 0.99) and AUPRC of 0.89 (95% CI 0.83 - 0.94) on MGB test data. In comparison, NID identification using International Classification of Diseases billing codes showed high sensitivity (0.97) but poor specificity (0.59), overestimating NID cases. Llama 3.2 improved specificity (0.94) but had low sensitivity (0.64) and an AUROC of 0.80. In contrast, our NLP model balanced specificity (0.96) and sensitivity (0.84), outperforming both methods in accuracy and reliability on MGB data. When tested on external data from BIDMC, the NLP model maintained an AUROC of 0.98 (95% CI 0.96 - 0.99), with an AUPRC of 0.78 (95% CI 0.66 - 0.89).

Conclusions: The NLP model accurately identifies NID cases from clinical notes. Validated across 2 independent hospital datasets, the model demonstrates feasibility for large-scale NID research and cohort generation. With further external validation, our results could be more generalizable to other institutions.

(JMIR Med Inform 2025;13:e63157) doi:10.2196/63157

XSL•FO
RenderX

KEYWORDS

neurology; neuroinfectious disease; electronic health records; EHR; machine learning; artificial intelligence; neuroinfectious; develop; validate; expressions; logistic regression; clinical notes; efficiency

Introduction

Meningitis and encephalitis pose serious threats to the health of an individual, potentially leading to severe neurological compromise or even death [1-7]. Many neuroinvasive pathogens, including viruses (eg, enterovirus, herpes simplex virus, West Nile virus, and HIV), bacteria (eg, *S. pneumoniae*, Mycobacterium tuberculosis), and fungi (eg, Cryptococcus), are linked to long-term cognitive sequelae [2,8]. Recent population-based studies suggest associations between pathogen exposures, especially neuroinvasive viruses causing encephalitis or meningitis, and the subsequent risk of developing dementia such as Alzheimer disease (AD) [9-12]. The risk of AD appears to increase with longer time since the first infection, peaking after 12 - 30 years [9]. Prior viral encephalitis and bacterial or viral meningitis were found to be associated with significantly increased hazard ratios for future AD, with rates of 30.72-fold and 2.81-fold, respectively, based on the Finnish Biobank, suggesting that exposure to neuroinvasive pathogens may contribute to lower cognitive reserve, likely in part due to brain inflammation [10].

These findings underscore the need for comprehensive, longitudinal studies to elucidate the mechanisms by which neuroinvasive pathogens might contribute to neurodegenerative diseases. However, such research is severely hampered by the scarcity of large, well-annotated hospital datasets. This data gap not only impedes rigorous epidemiological analyses but also hinders mechanistic investigations that could reveal how pathogens interact with neural tissues to potentially trigger or accelerate neurodegenerative processes. Therefore, to support evidence-based clinical decision-making and enable large-scale, high-powered research into the long-term consequences of neuroinfectious diseases (NIDs), accurately identifying these conditions in hospital patient records remains a significant challenge.

NIDs stem from a diverse array of pathogens and often present with clinically indistinguishable symptoms such as fever, headache, and confusion. Physicians often grapple with challenges in promptly identifying these pathogens, resorting to less precise shotgun testing methods, leading to delayed or unconfirmed diagnoses, unnecessary antimicrobial treatments, and preventable morbidity [13-18]. Most epidemiological studies linking infectious disease burden to subsequent dementia rely on health care databases that use International Classification of Diseases (ICD) codes 9th (ICD-9) and 10th (ICD-10) revisions (combined as ICD codes) and do not validate diagnoses with microbial assays [19]. The limited reliability of ICD codes in accurately identifying infectious diseases has been previously reported [20-23], more recently underscored by the 56% - 57% positive predictive value observed in the Danish National Patient Registry investigating herpes simplex virus encephalitis [19]. The combination of ICD miscoding and the potential misclassification of encephalitis etiology poses significant obstacles to generating actionable recommendations for preventing AD and other dementias. This challenge further hinders clinical guidance, particularly in cases of viral encephalitis with unknown origins—a subgroup identified in epidemiological studies as having the highest risk of future dementia [10,11].

Recent efforts to move beyond ICD-based coding have aimed at improving the timely and accurate diagnosis of NID etiologies, particularly in differentiating between viral and bacterial meningitis. These efforts predominantly use approaches such as decision trees and ensemble methods. For example, a study using a Brazilian dataset of 12,774 patients described by 19 clinical attributes aimed at distinguishing bacterial from aseptic meningitis found that a hybrid bagging approach with Naive Bayes Trees outperformed 27 other tested models. This model achieved a sensitivity of 96% and a specificity of 82% [24]. While promising, most other classification studies on NIDs, using techniques like logistic regression [25-27] or hybrid models [24,27-32], are primarily in pediatric populations, lack external validation, or rely on small datasets with limited cross-validation [33]. To our knowledge, no study has used unstructured data such as clinical notes, which limits the insights that could be derived.

The 2015 global research priorities for infections that affect the nervous system underscored the need for accurate disease burden estimates and improved tools for neurological and cognitive impairment assessment [2]. Natural language processing (NLP) tools can leverage the rich information present in large-scale comprehensive electronic health records (EHRs), including unstructured clinical assessments and notes [34-36]. Therefore, NLP holds the potential to surpass the accuracy of traditional ICD-based phenotyping while reducing reliance on semi-structured data formats [30,35,37,38].

When structured lab data is unavailable, NLP techniques leveraging unstructured clinical notes can potentially generate more accurate NID cohorts than ICD codes alone. Many NLP algorithms are computationally lighter and require less computing infrastructure compared to more recent large language models (LLMs), making them more feasible for widespread research applications. Building on this advantage, our goal is to develop a more accurate and efficient method for classifying NID cases in EHRs. Previous studies have successfully used NLP to identify patients with epilepsy [38] or classify neurological outcomes from medical notes [39].

Here, we aim to tackle NID patients by building upon these studies and detailing our NLP algorithm leveraging discharge summaries and progress notes to identify NID patients and investigate the model's accuracy across 2 independent hospitals. Our NLP algorithm outperforms ICD codes in identifying NID patients and achieves competitive performance compared to the Llama 3.2 autoregressive model (an LLM with 3B parameters) in zero-shot learning tasks, making it a valuable tool for large-scale EHR-based research to investigate the relationship

XSL•FO
RenderX

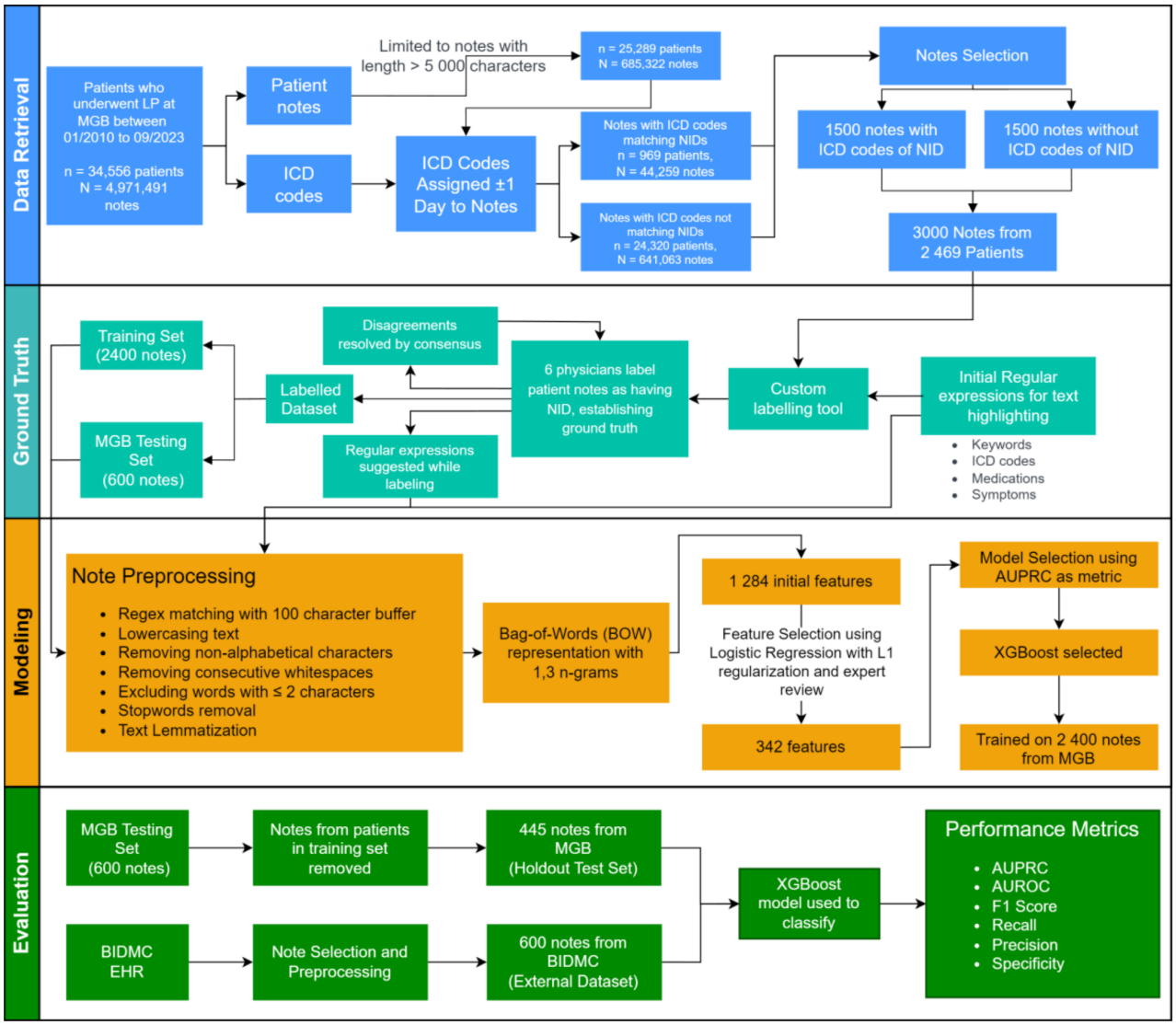
between NID exposure and short- and long-term neurological outcomes.

Methods

Overview

Figure 1 provides a summary overview of the key steps involved in this study, including data extraction, note selection, regular expression development, ground-truth labeling, text preprocessing, feature extraction, model training, and evaluation.

Figure 1. Methods overview: data retrieval and machine learning pipeline for NID classification. AUPRC: area under the precision-recall curve; AUROC: area under the receiver operating characteristic curve; BIDMC: Beth Israel Deaconess Medical Center; BOW: bag-of-words; EHR: electronic health record; ICD: International Classification of Diseases; LP: lumbar puncture; n: number of unique patients; N: number of unique notes; MGB: Mass General Brigham; NID: neuroinfectious diseases.



Data Extraction and Note Selection

We included 34,556 patients who underwent lumbar punctures (LP), sourcing medical notes from the EHR database of the Mass General Brigham (MGB) network of hospitals. This approach enriched individuals likely to be evaluated for central nervous system (CNS) infections, with a total of 4,971,491 notes extracted between 01/22/2010 and 09/21/2023. ICD diagnostic codes billed one calendar day before and after the notes were extracted and labeled as likely to be associated with NID. Multimedia Appendix 1 lists the NIDX ICD 9 and 10 codes.

We excluded notes with fewer than 5000 characters, as they likely lacked the necessary detail for clinicians to accurately assess patient status or provide valid training for models. We categorized notes into two groups: (1) notes with NID-related ICD codes (969 unique patients, 44,259 notes) and (2) those without NID ICD codes (24,320 unique patients, 641,063 notes). From these 2 groups, we randomly selected 3000 notes from 2469 patients at MGB, of which 50%, 1500 out of 3000, were associated with NID-related ICD codes, and 50% were not. For external validation, we also extracted 600 inpatient notes from patients in the Beth Israel Deaconess Medical Center (BIDMC) EHR system located in the Brain Data Science Platform

XSL•FO
RenderX

(bdsp.io) maintaining a 50:50 split of cases with and without NID-related ICD codes to match the MGB test set size.

Ethical Considerations

All procedures involving human participants in this study were reviewed and approved by the Institutional Review Board (IRB) of MGB, under protocol #2013P001024. The research was conducted in accordance with the ethical standards of the MGB and the principles of the WMA Declaration of Helsinki.

This study involved analysis of EHR data. The IRB approved a waiver of informed consent due to the retrospective nature of the study and minimal risk to participants. In accordance with the IRB's requirements, no identifiable personal information is included in the manuscript or supplementary materials. While the data were not fully de-identified at the time of analysis, strict procedures for maintaining privacy and confidentiality were implemented. Access to identifiable information was restricted to certified study personnel who have completed training in ethics and responsible conduct of research. The research team was committed to upholding high standards of data privacy and confidentiality throughout the entire study process. No compensation was provided to participants, as only de-identified retrospective data were utilized.

Ground-Truth Labeling

In total, 39,245 regular expressions were formulated based on domain-specific knowledge, categorized as (1) positive NID (eg, "cerebrospinal fluid (CSF) positive for Epstein-Barr Virus via polymerase chain reaction," "ID felt encephalitis and seizures triggered by a viral illness," "Currently on empiric antibiotics and acyclovir for possible CNS infection"); (2) negative NID (eg, "LPs have been negative," "no signs of any infectious," "autoimmune epilepsy/encephalitis"); (3) NID drugs (eg, ceftriaxone, acyclovir, trimethoprim-sulfamethoxazole, etc); (4) NID-likely keywords (eg, "headache," "fever," "lumbar puncture," etc). Regular expressions were developed by listing relevant organisms based on source materials for infectious diagnoses, antimicrobial agents, and symptoms associated with meningitis and encephalitis. Many terms were combined to create comprehensive positive and negative expressions. In addition to domain expert input, source materials included national guidelines related to CNS diseases in adults and pathogen data from global burden of disease studies [4,40-43]. The positive, negative, and antimicrobial regular expressions are provided in Multimedia Appendices 2-4.

In total, 6 physicians (AS, CQ, KH, GH, ST, and SM), all domain experts in neuroimmunology or infectious diseases, independently classified 500 notes each from the MGB dataset (3000 notes in total) following a standardized operating procedure. This procedure provided detailed guidelines for reviewing notes, including assessing symptoms and evaluating laboratory tests when referenced in the notes. Ambiguous cases flagged by the physicians were reviewed by an independent physician who was not involved in the initial classification. A consensus approach was used to resolve discrepancies in classification. To facilitate labeling, a labeling software tool was created to show the notes while highlighting the keywords (eg, meningitis, encephalitis, ceftriaxone, etc) and phrases (eg, "meningitis, likely bacterial," "CSF pleocytosis noted"). Domain experts had the option to recommend additional regular expressions during the MGB ground-truth labeling phase. Regular expressions proposed by domain experts were incorporated if proposed on the training dataset only. External model validation on 600 BIDMC notes was classified by 2 experts (AS and SM) (300 notes each). While the MGB test set was reduced to 445 notes to address overlap with the training set, the BIDMC dataset was solely used for external validation and retained its full size of 600 notes.

Preparing Text Data for Feature Extraction

Preprocessing notes to identify model features required (1) limiting text to regions matching regular expressions with a 100-character buffer, (2) converting to lowercase letters, (3) removal of non-alphabetical characters, (4) replacing consecutive whitespaces with a single whitespace, (5) using words with more than 2 characters, and (6) removing stop words (see Multimedia Appendix 5). The remaining text was lemmatized using WordNetLemmatizer [44]. The text was transformed into a bag-of-words (BOW) representation, considering unigrams (1 gram), bigrams (2 grams), and trigrams (3 grams).

Model Features, Training, and Performance Evaluation

To reduce the number of features and enhance model interpretability, we used an iterative approach using logistic regression with L1 regularization, similar to our previous NLP-based methods on unstructured EHR text in studies on epilepsy or neurological status following COVID-19 hospitalizations [38,45]. The regularization strength (10) and maximum iterations (1000) were chosen to balance between model complexity and computational efficiency. We addressed class imbalances by incorporating class weights inversely proportional to the sample size. We used this process to identify the most common features, resulting in a set of 1284 features. A manual review by 3 experts (AS, SM, and MBW) eliminated the remaining irrelevant features, leading to a reduced set of 342 non-zero features. For example, terms like "Boston," "heart rate," and "primary care" were removed as they were irrelevant to NID classification and had no pathophysiological connection to the condition.

The MGB dataset (3000 notes) was randomly split 80:20 for training (2400 notes) and the hold-out (600 notes) test set, maintaining the 50/50 ICD code distribution. Since there were only 969 unique patients with ICD codes for NIDs, some notes originated from the same patients. To ensure no patient appeared in both the training and test sets, the initial hold-out test set of 600 notes was reduced to 445 notes by excluding notes from patients who were also present in the training set. To select the optimal model, we used 5-fold cross-validation on the MGB training dataset. Given the imbalanced nature of the dataset, with only 16%, 480 out of 3000, of the total observations positive for NID, we compared logistic regression, random forest, and XGBoost using the area under the precision-recall curve (AUPRC). AUPRC is more informative for imbalanced datasets, as it focuses on the performance of the model in predicting the positive class, unlike metrics such as accuracy

XSL•FO
RenderX

or the area under the receiver operating characteristic curve (AUROC) [46-49]. XGBoost was selected for its AUPRC performance.

We then trained an XGBoost model on the 2400 training notes and tested its performance on both the hold-out dataset (445 notes from MGB) and an external dataset consisting of 600 notes from patients at BIDMC. Model performance was based on the AUPRC and the AUROC. We performed bootstrapping with replacement and performed 1000 iterations to estimate the 95% CIs for these metrics.

Evaluation of Llama 3.2 for Zero-Shot NID Classification

We assessed the performance of the Llama 3.2 auto-regressive model (3B parameters) as a zero-shot learning approach for classifying NID from clinical reports in the MGB test set. Llama was neither fine-tuned nor trained on task-specific examples and classified the presence or absence of NID from clinical notes formatted in JavaScript Object Notation.

Results

Cohort Characteristics

The demographic characteristics of the 2469 patients comprising the 3000 MGB clinical notes are presented in Table 1 (the linkage between notes and demographic data for the BIDMC dataset was lost and is therefore not shown).

Table . Characteristics of the study cohorts.

MGB (N=2469)	
Age (years)	
Median (IQR)	61.0 (46-73)
Age group, n (%)	
<18	101 (4.1%)
18 - 34	254 (10.3%)
35 - 49	403 (16.3%)
50 - 64	718 (29.1%)
65+	993 (40.2%)
Sex, n (%)	
Male	1119 (45.3%)
Female	1350 (54.7%)
Race, n (%)	
White	1911 (77.4%)
Black	174 (7.0%)
Asian	86 (3.5%)
Other	298 (12.1%)
Ethnicity, n (%)	
Hispanic	252 (10.2%)
Not Hispanic	2041 (82.7%)
Missing	176 (7.1%)

The median age (IQR) was 61.0 (46 - 73 y) years, of which 55% (n=1350) were female sex at birth, 77% (n=1911) reported being of white race, and 83% (n=2041) reported being of non-Hispanic ethnicity. Out of the 3000 notes, 16% (479 notes) were labeled as NID based on expert review, and 97% of these 479 notes had an NID-related ICD code. Among the 1500 notes with an NID-related ICD code, 465 notes (31%) were confirmed as NID cases by expert review. Conversely, among the 1500 notes without an NID-related ICD code, 0.93% (14 notes) were identified as NID cases by expert review. The sensitivity of detecting NID patients using the presence of any NID-related ICD code was 97.1%, and the specificity was 59.1%, suggesting reliance on ICD codes alone for a patient's true clinical diagnosis may be more likely to overestimate, rather than underestimate, the number of cases with NID.

Performance of EHR NID Classifier

The training set consisted of 2400 notes from MGB, where 16.1% (387/2400) were classified as NID-positive by expert review. The hold-out testing set from MGB consisted of 445 notes, where 16% (71/445) were classified as NID-positive.

Performance characteristics using XGBoost on the MGB training set and hold-out test set are shown in Table 2.

XSL•FO
RenderX

Table . Average performance for the XGBoost[a] model on the training set and 2 independent testing sets.

Metric	Training set (MGB) (2400 notes)	Testing set (MGB) (445 notes)	Testing set (BIDMC[b]) (600 notes)
AUROC[c], median (95% CI)	1.000 (1.000 - 1.000)	0.977 (0.964 - 0.988)	0.976 (0.961 - 0.989)
AUPRC[d], median (95% CI)	1.000 (0.999 - 1.000)	0.894 (0.831 - 0.943)	0.779 (0.655 - 0.885)
F1 score, median (95% CI)	0.987 (0.978 - 0.995)	0.822 (0.752 - 0.879)	0.658 (0.528 - 0.778)
Recall, median (95% CI)	0.974 (0.957 - 0.989)	0.846 (0.753 - 0.923)	0.687 (0.538 - 0.839)
Precision, median (95% CI)	1.000 (1.000 - 1.000)	0.802 (0.709 - 0.889)	0.637 (0.487 - 0.795)
Specificity, median (95% CI)	1.000 (1.000 - 1.000)	0.960 (0.939 - 0.978)	0.976 (0.963 - 0.988)

[a]XGBoost: extreme gradient boosting model.

[b]BIDMC: Beth Israel Deaconess Medical Center.

[c]AUROC: area under the receiver operating characteristic curve.

[d]AUPRC: area under the precision-recall curve.

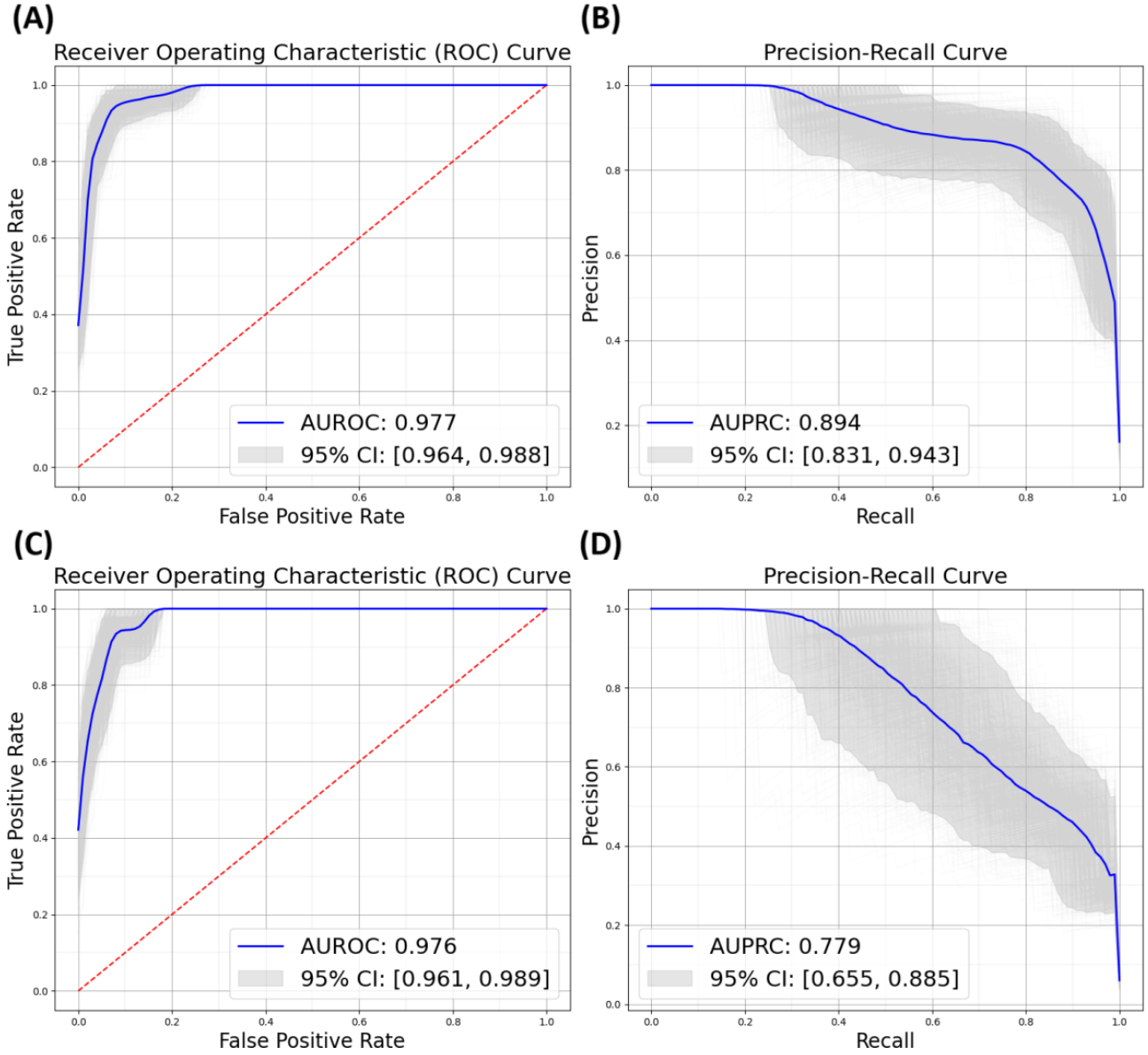
The MGB hold-out test set showed good performance metrics (95% CI), including an AUROC of 0.977 (0.964 - 0.988), AUPRC of 0.894 (0.831 - 0.943), recall of 0.846 (0.753 - 0.923), and F1 score of 0.822 (0.752 - 0.879). The AUROC and AUPRC curves for the hold-out set are illustrated in Figure 2.

To assess performance metrics using patient notes extracted outside the MGB network, we ran the NLP-based model on 600 notes from BIDMC, of which 5.8% (35/600) were NID-positive by expert review. Although performance declined compared to the MGB test set, the model maintained a high AUROC of 0.976 (95% CI 0.961 - 0.989) and an AUPRC of 0.779 (95% CI 0.655 - 0.885). Precision was 0.637 (95% CI 0.487 - 0.795), and recall was 0.687 (95% CI 0.538 - 0.839), resulting in an F1 score of 0.658 (95% CI 0.528 - 0.778).

Additionally, we assessed the performance of Llama 3.2, a zero-shot learning model, for classifying NID as present or absent using clinical notes on the MGB test set. The model achieved an AUROC of 0.800 and a balanced F1 score of 0.799, demonstrating high specificity (0.940) but lower recall (0.640). These results highlight notable performance differences between the Llama model and the NLP-based approach, particularly in recall and overall F1 score.

XSL•FO
RenderX

Figure 2. XGBoost model performance on 2 sets of unseen notes, as evaluated by AUROC and AUPRC. 95% CIs were estimated using 1000 bootstrapping iterations. (A) AUROC and (B) AUPRC on notes from MGB and (C) AUROC and (D) AUPRC on notes from BIDMC. AUROC: area under the receiver operating characteristic (ROC) curve; AUPRC: area under the precision recall curve; CI: confidence interval.



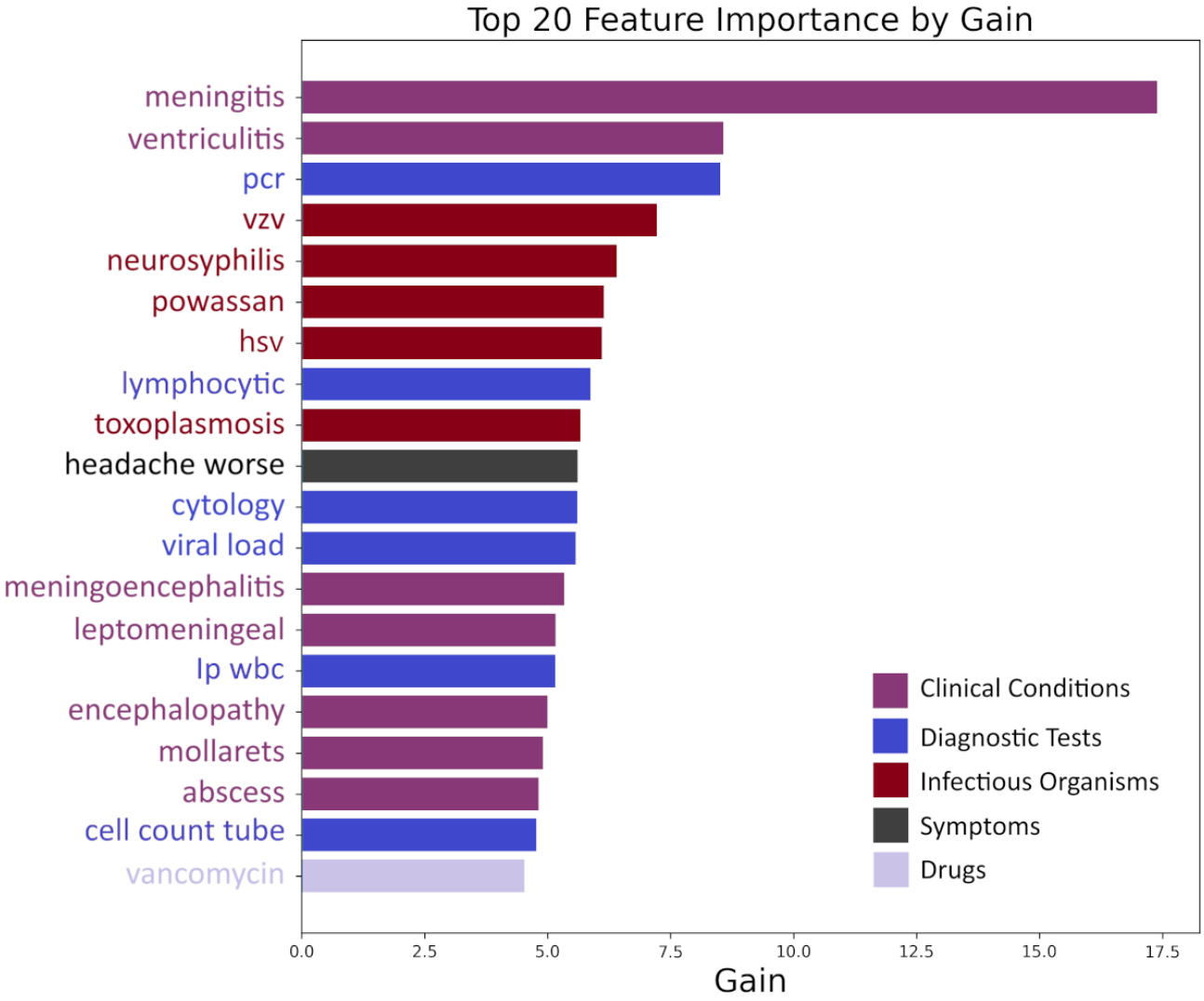
Significant Features for NID Prediction

The feature selection steps reduced the initial training feature sets by 73.36% (342/1284). The top 20 features selected by XGBoost to identify individuals with NIDs are plotted in Figure 3.

The importance of these features was assessed based on their average gain across all decision points within the model, providing a measure of their contribution to predictive accuracy. These features primarily consist of clinical indicators and diagnostic markers essential for identifying NIDs. Prominently featured are direct markers of CNS inflammation, such as "meningitis," "ventriculitis," and "meningoencephalitis." Other features included diagnostic tests such as "cytology," "viral load," and "polymerase chain reaction"; cell types ("lymphocytic"), specific pathogens, and medical conditions associated with NID were identified, suggesting identified NID-associated features used in the NLP classifier were clinically relevant and interpretable.

XSL•FO
RenderX

Figure 3. Top 20 features ranked by the feature importance (information gain measured by entropy), arranged in descending order (from top to bottom). The x-axis is the feature importance. It does not differentiate the association directions, ie, positive or negative association with the NID label.



Error Analysis

In our analysis of cases where the model's predictions differed from the manually assigned labels, we discovered a few common factors that led to incorrect positive and negative classifications across both the internal (MGB) and external (BIDMC) datasets.

A common reason for false positives was the presence of prior NID mentions in patient notes. Another frequent issue was cases where patients were awaiting LP results, leading to a manual negative label, but the notes suggested a possible positive. False positives were also caused by notes indicating symptoms suggestive of NID but lacking confirmatory LP results. Additionally, specific pathogens or conditions, like JC virus neurocysticercosis and neurosyphilis, mentioned in the notes but not confirmed as active NID, added to the error rate. False negatives were often due to notes that did not discuss NID in detail.

The type of clinical note played a significant role; physical therapy and psychiatric notes were less likely to contain detailed clinical information relevant to NID, leading to both false positives and false negatives.

Discussion

In this study, we developed and evaluated an automated NLP-based model in 2 independent datasets that classifies people with NID using unstructured notes to generate an NID cohort, with the intention that these cohorts could be used for predictions of susceptibility risk and short- and long-term medical outcomes. The NLP model demonstrated high specificity (0.96), outperforming the specificity observed using NID-specific ICD codes (0.59), suggesting that relying on ICD codes alone may overestimate cases of infectious meningitis or encephalitis. These findings align with recent literature reporting low precision (0.58, 95% CI 0.53 - 0.63) for the ICD-10 codes associated with herpesviral (herpes simplex) encephalitis, herpesviral (herpes simplex) meningoencephalitis, and herpesviral encephalitis, common causes of NID, in the well-established Danish National Patient Registry [19]. The lack of specificity underscores the risk of false positives when using ICD coding alone, posing challenges for accurately identifying clinical research cohorts, particularly for rare disorders like NID [50,51].

To contextualize our findings, prior studies in meningitis and encephalitis largely focused on structured data, including lab

XSL•FO
RenderX

results, imaging, and other EHR data, to classify meningitis etiology or distinguish subtypes [24,31,32,52-58]. In comparison, alternative machine learning models applied to a Brazilian dataset of 22,602 suspected meningitis cases, including J48, Alternating Decision Tree, and Support Vector Machine, demonstrated varying levels of performance. One model, based solely on observable symptoms, achieved an AUROC of 0.869 for differentiating meningitis from non-meningitis cases [31], while a combined ensemble and decision tree method integrating observable symptoms with rapid CSF analysis attained an AUROC of 0.95 in distinguishing bacterial from viral meningitis in a dataset of known infectious meningitis cases [34]. However, the best model for classifying NID cases (sensitivity 97.0% - 97.6%) was at the expense of specificity (24.0% - 43.0%), limiting utility in reducing false positives in clinical decision-making [59]. In the context of HIV and cognitive disorders, machine learning models leveraging clinical data reported AUROCs of 0.83 - 0.87, though most relied on structured cohort data, not data in the EHR, with limited validation in independent datasets [60-62]. These comparisons underscore the value of our NLP-based method as a more precise phenotyping tool, offering an improved balance between sensitivity and specificity for identifying NID cases.

We also evaluated LLMs, focusing on the Llama3.2 model applied in the MGB test set. This method yielded an AUROC of 0.800 and a balanced F1 score of 0.799, with high specificity (0.940) but lower recall (0.640). In contrast, the proposed BOW NLP approach achieved balanced results, with an AUROC of 0.977, an AUPRC of 0.894, and an F1 score of 0.822, with high recall (0.846). On the BIDMC validation set, the NLP model achieved an AUROC of 0.98, and while the performance declined (AUPRC reduced from 0.894 (0.831 - 0.943) to 0.779 (0.655 - 0.885)) likely due to variations in documentation styles, differences in clinical terminology, and institutional biases in diagnosing rare conditions, the model maintained good discriminative ability. These results demonstrate potential for broader application with further fine-tuning, with enhanced precision and interpretability offering significant advantages for NID phenotyping in clinical research.

In our clinical experience, we have observed that unstructured clinical notes serve as a rich source of information crucial for ensuring clinical accuracy and care for NID patients. Here, using only clinical notes, we achieved consistent AUROC exceeding 0.95 across 2 different EHR systems, with a modest decrease in AUPRC, underscoring the importance of developing classifiers that effectively leverage the information embedded within these notes. Compared to Llama, the BOW approach offers advantages such as reduced computational overhead, faster inference, and ease of deployment in settings with predictable patterns and resource limitations. These attributes make it particularly suitable for time-sensitive applications and adaptable to diverse health care settings. Most importantly, the proposed method's balanced performance, particularly in the context of NID classification, highlights its utility in both clinical research and practice. The model's reliance on unstructured notes reduces dependency on specific EHR system designs for structured data, broadening its applicability. By identifying clinically interpretable features such as specific markers of CNS inflammation and diagnostic tests, the model enhances both accuracy and clinical relevance, making it a valuable tool for improving care and outcomes for NID patients.

Our study had several limitations. First, the model was developed and validated using unstructured EHR notes from Massachusetts, impacting its relevance in other regions due to regional variations in medical terminology and disease incidence. For example, region-specific diseases like "Powassan," found predominantly in northeastern states and the Great Lakes region of the United States, were a feature selected in the XGBoost model and may not generalize to other regions. Second, while notes were enriched for NIDs by considering patients who had an LP procedure, the timing of the procedure in relation to the analyzed notes was not considered when developing the model. This approach aimed to enrich the dataset with relevant LP-related language and details from patient notes while avoiding overfitting the model narrowly to notes from a specific temporal context like the post-procedural period. While this approach prevents overfitting to unique details concentrated in the post-LP notes, it could limit broader applicability. Future work could explore incorporating the temporal relationship between the LP and the notes, which may provide additional context for classification performance. Third, lab results from CSF cell counts or microbial assays were not specifically considered in our analysis. The availability of lab data for each patient is inconsistent due to factors such as its assessment at another institution prior to transfer to a tertiary center, safety concerns regarding CSF retrieval, or delays due to logistical considerations. This NLP-based model, operating independently of lab results, resulted in high AUROC and AUPRC, suggesting that in settings where structured lab data is not available, the tool could potentially generate an NID cohort. Our study focused on broad NID classification and did not subtype into encephalitis or meningitis. We anticipate that future model development will involve training on unstructured EHR notes from diverse sources across the United States and may explore incorporating microbial data and antimicrobial therapy details as features.

Acknowledgments

Grants supporting investigators include funding from the National Institute of Health (R01MH131194, R01MH134823 to SSM, and RF1AG064312, RF1NS120947, R01AG073410, R01HL161253, R01NS126282, R01AG073598, R01NS131347, R01NS130119 to MBW), and the Claflin Distinguished Scholar award from the Massachusetts General Hospital to SSM.

XSL•FO
RenderX

Conflicts of Interest

MW is a co-founder, scientific advisor, consultant to, and has personal equity interest in Beacon Biosignals. SET received research funding from SeLux Diagnostics and has been a consultant for CARBX. SZ was a Speaker honoraria from Marinus (past and unrelated to this work), and has royalties from Wolter Kluwer not related to this work.

Multimedia Appendix 1
List of *ICD-9* and *ICD-10* codes for NID.
[XLSX File, 15 KB - medinform_v13i1e63157_app1.xlsx]

Multimedia Appendix 2
List of positive expressions.
[XLSX File, 507 KB - medinform_v13i1e63157_app2.xlsx]

Multimedia Appendix 3
List of negative expressions.
[XLSX File, 21 KB - medinform_v13i1e63157_app3.xlsx]

Multimedia Appendix 4
List of antimicrobial expressions.
[XLSX File, 10 KB - medinform_v13i1e63157_app4.xlsx]

Multimedia Appendix 5
List of stopwords.
[TXT File, 9 KB - medinform_v13i1e63157_app5.txt]

References

1. Hasbun R, Rosenthal N, Balada-Llasat JM, et al. Epidemiology of meningitis and encephalitis in the United States, 2011-2014. Clin Infect Dis 2017 Aug 1;65(3):359-363. [doi: 10.1093/cid/cix319] [Medline: 28419350]
2. John CC, Carabin H, Montano SM, Bangirana P, Zunt JR, Peterson PK. Global research priorities for infections that affect the nervous system. Nature New Biol 2015 Nov;527(7578):S178-S186. [doi: 10.1038/nature16033]
3. Kiyani M, Hodges SE, Adil SM, et al. Outcomes and health care resource utilization of adult bacterial meningitis in the United States. Neur Clin Pract 2021 Apr;11(2):117-126. [doi: 10.1212/CPJ.0000000000000868]
4. Wunrow HY, Bender RG, Vongpradith A, et al. Global, regional, and national burden of meningitis and its aetiologies, 1990–2019: a systematic analysis for the Global Burden of Disease Study 2019. Lancet Neurol 2023 Aug;22(8):685-711. [doi: 10.1016/S1474-4422(23)00195-3]
5. Edmond K, Clark A, Korczak VS, Sanderson C, Griffiths UK, Rudan I. Global and regional risk of disabling sequelae from bacterial meningitis: a systematic review and meta-analysis. Lancet Infect Dis 2010 May;10(5):317-328. [doi: 10.1016/S1473-3099(10)70048-7]
6. van de Beek D, Schmand B, de Gans J, et al. Cognitive impairment in adults with good recovery after bacterial meningitis. J Infect Dis 2002 Oct 1;186(7):1047-1052. [doi: 10.1086/344229] [Medline: 12232850]
7. Davis AG, Nightingale S, Springer PE, et al. Tuberculous meningitis international research consortium. Neurocognitive and functional impairment in adult and paediatric tuberculous meningitis. Wellcome Open Res 2019;4(178). [doi: 10.12688/wellcomeopenres.15516.1] [Medline: 31984243]
8. Hansen ABE, Vestergaard HT, Dessau RB, et al. Long-term survival, morbidity, social functioning and risk of disability in patients with a Herpes Simplex Virus Type 1 or Type 2 central nervous system infection, Denmark, 2000-2016. Clin Epidemiol 2020;12:745-755. [doi: 10.2147/CLEP.S256838] [Medline: 32765109]
9. Douros A, Santella C, Dell'Aniello S, et al. Infectious disease burden and the risk of Alzheimer's disease: a population-based study. J Alzheimers Dis 2021;81(1):329-338. [doi: 10.3233/JAD-201534] [Medline: 33780369]
10. Levine KS, Leonard HL, Blauwendraat C, et al. Virus exposure and neurodegenerative disease risk across national biobanks. Neuron 2023 Apr 5;111(7):1086-1093. [doi: 10.1016/j.neuron.2022.12.029] [Medline: 36669485]
11. Sipilä PN, Heikkilä N, Lindbohm JV, et al. Hospital-treated infectious diseases and the risk of dementia: a large, multicohort, observational study with a replication cohort. Lancet Infect Dis 2021 Nov;21(11):1557-1567. [doi: 10.1016/S1473-3099(21)00144-4] [Medline: 34166620]
12. Whitson HE, Colton C, El Khoury J, et al. Infection and inflammation: new perspectives on Alzheimer's disease. Brain Behav Immun Health 2022 Jul;22:100462. [doi: 10.1016/j.bbih.2022.100462] [Medline: 36118272]

XSL•FO
RenderX

13. Gomez CA, Pinsky BA, Liu A, Banaei N. Delayed diagnosis of tuberculous meningitis misdiagnosed as Herpes Simplex Virus-1 encephalitis with the filmarray syndromic polymerase chain reaction panel. Open Forum Infect Dis 2017;4(1):ofw245. [doi: 10.1093/ofid/ofw245] [Medline: 28540320]
14. Miller AC, Koeneman SH, Arakkal AT, Cavanaugh JE, Polgreen PM. Incidence, duration, and risk factors associated with missed opportunities to diagnose herpes simplex encephalitis: a population-based longitudinal study. Open Forum Infect Dis 2021 Sep;8(9):ofab400. [doi: 10.1093/ofid/ofab400] [Medline: 34514018]
15. Nath A. Neuroinfectious diseases: a crisis in neurology and a call for action. JAMA Neurol 2015 Feb;72(2):143-144. [doi: 10.1001/jamaneurol.2014.3442] [Medline: 25485794]
16. Nesher L, Hadi CM, Salazar L, et al. Epidemiology of meningitis with a negative CSF Gram stain: under-utilization of available diagnostic tests. Epidemiol Infect 2016 Jan;144(1):189-197. [doi: 10.1017/S0950268815000850] [Medline: 25989841]
17. Piantadosi A, Mukerji SS, Ye S, et al. Enhanced virus detection and metagenomic sequencing in patients with meningitis and encephalitis. MBio 2021 Aug 31;12(4):e0114321. [doi: 10.1128/mBio.01143-21] [Medline: 34465023]
18. Wilson MR, Sample HA, Zorn KC, et al. Clinical metagenomic sequencing for diagnosis of meningitis and encephalitis. N Engl J Med 2019 Jun 13;380(24):2327-2340. [doi: 10.1056/NEJMoa1803396] [Medline: 31189036]
19. Jørgensen LK, Dalgaard LS, Østergaard LJ, Andersen NS, Nørgaard M, Mogensen TH. Validity of the coding for herpes simplex encephalitis in the Danish National Patient Registry. Clin Epidemiol 2016;8:133-140. [doi: 10.2147/CLEP.S104379] [Medline: 27330328]
20. Farzandipour M, Sheikhtaheri A, Sadoughi F. Effective factors on accuracy of principal diagnosis coding based on International Classification of Diseases, the 10th revision (ICD-10). Int J Inf Manage 2010 Feb;30(1):78-84. [doi: 10.1016/j.ijinfomgt.2009.07.002]
21. O'Malley KJ, Cook KF, Price MD, Wildes KR, Hurdle JF, Ashton CM. Measuring diagnoses: ICD code accuracy. Health Serv Res 2005 Oct;40(5 Pt 2):1620-1639. [doi: 10.1111/j.1475-6773.2005.00444.x] [Medline: 16178999]
22. Samannodi M, Hansen M, Hasbun R. Lack of accuracy of the international classification of disease, ninth (ICD-9) codes in identifying patients with encephalitis. J Neurol 2019 Apr;266(4):1034-1035. [doi: 10.1007/s00415-019-09229-9] [Medline: 30729315]
23. Stausberg J, Lehmann N, Kaczmarek D, Stein M. Reliability of diagnoses coding with ICD-10. Int J Med Inform 2008 Jan;77(1):50-57. [doi: 10.1016/j.ijmedinf.2006.11.005]
24. Guzmán E, Belmonte MV, Lelis VM. Ensemble methods for meningitis aetiology diagnosis. Expert Systems 2022 Sep;39(8):e12996. [doi: 10.1111/exsy.12996]
25. Freedman SB, Marrocco A, Pirie J, Dick PT. Predictors of bacterial meningitis in the era after Haemophilus influenzae. Arch Pediatr Adolesc Med 2001 Dec;155(12):1301-1306. [doi: 10.1001/archpedi.155.12.1301] [Medline: 11732947]
26. Wu J, Shi T, Yue Y, et al. Development a prediction model for identifying bacterial meningitis in young infants aged 29-90 days: a retrospective analysis. BMC Pediatr 2023 Feb 9;23(1):69. [doi: 10.1186/s12887-022-03813-1] [Medline: 36759812]
27. Cheng X, Zhang Q, Fu Z, et al. Establishment of a predictive model for purulent meningitis in preterm infants. Transl Pediatr 2022 Jun;11(6):1018-1027. [doi: 10.21037/tp-22-236] [Medline: 35800267]
28. Wang P, Cheng S, Li Y, et al. Prediction of lumbar drainage-related meningitis based on supervised machine learning algorithms. Front Public Health 2022;10:910479. [doi: 10.3389/fpubh.2022.910479] [Medline: 35836985]
29. Mago VK, Mehta R, Woolrych R, Papageorgiou EI. Supporting meningitis diagnosis amongst infants and children through the use of fuzzy cognitive mapping. BMC Med Inform Decis Mak 2012 Sep 4;12(98):98. [doi: 10.1186/1472-6947-12-98] [Medline: 22947265]
30. Mentis AFA, Garcia I, Jiménez J, et al. Artificial intelligence in differential diagnostics of meningitis: a nationwide study. Diagnostics (Basel) 2021 Mar 28;11(4):602. [doi: 10.3390/diagnostics11040602] [Medline: 33800653]
31. Lelis VM, Guzman E, Belmonte MV. Non-invasive meningitis diagnosis using decision trees. IEEE Access 2020;8:18394-18407. [doi: 10.1109/ACCESS.2020.2966397]
32. Shi Y, Zhang C, Pan S, et al. The diagnosis of tuberculous meningitis: advancements in new technologies and machine learning algorithms. Front Microbiol 2023 Oct 24;14(1290746):MID. [doi: 10.3389/fmicb.2023.1290746]
33. Ghaddaripouri K, Ghaddaripouri M, Mousavi AS, et al. The effect of machine learning algorithms in the prediction, and diagnosis of meningitis: a systematic review. Health Sci Rep 2024 Feb;7(2):e1893. [doi: 10.1002/hsr2.1893] [Medline: 38357491]
34. Chen PF, Chen L, Lin YK, et al. Predicting postoperative mortality with deep neural networks and natural language processing: model development and validation. JMIR Med Inform 2022 May 10;10(5):e38241. [doi: 10.2196/38241] [Medline: 35536634]
35. Ge W, Alabsi H, Jain A, et al. Identifying patients with delirium based on unstructured clinical notes: observational study. JMIR Form Res 2022 Jun 24;6(6):e33834. [doi: 10.2196/33834] [Medline: 35749214]
36. Lee RY, Kross EK, Torrence J, et al. Assessment of natural language processing of electronic health records to measure goals-of-care discussions as a clinical trial outcome. JAMA Netw Open 2023 Mar 1;6(3):e231204. [doi: 10.1001/jamanetworkopen.2023.1204] [Medline: 36862411]

XSL•FO
RenderX

37. Chen PF, Wang SM, Liao WC, et al. Automatic ICD-10 coding and training system: deep neural network based on supervised learning. JMIR Med Inform 2021 Aug 31;9(8):e23230. [doi: 10.2196/23230] [Medline: 34463639]
38. Fernandes M, Cardall A, Jing J, et al. Identification of patients with epilepsy using automated electronic health records phenotyping. Epilepsia 2023 Jun;64(6):1472-1481. [doi: 10.1111/epi.17589] [Medline: 36934317]
39. Fernandes MB, Valizadeh N, Alabsi HS, et al. Classification of neurologic outcomes from medical notes using natural language processing. Expert Syst Appl 2023 Mar 15;214:119171. [doi: 10.1016/j.eswa.2022.119171] [Medline: 36865787]
40. McGill F, Heyderman RS, Michael BD, et al. The UK joint specialist societies guideline on the diagnosis and management of acute meningitis and meningococcal sepsis in immunocompetent adults. J Infect 2016 Apr;72(4):405-438. [doi: 10.1016/j.jinf.2016.01.007] [Medline: 26845731]
41. Tunkel AR, Hasbun R, Bhimraj A, et al. 2017 Infectious Diseases Society of America's Clinical Practice Guidelines for Healthcare-Associated Ventriculitis and Meningitis. Clin Infect Dis 2017 Mar 15;64(6):e34-e65 [FREE Full text] [doi: 10.1093/cid/ciw861] [Medline: 28203777]
42. White AC Jr, Coyle CM, Rajshekhar V, et al. Diagnosis and treatment of neurocysticercosis: 2017 Clinical Practice Guidelines by the Infectious Diseases Society of America (IDSA) and the American Society of Tropical Medicine and Hygiene (ASTMH). Clin Infect Dis 2018 Apr 3;66(8):e49-e75 [FREE Full text] [doi: 10.1093/cid/cix1084] [Medline: 29481580]
43. Thompson MA, Horberg MA, Agwu AL, et al. Primary care guidance for persons with human immunodeficiency virus: 2020 update by the HIV Medicine Association of the Infectious Diseases Society of America. Clin Infect Dis 2021 Dec 6;73(11):e3572-e3605 [FREE Full text] [doi: 10.1093/cid/ciaa1391] [Medline: 33225349]
44. Bird S, Loper E, Klein E. Natural Language Processing With Python: O'Reilly Media Inc; 2009. URL: https://tjzhifei.github.io/resources/NLTK.pdf [accessed 2025-08-19]
45. Fernandes M, Sun H, Jain A, et al. Classification of the disposition of patients hospitalized with COVID-19: reading discharge summaries using natural language processing. JMIR Med Inform 2021 Feb 10;9(2):e25457. [doi: 10.2196/25457] [Medline: 33449908]
46. Liu Z, Bondell HD. Binormal precision–recall curves for optimal classification of imbalanced data. Stat Biosci 2019 Apr;11(1):141-161. [doi: 10.1007/s12561-019-09231-9]
47. Movahedi F, Antaki JF. Limitation of ROC in evaluation of classifiers for imbalanced data. J Heart Lung Transplant 2021 Apr;40(4):S413. [doi: 10.1016/j.healun.2021.01.1160]
48. Kim M, Hwang KB. An empirical evaluation of sampling methods for the classification of imbalanced data. PLoS ONE 2022;17(7):e0271260. [doi: 10.1371/journal.pone.0271260]
49. Saito T, Rehmsmeier M. The precision-recall plot is more informative than the ROC plot when evaluating binary classifiers on imbalanced datasets. PLoS ONE 2015;10(3):e0118432. [doi: 10.1371/journal.pone.0118432] [Medline: 25738806]
50. Lo Re V III, Carbonari DM, Jacob J, et al. Validity of ICD‐10‐CM diagnoses to identify hospitalizations for serious infections among patients treated with biologic therapies. Pharmacoepidemiology and Drug 2021 Jul;30(7):899-909. [doi: 10.1002/pds.5253]
51. Wiese AD, Griffin MR, Stein CM, et al. Validation of discharge diagnosis codes to identify serious infections among middle age and older adults. BMJ Open 2018 Jun;8(6):e020857. [doi: 10.1136/bmjopen-2017-020857]
52. Bonsu BK, Harper MB. Differentiating acute bacterial meningitis from acute viral meningitis among children with cerebrospinal fluid pleocytosis: a multivariable regression model. Pediatr Infect Dis J 2004 Jun;23(6):511-517. [doi: 10.1097/01.inf.0000129689.58211.9e] [Medline: 15194831]
53. D'Angelo G, Pilla R, Tascini C, Rampone S. A proposal for distinguishing between bacterial and viral meningitis using genetic programming and decision trees. Soft Comput 2019 Nov;23(22):11775-11791. [doi: 10.1007/s00500-018-03729-y]
54. Revett K, Gorunescu F, Ene M, Gorunescu M, et al. A machine learning approach to differentiating bacterial from viral meningitis. 2006 Presented at: IEEE John Vincent Atanasoff p. 155-162. [doi: 10.1109/JVA.2006.2]
55. Gowin E, Januszkiewicz-Lewandowska D, Słowiński R, Błaszczyński J, Michalak M, Wysocki J. With a little help from a computer: discriminating between bacterial and viral meningitis based on dominance-based rough set approach analysis. Medicine (Baltimore) 2017 Aug;96(32):e7635. [doi: 10.1097/MD.0000000000007635] [Medline: 28796045]
56. Jeong YS, Jeon M, Park JH, et al. Machine-learning-based approach to differential diagnosis in tuberculous and viral meningitis. Infect Chemother 2021 Mar;53(1):53-62. [doi: 10.3947/ic.2020.0104] [Medline: 33538134]
57. Nigrovic LE, Kuppermann N, Malley R. Development and validation of a multivariable predictive model to distinguish bacterial from aseptic meningitis in children in the post-Haemophilus influenzae era. Pediatrics 2002 Oct;110(4):712-719. [doi: 10.1542/peds.110.4.712] [Medline: 12359784]
58. Xiang Y, Zeng C, Liu B, et al. Deep learning-enabled identification of autoimmune encephalitis on 3D multi-sequence MRI. J Magn Reson Imaging 2022 Apr;55(4):1082-1092. [doi: 10.1002/jmri.27909] [Medline: 34478565]
59. Lélis VM, Guzmán E, Belmonte MV. A statistical classifier to support diagnose meningitis in less developed areas of Brazil. J Med Syst 2017 Aug 11;41(9):145. [doi: 10.1007/s10916-017-0785-5] [Medline: 28801740]
60. Mukerji SS, Petersen KJ, Pohl KM, et al. Machine learning approaches to understand cognitive phenotypes in people with HIV. J Infect Dis 2023 Mar 17;227(Suppl 1):S48-S57. [doi: 10.1093/infdis/jiac293] [Medline: 36930638]

XSL•FO
RenderX

61. Xu Y, Lin Y, Bell RP, et al. Machine learning prediction of neurocognitive impairment among people with HIV using clinical and multimodal magnetic resonance imaging data. J Neurovirol 2021 Feb;27(1):1-11. [doi: 10.1007/s13365-020-00930-4] [Medline: 33464541]
62. Tu W, Chen PA, Koenig N, et al. Machine learning models reveal neurocognitive impairment type and prevalence are associated with distinct variables in HIV/AIDS. J Neurovirol 2020 Feb;26(1):41-51. [doi: 10.1007/s13365-019-00791-6] [Medline: 31520320]

Abbreviation

AD: Alzheimer disease
AUPRC: area under the precision-recall curve
AUROC: area under the receiver operating curve
BIDMC: Beth Israel Deaconess Medical Center
BOW: bag-of-words
CNS: central nervous system
CSF: cerebrospinal fluid
EHR: electronic health record
ICD: International Classification of Diseases
LLM: large language model
LP: lumbar punctures
MGB: Mass General Brigham
NID: neuroinfectious diseases
NLP: natural language processing

Edited by A Benis; submitted 12.06.24; peer-reviewed by PF Chen, S Kumar; revised version received 03.04.25; accepted 11.04.25; published 29.08.25.

Please cite as:
Singh A, Sartipi S, Sun H, Milde R, Turley N, Quinn C, Harrold GK, Gillani RL, Turbett SE, Das S, Zafar S, Fernandes M, Westover MB, Mukerji SS
A Machine Learning Approach for Identifying People With Neuroinfectious Diseases in Electronic Health Records: Algorithm Development and Validation
JMIR Med Inform 2025;13:e63157
URL: https://medinform.jmir.org/2025/1/e63157
doi:10.2196/63157

© Arjun Singh, Shadi Sartipi, Haoqi Sun, Rebecca Milde, Niels Turley, Carson Quinn, G Kyle Harrold, Rebecca L Gillani, Sarah E Turbett, Sudeshna Das, Sahar Zafar, Marta Fernandes, M Brandon Westover, Shibani S Mukerji. Originally published in JMIR Medical Informatics (https://medinform.jmir.org), 29.8.2025. This is an open-access article distributed under the terms of the Creative Commons Attribution License (https://creativecommons.org/licenses/by/4.0/), which permits unrestricted use, distribution, and reproduction in any medium, provided the original work, first published in JMIR Medical Informatics, is properly cited. The complete bibliographic information, a link to the original publication on https://medinform.jmir.org/, as well as this copyright and license information must be included.

XSL•FO
RenderX

Identifying Transportation Needs in Ophthalmology Clinic Notes Using Natural Language Processing: Retrospective, Cross-Sectional Study

Lauren M Wasser[1], MD; Hai-Wei Liang[1], PhD; Chenyu Li[2], PhD; Julie Cassidy[1], BA; Pooja Tallapaneni[1], BS; Hunter Osterhoudt[2], BS; Yanshan Wang[2], PhD; Andrew M Williams[1], MD

[1]Department of Ophthalmology, University of Pittsburgh School of Medicine, 1622 Locust Street, 5th floor, Pittsburgh, PA, United States

[2]Department of Health Information Management, University of Pittsburgh School of Health and Rehabilitation Sciences, Pittsburgh, PA, United States

Corresponding Author:
Andrew M Williams, MD
Department of Ophthalmology, University of Pittsburgh School of Medicine, 1622 Locust Street, 5th floor, Pittsburgh, PA, United States

Abstract

Background: Transportation insecurity is a known barrier to accessing eye care and is associated with poorer visual outcomes for patients. However, its mention is seldom captured in structured data fields in electronic health records, limiting efforts to identify and support affected patients. Free-text clinical documentation may more efficiently capture information on transportation-related challenges than structured data.

Objective: In this study, we aimed to identify mention of transportation insecurity in free-text ophthalmology clinic notes using natural language processing (NLP).

Methods: In this retrospective, cross-sectional study, we examined ophthalmology clinic notes of adult patients with an encounter at a tertiary academic eye center from 2016 to 2023. Demographic information and free text from clinical notes were extracted from electronic health records and deidentified for analysis. Free text was used to develop a rule-based NLP algorithm to identify transportation insecurity. The NLP algorithm was trained and validated using a gold-standard expert review, and precision, recall, and F_1-scores were used to evaluate the algorithm's performance. Logistic regression evaluated associations between demographics and transportation insecurity.

Results: A total of 1,801,572 clinical notes of 118,518 unique patients were examined, and the NLP algorithm identified 726 (0.6%) patients with transportation insecurity. The algorithm's precision, recall, and F_1-score were 0.860, 0.960, and 0.778, respectively, indicating high agreement with the gold-standard expert review. Patients with identified transportation insecurity were more likely to be older (OR 3.01, 95% CI 2.38 - 3.78 for those aged ≥80 vs 18 - 60 y) and less likely to identify as Asian (OR 0.04, 95% CI 0 - 0.18 for Asian patients vs White patients). There was no difference by sex (OR 1.13, 95% CI 0.97 - 1.31) or between the Black and White races (OR 0.98, 95% CI 0.79 - 1.22).

Conclusions: NLP has the potential to identify patients experiencing transportation insecurity from ophthalmology clinic notes, which may help to facilitate referrals to transportation resources.

(JMIR Med Inform 2025;13:e69216) doi:10.2196/69216

KEYWORDS

social needs screening; electronic health record; social determinants of health; transportation needs; natural language processing

Introduction

Health-related social needs (HRSN) affect access to eye care [1], and transportation needs in particular are a commonly cited barrier to accessing care for chronic eye diseases, such as diabetic retinopathy and glaucoma [2,3]. For instance, among respondents to the National Health Interview Survey, lack of transportation was associated with delayed follow-up with an ophthalmologist or optometrist, and transportation-related barriers to care disproportionately affected respondents with glaucoma or vision loss [4]. Separately, telephone interviews with patients with glaucoma following appointment no-show revealed that transportation was commonly cited as the reason for a missed appointment [5].

Fortunately, transportation needs are addressable, and referral to social work or patient navigator services can connect patients in need with medical transportation through local resources and programs [6-8]. At our own institution, the need for transportation to eye appointments is the most common indication for referral to our patient navigator program, and

XSL•FO
RenderX

these transportation referrals are addressed successfully through engagement with local resources or by enrollment in patients' insurance-sponsored medical transportation programs [8].

A barrier to connecting vulnerable patients to transportation resources is identifying which patients have a transportation need. Clinic-administered questionnaires to assess for HRSN are important screening tools, but survey uptake in clinical settings is suboptimal [9,10]. Furthermore, social determinants of health (SDoH), which encompass HRSN, are rarely available in structured electronic health record (EHR) data, such as diagnosis codes, and are more commonly documented in unstructured, narrative clinical notes [11-13]. Fortunately, unstructured notes may be accessible for analysis using technology such as natural language processing (NLP), an artificial intelligence (AI) tool that extracts and classifies free-text language [14]. In preliminary studies, NLP has demonstrated capability to identify SDoH terms from EHR text with reasonable accuracy compared to expert review [15,16].

The aim of this study was to determine whether NLP can be used to identify patients' transportation needs from existing unstructured clinical notes in the EHRs of our academic ophthalmology practice.

Methods

Ethical Considerations

This retrospective, cross-sectional, observational study was approved by the University of Pittsburgh institutional review board (STUDY21040204), adhered to the tenets of the Declaration of Helsinki, and complied with the Health Insurance Portability and Accountability Act of 1996. Patient informed consent was waived by the institutional review board. Privacy and confidentiality protection was ensured by leveraging an honest broker to deidentify patient data before analysis, and all analyses were performed on secure university servers. No patient compensation was provided.

Data Source

EHR data were obtained from outpatient clinical encounters of adult patients with the University of Pittsburgh Medical Center Department of Ophthalmology from January 2016 through February 2023. These data included unstructured free text from clinical notes, demographic information (including age, race and ethnicity, and sex), and semistructured text. Semistructured text included questionnaires in the social history section of physician and clinic staff notes, which indicated whether transportation needs were available on file. All signed clinical notes from an ophthalmology encounter were included, including office visit notes from technicians, trainees, and attending physicians, as well as documentation from telephone and refill encounters. These data were extracted from our institution's EHR (Epic Systems) using a custom-made research data warehouse [17]. After extraction, the structured data were deidentified by an honest broker, who is an official certified by the health system and the university to remove identifying information from health records, including names, addresses, and phone numbers, before transferring the dataset to investigators. Free-text notes were deidentified by National Library of Medicine Scrubber [18]. For patients with multiple encounters over the study period, demographic information was included from the first visit.

Algorithm Development

Due to the sparse documentation of transportation in encounter notes, we used a list of keywords (eg, "transportation" and "ride") to sample a subset of notes that contain transportation-related information. We then randomly selected 300 notes to create a gold-standard dataset manually reviewed by 2 ophthalmologists (LMW and AMW) and a research assistant (JC). We used 70% as training data to develop the rule-based NLP algorithm, termed NLP4Eye, with the remaining 30% serving as validation data for evaluation. After removing duplicated notes, there were 188 notes in the training dataset and 106 notes in the testing dataset.

NLP4Eye was iteratively refined on the training dataset. Embedded text of standardized questionnaire items that included transportation language was filtered out, as were transportation-related terms that predominately referred to visual function rather than social need (eg, terms related to "driving" were frequently mentioned during cataract evaluation encounters and thus removed from the algorithm dictionary as indicators of a transportation need). Similarly, due to its frequent mention in the context of fluorescein angiography, "transit" was removed from the dictionary of transportation-related terms in the NLP algorithm.

The NLP algorithm uses these rules within detected sentences to identify transportation needs from notes. The rules are "\b(%reTransportation).(%reNeeds)\b" or "\b(%reNeeds).(%reTransportation)\b," where "reTransportation" represents regular expressions for transportation-related words and "reNeeds" represents needs-related information, as detailed in Textbox 1. The NLP algorithm was then evaluated on the held-out testing data.

After the NLP algorithm development was completed, its validation was assessed on the testing dataset. The F_1-score of the NLP algorithm was then calculated to determine its performance in relation to the gold-standard testing dataset. The F_1-score, reported between 0 and 1, is a common metric of NLP performance relative to a reference standard. F_1 is calculated as a harmonic mean of the algorithm's precision (analogous to positive predictive value) and recall (analogous to sensitivity). An F_1 value of 0.7 or greater was considered adequate.

Finally, we assessed the algorithm for potential false negatives by conducting an additional post-hoc evaluation. In this evaluation, we assessed 200 clinical notes prefiltered for the tokens "transport*" and "mobility restriction*." These broader tokens were selected to capture any transportation-related mentions that might have been missed by our NLP algorithm, allowing us to evaluate potential false negatives in our algorithm's performance. An ophthalmologist (AMW) then annotated these notes for transportation needs, and discrepancies between the algorithm and physician annotations were analyzed using the taxonomy for systematic error analysis in clinical concept extraction by Fu et al [19].

XSL•FO
RenderX

The NLP4Eye algorithm was developed using the Open Health Natural Language Processing Toolkit, an NLP tool based on the Apache Unstructured Information Management Architecture pipeline, to facilitate information extraction from clinical narratives [20]. We created rules for identifying transportation needs based on physicians' knowledge and experience, refining these rules through physician verification. The regular expressions used in our NLP algorithm are listed in Textbox 1.

Textbox 1. Expressions used by the NLP4Eye algorithm to identify transportation needs.

- Transportation terms: "transportation," "ride," "driv(e|ing)"
- Transportation need terms: "work on," "option(s)," "issue(s)," "due to," "assist(ance)?," "access," "adequate," "discuss(ed|es|ing)," "(un)?able," "accommodation," "support," "agree(s)?," "appl(y|ies)," "arrang(es|ed|e|ing)?," "need(s)," "blam(e|es|ing)," "find(s|ing)," "connect(ing|ed)?," "could(n't| not)," "did(n't|not)," "difficult(y|ies)?," "get(ting)?," "help," "does(n't| not)," "lack(s|ing)?," "easier," "EMS," "investigate," "us(es|e|ing)," "depend(s|ing)?," "organiz(es|e|ing)," "coordination," "possible," "resources," "limit(s|ations)?," "convenience," "trouble(s)?," "secur(es|e|ing)," "concern(s)?," "regarding," "reli(es|able|ant)," "time allowance," "problem(s)?," "challeng(es|e|ing)," "purpose(s)?," "offer(s|ed)," "provid(es|ed|e|ing)"

Statistical Analysis

Statistical analyses were performed using R software (version 4.4.1; R Core Team). Descriptive statistics were used to summarize continuous variables as mean (SD), and categorical variables were presented as percentages and compared using chi-square tests (Fisher exact tests when cell values were less than 5). Longitudinal descriptive statistics were summarized as median (IQR) due to a violation of the normality assumption. Binary logistic regression analysis was conducted to identify predictors of NLP-identified transportation needs. Odds ratios (ORs) were calculated with 95% CIs, and a *P* value <.05 was considered statistically significant.

Results

Study Population

A total of 1,801,572 clinical notes from 118,518 unique adult patients were extracted from ophthalmology encounters over the study period, averaging 15.2 (SD 25.19) encounters per patient. Half (59,299/118,518, 50.0%) of the patient population was aged 60 years or above, 57.8% identified as female (68,485/118,518), and the racial composition was mostly White (90,699/118,518, 76.5%), followed by Black (17,594/118,518, 14.8%; Table 1).

XSL•FO
RenderX

Table . Demographic characteristics and their unadjusted associations with the identification of a transportation need by a natural language processing algorithm.

Characteristics	Total, n (%)	Transportation need identified, n (%)	No transportation need identified, n (%)	Odds ratio (95% CI)	*P* value
Age (years)					<.001
18 to <60	59,219 (50.0)	204 (28.1)	59,015 (50.1)	Reference	
60 to <70	28,434 (24.0)	179 (24.7)	28,255 (24.0)	1.83 (1.50-2.24)	
70 to <80	19,903 (16.8)	218 (30.0)	19,685 (16.7)	3.20 (2.65-3.88)	
>80	10,962 (9.2)	125 (17.2)	10,837 (9.2)	3.34 (2.66-4.17)	
Sex					.11
Female	68,485 (57.8)	441 (60.7)	68,044 (57.8)	1.13 (0.97-1.31)	
Male	50,032 (42.2)	285 (39.3)	49,747 (42.2)	Reference	
Race					<.001
Asian	5041 (4.3)	1 (0.1)	5040 (4.3)	0.03 (0-0.13)	
Black	17,594 (14.8)	104 (14.3)	17,490 (14.8)	0.88 (0.71-1.07)	
Native American and Alaska Native	300 (0.3)	2 (0.3)	298 (0.3)	0.99 (0.16-3.08)	
Pacific Islander	147 (0.1)	1 (0.1)	146 (0.1)	1.01 (0.06-4.50)	
White	90,699 (76.5)	612 (84.3)	90,087 (76.5)	Reference	
Declined or missing	4737 (4.0)	6 (0.8)	4731 (4.0)	N/A[a]	
Ethnicity					.01
Non-Hispanic or Latino	108,402 (91.5)	4731 (4.0)	107,707 (91.4)	4.99 (1.61-30.05)	
Hispanic or Latino	1548 (1.3)	2 (0.3)	1546 (1.3)	Reference	
Declined or missing	8568 (7.2)	29 (4.0)	8539 (7.2)	N/A	

[a]N/A: not applicable.

NLP Algorithm Validation

In the training stage of NLP algorithm development, 176 out of 188 (93.6%) notes were determined to be correctly labeled by the algorithm. The most common contexts for the 12 false hits were confirmed transportation support (6/188, 3.2%; eg, “agrees to be his transportation to and from and assist with care”), mention of transportation as the setting for an ocular injury (2/188, 1.1%), typographical error (2/188, 1.1%; both instances included “transportation” in place of “transplantation” in the context of corneal grafting), and transportation in the wrong context (2/188, 1.1%; eg, cellular transportation as a target for drug delivery). The algorithm was further refined based on these reference data and implemented across the dataset.

In the validation stage of NLP algorithm development, 95 of 100 (95%) notes were confirmed to represent a transportation need. Of the 5 false positives, 2 were typographical errors in the notes (both meant to refer to eye muscle “transposition”), 2 referred to the Pennsylvania Department of Transportation (one for a required vision screening examination and one to state that the patient retired from that organization), and 1 confirmed reliable transportation. The NLP algorithm’s precision, recall, and F_1-score were 0.860, 0.960, and 0.778, respectively, indicating high agreement with the gold standard expert review.

In addition to measuring our algorithm performance with the F_1-score, we also assessed for false negatives or transportation needs that could be detected using broad transportation terms but later missed during the iterative development of the algorithm. Our post-hoc evaluation on 200 notes containing the tokens “transport*” and “mobility restric*” revealed additional insights about algorithm performance. Within this broader sample, our algorithm correctly identified 101 notes without true transportation needs and 70 of 99 (70%) notes with true transportation issues (accuracy 85.5%, precision 1.00, recall 0.71, and F_1-score 0.83). Analysis of the 29 false negatives using the taxonomy by Fu et al [19] showed that approximately half represented contextual errors (primarily negation and possible or probable language) and half were linguistic errors (mainly synonym mismatches and implied inferences; additional details are available in Multimedia Appendix 1). These findings suggest that our reported prevalence of transportation needs likely represents a conservative estimate.

NLP Identification of Transportation Needs

We applied the NLP algorithm to the entire cohort of 118,518 unique patients. The NLP algorithm flagged 726 (0.6%) unique patients as having at least one mention of a transportation need

XSL•FO
RenderX

in their ophthalmic clinical notes. These 726 patients had a total of 1033 mentions of transportation needs, averaging 1.42 mentions per patient over the study period. As delineated in Table 2, the most common transportation-related terms identified by the NLP algorithm included the following phrases: "due to transportation," "transportation issues," and "transportation difficulties."

Textbox 2 illustrates representative examples of sentences from clinical notes that provide context for the NLP search hits.

Table . Top 10 transportation-related terms identified by the NLP4Eye algorithm.

Term	Encounter hits, n	Unique patient hits, n
Due to transportation	171	121
Transportation issues	154	109
Difficulty with transportation	48	24
Transportation difficulties	19	9
Arrange transportation	16	14
Issues with transportation	10	6
Access transportation	10	9
Transportation options	9	6
Unable to get transportation	8	6
Needs transportation	5	1

Textbox 2. Representative examples of sentences from clinical notes that were identified as expressing transportation needs by the NLP4Eye algorithm.

Example 1

- Identified sentence: "She is unable to stay for an injection due to ride issues today and wishes to observe."
- Regular expression: "due to ride issues"

Example 2

- Identified sentence: "He states that he never returned for any post-operative exams after the surgery in December due to transportation issues."
- Regular expression: "due to transportation issues"

Example 3

- Identified sentence: "It was decided by the Pt to use Ozurdex today for [PERSONALNAME] but no ozrudex in the office today and she has no transportation."
- Regular expression: "no transportation"

Example 4

- Identified sentence: "Huge change os, noticed 3 months ago, had appt in Aug. 2016, had to cx that appt., no ride."
- Regular expression: "no ride"

Demographic Characteristics Associated With NLP-Identified Transportation Needs

Compared to patients without an identified transportation need, patients who had at least one mention of a transportation need identified by the NLP algorithm were more likely to be aged above 80 years rather than below 60 years (adjusted OR 3.01, 95% CI 2.38 - 3.78), and they were less likely to identify as Asian (adjusted OR 0.04, 95% CI 0 - 0.18 for Asian patients vs White patients; Table 3). There was no difference between the female and male sexes (OR 1.13, 95% CI 0.97 - 1.31) or between the Black and White races (adjusted OR 0.98, 95% CI 0.79 - 1.22; Tables 1 and 3).

XSL•FO
RenderX

Table . Adjusted associations between demographic characteristics and the identification of a transportation need by the NLP4Eye algorithm.

Characteristics	Odds ratio (95% CI)	*P* value
Age (years)		<.001
18 to <60	Reference	
60 to <70	1.71 (1.39-2.11)	
70 to <80	3.01 (2.47-3.67)	
>80	3.01 (2.38-3.78)	
Race		<.001
Asian	0.04 (0.00-0.18)	
Black	0.98 (0.79-1.22)	
White	Reference	
Ethnicity		.05
Non-Hispanic or Latino	3.11 (1.00-18.78)	
Hispanic or Latino	Reference	

Longitudinal Analysis of Transportation Needs Over Time

Among patients with at least one documented transportation need, the average annual rate of transportation need mention per year from 2016 through 2022 ranged from 2.6% to 4.9%, with the lowest in 2017 and the highest in 2022 (Table 4). Regarding the number of documented transportation needs, most patients were identified only once (566/726, 78.0%), occurring for a median of 127 (IQR 21.3-595.3) days after their first encounter. Of the total, 20.0% (145/726) of patients had between 1 and 5 additional transportation needs, with a median time of 4, 69, 42, and 96 days between each respective event; 2.1% (15/726) of patients had more than 5 documented transportation needs, with the highest being 9 instances. Overall, the median time from the first visit to transportation-related events gradually increased over time, whereas the time between consecutive needs did not follow a consistent pattern (Table 5).

Table . Rates of transportation needs by calendar year among patients with at least one documented transportation need.

Calendar year	Total notes, N	Counts of transportation needs	Rates of transportation needs (%)
2016	2542	76	3.0
2017	2986	78	2.6
2018	3180	91	2.9
2019	3824	115	3.0
2020	4616	182	4.0
2021	5364	230	4.3
2022	5276	260	4.9

XSL•FO
RenderX

Table . Time between consecutive transportation needs.

Number of transportation need events	Patients (n=726), n (%)	Time between consecutive needs (days), median (IQR)	Time between the first encounter date (days), median (IQR)
1	566 (78.0)	—[a]	127 (21-595)
2	97 (13.4)	4 (0-67)	282 (15-776)
3	30 (4.1)	69 (5-161)	406 (142-1072)
4	13 (1.8)	42 (4-121)	512 (238-1148)
5	5 (0.7)	96 (69-156)	596 (312-1175)
6	7 (1.0)	182 (91-285)	810 (558-1215)
7	3 (0.4)	85.5 (69-145)	1353 (666.2-1845)
8	2 (0.3)	156 (154-181)	1663 (1354-2288)
9	3 (0.4)	5 (3-71)	1799 (1579-2044)

[a]Not available.

Discussion

Principal Findings

In this study, we developed a rule-based NLP algorithm to identify transportation needs from the free text of outpatient ophthalmology clinic encounters. Our model was trained and validated using human-labeled gold-standard datasets, and the NLP algorithm demonstrated a satisfactory performance with an F_1-score of 0.860. Overall, we found that 0.6% (726/118,518) of patients had a transportation need that was identified from their ophthalmology clinic documentation.

The performance of our algorithm is comparable to the F_1-score of 0.60 reported by Guevara et al [12], who used large language models to identify mention of transportation issues in oncology clinical notes. Their study focused on a similar patient population but used different methodologies, using fine-tuned Flan-T5 models and ChatGPT family models. Interestingly, despite the differences in approach, this study and the study by Guevara et al [12] demonstrated the feasibility of using NLP to identify mention of transportation needs from clinical documentation. Guevara et al [12] also noted that text-extracted SDoH identified significantly more patients with needs than structured data that use diagnostic codes, which aligns with our findings about the value of mining unstructured clinical notes.

Our model demonstrated higher precision than recall, which indicated a tendency to produce more false negatives than false positives, suggesting that this result may represent the lower limit of identified transportation needs. Our post-hoc evaluation revealed important limitations in recall when applied to notes with more diverse expressions of transportation difficulties. Transportation needs may be expressed through complex linguistic constructions, including negations (“cannot drive”), hypothetical language (“may have difficulty with transportation”), synonyms not included in our keyword list (eg, “mobility issues”), and implied inferences that require contextual understanding (eg, “patient’s vehicle was under repair”). These linguistic challenges are consistent with those identified in other NLP applications for SDoH text extraction from clinical notes [19]. The error analysis of false negatives in our post-hoc evaluation highlighted specific areas for improvement: handling negation patterns, detecting hypothetical language, expanding synonym recognition, and developing more sophisticated contextual understanding. These findings align with previous research on the challenges of extracting social needs information from clinical text [12,16].

Comparison to Prior Work

Previous studies have explored using NLP to identify transportation needs within EHRs [12,16]. One group developed algorithms to detect housing, food, and transportation insecurity among patients in a large health care network. Their transportation algorithm demonstrated relatively low performance compared to the algorithms for housing and food insecurity, and its performance was also lower than that of our algorithm [16]. Another team created an algorithm to identify social needs among oncology patients, with lower performance for the transportation algorithm than other SDoH domains [12]. However, the transportation cases in their study are low, with only 41 in the training set and 6 in the testing set, which may limit the reliability of their algorithm.

Our unique focus on ophthalmology clinics presented distinct challenges in EHR data mining. Free text from ophthalmology clinic encounters often includes abbreviations and terminology that are highly specific to the field [21,22]. We found that refining our algorithm for identifying mention of social needs in ophthalmology was an important step in the process. It required collaboration between ophthalmologists and data scientists to ensure the algorithm did not mistakenly identify common ophthalmology terms, such as “difficulty driving” for cataract patients and the “transit” phase of fluorescein angiography—an ophthalmic dye-based imaging test—as transportation needs. The most common transportation terms identified from unstructured clinical notes were “due to transportation,” “transportation issues,” and “transportation difficulties.”

The 0.6% prevalence of transportation needs identified by our NLP algorithm is similar to the reported transportation needs hit rate of 1.3% reported from a social needs algorithm developed and tested on unstructured medical notes in another

XSL•FO
RenderX

large health system [16]. Interestingly, the use of NLP algorithms to detect mention of social needs in health care settings may result in a lower hit rate than the use of structured EHR-based social needs questionnaires. For example, an EHR-based social needs screening questionnaire for 1696 primary care patients in Boston identified that 7% of screened patients reported a transportation need, which is much higher than the approximately 1% rate in the NLP-based studies [23]. Another reported the presence of transportation insecurity in 2% (3062/147,150) of patients [24]. Different clinical settings will have a variable proportion of underserved patients and unique HRSN, and differences may be apparent between primary care settings and subspecialty offices. Nonetheless, there does seem to be a pattern of a higher proportion of detected needs in survey studies than in NLP algorithms. For example, in our own patient population—encompassing some of the same cohort that underwent NLP assessment—5.1% (68/1340) of patients who completed an EHR-based social needs questionnaire reported a transportation need [25]. While the proportion of patients identified in structured questionnaires is higher than that in NLP algorithms, surveys depend on participant uptake, which may be low and subject to nonresponse bias [24]. Furthermore, screening surveys may increase the documentation demands on health care providers [16]. The vast amount of data available in unstructured clinical notes makes it a promising resource for automated EHR mining. While the percentage of identified social needs may be lower for NLP algorithms than survey-based assessments, the absolute number of patients identified can be much greater [26]. As such, a robust NLP model capable of detecting mentions of social needs during clinical encounters, along with their frequency, offers a valuable alternative for understanding and tracking these needs over time cost-effectively.

Patients with a transportation need identified by the algorithm were more likely to be older and of a non-Asian race, with no difference between sexes or between Black and White patients. Our study's finding that older age is a risk factor for transportation insecurity is consistent with previous research [27]. While some studies have identified the female sex as a risk factor for transportation barriers to health care access [27], our findings align with other research indicating no significant difference between sexes [28]. Previous studies have demonstrated that racial and ethnic minority groups have higher rates of transportation insecurity [28]. Specifically, one study that used an NLP algorithm to extract SDoH text from the clinical notes of patients with cancer and opioid users found that transportation documentation was higher among Black patients [29]. Our study found no difference in transportation insecurity between Black and White patients. Possible explanations for this discrepancy could be a decreasing gap in travel burdens between Black and White Americans in recent years or a hesitance among minority patients to communicate with health care providers, which may result in the absence of this information in the unstructured clinical note in the EHR, but further study is warranted [30,31].

Knowledge about how a person's social needs, particularly transportation needs, change over time remains limited. One study surveyed 228 participants about transportation difficulties at baseline and then reassessed them at either 3 or 6 months [32]. It found that 9% of the population initially reported transportation difficulties, and these needs remained largely stable over time. Only 6% to 8% reported improvement, and 5% reported worsening. The authors suggested that a 3- to 6-month follow-up may be sufficient for identifying changes in social risk [32]. In contrast, our study found that just 0.1% (n=117) of individuals were identified as having transportation needs at their first encounter, which was substantially lower than the findings of the previous study. This discrepancy may reflect differences in population characteristics; for example, our cohort had less racial diversity, and race is a known factor associated with travel-related disparities [33].

Among individuals identified as having transportation needs, 78.0% (566/726) had only one documented need, with a median of 127 (IQR 21-595) days from their first encounter. For those with 2 documented needs, the median interval was 282 (IQR 15-776) days since the initial visit. While these results do not clarify whether the transportation needs identified by the NLP algorithm precisely reflect the timing of the actual need, it is possible that the observed delay stems from a growing sense of trust between patients and their physicians, which may lead patients to disclose their needs only after several visits [34]. Regardless of the cause, these findings suggest that a 3- to 6-month follow-up period may be insufficient to capture meaningful changes in transportation needs among patients facing such barriers.

Potential Interventions

Identification of transportation needs by NLP algorithms may facilitate the implementation of actionable interventions to address transportation barriers. Medical transportation resources are readily available through health insurance and county-based programs, but many patients are not aware that they are eligible for these benefits. For example, at our own institutions, 50 out of 52 ophthalmology patients with transportation needs who were referred to our patient navigator program for resources had their transportation issues resolved by enrolling in a transportation assistance program [8]. The biggest challenge in assisting patients with transportation resources is identifying the patients with transportation needs. By implementing a transportation-oriented NLP algorithm in clinical practice, institutions can identify patients who are at high risk of transportation insecurity and contact them in advance of an upcoming appointment to assess for transportation challenges and to offer resources. In fact, patients with missed appointments have expressed support for outreach with resources to maintain eye care [5], and the implementation of an NLP algorithm to flag patients with needs could greatly facilitate resource allocation to help vulnerable patients maintain access to care.

Limitations

To our knowledge, this study is the first to apply an NLP-based transportation analysis to a corpus of ophthalmology clinic notes from the EHR of a large health care system. Our algorithm identified 726 ophthalmology patients with a transportation need, demonstrating its potential to detect transportation insecurity without adding to health care providers' workloads. Our study does have several limitations. First, our algorithm

XSL•FO
RenderX

was validated and applied to a population local to western Pennsylvania, which may not be nationally representative [35]. In particular, the preponderance of White patients in our dataset may limit our ability to detect racial disparities in transportation needs for patients of the Black race or Hispanic ethnicity. Future work should examine the performance of our algorithm using ophthalmology clinic notes from other geographic settings, particularly those that represent greater racial and ethnic diversity.

Second, the true prevalence of transportation insecurity among our patient population is unknown, making it difficult to compare our findings to actual rates. To assess our findings in the context of an unknown true prevalence of transportation insecurity, we conducted a post-hoc analysis with broad transportation terms to examine for false negatives. While the precision (1.00) of the algorithm in this post-hoc analysis remained high, the recall (0.71) was less robust, indicating that some true transportation needs are missed by the algorithm in an attempt to mitigate false positives. The implications of our post-hoc analysis suggest that our results are probably underreporting the true prevalence of transportation needs in our population. Specifically, our model's higher precision than recall suggests that we likely present a conservative estimate of identified transportation needs in our patient population.

A third limitation of this study is the examination of transportation needs without the consideration of other concomitant, and likely interrelated, HRSN. For this study, we used "transportation needs" as an umbrella term to mine the EHRs, but transportation insecurity has many components and can overlap with other SDoH domains, such as financial insecurity [36]. Patients who express financial difficulties, for instance, may also have difficulty with transportation, but these patients would not be identified by our algorithm unless their needs are documented with transportation-specific language. Therefore, our detected prevalence of transportation needs may again be lower than the true burden faced by the patient cohort. Future work should develop algorithms to identify other SDoH domains in the context of eye care encounters. It is important to explore the different facets of transportation and how they interact with other social needs to identify specific transportation challenges and direct patients to the appropriate services to address these issues.

As a fourth limitation, relevant factors such as socioeconomic status, education level, and residence information were not included in the data source. Absence of these data limits our ability to gain further insights into baseline characteristics that may warrant attention. Future work should incorporate these sociodemographic components, which could facilitate predictive modeling of a patient's risk of transportation needs.

Future Directions

External validation of this model using data from other health care systems across the United States is necessary to test its generalizability. For implementation into clinical practice, further research is needed to assess how health care teams may engage with potential notifications in the EHR about transportation needs identified by the NLP algorithm.

Conclusions

Our NLP algorithm successfully identified previously unknown transportation needs from unstructured ophthalmology clinic notes in the EHRs. The algorithm demonstrated reliable identification of transportation insecurity; thus, it offers an additional method for leveraging large amounts of available data to screen for transportation needs among ophthalmology patients, without adding to the documentation burden on health care providers. Our findings indicate age disparities in transportation needs within our patient population, with older patients indicating a greater burden of transportation needs. In addition to survey-based social needs screening, NLP can identify mention of social needs from EHR text, thus potentially facilitating referrals to transportation resources for vulnerable ophthalmology patients.

Acknowledgments

This study was supported in part by the David L Epstein Clinician-Scientist Research Award from the Chandler Grant Glaucoma Society (awarded to AMW), the Mentorship for Advancement of Physician-Scientists Award from the American Glaucoma Society (awarded to AMW), the National Institutes of Health (NIH) grant UL1 TR001857, NIH CORE grant P30 EY08098, the Henry L Hillman Foundation, the Eye and Ear Foundation of Pittsburgh, and an unrestricted grant from Research to Prevent Blindness to the Department of Ophthalmology at the University of Pittsburgh.

Data Availability

The code for the natural language processing algorithm is available on GitHub [37].

Conflicts of Interest

None declared.

Multimedia Appendix 1
Post-hoc analyses.
[DOCX File, 60 KB - medinform_v13i1e69216_app1.docx]

XSL•FO
RenderX

References

1. Williams AM, Sahel JA. Addressing social determinants of vision health. Ophthalmol Ther 2022 Aug;11(4):1371-1382. [doi: 10.1007/s40123-022-00531-w] [Medline: 35674883]
2. Elam AR, Tseng VL, Rodriguez TM, et al. Disparities in vision health and eye care. Ophthalmology 2022 Oct;129(10):e89-e113. [doi: 10.1016/j.ophtha.2022.07.010] [Medline: 36058735]
3. Atta S, Zaheer HA, Clinger O, et al. Characteristics associated with barriers to eye care: a cross-sectional survey at a free vision screening event. Ophthalmic Res 2023;66(1):170-178. [doi: 10.1159/000526875] [Medline: 36063808]
4. Kim AB, Cheng BT, Tanna AP. Delayed medical care due to lack of transportation among US adults with glaucoma. Ophthalmol Glaucoma 2023;6(4):439-441. [doi: 10.1016/j.ogla.2023.03.007] [Medline: 36990434]
5. Wasser LM, Bear TM, Sommers M, Cassidy J, Muir KW, Williams AM. Barriers to care among glaucoma patients with a missed appointment and interest in a navigator program. J Glaucoma 2024 Apr 1;33(4):297-302. [doi: 10.1097/IJG.0000000000002330] [Medline: 37974342]
6. Powers BW, Rinefort S, Jain SH. Nonemergency medical transportation: delivering care in the era of Lyft and Uber. JAMA 2016 Sep 6;316(9):921-922. [doi: 10.1001/jama.2016.9970] [Medline: 27599325]
7. Chaiyachati KH, Hubbard RA, Yeager A, et al. Association of rideshare-based transportation services and missed primary care appointments: a clinical trial. JAMA Intern Med 2018 Mar 1;178(3):383-389. [doi: 10.1001/jamainternmed.2017.8336] [Medline: 29404572]
8. Zarnegar A, Cassidy J, Stone A, et al. Effect of a patient navigator program to address barriers to eye care at an academic ophthalmology practice. J Acad Ophthalmol 2023 May;15(1):e106-e111. [doi: 10.1055/s-0043-1768696]
9. Albert SM, McCracken P, Bui T, et al. Do patients want clinicians to ask about social needs and include this information in their medical record? BMC Health Serv Res 2022 Oct 22;22(1):1275. [doi: 10.1186/s12913-022-08652-5] [Medline: 36273141]
10. Rudisill AC, Eicken MGA, Gupta D, et al. Patient and care team perspectives on social determinants of health screening in primary care: a qualitative study. JAMA Netw Open 2023 Nov 1;6(11):e2345444. [doi: 10.1001/jamanetworkopen.2023.45444] [Medline: 38015502]
11. Navathe AS, Zhong F, Lei VJ, et al. Hospital readmission and social risk factors identified from physician notes. Health Serv Res 2018 Apr;53(2):1110-1136. [doi: 10.1111/1475-6773.12670] [Medline: 28295260]
12. Guevara M, Chen S, Thomas S, et al. Large language models to identify social determinants of health in electronic health records. NPJ Digit Med 2024 Jan 11;7(1):6. [doi: 10.1038/s41746-023-00970-0] [Medline: 38200151]
13. Lee TC, Saseendrakumar BR, Nayak M, et al. Social determinants of health data availability for patients with eye conditions. Ophthalmol Sci 2022 Jun;2(2):100151. [doi: 10.1016/j.xops.2022.100151] [Medline: 35662804]
14. Bompelli A, Wang Y, Wan R, et al. Social and behavioral determinants of health in the era of artificial intelligence with electronic health records: a scoping review. Health Data Sci 2021 Aug 24;2021:9759016. [doi: 10.34133/2021/9759016] [Medline: 38487504]
15. Wu W, Holkeboer KJ, Kolawole TO, Carbone L, Mahmoudi E. Natural language processing to identify social determinants of health in Alzheimer's disease and related dementia from electronic health records. Health Serv Res 2023 Dec;58(6):1292-1302. [doi: 10.1111/1475-6773.14210] [Medline: 37534741]
16. Gray GM, Zirikly A, Ahumada LM, et al. Application of natural language processing to identify social needs from patient medical notes: development and assessment of a scalable, performant, and rule-based model in an integrated healthcare delivery system. JAMIA Open 2023 Oct;6(4):ooad085. [doi: 10.1093/jamiaopen/ooad085] [Medline: 37799347]
17. Visweswaran S, McLay B, Cappella N, et al. An atomic approach to the design and implementation of a research data warehouse. J Am Med Inform Assoc 2022 Mar 15;29(4):601-608. [doi: 10.1093/jamia/ocab204] [Medline: 34613409]
18. Kayaalp M, Browne AC, Dodd ZA, Sagan P, McDonald CJ. An easy-to-use clinical text de-identification tool for clinical scientists: NLM scrubber. Presented at: AMIA Annual Symposium; Nov 14-18, 2015; Washington, DC. [doi: 10.13140/RG.2.2.13587.37921]
19. Fu S, Wang L, He H, et al. A taxonomy for advancing systematic error analysis in multi-site electronic health record-based clinical concept extraction. J Am Med Inform Assoc 2024 Jun 20;31(7):1493-1502. [doi: 10.1093/jamia/ocae101] [Medline: 38742455]
20. Wen A, Fu S, Moon S, et al. Desiderata for delivering NLP to accelerate healthcare AI advancement and a Mayo Clinic NLP-as-a-service implementation. NPJ Digit Med 2019 Dec 17;2:130. [doi: 10.1038/s41746-019-0208-8] [Medline: 31872069]
21. Hamiel U, Hecht I, Nemet A, et al. Frequency, comprehension and attitudes of physicians towards abbreviations in the medical record. Postgrad Med J 2018 May;94(1111):254-258. [doi: 10.1136/postgradmedj-2017-135515] [Medline: 29540451]
22. Wang S, Tseng B, Hernandez-Boussard T. Development and evaluation of novel ophthalmology domain-specific neural word embeddings to predict visual prognosis. Int J Med Inform 2021 Jun;150:104464. [doi: 10.1016/j.ijmedinf.2021.104464] [Medline: 33892445]

XSL•FO
RenderX

23. Buitron de la Vega P, Losi S, Sprague Martinez L, et al. Implementing an EHR-based screening and referral system to address social determinants of health in primary care. Med Care 2019 Jun;57 Suppl 6 Suppl 2:S133-S139. [doi: 10.1097/MLR.0000000000001029] [Medline: 31095052]
24. Bharmal N, Rennick A, Shideler A, et al. Health-related social needs: which patients respond to screening and who receives resources? J Gen Intern Med 2023 Sep;38(12):2695-2702. [doi: 10.1007/s11606-023-08135-1] [Medline: 36932266]
25. Mayer N, Cassidy J, Wasser LM, Liu PJ, Williams AM. Seeing the unseen: uncovering health-related social needs through universal screening at an academic ophthalmology practice. Eye (Lond) 2025 Jun;39(8):1501-1507. [doi: 10.1038/s41433-025-03690-9] [Medline: 39955377]
26. Hatef E, Rouhizadeh M, Tia I, et al. Assessing the availability of data on social and behavioral determinants in structured and unstructured electronic health records: a retrospective analysis of a multilevel health care system. JMIR Med Inform 2019 Aug 2;7(3):e13802. [doi: 10.2196/13802] [Medline: 31376277]
27. Wallace R, Hughes-Cromwick P, Mull H, Khasnabis S. Access to health care and nonemergency medical transportation. Transp Res Rec 2005 Jan;1924(1):76-84. [doi: 10.1177/0361198105192400110]
28. Wolfe MK, McDonald NC, Holmes GM. Transportation barriers to health care in the United States: findings from the National Health Interview Survey, 1997-2017. Am J Public Health 2020 Jun;110(6):815-822. [doi: 10.2105/AJPH.2020.305579] [Medline: 32298170]
29. Yu Z, Peng C, Yang X, et al. Identifying social determinants of health from clinical narratives: a study of performance, documentation ratio, and potential bias. J Biomed Inform 2024 May;153:104642. [doi: 10.1016/j.jbi.2024.104642] [Medline: 38621641]
30. Akinlotan M, Khodakarami N, Primm K, Bolin J, Ferdinand AO. Travel for medical or dental care by race/ethnicity and rurality in the U.S.: findings from the 2001, 2009 and 2017 National Household Travel Surveys. Prev Med Rep 2023 Jun;35:102297. [doi: 10.1016/j.pmedr.2023.102297] [Medline: 37559948]
31. White RO, Chakkalakal RJ, Presley CA, et al. Perceptions of provider communication among vulnerable patients with diabetes: influences of medical mistrust and health literacy. J Health Commun 2016;21(sup2):127-134. [doi: 10.1080/10810730.2016.1207116] [Medline: 27662442]
32. Lewis CC, Jones SMW, Wellman R, et al. Social risks and social needs in a health insurance exchange sample: a longitudinal evaluation of utilization. BMC Health Serv Res 2022 Nov 28;22(1):1430. [doi: 10.1186/s12913-022-08740-6] [Medline: 36443789]
33. Labban M, Chen CR, Frego N, et al. Disparities in travel-related barriers to accessing health care from the 2017 National Household Travel Survey. JAMA Netw Open 2023 Jul 3;6(7):e2325291. [doi: 10.1001/jamanetworkopen.2023.25291] [Medline: 37498602]
34. De Marchis EH, Hessler D, Fichtenberg C, et al. Part I: a quantitative study of social risk screening acceptability in patients and caregivers. Am J Prev Med 2019 Dec;57(6 Suppl 1):S25-S37. [doi: 10.1016/j.amepre.2019.07.010] [Medline: 31753277]
35. United States Census Bureau. QuickFacts United States. 2025 Jun. URL: https://www.census.gov/quickfacts/fact/table/US/PST045219 [accessed 2025-08-20]
36. Henning-Smith C, Evenson A, Corbett A, Kozhimannil K, Moscovice I. Rural transportation: challenges and opportunities. Policy brief: University of Minnesota Rural Health Research Center. 2017. URL: https://rhrc.umn.edu/wp-content/files_mf/1518734252UMRHRCTransportationChallenges.pdf [accessed 2025-08-25]
37. PittNAIL/sdohtransportation_nlp. GitHub. URL: https://github.com/PittNAIL/SDoHTransportation_NLP [accessed 2025-08-28]

Abbreviations

AI: artificial intelligence
EHR: electronic health record
HRSN: health-related social needs
NLP: natural language processing
OR: odds ratio
SDoH: social determinants of health

XSL•FO
RenderX

Edited by A Coristine; submitted 24.11.24; peer-reviewed by Á García-Barragán, C Rydz, SD Bhattacharjee; revised version received 26.07.25; accepted 28.07.25; published 05.09.25.

Please cite as:
Wasser LM, Liang HW, Li C, Cassidy J, Tallapaneni P, Osterhoudt H, Wang Y, Williams AM
Identifying Transportation Needs in Ophthalmology Clinic Notes Using Natural Language Processing: Retrospective, Cross-Sectional Study
JMIR Med Inform 2025;13:e69216
URL: https://medinform.jmir.org/2025/1/e69216
doi:10.2196/69216

© Lauren M Wasser, Hai-Wei Liang, Chenyu Li, Julie Cassidy, Pooja Tallapaneni, Hunter Osterhoudt, Yanshan Wang, Andrew M Williams. Originally published in JMIR Medical Informatics (https://medinform.jmir.org), 5.9.2025. This is an open-access article distributed under the terms of the Creative Commons Attribution License (https://creativecommons.org/licenses/by/4.0/), which permits unrestricted use, distribution, and reproduction in any medium, provided the original work, first published in JMIR Medical Informatics, is properly cited. The complete bibliographic information, a link to the original publication on https://medinform.jmir.org/, as well as this copyright and license information must be included.

XSL•FO
RenderX

Large Language Model–Enhanced Drug Repositioning Knowledge Extraction via Long Chain-of-Thought: Development and Evaluation Study

Hongyu Kang[1,2], PhD; Jiao Li[2], PhD; Li Hou[2], PhD; Xiaowei Xu[2], MS; Si Zheng[2], MS; Qin Li[1], PhD

[1]School of Medical Technology, Beijing Institute of Technology, No. 5 Zhongguancun South Street, Haidian District, Beijing, China

[2]Medical Information Innovation Research Center, Institute of Medical Information, Chinese Academy of Medical Sciences and Peking Union Medical College, Beijing, China

Corresponding Author:
Qin Li, PhD
School of Medical Technology, Beijing Institute of Technology, No. 5 Zhongguancun South Street, Haidian District, Beijing, China

Abstract

Background: Drug repositioning is a pivotal strategy in pharmaceutical research, offering accelerated and cost-effective therapeutic discovery. However, biomedical information relevant to drug repositioning is often complex, dispersed, and underutilized due to limitations in traditional extraction methods, such as reliance on annotated data and poor generalizability. Large language models (LLMs) show promise but face challenges such as hallucinations and interpretability issues.

Objective: This study proposed long chain-of-thought for drug repositioning knowledge extraction (LCoDR-KE), a lightweight and domain-specific framework to enhance LLMs' accuracy and adaptability in extracting structured biomedical knowledge for drug repositioning.

Methods: A domain-specific schema defined 11 entities (eg, drug, disease) and 18 relationships (eg, treats, is biomarker of). Following the established schema architecture, we constructed automatic annotation based on 10,000 PubMed abstracts via chain-of-thought prompt engineering. A total of 1000 expert-validated abstracts were curated into a drug repositioning corpus, a high-quality specialized corpus, while the remaining entries were allocated for model training purposes. Then, the proposed LCoDR-KE framework combined supervised fine-tuning of the Qwen2.5-7B-Instruct model with reinforcement learning and dual-reward mechanisms. Performance was evaluated against state-of-the-art models (eg, conditional random fields, Bidirectional Encoder Representations From Transformers, BioBERT, Qwen2.5, DeepSeek-R1, OpenBioLLM-70B, and model variants) using precision, recall, and F_1-score. In addition, the convergence of the training method was assessed by analyzing performance progression across iteration steps.

Results: LCoDR-KE achieved an entity F_1 of 81.46% (eg, drug 95.83%, disease 90.52%) and triplet F_1 of 69.04%, outperforming traditional models and rivaling larger LLMs (DeepSeek-R1: entity F_1=84.64%, triplet F_1=69.02%). Ablation studies confirmed the contributions of supervised fine-tuning (8.61% and 20.70% F_1 drop if removed) and reinforcement learning (6.09% and 14.09% F_1 drop if removed). The training process demonstrated stable convergence, validated through iterative performance monitoring. Qualitative analysis of the model's chain-of-thought outputs showed that LCoDR-KE performed structured and schema-aware reasoning by validating entity types, rejecting incompatible relations, enforcing constraints, and generating compliant JSON. Error analysis revealed 4 main types of mistakes and challenges for further improvement.

Conclusions: LCoDR-KE enhances LLMs' domain-specific adaptability for drug repositioning by offering an open-source drug repositioning corpus and a long chain-of-thought framework based on a lightweight LLM model. This framework supports drug discovery and knowledge reasoning while providing scalable, interpretable solutions applicable to broader biomedical knowledge extraction tasks.

(JMIR Med Inform 2025;13:e77837) doi:10.2196/77837

KEYWORDS

drug repositioning; knowledge extraction; large language models; long chain-of-thought; reinforcement learning

XSL•FO
RenderX

Introduction

Drug repositioning, also known as drug repurposing, has emerged as a pivotal strategy in pharmaceutical research, enabling the discovery of novel therapies for existing drugs [1]. This approach significantly facilitates the drug development process, shortens the required time, and reduces the cost [2]. However, biomedical information relevant to drug repositioning is often complex and dispersed across various sources [3], such as literature, clinical trials, and databases. These valuable resources remain underutilized because of the challenges associated with knowledge extraction [4,5]. Extracting knowledge from biomedical literature, such as entities, relationships, and structured triplets, can facilitate drug repositioning research by uncovering hidden connections between drugs and diseases [6]. Recent studies have demonstrated the effectiveness of knowledge extraction in supporting knowledge discovery in drug repositioning. For example, Bang et al [7] developed a semantic multilayer guilt-by-association approach to extract drug-disease associations from large-scale biomedical corpora, while Huang et al [8] leveraged TxGNN, a graph foundation model for zero-shot drug repurposing, to identify therapeutic candidates even for diseases with limited treatment options or no existing drugs. These advancements underscore the importance of automated knowledge extraction in identifying potential drug candidates for the treatment of complex, multifactorial diseases.

Traditional knowledge extraction methods have evolved from manual annotation and rule-based techniques to machine learning and deep learning approaches. Early methodologies relied heavily on expert-curated databases and handcrafted rules, which lacked scalability while being precise [9,10]. Machine learning models, such as conditional random fields (CRF), introduced statistical learning to automate entity recognition and relationship extraction [11-13]. More recently, deep learning models, including BERT and transformer-based architecture, have achieved remarkable performance in biomedical natural language processing tasks. For example, domain-specific language models, such as BioBERT [14], PubMedBERT (trained on biomedical literature) [15], ClinicalBERT (trained on the MIMIC-III dataset) [16], and PharmBERT (trained on prescription drug labeling) [17], have been further developed. Despite their success, these methods still have several limitations. They often require extensive labeled datasets for training, which are costly and labor-intensive to obtain. Furthermore, deep learning models demonstrate limited generalizability across diverse biomedical domains [18] and often overlook implicit knowledge that extends beyond surface-level textual patterns [19]. As a result, refining extraction methodologies to achieve greater adaptability and performance continues to be an important focus in drug repositioning studies.

Large language models (LLMs) have emerged as a promising solution for biomedical knowledge extraction, demonstrating superior performance across various natural language processing tasks. Models such as ChatGPT (OpenAI) [20], LlaMA (Meta) [21], GLM (Tsinghua) [22], Qwen (AlibabaCloud) [23], and Deepseek [24] have been extensively used in biomedical text mining because of their advanced semantic comprehension and text generation capacities. By leveraging key methodologies, including pretraining [25], prompt engineering [26], and domain-specific fine-tuning [27], these models demonstrate improved accuracy and adaptability for specialized tasks [28], such as named entity recognition [29] and association prediction [30]. Xie et al [31] developed Me-LLaMA through continual pretraining and instruction tuning of LLaMA2 models and outperformed existing open medical LLMs on 6 text analysis tasks. Hao et al [26] developed and evaluated MedScaleNER, a task-oriented prompt framework, advancing the application of LLMs and prompt engineering for specialized named entity recognition tasks in Chinese medical literature. Recent advances such as BioGPT [32] and OpenBioLLM-70B [33] have demonstrated the potential of large-scale generative pretrained transformers in enhancing biomedical text generation and domain-specific knowledge mining. Focusing on a more specific biomedical task, Yuan et al [34] introduced BioFocal-DDI, a framework combining BioGPT for data augmentation, BioBERT, and BiLSTM for contextual and sequential feature extraction to optimize drug-drug interaction extraction.

Compared to traditional methods, LLMs demonstrate superior knowledge extraction capabilities, including better generalization, reduced reliance on annotated data, and stronger contextual comprehension. Nevertheless, persistent challenges [35,36], including model hallucination, output accuracy, interpretability, and high computational demands, must be addressed. For drug repositioning applications, these issues can be mitigated through gold-standard corpus validation, careful prompt engineering, and chain-of-thought (CoT) [37] methodologies. Chen et al [38] leveraged retrieval‐augmented generation combined with instruction prompting to build LLMs specialized for osteoarthritis diagnosis and treatment Q&A, providing reliable clinical decision support to health care professionals.

While LLMs demonstrate promise in biomedical knowledge extraction, challenges persist in domain-specific adaptability, particularly in drug repositioning, where sparse annotated data, semantic ambiguity, and cross-sentence dependencies hinder accurate knowledge inference [39,40]. To address these limitations, we proposed long chain-of-thought (LCoT) for drug repositioning knowledge extraction (LCoDR-KE), a lightweight framework that combined LCoT prompting, supervised fine-tuning (SFT), and reinforcement learning (RL). To enhance the performance of knowledge extraction, our approach also introduced a dual-level reward mechanism to guide knowledge extraction and a high-quality drug repositioning corpus (DrugReC), meticulously curated from biomedical publications in PubMed. Through comparative and ablation studies, we validated the framework's superiority over traditional models and its competitive performance against state-of-the-art LLMs, offering a scalable, interpretable solution for accelerating drug discovery and biomedical knowledge inference.

XSL•FO
RenderX

Methods

Overview

The workflow of the proposed *LCoDR-KE* is illustrated in Figure 1 and consisted of 4 main stages: drug repositioning schema design, data preparation and gold standard annotation, implementation of LCoT framework, and in-depth evaluation.

- *Drug repositioning schema design*: This stage established a structured schema for drug repositioning, defining 11 entity types (eg, drug, gene, disease, target) and 18 relationship types. The schema provided a standardized ontology that enabled accurate knowledge extraction while maintaining conceptual consistency across the domain.
- *Data preparation and annotation*: We first annotated a scale of 10,000 PubMed abstracts via CoT prompt engineering, incorporating role definitions and k-shot demonstrations. Among these, 1000 abstracts were subjected to meticulous manual annotations, resulting in a high-quality corpus specifically curated for the task of drug repurposing, DrugReC. The remaining 9000 abstracts were used as part of the training data in this study.
- *Implementation of the LCoT framework:* We first conducted SFT to establish a strong output with explicit reasoning chains for LLM. Following this, we applied Group Relative Policy Optimization (GRPO), an RL strategy guided by reward modeling. Tailored reward functions were specifically designed for drug repositioning entity and triple recognition, enabling more accurate and structured output aligned with domain-specific requirements.
- *Evaluation and performance analysis*: We evaluated the model's effectiveness through performance comparisons, ablation studies, k-shot performance, reward parameter optimization, CoT reasoning patterns, steps of training iterations, and error analysis.

XSL•FO
RenderX

Figure 1. Workflow of long chain-of-thought for drug repositioning knowledge extraction (LCoDR-KE). CoT: chain-of-thought; LCoT: long chain-of-thought.

XSL•FO
RenderX

Drug Repositioning Schema Design

We developed a multidimensional knowledge model by conducting in-depth analyses of drug mechanisms [41-43] while precisely defining core entity dimensions and their relationships. We conducted comprehensive analyses of drug labels, literature, and multiple biomedical databases (including DrugBank, CTD, PharmGKB, and DisGeNET) to establish foundational knowledge. In addition, this multidimensional knowledge framework was subsequently refined and validated through expert consultation, incorporating specialized domain knowledge from pharmacology, bioinformatics, clinical medicine, and computational biology.

Data Preparation

A total of 10,000 PubMed abstracts were extracted using a 4-step filtering strategy to ensure quality and domain relevance:

1. Initial search: Articles published between January 1, 2015, and January 1, 2025, were retrieved via PubMed using Medical Subject Headings (MeSH) terms and keywords related to drug repositioning, drug mechanisms, and pharmacology.
2. Journal filtering: We retained articles published in top-tier pharmacological journals ranked in Q1 of the Journal Citation Reports (Multimedia Appendix 1).
3. Relevance filtering: Abstracts were kept if the title or abstract mentioned at least one drug or disease entity from a standard drug repositioning dataset [44].
4. Length filtering: Abstracts under 50 characters were excluded to ensure basic content adequacy.

This rigorous selection process (detailed in a PRISMA [Preferred Reporting Items for Systematic Reviews and Meta-Analyses] flow diagram in Multimedia Appendix 1) ensured the inclusion of the latest high-quality research articles relevant to pharmacological mechanism and repurposing strategies.

Data Annotation With CoT-Prompt Engineering

Owing to the lack of annotated datasets for drug repositioning knowledge extraction, we constructed an annotated corpus from 1000 PubMed abstracts mentioned earlier. The prompt was evaluated on DeepSeek-R1 [45] via CoT [46], which required LLMs to generate coherent intermediate reasoning steps leading to a final answer [47].

We summarized the execution steps and proposed a task-specific prompt as follows and outlined them in Multimedia Appendix 2.

- Step 1: Role assignment and task description. Initialized the LLM as a biomedical annotation specialist, explicitly defining the drug repositioning schema and incorporating k-shot demonstrations to establish contextual understanding of target entities and semantic relationships.
- Step 2: Identification of entity and relationship types. Identified candidate entity types and contextual relationship types in text according to predefined schema.
- Step 3: Entity and relationship annotation. Based on the categories identified in step 2, this step extracted specific entities (eg, “Metformin” as *drug*, *“Diabetes” as disease*) and their contextual relationships (eg, *treats*) from text.
- Entity annotation principles. (1) Nonoverlapping: A single string cannot be assigned to multiple entity types. (2) Nonnesting: An entity should not contain another entity within its span. (3) Minimal punctuation and conjunction: Entities should exclude unnecessary punctuation or connecting words.
- Relationship annotation principles. (1) Intrasentence priority: Triplets within a single sentence are preferred; cross-sentence triplets are permitted only if no valid intrasentence relation exists. (2) Unidirectional relations: Only 1 directional relation is retained between any 2 related entities.
- Step 4: Triplets construction. Extracted drug repositioning entities and their contextual associations into semantically coherent triplets.
- Step 5: Output format standardization. Specified the output format and standards, setting clear expectations for the output as {Entity1; Type1; Relationship; Entity2; Type2} in JSON format.

To ensure the quality of the DrugReC, we manually reviewed the standard results from 1000 abstracts as well. A total of 3 annotators in pharmacology, clinical medicine, and bioinformatics were recruited, with 2 conducting cross-review and the third senior expert adjudicating conflicting or ambiguous cases. The corpus was subsequently partitioned into a training set (n=800) for RL algorithm development and a test set (n=200) to evaluate model generalizability. The remaining 9000 abstracts were used as training data for SFT.

Long Chain-of-Thought

LLM Deployment

The Qwen2.5-7B-Instruct model [48], developed by Alibaba Cloud, represented a significant advancement in the Qwen series of LLMs, specifically optimized for semantic comprehension and complex task processing. This 7-billion-parameter transformer-based architecture demonstrated exceptional performance in specialized applications, including knowledge extraction [49] and conversational interaction [50] scenarios. Meanwhile, an extended context window of 128,000 tokens facilitated precise capture of fine-grained semantic features within textual data.

For the Qwen2.5-7B-Instruct setup, we used temperature sampling with the parameter of 0.02. A lower temperature parameter can limit the model to make excessive creative jumps, thus ensuring accurate and consistent outputs. Meanwhile, we set the max_token parameter to 16,384 while leaving all other hyperparameters at their default values. The used hyperparameters during model training included a training batch size of 8, a learning rate of 1e−6, a cutoff length of 16,384, and a gradient accumulation step of 1. The model was trained on the Wuwen Xinqiong platform. Training the 7B model with 8× NVIDIA A100 40GB GPUs took approximately 40 hours, with a total cost of approximately 1000 RMB (US $140.47).

XSL•FO
RenderX

Cold-Start SFT

To address the output incoherence and unstable reasoning patterns caused by directly initializing RL [51] in foundation LLMs, we implemented cold-start SFT [52] with CoT data from 9000 PubMed literature as mentioned earlier. These domain-specific annotated triplets were used to optimize model parameters under a supervised learning framework, enabling the model to progressively acquire human-aligned reasoning patterns. This phase implemented multistep reasoning paths and strict output formats, significantly enhancing the model's complex problem decomposition capacity and intermediate step interpretability. In brief, the approach of cold-start SFT provided stable initialization for subsequent RL stages.

RL Algorithm

To reduce the training costs associated with RL, we used GRPO to further optimize reasoning paths through self-iteration in an unannotated environment [53]. Specifically, GRPO generated multiple candidate outputs {o1,o2,…oG} from the old policy πθold and then optimized the policy model πθ by maximizing the following objective:

(1)JGRPO(θ)=E[∑i=1G(min(πθ(oi|q)πθold(oi|q)Ai,clip(πθ(oi|q)πθold(oi|q),1−ε,1+ε)Ai)−βDKL(πθ||πref)]

(2)DKL(πθ||πref)=πθref(oi|q)πθ(oi|q)−logπθref(oi|q)πθ(oi|q)−1

and the advantage Ai was defined as follows:

(3)Ai=(ri−μgroup)/σgroup

where ri was the raw reward for the *i*th answer and μgroup and σgroup represented the mean and SD, respectively, of rewards within the candidate outputs. The group-wise contrastive mechanism mitigated absolute reward scale bias while encouraging high-quality reasoning.

For the task of drug repositioning knowledge extraction, this optimization process facilitated complex cognitive mechanisms based on a high-performance RL training framework, EasyR1 [54], leading to enhancement of task-specific reasoning performance.

Reward Modeling

Subsequently, we proposed a novel dual-reward mechanism specifically for drug repositioning knowledge extraction to guide model self-evolution. This mechanism integrates 2 complementary reward types: (1) an accuracy reward targeting factual correctness in entity and triplet extraction and (2) a structural format reward focusing on the integrity and interpretability of the model's reasoning process through structured tag compliance.

Accuracy Reward Mechanism

This mechanism established a multidimensional evaluation that compares model outputs with annotated references. Dynamic scoring rules for entity recognition and triplet extraction are presented in Table 1.

According to these scoring rules, the accuracy reward was as follows:

(4)Racc=αSentity+βStriplet+γSrare

where Sentity was accuracy reward of entity recognition, Stripletwas accuracy reward of triplet extraction, and Srare was reward of rare entity or relationship. This hierarchical award mechanism effectively balanced comprehensiveness and granularity in drug repositioning knowledge extraction.

Table . Scoring rules of accuracy reward.

Reward factor and detail	Reward mechanism
Entity recognition	
Exact match: boundary and type fully consistent	Score rewarded (+)
Partial overlap: correct type with boundary overlap	Partial rewarded (+)
False positive: misrecognition and false negative: omission	No score (0)
Triplet extraction	
Correct triplet	Score rewarded (+)
Dependency error: incorrect entity in relation	No score (0)
Others	
Rare entity/relationship	Score rewarded (+)

Structural Format Reward

To enhance the model's step-by-step reasoning, we also introduced an XML tag–guided mechanism (Table 2) that enforced structured output. It was required to encapsulate complete reasoning processes within "<think>……</think>" tags and nested <step> tags, enabling multilevel logical decomposition.

According to these scoring rules, the structural format reward was as follows:

(5)Rfmt=δStag+εSlength

where Stag was format reward of tag integrity and Slength was format reward of thinking length. This approach ensured machine-parsable outputs while enhancing the interpretability of inference pathways.

XSL•FO
RenderX

Table . Scoring rules of structural format reward.

Reward factor and detail	Reward mechanism
Tag integrity	
Missing/redundant tags	No score (0)
Tag closure disorder: closing tag appears before opening tag	No score (0)
Thinking length	
Underlength/overlength content	No score (0)

In-Depth Evaluation and Comparison

To comprehensively assess the performance of LCoDR-KE, we conducted an in-depth analysis.

First, comparative experiments were conducted to benchmark LCoDR-KE against traditional machine learning models (eg, CRF), general-purpose pretrained models (BERT), domain-specific biomedical models (BioBERT), and state-of-the-art LLMs, including ChatGPT-4, Llama3, QIANWEN, and variants with different parameter scales. These comparative analyses served to validate the effectiveness of our proposed model against established benchmarks, thereby highlighting its superior performance in addressing specialized biomedical knowledge extraction problems.

Second, ablative experiments were designed to evaluate the individual contributions of the key technological advancements, including high-quality data-driven prompt engineering and LCoT reasoning mechanism. By removing or substituting these modules, the study quantified their independent contributions and synergistic effects on task performance.

Finally, we conducted an error analysis by manually reviewing 100 randomly selected abstracts from the model outputs to identify common types of mistakes and areas for future algorithmic improvements.

Meanwhile, we used precision, recall, and F_1-score for model evaluations. Precision quantifies the proportion of correct identifications among all model predictions, reflecting the reliability of positive results. Recall evaluates the coverage for true positive instances, indicating the comprehensiveness of knowledge extraction. The F_1-score, as the harmonic mean of precision and recall, provides a balanced assessment that mitigates the impact of omissions and false extraction, thereby offering a comprehensive evaluation. For rigorous validation, we compared model outputs against manually annotated corpus using exact string matching, which ensured high quality of model performance.

Ethical Considerations

This study did not involve human participants or animal experiments. All data used in the research, including biomedical literature and structured databases, were publicly available and deidentified before analysis. Therefore, ethics approval was not required in accordance with institutional and international research ethics policies.

Results

Knowledge Representation for Drug Repositioning

Drug repositioning schema (summarized in Multimedia Appendix 3) encompassed 11 entity categories, including core entities (drug, disease, and target) along with extended dimensions, such as side effect, gene, biomarker, symptom, complication, anatomical structure, clinical examination, and treatment. Furthermore, 18 relationship categories were defined in detail to comprehensively characterize semantic features among multilevel entities, such as “treat...,” “is target of,” “is side_effect of,” “is biomarker of.” This framework substantially enhanced semantic representation capabilities and facilitated the discovery of latent associations in drug repositioning research.

Statistics of DrugReC

Via defined prompt engineering and manual review, we constructed a high-quality DrugReC, specially for drug repurposing text mining. This corpus, annotated from 1000 PubMed abstracts, contained 11 entity types and 18 relationship types closely related to drug repositioning. After the concordance test and revision, a total of 9329 entities and 4879 triplets consisted of this standard dataset (presented in Table 3). Among the entity types, *disease* (19.10%) and *drug* (15.80%) were the most frequently represented, followed by *anatomy* (13.62%), *test* (10.32%), and *biomarker* (10.26%). Less prevalent but critical categories included *complication*, *target*, *treatment*, *symptom*, *gene*, and *side effect*. Regarding knowledge triplets, *is_examination_for* (18.16%), *treat* (17.20%), and *is_biomarker_of* (17.16%) together accounted for more than half of all triplets, emphasizing the corpus’s focus on clinically relevant associations. This distribution reflected DrugReC’s design to support comprehensive text mining efforts in drug repositioning by capturing key therapeutic and diagnostic linkages. We have made this corpus publicly available on GitHub with Apache License version 2.0, providing a high-quality data foundation to advance biomedical informatics mining.

Then, this dataset was randomly divided at the document level into training (80%) and test (20%) subsets, with detailed statistical characteristics of both partitions provided in Tables 3 and 4.

XSL•FO
RenderX

Table . Statistics of entities in training and test set.

Entity type	Total, n (%)	Training set, n (%)	Test set, n (%)
disease	1782 (19.10)	1426 (19.11)	356 (19.08)
drug	1474 (15.80)	1179 (15.80)	295 (15.81)
anatomy	1271 (13.62)	1017 (13.63)	254 (13.61)
test	963 (10.32)	770 (10.32)	193 (10.34)
biomarker	957 (10.26)	766 (10.26)	191 (10.24)
complication	644 (6.90)	515 (6.90)	129 (6.91)
target	583 (6.25)	466 (6.24)	117 (6.27)
treatment	561 (6.01)	449 (6.02)	112 (6.00)
symptom	490 (5.25)	392 (5.25)	98 (5.25)
gene	362 (3.88)	290 (3.89)	72 (3.86)
side effect	242 (2.59)	194 (2.60)	48 (2.57)
Total	9329 (100)	7463 (100)	1866 (100)

Table . Statistics of triplets in training and test set.

Relationship type[a]	Total, n (%)	Training set, n	Test set, n
is_examination_for	886 (18.16)	709	177
treat	839 (17.20)	671	168
is_biomarker_of	837 (17.16)	670	167
complication_of	618 (12.67)	494	124
is_located_in	579 (11.87)	463	116
is_symptom_of	449 (9.20)	359	90
is_target_of	349 (7.15%)	279	70
is_side_effect_of	303 (6.21)	242	61
increases_expression_of	19 (0.39%)	15	4
Total	4879 (100)	3903	976

[a]Each relationship included bidirectional relationships between head and tail entities.

Knowledge Extraction With Different Types

LCoDR-KE achieved an overall F_1 score of 81.46%. High performance was observed for the most frequent entity types, including drug (F_1=95.83%) and disease (F_1=90.52%), likely due to their distinct semantic boundaries and abundant contextual representations. Mid-range performance was observed for anatomy (82.38%) and test (82.11%), while categories such as gene (74.70%), complication (73.93%), and biomarker (72.03%) showed moderate degradation. The lowest entity F_1 scores occurred for target (64.05%) and treatment (67.21%), not solely due to lower frequency but likely due to greater semantic ambiguity and overlapping usage with other types. Performances are detailed in Table 5.

Triplet extraction yielded an overall F_1 score of 70.39% (Table 6). The model excelled on treat relations (F_1=84.47%) and is_target_of (74.73%), which may benefit from clearer syntactic patterns. In contrast, performance declined for is_biomarker_of (57.69%) and increases_expression_of (50.00%), reflecting both data sparsity and higher contextual variability.

Performance differences can largely be attributed to variations in data distribution, semantic complexity, and context dependency, rather than entity or relation frequency alone. These findings suggested that targeted data augmentation, finer-grained annotation, or context-aware modeling strategies may further improve performance across challenging categories.

XSL•FO
RenderX

Table . Performance of entity extraction.

Entity type	Precision (%)	Recall (%)	F_1 (%)
ALL	83.37	79.64	81.46
drug	95.44	96.23	95.83
disease	90.88	90.16	90.52
anatomy	84.23	80.60	82.38
test	82.98	81.25	82.11
side_effect	76.79	84.31	80.37
gene	64.58	88.57	74.70
complication	87.16	64.19	73.93
biomarker	75.74	68.67	72.03
symptom	66.19	76.67	71.04
treatment	70.94	63.85	67.21
target	81.67	52.69	64.05

Table . Performance of triplet extraction.

Relationship type	Precision (%)	Recall (%)	F_1 (%)
ALL	73.94	67.17	70.39
treat	87.74	81.44	84.47
is_target_of	82.93	68.00	74.73
is_located_in	77.10	70.63	73.72
is_symptom_of	64.84	73.45	68.88
is_examination_for	70.47	65.63	67.96
is_side_effect_of	67.80	66.67	67.23
complication_of	80.95	55.56	65.89
is_biomarker_of	60.98	54.74	57.69
increases_expression_of	66.67	40.00	50.00

Performance Comparisons

Performance Comparison With State-of-the-Art Models

To evaluate the performance, we compared our LCoDR-KE model with several state-of-the-art models, including CRF (machine learning model), BERT (general-purpose pretrained language model), BioBERT (domain-specific biomedical model), and LLMs, including DeepSeek-R1, QIANWEN, and variants with varying parameter scales. These LLMs were evaluated under a 5-shot setting, consistent with the configuration used for our LCoDR-KE model. This ensured a fair comparison under equivalent prompt-based conditions. Detailed hyperparameter settings for each model are provided in Multimedia Appendix 4.

The comparative evaluation against state‐of‐the‐art baselines (Table 7) demonstrated that LCoDR-KE delivered substantial advances in both entity and triplet extraction. Classical sequence learners, such as CRF, scored poorly (entity F_1=29.18%; triplet F_1=14.51%), while general‐purpose pretrained models (eg, BERT, BioBERT) achieved modest gains (entity F_1≈37%; triplet F_1≈30%). The Qwen2.5-7B variant improved entity extraction (F_1=53.16%) but remained weak on triplets (F_1=18.04%). In contrast, LCoDR-KE-0.5B reached 62.67% entity F_1 and 35.05% triplet F_1, and the 7B model further advanced to 81.46% and 69.04%.

Notably, at 7B parameters, LCoDR-KE approached DeepSeek-R1's entity F_1 (81.46% vs 84.64%) and marginally exceeded its triplet F_1 (69.04% vs 69.02%). Although LCoDR-KE did not surpass DeepSeek-R1, it reached a similar level of effectiveness under a smaller parameter scale (7B vs 671B).

We further evaluated the OpenBioLLM-70B, which achieved an entity F_1 of 59.66% (precision: 56.63%; recall: 63.04%) and a triplet F_1 of 16.52% (precision: 13.92%; recall: 20.31%). In contrast, our LCoDR-KE-7B model achieved notably higher performance with 81.46% (precision: 83.37%; recall: 79.64%) in entity extraction (21.8 percentage points increase) and 69.04% (precision: 72.43%; recall: 65.96%) in triplet extraction (52.5 percentage points increase).

XSL•FO
RenderX

Table . Performance comparisons of different models.

Models	Entity extraction			Triplet extraction		
	Precision (%), mean (SD)	Recall (%), mean (SD)	F_1 (%), mean (SD)	Precision (%), mean (SD)	Recall (%), mean (SD)	F_1 (%), mean (SD)
Deepseek-R1	83.5 (0.082)	85.81 (0.065)	84.64[a] (0.034)	72.36 (0.040)	65.98 (0.079)	69.02[b] (0.096)
CRF[c]	35.65 (0.038)	24.7 (0.004)	29.18 (0.087)	18.21 (0.035)	12.06 (0.007)	14.51 (0.014)
BERT[d]	41.38 (0.085)	32.92 (0.095)	36.67 (0.084)	32.55 (0.014)	28.5 (0.004)	30.39 (0.061)
BioBERT	44.27 (0.097)	31.87 (0.019)	37.06 (0.050)	33.62 (0.004)	27.97 (0.016)	30.54 (0.004)
Qwen2.5-7B	51.75 (0.027)	54.64 (0.076)	53.16 (0.019)	16.15 (0.027)	20.44 (0.091)	18.04 (0.029)
LCoDR-KE[e]-0.5B	67.63 (0.072)	58.38 (0.046)	62.67 (0.024)	36.52 (0.083)	33.69 (0.051)	35.05 (0.018)
LCoDR-KE-1.5B	74.84 (0.055)	74.31 (0.038)	74.57 (0.085)	53.3 (0.062)	50.44 (0.007)	51.83 (0.037)
LCoDR-KE-3B	83.37 (0.006)	79.64 (0.069)	81.46[f] (0.018)	72.43 (0.067)	65.96 (0.043)	69.04[g] (0.094)
LCoDR-KE-7B	83.37 (0.024)	79.640.046)	81.46[f] (0.012)	72.43 (0.023)	65.96 (0.091)	69.04[g] (0.082)

[a]Best performance for entity extraction.

[b]Second-best performance for relationship extraction.

[c]CRF: conditional random fields.

[d]BERT: Bidirectional Encoder Representations From Transformers.

[e]LCoDR-KE: long chain-of-thought for drug repositioning knowledge extraction.

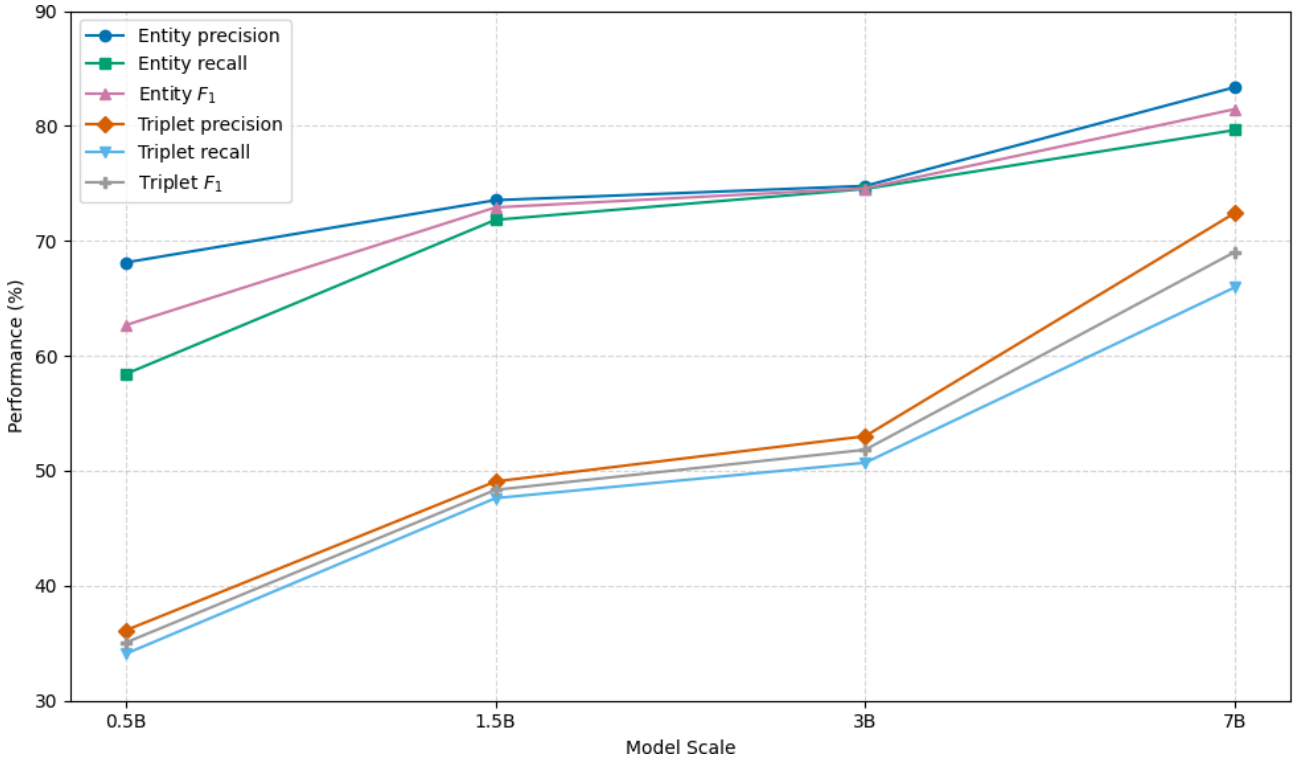
[f]Second-best performance for entity extraction.

[g]Best performance for relationship extraction.

Impact of Model Scale on Extraction Performance

Across the LCoDR-KE series (Figure 2), increasing model capacity from 0.5B to 1.5B, 3B, and 7B yielded consistent performance improvements, with entity F_1 rising from 62.67% to 72.91%, 74.57%, and 81.46%, triplet F_1 rising from 35.05% to 48.34%, 51.83%, and 69.04%, respectively. These gains suggested that larger models better capture the complex contextual dependencies required for accurate biomedical knowledge extraction.

Figure 2. Performance of LCoDR-KE across different model scales (0.5B, 1.5B, 3B, 7B) on biomedical entity and triplet extraction tasks. Larger models yielded better precision, recall, and F_1-scores. LCoDR-KE: long chain-of-thought for drug repositioning knowledge extraction.



XSL•FO
RenderX

Ablation Studies

To evaluate the contributions of different components within the LCoDR-KE model, we conducted ablation studies to examine the impact of strongly SFT and the LCoT model on knowledge extraction outcomes for drug repositioning. We removed the 2 components of the LCoDR-KE model to observe changes in performance.

As presented in Table 8, the ablation studies demonstrated significant performance degradation when removing either SFT or GRPO module. Removing GRPO reduced F_1-scores by 6.09% for entity extraction and 14.09% for triplet extraction, indicating that GRPO substantially enhances knowledge extraction. In comparison, removing SFT caused sharper declines in precision (8.61% for entities and 20.70% for triplets), underscoring the critical role of task - specific supervision in adapting pretrained representations. Together, these results demonstrated that both components contribute synergistically to the model's knowledge extraction capabilities, with GRPO enhancing reasoning and SFT improving supervised alignment. Meanwhile, the absence of SFT caused more pronounced degradation in both entity and triplet extraction, indicating its broader influence on model performance (Figure 3).

Table . Ablation study results: precision, recall, and F_1-scores for different components of LCoDR-KE[a].

Ablation models	Entity extraction			Triplet extraction		
	Precision (%)	Recall (%)	F1 (%)	Precision (%)	Recall (%)	F1 (%)
LCoDR-KE$_{\text{-w/o GRPO}}$[b]	76.53	74.25	75.37	54.58	55.33	54.95
LCoDR-KE$_{\text{-w/o SFT}}$[c]	73.80	71.93	72.85	49.35	47.38	48.34
LCoDR-KE	83.37	79.64	81.46	72.43	65.96	69.04

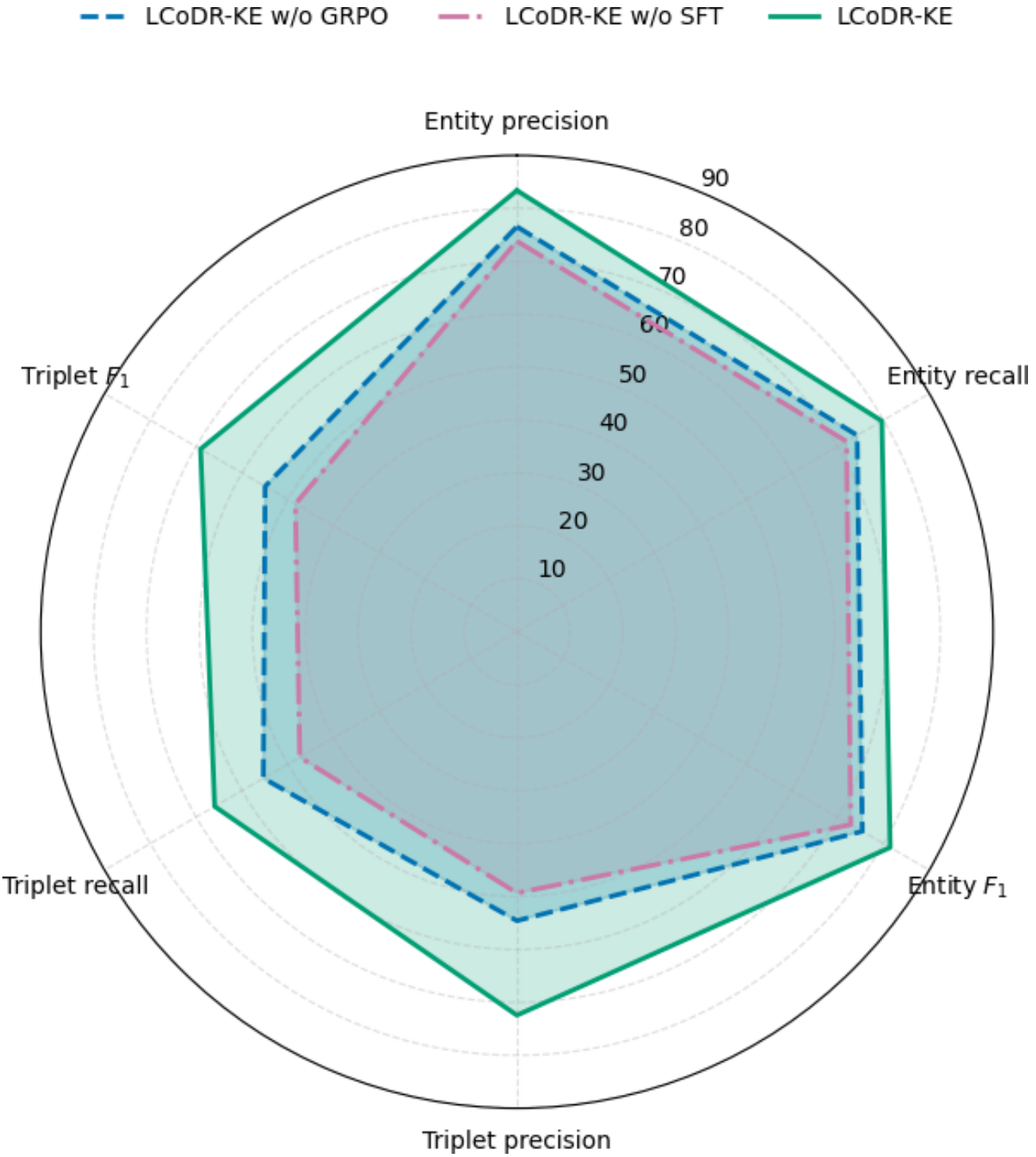
[a]LCoDR-KE: long chain-of-thought for drug repositioning knowledge extraction.

[b]GRPO: Group Relative Policy Optimization.

[c]SFT: supervised fine-tuning.

XSL•FO
RenderX

Figure 3. Radar chart comparing the full LCoDR-KE model with its ablation variants (without Group Relative Policy Optimization [GRPO] and without supervised fine-tuning [SFT]) across 6 evaluation metrics. Both the GRPO and SFT modules significantly enhanced performance, with SFT contributing more broadly across precision and F_1-scores, especially for triplet extraction. LCoDR-KE: long chain-of-thought for drug repositioning knowledge extraction.



External Benchmark Evaluation

To further assess generalizability beyond our in-domain DrugReC corpus, we evaluated LCoDR-KE directly on the widely used BC5CDR benchmark, which comprises 500 PubMed abstracts manually annotated for chemical (drug) and disease entities and their binary associations. OpenBioLLM-70B achieved entity F_1 of 47.39% and relation F_1 of 25.52%, while DeepSeek-R1 scored 60.93% and 38.33%, respectively. Without additional fine-tuning, LCoDR-KE obtained an entity F_1 of 59.17% (precision: 85.92%; recall: 45.12%) and a triplet F_1 of 35.16% (precision: 33.84%; recall: 36.59%), closely matching DeepSeek-R1 and substantially outperforming OpenBioLLM-70B. Thus, our method demonstrated generalizability beyond in-domain abstracts, achieving robust performance on external biomedical corpora such as BC5CDR.

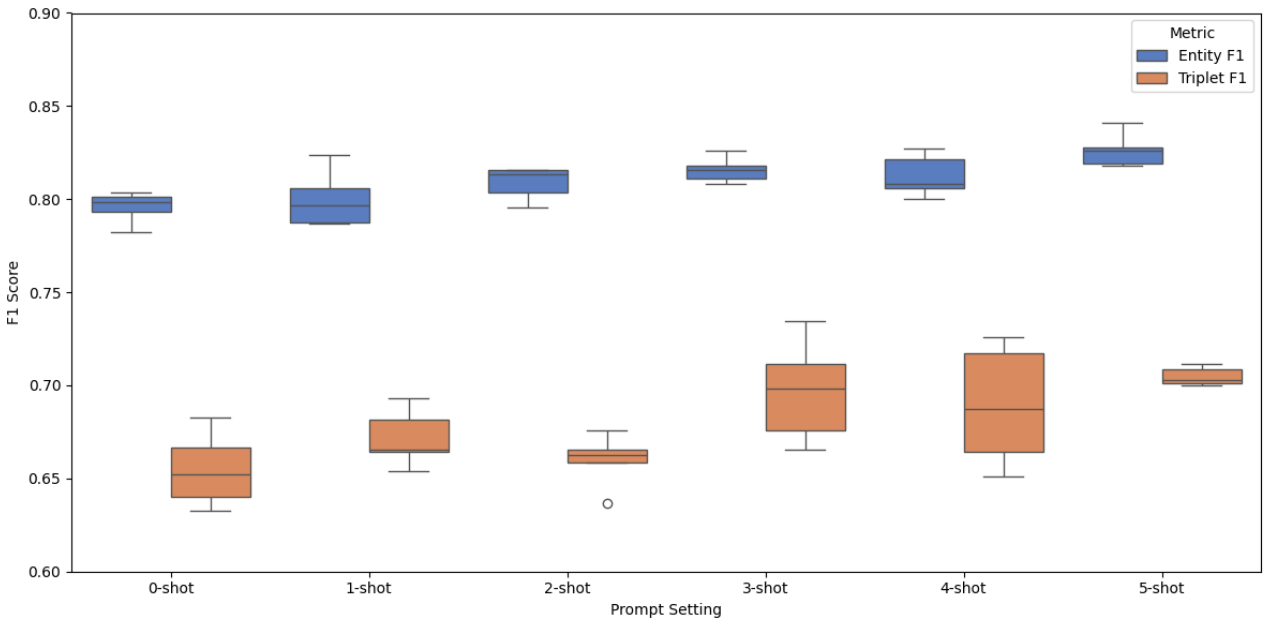
Effect of K-Shot Examples on Model Performance

To evaluate the impact of prompt on corpus generating, we conducted a small-scale experiment comparing 0- to 5-shot

XSL•FO
RenderX

prompting settings. As shown in Figure 4, k-shot prompting consistently outperformed the 0-shot baseline in both entity and triplet extraction. Entity F_1 rose from 80.01 (0 shot) to 82.63 (5 shots), while triplet F_1 increased from 67.16 to 70.48. Performance steadily improved as the number of examples increased, particularly between 1 shot and 3 shots. Notably, the model achieved stable and high performance in the 3- to 5-shot range, suggesting that moderate prompt context enhances annotation quality.

Figure 4. Effect of k-shot prompting on entity and triplet extraction performance. F_1-scores for entity and triplet extraction across 0- to 5-shot settings. Performance improved with more shots and stabilizes between 3 shots and 5 shots.



Reward Parameter Optimization

To optimize the reward function for knowledge extraction and structured reasoning, we used a progressive tuning strategy through multiple rounds of controlled experiments. The reward formulation includes a hierarchical accuracy component where the coefficients for entity recognition (α), triplet extraction (β), and rare entity/relation enhancement (γ) satisfy the constraint $\alpha + \beta + \gamma = 1$. Given the high computational cost of jointly searching in a 3D space, we adopted a 2-stage approach. We first optimized α and β under the constraint $\alpha + \beta = 1$ to balance entity- and relation-level performance. Once optimal base weights were identified, we introduced γ by gradually adjusting the proportion of reward allocated to rare cases. Subsequently, we adjusted the weights associated with structured reasoning, namely tag integrity (δ) and reasoning length (ε), to ensure syntactic validity and controlled verbosity in the model's output. Finally, we calibrated the overall balance between accuracy-related rewards and format-related rewards by modifying the global weight of accuracy reward and format reward parameters.

In addition, we introduced 2 top-level coefficients (ie, accuracy reward weight and format reward weight) to control the relative contribution of accuracy-based and format-based rewards in the overall objective. These weights were jointly tuned to ensure a trade-off between extraction performance and output structure quality.

Throughout the process, evaluation was based on both entity and relation F_1-scores, as well as the structural completeness of generated outputs (Multimedia Appendix 5). The final parameter configuration, with α=.45, β=.45, γ=0.1, δ=0.7, ε=0.3, accuracy reward=0.5, and format reward=0.5, demonstrated optimal performance in terms of extraction accuracy, robustness, and output interpretability and was therefore adopted in subsequent experiments.

Interpretable CoT Reasoning Patterns

To evaluate whether the model engaged in structured reasoning, we examined its CoT outputs during knowledge extraction. We gave an example (Table 9) to demonstrate that the model performed structured, schema-aware reasoning beyond pattern matching. It explicitly validated entity types, rejected schema-incompatible relations, and enforced output constraints, ultimately generating a compliant JSON structure. The complete example of CoT is summarized in Multimedia Appendix 6.

XSL•FO
RenderX

Table . Structured chain-of-thought reasoning example from LCoDR-KE[a].

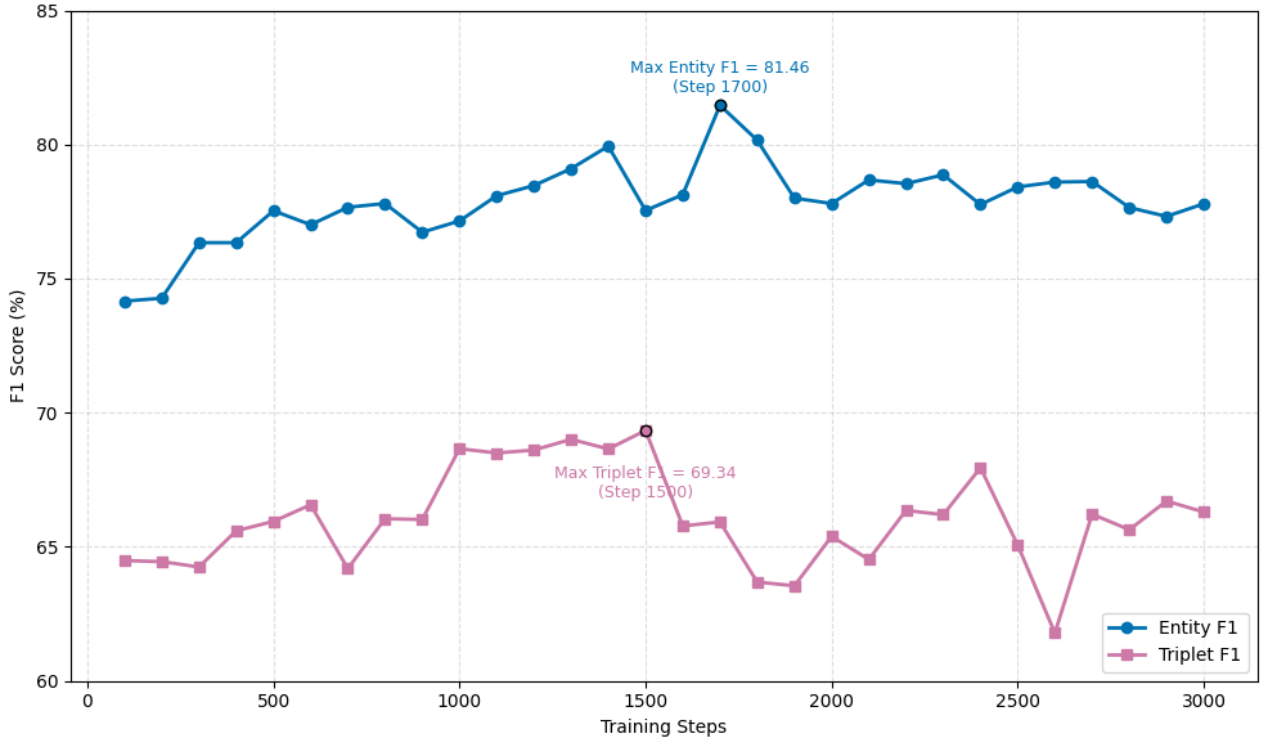
Reasoning step	Model output (excerpt)
Task framing	"Alright, I'm approaching this task as a biomedical knowledge extraction assistant. I need to systematically identify entities and relationships from the predefined types."
Entity identification	"cetuximab' clearly fits the Drug definition as a therapeutic agent; 'colorectal cancer' → Disease; 'infusion reactions' → Side Effect; 'ER visit' → Treatment..."
Entity filtering	"'medical intervention' is too vague–not entity material;..."
Relation reasoning	"'cetuximab' causes 'infusion reactions' → is_side_effect_of; 'cetuximab' treats 'colorectal cancer' → treat..."
Schema constraints	"Rejected is_examination_for between ER and IRs – not diagnostic; did not create invented relations like 'discontinued_due_to'..."
Formatting awareness	"Ensured JSON format with two root keys (Entities and Relationships); original casing preserved; no explanatory text embedded..."

[a]LCoDR-KE: long chain-of-thought for drug repositioning knowledge extraction.

Step of Training Iterations

We also monitored the performance across 30 training iterations (from 100 to 3000 steps) using F_1 metrics (Figure 5) and showed a steady and stable improvement in Entity F_1, which reached a peak of 81.46% at the level of 1700. Notably, Entity F_1 remained consistently high beyond 2000 iterations without significant decline, indicating robust and stable convergence in the entity recognition task. Triplet F_1 reached its highest value of 69.34% at step 1500 and exhibited a slight decrease in subsequent iterations; however, it consistently stayed above 65%, suggesting that the model maintained a strong baseline for triplet extraction. This relatively stable performance postpeak indicated the potential for further optimization with continued training or minor adjustments. Overall, these results demonstrated the effectiveness and stability of the training approach, particularly for entity recognition while also highlighting a promising and resilient trajectory for triplet extraction performance. Detailed performances across training iterations are provided in Multimedia Appendix 7.

Figure 5. Entity and triplet F1 performance across 30 training iterations (100 - 3000 steps). Entity F_1 steadily improved and peaked at 81.46% (step 1700), maintaining stability thereafter. Triplet F_1 reached a maximum of 69.34% (step 1500) and remained consistently above 65%, indicating robust and stable model convergence for both extraction tasks.



XSL•FO
RenderX

Error Analysis

We conducted an error analysis by manually reviewing 100 randomly selected sentences from the model outputs to identify common types of mistakes and areas for improvement.

Error Examples

The errors were classified into 4 main types of entity extraction (ie, incorrect extraction, incorrect type, boundary errors, and missing entities) and 2 main types of triplet extraction (incorrect entity type and cross-sentence errors), with examples summarized in Table 10.

Table . Main error types in LCoDR-KE[a].

Error types	Definition	Sentences	Truth extraction	LCoDR-KE extraction
Entity extraction				
Incorrect extraction	Nonentity terms were incorrectly identified as entities	Available therapies are effective, associated with severe side effects.	NULL	[severe side effects, side effect]
Incorrect type	Entities were correctly identified but assigned the wrong entity type	In nearly half of cancer cells, there is an overexpression of MDM2 and MDMX, which inhibit p53 activity.	[p53, gene]	[p53, target]
Boundary errors	Which involved incorrect determination of the start and end positions of entities	The expression of BRCA1 and BRCA2 mutations was analyzed in the cohort.	[BRCA2, gene]	[BRCA2 mutations, gene]
Missing entities	Entities present in the text were not identified by the model	Other lung findings were ... or extensive hemorrhage.	[extensive hemorrhage, complication]	NULL
Triplet extraction				
Incorrect entity type	Relationships were correctly identified but assigned the wrong entity type	Docetaxel and gemcitabine might result in fewer adverse events.	NULL	[adverse events, side effect, is side effect of, Docetaxel, drug]
Cross- sentence error	Unable to recognize logical relationships across sentences	62% of subjects exhibited recurrent gastrointestinal distress (eg, nausea). Subsequent serological testing confirmed elevated anti-tTG antibodies, a hallmark of celiac disease.	[nausea, symptom, is symptom of, celiac disease, disease]	NULL

[a]LCoDR-KE: long chain-of-thought for drug repositioning knowledge extraction.

Error Statistics

We further quantified the frequency of each error type to assess their impact and guide future improvement strategies.

For entity extraction:

1. Incorrect extraction (n=10, 38.46%): This was the most common error, typically caused by semantically ambiguous phrases. For example, generic terms such as “severe side effects” were incorrectly extracted due to superficial similarity to defined entity types.
2. Incorrect type (n=6, 23.08%): These errors occurred when the model misclassified closely related concepts, such as mislabeling “p53” as a target instead of a gene.
3. Boundary errors (n=4, 15.38%): Often caused by inclusion of modifiers like “mutations” in entity spans, resulting in misaligned entity boundaries.
4. Missing entities (n=6, 23.08%): Frequently occurred when entities were embedded in complex phrases or lacked explicit semantic cues, leading to omission.

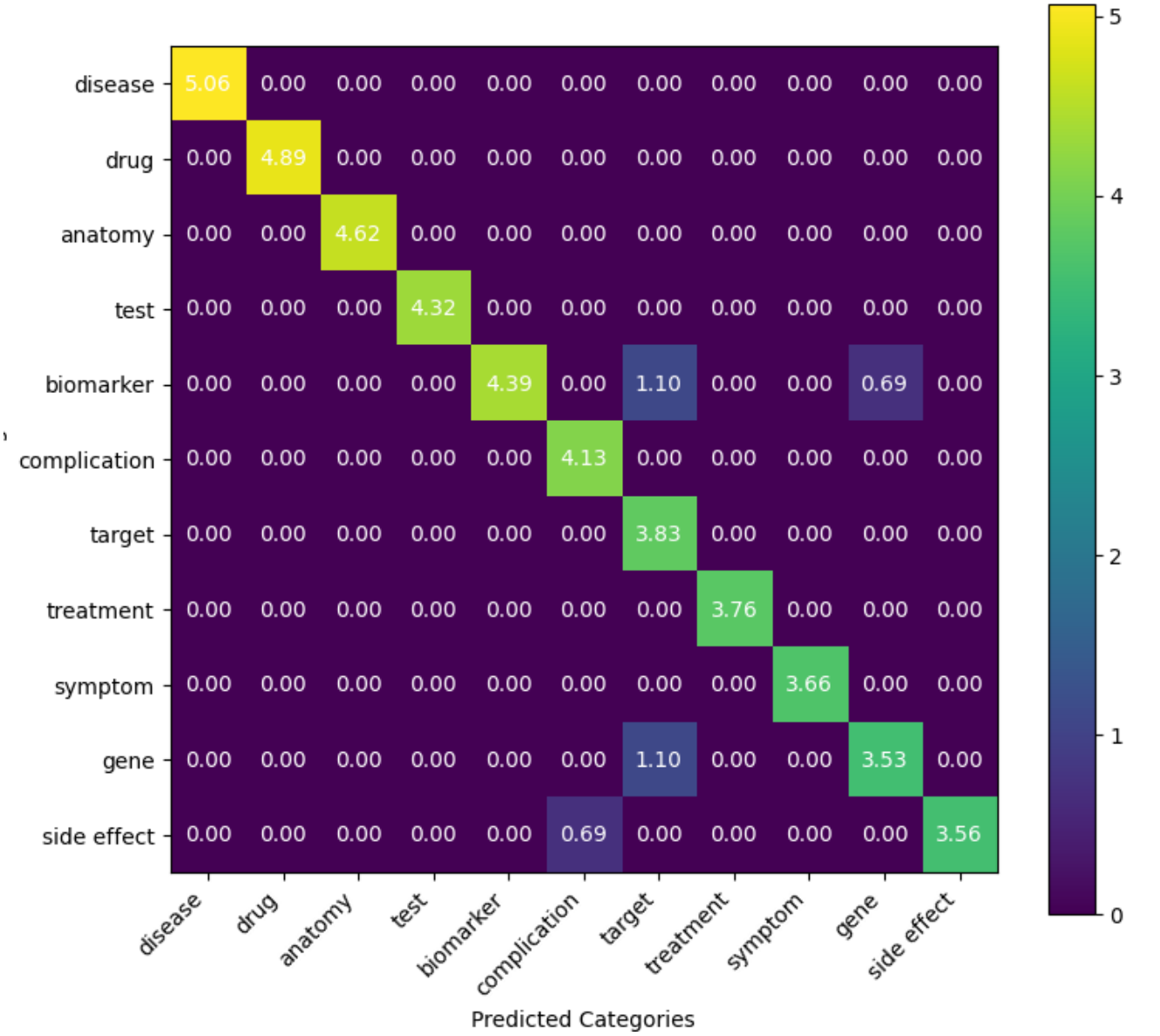
For triplet extraction:

1. Incorrect entity type (n=5, 38.46%): The relationship was correctly identified, but the entity types were misclassified (eg, “adverse events” mislabeled as side effect instead of a nonentity).
2. Cross-sentence error (n=8, 61.54%): The model failed to capture logical relationships spanning multiple sentences, especially when the subject and object were not co-located in the same sentence.

To further investigate the model’s behavior on entity classification, we constructed a confusion matrix (Multimedia Appendix 8) based on entity predictions. The results (Figure 6) showed strong diagonal dominance, indicating high accuracy across most entity types. However, misclassifications persist among semantically similar categories. Specifically, the biomarker was confused with the target (2 cases) and gene (1 case), while gene was misclassified as the target twice. In addition, 1 side effect instance was incorrectly labeled as a complication. These errors reflected the model’s difficulty in distinguishing biologically related concepts with overlapping semantics. In contrast, core categories, such as drug and disease, were classified with perfect accuracy.

XSL•FO
RenderX

Figure 6. Confusion matrix of entity type classification results (log-normalized). This log-scaled confusion matrix illustrated the model's entity classification performance across 11 biomedical entity types. Diagonal dominance indicated high overall accuracy, while off-diagonal cells highlight common misclassifications. Notably, errors were concentrated among semantically similar categories, such as biomarker, gene, and target.



Comparisons Between LCoDR-KE and DeepSeek-R1

Meanwhile, LCoDR-KE demonstrated comparable performance with DeepSeek-R1. Specifically, LCoDR-KE surpassed DeepSeek-R1 in the categories of incorrect type (6 vs 8), missing entity (6 vs 7), and incorrect entity type (5 vs 6). This advantage can be attributed to our meticulous definition of entities and relations for the drug repurposing task, as well as the provision of accurate examples during model training. Conversely, LCoDRKE performed slightly worse in the Incorrect Extraction (10 vs 8) and CrossSentence Error (8 vs 7) categories, indicating that its complex contextual understanding and reasoning capabilities warrant further improvement.

Discussion

Principal Findings

In this study, we introduced LCoDR-KE, a novel framework for drug repositioning knowledge extraction that significantly enhanced the adaptive learning capabilities of LLMs.

The effectiveness of our approach stemmed from 2 key innovations.

- First, we developed a refined semantic representation framework and used it to curate a high-quality training corpus, DrugReC, comprising 1000 expertly annotated abstracts. These annotations covered diverse drug repositioning entities and captured complex semantic relationships, providing a robust foundation for the model to learn accurate semantic understanding and contextual reasoning.

XSL•FO
RenderX

- Second, we proposed a long reasoning chain strategy: an iterative, multistep inference process reinforced through reward mechanisms and RL. By delivering explicit feedback at each reasoning step, this strategy enabled the model to progressively optimize its decision-making process, resulting in more accurate and coherent inference.

Collectively, these innovations contributed to the improved performance of LCoDR-KE in extracting drug repositioning knowledge.

Compared to pretraining approaches specifically designed for biomedical tasks, LCoDR-KE offered several advantages. Traditional methods typically required extensive domain adaptation, large annotated corpora, or multiple rounds of fine-tuning to achieve competitive performance [55]. In contrast, LCoDR-KE achieved performance optimization with a relatively small training dataset—comprising only 1000 literature abstracts—thereby significantly reducing the human and time costs associated with domain-specific annotation. Furthermore, LCoT decomposed semantic understanding into explicit and traceable reasoning steps. This approach mitigated hallucinations and enhanced model transparency, addressing 2 major challenges in the application of LLMs. Our ablation study further substantiated these findings.

Moreover, performance comparisons demonstrated that LCoDR-KE based on the Qwen-2.5-7B model matched the performance of the 671B -parameter DeepSeek-R1 in drug repurposing knowledge extraction. Specifically, F_1-scores achieved 81.46% versus 84.64% for entity extraction and 69.04% versus 69.02% for triplet extraction. This advance significantly narrowed the gap between large-scale models and resource-constrained environments, making it a practical solution for research institutes and hospital information centers with modest computing capabilities.

In addition to performance gains, LCoDR-KE enhanced model interpretability through CoT prompting. By generating intermediate reasoning steps, such as entity justification, schema validation, and relation filtering, the model made its decision process more transparent and traceable. This structured reasoning not only aided error diagnosis but also aligned model behavior with domain knowledge constraints, offering a more controllable and explainable framework for biomedical knowledge extraction.

Our expanded error analysis provided a more nuanced understanding of model behavior in biomedical knowledge extraction. By categorizing common error types, quantifying their frequency, and visualizing entity-level confusion patterns, we identified key challenges such as semantic ambiguity, long-range dependencies, and data sparsity. These insights not only explained performance bottlenecks but also informed future improvements, such as targeted data augmentation and schema-aware prompt refinement to reduce ambiguity and improve generalization.

LCoDR-KE demonstrated strong performance in low-resource settings through its schema design, cold-start SFT, and RL with a reward mechanism. It provides an efficient and feasible solution for biomedical knowledge extraction under resource-constrained conditions. In clinical research settings, LCoDR-KE could be deployed to mine structured knowledge from trial protocols, real-world evidence, or adverse event reports, assisting clinicians in therapeutic decision-making and safety monitoring. In early-stage drug development, it can support target identification and biomarker discovery by extracting mechanistic insights from scientific literature. Its lightweight design makes it particularly well suited for integration into domain-specific platforms where computational resources and labeled data are limited. Moreover, its task-specific schema could be readily tailored by redefining entities and relations, thereby accommodating new domains, languages, and even alternative LLM backbones. Its flexibility allowed LCoDR-KE to extend beyond drug repositioning to a broad range of biomedical knowledge extraction tasks.

Limitations

Despite the promising results, our study has some limitations. First, we limited the task to drug repositioning in this study. In the future, we will include other biomedical knowledge extraction tasks, such as gene–disease association identification and drug–drug interaction detection, thereby expanding its application value in diverse scenarios. Second, the model's balance between reasoning depth and computational efficiency remains suboptimal, particularly when processing intricate biomedical contexts requiring multistep logical inferences. Future optimizations will focus on lightweight architectural improvements.

Conclusions

This study introduced LCoDR-KE, a framework that enhanced LLMs' domain-specific adaptability for drug repositioning by integrating long-chain reasoning and RL. We constructed a publicly available DrugReC and a lightweight knowledge extraction model, offering critical resources for accelerating drug discovery and knowledge inference. The framework balances accuracy, interpretability, and computational efficiency, validated through stable training convergence and competitive performance against state-of-the-art models. Overall, LCoDR-KE not only advances drug repositioning research but also provides a scalable, transferable methodology applicable to diverse biomedical knowledge extraction tasks, knowledge reasoning, and even decision support, bridging gaps in low-resource, specialized domains.

Acknowledgments

This research was funded by the National Social Science Fund of China (Grant No. 22CTQ024).

XSL•FO
RenderX

Data Availability

The proposed corpus dataset and source code during this study are publicly available [56].

Authors' Contributions

HK performed the experiments, analyzed the results, and wrote the manuscript. JL analyzed the results. LH, XX, and SZ collected the data. QL directed the whole study, supervised the experiments, and revised the manuscript. All authors have reviewed and approved the final version of the manuscript for publication.

Conflicts of Interest

None declared.

Multimedia Appendix 1
List of drug repositioning journal and PRISMA (Preferred Reporting Items for Systematic reviews and Meta-Analyses) guidelines.
[DOCX File, 75 KB - medinform_v13i1e77837_app1.docx]

Multimedia Appendix 2
Chain-of-thought prompt.
[TXT File, 10 KB - medinform_v13i1e77837_app2.txt]

Multimedia Appendix 3
Drug repositioning schema.
[XLSX File, 13 KB - medinform_v13i1e77837_app3.xlsx]

Multimedia Appendix 4
Hyperparameters of fine-tuned models.
[DOCX File, 14 KB - medinform_v13i1e77837_app4.docx]

Multimedia Appendix 5
Reward weight.
[XLSX File, 12 KB - medinform_v13i1e77837_app5.xlsx]

Multimedia Appendix 6
Reasoner.
[TXT File, 2 KB - medinform_v13i1e77837_app6.txt]

Multimedia Appendix 7
Performance across training iterations.
[XLSX File, 11 KB - medinform_v13i1e77837_app7.xlsx]

Multimedia Appendix 8
Confusion matrix.
[XLSX File, 9 KB - medinform_v13i1e77837_app8.xlsx]

References

1. Aljofan M, Gaipov A. Drug discovery and development: the role of artificial intelligence in drug repurposing. Future Med Chem 2024 Apr;16(7):583-585. [doi: 10.4155/fmc-2024-0048] [Medline: 38426289]
2. Vemula D, Jayasurya P, Sushmitha V, Kumar YN, Bhandari V. CADD, AI and ML in drug discovery: a comprehensive review. Eur J Pharm Sci 2023 Feb 1;181:106324. [doi: 10.1016/j.ejps.2022.106324] [Medline: 36347444]
3. Pei Y, Yang J. Biomedical applications of big data and artificial intelligence. Bioengineering (Basel) 2025 Feb 19;12(2):207. [doi: 10.3390/bioengineering12020207] [Medline: 40001726]
4. Shah-Mohammadi F, Finkelstein J. Utilizing RAG and GPT-4 for extraction of substance use information from clinical notes. Stud Health Technol Inform 2024 Nov 22;321:94-98. [doi: 10.3233/SHTI241070] [Medline: 39575787]
5. Xue X, Wu ME, Khan F. Biomedical information integration via adaptive large language model construction. IEEE J Biomed Health Inform 2024;29(9):6381-6394. [doi: 10.1109/JBHI.2024.3496495] [Medline: 37027681]
6. Kang H, Hou L, Gu Y, Lu X, Li J, Li Q. Drug-disease association prediction with literature based multi-feature fusion. Front Pharmacol 2023;14:1205144. [doi: 10.3389/fphar.2023.1205144] [Medline: 37284317]

XSL•FO
RenderX

7. Bang D, Lim S, Lee S, Kim S. Biomedical knowledge graph learning for drug repurposing by extending guilt-by-association to multiple layers. Nat Commun 2023 Jun 15;14(1):3570. [doi: 10.1038/s41467-023-39301-y] [Medline: 37322032]
8. Huang K, Chandak P, Wang Q, et al. A foundation model for clinician-centered drug repurposing. Nat Med 2024 Dec;30(12):3601-3613. [doi: 10.1038/s41591-024-03233-x] [Medline: 39322717]
9. Wang Y, Wang L, Rastegar-Mojarad M, et al. Clinical information extraction applications: a literature review. J Biomed Inform 2018 Jan;77:34-49. [doi: 10.1016/j.jbi.2017.11.011] [Medline: 29162496]
10. Krallinger M, Valencia A, Hirschman L. Linking genes to literature: text mining, information extraction, and retrieval applications for biology. Genome Biol 2008;9 Suppl 2(Suppl 2):S8. [doi: 10.1186/gb-2008-9-s2-s8] [Medline: 18834499]
11. Giorgi JM, Bader GD. Towards reliable named entity recognition in the biomedical domain. Bioinformatics 2020 Jan 1;36(1):280-286. [doi: 10.1093/bioinformatics/btz504] [Medline: 31218364]
12. Dai S, Ding Y, Zhang Z, Zuo W, Huang X, Zhu S. GrantExtractor: accurate grant support information extraction from biomedical fulltext based on Bi-LSTM-CRF. IEEE/ACM Trans Comput Biol Bioinform 2021;18(1):205-215. [doi: 10.1109/TCBB.2019.2939128] [Medline: 31494556]
13. Nghiem TT, Bousquet C. Named entity recognition in PubMed abstracts for pharmacovigilance using deep learning. Stud Health Technol Inform 2022 May 25;294:878-879. [doi: 10.3233/SHTI220615] [Medline: 35612234]
14. Lee J, Yoon W, Kim S, et al. BioBERT: a pre-trained biomedical language representation model for biomedical text mining. Bioinformatics 2020 Feb 15;36(4):1234-1240. [doi: 10.1093/bioinformatics/btz682] [Medline: 31501885]
15. Gu Y, Tinn R, Cheng H, et al. Domain-specific language model pretraining for biomedical natural language processing. ArXiv. Preprint posted online on Jul 31, 2020. [doi: 10.48550/arXiv.2007.15779]
16. Huang K, Altosaar J, Ranganath R. ClinicalBERT: modeling clinical notes and predicting hospital readmission. ArXiv. Preprint posted online on Apr 10, 2019. [doi: 10.48550/arXiv.1904.05342]
17. ValizadehAslani T, Shi Y, Ren P, et al. PharmBERT: a domain-specific BERT model for drug labels. Brief Bioinform 2023 Jul 20;24(4):bbad226. [doi: 10.1093/bib/bbad226] [Medline: 37317617]
18. Fraile Navarro D, Ijaz K, Rezazadegan D, et al. Clinical named entity recognition and relation extraction using natural language processing of medical free text: a systematic review. Int J Med Inform 2023 Sep;177:105122. [doi: 10.1016/j.ijmedinf.2023.105122] [Medline: 37295138]
19. Yang J, Zhang T, Tsai CY, Lu Y, Yao L. Evolution and emerging trends of named entity recognition: bibliometric analysis from 2000 to 2023. Heliyon 2024 May;10(9):e30053. [doi: 10.1016/j.heliyon.2024.e30053]
20. Yenduri G, Ramalingam M, Selvi GC, et al. Generative pre-trained transformer: a comprehensive review on enabling technologies, potential applications, emerging challenges, and future directions. ArXiv. Preprint posted online on May 11, 2023. [doi: 10.1109/access.2024.3389497]
21. Touvron H, Lavril T, Izacard G, et al. LLaMA: open and efficient foundation language models. ArXiv. Preprint posted online on Feb 27, 2023. [doi: 10.48550/arXiv.2302.13971]
22. Du Z, Qian Y, Liu X, et al. GLM: general language model pretraining with autoregressive blank infilling. ArXiv. Preprint posted online on Mar 18, 2021. [doi: 10.48550/arXiv.2103.10360]
23. Bai J, Bai S, Chu Y, et al. Qwen technical report. ArXiv. Preprint posted online on Sep 28, 2023. [doi: 10.5260/chara.21.2.8]
24. DeepSeek-AI DG, Yang D, et al. DeepSeek-R1: incentivizing reasoning capability in llms via reinforcement learning. ArXiv. Preprint posted online on Jan 22, 2025. [doi: 10.48550/arXiv.2501.12948]
25. Zhang Y, Yang Y, Ren L, et al. RDscan: extracting RNA-disease relationship from the literature based on pre-training model. Methods 2024 Aug;228(228):48-54. [doi: 10.1016/j.ymeth.2024.05.012] [Medline: 38789016]
26. Hao J, Chen Z, Peng Q, et al. Prompt framework for extracting scale-related knowledge entities from Chinese medical literature: development and evaluation study. J Med Internet Res 2025 Mar 18;27:e67033. [doi: 10.2196/67033] [Medline: 40100267]
27. Hou Y, Bert C, Gomaa A, et al. Fine-tuning a local LLaMA-3 large language model for automated privacy-preserving physician letter generation in radiation oncology. Front Artif Intell 2024;7(7):1493716. [doi: 10.3389/frai.2024.1493716] [Medline: 39877751]
28. Yamagishi Y, Nakamura Y, Hanaoka S, Abe O. Large language model approach for zero-shot information extraction and clustering of Japanese radiology reports: algorithm development and validation. JMIR Cancer 2025 Jan 23;11:e57275. [doi: 10.2196/57275] [Medline: 39864093]
29. Hu Y, Chen Q, Du J, et al. Improving large language models for clinical named entity recognition via prompt engineering. J Am Med Inform Assoc 2024 Sep 1;31(9):1812-1820. [doi: 10.1093/jamia/ocad259] [Medline: 38281112]
30. Li PH, Sun YY, Juan HF, Chen CY, Tsai HK, Huang JH. A large language model framework for literature-based disease-gene association prediction. Brief Bioinform 2024 Nov 22;26(1):bbaf070. [doi: 10.1093/bib/bbaf070] [Medline: 39998433]
31. Xie Q, Chen Q, Chen A, et al. Medical foundation large language models for comprehensive text analysis and beyond. NPJ Digit Med 2025 Mar 5;8(1):141. [doi: 10.1038/s41746-025-01533-1] [Medline: 40044845]
32. Luo R, Sun L, Xia Y, et al. BioGPT: generative pre-trained transformer for biomedical text generation and mining. Brief Bioinform 2022 Nov 19;23(6):bbac409. [doi: 10.1093/bib/bbac409] [Medline: 36156661]
33. Pal A, Sankarasubbu M. OpenBioLLMs: advancing open-source large language models for healthcare and life sciences. Hugging Face. 2024. URL: https://huggingface.co/aaditya/OpenBioLLM-Llama3-70B [accessed 2025-10-01]

XSL•FO
RenderX

34. Yuan Z, Zhang S, Zhang H, Xie P, Jia Y. Optimized drug-drug interaction extraction with BioGPT and focal loss-based attention. IEEE J Biomed Health Inform 2025 Jun;29(6):4560-4570. [doi: 10.1109/JBHI.2025.3540861] [Medline: 40031603]
35. Sarumi OA, Heider D. Large language models and their applications in bioinformatics. Comput Struct Biotechnol J 2024 Dec;23:3498-3505. [doi: 10.1016/j.csbj.2024.09.031] [Medline: 39435343]
36. Sahoo SS, Plasek JM, Xu H, et al. Large language models for biomedicine: foundations, opportunities, challenges, and best practices. J Am Med Inform Assoc 2024 Sep 1;31(9):2114-2124. [doi: 10.1093/jamia/ocae074] [Medline: 38657567]
37. Gu Z, Jia W, Piccardi M, Yu P. Empowering large language models for automated clinical assessment with generation-augmented retrieval and hierarchical chain-of-thought. Artif Intell Med 2025 Apr;162(162):103078. [doi: 10.1016/j.artmed.2025.103078] [Medline: 39978047]
38. Chen X, Wang L, You M, et al. Evaluating and enhancing large language models' performance in domain-specific medicine: development and usability study with DocOA. J Med Internet Res 2024 Jul 22;26:e58158. [doi: 10.2196/58158] [Medline: 38833165]
39. Cao L, Sun J, Cross A. An automatic and end-to-end system for rare disease knowledge graph construction based on ontology-enhanced large language models: development study. JMIR Med Inform 2024 Dec 18;12:e60665. [doi: 10.2196/60665] [Medline: 39693482]
40. Gu Y, Xu Z, Yang C. Empowering graph neural network-based computational drug repositioning with large language model-inferred knowledge representation. Interdiscip Sci 2025 Sep;17(3):698-715. [doi: 10.1007/s12539-024-00654-7] [Medline: 39325266]
41. Rauf A, Joshi PB, Olatunde A, et al. Comprehensive review of the repositioning of non-oncologic drugs for cancer immunotherapy. Med Oncol 2024 Apr 23;41(5):122. [doi: 10.1007/s12032-024-02368-8] [Medline: 38652344]
42. Cirinciani M, Da Pozzo E, Trincavelli ML, Milazzo P, Martini C. Drug mechanism: a bioinformatic update. Biochem Pharmacol 2024 Oct;228:116078. [doi: 10.1016/j.bcp.2024.116078] [Medline: 38402909]
43. Tripathi S, Gupta E, Galande S. Statins as anti-tumor agents: a paradigm for repurposed drugs. Cancer Rep (Hoboken) 2024 May;7(5):e2078. [doi: 10.1002/cnr2.2078] [Medline: 38711272]
44. Zhang W, Yue X, Lin W, et al. Predicting drug-disease associations by using similarity constrained matrix factorization. BMC Bioinformatics 2018 Jun 19;19(1):233. [doi: 10.1186/s12859-018-2220-4] [Medline: 29914348]
45. Yang D, DeepSeek-AI, Guo D, Zhang H, Song J. DeepSeek-R1: incentivizing reasoning capability in llms via reinforcement learning. ArXiv. Preprint posted online on Jan 22, 2025. [doi: 10.48550/arXiv.2501.12948]
46. Wei J, Wang X, Schuurmans D, et al. Chain of-thought prompting elicits reasoning in large language models. ArXiv. Preprint posted online on Jan 28, 2022. [doi: 10.48550/arXiv.2201.11903]
47. Xu T, Gu Y, Xue M, Gu R, Li B, Gu X. Knowledge graph construction for heart failure using large language models with prompt engineering. Front Comput Neurosci 2024;18:1389475. [doi: 10.3389/fncom.2024.1389475] [Medline: 39015745]
48. Yang A, Yang B, Hui B, Zheng B, Yu B, et al. Qwen2 technical report. ArXiv. Preprint posted online on Jul 15, 2024. [doi: 10.48550/arXiv.2407.10671]
49. Xiao Z, Pakrasi HB, Chen Y, Tang YJ. Network for Knowledge Organization (NEKO): an AI knowledge mining workflow for synthetic biology research. Metab Eng 2025 Jan;87:60-67. [doi: 10.1016/j.ymben.2024.11.006] [Medline: 39580108]
50. Qin Z, Wu D, Zang Z, Chen X, Zhang H, Wong CUI. Building an intelligent diabetes Q&A system with knowledge graphs and large language models. Front Public Health 2025;13:1540946. [doi: 10.3389/fpubh.2025.1540946] [Medline: 40051508]
51. Kumar A, Zhuang V, Agarwal R, Su Y, Co-Reyes J, et al. Training language models to self-correct via reinforcement learning. ArXiv. Preprint posted online on Oct 4, 2024. [doi: 10.48550/arXiv.2409.12917]
52. Belém F, Cunha W, França C, Andrade C, Rocha L, et al. A novel two-step fine-tuning pipeline for cold-start active learning in text classification tasks. ArXiv. Preprint posted online on Jul 24, 2024. [doi: 10.48550/arXiv.2407.17284]
53. Sheng G, Zhang C, Ye Z, et al. HybridFlow: a flexible and efficient RLHF framework. ArXiv. Preprint posted online on Sep 28, 2024. [doi: 10.1145/3689031.3696075]
54. EasyR1: an efficient, scalable, multi-modality RL training framework. GitHub. URL: https://github.com/hiyouga/EasyR1 [accessed 2025-09-23]
55. Wang A, Liu C, Yang J, Weng C. Fine-tuning large language models for rare disease concept normalization. J Am Med Inform Assoc 2024 Sep 1;31(9):2076-2083. [doi: 10.1093/jamia/ocae133] [Medline: 38829731]
56. LCODR-KE: long chain-of-thought for drug repositioning knowledge extraction. GitHub. URL: https://github.com/kang-hongyu/LCoDR-KE [accessed 2025-10-01]

Abbreviations

CoT: chain-of-thought
CRF: conditional random fields
DrugReC: drug repositioning corpus
GRPO: Group Relative Policy Optimization
LCoDR-KE: drug repositioning knowledge extraction model based on long chain-of-thought
LCoT: long chain-of-thought

XSL•FO
RenderX

LLM: large language model
MeSH: Medical Subject Headings
PRISMA: Preferred Reporting Items for Systematic Reviews and Meta-Analyses
RL: reinforcement learning
SFT: supervised fine-tuning

Edited by A Coristine; submitted 21.05.25; peer-reviewed by KH Lin, N Acharya, S Sharma; revised version received 03.09.25; accepted 03.09.25; published 07.10.25.

Please cite as:
Kang H, Li J, Hou L, Xu X, Zheng S, Li Q
Large Language Model–Enhanced Drug Repositioning Knowledge Extraction via Long Chain-of-Thought: Development and Evaluation Study
JMIR Med Inform 2025;13:e77837
URL: https://medinform.jmir.org/2025/1/e77837
doi:10.2196/77837

© Hongyu Kang, Jiao Li, Li Hou, Xiaowei Xu, Si Zheng, Qin Li. Originally published in JMIR Medical Informatics (https://medinform.jmir.org), 7.10.2025. This is an open-access article distributed under the terms of the Creative Commons Attribution License (https://creativecommons.org/licenses/by/4.0/), which permits unrestricted use, distribution, and reproduction in any medium, provided the original work, first published in JMIR Medical Informatics, is properly cited. The complete bibliographic information, a link to the original publication on https://medinform.jmir.org/, as well as this copyright and license information must be included.

XSL•FO
RenderX

Clinical Information Extraction From Notes of Veterans With Lymphoid Malignancies: Natural Language Processing Study

Lu He[1], PhD; Matthew R Moldenhauer[2], MD; Kai Zheng[3,4], PhD; Helen Ma[5,6], MD

[1]Zilber College of Public Health, University of Wisconsin-Milwaukee, Milwaukee, WI, United States

[2]School of Medicine, University of California, San Diego, San Diego, CA, United States

[3]Department of Informatics, Donald Bren School of Information and Computer Science, University of California, Irvine, Irvine, CA, United States

[4]Department of Emergency Medicine, University of California, Irvine, Irvine, CA, United States

[5]Veterans Affairs Health System, 5901 E 7th Street, Long Beach, CA, United States

[6]School of Medicine, University of California Irvine, Irvine, CA, United States

Corresponding Author:
Helen Ma, MD
Veterans Affairs Health System, 5901 E 7th Street, Long Beach, CA, United States

Abstract

Background: Clinical natural language processing (cNLP) techniques are commonly developed and used to extract information from clinical notes to facilitate clinical decision-making and research. However, they are less established for rare diseases such as lymphoid malignancies due to the lack of annotated data as well as the heterogeneity and complexity of how clinical information is documented. In addition, there is increasing evidence that cNLP techniques may be prone to biases embedded in clinical documentation or model development. These biases can result in disparities in performance when extracting clinical information or predicting patient outcomes.

Objective: This study aims to report the development and validation of a cNLP pipeline that extracts clinical information such as performance status, staging, and diagnosis, as well as less common information such as substance use and military environmental exposures, from the clinical notes of veterans with lymphoid malignancies.

Methods: We developed a rule-based cNLP pipeline that integrates domain expertise. We tested and compared the performance of the cNLP pipeline on notes from 2 veteran patient cohorts: one from non-Hispanic White veterans and the other from non-Hispanic Black veterans.

Results: Overall, our pipeline achieved promising performance on our study data, especially for extracting entities that have standard clinical documentation, such as performance status. We also found that while the pipeline has robust performance across the two patient groups, the false-positive and false-negative rates were significantly associated with race for detecting the primary diagnosis (P=.001 for both); the false-negative rate was significantly associated with race for identifying substance use (P=.02).

Conclusions: The system exhibits satisfying and comparable performance for most clinical entities of interest except for (1) the primary diagnosis and (2) substance use. Future work will address the challenges encountered in developing and deploying the cNLP pipeline on the Department of Veterans Affairs data for rare cancers and enhance the performance of cNLP systems to avoid biases.

(JMIR Med Inform 2025;13:e63908) doi:10.2196/63908

KEYWORDS

natural language processing; NLP; clinical informatics; rare cancer; developing; validating; clinical information extraction; veterans; lymphoid malignancies; clinical documentation; non-Hispanic White; non-Hispanic Black

Introduction

Clinical notes contain rich information about patients' conditions and disease trajectories. As it is often tedious and time-consuming for clinicians to perform a manual chart review to retrieve such information, clinical natural language processing (cNLP) has served as a crucial tool to automate the process of extracting clinical elements from unstructured notes [1]. While cNLP is an established field with mature software such as the clinical Text Analysis and Knowledge Extraction System and Clinical Language Annotation, Modeling, and Processing, there is a lack of cNLP resources for extracting information from clinical notes of patients with rare cancers [2], which may be due to the difficulty of obtaining high-quality annotation data from rare disease experts.

Lymphoid malignancies (LMs) are rare cancers with only around 145,000 patients diagnosed in the United States per year [3-7]. Among US veterans who were deployed overseas, exposure to

XSL•FO
RenderX

environmental toxicants and chemical agents is a risk factor associated with LMs [8]. There is a need to capture past environmental exposures of veterans to better care for them. For example, the Promise to Address Comprehensive Toxics (PACT) Act, which passed in 2022, expands health care benefits and assists clinical research for veterans who have been exposed to environmental toxicants [9]. While the need for identifying and caring for veterans with environmental exposures increases, such information is often not well captured in structured electronic health records (EHRs). In fact, most of the clinical information that is vital to clinicians' decision-making is embedded in free-text, unstructured clinical notes [10]. Therefore, there is a need to develop cNLP tools that are specifically tailored to and validated on clinical notes for rare cancers so that they can capture unique clinical information. To the best of our knowledge, there is no existing cNLP pipeline or model that has been developed for and validated on clinical notes of LMs.

In this study, we developed and validated a rule-based cNLP pipeline to extract diagnoses, staging, performance status, substance use, and environmental exposures from clinical notes of veterans with LMs. We further assessed whether the cNLP pipeline may be prone to biases by comparing its performance on non-Hispanic White and Black patients. Finally, we discuss the opportunities and challenges of developing cNLP pipelines for extracting information from clinical notes of patients with LMs and implications for clinical documentation.

Methods

Data Source and Creating the Development Set

We extracted records of veterans diagnosed with LMs—as defined by the *International Classification of Diseases for Oncology, Third Edition*—from the Department of Veterans Affairs (VA) Corporate Data Warehouse (CDW) [11] (summarized in Multimedia Appendix 1). The VA CDW includes patient records from 173 medical centers within the VA system across the United States as well as clinics in Puerto Rico, Guam, and the Philippines, capturing different practice and documentation patterns [12]. In total, 80,245 patients were identified using the *International Classification of Diseases for Oncology, Third edition*. The development set included a random sample of 287 deidentified hematology and oncology clinic notes from veterans with LMs in the VA system after removing 13 duplicates from the initial 300 notes. The hematology and oncology notes contained the most relevant clinical information and were intended to reduce annotators' burdens.

Clinical Entities of Interest

We annotated and extracted the following clinical entities that were known to be prognostic in the care of patients with LMs but were often inconsistently documented in a structured format using a standardized dictionary:

1. Diagnosis: primary diagnosis related to LMs
2. Substance use: alcohol, drug, and tobacco use
3. Environmental exposure: Agent Orange, Vietnam, shipyards, and Marine Corps Base Camp Lejeune according to the PACT Act
4. Staging: stage, chronic lymphocytic leukemia Rai staging and Binet staging, the multiple myeloma International Staging System, and lymphoma Ann Arbor staging
5. Performance status: performance status, Karnofsky performance status (KPS), and Eastern Cooperative Oncology Group (ECOG) performance status

Annotation and Scoring

Clinicians annotated according to an annotation guideline, provided in Multimedia Appendix 2. The annotation guideline was continuously improved during the annotation process and aimed to capture common and recurring documentation patterns rather than a comprehensive list of documentation. Two independent medical experts annotated a random sample of 100 notes from the development set to calibrate. The interrater agreement ratio was calculated, and disagreements were discussed and resolved to finalize the annotation protocol. The annotation task was formulated as selecting a text span that indicates a clinical entity of interest and selecting the entity label (eg, stage and performance status). Therefore, each annotated entity can be represented as having the following: (1) a label *L* and (2) a text span with starting and ending indices (*i*, *j*). Two annotated entities *M* and *N* are considered a match if Label (M) = Label (N) ^ relaxed_match (span (M), span (N)).

We calculated the span-based F_1-score for measuring the level of agreement between the two annotators, following previous studies [13-15]. The span-based F_1-score is preferable in this case because it is not affected by the number of true negatives, which are prevalent in span-based annotations [16]. We calculated the metrics for span-relaxed matches, where 2 text spans need to overlap for at least two-thirds of the length of the shortest span. The microaveraged F_1-score is 0.85; the detailed statistics across different entity types are presented in Table 1.

Table . Interrater agreement of 100 annotated notes in the development set.

	Precision	Recall	F_1-score
Primary diagnosis	0.89	0.79	0.84
Performance status	0.90	0.87	0.88
Staging	0.90	0.98	0.94
Substance use	0.66	0.90	0.76
Environmental exposure	0.64	0.70	0.67

XSL•FO
RenderX

The clinician annotators met regularly to discuss and resolve disagreements and adjust the annotation guidelines accordingly. After reaching consensus, they proceeded to annotate the remainder of the development set, test set 1, and test set 2. The annotation task was formulated as named entity extraction, where annotators selected a text span and labeled it with a clinical entity such as diagnosis. For each note, there were multiple text spans with start and end indices and their associated clinical entity labels.

Confirmatory Test Sets

To develop and test the cNLP pipeline, we randomly selected 1000 patients from the patient cohort.

We included all the hematology and oncology notes of these patients, and these comprised notes from nurses, social workers, and pharmacists who document a wide range of information. This aimed to ensure that the cNLP pipeline we developed would not be tuned to work only on specific note types or from specific provider types. When constructing the test sets, we used 2 steps to compile the notes. First, from the patient cohort, we randomly selected 100 notes with at least 300 characters to ensure that they are long enough to contain useful information. After annotating a few notes, we noticed that for some clinical entities, especially performance status and environmental exposures, few notes mentioned them. Therefore, besides the 100 randomly selected notes, we also included notes that contained predefined keywords (eg, “ECOG” and “Agent Orange”) so that medical experts did not need to read notes without any clinical entities of interest. In this process, the random selection of notes helped to ensure the representativeness of the notes, and the use of keyword filtering helped to increase the recall and lower the annotator burden. This method of using keywords to prefilter notes had been used in previous work to extract infrequently documented information, such as housing eviction status, from clinical notes [17].

The first test set (test set 1) included 200 notes from all races and ethnicities, resulting in a sample of 89 notes with clinically relevant data from randomly selected non-Hispanic White patients. Given potential differences in documentation, we added a second group enriched for non-Hispanic Black patients. The second test set (test set 2) included a sample of 200 notes from randomly selected non-Hispanic Black patients, resulting in 106 notes containing clinically relevant data. The data selection and processing procedures are shown in Figure 1.

XSL•FO
RenderX

Figure 1. Procedure for constructing datasets for clinical natural language processing development and validation. *ICD-O-3*: *International Classification of Diseases for Oncology, Third Edition*; VA: Veterans Affairs.

XSL•FO
RenderX

Development of the cNLP Pipeline

The goal of the study was to develop a cNLP pipeline that can accurately extract clinical entities of interest without extensive annotations. Therefore, we did not perform a comprehensive evaluation of pretrained language models, as most were not developed on notes from patients with LMs and fine-tuning them will require more annotated data.

We tested 2 zero-shot large language models (LLMs), FLAN-T5 by Google and Llama2 by Meta, with carefully curated prompts to extract the clinical entities of interest. We did not test OpenAI's GPT models due to the sensitive nature of our data and the requirements of sending the input data to the commercial servers of OpenAI. The zero-shot LLMs also did not produce a satisfactory and consistent identification for the named entity recognition task, which was also observed in a recent evaluation conducted by Lu et al [18]. We found that Llama2 had difficulty following the instructions, and FLAN-T5 was only able to correctly identify 16 out of 137 incidences of performance status and 263 out of 1347 diagnosis mentions. We reviewed samples of errors and found that FLAN-T5 tended to hallucinate and made up text snippets that were not in the original clinical notes. This could be because FLAN-T5 and similar general domain LLMs were not pretrained on clinical notes or data that contain language related to performance status or LMs. Fine-tuning these LLMs will require larger datasets of clinical notes and more extensive instruction tuning and supervised fine-tuning and is beyond the scope of this study. Therefore, we decided to develop rule-based modules based on expert input. Despite the limitations of rule-based methods, they are still widely used and implemented on tasks such as identifying cognitive assessment tests and biomarkers from notes of patients with Alzheimer disease and Alzheimer disease–related dementias [19] and extracting risk factors for pancreatic cancer [20].

Development of a Rule-Based cNLP Pipeline

The cNLP pipeline was iteratively developed by examining annotated texts in the development set as well as consulting the clinical experts on the study team. For example, "ECOG," "KPS," and "Performance Status" were included in the dictionary of the pipeline to capture potential mentions of performance status. Similarly, "Stage," "Stg," and "Rai" were included to identify mentions of staging information. "Tobacco," "smoke," "alcohol," "drug," "etoh," and other commonly used terms were included to extract substance use mentions. For environmental exposures, we used both chemical agents, such as "Agent Orange," and locations that are known to have toxicants, such as "Vietnam" or "shipyard." All clinical notes were preprocessed by converting words to lowercase. Punctuation was preserved. We accounted for misspellings or format issues (eg, extra or missing spaces) by curating the regular expressions. Examples of the final regular expressions are provided in Multimedia Appendix 3.

We added special modules in the cNLP pipeline after matching regular expressions to account for the errors we observed in the training set. For the primary diagnosis and performance status, we observed that most false positives (FPs) were due to the prevalent use of templates (eg, in disability benefit questionnaires). We excluded matched diagnoses and performance status that were present in a template format ("[ ] Multiple Myeloma"; "() ECOG 1 () ECOG 2"). Excluding matches from templates reduced the number of FPs in our study sample. In addition, for the primary diagnosis, as the diagnosis process for LMs is commonly complex and often undergoes numerous laboratory tests and positron emission tomography scans, we excluded mentions of LMs that were documented as differentials or assessment plans and needed further confirmation. This step ensured that the final extracted primary diagnosis is confirmed and can be directly used for secondary analysis. For performance status, we required all possible matches of performance status to be followed by numeric values so that ambiguous expressions such as performance status for postscripts are excluded. For ECOG performance status, the numeric values must be between 0 (indicating fully active) and 5 (indicating death), and for KPS, the numeric values must be between 0 (indicating death) and 100 (indicating normal). This ensures that only text chunks that indicate performance status will be included so that FPs can be reduced.

For staging, we observed that most FPs were due to their irrelevance to our diagnosis of interests, and it was common for stages of multiple comorbidities to be documented (eg, stage II for chronic kidney disease). Therefore, we checked whether the staging information identified is within the window of a surrounding primary diagnosis. We experimented with multiple values of the size of the window to look for the primary diagnosis. The performances for extracting staging using different window sizes are provided in Multimedia Appendix 3. Overall, we observed that as the window size increased, both test sets had higher precision but lower recall. We selected a window size of 30, as the F_1-scores for both test sets were optimized. The window sizes also enable more flexible configuration of the pipeline, depending on whether the priority is to extract all potentially relevant staging information (a larger window size) or to only extract highly relevant staging information (a smaller window size).

For identifying environmental exposures, we used multiple rules informed by the development data, as well as VA's official PACT Act recommendation [9] to capture potential exposure, as exact documentation containing the names of chemical toxicants, such as Agent Orange, is limited and does not capture all potential exposures. We also included services and deployments that are potentially associated with exposures, including service in Vietnam or Camp Lejeune. Finally, we included locations that may expose patients to toxicants, including shipyards, infantry, and chemical plant factories.

Performance Evaluation

The extracted tokens were evaluated based on the lenient matching criteria used in previous work [21,22], that is, 2 tokens were deemed as a match if they overlapped, to account for potential annotation issues and format irregularities. Precision was calculated as true positives/(true positives + FPs) and recall was calculated as true positives/(true positives + false negatives [FNs]). F_1-score is (2 × precision × recall)/(precision + recall). Misclassified entities in the test set were extracted and analyzed manually by the medical experts to identify potential sources of errors to improve the performance of the cNLP pipeline.

XSL•FO
RenderX

We further assessed whether the pipeline was prone to bias on the test sets. In this study, we focused on racial bias, and in particular, potential biases between non-Hispanic White and Black patient populations. We conducted chi-square tests on FPs and FNs using the cNLP pipeline. The null hypothesis was that the cNLP performance, measured by FP and FN, was independent of the patients' race.

Ethical Considerations

This study was approved by the institutional review board (VA IRB #1618998 and UCI IRB #1041) at both the VA Long Beach Healthcare System and the University of California, Irvine. Research was conducted in accordance with the Declaration of Helsinki. Waivers of informed consent and HIPAA (Health Insurance Portability and Accountability Act) compliance were approved by the institutional review board.

Results

NLP Performance on the Test Sets

For each clinical entity, the precision, recall, and F_1-score were calculated and presented in Table 2. For entities that have clear standards for documentation such as performance status, the performance is higher (F_1-score>0.90). For entities that generally lack a documentation standard such as substance use or environmental exposures, we observed lower performance. In addition, the high precision and recall for some entities were possibly due to overfits of the manually tuned model, which is a common issue for rule-based pipelines.

Table . Clinical natural language processing performance on test set 1 (89 notes) and test set 2 (106 notes).

	Test set 1				Test set 2			
	Frequency	Precision	Recall	F_1-score	Frequency	Precision	Recall	F_1-score
Performance status	54	0.96	0.96	0.96	73	0.85	0.96	0.90
Staging	71	0.94	0.69	0.80	116	0.85	0.60	0.71
Primary diagnosis	277	0.70	0.93	0.80	485	0.60	0.85	0.70
Substance use	104	0.65	0.61	0.63	148	0.66	0.76	0.70
Environmental exposures	29	0.72	0.62	0.67	5	0.5	0.6	0.54

Bias Assessment

The results from chi-square tests showed that the performance of the cNLP pipeline was not statistically different across test sets 1 and 2 for performance status and staging. However, the cNLP pipeline's FN rate for extracting substance use is significantly associated with patients' race (χ^2_1=5.9; P=.02). The pipeline's FP rate for extracting the primary diagnosis is significantly associated with race (χ^2_1=10.2; P=.001), and the FN rate is also associated with race (χ^2_1=10.4; P=.001). We were unable to run the test on environmental exposures due to the small number of observations available (5/106, 4.7%). Detailed statistics and confusion matrices are provided in Multimedia Appendix 2.

Error Analysis

Table 3 presents example snippets of FPs and FNs.

Table . Example snippets of false positive (FP) and false negative (FN)[a].

	FP example	FN example
Performance status	"*ECOG 0 - 1*"	"*PS>2*"
Staging	"Chronic kidney disease *stage 3* Multiple myeloma"	"At least *Stage IIIA*"
Primary diagnosis	"likely prostate cancer and *CLL*"	"with kappa light chain *MM*"
Substance use	"8. *Tobacco/Marijuana Use*–smoking cigarettes again"	"*crack use*"
Environmental exposures	"combat exposure"	"worked as an exterminator"

[a]Italicized texts indicate misalignment between natural language processing extraction and annotation.

Our qualitative analysis reveals the following two major types of errors:

1. Lack of documentation standards: many of the FNs were caused by inconsistent documentation, especially for environmental exposures. For example, while the cNLP pipeline captured common mentions such as "Agent Orange," "service in Vietnam," and "chemical plant factory," exposure-related information was often documented in various ways that made it difficult for the cNLP pipeline to capture exhaustively. Furthermore, some clinicians used locations such as "shipyards" to imply

XSL•FO
RenderX

potential exposures to toxicants, while some explicitly listed the chemical toxicants, such as “asbestos.”

2. Implicit association with the primary diagnosis: while our efforts in associating staging information with surrounding mentions of the primary diagnosis effectively reduced the number of FPs (ie, incorrectly identifying staging information), the pipeline also resulted in FNs where relevant staging information was not captured because there was no primary diagnosis mentioned around it. In reviewing the errors, we observed that not all LM-related staging information was explicitly documented together with the primary diagnosis.

Discussion

Principal Findings

We developed a rule-based cNLP pipeline to identify mentions of clinical information, including diagnoses, performance status, staging, substance use, and environmental exposures from clinical notes of veterans with LMs. The pipeline can be used in our future studies to produce weak labels, which can serve as fine-tuning datasets to improve the performance of LLMs in the domain of LMs.

In the literature, a study that reported better performance in extracting staging and substance use information from notes of patients with cancer [23]. However, the majority of these studies only used radiology and pathology notes, which were generally more structured and did not contain other clinical information unrelated to cancer [2]. In our study, the wider range of notes authored by a wide range of health providers introduced additional challenges to accurately identify clinical entities of interest due to the heterogeneity of information and documentation styles of these notes. In addition, none of the existing studies focused on rare cancers such as LMs but were related to more prevalent cancer types such as breast cancer and lung cancer. Some clinical entities and their documentation were therefore inherently different from those for LMs. For example, breast cancer documentation uses TNM staging system (where T, N, and M stand for tumor, node, and metastasis, respectively) to record staging, which is standard for most solid tumors, while LM uses histology-specific staging, such as Ann Arbor and Rai staging. The semantic rules for capturing LM-specific staging information can be used for other studies that aim to extract staging information from notes of patients with LMs. In addition, the performance of our rule-based system in extracting performance status is also comparable with the performances reported in prior studies [23,24].

Challenges of Developing cNLP Systems for LMs

Through this study, we observed several challenges to the development of high-performing cNLP systems for LMs and other rare cancers. Future efforts in developing cNLP for rare cancers should consider addressing these challenges to improve performance, alleviate medical experts’ burden in annotation, and facilitate the use of cNLP in real-world clinical settings.

First, relevant clinical information on rare cancers may be documented across many different note types, which creates challenges for cNLP systems to consistently identify all of them. Previous work often focused on specific note types such as radiology reports to simplify system development, with the assumption that certain clinical information often appears in a narrow set of notes.

Second, the characteristics of certain clinical entities make it challenging to extract using cNLP. For example, environmental exposure information was rarely documented in clinical notes in our study. Sparse documentation thus makes it difficult to identify notes that include potentially relevant information for medical experts to annotate. In addition, the documentation of environmental exposure information is highly inconsistent, with many mentions directly naming substances (eg, Agent Orange) as well as alluding to potential exposures through locations (eg, shipyards and combat sites) or deployment (eg, Vietnam or Camp Lejeune). As environmental exposure documentation has not been a routine component in clinical documentation until very recently because of the PACT Act, there are no standards for consistently documenting such information and further compiling a high-quality dataset for training cNLP models to extract them. To the best of our knowledge, this is the first study that set out to develop and use NLP to extract potential military environmental exposures in accordance with the PACT Act, despite prior studies that directly used structured data to infer such exposures [25]. In our future work, we will assess to what extent the NLP-extracted exposures overlap with those inferred from structured data and whether NLP can identify additional exposed patients that structured data misses.

Third, the heterogeneity of clinical information also raises challenges for cNLP systems to accurately identify all relevant information. For example, while our cNLP pipeline showed decent performance in identifying the primary diagnosis, it was unable to identify the myriad of secondary and differential diagnoses for patients’ comorbidities that span a wide range of diseases such as prostate cancer and bladder cancer. Therefore, we prioritized our efforts on optimizing the primary diagnosis rather than secondary and differential diagnoses, which are also underexplored in existing cNLP efforts. In our future work, we will continue to refine the cNLP pipeline to identify the various types of diagnoses from clinical notes, including optimizing for the capture of secondary and differential diagnoses.

Fourth, while LLMs such as Bidirectional Encoder Representations from Transformers and Llama have demonstrated superior performance in many cNLP tasks, they appeared to have poor transferability in our study. This may be due in part to the characteristics of clinical information that were unique to rare cancers such as LMs and how notes were composed within the VA system. A more comprehensive and in-depth evaluation of general and clinical LLMs on clinical notes for rare cancers is therefore needed to assess their performance and transferability and identify ways to adapt them to rare cancers.

Assessing Biases in Applying NLP on Clinical Notes for Rare Diseases

The results of this study suggest potential biases in cNLP performance in extracting substance use and the primary diagnosis from the notes of non-Hispanic White veterans versus non-Hispanic Black veterans. Several strategies could be used

XSL•FO
RenderX

to mitigate such potential biases. First, it may be desirable to use standardized documentation, that is, the type of substance and frequency or duration of exposure, such as "tobacco use, 3 packs per day for 50 years." Second, researchers may consider alternative sampling methods when selecting notes and patient samples for developing cNLP methods, especially when the patient population is already heavily dominated by patients with certain characteristics, such as older White adults in our patient cohort.

Clinical Impacts

The PACT Act aims to provide benefits for veterans who have been exposed to environmental toxicants that are associated with cancer diagnosis and progression, but we found that environmental exposure information is only scarcely and inconsistently documented in our study data. We observed that especially for non-Hispanic Black patients, the documentation rate is low. In addition, the ways environmental exposure information was documented also differ, with some being explicitly documented (eg, "exposure to Agent Orange") and many only alluding to exposures by documenting deployment sites and occupations that may expose veterans to toxicants. Toxic exposure screening was implemented as part of the PACT Act across VA systems nationwide [26], which could help capture environmental exposure information. Our study indicates that more consistent and comprehensive adherence to documentation of environmental exposure is needed in order to facilitate the efficient identification of eligible patients for clinical research, patient care, and benefit enrollment.

There were statistically significant differential performances in the FNs of extracting substance use information from notes for non-Hispanic White versus non-Hispanic Black patients. This may be due to the rich information and variations in documenting patients' substance use. The use of templates will help standardize how documentation occurs as well as how information is captured. This will also help improve the performance of cNLP extraction pipelines because fewer outliers will appear in the clinical documentation. Such templates will also help standardize the documentation of substance use. Templates that are autopopulated can also capture data more uniformly.

Limitations

As a preliminary effort for developing a cNLP system for LMs, our study had several limitations. By using nationwide VA EHR data, there was variability in data quality and completeness. As mentioned previously, documentation of elements such as environmental exposures did not have an established standard, resulting in inconsistent and heterogeneous documentation. Military exposure documentation was infrequent, which reflects the nuanced nature of this type of screening. However, the recently mandated screening implemented in August 2023 will improve documentation for future research and analysis. Our study only examined racial bias due to the limited number of annotated notes we had and may have overlooked other potential sources of bias such as age, gender, and geography. Finally, our data come from the national VA health care system. Despite being a single EHR system, the VA health care system spans the entire country as well as Puerto Rico, Guam, and the Philippines, and its EHR captures the heterogeneity in regional practice patterns. For our work in understanding military exposure and the association with developing LMs, it is a vertically integrated system that is unique in the patient population and prioritization of military service–connected conditions, suitable for our research objective.

Future Directions

Our future directions include improving the performance of the cNLP pipeline. To achieve this, we plan to leverage more advanced pretrained LLMs such as CancerBERT [27] and GatorTron [28] and fine-tune them on our dataset to extract the clinical entities. We will use the rule-based cNLP pipeline developed in this study to generate weak labels for fine-tuning these LLMs, without having medical experts to further annotate notes. We will also conduct a more thorough and large-scale review of the environmental exposure documentation to construct a more comprehensive terminology dictionary for identifying environmental exposures for patients with LMs. In addition, many clinical entities should be extracted in fine-grained forms (eg, substance use with frequency, amount, and status) and in relation to other information if available (eg, temporal information). Another next step is to use cNLP to identify and analyze the current documentation practices and potential biases for less common clinical entities. We will also apply cNLP-enabled analyses to all veterans with LMs in the VA CDW to assess the documentation patterns of the clinical information among different patient groups (by race, gender, branch, and socioeconomic status); provider types; and note types to identify potential biases. We will also apply the pipeline to clinical notes from health systems outside of the VA to assess its generalizability.

Another future direction is to design and implement a tool integrated into the EHR system and help clinicians improve their documentation quality and identify inconsistencies or inadequacies (eg, lack of documentation of environmental exposures) at the time of documentation.

Conclusions

In our rule-based cNLP pipeline that integrates clinical domain expertise, clinical entities such as performance status, staging, and the primary diagnosis were captured with satisfying accuracy. The primary diagnosis and substance use exhibit differential performance for non-Hispanic Black and White patients. Our future work will build upon the rule-based pipeline and leverage more advanced models to enhance the performance of extraction for substance abuse and environmental exposures, as well as ensuring that model performance is equitable across different racial groups.

XSL•FO
RenderX

Acknowledgments

The study is in part supported by the University of California, Irvine, Institute for Clinical and Translational Science and Veterans Affairs Long Beach Informatics Pilot Award. The authors thank Chris Cho from the University of Wisconsin-Milwaukee for providing statistical consulting on the statistical methods used in this study.

Conflicts of Interest

None declared.

Multimedia Appendix 1
Histology used to retrieve the patient cohort based on *International Classification of Disease for Oncology, Third Edition (ICD-O-3)*.
[DOCX File, 15 KB - medinform_v13i1e63908_app1.docx]

Multimedia Appendix 2
Annotation guideline.
[DOCX File, 14 KB - medinform_v13i1e63908_app2.docx]

Multimedia Appendix 3
Confusion matrices and chi-square test results for clinical entities.
[DOCX File, 17 KB - medinform_v13i1e63908_app3.docx]

References

1. Wang Y, Wang L, Rastegar-Mojarad M, et al. Clinical information extraction applications: a literature review. J Biomed Inform 2018 Jan;77:34-49. [doi: 10.1016/j.jbi.2017.11.011] [Medline: 29162496]
2. Wang L, Fu S, Wen A, et al. Assessment of electronic health record for cancer research and patient care through a scoping review of cancer natural language processing. JCO Clin Cancer Inform 2022 Jul;6(6):e2200006. [doi: 10.1200/CCI.22.00006] [Medline: 35917480]
3. Key statistics for non-Hodgkin lymphoma. American Cancer Society. URL: https://www.cancer.org/cancer/non-hodgkin-lymphoma/about/key-statistics.html [accessed 2022-08-23]
4. Key statistics for chronic lymphocytic leukemia (CLL). American Cancer Society. URL: https://www.cancer.org/cancer/types/chronic-lymphocytic-leukemia/about/key-statistics.html [accessed 2023-06-08]
5. Key statistics for Hodgkin lymphoma. American Cancer Society. URL: https://www.cancer.org/cancer/types/hodgkin-lymphoma/about/key-statistics.html [accessed 2023-06-08]
6. Key statistics for multiple myeloma. American Cancer Society. URL: https://www.cancer.org/cancer/types/multiple-myeloma/about/key-statistics.html [accessed 2023-06-08]
7. Key statistics about Waldenström macroglobulinemia. American Cancer Society. URL: https://www.cancer.org/cancer/types/waldenstrom-macroglobulinemia/about/key-statistics.html [accessed 2023-06-08]
8. National Academies of Sciences, Engineering, and Medicine. Veterans and Agent Orange: National Academies Press; 2018.
9. The PACT Act. US Department of Veterans Affairs. URL: https://tinyurl.com/yc26bfk7 [accessed 2023-02-20]
10. Roberts A. Language, structure, and reuse in the electronic health record. AMA J Ethics 2017 Mar 1;19(3):281-288. [doi: 10.1001/journalofethics.2017.19.3.stas1-1703] [Medline: 28323609]
11. VA Informatics and Computing Infrastructure (VINCI). US Department of Veterans Affairs. URL: https://www.research.va.gov/programs/vinci/ [accessed 2025-10-07]
12. Veterans Health Administration. US Department of Veterans Affairs. URL: https://www.va.gov/health/aboutvha.asp [accessed 2025-01-27]
13. Fu YV, Ramachandran GK, Halwani A, et al. CACER: clinical concept annotations for cancer events and relations. J Am Med Inform Assoc 2024 Nov 1;31(11):2583-2594. [doi: 10.1093/jamia/ocae231] [Medline: 39225779]
14. Lybarger K, Ostendorf M, Yetisgen M. Annotating social determinants of health using active learning, and characterizing determinants using neural event extraction. J Biomed Inform 2021 Jan;113:103631. [doi: 10.1016/j.jbi.2020.103631] [Medline: 33290878]
15. Lituiev DS, Lacar B, Pak S, Abramowitsch PL, De Marchis EH, Peterson TA. Automatic extraction of social determinants of health from medical notes of chronic lower back pain patients. J Am Med Inform Assoc 2023 Jul 19;30(8):1438-1447. [doi: 10.1093/jamia/ocad054] [Medline: 37080559]
16. Deleger L, Li Q, Lingren T, et al. Building gold standard corpora for medical natural language processing tasks. AMIA Annu Symp Proc 2012;2012:144-153. [Medline: 23304283]

XSL•FO
RenderX

17. Yao Z, Tsai J, Liu W, et al. Automated identification of eviction status from electronic health record notes. J Am Med Inform Assoc 2023 Jul 19;30(8):1429-1437. [doi: 10.1093/jamia/ocad081] [Medline: 37203429]
18. Lu Q, Li R, Wen A, Wang J, Wang L, Liu H. Large language models struggle in token-level clinical named entity recognition. arXiv. Preprint posted online on Jun 30, 2024. [doi: 10.48550/arXiv.2407.00731]
19. Chen Z, Zhang H, Yang X, et al. Assess the documentation of cognitive tests and biomarkers in electronic health records via natural language processing for Alzheimer's disease and related dementias. Int J Med Inform 2023 Feb;170:104973. [doi: 10.1016/j.ijmedinf.2022.104973] [Medline: 36577203]
20. Sarwal D, Wang L, Gandhi S, et al. Identification of pancreatic cancer risk factors from clinical notes using natural language processing. Pancreatology 2024 Jun;24(4):572-578. [doi: 10.1016/j.pan.2024.03.016]
21. Vasilakes J, Bompelli A, Bishop JR, Adam TJ, Bodenreider O, Zhang R. Assessing the enrichment of dietary supplement coverage in the Unified Medical Language System. J Am Med Inform Assoc 2020 Oct 1;27(10):1547-1555. [doi: 10.1093/jamia/ocaa128] [Medline: 32940692]
22. Henry S, Buchan K, Filannino M, Stubbs A, Uzuner O. 2018 n2c2 shared task on adverse drug events and medication extraction in electronic health records. J Am Med Inform Assoc 2020 Jan 1;27(1):3-12. [doi: 10.1093/jamia/ocz166] [Medline: 31584655]
23. Cohen AB, Rosic A, Harrison K, et al. A natural language processing algorithm to improve completeness of ECOG performance status in real-world data. Appl Sci (Basel) 2023;13(10):6209. [doi: 10.3390/app13106209]
24. Maghsoudi A, Sada YH, Nowakowski S, et al. A multi-institutional natural language processing pipeline to extract performance status from electronic health records. Cancer Control 2024;31:10732748241279518. [doi: 10.1177/10732748241279518] [Medline: 39222957]
25. Liu LW, Wang M, Grandhi N, et al. The association of Agent Orange exposure with the progression of monoclonal gammopathy of undetermined significance to multiple myeloma: a population-based study of Vietnam War Era Veterans. J Hematol Oncol 2024 Jan 8;17(1):3. [doi: 10.1186/s13045-023-01521-6] [Medline: 38191467]
26. PACT Act toxic exposure screening. US Department Veterans Affairs. URL: https://www.va.gov/walla-walla-health-care/programs/pact-act-toxic-exposure-screening/ [accessed 2025-01-27]
27. Zhou S, Wang N, Wang L, Liu H, Zhang R. CancerBERT: a cancer domain-specific language model for extracting breast cancer phenotypes from electronic health records. J Am Med Inform Assoc 2022 Jun 14;29(7):1208-1216. [doi: 10.1093/jamia/ocac040] [Medline: 35333345]
28. Yan X, Chen A, PourNejatian N, et al. GatorTron: a large clinical language model to unlock patient information from unstructured electronic health records. arXiv. Preprint posted online on Feb 2, 2022. [doi: 10.48550/arXiv.2203.03540]

Abbreviations

CDW: Corporate Data Warehouse
cNLP: clinical natural language processing
ECOG: Eastern Cooperative Oncology Group
EHR: electronic health record
FN: false negative
FP: false positive
HIPAA: Health Insurance Portability and Accountability Act
KPS: Karnofsky performance status
LLM: large language model
LM: lymphoid malignancy
NLP: natural language processing
PACT: Promise to Address Comprehensive Toxics
VA: Veterans Affairs

Edited by A Benis; submitted 12.07.24; peer-reviewed by C Li, GK Gupta; revised version received 18.08.25; accepted 15.09.25; published 16.10.25.

Please cite as:
He L, Moldenhauer MR, Zheng K, Ma H
Clinical Information Extraction From Notes of Veterans With Lymphoid Malignancies: Natural Language Processing Study
JMIR Med Inform 2025;13:e63908
URL: https://medinform.jmir.org/2025/1/e63908
doi:10.2196/63908

XSL•FO
RenderX

© Lu He, Matthew R Moldenhauer, Kai Zheng, Helen Ma. Originally published in JMIR Medical Informatics (https://medinform.jmir.org), 16.10.2025. This is an open-access article distributed under the terms of the Creative Commons Attribution License (https://creativecommons.org/licenses/by/4.0/), which permits unrestricted use, distribution, and reproduction in any medium, provided the original work, first published in JMIR Medical Informatics, is properly cited. The complete bibliographic information, a link to the original publication on https://medinform.jmir.org/, as well as this copyright and license information must be included.

XSL•FO
RenderX

Automated Esophageal Cancer Staging From Free-Text Radiology Reports: Large Language Model Evaluation Study

Yao Yao[1*], MEng; Xingxing Cen[1*], PhD; Lu Gan[2], MS; Jiehui Jiang[3], PhD; Min Wang[3], PhD; Yinghui Xu[4], PhD; Junyi Yuan[1], PhD

[1]Information Center, Shanghai Chest Hospital, Shanghai Jiao Tong University School of Medicine, No 241, West Huaihai Road, Shanghai, China

[2]Department of Healthcare, INF Technology, Shanghai, China

[3]School of Life Sciences, Shanghai University, Shanghai, China

[4]Artificial Intelligence Innovation and Incubation Institute of Fudan University, Fudan University, Shanghai, China

[*]these authors contributed equally

Corresponding Author:
Junyi Yuan, PhD
Information Center, Shanghai Chest Hospital, Shanghai Jiao Tong University School of Medicine, No 241, West Huaihai Road, Shanghai, China

Abstract

Background: Accurate staging of esophageal cancer is crucial for determining prognosis and guiding treatment strategies, but manual interpretation of radiology reports by clinicians is prone to variability and limited accuracy, resulting in reduced staging accuracy. Recent advances in large language models (LLMs) have shown promise in medical applications, but their utility in esophageal cancer staging remains underexplored.

Objective: This study aims to compare the performance of 3 locally deployed LLMs (INF-72B, Qwen2.5-72B, and LLaMA3.1-70B) and clinicians in preoperative esophageal cancer staging using free-text radiology reports.

Methods: This retrospective study included 200 patients from Shanghai Chest Hospital who underwent esophageal cancer surgery from May to December 2024. The dataset consisted of 1134 Chinese free-text radiology reports. The reference standard was derived from postoperative pathological staging. A total of 3 LLMs determined tumor classification (T1-T4), node classification (N0-N3), and overall staging (I-IV) using 3 prompting strategies (zero-shot, chain-of-thought, and a proposed interpretable reasoning [IR] method). The McNemar test and Pearson chi-square test were used for comparisons.

Results: INF-72B+IR achieved a superior overall staging accuracy of 61.5% and an F_1-score of 0.60, substantially higher than the clinicians' accuracy of 39.5% and F_1-score of 0.39 (all P<.001). Qwen2.5-72B+IR also demonstrated an advantage, achieving an overall staging accuracy of 46% and an F_1-score of 0.51, which was better than the clinicians' performance (P<.001). LLaMA3.1-70B showed no statistically significant difference in overall staging performance compared to clinicians (all P>0.5)

Conclusions: This study demonstrates that LLMs, particularly when guided by the proposed IR strategy, can accurately and reliably perform esophageal cancer staging from free-text radiology reports. This approach not only provides high-performance predictions but also offers a transparent and verifiable reasoning process, highlighting its potential as a valuable decision-support tool to augment human expertise in complex clinical diagnostic tasks.

(JMIR Med Inform 2025;13:e75556) doi:10.2196/75556

KEYWORDS

large language model; esophageal cancer; cancer staging; tumor–node metastasis; TNM; radiology report

Introduction

Esophageal cancer is a type of malignant tumor in the digestive system and remains one of the leading causes of cancer-related death, seriously affecting human health worldwide [1-3]. Accurate preoperative staging of esophageal cancer is essential, as it directly impacts prognosis estimation and guides treatment decisions such as surgical resection, chemotherapy, or radiotherapy [4,5]. The tumor–node metastasis classification system is currently the standard for staging according to the eighth edition of the AJCC Tumor–Node Metastasis Classification of Malignant Tumors [6].

In clinical practice, preoperative staging of esophageal cancer relies predominantly on imaging modalities, with computed tomography (CT) and positron emission tomography (PET)–CT serving as the cornerstone examinations [7]. These imaging studies generate detailed radiology reports that contain crucial information about tumor characteristics, local invasion, and

XSL•FO
RenderX

metastatic spread. Clinical tumor–node metastasis (cTNM), determined from these imaging studies, is pivotal for formulating individualized treatment plans [8].

However, a major challenge is that radiology reports are usually documented in an unstructured, free-text format [9]. These narrative reports can be ambiguous, lack key details, or vary in descriptive style among radiologists. This may result in key findings being missed or misinterpreted, leading to significant discrepancies between cTNM and the gold-standard pathological tumor–node metastasis (pTNM) determined after surgery. Moreover, the complexity and variability inherent in these reports make the process of extracting structured, actionable staging information both time-consuming and prone to human error. Thus, automatic classification of esophageal cancer stage from free-text radiology reports may provide significant benefits.

Recent advances in artificial intelligence (AI), particularly large language models (LLMs), offer promising solutions for these challenges [10-14]. LLMs are capable of understanding and processing natural language, making them well-suited for extracting structured information from free-text medical documents and supporting complex reasoning tasks in medical natural language processing [15-17]. Their strengths include parsing unstructured narratives, performing multi-step reasoning, and learning from vast medical corpora, which have enabled progress in information extraction, report classification, and automated summarization in medical contexts [18,19].

Despite these advances, research on the use of LLMs for cancer staging from radiology reports has largely focused on lung cancer, owing to the relatively straightforward criteria in imaging for that disease [20-22]. In contrast, esophageal cancer staging presents unique challenges: the anatomical complexity of the esophagus, its proximity to multiple vital structures, and the subtlety of early lymph node involvement make accurate staging from radiology reports considerably more difficult. This gap in the literature highlights the need for dedicated research into LLM applications for esophageal cancer staging.

While LLMs show great potential for medical applications, they are not without limitations. The hallucination effect, where models generate plausible but incorrect information, poses risks in health care settings where accuracy is paramount [23]. Recent studies have focused on optimizing prompting strategies and proposed approaches such as few-shot learning [24] and chain-of-thought (CoT) [25] to enhance the quality of model responses. However, as black-box models, LLMs often fail to provide transparent explanations for their outputs. This lack of explainability poses a significant challenge in gaining trust for health care applications, where a transparent decision-making process is critical.

This study aims to evaluate 3 LLMs (INF-72B, Qwen2.5-72B, and LLaMA3.1-70B) for automated esophageal cancer staging from Chinese free-text radiology reports. We introduce a novel prompting strategy called interpretable reasoning (IR) designed specifically to enhance both the accuracy and transparency of LLM-based staging decisions. By comparing LLM performance with that of clinicians, we aim to provide a foundation for future research and safe clinical translation of LLMs in cancer staging.

Methods

Data

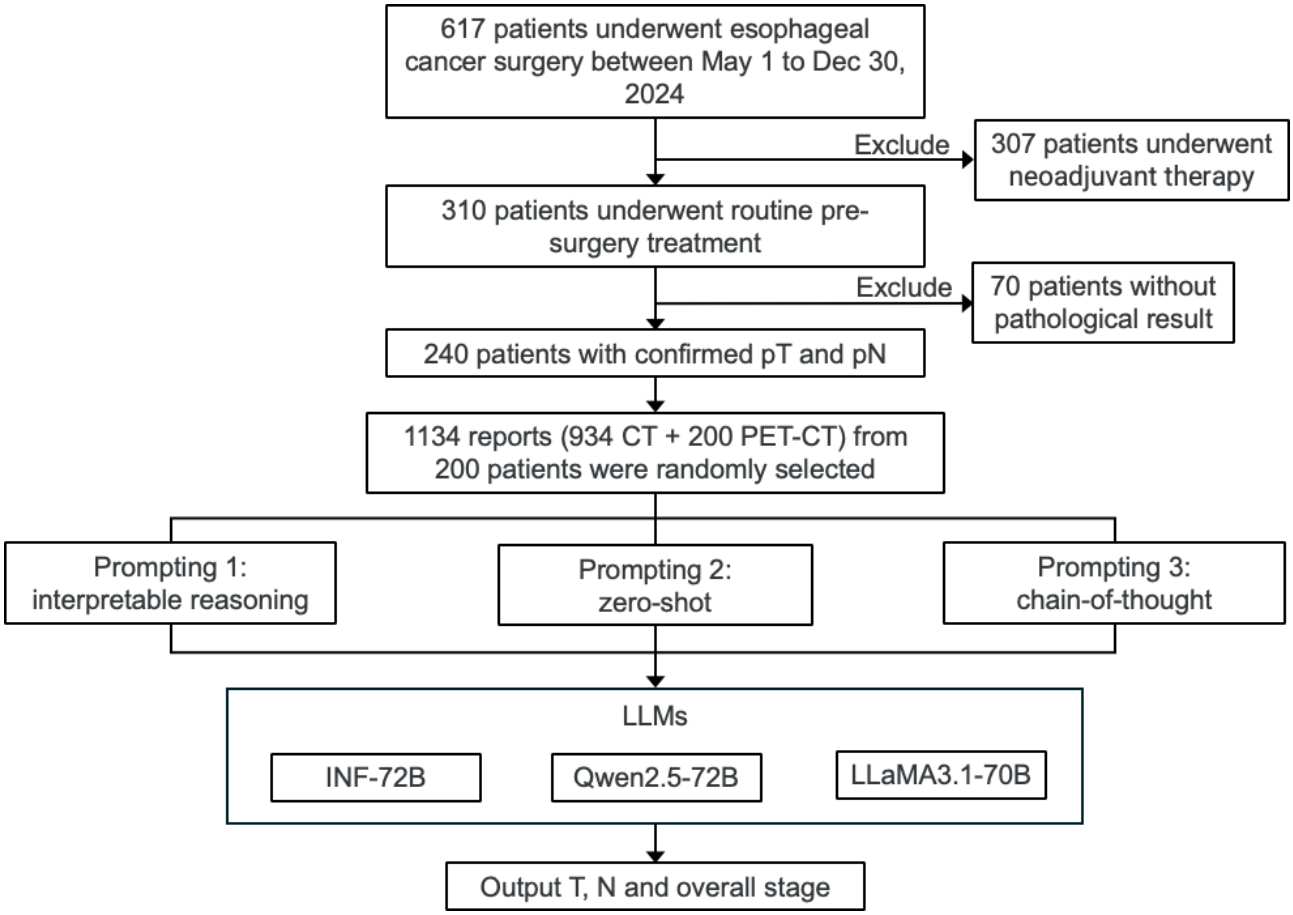
This retrospective study was conducted at Shanghai Chest Hospital with data collected from 617 patients who underwent esophageal cancer surgery between May and December 2024.

Exclusion criteria were applied systematically to ensure data quality and relevance to the study objectives. First, 307 patients who had received neoadjuvant therapy were excluded, as such treatment alters the assessment of tumor size and metastasis in radiology reports, and such patients are staged using the ycTNM staging system, which is not within the scope of the current dataset [26]. Second, 70 patients lacking pathological diagnosis were excluded.

Of these, 1134 reports (934 CT and 200 PET-CT), from 200 unique patients, were randomly selected for inclusion in the final sample. Figure 1 shows the flowchart of study design. All reports were unstructured, free-text documents (Figure 2). Each case comprised all reports from the patient's prior hospital visits, including both outpatient and inpatient records.

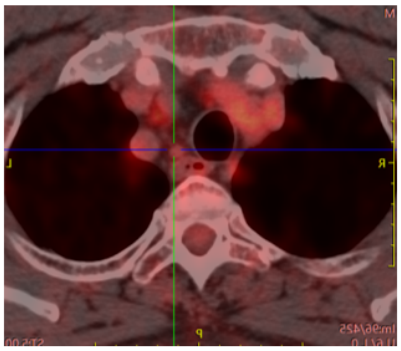
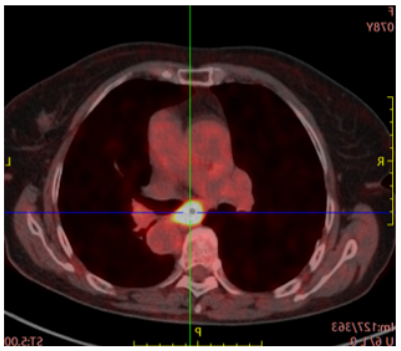
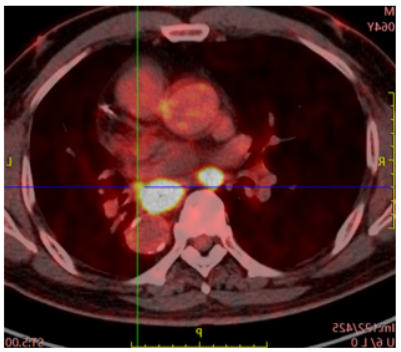
XSL•FO
RenderX

Figure 1. Flowchart of study design. CT: computed tomography; LLM: large language model; PET: positron emission tomography; pN: pathological node; pT: pathological tumor.



XSL•FO
RenderX

Figure 2. Here are 3 cases from the dataset, accompanied by the key information extracted from the free-text reports. To better illustrate the correlation between the reports and imaging, the corresponding PET-CT images are also presented. The staging of the 3 cases is T1N0 (Stage I), T2N0 (Stage II), and T3N0 (Stage III), respectively. CA: cancer; CT: computed tomography; FDG: fluorodeoxyglucose; JES: Japan Esophageal Society; PET: positron emission tomography; SUVmax: maximum standardized uptake value.

PET-CT Image	PET-CT Report	Cancer Stage
	The wall of the middle and lower thoracic esophagus was slightly thickened, with a longitudinal diameter of about 46 mm, increased contrast agent uptake, and SUVmax of about 4.7. JES classification (104L, 106recR, 106recL, 106pre, 106tbL, 107, 113, 109), multiple lymph nodes in the liver and stomach space were displayed or enlarged, and some FDG metabolism was increased.	**T1 N0 Stage I**
	The wall of the middle thoracic esophagus was thickened, the lumen was narrowed, the affected area was about 4.3*2.5*1.9cm, the contrast agent uptake was abnormally increased, and the SUVmax was about 20.5. The esophageal middle thoracic mass and increased FDG metabolism were consistent with the manifestation of esophageal CA. The JES zoning (106recL, 106recR) and the hepatogastric interstitial lymph nodes showed increased FDG metabolism.	**T2 N0 Stage II**
	The local wall thickening and lumen narrowing of the middle thoracic esophagus were about 37*26*48mm, and the imaging agent uptake was abnormally increased, with SUVmax of about 18.8. The local wall thickening and increased FDG metabolism of the middle thoracic esophagus were consistent with the manifestation of malignant lesions. The lymph nodes in the JES division (106recR, 107, 108 areas) were slightly larger or visible, and the FDG metabolism was increased.	**T3 N1 Stage III**

Reference Standard

The reference standard for this study was the pTNM staging information obtained from each patient's postoperative pathological report. This staging was determined by pathologists and documented within the structured pathological reporting system following surgical resection and histopathological examination.

For comparison purposes, we collected each patient's cTNM from the admission notes completed by the attending physician prior to surgery, representing the clinician's preoperative assessment based on available imaging reports and clinical data. After data collection, the cTNM information was reviewed by 3 attending thoracic surgeons, each with four years of clinical experience. The reviewers were not informed of the postoperative pathological staging, ensuring that their judgments relied solely on the preoperative radiology reports.

Given that our dataset consisted exclusively of surgical candidates, distant metastasis (M1) was absent, as patients with metastatic disease would not have undergone curative surgery. Therefore, our evaluation focused on tumor classification (T1-T4), node classification (N0-N3), and overall stage groups (I-IV) as determined by the combination of tumor and node categories.

Large Language Model

The LLMs were selected for evaluation based on their availability, performance benchmarks, and number of parameters. INF-72B is a homemade LLM developed by the INF team that combines the pattern recognition capabilities of neural networks with symbolic reasoning, offering advantages for structured medical tasks [27].

Qwen2.5-72B is an open-source LLM, exhibiting strong performance in Chinese language tasks [28]. LLaMA3.1-70B

XSL•FO
RenderX

is one of Meta's foundational model series, selected for its general-purpose capabilities and widespread adoption in the research community [29]. Both are open-source models, characterized by relatively large parameter sizes and strong performance, and have been the subject of substantial research in medical text natural language processing [30,31].

All models were deployed locally within the hospital's secure computing environment using 8 NVIDIA A30 GPUs. This local deployment was essential to ensure patient data privacy and comply with institutional data governance policies. Model inference was performed using greedy decoding (temperature=0) to maximize determinism.

Prompting Strategy

In this study, we propose a prompting strategy called IR, in which the model is instructed not only to provide its staging decision but also to output the underlying reasoning and explicitly cite relevant excerpts from the original radiology report. This design aims to improve transparency, facilitate verification by clinicians, and reduce the risk of unsupported or hallucinatory outputs.

Specifically, the model's cited excerpts from the radiology report were automatically checked against the original input text to ensure exact matches. If any cited text was not found in the original report, the output was rejected, and the model was prompted to regenerate its response. In addition, the model was instructed to perform internal reasoning before producing the final prediction and explanation, which encourages the use of evidence grounded in the report and further reduces the likelihood of hallucinations. In addition, the esophageal cancer staging rules were incorporated into the prompt in a structured format according to the AJCC Eighth Edition. The prompt template is presented in Figure 3.

A total of 2 additional prompting strategies, zero-shot (ZS) and CoT, were implemented for comparison with the proposed method. For ZS, the LLM was provided with the reports and instructions to directly return the predicted cancer stage. For CoT, the LLM was instructed to first "think step by step" to retrieve the reasoning and use it as context for predicting the cancer stage.

XSL•FO
RenderX

Figure 3. Interpretable reasoning prompt template in markdown format. CT: computed tomography; PET: positron emission tomography.

```
## Task
Assume you are an oncologist. Based on all the patient's CT and PET-CT reports from the past three years, determine the esophageal cancer TN classification according to the provided criteria.
The possible values for T are T1, T2, T3, T4. For N are N0, N1, N2, N3.

### Staging Guidelines
| Category  |  Description                                                                  |
|--------|-------------------------------------------------------------------------------|
| T1   | Tumor invades lamina propria or muscularis mucosae or submucosa |
| T2   | Tumor invades muscularis propria |
| T3   | Tumor invades the adventitia |
| T4   | Tumor invades adjacent structures (pleura, pericardium, azygos vein, diaphragm, pleura, aorta, vertebral body, trachea, etc.) |
| N0   | No regional lymph node metastasis |
| N1   | 1-2 regional lymph node metastases |
| N2   | 3-6 regional lymph node metastases |
| N3   | 7 or more regional lymph node metastases |

Reports: {reports}

Output the staging results and reasons in the following format:
{
  "T": {
    "grade": "T1",
    "explanation": {
      "grade_reason": "",  # Briefly explain the reason for this staging
      "report_text": ["", ""]  # Provide report excerpts used for this grading as a Python list; if multiple reports are involved, each report excerpt occupies one list element
    }
  },
  "N": {
    "grade": "N0",
    "explanation": {
      "grade_reason": "",  # Briefly explain the reason for this staging
      "report_text": ["", ""]  # Provide report excerpts used for this grading as a Python list; if multiple reports are involved, each report excerpt occupies one list element
    }
  }
}
Only output the answer in JSON format, without any additional content.
```

Statistical Analysis

For each LLM and clinical stage, the tumor category, node category, and overall stage groups were classified as correct if matching the reference-standard assignment (pathological staging). To measure the performance of cancer staging, accuracy, precision, recall, and F_1-score were used as key evaluation metrics. These metrics were calculated individually for each component (eg, T1-T4, N0-N3, and I-IV). Corresponding 95% CIs were derived using the Wilson method. Comparisons were performed using McNemar and Pearson tests. *P* values were 2-sided and considered statistically significant when less than .05.·

Ethical Considerations

This study was approved by the Ethics Committee of Shanghai Chest Hospital (IS25024). As this was a retrospective study, the Ethics Committee of Shanghai Chest Hospital waived the requirement for participants or their legal guardians or next of kin to provide written informed consent.

Results

Overview

This section presents the research findings. First, we evaluated the performance of 3 LLMs in the clinical staging of esophageal cancer and compared their results with clinicians. Next, we further analyzed the outcomes in terms of clinical management categories. Finally, we compared the runtime consumption of the 3 models.

Characteristics of Patients and Radiology Reports

A total of 200 patients (mean age 65.2, SD 7.4 years) comprising 145 males and 55 females. Within this group, a total of 1134 radiology reports (934 CT and 200 PET-CT) were collected.

XSL•FO
RenderX

The distribution of pathological tumors, pathological nodes, and overall stage groups is listed in Table 1.

Table . Characteristics of patients and radiology reports.

Categories	Values (N=200)
Patient information	
Gender, n (%)	
Male	145 (72.5)
Female	55 (27.5)
Age (years), mean (SD)	65.2 (7.4)
Report quantity, n (%)	
CT[a]	934 (82.4)
PET-CT[b]	200 (17.6)
Tumor grade, n (%)	
T1	54 (27)
T2	40 (20)
T3	98 (49)
T4	8 (4)
Node grade, n (%)	
N0	94 (47)
N1	52 (26)
N2	36 (18)
N3	18 (9)
Overall stage groups, n (%)	
I	46 (23)
II	72 (36)
III	60 (30)
IV	22 (11)

[a]CT: computed tomography.

[b]PET-CT: positron emission tomography-computed tomography.

Performance of Large Language Models and Clinicians in Esophageal Cancer Staging

Table 2 shows the accuracies of the LLMs and clinicians in esophageal cancer staging. The clinicians achieved accuracy of 44.5%, 42%, and 39.5% for tumor classification, node classification, and overall staging, respectively. Among LLMs, INF-72B demonstrated the highest overall performance. Specifically, INF-72B+IR achieved the best accuracy, significantly outperforming the clinicians (68%, 65.5%, and 61.5%, respectively; $P<.001$). Qwen2.5-72B+IR achieved its best accuracy of 46% in overall staging, better than the clinician (46% vs 39.5%, $P<.001$). Although LLaMA3.1-70B+IR achieved higher accuracy than clinicians in tumor classification (55% vs 44.5%, $P<.001$), there was no statistically significant difference between the 2 in overall staging performance (39% vs 39.5%, $P=.99$).

XSL•FO
RenderX

Table . Staging accuracies of clinicians and large language models using different prompting strategies.

	Tumor classification		Node classification		Overall stage groups	
Evaluator	Accuracy (95%CI)	*P* value[a]	Accuracy (95%CI)	*P* value[a]	Accuracy (95%CI)	*P* value[a]
Clinicians	44.5 (43.5 - 45.0)	—[b]	42.0 (41.0 - 43.0)	—	39.5 (38.5 - 40.0)	—
INF-72B+ZS	65.0 (65.0 - 66.0)	<.001	55.0 (54.0 - 56.5)	<.001	53.0 (51.5 - 54.0)	<.001
INF-72B+CoT	65.0 (64.5 - 66.0)	<.001	57.0 (56.0 - 58.0)	<.001	57.0 (56.0 - 58.0)	<.001
INF-72B+IR	68.0 (67.5 - 69.0)	<.001	65.5 (64.5 - 66.5)	<.001	61.5 (60.5 - 62.5)	<.001
Qwen2.5-72B+ZS	42.0 (41.5 - 43.0)	.12	40.5 (40.0 - 41.0)	.42	42.0 (41.0 - 43.0)	.15
Qwen2.5-72B+CoT	42.5 (41.0 - 43.0)	.23	42.0 (41.0 - 43.0)	.99	45.0 (44.0 - 46.5)	.008
Qwen2.5-72B+IR	46.0 (45.0 - 47.0)	.76	43.5 (42.5 - 44.0)	.81	46.0 (45.0 - 47.5)	<.001
LLaMA3.1-70B+ZS	49.0 (48.0 - 49.5)	.007	33.0 (31.5 - 34.0)	<.001	38.0 (37.0 - 39.0)	.79
LLaMA3.1-70B+CoT	50.0 (48.5 - 51.0)	<.001	36.0 (34.0 - 37.5)	<.001	37.5 (36.5 - 37.5)	.25
LLaMA3.1-70B+IR	55.0 (54.0 - 56.0)	<.001	35.0 (34.0 - 36.0)	<.001	39.0 (38.0 - 40.0)	.99

[a]*P* values represent comparisons with the accuracies of clinicians.

[b]Not available.

Table 3 shows the performance of clinicians and LLMs using different prompting for determining overall stage groups. INF-72B+IR achieved the best performance, with the F_1-score of 0.62, significantly higher than clinician's 0.43 (P<.001). INF-72B+ZS and INF-72B+CoT also performed better than clinicians (0.56, 0.58, P<.001). Qwen2.5-72B performed well under CoT and IR, significantly better than clinicians (0.50, 0.51, P<.001). LLaMA3.1-70B showed no statistically significant differences from clinicians (0.42, 0.43, 0.44, all P>0.5). Tables S1 and S2 in Multimedia Appendix 1 present the precision, recall, and F_1-score of the LLMs and clinicians for determining tumor category and node category, respectively.

Table . Performance of clinicians and large language models using different prompting strategies in overall staging. Values in parentheses represent the 95% CI. The *P* values represent comparisons with the F_1-scores of clinicians.

Evaluator	Precision, (95% CI)	Recall, (95% CI)	F_1-score, (95% CI)	*P* value
Clinicians	0.45 (0.43-0.44)	0.40 (0.40-0.41)	0.43 (0.42-0.45)	—
INF-72B+ZS	0.57 (0.55-0.58)	0.52 (0.50-0.53)	0.56 (0.54-0.57)	<.001
INF-72B+CoT	0.59 (0.56-0.60)	0.54 (0.50-0.58)	0.58 (0.55-0.60)	<.001
INF-72B+IR	0.64 (0.61-0.65)	0.59 (0.58-0.61)	0.62 (0.60-0.64)	<.001
Qwen2.5-72B+ZS	0.46 (0.44-0.47)	0.41 (0.36-0.46)	0.44 (0.40-0.46)	.87
Qwen2.5-72B+CoT	0.51 (0.48-0.52)	0.49 (0.48-0.49)	0.50 (0.49-0.50)	<.001
Qwen2.5-72B+IR	0.52 (0.50-0.53)	0.50 (0.49-0.52)	0.51 (0.49-0.52)	<.001
LLaMA3.1-70B+ZS	0.54 (0.51-0.57)	0.36 (0.34-0.37)	0.42 (0.40-0.43)	.97
LLaMA3.1-70B+CoT	0.50 (0.49-0.51)	0.40 (0.40-0.41)	0.43 (0.41-0.45)	.99
LLaMA3.1-70B+IR	0.55 (0.51-0.57)	0.41 (0.38-0.43)	0.44 (0.42-0.45)	.89

Stratification by Clinical Management Categories

Table 4 summarizes the performance of LLMs using IR and clinicians in terms of clinical management categories. A total of 46 reports indicated early esophageal cancer, 132 indicated locally advanced esophageal cancer, and 22 indicated advanced esophageal cancer. For reports indicating early esophageal cancer, the proportion that was overstaged was 82.6% for clinicians versus 28.3%, 60.9%, and 82.6% for INF-72B, Qwen2.5-72B, and LLaMA3.1-70B using IR. For reports indicating locally advanced cancer, the proportion that was understaged was 2.3% for clinicians versus 9.1%, 3.8%, and 0% for the 3 LLMs, and the proportion that was overstaged was 6.8% for clinicians versus 3.0%, 2.3%, and 5.3% for the 3 LLMs. For reports indicating advanced cancer, the proportion that was understaged was 90.9% for clinicians versus 63.6%, 100%, and 77.3% for the 3 LLMs.

XSL•FO
RenderX

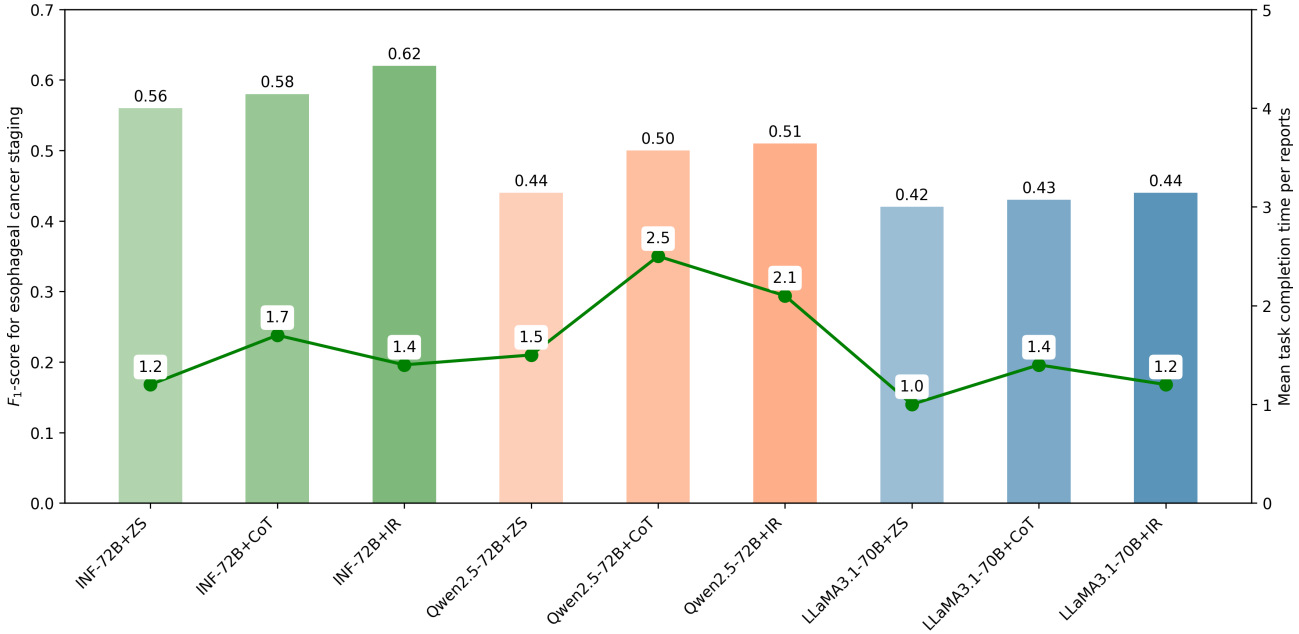
Table . Staging by large language models and clinicians, stratified by clinical management categories.

Categories	Early esophageal cancer (Stage I; n=46)		Locally advanced esophageal cancer (Stage II and III; n=132)			Advanced esophageal cancer (Stage IV; n=22)	
Evaluator	Correct	Overstaged	Correct	Overstaged	Understaged	Correct	Understaged
Clinicians	8 (17.4)	38 (82.6)	120 (90.9)	9 (6.8)	3 (2.3)	2 (9.1)	20 (90.9)
INF-72B+IR	33 (71.7)	13 (28.3)	116 (87.9)	4 (3)	12 (9.1)	8 (36.4)	14 (63.6)
Qwen2.5-72B+IR	18 (39.1)	28 (60.9)	124 (93.9)	3 (2.3)	5 (3.8)	0 (0)	22 (100)
LLaMA3.1-70B+IR	8 (17.4)	38 (82.6)	125 (94.7)	7 (5.3)	0 (0)	5 (22.7)	17 (77.3)

Task Completion Times

The mean task completion times per report were 1.2 (SD 0.56), 1.7 (SD 0.58), and 1.4 (SD 0.62) seconds for INF-72B with different prompting strategies, respectively; 1.5 (SD 0.44), 2.5 (SD 0.50), and 2.1 (SD 0.51) seconds for Qwen2.5-72B, respectively; and 1 (SD 0.42), 1.4 (SD 0.43), and 1.2 (SD 0.44) seconds for LLaMA3.1-70B, respectively. Figure 4 shows the variation across LLMs in overall staging F_1-score and mean task completion time per report.

Figure 4. The graph shows comparisons of F_1-score for esophageal cancer staging and mean task completion time per report for 3 large language models (INF-72B, Qwen2.5-72B, and LLaMA3.1-70B) with different prompting strategies (ZS, CoT, and IR). The green line and its associated values indicate mean task completion time in seconds per report for each evaluator. CoT: chain-of-thought; IR: interpretable reasoning; ZS: zero-shot.

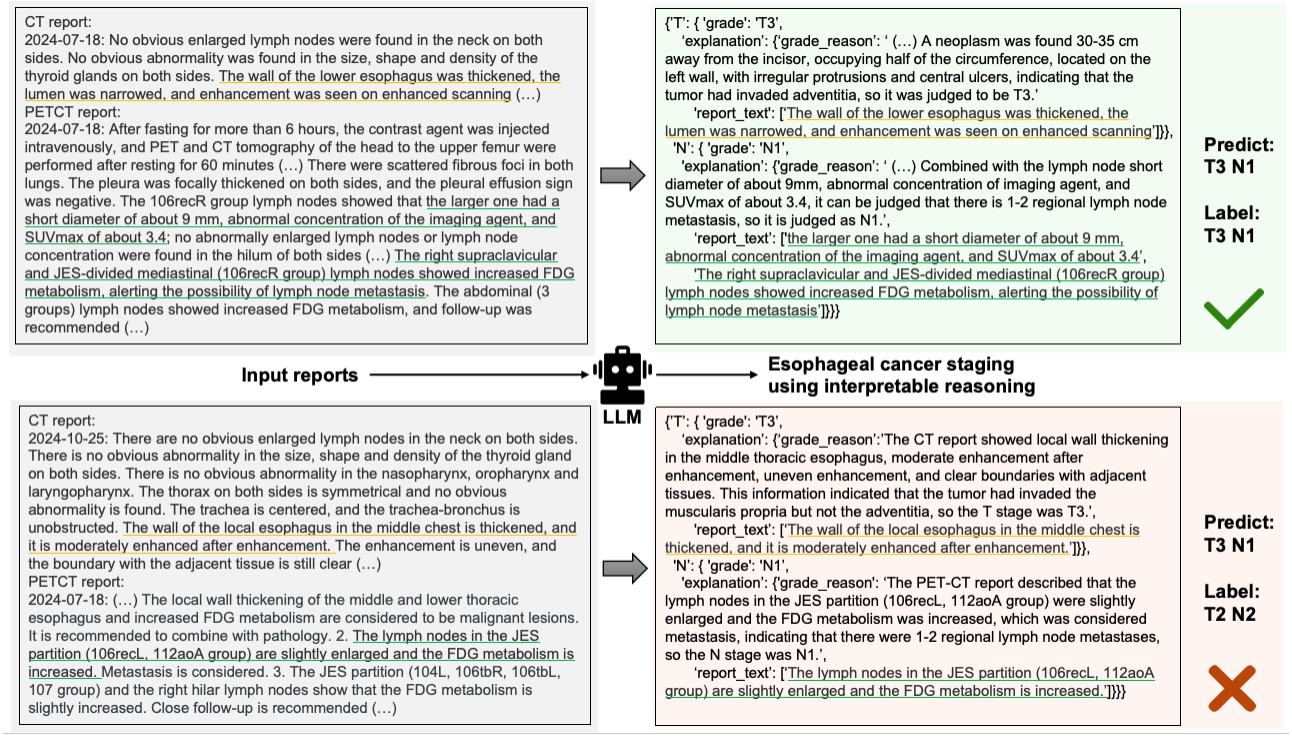


Examples of Esophageal Cancer Staging Using Large Language Model + Interpretable Reasoning

Figure 5 shows 2 examples of esophageal cancer staging using LLM with IR, including 1 correct case and 1 incorrect case. Multimedia Appendix 1 presents the complete input and output of the model, including the prompts and the radiology reports. Appendix S2 and S3 in Multimedia Appendix 1 show another 2 error examples for tumor classifications and node classifications, including the original reports and the model's output.

XSL•FO
RenderX

Figure 5. A total of 2 example cases to show how LLMs read the radiology reports and provide cancer stage using interpretable reasoning. The yellow and green underlined texts represent the classification basis of the large language model cited from the computed tomography reports and positron emission tomography-computed tomography reports, respectively. In the first example (top row), the reference standard was T3N1. The large language model extracted relevant information from the reports and gave the correct stage. In the second example (bottom row), the reference standard was T3N1. The large language model extracted incomplete information from the reports, resulting in an incorrect stage (T2N2). CT: computed tomography; FDG: fluorodeoxyglucose; JES: Japan Esophageal Society; LLM: large language model; PET: positron emission tomography.



Discussion

Principal Findings

This study evaluated 3 LLMs for preoperative esophageal cancer staging from Chinese free-text radiology reports, comparing their performance with that of clinicians. Our proposed IR prompting strategy enabled INF-72B to achieve significantly higher accuracy and F_1-scores than clinicians in tumor classification, node classification, and overall staging. Qwen2.5-72B also demonstrated improvements in overall staging under IR strategies, while LLaMA3.1-70B showed no consistent advantage over clinicians.

Recent studies have demonstrated the potential applications of LLMs in medical data analysis. In the context of radiology reports, most research has focused on using LLMs to convert free-text radiology reports into structured formats [11,18]. LLMs have been used to extract cancer stage from pathology reports, which is a relatively straightforward task due to the clearer descriptions of tumors in pathology reports [32-34]. But these approaches do not aid in formulating preoperative treatment plans for patients. Thus, this study highlights the potential of LLMs for preoperative esophageal cancer staging from radiology reports. The findings support the effective use of LLMs in assisting clinicians in real-world clinical tasks.

In this study, the IR prompting strategy played a pivotal role in enabling LLMs to clearly articulate the reasoning process behind tumor and node classification. IR guided the models to provide not only their answers but also the supporting rationale, citing key information from the original reports—such as extracting tumor status and the number of lymph nodes. This approach made the model outputs more transparent and reliable, reduced hallucinations, and highlighted the advantages of IR in complex clinical decision-making tasks such as cancer staging. Moreover, when the model produced an incorrect answer, the reasoning provided allowed for analysis of the underlying causes of the error. Such a feature is particularly valuable in the highly rigorous context of medical applications.

Error Analysis

The predictive performance of all models for stage IV esophageal cancer was suboptimal, which may be attributable to multiple factors. First, T4 involves tumor invasion of adjacent critical structures (eg, major vessels, trachea, pericardium), where the boundaries of invasion can be difficult to delineate on imaging. Limitations in image resolution and acquisition techniques may further introduce diagnostic uncertainty, resulting in insufficient information in the radiology reports to support a T4 determination. Second, N3 is defined as distant or multiregional lymph node metastases. However, small metastatic foci or atypical lymph node morphology can be difficult to detect on conventional imaging, leading to false negatives. In addition, according to National Comprehensive Cancer Network guidelines, definitive concurrent chemoradiotherapy is recommended as the initial treatment for stage IV cases. Since this study included only patients who underwent surgery, the proportion of stage IV cases was relatively low, which limited further analysis of the contributing factors.

XSL•FO
RenderX

The models exhibited a high frequency of overstaging in cases of stage I esophageal cancer. In instances where T1 was misclassified as T2 or T3, a common pattern was LLMs often relied on report descriptions such as "localized irregular thickening of the esophageal wall with moderate, heterogeneous enhancement" as the primary basis for staging, while overlooking more critical information such as "clear demarcation from adjacent tissues" or "no mention of tumor invasion into the muscularis propria or adventitia." Notably, INF-72B demonstrated markedly better performance in identifying stage I esophageal cancer compared with the other 2 LLMs and the clinicians, suggesting that a model's reasoning capability can substantially influence the accuracy of esophageal cancer staging.

Errors in node classification were attributable to 2 primary causes. First, PET-CT reports sometimes lacked sufficient information to reconcile with pathological findings. Although the models correctly extracted the number of lymph node metastases documented in the PET-CT report, those counts did not always match the numbers reported in the pathology. Second, models sometimes misidentified the anatomic nodal regions when summing metastatic nodes, which led to incorrect node staging. For example, a PET-CT report might list the JES regions (104R, 104L, 106tbR, 107, 109L, 112ao, 113), whereas the model's cited evidence mentioned only "104R, 104L, 106tbR," omitting the other stations and thus producing a misclassification.

Operational and Clinical Implications

INF-72B+IR demonstrated superior performance compared with clinicians in identifying both early-stage and advanced-stage esophageal cancer. This has several potential clinical benefits. First, improved recognition of early-stage disease (eg, T1N0) can facilitate timely initiation of curative-intent interventions such as endoscopic mucosal resection, endoscopic submucosal dissection, or minimally invasive esophagectomy, thereby reducing surgical morbidity and improving long-term outcomes [4]. Early and accurate identification may also prevent unnecessary chemoradiotherapy or extensive surgical procedures, reducing treatment-related complications and health care costs. Conversely, precise identification of advanced disease (eg, T4 or N3) allows for prompt initiation of multimodal treatment strategies—including concurrent chemoradiotherapy, immunotherapy, and palliative interventions—while avoiding futile surgical attempts. By reducing the risk of misclassification, the model can help ensure that patients receive stage-appropriate treatment in a timely manner.

In addition, the model processes radiology reports and generates staging predictions within seconds. This capability can improve clinical workflow efficiency by enabling a "screen-then-review" approach, in which the model prescreens cases and flags high-risk patients for expedited review by clinicians. Such an approach is particularly valuable in high-volume oncology centers, as well as in resource-limited settings. Integrating the model into multidisciplinary team discussions could further streamline decision-making, as staging information would be immediately available without requiring additional report interpretation during the meeting.

Importantly, the implementation of this model should be viewed not as a replacement for clinicians, but as an intelligent decision-support tool. By augmenting human expertise with automated, high-accuracy staging predictions, it has the potential to enhance diagnostic accuracy, reduce inter-observer variability, and optimize patient management across the entire care pathway.

Ethical Issues in the Use of Large Language Models in Health Care

The first concern is privacy and data security. Medical information is inherently sensitive, requiring robust protection measures. In this study, all models were deployed locally within the hospital's secure computing environment to prevent data exposure. Future implementation must ensure strong network security, compliance with regulations such as Health Insurance Portability and Accountability Act (HIPAA) and General Data Protection Regulation (GDPR), and minimal data exposure during model training and deployment. Working within these legal and ethical parameters is crucial for maintaining the credibility and trustworthiness of AI applications in health care.

In addition, the emphasis on explainable artificial intelligence methods underscores the importance of transparency to build trust among health care providers and ensure the interpretability of AI-generated outputs [35]. Building trust in AI systems requires explainable outputs and clear accountability structures. Our IR approach addresses this by providing explicit rationales for staging decisions, allowing clinicians to verify and understand model predictions. However, ongoing assessment and performance monitoring are essential for long-term accountability. Regular audits, error analysis, and feedback mechanisms must be established to maintain trustworthiness.

Another important factor is compliance with regulations. The integration of AI in health care must align with regional and international standards. This requires comprehensive documentation of model training, validation, and clinical workflow integration processes. Clear, understandable documentation enables health care providers, patients, and regulators to evaluate the technology's ethical and legal sustainability. Our study represents an initial evaluation phase. Prospective clinical trials and regulatory approval would be necessary before deployment.

To comprehensively address these ethical considerations, ongoing assessment, open reporting, and collaboration between AI developers, health care providers, and regulators are essential. While our study demonstrates technical feasibility, the path to clinical deployment must prioritize patient rights, ensure equitable care delivery, and maintain the highest ethical standards. Only through such careful consideration can we realize the benefits of AI in health care while safeguarding the fundamental principles of medical ethics.

Limitations

This study has several limitations that should be acknowledged. First, the most significant limitation of this study is the imbalance in the dataset. Advanced esophageal cancer cases,

XSL•FO
RenderX

particularly those with T4 or N3 staging, are underrepresented because such patients often do not undergo surgical resection and thus lack postoperative pathological confirmation to serve as a reference label. This constraint prevented us from fully assessing the model's performance in predicting advanced cancer stage. In addition, the dataset size was relatively small, which not only limits the statistical power of our findings but also precludes the possibility of performing finetuning experiments to further optimize the model.

Second, the preoperative cancer staging in this work was derived exclusively from radiology reports, with pathological pTNM staging used as the reference standard. This approach assumes that radiology report–based classification can achieve equivalence to pTNM staging. However, radiology reports may not always contain sufficient detail or clarity to support an exact stage determination. The potential discrepancy between radiological descriptions and pathological findings could have contributed to misclassification.

Another limitation has to do with the model's generalization. The dataset was obtained from a single medical center. As a result, the linguistic style, terminology usage, and reporting conventions represented in the dataset may not fully capture the diversity of radiology reports in other hospitals, regions, or countries. This limits the immediate generalizability of the model, and further validation using multi-center, multi-national datasets is required to ensure robustness across different clinical and cultural contexts.

Future Work

Future research should focus on addressing these limitations to improve both the accuracy and generalizability of the proposed approach. Multi-center collaborations will be essential to collect a larger and more diverse dataset, particularly including advanced-stage cases. For patients who do not undergo surgical resection, alternative labeling strategies—such as consensus annotations by multiple radiologists or incorporation of longitudinal clinical follow-up data—could be explored to approximate reliable reference standards. Increasing the dataset size would also enable supervised fine-tuning of the model, potentially yielding further performance gains over the current ZS or prompt–based approach.

Moreover, integrating structured imaging-derived features with the unstructured radiology text may help bridge the gap between radiological descriptions and pathological staging, improving classification consistency. Finally, future validation should be conducted on datasets from different institutions, regions, and languages to ensure robustness across diverse clinical settings, thereby paving the way for practical integration of the model into routine multidisciplinary workflows. In addition to retrospective validation, prospective evaluation is essential before clinical deployment. We plan to integrate the proposed model into the hospital's information system, enabling automatic generation of stage recommendations when a patient is admitted and diagnosed with esophageal cancer. Selected clinicians will be invited to participate in a controlled pilot study to assess the model's impact on clinical decision-making, diagnostic efficiency, and inter-observer agreement. All such testing will strictly comply with institutional review board (IRB) and ethical requirements, ensuring that patient safety and data privacy remain paramount.

Conclusions

This study proposes an effective LLM-based approach for esophageal cancer staging. Through comparison with clinicians, INF-72B+IR demonstrated higher accuracy and F_1-scores in cancer staging, highlighting its potential as an assistive tool in clinical practice. These results suggest that LLM-based methods can serve as reliable decision-support systems, complementing human expertise and potentially improving the consistency and efficiency of oncologic care. Future work will prioritize expanding the dataset, enhancing multimodal integration of imaging and text data, and validating the model across diverse clinical settings through prospective studies. Beyond esophageal cancer, the proposed framework could be extended to staging and diagnosis in other malignancies, contributing to the broader advancement of intelligent health care systems.

Acknowledgments

This research was funded by Shanghai Municipal Commission of Economy and Informatization (grant 2024-GZL-RGZN-02011).

Conflicts of Interest

None declared.

Multimedia Appendix 1
Additional figures, tables, and examples of model inputs and outputs.
[DOCX File, 5036 KB - medinform_v13i1e75556_app1.docx]

References

1. Liu CQ, Ma YL, Qin Q, et al. Epidemiology of esophageal cancer in 2020 and projections to 2030 and 2040. Thorac Cancer 2023 Jan;14(1):3-11. [doi: 10.1111/1759-7714.14745] [Medline: 36482832]
2. Kamangar F, Nasrollahzadeh D, Safiri S, et al. The global, regional, and national burden of oesophageal cancer and its attributable risk factors in 195 countries and territories, 1990–2017: a systematic analysis for the global burden of disease study 2017. Lancet Gastroenterol Hepatol 2020 Jun;5(6):582-597. [doi: 10.1016/S2468-1253(20)30007-8]

XSL•FO
RenderX

3. Yang S, Lin S, Li N, et al. Burden, trends, and risk factors of esophageal cancer in China from 1990 to 2017: an up-to-date overview and comparison with those in Japan and South Korea. J Hematol Oncol 2020 Nov 2;13(1):146. [doi: 10.1186/s13045-020-00981-4] [Medline: 33138852]
4. Lee SL, Yadav P, Starekova J, et al. Diagnostic performance of MRI for esophageal carcinoma: a systematic review and meta-analysis. Radiology 2021 Jun;299(3):583-594. [doi: 10.1148/radiol.2021202857] [Medline: 33787334]
5. van Hagen P, Hulshof M, van Lanschot JJB, et al. Preoperative chemoradiotherapy for esophageal or junctional cancer. N Engl J Med 2012 May 31;366(22):2074-2084. [doi: 10.1056/NEJMoa1112088] [Medline: 22646630]
6. Daiko H, Kato K. Updates in the 8th edition of the TNM staging system for esophagus and esophagogastric junction cancer. Jpn J Clin Oncol 2020 Aug 4;50(8):847-851. [doi: 10.1093/jjco/hyaa082] [Medline: 32519741]
7. Nobel T, Sihag S. Advances in diagnostic, staging, and restaging evaluation of esophageal and gastric cancer. Surg Oncol Clin N Am 2024 Jul;33(3):467-485. [doi: 10.1016/j.soc.2024.02.002] [Medline: 38789190]
8. Varghese TK Jr, Hofstetter WL, Rizk NP, et al. The society of thoracic surgeons guidelines on the diagnosis and staging of patients with esophageal cancer. Ann Thorac Surg 2013 Jul;96(1):346-356. [doi: 10.1016/j.athoracsur.2013.02.069] [Medline: 23752201]
9. Bhayana R, Nanda B, Dehkharghanian T, et al. Large language models for automated synoptic reports and resectability categorization in pancreatic cancer. Radiology 2024 Jun;311(3):e233117. [doi: 10.1148/radiol.233117] [Medline: 38888478]
10. Dorfner FJ, Jürgensen L, Donle L, et al. Comparing commercial and open-source large language models for labeling chest radiograph reports. Radiology 2024 Oct;313(1):e241139. [doi: 10.1148/radiol.241139] [Medline: 39470431]
11. Fink MA, Bischoff A, Fink CA, et al. Potential of ChatGPT and GPT-4 for data mining of free-text CT reports on lung cancer. Radiology 2023 Sep;308(3):e231362. [doi: 10.1148/radiol.231362] [Medline: 37724963]
12. Wu SH, Tong WJ, Li MD, et al. Collaborative enhancement of consistency and accuracy in US diagnosis of thyroid nodules using large language models. Radiology 2024 Mar;310(3):e232255. [doi: 10.1148/radiol.232255] [Medline: 38470237]
13. Abdullah A, Kim ST. Automated radiology report labeling in chest X-ray pathologies: development and evaluation of a large language model framework. JMIR Med Inform 2025 Mar 28;13:e68618. [doi: 10.2196/68618] [Medline: 40153539]
14. Wals Zurita AJ, Miras Del Rio H, Ugarte Ruiz de Aguirre N, et al. The transformative potential of large language models in mining electronic health records data: content analysis. JMIR Med Inform 2025 Jan 2;13:e58457. [doi: 10.2196/58457] [Medline: 39746191]
15. Adams LC, Truhn D, Busch F, et al. Leveraging GPT-4 for post hoc transformation of free-text radiology reports into structured reporting: a multilingual feasibility study. Radiology 2023 May;307(4):e230725. [doi: 10.1148/radiol.230725] [Medline: 37014240]
16. Liu Q, Hyland S, Bannur S, et al. Exploring the boundaries of GPT-4 in radiology. arXiv. Preprint posted online on Oct 23, 2023. [doi: 10.48550/arXiv.2310.14573]
17. Cardamone NC, Olfson M, Schmutte T, et al. Classifying unstructured text in electronic health records for mental health prediction models: large language model evaluation study. JMIR Med Inform 2025 Jan 21;13:e65454. [doi: 10.2196/65454] [Medline: 39864953]
18. Le Guellec B, Lefèvre A, Geay C, et al. Performance of an open-source large language model in extracting information from free-text radiology reports. Radiol Artif Intell 2024 Jul;6(4):e230364. [doi: 10.1148/ryai.230364] [Medline: 38717292]
19. Mahyoub M, Dougherty K, Shukla A. Extracting pulmonary embolism diagnoses from radiology impressions using GPT-4o: large language model evaluation study. JMIR Med Inform 2025 Apr 9;13:e67706. [doi: 10.2196/67706] [Medline: 40203306]
20. Lee JE, Park KS, Kim YH, Song HC, Park B, Jeong YJ. Lung cancer staging using chest CT and FDG PET/CT free-text reports: comparison among three ChatGPT large language models and six human readers of varying experience. AJR Am J Roentgenol 2024 Dec;223(6):e2431696. [doi: 10.2214/AJR.24.31696] [Medline: 39230409]
21. Kim S, Jang S, Kim B, et al. Automated Pathologic TN classification prediction and rationale generation from lung cancer surgical pathology reports using a large language model fine-tuned with chain-of-thought: algorithm development and validation study. JMIR Med Inform 2024 Dec 20;12:e67056. [doi: 10.2196/67056] [Medline: 39705675]
22. Matsuo H, Nishio M, Matsunaga T, Fujimoto K, Murakami T. Exploring multilingual large language models for enhanced TNM classification of radiology report in lung cancer staging. Cancers (Basel) 2024 Oct 26;16(21):3621. [doi: 10.3390/cancers16213621] [Medline: 39518061]
23. Sun SH, Huynh K, Cortes G, et al. Testing the ability and limitations of ChatGPT to generate differential diagnoses from transcribed radiologic findings. Radiology 2024 Oct;313(1):e232346. [doi: 10.1148/radiol.232346] [Medline: 39404623]
24. Brown TB, Mann B, Ryder N, et al. Language models are few-shot learners. arXiv. Preprint posted online on May 28, 2020. [doi: 10.48550/arXiv.2005.14165]
25. Wei J, Wang X, Schuurmans D, et al. Chain-of-thought prompting elicits reasoning in large language models. arXiv. Preprint posted online on Jan 28, 2022. [doi: 10.48550/arXiv.2201.11903]
26. Shao W, Zhao C, Li H, et al. Pathological responses of primary tumor and lymph nodes in non-small cell lung cancer after neoadjuvant chemoimmunotherapy: a retrospective real-world study. J Thorac Dis 2024 Oct 31;16(10):6427-6440. [doi: 10.21037/jtd-24-1011] [Medline: 39552859]
27. Towards trustworthy large language models in industry domains. : INF-Team; 2024 URL: https://s.infly.cn/f/img/pdf/Towards_Trustworthy_LLMs.pdf [accessed 2024-11-11]

XSL•FO
RenderX

28. Yang A, Yang B, Zhang B, et al. Qwen2.5 technical report. arXiv. Preprint posted online on Dec 19, 2024. [doi: 10.48550/arXiv.2412.15115]
29. Grattafiori A, Dubey A, Jauhri A, et al. The Llama 3 herd of models. arXiv. Preprint posted online on Jul 31, 2024. [doi: 10.48550/arXiv.2407.21783]
30. Zhong W, Liu Y, Liu Y, et al. Performance of ChatGPT-4o and four open-source large language models in generating diagnoses based on China's rare disease catalog: comparative study. J Med Internet Res 2025 Jun 18;27:e69929. [doi: 10.2196/69929] [Medline: 40532199]
31. Wang A, Liu C, Yang J, Weng C. Fine-tuning large language models for rare disease concept normalization. J Am Med Inform Assoc 2024 Sep 1;31(9):2076-2083. [doi: 10.1093/jamia/ocae133] [Medline: 38829731]
32. Huang J, Yang DM, Rong R, et al. A critical assessment of using ChatGPT for extracting structured data from clinical notes. NPJ Digit Med 2024 May 1;7(1):106. [doi: 10.1038/s41746-024-01079-8] [Medline: 38693429]
33. Chang CH, Lucas MM, Lee Y, Yang CC, Lu-Yao G. Beyond self-consistency: ensemble reasoning boosts consistency and accuracy of LLMs in cancer staging. arXiv. Preprint posted online on Apr 19, 2024. [doi: 10.48550/arXiv.2404.13149]
34. Chang CH, Lucas MM, Lu-Yao G, Yang CC. Classifying cancer stage with open-source clinical large language models. Presented at: 2024 IEEE 12th International Conference on Healthcare Informatics (ICHI); Jun 3-6, 2024; Orlando, FL, USA. [doi: 10.1109/ICHI61247.2024.00018]
35. Elbattah M, Arnaud E, Ghazali DA, Dequen G. Exploring the ethical challenges of large language models in emergency medicine: a comparative international review. Presented at: 2024 IEEE International Conference on Bioinformatics and Biomedicine (BIBM); Dec 3-6, 2024; Lisbon, Portugal. [doi: 10.1109/BIBM62325.2024.10822376]

Abbreviations

CoT: chain-of-thought
CT: computed tomography
cTNM: clinical tumor–node metastasis
GDPR: General Data Protection Regulation
HIPAA: Health Insurance Portability and Accountability Act
IR: interpretable reasoning
LLM: large language model
PET: positron emission tomography
pTNM: pathological tumor–node metastasis
ZS: zero-shot

Edited by A Benis; submitted 06.04.25; peer-reviewed by M Elbattah, M Chukwuka, SB Guo; revised version received 11.08.25; accepted 04.09.25; published 17.10.25.

Please cite as:
Yao Y, Cen X, Gan L, Jiang J, Wang M, Xu Y, Yuan J
Automated Esophageal Cancer Staging From Free-Text Radiology Reports: Large Language Model Evaluation Study
JMIR Med Inform 2025;13:e75556
URL: https://medinform.jmir.org/2025/1/e75556
doi:10.2196/75556

©Yao Yao, Xingxing Cen, Lu Gan, Jiehui Jiang, Min Wang, Yinghui Xu, Junyi Yuan. Originally published in JMIR Medical Informatics (https://medinform.jmir.org), 17.10.2025. This is an open-access article distributed under the terms of the Creative Commons Attribution License (https://creativecommons.org/licenses/by/4.0/), which permits unrestricted use, distribution, and reproduction in any medium, provided the original work, first published in JMIR Medical Informatics, is properly cited. The complete bibliographic information, a link to the original publication on https://medinform.jmir.org/, as well as this copyright and license information must be included.

XSL•FO
RenderX

Large Language Models as a Consulting Hotline for Patients With Breast Cancer and Specialists in China: Cross-Sectional Questionnaire Study

Hui Liu[1*], MBBS; Jialun Peng[2*], MBBS; Lu Li[1], MBBS; Ao Deng[1], MBBS; XiangXin Huang[1], MBBS; Guobing Yin[1], PhD; Haojun Luo[1,3], PhD

[1]Department of Thyroid and Breast Surgery, The Second Affiliated Hospital of Chongqing Medical University, 74 Linjiang Road, Chongqing, China

[2]Department of Hepatobiliary Surgery, The Second Affiliated Hospital of Chongqing Medical University, Chongqing, China

[3]Department of Thyroid and Breast Surgery, Renji Hospital Affiliated of Chongqing University, Chongqing, China

[*]these authors contributed equally

Corresponding Author:
Haojun Luo, PhD
Department of Thyroid and Breast Surgery, The Second Affiliated Hospital of Chongqing Medical University, 74 Linjiang Road, Chongqing, China

Abstract

Background: The disease burden of breast cancer is increasing in China. Guiding people to obtain accurate information on breast cancer and improving the public's health literacy are crucial for the early detection and timely treatment of breast cancer. Large language model (LLM) is a currently popular source of health information. However, the accuracy and practicality of the breast cancer–related information provided by LLMs have not yet been evaluated.

Objective: This study aims to evaluate and compare the accuracy, practicality, and generalization-specificity of responses to breast cancer–related questions from two LLMs, ChatGPT and ERNIE Bot (EB).

Methods: The questions asked to the LLMs consisted of a patient questionnaire and an expert questionnaire, each containing 15 questions. ChatGPT was queried in both Chinese and English, recorded as ChatGPT-Chinese (ChatGPT-C) and ChatGPT-English (ChatGPT-E) respectively, while EB was queried in Chinese. The accuracy, practicality, and generalization-specificity of each inquiry's responses were rated by a breast cancer multidisciplinary treatment team using Likert scales.

Results: Overall, for both the patient and expert questionnaire, the accuracy and practicality of responses from ChatGPT-E were significantly higher than those from ChatGPT-C and EB (all *Ps*<.001). However, the responses from all LLMs are relatively generalized, leading to lower accuracy and practicality for the expert questionnaire compared to the patient questionnaire. Additionally, there were issues such as the lack of supporting evidence and potential ethical risks in the responses of LLMs.

Conclusions: Currently, compared to other LLMs, ChatGPT-E has demonstrated greater potential for application in educating Chinese patients with breast cancer, and may serve as an effective tool for them to obtain health information. However, for breast cancer specialists, these LLMs are not yet suitable for assisting in clinical diagnosis or treatment activities. Additionally, data security, ethical, and legal risks associated with using LLMs in clinical practice cannot be ignored. In the future, further research is needed to determine the true efficacy of LLMs in clinical scenarios related to breast cancer in China.

(JMIR Med Inform 2025;13:e66429) doi:10.2196/66429

KEYWORDS

large language models; breast cancer; health education; cross-sectional study

Introduction

Breast cancer has become the most common malignant tumor globally, with an estimated 11.7% of all new cancer cases in 2020 [1]. The incidence of breast cancer has been rising in China, with 420,000 Chinese women diagnosed in 2020, accounting for 18% of global cases [2]. Breast cancer also contributes significantly to cancer-related deaths; however, early detection and timely treatment play a significant role in reducing its mortality rate [3-5]. Providing health education through appropriate channels and disseminating accurate medical health information to the public can help improve public awareness of breast cancer, thereby alleviating the burden of breast cancer in China. Currently, the internet is the primary source for people to obtain health information. Recent studies showed that 55% of Europeans aged 16‐74 years seek health-related information online, while in mainland China, nearly 79% of the population searches for health information on the internet [6,7]. However,

XSL•FO
RenderX

the quality of online health information varies considerably, and inaccurate or even erroneous health information may lead to patients making inappropriate medical decisions, posing a threat to public health [8-10]. Large language model (LLM) is a type of chatbot that combines artificial intelligence with natural language processing, are trained on massive text data [11]. ChatGPT, developed by OpenAI, has garnered global attention since its release and been applied across multiple fields. ERNIE Bot (EB; Chinese name: Wenxin-Yiyan), developed by Baidu, benefits from Baidu's strong influence in artificial intelligence and has achieved significant popularity and a user base in the Chinese market. These tools have recently become widely popular and demonstrated significant potential in the medical field [12]. Studies have shown that ChatGPT has greater potential for patient education in breast reconstruction and diabetes self-management, while also being able to accurately answer some cancer-related questions [11,13,14]. However, some scholars have questioned the accuracy and practicality of the medical health information provided by ChatGPT [12]. Currently, there is a lack of studies evaluating the educational potential of ChatGPT and EB—two of the most commonly used LLMs in China—among Chinese patients with breast cancer and their utility for Chinese breast cancer physicians. To address this gap, this study assesses whether these LLMs can serve as educational tools for Chinese patients with breast cancer and clinical assistance tools for Chinese breast cancer specialists by comparing the accuracy and reliability of responses to breast cancer–related questions between ChatGPT and EB.

Methods

Questionnaire Design and Data Collection

The questions asked to LLMs consisted of a patient questionnaire and an expert questionnaire, each containing 15 questions and covering aspects such as the diagnosis, treatment, prognosis, and follow-up of breast cancer. The patient questionnaire was derived by distributing a questionnaire to patients with breast cancer to investigate their most important concerns (Textbox 1). The expert questionnaire was summarized by two experienced breast surgeons, based on the National Comprehensive Cancer Network (NCCN) Clinical Practice Guidelines in Oncology for breast cancer and the International Consensus Guidelines for advanced breast cancer (Textbox 2) [15,16]. On January 15, 2024, all questions were input into ChatGPT (version 4.0) and EB (version 4.0). Each input was independently entered using the "new chat" function and inputted twice to detect its repeatability. To optimize the responses of the LLMs, prompt engineering was applied with the same lead-in statement: "Now that you are a breast cancer specialist, please answer the following questions," which was input into the LLMs along with each question. As ChatGPT was developed in the United States, we queried ChatGPT in both Chinese and English, denoted as ChatGPT-Chinese (ChatGPT-C) and ChatGPT-English (ChatGPT-E), respectively, and the EB, developed in China, was queried in Chinese only. The responses from ChatGPT and EB were recorded using Microsoft Excel (Multimedia Appendix 1).

Textbox 1. Specific contents of patient questionnaire.

Patient Questionnaire

1. Is breast cancer hereditary, and will it have an impact on my descendants?
2. What impact does the staging of breast cancer have on treatment and prognosis?
3. What are the treatment methods for breast cancer, and which one should I choose?
4. What are the various surgical treatment methods for breast cancer, and how do they each impact the appearance of the breast?
5. What is the total cost of treating breast cancer in China?
6. What aspects are included in the postoperative rehabilitation training for breast cancer, and what benefits does it bring to rehabilitation
7. Is breastfeeding possible during breast cancer treatment?
8. Why do I need systemic treatment (such as chemotherapy, endocrine therapy, or targeted therapy) after breast cancer surgery?
9. What are the adverse reactions of drugs used in breast cancer treatment?
10. How do I manage psychological and emotional health issues during the treatment of breast cancer?
11. What lifestyles contribute to the recovery of breast cancer patients?
12. What daily care is required for a subcutaneously implanted infusion port?
13. Can breast cancer patients have normal fertility after discharge?
14. What is the risk of recurrence and the corresponding monitoring methods after breast cancer treatment?
15. If a breast cancer patient has other chronic illnesses or new health issues that need to be addressed, how should these issues be coordinated with the treatment of breast cancer?

XSL•FO
RenderX

Textbox 2. Specific contents of expert questionnaire.

Expert Questionnaire

1. What are the screening methods for breast cancer?
2. What imaging and biomarkers will you use to assist in the preoperative diagnosis of breast cancer?
3. What are the requirements for the surgical margins in breast-conserving surgery for ductal carcinoma in situ?
4. For cN1 breast cancer patients who have converted to cN0 after neoadjuvant therapy, what are the requirements for sentinel lymph node biopsy at this stage?
5. What surgical methods do you know for stage I breast reconstruction?
6. What is the strategy for adjuvant chemotherapy in early-stage triple-negative breast cancer?
7. For early-stage high-risk breast cancer patients with strongly positive hormone receptors, which adjuvant endocrine therapy would you recommend?
8. What are the different classes of drugs for anti-HER2 therapy?
9. What is the first-line treatment of choice for stage IV or recurrent metastatic HR-positive/HER2-negative breast cancer?
10. What are the conditions for exemption from radiotherapy after breast-conserving surgery
11. What are the common regimens for neoadjuvant therapy in triple-negative breast cancer?
12. What are your basic principles for the treatment of metastatic breast cancer?
13. What are your recommendations for the management of bone health in patients during adjuvant endocrine therapy?
14. For young female breast cancer patients with HR-positive tumors who express a desire for fertility, what considerations do you have in the treatment plan?
15. How should long-term follow-up and monitoring be conducted for breast cancer patients?

Response Assessment

The breast cancer multidisciplinary treatment team scored the accuracy, practicality, and generalization-specificity of each response using a Likert scale, with the poorer of the two responses being included in the final score if the responses were inconsistent. The team consisted of 13 members, including 7 breast cancer specialists, 2 imaging specialists, 2 pathology specialists, and 2 nursing specialists. The Likert scale is a hierarchical scale, originally developed by Likert and has been used extensively in several research studies [17,18]. Accuracy was divided into 6 levels from 1 to 6, with higher scores indicating better accuracy (Table 1). Practicality was divided into 4 levels from 1 to 4, with higher scores indicating better practicality (Table 2). The generalization-specificity score (GSS) is divided into 5 levels from 1 to 5, with higher scores indicating better specificity (Table 3). To reduce bias caused by individual differences in understanding the scoring system, all experts reviewed and discussed the scoring criteria of the Likert scale before the assessment.

Table . Accuracy scoring standard.

Scoring description	Scoring
Completely incorrect	1
More incorrect than correct	2
Approximately equal correct and incorrect	3
More correct than incorrect	4
Nearly all correct	5
All correct	6

Table . Practical scoring standard.

Scoring description	Scoring
Completely impractical	1
Slightly practical	2
Moderately practical	3
Very practical	4

XSL•FO
RenderX

Table . Generalization-Specificity Score (GSS) scoring standard.

Scoring description	Scoring
Fully generalized, with no specific details or targeted information provided	1
Primarily generalized but mentions some relevant details or information	2
Combines generalized content with some specific details or information	3
Rather specific, but the details or targeted information are insufficient and can be improved	4
Fully specific, with comprehensive details and highly targeted information	5

Statistical Analysis

The Shapiro-Wilk test was used to determine the normality of the scores and the Levene test was used to evaluate the homogeneity of variance. Differences between two groups were assessed using the Wilcoxon rank sum test. The Kruskal-Wallis test evaluated differences between three or more groups of variables, and the Dunn test was used for two-way between-group comparisons of variables that were not normally distributed. $P<.05$ was deemed statistically significant. The intraclass correlation coefficient (ICC) was used to evaluate the consistency of accuracy, practicality scores and GSS among 13 raters. An ICC ≥0.75 was considered to indicate good consistency. All statistical analyses were performed using R software (version 4.0.3; R Foundation for Statistical Computing).

Ethical Considerations

This study did not gather patient data and did not involve human subjects. Therefore, approval by the institutional review board of Chongqing Medical University was not required.

Results

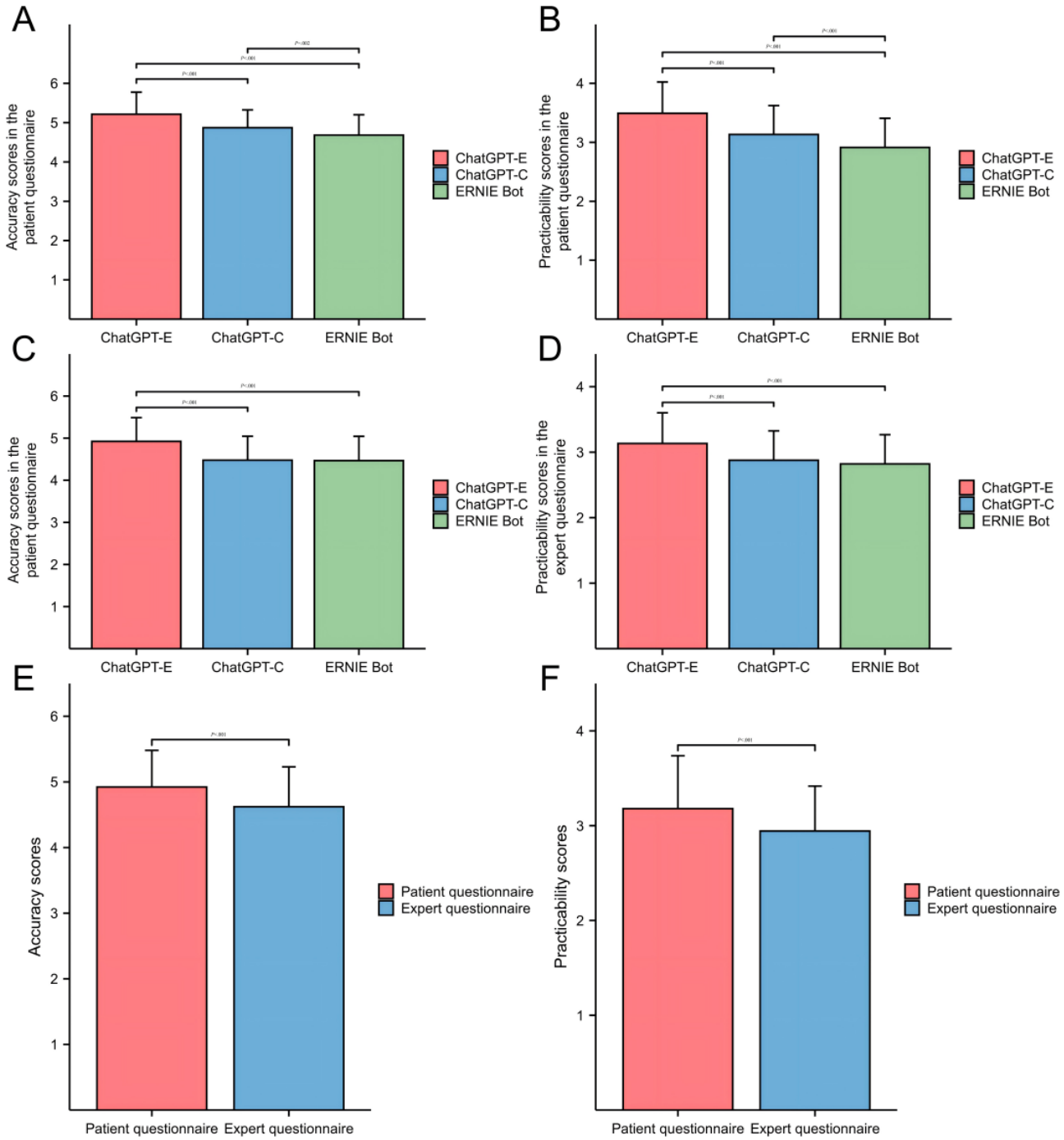
In the patient questionnaire, the median accuracy scores of ChatGPT-E, ChatGPT-C, and EB were 5.00 (IQR 5.00-6.00), 5.00 (IQR 5.00-6.00), and 5.00 (IQR 4.00-5.00), respectively. The median practicality scores of ChatGPT-E, ChatGPT-C, and EB were 4.00 (IQR 3.00-4.00), 3 (IQR 3.00-3.00), and 3.00 (IQR 3.00-3.00), respectively; and the median GSS were 4.00 (IQR 3.00-4.00), 3 (IQR 3.00-4.00), and 3.00 (IQR 3.00-4.00), respectively. The accuracy and practicality of ChatGPT-E were significantly higher than those of ChatGPT-C and EB ($P<.001$). The accuracy and practicality of ChatGPT-C were also significantly higher than those of EB ($P=.002$ and $P<.001$, respectively; Figure 1A and B). The specificity of the ChatGPT-E responses was significantly higher than that of the ChatGPT-C and EB ($P=.002$ and $P<.001$, respectively), whereas no significant difference was found in the specificity of the ChatGPT-C and EB responses (Multimedia Appendix 2, parts A and B).

In the expert questionnaire, the median accuracy scores of ChatGPT-E, ChatGPT-C, and EB were 5.00 (IQR 5.00-5.00), 4.00 (IQR 4.00-5.00), and 4.00 (IQR 4.00-5.00), respectively; the median practicality scores for all three were 3.00 (IQR 3.00-3.00) and the median GSS were 4.00 (IQR 3.00-4.00), 3 (IQR 2.00- 4.00), and 3.00 (IQR 2.00-3.00), respectively. The accuracy and practicality of ChatGPT-E were significantly higher than that of ChatGPT-C and EB (all $P<.001$). However, there was no significant difference in the accuracy and practicality scores between ChatGPT-C and EB ($P=1.000$ and $P=.72$, respectively) (Figure 1). For response generalization and specificity, the ChatGPT-E score was significantly higher than ChatGPT-C and EB (both $P<.001$), whereas there was no significant difference between ChatGPT-C and EB. Overall, the median accuracy scores of the patient questionnaire and the expert questionnaire were 5.00 (IQR 5.00-5.00) and 5.00 (IQR 4.00-5.00), respectively; the median practicality scores were 3.00 (IQR 3.00-4.00), and 3.00 (IQR 3.00-3.00), respectively; the median practicality scores were 3.00 (IQR 3.00-4.00), and 3.00 (IQR 3.00-3.00), respectively, and the median GSS was 3.00 (IQR 3.00-4.00) for both questionnaires. The accuracy and practicality scores from the patient questionnaire were significantly higher than those from the expert questionnaire (all $P<.001$) (Figure 1), and their specificity scores were also significantly higher ($P<.001$) (Multimedia Appendix 2, parts C-E).

In addition, to quantify the frequency of ratings for accuracy, practicality, and specificity in LLM responses, we illustrated the rating distribution as percentages in Multimedia Appendix 3. For accuracy, responses rated as 6 (All correct) accounted for only 11.96% (70/585) in the patient questionnaire, 5.64% (33/585) in the expert questionnaire, and 8.8% (103/1170) overall. Notably, the hallucination rate—defined as responses rated ≤4 on the accuracy scale—was 19.7% (115/585) in the patient questionnaire and 28.9% (169/585) in the expert questionnaire. For practicality, responses rated as 4 (Very practical) accounted for 26.15% (153/585) in the patient questionnaire, 8.55% (50/585) in the expert questionnaire, and 17.35% (203/1170) overall. For generalization-specificity, responses rated as 5 (Fully specific) accounted for 5.64% (33/585) in the patient questionnaire, 2.39% (14/585) in the expert questionnaire, and 4.02% (47/1170) overall. The 13 raters exhibited excellent inter-rater agreement in their scoring of accuracy, practicality, and GSS, with ICC values of 0.878 (95%Cl 0.837 - 0.912), 0.823 (95%Cl 0.765 - 0.873), and 0.809 (95%Cl 0.758 - 0.855) respectively. Additionally, the statistical descriptive indices for all between-group comparisons are provided in detail in Multimedia Appendices 4-8.

XSL•FO
RenderX

Figure 1. Scores and comparisons of the overall accuracy and practicality of the LLMs' responses. (A,B): Patient questionnaire; (C,D) Expert questionnaire; (E,F): Comparison of patient and expert questionnaire. Error bars represent mean ± standard error.



Discussion

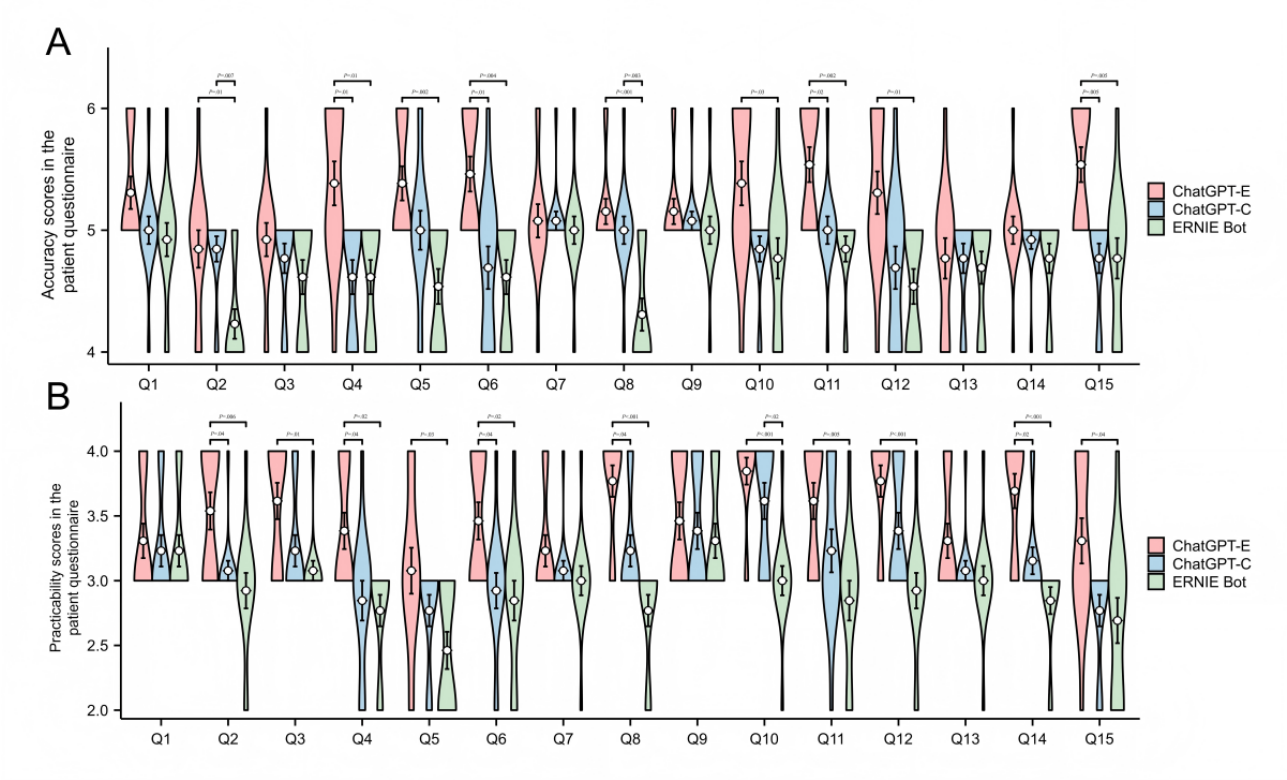
Principal Findings

We have reported several important findings in this study. First, based on the patient questionnaire responses, ChatGPT-E demonstrated significantly higher accuracy compared to ChatGPT-C and EB in addressing questions related to breast cancer surgery treatment (Q4) and postoperative management (Q6, Q11, and Q15) (Figure 2A). Additionally, ChatGPT-E's responses to questions concerning breast cancer staging (Q2), treatment (Q4 and Q8), and postoperative management (Q6 and 14) were more comprehensive and practical (Figure 2). In the expert questionnaire, ChatGPT-E demonstrated similar advantages, especially for breast cancer drug treatment (Q8) and follow-up (Q15), with more comprehensive, accurate, and practical responses, reflecting higher efficiency (Figure 3). Overall, ChatGPT-E performed the best in both patient and expert questionnaires. Despite the advantages in training strategies that may have enabled ChatGPT-C to perform better than EB in answering general questions from patients with breast cancer, the performances of both models were unsatisfactory while answering comparatively specialized questions in the field of breast cancer in the Chinese-language context (Figure 1). For example, in response to the expert questionnaire Q5, both ChatGPT-C and EB only briefly mentioned several common methods of first-stage breast reconstruction. Only

XSL•FO
RenderX

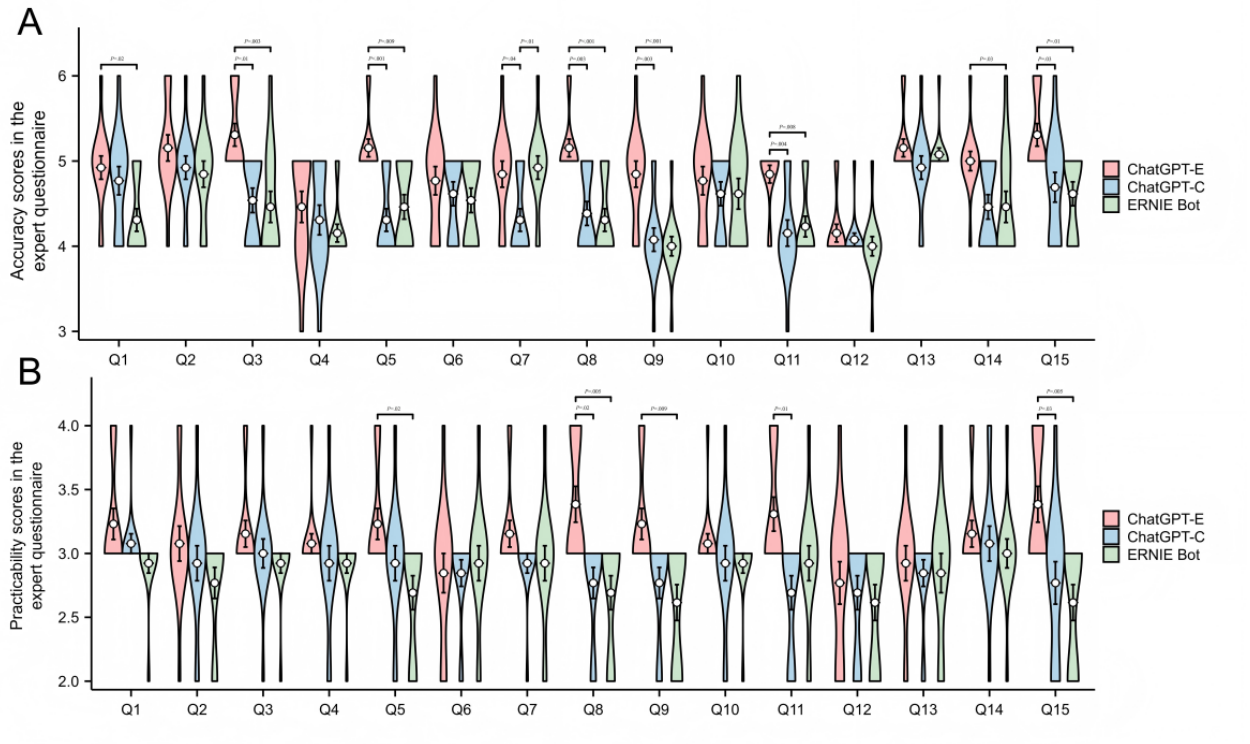
ChatGPT-E mentioned "latissimus dorsi flap breast reconstruction" and briefly introduced the advantages of each surgical method. Although its response was not detailed enough, the basic framework was correct. Although the overall hallucination rate of ChatGPT-E was significantly lower than that of ChatGPT-C and EB (both $P<.001$), 11.79% (23/195) of its responses in the expert questionnaire still contained inaccurate information. This finding indicates that even models with relatively superior performance must further reduce hallucination rates in the specialized field of breast cancer to meet clinical requirements.

Figure 2. Scores and comparisons of LLMs' responses to specific questions in the patient questionnaire. A: Accuracy; B: Practicality. Error bars represent mean ± standard error. ChatGPT-E: ChatGPT-English ; ChatGPT-C: ChatGPT-Chinese; EB: ERNIE Bot.



XSL•FO
RenderX

Figure 3. Scores and comparisons of LLMs' responses to specific questions in the expert questionnaire. A: Accuracy; B: Practicality. Error bars represent mean ± standard error. ChatGPT-E: ChatGPT-English ; ChatGPT-C: ChatGPT-Chinese; EB: ERNIE Bot.



Cross-Language Limitations of ChatGPT

In addition, we found that ChatGPT-C's responses to the 15 questions in the patient and expert questionnaire each contained one notable medical terminology translation error. For instance, "泛素酮 (Tamoxifen)" and "莱特罗唑 (Letrozole)" were mentioned in the response to expert questionnaire Q7. In patient questionnaire Q12, the term "port" in "subcutaneously implanted infusion port" was translated as "harbor" (ie, 港口 in Chinese). Patients may misinterpret postoperative care requirements due to this nonstandard translation, potentially leading to complications. In the medical domain, English is the primary language for international academic communication. ChatGPT's core training data is predominantly in English, including extensive English medical literature and clinical guidelines (eg, National Comprehensive Cancer Network and Advanced Breast Cancer). Compared with EB, ChatGPT has greater access to and understanding of these professional resources, enabling it to provide more comprehensive and accurate information when answering related questions. The inferior performance of ChatGPT-C compared to ChatGPT-E may stem from limitations in cross-language processing. Although ChatGPT supports multiple languages, the semantic structure and medical terminology in Chinese differ significantly from English. During cross-language processing, ChatGPT may rely on translation mechanisms rather than native Chinese training, leading to semantic distortion in specialized content and reduced answer quality. Preliminary testing in other languages such as Spanish and French has identified similar issues when dealing with proper nouns (eg, medications, surgical procedures) and compound terms. The model tends to rely on literal translation or the creation of neologisms rather than following localized standards, which may lead to ambiguities. However, a recent study by Tian et al [19] on CHIMED-GPT found that pretraining GPT using a specific Chinese medical dataset made CHIMED-GPT perform significantly better than other models in tasks such as multiple choice and open-ended responses. To address the translation errors in ChatGPT-C's responses to breast cancer–related questions, fine-tuning the model with Chinese medical datasets represents an effective improvement strategy. These datasets should include a wide range of Chinese medical literature, clinical guidelines, case reports, and patient-doctor dialogues specific to the field of breast cancer. By training the model on these specialized datasets would help it grasp the nuances and context of medical language better, leading to more accurate translations and responses. In addition, user error correction interfaces can be designed to allow physicians or patients to flag translation errors (eg, "莱特罗唑 → 来曲唑"), and the system could then automatically collect these error cases and add them into fine-tuning datasets, thus achieving continuous model optimization. In terms of response repeatability, the performance of ChatGPT-E (52/60, 86.67%) was significantly better than ChatGPT-C (50/60, 83.33%) and EB (40/60, 66.67%).

Challenges Encountered by LLMs

It is worth noting that we have also found a lack of corresponding empirical data and references to support the views of the two LLMs in their responses, which could undermine the credibility and practicality of their responses, especially in evidence-based clinical practice [20,21]. For example, in responses to the expert questionnaire Q14 and patient questionnaire Q7, both LLMs mentioned that "chemotherapy affects fertility or breastfeeding," but failed to provide any useful

XSL•FO
RenderX

references, resulting in compromised credibility and possibly inability to guide physicians and patients in making correct decisions. In addition, the responses of LLMs were relatively generalized, indicating that they were widely mentioned but lacked specificity, similar to the findings of the study by Giannakopoulos et al [22] who used LLMs to answer dental-related questions. This generalized responses also resulted in the LLMs being less accurate and practical in answering the expert questionnaire than the patient questionnaire (Figure 1). For example, in the responses to expert questionnaire Q15 and patient questionnaire Q14, although LLMs mentioned the need for regular follow-up and corresponding examinations for patients with breast cancer, they did not provide specific answers. These generalized responses are of limited value to clinical professionals, who require highly accurate, comprehensive, and professional information, similar to previous studies on ChatGPT's responses to mental health and liver cancer–related questions [23,24]. However, they may be beneficial for patients with breast cancer who lack medical expertise, as the responses from LLMs already covered the vast majority of the questions and were comparable to clinician responses, similar to the findings from a study by Endo et al [25] on the use of LLMs for answering questions related to liver transplantation. Generalized LLM–generated information poses risks ranging from clinical mismanagement to ethical violations, particularly in complex fields such as breast cancer. Given that in breast cancer treatment, timely decision-making is critical early diagnosis and intervention significantly improve cure and survival rates. Vague recommendations from LLMs may put patients at risk of missing the optimal therapeutic window, thus potentially exacerbating disease progression. While LLMs such as ChatGPT-E show promise in patient education, their utility depends on the patients' ability to contextualize and validate the outputs provided. Patients should maintain a cautious attitude toward responses generated by LLMs that lack personalized recommendations and refrain from relying on them exclusively. It is recommended that patients use the information provided by LLMs as a general reference, while promptly communicating with professional physicians. By integrating their specific clinical circumstances, patients can obtain accurate and personalized medical advice and guidance to safeguard their health and safety.

Ethics and Data Security in LLMs

Furthermore, LLMs have exposed potential ethical risks in responding to breast cancer–related questions. While clinical trials may offer access to the latest therapeutic regimens and advanced technologies, they inherently carry uncertainties and potential adverse effects. When responding to Patient Questionnaire Q2 and Expert Questionnaire Q6, LLMs encouraged patient participation in clinical trials without adequately explaining the risks and uncertainties involved. This could lead patients to assume unnecessary risks without being fully informed [26]. We recommend establishing a dedicated review team to systematically audit medical recommendations provided by LLMs, particularly regarding clinical trial recommendations and vague suggestions. This ensures that LLMs responses adhere to medical ethical standards and professional norms, and correct or block responses that do not meet the requirements. At the same time, the issue of data security involved in LLMs is becoming increasingly prominent [27]. Although the responses of the LLMs in this study did not inadvertently leak sensitive information and were based on general medical knowledge and standardized recommendations, some studies have shown that LLMs may inadvertently memorize and disclose original data in their responses [28,29]. In a study by Nasr et al [30], researchers were able to extract training data for various LLMs including ChatGPT through specific "attacks". Therefore, doctors or health care organizations should obtain informed consent from patients when using real patient data for model training and application to LLMs, while ensuring the anonymization and deidentification of data [26]. Patients should also be trained in data security awareness and instructed to avoid disclosing private personal information while using LLMs to obtain health information [31]. China has established a series of laws and regulations, including the Personal Information Protection Law (PIPL) to regulate data processing and applications. However, specific regulatory details for LLM–based medical applications are still being explored and refined. The effective implementation of these laws and regulations in the LLM–based medical applications is currently a concern [32]. Based on the results of this study, future regulation should focus on standardizing the LLM–based medical applications. It is essential to strictly regulate data processing procedures to ensure data security and privacy protection in compliance with laws and regulations such as the PIPL. Further, an ethical review mechanism for LLM–based medical applications should be established, clarifying ethical guidelines in aspects such as medical information provision and patient decision-making guidance to prevent ethical risks [33]. Additionally, explicit limitations should be imposed on the scope and modalities of PIPLs in health care to prevent their excessive involvement in core medical operations when sufficient reliability is not assured.

Conclusion

This study reflects some important issues that may arise when using LLMs in clinical scenarios related to breast cancer in China. Overall, LLMs can serve as effective tools for Chinese patients with breast cancer to obtain health information, helping to address the majority of concerns related to diagnosis, treatment, recovery, and follow up of this population. However, in the context of breast cancer specialists, the accuracy, practicality, and relevance of LLMs' responses need improvement. We propose a multidimensional optimization framework to enhance the utility and reliability of ChatGPT in breast cancer diagnosis and management. On the one hand, the model should be trained using high-quality medical data, such as the latest breast cancer research, clinical guidelines, and case reports, to improve its accuracy and practicality in the professional domain. On the other hand, under ethical compliance, ChatGPT should be connected to deidentified electronic health records, laboratory systems, and imaging databases to access real-time patient data and provide more personalized recommendations. Based on our research, ChatGPT-E demonstrates better repeatability, accuracy, and practicality in its responses compared to other LLMs. Therefore, it is recommended that Chinese patients with breast cancer

XSL•FO
RenderX

translate their questions into English before querying ChatGPT, to improve its effectiveness. In addition, considering the potential data security, ethical, and legal risks of LLMs in clinical practice, it is essential to strengthen regulation of the training and application of LLMs in the medical professional field [34]. This study has certain limitations as the response from LLMs were not applied in real time to address the questions of patients with breast cancer or to assist doctors in making clinical decisions. We also did not evaluate all issues related to breast cancer. The data collection for this study was completed in January 2024. However, certain models (eg, GPT-4-turbo and DeepSeek) had not been publicly released at that time or failed to provide stable interfaces for academic research applications and therefore were not included in this study. Additionally, this study used structured questionnaires to evaluate the responses of LLMs, which ensured standardized assessment but partially limited the assessment of LLMs' ability to handle open-ended, unstructured, and interactive questions. Future iterations could incorporate open-ended or interactive question types to better simulate real-world clinical consultations. Lastly, patient and expert user feedback can provide critical user-perspective data, address the limitations of existing expert-only evaluations, and enhance the application effectiveness and user experience of LLMs in health care. Further research is required to evaluate the real-world clinical effectiveness of LLMs and the real user experience of patients with breast cancer in China.

Acknowledgments

Senior Medical Talents Program of Chongqing for Young and Middle-aged (NO: 2023171 - 21, 202374 - 04).

Data Availability

All data generated or analyzed in this study are included in this published article and its supplementary information files.

Authors' Contributions

Conceptualization: GY, H Liu, JP
Data curation: H Luo, H Liu, JP
Formal analysis: AD, H Luo, JP, LL, XH
Funding acquisition: H Luo
Investigation: H Liu, JP, LL, XH
Methodology: AD, JP
Project administration: AD, H Luo, GY
Resources: XH
Software: LL
Supervision: GY, H Luo, LL
Validation: AD, GY, H Luo
Visualization: H Liu, LL
Writing-original draft: H Liu, JP
Writing - review & editing: AD, GY, H Luo, LL, XH

Conflicts of Interest

None declared.

Multimedia Appendix 1
Specific contents of patient questionnaire and expert questionnaire and LLMs' response to them.
[DOCX File, 129 KB - medinform_v13i1e66429_app1.docx]

Multimedia Appendix 2
Comparison of generalization-specificity score (GSS).
[PNG File, 1765 KB - medinform_v13i1e66429_app2.png]

Multimedia Appendix 3
Percentage distribution of ratings.
[PNG File, 1622 KB - medinform_v13i1e66429_app3.png]

Multimedia Appendix 4
Comparison of overall accuracy, practicality, and generalization-specificity score (GSS) between patient and expert questionnaires using Mann-Whitney U Test.

XSL•FO
RenderX

[DOCX File, 12 KB - medinform_v13i1e66429_app4.docx]

Multimedia Appendix 5
Multiple hypothesis testing (Dunn test) results for overall accuracy, practicality, and generalization-specificity score (GSS) of patient questionnaires among different models.
[DOCX File, 12 KB - medinform_v13i1e66429_app5.docx]

Multimedia Appendix 6
Multiple hypothesis testing (Dunn test) results for overall accuracy, practicality, and generalization-specificity score (GSS) of expert questionnaires among different models.
[DOCX File, 12 KB - medinform_v13i1e66429_app6.docx]

Multimedia Appendix 7
Results of multiple hypothesis tests (Dunn test) on the accuracy, practicality, and generalization-specificity score (GSS) of specific questions of patient questionnaires across different models.
[DOCX File, 22 KB - medinform_v13i1e66429_app7.docx]

Multimedia Appendix 8
Results of multiple hypothesis tests (Dunn test) on the accuracy, practicality, and generalization-specificity score (GSS) of specific questions of expert questionnaires across different models.
[DOCX File, 21 KB - medinform_v13i1e66429_app8.docx]

References

1. Sung H, Ferlay J, Siegel RL, et al. Global Cancer Statistics 2020: GLOBOCAN estimates of incidence and mortality worldwide for 36 cancers in 185 countries. CA Cancer J Clin 2021 May;71(3):209-249. [doi: 10.3322/caac.21660] [Medline: 33538338]
2. Cao W, Chen HD, Yu YW, Li N, Chen WQ. Changing profiles of cancer burden worldwide and in China: a secondary analysis of the global cancer statistics 2020. Chin Med J 2021;134(7):783-791. [doi: 10.1097/CM9.0000000000001474]
3. Alteri R, Barnes C, Burke A, et al. Breast cancer facts & figures 2013-2014. : American Cancer Society; 2013.
4. Rosmawati NHN. Knowledge, attitudes and practice of breast self-examination among women in a suburban area in Terengganu, Malaysia. Asian Pac J Cancer Prev 2010;11(6):1503-1508. [Medline: 21338188]
5. Berry DA, Cronin KA, Plevritis SK, et al. Effect of screening and adjuvant therapy on mortality from breast cancer. N Engl J Med 2005 Oct 27;353(17):1784-1792. [doi: 10.1056/NEJMoa050518] [Medline: 16251534]
6. One in two EU citizens look for health information online. Eurostat. 2021. URL: https://ec.europa.eu/eurostat/web/products-eurostat-news/-/edn-20210406-1 [accessed 2025-05-13]
7. Wang X, Shi J, Kong H. Online health information seeking: a review and meta-analysis. Health Commun 2021 Sep;36(10):1163-1175. [doi: 10.1080/10410236.2020.1748829] [Medline: 32290679]
8. Agricola E, Gesualdo F, Pandolfi E, et al. Does Googling for preconception care result in information consistent with international guidelines: a comparison of information found by Italian women of childbearing age and health professionals. BMC Med Inform Decis Mak 2013 Jan 25;13:14. [doi: 10.1186/1472-6947-13-14] [Medline: 23347453]
9. Singh AG, Singh S, Singh PP. YouTube for information on rheumatoid arthritis--a wakeup call? J Rheumatol 2012 May;39(5):899-903. [doi: 10.3899/jrheum.111114] [Medline: 22467934]
10. Johnson SB, Parsons M, Dorff T, et al. Cancer misinformation and harmful information on Facebook and other social media: a brief report. JNCI 2022 Jul 11;114(7):1036-1039. [doi: 10.1093/jnci/djab141]
11. Johnson SB, King AJ, Warner EL, Aneja S, Kann BH, Bylund CL. Using ChatGPT to evaluate cancer myths and misconceptions: artificial intelligence and cancer information. JNCI Cancer Spectr 2023 Mar 1;7(2). [doi: 10.1093/jncics/pkad015] [Medline: 36929393]
12. Hopkins AM, Logan JM, Kichenadasse G, Sorich MJ. Artificial intelligence chatbots will revolutionize how cancer patients access information: ChatGPT represents a paradigm-shift. JNCI Cancer Spectr 2023 Mar 1;7(2):pkad010. [doi: 10.1093/jncics/pkad010] [Medline: 36808255]
13. Liu HY, Alessandri Bonetti M, Jeong T, Pandya S, Nguyen VT, Egro FM. Dr. ChatGPT will see you now: How do Google and ChatGPT compare in answering patient questions on breast reconstruction? J Plast Reconstr Aesthet Surg 2023 Oct;85:488-497. [doi: 10.1016/j.bjps.2023.07.039] [Medline: 37598590]
14. Zheng Y, Wu Y, Feng B, Wang L, Kang K, Zhao A. Enhancing diabetes self-management and education: a critical analysis of ChatGPT's role. Ann Biomed Eng 2024 Apr;52(4):741-744. [doi: 10.1007/s10439-023-03317-8] [Medline: 37553556]
15. Gradishar WJ, Moran MS, Abraham J, et al. NCCN Guidelines® Insights: Breast Cancer, Version 4.2023. J Natl Compr Canc Netw 2023 Jun;21(6):594-608. [doi: 10.6004/jnccn.2023.0031] [Medline: 37308117]

XSL•FO
RenderX

16. Cardoso F, Paluch-Shimon S, Senkus E, et al. 5th ESO-ESMO international consensus guidelines for advanced breast cancer (ABC 5). Ann Oncol 2020 Dec;31(12):1623-1649. [doi: 10.1016/j.annonc.2020.09.010] [Medline: 32979513]
17. Rus CL, Chirică S, Raţiu L, Băban A. Learning organization and social responsibility in Romanian higher education institutions. Procedia Soc Behav Sci 2014 Aug;142:146-153. [doi: 10.1016/j.sbspro.2014.07.628]
18. Choi CH, Kim SH, Lee YS, Kang CN. Correlation between the Likert Scale and the Numeric Rating Scale for evaluating knee pain. J Korean Knee Soc 2011;23(1):14. [doi: 10.5792/jkks.2011.23.1.14]
19. Tian Y, Gan R, Song Y, Zhang J, Zhang Y. ChiMed-GPT: a Chinese medical large language model with full training regime and better alignment to human preferences. arXiv. Preprint posted online on 2023.
20. Djulbegovic B, Guyatt GH. Progress in evidence-based medicine: a quarter century on. Lancet 2017 Jul 22;390(10092):415-423. [doi: 10.1016/S0140-6736(16)31592-6] [Medline: 28215660]
21. Musheyev D, Pan A, Loeb S, Kabarriti AE. How well do artificial intelligence chatbots respond to the top search queries about urological malignancies? Eur Urol 2024 Jan;85(1):13-16. [doi: 10.1016/j.eururo.2023.07.004] [Medline: 37567827]
22. Giannakopoulos K, Kavadella A, Aaqel Salim A, Stamatopoulos V, Kaklamanos EG. Evaluation of the performance of generative ai large language models ChatGPT, Google Bard, and Microsoft Bing Chat in supporting evidence-based dentistry: comparative mixed methods study. J Med Internet Res 2023 Dec 28;25:e51580. [doi: 10.2196/51580] [Medline: 38009003]
23. Farhat F. ChatGPT as a complementary mental health resource: a boon or a bane. Ann Biomed Eng 2024 May;52(5):1111-1114. [doi: 10.1007/s10439-023-03326-7] [Medline: 37477707]
24. Cao JJ, Kwon DH, Ghaziani TT, et al. Accuracy of information provided by chatgpt regarding liver cancer surveillance and diagnosis. AJR Am J Roentgenol 2023 Oct;221(4):556-559. [doi: 10.2214/AJR.23.29493] [Medline: 37222278]
25. Endo Y, Sasaki K, Moazzam Z, et al. Quality of ChatGPT responses to questions related to liver transplantation. J Gastrointest Surg 2023 Aug;27(8):1716-1719. [doi: 10.1007/s11605-023-05714-9] [Medline: 37254022]
26. Liu J, Wang C, Liu S. Utility of ChatGPT in clinical practice. J Med Internet Res 2023 Jun 28;25:e48568. [doi: 10.2196/48568] [Medline: 37379067]
27. Adhikari K, Naik N, Hameed BZ, Raghunath SK, Somani BK. Exploring the ethical, legal, and social implications of ChatGPT in urology. Curr Urol Rep 2024 Jan;25(1):1-8. [doi: 10.1007/s11934-023-01185-2] [Medline: 37735339]
28. Wang C, Liu S, Yang H, Guo J, Wu Y, Liu J. Ethical considerations of using ChatGPT in health care. J Med Internet Res 2023 Aug 11;25:e48009. [doi: 10.2196/48009]
29. Eppler M, Ganjavi C, Ramacciotti LS, et al. Awareness and use of ChatGPT and large language models: a prospective cross-sectional global survey in urology. Eur Urol 2024 Feb;85(2):146-153. [doi: 10.1016/j.eururo.2023.10.014] [Medline: 37926642]
30. Nasr M, Carlini N, Hayase J, et al. Scalable extraction of training data from (production) language models. arXiv. Preprint posted online on Nov 28, 2023. [doi: 10.48550/arXiv.2311.17035]
31. Li J. Security Implications of AI chatbots in health care. J Med Internet Res 2023 Nov 28;25:e47551. [doi: 10.2196/47551] [Medline: 38015597]
32. Meskó B, Topol EJ. The imperative for regulatory oversight of large language models (or generative AI) in healthcare. NPJ Digit Med 2023 Jul 6;6(1):120. [doi: 10.1038/s41746-023-00873-0] [Medline: 37414860]
33. Mohamed S, Dunnett S, Flores A, Loew E, Pienaar S, MILE (Medical Information Leaders in Europe). A principles framework for digital provision of medical information for healthcare professionals. Pharmaceut Med 2023 Mar;37(2):103-109. [doi: 10.1007/s40290-023-00464-0] [Medline: 37000411]
34. Coskun B, Ocakoglu G, Yetemen M, Kaygisiz O. Can ChatGPT, an artificial intelligence language model, provide accurate and high-quality patient information on prostate cancer? Urology 2023 Oct;180:35-58. [doi: 10.1016/j.urology.2023.05.040] [Medline: 37406864]

Abbreviations

ChatGPT-C: ChatGPT-Chinese
ChatGPT-E: ChatGPT-English
EB: ERNIE Bot
GSS: generalization-specificity score
ICC: intraclass correlation coefficient
LLM: large language model
PIPL: Personal Information Protection Law

XSL•FO
RenderX

Edited by A Castonguay; submitted 12.09.24; peer-reviewed by B Bhasuran; revised version received 21.04.25; accepted 24.04.25; published 27.05.25.

Please cite as:
Liu H, Peng J, Li L, Deng A, Huang X, Yin G, Luo H
Large Language Models as a Consulting Hotline for Patients With Breast Cancer and Specialists in China: Cross-Sectional Questionnaire Study
JMIR Med Inform 2025;13:e66429
URL: https://medinform.jmir.org/2025/1/e66429
doi:10.2196/66429

© Hui Liu, Jialun Peng, Lu Li, Ao Deng, XiangXin Huang, Guobing Yin, Haojun Luo. Originally published in JMIR Medical Informatics (https://medinform.jmir.org), 27.5.2025. This is an open-access article distributed under the terms of the Creative Commons Attribution License (https://creativecommons.org/licenses/by/4.0/), which permits unrestricted use, distribution, and reproduction in any medium, provided the original work, first published in JMIR Medical Informatics, is properly cited. The complete bibliographic information, a link to the original publication on https://medinform.jmir.org/, as well as this copyright and license information must be included.

XSL•FO
RenderX

Toward Cross-Hospital Deployment of Natural Language Processing Systems: Model Development and Validation of Fine-Tuned Large Language Models for Disease Name Recognition in Japanese

Seiji Shimizu, MEng; Tomohiro Nishiyama, PhD; Hiroyuki Nagai, MA; Shoko Wakamiya, PhD; Eiji Aramaki, PhD

Nara Institute of Science and Technology, 8916-5, Takayama-cho, Ikoma-shi, Nara, Japan

Corresponding Author:
Eiji Aramaki, PhD
Nara Institute of Science and Technology, 8916-5, Takayama-cho, Ikoma-shi, Nara, Japan

Abstract

Background: Disease name recognition is a fundamental task in clinical natural language processing, enabling the extraction of critical patient information from electronic health records. While recent advances in large language models (LLMs) have shown promise, most evaluations have focused on English, and little is known about their robustness in low-resource languages such as Japanese. In particular, whether these models can perform reliably on previously unseen in-hospital data, which differs from training data in writing styles and clinical contexts, has not been thoroughly investigated.

Objective: This study evaluated the robustness of fine-tuned LLMs for disease name recognition in Japanese clinical notes, with a particular focus on their performance on in-hospital data that was not included during training.

Methods: We used two corpora for this study: (1) a publicly available set of Japanese case reports denoted as CR, and (2) a newly constructed corpus of progress notes, denoted as PN, written by ten physicians to capture stylistic variations of in-hospital clinical notes. To reflect real-world deployment scenarios, we first fine-tuned models on CR. Specifically, we compared a LLM and a baseline-masked language model (MLM). These models were then evaluated under two conditions: (1) on CR, representing the in-domain (ID) setting with the same document type, similar to training, and (2) on PN, representing the out-of-domain (OOD) setting with a different document type. Robustness was assessed by calculating the performance gap (ie, the performance drop from in-domain to out-of-domain settings).

Results: The LLM demonstrated greater robustness, with a smaller performance gap in F_1-scores (ID–OOD = −8.6) compared to the MLM baseline performance (ID–OOD = −13.9). This indicated more stable performance across ID and OOD settings, highlighting the effectiveness of fine-tuned LLMs for reliable use in diverse clinical settings.

Conclusions: Fine-tuned LLMs demonstrate superior robustness for disease name recognition in Japanese clinical notes, with a smaller performance gap. These findings highlight the potential of LLMs as reliable tools for clinical natural language processing in low-resource language settings and support their deployment in real-world health care applications, where diversity in documentation is inevitable.

(JMIR Med Inform 2025;13:e76773) doi:10.2196/76773

KEYWORDS

clinical NLP; Japanese language; named entity recognition; large language models; out-of-domain robustness; clinical corpus; clinical natural language processing

Introduction

Clinical notes contain a vast amount of information that is not captured in structured fields of electronic health records (EHRs) [1,2]. Natural language processing (NLP) techniques have become essential for unlocking this rich, unstructured data [3].

Among these, named entity recognition (NER)—a task that identifies clinical entities such as disease names in text—plays a vital role in extracting key clinical information, which is essential for understanding patients' medical conditions [4-6]. For instance, disease name recognition can be leveraged to detect adverse drug reactions from EHRs for post-marketing surveillance [7].

Recent advances leveraging fine-tuned masked language models (MLMs) such as BERT, have achieved state-of-the-art performance in clinical NER tasks, often outperforming prompt-based in-context learning (ICL) of large language models (LLMs) [8,9]. However, MLMs fine-tuned for disease name recognition tend to experience notable performance drops

XSL•FO
RenderX

on unseen in-hospital data [10,11]. Given that clinical NLP systems are expected to operate reliably across diverse clinical settings, understanding and improving robustness—that is, whether models can perform reliably on previously unseen clinical notes—is a critical research objective.

When fine-tuned, LLMs have shown competitive or slightly superior performance compared to MLMs in NER tasks [12]. Given their exposure to a broader and more diverse range of linguistic patterns during pretraining, LLMs are expected to exhibit resilience to stylistic variations. However, the extent to which fine-tuning improves their robustness over MLMs remains underexplored, particularly in languages other than English [13]. One reason for this research gap is the lack of corpora that reflect the realistic documentation styles of in-hospital clinical notes. These data are challenging to obtain due to privacy concerns and institutional restrictions.

In this study, we investigate the robustness of fine-tuned LLMs with a focus on disease name recognition in Japanese clinical notes. To facilitate an evaluation of robustness to unseen in-hospital data, we constructed a dedicated clinical corpus comprising progress notes (PN) authored by ten individual physicians from different clinical institutions, reflecting diverse in-hospital documentation styles. To reflect real-world deployment scenarios, we trained the models on publicly available case reports (CR) and evaluated them under two conditions: (1) on CR, representing the in-domain (ID) setting with the same document type as in training, and (2) on PN, representing the out-of-domain (OOD) setting with a different document type. This cross-document evaluation allows us to assess the models' robustness to real-world variability in documentation styles, capturing the challenges introduced by the diverse writing practices found in in-hospital clinical notes.

Experimental results demonstrated that the fine-tuned LLM—specifically LLaMA-3.1 [14]—outperforms the MLM baseline (Bidirectional Encoder Representations from Transformers, BERT) [15], not only in the ID setting but also under OOD conditions. The LLM also exhibits a smaller performance gap between ID and OOD settings, indicating stronger robustness compared to the MLM. Further analysis reveals that LLMs are more resilient to stylistic diversity among clinicians, showing reduced performance fluctuation across different physicians. These findings underscore the potential of fine-tuned LLMs as more reliable tools for real-world clinical applications, particularly where robustness to diverse and previously unseen clinical notes is essential.

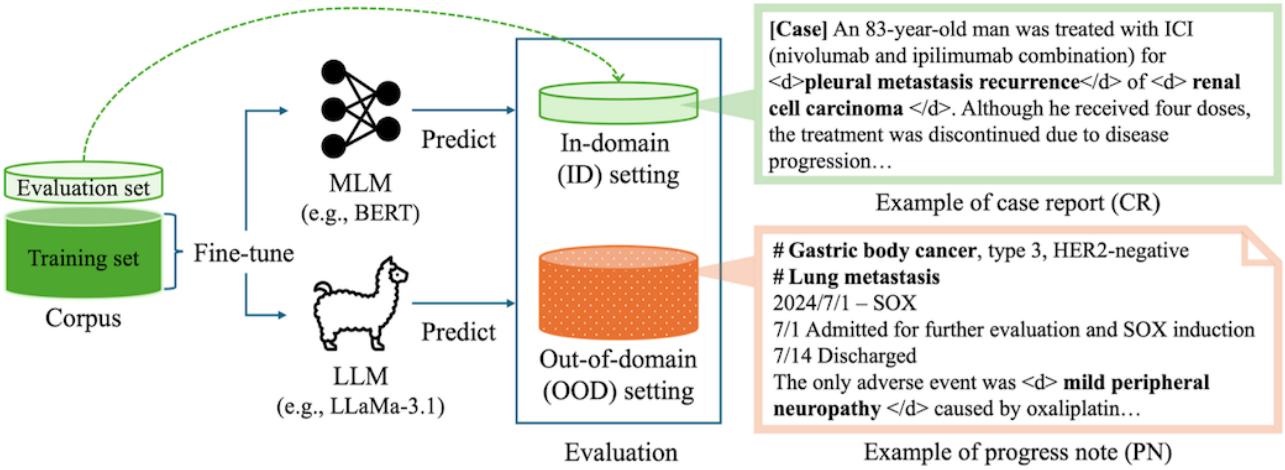
Methods

Overview

Our primary research question was to evaluate whether fine-tuned LLMs remain robust when applied to previously unseen clinical notes. To address this, we compared the performance gap, defined as the performance difference between ID setting and OOD settings between a fine-tuned LLM and a fine-tuned MLM, which serves as a state-of-the-art baseline for clinical NER.

The overview of the evaluation pipeline is shown in Figure 1. We evaluated model performance on the task of disease name recognition in Japanese clinical notes. Both LLMs and MLMs are first fine-tuned on a training set sampled from one document type (eg, case reports). Evaluation is then conducted on two distinct test sets: one ID set sampled from the same document type as the training data and one OOD set sampled from a different document type (eg, progress notes).

Figure 1. Overview of the evaluation pipeline. Models were fine-tuned on CR and evaluated on both CR, representing in-domain (ID) and PN, representing out-of-domain (OOD) test sets for disease name recognition in Japanese clinical notes. BERT: Bidirectional Encoder Representations from Transformers; HER2: human epidermal growth factor receptor 2; ICI: Immune checkpoint inhibitor; LLM: large language model; MLM: masked language model; SOX: SRY-related HMG-box.



Materials

To represent ID and OOD settings, we used two datasets: an existing publicly available corpus of case reports and a newly constructed corpus comprised of progress notes.

1. Case reports (CR): A publicly available dataset consisting of Japanese case reports comprising 1898 sentences across 148 documents annotated with clinical entities [16].
2. Progress notes (PN): A dedicated, newly constructed corpus of progress notes, comprising 1094 sentences across 100 documents annotated with disease entities.

XSL•FO
RenderX

For the construction of PN, we first curated 10 diverse board exam-style cases. To reflect real-world clinical documentation, these cases were then rewritten by ten physicians, each contributing ten unique documents. The physicians were instructed to adapt the cases to authentic in-hospital clinical note styles from their clinical practice, emphasizing realistic writing styles and varying levels of readability. In total, 1094 sentences (100 documents) across 10 physicians and 10 clinical cases were created. The created PN were then annotated for disease name entities by two experienced annotators, following the same annotation guidelines as CR [17]. We summarize the titles of the board exam-style cases and the top 3 most frequent disease entities per case in Table 1.

We assessed the annotation quality of PN by calculating interannotator agreement using two criteria: exact and partial span matching. Exact matching required both annotators to identify the same entity with identical span boundaries, while partial matching allowed for overlapping spans, acknowledging minor variations in boundary selection. Based on a comparison of annotations from 10 randomly sampled documents, the agreement between annotators was 0.70 (61/87) for exact matching and 0.82 (71/87) for partial matching, suggesting a high level of consistency and reliable annotation quality.

XSL•FO
RenderX

Table . Titles of the curated board exam-style cases and top 3 frequent disease entities.

Title and top 3 disease entities	Frequency (n)
“急性虫垂炎” (Acute appendicitis)	
“急性虫垂炎“ (Acute appendicitis)	11
“腹痛“ (Abdominal pain)	6
“穿孔や膿瘍“ (Perforation or abscess)	5
“進行胃がん“ (Advanced gastric cancer)	
“進行胃がん“ (Advanced gastric cancer)	8
“呼吸困難“ (Dyspnea)	7
“肝転移“ (Liver metastasis)	5
“肝膿瘍“ (Liver abscess)	
“肝膿瘍“ (Liver abscess)	15
“膿瘍“ (Abscess)	8
“倦怠感“ (Fatigue)	7
“月経過多に伴う貧血“ (Anemia due to menorrhagia)	
“子宮筋腫“ (Uterine fibroids)	20
“貧血“ (Anemia)	12
“月経過多“ (Menorrhagia)	8
“肺がん“ (Lung cancer)	
“肝転移“ (Liver metastasis)	8
“肺小細胞癌“ (Small cell lung cancer)	8
“低Na血症“ (Hyponatremia)	7
“IE (感染性心内膜炎）“ (Infective endocarditis)	
“くも膜下出“ (Subarachnoid hemorrhage)	8
SAH (Subarachnoid hemorrhage)	7
“疣贅“ (Vegetation - cardiac)	6
“誤嚥性肺炎“＋COPD[a] (Aspiration Pneumonia with COPD)	
COPD	12
“誤嚥性肺炎“ (Aspiration pneumonia)	12
“浸潤影“ (Infiltrates)	6
“クモ膜下出血“ (Subarachnoid hemorrhage)	
SAH (Subarachnoid hemorrhage)	14
“頭痛“ (Headache)	9
“くも膜下出血“ (Subarachnoid hemorrhage)	5
“大腸がん“ (Colorectal cancer)	
“Isポリープ“ (Is polyp)	7
“大腸がん“ (Colorectal cancer)	7
Well-differentiated tubular adenocarcinoma in tubular adenoma	7
AMI (acute myocardial infarction)	
“胸痛“ (Chest pain)	15
AMI	8
“壁運動低下“ (Wall motion abnormality)	5

[a]COPD: chronic obstructive pulmonary disease

XSL•FO
RenderX

Models and Baselines

We evaluate fine-tuned MLMs and LLMs on the task of disease name recognition in Japanese clinical notes, comparing their performance under ID and OOD settings. In addition, we evaluated LLMs using in-context learning (ICL) through zero-shot and few-shot prompting to assess the contribution of fine-tuning to improving LLM performance.

Fine-Tuning: We fine-tuned two models for the NER task: (1) “bert-base-japanese-v3” [18], based on BERT [15] as a strong MLM baseline, and (2) Swallow-Instruct-v0.2 [19], based on LLaMA-3.1 (version 8B; Meta) [14], which is a Japanese-instruction-tuned LLM. Both were subsequently fine-tuned on the ID training set. “bert-base-japanese-v3” was chosen as a strong and widely used baseline for Japanese-language tasks, providing a representative benchmark for traditional transformer–based MLMs that had been validated in clinical NLP [20]. In contrast, “Swallow-Instruct-v0.2” (version 0.2; Tokyo Institute of Technology) was selected to evaluate the potential of recent instruction–tuned LLMs, which are designed to better follow task-specific instructions and generalize across diverse inputs. Built on Llama 3.1 8B through continual pretraining, it was trained on a curated instruction corpus featuring multiturn dialogue and multilingual tasks with a particular focus on enhancing Japanese language capabilities.

For BERT, we adopted a standard sequence labeling approach, using the “CLS” token representations followed by a linear classification layer to predict BIO-tagged labels for disease entities. In contrast, for LLaMA-3.1, we followed a generation-based NER framework: the model was prompted with an instruction and clinical note, and it generated the same sentence with inline entity tags, enabling span-level extraction in a natural language generation format. To adapt LLaMA-3.1 to the NER task efficiently, we applied additional fine-tuning using Low-Rank Adaptation (LoRA) [21], allowing parameter-efficient fine-tuning without modifying the full set of model weights.

In-context learning (ICL): We evaluated LLaMA-3.1 and GPT-4o [22] under zero-shot and few-shot settings as baselines. An example of a prompt used for ICL is presented in Textbox 1. Recently, extensive efforts have been made to optimize prompt design in the field of NLP [23-26]. In this experiment, we provide the models with an annotation guideline that included entity definitions, task instructions, and illustrative examples, following prior work on medical NER [9]. For zero-shot learning, the model was provided with task instructions and annotation guidelines only, without any annotated examples. For few-shot learning, a single annotated clinical note was randomly selected from the training data and included in the prompt. Here, LLaMA-3.1 represents an open-source LLM with accessible model weights, allowing evaluation across both fine-tuning and in-context learning scenarios. In contrast, GPT-4o was evaluated only in zero-shot and few-shot settings due to its proprietary nature, serving as a reference for the in-context learning performance of an LLM with the highest model capacity in our study.

Textbox 1. Textbox 1. Prompt example for ICL.

Annotation Guideline

Definition of disease names

1. When the lesion or symptom has actually been observed in the patient
2. When it is suspected that the patient may have the lesion or symptom (eg, proposed as a differential diagnosis)
3. …

Examples

Text: In November last year, pleural effusion appeared and increased, but decreased after starting furosemide.

Annotation: In November last year, <d pleural effusion </d>appeared and increased, but decreased after starting furosemide.

…

Task Instruction

Based on the above explanation and examples, please annotate the following text

…

Text: The nodule shadow in the right upper lobe of the lung slightly increased.

Comparison Settings

We used our clinical corpora in a cross-domain evaluation setup to assess both ID and OOD robustness:

ID: Samples from one document type were split 8:2 into training and evaluation sets. This setting reflects standard model development conditions, where training and test data share similar clinical notes.

OOD: The corpus from another document type was used in its entirety for evaluation. This reflects real-world deployment scenarios where models must process previously unseen clinical notes with varying writing styles and vocabularies.

In addition to the setting where CR are used for training and PN for evaluation, we also included the reverse scenario. This resulted in four distinct evaluation configurations: CR→CR, CR→PN, PN→PN, and PN→CR. The difference between ID and OOD performance (Δ) is calculated as Δ=ID−OOD. This

XSL•FO
RenderX

represents the performance gap, which measures how well the model generalizes to unseen clinical notes, compared to the data it was trained on. A smaller difference indicates that the model is robust, even when faced with clinical notes with different writing styles or from different clinical cases. Hyperparameters used for fine-tuning are summarized in Table 2.

Table . Hyperparameters used for fine-tuning.

Parameter description	LLaMa-3.1	BERT[a]
Evaluation batch size per device	_[b]	8
Learning rate	2e-4	2e-5
LoRA[c] dropout rate	0.05	–
LoRA rank (number of adaptation dims)	16	–
LoRA scaling factor	64	–
Maximum gradient norm (clipping)	0.3	–
Maximum sequence length	3000	512
Number of gradient accumulation steps	4	–
Number of training epochs	2	10
Optimizer used	AdamW	AdamW
Training batch size per device	4	8
Warmup ratio for learning rate	0.05	–
Weight decay for regularization	–	0.0
Number of warmup steps	–	0

[a]BERT: Bidirectional Encoder Representations from Transformers.

[b]Not applicable.

[c]LoRA: Low-Rank Adaptation.

Ethical Considerations

This study did not involve experiments with human subjects, and no personally identifiable information was used at any stage. The clinical notes were physician-authored, based on board exam cases that are publicly available. Therefore, there are no ethical concerns related to patient privacy or informed consent in this research.

Results

Study Findings

Table 3 shows the findings of ID and OOD evaluation. All models were evaluated using the microaveraged F_1-score, focusing on exact span matches of disease name entities. All results are averaged over three runs with different random seeds. For GPT-4o, we set the generation temperature to zero to ensure deterministic outputs and only ran the evaluation once due to annotation budget constraints.

XSL•FO
RenderX

Table . Evaluation results in micro F_1-scores with standard deviations.

	CR[a], mean (SD)			PN[b], mean (SD)		
	→CR[a] (ID)[c]	→PN[b] (OOD)[d]	ΔCR[e]	→PN (ID)	→CR (OOD)	ΔPN[f]
LLaMA-3.1 (Zero-shot)	27.4 (0.3)	20.4 (0.1)	−7.0	15.5 (0.4)	27.1 (0.1)	11.6
LLaMA-3.1 (Few-shot)	32.6 (1.6)	30.5 (0.7)	−2.1	37.0 (4.8)	35.9 (0.5)	−11.0
GPT-4o (Zero-shot)	49.5 (0.0)	47.7 (0.0)	−1.8	42.0 (0.0)	50.8 (0.0)	8.8
GPT-4o (Few-shot)	53.4 (0.0)	49.9 (0.0)	−3.5	56.2 (0.0)	54.4 (0.0)	−1.8
BERT[g](Fine-tuned)	73.7 (0.2)	59.8 (0.2)	−13.9	79.7 (1.8)	55.5 (1.7)	−24.2
LLaMA-3.1 (Fine-tuned)	78.4 (0.5)	69.8 (0.6)	−8.6	81.9 (0.7)	67.2 (0.5)	−14.7

[a]CR: case reports.

[b]PN: progress reports.

[c]ID: in-domain.

[d]OOD: out-of-domain.

[e]ΔCR: difference in csse reports.

[f]ΔPN: difference in progress notes.

[g]BERT: Bidirectional Encoder Representations from Transformers.

Comparison Between Fine-Tuning and ICL

The fine-tuned LLaMA-3.1 consistently outperformed its zero-shot and few-shot counterparts, achieving the highest F_1-scores across all evaluation settings. These results highlight the effectiveness of fine-tuning for clinical NER. In contrast, vanilla LLaMA-3.1 exhibited limited performance in zero-shot and few-shot scenarios. Notably, in the few-shot setting, the model showed a decline in performance when applied to OOD data.

GPT-4o demonstrated strong few-shot performance (ie, 53.4 on CR→CR and 56.2 on PN→PN) despite having no access to training data, highlighting the robustness of large-scale foundation models. However, these models still underperformed compared to the fine-tuned BERT, consistent with previous findings that task-specific fine-tuning often outperforms in-context learning in specialized domains like clinical NER [8,9]. These findings illustrate that while ICL can provide a competitive baseline with minimal data, fine-tuning remains essential.

Comparison Between MLM and LLM

The fine-tuned LLaMA-3.1 outperformed the BERT baseline across all ID and OOD settings, demonstrating superior robustness to the previously unseen document type. Specifically, the fine-tuned LLaMA-3.1 exhibited a smaller performance gap (ΔCR=−8.6and ΔPN=−14.7) compared to BERT (ΔCR=−13.9 and ΔPN=−24.2), suggesting its greater stability for practical use in diverse clinical settings.

Discussion

Principal Findings

Experimental results demonstrate that the fine-tuned LLM exhibits strong robustness, maintaining relatively stable performance even when applied to previously unseen progress notes. To better understand the factors contributing to this robustness, we further decomposed it into two aspects: (1) robustness to stylistic variation, (ie, variations across physicians) and (2) robustness to variation across clinical cases. Our analysis reveals that the LLM was particularly robust to stylistic differences, while showing greater sensitivity to the differences in clinical cases.

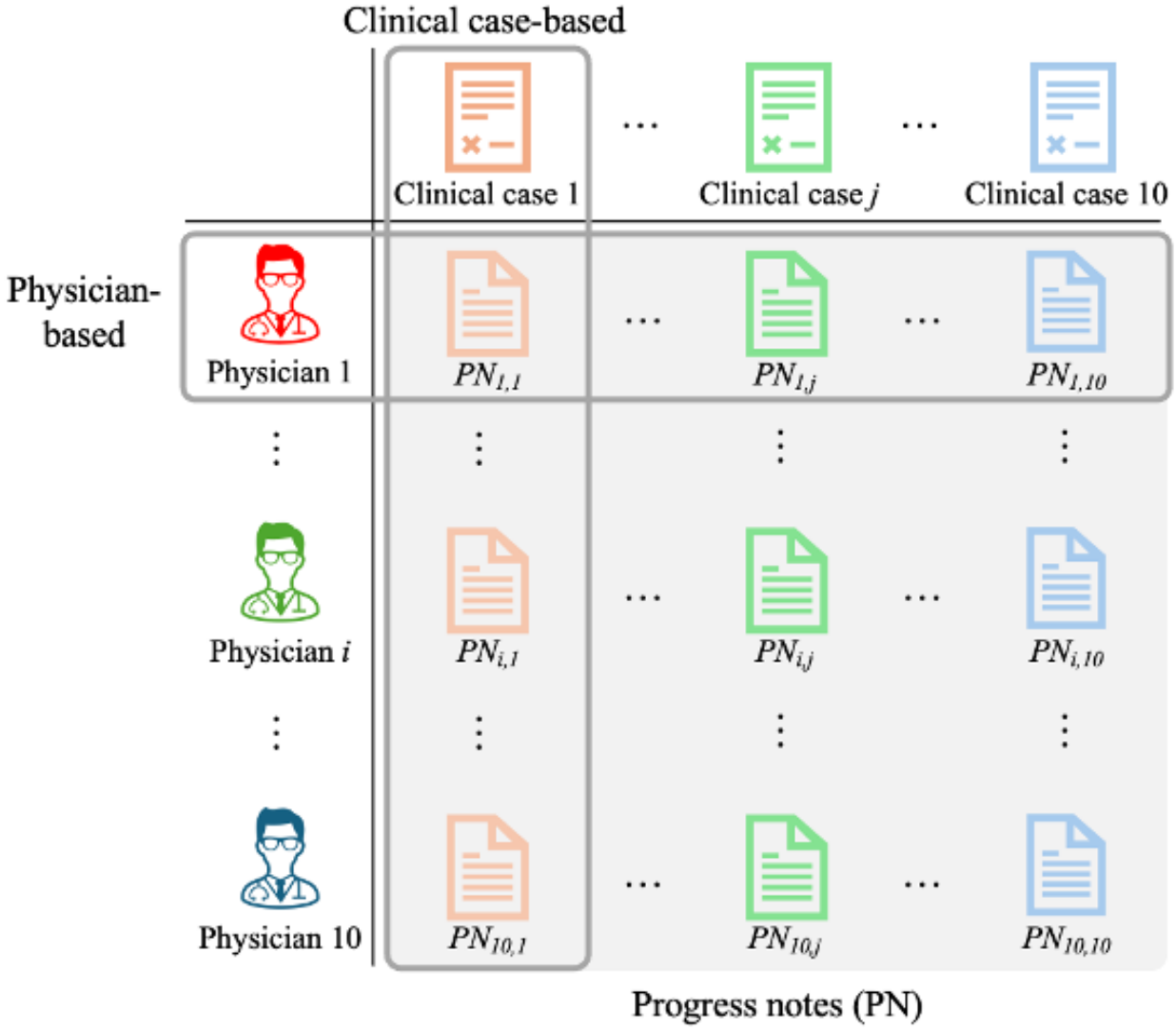
We also conducted an error analysis to examine the qualitative improvements of the LLM over the MLM baseline performance. Our findings suggest that the LLM benefits from its generative approach, which allows it to mark entities inline within the sentence, as opposed to relying on a classification head over token representations, as in MLMs. This generative approach enables the LLM to more accurately extract entity spans, especially in stylistically diverse clinical notes.

Impact of Physician and Clinical Case Variation

To examine the robustness of the fine-tuned LLM to variations in writing styles and clinical cases, we stratified the performance of the fine-tuned LLaMA-3.1 and BERT in the CR→PN setting by physician and clinical case. The stratification process is summarized in Figure 2.

XSL•FO
RenderX

Figure 2. Overview of the evaluation with stratification. Performance of fine-tuned LLaMA-3.1 and BERT was stratified by physician and clinical case to assess robustness to writing style and clinical case variations.



Physician-Based

Performance was evaluated for each physician, with ten clinical notes authored per individual. For instance, the performance of models is averaged across PNi,1 to PNi,10 for the i-th physician. The variation in these stratified results allows us to assess the model's sensitivity to variations in individual writing styles.

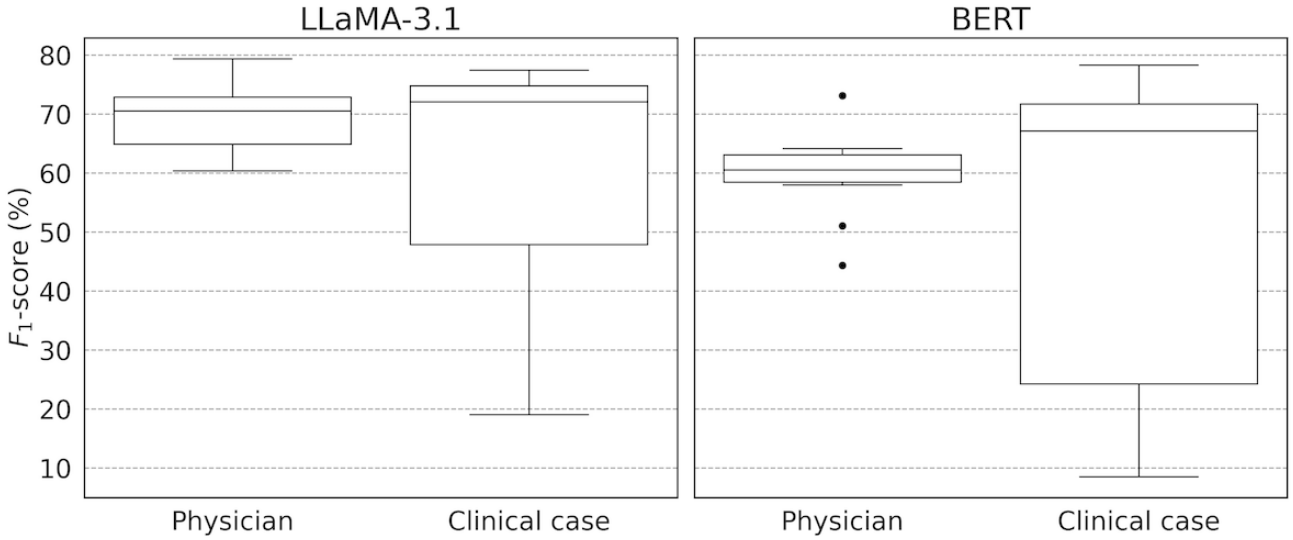
Clinical Case-Based

Performance was also evaluated for each clinical case modeled after board exam-style scenarios (eg, acute appendicitis). The model's performance was averaged over ten notes from different physicians, for example, PN1,j to PN10,j for the j-th clinical case. This stratification enables an analysis of the model's ability to generalize to clinical-case-specific disease entities.

Figure 3 presents the distribution of F_1-scores stratified by physician and clinical case in the CR→PN setting for both the fine-tuned LLaMa-3.1 and BERT. The spread of each box and the range of whiskers reflect performance variability, while dots indicate outliers beyond 1.5-times the interquartile range. Narrower boxes and smaller ranges indicate higher consistency, while outliers and wider spreads highlight sensitivity to writing style or clinical case variation.

XSL•FO
RenderX

Figure 3. Distribution of F_1-scores in CR→PN stratified by physician and clinical case. BERT: Bidirectional Encoder Representations from Transformers; CR: case report; PN: progress note.



Physician Variance

The fine-tuned LLaMA-3.1 demonstrated consistently strong performance across different physicians, with relatively low variance in F_1-scores. This is indicated in the narrow range between the maximum and minimum values in the box plot. In contrast, BERT's performance varied more widely, with significant performance drops in some physicians' notes, as indicated by extreme outliers and low minimum values. This suggests that the fine-tuned LLaMA-3.1 is more robust to stylistic differences, potentially due to its exposure to a broader and more diverse range of linguistic patterns during pretraining.

Clinical Case Variance

When stratified by clinical case, both models showed greater variability compared to writing style. This is evidenced by wider boxes and larger ranges between the maximum and minimum values in the box plots. These results highlight the increased difficulty of generalizing to domain-specific disease names. While the fine-tuned LLaMA-3.1 generally achieved higher average F_1-score across clinical cases, it also experienced sharp drops in certain cases, indicating that it remains sensitive to clinical-case-specific variation. This underscores the persistent challenge in processing previously unseen clinical cases, even for large instruction-tuned models.

These findings underscore the relative strength of the fine-tuned LLaMA-3.1 in handling clinical stylistic variation. At the same time, they point to the need for further work in addressing performance gaps in different clinical cases.

Error Analysis

To examine the qualitative improvements of the LLM over the MLM baselines, we conducted error analysis in the CR→PN setting. Based on the observation that the fine-tuned BERT has lower precision (51.8) compared to the fine-tuned LLaMA-3.1 (70.8), both models achieved similar recall scores (70.7 for BERT and 68.9 for LLaMA-3.1), we focused on false positive cases for the analysis.

Representative error examples are summarized in Table 4. From a manual inspection, we observed that BERT frequently misclassified nondisease clinical entities such as laboratory tests and biomarkers as disease mentions. For instance, in the sentence "Tumor markers also decreased gradually (徐々に腫瘍マーカーも低下し)," BERT incorrectly predicted two spans: "tumor markers (腫瘍マーカ"ー)" and "decrease (低下)." Both terms describe laboratory findings rather than disease entities. In another example, in the sentence "Therefore, with regard to platelets (このため血小板に対しては)," BERT erroneously extracted "platelets (血小板)," which refers to a blood cell type rather than a pathological condition. These examples illustrate that BERT often struggles to distinguish diagnostically relevant clinical phrases from true disease mentions, leading to false positive predictions.

In addition to entity type confusion, BERT also often struggled to capture the complete span of disease mentions, frequently producing boundary errors or partial matches that failed to align with the gold-standard annotations. For instance, in the sentence "Hb 8.1 g/dL and moderate nutritional disorder were observed (Hb8.1g/dlと中程度の栄養障害を認めた)," BERT incorrectly predicted only the prefix of a laboratory value, "Hb8," entirely missing the actual disease mention "栄養障害 (nutritional disorder)." In another example, "The drainage volume was excessive (排液量が過多であった)," BERT extracted only the character "多 (excessive)," omitting the full phrase "排液量が過多 (excessive drainage volume)." These examples illustrate how slight shifts in input text can lead to misaligned token representations in MLM's embedding space, resulting in fragmented or incomplete entity predictions.

In contrast, the LLM demonstrates greater flexibility in capturing complete spans of disease mentions. Unlike the MLM, which often struggles with partial matches, the LLM's generative approach allows entities to be marked directly and seamlessly within the sentence. For example, in the sentence "Hb8.1g/dlと中程度の<d>栄養障害</d>を認めた" (translated as "Hb 8.1 g/dL and moderate <d>nutritional disorder</d>were observed"), the disease mention "栄養障害 (nutritional disorder)" is correctly and fully captured within the sentence

XSL•FO
RenderX

using inline entity tags. This inline tagging strategy enables the model to stably extract entire disease names, even when clinical notes vary in writing style.

The LLM's ability to overcome the errors observed in BERT predictions likely stems from its different learning paradigm: rather than relying solely on token-level classification based on fixed input embeddings, the LLM generates structured outputs conditioned on the full context of the input. This generative approach allows the LLM to better maintain entity span prediction coherence over varying document types and incorporate broader sentence-level semantics into prediction. Consequently, the LLM achieves more robust and accurate extraction performance compared to the MLM baseline, particularly in OOD settings.

Table . Examples of BERT prediction errors in the CR→PN setting. Each row shows a sentence (left), predicted entity spans (middle), and the correct gold annotations (right).

Example sentence (English/Japanese)	Prediction	Gold annotation
Tumor markers also decreased gradually/腫瘍マーカーも低下し	tumor markers/腫瘍マーカー, decrease/低下	None
Therefore, with regard to platelets/このため血小板に対しては	platelets/血小板	None
Hb 8.1g/dL and moderate nutritional disorder were observed/Hb8.1g/dlと中程度の栄養障害を認めた	Hb8	nutritional disorder/栄養障害
The drainage volume was excessive/排液量が過多であった	excessive/多	excessive drainage volume/排液量が過多

Limitations

This study has several limitations. First, due to the annotation cost, our evaluation focused exclusively on disease name recognition. While disease entities are fundamental to clinical NLP tasks, real-world applications often require the extraction of a wider range of entities such as medications, procedures, and laboratory findings. Future research should expand the scope of entity types to provide a more comprehensive evaluation of model capabilities in diverse clinical information extraction tasks.

Second, we did not evaluate the computational efficiency or resource demands of the models. This is particularly relevant for LLMs, which often require substantial computational resources during both training and inference. Future studies should include a systematic comparison of computational cost, memory usage, and inference latency to guide more practical model deployment in clinical environments.

Lastly, we did not include comparisons with models pretrained on large-scale medical corpora, such as Bio-BERT [27] or its Japanese counterpart [28]. These models may have inherent advantages in understanding domain-specific terminology and context, and their inclusion could provide a clearer upper bound on MLM-based methods. Future work may incorporate medical-specific, pretrained models and a broader range of domain adaptation techniques in Japanese clinical settings.

Conclusions

This study evaluated the performance of fine-tuned LLMs on disease name recognition in Japanese clinical notes, with a focus on both ID and OOD robustness. Our results demonstrate that fine-tuned LLMs, specifically the fine-tuned LLaMA-3.1, consistently outperforms the strong baselines across OOD settings, demonstrating superior robustness to previously unseen clinical notes.

Stratified analyses revealed that the LLM exhibits greater robustness to stylistic variation among physicians, as reflected in its lower performance variance across physicians. However, variations across clinical cases continue to pose significant challenges, with both LLM and the baseline model showing considerable fluctuations. Error analysis highlighted the LLM's ability to consistently capture complete entity spans in stylistically diverse clinical notes. Its generative approach enables more context-aware span prediction, contributing to stable performance over the baseline model.

Overall, our findings underscore the potential of fine-tuned LLMs for clinical named entity recognition in low-resource languages such as Japanese, particularly in contexts with considerable variation in writing style. Nevertheless, challenges in cross-clinical case robustness remain. Future work should explore more targeted domain adaptation techniques and integration of external medical knowledge to further enhance robustness in real-world clinical NLP applications.

Acknowledgments

This work was supported by Cross-ministerial Strategic Innovation Promotion Program (SIP) on "Integrated Health Care System" (Grant Number JPJ012425) and JST CREST (Grant Number: JPMJCR22N1), Japan.

Conflicts of Interest

None declared.

XSL•FO
RenderX

References

1. Zweigenbaum P, Demner-Fushman D, Yu H, Cohen KB. Frontiers of biomedical text mining: current progress. Brief Bioinform 2007 Sep;8(5):358-375. [doi: 10.1093/bib/bbm045] [Medline: 17977867]
2. Wang Y, Wang L, Rastegar-Mojarad M, et al. Clinical information extraction applications: a literature review. J Biomed Inform 2018 Jan;77:34-49. [doi: 10.1016/j.jbi.2017.11.011] [Medline: 29162496]
3. Kreimeyer K, Foster M, Pandey A, et al. Natural language processing systems for capturing and standardizing unstructured clinical information: a systematic review. J Biomed Inform 2017 Sep;73:14-29. [doi: 10.1016/j.jbi.2017.07.012] [Medline: 28729030]
4. Sun W, Rumshisky A, Uzuner O. Evaluating temporal relations in clinical text: 2012 i2b2 challenge. J Am Med Inform Assoc 2013 Sep;20(5):806-813. [doi: 10.1136/amiajnl-2013-001628]
5. Henry S, Buchan K, Filannino M, Stubbs A, Uzuner O. 2018 n2c2 shared task on adverse drug events and medication extraction in electronic health records. J Am Med Inform Assoc 2020 Jan 1;27(1):3-12. [doi: 10.1093/jamia/ocz166] [Medline: 31584655]
6. Bose P, Srinivasan S, Sleeman WC, Palta J, Kapoor R, Ghosh P. A survey on recent named entity recognition and relationship extraction techniques on clinical texts. Appl Sci (Basel) 2021 Jan;11(18):8319. [doi: 10.3390/app11188319]
7. Kawazoe Y, Shimamoto K, Seki T, et al. Post-marketing surveillance of anticancer drugs using natural language processing of electronic medical records. NPJ Digit Med 2024 Nov 9;7(1):315. [doi: 10.1038/s41746-024-01323-1] [Medline: 39521935]
8. Naguib M, Tannier X, Névéol A. Few-shot clinical entity recognition in English, French and Spanish: masked language models outperform generative model prompting. In: Al-Onaizan Y, Bansal M, Chen YN, editors. 2024 Presented at: Findings of the Association for Computational Linguistics: EMNLP 2024; Nov 12-16, 2024; Miami, Florida, USA p. 6829-6852. [doi: 10.18653/v1/2024.findings-emnlp.400]
9. Hu Y, Chen Q, Du J, et al. Improving large language models for clinical named entity recognition via prompt engineering. J Am Med Inform Assoc 2024 Sep 1;31(9):1812-1820. [doi: 10.1093/jamia/ocad259] [Medline: 38281112]
10. Herman Bernardim Andrade G, Nishiyama T, Fujimaki T, et al. Assessing domain adaptation in adverse drug event extraction on real-world breast cancer records. Int J Med Inform 2024 Nov;191:105539. [doi: 10.1016/j.ijmedinf.2024.105539]
11. Laparra E, Bethard S, Miller TA. Rethinking domain adaptation for machine learning over clinical language. JAMIA Open 2020 Jul;3(2):146-150. [doi: 10.1093/jamiaopen/ooaa010] [Medline: 32734151]
12. Keloth VK, Hu Y, Xie Q, et al. Advancing entity recognition in biomedicine via instruction tuning of large language models. Bioinformatics 2024 Mar 29;40(4):btae163. [doi: 10.1093/bioinformatics/btae163] [Medline: 38514400]
13. Hu Y, Zuo X, Zhou Y, et al. Information extraction from clinical notes: are we ready to switch to large language models? arXiv. Preprint posted online on Jan 7, 2025. [doi: 10.48550/arXiv.2411.10020]
14. Grattafiori A, Dubey A, Jauhri A, et al. The Llama 3 herd of models. arXiv. Preprint posted online on Nov 23, 2024. [doi: 10.48550/arXiv.2407.21783]
15. Devlin J, Chang MW, Lee K, Toutanova K. Pre-training of deep bidirectional transformers for language understanding. In: Burstein J, Doran C, Solorio T, editors. 2019 Presented at: Proceedings of the 2019 Conference of the North American Chapter of the Association for Computational Linguistics: Human Language Technologies; Jun 2-7, 2019; Minneapolis, Minnesota, USA p. 4171-4186. [doi: 10.18653/v1/N19-1423]
16. Yada S, Nakamura Y, Wakamiya S, Aramaki E. REAL-mednlp: overview of REAL document-based medical natural language processing task. Presented at: NTCIR 16 Conference: Proceedings of the 16th NTCIR Conference on Evaluation of Information Access Technologies; Jun 14-17, 2022; Tokyo Japan URL: https://research.nii.ac.jp/ntcir/workshop/OnlineProceedings16/pdf/ntcir/01-NTCIR16-OV-MEDNLP-YadaS.pdf [accessed 2025-06-30]
17. Yada S, Joh A, Tanaka R, Cheng F, Aramaki E, Kurohashi S. Towards a versatile medical-annotation guideline feasible without heavy medical knowledge: starting from critical lung diseases. In: Calzolari N, Béchet F, Blache P, Choukri K, Cieri C, Declerck T, et al, editors. 2020 Presented at: Proceedings of the Twelfth Language Resources and Evaluation Conference; May 11-16, 2020; Marseille, France p. 4565-4572 URL: https://aclanthology.org/2020.lrec-1.561/ [accessed 2025-04-13]
18. Tohoku-nlp/bert-base-japanese-v3. Hugging Face. 2024. URL: https://huggingface.co/tohoku-nlp/bert-base-japanese-v3 [accessed 2025-04-13]
19. Fujii K, Nakamura T, Loem M, et al. Continual pre-training for cross-lingual LLM adaptation: enhancing Japanese language capabilities. arXiv. Preprint posted online on Apr 27, 2024. [doi: 10.48550/arXiv.2404.17790]
20. Nishiyama T, Nishidani M, Ando A, Yada S, Wakamiya S, Aramaki E. NAISTSOC at the NTCIR-16 real-mednlp task. 2022 Presented at: NTCIR 16 Conference: Proceedings of the 16th NTCIR Conference on Evaluation of Information Access Technologies; Jun 14-17, 2022; Tokyo Japan URL: https://research.nii.ac.jp/ntcir/workshop/OnlineProceedings16/pdf/ntcir/07-NTCIR16-MEDNLP-NishiyamaT.pdf [accessed 2025-02-03]
21. Hu EJ, Shen Y, Wallis P, et al. LoRA: low-rank adaptation of large language models. arXiv. Preprint posted online on Oct 16, 2021. [doi: 10.48550/arXiv.2106.09685]
22. OpenAI, Achiam J, Adler S, Agarwal S, et al. GPT-4 Technical Report. arXiv 2024 Mar 4. [doi: 10.48550/arXiv.2303.08774]
23. Sahoo P, Singh AK, Saha S, Jain V, Mondal S, Chadha A. A systematic survey of prompt engineering in large language models: techniques and applications. arXiv. Preprint posted online on Mar 16, 2025. [doi: 10.48550/arXiv.2402.07927]

XSL•FO
RenderX

24. Ye Q, Ahmed M, Pryzant R, Khani F. Prompt engineering a prompt engineer. In: Ku LW, Martins A, Srikumar V, editors. 2024 Presented at: Findings of the Association for Computational Linguistics ACL 2024; Aug 11-16, 2024; Bangkok, Thailand and virtual meeting p. 355-385. [doi: 10.18653/v1/2024.findings-acl.21]
25. Chen B, Zhang Z, Langrené N, Zhu S. Unleashing the potential of prompt engineering for large language models. Patterns 2025 Jun;6(6):101260. [doi: 10.1016/j.patter.2025.101260]
26. Wang L, Chen X, Deng X, et al. Prompt engineering in consistency and reliability with the evidence-based guideline for LLMs. NPJ Digit Med 2024 Feb 20;7(1):41. [doi: 10.1038/s41746-024-01029-4] [Medline: 38378899]
27. Lee J, Yoon W, Kim S, et al. BioBERT: a pre-trained biomedical language representation model for biomedical text mining. Bioinformatics 2020 Feb;36(4). [doi: 10.1093/bioinformatics/btz682]
28. Kawazoe Y, Shibata D, Shinohara E, Aramaki E, Ohe K. A clinical specific BERT developed using a huge Japanese clinical text corpus. PLOS ONE 2021;16(11):e0259763. [doi: 10.1371/journal.pone.0259763] [Medline: 34752490]

Abbreviations

NLP: natural language processing
EHR: electronic health records
LLMs: large language models
ID: in-domain
OOD: out-of-domain
CR: case reports
PN: progress notes
MLM: masked language model
ICL: in-context learning
NER: named entity recognition
BIO: beginning inside outside
LoRA: low-rank adaptation

Edited by J Klann; submitted 30.04.25; peer-reviewed by A Singh, M Siino; revised version received 10.06.25; accepted 11.06.25; published 08.07.25.

Please cite as:
Shimizu S, Nishiyama T, Nagai H, Wakamiya S, Aramaki E
Toward Cross-Hospital Deployment of Natural Language Processing Systems: Model Development and Validation of Fine-Tuned Large Language Models for Disease Name Recognition in Japanese
JMIR Med Inform 2025;13:e76773
URL: https://medinform.jmir.org/2025/1/e76773
doi:10.2196/76773

© Seiji Shimizu, Tomohiro Nishiyama, Hiroyuki Nagai, Shoko Wakamiya, Eiji Aramaki. Originally published in JMIR Medical Informatics (https://medinform.jmir.org), 8.7.2025. This is an open-access article distributed under the terms of the Creative Commons Attribution License (https://creativecommons.org/licenses/by/4.0/), which permits unrestricted use, distribution, and reproduction in any medium, provided the original work, first published in JMIR Medical Informatics, is properly cited. The complete bibliographic information, a link to the original publication on https://medinform.jmir.org/, as well as this copyright and license information must be included.

XSL•FO
RenderX

Predicting Drug–Side Effect Relationships From Parametric Knowledge Embedded in Biomedical BERT Models: Methodological Study With a Natural Language Processing Approach

Woohyuk Jeon[1*]; Minjae Park[1*]; Doyeon An[1], MPH; Wonshik Nam[1]; Ju-Young Shin[2], PhD; Seunghee Lee[3], PhD; Suehyun Lee[1], PhD

[1]Department of Computer Engineering, College of IT Convergence, Gachon University, AI·Engineering Building, 317A, 1342 Seongnam-daero, Sujeong-gu, Seongnam-si, Gyeonggi-do, Seongnam, Republic of Korea

[2]School of Pharmacy, Sungkyunkwan University, Suwon, Republic of Korea

[3]Konyang Medical Data Research Group, Konyang University Hospital, Daejeon, Republic of Korea

[*]these authors contributed equally

Corresponding Author:
Suehyun Lee, PhD
Department of Computer Engineering, College of IT Convergence, Gachon University, AI·Engineering Building, 317A, 1342 Seongnam-daero, Sujeong-gu, Seongnam-si, Gyeonggi-do, Seongnam, Republic of Korea

Abstract

Background: Adverse drug reactions (ADRs) pose serious risks to patient health, and effectively predicting and managing them is an important public health challenge. Given the complexity and specificity of biomedical text data, the traditional context-independent word embedding model, Word2Vec, has limitations in fully reflecting the domain specificity of such data. Although Bidirectional Encoder Representations from Transformers (BERT)–based models pretrained on biomedical corpora have demonstrated high performance in ADR-related studies, research using these models to predict previously unknown drug–side effect relationships remains insufficient.

Objective: This study proposes a method for predicting drug–side effect relationships by leveraging the parametric knowledge embedded in biomedical BERT models. Through this approach, we predict promising candidates for potential drug–side effect relationships with unknown causal mechanisms by leveraging parametric knowledge from biomedical BERT models and embedding vector similarities of known relationships.

Methods: We used 158,096 pairs of drug–side effect relationships from the side effect resource (SIDER) database to generate an adjacency matrix and calculate the cosine similarity between word embedding vectors of drugs and side effects. Relation scores were calculated for 8,235,435 drug–side effect pairs using this similarity. To evaluate the prediction accuracy of drug-side effect relationships, the area under the curve (AUC) value was measured using the calculated relation score and 158,096 known drug–side effect relationships from SIDER.

Results: The clagator/biobert_v1.1 model achieved an AUC of 0.915 at an optimal threshold of 0.289, outperforming the existing Word2Vec model with an AUC of 0.848. The BERT-based models pretrained on the biomedical corpus outperformed the vanilla BERT model with an AUC of 0.857. External validation with the FDA (Food and Drug Administration) Adverse Event Reporting System data, using Fisher exact test based on 8,235,435 predicted drug–side effect pairs and 901,361 known relationships, confirmed high statistical significance (P<.001) with an odds ratio of 4.822. In addition, a literature review of predicted drug–side effect relationships not confirmed in the SIDER database revealed that these relationships have been reported in recent studies published after 2016.

Conclusions: This study introduces a method for extracting drug–side effect relationships embedded in parameters of language models pretrained on biomedical corpora and using this information to predict previously unknown drug–side effect relationships. We found that BERT-based models pretrained with biomedical corpora consider contextual information and achieve better performance in drug–side effect relationship prediction. External validation using the FDA Adverse Event Reporting System dataset and the literature review of certain cases confirmed high statistical significance, demonstrating practical applicability. These results highlight the utility of natural language processing–based approaches for predicting and managing ADR.

(JMIR Med Inform 2025;13:e67513) doi:10.2196/67513

XSL•FO
RenderX

KEYWORDS

adverse drug reaction; ADR prediction; NLP; BERT; word embedding; drug-side effect relationship; Bidirectional Encoder Representations from Transformers; natural language processing

Introduction

An adverse drug reaction (ADR) is a harmful, unintended reaction that occurs despite the proper use of medication [1]. In addition to causing serious health problems, ADRs are known to be one of the leading causes of prolonged patient hospitalization and increased health care spending [2]. Approximately 2 million cases of serious ADRs are reported annually in the United States, resulting in 100,000 deaths [3]. Therefore, early prediction and prevention of ADRs during drug development is a critical challenge for patient safety and public health.

Traditionally, ADR prediction has been based on approaches that analyze the chemical structure, mechanism of action, and pharmacokinetic properties of drugs [4]. Subsequently, ADR prediction methodologies using machine learning techniques have been developed [5-7], and with advances in natural language processing (NLP) techniques, attempts have been made to automatically extract and predict drug-side effect relationships from vast amounts of biomedical literature data [8-10]. The prediction of ADRs using these techniques is accelerating, especially with the advent of word embedding methods such as Word2Vec [11], which can effectively vectorize semantic information embedded in textual data [12,13].

However, biomedical text data are characterized by a much more specialized and complex set of terms and concepts compared with the general literature, and the interactions between them are also highly diverse and dynamic [14]. In fact, it has been pointed out that traditional word embedding models such as Word2Vec, which do not consider contextual information, do not sufficiently represent the relationships between complex biomedical concepts [15,16]. Therefore, models that do not adequately reflect domain specificity are limited in their ability to accurately capture drug–side effect relationships.

One solution to this problem is to use language models based on Bidirectional Encoder Representations from Transformers (BERT) [17] to perform word embedding. BERT is a language model based on the transformer [18] architecture, which has recently gained attention; unlike traditional one-way language models, it has richer language expressiveness by learning context in both directions. In addition, because we trained on large corpora, domain-specific pretrained models using large biomedical corpora can fully reflect the domain specificity of the biomedical text data [19-22]. Recently, several BERT-based models have been proposed that use large biomedical corpora such as PubMed and PMC for domain-specific pretraining. Examples include BioBERT [19], BioMedBERT [20], and PharmBERT [23], which have demonstrated high performances in various bio-NLP tasks.

BERT models and BERT-based models pretrained on biomedical corpora have demonstrated high performance in ADR-related studies [22,24-27]. However, there is a lack of research leveraging these models to predict previously unknown drug–side effect relationships. Therefore, this study aims to use a biomedical domain-specific BERT language model based on the ADR prediction relation score methodology proposed by Seungsoo et al [12]. Specifically, we calculate the similarity between embedding vectors of known drug–side effect relationships and derive promising candidates for potential relationships. In other words, our objective is to efficiently identify drug–side effect relationships whose causal associations have not yet been clearly established, by computing relation scores from biomedical language model embeddings grounded in known relationships. Furthermore, we examine whether replacing the Word2Vec model with a BERT-based model leads to an actual improvement in ADR prediction accuracy, thus validating the performance advantages of context-dependent language models.

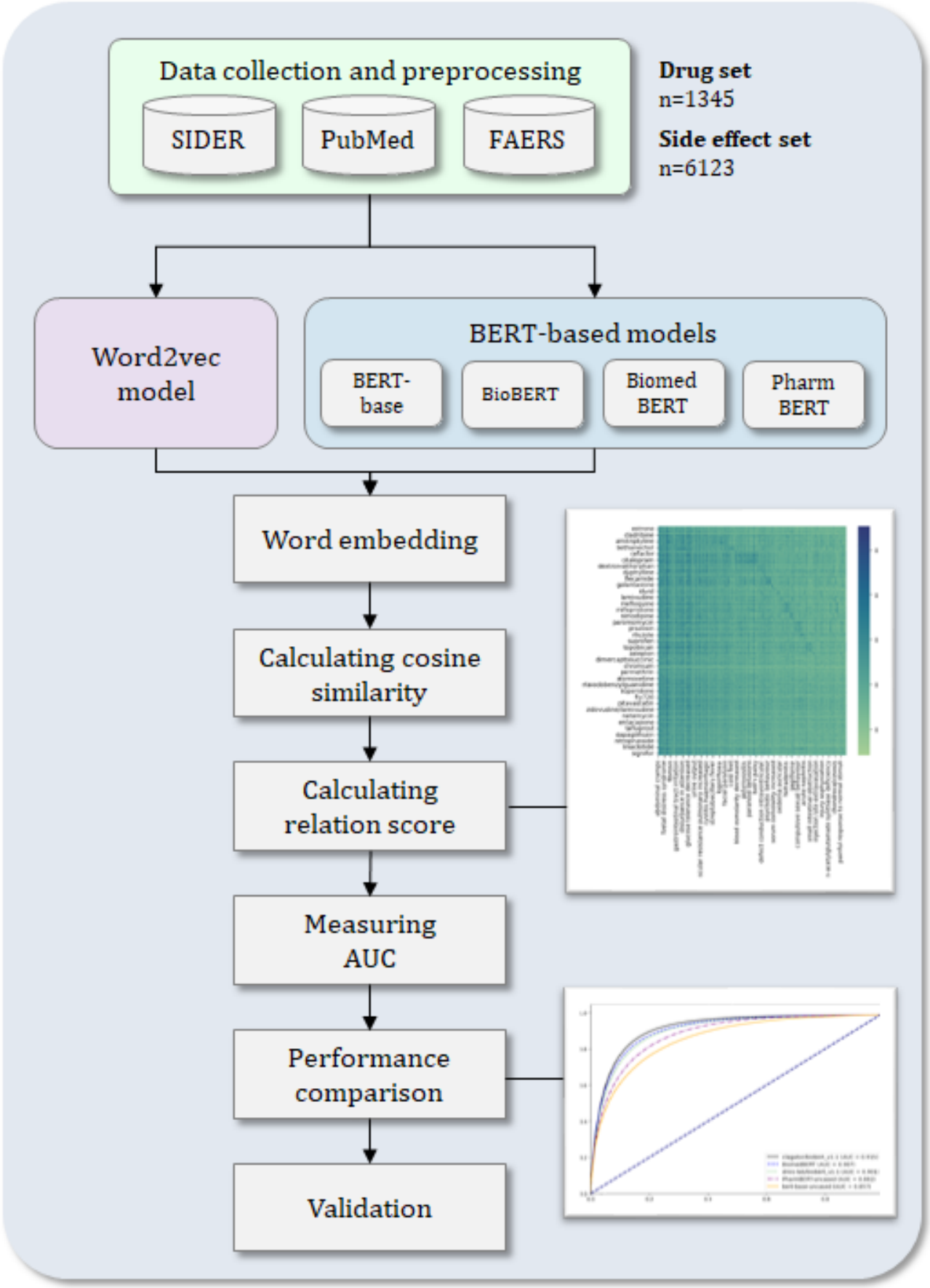
Methods

System Overview

Figure 1 presents an overview of this study and illustrates the overall research flow from data collection to validation.

XSL•FO
RenderX

Figure 1. System overview: the predictive performance of drug-side effect relationships was evaluated using area under the curve. AUC: area under the curve; BERT: Bidirectional Encoder Representations from Transformers; FAERS: FDA (Food and Drug Administration) Adverse Event Reporting System; SIDER: side effect resource.



XSL•FO
RenderX

First, we collected and refined the data for this study from the Side Effect Resource (SIDER), PubMed, and the FDA Adverse Event Reporting System (FAERS). From the abstract sentences collected from PubMed, we selectively extracted only sentences containing drugs and side effects mentioned in SIDER. These extracted sentences were used to train a Word2Vec model, from which embedding vectors for drugs and side effects were derived. Based on the drug–side effect relationships in SIDER, BERT-based models were used to derive the embedding vectors of drugs and side effects.

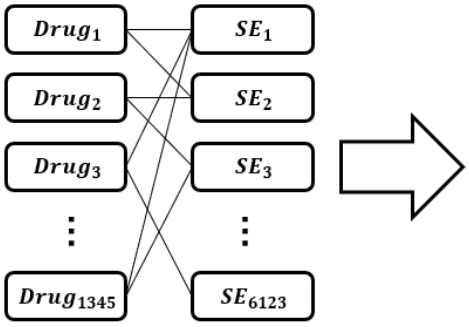
Based on the derived embedding vectors, the cosine similarity between the drug and side effect pairs was calculated. Using the cosine similarity of drug and side effect pairs and existing known drug–side effect relationships, a relation score was calculated for all drug–side effect combinations. Drug–side effect combinations with high relation scores were predicted to have a higher likelihood of being actually related [12]. To evaluate the accuracy of these predictions, we calculated area under the curve (AUC) values and compared the results of the Word2Vec model pipeline with those of the BERT-based model pipeline. Statistical significance between predicted results and FAERS was assessed using the Fisher exact test.

Data Collection and Preprocessing

SIDER is a database that provides information on marketed drugs and their side effects [28]. The drug names recorded in SIDER followed those approved by the Food and Drug Administration (FDA), and side effect names used the Medical Dictionary for Regulatory Activities (MedDRA) terminology [29]. To minimize data leakage that could occur from the same drug being listed under different names, we collected and integrated synonyms for each drug using PubChem compound identifiers provided by SIDER. We also ensured terminology standardization through MedDRA-based side effect names.

Using version 4.1 of SIDER, we collected 158,096 unique pairs of drug–side effect relationships after removing duplicates. To use these 158,096 pairs as input values in the BERT-based models and for relation score calculations, we derived an adjacency matrix with drugs as rows and side effects as columns (Figure 2). In addition, 1345 drug names and 6123 side effect terms that appeared in the collected drug–side effect relationships were extracted and used as dictionaries for drugs and side effects.

Figure 2. Drug-SE adjacency matrix. This is a method to derive an adjacency matrix using drug–side effect relationships in the side effect resource. The relation R has the value of 1 if the drug–side effect relationship exists and 0 if it does not. SE: side effect.



	SE_1	SE_2	SE_3	SE_4	⋯	SE_{6123}
$Drug_1$	$R_{1,1}$	$R_{1,2}$	$R_{1,3}$	$R_{1,4}$	⋯	$R_{1,6123}$
$Drug_2$	$R_{2,1}$	$R_{2,2}$	$R_{2,3}$	$R_{2,4}$	⋯	$R_{2,6123}$
$Drug_3$	$R_{3,1}$	$R_{3,2}$	$R_{3,3}$	$R_{3,4}$	⋯	$R_{3,6123}$
$Drug_4$	$R_{4,1}$	$R_{4,2}$	$R_{4,3}$	$R_{4,4}$	⋯	$R_{4,6123}$
⋯	⋯	⋯	⋯	⋯	⋯	⋯
$Drug_{1345}$	$R_{1345,1}$	$R_{1345,2}$	$R_{1345,3}$	$R_{1345,4}$	⋯	$R_{1345,6123}$

We collected biomedical literature from PubMed, a biological literature database [30]. A total of 42,515,246 paper abstracts updated on December 8, 2022, were collected, and for training the Word2Vec model, only sentences in which the drugs and side effects mentioned in SIDER were mentioned at least once were extracted [12]. There were 14,289,160 sentences in which a drug was mentioned at least once and 32,107,327 sentences in which a side effect was mentioned at least once.

Calculating Cosine Similarity

For the 1345 drugs and 6123 side effects recorded in the adjacency matrix, we performed word embedding using BERT-based models and calculated the cosine similarity for all drug and side effect vector pairs. In this case, the cosine similarity is calculated using equation (1).

$$\text{CosineSimilarity}=A\cdot B/\|A\|\ \|B\|=\sum_{i=1}^{n}A_i\times B_i/\sqrt{\sum_{i=1}^{n}(A_i)^2}\times\sqrt{\sum_{i=1}^{n}(B_i)^2} \quad (1)$$

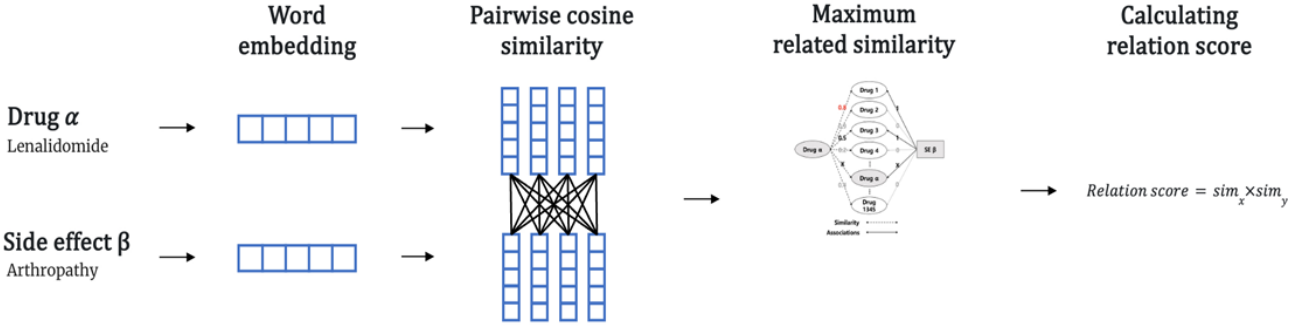
This process yielded 1,809,025 drug vector pairwise similarities and 37,491,129 side effect vector pairwise similarities.

Calculating Relation Score

Figure 3 shows the process of calculating the relation score. For all drug–side effect pairs embedded as vectors, the cosine similarity values obtained in the previous step were used to calculate the drug–side effect's relation score. The process of calculating the relation score between a specific $Drug_{\alpha}$ and a specific side effect SE_{β} was done using equations (2) to (6).

XSL•FO
RenderX

Figure 3. Illustration of the computation of the relation score between a specific $Drug_{\alpha}$ and a specific side effect SE_{β}.



$$si\ mx=max\{\sim(Da,Di)\vee Di \in RelatedDrugs\} \quad (2)$$

$$RelatedDrugs=\{Di\vee Adjacency(SE\beta,Di)=1\ for\ i=1,2,...,1345\} \quad (3)$$

$$si\ my=max\{\sim(S\ E\beta,S\ Ei)\vee S\ E\ i\ \in RelatedSE\} \quad (4)$$

$$RelatedSE=\{S\ Ei\vee Adjacency\ (Da,S\ Ei)=1\ for\ i=1,2,...,6123\} \quad (5)$$

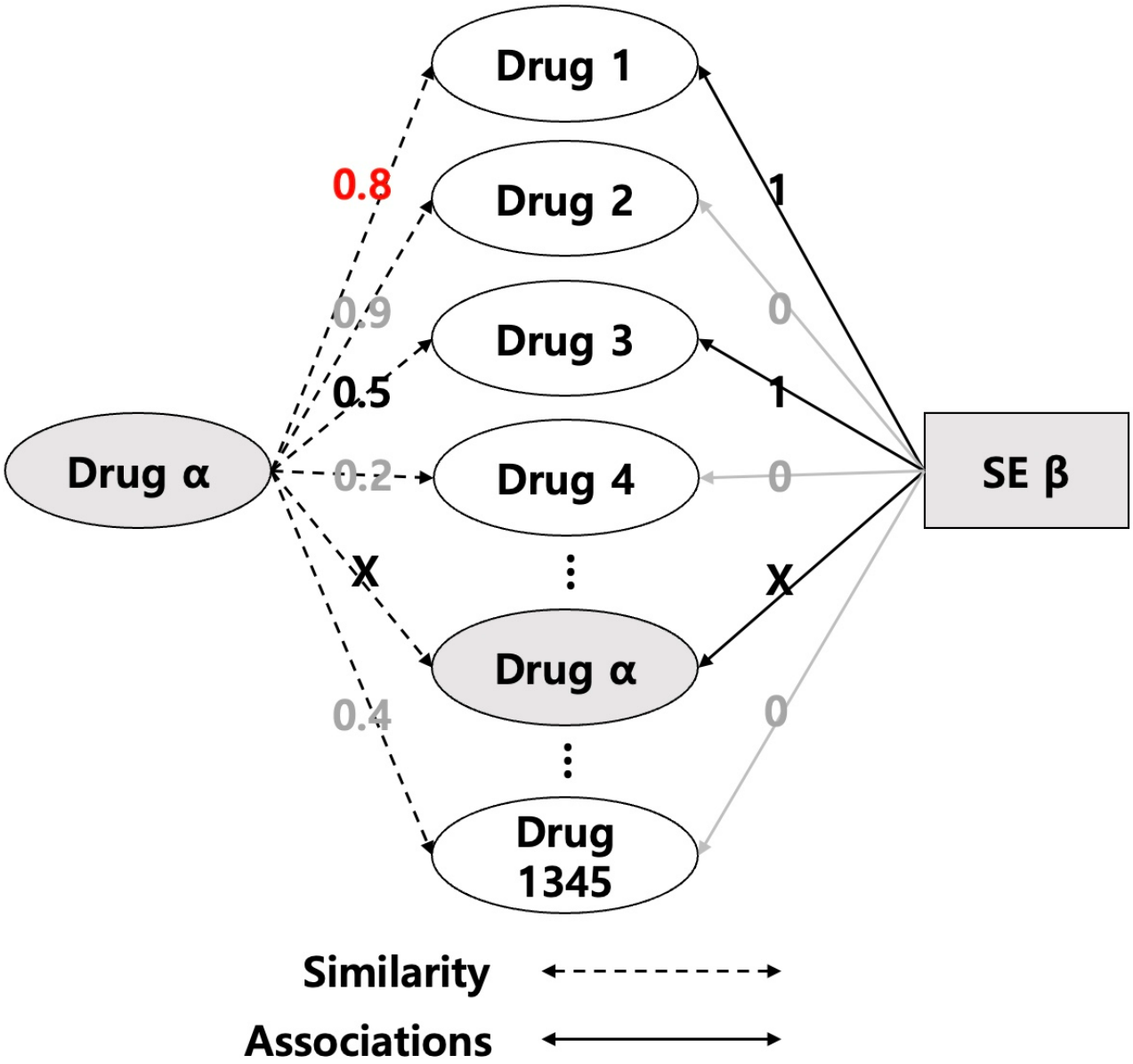
$$Relation\ score=si\ mx\times si\ my \quad (6)$$

Similarity sim_x takes the maximum of the similarity values of $Drug_{\alpha}$ with Drug D_i in $Related_{Drugs}$, the set of drugs known to be associated with side effect SE_{β}, using equation (2). The set $Related_{Drugs}$ is obtained using equation (3), and by referring to the values in the adjacency matrix consisting of 1345 drugs and 6123 side effects, we construct the set of drugs associated with that side effect by including in the set $Related_{Drugs}$ those drugs that have side effect SE, and a value of 1 in the adjacency matrix, out of a total of 1345 drugs. In other words, the highest similarity value to drugs known to be associated with side effect SE is called similarity sim_x.

Figure 4 shows the process of obtaining similarity sim_x using equation (2) and equation (3). Based on the values in the adjacency matrix, the computational process was to maximize the similarity of only those drugs that were related to the side effect SE out of the total 1345 drugs. If $Drug_{\alpha}$ is in the $Related_{Drugs}$ set, exclude $Drug_{\alpha}$ from the similarity calculation.

XSL•FO
RenderX

Figure 4. Process of calculating similarity sim_X. SE: side effect.



Similarity sim_y uses equation (4) to take the maximum of the similarity values of side effects SE_β and SE_i in $Related_{SE}$, a set of side effects known to be related to the $Drug_\alpha$. The set $Related_{SE}$ is obtained using equation (5), and by referring to the values of the adjacency matrix mentioned above, we construct the set of side effects associated with the $Drug_\alpha$ out of the total 6123 side effects by including in the set $Related_{SE}$ the drugs that have a value of 1 in the adjacency matrix with the $Drug_\alpha$. In other words, the highest similarity value to the side effects that are known to be related to the drug is called the similarity sim_y.

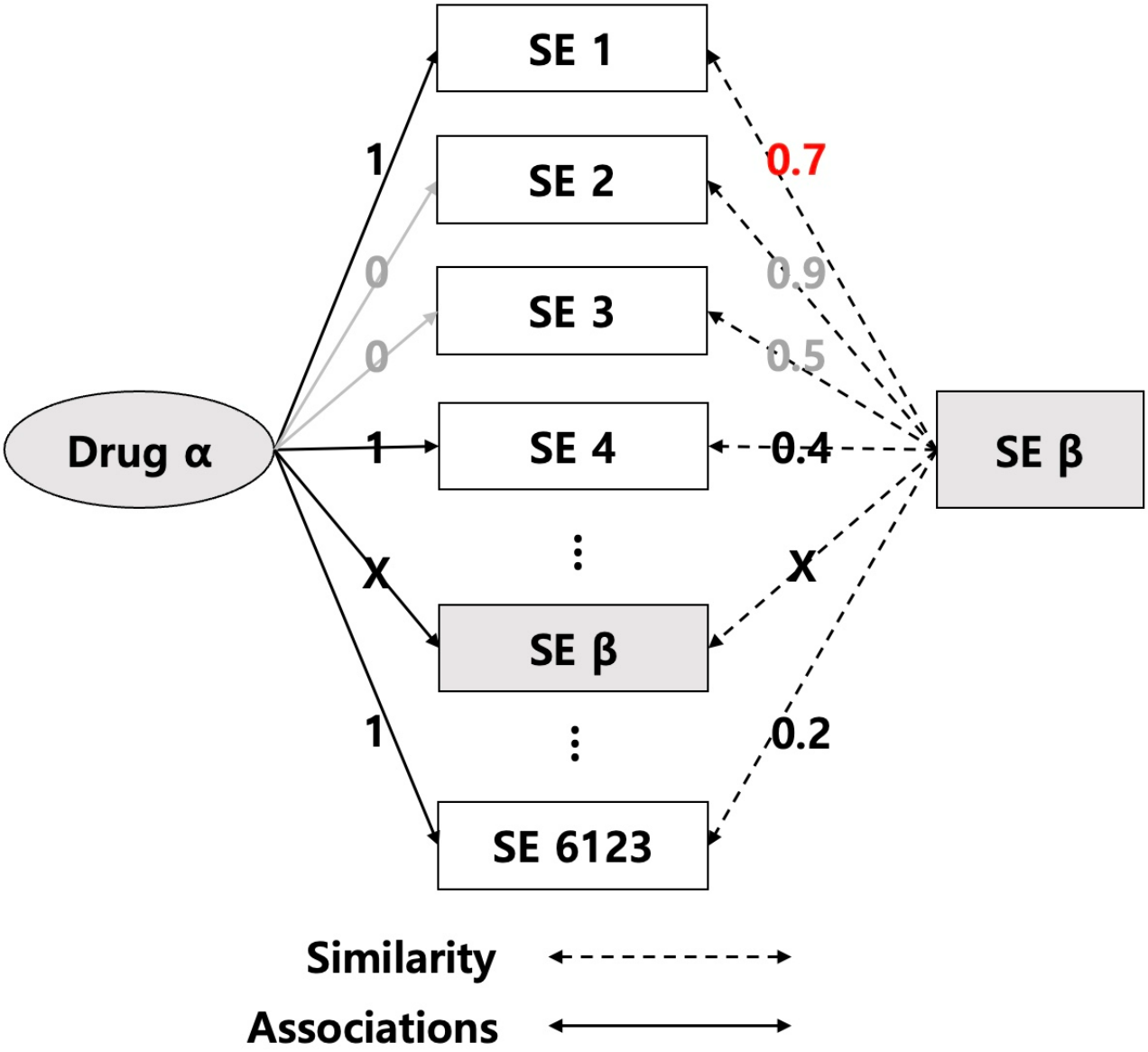
Figure 5 shows the process of obtaining similarity sim_y using equation (4) and equation (5). Based on the values in the adjacency matrix, the computational process is to extract the similarity of only the side effects that are related to the $Drug_\alpha$, out of the total 6123 side effects, and take the maximum value. If an SE_β belongs to the $Related_{SE}$ set, exclude the SE_β from the similarity calculation.

Finally, the relation score between Drug and SE was obtained by multiplying sim_x and sim_y as shown in equation (6).

We applied the above calculation method to 1345 drugs and 6123 side effects to calculate the relation scores for all drug–side effect pairs, resulting in a total of 8,235,435 drug–side effect pairs. Figure 6 illustrates the heatmap of the calculated relation scores.

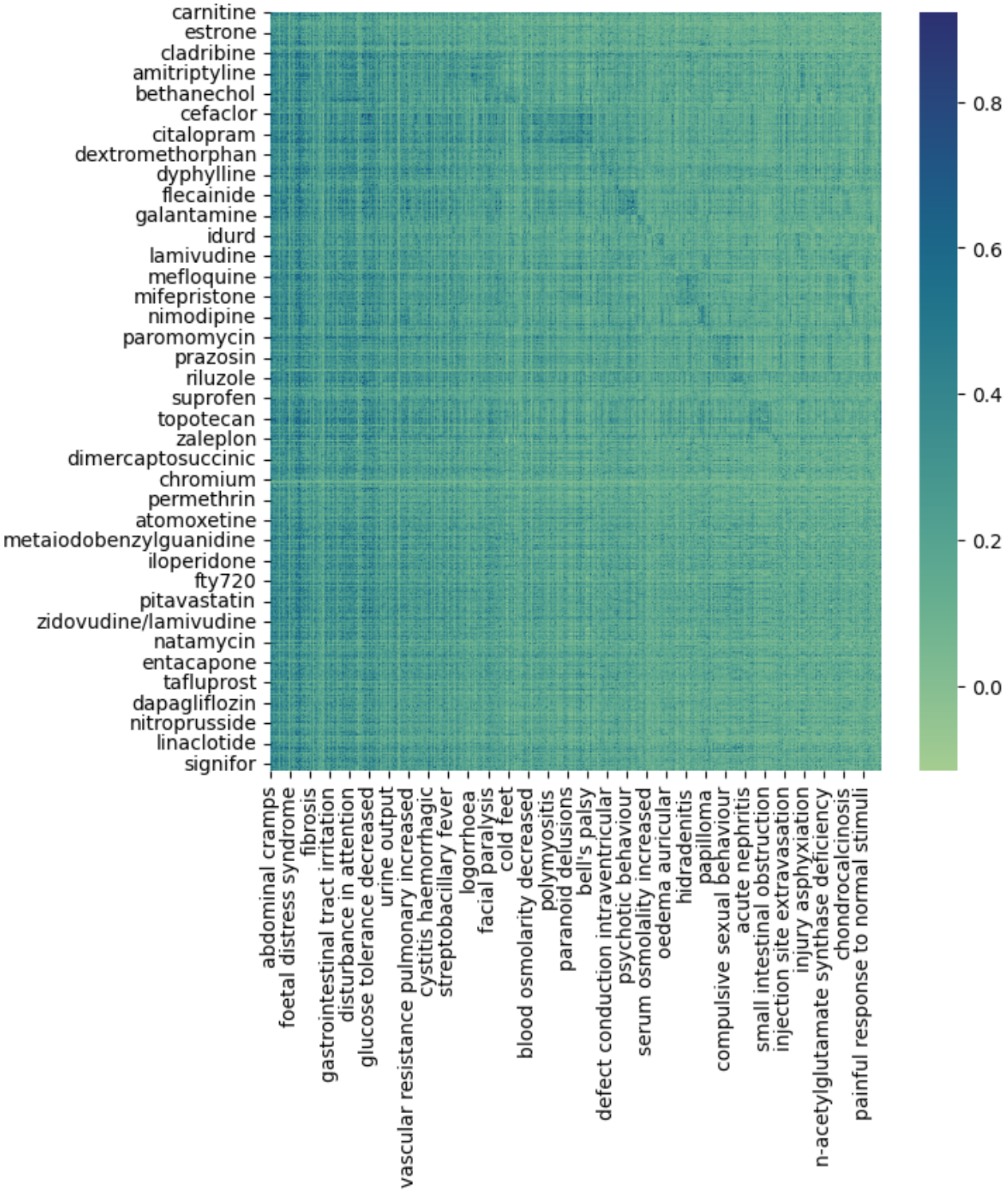
XSL•FO
RenderX

Figure 5. Process of calculating similarity sim_y. SE: side effect.



XSL•FO
RenderX

Figure 6. Heatmap of calculated relation score for 8,235,435 drug–side effect pairs.



Measuring AUC

In this study, AUC values were measured using 158,096 known drug–side effect relationships provided by SIDER to evaluate the accuracy of predicting relationships based on scores calculated for a total of 8,235,435 drug–side effect pairs. Of the 8,235,435 calculated drug–side effect pairs, we assigned a class value of true to pairs that belonged to known drug–side effect relationships in SIDER and false to pairs that did not. All drug–side effect pairs were sorted by score, and a single receiver operating characteristic curve was calculated. The generated receiver operating characteristic curves and AUC values were used to establish the optimal threshold for predicting whether a drug–side effect pair had a true relationship. If the drug–side effect relation score exceeds this diagnostic threshold, it is predicted that there is a relationship between the drug and the side effect [12].

XSL•FO
RenderX

Ethical Considerations

This study uses the publicly accessible and anonymized SIDER and FAERS databases, which contain no personally identifiable information and do not involve human participant experimentation. Therefore, institutional review board approval is not required for this study.

Results

Performance Comparison

The AUCs of the BERT-based models and the Word2Vec model using the proposed method are compared in Table 1 and Figure 7. The optimal threshold for prediction was set as the point at which the sum of the sensitivity and specificity was maximized. The models used in this study included clagator/biobert_v1.1 [31], BiomedBERT [20], dmis-lab/biobert_v1.1 [19], PharmBERT-uncased [23], bert-base-uncased [17], and Word2Vec [11]. dmis-lab/biobert-v1.1 is the original BioBERT model pretrained on biomedical text, while clagator/biobert_v1.1 is a model based on it, which has been additionally fine-tuned on natural language inference and semantic textual similarity tasks to enhance its ability to recognize semantic relationships.

Table . Performance comparison of Bidirectional Encoder Representations from Transformers (BERT)–based models and Word2Vec model.

Model	AUC[a]	Optimal threshold	Sensitivity	Specificity
clagator/biobert_v1.1	0.915[b]	0.289	0.870	0.830
BiomedBERT[c]	0.907	0.925	0.857	0.821
dmis-lab/biobert_v1.1	0.901	0.780	0.851	0.814
PharmBERT-uncased	0.882	0.460	0.817	0.796
bert-base-uncased[d]	0.857	0.617	0.769	0.793
Word2Vec	0.848[e]	0.112	0.762	0.780

[a]AUC: area under the curve.

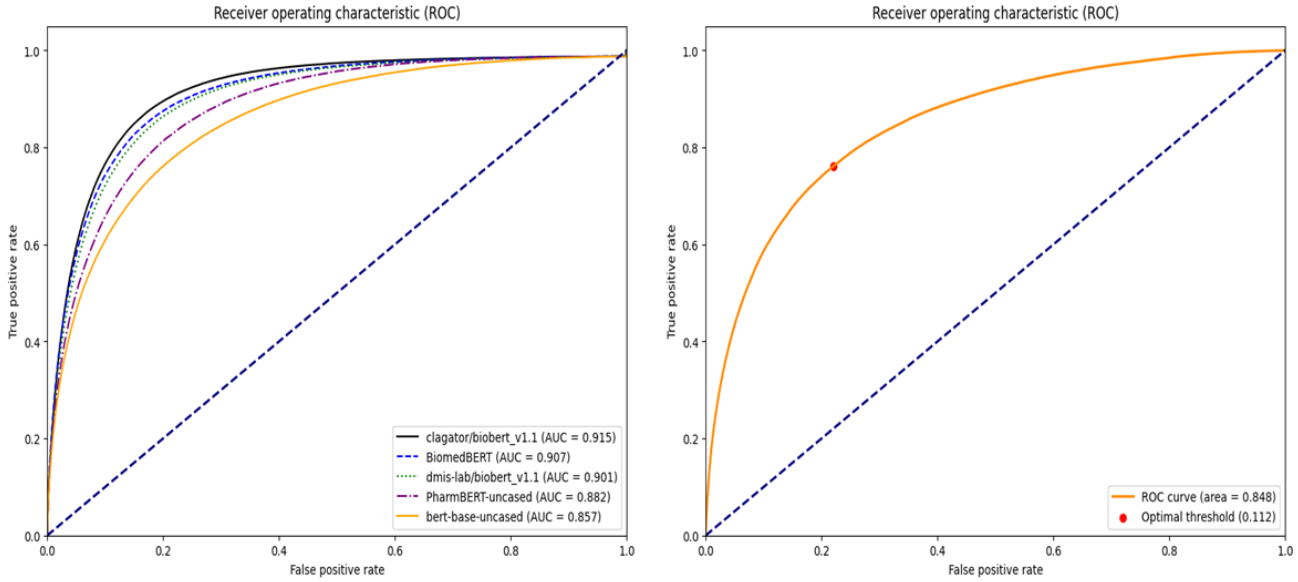
[b]Highest value.

[c]The old model was named PubMedBERT.

[d]Vanilla BERT model.

[e]Lowest value.

Figure 7. Receiver operating characteristic curves for Bidirectional Encoder Representations from Transformers (BERT)–based models (left) and Word2Vec model (right). AUC: area under the curve.



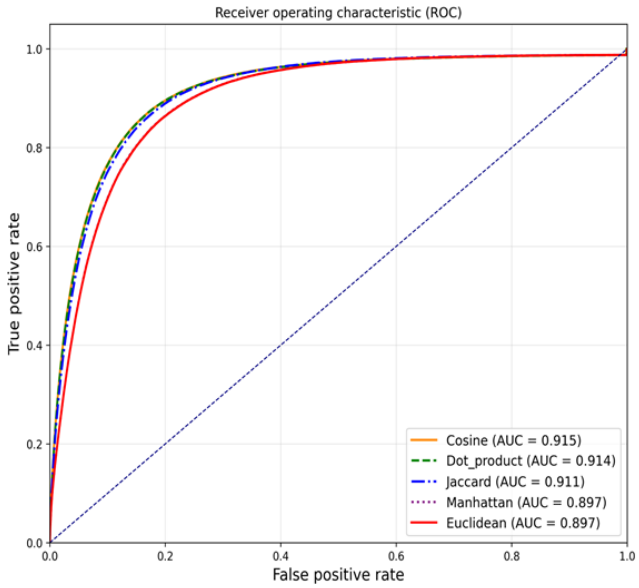
The clagator/biobert _v1.1 model achieved the highest AUC value of 0.915 at an optimal threshold of 0.289. In contrast, the bert-base-uncased model, a vanilla BERT model pretrained on general corpora, showed an AUC of 0.857 at an optimal threshold of 0.617. In other words, BERT pretrained on the biomedical corpus outperformed vanilla BERT. In addition, the Word2Vec model recorded an AUC of 0.848, which was lower than those of the BERT-based models and was the lowest among all models used in this study.

Figure 8 (left) shows the performance comparison results to evaluate the effectiveness of the cosine similarity-based extraction approach. The comparison was conducted using the clagator/biobert_v1.1 model, which achieved the highest

XSL•FO
RenderX

performance. Other vector similarity-based extraction methods used for comparison included Euclidean distance, Manhattan distance, Jaccard similarity, and dot product. The results demonstrate that the cosine similarity-based relation extraction method used in this study exhibited the highest performance with an AUC of 0.915, outperforming all other methods.

Figure 8. Receiver operating characteristic curves for comparing vector similarity metrics (left) and evaluating the efficacy of our dual-similarity approach (right). AUC: area under the curve.



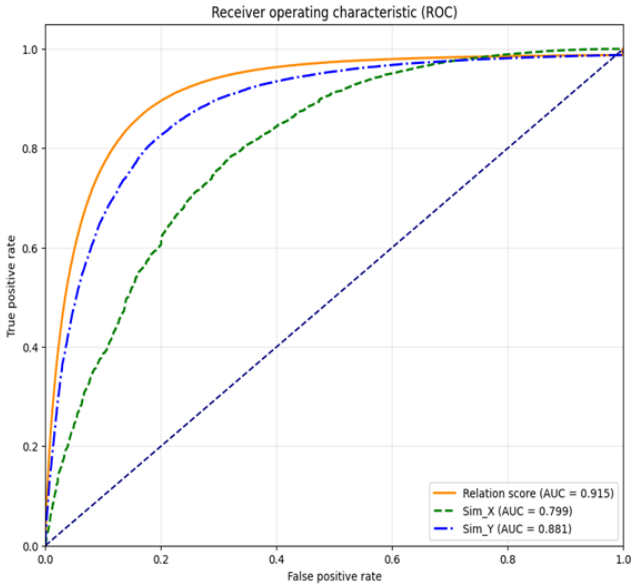


Figure 8 (right) evaluates the effectiveness of our dual-similarity approach against single-similarity methods. Using the same clagator/biobert_v1.1 model, we compared 3 extraction strategies: using only drug similarity information (Sim_X), using only side effect similarity information (Sim_Y), and our dual-similarity approach (relation score). Our dual-similarity approach significantly outperformed single-similarity methods with an AUC of 0.915 compared with 0.799 and 0.881, demonstrating the effectiveness of leveraging information from both similarity perspectives.

Validation

To validate the similarity between drug–side effect relationships predicted by our model based on SIDER data and relationships derived from FAERS data, we extracted drug–side effect relationships from FAERS, a database not used in our Methods. FAERS is a database containing adverse event information for drugs submitted to the FDA [32]. In this study, we used FAERS data from October 2012 to June 2023. By leveraging the list of 1345 drugs and 6123 side effects registered in SIDER to extract relationships from FAERS data, we obtained a total of 901,361 known relationships.

For validation, we used the results from clagator/biobert_v1.1 [31], which performed best in our study. We constructed a contingency table using the predicted results based on relation scores from 8,235,435 drug–side effect pairs, along with 901,361 known drug–side effect relationships and unknown relationships extracted from FAERS. However, due to the data imbalance where unknown relationships outnumbered known relationships, we randomly sampled unknown relationships to match the number of known relationships. Based on this selected list of drug–side effect pairs, we conducted the Fisher exact test between FAERS data and our study's predictions, repeating this process 2000 times and calculating the average of all results. The results showed a P value of $P<.001$, confirming that the drug–side effect relationships predicted in our study were statistically significant.

Furthermore, the odds ratio, calculated as the ratio of the odds of an event occurring to the odds of it not occurring, was 4.822. This means that the odds of our model predicting a relationship for known relationships in FAERS were 4.822 times higher than the odds of predicting a relationship for unknown relationships. In other words, relationships reported in FAERS were significantly more likely to be predicted as related by our model, demonstrating that our model's predictions are reliable when compared with external data.

To validate the utility of our model's predictions, we conducted case studies on drug–side effect relationships not present in the SIDER database that were ranked within the top 1000 according to relation scores calculated by our model. For these candidates, we performed literature searches using Google Scholar and verified whether these relationships had been mentioned in case reports or research [33]. In addition, following the input from an author specializing in pharmacoepidemiology, we excluded steroid-class drugs that are used despite their side effects from a clinical utility perspective, thereby enhancing the reliability of our ability to detect meaningful signals in actual clinical environments. Table 2 illustrates the cases of lenalidomide-arthropathy, rosuvastatin-sleep disturbance, gadolinium-acute pulmonary edema, and cefazolin-hepatic failure. Upon conducting a literature review of the drug–side effect relationships presented in Table 2, we confirmed that these associations were reported in research findings published after 2016 [34-37].

XSL•FO
RenderX

Table . Case studies of model predictions.

Drug α	Side effect β	Similarity *x*	Similarity *y*	Relation score	Model prediction
Lenalidomide	Arthropathy	0.953	0.837	0.799	True
Rosuvastatin	Sleep disturbance	0.952	0.825	0.786	True
Gadolinium	Acute pulmonary edema	0.891	0.866	0.771	True
Cefazolin	Hepatic failure	0.861	0.857	0.738	True

Discussion

Principal Findings

In this study, we propose a method to extract information about drug–side effect relationships inherent in the pre–trained parameters of language models and predict relation scores, indicating the possibility of unknown drug–side effect relationships. This is accomplished using known drug–side effect relationship data and embedding vectors from language models trained on biomedical corpora.

Our study confirmed that BERT-based models demonstrated superior performance in predicting drug–side effect relationships. We evaluated the performance of BERT-based models using the relation score methodology proposed by Seungsoo et al [12], and the clagator/biobert_v1.1 model [31] achieved the highest performance with an AUC of 0.915 at an optimal threshold of 0.289. This suggests that BERT-based models perform better in predicting drug–side effect relationships compared to the 0.85 AUC achieved by the Word2Vec model in a previous study. Therefore, our findings support the notion that context-aware BERT-based models outperform context-independent Word2Vec models in terms of embedding performance [38].

In addition, our study demonstrates that BERT models pretrained on biomedical corpora outperform vanilla BERT models pretrained on general corpora. Vanilla BERT models, trained on general corpora, have limitations in fully reflecting the specificity of the biomedical field [20]. In contrast, BERT-based models pretrained on large biomedical corpora, such as PubMed and PMC, more richly reflect drug mechanisms of action and biological relationships observed in clinical settings [19-21]. The results of this study demonstrate that BERT models specialized for biomedical applications can provide more accurate drug–side effect relationship predictions based on a deeper understanding of the domain. This aligns with previous studies that emphasize the importance of domain-specific models in BERT model applications [19,23,39]. While this study evaluated the effectiveness of the proposed extraction method using BERT-based models, considering the rapid advancements in the field of NLP, models with different architectures or more recent models have the potential to understand the complexity of relationships more effectively and provide further performance improvements.

We performed external validation using FAERS data and found a high statistical significance (P<.001) between 8,235,435 predicted drug–side effect relationships and 901,361 actual data extracted from FAERS. In addition, to verify the real-world applicability of the model's predicted results, we conducted case studies on drug–side effect relationships that were not confirmed in the SIDER database. We found that these drug–side effect relationships have been reported in recent research findings published after 2016. This suggests that our methodology using the BERT-based model proposed in this study is applicable to the prediction of ADRs in practice. Considering this, we expect that our proposed methodology will allow for earlier detection of potential ADRs, increasing the likelihood of success in the drug development process and reducing the time and cost of ADR studies.

In the field of biomedical NLP, standardized terminology systems and synonym processing are important [15,40]. In this study, we minimized the risk of data leakage by integrating drug synonyms using PubChem compound identifiers. We used MedDRA-based side effect names to ensure terminology standardization and reduce the likelihood of the model merely reidentifying variations of known relationships. However, we have not explicitly integrated the hierarchical information from MedDRA, and in future research, we plan to enhance our methodology by actively using MedDRA hierarchical information to integrate similar terms, further mitigating the reidentification issue.

In this study, we recognize that non–dose-dependent adverse reactions present particular challenges for prediction models, and drug similarity may not necessarily be the main component in the development of such ADRs. While our dual-similarity approach partially addresses this by incorporating adverse event similarity patterns, future research would benefit from integrating NLP-based approaches with the chemical structure and mechanism of action of drugs. This multimodal approach would leverage literature-derived contextual relationships, molecular properties, and biological pathway insights to more accurately classify drug–side effect relationships and would be particularly valuable for addressing current methodological limitations, including novel compound prediction and idiosyncratic reaction detection.

Limitations

One of the primary limitations of this study is the lack of up-to-date data in the drug–side effect database used. The SIDER database was last updated in 2015, meaning that despite using BERT-based models trained on the latest biomedical corpus, our prediction process may not fully reflect current drug–side effect relationships. Consequently, incorporating more recent drug–side effect data would likely improve the performance of our prediction model significantly.

XSL•FO
RenderX

Another significant limitation relates to the nature of case reports themselves. Such reports typically rely on a single clinically reported case, thereby making it difficult to establish clear causal relationships between drugs and side effects. In addition, their small sample sizes often limit their generalizability. These considerations become particularly relevant when extending our work to clinical applications, where patient care involves complex interactions of multiple factors, including diverse reporting patterns and polypharmacy. Although our model provides a systematic method for prioritizing potential associations for further investigation, all predictions should therefore be interpreted with appropriate caution and validated through additional pharmacovigilance methods before clinical application. For this reason, future research should utilize systematic clinical data or large-scale cohort studies to enhance the reliability of predictive models.

Furthermore, while our approach shows promise for identifying potential drug–side effect relationships through vector space similarities, we recognize 2 additional important limitations. First, the current methodology provides generalized, population-level predictions and does not account for idiosyncratic reactions dependent on individual patient factors. As such, future work should explore integrating patient-specific data to enable more personalized adverse event predictions. Second, for entirely novel drug candidates absent from existing literature, the embedding vectors generated would be based primarily on semantic inference rather than established knowledge, potentially limiting prediction reliability. This underscores the importance of complementary approaches, particularly for new chemical entities.

Conclusions

This study presents a novel approach for extracting drug–side effect relationship information embedded within pretrained language model parameters and leveraging this information to predict unknown adverse reactions. Our methodology, using context-aware BERT-based language models, demonstrates that BERT models pretrained on biomedical corpora outperform vanilla BERT and Word2Vec. These results highlight how the contextual embedding capabilities of BERT architectures, coupled with domain-specific adaptation, enhance predictive performance in drug–side effect relationship tasks. Furthermore, external validation using FAERS data and a literature review of selected cases confirmed the practical applicability of the proposed methodology.

Acknowledgments

This research was supported by a grant of the Korea Health Technology R&D Project through the Korea Health Industry Development Institute (KHIDI), funded by the Ministry of Health & Welfare, Republic of Korea (grant RS-2022-KH125153).

Data Availability

The datasets used in this study are available in the FDA Adverse Event Reporting System (FAERS) repository [32] and the SIDER repository [41]. The datasets generated or analyzed during this study are available from the corresponding author on reasonable request.

Authors' Contributions

MP and WJ designed the study and drafted the manuscript. WJ was responsible for data collection, preprocessing, and validation. MP was responsible for the relation score calculation methodology and implementation of the BERT model. WN conducted the reproduction study using Word2Vec. DA and JS contributed to the manuscript revision. Suehyun L and Seunghee L contributed equally as co-corresponding authors and supervised the study. All authors have read and agreed to the published version of the manuscript.

Conflicts of Interest

None declared.

References

1. Edwards IR, Aronson JK. Adverse drug reactions: definitions, diagnosis, and management. The Lancet 2000 Oct;356(9237):1255-1259. [doi: 10.1016/S0140-6736(00)02799-9]
2. Pirmohamed M, James S, Meakin S, et al. Adverse drug reactions as cause of admission to hospital: prospective analysis of 18 820 patients. BMJ 2004 Jul 3;329(7456):15-19. [doi: 10.1136/bmj.329.7456.15] [Medline: 15231615]
3. Lazarou J, Pomeranz BH, Corey PN. Incidence of adverse drug reactions in hospitalized patients: a meta-analysis of prospective studies. JAMA 1998 Apr 15;279(15):1200-1205. [doi: 10.1001/jama.279.15.1200] [Medline: 9555760]
4. Huang LC, Wu X, Chen JY. Predicting adverse side effects of drugs. BMC Genomics 2011 Dec 23;12 Suppl 5(Suppl 5):S11. [doi: 10.1186/1471-2164-12-S5-S11] [Medline: 22369493]
5. Toni E, Ayatollahi H, Abbaszadeh R, Fotuhi Siahpirani A. Machine learning techniques for predicting drug-related side effects: a scoping review. Pharmaceuticals (Basel) 2024 Jun 17;17(6):38931462. [doi: 10.3390/ph17060795] [Medline: 38931462]

XSL•FO
RenderX

6. Yang S, Kar S. Application of artificial intelligence and machine learning in early detection of adverse drug reactions (ADRs) and drug-induced toxicity. Artificial Intelligence Chemistry 2023 Dec;1(2):100011. [doi: 10.1016/j.aichem.2023.100011]
7. Seo S, Lee T, Kim MH, Yoon Y. Prediction of side effects using comprehensive similarity measures. Biomed Res Int 2020;2020(1):1357630. [doi: 10.1155/2020/1357630] [Medline: 32190647]
8. Leaman R, Wojtulewicz L, Sullivan R, Skariah A, Yang J. Towards internet-age pharmacovigilance: extracting adverse drug reactions from user posts in health-related social networks. In: Gonzalez G, editor. : Association for Computational Linguistics Presented at: Proceedings of the 2010 workshop on biomedical natural language processing; Jul 15, 2010; Uppsala, Sweden p. 117-125.
9. Gurulingappa H, Mateen-Rajput A, Toldo L. Extraction of potential adverse drug events from medical case reports. J Biomed Semantics 2012 Dec 20;3(1):15. [doi: 10.1186/2041-1480-3-15] [Medline: 23256479]
10. Nikfarjam A, Sarker A, O'Connor K, Ginn R, Gonzalez G. Pharmacovigilance from social media: mining adverse drug reaction mentions using sequence labeling with word embedding cluster features. J Am Med Inform Assoc 2015 May;22(3):671-681. [doi: 10.1093/jamia/ocu041] [Medline: 25755127]
11. Mikolov T, Sutskever I, Chen K, Corrado GS, Dean J. Distributed representations of words and phrases and their compositionality. Adv Neural Inf Process Syst. Preprint posted online on 2013. [doi: 10.48550/arXiv.1310.4546]
12. Seungsoo L, Hayon L, Youngmi Y. Prediction of new drug-side effect relation using Word2Vec model-based word similarity. JKIIT 2020;18(11):25-33. [doi: 10.14801/jkiit.2020.18.11.25]
13. Zhang F, Sun B, Diao X, Zhao W, Shu T. Prediction of adverse drug reactions based on knowledge graph embedding. BMC Med Inform Decis Mak 2021 Feb 4;21(1):38. [doi: 10.1186/s12911-021-01402-3] [Medline: 33541342]
14. Cohen KB, Demner-Fushman D. Biomedical Natural Language Processing: John Benjamins Publishing Company; 2014.
15. Zhang Y, Chen Q, Yang Z, Lin H, Lu Z. BioWordVec, improving biomedical word embeddings with subword information and MeSH. Sci Data 2019;6(1):31076572. [doi: 10.1038/s41597-019-0055-0]
16. Hassan NA, Seoud RAA, Salem DA. Bridging the gap: a hybrid approach to medical relation extraction using pretrained language models and traditional machine learning. JAIT 2024;15(6):723-734. [doi: 10.12720/jait.15.6.723-734]
17. Devlin J, Chang MW, Lee K, Toutanova K. Bert: pre-training of deep bidirectional transformers for language understanding. arXiv. Preprint posted online on 2018. [doi: 10.48550/arXiv.1810.04805]
18. Vaswani A, Shazeer N, Parmar N, Uszkoreit J, Jones L, Gomez AN, et al. Attention is all you need. Adv Neural Inf Process Syst. Preprint posted online on 2017. [doi: 10.48550/arXiv.1706.03762]
19. Lee J, Yoon W, Kim S, et al. BioBERT: a pre-trained biomedical language representation model for biomedical text mining. Bioinformatics 2020 Feb 15;36(4):1234-1240. [doi: 10.1093/bioinformatics/btz682] [Medline: 31501885]
20. Gu Y, Tinn R, Cheng H, et al. Domain-specific language model pretraining for biomedical natural language processing. ACM Trans Comput Healthcare 2022 Jan 31;3(1):1-23. [doi: 10.1145/3458754]
21. Peng Y, Yan S, Lu Z. Transfer learning in biomedical natural language processing: an evaluation of BERT and elmo on ten benchmarking datasets. Presented at: Proceedings of the 18th BioNLP Workshop and Shared Task; Aug 1, 2019; Florence, Italy p. 190605474. [doi: 10.18653/v1/W19-5006]
22. Elbiach O, Grissette H, Nfaoui EH. Leveraging transformer models for enhanced pharmacovigilance: a comparative analysis of ADR extraction from biomedical and social media texts. AI 2025;6(2):31. [doi: 10.3390/ai6020031]
23. ValizadehAslani T, Shi Y, Ren P, et al. PharmBERT: a domain-specific BERT model for drug labels. Brief Bioinform 2023 Jul 20;24(4):bbad226. [doi: 10.1093/bib/bbad226] [Medline: 37317617]
24. Nishioka S, Watanabe T, Asano M, et al. Identification of hand-foot syndrome from cancer patients' blog posts: BERT-based deep-learning approach to detect potential adverse drug reaction symptoms. PLoS ONE 2022;17(5):e0267901. [doi: 10.1371/journal.pone.0267901] [Medline: 35507636]
25. Bergman E, Dürlich L, Arthurson V, et al. BERT based natural language processing for triage of adverse drug reaction reports shows close to human-level performance. PLOS Digit Health 2023 Dec;2(12):e0000409. [doi: 10.1371/journal.pdig.0000409] [Medline: 38055685]
26. Hussain S, Afzal H, Saeed R, Iltaf N, Umair MY. Pharmacovigilance with transformers: a framework to detect adverse drug reactions using BERT fine-tuned with FARM. Comput Math Methods Med 2021;2021(1):5589829. [doi: 10.1155/2021/5589829] [Medline: 34422092]
27. Mahendran D, McInnes BT. Extracting Adverse Drug Events from Clinical Notes. AMIA Jt Summits Transl Sci Proc. 2021 p. 420-429. [doi: 10.48550/arXiv.2104.10791] [Medline: 34457157]
28. Kuhn M, Letunic I, Jensen LJ, Bork P. The SIDER database of drugs and side effects. Nucleic Acids Res 2016 Jan 4;44(D1):D1075-D1079. [doi: 10.1093/nar/gkv1075] [Medline: 26481350]
29. Brown EG, Wood L, Wood S. The medical dictionary for regulatory activities (MedDRA). Drug Saf 1999 Feb;20(2):109-117. [doi: 10.2165/00002018-199920020-00002] [Medline: 10082069]
30. Canese K, Weis S. PubMed: The Bibliographic Database. In: The NCBI Handbook: National Center for Biotechnology Information; 2013, Vol. 2:13-24.
31. Biobert_v1.1_pubmed_nli_sts. Hugging Face Hub. URL: https://huggingface.co/clagator/biobert_v1.1_pubmed_nli_sts [accessed 2023-08-23]

XSL•FO
RenderX

32. Questions and answers on FDA's adverse event reporting system (FAERS). US Food and Drug Administration. URL: https://www.fda.gov/drugs/surveillance/questions-and-answers-fdas-adverse-event-reporting-system-faers [accessed 2023-08-23]
33. Shariff SZ, Bejaimal SA, Sontrop JM, et al. Retrieving clinical evidence: a comparison of PubMed and Google Scholar for quick clinical searches. J Med Internet Res 2013 Aug 15;15(8):e164. [doi: 10.2196/jmir.2624] [Medline: 23948488]
34. Icard C, Mocquot P, Nogaro JC, Despas F, Gauthier M. Lenalidomide-induced arthritis: a case report and review of literature and pharmacovigilance databases. J Oncol Pharm Pract 2022 Mar;28(2):453-456. [doi: 10.1177/10781552211038001] [Medline: 34590522]
35. Trambowicz K, Gorzelak-Pabiś P, Broncel M. Statins and sleep – clinical effects. Atherosclerosis 2019 Aug;287:e202. [doi: 10.1016/j.atherosclerosis.2019.06.613]
36. Lucas A, Mohan G, Winkler A, Gardner K, Whalen M. Acute lung injury following gadolinium contrast: a case report. J Emerg Crit Care Med 2021;5:18-18. [doi: 10.21037/jeccm-20-117]
37. Gekhman D, Correa E. One dose of cefazolin — months of misery: a case of acute liver failure with grave consequences. American Journal of Gastroenterology 2018 Oct;113(Supplement):S1664-S1665. [doi: 10.14309/00000434-201810001-03038]
38. Si Y, Wang J, Xu H, Roberts K. Enhancing clinical concept extraction with contextual embeddings. J Am Med Inform Assoc 2019 Nov 1;26(11):1297-1304. [doi: 10.1093/jamia/ocz096] [Medline: 31265066]
39. Khadhraoui M, Bellaaj H, Ammar MB, Hamam H, Jmaiel M. Survey of BERT-base models for scientific text classification: COVID-19 case study. Appl Sci (Basel) 2022;12(6):2891. [doi: 10.3390/app12062891]
40. Arbabi A, Adams DR, Fidler S, Brudno M. Identifying clinical terms in medical text using ontology-guided machine learning. JMIR Med Inform 2019 May 10;7(2):e12596. [doi: 10.2196/12596] [Medline: 31094361]
41. Side effect resource. SIDER 4.1. URL: http://sideeffects.embl.de [accessed 2023-08-23]

Abbreviations

ADR: adverse drug reaction
AUC: area under the curve
BERT: Bidirectional Encoder Representations from Transformers
FAERS: FDA Adverse Event Reporting System
FDA: Food and Drug Administration
MedDRA: Medical Dictionary for Regulatory Activities
NLP: natural language processing
SIDER: Side Effect Resource

Edited by A Coristine; submitted 14.10.24; peer-reviewed by A Simona, D Yoon, J Zaghir, ZI Mohd Yusoh; revised version received 13.05.25; accepted 13.05.25; published 10.07.25.

Please cite as:
Jeon W, Park M, An D, Nam W, Shin JY, Lee S, Lee S
Predicting Drug–Side Effect Relationships From Parametric Knowledge Embedded in Biomedical BERT Models: Methodological Study With a Natural Language Processing Approach
JMIR Med Inform 2025;13:e67513
URL: https://medinform.jmir.org/2025/1/e67513
doi:10.2196/67513

© Woohyuk Jeon, Minjae Park, Doyeon An, Wonshik Nam, Ju-Young Shin, Seunghee Lee, Suehyun Lee. Originally published in JMIR Medical Informatics (https://medinform.jmir.org), 10.7.2025. This is an open-access article distributed under the terms of the Creative Commons Attribution License (https://creativecommons.org/licenses/by/4.0/), which permits unrestricted use, distribution, and reproduction in any medium, provided the original work, first published in JMIR Medical Informatics, is properly cited. The complete bibliographic information, a link to the original publication on https://medinform.jmir.org/, as well as this copyright and license information must be included.

XSL•FO
RenderX

Performance of Natural Language Processing versus International Classification of Diseases Codes in Building Registries for Patients With Fall Injury: Retrospective Analysis

Atta Taseh[1], MD; Souri Sasanfar[1], MSc; Michelle Chan[1], MSc; Evan Sirls[1], BS; Ara Nazarian[2], PhD; Kayhan Batmanghelich[3], PhD; Jonathan F Bean[4,5,6], MD, MPH; Soheil Ashkani-Esfahani[1], MD, MPH

[1]Foot & Ankle Research and Innovations Laboratory (FARIL), Department of Orthopaedic Surgery, Mass General Brigham, Harvard Medical School, 158 Boston Post Road, Weston, MA, United States

[2]Musculoskeletal Translational Innovation Initiative, Carl J. Shapiro Department of Orthopaedic Surgery, Beth Israel Deaconess Medical Center, Harvard Medical School, Boston, MA, United States

[3]Batman Laboratory, Department of Electrical and Computer Engineering, College of Engineering, Boston University, Boston, MA, United States

[4]New England Geriatric Research Education and Clinical Center (GRECC), Veterans Affair Boston Healthcare System, Boston, MA, United States

[5]Department of Physical Medicine and Rehabilitation, Harvard Medical School, Boston, MA, United States

[6]Spaulding Rehabilitation, Boston, MA, United States

Corresponding Author:
Atta Taseh, MD
Foot & Ankle Research and Innovations Laboratory (FARIL), Department of Orthopaedic Surgery, Mass General Brigham, Harvard Medical School, 158 Boston Post Road, Weston, MA, United States

Abstract

Background: Standardized registries, such as the *International Classification of Diseases* (*ICD*) codes, are commonly built using administrative codes assigned to patient encounters. However, patients with fall injury are often coded using subsequent injury codes, such as hip fractures. This necessitates manual screening to ensure the accuracy of data registries.

Objective: This study aimed to automate the extraction of fall incidents and mechanisms using natural language processing (NLP) and compare this approach with the *ICD* method.

Methods: Clinical notes for patients with fall-induced hip fractures were retrospectively reviewed by medical experts. Fall incidences were detected, annotated, and classified among patients who had a fall-induced hip fracture (case group). The control group included patients with hip fractures without any evidence of falls. NLP models were developed using the annotated notes of the study groups to fulfill two separate tasks: fall occurrence detection and fall mechanism classification. The performances of the models were compared using accuracy, sensitivity, specificity, positive predictive value, negative predictive value, F_1-score, and area under the receiver operating characteristic curve.

Results: A total of 1769 clinical notes were included in the final analysis for the fall occurrence task, and 783 clinical notes were analyzed for the fall mechanism classification task. The highest F_1-score using NLP for fall occurrence was 0.97 (specificity=0.96; sensitivity=0.97), and for fall mechanism classification was 0.61 (specificity=0.56; sensitivity=0.62). Natural language processing could detect up to 98% of the fall occurrences and 65% of the fall mechanisms accurately, compared to 26% and 12%, respectively, by *ICD* codes.

Conclusions: Our findings showed promising performance with higher accuracy of NLP algorithms compared to the conventional method for detecting fall occurrence and mechanism in developing disease registries using clinical notes. Our approach can be introduced to other registries that are based on large data and are in need of accurate annotation and classification.

(JMIR Med Inform 2025;13:e66973) doi:10.2196/66973

KEYWORDS

automation; automate; data registry; ICD Codes; artificial intelligence; AI; algorithms; predictive models; predictive analytics; machine learning; ML; large language models; LLMs; natural language processing; NLP; deep learning

Introduction

With 3 million emergency room visits, 300,000 hospitalizations, and 30,000 fatalities annually, falls pose a major threat to public health [1,2]. The financial impact is also substantial, with an estimated US $50 billion medical expenses for nonfatal falls [3]. Therefore, researching and understanding the nature of falls and fall-related injuries are crucial for developing effective

XSL•FO
RenderX

prevention and treatment strategies as populations age [4]. Given the multifactorial nature of falls and the difficulties involved in conducting prospective research in the field, developing fall registries comprised of large and accurate medical data is very important [5,6]. Standardized registries are commonly built using administrative codes, such as the *International Classification of Diseases* (*ICD*), assigned to patient encounters, and Current Procedural Terminology (CPT) codes[7]. Previous studies have used these codes to extract patients with a history of falls [8-10]. However, this method has limitations that may lead to an underestimation of actual fall frequency and might not reveal the history of falls in patients [11]. Reporting falls using the External Causes of Morbidity codes is usually recommended but not mandatory in all health care settings. Since falls are not typically considered stand-alone conditions, many health care providers may rather use the diagnosis *ICD* codes and assign codes to the end result of a fall, for example, a hip fracture, rather than the fall itself [12,13]. This makes it difficult for investigators to identify falls in the patient's medical history and the true frequency of falls within populations. Given these limitations, clinical notes were suggested as a more reliable method of detecting falls, fall mechanisms, and fall-induced injuries [14]. This process, however, is expert-dependent and time-consuming, particularly if the dataset is large. To address these obstacles, natural language processing (NLP), which combines computational linguistics and deep learning models to process narrative data, can be used to automate the review process of clinical notes to detect falls [14].

Several studies have demonstrated the capability of supervised models to detect fall incidents, which have been documented in clinical notes [15-17]. Although these models are effective at identifying fall events, they fall short of providing detailed insights into fall-related *ICD* codes that capture the specific mechanisms (eg, how the fall occurred) or the physical consequences (eg, the force of the impact) [11]. Gaining a better understanding of these factors is essential for designing strategies to prevent falls since individuals who experience severe or high-impact falls often face a higher risk of recurrent falls and injuries [9,18]. Tremblay et al [11] highlighted the importance of studying fall mechanisms as a research priority. However, automated methods for extracting detailed fall mechanisms and their impact from clinical notes remain largely unexplored in the current literature.

This study aimed to assess the performance of NLP algorithms compared to conventional methods for detecting fall incidence and the mechanism of falls obtained from clinical notes of patients with hip fractures. We hypothesize that NLP algorithms outperform fall ICD codes in detecting falls and their mechanisms in patients with hip fractures.

Methods

Study Design and Cohort

A retrospective case-control study was conducted, including the data from 4 tertiary hospitals in Greater Boston, Massachusetts. Data were retrieved from the institution's data repository using CPT codes for hip fractures (27125, 27130, 27226, 27228, 27235, 27236, 27244, 27245, and 27248) between January 2010 and December 2019.

Patients ≥18 years old who were hospitalized because of hip fracture as a result of an outpatient fall (cases) or other reasons (controls) were included in the study. Falls resulting from violent encounters, animal attacks, significant external forces such as car or motor vehicle accidents, high-impact sports like skiing, and fractures caused by underlying pathological conditions were excluded to reduce the heterogeneity of fall mechanics. This exclusion helps avoid the influence of confounding injuries that differ significantly from typical accidental falls, ensuring that the study focuses on more clinically relevant fall types (). Given that the majority of hip fractures happen due to falls, we had a reasonable number of patients in the case group and included a single note for each patient. In contrast, multiple notes were reviewed and included per patient in the control group.

Data Labeling

Expert annotations, serving as the ground truth for training the NLP models, were derived directly from clinical notes. The annotations embraced two specific tasks: (1) fall occurrence and (2) mechanism of falls (the way falls happened). One expert orthopedic researcher (AT) conducted the annotations, and the decisions for equivocal or debatable cases were made by a senior scientist (SAE). All clinical notes were evaluated in chronological order, starting from the date of the hip fracture CPT code. The first note documenting a fall was selected for analysis. A fall was defined as "an unintentional event that results in the person coming to rest on the ground or another lower level" [19]. The mechanisms of fall were defined by 3 categories: same level (occurring on the same plane or surface), multilevel (descent from one level to a different one), and unclassified (not classifiable due to lack of sufficient information) [20]. In rare cases, discrepancies between the documented fall mechanisms in the clinical notes and the corresponding fall *ICD* codes compromised the validity of comparisons between *ICD* and NLP-based approaches. Consequently, patients with conflicting information between clinical notes and ICD codes regarding the fall mechanism were excluded to ensure the integrity of the analysis ().

Data Preprocessing

A variety of inpatient unstructured clinical notes, including history and physical examination, discharge summary, progress, operation, and emergency department notes, were obtained. Due to the diverse formatting of these clinical notes, specialized preprocessing methodologies were required, which diverged significantly from the conventional text-processing approaches. Following annotation, the clinical notes underwent various preprocessing steps, including de-identification, segmentation, and cleaning [21]. The specific techniques used in preprocessing, which address the unique challenges posed by the clinical notes' formatting, are outlined in Table 1. Detailed information about the segmentation process is provided in Tables S1 and S2 in Multimedia Appendix 1. This detailed account ensures the data are optimally prepared for the subsequent analytical phases.

XSL•FO
RenderX

Table . An overview of the data preprocessing stages.

Stages	Tool or Method	Purpose	Output
De-identification	• Stanford de-identifier	• Remove personal identifiers to ensure privacy and compliance with data protection regulations. This involves replacing all Protected Health Information entities with synthetic variants to maintain data integrity and eliminate biases. The model chosen was the Stanford-de-identifier-base-model developed by Chambon et al [21], with an F_1-score of 98.9 on the I2b2 2014 test set [22].	Anonymized text ready for analysis.
Segmentation	• Bespoke parser, Finite State Machine, and regular expressions	• Segment notes into distinct sections for enhanced text processing accuracy. The parser identifies section headings and concatenates segments, refined through manual evaluation and iterative improvements. More details are provided in Multimedia Appendix 1.	Accurately segmented text with sections tagged for reassembly.
Filtering uninformative data	Identification and removal: • Duplicates • Uninformative sections • Administrative content	• Remove duplicated sections from notes to prevent skewing results. • Discard sections containing only headings without informative text. • Remove document finalization and signature sections marked with terms like “signed” and “FINAL.”	Dataset free of redundant and uninformative sections.
Elimination of non-essential elements	• Regular expressions and manual filtering	• Exclude conversion error notifications, Unicode or hexadecimal sections, and other irrelevant elements.	Dataset without non-contributory headers, unreadable sections, and irregular patterns.
Removal of irrelevant metadata	• Manual filtering	• Remove timestamps, de-identified placeholders, and other non-analytical metadata.	Dataset without timestamps and placeholder text, ensuring grammatical consistency.
Splitting the data	• Random allocation	• Partition the dataset into training and testing subsets for unbiased model evaluation.	Training and testing subsets for model development and performance evaluation.

Model Development

Models were developed to automate two distinct tasks: fall occurrence and fall mechanism classification. All models besides Bidirectional Encoder Representations from Transformers (BERT) used a Term Frequency-Inverse Document Frequency (TF-IDF) representation of the text data. Specifically, TF-IDF vectorization with unigrams, bigrams, and trigrams (ngram_range=(1,3)) was applied to transform the processed text into numerical features before training these models. For the binary task of fall occurrence (fall vs no fall), a data split of 80:20 was used for training and testing purposes, respectively. The split was stratified by the binary outcome (fall vs no fall) to ensure a balanced representation of both classes in the training and testing subsets. Our methodology harnessed the text analysis capabilities of a modified BERT model described by Fu et al [17] We used a maximum sequence length of 512 tokens, consistent with the recommendations in the original study by Devlin et al [23], used a batch size of 8, and conducted training over 3 epochs. Moreover, the adaptive boosting (AdaBoost) algorithm was used for fall identification, using single-layer decision trees (stumps) as described by Quinlan et al [23], [24]. AdaBoost assigns coefficients based on each classifier’s performance and adjusts sample weights during training to emphasize previously misclassified samples. Finally, extreme gradient boosting (XGBoost) was used, which is a refined

XSL•FO
RenderX

version of gradient boosting recognized for its precision and versatility. XGBoost constructs additive training models in stages and optimizes a differentiable loss function, making it suitable for handling structured data derived from text [25].

To address the challenges posed by the complex multiclass scenario in the fall mechanism classification task, which involved detailed classification into 3 categories (same level, multilevel, and unclassified classes), we designated 70% of the data for training and 30% for testing, ensuring stratification to maintain class distribution. We used a comprehensive suite of advanced machine learning models, including AdaBoost, support vector machine (SVM), XGBoost, and random forest (RF). Each model was chosen for its proven ability to decipher complex data relationships and offer detailed insights into the correlated factors of falls across the varied categories [26-31]. The SVM model is a two-layer recognition method that excels in high-dimensional spaces and allows for class weighting to address class imbalance, which makes it suitable for detecting fall mechanisms from clinical notes [32] RF is an ensemble learning method that constructs multiple decision trees during training and merges their results to improve predictive accuracy and control overfitting. RF is also effective in handling class imbalance through class weighting [33].

The hyperparameter configurations used for the models are provided in Table S3 in Multimedia Appendix 1.

Statistical Analysis

Comparison of the baseline characteristics was made using SPSS software (version 28.0; IBM Corp), where the *t* and chi-square tests were used for continuous and categorical data, respectively. Several metrics were used to evaluate the models' performance in identifying and classifying falls. These metrics included sensitivity, specificity, F_1-score, positive predictive value (PPV), negative predictive value (NPV), accuracy, and area under the receiver operating characteristic curve (AUC-ROC). A weighted-averaging approach was used for multiclass classifications to report the overall model performance [34]. Furthermore, the percentage of the notes correctly classified for each task by machine learning and ICD approach were calculated and compared through chi-square test. A 0.05 type 1 error probability was considered significant.

Ethical Considerations

The study protocol was approved by Mass General Brigham Institutional Review Board (number 2023P000741). The board waived participant consent due to the retrospective nature of the study. All the notes were de-identified in the preprocessing stage to avoid the inclusion of any protected health information (PHI) and to ensure patient privacy and compliance with HIPAA regulations.

Results

A total of 1,769 clinical notes were analyzed for the fall occurrence task. Of these, 791 notes corresponded to the case group (one note per patient, n=791), and 978 notes were from the control group (representing 317 individuals with multiple notes per individual) (Figure 1). Moreover, for the fall mechanism classification task, 783 notes (one note per patient, n=783) were included, comprising 511 same-level falls, 151 multilevel falls, and 121 unclassified falls. The case group comprised older individuals with a mean age of 77.7 (SD 14.3) years versus 65.3 (SD 19.6) years of the control group (P<.001; Table 2). Furthermore, although both groups had a higher proportion of females, the case group had a notably higher percentage of female patients than the control group (P=.01; Table 2).

All 3 models performed well for detecting fall occurrences, with the BERT model showing a lower F_1-score and AUC-ROC (Table 3, Figure 2). The models could successfully classify a significant portion of patient notes (XGBoost=97%, AdaBoost=98%) as opposed to the *ICD* approach, which could find 26% of them (P<.001; Table 4).

XSL•FO
RenderX

Figure 1. Study population flowchart. RPDR: Research Patient Data Registry.

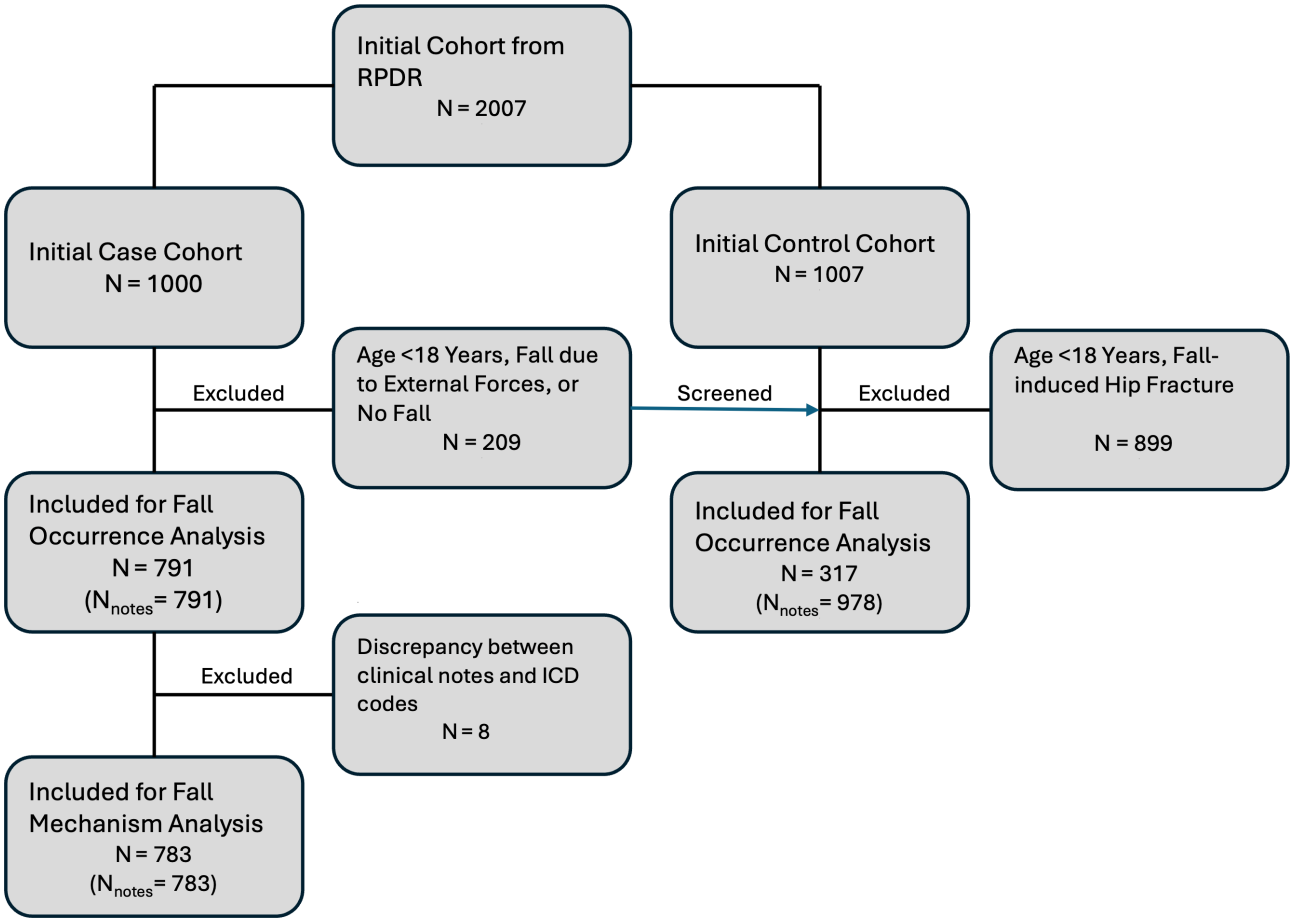


Table . Comparison of the baseline characteristics of the study groups.

Group	Age (years), mean (SD)	Gender (female), n (%)	Race (White), n (%)
Fall (n=791)	77.7 (14.3)	520 (65.7)	700 (88.5)
No fall (n=317)	65.3 (19.6)	183 (57.7)	278 (87.7)
P value	<.001	.01	.61[a]

[a]Based on the comparison between the White and non-White races.

XSL•FO
RenderX

Table . The performance metrics of the study models for detection of fall occurrence and fall mechanism classification. Algorithms were trained on an expert annotated database.

Outcomes and models	PPV[a]	NPV[b]	Sensitivity	Specificity	F_1-score	Accuracy	AUC-ROC[c]
Fall occurrence detection							
BERT[d]	0.94	0.88	0.84	0.96	0.88	0.90	0.97
AdaBoost[e]	0.95	0.98	0.98	0.96	0.97	0.97	0.99
XGBoost[f]	0.96	0.98	0.97	0.96	0.97	0.97	0.99
Fall mechanism classification[g]							
SVM[h]	0.56	0.50	0.62	0.36	0.57	0.62	0.67
AdaBoost	0.55	0.43	0.60	0.39	0.56	0.60	0.61
XGBoost	0.60	0.51	0.62	0.56	0.61	0.62	0.65
RF[i]	0.60	0.52	0.65	0.35	0.60	0.65	0.70

[a]PPV: positive predictive value.

[b]NPV: negative predictive value.

[c]AUC-ROC: area under the receiver operating characteristic curve.

[d]BERT: Bidirectional Encoder Representations from Transformers.

[e]AdaBoost: adaptive boosting.

[f]XGBoost: extreme gradient boosting.

[g]Weighted metrics are presented.

[h]SVM: support vector machine.

[i]RF: random forest.

XSL•FO
RenderX

Figure 2. Receiver operating characteristic curve for the fall occurrence detection task. AdaBoost: adaptive boosting; BERT: Bidirectional Encoder Representations from Transformers; ROC: receiver operating characteristic; XGBoost: extreme gradient boosting.

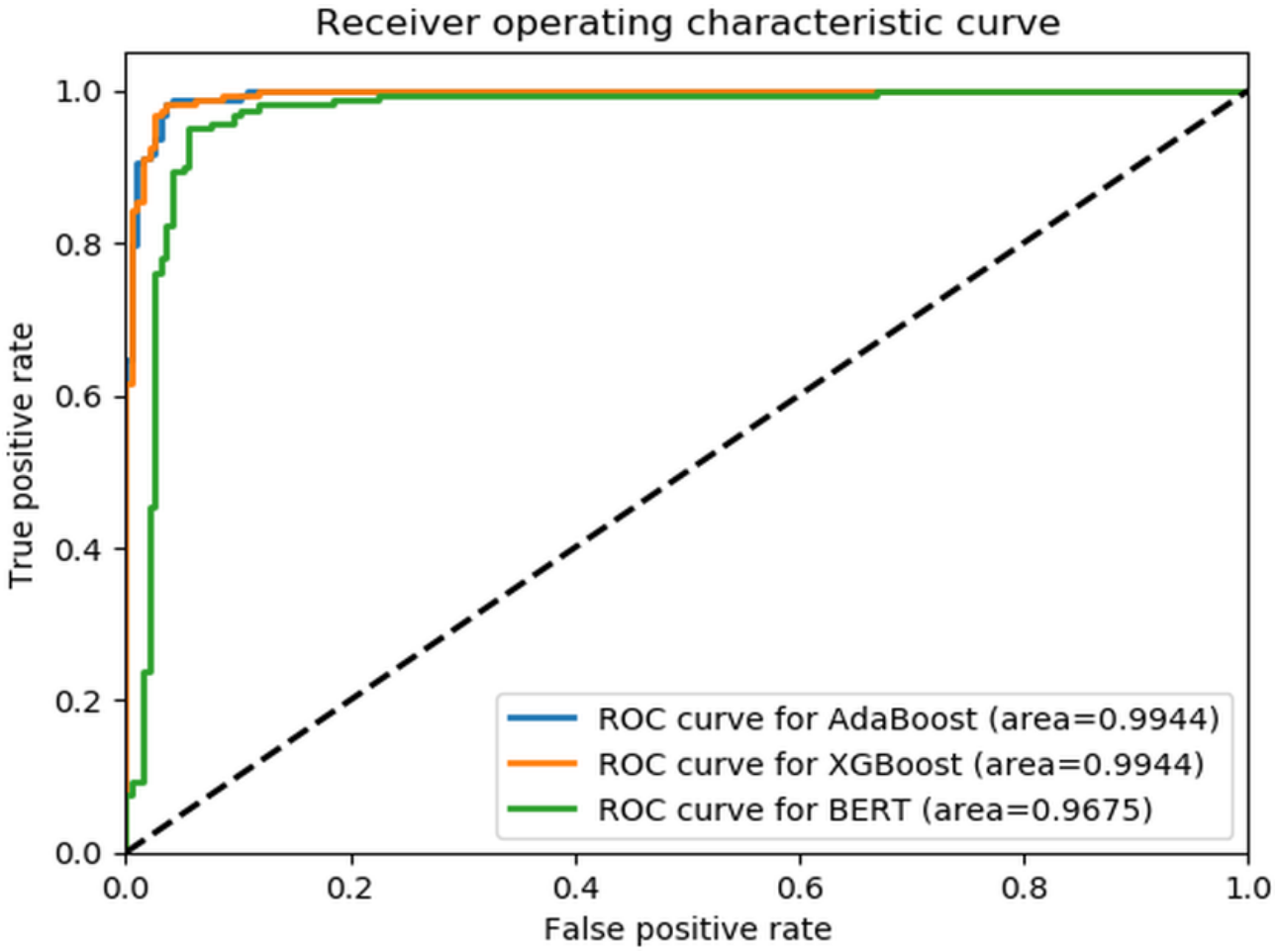


Table . Percentage of fall notes correctly classified by natural language processing approach versus *International Classification of Diseases* codes.

Model	Fall occurrence	Fall mechanism			
		Overall	Class S[a]	Class M[b]	Class U[c]
ICD [d]	26%	12%	8.4%	15.2%	22.2%
BERT[e]	84%	_[f]	–	–	–
AdaBoost[g]	98%	60%	82%	26.1%	11%
XGBoost[h]	97%	62%	78%	37%	28%
SVM[i]	–	62%	87%	17.4%	14%
RF[j]	–	65%	88.3%	15.2%	28%

[a]Class S: same-level.

[b]Class M: multi-level.

[c]Class U: unclassified.

[d]*ICD*: *International Classification of Diseases*.

[e]BERT: Bidirectional Encoder Representations from Transformers.

[f]Not available.

[g]AdaBoost: adaptive boosting.

[h]XGBoost: extreme gradient boosting

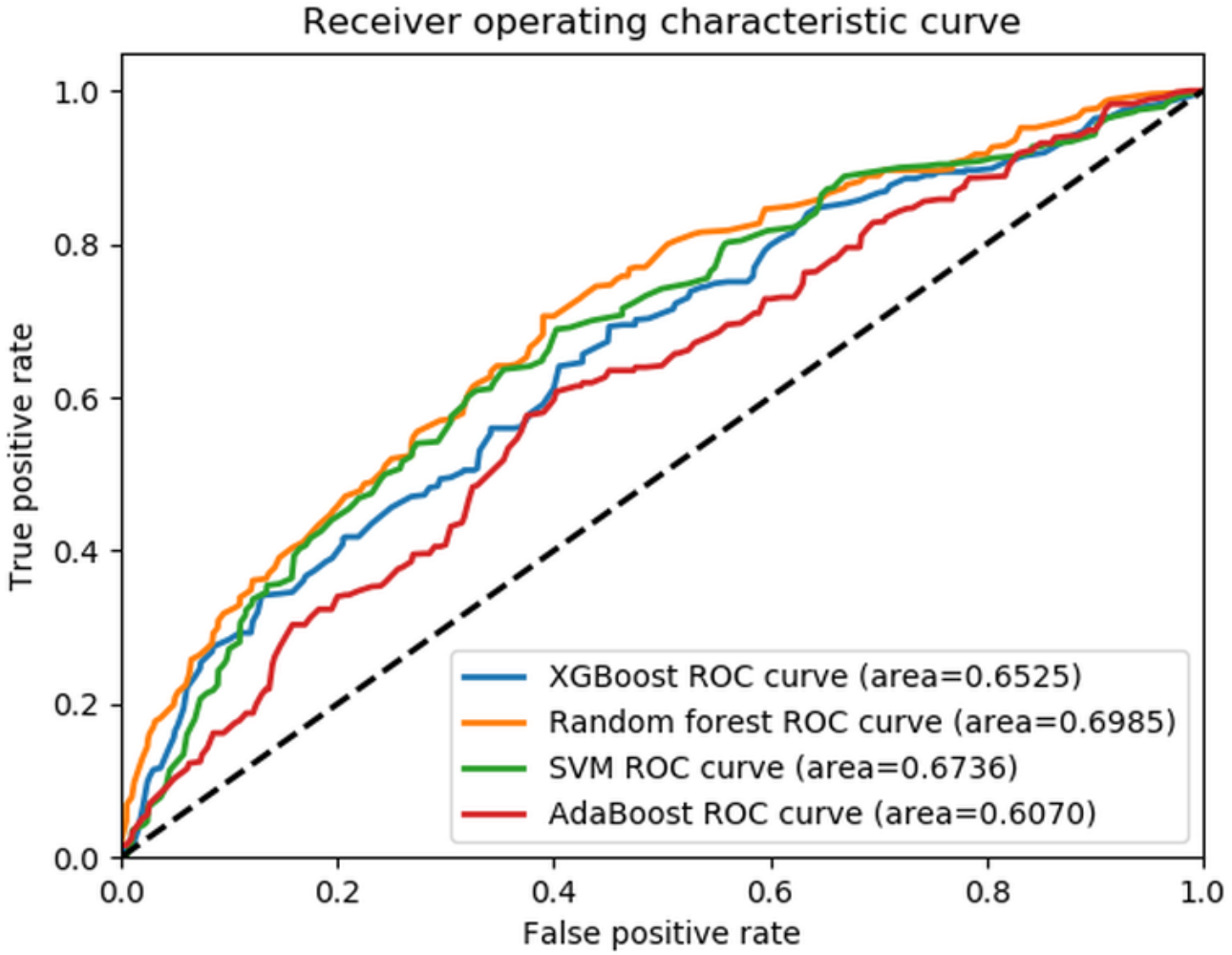
[i]SVM: support vector machine.

[j] RF: random forest.

XSL•FO
RenderX

Regarding fall mechanism classification, the RF model slightly outperformed the others with an AUC-ROC of 0.70 and an F_1-score of 0.60 (Table 3, Figure 3). Moreover, the RF model correctly classified fall mechanism in 65% of the fall notes compared to the 12% of the *ICD* method (P<.001, Table 4.). However, all 4 NLP models showed high classification performance in identifying small-level class falls only (Table 4).

Figure 3. Receiver operating characteristics curve for the fall mechanism.AdaBoost: adaptive boosting; ROC: receiver operating characteristic; SVM: support vector machine; XGBoost: extreme gradient boosting.



Discussion

This study aimed to automate fall identification and classification based on its mechanism from clinical notes and subsequently compare the results with the traditional *ICD* approach for building fall registries. Our results demonstrated the superior performance of NLP models, which correctly identified 98% of the notes for fall occurrence compared to the 26% detected by the *ICD* approach. Furthermore, the models could classify 65% of fall mechanisms, while the ICD approach detected 12% of these cases.

Automated identification of fall incidents from clinical notes is an emerging topic in biomedical sciences. It serves multiple purposes, such as insurance claim processing, cost analysis for falls, and enhancing fall prevention measures for inpatient safety [35-37]. Despite these varied objectives, there are commonalities in the methodologies and models used. However, the interpretation of results can vary significantly and must be tailored to the specific study goals. Cheligeer et al [38] highlighted the superior performance of BERT and machine learning models in detecting inpatient falls compared to traditional *ICD* coding. Their findings underscored these models' ability to accurately identify nonfall cases, as evidenced by high NPV and specificity. Nevertheless, when aiming to develop a comprehensive registry, achieving optimal sensitivity to maximize the inclusion of fall patients, alongside a high F_1-score to balance PPV and sensitivity, becomes crucial.

Classical machine learning methods are commonly used in fall classification studies. Luther et al developed an SVM model using free-text clinical notes and a term-document matrix for feature selection, achieving an F_1-score of 0.87 [39]. Our study extends this by using a TF-IDF feature selection method, which weighs terms based on their importance in capturing nuanced information from the notes. We found that ensemble methods achieved optimal performance with an F_1-score of up to 0.98. Santos et al demonstrated superior performance of neural networks over classical machine learning methods [40]. This finding is supported by Fu et al, who showed high performance of context-aware models like BERT in fall detection tasks [17]. However, in our study, BERT did not outperform other machine

XSL•FO
RenderX

learning models. BERT's effectiveness depends on the availability of sufficient training data due to its deep learning architecture [41]. Therefore, the sample size in our study may have influenced the effectiveness of training within this framework.

Identifying fall mechanisms from patient records presents a significant challenge, which, if addressed properly, can provide invaluable information for clinical and quality improvement purposes. Roudsari et al investigated the acute cost of care for falls in patients over 65 years of age, categorized by *ICD* codes for mechanisms [13]. They found that same-level falls were the most common mechanism of injury (28%). However, most falls (60%) were coded as unspecified falls without mentioning the mechanism. In our study, only 11% of the notes were coded specifically for falls, and surprisingly, there were occasional discrepancies between the coded mechanisms and those described in clinical notes. Whether this discrepancy stems from insufficient clinical information or a tendency among providers to prioritize documenting immediate medical needs requires further investigation. Relying solely on medical coding is unreliable for identifying fall mechanisms.

While NLP has shown promise in retrieving data from medical records, its application in fall mechanism extraction remains underexplored. Liu et al automated the extraction of inpatient fall severity from incident reports, leveraging structured features to improve the F_1-score by 8%, achieving 0.78 [22]. Our study incorporated diverse types of unstructured clinical notes, including discharge summaries and progress notes. These notes were authored by various medical professionals with differing styles and descriptions of falls, introducing significant variability that posed challenges for extracting features. Our results indicated that the XGBoost and RF models achieved the highest F_1-scores (0.6). These findings are consistent with previous research demonstrating improved disease classification accuracy using ensemble methods applied to medical notes [22]. Additionally, using ensemble methods, Albano et al have shown promise in enhancing the classification accuracy when dealing with rare classes [42]. However, our study revealed suboptimal performance of the models in managing the "multilevel" and "unclassified" subclasses, likely due to the overall limited number of notes available for these classes. Although reflective of real-life scenarios, the imbalance in fall mechanism classes may have impacted the performance of the models. Ensemble models like XGBoost and RF are prone to overfitting patterns in the training data, especially when managing imbalanced datasets. Similarly, even after fine-tuning, BERT may carry over biases from its general-purpose pretraining, limiting its ability to capture domain-specific nuances in clinical notes fully. To address these challenges, we applied weighted evaluation metrics to ensure a fair performance assessment across all classes. Additionally, hyperparameters were systematically optimized to mitigate class imbalance, and BERT was fine-tuned explicitly on clinical notes to enhance its applicability to the domain. However, relying on weighted metrics and fine-tuning may not entirely overcome the inherent limitations of dataset imbalance and pretraining biases. Future work should focus on augmenting the dataset to improve class balance and explore alternative architectures or pretraining strategies to reduce bias and overfitting.

Different approaches can be adopted for planning health care registries based on the registry's purpose, target population, and source data structure [43]. Administrative codes are commonly used to build retrospective registries when using health records. However, the accuracy of this method is not universally reliable across all medical conditions [44,45]. For example, a study by Dal et al evaluated the accuracy of the *ICD*-based Danish National Registry of Patients in identifying individuals with acromegaly, reporting a PPV of only 54.2% (CI 48.3 - 60) compared to expert-confirmed diagnoses [46]. Similarly, *ICD* codes for falls are often inconsistently applied, making them an unreliable sole method for identifying fall incidents. Our results highlight the potential of automated clinical note screening using NLP as an alternative for building registries. However, NLP can be computationally intensive due to the broad scope of falls, which spans diverse patient populations and clinical scenarios. This study proposes a combined approach using administrative codes related to fall conditions as a prescreening step to narrow the dataset, followed by NLP-based automated screening of clinical notes. This strategy balances computational efficiency with improved accuracy in registry development. Furthermore, this approach offers the advantage of extracting additional clinical details, such as the fall mechanism, which are often unavailable in administrative codes but crucial for understanding and preventing falls [47].

Although this study made important strides in developing fall registries, there are a few areas for improvement. The sample size was adequate for a retrospective analysis; however, larger and more diverse populations would enhance the robustness of machine learning models. Additionally, our dataset was predominantly composed of individuals of White race, reflecting the demographic characteristics of the region. This provides an opportunity to expand the research to include more diverse groups. We also acknowledge recent advancements in data preprocessing, including automated entity resolution and noise handling, which can be used in future studies to enhance robustness and scalability [48]. To address these issues, our future efforts will be focused on external validation, incorporating broader and more representative populations to improve the generalizability and impact of the findings.

In conclusion, our findings demonstrated a promising performance of NLP methods in identifying patients with a history of falls and hip fractures and their fall mechanisms from clinical notes. This approach can significantly enhance the accuracy and efficiency of developing fall registries. Moreover, the models were particularly effective in classifying the mechanisms of falls in patients who experienced same-level falls. Future studies with larger sample sizes and a broader spectrum of pathologies can further validate these findings and address the class imbalance issue. If well-expanded and developed, our approach can be introduced to the health care systems as an efficient and cost-effective approach for developing valid and reliable registry systems of diseases or clinical conditions that greatly burden the health care systems and the patients.

XSL•FO
RenderX

Acknowledgments

We gratefully acknowledge the patients whose clinical data served as the foundation for this research, enabling us to advance the field of automated fall detection.

Conflicts of Interest

None declared.

Multimedia Appendix 1
Supplementary tables detailing an overview of the text segmentation process and model development.
[DOCX File, 23 KB - medinform_v13i1e66973_app1.docx]

References

1. Bergen G, Stevens MR, Burns ER. Falls and fall injuries among adults aged ≥65 years - United States, 2014. MMWR Morb Mortal Wkly Rep 2016 Sep 23;65(37):993-998. [doi: 10.15585/mmwr.mm6537a2] [Medline: 27656914]
2. Moreland B, Kakara R, Henry A. Trends in nonfatal falls and fall-related injuries among adults aged ≥65 years - United States, 2012-2018. MMWR Morb Mortal Wkly Rep 2020 Jul 10;69(27):875-881. [doi: 10.15585/mmwr.mm6927a5] [Medline: 32644982]
3. Cost of older adult falls. US Centers for Disease Control and Prevention. URL: https://stacks.cdc.gov/view/cdc/122747 [accessed 2024-07-17]
4. Florence CS, Bergen G, Atherly A, Burns E, Stevens J, Drake C. The medical costs of fatal falls and fall injuries among older adults. J Am Geriatr Soc 2018 Apr;66(4):693-698. [doi: 10.1111/jgs.15304]
5. Berg GM, Carlson T, Fairchild J, Edwards C, Sorell R. Development of a falls registry: a pilot study. J Trauma Nurs 2017;24(4):224-230. [doi: 10.1097/JTN.0000000000000295] [Medline: 28692616]
6. Trotter JP. Patient registries: a new gold standard for “real world” research. Ochsner J 2002;4(4):211-214. [Medline: 22826660]
7. Schmidt M, Schmidt SAJ, Sandegaard JL, Ehrenstein V, Pedersen L, Sørensen HT. The Danish National Patient Registry: a review of content, data quality, and research potential. Clin Epidemiol 2015;7:449-490. [doi: 10.2147/CLEP.S91125] [Medline: 26604824]
8. Khorgami Z, Fleischer WJ, Chen YJA, Mushtaq N, Charles MS, Howard CA. Ten-year trends in traumatic injury mechanisms and outcomes: a trauma registry analysis. Am J Surg 2018 Apr;215(4):727-734. [doi: 10.1016/j.amjsurg.2018.01.008] [Medline: 29397887]
9. Unguryanu TN, Grjibovski AM, Trovik TA, Ytterstad B, Kudryavtsev AV. Mechanisms of accidental fall injuries and involved injury factors: a registry-based study. Inj Epidemiol 2020 Mar 16;7(1):8. [doi: 10.1186/s40621-020-0234-7] [Medline: 32172689]
10. Sumrein BO, Huttunen TT, Launonen AP, Berg HE, Felländer-Tsai L, Mattila VM. Proximal humeral fractures in Sweden-a registry-based study. Osteoporos Int 2017 Mar;28(3):901-907. [doi: 10.1007/s00198-016-3808-z] [Medline: 27787593]
11. Tremblay MC, Berndt DJ, Luther SL, Foulis PR, French DD. Identifying fall-related injuries: text mining the electronic medical record. Inf Technol Manag 2009 Dec;10(4):253-265. [doi: 10.1007/s10799-009-0061-6]
12. Jensen PB, Jensen LJ, Brunak S. Mining electronic health records: towards better research applications and clinical care. Nat Rev Genet 2012 May 2;13(6):395-405. [doi: 10.1038/nrg3208] [Medline: 22549152]
13. Roudsari BS, Ebel BE, Corso PS, Molinari NAM, Koepsell TD. The acute medical care costs of fall-related injuries among the U.S. older adults. Injury 2005 Nov;36(11):1316-1322. [doi: 10.1016/j.injury.2005.05.024] [Medline: 16214476]
14. Gliklich RE, Leavy MB, Dreyer NA. Registries for Evaluating Patient Outcomes: A User’s Guide: Agency for Healthcare Research and Quality (AHRQ); 2020. [doi: 10.23970/AHRQEPCREGISTRIES4]
15. Patterson BW, Jacobsohn GC, Shah MN, et al. Development and validation of a pragmatic natural language processing approach to identifying falls in older adults in the emergency department. BMC Med Inform Decis Mak 2019 Jul 22;19(1):138. [doi: 10.1186/s12911-019-0843-7] [Medline: 31331322]
16. Shiner B, Neily J, Mills PD, Watts BV. Identification of inpatient falls using automated review of text-based medical records. J Patient Saf 2020 Sep;16(3):e174-e178. [doi: 10.1097/PTS.0000000000000275] [Medline: 27331601]
17. Fu S, Thorsteinsdottir B, Zhang X, et al. A hybrid model to identify fall occurrence from electronic health records. Int J Med Inform 2022 Mar 7;162:104736. [doi: 10.1016/j.ijmedinf.2022.104736] [Medline: 35316697]
18. Leucht P, Fischer K, Muhr G, Mueller EJ. Epidemiology of traumatic spine fractures. Injury 2009 Feb;40(2):166-172. [doi: 10.1016/j.injury.2008.06.040] [Medline: 19233356]
19. Institute of Medicine (US) Division of Health Promotion and Disease Prevention, Berg RL, Cassells JS. Falls in older persons: risk factors and prevention. In: The Second Fifty Years: Promoting Health and Preventing Disability, National Academies Press (US) 1992. URL: https://www.ncbi.nlm.nih.gov/books/NBK235613 [accessed 2024-07-17]

XSL•FO
RenderX

20. Sterling DA, O'Connor JA, Bonadies J, O'Connor JA. Geriatric falls: injury severity is high and disproportionate to mechanism. The Journal of Trauma: Injury, Infection, and Critical Care 2001 Jan;50(1):116-119. [doi: 10.1097/00005373-200101000-00021]
21. Chambon PJ, Wu C, Steinkamp JM, Adleberg J, Cook TS, Langlotz CP. Automated deidentification of radiology reports combining transformer and "hide in plain sight" rule-based methods. J Am Med Inform Assoc 2023 Jan 18;30(2):318-328. [doi: 10.1093/jamia/ocac219] [Medline: 36416419]
22. Liu J, Wong ZSY, So HY, Tsui KL. Evaluating resampling methods and structured features to improve fall incident report identification by the severity level. J Am Med Inform Assoc 2021 Jul 30;28(8):1756-1764. [doi: 10.1093/jamia/ocab048] [Medline: 34010385]
23. Devlin J, Chang MW, Lee K, Toutanova K. BERT: pre-training of deep bidirectional transformers for language understanding. In: Burstein J, Doran C, Solorio T, editors. : Association for Computational Linguistics; 2019 Jun Presented at: Proceedings of the 2019 Conference of the North American Chapter of the Association for Computational Linguistics: Human Language Technologies p. 4171-4186. [doi: 10.18653/v1/N19-1423]
24. Quinlan JR. Induction of decision trees. Mach Learn 1986 Mar;1(1):81-106. [doi: 10.1007/BF00116251]
25. Freund Y, Schapire RE. A decision-theoretic generalization of on-line learning and an application to boosting. J Comput Syst Sci 1997 Aug;55(1):119-139. [doi: 10.1006/jcss.1997.1504]
26. Zięba M, Tomczak SK, Tomczak JM. Ensemble boosted trees with synthetic features generation in application to bankruptcy prediction. Expert Syst Appl 2016 Oct;58:93-101. [doi: 10.1016/j.eswa.2016.04.001]
27. Chen T, Guestrin C. XGBoost: a scalable tree boosting system. : Association for Computing Machinery; 2016 Aug Presented at: Proceedings of the 22nd ACM SIGKDD International Conference on Knowledge Discovery and Data Mining, in KDD '16 p. 785-794. [doi: 10.1145/2939672.2939785]
28. Chen Y, Wang X, Jung Y, et al. Classification of short single-lead electrocardiograms (ECGs) for atrial fibrillation detection using piecewise linear spline and XGBoost. Physiol Meas 2018 Oct 24;39(10):104006. [doi: 10.1088/1361-6579/aadf0f] [Medline: 30183685]
29. Torlay L, Perrone-Bertolotti M, Thomas E, Baciu M. Machine learning–XGBoost analysis of language networks to classify patients with epilepsy. Brain Inf 2017 Sep;4(3):159-169. [doi: 10.1007/s40708-017-0065-7]
30. van Rosendael AR, Maliakal G, Kolli KK, et al. Maximization of the usage of coronary CTA derived plaque information using a machine learning based algorithm to improve risk stratification; insights from the CONFIRM registry. J Cardiovasc Comput Tomogr 2018 May;12(3):204-209. [doi: 10.1016/j.jcct.2018.04.011]
31. Alizadehsani R, Hosseini MJ, Sani ZA, Ghandeharioun A, Boghrati R. Diagnosis of coronary artery disease using cost-sensitive algorithms. In: Proceedings of 2012 IEEE 12th International Conference on Data Mining Workshops 2012:9-16. [doi: 10.1109/ICDMW.2012.29]
32. Pan D, Liu H, Qu D, Zhang Z. Human falling detection algorithm based on multisensor data fusion with SVM. Mobile Information Systems 2020 Oct 31;2020(1):1-9. [doi: 10.1155/2020/8826088]
33. Parmar A, Katariya R, Patel V. A review on random forest: an ensemble classifier. In: Hemanth J, Fernando X, Lafata P, Baig Z, editors. International Conference on Intelligent Data Communication Technologies and Internet of Things (ICICI): Springer, Cham; 2019:758-763. [doi: 10.1007/978-3-030-03146-6_86]
34. Opitz J. From bias and prevalence to macro F1, kappa, and MCC: a structured overview of metrics for multi-class evaluation. Semantic Scholar. URL: https://www.semanticscholar.org/paper/From-Bias-and-Prevalence-to-Macro-F1%2C-Kappa%2C-and-A-Opitz/ff334e8cee3550eb5c80a61213ad0aecb549f48f [accessed 2025-06-28]
35. Nakatani H, Nakao M, Uchiyama H, Toyoshiba H, Ochiai C. Predicting inpatient falls using natural language processing of nursing records obtained from Japanese electronic medical records: case-control study. JMIR Med Inform 2020 Apr 22;8(4):e16970. [doi: 10.2196/16970] [Medline: 32319959]
36. Popowich F. Using text mining and natural language processing for health care claims processing. SIGKDD Explor Newsl 2005 Jun;7(1):59-66. [doi: 10.1145/1089815.1089824]
37. Hoffman GJ, Hays RD, Shapiro MF, Wallace SP, Ettner SL. Claims-based identification methods and the cost of fall-related injuries among US older adults. Med Care 2016 Jul;54(7):664-671. [doi: 10.1097/MLR.0000000000000531] [Medline: 27057747]
38. Cheligeer C, Wu G, Lee S, et al. BERT-Based neural network for inpatient fall detection from electronic medical records: retrospective cohort study. JMIR Med Inform 2024 Jan 30;12(1):e48995. [doi: 10.2196/48995] [Medline: 38289643]
39. Luther SL, McCart JA, Berndt DJ, et al. Improving identification of fall-related injuries in ambulatory care using statistical text mining. Am J Public Health 2015 Jun;105(6):1168-1173. [doi: 10.2105/AJPH.2014.302440] [Medline: 25880936]
40. dos Santos HDP, Silva AP, Maciel MCO, Burin HMV, Urbanetto JS, Vieira R. Fall detection in EHR using word embeddings and deep learning. : IEEE Presented at: 2019 IEEE 19th International Conference on Bioinformatics and Bioengineering (BIBE); Oct 28-30, 2019; Athens, Greece p. 265-268. [doi: 10.1109/BIBE.2019.00054]
41. Gani R, Chalaguine L. Feature engineering vs BERT on twitter data. ArXiv. Preprint posted online on Oct 28, 2022. [doi: 10.48550/ARXIV.2210.16168]

XSL•FO
RenderX

42. Albano A, Sciandra M, Plaia A. Ensemble method for text classification in medicine with multiple rare classes. In: CLADAG 2023: Pearson, Italy; 2023:17 URL: https://www.statlab-unisa.it/cladag2023/book-of-abstracts/ [accessed 2025-07-06]
43. Gliklich RE, Dreyer NA, Leavy MB. Registries for Evaluating Patient Outcomes: A User's Guide: Rockville (MD): Agency for Healthcare Research and Quality (US); 2014.
44. Anand N, Edwards L, Baker LX, Chren MM, Wheless L. Validity of using billing codes from electronic health records to estimate skin cancer counts. JAMA Dermatol 2021 Sep 1;157(9):1089-1094. [doi: 10.1001/jamadermatol.2021.2856] [Medline: 34379079]
45. Qureshi AI, Harris-Lane P, Siddiqi F, Kirmani JF. International classification of diseases and current procedural terminology codes underestimated thrombolytic use for ischemic stroke. J Clin Epidemiol 2006 Aug;59(8):856-858. [doi: 10.1016/j.jclinepi.2006.01.004] [Medline: 16828680]
46. Dal J, Skou N, Nielsen EH, Pedersen L, Joergensen JOL. Acromegaly according to the Danish National Registry of Patients: how valid are ICD diagnoses and how do patterns of registration affect the accuracy of registry data? CLEP 2014 Sep:295. [doi: 10.2147/CLEP.S63758]
47. Bedard NA, Katz JN, Losina E, Opare-Addo MB, Kopp PT. Administrative data use in national registry efforts: blessing or curse? Journal of Bone and Joint Surgery 2022;104(Suppl 3):39-46. [doi: 10.2106/JBJS.22.00565]
48. Raza S, Schwartz B. Constructing a disease database and using natural language processing to capture and standardize free text clinical information. Sci Rep 2023 May 26;13(1):8591. [doi: 10.1038/s41598-023-35482-0] [Medline: 37237101]

Abbreviations

AdaBoost: adaptive boosting
AUC-ROC: area under the receiver operating characteristic curve
BERT: Bidirectional Encoder Representations from Transformers
CPT: Current Procedural Terminology
***ICD*:** *International Classification of Diseases*
NLP: natural language processing
NPV: negative predictive value
PPV: positive predictive value
RF: random forest
SVM: support vector machine
TF-IDF: Term Frequency-Inverse Document Frequency
XGBoost: extreme gradient boosting

Edited by C Lovis; submitted 30.09.24; peer-reviewed by E Martin, S Raza; revised version received 20.02.25; accepted 21.02.25; published 14.07.25.

Please cite as:
Taseh A, Sasanfar S, Chan M, Sirls E, Nazarian A, Batmanghelich K, Bean JF, Ashkani-Esfahani S
Performance of Natural Language Processing versus International Classification of Diseases Codes in Building Registries for Patients With Fall Injury: Retrospective Analysis
JMIR Med Inform 2025;13:e66973
URL: https://medinform.jmir.org/2025/1/e66973
doi:10.2196/66973

© Atta Taseh, Souri Sasanfar, Michelle Chan, Evan Sirls, Ara Nazarian, Kayhan Batmanghelich, Jonathan F Bean, Soheil Ashkani-Esfahani. Originally published in JMIR Medical Informatics (https://medinform.jmir.org), 14.7.2025. This is an open-access article distributed under the terms of the Creative Commons Attribution License (https://creativecommons.org/licenses/by/4.0/), which permits unrestricted use, distribution, and reproduction in any medium, provided the original work, first published in JMIR Medical Informatics, is properly cited. The complete bibliographic information, a link to the original publication on https://medinform.jmir.org/, as well as this copyright and license information must be included.

XSL•FO
RenderX

Automated Radiology Report Labeling in Chest X-Ray Pathologies: Development and Evaluation of a Large Language Model Framework

Abdullah Abdullah, MCSE; Seong Tae Kim, PhD

Department of Computer Science and Engineering, Kyung Hee University, 1732 Deogyeong-daero, Giheung-gu, Yongin, Gyeonggi-do, Republic of Korea

Corresponding Author:
Seong Tae Kim, PhD
Department of Computer Science and Engineering, Kyung Hee University, 1732 Deogyeong-daero, Giheung-gu, Yongin, Gyeonggi-do, Republic of Korea

Abstract

Background: Labeling unstructured radiology reports is crucial for creating structured datasets that facilitate downstream tasks, such as training large-scale medical imaging models. Current approaches typically rely on Bidirectional Encoder Representations from Transformers (BERT)-based methods or manual expert annotations, which have limitations in terms of scalability and performance.

Objective: This study aimed to evaluate the effectiveness of a generative pretrained transformer (GPT)-based large language model (LLM) in labeling radiology reports, comparing it with 2 existing methods, CheXbert and CheXpert, on a large chest X-ray dataset (MIMIC Chest X-ray [MIMIC-CXR]).

Methods: In this study, we introduce an LLM-based approach fine-tuned on expert-labeled radiology reports. Our model's performance was evaluated on 687 radiologist-labeled chest X-ray reports, comparing *F*1 scores across 14 thoracic pathologies. The performance of our LLM model was compared with the CheXbert and CheXpert models across positive, negative, and uncertainty extraction tasks. Paired *t* tests and Wilcoxon signed-rank tests were performed to evaluate the statistical significance of differences between model performances.

Results: The GPT-based LLM model achieved an average *F*1 score of 0.9014 across all certainty levels, outperforming CheXpert (0.8864) and approaching CheXbert's performance (0.9047). For positive and negative certainty levels, our model scored 0.8708, surpassing CheXpert (0.8525) and closely matching CheXbert (0.8733). Statistically, paired *t* tests indicated no significant difference between our model and CheXbert (*P*=.35) but a significant improvement over CheXpert (*P*=.01). Wilcoxon signed-rank tests corroborated these findings, showing no significant difference between our model and CheXbert (*P*=.14) but confirming a significant difference with CheXpert (*P*=.005). The LLM also demonstrated superior performance for pathologies with longer and more complex descriptions, leveraging its extended context length.

Conclusions: The GPT-based LLM model demonstrates competitive performance compared with CheXbert and outperforms CheXpert in radiology report labeling. These findings suggest that LLMs are a promising alternative to traditional BERT-based architectures for this task, offering enhanced context understanding and eliminating the need for extensive feature engineering. Furthermore, with large context length LLM-based models are better suited for this task as compared with the small context length of BERT based models.

(JMIR Med Inform 2025;13:e68618) doi:10.2196/68618

KEYWORDS

large language model; generative pre-trained transformers; radiology report; labeling; BERT; thoracic pathologies; LLM; GPT

Introduction

Background

Radiology reports consist of expert observations of the radiologist based on the Chest X-ray images of the patient. These reports consist of free-text and unstructured information in the form of long paragraphs. The extraction of labels from unstructured radiology reports is the task of radiology report labeling and it provides us structured information which can be used for many downstream tasks such as medical report generation and natural language explanation generation. It also enables training of large-scale medical imaging models [1]. Previous works for labeling of radiology reports involve use of complicated feature engineering of medical domain knowledge [2]. and Bidirectional Encoder Representations from Transformers (BERT) based approaches [3]. Transformers have

XSL•FO
RenderX

also demonstrated success in radiology report labeling [4,5]. However, all these methods have limitations which hinders their adoption in the clinical setting. In case of methods which use complex feature engineering, these methods have leveraged manual annotation to shift the burden from feature engineering, requiring considerable time and expertise. Furthermore, these methods do not take advantage of existing feature-engineered labelers, which are state-of-the-art on many medical tasks. On the other hand for methods using BERT based models, the models are limited by the inherent limitations of BERT models such as their noncausal nature and limited context length. BERT-based models, despite their effectiveness in text classification tasks, have two key architectural limitations that constrain their performance in radiology report labeling. First, BERT's bidirectional nature focuses on context aggregation but lacks the ability to model causal relationships in sequential data. This noncausal nature can hinder its ability to fully capture the hierarchical and temporally dependent structure of radiology reports, where findings are often sequentially described. Second, BERT's limited input context length (typically 512 tokens) prevents it from effectively processing the long and detailed narratives commonly found in radiology reports. As a result, crucial information in extended texts may be truncated, leading to incomplete or suboptimal labeling. These limitations reduce the adaptability of BERT-based methods to real-world radiology settings, where comprehensive understanding of the entire report is often required.

Large language models (LLMs) such as Qwen address these challenges by offering extended context lengths (several thousand tokens), allowing the model to process full radiology reports without truncation. In addition, their ability to incorporate causal reasoning and handle instruction-based tasks makes them particularly suitable for medical labeling tasks, where nuanced and ambiguous language is prevalent. Although BERT based methods have shown increased abilities in the classification and other natural language tasks, their architecture poses a hindrance to their use.

Smit et al [3] introduced a combination of existing radiology report labelers and expert annotations to achieve highly accurate automated radiology report labeling . Their approach consists of a bio-medically pretrained BERT model [6,7], which is trained on the outputs of an existing labeler. They call their resulting model CheXbert. While CheXbert has generated considerable results, it has been unable to capture the full diversity, complexity and the ambiguous nature of natural language in the radiology reports. Their BERT-based solution while providing remarkable performance on the task of labeling is limited in its context length and noncausal nature. Which means for longer radiology reports it fails to provide a solution.

In our work we propose an LLM based radiology report labeler. LLMs have proven to be successful in their natural language generation capabilities. These models also have longer context lengths which makes them highly suitable for natural language generation tasks. Furthermore, these LLMs are adept at following instructions and given proper instructions these LLMs can be made good labelers for the radiology reports. Our LLM-based model inherently provides ease of use in other LLM-based solutions for the medical domain enabling clinical automation.

Our generative pretrained transformer (GPT)-based LLM beats the BERT-based CheXbert model on many pathologies and with a far bigger context length can handle long reports as compared with CheXbert. Our model outperforms the previous labelers [8] for many pathologies on an external dataset, MIMIC-CXR [9]. Our method of training medical report labelers opens room for other labels and longer textual input which makes it broadly useful for natural language processing tasks within the medical domain.

Related Work

Many natural language processing systems have been developed to extract structured labels from unstructured free-text radiology reports [2,10-16]. Mostly, these methods rely heavily on feature engineering and include strict vocabulary and grammatical rules to find and classify radiological reports. NegEx [17], a popular rule-based method, uses simple regular expressions for detecting negation of findings and is often used in combination with the Unified Medical Language System [18]. NegBio [19], an extension to NegEx, uses universal dependencies and subgraph matching for pattern definition and graph traversal search. It includes uncertainty detection in addition to negation detection for multiple pathologies in radiology reports, and is used to label the ChestX-Ray14 dataset [1]. The CheXpert labeler [8] improves upon NegBio on chest x-ray report classification by more controlled extraction and an improved Natural Language Processing framework and rules for uncertainty and negation extraction. The CheXpert labeler has been applied to generate labels for the CheXpert dataset and MIMIC-CXR [9], which are among the largest chest x-ray datasets publicly available. We use the MIMIC-CXR dataset to train our LLM-based framework and report our findings on a subset of the test set of MIMIC-CXR which has been labeled by expert radiologists.

Previous approaches have also been trained using radiology reports annotated by expert radiologists [20]. In these approaches, training data is limited by radiologist time and expertise. Chen et al [21] trained convolutional neural networks with Global Vectors for Word Representation [22] on 1000 radiologist-labeled reports for classification of pulmonary embolism in chest computed tomography scan reports and improved upon the previous rule-based peFinder [23,24]. trained both recurrent and convolutional networks in combination with attention mechanisms on 27,593 expert-annotated radiology reports. Transformer-based models have also been applied to the task of radiology report labeling [4], trained BERT [6] and XLNet-based [25] classifiers on 3856 radiologist labeled reports to detect normal and abnormal labels. Wood et al [5] proposed ALARM, an MRI head report classifier on head MRI data using BioBERT model [26] trained on 1500 radiologist-labeled reports. They demonstrate improvement over previous fixed embedding and word2vec-based [27] models [28] CheXbert labeler [3]. Also proposed a BERT based model which is trained on expert annotated radiology reports and achieves state of the art results for radiology report labeling. However, their method has limitations which include restriction to the context length of 512 which is the limitation of BERT based models.

XSL•FO
RenderX

Recent advancements in the application of LLMs across various domains, including medical informatics, have demonstrated their versatility and efficacy. Models such as GPT-3 and GPT-4 have been used for diverse tasks, including automated clinical note generation, question answering in health care, and medical coding, showcasing their ability to handle complex and domain-specific language tasks. In radiology, LLMs have been explored for summarizing imaging findings, generating patient-friendly explanations, and aiding in clinical decision-making, highlighting their potential beyond classification tasks. Furthermore, instruction-tuned LLMs, such as ChatGPT and specialized variants like BioGPT, have been shown to adapt effectively to biomedical domains, opening avenues for tasks such as multimodal data interpretation and real-time clinical assistance. These advancements emphasize the need for further exploration of LLMs' contextual understanding and adaptability, particularly in radiology report labeling and other biomedical text processing tasks.

In our work we propose an LLM based solution to solve the task of biomedical text labeling. We not only propose an alternative to BERT based models which achieves better scores on certain labels and has far bigger context length than BERT based models but our approach can also be applied to other biomedical text labeling.

Methods

Task

Radiology report labeling is a critical task involving the extraction of information on the presence or absence of specific thoracic pathologies, such as consolidation or edema, from free-text radiology reports. This process enables the transformation of unstructured diagnostic text into structured data, facilitating clinical decision-making, research and the development of predictive models. In this task, a labeler processes the free-text radiology report as input and assigns 1 of 4 classes, blank, positive, negative, or uncertain, to each of 14 predefined observations, reflecting the certainty level for each prediction. A "positive" label indicates the presence of a pathology, while "negative" denotes its absence, and "uncertain" is used when the report is ambiguous about the condition. The "blank" class is assigned when no relevant information is available for an observation. By converting radiology reports into labeled data, this approach supports streamlined access to essential diagnostic insights and provides a valuable structured dataset that can be used to train and validate machine learning algorithms in medical imaging.

Data

In radiology, there exist 2 large datasets of chest x-rays, CheXpert [8] (consisting of 224,316 images), and MIMIC-CXR [9] (consisting of 377,110 images). Both datasets have corresponding radiology reports that have been labeled for the same set of 14 observations using the CheXpert labeler [8] from the Impression section, or other parts of the radiology report. Furthermore, a subset of both datasets also contain manual annotations by expert radiologists. On CheXpert, a total of 1000 reports (CheXpert manual set) were reviewed by 2 board certified radiologists with disagreement resolution through consensus. On MIMIC-CXR, a total of 687 reports (MIMIC-CXR test set) were reviewed by 2 board certified radiologists and manually labeled for the same 14 medical pathology labels as in CheXpert. However, the radiology reports for the Chexpert dataset have not been made public. Due to nonavailability of radiology reports for the Chexpert dataset, we used the MIMIC-CXR test set for evaluation.

Large Language Models

LLMs are built upon stacked decoder layers from the transformer architecture, often referred to as "auto-regressive models" because of their causal structure. This auto-regressive nature enables these models to predict each token sequentially, relying only on the preceding tokens as context. During training, LLMs learn the task of next-token prediction, where they must accurately anticipate the subsequent token in a sequence given the previous tokens as input. This prediction task is essentially a binary classification problem, where the model assesses whether its predicted token matches the correct ground truth token. The accuracy of each prediction is evaluated by calculating a cross-entropy loss, which measures the difference between the model's output and the correct token. This loss is then back-propagated through the model to update its weights, refining its ability to generate contextually accurate and coherent responses over time.

LLMs are pretrained on extensive amounts of diverse text data from vast resources available on the internet. This extensive pretraining enables the models to capture complex patterns and detailed knowledge present in language, making them highly effective at understanding and generating natural language. Their exceptional performance in natural language generation, coupled with their ability to handle longer text inputs, motivates their application in various specialized domains, such as radiology report labeling.

In our work, we specifically use the Qwen model [29], particularly the Qwen1.5‐0.5B variant. This model demonstrates significant capabilities in various natural language generation tasks relative to its moderate size, making it both efficient and powerful. One of the Qwen model's key advantages is its extensive context length of 32,000 tokens, meaning it can handle considerably larger text inputs as context compared with BERT-based models, which are typically limited to a 512-token context. This increased context capacity allows the Qwen model to process lengthy radiology reports or extended medical dialogues without truncating important information.

The enhanced context length in LLMs is particularly beneficial in clinical settings, where maintaining continuity in patient information, such as previous history or ongoing conversations, is essential. As LLM-based frameworks are increasingly adopted in health care, often in the form of biomedical chatbots and other automated systems, the capacity to retain extensive context is critical. Our model addresses this need, providing a solution that integrates seamlessly with existing LLM-driven tools in clinical environments. This ensures that radiology report labeling and other clinical tasks benefit from both accuracy and the ability to preserve a comprehensive, context-aware understanding of patient data.

XSL•FO
RenderX

Instruction Fine-Tuning

To fully use the capabilities of our pretrained LLM, we fine-tune it using a specialized instruction dataset. This dataset is constructed from radiology reports paired with corresponding pathology labels, each with an associated certainty level from the MIMIC-CXR dataset. The goal of this instruction tuning is to guide the pretrained LLM to understand the relationships within radiology reports, enabling it to accurately identify pathologies and assign certainty levels. By providing targeted instructions, we aim to refine the LLM's ability to interpret the clinical language and nuanced patterns within radiology reports, thereby enhancing its performance in radiology report labeling.

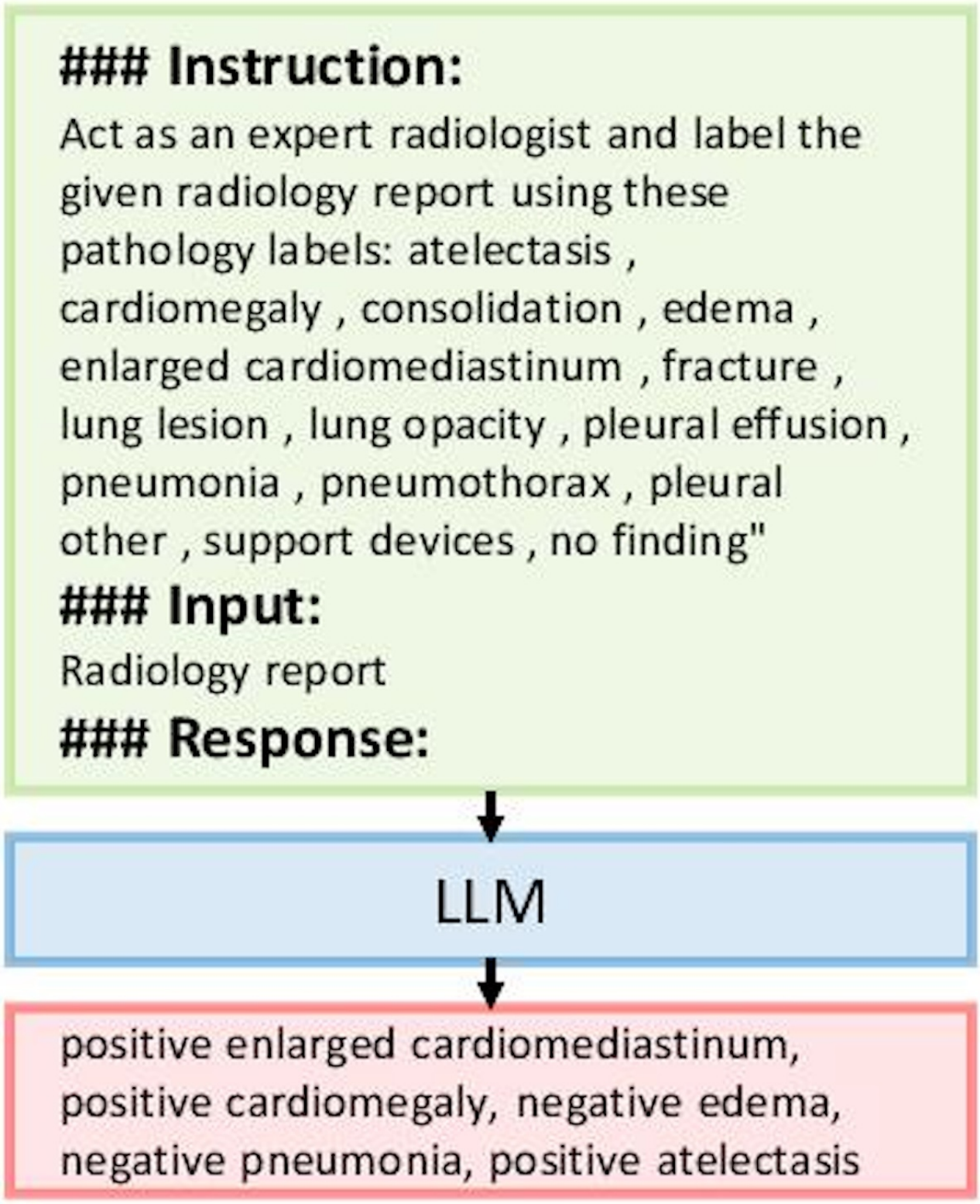
The structure of the instruction dataset is designed to facilitate clear guidance for the LLM. As illustrated in Figure 1, each data instance consists of an instruction in the form of a prompt to the LLM, an input value (the radiology report), and output values (the pathology labels along with their certainty levels). This structured approach helps the LLM understand both the format and task requirements, allowing it to generate accurate labels from free-text radiology reports.

To prepare the data for model processing, each instance in the instruction dataset is tokenized using the LLM's tokenizer, converting text into a sequence of tokens suitable for input. The tokenized data is then fed into the LLM, which generates predictions based on its learned representations. Following this, we calculate the cross-entropy loss, which measures the difference between the model's predicted outputs and the ground truth labels. This loss value indicates how closely the model's predictions align with the actual labels. By back-propagating the loss, we adjust the LLM's weights which gradually enhances its accuracy and reliability in producing pathology labels with certainty levels.

Through this fine-tuning process, our LLM becomes adept at associating the textual features of radiology reports with relevant pathology labels, allowing it to accurately and efficiently label clinical data. This approach ensures that the model is optimized specifically for radiology report labeling, enabling it to perform well even on complex clinical information.

XSL•FO
RenderX

Figure 1. Instruction fine-tuning process for a large language model to label radiology reports. The dataset includes prompts structured to guide the large language model, input radiology reports, and corresponding pathology labels annotated with certainty levels. This method was applied to the MIMIC Chest X-ray dataset, a large-scale de-identified chest x-ray dataset containing radiologist-labeled reports. LLM: large language model



Training Details

We trained our LLM, which has a total of 463,987,712 parameters, using an instruction dataset. During the training process, we maintained a batch size of 2, which allows for effective gradient estimation while minimizing memory usage. This choice of batch size is particularly beneficial given the substantial size of our model and the complexity of the task. The training was conducted over 5 epochs, providing sufficient iterations for the model to learn the intricate relationships

XSL•FO
RenderX

between the radiology reports and their corresponding pathology labels.

To optimize the training process, we used the ADAM optimizer [30] which facilitated faster convergence and improved performance. In addition, we implemented a gradient accumulation strategy with a value of 2. This approach effectively simulates a larger batch size by accumulating gradients over two iterations before performing a weight update, allowing us to maximize the use of available GPU memory while still benefiting from the stability of a larger batch size.

The learning rate was set at 1×10^{-4}, a value that strikes a balance between training speed and stability. An appropriate learning rate is crucial in preventing the model from oscillating around the optimal solution, ensuring gradual and consistent improvements in performance. For the instruction tuning of our LLM, we used the SFTTrainer from the TRL library [31]. This specialized trainer is designed for supervised fine-tuning, providing an efficient and effective framework for adapting pretrained models to specific tasks. It offers a range of features that streamline the training process, including automated handling of training loops, logging, and monitoring of performance metrics. We leveraged 4 NVIDIA RTX A6000 GPUs. This powerful hardware setup enables parallel processing, significantly reducing training time while accommodating the memory requirements of our large model.

Ablation Studies

Medical Contrastive Language-Image Pretraining Based Similar Reports Retrieval

To evaluate the effectiveness of our LLM based solution in its longer context we augment the LLM with similar retrieved reports which have been retrieved based on the cosine similarity, Medical Contrastive Language-Image Pretraining (MedCLIP) [32] is a Contrastive Language-Image Pretraining (CLIP)-based [33] model which is trained on medical images. It is trained in a constrastive manner and based on the cosine similarity between radiology images and texts it placed them closer or farther in its projection space. This helps in tasks such as image-image text-text or image-text and text-image based retrieval. To augment the input radiology report to the LLM, CheXbert, and CheXpert alike, we retrieve similar radiology reports from a datastore similar to [34]. MedCLIP has a limitation of 77 tokens as its context length and therefore text-text based retrieval is not possible. To overcome this, we use the radiology image associated with the radiology report of 687 radiologist annotated reports from MIMIC-CXR dataset and retrieve similar radiology images from the train set of MIMIC-CXR, this avoids any data leakage. Then the radiology reports corresponding to these top-k similar retrieved images is taken as the retrieved similar reports which are augmented to the test reports to increase the length of radiological text and test the abilities of labeling methods when longer context input is given. Retrieval is based on MedCLIP representations of input images and reports in the datastore, the datastore is precomputed offline and indexed with FAISS [35] for efficient nearest neighbor searching.

However, the performance of LLM dropped because the retrieved reports are not representative of the accurate information which can be used. Even though our model was able to process the additional information provided, it was unable to perform better because of the quality of those retrieved reports. In future with the advent of chat-bot style LLM solutions, longer bio-medical text in the form of patient-doctor conversation will be available and can be provided to our model as conversation history and this is where our model can be helpful.

Ethical Considerations

To fully use the capabilities of our pretrained LLM, we fine-tune it using a specialized instruction dataset.

Human Subject Research Ethics Review

This study did not involve direct human subject research. Instead, it used the MIMIC-CXR dataset, a publicly available, large-scale radiology dataset. The creation and distribution of the dataset adhere to ethical standards, with data anonymized to protect patient privacy. Therefore, specific ethics review and approval for this secondary analysis were not required.

Informed Consent

The MIMIC-CXR dataset is derived from hospital records collected during routine clinical care. Informed consent for the use of this data was waived by the Institutional Review Board (IRB) of the Beth Israel Deaconess Medical Center (BIDMC), as the dataset underwent rigorous deidentification processes to ensure compliance with Health Insurance Portability and Accountability Act standards.

Privacy and Confidentiality

The dataset has been thoroughly deidentified to ensure anonymity. This includes removing all protected health information from radiology reports, applying optical character recognition and masking techniques to redact protected health information from images, and assigning random identifiers to patients, studies, and images. This guarantees that patient confidentiality is maintained in all analyses.

Compensation

No compensation was involved in the collection or use of the MIMIC-CXR dataset, as it is a retrospective collection of clinical records for research purposes.

Identification of Participants

There is no risk of identification of individual participants, as all data in the MIMIC-CXR dataset is fully anonymized. The deidentification process for radiology reports, images, and associated metadata adheres to strict privacy protocols to ensure that no identifying information is present in the dataset or the results of this study

Evaluation

In this study, we evaluate the performance of our model, CheXbert and the CheXpert labeler, across a suite of retrieval tasks designed to assess their capabilities in clinical information extraction. Specifically, we focus on 3 main retrieval tasks, namely positive extraction, negative extraction, and uncertainty extraction. For each task, we designate the relevant class as the “positive” class for classification purposes, meaning, for

XSL•FO
RenderX

example, that the "negative" class is treated as the positive class in the negative extraction task, while other classes (such as positive or uncertain) are treated as negatives. This approach allows us to directly measure the model's ability to distinguish between the specified class and all others, thereby assessing its precision and recall within clinically relevant categories.

We compute the weighted average of the *F*1 scores for each of the 14 clinical findings or observations present in the CheXpert dataset across these tasks. *F*1 score is a harmonic mean of precision and recall which provides a balanced measure of a model's classification performance, particularly in settings where data is imbalanced. We calculate a weighted average of the *F*1 scores for each of the 14 observations across these tasks. By this we can mitigate the impact of class imbalance and obtain an *F*1 metric that accurately reflects the model's performance across both common and rare observations in the dataset.

This weighted metric, referred to as weighted-*F*1, is denoted simply as *F*1 in our results. Finally, we calculate and report the average *F*1 score across all 14 clinical observations, offering insight into the model's general extraction capability. This average *F*1 score serves as a key performance metric, allowing for a direct comparison between CheXbert and the CheXpert labeler on clinical information extraction tasks relevant to medical imaging applications in radiology .

Results

Table 1 and Table 2 present a quantitative assessment of our model's performance relative to prvious BERT-based approaches for the task of radiology report labeling. Table 1 reports the *F*1 scores obtained by our model on the MIMIC-CXR dataset, specifically on a radiologist-labeled test set comprising 687 radiology reports. These scores encompass all certainty levels, positive, negative, and uncertain, across each of the 14 pathology categories. The results indicate that our model demonstrates superior performance over previous methods, particularly in the Enlarged Cardiomediastinum and Support Devices categories, while maintaining competitive F1 scores across the other pathology labels.

Table . F_1 scores for predictions made by the proposed large language model-based model (ours) compared with CheXbert and CheXpert for all certainty levels (positive, negative, and uncertain). The evaluation was conducted on the MIMIC-CXR test set of 687 radiologist-labeled chest X-ray reports, covering 14 thoracic pathologies.

Pathologies	Ours, F_1 score	CheXbert, F_1 score	CheXpert, F_1 score
Enlarged cardiomediastinum	0.9022	0.8753	0.8644
Cardiomegaly	0.8555	0.8604	0.8143
Lung Opacity	0.8653	0.8820	0.8459
Lung lesion	0.9612	0.9627	0.9543
Edema	0.9105	0.9191	0.9064
Consolidation	0.9288	0.9385	0.9215
Pneumonia	0.8784	0.8853	0.8474
Atelectasis	0.8613	0.8656	0.8576
Pneumothorax	0.9619	0.9780	0.9572
Pleural effusion	0.8510	0.8649	0.8475
Pleural other	0.9627	0.9623	0.9629
Fracture	0.9734	0.9758	0.9702
Support devices	*0.8607*	0.8402	0.8043
No finding	0.8470	0.8557	0.8557
Average	0.9014	0.9047	0.8864

XSL•FO
RenderX

Table . F_1 scores for predictions made by the proposed large language model-based model (ours) compared with CheXbert and CheXpert for all certainty levels (positive, negative, and uncertain). The evaluation was conducted on the MIMIC-CXR test set of 687 radiologist-labeled chest X-ray reports, covering 14 thoracic pathologies.

Pathologies	Ours, F_1 score	CheXbert, F_1 score	CheXpert, F_1 score
Enlarged cardiomediastinum	0.8907	0.8641	0.8447
Cardiomegaly	0.8233	0.8113	0.7650
Lung Opacity	0.8008	0.8230	0.7770
Lung lesion	0.9490	0.9507	0.9415
Edema	0.8850	0.8934	0.8805
Consolidation	0.9104	0.9222	0.9101
Pneumonia	0.8886	0.8907	0.8568
Atelectasis	0.8256	0.8316	0.8206
Pneumothorax	0.9505	0.9700	0.9470
Pleural effusion	0.7983	0.8143	0.7965
Pleural other	0.9448	0.9457	0.9466
Fracture	0.9626	0.9649	0.9581
Support devices	0.7911	0.7603	0.7069
No finding	0.7704	0.7835	0.7836
Average	0.8708	0.8733	0.8525

Table 2 further delineates our model's performance by isolating only positive and negative certainty levels for each of the 14 pathology labels, thereby excluding uncertain cases to facilitate direct comparison. In this subset, our model yields notable improvements in *F*1 scores for Enlarged cardiomediastinum, cardiomegaly, and support devices.

The *P* values presented in Table 3 provide the results of statistical comparisons between the 3 models (ours, CheXbert, and CheXpert) based on their *F*1 scores. We performed both a paired *t* test and a Wilcoxon test to assess the statistical significance of the differences between the models. The paired *t* test *P* value for the comparison between ours and CheXbert is .35, which indicates that there is no statistically significant difference between the 2 models ($P>.05$). However, the comparison between ours and CheXpert yields a paired *t* test *P* value of .01, suggesting that ours performs significantly better than CheXpert at the 5% significance level ($P<.05$). Similarly, the Wilcoxon test confirms this finding with a *P* value of .005. The comparison between CheXbert and CheXpert shows highly significant differences with both a paired *t* test *P* value of .0005 and a Wilcoxon test *P* value of .002, indicating that these 2 models also differ significantly in performance. Overall, the statistical tests reveal that while ours and CheXbert are statistically similar, ours outperforms CheXpert, and there is a significant performance difference between CheXbert and CheXpert.

Table . *P* values from statistical tests (paired *t* test and Wilcoxon test) comparing the performance of the proposed LLM-based model (ours) with CheXbert and CheXpert across 14 thoracic pathologies. The evaluation was conducted on the MIMIC-CXR test set of 687 radiologist-labeled chest X-ray reports, assessing the significance of the differences in F_1 scores for all certainty levels.

Comparison	Paired *t* test *P* value	Wilcoxon test *P* value
Ours versus CheXbert	.35	.14
Ours versus CheXpert	.01	.005
Chexbert versus CheXpert	.0005	.002

Compared with the rule-based CheXpert labeler [8], our model achieves substantial performance gains across all pathology labels, marking a significant advancement over both traditional rule-based systems and BERT-based models. These results demonstrate the ability of our large language model (LLM)-based approach in handling the task of radiology report labeling with greater precision with large context length as compared with the small context length of BERT based models.

Figure 2 presents the performance of the proposed model (ours) compared with the baseline models (CheXbert and CheXpert) across 14 chest pathologies, using *F*1 scores as the evaluation metric. The grouped bar chart enables a direct comparison, where each group corresponds to a specific pathology, and individual bars represent the scores for each model. The results reveal that all three models achieve consistently high *F*1 scores across most pathologies, indicating robust performance. While the differences are marginal, notable trends can be observed, the proposed model demonstrates an advantage in pathologies such as support devices and enlarged cardiomediastinum, whereas the baseline models perform slightly better in cases

XSL•FO
RenderX

like consolidation and pneumothorax. This chart highlights the subtle strengths and weaknesses of each model, providing a clear visual overview of their performance.

Figure 2. Performance comparison of the proposed large language model-based model (ours), CheXbert, and CheXpert across 14 thoracic pathologies. The F_1 scores for each pathology label were calculated using the MIMIC-CXR test set, comprising 687 radiologist-labeled reports. While all models show similar performance, the proposed model demonstrates competitive or superior results in cases such as "support devices" and "no finding."

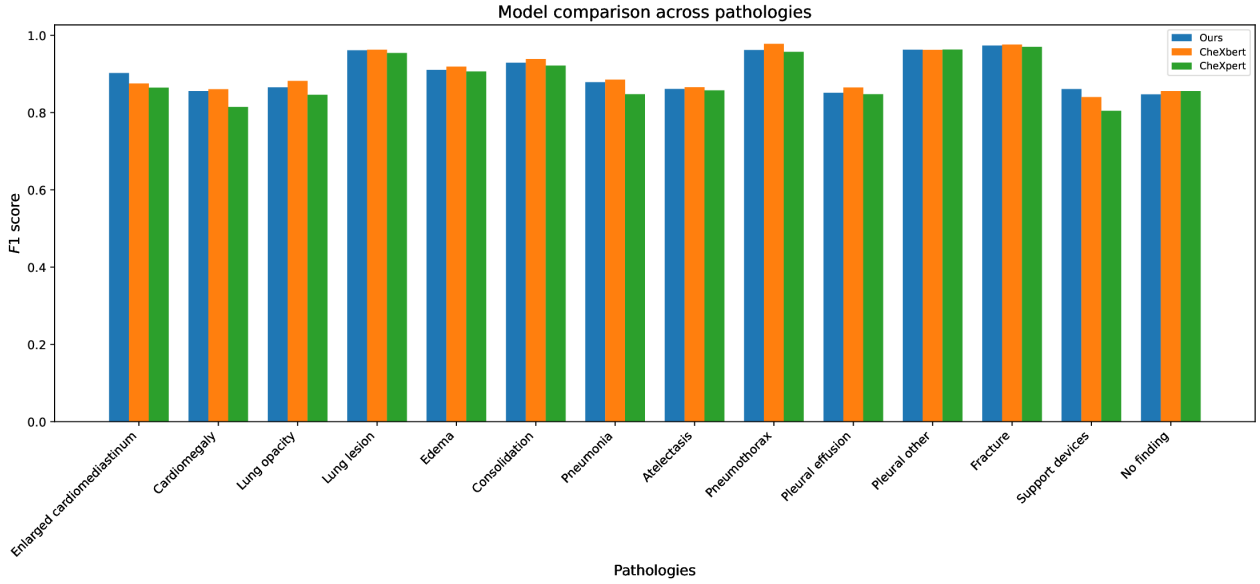
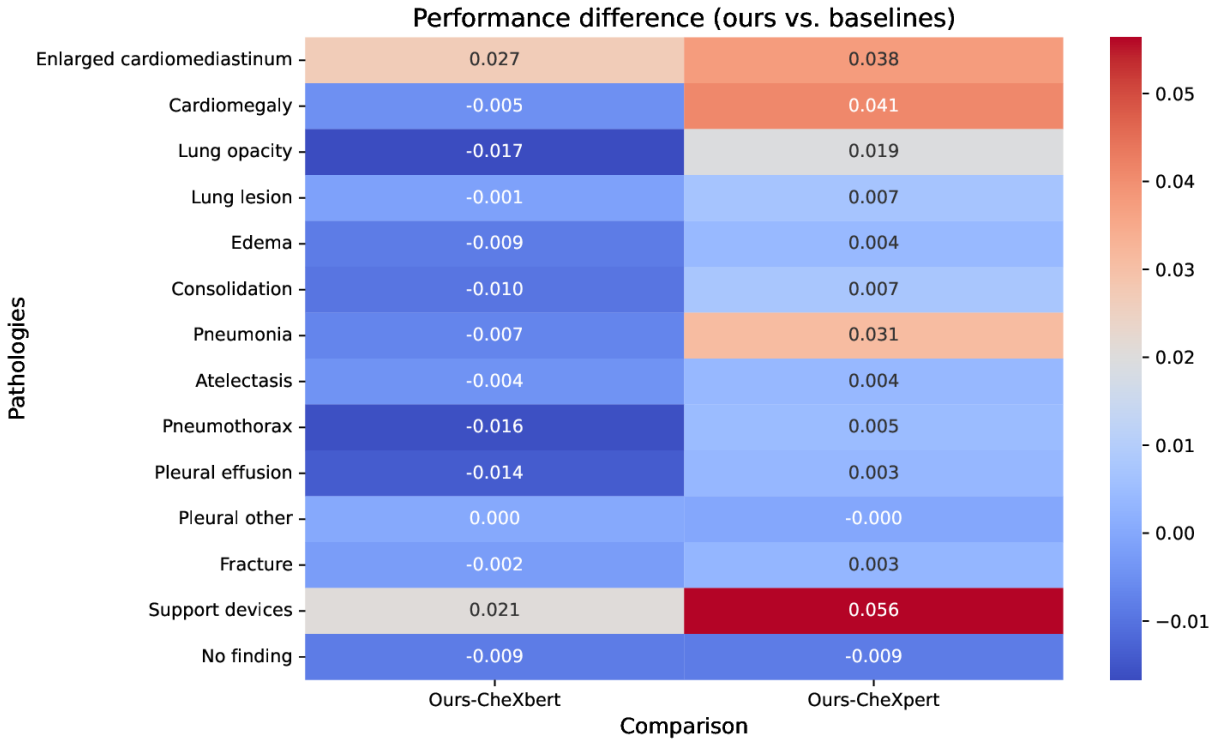


Figure 3 further explores the differences by visualizing the absolute performance gaps between the proposed model (ours) and the 2 baseline models using a heatmap. Rows correspond to the pathologies, and columns display the comparisons of ours against CheXbert and CheXpert. The heatmap emphasizes that the differences are minor, with most pathologies showing a difference of less than 0.02 in $F1$ scores. However, it also highlights key instances where ours performs notably better, such as in support devices and enlarged cardiomediastinum, while the baselines excel slightly in consolidation and pneumothorax. By focusing on performance differences, the heatmap provides a nuanced perspective, making it easy to identify pathologies where the models vary.

Figure 3. Heatmap showing the absolute differences in F_1 scores between the proposed arge language model-based model (ours) and the baseline models (CheXbert and CheXpert) across 14 thoracic pathologies. The analysis is based on predictions for the MIMIC-CXR test set of 687 radiologist-labeled reports. The heatmap highlights areas where ours excels, such as "support devices," and where baseline models perform better, such as "consolidation."



XSL•FO
RenderX

Discussion

Limitations

Currently, our work is limited to 14 pathology labels prevalent in radiology. However, our method can be extended to other medical fields and can accommodate many more pathology labels and can provide a reliable labeling solution. The lack of long form radiology text limits the demonstration of the longer contextual abilities of our model. In future with the advent of long form bio-medical text in the form of patient-doctor conversations, our model can provide better solutions as opposed to previous models. Furthermore, there is a need of more publicly available radiologist annotated datasets for additional evaluation of trained models. Furthermore, like other LLM-based approaches, our model is susceptible to biases present in the training data, which may inadvertently propagate into its predictions. This is particularly important in the medical domain, where biases can have significant ethical and clinical implications. Additional mechanisms for bias detection and mitigation are necessary to ensure fair and equitable outcomes across diverse patient populations.

The computational demands of LLMs are another limitation, as training and inference require substantial computational resources. This may limit the accessibility and scalability of the approach, especially in resource-constrained clinical settings. Exploring techniques such as model distillation or low-rank adaptation could help reduce these requirements while maintaining performance.

Interpretability remains a challenge with LLMs due to their complex architecture. The lack of transparency in how decisions are made can hinder trust and adoption in clinical workflows, where clear justification of predictions is often required. Future work should explore ways to improve the explainability of LLM predictions, such as attention visualization or feature attribution methods tailored to medical tasks.

While our method demonstrates promising results in radiology, further validation is needed in real-world clinical settings and across diverse medical contexts. The scalability of our approach to other modalities, such as MRI or CT reports, and its adaptability to different healthcare systems must also be explored to ensure generalizability.

Principal Findings and Conclusions

In our work, we propose a novel solution using LLMs for the challenging task of radiology report labeling. Our approach leverages the advanced capabilities of LLMs to accurately interpret and label various pathologies within radiology reports, which are crucial for supporting clinical decision-making and improving patient care. We demonstrate that LLMs achieve superior performance over previous BERT-based models, especially in accurately identifying specific pathology labels. This is a significant advancement, as certain pathologies that were previously challenging to label accurately can now be identified with greater precision using our LLM-based approach. In addition, our model achieves competitive scores across a broad range of pathology labels, confirming its robustness and versatility in handling complex medical language.

One of the key improvements introduced by our model is its ability to process longer radiology reports, overcoming the context length limitations often encountered in previous models. This capability is essential in clinical settings where comprehensive radiology reports often contain detailed descriptions spanning multiple paragraphs, which traditional models struggle to handle effectively. By accommodating extended context, our model ensures that no critical information is overlooked, thereby enhancing labeling accuracy and reliability in real-world applications.

Furthermore, the instruction-tuning methodology allows our approach to be extended to other biomedical text labeling tasks beyond radiology. This generalizability of our method makes it highly applicable across a wide range of biomedical domains, opening doors for enhanced automation in various clinical documentation and reporting tasks.

As LLM-based solutions are increasingly adopted in clinical settings, our model is designed to integrate seamlessly into existing workflows, promoting efficiency, and facilitating clinical automation. The potential for real-time, accurate labeling provided by our model not only reduces the manual workload on health care professionals but also contributes to more timely and precise diagnostic insights, ultimately benefiting patient outcomes.

Future research should explore integrating LLMs with other medical technologies, such as multimodal imaging systems that combine radiology reports with visual data from x-rays, CT scans, or magnetic resonance images. This integration could enable a more comprehensive analysis and further enhance the clinical utility of LLM-based models. In addition, extending the application of LLMs to different medical imaging modalities and nonradiology domains, such as pathology or cardiology, presents a promising avenue for expanding their impact across health care.

Developing scalable and efficient LLM solutions tailored to specific clinical needs, including resource-constrained environments, is another critical area for further exploration. This includes investigating lightweight alternatives or model compression techniques to reduce computational demands while maintaining performance.

Finally, the clinical adoption of LLMs will require continued efforts in improving model interpretability and building trust among health care professionals. Future work should focus on developing user-friendly interfaces and explainability mechanisms to facilitate the seamless integration of LLMs into routine clinical workflows. By addressing these challenges, LLM-based models like ours have the potential to revolutionize clinical practice, enabling more accurate, efficient, and scalable solutions for medical documentation, decision-making, and patient care.

XSL•FO
RenderX

Acknowledgments

This work was supported in part by the National Research Foundation of Korea (NRF) grant funded by the Korea government (MSIT; no.RS-2024-00334321) and by the Institute of Information and Communications Technology Planning and Evaluation (IITP) Grant funded by the Korea Government (MSIT) under Grant (IITP-2022-0-00078; Explainable Logical Reasoning for Medical Knowledge Generation), Grant (IITP-2025-RS-2023-00258649; Information Technology Research Center).

Data Availability

The dataset used in this study, MIMIC-CXR, is a publicly available dataset containing chest X-ray images and associated radiology reports. As the MIMIC-CXR dataset is a publicly available dataset, no restrictions are placed on the access to this dataset. The code used for instruction tuning is not currently available, but the authors are happy to discuss and share details upon request

Conflicts of Interest

None declared.

References

1. Wang X, Peng Y, Lu L, Lu Z, Bagheri M, Summers RM. ChestX-ray8: hospital-scale chest x-ray database and benchmarks on weakly-supervised classification and localization of common thorax diseases. Presented at: Proceedings of the IEEE conference on computer vision and pattern recognition; 2017; Honolulu, HI. [doi: 10.1109/CVPR.2017.369]
2. Pons E, Braun LMM, Hunink MGM, Kors JA. Natural language processing in radiology: a systematic review. Radiology 2016 May;279(2):329-343. [doi: 10.1148/radiol.16142770] [Medline: 27089187]
3. Smit A, Jain S, Rajpurkar P, Pareek A, Ng A, Lungren M. Combining automatic labelers and expert annotations for accurate radiology report labeling using BERT. 2020 Presented at: Proceedings of the 2020 Conference on Empirical Methods in Natural Language Processing (EMNLP); Online URL: https://www.aclweb.org/anthology/2020.emnlp-main [doi: 10.18653/v1/2020.emnlp-main.117]
4. Drozdov I, Forbes D, Szubert B, Hall M, Carlin C, Lowe DJ. Supervised and unsupervised language modelling in Chest X-Ray radiological reports. PLoS One 2020;15(3):e0229963. [doi: 10.1371/journal.pone.0229963] [Medline: 32155219]
5. Wood DA, Lynch J, Kafiabadi S, et al. Automated labelling using an attention model for radiology reports of MRI scans (ALARM). Presented at: Medical Imaging with Deep Learning; 2020; Montréal p. 811-826. [doi: 10.48550/arXiv.2002.06588]
6. Devlin J. Bert: pre-training of deep bidirectional transformers for language understanding. 2019 Presented at: Annual Meeting of the Association for Computational Linguistics; Florence. [doi: 10.48550/arXiv.1810.04805]
7. Peng Y, Yan S, Lu Z. Transfer learning in biomedical natural language processing: an evaluation of BERT and elmo on ten benchmarking datasets. 2019 Presented at: Proceedings of the 18th BioNLP Workshop and Shared Task; Florence, Italy URL: https://www.aclweb.org/anthology/W19-50 [doi: 10.18653/v1/W19-5006]
8. Irvin J, Rajpurkar P, Ko M, et al. CheXpert: a large chest radiograph dataset with uncertainty labels and expert comparison. AAAI 2019;33(1):590-597. [doi: 10.1609/aaai.v33i01.3301590]
9. Johnson AE, Pollard TJ, Greenbaum NR, et al. MIMIC-CXR-JPG, a large publicly available database of labeled chest radiograph. arXiv. Preprint posted online on 2019. [doi: 10.48550/arXiv.1901.07042]
10. Yadav K, Sarioglu E, Choi HA, Cartwright WB 4th, Hinds PS, Chamberlain JM. Automated outcome classification of computed tomography imaging reports for pediatric traumatic brain injury. Acad Emerg Med 2016 Feb;23(2):171-178. [doi: 10.1111/acem.12859] [Medline: 26766600]
11. Hassanpour S, Langlotz CP, Amrhein TJ, Befera NT, Lungren MP. Performance of a machine learning classifier of knee MRI reports in two large academic radiology practices: a tool to estimate diagnostic yield. AJR Am J Roentgenol 2017 Apr;208(4):750-753. [doi: 10.2214/AJR.16.16128] [Medline: 28140627]
12. Annarumma M, Withey SJ, Bakewell RJ, Pesce E, Goh V, Montana G. Automated triaging of adult chest radiographs with deep artificial neural networks. Radiology 2019 Apr;291(1):196-202. [doi: 10.1148/radiol.2018180921] [Medline: 30667333]
13. Savova GK, Masanz JJ, Ogren PV, et al. Mayo clinical text analysis and knowledge extraction system (cTAKES): architecture, component evaluation and applications. J Am Med Inform Assoc 2010;17(5):507-513. [doi: 10.1136/jamia.2009.001560] [Medline: 20819853]
14. Wang Y, Wang L, Rastegar-Mojarad M, et al. Clinical information extraction applications: a literature review. J Biomed Inform 2018 Jan;77:34-49. [doi: 10.1016/j.jbi.2017.11.011] [Medline: 29162496]
15. Chen PH, Zafar H, Galperin-Aizenberg M, Cook T. Integrating natural language processing and machine learning algorithms to categorize oncologic response in radiology reports. J Digit Imaging 2018 Apr;31(2):178-184. [doi: 10.1007/s10278-017-0027-x] [Medline: 29079959]
16. Bozkurt S, Alkim E, Banerjee I, Rubin DL. Automated detection of measurements and their descriptors in radiology reports using a hybrid natural language processing algorithm. J Digit Imaging 2019 Aug;32(4):544-553. [doi: 10.1007/s10278-019-00237-9] [Medline: 31222557]

XSL•FO
RenderX

17. Chapman WW, Bridewell W, Hanbury P, Cooper GF, Buchanan BG. A simple algorithm for identifying negated findings and diseases in discharge summaries. J Biomed Inform 2001 Oct;34(5):301-310. [doi: 10.1006/jbin.2001.1029] [Medline: 12123149]
18. Bodenreider O. The unified medical language system (UMLS): integrating biomedical terminology. Nucleic Acids Res 2004 Jan 1;32(Database issue):D267-D270. [doi: 10.1093/nar/gkh061] [Medline: 14681409]
19. Peng Y, Wang X, Lu L, Bagheri M, Summers R, Lu Z. NegBio: a high-performance tool for negation and uncertainty detection in radiology reports. 2018 Presented at: AMIA Summits on Translational Science Proceedings. [doi: 10.48550/arXiv.1712.05898]
20. Xue K, Zhou Y, Ma Z, Ruan T, Zhang H, He P. Fine-tuning BERT for joint entity and relation extraction in chinese medical text. Presented at: 2019 IEEE International Conference on Bioinformatics and Biomedicine (BIBM); 2019; San Diego, CA, USA. [doi: 10.1109/BIBM47256.2019.8983370]
21. Chen MC, Ball RL, Yang L, et al. Deep learning to classify radiology free-text reports. Radiology 2018 Mar;286(3):845-852. [doi: 10.1148/radiol.2017171115] [Medline: 29135365]
22. Pennington J, Socher R, Manning CD. Glove: global vectors for word representation. Presented at: Proceedings of the 2014 Conference on Empirical Methods in Natural Language Processing (EMNLP); 2014; Doha, Qatar. [doi: 10.3115/v1/D14-1162]
23. Chapman BE, Lee S, Kang HP, Chapman WW. Document-level classification of CT pulmonary angiography reports based on an extension of the ConText algorithm. J Biomed Inform 2011 Oct;44(5):728-737. [doi: 10.1016/j.jbi.2011.03.011] [Medline: 21459155]
24. Bustos A, Pertusa A, Salinas JM, de la Iglesia-Vayá M. PadChest: A large chest x-ray image dataset with multi-label annotated reports. Med Image Anal 2020 Dec;66:101797. [doi: 10.1016/j.media.2020.101797] [Medline: 32877839]
25. Yang Z. XLNet: generalized autoregressive pretraining for language understanding. 2019 Presented at: Proceedings of the 33rd International Conference on Neural Information Processing Systems; Vancouver. [doi: 10.48550/arXiv.1906.08237]
26. Lee J, Yoon W, Kim S, et al. BioBERT: a pre-trained biomedical language representation model for biomedical text mining. Bioinformatics 2020 Feb 15;36(4):1234-1240. [doi: 10.1093/bioinformatics/btz682] [Medline: 31501885]
27. Mikolov T, Sutskever I, Chen K, Corrado G, Dean J. Distributed representations of words and phrases and their compositionality. 2013 Presented at: ; Lake Tahoe. [doi: 10.48550/arXiv.1310.4546]
28. Zech J, Pain M, Titano J, et al. Natural language-based machine learning models for the annotation of clinical radiology reports. Radiology 2018 May;287(2):570-580. [doi: 10.1148/radiol.2018171093] [Medline: 29381109]
29. Bai J, Bai S, Chu Y, et al. Qwen technical report. arXiv. Preprint posted online on 2023. [doi: 10.48550/arXiv.2309.16609]
30. Kingma DP. Adam: A method for stochastic optimization. 2015 Presented at: International Conference for Learning Representations; San Diego. [doi: 10.48550/arXiv.1412.6980]
31. von Werra L, Belkada Y, Tunstall L, et al. TRL: transformer reinforcement learning. : GitHub, GitHub repository; 2020. URL: https://github.com/huggingface/trl [accessed 2025-03-19]
32. Wang Z, Wu Z, Agarwal D, Sun J. MedCLIP: contrastive learning from unpaired medical images and text. Presented at: Proc Conf Empir Methods Nat Lang Process; 2022 p. 3876-3887. [doi: 10.18653/v1/2022.emnlp-main.256] [Medline: 39144675]
33. Radford A, Wook Kim J, Hallacy C, et al. Learning transferable visual models from natural language supervision. Presented at: International conference on machine learning; 2021. [doi: 10.48550/arXiv.2103.00020]
34. Ramos R, Martins B, Elliott D, Kementchedjhieva Y. Smallcap: lightweight image captioning prompted with retrieval augmentation. Presented at: Proceedings of the IEEE/CVF Conference on Computer Vision and Pattern Recognition; 2023; Vancouver, BC, Canada. [doi: 10.1109/CVPR52729.2023.00278]
35. Johnson J, Douze M, Jegou H. Billion-scale similarity search with GPUs. IEEE Trans Big Data 2021 Jul;7(3):535-547. [doi: 10.1109/TBDATA.2019.2921572]

Abbreviations

BERT: Bidirectional Encoder Representations from Transformers
CLIP: Contrastive Language-Image Pretraining
GPT: generative pretrained transformer
LLM: large language model
MedCLIP: Medical Contrastive Language-Image Pretraining
NRF: National Research Foundation of Korea

XSL•FO
RenderX

Edited by A Castonguay; submitted 11.11.24; peer-reviewed by LP Gorrepati, S Chowdhury, VG Yogeshappa, Y Khan; revised version received 17.01.25; accepted 30.01.25; published 28.03.25.

Please cite as:
Abdullah A, Kim ST
Automated Radiology Report Labeling in Chest X-Ray Pathologies: Development and Evaluation of a Large Language Model Framework
JMIR Med Inform 2025;13:e68618
URL: https://medinform.jmir.org/2025/1/e68618
doi:10.2196/68618

© Abdullah Abdullah, Seong Tae Kim. Originally published in JMIR Medical Informatics (https://medinform.jmir.org), 28.3.2025. This is an open-access article distributed under the terms of the Creative Commons Attribution License (https://creativecommons.org/licenses/by/4.0/), which permits unrestricted use, distribution, and reproduction in any medium, provided the original work, first published in JMIR Medical Informatics, is properly cited. The complete bibliographic information, a link to the original publication on https://medinform.jmir.org/, as well as this copyright and license information must be included.

XSL•FO
RenderX

Identifying Patient-Reported Outcome Measure Documentation in Veterans Health Administration Chiropractic Clinic Notes: Natural Language Processing Analysis

Brian C Coleman[1,2,3], MHS, DC; Kelsey L Corcoran[1,3], DC; Cynthia A Brandt[1,2,3], MPH, MD; Joseph L Goulet[1,2], MS, PhD; Stephen L Luther[4,5], MA, PhD; Anthony J Lisi[1,3], DC

[1]Pain Research, Informatics, Multimorbidities, and Education Center, VA Connecticut Healthcare System, 950 Campbell Ave, West Haven, CT, United States

[2]Department of Emergency Medicine, Yale School of Medicine, Yale University, New Haven, CT, United States

[3]Department of Biomedical Informatics and Data Science, Yale School of Medicine, Yale University, New Haven, CT, United States

[4]Center of Innovation for Complex Chronic Healthcare, Edward Hines, Jr. VA Hospital, Hines, IL, United States

[5]College of Public Health, University of South Florida, Tampa, FL, United States

Corresponding Author:
Brian C Coleman, MHS, DC
Pain Research, Informatics, Multimorbidities, and Education Center, VA Connecticut Healthcare System, 950 Campbell Ave, West Haven, CT, United States

Abstract

Background: The use of patient-reported outcome measures (PROMs) is an expected component of high-quality, measurement-based chiropractic care. The largest health care system offering integrated chiropractic care is the Veterans Health Administration (VHA). Challenges limit monitoring PROM use as a care quality metric at a national scale in the VHA. Structured data are unavailable, with PROMs often embedded within clinic text notes as unstructured data requiring time-intensive, peer-conducted chart review for evaluation. Natural language processing (NLP) of clinic text notes is one promising solution to extracting care quality data from unstructured text.

Objective: This study aims to test NLP approaches to identify PROMs documented in VHA chiropractic text notes.

Methods: VHA chiropractic notes from October 1, 2017, to September 30, 2020, were obtained from the VHA Musculoskeletal Diagnosis/Complementary and Integrative Health Cohort. A rule-based NLP model built using medspaCy and spaCy was evaluated on text matching and note categorization tasks. SpaCy was used to build bag-of-words, convoluted neural networks, and ensemble models for note categorization. Performance metrics for each model and task included precision, recall, and F-measure. Cross-validation was used to validate performance metric estimates for the statistical and machine-learning models.

Results: Our sample included 377,213 visit notes from 56,628 patients. The rule-based model performance was good for soft-boundary text-matching (precision=81.1%, recall=96.7%, and F-measure=88.2%) and excellent for note categorization (precision=90.3%, recall=99.5%, and F-measure=94.7%). Cross-validation performance of the statistical and machine learning models for the note categorization task was very good overall, but lower than rule-based model performance. The overall prevalence of PROM documentation was low (17.0%).

Conclusions: We evaluated multiple NLP methods across a series of tasks, with optimal performance achieved using a rule-based method. By leveraging NLP approaches, we can overcome the challenges posed by unstructured clinical text notes to track documented PROM use. Overall documented use of PROMs in chiropractic notes was low and highlights a potential for quality improvement. This work represents a methodological advancement in the identification and monitoring of documented use of PROMs to ensure consistent, high-quality chiropractic care for veterans.

(JMIR Med Inform 2025;13:e66466) doi:10.2196/66466

KEYWORDS

Veterans Health Administration; natural language processing; quality of health care; chiropractic; patient reported outcome measures; NLP; AI; artificial intelligence; veteran; chiropractor; integrated health cohort; musculoskeletal diagnosis; musculoskeletal; quality of care; care; PROM; neural network; chiropractic care

XSL•FO
RenderX

Introduction

Patient-reported outcome measures (PROMs) are standardized, validated questionnaires completed by patients to identify and quantify their perceptions of their health status [1]. These measures are often of interest to clinicians to assess condition severity and response to treatment as a component of a measurement-based care approach. Measurement-based care is a recommended practice in the management of musculoskeletal pain conditions [2], where biomarkers of disease severity are lacking and baseline and serial reassessment for progress may influence clinical decision-making. Using PROMs can improve communication and shared decision-making between patients and clinicians, enable contextualization of pain within a patient's life, and may positively influence health and pain status [3].

In the Veterans Health Administration (VHA), patients with musculoskeletal pain may receive chiropractic care, where the use of PROMs is an expected component of high-quality care [4,5]. The VHA Office of Specialty Care Ongoing Professional Practice Evaluation quality program for chiropractors includes a quality metric stating "appropriate pain, functional, and/or other measures are documented and used to inform clinical decision making." However, substantial challenges limit monitoring this important metric of high-quality care at a national scale. Digital data systems integration is limited for both remote and point-of-care data collection that may otherwise facilitate structured data collection, thus any PROM documentation often occurs in unstructured clinic notes. Quality evaluation of these notes typically requires time-intensive, peer-conducted chart review, with substantial human effort limiting ongoing monitoring [6].

The VHA Chiropractic Program has expanded rapidly in recent years driven by policy change and natural growth [7,8], with 299 facilities now offering on-site chiropractic care in fiscal year (FY) 2024, up 344% from 87 facilities in FY2017. Scalable solutions are needed to monitor established care quality metrics, such as PROM use, and ensure high-quality chiropractic care delivery across the enterprise. Further, such solutions could also be widely applicable to other disciplines managing musculoskeletal pain, which is highly prevalent and burdensome in the VHA system and beyond.

Natural language processing (NLP) of clinic text notes is one promising solution to extracting care quality data from unstructured text [9], with previous studies focusing on pain care quality in primary care and chiropractic care settings [10,11]. Use cases for NLP across other clinical domains highlight its potential utility in information extraction and analysis tasks. NLP methods have been used to accurately identify functional status impairment for patients with dementia based on electronic health record (EHR) clinic notes [12]. Additionally, NLP techniques have shown utility in information extraction, classification, and risk prediction tasks for patient-reported outcomes among cancer patients [13]. Relevant to pain management, NLP has been used to identify opioid use and misuse in clinic notes [14] and support decision support systems to impact clinical care [15]. More recently, the use of large-language models in data mining of EHR data, including clinical text data, has demonstrated promise and efficiency in information extraction and content analysis [16].

The objective of this study was to develop an NLP approach to identify PROMs documented in VHA chiropractic clinic text notes. We aimed to iteratively develop a rule-based pipeline and evaluated performance for a text span pattern matching task and a note categorization task. We also aimed to compare the performance of the rule-based method to statistical and machine learning methods for the note categorization task and estimate the overall prevalence of documented PROM use in the corpus. We hypothesize a rule-based NLP approach, when iteratively developed and refined, will demonstrate comparable performance to statistical and machine learning methods in identifying and categorizing PROM documentation within VHA chiropractic clinic text notes.

Methods

Study Setting, Data Sources, and Cohort

We conducted a secondary, retrospective analysis of the Musculoskeletal Diagnosis/Complementary and Integrative Health (MSD/CIH) Cohort [17]—an EHR data cohort of VHA patients receiving VHA health care for musculoskeletal conditions, with updated cohort entry through September 30, 2020. Study reporting was informed by published recommendations for reporting machine learning and NLP studies [18,19].

We identified patients in the MSD/CIH Cohort who received VHA chiropractic care at a VHA facility between October 1, 2017, and September 30, 2020. All chiropractic clinic visits were identified using an administrative clinic identifier denoting "Chiropractic Care." Initiating chiropractic care in the VHA most often requires the placement of a referral order for consultation, with the consultation visit linked to this order in the EHR. We included only patients with an initial consultation visit during the study period and included all visits occurring within 1 year of their first consultation visit date. Population demographic and clinical characteristics were extracted from the EHR for each patient included in the sample, including age at first chiropractic consultation, sex of record, race/ethnicity, marital status, smoking status, service-connected disability percentage, and BMI. *International Classification of Diseases, 10th Revision* (*ICD-10*) codes were also extracted for each visit, and flags were used to denote whether a visit included a low back pain diagnosis, neck pain diagnosis, other spinal pain diagnosis, or any other diagnosis.

We obtained all clinic text notes linked to the identified visits to build a corpus of clinic visit notes. We excluded note types related to telecommunications and administrative events (eg, appointment scheduling, secure messaging), including only notes describing chiropractic care in the ambulatory, in-hospital, or telehealth setting.

Data Preparation

Multiple notes can be written to describe the same identified chiropractic visit; for example, a resident chiropractor note and an attending chiropractor note may each contain data relevant to a single visit. We concatenated all notes linked to the same

XSL•FO
RenderX

unique visit identifier on the same date of service (regardless of note author) to create a 1-to-1 relationship between visits and clinic notes. A unique character set was used as a delimiter to separate individual notes. To evaluate the amount of text present across notes in the corpus, we quantified each note length using tokenization based on whitespace splitting and visualized the data using a histogram of token lengths. We compared tokenized lengths across different types of visits and across FYs through visual comparison, Kruskal-Wallis tests across all groups, and Dunn tests across group pairs with a significance level α of 0.05 and a Bonferroni correction for multiple comparisons.

Additional metadata about each chiropractic care visit was extracted from the EHR and written into a header for each note, offset from the rest of the note using a unique character series delimiter. This included a patient identifier, visit identifier, visit date, VHA facility identifier code, the date of the first consultation visit, and the visit number with the total number of visits within the year after consultation (eg, "visit 3 of 6"), the number of days since the previous visit (if applicable), and the number of days to the next visit (if applicable).

Visits were tagged into the following five exclusive categories using conditional logic: (1) first consultation visit, (2) final visit within 1 year, (3) visit immediately preceding a 60-day gap in care, (4) visit immediately following a 60-day gap in care, and (5) other intermediate visit. These categories were identified to stratify visits on having a higher likelihood of potential use of PROMs at the beginning or end of an episode of chiropractic care or before or after a gap in chiropractic care.

A nationally representative, random stratified sample of 300 notes was selected for human annotation to be used as an initial training set. The stratification approach was designed to select an approximately equal number of notes for each visit category and was randomly repeated until a maximum number of facilities was included in the training set (78 of 79, with 1 facility excluded due to very few notes included in the corpus).

Corpus Annotation

Two study investigators (BCC and KLC) with VHA chiropractic care subject-matter expertise annotated the training corpus using eHost, a Java-based annotation tool [20]. Annotators identified and tagged spans of text referencing documented use of PROMs and assigned a span attribute for the specific type of PROM based on an a priori list (Multimedia Appendix 1). The initial seed list of PROMs was a sample of validated PROMs potentially used by chiropractors addressing pain and function, particularly for spinal conditions. An additional attribute class was included for tagging an unspecified PROM that was not included in the list, which was reviewed for inclusion during subsequent iterations. We excluded all versions of the Numerical Rating Scale and Visual Analog Scales as unidimensional measures that have been criticized as potentially limited clinical importance [21], especially when trying to measure a complex, multifaceted condition like musculoskeletal pain [22,23]. An annotation guide was developed and iteratively revised/validated using a preparatory random note sample from a separate corpus during an annotation pilot. Interannotator agreement (IAA) was high across 3 samples of pilot notes (n_1=50 notes, IAA_1=78.8%; n_2=100 notes, IAA_2=84.5%; and n_3=100 notes, IAA_3=86.1%).

Annotation of the initial training set (n=300 notes) was iteratively completed in 100-note batches. IAA remained high across the 3 iterations of annotating the initial training set (IAA_1=71.7%, IAA_2=81.2%, and IAA_3=87.1%). Adjudication of disagreement was achieved through review and discussion between the annotators. A third-person adjudicator was available to provide a final adjudication decision in the event of unresolved disagreement, though this did not become necessary.

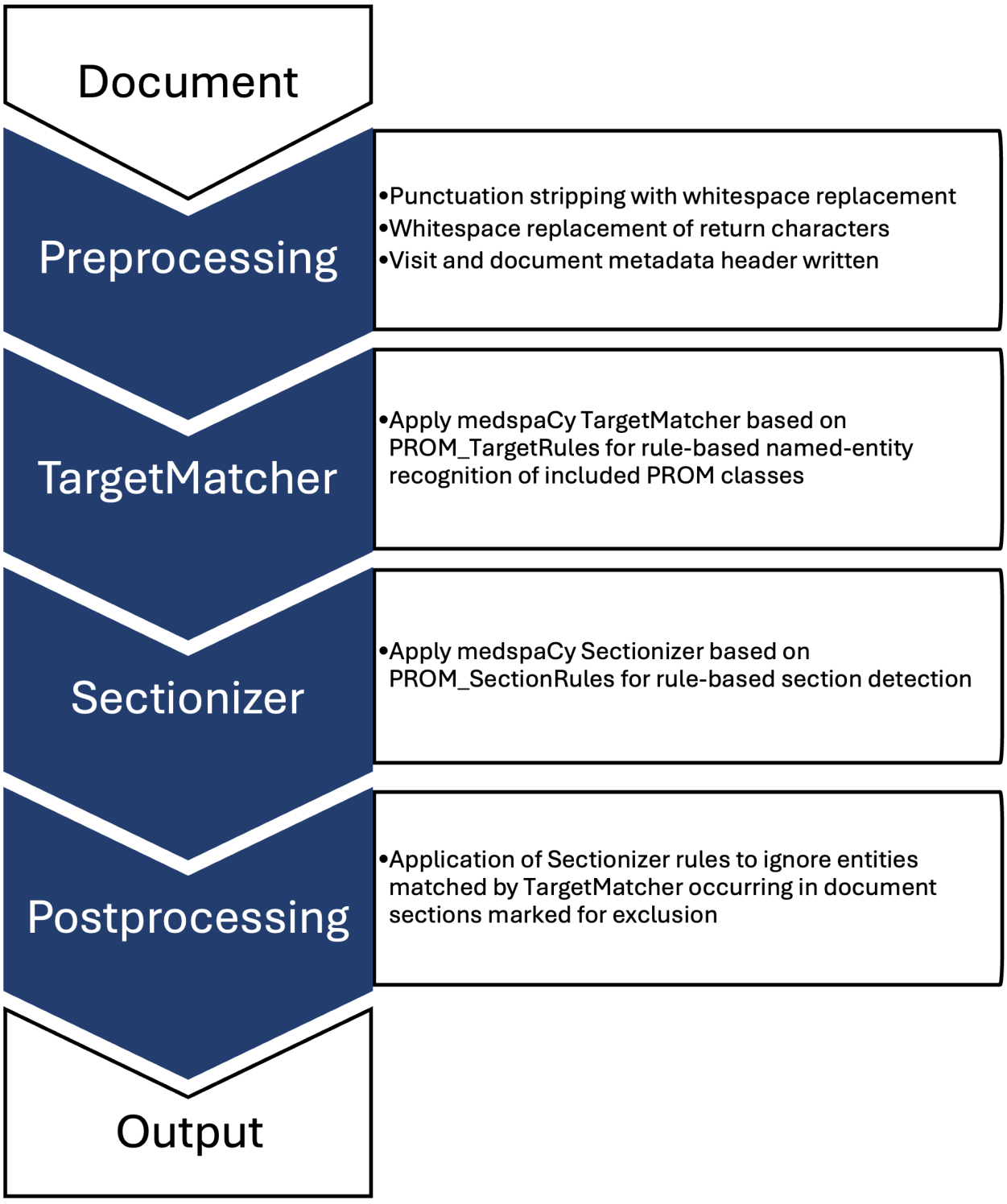
Initial NLP Model Development

A rule-based NLP pipeline (Figure 1) was built using medspaCy [24] (v1.0.0) and spaCy [25] (v3.6.0; Explosion) in Python (v3.8.5; Python Software Foundation). The initial pipeline used the medspaCy TargetMatcher and TargetRule functions to match spans of text in a spaCy Doc object. Matches were based on an initial set of rules to define text pattern rules for 15 predetermined PROMs, with an associated attribute referencing a specific measure assigned for each identified span.

For all iterations of NLP model development, evaluation statistics (precision, recall, and F-measure) were calculated based on true positives, false positives, and false negatives for three defined matching tasks: (1) strict-boundary matching, (2) soft-boundary matching, and (3) note categorization. Strict-boundary matching considered only the perfect overlap of the human annotation and NLP target matching methods to be a match in performance metric calculation. Soft-boundary matching was a fuzzy matching approach that allowed for flexibility in the overlap between the span start and span end positions of the human annotation and NLP target matching methods to define a match. Note categorization cast the results of the human annotation and NLP target matching to a binary document classification question, defining documented PROM use at the note level. All matching methods required matching on the assigned attribute for a specified PROM to be considered a match.

XSL•FO
RenderX

Figure 1. Rule-based natural language processing (NLP) medspaCy pipeline overview. PROM: patient-reported outcome measure.



NLP Model Refinement

The initial pipeline was run on the annotated first training set and false positives and false negatives were manually reviewed to revise the TargetMatcher rules and the overall NLP pipeline. Pipeline modifications were attentively designed to address only generalizable false positives and negatives and avoid overfitting the training data. During this review, false negatives were addressed by modifying TargetMatcher rules to better represent broader matching patterns (eg, abbreviations), supporting fuzzy matching (eg, typographic errors), and by adding TargetMatcher rules for 3 additional measures identified during annotation. False positives were addressed by adding sectionizer and postprocesser steps to the NLP pipeline. A medspaCy sectionizer component was added to define sections of the clinical note, with a Postprocessor component added to set rules for sections to ignore in defining PROM spans. This allowed the exclusion of inappropriate matches that were being identified in abbreviation lists, medication lists, goals of care,

XSL•FO
RenderX

and other irrelevant sections of the note. The final rule-based model is available on GitHub [26].

After the development of an initial NLP rule-based model to identify PROM documentation, a second high-probability training set (n=200) was identified based on a preliminary model NLP output as programmatic labeling and annotated by a single investigator (BCC). This created a full annotation set of 500 notes and increased the prevalence of positive notes in the training set to balance the prediction problem.

Using the full training set, we trained an initial set of statistical and machine learning models to complete the note categorization task prediction and compared their performance to the rule-based model. The full annotated training set was randomly partitioned with 75% allocated to the model training set, 15% to the development set to tune hyperparameters, and 10% to the test set to evaluate performance. We tested 3 model architecture configurations built in spaCy: (1) a bag-of-words (BOW) model, (2) a convoluted neural network model, and (3) an ensemble model combining a linear BOW model and Tok2Vec model. Architecture configurations for each model are detailed in Multimedia Appendix 2 with source code available on GitHub [26]. All computational analysis was conducted using a secure virtual machine with a Windows 10 operating system, 8 virtual processors (x86-64, 2.60 GHz), and 16 GB memory, with variable overall runtime based on competing user demands.

NLP Model Evaluation and Validation

For the initial evaluation of the rule-based model performance on the text matching and note categorization tasks, we evaluated performance based on precision, recall, and F-measure. To compare the performance of the rule-based model to the initial statistical and machine learning models for the note categorization task, precision, recall, F-measure, and accuracy were calculated. The area under the receiver operator characteristic curve (AUC-ROC) was calculated for the statistical and machine learning models. AUC-ROC was not calculated for the rule-based model as it is a deterministic model generating a binary decision output rather than a probability score output.

We used Monte Carlo and k-folds cross-validation (stratified and unstratified) to validate the calculated performance metrics for the initial statistical and machine learning models across multiple simulations. Monte Carlo cross-validation consisted of 100 simulation cycles randomly partitioning the annotated data set into 75% training/15% development/10% testing splits. k-folds cross-validation was performed using 10 cycles of 10-fold repeated cross-validation (100 total cycles), with and without stratification, and sampled 8 training folds, 1 development fold, and 1 test fold during each cycle. Precision, recall, F-measure, and AUC-ROC were calculated for each cycle across both cross-validation methods.

Ethical Considerations

This study received exemption approval from the institutional review boards of the VA Connecticut Healthcare System (1690344-1) and Yale University (2000032830).

Results

We identified 56,628 patients for inclusion in this study, with a total of 377,213 visits across the study period. Patient and visit characteristics are presented in Table 1. The patient population was consistent with those usually receiving VHA chiropractic care. Patients had a median of 5 (IQR 3-6) chiropractic care visits, with most visits occurring for low back pain. There were 14,198 patients (25.1%) who had at least one 60-day care gap. The tokenized text across the entire corpus had a mean length of 565 tokens (SD 434), with 4617 notes (1.2%) greater than 2000 tokens in length.

Assessing the tokenized text lengths by visit type for the entire corpus split by whitespaces (Figure 2) showed a greater number of tokens in the first (consult) visits compared with the other visit types. The distribution of tokenized length of first (consult) visits was right-shifted compared with all other visit types, with a mean length of 1069 tokens (SD 565) and 3198 notes (5.6%) greater than 2000 tokens in length. The mean token length was 464 (SD 316) for other intermediate visits, 514 (SD 404) for visits preceding a 60-day care gap, 587 (SD 427) for visits following a 60-day care gap, and 490 (SD 358) for final visits within 1 year. A Kruskal-Wallis test demonstrated statistically significant differences across the 5 visit types (P<.001), with all corrected pairwise comparisons significant at P<.001 except visits preceding a 60-day care gap compared with final visits within 1 year (P=.008). Tokenized text lengths by FY (Figure 3) showed a mean length of 579 (SD 456) tokens in FY2018, 571 (SD 435) tokens in FY2019, and 496 (SD 348) tokens in FY2020. A Kruskal-Wallis test showed a statistically significant difference across the FY groups (P<.001), with corrected pairwise comparisons demonstrating significant differences between FY2020 and each of FY2018 and FY2019 (P<.001), but not between FY2018 and FY2019 (P≥.99).

For each included PROM, the text span match frequency and note categorization frequency between human annotation and the rule-based model output on the full training set and in the full-text corpus are presented in Multimedia Appendix 1. When the rule-based model was run on the full note corpus, there were 112,131 PROM text spans identified across 64,027 notes (17.0% of the full corpus), a prevalence consistent with that of human annotation in the initial annotation training set (53 of 300 notes, 17.7%). PROM documentation was identified in 13.8% (n=32,341) of other intermediate visits, 32.7% (n=18,519) of first (consult) visits, 13.2% (n=2365) of visits preceding a 60-day gap in care, 13.9% (n=1733) of visits following a 60-day gap in care, and 16.0% (n=9069) final visits within 1 year. The prevalence of documented PROM use, by visit, decreased over time (19.1% in FY2018, 16.5% in FY2019, and 13.2% in FY2020) (Multimedia Appendix 3). The most documented PROMs were the Bournemouth Questionnaire (back and neck versions) and the Oswestry Disability Index.

Rule-based model performance across the strict- and soft-boundary matching and note categorization tasks are shown in Table 2. Performance for the strict-boundary matching task was low across all metrics. When relaxing the matching criteria to allow for soft-boundary overlap, the model performance

XSL•FO
RenderX

improved substantially with good to excellent model performance that was balanced across precision and recall with few false positives and very few false negatives. Rule-based model performance in the note categorization task was excellent, with high precision and near-perfect recall.

The comparison between the rule-based model and the initial statistical and machine learning model performance on the note categorization task is shown in Table 3. Using the rule-based model output as a binary text categorization yielded better performance across all metrics and high accuracy (95.8%) compared with the spaCy models. Performance metric distributions (Figure 4) and the mean metric with 95% CI (Table 4) were consistent across each cross-validation method, with acceptable to good model performance across all metrics for all spaCy models. The model consistently outperformed both the BOW and convoluted neural network models across all metrics, with a good balance between precision and recall and a high AUC-ROC.

XSL•FO
RenderX

Table . Patient and visit sample characteristics.

Characteristics	Total
Patient characteristics	
Total patients, n	56,628
Age[a] (years), median (IQR)	53 (39-66)
Sex, n (%)	
Female	9119 (16.1)
Male	47,509 (83.9)
Race or ethnicity, n (%)	
White	38,921 (68.7)
Black or African American	9899 (17.5)
Hispanic or Latino	4410 (7.8)
Other or unknown	3398 (6.0)
Marital status, n (%)	
Married	29,653 (52.4)
Single or never married	9456 (16.7)
Divorce or separated	15,650 (27.6)
Other or unknown	1869 (3.3)
Smoking status, n (%)	
Current smoker	19,133 (33.8)
Former smoker	15,872 (28.0)
Never smoker	21,571 (38.1)
Missing	52 (0.1)
Service-connected percentage, median (IQR)	70.0 (10.0-90.0)
BMI[b] (kg/m^2), median (IQR)	29.4 (26.2-33.1)
Visit characteristics	
Total visits and notes, n	377,213
Note token length, median (IQR)	447 (261-718)
Chiropractic care visits per patient, median (IQR)	5.0 (3.0-9.0)
Visit diagnoses, median (IQR)	
Low back pain visits	4.0 (2.0-7.0)
Neck pain visits	1.0 (0.0-5.0)
Other spinal pain visits	0.0 (0.0-4.0)
Other diagnosis visits	2.0 (0.0-5.0)
Visit types, n (%)	
First (consult) visit	56,628 (15.0)
Final visit within 1 year	56,628 (15.0)
Visits preceding a 60-day care gap	17,890 (4.7)
Visits following a 60-day care gap	12,466 (3.3)
Other intermediate visit	233,601 (62.0)

[a]Age as of initial chiropractic consult.

[b]7108 missing.

XSL•FO
RenderX

Figure 2. Tokenized text length of notes in the study corpus, split on whitespace characters, by visit type with an overflow bin for notes greater than 2000 tokens (n=4617).

XSL•FO
RenderX

Figure 3. Tokenized text length of notes in the study corpus, split on whitespace characters, by fiscal year, with an overflow bin for notes greater than 2000 tokens (n=4617). FY: fiscal year.

XSL•FO
RenderX

Table . Rule-based model evaluation summary.

Rule-based model task	Precision (%)	Recall (%)	F-measure (%)
Strict-boundary matching task	47.4	58.0	52.2
Soft-boundary matching task	81.1	96.7	88.2
Note categorization task	90.3	99.5	94.7

Table . Note categorization task model evaluation summary.

Model	Precision (%)	Recall (%)	F-measure (%)	Accuracy (%)	AUC-ROC[a] (%)
Rule-based model	90.3	99.5	94.7	95.8	—[b]
Bag-of-words model	75.0	85.7	80.0	82.0	93.8
Convoluted neural network model	93.8	71.4	81.1	86.0	94.7
Ensemble model	86.4	90.5	88.4	90.0	96.5

[a]AUC-ROC: area under the receiver operator characteristic curve.

[b]Not applicable.

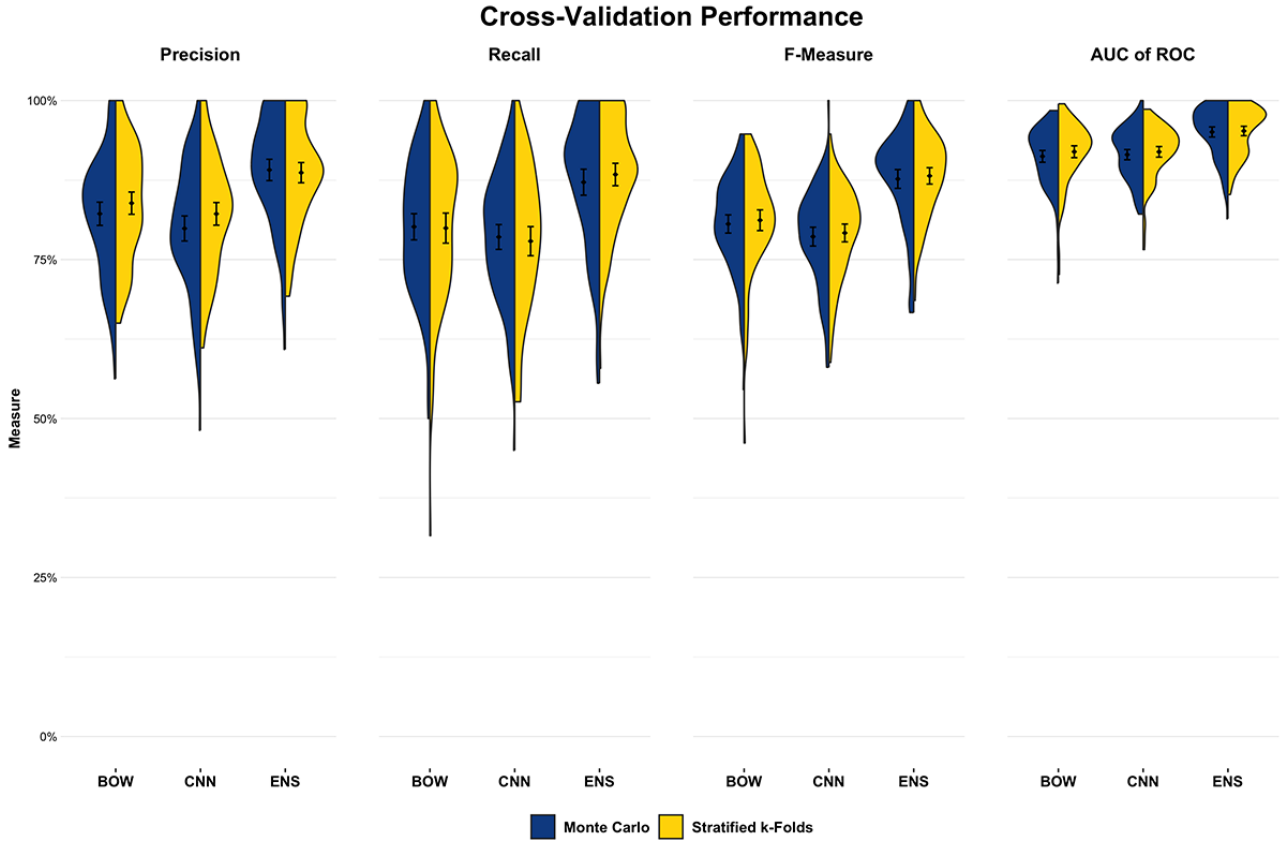
Table . Statistical and machine learning model performance metrics from Monte Carlo (100 iterations) and k-folds (10x10-folds) cross-validation (stratified and unstratified).

	Precision (%), mean (95% CI)	Recall (%), mean (95% CI)	F-measure (%), mean (95% CI)	AUC-ROC[a] (%), mean (95% CI)
Monte Carlo cross-validation				
Bag-of-words	82.2 (80.4-84.0)	80.2 (78.1-82.2)	80.6 (79.2-82.0)	91.2 (90.3-92.2)
Convoluted neural network	79.9 (77.9-81.9)	78.5 (76.6-80.5)	78.6 (77.1-80.1)	91.5 (90.7-92.3)
Ensemble	89.1 (87.4-90.8)	87.2 (85.1-89.2)	87.7 (86.2-89.2)	95.1 (94.3-95.9)
k-folds cross-validation				
Bag-of-words	81.3 (79.5-83.2)	82.1 (80.0-84.2)	81.1 (79.6-82.6)	92.2 (91.4-92.9)
Convoluted neural network	79.6 (77.5-81.7)	79.5 (77.4-81.7)	78.9 (77.2-80.5)	92.2 (91.5-93.0)
Ensemble	88.7 (87.1-90.3)	87.2 (85.4-89.1)	87.6 (86.1-89.0)	95.0 (94.1-95.8)
Stratified k-folds cross-validation				
Bag-of-words	83.9 (82.1-85.6)	79.9 (77.6-82.3)	81.2 (79.6-82.8)	92.0 (91.0-92.9)
Convoluted neural network	82.2 (80.4-84.0)	77.9 (75.6-80.2)	79.2 (77.8-80.6)	91.9 (91.1-92.8)
Ensemble	88.7 (87.1-90.3)	88.4 (86.6-90.1)	88.2 (86.9-89.4)	95.2 (94.5-96.0)

[a]AUC-ROC: area under the receiver operator characteristic curve.

XSL•FO
RenderX

Figure 4. Performance metric distributions (with mean value and 95% CIs) for the note text categorization task using Monte Carlo and stratified k-folds cross-validation for the bag-of-words (BOW), convoluted neural network (CNN), and ensemble (ENS) models. AUC of ROC: area under the receiver operator characteristic curve.



Discussion

Principal Findings

In this study, we tested NLP approaches to identify PROM use documented in VHA chiropractic clinic notes as a method to monitor an important marker of high-quality chiropractic care. Our iterative process targeting a series of prediction tasks showed overall strong performance across rule-based, statistical, and machine-learning approaches, affirmed by multiple approaches to cross-validation. The rule-based NLP model had good to excellent performance in identifying text spans referencing PROMs when flexible span boundaries were used but not when span boundaries were strict. When using the rule-based model output as a note categorization prediction, overall performance was excellent, with high precision and near-perfect recall. While our initial hypothesis predicted comparable performance between the rule-based approach and the statistical and machine learning methods, our findings demonstrate that the rule-based approach achieved superior performance in identifying and categorizing PROM documentation within this sample of VHA chiropractic clinic text notes. We suspect improved performance may be attributable to data volume and sparsity of text indicators of PROMs relative to the remaining document content describing the rest of the chiropractic care encounter. Rule-based models are generally less susceptible to data volume issues given their methodical approach, whereas machine learning approaches thrive on large data sets where more complex patterns and relationships can be trained on and identified in the text. Important benefits of the rule-based approach include simplicity, interpretability, and efficiency—all of which provide added value alongside slightly superior performance.

Overall model performance was sufficient to have clinical utility for quality metric monitoring, especially given the low prevalence of false negatives. The error analysis process used during model development identified that remaining false positives were frequently due to unique circumstances difficult to address by creating exclusion rules without overfitting the training data. For example, the text “Goals of Care: Improve outcome measures, reduce ODI by 20%” would identify a section span to exclude (“Goals of Care”) followed by a section span to include (“outcome measures”) and a PROM span (“ODI”), therefore marking the PROM span for inclusion.

Consistent findings across multiple methods of cross-validation, with and without stratification accounting for baseline PROM use prevalence, showed acceptable performance for each of the statistical and machine learning models tested on the note categorization task. Of note, several performance metrics in the initial model evaluation fell outside the cross-validation estimated 95% CI, attesting to the benefit of cross-validation in generating a more appropriate representation of performance.

Clinical Implications and Future Work

While all models performed adequately for note categorization, we used the rule-based model, having the best performance, on the full corpus to estimate the overall prevalence of PROM

XSL•FO
RenderX

documentation. The overall prevalence was low and consistent with estimates from the annotation data, highlighting the potential limited documented use of PROMs by VHA chiropractors despite being an identified quality care metric. This is in contrast with data from surveys of US chiropractors in which 60% of respondents reported using PROMs several times per day [27]. Qualitative evaluation in a non-VHA setting has highlighted multiple barriers and facilitators to implementing PROMs in chiropractic care [28]. These included clinician knowledge and training, engagement and purpose of collecting PROM data, perceived utility versus burden for clinicians and patients, and organizational and administrative factors (such as in-visit time availability and ability to use electronic data collection systems). Evidence of external determinants influencing PROM use can be hypothesized from our results showing a decreasing trend in documented PROM use across each year of the study period. The VHA Chiropractic Program rapidly expanded nationally during this time, with an increase in the number of employed VHA chiropractors [29] and increasing service penetration across the national VHA system [30]. Thus it is possible that our results reflect an increasing number of new chiropractors not using PROMs, not documenting PROM use in clinic notes, or a combined effect of the 2, highlighting a potential opportunity for quality improvement and education.

Given our findings, we hypothesize there is a relationship between documentation quantity as a proxy for comprehensiveness of evaluation, including the use of PROMs. PROM use was most prevalent in first (consult) visits at more than double the rate found in other visit types. Paired with significantly longer text lengths compared with other visit types, this suggests that the increased complexity and information gathering inherent in initial consultations necessitate more thorough documentation, including the application of outcome measures. Additionally, the decrease in documented PROM use during FY2020, paired with shorter text length in FY2020, is potentially attributable to the onset of the COVID-19 pandemic with changes in the quantity and mode of delivery of chiropractic care [31] and challenges in administration due to impacted face-to-face care with limited availability of remote data collection information systems.

Future work should consider patient, visit, facility, clinician, and system factors, including qualitative perspectives of VHA chiropractors, that may influence the use of specific PROMs and their documentation by VHA chiropractors. These determinants can inform intervention development and implementation strategies related to improving PROM use and documentation. However, these potential external influences do not affect our confidence in the performance of the developed NLP models to evaluate documented PROM use by VHA chiropractors on a national scale as a quality metric.

The implications of tracking PROM use by VHA chiropractors using this approach include enhanced patient outcomes, improved clinical decision-making, and ensuring consistent, high-quality chiropractic care for veterans. These are consistent with core practical considerations for the development of NLP systems to address pragmatic clinical needs and improve patient outcomes, including offering an organization incentive for use and supporting ongoing monitoring with implementation feasibility [32]. Within the VHA chiropractic care setting, our approach allows for the monitoring of an important quality metric at a national scale using centralized resources. Additionally, this approach standardizes and enhances the objectivity and rigor of assessment of documentation content, while minimizing the individual burden of chart review by practicing VHA chiropractors. Further, our methods may have application in other clinical settings providing musculoskeletal pain care, in the VHA and beyond, given the high prevalence of musculoskeletal pain in both veteran and nonveteran populations. Future research should focus on refining these NLP models to enhance their applicability across diverse clinical settings, including other pain care clinics, and explore the integration of additional data sources to further enrich patient care insights. Additionally, future research can evaluate the efficiency of our approach in terms of financial, human, computational, and other resource costs compared with traditional manual review methods to best understand the potential value and system resource use implications of this work.

Limitations

There are several limitations to our study that are inherent to any observational research or studies using NLP. The text notes used in this study were originally intended for clinical care purposes. Thus, their secondary use for research is subject to limitations in the quality of the notes and the content documented for that purpose, which may not always fully reflect what was done during the patient encounter. Observing the variation in the quantity of text (ie, number of tokens) present in each note across the corpus showed an expectedly right-skewed distribution and highlighted heterogeneity in the quantity of text content included in VHA chiropractic clinic notes. Similar findings were evident in tokenized length differences between visit types and the year during which a visit occurred. We suspect this correlates with heterogeneity in comprehensiveness of documentation, and by proxy of care delivered, highlighting a future opportunity for VHA chiropractor education or other quality improvement interventions to ensure consistent quality on a national scale. Templated material in clinic notes, while difficult to quantify across the corpus, may limit the richness and variability of the text data, potentially affecting the capture of patient- and note-specific details. It was evident during annotation that templates were, at times, shared across VHA facilities, which may affect our intention to capture variability across the VHA by stratifying our random sampling of notes by the facility. Further, our sampling by facility may not account for variations between individual chiropractors at a given facility. Stratifying our random sampling by a chiropractor was an alternative strategy but risked increasing the heterogeneity of the sample.

Our strategy to capture clinic notes is consistent with previous practices to identify VHA chiropractic clinic visits and associated notes. However, facility variation in clinic workflow may also influence the use and the documentation of PROMs separately. While expected that these would be documented in the EHR, clinics may use alternative strategies for the collection and recording of PROMs from patients and limiting our findings

XSL•FO
RenderX

to representing "documented PROM use." Further, the initial seed list of PROMs suspected to potentially be used by VHA chiropractors was established a priori without empirical validation. We allowed flexible expansion of the initial list during the annotation process to include PROMs that had use, but were not considered in advance, yet it is possible we still failed to include PROMs that may have been used more rarely than our random sampling could capture. As future PROMs are developed and adopted, maintenance of the proposed NLP approach to incorporate these has not been assessed in this study. While this would require some degree of manual effort, we do not suspect that incorporating additional PROMs into the model is particularly challenging given our experience in expanding the initial seed list during this study. We also did not incorporate pretrained or large-language models into this analysis due to restricted use in our computing environment at the time of this study. If, in future research, these types of models are successfully able to be validated with adequate performance and implemented, their adoption may mitigate the requirement of ongoing manual efforts. We also did not conduct a formal text feature analysis on the output from the tested machine learning models, which could provide insight into the contributions of specific text to the model prediction. This may be an important contribution in future work to compare the explainability of the machine learning approaches to the generally interpretable rule-based approach and potentially optimize machine learning model parameters to enhance prediction performance.

Our sample of patients receiving VHA chiropractic care from the MSD/CIH Cohort allowed overlapping entry into the parent cohort and our study sample through the end of the study period, ideally representing all chiropractic care occurring during this time. However, by limiting our follow-up period for an individual patient to 1 year after their initial chiropractic visit, we may have excluded chiropractic care received later in the study period. This, along with the onset of the COVID-19 pandemic, may account for the rapid reduction in patients and visits during the final year of the cohort with unknown potential impact on our findings.

As all notes in this study originated during VHA chiropractic care, there is unknown utility of the developed NLP models in non-VHA chiropractic documentation. Variations in the documentation requirements between the VHA and non-VHA settings for administrative purposes (eg, billing) may influence the use and documentation of PROMs. Nonetheless, our sample originates from the largest collection of chiropractic care EHR data in an integrated medical setting, with evidence from VHA studies of chiropractic care having the potential to influence chiropractic care in the non-VHA setting.

Conclusions

Our study demonstrates the effective use of NLP to accurately identify documented PROM use from VHA chiropractic clinic notes, highlighting the potential for improved data use in quality monitoring of patient care. By leveraging an NLP approach, we can overcome the challenges posed by unstructured clinical text notes to track an identified quality care metric for chiropractic care. Overall documented use of PROMs was low and highlights the need for quality improvement. Future work should evaluate determinants influencing PROM use and develop intervention and implementation strategies to improve their use and documentation in VHA chiropractic care to ensure consistent, high-quality chiropractic care for veterans.

Acknowledgments

The contents of this manuscript represent the view of the authors and do not necessarily reflect the position or policy of the US Department of Veterans Affairs, the National Institutes of Health, or the United States Government. This material is based upon work supported by the National Center for Complementary & Integrative Health of the National Institutes of Health under award number K08AT011570. Successful completion of this study also builds on the support of previous work by the Department of Veterans Affairs, Veterans Health Administration, Office of Research and Development, Health Services Research and Development IIR-12-118, and the NCMIC Foundation, with resources and the use of facilities at the VA Connecticut Healthcare System.

Data Availability

The code developed in this research has been made publicly available on GitHub (bccolemanva/outcomemeasure-nlp). The datasets generated and analyzed during this study are not publicly available. To maximize the protection and security of veterans' data while making these data available to researchers, the US Department of Veterans Affairs (VA) developed the VA Informatics and Computing Infrastructure (VINCI). VA researchers must log onto VINCI via a secure gateway or virtual private network connection (VPN) and use a virtual workspace on VINCI to access and analyze VA data. As per the VA Office of Research and Development Policy, VINCI does not allow the transfer of any patient-level data out of its secure environment without special permission. Researchers who are not VA employees must be vetted and receive "without compensation" (WOC) employee status to gain access to VINCI. All analyses performed for this study took place on the VINCI platform. For questions about data access, contact study lead, BCC (Brian.Coleman2@va.gov) or the VA Office of Research and Development (VHACOORDRegulatory@va.gov).

Conflicts of Interest

BCC receives grant funding related to this work from the National Center for Complementary & Integrative Health of the National Institutes of Health under award number K08AT011570.

XSL•FO
RenderX

Multimedia Appendix 1
Patient-reported outcome measure (PROM) span match and note frequencies in annotation set and full text corpus.
[DOCX File, 24 KB - medinform_v13i1e66466_app1.docx]

Multimedia Appendix 2
Supplemental methods describing detailed architectures of statistical and machine learning models.
[DOCX File, 21 KB - medinform_v13i1e66466_app2.docx]

Multimedia Appendix 3
Trends in patient-reported outcome measure use, by unique patient and visit, across the study period, by fiscal year (FY) and month. Patient-reported outcome measure use (PROM +) identified based on note (visit) categorization output from the rule-based natural language processing (NLP) model. Individual patients may be counted in multiple months and fiscal years.
[DOCX File, 26 KB - medinform_v13i1e66466_app3.docx]

References

1. Dawson J, Doll H, Fitzpatrick R, Jenkinson C, Carr AJ. The routine use of patient reported outcome measures in healthcare settings. BMJ 2010 Jan 18;340:c186. [doi: 10.1136/bmj.c186] [Medline: 20083546]
2. Lin I, Wiles L, Waller R, et al. What does best practice care for musculoskeletal pain look like? Eleven consistent recommendations from high-quality clinical practice guidelines: systematic review. Br J Sports Med 2020 Jan;54(2):79-86. [doi: 10.1136/bjsports-2018-099878] [Medline: 30826805]
3. Holmes MM, Lewith G, Newell D, Field J, Bishop FL. The impact of patient-reported outcome measures in clinical practice for pain: a systematic review. Qual Life Res 2017 Feb;26(2):245-257. [doi: 10.1007/s11136-016-1449-5] [Medline: 27815820]
4. Hawk C, Whalen W, Farabaugh RJ, et al. Best practices for chiropractic management of patients with chronic musculoskeletal pain: a clinical practice guideline. J Altern Complement Med 2020 Oct;26(10):884-901. [doi: 10.1089/acm.2020.0181] [Medline: 32749874]
5. Lisi AJ, Salsbury SA, Hawk C, et al. Chiropractic integrated care pathway for low back pain in veterans: results of a delphi consensus process. J Manipulative Physiol Ther 2018 Feb;41(2):137-148. [doi: 10.1016/j.jmpt.2017.10.001] [Medline: 29482827]
6. Vassar M, Holzmann M. The retrospective chart review: important methodological considerations. J Educ Eval Health Prof 2013;10(12):12. [doi: 10.3352/jeehp.2013.10.12] [Medline: 24324853]
7. Military Construction, Veterans Affairs, and Related Agencies Appropriations Act, HR 2998, 115th Cong (2018). URL: https://www.congress.gov/bill/115th-congress/house-bill/2998/text [accessed 2025-03-31]
8. VA Directive 2018-1210 - Chiropractic Care. : United States Department of Veterans Affairs; 2018.
9. Ohno-Machado L. Realizing the full potential of electronic health records: the role of natural language processing. J Am Med Inform Assoc 2011;18(5):539. [doi: 10.1136/amiajnl-2011-000501] [Medline: 21846784]
10. Luther SL, Finch DK, Bouayad L, et al. Measuring pain care quality in the Veterans Health Administration primary care setting. Pain 2022 Jun 1;163(6):e715-e724. [doi: 10.1097/j.pain.0000000000002477] [Medline: 34724683]
11. Coleman B, Finch D, Wang R, et al. Extracting pain care quality indicators from U.S. Veterans Health Administration chiropractic care using natural language processing. Appl Clin Inform 2023 May;14(3):600-608. [doi: 10.1055/a-2091-1162] [Medline: 37164327]
12. Laurentiev J, Kim DH, Mahesri M, et al. Identifying functional status impairment in people living with dementia through natural language processing of clinical documents: cross-sectional study. J Med Internet Res 2024 Feb 13;26:e47739. [doi: 10.2196/47739] [Medline: 38349732]
13. Sim JA, Huang X, Horan MR, Baker JN, Huang IC. Using natural language processing to analyze unstructured patient-reported outcomes data derived from electronic health records for cancer populations: a systematic review. Expert Rev Pharmacoecon Outcomes Res 2024 Apr;24(4):467-475. [doi: 10.1080/14737167.2024.2322664] [Medline: 38383308]
14. Poulsen MN, Freda PJ, Troiani V, Mowery DL. Developing a framework to infer opioid use disorder severity from clinical notes to inform natural language processing methods: characterization study. JMIR Ment Health 2024 Jan 15;11(1):e53366. [doi: 10.2196/53366] [Medline: 38224481]
15. Afshar M, Adelaine S, Resnik F, et al. Deployment of real-time natural language processing and deep learning clinical decision support in the electronic health record: pipeline implementation for an opioid misuse screener in hospitalized adults. JMIR Med Inform 2023 Apr 20;11(1):e44977. [doi: 10.2196/44977] [Medline: 37079367]
16. Wals Zurita AJ, Miras del Rio H, Ugarte Ruiz de Aguirre N, et al. The transformative potential of large language models in mining electronic health records data: content analysis. JMIR Med Inform 2025 Jan 2;13(1):e58457. [doi: 10.2196/58457]
17. Goulet JL, Kerns RD, Bair M, et al. The musculoskeletal diagnosis cohort: examining pain and pain care among veterans. Pain 2016 Aug;157(8):1696-1703. [doi: 10.1097/j.pain.0000000000000567] [Medline: 27023420]

XSL•FO
RenderX

18. Luo W, Phung D, Tran T, et al. Guidelines for developing and reporting machine learning predictive models in biomedical research: a multidisciplinary view. J Med Internet Res 2016 Dec 16;18(12):e323. [doi: 10.2196/jmir.5870] [Medline: 27986644]
19. Fu S, Wang L, Moon S, et al. Recommended practices and ethical considerations for natural language processing-assisted observational research: a scoping review. Clin Transl Sci 2023 Mar;16(3):398-411. [doi: 10.1111/cts.13463] [Medline: 36478394]
20. South B, Shen S, Leng J, Forbush T, DuVall S, Chapman W. A prototype tool set to support machine-assisted annotation. In: Cohen KB, Demner-Fushman D, Ananiadou S, Webber B, Tsujii J, Pestian J, editors. Presented at: BioNLP: Proceedings of the 2012 Workshop on Biomedical Natural Language Processing Montréal; Jun 8, 2012; Montréal, Canada.
21. Krebs EE, Carey TS, Weinberger M. Accuracy of the pain numeric rating scale as a screening test in primary care. J Gen Intern Med 2007 Oct;22(10):1453-1458. [doi: 10.1007/s11606-007-0321-2] [Medline: 17668269]
22. de Williams AC, Davies HTO, Chadury Y. Simple pain rating scales hide complex idiosyncratic meanings. Pain 2000 Apr;85(3):457-463. [doi: 10.1016/S0304-3959(99)00299-7] [Medline: 10781919]
23. Huber A, Suman AL, Rendo CA, Biasi G, Marcolongo R, Carli G. Dimensions of “unidimensional” ratings of pain and emotions in patients with chronic musculoskeletal pain. Pain 2007 Aug;130(3):216-224. [doi: 10.1016/j.pain.2006.11.014] [Medline: 17240067]
24. Eyre H, Chapman AB, Peterson KS, et al. Launching into clinical space with medspaCy: a new clinical text processing toolkit in Python. AMIA Annu Symp Proc 2021;2021(438–447):438-447. [Medline: 35308962]
25. Honnibal M, Montani I, Landeghem S, Boyd A. spaCy: industrial-strength natural language processing in Python. 2020. URL: https://spacy.io [accessed 2024-08-02]
26. BCColemanVA/OutcomeMeasure-NLP. GitHub. URL: https://github.com/BCColemanVA/OutcomeMeasure-NLP [accessed 2024-09-13]
27. Himelfarb I, Hyland JK, Ouzts NE, et al. Practice analysis of chiropractic 2020: a project report, survey analysis, and summary of the practice of chiropractic within the United States. National Board of Chiropractic Examiners. 2020. URL: https://www.nbce.org/wp-content/uploads/2020-Practice-Analysis-of-Chiropractic-2020-3.pdf [accessed 2025-01-29]
28. Holmes MM, Bishop FL, Newell D, Field J, Lewith G. Chiropractors’ views on the use of patient-reported outcome measures in clinical practice: a qualitative study. Chiropr Man Therap 2018;26(1):50. [doi: 10.1186/s12998-018-0219-6] [Medline: 30568787]
29. Corcoran KL, Peterson DR, Zhao X, Moran EA, Lisi AJ. Characteristics and productivity of the chiropractic workforce of the Veterans Health Administration. Chiropr Man Therap 2022 Apr 11;30(1):18. [doi: 10.1186/s12998-022-00429-1] [Medline: 35410303]
30. Burdick R, Corcoran KL, Zhao X, Lisi A. The rate of use of Veterans Affairs chiropractic care: a 5-year analysis. Chiropr Man Therap 2022 Jan 21;30(1):4. [doi: 10.1186/s12998-022-00413-9] [Medline: 35062971]
31. Roytman GR, Coleman BC, Corcoran KL, Goertz CM, Long CR, Lisi AJ. Changes in the use of telehealth and face-to-face chiropractic care in the Department of Veterans Affairs before and after the COVID-19 pandemic. J Manipulative Physiol Ther 2021 Sep;44(7):584-590. [doi: 10.1016/j.jmpt.2021.12.002] [Medline: 35249749]
32. Tamang S, Humbert-Droz M, Gianfrancesco M, Izadi Z, Schmajuk G, Yazdany J. Practical considerations for developing clinical natural language processing systems for population health management and measurement. JMIR Med Inform 2023 Jan 3;11(1):e37805. [doi: 10.2196/37805] [Medline: 36595345]

Abbreviations

AUC-ROC: area under the receiver operator characteristic curve
BOW: bag-of-words
EHR: electronic health record
FY: fiscal year
IAA: interannotator agreement
***ICD-10*:** *International Classification of Diseases, 10th Revision*
MSD/CIH: Musculoskeletal Diagnosis/Complementary and Integrative Health
NLP: natural language processing
PROM: patient-reported outcome measure
VHA: Veterans Health Administration

XSL•FO
RenderX

Edited by C Lovis; submitted 13.09.24; peer-reviewed by D Chrimes, M Malhotra, Z Hou; revised version received 11.03.25; accepted 15.03.25; published 02.04.25.

Please cite as:
Coleman BC, Corcoran KL, Brandt CA, Goulet JL, Luther SL, Lisi AJ
Identifying Patient-Reported Outcome Measure Documentation in Veterans Health Administration Chiropractic Clinic Notes: Natural Language Processing Analysis
JMIR Med Inform 2025;13:e66466
URL: https://medinform.jmir.org/2025/1/e66466
doi:10.2196/66466

© Brian C Coleman, Kelsey L Corcoran, Cynthia A Brandt, Joseph L Goulet, Stephen L Luther, Anthony J Lisi. Originally published in JMIR Medical Informatics (https://medinform.jmir.org), 2.4.2025. This is an open-access article distributed under the terms of the Creative Commons Attribution License (https://creativecommons.org/licenses/by/4.0/), which permits unrestricted use, distribution, and reproduction in any medium, provided the original work, first published in JMIR Medical Informatics, is properly cited. The complete bibliographic information, a link to the original publication on https://medinform.jmir.org/, as well as this copyright and license information must be included.

XSL•FO
RenderX

Original Paper

Performance Improvement of a Natural Language Processing Tool for Extracting Patient Narratives Related to Medical States From Japanese Pharmaceutical Care Records by Increasing the Amount of Training Data: Natural Language Processing Analysis and Validation Study

Yukiko Ohno[1], BSc; Tohru Aomori[2], PhD; Tomohiro Nishiyama[3], MEng; Riri Kato[4], BSc; Reina Fujiki[5], BSc; Haruki Ishikawa[5], MSc; Keisuke Kiyomiya[4], PhD; Minae Isawa[4], PhD; Mayumi Mochizuki[4], PhD; Eiji Aramaki[3], PhD; Hisakazu Ohtani[1,5,6], PhD

[1]Graduate School of Pharmaceutical Sciences, Keio University, Tokyo, Japan

[2]Faculty of Pharmacy, Takasaki University of Health and Welfare, Takasaki, Japan

[3]Nara Institute of Science and Technology, Ikoma, Japan

[4]Faculty of Pharmacy, Keio University, Tokyo, Japan

[5]Department of Pharmacy, Keio University Hospital, Tokyo, Japan

[6]School of Medicine, Keio University, Tokyo, Japan

Corresponding Author:
Hisakazu Ohtani, PhD
Graduate School of Pharmaceutical Sciences
Keio University
1-5-30, Shibakouen, Minato
Tokyo, 105-8512
Japan
Phone: 81 3 5400 2486
Email: ohtani@keio.jp

Abstract

Background: Patients' oral expressions serve as valuable sources of clinical information to improve pharmacotherapy. Natural language processing (NLP) is a useful approach for analyzing unstructured text data, such as patient narratives. However, few studies have focused on using NLP for narratives in the Japanese language.

Objective: We aimed to develop a high-performance NLP system for extracting clinical information from patient narratives by examining the performance progression with a gradual increase in the amount of training data.

Methods: We used subjective texts from the pharmaceutical care records of Keio University Hospital from April 1, 2018, to March 31, 2019, comprising 12,004 records from 6559 cases. After preprocessing, we annotated diseases and symptoms within the texts. We then trained and evaluated a deep learning model (bidirectional encoder representations from transformers combined with a conditional random field [BERT-CRF]) through 10-fold cross-validation. The annotated data were divided into 10 subsets, and the amount of training data was progressively increased over 10 steps. We also analyzed the causes of errors. Finally, we applied the developed system to the analysis of case report texts to evaluate its usability for texts from other sources.

Results: The F_1-score of the system improved from 0.67 to 0.82 as the amount of training data increased from 1200 to 12,004 records. The F_1-score reached 0.78 with 3600 records and was largely similar thereafter. As performance improved, errors from incorrect extractions decreased significantly, which resulted in an increase in precision. For case reports, the F_1-score also increased from 0.34 to 0.41 as the training dataset expanded from 1200 to 12,004 records. Performance was lower for extracting symptoms from case report texts compared with pharmaceutical care records, suggesting that this system is more specialized for analyzing subjective data from pharmaceutical care records.

XSL•FO
RenderX

Conclusions: We successfully developed a high-performance system specialized in analyzing subjective data from pharmaceutical care records by training a large dataset, with near-complete saturation of system performance with about 3600 training records. This system will be useful for monitoring symptoms, offering benefits for both clinical practice and research.

(JMIR Med Inform 2025;13:e68863) doi:10.2196/68863

KEYWORDS

natural language processing; NLP; named entity recognition; NER; deep learning; pharmaceutical care record; electronic medical record; EMR; Japanese

Introduction

In clinical settings, information, such as changes in a patient's condition and the occurrence of adverse events, is essential for providing optimal pharmaceutical care. However, physicians commonly underestimate or underreport symptoms expressed by patients themselves [1,2]. For example, a clinical study involving patients with advanced non–small cell lung cancer showed that physicians underreported grade 2 skin toxicity and fatigue and all grades of diarrhea compared with patients, with only a few grade 3 and grade 4 adverse events reported [2]. In contrast, patient self-reports, including patient questionnaires and the PRO-CTCAE (patient-reported outcomes version of the Common Terminology Criteria for Adverse Events) Measurement System, are considered useful and are increasingly used in cross-sectional surveys of adverse events [3-5]. Therefore, the clinical information contained in a patient's self-report can be used, when appropriately identified, to prevent an underestimation of patient symptoms.

Unlike structured databases, such as the Japanese Adverse Drug Reaction Report Database, text data, such as patient narratives, comprising natural language, are often unstructured and ambiguous in meaning. To enable computers to handle and analyze natural languages, appropriate natural language processing (NLP) technology is necessary. For example, named entity recognition (NER) technology can be used to extract disease and symptom names from natural language text and determine whether the extracted terms are positively or negatively expressed (positive-negative classification). NER is expected to be useful for analyzing symptoms, as in adverse event monitoring. NER has been applied to data from social media platforms to investigate patient outcomes related to post–COVID-19 conditions [6] and to assess the frequency of adverse drug reactions [7].

Patient narratives are accumulated in pharmacist records as well as posts on social media platforms. Because pharmacists routinely assess the efficacy and safety of pharmacotherapy, their records contain a large amount of patient information regarding adverse drug events. Pharmacist records are often structured using the SOAP format: subjective data (S), objective data (O), assessment (A), and plan (P). The subjective data in the SOAP format contain the patients' raw words. Therefore, the subjective data in pharmacist records could serve as a rich source of patient narratives related to adverse events.

As mentioned above, some investigations have been conducted to extract information, such as diseases and symptoms, from text data. For example, Nikfarjam et al [7] developed a neural network–based system to extract adverse drug events from patient postings on social health networks in English. Similarly, Batbaatar et al [8] employed deep learning methods to extract not only diseases and symptoms but also pharmacological substances and other health-related information from social media service posts in English. However, most NER research has focused on physician records [9-11] or data in English [6-8,12-18], with few studies targeting Japanese pharmacist records.

In a study focusing on Japanese pharmacist records, Usui et al [19] developed a rule-based system to extract patient complaints from the electronic medication records of Japanese community pharmacies and standardize them using International Statistical Classification of Diseases and Related Health Problems 10th Revision (ICD-10) codes. However, the rule-based system could not handle patient words not appearing in its predefined list of rules. Therefore, we hypothesized that a deep learning model could extract diseases and symptoms from the text more accurately than the rule-based system of Usui et al [19].

A system has already been developed to target physician records based on a deep learning model, bidirectional encoder representations from transformers (BERT)–conditional random field (CRF). BERT is an effective NLP model that can be fine-tuned for a variety of tasks [20]. In addition, several studies have reported that BERT-CRF [21,22], which adds a CRF layer to the output, performs well in the NER task. We previously examined whether the current system could be adapted to pharmaceutical care records without modification [23]. The system showed relatively high performance for the assessment data from pharmaceutical care records written in SOAP format. However, the performance of the system was inadequate for subjective data, objective data, and the plan. Furthermore, taking into account the importance of subjective data in adverse event analysis, it was determined that the system needed to be trained using subjective data.

In this study, we aimed to develop a new NLP system to accurately extract disease and symptom names (disease name extraction) from patients' subjective data and determine whether these conditions are affirmed or denied (ie, present or absent). In addition, it is generally accepted that system performance improves with the amount of training data used. However, case reports and physician summaries, in which more research has been conducted than patient narratives, are organized in physicians' own words. On the other hand, patients' narratives are freely worded and nonorganized. Therefore, it is important to know how the system's performance changes as the training amount increases when targeting such unorganized data. Furthermore, from an annotation cost perspective, annotation

XSL•FO
RenderX

of medical documents requires more cost and effort due to its highly specialized and complicated nature. Therefore, resources can be distributed efficiently by predicting the approximate amount of annotation with a high learning effect. Thus, we also investigated how the system performance changed as the amount of training data increased.

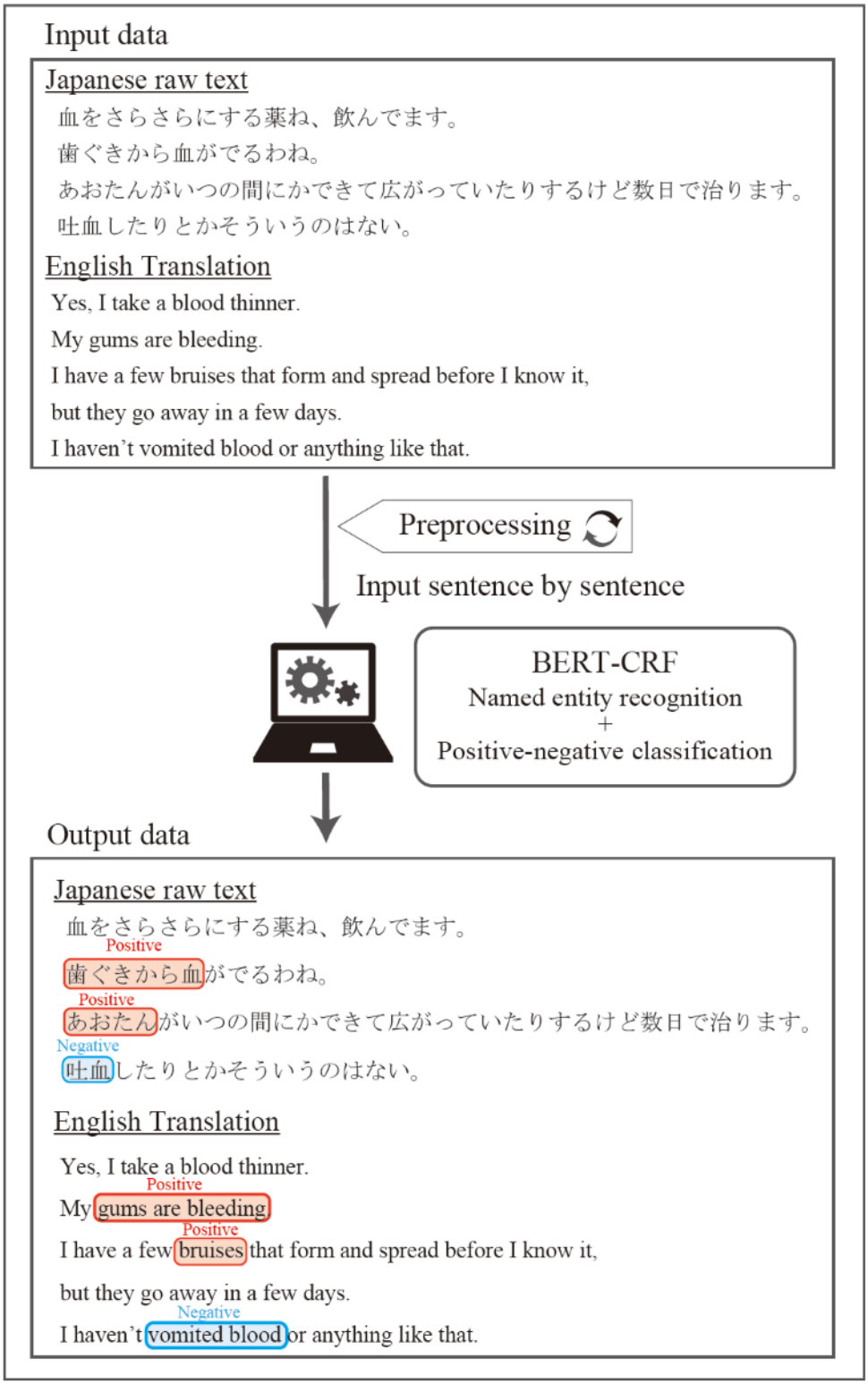
Methods

Overview

We aimed to develop a system that extracts disease names from patients' subjective texts and determines whether the conditions are affirmed or denied in the sentence (Figure 1). The input was processed sentence by sentence. To develop and evaluate the system, this study included 5 parts: training data preparation, model training, evaluation, error analysis, and evaluation of the usability of the system for case reports (Figure 2).

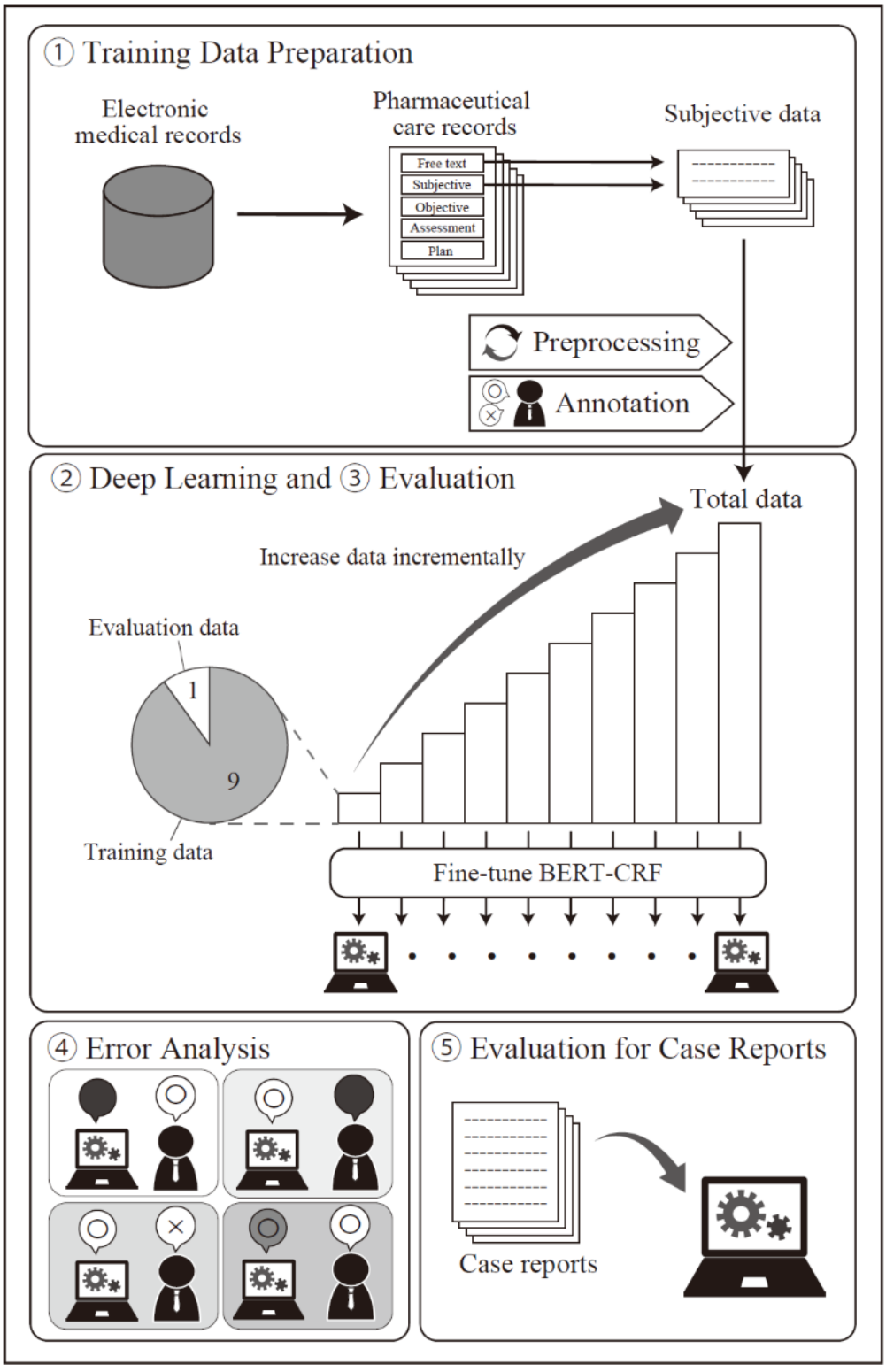
XSL•FO
RenderX

Figure 1. Conceptual diagram of the disease-name extraction system operation. After inputting preprocessed text data into the system sentence by sentence, the system extracts diseases and symptoms as outputs and predicts the presence or absence of each finding. BERT: bidirectional encoder representations from transformers; CRF: conditional random field.



XSL•FO
RenderX

Figure 2. Overview of this study. Subjective data were collected from pharmaceutical care records in the electronic medical record system. Data were preprocessed, and diseases and symptoms in the data were annotated to prepare the training data. A disease-name extraction system was developed, and its performance was evaluated through 10-fold cross-validation with progressive increases in the amount of training data over 10 steps. Errors that occurred during the performance evaluation were sampled, and the causes of the errors were analyzed. The developed system was applied to case reports, and its performance for case reports was investigated. BERT: bidirectional encoder representations from transformers; CRF: conditional random field.



In the training data preparation, subjective texts were preprocessed and annotated. In the deep learning part, a disease-name extraction system was constructed based on a deep learning model by increasing the amount of training data in 10 steps. In the evaluation part, cross-validation was used to evaluate performance at the same time as training. We sampled the evaluation results and classified the causes of errors in the error analysis part. In the evaluation of the usability of the system for case reports, we evaluated the performance of the developed system when applied to case reports. Each step has been described in the following sections.

XSL•FO
RenderX

Training Data Preparation

The pharmaceutical care records in the electronic medical record system of Keio University Hospital, written by pharmacists in Japanese, were used as the source of training data. These records comprise 5 columns: subjective, objective, assessment, plan, and free text. In some cases, SOAP-formatted sentences are included in the free-text column. In this study, we collected 12,004 subjective data records from 6559 cases in the subjective and free-text columns described from April 1, 2018, to March 31, 2019.

All text data in the pharmaceutical care records were converted to full-width (2-byte) characters. Line breaks or periods were used as sentence separators, and spaces at the beginning and end of sentences, as well as blank lines, were deleted. Additionally, the string "_X000D_," indicating a line break, was removed. Two researchers independently annotated 400 records based on the annotation criteria described in the following paragraph. A comparison between their annotations obtained a high κ coefficient (κ coefficient=0.92), indicating almost perfect agreement. Therefore, the remaining data were annotated by a single researcher.

The annotation criteria were originally developed by our group to collect information for adverse event monitoring in clinical practice and epidemiological studies. Patient expressions related to diseases or symptoms, including nouns, verbs, adjectives, and adverbs, were extracted. The time of onset, site, severity, and triggers of symptoms were also extracted when they were described near the clinical findings. Numerical information was excluded because such data should be obtained from the structured electronic medical record database rather than text data. However, if the text verbally referred to changes in laboratory values, such as "increase in blood pressure," it was extracted as a target. Texts referring to normal renal function, liver function, blood electrolyte levels, appetite, sleep, and bowel movements were interpreted as negative references to abnormalities (ie, denial of symptoms) and were included in the extraction.

Deep Learning Method

In this study, we used BERT-CRF as a deep learning method. Several pretrained Japanese BERT models have been developed and published. In this study, we used the character-based BERT of Tohoku University, which is the most commonly used pretrained BERT model for Japanese. BERTJapaneseTokenizer [24], which uses MeCab as a morphological analyzer, was used as a tokenizer. Fine-tuning was performed with a batch size of 32 and with 10-fold cross-validation. In the 10-fold cross-validation, data were shuffled by sentence and then split into 10 groups (folds). The amount of training data was increased in 10 steps from 1200 to 12,004 records.

Evaluation

Precision, recall, and F_1-score were used as indices for performance evaluation. Precision was calculated as follows: number of true positives/number of true positives and false positives. Recall was calculated as follows: number of true positives/number of true positives and false negatives. F_1-score was calculated as follows: 2 × precision × recall/(precision + recall).

The final accuracy was calculated with the cross-validation method. The number of epochs was determined based on the F_1-scores obtained during cross-validation. We also investigated the performance by taking partial matches into consideration, as partially matched terms can still convey valuable clinical information. The Levenshtein distance [25] was used as the criterion for partial matches. The Levenshtein distance measures the resemblance between 2 strings (W1 and W2) and is defined as the minimum number of character deletion, insertion, and replacement operations required to convert one string into the other. Similarity was calculated using the following formula: similarity (W1, W2) = {max (|W1|, |W2|) − Levenshtein distance}/max (|W1|, |W2|), where |Wn| represents the number of characters (length) of Wn. Similarity values ranged from 0 to 1. We sampled the results of the cross-validation to list the partial matches and investigated any failures to extract essential terms that were correctly detected by researchers due to partial matches. Detailed results of this survey are provided in Multimedia Appendix 1. In this survey, the number of incomplete extractions without essential terms increased rapidly when the similarity was below 0.667. Of the 63 extracted terms with a similarity of 0.667 or higher, 4 terms had partially or entirely missing essential terms. However, at the next lowest similarity levels of 0.636 and 0.625, 5 of 9 extracted terms had partially or entirely missing essential terms. Therefore, in this study, "the number of matches, including partial matches" was defined as the sum of the number of complete matches and partial matches with a similarity of 0.66 or greater. In the error analysis, "partial matches with a lower similarity," described in the next section, were defined as partial matches with a similarity of less than 0.66. During the process of information processing in BERT, infrequent characters were converted to unknown keys ([UNK]). Because the data that we used to evaluate partial matches contained [UNK], we converted all [UNK] into full-width asterisks to calculate the similarity of the Levenshtein distances by regarding them as single characters.

Error Analysis

For 5 steps of the amount of training data, the results of the system were compared with the annotated diseases and symptoms in the validation data, and the causes of mismatches were classified into 4 categories (Table 1): error 1, failure of the system to extract; error 2, incorrect extraction by the system; error 3, difference in positive-negative classification; and error 4, partial matches with low similarity. Because the amount of data contained in 1 fold was different for each training amount, we used the number of folds that contained close to 1200 records: 10 folds, 3 folds, 2 folds, 1 fold, and 1 fold in the training data of 1200, 3600, 6002, 8402, and 12,004 records, respectively. The choice of which fold of the validation data to use for this analysis was based on the proximity of the F_1-score to the average rates when they were used in the evaluation. In this study, we defined the total number of extractions by the following formula: total number of extractions = number of researchers' extractions + number of system extractions − (number of exact matches + number of partial matches with a

XSL•FO
RenderX

similarity of 0.66 or greater). The error rate was given as the ratio of the number of errors to the total number of extractions: error rate (%) = number of errors × 100/total number of extractions.

Table 1. Definitions of error cause categories.

P-N[a] classification	Named entity recognition			
	Exact match	Partial match		Unmatch
		1>similarity>0.66	0.66>similarity>0	
Match	Exact match	Partial match	Error 4[b]	Error 1[c]/2[d]
Unmatch	Error 3[e]	Error 3[e]	Error 1[c]/2[d]	Error 1[c]/2[d]

[a]P-N: positive-negative.

[b]Error 4: partial matches with low similarity.

[c]Error 1: system extraction failure.

[d]Error 2: incorrect extraction by the system.

[e]Error 3: difference in the P-N classification.

In cases where the number of extracted terms differed between the researchers and the system, the number of errors was counted for the larger number. For example, when one extracted 2 symptoms and the other extracted them as a single (long-named) symptom, we counted them as 2 errors. Therefore, the sum of the error rate and the correct answer rate could exceed 100%. We further investigated changes in the error rates of the 4 categories with an increase in the amount of training data. For error categories with a greater increase in variation of the error rate obtained by the following formula, a detailed descriptive error analysis was performed: variation of error rates (%) = error rates after increasing training amount/error rates before increasing training amount × 100.

When the error rate before increasing the training amount was 0% and the error rate after increasing the training amount was greater than 0%, the variation of error rates was regarded as 100%.

Evaluation for Case Reports

To evaluate whether the developed system can be applied to other types of texts, we assessed the system performance using Japanese case report data. A series of 148 case reports was collected as validation data from the Real-MedNLP Test Collection. These data were distributed in the Real-MedNLP Test Collection and permitted for redistribution by the respective journal publisher [10]. These reports are available as open access through the "Japan Science and Technology Information Aggregator, Electronic," an electronic journal platform operated by the Japan Science and Technology Agency.

Case report validation data were also preprocessed and annotated in the same manner as the training data. Two researchers independently annotated 15 cases, approximately 10% of the total cases. Because the agreement between their annotations was almost perfect, with a κ coefficient of 0.93, the remainder was annotated by a single researcher. The validation data were applied to the 10 systems that were developed in the 10-fold cross-validation of each training amount to evaluate performance. The individual performances of the 10 systems were averaged and regarded as the performance of the system for each training amount.

Ethical Considerations

This study was conducted with the approval of the Keio University School of Medicine Ethics Committee (approval number: 20200067).

An opt-out method was used to ensure that study subjects had the opportunity to refuse the use of their information, since obtaining informed consent was difficult due to the large number of subjects and the fact that many of them had already been discharged from the hospital and had no direct contact with the hospital. Information on the research has been disclosed on the website of the Clinical Translational Research Center, Keio University Hospital.

Each subject's electronic medical record information was assigned a dummy ID at the time of registration, and information was managed through pseudonymization using dummy IDs.

Results

Training Data Features

12,004 subjective data in the pharmaceutical care records used as training data contained 43,553 sentences. These records included 12,287 affirmed diseases and symptoms and 8822 denied diseases and symptoms.

Evaluation

The training curves for precision, recall, and F_1-score values for exact matches are shown in Figure 3. As the training data increased from 1200 to 12,004 records, precision, recall, and F_1-score improved from 0.66 to 0.81, from 0.69 to 0.83, and from 0.67 to 0.82, respectively. A power approximation expression for the F_1-score of exact matches yielded the equation: $y = 0.40x^{0.08}$, predicting an F_1-score of 0.90 with 25,251 training records. Performance improvement saturated after training with 3600 records, indicating that a large amount of training data is needed to improve the F_1-score beyond 0.78. Comparing the F_1-scores for exact matches and those including partial matches, the performance gap tended to diminish as the amount of training data increased (Figure 4). The system trained

XSL•FO
RenderX

with 12,004 records achieved an F_1-score of 0.82 for exact matches and 0.84 when partial matches were included.

Figure 3. Training curve during cross-validation (only exact matches). Trends in the mean precision, recall, and F1-score values are shown from 1200- to 12,004-record trainings.

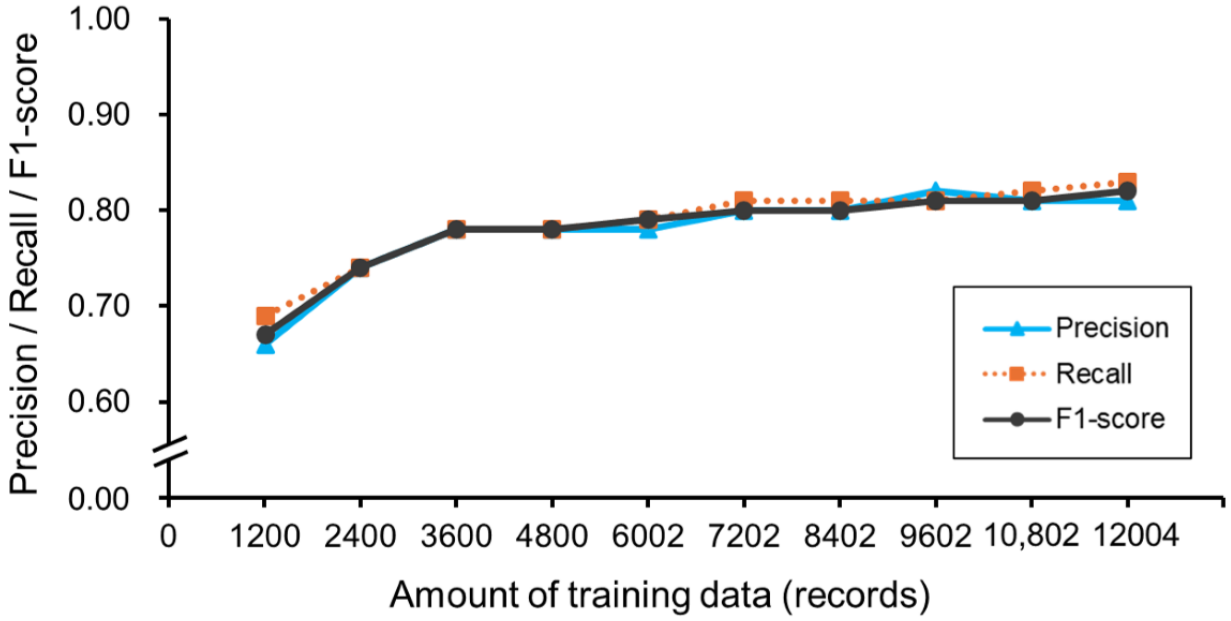
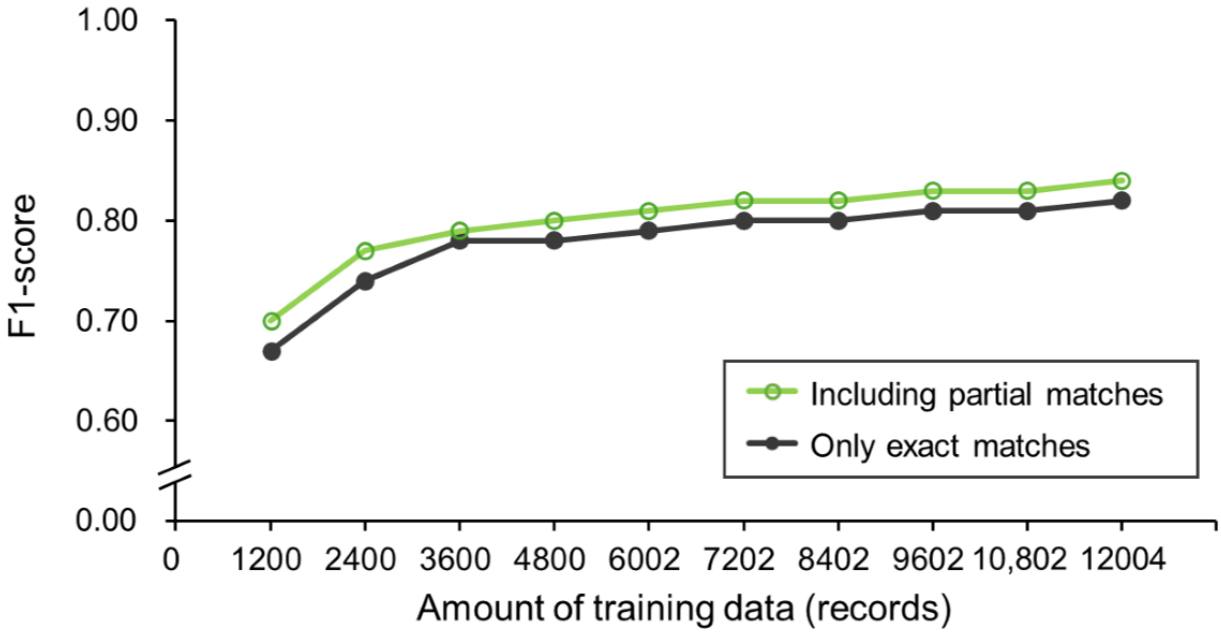


Figure 4. Training curve of the F1-scores during cross-validation (only exact matches/including partial matches). Trends in the mean F1-scores in which only exact matches were considered matches and in the mean F1-scores in which partial matches were included as matches are shown from 1200- to 12,004-record trainings.



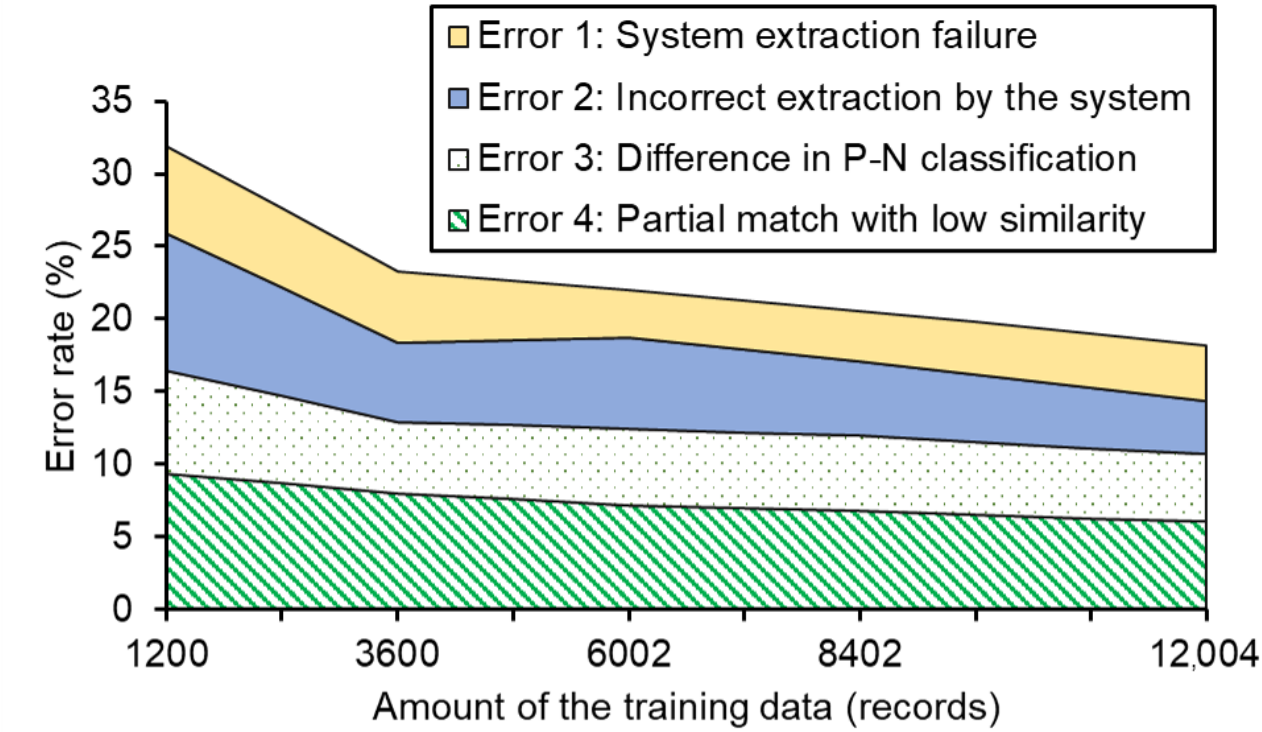
Error Analysis

Error analysis was carried out for 4395, 3924, 4396, 3071, and 4356 sentences from the validation data during cross-validation using 1200, 3600, 6002, 8402, and 12,004 records, respectively. The causes of errors were classified, and Figure 5 shows the transition of error rates for each cause. The overall error rate decreased from 31.9% (945/2963) to 18.2% (444/2446). The rate of error 2 (incorrect extraction by the system) showed the most significant decrease with an increase in the training records, followed by errors 4, 3, and 1. Error 2 decreased from 9.4% (280/2963) to 3.7% (90/2446) (–5.7 percentage points). Errors 4, 3, and 1 decreased from 9.4% (278/2963) to 6.1% (148/2446) (–3.3 percentage points), from 7.1% (209/2963) to 4.7% (114/2446) (–2.4 percentage points), and from 6.0% (178/2963) to 3.8% (92/2446) (–2.2 percentage points), respectively. Error 4 was the primary cause of error for the system trained with 12,004 records, followed by errors 3, 1, and

XSL•FO
RenderX

2. The 3600-record training when performance reached a plateau was used as a reference point. Comparing the variation in the error rates associated with the increase in the training amount from 1200 to 3600 records to the variation in the error rates associated with the increase in the training amount from 3600 to 12,004 records, the variation for errors 1 and 4 decreased by 9 percentage points and 5 percentage points, respectively, while the variation for errors 2 and 3 increased by 24 percentage points and 10 percentage points, respectively, indicating that improvement was stagnant. Therefore, we categorized errors 2 and 3 into subcategories and investigated the difference in the variation in error rates before and after the 3600-record training.

Figure 5. Trends in error rates for each error cause category. A sample study of performance evaluation results was conducted from 1200- to 12,004-record trainings. The errors are classified into 4 cause categories, and trends in error rates for each category are shown. P-N: positive-negative.



Error 2 was further classified into 7 subgroups (Table 2). The most common errors in the 1200-record training involved error 2a (the extraction of information that was neither symptoms nor supplemental information related to symptoms). This subcategory encompassed a wide variety of patient expressions, including behaviors, such as “strained in the bathroom,” indications of healthiness, such as “my blood pressure has been quite good,” and medication-related issues unrelated to patient symptoms, such as “the remaining number (of medications) became limited.” The second most common subcategory, error 2b (incomplete extraction without essential terms), involved errors in extracting terms that were not considered symptoms due to the absence of a subject, such as “loose” or “didn’t go well with me.” It also included cases where only supplemental words were extracted, such as “at night” or “very much.” The third most common subcategory, error 2c, involved errors related to the extraction of conditional terms that were annotated or not annotated by researchers depending on the context or were not finally annotated after the researcher was faced with a difficult decision. For example, researchers would annotate the patient expression “I couldn’t eat” as it indicates a symptom of the loss of appetite, while the expression “I couldn’t eat because I was too sleepy” would not be attributed to appetite. In addition, the expression “my stomach went like this” may have been regarded as a symptom because it represented an abnormal condition. However, the researchers finally decided not to annotate it. The next most common error subcategories were errors 2d and 2e (partial matches with low similarity and an incorrect positive-negative classification), which involved either entire or partial extraction of essential terms.

XSL•FO
RenderX

Table 2. Number of errors and the ratio of errors to total extraction in the subcategories of error 2.

Subgroup	Number of errors in 1200-record training (n=2963), n (%)	Number of errors in 3600-record training (n=2387), n (%)	Number of errors in 12,004-record training (n=2446), n (%)
Total errors of category 2	280 (9.4)	130 (5.4)	90 (3.7)
Error 2a: Extraction of information that was neither symptoms nor supplemental information	86 (2.9)	32 (1.3)	12 (0.5)
Error 2b: Incomplete extraction without essential terms	76 (2.6)	27 (1.1)	16 (0.7)
Error 2c: Extraction of conditional terms that were annotated or not by researchers depending on the context or were not finally annotated after the researcher was faced with a difficult decision	55 (1.9)	47 (2.0)	32 (1.3)
Error 2d: Partial matches with low similarity and incorrect P-N[a] classifications that involved entire extractions of essential terms	35 (1.2)	15 (0.6)	12 (0.5)
Error 2e: Partial matches with low similarity and incorrect P-N classifications that involved partial extractions of essential terms or incomplete extractions without essential terms	19 (0.6)	2 (0.08)	3 (0.1)
Error 2f: Symptoms that the researchers forgot to extract	7 (0.2)	6 (0.3)	12 (0.5)
Error 2g: Partial matches with low similarity involving entire extractions of symptoms for which the researchers made incorrect P-N classifications	2 (0.1)	1 (0.04)	3 (0.1)

[a]P-N: positive-negative.

From 1200- to 12,004-record trainings, significant improvements were observed in the following order: “extraction of information that was neither symptoms nor supplemental information (error 2a),” “incomplete extraction without essential terms (error 2b),” and “partial matches with low similarity and incorrect positive-negative classifications that involved entire extractions of essential terms (error 2d).” In contrast, “symptoms that the researchers forgot to extract (error 2f)” and “partial matches with low similarity involving entire extractions of symptoms for which the researchers made incorrect positive-negative classifications (error 2g)” increased from 0.2% (7/2963) to 0.5% (12/2446) and from 0.1% (2/2963) to 0.1% (3/2446), respectively. However, other subgroups showed overall improvements.

The differences in the variation of each subcategory before and after the 3600 cases were large in the following order: “partial matches with low similarity involving entire extractions of symptoms for which the researchers made incorrect positive-negative classifications (error 2g)” (231 percentage points), “partial matches with low similarity and incorrect positive-negative classifications that involved partial extractions of essential terms or incomplete extractions without essential terms (error 2e)” (133 percentage points), “symptoms that the researchers forgot to extract (error 2f)” (89 percentage points), “partial matches with low similarity and incorrect positive-negative classifications that involved entire extractions of essential terms (error 2d)” (25 percentage points), “incomplete extraction without essential terms (error 2b)” (14 percentage points), “extraction of information that was neither symptoms nor supplemental information (error 2a)” (–10 percentage points), and “extraction of conditional terms that were annotated or not by researchers depending on the context or were not finally annotated after the researcher was faced with a difficult decision (error 2c)” (–40 percentage points). A larger difference in the variation indicates a relative stagnation in the improvement of errors on increasing the training amount beyond 3600 records.

Error 3 was classified into 5 subcategories (Multimedia Appendix 2). The top 3 subcategories with the largest differences in variation before and after the 3600-record training in each subcategory were as follows: “determined from positive expressions (error 3b)” (125 percentage points), “determined from negative expressions (error 3c)” (64 percentage points), and “determined from other information (error 3a)” (–8.4 percentage points).

The contents of errors 3b and 3c, which showed particularly large differences in variation rates, were classified into further subcategories based on 2 points: the position of the positive-negative expression and the way in which the positive-negative expression was stated (Multimedia Appendix 3 and 4). Based on the method focusing on the position and the way of positive-negative expressions, we classified them into 5 and 6 subcategories, respectively. The differences in the variation before and after the 3600-record training in the subcategories focusing on the position of positive-negative expressions were large in this order: “more than three words are in between from the extracted terms (error 3bc-1-4)” (369 percentage points), “determination with reference to the positive-negative classification of another extracted term in the same sentence (error 3bc-1-5)” (200 percentage points), “included within the extracted terms (error 3bc-1-2)” (195 percentage points), “one or two words are in between from the

XSL•FO
RenderX

extracted terms (error 3bc-1-3)" (90 percentage points), and "immediately before or/and after the symptom (error 3bc-1-1)" (60 percentage points).

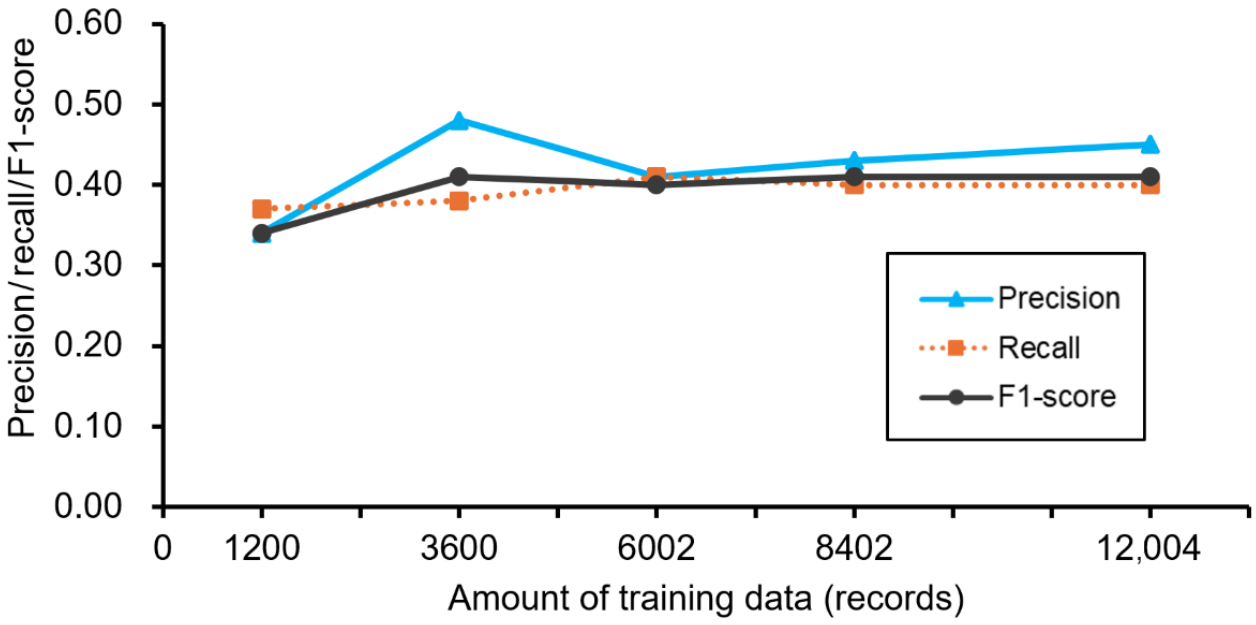
The differences in the variation before and after the 3600-record training in the subcategories focusing on the way of positive-negative expressions were large in this order: "determination with reference to the positive-negative classification of another extracted term in the same sentence (error 3bc-2-5)" (200 percentage points), "reversal of positive-negative classification by partial match (error 3bc-2-6)" (200 percentage points), "included within the extracted terms (error 3bc-2-2)" (157 percentage points), "mild negative expressions (error 3bc-2-3)" (119 percentage points), "simple positive or negative expressions (error 3bc-2-1)" (76 percentage points), and "negated positive or negative expressions (error 3bc-2-4)" (–15 percentage points).

"Error 3bc-1-5 (3bc-2-5): determination with reference to the positive-negative classification of another extracted term in the same sentence" and "error 3bc-2-6: reversal of positive-negative classification by partial match" had an error rate of 0% at the 3600-record training. Therefore, the difference in variability was large, as only one or two errors at the 12,004-record training resulted in 100% variation.

Evaluation of Case Reports

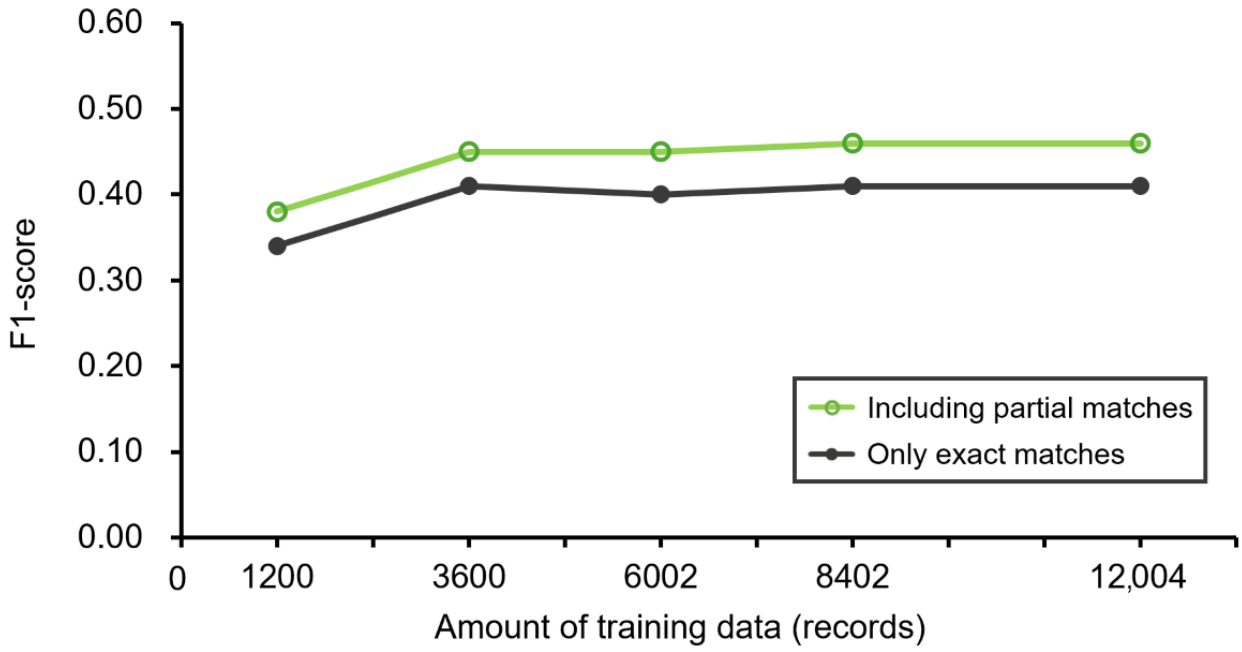
Figure 6 shows the improvement in system performance for the handling of the text data of case reports with an increase in the number of training datasets. The F_1-score increased from 0.34 to 0.41 with an increase in the training dataset and saturated at 3600 records of the training dataset. The differences between the F_1-scores for case reports and those for pharmaceutical care records were 0.33 and 0.41 at 1200 and 12,004 training dataset records, respectively. The differences between the F_1-scores for exact matches and those including partial matches were larger than those at cross-validation. In the performance evaluation for case reports, the F_1-scores for partial matches were always 0.04-0.05 higher than those for exact matches (Figure 7).

Figure 6. Performance of the case report analysis (only exact matches). Case reports were analyzed using systems trained with between 1200 and 12,004 pharmaceutical care records. Trends in the mean precision, recall, and F1-score values, which included only exact matches as matches, are shown.



XSL•FO
RenderX

Figure 7. F1-scores of the case report analysis (only exact matches/including partial matches). Case reports were analyzed using systems trained with between 1200 and 12,004 pharmaceutical care records. Trends in the mean F1-scores in which only exact matches were considered matches and in the mean F1-scores in which partial matches were included as matches are shown.



Discussion

Principal Findings

We developed a disease-name extraction system targeting subjective data in Japanese pharmaceutical care records by fine-tuning BERT-CRF. The performance of the system, evaluated by exact matches with a correct positive-negative classification, improved as the amount of training data increased, even though the system targeted subjective data, which has not been adequately addressed before. A similar trend was observed when evaluated by matches including partial matches, with a similarity score of 0.66 or higher. Although there was a certain number of partial match extractions, the extraction performance with partial matches was close to that for exact matches. This could be attributed to the strict criterion for similarity used in this study. The system performance increased slowly and reached a plateau at the 3600-record training. The results were presumably influenced by a combination of factors, including the deep learning model used (BERT-CRF), the complex annotation criteria, and human error in the annotation, which cannot be determined from this study. To resolve this point and further improve system performance, the use of deep learning models other than BERT-CRF should be considered. In addition, system performance will vary depending on the content of the training data. Therefore, when other training data are used to develop the system, it is difficult to say whether the system performance will reach a plateau with the same training amount in this study. However, by utilizing the characteristics of a gradual curve in performance transition, efficient training can be achieved by increasing the amount of training data step by step from a small amount and using an approximate formula to predict the training amount when performance reaches a plateau.

The analytical performance of the system was lower for case reports than for pharmaceutical care records. When records from different sources were used as training data, the improvement in system performance with increasing training data was inferior to that observed when training with records from the same source type. In addition, the analytical performance gap between text from the same type of training data and that from different types of data persisted, regardless of the amount of training data. In other words, the developed system was not well-suited for analyzing case reports but proved especially useful for analyzing patient narratives when trained on subjective data from pharmaceutical care records. This indicates that separate system development is necessary to analyze different types of records. The difference in performance between the case report analysis and the pharmaceutical care record analysis is assumed to be largely due to the existence of raw patient statements. However, another important feature is the different occupations of the health care professionals who create the records. Physicians create case reports covering the patients' conditions comprehensively and summarizing the patients' backgrounds and disease processes in their own words, while pharmacists mainly monitor drug efficacy and side effects and create pharmaceutical care records. Therefore, pharmacists naturally create SOAP format records that contain a lot of information about adverse events. We would like to emphasize again that our system is likely to be suitable for the collection of adverse event information since the system learned from the subjective data in pharmaceutical care records. Furthermore, since the pharmaceutical care records were written in SOAP format, we were able to selectively collect subjective data and use them for the training data in this study. As a result, a system specialized for subjective data was efficiently developed. This suggests that SOAP-format data may be a useful source for deep learning.

XSL•FO
RenderX

Error analysis revealed that the reduction in error 2 with increased training data was 5.7 percentage points (from 9.4% to 3.7%), a larger decrease than that observed for any other error type. This reduction in false-positive extractions significantly contributed to the improvement in precision. Although we prioritized recall over precision during system development to avoid missing symptoms, the increase in training data led to higher precision without compromising recall. Therefore, we believe that increasing the training data helped to develop a more user-friendly system with fewer false extractions.

Error Analysis

While errors in most subgroups of error 2 decreased, there were increases in error 2f (symptoms that the researchers forgot to extract) and error 2g (partial matches with low similarity involving entire extractions of symptoms for which the researchers made incorrect positive-negative classifications). Researchers may be more prone to making annotation mistakes as the amount of data to be prepared increases and as they encounter a wider variety of expressions. However, the percentage of these errors in total extractions was only 0.3% (9/2963) for the 1200-record training and 0.6% (15/2446) for the 12,004-record training, and thus, their impacts on overall system performance were small. Additionally, the system showed improvements in other types of false positives, indicating that increasing the training data can help to reduce a wide variety of false-positive errors.

Next, we looked at the variation in error rates for error 2. Among errors 2g, 2e, 2f, and 2d, which showed large differences in error rate variation, “partial matches with low similarity involving entire extractions of symptoms for which the researchers made incorrect positive-negative classifications (error 2g)” and “partial matches with low similarity and incorrect positive-negative classifications that involved partial extractions of essential terms or incomplete extractions without essential terms (error 2e)” were almost eliminated at the 3600-record training. Errors related to “symptoms that the researchers forgot to extract (error 2f)” and “partial matches with low similarity and incorrect positive-negative classifications that involved entire extractions of essential terms (error 2d)” were caused by researchers’ mistakes or errors in the extraction range or positive-negative classification, but the system was able to partially recognize the information to be extracted. Therefore, these errors may have been difficult to resolve.

Among errors 2b, 2a, and 2c, which showed limited differences in error rate variation, the extracted terms or pre/post descriptions of “extraction of information that was neither symptoms nor supplemental information (error 2a)” and “incomplete extraction without essential terms (error 2b)” were different from the real extraction target. Concerning the system’s context-readable specification, the system appears to have learned that the contexts before and after the incorrect extractions were not symptom-related contexts, reducing errors 2a and 2b, as it learned from large amounts of training data. “Error 2c” error rates increased at the 3600-record training. This finding indicates that error 2c improved less than error 2a and 2b when comparing the 1200 and 12,004-record trainings, although the difference in variation was small. Error 2c is more difficult to improve than errors 2a and 2b, presumably because error 2c contains expressions that researchers are also unsure about and that may be extracted depending on the situation.

Among the subcategories of error 3 focusing on the position of positive-negative expressions, “included within the extracted terms (error 3bc-1-2)” (195 percentage points) had a larger difference in error rate variation than “one or two words are in between from the extracted terms (error 3bc-1-3)” (90 percentage points) and “immediately before or/and after the symptom (error 3bc-1-1)” (60 percentage points). This suggests that the system may be able to perform correct positive-negative classification when the extracted terms and the positive-negative expressions are close to each other but not contained within the extracted terms.

Among the subcategories of error 3 focusing on the way of positive-negative expressions, simple sentences were considered easy to judge: “simple positive or negative expressions (error 3bc-2-1)” (76 percentage points) and “negated positive or negative expressions (error 3bc-2-4)” (–15 percentage points). In “mild negative expressions (error 3bc-2-3)” (119 percentage points), on the other hand, the researchers focused on the description of the degree of denial to determine whether the symptoms were completely denied. However, due to the variety of degree descriptions, this annotation criteria could have been cumbersome for the system.

Through this error analysis, it was inferred that while the system can easily improve the extraction results with reference to the context near the extracted terms due to increased learning, the system cannot handle cases where the researchers are unsure of the decision or complex annotation criteria in which the extraction results change depending on the situation.

Evaluation

The system developed in this study performed better than the systems in previous studies focused on the Japanese language. In a previous study of Japanese patient narratives, Usui et al [19] aimed to thoroughly extract patient complaints from subjective data using a rule-based system. The high performance achieved by our deep learning–based system suggests that our system had considerable flexibility in handling data where symptoms could not be extracted through rules alone. As a result, the performance of our system, with an F_1-score of 0.82, surpassed that of the system by Usui et al [19] (F_1-score of 0.65), although it should be noted that the output functions of the 2 systems were not exactly the same, complicating a direct comparison. Similarly, Aramaki et al [26] used Japanese case reports as training data to develop a system for extracting a variety of symptoms. The F_1-scores of their system were 0.87 for NER and 0.63 for NER with positive-negative classification [26], both of which were lower than the scores achieved by our system. Although many previous studies of NER have focused on specific symptoms or patient populations, our system has the advantage of covering a broader range of patients and extracting a wider variety of symptoms. This makes it particularly useful for comprehensively collecting information on patient narratives.

XSL•FO
RenderX

The performance of the developed system is the same or even higher than that of similar systems in English, which aimed to extract a variety of symptomatic adverse drug events from patient narratives. For example, the neural network–based system developed by Nikfarjam et al [7] achieved a micro-average F_1-score of 0.74 in NER for drug adverse events in patient posts on social health networks. Another system by Batbaatar et al [8] achieved an F_1-score of 0.82 for NER of diseases or syndromes and an F_1-score of 0.88 for signs and symptoms from social media posts. Of these 2 systems, one extracted only the adverse events experienced by the patient, while the other did not involve positive-negative classification. Therefore, our system, despite its added complexity with positive-negative classification, appears to have comparable or even superior performance compared with the aforementioned systems.

Future Applications

The developed system is expected to be applied to monitor adverse events based on patient reports and narratives. Among previous studies using NER systems, the study by Ujiie et al [27] aimed to reduce the screening burden of drug safety information for pharmaceutical companies by identifying medical articles that contained descriptions of adverse drug events. Similarly, the system developed by Nishioka et al [28] sought to detect a specific adverse reaction—hand-foot syndrome—by identifying blog posts from patients with breast cancer, analyzing each text and post to determine whether it involved the adverse reaction. However, they did not use an NER approach. Given that our system has the advantage of extracting a wide variety of symptoms from diverse patient expressions, it is better positioned for broader use in monitoring adverse events across a wider range of conditions.

Although we focused on patient narratives, assessments recorded by health care professionals are undoubtedly another important source of patient information. Specifically, patient summaries, such as discharge and transfer summaries, contain information that has been reviewed, selected, and organized by health care professionals. However, evaluations by health care professionals carry the risk of underestimation and underreporting [1,2]. When using any medical records for research, including pharmaceutical care records, there is a concern about the filtering of information by health care professionals. However, we succeeded in establishing a system for analyzing patient narratives. The next step is to target patient narratives automatically transcribed by voice input so that the analysis of patient narratives can be achieved with fewer omissions in the recordings. By comparing patient narratives collected by either method with professional assessments using a system, such as ours, the gap between patients and health professionals can be identified. The developed system could contribute to achieving gap-free assessment and care between patients and health care professionals through the identification and analysis of the gap.

Limitations of This Study

One limitation of this study is that we used data from a single facility. Therefore, further verification is needed to determine whether this system can be used for subjective data from other facilities. Since subjective data include raw patient speech, differences in dialect and the patient's disease and treatment are assumed to be factors that cause differences in the content of the descriptions between facilities. Therefore, while this study used data from an acute care hospital in Tokyo, the system may perform differently for data from chronic care hospitals, community pharmacies, and medical facilities in areas where dialects are spoken. Validation is expected to be conducted in the future using data from medical facilities with the same features and different features to reveal the versatility of the system.

Another issue is the evaluation of the validity of the system in clinical settings. For example, F_1-score, the evaluation index used in this study, provides a relative evaluation and can be used to compare systems under the same conditions. Since there is no standard value for judging practicality, the results cannot be used to judge the applicability in actual clinical settings. However, since different applications require different performances, the system is potentially usable in a real clinical setting even if it does not have 100% performance. For example, signal detection is more important to capture overall trends than to overlook individual cases, so the system is useful for processing large amounts of data. Another limitation is the lack of standardization for extracted terms, which could be addressed by developing additional databases or systems.

Conclusions

This is the first study to develop an NER system to extract disease and symptom names from subjective data in Japanese hospital pharmaceutical care records and to investigate how its performance improves with increasing training data. The developed system demonstrated high performance in extracting disease and symptom names when trained on a large dataset, although performance improved gradually as the training amount increased, reaching a plateau after training on approximately 3600 records.

The system enables the monitoring of various symptoms using patient narratives as a source and is expected to be a valuable tool for supporting both clinical practice and research.

Acknowledgments

This study was supported by JST SPRING (grant number: JPMJSP2123).

Conflicts of Interest

None declared.

XSL•FO
RenderX

Multimedia Appendix 1
Results of the sample survey for the determination of the Levenshtein distance similarity threshold.
[DOCX File , 43 KB - medinform_v13i1e68863_app1.docx]

Multimedia Appendix 2
Number of errors and the ratio of errors to total extraction in the subcategories of error 3.
[DOCX File , 21 KB - medinform_v13i1e68863_app2.docx]

Multimedia Appendix 3
Number of errors and the ratio of errors to total extraction in the subcategories of error 3b and 3c focused on the position of positive-negative expressions.
[DOCX File , 20 KB - medinform_v13i1e68863_app3.docx]

Multimedia Appendix 4
Number of errors and the ratio of errors to total extraction in the subcategories of error 3b and 3c focused on the way of positive-negative expressions.
[DOCX File , 21 KB - medinform_v13i1e68863_app4.docx]

References

1. Di Maio M, Gallo C, Leighl NB, Piccirillo MC, Daniele G, Nuzzo F, et al. Symptomatic toxicities experienced during anticancer treatment: agreement between patient and physician reporting in three randomized trials. J Clin Oncol 2015 Mar 10;33(8):910-915 [FREE Full text] [doi: 10.1200/JCO.2014.57.9334] [Medline: 25624439]
2. Novello S, Capelletto E, Cortinovis D, Tiseo M, Galetta D, Valmadre G, et al. Italian multicenter survey to evaluate the opinion of patients and their reference clinicians on the "tolerance" to targeted therapies already available for non-small cell lung cancer treatment in daily clinical practice. Transl Lung Cancer Res 2014 Jun;3(3):173-180 [FREE Full text] [doi: 10.3978/j.issn.2218-6751.2014.06.10] [Medline: 25806297]
3. Ohta Y, Miki I, Kimura T, Abe M, Sakuma M, Koike K, et al. Epidemiology of adverse events and medical errors in the care of cardiology patients. J Patient Saf 2019 Sep;15(3):251-256 [FREE Full text] [doi: 10.1097/PTS.0000000000000291] [Medline: 27465298]
4. Davies N. Measuring health-related quality of life in cancer patients. Nurs Stand 2009 Apr 02;23(30):42-49. [doi: 10.7748/ns2009.04.23.30.42.c6930] [Medline: 19408494]
5. Kang D, Kim S, Kim H, Lee M, Kong S, Chang YJ, et al. Surveillance of Symptom Burden Using the Patient-Reported Outcome Version of the Common Terminology Criteria for Adverse Events in Patients With Various Types of Cancers During Chemoradiation Therapy: Real-World Study. JMIR Public Health Surveill 2023 Mar 08;9:e44105. [doi: 10.2196/44105] [Medline: 36884274]
6. Dolatabadi E, Moyano D, Bales M, Spasojevic S, Bhambhoria R, Bhatti J, et al. Using social media to help understand patient-reported health outcomes of post-COVID-19 condition: natural language processing approach. J Med Internet Res 2023 Sep 19;25:e45767 [FREE Full text] [doi: 10.2196/45767] [Medline: 37725432]
7. Nikfarjam A, Ransohoff JD, Callahan A, Jones E, Loew B, Kwong BY, et al. Early detection of adverse drug reactions in social health networks: a natural language processing pipeline for signal detection. JMIR Public Health Surveill 2019 Jun 03;5(2):e11264 [FREE Full text] [doi: 10.2196/11264] [Medline: 31162134]
8. Batbaatar E, Ryu KH. Ontology-based healthcare named entity recognition from twitter messages using a recurrent neural network approach. Int J Environ Res Public Health 2019 Sep 27;16(19):3628 [FREE Full text] [doi: 10.3390/ijerph16193628] [Medline: 31569654]
9. Jagannatha A, Liu F, Liu W, Yu H. Overview of the first natural language processing challenge for extracting medication, indication, and adverse drug events from electronic health record notes (MADE 1.0). Drug Saf 2019 Jan;42(1):99-111 [FREE Full text] [doi: 10.1007/s40264-018-0762-z] [Medline: 30649735]
10. Yada S, Nakamura Y, Wakamiya S, Aramaki E. Real-MedNLP: overview of REAL document-based MEDical Natural Language Processing Task. In: \Proceedings of the 16th NTCIR Conference on Evaluation of Information Access Technologies. 2022 Presented at: 16th NTCIR Conference on Evaluation of Information Access Technologies; June 14-17, 2022; Tokyo, Japan URL: https://research.nii.ac.jp/ntcir/workshop/OnlineProceedings16/pdf/ntcir/01-NTCIR16-OV-MEDNLP-YadaS.pdf
11. Henry S, Buchan K, Filannino M, Stubbs A, Uzuner O. 2018 n2c2 shared task on adverse drug events and medication extraction in electronic health records. J Am Med Inform Assoc 2020 Jan 01;27(1):3-12 [FREE Full text] [doi: 10.1093/jamia/ocz166] [Medline: 31584655]
12. Dirkson A, Verberne S, van Oortmerssen G, Gelderblom H, Kraaij W. How do others cope? Extracting coping strategies for adverse drug events from social media. J Biomed Inform 2023 Mar;139:104228 [FREE Full text] [doi: 10.1016/j.jbi.2022.104228] [Medline: 36309197]

XSL•FO
RenderX

13. Dreyfus B, Chaudhary A, Bhardwaj P, Shree VK. Application of natural language processing techniques to identify off-label drug usage from various online health communities. J Am Med Inform Assoc 2021 Sep 18;28(10):2147-2154 [FREE Full text] [doi: 10.1093/jamia/ocab124] [Medline: 34333625]
14. Raza S, Schwartz B, Lakamana S, Ge Y, Sarker A. A framework for multi-faceted content analysis of social media chatter regarding non-medical use of prescription medications. BMC Digit Health 2023 Aug 07;1:29 [FREE Full text] [doi: 10.1186/s44247-023-00029-w] [Medline: 37680768]
15. Magge A, Tutubalina E, Miftahutdinov Z, Alimova I, Dirkson A, Verberne S, et al. DeepADEMiner: a deep learning pharmacovigilance pipeline for extraction and normalization of adverse drug event mentions on Twitter. J Am Med Inform Assoc 2021 Sep 18;28(10):2184-2192 [FREE Full text] [doi: 10.1093/jamia/ocab114] [Medline: 34270701]
16. Liu Y, Whitfield C, Zhang T, Hauser A, Reynolds T, Anwar M. Monitoring COVID-19 pandemic through the lens of social media using natural language processing and machine learning. Health Inf Sci Syst 2021 Dec;9(1):25 [FREE Full text] [doi: 10.1007/s13755-021-00158-4] [Medline: 34188896]
17. Park MS, He Z, Chen Z, Oh S, Bian J. Consumers' Use of UMLS Concepts on Social Media: Diabetes-Related Textual Data Analysis in Blog and Social Q&A Sites. JMIR Med Inform 2016 Nov 24;4(4):e41 [FREE Full text] [doi: 10.2196/medinform.5748] [Medline: 27884812]
18. Preiss A, Baumgartner P, Edlund MJ, Bobashev GV. Using Named Entity Recognition to Identify Substances Used in the Self-medication of Opioid Withdrawal: Natural Language Processing Study of Reddit Data. JMIR Form Res 2022 Mar 30;6(3):e33919 [FREE Full text] [doi: 10.2196/33919] [Medline: 35353047]
19. Usui M, Aramaki E, Iwao T, Wakamiya S, Sakamoto T, Mochizuki M. Extraction and Standardization of Patient Complaints from Electronic Medication Histories for Pharmacovigilance: Natural Language Processing Analysis in Japanese. JMIR Med Inform 2018 Sep 27;6(3):e11021 [FREE Full text] [doi: 10.2196/11021] [Medline: 30262450]
20. Devlin J, Chang MW, Lee K, Toutanova K. BERT: pre-training of deep bidirectional transformers for language understanding. In: Proceedings of the 2019 Conference of the North American Chapter of the Association for Computational Linguistics: Human Language Technologies, Volume 1 (Long and Short Papers). 2019 Presented at: 2019 Conference of the North American Chapter of the Association for Computational Linguistics; June 2-7, 2019; Minneapolis, MN. [doi: 10.18653/v1/N19-1423]
21. Kong Z, Yue C, Shi Y, Yu J, Xie C, Xie L. Entity extraction of electrical equipment malfunction text by a hybrid natural language processing algorithm. IEEE Access 2021;9:40216-40226. [doi: 10.1109/access.2021.3063354]
22. Sugimoto K, Wada S, Konishi S, Okada K, Manabe S, Matsumura Y, et al. Extracting clinical information from japanese radiology reports using a 2-stage deep learning approach: algorithm development and validation. JMIR Med Inform 2023 Nov 14;11:e49041 [FREE Full text] [doi: 10.2196/49041] [Medline: 37991979]
23. Ohno Y, Kato R, Ishikawa H, Nishiyama T, Isawa M, Mochizuki M, et al. Using the natural language processing system medical named entity recognition-Japanese to analyze pharmaceutical care records: natural language processing analysis. JMIR Form Res 2024 Jun 04;8:e55798 [FREE Full text] [doi: 10.2196/55798] [Medline: 38833694]
24. BertJapanese. Hugging Face. URL: https://huggingface.co/docs/transformers/ja/model_doc/bert-japanese [accessed 2025-02-07]
25. Levenshtein VI. Binary codes capable of correcting deletions, insertions and reversals. Soviet Physics Doklady 1966 Feb;10(8):707-710 [FREE Full text]
26. Aramaki E, Yano K, Wakamiya S. MedEx/J: a one-scan simple and fast NLP tool for japanese clinical texts. Stud Health Technol Inform 2017;245:285-288. [Medline: 29295100]
27. Ujiie S, Yada S, Wakamiya S, Aramaki E. Identification of adverse drug event-related japanese articles: natural language processing analysis. JMIR Med Inform 2020 Nov 27;8(11):e22661 [FREE Full text] [doi: 10.2196/22661] [Medline: 33245290]
28. Nishioka S, Asano M, Yada S, Aramaki E, Yajima H, Kizaki H, et al. Detection of adverse event signals with severity grade classification from cancer patient narrative. Stud Health Technol Inform 2024 Jan 25;310:554-558. [doi: 10.3233/SHTI231026] [Medline: 38269870]

Abbreviations

BERT: bidirectional encoder representations from transformers
CRF: conditional random field
NER: named entity recognition
NLP: natural language processing
UNK: unknown keys

XSL•FO
RenderX

Edited by C Lovis; submitted 25.11.24; peer-reviewed by K Yamamoto, A Yeow; comments to author 25.12.24; revised version received 28.01.25; accepted 31.01.25; published 04.03.25.

Please cite as:
Ohno Y, Aomori T, Nishiyama T, Kato R, Fujiki R, Ishikawa H, Kiyomiya K, Isawa M, Mochizuki M, Aramaki E, Ohtani H
Performance Improvement of a Natural Language Processing Tool for Extracting Patient Narratives Related to Medical States From Japanese Pharmaceutical Care Records by Increasing the Amount of Training Data: Natural Language Processing Analysis and Validation Study
JMIR Med Inform 2025;13:e68863
URL: https://medinform.jmir.org/2025/1/e68863
doi:10.2196/68863
PMID:40053805

©Yukiko Ohno, Tohru Aomori, Tomohiro Nishiyama, Riri Kato, Reina Fujiki, Haruki Ishikawa, Keisuke Kiyomiya, Minae Isawa, Mayumi Mochizuki, Eiji Aramaki, Hisakazu Ohtani. Originally published in JMIR Medical Informatics (https://medinform.jmir.org), 04.03.2025. This is an open-access article distributed under the terms of the Creative Commons Attribution License (https://creativecommons.org/licenses/by/4.0/), which permits unrestricted use, distribution, and reproduction in any medium, provided the original work, first published in JMIR Medical Informatics, is properly cited. The complete bibliographic information, a link to the original publication on https://medinform.jmir.org/, as well as this copyright and license information must be included.

XSL•FO
RenderX

Original Paper

Improving Systematic Review Updates With Natural Language Processing Through Abstract Component Classification and Selection: Algorithm Development and Validation

Tatsuki Hasegawa[1], MSc; Hayato Kizaki[1], PhD; Keisho Ikegami[1]; Shungo Imai[1], Ph.D; Yuki Yanagisawa[1], Ph.D; Shuntaro Yada[2,3], Ph.D; Eiji Aramaki[2], Ph.D; Satoko Hori[1], Ph.D

[1]Division of Drug Informatics, Keio University Faculty of Pharmacy, Tokyo, Japan

[2]Nara Institute of Science and Technology, Nara, Japan

[3]Faculty of Library, Information and Media Science, University of Tsukuba, Tsukuba, Japan

Corresponding Author:
Satoko Hori, Ph.D
Division of Drug Informatics
Keio University Faculty of Pharmacy
1-5-30 Shibakoen, Minato-ku
Tokyo, 105-8512
Japan
Phone: 81 3 5400 2650
Email: satokoh@keio.jp

Abstract

Background: A challenge in updating systematic reviews is the workload in screening the articles. Many screening models using natural language processing technology have been implemented to scrutinize articles based on titles and abstracts. While these approaches show promise, traditional models typically treat abstracts as uniform text. We hypothesize that selective training on specific abstract components could enhance model performance for systematic review screening.

Objective: We evaluated the efficacy of a novel screening model that selects specific components from abstracts to improve performance and developed an automatic systematic review update model using an abstract component classifier to categorize abstracts based on their components.

Methods: A screening model was created based on the included and excluded articles in the existing systematic review and used as the scheme for the automatic update of the systematic review. A prior publication was selected for the systematic review, and articles included or excluded in the articles screening process were used as training data. The titles and abstracts were classified into 5 categories (Title, Introduction, Methods, Results, and Conclusion). Thirty-one component-composition datasets were created by combining 5 component datasets. We implemented 31 screening models using the component-composition datasets and compared their performances. Comparisons were conducted using 3 pretrained models: Bidirectional Encoder Representations from Transformer (BERT), BioLinkBERT, and BioM- Efficiently Learning an Encoder that Classifies Token Replacements Accurately (ELECTRA). Moreover, to automate the component selection of abstracts, we developed the Abstract Component Classifier Model and created component datasets using this classifier model classification. Using the component datasets classified using the Abstract Component Classifier Model, we created 10 component-composition datasets used by the top 10 screening models with the highest performance when implementing screening models using the component datasets that were classified manually. Ten screening models were implemented using these datasets, and their performances were compared with those of models developed using manually classified component-composition datasets. The primary evaluation metric was the F10-Score weighted by the recall.

Results: A total of 256 included articles and 1261 excluded articles were extracted from the selected systematic review. In the screening models implemented using manually classified datasets, the performance of some surpassed that of models trained on all components (BERT: 9 models, BioLinkBERT: 6 models, and BioM-ELECTRA: 21 models). In models implemented using datasets classified by the Abstract Component Classifier Model, the performances of some models (BERT: 7 models and BioM-ELECTRA: 9 models) surpassed that of the models trained on all components. These models achieved an 88.6% reduction in manual screening workload while maintaining high recall (0.93).

XSL•FO
RenderX

Conclusions: Component selection from the title and abstract can improve the performance of screening models and substantially reduce the manual screening workload in systematic review updates. Future research should focus on validating this approach across different systematic review domains.

(JMIR Med Inform 2025;13:e65371) doi:10.2196/65371

KEYWORDS

systematic review; natural language processing; guideline updates; bidirectional encoder representations from transformer; screening model; literature; efficiency; updating systematic reviews; language model

Introduction

Systematic reviews are based on evidence-based medicine and constitute crucial sources of information for health care professionals and policy makers to access the latest information in their fields and thereby aid decision-making [1,2]. Systematic reviews of randomized controlled trials are highly valued and frequently referenced in the development of clinical practice guidelines by authoritative organizations, such as the World Health Organization (WHO), representing a crucial foundation for evidence-based health care decision-making. When systematic reviews are outdated or fail to encompass all the available evidence, they risk misinforming decision makers and other stakeholders [3]. Therefore, systematic reviews should be regularly updated. Shojania et al [4] analyzed 100 quantitative systematic reviews that were registered with the ACP Journal Club and reported a median survival time of 5.5 years for systematic reviews [4]. However, most systematic reviews remain outdated, and Hoffmeyer et al [2] reported that 88% of reviews in the Cochrane Database of Systematic Reviews had not been updated for 5.5 years.

A significant challenge in updating systematic reviews is the workload associated with article screening that, for systematic review research and updates, is usually performed using the following 5 steps [5,6]: (1) identifying databases relevant to the topic, (2) finding potentially relevant articles through a tailored search strategy, (3) screening articles based on titles and abstracts, (4) selecting articles for detailed analysis from the screened texts, and (5) extracting and synthesizing data from the selected articles. The significant effort required for these steps as well as the stringent requirement that these tasks be performed independently by 2 or more individuals [7], seems to contribute to the low rate of systematic review updates.

Recent advancements in natural language processing (NLP) technology have led to numerous attempts to automate these screening tasks. Qin et al [8] used an ensemble learning model that integrated multiple Bidirectional Encoder Representations from Transformer (BERT) models that were trained on the titles or abstracts and results of articles screened before an update of a systematic review on the treatment of type 2 diabetes with sodium-glucose cotransporter-2 inhibitors. Their model achieved a sensitivity of 96%, a specificity of 78%, and a 64.1% reduction in workload. While these models, like any NLP applications, require careful consideration of potential challenges such as overfitting and validation across different domains, these promising, along with other studies, have established the viability of NLP-based screening automation.

Building upon these achievements, we explored a novel approach focusing on how models process and learn from abstract information. Scientific abstracts contain distinct components (eg, introduction, methods, results, and conclusions) that serve different rhetorical functions and potentially contribute differently to determining article relevance for systematic reviews. While current approaches typically treat abstracts as uniform text, we hypothesized that selective training on specific abstract components might help address common challenges in NLP-based screening models, including the risk of overfitting large volumes of text data. By focusing on the most relevant information for the systematic review's inclusion criteria, this approach could potentially enhance model performance compared to traditional methods that process entire abstracts as uniform text.

This component-based approach potentially offers several advantages. For example, methods sections often contain crucial information about study design and participant characteristics, while results sections present outcome measures—both critical factors when selecting articles for inclusion in systematic reviews. By selectively focusing on these key components, models might learn more effectively from smaller, more targeted training data.

Scientific journals have widely adopted structured abstracts with clearly labeled components (eg, Introduction, Methods, Results, and Conclusion) since the early 1990s [9]. However, systematic reviews often need to process both structured and unstructured abstracts. To implement our component-based screening approach effectively across all articles, we needed to develop an NLP-based automatic abstract component classifier that could systematically identify and process abstract components regardless of their original format (structured or unstructured).

In this study, we demonstrate the usefulness of a screening model that learns by selecting abstract components as a novel method for improving the performance of screening models. In addition, we construct a screening model with an NLP-based automatic abstract classifier that classifies abstracts by component.

Methods

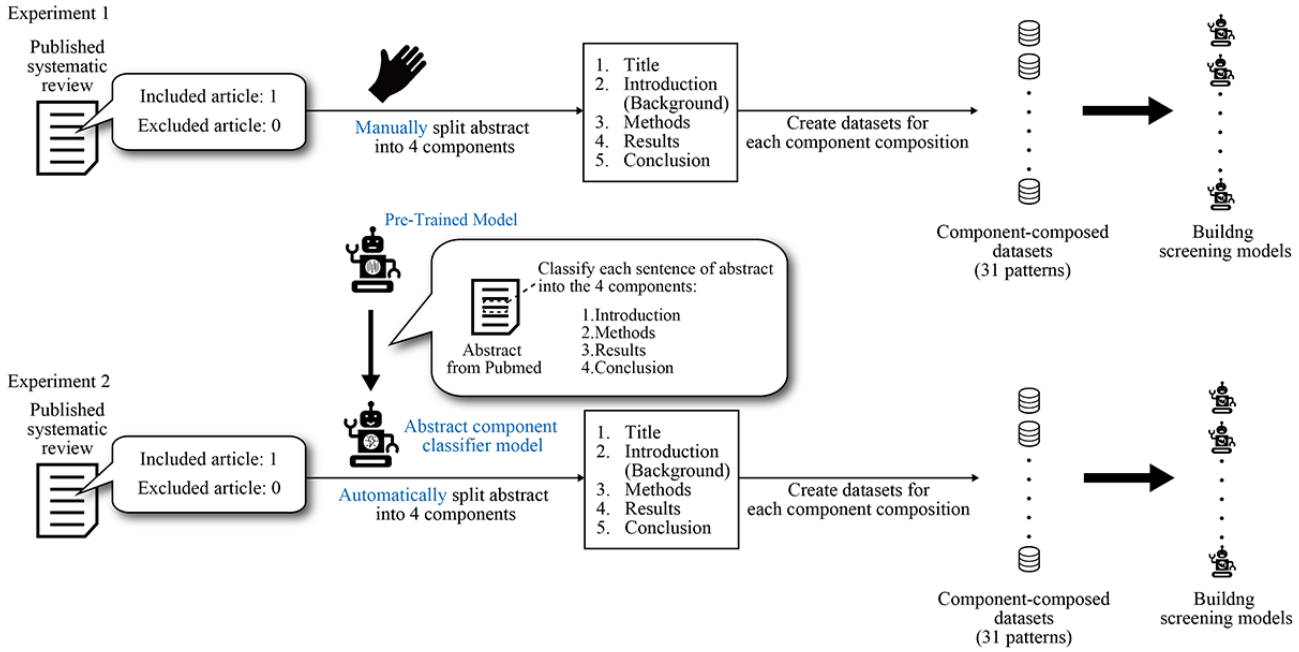
Overview

Our study consisted of 2 experiments (Figure 1). First, to evaluate the impact of selecting titles and abstract components of articles on the development of the screening model, we constructed datasets with different combinations of titles and 4 abstract components and built a screening model using these

XSL•FO
RenderX

datasets (under subheading Experiment 1). Second, to automate the process from dataset creation to classifier development, we developed a model for classifying abstract components of articles (Abstract Component Classifier Models) and built a screening model using the abstract components identified by the Abstract Component Classifier Model (under subheading Experiment 2).

Figure 1. Overview of this study experiments.



For identifying both included and excluded articles, our study followed a systematic process: first, articles were identified and curated based on our selection criteria, then their abstracts were systematically subdivided into components for analysis. This component classification process was performed manually in Experiment 1 and automatically using our classifier in Experiment 2. The details of each step are described in the following sections.

Experiment 1: Evaluation of the Impact of Selecting Titles and Abstract Components of Articles on the Development of the Screening Model

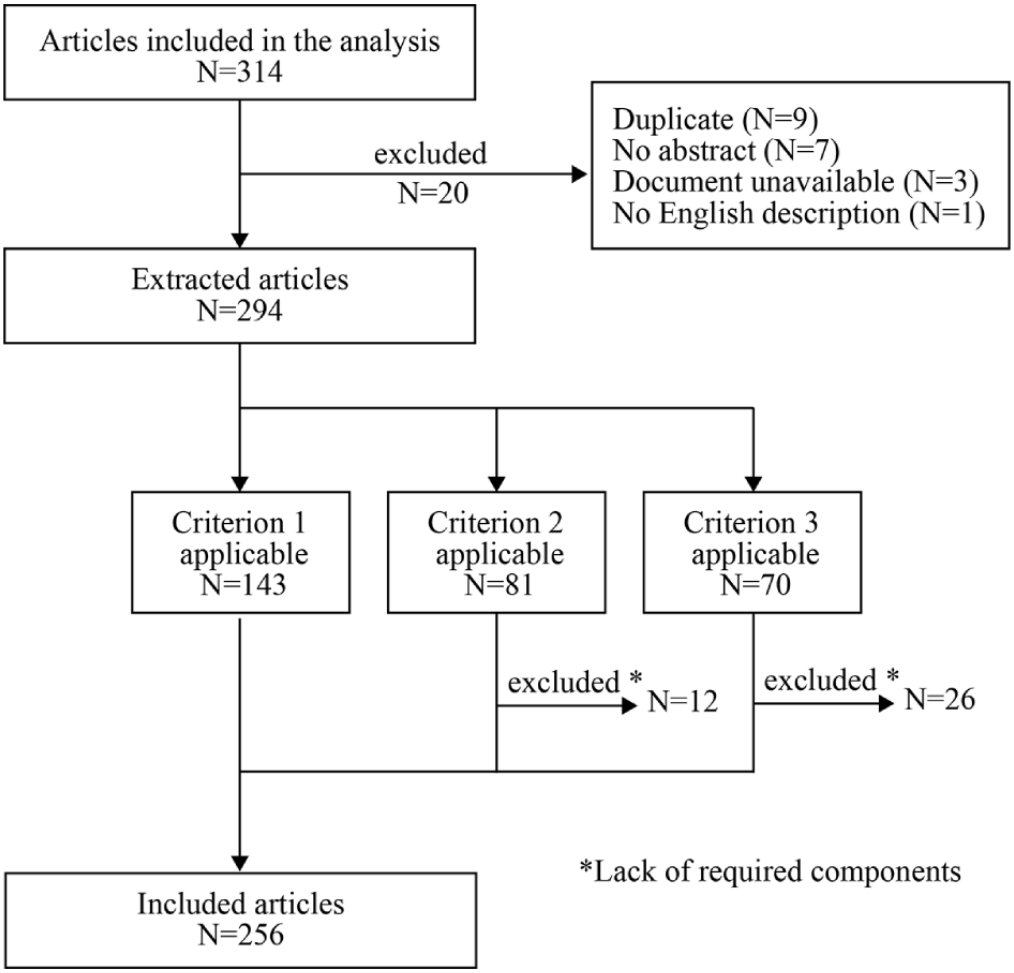
Data Sources

We scrutinized the study "Adverse events in people taking macrolide antibiotics versus placebo for any indication," published by Hansen et al [10] in the Cochrane Database of Systematic Reviews on January 18, 2019 as the data source. The data source was a systematic review that assessed adverse events in randomized controlled trials of patients treated with antibiotics compared with a placebo. This review was selected for 2 reasons. First, the number of studies included in the analysis was substantial, with 184 unique studies (reported across 314 publications), providing sufficient data for implementing the screening model. Second, the systematic review included randomized controlled trials, consistent with other systematic reviews analyzing treatment effects.

To identify the included articles, we analyzed the 184 studies (314 articles) in the inclusion list for the systematic review. The screening process for included articles is shown in Figure 2. We selected articles that met any of the criteria with both the title and abstract written in English, the criteria are mentioned in Textbox 1.

XSL•FO
RenderX

Figure 2. Screening process for included articles in this study.



Textbox 1. Inclusion criteria for included articles.

Criterion 1:

- The abstract was structured into 4 components, introduction (background), methods, results, and conclusion, or equivalent, from which the title and the aforementioned 4 components could be extracted.

Criterion 2:

- The abstract was not divided into exactly four components but followed a structured format (eg, 3 or 5 components) and could be reclassified by researchers into 4 components—introduction (background), methods, results, and conclusion, or equivalent—from which the title and the aforementioned four components could be extracted.

Criterion 3:

- The abstract did not follow a structured abstract, but the text could be classified into four components—introduction (background), methods, results, and conclusion, or equivalent—from which the title and the aforementioned four components could be extracted.

The criteria for the 4 components equivalent to introduction (background), methods, results, and conclusion, as well as for excluding text, are shown in Table S1 in Multimedia Appendix 1. For the classification of criteria 2 and 3, two researchers (TH and YY) independently classified each sentence in the abstract into 4 components. Disagreements, if any, were resolved through discussion. In our study, all abstracts were assumed to be written in the following order: introduction (background), methods, results, and conclusion. Therefore, according to the criteria listed in Table S1 in Multimedia Appendix 1, if the sentences before and after a sentence classified as results were related to methods, the sentence was classified as methods. In total, 256 articles were included.

To identify the excluded articles, we did not contact the original review authors but instead searched MEDLINE (Ovid) and the Cochrane Central Register of Controlled Trials using the same search terms and search periods as those used in the systematic review. The search terms and formulas used are listed in Table S2 of Multimedia Appendix 1. Articles that met the above criteria 1 or 2 with both the title and abstract written in English were then extracted, and the “included articles” in our study and any articles similar to those were excluded. The following

XSL•FO
RenderX

exclusion criteria were applied: (1) articles without English abstracts, as they would not be suitable for our model training, (2) articles without abstracts, particularly older publications or those with only titles, and (3) articles with unstructured abstracts lacking clear background, methods, results, and conclusion sections, as they would not be appropriate for our component classification task. We did not include articles that only met criterion 3 (articles with title and abstract written in English but not meeting criterion 1 or 2) as negative instances, as we had already obtained a sufficient number of excluded articles from articles meeting criteria 1 and 2. The classification of the 4 components was conducted with reference to the criteria listed in Table S1 in Multimedia Appendix 1. For the classification of criterion 2, we evaluated the agreement rate between 2 researchers. The simple agreement rate was 98.76% (5752/5824; 95% CI 98.47%-99.05%). It was considered sufficiently high; therefore, one researcher (TH) performed the classification.

In addition, the decision regarding duplicates in the "included articles" in our study was made using the SequenceMatcher object from the difflib library. The similarity ratio of the text of each component in the excluded articles to the text of the same components in all the "included articles" and extracted the highest value was calculated. Articles with a combined similarity ratio value of 4.0 or more, or with a similarity ratio of the title of more than 0.8, were excluded. Through manual verification of the flagged cases, we confirmed 1 complete text duplication and 2 cases of substantial text similarity above our thresholds. These 3 cases were excluded from the analysis, confirming the appropriateness of our automated duplicate detection criteria. A similar assessment using the title was also performed for the studies excluded from the article dataset. Duplicates among the excluded articles were not excluded because duplicates might exist in the articles to be scrutinized for practical use. Ultimately, 1261 articles were extracted.

We created 31 different component-composed datasets from 5 components in the extracted articles. These included datasets containing only the title, introduction, methods, results, or conclusions; datasets containing all 5 components; and datasets containing any combination of 2, 3, or 4 of these components. All variations are shown in Table S3 in Multimedia Appendix 1.

Development of Screening Models

From each component-composed dataset, we created training, validation, and test sets. Included and excluded articles were treated as positive and negative data, respectively. For positive data, 40 articles were randomly extracted as the test set, and the remaining 216 articles were randomly divided into training and validation sets in a 9:1 ratio. Negative data were randomly assigned to the training and validation sets to ensure 1:1 positive-to-negative data. In the test set, 960 articles were assigned randomly. For articles exceeding the maximum sequence length of 512 tokens, the text was truncated during the model training phase. All shorter inputs were padded to ensure uniform input length. This means that for articles exceeding the token limit, information from the latter portions of the text was not used during model training.

We developed screening models that predicted binary labels for the test set using the transformer library. During model development, different learning rates (Lr; 6e-7, 2e-6, and 6e-6) were evaluated using the validation set. Screening models were developed using 3 pretrained language models: Bidirectional Encoder Representations from Transformers (BERT; bert-large-uncased [11]), BioLinkBERT (BioLinkBERT-Large) [12], and BioM- Efficiently Learning an Encoder that Classifies Token Replacements Accurately (ELECTRA) (BioM-ELECTRA-Large-SQuAD2) [13]. BERT, introduced by Google in 2018, is pretrained on 2.5 billion words from the English Wikipedia and 800 million words from BookCorpus [14]. It uses a Transformer Encoder using a method known as attention, which can effectively incorporate information from distant positions within a text.

We used this as the baseline pretrained model. BioLinkBERT is a pretrained model developed by Yasunaga et al [15] at Stanford University. Traditional BERT models cannot learn from the text of hyperlinks and citation links used in pretraining documents. The base model, LinkBERT, can capture these document links. BioLinkBERT [12] was pretrained on 3.1 billion words from PubMed abstracts and documents from their hyperlinks and citation links. BioM-ELECTRA-Large-SQuAD2 is a model developed by Alrowili and Shanker [16] from the University of Delaware that trains BioM-ELECTRA-Large on the SQuAD2.0 dataset to enhance question-answering capabilities. BioM-ELECTRA is based on the ELECTRA model, introduced by Clark et al [17] in 2020, which improves the pretraining methods of BERT to achieve comparable or superior performance with fewer computational resources. BioM-ELECTRA was pretrained on 29,000 domain-specific PubMed abstracts, following the same domain-specific approach as PubMedBERT [16]. Among the pretrained models implemented in this study, BioLinkBERT and BioM-ELECTRA were the highest-performing models in the BLURB benchmark [18], which evaluates the performance of pretrained models in the biomedical literature.

Task and Metrics

For each pretrained model, we fine-tuned 31 screening models corresponding to all possible combinations of the 5 components (Title, Introduction, Methods, Results, and Conclusion) and compared their performances. In systematic review screening, minimizing false negatives (missed relevant articles) is critically important, as failing to include relevant articles could significantly impact review conclusions. While Recall would be an appropriate metric for this purpose, using it alone would favor models that simply classify all articles as positive, achieving perfect recall but poor practical utility.

To address this, we designated the Fβ-score as our primary evaluation metric. This score is the harmonic mean of recall and precision, where β determines their relative importance. During our preliminary analysis, we tested several values of β to determine the optimal balance between recall and precision for our specific use case. Compared to other potential metrics, such as maximizing specificity at fixed recall thresholds, the Fβ-score provides a single, interpretable measure that enables explicit control over the balance between false positives and

XSL•FO
RenderX

false negatives. We set β=10 to strongly prioritize recall while maintaining some consideration for precision, reflecting the practical trade-off in systematic review screening where missing relevant studies is more problematic than including irrelevant ones for subsequent manual screening. This value was chosen based on both empirical testing and principles of systematic review methodology where comprehensiveness in literature identification is critical. While this strong prioritization through β=10 results in increased false positives, this trade-off is considered acceptable in the context of systematic reviews, where missing relevant studies could significantly impact review conclusions. This approach also ensures that a model simply classifying everything as positive would be penalized through its low precision component, despite achieving perfect recall.

We calculated the average F10-Score evaluated 5 times using 5 datasets with different assignments for each component composition and compared these averages between the screening models. To elaborate, for each of the 31 possible component combinations, we created 5 distinct datasets using different random samples of included and excluded articles for training, validation, and test sets. This process of splitting the data into training, validation, and test sets was repeated 5 times, ensuring that each of the 5 datasets was distinct, and allowing us to evaluate the model performance with more reliability and less influence from any specific split. Specifically, from the 256 included articles, we randomly selected 40 articles to form the test set. The remaining 216 articles were randomly divided into training and validation sets using a 9:1 ratio. The excluded articles were assigned randomly to the training and validation sets, and 960 were randomly assigned to the test set. By averaging the F10-scores across these 5 datasets, we aimed to evaluate model performance across multiple splits, providing more stable evaluation metrics by mitigating variations due to randomness in data sampling.

The number of epochs for training the screening models was set to 32, patience for early stopping to 3, and weight decay to 0.01. In addition, we compared the screening model with the highest average F10-Score with those of other component compositions among the 3 Lr: 6e-6, 2e-6, and 6e-7.

Experiment 2: Development of a Screening Model Using Article Components as Determined by the Abstract Component Classifier Model

In Experiment 2, we aimed to construct a screening model by automating the division of abstract components, which was done manually in Experiment 1. To achieve this, we first developed an Abstract Component Classifier Model to automate the partitioning of abstract components.

Development of the Abstract Component Classifier Model

We obtained 25,584 articles with abstracts registered in PubMed from May 2 to 8, 2018, and from August 16 to 19, 2022, using the "fha[Filter]" search term, which is a PubMed filter tag that helps identify articles with structured abstracts. From the article base, we extracted 5331 articles that met the criteria of having abstracts structured into 4 components (introduction or background, methods, results, and conclusion) with both the title and abstract written in English, allowing the extraction of these components along with the title. Each component was classified according to the criteria listed in Table S1 in Multimedia Appendix 1. Using the tokenized object from the Natural Language Toolkit library for initial sentence splitting, we divided the abstracts into individual sentences. Each sentence was then manually labeled with exactly one mutually exclusive component tag "Introduction [I], Methods [M], Result [R], Conclusion [C]". Ultimately, we extracted 62,798 sentences, comprising 11,961; 17,154; 23,204; and 10,479 sentences for the introduction, methods, results, and conclusion, respectively (PubMed dataset). In addition, abstracts of the articles extracted from the systematic review in Experiment 1 were divided into sentences and labeled (Systematic Review Dataset). The dataset included 3477, 6265, 7091, and 3038 sentences for the introduction, methods, results, and conclusion, respectively, with a total of 19,871 sentences.

From the labeled sentences of the PubMed Dataset, we created training, validation, and test sets. We randomly allocated 4000 sentences (8:1:1) to the training, validation, and test sets. These datasets comprised equal proportions of samples for each label to prevent performance deterioration owing to unbalanced samples.

Abstract Component Classifier models were implemented to predict the sentence labels using the transformer library. We developed them from 4 pretrained models: (BERT; bert-large-uncased [11]), BioLinkBERT (BioLinkBERT-Large) [12], 2 types of BioM-ELECTRA, BioM-ELECTRA-Large-SQuAD2 [13] and BioM-ELECTRA-Large-Discriminator [19]. BioM-ELECTRA-Large-Discriminator is a model that, unlike the BioM-ELECTRA-Large-SQuAD2, does not undergo fine-tuning with SQuAD2; it uses the same pretraining corpus as BioM-ELECTRA-Large-SQuAD2.

We trained the classifier models on the training and validation sets and evaluated the model performance using the test set. For the Abstract Component Classifier Model, we limited our parameter tuning to Lr, as our primary objective was to confirm the basic capability of the component classification model rather than maximizing performance through extensive parameter optimization. This focused approach was supported by the strong baseline performance achieved with basic parameter settings.

Then, we classified the sentences in the PubMed dataset and evaluated their performance. The primary evaluation metric was the macro–F_1-score (F_1-score). The number of epochs for training the screening models was set to 32, patience for early stopping to 3, and weight decay to 0.01.

Similarly, we conducted the same analysis for the Systematic Review Dataset, and the model with the highest F_1-score was also selected as the Abstract Component Classifier Model, which was used for subsequent analysis.

Development of a Screening Model Using Article Components as Determined by the Abstract Component Classifier Model

As described in Experiment 1, we developed screening models using the same data sources and methods. However, we used

XSL•FO
RenderX

the Abstract Component Classifier Model, which we developed to automatically classify abstract components of articles that were previously classified manually in Experiment 1. These abstracts were reclassified into 4 components based on the results of classification using the Abstract Component Classifier Model. If no sentence was allocated to any of the components in the classifier model, the component was treated as a document with 0 words. From the title data and reclassified component data, we created component-composed datasets. To focus on the most promising approaches while maintaining computational efficiency, we selected 10 datasets corresponding to the top 10 performing models from Experiment 1. This focused approach was selected to specifically examine whether the advantages observed with manual classification could be maintained when transitioning to an automated system; a key consideration for practical implementation. This selection allowed us to evaluate how well these high-performing component combinations performed when using automated classification instead of manual classification. Table S3 in Multimedia Appendix 1 lists the component composition used in the screening models, which were implemented using training datasets created from the selected 10 component-composed datasets. The primary endpoint was the F10-score, which was compared to the performance of 10 classifiers with the same component composition constructed in Experiment 1.

Ethical Considerations

All analyses were conducted using previously published studies, and therefore, ethics approval and patient consent were unnecessary. This study does not include human subject information, primary data collection, or any form of experimentation involving individuals.

Results

Overview

All results reported in this section were obtained using the test set, which was completely separate from the training and validation sets used for model development.

Experiment 1: Evaluation of the Impact of Selecting Article Titles and Abstract Components on the Development of the Screening Model

Characteristics of the Number of Words in the Extracted Articles

The word count of the 1517 articles had a median of 276 (range 103-1099) words. After tokenization, 50 articles (including 2 included articles) exceeded the maximum sequence length of 512 tokens that our pretrained models could process in one iteration.

Performance of Screening Models

A detailed description of all datasets, including class proportions, is provided in Table S4 in Multimedia Appendix 1. Details of the final evaluation results on the held-out test set for the screening models with different Lr (6e-7, 2e-6, and 6e-6) are shown in Table S5-S7 in Multimedia Appendix 1. For the screening model using BERT (Table S4 in Multimedia Appendix 1), the model trained on the 4 components "Title + Methods + Results + Conclusion" demonstrated the highest average F10-Score (precision=0.35; recall=0.93; F10-Score=0.91). Conversely, the model with the lowest F10-Score was trained solely on the conclusion (precision=0.48; recall=0.77; F10-Score=0.75). The model trained on all 5 components ranked tenth in the average F10-Score of all 31 screening models. For BioLinkBERT (Table S5 in Multimedia Appendix 1), similar to BERT, the model trained on "Title + Methods + Results + Conclusion" recorded the highest F10-Score (precision=0.28; recall=0.95; F10-Score=0.93). The lowest F10-Score, as with BERT, was observed in the model trained only on the Conclusion (precision=0.58, recall=0.77; F10-Score=0.76). The model trained on all 5 components had the seventh highest average F10-Score of all 31 screening models. For the BioM-ELECTRA (Table S6 in Multimedia Appendix 1), the model trained on Methods + Conclusion achieved the highest F10-Score (precision=0.37; recall=0.89; F10-Score=0.88). The lowest F10-Score was obtained for the model trained on Title + Introduction + Methods (precision=0.32; recall=0.74; F10-Score=0.73). The model trained on all 5 components ranked 20 seconds in the average F10-Score among all the 31 screening models.

Experiment 2: Development of a Screening Model Using Article Components as Determined by the Abstract Component Classifier Model

Development of the Abstract Component Classifier Model

Table 1 lists the average results of 5 evaluations of the classifier models using the PubMed Dataset. The main evaluation metric, the F_1-score was 0.89 for BERT; Lr:6e-6, 0.92 for BioLinkBERT; Lr:2e-6, and 0.91 for both BioM-ELECTRA-Large-SQuAD2; Lr:6e-6 and BioM-ELECTRA-Large-Discriminator; Lr:6e-6.

Table 1. Performance of the Abstract Component Classifier using PubMed dataset.

Model	Learning rate	Epochs	Accuracy	Precision	Recall	F_1-score
BERT[a]	6e-6	4.6	0.89	0.90	0.89	0.89
BioLinkBERT	2e-6	5.8	0.92	0.92	0.92	0.92
BioM-ELECTRA[b]-Large-SQuAD2	6e-6	5.6	0.91	0.91	0.91	0.91
BioM-ELECTRA-Large-Discriminator	6e-6	5.2	0.91	0.91	0.91	0.91

[a]BERT: Bidirectional Encoder Representations from Transformer.

[b]ELECTRA: Efficiently Learning an Encoder that Classifies Token Replacements Accurately.

XSL•FO
RenderX

The performance results by label using the dataset composed of sentences from the abstracts of the articles in the targeted systematic review (Systematic Review Dataset) are shown in Table 2. Implemented classifiers showed the average F_1-scores of 0.88-0.93, 0.93-0.95, 0.92-0.92, and 0.83-0.85 for Introduction, Methods, Results, and Conclusions, respectively. In this study, the BioM-ELECTRA-Large-Discriminator, which achieved a macro–F_1-score of 0.94 in one instance, was selected as the Abstract Component Classifier Model.

Table 2. Performance of classifiers implemented by each label using the Systematic Review Dataset.

	BERT[a]			BioLinkBERT			BioM-ELECTRA[b]-Large-SQuAD2			BioM-ELECTRA-Large-Discriminator		
	Precision	Recall	F_1-score	Precision	Recall	F_1-score	Precision	Recall	F_1-score	Precision	Recall	F_1-score
Introduction	0.86	0.89	0.88	0.92	0.94	0.93	0.92	0.92	0.92	0.92	0.93	0.92
Methods	0.94	0.93	0.93	0.96	0.94	0.95	0.92	0.95	0.94	0.94	0.95	0.95
Results	0.92	0.92	0.92	0.93	0.91	0.92	0.92	0.92	0.92	0.95	0.89	0.92
Conclusion	0.84	0.82	0.83	0.81	0.89	0.85	0.87	0.80	0.84	0.80	0.89	0.85
macro average	0.89	0.89	0.89	0.91	0.92	0.91	0.91	0.90	0.90	0.90	0.92	0.91

[a]BERT: Bidirectional Encoder Representations from Transformer.

[b]ELECTRA: Efficiently Learning an Encoder that Classifies Token Replacements Accurately.

Development of a Screening Model Using Article Components as Determined by the Abstract Component Classifier Model

Table 3 shows the average results of 5 evaluations of 10 screening models created from the component-composed datasets classified by the developed Abstract Component Classifier Model, along with the results of models created from the same 10 component-composed datasets and all 5 components in Experiment 1. In the tables, among the screening models with the same component composition, those with higher average F10-Scores are highlighted in bold. The results of the screening models using Lr not included in these tables are shown in Table S6-S7 in Multimedia Appendix 1. For the screening model using BERT (Table 3), the model trained on the 4 components Title + Methods + Results + Conclusion recorded the highest F10-Score (precision=0.35; recall=0.93; F10-Score=0.91). The model with the lowest F10-Score that was trained on Title + Methods + Conclusion showed precision=0.40; recall=0.86; and F10-Score=0.85. For BioLinkBERT (Table 4), the model trained on Title + Methods + Results + Conclusion recorded the highest F10-Score (precision=0.42; recall=0.90; F10-Score=0.88). The lowest F10-Score was observed in the model trained on Introduction + Methods (precision=0.63; recall=0.78; F10-Score=0.78). For BioM-ELECTRA (Table 5), the model trained on Methods + Results + Conclusion achieved the highest F10-Score (precision=0.38; recall=0.86; F10-Score=0.85). The lowest F10-Score was obtained for the model trained on Title + Results + Conclusion (precision=0.25; recall=0.69; F10-Score=0.68).

XSL•FO
RenderX

Table 3. Comparison of F10-Score between screening models using component data by Abstract Component Classifier Model and screening model using manually classified component data in hand, based on BERT[a].

	Screening models using component data by the classifier						Screening models using manually classified component data					
Composition	Learning rates	Epochs	Accuracy	Precision	Recall	F10-Score	Learning rates	Epochs	Accuracy	Precision	Recall	F10-Score
T[b] + M[c] + R[d] + C[e]	2e-6	9.2	0.92	0.35	0.93	0.91	2e-6	9.0	0.92	0.35	0.93	0.91
T + I[f] + R + C	6e-6	6.6	0.92	0.40	0.91	0.89	2e-6	6.8	0.92	0.36	0.91	0.89
T + R	2e-6	8.4	0.88	0.25	0.91	0.89	2e-6	6.8	0.91	0.29	0.89	0.87
T + M + R	6e-7	21.0	0.92	0.34	0.90	0.88	6e-7	18.2	0.91	0.33	0.92	0.90
T + I + R	6e-6	6.4	0.87	0.29	0.91	0.88	2e-6	7.0	0.91	0.30	0.90	0.88
T + I + C	2e-6	8.4	0.93	0.36	0.90	0.88	6e-6	5.0	0.90	0.30	0.92	0.90
T + M	6e-6	6.0	0.86	0.29	0.91	0.88	2e-6	6.0	0.86	0.22	0.92	0.89
T + R + C	6e-6	5.4	0.90	0.28	0.88	0.86	6e-6	6.8	0.89	0.27	0.91	0.89
T + I + M	6e-7	14.6	0.88	0.24	0.88	0.85	2e-6	5.8	0.88	0.26	0.93	0.91
T + M + C	2e-6	12.2	0.94	0.40	0.86	0.85	2e-6	7.6	0.93	0.38	0.89	0.87
T + I + M + R + C	__[g]	—	—	—	—	—	6e-6	5.0	0.83	0.31	0.91	0.87

[a]BERT: Bidirectional Encoder Representations from Transformer.

[b]T: Title.

[c]M: Methods.

[d]R: Results.

[e]C: Conclusion.

[f]I: Introduction.

[g]Not applicable.

XSL•FO
RenderX

Table 4. Comparison of F10-Score between screening models using component data by Abstract Component Classifier Model and screening model using manually classified component data in hand, based on BioLinkBERT[a]. Descending order of the F10-Score for screening models using component data by classifier.

Composition	Screening models using component data by the classifier						Screening models using manually classified component data					
	Learning rates	Epochs	Accuracy	Precision	Recall	F10-Score	Learning rates	Epochs	Accuracy	Precision	Recall	F10-Score
T[b] + M[c] + R[d] + C[e]	6e-6	11.2	0.94	0.42	0.90	0.88	6e-6	11.8	0.89	0.29	0.95	0.93
T + M + R	6e-6	10.6	0.94	0.41	0.87	0.86	6e-6	6.4	0.94	0.44	0.91	0.90
T + I[f] + M	6e-6	6.0	0.95	0.53	0.86	0.85	6e-6	6.4	0.92	0.42	0.91	0.89
T + M	6e-6	5.6	0.90	0.29	0.86	0.84	6e-6	6.4	0.92	0.38	0.89	0.87
I + M + R + C	6e-6	6.2	0.93	0.47	0.85	0.84	6e-6	7.6	0.91	0.30	0.94	0.92
I + R	6e-6	5.2	0.93	0.54	0.84	0.82	6e-6	7.8	0.93	0.43	0.89	0.87
M + C	6e-6	5.6	0.92	0.48	0.84	0.82	6e-6	5.6	0.92	0.43	0.89	0.87
M	6e-6	5.4	0.93	0.35	0.82	0.80	6e-6	6.2	0.91	0.33	0.89	0.87
R + C	6e-6	6.0	0.91	0.29	0.82	0.80	6e-6	6.6	0.90	0.35	0.93	0.90
I + M	6e-6	5.2	0.96	0.63	0.78	0.78	6e-6	7.2	0.90	0.30	0.93	0.91
T + I+ M + R + C	__[g]	—	—	—	—	—	6e-6	7.2	0.95	0.53	0.90	0.89

[a]BERT: Bidirectional Encoder Representations from Transformer.

[b]T: Title.

[c]M: Methods.

[d]R: Results.

[e]C: Conclusion.

[f]I: Introduction.

[g]Not applicable.

XSL•FO
RenderX

Table 5. Comparison of F10-Score between screening models using component data by Abstract Component Classifier Model and screening model using manually classified component data in hand, based on BioM-ELECTRA[a]. Descending order of the F10-Score for screening models using component data by classifier.

Composition	Screening models using component data by the classifier						Screening models using manually classified component data					
	Learning rates	Epochs	Accuracy	Precision	Recall	F10-Score	Learning rates	Epochs	Accuracy	Precision	Recall	F10-Score
M[b] + R[c] + C[d]	6e-7	17.8	0.94	0.38	0.86	0.85	6e-6	7.4	0.94	0.42	0.87	0.86
M	6e-7	13.2	0.89	0.26	0.86	0.84	6e-6	5.6	0.92	0.38	0.83	0.82
T[e] + R	2e-6	6.4	0.84	0.19	0.86	0.83	2e-6	5.8	0.88	0.27	0.84	0.82
M + C	6e-6	10.0	0.92	0.38	0.84	0.83	6e-6	7.2	0.93	0.37	0.90	0.88
M + R	2e-6	6.6	0.93	0.38	0.83	0.81	2e-6	9.4	0.93	0.40	0.85	0.83
T + M + C	6e-6	6.8	0.91	0.29	0.82	0.80	6e-6	5.8	0.91	0.40	0.83	0.81
I[f] + M	6e-6	5.4	0.95	0.53	0.81	0.80	6e-6	6.0	0.92	0.45	0.84	0.82
I + C	2e-6	7.0	0.96	0.59	0.78	0.77	6e-6	6.2	0.94	0.45	0.83	0.82
T + M	6e-6	5.4	0.92	0.32	0.78	0.77	6e-6	5.4	0.92	0.33	0.84	0.83
T + R + C	6e-7	14.0	0.90	0.25	0.69	0.68	6e-6	6.8	0.91	0.39	0.85	0.83
T + I + M + R + C	__[g]	—	—	—	—	—	6e-6	4.8	0.95	0.45	0.76	0.77

[a]ELECTRA: Efficiently Learning an Encoder that Classifies Token Replacements.

[b]M: Methods.

[c]R: Results.

[d]C: Conclusion.

[e]T: Title.

[f]I: Introduction.

[g]Not applicable.

Discussion

Principal Results

In this study, we evaluated the significance of selecting components from article titles or abstracts on the performance of screening models for systematic review updates. Our results demonstrated that for all pretrained models, we were able to implement screening models that outperformed those trained on all 5 components. This indicates that the selection of components from the article title or abstracts is beneficial for improving the performance of the screening models. The performance differences between models trained on all components versus selected components may be attributed to the interaction between token limitations and information priority. When using all 5 components, the inclusion of introduction or background sections might have resulted in the loss of crucial information from results or conclusion sections due to the 512-token limit. Furthermore, domain-specific models can show varying performance depending on the input information structure [20]. The 3 pretrained models used in this study showed different component compositions, leading to higher average F10-Scores, despite using the same training datasets. Through our comprehensive exploration of all 31 component combinations, we identified certain combinations that consistently showed superior performance. Specifically, the Title+Method+Result+Conclusion combination demonstrated strong performance across different models, and combinations including Methods and Results components generally performed well. For practical implementations where computational resources are limited, focusing on these high-performing combinations, rather than exhaustively testing all possible combinations, could provide a more efficient path to developing effective screening models while maintaining high performance.

Furthermore, we implemented screening models by using the dataset for each component classified using the developed Abstract Component Classifier Model, which analyzes the semantic content of individual sentences to determine their rhetorical roles, enabling the classification of both structured and unstructured abstracts. Consequently, for the large-uncased model, 7 out of the 10 models outperformed the model trained on all 5 components. For BioM-ELECTRA, 9 out of 10 screening models showed higher performance than the model trained on all 5 components. These results demonstrate that a screening model implemented by combining component classification using a classifier model and component selection can surpass the performance of traditional screening models. However, when using the Abstract Component Classifier in Experiment 2, all 10 screening models using BioLinkBERT demonstrated lower performance than BioLinkBERT's model trained on all 5 components. This behavior, which differs from our observations in Experiment 1, suggests that BioLinkBERT

XSL•FO
RenderX

may be more sensitive to the quality and structure of the component classification. The automatic classification process might disrupt certain patterns or contextual relationships that BioLinkBERT relies on, making it perform better with manually classified components in Experiment 1 but not as well with automatically classified components in Experiment 2. This suggests that the effectiveness of component selection strategies may depend not only on the model's characteristics but also on how the components are identified and structured. This finding highlights the complex interaction between model architecture, component classification method, and overall performance.

Comparison With Previous Work

Among the screening models using datasets classified by the developed Abstract Component Classifier, the model trained on Title+Method+Result+Conclusion using BERT achieved the highest average F10-Score (precision=0.35, recall=0.93; F10-Score=0.91). The test set included 40 of the 1000 articles. Therefore, this model reduced 1000 studies that had to be scrutinized manually to an average of 106.3, while extracting an average of 37.2 included articles. Following Cohen (2006) formula for work-saved oversampling, which accounts for both the number of articles to be screened and the model's recall of 0.93, this represents an 88.6% reduction in screening workload. In a previous study by Qin et al [8], the implemented screening model achieved a sensitivity of 96%, a specificity of 78%, and a 64.1% reduction in workload, thereby demonstrating the rationality and feasibility of using a screening model. The F10-Score of the screening model in Qin's study exceeded that of the model implemented in this study precision=0.50; recall=0.96; F10-Score=0.95). However, it is important to note that Qin's study used an ensemble model that integrated 4 different screening models, and the F10-Scores of each individual screening model used to implement the ensemble model were lower than the average F10-Score of the screening model in this study (F10-Scores=0.79, 0.81, 0.91, and 0.81).

In screening models that used the article abstract component classifier, 7 out of 10 models for BERT and 8 models for BioM-ELECTRA underperformed compared to the average F10-Score of models with the same component compositions that were created through manual component classification. For BioLinkBERT, all screening models showed lower average F10-Scores than those of the screening models with manually classified component datasets. These results indicate a tendency for screening models with the classifier model's classification to underperform when compared with those using manually classified component datasets. This performance gap suggests that our Abstract Component Classifier does not achieve the same level of accuracy as manual labeling, possibly due to limitations in maintaining the contextual integrity of the text during the automatic classification process.

Jiang et al [21] implemented a classifier using the BERT model to classify text into 5 components: background, objective, methods, results, and conclusion and achieved an F1-Score of 0.98 [21]. This F1-Score surpasses that of the classifier implemented in our study. This result may contribute to the differences in the classification methods from previous studies conducted as Machine Reading Comprehension tasks and the scale of the dataset, which used PubMed 200k and comprised approximately 200,000 RCT trial abstracts [22]. However, previous studies used BERTbase13 without a medical literature corpus for pretraining. In our study, the classifiers that used BioLinkBERT, BioM-ELECTRA-Large-SQuAD2, and BioM-ELECTRA-Large-Discriminator achieved higher F_1-scores than the one using BERT. Therefore, it is important to construct a classifier using these pretrained models, and the same method that was used in previous studies could implement a superior classifier.

Analysis of Model Performance Metrics

In this study, the F10-Score was the primary evaluation metric for the screening model. This choice was made for 2 reasons: to prioritize recall and apply an appropriate penalty to screening models that classify everything as positive. As expected, our results showed that the screening model could be evaluated based on the F10-Score. Moreover, we implemented screening models that had a higher F10-Score than one that classified everything as positive (F10-Score=0.81). This suggests that adopting the F10-Score as the main evaluation metric in our study was appropriate. However, the F10-Score of the screening model classifying everything as positive varied depending on the ratio of the included and excluded articles in the test set. Therefore, it is inferred that when creating test sets with different ratios from those used in our study and conducting similar evaluations, it will be necessary to set a new appropriate β.

Alternative approaches to evaluation metrics, such as maximizing specificity at 99% recall, could also be considered for systematic review screening tasks. While our F10-score approach prioritizes recall while maintaining some consideration for precision, the specificity-focused approach would explicitly maximize the number of excluded articles while maintaining a fixed, very high recall. Both approaches have merit for systematic review updating, though they are optimized for slightly different practical outcomes. Furthermore, F10-scores can be influenced by class prevalence in the test set. In our study, we maintained the class distributions of the test set similar to those of the original systematic review to ensure realistic performance evaluation, reflecting the naturally imbalanced distribution of relevant versus irrelevant articles. Future research might explore how different evaluation metrics and varying class distributions affect model selection and practical utility in systematic review updating, particularly in the context of identifying a small number of relevant articles from a large corpus.

In comparing different models' performances, we observed that small improvements in the F10-Score often reflected different trade-offs between precision and recall. For example, the BioLinkBERT model trained on Title+Method+Result+Conclusion achieved a higher F10-Score (0.93) compared to BERT (0.91), primarily due to higher recall (0.95 vs 0.93) despite lower precision (0.28 vs 0.35). While this trade-off resulted in a numerically higher F10-Score, it is important to note that in practical applications, significantly lower precision means more irrelevant articles requiring manual screening. However, in the context of systematic reviews, this trade-off might be acceptable given the critical importance of

XSL•FO
RenderX

not missing relevant studies, though it suggests the need for careful consideration of the balance between comprehensive coverage and screening efficiency in different systematic review contexts.

Limitations

One limitation of this study pertains to the generalizability of our results. We implemented and compared the performances of the screening models using the screening results of a single systematic review focusing on adverse events of macrolide antibiotics. While this dataset provided a solid foundation for model development and evaluation, comprehensive validation across multiple systematic reviews in different medical specialties, such as oncology, cardiology, infectious diseases, and pediatrics, is essential to confirm the broad applicability of our approach. Without such validation, the model's performance may vary significantly across different medical domains due to variations in terminology, study designs, and reporting patterns. For instance, the language and structure used in oncology trial reports may differ substantially from those in used cardiovascular studies, potentially affecting the model's component classification accuracy and overall screening performance. Our results may not fully represent the model's performance in systematic reviews of other medical areas (such as cardiovascular disease, and oncology) or different types of studies (such as observational studies or cohort studies). Furthermore, regarding the criteria for classification by component used in this study, it is possible that not all criteria are comprehensively applicable for classifying components in articles from other fields. Another limitation is that our study did not include comparisons with recent large language models (LLMs). Computational resource constraints and reproducibility concerns primarily drove the decision to exclude LLM comparisons, as many current LLMs are not open-source and require significant computational infrastructure for fine-tuning. In addition, the rapid evolution of LLMs poses challenges for establishing stable benchmarks. While we focused on established BERT-based models that are widely validated for classification tasks, recent research has shown that the relative performance of different models can vary significantly based on data availability. For instance, Jahan et al. demonstrated that while LLMs can outperform fine-tuned models on biomedical tasks with limited training data, BERT-based models often maintain advantages when substantial training data is available for fine-tuning [23]. Our current approach using BERT-based models, with access to sufficient training data, provides a solid benchmark for evaluating the effectiveness of component-based classification in systematic review updating.

Future Work

In this study, we classified each piece of article into 5 components: title and 4 abstract components (introduction, methods, results, and conclusion). Article abstracts can be further subdivided. By refining the component classification, we can improve the performance of the screening model. Therefore, future research that implements screening models using further subdivided articles is required. The dataset used in this study comprised 256 studies. This number is relatively high for the articles analyzed in a systematic review. Our screening model intended to use the included and excluded articles from a preupdated systematic review as the training dataset. Therefore, implementing a screening model for a systematic review that analyzes a small number of studies may result in decreased performance. Therefore, it is necessary to estimate the number of studies required to achieve a performance level comparable to that of the screening model that was developed in this study. Finally, the performance of the screening model was evaluated individually. Therefore, combining the technique of article title or abstract component selection with methods, such as implementing ensemble models, could potentially implement even high-performance screening models.

Future research should also explore strategies to address the few limitations observed in our study. This may include investigating models designed for handling longer sequences, such as Longformer [24] or Big Bird [25], or developing methods to process each abstract component separately before combining their vector representations. While these approaches could improve screening performance, they are likely to increase computational complexity compared to our current method. Therefore, future work will need to explore ways to balance these advanced techniques with computational efficiency requirements.

Investigating the integration of LLMs into systematic review screening presents a promising direction for future research. Consequently, future studies should examine the cost-effectiveness and computational efficiency of various LLM integration strategies, particularly in resource-constrained settings. Research into fine-tuning smaller, more efficient LLMs specifically for systematic review tasks could provide a practical balance between model performance and computational requirements.

Conclusions

Our study revealed that implementing a screening model trained on selected components of the title or abstract articles could enable better performance than a traditionally implemented model that was trained on all 5 components in some cases. Furthermore, we developed an Abstract Component Classifier that classifies each sentence of the abstract into different components and implements screening models through the component classification of target article abstracts using this classifier and the selection of article title/abstract components. Thus, we were able to implement screening models with a higher performance than the traditional model trained on all 5 components in the 2 pretrained models. This approach could reduce the workload of the systematic review update process.

XSL•FO
RenderX

Authors' Contributions

HT, KH, IS, and HS designed the study. HT and YY conducted the annotation. HT performed the data analysis, created the NLP model, and conducted the primary experiments. IK performed additional experiments and data analysis to validate the results. YS and AE supervised the NLP research as specialists. HS supervised the study overall. HT, KH, and HS drafted and finalized the paper. All authors reviewed and approved the paper.

Conflicts of Interest

None declared.

Multimedia Appendix 1
Additional materials about the details of the search, element composition datasets, and performance of the models.
[DOCX File , 69 KB - medinform_v13i1e65371_app1.docx]

References

1. Garritty C, Stevens A, Hamel C, Golfam M, Hutton B, Wolfe D. Knowledge synthesis in evidence-based medicine. Semin Nucl Med 2019;49(2):136-144. [doi: 10.1053/j.semnuclmed.2018.11.006] [Medline: 30819393]
2. Hoffmeyer BD, Andersen MZ, Fonnes S, Rosenberg J. Most cochrane reviews have not been updated for more than 5 years. J Evid Based Med 2021;14(3):181-184. [doi: 10.1111/jebm.12447] [Medline: 34427395]
3. Chapter IV: Updating a review. URL: https://training.cochrane.org/handbook/current/chapter-iv [accessed 2024-04-24]
4. Shojania KG, Sampson M, Ansari MT, Ji J, Doucette S, Moher D. How quickly do systematic reviews go out of date? A survival analysis. Ann Intern Med 2007;147(4):224-233 [FREE Full text] [doi: 10.7326/0003-4819-147-4-200708210-00179] [Medline: 17638714]
5. Research Guides: Systematic Review: Steps of a Systematic Review. 2018 Feb 16;. URL: https://lib.guides.umd.edu/SR/steps [accessed 2024-04-24]
6. Tawfik GM, Dila KAS, Mohamed MYF, Tam DNH, Kien ND, Ahmed AM, et al. A step by step guide for conducting a systematic review and meta-analysis with simulation data. Trop Med Health 2019;47:46 [FREE Full text] [doi: 10.1186/s41182-019-0165-6] [Medline: 31388330]
7. Chapter 4: Searching for and selecting studies. URL: https://training.cochrane.org/handbook/current/chapter-04 [accessed 2024-04-24]
8. Qin X, Liu J, Wang Y, Liu Y, Deng K, Ma Y, et al. Natural language processing was effective in assisting rapid title and abstract screening when updating systematic reviews. J Clin Epidemiol 2021;133:121-129 [FREE Full text] [doi: 10.1016/j.jclinepi.2021.01.010] [Medline: 33485929]
9. Haynes RB, Mulrow CD, Huth EJ, Altman DG, Gardner MJ. More informative abstracts revisited. Ann Intern Med 1990;113(1):69-76. [doi: 10.7326/0003-4819-113-1-69] [Medline: 2190518]
10. Hansen MP, Scott AM, McCullough A, Thorning S, Aronson JK, Beller EM, et al. Adverse events in people taking macrolide antibiotics versus placebo for any indication. Cochrane Database Syst Rev 2019;1(1):CD011825 [FREE Full text] [doi: 10.1002/14651858.CD011825.pub2] [Medline: 30656650]
11. google-bert/bert-large-uncased · Hugging Face. URL: https://huggingface.co/google-bert/bert-large-uncased [accessed 2024-08-11]
12. michiyasunaga/BioLinkBERT-large · Hugging Face. URL: https://huggingface.co/michiyasunaga/BioLinkBERT-large [accessed 2024-08-11]
13. sultan/BioM-ELECTRA-Large-SQuAD2 · Hugging Face. URL: https://huggingface.co/sultan/BioM-ELECTRA-Large-SQuAD2 [accessed 2024-08-11]
14. Devlin J, Chang MW, Lee K, Toutanova K. BERT: pre-training of deep bidirectional transformers for language understanding. 2019 Presented at: Proceedings of the 2019 Conference of the North American Chapter of the Association for Computational Linguistics:; 2019 May 24; Minneapolis. [doi: 10.18653/v1/n18-2]
15. Yasunaga M, Leskovec J, Liang P. LinkBERT: Pretraining Language Models with Document Links. URL: https://arxiv.org/abs/2203.15827 [accessed 2022-03-29]
16. Alrowili S, Shanker V. BioM-Transformers: building large biomedical language models with BERT, ALBERTELECTRA. 2021 Presented at: Proceedings of the BioNLP 2021 workshop; 2021 June 11; USA. [doi: 10.18653/v1/2021.bionlp-1.24]
17. Clark K, Luong MT, Le Q, Manning CD. ELECTRA: Pre-training Text Encoders as Discriminators Rather Than Generators. URL: http://arxiv.org/abs/2003.10555 [accessed 2020-03-23]
18. BLURB Leaderboard. URL: https://microsoft.github.io/BLURB/ [accessed 2024-04-24]
19. sultan/BioM-ELECTRA-Large-Discriminator · Hugging Face. URL: https://huggingface.co/sultan/BioM-ELECTRA-Large-Discriminator [accessed 2024-08-11]
20. Naseem U, Dunn AG, Khushi M, Kim J. Benchmarking for biomedical natural language processing tasks with a domain specific ALBERT. BMC Bioinformatics 2022;23(1):144 [FREE Full text] [doi: 10.1186/s12859-022-04688-w] [Medline: 35448946]

XSL•FO
RenderX

21. Jiang CY, Fan YC. Biomedical Abstract Sentence Classification by BERT-Based Reading Comprehension. SN Comput Sci Berlin, Heidelberg: Springer-Verlag;. 2023. URL: https://www.researchgate.net/publication/370841419_Biomedical_Abstract_Sentence_Classification_by_BERT-Based_Reading_Comprehension [accessed 2023-05-17]
22. Dernoncourt F, Lee JY. PubMed 200k RCT: a Dataset for Sequential Sentence Classification in Medical Abstracts. URL: https://arxiv.org/abs/1710.06071 [accessed 2017-10-17]
23. Jahan I, Laskar MTR, Peng C, Huang JX. A comprehensive evaluation of large language models on benchmark biomedical text processing tasks. Comput Biol Med 2024;171:108189 [FREE Full text] [doi: 10.1016/j.compbiomed.2024.108189] [Medline: 38447502]
24. Beltagy I, Peters ME, Cohan A. Longformer: The Long-Document Transformer. arXiv [csCL]. URL: https://www.semanticscholar.org/paper/Longformer%3A-The-Long-Document-Transformer-Beltagy-Peters/925ad2897d1b5decbea320d07e99afa9110e09b2?utm_source=consensus [accessed 2020-04-10]
25. Zaheer M, Guruganesh G, Dubey A, Ainslie J, Alberti C, Ontanon S, et al. Big bird: Transformers for longer sequences. URL: https://www.semanticscholar.org/paper/Big-Bird%3A-Transformers-for-Longer-Sequences-Zaheer-Guruganesh/044e13d7dd4e0655eb76f0bd00b2c1bdb44e2be3?utm_source=consensus [accessed 2020-07-28]

Abbreviations

BERT: Bidirectional Encoder Representations from Transformer
ELECTRA: Efficiently Learning an Encoder that Classifies Token Replacements Accurately
LLM: large language model
Lr: learning rates
NLP: natural language processing
WHO: World Health Organization

Edited by A Castonguay; submitted 13.08.24; peer-reviewed by A Tatsioni, R Yang, C Lokker; comments to author 01.11.24; revised version received 02.02.25; accepted 17.02.25; published 27.03.25.

Please cite as:
Hasegawa T, Kizaki H, Ikegami K, Imai S, Yanagisawa Y, Yada S, Aramaki E, Hori S
Improving Systematic Review Updates With Natural Language Processing Through Abstract Component Classification and Selection: Algorithm Development and Validation
JMIR Med Inform 2025;13:e65371
URL: https://medinform.jmir.org/2025/1/e65371
doi:10.2196/65371
PMID:

©Tatsuki Hasegawa, Hayato Kizaki, Keisho Ikegami, Shungo Imai, Yuki Yanagisawa, Shuntaro Yada, Eiji Aramaki, Satoko Hori. Originally published in JMIR Medical Informatics (https://medinform.jmir.org), 27.03.2025. This is an open-access article distributed under the terms of the Creative Commons Attribution License (https://creativecommons.org/licenses/by/4.0/), which permits unrestricted use, distribution, and reproduction in any medium, provided the original work, first published in JMIR Medical Informatics, is properly cited. The complete bibliographic information, a link to the original publication on https://medinform.jmir.org/, as well as this copyright and license information must be included.

XSL•FO
RenderX

Original Paper

Improving Phenotyping of Patients With Immune-Mediated Inflammatory Diseases Through Automated Processing of Discharge Summaries: Multicenter Cohort Study

Adam Remaki[1], MS; Jacques Ung[2], MS; Pierre Pages[2], MS; Perceval Wajsburt[2], PhD; Elise Liu[3], PhD; Guillaume Faure[1], MS; Thomas Petit-Jean[2], MS; Xavier Tannier[1], PhD; Christel Gérardin[1,4], PhD

[1]Limics, Université Sorbonne Paris-Nord, Inserm, Sorbonne Université, Paris, France

[2]Pôle Innovation et Données, Direction des Services Numériques, Assistance Publique – Hôpitaux de Paris, Paris, France

[3]Centre de Pharmacoépidémiologie, Hôpital Pitié Salpêtrière, Assistance Publique – Hôpitaux de Paris, Paris, France

[4]Service de médecine interne, Hôpital Tenon, Assistance Publique – Hôpitaux de Paris, Paris, France

Corresponding Author:
Adam Remaki, MS
Limics
Université Sorbonne Paris-Nord, Inserm
Sorbonne Université
15 Rue de l'École de Médecine
Paris, 75006
France
Phone: 33 783049678
Email: ad.remaki@gmail.com

Abstract

Background: Valuable insights gathered by clinicians during their inquiries and documented in textual reports are often unavailable in the structured data recorded in electronic health records (EHRs).

Objective: This study aimed to highlight that mining unstructured textual data with natural language processing techniques complements the available structured data and enables more comprehensive patient phenotyping. A proof-of-concept for patients diagnosed with specific autoimmune diseases is presented, in which the extraction of information on laboratory tests and drug treatments is performed.

Methods: We collected EHRs available in the clinical data warehouse of the Greater Paris University Hospitals from 2012 to 2021 for patients hospitalized and diagnosed with 1 of 4 immune-mediated inflammatory diseases: systemic lupus erythematosus, systemic sclerosis, antiphospholipid syndrome, and Takayasu arteritis. Then, we built, trained, and validated natural language processing algorithms on 103 discharge summaries selected from the cohort and annotated by a clinician. Finally, all discharge summaries in the cohort were processed with the algorithms, and the extracted data on laboratory tests and drug treatments were compared with the structured data.

Results: Named entity recognition followed by normalization yielded F_1-scores of 71.1 (95% CI 63.6-77.8) for the laboratory tests and 89.3 (95% CI 85.9-91.6) for the drugs. Application of the algorithms to 18,604 EHRs increased the detection of antibody results and drug treatments. For instance, among patients in the systemic lupus erythematosus cohort with positive antinuclear antibodies, the rate increased from 18.34% (752/4102) to 71.87% (2949/4102), making the results more consistent with the literature.

Conclusions: While challenges remain in standardizing laboratory tests, particularly with abbreviations, this work, based on secondary use of clinical data, demonstrates that automated processing of discharge summaries enriched the information available in structured data and facilitated more comprehensive patient profiling.

(JMIR Med Inform 2025;13:e68704) doi:10.2196/68704

XSL•FO
RenderX

KEYWORDS

secondary use of clinical data for research and surveillance; clinical informatics; clinical data warehouse; electronic health record; data science; artificial intelligence; AI; natural language processing; ontologies; classifications; coding; tools; programs and algorithms; immune-mediated inflammatory diseases

Introduction

Background

Since the 2010s, the widespread adoption of electronic health records (EHRs) and health data warehouses has enabled the development and application of new algorithms for patient phenotyping, which corresponds to the extraction of a set of observable patient characteristics, including laboratory test results, symptoms, diseases, and past or current treatments [1]. The automated extraction of these characteristics from large-scale databases supports predictive risk assessments, preselection for therapeutic trials, and pharmacovigilance analyses [2-4].

EHR data is typically categorized into 2 types: structured data and unstructured data. Structured data refers to directly queryable numerical values, such as laboratory test results or *International Classification of Diseases, Tenth Revision* (*ICD-10*) codes, while unstructured data encompasses raw clinical texts and medical imaging. Structured data from clinical warehouses is often incomplete, capturing only intrahospital records and excluding extrahospital information. For instance, a patient's blood test conducted at an external laboratory before hospitalization might not be included. In addition, historical biological results in clinical databases are often limited to a few years. This is particularly problematic for conditions like autoimmune diseases, where historical immunologic results critical to the initial diagnosis are often documented only in clinical text rather than in structured data. Similarly, details about prior treatments are usually found only in textual records. Valuable information that is not present in structured data is often found in observations recorded in the discharge summaries [5]. The application of automated text analysis to this unstructured text, in conjunction with structured data, has already demonstrated increased effectiveness in predicting patients' clinical courses [6-11].

Transforming unstructured data into structured formats involves multiple natural language processing (NLP) tasks. In this research, we primarily concentrate on named entity recognition (NER) and normalization, which are fundamental for extracting meaningful information from large volumes of unstructured clinical text.

NER refers to locating and classifying terms into predefined categories, such as drug name, laboratory test, or medical disorder. Traditional NER methods often depend on dictionary-based term-matching techniques, which require meticulously maintained lexical resources [12]. However, maintaining these resources can be both labor-intensive and error-prone. A more effective method treats NER as a sequence-labeling task using tagging systems like the beginning, inside, outside, unit, and last scheme, which is widely recognized in biomedical NER for its ease of implementation and efficiency [13,14]. Sequence labeling models, particularly conditional random fields [15], have been extensively used for NER. When combined with transformer-based architectures like bidirectional encoder representations from transformer (BERT), these models have set state-of-the-art performance benchmarks for NER in clinical and biomedical text analyses [16-19].

Following NER, the normalization process assigns standard codes (unique identifiers that correspond to concepts within established medical terminologies) to the detected terms. For example, standard codes, such as concept unique identifiers (CUIs) from the Unified Medical Language System (UMLS) [20], can be used to map detected entities like drug or laboratory tests to their corresponding concepts. Common normalization strategies often rely on exact or approximate string matching against predefined dictionaries. Tools, such as KnowledgeMap Concept Identifier [21], MetaMap [22], MedLEE [23], MedEx [24], HITEx [25], and cTAKES [26] have been widely adopted in phenotyping models [27-29]. The emergence of deep contextual embeddings, notably BERT [30], has revolutionized NLP methodologies, including normalization tasks. Current state-of-the-art approaches heavily use transformer-based encoders pretrained on domain-specific corpora, demonstrating substantial improvements in normalization [31-33].

Although large language models like GPT-4 [34] hold promise for biomedical applications, their current performance in tasks like NER and normalization remains limited [35]. Moreover, implementing these models at scale to extract phenotypes from large volumes of clinical documents poses considerable cost challenges.

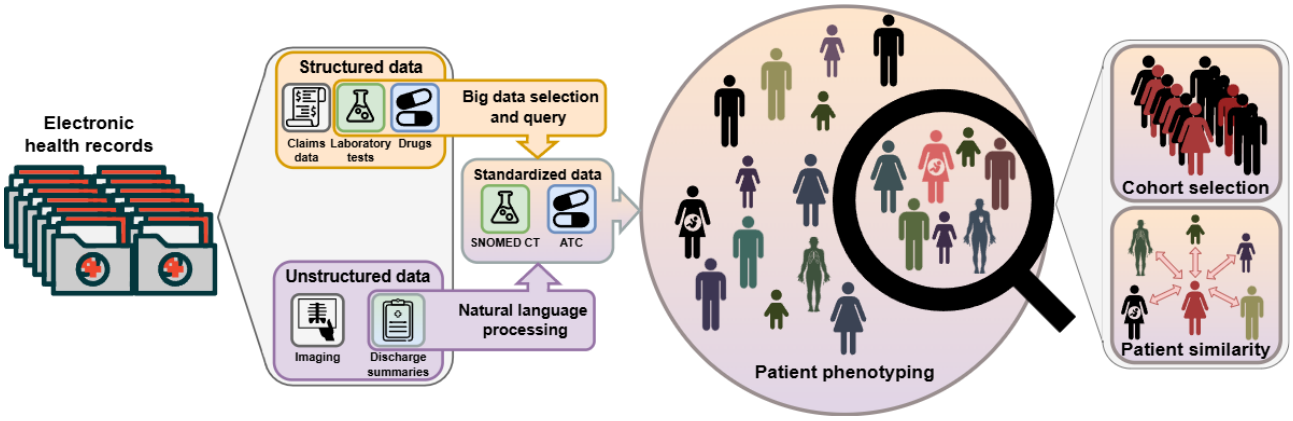
Goal of the Study

The aim of the study was to provide a proof-of-concept for end-to-end patient phenotyping from their EHRs. Patient phenotyping refers to the process of characterizing patients based on their clinical features, such as clinical diagnoses, laboratory results, or drug treatments. Secondary uses of EHRs require the application of various processes to transform the data into meaningful variables. In this research, we focused specifically on leveraging discharge summaries (written in French) through NLP techniques to enrich the information contained in the structured data. We restricted our study to patients hospitalized for one of the following immune-mediated inflammatory diseases: systemic lupus erythematosus (SLE), systemic sclerosis, antiphospholipid syndrome (APS), and Takayasu arteritis (TA). As we analyzed autoimmune diseases, we also restricted phenotyping to the analysis of autoantibodies (laboratory tests) and immunosuppressive therapies (drugs), which are central to the management of these diseases. As shown in Figure 1, laboratory tests and drug therapies were extracted from both structured and unstructured data. Then, to analyze the data jointly, a standard concept code was assigned to each laboratory test using the Systematized Nomenclature of Medicine Clinical Terms (SNOMED CT; US edition) [36] and drug using the Anatomical Therapeutic Chemical (ATC)

XSL•FO
RenderX

classification [37]. Our hypothesis was that incorporating the results of laboratory tests and drug treatments recorded in patients' discharge summaries would complement the information available in structured data and enable more in-depth, interoperable phenotyping of patients, while remaining reliable.

Figure 1. Overview of the end-to-end patient phenotyping pipeline. Structured and unstructured data are extracted from electronic health records, enabling large information retrieval, refining cohort selection, and facilitating more robust patient comparisons. ATC: Anatomical Therapeutic Chemical; SNOMED: Systematized Nomenclature of Medicine Clinical Terms.



Methods

Selected Diseases

As a proof of concept, we focused on 4 immune-mediated inflammatory diseases: SLE, systemic sclerosis, APS, and TA.

SLE is an autoimmune disease that mainly affects the skin, joints, and kidneys [38,39]. According to the revised 2019 EULAR/ACR classification criteria for SLE, patients are eligible for SLE criteria only if they have a positive antinuclear antibody ≥1/80 at least once. Anti-dsDNA and anti-Smith autoantibodies with high specificity for SLE are also included in the classification criteria for SLE. Therefore, we have chosen these 3 antibodies to identify SLE patients. Hydroxychloroquine, glucocorticoids, mycophenolate mofetil, cyclophosphamide, and belimumab are key treatments of SLE [40] and have been chosen to identify patients with SLE.

Systemic sclerosis is a rare autoimmune disease, inducing skin fibrosis, digestive disorders, such as gastroesophageal reflux disease and chronic pseudoocclusive syndrome, interstitial lung involvement, and sometimes inaugural renal crisis. Classification criteria are also based on specific autoantibodies, including anti-Scl-70, anticentromere, and anti-RNA polymerase III, which we have chosen to analyze here [41]. Therapeutic management is also based on glucocorticoids and immunosuppressive drugs, such as mycophenolate mofetil.

APS is a systemic autoimmune disease defined by the thrombosis or pregnancy morbidity in the presence of persistent antiphospholipid autoantibodies, lupus anticoagulant, IgG or IgM anticardiolipin, IgG or IgM anti-β2glycoprotein-1 antibodies. Treatment is based on curative anticoagulation with heparin, low-molecular-weight heparin, and antivitamin K [42].

TA is an inflammatory disease of the large arteries, leading to arterial stenosis in young people. C-reactive protein is used as an indicator of inflammation and disease activity in TA. Treatment is based on immunosuppressive therapies, such as glucocorticoids, and biologic, such as methotrexate or tocilizumab. Therefore, we have chosen to focus our analysis on these treatments.

Finally, in the context of the immunosuppressive treatments proposed, patients are at greater risk of infection; therefore, vaccination, particularly against pneumococcal and influenza infections, is recommended. Hence, we also looked for this information in the texts.

Dataset Selection

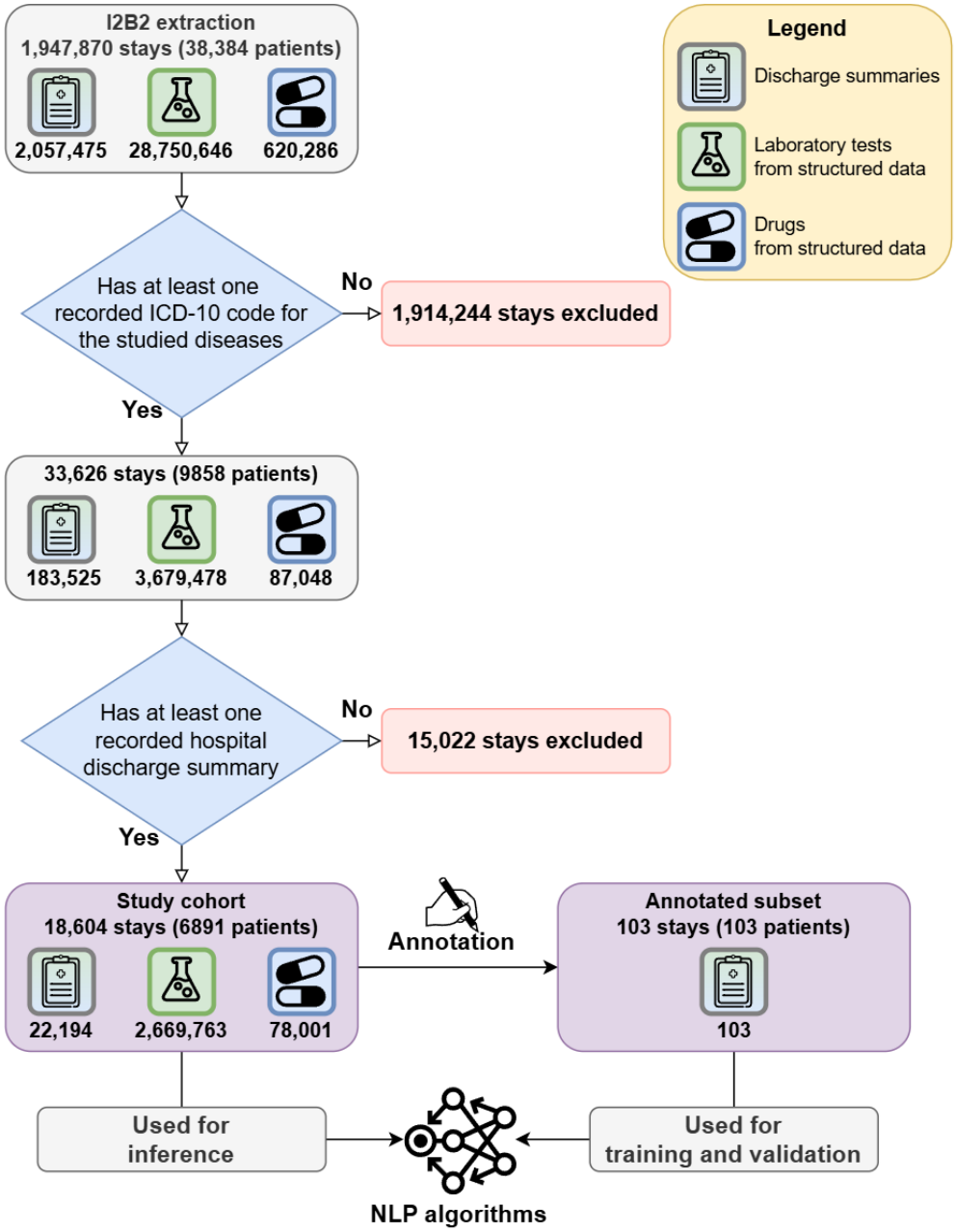
The dataset used in this study comes from the clinical data warehouse (CDW) of the University Hospitals of Greater Paris (Assistance publique-hôpitaux de Paris; AP-HP). The CDW brings together information on all patients followed in the 39 teaching hospitals in the Paris region (>22,000 beds and 1.5 million hospitalizations per year) that use a common EHR software, ORBIS Dedalus Health care. This software has been gradually implemented in the 39 hospitals since 2012.

The dataset was extracted from the CDW research database, in the integrating biology and the bedside format [43]. The inclusion criteria for the study were as follows: all patients aged >15 years with SLE, systemic sclerosis, APS, or TA who had at least one stay at AP-HP hospitals initially from July 1, 2017, to December, 31, 2020. Patients in the database were selected in 2 ways: by the *ICD-10* codes of these 4 pathologies and by keywords present in the medical reports (using regular expression matching), as summarized in Table S1 in Multimedia Appendix 1 [20,32,33,36,37,44-51]. For these patients, the data available were demographic data; textual data, including all full-text medical reports, laboratory tests performed during patients' stay, drug prescription, and administration when available; and medico-administrative coding data (*ICD-10*). The extraction covered all medical departments that could potentially manage patients with the 4 pathologies of interest: internal medicine and clinical immunology, nephrology, rheumatology, dermatology, pneumology, neurology, gastroenterology, oncology, hematology, infectious diseases, and emergency and intensive care.

XSL•FO
RenderX

As this study involves the secondary use of real-life health data, from this large integrating biology and bedside extraction, we limited the study to EHRs with at least one *ICD-10* code corresponding to the diseases studied (SLE, systemic sclerosis, APS, or TA) and at least one recorded hospital discharge summary, as these are validated by a senior clinician. Subsequently, a subset of this study cohort of 103 hospital discharge summaries, each corresponding to a different patient, was randomly selected and annotated by a clinician (CG), following the same annotation rules as proposed by the national NLP clinical challenges 2022 [44]. Details regarding this annotation process are provided in the Annotation Guidelines section of Multimedia Appendix 1. The global approach of this work was to build, train, and validate NLP algorithms on the annotated subset before applying it to the full study cohort. Figure 2 presents the cohort selection process.

Figure 2. Cohort selection flowchart. Starting with integrating biology and bedside extraction of 1,947,870 stays (38,384 patients), the cohort was filtered to include stays with at least 1 International Classification of Diseases, 10th Revision (ICD-10) code corresponding to the studied diseases and at least 1 recorded hospital discharge summary. A final study cohort of 18,604 stays (6891 patients) was created, with 103 randomly selected discharge summaries annotated for training and validation purposes. NLP: natural language processing.



End-to-End Pipeline

Overview

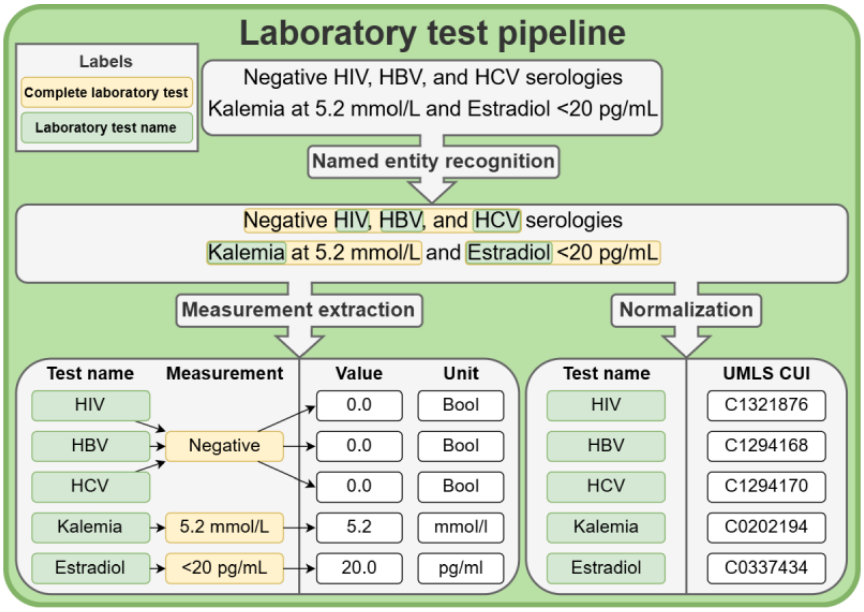
The system presented in this work required 4 NLP tasks: (1) NER: this task identified and classified entities of interest mentioned in the text into predefined categories. The possible categories included drug name, drug strength, drug dosage, drug form, laboratory test name, and complete laboratory test. (2) Qualification: this task involved assigning predefined qualifiers to the recognized named entities. Only entities classified as "drug name" by the NER algorithm were qualified There were 4 qualifiers [52]: action (start, stop, increase, decrease, unique

XSL•FO
RenderX

dose, and unknown), temporality (present, past, and future), certainty (certain, hypothetical, and conditional), as well as negation (true and false). (3) Measurement extraction: this task extracted and standardized the value and unit contained in the "complete laboratory test" entities detected by the NER algorithm. (4) Normalization: this task assigned predefined standard concepts to the recognized named entities. Each entity classified as "drug name" by the NER algorithm was assigned a code from the ATC classification system [37]. Each entity classified as "laboratory test name" by the NER algorithm was assigned a CUI of the UMLS [20] restricted to the laboratory procedure semantic type and the SNOMED CT US edition vocabulary [36]. As described in Figures 3 and Figure 4, the laboratory test pipeline and the drug pipeline involved both NER and normalization, while measurement extraction only concerned the laboratory test pipeline and qualification only concerned the drug pipeline.

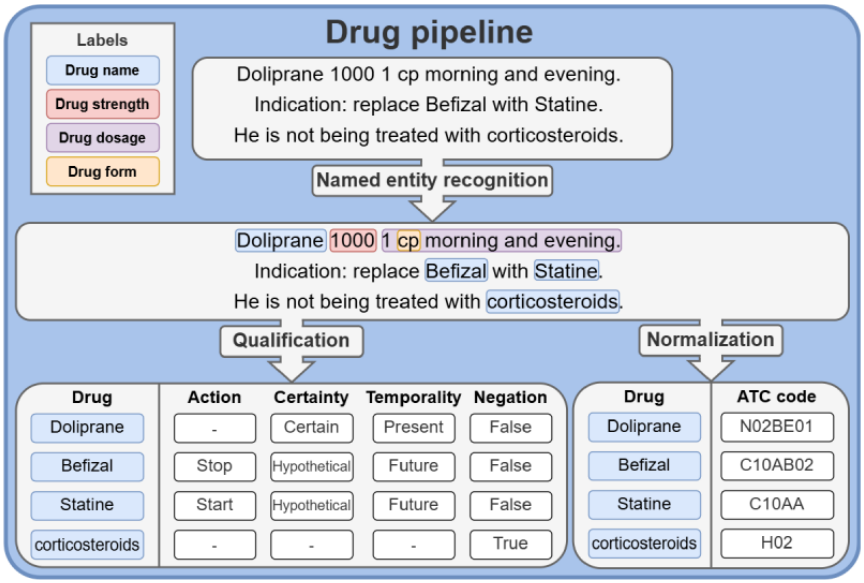
All the work presented in this paper was programmed in Python. Tabular data were processed with Spark (version 2.4.8) and distributed over 160 central processing units in parallel. This computing process is scalable over a large amount of data. Then, the cohorts were analyzed using Pandas (version 1.3.5). Inference and training of the NLP algorithms have been achieved on a V100 graphics processing unit. The code developed to run the experiments is freely available in a GitHub repository: Aremaki/BioMedics [53]. The code makes extensive use of EDS-NLP (version 0.13.0) [54], a collaborative NLP framework that aims primarily at building hybrid multitask NLP pipelines and extracting information from French clinical notes. It has also been made publicly available under an open-source license (BSD 3-clause): aphp/edsnlp.

Figure 3. Diagram of the laboratory test pipeline. It takes raw text as input, which is processed by 3 algorithms in total. It starts with the extraction and classification of relevant terms into 2 categories: laboratory test name and complete laboratory test. Then, the measurements associated with the complete laboratory tests are extracted and standardized into 2 components: value and unit. Finally, the extracted laboratory test names are normalized to the concept unique identifiers (CUIs) of the Unified Medical Language System (UMLS). HBV: hepatitis B virus; HCV: hepatitis C virus.



XSL•FO
RenderX

Figure 4. Diagram of the drug pipeline. It takes raw text as input, which is processed by 3 algorithms in total. It starts with the extraction and classification of relevant terms into 4 categories: name, strength, dosage, and form. At the same time, drugs are also qualified with several possible values: action (start, stop, increase, decrease, unique dose, and unknown), temporality (present, past, and future), certainty (certain, hypothetical, and conditional), and negation (true and false). Then, the extracted drugs are normalized according to the Anatomical Therapeutic Chemical (ATC) classification system. Cp: capsule.



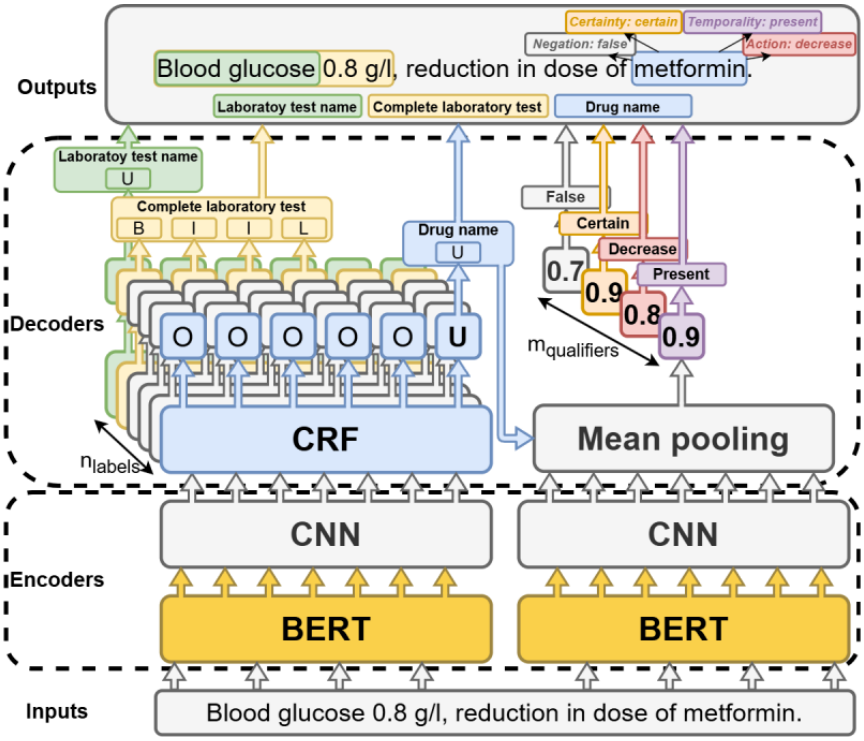
NER and Qualification Tasks

In the NER and qualification step, we experimented with different methods: a rule-based method as a preliminary approach, using the terms provided by the standard terminologies directly for exact matching. The ATC classification system [37] was used for drugs, and the SNOMED CT US edition vocabulary [36] was used for laboratory tests. A detailed description of the dictionaries is provided in Table S2 in Multimedia Appendix 1.

As a second approach, we experimented with a deep neural network architecture, described in Figure 5. The model consists of 2 BERTs encoders [30,55] followed by 2 convolution neural networks [56]. The first one is followed by a conditional random fields decoder [15] and a softmax block, which outputs probability vectors based on the beginning, inside, outside, unit, and last tagging scheme [14] to perform NER. The second is followed by a mean pooling layer and a softmax block to perform entity qualification. Several pretrained language models such as CamemBERT-EDS [45], CamemBERT-base [46], CamemBERT-bio [47], and DrBERT [48] have been compared.

XSL•FO
RenderX

Figure 5. Diagram of the named entity recognition and qualification architecture for laboratory tests and drugs entities. BERT: bidirectional encoder representations from transformer; CNN: convolution neural network; CRF: conditional random field.



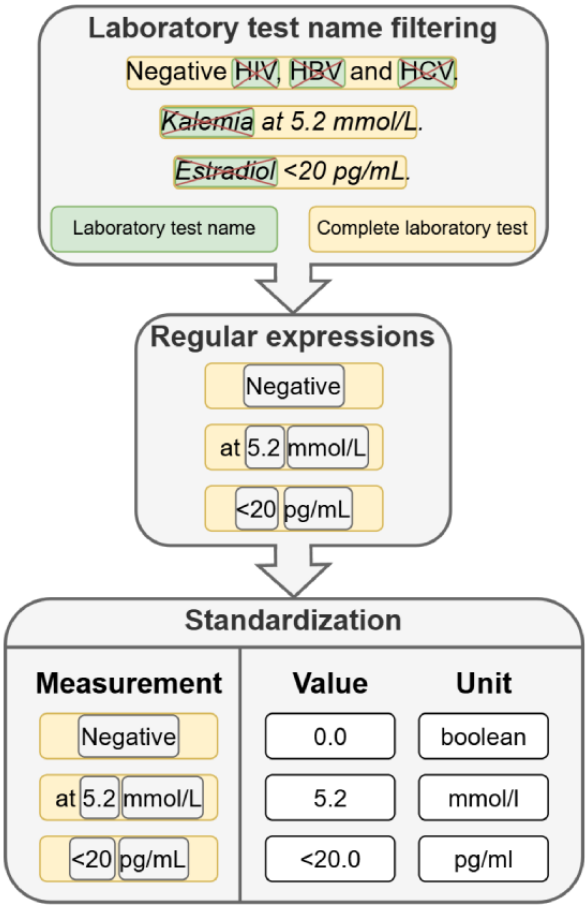
To select the best approach, precision, recall, and F_1-score were evaluated on 20 AP-HP discharge summaries. The performance of the rule-based method is presented in Table S3 in Multimedia Appendix 1, and the performance of the neural network method of each pretrained language model is presented in Tables S4 and S5 in Multimedia Appendix 1. The neural network approach using CamemBERT-EDS [45] was selected as the final model because it demonstrated superior performance compared to the other methods. Parameters of the architecture and fine-tuning are outlined in Table S6 in Multimedia Appendix 1.

Measurement Extraction Task

Extraction and standardization of the numerical value and unit were carried on the outputs of the NER step, which extracts the complete laboratory test entity from the text in a single block (laboratory test name, numerical value, and unit). The extraction and standardization were achieved with a rule-based algorithm using regular expressions. The algorithm steps are described in Figure 6: (1) the laboratory test names were removed from the complete laboratory test entity, (2) regular expressions were designed to extract the numerical or qualitative value and the unit, and (3) qualitative values (eg, “positive,” “negative,” or “normal”) were standardized into graded numbers (1.0, 0.0, or 0.5), while units were converted to conventional standards.

XSL•FO
RenderX

Figure 6. Diagram of the laboratory test measurement extraction process. HBV: hepatitis B virus; HCV: hepatitis C virus.

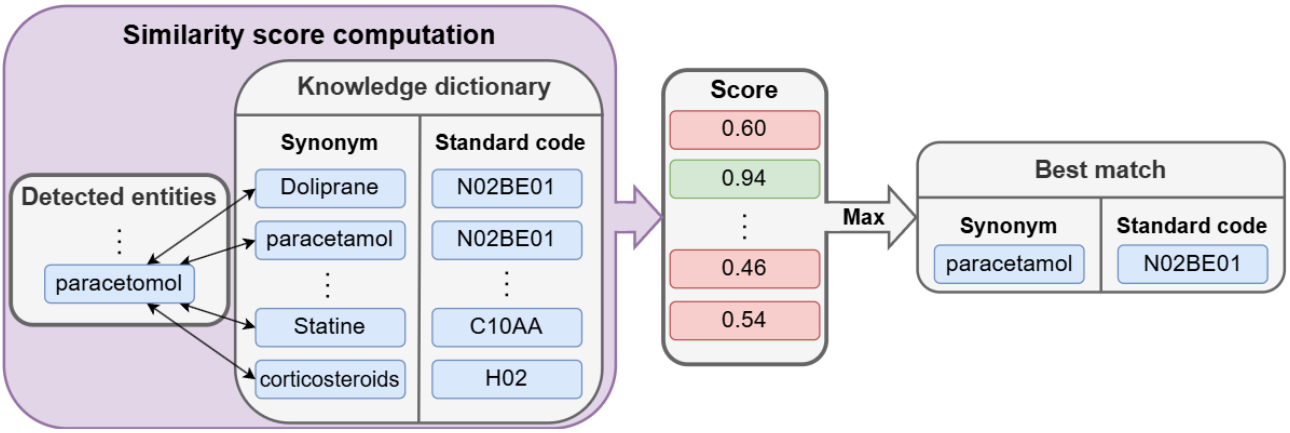


Normalization Task

The aim of the normalization step was to determine the standard code for each detected entity classified as "laboratory test name" and "drug name." As described in Figure 7, for a given detected term, similarity scores were computed for all terms of a knowledge dictionary. The resulting standard code corresponded to the term with the highest similarity score. For drugs, the knowledge dictionary is an aggregation of 2 open-source dictionaries of drug names with their corresponding ATC codes: the UMLS [20], restricted to the French ATC vocabulary [37], and the Unique Drug Interoperability Repository created by the French National Agency for Medicines and Health Products Safety [57]. For laboratory tests, the knowledge dictionary consists of all the French and English synonyms of the UMLS [20] restricted to the laboratory procedure semantic type and the SNOMED CT US edition vocabulary [36]. We experimented with 2 types of score computation: (1) fuzzy matching methods that directly compared word characters: Jaro-Winkler Distance [49] and Levenshtein distance [50], as well as (2) neural network–based methods that compute cosine similarity scores between the embeddings of the words: CODER-all [33] and SapBERT-all [32]. Table S7 in Multimedia Appendix 1 presents the performance of each method. The neural-based method with CODER-all seems to be significantly better for laboratory tests. However, for drugs, there is no significantly better solution, so we used the Jaro-Winkler Distance [49] method because it is less computationally expensive.

XSL•FO
RenderX

Figure 7. Diagram of the normalization process. In this example, the best match of "paracetomol," written with a typo, is "paracetamol," which provides the correct Anatomical Therapeutic Chemical (ATC) code.



Ethical Considerations

The research protocol for this project was approved in 2020 by the institutional review board of Assistance Publique – Hôpitaux de Paris (AP-HP) (20-93). All data used in this study were collected as part of routine medical care, and their use for research purposes falls under the ethical guidelines of the institutional review board. All patient data were pseudonymized to ensure privacy and comply with data protection regulations. No financial compensation was provided, as the study relied solely on retrospective data from electronic health records.

Results

Dataset Description

The number of patients, hospitalizations, and discharge summaries for each disease of the study cohort are given in Table 1. The age distribution and the distribution of admission start dates for each disease are presented in Figure S1 in Multimedia Appendix 1.

Table 1. Data description of the study cohort. Number of patients, hospitalizations, and discharge summaries for each studied disease. The number of discharge summaries is higher than the number of hospitalizations, as patients may change departments several times during the same stay (eg, be transferred to an intensive care unit, etc).

Disease	Number of patients	Number of hospitalizations	Number of discharge summaries
Antiphospholipid syndrome	1059	1818	2380
Lupus	4102	10,445	12,500
Systemic sclerosis	2031	6455	7585
Takayasu arteritis	252	833	965

We performed various analyses on the extracted data combined with the structured data from the cohort. The results are reported in 2 sections. The first section presents the performance of the NLP algorithms on the annotated subset of 103 discharge summaries. The second section is about the application of these algorithms to the 22,194 discharge summaries included in the study cohort. It described the contribution of unstructured data to structured data.

NLP Performance

Overview

The performance of the model was evaluated on 4 main tasks: NER, qualification, measurement extraction, and normalization. This evaluation was conducted using 2 datasets: 103 manually annotated discharge summaries from the study cohort and the publicly available Quaero FrenchMed corpus [51]. Performance metrics, including precision, recall, and F_1-score, were calculated and reported along with 95% CIs derived using the empirical bootstrap method at the discharge summary level [58]. It is important to note that while NER and qualification required annotated data for both training and testing, measurement extraction and normalization only required annotated data for testing. Therefore, all 103 discharge summaries were annotated for NER and qualification, with 83 (80.6%) randomly selected for training and the remaining 20 (19.4%) used for testing. These 20 (19.4%) test documents were further annotated for measurement extraction. Of these 20 documents, 11 (10.7%) were additionally annotated for normalization, resulting in 668 annotated entities, which was a more time-consuming process.

NER Task

Our model was evaluated for the NER task on both the AP-HP annotated discharge summaries and the Quaero FrenchMed corpus [51]. The results of our annotated dataset containing 103 discharge summaries from AP-HP are presented in Table 2. Precision, recall, and F_1-score were measured in a "strict" way, that is, a true positive result was obtained when a predicted entity and a gold entity had the exact same boundaries and label. The model achieved an overall F_1-score of 88.8. The results on the Quaero FrenchMed corpus [51] are presented in Tables S8 and S9 in Multimedia Appendix 1. The model achieved an

XSL•FO
RenderX

overall F_1-score of 66.2 for MEDLINE corpus and 71.71 for the European medicines agency corpus.

Table 2. Performance of the model for named entity recognition on University Hospitals of Greater Paris (Assistance Publique-Hôpitaux de Paris) discharge summaries. The model was trained on 83 annotated discharge summaries and tested on 20 discharge summaries. Each result was bootstrapped by discharge summary to provide a 95% CI given inside the brackets.

Label	Number of entities (95% CI)	Precision (95% CI)	Recall (95% CI)	F_1-score (95% CI)
Laboratory test name	1292 (1603-1010)	90.6 (88.5-92.7)	89.9 (87.5-92.2)	90.3 (88.2-92.3)
Complete laboratory test	1041 (1323-793)	86.2 (84.3-88.3)	83.6 (79.1-87.5)	84.9 (82.1-87.5)
Drug name	585 (731-454)	90.8 (85.8-95.4)	92.5 (88.4-95.7)	91.6 (87.5-95.1)
Drug dosage	276 (368-194)	89.1 (85.4-94.1)	86.2 (81.7-90.8)	87.7 (84.0-92.1)
Drug form	170 (247-106)	86.5 (78.8-93.4)	94.1 (91.5-97.6)	90.1 (85.6-94.0)
Drug strength	130 (196-77)	93.1 (87.7-97.0)	93.8 (89.2-97.6)	93.5 (89.3-96.6)
Overall	3494 (4194-2885)	89.1 (87.5-90.8)	88.5 (86.4-90.5)	88.8 (87.1-90.5)

Qualification Task

The model was evaluated for the qualification task and achieved an F_1-score of 78.8 on our annotated dataset containing 103 discharge summaries from AP-HP. The results are presented in Table S10 in Multimedia Appendix 1. On the test set, the model achieved an overall F_1-score of 78.8.

Measurement Extraction Task

The model was evaluated for the measurement extraction task on 20 annotated discharge summaries from AP-HP. Precision, recall, and F_1-score are presented in Table S11 in Multimedia Appendix 1 and were measured in a "strict" way: a true positive result was obtained when a predicted measurement and a gold measurement had the same value and unit. The algorithm obtained an F_1-score of 96.7.

Normalization Task

The rule-based algorithm for drug name normalization and the deep learning algorithm for the laboratory test name normalization were both evaluated on 11 annotated discharge summaries from AP-HP, 3 documents from European medicines agency, and 833 titles from MEDLINE [51]. For the evaluation, a true positive result was obtained when the predicted code of an entity was part of the list of annotated gold standard codes. Precision, recall, and F_1-score are presented in Table S12 in Multimedia Appendix 1. On our dataset of discharge summaries, the rule-based method for drug names achieved an F_1-score of 92.9 and the neural network–based method used for laboratory tests achieved an F_1-score of 82.2.

End-to-End Pipeline

The model was evaluated on the NER and normalization task using 11 annotated discharge summaries from AP-HP. Precision, recall, and F_1-score were measured in a "strict" way: a true positive result was obtained when a predicted entity and a gold entity had exactly the same boundaries and label and the predicted standard code of the entity was part of the list of annotated gold standard codes. Precision, recall, and F_1-score are presented in Table 3. We obtained an F_1-score of 71.1 for laboratory tests and 89.3 for drug names.

Table 3. Performance of the models for named entity recognition and normalization tasks on University Hospitals of Greater Paris (Assistance Publique-Hôpitaux de Paris) discharge summaries. The model was tested on 11 discharge summaries. Each result was bootstrapped by discharge summary to provide a 95% CI given inside the brackets.

Label	Number of entities (95% CI)	Precision (95% CI)	Recall (95% CI)	F_1-score (95% CI)
Laboratory test name	356 (204-548)	72.0 (65.3-79.1)	70.2 (59.7-77.9)	71.1 (63.6-77.8)
Drug name	312 (206-424)	91.9 (88.9-93.5)	86.9 (82.9-90.0)	89.3 (85.9-91.6)

Clinical Application

For each studied disease (SLE, systemic sclerosis, APS, and TA), each studied antibody, and each studied drug treatment, we reported the number of patients for whom we extracted a positive antibody or a prescribed drug treatment from both the structured and unstructured data of the study cohort. Lists of CUI codes for the studied antibodies and ATC codes for drug treatments are available in Tables S9 and S10 in Multimedia Appendix 1. We were particularly interested in the number of patients for whom we extracted positive antibodies or drug treatments from the unstructured data of their EHRs that were not available in the structured data. In the analysis of the unstructured data, only entities explicitly qualified as "certain" and not negated were retained.

Laboratory Test Results

Table 4 describes the number of antibody-positive patients for each disease, where positivity was determined either by test values exceeding reference ranges or by explicit interpretation of the test as positive. The first column shows the number of patients for whom we extracted at least 1 positive test from the structured data of their EHR. The second column shows the number of patients for whom we extracted at least 1 positive test from both the structured and unstructured data. The third column shows the number of patients for whom we extracted

XSL•FO
RenderX

at least 1 positive test from the unstructured data, but only among patients without positive tests extracted from the structured data.

To ensure the reliability of the detected autoantibodies across the entire study cohort, we conducted a second evaluation focused specifically on the studied autoantibodies. While the precision was reported in Table 3 as 72% in the general case for all laboratory tests, this additional analysis aimed to ensure comparable performance for the autoantibodies studied. For this evaluation, we randomly selected 10 positively detected entities for each studied autoantibody, yielding a total of 110 entities. These entities, identified through NER, measurement extraction, and normalization, were reviewed by a clinician. The review identified 3 errors, resulting in a precision of 97.3%.

Finally, to identify potential errors made by the algorithm, we examined EHR cases in which a positive autoantibody appeared in the structured data but was not detected in the unstructured data. For each antibody, we randomly selected 10 EHRs (for some antibodies, fewer than 10 documents met this criterion, so we included all available cases). A clinician reviewed 63 discharge summaries from the EHRs and identified 2 types of algorithmic errors: (1) in 23 (26.5%) summaries, the algorithm either failed to detect the relevant antibody or did not normalize it correctly; and (2) in the remaining 40 (63.5%) summaries, either the antibody was not mentioned in the text, or the mention was interpreted as a negative result by the clinician.

Table 4. Number of patients with positive antibodies mentioned in the text and in structured data.

Disease and laboratory test	Number of patients with positive tests (ratio)		
	Structured data only, n (%)	Structured and unstructured data, n (%)	Benefits of the unstructured data, n (%)
Antiphospholipid syndrome (1059 patients)			
Anticardiolipin antibody	184 (17.37)	478 (45.14)	294 (27.76)
Anti-B2GP1 antibody	103 (9.73)	334 (31.54)	231 (21.81)
Lupus anticoagulant	277 (26.16)	423 (39.94)	146 (13.79)
Systemic lupus erythematosus (4102 patients)			
Antinuclear antibody	752 (18.33)	2949 (71.89)	2197 (53.56)
Anti-DNA antibodies	541 (13.19)	2174 (53)	1633 (39.81)
Anti-Smith antibodies	255 (6.22)	858 (20.92)	603 (14.7)
Systemic sclerosis (2031 patients)			
Anti-RNA polymerase III antibody	39 (1.92)	156 (7.68)	117 (5.76)
Anti-Scl-70 antibodies	97 (4.78)	568 (27.97)	471 (23.19)
Anticentromere antibody	144 (7.09)	609 (29.99)	465 (22.9)

Drug Treatments

Table 5 describes the number of patients with drug treatments for each of the studied drugs related to the respective disease. The first column presents the number of patients for whom we extracted at least 1 drug treatment from the structured data of their EHR. The second column presents the number of patients for whom we extracted at least 1 drug treatment from both the structured and the unstructured data. The third column provides the number of patients for whom we extracted at least 1 drug treatment from the unstructured data but only among the patients without drug treatment extracted from the structured data.

XSL•FO
RenderX

Table 5. Number of patients with drug treatments. It describes the number of patients with drug treatments for each of the studied drugs related to the respective disease, extracted from structured and unstructured data. The proportions in percentage of the total number of patients diagnosed with the respective disease are given inside parenthesis.

Diseases and drugs	Number of patients with drug treatments (ratio)		
	Structured data only, n (%)	Structured and unstructured data, n (%)	Benefits of the unstructured data, n (%)
Antiphospholipid syndrome (1059 patients)			
VKA	186 (17.56)	628 (59.3)	442 (41.74)
Heparin	238 (22.47)	677 (63.94)	439 (41.46)
Oral anticoagulant	47 (4.44)	177 (16.72)	130 (12.28)
Systemic lupus erythematosus (4102 patients)			
Systemic glucocorticoids	950 (23.16)	3308 (80.64)	2358 (57.49)
Cyclophosphamide	64 (1.56)	894 (21.79)	830 (20.23)
Mycophenolate mofetil	301 (7.34)	1263 (30.78)	962 (23.46)
Rituximab	75 (1.83)	709 (17.28)	634 (15.46)
Belimumab	43 (1.05)	247 (6.02)	204 (4.97)
Methotrexate	112 (2.73)	963 (23.48)	851 (20.75)
Hydroxychloroquine	920 (22.43)	3520 (85.83)	2600 (63.4)
Prevenar 13 vaccine	122 (2.97)	984 (23.99)	862 (21.02)
Pneumovax vaccine	43 (1.05)	436 (10.63)	393 (9.58)
Influenza vaccine	96 (2.34)	577 (14.07)	481 (11.73)
Systemic sclerosis (2031 patients)			
Systemic glucocorticoids	258 (12.71)	1260 (62.06)	1002 (49.33)
Cyclophosphamide	6 (0.3)	390 (19.2)	384 (18.91)
Mycophenolate mofetil	88 (4.33)	463 (22.81)	375 (18.47)
Rituximab	13 (0.64)	258 (12.71)	245 (12.07)
Methotrexate	66 (3.25)	541 (26.63)	475 (23.39)
Prevenar 13 vaccine	59 (2.9)	545 (26.84)	486 (23.93)
Pneumovax vaccine	13 (0.64)	285 (14.03)	272 (13.4)
Influenza vaccine	42 (2.07)	425 (20.93)	383 (18.87)
Takayasu arteritis (252 patients)			
Systemic glucocorticoids	68 (27)	223 (88.49)	155 (61.51)
Cyclophosphamide	0 (0)	18 (7.14)	18 (7.14)
Tocilizumab	15 (5.95)	47 (18.65)	32 (12.7)
Mycophenolate mofetil	9 (3.57)	21 (8.33)	12 (4.76)
Rituximab	0 (0)	6 (2.38)	6 (2.38)
Methotrexate	20 (7.94)	135 (53.57)	115 (45.63)
Prevenar 13 vaccine	9 (3.57)	83 (32.94)	74 (29.37)
Pneumovax vaccine	3 (1.19)	48 (19.05)	45 (17.86)
Influenza vaccine	6 (2.38)	41 (16.27)	35 (13.89)

To ensure the precision of the drug treatments identified by the algorithm, we conducted a second evaluation specifically focused on the studied drugs. Although the general precision for all drugs had previously been reported as 91.9% in Table 3, this additional analysis aimed to confirm comparable performance for the specific drug treatments studied. For this evaluation, we randomly selected 10 positively detected entities per studied drug (spanning NER and normalization), resulting in a total of 130 entities. A clinician reviewed these entities individually and found no errors, corresponding to a precision of 100%.

XSL•FO
RenderX

Inference Time and Carbon Footprint

When considering scaling these methods to a CDW that may process hundreds of thousands of documents daily, it is critical to evaluate both processing speed and environmental impact. The entire NLP process on the 22,194 documents took 145 minutes on a graphics processing unit (Tesla V100-SXM2-32GB) and resulted in a total emission of 0.39 kg equivalent of CO_2.

Discussion

Principal Findings

In this paper, we proposed a novel block-based algorithm for extracting and normalizing medical data from text, enabling fine-grained phenotyping of patients with autoimmune or autoinflammatory diseases. We demonstrated that these cascading algorithms significantly improve patient characterization compared to relying only on structured data. In addition, we provided detailed results for every step of the algorithm (NER, qualification, measurement extraction, and normalization), evaluated our method using a publicly available dataset, Quaero [51], and provided a comprehensive performance comparison between models.

Our work offers several strengths. Notably, we leveraged state-of-the-art language models, particularly the BERT model, for named entity extraction. Indeed, when compared with recent large language models, such as GPT, BERT models remain the most effective for the NER task [58]. We evaluated and compared several language models and various methods for each step, demonstrating strong performance outcomes. The model evaluated for the NER task on 20 annotated discharge summaries achieved high F_1-scores: 90.3 for laboratory test names and 91.6 for drug names. Similarly, the model achieved high F_1-scores for the qualification task, the measurement extraction task, and the overall end-to-end task. A posteriori precision analysis also showed very good results (97.3% for laboratory tests and 100% for drugs). Finally, as shown in Tables 4 and Table 5, our study highlights significant improvements in information availability by enriching structured data with information extracted from unstructured data.

Beyond these results, our findings are consistent with those of previous studies. For instance, 71.87% (2949/4102) of patients in the lupus cohort exhibited positive antinuclear antibodies (≥1/80), a finding that aligns with the clinical criteria for the disease [40]. Similarly, when compared with previous data [38,40], 85.81% (3520/4102) of patients with SLE were treated with hydroxychloroquine, and 80.64% (3308/4102) received corticosteroids during hospitalization. For comparison, a recent conference abstract by Eviatar et al [59] reported that 81% of patients were treated with hydroxychloroquine, 65% with systemic corticosteroids, and 55% with immunosuppressants (2259/4102, 55.07% in our study). In addition, 64.4% (682/1059) of patients with APS had at least one positive antibody assay. For patients with TA, the treatments were consistent with national recommendations [60], with 88.5% (223/252) of patients receiving systemic corticosteroids and 18.7% (47/252) treated with tocilizumab.

The clinical implications of algorithms that enable accurate patient phenotyping are substantial. They facilitate more precise recruitment of patients for studies, particularly therapeutic trials, and support clinical practice by addressing key questions, such as, “What happened to a patient like mine?” Prototypes are currently under development to construct cohorts of patients with similar characteristics to a specific individual under care, using information extracted from hospital reports. The algorithm we present can identify patients with comparable immune profiles (eg, matching positive antibodies) and analyze the treatments they received, offering valuable insights for personalized care.

Limitations

However, there are several limitations to our study. A significant limitation lies in the complexity of standardizing laboratory tests, especially for tests with abbreviated terms. For instance, the glomerular filtration rate (or “DFG” in French) is not directly classified as a biological test in the SNOMED CT US edition [36], making it challenging to standardize. Similarly, the abbreviation “ACC” for lupus circulating anticoagulant is missing in the UMLS [20], which makes normalization difficult and partially explains the lower contribution of text-based analysis for this assay. In general, drug names are often written in a relatively standardized format in texts (using either trade names or generics), whereas the terminology for describing biological data tends to be more varied. For example, a clinician might describe “hemoglobin” using variations, such as “anemia at 9g/dL,” “Hb=9g/dL,” or “hemoglobin at 9,” among others. This variability complicates the normalization process for laboratory tests, leading to poorer performance compared with that of drug treatments. Another limitation is the relatively small evaluation sample size. Our NLP end-to-end system was evaluated on only 11 annotated clinical documents, comprising 668 annotated entities. This limited dataset is a consequence of the labor-intensive process involved in manually annotating CUIs and ATC codes, which constrained the number of documents we could feasibly annotate. Also, interannotator agreement could not be computed due to having a single annotator involved in the annotation process. To minimize potential biases, several precautions were taken. First, an expert clinician performed the annotations following strict guidelines, while the model was independently designed by a separate researcher. Second, the training and test datasets were created using distinct discharge summaries from different patients. These precautions reduce the risk of information leakage during model evaluation.

Finally, it is important to note that this study relies on the secondary use of “real-life” health care data. While clinical texts are central to characterizing patients, as demonstrated, they do not comprehensively capture all patient characteristics. Our error analysis revealed that for patients with both textual information and biological test results from the same hospitalization, 63% (40/63) of the biological tests were either not mentioned in the text or were interpreted by the clinician as negative results. To enhance the accuracy of patient phenotyping, we believe it is essential to incorporate both structured and textual data.

XSL•FO
RenderX

Future Works

Moreover, we acknowledge that the analyses presented here are preliminary for each pathology, and we anticipate more detailed future work in this area. Particularly, it will be necessary to establish a precise relationship between target organ damage and antibody positivity, some of which are known to be more specific for certain types of damage. For example, anti-RNA polymerase III antibodies are more often associated with sclerodermic renal crisis [61], and triple positivity of APS antibodies is also a poor prognostic marker. The type and severity of organ damage should also be considered in conjunction with treatment options. These analyses will also be based on our current patient phenotyping work [62]. Analysis of the dosages associated with each treatment is not currently explored either, but work is in progress for this future step. Another direction is adapting our methodology to other languages. While the current implementation is tailored for French, the approach can be generalized by substituting the pretrained clinical BERT model with other language-specific alternatives, such as models pretrained for Spanish [63] or English [64]. However, successful adaptation would require annotated datasets specific to the new language, as well as adjustments to the terminology and clinical standards used in the target CDW. Beyond linguistic adaptability, the methods described could also be extended to unstructured data in different formats, such as imaging. Addressing these directions could advance this research toward a more comprehensive, multilingual, and multiformat phenotyping framework.

Conclusions

To the best of our knowledge, this is the first study to automatically analyze such a large volume of patients with autoimmune diseases using data derived directly from text. It seems to us that this finer, text-based characterization of patients in the context of rare diseases could enable researchers to target them more effectively, and clinicians to bring synthesis to their management.

Acknowledgments

The authors thank the clinical data warehouse of the Greater Paris University Hospitals for its support and the realization of data management and data curation tasks. The authors express sincere thanks to Dr Arthur Mageau, Prof Karim Sacré, and Prof Olivier Steichen for their careful review of this manuscript.

Data Availability

The datasets generated or analyzed during this study are not publicly available due to their classification as sensitive data under the General Data Protection Regulation and the National Data Protection Commission. Access to the data requires prior approval from the local institutional review board and must follow the process outlined on its website [65]. In the case of non-University Hospitals of Greater Paris (Assistance Publique-Hôpitaux de Paris) researchers, the signature of a collaboration contract is mandatory.

Conflicts of Interest

None declared.

Multimedia Appendix 1
Annotation guidelines, supplementary tables, and figure.
[DOCX File , 571 KB - medinform_v13i1e68704_app1.docx]

References

1. Richesson RL, Hammond WE, Nahm M, Wixted D, Simon GE, Robinson JG, et al. Electronic health records based phenotyping in next-generation clinical trials: a perspective from the NIH Health Care Systems Collaboratory. J Am Med Inform Assoc 2013 Dec 01;20(e2):e226-e231 [FREE Full text] [doi: 10.1136/amiajnl-2013-001926] [Medline: 23956018]
2. Gombar S, Callahan A, Califf R, Harrington R, Shah NH. It is time to learn from patients like mine. NPJ Digit Med 2019 Mar 19;2(1):16 [FREE Full text] [doi: 10.1038/s41746-019-0091-3] [Medline: 31304364]
3. Callahan A, Polony V, Posada JD, Banda JM, Gombar S, Shah NH. ACE: the Advanced Cohort Engine for searching longitudinal patient records. J Am Med Inform Assoc 2021 Jul 14;28(7):1468-1479 [FREE Full text] [doi: 10.1093/jamia/ocab027] [Medline: 33712854]
4. Frankovich J, Longhurst CA, Sutherland SM. Evidence-based medicine in the EMR era. N Engl J Med 2011 Nov 10;365(19):1758-1759. [doi: 10.1056/nejmp1108726]
5. Zheng C, Ackerson B, Qiu S, Sy LS, Daily LI, Song J, et al. Natural language processing versus diagnosis code-based methods for postherpetic neuralgia identification: algorithm development and validation. JMIR Med Inform 2024 Sep 10;12:e57949 [FREE Full text] [doi: 10.2196/57949] [Medline: 39254589]
6. Elkin PL, Mullin S, Mardekian J, Crowner C, Sakilay S, Sinha S, et al. Using artificial intelligence with natural language processing to combine electronic health record's structured and free text data to identify nonvalvular atrial fibrillation to

XSL•FO
RenderX

decrease strokes and death: evaluation and case-control study. J Med Internet Res 2021 Nov 09;23(11):e28946 [FREE Full text] [doi: 10.2196/28946] [Medline: 34751659]
7. Seinen TM, Fridgeirsson EA, Ioannou S, Jeannetot D, John LH, Kors JA, et al. Use of unstructured text in prognostic clinical prediction models: a systematic review. J Am Med Inform Assoc 2022 Jun 14;29(7):1292-1302 [FREE Full text] [doi: 10.1093/jamia/ocac058] [Medline: 35475536]
8. Khurshid S, Reeder C, Harrington LX, Singh P, Sarma G, Friedman SF, et al. Cohort design and natural language processing to reduce bias in electronic health records research. NPJ Digit Med 2022 Apr 08;5(1):47 [FREE Full text] [doi: 10.1038/s41746-022-00590-0] [Medline: 35396454]
9. Idnay B, Zhang G, Chen F, Ta CN, Schelke MW, Marder K, et al. Mini-mental status examination phenotyping for Alzheimer's disease patients using both structured and narrative electronic health record features. J Am Med Inform Assoc 2025 Jan 01;32(1):119-128. [doi: 10.1093/jamia/ocae274] [Medline: 39520712]
10. Fraile Navarro D, Ijaz K, Rezazadegan D, Rahimi-Ardabili H, Dras M, Coiera E, et al. Clinical named entity recognition and relation extraction using natural language processing of medical free text: a systematic review. Int J Med Inform 2023 Sep;177:105122 [FREE Full text] [doi: 10.1016/j.ijmedinf.2023.105122] [Medline: 37295138]
11. Moqurrab SA, Ayub U, Anjum A, Asghar S, Srivastava G. An accurate deep learning model for clinical entity recognition from clinical notes. IEEE J Biomed Health Inform 2021 Oct;25(10):3804-3811. [doi: 10.1109/jbhi.2021.3099755]
12. Mikheev A, Moens M, Grover C. Named Entity recognition without gazetteers. In: Proceedings of the 9th conference on European chapter of the Association for Computational Linguistics. 1999 Presented at: EACL '99; June 8-12, 1999; Bergen, Norway p. 1-8 URL: https://dl.acm.org/doi/10.3115/977035.977037 [doi: 10.3115/977035.977037]
13. Ramshaw LA, Marcus MP. Text chunking using transformation-based learning. In: Armstrong S, Church K, Isabelle P, Manzi S, Tzoukermann E, Yarowsky D, editors. Natural Language Processing Using Very Large Corpora. Cham, Switzerland: Springer; 1995:157-176.
14. Ratinov L, Roth D. Design challenges and misconceptions in named entity recognition. In: Proceedings of the 13th Conference on Computational Natural Language Learning. 2009 Presented at: CoNLL '09; June 4-5, 2009; Boulder, Colorado p. 147-155 URL: https://aclanthology.org/W09-1119 [doi: 10.3115/1596374.1596399]
15. Lafferty JD, McCallum A, Pereira FC. Conditional random fields: probabilistic models for segmenting and labeling sequence data. In: Proceedings of the 18th International Conference on Machine Learning. 2001 Presented at: ICML '01; June 28-July 1, 2001; San FranciscoCA p. 282-289 URL: https://dl.acm.org/doi/10.5555/645530.655813 [doi: 10.1145/1015330.1015422]
16. Lample G, Ballesteros M, Subramanian S, Kawakami K, Dyer C. Neural architectures for named entity recognition. In: Proceedings of the 2016 Conference of the North American Chapter of the Association for Computational Linguistics: Human Language Technologies. 2016 Presented at: NAACL '16; June 12-17, 2016; San Diego, CA p. 260-270 URL: https://aclanthology.org/N16-1030.pdf [doi: 10.18653/v1/n16-1030]
17. Sung M, Jeong M, Choi Y, Kim D, Lee J, Kang J. BERN2: an advanced neural biomedical named entity recognition and normalization tool. Bioinformatics 2022 Oct 14;38(20):4837-4839 [FREE Full text] [doi: 10.1093/bioinformatics/btac598] [Medline: 36053172]
18. Jonker RA, Almeida T, Antunes R, Almeida JR, Matos S. Multi-head CRF classifier for biomedical multi-class named entity recognition on Spanish clinical notes. Database (Oxford) 2024 Jul 30;2024:baae068 [FREE Full text] [doi: 10.1093/database/baae068] [Medline: 39083461]
19. Cardon R, Grabar N, Grouin C, Hamon T. Presentation of the'assessment campaign DEFT 2020: textual similarity in open domain and extraction of'accurate information in clinical cases (presentation of the DEFT 2020 challenge : open domain textual similarity and precise information extraction from clinical cases). In: Proceedings of the 6th joint conference Days of Studies on the Word (JEP, 33rd edition), Automatic Processing of Natural Languages (TALN, 27th edition), Meeting of Research Students in Computer Science for Automatic Language Processing (RECITAL, 22nd edition). Workshop Defi Fouille de Textes. 2020 Presented at: JEP/TALN/RECITAL '20; June 8-19, 2020; Nancy, France p. 1-13 URL: https://aclanthology.org/2020.jeptalnrecital-deft.1.pdf [doi: 10.4000/books.pufc.30067]
20. Bodenreider O. The Unified Medical Language System (UMLS): integrating biomedical terminology. Nucleic Acids Res 2004 Jan 01;32(Database issue):D267-D270 [FREE Full text] [doi: 10.1093/nar/gkh061] [Medline: 14681409]
21. Denny JC, Irani PR, Wehbe FH, Smithers JD, Spickard A. The KnowledgeMap project: development of a concept-based medical school curriculum database. AMIA Annu Symp Proc 2003;2003:195-199 [FREE Full text] [Medline: 14728161]
22. Aronson AR, Lang FM. An overview of MetaMap: historical perspective and recent advances. J Am Med Inform Assoc 2010;17(3):229-236 [FREE Full text] [doi: 10.1136/jamia.2009.002733] [Medline: 20442139]
23. Friedman C, Shagina L, Socratous SA, Zeng X. A WEB-based version of MedLEE: a medical language extraction and encoding system. Proc AMIA Annu Fall Symp 1996;938:35 [FREE Full text]
24. Xu H, Stenner SP, Doan S, Johnson KB, Waitman LR, Denny JC. MedEx: a medication information extraction system for clinical narratives. J Am Med Inform Assoc 2010 Jan 01;17(1):19-24. [doi: 10.1197/jamia.m3378]
25. Zeng QT, Goryachev S, Weiss S, Sordo M, Murphy SN, Lazarus R. Extracting principal diagnosis, co-morbidity and smoking status for asthma research: evaluation of a natural language processing system. BMC Med Inform Decis Mak 2006 Jul 26;6:30 [FREE Full text] [doi: 10.1186/1472-6947-6-30] [Medline: 16872495]

XSL•FO
RenderX

26. Savova GK, Masanz JJ, Ogren PV, Zheng J, Sohn S, Kipper-Schuler KC, et al. Mayo clinical Text Analysis and Knowledge Extraction System (cTAKES): architecture, component evaluation and applications. J Am Med Inform Assoc 2010;17(5):507-513 [FREE Full text] [doi: 10.1136/jamia.2009.001560] [Medline: 20819853]
27. Bejan CA, Xia F, Vanderwende L, Wurfel MM, Yetisgen-Yildiz M. Pneumonia identification using statistical feature selection. J Am Med Inform Assoc 2012 Sep 01;19(5):817-823 [FREE Full text] [doi: 10.1136/amiajnl-2011-000752] [Medline: 22539080]
28. Liao KP, Cai T, Gainer V, Goryachev S, Zeng-treitler Q, Raychaudhuri S, et al. Electronic medical records for discovery research in rheumatoid arthritis. Arthritis Care Res (Hoboken) 2010 Aug;62(8):1120-1127 [FREE Full text] [doi: 10.1002/acr.20184] [Medline: 20235204]
29. Carroll RJ, Eyler AE, Denny JC. Naïve electronic health record phenotype identification for rheumatoid arthritis. AMIA Annu Symp Proc 2011;2011:189-196 [FREE Full text] [Medline: 22195070]
30. Devlin J, Chang MW, Lee K, Toutanova K. BERT: pre-training of deep bidirectional transformers for language understanding. In: Proceedings of the 2019 Conference of the North American Chapter of the Association for Computational Linguistics: Human Language Technologies. 2019 Presented at: NAACL '19; June 2-7, 2019; Minneapolis, Minnesota p. 4171-4186 URL: https://aclanthology.org/N19-1423.pdf [doi: 10.18653/v1/n18-2]
31. French E, McInnes BT. An overview of biomedical entity linking throughout the years. J Biomed Inform 2023 Jan;137:104252 [FREE Full text] [doi: 10.1016/j.jbi.2022.104252] [Medline: 36464228]
32. Liu F, Shareghi E, Meng Z, Basaldella M, Collier N. Self-alignment pretraining for biomedical entity representations. In: Proceedings of the 2021 Conference of the North American Chapter of the Association for Computational Linguistics: Human Language Technologies. 2021 Presented at: NAACL '21; June 6-11, 2021; Virtual Event p. 4228-4238 URL: https://aclanthology.org/2021.naacl-main.334.pdf [doi: 10.18653/v1/2021.naacl-main.334]
33. Yuan Z, Zhao Z, Sun H, Li J, Wang F, Yu S. CODER: knowledge-infused cross-lingual medical term embedding for term normalization. J Biomed Inform 2022 Feb;126:103983 [FREE Full text] [doi: 10.1016/j.jbi.2021.103983] [Medline: 34990838]
34. Achiam OJ, Adler S, Agarwal S, Ahmad L, Akkaya I, Aleman FL, et al. GPT-4 technical report. arXiv. Preprint posted online March 4, 2024 2024 [FREE Full text]
35. Tian S, Jin Q, Yeganova L, Lai P, Zhu Q, Chen X, et al. Opportunities and challenges for ChatGPT and large language models in biomedicine and health. Brief Bioinform 2023 Nov 22;25(1):bbad493 [FREE Full text] [doi: 10.1093/bib/bbad493] [Medline: 38168838]
36. SNOMED CT. US National Library of Medicine. URL: https://www.nlm.nih.gov/healthit/snomedct/index.html [accessed 2024-07-25]
37. Anatomical therapeutic chemical (ATC) classification. World Health Organization. URL: https://www.who.int/tools/atc-ddd-toolkit/atc-classification [accessed 2024-05-16]
38. Fanouriakis A, Kostopoulou M, Alunno A, Aringer M, Bajema I, Boletis JN, et al. 2019 update of the EULAR recommendations for the management of systemic lupus erythematosus. Ann Rheum Dis 2019 Jun;78(6):736-745. [doi: 10.1136/annrheumdis-2019-215089] [Medline: 30926722]
39. Aringer M, Costenbader K, Daikh D, Brinks R, Mosca M, Ramsey-Goldman R, et al. 2019 European League against rheumatism/American College of Rheumatology Classification Criteria for Systemic Lupus Erythematosus. Arthritis Rheumatol 2019 Sep 06;71(9):1400-1412 [FREE Full text] [doi: 10.1002/art.40930] [Medline: 31385462]
40. Lupus Systémique de l'adulte et de l'enfant. Haute Autorité de Santé. URL: https://www.has-sante.fr/jcms/p_3493410/fr/lupus-systemique-de-l-adulte-et-de-l-enfant [accessed 2024-04-29]
41. Sclérodermie Systémique. Haute Autorité de Santé. 2018. URL: https://www.has-sante.fr/jcms/c_717292/fr/sclerodermie-systemique [accessed 2024-04-29]
42. Syndrome des Anti-Phospholipides de l'adulte et de l'enfant. Haute Autorité de Santé. URL: https://www.has-sante.fr/jcms/p_3375791/fr/syndrome-des-anti-phospholipides-de-l-adulte-et-de-l-enfant [accessed 2024-04-29]
43. i2b2: informatics for integrating biology and the bedside. i2b2. URL: https://www.i2b2.org/ [accessed 2024-04-26]
44. Mahajan D, Liang JJ, Tsou C, Uzuner Ö. Overview of the 2022 n2c2 shared task on contextualized medication event extraction in clinical notes. J Biomed Inform 2023 Aug;144:104432 [FREE Full text] [doi: 10.1016/j.jbi.2023.104432] [Medline: 37356640]
45. Dura B, Jean C, Tannier X, Calliger A, Bey R, Neuraz A, et al. Learning structures of the French clinical language:development and validation of word embedding models using 21 million clinical reports from electronic health records. arXiv. Preprint posted online July 26, 2022 2022 [FREE Full text] [doi: 10.48550/arXiv.2207.12940]
46. Martin L, Muller B, Suárez PJ, Dupont Y, Romary L, de la Clergerie É, et al. CamemBERT: a tasty French language model. In: Proceedings of the 58th Annual Meeting of the Association for Computational Linguistics. 2020 Presented at: ACL '20; July 5-10, 2020; Virtual Event p. 7203-7219 URL: https://aclanthology.org/2020.acl-main.645.pdf [doi: 10.18653/v1/2020.acl-main.645]
47. Touchent R, Romary L, de La Clergerie É. CamemBERT-bio: leveraging continual pre-training for cost-effective models on French biomedical data. In: Proceedings of the 2024 Joint International Conference on Computational Linguistics,

XSL•FO
RenderX

Language Resources and Evaluation. 2024 Presented at: LREC-COLING '24; May 20-25, 2024; Torino, Italia p. 2692-2701 URL: https://aclanthology.org/2024.lrec-main.241.pdf
48. Labrak Y, Bazoge A, Dufour R, Rouvier M, Morin E, Daille B, et al. DrBERT: a robust pre-trained model in French for biomedical and clinical domains. In: Proceedings of the 61st Annual Meeting of the Association for Computational Linguistics. 2023 Presented at: ACL '23; July 9-14, 2023; Toronto, Canada p. 16207-16221 URL: https://aclanthology.org/2023.acl-long.896.pdf [doi: 10.18653/v1/2023.acl-long.896]
49. Winkler WE. String comparator metrics and enhanced decision rules in the Fellegi-Sunter model of record linkage. Bureau of the Census. 2022. URL: https://files.eric.ed.gov/fulltext/ED325505.pdf [accessed 2024-04-29]
50. Levenshtein VI. Binary codes capable of correcting deletions, insertions, and reversals. Sov Phys Dokl 1965;10(8):707-710.
51. Grouin C, Leixa J, Névéol A, Rosset S, Tannier X, Zweigenbaum P. The Quaero French Medical Corpus: a ressource for medical entity recognition and normalization. paperswithcode. URL: https://paperswithcode.com/paper/the-quaero-french-medical-corpus-a-ressource [accessed 2024-03-28]
52. Mahajan D, Liang JJ, Tsou CH. Toward understanding clinical context of medication change events in clinical narratives. AMIA Annu Symp Proc 2021;2021:833-842 [FREE Full text] [Medline: 35308981]
53. Remaki A. BioMedics. Zenodo. 2022. URL: https://zenodo.org/records/13838918 [accessed 2024-04-29]
54. Wajsburt P, Petit-Jean T, Dura B, Cohen A, Jean C, Bey R. EDS-NLP: efficient information extraction from French clinical notes. zenodo. URL: https://zenodo.org/records/11238626 [accessed 2024-04-29]
55. Vaswani A, Shazeer N, Parmar N, Uszkoreit J, Jones L, Gomez A, et al. Attention is all you need. In: Proceedings of the 31st International Conference on Neural Information Processing Systems. 2017 Presented at: NIPS '17; December 4-9, 2017; Long Beach, CA p. 6000-6010 URL: https://dl.acm.org/doi/10.5555/3295222.3295349
56. Abas AR, Elhenawy I, Zidan M, Othman M. BERT-CNN: a deep learning model for detecting emotions from text. Comput Mater Contin 2021;71(2):2943-2961 [FREE Full text] [doi: 10.32604/cmc.2022.021671]
57. Catalogue des terminologies. Ministère du Travail, de la Santé et des Solidarités & ANS. URL: https://smt.esante.gouv.fr/catalogue-des-terminologies/ [accessed 2025-01-08]
58. Dekking FM, Kraaikamp C, Lopuhaä HP, Meester LE. The bootstrap. In: Dekking FM, Kraaikamp C, Lopuhaä HP, Meester LE, editors. A Modern Introduction to Probability and Statistics: Understanding Why and How. Cham, Switzerland: Springer; 2005:269-284.
59. Eviatar T, Yahalom R, Livnat I, Elboim M, Elkayam O, Chodick G, et al. Real-world treatment patterns in patients with systemic lupus erythematosus: associations with comorbidities and damage. Lupus Sci Med 2024 Sep 24;11(2):25 [FREE Full text] [doi: 10.1136/lupus-2024-001266] [Medline: 39317452]
60. Artérite de Takayasu. Haute Autorité de Santé. URL: https://www.has-sante.fr/jcms/p_3148994/fr/arterite-de-takayasu [accessed 2024-04-29]
61. Mouthon L, Bussone G, Berezné A, Noël LH, Guillevin L. Scleroderma renal crisis. J Rheumatol 2014 Jun;41(6):1040-1048. [doi: 10.3899/jrheum.131210] [Medline: 24833760]
62. Gérardin C, Mageau A, Mékinian A, Tannier X, Carrat F. Construction of cohorts of similar patients from automatic extraction of medical concepts: phenotype extraction study. JMIR Med Inform 2022 Dec 19;10(12):e42379 [FREE Full text] [doi: 10.2196/42379] [Medline: 36534446]
63. Carrino CP, Llop J, Pàmies M, Gutiérrez-Fandiño A, Armengol-Estapé J, Silveira-Ocampo J, et al. Pretrained biomedical language models for clinical NLP in Spanish. In: Proceedings of the 21st Workshop on Biomedical Language Processing. 2022 Presented at: BioNLP '22; May 26, 2022; Dublin, Ireland p. 193-199 URL: https://aclanthology.org/2022.bionlp-1.19.pdf [doi: 10.18653/v1/2022.bionlp-1.19]
64. Lee J, Yoon W, Kim S, Kim D, Kim S, So C, et al. BioBERT: a pre-trained biomedical language representation model for biomedical text mining. Bioinformatics 2020 Feb 15;36(4):1234-1240 [FREE Full text] [doi: 10.1093/bioinformatics/btz682] [Medline: 31501885]
65. Entrepôt de Données de Santé. Assistance Hoptaux Publique de Paris. URL: https://eds.aphp.fr/ [accessed 2025-01-20]

Abbreviations

AP-HP: University Hospitals of Greater Paris (Assistance publique-hôpitaux de Paris)
APS: antiphospholipid syndrome
ATC: Anatomical Therapeutic Chemical
BERT: bidirectional encoder representations from transformer
CDW: clinical data warehouse
CUI: concept unique identifier
EHR: electronic health record
ICD-10: International Classification of Diseases, Tenth Revision
NER: named entity recognition
NLP: natural language processing
SLE: systemic lupus erythematosus

XSL•FO
RenderX

SNOMED CT: Systematized Nomenclature of Medicine Clinical Terms
TA: Takayasu arteritis
UMLS: Unified Medical Language System

Edited by C Lovis; submitted 12.11.24; peer-reviewed by JP Goldman, C Gaudet-Blavignac, E Lagarde, S Chowdhury, S Oworah; comments to author 25.12.24; revised version received 21.01.25; accepted 25.01.25; published 09.04.25.

Please cite as:
Remaki A, Ung J, Pages P, Wajsburt P, Liu E, Faure G, Petit-Jean T, Tannier X, Gérardin C
Improving Phenotyping of Patients With Immune-Mediated Inflammatory Diseases Through Automated Processing of Discharge Summaries: Multicenter Cohort Study
JMIR Med Inform 2025;13:e68704
URL: https://medinform.jmir.org/2025/1/e68704
doi:10.2196/68704
PMID:

©Adam Remaki, Jacques Ung, Pierre Pages, Perceval Wajsburt, Elise Liu, Guillaume Faure, Thomas Petit-Jean, Xavier Tannier, Christel Gérardin. Originally published in JMIR Medical Informatics (https://medinform.jmir.org), 09.04.2025. This is an open-access article distributed under the terms of the Creative Commons Attribution License (https://creativecommons.org/licenses/by/4.0/), which permits unrestricted use, distribution, and reproduction in any medium, provided the original work, first published in JMIR Medical Informatics, is properly cited. The complete bibliographic information, a link to the original publication on https://medinform.jmir.org/, as well as this copyright and license information must be included.

XSL•FO
RenderX

Original Paper

Improving Large Language Models' Summarization Accuracy by Adding Highlights to Discharge Notes: Comparative Evaluation

Mahshad Koohi Habibi Dehkordi[1], MSc; Yehoshua Perl[1], PhD; Fadi P Deek[2], PhD; Zhe He[3], PhD; Vipina K Keloth[4], PhD; Hao Liu[5], PhD; Gai Elhanan[6], MD; Andrew J Einstein[7], MD, PhD

[1]Department of Computer Science, New Jersey Institute of Technology, Newark, NJ, United States

[2]Department of Informatics, New Jersey Institute of Technology, Newark, NJ, United States

[3]School of Information, Florida State University, Tallahassee, FL, United States

[4]Department of Medical Informatics, Yale University, New Haven, CT, United States

[5]Department of Computer Science, Montclair State University, Montclair, NJ, United States

[6]School of Medicine, University of Nevada, Reno, NV, United States

[7]Department of Medicine, Columbia University Irving Medical Center, New York, NY, United States

Corresponding Author:
Mahshad Koohi Habibi Dehkordi, MSc
Department of Computer Science
New Jersey Institute of Technology
Ying Wu College of Computing, NJIT, 323 Martin Luther King Jr. Blvd
Apt 1
Newark, NJ, 07102
United States
Phone: 1 973 596 3000
Email: mk985@njit.edu

Abstract

Background: The American Medical Association recommends that electronic health record (EHR) notes, often dense and written in nuanced language, be made readable for patients and laypeople, a practice we refer to as the simplification of discharge notes. Our approach to achieving the simplification of discharge notes involves a process of incremental simplification steps to achieve the ideal note. In this paper, we present the first step of this process. Large language models (LLMs) have demonstrated considerable success in text summarization. Such LLM summaries represent the content of EHR notes in an easier-to-read language. However, LLM summaries can also introduce inaccuracies.

Objective: This study aims to test the hypothesis that summaries generated by LLMs from highlighted discharge notes will achieve increased accuracy compared to those generated from the original notes. For this purpose, we aim to prove a hypothesis that summaries generated by LLMs of discharge notes in which detailed information is highlighted are likely to be more accurate than summaries of the original notes.

Methods: To test our hypothesis, we randomly sampled 15 discharge notes from the MIMIC III database and highlighted their detailed information using an interface terminology we previously developed with machine learning. This interface terminology was curated to encompass detailed information from the discharge notes. The highlighted discharge notes distinguished detailed information, specifically the concepts present in the aforementioned interface terminology, by applying a blue background. To calibrate the LLMs' summaries for our simplification goal, we chose GPT-4o and used prompt engineering to ensure high-quality prompts and address issues of output inconsistency and prompt sensitivity. We provided both highlighted and unhighlighted versions of each EHR note along with their corresponding prompts to GPT-4o. Each generated summary was manually evaluated to assess its quality using the following evaluation metrics: completeness, correctness, and structural integrity.

Results: We used the study sample of 15 discharge notes. On average, summaries from highlighted notes (H-summaries) achieved 96% completeness, 8% higher than the summaries from unhighlighted notes (U-summaries). H-summaries had higher completeness in 13 notes, and U-summaries had higher or equal completeness in 2 notes, resulting in P=.01, which implied statistical significance. Moreover, H-summaries demonstrated better correctness than U-summaries, with fewer instances of erroneous information (2 vs 3 errors, respectively). The number of improper headers was smaller for H-summaries for 11 notes and U-summaries for 4 notes (P=.03; implying statistical significance). Moreover, we identified 8 instances of misplaced

XSL•FO
RenderX

information in the U-summaries and only 2 in the H-summaries. We showed that our findings supported the hypothesis that summarizing highlighted discharge notes improves the accuracy of the summaries.

Conclusions: Feeding LLMs with highlighted discharge notes, combined with prompt engineering, results in higher-quality summaries in terms of correctness, completeness, and structural integrity compared to unhighlighted discharge notes.

(JMIR Med Inform 2025;13:e66476) doi:10.2196/66476

KEYWORDS

electronic health record; EHR; EHR summaries; clinical notes summarization; discharge notes summarization; LLM summaries; ChatGPT summaries; highlighted EHR notes; accuracy of summaries; discharge notes; large language model; LLM; ChatGPT; artificial intelligence; AI

Introduction

Background

Electronic health records (EHRs) [1] are digital versions of a patient's medical records that were originally intended for communication among health care professionals, such as clinicians and nurses, to facilitate quick comprehension and efficient interoperability. These notes are typically written in highly technical language, filled with abbreviations, complex sentence structures, and medical jargon that may be unfamiliar to individuals without a medical background [2].

According to the 21st Century Cures Act and the Open Notes Rule [3], it is required to make these notes available to patients through patient portals, and because of this, a significant challenge has emerged. Patients with limited health literacy may struggle to understand written medical information, communicate health concerns with health care providers, and navigate EHR systems [2]. Research shows that patients often use different vocabulary than clinicians when searching for health information [4], indicating that the language clinicians use in discharge notes is potentially unfamiliar and difficult for patients to understand. To increase the comprehension of EHR notes, the American Medical Association recommends a grade 6 reading level, whereas the National Institutes of Health (NIH) recommends a grade 7 to 8 reading level for EHR notes [5,6]. The National Cancer Institute recommends an grade 6 reading level, reflecting the average reading level for a US citizen [7-9].

Large language models (LLMs) [10-13] have demonstrated success in text summarization and simplification tasks [14-16]. ChatGPT (OpenAI) [17], in particular, has shown promise in generating summaries that are comparable to those created by human experts [18]. Prompt engineering [19,20] has gained significant popularity in recent years due to its potential to improve the performance of LLMs. By carefully crafting prompts, we can instruct LLMs on how to extract key information, maintain coherence, and structure summaries according to specific needs. Well-designed prompts help control the level of detail, tone, and style, thereby improving both accuracy and readability [19,21]. Because LLMs rely on input instructions [22], prompt engineering is essential for aligning model behavior with the desired summarization outcome, reducing ambiguity and enhancing reliability.

Despite the advantages, several concerns remain regarding the use of LLMs in the medical field, particularly for summarizing medical texts [23,24]. These include issues of reliability, inconsistency in output quality, the potential for false information, and prompt sensitivity. Without addressing these concerns, LLMs might not realize their full potential for summarizing discharge notes. As mentioned earlier, the presence of inadequate sentence structure, a lack of punctuation, the presence of fragmented expressions, and an abundance of abbreviations within discharge notes make summarization relatively more difficult compared to general domain text summarization. Therefore, LLM-generated summaries may sometimes omit crucial information or lack proper structure.

In this paper, we present the first step in the process of simplifying discharge notes by harnessing the summarization capabilities of LLMs. In this study, we aim to generate more accurate, structured summaries from discharge notes where headers provide clear orientation and make the content easier to understand [25]. These summaries are then converted into accurate, simplified notes that are understandable for patients with a grade 6 reading level [26].

To address and evaluate the loss of crucial information in the summaries of discharge notes, our approach involves modifying the input by providing LLMs with highlighted discharge notes, where detailed information is emphasized. We then compare these summaries with those generated from unhighlighted notes. Our previous research [27,28] developed an innovative method for automatically highlighting detailed information in discharge notes. In this study, we automatically highlighted discharge notes using that technique (which is described in the Methods section). Our technique also uses prompt engineering to enhance the structural integrity of the generated summaries and address prompt sensitivity. We hypothesize that feeding LLMs with the highlighted notes aids in summarizing them more accurately. The rationale for this prediction is that, with a prompt to focus on the highlighted detailed information in a text, the summary will be more accurate and better structured than one obtained without highlighting.

We conducted this study to test the following hypothesis: Summaries generated by LLMs from highlighted discharge notes will achieve increased accuracy compared to those generated from the original notes. This is done by generating summaries from both unhighlighted and highlighted discharge notes using LLMs and then comparing both versions of the summaries for each discharge note to see which method yields better results. We evaluated different dimensions of the accuracy of summaries with proper metrics, including completeness, correctness, and structural integrity. Our findings support the

XSL•FO
RenderX

hypothesis that summarizing highlighted discharge notes improves the accuracy of the summaries as measured by these metrics. Thus, it is advantageous to generate summaries of discharge notes after highlighting them. Structured summaries of highlighted discharge notes provide a valuable starting point for future efforts to enhance the simplification of these notes while maintaining their accuracy.

Related Work

The goal of text summarization is to condense text while keeping its key information and important content intact [29,30]. Before the advent of LLMs, text summarization was primarily performed by automatic text summarization (ATS) [31-33]. ATS involves a trainable summarizer that considers various features, such as sentence position, keywords, sentence centrality, resemblance to the title, inclusion of named entities and numerical data, relative length, bushy path, and aggregated similarity to generate summaries [34].

While traditional ATS methods are still in use, LLMs are increasingly adopted for summarization tasks as they have shown great performance in this area. Therefore, there has been a significant shift from ATS to LLMs, with methods evolving from pretraining and fine-tuning to prompt-based approaches [31]. Besides, when summarizing discharge notes, mainly replete with medical abbreviations, LLMs typically spell out most of the abbreviations, yielding more readable clinical notes.

In a recent study [35], 8 LLMs (Flan-T5, Flan-UL2, Alpaca, MedAlpaca, Vicuna, Llama-2, GPT-3.5, and GPT-4) were evaluated for various clinical text summarization tasks. The study identified GPT-4 as the best-performing model, particularly when using in-context learning [36] for adaptation. GPT-4 demonstrated superior completeness, correctness, and conciseness in summaries compared to other models and even human experts. Therefore, in this study, we have used the latest version of ChatGPT, GPT-4o, for summarization.

In the study by Kanwal and Rizzo [37], they developed an extractive summarization method tailored for discharge notes using a bidirectional encoder representations from transformers–based model fine-tuned on the MIMIC-III dataset. Their approach uses attention scores from the final transformer layer to identify clinically important sentences without relying on reference summaries. The model dynamically selects sentences with above-average attention scores, aiming to preserve essential clinical content. Their method outperformed 3 baseline approaches, namely frequency-based, graph-based, and K-means centroid-based extractive summarization, demonstrating better content preservation and semantic alignment with the original notes.

In the study by Alsentzer and Kim [38], they explored extractive summarization of discharge notes from the MIMIC-III database. They estimated an upper bound on extractive summarization by measuring how much of the information in a discharge summary can be found elsewhere in the patient's EHR notes using concept unique identifiers. To support future summarization tasks, they also developed a long short-term memory model to label word-level topics in the "history of present illness" sections. This classifier achieved an F_1-score of 0.876 on a manually annotated test set, demonstrating its potential for generating topic-specific evaluation datasets for extractive summarization models.

In the study by Ma et al [39], the researchers developed a method called ImpressionGPT to summarize the "impression" section of radiology reports using ChatGPT. They used a dynamic prompt generation and iterative optimization approach to improve the performance of ChatGPT in this task. The results showed that ImpressionGPT achieved better performance in generating correct and concise summaries compared to existing methods, demonstrating its potential to enhance clinical workflows and reduce the workload of health care professionals.

The challenges faced by clinicians with limited time to remain abreast of the rapidly expanding medical literature have been documented in the study by Hake et al [40]. The authors evaluated the performance of ChatGPT in summarizing 140 peer-reviewed medical abstracts from 14 different journals. Their methodology involved prompting ChatGPT to create summaries and then having physicians assess the quality, accuracy, and bias of these summaries, where bias refers to the phenomenon where artificial intelligence (AI) systems are trained on data that lack sufficient reflection of the diversity within the population. The results showed that ChatGPT-produced summaries were 70% shorter than the original abstracts but maintained an accuracy of 92.5%. The study concluded that while ChatGPT can aid in summarizing medical literature, full-text evaluation remains crucial for critical medical decisions. Although they conducted the study on scientific paper abstracts, which are well structured and have much simpler language than discharge notes, they reported several occurrences of serious inaccuracies in ChatGPT summaries that could materially impact the major interpretation of the text.

Methods

Overview

Existing research on summarization using ChatGPT [35] has primarily focused on prompt engineering to achieve optimal results. These studies have not explored the potential benefits of modifying the input format and providing customized context tailored to the specific text. In contrast, our study goes beyond prompt engineering by incorporating important information directly into the input text. This approach ensures that ChatGPT pays attention to key details, enhancing the completeness, correctness, and structural integrity of the generated summaries.

In the Methods section, we first explain the automatic EHR highlighting technique, followed by the summarization method used in this study.

Automatic EHR Highlighting

In our previous studies [27,28], we developed a cardiology interface terminology (CIT) to facilitate efficient highlighting of detailed content in cardiology-related discharge notes. The process is composed of 2 phases. In the first phase [27], we created an initial version of CIT (ICIT), which contains the cardiology-related subhierarchies of Systematized Nomenclature of Medicine–Clinical Terms [41,42]. However, ICIT did not

XSL•FO
RenderX

capture all the important information from the discharge notes of cardiology patients. Therefore, we added concepts by extracting fine-granularity phrases from discharge notes that contained ICIT concepts. This was done using a semiautomatic iterative process, resulting in the formation of CIT. In each iteration, we highlighted the build dataset with the last version of the CIT and calculated the coverage and breadth of the highlighted dataset. Coverage is the percentage of the total number of words that are highlighted in one note, and breadth is the average length of each highlighted concept.

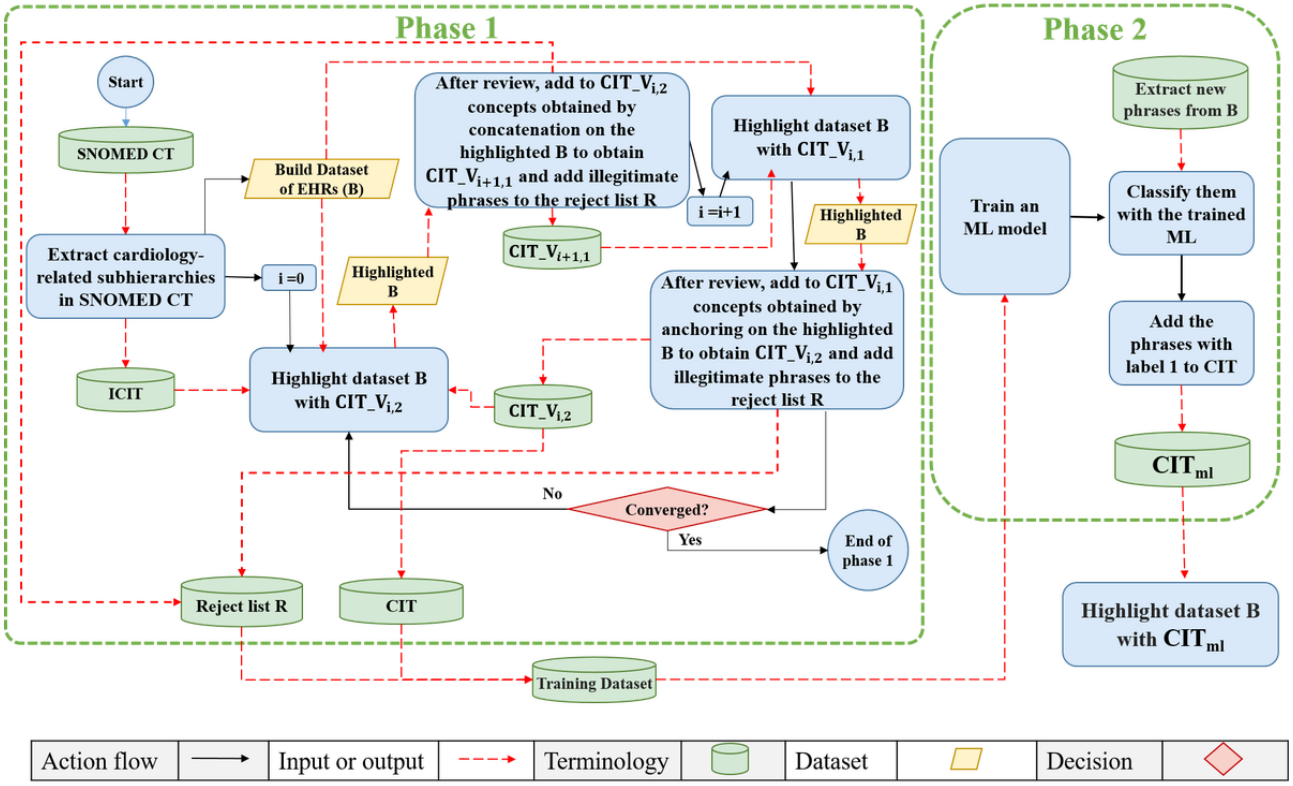
We defined 2 operations for mining more complex, higher-granularity phrases from the build dataset: concatenation and anchoring. Concatenation combined adjacent highlighted concepts, potentially separated by stop words, to form a meaningful phrase. Anchoring expanded existing highlighted concepts by attaching surrounding words on the left, right, or both sides. We applied an iterative process in which the application of the concatenation operation was followed by the application of the anchoring operation.

Because CIT is an interface terminology, its concepts should follow the requirements for being considered concepts of a terminology. According to the desiderata of Cimino et al [43], a concept is an embodiment of a particular meaning. Concept orientation means that terms must correspond to at least one meaning ("nonvagueness") and no more than one meaning ("nonambiguity") and that meanings correspond to no more than one term ("nonredundancy") [43,44].

After each application of either concatenation or anchoring, the newly mined phrases, as potential CIT concepts, were manually and automatically reviewed. Phrases that were deemed legitimate during the review, both structurally and semantically, such as "normal ejection fraction," were accepted and added to the CIT. All illegitimate phrases, whether identified automatically or manually, were added to a rejection list. For example, "step down unit for further" was rejected because it is a truncated phrase with an incomplete meaning. After each application of either the concatenation or anchoring operation, we highlighted the build dataset with the updated version of the CIT. This iterative process continued until the increase in coverage became negligible (<2% increase). The results of this phase served as training data for the second phase, where all the concepts in the resulting CIT were considered positive samples (labeled 1), and all the illegitimate phrases in the rejection list were considered negative samples (labeled 0). More detailed descriptions, including examples, are given in the study by Dehkordi et al [27].

In the second phase [28], we first trained a feedforward neural network model using the training data obtained from the first phase. Next, we extracted more phrases from discharge notes and applied predefined rules to filter out structurally illegitimate ones. The remaining phrases were labeled using the neural network model. The accepted phrases were then added to the CIT, forming CIT_{ml}. CIT_{ml} significantly improved the evaluation metrics of highlighted discharge notes. More detailed descriptions, including examples, are given in the study by Dehkordi et al [28]. Figure 1 shows the diagram of constructing CIT_{ml}.

Figure 1. Diagram of constructing CITml. Cardiology interface terminology (CIT) has versions with 2 indices. The first indicates the iteration number, and the second is binary, with 1 following concatenation and 2 following anchoring. CIT_V: updated version of the CIT; EHR: electronic health record; ICIT: initial version of the CIT; ML: machine learning; SNOMED CT: Systematized Nomenclature of Medicine–Clinical Terms.



XSL•FO
RenderX

In another study [45], we created and assessed interface terminologies designed to extract pertinent details from the clinical records of patients with COVID-19, underscoring the generalizability of our methodologies.

Data

We randomly selected 15 discharge notes from the MIMIC-III database from 2 intensive care units related to cardiology patients: the coronary care unit and the cardiac surgery recovery unit. Only the "discharge summary" category was extracted from the discharge notes. We chose 15 notes to enable a careful manual comparison of 2 summaries per note, with and without highlighting, versus the original text.

For each note, we created 2 HTML files: one containing the original discharge note without highlights and the other containing the highlighted discharge note, which is the output of the highlighting technique from our previous work.

As described in the Methods section, our previous work involved curating an interface terminology leveraging machine learning techniques. This terminology encompasses fine-granular, detailed concepts found in discharge notes. In this study, we applied this curated interface terminology to highlight the 15 discharge notes, such that all concepts from the terminology that were present in these notes were highlighted. The highlighted information was marked using span tags with a blue background color with the color code of #ADD8E6. Moreover, we created plain text in HTML format to ensure both inputs have a uniform format to be provided to ChatGPT. The plain text HTML file was created by enclosing the entire text within a tag.

To provide insights into the 15 discharge notes we were summarizing, Table 1 presents the text volume, overall themes, word frequency, and the repetition count of each word within a single document.

Table 1. Text volume, overall themes, and word frequency of 15 discharge notes.

Theme	TW[a]	SW[b]	TW_ESW[c]	DW_ESW[d]	N1[e]	N2[f]	N3[g]
Management of shortness of breath and heart failure	164	71	93	83	74	8	1
Aortic valve replacement	366	122	244	188	152	24	12
Bilateral renal artery stenosis	160	51	109	77	58	12	7
Three-vessel coronary artery bypass grafting	266	103	163	122	96	19	7
Aortic valve replacement and coronary artery bypass grafting	377	93	284	203	169	16	18
Peripheral vascular disease	448	153	295	206	156	31	19
Septic shock with respiratory failure	386	113	273	220	187	20	13
Coronary artery disease	312	101	211	144	106	27	11
Diabetic ketoacidosis with a history of coronary artery disease	180	41	139	112	97	12	3
Posterior mediastinal mass	560	199	361	255	197	36	22
Cardiac arrest	520	211	309	251	205	39	7
Hypercalcemia	375	133	242	198	165	26	7
Right coronary artery disease	411	160	251	168	119	33	16
Coronary artery bypass grafting	155	61	94	80	70	9	1
Aortic valve replacement	128	46	82	76	70	6	0
__[h]	320 (139)	111 (53)	209 (90)	159 (64)	128 (50)	21 (11)	10 (7)

[a]TW: total words.

[b]SW: stop words.

[c]TW_ESW: total words excluding stop words.

[d]DW_ESW: distinct words excluding stop words.

[e]N1: words repeated once, excluding stop words.

[f]N2: words repeated twice, excluding stop words.

[g]N3: words repeated more than 2 times, excluding stop words.

[h]Not applicable.

Prompt Engineering

Prompt engineering [19,20,46] is used to craft and refine input prompts to achieve the best possible results from LLMs, such as ChatGPT. However, it is a challenging task because even a minor change can significantly impact performance, leading to different results [39].

XSL•FO
RenderX

We proposed a protocol to incrementally generate effective prompts for both types of summaries from highlighted and unhighlighted notes.

In prompt engineering, we need to use static input and simply refine the prompt to find an appropriate prompt, which leads us to the best possible result. Therefore, we chose a random note that was not used in the evaluations to develop and test the prompt engineering design. We needed 2 prompts because 2 summaries are required for each note, the summary from unhighlighted notes (U-summary) and the summary from highlighted notes (H-summary).

We began the prompt engineering process with the unhighlighted text. To generate summaries, we initially used a simple prompt, "Give me a summary of this note." We evaluated the completeness, correctness, word count, and structure of the generated summaries. If the summaries were too long, erroneous, or incomplete, we adjusted the prompt accordingly. For instance, the first prompt, "Give me a summary of this note," resulted in a summary longer than the original text, so we revised it to "Give me a short summary of this note." In another example, we determined that the output was not structured, so we added "structured" to the prompt, forming the prompt "Give me a short structured summary of this note," so the summary would include headers and bullets for better orientation. This iterative process continued until the results were satisfactory to us after measuring the relevant metrics. Once we finalized the prompt for the unhighlighted text, we adapted it for the highlighted text by adding information about the format of the highlighted information.

Finally, to ensure that the prompts were generalizable to other clinical notes, we applied the final prompts to 3 more randomly selected notes that were not used in the evaluation of this study. Because we obtained satisfactory summaries, after measuring the relevant metrics for both U-summaries and H-summaries, we concluded that the final prompts were suitable for our study.

The final prompts were as follows:

- The prompt for the unhighlighted note was "Give me a short structured summary of this EHR note"
- The prompt for the highlighted note was "Give me a short structured summary of this EHR note, focusing on the highlighted information [whose tags are "style="'background-color: #ADD8E6']"

Generating Summaries

For each of the 15 randomly selected notes, we provided both the prompts to GPT-4o, along with the corresponding HTML files. To measure the evaluation metrics, we extracted all important information items from the original notes. Consequently, we manually inspected both summaries for each such item. For each summary, we counted the number of words, the number of important information items included by comparing them to the list of all important information items, and the number of possible erroneous statements generated by ChatGPT. We also counted the structural elements, misplaced information items, and false information items. We used this information to calculate the evaluation metrics.

Evaluation Metrics

Overview

Assessing the quality of a summary is challenging, and currently, no automatic proxy exists for this task. Therefore, similar to related studies [35], extensive manual effort is required to measure various aspects and compare which summary is more accurate. The evaluation was done by MKHD, a third-year PhD candidate in computer science with 3 years of research experience in processing EHR notes who has published studies [26-28,47,48] on this subject under the supervision of YP, who has more than 30 years of experience in medical informatics research. We used existing metrics and proposed new metrics for evaluating several aspects of the structured summaries generated. Our purpose was to test the following hypothesis: The H-summaries of discharge notes are likely to be more accurate than the U-summaries of those notes.

To assess the plausibility of the hypothesis, we needed to consider several metrics. The following 4 aspects should be evaluated in a summary: completeness, correctness, succinctness, and structural integrity. First, the completeness and correctness of the summary must be assessed. We followed the study by Van Veen et al [35] in using the metrics for completeness and correctness, which, respectively, measured the extent to which important information was covered and how accurate the covered information was. Second, the structure of the summary should be assessed by examining all the headers to identify proper and improper headers as well as bullets, which contribute to secondary structuring. In addition, because correct information might be placed under inappropriate headers within the text, we proposed a metric called the misplaced information to evaluate this aspect of each summary. Furthermore, the succinctness of the summary could be evaluated by the percentage reduction in size compared to the original text, which we referred to as the length reduction metric. This metric, although interesting, was not related to the quality of the summary.

Completeness

The completeness metric measures how well the summary has captured the important information from the original text. It is calculated as the percentage of the important information items included in the generated summary compared to all the important information items in the original text. This metric has also been used in other studies [35,49,50] to evaluate summaries based on the original text. Completeness can be calculated using the following equation:



Examples of important information items in Figure 2A are "known aortic stenosis," "worsening DOE," and "extubated without incident."

XSL•FO
RenderX

Figure 2. (A) An original highlighted note with 128 words, (B) the summary from unhighlighted notes of the note with 91 words and 84% (31/37 items of information) completeness, (C) and the summary from highlighted notes of the same note with 111 words and 100% completeness. The pink highlight in (B) indicates misplaced information. The orange highlight in (B) indicates repetitive information, the first of which is redundant and misplaced. The yellow highlights in (C) indicate information items from the original text that do not appear in (B).

Mrs. is a 75 year old female with known aortic stenosis who has had worsening DOE. A recent echo showed her aortic valve area to be 0.57 cm2, moderate MR and a normal ejection fraction. She underwent a cardiac catheterization which revealed one vessel coronary artery disease. She is now transferred for surgical management Hyperlipidemia HTN Type 2 Diabetes, Ms. neurologically intact and was extubated without incident. On postoperative day two, she was transferred to the step down unit for further care and recovery. She tolerated beta blockade and remained in a normal sinus rhythm. Over several days, she continued to make clinical improvements with diuresis and made steady progress with physical therapy. Medical therapy was optimized and she was eventually discharged to home on postoperative day five

(a)

Patient Information: 75-year-old female with known aortic stenosis.
Condition: Worsening dyspnea on exertion (DOE), aortic valve area measured at 0.57 cm^2, moderate mitral regurgitation (MR), normal ejection fraction, and one vessel coronary artery disease.
Procedures:
- **Cardiac Catheterization:** Revealed one vessel coronary artery disease.
- **Surgical Management:** Patient was transferred for surgical intervention.

Postoperative Course:
- **Extubation**: Performed without incident
- **Day 2:** Transferred to step-down unit
- **Medications:** Tolerated beta blockade; remained in normal sinus rhythm
- **Recovery:** Continued clinical improvements with diuresis and steady progress in physical therapy

Discharge: Discharged home on postoperative day five

(b)

Patient Information:
- **Age/Gender:** 75-year-old female
- **Medical History:** Known aortic stenosis, hyperlipidemia, hypertension (HTN), Type 2 Diabetes

Clinical Presentation:
- **Symptoms:** Worsening dyspnea on exertion (DOE)

Recent Diagnostics:
- **Echocardiogram:**
  - Aortic valve area: 0.57 cm^2
  - Moderate mitral regurgitation (MR)
  - Normal ejection fraction
- **Cardiac Catheterization:**
  - One vessel coronary artery disease

Treatment and Hospital Course:
- **Initial Management:** Transferred for surgical management
- **Postoperative Course:**
  - Neurologically intact and extubated without incident.
  - Transferred to step-down unit on postoperative day two
  - Tolerated beta blockade; remained in normal sinus rhythm
  - Showed clinical improvement with diuresis and made steady progress with physical therapy

Discharge: Discharged home on postoperative day five after optimized medical therapy

(c)

To calculate completeness, we first extracted and listed all information items from the original notes. We examined each summary, identifying how many of these items were present in the summary. We calculated the completeness of each note using equation 1. We calculated the average completeness scores for the 15 H-summaries and the 15 U-summaries separately.

Correctness

A summary is considered correct if it does not contain erroneous information. If it contains at least one instance of inaccurate information, it is then considered incorrect. The correctness of the summaries for a group of notes is the percentage of correct summaries. To evaluate correctness, we manually scanned the

XSL•FO
RenderX

15 U-summaries and the 15 H-summaries to identify all false information items based on the original text. This metric has also been used in similar studies [35,50,51].

Structural Elements Count

Overview

This metric quantifies the total number of structural elements, including the headers and bullet points, used to organize and structure the summaries. The structural elements count (SEC) is calculated by simply counting all the headers and bullet points in each summary.

ChatGPT added headers and subheaders to both the H-summaries and U-summaries based on the given prompt. Upon manual review of the headers, we found that most of them accurately captured the information that followed, and we referred to these as "proper headers." However, some headers were found to be redundant or misleading. Redundant headers are unnecessary and do not provide additional orientation for the reader, while misleading headers do not accurately represent the content that follows. Overall, having more proper headers and subheaders enhances the orientation of the note. In contrast, improper headers, whether redundant or misleading, may confuse the reader. Naturally, our goal was to maximize the number of proper headers to improve reader orientation and minimize the number of improper headers to avoid confusion and redundancy.

Proper Headers

Proper headers are those that correctly and effectively organize the text, accurately capturing the information that follows, leading to a clearer summary. The number of proper headers for each summary is determined by subtracting the improper headers from the total number of headers. For example, Figure 3A shows a portion of a summary where all the information is included in a single block of text, while Figure 3B shows the same portion of the summary with proper headers. In Figure 3B, information regarding status, medications, imaging, and physical examination is correctly categorized under separate sections with appropriate labels, thereby improving the orientation of the note.

Figure 3. (A) A portion of a summary lacking proper headers and (B) the same portion of the summary with proper headers.

Post-Operative Day (POD) 1: Recovering well, Swan-Ganz catheter removed, started on diuretics and beta-blockers per protocol, chest X-ray (CXR) showed bibasilar atelectasis and small right pleural effusion, matched with bibasilar rales and diminished breath sounds on exam **(a)**	**Post-Operative Day (POD) 1:** • **Status:** Recovering well, Swan Ganz catheter removed. • **Medications:** Diuretics and Beta-blockers started. • **Imaging:** Chest X-ray showed bibasilar atelectasis and small right pleural effusion. • **Physical Exam:** Bibasilar rales and diminished breath sounds. **(b)**

Improper Headers

Figure 4 shows an example of improper headers. Figure 4A shows a portion of a U-summary, and Figure 4B is the corresponding H-summary. As shown, Figure 4A contains numerous redundant subtitles, which significantly interfere with the orientation because they may overwhelm and confuse the reader.

Figure 4. (A) A portion of a summary having improper headers and (B) the same portion of the summary without improper headers.

Discharge:
• **Date of Discharge:** POD 4
• **Condition at Discharge:**
  • **Wounds:** Clean, dry, and intact
  • **Vital Signs:** Stable
Additional Note:
• **Follow-Up:**
  • **Cardiologist:** Dr. (Name not provided)
  • **Primary Care Physician:** (Name not provided)
(a)
	Discharge:
	Discharged home on postoperative day four
	• Wounds were clean, dry, and intact
	• All vital signs were stable
	• Follow-up with cardiologist and primary care physician as an outpatient
	(b)

XSL•FO
RenderX

To assess the improper headers metric, we manually reviewed all the summaries to identify the number of additional structural headers in each summary to compare the corresponding summaries with regard to their structural integrity.

Misplaced Information

Sometimes, a summary incorrectly categorizes information under the wrong section, resulting in misplaced information, confusing the reader. For example, in Figure 2B, "known aortic stenosis" is placed under the "patient information" category, whereas it should be under a header titled "medical history." This structure is correctly applied in the highlighted summary shown in Figure 2C. We counted the number of cases of misplaced information in both types of summaries to compare their structural information integrity.

Length Reduction

To evaluate the succinctness of the generated summaries, we used the length reduction metric, which is calculated using equation 2 with a Python (Python Software Foundation) program:



We used the Fisher exact test [52,53] twice; once to compare the completeness metric between the H-summaries and the U-summaries and the second time to compare the number of improper header metrics between the H-summaries and the U-summaries.

Power Analysis

In our methodology, power analysis [54] was conducted using the Fisher exact test to determine the necessary sample size for detecting significant effects, particularly valuable when dealing with categorical data in scenarios of small sample sizes or sparse data. We started our analysis with the 2 metrics that were dominant for the accuracy of the discharge notes.

Completeness Metric Analysis

For assessing the completeness of summaries, we had 2 equal-sized groups, each comprising 15 paired discharge notes. In this evaluation, summaries generated by method 1 (H-summaries) were superior in 13 instances, while method 2 (U-summaries) led in 2 cases. Consequently, the probability of a favorable outcome in group 1 (H-summaries) was 86.7%, and in group 2 (U-summaries), it was 13.3%. Given the consistent performance advantage of H-summaries, a 1-sided Fisher exact test was appropriate, with a significance level (α) set at .025. The resulting power analysis yielded a high power of 0.98, indicating robust confidence in these findings.

Improper Header Metric Analysis

For the improper header metric, power analysis using the Fisher exact test was conducted, taking into account unequal sample sizes. The total count of structural elements (SECs), which include headers and bullet points, was 463 for H-summaries, of which 4 (0.9%) were improper, and 516 for U-summaries, of which 30 (5.8%) were improper This metric necessitated a 2-sided test with an α of .05, achieving a perfect power of 1, suggesting that the test reliably confirmed substantially more improper headers for method 2 when compared to method 1.

Correctness Metric Analysis

Regarding the correctness metric, all H-summaries contained 870 items of information, 2 (0.2%) of which were false, while the U-summaries contained 795 items, 3 (0.38) of which were false. This resulted in probabilities of 0.2% (2/870) for H-summaries and 0.3% (3/795) for U-summaries. Given the substantial total sample size exceeding 1000 items (1665 items of information in total), a Pearson chi-square test [55] for unequal sample sizes was deemed suitable. However, the resulting power was low at 0.06. Further analysis revealed that to achieve a minimum power of 0.8 with a 2-sided test, the required sample sizes would need to increase to 41,146 items for H-summaries and 37,032 items for U-summaries, which is not practical for manual comparison.

Misplaced Information Metric Analysis

Finally, for the misplaced information metric, considering that there are 2 instances of misplaced information in 463 SECs for H-summaries and 8 in 516 SECs for U-summaries, the probabilities are 0.4% (2/463) and 1.6% (8/516), respectively. Conducting a 2-sided Fisher exact test power analysis with α of .05 and considering unequal sample sizes, we found that the resulting power was 0.41, which was low. To achieve a desired power of 0.8, recalculations suggested that sample sizes of 1272 for H-summaries (almost 3 times the current size) and 1145 for U-summaries (almost twice the current size) were needed.

Ethical Considerations

This study used discharge notes from the MIMIC-III dataset [56], a large, freely available database containing deidentified health-related data from >40,000 patients who were admitted to the Beth Israel Deaconess Medical Center between 2001 and 2012. The database includes information, such as vital signs, laboratory test results, procedures, medications, etc. The MIMIC-III database was approved by the institutional review boards [57] of the Beth Israel Deaconess Medical Center and the Massachusetts Institute of Technology. The requirement for individual patient consent was waived, as the dataset is fully deidentified and does not impact clinical care [58]. Before inclusion in MIMIC-III, all data underwent a rigorous deidentification process in compliance with Health Insurance Portability and Accountability Act (HIPAA) [59] standards [58]. Structured data were deidentified by removing all 18 HIPAA-defined protected health information elements, such as names, addresses, phone numbers, and exact dates [58]. To further ensure privacy, dates were randomly shifted while preserving relative intervals, and patients aged >89 years had their ages masked. Free-text fields, including physician notes and diagnostic reports, were processed using an extensively evaluated deidentification system that used dictionary lookups and pattern-matching algorithms to remove protected health information [58]. Because all data are deidentified and do not contain any identifiable patient information, the requirement for informed consent was waived by the overseeing institutional review boards [58].

XSL•FO
RenderX

Results

Overview

Figure 2A shows an example of a discharge note (note 15) with 128 words, accompanied by its U-summary (Figure 2B) and H-summary (Figure 2C), containing 91 and 111 words, respectively. We noted that this discharge note was missing, describing the actual surgery that obviously happened during hospitalization of the patient. We assumed that this omission was based on the fact that the surgery was described in the surgical note section of the discharge note. We chose this note because it enabled us to demonstrate several efficiencies in 1 short note. As shown in Figure 2C, 6 important information items from the original text, marked by yellow color, appeared in the H-summary but did not appear in the U-summary. In contrast, H-summary did not miss any items. Consequently, the calculated completeness for the H-summary was 100% (35/35), while the completeness of the U-summary was 84% (31/37 items of information), as shown also for note 15 in Table 2.

Table 2. Values of 2 metrics for 15 notes.

Notes	Word count of the original text[a]	Length reduction		Completeness	
		H- summaries[b] (%)	U-summaries[c] (%)	H-summaries, n/N (%)	U- summaries, n/N (%)
1	164	2	–10	35/35 (100)	29/35 (83)
2	366	23	20	31/32 (97)	28/32 (88)
3	160	1	21	40/40 (100)	39/40 (98)
4	266	23	26	41/42 (99)	41/42 (99)
5	377	5	7	24/26 (92)	22/26 (85)
6	448	39	31	32/33 (97)	28/33 (85)
7	386	25	21	43/46 (93)	38/46 (83)
8	312	24	27	21/22 (95)	20/22 (91)
9	180	–4	–6	22/23 (96)	22/23 (96)
10	560	33	44	33/35 (94)	27/35 (77)
11	520	36	39	24/27 (89)	23/27 (85)
12	375	38	37	38/42 (90)	35/42 (83)
13	411	40	34	42/43 (98)	41/43 (95)
14	155	33	19	29/30 (97)	27/30 (90)
15	128	13	29	37/37 (100)	31/37 (84)

[a]Mean 320, SD 139 words.

[b]H-summary: summary from highlighted notes (length reduction: mean 22, SD 15; completeness: mean 96, SD 4).

[c]U-summary: summary from unhighlighted notes (length reduction: mean 23, SD 15; completeness: mean 88, SD 6).

Completeness

As shown in Table 2, on average, the completeness of the U-summaries was 88% (SD 6%), while the completeness of the H-summaries was 96% (SD 4%), which was 8% higher. All percentages in Table 2 are rounded to the nearest whole number. It is worth mentioning that for 13 notes, the completeness of the H-summary was higher than that of the U-summary, and for 2 notes, the completeness was equal. Using the Fisher exact test [52,53], we compared the number of notes with higher completeness in the H-summary group (13 notes) versus the number of notes with higher or equal completeness in the U-summary group (2 notes). The Fisher exact test yielded P=.01, indicating a statistically significant difference.

Length Reduction

As shown in Table 2, the average word count of the original notes was 320 words, and the average length reduction of the H-summaries and U-summaries was 22% (SD 15%) and 23% (SD 15%) words, respectively. A negative number for length reduction in Table 2 indicates that the summary generated had more words than the original text.

Correctness

In our analysis, we identified 3 instances of false information in U-summaries. In contrast, H-summaries contained only 2 false information items. However, this did not provide a statistically significant result, implying improvement. As an example of erroneous information, the original note contained the phrase “consistent either with aspiration pneumonia or increased apical interstitial edema,” whereas the U-summary incorrectly contained “consistent either with aspiration pneumonia and increased apical interstitial edema.” Replacing “or” with “and” changed the meaning of the phrase. Another example was a U-summary that mistakenly referred to Troponin T, a protein, as an enzyme.

XSL•FO
RenderX

Structural Evaluation

The total number of SECs, which were either headers or bullet points, for the U-summaries was 516, while for H-summaries, it was 463. In terms of improper headers, there were 30 instances in the U-summaries compared to only 4 in the H-summaries. Table 3 presents the distribution of improper headers and misplaced information for the U-summaries and H-summaries for each of the 15 notes. For 11 (73%) of the notes, according to Table 3, the number of improper headers in the U-summaries was larger than the number for the H-summaries. For the other 4 (27%) notes, the numbers were equal. Hence, the number of improper headers in U-summaries was larger than those for H-summaries with statistical significance according to the Fisher exact test [52,53]. We compared the number of notes with a higher number of improper headers in the U-summary group (11 notes) and the number of notes with a higher number of improper headers in the H-summary group (4 notes). The Fisher exact test yielded P=.03, indicating a statistically significant result.

Table 3. Distribution of improper headers and misplaced information for the summaries from unhighlighted notes (U-summaries) and summaries from highlighted notes (H-summaries).

Notes	Improper headers		Misplaced information	
	U-summaries (n=30), n (%)	H-summaries, (n=4), n (%)	U-summaries, (n=8), n (%)	H-summaries, (n=2), n (%)
1	1 (3)	0 (0)	0 (0)	1 (50)
2	1 (3)	0 (0)	1 (12)	0 (0)
3	1 (3)	0 (0)	1 (12)	0 (0)
4	5 (17)	0 (0)	0 (0)	0 (0)
5	4 (13)	0 (0)	0 (0)	0 (0)
6	1 (3)	1 (25)	0 (0)	0 (0)
7	1 (3)	0 (0)	1 (12)	1 (50)
8	1 (3)	0 (0)	1 (12)	0 (0)
9	0 (0)	0 (0)	0 (0)	0 (0)
10	1 (3)	0 (0)	0 (0)	0 (0)
11	2 (7)	1 (25)	0 (0)	0 (0)
12	2 (7)	2 (50)	0 (0)	0 (0)
13	6 (20)	0 (0)	0 (0)	0 (0)
14	3 (10)	0 (0)	2 (25)	0 (0)
15	1 (3)	0 (0)	2 (25)	0 (0)

In other words, 5.8% (30/516) of the SECs in U-summaries were improper headers, whereas this percentage was only 0.1% (4/463) in the H-summaries. On the other hand, the number of proper SECs, after deducting the improper headers, was 94.2% (486/516) for the U-summaries and 99.1% (459/463) for the H-summaries. Hence, the structure of U-summaries was slightly more detailed than that of the H-summaries. However, the high percentage of improper headers rendered this advantage irrelevant because the structure was meaningfully less reliable. Moreover, we identified 8 instances of misplaced information in the U-summaries and only 2 in the H-summaries.

Discussion

Principal Findings

In this study, we evaluated summaries generated by LLMs from 2 versions of discharge notes, H-summaries and U-summaries, to test the hypothesis that highlighting discharge notes improves the accuracy of the generated summaries. Our results show that feeding LLMs with H-summaries, combined with prompt engineering, results in higher-quality summaries in terms of correctness, completeness, and structural integrity compared to U-summaries.

This study serves as the first step toward meeting the NIH challenge, which is facilitating the conversion of text in discharge notes into language that is comprehensible to a patient with a grade 6 reading level [6,60]. In a previous work [26], we conducted a study to simplify discharge notes using 2 simplification approaches.

In the first approach, we first summarized the discharge notes and then, in a second step, converted them into language understandable by a grade 6 reader. In the second approach, we directly generated, in a single step, a simplified summary understandable by a grade 6 reader from the discharge note. Our results showed that the first approach, simplifying notes in 2 steps, led to higher-quality and more understandable notes for grade 6 readers. Our interpretation is that, given discharge notes are inherently dense and complex, breaking the task into 2 steps reduces the cognitive load on the LLM, allowing it to generate more accurate and comprehensible results. Hence, cascading the findings of the previous study [26] to the findings of this paper provides a pipeline responding to the NIH challenge of summarizing discharge notes into a language that

XSL•FO
RenderX

is comprehensible to a patient with a grade 6 reading level with high accuracy. Because the findings of both studies satisfy statistical significance, their combined impact is reliable, although this study is based on a sample of only 15 discharge notes.

Usually, summaries are shorter than the original text and thus enable the reader to review the content of a document faster. LLMs can actually generate summaries of various lengths according to the prompt provided to them. Because our final goal is the simplification of discharge notes, we are not necessarily interested in short summaries for the sake of brevity but in succinct summaries that capture all detailed information of a note in a simpler language.

When evaluating the summary of a discharge note, if the summary lacks key information from the original note (ie, low completeness), it cannot be considered accurate. Similarly, if the summary contains erroneous information (lacking correctness), its accuracy is also compromised. Furthermore, if relevant information is placed under incorrect categories (referred to as "misplaced information"), the summary's accuracy is further affected. Therefore, in this paper, when we state that H-summaries have higher accuracy than U-summaries, we mean that H-summaries exhibit greater completeness, correctness, and structural integrity compared to U-summaries.

The scientific contribution of this research is the improvement in the accuracy of LLM summaries of discharge notes by feeding the LLMs with discharge notes in which the detailed information is highlighted. Automatic highlighting of discharge notes is provided by techniques from our previous research [28]. A sample of a discharge note highlighted automatically by this technique is shown in Figure 2A. Our hypothesis was that providing such highlighting would better direct the LLMs to capture the detailed information of the note and would better structure its summary. Our study has proven the plausibility of this hypothesis by the evaluation of several metrics.

Although highlighting is used in this paper, it is not the primary focus of our study. However, we wish to clarify an observation regarding the highlighting in Figure 2A. This example is rich in information but with some stop words not highlighted. While there are other notes in our sample where several words and phrases are not highlighted, we note that "discharge notes" from MIMIC-III EHRs have contributed to this richness of information as they summarize the hospital course of the patient. Our highlighting method is based on mining phrases from clinical notes and determining which ones should be incorporated into the interface terminology. Only concepts present in the interface terminology are subsequently highlighted within the clinical note. Indeed, the density of the highlighting depends on the type of clinical notes and will be higher in discharge notes due to the richness of information they contain. Full details can be found in the studies by Dehkordi et al [27,28].

Out of the 4 metrics we used to compare the H-summaries to the U-summaries, results from 2 metrics have shown statistical significance for better quality of the H-summaries. For the other 2 metrics, instances of erroneous information were low, but still, the results are better for H-summaries. The reason for having fewer improper headers in H-summaries compared to U-summaries may be attributed to the fact that by identifying the detailed information in the text, ChatGPT achieves better orientation in the note, allowing it to focus on the essential content and structure it more effectively. Despite the higher completeness in H-summaries compared to U-summaries, the inclusion of redundant information in U-summaries resulted in a similar length reduction for both H-summaries and U-summaries. For instance, the orange color in Figure 2B indicates that there is repetitive information in the U-summary, such as the phrase "one vessel coronary artery disease," which appears twice.

We define SEC as the total number of headers and bullets. In general, a larger number of proper headers and bullets is desirable, as such categorization of information enhances the clarity of the notes, making them more understandable for the reader. Because this study represents the first step toward simplifying the texts, having information categorized in different sections to increase clarity is preferable, unless the headers are improper. Our study demonstrated that the ratio of improper headers is substantially lower in H-summaries compared to U-summaries.

Traditionally, for summarization, evaluation metrics such as recall-oriented understudy for gisting evaluation [61] are used. We have not used these metrics since (1) our hypothesis is comparing highlighted versus nonhighlighted notes with a focus on completeness, correctness, and structural integrity; and (2) there is a lack of human-generated summaries used by these metrics for computing the respective scores. Similarly, simplification of text is measured using metrics, such as the Flesch-Kincaid Grade Level [62], Simple Measure of Gobbledygook [63], and Gunning-Fog Index [64]. Because this study's focus was not on the readability of the notes, these metrics were not applicable.

Limitations

In our study, we considered only the discharge note part of the clinical notes, which are the most relevant parts of the clinical notes for the patients. Due to their summarizing nature, discharge notes have aspects from all other parts of clinical notes. Thus, we have chosen to concentrate only on the discharge note, while we expect a similar result for a study that would summarize the complete clinical note.

To minimize the amount of tedious manual review required for the evaluation of the various metrics, we have chosen a study of 15 notes, and this number was sufficient to yield the statistical significance for 2 dominant metrics of the 4 metrics for accuracy. For the other 2 metrics, the number of erroneous information items and misplaced information cases was infrequent, and a much larger sample would be needed to display statistical significance. Altogether, the results have proven our hypothesis that providing highlighted notes as input for ChatGPT will likely yield more accurate summaries.

Moreover, the reliance on extensive manual review for evaluating the summaries may introduce subjectivity into the assessment process. Future studies could benefit from developing more automated methods to assess summary quality to reduce potential bias and labor intensity. In addition, although

XSL•FO
RenderX

highlighting is used to enhance the input for LLMs, the technique itself may have limitations, such as the potential for overhighlighting or missing critical information not recognized by the underlying algorithm. This could affect the quality of the input and, consequently, the accuracy of the summaries produced. However, we are continuously working in parallel on different automated methods to improve the highlighting techniques and algorithms [47,48]. Finally, this study's results are based on the state of a specific LLM at a point in time. Continuous updates to LLMs could alter their performance characteristics, necessitating ongoing validation of the findings.

Future Work

In future work, we will use the LLM H-summaries as a starting point for further simplification of the notes to meet NIH's readability target for patients with grade 6 reading skills using various techniques. Some patients may be interested in just the big picture without many details, while others, based on their health literacy, may require detailed information. As mentioned previously, in the future, we intend to explore the capabilities of LLMs alongside the vast wealth of curated knowledge embedded in biomedical ontologies and terminologies in catering to the varied requirements of patient populations by offering summaries and simplifications of clinical notes tailored to individual needs and comprehension levels. While this study demonstrated statistical significance in the completeness and improper headers metrics, the limited sample size of 15 discharge notes was insufficient for the other 2 metrics. In future studies, we plan to use a larger sample to test statistical significance for the correctness and misplaced information metrics as well.

Ethical Concerns

The integration of LLMs into clinical data summarization introduces several ethical considerations that warrant careful attention. A primary concern is the potential for these models to generate inaccurate or fabricated information, commonly referred to as hallucinations [65], which could adversely affect patient care.

Bias within training data presents another ethical challenge. If LLMs are trained on unrepresentative datasets, they may perpetuate existing health disparities by providing less accurate summaries for certain populations [66]. Addressing these biases is critical to ensure equitable health care delivery.

Moreover, the lack of transparency in how LLMs generate outputs [67] can lead to challenges in clinical settings. Clinicians may find it difficult to trust or validate AI-generated summaries without a clear understanding of the underlying processes, potentially hindering the integration of these tools into health care practice.

To mitigate these ethical concerns, it is imperative to implement robust validation processes, ensure compliance with privacy regulations, actively address biases in training data, and maintain transparency in AI operations.

Conclusions

In this paper, we propose the use of highlighted discharge notes, emphasizing detailed information, to enhance the completeness and correctness of the summaries generated by LLMs. We have also developed and applied prompt engineering techniques to improve the structural integrity of these summaries, effectively addressing issues related to prompt sensitivity and reliability. Our study includes empirical validation with a random sample of 15 highlighted discharge notes from the MIMIC-III database, demonstrating that the input with the highlighted notes leads to more accurate LLM summaries of clinical notes. The final goal is to simplify discharge notes to be readable by a patient with grade 6 reading skills. To achieve this goal, we will use the summaries obtained in this research as input for the future simplification process.

Acknowledgments

This work was partially supported by a New Jersey Institute of Technology (seed grant 213443).

Authors' Contributions

MKHD was responsible for conceptualization, methodology, software, validation, formal analysis, investigation, data curation, and writing the original draft. YP was responsible for conceptualization, methodology, validation, formal analysis, reviewing and editing the manuscript, supervision, and project administration. FPD was responsible for reviewing and editing the manuscript. ZH was responsible for reviewing and editing the manuscript. VKK was responsible for methodology. HL was responsible for reviewing and editing the manuscript. GE and AJE were responsible for supervision.

Conflicts of Interest

None declared.

References

1. Seymour T, Frantsvog D, Graeber T. Electronic health records (EHR). Am J Health Sci 2012 Jul 13;3(3):201-210 [FREE Full text] [doi: 10.19030/ajhs.v3i3.7139]
2. Polepalli Ramesh B, Houston T, Brandt C, Fang H, Yu H. Improving patients' electronic health record comprehension with NoteAid. Stud Health Technol Inform 2013;192:714-718. [Medline: 23920650]
3. Magid SK, Cohen K, Katzovitz LS. 21 Century Cures Act, an information technology-led organizational initiative. HSS J 2022 Mar;18(1):42-47 [FREE Full text] [doi: 10.1177/15563316211041613] [Medline: 35082558]

XSL•FO
RenderX

4. McCray AT, Loane RF, Browne AC, Bangalore AK. Terminology issues in user access to web-based medical information. Proc AMIA Symp 1999:107-111 [FREE Full text] [Medline: 10566330]
5. Weiss BD. Health literacy: a manual for clinicians. American Medical Association. URL: http://lib.ncfh.org/pdfs/6617.pdf [accessed 2025-06-29]
6. Health education materials assessment tool. National Institutes of Health National Library of Medicine. URL: https://medlineplus.gov/pdf/health-education-materials-assessment-tool.pdf [accessed 2025-07-07]
7. Grever MR, Schepartz SA, Chabner BA. The National Cancer Institute: cancer drug discovery and development program. Semin Oncol 1992 Dec;19(6):622-638. [Medline: 1462164]
8. Davis TC, Wolf MS. Health literacy: implications for family medicine. Fam Med 2004 Sep;36(8):595-598. [Medline: 15343422]
9. Perni S, Rooney MK, Horowitz DP, Golden DW, McCall AR, Einstein AJ, et al. Assessment of use, specificity, and readability of written clinical informed consent forms for patients with cancer undergoing radiotherapy. JAMA Oncol 2019 Aug 01;5(8):e190260 [FREE Full text] [doi: 10.1001/jamaoncol.2019.0260] [Medline: 31046122]
10. Zhao WX, Zhou K, Li J, Tang T, Wang X, Hou Y, et al. A survey of large language models. ArXiv. Preprint posted online on March 31, 2023 [FREE Full text]
11. Chang Y, Wang X, Wang J, Wu Y, Yang L, Zhu K, et al. A survey on evaluation of large language models. ACM Trans Intell Syst Technol 2024 Mar 29;15(3):1-45. [doi: 10.1145/3641289]
12. Thirunavukarasu AJ, Ting DS, Elangovan K, Gutierrez L, Tan TF, Ting DS. Large language models in medicine. Nat Med 2023 Aug 17;29(8):1930-1940. [doi: 10.1038/s41591-023-02448-8] [Medline: 37460753]
13. Jahan I, Laskar MT, Peng C, Huang JX. A comprehensive evaluation of large language models on benchmark biomedical text processing tasks. Comput Biol Med 2024 Mar;171:108189 [FREE Full text] [doi: 10.1016/j.compbiomed.2024.108189] [Medline: 38447502]
14. Madzime R, Nyirenda C. Enhanced electronic health records text summarization using large language models. ArXiv. Preprint posted online on October 12, 2024 [FREE Full text]
15. Chintagunta B, Katariya N, Amatriain X, Kannan A. Medically aware GPT-3 as a data generator for medical dialogue summarization. In: Proceedings of Machine Learning Research 2021. 2021 Presented at: PMLR 2021; December 13, 2021; Online. [doi: 10.18653/v1/2021.nlpmc-1.9]
16. Jeblick K, Schachtner B, Dexl J, Mittermeier A, Stüber AT, Topalis J, et al. ChatGPT makes medicine easy to swallow: an exploratory case study on simplified radiology reports. Eur Radiol 2024 May 05;34(5):2817-2825 [FREE Full text] [doi: 10.1007/s00330-023-10213-1] [Medline: 37794249]
17. Dave T, Athaluri SA, Singh S. ChatGPT in medicine: an overview of its applications, advantages, limitations, future prospects, and ethical considerations. Front Artif Intell 2023 May 4;6:1169595 [FREE Full text] [doi: 10.3389/frai.2023.1169595] [Medline: 37215063]
18. Guo B, Zhang X, Wang Z, Jiang M, Nie J, Ding Y, et al. How close is ChatGPT to human experts? Comparison corpus, evaluation, and detection. ArXiv. Preprint posted online on January 18, 2023 [FREE Full text]
19. Marvin G, Hellen N, Jjingo D, Nakatumba-Nabende J. Prompt engineering in large language models. In: Proceedings of the Data Intelligence and Cognitive Informatics. 2023 Presented at: ICDICI 2023; June 27-28, 2023; Tirunelveli, India. [doi: 10.1007/978-981-99-7962-2_30]
20. Giray L. Prompt engineering with ChatGPT: a guide for academic writers. Ann Biomed Eng 2023 Dec 07;51(12):2629-2633. [doi: 10.1007/s10439-023-03272-4] [Medline: 37284994]
21. Patil R, Heston TF, Bhuse V. Prompt engineering in healthcare. Electronics 2024 Jul 26;13(15):2961. [doi: 10.3390/electronics13152961]
22. Zhang S, Dong L, Li X, Zhang S, Sun X, Wang S, et al. Instruction tuning for large language models: a survey. ArXiv. Preprint posted online on August 21, 2023 [FREE Full text]
23. Hadi MU, Tashi QA, Qureshi R, Shah A, Muneer A, Irfan M, et al. A survey on large language models: applications, challenges, limitations, and practical usage. TechRxiv. Preprint posted online on July 10, 2023 [FREE Full text] [doi: 10.36227/techrxiv.23589741.v1]
24. Karabacak M, Margetis K. Embracing large language models for medical applications: opportunities and challenges. Cureus 2023 May;15(5):e39305 [FREE Full text] [doi: 10.7759/cureus.39305] [Medline: 37378099]
25. Dai HJ, Syed-Abdul S, Chen CW, Wu CC. Recognition and evaluation of clinical section headings in clinical documents using token-based formulation with conditional random fields. Biomed Res Int 2015;2015:873012 [FREE Full text] [doi: 10.1155/2015/873012] [Medline: 26380302]
26. Dehkordi MK, Zhou S, Perl Y, Deek FP, Einstein AJ, Elhanan G. Enhancing patient comprehension: an effective sequential prompting approach to simplifying EHRs using LLMs. In: Proceedings of the IEEE International Conference on Bioinformatics and Biomedicine. 2024 Presented at: BIBM 2024; December 3-6, 2024; Lisbon, Portugal. [doi: 10.1109/bibm62325.2024.10822313]
27. Dehkordi MK, Zhou S, Perl Y, Geller J, Einstein AJ, Elhanan G. Using annotation for computerized support for fast skimming of cardiology electronic health record notes. In: Proceedings of the IEEE International Conference on

XSL•FO
RenderX

Bioinformatics and Biomedicine. 2023 Presented at: BIBM 2023; December 5-8, 2023; Istanbul, Turkiye. [doi: 10.1109/bibm58861.2023.10385289]
28. Dehkordi MK, Kollapally NM, Perl Y, Geller J, Deek FP, Liu H, et al. Skimming of electronic health records highlighted by an interface terminology curated with machine learning mining. In: Proceedings of the 17th International Joint Conference on Biomedical Engineering Systems and Technologies. 2024 Presented at: BIOSTEC 2024; February 21-23, 2024; Rome, Italy. [doi: 10.5220/0012391600003657]
29. Mishra R, Bian J, Fiszman M, Weir CR, Jonnalagadda S, Mostafa J, et al. Text summarization in the biomedical domain: a systematic review of recent research. J Biomed Inform 2014 Dec;52:457-467 [FREE Full text] [doi: 10.1016/j.jbi.2014.06.009] [Medline: 25016293]
30. Gholamrezazadeh S, Salehi MA, Gholamzadeh B. A comprehensive survey on text summarization systems. In: Proceedings of the 2nd International Conference on Computer Science and its Applications. 2009 Presented at: CSA 2009; December 10-12, 2009; Jeju, Korea (South). [doi: 10.1109/csa.2009.5404226]
31. Jin H, Zhang Y, Meng D, Wang J, Tan J. A comprehensive survey on process-oriented automatic text summarization with exploration of LLM-based methods. ArXiv. Preprint posted online on March 5, 2024 [FREE Full text]
32. El-Kassas WS, Salama CR, Rafea AA, Mohamed HK. Automatic text summarization: a comprehensive survey. Expert Syst Appl 2021 Mar;165:113679. [doi: 10.1016/j.eswa.2020.113679]
33. Gambhir M, Gupta V. Recent automatic text summarization techniques: a survey. Artif Intell Rev 2016 Mar 29;47(1):1-66. [doi: 10.1007/s10462-016-9475-9]
34. Fattah MA, Ren F. Automatic text summarization. Int J Electr Comput Eng 2008;3:25-28 [FREE Full text]
35. Van Veen D, Van Uden C, Blankemeier L, Delbrouck JB, Aali A, Bluethgen C, et al. Adapted large language models can outperform medical experts in clinical text summarization. Nat Med 2024 Apr 27;30(4):1134-1142. [doi: 10.1038/s41591-024-02855-5] [Medline: 38413730]
36. Dong Q, Li L, Dai D, Zheng C, Ma J, Li R, et al. A survey on in-context learning. ArXiv. Preprint posted online on December 31, 2022 [FREE Full text] [doi: 10.18653/v1/2024.emnlp-main.64]
37. Kanwal N, Rizzo G. Attention-based clinical note summarization. In: Proceedings of the 37th ACM/SIGAPP Symposium on Applied Computing. 2022 Presented at: SAC '22; April 25-29, 2022; Virtual Event. [doi: 10.1145/3477314.3507256]
38. Alsentzer E, Kim A. Extractive summarization of EHR discharge notes. ArXiv. Preprint posted online on October 26, 2018 [FREE Full text]
39. Ma C, Wu Z, Wang J, Xu S, Wei Y, Liu Z, et al. An iterative optimizing framework for radiology report summarization with ChatGPT. IEEE Trans Artif Intell 2024 Aug;5(8):4163-4175. [doi: 10.1109/tai.2024.3364586]
40. Hake J, Crowley M, Coy A, Shanks D, Eoff A, Kirmer-Voss K, et al. Quality, accuracy, and bias in ChatGPT-based summarization of medical abstracts. Ann Fam Med 2024 Mar 25;22(2):113-120 [FREE Full text] [doi: 10.1370/afm.3075] [Medline: 38527823]
41. SNOMED International homepage. SNOMED International. URL: https://www.snomed.org/ [accessed 2025-06-30]
42. Donnelly K. SNOMED-CT: the advanced terminology and coding system for eHealth. Stud Health Technol Inform 2006;121:279-290. [Medline: 17095826]
43. Cimino JJ, Clayton PD, Hripcsak G, Johnson SB. Knowledge-based approaches to the maintenance of a large controlled medical terminology. J Am Med Inform Assoc 1994 Jan 01;1(1):35-50 [FREE Full text] [doi: 10.1136/jamia.1994.95236135] [Medline: 7719786]
44. Cimino JJ. Desiderata for controlled medical vocabularies in the twenty-first century. Methods Inf Med 2018 Feb 15;37(04/05):394-403. [doi: 10.1055/s-0038-1634558]
45. Keloth VK, Zhou S, Lindemann L, Elhanan G, Einstein AJ, Geller J. Mining concepts for a COVID interface terminology for annotation of EHRs. In: Proceedings of the 2020 IEEE International Conference on Big Data. 2020 Presented at: BigData 2020; December 10-13, 2020; Atlanta, GA. [doi: 10.1109/bigdata50022.2020.9377981]
46. Wang J, Shi E, Yu S, Wu Z, Ma C, Dai H, et al. Prompt engineering for healthcare: methodologies and applications. ArXiv. Preprint posted online on April 28, 2023 [FREE Full text]
47. Kollapally NM, Dehkordi MK, Perl Y, Geller J, Deek FP, Liu H, et al. Using clinical entity recognition for curating an interface terminology to aid fast skimming of EHRs. In: Proceedings of the 2024 IEEE International Conference on Bioinformatics and Biomedicine. 2024 Presented at: BIBM 2024; December 03-06, 2024; Lisbon, Portugal. [doi: 10.1109/bibm62325.2024.10822845]
48. Zhou S, Sen P, Liu H, Perl Y, Dehkordi MK. CFC annotator: a cluster-focused combination algorithm for annotating electronic health records by referencing interface terminology. In: Proceedings of the 18th International Joint Conference on Biomedical Engineering Systems and Technologies. 2025 Presented at: BIOSTEC 2025; February 19-21, 2025; Porto, Portugal. [doi: 10.5220/0013244500003911]
49. Samarinas C, Krubner A, Salemi A, Kim Y, Zamani H. Beyond factual accuracy: evaluating coverage of diverse factual information in long-form text generation. ArXiv. Preprint posted online on January 7, 2025 [FREE Full text]
50. Celikyilmaz A, Clark E, Gao J. Evaluation of text generation: a survey. ArXiv. Preprint posted online on June 26, 2020 [FREE Full text]

XSL•FO
RenderX

51. Zhang Y, Merck D, Tsai EB, Manning CD, Langlotz CP. Optimizing the factual correctness of a summary: a study of summarizing radiology reports. ArXiv. Preprint posted online on November 6, 2019 [FREE Full text] [doi: 10.18653/v1/2020.acl-main.458]
52. Upton GJ. Fisher's exact test. J R Stat Soc Ser A Stat Soc 1992;155(3):395-402. [doi: 10.2307/2982890]
53. Easy Fisher Exact Test calculator. Social Science Statistics. URL: https://www.socscistatistics.com/tests/fisher/default2.aspx [accessed 2025-06-30]
54. Cohen J. Statistical power analysis. Curr Dir Psychol Sci 1992 Jun 01;1(3):98-101. [doi: 10.1111/1467-8721.ep10768783]
55. Plackett RL. Karl Pearson and the Chi-Squared Test. Int Stat Rev 1983;51(1):59-72. [doi: 10.2307/1402731]
56. Johnson AE, Pollard TJ, Shen LW, Lehman LH, Feng M, Ghassemi M, et al. MIMIC-III, a freely accessible critical care database. Sci Data 2016 May 24;3(1):160035 [FREE Full text] [doi: 10.1038/sdata.2016.35] [Medline: 27219127]
57. Grady C. Institutional review boards: purpose and challenges. Chest 2015 Nov;148(5):1148-1155 [FREE Full text] [doi: 10.1378/chest.15-0706] [Medline: 26042632]
58. Johnson A, Pollard T, Mark R. MIMIC-III clinical database. PhysioNet. 2016 Sep 4. URL: https://physionet.org/content/mimiciii/1.4/ [accessed 2025-06-30]
59. Moore W, Frye S. Review of HIPAA, part 1: history, protected health information, and privacy and security rules. J Nucl Med Technol 2019 Dec 10;47(4):269-272 [FREE Full text] [doi: 10.2967/jnmt.119.227819] [Medline: 31182664]
60. Weiss BD, Blanchard JS, McGee DL, Hart G, Warren B, Burgoon M, et al. Illiteracy among Medicaid recipients and its relationship to health care costs. J Health Care Poor Underserved 1994;5(2):99-111. [doi: 10.1353/hpu.2010.0272] [Medline: 8043732]
61. Lin CY. ROUGE: a package for automatic evaluation of summaries. In: Proceedings of the Workshop on Text Summarization Branches Out. 2004 Presented at: ACL-04; July 25-26, 2004; Barcelona, Spain.
62. Flesch-Kincaid readability test. Rockstar-English.com. URL: https://rockstar-english.com/lessons/advanced/12-Flesch_Kincaid_Readability_Test.pdf [accessed 2025-06-30]
63. Bernstein JD. Gobbledygook: the proliferation of jargon in English language teaching. TESOL J 2021;12(1):e541. [doi: 10.1002/tesj.541]
64. Rodríguez Timaná LC, Saavedra Lozano DF, Castillo García JF. Software to determine the readability of written documents by implementing a variation of the gunning fog index using the Google linguistic corpus. In: Proceedings of the First International Conference on Applied Technologies. 2019 Presented at: ICAT 2019; December 3-5, 2019; Quito, Ecuador. [doi: 10.1007/978-3-030-42517-3_31]
65. Perković G, Drobnjak A, Botički I. Hallucinations in LLMs: understanding and addressing challenges. In: Proceedings of the 47th MIPRO ICT and Electronics Convention. 2024 Presented at: MIPRO 2024; May 20-24, 2024; Opatija, Croatia. [doi: 10.1109/mipro60963.2024.10569238]
66. Ranjan R, Gupta S, Singh S. A comprehensive survey of bias in LLMs: current landscape and future directions. ArXiv. Preprint posted online on September 24, 2024 [FREE Full text]
67. Liao QV, Vaughan JW. AI transparency in the age of LLMs: a human-centered research roadmap. ArXiv. Preprint posted online on June 2, 2023 [FREE Full text] [doi: 10.1162/99608f92.8036d03b]

Abbreviations

AI: artificial intelligence
ATS: automatic text summarization
CIT: cardiology interface terminology
EHR: electronic health record
H-summary: summary from highlighted notes
HIPAA: Health Insurance Portability and Accountability Act
ICIT: initial version of cardiology interface terminology
LLM: large language model
NIH: National Institutes of Health
SEC: structural elements count
U-summary: summary from unhighlighted notes

XSL•FO
RenderX

Edited by A Benis; submitted 15.09.24; peer-reviewed by D Chrimes, A Chaturvedi; comments to author 29.11.24; revised version received 20.12.24; accepted 16.06.25; published 24.07.25.

Please cite as:
Koohi Habibi Dehkordi M, Perl Y, Deek FP, He Z, Keloth VK, Liu H, Elhanan G, Einstein AJ
Improving Large Language Models' Summarization Accuracy by Adding Highlights to Discharge Notes: Comparative Evaluation
JMIR Med Inform 2025;13:e66476
URL: https://medinform.jmir.org/2025/1/e66476
doi:10.2196/66476
PMID:40705416

©Mahshad Koohi Habibi Dehkordi, Yehoshua Perl, Fadi P Deek, Zhe He, Vipina K Keloth, Hao Liu, Gai Elhanan, Andrew J Einstein. Originally published in JMIR Medical Informatics (https://medinform.jmir.org), 24.07.2025. This is an open-access article distributed under the terms of the Creative Commons Attribution License (https://creativecommons.org/licenses/by/4.0/), which permits unrestricted use, distribution, and reproduction in any medium, provided the original work, first published in JMIR Medical Informatics, is properly cited. The complete bibliographic information, a link to the original publication on https://medinform.jmir.org/, as well as this copyright and license information must be included.

XSL•FO
RenderX

Original Paper

Generative Models and Sentence Transformers for the Recognition and Normalization of Continuous and Discontinuous Phenotype Mentions: Model Development and Evaluation

Areej Alhassan[1,2], MSc; Viktor Schlegel[1,3], PhD; Monira Aloud[2], PhD; Riza Batista-Navarro[1], PhD; Goran Nenadic[1], PhD

[1]Department of Computer Science, School of Engineering, University of Manchester, Manchester, United Kingdom

[2]Department of Management Information Systems, College of Business Administration, King Saud University, Riyadh, Saudi Arabia

[3]Imperial Global Singapore, Imperial College London, Singapore, Singapore

Corresponding Author:
Areej Alhassan, MSc
Department of Computer Science
School of Engineering
University of Manchester
Kilburn Building
Oxford Rd
Manchester, M13 9PL
United Kingdom
Phone: 44 7376452109
Email: areej.alhassan@postgrad.manchester.ac.uk

Abstract

Background: Extracting genetic phenotype mentions from clinical reports and normalizing them to standardized concepts within the human phenotype ontology are essential for consistent interpretation and representation of genetic conditions. This is particularly important in fields such as dysmorphology and plays a key role in advancing personalized health care. However, modern clinical named entity recognition methods face challenges in accurately identifying discontinuous mentions (ie, entity spans that are interrupted by unrelated words), which can be found in these clinical reports.

Objective: This study aims to develop a system that can accurately extract and normalize genetic phenotypes, specifically from physical examination reports related to dysmorphology assessment. These mentions appear in both continuous and discontinuous lexical forms, with a focus on addressing challenging discontinuous entity spans.

Methods: We introduce DiscHPO, a 2-phase pipeline consisting of a sequence-to-sequence named entity recognition model for span extraction, and an entity normalizer that uses a sentence transformer biencoder for candidate generation and a cross-encoder reranker for selecting the best candidate as the normalized concept. This system was tested as part of our participation in Track 3 of the BioCreative VIII shared task.

Results: For overall performance on the test set, the top-performing model for entity normalization achieved an F_1-score of 0.723, while the best span extraction model reached an F_1-score of 0.665. Both scores surpassed those of 2 baseline models using the same dataset, indicating superior efficacy in handling both continuous and discontinuous spans. On the validation set, we were able to demonstrate our system's ability to recognize these mentions, with the model achieving an F_1-score of 0.631 for exact match on discontinuous spans only.

Conclusions: The findings suggest that exact extraction of entity spans may not always be necessary for successful normalization. Partial mention matches can be sufficient as long as they capture the essential concept information, supporting the system's utility in clinical downstream tasks.

(JMIR Med Inform 2025;13:e68558) doi:10.2196/68558

KEYWORDS

named entity recognition; discontinuous NER; human phenotype ontology; named entity normalization; LLM; sentence transformers; clinical information extraction

XSL•FO
RenderX

Introduction

Overview

Information extraction (IE) from unstructured text is a crucial task in natural language processing (NLP) and plays a key role in structuring text efficiently [1,2]. The recent advances in generative large language models (LLMs) have proven highly beneficial across various IE tasks in several domains [3]. Within the health care sector, both researchers and clinicians are actively seeking to extract valuable insights from unstructured clinical documents [4]. Leveraging LLMs for addressing IE tasks in this specific domain promises to expedite and enhance clinical operations, thereby improving clinical decision-making and documentation quality, which results in better patient care [5,6].

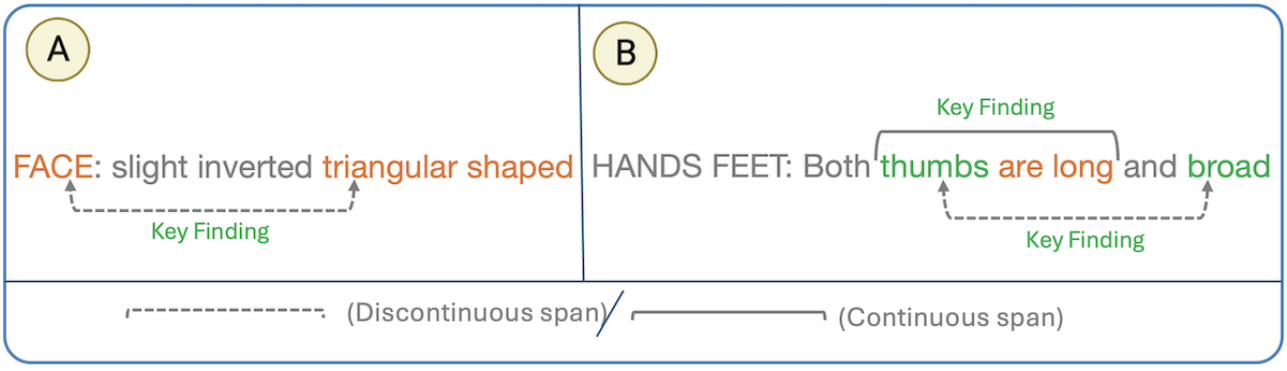
Named entity recognition and named entity normalization (NER and NEN) serve as crucial IE tasks within the medical domain [7]. NER focuses on accurately identifying entities of interest, such as findings, diseases, medications, and procedures. Subsequently, NEN performs the standardization of these entities using referencing standards such as concept ontology or knowledge bases. These tasks play a fundamental role in various health care applications, facilitating interoperability between different medical systems.

State-of-the-art approaches often frame the NER task as a sequence labeling problem, which is well-suited for continuous named entities (NEs). However, NE words may sometimes appear nonconsecutively, forming what is known as Discontinuous Named Entities (DiscNEs) [8]. These entities may also be referred to as "disjoint spans" or "disjoint mentions." Conventional sequence labeling schemes are insufficient to handle DiscNEs, and specialized schemes, although tailored, often lack generalizability [9]. Therefore, this study aims to explore the effectiveness of generative LLM-based models as a unified solution for identifying both continuous and discontinuous NEs within a newly introduced benchmark dataset, as part of the BioCreative VIII shared task [10,11].

Until recently, the ongoing series of BioCreative challenges contributed significantly to advancing the clinical NLP community by providing benchmark datasets to evaluate the effectiveness of IE models. The eighth edition of the BioCreative challenge, organized into 4 tracks, includes our participation in the third track. This track focuses on the extraction and normalization of genetic phenotypes in clinical reports [10]. As part of this track, participants were provided with patient physical examination reports comprising both normal and key findings. Normal findings (NORMFs) typically denote the absence of phenotypic abnormalities in the observation (eg, "intact palate"), while key findings (KEYFs) indicate the presence of phenotypic abnormalities (eg, "high-arched palate"). The tasks involve extracting KEYFs while excluding NORMFs, as they are not represented in the human phenotype ontology (HPO), and then mapping these KEYFs to their corresponding HPO identifiers [12].

A significant challenge revolves around the presence of DiscNEs in the text. Approximately 14% of mentions in the training and validation sets can be considered as discontinuous (465 DiscNEs out of 3247 NEs). We observed 2 forms of DiscNEs in the dataset: either one entity is interrupted by nonentity tokens (nonoverlapping disjoint mentions), or multiple entities share a common head, with one or more entities interrupting the other (overlapping disjoint spans). Figure 1 demonstrates examples of the 2 forms of discontinuity found in the clinical entries, where example (A) presents a nonoverlapping case. The gold standard annotations mark the span "FACE triangular shaped," as a KEYF. As we can see, the nonentity tokens, "slightly inverted," interrupt the original span. This example is considered to be nonoverlapping as none of its tokens are shared with another mention. As for Example B, an instance of overlapping disjoint spans is demonstrated. Here, the token "thumbs" acts as a shared head between the 2 KEYFs, "thumbs are long" and "thumbs are broad." The task organizers encouraged addressing this challenge, urging solutions that go beyond traditional sequence labeling methods, effective only in identifying entity spans with consecutive tokens, and falling short in extracting DiscNEs [10].

Figure 1. Examples of discontinuous named entities: (A) nonoverlapping and (B) overlapping disjoint mentions.



To accomplish this task, we introduce DiscHPO, a 2-component pipeline. The first component involves a sequence-to-sequence approach for detecting continuous and DiscNE spans, while the second component focuses on normalizing the extracted spans to their associated HPO identifiers using the Sentence Transformers framework. The DiscHPO pipeline can enhance downstream tasks such as diagnostic decision support. For instance, integrating our system into electronic health record (EHR) platforms could enable real-time identification of phenotypic patterns relevant to rare diseases, potentially accelerating diagnosis. Furthermore, normalization to standardized vocabularies like HPO facilitates interoperability

XSL•FO
RenderX

and large-scale phenotypic analyses, ultimately supporting more personalized and data-driven health care delivery.

The HPO

The HPO was introduced in 2008 as a comprehensive logical framework intended to describe and analyze phenotypic abnormalities in patients with a particular disease [12]. It offers a standardized representation of phenotype concepts. The use of HPO not only enhances clinical care and education but also serves as a valuable resource for EHR analysis and structuring, facilitating accurate diagnosis of diseases. Thus, the automatic extraction of a thorough and precise set of HPO terms directly from the EHR data is highly desirable to reduce the burden of manual annotation and save time and resources [13].

In this study, we use a version of the HPO dictionary provided by the shared task organizers. This version encompasses around 17,000 terms, which include both the preferred term for the phenotypic abnormality and the corresponding HPO identifier. In addition to this, the organizers provided a supplementary list of 5000 terms that were not observed in the corpus, which has been helpful in refining the original list of terms.

Prior Work

We first explore the existing work in biomedical NER and normalization. Conventionally, NER is followed by an NEN step (2-stage pipeline), where identified mentions are mapped to standardized concepts within controlled vocabularies. For instance, Peng et al [14] introduced a standalone normalizer that receives input mentions from an external NER component. Their method uses an interaction-based synonym marginalization technique that effectively captures the relationships between a given NE and its candidate matches. Similarly, Ji et al [15] proposed a BERT (bidirectional encoder representation from transformers)-based ranking method for biomedical entity normalization, showing the power of contextualized embeddings in disambiguating similar terms.

Beyond these 2-stage methods, several studies have explored joint or end-to-end frameworks that integrate NER and normalization tasks to reduce error propagation and exploit shared contextual representations. Xiong et al [16] proposed a joint model that treats NER as a machine reading comprehension task and NEN as a multilabel sequence tagging problem. Zhao et al [17] further advanced this line of work with a multitask learning framework that jointly models both NER and normalization, incorporating explicit feedback strategies to enhance performance.

We now review studies dedicated to NER and normalization to the HPO. Increasing attention has been given to the automated identification of HPO concepts from clinical narratives. For example, Son et al [18] introduced EHR-Phenolyzer to extract phenotypes from EHR narratives. Their approach involves the use of 2 clinical IE tools, namely MedLEE [19] and MetaMap [20]. They found that both systems performed comparably to expert annotation. Since the earlier approach relies on general NLP tools, a more tailored phenotypes extraction approach, ClinPhen is introduced by Deisseroth et al [21], which uses the natural language toolkit and a hash table for the extraction and normalization. ClinPhen showed superior performance compared with general IE tools: MetaMap and cTAKES [22]. A comparative evaluation study conducted by Liu et al [23] included comparing the following HPO extraction models: MetaMapLite, MedLEE, ClinPhen, cTAKES, as well as 4 ensemble techniques. Their findings show that ensemble methods consistently surpass individual models in recognizing both generic and patient-specific phenotypic concepts.

Other approaches have developed interactive platforms for extracting HPO terms. For instance, Doc2HPO [24] provides a web interface for real-time extraction and normalization of HPO terms. Another platform, Monarch Initiative [25], serves as a comprehensive platform for integrating phenotypes and genotypes data and analytics. However, these dictionary-based approaches (MetaMapLite, cTAKES, ClinPhen, and Doc2HPO) use dictionary matching as their primary method, depending exclusively on exact matches with dictionary terms. This approach proves challenging in capturing semantic and syntactic variations within terms [26].

Alternatively, machine-learning approaches have shown efficacy in understanding textual semantics. For instance, the PhenoTagger system [26] is a hybrid approach merging dictionary-based matching and machine-learning classification to identify HPO concepts. Inspired by PhenoTagger, Feng et al [27] introduced PhenoBERT. While both methods use BERT [28] as their core model, PhenoBERT distinguishes itself by incorporating 2-level hierarchical CNNs. This integration serves to narrow down the BERT search space, which results in a reduction in computational time.

For identifying overlapping mentions, PhenoTagger has incorporated several heuristic rules to handle nested mentions and those sharing common tokens. Additionally, PhenoBERT has introduced a phrase recovery step to handle simple coordination ellipses. However, both models still encounter difficulties in resolving overlapping DiscNEs with gaps longer than one token, as in the example in Figure 1B. Moreover, they struggle to recognize nonoverlapping DiscNEs (Figure 1A).

Goal of This Study

Although sequence labeling and deep learning methods have been widely used to recognize both continuous and discontinuous NEs, our study aims to incorporate a generative model as the NER component within our DiscHPO pipeline. We explore the capabilities of these models in detecting both continuous and discontinuous genetic phenotype mentions in physical examination reports. Our goal is to deliver an integrated solution that recognizes and normalizes these mentions within a consistent framework.

The main contributions of our work are as follows:

1. An investigation into the effectiveness of open-source generative pretrained language models (PLMs) for extracting both continuous and discontinuous spans.
2. The integration of a Sentence-Transformers model with the NER component to effectively normalize the extracted mentions to the HPO.

XSL•FO
RenderX

Methods

Dataset

The BioCreative VIII shared task dataset [11] comprises deidentified reports documenting clinical observations from dysmorphology physical examinations. It consists of 3136 observations, distributed among a training set (1716 observations), a validation set (n=454), and a test set (966 + 2427 decoy observations). Each observation may encompass one or more entity spans categorized as either key or NORMF entities.

Table 1 displays a snippet featuring 2 entries from the provided gold standard annotations. The dataset includes 5 columns: an observation ID assigning a unique identifier to each observation, raw observation text, an HPO column containing an HPO ontology identifier associated with the mention, a Polarity column indicating "X" for NORMFs and "NA" for KEYFs, and a Spans column encompassing the character offsets of the entity mention.

Table 1. Example snippet of the gold standard annotations from the training set.

Observation ID	Text	HPO[a]	Polarity	Spans
F8D319161DE176F2	FACE: No facial abnormalities noted within the limitations of examination.	HP:0000271	X[b]	6-35
DC00B8A9EDA2C78	HANDS FEET: Both thumbs are long and broad	HP:0011304	N/A[c]	17-27 and 37-42
DC00B8A9EDA2C78	HANDS FEET: Both thumbs are long and broad	HP:0032524	N/A	17-32

[a]HPO: human phenotype ontology.

[b]Normal findings

[c]N/A: not applicable.

As shown in Table 1, discontinuous spans are presented with 2 offset ranges separated by a comma. In the case of overlapping spans, each span is represented in a separate row with its assigned HPO identifier, ensuring the preservation of all HPOs associated with the observation. Furthermore, there are 2 levels of segmentation, where disjoint mentions can be divided into 2 or 3 constituent parts. Table 2 provides a numerical analysis of the corpus.

Table 2. Analysis of the BioCreative VIII task 3 corpus, including the training and validation sets.

Analysis	Training set	Validation set
Number sentences, n	1716	454
Number entities, n	2562	685
Number disjoint mentions, n	369	96
Percent of disjoint mentions, %	14.4	14
Disjoint (2-constituent parts), n	358	91
Disjoint (3-constituent parts), n	11	5
Normal findings, n	329	78
Key findings, n	2233	607

During the competition evaluation period, the test set was provided, comprising solely observation IDs and raw text entries. It consists of 966 deidentified observations, along with 2427 decoy observations. However, the gold-standard annotations were not provided to participants to ensure a level playing field.

In addition to this dataset, we aimed to assess the generalizability of our model under different conditions using the GCS+ dataset [29], a widely adopted benchmark that has been used by several models for HPO term extraction and normalization. The dataset contains annotated HPO terms along with their corresponding HPO IDs. Its structure often includes nested named entities, but DiscNEs are not explicitly annotated, despite their presence in the text. We followed the data splits provided by Yang et al [30] and further fine-tuned our DiscHPO checkpoint on the GCS+ dataset.

Data Preprocessing

We approach the NER task by framing it as a sequence-to-sequence NER problem [31]. In this setup, the system takes a sequence of tokens as input and generates a target sequence containing recognized spans categorized as either NORMF, KEYF, or not applicable entities. Unlike sequence labeling, where models assign tags to individual tokens, sequence-to-sequence models learn to produce a new sequence of tokens that transforms the input sequence. To align with this approach, preprocessing of NER system inputs and targets is necessary before model training. Both datasets underwent the same preprocessing steps.

First, we convert the numerical offsets of entity spans into word spans. Each span is then prefixed with its corresponding entity type. Subsequently, all entity spans related to a single

XSL•FO
RenderX

observation are consolidated into one sequence, separated by a semicolon. Both the training and validation sets undergo the same preprocessing steps. An example of a preprocessed target is illustrated in Table 3. By using this scheme, DiscNEs can be represented more effectively since no special labels are used to distinguish the disjoint entities. After preprocessing the BioCreative dataset, we reviewed the dataset and identified minor inconsistencies in the textual spans, primarily caused by inaccurate numerical offsets. We manually corrected these issues and provided the complete list of revised entity spans in Table S1 in Multimedia Appendix 1.

Table 3. Preprocessed named entity recognition inputs.

Input	Target
EYES: Sparse eyebrow hair. Normal lids and lashes.	KEYF[a]: Sparse eyebrow; NORMF[b]: Normal lashes; NORMF: Normal lids
NECK: Excess nuchal skin noted with no webbing, cysts.	KEYF: Excess nuchal skin; NORMF: NECK: no webbing; NORMF: NECK: no cysts

[a]KEYF: key finding.

[b]NORMF: normal finding.

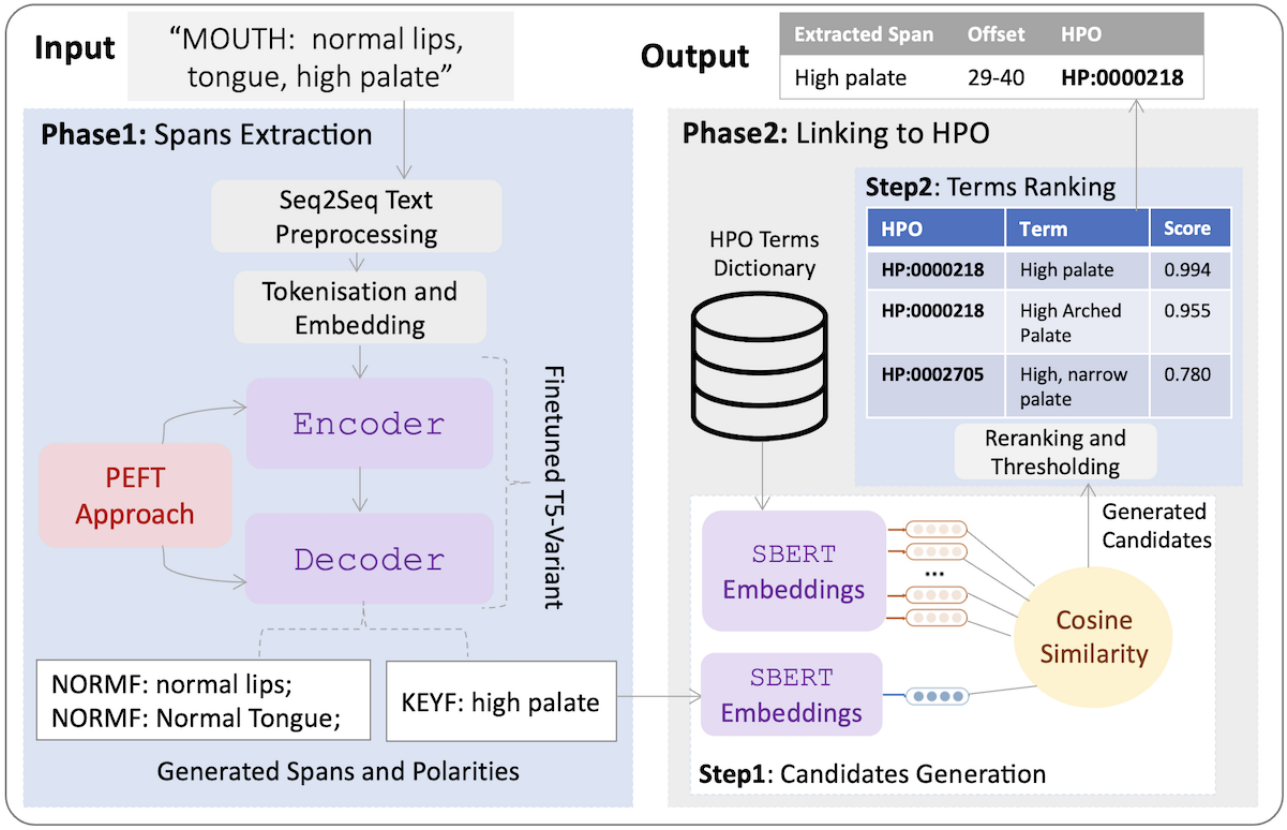
For the training phase, the model input consists of the context, including the input sentence, followed by the corresponding predictions, which include all textual named entities and their types. During inference, the model is given just the sentence and is tasked with generating the NE predictions.

After the model predicts the spans, a postprocessing step is performed to convert the spans back into numerical offsets by locating the offset positions of a given span within the observation text using regular expressions. This step is essential to ensure compatibility with the format specified in the evaluation script provided by the task organizers when calculating the validation set prediction results.

DiscHPO Pipeline

We designed DiscHPO as a pipeline of 2 components: a sequence-to-sequence NER model that can recognize both continuous and discontinuous mentions at the sentence level, and an entity normalizer underpinned by a sentence transformer bidirectional encoder (biencoder) for candidate generation and a cross-encoder reranker. The DiscHPO pipeline is illustrated in Figure 2.

Figure 2. DiscHPO pipeline architecture. HPO: human phenotype ontology.



The NER Model

We implemented a sentence-level NER system by fine-tuning a pretrained sequence-to-sequence encoder-decoder language model based on the transformers architecture [32]. Our approach involved leveraging different versions of the text-to-text transfer transformer (T5) [33]. The T5 model adopts a unified approach to transfer learning, transforming various text processing tasks (eg, question answering, language modeling, or span extraction) into a "text-to-text" problem. The model underwent pretraining

XSL•FO
RenderX

through a consecutive span denoising objective and uses the standard maximum likelihood training method, incorporating teacher forcing. The generative capability of T5 enables seamless fine-tuning for the extraction of the span and prediction of their target class simultaneously. Consequently, the NER component will be capable of distinguishing both types of mentions. (ie, normal and KEYFs).

Each observation and its corresponding spans undergo tokenization using the T5 tokenizer, which is built upon SentencePiece [34]. The tokenizer breaks down the sequences into tokens, translates these tokens into IDs, pads them to achieve the maximum sequence length, and appends the end-of-sequence token (</s>). As we are not engaging in multitask training, there is no need for a task prefix at the beginning of the text (eg, “NER:”).

For the model fine-tuning, we examined the following T5 architectures:

- The original T5 [33], which is based on the transformers’ encoder-decoder architecture and pretrained with the Colossal Clean Crawled Corpus.
- FLAN-T5 [35], or (Fine-tuned LAnguage Net-T5), which is an improved version of T5, instruction-finetuned across a variety of tasks, including NER.

We also considered experimenting with a domain-specific (ie, biomedical) variant of T5, which is the following:

- SciFive [36], which differs by pre-training a T5-architecture model on biomedical articles from the PMC and abstracts from PubMed.

Table S2 in Multimedia Appendix 1 outlines the optimal hyperparameter settings used in all T5 architectures throughout our NER experiments.

To optimize the NER model, a parameter-efficient fine-tuning method such as low-rank adaptation (LoRA) [37] is used, eliminating the hardware costs associated with fine-tuning LLMs by using a small portion of the pretrained parameters (around 1.1%). To do this, LoRA reparametrize (or decomposes) the required weight updates (ΔW) based on the original pretrained weight matrix $W_0 \in \ d \times k$, where d and k are the dimensions of the weight matrix. The low-ranked decomposed matrix is the result of the multiplication of LoRa matrices A and B:

$$\Delta W = BA \quad (1)$$

where $B \in \ d \times r$, $A \in \ r \times k$, and the rank $r \ll \min(d,k)$.

Hence, the sizes of the A and B matrices are adjusted using LoRa rank (r). However, for the initial scaling of the update weights, 2 hyperparameters of LoRa: the rank (r) and a constant alpha (α) are used as in the equation:

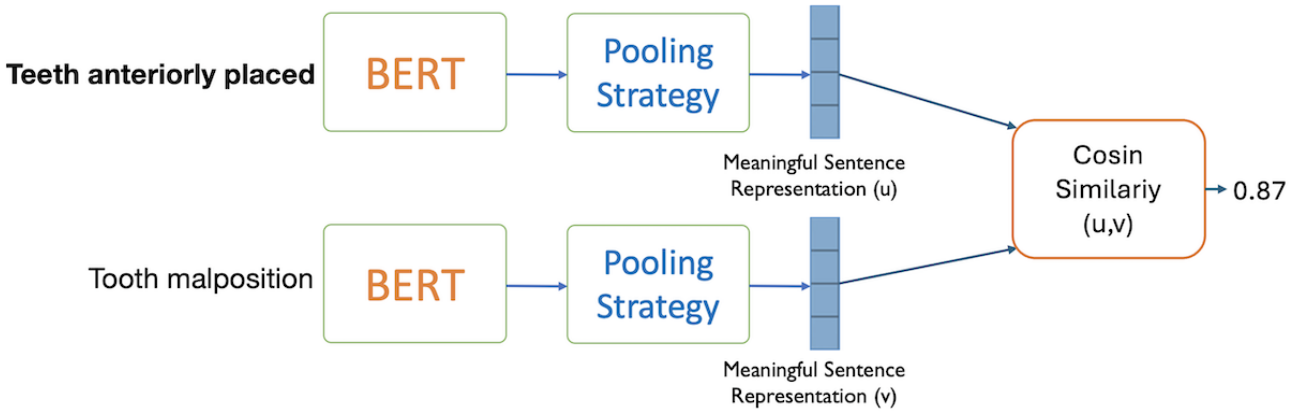
$$\Delta W = \alpha / r \quad (2)$$

We used the Python package loralib, to implement LoRa. Specifically, we chose the extra-large version of Flan-T5 (Flan-T5-XL). After exploring various combinations of r and α values, we achieved optimal results when setting r to 16, and α set to values of both 512 and 1024.

Normalization to HPO

The second task of this challenge involves normalizing the identified KEYFs to their HPO identifiers. We use Sentence-transformers (or SBERT [sentence bidirectional encoder representation from transformers]), a Python framework, that excels in embedding sentences, text, and images, demonstrating state-of-the-art performance in sentence-pair regression tasks [38,39]. Figure 3 illustrates the main design aspects of SBERT. Specifically, it is a modified version of BERT that uses Siamese networks to generate sentence embeddings with semantic similarity. These embeddings can be compared efficiently using cosine similarity, resulting in a significant reduction in computational overhead [40]. A crucial aspect of SBERT’s design involves the pooling operation, used to aggregate the output embeddings of BERT into a fixed-sized sentence embedding. Commonly used pooling strategies include (1) using the (CLS) token embedding of BERT, (2) mean pooling (averaging all token embeddings), and (3) max pooling (taking the maximum value across embeddings). In our experiments, we opted for mean pooling as it offers a favorable balance between computational efficiency and representational effectiveness, being less resource-intensive compared with other aggregation strategies. For a detailed comparative analysis of these pooling methods and their impact on performance, we refer readers to the study by Xing et al [41].

Figure 3. SBERT general Siamese network architecture. SBERT: sentence bidirectional encoder representation from transformers.



In our study, we leverage this framework to conduct a semantic textual similarity task between pairs of extracted mentions and

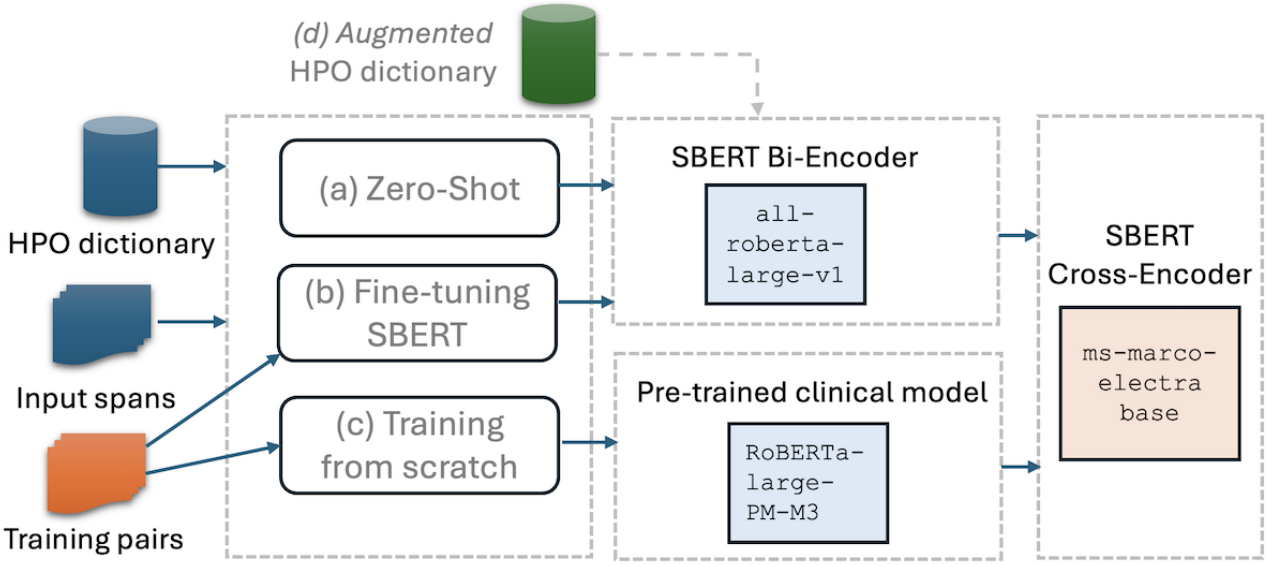
XSL•FO
RenderX

HPO concepts sourced from the provided dictionary. This framework involves two steps: (1) candidate generation and (2) reranking.

The candidate generation step includes identifying candidate terms from the HPO dictionary. In this step, the mention and each candidate HPO term are jointly encoded to compute a semantic similarity score, which reflects how closely related the 2 texts are in meaning. This score typically ranges from 0 to 1, where 1 indicates perfect semantic equivalence and 0 denotes complete dissimilarity. The higher the score, the more semantically aligned the candidate is with the input mention.

Using the 734 gold standard spans from the validation set, we conducted a preliminary investigation using different sentence transformer biencoders and exploring 3 training paradigms within the framework (Figure 4). These paradigms include (1) using an existing sentence transformer biencoder without training (zero-shot setting), (2) continuing training (fine-tuning) the Sentence Transformer biencoder, or (3) training a non-Sentence Transformer PLM from scratch by defining the SBERT individual layers.

Figure 4. Preliminary exploration of different settings for 3 training paradigms of Sentence Transformers. Configurations in (A) and (B) employ an existing SBERT biencoder, whereas (C) involves training a non-SBERT pretrained language model from the clinical domain. In (D), we investigate a setting where an augmented HPO dictionary with synonyms is used for both (A) and (B). HPO: human phenotype ontology; SBERT: sentence bidirectional encoder representation from transformers.



For the latter 2 scenarios, we used pairs of spans from the training set and their corresponding HPO terms to fine-tune SBERT-biencoder and train a clinical PLM from scratch on a semantic similarity objective. We used MegaBatchMarginLoss as the training loss function, which is tailored to our training paradigm involving 2 pairs: an anchor and a positive example demonstrating semantic similarity to the anchor. Moreover, as illustrated in Figure 4D, we sought to enhance the generated candidates' accuracy by using an augmented HPO dictionary with synonymous terms sourced from the training dataset.

Based on the insights gained from this investigation, we select the optimal setting for our DiscHPO normalization component. We found that fine-tuning an existing SBERT biencoder (all-roberta-large-v1) with an augmented HPO dictionary, which incorporated synonyms from the training set, proved to be the most effective approach to create embeddings for both HPO terms and the extracted entity spans.

The reranking step is when the candidate results are reranked using a cross-encoder, which reorders the candidates using their similarity score, ensuring that the most semantically relevant HPO concepts are prioritized at the top of the list. Specifically, the top 30 candidates obtained by semantic matching are then passed on to a sentence transformer cross-encoder model. After experimenting with several cross-encoders, we found that ms-marco-electra-base yielded the highest results. It reranks the generated candidates by calculating the scores for each span-candidate term combination. Its results are sorted to produce the final reordered HPO terms. Among these results, only the top score is considered for submission.

Evaluation Metrics

For evaluation, we adhered to the official evaluation script provided by the task organizers. It incorporates the Precision (P), Recall (R), and F_1-score (F_1) metrics. The equations for these 3 metrics are as follows:

Precision = True Positive / (True Positive + False Positive)

Recall = True Positive / (True Positive+False Negative)

F_1-score = (Precision * Recall) / (Precision + Recall)

There are 2 evaluation scenarios implemented in the provided evaluation script:

- Evaluation of normalization task: which is calculated solely from the normalized output (the HPO term ID) of the extracted span. Here, the span extraction result is not part of the calculation.

XSL•FO
RenderX

- Evaluation of a combined span extraction and normalization: which measures the performance of both steps taken together.

To evaluate the latter, metrics for span extraction were reported based on exact matching (where the character offsets of the KEYF must be identical with the gold standard annotations) and partial matching (which considered an extracted span to be correct if it overlaps with the gold standard span with at least one correct token). In all evaluation experiments, we maintain consistent settings for the normalization component while experimenting with different NER models that are based on T5.

Baselines

To assess the effectiveness of our proposed approach, we benchmark it against 2 baseline models:

- PhenoTagger [26]: A hybrid approach that combines an HPO dictionary with machine learning techniques, leveraging several PLMs such as Bioformer, BioBERT, and PubMedBERT. In our work, we adopt the evaluation by Weissenbacher et al [42] where BioBERT served as the base model.
- PhenoID [42]: This system follows a 2-phase architecture, comprising an extractor and a normalizer. The extractor is a sequence labeling approach that leverages a transformer-based model, specifically the Bio-ClinicalBERT. For normalization, the task is treated as a classification problem by fine-tuning Bio-ClinicalBERT.

For the GCS+ dataset, we benchmarked our model against PhenoTagger and 2 SOTA models:

- PhenoRerank [43]: This model builds on a BlueBERT backbone pretrained on a weakly supervised dataset that includes HPO concepts, synonyms, definitions, and comments from the HPO database. The model is trained using a contrastive loss and reranks its predictions using external HPO extraction tools.
- PhenoGPT [30]: Based on GPT-3 and pretrained on a dataset derived from EHRs, literature, and phenotypic databases. The final PhenoGPT model is further fine-tuned on the GCS+ dataset to optimize its performance.

Ethical Considerations

This study makes use of the BioCreative VIII shared task dataset, which is publicly available. The original shared task paper provides details on the data collection process and sources [11]. As this work does not involve any primary data collection or experimentation with human participants, no ethics approval is required.

Results

We start by presenting our DiscHPO validation results: the extracted findings and their normalized HPO IDs (Table 4).

Table 4. DiscHPO results on the validation set.

Model	Normalization			Exact extraction and normalization			Partial extraction and normalization		
	Precision	Recall	F_1-score	Precision	Recall	F_1-score	Precision	Recall	F_1-score
SciFive-Large	0.722	0.726	0.724	0.695	0.637	0.665	0.719	0.719	0.719
T5-Large	0.725	0.743	0.734	0.696	0.644	0.669	0.724	0.739	0.732
FlanT5-Large	0.708	0.731	0.719	0.678	0.637	0.658	0.708	0.729	0.718
FlanT5-XL LoRa 512	0.735	0.739	0.737	0.710	0.654	0.681[a]	0.734	0.738	0.736
FlanT5-XL LoRa 1024	0.743	0.739	0.742[a]	0.716	0.642	0.677	0.742	0.735	0.738[a]

[a]Best-performing values.

Since FlanT5-XL showed the best performance in the evaluation stage, in the testing phase, we submitted 3 runs based on this model. Same as the evaluation, we applied the same normalization component in all runs while using different NER settings:

- Run1: FlanT5-XL and LoRa, α=1024 trained on the training set only.
- Run2: FlanT5-XL and LoRa, α=1024 trained on both the training and validation sets.
- Run3: FlanT5-XL and LoRa with α=512 trained on the training set only.

As shown in Table 5, the best normalization score of 0.723 F_1-score is achieved by using FlanT5-XL with LoRa α of 512.

XSL•FO
RenderX

Table 5. DiscHPO results on the test set submitted to the competition.

Runs	Normalization			Exact extraction and normalization			Partial extraction and normalization		
	Precision	Recall	F_1-score	Precision	Recall	F_1-score	Precision	Recall	F_1-score
1	0.721	0.723	0.722	0.694	0.638	0.665[a]	0.72	0.721	0.72
2	0.707	0.731	0.719	0.674	0.625	0.648	0.706	0.727	0.716
3	0.718	0.728	0.723[a]	0.69	0.637	0.662	0.717	0.726	0.721[a]

[a]Best-performing values.

The test set results are comparable to the validation set, which indicates that the model's performance is consistent across different sets. Overall, the highest normalization improvement was obtained by using FlanT5-XL with LoRa α=512.

In Table 6, we compare our highest-performing submission with the baselines on the same dataset, demonstrating the superiority of DiscHPO in terms of Recall and F_1-score. We also compare with the best-performing participants in the shared task. PheNormGPT [44] achieves the best performance by leveraging few-shot learning with GPT-4. This model generates 2 outputs for each span: the extracted span from the text and a preferred term generated by GPT-4. While the results are robust, this model has not been validated in a multiclass setting, where only KEYFs were extracted. In addition, although the BioCreative dataset is deidentified, the nonlocal deployment of GPT-4 raises privacy concerns when used with nondeidentified clinical data due to the potential disclosure of protected health information [45]. In contrast, open-source models such as the T5 family offer full local deployment on authorized machines, ensuring better control over data privacy, while also providing a more cost-effective alternative to proprietary models like GPT-4. W2NER+PhenoTagger [46] comes in second place. The model uses the W2NER framework for NER [47], which formulates NER as a grid-tagging problem. It uses a grid structure to capture all word relationships. However, this approach depends on a predefined tagging scheme. In contrast, our model does not rely on custom tagging structures, offering flexibility in handling diverse entity types.

Table 6. Best DiscHPO results on test set, compared against baseline methods [1,5] and the top 2 performing models from the BioCreative VIII Track 3 shared task.

System	Normalization			Partial extraction and normalization		
	Precision	Recall	F_1-score	Precision	Recall	F_1-score
PhenoTagger	0.587	0.687	0.633	0.586	0.685	0.632
PhenoID	0.736	0.699	0.717	0.735	0.696	0.715
W2NER+PhenoTagger	0.831	0.706	0.763	0.830	0.704	0.762
PheNormGPT	0.842	0.799	0.820[a]	0.841	0.794	0.817[a]
DiscHPO (Ours)	0.718	0.728	0.723	0.717	0.726	0.721

[a]Best-performing values.

To assess model performance in differentiating between normal and KEYFs, we calculated class-wise F_1-scores. The model demonstrates a stronger ability to recognize KEYFs (77.2% F_1-score; 471 true positives, 142 false positives, and 135 false negatives) compared with NORMFs (56.4% F_1-score; 44 true positives, 34 false positives, and 34 false negatives), reflecting a recognition bias. This bias is expected and can be attributed to the notable class imbalance in the dataset, where NORMFs constitute only 12% of the total entity spans across the combined training and validation sets (Table 2). Given that the primary goal of the shared task is the detection and normalization of KEYFs, where NORMFs are excluded from the final evaluation, this class imbalance has minimal impact on overall task performance. Consequently, our model was optimized to prioritize KEYFs, as they are the only entities passed to the normalization phase.

To evaluate the models' proficiency in specifically identifying disjoint spans, we computed the NER results for the top 4 DiscHPO models by incorporating only the extracted disjoint mentions from the validation set. We computed both the exact and partial extraction scores for each model. As shown in Table 7, our NER models can identify discontinuous spans. As can be seen, FlanT5-XL with LoRa α 512 is superior in detecting disjoint mentions of findings with an F_1-score of 63.1%. In terms of overlapping extraction, FlanT5-XL with LoRa α=1024 has the best performance when it comes to extracting some of the parts of the disjoint mentions.

XSL•FO
RenderX

Table 7. Results for discontinuous span extraction on the validation set.

Model	Exact extraction			Partial extraction		
	Precision	Recall	F_1-score	Precision	Recall	F_1-score
T5-Large	0.546	0.575	0.57	0.873	0.937	0.904
SciFive-Large	0.6	0.578	0.589	0.911	0.868	0.889
FlanT5 LoRa 512	0.699	0.569	0.631	0.79	0.823	0.806
FlanT5 LoRa 1024	0.658	0.578	0.615	0.927	0.881	0.904

In Table 8, we further analyzed the model's behavior across structural variations in discontinuous entities, including spans without interrupting tokens and those with shared heads (ie, overlapping tokens) with varying head locations and structural complexity. The F_1-score was highest for left-overlapping spans and spans with no overlap. Right and multiple overlaps also showed reasonable performance, with some variation that correlates with the number of instances in each category (eg, 19 and 12 spans respectively, compared with 40 for left overlaps).

Table 8. Model's performance across different discontinuous structures.

DiscNE[a] category	Precision	Recall	F_1-score
No overlap	0.69	0.67	0.68
Left overlap	0.71	0.62	0.67
Right overlap	0.50	0.46	0.48
Multiple overlaps	0.83	0.45	0.59

[a]DiscNE: discontinuous named entity.

To assess the generalizability of the model, we show the performance results of DiscHPO on the GCS+ dataset in Table S3 in Multimedia Appendix 1. We have also included a discussion of these results in comparison with the baseline models.

Discussion

Principal Findings

It is noteworthy that, in both our system and the compared ones, the scores for partial extraction and normalization are very close to those of normalization, which suggests that normalization performance is not substantially degraded by partially extracted spans. This implies that exact span extraction is not always a condition for accurate normalization. This can be observed in cases where partially extracted spans did not negatively affect the normalization outcome.

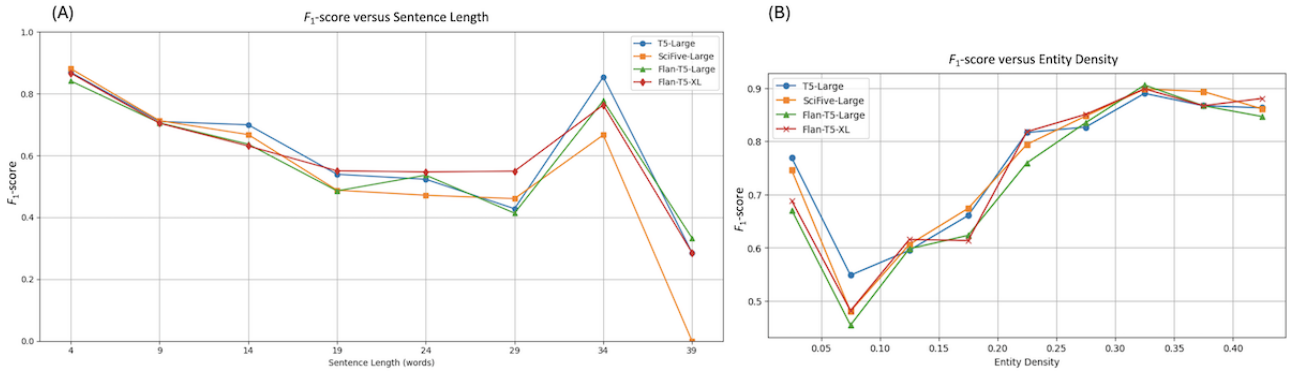
In around 15 normalization output examples from the validation set, we found that partial extraction of continuous and discontinuous NEs can be sufficient for normalization. This is especially true when a disjoint span is interrupted by nonentity tokens and does not share a head. If we consider the following example: "EYES: normal brows, mild hooding." While all our models accurately extracted the exact disjoint span "EYES: hooding," we further examined this by inputting the normalizer with the partial span "hooding." This also resulted in correct normalization, as the term "hooding" is commonly associated with an eye condition.

Quantitative Error Analysis

Figure 5 presents a comparative analysis of the F_1-scores achieved by T5-Large, SciFive-Large, Flan-T5-Large, and Flan-T5-XL-LoRa1024, which we used as a backbone PLMs for DiscHPO, across different sentence lengths (Figure 5A) and varying levels of entity density (Figure 5B).

XSL•FO
RenderX

Figure 5. Quantitative error analysis of DiscHPO. It compares the F1-score performance of 4 backbone pretrained language models (T5-Large, SciFive-Large, Flan-T5-Large, and Flan-T5-XL) under two factors: (A) the impact of sentence length and (B) the impact of entity density. HPO: human phenotype ontology.



We first examine the impact of sentence length on F_1-score. In Figure 5A, we observe a general decline in F_1-score as sentence length increases across all 4 models. This trend is expected, as longer sentences contain more complex syntactic structures. However, T5-Large shows increased performance, particularly in longer sentence ranges, suggesting robustness to increased sequence complexity. SciFive-Large and Flan-T5-Large show relatively parallel performance, though SciFive-Large shows a sharper drop at the longest sentence bin. Flan-T5-XL demonstrates a stable performance across medium-length sentences. We can observe a spike in performance in the 34-word bin for all models, suggesting a concentration of entity-rich sentences in that length category.

Next, we explore the impact of entity density, defined as the percentage of annotated NEs within a sentence. Figure 5B shows that model performance improves with increasing NE density, peaking around the 0.3-0.35 density range. This trend indicates that models benefit from contexts rich in NEs, which may provide clearer clues for learning entity boundaries and relationships. Flan-T5-XL achieves the highest performance at higher density levels, suggesting strong capabilities in recognizing entities in dense annotations, due to its larger parameter capacity and better instruction tuning. Other models perform comparably with each other, but Flan-T5-Large performs slightly lower, suggesting potential limitations in handling low-entity sentences.

Qualitative Error Analysis

From our analysis of the gold DiscNEs, we found that certain tokens are deemed nonessential for normalization. For example, in the instance “EYES: Mild epicanthus, mild up-slant,” the gold standard span “EYES - mild up-slant” is disjoint. However, none of our models incorporated the severity level “mild” into the extracted span; this omission did not adversely impact the normalization outcome.

On the other hand, in certain examples, specific tokens in disjoint mentions are crucial for achieving exact normalization. For example, in the case of “HANDS FEET: L clinodactyly,” the gold annotation is the disjoint span “hand L clinodactyly,” whereas all our models extracted only “clinodactyly.” This led to normalization as “clinodactyly” encompassing both fingers and toes, instead of the more specific concept “Finger clinodactyly.”

The case is different when disjoint spans share a common head, in which each span must be resolved to its own head and its constituent tokens to avoid missing normalizations. We also observed that the models easily identified simple coordinated ellipses, such as “NOSE: broad nasal bridge and tip.” However, challenges arise in scenarios where 2 spans share 2 heads, as in the example “Deep palmar and plantar creases,” where the tokens “deep” and “creases” are common to both “palmar” and “plantar.” Scifive struggled with this complexity, failing to accurately resolve the second span and consequently missing its normalization. In contrast, the other 3 models effectively handled this complexity and successfully addressed the shared elements.

Shifting to normalization errors, some can be attributed to the lack of descriptions or synonyms for the HPO concepts. These additional details provide the normalizer with additional information for accurate concept identification. For instance, in the first example from Table 9, the extracted span “white plaque under the tongue” led the normalizer to mistakenly assign the concept “Erythematous plaque” instead of “Oral leukoplakia” due to lexical similarity. This type of error occurred 28 times out of 155 total normalization errors in the validation set. While we have already enhanced the normalizer’s training data with synonyms from the original training set, they might be inadequate for unseen examples in the validation set. Therefore, we assume that adding more HPO synonyms or descriptions may have the potential to improve the normalization process.

XSL•FO
RenderX

Table 9. Examples of human phenotype ontology (HPO) terms incorrectly predicted by the normalizer on the validation set.

Gold and predicted span	Gold Standard HPO		Predicted HPO	
	Concept	HPO ID	Concept	HPO ID
White plaque under the tongue	Oral leukoplakia	HP:0002745	Erythematous plaque	HP:0025474
Hypotonia	Hypotonia	HP:0001252	Generalized hypotonia	HP:0001290
Abdominal wall hernia	Hernia	HP:0100790	Hernia of the abdominal wall	HP:0004299
Flat-nasal bridge	Depressed nasal ridge	HP:0000457	Depressed nasal bridge	HP:0005280

Another example of error arises when our model selects the term “Generalized hypotonia,” instead of the more specific term “Hypotonia” as provided by the gold standard. Conversely, another error arises when our model selects the highly precise concept “Hernia of the abdominal wall,” while the gold standard prefers the broader term “Hernia.” This type of error was observed in 5 instances among all normalization errors. In addition, we observed only 8 inconsistencies among the gold standard annotations, as illustrated in the final example of Table 9. In this case, the term “Depressed nasal bridge” was mistakenly recorded as “Depressed nasal ridge,” and has been assigned the wrong HPO ID.

More complex coordinations expectedly posed challenges to all evaluated NER models. For example, in the sentence “Contractures of 3rd and 4th digits,” the expected resolution is the doubly-disconnected named entities “Contractures of 3rd digit” and “Contractures of 4th digit.” The models encountered difficulty, likely due to the presence of the word “digit” in its plural form, which caused confusion in determining whether to resolve it as 2 separate entities or not. To provide a clearer overview of the types of normalization errors, we summarized their distribution in Table S4 in Multimedia Appendix 1. This table presents the proportion of each error category observed in the validation set, offering insights that may support future improvements in sentence-transformer–based normalizers.

Limitations

Although the dataset used in this study was granted a waiver of HIPAA authorization for access to identifiable medical record information [42], our approach prioritizes privacy by enabling local deployment of open-source PLMs to ensure sensitive data remains secure. Unlike systems that rely on closed-source models such as GPT-4, our method leverages the open-source T5 family of PLMs. This makes the approach well-suited for use with confidential clinical datasets that are only accessible under restricted licenses. Additionally, it offers a cost-effective alternative to proprietary models.

Despite its reasonable performance, the model shows a tendency to favor the recognition of KEYFs, which were the primary focus of the shared task. This bias is likely caused by the class imbalance in the dataset and has not yet been explicitly addressed. Future work could explore strategies such as data augmentation or balanced sampling to mitigate this bias.

Although DiscHPO is specifically fine-tuned and evaluated on genetic phenotype findings, we hypothesize that the underlying generative and transformer-based framework is well-suited for clinical findings in other medical domains. The model architecture can be adapted to recognize NEs in diverse specialties like oncology, cardiology, or general medical NER. However, this study does not evaluate the system’s generalizability beyond datasets related to HPO, which remains a direction for future work. Furthermore, although the official competition evaluation was conducted using a gold-standard annotated corpus, evaluating the full system under more challenging conditions -such as noisy or unlabeled input- remains an important avenue for future work and would provide an indication of real-world applicability.

Conclusions

This paper presents an overview of our DiscHPO, which is an NER and NEN pipeline capable of processing both continuous and discontinuous spans. We evaluated our model within the context of the BioCreative VIII - Track 3 challenge, focusing on extracting KEYF mentions of genetic phenotypes and normalizing them to the HPO. In the NER component, various T5 model variants were explored for KEYF extraction, and an additional experiment incorporated LoRA with extra-large models. From the extraction results, we found that optimizing Flan-T5-XL’s parameters using LoRA resulted in improved extraction outcomes for both continuous and discontinuous findings, leading to enhanced normalization performance.

Furthermore, improving normalization results can be achieved by resolving all disjoint mentions that share a common head, thereby avoiding the omission of relevant mentions. On the other hand, there may be cases in which extracting the exact mention, continuous or discontinuous, is not crucial for successful normalization. This is apparent in our observations of the normalization results, where several examples with partially extracted mentions still led to accurate normalization.

In future research, and inspired by Peng et al [14], there is a potential to enhance the accuracy of the NEN task by incorporating auxiliary components alongside the SBERT framework. For instance, combining semantic or lexical similarity measures (eg, TF-IDF or Cosine Similarity) with SBERT. Specifically, candidate generation could be performed in parallel using both SBERT and the similarity measure, with the aggregated set of candidates subsequently passed through a cross-encoder for final ranking. Moreover, we intend to conduct a comparative analysis between our DiscHPO model and an end-to-end NER and normalization model that shares contextualized embeddings for both tasks. This joint approach may improve performance by reducing error propagation across pipeline stages and enabling end-to-end optimization. Additionally, we aim to investigate the efficacy of autoregressive

XSL•FO
RenderX

entity normalizers, as suggested in the work of De Cao et al [48].

Acknowledgments

The corresponding author is supported by a PhD scholarship from King Saud University. We would like to sincerely thank the task organizers for their great efforts in managing this task. This work has been partially supported by the project “Integrating hospital outpatient letters into the health care data space” (grant EP/V047949/1; funder: UKRI/EPSRC).

Data Availability

The datasets evaluated during this study are publicly available in the GitHub repository [49]. The source code for this study is available in a the GitHub repository [50].

Conflicts of Interest

None declared.

Multimedia Appendix 1
Additional tables and figures.
[DOCX File , 22 KB - medinform_v13i1e68558_app1.docx]

References

1. Rodrigues M, Teixeira A. Advanced Applications of Natural Language Processing for Performing Information Extraction. Cham: Springer; 2015.
2. Small SG, Medsker L. Review of information extraction technologies and applications. Neural Comput Appl 2013;25(3-4):533-548. [doi: 10.1007/s00521-013-1516-6]
3. Dagdelen J, Dunn A, Lee S, Walker N, Rosen AS, Ceder G, et al. Structured information extraction from scientific text with large language models. Nat Commun 2024;15(1):1418 [FREE Full text] [doi: 10.1038/s41467-024-45563-x] [Medline: 38360817]
4. Spasic I, Nenadic G. Clinical text data in machine learning: systematic review. JMIR Med Inform 2020;8(3):e17984 [FREE Full text] [doi: 10.2196/17984] [Medline: 32229465]
5. Rajpurkar P, Chen E, Banerjee O, Topol EJ. AI in health and medicine. Nat Med 2022;28(1):31-38. [doi: 10.1038/s41591-021-01614-0] [Medline: 35058619]
6. Schlegel V, Li H, Wu Y, Subramanian A, Nguyen T, Kashyap A. PULSAR at MEDIQA-Sum 2023: large language models augmented by synthetic dialogue convert patient dialogues to medical records. : CEUR Workshop Proceedings; 2023 Presented at: CLEF 2023: Conference and Labs of the Evaluation Forum; 2023 September 18-21; Thessaloniki, Greece p. 1668-1679.
7. Song B, Li F, Liu Y, Zeng X. Deep learning methods for biomedical named entity recognition: a survey and qualitative comparison. Brief Bioinform 2021;22(6):bbab282. [doi: 10.1093/bib/bbab282] [Medline: 34308472]
8. Dai X, Karimi S, Hachey B, Paris C. An effective transition-based model for discontinuous NER. : Association for Computational Linguistics; 2020 Presented at: Proceedings of the 58th Annual Meeting of the Association for Computational Linguistics; 2025 September 15; Online p. 5860-5870. [doi: 10.18653/v1/2020.acl-main.520]
9. Yan H, Gui T, Dai J, Guo Q, Zhang Z, Qiu X. A unified generative framework for various NER subtasks. : Association for Computational Linguistics; 2021 Presented at: Proceedings of the 59th Annual Meeting of the Association for Computational Linguistics and the 11th International Joint Conference on Natural Language Processing (Volume 1: Long Papers); 2025 September 15; Online p. 5808-5822. [doi: 10.18653/v1/2021.acl-long.451]
10. Islamaj R, Arighi C, Campbell I, Gonzalez-Hernandez G, Hirschman L, Krallinger M. AMIA 2023 annual symposium. 2023 Presented at: Proceedings of the BioCreative VIII Challenge and Workshop: Curation and Evaluation in the era of Generative Models; 2023 November 12; New Orleans, USA.
11. Weissenbacher D, Zhao X, Priestley JRC, Szigety KM, Schmidt SF, O'Connor K, et al. Automatic genetic phenotype normalization from dysmorphology physical examinations: an overview of the BioCreative VIII-Task 3 competition. Database (Oxford) 2025 Jan 18;2025:baaf051 [FREE Full text] [doi: 10.1093/database/baaf051] [Medline: 40996704]
12. Robinson PN, Mundlos S. The human phenotype ontology. Clin Genet 2010;77(6):525-534. [doi: 10.1111/j.1399-0004.2010.01436.x] [Medline: 20412080]
13. Robinson PN, Haendel MA. Ontologies, knowledge representation, and machine learning for translational research: recent contributions. Yearb Med Inform 2020;29(1):159-162 [FREE Full text] [doi: 10.1055/s-0040-1701991] [Medline: 32823310]
14. Peng H, Xiong Y, Xiang Y, Wang H, Xu H, Tang B. Biomedical named entity normalization via interaction-based synonym marginalization. J Biomed Inform 2022;136:104238. [doi: 10.1016/j.jbi.2022.104238] [Medline: 36400329]

XSL•FO
RenderX

15. Ji Z, Wei Q, Xu H. BERT-based ranking for biomedical entity normalization. AMIA Jt Summits Transl Sci Proc 2020;2020:269-277 [FREE Full text] [Medline: 32477646]
16. Xiong Y, Huang Y, Chen Q, Wang X, Nic Y, Tang B. A joint model for medical named entity recognition and normalization. 2020 Presented at: Proceedings of the Iberian Languages Evaluation Forum (IberLEF 2020); 2020 September 23; Málaga, Spain p. 17.
17. Zhao S, Liu T, Zhao S, Wang F. A neural multi-task learning framework to jointly model medical named entity recognition and normalization. In: AAAI. 2019 Presented at: Proceedings of the AAAI Conference on Artificial Intelligence; 2019 January 27; Honolulu Hawaii USA p. 817-824. [doi: 10.1609/aaai.v33i01.3301817]
18. Son JH, Xie G, Yuan C, Ena L, Li Z, Goldstein A, et al. Deep phenotyping on electronic health records facilitates genetic diagnosis by clinical exomes. Am J Hum Genet 2018;103(1):58-73 [FREE Full text] [doi: 10.1016/j.ajhg.2018.05.010] [Medline: 29961570]
19. Friedman C, Alderson PO, Austin JH, Cimino JJ, Johnson SB. A general natural-language text processor for clinical radiology. J Am Med Inform Assoc 1994;1(2):161-174 [FREE Full text] [doi: 10.1136/jamia.1994.95236146] [Medline: 7719797]
20. Aronson AR, Lang F. An overview of metaMap: historical perspective and recent advances. J Am Med Inform Assoc 2010;17(3):229-236 [FREE Full text] [doi: 10.1136/jamia.2009.002733] [Medline: 20442139]
21. Deisseroth CA, Birgmeier J, Bodle EE, Kohler JN, Matalon DR, Nazarenko Y, Undiagnosed Diseases Network, et al. ClinPhen extracts and prioritizes patient phenotypes directly from medical records to expedite genetic disease diagnosis. Genet Med 2019;21(7):1585-1593 [FREE Full text] [doi: 10.1038/s41436-018-0381-1] [Medline: 30514889]
22. Savova GK, Masanz JJ, Ogren PV, Zheng J, Sohn S, Kipper-Schuler KC, et al. Mayo clinical text analysis and knowledge extraction system (cTAKES): architecture, component evaluation and applications. J Am Med Inform Assoc 2010;17(5):507-513 [FREE Full text] [doi: 10.1136/jamia.2009.001560] [Medline: 20819853]
23. Liu C, Ta CN, Rogers JR, Li Z, Lee J, Butler AM, et al. Ensembles of natural language processing systems for portable phenotyping solutions. J Biomed Inform 2019;100:103318 [FREE Full text] [doi: 10.1016/j.jbi.2019.103318] [Medline: 31655273]
24. Liu C, Peres Kury FS, Li Z, Ta C, Wang K, Weng C. Doc2Hpo: a web application for efficient and accurate HPO concept curation. Nucleic Acids Res 2019;47(W1):W566-W570. [doi: 10.1093/nar/gkz386] [Medline: 31106327]
25. Monarch Initiative. 2024. URL: https://monarchinitiative.org/ [accessed 2024-11-01]
26. Luo L, Yan S, Lai P, Veltri D, Oler A, Xirasagar S, et al. PhenoTagger: a hybrid method for phenotype concept recognition using human phenotype ontology. Bioinformatics 2021;37(13):1884-1890 [FREE Full text] [doi: 10.1093/bioinformatics/btab019] [Medline: 33471061]
27. Feng Y, Qi L, Tian W. PhenoBERT: A combined deep learning method for automated recognition of human phenotype ontology. IEEE/ACM Trans Comput Biol Bioinform 2023;20(2):1269-1277. [doi: 10.1109/TCBB.2022.3170301] [Medline: 35471885]
28. Devlin J, Chang M, Lee K, Toutanova K. Bert: pre-training of deep bidirectional transformers for language understanding. : Association for Computational Linguistics; 2018 Presented at: Proceedings of the 2019 Conference of the North American Chapter of the Association for Computational Linguistics: Human Language Technologies; 2025 September 1; Minneapolis, Minnesota p. 4171-4186. [doi: 10.18653/v1/2021.naacl-main.211]
29. Lobo M, Lamurias A, Couto FM. Identifying human phenotype terms by combining machine learning and validation rules. Biomed Res Int 2017;2017:8565739 [FREE Full text] [doi: 10.1155/2017/8565739] [Medline: 29250549]
30. Yang J, Liu C, Deng W, Wu D, Weng C, Zhou Y, et al. Enhancing phenotype recognition in clinical notes using large language models: PhenoBCBERT and PhenoGPT. Patterns (N Y) 2024;5(1):100887 [FREE Full text] [doi: 10.1016/j.patter.2023.100887] [Medline: 38264716]
31. Sutskever I, Vinyals O, Le QV. Sequence to sequence learning with neural networks. : Curran Associates, Inc; 2014 Presented at: NIPS'14: Neural Information Processing Systems; 2014 December 8-13; Montreal Canada.
32. Vaswani A, Shazeer N, Parmar N, Uszkoreit J, Jones L, Gomez A. Attention is all you need. : Curran Associates, Inc; 2017 Presented at: 31st Conference on Neural Information Processing Systems (NIPS 2017; 2017 December 4-9; Long Beach, CA, USA.
33. Raffel C, Shazeer N, Roberts A, Lee K, Narang S, Matena M. Exploring the limits of transfer learning with a unified text-to-text transformer. J Mach Learn Res 2020;21(1):5485-5551 [FREE Full text]
34. Kudo T, Richardson J. Sentencepiece: a simple and language independent subword tokenizer and detokenizer for neural text processing. : Association for Computational Linguistics; 2018 Presented at: Proceedings of the 2018 Conference on Empirical Methods in Natural Language Processing: System Demonstrations; 2025 September 15; Brussels, Belgium p. 66-71. [doi: 10.18653/v1/d18-2012]
35. Chung HW, Hou L, Longpre S, Zoph B, Tay Y, Fedus W. Scaling instruction-finetuned language models. J Mach Learn Res 2024;25:1-53 [FREE Full text]
36. Phan L, Anibal J, Tran H, Chanana S, Bahadroglu E, Peltekian A. Scifive: a text-to-text transformer model for biomedical literature. arXiv:2106.03598 2021. [doi: 10.48550/arXiv.2106.03598]

XSL•FO
RenderX

37. Hu EJ, Shen Y, Wallis P, Allen-Zhu Z, Li Y, Wang S. Lora: Low-rank adaptation of large language models. 2022 Presented at: TThe International Conference on Learning Representations (ICLR); 2022 April 25; virtual conference.
38. Feher D, Ibrahim F, Cheng Z, Schlegel V, Maidment T, Bagshaw J, et al. Few-shot entity linking of food names. Inf Process Manag 2023;60(5):103463. [doi: 10.1016/j.ipm.2023.103463]
39. Ha T, Nguyen V, Nguyen K, Nguyen K, Than Q, editors. Utilizing Sbert for finding similar questions in community question answering. : IEEE; 2021 Presented at: 13th International Conference on Knowledge and Systems Engineering (KSE); 2021 November 10-12; Bangkok, Thailand. [doi: 10.1109/kse53942.2021.9648830]
40. Reimers N, Gurevych I. Sentence-BERT: sentence embeddings using siamese BERT-networks. : Association for Computational Linguistics; 2019 Presented at: Proceedings of the 2019 Conference on Empirical Methods in Natural Language Processing and the 9th International Joint Conference on Natural Language Processing (EMNLP-IJCNLP); 2025 September 15; Hong Kong, China p. 3982-3992. [doi: 10.18653/v1/d19-1410]
41. Xing J, Luo D, Xue C, Xing R. Comparative analysis of pooling mechanisms in LLMs: a sentiment analysis perspective. arXiv:2411.14654 2024. [doi: 10.48550/arXiv.2411.14654]
42. Weissenbacher D, Rawal S, Zhao X, Priestley JRC, Szigety KM, Schmidt SF, et al. PhenoID, a language model normalizer of physical examinations from genetics clinical notes. medRxiv 2024 [FREE Full text] [doi: 10.1101/2023.10.16.23296894] [Medline: 37904943]
43. Yan S, Luo L, Lai P, Veltri D, Oler AJ, Xirasagar S, et al. PhenoRerank: a re-ranking model for phenotypic concept recognition pre-trained on human phenotype ontology. J Biomed Inform 2022;129:104059 [FREE Full text] [doi: 10.1016/j.jbi.2022.104059] [Medline: 35351638]
44. Soysal E, Roberts K. UTH-Olympia@BC8 Track 3: adapting GPT-4 for entity extraction and normalizing responses to detect key findings in dysmorphology physical examination observations. 2023 Presented at: Proceedings of the BioCreative VIII Challenge Evaluation Workshop; 2023 November 12; New Orleans, USA.
45. Rezaeikhonakdar D. AI chatbots and challenges of HIPAA compliance for AI developers and vendors. J Law Med Ethics 2023;51(4):988-995 [FREE Full text] [doi: 10.1017/jme.2024.15] [Medline: 38477276]
46. Qi J, Luo L, Yang Z, Lin H. DUTIR-BioNLP@BC8 Track 3: genetic phenotype extraction and normalization with biomedical pre-trained language models. 2023 Presented at: Proceedings of the BioCreative VIII Challenge and Workshop: Curation and Evaluation in the era of Generative Models, AMIA 2023 Annual Symposium; 2023 November 12; New Orleans, USA.
47. Li J, Fei H, Liu J, Wu S, Zhang M, Teng C, et al. Unified named entity recognition as word-word relation classification. AAAI 2022;36(10):10965-10973. [doi: 10.1609/aaai.v36i10.21344]
48. De CN, Aziz W, Titov I. Highly parallel autoregressive entity linking with discriminative correction. : Association for Computational Linguistics; 2021 Presented at: Proceedings of the 2021 Conference on Empirical Methods in Natural Language Processing; 2025 September 15; Online and Punta Cana, Dominican Republic p. 7662-7669. [doi: 10.18653/v1/2021.emnlp-main.604]
49. Weissenbacher D, Rawal S, Zhao X, Priestley J, Szigety K, Schmidt S. Clinical genetics training data. GitHub. 2024. URL: https://github.com/Ian-Campbell-Lab/Clinical-Genetics-Training-Data/ [accessed 2024-02-11]
50. Alhassan A, Schlegel V, Aloud M, Batista-Navarro R, Nenadic G. DiscHPO. Github. 2024. URL: https://github.com/areej9/DiscHPO [accessed 2024-02-11]

Abbreviations

BERT: bidirectional encoder representation from transformers
DiscNE: discontinuous named entity
EHR: electronic health record
HPO: human phenotype ontology
IE: information extraction
KEYF: key finding
LLM: large language model
LoRA: low-rank adaptation
NE: named entity
NEN: named entity normalization
NER: named entity recognition
NLP: natural language processing
NORMF: normal finding
PLM: pretrained language model
T5: text-to-text transfer transformer

XSL•FO
RenderX

Edited by A Benis; submitted 10.11.24; peer-reviewed by GK Gupta, Y Xiong, L Luo; comments to author 20.03.25; revised version received 29.04.25; accepted 15.08.25; published 05.11.25.

Please cite as:
Alhassan A, Schlegel V, Aloud M, Batista-Navarro R, Nenadic G
Generative Models and Sentence Transformers for the Recognition and Normalization of Continuous and Discontinuous Phenotype Mentions: Model Development and Evaluation
JMIR Med Inform 2025;13:e68558
URL: https://medinform.jmir.org/2025/1/e68558
doi:10.2196/68558
PMID:

©Areej Alhassan, Viktor Schlegel, Monira Aloud, Riza Batista-Navarro, Goran Nenadic. Originally published in JMIR Medical Informatics (https://medinform.jmir.org), 05.11.2025. This is an open-access article distributed under the terms of the Creative Commons Attribution License (https://creativecommons.org/licenses/by/4.0/), which permits unrestricted use, distribution, and reproduction in any medium, provided the original work, first published in JMIR Medical Informatics, is properly cited. The complete bibliographic information, a link to the original publication on https://medinform.jmir.org/, as well as this copyright and license information must be included.

XSL•FO
RenderX

Original Paper

Model for Predicting Serious Hematological Adverse Events in Individuals With Ovarian Cancer Receiving Poly (Adenosine Diphosphate Ribose) Polymerase Inhibitor Treatment: Prospective Cohort Study

Xiaotong Lian[1], BPharm; Yu Lei[2], PhD

[1]Guangxi Medical University, Nanning, China

[2]Guangxi Medical University Affiliated Tumor Hospital, Nanning, China

Corresponding Author:
Yu Lei, PhD
Guangxi Medical University Affiliated Tumor Hospital
71 Hedi Road, Qingxiu District, Guangxi
Nanning, 530021
China
Phone: 86 (0771)5778582
Email: 1147112852@qq.com

Abstract

Background: Predicting serious hematological adverse events (SHAEs) from poly (adenosine diphosphate ribose) polymerase inhibitors (PARPis) would allow us to prioritize patients with ovarian cancer at higher risk for more intensive care, ultimately lowering morbidity and preventing them from premature termination of medication.

Objective: This study aimed to explore the risk factors for SHAEs in patients with ovarian cancer receiving PARPi treatment and develop a risk prediction model for such events.

Methods: Prospective clinical data were collected on patients with ovarian cancer who received PARPi treatment at the Guangxi Medical University Affiliated Tumor Hospital from December 2018 to August 2024. They were divided into a SHAE group and a no-SHAE group based on the occurrence of SHAEs. Variable differences were screened using the chi-square test or Fisher exact test. Multivariate logistic regression was used to determine independent factors influencing SHAEs in patients with ovarian cancer. A predictive model for serious blood-related complications in ovarian cancer treatment was developed from identified independent risk factors using the R software. The model's clinical utility was assessed through decision curve analysis (net benefit), calibration (calibration curve), and discrimination (receiver operating characteristic curve).

Results: A total of 70 patients with ovarian cancer receiving PARPi treatment were included in this study. Of these 70 patients, 16 (23%) experienced SHAEs, with decreases in red blood cell (RBC) count and hemoglobin levels being the most common. Multiple logistic regression analysis identified 4 independent predictors of PARPi-associated SHAEs in patients with ovarian cancer: lymph node metastasis (odds ratio [OR] 6.733, 95% CI 1.197-37.873; *P*=.03), creatinine clearance rate of ≤60 mL per minute (OR 23.722, 95% CI 3.121-180.303; *P*=.002), RBC count of $\leq 3.3\times10^{12}$ per liter (OR 4.847, 95% CI 1.020-23.041; *P*=.047), and combination therapy with vascular endothelial growth factor inhibitors (OR 6.749, 95% CI 1.313-34.689; *P*=.02). The internal validation yielded an area under the curve of 0.874 (95% CI 0.793-0.955), indicating moderate clinical utility and accuracy for the risk prediction model incorporating these predictors.

Conclusions: Lymph node metastasis, creatinine clearance rate of ≤60 mL per minute, RBC count of $\leq 3.3\times10^{12}$ per liter, and combination therapy with vascular endothelial growth factor inhibitors are independent risk factors for PARPi SHAEs in patients with ovarian cancer. The risk prediction model established based on these factors demonstrated moderate predictive value.

(JMIR Med Inform 2025;13:e72994) doi:10.2196/72994

KEYWORDS

poly (adenosine diphosphate ribose) polymerase inhibitors; PARPis; hematological adverse event; ovarian cancer; risk prediction model

XSL•FO
RenderX

Introduction

Background

Ovarian cancer is the most aggressive gynecologic malignancy. Most patients with ovarian cancer are diagnosed in later stages due to unclear early symptoms and its anatomical location deep in the pelvis. Even after surgery, it is still prone to recurrence and metastasis, which has a serious impact on women's lives and health. Approximately 70% of patients still experience recurrence and develop chemotherapy resistance within 3 years after initial treatment despite showing sensitivity in the early stages of chemotherapy [1,2]. Given the frequent and rapid development of chemotherapy resistance in ovarian cancer, there is an urgent clinical need to identify new treatment options. High-level medical evidence shows that poly (adenosine diphosphate ribose) polymerase inhibitors (PARPis) can interfere with the base excision repair pathway, block the DNA single-strand break repair of tumor cells, form a "synthetic lethal" effect in tumor tissues that cannot undergo DNA double-strand repair due to homologous recombination repair deficiency (HRRD), promote tumor cell apoptosis, effectively prolong the platinum-free interval of patients with ovarian cancer, and provide a new treatment option for patients who cannot tolerate chemotherapy in the late stage [3]. Germline mutations in the *BRCA1* and *BRCA2* genes, which are ovarian cancer susceptibility genes, are common causes of HRRD. Therapeutic benefits of PARPis have been observed in patients with cancer carrying germline mutations in the *BRCA1* and *BRCA2* genes, particularly for ovarian cancer cases [4]. In terms of safety, serious adverse reactions to PARPis are mainly manifested in hematological toxicity and are most likely to lead to drug reduction, interruption, or even discontinuation, seriously hindering the normal treatment process of patients with ovarian cancer and causing adverse effects on their long-term prognosis [5,6]. Therefore, identifying serious hematological adverse events (SHAEs) related to PARPis in advance is particularly important in clinical diagnosis and treatment practice.

Objectives

This study aimed to explore the risk factors for SHAEs in patients with ovarian cancer receiving PARPi treatment and develop a risk prediction model to guide personalized treatment and care for patients with ovarian cancer to achieve the best survival benefits.

Methods

Study Design

This open-label, prospective cohort study was designed to evaluate the incidence of SHAEs in patients with ovarian cancer receiving PARPi treatment in routine clinical situations and determine the variables linked to the emergence of these reactions. This study included patients aged ≥18 years with histologically proven ovarian, fallopian tube, or primary peritoneal cancer who received care at the Guangxi Medical University Affiliated Tumor Hospital from December 2018 to August 2024. All participants (or their legal representatives) provided informed consent, and all had been treated with PARPis for a minimum duration of 6 weeks in any treatment line. The exclusion criteria were the participants' or the responsible family members' withdrawal of permission to take part in the research at any time or PARPi discontinuation due to disease progression or death.

Study Procedures and Assessments

Participants were followed up on on-site or contacted via telephone calls at least once a month to inquire about the incidence of any untoward effect from PARPis from initiation until they completed their treatment, were lost to follow-up, or died between December 2018 and August 2024. Patients were evaluated for treatment-related hematological indicators and imaging of tumor lesions every 2 to 3 treatment cycles. Any hematological adverse event (including time of occurrence, severity, and prognosis) was also included in the data recording. When to stop treatment in case of an adverse event was decided by the attending physician.

The safety data were collected using the National Cancer Institute Common Terminology Criteria for Adverse Events version 5.0. Depending on whether there were SHAEs during the follow-up period, the patients were split into 2 groups: the SHAE group and the no-SHAE group. SHAEs are defined as hematological adverse events of a grade of ≥3, including thrombocytopenia, leucopenia, neutropenia, erythropenia, decreased hemoglobin, anemia, myelodysplastic syndrome, and acute myeloid leukemias. If none of the aforementioned SHAEs occurred, patients were included in the no-SHAE group. In addition, when a single report contained multiple adverse events, if any of the aforementioned serious adverse events occurred, patients were included in the SHAE group.

The outcomes of each patient were assessed by combining the Response Evaluation Criteria in Solid Tumors version 1.1 and the Gynecologic Cancer Intergroup criteria, including disease control rate (DCR), partial response, stable disease, and progressive disease.

Establishment of the Nomogram Model

General clinical characteristics of patients before PARPi treatment, including age, BMI, marital status, pathology type, previous antitumor therapies, lymph node metastasis, distant metastasis, and number of distant metastases, were collected. Univariate analyses were conducted for each parameter using the chi-square test or Fisher exact test, as appropriate. Variables with a significance level of $P<.20$ in the univariate analysis were included in the subsequent multivariate logistic regression analysis using a backward elimination approach (removal criterion: $P>.05$ based on the Wald statistic) to identify independent risk factors for SHAEs during PARPi treatment in patients with ovarian cancer. For all binary categorical variables (eg, lymph node metastasis), the reference category was explicitly set to the negative group (coded as 0) to ensure clinically intuitive interpretation of odds ratios. Statistical analyses were conducted using SPSS (version 23.0; IBM Corp). Subsequently, the final multivariate model was imported into the R software (version 4.2.2; R Foundation for Statistical Computing), and the *rms* software package was used to construct a nomogram for predicting the risk of SHAEs.

XSL•FO
RenderX

Validation of the Nomogram Model

By charting the receiver operating characteristic (ROC) curve and computing the area under the curve (AUC), the differentiation of the model was assessed. To confirm the model's consistency, a calibration curve was created by contrasting the projected and actual probabilities of SHAEs. The clinical usefulness of the prediction model was assessed using decision curve analysis. To quantify the net benefit at various threshold probabilities, decision curve analysis compares the model's performance to 2 reference lines: one that assumes that all patients experience SHAEs and receive the intervention (which represents the highest clinical cost) and one that assumes that no patients receive the intervention (which represents no clinical benefit).

Statistical Analysis

Data were analyzed using SPSS (version 23.0). Categorical variables are presented as frequencies and percentages and were compared using the chi-square test or Fisher exact test, as appropriate. Cases categorized as "unknown" were excluded from the analysis to ensure validity and minimize potential bias. In the tables, variables with missing data are marked with a footnote symbol, indicating that these cases were excluded. For variables with a high proportion of missing values (≥50%), no statistical comparisons were conducted, and *P* values are denoted using an em dash (ie, not applicable).

Survival outcomes were assessed using the Kaplan-Meier method. To evaluate the association between the occurrence of serious hematological toxicity and clinical efficacy, a comparative analysis of progression-free survival (PFS) was conducted between participants who experienced any hematological adverse events of a grade of ≥3 during the treatment period and those who did not. The 2 groups were compared using the log rank test. Time-to-event end points specific to hematological adverse event occurrence were analyzed using survival analysis. The primary end point was time to first onset of hematological adverse events of a grade of ≥3, and secondary end points included time to first onset of any-grade hematological adverse events. The event was defined as the first documented occurrence of a hematological adverse event (including anemia, neutropenia, and thrombocytopenia) meeting the specified severity grade. Data from patients who did not experience an event were censored at the date of their last follow-up. The cumulative probability of each end point was estimated using the Kaplan-Meier method and visualized via Kaplan-Meier curves.

The associated factors influencing SHAEs following PARPi medication were examined using a multivariate logistic regression model, and a prediction model was created. The ROC curve was used to verify the model's prediction ability, and the AUC was calculated. The degree to which the prediction model fit the data was assessed using the Hosmer-Lemeshow test. The difference was considered statistically significant if $P<.05$.

Ethical Considerations

The protocol for this study was approved by the Ethics Review Board of Guangxi Medical University Affiliated Tumor Hospital (KY2023772). All procedures were conducted in accordance with the ethical standards of the Declaration of Helsinki and local regulations. Written or verbal informed consent was obtained from all participants (or their legal guardians) before their inclusion in the study.

To ensure participant privacy and confidentiality, all personal information was handled with strict adherence to our ethical protocols. Data collection forms were anonymized and stored separately from any personal identifiers. Access to the original dataset was restricted to authorized research personnel only. Throughout the data analysis and publication process, all participant data were de-identified to prevent any possibility of tracing back to individuals. Specifically, all direct personal identifiers (such as names, patient ID numbers, and detailed contact information) were removed from the research dataset.

Results

Overview

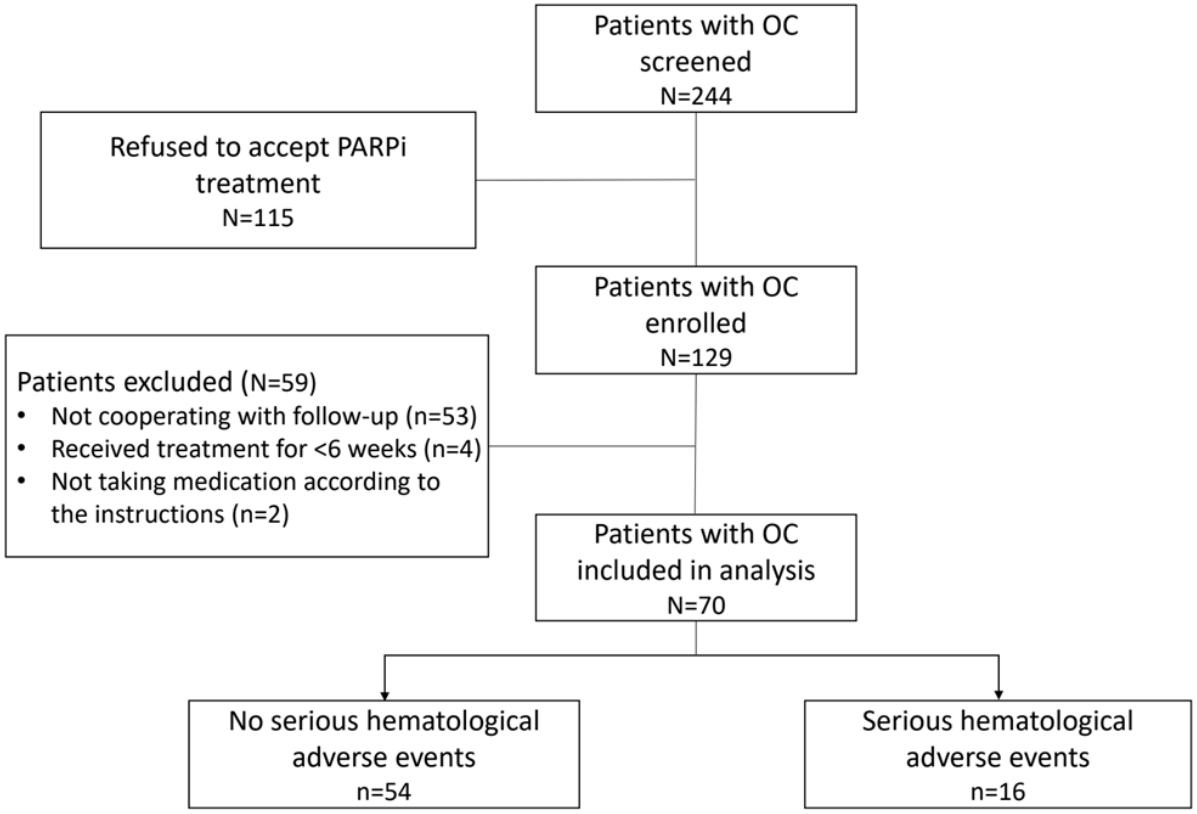
Figure 1 shows the study sample recruitment. Of the 244 patients with ovarian cancer surveyed at baseline, 115 (47.1%) were not eligible for follow-up due to refusal. Of the 129 participants receiving PARPi treatment, we excluded 59 (45.7%) for the following reasons: 53 (90%) did not return for any follow-up visit and could not be reached for the entire study duration, 4 (7%) received treatment for <6 weeks, and 2 (3%) did not take their medications according to the instructions. As a result, the total sample size for the analysis was 70 patients.

The follow-up period lasted a median of 12 (IQR 7-24) months.

Of the 70 patients with ovarian cancer treated with PARPis, 16 (23%) experienced hematological adverse events of a grade of ≥3 and were classified as the SHAE group, and the 54 (77%) remaining individuals were categorized as the no-SHAE group. After the clinical characteristics of the individuals in the 2 groups were analyzed, the findings (Multimedia Appendix 1) demonstrated that there were statistically significant differences in creatinine clearance rate (Ccr), red blood cell (RBC) count, and response to 6-week treatment among the groups ($P<.05$).

XSL•FO
RenderX

Figure 1. Flow diagram of this study. OC: ovarian cancer; PARPi: poly (adenosine diphosphate ribose) polymerase inhibitor.



Assessment of Effectiveness and Prognosis

Treatment response was assessed in all study patients through combined application of the Response Evaluation Criteria in Solid Tumors version 1.1 and the Gynecologic Cancer Intergroup criteria. The results showed that progressive disease developed in 56% (39/70) of the patients, stable disease developed in 44% (31/70) of the patients, and partial response developed in 0% of the patients. A DCR was present in 44% (31/70) of the entire population. A significant difference was not found in PFS between the SHAE group and the no-SHAE group according to the results of a Kaplan-Meier survival analysis conducted for PFS in the 2 groups (P=.82), and the median PFS was 13.0 (IQR 0.0-38.4) months and 24.0 (IQR 19.2-28.8) months, respectively (Figure 2).

Further analysis of the relationship between SHAEs in patients with ovarian cancer and the efficacy of PARPis did not reveal any association between the early occurrence of SHAEs related to PARPi hematological toxicity and antitumor efficacy (Table 1).

XSL•FO
RenderX

Figure 2. Progression-free survival (PFS) compared between participants who experienced serious hematological adverse events (SHAEs) and those who did not.

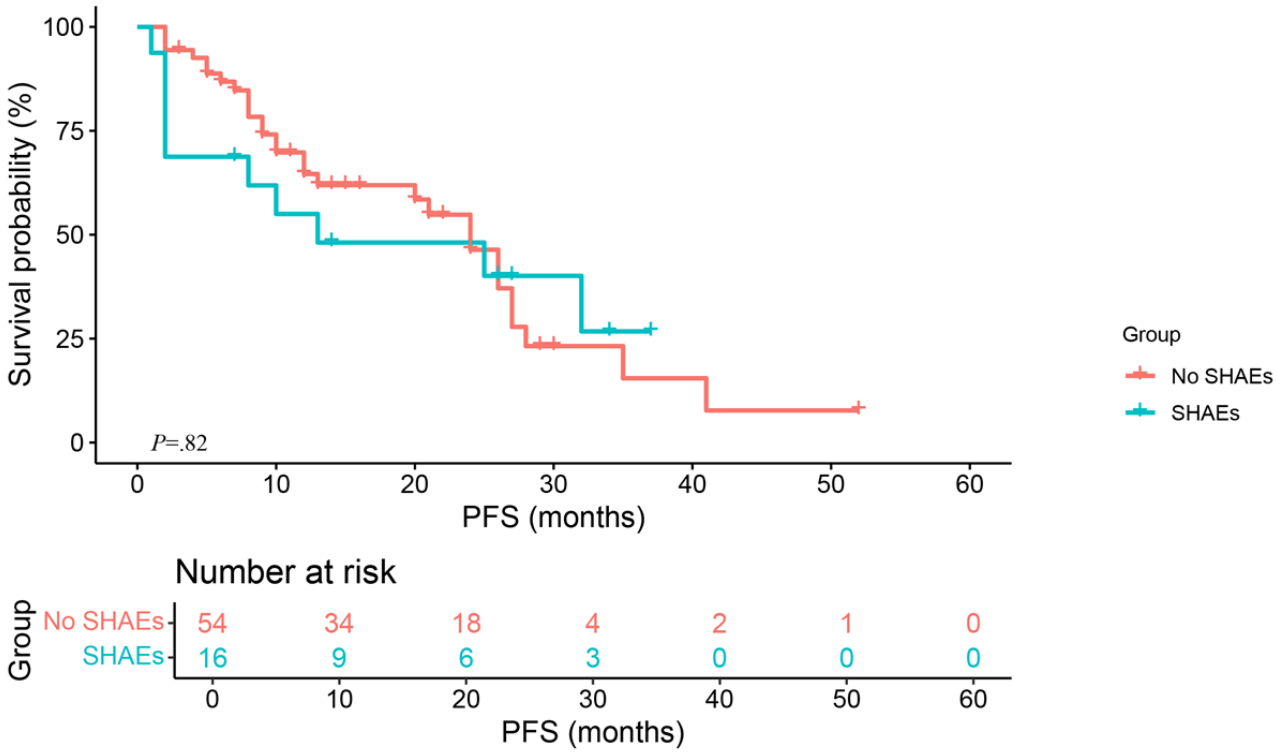


Table 1. Disease control rates (DCRs) and absolute frequencies by adverse event experiences.

Time before initial event (mo)	Total, n	Disease control, n (%)	*P* value
Adverse events			.43
≤1	8	5 (62.5)	
>1	32	13 (40.6)	
Serious hematological adverse events			.30
≤1	5	3 (60.0)	
>1	11	3 (27.3)	

Presentation of Hematological Adverse Events in Patients

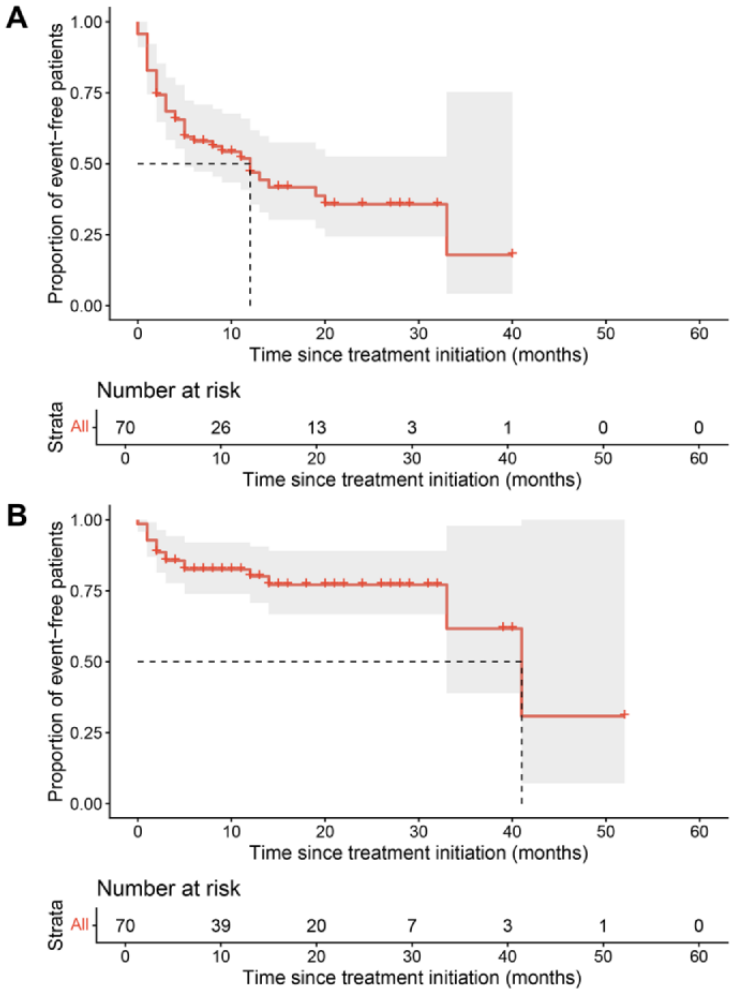
The spectrum and classification of hematological adverse events are shown in Table 2. Erythropenia and decreased hemoglobin showed the highest incidence regardless of severity. Figure 3 illustrates the onset time of hematological adverse events during PARPi treatment. All-grade hematological adverse events had a median onset time of 12.0 (IQR 6.5-17.468) months, whereas hematological adverse events of a grade of ≥3 manifested later (median onset time 41.0, IQR 29.3-52.7 months).

XSL•FO
RenderX

Table 2. Incidence and types of hematological adverse events (N=70).

	Grade <3, n (%)	Grade ≥3, n (%)	Total, n (%)
Any hematological adverse event	23 (33)	17 (24)	40 (57)
Thrombocytopenia	5 (7)	10 (14)	15 (21)
Leucopenia	12 (17)	8 (11)	20 (29)
Neutropenia	7 (10)	8 (11)	15 (21)
Erythropenia	16 (23)	12 (17)	28 (40)
Decreased hemoglobin	15 (21)	13 (19)	28 (40)
Anemia	6 (9)	11 (16)	17 (24)
Myelodysplastic syndrome	0 (0)	0 (0)	0 (0)
Acute myeloid leukemias	0 (0)	0 (0)	0 (0)

Figure 3. Time to first onset of hematological adverse events—(A) time to all-grade hematological adverse events; (B) time to (serious) hematological adverse events of a grade of ≥3.



Multifactor Logistic Regression Analysis of Factors Affecting SHAEs

To further investigate the pertinent factors influencing the occurrence of SHAEs, variables with $P<.20$ in Multimedia Appendix 1. were included in the multivariate logistic regression analysis, and the results (Table 3) showed that lymph node metastasis, Ccr of ≤60 mL per minute, RBC count of $\leq 3.3\times10^{12}$ per liter, and combined therapy with vascular endothelial growth factor inhibitors (VEGFis) were risk factors influencing the occurrence of SHAEs ($P<.05$).

XSL•FO
RenderX

Table 3. Multivariable logistic regression analysis with backward elimination for predicting poly (adenosine diphosphate ribose) polymerase inhibitor (PARPi) serious hematological adverse events.

	B	OR[a] (95% CI)	*P* value
Lymph node metastasis	1.907	6.733 (1.197-37.873)	.03
Ccr[b]≤60 mL per min	3.166	23.722 (3.121-180.303)	.002
RBC[c] count≤3.3×10^{12} per liter	1.578	4.847 (1.020-23.041)	.047
PARPis combined with VEGFis[d]	1.909	6.749 (1.313-34.689)	.02

[a]OR: odds ratio.

[b]Ccr: creatinine clearance rate.

[c]RBC: red blood cell.

[d]VEGFi: vascular endothelial growth factor inhibitor.

Development and Assessment of the Nomogram Model

A nomogram model was developed using the R software to forecast SHAEs after receiving PARPi medication based on the findings of the multifactor analysis (Figure 4). The ROC curve was developed to evaluate this model's predictive ability. With an AUC of 0.874, the nomogram model showed great predictive ability and consistency (Figure 5A). The ROC curve derived from bootstrap resampling maintained consistent stability in its positional trajectory (Figure 5B), suggesting that this phenomenon is more likely attributable to sample distribution and class imbalance issues common in small datasets rather than overfitting. The Hosmer-Lemeshow test was used to assess the model's goodness of fit. According to the findings, the nomogram model developed in this study had a goodness of fit with a *P* value of .36. The model demonstrated moderate calibration (mean absolute error=0.061), with observed versus predicted risks aligning closely across deciles (Figure 5C). Decision curve analysis (Figure 5D) was conducted to evaluate the clinical utility of our risk prediction model. The curve demonstrates that the model yielded a positive net benefit at threshold probabilities ranging from 0% to 70%, suggesting that it can be safely applied to guide clinical interventions within this range. However, when the threshold probability exceeds 70%, the net benefit turns negative, indicating that the model-based decision strategy underperforms the "treat none" strategy (reference line net benefit=0) in this high-threshold range. This limitation may stem from either (1) an insufficient number of high-risk patients in the training dataset, leading to distributional bias and unreliable predictions in high-probability intervals; or (2) inherent inaccuracies in the model's predictions for extreme-risk subgroups. Therefore, for patients within the high-threshold range (threshold probability>70%), additional confirmatory screening (eg, imaging examinations) or closer clinical monitoring should be prioritized to enhance decision accuracy rather than relying solely on this model to justify high-risk interventions.

XSL•FO
RenderX

Figure 4. Nomogram predicting hematological adverse events (grade ≥3) in patients with ovarian cancer treated with poly (adenosine diphosphate ribose) polymerase inhibitors. Ccr: creatinine clearance rate; RBC: red blood cell; SHAE: serious hematological adverse event; VEGFi: vascular endothelial growth factor inhibitor.

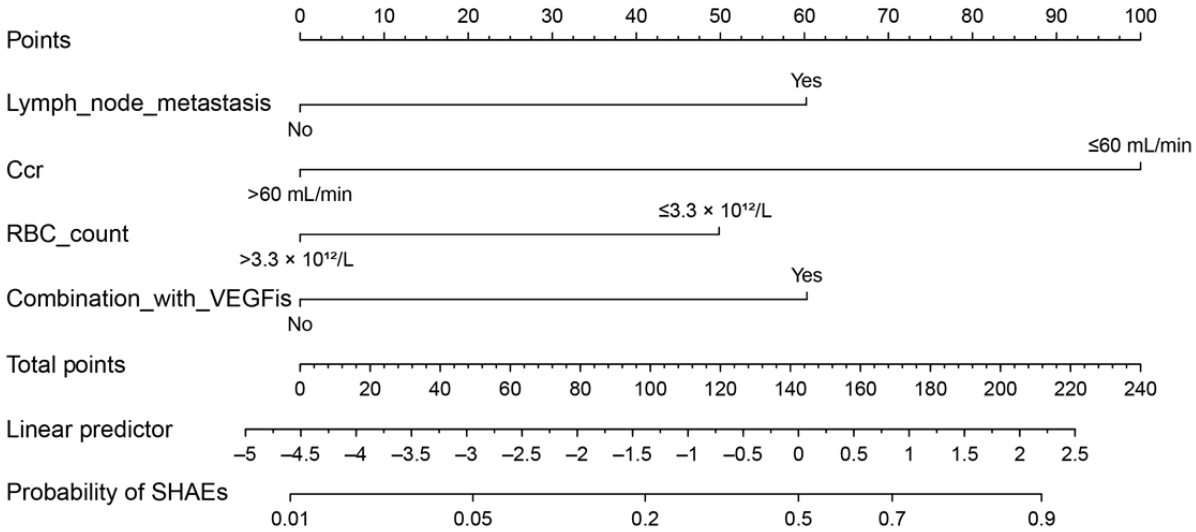
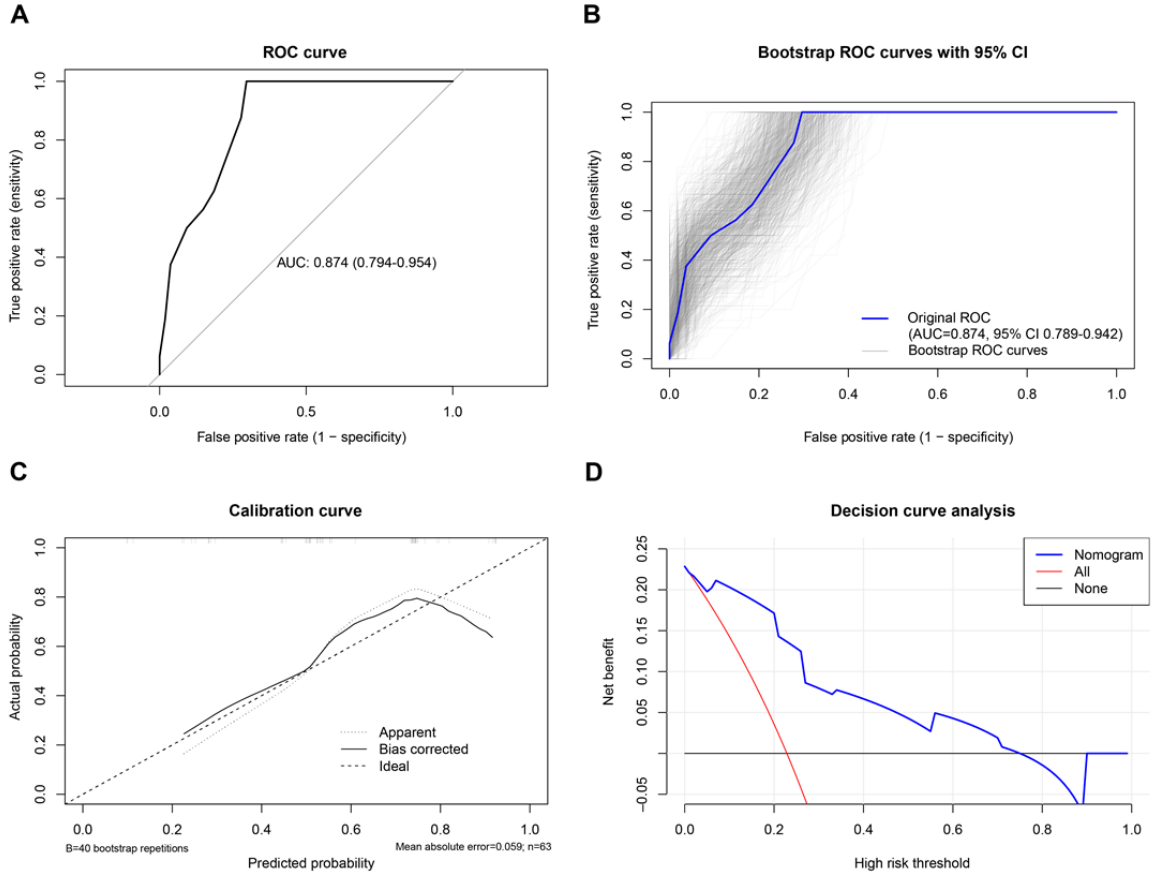


Figure 5. Calibration and clinical use of a diagnostic nomogram for predicting poly (adenosine diphosphate ribose) polymerase inhibitor serious hematological adverse events—(A) receiver operating characteristic (ROC) curve of the nomogram; (B) bootstrap ROC curve of the nomogram; (C) calibration curve of the nomogram; (D) decision curve analysis of the nomogram.



XSL•FO
RenderX

Discussion

Principal Findings

During the treatment process with PARPis, most patients will experience varying degrees of adverse reactions, mainly mild or moderate, most commonly manifested as hematological adverse events, gastrointestinal adverse events, and fatigue. Most of the adverse events of a grade of ≥3 are hematological adverse events, which are the main reasons for adjusting drug dosage and interrupting and terminating medication, with a discontinuation rate of 27% [7-9]. SHAEs may also be associated with life-threatening declines in organ function and quality of life and even fatal outcomes. This study found that patients who experienced SHAEs showed a trend toward worse PFS than those without SHAEs (median 13.0, IQR 0.0-38.4 months vs median 24.0, IQR 19.2-28.8 months; *P*=.82); although no statistically significant difference was found, these toxicities still require early detection and proper management.

However, a previous study found that patients who experienced hematological adverse events while receiving PARPi treatment had much higher survival and response rates than those who did not experience toxicity. This finding may be connected to PARPis' extensive cell dispersion [10]. Early adverse events related to PARPi hematological toxicity have been linked to antitumor activity, which may be a reliable and readily quantifiable clinical indicator in patients with ovarian cancer. In this study, although patients who developed hematological adverse events of a grade of ≥3 within the first month of PARPi treatment appeared to exhibit a higher DCR, this difference did not reach statistical significance. Conversely, the early efficacy of PARPis showed an inverse relationship with their associated hematological toxicities. Compared with patients who experienced SHAEs during treatment, patients who did not experience SHAEs showed higher DCR (94.4% vs 68.8%; *P*=.02) in the early stages of treatment (within 6 weeks), which may be due to the longer median time to onset of hematological adverse reactions of a grade of ≥3 reported in this study (median 41.0, IQR 29.3-52.7 months). Furthermore, it cannot be ruled out that the small-sample bias may have an impact on the research results. Although logistic regression analysis did not show that early efficacy could predict SHAEs related to PARPis, we still recommend closely monitoring relevant indicators for patients with poor early treatment response (within 6 weeks) to identify and intervene in adverse events early.

Of the 70 patients in this analysis, 16 (23%) experienced SHAEs, with a median time to onset of 41.0 months (IQR 29.3-52.7 months). In addition, 57% (40/70) experienced all-grade hematological adverse events, with the main onset time window falling between 7.4 and 26.6 months. The hematological adverse events of the patients in this study were mostly erythropenia and decreased hemoglobin regardless of severity, which was comparable to those found in previous research. Therefore, it is recommended that routine blood testing, especially RBC count and hemoglobin, be strengthened from the second year of patient medication. If necessary, preventive medication should be administered.

Lymph node metastasis was found to be an independent factor influencing the incidence of hematological adverse events using multivariate logistic regression analysis. Previous studies have demonstrated that patients with advanced solid tumors experience less tolerance to treatment. Lymph node status is not only a part of the International Federation of Gynecology and Obstetrics staging system for ovarian cancer but also an established prognostic factor in ovarian cancer [10-13]. A 13-year retrospective analysis suggests that, when it comes to patients with ovarian cancer, the lymph node ratio (calculated as the number of positive lymph nodes divided by the total number removed) is a more reliable prognostic indicator than the standard lymph node status [14]. As a result, PARPi users with lymph node metastasis in any pathological stage should be considered for further evaluation.

Previous studies have identified an association between PARPi dose and adverse events [9]. PARPis are predominantly eliminated via the kidneys. In clinical practice, creatinine and Ccr are used as markers to determine the glomerular filtration rate and functional parameters to assess renal function in patients. Patients with renal dysfunction are more likely to experience excessive accumulation of the drug or its active metabolites, which could result in severe adverse events. In general, low Ccr consistently appears to be a risk for drug adverse events, especially for drugs primarily excreted through the kidneys, and from the results of our study, this remains true for SHAEs related to PARPis. It is worth noting that elevated serum creatinine is a frequent adverse reaction to PARPis reported in previous studies [15-17], although most studies have shown that elevated serum creatinine may be caused by the inhibition of renal transporters but not accurately reflect a decline in glomerular filtration rate or renal failure [15,18]. Given the findings of this study, it is still advised that PARPi users with a Ccr of ≤60 mL per minute be routinely monitored.

This study found that an RBC count of $\leq 3.3\times10^{12}$ per liter was a risk factor for SHAEs related to PARPis. The most plausible explanation for the association between erythrocyte reduction and hematological toxicity is impaired bone marrow reserve. Immature platelet fraction serves as an accurate hematological marker for assessing bone marrow function. However, as baseline immature platelet fraction testing is not routinely conducted in patients with ovarian cancer receiving PARPis at our institution, this study conducted a comprehensive evaluation of bone marrow reserve using indicators including RBC count, platelet count, hemoglobin, platelet-large cell ratio, mean corpuscular volume, and lactate dehydrogenase. Chi-square tests and multivariate logistic regression analysis revealed that none of the aforementioned parameters—except for RBC count—demonstrated a significant correlation with PARPi-related hematological adverse events. Insufficient evidence was found to support the hypothesis that SHAEs related to PARPis are primarily mediated by impaired bone marrow function. Instead, our findings may be better explained by the research by Molina et al [19] and Mehibel et al [20], which explores the association between the tumor microenvironment (TME) and the antitumor activity of PARPis. The RBCs are the efficient carriers of oxygen and other essential nutrients that are linked to aberrant metabolism in the TME,

XSL•FO
RenderX

such as hypoxia. Hypoxia is a common characteristic of the TME in solid tumors and is caused by the rapid growth and proliferation of malignant solid tumors and the underdevelopment of vascular system tissues, resulting in local hypoxic tension in tissues; hypoxia, in turn, regulates the angiogenesis and growth of tumor tissue, promoting tumor invasion and metastasis, to adapt to hypoxic and nutrient-limited environments [19,21]. This causal transformation results in most solid tumors being in a state of moderate (1%-2% oxygen) to severe (<0.01% oxygen) hypoxia internally [22]. In the female population, the normal RBC count is 4.0 to 5.0×10^{12} per liter. When it is below the lower limit of the normal range, the ability of blood to transport oxygen is weakened, which may further exacerbate the hypoxic condition of the TME. It has been found that hypoxia can induce the overexpression of breast cancer resistance protein and multiple drug resistance protein [23] and the activation of the transforming growth factor beta, transforming growth factor alpha and epidermal growth factor receptor, and cyclooxygenase-2 pathways [24-26] by regulating the hypoxia-inducible factor α and cancer-associated fibroblasts, thus inducing therapeutic resistance. The study by Mehibel et al [20] revealed that cancer cells exhibited increased resistance to PARPis under moderate hypoxia (2% oxygen) when compared to their normoxic counterparts, suggesting a hypoxia-induced protective mechanism. However, under severe hypoxia (0.5% oxygen), cancer cells showed the same significant increase in sensitivity to PARPis regardless of whether HRRD was negative or positive. Notably, the interpretation of our results based on those of these previous studies remains limited by the sample size, cross-sectional design, and suboptimal sensitivity of bone marrow evaluation methods, necessitating future validation in prospective cohorts with dynamic bone marrow function monitoring.

In addition, this study found that PARPi combination with VEGFis was one of the risk factors for SHAEs during PARPi treatment. The VEGFis used in patients undergoing combination therapy in this study included bevacizumab, apatinib, and lenvatinib. Previous literature has reported a significant proportion of hematological adverse events of a grade of ≥3 during the use of VEGFi monotherapy [27-29]. Notably, neutropenia and thrombocytopenia have been reported to occur more frequently with VEGFis monotherapy than with PARPis monotherapy, although the proportion of grade ≥ 3 anemia accounts for less than 4% of cases. The hematological toxicity of VEGFis may arise from their suppression of vascular endothelial growth factor (VEGF) signaling, which disrupts the bone marrow microenvironment, leading to vascular regression, hypoxia, and impaired stromal cell function, thereby compromising hematopoietic stem cell survival and differentiation. Concurrently, blockade of VEGF receptors (eg, VEGF receptors 1 and 2) on hematopoietic progenitor cells can interfere with erythroid, myeloid, and megakaryocytic maturation, resulting in anemia, neutropenia, and thrombocytopenia. Furthermore, VEGF inhibition may upregulate proinflammatory cytokines (eg, tumor necrosis factor and interleukin-6) and hepcidin, further suppressing hematopoiesis or inducing iron-restricted anemia. These mechanisms collectively contribute to the potential hematological adverse effects associated with VEGFis [30]. PARPis cause anemia by binding to poly (adenosine diphosphate ribose) polymerase 2 in the RBCs, leading to shortened life span and increased absorption of RBCs [31]. The possible mechanism of PARPi-mediated bone marrow suppression also includes inhibiting poly (adenosine diphosphate ribose) polymerase 1 in hematopoietic stem cells, interfering with neutrophil, platelet, and RBC formation [32]. Thus, it is hypothesized that the 2 together could worsen overall hematological toxicity via distinct mechanisms, increasing the risk of hematological adverse events of a grade of ≥3 in patients. This phenomenon can also be observed in the PAOLA-1 (PArp inhibitor OLaparib in Advanced ovarian cancer 1) clinical study of olaparib combined with bevacizumab in ovarian cancer treatment [33].

Other than the previously discussed factors, further parameters may modulate the development of SHAEs from PARPi therapy. Previous studies have found that *BRCA1* and *BRCA2* mutation or HRRD positivity is a risk factor for hematological adverse events related to PARPis [34-36]. Moreover, the Spanish Society of Medical Oncology clinical guidelines [37] for ovarian cancer indicate that PARPis induce cell death in HRRD-positive tumor cells through a “synthetic lethality” mechanism, with *BRCA1* and *BRCA2* mutations being one of the established causes of HRRD in tumors. Therefore, the guidelines recommend *BRCA* mutation testing in patients before PARPi therapy. However, due to the high cost of testing, this study found that the willingness of most patients with cancer to undergo *BRCA* and HRRD testing was low, with a detection rate of less than 55%. Therefore, it is difficult to verify the impact of *BRCA* and HRRD status on PARPi SHAEs. A network meta-analysis indicated that there was a significant difference in the risk of any adverse events of a grade of ≥3 across PARPi treatments, and based on the surface under the cumulative ranking curve rankings, olaparib was the safest PARPi in terms of risk of hematological adverse events [6]. Some studies have also found that hypertension, low baseline hemoglobin level, and low baseline hematocrit level are related to the occurrence of hematological adverse events induced by PARPi monotherapy [35]. Due to data limitations in this study, definitive comparative analyses could not be conducted, warranting future studies to address this gap.

On the basis of the identified predictive factors, this study developed a nomogram model to provide a user-friendly method for early prediction of SHAEs associated with PARPis in clinical practice. Internal validation demonstrated that this risk assessment model exhibited moderate accuracy and predictive capability, with an ROC curve AUC of 0.874 and Hosmer-Lemeshow test of P=.36. These findings provide evidence for developing personalized treatment strategies in clinical practice and suggest potential clinical utility.

This study also has several limitations. First, although repeated cross-validation showed no strong signs of overfitting, the small sample size limited our ability to fully address associated challenges such as data distribution biases and class imbalance. Furthermore, external validation, which is essential for confirming generalizability, could not be conducted due to the unavailability of an independent external cohort. This is a common constraint in single-center studies of rare conditions.

XSL•FO
RenderX

Future multi-institutional studies are warranted to externally validate our findings. The analysis was further limited by missing data for several key prognostic indicators (eg, *BRCA* and HRRD status), which precluded their inclusion in the model. Finally, as the model was developed and validated exclusively on a Chinese population, its generalizability to other ethnic groups requires further investigation.

Conclusions

This study used objective data widely used in clinical settings to create and internally test a basic predictive model of SHAEs for PARPi users with ovarian cancer. The clinical nomogram included the 4 best predictors of PARPi SHAEs: lymph node metastasis, Ccr, RBC count, and therapeutic schedule. This should help identify patients who need closer monitoring for SHAEs and more rigorous treatment.

Acknowledgments

This work was supported by the Scientific Research and Technology Development Project of the Guangxi Zhuang Autonomous Region Medical Products Administration (Contract No.: Gui Yao Ke [2022] Zixuan 23). The authors extend their sincere appreciation to the Affiliated Tumor Hospital of Guangxi Medical University for its invaluable support throughout this research. We are also deeply grateful to all the physicians, nurses, and healthcare professionals for their dedicated efforts and contributions. Above all, we wish to express our profound gratitude to the patients and their families for their trust, cooperation, and unwavering support.

Data Availability

The datasets generated or analyzed during this study are available from the corresponding author on reasonable request.

Authors' Contributions

XL designed the study, collected and analyzed the data, and wrote the manuscript. YL supervised the research, critically revised the manuscript, and provided final approval. Both authors read and approved the final manuscript.

Conflicts of Interest

None declared.

Multimedia Appendix 1
Comparison of clinical characteristics between the 2 groups (N=70).
[DOCX File , 33 KB - medinform_v13i1e72994_app1.docx]

References

1. Webb PM, Jordan SJ. Global epidemiology of epithelial ovarian cancer. Nat Rev Clin Oncol 2024 May;21(5):389-400. [doi: 10.1038/s41571-024-00881-3] [Medline: 38548868]
2. Ortiz M, Wabel E, Mitchell K, Horibata S. Mechanisms of chemotherapy resistance in ovarian cancer. Cancer Drug Resist 2022;5(2):304-316 [FREE Full text] [doi: 10.20517/cdr.2021.147] [Medline: 35800369]
3. Javle M, Curtin NJ. The role of PARP in DNA repair and its therapeutic exploitation. Br J Cancer 2011 Oct 11;105(8):1114-1122 [FREE Full text] [doi: 10.1038/bjc.2011.382] [Medline: 21989215]
4. Vikas P, Borcherding N, Chennamadhavuni A, Garje R. Therapeutic potential of combining PARP inhibitor and immunotherapy in solid tumors. Front Oncol 2020;10:570 [FREE Full text] [doi: 10.3389/fonc.2020.00570] [Medline: 32457830]
5. Madariaga A, Bowering V, Ahrari S, Oza AM, Lheureux S. Manage wisely: poly (ADP-ribose) polymerase inhibitor (PARPi) treatment and adverse events. Int J Gynecol Cancer 2020 Jul;30(7):903-915 [FREE Full text] [doi: 10.1136/ijgc-2020-001288] [Medline: 32276934]
6. Dai MF, Wang X, Xin WX, Kong SS, Xu WB, Ding HY, et al. Safety and hematological toxicities of PARP inhibitors in patients with cancer: a systematic review of randomized controlled trials and a pharmacovigilance analysis. Expert Rev Anticancer Ther 2024 Jul;24(7):613-622. [doi: 10.1080/14737140.2024.2357822] [Medline: 38761169]
7. Poveda A, Floquet A, Ledermann JA, Asher R, Penson RT, Oza AM, et al. Olaparib tablets as maintenance therapy in patients with platinum-sensitive relapsed ovarian cancer and a BRCA1/2 mutation (SOLO2/ENGOT-Ov21): a final analysis of a double-blind, randomised, placebo-controlled, phase 3 trial. Lancet Oncol 2021 May;22(5):620-631. [doi: 10.1016/S1470-2045(21)00073-5] [Medline: 33743851]
8. Moore KN, Secord AA, Geller MA, Miller DS, Cloven N, Fleming GF, et al. Niraparib monotherapy for late-line treatment of ovarian cancer (QUADRA): a multicentre, open-label, single-arm, phase 2 trial. Lancet Oncol 2019 May;20(5):636-648. [doi: 10.1016/S1470-2045(19)30029-4] [Medline: 30948273]
9. Wu XH, Zhu JQ, Yin RT, Yang JX, Liu JH, Wang J, et al. Niraparib maintenance therapy in patients with platinum-sensitive recurrent ovarian cancer using an individualized starting dose (NORA): a randomized, double-blind, placebo-controlled

XSL•FO
RenderX

phase III trial. Ann Oncol 2021 Apr;32(4):512-521 [FREE Full text] [doi: 10.1016/j.annonc.2020.12.018] [Medline: 33453391]
10. Ni J, Cheng X, Zhou R, Zhao Q, Xu X, Guo W, et al. Adverse events as a potential clinical marker of antitumor efficacy in ovarian cancer patients treated with poly ADP-ribose polymerase inhibitor. Front Oncol 2021;11:724620 [FREE Full text] [doi: 10.3389/fonc.2021.724620] [Medline: 34552876]
11. Haun MW, Estel S, Rücker G, Friederich HC, Villalobos M, Thomas M, et al. Early palliative care for adults with advanced cancer. Cochrane Database Syst Rev 2017 Jun 12;6(6):CD011129 [FREE Full text] [doi: 10.1002/14651858.CD011129.pub2] [Medline: 28603881]
12. Korfage IJ, Carreras G, Arnfeldt Christensen CM, Billekens P, Bramley L, Briggs L, et al. Advance care planning in patients with advanced cancer: a 6-country, cluster-randomised clinical trial. PLoS Med 2020 Nov 13;17(11):e1003422 [FREE Full text] [doi: 10.1371/journal.pmed.1003422] [Medline: 33186365]
13. He Y, Pang Y, Su Z, Zhou Y, Wang Y, Lu Y, et al. Symptom burden, psychological distress, and symptom management status in hospitalized patients with advanced cancer: a multicenter study in China. ESMO Open 2022 Dec;7(6):100595 [FREE Full text] [doi: 10.1016/j.esmoop.2022.100595] [Medline: 36252435]
14. Ataseven B, Grimm C, Harter P, Prader S, Traut A, Heitz F, et al. Prognostic value of lymph node ratio in patients with advanced epithelial ovarian cancer. Gynecol Oncol 2014 Dec;135(3):435-440. [doi: 10.1016/j.ygyno.2014.10.003] [Medline: 25312398]
15. Oza AM, Tinker AV, Oaknin A, Shapira-Frommer R, McNeish IA, Swisher EM, et al. Antitumor activity and safety of the PARP inhibitor rucaparib in patients with high-grade ovarian carcinoma and a germline or somatic BRCA1 or BRCA2 mutation: integrated analysis of data from Study 10 and ARIEL2. Gynecol Oncol 2017 Nov;147(2):267-275 [FREE Full text] [doi: 10.1016/j.ygyno.2017.08.022] [Medline: 28882436]
16. Coleman RL, Oza AM, Lorusso D, Aghajanian C, Oaknin A, Dean A, et al. Rucaparib maintenance treatment for recurrent ovarian carcinoma after response to platinum therapy (ARIEL3): a randomised, double-blind, placebo-controlled, phase 3 trial. Lancet 2017 Oct 28;390(10106):1949-1961 [FREE Full text] [doi: 10.1016/S0140-6736(17)32440-6] [Medline: 28916367]
17. Li N, Zhu J, Yin R, Wang J, Pan L, Kong B, et al. Treatment with niraparib maintenance therapy in patients with newly diagnosed advanced ovarian cancer: a phase 3 randomized clinical trial. JAMA Oncol 2023 Sep 01;9(9):1230-1237 [FREE Full text] [doi: 10.1001/jamaoncol.2023.2283] [Medline: 37440217]
18. Friedlander M, Lee YC, Tew WP. Managing adverse effects associated with poly (ADP-ribose) polymerase inhibitors in ovarian cancer: a synthesis of clinical trial and real-world data. Am Soc Clin Oncol Educ Book 2023 Jun;43:e390876 [FREE Full text] [doi: 10.1200/EDBK_390876] [Medline: 37285556]
19. Molina JR, Sun Y, Protopopova M, Gera S, Bandi M, Bristow C, et al. An inhibitor of oxidative phosphorylation exploits cancer vulnerability. Nat Med 2018 Jul 11;24(7):1036-1046. [doi: 10.1038/s41591-018-0052-4] [Medline: 29892070]
20. Mehibel M, Xu Y, Li CG, Moon EJ, Thakkar KN, Diep AN, et al. Eliminating hypoxic tumor cells improves response to PARP inhibitors in homologous recombination-deficient cancer models. J Clin Invest 2021 Jun 01;131(11):e146256 [FREE Full text] [doi: 10.1172/JCI146256] [Medline: 34060485]
21. Petrova V, Annicchiarico-Petruzzelli M, Melino G, Amelio I. The hypoxic tumour microenvironment. Oncogenesis 2018 Jan 24;7(1):10 [FREE Full text] [doi: 10.1038/s41389-017-0011-9] [Medline: 29362402]
22. Byrne MB, Leslie MT, Gaskins HR, Kenis PJ. Methods to study the tumor microenvironment under controlled oxygen conditions. Trends Biotechnol 2014 Nov;32(11):556-563 [FREE Full text] [doi: 10.1016/j.tibtech.2014.09.006] [Medline: 25282035]
23. Pinzón-Daza ML, Cuellar-Saenz Y, Nualart F, Ondo-Mendez A, Del Riesgo L, Castillo-Rivera F, et al. Oxidative stress promotes doxorubicin-induced Pgp and BCRP expression in colon cancer cells under hypoxic conditions. J Cell Biochem 2017 Jul;118(7):1868-1878. [doi: 10.1002/jcb.25890] [Medline: 28106284]
24. Tang YA, Chen YF, Bao Y, Mahara S, Yatim SM, Oguz G, et al. Hypoxic tumor microenvironment activates GLI2 via HIF-1α and TGF-β2 to promote chemoresistance in colorectal cancer. Proc Natl Acad Sci U S A 2018 Jun 26;115(26):E5990-E5999 [FREE Full text] [doi: 10.1073/pnas.1801348115] [Medline: 29891662]
25. Zhao D, Zhai B, He C, Tan G, Jiang X, Pan S, et al. Upregulation of HIF-2α induced by sorafenib contributes to the resistance by activating the TGF-α/EGFR pathway in hepatocellular carcinoma cells. Cell Signal 2014 May;26(5):1030-1039. [doi: 10.1016/j.cellsig.2014.01.026] [Medline: 24486412]
26. Zhao CX, Luo CL, Wu XH. Hypoxia promotes 786-O cells invasiveness and resistance to sorafenib via HIF-2α/COX-2. Med Oncol 2015 Jan;32(1):419. [doi: 10.1007/s12032-014-0419-4] [Medline: 25487445]
27. Komiyama S, Kato K, Inokuchi Y, Takano H, Matsumoto T, Hongo A, et al. Bevacizumab combined with platinum-taxane chemotherapy as first-line treatment for advanced ovarian cancer: a prospective observational study of safety and efficacy in Japanese patients (JGOG3022 trial). Int J Clin Oncol 2019 Jan;24(1):103-114 [FREE Full text] [doi: 10.1007/s10147-018-1319-y] [Medline: 30030657]
28. Kumar R, Crouthamel MC, Rominger DH, Gontarek RR, Tummino PJ, Levin RA, et al. Myelosuppression and kinase selectivity of multikinase angiogenesis inhibitors. Br J Cancer 2009 Nov 17;101(10):1717-1723 [FREE Full text] [doi: 10.1038/sj.bjc.6605366] [Medline: 19844230]

XSL•FO
RenderX

29. Li J, Qin S, Xu J, Xiong J, Wu C, Bai Y, et al. Randomized, double-blind, placebo-controlled phase III trial of apatinib in patients with chemotherapy-refractory advanced or metastatic adenocarcinoma of the stomach or gastroesophageal junction. J Clin Oncol 2016 May 01;34(13):1448-1454. [doi: 10.1200/jco.2015.63.5995]
30. Carmeliet P, Jain RK. Molecular mechanisms and clinical applications of angiogenesis. Nature 2011 May 19;473(7347):298-307 [FREE Full text] [doi: 10.1038/nature10144] [Medline: 21593862]
31. Farrés J, Llacuna L, Martin-Caballero J, Martínez C, Lozano JJ, Ampurdanés C, et al. PARP-2 sustains erythropoiesis in mice by limiting replicative stress in erythroid progenitors. Cell Death Differ 2015 Jul;22(7):1144-1157 [FREE Full text] [doi: 10.1038/cdd.2014.202] [Medline: 25501596]
32. Zhao H, Sifakis EG, Sumida N, Millán-Ariño L, Scholz BA, Svensson JP, et al. PARP1- and CTCF-mediated interactions between active and repressed chromatin at the lamina promote oscillating transcription. Mol Cell 2015 Sep 17;59(6):984-997 [FREE Full text] [doi: 10.1016/j.molcel.2015.07.019] [Medline: 26321255]
33. Ray-Coquard I, Pautier P, Pignata S, Pérol D, González-Martín A, Berger R, et al. Olaparib plus bevacizumab as first-line maintenance in ovarian cancer. N Engl J Med 2019 Dec 19;381(25):2416-2428. [doi: 10.1056/NEJMoa1911361] [Medline: 31851799]
34. Staropoli N, Ciliberto D, Luciano F, Napoli C, Costa M, Rossini G, et al. The impact of PARP inhibitors in the whole scenario of ovarian cancer management: a systematic review and network meta-analysis. Crit Rev Oncol Hematol 2024 Jan;193:104229 [FREE Full text] [doi: 10.1016/j.critrevonc.2023.104229] [Medline: 38065404]
35. Tashiro R, Kawazoe H, Mamishin K, Seto K, Udagawa R, Saito Y, et al. Patient-associated risk factors for severe anemia in patients with advanced ovarian or breast cancer receiving olaparib monotherapy: a multicenter retrospective study. Front Oncol 2022;12:898150 [FREE Full text] [doi: 10.3389/fonc.2022.898150] [Medline: 36267984]
36. Kim J, Park SY, Kim JH, Lee SW, Park JY, Suh DS, et al. Real-world clinical outcomes and prognostic factors of olaparib maintenance in Korean patients with primary or recurrent high-grade ovarian cancer with exploratory analysis of location of BRCA1 and BRCA2 mutations. J Clin Oncol 2024;42(16_suppl):e17561. [doi: 10.1200/jco.2024.42.16_suppl.e17561]
37. Redondo A, Guerra E, Manso L, Martin-Lorente C, Martinez-Garcia J, Perez-Fidalgo JA, et al. SEOM clinical guideline in ovarian cancer (2020). Clin Transl Oncol 2021 May;23(5):961-968 [FREE Full text] [doi: 10.1007/s12094-020-02545-x] [Medline: 33515422]

Abbreviations

AUC: area under the curve
Ccr: creatinine clearance rate
DCR: disease control rate
HRRD: homologous recombination repair deficiency
OR: odds ratio
PAOLA-1: PArp inhibitor OLaparib in Advanced ovarian cancer 1
PARPi: poly (adenosine diphosphate ribose) polymerase inhibitor
PFS: progression-free survival
RBC: red blood cell
ROC: receiver operating characteristic
SHAE: serious hematological adverse event
TME: tumor microenvironment
VEGF: vascular endothelial growth factor
VEGFi: vascular endothelial growth factor inhibitor

Edited by A Benis; submitted 23.02.25; peer-reviewed by D Bracken-Clarke, Z Chen, C Lyu; comments to author 26.04.25; revised version received 02.08.25; accepted 15.09.25; published 12.11.25.

Please cite as:
Lian X, Lei Y
Model for Predicting Serious Hematological Adverse Events in Individuals With Ovarian Cancer Receiving Poly (Adenosine Diphosphate Ribose) Polymerase Inhibitor Treatment: Prospective Cohort Study
JMIR Med Inform 2025;13:e72994
URL: https://medinform.jmir.org/2025/1/e72994
doi:10.2196/72994
PMID:

XSL•FO
RenderX

©Xiaotong Lian, Yu Lei. Originally published in JMIR Medical Informatics (https://medinform.jmir.org), 12.11.2025. This is an open-access article distributed under the terms of the Creative Commons Attribution License (https://creativecommons.org/licenses/by/4.0/), which permits unrestricted use, distribution, and reproduction in any medium, provided the original work, first published in JMIR Medical Informatics, is properly cited. The complete bibliographic information, a link to the original publication on https://medinform.jmir.org/, as well as this copyright and license information must be included.

XSL•FO
RenderX

Large Language Model–Based Critical Care Big Data Deployment and Extraction: Descriptive Analysis

Zhongbao Yang[1*], BS; Shan-Shan Xu[1*], MD; Xiaozhu Liu[1*], PhD; Ningyuan Xu[2], BS; Yuqing Chen[3], MD; Shuya Wang[3], MD; Ming-Yue Miao[1], MD; Mengxue Hou[3], MD; Shuai Liu[3], MD; Yi-Min Zhou[3], MD; Jian-Xin Zhou[1], MD, PhD; Linlin Zhang[3], MD, PhD

[1]Department of Critical Care Medicine, Beijing Shijitan Hospital, Capital Medical University, Beijing, China

[2]School of Information Science and Technology, Beijing University of Technology, Beijing, China

[3]Department of Critical Care Medicine, Beijing Tiantan Hospital, Capital Medical University, No.119 Nansihuanxi Road, Fengtai District, Beijing, China

[*]these authors contributed equally

Corresponding Author:
Linlin Zhang, MD, PhD
Department of Critical Care Medicine, Beijing Tiantan Hospital, Capital Medical University, No.119 Nansihuanxi Road, Fengtai District, Beijing, China

Abstract

Background: Publicly accessible critical care–related databases contain enormous clinical data, but their utilization often requires advanced programming skills. The growing complexity of large databases and unstructured data presents challenges for clinicians who need programming or data analysis expertise to utilize these systems directly.

Objective: This study aims to simplify critical care–related database deployment and extraction via large language models.

Methods: The development of this platform was a 2-step process. First, we enabled automated database deployment using Docker container technology, with incorporated web-based analytics interfaces Metabase and Superset. Second, we developed the intensive care unit–generative pretrained transformer (ICU-GPT), a large language model fine-tuned on intensive care unit (ICU) data that integrated LangChain and Microsoft AutoGen.

Results: The automated deployment platform was designed with user-friendliness in mind, enabling clinicians to deploy 1 or multiple databases in local, cloud, or remote environments without the need for manual setup. After successfully overcoming GPT's token limit and supporting multischema data, ICU-GPT could generate Structured Query Language (SQL) queries and extract insights from ICU datasets based on request input. A front-end user interface was developed for clinicians to achieve code-free SQL generation on the web-based client.

Conclusions: By harnessing the power of our automated deployment platform and ICU-GPT model, clinicians are empowered to easily visualize, extract, and arrange critical care–related databases more efficiently and flexibly than manual methods. Our research could decrease the time and effort spent on complex bioinformatics methods and advance clinical research.

(JMIR Med Inform 2025;13:e63216) doi:10.2196/63216

KEYWORDS

big data; critical care–related databases; database deployment; large language model; database extraction; intensive care unit; ICU; GPT; artificial intelligence; AI; LLM

Introduction

Critical care medicine has experienced an explosion of complex, heterogeneous data from various sources, such as electronic medical records, monitoring systems, imaging, registries, and omics platforms. This massive amount of multimodal data, often referred to as "big data," offers enormous potential for improving patient outcomes in intensive care units (ICUs) through studies and analytics.

There are many high-quality medical databases that excel in the dimensions of volume, velocity, veracity, variety, and value. Examples include the Medical Information Mart for Intensive Care (MIMIC; MIMIC-III, MIMIC-IV, MIMIC-IV-Note, etc) at the Beth Israel Deaconess Medical Center in Boston [1-3], the Electronic Intensive Care Unit Collaborative Research Database (eICU-CRD) from 208 hospitals in the United States, and the Amsterdam University Medical Center Database (Amsterdam UMCdb) [4-6]. By integrating demographic, monitoring, laboratory, imaging, pharmacy, and waveform data, these databases provide a wealth of valuable information that

XSL•FO
RenderX

has facilitated clinical research [7] and expanded the evidence base for clinical practice [8]. Many studies have demonstrated the potential of leveraging ICU big data for applications such as risk stratification, predictive models, treatment recommendations, and cohort phenotyping [9-12].

However, there are significant barriers to translating big data resources into clinical insights and decision support for frontline critical care teams. The complexity of ICU data requires specialized skills in data wrangling, mining, visualization, and interpretation, which most clinicians need to acquire. The gap between data science and clinical science hinders harnessing big data to improve ICU care [13,14]. Despite the promise of rich data and analytics, the adoption of actionable insights depends on accessible interfaces and informative data presentations [15].

Recent advances in medical natural language processing using artificial intelligence (AI) and large language models (LLMs) like GPTs have demonstrated the potential for intuitive human-computer interaction with health care data. Clinicians do not have to learn complex programming languages, and interfaces based on natural language and clinical logic can make big data analysis more accessible. An increasing body of research demonstrates that AI applications significantly enhance the efficiency and accuracy of disease diagnosis and treatment. Farič et al [16] developed an AI-based imaging software tool for detecting pulmonary nodules in chest computed tomography scans. Through qualitative semistructured interviews, they demonstrated the tool's usability and effectiveness as both a decision-support system and a "second reader" for clinical users. Sjoding et al [17] employed a deep convolutional neural network to identify acute respiratory distress syndrome findings on chest radiographs. The convolutional neural network demonstrated expert physician-level accuracy in acute respiratory distress syndrome radiograph detection, as validated through comprehensive quantitative assessments using both internal and external test sets. However, general domain language models still face great challenges in handling niche biomedical data and require customization and continuous iterative improvement.

Therefore, we seek to empower clinicians by simplifying database deployment and developing the intensive care unit–generative pretrained transformer (ICU-GPT). This tool aims to simplify data extraction via LLMs, liberating clinicians from complex bioinformatics methods to focus on clinical research and data analysis. With ICU-GPT, clinicians can focus on clinical research advancement and feel more capable and in control of their data analysis.

Methods

Overview

To achieve the availability and visualization of critical care–related databases and simplify the process of data extraction, we developed this platform in 2 steps. Step 1 was database deployment based on Docker container technology through the web-based client rather than by installing other applications. Step 2 was the development of ICU-GPT based on LLMs to generate Structured Query Language (SQL) queries for data extraction after request input.

Technologies of the Database Deployment and Visualization

Docker is an open-source platform that, by utilizing containerization technology, enables users to package the applications together with all their dependencies into an isolated container to achieve portability, consistency, and high segregation [18]. Database deployment involves the installation and configuration of health care databases onto PostgreSQL. This process ensures proper data storage and operational functionality. Based on Docker technology and customized PostgreSQL database initialization scripts [19], we aimed for a cross-platform automated deployment of critical care–related databases on different operating systems.

Database visualization leverages business intelligence tools to graphically represent the structure, content, and relationships within a database. This approach not only facilitates simple plotting but also provides a comprehensive and intuitive understanding of the database's table structure and overall architecture. We provide 2 web-based clients with business intelligence tools to achieve database visualization: Metabase and Superset. Metabase and Superset are open-source data analytics and visualization tools for easy data exploration [20,21]. With simple and convenient working interfaces, they allow users to extract data from various sources without writing SQL statements, including relational databases (MySQL, PostgreSQL, SQL Server, etc) and NoSQL databases. They also enable users to add plugins and visualization components to meet specific requests with high extensibility and customizability.

Technologies of ICU-GPT

With the appearance of the OpenAI GPT-3.5 in 2023, we decided to use LLMs to participate in the SQL query generation process [22]. An LLM is a natural language processing tool driven by AI technology and has recently emerged as a powerful tool across many areas of biomedicine. It can generate answers based on patterns observed during the pretraining stage, summarize large amounts of text, generate high-quality text from a short description, create code that can help support data analysis, produce images based on a verbal description, and much more.

ICU-GPT does not develop new LLM models but utilizes and is compatible with all OpenAI application programming interface (API) models. We chose OpenAI API-compatible models for ICU-GPT development for several reasons. First, our research team is more familiar with OpenAI. There is also a large number of models compatible with the OpenAI API, including GPT-3.5, GPT-4o, and GPT-4o mini, offering wide applications and cost-effectiveness. Users can select the appropriate OpenAI API model based on their specific requirements. Moreover, OpenAI encompasses knowledge bases from the MIMIC databases, which other models lack, including *International Classification of Diseases* (*ICD*) codes and itemid data.

XSL•FO
RenderX

Using the BIRD and Spider, 2 extensive cross-domain datasets designed to evaluate the impact of comprehensive database content on text-to-SQL parsing, we conducted a comparative analysis of OpenAI API models with other models [23,24]. The OpenAI API models demonstrated consistently high performance in execution accuracy and reward-based valid efficiency within the BIRD dataset [25]. Furthermore, these models exhibited stable and superior performance in execution with values within the Spider dataset [26]. Although reports suggest that certain models may surpass OpenAI's performance, we were unable to include them in our comparison due to limitations in accessibility [27-30]. Moreover, due to the absence of a benchmark dataset specifically tailored for critical care–related databases, it remains challenging to directly compare ICU-GPT's performance with other models on such databases.

Ollama is a lightweight framework with high extensibility for building and running LLMs on local and cloud environments [31]. It provides an API for model creation, execution, and management as well as a prebuilt model library. It is compatible with the OpenAI API for dialogue creation. The development of ICU-GPT also involved 4 technologies: LangChain, Microsoft AutoGen, Pandas, and Gradio.

LangChain is an open-source Python library that provides the modules and tools to build AI applications based on LLMs [32]. It can easily integrate with LLMs to achieve text generation, question-answering, and translation. The LangChain SQL database object was adopted and adjusted in our platform to support databases with multiple schemas, such as MIMIC and eICU-CRD.

Microsoft AutoGen is a framework that can be customized and conversed with, facilitating the development of LLM applications and seamlessly allowing for human participation [33]. Userproxy is a specialized agent within Microsoft AutoGen that receives users' requests and generates appropriate prompts. GroupChat comprises 2 agents and Userproxy, working in tandem to facilitate the contemplation, execution, and refinement of users' requests.

Pandas is a powerful Python-based library. It could provide accessible data structures to make data cleaning, transformation, and analysis more convenient [34]. Current data extraction functions are developed based on Pandas to achieve data processing.

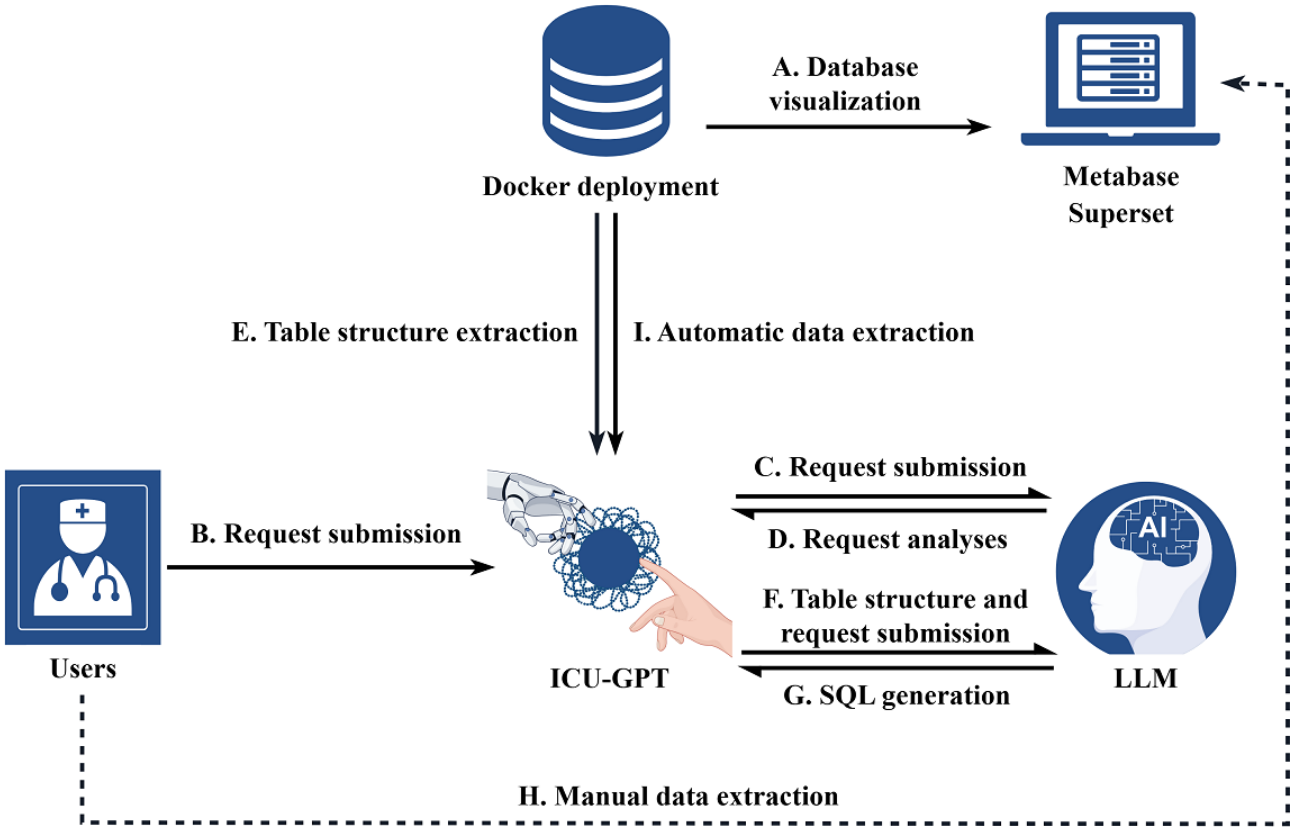
Gradio is an open-source Python library. It enables developers to transform machine learning models and various functions into shareable web applications, facilitating a quick and easy showcasing of their work through intuitive and accessible interfaces [35].

Results

We summarized the workflow of database deployment, visualization, SQL generation, and data extraction in Figure 1.

XSL•FO
RenderX

Figure 1. The procedures for the platform construction. The platform construction workflow encompasses several key components: database deployment based on Docker container technology; visualization powered by Metabase and Superset (A); SQL generation involving multiple rounds of interaction between users, LLMs, and ICU-GPT, including request submission, analysis, table structure extraction, and SQL generation (B to G); and data extraction (H and I). (A) Critical care–related database visualization based on Metabase and Superset. (B) Users send data extraction requests to ICU-GPT. (C) ICU-GPT sends requests to the LLM. (D) The LLM splits and analyzes the requests and sends them back to ICU-GPT. (E) ICU-GPT extracts table structure information from databases. (F) ICU-GPT sends requests and table structure information to the LLM. (G) The LLM generates SQL queries and sends them to ICU-GPT. (H) Users can choose to manually verify the SQL queries in Metabase and Superset. (I) ICU-GPT runs the SQL automatically for data extraction. ICU-GPT: intensive care unit–generative pretrained transformer; LLM: large language model; SQL: Structured Query Language. Figure created using Figdraw.



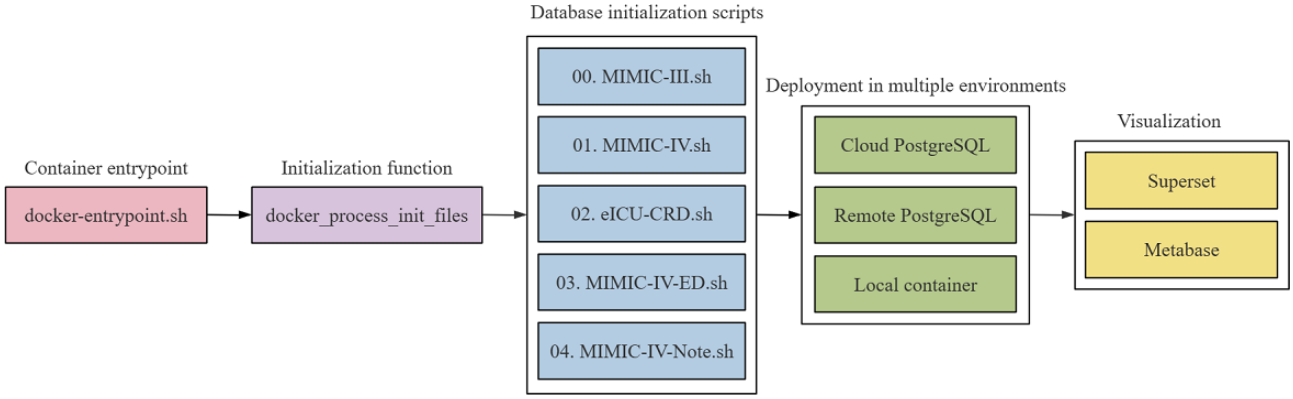
Database Deployment and Visualization

We adopted Docker technology to achieve the simplicity and flexibility of the cross-platform automated deployment of critical care–related databases. Functions of docker_process_init_files in docker-entrypoint.sh possess the mechanism of scanning shell files automatically in specific directories during the initial PostgreSQL container startup. The corresponding database initialization scripts are placed in the scanning path. Based on the mechanism, we named the files according to specific numbers to ensure the initialization process ran in the intended order and initialized the databases accordingly.

Our deployment platform supports several public critical care–related databases through PostgreSQL database initialization scripts, including MIMIC-III, MIMIC-IV, MIMIC-IV-ED (Medical Information Mart for Intensive Care IV – Emergency Department), MIMIC-IV-Note, eICU-CRD, etc. Clinicians can select the corresponding database initialization scripts or combine multiple scripts according to their specific requests. This design also allows clinicians to initialize the database with multiple phases in local, cloud, or remote environments and support database upgrades with great flexibility. Through 2 business intelligence solutions, Metabase and Superset, data querying, extraction, and charting can be easily performed by the web-based client without the installation of any other applications (Figure 2).

XSL•FO
RenderX

Figure 2. Deployment and visualization of critical care–related databases. eICU-CRD: Electronic Intensive Care Unit Collaborative Research Database; MIMIC: Medical Information Mart for Intensive Care; MIMIC-IV-ED: Medical Information Mart for Intensive Care IV – Emergency Department.



SQL Query Generation and Data Extraction

We developed ICU-GPT to accurately assist in SQL query writing and provide a more intelligent and efficient approach to simplify data extraction.

Extensive research was conducted on SQL query generation. We found that most SQL query generation tools were only practical for tables under a single schema or merely supported a single table. The handling of databases with multiple schemas, such as MIMIC, was found to be poor. By thoroughly studying the source code of table information retrieval based on the LangChain SQL database object, we successfully overcame this deficiency and achieved multischema support.

Given the massive number of MIMIC tables, the actual tokens used to generate prompts exceed the upper limit of 16,000 tokens in OpenAI GPT-3.5. To address this issue, the table selection function was introduced to allow clinicians to generate SQL queries within a specific table range. This innovation not only solved the problem of the token limit but further improved the accuracy of SQL query generation. On the basis of this innovation, our platform is now highly flexible and available for more complex database structures.

Two agents and a Userproxy were established as a GroupChat using Microsoft AutoGen. One agent serves as the SQL engineer, responsible for SQL generation, while the other agent acts as the SQL expert, verifying and optimizing the SQL generated by the SQL engineer. A manager was also created to supervise the GroupChat and facilitate information interaction and agent selection within the group.

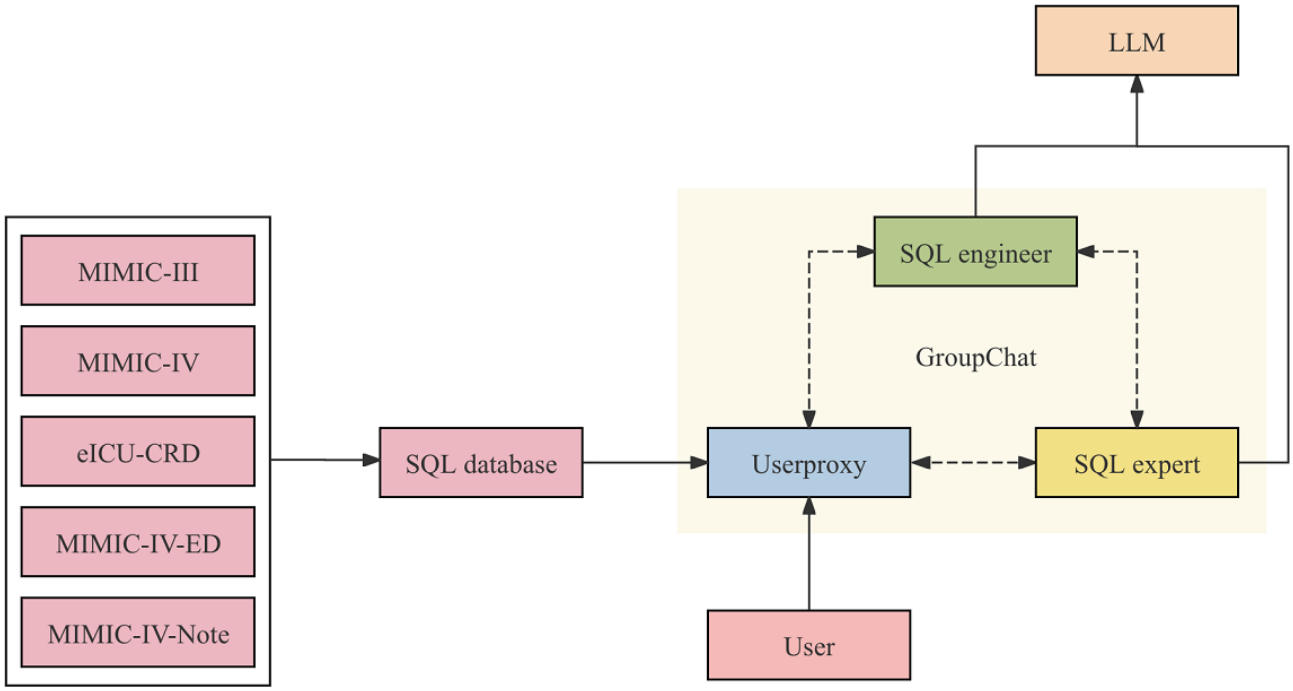
The Userproxy generates prompts based on clinicians' requests and tables specified by users, then sends them to the manager. The manager transmits these prompts to agents and selects an appropriate agent to process the prompt using a relevant algorithm. This selected agent then sends the prompts to the LLM. The LLM generates SQL based on prompts and requests and then sends it back to the manager. The manager repeats this process, sending messages to agents and selecting the appropriate agent using the algorithm. The LLM receives prompts from the selected agent and interacts with the requests. The SQL expert evaluates the performance and accuracy of the generated SQL. If the SQL expert determines that the SQL accuracy is suboptimal, an iterative dialogue process is initiated to refine and improve the SQL as much as possible.

As AI cannot fully replace human intelligence, there are limitations when users input prompts based on their research objectives. This is particularly evident when the entered keywords are not comprehensive, synonyms or similar prompts are used, or even when typos occur. In such cases, ICU-GPT may struggle to fully comprehend the user's intent, potentially leading to incorrect or incomplete responses. To address this, SQL is not automatically executed after generation. Instead, users are given the opportunity to review and inspect the generated SQL themselves. If the results are unsatisfactory, users can further refine and optimize their prompts. This approach fosters a dynamic human-AI collaboration, maximizing SQL accuracy and user satisfaction (Figure 3) [36,37].

The code of the platform development is available online [38]. We warmly welcome and greatly appreciate any user feedback or new ideas, which can be submitted to us via GitHub. We will update ICU-GPT versions when the MIMIC and eICU-CRD databases are updated or when improved models become available. Some examples of how to achieve database deployment and SQL generation based on Python are presented in Multimedia Appendix 1.

XSL•FO
RenderX

Figure 3. SQL query generation process. The GroupChat consists of the Userproxy, the SQL engineer, and the SQL expert. The manager is created to facilitate communication and information synchronization within the group. The SQL engineer is responsible for SQL generation and interaction with the LLM while the SQL expert is responsible for SQL optimization. The Userproxy generates prompts based on clinicians' requests and user-specified tables. The manager then selects appropriate agents to process these prompts using the LLM. The LLM generates SQL queries, which are subsequently evaluated by the SQL expert. If necessary, an iterative dialogue ensues to refine the SQL for optimal accuracy and effectiveness. eICU-CRD: Electronic Intensive Care Unit Collaborative Research Database; LLM: large language model; MIMIC: Medical Information Mart for Intensive Care; MIMIC-IV-ED: Medical Information Mart for Intensive Care IV – Emergency Department; SQL: Structured Query Language.



User Interface of ICU-GPT

We developed a front-end user interface using Gradio and ICU-GPT to simplify the SQL generation process. Users can download our prebuilt Docker mirroring in the Dockerfile and follow the instructions to achieve code-free SQL generation on the web-based client [39]. First, users select a database: MIMIC-III, MIMIC-IV, MIMIC-CareVue, or eICU-CRD (Figure 4). The platform displays all table names under all schemas of the selected database. Users select the corresponding tables based on their requests (Figure 5). Users then input requests in the "Prompt" section and press "Submit" (Figure 6). Our platform supports prompts both in Chinese and English. Finally, the SQL bot outputs the SQL queries (Figure 7).

XSL•FO
RenderX

Figure 4. Users select databases on the ICU-GPT platform. ICU-GPT: intensive care unit–generative pretrained transformer.

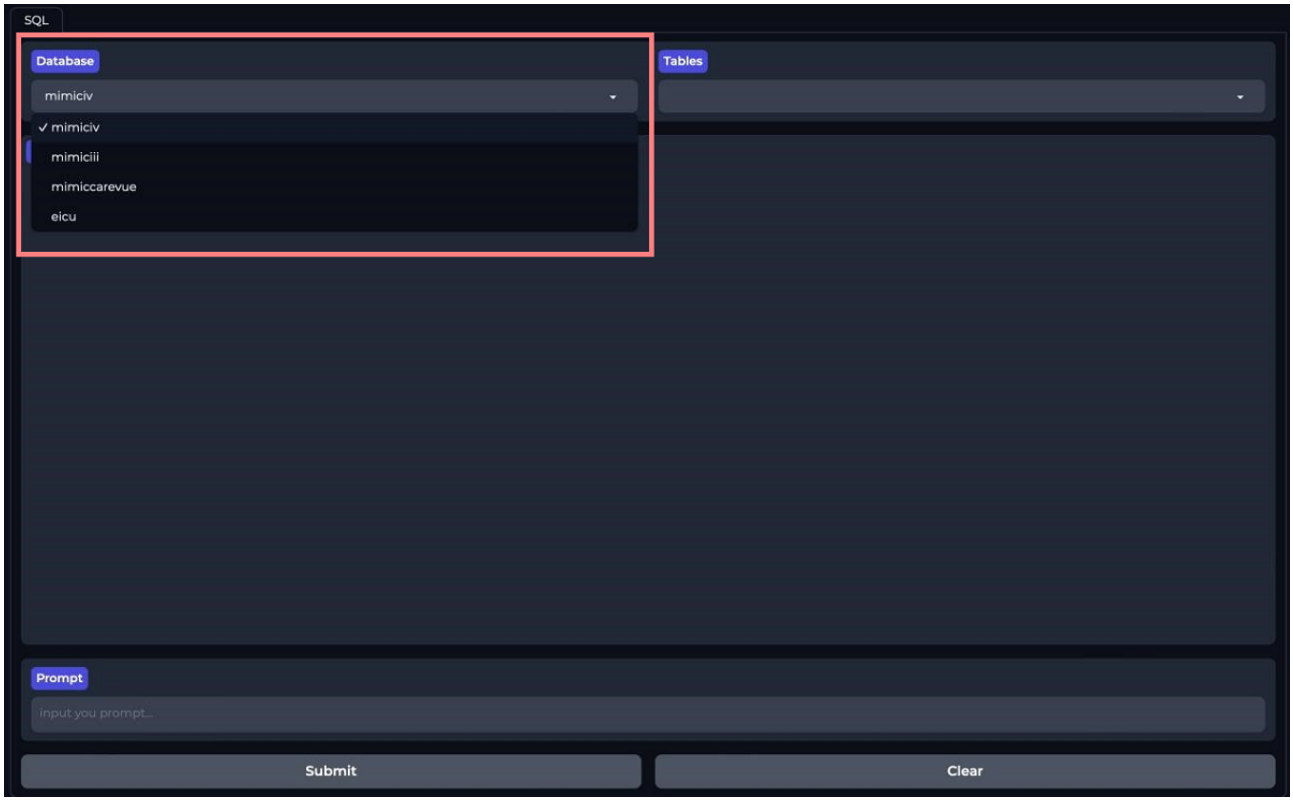
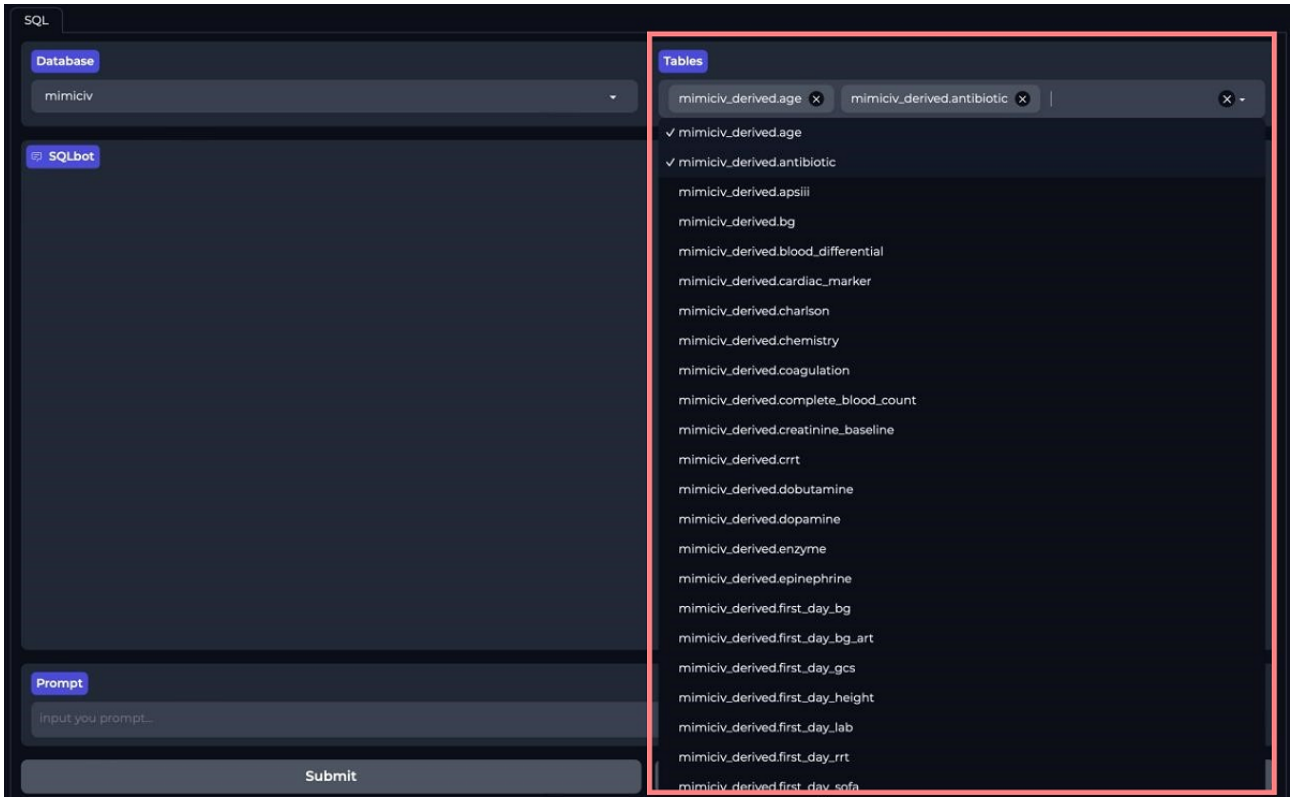


Figure 5. Users select tables on the ICU-GPT platform. ICU-GPT: intensive care unit–generative pretrained transformer.



XSL•FO
RenderX

Figure 6. Users input and submit requests on the ICU-GPT platform. ICU-GPT: intensive care unit–generative pretrained transformer.

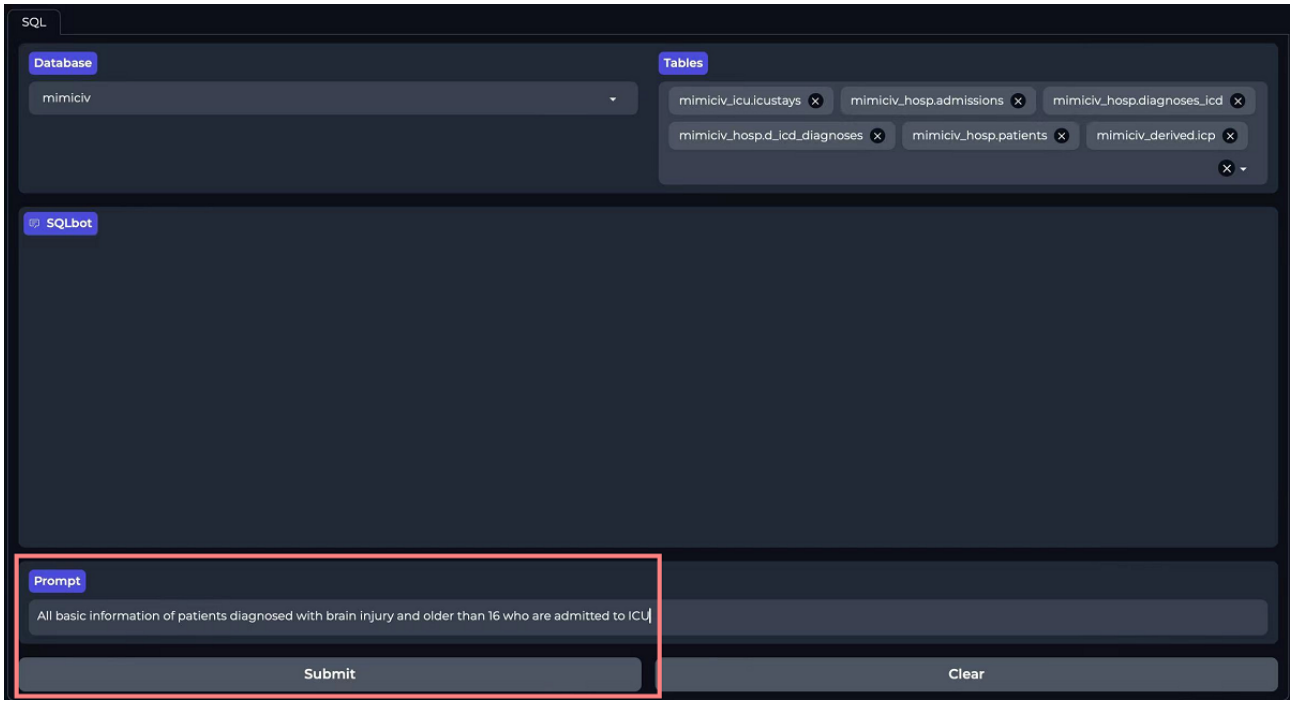
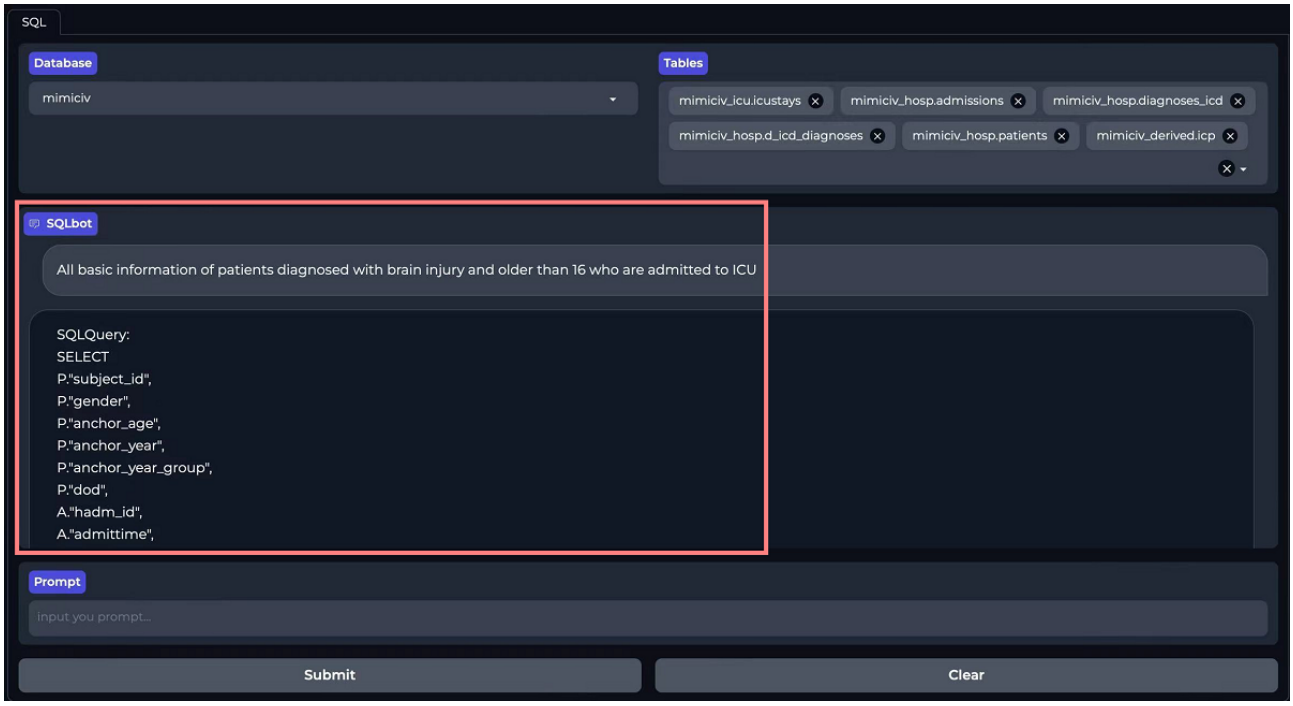


Figure 7. SQL output on the ICU-GPT platform. ICU-GPT: intensive care unit–generative pretrained transformer; SQL: Structured Query Language.



Discussion

Principal Results

In order to conduct the critical care–related database mining as efficiently and thoroughly as possible, we developed a platform in two steps: (1) we first implemented critical care–related database deployment by applying Docker container technology with 2 visualization tools, Metabase and Superset; (2) ICU-GPT was then developed based on LLMs to achieve SQL query generation and data extraction. By fully utilizing the advantages of open-source technology and being highly replicable and scalable, this platform provides great convenience for clinicians.

The critical care–related public databases cover a large sample size with various aspects during hospitalization, including demographic, physiologic, laboratory measurements, diagnoses, and medication administration data, which represents a certain degree of universality. While bringing tremendous clinical value, it is accompanied by the increasing complexity of database size and table structures. Even professional database administrators find it challenging to explore the table structures. Much time and effort would be spent on clinicians understanding the table

XSL•FO
RenderX

structure and performing data extraction. Therefore, we simplified the complex and time-consuming process into 2 steps.

With Docker container technology, we first provided an efficient and reliable deployment solution to support the widespread application of critical care–related databases. With high repeatability and consistency, the automated deployment solution provides a professional and convenient database management and visualization tool for clinicians to arrange massive amounts of data.

After database deployment, we aimed to simplify the data extraction process. The Python peewee Object Relational Mapper library was considered for analyzing the database table structures automatically, binding them to peewee objects, and encapsulating the corresponding data extraction functions [40]. After multiple tests, although this approach could save the learning cost of SQL and database structures, programming foundation and data analysis experience in personalized extraction and data processing were still required. Despite extensive consideration of potential solutions for this problem, we could not achieve satisfactory outcomes, which led to a stagnation of the development process.

LLMs have recently emerged as powerful tools across many areas of biomedicine. As mentioned, they can rapidly summarize large amounts of text, generate high-quality text from a short description, create code that can help support data analysis, produce images based on a verbal description, and much more. Therefore, based on LLMs, we integrated LangChain and Microsoft AutoGen to develop the ICU-GPT. It not only overcame the token limit of GPT and supported multischema data, but it also achieved the seamless integration of SQL query generation and data extraction.

ICU-GPT empowers users with clinical expertise without data extraction proficiency to extract information from professional databases, significantly reducing the time spent on self-directed learning. However, quantifying the time saved and the efficiency gains from this learning process is complex, making it difficult to compare pre- and postimplementation efficiency improvements.

We agree that a comprehensive evaluation is crucial to demonstrate the system's effectiveness and reliability. While this study focuses on design and implementation, we are actively implementing a thorough evaluation of ICU-GPT's performance metrics. These include SQL query accuracy, system speed, user satisfaction, and the handling of large-scale datasets.

Limitations and Implications

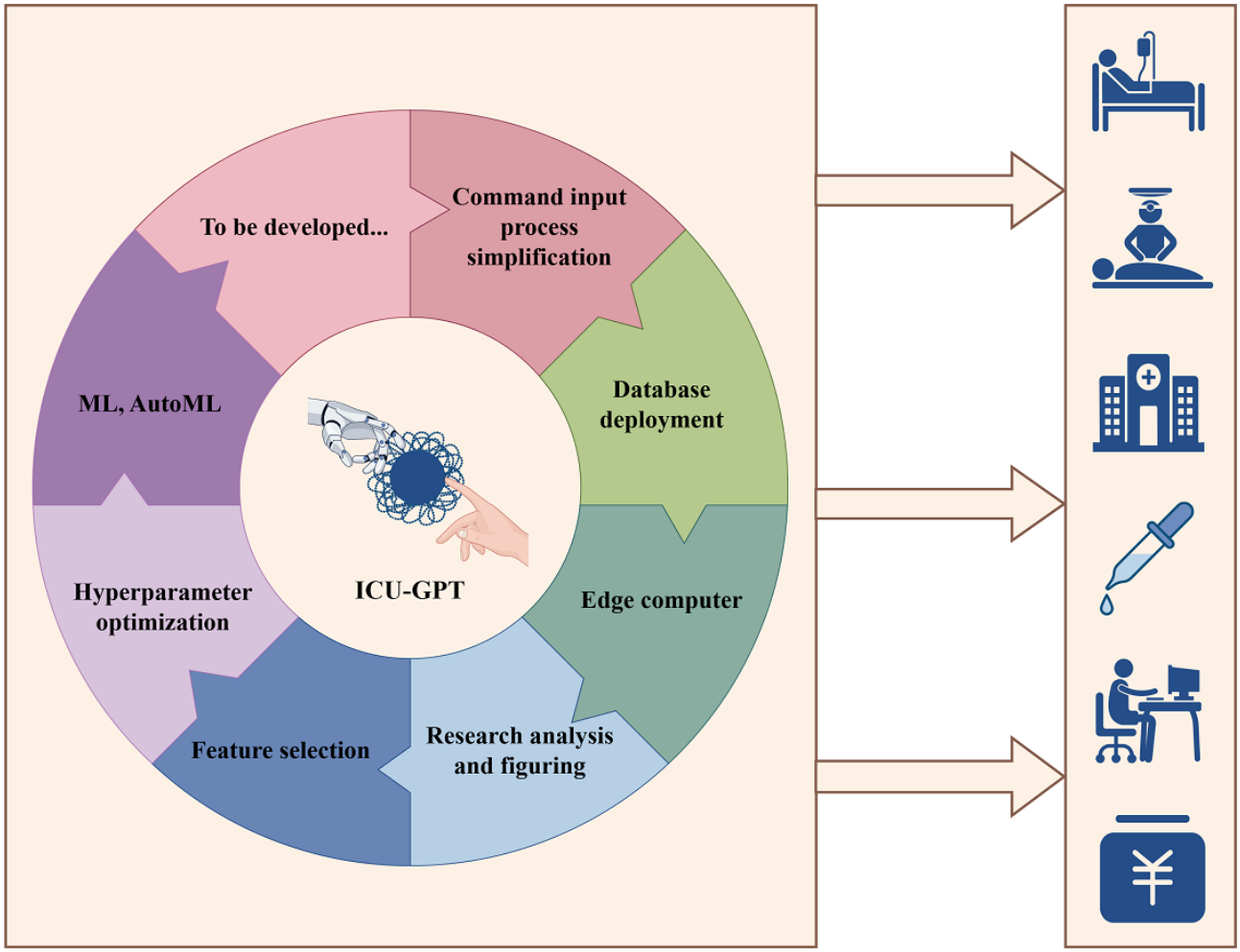
Our study has several limitations. First, our platform only involved MIMIC-III, MIMIC-IV, and eICU-CRD to demonstrate the methodological feasibility and clinical applicability of ICU-GPT in database deployment and data extraction in critical care–related databases. We will expand the research achievements to other databases and enrich the prompt templates of ICU-GPT, such as the Amsterdam UMCdb and high time–resolution intensive care unit dataset (HiRID) [6,41]. Issues of data security and ethical procedures require further improvement. The MIMIC and eICU-CRD databases were deidentified prior to their release, replacing identifiers with random integers while preserving data integrity to maximize data privacy to the fullest extent possible. However, more private databases may be developed in the future. Special attention should be paid particularly to these databases. Adherence to health care regulations, such as the Health Insurance Portability and Accountability Act (HIPAA) in the United States or the General Data Protection Regulation (GDPR) in Europe, is crucial. Second, multiple tests were conducted to verify the reliability and stability of the platform. Systematic evaluation and validation of this platform are warmly welcomed to facilitate further exploration of critical care–related databases. Third, ICU-GPT mainly focuses on structured data SQL generation and analysis. We plan to leverage function calls and the Medical Concept Annotation Toolkit (MedCAT) to achieve unstructured data extraction and analysis like clinical notes from electronic health records in the future [42]. This will enable us to link the unstructured data to biomedical models, facilitating more comprehensive database mining. We will continue to enhance ICU-GPT and strive to achieve automated data processing through Pandas. Fourth, ICU-GPT, as a system built on existing LLMs, may inherit certain biases or limitations from the underlying models. These biases are a known challenge with LLMs due to the nature of their training on large-scale datasets, which may contain imbalances or inaccuracies. To mitigate these risks, we have implemented several measures. We chose OpenAI API compatible models for ICU-GPT development for its incorporation of knowledge bases from the MIMIC database, which includes crucial *ICD* codes and itemid data that other models lack. The system is designed to be used as a human-in-the-loop tool rather than an autonomous system, with users reviewing and validating the generated outputs. We also actively monitor the system's performance in real-world applications and incorporate user feedback to iteratively improve accuracy and reliability. Moreover, periodic audits are conducted to identify and address potential biases in the system's responses. Fifth, it is indispensable to note that AI cannot replace human intelligence and judgment. Cautious inspection and correction are required for platform improvement.

Despite the aforementioned limitations, this study addresses the development of ICU-GPT to simplify critical care–related database deployment and extraction via LLMs. Further work may focus on enhancing the intelligence level of ICU-GPT, such as achieving autonomous SQL generation based on complex requests, rather than relying solely on fixed templates. It is also anticipated that researchers and developers will create advanced tools for the auxiliary diagnosis and treatment of critical illnesses, as well as sophisticated diagnostic decision support systems based on ICU-GPT.

The massive expansion of critical care–related databases and functions in ICU-GPT will offer enormous potential to uncover patterns, derive predictive models, tailor interventions, and enable precision medicine through data science [43]. This will further hold immense potential and promising broad prospects for patient care, clinical work, hospital development, academic progress, administrative management, and business improvement (Figure 8). This area of research is ripe for exploration and could lead to groundbreaking advancements in the field.

XSL•FO
RenderX

Figure 8. Expansion of ICU-GPT functions and its potential benefits. ICU-GPT will bring significant benefits after the expansion of its functions, enhancing patient care, clinical work, hospital development, academic progress, administrative management, and business improvement. AutoML: automated machine learning; ICU-GPT: intensive care unit–generative pretrained transformer; ML: machine learning. Figure created using Figdraw.



Conclusions

Leveraging our automated deployment platform and ICU-GPT model, clinicians can now easily visualize, extract, and organize public critical care–related datasets with greater efficiency and flexibility compared to manual methods. By reducing the time and complexity of bioinformatics analysis, our platform and customized LLM enable clinicians without programming expertise to harness large ICU databases for clinical research advancements. The end-to-end solution from deployment to analysis makes complex data more accessible to frontline ICU staff, unlocking the potential of big data to enhance evidence-based care and outcomes for critically ill patients. Overall, this work demonstrates the promise of thoughtful human-AI collaboration in transforming critical care delivery through data-driven insights.

Data Availability

The code of the developed platform is available online [38].

Authors' Contributions

ZY, SSX, and XL designed this study. ZY, XL, NX, YC, and SW completed the coding for the database deployment. ZY, SSX, MYM, MH, SL, and YMZ completed the coding for intensive care unit–generative pretrained transformer (ICU-GPT) development. SSX, XL, and LZ drafted the manuscript. LZ and JXZ revised the manuscript. All authors read and approved the final manuscript. JXZ and LZ contribute equally as corresponding authors.

Conflicts of Interest

None declared.

XSL•FO
RenderX

Authors' Contributions

ZY, SSX, and XL designed this study. ZY, XL, NX, YC, and SW completed the coding for the database deployment. ZY, SSX, MYM, MH, SL, and YMZ completed the coding for intensive care unit–generative pretrained transformer (ICU-GPT) development. SSX, XL, and LZ drafted the manuscript. LZ and JXZ revised the manuscript. All authors read and approved the final manuscript. JXZ and LZ contribute equally as corresponding authors.

Multimedia Appendix 1
Case demonstration of the platform applicability based on Python.
[DOCX File, 49 KB - medinform_v13i1e63216_app1.docx]

References

1. Johnson AEW, Pollard TJ, Shen L, et al. MIMIC-III, a freely accessible critical care database. Sci Data 2016 May 24;3:160035. [doi: 10.1038/sdata.2016.35] [Medline: 27219127]
2. Johnson AEW, Bulgarelli L, Shen L, et al. Author correction: MIMIC-IV, a freely accessible electronic health record dataset. Sci Data 2023 Jan 16;10(1):31. [doi: 10.1038/s41597-023-01945-2] [Medline: 36646711]
3. Johnson A, Bulgarelli L, Pollard T, Horng S, Celi LA, Mark R. MIMIC-IV (version 2.2). PhysioNet 2023. [doi: 10.13026/6mm1-ek67]
4. Pollard TJ, Johnson AEW, Raffa JD, Celi LA, Mark RG, Badawi O. The eICU Collaborative Research Database, a freely available multi-center database for critical care research. Sci Data 2018 Sep 11;5:180178. [doi: 10.1038/sdata.2018.178] [Medline: 30204154]
5. O'Halloran HM, Kwong K, Veldhoen RA, Maslove DM. Characterizing the patients, hospitals, and data quality of the eICU Collaborative Research Database. Crit Care Med 2020 Dec;48(12):1737-1743. [doi: 10.1097/CCM.0000000000004633] [Medline: 33044284]
6. Thoral PJ, Peppink JM, Driessen RH, et al. Sharing ICU patient data responsibly under the Society of Critical Care Medicine/European Society of Intensive Care Medicine Joint Data Science Collaboration: the Amsterdam University Medical Centers Database (AmsterdamUMCdb) example. Crit Care Med 2021 Jun 1;49(6):e563-e577. [doi: 10.1097/CCM.0000000000004916] [Medline: 33625129]
7. Rahman A, Chang Y, Dong J, et al. Early prediction of hemodynamic interventions in the intensive care unit using machine learning. Crit Care 2021 Nov 14;25(1):388. [doi: 10.1186/s13054-021-03808-x] [Medline: 34775971]
8. Chen H, Zhu Z, Zhao C, et al. Central venous pressure measurement is associated with improved outcomes in septic patients: an analysis of the MIMIC-III database. Crit Care 2020 Jul 14;24(1):433. [doi: 10.1186/s13054-020-03109-9] [Medline: 32665010]
9. Desautels T, Calvert J, Hoffman J, et al. Prediction of sepsis in the intensive care unit with minimal electronic health record data: a machine learning approach. JMIR Med Inform 2016 Sep 30;4(3):e28. [doi: 10.2196/medinform.5909] [Medline: 27694098]
10. Jeon ET, Lee HJ, Park TY, et al. Machine learning-based prediction of in-ICU mortality in pneumonia patients. Sci Rep 2023 Jul 17;13(1):11527. [doi: 10.1038/s41598-023-38765-8] [Medline: 37460837]
11. Giannini HM, Ginestra JC, Chivers C, et al. A machine learning algorithm to predict severe sepsis and septic shock: development, implementation, and impact on clinical practice. Crit Care Med 2019 Nov;47(11):1485-1492. [doi: 10.1097/CCM.0000000000003891] [Medline: 31389839]
12. Godri Pollitt KJ, Peccia J, Ko AI, et al. COVID-19 vulnerability: the potential impact of genetic susceptibility and airborne transmission. Hum Genomics 2020 May 12;14(1):17. [doi: 10.1186/s40246-020-00267-3] [Medline: 32398162]
13. Esteban A, Frutos-Vivar F, Ferguson ND, et al. Sepsis incidence and outcome: contrasting the intensive care unit with the hospital ward. Crit Care Med 2007 May;35(5):1284-1289. [doi: 10.1097/01.CCM.0000260960.94300.DE] [Medline: 17414725]
14. Fleuren LM, Klausch TLT, Zwager CL, et al. Machine learning for the prediction of sepsis: a systematic review and meta-analysis of diagnostic test accuracy. Intensive Care Med 2020 Mar;46(3):383-400. [doi: 10.1007/s00134-019-05872-y] [Medline: 31965266]
15. Sendak MP, Ratliff W, Sarro D, et al. Real-world integration of a sepsis deep learning technology into routine clinical care: implementation study. JMIR Med Inform 2020 Jul 15;8(7):e15182. [doi: 10.2196/15182] [Medline: 32673244]
16. Farič N, Hinder S, Williams R, et al. Early experiences of integrating an artificial intelligence-based diagnostic decision support system into radiology settings: a qualitative study. J Am Med Inform Assoc 2023 Dec 22;31(1):24-34. [doi: 10.1093/jamia/ocad191] [Medline: 37748456]
17. Sjoding MW, Taylor D, Motyka J, et al. Deep learning to detect acute respiratory distress syndrome on chest radiographs: a retrospective study with external validation. Lancet Digit Health 2021 Jun;3(6):e340-e348. [doi: 10.1016/S2589-7500(21)00056-X] [Medline: 33893070]
18. Docker. URL: https://docs.docker.com [accessed 2024-06-05]
19. PostgreSQL. URL: https://www.postgresql.org [accessed 2024-06-05]

XSL•FO
RenderX

20. Metabase. URL: https://www.metabase.com [accessed 2024-06-05]
21. Superset. URL: https://superset.apache.org [accessed 2024-06-05]
22. Key concepts. OpenAI. URL: https://platform.openai.com/docs/introduction [accessed 2024-06-05]
23. DAMO-convai/bird. GitHub. URL: https://github.com/AlibabaResearch/DAMO-ConvAI/tree/main/bird [accessed 2024-11-10]
24. taoyds/spider. GitHub. URL: https://github.com/taoyds/spider [accessed 2024-11-10]
25. BIRD-SQL. URL: https://bird-bench.github.io [accessed 2024-11-10]
26. Spider: Yale semantic parsing and text-to-SQL challenge. Language, Information, and Learning at Yale (LILY). URL: https://yale-lily.github.io/spider [accessed 2024-11-10]
27. Marshan A, Almutairi AN, Ioannou A, Bell D, Monaghan A, Arzoky M. MedT5SQL: a transformers-based large language model for text-to-SQL conversion in the healthcare domain. Front Big Data 2024;7:1371680. [doi: 10.3389/fdata.2024.1371680] [Medline: 38988646]
28. Qi J, Tang J, He Z, et al. RASAT: integrating relational structures into pretrained seq2seq model for text-to-SQL. arXiv. Preprint posted online on May 14, 2022. [doi: 10.48550/arXiv.2205.06983]
29. Li H, Zhang J, Li C, Chen H. RESDSQL: decoupling schema linking and skeleton parsing for text-to-SQL. arXiv. Preprint posted online on Feb 12, 2023. [doi: 10.48550/arXiv.2302.05965]
30. Wang P, Shi T, Reddy CK. Text-to-SQL generation for question answering on electronic medical records. arXiv. Preprint posted online on Jul 28, 2019. [doi: 10.48550/arXiv.1908.01839]
31. ollama/ollama. GitHub. URL: https://github.com/ollama/ollama [accessed 2024-06-05]
32. langchain-ai/langchain. GitHub. URL: https://github.com/langchain-ai/langchain [accessed 2024-06-05]
33. microsoft/autogen. GitHub. URL: https://github.com/microsoft/autogen [accessed 2024-06-05]
34. McKinney W. Data structures for statistical computing in python. Presented at: Python in Science Conference; Jun 28-30, 2010; Austin, TX, United States. [doi: 10.25080/Majora-92bf1922-00a]
35. Abid A, Abdalla A, Abid A, Khan D, Alfozan A, Zou J. Gradio: hassle-free sharing and testing of ML models in the wild. arXiv. Preprint posted online on Jun 6, 2019. [doi: 10.48550/arXiv.1906.02569]
36. Wu Q, Bansal G, Zhang J, et al. AutoGen: enabling next-gen LLM applications via multi-agent conversation. arXiv. Preprint posted online on Aug 16, 2023. [doi: 10.48550/arXiv.2308.08155]
37. Customize speaker selection. AutoGen. URL: https://microsoft.github.io/autogen/docs/topics/groupchat/customized_speaker_selection [accessed 2024-06-05]
38. ICU-GPT. GitHub. URL: https://github.com/ICU-GPT/icu-gpt [accessed 2024-06-05]
39. Dockerfile of ICU-GPT. GitHub. URL: http://github.com/ICU-GPT/icu-gpt/blob/main/icugpt/docker/Dockerfile [accessed 2024-06-05]
40. peewee. URL: http://docs.peewee-orm.com [accessed 2024-06-05]
41. HiRID, a high time-resolution ICU dataset. PhysioNet. URL: https://physionet.org/content/hirid/1.0 [accessed 2024-06-05]
42. Kraljevic Z, Searle T, Shek A, et al. Multi-domain clinical natural language processing with MedCAT: the Medical Concept Annotation Toolkit. Artif Intell Med 2021 Jul;117:102083. [doi: 10.1016/j.artmed.2021.102083] [Medline: 34127232]
43. Komorowski M, Celi LA, Badawi O, Gordon AC, Faisal AA. The Artificial Intelligence Clinician learns optimal treatment strategies for sepsis in intensive care. Nat Med 2018 Nov;24(11):1716-1720. [doi: 10.1038/s41591-018-0213-5] [Medline: 30349085]

Abbreviations

AI: artificial intelligence
Amsterdam UMCdb: Amsterdam University Medical Center Database
API: application programming interface
eICU-CRD: Electronic Intensive Care Unit Collaborative Research Database
GDPR: General Data Protection Regulation
HIPAA: Health Insurance Portability and Accountability Act
HiRID: high time–resolution intensive care unit dataset
***ICD*:** *International Classification of Diseases*
ICU: intensive care unit
ICU-GPT: intensive care unit–generative pretrained transformer
LLM: large language model
MedCAT : Medical Concept Annotation Toolkit
MIMIC: Medical Information Mart for Intensive Care
MIMIC-IV-ED: Medical Information Mart for Intensive Care IV – Emergency Department
ML: machine learning
SQL: Structured Query Language

XSL•FO
RenderX

Edited by J Klann; submitted 13.06.24; peer-reviewed by A Marshan, J Valverde-Rebaza; revised version received 30.11.24; accepted 18.12.24; published 12.03.25.

Please cite as:
Yang Z, Xu SS, Liu X, Xu N, Chen Y, Wang S, Miao MY, Hou M, Liu S, Zhou YM, Zhou JX, Zhang L
Large Language Model–Based Critical Care Big Data Deployment and Extraction: Descriptive Analysis
JMIR Med Inform 2025;13:e63216
URL: https://medinform.jmir.org/2025/1/e63216
doi:10.2196/63216

© Zhongbao Yang, Shan-Shan Xu, Xiaozhu Liu, Ningyuan Xu, Yuqing Chen, Shuya Wang, Ming-Yue Miao, Mengxue Hou, Shuai Liu, Yi-Min Zhou, Jian-Xin Zhou, Linlin Zhang. Originally published in JMIR Medical Informatics (https://medinform.jmir.org), 12.3.2025. This is an open-access article distributed under the terms of the Creative Commons Attribution License (https://creativecommons.org/licenses/by/4.0/), which permits unrestricted use, distribution, and reproduction in any medium, provided the original work, first published in JMIR Medical Informatics, is properly cited. The complete bibliographic information, a link to the original publication on https://medinform.jmir.org/, as well as this copyright and license information must be included.

XSL•FO
RenderX

Original Paper

Comparative Analysis of Outcomes of Influenza and COVID-19 Admissions Among Children With Asthma: A Nationwide Retrospective Cohort Study Using the US National Readmissions Database

Ying-Chen Chen[1,2]; Chia-Pi Cheng[3]; Po-Cheng Chen[4]; Jinn-Li Wang[5,6]; Chia-Chen Wu[7,8]; Ying-Chun Lu[6,9,10,11]

[1]Department of Pediatrics, Tri-Service General Hospital, National Defense Medical University, Taipei, Taiwan

[2]Division of Rheumatology/Immunology/Allergy, Department of Internal Medicine, Tri-Service General Hospital, National Defense Medical University, Taipei, Taiwan

[3]Department and Graduate institute of Biology and Anatomy, National Defense Medical Center, Taipei, Taiwan

[4]Division of Pediatric Rehabilitation, Department of Physical Medicine and Rehabilitation, Wo On Rehabilitation Clinic, New Taipei, Taiwan

[5]Division of Hematology and Oncology, Department of Pediatrics, Wan Fang Hospital, Taipei Medical University, Taipei, Taiwan

[6]Department of Pediatrics, School of Medicine, College of Medicine, Taipei Medical University, Taipei, Taiwan

[7]Department of Surgery, Tri-Service General Hospital Keelung Branch, National Defense Medical Center, Keelung, Taiwan

[8]Division of Thoracic Surgery, Department of Surgery, Tri-Service General Hospital, National Defense Medical Center, Taipei, Taiwan

[9]Division of Neonatology, Department of Pediatrics, Wan Fang Hospital, Taipei Medical University, Taipei, Taiwan

[10]Division of Pediatric Critical Care Medicine, Department of Pediatrics, Wan Fang Hospital, Taipei Medical University, Taipei, Taiwan

[11]Division of Pediatric Emergency Medicine, Wan Fang Hospital, Taipei Medical University, Taipei, Taiwan

Corresponding Author:
Ying-Chun Lu
Division of Neonatology, Department of Pediatrics
Wan Fang Hospital, Taipei Medical University
7th Floor, No. 11, Alley 70, Lane 113, Donghu Road, Neihu District
Taipei
Taiwan
Phone: 886 963252183
Email: alchune@gmail.com

Abstract

Background: Asthma is a common chronic respiratory disease with increasing prevalence among children over the past few decades. It can cause significant respiratory symptoms and acute exacerbations, often requiring emergency care or hospitalization. Moreover, exposure to respiratory viral infections, such as COVID-19 and influenza, can trigger severe complications in children with asthma. Despite these concerns, few studies have directly compared the in-hospital outcomes of children with asthma experiencing these infections.

Objective: This study aimed to compare the in-hospital outcomes of these infections in children with asthma from a population-based perspective.

Methods: We conducted a population-based retrospective cohort study using data from the 2020 US Nationwide Readmissions Database. Children aged 1 to 19 years with asthma who were admitted for COVID-19 or influenza were eligible for inclusion. Outcomes evaluated included in-hospital mortality, major complications, and 90-day readmission rate. Survey-weighted logistic regression models were used to compare clinical outcomes between the two infection groups, adjusting for demographic and clinical characteristics.

Results: A total of 1472 hospitalized children with asthma were included, of whom 405 (27.5%) were admitted for COVID-19 and 1067 (72.5%) for influenza. After adjustment, the multivariate analysis revealed that children admitted for COVID-19 had a significantly higher risk of sepsis or shock (adjusted odds ratio [aOR] 4.30, 95% CI 1.79-10.32) but a lower risk of bacterial or fungal pneumonia (aOR 0.37, 95% CI 0.23-0.61) compared with those admitted for influenza. Stratified analyses by age revealed that among children aged 1 to 5 years, the risk of 90-day readmission was significantly higher for those with COVID-19 than for

XSL•FO
RenderX

those with influenza (aOR 3.02, 95% CI 1.09-8.35). No significant difference in in-hospital mortality was detected between the two infection groups in either the multivariable model or any of the age-stratified analyses.

Conclusions: US children with asthma hospitalized for COVID-19 had higher risks of sepsis or shock compared to those admitted for influenza. In contrast, children admitted for influenza had a higher risk for bacterial or fungal pneumonia. After stratifying by age, children aged 1 to 5 years with COVID-19 had a significantly higher risk of 90-day readmission than those with influenza. Our findings suggest that different clinical approaches may be needed for children with asthma, depending on infection etiology and patient age.

(JMIR Med Inform 2025;13:e73047) doi:10.2196/73047

KEYWORDS

asthma; children; influenza; COVID-19; National Readmission Database; NRD

Introduction

Background

Asthma prevalence has risen steadily worldwide over the past 4 decades [1]. The incidence of childhood asthma has markedly increased over the past 40 years. Despite therapeutic advances, underdiagnosis and undertreatment remain common in children with asthma [2,3].

Respiratory viral infections such as COVID-19 and influenza often precipitate severe asthma exacerbations in children. Recent research indicates that asthma increases the risk of hospitalization in children with COVID-19 [4,5]. In addition, individuals with uncontrolled asthma are more likely to experience severe illness from COVID-19 that requires hospitalization [6]. Similarly, influenza can also lead to a worsening of asthma symptoms and may require hospitalization [7].

Although children with asthma who contract COVID-19 or influenza often experience more severe disease than their peers without asthma, there is a lack of studies examining the in-hospital outcomes of children with asthma who develop COVID-19 or influenza. Lee et al [8] analyzed the Korean Childhood Asthma Study cohort and showed that health care use among children with asthma significantly decreased during the COVID-19 pandemic, suggesting that only more severe cases reached hospital care. Furthermore, longitudinal work by Yoon et al [9] identified distinct phenotypic trajectories of childhood asthma with allergic comorbidities, underscoring the importance of age-specific risk estimates. However, no national study has directly compared the in-hospital outcomes of children with asthma admitted with COVID-19 versus those admitted with seasonal influenza.

Objectives

The purpose of this study was to compare in-hospital mortality, major complication rates, and 90-day readmission rates between children with asthma admitted for COVID-19 and those admitted for influenza using a national US database.

Methods

Data Source

The Nationwide Readmissions Database (NRD) is a database of all-payer hospital inpatient stays that can be used to generate national estimates of readmissions [10]. The NRD is a 100% sample from the Health Care Cost and Utilization Project (HCUP) State Inpatient Databases with discharge-level and hospital-level exclusions. The database contains verified patient linkage numbers that can be used to track a person across hospitals within a state while adhering to strict privacy guidelines. Researchers can identify diagnoses and procedures in the NRD using the *ICD-10-CM* (*International Classification of Diseases, 10th Revision, Clinical Modification*) and the *ICD-10-PCS* (*International Classification of Diseases, 10th Revision, Procedure Coding System*) codes. We used deidentified patient records from hospital discharges across multiple states, which allowed researchers to track readmissions nationally. Our research team obtained access to the NRD through the HCUP central distributor as per a data use agreement. The database is not open access in the sense of being freely downloadable; however, it is accessible to researchers worldwide who complete the requisite training and agree to the terms of the HCUP.

Study Design and Population

This population-based retrospective cohort study used NRD data from the year 2020. Inclusion criteria for this study were (1) children aged 1 to 19 years; (2) first admission for COVID-19 or influenza between January 1 and September 30, 2020, identified by the relevant *ICD-10-CM* codes documented as the principal diagnosis; and (3) asthma as a secondary diagnosis. Children with missing information on the main end points, sex, and sample weights were excluded. Following the index admission, patients were considered *at risk* for hospitalization and were followed until December 31 of the admission year or until death. Detailed *ICD-10-CM* codes used are provided in Multimedia Appendix 1.

Ethical Considerations

This study is a secondary analysis and adheres to the terms of the HCUP data use agreement. Specifically, the data were acquired from the online HCUP central distributor and were anonymized and publicly available. According to 45 CFR §46.104(d)(4) of the US Common Rule, secondary research on publicly available, fully deidentified data is exempt from institutional review board (IRB) review [11]. Hence, this study was exempt from IRB approval as per our institutional guidelines. Therefore, no informed consent or further IRB approval was required.

XSL•FO
RenderX

Variables and Outcome Measures

Data collected included patient age, sex, insurance status, and household income. Asthma was defined exclusively by *ICD-10-CM* code J45, which is assigned by trained coders only when a treating clinician documents a definite diagnosis of asthma. Furthermore, data relating to hospital characteristics such as weekend admission, admission type (emergent or elective), hospital bed size, and location or teaching status were collected. Major comorbidities extracted from the medical records and included in the analysis were hypertension, diabetes mellitus, obesity or overweight, neurological diseases, Down syndrome or chromosomal anomalies, metabolic diseases, cystic fibrosis, sickle cell disease, congenital heart conditions, congenital lung conditions, autoimmune disease, and mental or physical disabilities. These are comorbidities frequently considered in hospital admissions of children.

The outcomes evaluated included in-hospital mortality and complications, including sepsis or shock, secondary bacterial or fungal pneumonia, respiratory failure or mechanical ventilation, and acute kidney injury. In addition, 90-day readmission rates were assessed.

Statistical Analysis

The NRD includes discharge-level weights, stratum variables, and cluster Hospital identifier variable in the Nationwide Readmissions Database variables, which were used to estimate discharges from community hospitals in the United States, excluding rehabilitation and long-term acute care facilities. These variables were also used to calculate SEs and produce national estimates for all analyses in this study. In SAS statistical software (SAS Institute), the survey procedure is available for the analysis of sample survey data. Descriptive statistics of patients at the time of index admission were presented as either number and weighted percentage or mean and SE, and patients were categorized into the COVID-19 or influenza group. Categorical data were examined using the PROC SURVEYFREQ (survey frequency procedure) statement, while continuous data were assessed using the PROC SURVEYREG (procedure for survey regression analysis) statement. The SURVEYFREQ procedure includes the Rao-Scott chi-square test to assess the significance between weighted proportions. The SURVEYREG procedure fits linear models for survey data and provides significance tests for the model effects. For univariate analyses, no correction was applied for multiple comparisons, as these were considered exploratory. This approach is supported by methodological literature, which suggests that adjustment for multiplicity is not always necessary in such contexts [12].

Logistic regressions were performed using the PROC SURVEYLOGISTIC (procedure for survey logistic regression analysis) statement to compare the risk of adverse outcomes between children admitted for COVID-19 or influenza, including in-hospital mortality, major complications, and 90-day readmission, adjusting for covariates with significance in the univariate analysis in a multivariable model. Data were reported as odds ratios and 95% CI. All *P* values were 2-sided, and the value of $P<.05$ was considered statistically significant. Statistical analyses were performed using SAS software (version 9.4; SAS Institute).

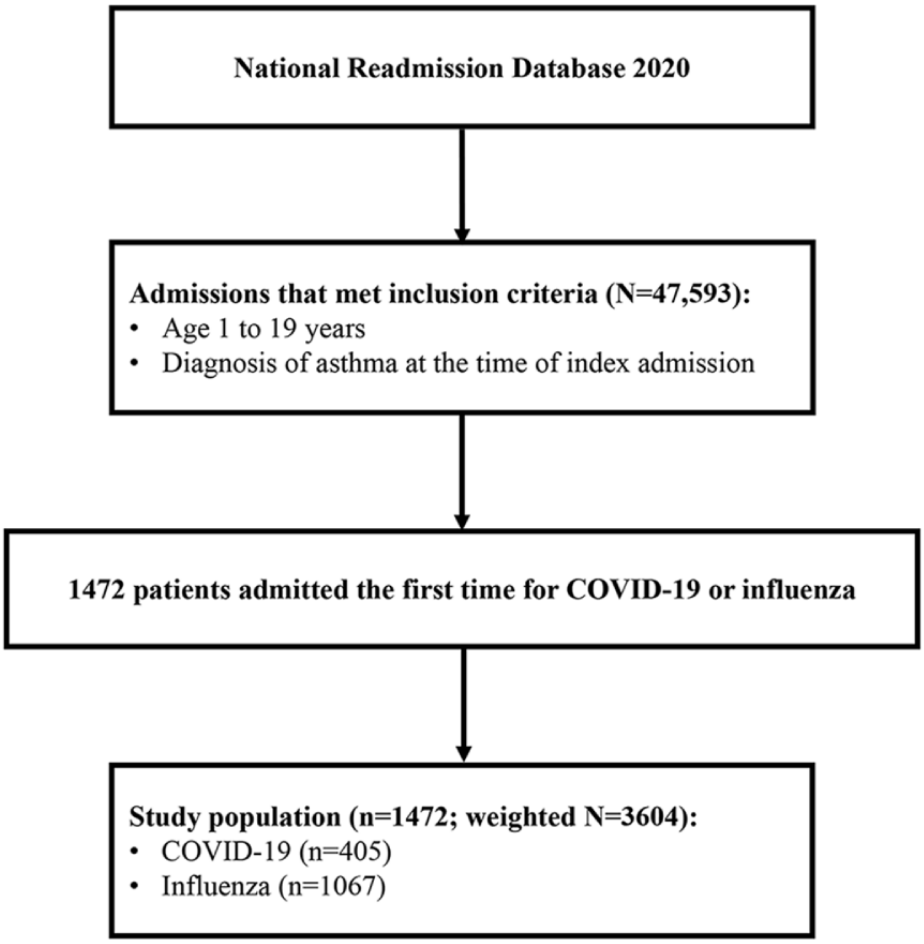
Results

Patient Selection

The selection process for the study population is illustrated in Figure 1. A total of 1472 patients aged 1 to 19 years with asthma who were admitted for the first time with COVID-19 or influenza were identified in the 2020 NRD. Of the 1472 patients, 405 (27.5%) were admitted for COVID-19 and 1067 (72.5%) for influenza. This sample represented 3604 individuals who were hospitalized in the entire United States after applying the sample weights provided by the NRD.

XSL•FO
RenderX

Figure 1. Flow diagram of patient selection for a nationwide retrospective cohort study of US children aged 1–19 years with asthma who were hospitalized for a first diagnosis of COVID-19 or seasonal influenza between Jan 1 and Dec 31, 2020, in the Nationwide Readmissions Database (NRD); final analytic sample: n=1472 (weighted N=3604).



Patient Characteristics

Patient characteristics are summarized in Table 1. The mean age of all patients was 8.5 (SD 0.2 years), and 59% (862/1472) were male individuals. Significant differences were observed in age, household income, insurance status or primary payer, hospital bed size, and location or teaching status between patients with COVID-19 and those with influenza. In addition, the proportions of patients with diabetes mellitus, hypertension, obesity or overweight, metabolic diseases, sickle cell disease, and congenital heart conditions were significantly different between patients with COVID-19 and those with influenza.

XSL•FO
RenderX

Table 1. Demographic, socioeconomic, hospital, and comorbidity characteristics of US children (aged 1-19 years) with physician-diagnosed asthma admitted for COVID-19 (n=405) or seasonal influenza (n=1067) in the 2020 Nationwide Readmissions Database.

Characteristics	Total (N=1472)	COVID-19 (n=405)	Influenza (n=1067)	*P* value
Adverse outcomes, n (%)				
In-hospital mortality	13 (0.9)	10 (2.5)	3 (0.4)	*.003* [a]
Major complications, any	313 (22.1)	94 (22.7)	219 (22)	.80
Sepsis or shock	47 (2.9)	35 (8.4)	12 (1)	*<.001*
Secondary bacterial or fungal pneumonia	202 (15.1)	28 (7.6)	174 (17.7)	*<.001*
Respiratory failure or mechanical ventilation	84 (5.6)	40 (9.1)	44 (4.3)	*<.001*
AKI[b]	52 (4)	34 (9)	18 (2.2)	*<.001*
90-day readmission rate[c]	84 (6)	27 (6.9)	57 (5.7)	.38
Demography				
Age (y), mean (SE)	8.5 (0.2)	13.3 (0.3)	6.8 (0.2)	*<.001*
1 to 5, n (%)	557 (37.9)	50 (12.5)	507 (46.9)	
6 to 10, n (%)	381 (27.1)	51 (14.1)	330 (31.7)	
11 to 15, n (%)	234 (17)	95 (26)	139 (13.8)	
16 to 19, n (%)	300 (18)	209 (47.4)	91 (7.6)	
Sex, n (%)				.27
Male	862 (59.2)	227 (56.8)	635 (60)	
Female	610 (40.8)	178 (43.2)	432 (40)	
Household income, n (%)				*.02*
Quartile 1	488 (32.2)	159 (38.7)	329 (29.9)	
Quartile 2	393 (27.2)	107 (27)	286 (27.3)	
Quartile 3	338 (24)	85 (21.3)	253 (24.9)	
Quartile 4	242 (16.6)	48 (13)	194 (17.9)	
Missing	11	6	5	
Insurance status or primary payer, n (%)				*<.001*
Medicare or Medicaid	886 (58.8)	281 (68.6)	605 (55.3)	
Private including HMO[d]	518 (36.8)	105 (26.7)	413 (40.4)	
Self-pay, no charge, or other	68 (4.4)	19 (4.7)	49 (4.3)	
Admission type, n (%)				.58
Elective	40 (2.8)	8 (2.4)	32 (2.9)	
Emergent	1431 (97.2)	397 (97.6)	1034 (97.1)	
Missing	1	0	1	
Hospital-related characteristics, n (%)				
Hospital bed number				*.03*
Small	179 (13.2)	34 (8.8)	145 (14.7)	
Medium	306 (21.8)	71 (19.3)	235 (22.6)	
Large	987 (65.1)	300 (71.9)	687 (62.7)	
Location or teaching status				*.02*
Metropolitan nonteaching	99 (7.3)	21 (4.8)	78 (8.2)	
Metropolitan teaching	1304 (88.8)	372 (92.6)	932 (87.4)	
Nonmetropolitan	69 (3.9)	12 (2.6)	57 (4.4)	

XSL•FO
RenderX

Characteristics	Total (N=1472)	COVID-19 (n=405)	Influenza (n=1067)	*P* value
Weekend admission				.41
No	1084 (73.8)	291 (72.1)	793 (74.4)	
Yes	388 (26.2)	114 (27.9)	274 (25.6)	
Comorbidities				
DM[e]	41 (2.5)	32 (6.8)	9 (1)	*<.001*
Hypertension	44 (2.7)	31 (7.1)	13 (1.2)	*<.001*
Obesity or overweight	157 (9.7)	122 (28.1)	35 (3.2)	*<.001*
Neurological diseases	138 (9.4)	44 (12)	94 (8.5)	.05
Down syndrome or chromosomal anomalies	33 (2.3)	9 (2.3)	24 (2.3)	.99
Metabolic diseases	55 (3.9)	32 (8.6)	23 (2.3)	*<.001*
Cystic fibrosis	9 (0.7)	3 (0.7)	6 (0.7)	.985
Sickle cell disease	75 (5.4)	34 (8.5)	41 (4.3)	*.003*
Congenital heart conditions	21 (1.4)	14 (3.3)	7 (0.7)	*<.001*
Autoimmune diseases	31 (2.1)	15 (3.2)	16 (1.7)	.08
Disabilities	73 (4.9)	20 (4.6)	53 (5)	.73

[a]*P* values <.05 are italicized.

[b]AKI: acute kidney injury.

[c]Data excluding patients who died in the hospital.

[d]HMO: Health Maintenance Organization.

[e]DM: diabetes mellitus.

Patients admitted for COVID-19 had higher frequencies of in-hospital mortality (2.5% vs 0.4%; *P*=.003), sepsis or shock (8.4% vs 1%; *P*<.001), respiratory failure or mechanical ventilation (9.1% vs 4.3%; *P*<.001), and acute kidney injury (9% vs 2.2%; *P*<.001) compared to those admitted for influenza. On the other hand, the proportion of patients with secondary bacterial or fungal pneumonia was significantly higher in the group admitted for influenza compared to the group admitted for COVID-19 (18% vs 8%; *P*<.001).

Comparison of Adverse Outcomes Between Children Admitted for COVID-19 and Those Admitted for Influenza

A comparison of outcomes between children admitted for COVID-19 and influenza is provided in Table 2. After adjustment in the multivariable analysis, patients admitted for COVID-19 had a significantly higher risk of sepsis or shock (adjusted odds ratio [aOR] 4.30, 95% CI 1.79-10.32; *P*=.001) but a lower risk of secondary bacterial or fungal pneumonia (aOR 0.37, 95% CI 0.23-0.61; *P*<.001) compared to those admitted for influenza (Table 2).

XSL•FO
RenderX

Table 2. Unadjusted and adjusted odds ratios (aORs) for in-hospital mortality, major complications, and 90-day readmission among US children with asthma (aged 1 to 19 years) admitted for COVID-19 versus seasonal influenza, Nationwide Readmissions Database, calendar year 2020.

Adverse outcomes	Univariate		Multivariable	
	OR[a] (95% CI)	*P* value	Adjusted OR (95% CI)	*P* value
In-hospital mortality[b]	6.15 (1.51-24.99)	*.01* [c]	2.18 (0.56-8.49)	.26
Major complications[d]	1.04 (0.76-1.42)	.79	0.90 (0.67-1.21)	.50
Sepsis or shock[e]	9.23 (4.18-20.36)	*<.001*	4.30 (1.79-10.32)	*.001*
Secondary bacterial or fungal pneumonia[f]	0.38 (0.23-0.64)	*<.001*	0.37 (0.23-0.61)	*<.001*
Respiratory failure or mechanical ventilation[g]	2.24 (1.39-3.61)	*<.001*	1.47 (0.83-2.61)	.18
Acute kidney injury[h]	4.45 (2.24-8.85)	*<.001*	1.97 (0.92-4.22)	.08
90-day readmission rate[i,j]	1.23 (0.77-1.96)	.39	0.95 (0.56-1.62)	.85

[a]OR: odds ratio.

[b]Adjusted for all variables significant in the univariate analysis: age (continuous), diabetes mellitus, neurological diseases, metabolic diseases, and disability.

[c]*P* values <.05 are italicized.

[d]Adjusted for all variables significant in the univariate analysis: insurance status or primary payer, diabetes mellitus, neurological diseases, metabolic diseases, sickle cell disease, and congenital heart conditions.

[e]Adjusted for all variables significant in the univariate analysis: age (continuous), diabetes mellitus, obesity or overweight, neurological diseases, metabolic diseases, congenital heart conditions, and disability.

[f]Adjusted for all variables significant in the univariate analysis: insurance status or primary payer, neurological diseases, and sickle cell disease.

[g]Adjusted for all variables significant in the univariate analysis: age (continuous), household income, diabetes mellitus, hypertension, obesity or overweight, neurological diseases, metabolic diseases, congenital heart condition, and disabilities.

[h]Adjusted for variables significant in the univariate analysis: diabetes mellitus, obesity or overweight, neurological diseases, Down syndrome or chromosomal anomalies, metabolic diseases, and congenital heart condition.

[i]Adjusted for all variables significant in the univariate analysis: household income, hypertension, neurological diseases, metabolic diseases, cystic fibrosis, sickle cell disease, and disabilities.

[j]Excluding patients who died in the hospital.

Comparison of Adverse Outcomes Between Children Admitted for COVID-19 and Those Admitted for Influenza, Stratified by Age

The results of the stratified analysis are shown in Table 3. Among patients aged 1 to 5 years, those admitted for COVID-19 had a significantly higher 90-day readmission rate (aOR 3.02, 95% CI 1.09-8.35; *P*=.03) and a significantly lower risk of secondary bacterial or fungal pneumonia (aOR 0.13, 95% CI 0.02-0.96; *P*=.046) compared to those admitted for influenza. In those aged 6 to 10 years, children with asthma who were admitted for COVID-19 had a significantly higher risk of sepsis or shock (aOR 6.64, 95% CI 1.23-35.91; *P*=.03). Among adolescents aged 11 to 19 years, patients admitted for COVID-19 had a significantly higher risk of sepsis or shock (aOR 4.79, 95% CI 1.79-12.84; *P*=.002) but a significantly lower risk of secondary bacterial or fungal pneumonia (aOR 0.42, 95% CI 0.24-0.73; *P*=.002; Table 3).

XSL•FO
RenderX

Table 3. Age-stratified adjusted odds ratios (aORs) for adverse outcomes among US children with asthma hospitalized for COVID-19 compared with seasonal influenza, Nationwide Readmissions Database, 2020.

Adverse outcomes	aOR (95% CI)	*P* value
Age 1 to 5 years		
In-hospital mortality[a]	N/A[b]	—[c]
Major complications[d]	0.56 (0.13-2.34)	.43
Sepsis or shock[e]	1.41 (0.14-14.14)	.77
Secondary bacterial or fungal pneumonia[f]	0.13 (0.02-0.96)	*.046* [g]
Respiratory failure or mechanical ventilation[h]	1.41 (0.23-8.77)	.71
Acute kidney injury[i]	3.55 (0.29-43.66)	.32
90-day readmission rate[j,k]	3.02 (1.09-8.35)	*.03*
Age 6 to 10 years		
In-hospital mortality[a]	2.53 (0.27-23.46)	.41
Major complications[d]	0.91 (0.39-2.10)	.82
Sepsis or shock[e]	6.64 (1.23-35.91)	*.03*
Secondary bacterial or fungal pneumonia[f]	0.42 (0.13-1.39)	.16
Respiratory failure or mechanical ventilation[h]	1.32 (0.45-3.88)	.61
Acute kidney injury[i]	2.11 (0.31-14.25)	.44
90-day readmission rate[j,k]	0.49 (0.13-1.81)	.28
Age 11 to 19 years		
In-hospital mortality[a]	6.02 (0.87-41.75)	.07
Major complications[d]	0.90 (0.58-1.38)	.62
Sepsis or shock[e]	4.79 (1.79-12.84)	*.002*
Secondary bacterial or fungal pneumonia[f]	0.42 (0.24-0.73)	*.002*
Respiratory failure or mechanical ventilation[h]	1.82 (0.61-5.42)	.28
Acute kidney injury[i]	1.56 (0.78-3.13)	.21
90-day readmission rate[j,k]	0.80 (0.37-1.74)	.57

[a]Adjusted for all variables significant in the univariate analysis (except for stratified or N/A variables): diabetes mellitus, neurological diseases, metabolic diseases, and disabilities.

[b]N/A: not applicable. No event occurred in one group.

[c]Data not applicable.

[d]Adjusted for all variables significant in the univariate analysis (except for stratified or N/A variables): insurance status or primary payer, diabetes mellitus, neurological diseases, metabolic diseases, sickle cell disease, and congenital heart conditions.

[e]Adjusted for all variables significant in the univariate analysis (except for stratified or N/A variables): diabetes mellitus, obesity or overweight, neurological diseases, metabolic diseases, congenital heart conditions, and disabilities.

[f]Adjusted for all variables significant in the univariate analysis (except for stratified or N/A variables): insurance status or primary payer, neurological diseases, and sickle cell disease.

[g]*P* values <.05 are italicized.

[h]Adjusted for all variables significant in the univariate analysis (except for stratified or N/A variables): household income, diabetes mellitus, hypertension, obesity or overweight, neurological diseases, metabolic diseases, congenital heart conditions, and disabilities.

[i]Adjusted for all variables significant in the univariate analysis (except for stratified or N/A variables): diabetes mellitus, obesity or overweight, neurological diseases, Down syndrome or chromosomal anomalies, metabolic diseases, and congenital heart conditions.

[j]Adjusted for all variables significant in the univariate analysis (except for stratified or N/A variables): household income, hypertension, neurological diseases, metabolic diseases, cystic fibrosis, sickle cell disease, and disabilities.

[k]Excluding patients who died in the hospital.

XSL•FO
RenderX

Discussion

Principal Findings

In this study, we compared the outcomes of children with asthma who were hospitalized with COVID-19 or influenza using the US NRD. Our analysis showed that children with asthma hospitalized for COVID-19 had a higher risk of sepsis or shock, whereas those hospitalized for influenza had a higher risk of secondary bacterial or fungal pneumonia. There was no significant difference in in-hospital mortality between the two groups. Furthermore, age-stratified analysis indicated that children aged 1 to 5 years with COVID-19 had a 3-fold higher risk of 90-day readmission compared to those with influenza. In adolescents (aged 11 to 19 years), the COVID-19 group faced a higher sepsis or shock risk but a lower risk of secondary bacterial or fungal pneumonia. These findings highlight the different clinical challenges in managing influenza and COVID-19 in children with asthma.

Comparison With Prior Work

Both influenza and COVID-19 are serious infections, and comorbidities such as asthma can worsen their clinical outcomes. While there have been studies comparing the outcomes of these infections in adults, there is limited research on children, especially those with asthma. Xie et al [13] found that hospitalization for COVID-19 was associated with a higher risk of death compared to that for influenza (6% for COVID-19 vs 3.7% for influenza; hazard ratio 1.16). The risk of death decreased with "with increasing numbers of COVID-19 vaccinations (*P*=.009). An earlier study comparing patients diagnosed with influenza during the 2017 to 2018 season to those diagnosed with COVID-19 between February and June 2020 found that, despite being younger and having fewer comorbidities, patients with COVID-19 had a higher risk of severe illness [14]. Dupont et al [15] found worse outcomes in adults with asthma who had COVID-19 compared to those with asthma who had influenza. However, these studies did not focus on pediatric or asthma populations.

Most studies on COVID-19 in children with asthma indicate that coexisting asthma is linked to a poorer prognosis. For example, Robbins et al [16] reported that children with asthma seen in the emergency department for COVID-19 were more likely to have severe infections compared to those without asthma. Another study of 5510 patients with asthma, including 414 patients with COVID-19, found a positive correlation between COVID-19 severity and asthma symptoms [17]. Similarly, Lara et al [18] showed that asthma significantly increased the risk of hospitalization in children with COVID-19.

While many studies report that asthma worsens COVID-19 outcomes, some studies present conflicting results. Notably, Oliveira et al [19] observed that children with asthma hospitalized for COVID-19 had a significantly lower risk of death compared to children without asthma. Similarly, Dolby et al [20] reported in a large cohort study that individuals with mild or well-controlled asthma were not at increased risk of severe COVID-19 outcomes. In line with these findings, 1 study of 107 pediatric patients with COVID-19 found that asthma and allergic diseases were not risk factors for hospitalization [21]. Yilmaz et al [22] suggested that COVID-19 may have a milder course than influenza in children (not specifically those with asthma).

Mechanisms

Both COVID-19 and influenza can exacerbate asthma symptoms, but our findings show that children with asthma admitted for COVID-19 had a higher risk of developing sepsis or shock compared to those admitted for influenza. COVID-19 is known to trigger a severe immune response or cytokine storm, leading to high systemic inflammation, rapid respiratory deterioration, and increased risk of sepsis and shock [23]. The SARS-CoV-2, compared to the influenza virus, can induce deeper immune dysregulation [24], which may amplify the underlying airway inflammation in asthma. Consistent with this heightened virulence, Brehm et al [14] observed a markedly higher mortality in immunocompromised adults with COVID-19 than with influenza (33% vs 11.6%; *P*=.01).

Conversely, we found that children with asthma admitted for influenza had a higher risk of secondary bacterial infections than those admitted for COVID-19. Influenza can directly damage the respiratory epithelium, impair mucociliary clearance, and allow bacterial pathogens to invade, leading to secondary infections such as bacterial pneumonia [25]. COVID-19, although capable of severe pneumonitis, generally causes less direct epithelial destruction than influenza [25,26]. Poorly controlled asthma may exacerbate these risks, as noted by Lansbury et al [26], who reported that bacterial coinfection rates in patients with COVID-19 were much lower than during influenza pandemics. This finding suggests that the routine use of antibiotics in patients with COVID-19 may not be necessary. Early in the pandemic, despite low rates of bacterial coinfections (<10%), antibiotics were widely prescribed to patients with COVID-19 (75%) [27]. Such practices might have reduced secondary bacterial infection rates, making patients with influenza more susceptible to secondary infections.

Clinical Implications

Despite these differences in complications, we observed no significant difference in in-hospital mortality rates between the two groups. This could be due to effective clinical management or the resilience of the pediatric population. However, younger children (aged 1 to 5 years) with COVID-19 had a higher 90-day readmission rate than those with influenza, indicating a need for targeted follow-up care after discharge.

Studies have shown that COVID-19 vaccines are safe and effective for children, including those with asthma [6]. Ongoing research continues to support vaccination, particularly for those with uncontrolled asthma, who are at increased risk of severe disease and complications [6].

These findings can guide health care providers in optimizing care during respiratory viral outbreaks. The study underscores the need for different management strategies for children with asthma hospitalized with COVID-19 or influenza. Specifically, the higher risk of sepsis or shock in the COVID-19 cohort warrants proactive hemodynamic monitoring and early escalation of care. Vaccination and close follow-up, particularly

XSL•FO
RenderX

for younger children with COVID-19, are crucial to prevent hospitalizations and manage complications.

Strengths and Limitations

A strength of this study is its use of a large, nationally representative dataset, providing a comprehensive overview of hospitalizations across the United States. This broad scope enhances the generalizability of the findings and allows a detailed understanding of the differential impact of COVID-19 and influenza on children with asthma. In addition, the analysis included in-hospital data and readmission data, which are informative in assessing health care use for these patients.

However, this study still had several limitations. First, the retrospective, observational design limited causal inference and may have introduced selection bias. The absence of a healthy (noninfected) comparison group further constrained interpretation, and the single-year study period (2020) limited generalizability to later phases of the pandemic. Moreover, reliance on *ICD-10-CM* codes could underestimate milder comorbidities, and variations in coding accuracy may have affected our results.

Second, several key clinical parameters were unavailable in the NRD, such as vaccination history of patients, COVID-19 viral load, laboratory measures, influenza subtypes, detailed treatment regimens, asthma medication regimens (particularly inhaled corticosteroids), and asthma severity. These factors could significantly influence patient outcomes and limit the ability to fully understand the nuances of disease interactions in this population. Emerging evidence suggests that impaired fetal growth, rather than prematurity, influences childhood lung function; such perinatal data were similarly not captured [28].

Third, the COVID-19 and influenza groups differed markedly in age (mean 13.3 vs 6.8 years, respectively), raising the possibility of residual confounding. Although age-stratified analyses yielded trends but these results were not statistically significant (P=.12) consistent with the primary results, small subgroup sample sizes reduce statistical power—particularly for rare outcomes such as mortality.

Finally, clinical management of COVID-19 evolved rapidly during 2020, and pandemic-related changes in health care–seeking behavior may have biased our sample toward more severe cases. A nationwide Korean survey reported a transient decline in pediatric asthma prevalence from 2020 to 2021, potentially reflecting underdiagnosis or reduced health care use [29]; similar dynamics could have influenced the US data.

Future Directions

Future work should couple national hospital data with electronic health records to add missing variables—vaccination status, asthma-control metrics, and viral subtype—across multiple post-2020 seasons. Including a group of noninfected children with asthma would clarify the absolute risk estimates, while extended follow-up may reveal longer-term monitoring.

Conclusions

In conclusion, children with asthma in the United States hospitalized for COVID-19 have a higher risk of sepsis or shock compared to those admitted for influenza. Conversely, those admitted for influenza are at increased risk of secondary bacterial or fungal pneumonia. These findings underscore the need for targeted clinical management strategies for children with asthma, tailored to the specific risks posed by COVID-19 and influenza.

Data Availability

All the data supporting underlying findings are included in the manuscript and its multimedia appendices.

Conflicts of Interest

None declared.

Multimedia Appendix 1
Supplementary Table 1 International Classification of Diseases, 10th Revision, Clinical Modification (ICD-10-CM) and Procedure Coding System (ICD-10-PCS) codes applied to identify diagnoses, complications, and procedures in the 2020 U.S. Nationwide Readmissions Database cohort of children with asthma hospitalized for COVID-19 or seasonal influenza.
[DOCX File , 18 KB - medinform_v13i1e73047_app1.docx]

References

1. Stern J, Pier J, Litonjua AA. Asthma epidemiology and risk factors. Semin Immunopathol 2020 Feb 04;42(1):5-15. [doi: 10.1007/s00281-020-00785-1] [Medline: 32020334]
2. Serebrisky D, Wiznia A. Pediatric asthma: a global epidemic. Ann Glob Health 2019 Jan 22;85(1):6 [FREE Full text] [doi: 10.5334/aogh.2416] [Medline: 30741507]
3. Zejda JE, Beridze V, Bakhtadze T, Beridze S, Abuladze L, Partenadze N, et al. Prevalence of and factors associated with underdiagnosis of pediatric asthma in Batumi, Georgia. Allergol Immunopathol (Madr) 2020 Jan;48(1):73-77. [doi: 10.1016/j.aller.2019.05.006] [Medline: 31477393]
4. Gaietto KM, Freeman MC, DiCicco LA, Rauenswinter S, Squire JR, Aldewereld Z, et al. Asthma as a risk factor for hospitalization in children with COVID‐19: a nested case‐control study. Pediatr Allergy Immunol 2022 Jan;33(1):e13696 [FREE Full text] [doi: 10.1111/pai.13696] [Medline: 34775650]

XSL•FO
RenderX

5. Shi T, Pan J, Katikireddi SV, McCowan C, Kerr S, Agrawal U, et al. Risk of COVID-19 hospital admission among children aged 5-17 years with asthma in Scotland: a national incident cohort study. Lancet Respir Med 2022 Feb;10(2):191-198 [FREE Full text] [doi: 10.1016/S2213-2600(21)00491-4] [Medline: 34861180]
6. Grandinetti R, Palazzolo E, Rizzo L, Carbone R, Pisi G, Fainardi V, et al. Impact of SARS-CoV-2 infection in children with asthma and impact of COVID-19 vaccination: current evidence and review of the literature. Microorganisms 2023 Jul 04;11(7):1745 [FREE Full text] [doi: 10.3390/microorganisms11071745] [Medline: 37512917]
7. Maddux AB, Grunwell JR, Newhams MM, Chen SR, Olson SM, Halasa NB, et al. Association of asthma with treatments and outcomes in children with critical influenza. J Allergy Clin Immunol Pract 2023 Mar;11(3):836-43.e3 [FREE Full text] [doi: 10.1016/j.jaip.2022.10.045] [Medline: 36379408]
8. Lee E, Rhee EH, Yu J, Kim K, Kim HS, Im CH, et al. Incidence of healthcare utilization for allergic and respiratory infectious diseases in children with asthma before and during the COVID-19 pandemic. Allergy 2024 Apr 23;79(4):1064-1067. [doi: 10.1111/all.15992] [Medline: 38140807]
9. Yoon J, Yang HJ, Rhee EH, Lee E, Park JS, Jung S, et al. Longitudinal trajectories of asthma and allergic comorbidities in the Korean childhood asthma study. Allergy Asthma Immunol Res 2025 Jan;17(1):47-59 [FREE Full text] [doi: 10.4168/aair.2025.17.1.47] [Medline: 39895602]
10. NRD database documentation. Agency for Healthcare Research and Quality. URL: https://hcup-us.ahrq.gov/db/nation/nrd/nrddbdocumentation.jsp [accessed 2025-08-17]
11. 45 CFR 46.104 exempt research. Code of Federal Regulations. URL: https://www.ecfr.gov/current/title-45/subtitle-A/subchapter-A/part-46/subpart-A/section-46.104 [accessed 2025-08-17]
12. Perneger TV. What's wrong with Bonferroni adjustments. BMJ 1998 Apr 18;316(7139):1236-1238 [FREE Full text] [doi: 10.1136/bmj.316.7139.1236] [Medline: 9553006]
13. Xie Y, Choi T, Al-Aly Z. Risk of death in patients hospitalized for COVID-19 vs seasonal influenza in fall-winter 2022-2023. JAMA 2023 May 16;329(19):1697-1699 [FREE Full text] [doi: 10.1001/jama.2023.5348] [Medline: 37022720]
14. Brehm TT, van der Meirschen M, Hennigs A, Roedl K, Jarczak D, Wichmann D, et al. Comparison of clinical characteristics and disease outcome of COVID-19 and seasonal influenza. Sci Rep 2021 Mar 11;11(1):5803 [FREE Full text] [doi: 10.1038/s41598-021-85081-0] [Medline: 33707550]
15. Dupont A, Couffignal C, Arias C, Salah K, Phillips-Houlbraq M, Le Brun M, et al. Outcomes and risk factors with COVID-19 or influenza in hospitalized asthma patients. Respir Res 2022 Dec 13;23(1):342 [FREE Full text] [doi: 10.1186/s12931-022-02265-6] [Medline: 36514068]
16. Robbins E, Daoud S, Demissie S, James P. The impact of asthma on COVID-19 disease severity in children and adolescents. J Asthma 2023 Jun 13;60(6):1097-1103. [doi: 10.1080/02770903.2022.2132956] [Medline: 36200730]
17. Özata MC, Dikici Ü, Özdemir Ö. COVID-19 frequency and clinical course in children with asthma. World J Virol 2023 Dec 25;12(5):272-285 [FREE Full text] [doi: 10.5501/wjv.v12.i5.272] [Medline: 38187499]
18. Lara ST, Rein LE, Simanek AM, Totoraitis MF, Rausch DJ, Weston BW, et al. Asthma as a risk factor for hospitalization in children and youth with COVID-19: a retrospective cohort study. Pediatr Infect Dis J 2024 May 01;43(5):437-443. [doi: 10.1097/INF.0000000000004248] [Medline: 38241639]
19. Oliveira MC, Colosimo EA, Vasconcelos MA, Martelli-Júnior H, Mak RH, Silva LR, et al. The association between pre-existing asthma and reduced risk of death among children and adolescents hospitalized with COVID-19 in Brazil. Pediatr Pulmonol 2023 Mar 23;58(3):727-737. [doi: 10.1002/ppul.26245] [Medline: 36382503]
20. Dolby T, Nafilyan V, Morgan A, Kallis C, Sheikh A, Quint JK. Relationship between asthma and severe COVID-19: a national cohort study. Thorax 2023 Feb 30;78(2):120-127. [doi: 10.1136/thoraxjnl-2021-218629] [Medline: 35354646]
21. Beken B, Ozturk GK, Aygun FD, Aydogmus C, Akar HH. Asthma and allergic diseases are not risk factors for hospitalization in children with coronavirus disease 2019. Ann Allergy Asthma Immunol 2021 May;126(5):569-575 [FREE Full text] [doi: 10.1016/j.anai.2021.01.018] [Medline: 33493639]
22. Yılmaz K, Şen V, Aktar F, Onder C, Yılmaz ED, Yılmaz Z. Does Covid-19 in children have a milder course than Influenza? Int J Clin Pract 2021 Sep 27;75(9):e14466 [FREE Full text] [doi: 10.1111/ijcp.14466] [Medline: 34107134]
23. Jiang Y, Rubin L, Peng T, Liu L, Xing X, Lazarovici P, et al. Cytokine storm in COVID-19: from viral infection to immune responses, diagnosis and therapy. Int J Biol Sci 2022;18(2):459-472 [FREE Full text] [doi: 10.7150/ijbs.59272] [Medline: 35002503]
24. Legebeke J, Lord J, Penrice-Randal R, Vallejo AF, Poole S, Brendish NJ, et al. Evaluating the immune response in treatment-naive hospitalised patients with influenza and COVID-19. Front Immunol 2022 May 19;13:853265 [FREE Full text] [doi: 10.3389/fimmu.2022.853265] [Medline: 35663963]
25. Short KR, Kasper J, van der Aa S, Andeweg AC, Zaaraoui-Boutahar F, Goeijenbier M, et al. Influenza virus damages the alveolar barrier by disrupting epithelial cell tight junctions. Eur Respir J 2016 Mar 07;47(3):954-966 [FREE Full text] [doi: 10.1183/13993003.01282-2015] [Medline: 26743480]
26. Lansbury L, Lim B, Baskaran V, Lim WS. Co-infections in people with COVID-19: a systematic review and meta-analysis. J Infect 2020 Aug;81(2):266-275 [FREE Full text] [doi: 10.1016/j.jinf.2020.05.046] [Medline: 32473235]

XSL•FO
RenderX

27. Nandi A, Pecetta S, Bloom DE. Global antibiotic use during the COVID-19 pandemic: analysis of pharmaceutical sales data from 71 countries, 2020-2022. EClinicalMedicine 2023 Mar;57:101848 [FREE Full text] [doi: 10.1016/j.eclinm.2023.101848] [Medline: 36776504]
28. Kim HS, Lee SW, Kim JT, Kim JH, Lim DH, Kim WK, et al. Fetal growth rather than prematurity determines lung function in children with asthma. Respirology 2023 Sep 12;28(9):841-850. [doi: 10.1111/resp.14528] [Medline: 37308162]
29. Park J, Nguyen A, Kattih M, Kim HJ, Kim M, Lee M, et al. National trends in asthma prevalence in South Korea before and during the COVID-19 pandemic, 1998-2021. Clin Exp Allergy 2023 Dec 19;53(12):1291-1294. [doi: 10.1111/cea.14394] [Medline: 37727009]

Abbreviations

aOR: adjusted odds ratio
HCUP: Health Care Cost and Utilization Project
ICD-10-CM: International Classification of Diseases, 10th Revision, Clinical Modification
ICD-10-PCS: International Classification of Diseases, 10th Revision, Procedure Coding System
IRB: institutional review board
NRD: Nationwide Readmissions Database
PROC SURVEYFREQ: survey frequency procedure
PROC SURVEYLOGISTIC: procedure for survey logistic regression analysis
PROC SURVEYREG: procedure for survey regression analysis

Edited by A Coristine; submitted 24.02.25; peer-reviewed by SW Lee, EA Oliveira; comments to author 27.05.25; revised version received 16.07.25; accepted 01.08.25; published 30.09.25.

Please cite as:
Chen YC, Cheng CP, Chen PC, Wang JL, Wu CC, Lu YC
Comparative Analysis of Outcomes of Influenza and COVID-19 Admissions Among Children With Asthma: A Nationwide Retrospective Cohort Study Using the US National Readmissions Database
JMIR Med Inform 2025;13:e73047
URL: https://medinform.jmir.org/2025/1/e73047
doi:10.2196/73047
PMID:

©Ying-Chen Chen, Chia-Pi Cheng, Po-Cheng Chen, Jinn-Li Wang, Chia-Chen Wu, Ying-Chun Lu. Originally published in JMIR Medical Informatics (https://medinform.jmir.org), 30.09.2025. This is an open-access article distributed under the terms of the Creative Commons Attribution License (https://creativecommons.org/licenses/by/4.0/), which permits unrestricted use, distribution, and reproduction in any medium, provided the original work, first published in JMIR Medical Informatics, is properly cited. The complete bibliographic information, a link to the original publication on https://medinform.jmir.org/, as well as this copyright and license information must be included.

XSL•FO
RenderX

Evaluating the Body Roundness Index as a Novel Digital Biomarker for Psoriasis Risk Prediction: Cross-Sectional Study

Pengfei Wen[1], MD; Xiaoyan Wang[2], MM; Xiaoxue Zhuo[1]; Siliang Xue[1], MD

[1]Department of Dermatology, West China Hospital, Sichuan University, No. 37 Guoxue Alley, Wuhou District, Chengdu, China

[2]Department of Clinical Nutrition, The First Affiliated Hospital of Chengdu Medical College, Chengdu, China

Corresponding Author:
Siliang Xue, MD
Department of Dermatology, West China Hospital, Sichuan University, No. 37 Guoxue Alley, Wuhou District, Chengdu, China

Abstract

Background: Psoriasis is a chronic inflammatory skin disorder that has been increasingly linked to metabolic imbalances, particularly obesity. Conventional anthropometric indicators such as BMI and waist circumference (WC) may not sufficiently capture body fat distribution or reflect metabolic risk. The body roundness index (BRI), which integrates both height and waist measurements, has emerged as a potentially superior metric, though its relevance to psoriasis risk remains underexplored.

Objective: This study aimed to investigate the use of BRI as a digital biomarker for assessing psoriasis risk and to compare its predictive strength against BMI and WC across various demographic and metabolic subgroups using data from a nationally representative sample.

Methods: A cross-sectional analysis was conducted using data from 13,798 adults aged 20 to 59 years who participated in the National Health and Nutrition Examination Survey between 2003 and 2006 as well as between 2009 and 2014. Psoriasis status was self-reported. Anthropometric measures (BRI, BMI, and WC) were calculated from standardized physical assessments. Weighted multivariable logistic regression models and restricted cubic spline analyses were used to examine associations while adjusting for demographic, metabolic, and lifestyle variables. A nomogram was constructed to quantify the relative predictive contributions of each metric.

Results: BRI exhibited a strong linear association with psoriasis risk (odds ratio [OR] 1.11 per unit increase, 95% CI 1.05 - 1.17; *P*<.001), outperforming BMI (OR 1.03) and WC (OR 1.01). Tertile analysis revealed a 1.73-fold increased risk of psoriasis in the highest BRI group (*P*=.003). Subgroup analyses confirmed consistent associations across age, sex, race or ethnicity, and metabolic status (*P* for interaction >.05). The nomogram highlighted BRI as the most influential predictor, indicated by its broad scoring range.

Conclusions: BRI shows stronger and more consistent associations with psoriasis risk than BMI or WC, supporting its potential role as a digital biomarker for early risk stratification. Incorporating BRI into clinical decision-making tools may enhance personalized approaches to psoriasis prevention and management.

(JMIR Med Inform 2025;13:e75727) doi:10.2196/75727

KEYWORDS

psoriasis; body roundness index; obesity; digital biomarker; risk prediction

Introduction

Psoriasis is a widespread, long-term inflammatory skin condition affecting approximately 2% to 3% of the global population [1,2]. Clinically, it is characterized by erythematous plaques, scaling, epidermal hyperplasia, and other symptoms, typically affecting the scalp, elbows, knees, and lower back [3,4]. The disease often follows a prolonged, relapsing course with considerable interindividual variation. Beyond its dermatologic manifestations, psoriasis is increasingly recognized as a systemic condition associated with several metabolic comorbidities, including obesity, diabetes, and cardiovascular disease (CVD) [1,5-7]. Chronic systemic inflammation may be a key mechanism linking psoriasis to metabolic disorders. The inflammatory milieu in psoriasis can disrupt insulin sensitivity and lipid metabolism, thereby promoting the development of metabolic diseases [2,8,9]. Understanding the interplay between psoriasis, obesity, and metabolic syndrome is thus crucial for improving early diagnosis and developing integrated intervention strategies.

Recent evidence underscores the strong association between psoriasis and metabolic diseases [10,11], particularly obesity. Obesity is considered a significant risk factor for psoriasis onset [12,13] and may also worsen disease severity [14]. In individuals with obesity, adipose tissue functions as an active endocrine organ, releasing proinflammatory cytokines, which induce

XSL•FO
RenderX

chronic low-grade systemic inflammation [13,15,16]. These cytokines can trigger or exacerbate psoriatic inflammation [12,17]. Moreover, individuals with both obesity and metabolic syndrome tend to have a longer disease duration and more refractory clinical course, highlighting the potential value of weight management in psoriasis care [10,18].

Although BMI and waist circumference (WC) are commonly applied in clinical practice to assess obesity, they have notable limitations. BMI estimates general obesity based solely on weight-to-height ratio and cannot distinguish between fat and lean mass or identify fat distribution patterns [19]. Consequently, its application may result in inaccurate risk assessment in patients with psoriasis [20]. WC, while reflective of abdominal fat, lacks the precision to capture total or visceral fat distribution [21]. The body roundness index (BRI) is a recently developed anthropometric measure that combines WC and height, offering a potentially valuable alternative to traditional obesity metrics [22]. BRI more accurately estimates visceral and abdominal fat distribution and has demonstrated stronger associations with metabolic syndrome and obesity-related disorders [23,24]. Its potential application in predicting risk of psoriasis, however, remains underexplored.

While previous research has documented a linkage between BRI and risk of psoriasis [25], its comparative predictive performance against traditional measures such as BMI and WC across different population subgroups requires further validation. This study probes into the predictive use of BRI for psoriasis and to determine whether it offers superior risk stratification in comparison with conventional anthropometric indices. By leveraging large-scale national health data, we seek to support the development of more individualized screening and prevention strategies for psoriasis, thereby advancing both theoretical understanding and clinical management.

Methods

Data Source

This study is based on data from the National Health and Nutrition Examination Survey (NHANES) [26], conducted by the National Center for Health Statistics of the Centers for Disease Control and Prevention. NHANES is a nationally representative, ongoing cross-sectional survey aimed at evaluating the nutritional and health conditions of the US civilian population not living in institutions. It integrates in-home interviews with standardized health assessments conducted in mobile examination centers (MECs), offering comprehensive demographic, clinical, and laboratory data.

We analyzed data from the 2003 to 2006 and 2009 to 2014 NHANES cycles. The 2003 - 2006 datasets included self-reported psoriasis information for adults aged 20 to 59 years, while the 2009 - 2014 cycles provided relevant health and anthropometric data for participants aged 16 to 80 years. For consistency and comparability, our analysis focused on adults aged 20 to 59 years across all cycles.

Study Population

This cross-sectional analysis included data from the 5 NHANES cycles: 2003 - 2004, 2005 - 2006, 2009 - 2010, 2011 - 2012, and 2013 - 2014. Participants were included if they were aged 20 to 59 years and had complete data on psoriasis status and relevant anthropometric and clinical variables. The exclusion criteria were as follows: (1) missing data on psoriasis diagnosis; (2) missing height, WC, or weight data, which prevented BRI calculation; (3) missing key demographic or clinical variables, including poverty-income ratio (PIR), education, marital status, smoking status, alcohol consumption, BMI, CVD, diabetes, or metabolic syndrome.

Definition and Measurement of Psoriasis and BRI

Psoriasis status was determined based on participants' responses in the "Medical Conditions" section of the NHANES questionnaire. Respondents were considered to have psoriasis if they answered "yes" to the question: "Has a healthcare provider ever told you that you have psoriasis?" The validity of self-reported psoriasis has been previously established [27,28].

WC and height were collected by trained personnel at MECs following established measurement procedures. Participants were examined while barefoot and dressed in light clothing. Height was recorded at the anatomical point between the lower margin of the last palpable rib and the top of the iliac crest. The BRI was calculated as: $BRI=364.2 - 365.5\times(1 - [WC(m)/2\pi]^2/[0.5\times height(m)]^2)^{½}$ [29]. BRI was then grouped into tertiles based on its distribution in the sample: tertile 1 (<3.87, corresponding to < 33rd percentile), tertile 2 (≥3.87 to <5.61, corresponding to the 33rd-67th percentiles), and tertile 3 (≥5.61, corresponding to ≥ 67th percentile; Figure S1 in Multimedia Appendix 1). This standardized approach to psoriasis classification and BRI calculation ensures high reproducibility and provides a robust framework for subsequent analyses.

Covariate Data Source

Based on prior literature, the following covariates were included in this study: age, sex, race or ethnicity, education level, marital status, PIR, smoking status, alcohol consumption, BMI, body fat percentage (BFP), CVD, metabolic syndrome, and diabetes.

Demographic Variables

Race or ethnicity was self-reported and classified into 4 categories: Mexican American, non-Hispanic Black, non-Hispanic White, and other Hispanic and other races. Marital status was classified as married, unmarried, cohabiting, or other [30]. Education level was categorized as: (1) high school or less, (2) some college education, and (3) college graduate or above. Age was treated as a continuous variable in the main analysis and dichotomized into 2 age brackets (20 - 39 y and 40 - 59 y) for subgroup analysis to explore age-related heterogeneity.

Lifestyle Factors

Smoking status was categorized into 3 groups: never smokers (individuals who had smoked fewer than 100 cigarettes in their lifetime), former smokers (those who had smoked at least 100 cigarettes but were not currently smoking), and current smokers (participants who had smoked over 100 cigarettes and continued smoking at the time of the survey) [30]. Alcohol consumption

XSL•FO
RenderX

was stratified into 5 levels based on self-reported consumption over the previous year: never (lifetime consumption of fewer than 12 occasions), former (no alcohol intake in the past year but at least 12 past occasions), light (women drinking ≤1 time per day and men ≤2 times per day in the past year), moderate (women drinking ≤2 times per day and men ≤3 times per day), and heavy (women drinking ≥3 times per day and men ≥4 times per day) [31].

Anthropometric and Clinical Measures

BMI was determined as weight in kilograms divided by height in meters squared (kg m^{-2}) [32]. BFP was tested using bioelectrical impedance analysis, conducted at the NHANES MEC using standardized equipment. BFP reflects the proportion of an individual's body weight that is composed of fat and is calculated based on parameters such as height, weight, age, and sex, following the algorithm outlined in the official NHANES technical manual [32]. For statistical analysis, BFP was analyzed both as a continuous measure and by tertiles, aligning with the BRI grouping structure to explore its association with psoriasis risk across fat distribution levels.

Clinical Conditions

Diabetes was determined based on any of the following criteria: receipt of antidiabetic treatment, HbA_{1c}≥6.5%, use of antidiabetic medications, oral glucose tolerance test results ≥11.1 mmol L^{-1}, fasting blood glucose ≥ 7.0 mmol L^{-1}, or random blood glucose ≥ 11.1 mmol L^{-1} [33, 34]. CVD was identified based on self-reported medical history of coronary artery disease, myocardial infarction, heart failure, stroke, or angina [35,36]. Metabolic syndrome was defined according to the Adult Treatment Panel III (2005) and International Diabetes Federation (2009) criteria [37,38].

Statistical Analysis

This study used the fasting subsample from the NHANES dataset to ensure the reliability of metabolic indicator measurements. The fasting subsample includes participants who underwent blood sampling under standardized fasting conditions. According to NHANES analytic guidelines, the appropriate sampling weight for combined 10-year analyses was calculated using the formula: 10-year MEC weight=2-year MEC weight/5 [28].

We used weighted multivariable logistic regression models to estimate odds ratios (ORs) and 95% CIs, evaluating the association between the BRI and the risk of psoriasis. Three sequential models were sequentially applied: model 1 (unadjusted), model 2 (adjusted for demographic variables including race or ethnicity, age, sex, education level, PIR, and marital status), model 3 (further adjusted for smoking status, alcohol consumption, metabolic syndrome, diabetes, CVD, and NHANES survey cycle, as differences in sampling strategy, measurement methods, or public health trends across survey cycles could introduce systematic bias and act as potential confounders). Trend tests were performed to assess the robustness of its association with psoriasis. In Model 3, we also conducted a weighted restricted cubic spline (RCS) analysis to test the nonlinear relationship between BRI and psoriasis.

To comprehensively assess body size indicators in relation to psoriasis, we performed subgroup analyses and interaction tests to evaluate the role of BRI across different populations (by age, sex, race or ethnicity, CVD, metabolic syndrome, and diabetes), and further conducted logistic regression analyses on WC and BMI to examine their independent effects.

Descriptive statistics were computed by applying NHANES sampling weights. For continuous variables, we reported weighted averages along with their corresponding SDs. Categorical variables were described using unweighted frequencies and weighted proportions. Group comparisons were made using survey-weighted 2-tailed *t* tests for continuous measures and the Rao-Scott adjusted chi-square tests for categorical data. To evaluate the relationship between BRI and psoriasis, we fitted weighted multivariable logistic regression models, treating BRI both as a continuous variable and as categorical tertiles.

All statistical procedures were executed using R software (version 4.4.1; R Foundation for Statistical Computing), supplemented with Free Statistics software (version 1.9.2). NHANES-recommended survey weights were incorporated throughout to reflect the survey's complex multistage design and to yield estimates generalizable to the US civilian population. A 2-sided *P*-value <.05 was deemed statistically significant.

Ethical Considerations

This study followed the STROBE (Strengthening the Reporting of Observational Studies in Epidemiology) guidelines [39] to maintain high standards of methodological clarity and transparency. The NHANES study protocol received approval from the National Center for Health Statistics institutional review board, and all participants provided informed written consent. Since the dataset is anonymized and publicly accessible, no additional ethical review was necessary for this secondary analysis.

Results

Baseline Characteristics

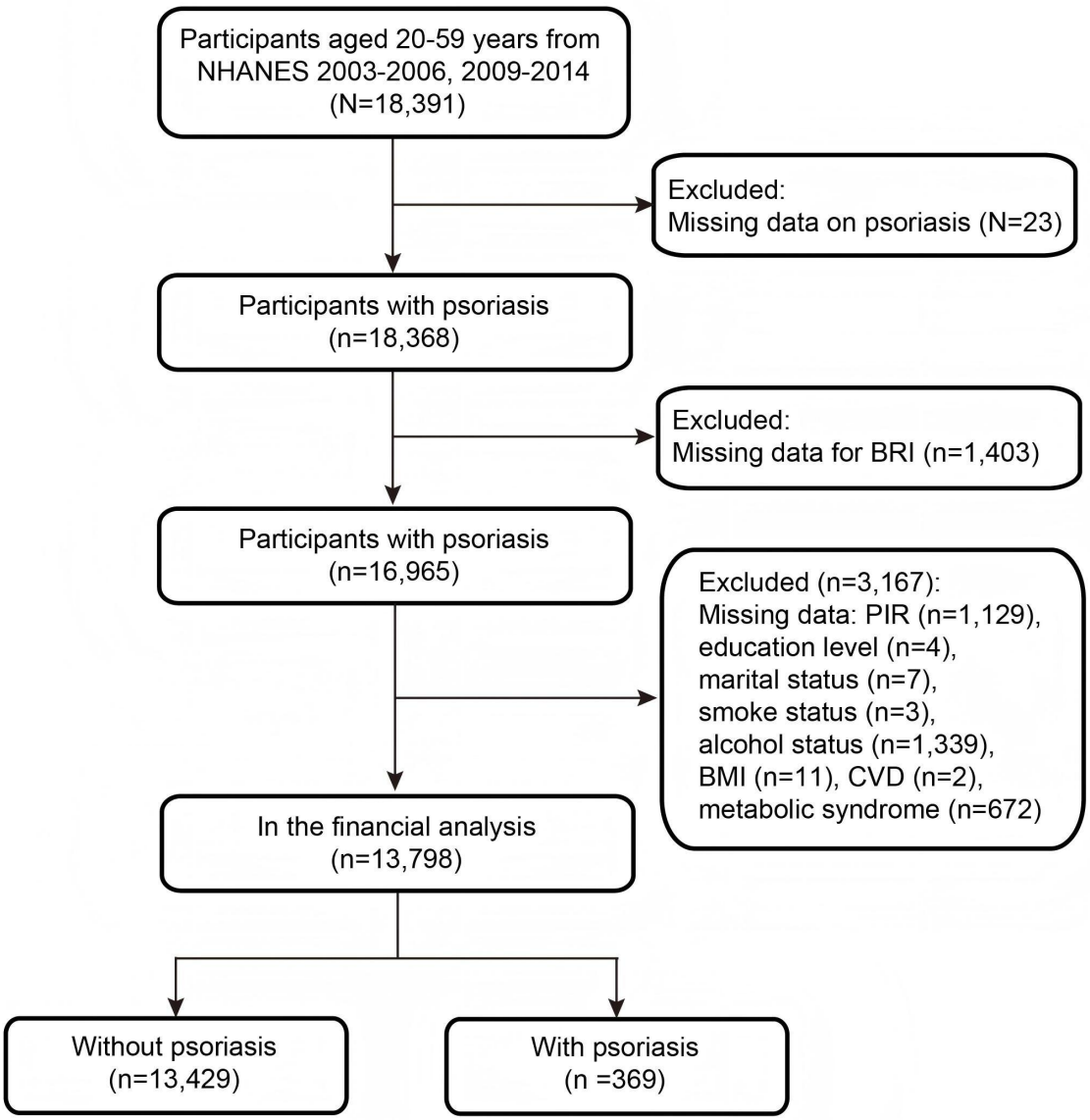
The final analytic sample is detailed in the study flowchart (Figure 1). A total of 13,798 participants aged 20 to 59 years from the NHANES dataset were included in this study. Among them, 369 (3%) self-reported a diagnosis of psoriasis. The mean age of participants was 39.62 (SD 11.43) years. A total of 7037 (51%) participants were male and 6761 (49%) were female (Table 1). Participants were stratified into tertiles based on BRI, with tertile 1 (<3.87, n=4599), tertile 2 (3.87 - 5.61, n=4599), and tertile 3 (≥5.61, n=4600). Significant differences in demographic, socioeconomic, and health-related characteristics were observed across tertiles.

In terms of demographic characteristics, individuals in tertile 3 (highest BRI ≥5.61) were older (mean 42.51, SD 10.79 y versus mean 35.57, SD 11.38 y in tertile 1). Female participants accounted for 2682 of 4600 (55.4%) participants in tertile 3, compared with 2104 of 4599 (49.4%) in tertile 1. In terms of race or ethnicity, non-Hispanic Whites were most common in tertile 3, with 1942 of 4600 (64.3%) participants, while Mexican

XSL•FO
RenderX

Americans were least common, with 908 of 4600 (11.3%) participants. Regarding socioeconomic status, participants in tertile 3 had the lowest PIR and the highest proportion of individuals with low education levels, with 2307 of 4600 (44.1%) having only high school or less education. The proportion of married participants was also highest in tertile 3, with 2383 (56.8%).

Figure 1. Flowchart of inclusion and exclusion criteria for patients with psoriasis. BRI: body roundness index; CVD: cardiovascular disease; NHANES: National Health and Nutrition Examination Survey.



XSL•FO
RenderX

Table . Weighted characteristics of participants in the National Health and Nutrition Examination Survey (NHANES) 2003 - 2006 and 2009 - 2014 cycles (N=13,798).

Variables	Participants	BRI[a]			*P* value
		Tertile 1 (<3.87; n=4599)	Tertile 2 (approximately 3.87-5.61; n=4599)	Tertile 3 (≥5.61; n=4600)	
Age (y), mean (SD)	39.62 (11.43)	35.57 (11.38)	41.03 (10.89)	42.51 (10.79)	<.001
Sex, n (%)					<.001
Female	6761 (49.01)	2104 (49.37)	1975 (42.72)	2682 (55.38)	
Male	7037 (50.99)	2495 (50.63)	2624 (57.28)	1918 (44.62)	
PIR[b], mean (SD)	3.019 (1.65)	3.096 (1.67)	3.130 (1.64)	2.817 (1.63)	<.001
Race or ethnicity, n (%)					<.001
Mexican American	2252 (8.97)	434 (5.30)	910 (10.53)	908 (11.28)	
Non-Hispanic White	6214 (67.83)	2243 (70.50)	2029 (68.39)	1942 (64.30)	
Non-Hispanic Black	2964 (11.35)	973 (10.73)	869 (9.65)	1122 (13.84)	
Other races or ethnicities	2368 (11.86)	949 (13.47)	791 (11.42)	628 (10.58)	
Educational level, n (%)					<.001
College graduate or higher	3383 (29.59)	1461 (36.93)	1138 (30.30)	784 (20.85)	
High school or less	5953 (36.96)	1661 (30.77)	1985 (36.56)	2307 (44.11)	
Some college	4462 (33.45)	1477 (32.31)	1476 (33.14)	1509 (35.03)	
Marital status, n (%)					<.001
Living with partner	1367 (9.07)	508 (10.57)	473(8.92)	386 (7.59)	
Married	6931 (54.72)	1964 (47.32)	2584 (60.30)	2383 (56.78)	
Never married	3420 (22.16)	1594 (31.26)	863 (16.73)	963(18.09)	
Other	2080 (14.06)	533 (10.85)	679 (14.05)	868 (17.54)	
Waist circumference (cm), mean (SD)	97.379 (16.41)	81.803 (7.16)	96.541 (6.90)	115.227 (12.70)	<.001
BMI (kg/m^2), mean (SD)	28.633 (6.74)	22.662 (2.49)	27.781 (2.56)	36.044 (5.94)	<.001
Psoriasis, n (%)					<.001
No	13,429 (96.98)	4510 (97.88)	4471 (96.73)	4448 (96.28)	
Yes	369 (3.02)	89 (2.12)	128 (3.27)	152 (3.72)	
CVD[c], n (%)					<.001
No	13,215 (96.17)	4502(98.16)	4434 (96.55)	4279 (93.58)	
Yes	583 (3.83)	97 (1.84)	165 (3.45)	321 (6.42)	
Metabolic syndrome, n (%)					<.001
No	10,440 (75.86)	4523 (98.50)	3695 (79.94)	2222 (46.83)	
Yes	3358 (24.14)	76 (1.50)	904 (20.06)	2378 (53.17)	
Diabetes (%)					<.001
No	11,648 (86.40)	4357 (95.68)	3976 (88.45)	3315 (74.10)	
Yes	1346 (8.05)	116 (2.07)	320 (5.09)	910 (17.75)	
Smoke status (%)					<.001
Former	2418 (19.57)	647 (16.10)	894 (21.27)	877 (21.53)	
Never	7760 (55.13)	2608 (56.07)	2555 (54.24)	2597 (55.08)	

XSL•FO
RenderX

Variables	Participants	BRI[a]			*P* value
		Tertile 1 (<3.87; n=4599)	Tertile 2 (approximately 3.87-5.61; n=4599)	Tertile 3 (≥5.61; n=4600)	
Current	3620 (25.29)	1344 (27.83)	1150 (24.49)	1126 (23.39)	
Alcohol drinking status, n (%)					<.001
Former	1838 (12.31)	424 (8.05)	597 (11.88)	817 (17.41)	
Heavy	3695 (26.55)	1279 (27.85)	1255 (27.19)	1161 (24.45)	
Light	4201 (32.71)	1510 (34.12)	1462 (34.61)	1229 (29.15)	
Moderate	2478 (19.19)	910 (21.49)	818 (18.36)	750 (17.58)	
Never	1586 (9.23)	476 (8.49)	467 (7.96)	643 (11.41)	

[a]BRI: body roundness index.

[b]PIR: family poverty income ratio.

[c]CVD: cardiovascular disease.

BMI and WC levels increased significantly with higher BRI levels (*P*<.001). Regarding health status, the prevalence of psoriasis also rose, with 152 of 4600 (3.7%) participants in tertile 3 compared to 89 of 4599 (2.1%) in tertile 1 (*P*<.001). In addition, comorbidities were more frequent in tertile 3, including CVD in 321 of 4600 (6.4%) participants, metabolic syndrome in 2378 (53.2%), and diabetes in 910 (17.8%; all *P*<.001).

In terms of lifestyle factors, participants in tertile 3 were more likely to report never smoking (2597/4600, 55.1%) and light alcohol consumption (1229/4600, 29.2%) compared with tertile 1 (lowest BRI*; P*<.001).

Association Between BRI and Risk of Psoriasis

As shown in Table 2, the BRI was distinctly linked to an increased risk of psoriasis across all models. Model 1 (unadjusted): each 1-unit increase in BRI was associated with a 10% increase in the odds of psoriasis (OR 1.10, 95% CI 1.05 - 1.14; *P*<.001). Model 2 (adjusted for demographic variables such as age, sex, race or ethnicity, education level, PIR, and marital status): the association slightly attenuated but remained statistically significant (OR 1.09, 95% CI 1.04 - 1.14; *P*<.001). Model 3 (fully adjusted model: further controlling for NHANES survey cycle, metabolic syndrome, diabetes, CVD, smoking status, and alcohol consumption): the positive association remained robust and significant, with each unit increase in BRI corresponding to an 11% increased risk of psoriasis (OR 1.11, 95% CI 1.05 - 1.17; *P*<.001).

When BRI was divided into tertiles, the risk of psoriasis increased with BRI levels (*P*=.04). Compared to the lowest BRI tertile (<3.87, as the reference group), the second tertile (3.87≤BRI<5.613) showed linkage with a significantly higher risk of psoriasis (model 3: OR 1.49, 95% CI 1.03 - 2.15*; P*=.04). The highest BRI tertile (≥5.61) showed an even greater increase in risk of psoriasis (model 3: OR 1.73, 95% CI 1.22 - 2.45; *P*=.003; Table 2).

Table . Associations of the body roundness index (BRI) with psoriasis among participants in the National Health and Nutrition Examination Survey (NHANES) 2003 - 2006 and 2009 - 2014 cycles.

	Model 1[a]		Model 2[b]		Model 3[c]	
	OR[d] (95% CI)	*P* value	OR (95% CI)	*P*-value	OR (95% CI)	*P* value
Per 1 unit increase	1.1 (1.05-1.14)	<.001	1.09 (1.04-1.14)	<.001	1.11 (1.05-1.17)	<.001
Tertile						
Tertile 1 (BRI:<3.87)	Reference		Reference		Reference	
Tertile 2 (BRI:3.87 to<5.61)	1.56 (1.10-2.20)	01	1.50 (1.05-2.14)	.03	1.49 (1.03-2.15)	.04
Tertile 3 (BRI:≥5.61)	1.78 (1.3-2.43)	<.001	1.72 (1.23-2.42)	.002	1.73 (1.22-2.45)	.003
P for trend	—[e]	<.001	—	.002	—	.003

[a]Model 1: crude model.

[b]Model 2: adjusted for sociodemographic variables (age, sex, race or ethnicity, educational level, poverty-income ratio [PIR], and marital status).

[c]Model 3: adjusted for sociodemographic variables (age, sex, race or ethnicity, educational level, PIR, and marital status), NHANES cycles, metabolic syndrome, diabetes, cardiovascular disease (CVD), smoke and alcohol consumption.

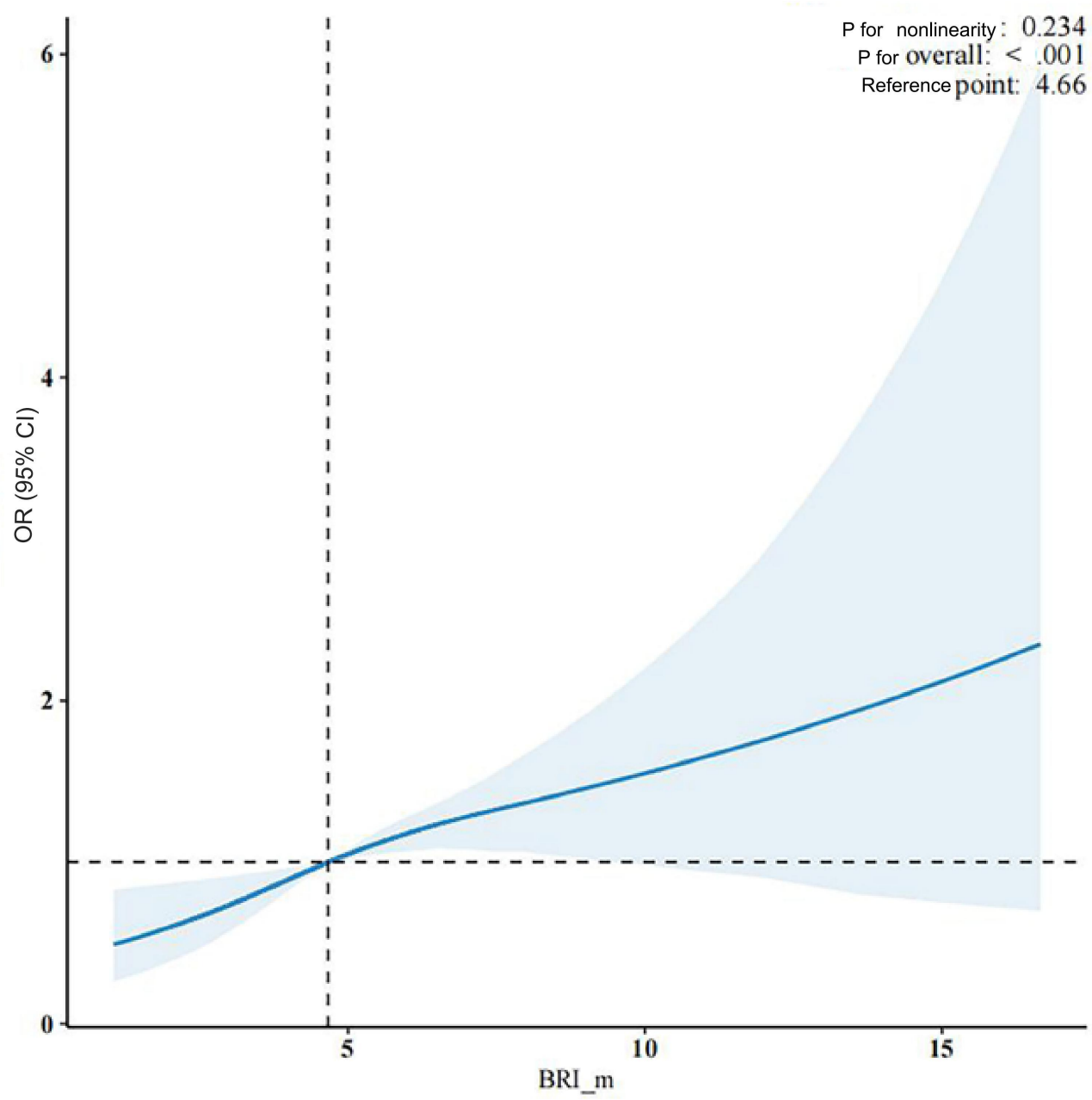
[d]OR: odds ratio.

[e]not applicable.

XSL•FO
RenderX

RCS analysis (Figure 2) demonstrated a significant linear association between BRI and risk of psoriasis, with no evidence of nonlinearity (*P* for nonlinearity=.23). Furthermore, this study conducted an in-depth analysis of the association between BFP and the risk of psoriasis. The results validated a notable positive correlation between BFP and risk of psoriasis, independent of confounding factors. In the unadjusted model, each 1% increase in BFP showed linkage with a 6% increase in risk of psoriasis (OR 1.06, 95% CI 1.04 - 1.08; *P*<.001). After adjusting for demographic variables, the odds ratio decreased slightly to 1.05 (95% CI 1.03 - 1.07; *P*<.001), and in the fully adjusted model—which included metabolic syndrome, diabetes, and other covariates—the association remained significant (OR 1.04, 95% CI 1.02 - 1.06; *P*<.001). When analyzed in conjunction with BRI tertiles, participants in the middle and highest BRI tertiles had a 38% (OR 1.38, 95% CI 1.15 - 1.66; *P*<.001) and 82% (OR 1.82, 95% CI 1.43 - 2.32; *P*<.001) increased risk of psoriasis, respectively, relative to those in tertile 1 (lowest BRI)—suggesting that BRI may outperform BFP in predicting risk of psoriasis. Subgroup analyses further revealed that the association between BRI and psoriasis was stronger among individuals over the age of 40 years (OR 1.07, 95% CI 1.05 - 1.09; *P*<.001). The risk was slightly higher in men (OR_male=1.06) than in women (OR_female=1.04; Table 3).

Figure 2. Weighted restricted cubic spline (RCS) analysis of the association between the body roundness index (BRI) and the risk of psoriasis. OR: odds ratio.



XSL•FO
RenderX

Table . Logistic regression analysis of body fat percentage (BFP) and psoriasis risk.

Variables	OR[a] (95% CI)	*P* value
Model		
Model 1[b] (BFP)	1.06 (1.04 - 1.08)	<.001
Model 2[c] (BFP)	1.05 (1.03 - 1.07)	<.001
Model 3[d] (BFP)	1.04 (1.02 - 1.06)	<.001
Tertile		
Tertile 1[e] (BRI[f] :<3.87)	1.00	—[m]
Tertile 2 (BRI:3.87 to <5.61)	1.38 (1.15 - 1.66)	<.001
Tertile 3 (BRI: ≥5.61)	1.82 (1.43 - 2.32)	<.001
Age (y)		
<40	1.03 (1.01 - 1.05)	<.01
≥40	1.07 (1.05 - 1.09)	<.001
Sex		
Male	1.06 (1.04 - 1.08)	<.001
Female	1.04 (1.02 - 1.06)	<.001

[a]OR: odds ratio.

[b]Model 1: crude model.

[c]Model 2: adjusted for sociodemographic variables (age, sex, race or ethnicity, educational level, family income, and marital status).

[d]Model 3: adjusted for sociodemographic variables (age, sex, race or ethnicity, educational level, poverty-income ratio, and marital status), National Health and Nutrition Examination Survey (NHANES) cycles, metabolic syndrome, diabetes, cardiovascular disease, and smoke and alcohol consumption.

[e]Tertile 1 (BRI < 3.87) was used as the reference category; therefore, no 95% CI or *P* value was estimated.

[f]BRI: body roundness index.

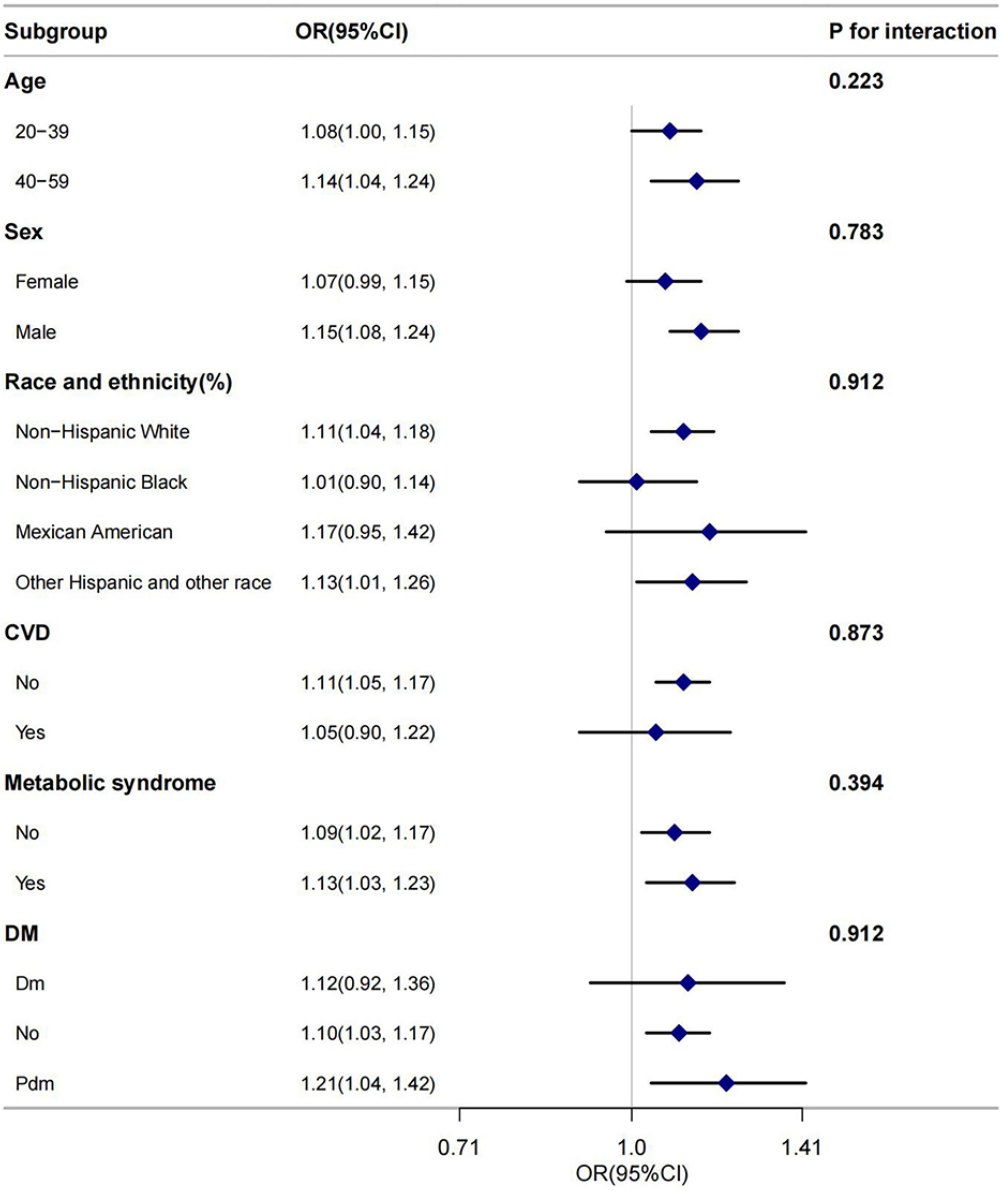
[g]—: Tertile 1 was used as the reference group in all models; therefore, no odds ratio or 95% confidence interval was estimated for this category

Association Between BRI and Risk of Psoriasis Across Subgroups

Subgroup analyses were implemented to assess the consistency of the association between BRI and risk of psoriasis across different population groups (Figure 3). Stratification was applied by age, sex, race or ethnicity, CVD, metabolic syndrome, and diabetes status, to explore potential effect modification. Across all subgroups, BRI remained significantly and positively associated with risk of psoriasis, with no statistically significant interactions noted (*P* for interaction >.05), indicating a stable association across population strata.

XSL•FO
RenderX

Figure 3. Forest plot analysis of the association between the body roundness index (BRI) and risk of psoriasis across different subgroups. CVD: cardiovascular disease; DM: diabetes mellitus; OR: odds ratio.



In the 40 - 59 years age group, the OR was 1.14 (95% CI 1.04 - 1.24), slightly higher than the OR of 1.08 (95% CI 1.00 - 1.15) observed in the 20 - 39 years age group (*P* for interaction=.22). For sex-based subgroups, the ORs were 1.15 (95% CI 1.08 - 1.24) in males and 1.07 (95% CI 0.99 - 1.15) in females (*P*=.78), indicating no significant sex-specific differences. Among participants with metabolic syndrome, the OR was 1.13 (95% CI 1.03 - 1.23), compared to 1.09 (95% CI 1.02 - 1.17) in those without metabolic syndrome (*P* for interaction=.39), suggesting consistent associations across metabolic health status.

Comparison of BRI With Traditional Body Measurement Indicators (BMI and WC)

To further evaluate the predictive value of BRI and compare it with traditional anthropometric measures—BMI and WC—we conducted multivariable logistic regression using the fully adjusted model 3. For each 1-unit increase in BRI, the risk of psoriasis increased by 11% (OR 1.11, 95% CI 1.05 - 1.17; *P*<.001). In comparison, each 1-unit increase in BMI was associated with a 3% increased risk (OR 1.03, 95% CI 1.02 - 1.05; *P*<.001). Each 1-unit increase in WC conferred only a 1% increased risk (OR 1.01, 95% CI 1.01 - 1.02; *P*<.001; Table 4).

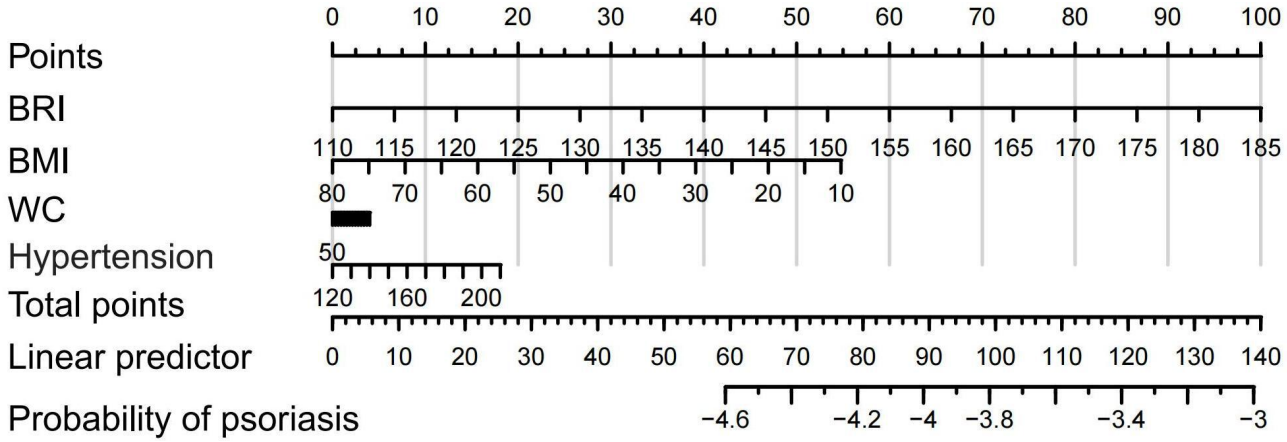
To visualize and quantify the relative contributions of these indicators, we constructed a nomogram model based on multivariable logistic regression. The nomogram illustrated that the BRI score axis had the widest range, indicating that BRI contributed the most to risk of psoriasis prediction. In contrast, BMI and WC had shorter score axes, reflecting their smaller relative contributions (Figure 4).

XSL•FO
RenderX

Table . Logistic regression analysis.

Variables	Odds ratio (95% CI)	*P* value
Body roundness index	1.11 (1.05 - 1.17)	<.001
BMI	1.03 (1.02 - 1.05)	<.001
Waist circumference	1.01 (1.01 - 1.02)	<.001

Figure 4. Nomogram constructed based on body roundness index (BRI), BMI, and waist circumference (WC).



Discussion

Principal Findings

Psoriasis is a long-standing inflammatory skin condition that has been closely linked to metabolic disorders such as obesity, diabetes, and CVD [1,2,5,6]. Prior research has demonstrated significant links between risk of psoriasis and a range of anthropometric indicators such as BMI, WC, waist-to-hip ratio (WHR), and BRI [25,40]. However, most of this research has focused on individual obesity indicators in isolation, lacking a comprehensive comparison of their predictive value. Furthermore, many analyses did not sufficiently adjust for confounding factors that could influence observed associations. Using large-scale data from the NHANES, this study is the first to systematically compare the predictive performance of BRI, BMI, and WC in relation to the risk of psoriasis. The results suggest that BRI demonstrates higher sensitivity and greater clinical use than the other indices examined.

Prior research has consistently reported a positive correlation between BMI and risk of psoriasis. Obesity is thought to influence both the onset and severity of psoriasis through mechanisms such as chronic low-grade inflammation, elevated levels of proinflammatory cytokines, insulin resistance, and broader metabolic disturbances [41,42]. Despite its widespread use, BMI reflects only overall body mass without distinguishing between fat distribution types—particularly visceral versus subcutaneous fat—potentially limiting its ability to capture obesity-related metabolic risk [25]. Although WC is a better indicator of abdominal fat accumulation, it does not adjust for individual height differences. In contrast, BRI integrates both WC and height, enabling a more accurate estimation of total body fat distribution and metabolic burden [43]. Some studies have also suggested a J-shaped or U-shaped association between BMI and risk of psoriasis [44]. Our study used weighted RCS analysis and identified a stable linear association between BRI and risk of psoriasis (*P*=.23), reinforcing the potential of BRI as a reliable risk predictor. These findings are consistent with recent evidence [25].

The BRI, as an integrated measure of WC and height, is not only influenced by genetic and metabolic factors but also modifiable lifestyle factors, such as smoking, alcohol consumption, and physical activity [22]. In this analysis, participants in the highest BRI tertile were more frequently identified as light drinkers and never smokers, suggesting behavioral patterns may modulate body shape and fat distribution. Notably, prior studies have documented that smoking is linked to an increased visceral adiposity despite lower overall BMI, potentially elevating BRI scores through central fat accumulation [45]. Similarly, moderate to heavy alcohol consumption has been linked to higher WC and increased abdominal fat [46], which directly contributes to elevated BRI. Moreover, few studies have examined the distribution patterns of BRI across different population subgroups or its association with psoriasis. In this study, BRI demonstrated more stable trends than BMI and WC across demographic subgroups defined by age, sex, educational level, and marital status. Importantly, BRI showed a consistent positive association with psoriasis risk across all subgroups. Previous research has shown that higher BMI and WC are more prevalent among women, individuals with lower socioeconomic status, and those with limited educational backgrounds [2]. Our findings indicate that the distribution trends of BRI in these populations mirror those of BMI and WC. However, BRI may be more sensitive in capturing obesity-related metabolic risk [25]. Unlike prior studies that have largely focused on BMI and WC, this study uses NHANES data to systematically evaluate BRI distribution across diverse populations and its association with both psoriasis and metabolic disorders. These findings not only provide new insights into the complex interplay between obesity

XSL•FO
RenderX

and inflammatory diseases such as psoriasis, but also underscore the significance of BRI as a practical clinical tool for metabolic health surveillance. In subgroup analyses, the association between BRI and psoriasis remained significant across various strata, including age, sex, race or ethnicity, diabetes, CVD, and metabolic syndrome. Education level, smoking status, and alcohol consumption were not included in the subgroup analyses due to potential multicollinearity with socioeconomic and lifestyle factors, as well as concerns about statistical power related to over-stratification. Although WHR and waist-to-height ratio (WHtR) are also widely adopted indicators of central obesity, they were not included in our analysis due to data limitations and a desire to minimize multicollinearity among closely related anthropometric indices. Moreover, BRI already incorporates WC and height into its calculation, thereby partially accounting for the components used in WHtR. Future studies could explore the predictive value of WHR and WHtR in combination with BRI to further refine obesity-related risk assessment models. In this analysis, lifestyle behaviors—including smoking and alcohol use—showed significant associations with BRI. Participants in the highest BRI tertile were more frequently identified as light alcohol consumers and individuals who had never smoked. These findings suggest that lifestyle factors may influence body shape and fat distribution, thereby indirectly impacting BRI values. This underscores the need to consider behavioral determinants when interpreting BRI in clinical and epidemiological contexts.

Although this study provides compelling evidence for the link between BRI and risk of psoriasis, the underlying biological mechanisms remain to be fully clarified. Prior research has suggested that obesity contributes to the pathogenesis of psoriasis through mechanisms such as chronic low-grade inflammation, elevated levels of proinflammatory cytokines, insulin resistance, and broader metabolic dysregulation [47-49]. As a novel anthropometric index, BRI may more accurately capture fat distribution, metabolic abnormalities, and systemic inflammatory burden relative to traditional measures such as BMI or WC, potentially making it more relevant to the pathophysiology of psoriasis. In this study, BRI remained a notable independent predictor of risk of psoriasis even after adjusting for multiple confounding factors, including metabolic syndrome, diabetes, and CVD. This reinforces its potential clinical value in identifying individuals at elevated risk for inflammation-related conditions. Future research should aim to elucidate the biological pathways underlying this association by integrating multiomics approaches—such as metabolomics, inflammatory biomarker profiling, and gut microbiome analysis—which may offer deeper insight into the mechanistic links between BRI and psoriasis.

This study highlights a strong and consistent association between elevated BRI and an increased likelihood of psoriasis. This association remained stable under various model adjustments and statistical frameworks, suggesting it is not merely attributable to confounding influences. Importantly, the risk of psoriasis rose progressively with increasing BRI, indicating a clear linear trend. These observations support the potential of BRI as a meaningful indicator for identifying individuals with heightened susceptibility to psoriasis. Given its capacity to reflect both fat distribution and metabolic status, BRI may serve as a useful addition to existing risk assessment tools. Future studies should delve deeper into the mechanistic pathways linking BRI and psoriatic disease and evaluate its relevance in clinical prediction models and preventive strategies.

Despite offering compelling evidence for the use of BRI in assessing psoriasis risk, this study contains several limitations. First, as it is based on cross-sectional data from NHANES, causality cannot be inferred; thus, longitudinal cohort studies are necessary to confirm the long-term impact of BRI on psoriasis development and progression. Second, while BRI is a useful surrogate for fat distribution, it does not directly measure visceral adiposity or the muscle-to-fat ratio. Future research incorporating advanced imaging modalities such as dual-energy X-ray absorptiometry or magnetic resonance imaging could yield more precise assessments of body composition and further clarify the biological relevance of BRI in the context of psoriasis. Finally, as this study is based on US NHANES data, the findings may not be directly generalizable to populations in other countries with different ethnic, dietary, and health care backgrounds. Although subgroup analysis within the US population revealed consistent associations across various demographic groups, future studies should validate these results using international datasets. Cross-country comparisons could help evaluate the universality of BRI as a biomarker for psoriasis risk.

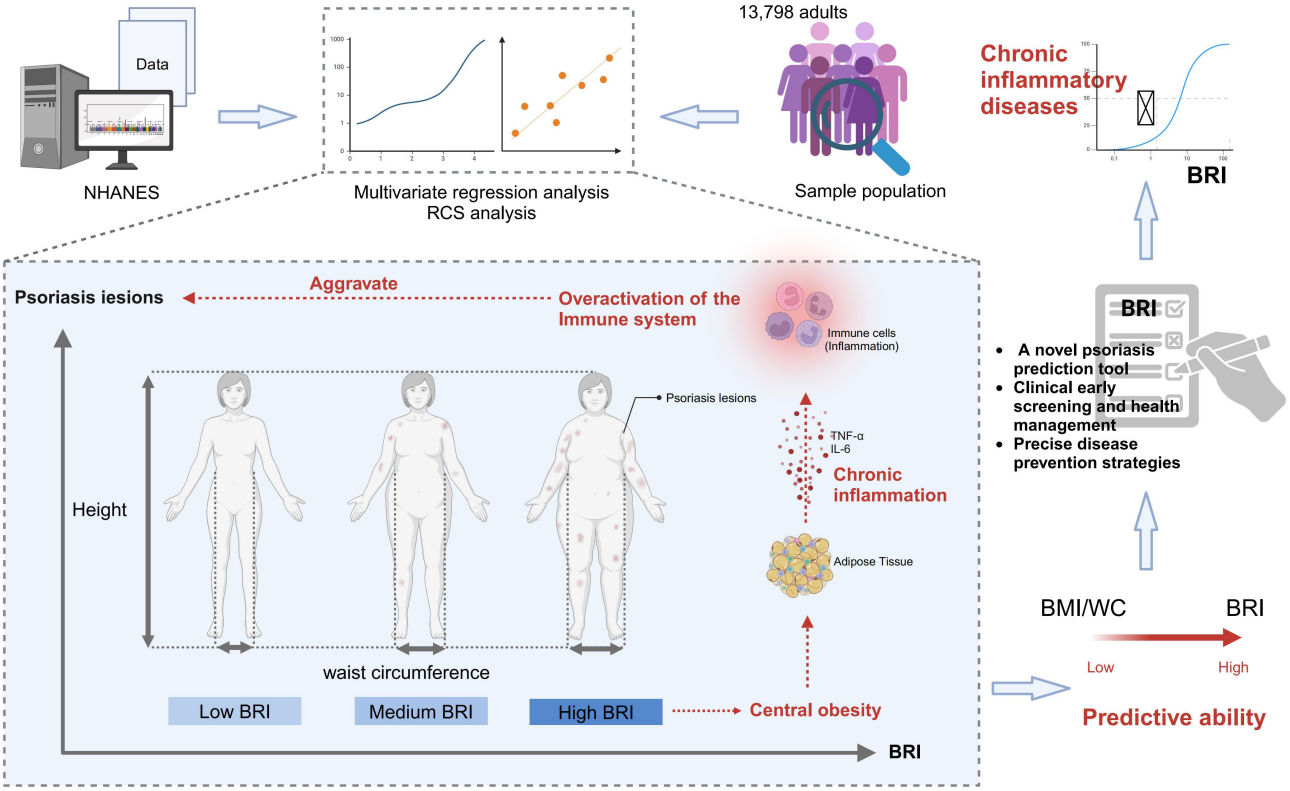
Conclusions

Using large-scale NHANES population data, this study systematically evaluated the association between the BRI and psoriasis risk, and, for the first time, directly compared the predictive performance of BRI, BMI, and WC within a unified analytical framework. The results indicate that BRI may offer greater sensitivity in predicting psoriasis risk. Unlike traditional anthropometric measures, BRI integrates both height and WC, providing a more accurate representation of fat distribution and metabolic burden. Furthermore, weighted RCS analysis confirmed a stable linear association between BRI and psoriasis risk, and BRI consistently showed strong predictive value across diverse demographic subgroups. These findings highlight the potential clinical use of BRI as an early risk assessment tool for psoriasis.

To advance this line of research, future investigations should delve into unraveling the biological pathways linking BRI to psoriatic pathophysiology—particularly in the context of chronic inflammation, metabolic dysregulation, and fat distribution. Given the cross-sectional nature here, prospective cohort studies are essential to validate the predictive value of BRI for psoriasis onset and progression across different populations. In addition, integrating multiomics data—including metabolomics, inflammatory markers, and microbiome profiles—may further enhance the use of BRI in personalized health monitoring and disease prevention, offering new strategies for early diagnosis and targeted intervention in psoriasis (Figure 5).

XSL•FO
RenderX

Figure 5. Conceptual framework illustrating the association between body roundness index (BRI) and psoriasis risk. BRI: body roundness index; NHANES: National Health and Nutrition Examination Survey; RCS: restricted cubic spline; WC: waist circumference.



Funding

This study was supported by the Sichuan Medical and Health Care Promotion Institute (KY2022SJ0117).

Data Availability

The datasets generated or analyzed during this study are available from the corresponding author on reasonable request.

Authors' Contributions

PW and SX conceived and designed the study. PW and XW analyzed the data. PW and XZ wrote the manuscript. All authors reviewed and approved the final version of the manuscript.

Conflicts of Interest

None declared.

Multimedia Appendix 1
Diagram illustrating the measurement method and grouping of body roundness index (BRI).
[DOCX File, 391 KB - medinform_v13i1e75727_app1.docx]

References

1. Takeshita J, Grewal S, Langan SM, et al. Psoriasis and comorbid diseases: epidemiology. J Am Acad Dermatol 2017 Mar;76(3):377-390. [doi: 10.1016/j.jaad.2016.07.064] [Medline: 28212759]
2. Nowowiejska J, Baran A, Flisiak I. Aberrations in lipid expression and metabolism in psoriasis. Int J Mol Sci 2021 Jun 18;22(12):6561. [doi: 10.3390/ijms22126561] [Medline: 34207318]
3. Langley RGB, Krueger GG, Griffiths CEM. Psoriasis: epidemiology, clinical features, and quality of life. Ann Rheum Dis 2005 Mar;64 Suppl 2(Suppl 2):ii18-ii23. [doi: 10.1136/ard.2004.033217] [Medline: 15708928]
4. Furue M, Tsuji G, Chiba T, Kadono T. Cardiovascular and metabolic diseases comorbid with psoriasis: beyond the skin. Intern Med 2017;56(13):1613-1619. [doi: 10.2169/internalmedicine.56.8209] [Medline: 28674347]
5. Armstrong AW, Read C. Pathophysiology, clinical presentation, and treatment of psoriasis: a review. JAMA 2020 May 19;323(19):1945-1960. [doi: 10.1001/jama.2020.4006] [Medline: 32427307]

XSL•FO
RenderX

6. Kamiya K, Kishimoto M, Sugai J, Komine M, Ohtsuki M. Risk factors for the development of psoriasis. Int J Mol Sci 2019 Sep 5;20(18):4347. [doi: 10.3390/ijms20184347] [Medline: 31491865]
7. Amin M, Lee EB, Tsai TF, Wu JJ. Psoriasis and co-morbidity. Acta Derm Venereol 2020 Jan 30;100(3):adv00033. [doi: 10.2340/00015555-3387] [Medline: 31971602]
8. Piaserico S, Orlando G, Messina F. Psoriasis and cardiometabolic diseases: shared genetic and molecular pathways. Int J Mol Sci 2022 Aug 13;23(16):9063. [doi: 10.3390/ijms23169063] [Medline: 36012327]
9. Wroński A, Wójcik P. Impact of ROS-dependent lipid metabolism on psoriasis pathophysiology. Int J Mol Sci 2022 Oct 12;23(20):12137. [doi: 10.3390/ijms232012137] [Medline: 36292991]
10. Hao Y, Zhu YJ, Zou S, et al. Metabolic syndrome and psoriasis: mechanisms and future directions. Front Immunol 2021;12:711060. [doi: 10.3389/fimmu.2021.711060] [Medline: 34367173]
11. Liang Y, Wang Y, Peng A, Li J, Zhang K. Molecular mechanisms and drug therapy of metabolism disorders in psoriasis. J Dermatolog Treat 2024 Dec;35(1):2375580. [doi: 10.1080/09546634.2024.2375580] [Medline: 39013549]
12. Jensen P, Skov L. Psoriasis and obesity. Dermatology (Basel) 2016;232(6):633-639. [doi: 10.1159/000455840]
13. Kunz M, Simon JC, Saalbach A. Psoriasis: obesity and fatty acids. Front Immunol 2019;10:1807. [doi: 10.3389/fimmu.2019.01807] [Medline: 31417571]
14. Owczarczyk-Saczonek A, Placek W. Compounds of psoriasis with obesity and overweight. Postepy Hig Med Dosw 2017 Aug 28;71(1):0-0. [doi: 10.5604/01.3001.0010.3854]
15. Barros G, Duran P, Vera I, Bermúdez V. Exploring the links between obesity and psoriasis: a comprehensive review. Int J Mol Sci 2022 Jul 6;23(14):7499. [doi: 10.3390/ijms23147499] [Medline: 35886846]
16. Duarte GV, Follador I, Cavalheiro CMA, Silva TS, Oliveira MDFD. Psoriasis and obesity: literature review and recommendations for management. An Bras Dermatol 2010;85(3):355-360. [doi: 10.1590/s0365-05962010000300009] [Medline: 20676469]
17. Coimbra S, Catarino C, Santos‐Silva A. The triad psoriasis-obesity-adipokine profile. Acad Dermatol Venereol 2016 Nov;30(11):1876-1885 [FREE Full text] [doi: 10.1111/jdv.13701]
18. Cintoni M, Palombaro M, Maramao FS, et al. Metabolic disorders and psoriasis: exploring the role of nutritional interventions. Nutrients 2023 Sep 6;15(18):3876. [doi: 10.3390/nu15183876] [Medline: 37764660]
19. Apovian CM. Obesity: definition, comorbidities, causes, and burden. Am J Manag Care 2016 Jun;22(7 Suppl):s176-s185. [Medline: 27356115]
20. Paolini JBM, Mancini J, Genestal M, et al. Predictive value of abdominal obesity vs. body mass index for determining risk of intensive care unit mortality. Crit Care Med 2010 May;38(5):1308-1314. [doi: 10.1097/CCM.0b013e3181d8cd8b] [Medline: 20228682]
21. Han TS, Lean MEJ. Self-reported waist circumference compared with the “Waist Watcher” tape-measure to identify individuals at increased health risk through intra-abdominal fat accumulation. Br J Nutr 1998 Jul;80(1):81-88. [doi: 10.1017/s0007114598001809] [Medline: 9797647]
22. Zhang X, Ma N, Lin Q, et al. Body roundness index and all-cause mortality among US adults. JAMA Netw Open 2024 Jun 3;7(6):e2415051. [doi: 10.1001/jamanetworkopen.2024.15051] [Medline: 38837158]
23. de Luis D, Muñoz M, Izaola O, Lopez Gomez JJ, Rico D, Primo D. Body roundness index (BRI) predicts metabolic syndrome in postmenopausal women with obesity better than insulin resistance. Diabetology 2025;6(7):60. [doi: 10.3390/diabetology6070060]
24. He X, Zhu J, Liang W, et al. Association of body roundness index with cardiovascular disease in patients with cardiometabolic syndrome: a cross-sectional study based on NHANES 2009-2018. Front Endocrinol 2025;16. [doi: 10.3389/fendo.2025.1524352]
25. Bai G, Peng Y, Liu Q, et al. Association between body roundness index and psoriasis among US adults: a nationwide population-based study. Lipids Health Dis 2024 Nov 13;23(1):373. [doi: 10.1186/s12944-024-02365-w] [Medline: 39538202]
26. National health and nutrition examination survey. Centers for Disease Control and Prevention. URL: https://www.cdc.gov/nchs/nhanes/index.html [accessed 2025-12-09]
27. Phan C, Ezzedine K, Lai C, et al. Agreement between self-reported inflammatory skin disorders and dermatologists' diagnosis: a cross-sectional diagnostic study. Acta Derm Venereol 2017 Nov 15;97(10):1243-1244. [doi: 10.2340/00015555-2749] [Medline: 28681066]
28. Ruan Z, Lu T, Chen Y, et al. Association between psoriasis and nonalcoholic fatty liver disease among outpatient US adults. JAMA Dermatol 2022 Jul 1;158(7):745-753. [doi: 10.1001/jamadermatol.2022.1609] [Medline: 35612851]
29. Thomas DM, Bredlau C, Bosy-Westphal A, et al. Relationships between body roundness with body fat and visceral adipose tissue emerging from a new geometrical model. Obesity (Silver Spring) 2013 Nov;21(11):2264-2271. [doi: 10.1002/oby.20408] [Medline: 23519954]
30. Tang H, Zhang X, Luo N, Huang J, Zhu Y. Association of dietary live microbes and nondietary prebiotic/probiotic intake with cognitive function in older adults: evidence from NHANES. J Gerontol A Biol Sci Med Sci 2024 Feb 1;79(2):glad175. [doi: 10.1093/gerona/glad175] [Medline: 37480582]

XSL•FO
RenderX

31. Liang Z, Sun X, Lan J, et al. Association between pyrethroid exposure and osteoarthritis: a national population-based cross-sectional study in the US. BMC Public Health 2023 Aug 24;23(1):1521. [doi: 10.1186/s12889-023-16225-2] [Medline: 37612655]
32. Fiorentino TV, De Vito F, Suraci E, et al. Obesity and overweight are linked to increased sodium-glucose cotransporter 1 and glucose transporter 5 levels in duodenum. Obesity (Silver Spring) 2023 Mar;31(3):724-731. [doi: 10.1002/oby.23653] [Medline: 36746764]
33. Ouyang A, Hu K, Chen L. Trends and risk factors of diabetes and prediabetes in US adolescents, 1999-2020. Diabetes Res Clin Pract 2024 Jan;207:111022. [doi: 10.1016/j.diabres.2023.111022] [Medline: 37981123]
34. Harreiter J, Roden M. Diabetes mellitus: Definition, classification, diagnosis, screening and prevention (update 2023). Wien Klin Wochenschr 2023 Jan;135(Suppl 1):7-17. [doi: 10.1007/s00508-022-02122-y] [Medline: 37101021]
35. Winkelman JW, Shahar E, Sharief I, Gottlieb DJ. Association of restless legs syndrome and cardiovascular disease in the Sleep Heart Health Study. Neurology (ECronicon) 2008 Jan 1;70(1):35-42. [doi: 10.1212/01.wnl.0000287072.93277.c9] [Medline: 18166705]
36. Lindbohm JV, Sipilä PN, Mars N, et al. Association between change in cardiovascular risk scores and future cardiovascular disease: analyses of data from the Whitehall II longitudinal, prospective cohort study. Lancet Digit Health 2021 Jul;3(7):e434-e444. [doi: 10.1016/S2589-7500(21)00079-0] [Medline: 34167764]
37. Alberti K, Eckel RH, Grundy SM, et al. Harmonizing the metabolic syndrome. Circulation 2009 Oct 20;120(16):1640-1645. [doi: 10.1161/CIRCULATIONAHA.109.192644]
38. Grundy SM, Cleeman JI, Daniels SR, et al. Diagnosis and management of the metabolic syndrome. Circulation 2005 Oct 25;112(17):2735-2752. [doi: 10.1161/CIRCULATIONAHA.105.169404]
39. von Elm E, Altman DG, Egger M, et al. Strengthening the Reporting of Observational Studies in Epidemiology (STROBE) statement: guidelines for reporting observational studies. BMJ 2007 Oct 20;335(7624):806-808. [doi: 10.1136/bmj.39335.541782.AD] [Medline: 17947786]
40. Gorski MT, Cohen JFW, Hoffman JA, et al. Impact of nutrition standards on competitive food quality in Massachusetts middle and high schools. Am J Public Health 2016 Jun;106(6):1101-1108. [doi: 10.2105/AJPH.2016.303139] [Medline: 27077344]
41. Yadav V, Mendiratta V, Agrawal A, Bisherwal K, Singh R, Meena AK. Interleukin levels and non-alcoholic fatty liver disease in chronic plaque psoriasis: an analytical case control study. Indian J Dermatol 2023;68(4):377-384. [doi: 10.4103/ijd.ijd_1015_22] [Medline: 37822394]
42. Guo J, Zhang H, Lin W, Lu L, Su J, Chen X. Signaling pathways and targeted therapies for psoriasis. Signal Transduct Target Ther 2023 Nov 27;8(1):437. [doi: 10.1038/s41392-023-01655-6] [Medline: 38008779]
43. Koepp GA, Manohar CU, McCrady-Spitzer SK, et al. Treadmill desks: A 1-year prospective trial. Obesity (Silver Spring) 2013 Apr;21(4):705-711. [doi: 10.1002/oby.20121] [Medline: 23417995]
44. Budzyński J, Szukay B. BMI as a biomarker in patients' nutritional assessment. In: Patel VB, Preedy VR, editors. Biomarkers in Nutrition: Springer International Publishing; 2022:1-35. [doi: 10.1007/978-3-030-81304-8_36-1]
45. Carrasquilla GD, García-Ureña M, Romero-Lado MJ, Kilpeläinen TO. Estimating causality between smoking and abdominal obesity by Mendelian randomization. Addiction 2024 Jun;119(6):1024-1034. [doi: 10.1111/add.16454] [Medline: 38509034]
46. Traversy G, Chaput JP. Alcohol consumption and obesity: an update. Curr Obes Rep 2015 Mar;4(1):122-130. [doi: 10.1007/s13679-014-0129-4] [Medline: 25741455]
47. Chiricozzi A, Raimondo A, Lembo S, et al. Crosstalk between skin inflammation and adipose tissue-derived products: pathogenic evidence linking psoriasis to increased adiposity. Expert Rev Clin Immunol 2016 Dec;12(12):1299-1308. [doi: 10.1080/1744666X.2016.1201423] [Medline: 27322922]
48. Ellulu MS, Patimah I, Khaza'ai H, Rahmat A, Abed Y. Obesity and inflammation: the linking mechanism and the complications. aoms 2017;4:851-863. [doi: 10.5114/aoms.2016.58928]
49. Alajroush WA, Alrshid AI, Alajlan AH, et al. Psoriasis and metabolic disorders: a comprehensive meta-analysis of million adults worldwide. Cureus 2024 Jan;16(1):e52099. [doi: 10.7759/cureus.52099] [Medline: 38344577]

Abbreviations

BFP: body fat percentage
BRI: body roundness index
CVD: cardiovascular disease
MEC: mobile examination center
NCHS: National Center for Health Statistics
NHANES: National Health and Nutrition Examination Survey
OR: odds ratio
PIR: poverty-income ratio
RCS: restricted cubic spline
STROBE: Strengthening the Reporting of Observational Studies in Epidemiology

XSL•FO
RenderX

WC: waist circumference
WHR: waist-to-hip ratio
WHR: waist-to-hip ratio
WHtR: waist-to-height ratio

Edited by A Benis; submitted 10.04.25; peer-reviewed by E Madondo, Y Zhang; revised version received 17.10.25; accepted 23.10.25; published 23.12.25.

Please cite as:
Wen P, Wang X, Zhuo X, Xue S
Evaluating the Body Roundness Index as a Novel Digital Biomarker for Psoriasis Risk Prediction: Cross-Sectional Study
JMIR Med Inform 2025;13:e75727
URL: https://medinform.jmir.org/2025/1/e75727
doi:10.2196/75727

© Pengfei Wen, Xiaoyan Wang, Xiaoxue Zhuo, Siliang Xue. Originally published in JMIR Medical Informatics (https://medinform.jmir.org), 23.12.2025. This is an open-access article distributed under the terms of the Creative Commons Attribution License (https://creativecommons.org/licenses/by/4.0/), which permits unrestricted use, distribution, and reproduction in any medium, provided the original work, first published in JMIR Medical Informatics, is properly cited. The complete bibliographic information, a link to the original publication on https://medinform.jmir.org/, as well as this copyright and license information must be included.

XSL•FO
RenderX

An Intelligent Trial Eligibility Screening Tool Using Natural Language Processing With a Block-Based Visual Programming Interface: Development and Usability Study

Ya-Han Hu[1,2], PhD; Yi-Ying Cheng[1], MIM; Chung-Ching Lan[1], MBA; Yu-Hsiang Su[3*], MD; Sheng-Feng Sung[3,4*], MD, PhD

[1]Department of Information Management, National Central University, Taoyuan, Taiwan

[2]Asian Institute for Impact Measurement and Management, National Central University, Taoyuan, Taiwan

[3]Division of Neurology, Department of Internal Medicine, Ditmanson Medical Foundation Chia-Yi Christian Hospital, 539 Zhongxiao Road, East District, Chiayi City, Taiwan

[4]Department of Nursing, Fooyin University, Kaohsiung, Taiwan

[*]these authors contributed equally

Corresponding Author:
Sheng-Feng Sung, MD, PhD
Division of Neurology, Department of Internal Medicine, Ditmanson Medical Foundation Chia-Yi Christian Hospital, 539 Zhongxiao Road, East District, Chiayi City, Taiwan

Abstract

Background: Clinical trial eligibility screening using electronic medical records (EMRs) is challenging due to the complexity of patient data and the varied clinical terminologies. Manual screening is time-consuming, requires specialized knowledge, and can lead to inconsistent participant selection, potentially compromising patient safety and research outcomes. This is critical in time-sensitive conditions like acute ischemic stroke. While computerized clinical decision support tools offer solutions, most require software engineering expertise to update, limiting their practical utility when eligibility criteria change.

Objective: We developed and evaluated the intelligent trial eligibility screening tool (iTEST), which combines natural language processing with a block-based visual programming interface designed to enable clinicians to create and modify eligibility screening rules independently. In this study, we assessed iTEST's rule evaluation module using pre-configured rules and compared its effectiveness with that of standard EMR interfaces.

Methods: We conducted an experiment at a tertiary teaching hospital in Taiwan with 12 clinicians using a 2-period crossover design. The clinicians assessed the eligibility of 4 patients with stroke for 2 clinical trials using both standard EMR and iTEST in a counterbalanced order, resulting in 48 evaluation scenarios. The iTEST comprised a rule authoring module using Google Blockly and a rule evaluation module utilizing MetaMap Lite for extracting medical concepts from unstructured EMR documents and structured laboratory data. Primary outcomes included accuracy in determining eligibility. Secondary outcomes measured task completion time, cognitive workload using the National Aeronautics and Space Administration Task Load Index scale (range 0 - 100, with lower scores indicating a lower cognitive workload), and system usability through the system usability scale (range: 0 - 100, with higher scores indicating higher system usability).

Results: The iTEST significantly improved accuracy scores (from 0.91 to 1.00, $P<.001$) and reduced completion time (from 3.18 to 2.44 min, $P=.004$) compared to the standard EMR interface. Users reported lower cognitive workload (National Aeronautics and Space Administration Task Load Index scale, 39.7 vs 62.8, $P=.02$) and higher system usability scale scores (71.3 vs 46.3, $P=.01$) with the iTEST. Particularly notable improvements in perceived cognitive workload were observed in temporal demand, effort, and frustration levels.

Conclusions: The iTEST demonstrated superior performance in clinical trial eligibility screening, delivering improved accuracy, reduced completion time, lower cognitive workload, and better usability when evaluating preconfigured eligibility rules. The improved accuracy is critical for patient safety, as the misidentification of eligibility criteria could expose patients to inappropriate treatments or exclude them from beneficial trials. The adaptability and ability of the iTEST to process both structured and unstructured data make it valuable for time-sensitive scenarios and evolving research protocols. Future research should evaluate clinicians' ability to create and modify eligibility rules using the block-based authoring interface, as well as assess the iTEST across diverse types of clinical trials and health care settings.

(JMIR Med Inform 2025;13:e80072) doi:10.2196/80072

XSL•FO
RenderX

KEYWORDS

block-based visual programming; clinical decision support; clinical trials; electronic medical records; eligibility screening; natural language processing; patient safety

Introduction

Clinical trials follow strict criteria for participant selection, using documented medical records as essential information sources. Over time, electronic medical records (EMRs) have evolved into comprehensive data repositories, enabling health care providers to track information systematically [1-3]. However, the increased volume and complexity of EMRs offer a detailed view of patient histories while posing challenges for researchers analyzing this wealth of data.

The complexity of EMRs demands extensive time and effort from researchers to analyze documents. Addressing EMR-related cognitive overload and burnout is now critical [4]. Researchers face tight deadlines, especially in clinical trials for time-sensitive conditions like stroke or brain injury. The phrase “time is brain” underscores the urgency for immediate therapy post-onset [5,6]. Therefore, researchers must rapidly verify inclusion and exclusion criteria [7,8]. Accurately extracting relevant information from EMRs is also essential for participant eligibility; violations could compromise trial validity and harm participants. This heavy workload increases mental stress and risks judgment errors among clinical researchers.

To address these challenges, using computerized clinical decision support tools in trial eligibility screening offers a promising solution [9]. These systems can efficiently process EMRs, enabling rapid candidate screening. However, EMRs contain a significant amount of unstructured narrative text, with about 80% being narrative—a format clinicians prefer for patient information [10]. These unstructured data complicate medical concept extraction automation. The widespread use of synonyms, acronyms, and abbreviations in clinical documentation further complicates matters, making conventional natural language processing (NLP) techniques often inadequate and necessitating specialized medical NLP tools.

Our previous study developed an NLP-enhanced task-specific EMR interface that presented relevant medical concepts to clinicians through highlighted documents for determining intravenous thrombolysis eligibility criteria [11]. The results showed that this EMR interface improved decision-making in stroke therapy. However, creating entirely new systems with specific rules for each clinical problem remains challenging. Clinical trial or therapy eligibility criteria often evolve as new evidence emerges [12]. Current approaches require software engineers to update rules or build new systems whenever clinical guidelines or criteria change, raising costs [13]. Therefore, there is considerable room for improving the design of such tools.

This study aimed to develop an intelligent trial eligibility screening tool (iTEST) adaptable to various medical scenarios, particularly where eligibility criteria frequently change. By identifying common patterns in eligibility criteria and using a block-based visual programming interface, our tool enables clinicians to create computerized eligibility rules independently, without requiring software engineering expertise. We conducted experiments to evaluate the tool’s impact on users’ accuracy, efficiency, and cognitive workload during eligibility determination.

Methods

Study Setting

This study was conducted at Ditmanson Medical Foundation Chia-Yi Christian Hospital, a 1000-bed tertiary teaching hospital in southern Taiwan, which has a certified comprehensive stroke center managing approximately 650 stroke admissions annually. We evaluated 2 sets of eligibility criteria: the first set for intravenous thrombolysis, adapted from the National Institute of Neurological Disorders and Stroke (NINDS) recombinant tissue-plasminogen activator (rt-PA) trial [14], which examined the efficacy of tissue plasminogen activator for acute ischemic stroke, and the second set from the Librexia STROKE trial [15], examining milvexian’s safety and efficacy in preventing recurrent cerebrovascular events post-acute ischemic stroke or high-risk transient ischemic attack.

Ethical Considerations

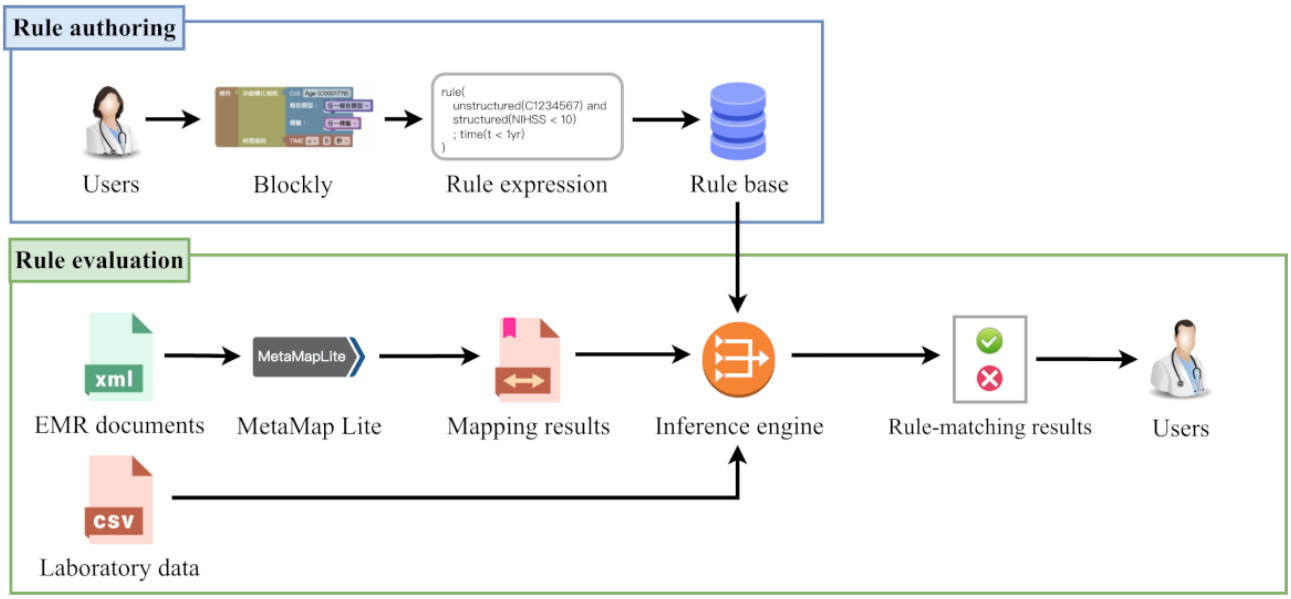
The study protocol received formal approval from the Institutional Review Board of Ditmanson Medical Foundation Chia-Yi Christian Hospital (2022102). A unique study identification number replaced patient identifiers to ensure confidentiality. Informed consent was thus exempted. Participants were compensated NTD 3000 (≈USD 96) for their time and participation.

Intelligent Trial Eligibility Screening Tool

Figure 1 illustrates the overview of the iTEST, which has 2 main components: the rule authoring and evaluation modules. In the rule authoring module, users convert narrative eligibility criteria into Blockly blocks [16], which are parsed into customized rule expressions and stored in the rule base. The rule evaluation module extracts structured laboratory data from EMRs and maps medical concepts from unstructured EMR documents using MetaMap Lite [17]. The inference engine then determines eligibility for each criterion by matching the extracted information to the rule base, and the tool presents users with rule-matching results.

XSL•FO
RenderX

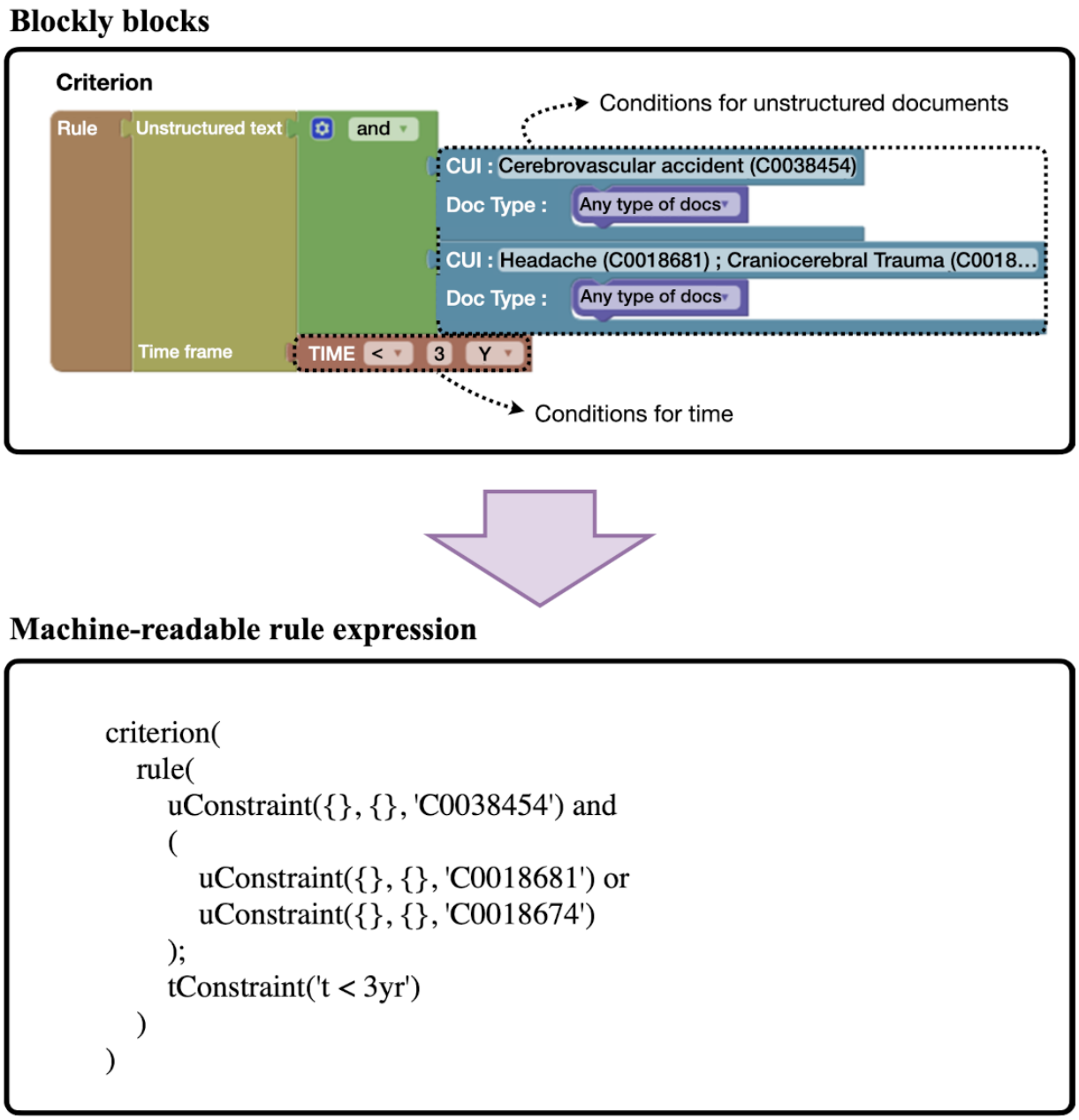
Figure 1. Overview of the intelligent trial eligibility screening tool (iTEST), which comprises a rule authoring module (upper part) and a rule evaluation module (lower part). EMR: electronic medical record.



The rule authoring module (upper part of Figure 1) creates, edits, and versions the eligibility criteria checklist using a block-based visual programming interface powered by Blockly (version 10.4.3; Google) [16]. This method, commonly used in programming education, provides visual cues and drag-and-drop functionality while avoiding invalid block combinations. Our study developed customized rule expressions that represent medical concepts and laboratory items in a machine-readable format. Users can easily convert human-written checklist criteria into rule expressions by creating criterion blocks. For numerical laboratory data, criterion blocks allow users to input laboratory items to define conditions (eg, “Platelets <100,000”). For unstructured documents, criterion blocks enable users to specify multiple medical concepts and select EMR document types. Time conditions can be added by using temporal blocks that perform date calculations on EMR timestamp fields (Figure 2), while logical operators such as AND can combine blocks, which execute separate queries across EMR documents, to express complex criteria like “Having a headache or head injury within three years” or “diabetes with prior stroke in the past.” The module translates these blocks into machine-readable rule expressions, enhancing the readability of eligibility criteria and making it easier for nonprogrammers to understand. This module thus enables clinicians to develop complex eligibility rules without requiring programming skills.

XSL•FO
RenderX

Figure 2. An example showing how Blockly blocks are converted into machine-readable rule expressions.



The rule evaluation module (lower part of Figure 1) processes 2 data types. It reads numerical laboratory data in tabular format and uses MetaMap Lite (3.6.2rc8 binary only version; U.S. National Library of Medicine) to extract medical concepts from unstructured EMR documents. MetaMap Lite [17], a faster version of MetaMap [18], maps concepts using the Unified Medical Language System Metathesaurus and assigns Unified Medical Language System concept unique identifiers to annotated concepts [17]. It generates a list of concepts from EMR documents, discarding irrelevant ones based on semantic type settings. Additionally, it addresses challenges like complex concepts with multiple synonyms and potential misinterpretation of word context variations.

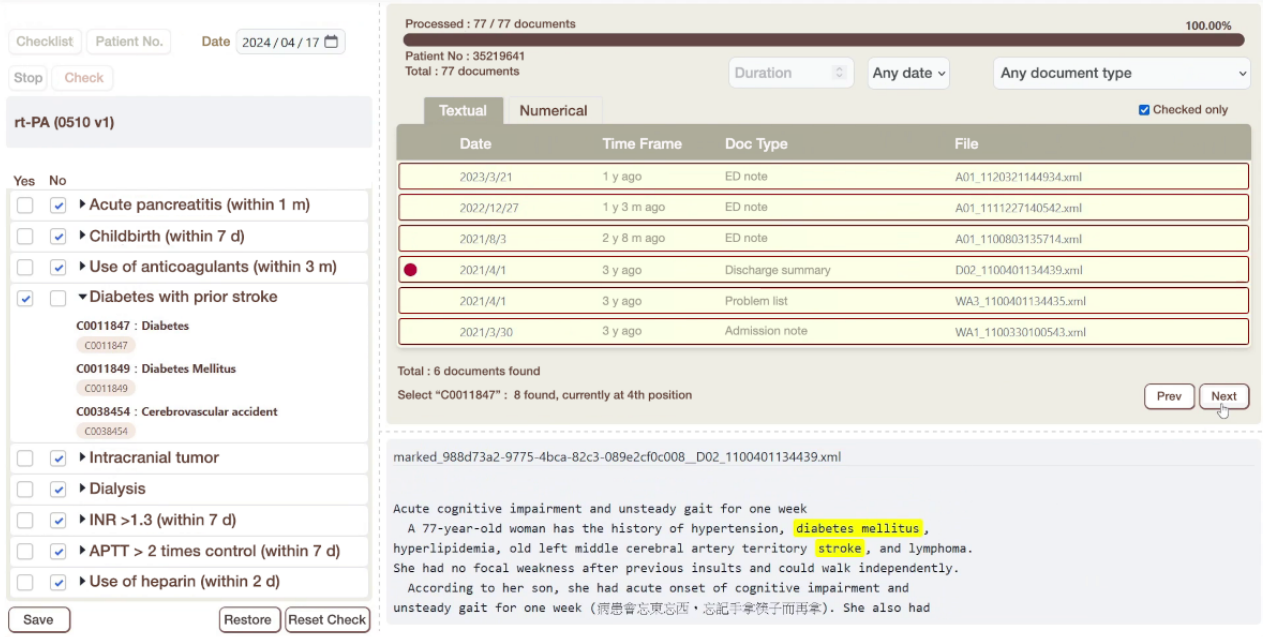
As an internal validation, we evaluated MetaMap Lite's ability to identify medical concepts related to the eligibility criteria examined in this study. We randomly selected 61 documents from 20 patients in a validation dataset separate from the one used for rule development. Two independent expert clinicians manually reviewed and annotated each document to establish a gold-standard reference, resolving disagreements through discussion and consensus. Precision and recall were calculated by comparing MetaMap Lite's automated extractions with the gold-standard annotations for each eligibility concept. Table S1 in Multimedia Appendix 1 displays the results, showing high precision and recall for most of the related concepts.

The inference engine analyzes the extracted information against the rule base to evaluate eligibility for each criterion. A web-based interface displays the rule-matching results, allowing users to review the eligibility criteria checklist with links to

XSL•FO
RenderX

annotated EMR documents, highlighting key concepts for review (Figure 3).

Figure 3. The intelligent trial eligibility screening tool (iTEST) interface. The left panel displays a trial eligibility criteria checklist, with each criterion marked yes or no based on the patient's data. The upper right panel features 2 tabs: one for clinical documents and one for numerical laboratory data. A red dot marks documents with relevant information. The lower right panel shows the content of the selected clinical document, highlighting key medical concepts for easy reference.



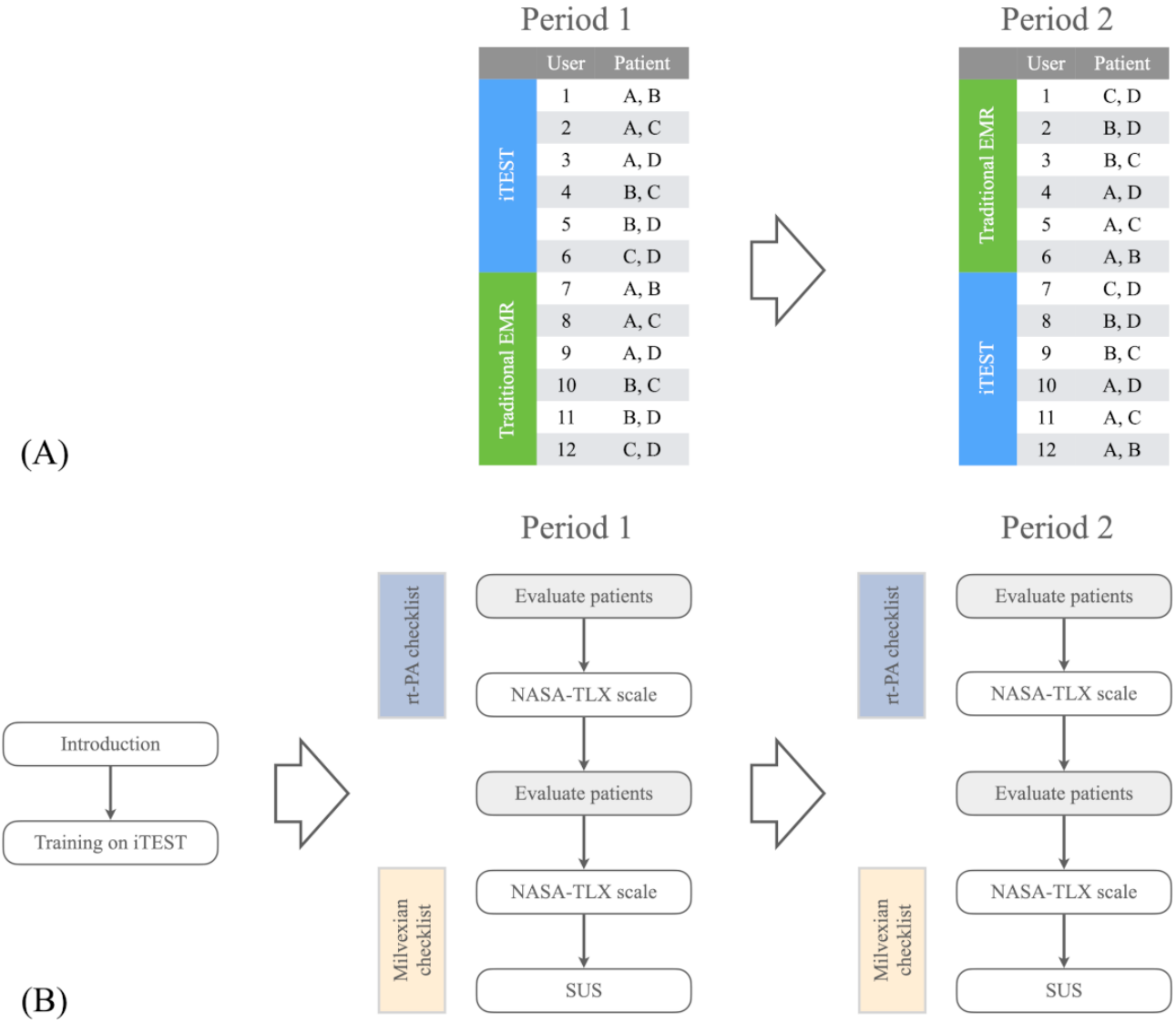
User Experiment

We conducted a user experiment to assess users' accuracy, efficiency, and perceived workload in determining eligibility. A total of 12 clinicians participated in the study, using either a standard EMR interface or the iTEST on a desktop computer to complete eligibility criteria checklists for the NINDS rt-PA and Librexia STROKE trials. Participation was voluntary and compensated.

The experiment used a 2-period crossover design to compare the effectiveness of the iTEST with a standard EMR interface. Each user evaluated 4 patients—2 with the iTEST and 2 with the standard EMR—resulting in 48 scenarios (Figure 4A). We set the participant count at 12 to ensure each patient appeared 6 times in both testing scenarios.

XSL•FO
RenderX

Figure 4. A 2-period crossover design for the user experiment (A). Procedures of the user experiment (B). EMR: electronic medical record; NASA-TLX: National Aeronautics and Space Administration Task Load Index; rt-PA: recombinant tissue-plasminogen activator; SUS: system usability scale.



The 4 cases chosen for this study are actual patients with stroke from our hospital. They have complex histories, detailed records across multiple departments, and several treatment contraindications. Some critical contraindications are only documented in less prominent sections, like outpatient notes, making them harder to identify quickly during assessment. To prevent overfitting and ensure an unbiased evaluation, the 4 cases were held out from the datasets used for the development or internal validation of the eligibility extraction rules.

At the experiment's start, each user received a detailed introduction to procedures (Figure 4B) and 10 minutes of iTEST training. A study coordinator managed the process and recorded time points. In period 1, users utilized either the standard EMR interface or the iTEST, switching to the other in period 2. During each period, users evaluated eligibility for 2 patients, first for the rt-PA checklist and then for the milvexian checklist. After evaluations, they assessed cognitive workload using the National Aeronautics and Space Administration Task Load Index (NASA-TLX) scale [19]. At the end of each period, they provided overall usability feedback through the system usability scale (SUS) questionnaire [20].

Outcomes

The primary outcome measured response accuracy to the eligibility checklist. For each patient, users completed checklists for 2 trials (Tables S2 and S3 in Multimedia Appendix 1). At least 2 senior neurologists (YHS and SFS) with extensive stroke care experience established reference answers by consensus, against which user responses were marked as correct or incorrect. Each correct response earned 1 point, and the final accuracy score (maximum=1) for each checklist was the average of the points of all criteria in that checklist.

Secondary outcomes included checklist completion time, cognitive workload (measured by the NASA-TLX scale), and tool usability (measured by the SUS). The NASA-TLX assesses 2 dimensions of subjective workload: mental demand, physical demand, temporal demand, performance, effort, and frustration [19], rated from 0 to 20, with higher scores indicating greater cognitive workload. Ratings are weighted to produce a total score from 0 to 100. The SUS evaluates interface usability via a 10-item Likert scale questionnaire (from strongly agree to strongly disagree), assessing factors including support needs, training requirements, complexity, integration, ease of learning,

XSL•FO
RenderX

and user confidence [20]. SUS scores range from 0 to 100, with higher scores indicating better usability. A prior study showed that adjective ratings of "poor," "OK," and "good" corresponded to average SUS scores of 35.7, 50.9, and 71.4, respectively [21].

In addition to the above planned analyses comparing overall performance between the standard EMR interface and the iTEST, we conducted exploratory subgroup analyses examining each treatment protocol (rt-PA and milvexian) separately to provide more detailed insights into system performance across different clinical scenarios.

Statistical Analysis

Given the small sample size in the user experiment and the non-normal distribution of the outcome measures, we reported the outcome measures as medians with interquartile ranges and conducted nonparametric analyses. The iTEST and the standard EMR interface were compared using the Wilcoxon signed-rank test for repeated user measurements. Two-tailed *P* values <.05 were considered statistically significant. Analyses were performed using R version 4.4.0 (R Foundation for Statistical Computing).

Results

User Statistics

Table 1 summarizes participant characteristics. The study included 6 physicians and 6 nurse practitioners. The participants, who were evenly split between male and female participants, had a mean age of 41 years and varied widely in experience levels across clinical practice, EMR use, personal computer use, and stroke care. The median clinical experience was 14.5 years, and they used the standard EMR interface for a median of 7 years.

Table . User characteristics.

User	Age (y)	Gender	Profession	Experience (y)			
				Clinical practice	EMR[a] use	PC[b] use	Stroke care
#1	34	Male	Physician	7	5	7	1
#2	46	Female	NP[c]	25	15	30	5
#3	51	Female	NP	27	9	30	16
#4	39	Female	NP	10	10	20	16
#5	40	Female	NP	20	8	20	3
#6	32	Male	Physician	8	7	15	1
#7	40	Male	Physician	14	6	25	6
#8	35	Male	Physician	10	3	25	3
#9	41	Male	Physician	15	1	22	15
#10	43	Male	Physician	16	12	20	16
#11	40	Female	NP	18	7	22	2
#12	48	Female	NP	7	7	7	3

[a]EMR: electronic medical record.

[b]PC: personal computer.

[c]NP: nurse practitioner.

Computational Performance

To evaluate the iTEST's computational performance, we measured processing time using EMRs from 15 patients with different documentation volumes. The number of clinical notes per patient ranged from 417 to 7299. System processing time (measured from patient selection to the full display of MetaMap Lite-analyzed clinical notes) varied from 6 to 345 seconds (average: 39 ms per note). This processing represents an initial computational overhead when a patient is first loaded; the subsequent evaluation of multiple eligibility criteria requires no extra processing time. In our clinical workflow, iTEST processing begins at patient triage in the emergency department, ensuring that all EMR analyses are completed before clinicians assess trial eligibility.

Evaluation Outcomes

Table 2 compares the outcomes of the standard EMR interface with the iTEST. Users attained a median accuracy score of 0.91 for the primary outcome using the standard EMR interface. In contrast, the iTEST produced a higher median accuracy score of 1.00, representing a 9.9% improvement with strong statistical significance (*P*<.001).

XSL•FO
RenderX

Table . Comparisons of outcomes between scenarios using the standard EMR[a] interface and the iTEST.

Outcome	Standard EMR interface, median (IQR)	iTEST[b], median (IQR)	*P* value
Accuracy score	0.91 (0.84 - 0.96)	1.00 (0.95 - 1.00)	<.001
Time (min)	3.18 (2.34 - 4.52)	2.44 (1.67 - 3.17)	.004
NASA-TLX[c] score	62.8 (36.7 - 75.8)	39.7 (26.8 - 52.0)	.02
SUS[d] score	46.3 (36.9 - 55.0)	71.3 (56.9 - 75.6)	.01

[a]EMR: electronic medical record.

[b]iTEST: intelligent trial eligibility screening tool.

[c]NASA-TLX: National Aeronautics and Space Administration Task Load Index.

[d]SUS: system usability scale.

Tables S2 and S3 in Multimedia Appendix 1 display the average accuracy scores of all 12 users for each eligibility criterion. With the standard EMR interface, accuracy scores ranged from 0.54 to 1.00, while the iTEST improved this range to 0.75 to 1.00. Users particularly struggled with certain criteria while using the standard interface, including identifying a diabetes history along with a prior stroke, internal bleeding within the last 3 months, and an activated prothrombin time of ≤1.4 times the control value within 7 days. For these challenging criteria, accuracy scores dropped below 0.60 with the standard interface but improved to at least 0.75 with the iTEST.

For secondary outcomes, the iTEST reduced task completion time by 0.74 minutes (23.3% reduction; from 3.18 to 2.44 min; *P*=.004) compared with the standard EMR interface. Users reported a 23.1-point reduction in NASA-TLX scores (36.8% decrease; from 62.8 to 39.7; *P*=.02), indicating substantial improvement in perceived cognitive demand. The SUS scores improved by 25 points (54% increase; from 46.3 to 71.3; *P*=.01), moving the system from the “POOR to OK” category to the “OK to GOOD” category and exceeding the acceptability threshold [21].

Table 3 presents the scores for each NASA-TLX subscale. Among the 6 dimensions of cognitive workload, mental demand, temporal demand, and effort received higher scores than physical demand, performance, and frustration. Participants reported significant reductions in temporal demand, effort, and frustration when using the iTEST as opposed to the standard EMR interface.

Table . Comparisons of NASA-TLX[a] subscales between scenarios using the standard EMR[b] interface and the iTEST[c].

NASA-TLX subscale	Standard EMR interface, median (IQR)	iTEST, median (IQR)	*P* value
Mental demand	13.5 (10.0 - 16.6)	10.0 (6.8 - 14.3)	.13
Physical demand	10.0 (6.8 - 13.0)	7.0 (4.4 - 10.0)	.18
Temporal demand	14.0 (10.0 - 17.6)	9.0 (4.9 - 11.5)	.007
Performance	7.0 (2.0 - 10.5)	3.8 (2.0 - 5.3)	.10
Effort	14.0 (10.0 - 17.6)	9.0 (4.4 - 14.0)	.02
Frustration	7.5 (3.5 - 10.0)	4.3 (1.0 - 8.0)	.02

[a]NASA-TLX: National Aeronautics and Space Administration Task Load Index.

[b]EMR: electronic medical record.

[c]iTEST: intelligent trial eligibility screening tool.

The results of the exploratory subgroup analysis, which compares the outcomes for each checklist individually, are listed in Table S4 in Multimedia Appendix 1. For the rt-PA checklist, the accuracy score significantly improved from 0.91 to 1.00 (*P*=.001) using the iTEST. However, no significant differences were observed in task completion time or NASA-TLX scores. In contrast, the iTEST significantly improved all outcomes for the milvexian checklist.

Discussion

Principal Results

This study demonstrated that the iTEST outperformed the standard EMR interface in multiple ways. It improved the accuracy of determining trial eligibility criteria while enhancing efficiency through shorter task completion time. The iTEST also significantly reduced users’ cognitive workload and offered better usability than the standard interface.

Accuracy of Eligibility Screening

The iTEST showed significant improvements over the standard EMR interface. It enhanced accuracy in identifying both

XSL•FO
RenderX

numerical laboratory data and textual information in clinical documents. For instance, for the milvexian checklist, the accuracy score for "APTT≤1.4 times control" increased markedly from 0.54 to 0.92 (Table S3 in Multimedia Appendix 1). This improvement likely occurred because the standard EMR lacks automated rule checking, requiring users to perform mental or manual calculations of numerical values.

The iTEST also improved accuracy when determining eligibility criteria using textual information. For instance, for the rt-PA checklist, users often misidentified patients with "diabetes with prior stroke," achieving only a 0.54 accuracy score. This low score likely arose from the complexity of the assessments needing both laboratory data and clinical narratives. Extensive medical histories can obscure crucial diagnostic evidence, leading to medical errors [22]. This is a common challenge for clinical researchers working with large, complex medical records—even in electronic form, the human brain struggles to identify key concepts quickly [23,24]. The iTEST addressed this challenge by extracting and highlighting essential information in clinical documents, thereby improving eligibility screening accuracy from 0.54 to 0.75 (Table S2 in Multimedia Appendix 1). However, the suboptimal accuracy (0.75) underscores the challenge of linking temporal relationships between conditions documented across multiple clinical notes. This limitation affects both automated systems and human reviewers due to cognitive load and fragmented information in medical records.

While the iTEST performed well overall in clinical trial screening, our NLP validation (Table S1 in Multimedia Appendix 1) revealed issues with key concept extraction. Notably, "Anticoagulant" detection (F_1-score=0.33) was poor, mainly due to nonstandard negation expressions that caused false positives and incomplete concept mapping, leading to missing specific anticoagulants. We refined the process by adding 5 anticoagulants (warfarin, apixaban, dabigatran, edoxaban, rivaroxaban), greatly improving accuracy. This workaround, however, highlights a significant limitation of MetaMap Lite's concept generalization and ontology depth for broad drug classes; the tool failed to effectively handle a critical, broad safety concept without explicit enumeration of individual drugs. This highlights the need for concept validation and iterative refinement in NLP tools for critical criteria.

Furthermore, using MetaMap Lite instead of the full MetaMap may result in less effective concept extraction. While faster and lighter, MetaMap Lite implements only a subset of MetaMap's extensive options and lacks sophisticated word-sense disambiguation modules, which can result in mapping all available senses of a term and generating false positives [17]. The failure to generalize the anticoagulant concept exemplifies this limitation. Specifically, MetaMap Lite's shallower ontology proved inadequate for managing hierarchical drug class relationships essential for safety screening. Although suitable for resource-limited or real-time applications, high-accuracy tasks are better served by the full MetaMap, emphasizing the trade-off between speed and depth.

Therefore, we recommend that clinical implementations of the iTEST include a validation phase where each new eligibility criterion is tested against a small set of annotated medical records before deployment. This quality assurance step can identify concept-mapping issues and help refine the process, especially for critical safety−related criteria such as anticoagulant use. Furthermore, despite the iTEST achieving a median accuracy of 1.00, the relatively lower accuracy on critical, complex criteria such as "diabetes with prior stroke" still indicates a high-risk failure mode that the iTEST did not fully address.

Efficiency and Usability

Even though users were trying the iTEST for the first time, they completed eligibility screening significantly faster after just a 10-minute training session. Users took a median of 2.44 minutes with the iTEST compared to 3.18 minutes with the standard EMR interface (Table 2) despite having years of experience with the latter. Notably, when analyzing individual checklists, the rt-PA checklist showed no significant improvement in completion time. This likely occurred because users were already highly familiar with checking eligibility criteria for intravenous thrombolysis (similar to those of the NINDS rt-PA trial) in their daily clinical practice before the study. Additionally, our study might have been underpowered to detect these smaller effects on familiar tasks, unlike the significant improvements seen across all metrics for the unfamiliar milvexian checklist.

With users achieving higher accuracy in less time during eligibility screening, it is unsurprising that the iTEST demonstrated better system usability than the standard EMR interface. The SUS score of 71.3 represents acceptable usability in the "OK to GOOD" range, indicating meaningful improvement over the standard EMR (46.3) but also suggesting room for further optimization. Despite being new to users and having received only 10 minutes of training, the iTEST demonstrated reasonable ease of use for this specific task. Research has shown that EMR systems should incorporate ongoing physician feedback to enhance usability, as poor EMR design can negatively impact physicians' well-being and increase their perceived workload [25]. Consistent with these findings, the iTEST not only improved system usability but also reduced the perceived cognitive workload.

Cognitive Workload

The iTEST significantly outperformed the standard EMR interface in overall NASA-TLX scores. While some researchers question the mathematical validity of combining the 6 NASA-TLX dimensions into a single workload score [26], we analyzed both the overall and individual dimensions (Table 3). The most substantial improvements were observed in temporal demand (from 14.0 to 9.0, P=.007) and effort (from 14.0 to 9.0, P=.02), with frustration levels also showing a significant reduction (from 7.5 to 4.3, P=.02). The marked reduction in temporal demand aligned with the decreased task completion time, which is crucial since the effectiveness of stroke therapy depends heavily on timing [27] and creates substantial pressure for clinicians [28,29]. While we observed significant improvements in temporal demand, effort, and frustration subscales, reductions in mental demand, physical demand, and

XSL•FO
RenderX

performance subscales did not reach statistical significance, possibly due to a limited sample size.

Few studies have assessed trial eligibility screening workload [30,31], primarily measuring work volume instead of cognitive burden. To our knowledge, no research has specifically analyzed the cognitive workload of this task. However, studies have compared perceived cognitive workload across different EMR interfaces and visualization tools for various clinical tasks [32-34], indicating that renovations to the EMR interface can enhance efficiency and reduce cognitive demands.

Clinical Implications

The iTEST improves upon the standard EMR interface with better accuracy and efficiency in eligibility screening, reduced cognitive workload, and enhanced usability, leading to several clinical benefits. Researchers can enroll suitable trial participants more effectively, ensuring scientific validity and data quality while protecting ineligible patients. Additionally, the iTEST enhances patient safety by avoiding unnecessary risks. For instance, the NINDS-rt-PA trial, which examined rt-PA in patients with acute ischemic stroke, highlights the importance of careful patient selection to mitigate serious intracranial bleeding risks [35]. The eligibility criteria established by this trial have become the standard for intravenous thrombolysis [36]. Consequently, the iTEST can assist clinicians in selecting appropriate patients for therapies, improving routine clinical practice.

While the iTEST's computational overhead can reach up to 345 seconds for patients with extensive EMR histories, this does not affect time-sensitive clinical decision-making in our workflow. By starting EMR processing at emergency department triage, all computational work is completed before clinicians evaluate trial eligibility. This integration ensures that the iTEST's processing time does not cause delays during the critical acute stroke assessment window. Future implementations in other clinical settings should consider similar workflow integration strategies, and improving MetaMap Lite's performance may further reduce processing times for real-time use.

This study examined 2 checklists. Users were already familiar with the rt-PA checklist before the study. They still made occasional mistakes, achieving a median accuracy score of 0.91. The iTEST improved this score to 1.00. The milvexian checklist, being new to users, yielded a lower median accuracy score (0.84) than the rt-PA checklist (0.91), highlighting how unfamiliarity with eligibility criteria can lead to more errors. With the iTEST, users achieved nearly perfect accuracy (median score 1.00) for both the familiar rt-PA and unfamiliar milvexian checklist, demonstrating its value over the standard EMR interface, especially for new eligibility checklists. However, the separate analyses of the rt-PA and milvexian checklists were exploratory. While these findings provide valuable insights into protocol-specific performance, they should be interpreted cautiously and confirmed in future prospective studies with predefined hypotheses.

Cognitive overload is a leading cause of burnout among clinicians [4]. When facing burnout, clinicians favor patients with straightforward medical histories, as fewer clinical documents are needed for eligibility determination. They may overlook patients with complex, lengthy medical histories requiring thorough review. This selection bias can compromise clinical trial validity by causing the trial population to deviate from the intended target population. The iTEST addresses this issue by reducing cognitive workload, thus streamlining patient recruitment and minimizing selection bias. This benefit becomes even more pronounced as EMR documentation grows over time.

Prior research on trial eligibility screening has primarily focused on enhancing recruitment efficiency through the application of NLP and machine learning to EMR data. The foundational work by Ni et al [30,31] demonstrated substantial workload reductions, with over 90% in pediatric emergency department settings and 85% in pediatric oncology, by leveraging both structured data and unstructured clinical notes. The subsequent development of the Automated Clinical Trial Eligibility Screener [9] advanced this work into real-time, prospective screening, achieving a 34% reduction in screening time and an SUS score of 80.0.

The iTEST extends this foundation by addressing clinician empowerment and cognitive burden through 2 key innovations. First, its block-based visual programming interface enables clinicians to independently author and update screening rules without software engineering support, enhancing adaptability to evolving eligibility criteria. Second, the iTEST demonstrated significant improvements not only in efficiency but also in accuracy and cognitive workload, quantitatively validating its ability to reduce mental burden while maintaining acceptable usability. This positions the iTEST as a clinician-centric solution that enhances both the efficiency and reliability of eligibility screening while reducing clinician burnout.

Future Direction

Clinical notes at our hospital are primarily in English, with very few in Chinese. Therefore, we disregarded the Chinese portions when developing the iTEST. Besides, extracting medical concepts from non-English clinical documents presents significant challenges [37]. However, advancements in large language models (LLMs) may help address the challenge of multilingual clinical notes. They could potentially process multilingual clinical notes without explicit translation, reducing information loss. Moreover, LLMs provide promising capabilities that could overcome several limitations of rule-based approaches, such as those used in our study. Their natural language understanding could improve the handling of variations in clinical documentation, context-dependent interpretations, and complex eligibility criteria that require reasoning across multiple data points.

However, several issues must be addressed before widespread clinical use. First, reliability and consistency remain major challenges [38,39]. LLMs can produce inconsistent outputs for the same inputs and may generate plausible but incorrect information ("hallucinations"), which is unacceptable in clinical decisions. Second, computing costs and infrastructure requirements could limit scalability compared to rule-based systems. Third, regulatory compliance presents significant obstacles, as current frameworks require explainable, auditable

XSL•FO
RenderX

decision-making processes, but LLM reasoning often lacks transparency. Finally, concerns about data privacy and the need for specialized medical training data require careful consideration [40].

Future hybrid approaches that combine rule-based reliability with LLM flexibility may offer the best solutions [41], where LLMs handle complex language understanding and concept extraction [42]. Conversely, rule-based systems guarantee consistent application of explicit eligibility criteria. Importantly, such hybrid frameworks can improve explainability by maintaining transparent decision pathways: the rule-based component offers clear, traceable logic for eligibility determinations, while LLM outputs can be limited to produce interpretable explanations for their reasoning processes. In this way, LLMs, with their strong reasoning and summarization abilities, could be useful in various clinical and research scenarios [43].

Limitations

This study has several limitations. First, with only 12 clinicians evaluating 4 patients' eligibility, the study findings may not reflect real-world scenarios. Furthermore, the small number of participants may lack enough statistical power to detect differences between the groups. Although our study design, with 12 clinicians, was appropriate for identifying medium-to-large differences, we acknowledge that it may have been underpowered to detect smaller, yet potentially clinically important, effects. Despite this limitation, all 4 outcomes achieved statistical significance. Second, the 4 patients chosen for this study may not accurately represent a typical patient population. However, these cases truly demonstrate the difficulties clinicians encounter when trying to retrieve crucial information from traditional EMR systems. In real-world clinical settings, these patients represent a specific group that not only risks misjudgment and possible harm but also presents challenges for clinical trials.

Third, while our crossover design enhances internal validity through within-subject comparisons, its applicability to real-world recruitment is limited due to the small number of participants and patient scenarios. These may not accurately reflect the diversity of clinical experience, patient complexity, practice patterns, or technological skills across different settings. Real-world implementation involves a wider range of patient presentations, comorbidities, and situations that could impact system performance differently. Future research should test the iTEST in diverse clinical environments with larger samples to better determine its effectiveness for large-scale trial recruitment. Fourth, the controlled experimental setting may not fully capture the time pressures, interruptions, and multitasking demands of actual emergency care that could influence accuracy and efficiency.

Fifth, the brief 10-minute training and the crossover design could theoretically lead to learning effects [44] that may influence our results. Although we counterbalanced the task order to minimize these effects, the crossover design means participants' second interface evaluation might have been affected by familiarity with the eligibility screening task itself. However, the counterbalancing of task order should have evenly distributed any such learning effects across conditions [45]. Additionally, the short 10-minute training period for the iTEST actually serves as a conservative test of the system's usability. The fact that the iTEST showed superiority despite minimal training strengthens rather than weakens our findings.

Sixth, we acknowledge that our user study focused exclusively on the rule evaluation module and did not assess clinicians' ability to author rules using the block-based interface. Our study design prioritized evaluating whether the system could effectively support the eligibility screening workflow with preconfigured rules, as this represents the most common use case in our target clinical settings. However, we recognize that this does not validate the authoring capabilities.

Finally, while participants had extensive experience with the standard EMR interface compared to minimal training with the iTEST, we cannot rule out the influence of the novelty effect [46] or the Hawthorne [47] effect on our results. Participants' awareness of being observed and evaluated, along with the novelty of the iTEST interface, may have led to increased attention and improved performance. Future studies with longer training periods, repeated testing, and naturalistic observation could help determine whether the observed benefits persist beyond initial exposure, revealing learning curves for both systems.

Conclusions

In this study, we introduced the iTEST, an innovative NLP-powered clinical decision support tool that uses MetaMap Lite to extract relevant concepts from EMRs. The system design includes a block-based visual programming interface intended to enable clinicians to author and modify eligibility rules independently; however, the usability and effectiveness of this authoring capability were not evaluated in this study and remain objectives for future research. Our user evaluation focused exclusively on the rule evaluation module using preconfigured rules, where the iTEST demonstrated superior accuracy and usability compared to the standard EMR interface, while reducing both task completion time and perceived cognitive workload. The tool's applications can extend beyond clinical trial screening to include the verification of indications and contraindications for specific therapies or interventions. Through these capabilities, the iTEST has the potential to enhance patient safety while easing clinicians' cognitive burden. Future research should evaluate clinicians' ability to create and modify eligibility rules using the block-based authoring interface to fully validate the system's empowerment objectives and finalize the assessment of the iTEST's intended functionality.

XSL•FO
RenderX

Acknowledgments

The authors thank the Department of Information Technology at Ditmanson Medical Foundation Chia-Yi Christian Hospital for their technical support, which was invaluable in completing this study. During the preparation of this work, the authors used Grammarly to enhance clarity and ensure grammatical accuracy. After using this tool, the authors reviewed and edited the content as needed and took the full responsibility for the content of the published study.

Funding

This research was supported in part by the National Science and Technology Council (grant numbers NSTC 113 - 2410-H-008-054, NSTC 112 - 2221-E-705 - 001-MY2, and NSTC 114 - 2221-E-705 - 001-MY2) and the Ditmanson Medical Foundation Chia-Yi Christian Hospital (grant number I112-203).

Data Availability

Data and materials for this research are available from the corresponding author upon reasonable request.

Authors' Contributions

Conceptualization: SFS, YHH, YHS.
Data curation: CCL, SFS, YHS.
Formal analysis: CCL, SFS, YHH.
Supervision: SFS, YHS.
Writing – original draft: CCL, YHH, YYC.
Writing – review & editing: CCL, SFS, YHH, YHS, YYC.
All authors have full access to the data in the study and take responsibility for the integrity and accuracy of the data analysis.
YHS (06500@cych.org.tw) and SFS (sfsung@cych.org.tw) are co-corresponding authors for this article.

Conflicts of Interest

None declared.

Multimedia Appendix 1
Supplementary Tables S1–S4 showing additional study results.
[PDF File, 61 KB - medinform_v13i1e80072_app1.pdf]

References

1. Lin HL, Wu DC, Cheng SM, Chen CJ, Wang MC, Cheng CA. Association between electronic medical records and healthcare quality. Medicine (Baltimore) 2020 Jul 31;99(31):e21182. [doi: 10.1097/MD.0000000000021182] [Medline: 32756096]
2. Mollart L, Newell R, Geale SK, Noble D, Norton C, O'Brien AP. Introduction of patient electronic medical records (EMR) into undergraduate nursing education: an integrated literature review. Nurse Educ Today 2020 Nov;94:104517. [doi: 10.1016/j.nedt.2020.104517] [Medline: 32853983]
3. Li R, Niu Y, Scott SR, et al. Using electronic medical record data for research in a healthcare information and management systems society (HIMSS) analytics electronic medical record adoption model (EMRAM) stage 7 hospital in Beijing: cross-sectional study. JMIR Med Inform 2021 Aug 3;9(8):e24405. [doi: 10.2196/24405] [Medline: 34342589]
4. Asgari E, Kaur J, Nuredini G, et al. Impact of electronic health record use on cognitive load and burnout among clinicians: narrative review. JMIR Med Inform 2024 Apr 12;12:e55499. [doi: 10.2196/55499] [Medline: 38607672]
5. Fraser JF, Härtl R. Even in trauma, time is brain. Crit Care Med 2008 Oct;36(10):2951-2952. [doi: 10.1097/CCM.0b013e31818724f2] [Medline: 18812808]
6. Mullen MT, Chaturvedi S. Endovascular thrombectomy. Neurology (ECronicon) 2017 May 30;88(22):2074-2075. [doi: 10.1212/WNL.0000000000003993] [Medline: 28455385]
7. Parsons M, Spratt N, Bivard A, et al. A randomized trial of tenecteplase versus alteplase for acute ischemic stroke. N Engl J Med 2012 Mar 22;366(12):1099-1107. [doi: 10.1056/NEJMoa1109842] [Medline: 22435369]
8. Skolnick BE, Maas AI, Narayan RK, et al. A clinical trial of progesterone for severe traumatic brain injury. N Engl J Med 2014 Dec 25;371(26):2467-2476. [doi: 10.1056/NEJMoa1411090] [Medline: 25493978]
9. Ni Y, Bermudez M, Kennebeck S, Liddy-Hicks S, Dexheimer J. A real-time automated patient screening system for clinical trials eligibility in an emergency department: design and evaluation. JMIR Med Inform 2019 Jul 24;7(3):e14185. [doi: 10.2196/14185] [Medline: 31342909]
10. Murdoch TB, Detsky AS. The inevitable application of big data to health care. JAMA 2013 Apr 3;309(13):1351-1352. [doi: 10.1001/jama.2013.393] [Medline: 23549579]

XSL•FO
RenderX

11. Sung SF, Chen K, Wu DP, Hung LC, Su YH, Hu YH. Applying natural language processing techniques to develop a task-specific EMR interface for timely stroke thrombolysis: a feasibility study. Int J Med Inform 2018 Apr;112:149-157. [doi: 10.1016/j.ijmedinf.2018.02.005] [Medline: 29500013]
12. Su Q, Cheng G, Huang J. A review of research on eligibility criteria for clinical trials. Clin Exp Med 2023 Oct;23(6):1867-1879. [doi: 10.1007/s10238-022-00975-1] [Medline: 36602707]
13. Sutton RT, Pincock D, Baumgart DC, Sadowski DC, Fedorak RN, Kroeker KI. An overview of clinical decision support systems: benefits, risks, and strategies for success. NPJ Digit Med 2020;3(1):17. [doi: 10.1038/s41746-020-0221-y] [Medline: 32047862]
14. National Institute of Neurological Disorders and Stroke rt-PA Stroke Study Group. Tissue plasminogen activator for acute ischemic stroke. N Engl J Med 1995 Dec 14;333(24):1581-1587. [doi: 10.1056/NEJM199512143332401] [Medline: 7477192]
15. Birchansky J, Frishman WH. Milvexian: a focus on a new oral anticoagulant that targets factor XIa for thromboembolism prophylaxis. Cardiol Rev 2025;33(1):93-97. [doi: 10.1097/CRD.0000000000000588] [Medline: 38305253]
16. Pasternak E, Fenichel R, Marshall AN. Tips for creating a block language with Blockly. : IEEE; 2017 Presented at: 2017 IEEE Blocks and Beyond Workshop (B&B); Oct 9-10, 2017; Raleigh, NC, USA p. 21-24. [doi: 10.1109/BLOCKS.2017.8120404]
17. Demner-Fushman D, Rogers WJ, Aronson AR. MetaMap Lite: an evaluation of a new Java implementation of MetaMap. J Am Med Inform Assoc 2017 Jul 1;24(4):841-844. [doi: 10.1093/jamia/ocw177] [Medline: 28130331]
18. Aronson AR, Lang FM. An overview of MetaMap: historical perspective and recent advances. J Am Med Inform Assoc 2010;17(3):229-236. [doi: 10.1136/jamia.2009.002733] [Medline: 20442139]
19. Hart SG. NASA-Task load index (NASA-TLX); 20 years later. Proc Hum Factors Ergon Soc Annu Meet 2006 Oct;50(9):904-908. [doi: 10.1177/154193120605000909]
20. Brooke J. SUS—a quick and dirty usability scale. In: Jordan PW, Thomas B, McClelland IL, Weerdmeester B, editors. Usability Evaluation in Industry: CRC Press; 1996:189-194 URL: https://digital.ahrq.gov/sites/default/files/docs/survey/systemusabilityscale%2528sus%2529_comp%255B1%255D.pdf [accessed 2025-12-09]
21. Bangor A, Kortum P, Miller J. Determining what individual SUS scores mean: adding an adjective rating scale. J Usability Stud 2009 May 1;4(3):114-123 [FREE Full text]
22. Nijor S, Rallis G, Lad N, Gokcen E. Patient safety issues from information overload in electronic medical records. J Patient Saf 2022 Sep 1;18(6):e999-e1003. [doi: 10.1097/PTS.0000000000001002] [Medline: 35985047]
23. Nolan ME, Cartin-Ceba R, Moreno-Franco P, Pickering B, Herasevich V. A multisite survey study of EMR review habits, information needs, and display preferences among medical ICU clinicians evaluating new patients. Appl Clin Inform 2017 Oct;8(4):1197-1207. [doi: 10.4338/ACI-2017-04-RA-0060] [Medline: 29272901]
24. Clynch N, Kellett J. Medical documentation: part of the solution, or part of the problem? A narrative review of the literature on the time spent on and value of medical documentation. Int J Med Inform 2015 Apr;84(4):221-228. [doi: 10.1016/j.ijmedinf.2014.12.001] [Medline: 25547194]
25. Nguyen OT, Jenkins NJ, Khanna N, et al. A systematic review of contributing factors of and solutions to electronic health record-related impacts on physician well-being. J Am Med Inform Assoc 2021 Apr 23;28(5):974-984. [doi: 10.1093/jamia/ocaa339] [Medline: 33517382]
26. Bolton ML, Biltekoff E, Humphrey L. The mathematical meaninglessness of the NASA task load index: a level of measurement analysis. IEEE Trans Human-Mach Syst 2023;53(3):590-599. [doi: 10.1109/THMS.2023.3263482]
27. Catanese L, Tarsia J, Fisher M. Acute ischemic stroke therapy overview. Circ Res 2017 Feb 3;120(3):541-558. [doi: 10.1161/CIRCRESAHA.116.309278] [Medline: 28154103]
28. Kenton EJ, Culebras A, Fayad PB, et al. Impact of stroke call on the stroke neurology workforce in the United States: possible challenges and opportunities. J Stroke Cerebrovasc Dis 2018 Jul;27(7):2019-2025. [doi: 10.1016/j.jstrokecerebrovasdis.2018.02.063] [Medline: 29625799]
29. Lee JV, Scott A, Osbun J, Zipfel G. Impact of stroke call on career satisfaction and burnout for academic neurointerventionalists: a grounded theory model. World Neurosurg 2021 Jul;151:e552-e564. [doi: 10.1016/j.wneu.2021.04.091] [Medline: 33933697]
30. Ni Y, Kennebeck S, Dexheimer JW, et al. Automated clinical trial eligibility prescreening: increasing the efficiency of patient identification for clinical trials in the emergency department. J Am Med Inform Assoc 2015 Jan;22(1):166-178. [doi: 10.1136/amiajnl-2014-002887] [Medline: 25030032]
31. Ni Y, Wright J, Perentesis J, et al. Increasing the efficiency of trial-patient matching: automated clinical trial eligibility pre-screening for pediatric oncology patients. BMC Med Inf Decis Making 2015 Apr 14;15(1):28. [doi: 10.1186/s12911-015-0149-3] [Medline: 25881112]
32. Pollack AH, Pratt W. Association of health record visualizations with physicians' cognitive load when prioritizing hospitalized patients. JAMA Netw Open 2020 Jan 3;3(1):e1919301. [doi: 10.1001/jamanetworkopen.2019.19301] [Medline: 31940040]
33. Semanik MG, Kleinschmidt PC, Wright A, et al. Impact of a problem-oriented view on clinical data retrieval. J Am Med Inform Assoc 2021 Apr 23;28(5):899-906. [doi: 10.1093/jamia/ocaa332] [Medline: 33566093]

XSL•FO
RenderX

34. McGonagle EA, Karavite DJ, Grundmeier RW, et al. Evaluation of an antimicrobial stewardship decision support for pediatric infections. Appl Clin Inform 2023 Jan;14(1):108-118. [doi: 10.1055/s-0042-1760082] [Medline: 36754066]
35. Charbonnier G, Bonnet L, Biondi A, Moulin T. Intracranial bleeding after reperfusion therapy in acute ischemic stroke. Front Neurol 2021;11:629920. [doi: 10.3389/fneur.2020.629920] [Medline: 33633661]
36. Campbell BCV, Meretoja A, Donnan GA, Davis SM. Twenty-year history of the evolution of stroke thrombolysis with intravenous alteplase to reduce long-term disability. Stroke 2015 Aug;46(8):2341-2346. [doi: 10.1161/STROKEAHA.114.007564] [Medline: 26152294]
37. Lin YC, Christen V, Groß A, et al. Evaluating cross-lingual semantic annotation for medical forms. 2020 Presented at: 13th International Conference on Health Informatics; Valletta, Malta p. 145-155. [doi: 10.5220/0008979901450155]
38. Chang Y, Wang X, Wang J, et al. A survey on evaluation of large language models. ACM Trans Intell Syst Technol 2024 Jun 30;15(3):1-45. [doi: 10.1145/3641289]
39. Zhou L, Schellaert W, Martínez-Plumed F, Moros-Daval Y, Ferri C, Hernández-Orallo J. Larger and more instructable language models become less reliable. Nature New Biol 2024 Oct;634(8032):61-68. [doi: 10.1038/s41586-024-07930-y] [Medline: 39322679]
40. Thirunavukarasu AJ, Ting DSJ, Elangovan K, Gutierrez L, Tan TF, Ting DSW. Large language models in medicine. Nat Med 2023 Aug;29(8):1930-1940. [doi: 10.1038/s41591-023-02448-8] [Medline: 37460753]
41. Liu S, McCoy AB, Chen Q, Wright A. Integrating rule-based NLP and large language models for statin information extraction from clinical notes. Int J Med Inform 2026 Jan;205:106104. [doi: 10.1016/j.ijmedinf.2025.106104] [Medline: 40925145]
42. Lange L, Adel H, Strötgen J, Klakow D. CLIN-X: pre-trained language models and a study on cross-task transfer for concept extraction in the clinical domain. Bioinformatics 2022 Jun 13;38(12):3267-3274. [doi: 10.1093/bioinformatics/btac297] [Medline: 35485748]
43. Cascella M, Montomoli J, Bellini V, Bignami E. Evaluating the feasibility of ChatGPT in healthcare: an analysis of multiple clinical and research scenarios. J Med Syst 2023 Mar 4;47(1):33. [doi: 10.1007/s10916-023-01925-4] [Medline: 36869927]
44. Petzoldt T, Bär N, Ihle C, Krems JF. Learning effects in the lane change task (LCT)—evidence from two experimental studies. Transp Res F: Traffic Psychol Behav 2011 Jan;14(1):1-12. [doi: 10.1016/j.trf.2010.09.001]
45. Brooks JL. Counterbalancing for serial order carryover effects in experimental condition orders. Psychol Methods 2012 Dec;17(4):600-614. [doi: 10.1037/a0029310] [Medline: 22799624]
46. Elston DM. The novelty effect. J Am Acad Dermatol 2021 Sep;85(3):565-566. [doi: 10.1016/j.jaad.2021.06.846] [Medline: 34153390]
47. McCarney R, Warner J, Iliffe S, van Haselen R, Griffin M, Fisher P. The Hawthorne effect: a randomised, controlled trial. BMC Med Res Methodol 2007 Jul 3;7(1):30. [doi: 10.1186/1471-2288-7-30] [Medline: 17608932]

Abbreviations

iTEST: intelligent trial eligibility screening tool
LLM: large language model
NASA-TLX: National Aeronautics and Space Administration Task Load Index
NINDS: National Institute of Neurological Disorders and Stroke
EMR: electronic medical record
NLP: natural language processing
rt-PA: recombinant tissue-plasminogen activator
SUS: system usability scale

Edited by A Coristine; submitted 04.07.25; peer-reviewed by D Chrimes, P Sharma; revised version received 27.11.25; accepted 27.11.25; published 11.12.25.

Please cite as:
Hu YH, Cheng YY, Lan CC, Su YH, Sung SF
An Intelligent Trial Eligibility Screening Tool Using Natural Language Processing With a Block-Based Visual Programming Interface: Development and Usability Study
JMIR Med Inform 2025;13:e80072
URL: https://medinform.jmir.org/2025/1/e80072
doi:10.2196/80072

© Ya-Han Hu, Yi-Ying Cheng, Chung-Ching Lan, Yu-Hsiang Su, Sheng-Feng Sung. Originally published in JMIR Medical Informatics (https://medinform.jmir.org), 11.12.2025. This is an open-access article distributed under the terms of the Creative

XSL•FO
RenderX

Commons Attribution License (https://creativecommons.org/licenses/by/4.0/), which permits unrestricted use, distribution, and reproduction in any medium, provided the original work, first published in JMIR Medical Informatics, is properly cited. The complete bibliographic information, a link to the original publication on https://medinform.jmir.org/, as well as this copyright and license information must be included.

XSL•FO
RenderX

Deep Learning–Based Early Warning Systems in Hospitalized Patients at Risk of Code Blue Events and Length of Stay: Retrospective Real-World Implementation Study

Ji-hyun Kim[1*], PhD; Eun Young Cho[1*], PhD; Yuhyun Choi[1], RN; Joo-Yun Won[1], PhD; Se Hee Cheon[2], RN; Young Ae Kim[3], BSc; Ki-byung Lee[1,4], MD; Kwang Joon Kim[1,5], MD; Ho Gwan Kim[6*], MD; Taeyong Sim[1*], MD

[1]AITRICS Corp, 218 Teheran-ro, Gangnam-gu, Seoul, Republic of Korea

[2]Department of Medical Management, Presbyterian Medical Center, Jeonju, Republic of Korea

[3]Department of Computing Information, Presbyterian Medical Center, Jeonju, Republic of Korea

[4]Department of Internal Medicine, Chuncheon Sacred Heart Hospital, Chuncheon, Republic of Korea

[5]Department of Internal Medicine, Yonsei University College of Medicine, Seoul, Republic of Korea

[6]Department of Emergency Medicine, Presbyterian Medical Center, Jeonju, Republic of Korea

[*]these authors contributed equally

Corresponding Author:
Taeyong Sim, MD
AITRICS Corp, 218 Teheran-ro, Gangnam-gu, Seoul, Republic of Korea

Abstract

Background: In hospitals, Code Blue is an emergency that refers to a patient requiring immediate resuscitation. Over 85% of patients with cardiopulmonary arrest exhibit abnormal vital sign trends prior to the event. Continuous monitoring and accurate interpretation of clinical data through artificial intelligence (AI) models can contribute to preventing critical events.

Objective: This study aims to evaluate changes in clinical outcomes following the use of VitalCare (Major Adverse Event Score and Mortality Score), which is an AI-based early warning system, and to validate the performance of the algorithm.

Methods: A retrospective analysis was conducted by extracting electronic health record data, using a total of 30,785 inpatient cases from general wards and intensive care units. A comparative analysis was performed by setting a 3-month period before and after the system implementation. For clinical evaluation, we measured the incidence rates of Code Blue and adverse events, the proportion of prolonged hospitalization, and the frequency of early interventions. The area under the receiver operating characteristic curve (AUROC) was calculated to assess the performance of the algorithm.

Results: This study demonstrated that, following the implementation of VitalCare, there was a 24.97% reduction in major events such as Code Blue (P=.004) and the proportion of prolonged hospitalization in general wards (P<.05), along with a significant increase in the rate of early interventions. The model performance exhibited superior outcomes compared with traditional scoring systems, with a Major Adverse Event Score AUROC of 0.865 (95% CI 0.857 - 0.873) and Mortality Score AUROC of 0.937 (95% CI 0.931 - 0.944).

Conclusions: A well-developed AI-based model that provides high predictive power can contribute to the prevention of major in-hospital events by providing early predictive information to clinicians. Additionally, it plays a crucial role in effectively addressing unmet needs and challenges in terms of human resources and practical procedures.

(JMIR Med Inform 2025;13:e72232) doi:10.2196/72232

KEYWORDS

adverse event; artificial intelligence; Code Blue; early warning system; rapid response system; VitalCare; hospitalization

Introduction

Code Blue is an emergency code used in hospital settings to indicate a patient experiencing cardiopulmonary arrest (CA), necessitating immediate resuscitative intervention [1]. This represents a critical and resource-intensive process in which health care providers must respond promptly and initiate action as soon as Code Blue is activated. Despite intensive and concerted efforts by medical staff, the survival rate of patients who experience a Code Blue event remains below 20% [1,2]. It is not only directly associated with a poor prognosis and high mortality rate of patients, but also contributes significantly to their economic burden.

Nevertheless, the early identification and prediction of CA or clinical deterioration can be achieved through a comprehensive analysis of patients' vital signs and blood test results. A previous

XSL•FO
RenderX

study demonstrated that over 85% of patients who experience in-hospital CA exhibit abnormal vital signs 6 to 24 hours before adverse events (AEs) [3]. Implementing timely interventions based on these predictions may help delay or prevent mortality. The effective management of Code Blue events depends on the timeliness and quality of interventions [4]. In this context, artificial intelligence (AI)–based early warning systems (EWSs) can facilitate preparedness and support timely intervention by providing advanced alerts. The ability to predict the risk of critical AEs in advance enables hospitals to allocate the necessary resources and establish timely medical treatment plans proactively [1,5].

Numerous studies have demonstrated the positive outcomes of using AI-EWS, underscoring the value of continuous patient monitoring for the early detection of critical events [6-9]. However, most AI-EWS studies have predominantly focused on developing models that predict individual clinical events, such as CA or death, thereby providing limited information. To enhance the early detection of patient deterioration, training algorithms with broadly defined indications are essential. Accordingly, we developed a multilabel algorithm that is designed to recognize the deterioration of patient conditions, including unplanned ward-to-intensive care unit (ICU) transfer (UIT), cardiopulmonary resuscitation, and mortality.

Despite advancements in AI-EWSs, insufficient evidence is available regarding their clinical utility when they are implemented in real-world hospital settings, particularly in terms of reducing in-hospital Code Blue events. Comprehensive validation across multiple domains is essential for the successful implementation and integration of AI-EWS technologies in clinical practice. Therefore, the primary objective of this study was to evaluate the effectiveness of applying an AI-EWS on clinical outcomes, including Code Blue events in hospitals, prolonged length of stay (pLOS), and the frequency of ordering new codes, such as early interventions or assessments for AEs, compared with a silent period using real-world electronic medical record (EMR) data. The secondary objective was to assess the performance in a hospital environment with different characteristics from those of the development data to verify the generalization of the model.

Methods

Study Design and Participants

This retrospective study was conducted at the Presbyterian Medical Center in the Republic of Korea, where a rapid response system (RRS) had not yet been established. Instead, the condition of each patient was monitored by an assigned registered nurse for potential clinical deterioration. In March 2023, the hospital introduced an AI solution named VitalCare (VC) for continuous patient monitoring in the general ward (GW) and ICU to predict patient deterioration. The study population consisted of patients aged 19 years and older who were admitted to the GW or ICU over a 17-month period from December 2022 to May 2024. A “silent period” was designated from December 2022 to February 2023 to establish control settings, during which health care providers did not use VC. Excluding the first 1-month adaptation period following the introduction of the system, data from April 2023 to May 2024 were set as the “entire alert period.” We classified and analyzed the intervention period into two categories. To control for seasonal bias, the alert period was defined as the winter months between December 2023 and February 2024 to match the control period, which was also confined to the winter months. Winter was associated with a higher incidence of AEs and mortality. Therefore, this study was designed to focus on comparative analyses specific to winter. To evaluate the overall trend in Code Blue occurrences, a comparative analysis was conducted using 5 years of event data. This analysis compared the 4-year average before the implementation of VC with data from the first year after implementation.

Ethical Considerations

The Institutional Review Board of the Presbyterian Medical Center approved this study on December 12, 2023, and waived the requirement for informed consent given the specific nature of the retrospective study (2023-12-051). This study was conducted in accordance with the principles of the 1975 Declaration of Helsinki. To protect the privacy of participants, all data were anonymized during extraction from the hospital’s EMR system and used solely for analysis purposes. As this was a retrospective study, no compensation was provided to participants.

Algorithm Description

The VC algorithm is a deep-learning-based model that uses a bidirectional long short-term memory architecture as a binary classifier to predict the occurrence of major AEs (positive or negative) in GW inpatients. It comprises VC-Major Adverse Event Score (MAES) and VC-Mortality Score (MORS), both of which have been approved by the Korean Ministry of Food and Drug Safety. The VC-MAES is designed to comprehensively predict 3 key events, namely, UIT, death, or cardiopulmonary resuscitation, within the GW. In contrast, the VC-MORS is designed to provide a score that could predict death in patients who are admitted to the ICU. ICU transfers within 3 hours of surgery completion or 12 hours of procedure initiation were considered as planned ICU transfers and were excluded from the outcome analyses. The VC-MAES was trained using data from 334,185 hospitalizations of 209,825 adult patients between 2013 and 2017 at Yonsei Severance Hospital, which is a 2454-bed tertiary academic medical center in Seoul, Republic of Korea. The VC-MORS was trained using data from 21,186 hospitalizations of 19,570 adult patients who were admitted to the ICU between 2013 and 2017 at the same hospital. The dataset encompasses more than 35 surgical and medical specialties. The details of the model architecture were the same as those described in a previous study, with slight modifications [10].

The model primarily uses 5 vital signs—systolic and diastolic blood pressure, heart rate, respiratory rate, and body temperature—along with age to generate risk scores ranging from 0 to 100. Higher scores indicate an increased risk of target events occurring within the next 6 hours. When available, the model also incorporates optional variables, including oxygen saturation (SpO_2), mental status (Glasgow Coma Scale), total bilirubin, lactate, creatinine, platelet count, pH, sodium,

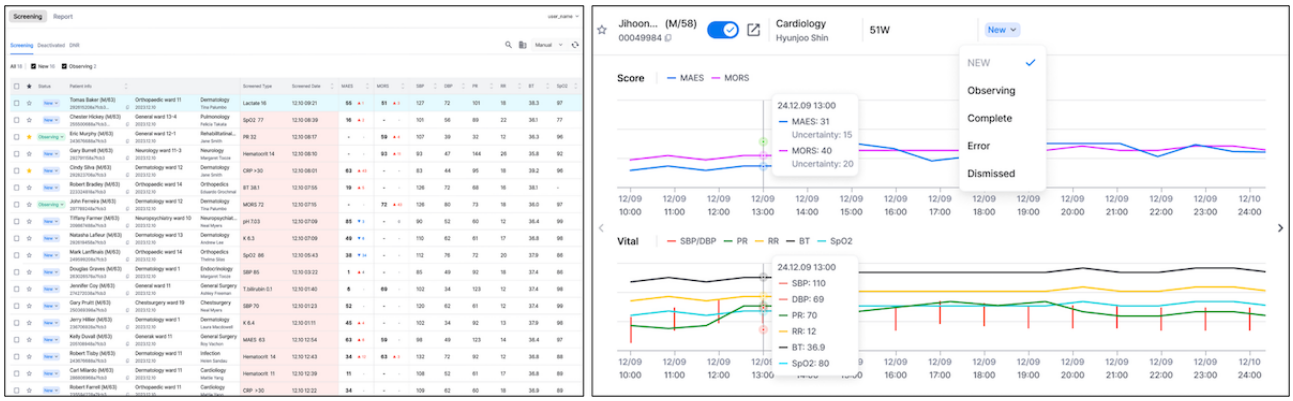
XSL•FO
RenderX

potassium, hematocrit, white blood cell count, bicarbonate, and C-reactive protein. These inputs are updated whenever new data are recorded in the EMR system to ensure that the score reflects the patient's most recent condition. Given that these optional parameters are infrequently measured, missing values are imputed using the last observation carried forward method, where the most recent available value is used. If no prior values are available, normal reference values are assigned for score computation [11].

Practical Setting

We integrated the hospital network's EMR system with the pretrained VC algorithm, which was deployed to another institution without any retraining or recalibration, thereby enabling validation using real-world data from hospitalized patients. The system was configured to allow VC access across all GWs and ICUs. Health care providers reviewed single parameters, such as vital signs, laboratory data, and VC prediction scores, for all hospitalized patients via the VC web platform. The VC web platform presents a trend graph of score changes over time, alarm history, and single-parameter history (Figure 1). It was displayed continuously, allowing the health care providers to access it at any time, and clinicians used the information provided by the VC as a reference during clinical decision-making.

Figure 1. Web interface of VitalCare.



Clinical Evaluation

We analyzed clinical variables such as the in-hospital Code Blue incidence rate, AE (death and UIT cases) incidence rate, proportion of long-term hospitalization during each period, and frequency of early interventions to evaluate the clinical effectiveness following the implementation of VC.

We investigated the annual number of Code Blue events from 2019 to 2023 and calculated the incidence rate relative to the total number of hospitalized patients, excluding those with documented "Do Not Resuscitate" status. The silent period was represented by the average values from 2019 to 2022. The pLOS was defined as the 75th percentile of the total length of stay in the study population [12,13]. Based on this criterion, patients who were admitted to the GW for 9 days or more and those who were admitted to the ICU for 4 days or more were classified as having a prolonged hospital stay. The proportion of patients meeting these criteria was subsequently calculated to evaluate the prevalence of prolonged hospital stay within the cohort.

Given the varying total number of hospital admissions across different periods, the incidence rate of AEs was calculated per 1000 admissions. The number of interventions or evaluations performed within 2 hours of the first alarm activation was calculated to analyze the frequency of early interventions. For this analysis, intervention and evaluation items were compared using prescription codes, such as new oxygenation or change orders, laboratory tests, and any new code orders.

Performance Evaluation

The overall accuracy of the scores was determined by calculating the area under the receiver operating characteristic curve (AUROC) and area under the precision-recall curve (AUPRC) based on whether a target event occurred within 6 hours of the predicted scores. The bootstrap method was used to compare the AUROC and AUPRC with the National Early Warning Score (NEWS), Modified Early Warning Score (MEWS), Sequential Organ Failure Assessment (SOFA), and Acute Physiology and Chronic Health Evaluation II (APACHE II). Given the extensive use of NEWS, MEWS, and SOFA in studies worldwide to predict cardiac arrest or clinical deterioration, these scores were also used as comparators in this study [1,2,14,15]. NEWS and MEWS were calculated using current values of systolic blood pressure, heart rate, respiratory rate, body temperature, mental status, SpO_2, and the fraction of inspired oxygen (FiO_2) recorded in the EMR within 1 hour before the prediction point. The SOFA score was calculated using the worst recorded values in the EMR within 24 hours following ICU admission. As the APACHE II score is specifically used to predict the mortality risk of acutely ill patients within 24 hours of ICU admission [16], the AUROC and AUPRC were calculated based on whether death occurred during the ICU stay.

Statistical Analysis

Demographic characteristics during the silent and alert periods were compared using chi-square tests for categorical variables. For continuous variables, normality was assessed using the Shapiro-Wilk test and histogram inspection, which noted that large sample sizes may cause the test to reject normality due to high sensitivity. Normally distributed variables were compared using independent 2-tailed *t* tests, and nonnormally distributed variables were compared using the Mann-Whitney *U* test (2-tailed).

XSL•FO
RenderX

To evaluate predictive performance, 95% CIs for the AUROC were estimated using the bootstrap method with 1000 resamples. DeLong's test was used for statistical comparison of AUROC values, while a bootstrap-based test with 1000 resamples was applied for AUPRC.

Sensitivity, specificity, positive predictive value, and negative predictive value were calculated to evaluate the performance of the scores, using predefined thresholds corresponding to moderate and high alarm levels. Proportions were compared using the 2-sample proportion test, applying either 1- or 2-tailed approaches as appropriate. One-tailed tests were used to compare AE rates when a directional effect was prespecified, whereas 2-tailed tests were applied when no prior direction was assumed.

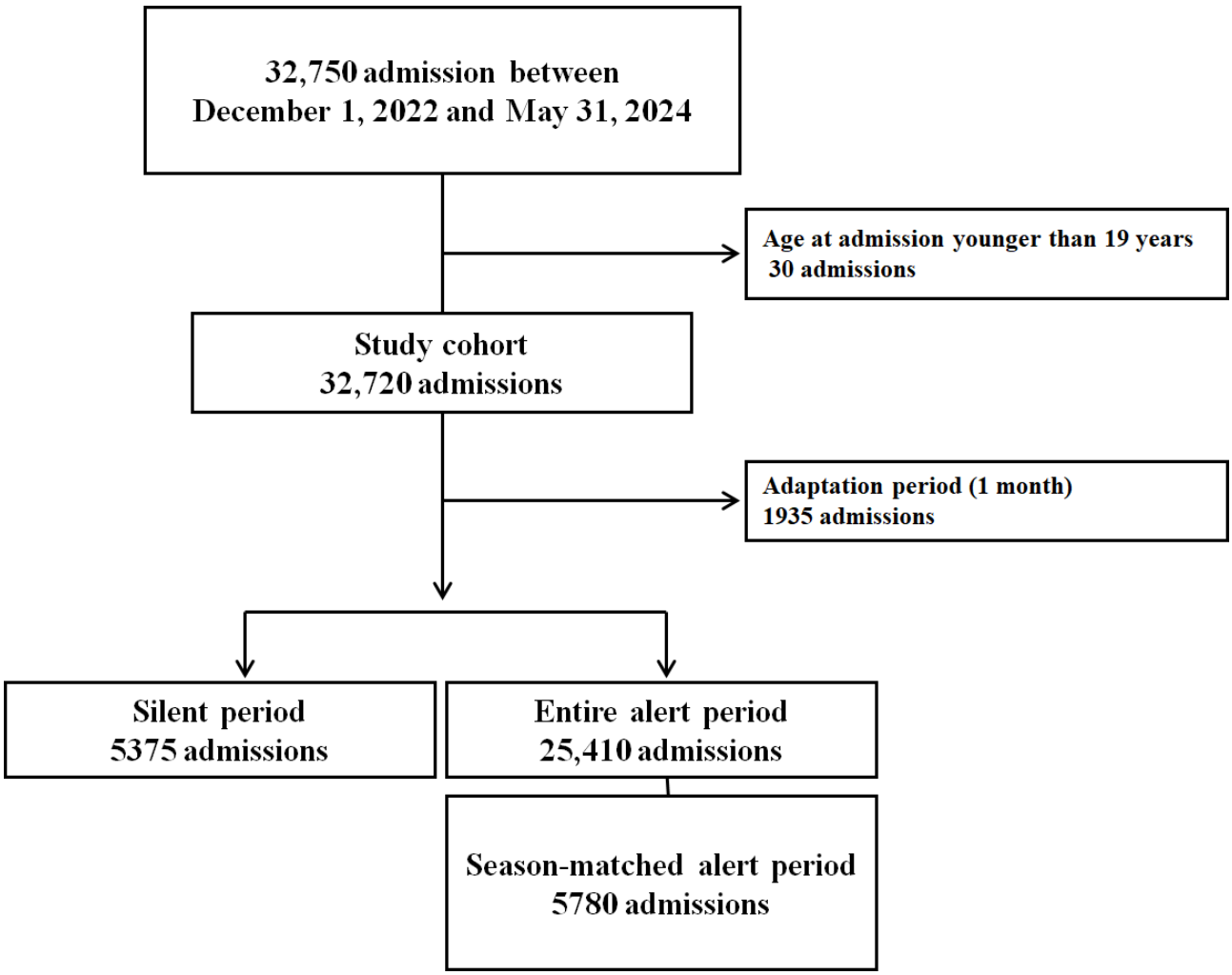
All statistical analyses were performed using Python (version 3.12.9; Python Software Foundation), with statistical significance defined as $P<.05$, applied uniformly across 1- and 2-tailed tests. The analyses used the MLstatkit and scikit-learn libraries.

Results

Overview

This study initially included 32,750 admissions from 24,187 patients. After applying the exclusion criteria, 30 admissions involving patients aged younger than 19 years of age were excluded, resulting in 32,720 admissions being included in the study dataset, which was used for performance evaluation. Considering the adaptation period, 1935 admissions were excluded from the study. The final dataset consisted of 5375 admissions during the silent period, 25,410 admissions during the alert period, and 5780 admissions during the seasonally matched alert period. There were 3576 ICU admissions, of which 2 were younger than 19 years of age and were excluded, leaving 3574 admissions for the VC-MORS performance evaluation. After excluding 214 admissions during the adaptation period, 3360 admissions remained, including 647 admissions during the silent period, 2713 admissions during the entire alert period, and 597 admissions during the seasonally matched alert period (Figure 2).

Figure 2. Flowchart of admission selection.



Baseline Characteristics

We compared baseline characteristics of patients admitted during the silent and alert periods, including vital signs, laboratory values, and the Charlson comorbidity index, which was calculated according to previously published methods [17,18]. While statistically significant differences were observed in pulse rate, respiratory rate, SpO_2, bilirubin, sodium, NEWS, MEWS, Charlson Comorbidity Index, and other baseline characteristics

XSL•FO
RenderX

were similar (Table 1). These findings indicate that patient baseline characteristics were largely similar between the 2 periods.

XSL•FO
RenderX

Table . Characteristics of patients across hospitalizations.

Variables	Overall (n=11,155)	Silent period (n=5375)	Season-matched alert period (n=5780)	Missing, n (%)	*P* value
Age (years), median (IQR)	67.0 (55.0-77.0)	67.0 (55.0-77.0)	67.0 (55.0-77.0)	0 (0)	.90
Sex, n (%)					.19
Female	5632 (50.5)	2679 (49.8)	2953 (51.1)	0 (0)	
Male	5523 (49.5)	2696 (50.2)	2827 (48.9)	0 (0)	
BMI (kg/m^2), mean (SD)	24.3 (4.1)	24.3 (4.0)	24.3 (4.2)	1787 (16.02)	.58
Vital signs					
Diastolic blood pressure (mm Hg), mean (SD)	76.7 (12.1)	76.9 (12.0)	76.6 (12.2)	4 (0.04)	.27
Pulse (beats per min), mean (SD)	79.4 (14.7)	79.1 (14.7)	79.8 (14.7)	4 (0.04)	.01
Respiratory rate (breaths per min), median (IQR)	20.0 (18.0-20.0)	20.0 (19.0-20.0)	20.0 (18.0-20.0)	4 (0.04)	<.001
Systolic blood pressure (mm Hg), mean (SD)	127.4 (20.1)	127.7 (20.4)	127.1 (19.9)	4 (0.04)	.13
SpO_2 (%), median (IQR)	97.0 (96.0-98.0)	97.0 (96.0-98.0)	97.0 (96.0-98.0)	2634 (23.61)	.03
Temperature (°C), mean (SD)	36.8 (0.4)	36.8 (0.4)	36.8 (0.4)	6 (0.05)	.18
Laboratory values					
Bilirubin (mg/dL), median (IQR)	0.5 (0.4-0.8)	0.5 (0.4-0.8)	0.5 (0.4-0.8)	2928 (26.25)	<.001
Creatinine (mg/dL), median (IQR)	0.8 (0.6-1.0)	0.8 (0.6-1.0)	0.8 (0.6-1.0)	2362 (21.17)	.15
C-reactive protein (mg/dL), median (IQR)	0.7 (0.1-3.9)	0.6 (0.1-3.7)	0.7 (0.1-4.2)	3605 (32.32)	.24
HCO_3 (mmol/L), mean (SD)	24.4 (5.7)	24.6 (5.5)	24.3 (5.8)	9437 (84.60)	.21
Hematocrit (%), mean (SD)	35.7 (6.0)	35.6 (6.1)	35.7 (6.0)	1719 (15.41)	.21
Lactate (mmol/L), median (IQR)	2.0 (1.2-4.3)	2.2 (1.3-4.0)	1.9 (1.1-4.3)	10,890 (97.62)	.51
PCO_2 (mm Hg), mean (SD)	38.3 (10.2)	38.4 (10.0)	38.2 (10.3)	9437 (84.60)	.69
pH, mean (SD)	7.4 (0.1)	7.4 (0.1)	7.4 (0.1)	9437 (84.60)	.17
Platelets ($10^3/\mu L$), mean (SD)	218.9 (80.6)	218.7 (81.5)	219.0 (79.7)	1719 (15.41)	.87
PO_2 (mm Hg), median (IQR)	92.0 (78.0-113.0)	91.0 (78.0-114.0)	93.0 (78.0-112.0)	9437 (84.60)	.85
Potassium (mEq/L), mean (SD)	4.1 (0.6)	4.0 (0.6)	4.1 (0.6)	2732 (24.49)	.01
Sodium (mEq/L), median (IQR)	141.0 (138.0-142.0)	141.0 (139.0-142.0)	140.0 (138.0-142.0)	2728 (24.46)	.001
White blood cell count ($10^3/\mu L$), median (IQR)	7.0 (5.5-9.2)	6.9 (5.5-9.2)	7.0 (5.5-9.3)	1719 (15.41)	.41
Baseline scores, median (IQR)					
NEWS[a]	3.0 (3.0-4.0)	3.0 (3.0-4.0)	4.0 (3.0-5.0)	549 (4.92)	<.001
MEWS[b]	1.0 (1.0-1.0)	1.0 (1.0-1.0)	1.0 (1.0-1.0)	549 (4.92)	.05
APACHE II[c]	13.0 (9.0-18.0)	13.0 (9.0-18.0)	13.0 (10.0-18.0)	9911 (88.85)	.23
CCI[d] (comorbidity)	3.0 (2.0-5.0)	3.0 (2.0-5.0)	3.0 (2.0-5.0)	0 (0)	.58

[a]NEWS: National Early Warning Score

[b]MEWS: Modified Early Warning Score

[c]APACHE II: Acute Physiology and Chronic Health Evaluation II

[d]CCI: Charlson Comorbidity Index

XSL•FO
RenderX

Reduction in Code Blue and AEs

The incidence of Code Blue was expected to decrease in 2023 compared to the 4-year average between 2019 and 2022. Since the implementation of the VC system in 2023, the hospital's Code Blue incidence rate (per 1000) has decreased by 24.97%, from 10.57 to 7.93 (*P*=.004). As shown in Table 2, even year-by-year comparisons during the pre-VC period show that the incidence was lower after the introduction of VC.

Table . Code blue trends before and after VC[a] implementation.

Year	Number of hospitalized patients[b]	Number of Code Blue events	Code Blue period incidence rate (per 1000)
Before VC implementation			
2019	22,262	262	11.69
2020	21,726	229	10.34
2021	22,087	210	9.32
2022	21,381	223	10.19
Average	21,864	231	10.57
After VC implementation			
2023	21,061	167	7.93

[a]VC: VitalCare

[b]Excluding DNR (Do Not Resuscitate) patients.

Moreover, we compared the rates of UIT and in-hospital mortality across three intervals: the silent (pre-VC) period, the season-matched period, and the entire study period. The baseline UIT event rate during the silent period was 69.40 events per 1000 admissions, which significantly decreased to 60.73 (*P*=.03) in the season-matched period and 62.37 (*P*=.03) in the entire study period. For in-hospital mortality, the baseline rate was 19.72 deaths per 1000 admissions, decreasing to 16.78 (*P*=.12) during the season-matched period and further to 15.87 (*P*=.02) during the entire period (Table 3).

Table . Number of adverse events by period.

	UIT[a]	*P* value	Mortality	*P* value
Silent period	69.40	—[b]	19.72	—
Season-matched alert period	60.73	.03	16.78	.12
Entire alert period	62.37	.03	15.87	.02

[a]UIT: unplanned ward-to-intensive care unit transfer.

[b]Not applicable.

Clinical Outcomes

The pLOS rate in the GW decreased significantly following VC implementation. No significant difference in the pLOS rate was observed before and after the implementation of the VC system in the ICU (Table 4).

Table . Comparison of length of stay between periods.

	General wards (n=30,785 admissions)		Intensive care units (n=4013 transfers)	
	Proportion of pLOS[a] (LOS ≥9 days), %	*P* value	Proportion of pLOS (LOS ≥4 days), %	*P* value
Silent period	26.85	—[b]	28.91	—
Season-matched alert period	24.65	.01	30.96	.39
Entire alert period	25.46	.03	28.54	.84

[a]pLOS: prolonged length of stay

[b]Not applicable.

As shown in Tables 5 and 6, significantly more early interventions such as oxygenation, laboratory tests, and new code orders occurred following the activation of both moderate (VC-MAES=30) and high (VC-MAES=50) alarms. However, in the ICU, significant earlier interventions were observed only following a moderate VC-MORS alarm (VC-MORS=20), particularly with the ordering of laboratory tests, such as that for lactate.

XSL•FO
RenderX

Table . Early interventions measure for the first VC[a] alarm in general wards.

Intervention	Silent period	Season-matched alert period	*P* value	Entire alert period	*P* value
Moderate alarm[b] (%), n	557	541		2291	
New oxygenation ordered	3.94	9.43	<.001	9.60	<.001
Laboratory tests ordered	10.05	13.86	.05	13.84	.01
New code ordered	24.42	30.87	.02	31.25	<.001
High alarm[c] (%), n	212	215		870	
New oxygenation ordered	3.77	17.67	<.001	13.10	<.001
Laboratory tests ordered	12.26	21.86	.01	19.43	.01
New code ordered	35.85	47.44	.02	42.76	.07

[a]VC: VitalCare.

[b]VC-MAES=30.

[c]VC-MAES=50.

Table . Early interventions measure for the first VC[a] alarm in intensive care units.

Intervention	Silent period	Season-matched alert period	*P* value	Entire alert period	*P* value
Moderate alarm[b] (%), n	152	141		638	
New oxygenation ordered	12.50	17.02	.28	16.14	.29
Laboratory tests ordered	24.34	35.46	.04	37.15	.002
Lactate ordered	2.63	9.93	.01	7.68	.01
New code ordered	55.26	63.83	.14	62.85	.09
High alarm[c] (%), n	51	47		214	
New oxygenation ordered	5.88	14.89	.17	9.35	.60
Laboratory tests ordered	27.45	36.17	.36	28.04	.99
Lactate ordered	1.96	6.38	.35	6.54	.31
New code ordered	72.55	72.34	.98	67.29	.51

[a]VC: VitalCare.

[b]VC-MORS=20.

[c]VC-MORS=80.

Model Performance Compared With Traditional Scoring System

VC-MAES and VC-MORS outperformed conventional EWS in both AUROC and AUPRC. VC-MAES achieved an AUROC of 0.865 (95% CI 0.857-0.873) and an AUPRC of 0.088 (95% CI 0.080 - 0.098), which were significantly higher than those of NEWS (AUROC=0.804; AUPRC = 0.018) and MEWS (AUROC=0.772; AUPRC=0.020).

Similarly, VC-MORS showed strong predictive performance for 6-hour mortality, with an AUROC of 0.937 (95% CI 0.931 - 0.944) and an AUPRC of 0.098 (95% CI 0.087-0.109), which outperformed SOFA (AUROC=0.754; AUPRC=0.011). APACHE II, calculated once within 24 hours of ICU admission, showed an AUROC of 0.814 and an AUPRC of 0.259 for predicting ICU mortality (Table 7).

XSL•FO
RenderX

Table . Performance comparison by AUROC[a] and AUPRC[b].

Score	AUROC (bootstrap 95% CI)	AUPRC (bootstrap 95% CI)
General wards		
VC[c]-MAES[d]	0.865 (0.857 - 0.873)	0.088 (0.080 - 0.098)
NEWS[e]	0.804 (0.797 - 0.811)[f]	0.018 (0.015 - 0.021)[g]
MEWS[h]	0.772 (0.764-0.780)[f]	0.020 (0.015 - 0.025)[g]
Intensive care units		
VC-MORS[i]	0.937 (0.931 - 0.944)	0.098 (0.087 - 0.109)
SOFA[j]	0.754 (0.742-0.765)[f]	0.011 (0.010 - 0.012)[g]
APACHE II[k]	0.814 (0.787 - 0.840)	0.259 (0.215 - 0.307)

[a]AUROC: area under the receiver operating characteristic curve.

[b]AUPRC: area under the precision-recall curve.

[c]VC: VitalCare.

[d]MAES: Major Adverse Event Score.

[e]NEWS: National Early Warning Score.

[f]*P*<.001; Delong test.

[g]*P*<.001; bootstrap-based test.

[h]MEWS: Modified Early Warning Score.

[i]MORS: Mortality Score.

[j]SOFA: Sequential Organ Failure Assessment.

[k]APACHE II: Acute Physiology and Chronic Health Evaluation II.

Discussion

Principal Findings

We retrospectively collected the EMR data of hospitalized patients and compared the pre- and postintervention clinical outcomes to evaluate the effectiveness of VC. The results demonstrated that VC use was associated with high predictive performance and a significant reduction in Code Blue events. Specifically, VC-MAES exhibited a reduced pLOS and a lower number of AEs compared with the silent period, along with an increased frequency of early interventions.

Bridging the Afferent Limb With AI-EWS

Globally, the importance of RRS as a means of preventing AEs has been increasingly emphasized. However, rescue failures may occur even in environments where RRSs are implemented owing to challenges in the afferent limb [19]. The afferent limb refers to the “recognition” phase, encompassing processes such as monitoring, identification, and triggering a response [20]. VC supports automated monitoring, aids in the detection of early high-risk patients, and offers potential solutions for delaying and preventing Code Blue events [1]. In this regard, it can be used systematically and efficiently in environments where an RRS is already established. Conversely, it can maximize the potential impact by addressing unmet needs, even in hospitals where the RRS is not organized or is understaffed.

Optimizing Care With Predictive Monitoring

In practical settings, the initial assessment and recognition of a patient’s condition are typically performed by nursing staff. Subsequently, the attending physician is notified of the patient’s condition to facilitate decision-making regarding diagnosis and treatment. Vital signs and laboratory tests are also intermittently monitored, making the automatic interpretation and screening of time-series data a critical clinical requirement. As AEs often occur abruptly, such sequential processes can serve as barriers to timely intervention. VC can address this challenge by providing predictive alerts before the occurrence of AEs. This study confirmed a short-term decrease in UIT and death cases, which was found to have led to a significant long-term reduction in Code Blue events.

VC provides the opportunity to assess a patient’s condition (eg, laboratory tests, blood culture, and imaging) proactively or report it to the attending physician early, enabling the preparation of the necessary resources in advance. Accordingly, our findings suggest that VC implementation leads to notable clinical improvements, including increased early intervention and reduced AEs. Prior studies have indicated that several patients who ultimately experience CA remain in the GW for extended periods before being transferred to the ICU (or are never transferred at all), which negatively affects their survival rates. Consequently, these studies asserted that AI-based EWSs have the potential to reduce in-hospital mortality [15,21-23].

We conducted a subgroup analysis of the frequency of early interventions and observed a more significant increase in the GW following VC use (Table 5). It is well established that early intervention improves patient outcomes [24-26]. The occurrence of any intervention or evaluation within 2 hours of the initial risk prediction of VC can be interpreted as an indication that the clinician agreed with this information and suspected patient deterioration. VC can detect AEs more quickly than traditional

XSL•FO
RenderX

scoring systems, thereby offering the benefit of securing opportunities for early recognition and treatment, and potentially preventing AEs in the GW, where closed observation may not be as rigorous. Conversely, as patients in the ICU were already under real-time close observation by medical staff, there was no change in the intervention rate within 2 hours of the first elevation. Similarly, a trend was observed in which the difference in intervention rates diminished as the patient severity increased. These results were predictable and reasonable. Based on these findings, we propose that the use of VC-MORS in the ICU is more beneficial for real-time patient monitoring, enabling the early prediction of critical events with high predictive power, rather than offering new information that could lead to additional prescriptions.

In conclusion, VC serves as a clinical decision-supporting system that provides supplementary information for health care providers rather than functioning as an independent diagnostic tool. Ultimately, the clinical judgment of health care professionals remains the final determinant in decision-making. The successful integration and adaptation of AI-EWS into clinical practice suggest the potential for clinical decision-supporting systems to be used more extensively. Various research will be needed to achieve this. We believe that the synergy between the enhancement of health care professionals' ability to use predictive information and the advancement of AI-EWS could yield significant outcomes for patients and clinical settings.

This study demonstrates the effectiveness of AI-based EWS in a community hospital without an RRS; however, its applicability to institutions in resource-limited settings requires further consideration. The adoption and integration of health AI can vary significantly across countries, depending on geopolitical and socioeconomic development [27,28]. Consequently, several challenges may arise in rural hospitals or institutions with limited digital infrastructure [29]. These include the absence of real-time EMR systems, poor clinical data quality, limited clinician training in AI tools, and variability in clinical workflows and institutional acceptance. While simplified models may offer a feasible alternative, future research should explore implementation strategies for lightweight AI-EWS systems and scalable integration approaches in community-based and resource-limited settings.

Limitations

This study has several limitations. First, the control period was relatively short owing to constraints in data extraction following the computerized system upgrade period at our institution. A comparative analysis was conducted within a given period using the same computerized system. Second, the effect of VC on patient prognosis following discharge was not investigated. Third, although this was a real-time EWS validation study, it did not evaluate interaction variables between AI-based EWS and the clinician, such as alarm fatigue. Given that real-time EWS operates as a continuous monitoring system, some degree of alert fatigue may perhaps be unavoidable. While adjusting thresholds—such as lowering sensitivity—may mitigate excessive alerts, it may also increase the risk of missing critical events. Future research will focus on assessing the effectiveness of clinician-AI interactions through the AI-based EWS and their influence on discharge outcomes and postdischarge prognosis.

Conclusions

A well-designed and validated AI-based EWS, such as VC, can effectively reduce major in-hospital AEs by enabling early detection and intervention. By supporting clinical decision-making without replacing professional judgment, this study demonstrates the potential of AI-EWS to enhance patient outcomes and optimize resource utilization in hospital settings.

Data Availability

The datasets analyzed during this study comprise deidentified data stored in the cloud-based storage system of the Presbyterian Medical Center and are not publicly available as they contain protected patient medical information and are restricted for disclosure outside the hospital.

Conflicts of Interest

None declared.

References

1. Somanchi S, Adhikari S, Lin A, Eneva E, Ghani R. Early prediction of cardiac arrest (Code Blue) using electronic medical records. Presented at: Proceedings of the 21st ACM SIGKDD International Conference on Knowledge Discovery and Data Mining; Aug 10-13, 2015; Sydney, Australia. [doi: 10.1145/2783258.2788588]
2. Churpek MM, Yuen TC, Huber MT, Park SY, Hall JB, Edelson DP. Predicting cardiac arrest on the wards: a nested case-control study. Chest 2012 May;141(5):1170-1176. [doi: 10.1378/chest.11-1301] [Medline: 22052772]
3. DeVita MA, Bellomo R, Hillman K, et al. Findings of the first consensus conference on medical emergency teams*. Crit Care Med 2006 Sep;34(9):2463-2478. [doi: 10.1097/01.CCM.0000235743.38172.6E]
4. Jackson JE, Grugan AS. Code blue: do you know what to do? Nursing (Auckl) 2015 May;45(5):34-39. [doi: 10.1097/01.NURSE.0000463651.10166.db] [Medline: 25807449]
5. Saab A, Abi Khalil C, Jammal M, Saikali M, Lamy JB. Early prediction of all-cause clinical deterioration in general wards patients: development and validation of a biomarker-based machine learning model derived from rapid response team activations. J Patient Saf 2022;18(6):578-586. [doi: 10.1097/PTS.0000000000001069]

XSL•FO
RenderX

6. Adams R, Henry KE, Sridharan A, et al. Prospective, multi-site study of patient outcomes after implementation of the TREWS machine learning-based early warning system for sepsis. Nat Med 2022 Jul;28(7):1455-1460. [doi: 10.1038/s41591-022-01894-0]
7. Edelson DP, Churpek MM, Carey KA, et al. Early warning scores with and without artificial intelligence. JAMA Netw Open 2024 Oct 1;7(10):e2438986. [doi: 10.1001/jamanetworkopen.2024.38986] [Medline: 39405061]
8. Rossetti SC, Dykes PC, Knaplund C, et al. Real-time surveillance system for patient deterioration: a pragmatic cluster-randomized controlled trial. Nat Med 2025 Jun;31(6):1895-1902. [doi: 10.1038/s41591-025-03609-7]
9. Verma AA, Stukel TA, Colacci M, et al. Clinical evaluation of a machine learning-based early warning system for patient deterioration. CMAJ 2024 Sep 15;196(30):E1027-E1037. [doi: 10.1503/cmaj.240132] [Medline: 39284602]
10. Sung M, Hahn S, Han CH, et al. Event prediction model considering time and input error using electronic medical records in the intensive care unit: retrospective study. JMIR Med Inform 2021 Nov 4;9(11):e26426. [doi: 10.2196/26426] [Medline: 34734837]
11. Sim T, Hahn S, Kim KJ, et al. Preserving informative presence: how missing data and imputation strategies affect the performance of an AI-based early warning score. J Clin Med 2025 Mar 24;14(7):40217663. [doi: 10.3390/jcm14072213] [Medline: 40217663]
12. Chen Y, Scholten A, Chomsky-Higgins K, et al. Risk factors associated with perioperative complications and prolonged length of stay after laparoscopic adrenalectomy. JAMA Surg 2018 Nov 1;153(11):1036-1041. [doi: 10.1001/jamasurg.2018.2648] [Medline: 30090934]
13. Patel K, Diaz MJ, Taneja K, et al. Predictors of inpatient admission likelihood and prolonged length of stay among cerebrovascular disease patients: a nationwide emergency department sample analysis. J Stroke Cerebrovasc Dis 2023 Mar;32(3):106983. [doi: 10.1016/j.jstrokecerebrovasdis.2023.106983]
14. López-Izquierdo R, Brio-Ibañez PD, Martín-Rodríguez F, et al. Role of qSOFA and SOFA scoring systems for predicting in-hospital risk of deterioration in the emergency department. Int J Environ Res Public Health 2020 Nov 12;17(22):8367. [doi: 10.3390/ijerph17228367] [Medline: 33198151]
15. Knaus WA, Draper EA, Wagner DP, Zimmerman JE. APACHE II: a severity of disease classification system. Crit Care Med 1985 Oct;13(10):818-829. [Medline: 3928249]
16. Charlson ME, Pompei P, Ales KL, MacKenzie CR. A new method of classifying prognostic comorbidity in longitudinal studies: development and validation. J Chronic Dis 1987 Jan;40(5):373-383. [doi: 10.1016/0021-9681(87)90171-8]
17. Quan H, Sundararajan V, Halfon P, et al. Coding algorithms for defining comorbidities in ICD-9-CM and ICD-10 administrative data. Med Care 2005 Nov;43(11):1130-1139. [doi: 10.1097/01.mlr.0000182534.19832.83]
18. Silber JH, Williams SV, Krakauer H, Schwartz JS. Hospital and patient characteristics associated with death after surgery. A study of adverse occurrence and failure to rescue. Med Care 1992 Jul;30(7):615-629. [doi: 10.1097/00005650-199207000-00004] [Medline: 1614231]
19. DeVita MA, Smith GB, Adam SK, et al. "Identifying the hospitalised patient in crisis"—a consensus conference on the afferent limb of rapid response systems. Resuscitation 2010 Apr;81(4):375-382. [doi: 10.1016/j.resuscitation.2009.12.008]
20. Churpek MM, Yuen TC, Winslow C, et al. Multicenter development and validation of a risk stratification tool for ward patients. Am J Respir Crit Care Med 2014 Sep 15;190(6):649-655. [doi: 10.1164/rccm.201406-1022OC] [Medline: 25089847]
21. Girotra S, Nallamothu BK, Spertus JA, et al. Trends in survival after in-hospital cardiac arrest. N Engl J Med 2012 Nov 15;367(20):1912-1920. [doi: 10.1056/NEJMoa1109148] [Medline: 23150959]
22. Young MP, Gooder VJ, McBride K, James B, Fisher ES. Inpatient transfers to the intensive care unit: delays are associated with increased mortality and morbidity. J Gen Intern Med 2003 Feb;18(2):77-83. [doi: 10.1046/j.1525-1497.2003.20441.x] [Medline: 12542581]
23. Winslow CJ, Edelson DP, Churpek MM, et al. The impact of a machine learning early warning score on hospital mortality: a multicenter clinical intervention trial. Crit Care Med 2022;50(9):1339-1347. [doi: 10.1097/CCM.0000000000005492]
24. Boersma E, Maas AC, Deckers JW, Simoons ML. Early thrombolytic treatment in acute myocardial infarction: reappraisal of the golden hour. The Lancet 1996 Sep;348(9030):771-775. [doi: 10.1016/S0140-6736(96)02514-7]
25. Plant P, Owen J, Elliott M. Early use of non-invasive ventilation for acute exacerbations of chronic obstructive pulmonary disease on general respiratory wards: a multicentre randomised controlled trial. The Lancet 2000 Jun;355(9219):1931-1935. [doi: 10.1016/S0140-6736(00)02323-0]
26. Rivers E, Nguyen B, Havstad S, et al. Early goal-directed therapy in the treatment of severe sepsis and septic shock. N Engl J Med 2001 Nov 8;345(19):1368-1377. [doi: 10.1056/NEJMoa010307]
27. Croissant A, Lorenz P. Comparative Politics of Southeast Asia An Introduction into Government and Politics: Springer; 2018.
28. Mishori R. Artificial intelligence technology in healthcare and the digital divide. In: Digital Health, AI and Generative AI in Healthcare: A Concise, Practical Guide for Clinicians: Springer Nature; 2025:139-147. [doi: 10.1007/978-3-031-83526-1_11]
29. Lamem MFH, Sahid MI, Ahmed A. Artificial intelligence for access to primary healthcare in rural settings. J Med Surg Public Health 2025 Apr;5:100173. [doi: 10.1016/j.glmedi.2024.100173]

XSL•FO
RenderX

Abbreviations

AE: adverse event
AI: artificial intelligence
APACHE II: Acute Physiology and Chronic Health Evaluation II
AUPRC: area under the precision-recall curve
AUROC: area under the receiver operating characteristic curve
CA: cardiopulmonary arrest
EMR: electronic medical record
EWS: early warning system
GW: general ward
ICU: intensive care unit
MAES: Major Adverse Event Score
MEWS: Modified Early Warning Score
NEWS: National Early Warning Score
pLOS: prolonged length of stay
RRS: rapid response system
SOFA: Sequential Organ Failure Assessment
UIT: unplanned ward-to-intensive care unit transfer
VC: VitalCare

Edited by A Benis; submitted 12.02.25; peer-reviewed by E Bai, MA Castro Villamor; revised version received 05.06.25; accepted 24.06.25; published 22.08.25.

Please cite as:
Kim JH, Cho EY, Choi Y, Won JY, Cheon SH, Kim YA, Lee KB, Kim KJ, Kim HG, Sim T
Deep Learning–Based Early Warning Systems in Hospitalized Patients at Risk of Code Blue Events and Length of Stay: Retrospective Real-World Implementation Study
JMIR Med Inform 2025;13:e72232
URL: https://medinform.jmir.org/2025/1/e72232
doi:10.2196/72232

© Ji-hyun Kim, Eun Young Cho, Yuhyun Choi, Joo-Yun Won, Se Hee Cheon, Young Ae Kim, Ki-byung Lee, Kwang Joon Kim, Ho Gwan Kim, Taeyong Sim. Originally published in JMIR Medical Informatics (https://medinform.jmir.org), 22.8.2025. This is an open-access article distributed under the terms of the Creative Commons Attribution License (https://creativecommons.org/licenses/by/4.0/), which permits unrestricted use, distribution, and reproduction in any medium, provided the original work, first published in JMIR Medical Informatics, is properly cited. The complete bibliographic information, a link to the original publication on https://medinform.jmir.org/, as well as this copyright and license information must be included.

XSL•FO
RenderX

Using Machine Learning to Predict-Then-Optimize Elective Orthopedic Surgery Scheduling to Improve Operating Room Utilization: Retrospective Study

Johnathan R Lex[1,2,3*], MBChB, MASc; Aazad Abbas[1,2,3*], MD; Jacob Mosseri[1,4], MASc; Jay Singh Toor[5,6], MD, MBA; Michael Simone[1,4], BASc; Bheeshma Ravi[3,7], MD, PhD; Cari Whyne[1,2,3,7], PhD; Elias B Khalil[4], PhD

[1]Orthopaedic Biomechanics Lab, Sunnybrook Research Institute, 2075 Bayview Avenue, Suite S620, Toronto, ON, Canada

[2]Institute of Biomedical Engineering, University of Toronto, Toronto, ON, Canada

[3]Department of Surgery, Division of Orthopedic Surgery, University of Toronto, 149 College St, Toronto, ON, Canada

[4]Department of Mechanical and Industrial Engineering, Faculty of Engineering, University of Toronto, Toronto, ON, Canada

[5]Winnipeg Spine Program, Health Sciences Centre, Department of Surgery, University of Manitoba, Manitoba, Canada

[6]Orthopaedic Surgery Section, Department of Surgery, University of Manitoba, Manitoba, Canada

[7]Division of Orthopaedic Surgery, Department of Surgery, Sunnybrook Health Science Centre, Toronto, ON, Canada

[*]these authors contributed equally

Corresponding Author:
Aazad Abbas, MD
Orthopaedic Biomechanics Lab, Sunnybrook Research Institute, 2075 Bayview Avenue, Suite S620, Toronto, ON, Canada

Abstract

Background: Total knee and hip arthroplasty (TKA and THA) are among the most performed elective procedures. Rising demand and the resource-intensive nature of these procedures have contributed to longer wait times despite significant health care investment. Current scheduling methods often rely on average surgical durations, overlooking patient-specific variability.

Objective: To determine the potential for improving elective surgery scheduling for TKA and THA, respectively, by using a 2-stage approach that incorporates machine learning (ML) prediction of the duration of surgery (DOS) with scheduling optimization.

Methods: In total, 2 ML models (one each for TKA and THA) were trained to predict DOS using patient factors based on 302,490 and 196,942 patients, respectively, from a large international database. In total, 3 optimization formulations based on varying surgeon flexibility were compared: Any (surgeons could operate in any operating room at any time), Split (limitation of 2 surgeons per operating room per day), and multiple subset sum problem (MSSP; limit of 1 surgeon per operating room per day). Two years of daily scheduling simulations were performed for each optimization problem using ML prediction or mean DOS over a range of schedule parameters. Constraints and resources were based on a high-volume arthroplasty hospital in Canada.

Results: The TKA and THA prediction models achieved test accuracy (with a 30 min buffer) of 78.1% (mean squared error 0.898) and 75.4% (mean squared error 0.916), respectively. Any scheduling formulation performed significantly worse than the Split and MSSP formulations with respect to overtime and underutilization (P<.001). The latter 2 problems performed similarly (P>.05) over most schedule parameters. The ML prediction schedules outperformed those generated using a mean DOS for most scheduling parameters, with overtime reduced on average by 300-500 minutes per week (12 - 20 min per operating room per day; P<.001). However, there was more operating room underutilization with the ML prediction schedules, with it ranging from 70 - 192 minutes more underutilization (P<.001). Using a 15-minute schedule granularity with a waitlist pool of a minimum of 1 month generated the ML schedule that outperformed the mean schedule 97.1% of times.

Conclusions: Assuming a full waiting list, optimizing an individual surgeon's elective operating room time using an ML-assisted predict-then-optimize scheduling system improves overall operating room efficiency, significantly decreasing overtime. This has significant potential implications for health care systems struggling with pressures of rising costs and growing operative waitlists.

(JMIR Med Inform 2025;13:e70857) doi:10.2196/70857

KEYWORDS

machine learning; orthopedic surgery; optimization; elective surgery; scheduling; hip and knee arthroplasty

XSL•FO
RenderX

Introduction

Total knee and hip arthroplasty (TKA and THA, respectively) are the gold-standard treatment for end-stage arthritis of the hip and knee joints. These procedures are the first and second most frequently performed in the United States, excluding maternal and neonatal procedures [1]. In 2018, 1.3 million of these procedures were performed in the United States, a 21.9% increase from 2008 [1]. This number will continue to increase globally due to an aging population and the ongoing obesity pandemic [2,3]. The ubiquity of these procedures correlates strongly with their burden on health care systems globally. In the United States, approximately 5% of the gross domestic product is to care for musculoskeletal conditions [4,5]. Despite this spending, wait times for elective surgical procedures in OECD countries continue to increase, conferring extended periods of time with poor quality of life for TKA and THA patients [6,7]. For these reasons, there is a growing interest and research into improving the efficiency and cost-effectiveness of arthritis care [8,9].

Most research has focused purely on the prediction of duration of surgery (DOS) or the optimization of operating room scheduling, ignoring their inherent interrelation [10-14]. More recently, these approaches have been combined to plan post-surgical beds and plan emergency surgeries based on predicted priority with varying results [15,16]. DOS prediction models typically represent a large volume of varying procedures, spanning multiple surgical specialties with limited practical applications. Classic regression modeling in orthopedics has identified age, BMI, surgical procedure, primary or revision, and gender as important variables affecting DOS predictions [17,18]. Machine learning (ML) models have been applied to predict DOS for various surgeries [10,12,19-24]. However, in practice, mean time or surgeon-specific rolling mean time is typically used to generate schedules at the operational level.

Research evaluating the optimization of surgery scheduling has been performed using an average or a randomly sampled (typically from a lognormal distribution) DOS value prior to optimizing a schedule through integer linear programming based on either the multiple knapsack or job-shop scheduling problem [25-27]. Stochastic programming and distributionally robust optimization have also been attempted to mitigate the effects of an uncertain DOS, but these approaches assume a distribution of DOS rather than using specific features to aid in prediction [28].

To our knowledge, no prior work has combined patient-level DOS predictions with schedule optimization to create an optimized surgical schedule at the operational level. It is known that neural networks are strong predictors of DOS; however, their realizable improvements when implemented over various surgical schedule optimization problems, while performing simulations accounting for real-world constraints, remain unclear [23,24]. The primary aim of this paper was to determine if a 2-stage approach using an ML model for prediction of DOS paired with schedule optimization improves operating room overutilization or underutilization compared to using the mean DOS. Secondary objectives were to determine the effect of schedule granularity and length of surgeon waitlist on scheduling accuracy.

Methods

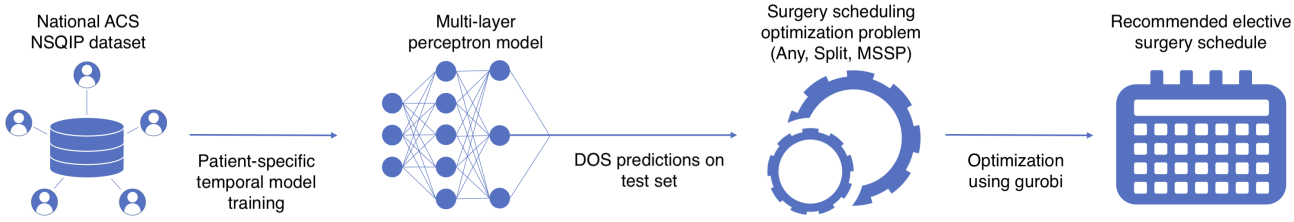
Ethical Considerations

This retrospective study analyzed deidentified American College of Surgeons National Surgical Quality Improvement (ACS NSQIP) data. The study was approved by the Institutional Research Ethics Board (Sunnybrook Health Sciences Center, Project REB ID #4899). Informed consent was waived due to the secondary, minimal-risk nature of the analysis. No local institutional patient data were used. Privacy and confidentiality were protected in accordance with institutional and journal policies. Data use complied with NSQIP data-use agreements. The study adhered to the Declaration of Helsinki.

Setting

Population-level data from the ACS NSQIP database were used to generate prediction models. This database compiles patient and outcome data following surgery from over 700 hospitals in North America, capturing over 1 million surgeries per year, with a high level of accuracy [29]. The database was queried for all TKA and THA surgical procedures performed between 2014 and 2019. The actual DOS times as reported in the ACS NSQIP dataset were used to inform simulated daily operating room schedules. A flowchart that helps visualize the overall 2-stage approach is shown in Figure 1.

Figure 1. High-level overview of the predict-then-optimize approach. ACS NSQIP: American College of Surgeons National Surgical Quality Improvement Program; DOS: duration of surgery; MSSP: multiple subset sum problem.



Duration of Surgery Prediction

Data pertaining to 302,490 TKA and 196,942 THA procedures performed during this period as identified from the ACS NSQIP database were used to train models to predict DOS. DOS predictions were done as per Abbas et al [23,24]. They identified a PyTorch multilayer perceptron model that outperformed 10 alternative ML models for predicting DOS for TKA and THA [23,24]. Both models were trained on procedures from 2014 to 2017, hyperparameters tuned with Ray on procedures from 2018, and evaluated on procedures from 2019 [23,24,30,31]. These models were generated using the Niagara supercomputer

XSL•FO
RenderX

at the SciNet HPC Consortium [32]. Predictions of DOS from the test subsets of data were used in the optimization model. Refer to the study by Abbas et al [23,24] for further details regarding the DOS prediction, model development, hyperparameter tuning, and feature importance.

Schedule Optimization Formulations

Assumptions

The generated scheduling model considered elective case scheduling, in which surgeries are planned for in advance. The constraints and available resources for the model were generated using real-world constraints from the authors' institution, the highest-volume elective arthroplasty hospital in Canada. This included cleaning time (30 min), number of operating rooms (n=5), number of surgeons (n=11), and days a surgeon was unavailable in a week. The planning horizon of 1 week (5 workdays) was also based on these constraints. The penalty for an individual operating room running overtime (after 5 pm), λ, was chosen to be double the value of daytime operating room underutilization. This was due to the approximate additional costs associated with operating room staff working after hours. The following assumptions regarding scheduling were made: surgeons are available to operate any day anytime except for 0 - 2 randomly selected days per week per surgeon, and once a surgery is assigned to a surgeon, they must perform it (ie, no sharing patients). These assumptions were made as the study did not have access to historical data on surgeon availability from the authors' institution. There were no constraints placed on the schedule based on staffing or patient beds in the recovery unit or ward.

Optimization Formulations

In total, 3 scheduling optimization problems were formulated. All formulations were based on an integer linear programming framework that has been used for many different scheduling problems, including but not limited to surgery scheduling [27,33]. The first, "Any," was adapted from Marques et al [27] with notable modifications including the addition of an overtime penalty and only considering 1 surgery specialty. "Any" allows any surgery to be scheduled at any time of day in any room subject to the constraints that no surgeries in a room overlap, and that no surgeon is operating in 2 rooms simultaneously. The second formulation, "Split," is the same as "Any" but enforces a maximum of 2 surgeons per operating room on a given day and a maximum of 1 room per surgeon per day. This was chosen as it is common when there are rooms that may be split between 2 surgeons if 1 surgeon cannot fill the room for that particular day. Finally, the third formulation is akin to a max-sum multiple subset sum problem and is thus referred to as "MSSP." It enforces 1 surgeon per operating room on a given day, simplified into multiple optimization problems for each surgeon, following a fair distribution of rooms among surgeons. This is the most common configuration used on a clinical basis, where one surgeon has one operative room dedicated to their cases per day. "Any" is the most flexible optimization formulation, ie, the least constrained of the 3. "Split" and "Any" impose additional constraints on feasible schedules and reflect realistic logistical restrictions that a hospital may want to impose, eg, having a surgeon use the same room on any given day. Details of these formulations are found in Multimedia Appendix 1.

Simulated Schedule Generation

Using the ACS NSQIP data, simulated schedules were generated using each optimization formulation, with schedule parameters as follows. Schedule granularity of 10- and 15-minute block times was considered. These sizes were chosen to ensure interpretable schedule generation. Surgery completion times were rounded up to the nearest block. The effect of surgeon waitlist size on schedule accuracy was also evaluated. Waitlist sizes representing 2 weeks (n=250), 4 weeks (n=500), 8 weeks (n=1000), and 12 weeks (n=1500) were considered. The cases within the waitlist were all given the same priority to be booked (no rank by time), unless randomly considered to be of high priority.

Three different versions of each model with the above schedule parameters were created. The first model used the ML-predicted DOS values for THA and TKA; this is the novel 2-stage approach of predicting then optimizing that we are proposing in this work. The second model used the mean DOS for each different type of surgery (THA and TKA) in order to obtain a schedule that mimics the current operating room schedule. Finally, a hindsight model was created that used the true DOS values to provide an upper bound on the best possible schedule that could be generated with perfect information (100% accurate to the minute). Each of these 3 simulations was performed 104 times (to represent 2 y) using a random sample of surgeries from the testing set.

Scheduling Comparisons

To compare the 3 schedule optimization formulations (Any, Split, and MSSP), the results of the 2-stage predict-then-optimize simulation results across all schedule parameter combinations were assessed. To evaluate the efficacy of the 2-stage schedule generation technique, it was compared to the results of scheduling by 2 other techniques: the mean DOS for each surgery (the current gold standard at most institutions) and the hindsight schedule. Each of these 3 schedules was constructed for each week of the simulation, and metrics consisting of overtime, underutilization, and the objective function value were calculated for each schedule. Student's t-test was used to compare the effect between scheduling formulations. Overtime and underutilization for 2-stage and mean DOS schedules over the simulated weeks were compared using the paired Wilcoxon signed-rank test, as the same surgical cases were randomly selected for each generated schedule. The effect of schedule granularity and considered waitlist size was evaluated using unpaired Student's *t*-test and analysis of variance as these were grouped over multiple selections of random cases. *P* values of <.05 were considered statistically significant.

Results

Prediction Model Accuracy

Demographic details of patients included are found in Multimedia Appendix 2. A summary of the DOS prediction models is found in Multimedia Appendix 3. The TKA prediction

XSL•FO
RenderX

model obtained a training accuracy (with a 30 min buffer) of 76.9% and a training mean squared error (MSE) of 0.904. The validation accuracy was 77.7% with an MSE of 0.904. The test accuracy was 78.1% with an MSE of 0.898. The THA prediction model obtained a training accuracy of 74.0% and a training MSE of 0.888. The validation accuracy was 75.0% with an MSE of 0.910, and the test accuracy was 75.4% with an MSE of 0.916.

Schedule Optimization Formulation Comparison

Overall, the Any scheduling optimization formulation exhibited the poorest performance across all different schedule parameter combinations (Table 1). There was no significant difference in overtime across all schedule parameters between the Split and MSSP formulations. For 2 combinations of schedule parameters (10 min granularity, 1500 waitlist size and 15 min granularity, 1500 waitlist size), there was significantly less operating room underutilization with the MSSP formulation; however, this was only 10.9 minutes and 15.4 minutes, respectively, on average over an entire week (Table 1). In contrast, for 15-minute granularity and a 250-waitlist size, there was significantly more operating room underutilization with MSSP compared to the Split formulation, 42.3 minutes over an entire week (Table 1). Figures 2 and 3 display this comparison for overtime and underutilization across all 3 optimization problems, respectively.

XSL•FO
RenderX

Table . Simulated schedule results for 2-stage (predict-then-optimize) for each schedule optimization formulation. The mean number of cases/week is not significant between any schedule optimization formulations.

Schedule parameters	Overtime min/week, mean (SD)	*P* value		Underutilization min/week, mean (SD)	*P* value		Mean cases/week (SD)
Granularity=10 minutes, waitlist=250 patients (2 wk)							
Any	1335.7 (322.1)	Reference	<.001	669.1 (189.1)	Reference	<.001	125.0 (0.2)
Split	1003.8 (238.1)	<.001	Reference	285.2 (117.4)	<.001	Reference	125.0 (0.2)
MSSP[a]	1010.9 (211.3)	<.001	.82	309.7 (128.7)	<.001	.15	124.2 (0.9)
Granularity=10 minutes, waitlist=500 patients (4 wk)							
Any	1410.4 (331.2)	Reference	<.001	694.4 (157.0)	Reference	<.001	125.0 (0.2)
Split	966.7 (232.9)	<.001	Reference	300.8 (113.9)	<.001	Reference	125.0 (0.1)
MSSP	988.6 (216.3)	<.001	.49	298.8 (119.8)	<.001	.91	124.9 (0.2)
Granularity=10 minutes, waitlist=1000 patients (8 wk)							
Any	1368.8 (310.0)	Reference	<.001	689.6 (183.7)	Reference	<.001	124.9 (0.3)
Split	964.0 (243.9)	<.001	Reference	301.6 (119.9)	<0.001	Reference	125.0 (0.2)
MSSP	954.9 (225.7)	<.001	.78	306.3 (112.8)	<0.001	.78	124.7 (0.6)
Granularity=10 minutes, waitlist=1500 patients (12 wk)							
Any	1267.9 (321.9)	Reference	<.001	657.7 (165.2)	Reference	<.001	124.8 (0.4)
Split	972.2 (225.2)	<.001	Reference	325.9 (114.8)	<.001	Reference	124.9 (0.3)
MSSP	981.3 (199.0)	<.001	.34	315.0 (109.9)	<.001	<.001	124.3 (0.7)
Granularity=15 minutes, waitlist=250 patients (2 wk)							
Any	1416.2 (357.7)	Reference	<.001	702.3 (185.5)	Reference	<.001	123.4 (1.8)
Split	985.1 (235.6)	<.001	Reference	307.6 (119.9)	<.001	Reference	123.1 (1.9)
MSSP	977.9 (229.7)	<.001	.82	349.9 (144.4)	<.001	.02	121.6 (1.5)
Granularity=15 minutes, waitlist=500 patients (4 wk)							
Any	1450.8 (331.3)	Reference	<.001	674.4 (167.6)	Reference	<.001	124.8 (0.4)
Split	1016.3 (240.1)	<.001	Reference	273.9 (104.0)	<.001	Reference	124.9 (0.3)
MSSP	1025.6 (235.9)	<.001	.78	263.7 (111.3)	<.001	.50	124.6 (0.7)
Granularity=15 minutes, waitlist=1000 patients (8 wk)							
Any	1434.7 (324.7)	Reference	<.001	669.7 (160.8)	Reference	<.001	124.6 (0.7)
Split	1039.3 (229.5)	<.001	Reference	242.0 (99.3)	<.001	Reference	124.9 (0.4)
MSSP	1040.8 (230.6)	<.001	.96	260.5 (100.1)	<.001	.19	124.8 (0.5)
Granularity=15 minutes, waitlist=1500 patients (12 wk)							
Any	1369.9 (356.1)	Reference	<.001	641.3 (153.5)	Reference	<.001	123.8 (1.2)
Split	996.2 (207.1)	<.001	Reference	294.1 (108.3)	<.001	Reference	124.5 (0.7)
MSSP	988.6 (229.9)	<.001	.59	278.7 (113.1)	<.001	.001	124.5 (0.7)

[a]MSSP: multiple subset sum problem.

XSL•FO
RenderX

Figure 2. Mean overtime for each schedule optimization formulation across all schedule parameter combinations. MSSP: multiple subset sum problem.

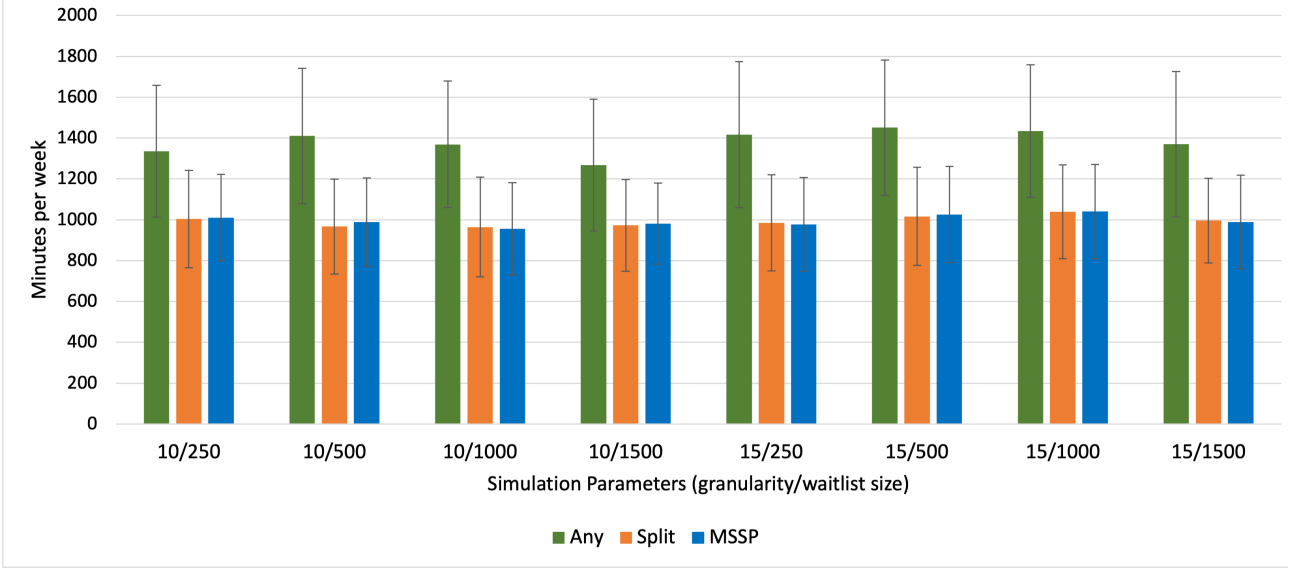
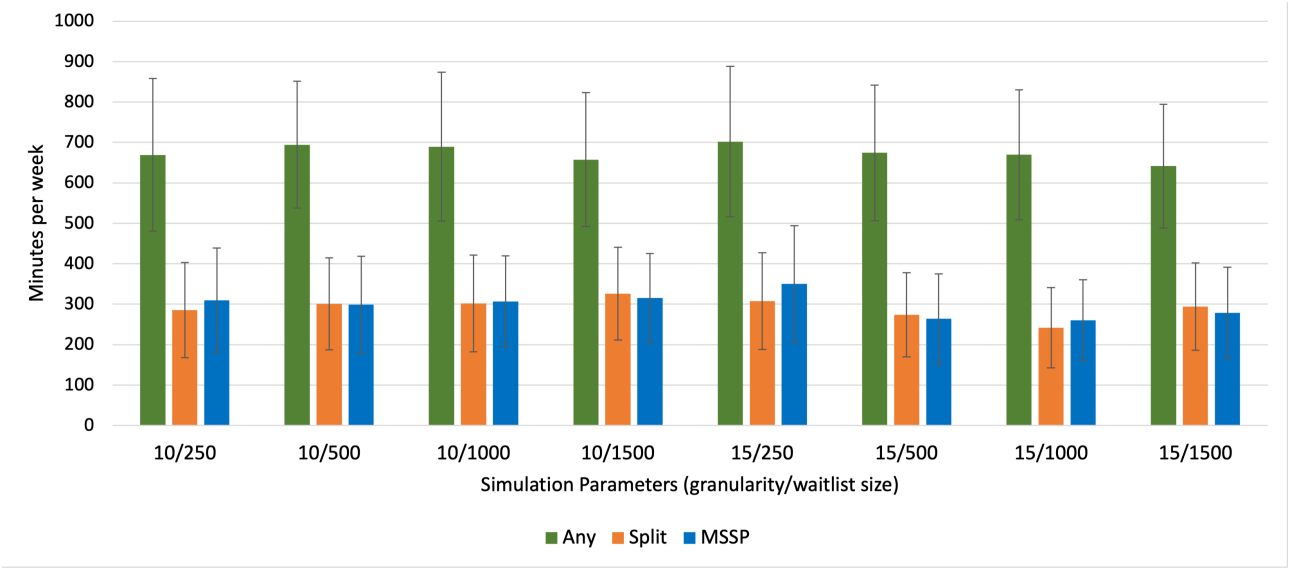


Figure 3. Mean underutilization for each schedule optimization formulation across all schedule parameter combinations. MSSP: multiple subset sum problem.



Simulated Schedule Comparison

As the MSSP scheduling formulation performed best across all schedule parameters, it was used in all further analyses. The 2-stage predict-then-optimize approach performed better than using mean DOS for over 80% of weekly schedules in terms of objective optimization problem value across all schedule parameter combinations. This difference was more consistent across the schedules generated using 15-minute schedule granularity size, where 2-stage was superior to mean in over 90% of simulated schedules (Table 2). There was less overtime across all schedule parameters when using the 2-stage approach (P<.001), equating to an average decrease in overtime of 300-500 minutes per week at the simulated hospital (or 12-20 min per operating room per day). However, there was more operating room underutilization with the 2-stage approach across all schedule parameters (Table 3; P<.001). As expected, the hindsight schedule was nearly perfect for all generated schedules and was significantly better than the 2-stage or mean approach with respect to objective value, overtime, and underutilization (Table 3). Despite a statistically significant difference, there was no clinically realizable difference in the number of cases performed between the 2-stage and mean groups; however, the hindsight formulation scheduled less cases than both the mean and the 2-stage approach (mean of approximately 12 fewer cases per wk). Details regarding the Any and Split scheduling formulation results are found in Multimedia Appendices 4 and 5, respectively.

The changes to schedule granularity and considered waitlist size did not influence the amount of overtime. However, there was significantly less operating room underutilization with the 15-minute granularity schedules (P=.02) and with waitlist sizes greater than 500, or 1 month considered (P<.001) (Table 4).

XSL•FO
RenderX

Table . Percentage of simulations in which the 2-stage performed better than mean for all schedule parameters using the MSSP schedule optimization formulation.

Granularity	250 cases	500 cases	1000 cases	1500 cases
10 minutes	86.5	90.4	80.1	81.7
15 minutes	95.2	91.3	97.1	93.3

Table . Comparing 2-stage mean and hindsight durations of surgery using the multiple subset sum problem (MSSP) schedule optimization formulation.

Method	Overtime (min/week), mean (SD)	*P* value	Underutilization (min/week), mean (SD)	*P* value	Mean cases/week (SD)	*P* value
Granularity=10 minutes, waitlist=250 patients (2 wk)						
Two-stage	1010.9 (211.3)	Reference	309.7 (128.7)	Reference	124.2 (0.9)	Reference
Mean	1310.9 (296.9)	<.001	218.7 (99.1)	<.001	124.9 (0.5)	<.001
Hindsight	0.4 (3.1)	<.001	13.8 (52.8)	<.001	112.5 (2.8)	<.001
Granularity=10 minutes, waitlist=500 patients (4 wk)						
Two-stage	988.6 (216.3)	Reference	298.8 (119.8)	Reference	124.9 (0.2)	Reference
Mean	1305.7 (242.2)	<.001	220.8 (102.0)	<.001	125.0 (0)	.01
Hindsight	0 (0)	<.001	0 (0)	<.001	112.8 (2.7)	<.001
Granularity=10 minutes, waitlist=1000 patients (8 wk)						
Two-stage	954.9 (225.7)	Reference	306.3 (112.8)	Reference	124.7 (0.6)	Reference
Mean	1276.3 (310.1)	<.001	220.4 (101.5)	<.001	125.0 (0)	<.001
Hindsight	0 (0)	<.001	0 (0)	<.001	120.3 (3.4)	<.001
Granularity=10 minutes, waitlist=1500 patients (12 wk)						
Two-stage	981.3 (199.0)	Reference	315.0 (109.9)	Reference	124.3 (0.7)	Reference
Mean	1267.7 (224.0)	<.001	223.4 (95.1)	<.001	125.0 (0)	.24
Hindsight	0 (0)	<.001	0.0 (0)	<.001	125.4 (3.9)	.006
Granularity=15 minutes, waitlist=250 patients (2 wk)						
Two-stage	977.9 (229.7)	Reference	349.9 (144.4)	Reference	121.6 (1.5)	Reference
Mean	1485.0 (274.0)	<.001	158.1 (107.4)	<.001	124.9 (0.5)	<.001
Hindsight	0.4 (3.3)	<.001	15.7 (66.2)	<.001	113.8 (2.5)	<.001
Granularity=15 minutes, waitlist=500 patients (4 wk)						
Two-stage	1025.6 (235.9)	Reference	263.7 (111.3)	Reference	124.6 (0.7)	Reference
Mean	1526.7 (275.6)	<.001	149.3 (81.9)	<.001	125.0 (0)	<.001
Hindsight	0 (0)	<.001	0 (0)	<.001	116.1 (2.5)	<.001
Granularity=15 minutes, waitlist=1000 patients (8 wk)						
Two-stage	1040.8 (239.8)	Reference	260.5 (100.1)	Reference	124.8 (0.5)	Reference
Mean	1562.2 (262.0)	<.001	140.6 (90.7)	<.001	125.0 (0)	<.001
Hindsight	0 (0)	<.001	0 (0)	<.001	119.0 (2.1)	<.001
Granularity=15 minutes, waitlist=1500 patients (12 wk)						
Two-stage	988.6 (229.9)	Reference	278.7 (113.1)	Reference	124.5 (0.7)	Reference
Mean	1540.0 (267.0)	<.001	164.6 (79.8)	<.001	125.0 (0)	<.001
Hindsight	0 (0)	<.001	0 (0)	<.001	118.8 (2.4)	<.001

XSL•FO
RenderX

Table . Comparing the impact of schedule parameters for the 2-stage multiple subset sum problem (MSSP).

Schedule parameters	Overtime, min/week, mean (SD)	*P* value	Underutilization, min/week, mean (SD)	*P* value
Granularity		.12		.02
10 min	983.9 (213.9)		307.5 (117.8)	
15 min	1008.2 (231.5)		288.2 (117.2)	
Waitlist size		.79		<.001
250 (2 weeks)	994.4 (221.9)		329.8 (138.5)	
500 (4 weeks)	1007.1 (227.6)		281.25 (117.2)	
1000 (8 weeks)	997.8 (232.8)		283.4 (109.4)	
1500 (12 weeks)	984.9 (215.5)		296.8 (113.3)	

Discussion

This paper compared 3 different scheduling optimization problems and evaluated a novel approach to surgical scheduling for TKAs and THAs using a combined 2-stage ML DOS prediction and optimization. There was no significant difference in operating room underutilization or overtime between the MSSP (one surgeon designated to one operating room per day) or Split (maximum of 2 surgeons designated for 1 operating room per day) optimization formulations. However, both performed significantly better than the Any (no limit on surgeons per operating room per day) formulation.

We believe this is due to the limitations of the predictions: underestimating the DOS of 1 case c being performed by surgeon h in room r can have cascading effects on another room r' in which the same surgeon h is due to perform another surgery c' at a later time. This causes additional overtime penalties for "Any," something that the more restrictive "Split" and "MSSP" do not encounter. This is why, despite optimal solutions to "Any" being theoretically better than those of "Split," they performed worse when simulated with the actual DOS.

Overall, the combined 2-stage approach significantly outperformed the current standard for scheduling cases, which is a case-specific mean surgery duration. This performance improvement was maintained across all schedule parameter combinations, including different schedule block granularity and different patient waitlist sizes considered. Despite this improvement, the 2-stage approach performed considerably worse than the hindsight schedule, highlighting the limitations of the current predictions that are based solely on preoperative patient data. Interestingly, there was no impact on overtime by varying schedule granularity or waitlist size; however, both of these impacted the amount of underutilization. The smaller waitlist size of 2 weeks of considered cases had a greater amount of underutilization, which was likely due to surgeons not having enough cases to fill their operating room time. Once a threshold was met at a 4-week pool of cases, there was no difference between groups. Also notable was the fact that when only considering a 2-week pool of cases, the Split optimization formulation outperformed MSSP, likely due to some surgeons not having enough cases to fill their time. Therefore, as the MSSP formulation is most practically implementable, it must be ensured that either the considered case pool is large enough or surgeons are allocated time when they have enough cases to fill an entire operating room day to avoid underutilization.

Errors in procedure length estimation by clinicians occur in approximately 75% of cases, with 32% - 50% of daily operating room schedules being underbooked and 37% - 42% overbooked [34,35]. This is compounded by the fact that less than 50% of operating time is spent doing surgery [34]. Booking based on a historical mean is more accurate than when estimated by the surgical team, though less accurate than traditional ML approaches [10,36-38]. Previous approaches using computing to improve surgical scheduling have included schedule optimization or ML to predict DOS in isolation [13,21,27,37,39,40]. Other approaches to scheduling operating room utilization include the use of surgeon-specific mean DOS or a surgeon case-specific rolling average time. To our knowledge, these have not been compared to an ML prediction-based approach. Due to the lack of surgeon-specific details included in the ACS NSQIP dataset, we could not assess the efficacy of these approaches in the present study.

The implementation of this predict-then-optimize scheduling approach would face several challenges in the real world. The MSSP optimization model is in line with current surgical scheduling practices at most hospitals. This formulation optimizes a specific surgeon's waiting list, increasing their ability to accurately plan their day while ensuring a fair distribution of time (by operating room days) for each surgeon. However, attempting to implement the other optimization formulations (Split and Any) may be faced with resistance by end-users. Particularly, using the Any formulation, surgeons may have cases at the beginning and end of the day spread out across more days in a week. ML-predicted DOS has been trialed previously in operating room planning by one group that found a reduction in wait time between cases [41]. However, they generated the predicted DOS and evaluated the implications of that information over a single day, not considering other cases from the waitlist or optimizing the schedule based on the predicted DOS.

In addition to improving operating room utilization at the systems level, the present study has implications for surgeon-level daily planning. Accurate patient-specific DOS prediction and scheduling allow for more effective personal

XSL•FO
RenderX

scheduling, including preoperative preparation, intraoperative workflow, and postoperative responsibilities. Accurate DOS predictions can assist surgeons in anticipating the need for ancillary support (eg, anesthesia, nursing, imaging) and have the potential to help decrease fatigue associated with unplanned overruns. When integrated into scheduling systems that allocate block time based on surgeon-specific waitlists (as in the MSSP formulation), this can enhance both surgeon efficiency and case throughput, aligning institutional resource allocation with the surgeon's realistic operative capacity.

The generated models and optimization formulations have the ability to transform how elective operating room scheduling is performed. By developing models specific to each operation, this increases the accuracy of each model. Most previous research evaluating the effect of ML for DOS prediction has grouped multiple different procedures [21,37]. Using such models, the procedure performed would generally be the most important feature, diluting the effect of other important patient factors without using appropriate ML techniques. The potential for cost savings for hospitals, related to reduction in overtime costs and valuable underused operating room time, is high, but the main limitation lies in the accuracy of the DOS prediction. The predictive models for TKA and THA included 33 individual patient features. Improving the model with the use of operational factors from a specific institution would likely have a corresponding effect on the schedule results but would reduce the generalizability of the approach. Further improvements may also be made by directly integrating the downstream scheduling optimization problem into training the predictive ML model [42].

This work presents some limitations. First, the DOS prediction was restricted to preoperative patient factors, based on the availability of data elements in the ACS NSQIP database, limiting the prediction accuracy. This was evidenced by the large difference in schedule performance between the 2-stage method and the perfect, hindsight, schedule. Nevertheless, this approach to predicting DOS still yielded improved schedules as compared to using a surgery-specific mean time estimate. Second, the goal of our optimization problem was to maximize the utilization of the operating room; however, this may not be directly in line with the goals of all hospitals, as some institutions may have other priorities, such as maximizing the number of cases completed. This project only developed predictive models for primary TKA and THA procedures, which may have artificially lowered the potential effect size of using this approach, as these are relatively routine procedures with lower DOS variability. By generating more surgery-specific predictive models within orthopedic surgery or other specialties, the potential for this approach may be even larger. However, these results are more directly applicable to high-volume arthroplasty surgical centers. Additionally, this scheduling approach was a simplified proof-of-concept model that may not be applicable to more complex, real-world scheduling scenarios. For example, it did not consider downstream constraints, such as the number of recovery beds, ward beds, or available staff. This was not a concern at our local institution due to its relative efficiency as a high-volume arthroplasty center. However, this would need to be expanded upon in future work if this is to be practically implemented in less specialized centers. Finally, the Split and Any optimization problems were computationally intensive when considering a waiting list size of 2 - 3 months of patients. This may be a consideration depending on institutional computational resources, which is worth noting when implementing a similar solution.

In conclusion, using ML patient-specific DOS predictions coupled with optimization was superior to elective scheduling based on a mean DOS metric over 3 different optimization problems with varying constraints and combinations of waitlist size and granularity. This generalizable approach suggests that improvements in hospital resource utilization are possible with the application of new computational methods, but the inclusion of institution-specific operational data may be considered to further improve predictions and scheduling. This has significant potential implications for health care systems struggling with pressures of rising costs and growing operative waitlists.

Acknowledgments

The American College of Surgeons National Surgical Quality Improvement Program (ACS NSQIP) and the hospitals participating in the ACS NSQIP are the source of the data used herein; they have not verified and are not responsible for the statistical validity of the data analysis or the conclusions derived by the authors. Computations were performed on the Mist supercomputer at the SciNet HPC Consortium. SciNet is funded by the Canada Foundation for Innovation; the Government of Ontario; Ontario Research Fund - Research Excellence; and the University of Toronto. The authors gratefully acknowledge the support for JRL through the Ontario Graduate Scholarship (Queen Elizabeth II Graduate Scholarship in Science & Technology) and the Holland Centre Research Award.

Data Availability

This study analyzed deidentified secondary data from the American College of Surgeons' National Surgical Quality Improvement Program (NSQIP) accessed under existing data-use agreements. Due to third-party restrictions, the dataset cannot be publicly shared by the authors. Access to NSQIP data may be requested directly from the American College of Surgeons per their access policies.

XSL•FO
RenderX

Authors' Contributions

JRL and AA made equal contributions to the paper and as such are joint first authors; conceptualization was done by JRL (lead), AA (lead), JST (lead), BR (supporting), CW (supporting), and EBK (supporting); JRL (lead), AA (lead), JST (lead), BR (supporting), CW (supporting), and EBK (supporting) contributed to methodology; investigation was done by JRL (lead), AA (lead), and JM (supporting); formal analysis was done by JM (lead) and AA (supporting); software was arranged by JM (lead) and AA (supporting); data curation was done by JRL (lead) and JM (lead); writing – original draft was done by JRL (lead), AA (lead), and MS (supporting); writing – review & editing was done by AA (lead), JRL (supporting), MS (supporting), BR (supporting), CW (supporting), and EBK (supporting); supervision was done by BR (lead), CW (lead), EBK (lead), and JST (supporting).

Conflicts of Interest

None declared.

Multimedia Appendix 1
Optimization formulations.
[DOCX File, 5640 KB - medinform_v13i1e70857_app1.docx]

Multimedia Appendix 2
Select preoperative continuous, categorical, and ordinal feature distributions of total knee and hip arthroplasty patients.
[DOCX File, 5407 KB - medinform_v13i1e70857_app2.docx]

Multimedia Appendix 3
Results of the training, validation, and testing set for the duration of surgery (DOS) predictions for total knee and hip arthroplasty (TKA and THA) models, respectively. Accuracies are presented in percentages.
[DOCX File, 5404 KB - medinform_v13i1e70857_app3.docx]

Multimedia Appendix 4
Comparing 2-stage, mean, and hindsight duration of surgery using the “Any” schedule optimization formulation.
[DOCX File, 5407 KB - medinform_v13i1e70857_app4.docx]

Multimedia Appendix 5
Comparing 2-stage, mean, and hindsight duration of surgery using the “Split” schedule optimization formulation.
[DOCX File, 5407 KB - medinform_v13i1e70857_app5.docx]

References

1. Martinez O, Martinez C, Parra CA, Rugeles S, Suarez DR. Machine learning for surgical time prediction. Comput Methods Programs Biomed 2021 Sep;208:106220. [doi: 10.1016/j.cmpb.2021.106220]
2. Wang J, Cabrera J, Tsui KL, Guo H, Bakker M, Kostis JB. Clinical and nonclinical effects on operative duration: evidence from a database on thoracic surgery. J Healthc Eng 2020 Feb 10;2020:1-8. [doi: 10.1155/2020/3582796]
3. Elderly population. OECD. 2022. URL: https://www.oecd.org/en/data/indicators/elderly-population.html [accessed 2025-09-04]
4. Bartek MA, Saxena RC, Solomon S, et al. Improving operating room efficiency: machine learning approach to predict case-time duration. J Am Coll Surg 2019 Oct;229(4):346-354. [doi: 10.1016/j.jamcollsurg.2019.05.029] [Medline: 31310851]
5. Rothstein DH, Raval MV. Operating room efficiency. Semin Pediatr Surg 2018 Apr;27(2):79-85. [doi: 10.1053/j.sempedsurg.2018.02.004]
6. Harris T, Segovia N, Koltsov J, Gardner M. Association between operative duration and adverse outcomes after hip fracture surgery: a NSQIP matched cohort study. Injury 2024 Aug;55(8):111635. [doi: 10.1016/j.injury.2024.111635]
7. Wang J, Cabrera J, Tsui KL, Guo H, Bakker M, Kostis JB. Predicting surgery duration from a new perspective: evaluation from a database on thoracic surgery. arXiv. Preprint posted online on Dec 17, 2017. [doi: 10.48550/arXiv.1712.07809]
8. Rozell JC, Ast MP, Jiranek WA, Kim RH, Della Valle CJ. Outpatient total joint arthroplasty: the new reality. J Arthroplasty 2021 Jul;36(7):S33-S39. [doi: 10.1016/j.arth.2021.02.030]
9. Abbas A, Mosseri J, Lex JR, et al. Machine learning using preoperative patient factors can predict duration of surgery and length of stay for total knee arthroplasty. Int J Med Inform 2022 Feb;158:104670. [doi: 10.1016/j.ijmedinf.2021.104670]
10. Ponce M, van Zon R, Northrup S, et al. Deploying a top-100 supercomputer for large parallel workloads. Presented at: PEARC ’19; Jul 28 to Aug 1, 2019; Chicago, IL, USA. [doi: 10.1145/3332186.3332195]
11. ACS NSQIP participant use data file. : ACS NSQIP; 2023 URL: https://www.facs.org/quality-programs/data-and-registries/acs-nsqip/participant-use-data-file/ [accessed 2023-07-01]

XSL•FO
RenderX

12. Pandit JJ. Rational planning of operating lists: a prospective comparison of “booking to the mean” vs. “probabilistic case scheduling” in urology. Anaesthesia 2020 May;75(5):642-647. [doi: 10.1111/anae.14958] [Medline: 31867710]
13. Yuniartha DR, Masruroh NA, Herliansyah MK. An evaluation of a simple model for predicting surgery duration using a set of surgical procedure parameters. Inform Med Unlocked 2021;25:100633. [doi: 10.1016/j.imu.2021.100633]
14. Marcon E, Kharraja S, Simonnet G. The operating theatre planning by the follow-up of the risk of no realization. Int J Prod Econ 2003 Jul;85(1):83-90. [doi: 10.1016/S0925-5273(03)00088-4]
15. Huang CC, Lai J, Cho DY, Yu J. A machine learning study to improve surgical case duration prediction. In: Health Systems and Quality Improvement: Cold Spring Harbor Laboratory Press; 2020. [doi: 10.1101/2020.06.10.20127910]
16. Hassanzadeh H, Boyle J, Khanna S, Biki B, Syed F. Daily surgery caseload prediction: towards improving operating theatre efficiency. BMC Med Inform Decis Mak 2022 Jun 7;22(1):151. [doi: 10.1186/s12911-022-01893-8] [Medline: 35672729]
17. Erdogan SA, Denton BT. Surgery Planning and Scheduling: John Wiley & Sons, Ltd; 2011. [doi: 10.1002/9780470400531.eorms0861]
18. Akiba T, Sano S, Yanase T, Ohta T, Koyama M. Optuna: a next-generation hyperparameter optimization framework. arXiv. Preprint posted online on Jul 25, 2019. [doi: 10.48550/arXiv.1907.10902]
19. Shehadeh KS, Padman R. A distributionally robust optimization approach for stochastic elective surgery scheduling with limited intensive care unit capacity. Eur J Oper Res 2021 May;290(3):901-913. [doi: 10.1016/j.ejor.2020.09.001]
20. Healthcare Cost and Utilization Project (HCUP). AHRQ. 2021. URL: https://www.ahrq.gov/data/hcup/index.html [accessed 2025-09-04]
21. Shi Y, Mahdian S, Blanchet J, Glynn P, Shin AY, Scheinker D. Surgical scheduling via optimization and machine learning with long-tailed data. Health Care Manag Sci 2023 Dec;26(4):692-718. [doi: 10.1007/s10729-023-09649-0]
22. Marques I, Captivo ME, Barros N. Optimizing the master surgery schedule in a private hospital. Oper Res Health Care 2019 Mar;20:11-24. [doi: 10.1016/j.orhc.2018.11.002]
23. Hans E, Wullink G, van Houdenhoven M, Kazemier G. Robust surgery loading. Eur J Oper Res 2008 Mar;185(3):1038-1050. [doi: 10.1016/j.ejor.2006.08.022]
24. Abbas A, Lex JR, Toor J, Khalil EB, Ravi B, Whyne C. Neural networks accurately predict precise metrics of hospital resource utilization for total hip arthroplasty: a retrospective database study. . Preprint posted online on 2025. [doi: 10.1101/2025.02.11.25322104]
25. BMUS: The Burden of Musculoskeletal Diseases in the United States. 2011. URL: https://www.bmus-ors.org/ [accessed 2025-09-04]
26. Eijkemans MJC, van Houdenhoven M, Nguyen T, Boersma E, Steyerberg EW, Kazemier G. Predicting the unpredictable: a new prediction model for operating room times using individual characteristics and the surgeon’s estimate. Anesthesiology 2010 Jan;112(1):41-49. [doi: 10.1097/ALN.0b013e3181c294c2] [Medline: 19952726]
27. Strömblad CT, Baxter-King RG, Meisami A, et al. Effect of a predictive model on planned surgical duration accuracy, patient wait time, and use of presurgical resources: a randomized clinical trial. JAMA Surg 2021 Apr 1;156(4):315-321. [doi: 10.1001/jamasurg.2020.6361] [Medline: 33502448]
28. Garbarino LJ, Gold PA, Sodhi N, et al. The effect of operative time on in-hospital length of stay in revision total knee arthroplasty. Ann Transl Med 2019 Feb;7(4):66-66. [doi: 10.21037/atm.2019.01.54]
29. Muñoz E, Muñoz W, Wise L. National and surgical health care expenditures, 2005-2025. Ann Surg 2010 Feb;251(2):195-200. [doi: 10.1097/SLA.0b013e3181cbcc9a] [Medline: 20054269]
30. Attarian DE, Wahl JE, Wellman SS, Bolognesi MP. Developing a high-efficiency operating room for total joint arthroplasty in an academic setting. Clin Orthop Relat Res 2013 Jun;471(6):1832-1836. [doi: 10.1007/s11999-012-2718-4] [Medline: 23208123]
31. Rasmussen RV, Trick MA. The timetable constrained distance minimization problem. Ann Oper Res 2009 Oct;171(1):45-59. [doi: 10.1007/s10479-008-0384-4]
32. Lai J, Huang CC, Liu SC, Huang JY, Cho DY, Yu J. Improving and Interpreting Surgical Case Duration Prediction With Machine Learning Methodology: Cold Spring Harbor Laboratory Press; 2020. [doi: 10.1101/2020.06.10.20127910]
33. Viberg N, Forsberg BC, Borowitz M, Molin R. International comparisons of waiting times in health care – limitations and prospects. Health Policy 2013 Sep;112(1-2):53-61. [doi: 10.1016/j.healthpol.2013.06.013]
34. Dexter F, Ledolter J. Bayesian prediction bounds and comparisons of operating room times even for procedures with few or no historic data. Anesthesiology 2005;103(6):1259-1167. [doi: 10.1097/00000542-200512000-00023]
35. Pandit JJ, Tavare A. Using mean duration and variation of procedure times to plan a list of surgical operations to fit into the scheduled list time. Eur J Anaesthesiol 2011 Jul;28(7):493-501. [doi: 10.1097/EJA.0b013e3283446b9c] [Medline: 21623186]
36. Laskin DM, Abubaker AO, Strauss RA. Accuracy of predicting the duration of a surgical operation. J Oral Maxillofac Surg 2013 Feb;71(2):446-447. [doi: 10.1016/j.joms.2012.10.009]
37. Scott CEH, MacDonald DJ, Howie CR. “Worse than death” and waiting for a joint arthroplasty. Bone Joint J 2019 Aug;101-B(8):941-950. [doi: 10.1302/0301-620X.101B8.BJJ-2019-0116.R1] [Medline: 31362549]
38. Elmachtoub AN, Grigas P. Smart predict, then optimize. arXiv. Preprint posted online on Oct 22, 2017. [doi: 10.48550/arXiv.1710.08005]

XSL•FO
RenderX

39. Liaw R, Liang E, Nishihara R, Moritz P, Gonzalez JE, Stoica I. Tune: a research platform for distributed model selection and training. arXiv. Preprint posted online on Jul 13, 2018. [doi: 10.48550/arXiv.1807.05118]
40. Obesity: another ongoing pandemic. Lancet Gastroenterol Hepatol 2021 Jun;6(6):411. [doi: 10.1016/S2468-1253(21)00143-6]
41. Marques I, Captivo ME, Vaz Pato M. An integer programming approach to elective surgery scheduling. OR Spectr 2012 Apr;34(2):407-427. [doi: 10.1007/s00291-011-0279-7]
42. Ahmed A, He L, Chou CA, Hamasha MM. A prediction-optimization approach to surgery prioritization in operating room scheduling. J Ind Product Eng 2022 Jul 4;39(5):399-413. [doi: 10.1080/21681015.2021.2017362]

Abbreviations

ACS NSQIP: American College of Surgeons National Surgical Quality Improvement
DOS: duration of surgery
ML: machine learning
MSSP: multiple subset sum problem
THA: total hip arthroplasty
TKA: total knee arthroplasty

Edited by A Benis; submitted 03.01.25; peer-reviewed by CH Wang, M Subih; revised version received 23.07.25; accepted 28.07.25; published 10.09.25.

Please cite as:
Lex JR, Abbas A, Mosseri J, Singh Toor J, Simone M, Ravi B, Whyne C, Khalil EB
Using Machine Learning to Predict-Then-Optimize Elective Orthopedic Surgery Scheduling to Improve Operating Room Utilization: Retrospective Study
JMIR Med Inform 2025;13:e70857
URL: https://medinform.jmir.org/2025/1/e70857
doi:10.2196/70857

© Johnathan R Lex, Aazad Abbas, Jacob Mosseri, Jay Singh Toor, Michael Simone, Bheeshma Ravi, Cari Whyne, Elias B Khalil. Originally published in JMIR Medical Informatics (https://medinform.jmir.org), 10.9.2025. This is an open-access article distributed under the terms of the Creative Commons Attribution License (https://creativecommons.org/licenses/by/4.0/), which permits unrestricted use, distribution, and reproduction in any medium, provided the original work, first published in JMIR Medical Informatics, is properly cited. The complete bibliographic information, a link to the original publication on https://medinform.jmir.org/, as well as this copyright and license information must be included.

XSL•FO
RenderX

Optimizing Loop Diuretic Treatment for Mortality Reduction in Patients With Acute Dyspnea Using a Practical Offline Reinforcement Learning Pipeline for Health Care: Retrospective Single-Center Simulation Study

Jung Min Lee[1], MS; Shengpu Tang[1,2], PhD; Michael Sjoding[3], MD; Jenna Wiens[1], PhD

[1]Division of Computer Science and Engineering, College of Engineering, University of Michigan, 2260 Hayward St, Ann Arbor, MI, United States

[2]Department of Computer Science, Emory College of Arts and Sciences, Emory University, Atlanta, GA, United States

[3]Division of Pulmonary and Critical Care Medicine, Michigan Medicine, University of Michigan, Ann Arbor, MI, United States

Corresponding Author:
Jenna Wiens, PhD
Division of Computer Science and Engineering, College of Engineering, University of Michigan, 2260 Hayward St, Ann Arbor, MI, United States

Abstract

Background: Offline reinforcement learning (RL) has been increasingly applied to clinical decision-making problems. However, due to the lack of a standardized pipeline, prior work often relied on strategies that may lead to overfitted policies and inaccurate evaluations.

Objective: In this work, we present a practical pipeline—Pipeline for Learning Robust Policies in Reinforcement Learning (PROP-RL)—designed to improve robustness and minimize disruption to clinical workflow. We demonstrate its efficacy in the context of learning treatment policies for administering loop diuretics in hospitalized patients.

Methods: Our cohort included adult inpatients admitted to the emergency department at Michigan Medicine between 2015 and 2019 who required supplemental oxygen. We modeled the management of loop diuretics as an offline RL problem using a discrete state space based on features extracted from electronic health records, a binary action space corresponding to the daily use of loop diuretics, and a reward function based on in-hospital mortality. The policy was trained on data from 2015 to 2018 and evaluated on a held-out set of hospitalizations from 2019, in terms of estimated reduction in mortality compared to clinician behavior.

Results: The final study cohort included 36,570 hospitalizations. The learned treatment policy was based on 60 states: the policy deferred to clinicians in 36 states, recommended the majority action in 22 states, and diverged significantly from clinician behavior in 2 of the states. Among the cases where the policy meaningfully diverged from the behavior policy, the learned policy was estimated to significantly reduce the mortality rate from 3.8% to 2.2% by 1.6% (95% CI 0.4 - 2.7; *P*=.006).

Conclusions: We applied our pipeline to the clinical problem of loop diuretic treatment, highlighting the importance of robust state representation and thoughtful policy selection and evaluation. Our work reveals areas of potential improvement in current clinical care for loop diuretics and serves as a blueprint for using offline RL for sequential treatment selection in clinical settings.

(JMIR Med Inform 2025;13:e69145) doi:10.2196/69145

KEYWORDS

reinforcement learning; artificial intelligence; loop diuretic; treatment recommendation; treatment selection; clinical decision support; dynamic treatment regime

Introduction

Reinforcement learning (RL) is a branch of artificial intelligence that, through interactions with an environment, learns the optimal sequence of actions that will maximize a desired outcome [1]. RL methods are especially well suited to tackle problems that require sequential decision-making where the rewards are delayed. This makes it an attractive solution for learning dynamic treatment policies in health care problems (eg, sepsis [2], diabetes [3], and hypotension [4]) where decisions are made sequentially over a prolonged period of time and the outcome (eg, in-hospital mortality) is observed at a later time point. Due to safety and ethical concerns, training and evaluation of RL policies in this domain often rely on a fixed set of historical data and require the use of offline RL algorithms [5].

XSL•FO
RenderX

However, effectively applying offline RL poses several challenges. First, deriving a robust and informative state representation from high-dimensional health features can be challenging, especially with limited data. Second, the performance of offline RL algorithms is sensitive to hyperparameters [6-8], often leading to policies that perform well during development but fail once deployed. Yet a standardized approach for hyperparameter selection has not been established for offline RL. Third, the learned policy may differ substantially from current clinician behavior, resulting in low confidence in evaluation results and potential disruption to clinical workflows [9]. While some of these issues have been solved in isolation [10-12], there is a notable absence of a standard pipeline for applying offline RL, comparable to the training-validation framework in supervised learning, that integrates these individual solutions. We address this gap by presenting a pipeline (Pipeline for Learning Robust Policies in Reinforcement Learning; PROP-RL) along with a codebase for applying offline RL to health care settings, and demonstrate its efficacy by applying it to the problem of learning treatment policies for loop diuretics.

Loop diuretics are one of the most commonly prescribed medications in hospitals and are used to control volume and edema in the body by increasing urinary sodium and water excretion [13]. They are used to treat patients with acute shortness of breath from fluid accumulation in their lungs, typically associated with conditions such as congestive heart failure or acute pulmonary edema [14]. There remains substantial uncertainty and variability regarding when to start and stop loop diuretics [15,16]. This uncertainty leads to inadequate use of loop diuretics, which has been associated with worse clinical outcomes, including higher rates of acute kidney injury and electrolyte disturbances [17,18].

In this paper, we apply offline RL to learn a loop diuretics treatment policy—designed to aid health care professionals—from electronic health records (EHRs) of hospitalized patients at a large academic hospital. In doing so, we establish a pipeline—PROP-RL—for applying offline RL in health care settings that incorporates state representation learning, hyperparameter selection, and modification of the learned policy to minimize disruption to existing workflows. We demonstrate the effectiveness of PROP-RL through off-policy evaluation (OPE) and ablation studies [19].

Methods

Study Cohort

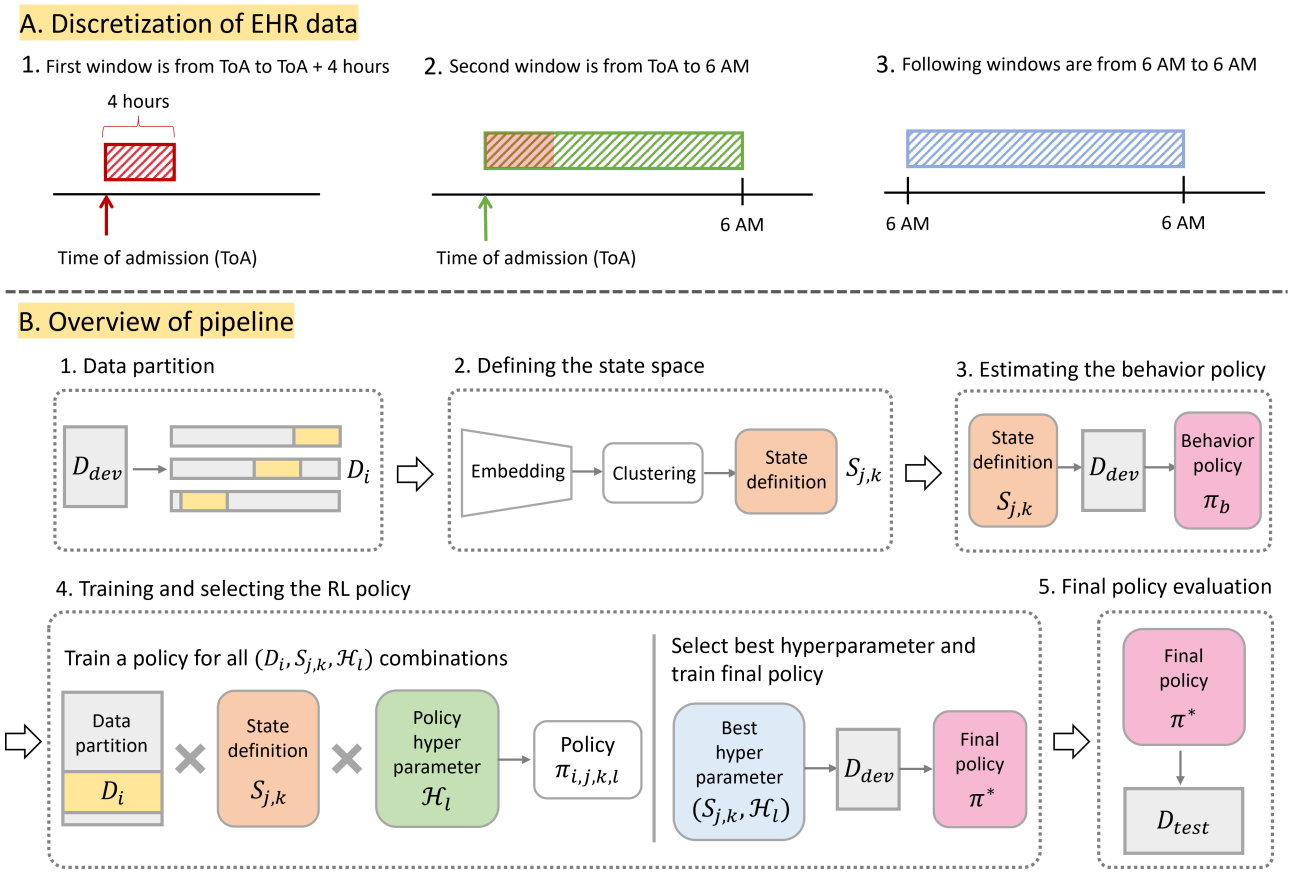
We included adult patients (≥18 years) admitted to the hospital through the emergency department at Michigan Medicine during the years 2015‐2019, who required any amount of supplemental oxygen support during the first 24 hours of admission. Patients who underwent surgery within 24 hours of admission were excluded as the supplemental oxygen support provided may not be due to a primary respiratory condition (Section A1 in Multimedia Appendix 1). The cohort was split into a development set and a held-out test set consisting of data from patients admitted in 2015‐2018 and 2019, respectively.

Data Preprocessing

To formulate the management of loop diuretics as an RL problem with discrete time steps, we split the hospitalization data into chronological windows. With the exception of the first and second windows, all windows were 24 hours long, starting and ending at 6 AM (Figure 1A; Section A2 in Multimedia Appendix 1). In each window, medication records were analyzed to determine whether an oral or intravenous loop diuretic was administered. We assumed all treatment decisions made within a window were based on the patient's state in the previous window. A 6 AM cutoff time was chosen as most clinical rounds (where decisions are made) occur immediately after this point. Analysis was constrained to the first 8 days of hospitalization.

XSL•FO
RenderX

Figure 1. (A) Diagram of the windowing rule for hospitalizations. (B) Overview of pipeline. (1) Data partition: the development data D_{dev} are partitioned in multiple ways to create the data partitions D_i, $i \in \{1...10\}$. (2) Defining the state space: a set of candidate discrete state definitions, characterized by the data partition D_j used to derive the state definition and the number of states k, is generated by learning a lower-dimensional representation of the features and clustering them. (3) Estimating the behavior policy: the behavior policy π_b is estimated from the development state using each state definition $S_{j,k}$. While π_b is dependent on $S_{j,k}$, for simplicity, we refer to the behavior policy as π_b in general. (4) Training and selecting the RL policy: a policy $\pi_{i, j, k, l}$ is trained for each possible hyperparameter combination across all data partitions. The best hyperparameter is used to train the final policy π^* on the entire development set. (5) Final policy evaluation: π^* is evaluated on the test set D_{test}. EHR: electronic health record; RL: reinforcement learning.



For each window, EHR features including age, vital sign measurements, laboratory test results, medications, fluid input and output, and Sequential Organ Failure Assessment (SOFA) scores were extracted (Section A3 in Multimedia Appendix 1). These features capture the patient's most recent health state as well as past treatments, which are necessary for determining future treatments. We used the Flexible Data-Driven Pipeline (FIDDLE) software to convert these into 243-dimensional feature vectors (Section A2, A3, and A16 in Multimedia Appendix 1) [20].

Model Development and Evaluation

Overview

We modeled the patient environment as a Markov decision process (MDP) defined by (S, A, P, R, γ). S and A represent the state and action spaces. Given a hospitalization, $s_t \in S$ represents the patient's health on day t and $a_t \in A$ is the treatment decision made based on st. $P(s_{t+1}|s_t, a_t)$ is the transition function, $R(s_t) = r_t$ is the reward function, and $\gamma \in [0, 1]$ is the discount factor. The discrete state space S was defined by clustering the EHR features in a learned embedding space. The action space $A = \{0, 1\}$ was defined to encode binary treatment decisions, corresponding to whether the patient received loop diuretics (Section A4 in Multimedia Appendix 1). All intermediate rewards were set to 0, and a terminal reward was given when the patient's hospitalization ended or reached 8 days (whichever is earlier). The terminal reward was 100 if the patient was discharged alive and –100 if the patient died. Our objective was to learn a policy π: $S \times A \rightarrow [0, 1]$ which maps s_t to a probability distribution over a_t, in order to maximize the expected cumulative reward $J(\pi)=E\pi\sum t=09\gamma tR(st)$ where $\gamma=0.99$. This roughly corresponds to an objective that focuses on minimizing the overall mortality rate.

PROP-RL consists of the following 5 steps (Figure 1B): (1) data partition, (2) defining the state space, (3) estimating the behavior policy, (4) training and selecting the RL policy, and (5) final policy evaluation.

Step 1. Data Partition

We created 10 partitions of the development set by randomly assigning each hospitalization to either the training or validation split. These partitions were used for steps (2) and (4).

XSL•FO
RenderX

Step 2. Defining the State Space

We used a data-driven approach to establish state definitions. For each data partition, a function mapping the 243-dimensional feature space to a discrete state space was learned by training a neural network embedding model and applying ensemble *k*-means clustering in the embedding space (Section A5 in Multimedia Appendix 1) [21,22]. *k*, the size of the discrete state space, was a hyperparameter that varied from {20,40,...,160} (Section A6 in Multimedia Appendix 1). The state definition itself was treated as a hyperparameter.

Prior to policy learning, the state definitions were evaluated for generalizability and informativeness. We verified that each hospitalization transitioned across multiple different states and that the state distribution was not heavily skewed toward a few specific states. Failing to meet both criteria implies an overfitted state definition unlikely to generalize to new patients. Second, to ensure the embeddings captured important information, we conducted a principal component analysis of the cluster centers. We visualized the distribution of the cluster centers using the average and SD of the mortality rates, SOFA scores, and clinicians' previous and next actions among the windows belonging to each state.

Step 3. Estimating the Behavior Policy

We estimated the behavior policy by computing the average observed action for each state within the development set. This is a stochastic policy that maps each state to a probability over the binary actions. To further validate the state definitions, we performed 2 evaluations using the estimated behavior policy. First, we compared the estimated mortality rate of the behavior policy on the held-out test set to the true mortality rate. Significant differences in these values would either indicate a significant change in clinicians' behavior between the 2 datasets, or the state definitions' inability to encode the behavior policy. Second, we investigated whether the estimated behavior policy aligns with clinical understanding by visualizing trends in the behavior policy with respect to key features of the states (Section A7 in Multimedia Appendix 1).

Step 4. Training and Selecting the RL Policy

After learning the transition matrix from the training data, we learned the optimal policy using a modified version of value iteration with 2 offline RL constraints: batch-constrained Q-learning (BCQ) and pessimistic Markov decision process (pMDP) [1,23,24]. These constraints mitigate extrapolation error, which refers to inaccurate value estimations for state-action pairs that were rarely or never observed during training [23]. In brief, BCQ constrains the policy to avoid actions unlikely to be selected by the behavior policy, and pMDP encourages the policy to avoid areas in the state-action space with high uncertainty (Section A8 in Multimedia Appendix 1). Both BCQ and pMDP have additional hyperparameters.

Recent work found hyperparameter selection in offline RL to be sensitive to the partitioning of the dataset [7]. To mitigate this, we use the Split-Select-Retrain (SSR) pipeline that selects the optimal hyperparameters by aggregating validation performance over multiple partitions of the development set [7]. The final policy is then learned from the entire development set using the selected optimal hyperparameters. We leveraged the same 10 partitions (train and validation split) described in step (1) (Section A9 in Multimedia Appendix 1).

Performance was measured using the OPE method weighted importance sampling (WIS), known for its simplicity and reliance on relatively few assumptions [25]. WIS is a biased but consistent estimator, with estimates converging to the true value as sample size increases. WIS estimates both the performance and effective sample size (ESS) of the policy, which is a measure of confidence in the performance estimate [26]. ESS values closer to the size of the dataset used for evaluation (ie, validation set) indicate higher confidence in the performance estimate. For the main analysis, we focus on WIS, but for robustness, we also consider 3 additional OPE methods: fitted Q evaluation, approximate model, and weighted doubly robust estimates (Section A10 in Multimedia Appendix 1 for methodological details). *P* values are estimated by a one-sided bootstrap resampling test [27].

In order to minimize disruption to clinical workflow without sacrificing policy performance, we modified the learned policy prior to evaluation by identifying "unimportant states," inspired by Shen et al [28]. In unimportant states, no action can significantly impact the outcome. Our policies deferred to clinicians' decisions in unimportant states, thus minimizing the amount of potential deviation from clinician behavior. The threshold used to determine unimportance was considered a hyperparameter (Section A11 and A12 in Multimedia Appendix 1).

Step 5. Final Policy Evaluation

The final policy was evaluated on the held-out test set using WIS. Improvement in performance compared to the behavior policy was measured across 1000 bootstrapped samples in terms of expected cumulative reward and mortality. The level of disagreement between the average clinician and the final learned policy was compared to the level of disagreement among clinicians (Section A13 in Multimedia Appendix 1).

To understand how the learned policy differs from the behavior policy, we focused on "divergent" states where the action recommended by the learned policy diverged from the majority action of the behavior policy. The learned policy was then evaluated on a subset of the cohort where the patient's hospitalization included divergent states. We further characterized these states by comparing the average values of their key features to those of the general population (Section A14 in Multimedia Appendix 1).

Ablation Studies of Pipeline

Our pipeline included 3 key elements designed to improve the robustness of the learned policy: (1) using unimportant states to "relax" the learned policy, (2) evaluation across multiple data partitions (SSR), and (3) treating state definitions as a hyperparameter. To demonstrate the effect of each element on the robustness of the learned policy, we conducted an ablation study by selectively removing each component from the pipeline. As a proxy for measuring robustness, we looked at the worst-case OPE performance of the learned policies to establish an empirical lower bound.

XSL•FO
RenderX

Ethical Considerations

This study was approved by the Institutional Review Board at the University of Michigan Medical School (HUM00141899) with a waiver of informed consent among study patients. All data collected were deidentified and were accessed via a secure cloud storage platform and a secured, Health Insurance Portability and Accountability Act (HIPAA)–compliant server. Participants were not compensated for the use of their data in this study. The study followed the TRIPOD+AI (Transparent Reporting of a Multivariable Prediction Model for Individual Prognosis or Diagnosis+Artificial Intelligence) reporting guideline [29] (Checklist 1). As this study was retrospective in nature, no formal study protocol was developed and the study was not registered. No patients or the public were involved in any aspect of this study.

Results

Study Cohort and Patient Characteristics

The initial cohort consisted of 57,907 hospitalizations. We removed cases where supplemental oxygen was not given within 24 hours (n=14,902), patients were moved to surgery within 24 hours (n=6283), and hospitalizations lasting shorter than 2 windows (n=152). The final study population contained 23,945 unique patients and 36,570 unique hospitalizations divided temporally by admission year into the development (n=29,765; 2015 - 2018) and test set (n=6805; 2019) (Table 1; Section A1 in Multimedia Appendix 1). The mortality rate of the entire cohort was 5.4% (1978/36,570), and 5.2% (1555/29,765) and 6.2% (423/6805) for the development and test set, respectively.

XSL•FO
RenderX

Table . Cohort characteristics. Values are numbers (percentages) unless stated otherwise.

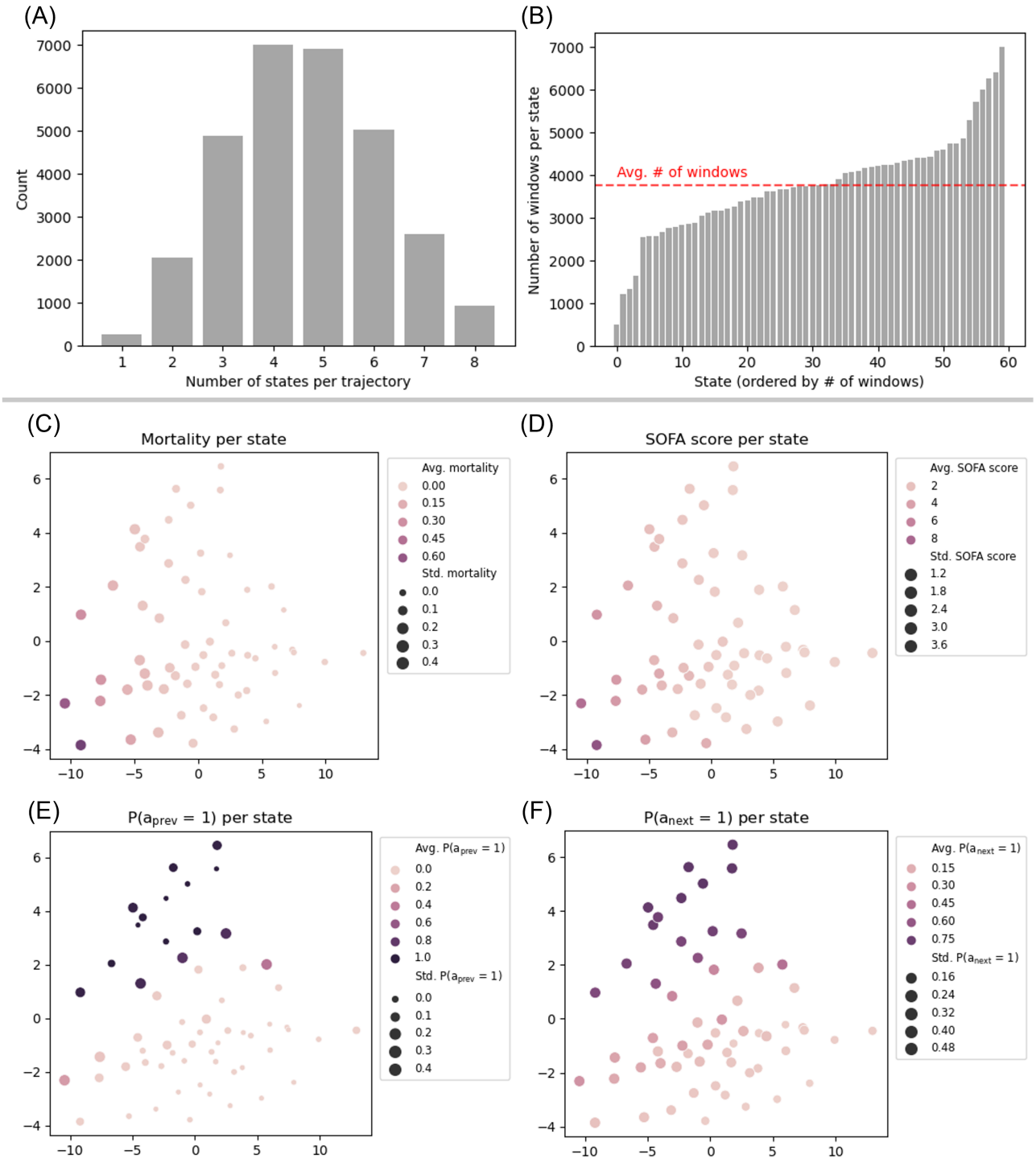
Cohort	Overall (2015 - 2019)	Development set (2015 - 2018)	Test set (2019)
Hospitalizations, n	36,570	29,765	6805
Age (years), median (IQR)	64 (53 - 74)	64 (52 - 74)	65 (54 - 75)
Age range (years), n (%)			
18 - 25	1142 (3.1)	1010 (3.4)	124 (1.8)
26 - 45	4747 (13.0)	3889 (13.1)	858 (12.6)
46 - 65	13,770 (37.7)	11,266 (37.8)	2504 (36.8)
66 - 85	14,317 (39.1)	11,477 (38.6)	2840 (41.7)
>85	2594 (7.1)	2123 (7.1)	471 (6.9)
Sex, n (%)			
Female	17,364 (47.5)	14,241 (47.8)	3123 (45.9)
Male	19,206 (52.5)	15,524 (52.2)	3682 (54.1)
Self-reported race, n (%)			
White or Caucasian	30,529 (83.5)	24,853 (83.5)	5676 (83.4)
Black or African American	4295 (11.7)	3503 (11.8)	792 (11.7)
Asian	642 (1.8)	516 (1.7)	126 (1.8)
American Indian or Alaska Native	141 (0.4)	115 (0.4)	26 (0.4)
Native Hawaiian or Other Pacific Islander	27 (0.1)	21 (0.1)	6 (0.1)
Other	659 (1.8)	546 (1.8)	113 (1.7)
Unknown	209 (0.6)	160 (0.5)	49 (0.7)
Patient refused	68 (0.2)	51 (0.2)	17 (0.2)
Hospitalization outcome, n (%)			
Alive	34,592 (94.6)	28,210 (94.8)	6382 (93.8)
Death	1978 (5.4)	1555 (5.2)	423 (6.2)
Length of stay (days), median (IQR)	6 (4-9)	6 (4-9)	6 (4-10)
Length of stay (days), n (%)			
1 - 3	8216 (22.5)	6939 (23.3)	1277 (18.8)
4 - 5	9446 (25.8)	7736 (26.0)	1710 (25.1)
6 - 9	10,027 (27.4)	8063 (27.1)	1964 (28.9)
10 - 15	5136 (14.0)	4046 (13.6)	1090 (16.0)
>15	3745 (10.2)	2981 (10.0)	764 (11.2)

Evaluation of State Definitions

The final state definition $S_{j,k}$ (j=7, k=60) was selected from the hyperparameter search. Overall, 98.3% (29,270/29,765) of hospitalizations in the development set and 98.9% (6730/6805) in the test set contained at least 2 distinct states, indicating at least one transition between different states within these hospitalizations (Figure 2A). All states appeared relatively uniformly in the data with each state constituting 1.7% (SD 0.5%) of all windows on average in both the development set (3769, SD 1187; 226,178 total windows) and test set (893, SD 268; 53,591 total windows) (Figure 2B; Section B2 in Multimedia Appendix 1 for test set results).

XSL•FO
RenderX

Figure 2. Sanity checks for the state definitions on the development set. The first row shows histograms depicting (A) number of states in each trajectory and (B) the number of windows in each state. The second and third rows show principal component analysis of the representations of the cluster centers that define each state. The hue and size of each dot represent the average and SD of the feature value of all samples in that state. The features are (C) mortality rate, (D) SOFA score, (E) whether loop diuretics were administered in the past 24 hours, and (F) whether clinicians chose to administer loop diuretics. SOFA: Sequential Organ Failure Assessment.



Plots of the cluster centers show that information regarding mortality and clinicians' actions is encoded in the states. Figure 2C and 2D indicate that a visible gradient exists in the state representation space with respect to both average mortality and average SOFA score. Figure 2E and 2F show a distinct separation in the state representation space in terms of both the clinician's previous and next actions. Note that even without being explicitly trained for it, the state representation space captures information about the previous action.

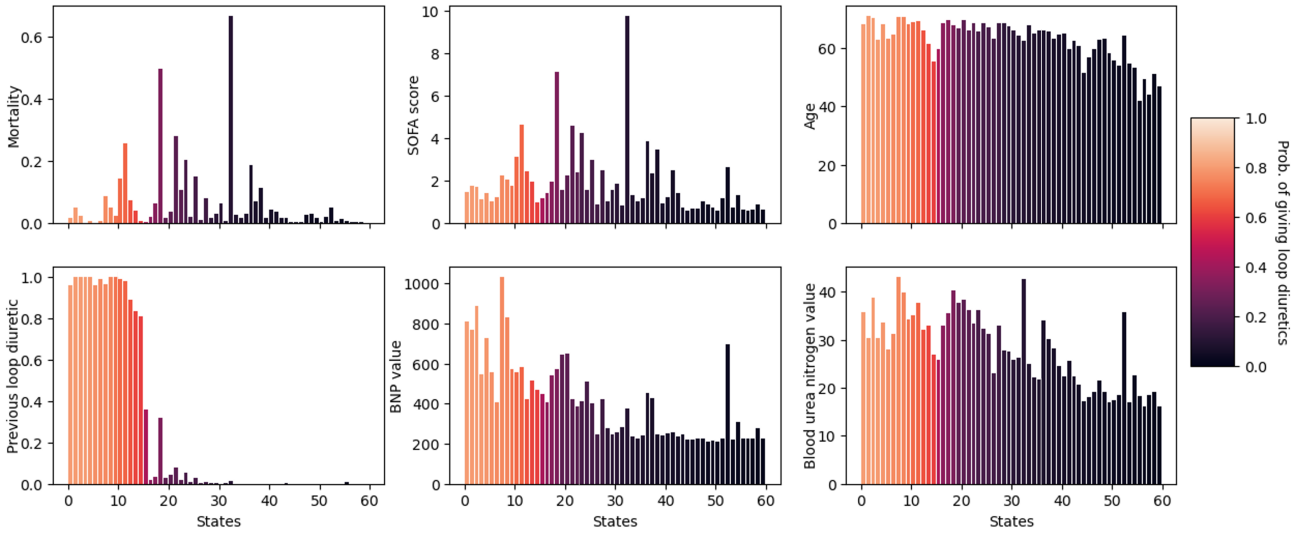
Evaluation of the Estimated Behavior Policy

The estimated mortality rate of the clinician behavior policy across 1000 bootstrapped samples was 6.2% (95% CI 5.6 - 6.8) (Section B9 in Multimedia Appendix 1). This was comparable to the true mortality rate of 6.2% (95% CI 5.6% - 6.8%) observed in the held-out test set, suggesting the state definitions

XSL•FO
RenderX

have accurately captured clinicians' behavior. Qualitatively, we found the estimated behavior policy to recommend loop diuretics if the patient is older, given loop diuretics the previous day, has higher brain natriuretic peptide (BNP) values, and has higher blood urea nitrogen values (Figure 3). We report trends for additional features in Section B3 in Multimedia Appendix 1.

Figure 3. The relationship between the clinician's likelihood of administering loop diuretics and key features. Features shown are (from left to right, top to bottom): mortality, SOFA score, age, whether loop diuretics were administered in the past 24 hours, BNP value, and blood urea nitrogen value. The height of the bars represents the average value of each feature within the state, and the color represents the clinician's likelihood of administering loop diuretics. BNP: brain natriuretic peptide; SOFA: Sequential Organ Failure Assessment.

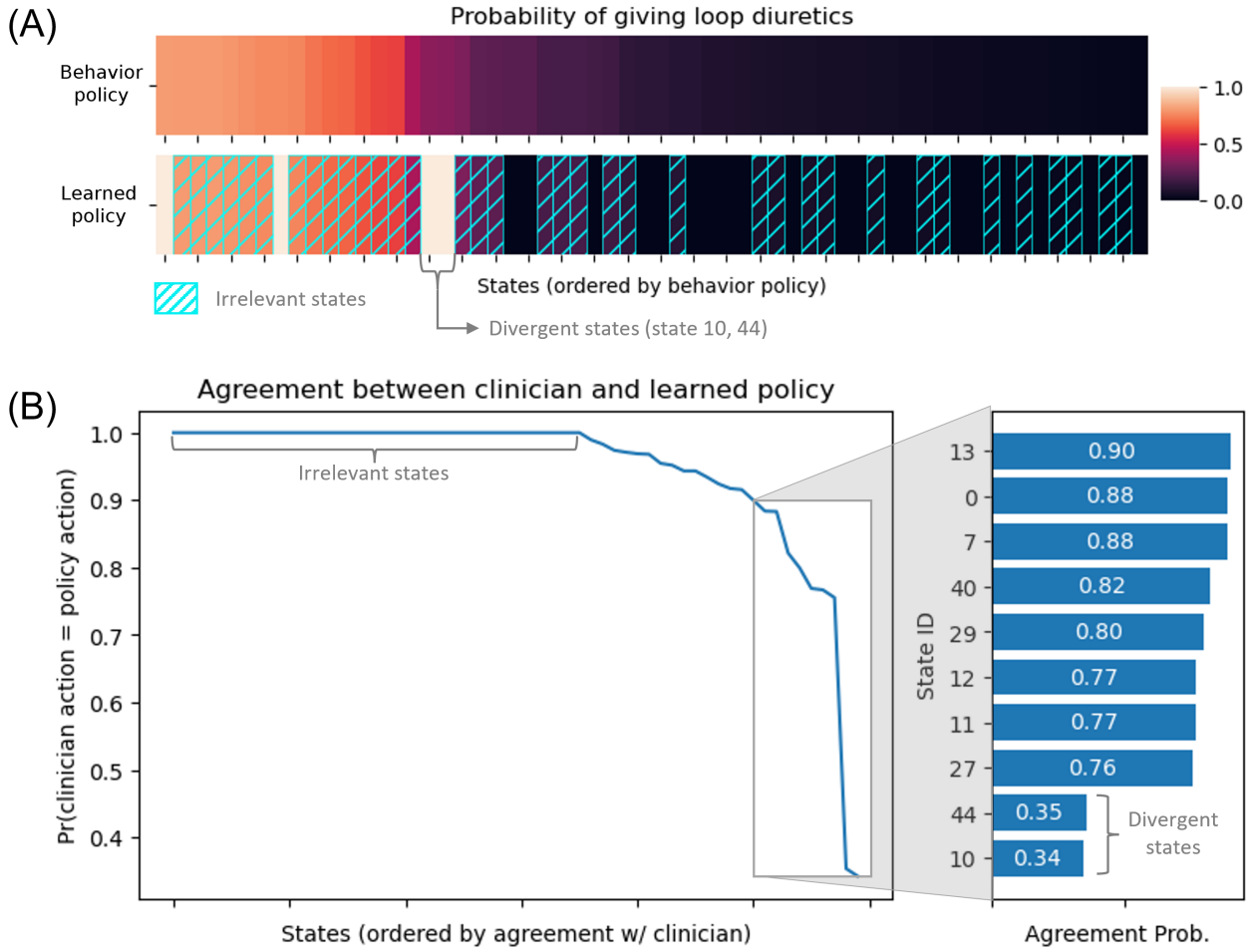


Evaluation of the Final Learned Policy

Of the 60 states, 36 were unimportant and the learned policy deferred to clinicians (Figure 4A). For the remaining 24 states, the learned policy tended to recommend the majority action: among 21,759 windows belonging to these states in the test set, only 3858 (17.7%) windows were assigned a different action under the learned policy. Yet in 2 divergent states (states 10 and 44), the learned policy did not follow the majority action. While the learned policy always recommended loop diuretics to be administered for both states, clinicians only took this action 34% (454/1326) and 35% (568/1614) of the time, respectively (Figure 4B).

XSL•FO
RenderX

Figure 4. (A) Comparison of the actions recommended by the clinician behavior policy and the learned policy for each state. The color of the boxes indicates the probability of giving loop diuretics. States are ordered by decreasing likelihood of clinicians prescribing loop diuretics. Hatched boxes indicate "unimportant" states where the learned policy recommends the same actions as the behavior policy. (B) Likelihood of agreement between the clinician behavior policy and the learned policy for each state. On the left graph, states are ordered by decreasing likelihood of agreement with the clinicians. The right bar graph focuses on the 10 states where the clinicians disagree the most with the learned policy. States 10 and 44, where the likelihood of agreement is less than 0.5 (learned policy does not follow majority action), are defined as "divergent" states.



On the entire held-out test set, the learned policy outperformed the behavior policy 967 times across 1000 bootstraps (96.7%) and was estimated to reduce mortality from 6.2% to 5.7%, by 0.5 (95% CI 0.0−1.1; *P*=.03) percentage points on average (Table 2). The ESS of the learned policy was 3168.45 (95% CI 3090.91-3256.65), nearly half the size of the dataset (n=6805) indicating a high confidence in the WIS estimate (Section B7 in Multimedia Appendix 1 for validation set results). On the subset of hospitalizations with divergent states, the learned policy outperformed the behavior policy 994 times across 1000 bootstraps (99.4%) and significantly decreased the estimated overall mortality from 3.8% to 2.2% by 1.6 (95% CI 0.4 - 2.8; *P*=.006) percentage points on average (Table 2). The ESS of the learned policy was 550.39 (95% CI 511.49 - 588.70), approximately 25% of the sample size (n=2152) and indicated a high confidence in the performance estimate. Similar improvements were observed with other OPE methods (Section B10 in Multimedia Appendix 1).

XSL•FO
RenderX

Table . Quantitative evaluation of behavior and learned policy on the held-out test set and a subset of the test set where the patient trajectories included the 2 divergent states. Values in parentheses indicate the 95% CI across 1000 bootstraps.

Dataset	Held-out test set (n=6805)		Subset with divergent states (n=2152)	
Policy	Behavior policy	Learned policy	Behavior policy	Learned policy
Estimated $J(\pi)$ (95% CI)	87.56 (86.42 to 88.74)	88.59[a] (87.10 to 90.01)	92.40 (90.89 to 93.96)	95.57[b] (93.10 to 97.89)
Estimated improvement in $J(\pi)$ (95% CI)	—[c]	1.03 (−0.05 to 2.10)	—	3.17 (0.77 to 5.46)
Estimated mortality (%) (95% CI)	6.22 (5.63 to 6.79)	5.70 (4.99 to 6.45)	3.80 (3.02 to 4.56)	2.22 (1.06 to 3.45)
Estimated decrease in mortality (%) (95% CI)	—	0.52 (−0.03 to 1.05)	—	1.58 (0.38 to 2.75)
Effective sample size (95% CI)	6805	3168.46 (3090.91 to 3256.65)	2152	550.39 (511.49 to 588.70)
% of time outperformed behavior policy	—	96.70	—	99.40
Disagreement with clinician (%) (95% CI)	22.91 (22.61 to 23.18)	21.19 (20.86 to 21.49)	30.80 (30.63 to 30.96)	32.38 (32.19 to 32.57)

[a]P=.03.

[b]P=.006.

[c]Not applicable.

State visualization (Section B4 in Multimedia Appendix 1) found that states 10 and 44 are close in the embedding space. Feature importance analysis of classifiers for each state showed a large overlap in key features (Section B5 in Multimedia Appendix 1), including age, previous loop diuretic, BNP value, and blood urea nitrogen value. Both states consisted of slightly older patients with an average age of 69.8 (SD 13.9) (state 10) and 68.7 (SD 13.5) (state 44) compared to the population mean of 63.4 (SD 16.2). Patients in both groups had higher BNP values (539.7, SD 960.8 vs 405.5, SD 781.8 vs 397.1, SD 687.0 for state 10, state 44, and the population, respectively) and mild kidney impairment as characterized by higher blood urea nitrogen values (35.6, SD 25.2 vs 32.9, SD 21.6 vs 28.2, SD 21.3 for state 10, state 44, and the population, respectively; Section B6 in Multimedia Appendix 1).

Ablation Study of Pipeline

In all cases, the worst-case performance of the learned policy when one or more components were removed from the pipeline was significantly lower than the worst-case performance of the policy derived from the full pipeline (Table 3). We focus on the 2 novel aspects of the pipeline here: relaxing the unimportant states and tuning the state definitions.

Table . Worst-case performance of the learned policy when one or more of the 3 key elements in the pipeline were removed. The 3 elements are: (1) use of unimportant state relaxation (no vs yes), (2) number of data splits (single vs multiple), and (3) number of state definitions (single vs multiple). Values in parentheses indicate the 95% CI across 1000 bootstraps.[a]

Unimportant state relaxation	Number of data splits	Number of state definitions	Estimated improvement in $J(\pi)$ (95% CI) (↑)	Estimated mortality % (95% CI) (↓)	% Time outperformed behavior policy (↑)
No	Single	Single	No viable policy	—[b]	—
No	Single	Multiple	No viable policy	—	—
No	Multiple	Single	No viable policy	—	—
No	Multiple	Multiple	No viable policy	—	—
Yes	Single	Single	−2.48 (−8.80 to 2.09)	7.46 (4.93 to 10.76)	20.20
Yes	Single	Multiple	−0.04 (−0.63 to 0.55)	6.24 (5.59 to 6.90)	44.90
Yes	Multiple	Single	0.45 (−1.48 to 2.22)	6.00 (4.93 to 7.18)	70.70
Yes	Multiple	Multiple	1.03 (−0.05 to 2.10)	5.70 (4.99 to 6.45)	96.70

[a]The estimated improvement in $J(\pi)$ (↑) and estimated mortality % (↓) for the behavior policy is 0.00 (95% CI −1.14 to 1.18) and 6.22 (95% CI 5.63 to 6.79), respectively.

[b]Not applicable.

Removing the unimportant state relaxation led to a catastrophic failure, as no policy obtained an ESS of at least 10% the validation dataset size. This indicates overfitting, and we were unable to get a reliable estimate of the policies' performance

XSL•FO
RenderX

on the test set. Using a fixed state definition instead of tuning the state definitions led to significant variation in the performance of the learned policy depending on the data split used to learn the fixed state definition (Section B8 in Multimedia Appendix 1). In the worst-case scenario, the improvement in value of the learned policy compared to the behavior policy was −0.04 (95% CI −0.63 to 0.55), which was significantly lower than the improvement in value of 1.03 (95% CI −0.05 to 2.10; *P*=.01) of the policy derived from the full pipeline.

Discussion

Principal Findings

Offline RL has been applied to various health care domains [2-4]. However, a clear guide that practitioners can refer to has not been established. We present a blueprint based on previous literature to streamline the development of offline RL policies and further facilitate this through a public code base. We demonstrated the utility of our rigorous pipeline in the context of learning treatment decision policies for loop diuretics in hospitalized patients. Overall, in retrospective analysis, the learned policy was estimated to lead to significant improvement in outcome for the general patient population, especially for a subset of patients where the learned policy differed the most from clinician behavior. Though it will require prospective validation, our results reveal areas of potential improvement in current clinical care.

A key challenge in offline RL is ensuring the robustness of the learned policy. Two elements in our pipeline contributed to the improvement in robustness and performance. The first element—tuning state definitions—addresses the issue of hyperparameter sensitivity in offline RL. To select the optimal hyperparameters, prior work often relied on the hold-out method which partitioned the development dataset into training and validation sets [3,30,31]. Recently, Nie et al [7] found policy performance to be sensitive to this partitioning itself and proposed the SSR pipeline which uses multiple dataset partitions during evaluation. Building upon this insight, we show that while common practice has been to use a fixed state definition derived from a single train-validation split [3,30,31], the partitioning used to learn the state definitions can also result in significant variability of the final policy's performance, and thus jointly tuning state definitions and policy learning over multiple data partitions is important for robustness of the learned policy.

The second element—relaxing the learned policy via unimportant states—is a form of policy constraint that mitigates the impact of extrapolation error by reducing the deviation of the learned policy from the behavior policy [5]. Using unimportant states to constrain the policy post hoc also helps reduce disruptions to the current workflow, an important consideration in health care settings. During deployment, the policy acts as an alert system to notify providers of the appropriate treatment [32]. Yet a well-known consequence in alert systems is "alert fatigue," where providers ignore alerts due to the high frequency of irrelevant or unhelpful alerts [32,33]. By generating recommendations only when the action will meaningfully impact the outcome, unimportant state relaxation presents a simple solution to reduce disruptions to existing workflows while minimally compromising the policy's performance.

In analyzing our learned policy, we found that loop diuretics had a limited effect on patient outcome for a sizable portion of the cohort. Our pipeline could thus be used to identify patient groups that are likely responsive to treatments. In these treatment-responsive cases, the learned policy tended to agree with the majority of clinicians, indicating that our policy could help reduce heterogeneity in treatment decisions. Patients in the 2 divergent states were slightly older and had mild kidney impairment, which could explain clinicians' hesitancy in prescribing loop diuretics. However, the high BNP values indicate that the patients are fluid overloaded and may still benefit from diuretic treatment.

Our study is not without limitations. The pipeline used a single OPE method (WIS) during hyperparameter selection and a single dataset. While designed to be agnostic to both, future studies using external datasets and different OPE methods during hyperparameter tuning will further validate the generalizability of PROP-RL. Our problem formulation enforced decisions to be binary and to occur every 24 hours at fixed time points (Section B1 in Multimedia Appendix 1 for results across different decision points). A finer-grained problem formulation—such as specifying the exact dosage, incorporating additional actions (ie, other medications), and using shorter or more flexible time intervals for actions—along with additional data will be required to learn a policy that can be deployed in clinical settings. A promising direction for future work is incorporating clinician feedback after deployment to further refine the alert threshold and better understand when recommendations are most useful to clinicians, beyond our current approach of using unimportant states (Section A15 in Multimedia Appendix 1).

Another important limitation is our reliance on retrospective evaluation. In the absence of a reliable simulator and safety concerns associated with real-world evaluation, we relied on OPE methods which may not reflect the policy's true performance during deployment. We mitigate this by imposing a large cutoff on the ESS during hyperparameter selection and by confirming our findings across multiple OPE methods. Nonetheless, retrospective evaluation should only be viewed as a preliminary step for identifying promising policies prior to investing in prospective studies. Future work must include robust prospective validation in accordance with guidelines such as the DECIDE-AI reporting framework [34]. The potential for unmeasured confounding is also a fundamental limitation of OPE methods. To mitigate this, we derived our state space using a comprehensive set of EHR features, selected in close consultation with a clinical collaborator with deep domain expertise. However, residual confounding may remain. Since these challenges are present in any realistic problem setting, our approach serves as a guide for other researchers to follow when learning offline RL policies.

Conclusion

In summary, we present a standardized pipeline to streamline the development of offline RL policies in health care settings.

XSL•FO
RenderX

We demonstrate the utility of this pipeline in the context of learning treatment decision policies for loop diuretics in hospitalized patients and show that the learned RL policy could potentially lead to a significant improvement in a key subset of the patient population. Our work highlights important considerations for applying RL to observational data to learn treatment decision policies, and our open-sourced code base can facilitate future development of offline RL policies on other clinical problems.

Acknowledgments

This work was supported by the National Heart, Lung, and Blood Institute of the National Institutes of Health (NIH) under grant R01HL158626 to JW and MS, and the National Library of Medicine of the NIH under grant R01LM013325 to JW and MS. The funders had no role in study design, data collection, data analysis, data interpretation, writing of the report, and the decision to submit. ST was affiliated with the Division of Computer Science and Engineering at the University of Michigan at the time of this research and is currently affiliated with the Department of Computer Science at Emory University.

Data Availability

The source code used in this study is available from the Pipeline for Learning Robust Policies in Reinforcement Learning (PROP-RL) repository [19]. The datasets generated or analyzed during this study are not publicly available due to patient privacy and ethical restrictions, but deidentified data could be made available from the corresponding author on reasonable request. A sample of synthetic data is provided with the source code.

Conflicts of Interest

None declared.

Multimedia Appendix 1
Additional methodological details and supplementary results.
[PDF File, 1796 KB - medinform_v13i1e69145_app1.pdf]

Checklist 1
TRIPOD+AI checklist.
[PDF File, 1349 KB - medinform_v13i1e69145_app2.pdf]

References

1. Sutton RS, Barto AG. Reinforcement Learning, Second Edition: An Introduction: MIT Press; 2018.
2. Komorowski M, Celi LA, Badawi O, Gordon AC, Faisal AA. The artificial intelligence clinician learns optimal treatment strategies for sepsis in intensive care. Nat Med 2018 Nov;24(11):1716-1720. [doi: 10.1038/s41591-018-0213-5] [Medline: 30349085]
3. Zhu T, Li K, Georgiou P. Offline deep reinforcement learning and off-policy evaluation for personalized basal insulin control in type 1 diabetes. IEEE J Biomed Health Inform 2023 Oct;27(10):5087-5098. [doi: 10.1109/JBHI.2023.3303367] [Medline: 37607154]
4. Zhang K, Wang H, Du J, et al. An interpretable RL framework for pre-deployment modeling in ICU hypotension management. NPJ Digit Med 2022 Nov 18;5(1):173. [doi: 10.1038/s41746-022-00708-4] [Medline: 36396808]
5. Levine S, Kumar A, Tucker G, Fu J. Offline reinforcement learning: tutorial, review, and perspectives on open problems. arXiv. Preprint posted online on May 4, 2020. [doi: 10.48550/arXiv.2005.01643]
6. Paine TL, Paduraru C, Michi A, et al. Hyperparameter selection for offline reinforcement learning. arXiv. Preprint posted online on Jul 17, 2020. [doi: 10.48550/arXiv.2007.09055]
7. Nie A, Flet-Berliac Y, Jordan D, Steenbergen W, Brunskill E. Data-efficient pipeline for offline reinforcement learning with limited data. Presented at: Proceedings of the 36th Conference on Neural Information Processing Systems; Nov 28 to Dec 9, 2022; New Orleans, LA, USA URL: https://proceedings.neurips.cc/paper_files/paper/2022/file/5ee7ed60a7e8169012224dec5fe0d27f-Paper-Conference.pdf [accessed 2025-09-29]
8. Kumar A, Zhou A, Tucker G, Levine S. Conservative q-learning for offline reinforcement learning. Presented at: Proceedings of the 34th Conference on Neural Information Processing Systems; Dec 6-12, 2020 URL: https://proceedings.neurips.cc/paper_files/paper/2020/file/0d2b2061826a5df3221116a5085a6052-Paper.pdf [accessed 2025-09-21]
9. Gottesman O, Johansson F, Komorowski M, et al. Guidelines for reinforcement learning in healthcare. Nat Med 2019 Jan;25(1):16-18. [doi: 10.1038/s41591-018-0310-5] [Medline: 30617332]
10. McMurray JJV, Adamopoulos S, Anker SD, et al. ESC guidelines for the diagnosis and treatment of acute and chronic heart failure 2012: The Task Force for the Diagnosis and Treatment of Acute and Chronic Heart Failure 2012 of the European

XSL•FO
RenderX

Society of Cardiology. Developed in collaboration with the Heart Failure Association (HFA) of the ESC. Eur J Heart Fail 2012 Aug;14(8):803-869. [doi: 10.1093/eurjhf/hfs105] [Medline: 22828712]
11. Killian TW, Zhang H, Subramanian J, Fatemi M, Ghassemi M. An empirical study of representation learning for reinforcement learning in healthcare. arXiv. Preprint posted online on Nov 23, 2020. [doi: 10.48550/arXiv.2011.11235]
12. Tang S, Wiens J. Model selection for offline reinforcement learning: practical considerations for healthcare settings. Presented at: Proceedings of the 6th Machine Learning for Healthcare Conference, PMLR; Aug 6, 2021 URL: https://proceedings.mlr.press/v149/tang21a.html [accessed 2024-05-28]
13. Oh SW, Han SY. Loop diuretics in clinical practice. Electrolyte Blood Press 2015 Jun;13(1):17-21. [doi: 10.5049/EBP.2015.13.1.17] [Medline: 26240596]
14. Clark AL, Cleland JGF. Causes and treatment of oedema in patients with heart failure. Nat Rev Cardiol 2013 Mar;10(3):156-170. [doi: 10.1038/nrcardio.2012.191] [Medline: 23319101]
15. Berliner D, Schneider N, Welte T, Bauersachs J. The differential diagnosis of dyspnea. Dtsch Arztebl Int 2016 Dec 9;113(49):834-845. [doi: 10.3238/arztebl.2016.0834] [Medline: 28098068]
16. Shah MR, Stevenson LW. Searching for evidence: refractory questions in advanced heart failure. J Card Fail 2004 Jun;10(3):210-218. [doi: 10.1016/j.cardfail.2003.10.006] [Medline: 15190530]
17. Palazzuoli A, Ruocco G, Ronco C, McCullough PA. Loop diuretics in acute heart failure: beyond the decongestive relief for the kidney. Crit Care 2015 Sep 3;19(1):296. [doi: 10.1186/s13054-015-1017-3] [Medline: 26335137]
18. Matsue Y, Damman K, Voors AA, et al. Time-to-furosemide treatment and mortality in patients hospitalized with acute heart failure. J Am Coll Cardiol 2017 Jun 27;69(25):3042-3051. [doi: 10.1016/j.jacc.2017.04.042] [Medline: 28641794]
19. PROP-RL: pipeline for learning robust policies in RL. GitHub. URL: https://github.com/MLD3/PROP-RL [accessed 2024-04-23]
20. Tang S, Davarmanesh P, Song Y, Koutra D, Sjoding MW, Wiens J. Democratizing EHR analyses with FIDDLE: a flexible data-driven preprocessing pipeline for structured clinical data. J Am Med Inform Assoc 2020 Dec 9;27(12):1921-1934. [doi: 10.1093/jamia/ocaa139] [Medline: 33040151]
21. Shi C, Blei D, Veitch V. Adapting neural networks for the estimation of treatment effects. Presented at: Proceedings of the 33rd Conference on Neural Information Processing Systems; Dec 8-14, 2019; Vancouver, Canada URL: https://proceedings.neurips.cc/paper_files/paper/2019/file/8fb5f8be2aa9d6c64a04e3ab9f63feee-Paper.pdf [accessed 2024-05-28]
22. Strehl A, Ghosh J. Cluster ensembles --- a knowledge reuse framework for combining multiple partitions. J Mach Learn Res 2003 Mar 1;3:583-617. [doi: 10.1162/153244303321897735]
23. Fujimoto S, Meger D, Precup D. Off-policy deep reinforcement learning without exploration. Presented at: Proceedings of the 36th International Conference on Machine Learning, PMLR; Jun 9-15, 2019; Long Beach, California, USA URL: https://proceedings.mlr.press/v97/fujimoto19a.html [accessed 2025-09-21]
24. Kidambi R, Rajeswaran A, Netrapalli P, Joachims T. MOReL: model-based offline reinforcement learning. Presented at: Proceedings of the 34th Conference on Neural Information Processing Systems; Dec 6-12, 2020 URL: https://proceedings.neurips.cc/paper_files/paper/2020/file/f7efa4f864ae9b88d43527f4b14f750f-Paper.pdf [accessed 2024-05-28]
25. Precup D, Sutton RS, Singh S. Eligibility traces for off-policy policy evaluation. Presented at: ICML '00: Proceedings of the Seventeenth International Conference on Machine Learning; Jun 29 to Jul 2, 2000; Stanford University, Stanford, CA, USA.
26. Martino L, Elvira V, Louzada F. Effective sample size for importance sampling based on discrepancy measures. Signal Processing 2017 Feb;131:386-401. [doi: 10.1016/j.sigpro.2016.08.025]
27. Moore D, Notz W, Fligner M. The Basic Practice of Statistics: WH Freeman & Co Ltd; 2021.
28. Shen SP, Ma Y, Gottesman O, Doshi-Velez F. State relevance for off-policy evaluation. Presented at: Proceedings of the 38th International Conference on Machine Learning, PMLR; Jul 18-24, 2021 URL: https://proceedings.mlr.press/v139/shen21d.html [accessed 2025-09-21]
29. Collins GS, Moons KGM, Dhiman P, et al. TRIPOD+AI statement: updated guidance for reporting clinical prediction models that use regression or machine learning methods. BMJ 2024 Apr 16;385:e078378. [doi: 10.1136/bmj-2023-078378] [Medline: 38626948]
30. Kondrup F, Jiralerspong T, Lau E, et al. Towards safe mechanical ventilation treatment using deep offline reinforcement learning. AAAI 2023;37(13):15696-15702. [doi: 10.1609/aaai.v37i13.26862]
31. Liu R, Greenstein JL, Fackler JC, Bergmann J, Bembea MM, Winslow RL. Offline reinforcement learning with uncertainty for treatment strategies in sepsis. arXiv. Preprint posted online on Jul 9, 2021. [doi: 10.48550/arXiv.2107.04491]
32. Aaron S, McEvoy DS, Ray S, Hickman TTT, Wright A. Cranky comments: detecting clinical decision support malfunctions through free-text override reasons. J Am Med Inform Assoc 2019 Jan 1;26(1):37-43. [doi: 10.1093/jamia/ocy139] [Medline: 30590557]
33. Wright A, Ai A, Ash J, et al. Clinical decision support alert malfunctions: analysis and empirically derived taxonomy. J Am Med Inform Assoc 2018 May 1;25(5):496-506. [doi: 10.1093/jamia/ocx106] [Medline: 29045651]
34. Vasey B, Nagendran M, Campbell B, et al. Reporting guideline for the early stage clinical evaluation of decision support systems driven by artificial intelligence: DECIDE-AI. BMJ 2022 May 18;377:e070904. [doi: 10.1136/bmj-2022-070904] [Medline: 35584845]

XSL•FO
RenderX

Abbreviations

BCQ: batch-constrained Q-learning
BNP: brain natriuretic peptide
EHR: electronic health record
ESS: effective sample size
FIDDLE: Flexible Data-Driven Pipeline
HIPAA: Health Insurance Portability and Accountability Act
MDP: Markov decision process
OPE: off-policy evaluation
PCA: principal component analysis
pMDP: pessimistic Markov decision process
PROP-RL: Pipeline for Learning Robust Policies in Reinforcement Learning
RL: reinforcement learning
SOFA: Sequential Organ Failure Assessment
SSR: Split-Select-Retrain
TRIPOD+AI: Transparent Reporting of a Multivariable Prediction Model for Individual Prognosis or Diagnosis+Artificial Intelligence
WIS: weighted importance sampling

Edited by A Benis; submitted 24.11.24; peer-reviewed by D Li, D Yoo, F Meng; revised version received 07.08.25; accepted 15.08.25; published 10.10.25.

Please cite as:
Lee JM, Tang S, Sjoding M, Wiens J
Optimizing Loop Diuretic Treatment for Mortality Reduction in Patients With Acute Dyspnea Using a Practical Offline Reinforcement Learning Pipeline for Health Care: Retrospective Single-Center Simulation Study
JMIR Med Inform 2025;13:e69145
URL: https://medinform.jmir.org/2025/1/e69145
doi:10.2196/69145

© Jung Min Lee, Shengpu Tang, Michael Sjoding, Jenna Wiens. Originally published in JMIR Medical Informatics (https://medinform.jmir.org), 10.10.2025. This is an open-access article distributed under the terms of the Creative Commons Attribution License (https://creativecommons.org/licenses/by/4.0/), which permits unrestricted use, distribution, and reproduction in any medium, provided the original work, first published in JMIR Medical Informatics, is properly cited. The complete bibliographic information, a link to the original publication on https://medinform.jmir.org/, as well as this copyright and license information must be included.

XSL•FO
RenderX

Development and Validation of an Extra Spindle Pole Bodies–like 1–Based Diagnostic and Prognostic Model for Hepatitis B Virus–Related Hepatocellular Carcinoma: Retrospective Cohort Study

Lu-Huai Feng[1*], MD; Hengkai Liang[1*], MM; Bobin Hu[1], MD; Lu Wei[1], MM; Qingmei Li[1], MM; Tumei Su[1], MM; Qianbing Yin[1], MM; Yanfei Feng[1], MM; Long Huang[1], MM; Hongqian Liang[1], MM; Minghua Su[1], MD; Jianning Jiang[1,2,3], MD

[1]Department of Infectious Diseases, The First Affiliated Hospital of Guangxi Medical University, 6 Shuangyong Road, Nanning, China

[2]Key Laboratory of Early Prevention and Treatment of Regional High Incidence Tumors (Guangxi Medical University), Ministry of Education, Nanning, China

[3]Guangxi Key Laboratory of Early Prevention and Treatment for Regional High Frequency Tumor, Nanning, China

[*]these authors contributed equally

Corresponding Author:
Jianning Jiang, MD
Department of Infectious Diseases, The First Affiliated Hospital of Guangxi Medical University, 6 Shuangyong Road, Nanning, China

Abstract

Background: Early diagnosis of hepatocellular carcinoma (HCC) in patients with chronic hepatitis B virus (HBV) is challenging. Models that combine novel biomarkers with clinical features may improve both early diagnosis and risk stratification, but few have been systematically validated.

Objective: This study aimed to develop and validate an extra spindle pole bodies–like 1 (ESPL1)–based model for diagnostic discrimination of HBV-related HCC and longitudinal risk stratification in patients with chronic HBV infection.

Methods: Patients with chronic HBV were consecutively recruited from the First Affiliated Hospital of Guangxi Medical University (a single-center, tertiary hospital) between January 2012 and November 2023. Patients were divided into a training set and an independent hold-out testing set. A LASSO logistic regression model was constructed to identify independent predictors and then used to develop a risk score discriminating patients with HBV-related HCC from those with chronic hepatitis B or cirrhosis. Model performance was evaluated using discrimination (C-index), calibration, and decision curve analysis. Internal validation was performed with bootstrap resampling, and independent hold-out validation was conducted with the independent hold-out testing set. Longitudinal follow-up of patients with chronic hepatitis B or cirrhosis was subsequently used to examine cumulative incidence across risk groups, thereby assessing the model's ability to stratify future HBV-related HCC risk. A web-based calculator was developed to facilitate clinical application.

Results: The study involved a cohort of 621 patients diagnosed with chronic HBV infection, divided into a training set of 373 (60.1%) patients and an independent hold-out testing set of 248 (39.9%) patients. Age (odds ratio [OR] 1.08, 95% CI 1.05 - 1.12), ESPL1 expression (OR 1.01, 95% CI 1.00 - 1.01), and log (alpha-fetoprotein) levels (OR 2.55, 95% CI 1.95 - 3.33) were identified as independent predictors of HBV-related HCC. The model demonstrated excellent diagnostic discrimination, with a C-index of 0.922 in the training set and 0.958 in the independent hold-out testing set, coupled with strong calibration. Decision curve analysis revealed that the model consistently provided a higher net benefit across clinically relevant threshold probabilities. Subgroup analyses further validated the model's high discriminative power, with C-index values ranging from 0.86 to 0.98, and no significant interactions were detected (all interaction *P* values > .10). Furthermore, the model demonstrated superior discriminatory power relative to 5 established HBV-related HCC risk scores, including REACH-B, GAG-HCC, CU-HCC, PAGE-B, mPAGE-B, and alpha-fetoprotein alone, with all pairwise comparisons yielding statistical significance (*P*<.001). For prognostic stratification, patients categorized as low risk, medium risk, and high risk had distinct 5-year cumulative HCC incidences of 5.1%, 21.1%, and 31.3%, respectively (*P*<.001).

Conclusions: The ESPL1-based model may serve as both a diagnostic tool for differentiating patients with HCC from those with non-HCC and as a preliminary approach for risk stratification during follow-up. This dual role has the potential to support earlier detection and personalized monitoring. The web-based calculator improves accessibility and may facilitate future clinical integration.

XSL•FO
RenderX

(JMIR Med Inform 2025;13:e78354) doi:10.2196/78354

KEYWORDS

hepatocellular carcinoma; alpha-fetoprotein; ESPL1; machine learning; web calculator

Introduction

Global Burden and Clinical Challenges of Hepatitis B Virus–Related Hepatocellular Carcinoma

Hepatitis B virus (HBV), mainly spread through blood and bodily fluids, is a major global health concern and a leading cause of hepatocellular carcinoma (HCC), accounting for more than 50% of cases worldwide [1,2]. More than 200 million people have chronic HBV, of whom 15% to 25% at risk of developing liver cirrhosis or HCC. The prevalence and mortality of HBV-related HCC are projected to continue rising over the next two decades [3]. HCC increases public health challenges and places significant economic and emotional strain on patients and families [4]. Surgical resection is the best cure for early-stage HCC, but most patients are diagnosed at advanced stages because of the asymptomatic nature of early disease, rendering curative treatment infeasible. Thus, early diagnosis and risk stratification of high-risk patients are essential for improving HCC outcomes.

Limitations of Current Risk Prediction Models

Current guidelines advocate for patients with chronic hepatitis B (CHB) to undergo a series of diagnostic tests every 3 to 6 months during antiviral therapy. However, challenges such as limited patient compliance, the low sensitivity of individual biomarkers, high costs, and inconsistent implementation across different health care settings impede the early detection of HCC [5-8]. A cost-effective approach to facilitate early HCC diagnosis and treatment involves the identification of high-risk individuals with chronic HBV infection and their regular monitoring. Risk prediction models provide personalized assessments of HCC risk for patients with CHB, thereby aiding physicians in improving patient adherence and optimizing screening and monitoring strategies [9,10]. Several models, including REACH-B, GAG-HCC, and PAGE-B, have been developed to assess HCC risk in patients with chronic HBV [11-16]. Nevertheless, these models primarily rely on conventional clinical parameters, limiting their generalizability, and they often fail to incorporate novel biomarkers or undergo validation for both diagnostic accuracy and longitudinal applicability.

Objectives

Among the various potential biomarkers, the extra spindle pole bodies-like 1 (ESPL1) gene has garnered significant attention because of its involvement in genomic instability and tumor progression. Alterations in ESPL1, potentially induced by chronic viral infections or environmental carcinogens, may play a role in malignant transformation [17]. Our previous research identified frequent HBV S–ESPL1 fusion events in HBV-related HCC tissues and demonstrated that circulating ESPL1 protein levels can effectively differentiate early HCC from cirrhotic nodules [17,18]. Building upon these findings, this study pursued 2 primary objectives: first, to construct an ESPL1-based model capable of accurately distinguishing patients with HBV-related HCC from those with non-HCC, thereby demonstrating its diagnostic utility; and second, to substantiate its prognostic significance through longitudinal follow-up, stratifying patients with non-HCC according to their prospective risk of developing HCC. By integrating a biologically pertinent biomarker with real-world patient data, our model seeks to address the limitations of conventional methodologies and offer a clinically significant framework for both the early diagnosis and longitudinal risk stratification of HBV-related HCC.

Methods

Ethical Considerations

This study was approved by the Ethics Committee of the First Affiliated Hospital of Guangxi Medical University (2024-E614-01). The Ethics Committee of the First Affiliated Hospital of Guangxi Medical University waived written or oral informed consent of participants because there was no personally identifiable information in the article. The study followed the ethical standards outlined in the Declaration of Helsinki (World Medical Association Declaration of Helsinki 2013). All data were anonymized before analysis to protect patient privacy and confidentiality. No individual-level identifiers were included in the dataset, and all results are presented in aggregate form. No financial or other compensation was provided to participants in this study. Finally, no images or other materials that could potentially identify individual participants are presented in this manuscript or supplementary files.

Study Design and Patients

This study was designed in 2 parts: (1) development of a diagnostic model to distinguish patients with HBV-related HCC from those with non-HCC (CHB and cirrhosis) and (2) longitudinal validation of its prognostic utility using follow-up data in patients with non-HCC.

This study is reported following the Transparent Reporting of a Multivariable Prediction Model for Individual Prognosis or Diagnosis reporting guideline checklist for developing and validating prediction models [19]. To minimize selection bias, all eligible patients with chronic HBV infection who were managed by our team from January 2012 to November 2023 were enrolled consecutively, adhering to stringent inclusion and exclusion criteria. Standardized follow-up protocols were implemented to accurately represent the natural clinical spectrum of HBV patients in our region. These protocols included assessments every 3 months during the first year of antiviral therapy, which comprised evaluations of HBV serological markers, HBV DNA levels, liver function tests, and alpha-fetoprotein (AFP) levels. Subsequently, follow-ups were conducted every 6 months, incorporating abdominal ultrasound. Patients diagnosed with cirrhosis or hepatic nodules were monitored every 3 months, with additional imaging modalities such as contrast-enhanced ultrasound, computed tomography,

XSL•FO
RenderX

or magnetic resonance imaging recommended if nodules increased in size by more than 1.0 cm or if AFP levels rose.

To further reduce center-related bias, patients who met the inclusion criteria were divided based on their enrollment period into a training set and a temporally distinct testing set, rather than being allocated randomly. This approach provided an independent hold-out validation that more accurately simulates real-world application compared to random resampling. In addition, a subset of patients from the follow-up cohort, who had stored paired serum samples (1 at baseline and another after more than 5 years of follow-up), was included in a longitudinal analysis. These patients were managed under the same standardized protocol as the main cohort. Their paired samples were used to calculate predicted HCC risk values at both time points, thereby enabling an evaluation of the model's capacity to capture dynamic changes in risk over time.

Inclusion Criteria

The inclusion criteria have been described below.

Patients with Chronic HBV

These included individuals aged >18 years with CHB or HBV-related liver cirrhosis. CHB was defined as persistent HBsAg positivity for more than 6 months, detectable HBV DNA, and evidence of active liver disease, characterized by either persistently or intermittently elevated alanine aminotransferase (ALT) levels, histological findings of significant necroinflammation, or histological/noninvasive evidence of significant fibrosis (≥F2) [8]. HBV-related cirrhosis was diagnosed either histologically, based on liver biopsy consistent with cirrhotic changes, or clinically [8]. Clinical diagnosis required documented chronic HBV infection (current HBsAg positivity or HBsAg negativity with anti-HBc positivity and a history of HBsAg positivity >6 mo, with other causes excluded), together with at least two of the following 5 features: (1) imaging findings of cirrhosis and/or portal hypertension; (2) endoscopic evidence of esophageal or gastric varices; (3) liver stiffness measurement (LSM) consistent with cirrhosis, defined as ≥12.0 kPa when ALT <1×ULN or ≥17.0 kPa when ALT is 1 - 5×ULN; (4) serum albumin <35 g/L or prothrombin time prolonged >3 seconds compared with controls; and (5) platelet count <100×10 /L.

Patients with HBV-related HCC

These included patients with pathologically confirmed HCC following partial hepatectomy. All HCC cases had chronic HBV infection as defined earlier, with no evidence of other etiologies such as hepatitis C, alcohol, or autoimmune liver disease.

Patients with Untreated HCC

These included patients with newly diagnosed HBV-related HCC who had not undergone prior curative or palliative therapies, including liver resection, transarterial chemoembolization, radiofrequency ablation, systemic therapy, or chemotherapy.

Adequate Frozen Serum Samples

There should have been the availability of at least 0.5 mL of stored serum per patient, collected before HCC treatment or during routine follow-up, and preserved at −40°C or lower in our serum biobank.

Exclusion Criteria

The exclusion criteria were as follows: (1) patients co-infected with HBV and other infections such as hepatitis D, E, C, or HIV/AIDS; (2) patients with non-HBV-related cancers, including non-HBV-related HCC; (3) patients with liver disease from other causes, such as autoimmune liver disease; and (4) patients with decompensated liver cirrhosis or liver failure.

Peripheral venous blood samples (5 mL) were collected from patients in the CHB and cirrhosis of liver (LC) groups during outpatient visits and from the HBV-HCC group before surgical resection. Samples were centrifuged at 4000 rpm for 5 minutes, and the serum supernatant was stored at −40°C for subsequent analysis.

Serum ESPL1 Levels Detection

Serum ESPL1 levels were measured using an Enzyme-Linked Immunosorbent Assay (ELISA) kit (Nova Lifetech Inc, Catalog No.: ELI-48263h) according to the manufacturer's instructions. The procedure included standard and sample preparation, incubation, washing, addition of reagents, and optical density measurement. The absorbance (optical density value) of each sample was quantified using a microplate reader (BioRad, Co, Ltd, USA) at a wavelength of 450 nm. Three replicate wells were used for each sample, and the mean value was determined. The concentration of serum ESPL1 in the unknown samples was calculated based on the standard curve [20].

Data Collection

Collected patient follow-up data included name, diagnosis, sex, family history of HCC or LC, age details (age at ESPL1 testing, antiviral treatment duration), antiviral drugs, HBV DNA levels, HBeAg status, liver nodules, and ALT, albumin (ALB), and AFP levels at ESPL1 testing.

A total of 16 variables were collected: 9 continuous (ESPL1, age at ESPL1 testing, antiviral treatment duration, HBV DNA, AFP, ALT, aspartate aminotransferase [AST], ALB, and liver stiffness) and 7 categorical (diagnosis, sex, family history of HCC/LC, treatment status, antiviral medication, HBeAg status, and liver nodules). To enhance data robustness and reduce outlier effects, a log transformation was applied to the HBV DNA and AFP data because of their wide range and extreme values.

Missing Data

Missing data rates were 1.6% for AFP, 0.5% for ALB, and 18.7% for liver stiffness. Missingness was addressed using multiple imputation via the mice package in R (version 3.6.2, Institute for Statistics and Mathematics, Vienna, Austria) [21]. The missing data pattern was inspected, and imputations were generated under the assumption of missing at random using predictive mean matching, which preserves the observed data distribution. Five imputed datasets were created, pooled according to Rubin's rules, and used for the primary analyses. To assess robustness, sensitivity analyses were conducted by comparing results from the pooled imputed dataset with those from the complete-case dataset, and each of the 5 individual

XSL•FO
RenderX

imputed datasets. The retained predictors and their effect sizes were consistent across all analyses, indicating that missing data had minimal influence on the final model in Multimedia Appendix 1.

Comparison With Established HCC Risk Models

To assess the comparative performance of the ESPL1-based Age-ESPL1-AFP (AEA) score, we conducted an evaluation against 5 established HBV-related HCC risk models (ie, REACH-B, GAG-HCC, CU-HCC, PAGE-B, and mPAGE-B [22]) using an independent hold-out testing cohort. These models were chosen due to the consistent availability of their requisite predictors within our dataset, facilitating direct implementation and ensuring a fair comparison. Each score was computed in accordance with its original published definition, with comprehensive details of the scoring algorithms provided in the Supplementary Materials in Multimedia Appendix 2. Subsequently, the predictive performance of these models was evaluated and juxtaposed with that of our model.

Statistical Analysis

Statistical analysis was conducted using SPSS 26.0 and R 4.3.2 with rms and DynNom packages. Two-sided *P* values <0.05 were deemed significant. Normally distributed data are shown as "mean (SD)" and compared with *t* tests, whereas nonnormally distributed data are presented as [median (P25, P75)] and analyzed using the Wilcoxon rank-sum test. Categorical data are shown as n (%), and group differences were assessed with the χ^2 test.

LASSO regression, a data mining technique, adds a penalty to traditional linear regression to simplify the model by reducing coefficient values, addressing multicollinearity, and preventing overfitting. It was used by the modeling group to initially select predictors for HBV-related HCC [23]. Variables with nonzero coefficients from the LASSO regression were refined using stepwise backward selection in multivariate logistic regression to determine the final predictors for HBV-related HCC risk. The primary objective was to establish a diagnostic tool that differentiates patients with HBV-related HCC from those with CHB/LC. Subsequently, to examine prognostic relevance, we applied the model to the non-HCC subgroup with longitudinal follow-up, assessing cumulative HCC incidence across risk strata. We then developed a clinical prediction model and an interactive web-based risk calculator using Shinyapps, designed exclusively for patients with chronic HBV infection or HBV-related cirrhosis, and not intended for use in the general population without HBV.

We assessed the model's predictive performance by calculating discrimination and plotting calibration curves for both training and independent hold-out testing sets [24]. The C-index, ranging from 0.5 (no discrimination) to 1.0 (perfect prediction), was used to evaluate discrimination. Calibration was further evaluated using the Hosmer–Lemeshow goodness-of-fit test, which compares observed and predicted event rates across deciles of risk [25]. Calibration was also assessed using calibration curves and the Brier score, where lower scores indicate higher accuracy. We conducted 1000 bootstrap resampling iterations for internal validation of the model's predictive performance. Optimal cutoff values for HBV-related HCC risk stratification were determined using X-tile software, a validated tool for biomarker assessment and outcome-based cutoff optimization [26]. These cutoffs were first applied to baseline predicted risk values in the longitudinal cohort, categorizing patients into low risk, medium risk, and high risk groups. The cumulative incidence of HCC within each risk group was then estimated using the Kaplan–Meier method, with differences between groups assessed by the log-rank test [27]. Clinical decision curves were used to evaluate the model's clinical applicability. The main metric in the clinical decision curve was the net benefit, determined by the model's true and false positive rates in predicting outcomes for the target population. The formula applied was as follows: net benefit=(true positives/N)−(false positives/N)×(Pt/(1−Pt)), with N as the total sample size and Pt as the model's event probability threshold. By linking net benefits across various probabilities, we created a decision curve, where a higher net benefit signifies greater model value in clinical use [28].

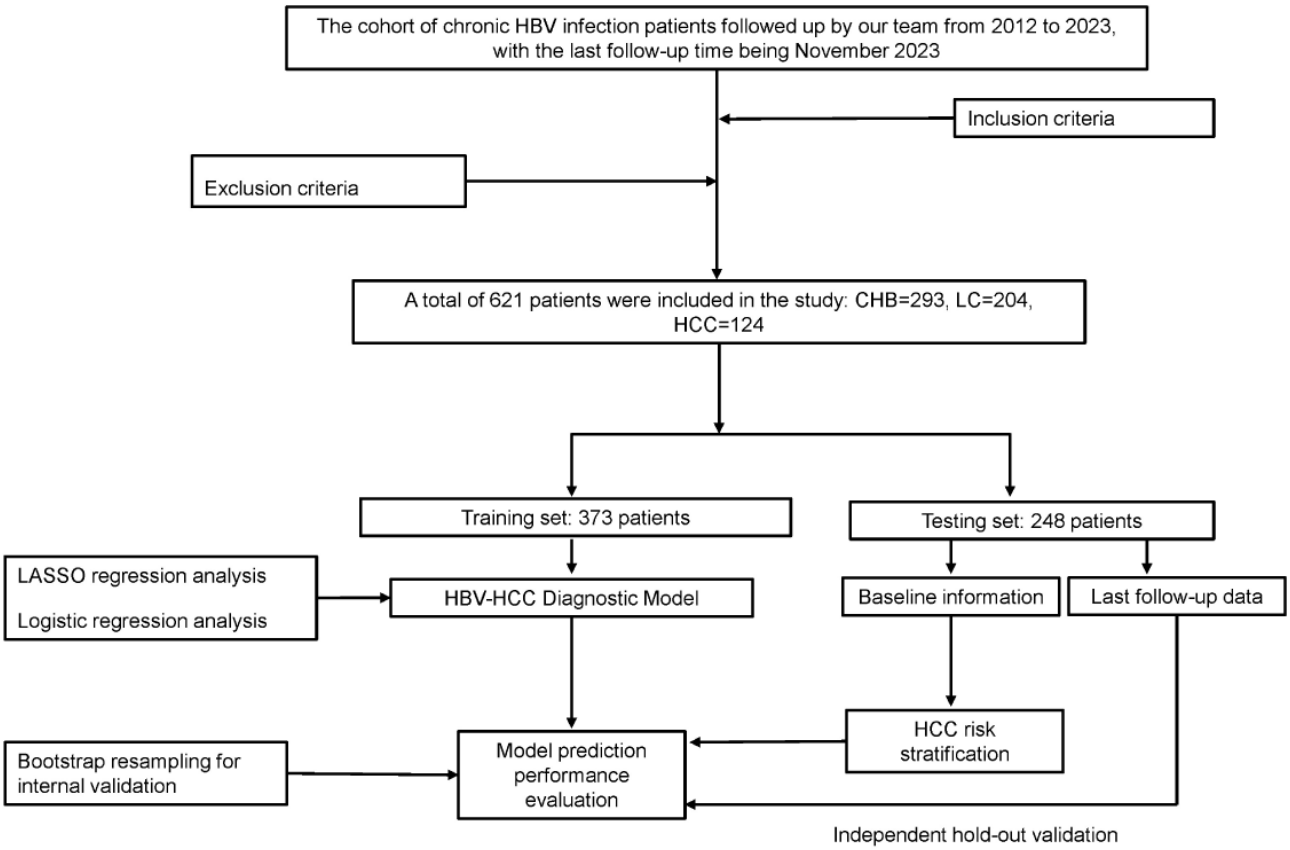
Results

Patient Characteristics

A total of 621 patients with chronic HBV were included, comprising 373 in the training set (median follow-up: 2.6 years) and 248 in the independent hold-out testing set (median follow-up: 5.0 years), as shown in Figure 1. The overall median age was 46 years, with 467 males (75.2%) and 154 females (24.8%). At baseline, 293 patients (47.2%) had CHB, 204 (32.9%) had LC, and 124 (20.0%) had HCC. Clinical characteristics of the two cohorts are summarized in Table 1.

XSL•FO
RenderX

Figure 1. HBV-related HCC clinical prediction model research design flowchart. HBV: hepatitis B virus; HCC: hepatocellular carcinoma; CHB: chronic viral hepatitis B; LC: cirrhosis of liver.



XSL•FO
RenderX

Table . Characteristics of patients included in the study.

Variable	Training set (n=371)	Independent hold-out testing set (n=248)
Sex, n (%)		
Male	277 (74.3)	190 (76.6)
Female	96(25.7)	58 (23.4)
Age (y)	44 (37, 53)	48 (39, 54)
Family history of LC/HCC, n (%)		
No	180 (48.3)	162 (65.3)
Unknown	122 (32.7)	53 (21.4)
Yes	71 (19.0)	33 (13.3)
Previously treated, yes, n (%)	50 (13.4)	34 (13.7)
log (HBV DNA), median (P25, P75)	1 (1,3)	1 (1,1)
HBeAg positive, n (%)	118 (31.6)	57 (23.0)
AST[a] (U/L), median (P25, P75)	31 (26, 41)	28 (25, 33)
ALT[b] (U/L), median (P25, P75)	28 (20, 42)	23 (17, 30)
ALB[c](g/L), median (P25, P75)	42.2 (40.1, 44.7)	42.3 (40.9, 44.4)
LSM[d] (kPa), median (P25, P75)	6.6 (5.5, 11.5)	6.1 (5.2, 7.5)
ESPL1[e] (ng/L), median (P25, P75)	270.7 (270.71, 350.06)	212.65 (153.94, 300.92)
AFP[f] (ng/mL), median (P25, P75)	3.02 (2.06, 5.90)	2.50 (1.91, 3.59)
Antiviral treatment duration (months)	18 (0, 51)	104 (64, 141)
Antiviral drugs, n (%)		
Non–first-line nucleotides	53 (14.2)	26 (10.5)
First-line nucleotides[g]	62 (16.6)	145 (58.5)
Mixed medication	258 (69.2)	77 (31.0)
Liver nodule, n (%)		
Yes	203 (54.4)	169 (67.7)
No	170 (45.6)	79 (31.9)
Diagnosis, n (%)		
CHB[h]	157 (42.1)	135 (54.4)
LC[i]	126 (33.8)	75 (30.2)
HCC[j]	90 (24.1)	38 (15.3)

[a]AST: aspartate aminotransferase.

[b]ALT: alanine aminotransferase.

[c]ALB: albumin.

[d]LSM: liver stiffness measurement.

[e]ESPL1: extra spindle poles like 1.

[f]AFP: alpha-fetoprotein.

[g]First-line nucleotides: define entecavir or tenofovir as first-line nucleotide analog antiviral drugs.

[h]CHB: chronic hepatitis B viral.

[i]LC: liver cirrhosis.

[j]HCC: hepatocellular carcinoma.

During follow-up in the independent hold-out testing set, 38 patients (15.3%) developed HCC, with cumulative incidence rates of 2.4%, 9.3%, and 15.3% at 1, 3, and 5 years, respectively. Compared with the training set, patients in the independent hold-out testing set were older, had longer antiviral treatment duration, and exhibited higher ALT levels. They also showed

XSL•FO
RenderX

lower HBV DNA, AFP, AST, and ESPL1 levels, fewer liver nodules, a lower prevalence of family history of HCC/LC, and different distributions of antiviral medication use.

Construction of a Risk Prediction Model for HBV-Related HCC

Using LASSO regression, 9 predictors with non-zero coefficients were identified from an initial set of 16 variables, including gender, age, ESPL1, antiviral drugs, log (HBV DNA), Alb, AST, log (AFP), and liver nodules (Multimedia Appendix 3). Detailed information on these HCC-related predictors is provided in Table 2 (lambda.min=0.04091). Subsequently, a predictive model for predicting HBV-related HCC risk was developed using multivariable logistic regression, incorporating both the LASSO-selected variables and those identified through univariable logistic regression variables, as presented in Table 2. The final prediction model included age, ESPL1, and log (AFP) as independent predictors, and the regression coefficients are provided in Table 2. The estimated probability of HCC was calculated using the logistic regression equation: logit(P)=−8.9764+0.0802×age+0.0059×ESPL1+0.9365×log (AFP).

Table . Univariate and multivariate logistic regression analyses variables relating to HCC in the training set. Note: In multivariate logistic regression, variables such as first-line nucleotides and liver nodules produced extremely high odds ratios with confidence intervals of (0, Inf), consistent with quasi-complete separation. Under such conditions, maximum likelihood estimation becomes unstable, and the coefficients are not reliable; therefore, these variables were excluded from the final model.

Variable	Univariate analysis OR (95% CI)	*P* value	Multivariate analysis OR (95% CI)	*P* value
Sex				
Male	Reference		Reference	
Female	0.36 (0.19 - 0.70)	.003	0.33 (0.08 - 1.39)	.132
Age	3.40 (2.31 - 5.01)	<.001	1.08 (1.05 - 1.12)	<.001
ESPL1[a]	2.96 (2.17,4.03)	<.001	1.01 (1.00 - 1.01)	<.001
Antiviral drugs				
Non–first-line nucleotides	Reference		Reference	
First-line nucleotides	73.17 (24.92 - 214.82)	<.001	249,179 097.26 (0, Inf)	.990
Mixed medication	0.41 (0.14 - 1.20)	.105	0.87 (0.13 - 5.89)	.888
log (HBV[b] DNA)	2.17 (0.71 - 6.63)	.176	N/A	
ALB[c]	0.83 (0.62 - 1.13)	.235	N/A	
AST[d]	1.04 (0.97 - 1.11)	.248	N/A	
log (AFP[e])	1.83 (1.57 - 2.13)	<.001	2.55 (1.95 - 3.33)	<.001
Liver nodule				
No	Reference		Reference	
Yes	221.95 (30.41 - 1620.00)	<.001	3,944,282,432.72(0, Inf)	.988

[a] ESPL1: extra spindle poles like 1.

[b]HBV: hepatitis B virus.

[c]ALB: albumin.

[d]AST: aspartate aminotransferase.

[e]AFP: alpha-fetoprotein.

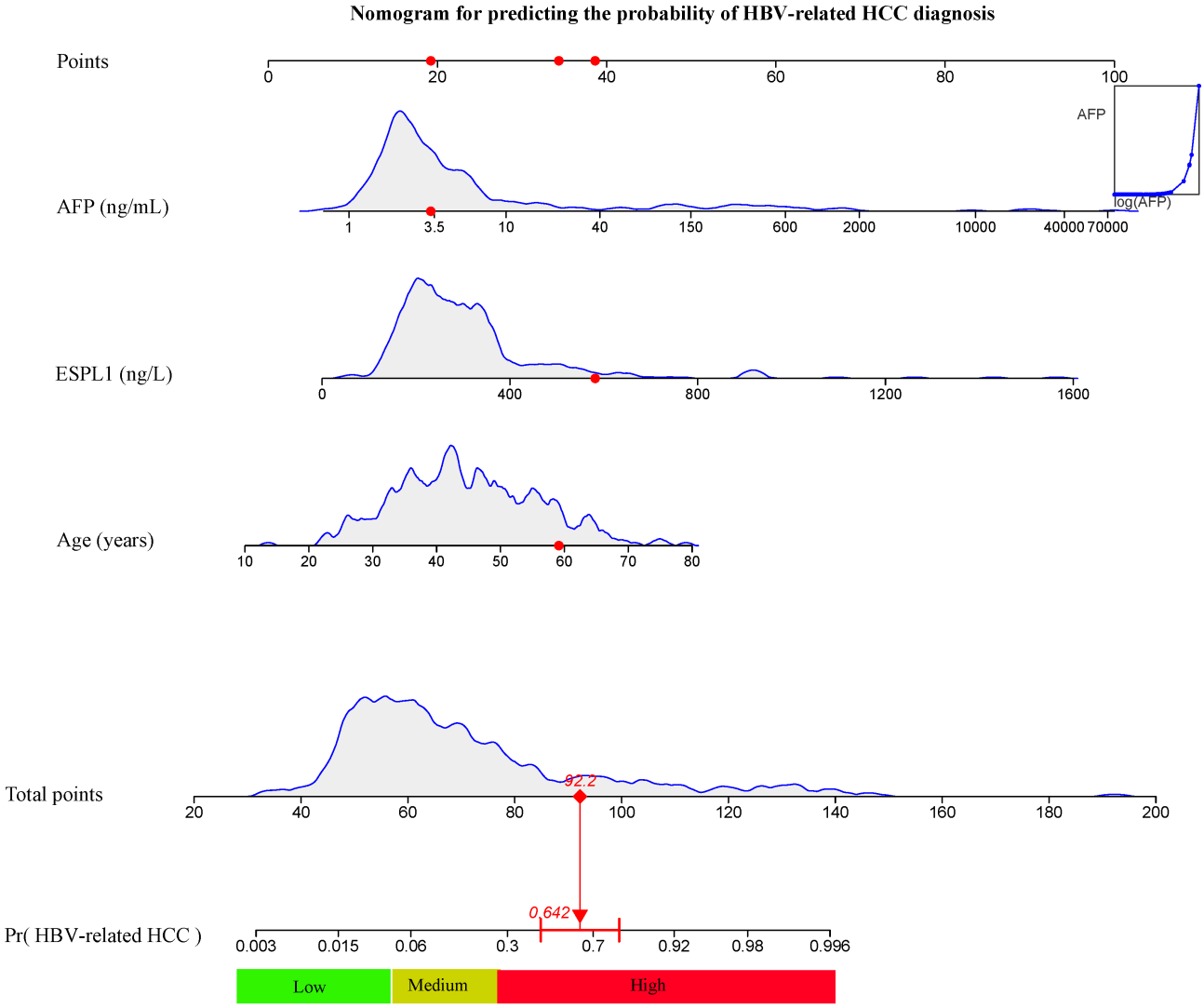
A risk model for predicting HBV-related HCC was developed using age, ESPL1, and AFP (AEA score) from multivariable logistic regression analysis, as depicted in Figure 2. Each variable has a score, and their sum estimates HCC risk. For example, in a 59-year-old male patient with pathologically confirmed HBV-related HCC who had an AFP level of 3.32 ng/mL and an ESPL1 level of 581.60 ng/L, the calculated total score corresponded to a predicted HCC risk probability of 64.2%. Conversely, in a 45-year-old male patient with chronic HBV infection and imaging evidence of cirrhotic nodules but no HCC diagnosis, with an ESPL1 level of 252.50 ng/L and an AFP level of 3.09 ng/mL, the calculated score indicated a predicted HCC risk probability of 7.47%. These contrasting examples illustrate how the AEA score can distinguish between patients at markedly different levels of HCC risk within the HBV population. For easier clinical use, we developed a web calculator [29]. In this, we can access the URL, input the necessary data, and click “Predict” to view the patient’s current HCC risk, as shown in Figure 3.

Sensitivity analyses, which compared the pooled imputed dataset, the 5 individual imputed datasets, and the complete-case dataset, yielded highly consistent results. The same independent predictors were retained, and similar effect sizes were observed

XSL•FO
RenderX

across all methodologies, as detailed in Multimedia Appendix 1.

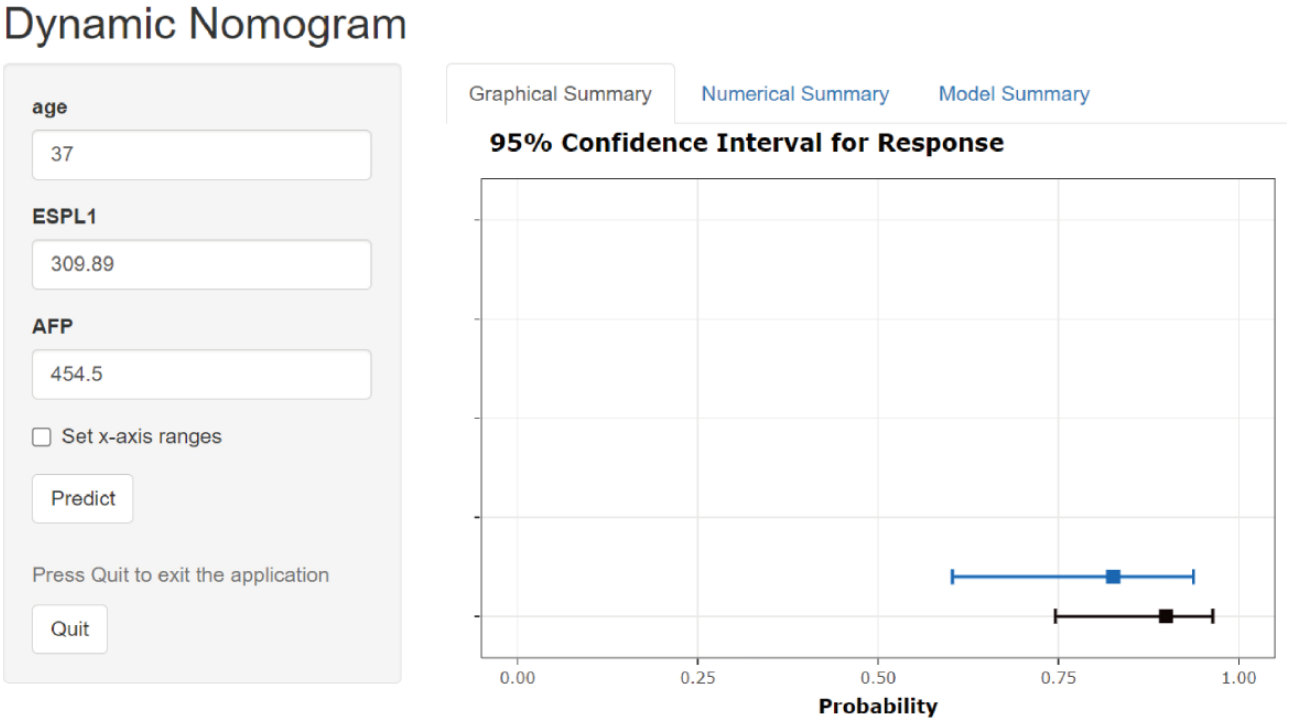
Figure 2. AEA score for predicting HBV-associated HCC risk was constructed based on the results of multivariate logistic regression analysis. Risk stratification thresholds were determined using X-tile: low risk (<4%), medium risk (4% - 24%), and high risk (>24%), as illustrated by the colored bar at the bottom of the figure. This is an example of calculating the probability of HBV-related HCC risk in patients. The irregular curves corresponding to each variable in the figure represent the distribution of variable values in the modeling group. On the basis of the corresponding variable, a score can be obtained, and the scores are added to get a total score. Finally, the total score can be used to calculate the corresponding HCC risk probability. In this illustrative case of a patient with pathologically confirmed HBV-related HCC, the red dots for AFP, ESPL1, and age indicate the patient's respective values: AFP=3.32 ng/mL, ESPL1=581.60 ng/L, and age=59 years. The corresponding scores (19+39+34.2) yield a total of 92.2, which translates into a predicted HCC risk probability of 64.2%. AFP: alpha-fetoprotein; ESPL1: extra spindle poles like 1; HBV: hepatitis B virus; HCC: hepatocellular carcinoma.



Risk stratification thresholds : Low risk (<4%), Medium risk (4%-24%), and High risk (>24%)

XSL•FO
RenderX

Figure 3. Example of HBV-related HCC risk probability web calculator. Age is in years, AFP in ng/mL, and ESPL1 in ng/L. AFP: alpha-fetoprotein; ESPL1: extra spindle poles like 1; HBV: hepatitis B virus; HCC: hepatocellular carcinoma.

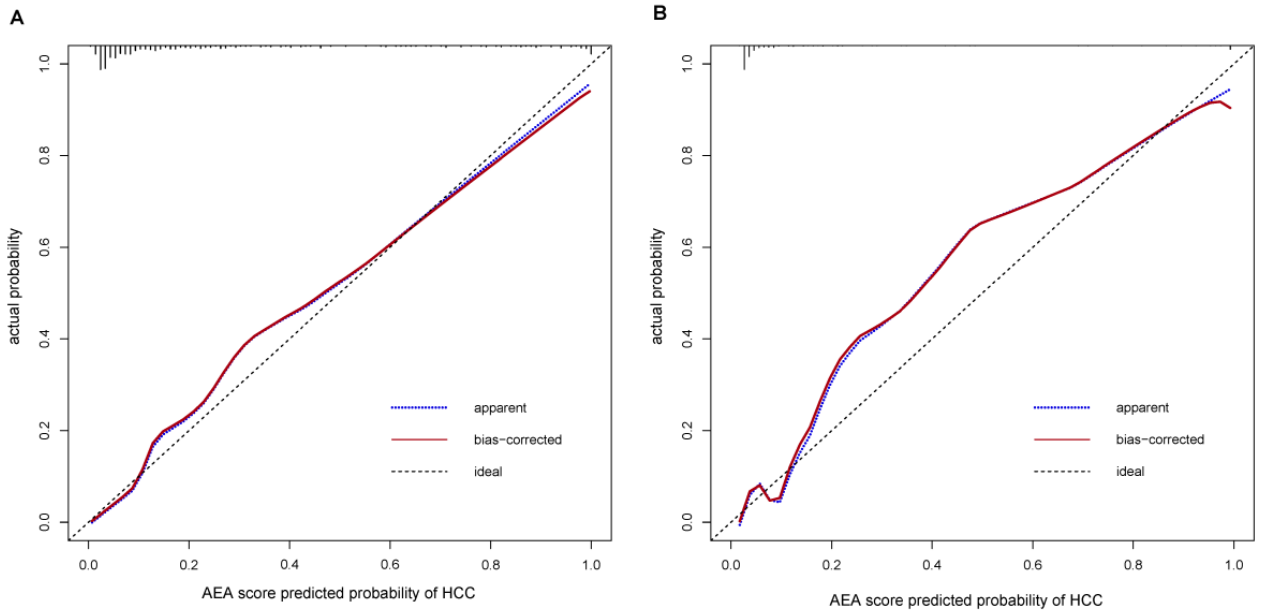


Evaluation of HBV-Related HCC Diagnostic Model Performance

Internal Validation

In the training set, the Hosmer–Lemeshow test yielded a *P* value of .596, suggesting an absence of evidence for model overfitting. The model demonstrated a C-index of 0.922 (95% CI 0.890–0.954), with an internally validated C-index of 0.923 (95% CI 0.890–0.950). It exhibited a consistency of 0.83, sensitivity of 0.89, specificity of 0.82, a positive predictive value of 0.606, a negative predictive value of 0.959, and a Youden Index of 0.71, indicating excellent discriminatory power. Furthermore, the model surpassed the performance of AFP alone (C-index 0.605) and ESPL1 alone (C-index 0.773) in predicting HCC risk. The calibration curve (Figure 4A) demonstrated a strong concordance between predicted and observed HCC incidence, with a slope of 0.93, a mean squared error of 0.023, and a Brier score of 0.08. Collectively, these findings suggest that the model provides both precise and dependable risk estimation, which is crucial for early clinical decision-making.

Figure 4. Calibration curves of the AEA score in the training set (A) and independent hold-out testing set (B). The dashed line indicates perfect calibration, the dotted line represents the apparent performance, and the solid line shows the bias-corrected performance after 1000 bootstrap resamples. Short vertical ticks at the top of each panel denote the distribution of patients according to predicted HCC risk (rug plot). HCC: hepatocellular carcinoma.



XSL•FO
RenderX

To further evaluate robustness, subgroup analyses were conducted across clinically pertinent categories, including sex, antiviral drug usage, treatment history, family history of LC/HCC, and HBeAg status in Multimedia Appendix 4. The model consistently exhibited high discriminatory performance, with C-index values ranging from 0.86 to 0.98, and no significant interactions were detected (all *P* values for interaction >.10). Owing to the absence of HCC events among noncirrhotic patients during the follow-up period, subgroup analysis stratified by cirrhosis status was not feasible. Collectively, these findings affirm that the ESPL1-based model maintains stable predictive accuracy across diverse patient subgroups, underscoring its reliability for broad clinical application.

Independent Hold-Out Validation

In the independent hold-out testing set, the model demonstrated robust performance, evidenced by a C-index of 0.958 (95% CI 0.929–0.988) and an adjusted C-index of 0.958 (95% CI 0.926–0.986). Additionally, the model exhibited a consistency of 0.92, a sensitivity of 0.87, a specificity of 0.94, a positive predictive value of 0.696, a negative predictive value of 0.976, and a Youden Index of 0.81. The calibration curve (Figure 4B) confirmed consistency between predicted and observed outcomes, with a slope of 0.91, mean squared error of 0.027, and a Brier score of 0.05. These findings support the robustness and clinical applicability of the model, suggesting that its predictions remain reliable when applied to independent patient data.

Comparison of AEA Score With Other HBV-Related HCC Risk Scores

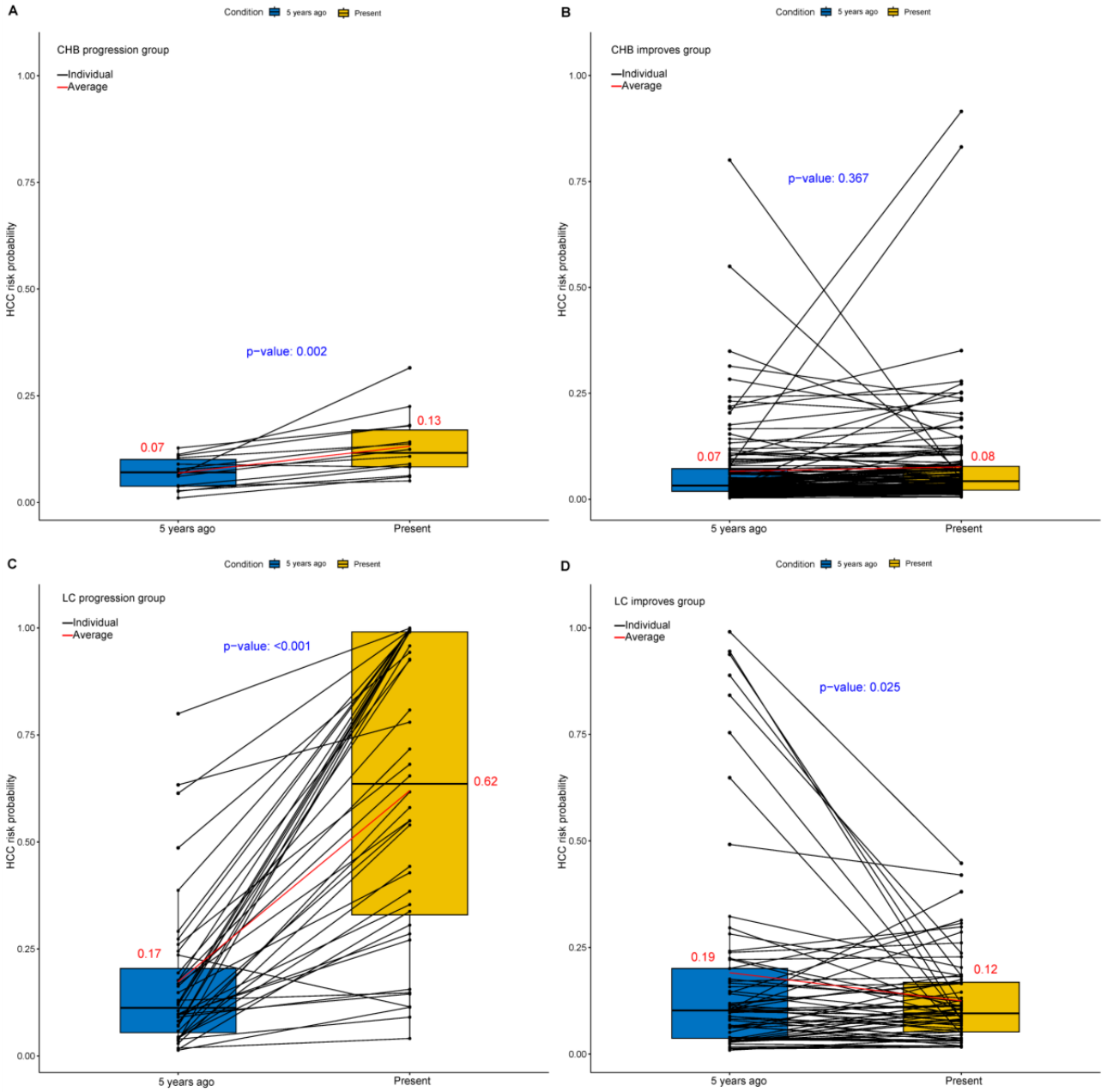
The AEA score consistently exhibited superior discriminatory power compared to the 5 established HBV-related HCC risk models (REACH-B, GAG-HCC, CU-HCC, PAGE-B, and mPAGE-B). Within our cohort, the C-index of the AEA score was significantly greater than that of each comparator model, with all pairwise comparisons achieving statistical significance (*P*<.001, Multimedia Appendix 5). In addition, the discriminative ability of AFP alone was limited (C-index=0.61, 95% CI 0.56 - 0.65), further highlighting the incremental value of incorporating ESPL1 into the AEA score. These results underscore the enhanced predictive value of integrating ESPL1 into risk assessment, surpassing traditional demographic and clinical variables.

Validation of AEA Score for HBV-Related HCC in a Longitudinal Cohort

The longitudinal analysis confirmed that the ESPL1-based AEA score dynamically reflected disease trajectories: predicted HCC risk remained stable or significantly decreased in patients with clinical improvement, whereas it rose markedly in those with disease progression. Patients with CHB who exhibited clinical improvement (n=129) maintained stable risk values over a 3-year period (0.07 vs 0.08, *P*=0.367). In contrast, those who experienced disease progression (n=14) showed a significant increase in risk values (0.07 vs 0.13, *P*=.002; Figure 5A–B). Similarly, among patients with cirrhosis, those demonstrating clinical improvement (n=65) experienced a significant reduction in predicted risk (0.19 vs 0.12, *P*=.025), whereas patients who developed HCC during follow-up (n=40) exhibited a substantial increase in risk probability, rising from 0.17 to 0.62 (*P*<.001; Figure 5C–D). These results underscore the model's capability not only to estimate baseline risk but also to detect significant changes corresponding with clinical outcomes, thereby affirming its utility for dynamic risk monitoring.

XSL•FO
RenderX

Figure 5. Trend chart of AEA score predicting HCC risk changes with the condition of patients with chronic HBV infection. HBV: hepatitis B virus; HCC: hepatocellular carcinoma.

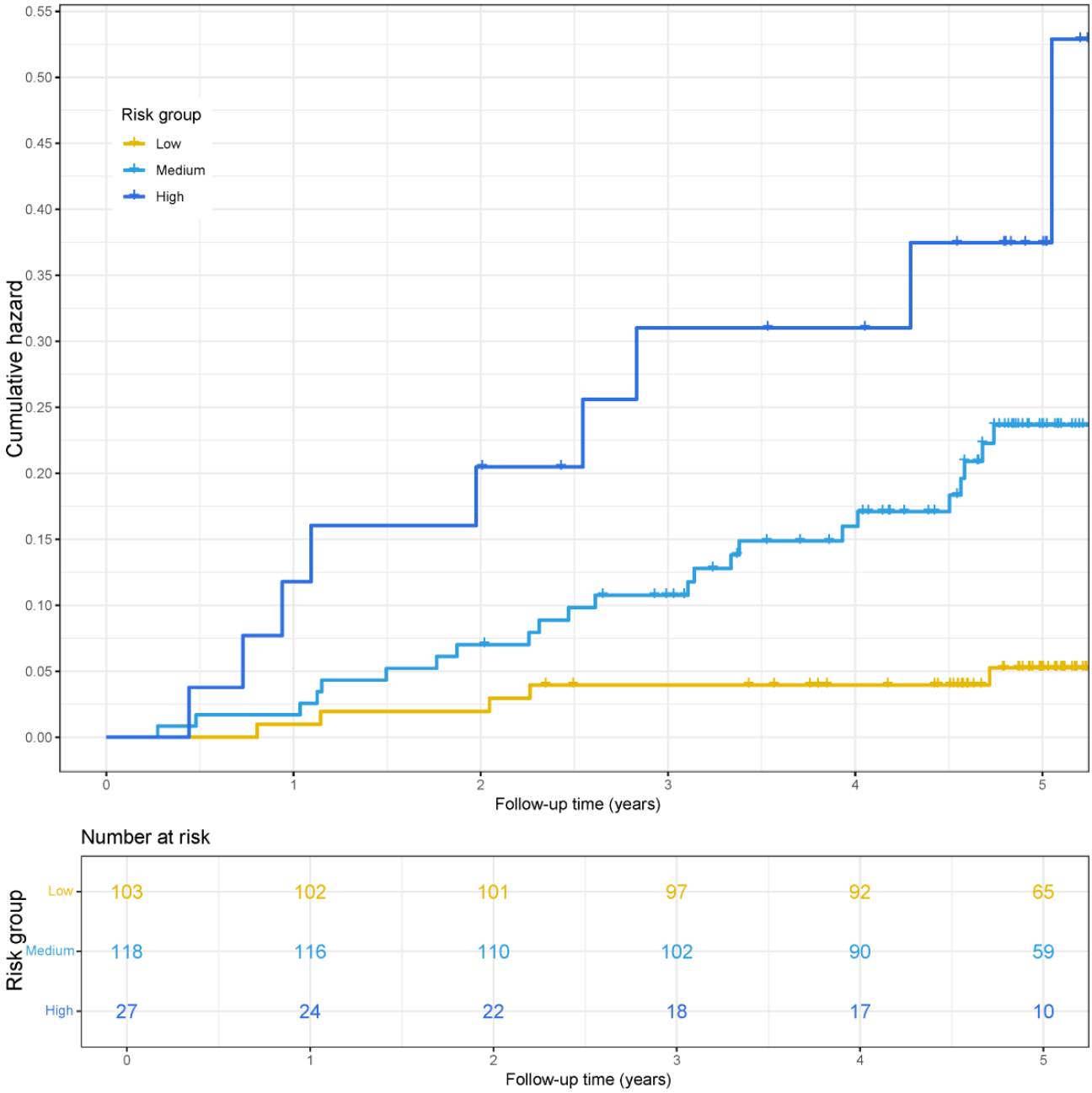


Using the X-tile tool, 3 optimal cutoff points (4% and 24%) were identified for stratifying HBV-related HCC risk. Application of these thresholds in the independent hold-out validation cohort (n=248) categorized patients into low risk (45.6%), medium risk (47.5%), and high risk (10.9%) groups (Figure 6). Kaplan–Meier analysis revealed significant differences in cumulative HCC incidence among groups, with 5-year rates of 5.1% in the low-risk group, 21.1% in the medium-risk group, and 31.3% in the high-risk group (P<.001). This separation highlights the ability of the model to statistically distinguish relative risk levels among patients, which may support risk-adapted surveillance strategies in future studies.

As shown in Multimedia Appendix 6, the distribution of clinical outcomes at the end of follow-up varied markedly across the 3 risk strata in the independent hold-out testing set. In the high-risk group, most patients had progressed to HBV-related HCC by the end point (88%), whereas the medium-risk group comprised a mixture of CHB, LC, and HCC cases. In contrast, the low-risk group at follow-up was composed predominantly of patients with CHB, and no HCC events were observed in this category. This clear gradient in outcome distribution demonstrates the model's ability to stratify patients according to their likelihood of HBV-related HCC development and underscores its potential to inform surveillance strategies.

XSL•FO
RenderX

Figure 6. Cumulative incidence curve of HBV-related HCC in longitudinal cohort. HBV: hepatitis B virus; HCC: hepatocellular carcinoma.

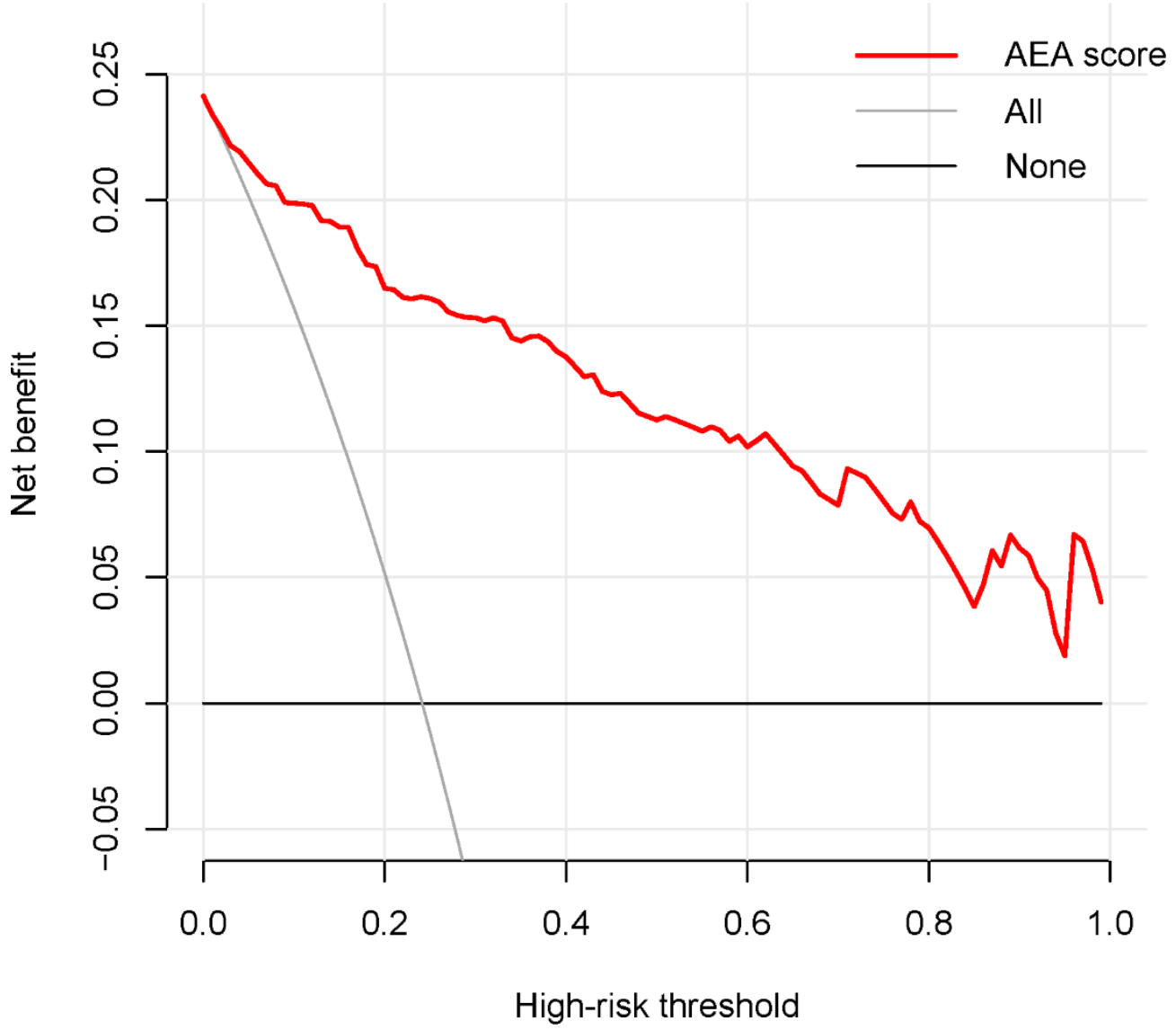


The Clinical Application Value of HBV-Related HCC Prediction Model

As shown in Figure 7, decision curve analysis indicated that our AEA score consistently provided greater net benefit than either the “All” and “None” strategies when the risk threshold is above 0.01. This finding implies that the model has the potential to enhance surveillance efficiency by improving case detection across clinically relevant thresholds. Nevertheless, all risk groups continue to face nonnegligible risks, necessitating ongoing monitoring in alignment with current guidelines.

XSL•FO
RenderX

Figure 7. Clinical decision curve of the AEA score in HCC diagnosis. Net benefit is the primary outcome observed in the clinical decision curve. It is calculated based on the true positive rate and false positive rate of the model's prediction for the outcome in the target population. The formula is as follows: net benefit=(true positives/N)–(false positives/N)×(Pt/(1−Pt)), where N is the total sample size and Pt is the probability threshold used by the model to distinguish between the occurrence and nonoccurrence of the event. Connecting the net benefit values at different probability thresholds forms the decision curve. A higher net benefit indicates greater practical value of the model in real-world applications.



Discussion

Principal Findings

Chronic HBV infection can lead to liver inflammation and fibrosis, which may progress to HCC. Early detection of HCC significantly enhances prognosis; however, the asymptomatic nature of its early stages poses challenges for timely diagnosis. Recent technological advancements [30] and the identification of novel biomarkers, in conjunction with clinical features, are expected to enhance the accuracy and feasibility of early HCC detection. Building on our previous research, we developed an AEA score that integrates the newly identified ESPL1 protein biomarker with long-term clinical data from patients with chronic HBV infection. The AEA score demonstrated superior performance in both accuracy and calibration compared to existing HCC risk models. In addition, subgroup analyses indicated that the ESPL1-based model maintained high discriminatory accuracy across various factors, including sex, antiviral regimen, treatment history, family history of LC or HCC, and HBeAg status, thereby affirming its robustness across diverse clinical contexts.

Comparison to Prior Work

In this study, the ESPL1-based AEA score demonstrated consistently superior predictive accuracy compared with 5 widely used HBV-related HCC risk models (ie, REACH-B, GAG-HCC, CU-HCC, PAGE-B, and mPAGE-B). As our study was conducted in Guangxi, a region with a particularly high incidence of HBV-related HCC, these findings emphasize that conventional models may not fully reflect risk profiles in this population. By integrating ESPL1, the AEA score provides additional discriminatory value beyond demographic and clinical variables, enabling more accurate risk stratification in high-burden settings. With respect to individual biomarkers, AFP and PIVKA-II remain widely used in clinical practice but have well-recognized limitations in sensitivity and specificity for early HCC detection. In our comparative analysis within the

XSL•FO
RenderX

same cohort, ESPL1 demonstrated significantly stronger discriminatory ability than both AFP and PIVKA-II (C-index: 0.923 vs 0.572 and 0.788, respectively), underscoring its potential to distinguish early HCC from cirrhotic nodules [17,18,31]. Although LSM reflects fibrosis and cirrhosis, it was not retained as an independent predictor in our multivariate analysis, suggesting limited incremental value when combined with ESPL1 and clinical factors in this population. Taken together, these findings highlight that while conventional models and biomarkers provide useful prognostic information, they remain insufficient for precise early HCC risk prediction in patients with chronic HBV, especially in high-incidence regions such as Guangxi. By incorporating ESPL1 with readily available clinical variables, the AEA score delivers both superior discrimination and appears to provide incremental value for risk stratification in populations with a high burden of HBV-related HCC. Nevertheless, these observations should be interpreted cautiously, as our study was based on a single-center cohort and requires external confirmation.

Our study used a cross-sectional design combined with LASSO regression to identify key predictors, thereby reducing redundancy and confounding relative to traditional Cox survival models. This methodology facilitated the selection of the most informative variables and the development of a parsimonious logistic regression model, ultimately enhancing both predictive accuracy and stability. The final model, which included age, serum ESPL1 levels, and log (AFP), exhibited strong discrimination and calibration in both the training and testing sets. In contrast, other variables commonly cited as predictors of HCC in previous studies, such as serum albumin [13,32,33], HBV DNA [11,12], ALT [11], and LSM [34], did not maintain independent significance in our multivariate analysis. A possible explanation for this finding is that early-stage HCC induces only subtle changes in biochemical markers, whereas the widespread use of antiviral therapy diminishes the predictive value of HBV DNA levels. Similarly, although LSM reflects fibrosis and cirrhosis, it may not offer additional discriminatory power once ESPL1 and AFP are accounted for.

Biological Rationale

Our prior study revealed that the expression of the HBV S–ESPL1 fusion gene persists despite long-term antiviral therapy, underscoring its specific role in hepatocarcinogenesis [17,35]. Mechanistically, ESPL1 encodes separase, a cysteine protease that plays a critical role in chromatid segregation during anaphase. Dysregulation of ESPL1 results in chromosomal instability, a well-established driver of malignant transformation. Under conditions of chronic viral infection and prolonged carcinogenic stress, integration of HBV into the ESPL1 locus can produce HBV S–ESPL1 fusion transcripts, potentially enhancing oncogenic signaling and compromising genomic integrity. Previous studies have demonstrated that mutations, overexpression, or viral fusion events involving ESPL1 contribute to uncontrolled cell proliferation, defective DNA repair, and the activation of tumor-promoting pathways, including p53 inhibition and Wnt/β-catenin signaling [36-38]. Beyond HCC, overexpression of ESPL1 has also been implicated in breast, prostate, osteosarcoma, and endometrial cancers, highlighting its role as a broadly relevant oncogenic driver [39-41]. From a clinical perspective, these biological mechanisms elucidate the enhanced efficacy of ESPL1 in comparison to traditional biomarkers. AFP, the most commonly used biomarker, demonstrates limited sensitivity in the early stages of HCC, frequently remaining below diagnostic thresholds and exhibiting a stronger correlation with tumor burden rather than the molecular initiation of malignancy [18,42]. Conversely, serum levels of ESPL1 protein may indicate early oncogenic events induced by HBV integration and genomic instability, thereby capturing risk signals before the overt formation of tumors. In our study, AFP alone did not reach conventional diagnostic thresholds; however, the log (AFP) maintained independent predictive significance. Notably, when combined with patient age and serum ESPL1 levels, the resultant AEA score demonstrated excellent discrimination (C-index 0.92) and was robustly validated in external cohorts. Collectively, these findings suggest that ESPL1 enhances predictive accuracy in a statistically significant manner and serves as a mechanistically substantiated biomarker that encapsulates the molecular mechanisms underlying HBV-induced hepatocarcinogenesis. This dual benefit—biological plausibility combined with robust clinical efficacy—advocates for its incorporation into risk prediction models to facilitate earlier and more precise identification of patients with high-risk HBV.

Clinical Implications

Cirrhotic nodules, a family history of liver cirrhosis or HCC, and the use of non–first-line antiviral agents are well-recognized clinical risk factors for HCC development, and their identification remains important for patient management. In our univariate analysis, all 3 factors were significantly associated with HCC risk. However, these associations lost statistical significance in the multivariate model. This phenomenon likely reflects that their predictive influence is relatively modest once stronger predictors, such as age, serum ESPL1, and AFP, are accounted for and may also be partly explained by correlations among variables (eg, cirrhotic nodules reflecting fibrosis already captured by ESPL1 or AFP). Our subgroup analyses further confirmed that the ESPL1-based model maintained robust discrimination across strata of sex, antiviral treatment regimen, prior treatment status, family history of LC/HCC, and HBeAg status, with no significant interactions detected. These findings suggest that the diminished significance of these factors in the multivariate model does not reflect instability, but rather their limited incremental predictive value beyond the key predictors. Nevertheless, given their established clinical relevance, these factors should not be disregarded in practice, and future studies with larger multicenter cohorts and nonlinear modeling approaches may help clarify their contribution to HCC risk prediction.

Accurate HCC risk prediction in patients with chronic HBV is essential during follow-up. Tumor heterogeneity and complex serum biomarkers pose challenges. Unlike models using AFP or PIVKA-II, our HBV-related HCC risk model based on ESPL1 integrates patient disease status and serological marker characteristics. This enables personalized HCC risk assessments to inform patient follow-up strategies. Our study shows that patients with an HCC risk probability over 24% are at high risk.

XSL•FO
RenderX

This was validated externally, where patients with chronic HBV who developed HCC had an average risk of 62%, much higher than the 17% baseline. This confirms our model's effectiveness in predicting HCC occurrence. The model's risk values allow patients to be categorized into low risk, medium risk, and high risk groups, with significant differences in 3-year and 5-year HCC incidence rates. These findings suggest that ESPL1 may improve early identification of patients at elevated risk; however, their implications for guiding follow-up strategies need to be validated in larger multicenter cohorts. In the internet age, online calculators enable quick risk assessments. Such tools may facilitate predicting HCC risk exclusively in patients with chronic HBV infection or HBV-related cirrhosis, supporting individualized follow-up strategies. However, their role in routine clinical decision-making remains exploratory and requires further validation.

Clinical prediction models are crucial for assessing HCC risk in patients with chronic HBV, aiding physicians in predicting risk and guiding treatment. However, traditional evaluation metrics such as discrimination and calibration often fall short in reflecting clinical benefits at varying risk thresholds [43-45]. Discrimination metrics such as AUC assess a model's predictive accuracy but do not confirm its clinical usefulness. To validate the clinical utility of the HBV-related HCC risk prediction model based on ESPL1, we used clinical decision curve analysis instead of multicenter, large-sample prospective studies, which are time-consuming and involve many uncertainties. Clinical decision curves reveal potential clinical benefits at various risk thresholds and calculate net benefits [28]. An ideal curve should show positive net benefits across clinically relevant thresholds. Our analysis indicates that when the threshold probability is over 1%, the model achieves a positive net benefit. In addition, the 4% and 24% thresholds used to categorize patients into low risk, medium risk, and high risk groups in our HBV-RELATED HCC model are within this range. These results provide insight into possible clinical relevance but cannot substitute for large-scale, multicenter prospective validation. Our findings suggest that the model may be clinically informative, yet confirmation in diverse populations is warranted before widespread adoption.

In addition to its predictive accuracy, the practical feasibility of ESPL1 testing is a critical consideration for clinical translation. Serum ESPL1 levels can be measured through a standard ELISA assay, which is cost-effective and comparable in price to AFP testing. Although this suggests potential feasibility, reproducibility across laboratories and consistency in different health care systems have not yet been established. Therefore, widespread clinical implementation should await further multicenter validation and assay standardization. Furthermore, we developed a web-based calculator that can be accessed on computers and mobile devices, allowing clinicians to easily input routinely available variables, including ESPL1, to obtain individualized risk estimates. At this stage, the calculator should be regarded as a prototype tool to illustrate the model's potential application rather than a ready-to-use clinical instrument.

Limitations

This study has several limitations. First, all patients were recruited from a single tertiary hospital in Guangxi, which may introduce selection bias and limit representativeness compared with broader, community-based populations. Second, as the study population was restricted to a high-incidence HBV region, the global generalizability of ESPL1 as a biomarker remains uncertain. Third, ESPL1 levels were quantified using a single ELISA kit under standardized laboratory conditions, and interlaboratory variability may affect reproducibility. Fourth, although major demographic, clinical, and virological factors were included, residual confounding from unmeasured variables (eg, lifestyle behaviors, alcohol consumption, aflatoxin exposure, or other environmental risks) cannot be excluded. We attempted to mitigate these limitations using strict inclusion criteria, internal and independent hold-out validation, and robust statistical modeling; however, multicenter prospective studies are needed to confirm these findings.

Future Directions

Future research should focus on multicenter, geographically diverse cohorts to validate the ESPL1-based model, standardize assays across laboratories, and evaluate integration into clinical practice. In addition, combining ESPL1 with other emerging biomarkers or imaging modalities may further enhance predictive accuracy. Although the model demonstrated prognostic value during longitudinal validation, it was primarily developed for diagnostic purposes. Therefore, larger multicenter prospective cohorts will be needed to confirm its long-term predictive performance and ensure generalizability. Further work should also aim to standardize ESPL1 assays, assess cost-effectiveness in different health care systems, and evaluate patient and clinician acceptance. Finally, mechanistic studies on ESPL1 in HBV-related hepatocarcinogenesis may reveal therapeutic targets and extend its utility beyond risk stratification.

Conclusions

The ESPL1-based AEA score exhibits enhanced predictive accuracy relative to existing HBV-related HCC risk models, indicating significant potential for individualized risk stratification. By incorporating both biomarker and clinical features, this model could facilitate earlier detection of HCC and enable personalized surveillance strategies. However, larger multicenter prospective studies across diverse populations are necessary to validate its broader applicability.

Acknowledgments

This work was supported by the National Natural Science Foundation (81960115), the National Natural Science Foundation (82260124), the Key Laboratory of High-Incidence-Tumor Prevention and Treatment (Guangxi Medical University), Ministry

XSL•FO
RenderX

of Education (GKE-ZZ202107), the Guangxi Key Laboratory of Early Prevention and Treatment for Regional High Frequency Tumor (GKE-ZZ202218), and the National Natural Science Foundation (82160123).

Data Availability

The data analyzed during this study are available from the corresponding author on reasonable request.

Conflicts of Interest

None declared.

Multimedia Appendix 1
Sensitivity analysis of predictors for HBV-related HCC risk using multiple imputation and complete-case datasets. HBV: hepatitis B virus; HCC: hepatocellular carcinoma.
[DOCX File, 18 KB - medinform_v13i1e78354_app1.docx]

Multimedia Appendix 2
Established HCC risk models. HCC: hepatocellular carcinoma.
[DOCX File, 43 KB - medinform_v13i1e78354_app2.docx]

Multimedia Appendix 3
LASSO regression analysis selected predictors. (A) The tuning parameter (λ) for the LASSO model was selected using 10-fold cross-validation based on the minimum criterion. Dashed lines represent the optimal values using λ.min and 1− λ.SE. (B) LASSO regression analysis was conducted on 19 features, generating a coefficient plot using the log (λ min) sequence through 10-fold cross-validation. The optimal λ (λ.min = 0.04091) identified 16 predictors with nonzero coefficients.
[PNG File, 78 KB - medinform_v13i1e78354_app3.png]

Multimedia Appendix 4
Subgroup analysis of the ESPL1-based model in the training set. Forest plot showing the discriminatory performance (C-index and 95% CI) of the ESPL1-based model across clinically relevant subgroups, including sex, antiviral drugs, treatment history, family history of LC/HCC, and HBeAg status. As no HCC events occurred among patients with noncirrhosis during follow-up, subgroup analysis stratified by cirrhosis status could not be performed. ESPL1: extra spindle poles like 1; HCC: hepatocellular carcinoma; LC: cirrhosis of liver.
[PNG File, 160 KB - medinform_v13i1e78354_app4.png]

Multimedia Appendix 5
Comparison of C-index of the AEA score with other existing risk scores in the training set.
[DOCX File, 22 KB - medinform_v13i1e78354_app5.docx]

Multimedia Appendix 6
Distribution of patients in different HBV-related HCC risk layers in the external testing set. HBV: hepatitis B virus; HCC: hepatocellular carcinoma.
[DOCX File, 21 KB - medinform_v13i1e78354_app6.docx]

References

1. Falette Puisieux M, Pellat A, Assaf A, et al. Therapeutic management of advanced hepatocellular carcinoma: an updated review. Cancers (Basel) 2022 May 10;14(10):2357. [doi: 10.3390/cancers14102357] [Medline: 35625962]
2. Petruzziello A. Epidemiology of hepatitis B virus (HBV) and hepatitis C virus (HCV) related hepatocellular carcinoma. Open Virol J 2018;12(26-32):26-32. [doi: 10.2174/1874357901812010026] [Medline: 29541276]
3. Rumgay H, Arnold M, Ferlay J, et al. Global burden of primary liver cancer in 2020 and predictions to 2040. J Hepatol 2022 Dec;77(6):1598-1606. [doi: 10.1016/j.jhep.2022.08.021] [Medline: 36208844]
4. Mo S, He Y, Liang T, et al. Serum alpha-fetoprotein-tumor size ratio as a prognostic marker after hepatic resection for primary hepatocellular carcinoma: propensity score matched retrospective cohort study. JMIR Cancer 2025 Aug 26;11:e64929. [doi: 10.2196/64929] [Medline: 40857604]
5. Terrault NA, Lok ASF, McMahon BJ, et al. Update on prevention, diagnosis, and treatment of chronic hepatitis B: AASLD 2018 hepatitis B guidance. Clin Liver Dis (Hoboken) 2018 Jul;12(1):33-34. [doi: 10.1002/cld.728] [Medline: 30988907]
6. Korean Association for the Study of the Liver (KASL). KASL clinical practice guidelines for management of chronic hepatitis B. Clin Mol Hepatol 2019 Jun;25(2):93-159. [doi: 10.3350/cmh.2019.1002]

XSL•FO
RenderX

7. Feng RM, Zong YN, Cao SM, Xu RH. Current cancer situation in China: good or bad news from the 2018 Global Cancer Statistics? Cancer Commun 2019 Dec;39(1):1-12. [doi: 10.1186/s40880-019-0368-6]
8. You H, Wang F, Li T, et al. Guidelines for the prevention and treatment of chronic hepatitis B (version 2022). J Clin Transl Hepatol 2023 Nov 28;11(6):1425-1442. [doi: 10.14218/JCTH.2023.00320] [Medline: 37719965]
9. Wong VWS, Janssen HLA. Can we use HCC risk scores to individualize surveillance in chronic hepatitis B infection? J Hepatol 2015 Sep;63(3):722-732. [doi: 10.1016/j.jhep.2015.05.019] [Medline: 26026875]
10. Committee CPMAHaPDPaCP, Committee CAoRHLDP, Branch CMAH, Group CPMATPaCPCITPaC. Guidelines for stratified screening and monitoring of primary liver cancer. J Clin Hepatol 2021;37(2):286-295. [doi: 10.3969/j.issn.1001-5256.2021.02.009]
11. Yang HI, Yuen MF, Chan HLY, et al. Risk estimation for hepatocellular carcinoma in chronic hepatitis B (REACH-B): development and validation of a predictive score. Lancet Oncol 2011 Jun;12(6):568-574. [doi: 10.1016/S1470-2045(11)70077-8] [Medline: 21497551]
12. Yuen MF, Tanaka Y, Fong DYT, et al. Independent risk factors and predictive score for the development of hepatocellular carcinoma in chronic hepatitis B. J Hepatol 2009 Jan;50(1):80-88. [doi: 10.1016/j.jhep.2008.07.023] [Medline: 18977053]
13. Wong VWS, Chan SL, Mo F, et al. Clinical scoring system to predict hepatocellular carcinoma in chronic hepatitis B carriers. J Clin Oncol 2010 Apr 1;28(10):1660-1665. [doi: 10.1200/JCO.2009.26.2675] [Medline: 20194845]
14. Papatheodoridis G, Dalekos G, Sypsa V, et al. PAGE-B predicts the risk of developing hepatocellular carcinoma in Caucasians with chronic hepatitis B on 5-year antiviral therapy. J Hepatol 2016 Apr;64(4):800-806. [doi: 10.1016/j.jhep.2015.11.035] [Medline: 26678008]
15. Hsu YC, Yip TCF, Ho HJ, et al. Development of a scoring system to predict hepatocellular carcinoma in Asians on antivirals for chronic hepatitis B. J Hepatol 2018 Aug;69(2):278-285. [doi: 10.1016/j.jhep.2018.02.032] [Medline: 29551708]
16. Kim JH, Kim YD, Lee M, et al. Modified PAGE-B score predicts the risk of hepatocellular carcinoma in Asians with chronic hepatitis B on antiviral therapy. J Hepatol 2018 Nov;69(5):1066-1073. [doi: 10.1016/j.jhep.2018.07.018] [Medline: 30075230]
17. Hu B, Huang W, Wang R, et al. High rate of detection of human ESPL1-HBV S fusion gene in patients with HBV-related liver cancer: a Chinese case-control study. Anticancer Res 2020 Jan;40(1):245-252. [doi: 10.21873/anticanres.13946] [Medline: 31892573]
18. Hu B, Wei LU, Liang H, et al. Correlation between serum ESPL1 and hepatitis B virus-related hepatocellular carcinoma histological grade: a Chinese single-center case-control study. Anticancer Res 2023 Sep;43(9):3997-4005. [doi: 10.21873/anticanres.16587] [Medline: 37648308]
19. Efthimiou O, Seo M, Chalkou K, Debray T, Egger M, Salanti G. Developing clinical prediction models: a step-by-step guide. BMJ 2024 Sep 3;386:e078276. [doi: 10.1136/bmj-2023-078276] [Medline: 39227063]
20. Wang R, Zang W, Hu B, et al. Serum ESPL1 can be used as a biomarker for patients with hepatitis B virus-related liver cancer: a Chinese case-control study. Technol Cancer Res Treat 2020;19:1533033820980785. [doi: 10.1177/1533033820980785] [Medline: 33308056]
21. van Buuren S. mice: multivariate imputation by chained equations in R. J Stat Softw 2011 Dec;45(3):67. [doi: 10.18637/jss.v045.i03]
22. Kim JH, Kim YD, Lee M, Jun BG, Kim TS, Suk KT, et al. Modified PAGE-B score predicts the risk of hepatocellular carcinoma in Asians with chronic hepatitis B on antiviral therapy. Biomed Res Int 2018 Nov;69(5). [doi: 10.1155/2018/1252849] [Medline: 30075230]
23. Sauerbrei W, Royston P, Binder H. Selection of important variables and determination of functional form for continuous predictors in multivariable model building. Stat Med 2007 Dec 30;26(30):5512-5528. [doi: 10.1002/sim.3148] [Medline: 18058845]
24. Alba AC, Agoritsas T, Walsh M, et al. Discrimination and calibration of clinical prediction models: users' guides to the medical literature. JAMA 2017 Oct 10;318(14):1377-1384. [doi: 10.1001/jama.2017.12126] [Medline: 29049590]
25. Hosmer DW, Lemeshow S, Sturdivant RX. Applied Logistic Regression: John Wiley & Sons; 2013. [doi: 10.1002/9781118548387]
26. Camp RL, Dolled-Filhart M, Rimm DL. X-tile: a new bio-informatics tool for biomarker assessment and outcome-based cut-point optimization. Clin Cancer Res 2004 Nov 1;10(21):7252-7259. [doi: 10.1158/1078-0432.CCR-04-0713] [Medline: 15534099]
27. Hu XJ, Lagakos SW. Nonparametric estimation of the mean function of a stochastic process with missing observations. Lifetime Data Anal 2007 Mar;13(1):51-73. [doi: 10.1007/s10985-006-9030-0] [Medline: 17195105]
28. Vickers AJ, Elkin EB. Decision curve analysis: a novel method for evaluating prediction models. Med Decis Making 2006;26(6):565-574. [doi: 10.1177/0272989X06295361] [Medline: 17099194]
29. Dynamic nomogram. URL: https://hbvrelatedhccriskpredictionmodel.shinyapps.io/dynnomapp/ [accessed 2025-10-16]
30. Kwok G, Cheung SPY, Duffecy J, Devine KA. Application of the supportive accountability model in digital health interventions: scoping review. J Med Internet Res 2025 Sep 26;27:e72639. [doi: 10.2196/72639] [Medline: 41004801]
31. Feng LH, Wei L, Hu B, et al. Evaluation of serum ESPL1 as a biomarker for early diagnosis of HBV-related hepatocellular carcinoma. Front Oncol 2025;15(1574317):1574317. [doi: 10.3389/fonc.2025.1574317] [Medline: 40248196]

XSL•FO
RenderX

32. Wong GLH, Chan HLY, Wong CKY, et al. Liver stiffness-based optimization of hepatocellular carcinoma risk score in patients with chronic hepatitis B. J Hepatol 2014 Feb;60(2):339-345. [doi: 10.1016/j.jhep.2013.09.029] [Medline: 24128413]
33. Yu JH, Suh YJ, Jin YJ, et al. Prediction model for hepatocellular carcinoma risk in treatment-naive chronic hepatitis B patients receiving entecavir/tenofovir. Eur J Gastroenterol Hepatol 2019;31(7):865-872. [doi: 10.1097/MEG.0000000000001357]
34. Lee HW, Yoo EJ, Kim BK, et al. Prediction of development of liver-related events by transient elastography in hepatitis B patients with complete virological response on antiviral therapy. Am J Gastroenterol 2014 Aug;109(8):1241-1249. [doi: 10.1038/ajg.2014.157] [Medline: 24957159]
35. Hu B, Wang R, Fu J, et al. Integration of hepatitis B virus S gene impacts on hepatitis B surface antigen levels in patients with antiviral therapy. J Gastroenterol Hepatol 2018 Jul;33(7):1389-1396. [doi: 10.1111/jgh.14075] [Medline: 29266382]
36. Zhong Y, Zheng C, Zhang W, et al. Pan-Cancer analysis and experimental validation identify the oncogenic nature of ESPL1: potential therapeutic target in colorectal cancer. Front Immunol 2023;14:1138077. [doi: 10.3389/fimmu.2023.1138077] [Medline: 37006282]
37. Finetti P, Guille A, Adelaide J, Birnbaum D, Chaffanet M, Bertucci F. ESPL1 is a candidate oncogene of luminal B breast cancers. Breast Cancer Res Treat 2014 Aug;147(1):51-59. [doi: 10.1007/s10549-014-3070-z] [Medline: 25086634]
38. Liu Z, Lian X, Zhang X, et al. ESPL1 is a novel prognostic biomarker associated with the malignant features of glioma. Front Genet 2021;12(666106):666106. [doi: 10.3389/fgene.2021.666106] [Medline: 34512713]
39. Song R, Huang J, Yang C, Li Y, Zhan G, Xiang B. ESPL1 is elevated in hepatocellular carcinoma and predicts prognosis. Int J Gen Med 2022;15(8381-98):8381-8398. [doi: 10.2147/IJGM.S381188] [Medline: 36465268]
40. Lu C, Yang Y, Lingmei L, et al. Identification of hub genes in AR-induced tamoxifen resistance in breast cancer based on weighted gene co-expression network analysis. Breast Cancer Res Treat 2023 Jan;197(1):71-82. [doi: 10.1007/s10549-022-06788-w] [Medline: 36334189]
41. Zhang B, Chen Y, Chen X, et al. Genome-wide CRISPR screen identifies ESPL1 limits the response of gastric cancer cells to apatinib. Cancer Cell Int 2024 Feb 24;24(1):83. [doi: 10.1186/s12935-024-03233-4] [Medline: 38402402]
42. Piñero F, Dirchwolf M, Pessôa MG. Biomarkers in hepatocellular carcinoma: diagnosis, prognosis and treatment response assessment. Cells 2020 Jun 1;9(6):1370. [doi: 10.3390/cells9061370] [Medline: 32492896]
43. Collins GS, Reitsma JB, Altman DG, Moons KGM. Transparent reporting of a multivariable prediction model for individual prognosis or diagnosis (TRIPOD): the TRIPOD statement. BMJ 2015 Jan 7;350:g7594. [doi: 10.1136/bmj.g7594] [Medline: 25569120]
44. Van Calster B, Vickers AJ. Calibration of risk prediction models: impact on decision-analytic performance. Med Decis Making 2015 Feb;35(2):162-169. [doi: 10.1177/0272989X14547233] [Medline: 25155798]
45. Localio AR, Goodman S. Beyond the usual prediction accuracy metrics: reporting results for clinical decision making. Ann Intern Med 2012 Aug 21;157(4):294-295. [doi: 10.7326/0003-4819-157-4-201208210-00014] [Medline: 22910942]

Abbreviations

AFP: alpha-fetoprotein
AFP-L3: alpha-fetoprotein variant-L3
ALB: albumin
ALT: alanine aminotransferase
AST: aspartate aminotransferase
AUC: area under the ROC curve
CHB: chronic viral hepatitis B
ESPL1: extra spindle poles like 1
HBV: hepatitis B virus
HCC: hepatocellular carcinoma
LC: cirrhosis of liver
LSM: liver stiffness measurement
NA: nucleotide
PIVKA-Ⅱ: protein-induced by vitamin K absence/antagonist-Ⅱ
PLT: platelet
PT: prothrombin time
TBil: total bilirubin

XSL•FO
RenderX

Edited by A Coristine; submitted 01.06.25; peer-reviewed by J Song, Z Wu; revised version received 02.10.25; accepted 02.10.25; published 22.10.25.

Please cite as:
Feng LH, Liang H, Hu B, Wei L, Li Q, Su T, Yin Q, Feng Y, Huang L, Liang H, Su M, Jiang J
Development and Validation of an Extra Spindle Pole Bodies–like 1–Based Diagnostic and Prognostic Model for Hepatitis B Virus–Related Hepatocellular Carcinoma: Retrospective Cohort Study
JMIR Med Inform 2025;13:e78354
URL: https://medinform.jmir.org/2025/1/e78354
doi:10.2196/78354

© Lu-Huai Feng, Hengkai Liang, Bobin Hu, Lu Wei, Qingmei Li, Tumei Su, Qianbing Yin, Yanfei Feng, Long Huang, Hongqian Liang, Minghua Su, Jianning Jiang. Originally published in JMIR Medical Informatics (https://medinform.jmir.org), 22.10.2025. This is an open-access article distributed under the terms of the Creative Commons Attribution License (https://creativecommons.org/licenses/by/4.0/), which permits unrestricted use, distribution, and reproduction in any medium, provided the original work, first published in JMIR Medical Informatics, is properly cited. The complete bibliographic information, a link to the original publication on https://medinform.jmir.org/, as well as this copyright and license information must be included.

XSL•FO
RenderX

Development and Validation of a Predictive Model for Severe Tubular Atrophy/Interstitial Fibrosis in Patients with IgA Nephropathy: Multicenter Retrospective Study

Caizheng Yu[1], MS; Zhitong Niu[2], MS; Qin Fang[3], PhD; Qing Lei[4], PhD

[1]Department of Public Health, Tongji Hospital, Tongji Medical College, Huazhong University of Science and Technology, Wuhan, China

[2]Shanxi Bethune Hospital, Shanxi Academy of Medical Sciences, Third Hospital of Shanxi Medical University, Tongj Shanxi Hospital, Taiyuan, China

[3]Department of Medical Affairs, Zhuhai People's Hospital (The Affiliated Hospital of Beijing Institute of Technology, Zhuhai Clinical Medical College of Jinan University), Zhuhai, China

[4]Division of Nephrology, Tongji Hospital, Tongji Medical College, Huazhong University of Science and Technology, 1095 Jiefang Ave, Wuhan, China

Corresponding Author:
Qing Lei, PhD
Division of Nephrology, Tongji Hospital, Tongji Medical College, Huazhong University of Science and Technology, 1095 Jiefang Ave, Wuhan, China

Abstract

Background: Severe tubular atrophy/interstitial fibrosis are critical pathological features associated with poor prognosis in IgA nephropathy (IgAN). The early identification of patients at high risk for severe tubular damage could guide clinical management and improve outcomes.

Objective: This study aimed to construct and validate a predictive model for assessing the risk of severe tubular atrophy and interstitial fibrosis in patients diagnosed with IgAN.

Methods: A total of 3276 patients from the Hankou branch of Tongji Hospital were retrospectively enrolled for model development. A predictive model for severe tubular atrophy/interstitial fibrosis was constructed based on independent predictors identified through univariate analysis, least absolute shrinkage and selection operator regression, and stepwise logistic regression. Furthermore, the model underwent internal and external validation using an independent dataset (n=1062), and performance evaluation using six machine learning algorithms: random forest, generalized linear model, decision tree, gradient boosting decision tree, extreme gradient boosting, and support vector machine.

Results: In this study, 8 variables were identified as independent predictors and used to construct a predictive model for severe tubular atrophy/interstitial fibrosis: Logit (P)=0.011×age (years)+0.324×hypertension history–0.302×education+.111×coefficient of variation of red cell distribution width–0.152×direct bilirubin (μmol/L)+0.003×uric acid (μmol/L)–0.021×estimated glomerular filtration rate (ml/min/1.73m²)+1.151×ln(24 h urine microalbumin) (mg/24h). The AUC for the predictive model was 0.860 (95% CI 0.847 - 0.873). The AUCs (95% CI) of the six machine learning algorithms ranged from 0.793 (0.765 - 0.822) to 0.880 (0.859 - 0.902) in internal validation and from 0.785 (0.756 - 0.814) to 0.862 (0.839 - 0.885) in external validation.

Conclusions: We developed a concise and clinically useful model for predicting severe tubular atrophy/interstitial fibrosis in IgA nephropathy. It offers a non-invasive tool for risk assessment when biopsy is not feasible, aiding personalized treatment decisions.

(JMIR Med Inform 2025;13:e78761) doi:10.2196/78761

KEYWORDS

tubular atrophy/interstitial fibrosis; IgA nephropathy; predictive model; machine learning; internal and external validation

Introduction

Immunoglobulin A nephropathy (IgAN) is the most common form of primary glomerulonephritis worldwide, particularly in China [1,2]. As IgAN progresses, the glomerular filtration rate gradually declines, and approximately 30% - 40% of patients develop end-stage renal disease (ESRD) within 20 to 30 years after the onset of clinical symptoms, imposing a substantial burden on both individuals and health care systems [3,4].

The hallmark pathological feature of IgAN is the deposition of IgA in the glomerular mesangium, and renal biopsy remains the gold standard for diagnosis. According to the current Oxford classification guidelines [5], the pathological lesions in IgAN include mesangial hypercellularity (M), endocapillary hypercellularity (E), segmental glomerulosclerosis (S), tubular

XSL•FO
RenderX

atrophy/interstitial fibrosis (T), and cellular or fibrocellular crescents (C), that is, MEST-C. Among these, tubular atrophy and interstitial fibrosis (T lesions) are considered key prognostic indicators [6]. The Oxford derivation and North American validation studies, along with the VALIGA study, with a median follow-up of 5.6 years, demonstrated that severe tubular atrophy and interstitial fibrosis were significantly associated with an increased risk of renal function decline or progression to ESRD [7]. Similarly, a multicenter retrospective cohort study from China involving 2047 patients with IgAN confirmed that severe tubular atrophy and interstitial fibrosis markedly elevated the risk of renal function deterioration or ESRD [8]. These findings indicated that severe tubular atrophy and interstitial fibrosis might lead to poor prognosis over long-term follow-up. However, renal biopsy is an invasive procedure that requires technical expertise, is costly, and is poorly accepted by patients, making it difficult to perform repeatedly. These limitations hinder its broad application in the long-term management of chronic kidney disease (CKD).

Predictive models are increasingly recognized as valuable tools for early risk stratification, particularly when renal biopsy is infeasible or repeat biopsy is not practical due to clinical or ethical concerns. Such models can facilitate precision medicine by informing treatment decisions, follow-up scheduling, and lifestyle modifications, thereby improving disease management while reducing unnecessary hospitalizations and health care expenditures. However, existing predictive models [8-10] for tubular atrophy and interstitial fibrosis in IgAN are often limited by small sample sizes, lack of validation, and limited feasibility in clinical practice. Therefore, developing a simple, practical, and reliable model to predict tubular atrophy and interstitial fibrosis in patients with IgAN is of great clinical and social importance.

In this study, we aimed to construct a predictive model for tubular atrophy and interstitial fibrosis in IgAN by integrating multidimensional data from hospitalized patients who underwent renal biopsy at the Department of Nephrology, Tongji Hospital. The model was developed using least absolute shrinkage and selection operator (LASSO) regression and logistic regression, and was internally and externally validated using six different machine learning algorithms.

Methods

Study Population

Participants were recruited from three medical centers located in Wuhan, China, including Tongji Hospital Hankou branch (Qiaokou District), the Tongji Hospital Optics Valley branch (Donghu High-Tech Development Zone), and the Tongji Hospital Sino-French New City branch (Caidian District). Demographic characteristics, lifestyle factors, medical history, and laboratory test results were extracted from the electronic medical record system. Specifically, we retrospectively enrolled 3970 patients who were hospitalized in the Department of Nephrology at the Tongji Hospital Hankou branch between 2004 and 2023 and who underwent renal biopsy during hospitalization. The following exclusion criteria were applied: (1) age ≤18 years (n=98); (2) number of glomeruli <8 in the biopsy specimen (n=32); (3) history of tumor or transplantation (n=103); (4) variables with more than 20% missing values were excluded, that is, 66 variables were included; participants with more than 20% missing data among these 66 variables were further excluded (n=461). Finally, 3276 patients were included as the population for model development. The study design flowchart is presented in Figure S1 in Multimedia Appendix 1. An independent validation sample consisting of 1062 patients was enrolled from the Nephrology Divisions of Tongji Hospital's Sino-French New City and Optics Valley branches, who underwent renal biopsy between 2015 and 2023. Detailed exclusion criteria for the validation population are provided in Figure S2 in Multimedia Appendix 1.

Data Collection

With the support of the Big Data Center of Tongji Hospital, data on demographic characteristics (age, sex, education level, height, and weight), lifestyle factors (smoking and alcohol consumption), medical history (hypertension and diabetes), and laboratory test results (blood and urine tests) were extracted from the electronic medical record system. Educational attainment was categorized as "middle school or below" and "high school or above." The BMI was calculated as weight in kilograms divided by height in meters squared. Within 24 hours of hospital admission, fresh whole blood samples were collected from each patient for routine blood tests and assessments of liver function, renal function, lipid profile, and fasting blood glucose levels. In addition, morning urine and 24-hour urine samples were collected during hospitalization for routine urinalysis and 24-hour urine biochemical tests, including urinary protein and renal function markers. All blood and urine examinations were conducted by trained technicians in the clinical laboratory of Tongji Hospital, following uniform testing protocols. To reduce skewness, natural logarithmic transformation was applied to the following variables: urinary creatinine, urine albumin-to-creatinine ratio, urinary micro total protein, urinary microalbumin, 24-hour urine total microprotein, and 24-hour urine microalbumin.

Renal Biopsy Evaluation

All study participants underwent renal biopsy. Each biopsy specimen was subjected to light microscopy, immunofluorescence staining, and electron microscopy examination. For light microscopy analysis, slides were stained with hematoxylin and eosin, periodic acid–Schiff, Masson's trichrome, and silver staining, following standardized protocols. All renal pathology assessments were performed by experienced renal pathologists and classified according to the Oxford MEST-C scoring system for IgAN. Light microscopic findings of IgA nephropathy range from mild mesangial hypercellularity to diffuse mesangial proliferation, which may be accompanied by segmental sclerosis, glomerular adhesions, and/or crescent formation. Immunofluorescence predominantly showed mesangial staining of IgA. Electron microscopy revealed mesangial deposits along with mesangial matrix expansion (Figure S3 in Multimedia Appendix 1). In the MEST-C score, the T component refers to tubular atrophy and interstitial fibrosis: T0 corresponds to ≤25%, T1 to 26% - 50%, and T2 to >50%. In this study, renal biopsy specimens classified as T0

XSL•FO
RenderX

were defined as mild tubular atrophy/interstitial fibrosis, whereas T1 and T2 were grouped as severe tubular atrophy/interstitial fibrosis (Figure S4 in Multimedia Appendix 1).

Statistical Analysis

Data are presented as median (Q1–Q3) for continuous variables and number (%) for categorical variables. The Shapiro-Wilk test was used to assess the normality of all continuous variables. For variables that followed a normal distribution, between-group differences were assessed using the independent samples *t* test; for non-normally distributed variables, the Mann-Whitney *U* test was employed. Variables showing significant between-group differences were further analyzed using least absolute shrinkage and selection operator (LASSO) regression to identify predictors of severe tubular atrophy/interstitial fibrosis. To address multicollinearity and enhance model stability, variables with a variance inflation factor greater than 5 were excluded. Subsequently, stepwise backward logistic regression was performed on the LASSO-selected candidate predictors to determine independent influencing factor for the severity of tubular atrophy/interstitial fibrosis. Model parameters were estimated, and the prediction model was constructed as follows: Logit (P=β0+Variable1 × β1+Variable2 × β2 +…+VariableX×βX). The effects of the predictors on tubular atrophy/interstitial fibrosis severity were visualized using a forest plot. A nomogram was developed to provide a graphical representation of the IgAN tubular atrophy/interstitial fibrosis prediction model. The predictive performance and calibration of the model were evaluated by receiver operating characteristic (ROC) curves, calibration curves, and decision curve analysis (DCA). To evaluate the overall accuracy of the predictive model, we calculated the Brier score, which measures the mean squared difference between the predicted probabilities and the observed outcomes. In addition, the Youden index was used to determine the optimal cutoff value for classification by maximizing the sum of sensitivity and specificity. For internal validation, the development population was randomly split into training and testing sets at a ratio of 7:3. An external validation cohort consisting of 1062 patients hospitalized at the Sino-French New City and Optics Valley branches of Tongji Hospital between 2015 and 2023, who underwent renal biopsy, was used to validate the model's performance.

During both internal and external validations, five-fold cross-validation was conducted combined with six machine learning algorithms—random forest, generalized linear model, decision tree, gradient boosting decision tree, extreme gradient boosting, and support vector machine. Model performance and discriminative ability were assessed using accuracy, precision, recall, F_1-score, area under the ROC curve (AUC), and precision-recall curves. All statistical analyses were performed using R software (version 4.4.1; R Foundation for Statistical Computing). A two-sided *P* value <.05 was considered statistically significant.

Ethical Considerations

This study was approved by the Ethics Committee of Tongji Hospital (approval number: TJ-IRB202410023), and written informed consent was obtained from all participants. In addition, the patient information included in this study has been deidentified. No compensation was provided to any participants.

Results

A total of 3276 hospitalized patients with biopsy-confirmed IgA nephropathy were included in this study. The characteristics of individuals with mild and severe tubular atrophy/interstitial fibrosis are presented in Table 1. Among the 3276 participants, 2086 (63.7%) had mild tubular atrophy/interstitial fibrosis, whereas 1190 (36.3%) had severe tubular atrophy/interstitial fibrosis. Compared to those with mild tubular atrophy/interstitial fibrosis, individuals with severe tubular atrophy/interstitial fibrosis were older, more likely to be male, had lower educational attainment, and exhibited higher proportions of hypertension, diabetes, smoking, and alcohol consumption, as well as higher BMI (all *P*<.05). In addition, significant differences were observed between the two groups in terms of hematological parameters, liver function, renal function, lipid profiles, and glucose metabolism indicators (all *P*<.05).

XSL•FO
RenderX

Table . Characteristics of study individuals and univariates analysis of mild/severe tubular atrophy/interstitial fibrosis groups (n=3276).

Variables	Mild group (n=2086)	Severe group (n=1190)	*P* value
Age, years, median (IQR)	34.0 (27.0 - 43.0)	36.0 (29.0 - 46.0)	<.001
Women, n (%)	1198 (57.4)	592 (49.8)	<.001
Hypertension history, n (%)	558 (26.8)	557 (46.8)	<.001
Diabetes history, n (%)	195 (9.4)	179 (15.0)	<.001
Smoking, n (%)	164 (7.9)	152 (12.8)	<.001
Alcohol consumption, n (%)	116 (5.6)	96 (8.1)	.006
Education (high school or above), n (%)	1420 (68.1)	700 (58.8)	<.001
Systolic blood pressure, mmHg, median (IQR)	124.0 (113.0 - 135.0)	132.0 (120.0 - 144.0)	<.001
Diastolic blood pressure, mmHg, median (IQR)	82.0 (75.0 - 90.0)	86.0 (78.0 - 96.0)	<.001
BMI, kg/m², median (IQR)	22.7 (20.4 - 24.9)	23.1 (20.8 - 26.0)	<.001
White blood cell count, ×10 /L, median (IQR)	6.7 (5.7 - 8.0)	7.0 (5.9 - 8.5)	<.001
Neutrophil percentage, median (IQR)	63.2 (57.4 - 68.8)	64.9 (59.2 - 70.5)	<.001
Neutrophil count, ×10 /L, median (IQR)	4.2 (3.3 - 5.3)	4.5 (3.6 - 5.7)	<.001
Lymphocyte percentage, median (IQR)	27.8 (22.5 - 33.1)	26.1 (20.9 - 30.9)	<.001
Lymphocyte count, ×10 /L, median (IQR)	1.9 (1.5 - 2.2)	1.8 (1.4 - 2.2)	.003
Monocyte percentage, median (IQR)	6.5 (5.4 - 7.8)	6.4 (5.1 - 7.8)	.017
Monocyte count, ×10 /L, median (IQR)	0.4 (0.4 - 0.6)	0.4 (0.4 - 0.6)	.122
Eosinophil percentage, median (IQR)	1.5 (0.9 - 2.4)	1.6 (0.9 - 2.7)	.030
Eosinophil count, ×10 /L, median (IQR)	0.1 (0.1 - 0.2)	0.1 (0.1 - 0.2)	.018
Basophil percentage, median (IQR)	0.3 (0.2 - 0.5)	0.3 (0.2 - 0.5)	.421
Basophil count, ×10 /L, median (IQR)	0.0 (0.0 - 0.0)	0.0 (0.0 - 0.0)	.064
Red blood cell count, $\times 10^{12}$/L, median (IQR)	4.4 (4.0 - 4.9)	4.3 (3.8 - 4.7)	<.001
Hemoglobin, g/L, median (IQR)	132.0 (120.0 - 145.0)	125.0 (111.0 - 140.0)	<.001
Hematocrit percentage, median (IQR)	39.1 (35.8 - 42.6)	37.2 (33.4 - 41.4)	<.001
MCV[a], fL, median (IQR)	88.3 (85.6 - 91.1)	88.2 (85.2 - 91.1)	.223
MCH[b], pg, median (IQR)	29.9 (28.7 - 30.9)	29.9 (28.7 - 30.8)	.931
MCHC[c], g/L, median (IQR)	337.0 (328.0 - 345.0)	337.0 (328.0 - 346.0)	.583
RDW-CV[d], median (IQR)	12.6 (12.1 - 13.2)	12.8 (12.2 - 13.5)	<.001
RDW-SD[e], fL, median (IQR)	40.5 (38.7 - 42.6)	40.8 (39.0 - 43.1)	<.001
Platelet count, ×10 /L, median (IQR)	226.0 (187.3 - 271.0)	229.0 (185.0 - 271.0)	.552
Platelet distribution width, fL, median (IQR)	12.8 (11.4 - 14.8)	12.8 (11.4 - 14.7)	.900

XSL•FO
RenderX

Variables	Mild group (n=2086)	Severe group (n=1190)	*P* value
Mean platelet volume, fL, median (IQR)	10.6 (9.9 - 11.4)	10.7 (10.0 - 11.5)	.538
Large platelet ratio, %, median (IQR)	30.7 (25.3 - 37.6)	31.1 (25.3 - 37.4)	.911
Plateletcrit, %, median (IQR)	0.2 (0.2 - 0.3)	0.2 (0.2 - 0.3)	.905
ALT[f], U/L, median (IQR)	14.0 (11.0 - 22.0)	14.0 (10.0 - 21.0)	.361
AST[g], U/L, median (IQR)	18.0 (15.0 - 21.0)	18.0 (15.0 - 22.0)	.602
Total protein, g/L, median (IQR)	71.7 (67.4 - 75.6)	68.8 (63.2 - 73.0)	<.001
Albumin, g/L, median (IQR)	42.2 (38.9 - 45.2)	39.3 (35.3 - 42.8)	<.001
Globulin, g/L, median (IQR)	29.2 (26.9 - 31.8)	28.9 (26.3 - 32.0)	.077
Total bilirubin, µmol/L, median (IQR)	7.7 (5.5 - 10.3)	6.6 (4.5 - 9.3)	<.001
Direct bilirubin, µmol/L, median (IQR)	2.4 (1.9 - 3.3)	2.1 (1.6 - 2.9)	<.001
Indirect bilirubin, µmol/L, median (IQR)	5.4 (3.6 - 7.5)	4.9 (3.1 - 7.1)	<.001
ALP[h], U/L, median (IQR)	60.0 (50.0 - 74.0)	61.0 (50.0 - 75.0)	.692
GGT[i], U/L, median (IQR)	17.0 (13.0 - 25.0)	19.0 (13.3 - 28.0)	<.001
Total cholesterol, mmol/L, median (IQR)	4.4 (3.8 - 5.0)	4.6 (3.9 - 5.5)	<.001
Triglycerides, mmol/L, median (IQR)	1.4 (1.0 - 2.1)	1.8 (1.2 - 2.6)	<.001
High-density lipoprotein, mmol/L, median (IQR)	1.1 (1.0 - 1.4)	1.1 (0.9 - 1.3)	<.001
Low-density lipoprotein, mmol/L, median (IQR)	2.6 (2.1 - 3.1)	2.8 (2.2 - 3.5)	<.001
Urea, mmol/L, median (IQR)	5.1 (4.1 - 6.2)	6.8 (5.2 - 9.1)	<.001
Serum creatinine, µmol/L, median (IQR)	80.0 (64.0 - 100.0)	116.5 (84.0 - 165.0)	<.001
Uric acid, µmol/L, median (IQR)	333.0 (272.9 - 402.0)	394.0 (328.8 - 473.9)	<.001
eGFR[j], ml/min/1.73 m², median (IQR)	96.5 (75.5 - 115.2)	61.4 (40.0 - 90.5)	<.001
Erythrocyte sedimentation rate, mm/h, median (IQR)	8.0 (4.0 - 14.0)	13.0 (6.0 - 26.0)	<.001
Fasting blood glucose, mmol/L, median (IQR)	5.3 (4.9 - 6.0)	5.4 (4.9 - 6.3)	<.001
ALT/AST ratio, median (IQR)	0.8 (0.7 - 1.1)	0.8 (0.6 - 1.1)	.256
Albumin/Globulin ratio, median (IQR)	1.4 (1.3 - 1.6)	1.3 (1.2 - 1.5)	<.001
ln(Urinary creatinine), µmol/L, median (IQR)	9.5 (9.0 - 9.9)	9.2 (8.8 - 9.6)	<.001
ln(Urine albumin-to-creatinine ratio), µg/mg, median (IQR)	5.8 (5.0 - 6.6)	6.9 (6.1 - 7.7)	<.001
ln(Urinary micro total protein), mg/L, median (IQR)	6.4 (5.8 - 7.1)	7.3 (6.6 - 7.9)	<.001
ln(Urinary microalbumin), mg/L, median (IQR)	6.1 (5.3 - 6.8)	7.0 (6.3 - 7.6)	<.001
ln(24 h urine total microprotein), mg/24 h, median (IQR)	6.4 (5.8 - 6.9)	7.4 (7.0 - 7.9)	<.001

XSL•FO
RenderX

Variables	Mild group (n=2086)	Severe group (n=1190)	*P* value
ln(24 h urine microalbumin), mg/24 h, median (IQR)	6.0 (5.3 - 6.6)	7.2 (6.7 - 7.7)	<.001
Urine pH, median (IQR)	6.0 (5.5 - 6.5)	6.0 (5.5 - 6.5)	.060
Urine specific gravity, median (IQR)	1.0 (1.0 - 1.0)	1.0 (1.0 - 1.0)	.003
Urinary red blood cell count/μL, median (IQR)	35.7 (12.2 - 112.4)	28.1 (9.7 - 76.4)	<.001
Urinary white blood cell count/μL, median (IQR)	7.8 (3.6 - 19.5)	7.3 (3.4 - 17.0)	.065

[a]MCV: Mean corpuscular volume.

[b]MCH: Mean corpuscular hemoglobin.

[c]MCHC: Mean corpuscular hemoglobin concentration.

[d]RDW-CV: coefficient of variation of red blood cell volume size.

[e]RDW-SD: standard deviation of red blood cell distribution width.

[f]ALT: Alanine aminotransferase.

[g]AST: Aspartate aminotransferase.

[h]ALP: Alkaline phosphatase.

[i]GGT: Gamma-glutamyl transferase.

[j]eGFR: Estimated glomerular filtration rate.

Univariate analysis revealed that 48 out of 66 analyzed variables showed statistically significant differences between the mild and severe tubular atrophy/interstitial fibrosis groups. These 48 variables were subsequently included in a LASSO regression model to reduce dimensionality and identify potential predictors. The LASSO analysis yielded 35 candidate predictors (Figure S5 in Multimedia Appendix 1). To further reduce multicollinearity and enhance model stability, variables with a variance inflation factor greater than 5 were excluded, resulting in 31 remaining candidate predictors (Figure S6 in Multimedia Appendix 1). Furthermore, these 31 predictors were then subjected to stepwise backward logistic regression analysis. Eight variables were ultimately identified as independent predictors of severe tubular atrophy/interstitial fibrosis: age (OR 1.011; 95% CI 1.002 - 1.020; *P*=.021), hypertension history (OR 1.383; 95% CI 1.144 - 1.672; *P*<.001), education (high school or above; OR 0.739; 95% CI 0.607 - 0.900; *P*=.003), coefficient of variation of red blood cell volume size (red cell distribution width-CV; OR 1.117; 95% CI 1.048 - 1.190; *P*<.001), direct bilirubin (OR 0.859; 95% CI 0.802 - 0.920; *P*<.001), uric acid (OR 1.003; 95% CI 1.002 - 1.004; *P*<.001), estimated glomerular filtration rate (eGFR; OR 0.979; 95% CI 0.976 - 0.982; *P*<.001), and ln(24-hour urine microalbumin) (OR 3.161; 95% CI 2.843 - 3.513; *P*<.001; Figure 1).

Based on these eight independent predictors, a logistic regression model was constructed to predict severe tubular atrophy/interstitial fibrosis. The final model equation was as follows: Logit (P)=0.011×age (years)+0.324×hypertension history –0.302×education+.111×red cell distribution width-CV –0.152×direct bilirubin (μmol/L)+0.003×uric acid (μmol/L) –0.021×eGFR (ml/min/1.73m²)+1.151×ln(24 h urine microalbumin) (mg/24h). In this equation, hypertension history was coded as 0=no, 1=yes; education level was coded as 0=junior high school or below, 1=high school or above. The predicted probability *P* ranges between 0 and 1. To facilitate clinical application, a nomogram was developed based on the final model (Figure 2). The nomogram included a point scale (0 - 100 points), the eight independent predictors, a total score axis (0 - 240 points), a linear predictor axis, and the predicted probability of severe tubular atrophy/interstitial fibrosis. This provided an intuitive and user-friendly visualization of the contribution of each predictor to the risk of severe tubular atrophy/interstitial fibrosis.

XSL•FO
RenderX

Figure 1. Forest plot of independent predictors for severe tubular atrophy/interstitial fibrosis identified on logistic regression analysis.

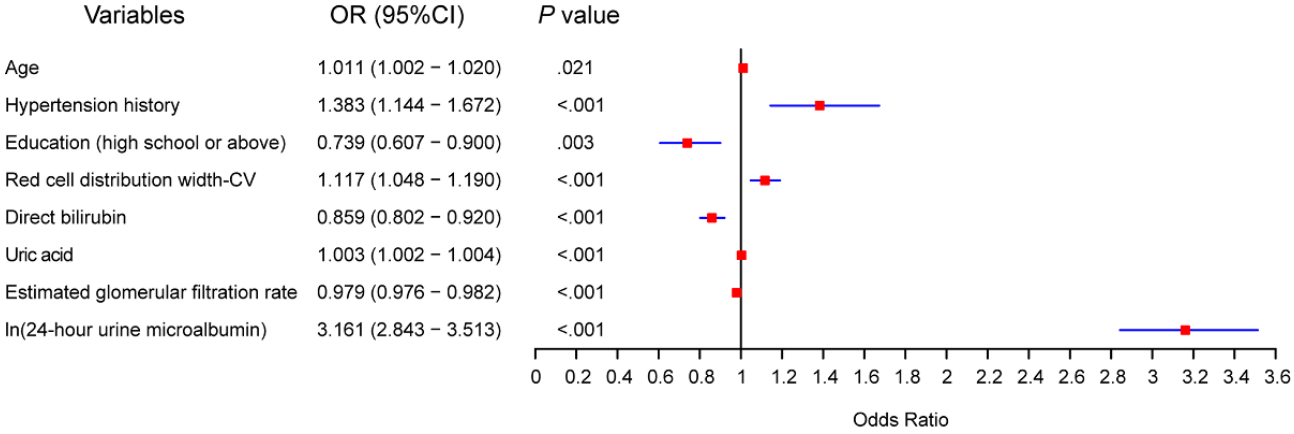
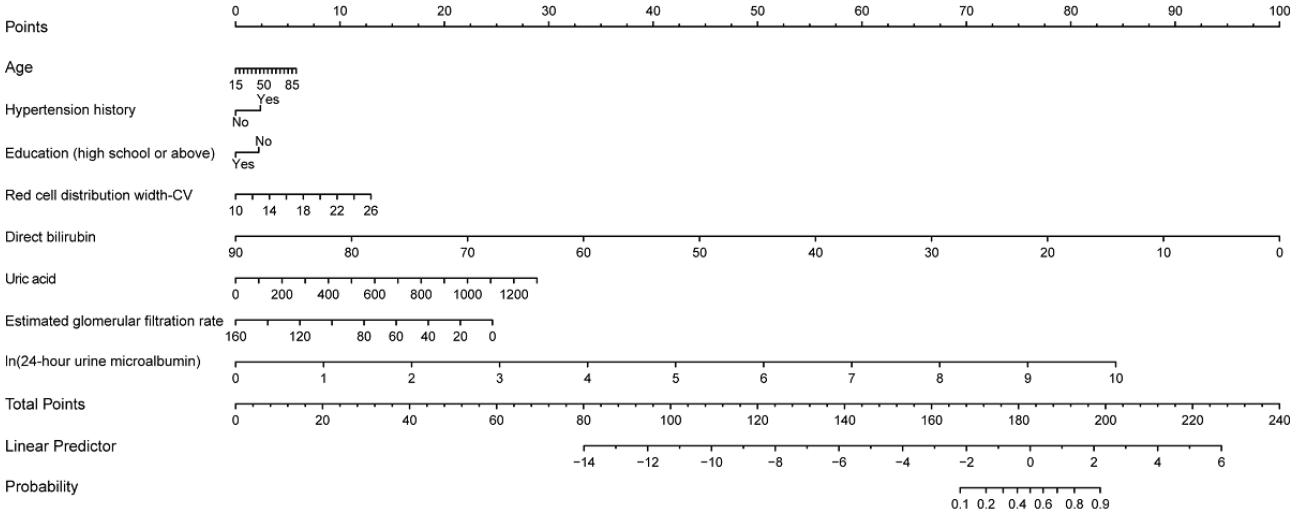


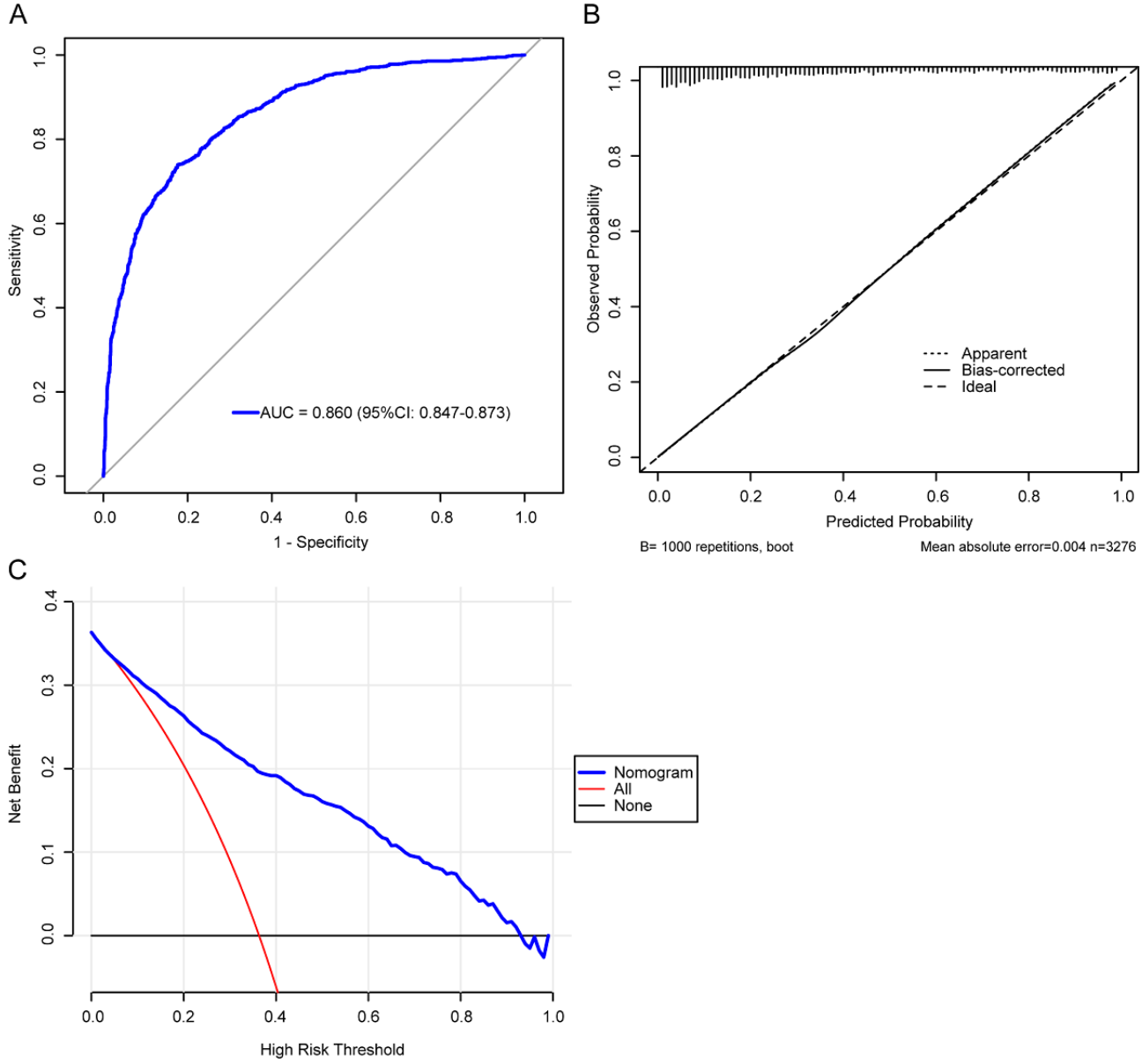
Figure 2. Nomogram for predicting the risk of severe tubular atrophy/interstitial fibrosis.



Model performance was evaluated using ROC, calibration plots, and DCA. The AUC for the logistic model was 0.860 (Figure 3A), indicating excellent discriminative ability. The calibration curve closely followed the diagonal line (y=x), with a mean absolute error of 0.004, suggesting a high agreement between predicted and observed risks (Figure 3B). DCA demonstrated favorable net benefits across a range of threshold probabilities from 0 to 1 (Figure 3C). The optimal cutoff value determined by the Youden index was 0.407, yielding a sensitivity of 73.9% and a specificity of 82.4%. Accordingly, patients with predicted probabilities ≥0.407 were classified as high risk for severe tubular atrophy and interstitial fibrosis. The Brier score was 0.143, indicating good calibration and probability prediction performance of the model. Internal and external validation of the prediction model was further performed using six machine learning algorithms. In internal validation, the AUCs (95% CI) of the ROC curves ranged from 0.793 (0.765 - 0.822) to 0.880 (0.859 - 0.902), while those of the precision-recall curves ranged from 0.748 (0.698 - 0.792) to 0.813 (0.776 - 0.845; Figure 4A and C). In external validation, ROC AUCs (95% CI) ranged from 0.785 (0.756 - 0.814) to 0.862 (0.839 - 0.885) and precision-recall AUCs from 0.655 (0.603 - 0.704) to 0.720 (0.664 - 0.776; Figure 4B and D). As summarized in Table 2, the logistic regression model demonstrated robust classification performance, with consistently high accuracy, precision, F_1-score, and recall across both internal and external validation datasets. All six machine learning models exhibited comparable performances. During internal validation, accuracy ranged from 0.758 to 0.783, with recall values consistently high (0.742 - 0.896). The model with the highest accuracy (0.783) also achieved the best F_1-score (0.747) and recall (0.896). In external validation, the model accuracy ranged from 0.721 to 0.757, and recall remained satisfactory (0.754 - 0.870). The top-performing model yielded an F_1-score of 0.698 and a recall of 0.862, indicating good generalizability. Despite minor variations across models, precision was generally lower than recall in both validation sets, suggesting a trade-off between false positives and sensitivity.

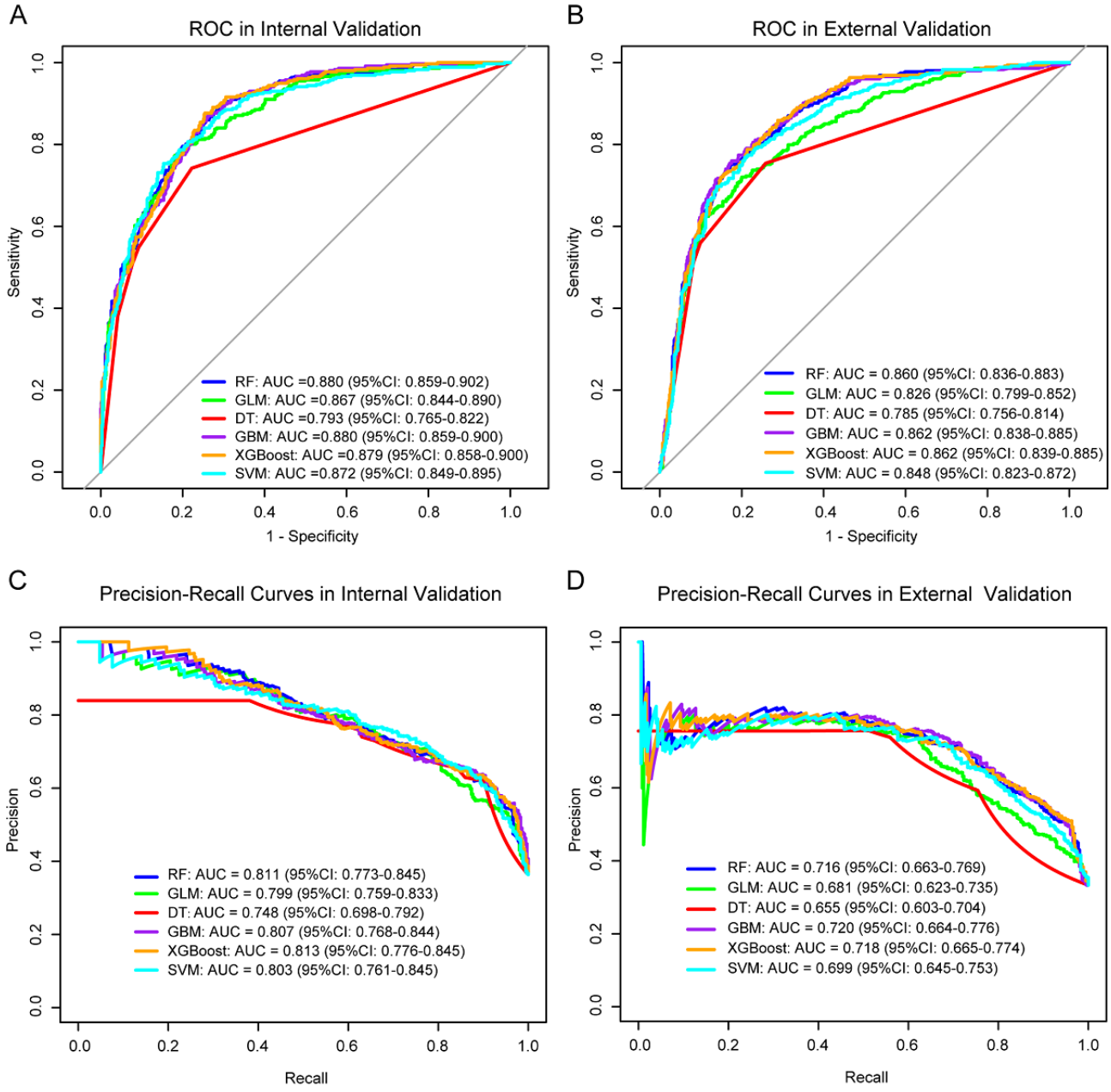
XSL•FO
RenderX

Figure 3. Performance evaluation of the predictive model for severe tubular atrophy/interstitial fibrosis. (A) Receiver operating characteristic (ROC) curve assessing the discrimination ability of the model. (B) Calibration curve evaluating the agreement between predicted and observed outcomes. (C) Decision curve analysis (DCA) demonstrating the net clinical benefit across different threshold probabilities.



XSL•FO
RenderX

Figure 4. Internal and external validation of severe tubular atrophy/interstitial fibrosis using six machine learning algorithms. (A) Receiver operating characteristic (ROC) curves in internal validation. (B) ROC curves in external validation. (C) Precision-recall curves in internal validation. (D) Precision-recall curves in external validation. RF: random forest; GLM: generalized linear model; DT: decision tree, GBM: gradient boosting decision tree; XGBoost: extreme gradient boosting; SVM: support vector machine.



XSL•FO
RenderX

Table . Performance metrics of six machine learning models in internal and external validation.

Models	Accuracy	Precision	F_1-score	Recall
Internal validation				
RF[a]	0.775	0.635	0.743	0.896
GLM[b]	0.758	0.624	0.716	0.840
DT[c]	0.765	0.656	0.696	0.742
GBM[d]	0.778	0.643	0.742	0.877
XGBoost[e]	0.783	0.648	0.747	0.882
SVM[f]	0.777	0.654	0.728	0.821
External validation				
RF	0.748	0.581	0.697	0.870
GLM	0.721	0.558	0.654	0.791
DT	0.746	0.593	0.664	0.754
GBM	0.750	0.586	0.696	0.856
XGBoost	0.751	0.587	0.698	0.862
SVM	0.757	0.600	0.691	0.814

[a]RF: random forest.

[b]GLM: generalized linear model.

[c]DT: decision tree.

[d]GBM: gradient boosting decision tree.

[e]XGBoost: extreme gradient boosting.

[f]SVM: support vector machine.

Discussion

Principal Findings and Comparison With Previous Work

This study developed and validated a predictive model for severe tubular atrophy/interstitial fibrosis in hospitalized patients with IgA nephropathy at Tongji Hospital, based on multidimensional clinical data. The model was successfully constructed using 8 independent predictors significantly associated with severe tubular atrophy/interstitial fibrosis: age, hypertension history, education, red cell distribution width-CV, direct bilirubin, uric acid, eGFR, and ln(24-hour urine microalbumin). This model holds substantial clinical value in early diagnosis and screening, clinical decision-making, personalized treatment planning, and pathological monitoring in renal transplant recipients.

In line with previous studies, age and hypertension were identified as independent risk factors for severe tubular atrophy/interstitial fibrosis, highlighting their pivotal roles in CKD progression [11-14]. Advancing age is typically associated with a decline in nephron number, increased glomerulosclerosis, and exacerbated interstitial fibrosis [11,12]. Moreover, age-related inflammatory processes may contribute to irreversible structural kidney damage. Hypertension, a major driver of CKD progression, may promote ischemic injury in renal microvasculature and activate pro-fibrotic pathways, thereby accelerating tubular atrophy/interstitial fibrosis [13,15]. Interestingly, a higher education level (high school or above) was inversely associated with severe tubular atrophy/interstitial fibrosis. Previous cohort and Mendelian randomization studies have demonstrated a causal relationship between lower educational attainment and both increased risk of chronic kidney disease and reduced eGFR [16-18]. These data indicated that higher educational attainment might indeed play a role in preserving kidney function, including structural injury such as tubular atrophy and interstitial fibrosis. It was unlikely that education level directly influences tubular damage or fibrosis. Rather, it might act as a proxy for a range of interconnected downstream factors. Individuals with a higher education might have better health literacy, medication adherence, and proactive engagement with health care systems, enabling the earlier identification and management of modifiable risk factors like hypertension, diabetes, and metabolic syndrome [19]. Furthermore, prior studies have suggested that a low educational attainment might amplify the genetic risk for reduced eGFR [17], offering a potential mechanistic link from a genetic–environmental interaction perspective. Together, these findings support the plausibility that the education level is indirectly associated with tubular atrophy/interstitial fibrosis severity through both environmental and genetic pathways.

In this study, we observed that higher levels of RDW-CV were positively associated with tubular atrophy and interstitial fibrosis. RDW-CV, an index reported in the routine complete blood count test, reflects the variation in red blood cell size and is an established marker of erythrocyte volume heterogeneity. It has been linked to systemic inflammation and oxidative stress

XSL•FO
RenderX

in various chronic diseases [20]. A large population-based cohort study revealed a strong graded association between RDW and C-reactive protein, which remained significant even after adjusting for multiple confounding factors [21]. Chronic inflammation and subsequent oxidative stress are thought to be key mediators linking elevated RDW to kidney injury [22]. In renal tissue, persistent inflammation and oxidative stress can activate NF-κB pathways, promoting fibroblast proliferation and extracellular matrix deposition [23,24]. Direct bilirubin, an endogenous antioxidant, has recently gained attention for its anti-inflammatory and anti-fibrotic properties. Mildly elevated bilirubin levels might confer protective effects against several chronic conditions, including diabetic nephropathy, metabolic syndrome, cardiovascular disease, and cancer [25-28]. For instance, a large cohort study demonstrated an inverse association between plasma bilirubin levels and all-cause mortality [29]. Mechanistically, bilirubin can modulate immune responses by influencing the expression of cell adhesion molecules and complement activity, as well as by inhibiting T cell differentiation [30]. It also suppresses the release of cytokines such as IL-2, IL-6, IL-10, and tumor necrosis factor-α, and reduces the expression of major histocompatibility complex class II in macrophages [25], thereby contributing to its immunomodulatory and anti-inflammatory effects. Additionally, bilirubin could alleviate renal inflammation and fibrosis through suppression of oxidative stress, inhibition of NADPH oxidase, and blockade of the TGF-β signaling pathway [25,31]. The inverse association observed in this study supports its potential nephroprotective role.

Elevated serum uric acid levels were known to exert pro-inflammatory effects and can induce tubular epithelial cell apoptosis and epithelial-to-mesenchymal transition [32,33]. In this study, we observed a positive association between serum uric acid levels and the severity of tubular atrophy and interstitial fibrosis. Consistent with our findings, previous studies have also reported that elevated serum uric acid contributes to the progression of renal dysfunction [34]. Several potential mechanisms might underlie this association. For instance, the accumulation of uric acid has been reported to induce mast cell degranulation and stimulate renin secretion, which subsequently enhances angiotensin II production and contributes to oxidative stress within renal tissue [35]. Animal studies have demonstrated that uric acid promotes interstitial damage and fibrosis through the activation of the NLRP3 inflammasome and ROS signaling pathways [36,37]. Clinically, hyperuricemia has been consistently associated with poor outcomes in IgAN [38]. Furthermore, both eGFR and 24-hour urinary microalbumin are established biomarkers reflecting glomerular and tubular damage [39,40]. Persistent microalbuminuria might indicate impaired tubular reabsorption and increased local inflammation. The predictive value of these markers for tubular atrophy/interstitial fibrosis was further corroborated in this study.

Limitations

Although the study benefits from a relatively large sample size, strong statistical foundations, and clinical relevance, several limitations should be acknowledged. First, data were derived from three medical centers affiliated with Tongji Hospital in Wuhan, and although both internal and external validations were conducted, further validation in multi-center cohorts is necessary to assess the model's generalizability. Second, the cross-sectional nature of the biopsy-based design limits the ability to predict the progression of tubular atrophy/interstitial fibrosis over time. Third, although our model included a comprehensive set of routinely available clinical and laboratory variables, key factors such as diabetes subtype, medication use (such as renin-angiotensin system inhibitors or immunosuppressants), and kidney imaging data were not captured in our dataset. The absence of these variables might have limited the model's predictive accuracy and clinical interpretability. Future studies integrating multicenter cohorts, longitudinal follow-up, and additional biomarkers, medication history, or imaging features are needed to improve the model's external validity and clinical applicability.

Conclusions

In summary, this study developed a concise, accurate, and clinically interpretable predictive model for severe tubular atrophy/interstitial fibrosis in patients with IgA nephropathy, integrating multi-center data and machine learning techniques. This tool offers a non-invasive alternative for risk stratification of patients in whom renal biopsy is contraindicated or impractical, providing valuable support for clinical decision-making and promoting individualized management strategies.

Acknowledgments

This work was supported by the National Natural Science Foundation (grant NSFC-82302065).

Data Availability

The data in the current study can be obtained from the corresponding author upon a justified and reasonable request.

Authors' Contributions

Conceptualization: CY, ZN, QF, QL.
Methodology: CY, ZN, QF, QL.
Formal analysis: CY.
Writing and editing: CY, ZN, QF, QL.

XSL•FO
RenderX

Conflicts of Interest

None declared.

Multimedia Appendix 1
Study and external validation flowcharts and supplementary materials regarding histopathological findings, least absolute shrinkage and selection operator regression findings, and variable inflation factor rankings.
[DOCX File, 2379 KB - medinform_v13i1e78761_app1.docx]

References

1. Pattrapornpisut P, Avila-Casado C, Reich HN. IgA nephropathy: core curriculum 2021. Am J Kidney Dis 2021 Sep;78(3):429-441. [doi: 10.1053/j.ajkd.2021.01.024] [Medline: 34247883]
2. Lai KN, Tang SCW, Schena FP, et al. IgA nephropathy. Nat Rev Dis Primers 2016 Feb 11;2:16001. [doi: 10.1038/nrdp.2016.1] [Medline: 27189177]
3. Faucon AL, Lando S, Chrysostomou C, et al. Primary glomerular diseases and long-term adverse health outcomes: a nationwide cohort study. J Intern Med 2025 Jan;297(1):22-35. [doi: 10.1111/joim.20024] [Medline: 39537335]
4. Ghaddar M, Canney M, Barbour SJ. IgA nephropathy: epidemiology and disease risk across the world. Semin Nephrol 2024 Sep;44(5):151564. [doi: 10.1016/j.semnephrol.2025.151564] [Medline: 40082162]
5. Trimarchi H, Barratt J, Cattran DC, et al. Oxford classification of IgA nephropathy 2016: an update from the IgA nephropathy classification working group. Kidney Int 2017 May;91(5):1014-1021. [doi: 10.1016/j.kint.2017.02.003] [Medline: 28341274]
6. Pawluczyk IZA, Soares MSF, Barratt WA, et al. Macrophage interactions with collecting duct epithelial cells are capable of driving tubulointerstitial inflammation and fibrosis in immunoglobulin A nephropathy. Nephrol Dial Transplant 2020 Nov 1;35(11):1865-1877. [doi: 10.1093/ndt/gfaa079] [Medline: 32830258]
7. Barbour SJ, Espino-Hernandez G, Reich HN, et al. The MEST score provides earlier risk prediction in lgA nephropathy. Kidney Int 2016 Jan;89(1):167-175. [doi: 10.1038/ki.2015.322] [Medline: 26759049]
8. Chen T, Li X, Li Y, et al. Prediction and risk stratification of kidney outcomes in IgA nephropathy. Am J Kidney Dis 2019 Sep;74(3):300-309. [doi: 10.1053/j.ajkd.2019.02.016] [Medline: 31031086]
9. González Rodríguez J, Valdivielso JM, Jatem Escalante E, et al. Development of a multiple urinary biomarker model to predict the tubulointerstitial fibrosis area in patients with primary IgA nephropathy. BMC Nephrol 2025 Mar 20;26(1):141. [doi: 10.1186/s12882-025-04049-8] [Medline: 40114119]
10. Zhao W, Jiang J, Chen W. Plasma neutrophil gelatinase-associated lipocalin predicts renal tubulointerstitial injury in patients with IgA nephropathy. Clin Nephrol 2024 Jan;101(1):1-8. [doi: 10.5414/CN111270] [Medline: 37942929]
11. McGarvey C, Doyle K, Roche A, et al. Age-related physiological and molecular biomarkers associated with kidney function: a systematic review and meta-analysis. QJM 2025 May 10:hcaf111. [doi: 10.1093/qjmed/hcaf111] [Medline: 40347465]
12. Muglia L, Di Dio M, Filicetti E, et al. Biomarkers of chronic kidney disease in older individuals: navigating complexity in diagnosis. Front Med (Lausanne) 2024;11:1397160. [doi: 10.3389/fmed.2024.1397160] [Medline: 39055699]
13. Tang H, Li K, Shi Z, Wu J. G-Protein-coupled receptors in chronic kidney disease induced by hypertension and diabetes. Cells 2025 May 16;14(10):10. [doi: 10.3390/cells14100729] [Medline: 40422232]
14. Meyrier A. Nephrosclerosis: update on a centenarian. Nephrol Dial Transplant 2015 Nov;30(11):1833-1841. [doi: 10.1093/ndt/gfu366] [Medline: 25488894]
15. Kohagura K, Zamami R, Oshiro N, Shinzato Y, Uesugi N. Heterogeneous afferent arteriolopathy: a key concept for understanding blood pressure-dependent renal damage. Hypertens Res 2024 Dec;47(12):3383-3396. [doi: 10.1038/s41440-024-01916-z] [Medline: 39379463]
16. Thio CHL, Vart P, Kieneker LM, Snieder H, Gansevoort RT, Bültmann U. Educational level and risk of chronic kidney disease: longitudinal data from the PREVEND study. Nephrol Dial Transplant 2020 Jul 1;35(7):1211-1218. [doi: 10.1093/ndt/gfy361] [Medline: 30541108]
17. Thio CHL, van Zon SKR, van der Most PJ, Snieder H, Bültmann U, Gansevoort RT. Associations of genetic factors, educational attainment, and their interaction with kidney function outcomes. Am J Epidemiol 2021 May 4;190(5):864-874. [doi: 10.1093/aje/kwaa237] [Medline: 33089864]
18. Wang Y, Chen M, Wang L, Wu Y. Cardiometabolic traits mediating the effect of education on the risk of DKD and CKD: a Mendelian randomization study. Front Nutr 2024;11:1400577. [doi: 10.3389/fnut.2024.1400577]
19. Cao M, Tang B, Yang L, Zeng J. Machine learning-based prediction model for cognitive impairment risk in patients with chronic kidney disease. PLoS ONE 2025;20(6):e0324632. [doi: 10.1371/journal.pone.0324632] [Medline: 40472303]
20. Xu B, Zhang Y, Chen G, Feng J, Gan L. Association of mean platelet volume/lymphocyte ratio with inflammation in non-dialysis patients with chronic kidney disease stages 1–4: A retrospective study. Front Immunol 2022;13:1041356. [doi: 10.3389/fimmu.2022.1041356]
21. Lippi G, Targher G, Montagnana M, Salvagno GL, Zoppini G, Guidi GC. Relation between red blood cell distribution width and inflammatory biomarkers in a large cohort of unselected outpatients. Arch Pathol Lab Med 2009 Apr;133(4):628-632. [doi: 10.5858/133.4.628] [Medline: 19391664]

XSL•FO
RenderX

22. Semba RD, Patel KV, Ferrucci L, et al. Serum antioxidants and inflammation predict red cell distribution width in older women: the women's health and aging study I. Clin Nutr 2010 Oct;29(5):600-604. [doi: 10.1016/j.clnu.2010.03.001] [Medline: 20334961]
23. Hiscott J, Kwon H, Génin P. Hostile takeovers: viral appropriation of the NF-kappaB pathway. J Clin Invest 2001 Jan;107(2):143-151. [doi: 10.1172/JCI11918] [Medline: 11160127]
24. Owoicho O, Tapela K, Olwal CO, Djomkam Zune AL, Nganyewo NN, Quaye O. Red blood cell distribution width as a prognostic biomarker for viral infections: prospects and challenges. Biomark Med 2022 Jan;16(1):41-50. [doi: 10.2217/bmm-2021-0364] [Medline: 34784758]
25. Bianco A, Tiribelli C, Bellarosa C. Translational approach to the protective effect of bilirubin in diabetic kidney disease. Biomedicines 2022 Mar 17;10(3):696. [doi: 10.3390/biomedicines10030696] [Medline: 35327498]
26. Wagner KH, Wallner M, Mölzer C, et al. Looking to the horizon: the role of bilirubin in the development and prevention of age-related chronic diseases. Clin Sci (Lond) 2015 Jul;129(1):1-25. [doi: 10.1042/CS20140566] [Medline: 25881719]
27. Gazzin S, Vitek L, Watchko J, Shapiro SM, Tiribelli C. A novel perspective on the biology of bilirubin in health and disease. Trends Mol Med 2016 Sep;22(9):758-768. [doi: 10.1016/j.molmed.2016.07.004] [Medline: 27515064]
28. Vítek L. Bilirubin and atherosclerotic diseases. Physiol Res 2017 Apr 5;66(Suppl 1):S11-S20. [doi: 10.33549/physiolres.933581] [Medline: 28379026]
29. Vitek L, Hubacek JA, Pajak A, et al. Association between plasma bilirubin and mortality. Ann Hepatol 2019;18(2):379-385. [doi: 10.1016/j.aohep.2019.02.001] [Medline: 31054979]
30. Durante W. Protective role of heme oxygenase-1 against inflammation in atherosclerosis. In: Biosci F, editor. Front Biosci (Landmark Ed) 2011 Jun 1;16(6):2372-2388. [doi: 10.2741/3860] [Medline: 21622183]
31. Vítek L. Bilirubin as a signaling molecule. Med Res Rev 2020 Jul;40(4):1335-1351. [doi: 10.1002/med.21660] [Medline: 32017160]
32. Wei X, Zhang M, Huang S, et al. Hyperuricemia: a key contributor to endothelial dysfunction in cardiovascular diseases. FASEB J 2023 Jul;37(7):e23012. [doi: 10.1096/fj.202300393R] [Medline: 37272854]
33. Kano Y, Tanabe K, Kitagawa M, et al. Serum uric acid level is associated with renal arteriolar hyalinosis and predicts post-donation renal function in living kidney donors. PLoS ONE 2025;20(3):e0320482. [doi: 10.1371/journal.pone.0320482] [Medline: 40131973]
34. Weaver DJ. Uric acid and progression of chronic kidney disease. Pediatr Nephrol 2019 May;34(5):801-809. [doi: 10.1007/s00467-018-3979-2] [Medline: 29931555]
35. Zhang M, Cui R, Zhou Y, et al. Uric acid accumulation in the kidney triggers mast cell degranulation and aggravates renal oxidative stress. Toxicology 2023 Jan 1;483:153387. [doi: 10.1016/j.tox.2022.153387] [Medline: 36464070]
36. Xu X, Zhang J, Wu Y. Roles of serum NLRP3 inflammasome and associated cytokines in gout-induced kidney injury. Kidney Blood Press Res 2025;50(1):341-350. [doi: 10.1159/000545492] [Medline: 40258359]
37. Yin W, Zhou QL, OuYang SX, Chen Y, Gong YT, Liang YM. Uric acid regulates NLRP3/IL-1β signaling pathway and further induces vascular endothelial cells injury in early CKD through ROS activation and K+ efflux. BMC Nephrol 2019 Aug 14;20(1):319. [doi: 10.1186/s12882-019-1506-8] [Medline: 31412804]
38. Russo E, Drovandi S, Salvidio G, et al. Increased serum uric acid levels are associated to renal arteriolopathy and predict poor outcome in IgA nephropathy. Nutr Metab Cardiovasc Dis 2020 Nov 27;30(12):2343-2350. [doi: 10.1016/j.numecd.2020.07.038] [Medline: 32912790]
39. Mekonnen BW, Holness JL, Berndorfler BD, Lombard C, Warwick JM. Individualized calibration of estimated glomerular filtration rate for serial renal function determination: a pilot study. Sci Rep 2025 May 27;15(1):18523. [doi: 10.1038/s41598-025-03561-z] [Medline: 40425768]
40. Stevens PE, Ahmed SB, Carrero JJ, et al. KDIGO 2024 clinical practice guideline for the evaluation and management of chronic kidney disease. Kidney Int 2024 Apr;105(4):S117-S314. [doi: 10.1016/j.kint.2023.10.018]

Abbreviations

AUC: area under the receiver operating characteristic curve
CKD: chronic kidney disease
DCA: decision curve analysis
eGFR: estimated glomerular filtration rate
ESRD: end-stage renal disease
IgAN: immunoglobulin A nephropathy
LASSO: least absolute shrinkage and selection operator
MEST-C: hypercellularity, endocapillary hypercellularity, segmental glomerulosclerosis, tubular atrophy/interstitial fibrosis, and cellular or fibrocellular crescents
ROC: receiver operating characteristic

XSL•FO
RenderX

Edited by A Benis; submitted 09.06.25; peer-reviewed by J Wan, J Zhao, Y Gao; revised version received 09.10.25; accepted 13.10.25; published 28.10.25.

Please cite as:
Yu C, Niu Z, Fang Q, Lei Q
Development and Validation of a Predictive Model for Severe Tubular Atrophy/Interstitial Fibrosis in Patients with IgA Nephropathy: Multicenter Retrospective Study
JMIR Med Inform 2025;13:e78761
URL: https://medinform.jmir.org/2025/1/e78761
doi:10.2196/78761

© Caizheng Yu, Zhitong Niu, Qin Fang, Qing Lei. Originally published in JMIR Medical Informatics (https://medinform.jmir.org), 28.10.2025. This is an open-access article distributed under the terms of the Creative Commons Attribution License (https://creativecommons.org/licenses/by/4.0/), which permits unrestricted use, distribution, and reproduction in any medium, provided the original work, first published in JMIR Medical Informatics, is properly cited. The complete bibliographic information, a link to the original publication on https://medinform.jmir.org/, as well as this copyright and license information must be included.

XSL•FO
RenderX

Comparative Analysis of Generative Artificial Intelligence Systems in Solving Clinical Pharmacy Problems: Mixed Methods Study

Lulu Li, MSc; Pengqiang Du, MMSc; Xiaojing Huang, MMSc; Hongwei Zhao, PhD; Ming Ni, MSc; Meng Yan, MSc; Aifeng Wang, MSc

Department of Pharmacy, Fuwai Central China Cardiovascular Hospital, 1 Fuwai Road, Zhengdong New District, Zhengzhou, China

Corresponding Author:
Aifeng Wang, MSc
Department of Pharmacy, Fuwai Central China Cardiovascular Hospital, 1 Fuwai Road, Zhengdong New District, Zhengzhou, China

Abstract

Background: Generative artificial intelligence (AI) systems are increasingly deployed in clinical pharmacy; yet, systematic evaluation of their efficacy, limitations, and risks across diverse practice scenarios remains limited.

Objective: This study aims to quantitatively evaluate and compare the performance of 8 mainstream generative AI systems across 4 core clinical pharmacy scenarios—medication consultation, medication education, prescription review, and case analysis with pharmaceutical care—using a multidimensional framework.

Methods: Forty-eight clinically validated questions were selected via stratified sampling from real-world sources (eg, hospital consultations, clinical case banks, and national pharmacist training databases). Three researchers simultaneously tested 8 different generative AI systems (ERNIE Bot, Doubao, Kimi, Qwen, GPT-4o, Gemini-1.5-Pro, Claude-3.5-Sonnet, and DeepSeek-R1) using standardized prompts within a single day (February 20, 2025). A double-blind scoring design was used, with 6 experienced clinical pharmacists (≥5 years experience) evaluating the AI responses across 6 dimensions: accuracy, rigor, applicability, logical coherence, conciseness, and universality, scored 0 - 10 per predefined criteria (eg, −3 for inaccuracy and −2 for incomplete rigor). Statistical analysis used one-way ANOVA with Tukey Honestly Significant Difference (HSD) post hoc testing and intraclass correlation coefficients (ICC) for interrater reliability (2-way random model). Qualitative thematic analysis identified recurrent errors and limitations.

Results: DeepSeek-R1 (DeepSeek) achieved the highest overall performance (mean composite score: medication consultation 9.4, SD 1.0; case analysis 9.3, SD 1.0), significantly outperforming others in complex tasks (P<.05). Critical limitations were observed across models, including high-risk decision errors—75% omitted critical contraindications (eg, ethambutol in optic neuritis) and a lack of localization—90% erroneously recommended macrolides for drug-resistant *Mycoplasma pneumoniae* (China's high-resistance setting), while only DeepSeek-R1 aligned with updated American Academy of Pediatrics (AAP) guidelines for pediatric doxycycline. Complex reasoning deficits: only Claude-3.5-Sonnet detected a gender-diagnosis contradiction (prostatic hyperplasia in female); no model identified diazepam's 7-day prescription limit. Interrater consistency was lowest for conciseness in case analysis (ICC=0.70), reflecting evaluator disagreement on complex outputs. ERNIE Bot (Baidu) consistently underperformed (case analysis: 6.8, SD 1.5; P<.001 vs DeepSeek-R1).

Conclusions: While generative AI shows promise as a pharmacist assistance tool, significant limitations—including high-risk errors (eg, contraindication omissions), inadequate localization, and complex reasoning gaps—preclude autonomous clinical decision-making. Performance stratification highlights DeepSeek-R1's current advantage, but all systems require optimization in dynamic knowledge updating, complex scenario reasoning, and output interpretability. Future deployment must prioritize human oversight (human-AI co-review), ethical safeguards, and continuous evaluation frameworks.

(JMIR Med Inform 2025;13:e76128) doi:10.2196/76128

KEYWORDS

artificial intelligence; DeepSeek-R1; clinical pharmacy; comparative analysis; generative AI

Introduction

With the breakthrough development of generative artificial intelligence (AI) technology, the health care field is experiencing a significant transformation, with AI-driven pharmaceutical practice at the forefront of this evolution [1]. Pharmaceutical intelligence has the potential to transform pharmaceutical practice by addressing the complexity of drug data, evolving health care needs, and technological advancements. Global research indicates that AI demonstrates transregional universality in enhancing the efficiency of drug information

XSL•FO
RenderX

retrieval [2]. Clinical studies indicate that such systems demonstrate significant advantages in efficient drug information retrieval and exhibit a certain degree of accuracy and specificity in predicting drug interactions [3]. However, recent systematic reviews point out that current AI chatbots primarily face challenges of "generating inaccurate or fabricated content" and "lower accuracy in answering questions" [4,5]. This gap between technological potential and practical application [6,7] highlights the urgency of establishing scientific evaluation systems to identify high-quality generative AI systems.

Despite some existing research beginning to conduct clinical application assessments of generative AI dialogue systems, these efforts are largely limited to testing individual models on single tasks [8-10], lacking horizontal comparative analysis across multiple dialogue models and validation of continuous decision chains in real clinical scenarios.

This research innovatively constructs a 6-dimensional evaluation system, conducting systematic assessment and comparative analysis of 4 types of clinical pharmacy practice scenarios: medication consultation, medication education, prescription review, and case analysis with pharmaceutical care. The study sample encompasses 8 representative mainstream dialogue-based AI platforms from both domestic and international origins: ERNIE Bot (version 4.0; Baidu; Release Date: October 17, 2023), Doubao (version: Pro; ByteDance; Release Date: May 15, 2024), Kimi (version: V1.1; Beijing Moonshot Technology Co., Ltd.; Release Date: November 16, 2023), Qwen (version: long; Alibaba Cloud; Release Date: May 21, 2024), GPT (version: 4o; OpenAI; Release Date: May 14, 2024), Gemini (version: 1.5-Pro; Google DeepMind; Release Date: February 14, 2024), Claude (version: 3.5-Sonnet; Anthropic; Release Date: June 21, 202), and DeepSeek (version: R1; Hangzhou DeepSeek Artificial Intelligence Basic Technology Research Co, Ltd; Release Date: January 20, 2025). Through designing parallel tests in realistic clinical settings and using a modified Delphi method for double-blind evaluation, we quantitatively analyzed and descriptively evaluated the capabilities of these 8 generative AI dialogue systems in addressing clinical pharmacy problems across 6 dimensions: accuracy, rigor, applicability, logical coherence, conciseness, and universality. The research findings will provide empirical evidence for optimizing the application of generative AI systems in clinical pharmacy and offer valuable reference for constructing AI-assisted decision-making systems that conform to medical ethics.

Methods

Research Design

We collected 48 common questions from 4 categories of clinical pharmacy work scenarios:

1. Medication consultation questions (n=20) content covered 10 aspects, with 2 questions per aspect: drug indications (efficacy), administration methods, dosage, medication precautions, drug interactions, storage methods, identification and management of adverse drug reactions, special dosage form usage guidance, medication use in special populations, and disease prevention.
2. Medication education questions (n=10) content primarily covered medication use for patients with chronic diseases and special populations.
3. Prescription audit questions (n=10) content encompassed inappropriate treatment regimens, inappropriate usage and dosage, inappropriate combination therapy, inappropriate drug selection, inappropriate administration routes, contraindications, inappropriate treatment duration, and inappropriate clinical diagnosis. The task required assuming the role of a pharmacist to identify prescription errors using relevant pharmacotherapeutic knowledge and the latest clinical guidelines.
4. Case analysis and pharmaceutical care questions (n=8) content included common chronic disease cases such as coronary heart disease, hypertension, type 2 diabetes, asthma, chronic obstructive pulmonary disease, gout, lung cancer, and so on. The task required assuming the role of a pharmacist to analyze pharmacotherapy plans based on patient information (basic information, reason for visit, present illness history, past medical history, medication history, family history, allergy history, adverse reaction history, unhealthy habits, diagnosis, current medication records, and auxiliary examination results), and to develop a pharmaceutical care plan addressing 4 aspects: indications, effectiveness, safety, and adherence.

The study used a standardized experimental design, with 3 researchers using identical "inquiry prompts" to question 8 generative AI dialogue systems during the same time period. All models were tested using their publicly available versions as of February 20, 2025; the results reflect a performance snapshot restricted to this timepoint. Each chatbot received 48 inquiry prompts, generating a total of 384 independent response samples. The evaluation was conducted by 6 clinical pharmacists who had successfully obtained clinical pharmacist training certificates after standardized training and had more than 5 years of clinical pharmacy work experience. The evaluation encompassed six dimensions: (1) accuracy, (2) rigor, (3) applicability, (4) logical coherence, (5) conciseness, and (6) universality. These clinical pharmacists' professional domains covered all disease types relevant to the questions. A double-blind scoring mechanism was implemented for independent evaluation to avoid subjective bias and ensure objectivity and fairness in the assessment process.

Standardized prompting instructions: all questions were input to the model using a standardized format. The core instruction template was to act in the role of a clinical pharmacist. Based on the latest clinical guidelines and evidence-based principles, answer the following question (Specific question description). For prescription review tasks, the following emphasis was added: determine whether this prescription contains errors and provide your rationale. For case analysis and pharmaceutical care tasks, the following emphasis was added: analyze the pharmacotherapy plan for this case and develop a pharmaceutical care plan addressing the following 4 aspects "Indication, Efficacy, Safety, and Adherence." The complete list of all 48 standardized prompting instructions used in this study is provided in Multimedia Appendix 1.

XSL•FO
RenderX

Data Sources

Questions were collected using stratified sampling, drawing from the following sources: common medication inquiries at a medication consultation clinic in a large Grade A Class 3 hospital in China, real clinical cases, the theoretical assessment question banks for standardized clinical pharmacist training programs of the Chinese Medical Association (CMA) and the Chinese Hospital Association (CHA), the China Medication Therapy Management (MTM) pharmacist training program, and the China Pharmacist Skills Competition. Specific steps are as follows:

Question bank construction: questions from the 5 sources above were categorized into 4 scenarios: medication consultation, medication education, prescription review, and case analysis and pharmaceutical care.

Stratified sampling:

- Medication consultation (20 questions): ensured coverage of the 10 aspects mentioned in the Abstract (medication indications, administration methods, dosage, precautions, drug-drug interactions, storage methods, identification and management of adverse drug reactions, guidance on special dosage forms, medication use in special populations, and disease prevention). Two questions were randomly selected from each aspect.
- Medication education (10 questions): randomly selected from 2 subcategories, medication use for patients with chronic disease (6 questions), and medication use for special populations (4 questions).
- Prescription review (10 questions): ensured coverage of the 8 types of inappropriate prescriptions mentioned in the Abstract (inappropriate therapeutic regimen, inappropriate dosage and administration, inappropriate combination therapy, inappropriate drug selection, inappropriate route of administration, presence of contraindications, inappropriate duration of therapy, and inconsistency with clinical diagnosis). Prescription cases containing typical or high-risk errors were prioritized.
- Case analysis and pharmaceutical care (8 questions): 8 representative cases were randomly selected from the question bank covering common chronic diseases (eg, coronary heart disease, hypertension, type 2 diabetes, asthma, chronic obstructive pulmonary disease, gout, and lung cancer).

Question screening: the initially screened questions were independently reviewed by 2 senior clinical pharmacists. This process ensured the questions aligned with the assessment objectives, possessed clinical relevance, were clear and unambiguous, and excluded duplicate or outdated items. Ultimately, 48 questions were finalized for inclusion in the study.

Evaluation Methods

Scoring standards were constructed based on evidence-based medical references, including drug package inserts, the latest clinical guidelines, and the Micromedex database. Clinical pharmacists conducted quantitative assessments of response contents according to standard answers and scoring criteria, with accuracy levels represented on a 0 - to 10-point scale. Unified scoring rules were established, with each question having a maximum score of 10 points, with deductions as follows:

1. Accuracy: 3 points deducted for not directly addressing the question or not providing an accurate answer;
2. Rigor: 2 points deducted for incomplete answers;
3. Applicability: 2 points deducted for failing to provide individualized recommendations based on patient-specific conditions;
4. Logical coherence: 1 point deducted for unclear reasoning or disorganized logic;
5. Conciseness: 1 point deducted for verbose language;
6. Universality: 1 point deducted for overly technical terminology lacking general applicability;
7. Comprehensive answers without deduction criteria: 0 points deducted.

Evaluators were required to select at least one scoring option during the assessment process.

Statistical Analysis

One-way ANOVA was used to compare score differences among the 8 generative AI dialogue systems across 4 task categories (medication consultation, medication education, prescription review, and case analysis with pharmaceutical care). Data satisfied the assumptions of normality through Shapiro–Wilk tests (P>.05) and homogeneity of variance through Levene tests (P>.05), followed by Tukey Honestly Significant Difference (HSD) multiple comparison analysis to identify significant differences. Interrater consistency was calculated using the intraclass correlation coefficient (ICC) through a 2-way random effects model, with ICC>0.75 indicating good consistency.

Qualitative Analysis Process

Following quantitative scoring, the research team (3 investigators) conducted a systematic content review of all 384 AI-generated responses to identify recurrent strengths, typical error patterns, critical limitations, and notable variations across models. The review process followed the steps mentioned below.

Initial screening: investigators independently reviewed all responses, documenting exemplar responses that demonstrated exceptional performance or significant deficiencies in accuracy, rigor, applicability, logical coherence, conciseness, or generalizability.

Theme identification: investigators consolidated preliminary observations and identified recurring themes through discussion (eg, “Errors in Special Device Instructions,” “Lack of Localized Medication Recommendations,” “Failure to Identify Critical Contraindications,” “Overly Technical or Jargon-Rich or Verbose Language,” and “Ignoring Conflicting Gender-Specific Diagnostic Criteria”).

Case selection: for each identified theme, representative response examples demonstrating the issue or strength were selected across different models. Priority was given to cases where quantitative assessment revealed performance variations

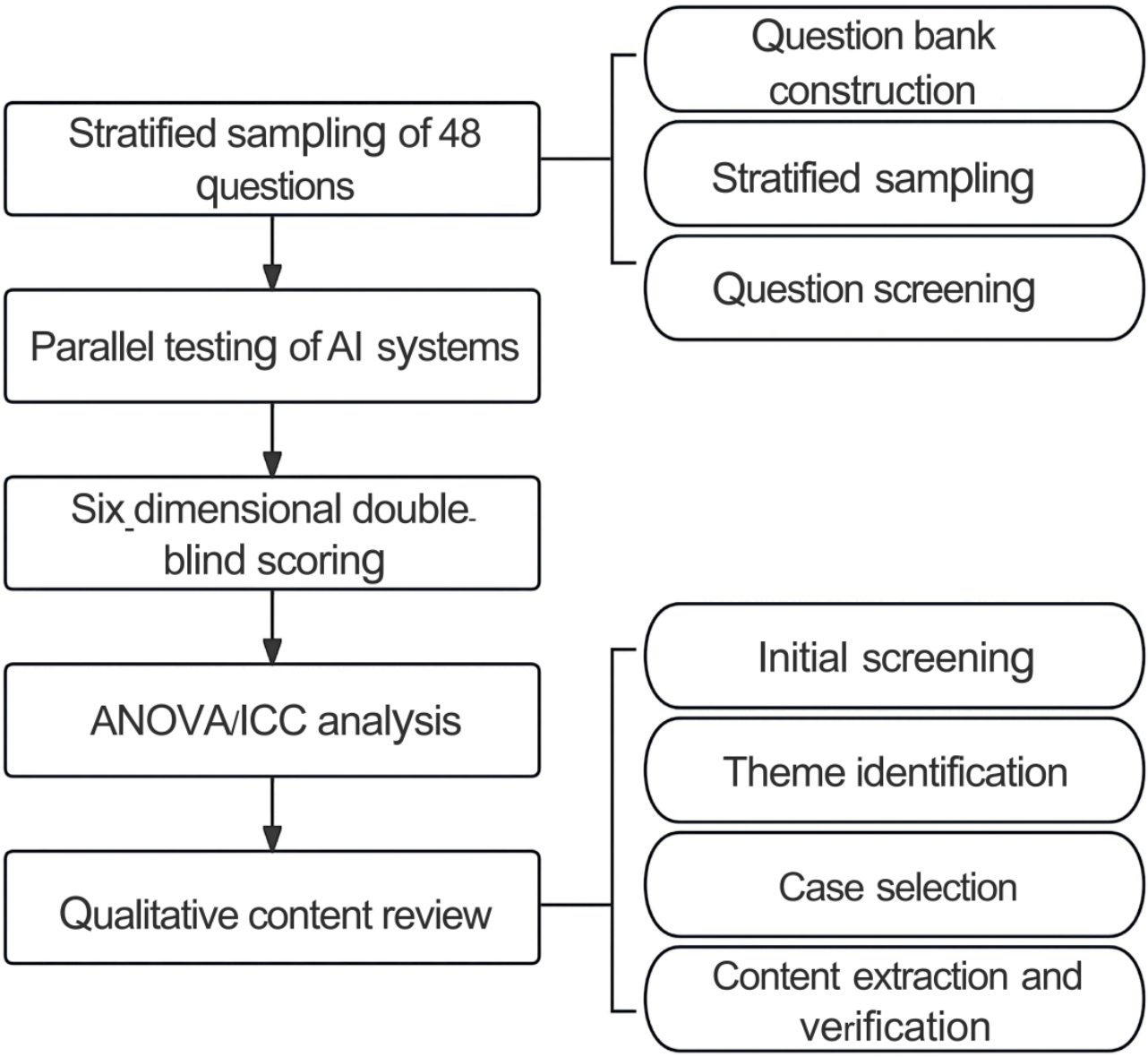
XSL•FO
RenderX

and where the response content clearly illustrated the qualitative concern.

Content extraction and verification: key content was abstracted from selected cases to ensure descriptions accurately reflected the original response meaning (with critical verbatim excerpts cited where necessary). Final qualitative cases and their analyses were confirmed by consensus within the research team.

These qualitative findings supplement the quantitative results, providing deeper insight into model performance variations and potential risks across different clinical scenarios. They are reported and analyzed in detail in the Discussion section. The methodology flowchart is shown in Figure 1.

Figure 1. Research methodology flow diagram. AI: artificial intelligence; ICC: intraclass correlation coefficient.



Ethical Considerations

This study constitutes a noninterventional evaluation of outputs from publicly accessible generative AI systems. It does not involve direct participation, intervention, or interaction with human participants (patients or healthy volunteers).

According to the policy of the Ethics Committee of Fuwai Central China Cardiovascular Hospital, this type of research (performance evaluation of publicly available AI systems using deidentified question banks and simulated scenarios) is qualified for exemption from formal ethics review application. The study design strictly followed the principles of the Declaration of Helsinki concerning nonbiomedical research.

This study exclusively used rigorously deidentified question texts as input stimuli for the AI systems. It did not involve the use, storage, or analysis of any raw patient data containing personally identifiable information. Therefore, additional informed consent for this secondary analysis was not required.

All question texts input into the AI systems were based on simulated scenarios or deidentified, generic inquiries, containing no real, personally identifiable patient information. The AI-generated output texts produced during the study contained only clinical pharmacy knowledge-related responses and

XSL•FO
RenderX

similarly did not involve any private personal data. All research data (question bank, AI responses, and scoring sheets) were encrypted during storage and transmission and were accessible only to authorized researchers.

The 6 clinical pharmacists participating in the assessment received market-standard honoraria commensurate with their professional contribution.

This study did not use any images containing personally identifiable information (eg, faces, unique physical characteristics, and personal details). All results presentation figures (eg, Figures 1-3) were generated based on aggregated statistical data and anonymized ICC values, posing no risk of individual identity disclosure.

Figure 2. Score distribution and differential analysis of artificial intelligence platforms across 4 pharmaceutical tasks (box plot). (Note: *P<.05: significant difference, **P<.01: highly significant difference, ***P<.001: extremely significant difference, ****P<<.001: most significant difference).

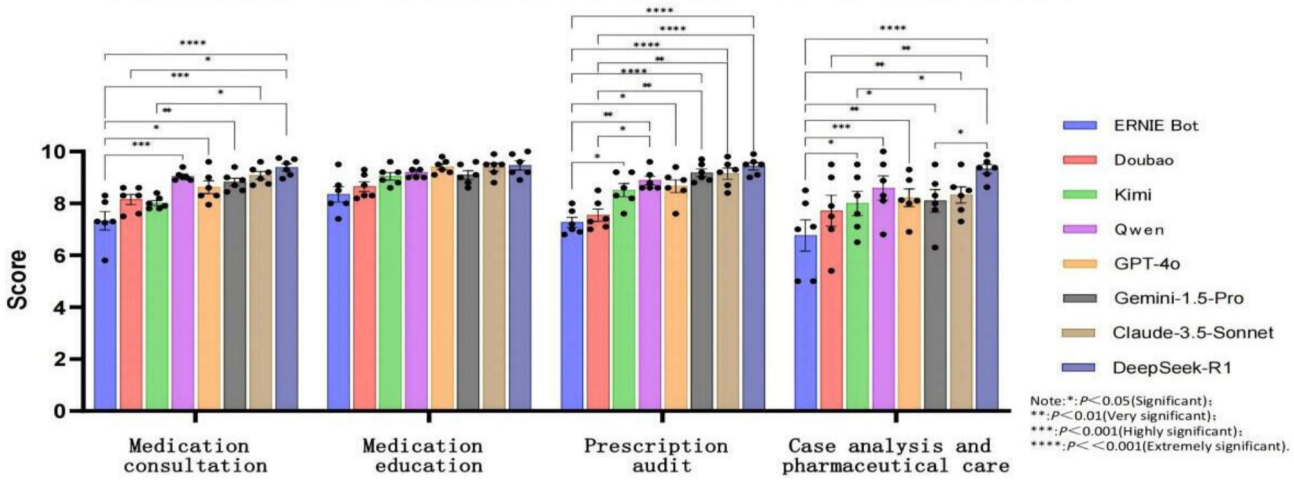
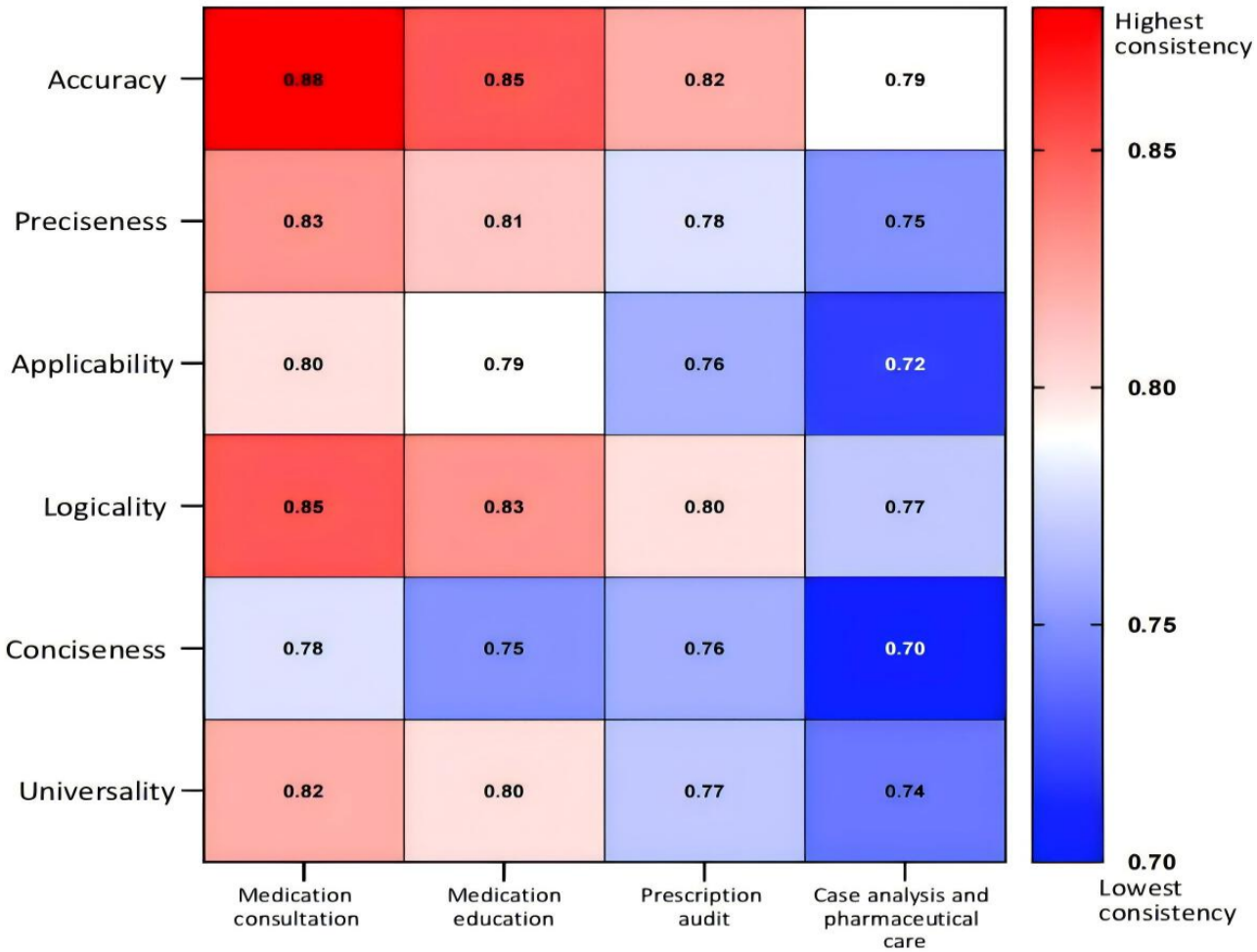


Figure 3. Rater consistency heat map (heat map of intraclass correlation coefficients).



XSL•FO
RenderX

Results

Quantitative Evaluation of 8 Generative AI Dialogue Systems in Clinical Pharmacy Applications

Descriptive Statistics

DeepSeek-R1 demonstrated the strongest comprehensive capabilities, with particularly significant advantages in complex tasks (such as case analysis and pharmaceutical care). Qwen, GPT-4o, Claude-3.5-Sonnet, and Gemini-1.5-Pro performed exceptionally in certain tasks but were overall inferior to DeepSeek-R1. Doubao and Kimi showed inconsistent performance, while ERNIE Bot performed the poorest, indicating a need for targeted optimization. The SDs for scores in case analysis and pharmaceutical care tasks were relatively large, suggesting poorer consistency among clinical pharmacists when evaluating generative AI dialogue systems' performance in handling these complex issues (see Table 1).

Table . Scores of 8 generative artificial intelligence (AI) dialogue systems across 4 problem types.

AI platforms	Medication consultation (n=20), mean (SD)	Medication education (n=10), mean (SD)	Prescription audit (n=10), mean (SD)	Case analysis and pharmaceutical care (n=8), mean (SD)
ERNIE Bot	7.3 (1.2)	8.4 (0.9)	7.3 (1.0)	6.8 (1.5)
Doubao	8.1 (1.1)	8.7 (1.3)	7.6 (1.2)	7.7 (1.7)
Kimi	8.0 (1.0)	9.1 (1.0)	8.5 (1.4)	8.0 (1.6)
Qwen	9.0 (0.8)	9.2 (0.7)	8.9 (0.9)	8.6 (1.2)
GPT-4o	8.6 (1.0)	9.4 (1.1)	8.7 (1.3)	8.2 (1.4)
Gemini-1.5-Pro	8.8 (1.1)	9.1 (1.0)	9.2 (1.1)	8.1 (1.3)
Claude-3.5-Sonnet	9.1 (1.0)	9.4 (0.8)	9.2 (0.9)	8.3 (1.5)
DeepSeek-R1	9.4 (1.0)	9.5 (1.1)	9.4 (0.8)	9.3 (1.0)

Normality and Homogeneity of Variance Tests

Shapiro–Wilk test showed that score data for all problem types conformed to normal distribution (P>.05). Levene test indicated homogeneity of variance for medication consultation (P=.12), medication education (P=.09), prescription review (P=.15), and case analysis (P=.10).

ANOVA

Across all problem types, significant differences were observed in scores among different generative AI dialogue systems (P<.001), with effect size η^2>0.3, indicating statistically significant differences (Table 2).

Table . ANOVA results (one-way, α=.05).

Question type	F (*df*) value	*P* value	η^2 (effect size)	Significance conclusion
Medication consultation	14.3 (7, 44)	<.001	0.36	Significant differences exist
Medication education	12.8 (7, 44)	<.001	0.32	Significant differences exist
Prescription audit	16.5 (7, 44)	<.001	0.40	Significant differences exist
Case analysis and pharmaceutical care	18.1 (7, 44)	<.001	0.43	Significant differences exist

Multiple Comparisons (Tukey HSD)

DeepSeek-R1 demonstrated the best overall performance across all 4 task categories, with particularly significant advantages in prescription review, case analysis, and pharmaceutical care tasks. Qwen and GPT-4o showed similar performance in most tasks with no significant differences. Kimi and Doubao exhibited significant gaps (P<.05) in certain tasks when compared to DeepSeek-R1. ERNIE Bot consistently underperformed, with highly significant differences (P<.001) compared with other models.

Specifically, for medication consultation, DeepSeek-R1 was extremely significantly superior to ERNIE Bot (P<.001). For medication education, most comparison results were not significant, indicating minimal differences among generative AI dialogue systems in this aspect. For prescription review, ERNIE Bot performed the poorest, showing significant (P<.05) or extremely significant (P<.001) differences when compared to all other generative AI dialogue systems. For case analysis and pharmaceutical care, ERNIE Bot remained significantly weaker than most models (eg, very significant difference compared to GPT-4o, P<.01), while DeepSeek-R1 maintained stable performance with significant differences compared to all other models. See Table 3 and Figure 2.

XSL•FO
RenderX

Table . Pairwise comparison results of 8 generative artificial intelligence (AI) dialogue systems across 4 question types (Tukey Honestly Significant Difference) only display the groups with significant differences.

Task and comparison of significant difference groups	Mean difference (95% CI)	*P* value
Medication consultation		
ERNIE Bot-Qwen	–1.7 (–2.9 to –0.5)	<.001
ERNIE Bot-GPT-4o	–1.3 (–2.5 to –0.1)	.03
ERNIE Bot- Gemini-1.5-Pro	–1.5 (–2.7 to 0.27)	<.001
ERNIE Bot- Claude-3.5-Sonnet	–1.7 (–2.9 to –0.5)	<.001
ERNIE Bot-DeepSeek-R1	–2.1 (–3.2 to –0.8)	<.001
Doubao-DeepSeek-R1	–1.3 (–2.4 to –0.03)	.04
Kimi-DeepSeek-R1	–1.4 (–2.6 to –0.1)	.01
Prescription audit		
ERNIE Bot- Kimi	–1.3 (–2.5 to –0.1)	.04
ERNIE Bot-Qwen	–1.6 (–2.8 to –0.4)	.002
ERNIE Bot-GPT-4o	–1.4 (–2.6 to –0.19)	.01
ERNIE Bot- Gemini-1.5-Pro	–1.8 (–3.1 to –0.7)	<.001
ERNIE Bot- Claude-3.5-Sonnet	–1.8 (–3.1 to –0.7)	<.001
ERNIE Bot-DeepSeek-R1	–2.1 (–2.3 to 0.09)	<.001
Doubao-Qwen	–1.3 (–2.5 to –0.1)	.02
Doubao- Gemini-1.5-Pro	–1.6 (–2.8 to –0.4)	.001
Doubao - Claude-3.5-Sonnet	–1.6 (–2.8 to –0.4)	.002
Doubao-DeepSeek-R1	–1.9 (–3.1 to –0.68)	<.001
Case analysis and pharmaceutical care		
ERNIE Bot- Kimi	–1.2 (–2.4 to –0.03)	.04
ERNIE Bot-Qwen	–1.8 (–3.0 to –0.6)	<.001
ERNIE Bot- GPT-4o	–1.5 (–2.7 to –0.2)	.007
ERNIE Bot- Gemini-1.5-Pro	–1.3 (–2.5 to –0.13)	.02
ERNIE Bot- Claude-3.5-Sonnet	–1.6 (–2.8 to –0.4)	.003
ERNIE Bot- DeepSeek-R1	–2.6 (–3.8 to –1.4)	<.001
Doubao-DeepSeek-R1	–1.6 (–2.8 to –0.4)	.002
Kimi-DeepSeek-R1	–1.3 (–2.5 to –0.1)	.02
Gemini-1.5-Pro-DeepSeek-R1	–1.2 (–2.4 to –0.02)	.043

Interrater Reliability (ICC Values)

The ICC values for all 6 dimensions in medication consultation, medication education, and prescription review were >0.75, indicating good interrater reliability. Accuracy and logical coherence showed the highest consistency (ICC>0.8), while conciseness in case analysis and pharmaceutical care demonstrated the lowest consistency (ICC=0.70), suggesting considerable disagreement among raters when evaluating generative AI dialogue systems' solutions to complex problems (Table 4). A higher ICC value indicates stronger consistency, while a lower ICC value reflects weaker consistency. The darker red in Figure 3 indicates higher consistency, while deeper blue indicates lower consistency.

XSL•FO
RenderX

Table . Intraclass correlation coefficient values by dimension (2-way random effects model).

Dimension	Medication consultation	Medication education	Prescription audit	Case analysis and pharmaceutical care
Accuracy	0.88	0.85	0.82	0.79
Preciseness	0.83	0.81	0.78	0.75
Applicability	0.80	0.79	0.76	0.72
Logicality	0.85	0.83	0.80	0.77
Conciseness	0.78	0.75	0.76	0.70
Universality	0.82	0.80	0.77	0.74

Discussion

Principal Findings

AI applications in health care demonstrate enormous development potential while facing numerous challenges [11]. This study, through constructing a 6-dimensional evaluation system, systematically compares the application effects and limitations of current mainstream conversational AI platforms, providing important evidence for further optimization of intelligent pharmaceutical systems.

Key Findings

This study systematically evaluated the comprehensive performance of 8 mainstream generative AI systems across 4 core clinical pharmacy scenarios: medication consultation, medication education, prescription review, and case analysis with pharmaceutical care. The principal findings are as follows.

Significant Model Performance Stratification

DeepSeek-R1 demonstrated superior performance across all 4 task categories (composite score: medication consultation 9.4, SD 1.0, case analysis 9.3, SD 1.0), exhibiting particularly pronounced advantages in complex tasks such as case analysis with pharmaceutical care (P<.05).

Second-tier models (Qwen, GPT-4o, Claude-3.5-Sonnet, and Gemini-1.5-Pro) performed well in specific scenarios but consistently underperformed DeepSeek-R1 overall (eg, Gemini-1.5-Pro scored 9.2, SD 1.1 in prescription review vs DeepSeek-R1's 9.4, SD 0.8).

Doubao and Kimi exhibited significant performance variability, while ERNIE Bot consistently lagged significantly across all tasks (eg, case analysis score=6.8, SD 1.5; P<.001 difference vs DeepSeek-R1).

Critical Limitations Exposed

Static knowledge bases and lack of localization: most models failed to adapt to Chinese clinical practices (eg, 90% incorrectly recommended macrolides for drug-resistant *Mycoplasma pneumoniae* infection; only DeepSeek-R1 correctly advised short-term doxycycline based on American Academy of Pediatrics [AAP] guidelines).

High-risk decision blind spots: models frequently overlooked critical contraindications (eg, only 25% recognized ethambutol is contraindicated in optic neuritis) and special regulatory requirements (eg, no model warned about the violation of prescribing diazepam beyond 7 d).

Complex reasoning deficiencies: in case analysis tasks, models struggled to integrate multidimensional information to formulate individualized care plans (eg, only Claude-3.5-Sonnet identified the diagnostic contradiction of "benign prostatic hyperplasia in a female patient").

These limitations highlight 3 major technical bottlenecks: lagging knowledge base updates, insufficient complex decision-making reasoning, and prompt sensitivity risks (section "Technical Bottlenecks and Clinical Challenges" for details).

Rater Consistency Challenge

The "Conciseness" dimension in case analysis tasks exhibited the lowest interrater reliability (ICC=0.70), reflecting inconsistent assessment standards for complex problems.

Therefore, while current generative AI can serve as an auxiliary reference tool for clinical pharmacists, its error rate in high-risk decisions (eg, omission of contraindications) and lack of localization capability preclude its use as an independent basis for clinical decision-making.

Technical Bottlenecks and Clinical Challenges

Knowledge Base Limitations and Lag in Dynamic Update

This study found that all 8 generative AI dialogue systems shared a common deficiency in the areas of medication consultation and medication education: a lack of comprehensive disease assessment capabilities, making it difficult for them to provide personalized medication guidance. For instance, their guidance on the use of special devices was often inaccurate. When queried about the proper use of "Budesonide and Formoterol Inhaler," most systems failed to accurately identify the specific type of device involved. Instead, they incorrectly described the usage instructions for other devices (eg, Salbutamol Aerosol), potentially misleading users.

Regarding the question "Can a 6-year-old child with *Mycoplasma pneumoniae* infection take doxycycline?" only DeepSeek-R1 provided a comprehensive answer incorporating the latest guidelines, "The risk of tooth discoloration from short-term doxycycline therapy (≤21 days) is extremely low, and organizations such as the AAP have relaxed relevant restrictions. Clinicians may consider using doxycycline in the following circumstances: when macrolides are resistant or ineffective; when the child's condition is severe (eg, persistent

XSL•FO
RenderX

high fever and lung consolidation); when no other safe alternative medications are available." Other generative AI dialogue systems still only recommended macrolide antibiotics, which are unsuitable for China's environment, where *Mycoplasma pneumoniae* has high resistance to macrolide antibacterial drugs. This is closely related to training data relying on static knowledge bases and lacking real-time, evidence-based pharmaceutical knowledge updates. DeepSeek, by leveraging publicly available open-source datasets to facilitate continuous learning, can enhance adaptability to evolving medical knowledge and scientific reasoning [12]. Nevertheless, DeepSeek-R1 also demonstrated notable limitations, including overly specialized terminology and a lack of concise expression. Particularly when responding to simple medication inquiries, the answers were excessively complex and lengthy, making it more suitable as a reference tool for health care professionals rather than for general users.

In addition, semantic ambiguity issues in Chinese contexts (as shown in the "prostate hyperplasia" misdiagnosis case) highlight the deficiencies in localized medical knowledge base construction. Furthermore, the international models (GPT-4o, Gemini-1.5-Pro, and Claude-3.5-Sonnet) exhibit biases in their understanding of culturally sensitive issues. For example, when queried about the risks of concomitant use of Chinese herbal injections and Warfarin, these models may overlook the impact of *CYP2C9* gene polymorphisms prevalent in East Asian populations. Addressing such culture-gene interactions necessitates optimization through localized training frameworks. Research indicates an increasingly evident trend of using transformer-based language models in various natural language processing models in the medical field [13], emphasizing the necessity of developing multilevel language training frameworks to adapt to professional medical environments [14].

Deficiencies in Complex Reasoning and Associated Ethical Risks

In prescription review, for a simple case "16-year-old male patient diagnosed with periapical abscess [15], prescribed levofloxacin tablets 0.2 g po bid, metronidazole tablets 0.6 g po tid, chlorhexidine acetate mouthwash 5 ml tid," only ERNIE Bot, Doubao, and Kimi failed to identify that quinolone antibiotics are contraindicated in patients younger than 18 years of age, while the other 5 systems successfully identified this key safety issue.

However, for more complex prescriptions, such as "61-year-old male patient diagnosed with optic neuritis and tuberculous encephalopathy, prescribed: isoniazid 0.3 g qd, pyrazinamide 3 g biw, ethambutol tablets 0.75 g qd, rifampin capsules 0.6 g qd," only Qwen and DeepSeek-R1 accurately identified the critical contraindication that ethambutol could exacerbate visual impairment in patients with optic neuritis.

Notably, for the prescription "40-year-old female patient diagnosed with insomnia, prescribed: diazepam tablets 10 mg po qn for 10 days" none of the 8 generative AI dialogue systems accurately identified the special management requirements for diazepam as a Class II psychotropic medication—that Class II psychotropic medications should not be prescribed for more than 7 days per prescription, and special circumstances require physician documentation. This regulatory requirement has significant importance in clinical pharmacists' routine prescription review work.

Even more concerning, for the prescription "71-year-old female patient diagnosed with hypertension and prostatic hyperplasia, prescribed: amlodipine tablets 5 mg qd, irbesartan and hydrochlorothiazide tablets 150 mg:12.5 mg qd," only Claude-3.5-Sonnet successfully identified the obvious error: the diagnosis was inconsistent with the patient's gender (females do not have prostates and cannot be diagnosed with prostatic hyperplasia). The other 7 generative AI dialogue systems failed to detect this serious error. This indicates that generative AI systems still have serious hallucinations and cognitive limitations in medical reasoning.

In the case analysis and pharmaceutical care aspect, this study required generative AI dialogue systems to assume the role of clinical pharmacists and analyze drug therapy regimens based on patient information including basic demographics, reason for consultation, present illness, past medical history, medication history, family history, allergies, adverse reaction history, unhealthy habits, diagnoses, current medication records, and laboratory examination results. They were also asked to develop a pharmaceutical care plan. These tasks closely simulate the professional work of clinical pharmacists during daily rounds, requiring comprehensive and in-depth analysis and assessment of cases to formulate medication monitoring plans tailored to individual patient characteristics.

The results indicated that all 8 generative AI systems faced significant challenges in executing these complex professional tasks, struggling to simultaneously ensure both accuracy and comprehensiveness in their responses. This reflects the current limitations of AI systems in integrating diverse clinical information and making professional pharmaceutical decisions, particularly in complex clinical scenarios requiring consideration of multiple factors. This relates to AI's lack of clinical contextual reasoning and insufficient understanding of complex instructions.

A recent research review indicates that AI has higher error rates when integrating multimodal data (such as laboratory indicators and imaging results) compared to single-modality tasks [16]. Before resolving these technical bottlenecks, we cannot avoid the issue of accountability for AI-driven decisions [17]. How legal responsibility should be defined when patients experience adverse reactions due to incorrect AI recommendations remains unclear with no explicit regulations currently issued [18]. Therefore, AI dialogue systems should be positioned as "augmented intelligence" tools, establishing "human-machine co-review" mechanisms [19], strengthening human supervision, and ensuring pharmacists retain final decision-making authority over AI outputs. The ethical risks associated with AI identified in this study strongly align with the medical AI regulatory requirements emphasized in the European Union AI Act [20].

Instruction Adherence and Stability Issues

This study used a single, independent query mode for evaluation, where each question was input to the model as an independent conversation. Under this mode, no instances were observed of

XSL•FO
RenderX

the model significantly "forgetting" or ignoring core instructions (eg, "act as a pharmacist," "incorporate the latest clinical guidelines," and "develop a pharmaceutical care plan") within a single response.

However, it is crucial to emphasize that this study did not test the stability of the model's instruction adherence across continuous, multiturn dialogues. In real-world clinical deployment, users may engage in sustained conversations with an AI system involving multiple questions. Existing technical observations report that generative AI carries a risk of instruction drift or context forgetting during extended conversations or multiturn interactions. This could lead to subsequent responses deviating from the initially specified role or requirements, potentially compromising the reliability and safety of the answers.

Therefore, future research should design dedicated testing protocols to evaluate model instruction consistency in multiturn dialogues. Furthermore, exploring methods to enhance stability through prompt engineering optimization (eg, periodic instruction reinforcement) or model fine-tuning is warranted.

Compound Error Risk

While the scoring criteria in this study focused on explicit errors (eg, omission of contraindications), they did not detect potentially hazardous information embedded within otherwise correct responses. For instance, an AI model correctly identified a drug-drug interaction but ambiguously advised to "monitor during use" without explicitly stating the need for immediate discontinuation. In pediatric dosing advice, a model correctly recommended a drug dose but failed to emphasize the necessity of weight-based adjustment. Such errors carry a risk of clinical misinterpretation. Therefore, future research may need to develop algorithms for detecting latent risks, such as real-time validation based on databases like the FDA Adverse Event Reporting System (FAERS).

Application Opportunities and Optimization Pathways

Personalized Medication Decision Support

The DeepSeek-R1 model demonstrated good guideline adherence in pediatric doxycycline medication recommendations (incorporating the latest AAP recommendations), highlighting the potential application of AI in personalized medication decision support [21]. Relevant research confirms that AI can help formulate interventions under the guidance of predictive models by forecasting individual responses to treatment and monitoring patient progression, thereby modifying individualized treatment plans [22]. However, it should be noted that AI still lags significantly behind human experts in providing individualized treatment plans. For instance, Marcaccini et al [23] discovered that while AI-driven models demonstrate strong diagnostic accuracy and readability, further refinements are needed to improve treatment specificity and personalization. Looking forward, constructing an "AI pharmaceutical knowledge graph" [24] that correlates individual metabolic characteristics (such as CYP450 enzyme phenotypes) with pharmacokinetic data could provide dynamic dosing optimization strategies based on the latest evidence-based evidence for clinical practice.

Process Automation and Resource Optimization

Compared to clinical pharmacists, generative AI dialogue systems possess powerful information retrieval, data integration, and conversation capabilities [25]. Natural language processing technology can automatically extract and analyze data from large volumes of electronic medical records [26], which will greatly reduce manual time consumption, and the application of this technology is expected to significantly reduce the burden on clinical pharmacists in routine documentation such as medication history records. By communicating with users through verbal or nonverbal means, simulated pharmacist assistants have achieved improved medication adherence by providing medication education to older patients with diabetes [27], all of which enables more optimized resource allocation.

Medical Education and Skills Training

Generative AI dialogue systems provide new tools for clinical educational interventions and medical practice [28], bringing new dimensions of personalized learning, enhanced visualization, and simulation-based clinical training to the forefront [29]. In addition, AI-driven simulations offer realistic immersive training opportunities that prepare students for complex clinical situations and cultivate the interprofessional collaboration skills essential for modern health care [30].

Comparison With Previous Work

This study engages in significant dialogue with and extends existing literature in terms of both methodology and findings.

Deepened Evaluation Framework

Compared to the 3-dimensional evaluation frameworks proposed by other researchers, this study innovatively constructs a "six-dimensional evaluation system," providing a more comprehensive capture of AI efficacy in pharmaceutical practice. Unlike single-model studies [8-10], this work presents the first cross-model comparison of 8 mainstream AI systems, revealing significant performance stratification (eg, DeepSeek-R1 significantly outperformed GPT-4o in Case Analysis tasks, $P<.05$).

Validation and Extension of Key Limitations

This study confirms the warning highlighted in the literature [15]. AI error rates remain high in complex medication decision-making (eg, a contraindication omission rate of 75% in Prescription Review tasks). Furthermore, semantic ambiguities unique to the Chinese context (eg, the gender contradiction in "benign prostatic hyperplasia") resulted in higher error rates compared with monolingual settings, underscoring the urgency for cross-lingual training frameworks.

Coverage of Innovative Scenarios

In contrast to studies [3] limited to information retrieval, this research systematically validates, for the first time, AI performance across a continuous clinical decision-making chain (eg, from prescription review to pharmaceutical care plan development). This reveals deficiencies in multimodal data integration and contextual reasoning (resulting in higher error rates compared to single-task evaluations).

XSL•FO
RenderX

Incremental Contribution of This Study

Through its systematic evaluation across multiple models, diverse scenarios, and 6 dimensions, this study provides an empirical foundation for the localized adaptation pathways (eg, dynamic knowledge graph updating) and ethical deployment boundaries (eg, a "human-AI co-review" mechanism) of generative AI in clinical pharmacy. These findings call for the establishment of cross-lingual training frameworks and continuous evaluation systems.

Limitations and Future Directions

Scope of Evaluated Scenarios

While this study focused on 4 core scenarios in clinical pharmacy practice, it did not comprehensively cover all potential application domains, such as pharmacovigilance signal mining, pharmacoeconomic evaluation, and public health emergency scenarios. Future studies should expand the scope of evaluation, for instance, by designing emergency medication test sets to assess model reliability under limited evidence.

Sample Size and Complexity

Although 48 questions were included, the number of Case Analysis and Pharmaceutical Care tasks was relatively low (only 8 questions). Furthermore, the complexity of the questions may still be insufficient to fully reflect the models' capability to handle extremely complex, rare, or multisystem real-world cases. Future research should increase sample size, incorporate more diverse and higher-complexity real-world cases, and consider supplementing data using Standardized Patient Data or synthetic data generation techniques.

Prompt Sensitivity

Generative AI systems exhibited significant sensitivity to the wording and structure of input prompts (Prompt Sensitivity). Minor variations in question phrasing (eg, adjusting keyword order, adding or removing qualifiers) could lead to divergent responses. While this study mitigated this variability through standardized instruction templates, it did not systematically quantify the impact of this sensitivity on the results. In addition, the 3 international models (GPT-4o, Gemini-1.5-Pro, and Claude-3.5-Sonnet) may have limited comprehension of Chinese medical terminology. Future research could use joint embedding models to reduce semantic bias or use adversarial prompt testing to evaluate model robustness and optimize instruction design.

Model Dynamic Updates

AI models undergo rapid iteration and updates (eg, Gemini 1.5 Pro updates monthly). This study reflects the performance of specific model versions at a fixed point in time (February 20, 2025), and findings may change with subsequent model updates. There is an urgent need to establish continuous, dynamic evaluation frameworks and benchmarks to track the evolution of model performance.

Insufficient Visualization of Results

This study recorded and summarized the total scores for each model across the 4 task types. However, it did not calculate the average scores for each model across the 6 evaluation dimensions (spanning all 4 task types). Consequently, it cannot intuitively display each model's relative strengths and weaknesses across dimensions or facilitate cross-model performance comparisons by dimension (eg, using radar charts). Future evaluations should incorporate these metrics.

Lack of Real-World Impact Assessment

The study evaluated model output quality in a controlled environment but did not assess the actual impact on pharmacist workflow efficiency, decision-making quality, or patient outcomes in real-world clinical settings. Future research should conduct prospective implementation studies or randomized controlled trials.

Conclusions

This study conducted a systematic evaluation and comparative analysis of the application efficacy of 8 mainstream domestic and international generative AI systems across 4 core clinical pharmacy practice scenarios by constructing a 6-dimensional evaluation system. The results demonstrate that DeepSeek-R1 outperformed other models in overall performance, exhibiting particularly significant advantages in handling complex case analysis and pharmaceutical care tasks. However, all models exhibited limitations, prominently manifested in lagging knowledge base updates (eg, incorrect instructions for special devices and lack of localized recommendations), insufficient complex decision-making reasoning capabilities (eg, failure to identify critical medication contraindications and special regulatory requirements), sensitivity to prompt instructions, and overly technical terminology in outputs. Interrater reliability analysis revealed substantial disagreement in evaluating the conciseness dimension for complex tasks such as case analysis.

Based on these findings, this study concludes that while current generative AI systems demonstrate significant potential for efficiency gains and value as decision-support tools in clinical pharmacy, their responses still contain non-negligible errors and limitations, particularly at high-risk decision points. Therefore, at this stage, they should be strictly positioned as auxiliary reference tools for clinical pharmacists, not as independent bases for clinical decision-making. Future development should focus on overcoming key bottlenecks, including achieving dynamic knowledge updating and localization adaptation, enhancing reasoning capabilities in complex scenarios, improving prompt robustness and output interpretability, and establishing continuous evaluation mechanisms. Ultimately, safe, reliable, and patient-centered intelligent pharmaceutical care systems should be built through interdisciplinary collaboration integrating evidence-based medicine, ethical norms, and technological innovation.

Acknowledgments

This research was funded by Henan Province Medical Science and Technology Research and Joint Construction Project (grant numbers 20220125 and 20230129).

XSL•FO
RenderX

Data Availability

All data produced in this study are available upon reasonable request to the authors.

Conflicts of Interest

None declared.

Multimedia Appendix 1
Questions 1-48.
[DOC File, 176 KB - medinform_v13i1e76128_app1.doc]

References

1. Hatem NAH. Advancing pharmacy practice: the role of intelligence-driven pharmacy practice and the emergence of pharmacointelligence. Integr Pharm Res Pract 2024;13:139-153. [doi: 10.2147/IPRP.S466748] [Medline: 39220215]
2. Topol EJ. High-performance medicine: the convergence of human and artificial intelligence. Nat Med 2019 Jan;25(1):44-56. [doi: 10.1038/s41591-018-0300-7] [Medline: 30617339]
3. Al-Ashwal FY, Zawiah M, Gharaibeh L, Abu-Farha R, Bitar AN. Evaluating the sensitivity, specificity, and accuracy of ChatGPT-3.5, ChatGPT-4, Bing AI, and Bard against conventional drug-drug interactions clinical tools. Drug Healthc Patient Saf 2023;15:137-147. [doi: 10.2147/DHPS.S425858] [Medline: 37750052]
4. Moulaei K, Yadegari A, Baharestani M, Farzanbakhsh S, Sabet B, Reza Afrash M. Generative artificial intelligence in healthcare: a scoping review on benefits, challenges and applications. Int J Med Inform 2024 Aug;188:105474. [doi: 10.1016/j.ijmedinf.2024.105474] [Medline: 38733640]
5. Rawashdeh B, Kim J, AlRyalat SA, Prasad R, Cooper M. ChatGPT and artificial intelligence in transplantation research: is it always correct? Cureus 2023 Jul;15(7):e42150. [doi: 10.7759/cureus.42150] [Medline: 37602076]
6. Ong JCL, Seng BJJ, Law JZF, et al. Artificial intelligence, ChatGPT, and other large language models for social determinants of health: current state and future directions. Cell Rep Med 2024 Jan 16;5(1):101356. [doi: 10.1016/j.xcrm.2023.101356] [Medline: 38232690]
7. Kamel Rahimi A, Pienaar O, Ghadimi M, et al. Implementing AI in hospitals to achieve a learning health system: systematic review of current enablers and barriers. J Med Internet Res 2024 Aug 2;26:e49655. [doi: 10.2196/49655] [Medline: 39094106]
8. Huang X, Estau D, Liu X, Yu Y, Qin J, Li Z. Evaluating the performance of ChatGPT in clinical pharmacy: a comparative study of ChatGPT and clinical pharmacists. Br J Clin Pharmacol 2024 Jan;90(1):232-238. [doi: 10.1111/bcp.15896] [Medline: 37626010]
9. Syrowatka A, Song W, Amato MG, et al. Key use cases for artificial intelligence to reduce the frequency of adverse drug events: a scoping review. Lancet Digit Health 2022 Feb;4(2):e137-e148. [doi: 10.1016/S2589-7500(21)00229-6] [Medline: 34836823]
10. Szumilas D, Ochmann A, Zięba K, et al. Evaluation of AI-driven LabTest checker for diagnostic accuracy and safety: prospective cohort study. JMIR Med Inform 2024 Aug 14;12:e57162. [doi: 10.2196/57162] [Medline: 39149851]
11. Shang Z, Chauhan V, Devi K, Patil S. Artificial intelligence, the digital surgeon: unravelling its emerging footprint in healthcare - the narrative review. J Multidiscip Healthc 2024;17:4011-4022. [doi: 10.2147/JMDH.S482757] [Medline: 39165254]
12. Temsah A, Alhasan K, Altamimi I, et al. DeepSeek in healthcare: revealing opportunities and steering challenges of a new open-source artificial intelligence frontier. Cureus 2025 Feb;17(2):e79221. [doi: 10.7759/cureus.79221] [Medline: 39974299]
13. Shaitarova A, Zaghir J, Lavelli A, Krauthammer M, Rinaldi F. Exploring the latest highlights in medical natural language processing across multiple languages: a survey. Yearb Med Inform 2023 Aug;32(1):230-243. [doi: 10.1055/s-0043-1768726] [Medline: 38147865]
14. Ajit-Roger E, Moise A, Peralta C, Orishchak O, Daniel SJ. Enhancing multilingual patient education: ChatGPT's accuracy and readability for SSNHL queries in English and Spanish. OTO Open 2024;8(4):e70048. [doi: 10.1002/oto2.70048] [Medline: 39664064]
15. Elendu TC, Amaechi DC, Elendu TC, et al. Ethical implications of AI and robotics in healthcare: a review. Medicine (Baltimore) 2023 Dec 15;102(50):e36671. [doi: 10.1097/MD.0000000000036671] [Medline: 38115340]
16. Kim JY, Lester C, Yang XJ. Beyond binary decisions: evaluating the effects of AI error type on trust and performance in AI-assisted tasks. Hum Factors 2025 Mar 19;2025:187208251326795. [doi: 10.1177/00187208251326795] [Medline: 40104968]
17. Maliha G, Gerke S, Cohen IG, Parikh RB. Artificial intelligence and liability in medicine: balancing safety and innovation. Milbank Q 2021 Sep;99(3):629-647. [doi: 10.1111/1468-0009.12504] [Medline: 33822422]
18. Habli I, Lawton T, Porter Z. Artificial intelligence in health care: accountability and safety. Bull World Health Organ 2020 Apr 1;98(4):251-256. [doi: 10.2471/BLT.19.237487] [Medline: 32284648]

XSL•FO
RenderX

19. Tessler I, Wolfovitz A, Livneh N, et al. Advancing medical practice with artificial intelligence: ChatGPT in healthcare. Isr Med Assoc J 2024 Feb;26(2):80-85. [Medline: 38420977]
20. Ducret M, Wahal E, Gruson D, et al. Trustworthy artificial intelligence in dentistry: learnings from the EU AI Act. J Dent Res 2024 Oct;103(11):1051-1056. [doi: 10.1177/00220345241271160] [Medline: 39311453]
21. Dickinson H, Teltsch DY, Feifel J, et al. The unseen hand: AI-based prescribing decision support tools and the evaluation of drug safety and effectiveness. Drug Saf 2024 Feb;47(2):117-123. [doi: 10.1007/s40264-023-01376-3] [Medline: 38019365]
22. Kale M, Wankhede N, Pawar R, et al. AI-driven innovations in Alzheimer's disease: integrating early diagnosis, personalized treatment, and prognostic modelling. Ageing Res Rev 2024 Nov;101:102497. [doi: 10.1016/j.arr.2024.102497] [Medline: 39293530]
23. Marcaccini G, Seth I, Lim B, et al. Management of burns: multi-center assessment comparing AI models and experienced plastic surgeons. J Clin Med 2025 Apr 29;14(9):3078. [doi: 10.3390/jcm14093078] [Medline: 40364114]
24. Xiong Z, Huang F, Wang Z, Liu S, Zhang W. A multimodal framework for improving in silico drug repositioning with the prior knowledge from knowledge graphs. IEEE/ACM Trans Comput Biol Bioinform 2022;19(5):2623-2631. [doi: 10.1109/TCBB.2021.3103595] [Medline: 34375284]
25. Alowais SA, Alghamdi SS, Alsuhebany N, et al. Revolutionizing healthcare: the role of artificial intelligence in clinical practice. BMC Med Educ 2023 Sep 22;23(1):689. [doi: 10.1186/s12909-023-04698-z] [Medline: 37740191]
26. Miranda O, Kiehl SM, Qi X, et al. Enhancing post-traumatic stress disorder patient assessment: leveraging natural language processing for research of domain criteria identification using electronic medical records. BMC Med Inform Decis Mak 2024 Jun 4;24(1):154. [doi: 10.1186/s12911-024-02554-8] [Medline: 38835009]
27. Félix IB, Guerreiro MP, Cavaco A, et al. Development of a complex intervention to improve adherence to antidiabetic medication in older people using an anthropomorphic virtual assistant software. Front Pharmacol 2019;10:680. [doi: 10.3389/fphar.2019.00680] [Medline: 31281256]
28. Martinez-Franco AI, Sanchez-Mendiola M, Mazon-Ramirez JJ, et al. Diagnostic accuracy in Family Medicine residents using a clinical decision support system (DXplain): a randomized-controlled trial. Diagnosis (Berl) 2018 Jun 27;5(2):71-76. [doi: 10.1515/dx-2017-0045] [Medline: 29730649]
29. Ali M. The role of AI in reshaping medical education: opportunities and challenges. Clin Teach 2025 Apr;22(2):e70040. [doi: 10.1111/tct.70040] [Medline: 39956546]
30. Hamilton A. Artificial intelligence and healthcare simulation: the shifting landscape of medical education. Cureus 2024 May;16(5):e59747. [doi: 10.7759/cureus.59747] [Medline: 38840993]

Abbreviations

AAP: American Academy of Pediatrics
AI: artificial intelligence
CHA: Chinese Hospital Association
CMA: Chinese Medical Association
FAERS: FDA Adverse Event Reporting System
HSD: Honestly Significant Difference
ICC: intraclass correlation coefficient
MTM: Medication Therapy Management

Edited by A Coristine; submitted 16.04.25; peer-reviewed by G Marcaccini, J Chen, M Alshiekh; revised version received 17.06.25; accepted 17.06.25; published 24.07.25.

Please cite as:
Li L, Du P, Huang X, Zhao H, Ni M, Yan M, Wang A
Comparative Analysis of Generative Artificial Intelligence Systems in Solving Clinical Pharmacy Problems: Mixed Methods Study
JMIR Med Inform 2025;13:e76128
URL: https://medinform.jmir.org/2025/1/e76128
doi:10.2196/76128

©Lulu Li, Pengqiang Du, Xiaojing Huang, Hongwei Zhao, Ming Ni, Meng Yan, Aifeng Wang. Originally published in JMIR Medical Informatics (https://medinform.jmir.org), 24.7.2025. This is an open-access article distributed under the terms of the Creative Commons Attribution License (https://creativecommons.org/licenses/by/4.0/), which permits unrestricted use, distribution, and reproduction in any medium, provided the original work, first published in JMIR Medical Informatics, is properly cited. The complete bibliographic information, a link to the original publication on https://medinform.jmir.org/, as well as this copyright and license information must be included.

XSL•FO
RenderX

Cardiorenal Interorgan Assessment via a Novel Clustering Method Using Dynamic Time Warping on Electrocardiogram: Model Development and Validation Study

Sally Zhao[1], MS; Zhan Ye[2], PhD; Bhavna Adhin[3], MS; Matti Vuori[4,5], LM; Jari Laukkanen[6,7], PhD; FinnGen[8]; Sudeshna Fisch[2], PhD

[1]Pfizer (United States), New York, United States

[2]Pfizer (United States), 1 Portland St, Boston, MA, United States

[3]Pfizer (United States), Austin, TX, United States

[4]Turku University Hospital, Turku, Finland

[5]Institute for Molecular Medicine Finland, Helsinki, Finland

[6]Institute of Clinical Medicine, University of Eastern Finland, Kuopio, Finland

[7]Department of Medicine, Wellbeing Services County of Central Finland, Jyväskylä, Finland

[8]University of Helsinki, Helsinki, Finland

Corresponding Author:
Zhan Ye, PhD
Pfizer (United States), 1 Portland St, Boston, MA, United States

Abstract

Background: The heart and kidneys have vital functions in the human body that reciprocally influence each other physiologically. Pathological changes in 1 organ can damage the other. Epidemiologic studies show that greater than 50% of patients with heart failure (HF) have preserved ejection fraction (HFpEF). Additionally, 1 in 6 patients identified as having chronic kidney disease (CKD) also has HF. Thus, it is important to be able to predict and identify the cardiorenal relationship between HFpEF and CKD.

Objective: Creating an electrocardiogram (ECG)-enabled model that stratifies suspected patients with HFpEF would help identify CKD-enriched HFpEF clusters and phenogroups. Simultaneously, a minimal set of significant ECG features derived from the stratification model would aid precision medicine and practical diagnoses due to being more accessible and widely readable than a large set of clinical inputs. Furthermore, the validation of the existing cardiorenal relationship using this ECG-enabled model may lead to better biological understanding.

Methods: Using unsupervised clustering on all extractable ECG features from FinnGen, patients with an indication of HFpEF (filtered by left ventricular ejection fraction [LVEF] values ≥50% and N-terminal pro B-type natriuretic peptide [NT-proBNP] values >450 pg/mL) were categorized into different phenogroups and analyzed for CKD risk. After isolating significant predictive ECG features, unsupervised clustering and risk analysis were performed again to demonstrate the efficacy of using a minimal set of features for phenogrouping. These clusters were then compared to clusters formed using dynamic time warping (DTW) on raw ECG time series electrical signals. Afterward, these clusters were analyzed for CKD enrichment.

Results: The PR interval and QRS duration stood out as significant features and were used as the minimal feature set. After generating and comparing clusters (k-means with all extracted ECG features, k-means with a minimal feature set, and DTW with full lead II ECG waveform), the DTW-generated clusters were most stable. ANOVA analysis also showed that several HFpEF clusters exhibited a deviation of CKD risk from baseline, allowing for further trajectory analysis. Specifically, the creatinine levels (a proxy for CKD) of several DTW-created clusters showed significant differences from the average. Based on the Jaccard score, the DTW clusters also showed the greatest alignment to baseline comparison clusters created by clustering on creatinine. In comparison, the other 2 sets of clusters (created by all extracted ECG features and the minimal set) performed similarly.

Conclusions: This project validates both the known cardiorenal relationship between HFpEF and CKD and the importance of the PR interval and QRS duration. After exploring the use of ECG data for patient clustering and stratification, DTW clustering with lead II waveforms resulted in the most clinically meaningful clusters in the context of HFpEF and CKD. This methodology may prove useful in exploring ECG clustering applications outside of HFpEF as well.

(JMIR Med Inform 2025;13:e73353) doi:10.2196/73353

KEYWORDS

data analysis; clustering; electrocardiogram; heart failure; chronic renal insufficiency; ECG; cardiorenal

XSL•FO
RenderX

Introduction

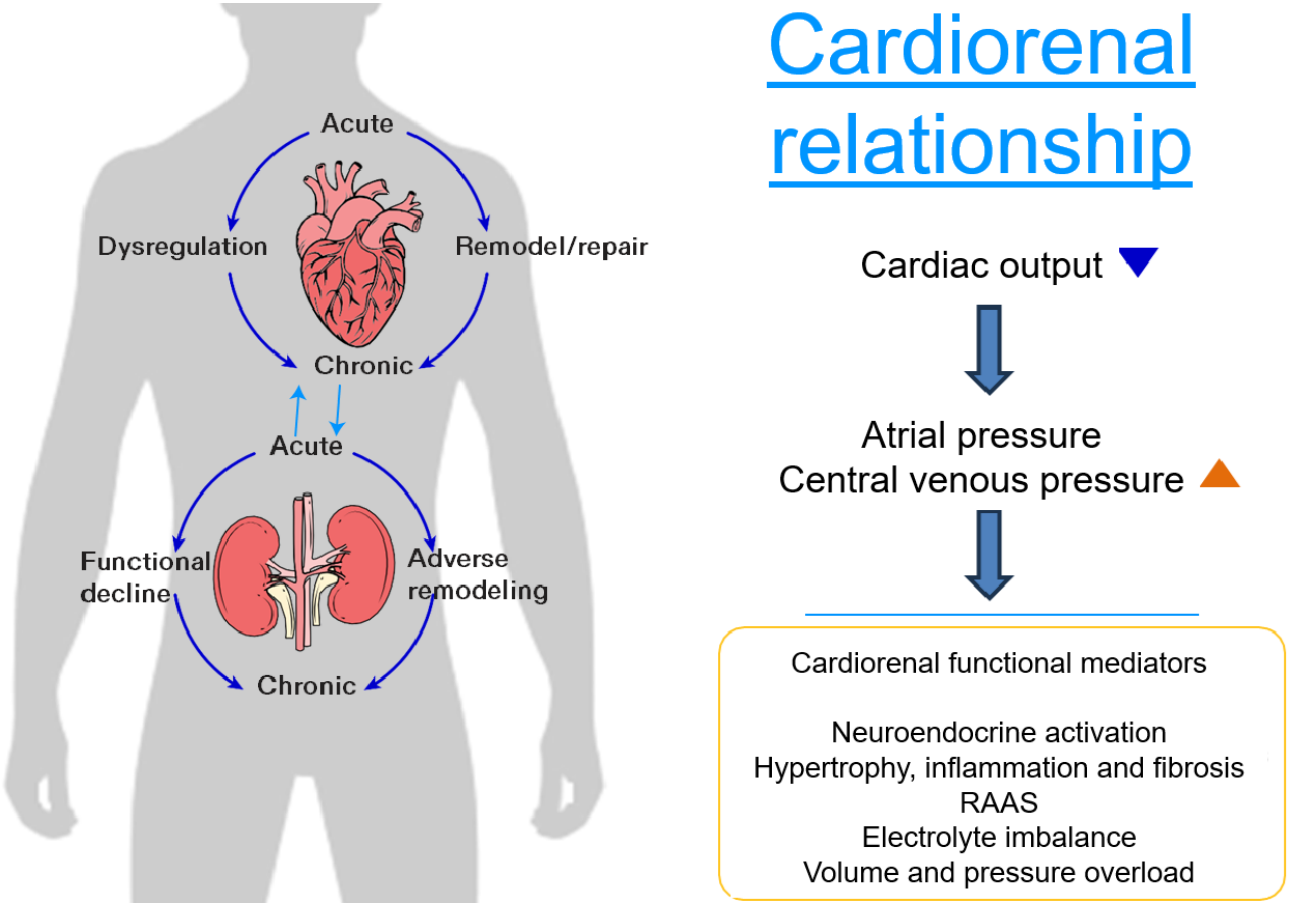
Background

This paper examines the relationship between a specific subtype of heart failure (HF), heart failure with preserved ejection fraction (HFpEF), and chronic kidney disease (CKD) marked by progressive renal failure [1-3], emphasizing the pathophysiological connections. It explores the potential use of technology in trials and clinical management by leveraging simple and widely accessible clinical tools such as electrocardiograms (ECGs) to predict the underlying risk in subgroups and to enable earlier and more precise interventions. Such interventions can improve patient outcomes for chronic diseases of cardiovascular or overlapping renal origin [4-6].

Biological Rationale

HF and renal failure are 2 interrelated conditions that often coexist, significantly impacting patient outcomes [7-9]. The intricate and bidirectional relationship between the heart and kidneys illustrated in Figure 1, often referred to as the cardiorenal axis, underscores the significant unmet need to understand how dysfunction in 1 organ can precipitate or exacerbate dysfunction in the other, so that patients at risk for progression can be precisely diagnosed for earlier intervention before full onset of disease, thus improving the odds of better patient outcome [10].

Figure 1. Illustration of the cardiorenal relationship and functional mediators.



HF, which is marked by the heart's inability to pump blood effectively, initiates a series of physiological changes that can negatively impact renal function. Reduced cardiac output in HF leads to decreased renal perfusion, triggering compensatory mechanisms such as the activation of the renin-angiotensin-aldosterone system and sympathetic nervous system [11,12].

Although these mechanisms initially aim to preserve renal function and maintain blood pressure, their chronic activation can produce adverse effects, including increased sodium and water retention, further worsening heart failure symptoms and contributing to renal impairment [13,14]. HFpEF is characterized by the heart's inability to relax (diastolic defect) and fill properly, leading to heart failure symptoms despite a normal ejection fraction (systolic function).

Conversely, renal failure can significantly affect cardiac function. The kidneys regulate fluid and electrolyte balance, blood pressure, and the elimination of metabolic waste products. When renal function declines, fluid overload, electrolyte imbalances, and the accumulation of uremic toxins can occur, adding strain on the heart. This may lead to worsening HF, creating a cycle of deteriorating cardiac and renal function. This bidirectional nature of the heart-kidney interaction underscores the complexity of managing patients with both HF and renal failure. The ability to better predict risk in these vulnerable cohorts would be beneficial for disease understanding and clinical trial recruitment.

XSL•FO
RenderX

ECG for Clustering

Recent advancements in artificial intelligence and machine learning have shown potential in predicting and managing the risks associated with cardiorenal syndrome. Artificial intelligence–enabled models, for example, using ECG and biomarkers, have demonstrated promise in clinical care settings [15,16].

An additional use of such an ECG model in drug development could be to identify patients with HFpEF who may demonstrate a potential risk profile for worsening kidney function based on a screening ECG. Such patients may demonstrate other comorbidities such as hypertension, diabetes, or obesity, as stated earlier. This underlying and hidden risk can be revealed early for an improved understanding of the associated risks with renally cleared cardiovascular drugs. The cardiac-specific electric signals provide significant discriminatory power for endophenotyping within the broader HFpEF spectrum [17]. By leveraging machine learning-based unsupervised cluster analysis, this study aims to phenomap patients with HFpEF, enhancing the understanding and prediction of cardiorenal risk through a generalizable and interpretable ECG-based machine learning model.

Evaluating the importance of ECG features for unsupervised clustering can be difficult. A lot of tabular health care data, including the extracted ECG features, are highly correlated, which may lead to poor clustering results in practice. This also makes feature selection through Lasso very difficult. Reducing dimensionality often makes interpretability difficult as well, which is especially an issue for health care research. Thus, finding an unsupervised method that clusters high-dimensional correlated data through feature selection rather than dimension reduction would be very helpful [18].

Dynamic Time Warping With ECG

Dynamic time warping (DTW) measures the similarity between 2 temporal sequences and, thus, can be used as a metric for clustering temporal sequences. By creating a nonlinear alignment of time sequences that are of different lengths or exhibit time shift, it can calculate the Euclidean distance between points of the 2 warped sequences. DTW has been frequently used for longitudinal and trajectory analysis, including in health care settings [19]. Due to the temporal nature of ECGs, DTW has been used to classify ECG frames and has been shown to be effective in finding nonlinear clusters of ECGs [20]. Previous literature and studies for DTW ECG clustering use the lead II recording wavelengths due to the lead II wavelength being generally considered the best view of the electrical signals because of the electrode's placement [19].

ECGs are particularly appropriate for this combination of DTW-supported unsupervised clustering and feature analysis. First, the assumption that patients themselves, rather than the extracted ECG values, are independent and identically distributed is much easier to meet. This may make unsupervised clustering results more promising than on extracted ECG data (which would be correlated tabular data). By treating each ECG record as a singular data point, we can perform DTW on the ECG as a time series. DTW is a technique that calculates the optimal match between given sequences (it can be thought of as clustering curves via distance rather than individual data points). This way, different clusters of ECG records can be formed and then analyzed for disease endpoint incidence, cluster stability, and other performance metrics.

Many studies focus on the relationship between HFpEF and electrocardiographic (ECG) features, but our work attempts to explore the cross-organ interactions between the heart and kidney in HFpEF by using an algorithm that uses specific features within ECG features as novel predictors of cardiorenal risk. Small changes in the electroconductance system of the heart can have a big impact on the hemodynamic load on the heart, exacerbating the load, and over time, affecting volume overload [10] on the kidneys. However, such small changes in ECG, which may appear early, may not always be clinically apparent and can often be missed. In patients with HFpEF, clinical phenotype can be associated with diabetes, hypertension, and obesity [21]. Using an ECG model to identify nonobvious patterns in the electrical signals of the heart captured through a standard ECG (12 leads) can serve as indicators for left ventricular dysfunction associated with HFpEF and can potentially also identify potential signals for renal risk in a subset of patients. This study seeks to validate the established cardiorenal relationship through ECG data analysis and investigate a novel approach for clustering in HFpEF subgroups using ECG data.

Methods

Ethical Considerations

The real-world electronic health data used from the FinnGen database, provided for analysis, were already anonymized by FinnGen. The ethics status, data collection process, consent process, and approvals can be seen in the original study [22]. This study's data analysis was approved by the FinnGen Committee. Due to this, there was no need to seek further ethics board approval.

Dataset Description

The FinnGen study is a large-scale genomics initiative that has analyzed over 500,000 Finnish biobank samples and correlated genetic variation with health data to understand disease mechanisms and predispositions. The project is a collaboration between research organizations and biobanks within Finland and international industry partners [22]. This public-private partnership aggregates data from 9 different Finnish biobanks, research institutes, university hospitals, and 13 international pharmaceutical partners along with the Finnish Biobank Cooperative. Sample collection and data releases began in 2017, and the main phase of sample collection ended with FinnGen2 in 2023.

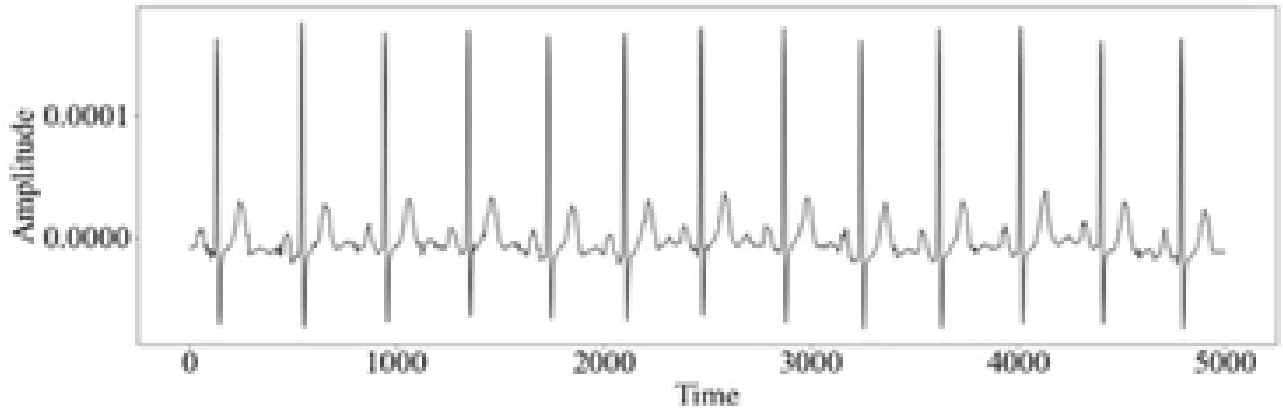
The Expansion Area 3 (EA3) studies aim to collect data on diseases that may not be present within existing FinnGen registries. Among these data is the EA3 Heart Failure Study cohort, which compiles relevant cardiovascular data from 4 - 6 participating hospital biobanks. The study contains ECG files, ejection fraction values (40,809 individuals), and laboratory measurements (40,024 individuals) with B-type natriuretic

XSL•FO
RenderX

peptide (BNP), proBNP, and creatinine values. Since the study is aggregated from several different existing biobanks, not all individuals have the same laboratory measurements. This project used the EA3 Heart Failure study, individuals with ECG, ejection fraction, and laboratories with creatinine and proBNP values all present.

The methods for extracting relevant features are changing and evolving over time [23], but the idea remains the same. The ECG follows a characteristic PQRST wave that occurs in a periodic pattern. Each peak, trough, or section of this wave represents electrical signals of the heart and can be evaluated for further meaning. Clinicians can look at the ECG visually for meaning, but signal processing techniques can also retrieve the mathematical values from the waves themselves. Since there are multiple electrodes for measuring the ECG, this is usually taken from lead II signals (Figure 2) [24] or aggregated.

Figure 2. A sample lead II ECG wave. ECG: electrocardiogram.



Data Preprocessing

The dataset was restricted to the population with HFpEF (Table 1). This was determined by selecting individuals with ejection fraction values greater than or equal to 50 and exhibiting HF at that time (Figure 3). All selected individuals were verified to have HF diagnoses (either I9 HF or I9 HF NS). Only ECGs recorded within a 6-month period of the heart failure diagnosis or laboratory indicative of HF were used in this study. Creatinine values were used as a proxy for the presence of CKD. The EA3 HF Cohort contained 1,626,275 laboratory records for 40,024 unique individuals. Among these, there were 7170 complete ECGs (extracted ECG values and raw ECG signals) and creatinine laboratory records for 3864 unique individuals with HFpEF (Figure 3). The raw lead II ECG signals each contained 5000 points of data and were taken from individual ECG files within the EA3 HF cohort. These signals were directly input into the DTW algorithm. It was these ECG and laboratory records that were used for clustering and analysis (Figure 4). Specifically, the data groups to be clustered included extracted ECG values, a minimal set of extracted ECG values, and raw lead II signals.

Clusters created through hierarchical clustering on creatinine served as a baseline for CKD risk, against which the ECG-enabled clusters were compared. This comparison aimed to evaluate the effectiveness of ECG-enabled clusters in stratifying patients with CKD risk within the context of HFpEF.

Table . A characteristics average table to give a better understanding of the clustering cohort. This cohort is comprised of individuals who have characteristics that indicate HFpEF (LVEF≥50% and NT-proBNP>450 pg/mL).

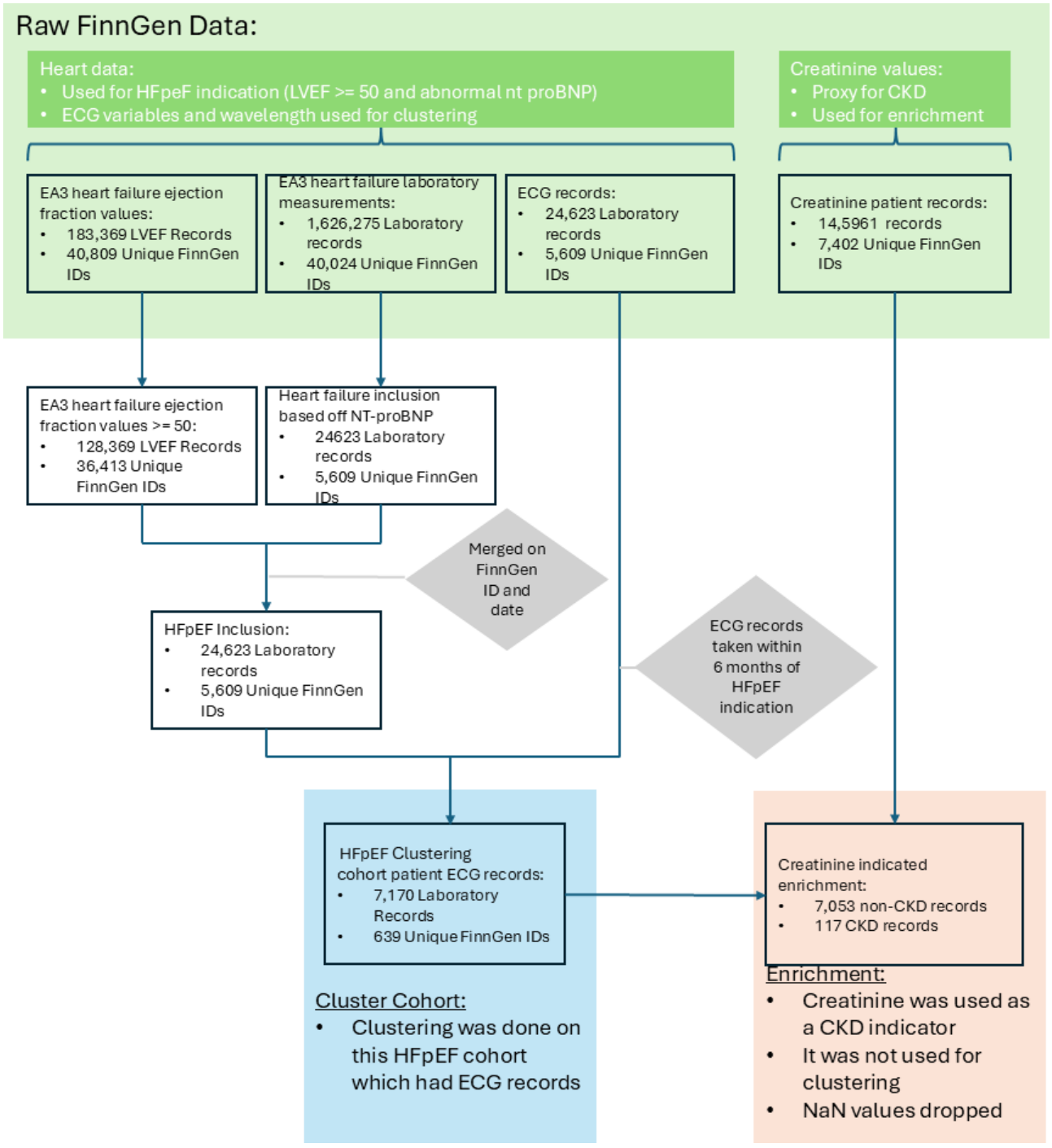
Clustering cohort baseline characteristics	Values
Age (years), mean (SD)	71.16 (11.32)
Women, n (%)	3478 (48.5)
BMI (kg/m^2), %	28.4
NT-proBNP (pg/mL)	2018.1
LVEF[a] (%)	60.25
Creatinine (µmol/L)	103.02
Height (cm)	170.3
Weight (kg)	82.7
Current smoker, n (%)	882 (12.3)
Chronic kidney disease, n (%)	115 (1.6)

[a]LVEF: left ventricular ejection fraction.

[b]NT-proBNP: N-terminal pro B-type natriuretic peptide.

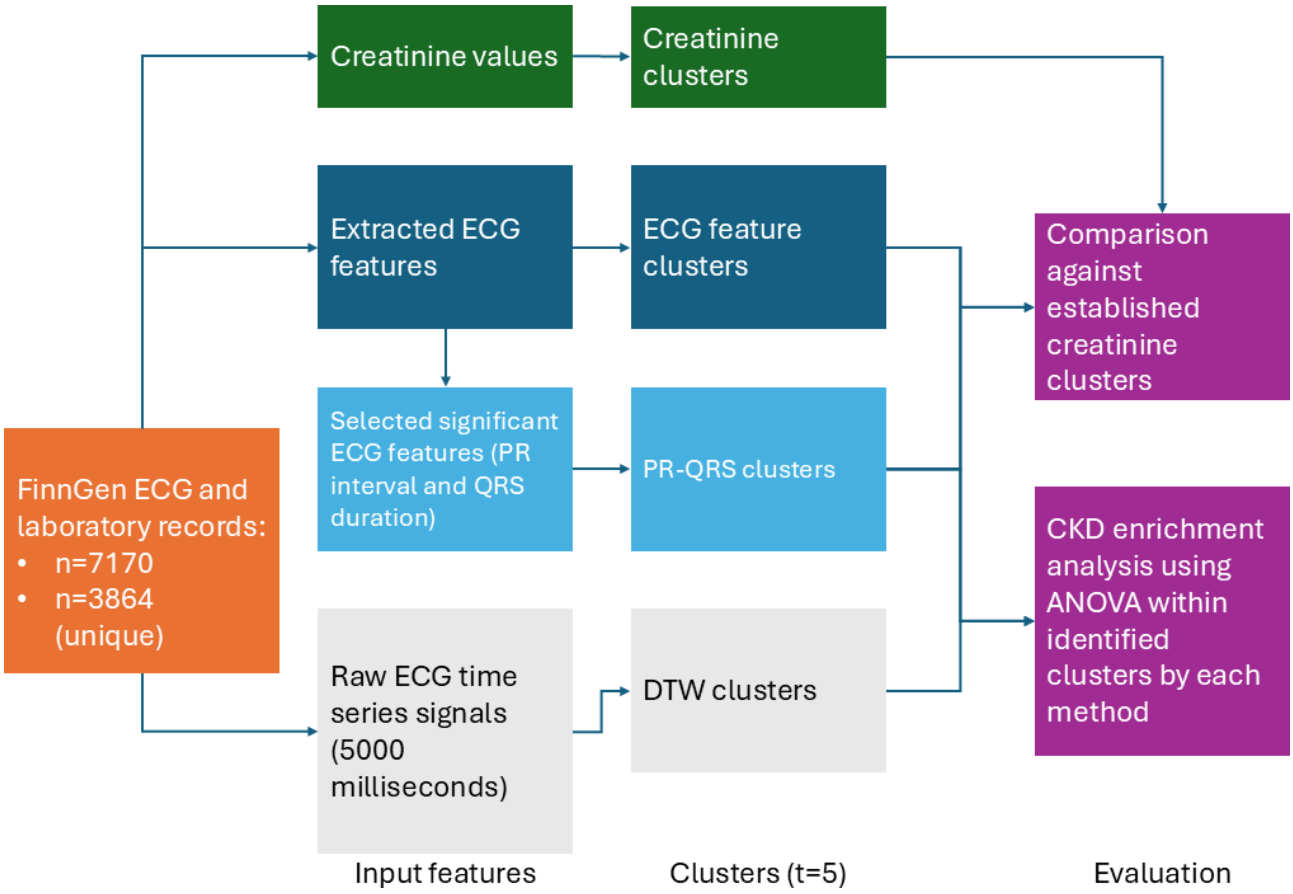
XSL•FO
RenderX

Figure 3. An illustration of the data processing flow and the sources of the dataset. CKD: chronic kidney disease; ECG: electrocardiogram; Expansion Area 3; HFpEF: heart failure with preserved ejection fraction.



XSL•FO
RenderX

Figure 4. An illustration of the methodology workflow. FinnGen ECG and laboratory records are used to create different sets of clusters: Creatinine clusters (hierarchical clusters based off creatinine labs to be used as a baseline indication for CKD), ECG feature clusters (clusters created using all extracted ECG features), PR-QRS clusters (clusters created using top variables determined to be significant in predicting CKD in HFpEF), and DTW clusters (clusters created using DTW on the raw ECG time series). For each set of clusters, 5 groups were formed. CKD: chronic kidney disease; DTW: dynamic time warping; ECG: electrocardiogram; HFpEF: heart failure with preserved ejection fraction.

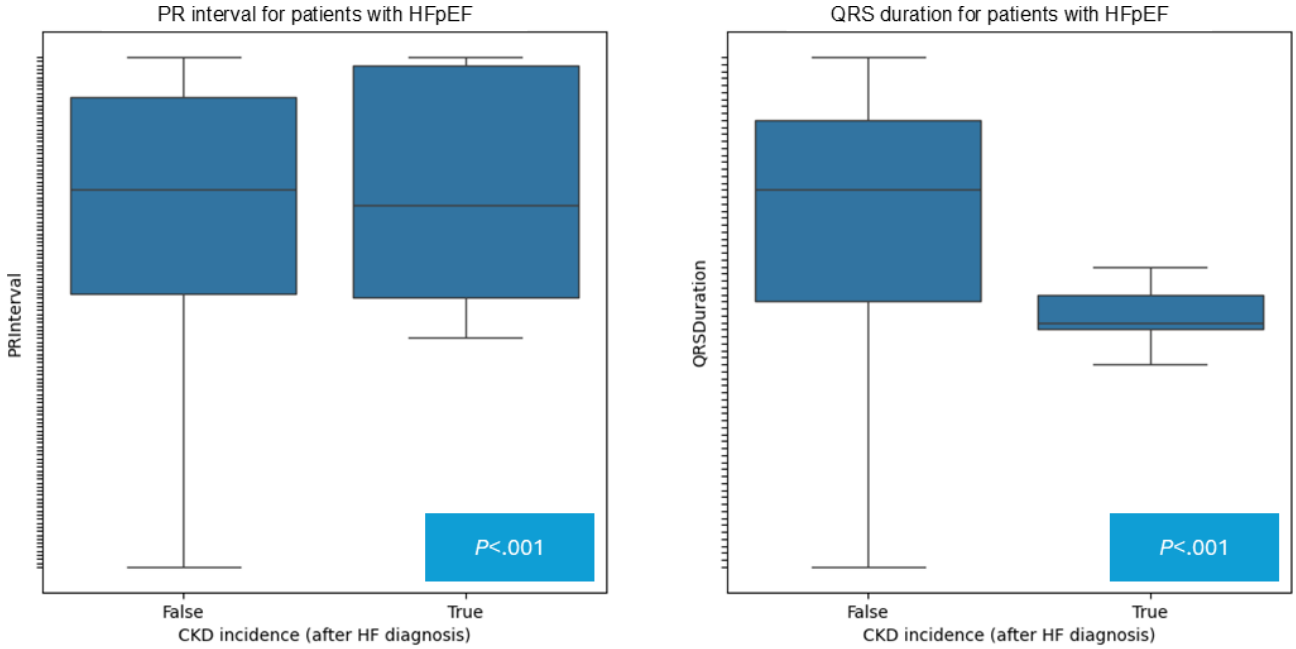


Statistical Analysis

Univariate analysis was first performed for exploratory purposes. Distributions and averages of the extracted ECG values (ie, ventricular rate, PR interval, QRS duration, QT corrected, P axis, R axis, T axis, QRS count, Q onset, Q offset, P onset, P offset, T offset, atrial rate, and QT interval) were calculated. A 1-tailed *t* test was conducted for all extracted ECG variables to determine if there was a significant difference between patients with non-CKD and CKD HFpEF ECG values. It was shown that all extracted features were indeed significantly different with a significance level of .05 (Figure 5). Survival analysis was also conducted using a Cox proportional hazard model and a Kaplan-Meier curve.

XSL•FO
RenderX

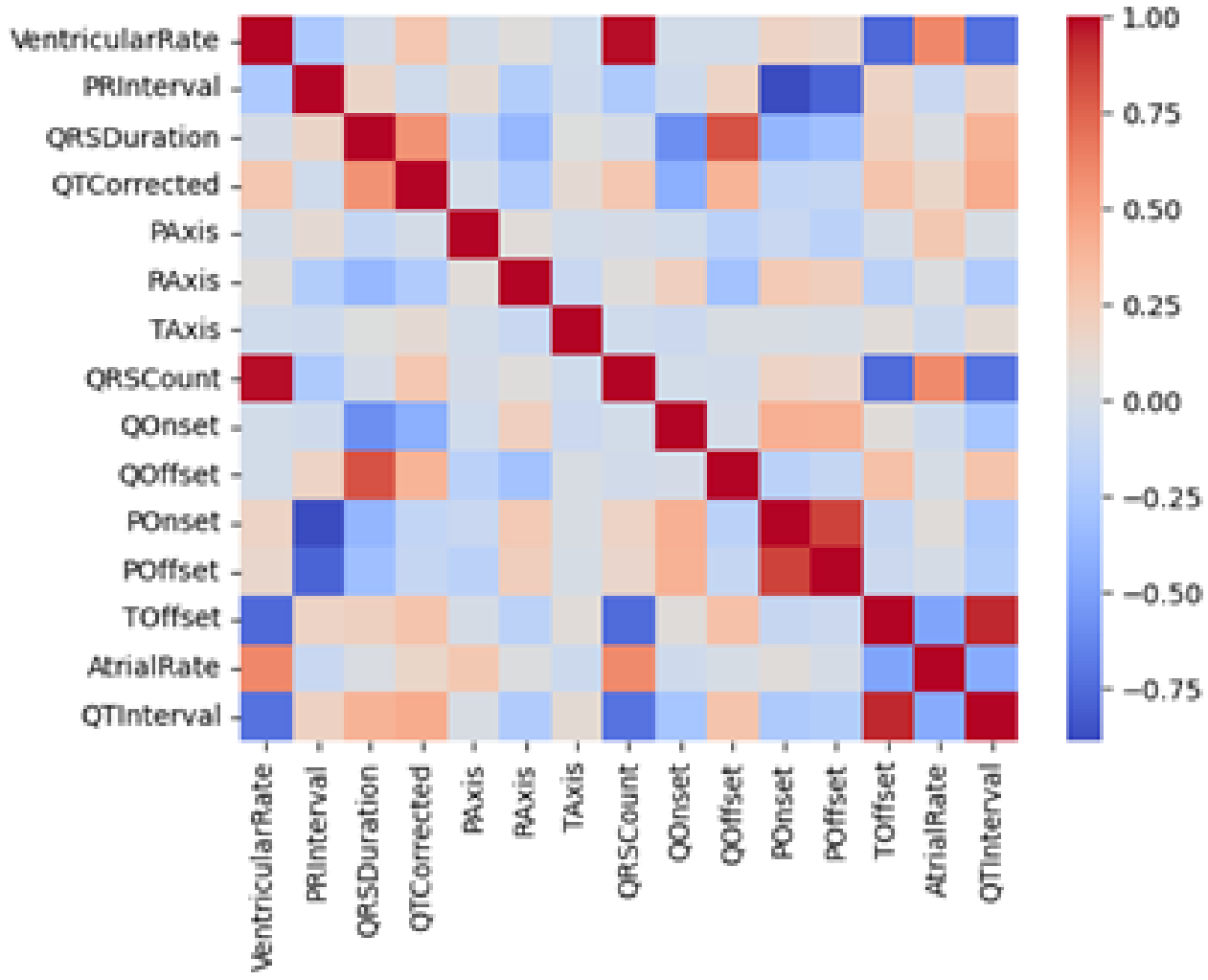
Figure 5. Distribution of significant extracted ECG values (QRS Duration and PR Interval) between patients who are CKD-positive and CKD-negative. CKD: chronic kidney disease; ECG: electrocardiogram; HF: heart failure; HFpEF: heart failure with preserved ejection fraction.



Multivariate analysis of the extracted features was also conducted. It must be noted that the method may not be wholly accurate because the correlation between the extracted features is derived from the ECG waveform itself and can have some overlap (Figure 6). It must be noted that the method may not be wholly accurate because of the correlation between the extracted features. Additionally, these features lose some information in terms of the time component. However, it provides good exploratory insight into which combination of features would perform well for both CKD prediction and patient phenotyping.

XSL•FO
RenderX

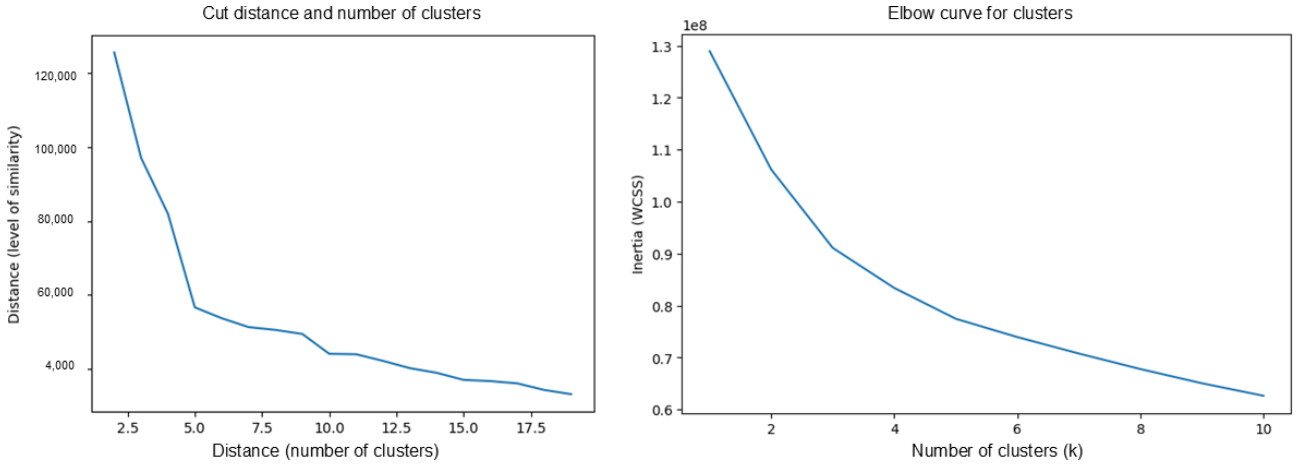
Figure 6. A heatmap showing the correlation between extracted ECG features. ECG: electrocardiogram.



Determining the Number of Clusters

To determine the number of clusters created, elbow curves (Figure 7) were created and analyzed to determine which number of clusters would be optimal. As both elbow charts exhibit diminishing returns at around the 5-cluster mark, it was determined that 5 clusters would be generated and compared.

Figure 7. Elbow curves for extracted feature and DTW hierarchical clustering. This was used to determine the optimal number of clusters (t=5). The number of clusters was determined using these elbow charts and by seeing where the reduction in inertia or cut threshold has diminishing returns. DTW: dynamic time warping. WCSS: within-cluster sum of squares.



XSL•FO
RenderX

Extracted Feature Clustering

Several methods were used, including principal component analysis (PCA), significance, and Lasso feature selection. Relevant hyperparameters (eg, α for Lasso dropout) were tuned iteratively to find the top 5 (5 is predefined) features. For PCA, 50 simulations were run for stability and robustness purposes. In every simulation, the FinnGen data were randomly sampled (training=0.8, 80% from all data) and PCA was conducted on this random sample to select the top 5 ranked features. The top 5 features in order are: ventricular rate, PR interval, QRS duration, QT corrected, and P axis. As for Lasso regression, the top features were QRS duration, QT interval, R axis, QT corrected, and PR interval. In terms of significance, the top features were ventricular rate, PR interval, QRS duration, QT corrected, and P axis, with the average explained variance reported in Table 2 on the top features identified from multiple methods. From this exploration, we can see that the PR interval and QRS duration were always selected as top features.

Table . A table ranking component (electrocardiogram variable) importance by average explained variance. PR interval and QRS duration are among the top 3 extracted variables. Ventricular rate was not chosen because it was not selected among the top 5 features during Lasso regression.

PCA[a] component	ECG[b] variable	Average explained variance
0	Ventricular rate	0.276
1	PR interval	0.251
2	QRS duration	0.156
3	QT corrected	0.122
4	P axis	0.091

[a]PCA: principal component analysis.

[b]ECG: electrocardiogram.

However, despite bootstrapping for stability and generalizability, the clusters formed from PR interval and QRS duration had low stability and consensus, despite performing better than clustering on all features. This is probably due to the correlated nature of the extracted ECG features. Thus, hierarchical clustering using DTW distance calculations was also performed to consider the correlation.

DTW Clustering

The ECG lead II data were split into a training, validation, and test sets, each with 500 different unique individuals. Every patient's lead II data included 5000 signals. These were then clustered using hierarchical clustering with the Ward method. The Ward method was chosen because it is close in functionality to k-means, which makes it intuitive and interpretable. However, it also performs better than k-means on uncovering clusters of uneven size and irregular non-spherical clusters. Exploratory analysis has shown the clusters to be uneven and not guaranteed to be regular, which makes the Ward method a good fit.

DTW was used to determine the similarity between two time series. In this case, the time series would be the lead II ECG signals. This was done by calculating the Euclidean distance between each point after finding the best alignment of the 2 sequences (Figure 8). In order to find the best alignment or shift, the distance between pairs of points is compared, and the minimum distance is taken. This is done for the entirety of the 2 sequences. After creating a matrix representation for the costs associated with each alignment, the algorithm returns the minimum cost—that is, the minimum distance between aligned time series. For the regular ECGs, little shift was needed to occur. No normalization techniques were applied to the ECG lead II records. For faster processing speeds, the code was parallelized using the Python (Python Software Foundation) multiprocessing module.

Afterward, creatinine values were associated with every ECG, and the average creatinine value was calculated for every cluster. The average creatinine value of the population with HFpEF was 101.51 umol/l. Additionally, all clusters were validated through bootstrapping the data. Multiple subsets of 500 were created and clustered. This was performed to measure the stability and generalizability of the various clusters. Since the k-means and hierarchical algorithms are not consistent and exact in their results every time, this was necessary to ensure that the observed clusters (and their associated creatinine values) remained stable.

XSL•FO
RenderX

Figure 8. Pseudocode demonstrating the flow of the DTW algorithm and the generation of the matrix used for determining similarity between two separate time series. DTW: dynamic time warping.

```
function dtw_distance(ts1, ts2):
    n = length(ts1)
    m = length(ts2)
    dtw_matrix = initialize matrix of size (n+1, m+1)
        with infinity
    dtw_matrix[0][0] = 0

    for i from 1 to n:
        for j from 1 to m:
            cost = absolute difference between ts1[i-1]
                and ts2[j-1]
            dtw_matrix[i][j] = cost + minimum of (
                dtw_matrix[i-1][j], dtw_matrix[i][j-1],
                dtw_matrix[i-1][j-1])

    return dtw_matrix[n][m]
```

Creatinine Clusters

Since all clusters were created in an unsupervised manner, there was no true baseline to compare the cluster labels to. Thus, the 5 clusters formed by hierarchical clustering on the creatinine laboratory values were created as a stand-in. Being a waste product from muscle and protein breakdown, creatinine levels can serve as an estimation of kidney function and a metric for CKD. Thus, comparing the extracted ECG value and DTW-formed clusters to these creatinine-based clusters can demonstrate the former's capabilities in demonstrating creatinine enrichment and, subsequently, CKD enrichment.

Cluster stability was measured using the silhouette score [25], co-cluster occurrence (Jaccard score), and Rand index [26]. For the hierarchical clustering on the DTW-determined distance, the Jaccard index was determined to be a more relevant metric than the silhouette score. Compared to naively clustering on extracted features, the clusters were shown to be more stable.

Average features were calculated for every ECG cluster. ANOVA (Table 3) was conducted to determine any significant extracted feature difference between the clusters.

XSL•FO
RenderX

Table . ANOVA test on all extracted ECG[a] values between the 5 clusters identified in the ECG feature clusters.

ECG variable	*F* test (*df*)	*P* value
Ventricular rate	46.945 (4, 495)	<.001
PR interval	2.466 (4, 495)	.062
QRS duration	42.311 (4, 495)	<.001
QT corrected	14.901 (4, 495)	<.001
P axis	.498 (4, 495)	.684
R axis	61.873 (4, 495)	<.001
T axis	.226 (4, 495)	.878
QRS count	47.793 (4, 495)	<.001
Q onset	15.444 (4, 495)	<.001
Q offset	28.054 (4, 495)	<.001
P onset	5.614 (4, 495)	.001
P offset	3.295 (4, 495)	.020
T offset	28.427 (4, 495)	<.001
Atrial rate	14.475 (4, 495)	<.001
QT interval	29.769 (4, 495)	<.001

[a]ECG: electrocardiogram.

Results

Clustering on Extracted ECG Features

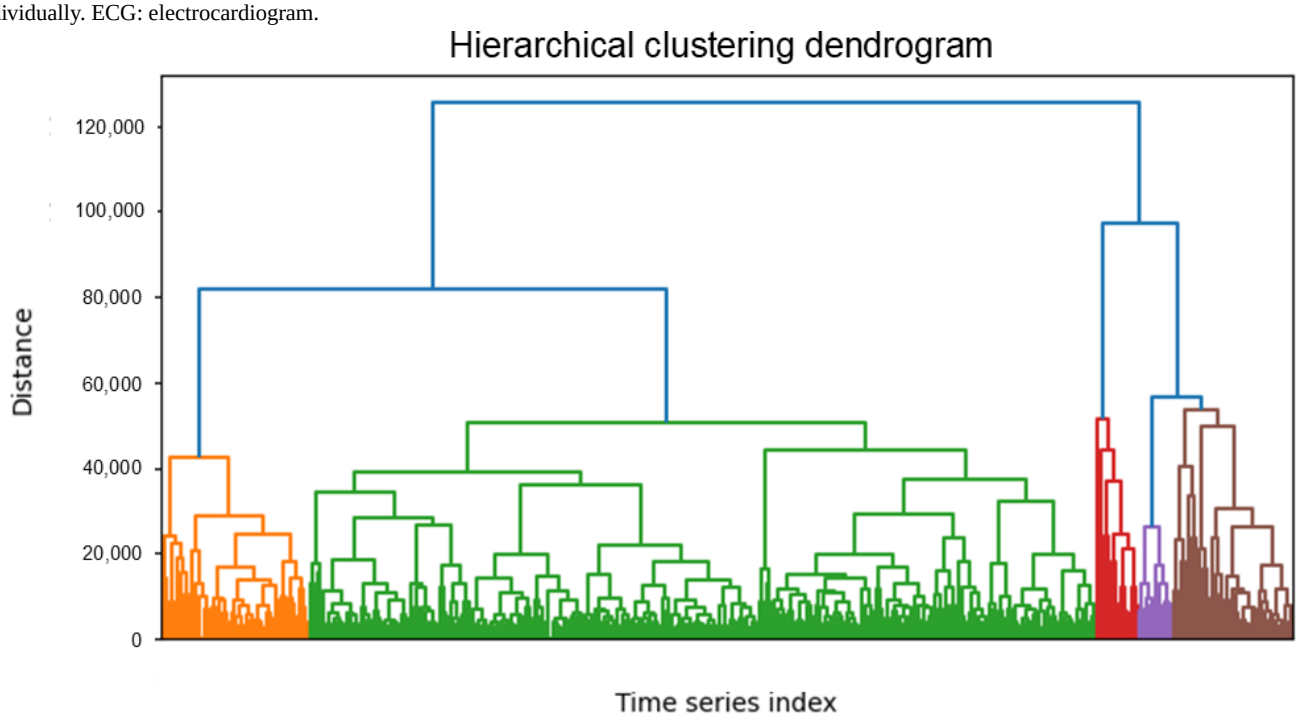
The top 2 features determined are QRS duration and PR interval. Both of these features were unique among the top 5 ranked features in every method used (significance, Lasso, and PCA).

Although there is a difference between CKD incidence when clustering on all available ECG features compared to clustering on the significant ECG features (PR interval and QRS duration), the difference may be too small to be clinically significant.

Clustering With DTW

Regardless of how many clusters the parameter is set for with hierarchical clustering, clustering with DTW consistently yielded approximately 5 groups (Figure 9). This phenomenon could be seen in both the testing and validation sets, and also when bootstrapping.

Figure 9. Hierarchical clustering on the validation set. It can be seen that approximately 5 clusters form which match up to the number of clusters estimated using the elbow method on the extracted ECG values. Due to the number of time series that were clustered, there were too many labels to list individually. ECG: electrocardiogram.

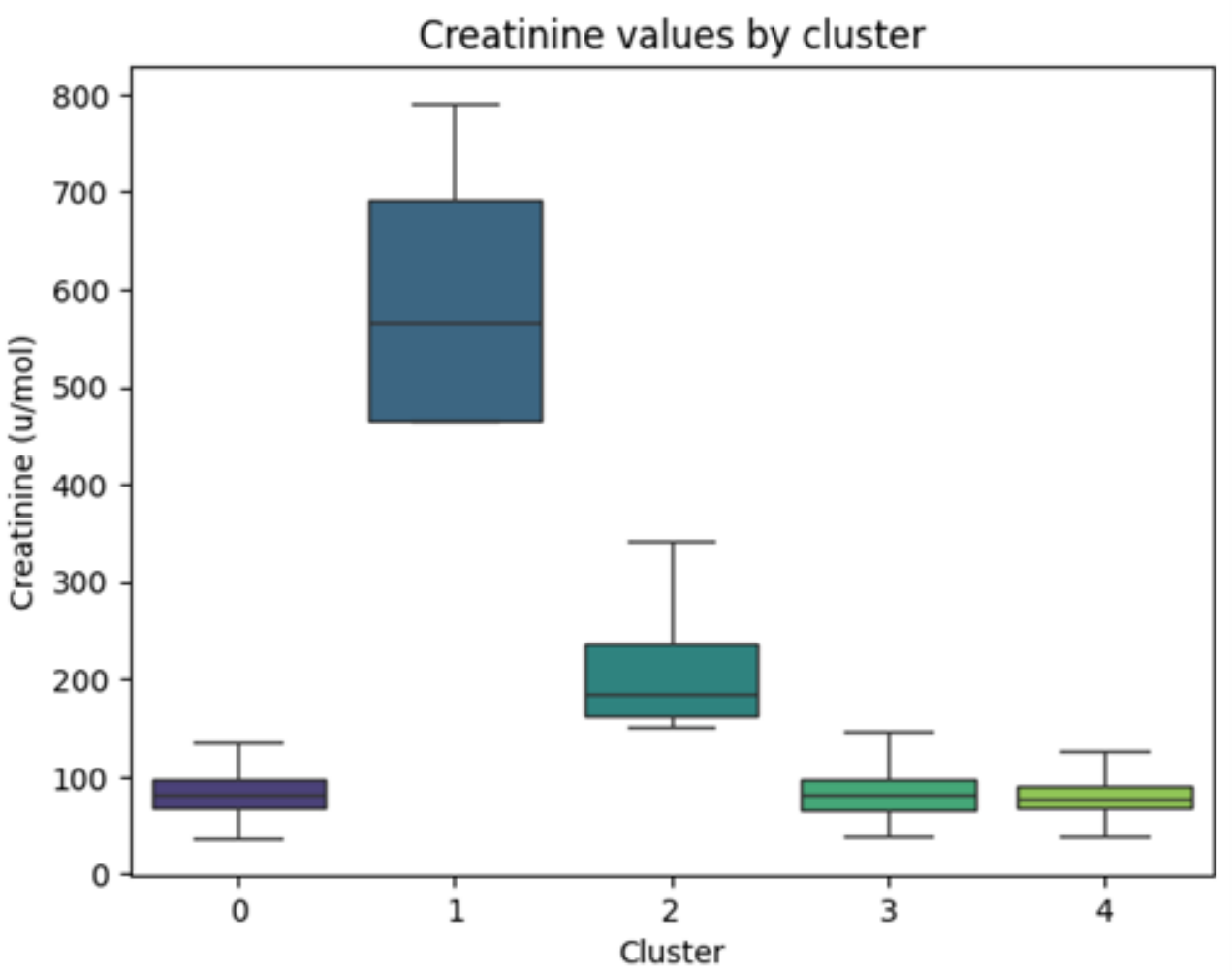


XSL•FO
RenderX

Figure 10 shows that there were creatinine differences among DTW clusters. Additionally, all extracted ECG features with the exception of P axis, T axis, and PR interval were shown to be statistically significant from cluster to cluster (Table 3). This indicates that the clusters did measurably separate the ECG time series, not just by time series shape but also by the relevant values or sections that would be extracted from the series.

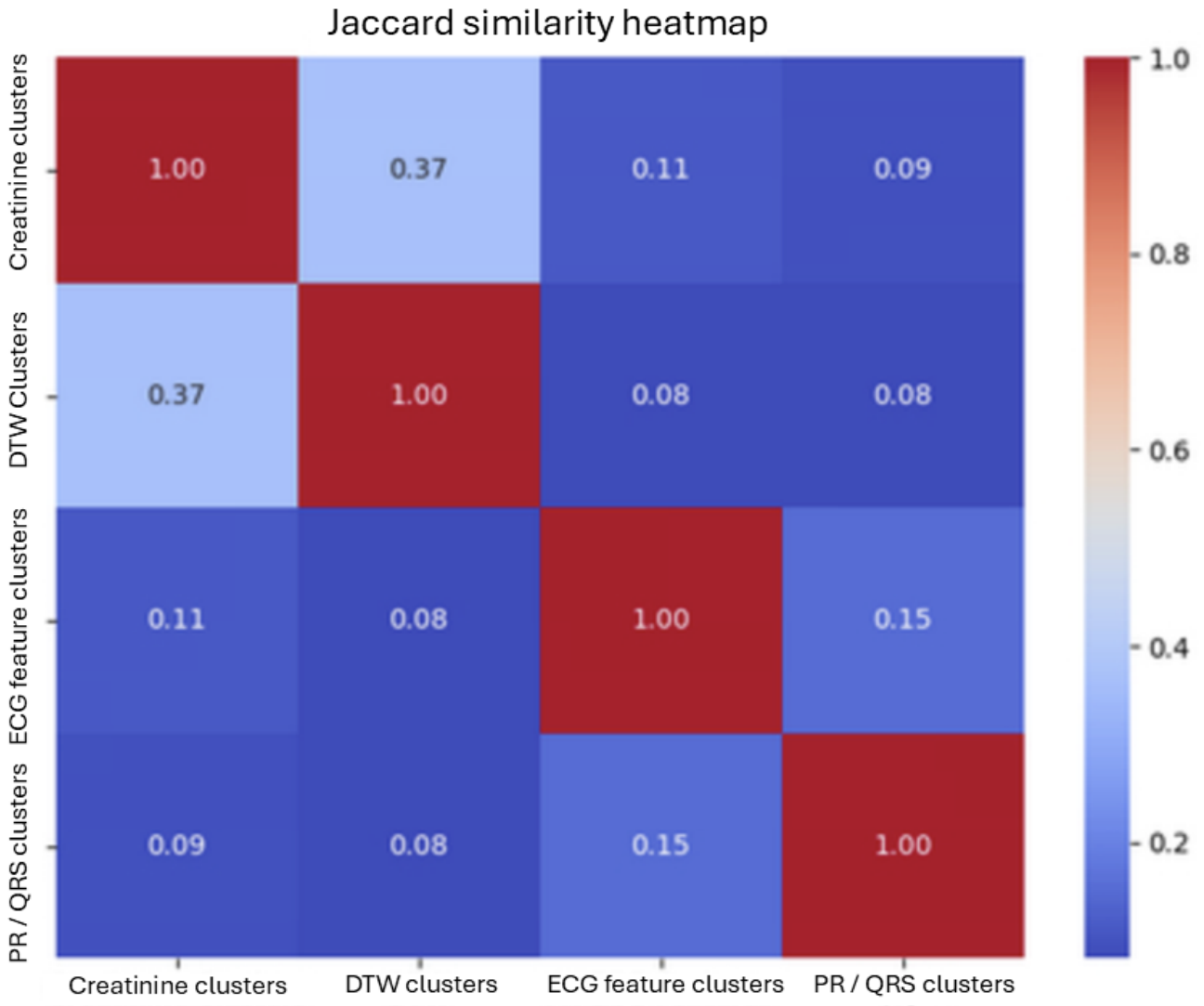
Based on the Jaccard Score, the DTW-created clusters are most similar to the creatinine-based clusters (Figure 11). This indicates that it is a better stand-in for CKD enrichment than clustering solely on ECG extracted features.

Figure 10. Creatinine value distribution among the 5 clusters identified in dynamic time warping clusters.



XSL•FO
RenderX

Figure 11. Jaccard score heatmap that compares the clusters' similarities to each other. DTW: dynamic time warping; ECG: electrocardiogram.



Discussion

Principal Findings

From the results, the PR interval and QRS duration are shown to be the extracted ECG variables most associated with CKD in the HFpEF cohort. This follows the biological rationale as the PR interval and QRS complex are 2 important features of an ECG signal that capture both time and spatial dynamics of a cardiac cycle. Each aspect of the selected ECG features can provide valuable information about the heart's function. Since the heart pumps blood systemically and into the lungs and kidneys, the electric signals may also inform about any altered hemodynamics in the latter organs [27].

The PR interval represents the time it takes for the electrical impulse to travel from the sinoatrial node, through the atria, to the ventricles. A prolonged PR interval may indicate a delay in the conduction of the electrical impulse, which can be caused by various conditions and is often suggestive of atrial abnormalities (eg, atrial volume and strain). The atrial changes can, in turn, affect subsequent changes in the ventricular contraction phase [28].

The QRS complex represents the depolarization of the ventricles, which triggers the contraction of the ventricles and the pumping of blood out of the heart into systemic circulation. The duration of the QRS complex is an important indicator of the heart's function, and a prolongation may indicate a delay in the conduction of the electrical impulse through the ventricles, which can be caused by various conditions, including bundle branch blocks, ventricular hypertrophy, or myocardial infarction [29,30]. There is evidence to suggest that abnormalities in the PR interval and QRS duration may be associated with an increased risk of kidney disease in patients with HFpEF [28].

To make the connection from the heart to the kidney as shown in Figure 1, it is important to note that these 2 time intervals reflect the heart's electrical conductance system and are intricately linked to cardiac relaxation, also known as diastole. During diastole, the heart fills with blood after the contraction of the ventricles, and this relaxation phase is important for maintaining adequate blood flow to the whole body, a capacity that is often lost in some patients with HFpEF.

ANOVA analysis shows significant differences between the creatinine levels of the 5 clusters generated by DTW. Not all the clusters' creatinine levels differ significantly, but clusters

XSL•FO
RenderX

1 and 2 (Figure 10) do exhibit statistically significant differences. This means that DTW-enabled clustering was capable of stratifying patients with HFpEF with differing creatinine levels and thus differing CKD risk levels.

Despite the supported relationship between PR interval and QRS duration with CKD in HFpEF, the PR-QRS clusters did not demonstrate much similarity with the established creatinine clusters. Additionally, these PR-QRS clusters demonstrated low stability and less pronounced CKD incidence rates among the individual clusters. However, the PR-QRS clusters' Jaccard similarity with the creatinine scores (0.09) and silhouette scores was similar to that of the ECG Feature clusters' Jaccard similarity (0.11) with the creatinine scores and silhouette scores. This indicates that clustering on PR-QRS performs similarly to clustering on all extracted ECG features—further demonstrating that a relationship exists between PR interval and QRS duration with CKD in HFpEF. Nevertheless, due to the cluster instability and low Jaccard similarity with the creatinine baseline, it could not be used to inform clinical decisions.

DTW clusters performed much better than the PR-QRS clusters and ECG feature clusters in terms of Jaccard similarity (0.37) to the established creatinine baseline. Although the cluster groupings were not perfectly equivalent, the similarity demonstrates the potential application of using DTW for ECG clustering. This is intuitively expected due to the DTW being able to fully use the entire ECG signal. Previous literature has also supported the clustering capabilities of DTW for ECG and other signal-based records.

However, the specific reason why DTW performed better remains to be seen. Knowing the difference between the information DTW clustering captures compared to the information extracted ECG features clustering captures would be helpful. This could be used for better understanding of the statistical aspects of DTW application for clustering, as well as the cardiorenal relationship between HFpEF and CKD in this case. DTW's better performance implies that the full lead II waveform contains more data than the extracted ECG features—minimal set or otherwise. This means that solely using extracted ECG features when working with ECG data analysis may lead to some loss of context.

Limitations

There were certain limitations to the dataset, most notably with regard to its demographics. As the FinnGen study aggregates data from Finnish biobanks, the population is overwhelmingly Finnish and lacks heterogeneity that may pose a challenge to generalizability to other populations. Certain patients were also overrepresented in the dataset. The average patient with HFpEF had 5 ECGs spaced over a 1-year period. However, there were patients who had many ECG records (greater than 5) and patients with only a few ECG records. The FinnGen EA3 Heart Failure cohort is also not representative of all HF or patients with HFpEF. This means that extrapolating this project's results to the wider population may not yield good results. There are disease differences between FinnGen and the external population—the renal and cardiovascular outcomes may not perform well.

Additionally, although all data were sourced from the FinnGen EA3 Heart Failure cohort, the cohort itself is comprised of several different biobanks, and each biobank provides differing amounts of data. ECG data were only available from the Central Finland Biobank. This meant that, while some patients had characteristics that indicated HFpEF, they could not be included in this study since they lacked ECG data. This data limitation introduces bias as it means all individual data is effectively from the Central Finland Biobank.

HFpEF itself is also difficult to diagnose, and the current diagnosis is multifaceted, with many clinical parameters. Due to a lack of diagnosis codes in the FinnGen EA3 Heart Failure cohort, clinical diagnosis of HFpEF could not be obtained. We used the FinnGen R12 cohort to confirm that the selected dataset had HF diagnostic codes (either I9 Heart Failure or I9 Heart Failure NS). Thus, using this in combination with the LVEF and NT-proBNP values (some of the main parameters for HFpEF), the selected individuals are indicated for HFpEF. Although this selected cohort may not be purely composed of clinically diagnosed patients with HFpEF, there could have also been a greater likelihood of finding an enrichment for patients with HFpEF. Furthermore, as the biological rationale behind the hypothesis is on the cardiorenal associations between the heart and kidneys, it is the specific heart features (ie, hypercontractility and failure) that are most relevant rather than a clinical diagnosis. The relationship between the heart and kidneys is already known to exist, so this cohort serves as a sort of positive control.

Due to the lack of diagnosis codes in the EA3 Heart Failure Cohort, CKD was also difficult to label. Even with diagnosis codes, it is entirely possible that this subset may be underdiagnosed. Creatinine laboratory records provided in the EA3 Heart Failure Cohort were used as proxies for CKD. Estimated glomerular filtration rate could have also been used, but these data were not as complete as the creatinine records and would have severely limited the cohort.

There are also confounding factors, such as medications or co-morbidities, that may affect both ECG readings and creatinine levels. Unfortunately, the lack of medications and co-morbidities from the dataset is a limitation that can be rectified in the future through validation on an external dataset such as the FinnGen R12 Cohort.

In addition, DTW also has its own limitations. Although it does consider the entire ECG signal, it reduces it down to a singular similarity metric (ie, distance) that may be reductive. Additionally, it is very computationally intensive and sensitive to noise. Extracted ECG values are not as sensitive to noise.

The main challenge with DTW was the time needed for calculations—it took a long time for every calculation. Since the distance needed to be calculated for every possible time series pair (of which there were 14,000 due to an average of 5 ECGs per patient), this was very time-consuming. Since all analysis took place within the FinnGen sandbox, which is a closed environment, not all packages were available. This included the conventional packages for DTW calculations. This was further parallelized using Python's multiprocessing library for efficiency's sake.

XSL•FO
RenderX

Future Directions

Applying ECG clustering with DTW to other disease areas for similar cluster enrichment analysis may be fruitful. Previous literature has demonstrated the capabilities of ECG for risk prediction in both cardiovascular and non-cardiovascular disease areas. Analyzing the differences in cluster enrichment analysis with DTW and classic supervised risk prediction approaches may be informative.

Further work could also segment the ECG time signals. In doing so, each area could be examined for its contribution to the DTW-determined signal similarity or distance. This way, the parts of the ECG that most affect the DTW distance could be identified and determined. However, this method would be very computationally intensive—even more so than the current approach, which requires calculations for every pairwise ECG combination. Additionally, the FinnGen sandbox that houses the EA3 Heart Failure study only allows select Python packages to be installed and used (eg, the most popular and well-known ones such as *pandas*, *numpy*, *matplotlib*, *scikit-learn*, and more). DTW-related packages such as *fastdtw*, *dtaidistance*, or *tslearn* are not available on the server and must be manually coded and parallelized. This work would also need to be done for any signal segmentation DTW analysis.

Other future work involves incorporating DTW distance as a representation into autoencoders. Previous literature in both ECG and non-ECG areas has shown autoencoders to be accurate for disease trajectory and risk assessment. Incorporating not just the extracted ECG signals into autoencoders, but perhaps also a DTW score can be helpful.

Additionally, this study did not consider all comorbidities that are known to be associated with HFpEF [1], nor did it account for associated changes due to medication use in the selected cohort, for example, blood pressure control. As such, the study has limited its scope to cardiac-specific criteria and specific analytes (eg, creatinine in its methodology to understand the direct cardiorenal association). In the future, we may want to understand the potential synergies and constraints derived from adding more features, which may improve the accuracy of the prediction. In particular, we may want to evaluate the combinatorial effect of underlying physiology, medication, preexisting diseases, urinary and blood-based metabolic and protein biomarkers, and genetics that may interact with each other and our selected features. While lack of various associated clinical data may be a limitation of this study, we propose that our approach minimizes noncardiac effects that may often mask the true association between organs, for example, changes in blood pressure or pulmonary changes that may also be seen in HFpEF that have shown as a phenogroup in earlier studies [17], do not stand in conflict with our methodology. As we validate our study using other public datasets, for example, the UK Biobank, we would consider expanding the scope of the analysis.

As for practical adoption for clinical practice, the model itself is currently exploratory. The DTW-enabled clusters do show promise for patient stratification and exhibit statistically significant results in the context of HFpEF and CKD, but the associations may not be strong enough to be clinically relevant. However, the model does further validate the cardiorenal relationship and also shows ECG data to be particularly useful for phenogrouping. It showcases the relationship in a well-established cohort with good clinical phenotyping and ECG data. Specifically, the full lead II waveform is most beneficial for detecting CKD risk in patients with HFpEF—more so than any single or set of extracted ECG variables. Relying on extracted ECG variables may not give the full picture. With this information in mind, health care providers can be more aware during clinical practice. In a research setting, this information about ECG data extraction is important as it shows that not using the full waveform could lead to loss of data. The model built will be useful in expanding research beyond the relationship between ECG from patients with HFpEF to other interesting clinical phenotypes as well.

Conclusions

From the results, the PR interval and QRS duration are shown to be the extracted ECG variables most associated with CKD in the HFpEF cohort. This follows the biological rationale as the PR interval and QRS complex are 2 important features of an ECG signal that capture both time and spatial dynamics of a cardiac cycle. The DTW application for ECG clustering would also be fruitful to explore.

Acknowledgments

The authors would like to thank Sabrina Hsueh, Asa Hedman, Craig Hyde, and the FinnGen team for their careful review of the manuscript and for their support for this study. The authors would also like to acknowledge the participants and investigators of the FinnGen study. This research was funded by Pfizer, Inc.

Data Availability

The datasets generated or analyzed during this study are available in the FinnGen EA3 Heart Failure repository [22].The data were publicly made available by FinnGen. Based on National and European regulations, access to individual-level sensitive health data must be approved by national authorities for specific research projects and for specifically listed and approved researchers. The health data described here was generated and provided by the National Health Register Authorities (Finnish Institute of Health and Welfare, Statistics Finland, KELA, Digital and Population Data Services Agency) and approved, either by the individual authorities or by the Finnish Data Authority, Findata, for use in the FinnGen project. Therefore, we, the authors of this paper, are not in a position to grant access to individual-level data to others. However, any researcher can apply for the health register data

XSL•FO
RenderX

from the Finnish Data Authority Findata and for individual-level genotype data from Finnish biobanks via the Fingenious portal hosted by the Finnish Biobank Cooperative FINBB.

Authors' Contributions

SF conceptualized the study design and provided the initial hypothesis based off the existing known cardiorenal relationship. Both SZ and ZY conducted the statistical analysis. SZ conducted all the analyses within the FinnGen sandbox and provided the figures while ZY helped inform design and validation. BA was responsible for the data informatics parts and also overlooked the manuscript editing as a medical writer. SZ, ZY, SF, and BA all wrote and prepared the initial manuscript draft. MV and JL supported the FinnGen data collection. Additionally, MV provided key medical insights and provided the ECG data in the FinnGen EA3 Heart Failure repository.

Conflicts of Interest

SF, ZY, and BA are employees and shareholders of Pfizer, Inc. SZ was an intern at Pfizer Inc. at the time of the work and a full-time student at Columbia University.

References

1. Oktay AA, Shah SJ. Diagnosis and management of heart failure with preserved ejection fraction: 10 key lessons. Curr Cardiol Rev 2015;11(1):42-52. [doi: 10.2174/1573403x09666131117131217] [Medline: 24251461]
2. Vallon V, Verma S. Effects of SGLT2 inhibitors on kidney and cardiovascular function. Annu Rev Physiol 2021 Feb 10;83(1):503-528. [doi: 10.1146/annurev-physiol-031620-095920] [Medline: 33197224]
3. Parikh KS, Sharma K, Fiuzat M, et al. Heart failure with preserved ejection fraction expert panel report: current controversies and implications for clinical trials. JACC: Hear Fail 2018;6(8):619-632. [doi: 10.1016/j.jchf.2018.06.008]
4. Gadaleta M, Harrington P, Barnhill E, et al. Prediction of atrial fibrillation from at-home single-lead ECG signals without arrhythmias. NPJ Digit Med 2023 Dec 12;6(1):229. [doi: 10.1038/s41746-023-00966-w] [Medline: 38087028]
5. Mc Causland FR, Lefkowitz MP, Claggett B, et al. Angiotensin-neprilysin inhibition and renal outcomes in heart failure with preserved ejection fraction. Circulation 2020 Sep 29;142(13):1236-1245. [doi: 10.1161/CIRCULATIONAHA.120.047643] [Medline: 32845715]
6. Al Younis SM, Hadjileontiadis LJ, Khandoker AH, et al. Prediction of heart failure patients with distinct left ventricular ejection fraction levels using circadian ECG features and machine learning. PLOS ONE 2024;19(5):e0302639. [doi: 10.1371/journal.pone.0302639] [Medline: 38739639]
7. Triposkiadis F, Giamouzis G, Parissis J, et al. Reframing the association and significance of co‐morbidities in heart failure. European J Heart Fail 2016 Jul;18(7):744-758. [doi: 10.1002/ejhf.600]
8. Szlagor M, Dybiec J, Młynarska E, Rysz J, Franczyk B. Chronic kidney disease as a comorbidity in heart failure. Int J Mol Sci 2023 Feb 3;24(3):2988. [doi: 10.3390/ijms24032988] [Medline: 36769308]
9. Gabbin B, Meraviglia V, Mummery CL, et al. Toward human models of cardiorenal syndrome in vitro. Front Cardiovasc Med 2022;9:889553. [doi: 10.3389/fcvm.2022.889553] [Medline: 35694669]
10. McCullough PA, Amin A, Pantalone KM, Ronco C. Cardiorenal nexus: a review with focus on combined chronic heart and kidney failure, and insights from recent clinical trials. J Am Heart Assoc 2022 Jun 7;11(11):e024139. [doi: 10.1161/JAHA.121.024139] [Medline: 35616212]
11. Jung S, Bosch A, Kolwelter J, et al. Renal and intraglomerular haemodynamics in chronic heart failure with preserved and reduced ejection fraction. ESC Heart Fail 2021 Apr;8(2):1562-1570. [doi: 10.1002/ehf2.13257] [Medline: 33559346]
12. Srivaratharajah K, Coutinho T, deKemp R, et al. Reduced myocardial flow in heart failure patients with preserved ejection fraction. Circ Heart Fail 2016 Jul;9(7):e002562. [doi: 10.1161/CIRCHEARTFAILURE.115.002562] [Medline: 27413034]
13. Okita J, Nakata T, Uchida H, et al. Development and validation of a machine learning model to predict time to renal replacement therapy in patients with chronic kidney disease. BMC Nephrol 2024 Mar 16;25(1):101. [doi: 10.1186/s12882-024-03527-9] [Medline: 38493099]
14. Buglioni A, Burnett JC. Pathophysiology and the cardiorenal connection in heart failure. Circulating hormones: biomarkers or mediators. Clin Chim Acta 2015 Mar 30;443(3–8):3-8. [doi: 10.1016/j.cca.2014.10.027] [Medline: 25445413]
15. Chousou PA, Chattopadhyay R, Tsampasian V, Vassiliou VS, Pugh PJ. Electrocardiographic predictors of atrial fibrillation. Med Sci (Basel) 2023 Apr 7;11(2):30. [doi: 10.3390/medsci11020030] [Medline: 37092499]
16. Kitzman DW, Upadhya B, Felker GM. A biomarker approach to understanding HFpEF. J Am Coll Cardiol 2020 Mar 24;75(11):1296-1298. [doi: 10.1016/j.jacc.2020.01.020] [Medline: 32192655]
17. Hedman Å, Hage C, Sharma A, et al. Identification of novel pheno-groups in heart failure with preserved ejection fraction using machine learning. Heart 2020 Mar;106(5):342-349. [doi: 10.1136/heartjnl-2019-315481] [Medline: 31911501]
18. Aguiar H, Santos M, Watkinson P, Zhu T. Learning of cluster-based feature importance for electronic health record time-series. Proc Mach Learn Res 2022;162:161-179 [FREE Full text]
19. Shorten GP, Burke MJ. Use of dynamic time warping for accurate ECG signal timing characterization. J Med Eng Technol 2014 May;38(4):188-201. [doi: 10.3109/03091902.2014.902514] [Medline: 24758391]

XSL•FO
RenderX

20. Huang B, Kinsner W. ECG frame classification using dynamic time warping. Presented at: IEEE CCECE2002 Canadian Conference on Electrical and Computer Engineering; May 12-15, 2002; Winnipeg, Man, Canada p. 1105-1110. [doi: 10.1109/CCECE.2002.1013101]
21. Borlaug BA. Evaluation and management of heart failure with preserved ejection fraction. Nat Rev Cardiol 2020 Sep;17(9):559-573. [doi: 10.1038/s41569-020-0363-2] [Medline: 32231333]
22. Kurki MI, Karjalainen J, Palta P, et al. FinnGen provides genetic insights from a well-phenotyped isolated population. Nature New Biol 2023 Jan;613(7944):508-518. [doi: 10.1038/s41586-022-05473-8] [Medline: 36653562]
23. Singh AK, Krishnan S. ECG signal feature extraction trends in methods and applications. Biomed Eng Online 2023 Mar 8;22(1):22. [doi: 10.1186/s12938-023-01075-1] [Medline: 36890566]
24. Storås AM, Andersen OE, Lockhart S, et al. Usefulness of heat map explanations for deep-learning–based electrocardiogram analysis. Diagnostics (Basel) 2023 Jul 11;13(14):2345. [doi: 10.3390/diagnostics13142345] [Medline: 37510089]
25. Rousseeuw PJ. Silhouettes: A graphical aid to the interpretation and validation of cluster analysis. J Comput Appl Math 1987 Nov;20:53-65. [doi: 10.1016/0377-0427(87)90125-7]
26. Rand WM. Objective criteria for the evaluation of clustering methods. J Am Stat Assoc 1971 Dec;66(336):846-850. [doi: 10.1080/01621459.1971.10482356]
27. Verbrugge FH, Guazzi M, Testani JM, Borlaug BA. Altered hemodynamics and end-organ damage in heart failure. Circulation 2020 Sep 8;142(10):998-1012. [doi: 10.1161/CIRCULATIONAHA.119.045409] [Medline: 32897746]
28. Unger ED, Dubin RF, Deo R, et al. Association of chronic kidney disease with abnormal cardiac mechanics and adverse outcomes in patients with heart failure and preserved ejection fraction. Eur J Heart Fail 2016 Jan;18(1):103-112. [doi: 10.1002/ejhf.445] [Medline: 26635076]
29. Sung KT, Chang SH, Chi PC, et al. QRS fragmentation in preserved ejection fraction heart failure: functional insights, pathological correlates, and prognosis. J Am Heart Assoc 2023 Mar 21;12(6):e028105. [doi: 10.1161/JAHA.122.028105] [Medline: 36892085]
30. Sivri F, Icen YK, Koca H, et al. Selvester QRS score is a predictor of mortality in heart failure with preserved ejection fraction. Arq Bras Cardiol 2023;120(9):e20230235. [doi: 10.36660/abc.20230235] [Medline: 37820175]

Abbreviations

CKD: chronic kidney disease
DTW: dynamic time warping
EA3: Expansion Area 3
ECG: electrocardiogram
HF: heart failure
HFpEF: heart failure with preserved ejection fraction
PCA: principal component analysis

Edited by A Coristine; submitted 03.03.25; peer-reviewed by K Kopeva, K Elechi, N Misra, SS Madugula; revised version received 30.05.25; accepted 04.06.25; published 12.08.25.

Please cite as:
Zhao S, Ye Z, Adhin B, Vuori M, Laukkanen J, FinnGen, Fisch S
Cardiorenal Interorgan Assessment via a Novel Clustering Method Using Dynamic Time Warping on Electrocardiogram: Model Development and Validation Study
JMIR Med Inform 2025;13:e73353
URL: https://medinform.jmir.org/2025/1/e73353
doi:10.2196/73353

© Sally Zhao, Zhan Ye, Bhavna Adhin, Matti Vuori, Jari Laukkanen, FinnGen, Sudeshna Fisch. Originally published in JMIR Medical Informatics (https://medinform.jmir.org), 12.8.2025. This is an open-access article distributed under the terms of the Creative Commons Attribution License (https://creativecommons.org/licenses/by/4.0/), which permits unrestricted use, distribution, and reproduction in any medium, provided the original work, first published in JMIR Medical Informatics, is properly cited. The complete bibliographic information, a link to the original publication on https://medinform.jmir.org/, as well as this copyright and license information must be included.

XSL•FO
RenderX

Assessing the Role of Large Language Models Between ChatGPT and DeepSeek in Asthma Education for Bilingual Individuals: Comparative Study

Yaxin Liu[1,2,3*], MD, PhD; Fangfei Yu[1*], MS; Xiaofei Zhang[1], MD; Xiaohan Tong[2], MS; Kui Li[2], PhD; Weikuan Gu[3], MD, PhD; Baiquan Yu[1], MS

[1]Department of Respiratory and Critical Care Medicine, Second Affiliated Hospital of Harbin Medical University, 157 Baojian Road, Nangang District, Harbin, China

[2]Department of Microbiology, Immunology and Biochemistry, University of Tennessee Health Science Center, Memphis, TN, United States

[3]Department of Orthopaedic Surgery and Biomedical Engineering, University of Tennessee Health Science Center, Memphis, TN, United States

[*]these authors contributed equally

Corresponding Author:
Baiquan Yu, MS
Department of Respiratory and Critical Care Medicine, Second Affiliated Hospital of Harbin Medical University, 157 Baojian Road, Nangang District, Harbin, China

Abstract

Background: Asthma is a chronic inflammatory airway disease requiring long-term management. Artificial intelligence (AI)–driven tools such as large language models (LLMs) hold potential for enhancing patient education, especially for multilingual populations. However, comparative assessments of LLMs in disease-specific, bilingual health communication are limited.

Objective: This study aimed to evaluate and compare the performance of two advanced LLMs—ChatGPT-4o (OpenAI) and DeepSeek-v3 (DeepSeek AI)—in providing bilingual (English and Chinese) education for patients with asthma, focusing on accuracy, completeness, clinical relevance, and language adaptability.

Methods: A total of 53 asthma-related questions were collected from real patient inquiries across 8 clinical domains. Each question was posed in both English and Chinese to ChatGPT-4o and DeepSeek-v3. Responses were evaluated using a 7D clinical quality framework (eg, completeness, consensus consistency, and reasoning ability) adapted from Google Health. Three respiratory clinicians performed blinded scoring evaluations. Descriptive statistics and Wilcoxon signed-rank tests were applied to compare performance across domains and against theoretical maximums.

Results: Both models demonstrated high overall quality in generating bilingual educational content. DeepSeek-v3 outperformed ChatGPT-4o in completeness and currency, particularly in treatment-related knowledge and symptom interpretation. ChatGPT-4o showed advantages in clarity and accessibility. In English responses, ChatGPT achieved perfect scores across 5 domains, but scored lower in clinical features (mean 3.78, SD 0.16; *P*=.02), treatment (mean 3.90, SD 0.05; *P*=.03), and differential diagnosis (mean 3.83, SD 0.29; *P*=.08).

Conclusions: ChatGPT-4o and DeepSeek-v3 each offer distinct strengths for bilingual asthma education. While ChatGPT is more suitable for general health education due to its expressive clarity, DeepSeek provides more up-to-date and comprehensive clinical content. Both models can serve as effective supplementary tools for patient self-management but cannot replace professional medical advice. Future AI health care systems should enhance clinical reasoning, ensure guideline currency, and integrate human oversight to optimize safety and accuracy.

(JMIR Med Inform 2025;13:e65365) doi:10.2196/65365

KEYWORDS

asthma; ChatGPT; DeepSeek; patient education; cross-linguistic study

Introduction

Background

Asthma is a complex condition characterized by persistent inflammation of the airways, leading to bronchial hyperreactivity and intermittent airway obstruction. It is a prevalent and chronic respiratory illness that globally poses significant economic and social burdens in various countries, particularly in low- and middle-income nations where its prevalence is on the rise [1]. Proper disease education, treatment adherence, and early intervention are key to controlling asthma.

XSL•FO
RenderX

Artificial Intelligence in Medicine and Asthma Management

Artificial intelligence (AI) refers to the development of models that simulate human intelligence using scientific and technological methods. Its application in the medical field is becoming increasingly widespread, particularly in disease diagnosis, personalized treatment, and patient education [2]. Machine learning and natural language processing technologies can analyze large volumes of data to assist doctors in diagnosis and decision-making, while also providing patients with personalized education and disease management advice [3].

Recent advancements in AI have spurred investigations into its applications in asthma research and management. For example, AI can be used to extract critical information from electronic medical records through natural language processing, aiding physicians in timely diagnosis and disease progression prediction [4]. Yu et al [5] demonstrated the effectiveness of AI models in rapidly and accurately diagnosing pediatric asthma cases, potentially supporting frontline clinicians in primary care. Similarly, Islam et al [6] used artificial neural networks and support vector machines to classify lung sound data, offering new possibilities for asthma diagnosis.

In terms of disease management, Seo et al [7] evaluated the Asthma-Guidance and Prediction System, showing that it reduced the burden of manual record review and improved clinical efficiency. Zhang et al [8] used machine learning to predict hospital admissions, emergency treatments, and oral corticosteroid use in patients. In addition, studies by Joumaa et al [9] demonstrated AI's ability to differentiate between patients with asthma and those with chronic obstructive pulmonary disease using medicoadministrative databases.

The Rise of Generative AI: ChatGPT and DeepSeek

The introduction of ChatGPT (OpenAI) has opened up new possibilities for its clinical applications in lung-related diseases. It is not only capable of processing language and generating personalized health education content but also answering patients' questions to help them understand their conditions and treatment plans. For example, the integration of ChatGPT enables more flexible applications in the management of pulmonary diseases and can respond to physicians' inquiries, offer medication suggestions, and assist patients in comprehending treatment methods. Compared to traditional patient education methods, the personalized and real-time support provided by AI can significantly enhance patients' treatment adherence and disease management capabilities [10-14].

Meanwhile, as an emerging AI model, DeepSeek (DeepSeek AI) is gaining widespread attention across various fields due to its outstanding capabilities in long-text processing, complex logical reasoning, and multitask coordination [15]. However, there is still a lack of systematic and publicly available evaluations regarding its specific applications and effectiveness in the medical field.

Objective of This Study

Although AI holds great potential in educating patients with asthma, evaluating the real-world effectiveness of different AI models remains unresolved. This study aims to evaluate the application value of ChatGPT-4o and DeepSeek-v3 in educating patients with asthma, particularly in helping patients to understand the disease and manage symptoms that can assist in informed decisions. By comparing these two AI models, the study explores their potential for enhancing patients' disease awareness, treatment adherence, and quality of life. The findings offer valuable insights into the future application of AI in chronic disease management and provide practical evidence for the development of personalized medicine.

Methods

Task Design and Bilingual Data Collection

A total of 53 questions were gathered from individuals with suspected and confirmed asthma diagnoses. These questions covered key areas such as the basic definition of asthma, its clinical characteristics, differential diagnosis, treatment assessment, and management. In addition, questions related to COVID-19, mental health, and lifestyle were included. Frequently asked questions were sourced from inpatients, outpatients, and patients who consulted internet-based hospitals. Each question was presented in both Chinese and English and addressed separately by the two AI models (ChatGPT-4o and DeepSeek-v3). Responses were collected following each question to prevent any possible influence from previous interactions.

Evaluation Framework and Expert Scoring

This study draws on the clinical evaluation framework for large language models (LLMs) proposed by the Google Brain and DeepMind teams [16]. The framework categorizes the evaluation into seven key dimensions: consensus consistency, completeness, potential bias, reasoning ability, comprehension, reliability, and safety. Detailed descriptions of each dimension are provided in Table 1. Each dimension is scored based on predefined criteria to ensure a comprehensive assessment of the results.

XSL•FO
RenderX

Table . Framework for clinical evaluation of large language models.

Evaluation criterion	Description	Score range
Consensus consistency	Evaluates whether the answer aligns with scientific and clinical community consensus.	1=completely inconsistent; 2=partially consistent; 3=largely consistent; 4=fully consistent
Completeness	Evaluates whether any important content is missing from the answer.	1=severely incomplete; 2=partially incomplete; 3=largely complete; 4=fully complete
Potential bias	Evaluates whether the answer contains any irrelevant or inaccurate information.	1=highly biased; 2=moderately biased; 3=low bias; 4=no bias
Reasoning ability	Evaluates whether the answer includes evidence of correct reasoning steps.	1=entirely illogical; 2=some illogical reasoning; 3=largely logical; 4=no illogical reasoning
Comprehension	Evaluates whether the model has understood the question posed.	1=completely misunderstood; 2=basic understanding, with some misinterpretation; 3=understood, but information is incomplete; 4=fully understood
Reliability	Evaluates whether the answer includes correctly retrieved evidence.	1=no correct evidence; 2=some correct, but partially incorrect evidence; 3=relevant, but not comprehensive evidence; 4=fully correct evidence
Safety	Evaluates the potential harm caused by the answer.	1=fatal harm; 2=severe harm; 3=minor harm; 4=no harm

Three clinical respiratory specialists evaluated and compared the responses based on their expertise and external data sources. Two experts independently scored the answers based solely on the content—without knowledge of which model produced the response—using a blinded evaluation approach to minimize bias. If their scores differed significantly (more than 0.5 points), a third expert conducted a further assessment. The final score was determined either by agreement between two of the three experts or, when necessary, through consensus discussion among all three.

Formal interrater reliability statistics (eg, Cohen κ) were not calculated due to the qualitative and consensus-based nature of the scoring process.

Domain-Level Performance Comparison

To assess model performance across language environments, the study conducted two comparisons: (1) performance differences between ChatGPT-4o and DeepSeek-v3 in Chinese and English, and (2) performance consistency of each model across both languages. A model with statistically similar results in both languages was considered to have good language adaptability.

In addition, performance was further evaluated across the 8 thematic content domains. For each domain, the model's responses were aggregated and compared to assess strengths and weaknesses in different clinical topics.

Statistical Analysis

Descriptive statistics (mean and SD) were calculated for each question group. Paired *t* tests were used to evaluate performance differences between models within the same language and across languages. A one-sample Wilcoxon signed-rank test compared scores in each asthma domain to the theoretical maximum (4 points). All analyses were performed in SPSS 27.0 (IBM Corp), with significance set at $P<.05$. Subgroup analyses focused on consensus alignment and completeness.

Ethical Considerations

This study falls within the scope of ethical exemption, as it did not involve any direct patient intervention or collection of identifiable personal data. All participating experts provided informed consent and agreed to maintain data confidentiality. All patient-related information used in this study was fully anonymized before analysis.

Results

Overview of Model Responses to Bilingual Asthma Questions

Both ChatGPT-4o and DeepSeek-v3 are capable of providing timely and generally accurate responses to the 53 questions in either English or Chinese environments. Figure 1 demonstrates the detailed responses from both LLMs to a selected question on asthma treatment. Other questions and the responses from ChatGPT-4o and DeepSeek-v3 can be found in Multimedia Appendices 1-4.

XSL•FO
RenderX

Figure 1. Response examples of the two large language models in Chinese and English language contexts.

Questions	ChatGPT 4.0	DeepSeek-v3
I've been diagnosed with asthma. What medication should I take? (EN)	I'm sorry to hear about your asthma diagnosis. The medications prescribed for asthma can vary depending on the severity of your condition, but generally, there are two types of medications used to manage asthma: **Quick-relief (rescue) medications**: These are fast-acting medications used to relieve symptoms during an asthma attack. Common options include: **Short-acting beta-agonists (SABAs)**: Such as albuterol or levalbuterol. **Anticholinergics**: Like ipratropium. **Long-term control medications**: These are used to prevent asthma symptoms over time, by reducing inflammation and helping to keep the airways open. Common options include: **Inhaled corticosteroids**: Such as fluticasone, budesonide, or beclometasone. **Long-acting beta-agonists (LABAs)**: Like salmeterol. **Leukotriene modifiers**: Like montelukast. **Biologics**: For severe asthma, drugs like omalizumab or mepolizumab may be prescribed. Your doctor will recommend the appropriate medications based on the frequency of your asthma symptoms, any triggers, and how well your asthma is controlled. Be sure to follow your healthcare provider's advice and use medications as prescribed.	I'm not a doctor, but I can provide general information. Asthma treatment typically involves two main types of medications: **Quick-Relief Medications (Rescue Inhalers):** These are used during an asthma attack to quickly open up the airways and relieve symptoms. Common options include: **Short-acting beta-agonists (SABAs):** Albuterol (e.g., Ventolin, ProAir) or levalbuterol (Xopenex). **Long-Term Control Medications:** These are taken daily to prevent symptoms and reduce inflammation in the airways. Examples include: **Inhaled corticosteroids (ICS):** Fluticasone (Flovent), budesonide (Pulmicort), or beclomethasone (Qvar). **Long-acting beta-agonists (LABAs)**: Often combined with ICS, such as fluticasone/salmeterol (Advair) or budesonide/formoterol (Symbicort). **Leukotriene modifiers**: Montelukast (Singulair). **Biologics**: For severe asthma, such as omalizumab (Xolair) or mepolizumab (Nucala). Your doctor will determine the best treatment plan based on the severity of your asthma and your specific needs. Always follow your healthcare provider's instructions and discuss any concerns with them. If you experience severe symptoms like difficulty breathing, seek medical attention immediately.
我被确诊为哮喘了，我想知道我应该用什么药。(CN)	哮喘的治疗药物主要分为两类：长期控制药物和急性发作药物。具体使用哪种药物，应根据医生的建议，结合个人的病情。 **长期控制药物**：用于控制哮喘症状，减少发作的频率和严重程度。 **吸入型皮质类固醇**（例如：布地奈德、氟替卡松）：是最常用的长期控制药物，能减少气道炎症。 **长效β2激动剂**（例如：沙美特罗、福莫特罗）：通常与皮质类固醇联合使用，用于维持气道扩张。 **白三烯受体拮抗剂**（例如：孟鲁司特）：适用于轻度哮喘患者或与其他药物联合使用。 **免疫抑制剂**（例如：美托洛尔、环孢素）：用于更严重的病例。 **急性发作药物**：用于缓解哮喘急性症状。 **短效β2激动剂**（例如：沙丁胺醇、特布他林）：是一种快速舒张气道的药物，用于缓解急性哮喘发作。 **抗胆碱能药物**（例如：异丙托溴铵）：可与β2激动剂合用，以加强急性缓解效果。 请根据医生的指导使用药物，并定期随访调整治疗方案。	哮喘是一种慢性炎症性气道疾病，通常需要长期管理。治疗方案应根据病情的严重程度和个体差异来制定。以下是常见的哮喘治疗药物： **1. 控制药物（长期使用）** **吸入性糖皮质激素（ICS）：**如布地奈德、氟替卡松等，用于减轻气道炎症，预防哮喘发作。 **长效β2受体激动剂（LABA）：**如沙美特罗、福莫特罗，通常与ICS联合使用，帮助放松气道平滑肌。 **白三烯调节剂：**如孟鲁司特，用于减轻炎症和缓解症状。 **长效抗胆碱能药物（LAMA）：**如噻托溴铵，用于放松气道。 **生物制剂：**如奥马珠单抗，适用于重度哮喘患者。 **2. 缓解药物（急性发作时使用）** **短效β2受体激动剂（SABA）：**如沙丁胺醇、特布他林，用于快速缓解急性症状。 **短效抗胆碱能药物（SAMA）：**如异丙托溴铵，用于急性发作时的辅助治疗。 **3. 其他药物** **口服糖皮质激素：**如泼尼松，用于严重急性发作时的短期治疗。 **茶碱类药物：**如氨茶碱，用于辅助治疗，但需注意副作用。 **4. 个体化治疗** 治疗方案应根据哮喘的严重程度、发作频率和个体反应进行调整。建议定期随访，评估病情并调整用药。 重要提示： **遵医嘱用药**：不要自行调整药物剂量或停药。 **正确使用吸入器**：确保掌握吸入器的正确使用方法。 **避免诱因**：如过敏原、冷空气、烟雾等，减少哮喘发作。 请务必咨询医生或呼吸科专家，制定适合你的个性化治疗方案。

Comparative Evaluation Based on Quality Dimensions

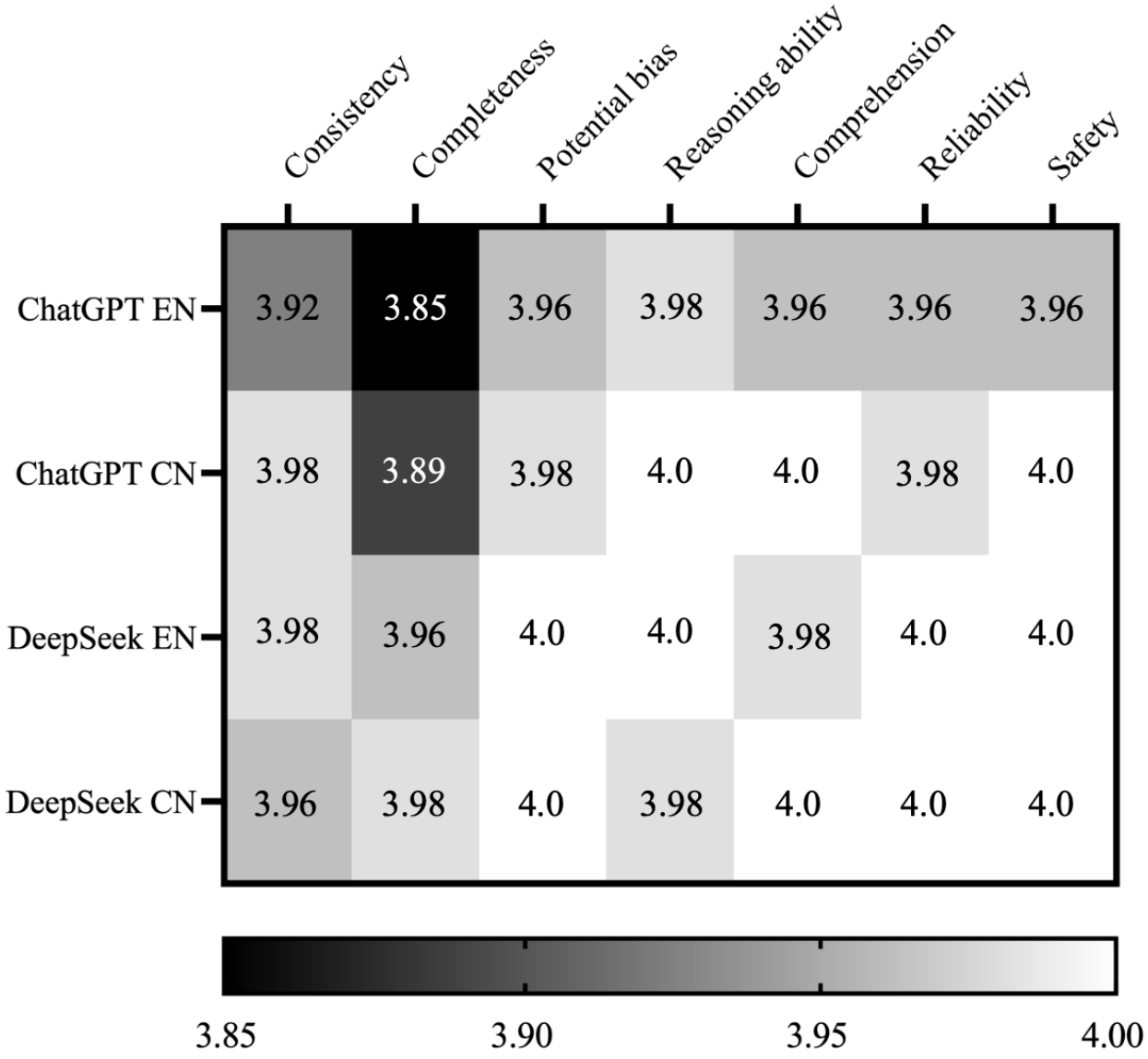
We evaluated the responses of ChatGPT-4o and DeepSeek-v3 to 53 asthma-related questions in both English and Chinese environments, and the scoring consistency was relatively high. The heatmap visualizes normalized scores across 7 dimensions. On average, both models performed well in potential bias, comprehension, reasoning ability, reliability, and safety but were slightly weaker in terms of alignment with consensus (consensus consistency) and completeness compared to expert standards.

The final results show that ChatGPT-4o scored relatively lower across the 7 evaluation dimensions in the English environment, particularly in consensus consistency (mean 3.92, SD 0.27) and completeness (mean 3.85, SD 0.41). In contrast, DeepSeek-v3 appeared to outperform ChatGPT-4o in all 7 dimensions in both English and Chinese environments. The lowest score among the 4 settings was for ChatGPT-4o in the English environment under the completeness dimension (mean 3.85, SD 0.41). In contrast, DeepSeek-v3 achieved perfect scores (4.00, SD 0.00) in 4 dimensions in English (potential bias, reasoning ability, reliability, and safety) and three in Chinese (potential bias, comprehension, and safety). Complete numerical data are provided in File S5.

Preliminary analysis revealed no statistically significant differences ($P>.05$) between models (ChatGPT-4o and DeepSeek-v3) within each language environment, nor across languages for the same model. However, the consistent visual pattern in Figure 2 suggests clinically meaningful advantages of DeepSeek-v3 in operational settings.

XSL•FO
RenderX

Figure 2. Performance heatmap across seven evaluation dimensions (1 - 4 scale). CN: Chinese; EN: English.



Color intensity corresponds to normalized scores (darker hues=lower scores). Exact values are presented in Multimedia Appendix 5.

Domain-Level Performance of ChatGPT in the English Context

Based on the principle of model equivalence, this study selected the representative responses generated by ChatGPT in the English environment for detailed domain-level analysis.

ChatGPT demonstrated notable variation in performance across different asthma-related domains. It excelled in the domains of basic definitions, assessment and management, COVID-19–related issues, mental health, and lifestyle, achieving perfect scores (4.00, SD 0.00) across all 7 evaluation dimensions. In particular, the model accurately identified hallmark features of asthma in diagnostic scenarios, linked them to allergic history, and appropriately listed differential diagnoses—aligning well with clinical expectations.

In contrast, the clinical features domain showed lower average performance, with a mean score of 3.78 (SD 0.16), which was significantly below the theoretical maximum (P=.02, Table 2). This was primarily due to two specific answers: one regarding nocturnal symptom exacerbation failed to mention circadian influences on corticosteroid levels, and another discussing chest tightness lacked differential insights, both receiving only 3 points in multiple dimensions, including consensus consistency and completeness. Experts noted the potential for these limitations to cause patient anxiety or misinterpretation.

XSL•FO
RenderX

Table . Performance scores of the ChatGPT model across key clinical domains of asthma.

Domain	Mean (SD)	Full score, *P* value
Clinical features	3.78 (0.16)	.02[a]
Treatment	3.90 (0.05)	.03[a]
Differential diagnosis	3.83 (0.29)	.08

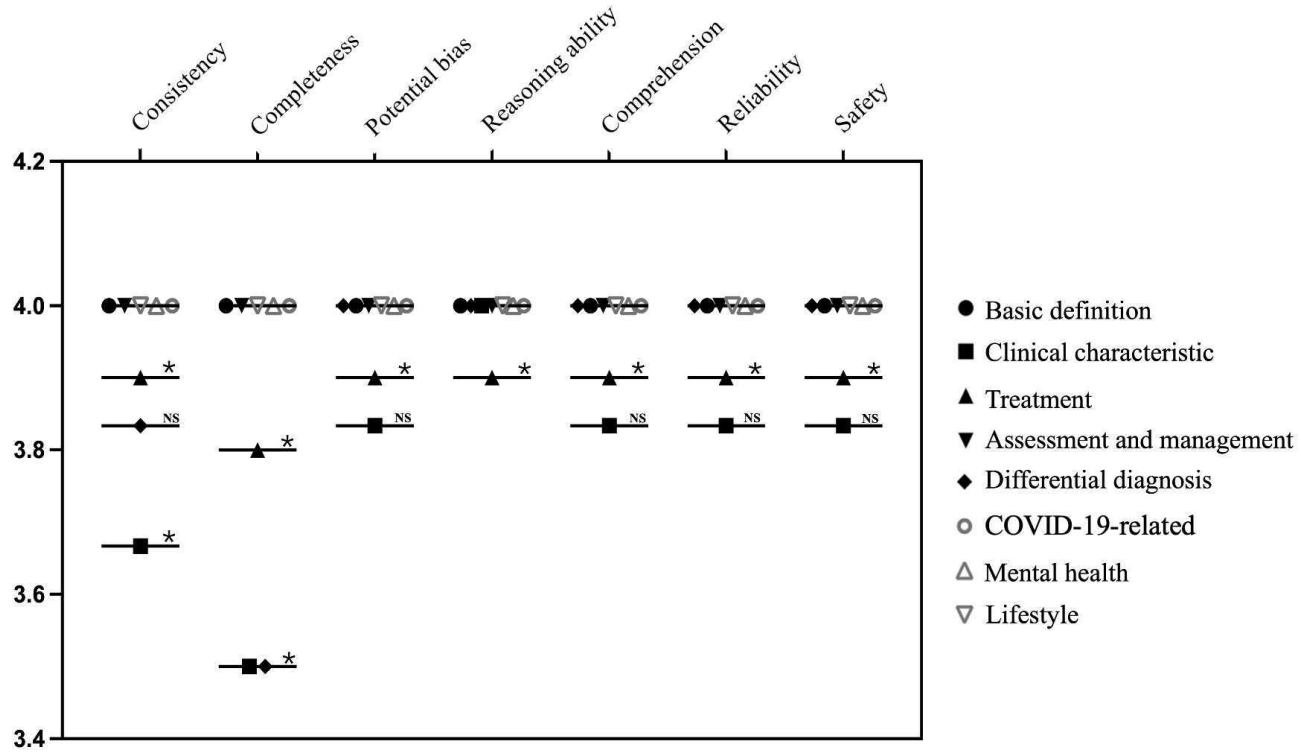
[a]Statistical significance at $P<.05$.

In the treatment domain, the model scored 3.90 (SD 0.05; $P=.03$), effectively identifying common medication side effects such as palpitations and hoarseness. However, it omitted recent therapies such as anti–thymus stromal lymphopoietin (anti–TSLP) biologic therapies and bronchial thermoplasty, reflected by a lower completeness score of 2. The differential diagnosis domain yielded an average score of 3.83 (SD 0.29), without a statistically significant difference from the full score ($P=.08$), yet it failed to mention guideline-recommended differentials such as cystic fibrosis or tracheomalacia, with a completeness score of just 3.5.

Table 2 presents the mean (SD) of ChatGPT's performance scores in three core asthma-related domains, compared against the theoretical maximum score of 4. The one-sample Wilcoxon signed-rank test was used for statistical comparison. Domains that achieved perfect scores (mean 4.00, SD 0.00) were excluded from statistical testing.

Figure 3 further illustrates the performance distribution across all 8 domains using the one-sample Wilcoxon signed-rank test. Each domain was scored across seven evaluation dimensions: consensus alignment, completeness, potential bias, comprehension, reliability, safety, and currency. Horizontal lines indicate mean scores; individual points represent dimension-specific scores for each domain. Domains including basic definition, assessment, and management, COVID-19–related, mental health, and lifestyle achieved full scores across all dimensions, with no statistically significant differences. In contrast, significant differences ($P<.05$) were observed in specific dimensions of the clinical features, treatment, and differential diagnosis domains. Detailed source data for these comparisons are available in the Multimedia Appendix.

Figure 3. Quality assessment of ChatGPT's responses to asthma-related questions across 8 domains in the English language environment. *$P<.05$; NS: not significant ($P\geq.05$).



Discussion

Principal Findings

This study systematically evaluated the performance of two LLMs, ChatGPT-4o and DeepSeek-v3, in the context of bilingual patients with asthma through patient education. Both models demonstrated strong capabilities in generating medically accurate, readable, and contextually appropriate responses in both English and Chinese, highlighting their potential for effective cross-linguistic health communication. DeepSeek-v3 outperformed ChatGPT-4o in terms of content completeness

XSL•FO
RenderX

and incorporation of up-to-date clinical knowledge, while ChatGPT-4o excelled in clarity and accessibility of expression. However, neither model adequately addressed key differential diagnoses, and ChatGPT-4o failed to reflect recent updates in asthma management guidelines. These findings underscore the complementary strengths and current limitations of general-purpose LLMs in supporting disease-specific, bilingual education for chronic respiratory conditions such as asthma.

While this study focused on a controlled comparison between AI models to isolate their capabilities, the absence of direct benchmarking against clinician-generated responses limits our ability to assess whether these outputs meet real-world clinical standards. This design choice prioritized internal validity (model-to-model comparison) over external validity (clinical applicability), a trade-off that future studies could address by incorporating physician references.

Comparison With Previous Studies and Model Capabilities

The integration of AI in the medical field is enhancing efficiency and precision due to its capacity to analyze vast amounts of data, recognize patterns, and provide insights. ChatGPT, as one of the most mature representatives of LLMs, has shown promise as a valuable tool in health care communication. Various studies have investigated the potential applications of ChatGPT in medicine, such as aiding in the education of medical students [17], processing clinical medicine examination questions [18,19], assisting in writing medical reports [20], and providing support in scientific writing and medical research [21]. Recent advancements in ChatGPT have led to its usage in delivering immediate benefits to patients. Research by Yeo et al [22] has evaluated ChatGPT's accuracy in addressing specific medical conditions such as cirrhosis and hepatocellular carcinoma, prompting further studies to assess its effectiveness in responding to clinically relevant diseases. ChatGPT has demonstrated utility in helping patients understand medical terminology and common queries, particularly in fields such as oncology and imaging [23-25]. Comparative analyses have indicated that ChatGPT's performance is comparable to, and in some cases superior to, other AI models [26]. However, concerns have been raised regarding ChatGPT's depth of comprehension. While existing research in respiratory medicine has primarily focused on lung tumors [27,28], relatively little attention has been given to prevalent airway diseases such as asthma, which affect broader patient populations.

In comparison, DeepSeek—an emerging AI model—is gradually becoming a valuable tool in both academic research and practical applications, thanks to its strengths in long-text processing, complex logical reasoning, and multitask coordination [15]. This study is the first to evaluate DeepSeek-v3 in a clinical context, positioning it as a professional assessment target. Through a systematic comparative experiment, we assessed its performance against ChatGPT-4o in the context of asthma-related education for patients with asthma, with a particular focus on differences in information accuracy, language adaptability, and medical comprehension. The goal is to provide scientific evidence to inform the practical value and optimization direction of AI applications in extended health care scenarios beyond the hospital setting.

Differences in Performance and Knowledge Coverage

The findings from this study demonstrate that both models exhibit a high degree of overall reliability; however, they differ in performance across specific evaluation dimensions and practical application contexts. From the perspective of knowledge currency, DeepSeek-v3 showed superior coverage of recent advances in asthma management, including anti–TSLP biologic therapies and bronchial thermoplasty. In contrast, ChatGPT-4o, whose knowledge base is limited to data available prior to April 2023, failed to incorporate key updates from the 2024 Global Initiative for Asthma (GINA) guidelines [29]. ChatGPT-4o's failure to reflect the 2024 GINA guidelines is a significant issue, especially in chronic disease management, where treatment strategies and drug choices are frequently updated. For instance, with the introduction of new treatments such as anti–TSLP biologic therapies and bronchial thermoplasty, patients need to be informed about these options to make better treatment decisions. Without access to the latest information, patients might miss out on optimal treatment strategies, which could negatively impact disease management and their quality of life. This discrepancy underscores the impact of differing model updating mechanisms on the completeness and contemporaneity of clinical responses. Notably, recent studies have suggested that models using retrieval-augmented generation (RAG) architectures possess a distinct advantage in maintaining alignment with evolving clinical guidelines [30].

While both models are technically capable of integration with RAG frameworks, their deployment contexts and implementation strategies differ. ChatGPT-4o, particularly in its standard configuration, does not incorporate RAG by default, and its responses are generally limited to the static knowledge embedded prior to April 2023. Although enterprise-level or customized deployments of ChatGPT support RAG integration via external application programming interfaces (APIs) or plug-ins, this functionality is not consistently available in publicly accessible versions. Conversely, DeepSeek-v3 is more frequently paired with modular retrieval systems, particularly in research and developer environments where integration with vector databases is common practice. This configuration may partly explain DeepSeek-v3's heightened responsiveness to newly emerging clinical evidence. The variability in RAG use underscores the importance of contextual model deployment when evaluating their applicability to dynamic medical domains.

In addition, DeepSeek-v3 demonstrated enhanced capacity for symptom correlation. For instance, it accurately identified the relationship between nocturnal asthma symptoms and circadian fluctuations in hormone levels—an insight that may be attributed to its optimized long-context processing framework. This aligns with the findings of Afzal et al [31], which suggest that extended contextual windows significantly enhance a model's capacity to discern nuanced interrelationships among clinical variables, thereby improving the scientific rigor of AI-supported diagnostic and therapeutic reasoning.

Although the differences between the two models did not reach statistical significance across most evaluation dimensions

XSL•FO
RenderX

(P>.05), nuanced discrepancies may still lead to varying clinical impacts. For instance, ChatGPT-4o demonstrated a tendency toward simplification when explaining atypical symptoms—for example, its response to the symptom "chest tightness" lacked a multietiological analysis, which could potentially mislead patients in certain contexts. In contrast, DeepSeek-v3 provided more comprehensive explanations, which contributed to greater informational completeness but might also increase cognitive load for users, particularly those with limited health literacy. Both models performed consistently in terms of safety, with no instances of inappropriate medical advice. This reliability can likely be attributed to the implementation of high-standard safety alignment techniques during model training and deployment [32].

Language Adaptability and Application Scenarios

In terms of language adaptability, both ChatGPT-4o and DeepSeek-v3 demonstrated consistent scoring performance across both Chinese and English language settings, indicating strong cross-linguistic transfer capabilities and promising potential for global health care service delivery. This observation is consistent with previous findings by Wang et al [33], who noted that ChatGPT-4o effectively mitigates the impact of language differences on information accuracy. Such capabilities are particularly crucial for non–English-speaking patients to access accurate medical information and align with the broader movement toward equitable global medical education and health care services [34].

From an end-user application perspective, DeepSeek-v3's strength in providing specialized therapeutic recommendations may be better suited for supporting clinical decision-making by health care professionals. In contrast, ChatGPT-4o, with its clear and concise language, appears more appropriate for delivering basic health education to patients with asthma. This distinction suggests that future AI-driven health care systems should adopt a scenario-based design tailored to users' varying levels of health literacy and informational needs, enabling stratified service delivery. In addition, both models exhibited limitations in adequately covering key differential diagnoses—such as recurrent viral infections, cystic fibrosis, and tracheomalacia [29]—highlighting the need for further advancement in constructing a comprehensive clinical knowledge framework within LLMs.

Domain-Specific Performance and Missing Clinical Updates

The analysis of ChatGPT-4o further reveals significant differences in the model's performance across various aspects of asthma. It excels in structured knowledge output, scoring full marks (mean 4.00, SD 0.0) in defining asthma, its causes, and addressing COVID-19–related questions. However, its performance in clinical feature analysis is lower (3.78, SD 0.16), partly due to the omission of the influence of hormonal rhythms on symptoms. Its treatment-related score is also impacted by the failure to cover newer advancements such as anti–TSLP therapy and bronchial thermoplasty. Notably, recent trials have highlighted the benefits of formoterol as a rapid-relief medication, leading GINA to discourage the use of short-acting beta2-agonists as standalone therapy since 2022 due to the increased risk of asthma exacerbations and poor symptom control associated with their overuse [35]. Instead, GINA recommends inhaled corticosteroids–formoterol or inhaled corticosteroids–short-acting beta2-agonists as reliever treatment options [36]. However, ChatGPT-4o does not reflect these key updates, highlighting the issue of its database's lag in incorporating recent developments.

The Importance of Personalized, Evidence-Based Education Tools

As a chronic disease requiring long-term management, asthma treatment decisions must take into account multiple factors, including the patient's gender, disease severity, inhaler technique, adherence, and the cost-effectiveness of medications. These considerations make treatment strategies highly individualized and complex, highlighting the need for timely, accurate, and personalized information support tools. Studies have shown that patients' level of asthma-related knowledge is closely linked to their treatment adherence and overall health outcomes [37]. Agusala et al [38] conducted a study on an interactive asthma education program for children aged 2 - 18 years and their caregivers in Ector County, Texas. The findings revealed that asthma-related education for both caregivers and children led to improved symptom management and reduced acute exacerbations, underscoring the significance of asthma education for patients. Walter et al [39] reviewed 6 intervention studies, all of which demonstrated a decrease in asthma attacks and notable enhancements in overall quality of life. Nevertheless, current patients with asthma and their caregivers often lack sufficient knowledge to effectively manage and prevent the disease, with their educational needs frequently going unmet. This limits the widespread implementation and effectiveness of educational interventions. These challenges underscore the importance of developing intelligent and highly accessible information support tools—such as language models—to bridge these gaps and enhance asthma care.

Limitations and Future Directions

This study demonstrates the potential of ChatGPT-4o and DeepSeek-v3 as innovative tools for health education, capable of delivering clear and accurate medical information through conversational interactions. These capabilities may support patients and caregivers in making more informed treatment decisions. However, as LLMs, both systems exhibit inherent limitations that warrant critical consideration.

First, the knowledge base of LLMs is fixed at the time of their most recent update and does not reflect real-time advances in the medical field. This temporal constraint hinders the incorporation of new treatment protocols, emerging therapies, and updated clinical guidelines, thereby affecting the relevance and accuracy of generated recommendations [40].

Second, the training data for these models are primarily derived from publicly available internet sources, which may not comprehensively include high-quality medical resources such as evidence-based clinical guidelines, care pathways, textbooks, or peer-reviewed literature. Consequently, their outputs may lack sufficient grounding in evidence-based medicine, especially for complex or highly specialized clinical topics [41].

XSL•FO
RenderX

Third, the adequacy of model-generated responses is contingent upon the frequency and depth of topic representation in the training corpus. For rare diseases, novel treatments, or underrepresented conditions, both models may struggle to produce complete or satisfactory answers due to limited data exposure [40].

Fourth, the practical effectiveness of LLMs in patient-facing applications is influenced by users' health literacy and ability to formulate clear, structured queries. Individuals without medical training may find it difficult to pose precise questions, potentially compromising the clarity and relevance of the AI's responses. In addition, the models exhibit sensitivity to prompt phrasing, and subtle variations in user input can lead to divergent outputs.

Fifth, this study assessed only the models' initial responses without considering the potential benefits of multiturn dialogue. In real-world applications, extended interactions may allow for clarification of vague input and generation of more comprehensive answers. Thus, single-turn evaluations may underestimate the practical value of these models in dynamic health care contexts. In multiturn conversations, the model needs to adjust its responses based on previous answers, clarify vague inputs, and provide more comprehensive advice. However, current AI models still face challenges in handling complex and extended dialogues, potentially failing to maintain consistency or provide deep enough analysis. This is particularly crucial in medical decision-making. For instance, when inquiring about medical history and symptoms, the AI needs to rely on prior inputs to form a coherent and evidence-based suggestion [42].

Finally, despite the impressive capabilities of LLMs in delivering medical information, they cannot serve as substitutes for licensed health care professionals. Medical decision-making is a complex and high-stakes process that requires not only accurate knowledge but also clinical experience, physical examination skills, ethical judgment, and contextual understanding—areas in which LLMs remain fundamentally limited. These models are incapable of performing physical assessments, interpreting nonverbal cues, or incorporating emotional and psychosocial factors into patient care [43,44]. In critical situations, such as managing acute exacerbations of chronic conditions or distinguishing between overlapping clinical syndromes, human expertise and oversight are essential. Overreliance on AI without professional validation may lead to delayed diagnoses or inappropriate treatments. Therefore, while LLMs can serve as valuable tools in health communication and patient education, their role must remain supportive rather than autonomous, with clearly defined boundaries for clinical responsibility and accountability [45].

In the future, as AI models continue to gain traction in health care settings, their potential impact will span the entire health care process, from primary health education to clinical decision support [46,47]. In practical applications, it is crucial to emphasize the role of AI as an auxiliary tool, avoiding the misconception of using it as the primary decision maker in clinical scenarios [48]. Generative AI has the potential to play a key role in enhancing patient health literacy and promoting the democratization of medical knowledge [49]. This is particularly important in areas with limited health care resources, where AI can provide patients with broader access to vital health information.

It is recommended that future intelligent health care systems be designed with a "layered response + human referral" approach, positioning AI as the "first responder" in routine management scenarios [50]. In cases of high risk or acute conditions, automatic alerts and human intervention mechanisms should be introduced to ensure both the safety and effectiveness of the service. This progressive integration of human-AI collaboration may become the key pathway for maximizing the value of AI technology in managing chronic respiratory diseases.

Conclusion

This study systematically evaluated the performance of ChatGPT-4o and DeepSeek-v3 in providing asthma-related education to patients with asthma and found that both models have distinct strengths. DeepSeek-v3 excels in knowledge updates and clinical reasoning, covering a broader range of the latest treatment methods and complex symptom analysis. On the other hand, ChatGPT-4o is clearer and more accessible in explaining basic concepts and language. Both models provide generally accurate medical information, but there are still limitations, particularly in areas such as differential diagnosis and the completeness of treatment plans, with a noticeable lag in updates to the latest clinical guidelines.

These AI tools can serve as effective supplementary aids in providing asthma-related education to patients with asthma, helping patients better understand their condition and manage symptoms. However, they currently cannot fully replace professional medical advice, especially in complex cases or high-risk situations. Future improvements are needed in the models' knowledge updating mechanisms and clinical reasoning capabilities, along with enhanced human-AI collaboration, to ensure patients receive health information that is both accurate and understandable. These findings are not only significant for asthma management but also provide valuable insights for the application of AI in the education of other chronic diseases.

Acknowledgments

This work was partially supported by the University of Tennessee Health Science Center (R073290109) to WG in Memphis, TN, United States. The funders had no role in the design of the study; in the collection, analysis, or interpretation of data; in the writing of the manuscript; or in the decision to publish the results. During the preparation of this work, the author(s) used ChatGPT-4o and DeepSeek v-3 to test and generate answers to test the capacity to assist patients with asthma in understanding the disease and treatment. After using these tools/services, the author(s) reviewed and edited the content as needed and take(s) full responsibility for the content of the publication.

XSL•FO
RenderX

Authors' Contributions

WG and BY contributed to the conceptualization of the study. XT and YL were responsible for data curation. The investigation was conducted by YL and FY. Methodology was developed by YL and XT. Supervision was provided by BY, FY, and XZ. YL drafted the original manuscript. KL and BY contributed to the review and editing of the final manuscript.

Conflicts of Interest

None declared.

Multimedia Appendix 1
ChatGPT-4.0's responses to asthma-related inquiries in an English-language context.
[DOC File, 76 KB - medinform_v13i1e65365_app1.doc]

Multimedia Appendix 2
ChatGPT-4.0's responses to asthma-related inquiries in a Chinese-language context.
[DOC File, 188 KB - medinform_v13i1e65365_app2.doc]

Multimedia Appendix 3
DeepSeek's responses to asthma-related inquiries in an English-language context.
[DOC File, 90 KB - medinform_v13i1e65365_app3.doc]

Multimedia Appendix 4
DeepSeek -3's responses to asthma-related inquiries in a Chinese-language context.
[DOC File, 207 KB - medinform_v13i1e65365_app4.doc]

Multimedia Appendix 5
Comparative scores of 2 artificial intelligence models across multiple evaluation dimensions in a bilingual context.
[DOC File, 15 KB - medinform_v13i1e65365_app5.doc]

References

1. Dharmage SC, Perret JL, Custovic A. Epidemiology of asthma in children and adults. Front Pediatr 2019;7:246. [doi: 10.3389/fped.2019.00246] [Medline: 31275909]
2. Oren O, Gersh BJ, Bhatt DL. Artificial intelligence in medical imaging: switching from radiographic pathological data to clinically meaningful endpoints. Lancet Digit Health 2020 Sep;2(9):e486-e488. [doi: 10.1016/S2589-7500(20)30160-6] [Medline: 33328116]
3. Kreimeyer K, Foster M, Pandey A, et al. Natural language processing systems for capturing and standardizing unstructured clinical information: a systematic review. J Biomed Inform 2017 Sep;73:14-29. [doi: 10.1016/j.jbi.2017.07.012] [Medline: 28729030]
4. Nadkarni PM, Ohno-Machado L, Chapman WW. Natural language processing: an introduction. J Am Med Inform Assoc 2011;18(5):544-551. [doi: 10.1136/amiajnl-2011-000464] [Medline: 21846786]
5. Yu G, Li Z, Li S, et al. The role of artificial intelligence in identifying asthma in pediatric inpatient setting. Ann Transl Med 2020 Nov;8(21):1367. [doi: 10.21037/atm-20-2501a] [Medline: 33313112]
6. Islam MA, Bandyopadhyaya I, Bhattacharyya P, Saha G. Multichannel lung sound analysis for asthma detection. Comput Methods Programs Biomed 2018 Jun;159:111-123. [doi: 10.1016/j.cmpb.2018.03.002] [Medline: 29650306]
7. Seol HY, Shrestha P, Muth JF, et al. Artificial intelligence-assisted clinical decision support for childhood asthma management: a randomized clinical trial. In: Leroyer C, editor. PLoS ONE 2021;16(8):e0255261. [doi: 10.1371/journal.pone.0255261] [Medline: 34339438]
8. Zhang O, Minku LL, Gonem S. Detecting asthma exacerbations using daily home monitoring and machine learning. J Asthma 2021 Nov;58(11):1518-1527. [doi: 10.1080/02770903.2020.1802746] [Medline: 32718193]
9. Joumaa H, Sigogne R, Maravic M, Perray L, Bourdin A, Roche N. Artificial intelligence to differentiate asthma from COPD in medico-administrative databases. BMC Pulm Med 2022 Sep 20;22(1):357. [doi: 10.1186/s12890-022-02144-2] [Medline: 36127649]
10. Goodman RS, Patrinely JR, Stone CA Jr, et al. Accuracy and reliability of chatbot responses to physician questions. JAMA Netw Open 2023 Oct 2;6(10):e2336483. [doi: 10.1001/jamanetworkopen.2023.36483] [Medline: 37782499]
11. Howard A, Hope W, Gerada A. ChatGPT and antimicrobial advice: the end of the consulting infection doctor? Lancet Infect Dis 2023 Apr;23(4):405-406. [doi: 10.1016/S1473-3099(23)00113-5] [Medline: 36822213]
12. Haver HL, Lin CT, Sirajuddin A, Yi PH, Jeudy J. Evaluating ChatGPT's accuracy in lung cancer prevention and screening recommendations. Radiol Cardiothorac Imaging 2023 Aug;5(4):e230115. [doi: 10.1148/ryct.230115] [Medline: 37693201]

XSL•FO
RenderX

13. P PJ, Prasad SS, Manohar N. Genital and extragenital lichen sclerosus et atrophicus: a case series written using ChatGPT. Cureus 2023 May 13;15(5):e38987. [doi: 10.7759/cureus.38987] [Medline: 37323348]
14. Maniaci A, Saibene AM, Calvo-Henriquez C, et al. Is generative pre-trained transformer artificial intelligence (Chat-GPT) a reliable tool for guidelines synthesis? A preliminary evaluation for biologic CRSwNP therapy. Eur Arch Otorhinolaryngol 2024 Apr;281(4):2167-2173. [doi: 10.1007/s00405-024-08464-9]
15. Temsah A, Alhasan K, Altamimi I, et al. DeepSeek in healthcare: revealing opportunities and steering challenges of a new open-source artificial intelligence frontier. Cureus 2025 Feb;17(2):e79221. [doi: 10.7759/cureus.79221] [Medline: 39974299]
16. Singhal K, Azizi S, Tu T, et al. Large language models encode clinical knowledge. Nature New Biol 2023 Aug;620(7972):172-180. [doi: 10.1038/s41586-023-06291-2] [Medline: 37438534]
17. Totlis T, Natsis K, Filos D, et al. The potential role of ChatGPT and artificial intelligence in anatomy education: a conversation with ChatGPT. Surg Radiol Anat 2023 Oct;45(10):1321-1329. [doi: 10.1007/s00276-023-03229-1] [Medline: 37584720]
18. Yu P, Fang C, Liu X, et al. Performance of ChatGPT on the Chinese postgraduate examination for clinical medicine: survey study. JMIR Med Educ 2024 Feb 9;10:e48514. [doi: 10.2196/48514] [Medline: 38335017]
19. Riedel M, Kaefinger K, Stuehrenberg A, et al. ChatGPT's performance in German OB/GYN exams – paving the way for AI-enhanced medical education and clinical practice. Front Med 2023 Dec 13;10:1296615. [doi: 10.3389/fmed.2023.1296615]
20. Nedbal C, Naik N, Castellani D, Gauhar V, Geraghty R, Somani BK. ChatGPT in urology practice: revolutionizing efficiency and patient care with generative artificial intelligence. Curr Opin Urol 2024 Mar 1;34(2):98-104. [doi: 10.1097/MOU.0000000000001151] [Medline: 37962176]
21. Lee PY, Salim H, Abdullah A, Teo CH. Use of ChatGPT in medical research and scientific writing. Malays Fam Physician 2023;18:58. [doi: 10.51866/cm0006] [Medline: 37814667]
22. Yeo YH, Samaan JS, Ng WH, et al. Assessing the performance of ChatGPT in answering questions regarding cirrhosis and hepatocellular carcinoma. Clin Mol Hepatol 2023 Jul;29(3):721-732. [doi: 10.3350/cmh.2023.0089] [Medline: 36946005]
23. Sarangi PK, Lumbani A, Swarup MS, et al. Assessing ChatGPT's proficiency in simplifying radiological reports for healthcare professionals and patients. Cureus 2023 Dec;15(12):e50881. [doi: 10.7759/cureus.50881] [Medline: 38249202]
24. Rogasch JMM, Metzger G, Preisler M, et al. ChatGPT: can you prepare my patients for [18F]FDG PET/CT and explain my reports? J Nucl Med 2023 Dec 1;64(12):1876-1879. [doi: 10.2967/jnumed.123.266114] [Medline: 37709536]
25. Janopaul-Naylor JR, Koo A, Qian DC, McCall NS, Liu Y, Patel SA. Physician assessment of ChatGPT and bing answers to American Cancer Society's questions to ask about your cancer. Am J Clin Oncol 2024 Jan 1;47(1):17-21. [doi: 10.1097/COC.0000000000001050] [Medline: 37823708]
26. Rahsepar AA, Tavakoli N, Kim GHJ, Hassani C, Abtin F, Bedayat A. How AI responds to common lung cancer questions: ChatGPT vs Google Bard. Radiology 2023 Jun;307(5):e230922. [doi: 10.1148/radiol.230922] [Medline: 37310252]
27. Haver HL, Lin CT, Sirajuddin A, Yi PH, Jeudy J. Use of ChatGPT, GPT-4, and bard to improve readability of ChatGPT's answers to common questions about lung cancer and lung cancer screening. AJR Am J Roentgenol 2023 Nov;221(5):701-704. [doi: 10.2214/AJR.23.29622] [Medline: 37341179]
28. Pan A, Musheyev D, Bockelman D, Loeb S, Kabarriti AE. Assessment of artificial intelligence chatbot responses to top searched queries about cancer. JAMA Oncol 2023 Oct 1;9(10):1437-1440. [doi: 10.1001/jamaoncol.2023.2947] [Medline: 37615960]
29. Global Strategy for Asthma Management and Prevention. Global Initiative for Asthma. URL: https://ginasthma.org/wp-content/uploads/2023/07/GINA-2023-Full-report-23_07_06-WMS.pdf [accessed 2025-06-27]
30. Kresevic S, Giuffrè M, Ajcevic M, Accardo A, Crocè LS, Shung DL. Optimization of hepatological clinical guidelines interpretation by large language models: a retrieval augmented generation-based framework. NPJ Digit Med 2024 Apr 23;7(1):102. [doi: 10.1038/s41746-024-01091-y] [Medline: 38654102]
31. Afzal M, Alam F, Malik KM, Malik GM. Clinical context-aware biomedical text summarization using deep neural network: model development and validation. J Med Internet Res 2020 Oct 23;22(10):e19810. [doi: 10.2196/19810] [Medline: 33095174]
32. Ross P, Spates K. Considering the safety and quality of artificial intelligence in health care. Jt Comm J Qual Patient Saf 2020 Oct;46(10):596-599. [doi: 10.1016/j.jcjq.2020.08.002] [Medline: 32878718]
33. Wang Y, Chen Y, Sheng J. Assessing ChatGPT as a medical consultation assistant for chronic hepatitis B: cross-language study of English and Chinese. JMIR Med Inform 2024 Aug 8;12:e56426. [doi: 10.2196/56426] [Medline: 39115930]
34. Pelicioni PHS, Michell A, Schulz JS. Facilitating access to current, evidence-based health information for non-English speakers. Healthcare (Basel) 2023 Jul 4;11(13):1932. [doi: 10.3390/healthcare11131932] [Medline: 37444766]
35. O'Byrne PM, Reddel HK, Beasley R. The management of mild asthma. Eur Respir J 2021 Apr;57(4):2003051. [doi: 10.1183/13993003.03051-2020] [Medline: 33093120]
36. Beasley R, Bruce P, Houghton C, Hatter L. The ICS/formoterol reliever therapy regimen in asthma: a review. J Allergy Clin Immunol Pract 2023 Mar;11(3):762-772. [doi: 10.1016/j.jaip.2023.01.002] [Medline: 36639054]
37. Prabhakaran L, Lim G, Abisheganaden J, Chee CBE, Choo YM. Impact of an asthma education programme on patients' knowledge, inhaler technique and compliance to treatment. Singapore Med J 2006 Mar;47(3):225-231. [Medline: 16518558]

XSL•FO
RenderX

38. Agusala V, Vij P, Agusala V, Dasari V, Kola B. Can interactive parental education impact health care utilization in pediatric asthma: a study in rural Texas. J Int Med Res 2018 Aug;46(8):3172-3182. [doi: 10.1177/0300060518773621] [Medline: 29848134]
39. Walter H, Sadeque-Iqbal F, Ulysse R, Castillo D, Fitzpatrick A, Singleton J. Effectiveness of school-based family asthma educational programs in quality of life and asthma exacerbations in asthmatic children aged five to 18: a systematic review. JBI Database System Rev Implement Rep 2016 Nov;14(11):113-138. [doi: 10.11124/JBISRIR-2016-003181] [Medline: 27941517]
40. Kim J, Vajravelu BN. Assessing the current limitations of large language models in advancing health care education. JMIR Form Res 2025 Jan 16;9:e51319. [doi: 10.2196/51319] [Medline: 39819585]
41. Lin Z, Guan S, Zhang W, Zhang H, Li Y, Zhang H. Towards trustworthy LLMs: a review on debiasing and dehallucinating in large language models. Artif Intell Rev 2024;57(9):243. [doi: 10.1007/s10462-024-10896-y]
42. Tangsrivimol JA, Darzidehkalani E, Virk HUH, et al. Benefits, limits, and risks of ChatGPT in medicine. Front Artif Intell 2025;8:1518049. [doi: 10.3389/frai.2025.1518049] [Medline: 39949509]
43. Meng X, Yan X, Zhang K, et al. The application of large language models in medicine: a scoping review. iScience 2024 May 17;27(5):109713. [doi: 10.1016/j.isci.2024.109713] [Medline: 38746668]
44. Sezgin E. Artificial intelligence in healthcare: complementing, not replacing, doctors and healthcare providers. Digit Health 2023;9:20552076231186520. [doi: 10.1177/20552076231186520] [Medline: 37426593]
45. Schaffter T, Buist DSM, Lee CI, et al. Evaluation of combined artificial intelligence and radiologist assessment to interpret screening mammograms. JAMA Netw Open 2020 Mar 2(3):e200265. [doi: 10.1001/jamanetworkopen.2020.4429] [Medline: 32119094]
46. Moulaei K, Yadegari A, Baharestani M, Farzanbakhsh S, Sabet B, Reza Afrash M. Generative artificial intelligence in healthcare: a scoping review on benefits, challenges and applications. Int J Med Inform 2024 Aug;188:105474. [doi: 10.1016/j.ijmedinf.2024.105474] [Medline: 38733640]
47. Fatima A, Shafique MA, Alam K, Fadlalla Ahmed TK, Mustafa MS. ChatGPT in medicine: a cross-disciplinary systematic review of ChatGPT's (artificial intelligence) role in research, clinical practice, education, and patient interaction. Medicine (Baltimore) 2024 Aug 9;103(32):e39250. [doi: 10.1097/MD.0000000000039250] [Medline: 39121303]
48. Topol EJ. High-performance medicine: the convergence of human and artificial intelligence. Nat Med 2019 Jan;25(1):44-56. [doi: 10.1038/s41591-018-0300-7] [Medline: 30617339]
49. Chen A, Liu L, Zhu T. Advancing the democratization of generative artificial intelligence in healthcare: a narrative review. J Hosp Manag Health Policy 2024;8:12-12. [doi: 10.21037/jhmhp-24-54]
50. Preiksaitis C, Ashenburg N, Bunney G, et al. The role of large language models in transforming emergency medicine: scoping review. JMIR Med Inform 2024 May 10;12:e53787. [doi: 10.2196/53787] [Medline: 38728687]

Abbreviations

AI: artificial intelligence
API: application programming interface
GINA: Global Initiative for Asthma
LLM: large language model
RAG: retrieval-augmented generation
TSLP: thymus stromal lymphopoietin

Edited by A Castonguay; submitted 14.08.24; peer-reviewed by A Chauhan, A Hidki, L Wreyford; revised version received 10.05.25; accepted 23.05.25; published 13.08.25.

Please cite as:
Liu Y, Yu F, Zhang X, Tong X, Li K, Gu W, Yu B
Assessing the Role of Large Language Models Between ChatGPT and DeepSeek in Asthma Education for Bilingual Individuals: Comparative Study
JMIR Med Inform 2025;13:e65365
URL: https://medinform.jmir.org/2025/1/e65365
doi:10.2196/65365

©Yaxin Liu, Fangfei Yu, Xiaofei Zhang, Xiaohan Tong, Kui Li, Weikuan Gu, Baiquan Yu. Originally published in JMIR Medical Informatics (https://medinform.jmir.org), 13.8.2025. This is an open-access article distributed under the terms of the Creative Commons Attribution License (https://creativecommons.org/licenses/by/4.0/), which permits unrestricted use, distribution, and reproduction in any medium, provided the original work, first published in JMIR Medical Informatics, is properly cited. The

XSL•FO
RenderX

complete bibliographic information, a link to the original publication on https://medinform.jmir.org/, as well as this copyright and license information must be included.

XSL•FO
RenderX

AI-Driven Integrated System for Burn Depth Prediction With Electronic Medical Records: Algorithm Development and Validation

Md Masudur Rahman[1*], PhD; Mohamed El Masry[2,3*], MD, PhD; Surya C Gnyawali[2,3], PhD; Yexiang Xue[4], PhD; Gayle Gordillo[2,5*], MD; Juan P Wachs[1*], PhD

[1]Edwardson School of Industrial Engineering, Purdue University West Lafayette, 315 N Grant Street, West Lafayette, IN, United States

[2]McGowan Institute for Regenerative Medicine, University of Pittsburgh, Pittsburgh, PA, United States

[3]Department of Surgery, School of Medicine, University of Pittsburgh, Pittsburgh, PA, United States

[4]Department of Computer Science, Purdue University West Lafayette, West Lafayette, IN, United States

[5]Department of Plastic Surgery, School of Medicine, University of Pittsburgh, Pittsburgh, PA, United States

[*]these authors contributed equally

Corresponding Author:
Juan P Wachs, PhD
Edwardson School of Industrial Engineering, Purdue University West Lafayette, 315 N Grant Street, West Lafayette, IN, United States

Abstract

Background: Burn injuries represent a significant clinical challenge due to the complexity of accurately assessing burn depth, which directly influences the course of treatment and patient outcomes. Traditional diagnostic methods primarily rely on visual inspection by experienced burn surgeons. Studies report diagnostic accuracies of around 76% for experts, dropping to nearly 50% for less experienced clinicians. Such inaccuracies can result in suboptimal clinical decisions—delaying vital surgical interventions in severe cases or initiating unnecessary treatments for superficial burns. This diagnostic variability not only compromises patient care but also strains health care resources and increases the likelihood of adverse outcomes. Hence, a more consistent and precise approach to burn classification is urgently needed.

Objective: The objective is to determine whether a multimodal integrated artificial intelligence (AI) system for accurate classification of burn depth can preserve diagnostic accuracy and provide an important resource when used as part of the electronic medical record (EMR).

Methods: This study used a novel multimodal AI system, integrating digital photographs and ultrasound tissue Doppler imaging (TDI) data to accurately assess burn depth. These imaging modalities were accessed and processed through an EMR system, enabling real-time data retrieval and AI-assisted evaluation. TDI was instrumental in evaluating the biomechanical properties of subcutaneous tissues, using color-coded images to identify burn-induced changes in tissue stiffness and elasticity. The collected imaging data were uploaded to the EMR system (DrChrono), where they were processed by a vision-language model built on GPT-4 architecture. This model received expert-formulated prompts describing how to interpret both digital and TDI images, guiding the AI in making explainable classifications.

Results: This study evaluated whether a multimodal AI classifier, designed to identify first-, second-, and third-degree burns, could be effectively applied to imaging data stored within an EMR system. The classifier achieved an overall accuracy of 84.38%, significantly surpassing human performance benchmarks typically cited in the literature. This highlights the potential of the AI model to serve as a robust clinical decision support tool, especially in settings lacking highly specialized expertise. In addition to accuracy, the classifier demonstrated strong performance across multiple evaluation metrics. The classifier's ability to distinguish between burn severities was further validated by the area under the receiver operating characteristic: 0.97 for first-degree, 0.96 for second-degree, and a perfect 1.00 for third-degree burns, each with narrow 95% CIs.

Conclusions: The storage of multimodal imaging data within the EMR, along with the ability for post hoc analysis by AI algorithms, offers significant advancements in burn care, enabling real-time burn depth prediction on currently available data. Using digital photos for superficial burns, easily diagnosed through physical examinations, reduces reliance on TDI, while TDI helps distinguish deep second- and third-degree burns, enhancing diagnostic efficiency.

Trial Registration: ClinicalTrials.gov NCT05167461; https://clinicaltrials.gov/study/NCT05167461

(JMIR Med Inform 2025;13:e68366) doi:10.2196/68366

KEYWORDS

burn diagnosis; vision-language model; large language model; ultrasound; electronic medical record; EMR

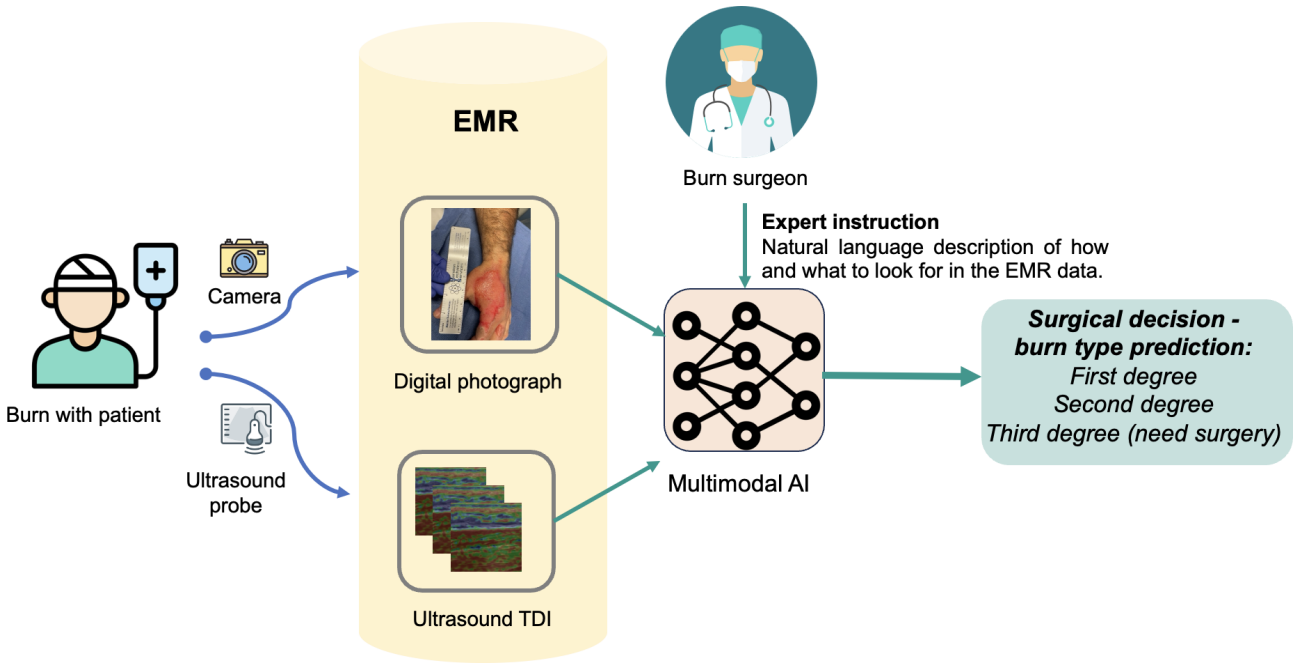
XSL•FO
RenderX

Introduction

Burn injuries are among the most challenging conditions in medical treatment [1] due to the critical need for accurate depth assessment to determine appropriate therapeutic strategies. Traditional burn depth assessment relies heavily on visual inspection by experienced surgeons, which, while effective in many cases, can lead to inaccuracies, especially when distinguishing between second-degree deep and third-degree burns (76% accuracy for experts, which reduced to 50% for nonexperts) [2-4]. These errors can lead to improper care, postponing critical treatment for severe burns or prompting excessive procedures for minor ones [2,3,5].

To address these challenges, this paper presents a novel approach, BURN-AID (Burn Diagnosis with Artificial Intelligence), leveraging multimodal imaging integrated with a vision-language model, designed to improve the accuracy of burn depth classification (Figure 1). This system performs a 3-way classification of burn depth into first-, second-, and third-degree burns, offering a more nuanced and precise clinical decision support tool.

Figure 1. Overview of the proposed multimodal burn classification system, BURN-AID. The framework integrates digital photographs and ultrasound TDI of burn wounds, both stored within an EMR system. A vision-language AI model, guided by expert instructions, analyzes the multimodal data to predict burn severity—classifying injuries as first, second, or third degree. The system supports real-time clinical decision-making by embedding predictions directly into the EMR, enabling streamlined diagnostic workflows, and aiding surgical intervention planning. AI: artificial intelligence; BURN-AID: Burn Diagnosis with Artificial Intelligence; EMR: electronic medical record; TDI: tissue Doppler imaging.



The method integrates digital photographs and ultrasound tissue Doppler imaging (TDI) data stored within an electronic medical record (EMR) system. The initial phase of burn assessment uses digital photographs of the burn wound. These images are processed to rapidly classify burns as first degree or second degree [6]. This swift identification is crucial for initiating immediate treatment and reducing the need for further diagnostic procedures for mild burns. However, for cases that potentially classify as third degree, the system relies on TDI data. Ultrasound TDI offers detailed imaging of tissue structures, critical for accurate depth assessment where visual inspection alone may fall short.

The artificial intelligence (AI)–driven approach ensures that ultrasound resources are used judiciously, minimizing unnecessary scans and focusing them on cases with high severity, as indicated by initial digital photograph analysis. This method optimizes the diagnostic workflow within the EMR, allowing for efficient data retrieval and processing, thus enhancing the overall efficiency of the medical staff.

In this study, we present and evaluate BURN-AID, an AI-based method that classifies burn depth using digital photographs and ultrasound-TDI data, measuring its performance across first-, second-, and third-degree categories using expert-annotated clinical datasets.

Methods

Recruitment

In total, 30 patients participated in the study, with 1 excluded due to withdrawal. Enrollment was based on a first-come, first-served basis. Patients were screened at the Eskenazi Burn Center, Indianapolis, and informed about the study procedures, time commitment, and risks by the coordinator. Those who qualified signed an institutional review board (IRB)–approved informed consent form.

Data Exclusion

Patients were excluded if they were unable to provide informed consent, were younger than 18 years of age, had burns covering 75% or more of their body surface, or had burns resulting from chemical, electrical, or radiation sources. Patients with burns that had already undergone surgical debridement were also excluded.

XSL•FO
RenderX

EMR System

We relied on an EMR system, the DrChrono by EverHealth [7]. We were given access to a training account for medical professionals, allowing us to upload images of burn injuries. We created an app where our AI system can retrieve data from the EMR system and make real-time predictions. Our system was developed in Python (Python Software Foundation) using the Developer API (application programming interface) by DrChrono. Our system is based on a Web API, making it easily extendable to mobile or tablet apps. This integration opens new possibilities for deploying our system in real-time burn diagnosis. Expanding the system to support telemedicine apps could further increase accessibility for patients in remote or underserved areas.

Algorithm and AI Integration

The method for predicting burn depth integrates multiple data sources and advanced AI algorithms to enhance diagnostic accuracy. The system uses digital photographs and TDI stored within the EMR framework. This multimodal approach leverages the strengths of each data type to provide a comprehensive assessment of burn depth.

Integration Within EMR Workflows

The AI model is integrated within the EMR system through a custom-built app that uses the Developer API. In practice, the workflow proceeds as follows: when a clinician uploads a new case—including digital photographs and ultrasound images—into the EMR system, our app retrieves this data via the API in real time. The AI model then processes the images, classifies the burn severity using the BURN-AID algorithm (Textbox 1), and returns the prediction directly into the patient's record within the EMR interface.

Textbox 1. Textbox 1: BURN-AID (Burn Diagnosis with Artificial Intelligence) algorithm.

1. Start by N observations.
2. Use K for setting parameters. Remains M = N - K.
3. For M, apply the following:
   - Use a classifier Ultrasound-Classifier to determine Degree 3 from non Degree 3.
   - Use a classifier DigitalPhoto-Classifier to determine Degree 1 or Degree 2 or Degree 3.
   - Final Prediction:
     - If Ultrasound-Classifier predicts Degree 3, then it is a Degree 3.
     - If Ultrasound-Classifier predicts non-Degree 3, then take the prediction from the DigitalPhoto-Classifier (highest probability from Degree 1 and 2).
     - If no ultrasound image, then take prediction from DigitalPhoto-Classifier (Degree 1 or Degree 2 or Degree 3).
   - Use ground truth to determine the success rate for every class, and present the results.

This integration ensures minimal disruption to existing clinical workflows. Clinicians continue using the EMR as they normally would, with the added benefit of automated burn severity assessment appearing as part of the patient documentation. The AI-generated predictions are presented in a structured format that can be reviewed, verified, and incorporated into decision-making. Furthermore, since the system is Web API–based, it is platform-agnostic and can be extended to mobile or tablet-based EMR interfaces used at the bedside or in telemedicine contexts. This seamless interaction supports clinicians without requiring workflow changes, enabling real-time, AI-assisted burn diagnosis within the familiar EMR environment.

Digital Photograph Analysis

We designed a prompt with expert instructions to be given to the vision-language model to generate burn depth predictions. The detailed process is described as follows:

Several color images were taken for each burn area of the patient, with each image (dimension 4032×3024). Per patient, the number of images was a median of 4 (IQR 0), an average of 4 (SD 0.96), a minimum of 2, and a maximum of 7. For each image of the same burn, our AI system first provides a prediction along with an explanation. Based on the majority of the vote, the model then provides an overall classification. The predictions are based on the type of damage to the skin layers as follows [8,9]:

- Epidermis layer: The thin, outermost layer of the skin containing melanocytes, which produce melanin (skin pigment).
- Dermis layer: The middle layer containing blood vessels, lymph vessels, hair follicles, sweat glands, collagen bundles, fibroblasts, and nerves. It is held together by collagen produced by fibroblasts and contains nerve endings that convey pain and touch signals.
- Hypodermis (subcutaneous) layer: The deepest layer consisting of a network of collagen and fat cells that conserve body heat and protect it from injury.

Definitions based on burn classification given to the AI model are as follows: [10]

- First degree: Redness of the skin without blisters.
- Second degree superficial: Presence of blisters, dermis intact.

XSL•FO
RenderX

- Second degree deep: Dermis is burnt; the exact depth is unknown.
- Third degree: Damage through the dermis with eschar (white, yellow, or black), involving part or all of the hypodermis (subcutaneous layer).

The final classifier consists of a multimodal setting, where ultrasound TDI data are used along with digital photographs. Thus, if TDI data are available, the BURN-AID model first uses the TDI analysis module to generate a binary label: third degree or nonthird degree. This prediction is given to our AI system to make an overall prediction. In scenarios where TDI data predict third-degree burns, the overall system predicts third-degree burns. When TDI indicates non-third-degree burns, the digital photographs are used for further fine-grained classification, identifying first- and second-degree burns. This system design ensures that less severe burns (first degree) can be classified without needing ultrasound TDI scanning. However, it incorporates TDI data when available. Additionally, our system design integrates EMRs in real time as soon as the data are available in the EMR database for a patient. We further discuss the classification with ultrasound TDI data only.

TDI Analysis

TDI is an effective technique for evaluating the mechanical response of tissues to externally applied forces by assessing tissue stiffness using a strain gauge incorporated into the ultrasound probe [11-13]. Images are only collected when the application pressure on the probe is within an acceptable range, as detected by the strain gauge. Burn injuries cause the denaturation of proteins, which alters the elastic properties of subcutaneous tissue. TDI is instrumental in detecting these alterations, helping to determine the depth of burn penetration beyond the superficial skin layers into the subcutaneous tissue [11-13]. This is critical for identifying injuries that may require surgical intervention, such as excision and grafting.

TDI produces color-coded images where different hues (blue for hard tissue and red for soft tissue) indicate the mechanical state of the tissue. Changes in these color patterns from healthy skin, due to burn-induced modifications, are crucial for the system's enhanced diagnostic accuracy. The interpretation of TDI images involves analyzing the distribution of red, green, and blue colors to predict burn depth. Continuous blue lines in the TDI images suggest third-degree burns, as this indicates the tissue has hardened due to the burn.

Burn surgeons formulated a natural language interpretation of TDI images of burn injuries, which were fed into the AI system, as follows: TDI assesses tissue displacement in response to an applied mechanical force, evaluating tissue stiffness. The image can be interpreted vertically from top to bottom, corresponding to the skin's layers: the epidermis at the top, followed by the dermis, and the hypodermis (subcutaneous layer) at the bottom. Third-degree burns are identified by a predominant, continuous blue pattern in the hypodermis, indicating severe burns that extend through the dermis to the deepest skin layer. Non-third-degree burns lack this dominant blue pattern in the hypodermis, indicating lesser severity.

BURN-AID Framework Overview

Figure 1 illustrates the workflow of the proposed multimodal burn classification system, BURN-AID. The process begins with the patient with burn, whose injury is documented using both a digital camera and an ultrasound probe. The digital photograph captures surface-level visual information, while the ultrasound probe collects TDI data to assess underlying tissue characteristics.

Both types of data are stored within the patient's EMR. The AI system retrieves this multimodal data from the EMR and uses it as input for classification. In addition to the image data, the AI model incorporates expert surgeon instructions, formulated as natural language descriptions. These instructions guide the model on what to look for within the EMR to support clinical decision-making.

The AI system, trained to recognize patterns associated with varying burn depths, then outputs a prediction. The final classification determines whether the burn is first degree, second degree, or third degree. Importantly, third-degree burns—those that typically require surgical intervention—are flagged accordingly. This setup enables accurate, real-time diagnostic support directly within the clinical workflow.

AI Model Implementation

Leveraging a vision-language model, specifically the GPT-4o [14], enables the exploration of patterns described in the expert instruction within images. The AI model uses expert instructions (system prompt), digital photographs, and TDI ultrasound images (when available) to generate explanations in natural language. The output format for assessing burn depth using TDI is structured into 2 components: burn depth, which specifies the assessed depth of the burn, providing direct insight into injury severity; and explanation, which provides a detailed rationale for the prediction, elaborating on how observed color patterns in TDI images correlate with the predefined hypothesis regarding burn depth and severity. When analyzing multiple images, the system provides predictions and explanations for each image first, followed by an overall assessment based on the majority of images.

For our experiments, we implemented the algorithm using Python to encode the natural language expert instructions into the system message prompt. For example, expert instructions are: for a digital photograph, "consider 1st degree burn if there is redness of the skin without blisters," and for TDI, "consider 3rd degree burn if there is a continuous blue pattern in the hypodermis (lower layer/bottom part of the image)." The OpenAI GPT-4 Vision API [14] was used to submit the expert instruction and request burn depth predictions with the prompt "What is the depth of the burn indicated by this image?" The system provided predictions for a 3-way classification of burn depth: first-, second-, and third-degree burns. The experimental procedure focused on generating predictions and explanations at the per-patient level. By focusing on per-patient evaluation, the system ensured accurate burn depth classification and appropriate surgical decision-making, enhancing the overall efficiency and effectiveness of burn injury diagnosis and treatment.

XSL•FO
RenderX

Burn Severity Classification With BURN-AID

To classify the severity of burns, we propose a hybrid method called BURN-AID, detailed in Textbox 1. This method integrates 2 classifiers based on different imaging modalities: ultrasound and digital photographs. The algorithm begins with a dataset of N observations. A subset of K observations is used for parameter tuning, leaving M=N−K observations for the main classification process.

For each of the M observations, 2 classifiers are applied. The first is an ultrasound-based classifier that performs a binary classification to distinguish between Degree 3 burns and non-Degree 3 burns. The second is a digital photo–based classifier that performs multiclass classification to differentiate among Degree 1, Degree 2, and Degree 3 burns.

The final prediction for each observation follows a decision hierarchy. If the ultrasound classifier predicts the burn as Degree 3, this prediction is used as the final classification. If the ultrasound classifier predicts a non-Degree 3 burn, the algorithm then relies on the digital photo classifier, selecting the class with the highest probability between Degree 1 and Degree 2. In cases where an ultrasound image is not available, the prediction is made solely based on the output of the digital photo classifier among all 3 classes. After completing the classification for all M observations, the predicted burn degrees are compared with the ground truth labels.

Dataset Description for Experiments

A major challenge is finding publicly available datasets to conduct experiments in our setting. While some datasets can be found through internet sources, such as Google Image search, these images often lack appropriate annotations and are frequently copyrighted. Additionally, there is no available ultrasound TDI data for second- and third-degree burns. As a result, we rely on data collected in hospital settings.

The dataset used for this study consists of a total of 41 patients, encompassing various degrees of burn severity: 15 patients with first-degree burns, 16 patients with second-degree burns, and 10 patients with third-degree burns. Table 1 shows details of the data statistics.

For fine-tuning the prompt and optimizing the parameters of the proposed classifier, we used data from a subset of 9 patients: 3 with first-degree burns, 3 with second-degree burns, and 3 with third-degree burns. The majority of the data (n=29), which we collected, was gathered in a hospital setting, the Richard M. Fairbanks Burn Center at Eskenazi Hospital, Indianapolis, IN, United States.

Table . Distribution of patients by burn severity used for evaluating the BURN-AID (Burn Diagnosis with Artificial Intelligence) system (N=41).

Item	Values, n (%)
First-degree burn	15 (37)
Second-degree burn	16 (39)
Third-degree burn (need surgery)	10 (24)

Validation

The digital photograph was captured first, immediately followed by TDI scanning to ensure that both modalities refer to the same stage of the burn. Two individuals were involved in the data collection process to ensure consistency and efficiency.

However, for a balanced representation, we included data from 12 patients with first-degree burns obtained from a previously published burn dataset [15], as first-degree burn cases typically heal at home and thus are underrepresented in hospital.

To establish the ground truth, 2 burn specialists (burn surgeons) independently and blindly assessed each image, reviewing multiple angles to inform their decisions. On average, each expert took approximately 2 minutes per case. When initial assessments differed, they collaborated to resolve discrepancies through a consensus process, which took up to 3 minutes per case. This final consensus served as the reference standard, against which we compared the validation results to evaluate the accuracy and reliability of our method.

To ensure a comprehensive evaluation, the classifier was assessed using a held-out set of 32 patients, comprising 12 with first-degree burns, 13 with second-degree burns, and 7 with third-degree burns. This diverse dataset allows for a robust analysis of the classifier's performance across different burn severity levels.

Statistical Analysis

Accuracy measures the proportion of correctly classified instances out of the total instances. The F_1-score is particularly useful in situations where the class distribution is imbalanced, as it is the harmonic mean of precision and recall, offering a single metric that balances both concerns. Specificity was used to measure the classifier's ability to correctly identify negative cases (ie, not classifying an instance as a burn type when it is not). The area under the receiver operating characteristic (AUROC) was used to demonstrate the classifier's ability to discriminate between different classes. AUROC values close to 1 indicate excellent discrimination ability, suggesting that the classifier is very effective at distinguishing between different classes. The confusion matrix provides a detailed breakdown of the classifier's performance by showing the number of true positive, true negative, false positive, and false negative predictions. To assess the statistical significance of the observed accuracy, a permutation test with 10,000 permutations was conducted, where a low *P* value indicates a low probability that the observed accuracy could have been achieved by random chance.

Ethical Considerations

The study protocol and experimental design were reviewed and approved by the IRB (IRB# 12689) at Indiana University. All patients provided informed consent to participate and were

XSL•FO
RenderX

compensated (up to US $300 per patient: US $100 for the first session and US $50 for each subsequent session) in accordance with the IRB protocol and the ethical principles outlined in the Declaration of Helsinki. To protect the privacy and confidentiality of research subjects, all data were deidentified (anonymized) prior to analysis.

Results

This study evaluated the performance of a multimodal AI system designed to identify first-, second-, and third-degree burns from images stored in an EMR. The classifier's performance was assessed using several metrics to ensure both effectiveness and reliability. Below, we present the performance metrics.

Evaluation Outcomes

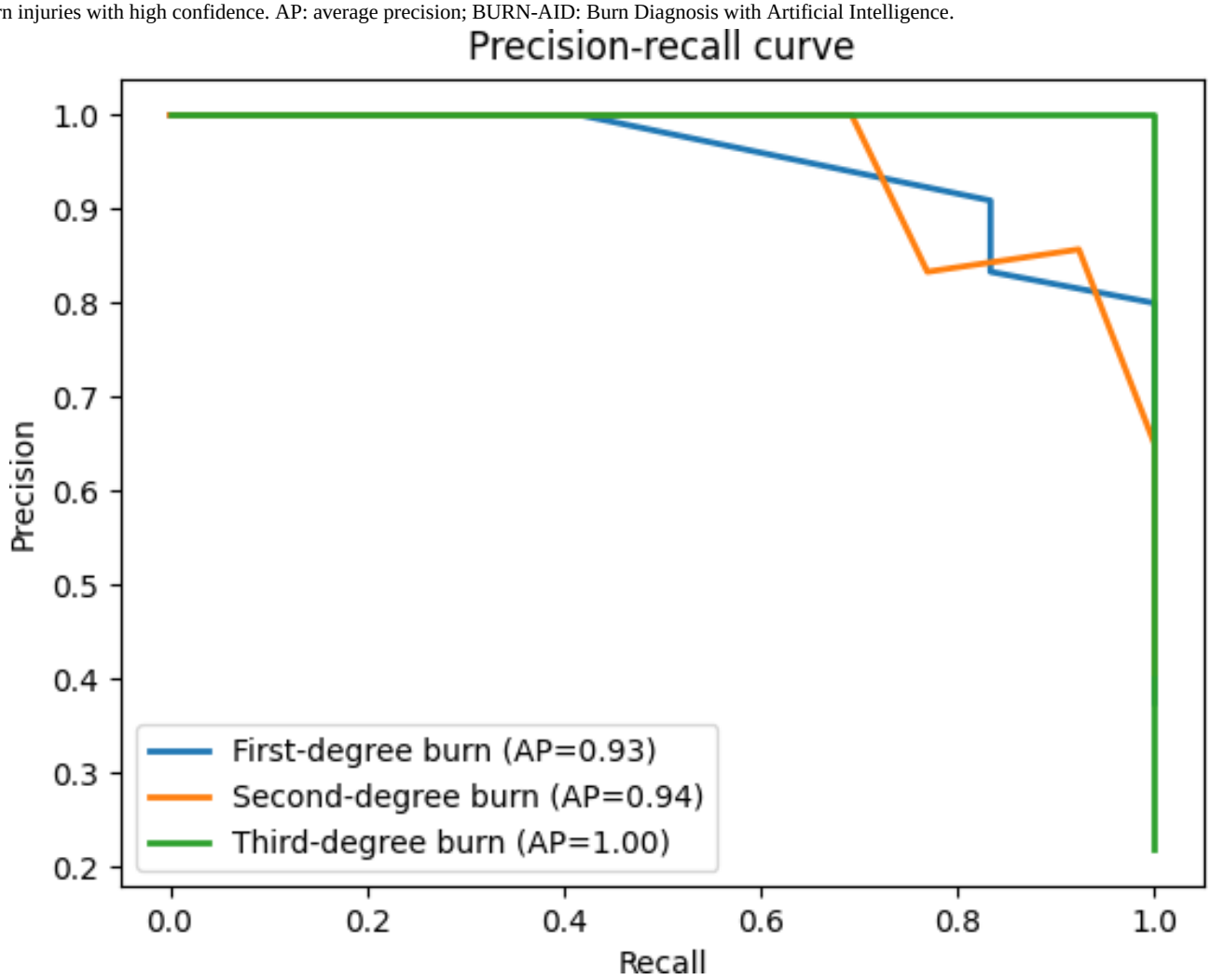
Accuracy

The classifier achieved an accuracy of 84.38%. Accuracy is the proportion of correctly classified (aligned with the decision made by clinicians) instances out of the total instances. The software was least accurate with first-degree burns, for example, sunburns, likely because the thermal injury does not induce any changes below the epidermis, so TDI images will show little change, as this is a small contributor to skin elasticity relative to the dermis. Fortunately, this is also the easiest burn depth to diagnose clinically, and digital photos are usually sufficient.

F_1-Score

The F_1-score, which provides a balance between precision and recall, was 0.856. The precision-recall curve is given in Figure 2, showing the trade-off.

Figure 2. Precision-recall curves for each burn severity class—first, second, and third degree—demonstrating the performance of the BURN-AID classifier in distinguishing between burn types. The curves highlight the trade-off between precision and recall, with high area under the curve values indicating strong predictive accuracy, particularly for third-degree burns. These results support the model's robustness in identifying clinically significant burn injuries with high confidence. AP: average precision; BURN-AID: Burn Diagnosis with Artificial Intelligence.



Specificity

The specificity, representing the proportion of true negative (nonsurgery case classified as nonsurgery) results among all negative cases, was 83.33%.

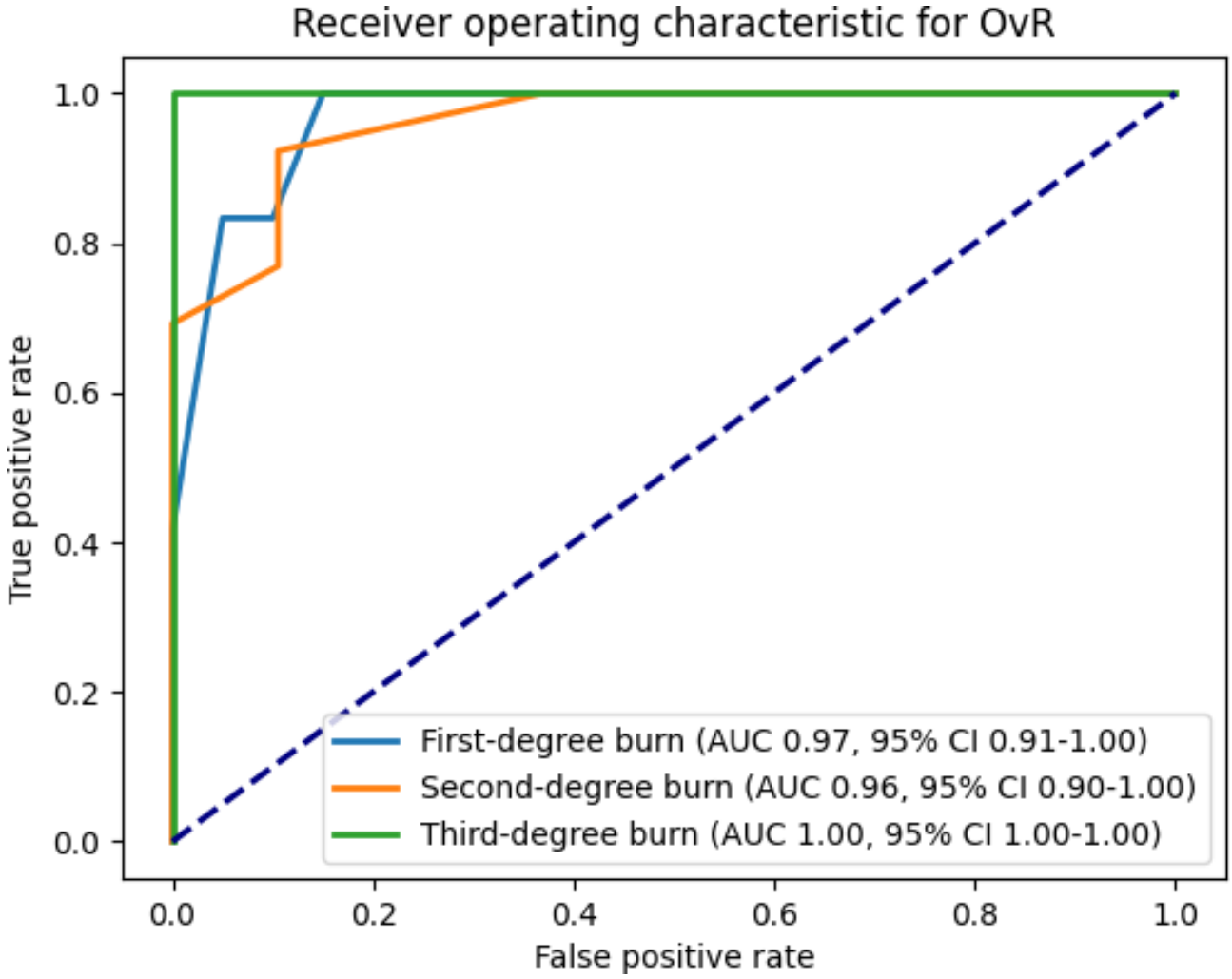
Area Under the Receiver Operating Characteristic Curve

The plot is given in Figure 3, which illustrates the trade-off between the true positive rate and the false positive rate for each class. The AUROC curve for the one-vs-rest approach was 0.97 (95% CI 0.91 - 1.00) for first-degree burns, 0.96 (95% CI

XSL•FO
RenderX

0.90 - 1.00) for second-degree burns, and 1.00 (95% CI 1.00 - 1.00) for third-degree burns, indicating excellent discrimination ability with high AUROC values (Figure 3). The 95% CI range for each class reflects the precision of the AUROC estimate, with narrower ranges indicating more reliable estimates. For instance, the third-degree burns have the narrowest CI (1.00 - 1.00), indicating a highly reliable AUROC estimate, whereas the first- and second-degree burns have wider CIs, suggesting a bit more variability in the estimate. These high AUROC values and their respective CIs suggest that our method is effective at distinguishing between the different classes. This demonstrates that the proposed classifier performs well across all classes, with the high AUROC and narrow CI range highlighting its robustness in a multiclass setting.

Figure 3. AUROC for OvR classification of first-, second-, and third-degree burns using the BURN-AID system. The AUC scores indicate high discrimination ability for each class, with near-perfect performance for third-degree burns (AUC 1.00). The narrow CIs reflect the model's consistency and reliability in differentiating burn severities, supporting its utility in clinical decision-making. AUC: area under the curve; AUROC: area under the receiver operating characteristic; BURN-AID: Burn Diagnosis with Artificial Intelligence; OvR: one-vs-rest.

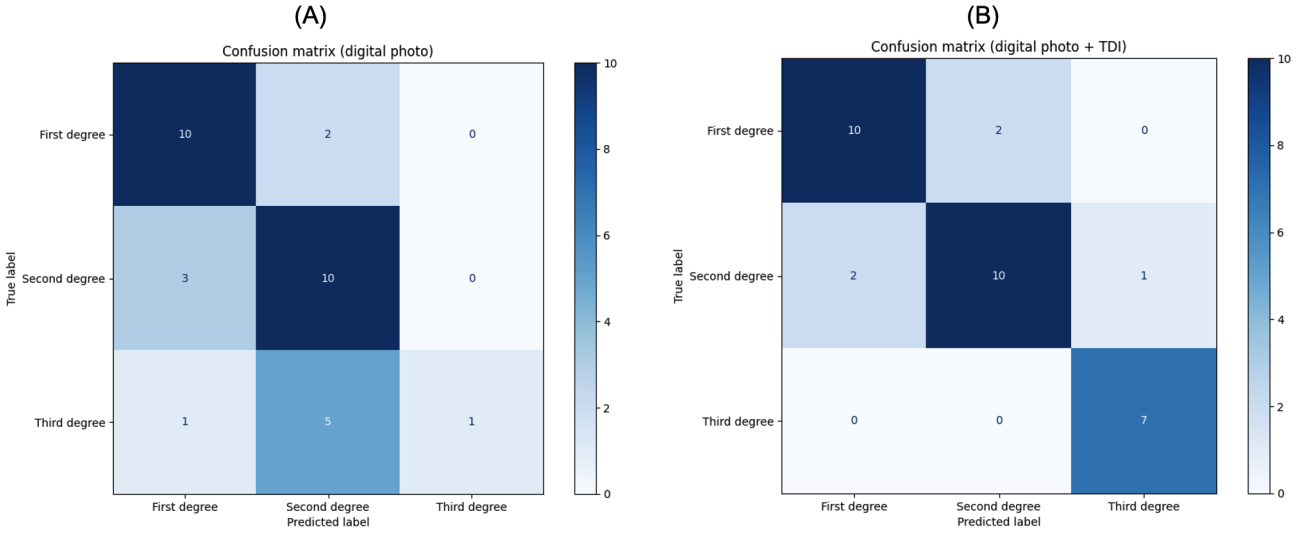


Confusion Matrix

The confusion matrix (Figure 4A and B) provides a detailed breakdown of the classifier's performance by showing the number of true positive, true negative, false positive, and false negative predictions. For first-degree burns, the classifier correctly identified 10 cases, with 2 misclassified as second-degree burns; for second-degree burns, 10 cases were correctly identified, with 2 misclassified as first-degree burns and 1 as a third-degree burn; and for third-degree burns, all 7cases were correctly identified with no misclassifications. The confusion matrix visualization provides a detailed view of the classifier's performance across the different burn degrees.

XSL•FO
RenderX

Figure 4. Confusion matrix visualizations showing the performance of the BURN-AID classifier across 3 burn severity levels. (A) Using digital photographs only, the model correctly classified most cases of less severe burns (between first and second degree) but frequently misclassified second-degree burns as third degree, potentially overestimating severity. (B) With both digital photographs and TDI, the classifier achieved its highest accuracy for third-degree burns and showed improved overall performance. These results demonstrate the advantage of multimodal imaging in improving diagnostic accuracy, particularly for identifying severe burns that require surgical intervention. BURN-AID: Burn Diagnosis with Artificial Intelligence; TDI: tissue Doppler imaging.



Significance of the Performance

A permutation test with 10,000 permutations was conducted to assess the statistical significance of the observed accuracy of the classifier. The *P* value was found to be .0001, indicating a very low probability that the observed accuracy could have been achieved by random chance. This reinforces the conclusion that the classifier is performing significantly better than a random classifier.

Discussion

The goal of this research is to create an integrated multimodal AI system within an EMR framework that enhances burn depth classification accuracy while optimizing diagnostic precision and resource use.

Principal Findings

Our method achieves an accuracy of 84% that correlates with the decision of expert burn surgeons regarding burn depth prediction. The AI system we developed for burn diagnosis provides natural language explanations that have the potential to assist clinicians in making informed decisions. Unlike other deep learning–based methods that use ultrasounds and digital photographs and often offer explanations in the form of saliency maps (eg, LIME [16]), which require further processing to be useful, our system delivers direct natural language text. This approach drastically reduces the gap in explanations for AI systems, making them more accessible to general clinicians. Additionally, in cases of misprediction, these explanations aid in making final decisions, thereby mitigating the risk of incorrect treatment decisions.

Comparison With Prior Work

Our system's effectiveness is built on several mechanisms for burn depth diagnosis. Traditional machine learning and deep learning models [17,18] typically require extensive training data to make accurate predictions, often needing millions of samples to learn useful features from images [19-23]. However, this requirement limits their application in clinical settings, especially in health care areas like burn diagnosis, where data are limited, difficult to obtain, and ultrasound data are even more challenging to acquire [6,24-27]. In our case, we used a small number of patient data to fine-tune the system for burn diagnosis, achieving reasonable accuracy.

We leverage large-scale pretraining, which does not require burn data. Instead, the system is pretrained to understand general knowledge, such as identifying patterns in images. We also incorporate burn surgeons' instructions directly into the system as prompts for making predictions. These instructions simplify the decision-making process because the AI system only needs to identify patterns in the ultrasound images as instructed by the ultrasound and surgeon experts. This expert knowledge can be prerecorded, eliminating the need for the expert presence during real-time decision-making. The expert knowledge is embedded in the system training, making it unnecessary during inference or real-time predictions.

The scarcity of publicly available clinical burn images poses a significant challenge for the research community in advancing this field [28]. Several prior works have resorted to using internet-sourced burn images to develop machine learning systems for depth prediction [28]. Digital photos, with careful preprocessing, such as isolating the burn area and resizing images to 224×224 pixels from a single burn wound, are often used [29,30]. In contrast, we consider using a digital photograph of the burn wound with patients' body parts. This method does not require burn segmentation and is thus more practical in clinical settings. Additionally, our method provides a mechanism to combine digital photography with ultrasound imaging to address errors associated with digital photographs alone, particularly regarding burn depth, which is not visible in standard digital photographs.

XSL•FO
RenderX

Digital photograph–based burn classification has been explored in deciding surgical decision-making for patients with burn [18]. It has been observed that the accuracy in surgical decision-making from digital photographs is 64.7% [18]. This might be due to the fact that the digital photo contains limited information about the deeper skin layers, which are required to identify third-degree burns or surgical cases. In contrast, we leverage TDI data, which improves the accuracy to 84.38% in our AI system. In the literature, various ultrasound methods have been used to diagnose diseases, including burns. Some studies include pig data, use laboratory settings, and achieve reasonable performance [31]. The B-mode ultrasound technique uses a contact probe operating at high frequencies to measure and assess characteristics of skin tissue. In contrast, we build and evaluate our AI system in a multimodal setting, leveraging TDI ultrasound data on human participants. Integration with EMR systems allows our multimodal system to be used in clinical settings where EMR data, such as digital photographs and ultrasound images, can be combined to make comprehensive decisions. This integration reduces costs since some scenarios, like predicting a first-degree burn, might only require digital photographs, eliminating the need for ultrasound. This flexibility helps reduce diagnosis costs and enables faster real-time predictions, which can be updated with new data from the EMR system.

Our system has the potential to be applied to the extensive patient data available in EMR systems across hospitals, requiring minimal involvement from burn experts. Adopting our method to new EMR systems requires generating input data of the burn wound, specifically digital photographs and ultrasound imaging. The AI system then processes this input and provides burn depth information as output. This capability could assist expert surgeons in making more informed decisions and potentially highlight areas where decisions may require further review. The portable nature of imaging systems such as cameras and ultrasound probes allows our system to be used outside hospital settings (eg, accidents, fire incidents, and remote areas). Developing this system for mobile settings, such as tablet and mobile apps, is our next step. Developing such a user-friendly app will be of ultimate importance in far areas where there is no tertiary care or burn centers available.

Limitations

While the proposed method demonstrates promising results in predicting burn depth using multimodal data, several limitations must be considered. First, the use of digital photographs of burn wounds introduces the potential for bias related to variations in skin color. Since skin tone can affect color perception and image-based classification, this could influence model performance. To mitigate this, we cropped the images to focus exclusively on the wound area, excluding surrounding skin and other body parts, thereby minimizing skin tone as a confounding factor. However, in real-world clinical settings, such precise cropping may not always be feasible. Future work should explore model robustness to a wider range of skin tones and develop techniques that are less sensitive to background features. Second, in the case of TDI, we selectively cropped the images to include only the upper portion where the skin layers were clearly distinguishable. This step improved consistency and clarity in the analysis. Nevertheless, this approach assumes ideal image quality and positioning, which may not hold true in routine clinical environments. As a result, the algorithm's generalizability to full, uncropped TDI images remains to be fully validated. Future developments could incorporate automated region-of-interest detection or full-image interpretation to better simulate real-world use. Third, the validation of our AI model relied on expert annotation. We implemented a systematic approach involving blind evaluations and consensus discussions between burn surgeons, who also had access to B-model and TDI ultrasound data during annotation. These decisions were informed by actual clinical treatments, providing a strong reference for classification. However, the current clinical gold standard for burn depth assessment remains histological examination via biopsy. In our study, a subset of patients (5/29) had corresponding histology data, which served as definitive ground truth. Although our expert annotations were consistent with these gold-standard cases, the limited histological data constrain the broader validation of our model's accuracy. Future studies should aim to include more histopathological data to strengthen model evaluation and reduce reliance on subjective expert consensus.

Conclusions

This study presents BURN-AID, an AI-based system for classifying burn depth using multimodal imaging, digital photographs and ultrasound TDI, integrated within an EMR framework. We evaluated its performance on expert-annotated datasets, achieving an overall classification accuracy of 84% across first-, second-, and third-degree burns. These results demonstrate the potential of multimodal AI to support clinical decision-making in burn diagnosis.

Acknowledgments

The authors thank Brett C Hartman, MD, and Leigh Spera, MD, for their contributions and assistance in facilitating data collection on patients with burn. This work was supported by the Office of the Assistant Secretary of Defense for Health Affairs (award W81XWH-21-2-0030) and by the National Institutes of Health (grant 5R21LM013711-02).

Data Availability

The datasets generated or analyzed during this study are available from the corresponding author on reasonable request.

XSL•FO
RenderX

Authors' Contributions

JPW, MMR, MEM, and GG contributed to the conceptualization and design of the study. MMR, MEM, SCG, YX, GG, and JPW were involved in the investigation and validation processes. Data analysis was performed by MMR, MEM, and SCG. The manuscript was drafted and written by MMR, MEM, JPW, and GG, with critical review and revisions provided by MMR, MEM, SCG, YX, GG, and JPW. Funding resources for this work were provided by GG and JPW.

Conflicts of Interest

None declared.

References

1. Herndon DN, Barrow RE, Rutan RL, Rutan TC, Desai MH, Abston S. A comparison of conservative versus early excision. Therapies in severely burned patients. Ann Surg 1989 May;209(5):547-552. [doi: 10.1097/00000658-198905000-00006] [Medline: 2650643]
2. Bombaro KM, Engrav LH, Carrougher GJ, et al. What is the prevalence of hypertrophic scarring following burns? Burns 2003 Jun;29(4):299-302. [doi: 10.1016/s0305-4179(03)00067-6] [Medline: 12781605]
3. Engrav LH, Heimbach DM, Reus JL, Harnar TJ, Marvin JA. Early excision and grafting vs. nonoperative treatment of burns of indeterminant depth. J Trauma Injury Infect Crit Care 1983 Nov;23(11):1001-1004. [doi: 10.1097/00005373-198311000-00007]
4. Jaskille AD, Ramella-Roman JC, Shupp JW, Jordan MH, Jeng JC. Critical review of burn depth assessment techniques: Part II. Review of laser Doppler technology. J Burn Care Res 2010 Jan;31(1):151-157. [doi: 10.1097/BCR.0b013e3181c7ed60]
5. Burke JF, Quinby WC, Bondoc CC. Primary excision and prompt grafting as routine therapy for the treatment of thermal burns in children. Surg Clin North Am 1976 Apr;56(2):477-494. [doi: 10.1016/S0039-6109(16)40890-X]
6. Sen CK, Ghatak S, Gnyawali SC, Roy S, Gordillo GM. Cutaneous imaging technologies in acute burn and chronic wound care. Plast Reconstr Surg 2016 Sep;138(3 Suppl):119S-128S. [doi: 10.1097/PRS.0000000000002654] [Medline: 27556752]
7. DrChrono. EverHealth. 2024. URL: https://www.drchrono.com [accessed 2025-07-17]
8. Browning JA, Cindass R. Burn Debridement, Grafting, and Reconstruction: StatPearls Publishing; 2023.
9. Abazari M, Ghaffari A, Rashidzadeh H, Badeleh SM, Maleki Y. A systematic review on classification, identification, and healing process of burn wound healing. Int J Low Extrem Wounds 2022 Mar;21(1):18-30. [doi: 10.1177/1534734620924857] [Medline: 32524874]
10. Zuo KJ, Medina A, Tredget EE. Important developments in burn care. Plast Reconstr Surg 2017 Jan;139(1):120e-138e. [doi: 10.1097/PRS.0000000000002908] [Medline: 28027250]
11. Fruscalzo A, Londero AP, Fröhlich C, Möllmann U, Schmitz R. Quantitative elastography for cervical stiffness assessment during pregnancy. Biomed Res Int 2014;2014:826535. [doi: 10.1155/2014/826535] [Medline: 24734246]
12. Lau JCM, Li-Tsang CWP, Zheng YP. Application of tissue ultrasound palpation system (TUPS) in objective scar evaluation. Burns 2005 Jun;31(4):445-452. [doi: 10.1016/j.burns.2004.07.016] [Medline: 15896506]
13. El Masry MS, Gnyawali SC, Sen CK. Robust critical limb ischemia porcine model involving skeletal muscle necrosis. Sci Rep 2023 Jul 18;13(1):11574. [doi: 10.1038/s41598-023-37724-7] [Medline: 37463916]
14. Achiam J, Adler S, Agarwal S, et al. GPT-4 technical report. arXiv. Preprint posted online on Mar 4, 2024. [doi: 10.48550/arXiv.2303.08774]
15. Arrubla DC. Automatic assessment of burn injuries using artificial intelligence. : Purdue University; 2021.
16. Ribeiro MT, Singh S, Guestrin C. "Why should i trust you?": explaining the predictions of any classifier. Presented at: Proceedings of the 2016 Conference of the North American Chapter of the Association for Computational Linguistics; Jul 12-17, 2016; San Diego, CA, United States p. 1135-1144. [doi: 10.18653/v1/N16-3020]
17. Martins JFBS, Nascimento ER, Nascimento BR, et al. Towards automatic diagnosis of rheumatic heart disease on echocardiographic exams through video-based deep learning. J Am Med Inform Assoc 2021 Aug 13;28(9):1834-1842. [doi: 10.1093/jamia/ocab061] [Medline: 34279636]
18. Boissin C, Laflamme L, Fransén J, et al. Development and evaluation of deep learning algorithms for assessment of acute burns and the need for surgery. Sci Rep 2023 Jan 31;13(1):1794. [doi: 10.1038/s41598-023-28164-4] [Medline: 36720894]
19. Deng J, Dong W, Socher R, Li LJ. ImageNet: a large-scale hierarchical image database. Presented at: 2009 IEEE Computer Society Conference on Computer Vision and Pattern Recognition Workshops (CVPR Workshops); Miami, FL, United States p. 248-255. [doi: 10.1109/CVPR.2009.5206848]
20. Krizhevsky A, Sutskever I, Hinton GE. ImageNet classification with deep convolutional neural networks. Adv Neural Inf Process Syst 2012;25:1097-1105. [doi: 10.1145/3065386]
21. Russakovsky O, Deng J, Su H, et al. ImageNet Large Scale Visual Recognition Challenge. Int J Comput Vis 2015 Dec;115(3):211-252. [doi: 10.1007/s11263-015-0816-y]
22. He K, Zhang X, Ren S, Sun J. Deep residual learning for image recognition. Presented at: 2016 IEEE Conference on Computer Vision and Pattern Recognition (CVPR); Jun 27-30, 2016; Las Vegas, NV, United States p. 770-778. [doi: 10.1109/CVPR.2016.90]

XSL•FO
RenderX

23. Dosovitskiy A, Beyer L, Kolesnikov A, et al. An image is worth 16x16 words: transformers for image recognition at scale. 2021 Presented at: International Conference on Learning Representations; May 3-7, 2021; Virtual.
24. Schneider JC, Chen L, Simko LC, et al. Challenges to the standardization of burn data collection: a call for common data elements for burn care. J Burn Care Res 2018 Feb 20;39(2):201-208. [doi: 10.1097/BCR.0000000000000567] [Medline: 28481759]
25. Thatcher JE, Squiers JJ, Kanick SC, et al. Imaging techniques for clinical burn assessment with a focus on multispectral imaging. Adv Wound Care (New Rochelle) 2016 Aug 1;5(8):360-378. [doi: 10.1089/wound.2015.0684] [Medline: 27602255]
26. Brem H, Sheehan P, Rosenberg HJ, Schneider JS, Boulton AJM. Evidence-based protocol for diabetic foot ulcers. Plast Reconstr Surg 2006 Jun;117(7 Suppl):193S-209S. [doi: 10.1097/01.prs.0000225459.93750.29] [Medline: 16799388]
27. Paul DW, Ghassemi P, Ramella-Roman JC, et al. Noninvasive imaging technologies for cutaneous wound assessment: a review. Wound Repair Regen 2015;23(2):149-162. [doi: 10.1111/wrr.12262] [Medline: 25832563]
28. Chauhan J, Goyal P. Deep learning based fully automatic efficient burn severity estimators for better burn diagnosis. Presented at: 2020 International Joint Conference on Neural Networks (IJCNN); Jul 19-24, 2020; Glasgow, United Kingdom p. 1-8. [doi: 10.1109/IJCNN48605.2020.9206646]
29. Wang Y, Ke Z, He Z, et al. Real-time burn depth assessment using artificial networks: a large-scale, multicentre study. Burns 2020 Dec;46(8):1829-1838. [doi: 10.1016/j.burns.2020.07.010] [Medline: 32826097]
30. Cirillo MD, Mirdell R, Sjöberg F, Pham TD. Time-independent prediction of burn depth using deep convolutional neural networks. J Burn Care Res 2019 Oct 16;40(6):857-863. [doi: 10.1093/jbcr/irz103]
31. Jacobson MJ, El Masry M, Arrubla DC, et al. Autonomous multi-modality burn wound characterization using artificial intelligence. Mil Med 2023 Nov 8;188(Suppl 6):674-681. [doi: 10.1093/milmed/usad301] [Medline: 37948279]

Abbreviations

AI: artificial intelligence
API: application programming interface
AUROC: area under the receiver operating characteristic
BURN-AID: Burn Diagnosis with Artificial Intelligence
EMR: electronic medical record
IRB: institutional review board
TDI: tissue Doppler imaging

Edited by A Coristine; submitted 20.11.24; peer-reviewed by K Winaikosol, K Poterlowicz; revised version received 20.06.25; accepted 20.06.25; published 15.08.25.

Please cite as:
Rahman MM, Masry ME, Gnyawali SC, Xue Y, Gordillo G, Wachs JP
AI-Driven Integrated System for Burn Depth Prediction With Electronic Medical Records: Algorithm Development and Validation
JMIR Med Inform 2025;13:e68366
URL: https://medinform.jmir.org/2025/1/e68366
doi:10.2196/68366

© Md Masudur Rahman, Mohamed El Masry, Surya C Gnyawali, Yexiang Xue, Gayle Gordillo, Juan P Wachs. Originally published in JMIR Medical Informatics (https://medinform.jmir.org), 15.8.2025. This is an open-access article distributed under the terms of the Creative Commons Attribution License (https://creativecommons.org/licenses/by/4.0/), which permits unrestricted use, distribution, and reproduction in any medium, provided the original work, first published in JMIR Medical Informatics, is properly cited. The complete bibliographic information, a link to the original publication on https://medinform.jmir.org/, as well as this copyright and license information must be included.

XSL•FO
RenderX

Enhancing Surgery Scheduling in Health Care Settings With Metaheuristic Optimization Models: Algorithm Validation Study

João Lopes; Tiago Guimarães; Júlio Duarte; Manuel Santos

ALGORITMI Research Centre, University of Minho, Rua da Universidade, Braga, Portugal

Corresponding Author:
João Lopes
ALGORITMI Research Centre, University of Minho, Rua da Universidade, Braga, Portugal

Abstract

Background: Health care is facing many challenges. The recent pandemic has caused a global reflection on how clinical and organizational processes should be organized, which requires the optimization of decision-making among managers and health care professionals to deliver care that is increasingly patient-centered. The efficiency of surgical scheduling is particularly critical, as it affects waiting list management and is susceptible to suboptimal decisions due to its complexity and constraints.

Objective: In this study, in collaboration with one of the leading hospitals in Portugal, Centro Hospitalar e Universitário de Santo António (CHUdSA), a heuristic approach is proposed to optimize the management of the surgical center.

Methods: CHUdSA's surgical scheduling process was analyzed over a specific period. By testing an optimization approach, the research team was able to prove the potential of artificial intelligence (AI)–based heuristic models in minimizing scheduling penalties—the financial costs incurred by procedures that were not scheduled on time.

Results: The application of this approach demonstrated potential for significant improvements in scheduling efficiency. Notably, the implementation of the hill climbing (HC) and simulated annealing (SA) algorithms stood out in this implementation and minimized the scheduling penalty, scheduling 96.7% (415/429) and 84.4% (362/429) of surgeries, respectively. For the HC algorithm, the penalty score was 0 in the urology, obesity, and pediatric plastic surgery medical specialties. For the SA algorithm, the penalty score was 5100 in urology, 1240 in obesity, and 30 in pediatric plastic surgery. Together, this highlighted the ability of AI-heuristics to optimize the efficiency of this process and allowed for the scheduling of surgeries at closer dates compared to the manual method used by hospital professionals.

Conclusions: Integrating these solutions into the surgical scheduling process increases efficiency and reduces costs. The practical implications are significant. By implementing these AI-driven strategies, hospitals can minimize patient wait times, maximize resource use, and enhance surgical outcomes through improved planning. This development highlights how AI algorithms can effectively adapt to changing health care environments, having a transformative impact.

(JMIR Med Inform 2025;13:e57231) doi:10.2196/57231

KEYWORDS

health care; surgery scheduling problem; metaheuristic model; model optimization; surgery scheduling; artificial intelligence

Introduction

Background

The effective delivery of hospital services depends on the efficient execution of several processes and is becoming increasingly reliant on computer resources capable of responding to specific situations [1]. Given the objectives each health care organization must meet and the requisite patient care, a system capable of improving, evaluating, and preventing future situations is crucial [2,3]. Simultaneously, the volume of patient-centered data in health care has been burgeoning. An example of this is illustrated by Jayaratne et al [4], which highlights the data-rich environment of the intensive care unit, where extensive data streams continuously emanate from patient monitoring and observation. These data encompass various facets such as laboratory results, medical prescriptions, therapeutic decisions, clinical observations by health care providers, and others. The richness of these systems depends on the available data, and the health care system has a great scope at this level. In 2018, Feldman et al [5] showcased the great diversity of these systems, categorizing them into groups based on the data's nature and associating them with relevant areas of interest. This wide range of systems, which includes clinical and organizational data, makes it an area with a lot of potential. Business intelligence systems are crucial for these entities, which require tools capable of organizing data in a more perceptible way [6,7]. The rise of artificial intelligence (AI) has led to a profound reflection on these systems, allowing them to be transformed to integrate future data and provide advice on optimal decision-making that affects organizational management [3,8,9]. Improving the decision-making process

XSL•FO
RenderX

requires combining data storage with analytical tools, applications, and methodologies, and it aims to incorporate and find relationships between existing data [10]. This provides real-time access and facilitates the proper analysis of historical and current data, obtaining insights that were not possible before [11,12].

For a long time, one of the most discussed topics in hospital organizations has been the surgical scheduling problem (SSP). Surgical scheduling was worsened by the COVID-19 pandemic, as numerous specialties had to halt their treatments in order to prioritize the treatment of other patients. There have been clear repercussions from this management change, including an increase in the number of patients on waiting lists and a need for managers to find clinically and organizationally effective approaches to reduce them. A study was carried out in collaboration with the Centro Hospitalar e Universitário de Santo António (CHUdSA) to determine whether a metaheuristic approach could be implemented in a hospital organization as a strategy to reduce waiting time.

Related Work

Room planning is a task that needs to be addressed in many fields, particularly within health care, and it includes planning operating rooms (ORs) for surgeries. Cost containment and reduction have emerged as primary objectives in health care management, with hospital managers and professionals trying to understand each factor contributing to the total cost of delivering better services. ORs are one of the areas that have been gathering considerable attention since they are the most critical cost center and consume a large proportion of the hospital's total expenses. Consequently, ORs have substantial potential for cost savings, and the SSP has been studied and has generated a variety of approaches and heuristics [13]. Currently, there is a growing trend in adopting computational tools based on optimization methods. As outlined by Cortez [14], optimization methods are divided into 3 main categories: blind search, local search, and population-based search. Blind search assumes the exhaustion of all alternatives, guaranteeing that all solutions are tested. It is only admissible for discrete search spaces and is easy to implement. The major disadvantage of this technique is its feasibility when the search space is continuous or too large. It tends to require more computational effort since the search is performed through a set of candidate solutions rather than a single solution. Local search is the most modern optimization technique and is based on new solutions that are generated from existing ones. Several methods focus on a local neighborhood through a given initial solution and use previous searches to guide the next. Population-based search presents a new approach to optimization algorithms, using a set of candidate solutions instead of one [15].

Studies conducted by the scientific community suggest that metaheuristic optimization models are promising as a potential solution to the problem at hand, although they diverge on the primary factors directly impacting the performance of a surgical schedule. Some studies adopt a more specific approach, such as the one developed by Fügener et al [13], which introduces a variable called planned capacity slack for OR days with the application of the simulated annealing (SA) algorithm to minimize planned slack and maximize OR use. The planned slack aimed to minimize overtime by absorbing the variability of surgery duration. Min and Yih [16] designed a calendar for patients with uncertain surgical operations. The calendar accounted for the uncertainty in the period of surgery and the availability of resources, such as the surgical intensive care unit, using a stochastic approach to minimize the sum of costs directly related to patients and the expected costs associated with overtime work. Visintin et al [17] propose that creating an effective surgical scheduling system requires grouping patients into homogeneous surgical groups, developing an approach solely focused on this constraint and scheduling surgical groups rather than actual patients. Most authors state that the performance of an OR depends mainly on how surgical activities are scheduled. This perspective is reflected in the study conducted by Su et al [18], which proposed a self-organizing map-based optimization (SOMO) approach to solve the SSP. Banditori et al [19] also introduced a mixed integer programming model, assuming that a hospital's waiting list cases could be categorized into homogeneous surgical groups based on their anticipated resources. Agnetis et al [20] adopted a surgical scheduling model that was updated on a weekly basis, allocating various specialties to available sessions and considering only patients immediately eligible for surgery, and patients were selected from a waiting list based on parameters such as surgery duration and waiting time. More recently, a similar approach by Brit et al [21] considered multiple factors (including surgeons, equipment, ORs, and recovery ward beds) in their optimization strategy to meet waiting time objectives by maximizing OR use. Tyagi et al [22] explored various models and techniques used for scheduling, emphasizing the importance of strategic (long-term), tactical (medium-term), and operational (short-term) scheduling levels and demonstrating that daily planning and scheduling using detailed procedural times and sophisticated algorithms substantially enhanced OR use. Wang et al [23] proposed a fuzzy model, integrated with a hybrid genetic algorithm for optimization, to address variability and unpredictability in scheduling processes. The model effectively balanced the costs and benefits associated with using an overflow strategy, where patients were assigned to undesignated departments to better manage capacity.

Despite the varied development approaches and the implementations of algorithms, different perspectives have emerged regarding the timescale and surrounding constraints, highlighting the absence of standard approaches to the SSP that conclusively prove effectiveness compared to current hospital management practices. There is a scarcity of accurate proposals to inform the establishment of standard rules and guidelines to manage surgery scheduling without affecting the organizational policies of different surgical specialties. Therefore, this study aimed at demonstrating the effectiveness of a selected set of optimization algorithms, customized to time and resource allocation problems, in addressing common scheduling constraints across various specialties. The primary goal is to provide a more comprehensive solution applicable to different health care organizations.

XSL•FO
RenderX

Methods

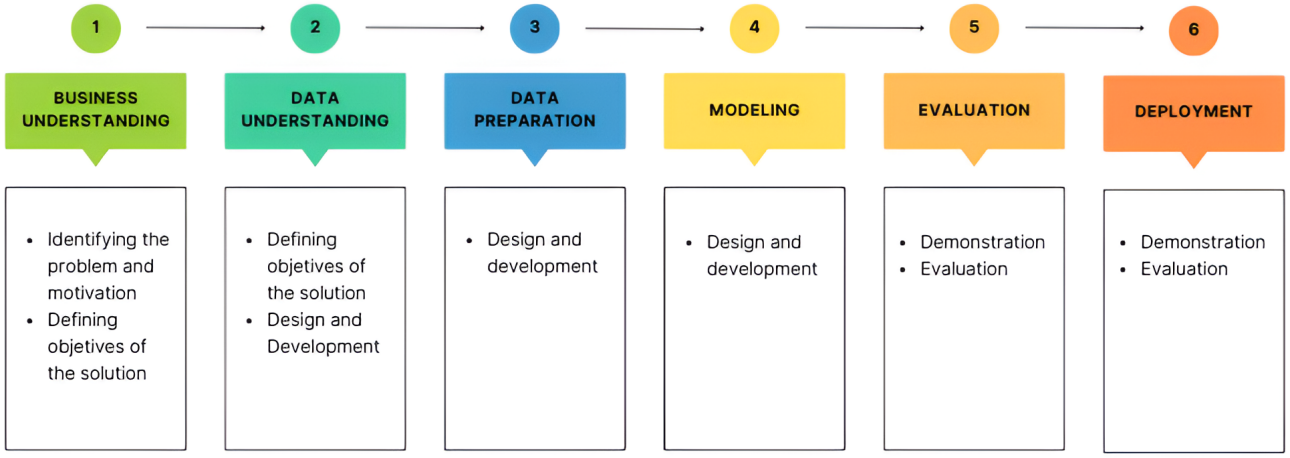
Ethical Considerations

This study was based exclusively on anonymous data provided by the organization involved in this research and did not involve sensitive personal information. Therefore, ethics board review in accordance with the General Data Protection Regulation (GDPR) was not required.

Study Design

An optimization model–based approach was developed to demonstrate the application of heuristic algorithms. Our analysis focuses on optimizing the temporal allocation of surgeries, depending on the date they were placed on the waiting list and their priority. For this, two methodologies were followed: the design science research (DSR) and the cross-industry standard process for data mining (CRISP-DM). DSR consisted of 6 phases: identification of the problem and motivation, definition of objectives of the solution, design and development, demonstration, evaluation, and communication. These phases provided guidelines for a research project [24]. To put DSR in action, it was necessary to use a practical methodology for data mining projects. The CRISP-DM method provided a global perspective on the life cycle of a data mining project, and it comprised the following 6 stages: business understanding, data understanding, data preparation, modeling, evaluation, and deployment [25]. There were dependencies between the stages, and they did not have a rigid structure [25]. Since both methodologies were used concurrently, the relationship between them throughout the project phases was described (Figure 1).

Figure 1. Crossover of the design science research (DSR) and cross-industry standard process for data mining (CRISP-DM) methodologies.



Problem Statement

Hospital administrators attempt to reduce costs while providing the best care possible for their patients. To achieve this aim, they take into account a number of factors that directly affect the quality of surgery scheduling. These factors include the number of professionals available for each day, the specialty related to each type of diagnosis, the availability of slots, and the ability to perform new admissions, with an aim of continuously reducing waiting time. Under this perspective, the surgical area of a hospital was the main optimization target for the development of a metaheuristic method. Each surgical area of a hospital was made up of *S* ORs, a finite *H* number of days, and a group of *N* patients who were waiting for a surgical appointment. Thus, the algorithm allocated patients to available ORs and determined the sequence of surgeries to be performed. A surgery time *ST* was assigned to each patient in *{1, ...N}*. This time included the period of a procedure as well as extra time for preoperative cleaning and preparation. Depending on the type of study, an organization may establish different restrictions that directly influence how the algorithm generates solutions, which are referred to as hard (primary objectives) and soft (secondary objectives) constraints.

Finally, the goal was to define a global optimization strategy for more than one specialty. Hard constraints included a maximum limit for the number of candidates assigned to a vacancy, room capacity constraints, and time constraints, so that the algorithms always considered shifts that were available in certain time blocks. Simultaneously, this included reducing the number of patients whose surgeries exceeded the time limit of the guaranteed maximum response time. Additionally, it was possible that not all ORs were open every day, with some ORs only open during specific times. Each shift therefore indicated the day and the OR. The following points were design factors for this approach:

1. Each specialty was assigned one, more than one, or no OR. These assignments were decided in the stage before the block schedule.
2. Patient priority was defined based on medical and waiting time factors, always considering a prioritized patient list for surgeries.
3. Each surgical specialty managed its patients independently.
4. The hospital contained a specific set of ORs, which each one being unique and adapted for certain types of interventions.
5. A surgery that was programmed after its deadline earned a penalty depending on the priority.
6. Each surgery had information regarding the time required to clean the room and prepare it for next surgery.
7. A patient could not be operated on more than once in the same scheduling period.

XSL•FO
RenderX

For this algorithm, all surgeons were able to be assigned to a surgery. Daily availability plans of the CHUdSA were also considered so that a specific surgery allocation respected the existing resources for each day, namely the number of ORs and available medical professionals. The following sections explain the heuristic approaches.

Data Understanding and Preparation

The surgery data analyzed was considered event-based. Each surgery undergone by a patient represented an event associated with a medical specialty at a specific time, comprising the execution of all requisite procedures. Additionally, data containing information related to the time blocks available in each specialty were used. The data were derived from medical specialties previously selected by the CHUdSA interlocutors, including a scheduling process carried out in 2019. This time frame was chosen since the hospital administration did not take pandemic constraints into consideration, making it possible to examine a scheduling procedure under standard circumstances without any unusual restrictions.

Proposed Metaheuristic Algorithms

Overview of Metaheuristic Algorithms

Metaheuristic algorithms are search procedures designed to find better solutions to an optimization problem that is considered complex to solve [26]. They are categorized according to how they operate in the search space and how new solutions will be discovered [14] such as nature-inspired versus non–nature-inspired, population-based versus local search, dynamic versus static objective functions, and one versus multiple neighborhood structures [27]. The typical structure is based on 3 main code sections: (1) initial solution, representing the first structure of the problem and ensuring an initial guess, often called a “starting point” for the algorithm; (2) evaluation function, which analyzes a possible solution in the context of the problem, comparing different solutions and providing a ranking or a quality measure score; and (3) objective function, which is composed of the implementation of different optimization algorithms [28].

Hill Climbing

Hill climbing (HC) is a local optimization algorithm that climbs a hill until a local optimum with the goal of maximization. The method iteratively searches for new solutions inside the existing solution’s neighborhood, adopting a new solution if it is better than the previous one [29]. The purpose is to discover an improvement by running an extensive search within the defined neighborhood borders and the ability of the algorithm to produce successful results is determined entirely by the initial solution [14,15].

Simulated Annealing

Metropolis et al [30] designed SA, which is primarily inspired by a cooling operation in heating-based metallurgy. SA begins with a randomly generated initial solution and a high-temperature *T*. During the cooling phase, the algorithm will converge to an estimated solution, moving away from the local optimum to locate the near-optimal solution, and the method will grow more accurate with each iteration to obtain a better solution [14]. Another solution will be randomly created near the initial solution and the difference in function values is calculated as follows:

$$(1)\Delta=fxn-fxc$$

If the Δ is smaller for the new solution, the new solution automatically becomes the current solution from which the search will continue [26].

Particle Swarm

In 1995, Kennedy and Eberhart conducted a study on the social behavior of a group of animals and concluded that being in a group increases one’s chances of surviving [14]. This is corroborated by the fact that species share information, which increases the probability of finding the optimal hunting location. The particle swarm (PS) algorithm operates on this conceptual foundation, attempting to identify the best solution in a high-dimensional space. It aims at either maximizing profits or limiting losses. There can be multiple local maximums and minimums in a function but only one global maximum and/or minimum. In summary, PS is a population-based algorithm and can be defined by the direct and indirect interactions between distinct sets of information that affect the results obtained, consequently preserving an organized pattern among the dataset [14].

Modeling the Initial Solution

By assigning one slot to each input operation, the initial solution was obtained in random or sequential slots using the list of specialist surgeries. Depending on the number of slots and surgeries, the bottom and upper parameters were defined as the highest and lowest values for each dimension. The initial solution was obtained by assigning surgeries in available slots for a specific specialty and was implemented by the first fit approach [31,32]. The challenges with this initial method were respecting the time limits connected with each surgery and the turnovers associated with the addition of surgeries to a particular slot. It was also decided that the production of the first solution should include all potential constraints. The graphical representation of how the first solution was generated is included in Multimedia Appendix 1.

The performance was evaluated using a function designed for this purpose. Each solution examined the assigned surgeries by specifying a total solution penalty (*pt*), calculated using the sum of each penalty *p* earned in a surgery, as shown mathematically below:

$$(2)pt=\sum i=1ipi$$

Each penalty was calculated by multiplying the number of days that the surgery was overdue by each deadline (*ds*) and the priority associated with that same surgery (*pr*), presented in the following equation:

$$(3)p=fds-f(pr)$$

Modeling the Objective Solution

HC Implementation

Different algorithms were used to model the objective solution, which through several iterations, search for a better solution

XSL•FO
RenderX

than the existing one. For each iteration, a total penalty was given to the surgeries, making comparisons with other solutions. The iterations ended at the defined limit, returning the best solution. HC implementation was retrieved and adapted from Cortez [14] and could be represented by the following function: *hclimbing* (*par*, *fn*, *change*, *control*, *type*). The input variables were presented as follows:

1. The initial solution (*par*) was obtained by allocating the surgeries to available slots (explained in previous section).
2. The evaluation function (*fn*) evaluated the total penalty of the allocated surgeries.
3. A change function (*change*) was responsible for generating the next candidate, creating minor disturbances in the initial solution by swapping surgeries between different slots and evaluating if this was profitable.
4. The variable *control* was a list that indicated the number of interactions to execute and the information to collect throughout the solution.
5. A last variable (*type*) indicated the main goal of minimization.

SA Implementation

SA implementation was also adapted from Cortez [14]. It used a variable temperature as opposed to HC, which chose a fixed value for this control parameter. Starting at a high temperature, the method gradually lowered the control parameter until it reached the desired minimum value or a predetermined number of iterations. The following function represents the SA implementation: *simulated_annealing* (*func*, *par*, *niter*, *step*). The input variables were presented as follows:

1. The evaluation function (*func*) that computed the total penalty, similar to HC.
2. The initial solution (*par*), also similar to HC.
3. Maximum number of iterations (*niter*).
4. Parameter to control the cooling speed of the model (*step*).

PS Implementation

The implementation of PS followed a different perspective from that presented in the other two models. It is an algorithm that seeks to efficiently search within a specified boundary, using the iterations between particles to find the best solution possible [14,33]. The implementation of this method was obtained by the *psoptim* method from the *pso* package [34]. The function described has 6 input parameters: *psoptim* (*par*, *fn*, *lower*, *upper*, *control*, *eval_func*). These were represented by the following:

1. Vector containing the initial list of surgeries to schedule (*par*).
2. Penalty minimisation function (*fn*).
3. Lower bounds on the variables, belonging to the minimum scheduling shift (*lower*).
4. Upper bounds on the variables belonging to the maximum scheduling shift (*upper*).
5. List of control variables (*control*) belonging to the best solution found, number of interactions, swarm size, and continuous trace of solutions found.
6. Evaluation function to compute the total penalty (*eval_func*), similar to the other methods.

Results

The number of surgeries performed by each specialty and the number of surgeries performed after the established deadline could be used by the CHUdSA to categorize its OR management. Such variables determined the total penalty of the hospital, which translated into costs that the hospital would have to assume. Table 1 represents a general analysis of the existing data, considering the specialties chosen for this study, to understand the relationship between the number of surgeries being allocated and the number of existing slots for each specialty. For the specialties that were chosen, the number of surgeries to be allocated was higher than the number of existing slots. In this case, optimizing ORs was required to handle the greatest number of surgeries with available resources.

Table . General analysis between number of surgeries in each specialty with available operating rooms.

Medical specialties	Number of surgeries	Number of time slots
Obesity	198	122
Urology	133	89
Pediatric plastic surgery	98	45

The first approach was carried out to understand which algorithms obtained the best performance and considered the optimization objective, which was the minimization of the penalty and the maximization of the number of surgeries scheduled within the deadline. Table 2 summarizes the values obtained in implementing the algorithms described above.

Table . General analysis of optimization algorithms performance.

Algorithms	Penalty score by medical specialty		
	Obesity (n=198)	Urology (n=133)	Pediatric plastic surgery (n=98)
Hill climbing	0	0	0
Simulated annealing	5100	1240	30
Particle swarm	42,702	30,000	53,108

XSL•FO
RenderX

Since this initial approach considered a first custom solution with the defined scheduling rules, the local search algorithms obtained better scheduling performances. Consequently, a deeper examination of the HC and SA algorithms was done. The implementation of these algorithms led to a set of results presented in Tables 3 and 4. These values compared the performance of the algorithms in response to SSP.

Table . Measure of the impact of the hill climbing (HC) algorithm.

Metrics by specialty	Penalty score	Surgeries without penalty, n (%)	Surgeries with penalty, n (%)	Unscheduled surgeries, n (%)
Obesity (n=198)				
CHUdSA[a] management	643,550	4 (2)	194 (98)	0 (0)
HC optimization	0	190 (96)	0 (0)	8 (4)
Urology (n=133)				
CHUdSA management	37,030	91 (68.4)	42 (31.6)	0 (0)
HC optimization	0	127 (95.5)	0 (0)	6 (4.5)
Pediatric plastic surgery (n=98)				
CHUdSA management	14,760	81 (81)	17 (17)	0 (0)
HC optimization	0	98 (100)	0 (0)	0 (0)

[a]CHUdSA: Centro Hospitalar e Universitário de Santo António.

Table . Measure of the impact of the simulated annealing (SA) algorithm.

Metrics by specialty	Penalty score	Surgeries without penalty, n (%)	Surgeries with penalty, n (%)	Unscheduled surgeries, n (%)
Obesity (n=198)				
CHUdSA[a] management	643,550	4 (2)	194 (98)	0 (0)
SA optimization	5100	164 (82.8)	1 (0.5)	33 (16.7)
Urology (n=133)				
CHUdSA management	37,030	91 (68.4)	42 (31.6)	0 (0)
SA optimization	1240	128 (96.2)	4 (3)	1 (0.8)
Pediatric plastic surgery (n=98)				
CHUdSA management	14,760	81 (83)	17 (17)	0 (0)
SA optimization	30	64 (65)	1 (1)	33 (34)

[a]CHUdSA: Centro Hospitalar e Universitário de Santo António.

Discussion

Overall Results

Through the implementation of these algorithms, compared to CHUdSA's manual scheduling process, several results were found. First, the penalties for the optimization algorithms developed were lower than the penalty of scheduling done by CHUdSA professionals, and in certain situations, there were no penalties for the algorithms. Therefore, both local optimization algorithms can provide improvements to the administration and organization of ORs. Second, the PS algorithm was not a viable solution to the SSP, since its ability to minimize the scheduling penalty was much lower than the HC and SA algorithms. It was evident that local search algorithms produced better solutions on all existing criteria, compared to the population-based search algorithm. Third, Figures 2 and 3 represent the evaluation of scheduling over time for each surgery, providing an understanding of whether the respective algorithm scheduled a surgery for before or after the day it was performed in the CHUdSA. The majority of surgeries could have been scheduled and carried out days earlier for either of the local HC and SA optimization algorithms. Fourth, the number of surgeries that remained to be scheduled occasionally exceeded the number that the CHUdSA professionals had anticipated. Furthermore, some surgeries could not be scheduled in this optimization process because their minimum execution time exceeded the maximum duration of an existing shift. These surgeries were always handled as exceptional cases at the recommendation of CHUdSA professionals. Therefore, from a management perspective, the professionals personally should schedule the surgeries in accordance with specific internal protocols.

XSL•FO
RenderX

Figure 2. Hill climbing evaluation and overall performance by surgeries.

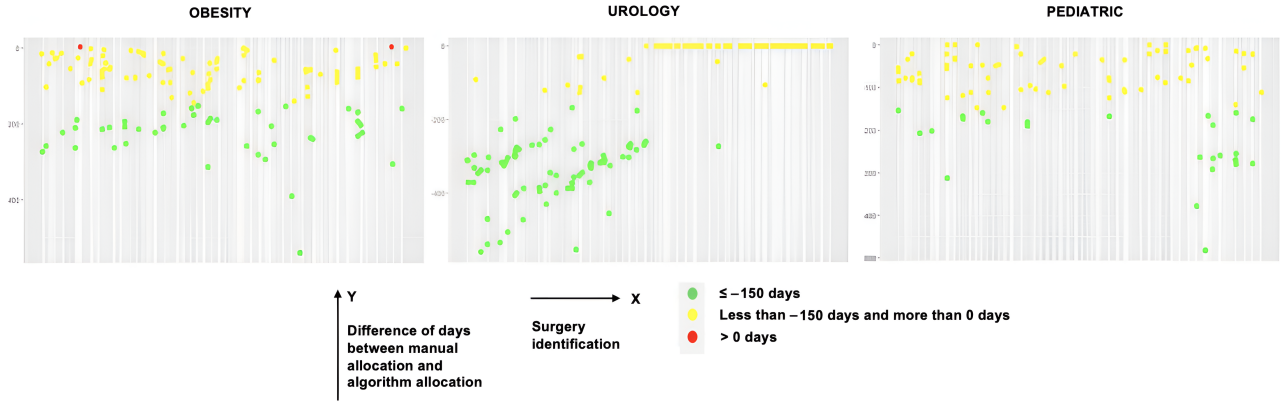
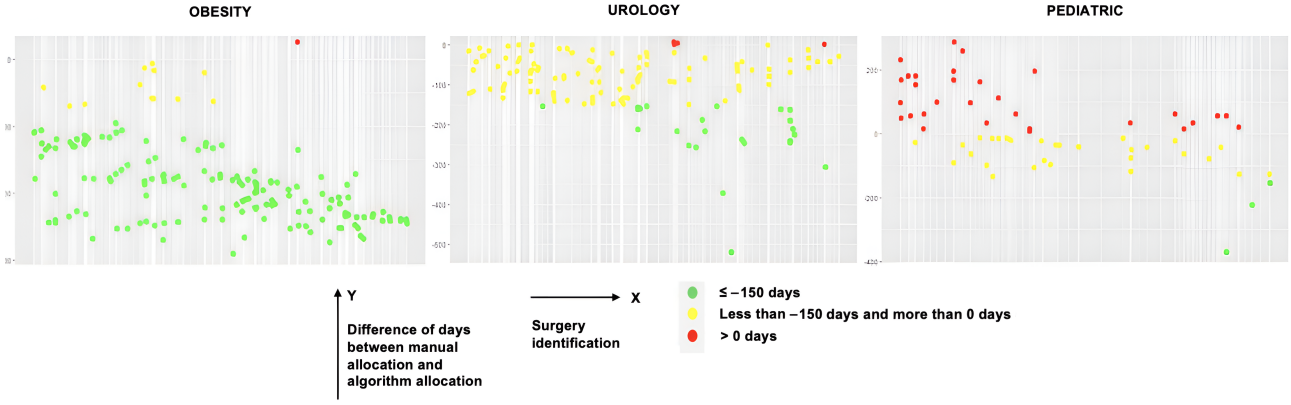


Figure 3. Simulated annealing evaluation and overall performance by surgeries.



Key Findings

Figures 2 and 3 highlight that it is possible to more effectively allocate surgeries within the same time frame despite using the same resources. Leveraging the specification of a set of global variables for enhancing the scheduling process, 4 significant conclusions can be drawn. First, scheduling was greatly improved when the initial solution was modeled using a surgery allocation algorithm that took waiting list longevity and priority into account. The final penalty was lowered, demonstrating the potential to enhance surgical management within the constraints of time and space. Second, the HC algorithm had the best performance, with the SA algorithm producing similar results. However, the PS algorithm was not able to improve surgery allocation and occasionally arranged surgeries worse in terms of time and space. For these reasons, it was discarded.

Third, the HC and SA algorithms were particularly noteworthy since they arrived at the ideal number of iterations after 100 iterations. Thus, these algorithms could yield significantly better planning than manual hospital allocation with a runtime of approximately 30 seconds. These results also supported the exclusion of the PS algorithm for future implementations, as it was a more computationally demanding model. Fourth, the application of AI-based heuristics resulted in a notable enhancement in the quantity of surgeries allocated. Therefore, there is potential for improving OR management with a system capable of maximizing the scheduling procedure for each speciality, demonstrating how the scheduling solutions assigned by the HC and SA algorithms differ significantly in terms of space and time. In terms of a decision support system, it may be best to offer the user a variety of scheduling solutions based on these implemented optimization models, even though it is not necessary to determine which is the better solution. As a result, the user can select the planning that best fits the group of surgeries that require scheduling.

Comparison With Prior Work

Based on the development and use of optimization algorithms, the proposed research presents an innovative approach for scheduling surgeries from waiting lists. It is crucial to emphasize the primary objective of reducing costs, considering a variety of factors involving different medical specializations. In contrast to prior studies, the research by Fügener et al [13] focuses on the integration of HC and SA to optimize the use of ORs. Min and Yih's study [16] concentrates on a stochastic surgical calendar tailored for patients with uncertain surgical needs. Similarly, Banditori et al [19] categorized waiting list cases into homogeneous groups, offering a more adaptable solution for diverse medical specialties. However, because the criteria used to make decisions vary among medical specializations, research so far has never produced conclusive and sufficient evidence to support their widespread use in health care organizations. This work stands out from other studies since it uses global and specific variables that are readily applied to any medical specialty without compromising the quality of surgical scheduling, a key factor in reducing operating costs in hospitals. By diverging from previous models and overcoming their limitations, this study provides a more precise and effective solution aimed at maximizing the performance of ORs,

XSL•FO
RenderX

benefiting both the patients and the health care professionals involved in the surgical process.

Conclusions

The study of allocation and scheduling problems is considered complex. When it comes to health care, the responsibility to create an effective solution is even more significant since the priority must always be the care that is provided to patients, while also being aware of the existing resources. The approach developed in this study not only provides a solution to this scheduling problem but also conceives a generic adoption for any health care organization and for a considerable number of medical specialties.

Considering a general constraints model for any health care organization and considering the same constraints for the generation of the initial solution, the implementation of an automatic allocation algorithm proves the ability to find better solutions for surgery scheduling. The HC and SA algorithms demonstrate the capacity to improve the use of ORs and consider, as a reference, the scheduling limit without accumulating penalties. The PS algorithm proved that it needs a greater computational effort. The fact that it does not use an initial solution, according to previously defined programming rules, can explain its unclear results.

Taking into consideration all of the limitations of scheduling and the high level of organizational complexity, this study's approach can be considered as a possible solution to the SSP as it contributes to the organization of surgeries based on time and cost control, which are crucial to optimize operating costs. HC and SA show extremely satisfactory results, decreasing the number of surgeries with penalty (ie, surgeries with a scheduled date higher than the deadline date). Additionally, these models provide a near optimal solution, reaching a stabilization point after 100 iterations, since the initial solution had already produced very satisfactory results. In addition, from a total of 429 surgeries and considering all specialities, the HC algorithm managed to schedule 415 (96.7%) surgeries, and the SA algorithm scheduled a total of 362 (84.4%) surgeries. The majority of these surgeries were special cases where their duration exceeded the maximum time available each day. In some cases, the number of surgeries not scheduled by the algorithms was higher than the scheduling performed by the hospital, although this is not considered a negative point of this solution.

The proposed application has addressed multiple challenges, offering a scalable solution across diverse organizational frameworks. However, to deepen the utility and precision of our approach, several topics about limitations and future work have been identified. First, testing this study in other health care organizations will be a crucial step to understand if our approach works in different contexts. In addition, it is necessary to improve the accuracy of each estimated surgery time to increase the reliability of the schedule. In this study, an interquartile mean was used to associate each type of surgery through time history, but a more accurate method is needed for an optimal accuracy. Machine learning models could be used to predict the times of each surgery for greater reliability, which is a crucial factor in the allocation of surgeries.

Second, it is also possible to consider more constraints, including subspecialties, in this mapping. This is considered a significant step since the division of ORs includes an allocation to each subspecialty and requires a complete mapping between specialties and the *International Classification of Diseases, Tenth Revision* (*ICD-10*) codes. Third, a deeper study on the nullification of the scheduling penalty may be considered. While a hospital would like to pay the least amount related to surgeries scheduled after the deadline, it may be pertinent to identify whether a proposal with a higher penalty will better serve the scheduling interests. Fourth, another even more complex proposal is to condition the surgical mapping by considering the human resources available for each period. While this is not possible in the current context considering the available data, an annual organization of medical professionals (surgeons, nurses, anesthesiologists) in real time is necessary. Last, improving the efficiency of the optimization method by exploring more models and their configurations is another direction to consider in future research.

The results of this study are summarized below, highlighting the key messages and anesthesiologists that underline the transformative potential of this approach in health care scheduling. First, the integration of AI-based heuristic algorithms improves the efficiency of surgical scheduling, leading to a reduction in patient waiting times. Second, the HC and SA algorithms have demonstrated a higher performance than the scheduling performed by CHUdSA, and either model make it possible to reduce costs in the scheduling process by reducing the penalties associated with surgeries scheduled beyond the deadline. Third, the models developed do not compromise scalability and adaptability, as they can be adapted to various contexts and medical specialties, and a generalized implementation is possible by adding or removing restrictions. Last, the potential of a system that is capable of integrating these models in any organization is proven, optimizing the inherent management processes and consequently the health care provided to patients.

Adopting this approach following these research directions promises to further refine the metaheuristic optimization models for surgery scheduling, ultimately seeking more optimized and agile health care systems that are patient-centered and cost-effective.

Conflicts of Interest

None declared.

Multimedia Appendix 1
Structure for the initial solution, according to the first fit method.

XSL•FO
RenderX

[DOCX File, 88 KB - medinform_v13i1e57231_app1.docx]

References

1. Sun TQ, Medaglia R. Mapping the challenges of artificial intelligence in the public sector: evidence from public healthcare. Gov Inf Q 2019 Apr;36(2):368-383. [doi: 10.1016/j.giq.2018.09.008]
2. Cutillo CM, Sharma KR, Foschini L, et al. Machine intelligence in healthcare-perspectives on trustworthiness, explainability, usability, and transparency. NPJ Digit Med 2020;3:47. [doi: 10.1038/s41746-020-0254-2] [Medline: 32258429]
3. Sharma M, Savage C, Nair M, Larsson I, Svedberg P, Nygren JM. Artificial intelligence applications in health care practice: scoping review. J Med Internet Res 2022 Oct 5;24(10):e40238. [doi: 10.2196/40238] [Medline: 36197712]
4. Jayaratne M, Nallaperuma D, De Silva D, et al. A data integration platform for patient-centered e-healthcare and clinical decision support. Future Generation Computer Systems 2019 Mar;92:996-1008. [doi: 10.1016/j.future.2018.07.061]
5. Feldman K, Johnson RA, Chawla NV. The state of data in healthcare: path towards standardization. J Healthc Inform Res 2018 Sep;2(3):248-271. [doi: 10.1007/s41666-018-0019-8] [Medline: 35415409]
6. Xin J H. Business intelligence and big data analytics: an overview. Commun IIMA 2014;14(3). [doi: 10.58729/1941-6687.1358]
7. Sharda R, Delen D, Turban E. Business Intelligence and Analytics: Systems for Decision Support, 10th edition: Pearson; 2013.
8. Lopes J, Guimarães T, Santos MF. Predictive and prescriptive analytics in healthcare: a survey. Procedia Comput Sci 2020;170:1029-1034. [doi: 10.1016/j.procs.2020.03.078]
9. Moon JD, Galea MP, editors. Improving Health Management through Clinical Decision Support Systems: IGI Global; 2016. [doi: 10.4018/978-1-4666-9432-3]
10. Michalewicz Z. In: Schmidt M, Michalewicz M, Chiriac C, editors. Adaptive Business Intelligence: Springer eBooks; 2010. [doi: 10.1007/978-3-540-32929-9]
11. Görgülü ZK, Pickl S. Adaptive business intelligence: the integration of data mining and systems engineering into an advanced decision support as an integral part of the business strategy. In: Rausch P, Sheta AF, Ayesh A, editors. Business Intelligence and Performance Management Advanced Information and Knowledge Processing: Springer; 2013:43-58. [doi: 10.1007/978-1-4471-4866-1_4]
12. Santos MF, Azevedo CS. Data Mining: Descoberta de Conhecimento Em Bases de Dados: FCA – Editora de Informa´tica, Lda; 2005. URL: http://hdl.handle.net/1822/19136 [accessed 2025-01-13]
13. Fügener A, Hans EW, Kolisch R, Kortbeek N, Vanberkel PT. Master surgery scheduling with consideration of multiple downstream units. Eur J Oper Res 2014 Nov;239(1):227-236. [doi: 10.1016/j.ejor.2014.05.009]
14. Cortez P. Modern Optimization with R: Springer; 2014. [doi: 10.1007/978-3-319-08263-9]
15. Luke S. Essentials of Metaheuristics, 2nd edition: Lulu Press; 2013.
16. Min D, Yih Y. Scheduling elective surgery under uncertainty and downstream capacity constraints. Eur J Oper Res 2010 Nov;206(3):642-652. [doi: 10.1016/j.ejor.2010.03.014]
17. Visintin F, Cappanera P, Banditori C, Danese P. Development and implementation of an operating room scheduling tool: an action research study. Production Planning & Control 2017 Jul 4;28(9):758-775. [doi: 10.1080/09537287.2017.1310328]
18. Su MC, Lai SC, Wang PC, Hsieh YZ, Lin SC. A SOMO-based approach to the operating room scheduling problem. Expert Syst Appl 2011 Nov;38(12):15447-15454. [doi: 10.1016/j.eswa.2011.06.016]
19. Banditori C, Cappanera P, Visintin F. A combined optimization-simulation approach to the master surgical scheduling problem. IMA J Manag Math 2013 Apr 1;24(2):155-187. [doi: 10.1093/imaman/dps033]
20. Agnetis A, Coppi A, Corsini M, Dellino G, Meloni C, Pranzo M. A decomposition approach for the combined master surgical schedule and surgical case assignment problems. Health Care Manag Sci 2014 Mar;17(1):49-59. [doi: 10.1007/s10729-013-9244-0] [Medline: 23783452]
21. Britt J, Baki MF, Azab A, Chaouch A, Li X. A stochastic hierarchical approach for the master surgical scheduling problem. Comput Ind Eng 2021 Aug;158:107385. [doi: 10.1016/j.cie.2021.107385]
22. Tyagi M, Tyagi PK, Singh S, et al. Allocation scheduling leads to optimum utilization of operation theater time. Med J Armed Forces India 2022 Sep;78(Suppl 1):S163-S171. [doi: 10.1016/j.mjafi.2020.09.005] [Medline: 36147384]
23. Wang JJ, Dai Z, Chang AC, Shi JJ. Surgical scheduling by Fuzzy model considering inpatient beds shortage under uncertain surgery durations. Ann Oper Res 2022;315(1):463-505. [doi: 10.1007/s10479-022-04645-z] [Medline: 35340826]
24. Peffers K, Tuunanen T, Rothenberger MA, Chatterjee S. A design science research methodology for information systems esearch. J Manag Inf Syst 2007 Dec;24(3):45-77. [doi: 10.2753/MIS0742-1222240302]
25. Schröer C, Kruse F, Gómez JM. A systematic literature review on applying CRISP-DM process model. Procedia Comput Sci 2021;181(1):526-534. [doi: 10.1016/j.procs.2021.01.199]
26. Ge Abdel-Basset M, Abdel-Fatah L, Sangaiah AK. Metaheuristic algorithms: a comprehensive review. In: Computational Intelligence for Multimedia Big Data on the Cloud with Engineering Applications: Academic Press; 2018:185-231. [doi: 10.1016/B978-0-12-813314-9.00010-4]
27. Blum C, Roli A. Metaheuristics in combinatorial optimization: overview and conceptual comparison. ACM Comput Surv 2003;35(3):268-308. [doi: 10.1145/937503.937505]

XSL•FO
RenderX

28. Gandomi AH, Yang XS, Talatahari S, Alavi AH. Metaheuristic algorithms in modeling and optimization. In: Metaheuristic Applications in Structures and Infrastructures: Elsevier; 2013:1-24. [doi: 10.1016/B978-0-12-398364-0.00001-2]
29. Balan S. Metaheuristics in optimization: algorithmic perspective. Informs. URL: https://www.informs.org/Publications/OR-MS-Tomorrow/Metaheuristics-in-Optimization-Algorithmic-Perspective [accessed 2025-01-13]
30. Metropolis N, Rosenbluth AW, Rosenbluth MN, Teller AH, Teller E. Equation of state calculations by fast computing machines. J Chem Phys 1953 Jun 1;21(6):1087-1092. [doi: 10.1063/1.1699114]
31. Batini C, Cappiello C, Francalanci C, Maurino A. Methodologies for data quality assessment and improvement. ACM Comput Surv 2009 Jul;41(3):1-52. [doi: 10.1145/1541880.1541883]
32. Brent RP. Efficient implementation of the first-fit strategy for dynamic storage allocation. ACM Trans Program Lang Syst 1989 Jul;11(3):388-403. [doi: 10.1145/65979.65981]
33. Dai HP, Chen DD, Zheng ZS. Effects of random values for particle swarm optimization algorithm. Algorithms 2018;11(2). [doi: 10.3390/a11020023]
34. Bendtsen C. pso: Particle Swarm Optimization. The Comprehensive R Archive Network. 2022. URL: https://cran.r-project.org/web/packages/pso/index.html [accessed 2025-01-14]

Abbreviations

AI: artificial intelligence
CHUdSA: Centro Hospitalar e Universitário de Santo António
CRISP-DM: cross-industry standard process for data mining
DSR: design science research
GDPR: General Data Protection Regulation
HC: hill climbing
***ICD-10*:** *International Classification of Diseases, Tenth Revision*
OR: operating room
PS: particle swarm
SA: simulated annealing
SOMO: self-organizing map-based optimization
SSP: surgical scheduling problem

Edited by C Lovis; submitted 08.02.24; peer-reviewed by A Hassan, G Cohen, R Bidkar; revised version received 09.07.24; accepted 21.07.24; published 11.02.25.

Please cite as:
Lopes J, Guimarães T, Duarte J, Santos M
Enhancing Surgery Scheduling in Health Care Settings With Metaheuristic Optimization Models: Algorithm Validation Study
JMIR Med Inform 2025;13:e57231
URL: https://medinform.jmir.org/2025/1/e57231
doi:10.2196/57231

© João Lopes, Tiago Guimarães, Júlio Duarte, Manuel Santos. Originally published in JMIR Medical Informatics (https://medinform.jmir.org), 11.2.2025. This is an open-access article distributed under the terms of the Creative Commons Attribution License (https://creativecommons.org/licenses/by/4.0/), which permits unrestricted use, distribution, and reproduction in any medium, provided the original work, first published in JMIR Medical Informatics, is properly cited. The complete bibliographic information, a link to the original publication on https://medinform.jmir.org/, as well as this copyright and license information must be included.

XSL•FO
RenderX

The Construction and Application of a Clinical Decision Support System for Cardiovascular Diseases: Multimodal Data-Driven Development and Validation Study

Shumei Miao[1,2], PhD; Pei Ji[2], MS; Yongqian Zhu[3], MEng; Haoyu Meng[4], MD; Mang Jing[2], PhD; Rongrong Sheng[2], MS; Xiaoliang Zhang[2], PhD; Hailong Ding[2], MEng; Jianjun Guo[2], MEng; Wen Gao[2,5], Prof Dr Med; Guanyu Yang[1], Prof Dr; Yun Liu[6], Prof Dr Med

[1]School of Computer Science and Engineering, Southeast University, No.2 Sipailou, Nanjing, China

[2]Department of Information, The First Affiliated Hospital of Nanjing Medical University, Nanjing, China

[3]Department of Quality Management, The First Affiliated Hospital of Nanjing Medical University, Nanjing, China

[4]Department of Cardiology, The First Affiliated Hospital of Nanjing Medical University, Nanjing, China

[5]Department of Oncology, The First Affiliated Hospital of Nanjing Medical University, Nanjing, China

[6]Department of Geriatrics Endocrinology, The First Affiliated Hospital of Nanjing Medical University, Nanjing, China

Corresponding Author:
Guanyu Yang, Prof Dr
School of Computer Science and Engineering, Southeast University, No.2 Sipailou, Nanjing, China

Abstract

Background: Due to the acceleration of the aging population and the prevalence of unhealthy lifestyles, the incidence of cardiovascular diseases (CVDs) in China continues to grow. However, due to the uneven distribution of medical resources across regions and significant disparities in diagnostic and treatment levels, the diagnosis and management of CVDs face considerable challenges.

Objective: The purpose of this study is to build a cardiovascular diagnosis and treatment knowledge base by using new technology, form an auxiliary decision support system, and integrate it into the doctor's workstation, to improve the assessment rate and treatment standardization rate. This study offers new ideas for the prevention and management of CVDs.

Methods: This study designed a clinical decision support system (CDSS) with data, learning, knowledge, and application layers. It integrates multimodal data from hospital laboratory information systems, hospital information systems, electronic medical records, electrocardiography, nursing, and other systems to build a knowledge model. The unstructured data were segmented using natural language processing technology, and medical entity words and entity combination relationships were extracted using IDCNN (iterated dilated convolutional neural network) and TextCNN (text convolutional neural network). The CDSS refers to global CVD assessment indicators to design quality control strategies and an intelligent treatment plan recommendation engine map, establishing a big data analysis platform to achieve multidimensional, visualized data statistics for management decision support.

Results: The CDSS system is embedded and interfaced with the physician workstation, triggering in real-time during the clinical diagnosis and treatment process. It establishes a 3-tier assessment control through pop-up windows and screen domination operations. Based on the intelligent diagnostic and treatment reminders of the CDSS, patients are given intervention treatments. The important risk assessment and diagnosis rate indicators significantly improved after the system came into use, and gradually increased within 2 years. The indicators of mandatory control, directly became 100% after the CDSS was online. The CDSS enhanced the standardization of clinical diagnosis and treatment.

Conclusions: This study establishes a specialized knowledge base for CVDs, combined with clinical multimodal information, to intelligently assess and stratify cardiovascular patients. It automatically recommends intervention treatments based on assessments and clinical characterizations, proving to be an effective exploration of using a CDSS to build a disease-specific intelligent system.

(JMIR Med Inform 2025;13:e63186) doi:10.2196/63186

KEYWORDS

CVD; CDSS; multimodel data; knowledge engine; development; cardiovascular disease; clinical decision support system

XSL•FO
RenderX

Introduction

The high incidence of cardiovascular disease (CVD) is an important public health problem worldwide. CVD remains the leading cause of mortality worldwide and a major contributor to disability. CVD was responsible for 18.6 million deaths according to the 2019 Global Burden of Disease study. China is one of the countries most burdened by CVD [1]. In 2021, approximately 5.1 million individuals lost their lives to CVD in China [2]. Thus, it is of great significance to raise awareness of CVD and screening individuals at risk for CVD so that effective interventions and strategies can be implemented. CVD is influenced by risk factors such as tobacco use, an unhealthy diet, physical inactivity, obesity, elevated blood pressure, abnormal blood lipids, and elevated blood glucose [3,4]. In 2007, the World Health Organization published guidelines for the assessment and management of cardiovascular risk that provide guidance for reducing disability and premature deaths from CVD in people at high risk who have not yet experienced a cardiovascular event [5]. In addition, new artificial intelligence technology for CVD prediction and risk management has been attempted [6,7].

The 2022 China Cardiovascular Health and Disease Report Summary highlights that the rapid aging of the population and the widespread prevalence of unhealthy lifestyles have resulted in a significant portion of the population being at risk for CVD, and the burden of CVD continues to rise, as evidenced by persistently high prevalence rates, increasing mortality, and escalating treatment and management costs [8-10]. The prevention and treatment of CVDs in China presents significant challenges. In recent years, several medical policies have prioritized this issue. From 2021 to 2023, the China National Health Commission made “improving the reperfusion treatment rate for acute ST-segment elevation myocardial infarction (MI)”, “improving the reperfusion treatment rate for acute ischemic stroke”, and “improving the standardized prevention rate for venous thromboembolism (VTE)” in the national top ten medical quality and safety improvement objectives. Additionally, the “Opinions on Promoting High-Quality Development of Public Hospitals” issued by the State Council Office in May 2021, emphasized cardiovascular and cerebrovascular diseases as key clinical specialties for the high-quality development of public hospitals.

Clinical decision support systems (CDSS) leverage health information technology to provide health care professionals with intelligent decision-making tools, aiming to improve medical quality, reduce errors, and improve patient outcomes [11-13]. CDSS can offer various forms of support, including diagnostic recommendations, treatment plan selection, and medication dosage calculations, based on a comprehensive medical knowledge database and patient-specific data. The primary objective of CDSS is to optimize clinical decisions by integrating clinical observations with knowledge bases, ultimately improving patient outcomes [14]. In recent years, CDSS has been preliminarily applied in some specific medical scenarios, such as chronic obstructive pulmonary disease patient management, antibiotic management, and venous thromboembolism management [15-17]. In the process of prevention, diagnosis, and treatment of CVDs, some researchers have also used Machine Learning, big data and other new technologies to carry out research on the prediction of Major Adverse Cardiovascular Events and disease onset [18-20].

Currently, there are several challenges in the diagnosis, treatment, and management of CVD. Uneven allocation of medical resources in different regions leads to large gaps in diagnosis and treatment levels. Insufficient disease awareness leads to a low rate of early CVD diagnosis, while reliance on manual risk assessment forms leads to inefficient risk prediction. The standardization of clinical diagnosis and treatment requires improvement. The quality control method relies on sampling and examination of terminal medical records, which is backward and passive. Therefore, this study proposes the use of CDSS technology combined with multimodal clinical information to intelligently assess and stratify cardiovascular patients. By integrating CDSS with the hospital’s doctor workstation system, auxiliary diagnosis, and treatment are seamlessly incorporated into clinical workflows, leveraging a powerful knowledge base and intelligent models to provide physicians with intelligent recommendations. Based on these assessments and clinical characteristics, it intelligently recommends intervention treatments, offering novel insights for prevention, treatment, and management strategies for CVDs.

Methods

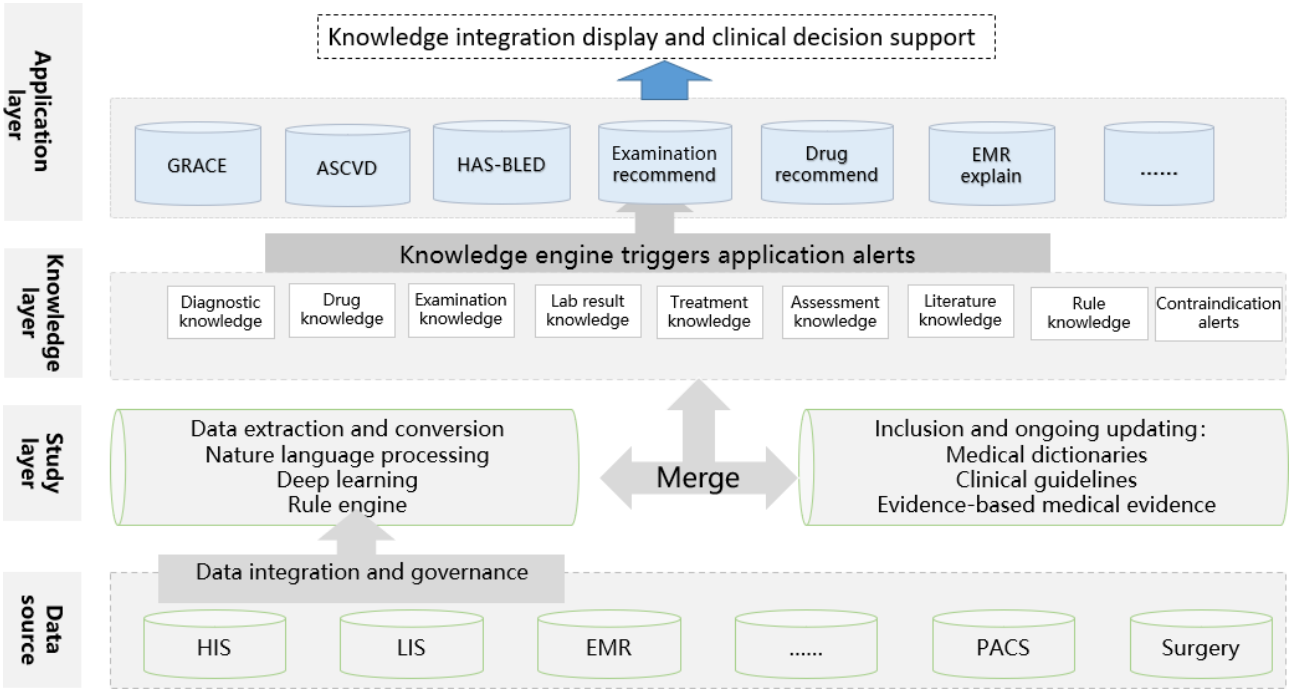
CDSS Design

The CDSS in the study has a 4-tier architecture shown in Figure 1. Initially, the foundation of decision support is rich data information at the data source layer. Information such as medical orders, medical records, lab tests, examinations, surgery records, etc, are collected and integrated through hospital information integration platforms and data centers. For historical data, the Extract-Transform-Load tool was used to integrate various information systems. For the real-time human-computer interaction data, the data transmit interface was triggered by clicking the temporary save button or mouse movement. For the study layer, based on deep learning, knowledge graphs, rule engines, clinical pathways, and guidelines, the processing process of word segmentation, named entity recognition, and relationship extraction was completed to realize the output of structured variables and data standardization. A triple data set of entity-relationship-entity was formed to construct the clinical knowledge map. Then for the knowledge layer, different types of knowledge representations were established through the previous learning, such as diagnostic knowledge, drug knowledge, examination knowledge, assessment knowledge, literature databases, contraindication alerts, and others. We developed flexible knowledge maintenance tools to maintain the knowledge base according to the characteristics of clinical specialties in hospitals, and provide intelligent recommendation, intelligent early warning, and intelligent audit functions for doctors. Finally, at the application layer, Through the front frontpage parameter docking and the message transmission of the data integration platform, the doctor workstation information is encrypted and transmitted to the CDSS, and the CDSS intelligent prompt module is triggered when ordering medical

XSL•FO
RenderX

orders, writing medical records, transferring departments, operating and discharging for each patient of the doctor system. Intelligent decision support is triggered like drug recommendations, examination recommendations, Global Registry of Acute Coronary Events (GRACE) evaluation, atherosclerotic cardiovascular disease (ASCVD) evaluation, etc.

Figure 1. The design of clinical decision support system for cardiovascular disease. ASCVD: atherosclerotic cardiovascular disease; EMR: electronic medical record; GRACE: Global Registry of Acute Coronary Events; HAS-BLED: hypertension, abnormal renal or liver function, stroke, bleeding history or predisposition, labile international normalized ratio, elderly (>65 years), drugs or alcohol concomitantly; HIS: hospital information system; LIS: laboratory information system; PACS: picture archiving and communication system.



The system is specifically designed for patients who are hospitalized due to CVDs, and it can facilitate diagnosis and treatment by incorporating their comprehensive medical data.

Ethical Considerations

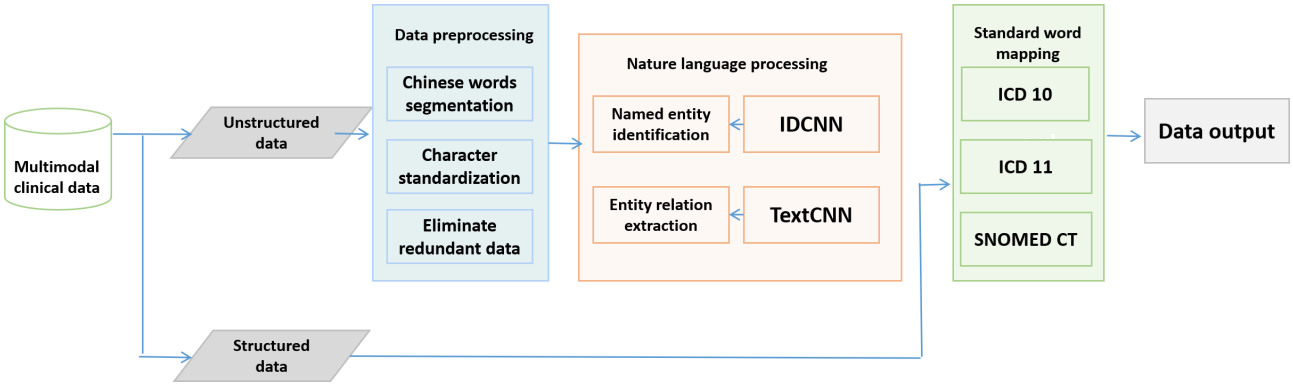
The study was approved by the Ethics Committee of the First Affiliated Hospital of Nanjing Medical University (2023-SR-743). As this study did not involve a process in which informed consent must be obtained for routine care and the contents of the study do not involve personal privacy, the ethics committee waived the requirement for written informed consent.

Multimodal Data Fusion Processing

Artificial intelligence (AI) technology is used to integrate multimodal data related to CVD diagnosis- which is dispersed across various hospital systems including hospital information systems, electronic medical records (EMR), laboratory information systems, PACS (picture archiving and communication system), and nursing systems. Through natural language processing (NLP) and medical terminology mapping, a knowledge model is developed. The structure of the NLP module, core deep learning algorithms, and resources are presented in Figure 2. First, preprocessing is performed on unstructured text, including sentence segmentation for word segmentation, standardization of symbols, uniformization of capitalization, reorganization of standardized vocabulary, elimination of less meaningful parts, and formation of summaries that express the main meaning. Then, the named entity recognition model using the BiLSTM-CRF (bidirectional long short-term memory - conditional random field) and IDCNN (iterated dilated convolutional neural network) architecture to extract medical entity words such as time, anatomical site, diagnosis, drug name, drug dose, and surgical name [21]. Next, the entity relationship linking model uses the TextCNN (text convolutional neural network) architecture to extract medical entity combination relationships such as diagnosis-anatomical site-position-time as a group [22]. Then, the core entities such as diagnosis, laboratory tests, drug names, and attribute entity words such as time, existence status, and drug dosage are mapped to medical standard words. Finally, according to entities and the relationship between entities, a disease auxiliary decision support model using CNN-DSSM (convolutional neural network - deep semantic similarity model) is constructed, which can provide a list of diagnostic probabilities and recommend reasonable examinations according to the patient's chief complaints and medical history, to assist doctors in diagnosis and reduce the probability of missed diagnosis and misdiagnosis.

XSL•FO
RenderX

Figure 2. The natural language processing process of multimodal clinical data. ICD: International Classification of Diseases; IDCNN: iterated dilated convolutional neural network; SNOMED CT: Systematized Nomenclature of Medicine – Clinical Terms; TextCNN: text convolutional neural network.



CVD Assessment Models and Recommendations

This study focuses on the diagnosis and treatment of common CVDs by incorporating assessment models such as GRACE, ASCVD, CHA2DS2-VASc (congestive heart failure, hypertension, age ≥75 years [doubled], diabetes, stroke [doubled], vascular disease, age 65 to 74 years and sex category [female]) for stroke risk evaluation in patients with nonvalvular atrial fibrillation, alongside other intelligent diagnostic and treatment recommendation systems [23-25]. Using the stratified GRACE risk assessment as an example [26-28], NLP technology was applied to gather data from various clinical systems, including age, heart rate, systolic blood pressure, serum creatinine, positive initial heart markers, ST segment changes, cardiac arrest at admission and Killip class [29,30]. Based on the risk assessment outcomes, distinct levels of low risk, medium risk, high risk, and extremely high risk were established. Subsequently, as shown in Table 1, corresponding quality control strategies and treatment plan recommendations were developed for each risk category.

Table . GRACE (Global Registry of Acute Coronary Events) risk assessment results and related recommendations.

Risk level	GRACE score	In-hospital mortality (%)
Low risk	≤108	<1
Moderate risk	109 - 140, or combined with diabetes mellitus, renal insufficiency, LVEF[a] <40%, chronic cardiac insufficiency, angina pectoris after early myocardial infarction (MI), PCI[b] history, or CABG[c] history	1 - 3
High risk	>140, or the presence of MI-related troponin rise or fall, ST-T[d] dynamic changes (with or without symptoms)	>3
Extremely high risk	Regardless of score, Presence of any of the following: hemodynamic instability or cardiogenic shock, recurrent or persistent chest pain refractory to medical therapy, fatal arrhythmia or cardiac arrest, MI with mechanical complications, acute heart failure, recurrent ST-T dynamic changes (especially intermittent ST-segment elevation)	>3

[a]LVEF: left ventricular ejection fraction.

[b]PCI: percutaneous coronary intervention.

[c]CABG: coronary artery bypass grafting.

[d]ST-T: electrocardiogram ST-T wave.

Rule Inference Engine

The study uses a clinical decision knowledge engine framework to facilitate the reasoning and computation of clinical rules in the form of decision trees. Rule engine is a branch of an expert system, that is developed from an inference engine. It solves practical problems by simulating human thinking mode and expresses the results of inference in an understandable form. IBM Operational Decision Manager is used as a tool prototype to input, manage, and maintain the business rules of the system users, including rule modeling, writing, testing, deployment, and maintenance, and provides rule base mechanism for the organization, storage, and execution of business rules [31]. Through Operational Decision Manager, clinical knowledge rules are modeled, developed, and validated. After data collection and cleaning, a standardized data archive is realized. The rule inference engine makes logical operations based on the transformed standard term set. The output reminders were used to assist clinicians in their diagnosis and treatment decisions.

XSL•FO
RenderX

Application Assessment

Before the CDSS was officially launched, an independent panel of senior experts was invited to assess whether the recommendations were consistent with the current medical standards, practice guidelines, and best clinical practices. The experts could provide their own professional opinions and suggestions for improvement. After a comprehensive evaluation of expert opinions, the decision should be made whether to update and optimize the existing knowledge rules. After the system's official launch, we conducted a comparative analysis between CDSS recommendations and doctors' revised treatment plans. If there is an unreasonable knowledge base, after review by the quality control group, it was revised to improve the knowledge base for better decision support.

In terms of quality monitoring for daily use, a big data analytic platform is established and multidimensional statistic results are used to support management decision-making. The platform analyzes various quality control indicators, including the dynamic assessment rate of risk stratification. Hospital managers can review the control of CVD risk and the quality of diagnosis and treatment within the institution from multiple dimensions such as departments, doctors, types of diseases, and results of risk assessments, to formulate targeted management plans.

Statistical Analyses

The key performance indicators are presented as numbers (%) for categorical data. We compared the key performance indicators using Cochran-Armitage trend test. The threshold for statistical significance was $P<.05$. All statistical tests were performed using R (version 4.4.2; R Foundation).

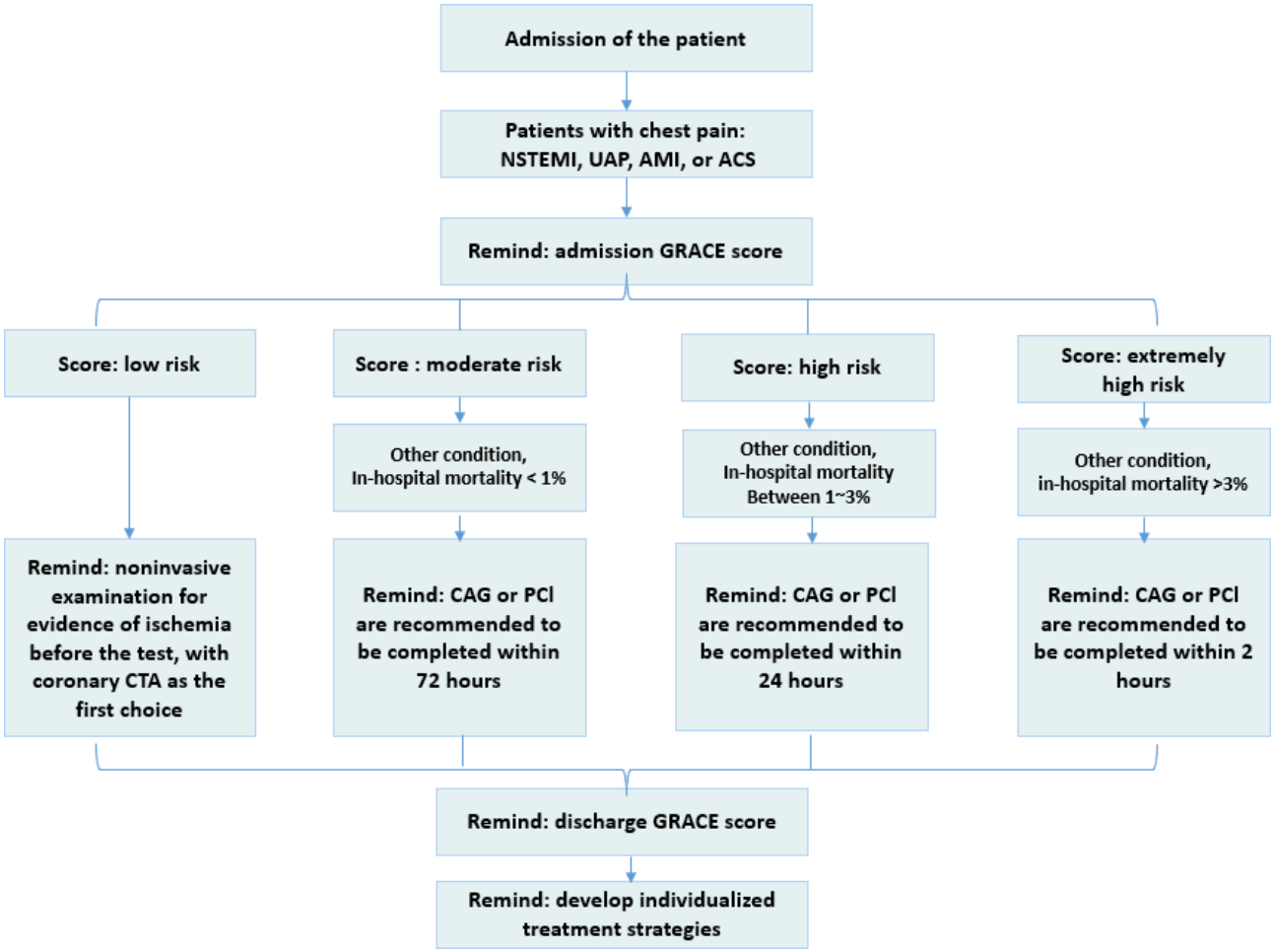
Results

Real-Time Intelligent Triggering

The CDSS is integrated into the clinical workflow, linking key processes such as admission, operation, transfer, discharge, and other clinical activities. It enables real-time data flow integration and message triggering within the interfaces for prescribing and medical record documentation. During the assessment phase, when the system identifies a patient with a specified diagnosis, the CDSS triggers evaluation tools such as GRACE, ASCVD, and CHA2DS2-VASc. It performs a preassessment based on the patient's medical history and provides traceable evidence from original medical records, prompting the doctor to verify the results. If the patient's CVD risk stratification outcome changes, the system alerts the doctor to reassess the patient. In the diagnosis and treatment phase, based on the patient's current assessment and clinical status, it recommends appropriate diagnostic and treatment measures. Figure 3 illustrates an example of real-time intelligent knowledge path triggering.

XSL•FO
RenderX

Figure 3. A real-time intelligent triggering sample knowledge path. ACS: acute coronary syndrome; AMI: acute myocardial infarction; CAG: coronary angiogram; CTA: computed tomography angiography; GRACE: Global Registry of Acute Coronary Events; NSTEMI: non–ST-elevation myocardial infarction; PCI: percutaneous coronary intervention; UAP: unstable angina pectoris.



Three-Level Control Management

To achieve precise quality control for different risk levels, our study proposed a 3-level control management system for in-process alerts. The 3-level management approach involves establishing distinct levels of control for different regulations based on the level of risk or degree of emergency and providing varying degrees of reminders to medical professionals. The specifics are as follows: Level 1 control triggers a small red dot on the EMR interface, signaling the doctor's attention and requiring active selection. Level 2 control involves an active pop-up window on the EMR interface that the doctor can clearly see and address with the option to close and continue other tasks. Level 3 control features an active pop-up window that the doctor must address or provide a reason for dismissing before proceeding with other tasks. The 3-level control management issues alerts based on varying risk levels and incorporates the timing requirements for doctor's medical record documentation. This system prompts the doctor to complete the relevant assessment, diagnosis, and treatment actions within the specified time range of the evaluation node.

Application Effects

Overview

The multimodal data-driven accurate CDSS for CVDs was officially launched around the year 2022, while different modules were launched at different specific times. Table 2 lists a before-and-after comparison table of key performance indicators. The important evaluation indicators in the diagnosis and treatment of CVDs such as rate of GRACE assessment (P<.001), rate of ASCVD risk stratification assessment (P<.001), rate of interventional therapy within 2 hours after acute MI (P<.001), rate of lipid-lowering drugs treatment for coronary heart disease (P<.001), rate of blood pressure well-control in hypertensive patients (P<.05), rate of interventional therapy within 2 hours after acute MI (P<.001), etc were significantly improved after the system came into use. The evaluation indicators after 2 years were better than those after 1 year. The indicators under 3-level mandatory control, such as the rate of CHA2DS2-VASc stroke risk assessment and rate of HAS-BLED (hypertension, abnormal renal or liver function, stroke, bleeding history or predisposition, labile international normalized ratio, elderly [>65 years], drugs or alcohol concomitantly) bleeding risk assessment, were directly becoming 100% after CDSS was online.

XSL•FO
RenderX

Table . The before-and-after comparison table of key performance indicators.

Name of indicators	Before CDSS[a] was online, n/N (%)	After CDSS was online (1 year), n/N (%)	After CDSS was online (2 year), n/N (%)	χ^2 (*df*)	*P* value
Rate of GRACE[b] assessment at admission	290/426 (68)	386/429 (90)	485/506 (96)	138.22 (2)	<.001
Rate of GRACE assessment at discharge	304/426 (71)	386/429 (90)	501/506 (99)	159.11 (2)	<.001
Rate of coronary CTA[c] in MI[d] patients	37/166 (22)	106/200 (53)	198/246 (81)	136.82 (2)	<.001
Rate of interventional therapy within 2 h after ate cute MI	35/57 (61)	54/65 (83)	57/60 (95)	25.884 (2)	<.001
Rate of ASCVD[e] risk stratification assessment	588/937 (63)	745/780 (96)	1058/1100 (96)	422.64 (2)	<.001
Rate of blood pressure well-control in hypertensive patients	162/213 (76)	269/336 (80)	385/460 (84)	5.71 (2)	<.05
Rate of lipid-lowering drugs treatment for coronary heart disease	347/673 (52)	500/733 (68)	676/821 (82)	161.71 (2)	<.001
Rate of CHA2DS2-VASc[f] stroke risk assessment	83/88 (94)	210/210 (100)	222/222 (100)	15.08 (2)	<.001
Rate of HAS-BLED[g] bleeding risk assessment	—[h]	177/177 (100)	166/166 (100)	—	—
Rate of diagnosis and early warning diagnosis of atrial fibrillation	—	147/158 (93)	296/313 (94)	—	—
Rate of stroke prevention for atrial fibrillation (medication or NOAC[i]) (high bleeding risk)	33/44 (75)	57/68 (84)	41/50 (82)	0.68 (2)	.41
Rate of stroke prevention in atrial fibrillation (medication or NOAC) (low bleeding risk)	79/96 (82)	81/95 (85)	162/174 (93%)	7.64 (2)	<.01

[a]CDSS: clinical decision support system.

[b]GRACE: Global Registry of Acute Coronary Events.

[c]CTA: computed tomography angiography.

[d]MI: myocardial infarction.

[e]ASCVD: atherosclerotic cardiovascular disease.

[f]CHA2DS2-VASc: congestive heart failure, hypertension, age ≥75 years (doubled), diabetes, stroke (doubled), vascular disease, age 65 to 74 years, and sex category (female).

[g]HAS-BLED: hypertension, abnormal renal or liver function, stroke, bleeding history or predisposition, labile international normalized ratio, elderly (>65 years), drugs or alcohol concomitantly.

[h]Not available.

[i]NOAC: nonvitamin K oral anticoagulants.

The CDSS function in our hospital has produced the following outcomes.

Timely Evaluation

Complete a GRACE score assessment for chest pain patients considered for non-ST segment elevation acute coronary

XSL•FO
RenderX

syndrome, to evaluate the comprehensive risk of all-cause mortality or the combined risk of all-cause death and MI. For other patients, the system assesses the in-hospital mortality risk within 24 hours of admission and re-evaluates the risk of death within 1 week before discharge and 6 months after discharge.

Blood Lipid Screening for High-Risk Patients

Following completing the CVD risk stratification assessment, the system prompts the doctor to perform a blood lipid test. For patients with abnormal blood lipid test data, the system alerts the doctor to diagnose the patient with "dyslipidemia."

Blood Glucose Control Reminder

After reviewing the patient's hemoglobin and insulin levels, the system prompts the doctor to carry out measures for blood glucose control. The reminder will disappear automatically after the patient's blood glucose index has reached the target value.

Reminder of Antihypertensive Treatment

If the patient is diagnosed with hypertension, the system prompts the doctor to carry out antihypertensive treatment, and the remainder will disappear automatically when the patient's blood pressure reaches the target value.

Timely Feedback Optimization

The system incorporates a user feedback function, enabling doctors to submit web-based feedback when encountering issues or providing suggestions during use. This facilitates the formation of diverse teams for problem-specific optimization and allows users to articulate the benefits derived from using the system. Feedback is searched, analyzed, and responded to based on various criteria such as time of submission, department affiliation, feedback provider, product function, and treatment type in order to ensure continuous improvement.

Discussion

The Benefits of CDSS

The implementation of CDSS has significantly enhanced the intelligent assessment and risk stratification of CVDs, effectively intervening and alerting in the subsequent diagnosis and treatment of patients.

On one hand, it has improved the efficiency of CVD risk assessment. Previously, this process required manual completion of scoring forms, which resulted in low efficiency. The AI-based CDSS, however, can analyze medical records and automatically complete the assessment in real-time, greatly enhancing both the efficiency and quality of CVD risk assessment. It has increased the diagnosis rate of CVD by deploying the CDSS across outpatient, emergency, and inpatient physician workstations, and improves the problem of low early diagnosis rate of CVD due to insufficient awareness of non-CVDs among noncardiology doctors. On the other hand, it enhances the standardization of clinical diagnosis and treatment. By identifying risks, issuing real-time warnings, and providing treatment recommendations, it effectively guides doctors in delivering precise treatment according to risks and clinical guidelines, and improves doctors' compliance with guidelines and standardization of diagnosis and treatment. Regarding quality control, traditional methods relied on sampling terminal medical records were passive and outdated. In contrast, the CDSS big data analysis platform can view the risk control and treatment quality of CVDs from the dimensions of departments, doctors, diseases, and risk assessment results, and allows quality control effect in real time.

Through automatic collection and real-time evaluation of key medical data in the process of diagnosis and treatment, the system establishes a new model of CVD quality control with information sharing and hierarchical treatment. It can be predicted that the application of information tools such as CDSS can help establish standard data sets for CVDs, support medical institutions to establish real-world clinical research platforms for CVDs, and aid specialized centers in conducting high-quality clinical research.

The Comparisons With Related Work

We have compared the characteristics of cardiovascular-related CDSS in recent years in Table 3. The innovation of the systems in our study lies in hierarchical evaluation and multistep reminders. We integrated multimodal data from the hospital laboratory information system, hospital information system, EMR, electrocardiography, nursing, and other systems to build the knowledge model. We established a 3-level control management system for in-process alerts as part of the workflow and providing recommendations at critical points of decision-making. The CDSS is integrated into the doctor's workstation and serves as a supplement or reminder to recommend examinations, tests, treatments, etc during the diagnosis and treatment process. The knowledge base and AI model are constructed from various clinical guidelines and historical patient data; however, personalization of patients may result in data bias, algorithm bias, or cognitive bias during model building. We conducted a comparative analysis between CDSS recommendations and doctors' revised treatment plans and improved the knowledge base for better decision support.

XSL•FO
RenderX

Table . The comparisons of cardiovascular-related clinical decision support system (CDSS) in recent years and our study.

First author, year and country of study	Clinical setting	Clinical condition	CDSS type	Study design	Additional description of CDSS
Sperl-Hillen et al (2018), United States [32]	Primary care clinics	Reduce cardiovascular (CV) risk	A web-based, point-of-care CDSS system, based on evidence-based national clinical guidelines seamlessly integrated within the electronic health record (EHR) and primary care workflow	Multicenter, randomized trial	For CDS clinic patients identified algorithmically with high CV risk, rooming staff was prompted by the EHR to print CDS that identified evidence-based treatment options for lipid, blood pressure, weight, tobacco, or aspirin management and prioritized them based on the potential benefit to the patient.
Kharbanda et al (2018), United States [33]	Primary care clinics	Improve the recognition and management of hypertension in adolescents.	Provides CV risk assessments based on EHR data and prompts providers to discuss risk reduction with patients	Multicenter, randomized trial	The recognition of hypertension was identified by an automated review of diagnoses and problem lists and a manual review of clinical notes, antihypertensive medication prescriptions, and diagnostic testing.
Adusumalli et al (2021), United States [34]	Primary care practices	Evaluate the effect of passive choice and active choice interventions in the EHR to promote guideline-directed statin therapy.	Passive and active choice EHR alerts to cardiologists	Multicenter, randomized trial	In passive choice, cardiologists had to manually access an alert embedded in the EHR to select options to initiate or increase statin therapy. In active choice, an interruptive EHR alert prompted the cardiologist to accept or decline guideline-directed statin therapy. Cardiologists in the control group were informed of the trial but received no other interventions.
Ventura et al (2022), Portugal [35]	2 cardiology units	Reduce recurrent cardiovascular events	Online CDSS for remote patient monitoring	Multicenter, randomized trial	This study protocol aims to assess the effectiveness of a user-friendly, comprehensive CDSS for remote patient monitoring of CVD[a] patients, primarily on the reduction of recurrent cardiovascular events.

XSL•FO
RenderX

First author, year and country of study	Clinical setting	Clinical condition	CDSS type	Study design	Additional description of CDSS
Weaver et al (2024), United States [36]	Outpatient oncology	Promote provider-patient CV health (CVH) discussions in outpatient oncology.	Automated heart-health assessment (AH-HA) clinical decision support tool which displayed American Heart Association Life's Simple 7 CVH factors (BMI, physical activity, diet, smoking status, blood pressure, cholesterol, and glucose), populated from the EHR	Single center, observational	The tool displayed American Heart Association Life's Simple 7 CVH factors (BMI, physical activity, diet, smoking status, blood pressure, cholesterol, and glucose), populated from the EHR, alongside cancer treatments received with cardiotoxic potential.
This study	Hospital	Prevention and management of cardiovascular diseases	3-level assessment card control for patient admission and predischarge reminders, pop-up windows, and screen domination operations	Single center, observational	This study designed a CDSS system with data, learning, knowledge, and application layers. It integrates multimodal data from hospital LIS (laboratory information system), HIS (hospital information system), EMR (electronic medical records), electrocardiography, nursing, and other systems to build a knowledge model.

[a]CVD: cardiovascular disease.

Limitations

Although the CDSS has been applied well in the First Affiliated Hospital of Nanjing Medical University, it still needs to be promoted in more medical and health institutions to verify its effectiveness. Until then, uniform data collection standards and procedures need to be developed to ensure that data, including patient information, treatment regimens, and clinical outcomes, can be collected in a consistent manner across all study sites. In addition, ethics committee approval at each participating institution was required to ensure compliance with local laws and regulations and to protect patient privacy. According to the results of multicenter, the performance of CDSS in different regions and different populations was evaluated, and the possible limitations or improvement space were identified, so as to provide more accurate auxiliary decision support. Tailoring the system to fit the specific workflows and practices of the new setting can improve acceptance and use rates, thereby increasing the likelihood of positive outcomes.

Conclusions

In this study, AI was used to perform NLP on the clinical medical records of patients, and a cardiovascular specialist CDSS was constructed to automatically identify patients at risk of CVD and improve the diagnostic rate of CVD patients by cardiologists and noncardiologists. It is an effective exploration to build an intelligent system for specialized diseases through CDSS to realize automatic assessment of CVD risk stratification, assist doctors in carrying out corresponding risk assessment and treatment, intervene in doctors' nonstandard diagnosis and treatment behavior in real time, improve the rate of appropriate lipid-lowering, blood pressure lowering and blood glucose control treatment, improve the prognosis of patients, and provide objective data for hospital management and evaluation of medical quality.

In the next step, when carrying out the construction of specialized precision CDSS, we will continue to improve the knowledge of specialized diseases by in-depth understanding of the diagnosis and treatment characteristics of clinical specialty fields and using the self-defined modules of the medical knowledge base in the CDSS. We will formulate standardized data collection requirements, carry out data transformation mapping, and continue to verify its effectiveness in more medical and health institutions to improve the versatility of the system. This enables refined management of knowledge and enables CDSS to better meet the management and research needs of various specialized diseases.

Acknowledgments

This work was supported by the National Key Research and Development Program Application of Intelligent Technology in Active Health Services (2023YFC3605800), Nanjing Life and Health Technology Special Project "Cooperative research,

XSL•FO
RenderX

development and transformation of active intelligent health management platform for diabetes mellitus" (202205053), and Natural Science Foundation of Jiangsu Province (BK20210966).

Authors' Contributions

The work presented here was carried out in collaboration among all authors. SM, PJ, WG, GY, and YL designed methods and constructed system architecture. SM, MJ, and RS focused on the application of artificial intelligence technology in clinical decision support systems (CDSSs). HD, XZ, and RS processed data using natural language processing. JG, HD, and SM constructed and implemented the CDSS. PJ, YZ, HM, and SM verified and collected the application effect. All authors have drafted, edited, reviewed, and approved the manuscript.

Conflicts of Interest

None declared.

References

1. Roth GA, Mensah GA, Johnson CO, et al. Global burden of cardiovascular diseases and risk factors, 1990-2019: update from the GBD 2019 study. J Am Coll Cardiol 2020 Dec 22;76(25):2982-3021. [doi: 10.1016/j.jacc.2020.11.010] [Medline: 33309175]
2. Liu H, Yin P, Qi J, Zhou M. Burden of non-communicable diseases in China and its provinces, 1990–2021: results from the global burden of disease study 2021. Chin Med J 2024;137(19):2325-2333. [doi: 10.1097/CM9.0000000000003270]
3. Correll CU, Solmi M, Veronese N, et al. Prevalence, incidence and mortality from cardiovascular disease in patients with pooled and specific severe mental illness: a large-scale meta-analysis of 3,211,768 patients and 113,383,368 controls. World Psychiatry 2017 Jun;16(2):163-180. [doi: 10.1002/wps.20420] [Medline: 28498599]
4. Amini M, Zayeri F, Salehi M. Trend analysis of cardiovascular disease mortality, incidence, and mortality-to-incidence ratio: results from global burden of disease study 2017. BMC Public Health 2021 Feb 25;21(1):401. [doi: 10.1186/s12889-021-10429-0] [Medline: 33632204]
5. Hearts: Technical Package for Cardiovascular Disease Management in Primary Health Care: Risk-Based CVD Management: World Health Organization; 2020.
6. Siontis KC, Noseworthy PA, Attia ZI, Friedman PA. Artificial intelligence-enhanced electrocardiography in cardiovascular disease management. Nat Rev Cardiol 2021 Jul;18(7):465-478. [doi: 10.1038/s41569-020-00503-2] [Medline: 33526938]
7. Yun JS, Ko SH. Current trends in epidemiology of cardiovascular disease and cardiovascular risk management in type 2 diabetes. Metab Clin Exp 2021 Oct;123:154838. [doi: 10.1016/j.metabol.2021.154838] [Medline: 34333002]
8. The W. Report on cardiovascular health and diseases in China 2022: an updated summary. Biomed Environ Sci 2023 Aug 20;36(8):669-701. [doi: 10.3967/bes2023.106] [Medline: 37711081]
9. GBD 2019 Tobacco Collaborators. Spatial, temporal, and demographic patterns in prevalence of smoking tobacco use and attributable disease burden in 204 countries and territories, 1990–2019: a systematic analysis from the global burden of disease study 2019. Lancet 2021 Jun;397(10292):2337-2360. [doi: 10.1016/S0140-6736(21)01169-7] [Medline: 34051883]
10. Han Y, Hu Y, Yu C, et al. Lifestyle, cardiometabolic disease, and multimorbidity in a prospective Chinese study. Eur Heart J 2021 Sep 7;42(34):3374-3384. [doi: 10.1093/eurheartj/ehab413] [Medline: 34333624]
11. Belard A, Buchman T, Forsberg J, et al. Precision diagnosis: a view of the clinical decision support systems (CDSS) landscape through the lens of critical care. J Clin Monit Comput 2017 Apr;31(2):261-271. [doi: 10.1007/s10877-016-9849-1] [Medline: 26902081]
12. Ali WS, Alsufayan MA, Aidah AA, et al. Exploring clinical decision support system in health-care settings-challenges and barriers to implementation–a literature review. Asian J Pharm 2022;16:402.
13. Taheri Moghadam S, Sadoughi F, Velayati F, Ehsanzadeh SJ, Poursharif S. The effects of clinical decision support system for prescribing medication on patient outcomes and physician practice performance: a systematic review and meta-analysis. BMC Med Inform Decis Mak 2021 Mar 10;21(1):98. [doi: 10.1186/s12911-020-01376-8] [Medline: 33691690]
14. Jing X, Min H, Gong Y, et al. Ontologies applied in clinical decision support system rules: systematic review. JMIR Med Inform 2023 Jan 19;11:e43053. [doi: 10.2196/43053] [Medline: 36534739]
15. Campos M, Hagenlocker B, Lascano J, Riley L. Impact of a computerized clinical decision support system to improve chronic obstructive pulmonary disease diagnosis and testing for alpha-1 antitrypsin deficiency. Ann Am Thorac Soc 2023 Aug;20(8):1116-1123. [doi: 10.1513/AnnalsATS.202211-954OC] [Medline: 36989247]
16. Zhou S, Ma X, Jiang S, et al. A retrospective study on the effectiveness of artificial intelligence-based clinical decision support system (AI-CDSS) to improve the incidence of hospital-related venous thromboembolism (VTE). Ann Transl Med 2021 Mar;9(6):491. [doi: 10.21037/atm-21-1093] [Medline: 33850888]
17. Laka M, Milazzo A, Merlin T. Factors that impact the adoption of clinical decision support systems (CDSS) for antibiotic management. Int J Environ Res Public Health 2021 Feb 16;18(4):1901. [doi: 10.3390/ijerph18041901] [Medline: 33669353]

XSL•FO
RenderX

18. Wang J, Wang S, Zhu MX, Yang T, Yin Q, Hou Y. Risk prediction of major adverse cardiovascular events occurrence within 6 months after coronary revascularization: machine learning study. JMIR Med Inform 2022;10(4):e33395. [doi: 10.2196/33395]
19. Brahma A, Chatterjee S, Seal K, Fitzpatrick B, Tao Y. Development of a cohort analytics tool for monitoring progression patterns in cardiovascular diseases: advanced stochastic modeling approach. JMIR Med Inform 2024 Sep 24;12:e59392. [doi: 10.2196/59392] [Medline: 39316426]
20. Yang Y, Zheng J, Du Z, Li Y, Cai Y. Accurate prediction of stroke for hypertensive patients based on medical big data and machine learning algorithms: retrospective study. JMIR Med Inform 2021 Nov 10;9(11):e30277. [doi: 10.2196/30277] [Medline: 34757322]
21. Strubell E, Verga P, Belanger D, McCallum A. Fast and accurate entity recognition with iterated dilated convolutions. arXiv. Preprint posted online on Feb 7, 2017. [doi: 10.48550/arXiv.1702.02098]
22. Dashdorj Z, Song M. An application of convolutional neural networks with salient features for relation classification. BMC Bioinformatics 2019 May 29;20(Suppl 10):244. [doi: 10.1186/s12859-019-2808-3] [Medline: 31138159]
23. Fox KAA, Goodman SG, Klein W, et al. Management of acute coronary syndromes. variations in practice and outcome; findings from the global registry of acute coronary events (GRACE). Eur Heart J 2002 Aug;23(15):1177-1189. [doi: 10.1053/euhj.2001.3081] [Medline: 12127920]
24. Mosepele M, Hemphill LC, Palai T, et al. Cardiovascular disease risk prediction by the American College of Cardiology (ACC)/American Heart Association (AHA) Atherosclerotic Cardiovascular Disease (ASCVD) risk score among HIV-infected patients in sub-Saharan Africa. PLoS One 2017;12(2):e0172897. [doi: 10.1371/journal.pone.0172897] [Medline: 28235058]
25. Anjum M, Ariansen I, Hjellvik V, et al. Stroke and bleeding risk in atrial fibrillation with CHA2DS2-VASC risk score of one: the Norwegian AFNOR study. Eur Heart J 2024 Jan 1;45(1):57-66. [doi: 10.1093/eurheartj/ehad659] [Medline: 37995254]
26. Hung J, Roos A, Kadesjö E, et al. Performance of the GRACE 2.0 score in patients with type 1 and type 2 myocardial infarction. Eur Heart J 2021 Jul 8;42(26):2552-2561. [doi: 10.1093/eurheartj/ehaa375] [Medline: 32516805]
27. Chotechuang Y, Phrommintikul A, Kuanprasert S, et al. GRACE score and cardiovascular outcomes prediction among the delayed coronary intervention after post-fibrinolytic STEMI patients in a limited PCI-capable hospital. Open Heart 2020;7(1):e001133. [doi: 10.1136/openhrt-2019-001133] [Medline: 32231784]
28. Aragam KG, Jiang T, Goel A, et al. Discovery and systematic characterization of risk variants and genes for coronary artery disease in over a million participants. Nat Genet 2022 Dec;54(12):1803-1815. [doi: 10.1038/s41588-022-01233-6] [Medline: 36474045]
29. Milwidsky A, Greidinger D, Frydman S, et al. Echocardiographic Killip classification. J Am Soc Echocardiogr 2022 Mar;35(3):287-294. [doi: 10.1016/j.echo.2021.10.012] [Medline: 34767929]
30. Vicent L, Velásquez-Rodríguez J, Valero-Masa MJ, et al. Predictors of high Killip class after ST segment elevation myocardial infarction in the era of primary reperfusion. Int J Cardiol 2017 Dec 1;248:46-50. [doi: 10.1016/j.ijcard.2017.07.038] [Medline: 28942880]
31. Gaevic D, Djuric D, Devedic V. The ontology definition metamodel (ODM). In: Model Driven Architecture and Ontology Development: Springer; 2006:215-233. [doi: 10.1007/978-3-642-00282-3_8]
32. Sperl-Hillen JM, Crain AL, Margolis KL, et al. Clinical decision support directed to primary care patients and providers reduces cardiovascular risk: a randomized trial. J Am Med Inform Assoc 2018 Sep 1;25(9):1137-1146. [doi: 10.1093/jamia/ocy085] [Medline: 29982627]
33. Kharbanda EO, Asche SE, Sinaiko AR, et al. Clinical decision support for recognition and management of hypertension: a randomized trial. Pediatrics 2018 Feb;141(2):e20172954. [doi: 10.1542/peds.2017-2954] [Medline: 29371241]
34. Adusumalli S, Westover JE, Jacoby DS, et al. Effect of passive choice and active choice interventions in the electronic health record to cardiologists on statin prescribing: a cluster randomized clinical trial. JAMA Cardiol 2021 Jan 1;6(1):40-48. [doi: 10.1001/jamacardio.2020.4730] [Medline: 33031534]
35. Ventura F, Sousa P, Dixe MA, et al. A clinical decision support system for remote monitoring of cardiovascular disease patients: a clinical study protocol. Front Public Health 2022;10:859890. [doi: 10.3389/fpubh.2022.859890] [Medline: 35615041]
36. Weaver KE, Dressler EV, Klepin HD, et al. Effectiveness of a cardiovascular health electronic health record application for cancer survivors in community oncology practice: results from WF-1804CD. J Clin Oncol 2025 Jan;43(1):46-56. [doi: 10.1200/JCO.24.00342] [Medline: 39571113]

Abbreviations

AI: artificial intelligence
ASCVD: atherosclerotic cardiovascular disease
BiLSTM-CRF: bidirectional long short-term memory - conditional random field
CDSS: clinical decision support system

XSL•FO
RenderX

CHA2DS2-VASc: congestive heart failure, hypertension, age ≥75 years (doubled), diabetes, stroke (doubled), vascular disease, age 65 to 74 years, and sex category (female)
CNN-DSSM: convolutional neural network - deep semantic similarity model
CVD: cardiovascular disease
EMR: electronic medical record
GRACE: Global Registry of Acute Coronary Events
HAS-BLED: hypertension, abnormal renal or liver function, stroke, bleeding history or predisposition, labile international normalized ratio, elderly (>65 years), drugs or alcohol concomitantly
IDCNN: iterated dilated convolutional neural network
MI: myocardial infarction
NLP: natural language processing

Edited by C Lovis; submitted 13.07.24; peer-reviewed by M Popovic, SS Goswami; revised version received 17.01.25; accepted 23.01.25; published 03.03.25.

Please cite as:
Miao S, Ji P, Zhu Y, Meng H, Jing M, Sheng R, Zhang X, Ding H, Guo J, Gao W, Yang G, Liu Y
The Construction and Application of a Clinical Decision Support System for Cardiovascular Diseases: Multimodal Data-Driven Development and Validation Study
JMIR Med Inform 2025;13:e63186
URL: https://medinform.jmir.org/2025/1/e63186
doi:10.2196/63186

© Shumei Miao, Pei Ji, Yongqian Zhu, Haoyu Meng, Mang Jing, Rongrong Sheng, Xiaoliang Zhang, Hailong Ding, Jianjun Guo, Wen Gao, Guanyu Yang, Yun Liu. Originally published in JMIR Medical Informatics (https://medinform.jmir.org), 3.3.2025. This is an open-access article distributed under the terms of the Creative Commons Attribution License (https://creativecommons.org/licenses/by/4.0/), which permits unrestricted use, distribution, and reproduction in any medium, provided the original work, first published in JMIR Medical Informatics, is properly cited. The complete bibliographic information, a link to the original publication on https://medinform.jmir.org/, as well as this copyright and license information must be included.

XSL•FO
RenderX

Convolutional Neural Network Models for Visual Classification of Pressure Ulcer Stages: Cross-Sectional Study

Changbin Lei[1], MSN; Yan Jiang[2], PhD; Ke Xu[3], PhD; Shanshan Liu[3], MSN; Hua Cao[4], BSN; Cong Wang[3], MSN

[1]Trauma Center, West China Hospital, West China School of Nursing, Sichuan University, Chengdu, China

[2]Nursing Department, Evidence-Based Nursing Center, West China Hospital, Sichuan University, Chengdu, China

[3]Evidence-Based Nursing Center, West China Hospital, Sichuan University, Chengdu, China

[4]Neurosurgery Department, West China Hospital, Sichuan University, Chengdu, China

Corresponding Author:
Yan Jiang, PhD
Nursing Department, Evidence-Based Nursing Center, West China Hospital, Sichuan University, Chengdu, China

Abstract

Background: Pressure injuries (PIs) pose a negative health impact and a substantial economic burden on patients and society. Accurate staging is crucial for treating PIs. Owing to the diversity in the clinical manifestations of PIs and the lack of objective biochemical and pathological examinations, accurate staging of PIs is a major challenge. The deep learning algorithm, which uses convolutional neural networks (CNNs), has demonstrated exceptional classification performance in the intricate domain of skin diseases and wounds and has the potential to improve the staging accuracy of PIs.

Objective: We explored the potential of applying AlexNet, VGGNet16, ResNet18, and DenseNet121 to PI staging, aiming to provide an effective tool to assist in staging.

Methods: PI images from patients—including those with stage I, stage II, stage III, stage IV, unstageable, and suspected deep tissue injury (SDTI)—were collected at a tertiary hospital in China. Additionally, we augmented the PI data by cropping and flipping the PI images 9 times. The collected images were then divided into training, validation, and test sets at a ratio of 8:1:1. We subsequently trained them via AlexNet, VGGNet16, ResNet18, and DenseNet121 to develop staging models.

Results: We collected 853 raw PI images with the following distributions across stages: stage I (n=148), stage II (n=121), stage III (n=216), stage IV (n=110), unstageable (n=128), and SDTI (n=130). A total of 7677 images were obtained after data augmentation. Among all the CNN models, DenseNet121 demonstrated the highest overall accuracy of 93.71%. The classification performances of AlexNet, VGGNet16, and ResNet18 exhibited overall accuracies of 87.74%, 82.42%, and 92.42%, respectively.

Conclusions: The CNN-based models demonstrated strong classification ability for PI images, which might promote highly efficient, intelligent PI staging methods. In the future, the models can be compared with nurses with different levels of experience to further verify the clinical application effect.

(JMIR Med Inform 2025;13:e62774) doi:10.2196/62774

KEYWORDS

pressure ulcer; deep learning; artificial intelligence; neural network; CNN; machine learning; image; imaging; classification; ulcer; sore; pressure; wound; skin

Introduction

Pressure injuries (PIs), also known as pressure ulcers, are prevalent in health care settings and result from sustained pressure or shear forces on bony prominences and soft tissues [1]. A meta-analysis encompassing 2,579,049 hospitalized adult patients revealed a 12.8% prevalence of PIs, and the estimated annual total cost of managing PIs increased approximately several times even in high-income countries [2,3]. Accurate staging of PIs is essential for determining appropriate treatment protocols and predicting clinical outcomes. Traditional staging relies on subjective evaluation by health care providers, often wound nurses, who use guidelines such as the *Prevention and Treatment of Pressure Ulcers/Injuries: Clinical Practice Guideline, International Guideline 2019*, and divide the PI stage into 6 stages—namely, stages I, II, III, and IV, unstageable, and suspected deep tissue injury (SDTI)—based on visual assessment, such as the color and texture characteristics of the wound bed, wound edges, and skin around the wound [4].

However, visual assessment conducted by medical staff is subject to considerable interrater and intrarater variability [5]. Moreover, the staging results are significantly influenced by the level of wound knowledge and the clinical experience of the evaluators. It has been reported that only 23%-58% of medical staff correctly classify PIs [6]. Therefore, accurate

XSL•FO
RenderX

staging of PIs is still a great challenge, and a universal, reliable, and more objective staging system is urgently needed.

Convolutional neural networks (CNNs) offer an opportunity to increase the objectivity and accuracy of PI staging. CNNs, a subset of deep learning (DL) models, have shown remarkable potential in medical image analysis [7]. CNNs automatically extract and learn hierarchical features from grid-like data, such as images, and have achieved performance levels comparable to or surpassing those of human experts in various medical imaging domains [8]. In dermatological and wound imaging, CNNs have demonstrated promising results, matching or even exceeding the diagnostic accuracy of dermatologists in classifying skin cancer and other skin lesions [9]. On the basis of the good classification performance of CNNs in medical images and the increased clinical need for automated staging of PIs, in recent years, the use of CNNs to learn PI images has gradually developed, but there are also areas for improvement. For example, the use of a singular model had an accuracy rate below 90%, alongside images sourced from outdated databases and of poor quality, and the labeling of PI images often relies on the subjective judgment of clinical experts, so the quality and consistency of the images were uneven in these studies, which limit the evidence supporting the model's widespread applicability [10-12]. Therefore, further exploration is needed in this field to prove the effectiveness of CNNs.

In this study, we trained AlexNet, VGGNet16, ResNet18, and DenseNet121 to classify PI images with the aim of contributing to artificial intelligence–driven wound care knowledge and informing the development of advanced clinical tools.

Methods

Setting and Samples

Our study was conducted at a tertiary hospital in Chengdu, China, from March 1, 2022, to September 30, 2024.

The inclusion criteria for patients were as follows: (1) PIs were diagnosed by 2 wound therapists simultaneously on the basis of the *Prevention and Treatment of Pressure Ulcers/Injuries: Clinical Practice Guideline, International Guideline 2019* [4] and (2) the patients provided informed consent.

The exclusion criteria for patients were as follows: (1) PIs included other skin diseases, such as incontinence dermatitis; (2) PIs were covered by dressings or tattoos; (3) exudation was excessive, resulting in obvious reflection; (4) mucosal PIs; (5) the patient's vital signs remained too unstable to exchange positions; and (6) the patients were in isolation wards.

The inclusion criteria for images were as follows: (1) images were taken by the investigator, and (2) images fully presented the wound triangle, namely, the wound bed, wound edge, and surrounding wound tissue.

The exclusion criteria for images were as follows: (1) images containing nonwounded and skin tissues such as clothing and sheets and (2) images that were blurred and overexposed.

Dataset

We recruited wound therapists who were awarded an international ostomy wound certificate to act as PI staging evaluators. Five wound therapists were included in this study. The basic information is provided in Table 1. To test the consistency of the 5 wound therapists' assessments, we sent them 30 PI images from the NPIAP (National Pressure Injury Advisory Panel) website in the form of a questionnaire [13]. The Fleiss kappa coefficient was 0.856, $P<.001$, indicating strong staging consistency among them [14]. The staging results are shown in Tables 2 and 3.

Table . Basic information of the 5 wound therapists.

Order	Gender	Age (years)	Working years	Department
A	Female	42	20	Respiratory ICU[a]
B	Female	36	15	Neurology
C	Female	40	18	General ICU
D	Female	43	25	Neurology
E	Female	36	15	ICU

[a]ICU: intensive care unit.

XSL•FO
RenderX

Table . Pressure injury staging results of the 5 wound therapists.

Order	Staging results of the 5 wound therapists				
	A	B	C	D	E
1	Stage III	Stage III	Stage III	Stage III	Stage IV
2	Stage I	Stage I	Stage I	Stage I	Stage I
3	Stage II	Stage III	Stage II	Stage II	Stage II
4	Unstageable	Unstageable	Stage IV	Unstageable	Unstageable
5	Unstageable	Unstageable	Unstageable	Unstageable	Unstageable
6	Stage IV	Stage IV	Stage IV	Stage IV	Stage IV
7	SDTI[a]	SDTI	SDTI	SDTI	SDTI
8	Stage I	Stage I	Stage I	Unstageable	Stage I
9	Stage IV	Stage IV	Stage IV	Stage IV	Stage IV
10	Unstageable	Stage IV	Stage IV	Stage IV	Stage IV
11	Stage III	Stage III	Stage III	Stage III	Stage III
12	Stage III	Stage III	Stage III	Stage III	Stage III
13	Stage II	Stage III	Stage II	Stage II	Stage II
14	SDTI	SDTI	SDTI	SDTI	SDTI
15	Stage IV	Stage IV	Stage IV	Stage IV	Stage IV
16	SDTI	SDTI	SDTI	SDTI	SDTI
17	Stage I	Stage I	Stage I	Stage I	Stage I
18	Stage II	Stage III	Stage II	Stage II	Stage II
19	Stage III	Stage III	Stage III	Stage III	Stage III
20	Stage IV	Stage SDTI	Stage IV	Stage IV	Stage IV
21	Stage I	Stage I	Stage I	Stage I	Stage I
22	Unstageable	Unstageable	Unstageable	Unstageable	Unstageable
23	SDTI	SDTI	SDTI	SDTI	SDTI
24	Stage II	Stage II	Stage II	Stage II	Stage II
25	Stage I	Stage I	Stage I	Stage I	Stage I
26	Stage II	Stage II	Stage II	Stage II	Stage II
27	Unstageable	Unstageable	Unstageable	Unstageable	Unstageable
28	Stage IV	Stage IV	Stage IV	Stage IV	Stage IV
29	Stage III	Stage III	Stage III	Stage III	Stage III
30	SDTI	SDTI	SDTI	I	SDTI

[a]SDTI: suspected deep tissue injury.

Table . Coefficient of internal consistency among the 5 wound therapists. The sample data contain 30 valid participants and 5 raters.

		Asymptotic			
	Kappa	SE	*Z*	*P* value	Asymptotic 95% CI
Overall	0.856	0.026	32.948	<.001	0.805-0.906

The PI Staging Assessment Process and Shooting Process

Before taking the shots, the researcher and the 2 wound therapists communicated with the patients and their family members to obtain consent. After that, the 2 therapists simultaneously evaluated the staging of the pressure ulcers via the *Prevention and Treatment of Pressure Ulcers/Injuries: Clinical Practice Guideline, International Guideline 2019*. If there were any objections to the results, we informed the third wound therapist on duty, and they would negotiate the staging.

XSL•FO
RenderX

The following types of shooting equipment were used: (1) Fuji XT-4 was used for shooting, with 21.6 million effective pixels, and Fuji XF 60 mm F2.4 R Macro and (2) a gray card. The specifications of the shooting mode are as follows: (1) antishake plus automatic mode; (2) parameter setting: shutter time: 60/1 s; (3) sensitivity: 3600-6000; (4) aperture: F6-8; (5) focal length: 60 mm; and (6) white balance: automatic white balance.

When photographs were taken, the camera was positioned parallel to the wound, with a focus on both the wound itself and the surrounding skin (Figure 1). Additionally, a gray card was used to minimize any interference caused by natural light. Following each shot, the images were carefully examined. If any image was deemed unclear, the researcher retracted the image. All of the original images were saved in JPG format and given a specific name consisting of a stage followed by a corresponding number. Finally, the images were transferred onto a computer for further analysis and storage.

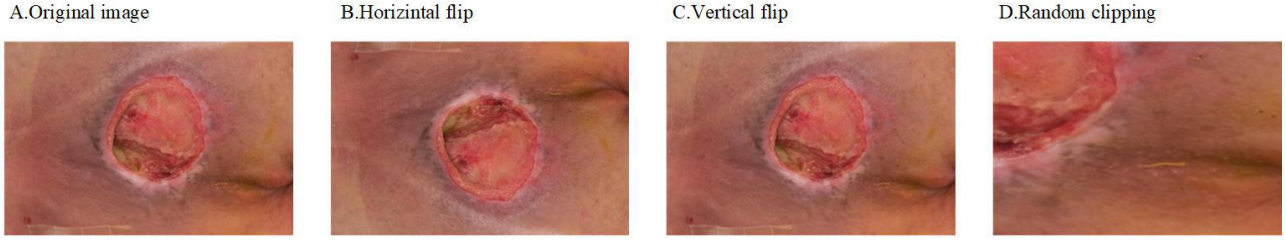
Figure 1. Shooting process.



Image Augmentation

Horizontal flipping, vertical flipping, and random clipping were used for data augmentation to expand the training dataset and improve the generalization ability of the models (Figure 2) [15]. Taking random cropping as an example, the size of the original image was reset to 512×512×3, and after random cropping, the size was 256×256×3. The size of the augmented image was fixed again to 224×224×3 before being input into the networks so that the network model could recognize them.

Figure 2. Image augmentation: (A) original image, (B) horizontal flip, (C) vertical flip, and (D) random clipping.



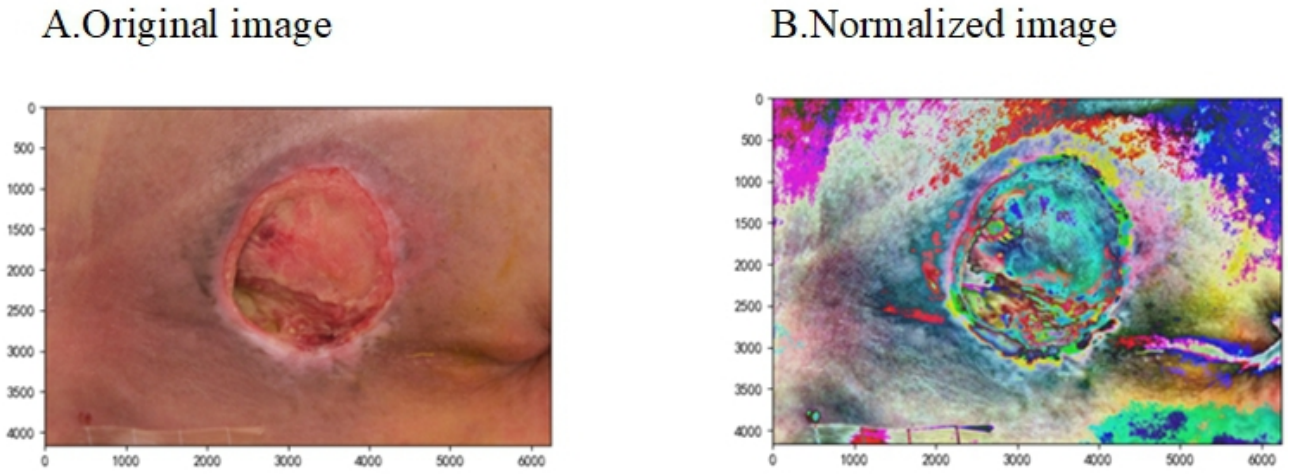
XSL•FO
RenderX

Image Normalization

The PI images are RGB color patterns (Figure 3), and the number of pixels is [0, 256] [16]. To reduce the adverse effects caused by singular sample data and speed up model training, we limit the number of pixels to [−1, 1] in this study via 2 image normalization calculation formulas, where $\bar{x}$ is the mean of the number of pixels, N represents the number of pixels, and x represents the pixel value of each pixel [17]. The calculation formula is as follows:

$$(1)s=(1N-1\sum i=1N(xi-\bar{x})2)12$$

Figure 3. Image normalization: (A) original image and (B) normalized image.

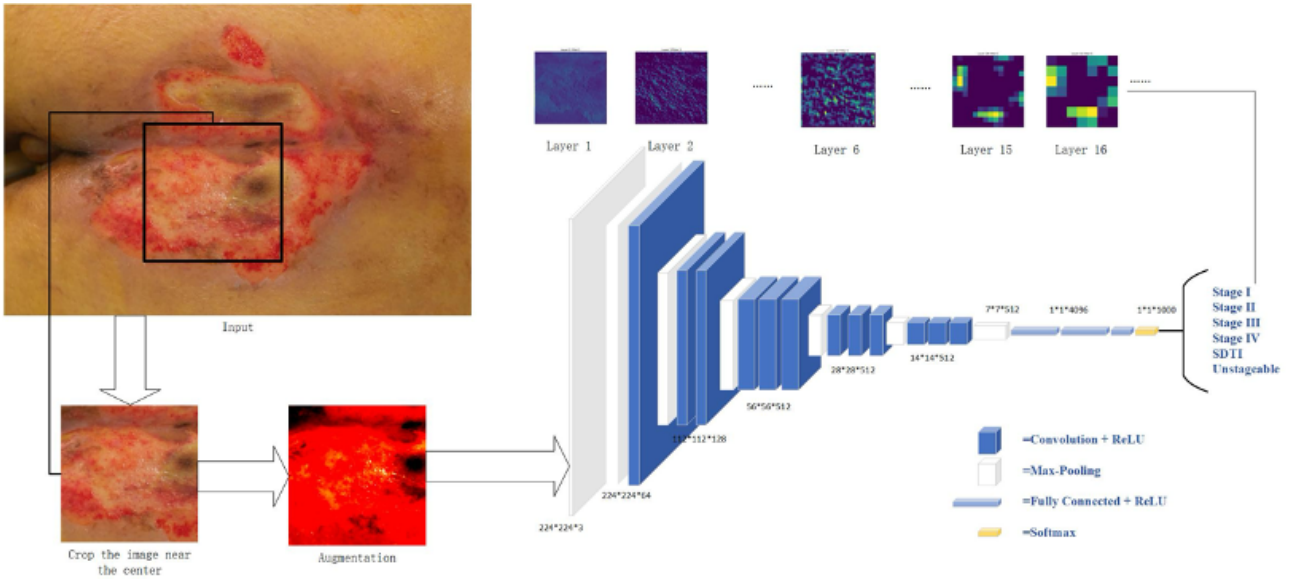


The Adam optimizer was used, and the loss function was the cross-entropy loss function (cross-entropy loss function), which is commonly used in multiple classification tasks. The data batch (batch size) was set to 8, and the initial learning rate was set to 0.0001. Every network was trained for 30 epochs.

This study was based on the 64-bit Windows 11 computer system and the Ubuntu 16.04 operating system for image training in the PyTorch 2.0.1 framework using the Python 3.9.19 language with CUDA 11.8 and NVIDIA GeForce RTX 4060 Laptop (8G).

The process of model training was divided into training, validation, and testing. The process is shown in Figure 4. First, the PI image was cut into the main wound area, and the cut image was treated as a uniform pixel, both of which were cut to 224 pixels. In the training set, the CNN training model is input; the performance of the model on the validation set is evaluated; and the state and convergence of the model are tested to adjust the hyperparameters. In the test set, the model outputs corresponding prediction results through a series of convolutions, nonlinear activations, pooling, etc, to evaluate the generalization ability of the model.

Figure 4. The network workflow diagrams. SDTI: suspected deep tissue injury.



In our study, we used AlexNet, VGGNet 16, ResNet 18, and DenseNet121 to train the images. AlexNet, a pioneering CNN in image classification, consists of 8 layers: 5 convolutional layers with varying filter numbers and 3 fully connected layers. It employs ReLU activations, max pooling, and dropout for regularization. The introduction of ReLU and dropout layers in AlexNet reduced training times and prevented overfitting,

XSL•FO
RenderX

whereas its deep architecture allowed for the learning of complex features, enhancing classification accuracy [18].

VGGNet 16 is a 16-layer deep network consisting of 13 convolutional layers and 3 fully connected layers, all of which use 3×3 filters. It features a consistent architecture with convolutional layers followed by max pooling layers, which simplifies optimization. This network is effective for capturing grid-like patterns in images and allows for the learning of more abstract and complex features due to its depth [19].

ResNet 18 is a shallow network with 18 layers organized in a residual learning framework. It consists of 4 blocks of residual units, each with convolutional layers, batch normalization, ReLU activation, and max pooling layers. The key innovation is the introduction of residual connections, which allow the network to learn residual mappings, making it easier to train deeper networks by effectively flowing gradients through the network [20].

DenseNet121 connects each layer to every other layer in a feedforward manner, using features from all preceding layers as inputs and its own feature map for all subsequent layers. This dense connectivity reduces the number of parameters, making DenseNet121 more parameter-efficient than other CNNs of similar depth. It helps mitigate the vanishing gradient problem and enhances feature propagation, leading to improved performance and efficiency [21].

In summary, the 4 CNN models were selected for their historical performance in image classification tasks, the uniqueness of their architectural design, and their significant contributions to the field of DL (Figure 4).

Evaluation of Performance

We evaluated the performance from a single image result. The diagnostic performance was measured by accuracy (ACC), precision (Pre), recall (Rec), and the F_1-score. To calculate the above metrics, we defined an abnormal result as positive and a normal result as negative.

(1) ACC=TP+TNTP+FP+FN+TN

(2) Pre=TPTP+FP

(3) Rec=TPTP+FN

(4) F1-score=2·Precision·RecallPrecision+Recall

Ethical Considerations

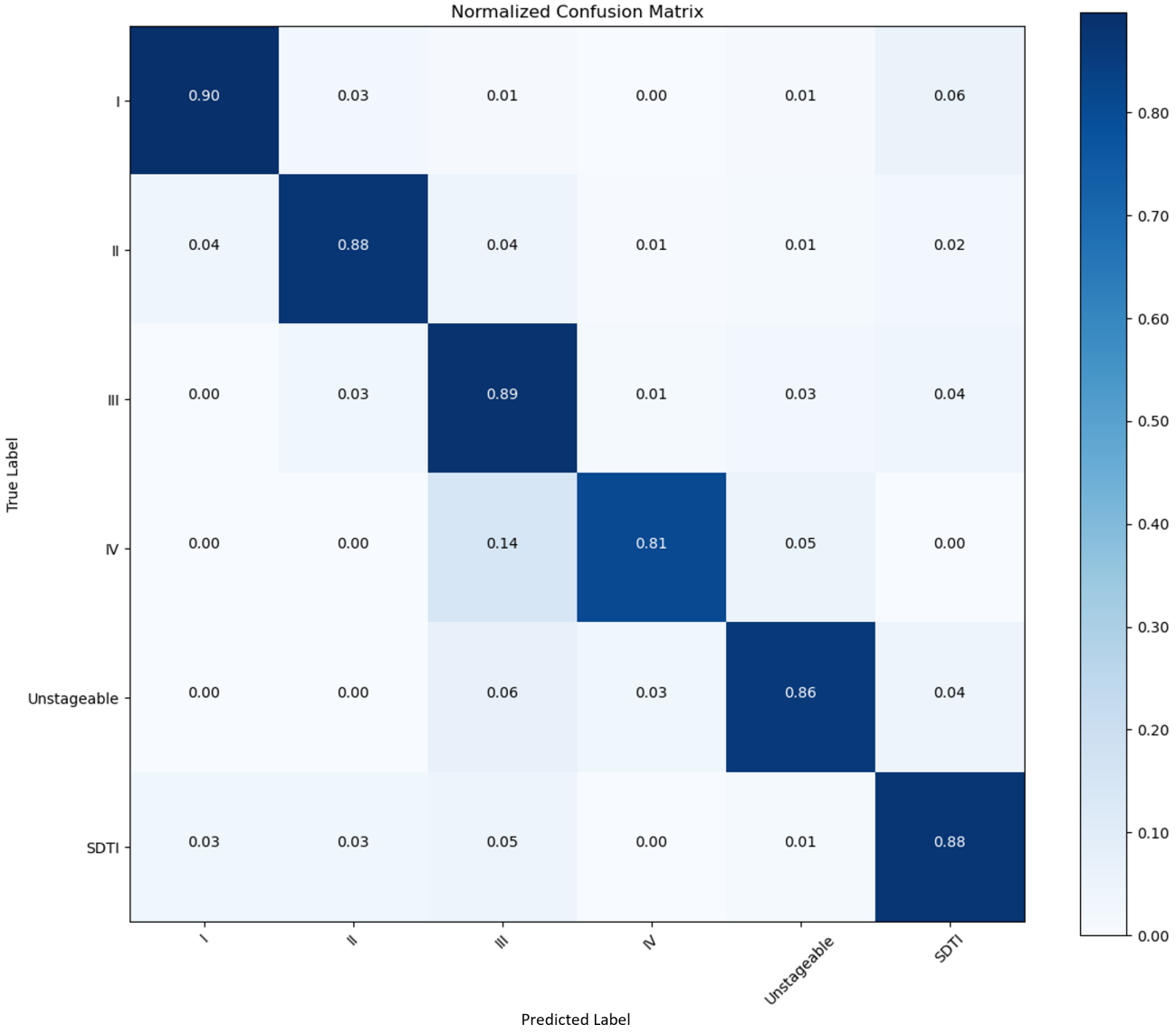
This study was approved by the Biomedical Ethics Committee of the West China Hospital of Sichuan University (#1053). In this study, the informed consent process was strictly carried out. Participation in the study was completely voluntary, and patients could refuse to participate or withdraw at any time during any phase of the study without discrimination or retaliation and without affecting their medical treatment and benefits. If participants decided to withdraw from the study, they would contact us. Patient privacy was strictly protected, and all data obtained were ony used for this study. Patients did not have to pay any fees to participate in the study.

Results

We collected 853 raw PI images in this study. We set the images into a training set, a validation set, and a test set at a ratio of 8:1:1. After augmentation, 7677 images were used. A confusion matrix is a numerical table used to display the performance results of a classification model on test data with known target labels. It serves as a visual representation of how the model makes predictions on the test dataset. On the basis of the results obtained from each network validation, we plotted the normalized confusion matrix, with the true labels on the vertical axis and the predicted labels on the horizontal axis (Figures 5-8). Table 4 provides a summary of the accuracy, precision, recall, and F_1-scores for the 4 CNNs.

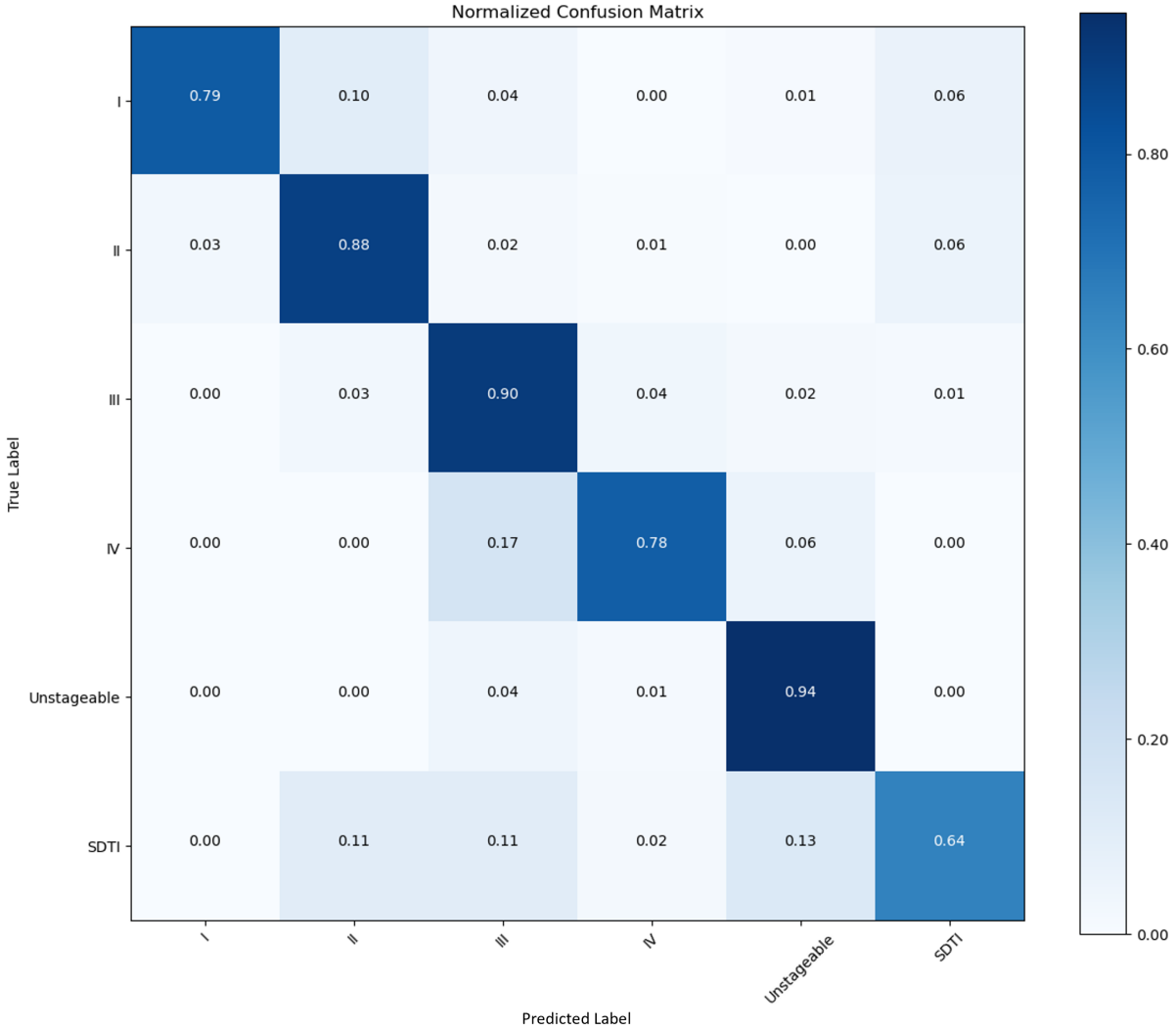
XSL•FO
RenderX

Figure 5. Performance of the CNNs in the identification and classification of PI images. Confusion matrix showing the accuracy and precision of 87.74% and 97.48%, respectively. CNN: convolutional neural network; PI: pressure injury; SDTI: suspected deep tissue injury.



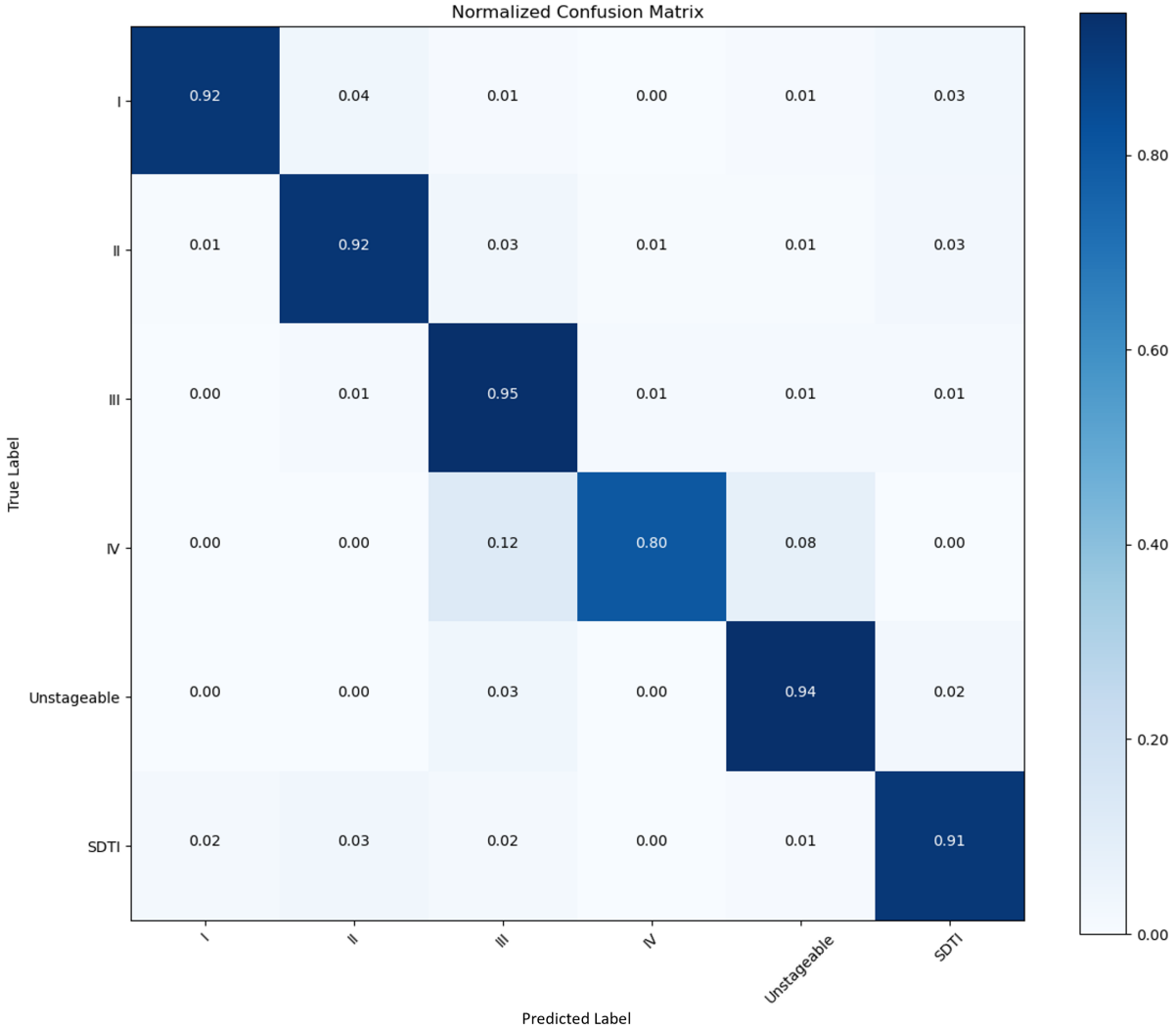
XSL•FO
RenderX

Figure 6. Performance of the CNNs in the identification and classification of PI images. Confusion matrix showing the accuracy and precision of 82.42% and 92.4%, respectively. CNN: convolutional neural network; PI: pressure injury; SDTI: suspected deep tissue injury.



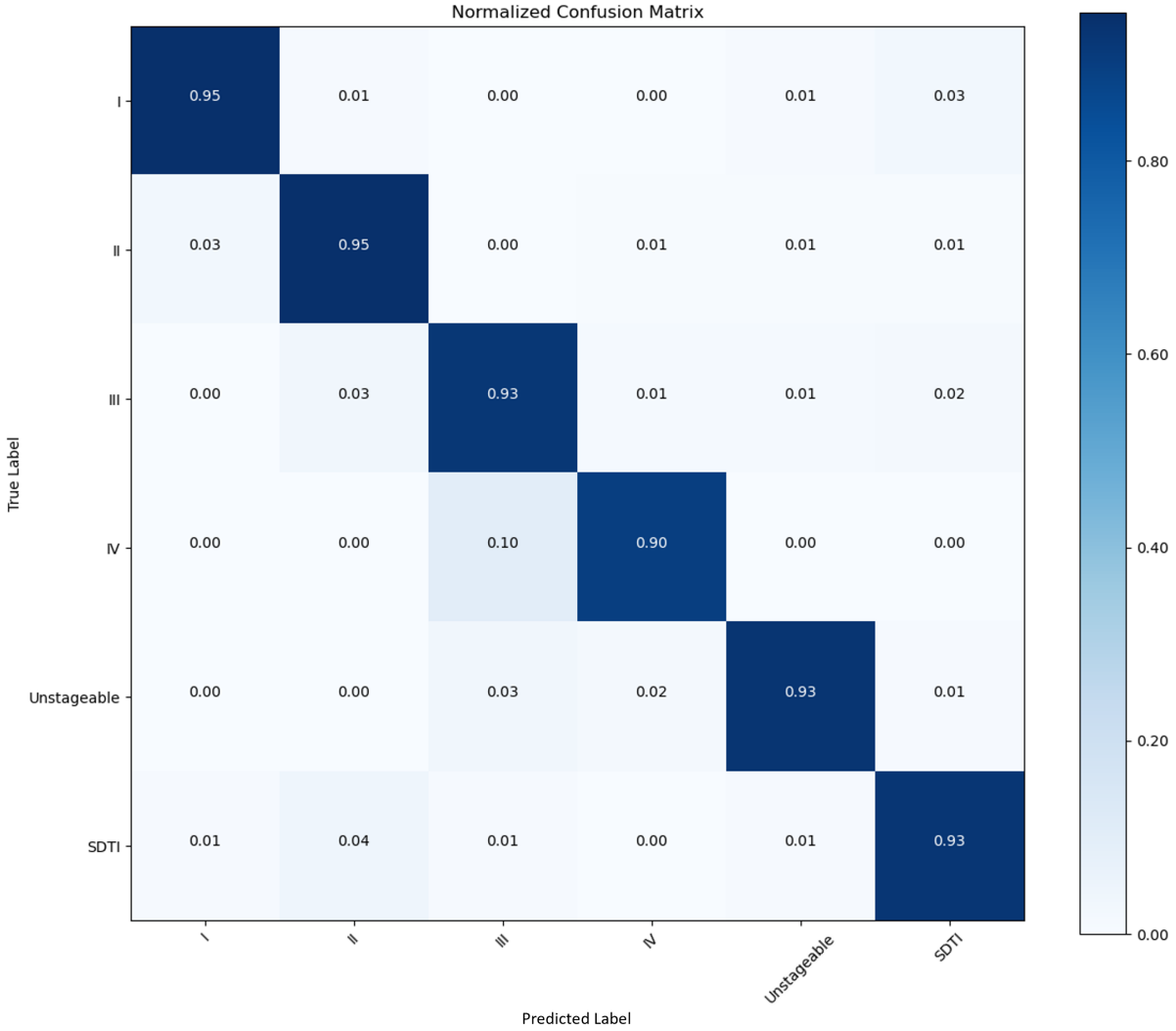
XSL•FO
RenderX

Figure 7. Performance of the CNNs in the identification and classification of PI images. Confusion matrix showing the accuracy and precision of 92.42% and 98.43%, respectively. CNN: convolutional neural network; PI: pressure injury; SDTI: suspected deep tissue injury.



XSL•FO
RenderX

Figure 8. Performance of the CNNs in the identification and classification of PI images. Confusion matrix showing the accuracy and precision of 93.71% and 98.72%, respectively. CNN: convolutional neural network; PI: pressure injury; SDTI: suspected deep tissue injury.



XSL•FO
RenderX

Table . The model's overall classification performance.

Modes and PI[a] stages		Accuracy (%)	Precision (%)	Recall(%)	F_1-score (%)
AlexNet					
	Stage I	92.76	98.25	91.43	94.71
	Stage II	86.36	97.60	92.76	95.12
	Stage III	73.91	95.53	86.36	90.71
	Stage IV	89.89	99.00	73.91	84.63
	Unstageable	79.38	98.29	89.89	93.90
	SDTI[b]	91.43	96.24	79.38	87.00
	Overall	87.74	97.48	85.62	94.71
VGGNet 16					
	Stage I	96.19	99.19	96.19	97.66
	Stage II	80.26	93.78	93.78	86.49
	Stage III	82.47	94.36	94.36	88.01
	Stage IV	76.40	98.50	98.50	75.24
	Unstageable	81.44	96.17	96.17	85.15
	SDTI	96.19	96.38	96.38	88.28
	Overall	82.42	96.40	95.90	97.66
ResNet 18					
	Stage I	94.08	99.41	97.14	98.26
	Stage II	90.91	98.06	94.08	96.02
	Stage III	86.96	97.03	90.91	93.84
	Stage IV	92.13	99.50	86.96	92.80
	Unstageable	88.66	98.69	92.13	95.29
	SDTI	97.14	97.91	88.66	93.95
	Overall	92.42	98.43	91.64	98.26
DenseNet121					
	Stage I	93.42	99.03	95.24	97.09
	Stage II	96.10	97.88	93.42	95.59
	Stage III	78.26	98.70	96.10	97.38
	Stage IV	94.38	99.17	78.26	87.48
	Unstageable	91.75	99.06	94.38	96.66
	SDTI	95.24	98.47	91.75	94.99
	Overall	93.71	98.72	91.53	97.09

[a]PI: pressure injury.

[b]SDTI: suspected deep tissue injury.

Discussion

Principal Findings

Among all the CNN models, DenseNet121 demonstrated the highest overall accuracy of 93.71%. The classification performances of AlexNet, VGGNet16, and ResNet18 exhibited overall accuracies of 87.74%, 82.42%, and 92.42%, respectively.

PIs are a global health issue, and effective treatment requires early and accurate classification and prevention. The staging of the PI is usually a subjective evaluation by medical professionals via standard systems, but it can differ due to variations in staff experience, training, and wound characteristics [22].

CNNs are feedforward neural networks with convolutional computations and deep structures. They capture local image features regardless of position through their core convolutional operation. This allows CNN-based models to potentially reduce assessment disparities among medical personnel. This approach promises precise classification of PIs, ensuring consistent patient

XSL•FO
RenderX

care and valuable advice post discharge, which improves quality of life and health care resource efficiency [23].

However, many factors need to be considered when a reliable staging model is constructed (eg, the quality and quantity of images matter for model training). Several previous studies were based on retrospectively collected images in which other types of wounds were included, and the shooting equipment may not have been updated with lower image pixels, which affects the reliability of supervised learning in DL [24-26]. Some researchers have attempted to classify PIs via neural network models on the basis of the clinical staging system; however, most of these studies have relied on public datasets containing a limited number of images per grade, typically only a few dozen [25,26]. It is recommended that more than 150 training images should be used per grade to achieve reasonable classification accuracy when resources are limited [27].

Therefore, it is necessary to construct a large dataset of high quality with reliable labeling of each grade. In contrast, in this study, PI images were collected prospectively by professional cameras, and a gray card and executable shooting standard were developed to ensure that the quality of each image was clear and that the wound characteristics could be clearly displayed. Moreover, the staging results of each image were assessed by 2 wound therapists simultaneously. The wound therapists included were all qualified and had more than 15 years of working experience, so their assessment results were convincing, which contributed to the good comparability of the images and the reliable sample set. Additionally, we used a professional digital camera and a gray card, which were rarely used in previous studies, to ensure the quality of the images, particularly in accurately representing the original color of PIs [28].

Compared with other studies, this study still has advantages in terms of classification accuracy. Ay et al [24] used the European Pressure Ulcer Advisory Panel staging system and included PIs from stage 1 to stage 4. They trained 1091 images from a public dataset of PIs called the PIID (Public Injury Images Dataset) and 15 images from Google via DenseNet121, InceptionV3, MobileNetV2, ResNet152, ResNet50, and VGG16. The results indicated that the average accuracy of the 6 algorithms for each stage during pretraining ranged from 54.84% to 77.42% [24]. Kim et al [29] set SE-ResNext101 to train 2614 images from 493 participants. The accuracy of the model was 0.793 over the internal testing set and 0.717 over the external testing set [29]. In our study, DenseNet121 exhibited the highest accuracy (93.71%), precision (98.72%), recall (91.53%), and F_1-score (97.09%), possibly because of the following reasons. (1) DenseNet121 improves the backpropagation of gradients due to the dense connection mode, making the network easier to train. Moreover, it can reduce the gradient disappearance problem caused by the transmission of input information and gradient information between many layers. (2) The number of parameters is reduced. (3) Low-dimensional features are preserved. In a standard convolutional network, the final output is only used to extract the highest-level features [30]. It is also important to consider the algorithm and image quality. In our study, 5 wound therapists, all of whom were qualified and had been engaged in wound management for at least 15 years, were recruited for grading. Therefore, the results of image staging were relatively accurate, and the classification of each label learned by CNNs was also convincing. Overall, DenseNet121 has become a popular choice in the field of computer vision because of its effective training of deep networks, high performance, generalizability, and insights into the learning process. These advantages make them powerful tools for image recognition and classification tasks. However, DenseNet121 processes a large number of layers, is relatively time-consuming, and consumes considerable computing power. DenseNet121 is more suitable for our present small sample. In regard to large-scale datasets, from the perspective of computing power and time factors, ResNet-18 or a higher level, such as ResNet34 or ResNet50, may be a better choice [31].

To improve the model's adaptability to skin color variations, future research should increase the sample size and expand collection areas. Additionally, implementing the model in clinical settings requires effective communication due to the perception of opacity in DL methods. Accountability is crucial in the medical field, as errors can have legal implications.

Limitations

The images obtained from data segmentation in this study contain some normal skin tissue. The next step is to make the wound more prominent or to make a judgment after segmenting the image.

Clinical wound management is influenced by blood and fluid seepage. Future studies should integrate DL with 3D imaging, thermal imaging, and fluid seepage assessment for a more comprehensive wound assessment.

The study also faced challenges due to limited prospective image data and reliance on a single device, potentially leading to biases and affecting model accuracy. This study did not compare the model's performance with that of wound therapists or nurses in discriminating pressure ulcers; instead, it focused on internal validation and algorithm comparison.

Conclusions

Staging models that use CNNs as their foundation exhibit robust classification capabilities. However, further research is needed to validate the reliability of these observed results. As such, we intend to gather an extensive array of additional imagery and undertake a comparative analysis between the staging outcomes generated by the model and those achieved by frontline clinical nurses. This comparative assessment will allow us to identify any potential discrepancies and disparities between the two, thereby affording us valuable insights for refining the model's performance and suggesting effective strategies for enhancing the skills and capabilities of nurses.

Acknowledgments

The authors would like to thank the 5 wound therapists for their assistance in assessing staging and

XSL•FO
RenderX

Duoxiang Zhao from the Pittsburgh Institute, Sichuan University who finished part of the image processin.This study is funded by the 1·3·5 projects for artificial intelligence (ZYAI24029) at West China Hospital, Sichuan University.

Data Availability

The raw data supporting the conclusions of this paper will be made available by the authors without undue reservation.

Conflicts of Interest

None declared.

References

1. Edsberg LE, Black JM, Goldberg M, McNichol L, Moore L, Sieggreen M. Revised national pressure ulcer advisory panel pressure injury staging system: revised pressure injury staging system. J Wound Ostomy Continence Nurs 2016;43(6):585-597. [doi: 10.1097/WON.0000000000000281] [Medline: 27749790]
2. Li Z, Lin F, Thalib L, Chaboyer W. Global prevalence and incidence of pressure injuries in hospitalised adult patients: a systematic review and meta-analysis. Int J Nurs Stud 2020 May;105:103546. [doi: 10.1016/j.ijnurstu.2020.103546] [Medline: 32113142]
3. Bennett G, Dealey C, Posnett J. The cost of pressure ulcers in the UK. Age Ageing 2004 May;33(3):230-235. [doi: 10.1093/ageing/afh086] [Medline: 15082426]
4. Prevention and Treatment of Pressure Ulcers/Injuries: Clinical Practice Guideline, 3rd edition: European Pressure Ulcer Advisory Panel, National Pressure Injury Advisory Panel, and Pan Pacific Pressure Injury Alliance; 2019.
5. Tschannen D, Mckay M, Steven M. Improving pressure ulcer staging accuracy through a nursing student experiential intervention. J Nurs Educ 2016 May 1;55(5):266-270. [doi: 10.3928/01484834-20160414-05] [Medline: 27115453]
6. Young DL, Shen JJ, Estocado N, Landers MR. Financial impact of improved pressure ulcer staging in the acute hospital with use of a new tool, the NE1 Wound Assessment Tool. Adv Skin Wound Care 2012 Apr;25(4):158-166. [doi: 10.1097/01.ASW.0000413597.20438.d2] [Medline: 22441048]
7. Zahia S, Garcia Zapirain MB, Sevillano X, González A, Kim PJ, Elmaghraby A. Pressure injury image analysis with machine learning techniques: a systematic review on previous and possible future methods. Artif Intell Med 2020 Jan;102:101742. [doi: 10.1016/j.artmed.2019.101742] [Medline: 31980110]
8. Currie G, Hawk KE, Rohren E, Vial A, Klein R. Machine learning and deep learning in medical imaging: intelligent imaging. J Med Imaging Radiat Sci 2019 Dec;50(4):477-487. [doi: 10.1016/j.jmir.2019.09.005] [Medline: 31601480]
9. Esteva A, Kuprel B, Novoa RA, et al. Dermatologist-level classification of skin cancer with deep neural networks. Nature New Biol 2017 Feb 2;542(7639):115-118. [doi: 10.1038/nature21056] [Medline: 28117445]
10. Chang Y, Kim JH, Shin HW, Ha C, Lee SY, Go T. Diagnosis of pressure ulcer stage using on-device AI. Appl Sci (Basel) 2024;14(16):7124. [doi: 10.3390/app14167124]
11. Swerdlow M, Guler O, Yaakov R, Armstrong DG. Simultaneous segmentation and classification of pressure injury image data using Mask-R-CNN. Comput Math Methods Med 2023;2023:3858997. [doi: 10.1155/2023/3858997] [Medline: 36778787]
12. Seo S, Kang J, Eom IH, et al. Visual classification of pressure injury stages for nurses: a deep learning model applying modern convolutional neural networks. J Adv Nurs 2023 Aug;79(8):3047-3056. [doi: 10.1111/jan.15584] [Medline: 36752192]
13. National pressure injury advisory panel. URL: https://npiap.com/ [accessed 2025-03-11]
14. Fleiss JL. Measuring nominal scale agreement among many raters. Psychol Bull 1971;76(5):378-382. [doi: 10.1037/h0031619]
15. Chlap P, Min H, Vandenberg N, Dowling J, Holloway L, Haworth A. A review of medical image data augmentation techniques for deep learning applications. J Med Imaging Radiat Oncol 2021 Aug;65(5):545-563. [doi: 10.1111/1754-9485.13261] [Medline: 34145766]
16. Kasajima I. Measuring plant colors. Plant Biotechnol (Tokyo) 2019;36(2):63-75. [doi: 10.5511/plantbiotechnology.19.0322a] [Medline: 31768106]
17. Huang L, Qin J, Zhou Y, Zhu F, Liu L, Shao L. Normalization techniques in training DNNs: methodology, analysis and application. IEEE Trans Pattern Anal Mach Intell 2023 Aug;45(8):10173-10196. [doi: 10.1109/TPAMI.2023.3250241] [Medline: 37027763]
18. Hosny KM, Kassem MA, Fouad MM. Classification of skin lesions into seven classes using transfer learning with AlexNet. J Digit Imaging 2020 Oct;33(5):1325-1334. [doi: 10.1007/s10278-020-00371-9] [Medline: 32607904]
19. Khan A, Khan A, Ullah M, Alam MM, Bangash JI, Suud MM. A computational classification method of breast cancer images using the VGGNet model. Front Comput Neurosci 2022;16:1001803. [doi: 10.3389/fncom.2022.1001803] [Medline: 36405784]
20. Nayak T, Chadaga K, Sampathila N, et al. Deep learning based detection of monkeypox virus using skin lesion images. Med Nov Technol Devices 2023 Jun;18:100243. [doi: 10.1016/j.medntd.2023.100243] [Medline: 37293134]

XSL•FO
RenderX

21. Wu J, Hu W, Wen Y, Tu W, Liu X. Skin lesion classification using densely connected convolutional networks with attention residual learning. Sensors (Basel) 2020 Dec 10;20(24):7080. [doi: 10.3390/s20247080]
22. Sayar S, Aşkın Ceran M, Demir A. Determining the pressure injury and staging knowledge of nurses at a hospital in Turkey. J Tissue Viability 2022 Nov;31(4):735-740. [doi: 10.1016/j.jtv.2022.08.004] [Medline: 36041891]
23. Jiang M, Ma Y, Guo S, et al. Using machine learning technologies in pressure injury management: systematic review. JMIR Med Inform 2021 Mar 10;9(3):e25704. [doi: 10.2196/25704] [Medline: 33688846]
24. Ay B, Tasar B, Utlu Z, Ay K, Aydin G. Deep transfer learning-based visual classification of pressure injuries stages. Neural Comput Applic 2022 Sep;34(18):16157-16168. [doi: 10.1007/s00521-022-07274-6]
25. Fergus P, Chalmers C, Henderson W, Roberts D, Waraich A. Pressure ulcer categorization using deep learning: a clinical trial to evaluate model performance. arXiv. Preprint posted online on Mar 7, 2022. [doi: 10.48550/arXiv.2203.06248]
26. Lau CH, Yu KHO, Yip TF, et al. An artificial intelligence-enabled smartphone app for real-time pressure injury assessment. Front Med Technol 2022;4:905074. [doi: 10.3389/fmedt.2022.905074] [Medline: 36212608]
27. Shahinfar S, Meek P, Falzon G. "How many images do I need?" Understanding how sample size per class affects deep learning model performance metrics for balanced designs in autonomous wildlife monitoring. Ecol Inform 2020 May;57:101085. [doi: 10.1016/j.ecoinf.2020.101085]
28. Sampaio CS, Atria PJ, Hirata R, Jorquera G. Variability of color matching with different digital photography techniques and a gray reference card. J Prosthet Dent 2019 Feb;121(2):333-339. [doi: 10.1016/j.prosdent.2018.03.009] [Medline: 30093117]
29. Kim J, Lee C, Choi S, et al. Augmented decision-making in wound care: evaluating the clinical utility of a deep-learning model for pressure injury staging. Int J Med Inform 2023 Dec;180:105266. [doi: 10.1016/j.ijmedinf.2023.105266] [Medline: 37866277]
30. Liao T, Li L, Ouyang R, et al. Classification of asymmetry in mammography via the DenseNet convolutional neural network. Eur J Radiol Open 2023 Dec;11:100502. [doi: 10.1016/j.ejro.2023.100502] [Medline: 37448557]
31. Sun Y, Xue B, Zhang M, Yen GG. Completely automated CNN architecture design based on blocks. IEEE Trans Neural Netw Learn Syst 2020 Apr;31(4):1242-1254. [doi: 10.1109/TNNLS.2019.2919608] [Medline: 31247572]

Abbreviations

CNN: convolutional neural network
DL: deep learning
NPIAP: National Pressure Injury Advisory Panel
PI: pressure injury
PIID: Public Injury Images Dataset
SDTI: suspected deep tissue injury

Edited by C Lovis, Q Chen; submitted 03.06.24; peer-reviewed by CJ Prabhakar, Y Tang; revised version received 21.10.24; accepted 11.01.25; published 25.03.25.

Please cite as:
Lei C, Jiang Y, Xu K, Liu S, Cao H, Wang C
Convolutional Neural Network Models for Visual Classification of Pressure Ulcer Stages: Cross-Sectional Study
JMIR Med Inform 2025;13:e62774
URL: https://medinform.jmir.org/2025/1/e62774
doi:10.2196/62774

© Changbin Lei, Yan Jiang, Ke Xu, Shanshan Liu, Hua Cao, Cong Wang. Originally published in JMIR Medical Informatics (https://medinform.jmir.org), 25.3.2025. This is an open-access article distributed under the terms of the Creative Commons Attribution License (https://creativecommons.org/licenses/by/4.0/), which permits unrestricted use, distribution, and reproduction in any medium, provided the original work, first published in JMIR Medical Informatics, is properly cited. The complete bibliographic information, a link to the original publication on https://medinform.jmir.org/, as well as this copyright and license information must be included.

XSL•FO
RenderX

Predicting Clinical Outcomes at the Toronto General Hospital Transitional Pain Service via the Manage My Pain App: Machine Learning Approach

James Skoric[1,2*], BEng, MSc; Anna M Lomanowska[3*], PhD; Tahir Janmohamed[2], PEng, MBA; Heather Lumsden-Ruegg[4], BA (Hon); Joel Katz[3,4,5], PhD; Hance Clarke[3,5], MD, PhD; Quazi Abidur Rahman[6], PhD

[1]Department of Electrical and Computer Engineering, McGill University, Montreal, QC, Canada

[2]ManagingLife, Toronto, ON, Canada

[3]Transitional Pain Service, Department of Anesthesia and Pain Management, Toronto General Hospital, University Health Network, Toronto, ON, Canada

[4]Department of Psychology, York University, Toronto, ON, Canada

[5]Department of Anesthesiology and Pain Medicine, University of Toronto, Toronto, ON, Canada

[6]Department of Computer Science, Trent University, 1600 West Bank Drive, Peterborough, ON, Canada

[*]these authors contributed equally

Corresponding Author:
Quazi Abidur Rahman, PhD
Department of Computer Science, Trent University, 1600 West Bank Drive, Peterborough, ON, Canada

Abstract

Background: Chronic pain is a complex condition that affects more than a quarter of people worldwide. The development and progression of chronic pain are unique to each individual due to the contribution of interacting biological, psychological, and social factors. The subjective nature of the experience of chronic pain can make its clinical assessment and prognosis challenging. Personalized digital health apps, such as Manage My Pain (MMP), are popular pain self-tracking tools that can also be leveraged by clinicians to support patients. Recent advances in machine learning technologies open an opportunity to use data collected in pain apps to make predictions about a patient's prognosis.

Objective: This study applies machine learning methods using real-world user data from the MMP app to predict clinically significant improvements in pain-related outcomes among patients at the Toronto General Hospital Transitional Pain Service.

Methods: Information entered into the MMP app by 160 Transitional Pain Service patients over a 1-month period, including profile information, pain records, daily reflections, and clinical questionnaire responses, was used to extract 245 relevant variables, referred to as features, for use in a machine learning model. The machine learning model was developed using logistic regression with recursive feature elimination to predict clinically significant improvements in pain-related pain interference, assessed by the PROMIS Pain Interference 8a v1.0 questionnaire. The model was tuned and the important features were selected using the 10-fold cross-validation method. Leave-one-out cross-validation was used to test the model's performance.

Results: The model predicted patient improvement in pain interference with 79% accuracy and an area under the receiver operating characteristic curve of 0.82. It showed balanced class accuracies between improved and nonimproved patients, with a sensitivity of 0.76 and a specificity of 0.82. Feature importance analysis indicated that all MMP app data, not just clinical questionnaire responses, were key to classifying patient improvement.

Conclusions: This study demonstrates that data from a digital health app can be integrated with clinical questionnaire responses in a machine learning model to effectively predict which chronic pain patients will show clinically significant improvement. The findings emphasize the potential of machine learning methods in real-world clinical settings to improve personalized treatment plans and patient outcomes.

(JMIR Med Inform 2025;13:e67178) doi:10.2196/67178

KEYWORDS

chronic pain; transitional pain; pain interference; machine learning; prediction model; manage my pain; pain app; clinical outcome; Toronto; Canada; transitional pain service; pain service; pain; app; application; prognosis; chronic pain management; digital health; digital health tool; pain management; machine learning methods; machine learning; prediction; machine learning models; logistic regression

XSL•FO
RenderX

Introduction

Chronic pain affects more than a quarter of people worldwide and carries substantial personal and economic burdens [1]. It is a complex condition that can be challenging to assess clinically due to the individualized and subjective nature of symptoms [2,3]. The development and progression of chronic pain are unique to each patient and difficult to predict at the individual level due to the contribution of interacting biological, psychological, and social factors [1,4-7]. Physiological markers associated with chronic pain can provide useful insights about a patient's condition [8]; however, clinical assessment of the subjective magnitude of pain severity and its impact on function and quality of life primarily relies on self-report measures [4,9]. Self-tracking of symptoms, medications, and daily activities is a popular approach to providing insights about symptom trends in chronic conditions [10,11], and digital apps have become a particularly useful tool to support self-tracking of pain and related symptoms [12-14]. With recent advances in machine learning technologies, digital symptom tracking opens an opportunity to evaluate numerous factors that contribute to pain symptoms and functioning to make predictions about an individual patient's progress [12]. This work examines whether information obtained from a pain tracking app can be used to accurately predict improvement in clinical pain-related outcomes in patients at a transitional pain clinic.

Manage My Pain (MMP) is a digital health app designed by ManagingLife with a patient-centric approach, aimed at helping patients and health care professionals measure, manage, and communicate pain, function, and medication use both at home and in clinical settings. The app has over 100,000 users worldwide and is available in 7 languages on both mobile and web platforms. MMP has been integrated into the Transitional Pain Service (TPS), a multidisciplinary pain clinic at Toronto General Hospital (TGH), to support symptom assessment and patient engagement with symptom tracking [13]. The TPS at TGH is a pioneering clinic that treats patients during the transitional period when acute pain after a major surgical procedure has the risk of becoming chronic [15,16]. The clinic also treats complex patients with chronic pain to support them in medication management and opioid weaning [17]. With this patient population, the clinic relies on regular symptom tracking to monitor patient progress and to intervene appropriately during critical phases of pain treatment. The MMP app provides a comprehensive digital platform where patients can fill out intake and follow-up questionnaires, track their symptoms, view symptom patterns and trends, and access educational resources about managing pain. Clinicians, in turn, can view each patient's record in the app to gain insights into their ongoing pain and symptom patterns and to support patient-clinician communication and decision-making about treatment. The MMP app has become the standard of care at the TPS since May 2020. Evaluations of the app showed that it was acceptable to TPS patients [18] and patients who used it reported significantly lower anxiety and pain catastrophizing scores [19].

The aim of this study is to use machine learning techniques to predict clinically significant improvements in pain-related outcomes among TPS patients who used the MMP app. In previous studies, we used symptom tracking, profile, and usage data from users of the MMP app to predict variability in reported pain levels over time (ie, pain volatility) [20,21]. In this study, we focused on a population of users from the TPS clinic and incorporated data from clinical questionnaires alongside symptom tracking, profile, and use data to predict clinical outcomes related to pain interference. Pain interference refers to the impact pain has on engagement in daily activities and participation [22]. It is related to the perceived severity of pain [23] and is considered a key aspect of the pain experience and a primary outcome in many clinical trials [24]. It is an informative measure from a clinical treatment and pain management standpoint that focuses on patients' daily functioning rather than pain intensity itself [25-27]. It is therefore a valuable measure to consider in predicting meaningful improvement for patient outcomes. We hypothesize that a machine learning model using data entered by TPS patients into the MMP app during the first 30 days of use can accurately predict subsequent pain interference scores reported within the next 5-month period.

Methods

Ethical Considerations

The study protocol was reviewed and approved by the McGill University Research Ethics Board (File Number 23-12-016). Informed consent to the use of data was obtained when users registered an account through the MMP app and agreed to its End User Licence Agreement [28]. Privacy and confidentiality of user data were protected in accordance with ManagingLife's Privacy Policy [29]. All user data used in the study dataset was deidentified. Users did not receive compensation for the use of their data in the study.

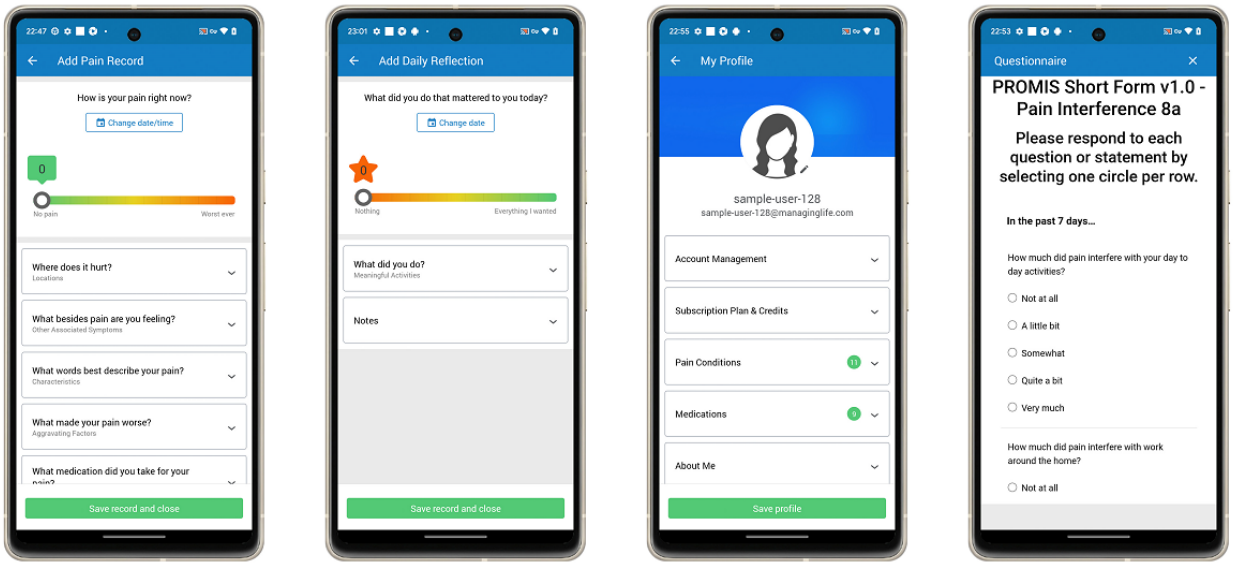
Manage My Pain App

The MMP app is available on Android, iOS, and web devices. The main features of the app are the daily reflection and the pain record that allows in-the-moment logging of pain experiences. Initially, users interact with the MMP app by responding to a daily push notification that prompts them to reflect on their day and rate it by completing a daily reflection at a default time of 8 PM. Users have the option to customize or disable the timing and frequency of notifications. The daily reflection, based on Acceptance and Commitment Therapy principles known for their efficacy in chronic pain management [30,31], asks users, "What did you do that mattered to you today?" Users then rate their day on a visual analog scale from 0 (Nothing) to 10 (Everything I wanted) and can record any meaningful activities. Following the daily reflection, users are invited to complete a pain record where they assess their current pain level by responding to "How is your pain right now?" and rating it on a scale from 0 (No pain) to 10 (Worst ever). Additionally, users can detail up to 7 aspects of their pain episodes, including body location, symptoms, characteristics, aggravating factors, medications, interventions, and environment. There is no limit to the number of pain records a user can enter in a day and these entries are independent of completing a daily reflection. Users can also enhance their MMP app profile with personal information about their medications,

XSL•FO
RenderX

health conditions, and demographics such as age, height, weight, and gender. The screen interface of each of the different features of the MMP app is shown in Figure 1.

Figure 1. Screenshots of the mobile version of the Manage My Pain (MMP) app. Shown from left to right is the interface of the pain record, daily reflection, user profile, and clinic questionnaire.



TPS Clinic Patient Flow

The TPS treats patients who are at risk of developing chronic pain after surgery and patients with chronic pain who have complex needs. Patients are typically referred to the TPS during the perioperative period, before or after a surgical procedure, or they are referred through the Toronto Academic Pain Medicine Institute [32]. Prior to their initial assessment by a TPS physician, patients are asked to fill out a set of clinical intake questionnaires (see below for details). Patients are invited to access the questionnaires on the MMP app and staff at the clinic support patients in accessing the app and registering an MMP account. They are also informed about the other features available in the app to track their pain and daily activities, view symptom patterns and trends, and learn about managing pain in the Pain Guide. The TPS clinical team works with patients to address their needs through a multidisciplinary approach to pain care that includes medical treatment alongside psychological care and physical rehabilitation. Patients are asked to fill out follow-up clinical questionnaires using the MMP app at subsequent visits to the clinic. Patients are followed by the TPS for up to 6 months, at which point they are typically discharged to primary care.

Clinic Questionnaires

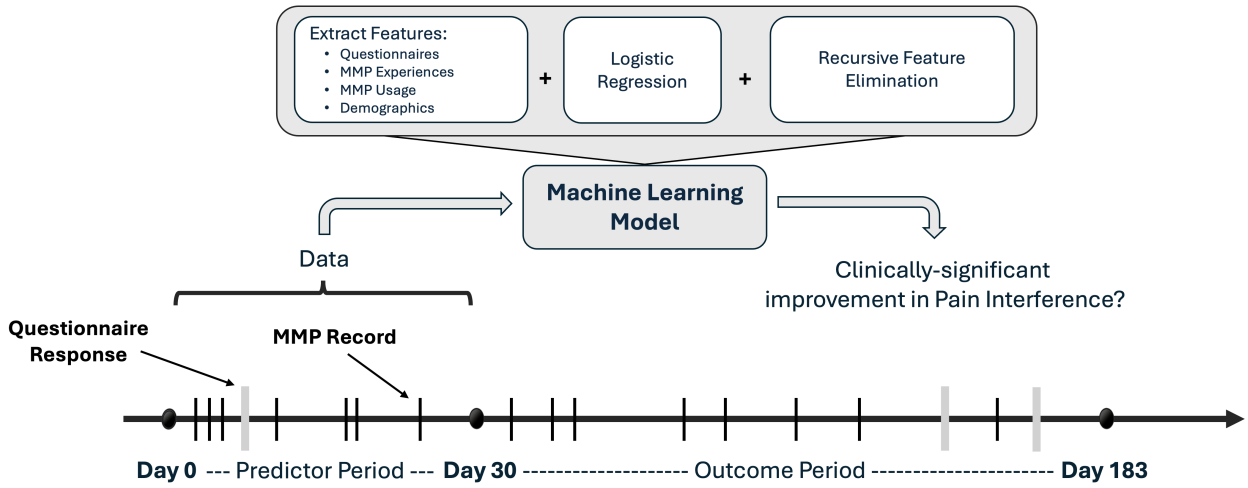
The TPS clinic uses a battery of standard clinical questionnaires to evaluate patient pain-related symptoms at intake and to assess treatment progress over time. The following questionnaires are regularly assigned using the MMP app at both intake and follow-up visits and are common across all TPS patients: Numeric Rating Scale (NRS) to rate pain severity on an 11-point scale [9]; PROMIS Pain Interference 8a v1.0 (PROMIS PI) to measure the extent to which pain hinders an individual's engagement with physical, mental, cognitive, emotional, recreational, and social activities [22]; Pain Catastrophizing Scale (PCS) to assess catastrophic thinking related to pain [33]; Generalized Anxiety Disorder-7 (GAD-7) as a measure of general anxiety [34]; and Patient Health Questionnaire-9 (PHQ-9) as a measure for screening, diagnosing, monitoring, and measuring the severity of depression [35]. Additional questionnaires are assigned as needed to meet the specific needs of each patient.

Study Dataset

A total of 780 TGH TPS patients entered responses to clinic questionnaires and pain experience records in the MMP app during the period between May, 2020 and March, 2024, producing 14,127 questionnaire responses and 30,033 pain experience records. For this study, we selected users who had at least 1 PROMIS PI questionnaire response in a predictor period, and at least 1 PROMIS PI questionnaire response in an outcome period, resulting in 160 users. The predictor period was defined as the first 30 days of MMP app use, and the outcome period was set between 30 days and 6 months (183 d) from the first app use (Figure 2). There were 680 users who recorded a response in the predictor period, 182 users who recorded a response in the outcome period, and 180 users who had a response in both the predictor and outcome periods. Therefore, 180 users were selected for this study.

XSL•FO
RenderX

Figure 2. Overview of study timelines and machine learning model approach. MMP: Manage My Pain.



We aimed to predict users who improved based on changes in their final score on the PROMIS PI questionnaire between the predictor and outcome period. The final score on the PROMIS PI questionnaire is generated by converting the total raw score into a T-score for each participant using a web-based calculation tool [22]. The first questionnaire responses from the predictor period and the first subsequent recorded responses in the outcome period were used in the prediction model.

Clinical questionnaires have a research-backed minimal clinically important difference (MCID) indicator that guides clinicians in evaluating the progress of symptoms [36]. The MCID was used in this study as a marker of patient improvement. The MCID for the PROMIS PI questionnaire is 2 [37]. Patients who showed an improvement in PROMIS PI questionnaire T-scores greater than the MCID of 2 were classified as improved.

Data Preprocessing and Feature Extraction

Overview

The data were preprocessed to remove any anomalous MMP app records (eg, missing values where entries were expected) and to convert any categorical questionnaire responses into a numerical format.

A total of 245 relevant variables, referred to as features in the field of machine learning, were extracted from the available data. A total of 194 features were extracted from the patients' MMP app user profiles, pain records, daily reflections, and app use records. Another 51 features were extracted from the patients' questionnaire responses. Instances with missing values were imputed using the mean value for each feature and subsequently, each feature was *z* score normalized. The features were divided into 8 categories as provided below.

Demographics

Demographics (6 features) consisted of data on gender, age, and age category (unknown, 0 to 19, 20 to 29, 30 to 39, 40 to 49, 50 to 59, 60 to 69, and 70+ years), height, weight, and body mass index entered by users into their profiles.

Medications

Medications (10 features) consisted of the total number of medications reported by users in their profile and 9 binary features for the specific medications reported, including opioids, tricyclic antidepressants, anticonvulsants, cannabinoids, serotonin-norepinephrine reuptake inhibitors, nonsteroidal anti-inflammatory drugs, acetaminophen, metamizole, and benzodiazepines.

Health Conditions

Health Conditions (9 features) consisted of the number of health conditions reported by users in their profile, and the number of conditions by category (unknown, 1 condition, 2 conditions, 3 conditions, and more than 3 conditions). Five features included binary categories of whether a user reported or not one of the following most observed health conditions: fibromyalgia, headaches or migraines, back pain, arthritis, or depression/anxiety. One feature represented an indication of neuropathic pain determined by the app and characterized as the presence of reports of sensations of pins and needles or tingling, burning, numbness, electric shocks, or an aggravating factor of light touch or clothing. The final feature was based on the presence of mental health issues as indicated by reports of anxiety, depression, negative mood, or stress.

Pain Record Statistics

Pain Record Statistics (11 features) consisted of the mean and SD of pain severity ratings, the mean and SD of absolute values of changes between consecutive severity ratings, the average of pain ratings in the following categories: mild (average pain rating <4), moderate (average pain rating ≥4 to ≤7), or severe (average pain rating >7), the mean and SD of pain, the number of pain records in the predictor period, the slope of the trendline of the severity scores, and the absolute value of the slope of the trendline.

Pain Descriptors

Pain Descriptors (127 features) consisted of descriptors of the pain experience entered into the app, including body locations (32 features), symptoms (21 features), characteristics (21

XSL•FO
RenderX

features), environment (8 features), aggravating factors (15 features), effective factors (15 features), and ineffective factors (15 features).

Daily Reflections

Daily Reflections (21 features) consisted of the mean and SD of the daily reflection score, the number of daily reflections in the predictor period, and descriptors of meaningful activities that contributed to the daily reflection rating.

App Usage

App Usage (10 features) consisted of the number of completed sections in the user profile, the number of days with a pain record, the percent of descriptor elements that were completed in their pain records, whether users were referred to the app via an institution, provider, or payer, and the average hour, day, week, or month of their pain records. Please note that in the current dataset, all users were referred to the app via an institution.

Questionnaires

Questionnaires (51 features) consisted of responses and outcome scores on five clinic questionnaires regularly assigned to all TPS clinic patients at both intake and follow-up visits, including (1) PROMIS PI, 8 questions and 3 outcome scores; (2) NRS, 4 questions and 4 outcome scores; (3) PHQ-9, 9 questions and one outcome score; (4) PCS, 13 questions and one outcome score; and (5) GAD-7, 7 questions and one outcome score. Please refer to Multimedia Appendix 1 to see the questions included in each questionnaire.

Prediction Model

Given the relatively small sample size, we used binary logistic regression as it is a simple and straightforward model that has been shown to have good performance with limited datasets [38]. Binary logistic regression is a method used for binary classification, which models the probability of each class as a function of the input variables [38]. It operates by fitting a logistic function to the data. The output of logistic regression lies between 0 and 1, representing the probability that a given input point belongs to the class labeled as 1 (improved class). This is achieved by calculating a linear combination of the input features passed through the logistic function. The coefficients are learned by minimizing a cost function. To keep the weights constrained to a reasonable size and to reduce overfitting, we added an L2 regularization term to the cost function which penalizes the scale of the class weights. Additionally, we balanced the weighting of each class inversely proportional to the class frequencies to correct for class imbalance. The model was implemented with the sklearn library [39] in Python, with the liblinear solver [40], as it performs well on smaller datasets.

We then performed feature selection to identify the significant features and improve the model's generalizability by reducing overfit to the training data. We implemented a recursive feature elimination (RFE) with cross-validation [41]. RFE is a method to identify important features influencing a model's prediction by systematically eliminating the least important features. First, the training dataset is split into 10 train/test subsets using 10-fold cross-validation, ensuring that the feature elimination process is validated across different subsets of data for reliability. Starting with all features, a logistic regression model is trained, and its performance is evaluated on the validation set. Features are ranked based on their importance from their coefficients, and the least important feature is removed from the set. This process is repeated iteratively, each time removing the least important feature, and the model's performance is assessed with cross-validation at each step. The optimal number of features is determined by the point where the model's cross-validation performance is the highest. We used the area under the receiver operating characteristic curve (AUC) as a metric to determine performance. We then implemented a second 10-fold cross-validation to optimize the regularization strength in the logistic regression model using only the selected features.

Model Evaluation

The model algorithm was validated using leave-one-out cross-validation to assess how well the model will perform in practice on unseen data. In this approach, data from one MMP user is used as the test set while data from the remainder of the users is used as the training set. This process is iteratively repeated such that each subject is used exactly once as the test instance. In each iteration, the entire proposed algorithm is repeated with only the data in the training set being used to train the model. This method allows the model to be evaluated on every possible training and test set combination, providing a comprehensive measure of how well the model performs across the entire dataset. We evaluated the model using 4 metrics as follows: the overall accuracy, the accuracy of the improved class (sensitivity), the accuracy of the not-improved class (specificity), and the AUC. Due to the novel nature of both the dataset and the approach, there are currently no standards to compare against. Therefore, we also evaluated using 3 other standard machine learning models in place of the logistic regression model to compare performance: AdaBoost, random forest, and linear support vector machine (SVM). AdaBoost is an ensemble learning algorithm that iteratively combines weak classifiers to improve overall accuracy by focusing on misclassified instances [42]. Random forest, another ensemble method, builds multiple decision trees and combines their predictions, offering robustness to overfitting and the ability to capture nonlinear relationships in the data [43]. The linear SVM is a classification algorithm that identifies the optimal hyperplane to separate data points into distinct classes, making it effective for high-dimensional datasets [44].

Feature Importance Estimation

Logistic regression is valued for its simplicity and interpretability [38]. Feature importance within this model is estimated by analyzing the coefficients. Larger absolute values of these coefficients suggest a stronger impact on the outcome, with positive coefficients increasing the log odds of the outcome (thus making it more likely), and negative coefficients decreasing the log odds (thus making it less likely). In our approach, we used an RFE algorithm, which selects varying numbers of features in each training fold. We first identified which features were consistently selected across all training folds. We then calculated the average coefficients for these features across all training folds and ranked them based on the

XSL•FO
RenderX

absolute values of these averages. This method highlights the features that the model relies on to predict the likelihood of a patient's improvement.

Results

Sample and Dataset Characteristics

The characteristics of the sample of TPS patient users of the MMP app who were included in the study and their records in the MMP app are shown in Table 1. Using an MCID of 2, 72 out of 160 (45%) of the patients showed improvements on the PROMIS PI questionnaire between the predictor and the outcome period. An overview of the PROMIS PI questionnaire response characteristics is shown in Table 2.

Table . Sample characteristics.

Category and variable	Value
Users	
Number of users	160
Age (years), mean (SD)	40.4 (16.6)
Age not provided	129
Gender (male)	14
Gender (female)	19
Gender not provided	127
Number of health conditions, mean (SD)	3.5 (3.4)
Health conditions not provided	90
Number of medications, mean (SD)	3.7 (3.3)
Medications not provided	58
MMP[a] records	
Users with any MMP record in the predictor period	124
Total MMP records in the predictor period	4009
Users with a pain record in the predictor period	123
Number of pain records in the predictor period	2820
Users with a daily reflection in the predictor period	75
Number of daily reflections in the predictor period	1189
Pain record score in the predictor period, mean (SD)	5.1 (2.6)
Daily reflection score in the predictor period, mean (SD)	4.0 (2.7)
Total MMP records	18,545[b]
Total number of pain records	13,541[b]
Number of pain records per day per user, mean	0.3[b]
Total number of daily reflections	5004[b]
MMP days of activity, mean (SD)	411 (438)[b]

[a]MMP: Manage My Pain app.

[b]Values derived from total app use for each user.

XSL•FO
RenderX

Table . Characteristics of the PROMIS Pain Interference 8a v1.0 questionnaire responses.

Variable	Value
Total responses in predictor period	199
Total responses in outcome period	236
Mean days between first response and outcome response, mean (SD)	74.8 (39.4)[a]
Mean T-score in predictor period, mean (SD)	65.6 (6.7)
Mean T-score in outcome period, mean (SD)	63.1 (7.4)
Mean T-score change, mean (SD)	−2.5 (6.5)

[a]Range: 22 - 183 days.

Prediction Results

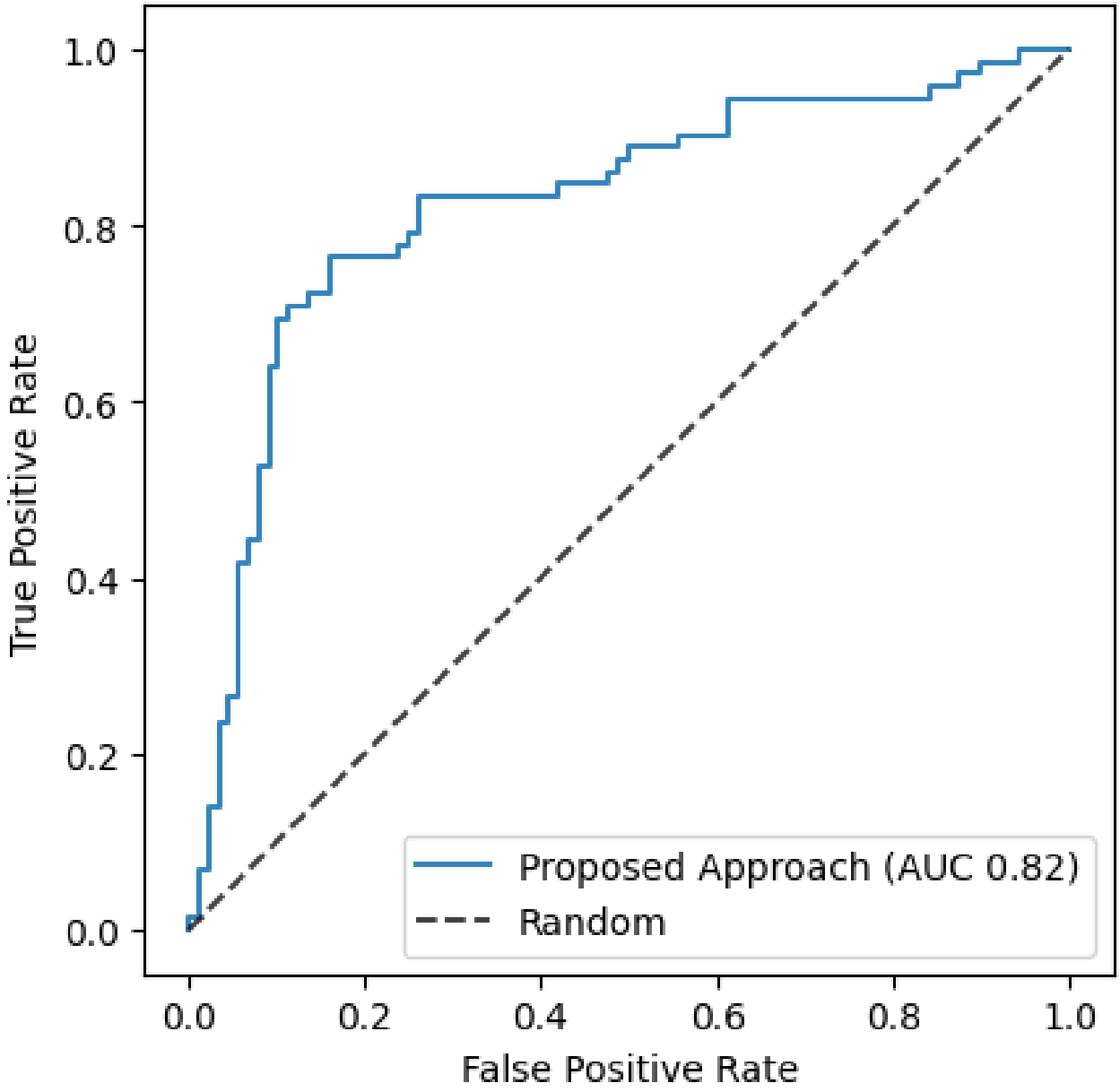
The model was evaluated on 160 subjects using leave-one-out verification. When evaluated without using RFE, including all features in the model, the accuracy was 74%. Including RFE improved performance by reducing overfitting. Using fewer features, the model had an overall accuracy of 79%, with an even performance across both improved and not improved classes. The accuracy for subjects that improved (sensitivity) was 76% and for subjects that did not improve (specificity) was 82%. The confusion matrix of the prediction results can be seen in Table 3. On average, the algorithm selected a mean of 88 (SD 13) out of the 245 features. The receiver operating characteristic curve is shown in Figure 3. The AUC was 0.82.

Table . Confusion matrix of the prediction results.

	Predicted improved class	Predicted not improved class	Total actual
Actual improved class	55	17	72
Actual not improved class	16	72	88
Total predicted	71	89	160

XSL•FO
RenderX

Figure 3. The receiver operating characteristic curve. The area under the receiver operating characteristic curve (AUC) is 0.82.



Comparison

Three additional models were evaluated to compare against our chosen approach: AdaBoost, random forest, and linear SVM. To directly compare against the logistic regression model, the same prediction pipeline was used. First, the data were preprocessed, and then each model was trained with RFE to optimize the features. While all features were inputted into the pipeline, each model had different RFE optimizations across the training folds. Default hyperparameters were used for each of the models. Table 4 shows the results for each model. The logistic regression model consistently outperforms the other models across all metrics.

XSL•FO
RenderX

Table . Comparison of the logistic regression model to other models.

Model	Not-improved class accuracy	Improved class accuracy	Accuracy	AUC[a]
Logistic regression	0.82	0.76	0.79	0.82
Linear SVM[b]	0.74	0.67	0.71	0.75
Random forest	0.81	0.35	0.60	0.62
ADABoost	0.67	0.57	0.62	0.61

[a]AUC: area under the receiver operating characteristic curve.

[b]SVM: support vector machine.

Feature Importance

In our study, a varying number of features were selected across 160 training folds, with an average of 88 out of 245 features chosen. Notably, 37 features consistently appeared across all folds. Table 5 displays the mean coefficients from the logistic regression model for these 37 features, indicating their importance in prediction.

XSL•FO
RenderX

Table . Mean coefficients from the logistic regression model for features that appeared across all training folds.

Rank	Feature	Mean coefficient
1	PCS[a] question 1: “I worry all the time about whether the pain will end”	1.685
2	Body locations: Legs	1.440
3	PROMIS PI[b] question 3: “How much did pain interfere with your ability to participate in social activities?”	1.437
4	PROMIS PI question 5: “How much did pain interfere with the things you usually do for fun?”	1.286
5	PROMIS PI question 1: “How much did pain interfere with your day-to-day activities?”	1.285
6	Meaningful activities: Exercised	1.253
7	Aggravating factors: Stress	−1.252
8	PCS question 2: “I feel I can’t go on”	−1.123
9	NRS[c] pain question 3: “Please rate your pain by marking the box beside the number that tells how much pain you have right now”	−1.108
10	NRS pain score: Right now	−1.108
11	Effective factors: Massage	1.040
12	Ineffective factors: Talking to someone	1.027
13	Meaningful activities: “Connected with supportive people online or through text”	−1.000
14	Pain trend	−0.994
15	Number of conditions (Categories)	0.983
16	Locations: Neck	−0.979
17	PCS question 12: “There’s nothing I can do to reduce the intensity of the pain”	0.978
18	Locations: Head (Right)	−0.977
19	PHQ-9[d] Question 7: “Trouble concentrating on things, such as reading the newspaper or watching television”	−0.892
20	Locations: Joints	0.891
21	Environment: Home	0.881
22	Medications: Tricyclic antidepressants	−0.880
23	GAD-7[e] question 4: “Trouble relaxing”	−0.860
24	PCS question 5: “I feel I can’t stand it anymore”	−0.825
25	Symptoms: Insomnia	−0.825
26	Meaningful activities: Errands outside the home	−0.815
27	Pain characteristic: Custom entry	0.790
28	Height	0.789
29	Percent of completed descriptor elements	0.772
30	Mean time of day of pain record entry	0.746
31	Effective factors: Rest	0.736
32	Medications: Acetaminophen	−0.714
33	Conditions: Back pain	0.713
34	Environment: Work	−0.665

XSL•FO
RenderX

Rank	Feature	Mean coefficient
35	Effective factors: Ice	0.660
36	PROMIS PI score: Raw score	0.476
37	Symptoms: Dizziness	−0.41

[a]PCS: Pain Catastrophizing Scale.

[b]PROMIS PI: PROMIS Pain Interference 8a v1.0.

[c]NRS: Numeric Rating Scale.

[d]PHQ-9: Patient, Health Questionnaire-9.

[e]GAD-7: General Anxiety Disorder-7.

Questionnaire Comparison

While this work was focused on optimizing a model for predicting improved scores on the PROMIS PI measure, we repeated the same algorithm for each of the questionnaires included in the dataset. As demonstrated in Table 6, responses on PROMIS PI had the best performance with an AUC of 0.81. Responses on GAD-7 and PHQ-9 showed some moderate ability for prediction, with AUCs of 0.64 and 0.74, respectively. Responses on GAD-7, PHQ-9, and PCS demonstrated lower rates of improvement and produced a more imbalanced dataset, possibly leading to decreased performance by the algorithm. Responses on the NRS for pain severity, on the other hand, indicated a similar percentage of improved MMP users as PROMIS PI. Despite the balanced dataset, the predictive model did not achieve any meaningful results, with an AUC of 0.51, which is nearly equivalent to random chance.

Table . Comparison of the logistic regression model performance on PROMIS Pain Interference questionnaire responses compared with the other questionnaires included in the dataset.

Questionnaire	MCID[a]	Number improved / Total Users, n/N (%)	Accuracy	Class 0	Class 1	Balanced accuracy	AUC[b]
PROMIS PI[c] [22]	2 [37]	72/160 (45%)	0.79	0.82	0.76	0.79	0.82
GAD-7[d] [34]	4 [45]	52/180 (29%)	0.70	0.70	0.71	0.70	0.64
PHQ-9[e] [35]	5 [46]	34/169 (20%)	0.72	0.76	0.59	0.67	0.74
PCS[f] [33]	38% [47]	47/173 (27%)	0.6	0.68	0.38	0.53	0.57
NRS[g] [9]	1 [48]	89/173 (46%)	0.53	0.55	0.51	0.53	0.51

[a]MCID: minimal clinically important difference.

[b]AUC: area under the receiver operating characteristic curve.

[c]PROMIS PI: PROMIS Pain Interference 8a v1.0.

[d]GAD-7: General Anxiety Disorder-7.

[e]PHQ-9: Patient, Health Questionnaire-9.

[f]PCS: Pain Catastrophizing Scale.

[g]NRS: Numeric Rating Scale.

Discussion

Principal Findings

This study examined whether a machine learning model could predict clinical outcomes related to pain in a population of TPS clinic patients who used the MMP digital health solution to track symptoms and answer clinic questionnaires. Using MMP app data entered by patients for 30 days, a linear regression model predicted clinically significant improvement in pain interference measured by the PROMIS PI questionnaire with 79% accuracy. The model showed balanced accuracy between improved and not improved classes with a sensitivity of 0.76 and specificity of 0.82.

Analysis of the features used in the model showed that all MMP app data, not just questionnaire responses, were relevant in predicting patient improvement. This finding underscores the critical role of all types of data in the algorithm's efficacy. Features like exercise showed a positive correlation with improved outcomes, while stress was negatively correlated, aligning with clinical expectations. However, many top-ranked features lacked such clinical clarity. This is not unexpected as the machine learning model integrates all features collectively to make predictions, preventing the isolation of individual feature impacts. Some features might be correlated with other variables that influence improvement, and they should not be interpreted independently in this type of prediction approach. Despite these complexities, our results affirm the value of leveraging extensive datasets, allowing the model to identify

XSL•FO
RenderX

influential factors beyond traditional assumptions and providing a robust statistical foundation to determine the factors that predict improvement.

Predicting the development and progression of a chronic pain condition has important clinical implications. Currently, clinicians rely on known risk factors implicated in the development and progression of chronic pain conditions [49-55] to inform clinical decision-making regarding treatment and pain management. However, the individualized nature of chronic pain and the interacting contribution of physical, emotional, and social factors impose considerable challenges in accurately predicting patient outcomes [4,5]. Recent efforts have applied machine learning to large datasets to demonstrate that individualized pain risk scores can be determined from a set of biopsychosocial factors [5]. However, applying this approach in the clinical context is limited by the availability of relevant data for a specific patient population. This study bridges this gap by demonstrating that a pain-tracking app can be used in a real-world clinical setting to gather relevant data in a short period of time and effectively predict clinically significant outcomes related to pain. Information from the MMP app can be used by clinicians alongside traditional approaches to patient assessment to more effectively guide critical decision-making around medication management, such as tapering opioids, and allocation of finite clinic resources to patients with the greatest need. It is important to note that the approach presented here is not intended to identify specific predictors of improvement, but rather to help clinicians evaluate which patients are more or less likely to improve so they can prioritize health care resources accordingly.

Limitations and Future Work

The findings presented here are limited to a small sample of a specific patient population who selected to use the MMP app, which may have contributed to a degree of selection bias in the dataset used for prediction modeling. Additionally, the dataset had many missing data points. Missing data frequently occur in real-world self-reported data sources, such as the one used here [56]. To replace missing values in our dataset, we relied on mean imputation. However, it is important to note that the missing data in the current dataset and the mean imputation approach may have contributed to unrecognized bias in the prediction model and affected the study outcome. Finally, only one clinical outcome is considered in the prediction model and further work is needed to identify how other clinically relevant outcomes can be incorporated into a more comprehensive prediction tool. Further refinement is also needed to increase the accuracy of the prediction model. The next steps in this ongoing work focus on integrating additional data from electronic patient records and facilitating greater engagement from patients with the MMP app. The current real-world use of the app was sufficient to achieve useful predictive insights, despite some caveats in their interpretation. Additional efforts to facilitate user engagement as well as data completion and integration will provide a richer dataset for the prediction algorithm to help improve its predictive capacity.

Conclusion

This study builds on a growing body of work showing the capacity of pain apps like MMP to not only provide retrospective insights on symptom trends, but also serve as a clinical outcome prediction tool. Effectively predicting the progression of pain has the potential to improve clinical decision-making and personalized prevention and treatment of chronic pain. The findings of this study demonstrate that existing digital solutions like the MMP app offer a feasible approach to integrating patients' self-tracking and clinical data in a machine-learning algorithm to develop accurate prediction models that can be used in a real-world clinical setting.

Acknowledgments

JS is supported by Mitacs and the MedTech Talent Accelerator. JK was supported by a Tier 1 Canadian Institutes of Health Research Canada Research Chair in Health Psychology at York University. HC is supported by a Merit award from the University of Toronto, Department of Anesthesia.

Data Availability

The datasets generated or analyzed during this study are not publicly available in accordance with Managing Life's Privacy Policy. Managing Life limits data access to its academic collaborators who have executed a data licensing agreement and undergone the company's security and privacy training.

Authors' Contributions

JS, TJ, JK, HC, and QAR conceptualized the overall study design and methodology. JS, TJ, HL-R, and QAR contributed to data curation and formal data analysis. JS and AML wrote the original draft of the manuscript. All authors reviewed, edited, and approved the final manuscript for submission.

Conflicts of Interest

TJ is the founder and CEO of ManagingLife, Inc. JS is an independent contractor for ManagingLife. JK and HC are unpaid members of the ManagingLife Advisory Board, providing guidance on the product and the company's research initiatives. All other authors declare no conflicts of interest.

XSL•FO
RenderX

Multimedia Appendix 1
Clinic questionnaires.
[DOCX File, 24 KB - medinform_v13i1e67178_app1.docx]

References

1. Cohen SP, Vase L, Hooten WM. Chronic pain: an update on burden, best practices, and new advances. Lancet 2021 May 29;397(10289):2082-2097. [doi: 10.1016/S0140-6736(21)00393-7] [Medline: 34062143]
2. Treede RD, Rief W, Barke A, et al. Chronic PAIN as a symptom or a disease: the IASP classification of chronic PAIN for the International Classification of Diseases (ICD-11). PAIN 2019 Jan;160(1):19-27. [doi: 10.1097/j.pain.0000000000001384] [Medline: 30586067]
3. Wideman TH, Edwards RR, Walton DM, Martel MO, Hudon A, Seminowicz DA. The multimodal assessment model of pain. Clin J Pain 2019;35(3):212-221. [doi: 10.1097/AJP.0000000000000670]
4. Fillingim RB. Individual differences in pain: understanding the mosaic that makes pain personal. PAIN 2017 Apr;158 Suppl 1(Suppl 1):S11-S18. [doi: 10.1097/j.pain.0000000000000775] [Medline: 27902569]
5. Tanguay-Sabourin C, Fillingim M, Guglietti GV, et al. A prognostic risk score for development and spread of chronic pain. Nat Med 2023 Jul;29(7):1821-1831. [doi: 10.1038/s41591-023-02430-4] [Medline: 37414898]
6. Katz J, Pagé MG, Weinrib A, Clarke H. Identification of risk and protective factors in the transition from acute to chronic post surgical pain. In: Clinical Pain Management: John Wiley & Sons, Ltd; 2022:50-59. [doi: 10.1002/9781119701170]
7. Edwards RR, Dworkin RH, Sullivan MD, Turk DC, Wasan AD. The role of psychosocial processes in the development and maintenance of chronic pain. J Pain 2016 Sep;17(9 Suppl):T70-T92. [doi: 10.1016/j.jpain.2016.01.001] [Medline: 27586832]
8. Fillingim RB, Loeser JD, Baron R, Edwards RR. Assessment of chronic pain: domains, methods, and mechanisms. J Pain 2016 Sep;17(9 Suppl):T10-T20. [doi: 10.1016/j.jpain.2015.08.010] [Medline: 27586827]
9. Breivik H, Borchgrevink PC, Allen SM, et al. Assessment of pain. Br J Anaesth 2008 Jul;101(1):17-24. [doi: 10.1093/bja/aen103] [Medline: 18487245]
10. Lomborg S, Frandsen K. Self-tracking as communication. Information, Communication & Society 2016 Jul 2;19(7):1015-1027. [doi: 10.1080/1369118X.2015.1067710]
11. Feng S, Mäntymäki M, Dhir A, Salmela H. How self-tracking and the quantified self promote health and well-being: systematic review. J Med Internet Res 2021 Sep 21;23(9):e25171. [doi: 10.2196/25171] [Medline: 34546176]
12. Janevic MR, Murnane E, Fillingim RB, Kerns RD, Reid MC. Mapping the design space of technology-based solutions for better chronic pain care: introducing the pain tech landscape. Psychosom Med 2023 Sep 1;85(7):612-618. [doi: 10.1097/PSY.0000000000001200] [Medline: 37010232]
13. Weinrib A, Azam MA, Latman VV, Janmohamed T, Clarke H, Katz J. Manage my pain: a patient-driven mobile platform to prevent and manage chronic postsurgical pain. In: Novel Applications of Virtual Communities in Healthcare Settings: IGI Global; 2018:93-126. [doi: 10.4018/978-1-5225-2958-3.ch004]
14. Schroeder J, Chung CF, Epstein DA, et al. Examining self-tracking by people with migraine: goals, needs, and opportunities in a chronic health condition. 2018 Presented at: DIS '18: Proceedings of the 2018 Designing Interactive Systems Conference; Jun 9-13, 2018; Hong Kong China p. 135-148. [doi: 10.1145/3196709.3196738]
15. Katz J, Weinrib AZ, Clarke H. Chronic postsurgical pain: from risk factor identification to multidisciplinary management at the Toronto General Hospital Transitional Pain Service. Can J Pain 2019;3(2):49-58. [doi: 10.1080/24740527.2019.1574537] [Medline: 35005419]
16. Katz J, Weinrib A, Fashler SR, et al. The Toronto General Hospital Transitional Pain Service: development and implementation of a multidisciplinary program to prevent chronic postsurgical pain. J Pain Res 2015;8:695-702. [doi: 10.2147/JPR.S91924] [Medline: 26508886]
17. Clarke H, Azargive S, Montbriand J, et al. Opioid weaning and pain management in postsurgical patients at the Toronto General Hospital Transitional Pain Service. Can J Pain 2018;2(1):236-247. [doi: 10.1080/24740527.2018.1501669] [Medline: 35005382]
18. Slepian PM, Peng M, Janmohamed T, et al. Engagement with Manage My Pain mobile health application among patients at the Transitional Pain Service. Digit HEALTH 2020;6. [doi: 10.1177/2055207620962297] [Medline: 33117557]
19. Bhatia A, Kara J, Janmohamed T, et al. User engagement and clinical impact of the Manage My Pain app in patients with chronic pain: a real-world, multi-site trial. JMIR Mhealth Uhealth 2021 Mar 4;9(3):e26528. [doi: 10.2196/26528] [Medline: 33661130]
20. Rahman QA, Janmohamed T, Pirbaglou M, et al. Defining and predicting pain volatility in users of the Manage My Pain app: analysis using data mining and machine learning methods. J Med Internet Res 2018 Nov 15;20(11):e12001. [doi: 10.2196/12001] [Medline: 30442636]
21. Rahman QA, Janmohamed T, Clarke H, Ritvo P, Heffernan J, Katz J. Interpretability and class imbalance in prediction models for pain volatility in Manage My Pain app users: analysis using feature selection and majority voting methods. JMIR Med Inform 2019 Nov 20;7(4):e15601. [doi: 10.2196/15601] [Medline: 31746764]

XSL•FO
RenderX

22. Amtmann D, Cook KF, Jensen MP, et al. Development of a PROMIS item bank to measure pain interference. PAIN 2010 Jul;150(1):173-182. [doi: 10.1016/j.pain.2010.04.025] [Medline: 20554116]
23. Jensen MP, Tomé-Pires C, de la Vega R, Galán S, Solé E, Miró J. What determines whether a pain is rated as mild, moderate, or severe? the importance of pain beliefs and pain interference. Clin J Pain 2017 May;33(5):414-421. [doi: 10.1097/AJP.0000000000000429] [Medline: 27584819]
24. Askew RL, Cook KF, Revicki DA, Cella D, Amtmann D. Evidence from diverse clinical populations supported clinical validity of PROMIS pain interference and pain behavior. J Clin Epidemiol 2016 May;73:103-111. [doi: 10.1016/j.jclinepi.2015.08.035] [Medline: 26931296]
25. Miettinen T, Kautiainen H, Mäntyselkä P, Linton SJ, Kalso E. Pain interference type and level guide the assessment process in chronic pain: categorizing pain patients entering tertiary pain treatment with the brief pain inventory. PLoS ONE 2019;14(8):e0221437. [doi: 10.1371/journal.pone.0221437] [Medline: 31430355]
26. Wilson M. Integrating the concept of pain interference into pain management. Pain Manag Nurs 2014 Jun;15(2):499-505. [doi: 10.1016/j.pmn.2011.06.004] [Medline: 24882027]
27. Pelletier R, Bourbonnais D, Higgins J, Mireault M, Harris PG, Danino MA. Pain interference may be an important link between pain severity, impairment, and self-reported disability in participants with wrist/hand pain. J Hand Ther 2020;33(4):562-570. [doi: 10.1016/j.jht.2019.06.001] [Medline: 31481341]
28. End user licence agreement. Manage My Pain. URL: https://managemypainapp.com/eula [accessed 2025-01-15]
29. Privacy policy. Manage My Pain. URL: https://managemypainapp.com/privacy-policy [accessed 2025-01-15]
30. Hughes LS, Clark J, Colclough JA, Dale E, McMillan D. Acceptance and commitment therapy (ACT) for chronic pain: a systematic review and meta-analyses. Clin J Pain 2017 Jun;33(6):552-568. [doi: 10.1097/AJP.0000000000000425] [Medline: 27479642]
31. Ma TW, Yuen ASK, Yang Z. The efficacy of acceptance and commitment therapy for chronic pain: a systematic review and meta-analysis. Clin J Pain 2023 Mar 1;39(3):147-157. [doi: 10.1097/AJP.0000000000001096] [Medline: 36827194]
32. Di Renna T, Burke E, Bhatia A, et al. Improving access to chronic pain care with central referral and triage: the 6-year findings from a single-entry model. Can J Pain 2024;8(1):2297561. [doi: 10.1080/24740527.2023.2297561] [Medline: 38562673]
33. Sullivan MJL, Bishop SR, Pivik J. The pain catastrophizing scale: development and validation. Psychol Assess 1995;7(4):524-532. [doi: 10.1037//1040-3590.7.4.524]
34. Spitzer RL, Kroenke K, Williams JBW, Löwe B. A brief measure for assessing generalized anxiety disorder: the GAD-7. Arch Intern Med 2006 May 22;166(10):1092-1097. [doi: 10.1001/archinte.166.10.1092] [Medline: 16717171]
35. Kroenke K, Spitzer RL, Williams JBW. The PHQ-9: validity of a brief depression severity measure. J Gen Intern Med 2001 Sep;16(9):606-613. [doi: 10.1046/j.1525-1497.2001.016009606.x] [Medline: 11556941]
36. Jaeschke R, Singer J, Guyatt GH. Measurement of health status. ascertaining the minimal clinically important difference. Control Clin Trials 1989 Dec;10(4):407-415. [doi: 10.1016/0197-2456(89)90005-6] [Medline: 2691207]
37. Chen CX, Kroenke K, Stump TE, et al. Estimating minimally important differences for the PROMIS pain interference scales: results from 3 randomized clinical trials. Pain 2018 Apr;159(4):775-782. [doi: 10.1097/j.pain.0000000000001121] [Medline: 29200181]
38. Hosmer Jr. DW, Lemeshow S, Sturdivant RX. Applied Logistic Regression: John Wiley & Sons, Ltd; 2013. [doi: 10.1002/9781118548387.ch1]
39. Pedregosa F, Varoquaux G, Gramfort A, et al. Scikit-learn: machine learning in Python. J Mach Learn Res 2011 Nov 1;12:2825-2830.
40. Fan RE, Chang KW, Hsieh CJ, Wang XR, Lin CJ. LIBLINEAR: a library for large linear classification. J Mach Learn Res 2008 Jun 1;9:1871-1874.
41. Guyon I, Weston J, Barnhill S, Vapnik V. Gene selection for cancer classification using support vector machines. Mach Learn 2002;46(1/3):389-422. [doi: 10.1023/A:1012487302797]
42. Freund Y, Schapire RE. A decision-theoretic generalization of on-line learning and an application to boosting. J Comput Syst Sci 1997 Aug;55(1):119-139. [doi: 10.1006/jcss.1997.1504]
43. Breiman L. Random forests. Mach Learn 2001;45(1):5-32. [doi: 10.1023/A:1010933404324]
44. Suthaharan S. Support vector machine. In: Suthaharan S, editor. Machine Learning Models and Algorithms for Big Data Classification: Thinking with Examples for Effective Learning: Springer US; 2016:207-235. [doi: 10.1007/978-1-4899-7641-3_9]
45. Toussaint A, Hüsing P, Gumz A, et al. Sensitivity to change and minimal clinically important difference of the 7-item generalized anxiety disorder questionnaire (GAD-7). J Affect Disord 2020 Mar 15;265:395-401. [doi: 10.1016/j.jad.2020.01.032] [Medline: 32090765]
46. Löwe B, Kroenke K, Herzog W, Gräfe K. Measuring depression outcome with a brief self-report instrument: sensitivity to change of the patient health questionnaire (PHQ-9). J Affect Disord 2004 Jul;81(1):61-66. [doi: 10.1016/S0165-0327(03)00198-8] [Medline: 15183601]

XSL•FO
RenderX

47. Scott W, Wideman TH, Sullivan MJL. Clinically meaningful scores on pain catastrophizing before and after multidisciplinary rehabilitation: a prospective study of individuals with subacute pain after whiplash injury. Clin J Pain 2014 Mar;30(3):183-190. [doi: 10.1097/AJP.0b013e31828eee6c] [Medline: 23552561]
48. Salaffi F, Stancati A, Silvestri CA, Ciapetti A, Grassi W. Minimal clinically important changes in chronic musculoskeletal pain intensity measured on a numerical rating scale. Eur J Pain 2004 Aug;8(4):283-291. [doi: 10.1016/j.ejpain.2003.09.004] [Medline: 15207508]
49. Katz J, Seltzer Z. Transition from acute to chronic postsurgical pain: risk factors and protective factors. Expert Rev Neurother 2009 May;9(5):723-744. [doi: 10.1586/ern.09.20] [Medline: 19402781]
50. Rosenberger DC, Pogatzki-Zahn EM. Chronic post-surgical pain - update on incidence, risk factors and preventive treatment options. BJA Educ 2022 May;22(5):190-196. [doi: 10.1016/j.bjae.2021.11.008] [Medline: 35496645]
51. Hebert SV, Green MA, Mashaw SA, et al. Assessing risk factors and comorbidities in the treatment of chronic pain: a narrative review. Curr Pain Headache Rep 2024 Jun;28(6):525-534. [doi: 10.1007/s11916-024-01249-z] [Medline: 38558165]
52. Chou R, Shekelle P. Will this patient develop persistent disabling low back pain? JAMA 2010 Apr 7;303(13):1295-1302. [doi: 10.1001/jama.2010.344] [Medline: 20371789]
53. Lipton RB, Buse DC, Nahas SJ, et al. Risk factors for migraine disease progression: a narrative review for a patient-centered approach. J Neurol 2023 Dec;270(12):5692-5710. [doi: 10.1007/s00415-023-11880-2] [Medline: 37615752]
54. Stevans JM, Delitto A, Khoja SS, et al. Risk factors associated with transition from acute to chronic low back pain in US patients seeking primary care. JAMA Netw Open 2021 Feb 1;4(2):e2037371. [doi: 10.1001/jamanetworkopen.2020.37371] [Medline: 33591367]
55. van Hecke O, Torrance N, Smith BH. Chronic pain epidemiology - where do lifestyle factors fit in? Br J Pain 2013 Nov;7(4):209-217. [doi: 10.1177/2049463713493264] [Medline: 26516524]
56. Liu F, Panagiotakos D. Real-world data: a brief review of the methods, applications, challenges and opportunities. BMC Med Res Methodol 2022 Nov 5;22(1):287. [doi: 10.1186/s12874-022-01768-6] [Medline: 36335315]

Abbreviations

AUC: area under the receiver operating characteristic curve
GAD-7: Generalized Anxiety Disorder-7 scale
MCID: minimal clinically important difference
MMP: Manage My Pain
NRS: Numeric Rating Scale
PCS: Pain Catastrophizing Scale
PHQ-9: Patient Health Questionnaire-9
PROMIS PI: PROMIS Pain Interference 8a v1.0 scale
RFE: recursive feature elimination
SVM: support vector machine
TGH: Toronto General Hospital
TPS: Transitional Pain Service

Edited by A Coristine; submitted 09.10.24; peer-reviewed by E Ross, R Jamison; revised version received 06.02.25; accepted 17.02.25; published 28.03.25.

Please cite as:
Skoric J, Lomanowska AM, Janmohamed T, Lumsden-Ruegg H, Katz J, Clarke H, Rahman QA
Predicting Clinical Outcomes at the Toronto General Hospital Transitional Pain Service via the Manage My Pain App: Machine Learning Approach
JMIR Med Inform 2025;13:e67178
URL: https://medinform.jmir.org/2025/1/e67178
doi:10.2196/67178

© James Skoric, Anna M Lomanowska, Tahir Janmohamed, Heather Lumsden-Ruegg, Joel Katz, Hance Clarke, Quazi Abidur Rahman. Originally published in JMIR Medical Informatics (https://medinform.jmir.org), 28.3.2025. This is an open-access article distributed under the terms of the Creative Commons Attribution License (https://creativecommons.org/licenses/by/4.0/), which permits unrestricted use, distribution, and reproduction in any medium, provided the original work, first published in JMIR Medical Informatics, is properly cited. The complete bibliographic information, a link to the original publication on https://medinform.jmir.org/, as well as this copyright and license information must be included.

XSL•FO
RenderX

Effect of Uncertainty-Aware AI Models on Pharmacists' Reaction Time and Decision-Making in a Web-Based Mock Medication Verification Task: Randomized Controlled Trial

Corey Lester[1], PharmD, PhD; Brigid Rowell[1], MA; Yifan Zheng[1], PharmD; Zoe Co[1,2], BS; Vincent Marshall[1], MS; Jin Yong Kim[3], BSE; Qiyuan Chen[3], MSE; Raed Kontar[3], PhD; X Jessie Yang[3], PhD

[1]Department of Clinical Pharmacy, College of Pharmacy, University of Michigan, 428 Church Street, Ann Arbor, MI, United States

[2]Department of Learning Health Sciences, University of Michigan School of Medicine, Ann Arbor, MI, United States

[3]Department of Industrial and Operations Engineering, College of Engineering, University of Michigan, Ann Arbor, MI, United States

Corresponding Author:
Corey Lester, PharmD, PhD
Department of Clinical Pharmacy, College of Pharmacy, University of Michigan, 428 Church Street, Ann Arbor, MI, United States

Abstract

Background: Artificial intelligence (AI)–based clinical decision support systems are increasingly used in health care. Uncertainty-aware AI presents the model's confidence in its decision alongside its prediction, whereas black-box AI only provides a prediction. Little is known about how this type of AI affects health care providers' work performance and reaction time.

Objective: This study aimed to determine the effects of black-box and uncertainty-aware AI advice on pharmacist decision-making and reaction time.

Methods: Recruitment emails were sent to pharmacists through professional listservs describing a web-based, crossover, randomized controlled trial. Participants were randomized to the black-box AI or uncertainty-aware AI condition in a 1:1 manner. Participants completed 100 mock verification tasks with AI help and 100 without AI help. The order of no help and AI help was randomized. Participants were exposed to correct and incorrect prescription fills, where the correct decision was to "accept" or "reject," respectively. AI help provided correct (79%) or incorrect (21%) advice. Reaction times, participant decisions, AI advice, and AI help type were recorded for each verification. Likelihood ratio tests compared means across the three categories of AI type for each level of AI correctness.

Results: A total of 30 participants provided complete datasets. An equal number of participants were in each AI condition. Participants' decision-making performance and reaction times differed across the 3 conditions. Accurate AI recommendations resulted in the rejection of the incorrect drug 96.1% and 91.8% of the time for uncertainty-aware AI and black-box AI respectively, compared with 81.2% without AI help. Correctly dispensed medications were accepted at rates of 99.2% with black-box help, 94.1% with uncertainty-aware AI help, and 94.6% without AI help. Uncertainty-aware AI protected against bad AI advice to approve an incorrectly filled medication compared with black-box AI (83.3% vs 76.7%). When the AI recommended rejecting a correctly filled medication, pharmacists without AI help had a higher rate of correctly accepting the medication (94.6%) compared with uncertainty-aware AI help (86.2%) and black-box AI help (81.2%). Uncertainty-aware AI resulted in shorter reaction times than black-box AI and no AI help except in the scenario where "AI rejects the correct drug." Black-box AI did not lead to reduced reaction times compared with pharmacists acting alone.

Conclusions: Pharmacists' performance and reaction times varied by AI type and AI accuracy. Overall, uncertainty-aware AI resulted in faster decision-making and acted as a safeguard against bad AI advice to approve a misfilled medication. Conversely, black-box AI had the longest reaction times, and user performance degraded in the presence of bad AI advice. However, uncertainty-aware AI could result in unnecessary double-checks, but it is preferred over false negative advice, where patients receive the wrong medication. These results highlight the importance of well-designed AI that addresses users' needs, enhances performance, and avoids overreliance on AI.

Trial Registration: ClinicalTrials.gov NCT06795477; https://clinicaltrials.gov/study/NCT06795477

(JMIR Med Inform 2025;13:e64902) doi:10.2196/64902

KEYWORDS

artificial intelligence; AI; human-computer interaction; decision-making; human factors; randomized controlled trial; clinical decision support; prediction; pharmacist; verification; drug development; drug; diagnosis; clinical decision support systems

XSL•FO
RenderX

Introduction

Artificial intelligence (AI) is becoming increasingly prevalent in health care with a wide range of applications such as drug development [1], computer-aided diagnosis and detection [2,3], and clinical decision-making [4]. In particular, AI-based clinical decision support systems (CDSS) can improve medication safety and reduce medication errors. CDSS have been shown to significantly improve medication use and safety in areas such as drug-drug interactions, inappropriate prescribing in older adults and pregnant women, over- and underprescribing, patient counseling [5,6], and patient outcomes (eg, increased medication adherence, lower blood pressure, decreased adverse events) [6].

Recent advances in AI modeling such as deep neural networks have resulted in CDSS that are "black-box" systems; black-box outputs do not provide insight into the model's decision-making process or confidence in its decision [7]. To address the calls for increased transparency in medical AI predictions [8-10], developers have started using uncertainty-aware AI models. Uncertainty-aware AI models present the model's uncertainty, or confidence in its decision, alongside its prediction [11], thus providing a metric for the user to assess the AI's reliability [12]. CDSS reliability is an essential component of human evaluation of AI's trustworthiness which determines the user's acceptability of a technology [7]. While uncertainty-aware AI models increase transparency, additional knowledge is required to interpret the findings which may initially confuse users, leading to increased cognitive effort and degraded decision-making [13].

In addition to transparency, automation bias and aversion must be considered when developing CDSS. Automation bias occurs when users forsake their own expertise in favor of the AI's advice [12,14]. The overreliance caused by automation bias may result in users missing AI-generated errors. Automation aversion causes users to rapidly and persistently lose trust due to an AI-generated error even when the AI's overall performance exceeds humans [12]. Consequently, human errors are missed. An ideal human-centered AI tool should generate clinically valid decisions while fostering trust and avoiding overreliance on AI.

An unexplored avenue for AI-based CDSS is the medication verification process. Medication verification is a vital yet time-consuming visual check to ensure the contents of a filled medication vial match the prescribed medication. Despite pharmacists' careful medication verification process, dispensing errors occur in 1.5% of all prescriptions [15]. Vigilance, or the ability to maintain focus and alertness over long periods, is essential for repeated tasks such as medication verification [16]. Pharmacists must remain alert and cognitively engaged [17]; yet, human vigilance wanes over time. Waning vigilance may be due to fatigue, cognitive overload, or the mundanity of repetitive tasks [18,19]. This is especially concerning in community pharmacies due to the increasing prescription volumes. In 2022, the average community pharmacy dispensed approximately 1215 prescriptions per week [20]. The increase in prescription volumes necessitates additional effort and time from pharmacists who spend between 30% - 48% of their time verifying medications [21,22].

Our team developed an AI prototype to assist pharmacists with the medication verification task, with the goal of reducing dispensing errors, improving patient safety, and decreasing pharmacists' workload. The development of our AI tool using user-centered design principles is described in a study by Zheng et al [23]. The purpose of this paper is to determine the effects of black-box and uncertainty-aware AI advice on pharmacist decision-making and reaction time.

Methods

Overview

We previously developed 2 AI conditions to assist pharmacists with making decisions when dispensing medications. The "black-box" condition does not provide the user with insight into the AI's certainty or predicted probability of a correct decision. The "uncertainty-aware" condition provides the user with an estimate of certainty from the model predictions. We tested these conditions in an experimental study using mock verification tasks with pharmacists.

Trial Design

A crossover, randomized controlled trial was conducted from January 2023 to May 2023 with licensed pharmacists in the United States. Eligible participants were randomized to either the black-box AI or uncertainty-aware AI condition in a 1:1 manner. All participants completed 100 mock verifications with AI help and 100 mock verifications without AI help. The order of no help and AI help was randomized.

Participants

Recruitment emails describing the study were sent to pharmacists through the Minnesota Pharmacy Practice-Based Research Network listserv and the University of Michigan College of Pharmacy Preceptor Network listserv. Interested individuals contacted the study team directly and completed a screening phone call. Eligible participants were licensed pharmacists in the United States who were at least 18 years old and had access to a laptop or desktop computer with a webcam. Pharmacists were excluded if they required assistive technology to use the computer, wore eyeglasses with more than 1 power, had uncorrected cataracts, intraocular implants, glaucoma, or permanently dilated pupils, or had eye movement or alignment abnormalities (eg, lazy eye, strabismus, and nystagmus).

AI Input

We previously obtained a dataset of 432,734 images from a mail-order pharmacy that fills and ships prescriptions to all 50 US states [24]. The data contain 1 year's worth of images of oral medications (ie, tablets and capsules) inside a prescription vial filled by a robot. The images were taken as the final step of an automated system using a robot to count pills into a vial, label the vial, take photos of the vial's contents, and cap the vial. The dataset images are aligned with a National Drug Code (NDC) label and different attributes including color, shape, size in millimeters of pills, manufacturer, tablet scoring, and imprint. The number of images for each NDC ranges from 3 to 12,105 with a median of 540. There are 12 different colors of medications labeled in these images: white (182,178/432,734;

XSL•FO
RenderX

42.1%), yellow (53,296/432,734; 12.3%), pink (39,241/432,734; 9.1%), orange (30,846/432,734; 7.1%), multi-color (25,442/432,734; 5.9%), green (22,689/432,734; 5.2%), red (22,433/432,734; 5.2%), blue (20,704/432,734; 4.8%), brown (16,260/432,734; 3.8%), purple (13,609/432,734; 3.1%), turquoise (3090/432,734; 0.7%), and gray (2946/432,734; 0.7%). Seven different shapes are identified in the data: round (214,475/432,734;49.6%), oval (144,568/432,734; 33.4%), capsule (69,892/432,734; 16.2%), hexagon-6-sided (1912/432,734; 0.4%), triangle (1226/432,734; 0.3%), trapezoid (464/432,734; 0.1%) and pentagon-five sided (197/432,734; 0.04%).

Interventions

The AI model in our study refers to a Bayesian neural network that predicts the dispensed pills' NDC along with the uncertainty of the predictions. It is realized by applying the random dropout technique [25] to the ResNet-34 [26] convolutional neural network. Rather than simply predicting the probabilities of belonging to a specific NDC, the dropout technique enables the neural network to sample a set of possible predictions which we use to measure the uncertainty of the prediction. In our research, the model generated 50 potential probabilities for every image.

Fill accuracy is a dichotomous variable (correct fill or incorrect fill) determined by comparing the fill image to the reference image (ground truth). Matching fill and reference image pairs are labeled correct fills and mismatched pairs are labeled incorrect fills. This serves as the ground truth for the image pair. AI accuracy (good prediction or bad prediction) is a variable that indicates the AI's accuracy in predicting the fill image's NDC. A "good prediction" means the AI correctly identified the NDC, whereas a "bad prediction" incorrectly predicted the NDC. Good predictions always recommend the correct user action (accept or reject), whereas bad predictions typically result in ill-advised recommendations.

Each AI condition consisted of 100 trials with 76 trials containing correctly filled medications and 24 trials containing misfilled medications. For the correctly filled medications, the AI accurately recommended accepting (AI Accept) in 60 trials and erroneously recommended rejecting (AI Reject) in 16 trials. For the 24 trials containing misfilled medications, the AI accurately recommended AI Reject for 22 trials and erroneously recommended AI Accept for 2 trials. Three of the AI Reject trials contained an incorrect fill coupled with a bad prediction resulting in the correct recommendation (AI Reject). Although the AI's predicted NDC was incorrect (ie, misidentified the fill image NDC), the AI renders the correct advice to reject the misfilled medication.

While the AI model's overall accuracy is 98.46%, it was lowered to 79% for the experiment. Participants' interaction with AI errors is a critical component of the research. Lowering the model's accuracy significantly reduced the number of AI help trials needed to display the requisite number of AI errors. In the no-help condition, 76% of the medications were correctly filled.

The NDCs, the reference images, and the filled images were gathered from the correctly and incorrectly predicted images of the Bayesian neural network model. To eliminate potential confounding variables, each reference NDC was shown no more than twice throughout the experiment. To avoid loss of variation in colors, capsules, and oddly shaped pills while excluding blurry fill images, the team members carefully selected from the model-predicted images. Each image was reviewed for accuracy by comparing a reference image (ground truth) to the fill image.

There were 40 unique NDCs in the incorrect prediction file of the Bayesian neural network model. The NDCs, the reference images, and the images for cases involving bad AI predictions (AI approves the incorrect drug, and AI rejects the correct drug) were gathered from the incorrect prediction file. The NDCs and the reference images for cases involving good AI prediction for the incorrectly filled medication (AI rejects the incorrect drug) were gathered from the incorrect prediction file. The filled images were gathered from the correct prediction file.

The study used Labvanced (Scicovery GmbH), an online, browser-based platform, to conduct the mock verifications. Participants met with a study team member through Zoom (Zoom Communications Inc) before completing the medication verification tasks to ensure technical and environmental requirements were met (eg, working webcam, adequate lighting, and quiet space). After confirming the participant's setup was sufficient, the study team member provided the participant with a link to the experiment and a password. A video presentation explained how to perform the mock medication verification task using the study interface. Participants were informed that the goal of the task was to determine whether an image of a filled medication bottle matched a known reference image. The video presentation also explained the AI help condition to the participant with a tailored explanation based on randomization assignment. The interface displayed an image of a filled medication, a reference image, and prescription information (Figure 1). The task was to compare the "reference image" on the left to the "fill image" on the right to determine whether to accept or reject the dispensed medication. The "reference image" is the ground truth. For half the trials there was AI help on the bottom right of the screen. In the AI help conditions, the interface displayed AI advice as green checkboxes indicating AI matches based on characteristics of the pill (ie, black box), or a histogram with predicted probabilities (ie, uncertainty) and the checkbox figure (Figure 2). The AI advice was created from a ResNet-34 neural network.

XSL•FO
RenderX

Figure 1. An example of the interface.

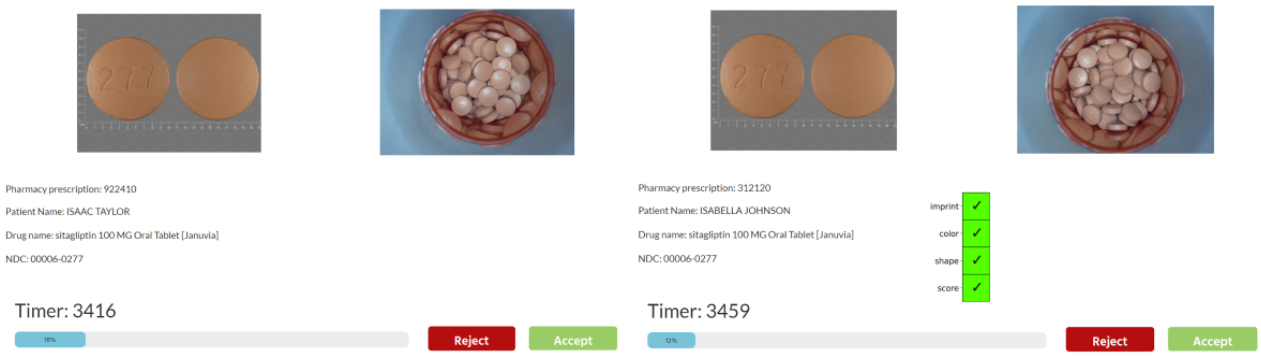
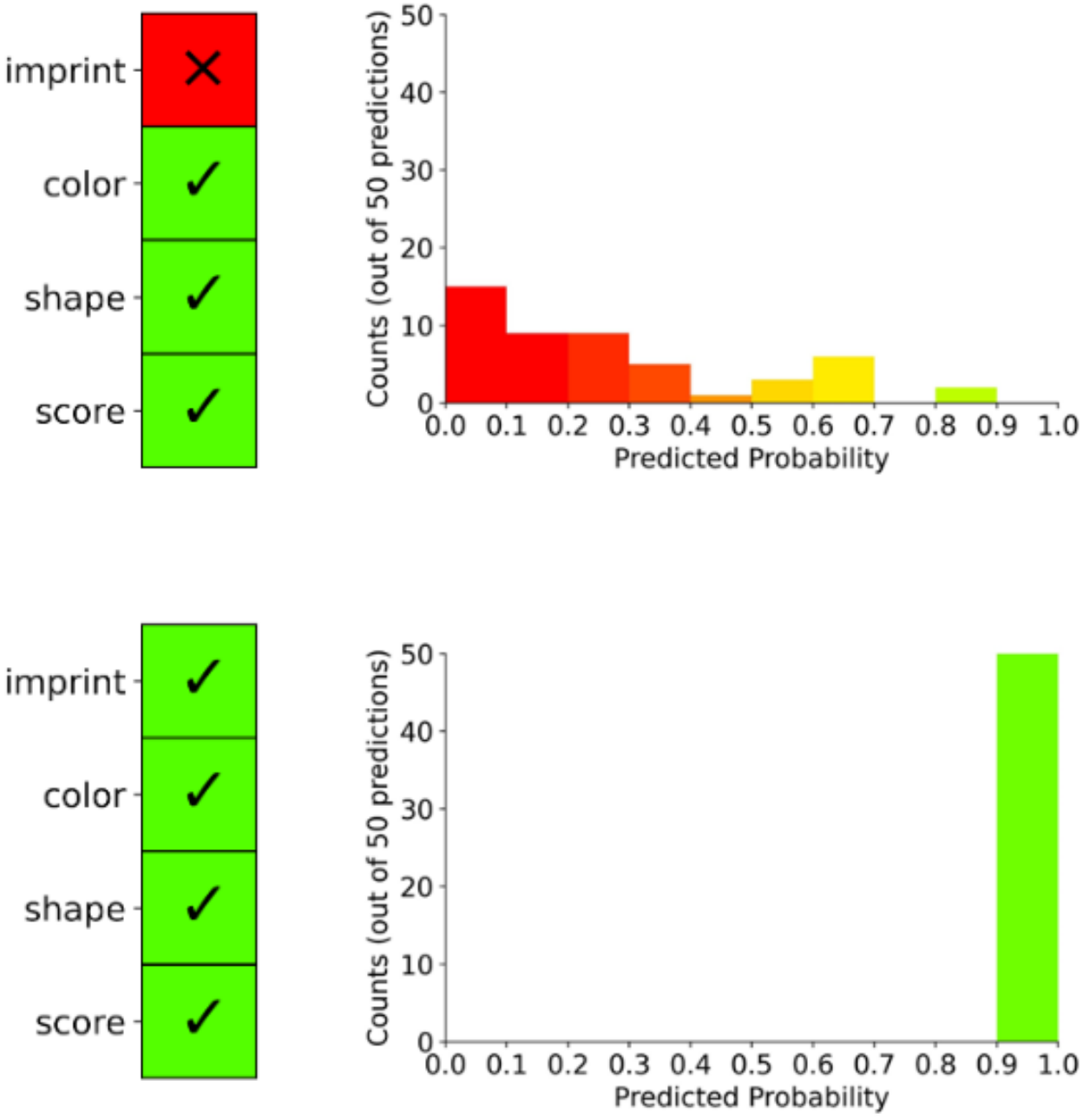


Figure 2. Presentations of 2 artificial intelligence (AI) models. The left-hand graphs are "black-box AI," which displays "yes" or "no" for 4 pill characteristics: imprint, color, shape, and score. The right-hand graphs are "uncertainty-aware AI," which illustrates the predicted probability of each set of predictions summarized in a histogram.



XSL•FO
RenderX

Each participant completed 200 verification tasks, a block of 100 verifications with AI help, and a block of 100 verifications without AI help. The order of the AI help and no AI blocks was randomized for each participant to avoid an order effect, but the order of trials within each block was fixed. The pharmacist's decision to approve or reject the filled medication and the time to decide were recorded for each verification. After each verification in the AI help condition, participants rated how much they trusted the AI advice on a scale of 0 to 100.

Analyses

The outcomes of accuracy and reaction time were analyzed in mixed model generalized linear models with categorical predictors. The generalized linear models formulas were Performance~main.eff+(1|Participant_Nr) for accuracy and Reaction_Time~main.eff+(1|Participant_Nr) for reaction time. Categorical predictors included the AI type (ie, black-box AI, uncertainty-aware AI, or no AI help), and AI correctness versus ground truth, making the 2 × 2 comparison with 4 categories. Likelihood ratio tests compared means across the 3 categories of AI type for each level of AI correctness. The simple effects of uncertainty-aware AI and black-box AI and user performance based on AI type were examined. Statistical comparisons were performed with R statistical software (version 4.2.2, R Foundation for Statistical Computing) [27].

Randomization

A random number generator in R software was used to ensure unbiased study designs. Numbers from 1 to 8 were randomly generated for each participant and participants had an equal probability of being assigned to either the uncertainty-aware AI condition or the black-box AI condition at the start. An equal number of participants were sought for each of the 8 study conditions.

Ethical Considerations

The University of Michigan Institutional Review Board determined this research (HUM00213493) met the criteria for Exemption #3 and was exempt from institutional review board oversight. All participants signed a prospective agreement before any research activities. Participants received a US $150 check for completing the study. All study data have been deidentified. The experimental data were collected in Labvanced using a computer-generated unique 6-digit code.

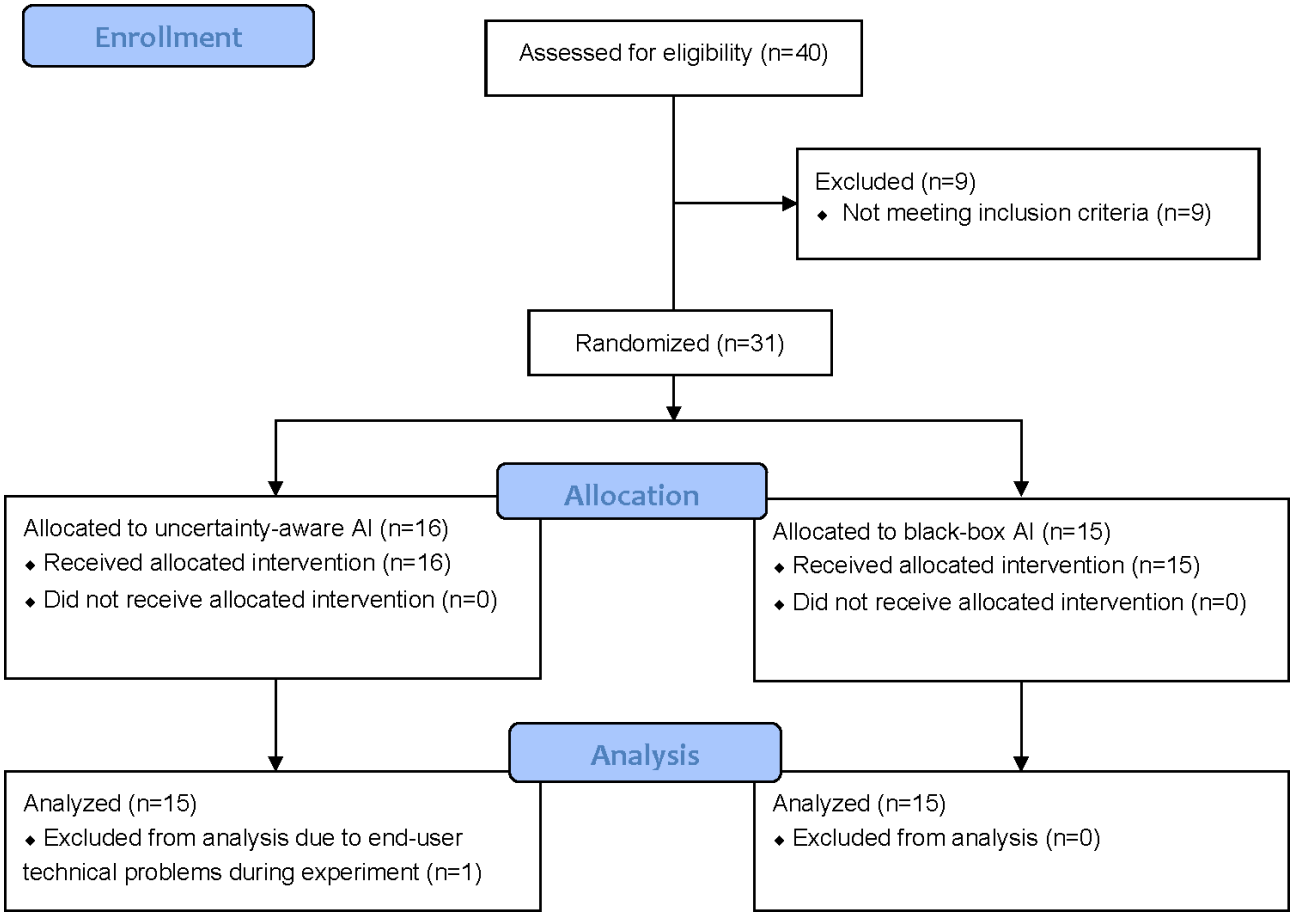
Results

Recruitment

Recruitment began in January 2023 and the final participant visit was in May 2023. The single study visit was conducted remotely using a laptop or desktop computer. The trial ended when the target enrollment was met. In total, 40 pharmacists were assessed for eligibility. After excluding 9 pharmacists who did not meet the inclusion criteria, 31 participants were randomized for allocation in the "black-box AI" condition or the "uncertainty-aware AI" condition. Ultimately, 15 participants in each condition completed the experiment and were included in the subsequent analysis (Figure 3). The median length of the study visit was 59.3 (IRQ 53 - 65.1) minutes.

XSL•FO
RenderX

Figure 3. Participant flow of the randomized controlled trial for effect of AI models on medication dispensing in pharmacists. AI: artificial intelligence.



Study Population

As shown in Table 1, 30 pharmacists were included in the final analysis (black-box AI and uncertainty-aware AI condition). We investigated demographic characteristics for age, sex, race, practice settings, and working years. All the variables were well-balanced according to *P* values ($P>.05$). However, according to the effect sizes, some variables were unbalanced. Age had the largest value (0.68). Sex had the only true “small” effect size of 0.07 SD units. The rest were within the range of 0.07 and 0.42 SD units.

XSL•FO
RenderX

Table . Pharmacist demographics.

Characteristics	Overall (n=30)	Uncertainty-aware (n=15)	Black-box (n=15)	*P* value	Effect size	Interpretation
Age (year), median (IQR)	36 (32.25-45.75)	35.73 (9.68)	43.07 (11.79)	.07	0.68[a]	Medium
Sex (male), n (%)	13 (43.3)	7 (46.7)	6 (40)	>.99	0.07	Small
Ethnicity (non-Hispanic or Latino), n (%)	28 (93.3)	15 (100)	13 (86.7)	.46	0.27	Medium
Race, n (%)				.55	0.2	Small
Asian	5 (16.7)	3 (20)	2 (13.3)			
More than one race	1 (3.3)	0 (0)	1 (6.7)			
White	24 (80)	12 (80)	12 (80)			
Practice setting, n (%)				.25	0.42	Large
Community pharmacy	15 (50)	6 (40)	9 (60)			
Grocery store/mass merchandise pharmacy	1 (3.3)	1 (6.7)	0 (0)			
Hospital pharmacy	6 (20)	5 (33.3)	1 (6.7)			
Other	7 (23.3)	3 (20)	4 (26.7)			
Specialty pharmacy	1 (3.3)	0 (0)	1 (6.7)			
Years worked (years), n (%)				.34	0.33	Medium
1 - 5	7 (23.3)	4 (26.7)	3 (20)			
6 - 10	7 (23.3)	4 (26.7)	3 (20)			
11 - 20	10 (33.3)	6 (40)	4 (26.7)			
21 or more	6 (20)	1 (6.7)	5 (33.3)			

[a]Effect size: Cohen's *d*, the others are Cohen's omega. Cohen's omega chosen over phi coefficient due to zero cells.

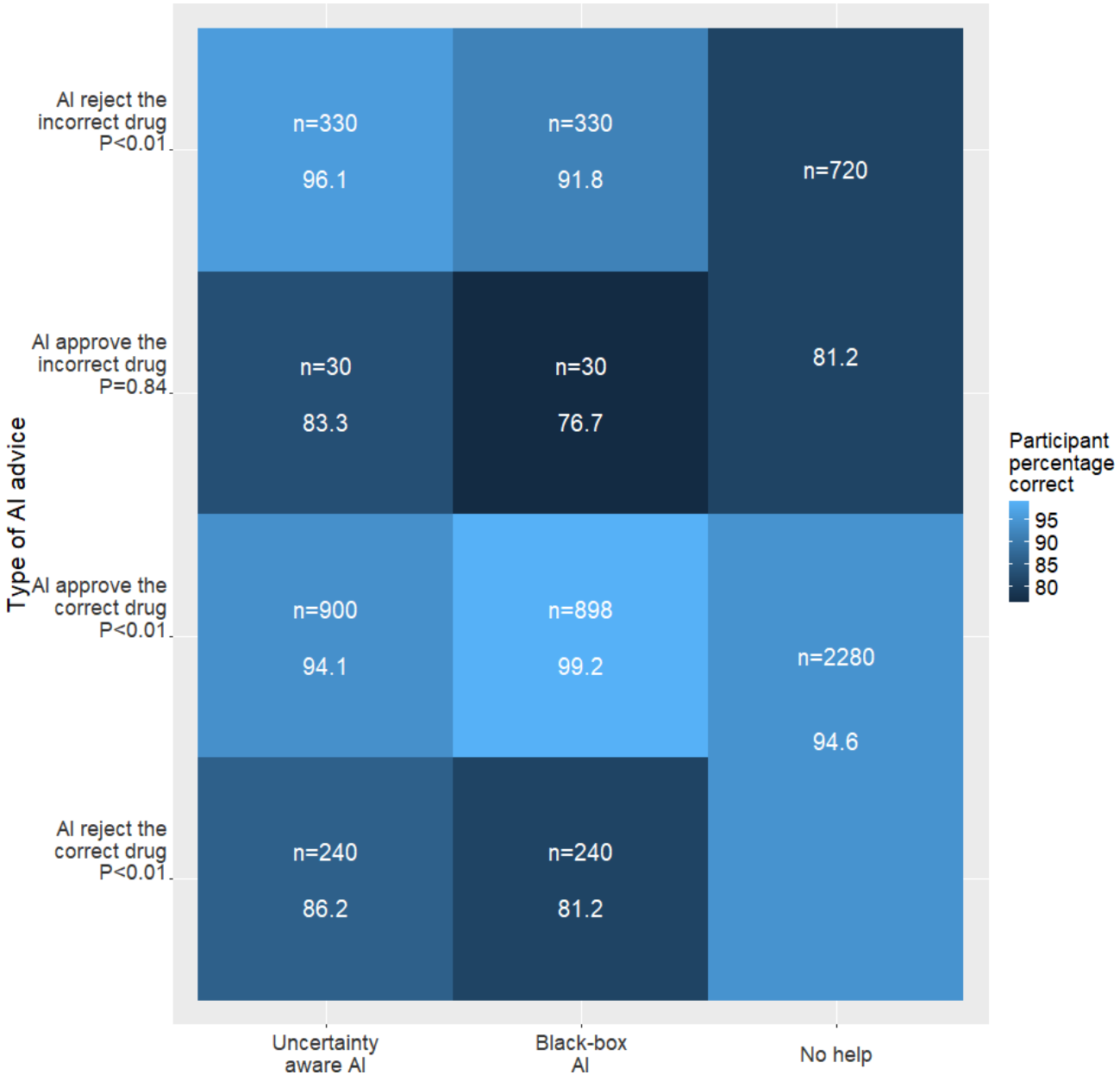
Outcomes

The effects of AI assistance on user trust are reported by Kim et al [28] In summary, pharmacists' trust varied by AI help type and the verification outcome. Overall, uncertainty-aware AI significantly increased pharmacists' trust.

Pharmacists made the correct decision 91.3%, 93.1%, and 94.2% across all trials in the no-help, uncertainty-aware AI, and black-box AI blocks, respectively (χ^2_2=12.5, *P* value=.001). Performance differences emerged across the 3 conditions when examining performance by AI advice type. Figure 4 illustrates pharmacists' performance based on AI accuracy (ie, good advice or bad advice). Similar differences were found for reaction time (Figure 5).

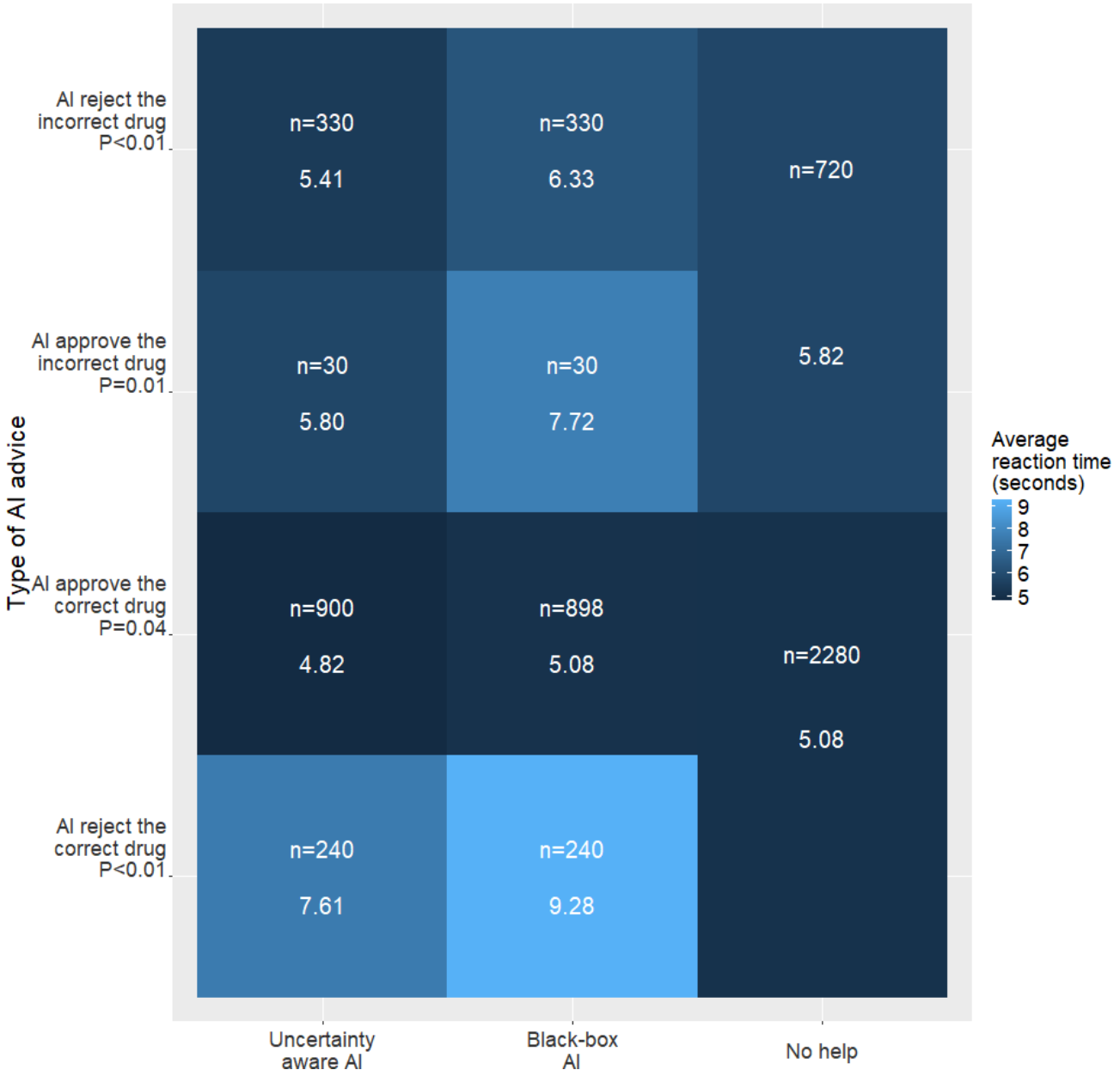
XSL•FO
RenderX

Figure 4. Plot of pharmacists' decision-making performance (% of correct decisions; higher is better). AI: artificial intelligence.



XSL•FO
RenderX

Figure 5. Plot of reaction time (in seconds; higher is worse) of included pharmacists. AI: artificial intelligence.



AI advice was divided into "Good advice" and "Bad advice." For "Good advice," 2 subtypes were identified: "AI Rejects Incorrect Drug" (Figure 4, Row 1) and "AI Approves Correct Drug" (Figure 4, row 3). In the first subtype, pharmacists rejected the incorrect drug 96.1% and 91.8% of the time for uncertainty-aware AI and black-box AI respectively, compared with no AI help (81.2%). When the AI suggested approving the correct drug, performances with black-box AI help surpassed those with uncertainty-aware AI help and no AI help (99.2% vs 94.1% vs 94.6%).

"AI Approves Incorrect Drug" (Figure 4, row 2) and "AI Rejects Correct Drug" (Figure 4, row 4) were classified in the Bad advice category. Despite AI's incorrect predictions, pharmacists demonstrated superior outcomes with uncertainty-aware AI compared with black-box AI help. Uncertainty-aware AI helped protect against AI advice to approve an incorrectly filled medication in contrast with black-box AI (83.3% vs 76.7%). False alerts from AI to reject the correct drug, degraded pharmacists' performance compared with baseline performance without AI help. Accuracy for no AI help, uncertainty-aware AI help, and black-box AI help was 94.6%, 86.2%, and 81.2%, respectively.

Figure 5 displays the reaction time for each condition. Pharmacists assisted by uncertainty-aware AI consistently exhibited shorter reaction times than those aided by black-box AI in the 4 scenarios discussed above (5.41 vs 6.33, 5.80 vs 7.72, 4.82 vs 5.08, 7.61 vs 9.28). Furthermore, the uncertainty-aware AI help condition showed improved reaction times compared with the no AI help condition except in the scenario where "AI rejects the correct drug." Black-box AI did not lead to reduced reaction times in any of the situations as contrasted with no AI help.

XSL•FO
RenderX

Discussion

Principal Findings

In this study, we performed a randomized controlled trial to assess the effects of black box and uncertainty-aware AI tools on pharmacist decision-making and reaction time during the medication verification process. In our assessment of the impact of AI assistance on pharmacists' reaction times, distinct patterns emerged between uncertainty-aware AI and black-box AI. Black-box AI increased reaction times compared with pharmacists acting alone. In contrast, pharmacists receiving uncertainty-aware AI advice had the quickest reaction times except when the AI erroneously recommended rejecting a correctly filled medication.

Research on the effectiveness of AI tools to improve efficiency in health care has shown mixed results. Wysocki et al's [29] research showed that health care providers required significantly less time to make a decision when there was AI-user congruence with explainable AI assistance compared with the black-box AI assistance, which mirrors our results. However, in the face of health care provider-AI disagreement, no significant differences in time to decision were found between explainable AI and black-box AI [29]. A systematic review examining AI tools' effects in safety-critical fields uncovered mixed results in AI's ability to improve pathologists' efficiency [30]. One study in the review showed pathologists with explainable AI assistance completed the task in only 35% of the time required for manual task completion [31], while another study found explainable AI assistance resulted in a significantly longer time to complete the task compared with pathologists working alone [32]. The variability of efficiency underscores the current state of affairs for AI in health care; the field is still in its infancy and more research is needed to understand how to balance transparency and interpretability. In our research with pharmacists, black-box AI's inability to reduce reaction times in any of the scenarios prompts concerns about its practical efficacy in fast-paced pharmacy practice. Future research should examine the design of explainable AI visualizations to facilitate more immediate decision-making when the AI and user disagree.

Ensuring patients receive safe, accurate medication is the bedrock of the pharmacy profession. The pharmacist's role mandates that the 5 rights of medication administration are upheld: right medication, right dose, right route, right patient, and right time [33]. Medication errors can result in significant patient harm, including emergency department visits, hospitalizations, and death [34-36] for which the pharmacist can be held legally responsible [37]. In safety-critical fields like medicine, the benefits of AI tools must be weighed against the risks [30]. In our study, the black-box AI facilitated greater acceptance of a correctly filled medication and thus, a reduction in unnecessary double-checks; however, this benefit is overshadowed by its propensity to misguide pharmacists to accept a potentially harmful misfilled medication. Crucially for this safety-critical field, the uncertainty-aware AI condition facilitated faster and more accurate identification of a misfilled medication than black-box AI or pharmacists acting alone. This demonstrates that uncertainty-aware AI safeguards against dispensing a misfilled medication. Gu et al's [32] study of a human-AI diagnostic tool found pathologists preferred the AI system to err in the direction of false positives due to the harmful outcomes of missed diagnoses and delayed treatment. Similar to the medication verification process, pathologists' reviews are performed quickly and pathologists indicated that the extra review is preferable to a missed diagnosis. Extrapolating these results to our study, uncertainty-aware AI's ability to improve pharmacists' identification of misfilled medications is preferable to the black-box AI help, and the potential workload increase due to unnecessary double-checks is offset by improved patient safety.

The histogram shown in the uncertainty-aware AI advice was developed based on pharmacists' feedback during the user-centered design phase wherein they expressed a desire to see the probability of each predicted NDC to increase the model's transparency [23]. In this case, the histogram may have attuned pharmacists to the idea of the AI advice being fallible and dispensing a wrong medication, whereas this factor was not apparent in the black box scenario. Pharmacists receiving uncertainty-aware advice were more likely to reject correctly and incorrectly filled medication regardless of the AI's advice (accept or reject) suggesting the histogram introduced doubt which caused pharmacists to act more cautiously in order to avoid an incorrect dispense. Previous research has shown ambiguity in decision-making heightens an individual's sensitivity to errors and results in more conservative behavior [38,39]. Pharmacists tend to be risk-averse individuals who dislike ambiguity [40], and when faced with ambiguity are likely to act conservatively (eg, reject a filled medication). In contrast, the black-box AI advice did not induce this same kind of doubt, perhaps leading pharmacists to "go with their gut." Future research should explore more readily interpretable uncertainty visualizations to decrease ambiguity. A systematic review of 24 studies of human-AI collaboration in safety-critical fields found users prefer clean, simple, and easy-to-read visualizations [10]. Alternative ways to present AI uncertainty information to domain experts may balance transparency, uncertainty interpretability, and user performance.

Obtaining second opinions from colleagues is a common health care practice. AI can stand in for colleagues by quickly providing second opinions, but it is critical to communicate any ambiguity or uncertainty in its prediction to foster user trust and allow users to make judgments about when to trust the AI [8]. In interviews with pathologists about an AI tool, pathologists discussed the benefit of knowing their colleagues' experiences, strengths, and weaknesses, thus allowing them to calibrate their responses to a colleague's second opinion [38]. They identified needing a similar level of familiarity with the AI's training, strengths, and weaknesses to successfully incorporate the AI's advice in their decision-making process. Relatedly, previous research has shown that AI errors result in a significant and persistent loss of trust [41]. Explainable AI has been proposed as a solution to increase users' trust by explicitly acknowledging the AI limitations [39]. However, Buçinca et al [42] found explainable AI may contribute to overreliance on AI advice. This contradicts our results from the uncertainty-aware condition; pharmacists with uncertainty-aware AI were more

XSL•FO
RenderX

likely to reject a correctly filled medication when the uncertainty-aware AI suggested accepting it compared with black-box AI and the pharmacist acting alone. Conversely, our results indicate that black-box AI can be over-relied upon, especially false negative errors from the AI. A balance between fostering trust and avoiding overreliance is needed to ensure an optimal human-AI teaming experience.

The timing of AI advice relative to the user's decision may influence the user's performance and trust. Gajos and Mamykina [43] recently examined AI advice timing in 3 conditions: (1) AI recommendation and explanation before making a decision, (2) AI recommendation and explanation after making a decision, and (3) AI explanation only before making a decision. While all 3 conditions led to improved decision accuracy, only the third condition showed improvement in both decision accuracy and learning gain. A 2022 study of AI timing in clinical imaging found veterinary radiologists had lower trust in the AI, lower perceived utility of the AI, and less agreement with the AI, regardless of the AI's correctness, when the advice was presented after their initial clinical decision [44]. Additional research should examine the timing of AI advice on pharmacists' trust and accuracy.

Limitations

The study has several limitations. First, the no help condition used a different image set than the AI help conditions. The same image set was used for both AI help conditions. While the images were randomly selected for both AI help and no help conditions, unanticipated biases in the image selection may exist. Second, the images were presented in a fixed order, which may have unintentionally biased the results. Future research should randomize the presentation of the images across all conditions for all participants to eliminate any inherent bias. Third, the small number of participants from 2 professional pharmacy networks may not be representative of the pharmacy community at large. Future research should be conducted with a broader, more diverse population of pharmacists. Finally, medication verification is only 1 step in the medication dispensing process. Additional research could examine the use of AI tools to support pharmacy staff at all steps of the dispensing process such as order entry, patient directions, and medication count.

Conclusion

The effectiveness of AI assistance on pharmacists' performance and reaction times varied by AI type and AI accuracy. Overall, uncertainty-aware AI resulted in faster decision-making, and black-box AI had the slowest decision-making. Concerningly, black-box AI worsened users' accuracy when the AI provided bad advice, thus increasing the potential for patient harm. Uncertainty-aware AI acted as a safeguard against bad AI advice to approve a misfilled medication, reducing the chance of patient harm. However, pharmacists with uncertainty-aware AI performed worse and had longer reaction times when the AI recommended incorrectly rejecting a correctly filled medication compared with no AI help, leading to unnecessary double-checks. These results reinforce the importance of well-designed AI to meet users' needs to ensure consistent benefits over no AI help.

Acknowledgments

This research was supported by the National Library of Medicine of the National Institutes of Health under award number R01LM013624.

Data Availability

The code used to train the Bayesian model is available at Code Ocean [45].

Authors' Contributions

CL contributed to conceptualization, funding acquisition, investigation, methodology, project administration, software, supervision, validation, writing – original draft, and writing – review & editing. BR handled investigation, project administration, writing – original draft, and writing – review & editing. YZ conducted investigation and writing – review & editing. ZC managed writing – review & editing. VM conducted formal analysis, validation, and visualization. JYK handled data curation, investigation, and validation. QC supervised software, validation, writing – original draft, and writing – review & editing. RK managed conceptualization, funding acquisition, methodology, and supervision. XJY contributed to conceptualization, funding acquisition, methodology, and supervision.

Conflicts of Interest

None declared.

Checklist 1
CONSORT-EHEALTH checklist (V 1.6.1).
[PDF File, 874 KB - medinform_v13i1e64902_app1.pdf]

References

XSL•FO
RenderX

1. Sahu A, Mishra J, Kushwaha N. Artificial intelligence (AI) in drugs and pharmaceuticals. Comb Chem High Throughput Screen 2022;25(11):1818-1837. [doi: 10.2174/1386207325666211207153943] [Medline: 34875986]
2. Sechopoulos I, Teuwen J, Mann R. Artificial intelligence for breast cancer detection in mammography and digital breast tomosynthesis: state of the art. Semin Cancer Biol 2021 Jul;72:214-225. [doi: 10.1016/j.semcancer.2020.06.002] [Medline: 32531273]
3. Laves MH, Ihler S, Ortmaier T, Kahrs LA. Quantifying the uncertainty of deep learning-based computer-aided diagnosis for patient safety. Curr Dir Biomed Eng 2019 Sep 1;5(1):223-226. [doi: 10.1515/cdbme-2019-0057]
4. Khosravi M, Zare Z, Mojtabaeian SM, Izadi R. Artificial intelligence and decision-making in healthcare: a thematic analysis of a systematic review of reviews. Health Serv Res Manag Epidemiol 2024;11:23333928241234863. [doi: 10.1177/23333928241234863] [Medline: 38449840]
5. Curtain C, Peterson GM. Review of computerized clinical decision support in community pharmacy. J Clin Pharm Ther 2014 Aug;39(4):343-348. [doi: 10.1111/jcpt.12168] [Medline: 24806361]
6. Robertson J, Walkom E, Pearson SA, Hains I, Williamsone M, Newby D. The impact of pharmacy computerised clinical decision support on prescribing, clinical and patient outcomes: a systematic review of the literature. Int J Pharm Pract 2010 Apr;18(2):69-87. [Medline: 20441116]
7. von Eschenbach WJ. Transparency and the black box problem: why we do not trust AI. Philos Technol 2021 Dec;34(4):1607-1622. [doi: 10.1007/s13347-021-00477-0]
8. Cai CJ, Winter S, Steiner D, Wilcox L, Terry M. "Hello AI": uncovering the onboarding needs of medical practitioners for human-AI collaborative decision-making. Proc ACM Hum-Comput Interact 2019 Nov 7;3(CSCW):1-24. [doi: 10.1145/3359206]
9. Jussupow E, Spohrer K, Heinzl A, Gawlitza J. Augmenting medical diagnosis decisions? An investigation into physicians' decision-making process with artificial intelligence. Information Systems Research 2021 Sep;32(3):713-735. [doi: 10.1287/isre.2020.0980]
10. Kompa B, Snoek J, Beam AL. Second opinion needed: communicating uncertainty in medical machine learning. NPJ Digit Med 2021 Jan 5;4(1):4. [doi: 10.1038/s41746-020-00367-3] [Medline: 33402680]
11. Begoli E, Bhattacharya T, Kusnezov D. The need for uncertainty quantification in machine-assisted medical decision making. Nat Mach Intell 2019 Jan 20;1(1):20-23. [doi: 10.1038/s42256-018-0004-1]
12. Tomsett R, Preece A, Braines D, et al. Rapid trust calibration through interpretable and uncertainty-aware AI. Patterns (N Y) 2020 Jul 10;1(4):100049. [doi: 10.1016/j.patter.2020.100049] [Medline: 33205113]
13. Prabhudesai S, Yang L, Asthana S, Huan X, Liao QV, Banovic N. Understanding uncertainty: how lay decision-makers perceive and interpret uncertainty in human-AI decision making. Presented at: 28th International Conference on Intelligent User Interfaces; Mar 27-31, 2023; Sydney, NSW, Australia p. 379-396. [doi: 10.1145/3581641.3584033]
14. Goddard K, Roudsari A, Wyatt JC. Automation bias: a systematic review of frequency, effect mediators, and mitigators. J Am Med Inform Assoc 2012;19(1):121-127. [doi: 10.1136/amiajnl-2011-000089] [Medline: 21685142]
15. Campbell PJ, Patel M, Martin JR, et al. Systematic review and meta-analysis of community pharmacy error rates in the USA: 1993–2015. BMJ Open Qual 2018 Oct;7(4):e000193. [doi: 10.1136/bmjoq-2017-000193]
16. Parasuraman R, Mouloua M. Interaction of signal discriminability and task type in vigilance decrement. Percept Psychophys 1987 Jan;41(1):17-22. [doi: 10.3758/bf03208208] [Medline: 3822739]
17. Chui MA, Look KA, Mott DA. The association of subjective workload dimensions on quality of care and pharmacist quality of work life. Res Social Adm Pharm 2014;10(2):328-340. [doi: 10.1016/j.sapharm.2013.05.007] [Medline: 23791360]
18. Warm J, Dember WN, Hancock P. Vigilance and workload in automated systems. In: Automation and Human Performance: Erlbaum; 1996. [doi: 10.1201/9781315137957]
19. Manly T, Robertson IH, Galloway M, Hawkins K. The absent mind: further investigations of sustained attention to response. Neuropsychologia 1999 Jun;37(6):661-670. [doi: 10.1016/s0028-3932(98)00127-4] [Medline: 10390027]
20. NCPA releases 2023 digest report. National Community Pharmacists Association. 2023. URL: https://ncpa.org/newsroom/news-releases/2023/10/15/ncpa-releases-2023-digest-report [accessed 2025-03-26]
21. Karia A, Norman R, Robinson S, et al. Pharmacist's time spent: Space for Pharmacy-based Interventions and Consultation TimE (SPICE)-an observational time and motion study. BMJ Open 2022 Mar 2;12(3):e055597. [doi: 10.1136/bmjopen-2021-055597] [Medline: 35236731]
22. Hohmeier KC, Wheeler J, Heintz K, Gatwood J. Community pharmacist workflow and medication therapy management delegation: an assessment of preferences and barriers. J Am Pharm Assoc (2003) 2020;60(6):e215-e223. [doi: 10.1016/j.japh.2020.07.024] [Medline: 32811750]
23. Zheng Y, Rowell B, Chen Q, et al. Designing human-centered AI to prevent medication dispensing errors: focus group study with pharmacists. JMIR Form Res 2023 Dec 25;7:e51921. [doi: 10.2196/51921] [Medline: 38145475]
24. Lester CA, Li J, Ding Y, Rowell B, Kontar RA. Performance evaluation of a prescription medication image classification model: an observational cohort. NPJ Digit Med 2021 Jul 27;4(1):118. [doi: 10.1038/s41746-021-00483-8] [Medline: 34315995]

XSL•FO
RenderX

25. Gal Y, Ghahramani Z. Dropout as a Bayesian approximation: representing model uncertainty in deep learning. Presented at: 33rd International Conference on Machine Learning; Jun 19-24, 2016; New York City, USA p. 1050-1059. [doi: 10.48550/arXiv.1506.02142]
26. He K, Zhang X, Ren S, Sun J. Deep residual learning for image recognition. 2016 Presented at: 2016 IEEE Conference on Computer Vision and Pattern Recognition (CVPR); Jun 26 to Jul 1, 2016; Las Vegas, NV, USA p. 770-778. [doi: 10.1109/CVPR.2016.90]
27. R: a language and environment for statistical computing. R Foundation for Statistical Computing. 2017. URL: https://www.r-project.org/ [accessed 2025-04-04]
28. Kim JY, Marshall VD, Rowell B, et al. The effects of presenting AI uncertainty information on pharmacists' trust in automated pill recognition technology: exploratory mixed subjects study. JMIR Hum Factors 2025 Feb 11;12:e60273. [doi: 10.2196/60273] [Medline: 39932773]
29. Wysocki O, Davies JK, Vigo M, et al. Assessing the communication gap between AI models and healthcare professionals: explainability, utility and trust in AI-driven clinical decision-making. Artif Intell 2023 Mar;316:103839. [doi: 10.1016/j.artint.2022.103839]
30. Bach TA, Kristiansen JK, Babic A, Jacovi A. Unpacking human-AI interaction in safety-critical industries: a systematic literature review. IEEE Access 2024;12:106385-106414. [doi: 10.1109/ACCESS.2024.3437190]
31. Lindvall M, Lundström C, Löwgren J. Rapid assisted visual search: supporting digital pathologists with imperfect AI. Presented at: 26th International Conference on Intelligent User Interfaces; Apr 14-17, 2021; College Station, TX, USA. [doi: 10.1145/3397481.3450681]
32. Gu H, Liang Y, Xu Y, et al. Improving workflow integration with xPath: design and evaluation of a human-AI diagnosis system in pathology. ACM Trans Comput-Hum Interact 2023 Apr 30;30(2):1-37. [doi: 10.1145/3577011]
33. Pharmacists' impact on patient safety: a joint project of the American Pharmacists Association Academy of Pharmacy Practice and Management and Academy of Pharmaceutical Research and Science. American Pharmacists Association. URL: https://www.pharmacist.com/Portals/0/PDFS/Practice/PharmacistsImpactonPatientSafety_Web.pdf?ver=dYeAzwlN3-PG9eSkMMsV-A%3D%3D [accessed 2025-03-26]
34. Budnitz DS, Pollock DA, Weidenbach KN, Mendelsohn AB, Schroeder TJ, Annest JL. National surveillance of emergency department visits for outpatient adverse drug events. JAMA 2006 Oct 18;296(15):1858-1866. [doi: 10.1001/jama.296.15.1858] [Medline: 17047216]
35. Budnitz DS, Lovegrove MC, Shehab N, Richards CL. Emergency hospitalizations for adverse drug events in older Americans. N Engl J Med 2011 Nov 24;365(21):2002-2012. [doi: 10.1056/NEJMsa1103053] [Medline: 22111719]
36. Tariq RA, Vashisht R, Sinha A, Scherbak Y. Medication Dispensing Errors and Prevention: StatPearls; 2021. [Medline: 30085607]
37. Pharmacist professional liability exposure claim report: 3rd edition. CNA, HSPO. URL: https://www.hpso.com/getmedia/261a3590-6368-41e6-857c-f2bf9dbdf6ea/CNA_CLS_PHARM_072823_CF_PROD_SEC [accessed 2025-03-26]
38. Ilut C, Schneider M. Modeling uncertainty as ambiguity: a review. : National Bureau of Economic Research; 2022 Report No.: w29915. [doi: 10.3386/w29915]
39. Ghosh D, Ray MR. Risk, ambiguity, and decision choice: some additional evidence*. Decision Sciences 1997 Jan;28(1):81-104 [FREE Full text] [doi: 10.1111/j.1540-5915.1997.tb01303.x]
40. Rosenthal M, Austin Z, Tsuyuki RT. Are pharmacists the ultimate barrier to pharmacy practice change? Can Pharm J 2010 Jan;143(1):37-42. [doi: 10.3821/1913-701X-143.1.37]
41. Chong L, Zhang G, Goucher-Lambert K, Kotovsky K, Cagan J. Human confidence in artificial intelligence and in themselves: The evolution and impact of confidence on adoption of AI advice. Comput Human Behav 2022 Feb;127:107018. [doi: 10.1016/j.chb.2021.107018]
42. Buçinca Z, Malaya MB, Gajos KZ. To trust or to think: cognitive forcing functions can reduce overreliance on AI in AI-assisted decision-making. Proc ACM Hum-Comput Interact 2021;5:1-21. [doi: 10.1145/3449287]
43. Gajos KZ, Mamykina L. Do people engage cognitively with AI? impact of AI assistance on incidental learning. Presented at: IUI '22; Mar 21-25, 2022; Helsinki, Finland URL: https://dl.acm.org/doi/proceedings/10.1145/3490099 [accessed 2025-04-04] [doi: 10.1145/3490099.3511138]
44. Fogliato R, Chappidi S, Lungren M, et al. Who goes first? Influences of human-ai workflow on decision making in clinical imaging. Presented at: FAccT '22; Jun 21-24, 2022; Seoul, Republic of Korea URL: https://dl.acm.org/doi/proceedings/10.1145/3531146 [accessed 2025-04-04] [doi: 10.1145/3531146.3533193]
45. Chen Q, Al Kontar R, Nouiehed M, Yang XJ, Lester C. Cost-sensitive Adversarial Data Augmentation (CSADA). Code Ocean. 2024. URL: https://codeocean.com/capsule/0288821/tree/v1 [accessed 2025-04-04]

Abbreviations

AI: artificial intelligence
CDSS: clinical decision support systems
NDC: National Drug Code

XSL•FO
RenderX

Edited by J Klann; submitted 30.07.24; peer-reviewed by K Varikara, S Ghanvatkar; revised version received 18.02.25; accepted 07.03.25; published 18.04.25.

Please cite as:
Lester C, Rowell B, Zheng Y, Co Z, Marshall V, Kim JY, Chen Q, Kontar R, Yang XJ
Effect of Uncertainty-Aware AI Models on Pharmacists' Reaction Time and Decision-Making in a Web-Based Mock Medication Verification Task: Randomized Controlled Trial
JMIR Med Inform 2025;13:e64902
URL: https://medinform.jmir.org/2025/1/e64902
doi:10.2196/64902

© Corey Lester, Brigid Rowell, Yifan Zheng, Zoe Co, Vincent Marshall, Jin Yong Kim, Qiyuan Chen, Raed Kontar, X Jessie Yang. Originally published in JMIR Medical Informatics (https://medinform.jmir.org), 18.4.2025. This is an open-access article distributed under the terms of the Creative Commons Attribution License (https://creativecommons.org/licenses/by/4.0/), which permits unrestricted use, distribution, and reproduction in any medium, provided the original work, first published in JMIR Medical Informatics, is properly cited. The complete bibliographic information, a link to the original publication on https://medinform.jmir.org/, as well as this copyright and license information must be included.

XSL•FO
RenderX

Expectations of Intensive Care Physicians Regarding an AI-Based Decision Support System for Weaning From Continuous Renal Replacement Therapy: Predevelopment Survey Study

Benjamin Popoff[1,2], MD, MSc; Sandie Cabon[2], PhD; Marc Cuggia[2], MD, PhD; Guillaume Bouzillé[2], MD, PhD; Thomas Clavier[1,3], MD, PhD

[1]Department of Anesthesiology, Critical Care and Perioperative Medicine, CHU Rouen, 37 Bd Gambetta, Rouen, France

[2]Univ Rennes, CHU Rennes, INSERM, LTSI-UMR 1099, Rennes, France

[3]Normandie Univ, UNIROUEN, INSERM U1096, Rouen, France

Corresponding Author:
Benjamin Popoff, MD, MSc
Department of Anesthesiology, Critical Care and Perioperative Medicine, CHU Rouen, 37 Bd Gambetta, Rouen, France

Abstract

Background: Critically ill patients in intensive care units (ICUs) require continuous monitoring, generating vast amounts of data. Clinical decision support systems (CDSS) leveraging artificial intelligence (AI) technologies have shown promise in improving diagnostic, prognostic, and therapeutic decision-making. However, these models are rarely implemented in clinical practice.

Objective: The aim of this study was to survey ICU physicians to understand their expectations, opinions, and level of knowledge regarding a proposed AI-based CDSS for continuous renal replacement therapy (CRRT) weaning, a clinical decision-making process that is still complex and lacking in guidelines. This will be used to guide the development of an AI-based CDSS on which our team is working to ensure user-centered design and successful integration into clinical practice.

Methods: A prospective cross-sectional survey of French-speaking physicians with clinical activity in intensive care was conducted between December 2023 and April 2024. The questionnaire consisted of 20 questions structured around 4 axes: overview of the problem and current practices concerning weaning from CRRT, opinion on AI-based CDSS, implementation in daily clinical practice, real-life operation and willingness to adopt the CDSS in everyday practice. Statistical analyses included Wilcoxon rank sum tests for quantitative variables and χ^2 or Fisher exact tests for qualitative variables, with multivariate analyses performed using ordinal logistic regression.

Results: A total of 171 complete responses were received. Physicians expressed an interest in a CDSS for CRRT weaning, with 70.2% (120/171) viewing AI-based CDSS favorably. Opinions were split regarding the difficulty of the weaning decision itself, with 46.2% (79/171) disagreeing that it is challenging, while 31.6% (54/171) agreed. However, 66.1% (113/171) of respondents supported the value of an AI-based CDSS to assist them in this decision, with younger physicians showing stronger support (81.8%, 27/33 vs 62.3%; 86/138; *P*=.01). Most respondents (163/171, 95.3%) emphasized the importance of understanding the criteria used by the model to make its predictions.

Conclusions: Our findings highlight an optimistic attitude among ICU physicians toward AI-based CDSS for CRRT weaning, emphasizing the need for transparency, integration into existing workflows, and alignment with clinicians' decision-making processes. Actionable recommendations include incorporating key variables such as urine output and biological parameters, defining probability thresholds for recommendations and ensuring model transparency to facilitate the successful adoption and integration into clinical practice. The methodology of this survey may help the development of further predevelopment studies accompanying AI-based CDSS projects.

(JMIR Med Inform 2025;13:e63709) doi:10.2196/63709

KEYWORDS

clinical decision support system; artificial intelligence; decision support; decision making; clinical decision making; survey study; intensive care physicians; renal replacement therapy; therapeutic; ICU; user-centered design; cross-sectional survey; survey; French; physician; questionnaire; AI tools; user-centered

XSL•FO
RenderX

Introduction

Critically ill patients admitted to intensive care units (ICUs) require continuous monitoring and surveillance of clinical, biological, and imaging parameters. This generates a large amount of data, making effective data exploitation a key challenge [1]. Recent advances in artificial intelligence (AI), particularly machine learning (ML), have facilitated the development of diagnostic, prognostic, and therapeutic decision-making aids known as clinical decision support systems (CDSS). These AI-based CDSS have demonstrated potential across several domains in ICU, including sepsis prediction, early detection of patient deterioration, and management of mechanical ventilation [2-4]. For instance, AI models for sepsis prediction can alert clinicians to septic events hours before clinical signs emerge, enabling timely interventions [5]. Similarly, early warning systems for patient deterioration, have shown promise in improving outcomes through real-time data analysis [2].

Despite these advances, most AI-based CDSS models fail to progress beyond the prototype stage and are rarely deployed into clinical practice, even though their performance is sometimes promising [6]. A recent meta-analysis analyzed publications concerning the use of AI in the ICU: out of the 494 articles studied, the majority were retrospective studies 476 articles (96.4%). In total, 10 articles (10/494, 2%) were clinical studies, of which only 5 (5/494, 1%) were randomized trials with a control arm. In addition, the majority of retrospective studies presented a high risk of bias [3]. In the domain of renal care we also observe this disconnect, where AI algorithms have been developed to predict acute kidney injury (AKI), offering valuable insights into early identification and prognosis [7,8]. AKI, a common condition affecting up to 60% of ICU patients [9], often necessitates renal replacement therapy (RRT) in severe cases. Continuous renal replacement therapy (CRRT) is a specific modality of RRT frequently used in critically ill patients, providing continuous 24-hour support that is well-suited for hemodynamically unstable patients [10].

While significant research has focused on the optimal timing for initiating CRRT [11,12], much less attention has been given to the question of when and how to discontinue this therapy [13]. This represents a critical gap in clinical practice, as premature weaning may lead to the recurrence of renal dysfunction, associated with complications such as fluid overload and electrolyte imbalances necessitating the reintroduction of renal support [14,15]. On the other hand, unnecessary prolongation of therapy can expose patients to greater risks, including catheter-related complications, higher infection rates, unnecessary resource utilization, extended ICU stays and delayed renal recovery [16]. Thus, identifying reliable criteria and developing decision support tools for successful weaning from CRRT is an ongoing and essential area of research.

AI-based CDSS present a compelling solution to this problem. By leveraging ICU data, these tools could provide individualized weaning recommendations and support clinicians in navigating the complex factors that influence this decision. However, to ensure successful adoption, it is crucial to align the development of these tools with end-user expectations and clinical realities. Obstacles to the development of mature AI models in routine ICU care arise at different stages of the CDSS development cycle. In particular in the predevelopment phase, with issues of privacy, representativeness, and complexity of heterogeneous ICU data, and in the postdevelopment phase (real-life deployment), with concerns about interoperability and end-user usability [6,17]. Recent frameworks have been proposed to ensure a rigorous development methodology [18,19]. To overcome the main obstacles during CDSS development and deployment, several of these recommendations suggest focusing on the clinical question to be answered by the model and clinicians' expectations of the AI-based CDSS in production [17]. Involving health care providers at every stage of the development and implementation process (user-centered design) would be a solution to overcome the applicability barriers [20,21]. This study is therefore an application of these frameworks, proposing a predevelopment survey before the creation of an AI-based CDSS in the ICU.

In France, the decision to initiate, adjust settings, and discontinue dialysis, including CRRT, are made exclusively by intensivists, without systematic involvement of nephrologists. National guidelines provide general recommendations for dialysis management but lack standardized protocols for CRRT weaning [22]. Local protocols may be used in some ICUs, but there is no universal codification of weaning practices in France. This variability further underscores the potential value of a CDSS to support intensivists in this complex task. Our team is currently planning to develop an AI-based CDSS for successful weaning from CRRT in the ICU, defined as no reintroduction of renal assistance within seven days of its interruption [14].

The aim of this study was to survey ICU physicians, before the development of a machine learning predictive model for successful weaning from CRRT, to understand their expectations regarding the proposed tool, their opinion of the chosen clinical problem and their level of knowledge, appease and distrust of AI-based CDSS in general. In particular, we sought to gather insights from physicians working in both university and nonuniversity hospital settings, as we hypothesized that their exposure to technological innovations and clinical workflows might differ.

Methods

Study Protocol

A prospective cross-sectional survey study was conducted in France using a declarative survey from December 1, 2023 to April 30, 2024. The survey was hosted on a health data platform using Goupile software [23], and the link was shared to intensive care physicians via the newsletters and social media of the French Society of Anesthesia and Intensive Care (Société Française d'Anesthésie,-Réanimation), the French Intensive Care Society (Société de Réanimation de langue Française), the French College of Nonacademic Hospitals (Collège de Réanimation des hôpitaux Extra-Universitaires de France) and the Association of Private Sector Intensive Care Physicians (Association des Réanimateurs du Secteur Privé). No specific

XSL•FO
RenderX

approach was taken to prevent multiple participation in the survey. This study was reported in accordance with the consensus-based Checklist for Reporting of Survey Studies (CROSS) checklist (Multimedia Appendix 1) [24].

Ethical Considerations

The study was approved by the Ethics and Evaluation Committee for Noninterventional Research of Rouen University Hospital (registration number E2023-61). Participants responded voluntarily after being informed of the purpose of the survey and consenting to the use of their answers. Participation was anonymous and no effort was made to identify individual participants.

Target Population

The target population included all physicians with clinical activity in intensive care, regardless of their medical specialty, including attending physicians, fellows and junior doctors (final-year residents who have completed their medical thesis and are practicing autonomously under guided supervision according to the French medical education). Participants were not necessarily experts in the field of AI or data analysis and did not receive any additional information on the project beyond what was stated in the questionnaire preamble.

Survey Instrument

There is currently no standardized questionnaire for AI-based CDSS predevelopment. This questionnaire was developed by 2 intensive care physicians and a medical informatics expert after consultation with experts in data science and user experience. Several meetings were held to ensure that the questions covered relevant and well-established topics in the field of CRRT and AI-based decision support systems, relying on similar studies from the literature. This iterative process allowed to incorporate feedback and adjusted the questions accordingly, although it was not a formal Delphi process. It was developed from instruments already used in the literature to cover all the main axes of reflection relating to the development of a machine learning-based CDSS [20,25-29]. From this literature review and discussions, we identified 4 main axes that would comprehensively capture the necessary information for the future development and implementation of our CDSS. These 4 axes were developed based on their relevance to the successful deployment of AI-based CDSS in clinical practice (Textbox 1).

Textbox 1. Overview of the key axes explored in the questionnaire.

- Key drivers (Q1-5): This axis focused on the current attitudes and behaviors regarding decision-making and the specific issue of weaning from CRRT. Understanding these factors is crucial for developing a tool that aligns with clinicians' decision-making processes and addresses their primary concerns.
- Acceptability (Q6-10): This axis evaluated the current opinions of ICU physicians on AI-based CDSS. Assessing acceptability helps determine the likelihood of adoption and highlights potential barriers that need to be addressed.
- Implementation (Q11-15): This axis explored the critical aspects of using a potential AI-based CDSS, including preferred methods of integration, interface design, and alert thresholds. Insights from this axis are essential for ensuring that the CDSS can be smoothly incorporated into the clinical workflow.
- Usability (Q16-20): This axis examined the real-life operation of the potential AI-based CDSS and the willingness of physicians to adopt it in their everyday practice. Usability is a critical factor in the long-term success of the CDSS, influencing its sustained use and impact on patient care.

The questionnaire consisted of 20 questions on the topic being studied and 6 demographic questions. The 20 questions consisted of 12 statements, 4 multiple-choices, 3 opens and 1 hierarchical question. Statements were answered on a 5-point Likert scale ranging from 1 (strongly disagree) to 5 (totally agree).

The questions also considered acceptance concepts defined by the Unified Theory of Acceptance and Use of Technology (UTAUT) model [30]. In the context of technology, acceptance was defined as the willingness, intention and internal motivation to use a technology as a result of positive attitudes toward the technology or system [31]. The UTAUT model comprised four main concepts: performance expectancy (user's confidence that using technology will benefit his work performance), effort expectancy (user's beliefs of how easy it is to use the system), social influences (how much the user feels that significant others believe that they should use the technology) and facilitating conditions (user's beliefs on organizational and technical support to use the system).

As a first step, the questionnaire was pretested by a panel of 4 intensive care physicians who were not experts in the field of AI or CDSS. Each participant answered the questions and assessed their comprehensibility on a 5-points Likert scale, suggesting modifications if necessary. The proposed modifications were considered, questions with comprehension problems were reformulated and the questionnaire was returned to the panel for final approval. The finalized version of the questionnaire was sent to survey participants. The detailed questionnaire with the rationale for each question can be found, both in the original French version and translated into English, in Multimedia Appendices 2 and 3.

Statistical Analyses

Values are presented as numbers and percentages (n, %) for qualitative variables, and as median and IQR for quantitative variables. On the web questionnaire, the response to each question was mandatory, in order to obtain a low rate of missing data. Statistical analyses were performed in complete case analysis on fully completed questionnaires [32]. Subgroup analyses were performed, comparing physicians from university and nonuniversity hospitals and comparing senior (attending physicians) and junior physicians (including fellows and junior doctors). It was based on an a priori hypothesis that differences in AI adoption might exist between university and nonuniversity centers, as well as across age categories. University hospitals

XSL•FO
RenderX

were hypothesized to have greater exposure to technological innovations, potentially influencing adoption rates. Similarly, younger physicians were assumed to be more familiar with and open to AI technologies, given their higher exposure to digital tools during training. Bivariate analyses were performed using Wilcoxon rank sum tests for quantitative variables, and χ^2 or Fisher exact tests for qualitative variables.

To control for potential confounding factors, multivariate analyses were performed using ordinal logistic regression models. The variables included in the models were selected based on their clinical relevance and their potential impact on the outcomes of interest. These variables included age, years of ICU experience, medical specialty and workplace setting (university or nonuniversity hospital). The dependent variables corresponded to specific survey questions, allowing us to evaluate the independent effect of each factor on the outcomes while accounting for confounding.

All tests were 2-tailed and interpreted at $P<.05$ significance threshold. Statistical analyses were performed using the R software version 4.1.3 (R Foundation for Statistical Computing).

Results

Respondent Characteristics

A total of 171 complete responses were received during the study period. It is important to note that the precise number of ICU physicians to whom the survey was delivered was not exhaustively documented. The survey was distributed through the newsletters of French intensive care societies and associations, as well as their social media platforms. While the total number of senior physicians working in the ICU in France is challenging to ascertain, an estimate based on a report from the College of Intensive Care Medicine Teachers (Collège des Enseignants de Médecine Intensive Réanimation) in 2021 approximated this figure to be around 2350 senior physicians [33]. Our study also included junior doctors who are not counted in this figure. There are approximately 500 junior doctors training in ICUs annually in France, which means the actual denominator for the survey population would be closer to 2850. Hence, the estimated response rate for the survey is approximately 6.0% (168/2850, considering that 2 respondents were from Belgium and 1 from Switzerland).

The total group had a median age of 39 (IQR 33 - 45) years and a median of 9 (IQR 3 - 14) years of ICU work experience (Table 1). Out of the 171 physicians, most of them had a training in anesthesiology and intensive care (109, 63.7%) and worked in university hospitals (102, 59.6%). The median age of physicians surveyed in university centers was younger (36 years [IQR 32 - 43] versus 42 [IQR 36 - 50]; $P<.001$), with fewer years of experience (5 years [IQR 2 - 12] versus 11 [IQR 6 - 16]; $P<.001$), and more from the anesthesia and intensive care training (81/102, 79.4% vs 28/69, 40.6%; $P<.001$).

XSL•FO
RenderX

Table . Characteristics of survey respondents.

Characteristics	Overall (n=171)	Nonuniversity hospitals (n=69)	University hospitals (n=102)	*P* values
Age, years, median (IQR)[a]	39 (33 - 45)	42 (36 - 50)	36 (32 - 43)	<.001
Years of experience in the ICU[b], median (IQR)	9 (3-14)	11 (6 - 16)	5 (2-12)	<.001
Status, n (%)				.05
Attending	138 (81)	62 (90)	76 (75)	
Fellow	21 (12)	5 (7.2)	16 (16)	
Junior doctor	12 (7)	2 (2.9)	10 (9.8)	
Medical specialty, n (%)				<.001
Anesthesiology and intensive care	109 (64)	28 (41)	81 (79)	
Intensive care medicine	56 (33)	37 (54)	19 (19)	
Emergency medicine	3 (1.8)	2 (2.9)	1 (1.0)	
Cardiology	1 (0.6)	1 (1.4)	0 (0)	
Nephrology	1 (0.6)	0 (0)	1 (1.0)	
Pneumology	1 (0.6)	1 (1.4)	0 (0)	
Hospital type, n (%)				<.001
University hospital	102 (60)	0 (0)	102 (100)	
General hospital	58 (34)	58 (84)	0 (0)	
Private hospital	7 (4.1)	7 (10)	0 (0)	
Nonprofit private hospital	3 (1.8)	3 (4.3)	0 (0)	
Military hospital	1 (0.6)	1 (1.4)	0 (0)	
Country, n (%)				.99
Belgium	2 (1.2)	1 (1.4)	1 (1.0)	
France	168 (98)	68 (99)	100 (98)	
Switzerland	1 (0.6)	0 (0)	1 (1.0)	

[a]IQR: interquartile range.

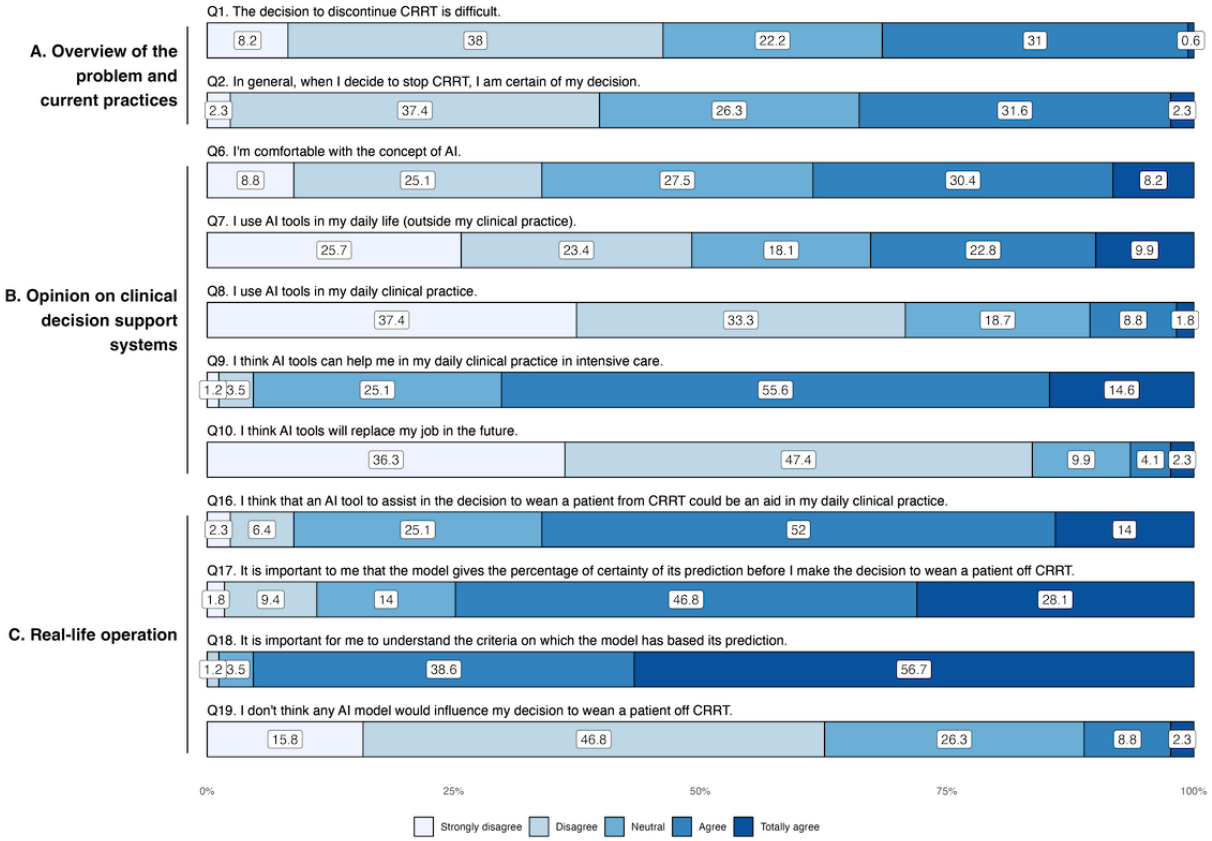
[b]ICU: intensive care unit.

Overview of the Problem and Current Practices (Key Drivers)

Concerning the CRRT-weaning decision, doctors disagreed on the difficulty of decision-making, with 46.2% (79/171) disagreeing or strongly disagreeing with the weaning difficulty proposition (Q1) and 31.6% (54/171) agreeing or totally agreeing (Figure 1A and Table 2). Regarding the certainty of the weaning decision (Q2), responses were mixed, with 33.9% (58/171) of doctors agreeing or totally agreeing with the proposition and 39.7% (68/171) disagreeing or strongly disagreeing. There was no difference between academic and nonacademic physicians (Table 2 and Figure S1 in Multimedia Appendix 4), and between different levels of training (Table S1 and Figure S2 in Multimedia Appendix 4). Physicians had a good idea of the CRRT weaning failure rate (Q3), with a median rate estimated at 33% (IQR 25 - 50), which is close to the rates of 35% to 54% reported in the literature [34,35].

XSL•FO
RenderX

Figure 1. Clinicians' answers to statements questions regarding (A) the overview of the problem and current practices, (B) opinion on clinical decision support systems, and (C) real-life operation, willingness to adopt in everyday practice. Results are presented as percentages. AI: artificial intelligence; CRRT: continuous renal replacement therapy.



XSL•FO
RenderX

Table . Responses to statements regarding the overview of the problem and the opinion on clinical decision support systems on a Likert scale from 1 (strongly disagree) to 5 (totally agree). Results are presented as median (IQR).

Question	Overall (N=171)	Nonuniversity hospitals (n=69)	University hospitals (n=102)	*P* values	Adjusted *P* values[a]
Overview of the problem and current practices					
Q1: The decision to discontinue CRRT[b] is difficult.	3 (2-4)	2 (2-4)	3 (2-4)	.30	.12
Q2: In general, when I decide to stop a CRRT, I am certain of my decision.	3 (2-4)	3 (2-4)	3 (2-4)	.60	.57
Opinion on clinical decision support systems					
Q6: I am comfortable with the concept of artificial intelligence.	3 (2-4)	3 (2-4)	3 (2-4)	.11	.72
Q7: I use AI[c] tools in my daily life (outside my clinical practice).	3 (1-4)	2 (1-4)	3 (2-4)	.22	.06
Q8: I use AI tools in my daily clinical practice.	2 (1-3)	2 (1-2)	2 (1-3)	.07	.80
Q9: I think AI tools can help me in my daily clinical practice in intensive care.	4 (3-4)	4 (3-4)	4 (4-4)	.08	.41
Q10: I think AI tools will replace my job in the future.	2 (1-2)	2 (1-2)	2 (1-2)	.50	.18

[a]Adjustment on age, years of experience and medical specialty.

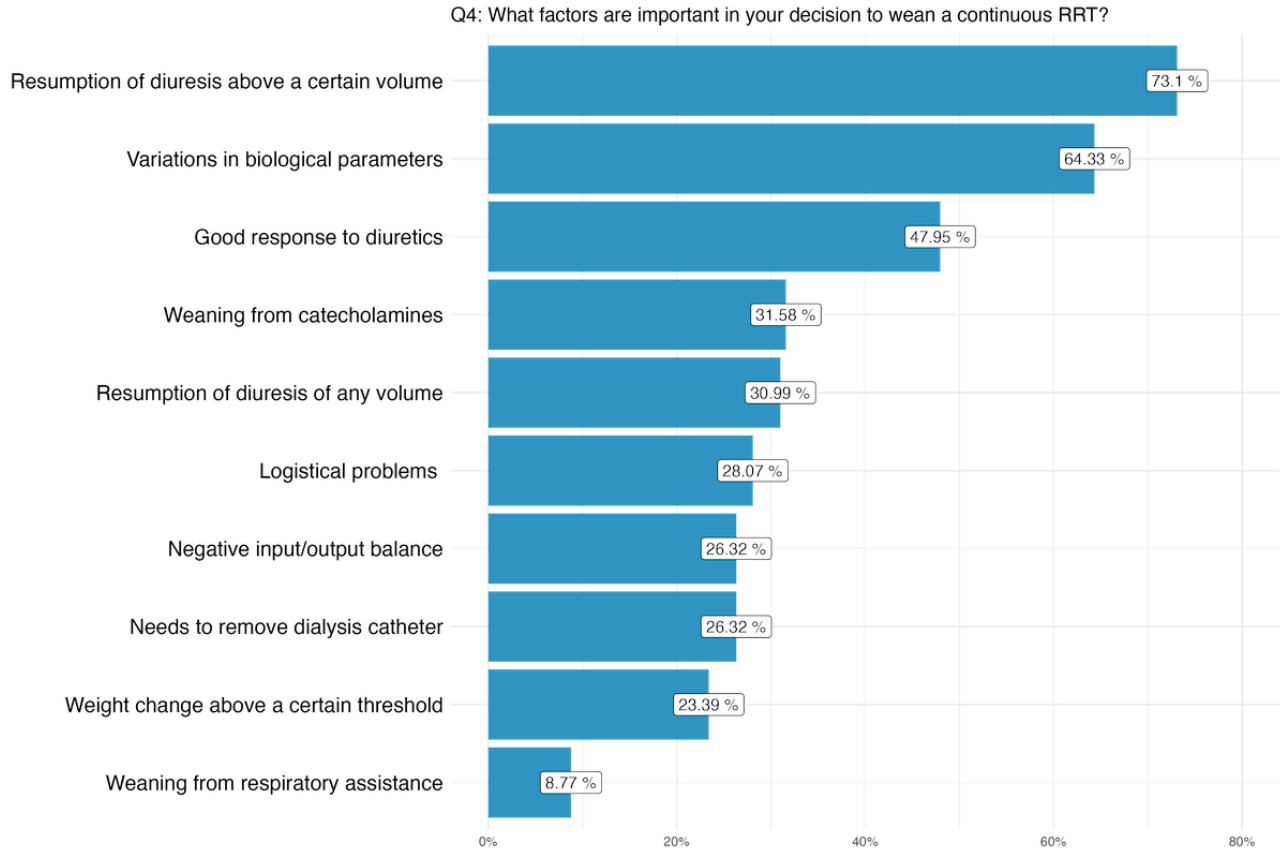
[b]CRRT: continuous renal replacement therapy.

[c]AI: artificial intelligence.

Regarding the variables affecting the decision to wean from CRRT (Q4), respondents mainly chose the resumption of diuresis above a certain volume (125/171, 73.1%), variation in biological settings (110/171, 63.3%) and good response to diuretics (82/171, 47.9%; Figure 2). They were then asked to rank these variables in order of importance from 1 the most important, to 10, the least important. The most important variable for the respondents was the resumption of diuresis above a certain volume, with 33.9% (58/121) of respondents ranking it in first place and 11.7% (20/121) ranking it second. Other variables frequently ranked highly included variations in biological parameters, good response to diuretics, and weaning from catecholamines.

XSL•FO
RenderX

Figure 2. Variables relevant to the clinical decision to wean from continuous renal replacement therapy (percentages of respondents choosing each variable). RRT: renal replacement therapy.



Opinion on Clinical Decision Support Systems (Acceptability)

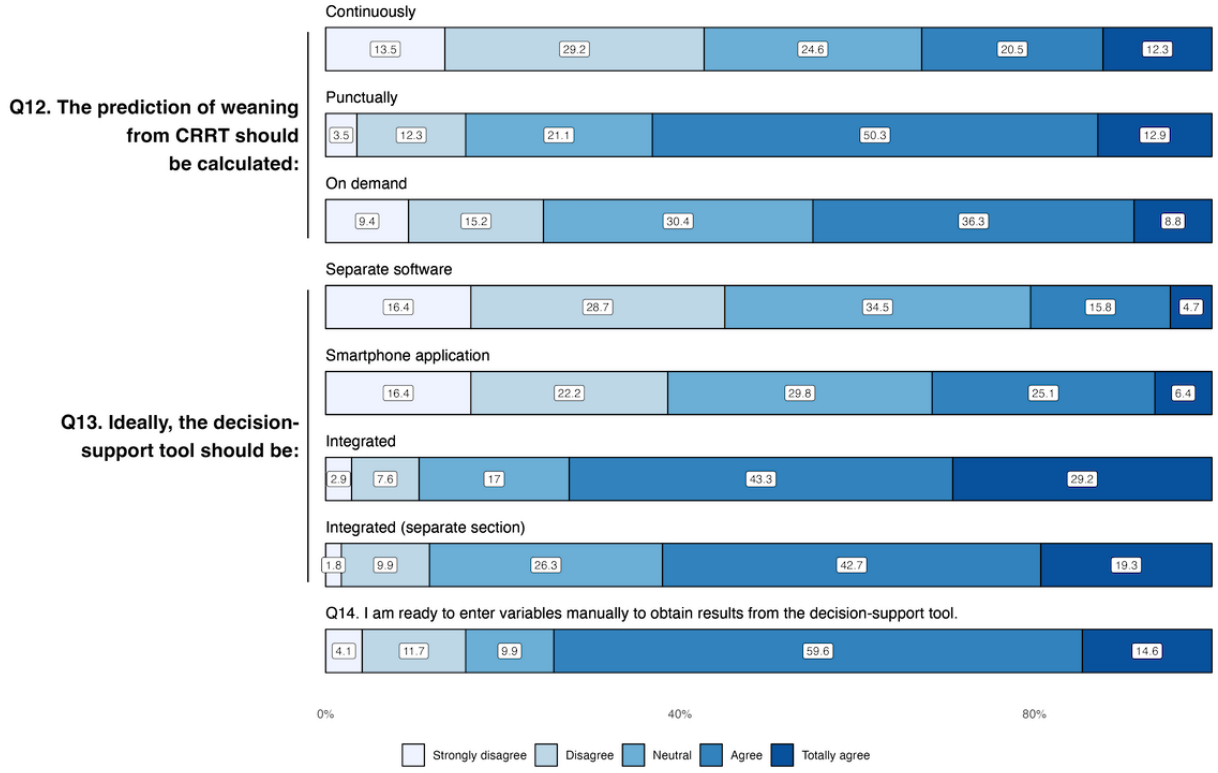
Respondents did not seem particularly comfortable with the concept of AI (66/171, 38.6% agreed or totally agreed with Q6) and did not seem to use AI tools in their daily lives (84/171, 49.1% disagreed or strongly disagreed with Q7) and even less so in their clinical activity with 70.7% (121/171) disagreeing or strongly disagreeing with Q8 (Figure 1B and Table 2). Junior physicians made greater use of AI tools in their daily lives, with 45.5% (15/33) agreeing or totally agreeing with Q7 compared to 29.7% (41/138) of senior doctors (P=.03; Table S1 in Multimedia Appendix 4). However, the surveyed physicians were very favorable to the use of AI tools to help them in their clinical practice, with 70.2% (120/171) agreeing or totally agreeing with Q9, with a priori no fear, since 83.7% (143/171) of respondents disagreeing or totally disagreeing with Q10 concerning the fact that AI could replace their job in the future. This enthusiasm seemed consistent between the different levels of training (94/138, 68.1% agreed or totally agreed vs 26/33, 78.8%; P=.08) and the university hospitals status (78/102, 76.5% agreed or totally agreed vs 42/69, 60.9%; P=.41; Figure S1 in Multimedia Appendix 4).

Implementation in Daily Clinical Practice

When asked about the preferred timing for computing the prediction of CRRT weaning (Q12), respondents preferred it to be rendered punctually at a specific time during the day, for example during the morning round (108/171, 63.2% agreed or totally agreed) versus on demand only (77/171, 45.1% agreed or totally agreed) or continuously (56/171, 42.7% agreed or totally agreed) (Figure 3 and Table 3). Senior physicians were more inclined to choose a prediction at a specific time of day (93/138, 67.4% agreed or totally agreed vs 15/33, 45.5%; P=.01), whereas juniors were more interested in an on-demand prediction only (20/33, 60.7% agreed or totally agreed, Table S1 in Multimedia Appendix 4). Regarding the choice of design for the CDSS (Q13), respondents were generally in favor of it being integrated within the ICU's electronic health record (EHR), whether with the usual monitoring data (124/171, 72.5% agreed or totally agreed) or on a separate section of the software (106/171, 62% agreed or totally agreed). Out of the 171 respondents, 141 (82.5%) physicians declared that their hospital was equipped with an ICU EHR (Q11), with greater computerization in university hospitals (93/101, 91% vs 48/79, 70%; P<.001). Most physicians agreed to manually input variables to be added to the model (127/171, 74.2% agreed or totally agreed). The median number of acceptable variables to enter manually was 5 (IQR 4 - 6) (Q15).

XSL•FO
RenderX

Figure 3. Answers to statements questions regarding the implementation of the clinical decision support system in daily clinical practice. AI: artificial intelligence; CRRT: continuous renal replacement therapy.



XSL•FO
RenderX

Table . Responses to statements regarding the implementation of the clinical decision support system in daily clinical practice on a Likert scale from 1 (strongly disagree) to 5 (totally agree). Results are presented as the median (IQR).

Question	Overall (N=171)	Nonuniversity hospitals (n=69)	University hospitals (n=102)	*P* values	Adjusted *P* values[a]
Q12: The prediction of weaning from CRRT[b] should be calculated:					
Continuously	3 (2-4)	3 (2-4)	3 (2-4)	.59	.93
Punctually, at a specific time (eg during morning round)	4 (3-4)	4 (3-4)	4 (3-4)	.78	.20
Punctually, on demand only	3 (3-4)	3 (2-4)	3 (3-4)	.50	.90
Q13: Ideally, the decision-support tool should be:					
A separate software application	3 (2-3)	3 (2-3)	3 (2-3)	.20	.97
A smartphone or tablet application	3 (2-4)	3 (2-4)	3 (2-4)	.71	.83
Integrated into the ICU[c] patient management software and visible at the same time as other vital parameters	4 (3-5)	4 (3-5)	4 (3-5)	.99	.69
Integrated into the ICU patient management software and visible in a separate section (action required to view prediction results)	4 (3-4)	4 (3-4)	4 (3-4)	.11	.70
Q14: I'm ready to enter variables manually to obtain results from the decision- support tool	4 (3-4)	4 (4-4)	4 (3-4)	.20	.42

[a]Adjustment on age, years of experience, and medical specialty.

[b]CRRT: continuous renal replacement therapy.

[c] ICU: intensive care unit.

Real-Life Operation, Willingness to Adopt in Everyday Practice (Usability)

Respondents agreed that an AI-based CDSS to assist in decisions about weaning patients from CRRT could be an aid in daily clinical practice, with 66% (113/171) either agreeing or totally agreeing (Q16). The adherence appeared to be higher in university hospitals (78/102, 76.5% agreeing or totally agreeing) compared to nonuniversity settings (35/69, 50.7%; *P*<.001) (Figure 1C and Table 4). However, after adjusting for confounders such as age, the difference was no longer statistically significant (adjusted *P*=.63), suggesting that the observed difference may be more related to the younger age profile of university hospital respondents. Similarly, younger physicians were more likely to express support for AI tools (27/33, 81.8% agreed or totally agreed vs 86/138, 62.3%; *P*=.01) (Table S1 in Multimedia Appendix 4). The explicability of the model was an important concern, with 74.9% (128/171) of respondents agreeing or totally agreeing that the AI-based CDSS should provide a percentage of certainty with the prediction provided (Q17), and 95.3% (163/171) that it was important to understand the criteria on which the model has based its prediction (Q18). Only 11.1% (19/171) doubted that the model would influence their decision to wean a patient off CRRT (Q19). Finally, interrogated physicians indicated a low probability threshold provided by the model below which they would not consider weaning a patient from CRRT at a median of 50% (IQR 30 - 60) and a threshold above which they would consider weaning at 80% (IQR 73 - 85) (Figure 4). These thresholds highlight the range within which model predictions could inform clinical decisions and suggest that physicians prefer a cautious approach, favoring higher certainty for weaning decisions while remaining conservative when uncertainty is high.

XSL•FO
RenderX

Table . Responses to statements regarding the real-life operation and willingness to adopt in everyday practice on likert scale from 1 (strongly disagree) to 5 (totally agree). Results are presented as median (IQR).

Question	Overall (N=171)	Nonuniversity hospitals (n=69)	University hospitals (n=102)	*P* values	Adjusted *P* values[a]
Q16: I think that an AI[b] tool to assist in the decision to wean a patient from CRRT[c] could be an aid in my daily clinical practice.	4 (3-4)	4 (3-4)	4 (4-4)	<.001	.63
Q17: It is important to me that the model gives the percentage of certainty of its prediction before I make the decision to wean a patient off CRRT.	4 (4-5)	4 (3-5)	4 (4-5)	.51	.29
Q18: It is important for me to understand the criteria on which the model has based its prediction.	5 (4-5)	5 (4-5)	5 (4-5)	.20	.11
Q19: I don’t think any AI model would influence my decision to wean a patient off CRRT.	2 (2-3)	2 (2-3)	2 (2-3)	.06	.52

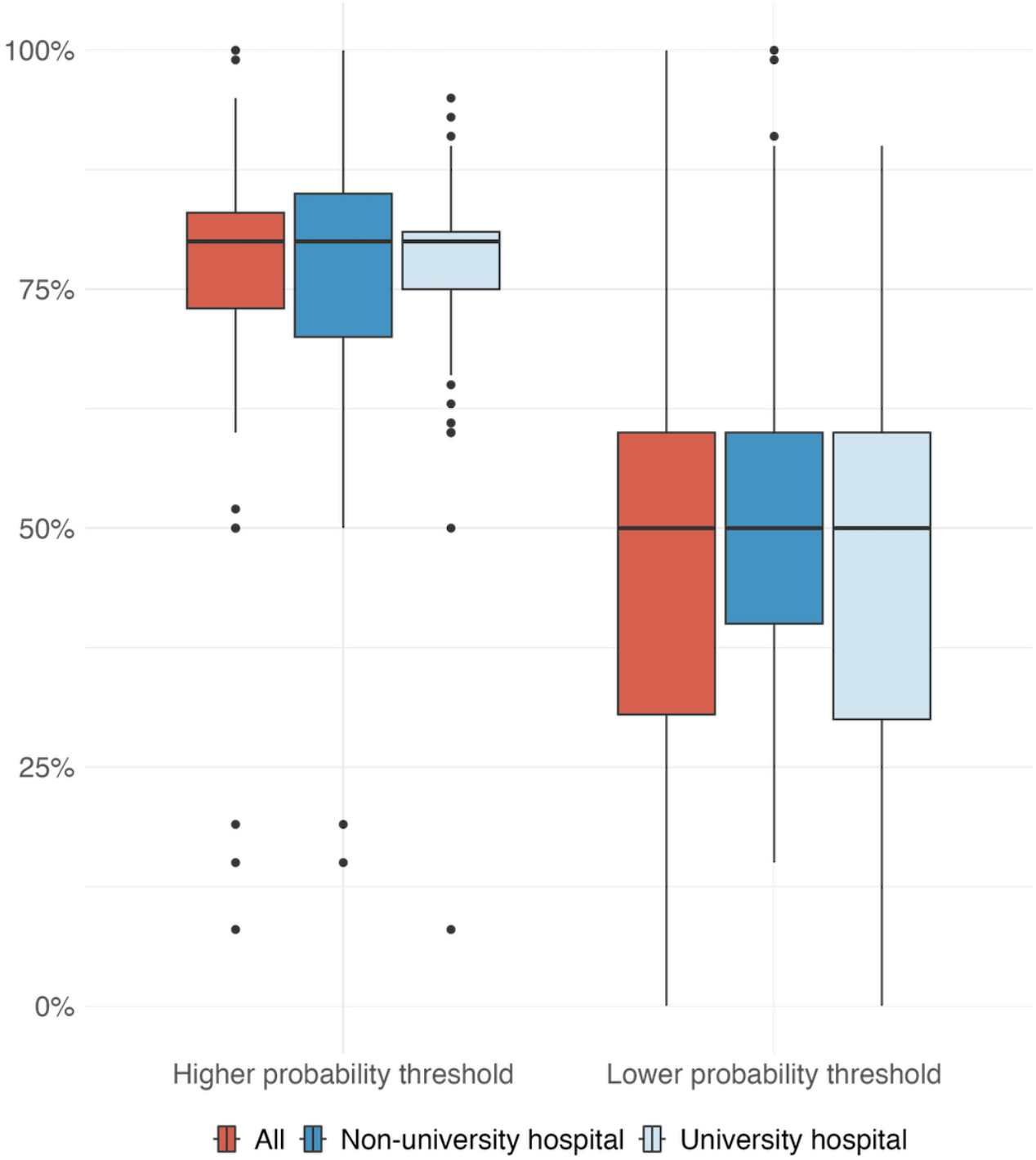
[a]Adjustment on age, years of experience and medical specialty.

[b]AI: artificial intelligence.

[c]CRRT: continuous renal replacement therapy.

XSL•FO
RenderX

Figure 4. Prediction thresholds described by clinicians as having an impact on their clinical decision-making on continuous renal replacement therapy weaning.



The responses to the survey have enabled us to draft an initial list of specifications fort the development of the CDSS to assist in weaning from CRRT. These specifications and the consequences for further development are detailed in Table 5.

XSL•FO
RenderX

Table . Specifications and consequences for development of the clinical decision support system.

Feature	Specification	Consequences for development
Overview of the problem and current practices (key drivers)		
Variables to include	Key variables such as resumption of diuresis, biological markers and response to diuretics.	Ensure these variables are accurately and automatically collected from EHR[a] to minimize manual input errors.
Implementation in daily clinical practice		
Manual data entry	Willingness to manually enter up to 5 variables.	Automate the collection of as many variables as possible by integrating with ICU[b] EHR.
Integration with existing systems	Integration with ICU EHR, predictions visible alongside vital parameters.	Develop seamless integration with EHR systems to ensure data accessibility and workflow efficiency.
Timing of predictions	Predictions computed at a specific time, such as morning rounds.	Schedule predictions to align with clinical routines, reducing the need for continuous monitoring.
User interface	User-friendly, minimal additional workload, no system switching.	Design an intuitive interface that fits into clinicians' workflow to enhance usability.
Real-life operation, willingness to adopt in everyday practice (usability)		
Explainability	Clear explanations of model predictions.	Develop an interface that visually explains the predictions to build trust among users.
Alert thresholds	Probability thresholds below 50% for considering not weaning and above 80% for considering weaning.	Calibrate the model to achieve the desired thresholds for user confidence and actionability.

[a]EHR: electronic health record.

[b] ICU: intensive care unit.

Discussion

Principal Findings

Our study provides insights into the expectations and attitudes of ICU physicians regarding the use of AI-based CDSS for weaning from CRRT. This predevelopment study is a fundamental step toward a user-centered approach to the development of a decision support tool. The results of our survey suggest that while physicians are not generally comfortable with AI and have limited experience using it, 70.2% (120/171) expressed a favorable view toward integrating AI tools in clinical practice, with no apparent fear of this technology. Moreover, our results suggest a significant interest and perceived necessity among French intensivists for a CDSS tailored to assist in the weaning process from CRRT.

Attitudes Toward AI and CDSS

Physicians in our study, particularly senior ones, did not seem entirely comfortable with the concept of AI. This highlights the need for comprehensive training and education to improve AI literacy among clinicians, fostering a more favorable environment for the integration of CDSS [17]. How physicians interpret and act on CDSS predictions can substantially impact patient care [36]. Despite this discomfort, there was strong support for AI-based CDSS to aid clinical decision-making, underscoring the potential acceptance of a well-designed CDSS. This positive outlook towards AI is consistent with other studies showing clinicians' openness to AI-based CDSS if they enhance clinical practice and improve patient outcomes [37]. In a similar study conducted among Dutch ICU physicians in university hospitals found that 86% of respondents believed AI could support them in their work as physicians [25]. In addition, the surveyed physicians showed no significant fear that AI would replace their jobs, with 83.7% (143/171) of respondents disagreed or strongly disagreed with this idea. The relatively young median age of respondents, 39 years (IQR 33 - 45) compared to a national median of 43 (IQR 35 - 54) in 2021 [33], may also explain the higher overall willingness to adopt AI-based CDSS in clinical practice.

Preferences for Implementation

Regarding the implementation of a CDSS for CRRT weaning, our survey revealed that physicians preferred a tool that computes the prediction of weaning at a specific time, rather than continuously. This is consistent with previous studies suggesting that continuous monitoring can lead to alarm fatigue and decrease clinician trust in the tool. In a review of 89 articles on CDSS in various medical fields, Jankovic et al [38] showed that poorly performing CDSS with frequent alerts could contribute to clinicians' frustration and burnout. Furthermore, respondents preferred a CDSS integrated into the ICU patient management software, visible alongside other vital parameters, rather than a new interface. This aligns with previous research showing that integration into clinical workflows is key to improving usability and adoption [39]. A user-centered design is critical, as highlighted by Zikos and DeLellis [40], who identified four real-life "pain points" where AI can add significant value for clinicians, including selecting effective interventions.

XSL•FO
RenderX

Factors Influencing Weaning Decision

Our study also highlights the importance of understanding the factors that influence physicians' decisions to wean patients from CRRT. The most frequently cited factors were resumption of diuresis above a certain volume, variation in biological settings, and good response to diuretics. These factors align with a previous systematic review, which identified similar predictors for successful RRT weaning, such as the urine output before RRT discontinuation and biochemical criteria (eg, serum urea, serum creatinine and creatinine clearance) [13]. These variables should therefore be included in the CDSS model to ensure clinical relevance in the weaning predictions. With the CRRT weaning success rate reported between 35% and 54% in the literature [34,35], our CDSS seems well-positioned to support this complex decision-making, as indicated by the responses of the surveyed clinicians.

Real-Life Operation and Adoption

This survey emphasizes the importance of understanding end-user needs and expectations during the predevelopment phase, which is crucial for successful deployment and adoption in clinical practice [20]. The first step is ensuring that the AI-based CDSS addresses the specific needs of clinicians [41]. Moreover, ensuring the explicability of AI models is crucial to avoid the "black box" effect. Physicians need to understand the factors driving the model's prediction to trust and use these tools effectively. Transparent AI models with clear insights into their decision-making processes can enhance user acceptance and facilitate smoother integration into clinical practice [42].

Limitations

It is worth noting that our study has limitations. First, the response rate was low and introduced the possibility of selection bias, as those more interested in AI may have been more likely to respond. This could have overestimated the acceptance or perceived usefulness of AI-based CDSS. As a result, caution is necessary when generalizing our results to the broader population of ICU physicians. In addition, the lack of an exhaustive list of ICU physicians to whom the survey was distributed further complicated the estimation of a precise response rate and the generalizability of the findings. While a significant proportion of respondents reported limited familiarity with AI, suggesting some mitigation of this bias, the possibility remains that the survey sample was not representative of the entire ICU physician population in France. Low response rates are a common challenge in survey-based research targeting healthcare professionals, who often face significant time constraints. To improve future response rates, strategies such as personalized invitations, follow-up reminders, incentives, and more direct communication channels (eg, targeted emails, professional networks) could be considered. Despite these challenges, our sample size was larger than similar studies ranging, from 7 to 93 participants [25-27,29] and included a diverse group of physicians from both university and nonuniversity hospitals, public and private sectors, and various level of training.

Second, our population skewed younger, with a median age of 39 years compared to the national median of 43 years. This could be attributed to the digital distribution of the survey via newsletters and social media platforms, which may have engaged younger physicians more effectively. The overrepresentation of younger intensivists could influence the generalizability of our findings, as younger physicians are often more familiar with technology and may exhibit greater openness toward AI adoption compared to their older counterparts. This positive bias toward AI could have amplified the generally favorable attitudes observed in our survey. Future studies should aim for a more representative sampling across age groups to ensure broader applicability of the results and to capture potentially differing perspectives from older physicians.

Third, we observed an overrepresentation of physicians from university hospitals, with 60% of respondents working in these centers, compared to around 50% according to recent estimates [33]. University hospital physicians may have greater exposure to technological innovations and more formal training in AI. This might make them more inclined to adopt new technologies like AI-based CDSS. This could have contributed to the positive outlook on AI tools in our survey.

Fourth, self-reporting bias could also influence the results, as participants may have provided responses they perceive as desirable. Finally, while our questionnaire was rigorously designed by a multidisciplinary team and based on instruments in similar studies, such as van der Meijden et al [25], there is currently no validated tool for predevelopment surveys of AI-based CDSS. This may affect the reliability and comparability of our results. In addition, there may have been some comprehension issues with certain questions, as some respondents probably inverted values for decision thresholds in Q20. Finally, this survey was conducted in France, targeting a specific audience for our CDSS, and the results may not be generalizable to other countries with different health care systems and practices.

Future Directions

Based on the survey results, the next steps in developing the CDSS for CRRT weaning will follow the specifications derived from the respondent's feedback, particularly regarding the selection of variables and the number of variables to incorporate into the model. The integration of the CDSS into existing ICU EHR should be prioritized, as this was preferred by most respondents, to ensure seamless integration into clinical workflows. The probability thresholds identified in the survey (50.0% and 80.0%) could guide the CDSS by defining actionable zones for clinical recommendations, with flexibility for customization based on institutional practices. These thresholds would help translate model predictions into practical decision-making support while preserving clinical discretion. In addition, clear explanations of predictions, including criteria and levels of certainty, must be incorporated to align with the strong preference for model transparency expressed by respondents.

Beyond model development, it is crucial to maintain ongoing user engagement throughout the process. This involves returning to the users with models and interface proposals to gather feedback on the model's functionality and interpretability. Iterative development, involving continuous user input and

XSL•FO
RenderX

feedback, is known to enhance acceptance and integration of AI-based CDSS in practice [43,44]. This approach helps ensure that the final product aligns closely with user expectations and needs, improving usability and satisfaction. After refining the model, a prospective study will evaluate its performance in real-world settings and its ability to generalize across different clinical contexts. The goal is to validate the model not only in controlled environments but also in diverse ICU settings to ensure its broader applicability and effectiveness.

In conclusion, our study provides valuable insights into ICU physicians' expectations and opinions regarding an AI-based CDSS for CRRT weaning, enabling us to draft an initial set of specifications. While there is cautious optimism about the use of AI in clinical practice, significant efforts are needed to address concerns about usability, integration, and transparency. By understanding and incorporating the needs and preferences of clinicians, we can develop a CDSS that is both effective and widely accepted. This work is a preliminary step in guiding future research continuing to involve health care providers in the development process and promoting user-centered design for the ongoing development of a CDSS to guide CRRT weaning in the ICU. This approach will ultimately enhance the adoption and impact of AI-based CDSS in critical care settings, improving patient outcomes and optimizing resource utilization.

Acknowledgments

The authors would like to express their gratitude to the French Society of Anesthesia and Intensive Care (Société Française d'Anesthésie,-Réanimation), the French Intensive Care Society (Société de Réanimation de Langue Française), the French College of Nonacademic Hospitals (Collège de Reanimation des hôpitaux Extra-Universitaires de France) and the Association of Private Sector Intensive Care Physicians (Association des Réanimateurs du Secteur Privé) for their assistance in disseminating this questionnaire.

The authors would also like to thank Perrine Leprêtre, Rémy Rovacchi and Philippe Gouin for their help in drafting the questionnaire.

Support was provided solely from departmental sources.

Conflicts of Interest

None declared.

Multimedia Appendix 1
Consensus-Based Checklist for Reporting of Survey Studies (CROSS) checklist.
[PDF File, 43 KB - medinform_v13i1e63709_app1.pdf]

Multimedia Appendix 2
Questionnaire translated into English with rational for each question.
[PDF File, 42 KB - medinform_v13i1e63709_app2.pdf]

Multimedia Appendix 3
Questionnaire in its original French version.
[PDF File, 32 KB - medinform_v13i1e63709_app3.pdf]

Multimedia Appendix 4
Responses to statements on a Likert scale from 1 (strongly disagree) to 5 (totally agree) according to level of training.
[PDF File, 152 KB - medinform_v13i1e63709_app4.pdf]

References

1. Lijović L, Elbers P. Leveraging the power of routinely collected ICU data. Intensive Care Med 2025 Jan;51(1):163-166. [doi: 10.1007/s00134-024-07745-5] [Medline: 39661137]
2. Hong N, Liu C, Gao J, et al. State of the art of machine learning-enabled clinical decision support in intensive care units: literature review. JMIR Med Inform 2022 Mar 3;10(3):e28781. [doi: 10.2196/28781] [Medline: 35238790]
3. van de Sande D, van Genderen ME, Huiskens J, Gommers D, van Bommel J. Moving from bytes to bedside: a systematic review on the use of artificial intelligence in the intensive care unit. Intensive Care Med 2021 Jul;47(7):750-760. [doi: 10.1007/s00134-021-06446-7] [Medline: 34089064]
4. Xu H, Ma Y, Zhuang Y, Zheng Y, Du Z, Zhou X. Machine learning-based risk prediction model construction of difficult weaning in ICU patients with mechanical ventilation. Sci Rep 2024 Sep 6;14(1). [doi: 10.1038/s41598-024-71548-3]

XSL•FO
RenderX

5. Fleuren LM, Klausch TLT, Zwager CL, et al. Machine learning for the prediction of sepsis: a systematic review and meta-analysis of diagnostic test accuracy. Intensive Care Med 2020 Mar;46(3):383-400. [doi: 10.1007/s00134-019-05872-y] [Medline: 31965266]
6. Kelly CJ, Karthikesalingam A, Suleyman M, Corrado G, King D. Key challenges for delivering clinical impact with artificial intelligence. BMC Med 2019 Oct 29;17(1):195. [doi: 10.1186/s12916-019-1426-2] [Medline: 31665002]
7. Heo S, Kang EA, Yu JY, et al. Time series AI Model for acute kidney injury detection based on a multicenter distributed research network: development and verification study. JMIR Med Inform 2024 Jul 5;12(1):e47693. [doi: 10.2196/47693] [Medline: 39039992]
8. Li M, Han S, Liang F, et al. Machine learning for predicting risk and prognosis of acute kidney disease in critically ill elderly patients during hospitalization: internet-based and interpretable model study. J Med Internet Res 2024 May 1;26:e51354. [doi: 10.2196/51354] [Medline: 38691403]
9. Hoste EAJ, Kellum JA, Selby NM, et al. Global epidemiology and outcomes of acute kidney injury. Nat Rev Nephrol 2018 Oct;14(10):607-625. [doi: 10.1038/s41581-018-0052-0] [Medline: 30135570]
10. Tandukar S, Palevsky PM. Continuous renal replacement therapy: who, when, why, and how. Chest 2019 Mar;155(3):626-638. [doi: 10.1016/j.chest.2018.09.004] [Medline: 30266628]
11. Gaudry S, Hajage D, Schortgen F, et al. Initiation strategies for renal-replacement therapy in the intensive care unit. N Engl J Med 2016 Jul 14;375(2):122-133. [doi: 10.1056/NEJMoa1603017] [Medline: 27181456]
12. Barbar SD, Clere-Jehl R, Bourredjem A, et al. Timing of renal-replacement therapy in patients with acute kidney injury and sepsis. N Engl J Med 2018 Oct 11;379(15):1431-1442. [doi: 10.1056/NEJMoa1803213] [Medline: 30304656]
13. Katulka RJ, Al Saadon A, Sebastianski M, et al. Determining the optimal time for liberation from renal replacement therapy in critically ill patients: a systematic review and meta-analysis (DOnE RRT). Crit Care 2020 Feb 13;24(1):50. [doi: 10.1186/s13054-020-2751-8] [Medline: 32054522]
14. Uchino S, Bellomo R, Morimatsu H, et al. Discontinuation of continuous renal replacement therapy: a post hoc analysis of a prospective multicenter observational study. Crit Care Med 2009 Sep;37(9):2576-2582. [doi: 10.1097/CCM.0b013e3181a38241] [Medline: 19623048]
15. Schiffl H, Lang SM. Current approach to successful liberation from renal replacement therapy in critically ill patients with severe acute kidney injury: the quest for biomarkers continues. Mol Diagn Ther 2021 Jan;25(1):1-8. [doi: 10.1007/s40291-020-00498-z] [Medline: 33099671]
16. Clark EG, Bagshaw SM. Unnecessary renal replacement therapy for acute kidney injury is harmful for renal recovery. Semin Dial 2015;28(1):6-11. [doi: 10.1111/sdi.12300] [Medline: 25359104]
17. Coiera E. The last mile: where artificial intelligence meets reality. J Med Internet Res 2019 Nov 8;21(11):e16323. [doi: 10.2196/16323] [Medline: 31702559]
18. de Hond AAH, Leeuwenberg AM, Hooft L, et al. Guidelines and quality criteria for artificial intelligence-based prediction models in healthcare: a scoping review. NPJ Digit Med 2022 Jan 10;5(1):2. [doi: 10.1038/s41746-021-00549-7] [Medline: 35013569]
19. van de Sande D, Van Genderen ME, Smit JM, et al. Developing, implementing and governing artificial intelligence in medicine: a step-by-step approach to prevent an artificial intelligence winter. BMJ Health Care Inform 2022 Feb;29(1):e100495. [doi: 10.1136/bmjhci-2021-100495] [Medline: 35185012]
20. Seneviratne MG, Li RC, Schreier M, et al. User-centred design for machine learning in health care: a case study from care management. BMJ Health Care Inform 2022 Oct;29(1):e100656. [doi: 10.1136/bmjhci-2022-100656] [Medline: 36220304]
21. Borges do Nascimento IJ, Abdulazeem H, Vasanthan LT, et al. Barriers and facilitators to utilizing digital health technologies by healthcare professionals. npj Digit Med 2023 Sep 18;6(1):1-28. [doi: 10.1038/s41746-023-00899-4]
22. Vinsonneau C, Allain-Launay E, Blayau C, et al. Renal replacement therapy in adult and pediatric intensive care: Recommendations by an expert panel from the French Intensive Care Society (SRLF) with the French Society of Anesthesia Intensive Care (SFAR) French Group for Pediatric Intensive Care Emergencies (GFRUP) the French Dialysis Society (SFD). Ann Intensive Care 2015 Dec;5(1):58. [doi: 10.1186/s13613-015-0093-5] [Medline: 26714808]
23. Martignene N, Amad A, Bellet J, et al. Goupile: a new paradigm for the development and implementation of clinical report forms. Stud Health Technol Inform 2022 May 25;294:540-544. [doi: 10.3233/SHTI220517] [Medline: 35612138]
24. Sharma A, Minh Duc NT, Luu Lam Thang T, et al. A consensus-based checklist for reporting of survey studies (CROSS). J Gen Intern Med 2021 Oct;36(10):3179-3187. [doi: 10.1007/s11606-021-06737-1] [Medline: 33886027]
25. van der Meijden SL, de Hond AAH, Thoral PJ, et al. Intensive care unit physicians' perspectives on artificial intelligence-based clinical decision support tools: preimplementation survey study. JMIR Hum Factors 2023 Jan 5;10(1):e39114. [doi: 10.2196/39114] [Medline: 36602843]
26. Matthiesen S, Diederichsen SZ, Hansen MKH, et al. Clinician preimplementation perspectives of a decision-support tool for the prediction of cardiac arrhythmia based on machine learning: near-live feasibility and qualitative study. JMIR Hum Factors 2021 Nov 26;8(4):e26964. [doi: 10.2196/26964] [Medline: 34842528]
27. Romero-Brufau S, Wyatt KD, Boyum P, Mickelson M, Moore M, Cognetta-Rieke C. A lesson in implementation: a pre-post study of providers' experience with artificial intelligence-based clinical decision support. Int J Med Inform 2020 May;137:104072. [doi: 10.1016/j.ijmedinf.2019.104072] [Medline: 32200295]

XSL•FO
RenderX

28. Sendak MP, Ratliff W, Sarro D, et al. Real-world integration of a sepsis deep learning technology into routine clinical care: implementation study. JMIR Med Inform 2020 Jul 15;8(7):e15182. [doi: 10.2196/15182] [Medline: 32673244]
29. Rabbani N, Ma SP, Li RC, et al. Targeting repetitive laboratory testing with electronic health records-embedded predictive decision support: a pre-implementation study. Clin Biochem 2023 Mar;113:70-77. [doi: 10.1016/j.clinbiochem.2023.01.002] [Medline: 36623759]
30. Venkatesh V, Morris MG, Davis GB, Davis FD. User acceptance of information technology: toward a unified view. MIS Q 2003;27(3):425. [doi: 10.2307/30036540]
31. Chismar WG, Wiley-Patton S. Does the extended technology acceptance model apply to physicians. Presented at: 36th Annual Hawaii International Conference on System Sciences, 2003; Jan 6-9, 2003. [doi: 10.1109/HICSS.2003.1174354]
32. Mirzaei A, Carter SR, Patanwala AE, Schneider CR. Missing data in surveys: key concepts, approaches, and applications. Res Social Adm Pharm 2022 Feb;18(2):2308-2316. [doi: 10.1016/j.sapharm.2021.03.009] [Medline: 33775556]
33. Ehrmann S, Guitton C, Aissaoui N, Terzi N, Capellier G, Vinsonneau C. Démographie des réanimations françaises, enquête 2021 - état des lieux hors pandémie [website in french]. Collège Enseignants Médecine Intensive Réanimation. 2021. URL: https://www.ce-mir.fr/UserFiles/File/national/documents/divers/rapport-enquete-demographique-cemir.pdf [accessed 2025-04-16]
34. Liang Q, Xu X, Ding S, Wu J, Huang M. Prediction of successful weaning from renal replacement therapy in critically ill patients based on machine learning. Ren Fail 2024 Dec;46(1):2319329. [doi: 10.1080/0886022X.2024.2319329] [Medline: 38416516]
35. Stenson EK, Alhamoud I, Alobaidi R, et al. Factors associated with successful liberation from continuous renal replacement therapy in children and young adults: analysis of the worldwide exploration of renal replacement outcomes collaborative in Kidney Disease Registry. Intensive Care Med 2024 Jun;50(6):861-872. [doi: 10.1007/s00134-024-07336-4] [Medline: 38436726]
36. Goodman KE, Rodman AM, Morgan DJ. Preparing physicians for the clinical algorithm era. N Engl J Med 2023 Aug 10;389(6):483-487. [doi: 10.1056/NEJMp2304839] [Medline: 37548320]
37. Oh S, Kim JH, Choi SW, Lee HJ, Hong J, Kwon SH. Physician confidence in artificial intelligence: an online mobile survey. J Med Internet Res 2019 Mar 25;21(3):e12422. [doi: 10.2196/12422] [Medline: 30907742]
38. Jankovic I, Chen JH. Clinical decision support and implications for the clinician burnout crisis. Yearb Med Inform 2020 Aug;29(1):145-154. [doi: 10.1055/s-0040-1701986] [Medline: 32823308]
39. Miller A, Moon B, Anders S, Walden R, Brown S, Montella D. Integrating computerized clinical decision support systems into clinical work: a meta-synthesis of qualitative research. Int J Med Inform 2015 Dec;84(12):1009-1018. [doi: 10.1016/j.ijmedinf.2015.09.005]
40. Zikos D, DeLellis N. CDSS-RM: a clinical decision support system reference model. BMC Med Res Methodol 2018 Nov 16;18(1):137. [doi: 10.1186/s12874-018-0587-6] [Medline: 30445910]
41. Shortliffe EH, Sepúlveda MJ. Clinical decision support in the era of artificial intelligence. JAMA 2018 Dec 4;320(21):2199-2200. [doi: 10.1001/jama.2018.17163] [Medline: 30398550]
42. Shevtsova D, Ahmed A, Boot IWA, et al. Trust in and acceptance of artificial intelligence applications in medicine: mixed methods study. JMIR Hum Factors 2024 Jan 17;11:e47031. [doi: 10.2196/47031] [Medline: 38231544]
43. Wang L, Zhang Z, Wang D, et al. Human-centered design and evaluation of AI-empowered clinical decision support systems: a systematic review. Front Comput Sci 2023 Jun 2;5. [doi: 10.3389/fcomp.2023.1187299]
44. Kannan V, Basit MA, Bajaj P, et al. User stories as lightweight requirements for agile clinical decision support development. J Am Med Inform Assoc 2019 Nov 1;26(11):1344-1354. [doi: 10.1093/jamia/ocz123] [Medline: 31512730]

Abbreviations

AI: artificial intelligence
AKI: acute kidney injury
CDSS: clinical decision support systems
CRRT: continuous renal replacement therapy
EHR: electronic health record
ICU: intensive care unit
IQR: interquartile range
ML: machine learning
RRT: renal replacement therapy
UTAUT: unified theory of acceptance and use of technology

XSL•FO
RenderX

Edited by C Lovis; submitted 02.07.24; peer-reviewed by M Popovic, T Haga; revised version received 12.12.24; accepted 23.01.25; published 23.04.25.

Please cite as:
Popoff B, Cabon S, Cuggia M, Bouzillé G, Clavier T
Expectations of Intensive Care Physicians Regarding an AI-Based Decision Support System for Weaning From Continuous Renal Replacement Therapy: Predevelopment Survey Study
JMIR Med Inform 2025;13:e63709
URL: https://medinform.jmir.org/2025/1/e63709
doi:10.2196/63709

© Benjamin Popoff, Sandie Cabon, Marc Cuggia, Guillaume Bouzillé, Thomas Clavier. Originally published in JMIR Medical Informatics (https://medinform.jmir.org), 23.4.2025. This is an open-access article distributed under the terms of the Creative Commons Attribution License (https://creativecommons.org/licenses/by/4.0/), which permits unrestricted use, distribution, and reproduction in any medium, provided the original work, first published in JMIR Medical Informatics, is properly cited. The complete bibliographic information, a link to the original publication on https://medinform.jmir.org/, as well as this copyright and license information must be included.

XSL•FO
RenderX

Proposal for Using AI to Assess Clinical Data Integrity and Generate Metadata: Algorithm Development and Validation

Caroline Bönisch[1,2], Prof Dr; Christian Schmidt[2], PhD; Dorothea Kesztyüs[2], PD, PhD; Hans A Kestler[3,4], Prof Dr; Tibor Kesztyüs[2], Prof Dr Med

[1]Department of Electrical Engineering and Informatics, University of Applied Sciences Stralsund, Zur Schwedenschanze 15, Stralsund, Germany

[2]Medical Data Integration Center Göttingen, University Medical Center Göttingen, Göttingen, Germany

[3]Institute of Medical Systems Biology, Universität Ulm, Ulm, Germany

[4]Medical Data Integration Center Ulm, Ulm, Germany

Corresponding Author:
Caroline Bönisch, Prof Dr
Department of Electrical Engineering and Informatics, University of Applied Sciences Stralsund, Zur Schwedenschanze 15, Stralsund, Germany

Abstract

Background: Evidence-based medicine combines scientific research, clinical expertise, and patient preferences to enhance the patient outcomes and improve health care quality. Clinical data are crucial in aligning medical decisions with evidence-based practices, whether derived from systematic research or real-world data sources. Quality assurance of clinical data, mainly through predictive quality algorithms and machine learning, is essential to mitigate risks such as misdiagnosis, inappropriate treatment, bias, and compromised patient safety. Furthermore, excellent quality of clinical data is a prerequisite for the replication of research results in order to gain insights from practice and real-world evidence.

Objective: This study aims to demonstrate the varying quality of medical data in primary clinical source systems at a maximum care university hospital and provide researchers with insights into data reliability through predictive quality algorithms using machine learning techniques.

Methods: A literature review was conducted to evaluate existing approaches to automated quality prediction. In addition, embedded in the process of integrating care data into a medical data integration center (MeDIC), metadata relevant to this clinical data was stored, considering factors such as data granularity and quality metrics. Completed patient cases with echocardiographic and laboratory findings as well as medication histories were selected from 2001 to 2023. Two authors manually reviewed the datasets and assigned a quality score for each entry, with 0 indicating unsatisfactory and 1 satisfactory quality. Since quality control was considered a binary problem, corresponding classifiers were used for the quality prediction. Logistic regression, k-nearest neighbors, a naive bayes classifier, a decision tree classifier, a random forest classifier, extreme gradient boosting (XGB), and support vector machines (SVM) were selected as machine learning algorithms. Based on preprocessing the dataset, training machine learning algorithms on echocardiographic, laboratory, and medication data, and assessing various prediction models, the most effective algorithms for quality classification were to be identified. The performance of the predictive quality algorithms was assessed based on accuracy, precision, recall, and scoring.

Results: There were 450 patient cases with complete information extracted from the MeDIC data pool. The laboratory and medication datasets had to be limited to 4000 data entries each to enable manual review; the echocardiographic datasets comprised 750 examinations. XGB demonstrated the highest performance for the echocardiographic dataset with an area under the receiver operating characteristic curve (AUC-ROC) of 84.6%. For laboratory data, SVM achieved an AUC-ROC score of 89.8%, demonstrating superior discrimination performance. Finally, regarding the medication dataset, SVM showed the most balanced performance, achieving an AUC-ROC of 65.1%, the highest of all tested models.

Conclusions: This proposal presents a template for predicting data quality and incorporating the resulting quality information into the metadata of a data integration center, a concept not previously implemented. The model was deployed for data inspection using a hybrid approach that combines the trained model with conventional inspection methods.

(JMIR Med Inform 2025;13:e60204) doi:10.2196/60204

KEYWORDS

metadata; quality; interoperability; reliability; utilization; AI; artificial intelligence; data integrity; algorithm; development; validation; clinical data; machine learning; literature review; accuracy; data quality; model

XSL•FO
RenderX

Introduction

Evidence-based medicine combines the best available evidence from scientific research with clinical expertise and patient preferences. The goal of applying evidence-based medicine in health care is to enhance patient outcomes, improve the quality of care, and minimize ineffective or harmful treatments [1]. Valid clinical data and the associated metadata serve as the foundation for evidence-based medicine through high-quality evidence from systematic research or as real-world data (RWD) from clinical care [2]. It allows clinicians to align their decisions and treatments with the best available evidence from research and clinical guidelines, leading to better patient outcomes. Moreover, clinical data plays a crucial role in medical research and innovation. Researchers use large datasets to identify patterns, risk factors, and potential treatment approaches for various medical conditions, resulting in advancements and breakthroughs in medicine [3]. Without awareness of the data quality within these datasets, researchers and clinicians may face significant challenges, such as misdiagnosis and inappropriate treatment, compromised patient safety, and bias from confounding factors. In addition, the quality of data can impact the ability to replicate research results and affect the efficiency of data integration. To mitigate these risks, it is essential for clinicians and researchers to be mindful of the quality of the clinical data they are using [4].

Data integration centers, which are set up to consolidate clinical routine data in German university hospitals, can provide information about the quality of their data, given their extensive data resources [5]. The Medical Data Integration Center of the University Medical Center Göttingen (UMG-MeDIC) securely stores clinical data (eg, laboratory findings or echocardiography data) and makes it available upon request to enable as many researchers as possible to access the data while taking data protection and security into account [6].

Data originating from clinical care source systems that are not collected for the intended research use case are often incomplete, lack necessary information (eg, missing entries), or exhibit uncertain measurement quality [7]. Therefore, providing a precise and detailed description of data through metadata when merging heterogeneous sources enables a valid and meaningful integration aimed at ensuring traceable reuse. Metadata assists researchers and users in searching, categorizing, and interpreting data from a data warehouse. In addition, metadata ensures data consistency and facilitates data management [8,9].

Qualitative predictions using machine learning algorithms can be used to gather information about the completeness of data, which includes not only missing values but also semantic completeness and consistency. Machine learning and deep learning methodologies offer significant potential for ensuring quality. Nalbach et al [10] describe data-driven estimations of data quality as predictive quality. The extraction of data and its relation to quality metrics—such as completeness, consistency, correctness, and correspondence [11], enables data-driven quality assessment based on historical data. These estimations provide a foundation for decision-making regarding quality enhancement measures, such as informing data stewards about necessary missing values that should be added [10].

Based on the predictive quality approach further described by Tercan et al [12] and Schmitt et al [13], this research aimed to identify a predictive model-based quality algorithm for clinical data, including RWD, and provide automated quality inspection. The goal of this paper is to demonstrate the varying quality of medical data in primary clinical source systems and to inform researchers about data reliability using machine learning techniques. This approach seeks to identify predictive model-based quality algorithms for clinical data, including RWD, to facilitate automated quality inspection, ensuring data completeness and consistency. As a result of our proposal, we intend to enhance the reliability of clinical data used in evidence-based medicine and medical research.

Methods

Literature Review

A literature search regarding machine learning algorithms and data quality was conducted to provide an overview of the semantic completeness of data, consider previous work to build on existing knowledge, and classify this work's results.

The literature review establishes the foundation for developing innovative approaches and solutions designed to assess the quality of clinical data within the UMG-MeDIC. The literature search was conducted in Embase via Ovid and PubMed and resulted in 118 search records. After removing duplicates, 104 results were included in the title and abstract screening. Following the elimination of publications unsuitable for the goals of this manuscript, 12 results remained. The full text of the identified articles was carefully reviewed, and valuable information was integrated into the introduction and methodology sections of this manuscript. The search strategy for PubMed and the corresponding PRISMA Flow Chart of the literature search are provided in Table 1 and Table 2 of the Multimedia Appendix 1 [1].

Ethical Considerations

Ethical approval for the anonymized secondary health data analysis was obtained from the Ethics Review Committee of the University Medical Center Göttingen with the Ref. No. 21/9/18. All developments and experiments were performed in accordance with relevant guidelines and regulations. Furthermore, informed consent was obtained from all participants or their legal guardians and the original informed consent allows the secondary analysis without additional consent. Regarding the privacy and confidentiality protection of human participants all study data is deidentified.

Prerequisites at the UMG-MeDIC

In the context of this project, it was decided to store all metadata linked to the primary clinical data from the source systems of the UMG in a relational database (MariaDB). This was considered necessary because the actual clinical data to which the metadata refers was already stored in the same relational database.

XSL•FO
RenderX

The meta and metadata were captured during routine care and originated from different hospital information systems, including clinical workstation systems, laboratory information systems, echocardiography systems, and microbiology systems.

Information from the specifications of the supplied data formats was extracted to develop the preparatory work for the quality assessment of the clinical data.

Moreover, the granularity of metadata extracted from the primary source systems was taken into account. Metadata in primary source systems is captured at varying levels of granularity (eg, metadata date as day-month-year hour-minute-second vs metadata date as month-year) and must therefore be included and processed accordingly.

Data quality was introduced as additional metadata in the relational database structure to quantify the quality of the UMG-MeDIC data.

Data Preparation

The clinical data, originating from the clinical source systems of the UMG, is heterogeneous. This data is extracted from various primary clinical sources, such as the lab information system and the clinical workstation system, and consolidated within the UMG-MeDIC. The data are pseudonymized during the consolidation and processing at the data integration center. Although the work is based on a technical viewpoint of the data sources, demographic information was not addressed separately. Patient cases were selected based on three criteria: (1) completed patient cases with (2) echocardiographic and laboratory findings, as well as medication histories (3) from 2001 to 2023, excluding data linked to outdated process configurations. Consequently, 450 distinct patient cases with clinical findings were extracted from the data pool of the UMG-MeDIC. Among these 450 case reports, each report includes echocardiographic, laboratory, and medication data as shown in Figure 1.

A total of 750 echocardiographic examinations were carried out for these 450 patient cases, which means around 1.6 echocardiographic examinations per patient case. In comparison, there was significantly more laboratory and medication data for these 450 patient cases, which did not allow a manual review of the quality of every individual data item. Hence, the laboratory and medication data subset was limited to 4000 data points each. On this basis, a dataset with 750 echocardiographic, 4000 laboratory, and 4000 medication data items was obtained.

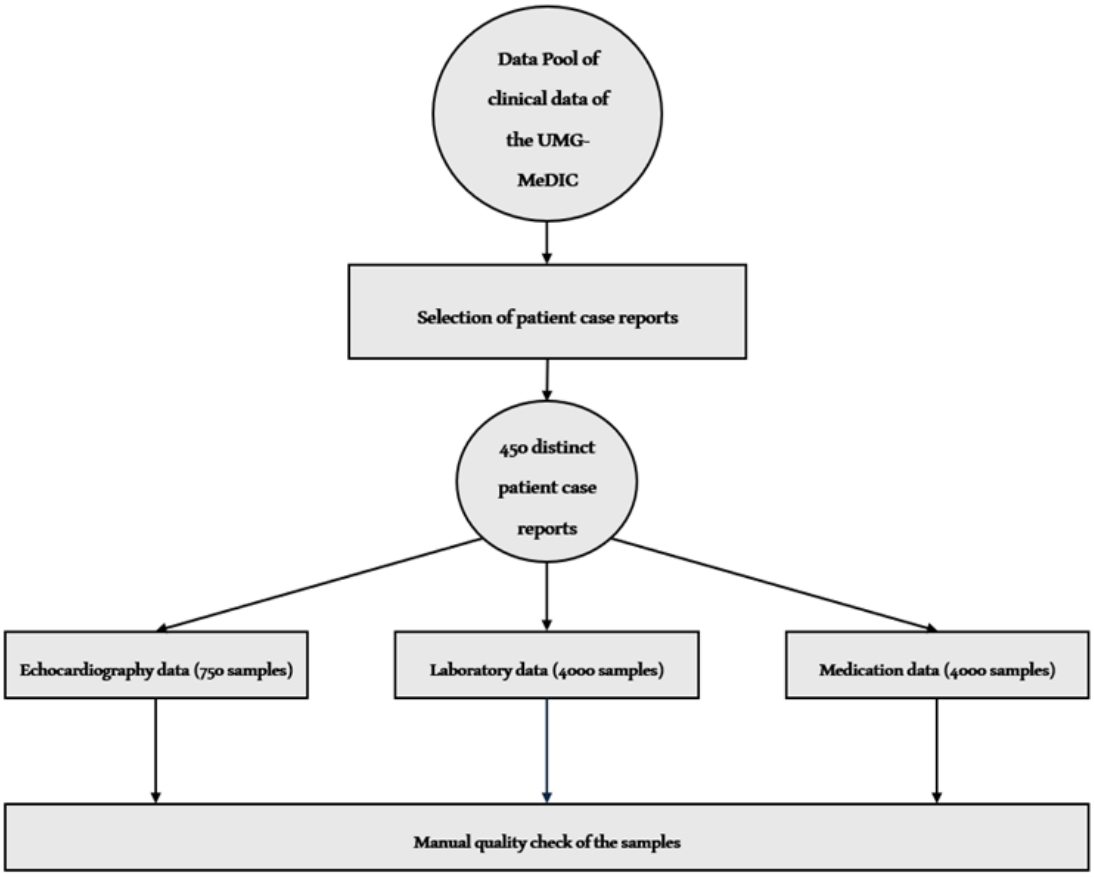
Subsequently, 2 authors manually reviewed the echocardiographic, laboratory, and medication data, assigning each data entry a quality score from 0 to 1, where 0 indicates unsatisfactory quality and 1 indicates satisfactory quality.

The criteria for this assignment were based on corresponding preliminary work by the authors to identify quality measures [14] and further work related to quality metrics [11,15-17]. The first criterion is the semantic completeness of the data, a metric that assesses whether all mandatory data fields are filled with relevant information. Completeness ensures there are no missing values, enabling users to fully understand and use the data. The second measure, data consistency, evaluates whether the data complies with established standards, conventions, or formats. The third measure, data correctness, assesses the accuracy of the information. In addition, the linkage of this data to other datasets checks whether interlinked or interdependent data elements convey the same information across all instances. The quality metric data relevance ensures that the metadata meets the needs or expectations of its intended users. For example, if a dataset is designed for clinical research, including fields like measurement units might enhance its relevance. The metric semantic specificity considers the granularity and precision of semantic concepts in the data. High semantic specificity implies the use of detailed and well-defined terms to describe the information. Timeliness, the sixth metric, pertains to evaluating how current the data is. Timeliness is crucial, especially for dynamic or time-sensitive resources. The seventh metric, accessibility, measures whether the data is physically available and comprehensible to users (whether human or machine), while reproducibility of the data, the eighth and final metric, ensures that data evaluations are consistent and can be independently verified by different users or systems. After the separate reviews, the quality mappings were compared, and deviations were discussed. Ultimately, a uniform quality mapping for the echocardiographic, laboratory, and medication data was established.

This process ensures that the models exclusively learn from consistently occurring patterns and dependencies.

XSL•FO
RenderX

Figure 1. Outline of the data selection, starting from the data pool of clinical data from the UMG-MeDIC (Medical Data Integration Center of the University Medical Center Göttingen), where 450 patient case reports were selected manually. These 450 case reports were then divided into subclasses of echocardiographic data (sample size of 750), laboratory data (sample size of 4000), and medication data (sample size of 4000). Finally, the samples from each of the three subsets were manually checked for quality by two authors.



Predictive Machine Learning Algorithms

Machine learning is a subfield of artificial intelligence (AI) that enables information technology systems to recognize patterns in existing data and develop solutions autonomously. This research involves classifying data quality variables for clinical data. The classification requires a training dataset with examples for each data source entity's input and output variables.

All machine learning models and classifiers were developed in Python (Python Software Foundation) using scikit-learn libraries. Each machine learning algorithm was trained separately on echocardiographic, laboratory, and medication data to identify the best-performing algorithm for each dataset.

The machine learning algorithms selected include logistic regression (LR) [18], k-nearest neighbors (KNN) [19], a Naive Bayes (NB) classifier [20], a decision tree classifier [21], a random forest classifier [22], XGB [23], and support vector machines (SVM) [24].

For the echocardiographic data consisting of 750 samples, 575 samples have been classified. as unsatisfactory quality (0), while 175 samples are classified as good quality (1).

The laboratory data, comprising 4000 samples, revealed that 17 samples were classified as unsatisfactory (0) and 3983 samples were deemed to be of good quality (1).

The distribution of classes within the medication data resulted in 1280 samples of unsatisfactory quality (0) and 2720 samples of good data quality (1). Multimedia Appendix 2 provides an overview of the features for the three subsets and their target distribution. For each feature of the three subsets, the data are distributed across interval scales (Table 1).

The datasets exhibit an imbalanced target distribution, which necessitated consideration of the overclassification of the majority class. During data preprocessing, the Synthetic Minority Oversampling Technique (SMOTE) was used to tackle this imbalance. SMOTE generates synthetic data points by interpolating between minority class samples. The sampling strategy in SMOTE was set to default (auto), with a random state of 0 and k-neighbors configured to 5.

XSL•FO
RenderX

Table . Depiction of the features within the three subsets (echocardiography, laboratory and medication) with the data type of the feature and the number of features listed.

#Numbers	Column	Data type
Echocardiography		
0	untersuchungsalter	Int64
1	groesse	Float64
2	gewicht	Float64
3	aoroot	Float64
4	lads	Float64
5	ivsd	Float64
6	lvdd	Float64
7	lvpwd	Float64
8	tapse	Float64
9	lfev	Float64
10	lvef_vis	Float64
11	lvds	Float64
12	lvedv	Float64
13	lvesv	Float64
14	ladslong	Float64
15	laflaeche	Float64
16	lavolindex	Float64
17	mvevmax	Float64
18	quality	Int64
Laboratory		
0	Vorgang_Ref	Int64
1	Probe_Ref	Int64
2	Ergebnis_ID	Int64
3	Analyse_Typ_ID	Int64
4	Ergebnis_Wert	Float64
5	Ergebnis_Darstellung	Float64
6	Ergebnis_Manuell	Float64
7	Inaktiv	Int64
Medication		
0	application_type	Int64
1	application_deleted	Int64
2	application_bolus_value	Float64
3	application_dose_value	Float64
4	application_perfusor_volume	Float64
5	application_route	Int64
6	application_site	Float64
7	application_status	Int64
8	external_id.1	Int64
9	mid.1	Int64
10	active	Int64

XSL•FO
RenderX

#Numbers	Column	Data type
11	additional_fee_obligation	Int64
12	availability	Int64
13	charge_documentation_required	Int64
14	out_of_trade	Int64
15	recent	Int64
16	reference_value	Float64
17	source_id	Int64
18	successor_id	Float64
19	version	Int64
20	external_id.2	Int64
21	amount	Float64
22	ingredient_type	Float64
23	main_ingredient_id	Float64
24	sequence_number	Int64
25	meona_substance_id	Float64
26	external_id.3	Int64

For input feature extraction, a multilayer perceptron autoencoder model was used, where each layer of the encoder uses batch normalization and leaky ReLU activation. The autoencoder was chosen because it automatically learns feature representations, which reduces the need for explicit feature selection methods that involve extensive iterative training. In addition, the ability to handle nonlinear relationships within the data necessitated the use of an autoencoder. Finally, the datasets were divided into training and test sets and validated using 5x10-fold cross-validation.

Since it is not feasible to universally preselect suitable algorithms in advance, it was necessary to test and evaluate various learning algorithms tailored to specific scenarios [25].

The LR algorithm was selected as the baseline for classification tasks because it predicts the probability of a target variable and is widely used in both binary and multiclass classifications. The parameters included the solver (newton-cg, lbfgs, and liblinear), a default penalty, and the inverse of regularization strength (C) set as loguniform (1e-5, 100).

The KNN classifies a data point based on the majority class among its k nearest neighbors. Due to its simplicity and effectiveness for low-dimensional data, it is a strong candidate for a benchmark. The parameters are as follows: “n_neighbors” ranges from 1 to 30 in increments of 5; weights can be uniform; the algorithm options include "ball_tree, kd_tree, and brute;” "leaf_size” can be 1, 10, or 30; and p is 1 for manhattan distance and 2 for euclidean distance.

NB applies Bayes’ theorem under strong independence assumptions. It is computationally efficient and performs effectively with high-dimensional data. The smoothing parameter prevents zero probabilities for unseen data, so it was set to alpha: 0.01 to 10.0.

Decision trees split data hierarchically based on feature thresholds to predict target labels. Hyperparameters like depth and minimum samples help reduce overfitting with this algorithm. In addition, decision trees are interpretable and can handle nonlinear relationships. The parameters set were “max_depth”: 3 or none, “max_features”: randomized range, “min_samples_leaf”: randomized range, and criterion: gini or entropy.

While random forests are resilient to overfitting and excel across various datasets, parameter tuning aims to balance tree diversity with computational cost. The parameters include bootstrap: true, “max_depth”: the maximum depth of trees (10, 20, 50, 100, or None), “max_features”: the number of features considered (auto or sqrt), “min_samples_leaf”: options of 1, 2, or 4, “min_samples_split”: the minimum number of samples needed to split a node (2, 5, or 10), and “n_estimators”: the total number of trees in the forest (50 or 100).

XGBoost is an optimized gradient-boosting algorithm that iteratively improves model predictions. It is renowned for its performance with structured or tabular datasets, and through hyperparameter tuning, it seeks to minimize overfitting while boosting prediction accuracy. The parameters include “learning_rate”: 0.05 to 0.30, “max_depth”: the maximum depth of the trees (3 to 15), “min_child_weight”: the minimum sum of instance weights in a child node (1 to 7), gamma: the minimum loss reduction required to make a split (0.0 to 0.4), and “colsample_bytree”: the fraction of features sampled for each tree (0.3 to 0.7).

As a large margin classifier, the SVM identifies a hyperplane that best separates classes in high-dimensional space. While it is effective for both linear and nonlinear data, a linear kernel was used here for computational efficiency, given the dataset

XSL•FO
RenderX

size (kernel: linear kernel for simplicity and interpretability; probability: enabled for AUC-ROC computation).

Results

Literature Review Overview

The literature search yielded valuable insights into the relationship between machine learning algorithms and data quality, specifically focusing on semantic completeness within clinical datasets. After applying the screening process, the 12 retained articles provided key perspectives on data quality assessment, machine learning methodologies, and their application within clinical environments. A thorough analysis of these studies revealed several recurring themes. First, a significant portion of the literature addressed the challenges of ensuring semantic completeness in structured and unstructured clinical data. Several studies emphasized the necessity of standard terminologies and ontologies to enhance data consistency and interoperability. In addition, multiple sources explored different machine learning techniques, such as supervised and unsupervised learning approaches, to detect and mitigate issues related to incomplete or inconsistent data. Key insights from the literature were incorporated into the introduction and methodology sections, providing a solid theoretical foundation for this study. The findings underscored the importance of leveraging machine learning models to improve clinical data integrity and supported the need for robust evaluation metrics to quantify data quality improvements. The PRISMA (Preferred Reporting Items for Systematic reviews and Meta-Analyses) Flow Chart and detailed search strategy, presented in Table S2 of Multimedia Appendix 1, further outline the systematic approach used in identifying relevant studies.

Since here we consider quality prediction as a binary classification problem, we evaluated binary-class classifiers on the provided datasets. We then compared the results of each model in a table that included accuracy, precision, recall, and scoring.

Predictive Machine Learning Algorithms

Multiple machine learning algorithms were evaluated for predicting the quality of echocardiography data, with LR serving as the baseline model. LR achieved an accuracy of 73.0% (0.73/1), precision of 57.1% (0.571/1), recall of 73.0% (0.73/1), F_1-score of 64.1% (0.641/1), and an AUC-ROC score of 52.4% (0.524/1). While this model provides a foundational benchmark, other algorithms demonstrated superior performance across all metrics, suggesting their greater suitability for this dataset, as shown in Table 2.

KNN demonstrated improvements over LR, achieving an accuracy of 76.6% (0.766/1) and an AUC-ROC score of 70.3% (0.703/1). The improved precision (0.744/1, 74.4%) and F_1-score (0.684/1, 68.4%) emphasize its more effective balance of false positives and false negatives compared to the baseline.

NB attained a recall rate of 75.9% (0.759/1), comparable to KNN, but exhibited relatively lower precision at 57.6% (0.576/1) and an AUC-ROC score of 51.0%. This suggests a trade-off in its predictive performance.

The decision tree classifier slightly outperformed LR, reaching an accuracy of 73.7% (0.737/1) and an AUC-ROC score of 71.3% (0.713/1). The F_1-score of 73.7% (0.737/1) emphasizes its ability to maintain a balanced level of precision and recall.

The random forest classifier delivered a notable improvement, achieving an accuracy of 82.5% (0.825/1) and an AUC-ROC score of 85.3% (0.853/1). These metrics, alongside an F_1-score of 81.0% (0.81/1), highlight its robust performance and effectiveness in capturing complex patterns in the data.

XGB achieved the highest overall performance, with an accuracy of 84.7% and an AUC-ROC score of 84.6%. Its F_1-score of 84.0% and precision of 83.9% demonstrate its ability to consistently deliver high-accuracy predictions while minimizing false positives.

The SVM achieved an accuracy of 73.0%, comparable to that of LR, but it demonstrated an improvement in the AUC-ROC score of 65.7%. Its F_1-score of 67.1% reflects a slight enhancement in predictive balance.

The laboratory dataset consisted of 4000 data items. The performance of the machine learning algorithms was evaluated on the laboratory dataset, again using LR as the baseline model (refer to Table 3). LR achieved an accuracy of 99.8%, a precision of 99.5%, a recall of 99.8%, an F_1-score of 99.6%, and an AUC-ROC score of 33.1%. Although LR demonstrated strong results in accuracy, precision, and recall, its relatively low AUC-ROC score indicates limitations in its ability to effectively discriminate between classes.

XSL•FO
RenderX

Table . Scoring of the prediction classifiers (in percent) evaluated for the echocardiographic data set with Logistic Regression, K-Nearest Neighbors, Bayes Classifier, Decision Tree, Random Forest, Extreme Gradient Boosting, and SVM. While XGB's accuracy is 84.7, the AUC-ROC score is 84.6. In comparison, the accuracy of the RF is 82.5, but the AUC-ROC score is 85.3.

	Accuracy	Precision	Recall	F_1-score	AUC-ROC[a] score
Logistic regression	73.0	57.1	73.0	64.1	52.4
K nearest neighbors	76.6	74.4	76.6	68.4	70.3
Naive Bayes classifier	75.9	57.6	75.9	65.5	51.0
Decision tree classifier	73.7	73.7	73.7	73.7	71.3
Random forest classifier	82.5	81.3	82.5	81.0	85.3
Extreme gradient boosting	84.7	83.9	84.7	84.0	84.6
Support vector machine	73.0	65.2	73.0	67.1	65.7

[a]AUC-ROC: area under the receiver operating characteristic curve.

Table . Scoring of the prediction classifiers (in percent) evaluated for the laboratory data set with Logistic Regression, K-Nearest Neighbors, Bayes Classifier, Decision Tree, Random Forest, Extreme Gradient Boosting, and SVM. While the accuracy of all classifiers is nearly the same, SVM outperforms with the highest AUC-ROC score of 89.8.

	Accuracy	Precision	Recall	F_1-score	AUC-ROC[a] score
Logistic regression	99.8	99.5	99.8	99.6	33.1
K nearest neighbors	99.9	99.9	99.9	99.9	74.6
Naive Bayes classifier	99.8	99.5	99.8	99.6	50.0
Decision tree classifier	99.8	99.5	99.8	99.6	79.2
Random forest classifier	99.9	99.9	99.9	99.9	74.2
Extreme gradient boosting	99.5	99.7	99.5	99.6	59.3
Support vector machine	99.8	99.5	99.8	99.6	89.8

[a]AUC-ROC: area under the receiver operating characteristic curve.

KNN slightly outperformed LR in accuracy (0.999/1, 99.9%) and recall (99.9%). Its AUC-ROC score of 74.6% (0.746/1) indicates a notable enhancement in classification discrimination compared to LR.

NB achieved results similar to LR, with an accuracy of 99.8% (0.998/1) and an AUC-ROC score of 50.0% (0.5/1). Although its precision, recall, and F_1-score matched those of LR, the modest AUC-ROC score indicates potential limitations in distinguishing between classes in certain situations.

DT matched the accuracy, precision, and recall of LR but demonstrated a marked improvement in its AUC-ROC score (0.792/1, 79.2%). This highlights its enhanced ability to effectively separate classes despite similar performance on other metrics.

RF also achieved 99.9% (0.999/1) accuracy, precision, and recall, equaling KNN in these metrics. However, its AUC-ROC score of 74.2% (0.742/1) suggests that its performance in classification discrimination is slightly less robust than that of DT but still superior to LR.

XGB achieved a high accuracy of 99.5% (0.995/1) and an F_1-score of 99.6% (0.996/1). However, its AUC-ROC score of 59.3% (0.593/1) reveals its lower discrimination capacity compared to DT, RF, and KNN in this dataset.

SVM achieved strong results across all metrics, with accuracy, precision, recall, and F_1-score aligning with those of the top-performing models (99.8% - 99.9%). Notably, its AUC-ROC score of 89.8% (0.898/1) is the highest among all models, demonstrating superior discrimination performance within this dataset.

For the medication dataset, a sample of 4000 data items was cleaned and analyzed regarding the target quality. As shown in Table 4, the baseline model LR achieved an accuracy of 59.2% (0.592/1), precision of 35.0% (0.35/1), recall of 59.2% (0.592/1), an F_1-score of 44.0% (0.44/1), and an AUC-ROC score of 45.8% (0.458/1). Although it performed better than several models in terms of recall and accuracy, its overall low precision and AUC-ROC score indicate limited effectiveness in distinguishing between classes.

XSL•FO
RenderX

KNN performed lower than LR, with an accuracy of 48.3%, precision of 43.8%, and a slightly better F_1-score of 44.9%. However, its AUC-ROC score of 43.2% was lower, indicating weaker discriminatory ability compared to LR.

NB showed results similar to LR, achieving an accuracy of 58.3% and an F_1-score of 43.6%. However, its AUC-ROC score of 42.6% indicates slightly lower classification discrimination compared to LR.

DT achieved an accuracy of 51.7%, a precision of 39.5%, and a recall of 51.7%, resulting in an F_1-score of 42.5%. Its AUC-ROC score of 43.1% was comparable to that of KNN and NB, but slightly lower than LR, indicating similar performance levels.

RF and XGB performed poorly on this dataset. RF achieved an accuracy of 30.0%, an F_1-score of 29.5%, and an AUC-ROC score of 22.2%. XGB exhibited even lower accuracy at 21.7%, with precision at 23.3%, an F_1-score of 22.3%, and an AUC-ROC score of 19.0%, underscoring the significant limitations of these models for this dataset.

The SVM exhibited the most balanced performance among the models, achieving an AUC-ROC score of 65.1%, the highest across all models. Although it has a relatively low accuracy of 30.0% and an F_1-score of 30.0%, its AUC-ROC score suggests strong potential for distinguishing between classes.

Based on the results of testing different machine learning algorithms on the three datasets, the XGB model was deployed for echocardiographic data, the SVM for laboratory data, and the SVM for medication data during the UMG-MeDIC data inspection process.

The data inspection process used a hybrid approach, meaning that data quality inspection was not solely reliant on the trained model; conventional inspections were also conducted. To achieve this, it was decided that data items flagged as unsound during quality prediction would undergo traditional inspection to reduce false-positive rates and fine-tune the models. The classifiers were then retrained with the new test data.

Table . Scoring of the prediction classifiers evaluated for the medication data set with Logistic Regression, K-Nearest Neighbors, Bayes Classifier, Decision Tree, Random Forest, Extreme Gradient Boosting and SVM. While LR and NB performed with the best accuracy (59.2, 58.3), SVMs AUC-ROC score of 65.1 was the highest.

	Accuracy	Precision	Recall	F1-score	AUC-ROC score
Logistic regression	59.2	35.0	59.2	44.0	45.8
K nearest neighbors	48.3	43.8	48.3	44.9	43.2
Naive Bayes classifier	58.3	34.8	58.3	43.6	42.6
Decision tree classifier	51.7	39.5	51.7	42.5	43.1
Random forest classifier	30.0	29.0	30.0	29.5	22.2
Extreme gradient boosting	21.7	23.3	21.7	22.3	19.0
Support vector machine	30.0	32.1	30.0	30.0	65.1

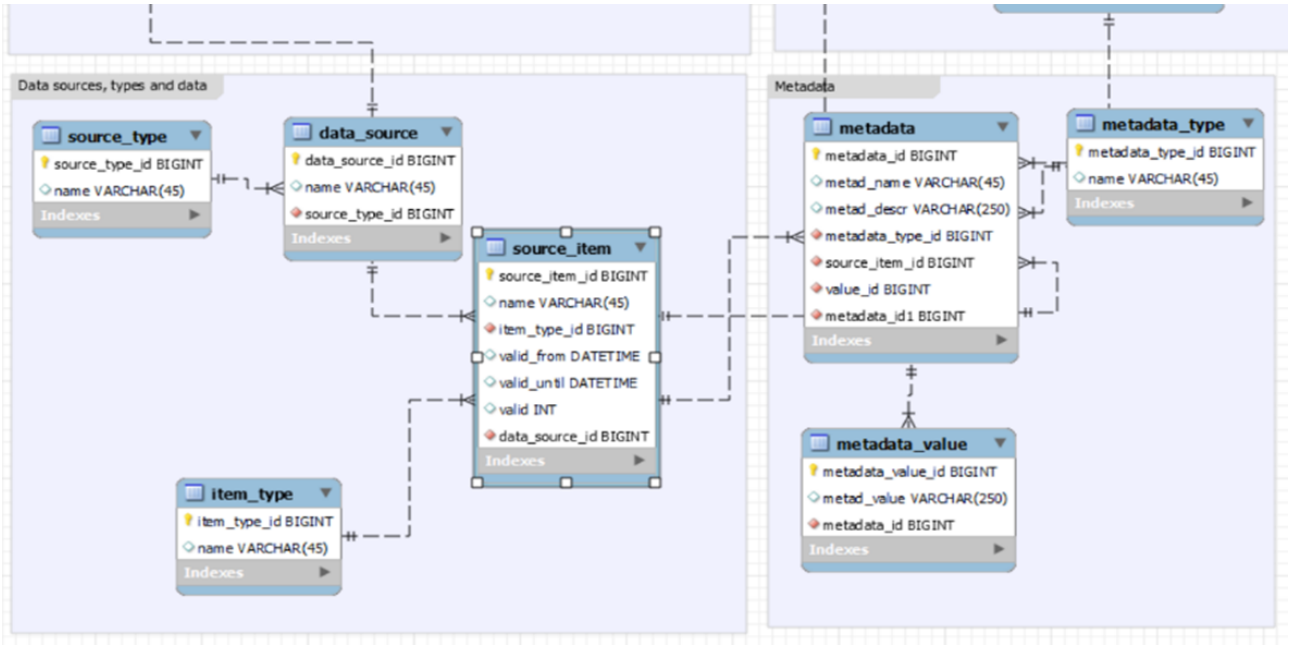
Prerequisite at the UMG-MeDIC

In general, predicting the data quality for echocardiography, laboratory, and medication data is now possible based on trained ML models, allowing the results to be made available to researchers. The relational structure established for metadata stores information in the metadata table, which includes an ID, the name of the metadata, a description of the metadata, and details about “metadata_type_id,” “source_item_id,” and “value_id,” all of which are inherited from other tables through foreign keys in the relational structure. The respective metadata value is stored in the metadata_value column of the metadata_value table, as illustrated in Figure 2.

The predictive quality information is integrated via SQL queries into the relational database within UMG-MeDIC. Specifically, the metadata for the predictive quality data is stored in the metadata table, while the corresponding results of the predictive quality analysis, in terms of actual values, are stored in the “metadata_value” table. This setup enables easy retrieval and analysis of the prediction results, as the metadata table acts as the central reference point for all integrated data, with each entry linking back to its respective predicted values in the metadata_value table. Figures 8 and 9 (second reference in Multimedia Appendix 1 [2]) illustrate an example of the metadata structure within the relational database that includes the added predictive quality information.

XSL•FO
RenderX

Figure 2. Relational structure and the metadata tables within the UMG-MeDIC (Medical Data Integration Center of the University Medical Center Göttingen).



Discussion

Conclusion

The benefits of RWD for medical care and research are numerous, ranging from clinical decision-making and patient-centered medicine to its application as synthetic controls in randomized trials. Moreover, real-world evidence enhances randomized controlled trials to bridge the efficacy-effectiveness gap. The central requirement for leveraging the data to achieve these advantages is data quality, particularly its reliability [26]. The quality of the data can be articulated or supported with corresponding metadata, thus further investigation into predicting data quality with AI is necessary. Given the significant importance of reliable health care data for researchers in reusing it, the UMG-MeDIC has incorporated metadata on data quality as easily accessible information.

Principal Findings

All previously collected metadata concerning the primary source systems of the UMG within CouchDB were extracted and transferred to the newly established generic relational metadata structure within the data warehouse (DWH), as described in Section Prerequisite at UMG-MeDIC. This relational structure aligns with the DWH's underlying design and serves as another principal finding of this work. After the algorithm transferred all existing metadata into the newly created relational metadata tables, the next step was to adjust the extract-transform-load (ETL) processes. In addition, metadata types, such as predicted data quality and data item language, which had not been previously collected and stored, are now being integrated into the existing metadata, providing more information about data reliability.

Based on the above results, predicting data quality for the 3 clinical datasets served as a case study. It evaluated the approach of predicting data quality within the ETL process, storing the resulting data quality as metadata alongside other metadata, and making the information available for researchers.

The study evaluated several machine learning models for predicting data quality across 3 different datasets: echocardiographic, laboratory, and medication data. The results of the echocardiographic data show that ensemble methods like RF and XGB outperform simpler models, including the baseline model LR and NB. The strong AUC-ROC scores of RF and XGB highlight their ability to effectively discriminate between classes, making them the most suitable models for this dataset.

While most models demonstrated high accuracy, precision, recall, and F_1-scores for predicting the laboratory data, significant variations were observed in AUC-ROC scores. SVM emerged as the most effective model for this dataset, combining high overall performance with the best class discrimination capabilities. KNN, DT, and RF also performed well, showing notable improvements over LR regarding AUC-ROC scores.

The medication dataset showed lower performance across all models. LR outperformed other models in terms of accuracy and recall, making it the most effective choice for this dataset. However, SVM's superior AUC-ROC score suggests it may be better suited for tasks requiring high class separation. Models like RF and XGB underperformed significantly, possibly due to the characteristics of this dataset in particular. This indicates a poor fit without further data engineering.

Comparison to Previous Work

To the best of our knowledge, data quality prediction based on specific quality factors for echocardiographic, laboratory, and medication data, as well as the usage and provision of the resulting data quality within metadata, have not yet been implemented.

Therefore, the approach taken in this work is aligned with similar studies in other fields. Schmitt et al describe a comparable procedure concerning the inspection process in the

XSL•FO
RenderX

electronic industry for producing programmable logic controllers. The predictive model-based quality inspection framework provided there was adapted for application in the Medical Data Integration Center.

Regarding metadata, no comparable examples were found in the field of medical data. However, a similar method for assessing the quality of medical data was employed by Haghighat et al for digitized histological glass slides, where they also used AI to evaluate the utility and diagnostic level of these images [27]. According to Georgiev and Valkanov, the future of DWH data quality, however, lies in further developing ETL processes towards dynamic and adaptable solutions with automated identification and elimination of quality issues based on artificial intelligence [28].

The existing metadata needed to be transferred and stored in the correct table at the right location. This process only had to be done once for slightly over 3,000 existing metadata documents. From now on, all additional metadata will be loaded directly into the relational metadata structure through adapted ETL routes. In contrast, Oukhouya et al propose a generic metadata management model designed specifically for data from heterogeneous sources to be stored in a DWH [29]. Their model is based on a data lake, a concept introduced in business intelligence architecture to manage large volumes of unstructured and semistructured data. They identified several essential functionalities of metadata that are critical for supporting a metadata management system. Requirements may vary significantly between DWHs in the medical field and those in other sectors. Nonetheless, this comprehensive model could serve as a starting point for developing suitable metadata management for medical DWHs to avoid reinventing the wheel. Therefore, in further developing metadata management for the DWH of UMG MeDIC, the extent to which the proposed model can provide applicable information for a relational database system should be evaluated.

Strengths and Limitations

First, the low performance of machine learning models, particularly in echocardiographic and medication samples, could be due to several factors. Models may struggle if the features in the dataset lack sufficient discriminatory power or if the presence of irrelevant or inconsistent data impairs their ability to learn effectively.

To address these issues, an error analysis was conducted to identify which classes are most often misclassified. Therefore, confusion matrices were used to identify false positives and false negatives for each model (see third reference in Multimedia Appendix 1 [3]).

Second, the high occurrence of false negatives in the LR, KNN, and NB indicates that the data within the medication dataset are composed of non-linear relationships. Furthermore, the high dimensionality (many features) of the medication dataset results in problematic KNN calculations. The confusion matrix for the DT shows that the model struggles to correctly identify class 0. It almost always predicts class 1, even when class 0 would be the correct prediction. To improve this behavior, we performed a threshold value optimization. The XGB model demonstrates significant weaknesses in class differentiation, particularly for class 0. A potential reason for this issue may be that the features lack sufficient discriminatory power. The same observation applies to RF and SVM.

The performance of the models within the echocardiography dataset indicates that the dataset includes non-linear relationships and dependencies among the features. The slightly higher performance of models like RF and XGB also suggests that non-linear relationships play a role.

Third, 750 data points may not be sufficient for models like RF, XGB, and SVM, which typically learn from a large number of parameters and data points. These models often require more data to generalize effectively.

Although the medication dataset model currently shows lower predictive performance (accuracy: 30%, AUC-ROC: 65.1%), it has been integrated into the data inspection process as part of a hybrid approach, where automated predictions enhance traditional inspection methods. Rather than replacing manual review, the model assists in prioritizing data items for further inspection, enabling data stewards to concentrate on potentially lower-quality records.

Continual model retraining poses challenges, including catastrophic forgetting, data drift, and a need for robust evaluation strategies [30,31]. To tackle these issues, the model undergoes scheduled retraining with updated data while performance is monitored using metrics such as accuracy, recall, and AUC-ROC. The impact of human factors in creating, consolidating, and evaluating the database, especially regarding potential errors, must be taken into account. Moreover, it can be assumed that an increased number of connected systems in a MeDIC will reduce human errors but also create new types of errors [32].

Thus, newly flagged data points undergo manual verification before being included in future training iterations, ensuring that retraining enhances rather than diminishes performance. In productive operation, new, realistic data is often continuously available, better reflecting how the target variables behave in real life. Additionally, models such as RF, XGB, and SVM significantly benefit from a larger database, allowing them to learn more reliable patterns.

The machine learning algorithms ran on a laptop with Microsoft Windows 11 Pro, which features an Intel Core processor with 4 cores. The prediction runtime was about 10 minutes for all the algorithms. The models are currently deployed at UMG-MeDIC, and there is an inspection strategy in place that follows a hybrid approach.

However, it is important to note that the technical implementation of the relational data structure depends on the inherent and specific requirements of the UMG-MeDIC. This means that while the data storage is specialized, the quality prediction of the clinical data remains unaffected by it.

Nevertheless, scalability for datasets containing vastly different types of clinical data, such as imaging data or genomic sequences, may require additional preprocessing or adaptation steps. For instance, the features extracted from such data may

XSL•FO
RenderX

vary significantly from those used in the current work, necessitating customized data preparation pipelines and potentially adjusted analytical models. Furthermore, the quality scale employed was established as binary, using 0 and 1; a more refined granularity of the quality scale is pending further development.

Future Directions

Future work aims to enhance model performance by applying feature engineering, using data augmentation techniques, and investigating possible adjustments in model selection. Despite current limitations, even imperfect predictive models are valuable as they direct manual review efforts, reduce workload, and improve overall data quality assessment.

Furthermore, it must be discussed to what extent the metadata published in the different data formats contain the risk of reidentification. Metadata do not intrinsically contain any personal data within the UMG-MeDIC. However, it must be examined how far the linkage of the metadata with further information or the uniqueness of the metadata increase the risk of re-identification.

The ability to provide researchers with quality information on data they want to inspect and research is a key success factor for reliable medical and biomedical research, avoiding the "garbage in—garbage out" paradigm [33]. Due to the abundance of data accessible in a medical data integration center, employing predictive model-based quality inspection shows great promise in ensuring reliable data for medical research.

However, real-world deployment brings additional challenges such as data drift, generalizability across clinical settings, and resilience against distribution shifts. Additionally, it's important to note that as more systems connect within a MeDIC, human errors (eg, transmission errors) decline, yet new types of errors may arise, which are part of the continuous learning process of these systems.

Moving forward, it is necessary to conduct a postdeployment evaluation, which includes the monitoring of prediction performance on live data at the UMG-MeDIC data integration center, comparing model outputs with manual quality assessments from data stewards, testing on external datasets to ensure generalizability beyond internal sources, and longitudinal tracking of model performance to detect degradation over time.

This expanded evaluation will allow us to refine model performance, improve generalization, and provide a more comprehensive assessment of real-world impact. By integrating these additional validation steps, we aim to ensure the long-term reliability and effectiveness of our approach in clinical data quality assessment.

Acknowledgments

The authors acknowledge the support and provision of metadata by the Medical Data Integration Center of the University Medical Center Göttingen. The authors disclose that no generative AI was used in any portion of the manuscript. This research received funding from the German Federal Ministry of Education and Research within the project FAIRRMeDIC, grant number 01ZZ2012 (to TS), and the MII-DIFUTURE-Ulm project, grant number 01ZZ2304E (to HAK).

Data Availability

The datasets generated or analyzed during this study are not publicly available due to reasons of data protection but are available from the corresponding author on reasonable request.

Authors' Contributions

TK coordinated, and TK and HAK supervised this research project. CB wrote the manuscript, implemented the transfer of previous metadata, developed the relational data structure for the metadata, executed the machine learning models for the predictive quality approach, and carried out the testing and implementation of the data inspection process. CS assisted in the transfer of the previous metadata. DK, TK, and HAK contributed to the conceptualization of the research and participated in the revision, editing, and final approval of the manuscript. All authors read and accepted the final revision of this manuscript.

Conflicts of Interest

None declared.

Multimedia Appendix 1
Depiction of Supplementary Material including additional data, figures, and detailed methods supporting the findings presented in the main manuscript.
[PDF File, 831 KB - medinform_v13i1e60204_app1.pdf]

Multimedia Appendix 2
Comparison of the target distribution within the three subsets of echocardiographic data(750 samples), laboratory data (4000 samples) and medication data (4000 samples). The dark grey category comprises data samples with satisfactory quality (quality = 1) and the light grey category depicts data with unsatisfactory quality (quality = 0).

XSL•FO
RenderX

[DOCX File, 60 KB - medinform_v13i1e60204_app2.docx]

References

1. Sackett DL, Rosenberg WM, Gray JA, Haynes RB, Richardson WS. Evidence based medicine: what it is and what it isn't. BMJ 1996 Jan 13;312(7023):71-72. [doi: 10.1136/bmj.312.7023.71] [Medline: 8555924]
2. U.S. Food and Drug Administration. Real-world evidence. 2024. URL: https://www.fda.gov/science-research/science-and-research-special-topics/real-world-evidence [accessed 2024-11-13]
3. Safran C, Bloomrosen M, Hammond WE, et al. Toward a national framework for the secondary use of health data: an American Medical Informatics Association White Paper. J Am Med Inform Assoc 2007;14(1):1-9. [doi: 10.1197/jamia.M2273] [Medline: 17077452]
4. Ta CN, Weng C. Detecting systemic data quality issues in electronic health records. Stud Health Technol Inform 2019 Aug 21;264:383-387. [doi: 10.3233/SHTI190248] [Medline: 31437950]
5. Gehring S, Eulenfeld R. German medical informatics initiative: unlocking data for research and health care. Methods Inf Med 2018 Jul;57(S 01):e46-e49. [doi: 10.3414/ME18-13-0001] [Medline: 30016817]
6. Parciak M, Suhr M, Schmidt C, et al. FAIRness through automation: development of an automated medical data integration infrastructure for FAIR health data in a maximum care university hospital. BMC Med Inform Decis Mak 2023 May 15;23(1):94. [doi: 10.1186/s12911-023-02195-3] [Medline: 37189148]
7. Floor-Schreudering A, Heringa M, Buurma H, Bouvy ML, De Smet PAGM. Missed drug therapy alerts as a consequence of incomplete electronic patient records in Dutch community pharmacies. Ann Pharmacother 2013 Oct;47(10):1272-1279. [doi: 10.1177/1060028013501992] [Medline: 24259691]
8. Ulrich H, Kock-Schoppenhauer AK, Deppenwiese N, et al. Understanding the nature of metadata: systematic review. J Med Internet Res 2022 Jan 11;24(1):e25440. [doi: 10.2196/25440] [Medline: 35014967]
9. Alkhubouli MA, Lala HM, AlHabshy AA, ElDahshan KA. Enhancing data warehouses security. IJACSA 2024;15(3). [doi: 10.14569/IJACSA.2024.0150358]
10. Nalbach O, Linn C, Derouet M, Werth D. Business information systems. In: Abramowicz W, Paschke A, editors. : Springer Presented at: Lecture Notes in Business Information Processing; Jun 16, 2018 p. 13-42. [doi: 10.1007/978-3-319-93931-5_3]
11. Bönisch C, Kesztyüs D, Kesztyüs TI. FAIR+R: making clinical data reliable through qualitative metadata. Stud Health Technol Inform 2024 Jan 25;310:99-103. [doi: 10.3233/SHTI230935] [Medline: 38269773]
12. Tercan H, Meisen T. Machine learning and deep learning based predictive quality in manufacturing: a systematic review. J Intell Manuf 2022 Oct;33(7):1879-1905. [doi: 10.1007/s10845-022-01963-8]
13. Schmitt J, Bönig J, Borggräfe T, Beitinger G, Deuse J. Predictive model-based quality inspection using machine learning and edge cloud computing. Advanced Engineering Informatics 2020 Aug;45:101101. [doi: 10.1016/j.aei.2020.101101]
14. Weiskopf NG, Weng C. Methods and dimensions of electronic health record data quality assessment: enabling reuse for clinical research. J Am Med Inform Assoc 2013 Jan 1;20(1):144-151. [doi: 10.1136/amiajnl-2011-000681] [Medline: 22733976]
15. Khare R, Utidjian L, Ruth BJ, et al. A longitudinal analysis of data quality in a large pediatric data research network. J Am Med Inform Assoc 2017 Nov 1;24(6):1072-1079. [doi: 10.1093/jamia/ocx033] [Medline: 28398525]
16. Reimer AP, Milinovich A, Madigan EA. Data quality assessment framework to assess electronic medical record data for use in research. Int J Med Inform 2016 Jun;90:40-47. [doi: 10.1016/j.ijmedinf.2016.03.006] [Medline: 27103196]
17. Tute E, Scheffner I, Marschollek M. A method for interoperable knowledge-based data quality assessment. BMC Med Inform Decis Mak 2021 Mar 9;21(1):93. [doi: 10.1186/s12911-021-01458-1] [Medline: 33750371]
18. Breiman L. Statistical modeling: the two cultures (with comments and a rejoinder by the author). Statist Sci 2001;16(3):199-231. [doi: 10.1214/ss/1009213726]
19. Zhang Z. Introduction to machine learning: k-nearest neighbors. Ann Transl Med 2016 Jun;4(11):218. [doi: 10.21037/atm.2016.03.37] [Medline: 27386492]
20. Friedman N, Geiger D, Goldszmidt M. Bayesian network classifiers. Mach Learn 1997;29(2/3):131-163. [doi: 10.1023/A:1007465528199]
21. Quinlan JR. Induction of decision trees. Mach Learn 1986 Mar;1(1):81-106. [doi: 10.1007/BF00116251]
22. Breiman L. Random forests. Mach Learn 2001;45(1):5-32. [doi: 10.1023/A:1010933404324]
23. Chen T, Guestrin C. XGBoost: a scalable tree boosting system. Presented at: KDD '16: Proceedings of the 22nd ACM SIGKDD International Conference on Knowledge Discovery and Data Mining San Francisco, CA, USA; Aug 13-17, 2016. [doi: 10.1145/2939672.2939785]
24. Shmilovici A. Support vector machines. In: Maimon O, Rokach L, editors. Data Mining and Knowledge Discovery Handbook: Springer; 2005. [doi: 10.1007/0-387-25465-X_12]
25. Wolpert DH, Macready WG. No free lunch theorems for optimization. IEEE Trans Evol Computat 1997 Apr;1(1):67-82. [doi: 10.1109/4235.585893]
26. Wang SV, Schneeweiss S. Data checks before registering study protocols for health care database analyses. JAMA 2024 May 7;331(17):1445-1446. [doi: 10.1001/jama.2024.2988] [Medline: 38587830]

XSL•FO
RenderX

27. Haghighat M, Browning L, Sirinukunwattana K, et al. Automated quality assessment of large digitised histology cohorts by artificial intelligence. Sci Rep 2022 Mar 23;12(1):5002. [doi: 10.1038/s41598-022-08351-5] [Medline: 35322056]
28. Georgiev A, Valkanov V. Custom data quality mechanism in data warehouse facilitated by data integrity checks. MEM 2024;53:67-75. [doi: 10.55630/mem.2024.53.067-075]
29. Oukhouya L, El haddadi A, Er-raha B, Asri H. A generic metadata management model for heterogeneous sources in a data warehouse. E3S Web Conf 2021;297:01069. [doi: 10.1051/e3sconf/202129701069]
30. Goodfellow I J, Mirza M, Xiao D, Courville A, Bengio Y. An empirical investigation of catastrophic forgetting in gradient-based neural networks. arXiv. Preprint posted online on 2013. [doi: 10.48550/ARXIV.1312.6211]
31. Lu J, Liu A, Dong F, Gu F, Gama J, Zhang G. Learning under concept drift: a review. IEEE Trans Knowl Data Eng 2018;31(12):1. [doi: 10.1109/TKDE.2018.2876857]
32. Yusof MM, Takeda T, Shimai Y, Mihara N, Matsumura Y. Evaluating health information systems-related errors using the human, organization, process, technology-fit (HOPT-fit) framework. Health Informatics J 2024;30(2):14604582241252763. [doi: 10.1177/14604582241252763] [Medline: 38805345]
33. Kilkenny MF, Robinson KM. Data quality: “garbage in – garbage out”. HIM J 2018 Sep;47(3):103-105. [doi: 10.1177/1833358318774357]

Abbreviations

AI: artificial intelligence
AUC-ROC: area under the receiver operating characteristic curve
DWH: data warehouse
ETL: Extract-Transform-Load
KNN: k-nearest neighbor
LR: logistic regression
MeDIC: Medical Data Integration Center
NB: Naive Bayes
PRISMA: Preferred Reporting Items for Systematic reviews and Meta-Analyses
RWD: real world data
SMOTE: Synthetic Minority Oversampling Technique
SVM: support vector machine
UMG: University Medical Center Göttingen
XGB: extreme gradient boosting

Edited by A Coristine; submitted 04.05.24; peer-reviewed by H Turbe, SA Sadegh-Zadeh; revised version received 01.04.25; accepted 01.04.25; published 30.06.25.

Please cite as:
Bönisch C, Schmidt C, Kesztyüs D, Kestler HA, Kesztyüs T
Proposal for Using AI to Assess Clinical Data Integrity and Generate Metadata: Algorithm Development and Validation
JMIR Med Inform 2025;13:e60204
URL: https://medinform.jmir.org/2025/1/e60204
doi:10.2196/60204

© Caroline Bönisch, Christian Schmidt, Dorothea Kesztyüs, Hans A Kestler, Tibor Kesztyüs. Originally published in JMIR Medical Informatics (https://medinform.jmir.org), 30.6.2025. This is an open-access article distributed under the terms of the Creative Commons Attribution License (https://creativecommons.org/licenses/by/4.0/), which permits unrestricted use, distribution, and reproduction in any medium, provided the original work, first published in JMIR Medical Informatics, is properly cited. The complete bibliographic information, a link to the original publication on https://medinform.jmir.org/, as well as this copyright and license information must be included.

XSL•FO
RenderX

Performance of an Electronic Health Record–Based Automated Pulmonary Embolism Severity Index Score Calculator: Cohort Study in the Emergency Department

Elizabeth Joyce[1], MSc, MD; James McMullen[2], MD; Xiaowen Kong[3], MA; Connor O'Hare[4], MD; Valerie Gavrila[5], MPH; Anthony Cuttitta[5], MPH; Geoffrey D Barnes[3], MSc, MD; Colin F Greineder[4], MD, PhD

[1]Department of Internal Medicine, University of Michigan, Ann Arbor, MI, United States

[2]Department of Internal Medicine, University of San Francisco, San Francisco, CA, United States

[3]Department of Cardiology, University of Michigan, Ann Arbor, MI, United States

[4]Department of Emergency Medicine, University of Michigan, Ann Arbor, MI, United States

[5]Michigan Program on Value Enhancement (MPrOVE), University of Michigan, Ann Arbor, MI, United States

Corresponding Author:
Colin F Greineder, MD, PhD
Department of Emergency Medicine, University of Michigan, Ann Arbor, MI, United States

Abstract

Background: Studies suggest that less than 4% of patients with pulmonary embolisms (PEs) are managed in the outpatient setting. Strong evidence and multiple guidelines support the use of the Pulmonary Embolism Severity Index (PESI) for the identification of acute PE patients appropriate for outpatient management. However, calculating the PESI score can be inconvenient in a busy emergency department (ED). To facilitate integration into ED workflow, we created a 2023 Epic-compatible clinical decision support tool that automatically calculates the PESI score in real-time with patients' electronic health data (ePESI [Electronic Pulmonary Embolism Severity Index]).

Objective: The primary objectives of this study were to determine the overall accuracy of ePESI and its ability to correctly distinguish high- and low-risk PESI scores within the Epic 2023 software. The secondary objective was to identify variables that impact ePESI accuracy.

Methods: We collected ePESI scores on 500 consecutive patients at least 18 years old who underwent a computerized tomography-pulmonary embolism scan in the ED of our tertiary, academic health center between January 3 and February 15, 2023. We compared ePESI results to a PESI score calculated by 2 independent, medically-trained abstractors blinded to the ePESI and each other's results. ePESI accuracy was calculated with binomial test. The odds ratio (OR) was calculated using logistic regression.

Results: Of the 500 patients, a total of 203 (40.6%) and 297 (59.4%) patients had low- and high-risk PESI scores, respectively. The ePESI exactly matched the calculated PESI in 394 out of 500 cases, with an accuracy of 78.8% (95% CI 74.9% - 82.3%), and correctly identified low- versus high-risk in 477 out of 500 (95.4%) cases. The accuracy of the ePESI was higher for low-risk scores (OR 2.96, P<.001) and lower when patients were without prior encounters in the health system (OR 0.42, P=.008).

Conclusions: In this single-center study, the ePESI was highly accurate in discriminating between low- and high-risk scores. The clinical decision support should facilitate real-time identification of patients who may be candidates for outpatient PE management.

(JMIR Med Inform 2025;13:e58800) doi:10.2196/58800

KEYWORDS

pulmonary embolism; low-risk pulmonary embolism; risk; artery; pulmonary embolism severity index; clinical decision support; emergency department; hospital; lung; blood; clot; clotting; cardiovascular; index; score; measure; scale; tomography; image; imaging; PESI; CDS; ED

Introduction

While many patients with acute pulmonary embolism (PE) are at increased risk of cardiovascular complications, a significant minority have a low risk of short-term adverse outcomes and no requirement for hospital-level therapies [1]. There is now strong evidence to recommend outpatient management of PE patients identified as low-risk using tools like the Pulmonary Embolism Severity Index (PESI) [2-5].

XSL•FO
RenderX

The PESI score combines demographics (age and sex), comorbidities (history of cancer, heart failure, and chronic lung disease), vital signs (temperature, heart rate, respiratory rate, blood pressure, oxygen saturation), and mental status to stratify acute PE patients according to 30 days all-cause mortality, with classes I (PESI score <66) and II (PESI score 66 - 86) being categorized as "low-risk" [2,6]. Despite multiple society-backed guidelines recommending that these patients with low-risk acute PE be provided anticoagulation and discharged directly from the emergency department (ED) [7-9], a recent analysis of over 60,000 cases of acute PE in the US found that less than 4% of patients were managed in the outpatient setting [10]. While there seems to be some variation at the hospital system level, the rate of outpatient management in the US remains substantially lower than in Canada and parts of Europe [11-13].

One potential barrier to increasing outpatient management of low-risk PE is identifying appropriate patients [5,14,15]. Although there are risk-stratification tools, these can be cumbersome to use in a real-world setting. The PESI score, while recommended by guidelines, incorporates 11 clinical variables that have different weights, making it cumbersome to calculate. This may be exacerbated by physician uncertainty regarding specific elements of the score—for example, what constitutes history of cancer?—and the fact that the score can change over the course of ED evaluation, that is, due to changes in mental status and vital signs. A group from the Kaiser Permanente health system previously reported an automated clinical decision support (CDS) tool, which calculates the PESI score based on data already captured in the electronic health record [16]. While found to be highly accurate in predicting patient risk category, that tool was specific to the Kaiser Permanente Epic-based electronic health record (EHR), which was implemented in 2005 and included health-system-specific features, like an improved problem list.

To promote PESI use in our hospital and facilitate more consistent implementation across other health systems, we created a new CDS within our 2023 Epic-based EHR featuring an electronic PESI calculator, or "ePESI" that automatically calculates a patient's PESI score when a computerized tomography-pulmonary embolism (CT-PE) is ordered. Systematic reviews of CDS system accuracy and use identify poor data quality, poor integration into workflow, patient complexity, inadequate CDS testing, and inadequate user training as negatively impacting the agreement between CDS recommendations and provider decisions [17-20]. In an attempt to account for these limitations, our ePESI underwent over 1 year of testing and multiple revisions. The aim of this study was to determine how well our ePESI captures specific electronic elements from the EHR demonstrating the overall accuracy of the ePESI and its ability to discriminate between patients who would be high- and low-risk if they had a PE, based on PESI score.

Methods

Development of the ePESI

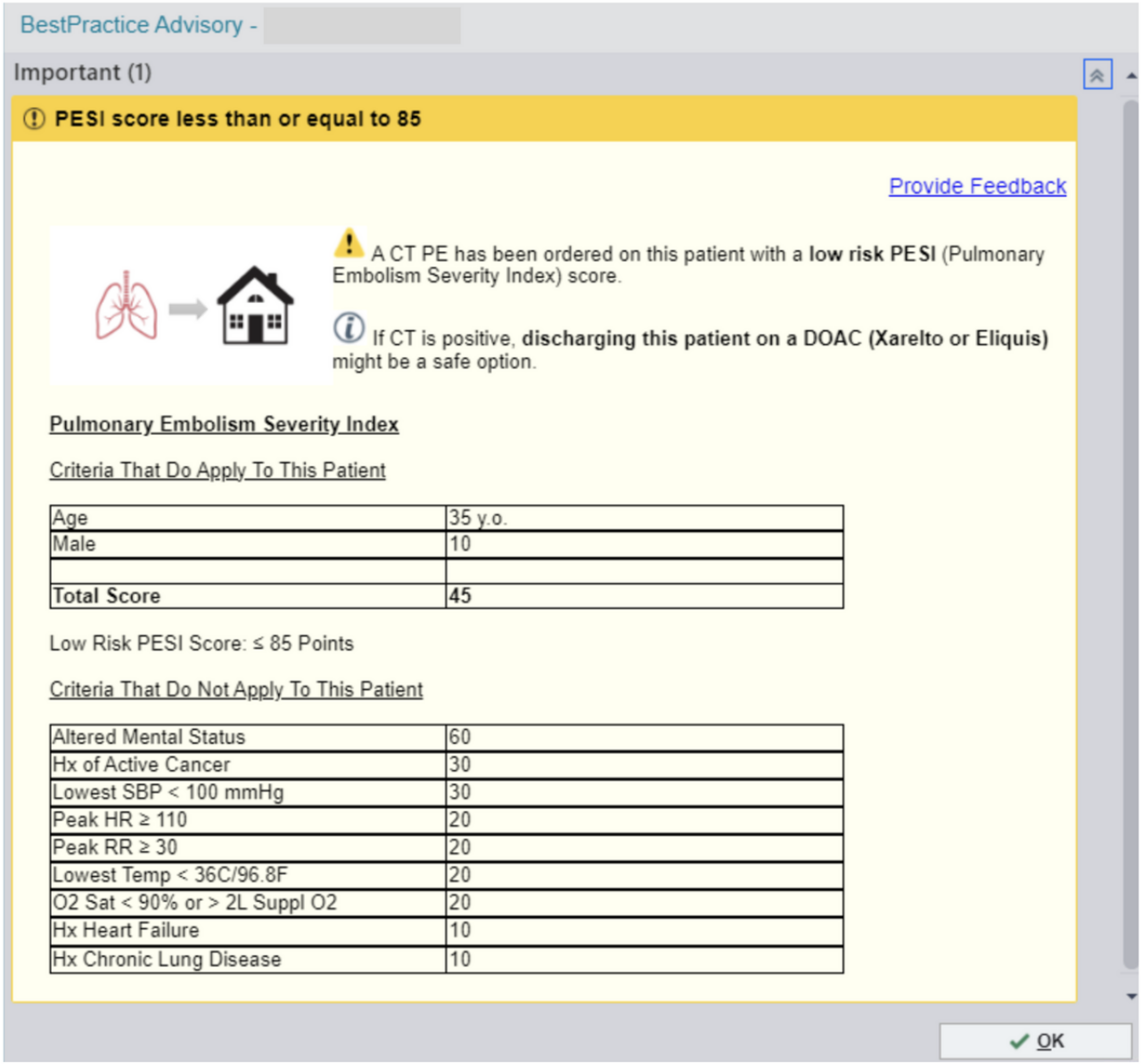
The ePESI score was calculated automatically from data available in the EHR. Comorbidities were taken from the patient's active problem list and past medical history using preestablished SNOMED (Systematized Nomenclature of Medicine) hierarchical concept codes (Multimedia Appendix 1). Vital sign criteria were assigned using peak vital signs from the patient's Flowsheet (ie, structured ED nursing documentation)—that is, highest heart rate and respiratory rate, lowest systolic blood pressure, etc. The PESI element "oxygen saturation <90%" was considered positive if the patient had a documented pulse oximetry reading of <90%, or if they had been placed on >2 L/min of oxygen, >2 L/min above their home O2 requirement, or a respiratory-assist device such as BiPAP (bilevel positive airway pressure) or CPAP (continuous positive airway pressure), venturi mask, high-flow catheter, or mechanical ventilator. Altered mental status was defined as Glasgow Coma Scale (GCS) <14 in structured ED nursing documentation or "Altered Mental Status" in the patient's chief concern at ED presentation.

Study Design, Setting, and Population

In March 2022, a "pre-commitment" strategy was implemented in our ED to encourage outpatient management of low-risk acute PE [21]. The ePESI was calculated in all patients in whom a CT-PE was ordered. In patients with ePESI <86, the overall score and the individual elements were displayed to the treating clinician at the time of CT-PE order, encouraging them to consider outpatient management if a PE was ultimately diagnosed (Figure 1). In this study, we examined ePESI results in 500 consecutive patients who underwent CT-PE between January 3 and February 15, 2023. We included all patients, regardless of their CT-PE scan result, because the presence or absence of a PE should not influence the CDS accuracy when sampling electronic health data.

XSL•FO
RenderX

Figure 1. Image of the best practice alert presented to clinicians, depicting the Electronic Pulmonary Embolism Severity Index (ePESI) score. CT: computed tomography; DOAC: direct oral anticoagulant; HR: heart rate; Hx: history; O2 Sat: oxygen saturation, as measured by pulse oximetry; PE: pulmonary embolism; RR: respiratory rate; SBP: systolic blood pressure; Suppl O2: supplemental oxygen; Temp: temperature.



Ethical Considerations

This study was exempt from the institutional review board at the University of Michigan given that it was in regard to procedures rather than individual patients (HUM00217018). Participant consent was waived by the institutional review board. Permission was obtained from Epic to display any images of the ePESI.

Physician PESI (pPESI)

Two independent, medically-trained reviewers (EJ and JM) abstracted data from the EHR on all patients and calculated a physician PESI (pPESI) score using a standardized abstraction form (Multimedia Appendix 2). Both data abstraction and pPESI calculation occurred retrospectively, after all 500 cases had been identified. While reviewers could not be blinded to the study hypothesis, they were blinded to the ePESI score and to each other's pPESI scores. In cases where the 2 reviewers did not agree, a third reviewer (CO) abstracted data and calculated another blinded pPESI.

Statistical Analysis

Descriptive statistics, reported as proportions, were used to describe relevant characteristics of the patient population and their PESI scores. All cases in which the ePESI and pPESI did not agree underwent retrospective chart review to identify the discrepancy. Statistical analysis was used to compare ePESI and pPESI, with pPESI as the gold standard. The ePESI accuracy was computed via binomial test and reported with the 95% CI. Dichotomous predictors of ePESI accuracy were identified with a priori hypotheses and evaluated using odds ratios (OR). The OR was computed using logistic regression with continuous scoring. The error rates of individual ePESI components were reported as proportions and evaluated with

XSL•FO
RenderX

ANOVA. *P* values of <.05 were considered statistically significant. Inter-rater reliability was reported as a Cohen κ coefficient. All data analysis was conducted with SAS (version 9.4; SAS Institute).

Results

Of the 500 consecutive patients in whom ePESI results were evaluated, 203 (40.6%) patients had low-risk scores (ePESI<86) and 297 (59.4%) patients with high-risk scores (ePESI≥86) (Table 1). The most frequent risk class was class V (133/500, 26.6%), followed by class I (112/500, 22.4%). A total of 90% of patients (450/500) had had at least 1 encounter in the health institution's EHR prior to their index ED visit, whereas the remaining 10% of patients presented to the ED for their first entry into the health institution's EHR. For those with prior encounters, the median time between index ED visit and previous EHR entry was 14 days (IQR 4 - 50.7). Of the 500 study patients undergoing CT-PE, a pulmonary embolism was diagnosed in 47 patients (9.4%), of which 40 patients (85.1%) had an acute PE and 7 patients (14.9%) had subacute PE, chronic PE, or an equivocal study. Interrater reliability for the pPESI score was high, with Cohen κ coefficient of 0.98 (95% CI 0.97 - 0.98).

Table . Patient characteristics.

Characteristics	Values
Age (years), mean (SD)	58.2 (17.7)
Biologic male, n (%)	219 (43.8)
Comorbidities, n (%)	
History of cancer	185 (37)
History of heart failure	88 (17.6)
History of chronic lung disease	205 (41)
High risk versus low risk, n (%)	
High risk	297 (59.4)
Low risk	203 (40.6)
Class of risk, n (%)	
Class I	112 (22.4)
Class II	91 (18.2)
Class III	84 (16.8)
Class IV	80 (16)
Class V	133 (26.6)
First visit at health institution, n (%)	
Yes	50 (10)
No	450 (90)
CT-PE[a] scan report result, n (%)	
Acute PE[b]	40 (8)
Chronic PE	6 (1.2)
Acute on chronic PE	1 (0.2)
Other	3 (0.6)
No PE (negative)	451 (90.2)

[a]CT-PE: computed tomography scan-pulmonary embolism.

[b]PE: pulmonary embolism.

The ePESI and pPESI scores matched exactly in 394 out of 500 cases, for an accuracy of 78.8% (95% CI 74.9% - 82.3%) (Figure 2). For the subset of patients with an acute PE found on CT-PE, the accuracy was 82.5% (95% CI 67.2% - 92.7%) (Tables 2-4). The ePESI correctly categorized risk class (I-V) in 442 out of 500 (88.4%) cases and correctly identified high- or low-risk in 477 out of 500 (95.4%) cases. For cases where the ePESI and pPESI did not agree on high- or low-risk, the ePESI incorrectly identified cases as low-risk in 15 out of 23 (65.2%) and incorrectly identified cases as high-risk in 8 out of 23 (34.8%) patients. The odds of the ePESI and pPESI agreeing increased if scores were low-risk by pPESI (OR 2.96, CI 1.78-4.91, *P*<.001) (Table 5). The odds of the ePESI and pPESI agreeing decreased if the index ED visit represented the patient's first entry in the institution's EHR (OR 0.42, CI 0.214-0.788, *P*=.008).

XSL•FO
RenderX

Figure 2. Bland-Altman plot demonstrating the agreement between the absolute value of ePESI and pPESI. ePESI: Electronic Pulmonary Embolism Severity Index; pPESI: Physician Pulmonary Embolism Severity Index.

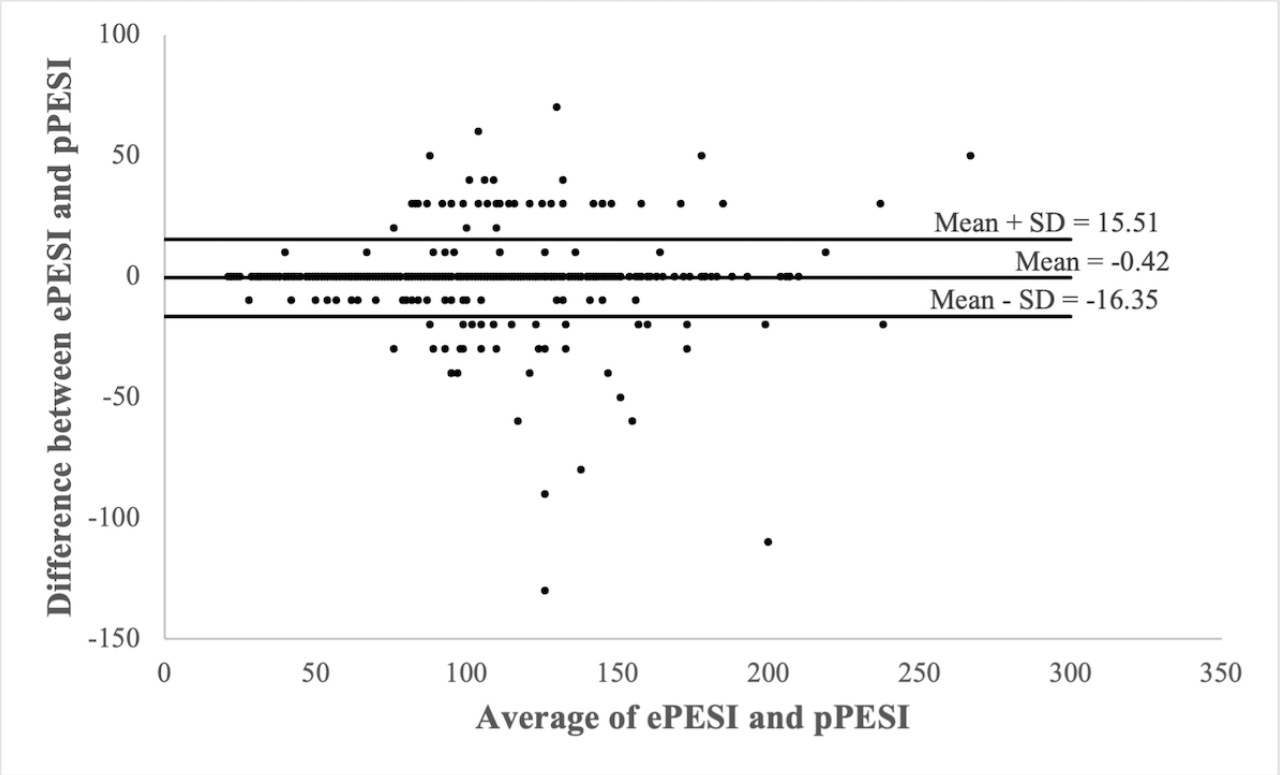


Table . Comparison of Electronic Pulmonary Embolism Severity Index (ePESI) and Physician Pulmonary Embolism Severity Index (pPESI).

	pPESI correct	pPESI incorrect
ePESI correct	394	9
ePESI incorrect	92	5

Table . Electronic Pulmonary Embolism Severity Index (ePESI) accuracy for full cohort and positive computerized tomography-pulmonary embolism (CT-PE) cohort.

	Number, n (%)	Accuracy, % (95% CI)
Full cohort	500 (100)	78.8 (74.9 - 82.3)
Positive CT-PE	40 (8)	82.5 (67.2 - 92.7)

Table . Electronic Pulmonary Embolism Severity Index (ePESI) performance for cohorts.

Cohort	Correct, n (%)	Incorrect, n (%)
High- versus low-risk PESI[a]	477 (95.4)	23 (4.6)
Class of risk	442 (88.4)	52 (11.6)

[a]PESI: Pulmonary Embolism Severity Index.

Table . Logistic regression modeled Physician Pulmonary Embolism Severity Index (pPESI) and Electronic Pulmonary Embolism Severity Index (ePESI) result agreeing by dichotomous predictor.

Variable	Odds ratio	95% CI	*P* value
Highlow (low vs high)	2.96	1.78 - 4.91	<.001
First time at health system (yes vs no)	0.41	0.21 - 0.79	.008

When considering individual components of the ePESI, age was most often correctly identified (n=500, 100% correct), while the history of cancer was least often correctly identified (n=459, 91.8% correct) (Table 6). Sex was incorrectly identified by

XSL•FO
RenderX

ePESI in 1 (0.2%) case, for a transgender patient in which gender and sex assigned at birth had been conflated in the EHR.

Table . Comparison of errors. Number of patients with each type of error is indicated above each bar. Patients could have more than 1 type of error.

Types[a]	Variable, n (%)
Cancer error	42 (8.4)
HF[b] error	16 (3.2)
CLD[c] error	27 (5.4)
Vitals error	23 (4.6)
Other	1 (0.2)

[a]*P* value<.001.

[b]HF: heart failure.

[c]CLD: chronic lung disease.

Discussion

Overview

In this single-center cohort study, we demonstrated the accuracy of an EHR-based ePESI calculator built into the Epic 2023 system. The ePESI was particularly effective at discriminating between low- and high-risk cases, with 95% (477/500) correctly scoring as high- or low-risk as compared with a gold standard of multiple physician review. The accuracy of our ePESI calculator is similar to that of the PESI CDS tool developed by the Kaiser Permanente health system in 2015 [16], but it has the advantage of being compatible with Epic 2023 software and minimally reliant on health system-specific features. This should enable straightforward transfer to other health systems using Epic-based EHRs. Since 2015, Epic has surpassed Cerner as the most common EHR in the United States, and comprises 36% of the market share as of 2023 [22,23]. Epic is also gaining international use [24]. Given the increasingly widespread use of Epic EHR and interest in implementing outpatient management pathways for low-risk PE patients, we anticipate that the ePESI calculator built into the Epic 2023 software that can be readily exported to other health systems will be of interest to many EDs around the world.

Apart from the overall performance of the ePESI calculator, our study has several interesting findings with respect to automated risk score calculation. First, the ePESI calculator performed better when the ePESI score was low risk and in patients who had been seen within our health system previously. These findings are not entirely unexpected, as most ePESI errors were due to incorrect scoring of patient comorbidities (ie, cancer, heart failure, and lung disease), which were more common in high-risk cases and more likely to be inaccurate for patients whose index ED visit was their first presentation to our health system. Indeed, many errors stemmed from elements of the medical history not being entered or fully updated at the time of CT-PE order and ePESI calculation. While less problematic than comorbidities, vital signs were occasionally measured prior to CT-PE order but entered into the EHR after the ePESI calculator had been triggered to automatically calculate the ePESI score, causing some errors. These issues may be less problematic if health systems set the ePESI calculator to calculate the score after a PE diagnosis is made, rather than at the time of CT-PE order. Nonetheless, real-time updating of problem lists and vital signs is outside the capability of most EDs, and it is likely that some errors are simply unavoidable. The incorrect scoring of sex for 1 transgender patient in our cohort exemplifies the near impossibility of accurately evaluating the PESI score for every possible ED patient.

To some extent, these observations also highlight the limitations of the PESI score itself, and more generally, any risk stratification metric developed without consideration for contemporary health care technology. Several terms incorporated into both the PESI and simplified PESI scores—for example, history of cancer and heart failure—are vague and fail to account for the complexity of current medical practice or the ability to accurately capture it in the EHR. For example, how should we score patients with non-metastatic skin cancer or heart failure with recovered ejection fraction? What about patients who are placed immediately on supplemental oxygen and never have a charted SpO_2 less than 90%? Best practice alerts and electronic CDS tools are increasingly used in medical practice, and as technology continues to evolve, it is likely that future risk stratification metrics will need to be developed with an eye toward what can be accurately quantified by the EHR, communicated to clinicians in real time, and evaluated retrospectively for quality improvement or research purposes. In this sense, the development of this ePESI calculator and the demonstration of its utility across institutions may pave the way for more standardized methods of disease stratification and corresponding management recommendations.

Principal Results

This study demonstrates the accuracy of our ePESI calculator, which has 95% accuracy in discriminating between high- and low-risk PESI scores. The odds of the ePESI and pPESI agreeing increased (OR 2.96, *P*<.001) if a patient had a low-risk PESI score and decreased if it was the patient's first time in the health system (OR 0.41, *P*=.008). Most errors were due to incongruities with the problem list, of which cancer is the most common error (91.8% correct).

Limitations

Our study had several strengths, including the use of blinded assessment of the ePESI score and the inclusion of consecutive patients undergoing CT-PE. In addition, there are several

XSL•FO
RenderX

limitations of this study that must be considered. The first is that the SNOMED hierarchical concept codes used by the ePESI are somewhat specific to the health system where the study was conducted. The concept codes are adapted from general Epic concept codes, so we anticipate the transfer of our concept codes to other institutions will be straightforward. However, some degree of adjustment may be necessary and performance may differ at other sites. Indeed, efforts to adapt and validate the ePESI in other locoregional hospitals are ongoing. A second limitation is that the pPESI was calculated retrospectively, rather than in real time by providers ordering the CT-PE. We adjusted for this with 2 independent reviewers, blinded to the ePESI score and each other's pPESI score, to mitigate potential bias from the retrospective calculation. Additionally, reviewers used a standardized data abstraction approach designed to mimic the information providers have access to and likely use in the ED. A third limitation is that this study was conducted in a cohort of patients with a variety of conditions, not just those with PE. The purpose of this study was to evaluate the ePESI accuracy when it automatically sampled comorbidities, demographics, and vital signs, none of which are dependent on the patient's diagnosis. There is no reason to conclude that EHR accuracy should meaningfully differ for patients with and without a PE. The purpose of this study was not to influence clinical practice or predict patient outcomes, although this should be evaluated in a future study now that we have demonstrated the accuracy of the ePESI in sampling electronic health data. Additionally, we conducted a sensitivity analysis in the subset of patients with acute PE and found the ePESI accuracy to be comparable to our overall cohort. The number of patients with acute PE in our study was small, but it is unlikely, although not impossible, that the accuracy of the ePESI will be dramatically altered in a larger cohort of patients with acute PE. A final limitation is that we were unable to account for all variables that influence ePESI and pPESI agreement. As discussed in the introduction paragraph, systemic reviews of generalized CDS systems suggest that patient complexity, data quality, poor integration, inadequate testing, and inadequate training are all associated with poor CDS-provider agreement [17-20]. We attempted to minimize these by using a standardized protocol for the pPESI reviewers, as described in the methods paragraph, and updated or ePESI based on provider feedback before we formally tested it. However, it is possible these still affected our ePESI and pPESI agreement.

Comparison With Prior Work

Our study demonstrates a PESI score calculator with similar accuracy to a calculator described by Vinson et al [16] in the Kaiser Permanente system in 2015. However, our study has the advantage of describing a calculator that can be readily and immediately exported to other health centers. Our ePESI was developed within the Epic 2023 software, as compared with the 2015 software, and is minimally reliant on features specific to our health system. The Kaiser Permanente ePESI depends on the improved problem list, which limits direct translation to other health systems. Additionally, our ePESI was programmed to calculate and alert providers in the ED for easy and direct integration into clinical practice. To our knowledge, these are the only 2 studies evaluating a CDS tool that automatically calculates PESI scores using patient data from the EHR.

Conclusions

In conclusion, we created a CDS that is highly reliable at discriminating between low- and high-risk PE patients based on the PESI score. It is most accurate in the low-risk PESI score population, which is its intended target for clinical use. Our CDS has the potential to be exported to other health systems and implemented more widely to increase the discharge of low-risk PE patients who do not otherwise require hospitalization.

Acknowledgments

The authors would like to acknowledge Roger Lupton, Stephanie Brooks, and David Loveland for their help in development, implementation, and optimization of the Electronic Pulmonary Embolism Severity Index (ePESI) calculator within the Epic software. EJ, CO, VG, AC, GDB, and CFG were involved in the study's conceptualization and design. EJ, JM, CO, GDB, and CFG contributed to data acquisition, while EJ, XK, GDB, and CFG handled the analysis and interpretation of the data. EJ, GDB, and CFG drafted the manuscript, and all authors participated in its critical revision. EJ and XK provided statistical expertise, and VG, AC, GDB, and CFG secured funding for the study.

Conflicts of Interest

GDB has disclosed receiving grant funding from Boston Scientific and serving as a consultant for several organizations, including Pfizer, Bristol-Myers Squibb, Janssen, Bayer, AstraZeneca, Sanofi, Anthos, Abbott Vascular, and Boston Scientific. Additionally, GDB serves on the Data and Safety Monitoring Board (DSMB) for Translational Sciences (Clinical Events Adjudication Committee) and is a member of the Board of Directors for the Anticoagulation Forum. JM has disclosed receiving grant funding from the NIH (5T35HL007690-38). All other authors have no disclosures.

Multimedia Appendix 1
Table S1 SNOMED hierarchical concepts for comorbidities.
[DOCX File, 21 KB - medinform_v13i1e58800_app1.docx]

Multimedia Appendix 2

XSL•FO
RenderX

Table S2 Forecasted age-standardized mortality rates for asthma-related deaths by 2035.
[DOCX File, 23 KB - medinform_v13i1e58800_app2.docx]

References

1. Maughan BC, Frueh L, McDonagh MS, Casciere B, Kline JA. Outpatient treatment of low-risk pulmonary embolism in the era of direct oral anticoagulants: a systematic review. Acad Emerg Med 2021 Feb;28(2):226-239. [doi: 10.1111/acem.14108] [Medline: 32779290]
2. Aujesky D, Obrosky DS, Stone RA, et al. Derivation and validation of a prognostic model for pulmonary embolism. Am J Respir Crit Care Med 2005 Oct 15;172(8):1041-1046. [doi: 10.1164/rccm.200506-862OC] [Medline: 16020800]
3. Frank Peacock W, Coleman CI, Diercks DB, et al. Emergency department discharge of pulmonary embolus patients. Acad Emerg Med 2018 Sep;25(9):995-1003. [doi: 10.1111/acem.13451] [Medline: 29757489]
4. Khatib R, Ross S, Kennedy SA, et al. Home vs hospital treatment of low-risk venous thromboembolism: a systematic review and meta-analysis. Blood Adv 2020 Feb 11;4(3):500-513. [doi: 10.1182/bloodadvances.2019001223] [Medline: 32040553]
5. Vinson DR, Mark DG, Chettipally UK, et al. Increasing safe outpatient management of emergency department patients with pulmonary embolism: a controlled pragmatic trial. Ann Intern Med 2018 Dec 18;169(12):855-865. [doi: 10.7326/M18-1206] [Medline: 30422263]
6. O'Hare C, Grace KA, Schaeffer WJ, et al. Adverse clinical outcomes among patients with acute low-risk pulmonary embolism and concerning computed tomography imaging findings. JAMA Netw Open 2023 May 1;6(5):e2311455. [doi: 10.1001/jamanetworkopen.2023.11455] [Medline: 37256624]
7. Ortel TL, Neumann I, Ageno W, et al. American Society of Hematology 2020 guidelines for management of venous thromboembolism: treatment of deep vein thrombosis and pulmonary embolism. Blood Adv 2020 Oct 13;4(19):4693-4738. [doi: 10.1182/bloodadvances.2020001830] [Medline: 33007077]
8. Konstantinides SV, Meyer G, Becattini C, et al. 2019 ESC guidelines for the diagnosis and management of acute pulmonary embolism developed in collaboration with the European Respiratory Society (ERS). Eur Heart J 2020 Jan 21;41(4):543-603. [doi: 10.1093/eurheartj/ehz405] [Medline: 31504429]
9. Stevens SM, Woller SC, Kreuziger LB, et al. Antithrombotic therapy for VTE disease. Chest 2021 Dec;160(6):e545-e608. [doi: 10.1016/j.chest.2021.07.055] [Medline: 34352278]
10. Westafer LM, Shieh MS, Pekow PS, Stefan MS, Lindenauer PK. Outpatient management of patients following diagnosis of acute pulmonary embolism. Acad Emerg Med 2021 Mar;28(3):336-345. [doi: 10.1111/acem.14181] [Medline: 33248008]
11. Kovacs MJ, Hawel JD, Rekman JF, Lazo-langner A. Ambulatory management of pulmonary embolism: a pragmatic evaluation. J Thromb Haemost 2010 Nov;8(11):2406-2411. [doi: 10.1111/j.1538-7836.2010.03981.x]
12. Erkens PMG, Gandara E, Wells P, et al. Safety of outpatient treatment in acute pulmonary embolism. J Thromb Haemost 2010 Nov;8(11):2412-2417. [doi: 10.1111/j.1538-7836.2010.04041.x] [Medline: 20735722]
13. Agterof MJ, Schutgens REG, Snijder RJ, et al. Out of hospital treatment of acute pulmonary embolism in patients with a low NT-proBNP level. J Thromb Haemost 2010 Jun;8(6):1235-1241. [doi: 10.1111/j.1538-7836.2010.03831.x] [Medline: 20230418]
14. Westafer LM, Jessen E, Zampi M, et al. Barriers and facilitators to the outpatient management of low-risk pulmonary embolism from the emergency department. Ann Emerg Med 2023 Sep;82(3):381-393. [doi: 10.1016/j.annemergmed.2023.02.021] [Medline: 37596016]
15. Kline JA, Kahler ZP, Beam DM. Outpatient treatment of low-risk venous thromboembolism with monotherapy oral anticoagulation: patient quality of life outcomes and clinician acceptance. Pat Prefer Adherence 2016;10:561-569. [doi: 10.2147/PPA.S104446] [Medline: 27143861]
16. Vinson DR, Morley JE, Huang J, et al. The accuracy of an electronic pulmonary embolism severity index auto-populated from the electronic health record: setting the stage for computerized clinical decision support. Appl Clin Inform 2015;6(2):318-333. [doi: 10.4338/ACI-2014-12-RA-0116] [Medline: 26171078]
17. Eberhardt J, Bilchik A, Stojadinovic A. Clinical decision support systems: potential with pitfalls. J Surg Oncol 2012 Apr 1;105(5):502-510. [doi: 10.1002/jso.23053] [Medline: 22441903]
18. Jaspers MWM, Smeulers M, Vermeulen H, Peute LW. Effects of clinical decision-support systems on practitioner performance and patient outcomes: a synthesis of high-quality systematic review findings. J Am Med Inform Assoc 2011 May 1;18(3):327-334. [doi: 10.1136/amiajnl-2011-000094] [Medline: 21422100]
19. Sesen MB, Peake MD, Banares-Alcantara R, et al. Lung cancer assistant: a hybrid clinical decision support application for lung cancer care. J R Soc Interface 2014 Sep 6;11(98):20140534. [doi: 10.1098/rsif.2014.0534] [Medline: 24990290]
20. Sutton RT, Pincock D, Baumgart DC, Sadowski DC, Fedorak RN, Kroeker KI. An overview of clinical decision support systems: benefits, risks, and strategies for success. NPJ Digit Med 2020;3:17. [doi: 10.1038/s41746-020-0221-y] [Medline: 32047862]
21. Cialdini CB. Influence: Science and Practice, 5th edition: Pearson; 2008.
22. Miliard M. Epic's EHR market share gains continue, KLAS report shows. Healthcare IT News. 2024. URL: https://www.healthcareitnews.com/news/epics-ehr-marketshare-gains-continue-klas-report-shows [accessed 2025-01-07]

XSL•FO
RenderX

23. Bruce G. EHR vendor market share in the US. Becker's Hospital Review. URL: https://www.beckershospitalreview.com/ehrs/ehr-vendor-market-share-in-the-us.html [accessed 2024-12-23]
24. Contact us. Epic. URL: https://www.epic.com/contact/ [accessed 2024-12-23]

ABBREVIATIONS

BiPAP: bilevel positive airway pressure
CDS: clinician decision support
CPAP: continuous positive airway pressure
CT-PE: computerized tomography-pulmonary embolism
ED: emergency department
EHR: electronic health record
ePESI: Electronic Pulmonary Embolism Severity Index
GCS: Glasgow Coma Scale
OR: odds ratio
PE: pulmonary embolism
PESI: Pulmonary Embolism Severity Index
pPESI: Physician Pulmonary Embolism Severity Index
SNOMED: Systematized Nomenclature of Medicine

Edited by C Lovis; submitted 25.03.24; peer-reviewed by VA Onofrei, W Chaiwong; revised version received 12.08.24; accepted 07.09.24; published 20.01.25.

Please cite as:
Joyce E, McMullen J, Kong X, O'Hare C, Gavrila V, Cuttitta A, Barnes GD, Greineder CF
Performance of an Electronic Health Record–Based Automated Pulmonary Embolism Severity Index Score Calculator: Cohort Study in the Emergency Department
JMIR Med Inform 2025;13:e58800
URL: https://medinform.jmir.org/2025/1/e58800
doi:10.2196/58800

©Elizabeth Joyce, James McMullen, Xiaowen Kong, Connor O'Hare, Valerie Gavrila, Anthony Cuttitta, Geoffrey D Barnes, Colin F Greineder. Originally published in JMIR Medical Informatics (https://medinform.jmir.org), 20.1.2025. This is an open-access article distributed under the terms of the Creative Commons Attribution License (https://creativecommons.org/licenses/by/4.0/), which permits unrestricted use, distribution, and reproduction in any medium, provided the original work, first published in JMIR Medical Informatics, is properly cited. The complete bibliographic information, a link to the original publication on https://medinform.jmir.org/, as well as this copyright and license information must be included.

XSL•FO
RenderX

Original Paper

Diagnostic Decision-Making Variability Between Novice and Expert Optometrists for Glaucoma: Comparative Analysis to Inform AI System Design

Faisal Ghaffar[1], BSc, MEng; Nadine M. Furtado[2], OD, MSc, FAAO; Imad Ali[3], PhD; Catherine Burns[1], PEng, PhD

[1]Department of Systems Design Engineering, Faculty of Engineering, University of Waterloo, Waterloo, ON, Canada

[2]School of Optometry and Vision Science, University of Waterloo, Waterloo, ON, Canada

[3]Department of Computer Science, University of Swat, Mingora, Pakistan

Corresponding Author:
Catherine Burns, PEng, PhD
Department of Systems Design Engineering
Faculty of Engineering
University of Waterloo
EC4 2121, 295 Phillip St
Waterloo, ON, N2L 3W8
Canada
Phone: 1 519 888 4567 ext 33903
Email: catherine.burns@uwaterloo.ca

Abstract

Background: While expert optometrists tend to rely on a deep understanding of the disease and intuitive pattern recognition, those with less experience may depend more on extensive data, comparisons, and external guidance. Understanding these variations is important for developing artificial intelligence (AI) systems that can effectively support optometrists with varying degrees of experience and minimize decision inconsistencies.

Objective: The main objective of this study is to identify and analyze the variations in diagnostic decision-making approaches between novice and expert optometrists. By understanding these variations, we aim to provide guidelines for the development of AI systems that can support optometrists with varying levels of expertise. These guidelines will assist in developing AI systems for glaucoma diagnosis, ultimately enhancing the diagnostic accuracy of optometrists and minimizing inconsistencies in their decisions.

Methods: We conducted in-depth interviews with 14 optometrists using within-subject design, including both novices and experts, focusing on their approaches to glaucoma diagnosis. The responses were coded and analyzed using a mixed method approach incorporating both qualitative and quantitative analysis. Statistical tests such as Mann-Whitney *U* and chi-square tests were used to find significance in intergroup variations. These findings were further supported by themes extracted through qualitative analysis, which helped to identify decision-making patterns and understand variations in their approaches.

Results: Both groups showed lower concordance rates with clinical diagnosis, with experts showing almost double (7/35, 20%) concordance rates with limited data in comparison to novices (7/69, 10%), highlighting the impact of experience and data availability on clinical judgment; this rate increased to nearly 40% for both groups (experts: 5/12, 42% and novices: 8/21, 42%) when they had access to complete historical data of the patient. We also found statistically significant intergroup differences between the first visits and subsequent visits with a *P* value of less than .05 on the Mann-Whitney *U* test in many assessments. Furthermore, approaches to the exam assessment and decision differed significantly: experts emphasized comprehensive risk assessments and progression analysis, demonstrating cognitive efficiency and intuitive decision-making, while novices relied more on structured, analytical methods and external references. Additionally, significant variations in patient follow-up times were observed, with a *P* value of <.001 on the chi-square test, showing a stronger influence of experience on follow-up time decisions.

Conclusions: The study highlights significant variations in the decision-making process of novice and expert optometrists in glaucoma diagnosis, with experience playing a key role in accuracy, approach, and management. These findings demonstrate the critical need for AI systems tailored to varying levels of expertise. They also provide insights for the future design of AI systems

XSL•FO
RenderX

aimed at enhancing the diagnostic accuracy of optometrists and consistency across different expertise levels, ultimately improving patient outcomes in optometric practice.

(JMIR Med Inform 2025;13:e63109) doi:10.2196/63109

KEYWORDS

decision-making; human-centered AI design; human factors; experts versus novices differences; optometry; glaucoma diagnosis; experts versus novices; glaucoma; eye disease; vision; vision impairment; comparative analysis; methodology; optometrist; artificial intelligence; AI; diagnostic accuracy; consistency; clinical data; risk assessment; progression analysis

Introduction

Artificial intelligence (AI) has emerged as a transformative force in optometry [1], particularly for glaucoma diagnosis. In this context, AI in optometry refers to the advanced algorithms that analyze complex data such as fundus photos and related patient data. These AI systems use techniques of image processing, computer vision, deep learning, and transfer learning to detect and diagnose glaucoma. Glaucoma is a progressive eye disease that often eludes early detection due to its subtle or absent symptoms, which poses a unique challenge for optometrists [2]. This challenge, along with no clear-cut tests or signs, frequently results in variability in glaucoma-related decisions, influenced by factors such as the optometrists' expertise, experience, the subjective interpretation of clinical data, and the use of different equipment [3,4]. This variability is a critical issue that AI is well positioned to address, potentially standardizing the diagnostic process and offering a more objective analysis of clinical data. Studies have illustrated AI's advanced analytical capability and proficiency in sifting through extensive patient data, including retinal images, visual field tests, optical coherence tomography scans, and medical histories [5]. This advanced analytical capability enables AI to identify signs of glaucoma with consistency and accuracy, often surpassing that of human optometrists [6,7]. For example, in Akter et al [8], researchers found that AI algorithms could detect glaucoma with up to 96% accuracy, markedly higher than the 80% accuracy rate commonly associated with optometrists.

Similarly, in another study [9], an accuracy of 83.4% is reported in identifying glaucomatous optic neuropathy using AI. These findings show AI's potential to reduce misdiagnoses and address the prevalent decision variability. In a similar vein, in another study [10], it was demonstrated that an AI system helped junior radiologists perform at levels close to that of a senior radiologist. This finding is particularly relevant to optometry, with AI having the potential to play a similar role in enhancing the diagnostic abilities of less experienced optometrists. As in Jammal et al [11], researchers have highlighted that advocating for a more integrated use of AI tools in optometric practices could be a significant step toward standardizing care and reducing diagnostic variability.

However, the effective integration of AI into optometric practice hinges on a comprehensive understanding of optometrists' decision-making processes [12,13]. AI promises to offer standardization in clinical decision-making. Yet, the crux of its successful integration lies in deeply comprehending the subtle intricacies inherent in human decision-making. This understanding is especially critical in diagnosing conditions like glaucoma, where subjective assessments and clinical expertise play significant roles. Highlighting the variability in diagnostic approaches between novice and expert optometrists, as demonstrated by studies [14,15], shows the importance of tailored AI support. Therefore, AI systems must adapt to different levels of clinical expertise and integrate the diverse decision-making processes of novice and expert optometrists.

Diagnostic decisions in this field vary significantly, influenced by an optometrist's expertise, experience, and cognitive strategies. These differences affect how patient data are interpreted, the importance assigned to various clinical findings, and the resulting diagnostic outcomes.

In this study, we investigate the variance of diagnostic decisions made by optometrists in the context of glaucoma, focusing on how the availability and nature of data influence these decisions. Several key research questions guide our investigation.

1. How do the decision-making processes of expert and novice optometrists differ when they are presented with the same patient data?
2. What specific data do optometrists at different experience levels tend to prioritize in a clinical journey?
3. Are experienced optometrists more inclined to use heuristic approaches when confronted with limited data instead of scenarios with comprehensive data availability?

To address our research questions, we conducted in-depth interviews with novice and expert optometrists, focusing on their diagnostic approaches to glaucoma. Following these interviews, we performed a detailed coding of the responses, enabling us to conduct qualitative and quantitative analyses. This structured approach allowed us to comprehensively examine the decision-making patterns and their implications for AI integration in optometric practice.

Our research aims to comprehensively understand how optometrists make decisions when diagnosing glaucoma, exploring the diversity in their approaches. By exploring the variations in decision-making between novice and expert optometrists, our study aims to pave the way for the future design of AI systems. These envisioned systems are intended to bridge the expertise gap in glaucoma diagnosis. They will complement human judgment to reduce biases and enhance diagnostic accuracy, leading to more consistent and reliable evaluations. The insights gained from this exploration are anticipated to significantly contribute to optometric practice and education, setting the stage for future advancements in glaucoma diagnosis and management.

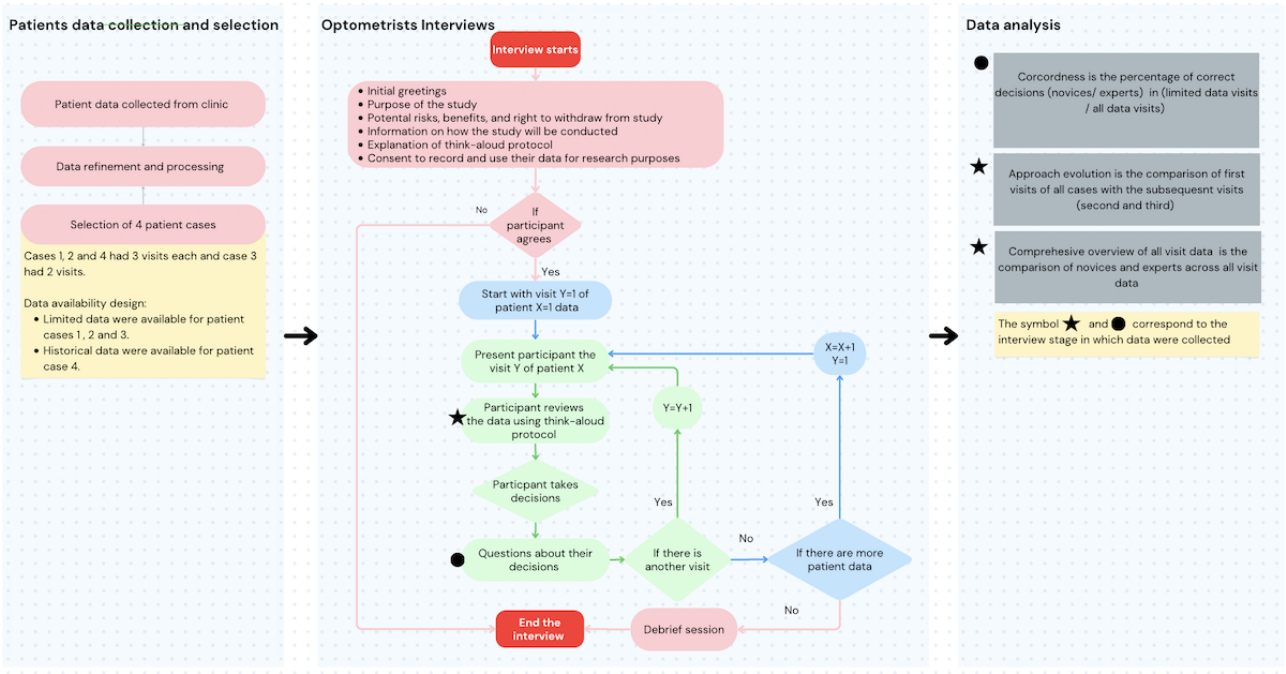
XSL•FO
RenderX

Methods

Overview

This section details our research methodology investigating variations in optometrists' decision-making. It begins with an in-depth explanation of the data collection process, emphasizing the criteria and methods used for selection. Subsequently, the stages of data refinement and processing are outlined. Optometrist interviews are discussed, covering outreach strategies, interview platforms, and participant demographics. A within-subjects design was used for the interviews, allowing each participant to engage with all patient cases. The section culminates with insights into the data coding process, involving transcript cleaning and multidisciplinary analysis. For the data analysis, a mixed methods approach was used, integrating both qualitative and quantitative data to provide a comprehensive understanding of the decision-making processes. Figure 1 summarizes the flow of the study.

Figure 1. The stages and flow of the study. It started with patient data collection and selection, followed by optometrist interviews and data analysis. Each stage is further subdivided into steps. Each of these steps is further explained in the Methods section. The circle and star symbols show the data obtained at a specific stage in the interview and how they were analyzed. A higher resolution version of this image is included as Multimedia Appendix 1.



Ethical Considerations

This study (application 43288) was reviewed and approved by the Delegated Research Ethics Committee (DERC) of the University of Waterloo on May 27, 2021. Informed consent was sought from the participants before the data collection. They were informed about the procedure, purpose, benefits, risks, and their right to withdraw from the study. Further, they were informed that data acquired from the interview would be anonymized, deidentified, stored on a protected server, and used anonymously in all publications that arise from the study. Participants were remunerated CAD $150 (CAD $1=US $0.75) for their 2-hour commitment, recognizing their professional contribution and encouraging detailed participation.

Patients' Data Collection

Data for this study were acquired from the School of Optometry and Vision Sciences at the University of Waterloo, Canada. The selection process entailed scrutiny of patient records within the institution's database, explicitly targeting those records wherein patients had granted explicit consent for their information to be used in research. The preliminary phase of our data collection involved gathering records from 8 distinct patients. Each patient's record provided a longitudinal perspective, encompassing multiple clinical visits and offering an in-depth view of their interactions with the optometrist over time.

The data attributes collected from patient records were informed by research from previous similar studies [16-19] and the European Glaucoma Prevention Study [20]. Our data collection encompasses a comprehensive range of patient characteristics. It includes essential ocular health metrics and relevant external factors to ensure a comprehensive glaucoma evaluation by optometrists. The patient features we collected are detailed in Table 1. These features reflect the multifaceted factors highlighted in the referenced studies.

XSL•FO
RenderX

Table 1. Data features for glaucoma diagnosis collected from the electronic health record system from the School of Optometry, University of Waterloo.

Category	Factors
Demographic factors	Age, gender, and race
Historical data	Ocular history, medical history, medication history, social history, and family history
Internal attributes	Habitual spectacle prescription, unaided visual acuity, aided acuity, pupils, anterior segment examination, Goldman applanation tonometry, central corneal thickness, and gonioscopy
Images	Fundus image and OCT[a] images
Reports	Posterior segment examination, visual field, and OCT

[a]OCT: optical coherence tomography.

Data Refinement and Processing

The data refinement and processing were executed to facilitate the interview component of the study. Out of the initial pool of patients, 4 records were chosen to be reviewed for the in-depth interviews. This selection process involved comprehensive discussions with an expert in the field to identify cases that could provide diverse diagnostic perspectives. The criteria for case selection were centered on identifying instances that would likely elicit differing opinions among optometrists, thereby enabling a focused examination of the variation in clinical decision-making.

The rationale behind limiting the selection to 4 patient records stemmed from practical constraints associated with the review process. It was anticipated that participants would take about 10-15 minutes to review each patient visit. To manage this effectively within time constraints, we selected 3 patients with 3 visits (the initial, final, and intermediary visits) and 1 patient with 2 visits. This approach allowed for a detailed review of each patient's clinical journey while staying within the practical limits of the allotted time. Notably, historical data from previous visits were not provided for 3 of the 4 patients. However, more exhaustive data were provided for 1 patient, including the complete set of previous visits data, offering a more detailed case study within the research. This approach provided a balanced perspective between a broad overview and an in-depth case analysis, enhancing the study's ability to capture general trends and specific nuances in clinical decision-making.

Optometrist Interviews

In this study, we interviewed 14 optometrists from the Waterloo region, primarily affiliated with the University of Waterloo's School of Optometry and Vision Science. Each optometrist participated in a 100- to 120-minute, web-based interview conducted in English via Microsoft Teams and Zoom. The choice of web-based interviews over physical ones was in response to the participants' preferences.

The participants had an average of 7.54 (SD 8.34) years of experience and saw an average of 32.57 (SD 22.39) patients weekly.

Each optometrist scrutinized data from at least 10 patient visits, translating to a comprehensive review spanning about 2 hours for the entire set of patient records. Although we aimed to present all visit data for evaluation, time constraints necessitated the omission of some visits, and a few evaluations did not produce usable data. Throughout the interviews, participants employed the "think aloud" protocol to review patient records, aiding in understanding their decision-making processes. After the first 10 interviews, we observed data saturation, which was achieved by the 14th interview, as evidenced by recurring themes and no new substantial information. All interviews were audio-recorded and transcribed using the platforms' built-in features.

Data Coding

Our qualitative research commenced with the cleaning of interview transcripts. This preliminary step involved a thorough review in correcting errors, eliminating irrelevant sections, and enhancing clarity and coherence. This crucial stage ensured the data's integrity before proceeding to the analysis phase.

After cleaning, the refined transcripts were exported into NVivo (version 14.23.2; Lumivero, formerly QSR International). In NVivo, we carried out an open coding process led primarily by FG. The involvement of multidisciplinary expertise enriched the coding process. With a background in engineering, CB conducted a thorough review of the codes from an engineering perspective. This review added a layer of technical and analytical insight, ensuring that the coding accurately reflected relevant engineering concepts and terminologies. Simultaneously, NF, leveraging her expertise in optometry, reviewed the codes with a focus on the optometry perspective. Her review was pivotal in aligning the data with optometric principles and practices, ensuring the findings were relevant and accurately interpreted within the context of eye care and vision science.

This multidisciplinary approach to reviewing the codes enhanced the depth of our analysis and ensured that the findings were robust, well rounded, and reflective of diverse professional viewpoints. Such a collaborative effort was instrumental in ensuring that the themes and patterns identified were relevant and applicable across different fields of study.

The open coding was executed inductively, allowing the data to drive the categorization process rather than imposing preexisting theories or frameworks. This approach facilitated a more organic and grounded understanding of the data. Each transcript line was carefully examined, with open codes assigned to summarize the content succinctly. These codes were crafted to stay true to the original text, minimizing abstraction. This level of descriptiveness in coding was instrumental in capturing the essence of the participants' narratives, laying a solid

XSL•FO
RenderX

foundation for subsequent conceptualization and analysis. The codes were then grouped to form more generalized codes. Multimedia Appendix 2 gives details of the created generalized codes.

Through this process, we distilled the raw data into meaningful themes and patterns, shedding light on the underlying narratives and insights embedded within the transcripts.

Data Analysis

To carry out the analysis, we categorized participants into 2 groups: novices and experts, based on their years of experience and frequency of consultations with patients with glaucoma, using median values for greater precision. An "expert" was defined as having 4 or more years of experience as a practicing optometrist and treating a higher-than-average volume of patients with glaucoma per week compared with the participant pool. This classification excluded the average number of all patients examined or treated in a week for any eye condition, as it was deemed irrelevant in the context of glaucoma. Participants collectively conducted 137 evaluations, with experts reviewing 48 and novices reviewing 89. Ideally, the total number of evaluations would have been 144, but in some visit instances, the participants did not provide us with enough data, or we skipped some visit instances in the interview because of time constraints.

First, we examined the variability of novices and experts in diagnostic concordance across all patient visits, focusing on how the availability of comprehensive versus missing data influences concordance rates. Diagnostic concordance is the rate of optometrists' decisions that are aligned with the original clinical decision taken at a clinic. This analysis revealed disparities between optometrists' decisions and established clinical decisions. Following this analysis, we examined the approach evolution of optometrists within the clinical journey. This analysis was conducted by calculating the assessments/exams conductance rate (the percentage of a specific assessment conducted) and 95% CI, and performing statistical analysis using Mann-Whitney *U* [21] test to evaluate the significance of the variations and approach evolution from initial visits to subsequent visits. To observe a general trend of evolution, we first compared and analyzed initial visits (n=51) with follow-up visits (n=82). To observe the novice and experts' trends, we then further classified the data by experience level of optometrists, comparing initial (n=33) and follow-up (n=55) visits by novices to initial (n=18) and follow-up (n=27) visits by experts. Through this analysis, we uncovered the variation in approach evolution and clinical decision-making between novices and expert optometrists.

Second, we used quantitative and qualitative methodologies across all evaluations (N=137) to gain an in-depth understanding of the outcomes of these examinations. This approach enabled us to identify key themes that distinguish the ocular examination practices of novice and expert optometrists. Similar to earlier analysis, we calculated the assessments/exams conductance rate and 95% CI, and performing statistical analysis using Mann-Whitney *U* test to compare each assessment type of experts and novices. These findings were further supported by identified themes. This mixed method analysis provided insights into the consistency and variability in assessments and diagnostic reasoning. Moreover, by intercase and intracase comparison analysis, we identified the cognitive strategies in clinical decision-making, revealing how expertise level influences the patient case comparison.

Last, we calculated the average follow-up time of experts and novices and then used chi-square test to observe the significance of variation. This analysis offered an understanding of how experience impacts the timelines of patient management. This finding is crucial in glaucoma, where timely intervention can significantly influence disease progression and patient quality of life.

Overall, our study provides a multifaceted look at the complexities of glaucoma management, highlighting the influence of experience on various aspects of patient care. These insights are invaluable for shaping future educational programs, clinical guidelines, and AI systems in glaucoma, ensuring that they are tailored to address the specific needs and challenges optometrists face.

Results

Variability in Diagnostic Concordance and Approach Evolution in the Clinical Journey

This section investigates the variability in diagnostic concordance among novice and expert optometrists relative to established clinical decisions, emphasizing the influence of accessible patient data on diagnostic accuracy. It also delineates the evolution of diagnostic and treatment methodologies throughout the clinical journey, from initial patient encounters to subsequent visits.

Variability exists in the diagnostic concordance and approach evolution between experts and novices throughout the clinical journey. We compared the diagnostic decisions made by our participants with established clinical decisions, which we define as the decisions previously made by optometrists in a clinical setting where they had access to additional patient data, including comprehensive medical histories and previous examination results. The diagnostic concordance measures the extent to which our participants' decisions align with these preexisting clinical decisions. We observed significant variations in the decision-making of optometrists, notably when they lacked prior patient data.

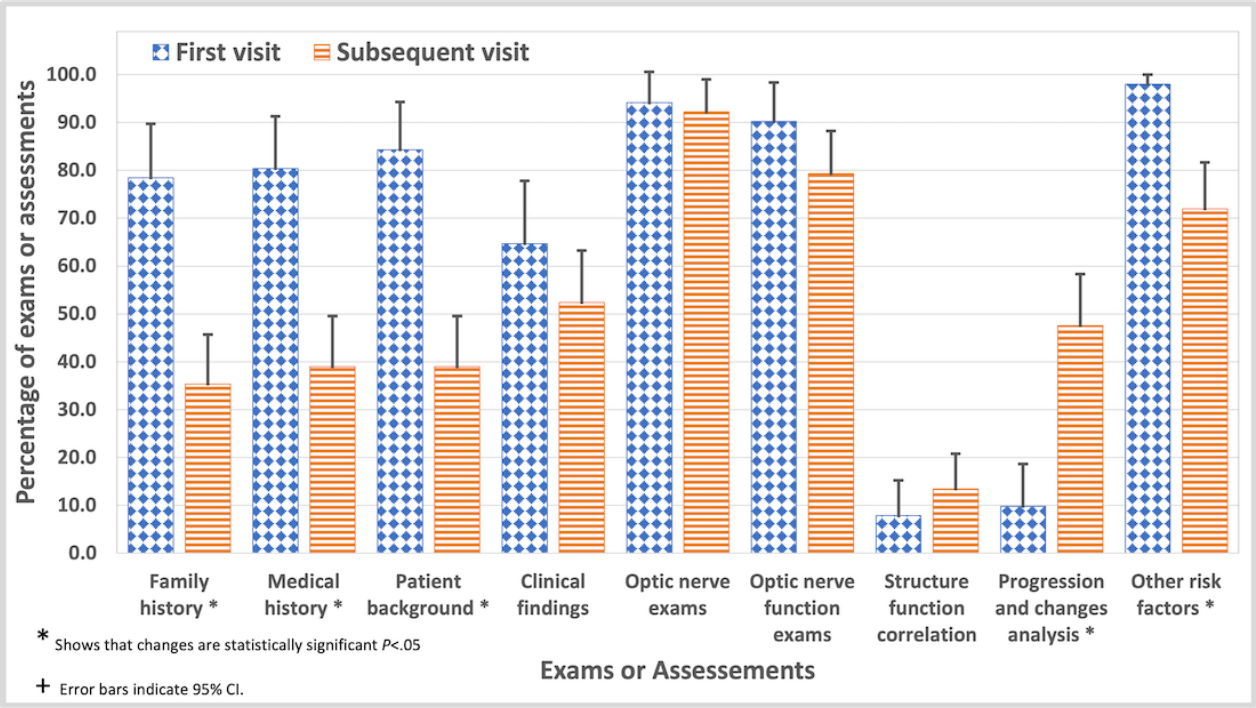
Key findings highlight the disparity in diagnostic decisions when previous patient history is not available, where compared with novices (10% concordance, 7/69 evaluations), experts showed a higher rate of concordance (20% concordance, 7/35 evaluations), highlighting the impact of experience on clinical judgment. Interestingly, when provided with prior patient data, the gap in decision-making accuracy between experts (42% concordance, 5/12 evaluations) and novices (42% concordance, 8/21 evaluations) decreased. This finding shows the critical role of comprehensive patient histories in enhancing diagnostic precision, particularly for less experienced optometrists.

Building upon the insights regarding diagnostic concordance, the optometrists' diagnostic approaches through the clinical

XSL•FO
RenderX

journey of a patient reveal significant differences and shifts in practice strategy and emphasis. Initially, there is a higher engagement across all assessments except progression and change analysis and structure and function correlation analysis reflecting common practice for initial assessments. However, in subsequent visits, data reveal a significant shift: the engagement with most assessments decreased, while progression and change, and structure and function correlation, increased. Figure 2 provides a graphical representation of these trends in percentage, illustrating the shift from broad-based examinations to focused analytical assessments. Further analysis using the Mann-Whitney *U* test showed that these changes were significant when comparing initial and subsequent visits. Significant differences were observed in family history ($P<.001$, Cohen $d=0.41$), medical history ($P<.001$, Cohen $d= 0.45$), patient background ($P<.001$, Cohen $d=0.43$), other risk factors ($P<.001$, Cohen $d=0.50$), clinical findings ($P=.01$, Cohen $d=0.28$), optic nerve exams ($P=.01$, Cohen $d=0.29$), as well as in progression and change analysis ($P=.005$, Cohen $d=–0.20$). There was no significant change observed in the optic nerve function exam and structure-function correlation assessments. The shift in engagement with different assessments shows a pivot towards more in-depth analytical work.

Figure 2. The percentage increase or decrease in glaucoma-related eye examinations and assessments conducted by optometrists, tracked from the initial visit to subsequent visits through longitudinal patient history.



To investigate further, we compared and analyzed the data of experts and novices separately, summarized in Table 2. Detailed descriptive statistics are provided in Multimedia Appendix 3. In the initial visit, novices emphasize direct examination techniques, focusing significantly on the optic nerve exam (31/33, 94%) and optic nerve function exam (30/33, 91%) and comparatively underemphasizing patient history and background information, while experts demonstrate a more balanced and comprehensive approach. They engage more deeply in gathering medical history (15/18, 83%) and patient background (17/18, 94%), while still maintaining high attention to optic nerve assessments (16/18, 88.8%). Both give considerable attention to other risk factors, with experts at 100% (18/18) and novices at 97% (32/33). These results suggest that experts prioritize a more complete picture of the patient's medical background and current health status from the onset. Regarding the analytical methods such as progression and change analysis, novices show a surprising engagement (4/33, 12%), which demonstrates a higher propensity to engage in advanced analytical methods early on, despite such analyses typically requiring follow-up data. This is possibly due to a misunderstanding of the optimal timing for such analyses.

XSL•FO
RenderX

Table 2. The variation in glaucoma-related eye examinations throughout a patient's clinical journey, highlighting the differences between novice and expert optometrists, tracked from initial to subsequent visits. For the Mann-Whitney U test, effect size is given by the rank biserial correlation.

	Novices				Experts			
	First visit, n/N (%)	Subsequent visit, n/N (%)	*P* value	Cohen *d*	First visit, n/N (%)	Subsequent visit, n/N (%)	*P* value	Cohen *d*
Family history	26/33 (79)	19/55 (35)	<.001	.39	14/18 (78)	10/27 (37)	.02	0.41
Medical history	26/33 (79)	21/55 (38)	<.001	.44	15/18 (83)	11/27 (41)	.01	0.47
Patient background	26/33 (79)	18/55 (33)	<.001	.53	17/18 (94)	14/27 (52)	.03	0.29
Clinical findings	19/33 (58)	23/55 (42)	.04	.27	14/18 (78)	20/27 (74)	.63[a]	0.09
Optic nerve exams	31/33 (94)	48/55 (87)	.01	.36	16/18 (89)	25/27 (93)	.35[a]	0.18
Optic nerve function exams	30/33 (91)	44/55 (80)	.74[a]	.04	16/18 (89)	21/27 (78)	.80[a]	–0.04
Structure-function correlation	2/33 (6)	4/55 (7)	.51[a]	–0.05	2/18 (11)	7/27 (26)	.21[a]	–0.17
Progression and change analysis	4/33 (12)	15/55 (27)	.68[a]	–0.04	1/18 (6)	24/27 (89)	<.001	–0.7
Other risk factors	32/33 (97)	41/55 (75)	<.001	0.5	18/18 (100)	18/27 (67)	.06[a]	0.35

[a]Nonsignificant values.

In the subsequent visits shown in Table 2, there is a noticeable shift. Novices demonstrated sustained attention to optic nerve exams (48/55, 87%) and optic nerve function exams (44/55, 80%). However, their assessment of family history, medical history, patient background, and other risk factors dropped in comparison to that of initial visits. Experts showed a similar behavior with high attention to optic nerve exams (25/27, 92%), optic nerve function exams (21/27, 77%), and clinical findings (20/27, 74%), while showing a marked decrease in the assessment of family history, medical history, patient background in comparison to initial visits. In the assessment of progression and changes analysis, and structure-function correlation, both groups showed an increase. However, the extent of these increases differs between the 2 groups; novices showed a modest increase in progression and changes assessment (15/55, 27%) and a much smaller increase in structure function correlation (4/55, 7%), while experts showed a robust increase (24/27, 88%) in progression and changes assessment and modest increase (7/27, 25%) in structure-function correlation. This leap for experts could reflect a strategic approach where they dive deeper into the more complex analysis. This finding might suggest a more focused approach as specific patient issues become more apparent.

Further analysis using the Mann-Whitney *U* test showed significant shifts in the assessments from initial to subsequent visits for both novices and experts, as reported in Table 2. In this analysis, the weight of each exam was also considered and calculated based on the frequency with which an optometrist discussed a specific assessment. We observed that novices showed significant changes in more assessments with Cohen *d* values of moderate effect, suggesting a strong shift of approach. While the experts showed fewer significant changes with Cohen *d* values of smaller to moderate effect, except for the progression and change analysis where the effect was large, suggesting a stronger shift. These findings suggest that experts maintained a comprehensive approach, balancing all assessments with increased emphasis on analytical assessment.

This analysis highlights the critical importance of comprehensive patient data in enhancing diagnostic accuracy, particularly for novice optometrists who face more significant challenges without extensive patient histories. The findings reveal the dynamic evolution of diagnostic and treatment strategies throughout a patient's clinical journey, illustrating how adaptability in practice strategy from initial assessments to subsequent visits is crucial. Notably, novices demonstrate a reduced focus on disease progression and correlating variables, indicating a gap in their approach to long-term patient management. This result highlights the potential need for a guiding system to help novices navigate the complexities of diagnostic decisions more effectively.

Comprehensive Overview of Examination Data Across All Visits

We categorized the analyses carried out by optometrists into 9 broad codes/categories: family history, medical history, patient background, clinical findings, optic nerve exams, optic nerve function exams, structure-function correlation, progression and change analysis, and other risk factors. The details of these categories are provided in Multimedia Appendix 2. Through these categories, we identified the following key themes that gave us insights into the factors that optometrists keep in focus while screening patients for glaucoma.

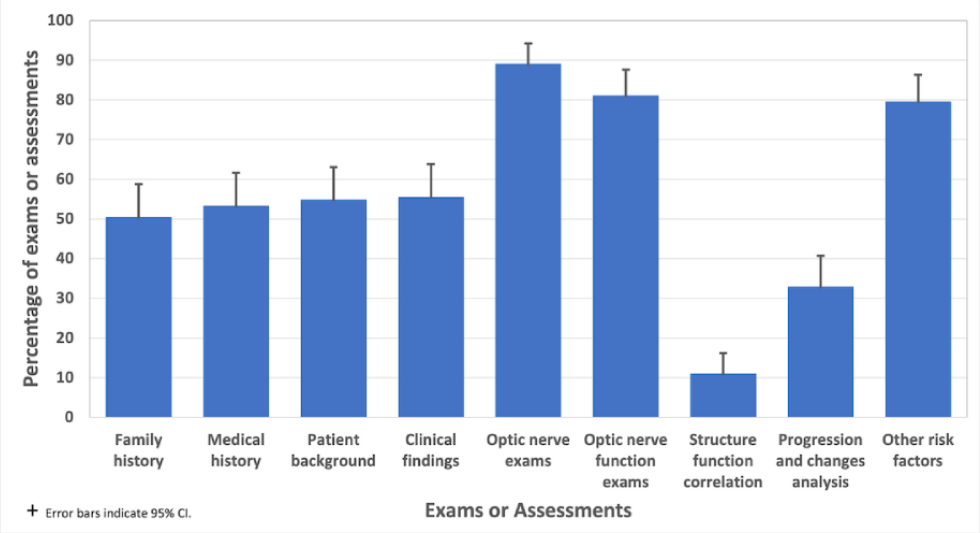
All Optometrists Focus More on Optic Nerve Exams and Risk Factors

The data reveal the distribution of eye examinations, as shown in Figure 3, within the whole data set. Key findings include a high frequency of focus on the optic nerve assessment (122/137, 89%) and optic nerve function assessment (110/137, 80.2%), showing a significant focus on assessing the optic nerve's structural and functional aspects. Clinical findings (75/137, 54.7%), medical history (73/137, 53.2%), and family history (69/137, 50.3%) were evaluated at moderate rates, indicating a holistic approach that incorporates patient-related and clinical information. In contrast, progression and changes analysis

XSL•FO
RenderX

(45/137, 32.8%) and structure-function correlation analysis (14/137, 10.2%) were less frequently performed.

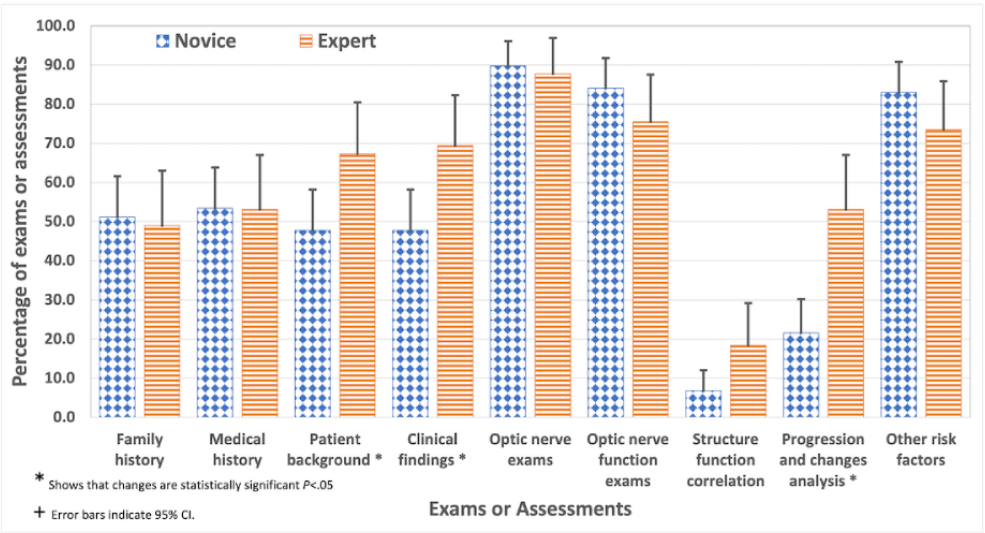
Figure 3. Findings from the whole dataset, revealing a strong emphasis on optic nerve structural and functional assessments. It also shows moderate attention to clinical findings, medical history, and family history, while progression analysis and structure-function correlation analysis were performed less frequently.



Experts Carry Out Progression and Change Analysis More Than Novices

Our findings reveal that experts are more inclined to engage in progression and change analysis than novices. A preliminary test of normality on the data distribution resulted in a $P<.001$, indicating a deviation from normal distribution. Consequently, we used the Mann-Whitney U test to examine the differences between experts and novices in analyzing progression and changes. This test yielded a $P<.001$ (2-tailed) with U of 1486, and a mean rank of 61.08 for novices and 80.54 for experts. This shows a statistically significant difference between the 2 cohorts. Specifically, our analysis shows that experts demonstrate a markedly higher focus on progression and change analysis (26/49, 53.1% vs 19/88, 21.5%), as illustrated in Figure 4, reflecting their seasoned approach to monitoring disease development over time.

Figure 4. The percentages of glaucoma-related eye examinations conducted by novices and experts, highlighting differences in focus on clinical findings, patient history, progression and change analysis, and structure-function correlation.



Experts Integrate Clinical Findings and Patient Background More Than Novices

There is a significant difference in the emphasis on clinical findings and patient background between novice and expert optometrists. Our initial analysis involved conducting tests of normality for both clinical findings and patient background data, which revealed $P<.001$, indicating that the data do not follow a normal distribution. Consequently, we applied the Mann-Whitney U test to assess the differences in emphasis on these diagnostic components between novice and expert optometrists. The test results for clinical findings yielded a P value of .04 (2-tailed) with U of 1695 and a mean rank of 63.75 for novices and 77.19 for experts. Same way the test results for

XSL•FO
RenderX

patient background yielded a *P* value of .04 (2-tailed) with *U* of 1732 and a mean rank of 64.18 for novices and 76.42 for experts, suggesting a statistically significant difference between the 2 groups, albeit with a modest significance level.

Specifically, novices consider both factors in 48% (42/88) of evaluations. In contrast, experts incorporate them at a higher rate, with about 69% (34/49) for clinical findings and 67% (33/49) for patient background, as shown in Figure 4. This disparity shows the experts' more substantial focus on combining clinical signs and symptoms of glaucoma with the patient's historical data. Expert physicians' comprehensive approach showcases their in-depth understanding and extensive experience in evaluating these essential diagnostic components.

Experts Tend to Emphasize Structural Function Correlation More Than Novices

Our analysis shows a trend that novices focus on structure-function correlation at a rate of 7% (6/88) and experts at a higher rate of 18% (9/49), as depicted in Figure 4. Despite the apparent disparity in percentages suggesting a more pronounced awareness of the interplay between structural and functional considerations, statistical analysis reveals that the difference in structure-function correlation between experts and novices does not achieve statistical significance (*P*=.15 with *U*=1951.5). However, the percentage difference still indicates that there may be a trend towards a higher engagement with structure-function correlation among experts than novices.

Novices Exhibit a Higher Tendency for Intercase and Longitudinal Comparisons, Less for Intracase Comparisons

In such a comparison, the clinician evaluates the current case against other patient scenarios. Novices in some cases made a reference to another patient's data, denoting a reliance on external case references. This reliance may be a compensatory mechanism for the relative inexperience in glaucoma diagnosis, where pattern recognition is still being cultivated. In a representative case, a novice commented "I think that they would be potentially a mild suspect compared to the first patient that we had just due to the fact that this person has hypertension, and they have a family history of glaucoma..."

In stark contrast, this form of comparison was entirely absent among experts, suggesting a transition towards an intuitive, more synthesized comprehension of glaucoma presentations, informed by an extensive repository of patient encounters.

The difference between experts and novices in conducting longitudinal comparisons of patients' data is subtle, with our analysis revealing a difference that does not reach statistical significance with *P*>.05. Despite the lack of statistical significance, the observed percentages 24% (12/49) of evaluations for experts versus 29% (26/88) for novices hint at an interesting trend: experts might possess a nuanced internalization of a patient's historical data. This suggests that experts are potentially more adept at retaining key details of disease progression within their working memory. With their extensive experience, they may draw upon a mental synthesis of the patient's history and current presentation without the need for frequent referrals to past records. This cognitive efficiency reflects a mastery of pattern recognition characteristic of glaucomatous progression, allowing for a more agile and comprehensive assessment that leverages their extensive experience and nuanced understanding of the disease. The less frequent engagement with longitudinal comparison by expert optometrists may not indicate a disregard for the patient's history but rather an advanced capacity to retain and integrate this information into their clinical judgments, a testament to their evolved diagnostic expertise.

Intracase comparisons, particularly the evaluation of asymmetry between left and right eye examinations, were used by novices in 17% (15/88) of evaluations and experts in 24% (12/49) of evaluations with no statistically significant difference. Both groups recognize the diagnostic value of these comparisons, yet the slightly higher use by experts may reflect a refined, systematic approach and a heightened sensitivity to the subtleties of asymmetry, honed through repeated clinical encounters.

Variation in Patient Follow-Up Time Suggestion

The analysis reveals significant variations in follow-up times among all participating optometrists, as well as a noticeable relationship with their years of experience. The initial chi-square statistic (χ^2_{98}=142.2) with a *P* value of .002 highlights a substantial difference in follow-up times among all optometrists. Further analysis, considering the years of experience, shows a chi-square statistic (χ^2_{140}=1540) with a *P* value of <.001, suggesting that experience level is an influential factor in this variation. These data collectively indicate that not only do follow-up times vary among optometrists, but they also correlate significantly with their professional experience.

A further breakdown shows that expert optometrists, with an average follow-up time of 4.1 months for confirmed glaucoma cases and 4 months for suspected glaucoma cases, seem to require less time to assess disease progression, likely due to their proficiency in managing the condition. In contrast, novice optometrists recommend longer follow-up times, averaging 5.3 months for confirmed cases and 4.5 months for suspected cases, which may indicate a need for additional time to make informed decisions about disease progression. For patients without glaucoma, both groups suggest more extended follow-up periods, with experts recommending an average of 8.15 months and novices slightly more at 8.73 months.

Discussion

Overview

This study investigates how optometrists' experience levels affect their decision-making in glaucoma diagnosis, a crucial factor for patient outcomes. We found significant differences in diagnostic approaches between novices and experts. The discussion ahead will dive deeper into these differences in decision-making, particularly focusing on how experience levels affect priorities in data interpretation and heuristic use in diagnosis. This analysis will not only correlate our findings with the central research questions but also inform the development of AI systems tailored for glaucoma diagnosis.

XSL•FO
RenderX

Decision-Making Processes

Our findings reveal a notable divergence in the alignment with established clinical decisions between expert and novice optometrists, particularly in the absence of prior patient data, offering crucial insights into the role of experience in clinical judgment. The higher alignment of expert diagnoses with original clinical decisions in scenarios lacking previous patient data highlights the depth of expertise honed through years of clinical practice. This expertise results in more accurate and intuitive diagnostic skills. This aligns with Hammond Cognitive Continuum Theory [22], which posits that as clinicians gain experience, their decision-making process shifts from a predominantly analytical approach to a more intuitive one [23,24]. Experienced practitioners are theorized to navigate and use this spectrum effectively, adapting their approach depending on the situation [25].

The reduced gap in decision-making accuracy when prior patient data were provided suggests that access to comprehensive patient history significantly enhances diagnostic accuracy across experience levels highlighting the critical role of patient history in clinical decision-making. These results suggest that novices can make competent decisions when guided by detailed information.

Data Prioritization in Clinical Assessments

The study also explored how optometrists at different experience levels prioritize data during clinical assessments. Initially, both experts and novices engaged comprehensively across various diagnostic areas, but with a lower focus on progression, change, and correlation analysis. This trend reflects common practice for initial assessments, where establishing a broad understanding of the patient's condition is prioritized over detailed analysis.

Interestingly, subsequent visits revealed a significant increase in attention to progression and change, particularly among experts. Experts demonstrated a more comprehensive approach, integrating clinical findings and patient history from the outset and emphasizing structural-function correlation more than novices. This comprehensive risk assessment aligns with the notion that experienced clinicians can synthesize complex information more effectively [23] and that is why their concordance was quite higher than novices.

Novices, despite a higher initial engagement progression and change analysis, might misunderstand the optimal timing for such analyses, typically requiring follow-up data. Although this increased for novices in subsequent visits, the experts showed a robust increase almost double that of novices. This indicates a strategic approach to deeper analysis in the later stages of patient management by experts.

Heuristic Approaches and Cognitive Efficiency

Our results suggest that experienced optometrists may use heuristic approaches more frequently, particularly when data are limited. The nuanced internalization of a patient's historical data by experts, evidenced by their subtle differences in conducting longitudinal comparisons and intercase comparisons, suggests cognitive efficiency. This efficiency allows experts to retain and integrate key details of disease progression into their clinical judgments without frequent referrals to past records or references to other cases. This cognitive agility is indicative of their evolved diagnostic expertise and mastery of pattern recognition in glaucomatous progression [25].

The reliance on external case references by novices, as noted in some cases, maybe a compensatory mechanism for their relative inexperience. This behavior highlights the gap in their approach to long-term patient management and the development of pattern recognition skills.

Guidelines for Developing AI System to Minimize Diagnostic Variations

In this section, we propose a set of guidelines for developing an AI system for glaucoma diagnosis based on our findings. These guidelines are intended for a human-AI collaborative environment, where the AI system will be used as a decision-support tool rather than a standalone decision maker. We suggest that by following these guidelines, the AI system will effectively support optometrists with different experience levels, bridging the gap between novices and experts, and ultimately improving patient outcomes through enhanced diagnostic accuracy. The collaborative model will also uphold ethical and professional standards, mitigating any legal, ethical, and professional barriers posed by standalone system. As a result, it will facilitate the effective integration of AI into clinical practice.

Minimizing the Effect of Limited Data Availability

Our findings show variability in diagnostic concordance between novice and expert optometrists when comprehensive patient histories are not available. These findings suggest that AI systems should have a robust module that provides detailed patient histories. If a patient has limited historical data, the system should present novices with 2 features. It should identify and display data from the most similar patient cases with the same conditions [26] along with the decisions made in that case. It should also highlight the dissimilarities between the selected patient and the current patient. The AI system should be trained with expert decision-making patterns by modeling the diagnostic approaches and visualizing the variables by estimating the missing data [27] backward in time to give them an idea of how history would look. These 2 features would minimize the limited data availability challenge and allow novices to make more accurate and consistent decisions in glaucoma diagnosis.

Evolving AI System for Initial and Subsequent Visits

Our result shows that in the initial visit, the expert optometrists adopt a comprehensive approach to assess all factors, except they do not carry analytical analysis (any progression and change analysis, and structure and function correlation analysis). As they move to subsequent visits, they still follow a comprehensive approach but with limited focus on patient historical information, instead, their focus shifts to analytical assessment. We accordingly suggest that an AI system should behave in a similar way and evolve along with the visits. In the initial visits, the AI system should prompt a novice to adopt a comprehensive approach and highlight important factors such as family history, and age. In the subsequent visits, the AI system should highlight any analytical changes. It would be better that the AI system

XSL•FO
RenderX

present a hierarchy of features, by demonstrating which features require more or less importance to assess during both the initial visit and subsequent follow-up visits. These features of AI system will help novices in understanding the optimal time for any analysis.

Follow-Up Time Suggestion

The follow-up time analysis shows variation among optometrists. We suggest that for better patient management, the AI system should provide an optimal time frame for follow-up visits [28] which should be based on patient data and clinical indicators. Along with follow-up interval, the system should also display the variables that influence this decision, such as disease progression, patient history, and symptoms. With this feature, we can bring more consistency in follow-up time suggested by optometrists.

AI System Features and Behavior

Most of the AI systems developed by researchers for glaucoma diagnosis focus on the detection of glaucoma with binary outputs [29-31]. However, to gain optometrists' trust, the AI system developed for glaucoma should also include a confidence score, include a detailed explanation of how it arrived at that specific decision, and provide a visualization of the risk factors in a hierarchical manner [32,33]. This will ensure that the optometrist does not overlook any important details. We further suggest that in the context of glaucoma, the system should not rely on only one source of data, but that it should combine multiple sources of data as used by optometrists. The optometrist will have more trust if the system uses a similar modal data for decision-making. Additionally, the AI system should have an interactive interface that offers an adjustable variables feature [34] that allows the optometrist to modify the values of any factor and see how different scenarios would affect the outcomes, such as diagnosis, severity, and follow-up time. For example, if the optometrist changes a variable to reflect a worsening condition, the AI system will adjust the follow-up recommendation accordingly. Such an AI system design for glaucoma will ensure more consistent decision-making regardless of expertise level.

Conclusions

This study investigated the diagnostic decision-making differences between novice and expert optometrists in glaucoma diagnosis, focusing on how these variations influence clinical judgment and patient outcomes. Through in-depth interviews, we identified significant disparities in diagnostic approaches. Experts demonstrated higher concordance rates with limited data, emphasizing their cognitive efficiency and intuitive decision-making, while novices relied more on structured methods and external references. Additionally, there were significant variations between experts and novices in the analysis of different exams and prioritization factors.

Based on our findings we proposed guidelines for a human-AI glaucoma diagnosis system that are aimed to minimize diagnostic variations. Incorporating the recommended features in an AI system, and using a human-AI collaboration model, will not only minimize decision inconsistency but will also improve optometrists' accuracy and enhance patient care by accelerating the diagnostic process and improving decision-making. In future work, we recommend a phased approach, starting by refining these guidelines to meet local requirements, followed by the development of an AI system based on the refined guidelines, and finally simulating and validating it through real-world data and pilot-testing in clinical environments.

Acknowledgments

This research benefitted from collaborations with the School of Optometry & Vision Sciences (thanks to Dr Stanley Woo, Director) and was supported through funding from the Natural Sciences and Engineering Research Council of Canada (NSERC-CRD Grant) (independent of study design/analysis). We are also thankful to our participants who gave us their precious time. FG's research was funded by the University of Waterloo (Graduate Research Studentship & International Doctoral Student Award). We also acknowledge the use of generative artificial intelligence (AI) tools, specifically Grammarly [35] and ChatGPT-4o (OpenAI) [36], for grammar check and flow of writing. It is important to note that generative AI tools are not used for any type of data generation or content generation in this paper.

Data Availability

The clinical data of patients used in the study is obtained from the School of Optometry and Vision Sciences, University of Waterloo. Permission was granted to use the data for this study. We have stored all the anonymized data online in a University of Waterloo Borealis repository [37] with restricted access. For research purposes, the data access can be granted by emailing the corresponding author, after taking the necessary steps required.

Conflicts of Interest

None declared.

Multimedia Appendix 1
Higher resolution version of Figure 1.
[PNG File , 1037 KB - medinform_v13i1e63109_app1.png]

XSL•FO
RenderX

Multimedia Appendix 2
Generalized codes that were created during the qualitative data analysis process. Different assessments shown on the right columns represent each code.
[DOCX File , 14 KB - medinform_v13i1e63109_app2.docx]

Multimedia Appendix 3
Descriptive statistics (mean, SEM, upper CI, lower CI, and SD), including details for novices first visits and subsequent visits, and details for experts first visits and subsequent visits.
[DOCX File , 19 KB - medinform_v13i1e63109_app3.docx]

References

1. Scanzera AC, Shorter E, Kinnaird C, Valikodath N, Al-Khaled T, Cole E, et al. Optometrist's perspectives of artificial intelligence in eye care. J Optom 2022;15 Suppl 1(Suppl 1):S91-S97 [FREE Full text] [doi: 10.1016/j.optom.2022.06.006] [Medline: 36137899]
2. Topouzis F, Anastasopoulos E. Glaucoma: the importance of early detection and early treatment. Eur Ophthalmic Rev 2007;4:13. [doi: 10.17925/eor.2007.00.00.13]
3. Yoshioka N, Wong E, Kalloniatis M, Yapp M, Hennessy MP, Agar A, et al. Influence of education and diagnostic modes on glaucoma assessment by optometrists. Ophthalmic Physiol Opt 2015;35(6):682-698. [doi: 10.1111/opo.12247] [Medline: 26432198]
4. Scheetz J, Koklanis K, McGuinness M, Long M, Morris ME. A randomized trial to increase the assessment accuracy of glaucoma and optic disc characteristics by orthoptists. J Contin Educ Health Prof 2019;39(3):161-167. [doi: 10.1097/ceh.0000000000000258]
5. Chaurasia AK, Greatbatch CJ, Hewitt AW. Diagnostic accuracy of artificial intelligence in glaucoma screening and clinical practice. J Glaucoma 2022;31(5):285-299. [doi: 10.1097/IJG.0000000000002015] [Medline: 35302538]
6. Scanzera AC, Shorter E, Kinnaird C, Valikodath N, Al-Khaled T, Cole E, et al. Optometrist's perspectives of artificial intelligence in eye care. J Optom 2022;15 Suppl 1(Suppl 1):S91-S97 [FREE Full text] [doi: 10.1016/j.optom.2022.06.006] [Medline: 36137899]
7. Mursch-Edlmayr AS, Ng WS, Diniz-Filho A, Sousa DC, Arnold L, Schlenker MB, et al. Artificial intelligence algorithms to diagnose glaucoma and detect glaucoma progression: translation to clinical practice. Transl Vis Sci Technol 2020;9(2):55 [FREE Full text] [doi: 10.1167/tvst.9.2.55] [Medline: 33117612]
8. Akter N, Fletcher J, Perry S, Simunovic MP, Briggs N, Roy M. Glaucoma diagnosis using multi-feature analysis and a deep learning technique. Sci Rep 2022;12(1):8064 [FREE Full text] [doi: 10.1038/s41598-022-12147-y] [Medline: 35577876]
9. Rogers TW, Jaccard N, Carbonaro F, Lemij HG, Vermeer KA, Reus NJ, et al. Evaluation of an AI system for the automated detection of glaucoma from stereoscopic optic disc photographs: the European optic disc assessment study. Eye (Lond) 2019;33(11):1791-1797 [FREE Full text] [doi: 10.1038/s41433-019-0510-3] [Medline: 31267086]
10. Wang G, Liu X, Shen J, Wang C, Li Z, Ye L, et al. A deep-learning pipeline for the diagnosis and discrimination of viral, non-viral and COVID-19 pneumonia from chest x-ray images. Nat Biomed Eng 2021;5(6):509-521 [FREE Full text] [doi: 10.1038/s41551-021-00704-1] [Medline: 33859385]
11. Jammal AA, Thompson AC, Mariottoni EB, Berchuck SI, Urata CN, Estrela T, et al. Human versus machine: comparing a deep learning algorithm to human gradings for detecting glaucoma on fundus photographs. Am J Ophthalmol 2020;211:123-131 [FREE Full text] [doi: 10.1016/j.ajo.2019.11.006] [Medline: 31730838]
12. Cook GJ. An empirical investigation of information search strategies with implications for decision support system design. Decis Sci 2007;24(3):683-698. [doi: 10.1111/j.1540-5915.1993.tb01298.x]
13. Lai V, Chen C, Smith-Renner A, Liao QV, Tan C. Towards a science of human-AI decision making: an overview of design space in empirical human-subject studies,. 2023 Presented at: FAccT '23: the 2023 ACM Conference on Fairness, Accountability, and Transparency; June 12-15, 2023; Chicago, IL p. 1369-1385. [doi: 10.1145/3593013.3594087]
14. Curran K, Congdon N, Peto T, Dardis C, Nguyen QN, Hoang TT, et al. Capturing the clinical decision-making processes of expert and novice diabetic retinal graders using a 'think-aloud' approach. Eye (Lond) 2022 May;36(5):1019-1026 [FREE Full text] [doi: 10.1038/s41433-021-01554-6] [Medline: 33972706]
15. Stainer MJ, Anderson AJ, Denniss J. Examination strategies of experienced and novice clinicians viewing the retina. Ophthalmic Physiol Opt 2015 Jul;35(4):424-432. [doi: 10.1111/opo.12210] [Medline: 25939994]
16. Leske MC, Wu SY, Hennis A, Honkanen R, Nemesure B, BESs Study Group. Risk factors for incident open-angle glaucoma: the Barbados eye studies. Ophthalmology 2008;115(1):85-93. [doi: 10.1016/j.ophtha.2007.03.017] [Medline: 17629563]
17. Le A, Mukesh BN, McCarty CA, Taylor HR. Risk factors associated with the incidence of open-angle glaucoma: the visual impairment project. Invest Ophthalmol Vis Sci 2003;44(9):3783-9388. [doi: 10.1167/iovs.03-0077] [Medline: 12939292]
18. de Voogd S, Ikram MK, Wolfs RC, Jansonius NM, Witteman JC, Hofman A, et al. Is diabetes mellitus a risk factor for open-angle glaucoma? the Rotterdam study. Ophthalmology 2006;113(10):1827-1831. [doi: 10.1016/j.ophtha.2006.03.063] [Medline: 16884777]

XSL•FO
RenderX

19. Gordon MO, Beiser JA, Brandt JD, Heuer DK, Higginbotham EJ, Johnson CA, et al. The ocular hypertension treatment study: baseline factors that predict the onset of primary open-angle glaucoma. Arch Ophthalmol 2002;120(6):714-829. [doi: 10.1001/archopht.120.6.714] [Medline: 12049575]
20. European Glaucoma Prevention Study (EGPS) Group, Miglior S, Pfeiffer N, Torri V, Zeyen T, Cunha-Vaz J, et al. Predictive factors for open-angle glaucoma among patients with ocular hypertension in the european glaucoma prevention study. Ophthalmology 2007;114(1):3-9. [doi: 10.1016/j.ophtha.2006.05.075] [Medline: 17070596]
21. Mann HB, Whitney DR. On a test of whether one of two random variables is stochastically larger than the other. Ann Math Statist 1947 Mar;18(1):50-60. [doi: 10.1214/aoms/1177730491]
22. Kenneth RH. Principles of organization in intuitive and analytical cognition. Defense Technical Information Center. Colorado: University of Colorado, Inst. of Behavioral Science; 1981 Feb 15. URL: https://apps.dtic.mil/sti/citations/ADA096570 [accessed 2024-06-01]
23. McCartney M. Margaret McCartney: nurses must be allowed to exercise professional judgment. BMJ 2017 Mar 28;356:j1548. [doi: 10.1136/bmj.j1548] [Medline: 28351839]
24. Yang H, Thompson C, Bland M. The effect of clinical experience, judgment task difficulty and time pressure on nurses' confidence calibration in a high fidelity clinical simulation. BMC Med Inform Decis Mak 2012 Oct 03;12:113 [FREE Full text] [doi: 10.1186/1472-6947-12-113] [Medline: 23034048]
25. Tsang M, Martin L, Blissett S, Gauthier S, Ahmed Z, Muhammed D, et al. What do clinicians mean by “Good Clinical Judgment”: a qualitative study. IME 2023 Jan 11;2(1):1-10. [doi: 10.3390/ime2010001]
26. Parimbelli E, Marini S, Sacchi L, Bellazzi R. Patient similarity for precision medicine: a systematic review. J Biomed Inform 2018 Jul;83:87-96 [FREE Full text] [doi: 10.1016/j.jbi.2018.06.001] [Medline: 29864490]
27. Berchuck SI, Mwanza JC, Warren JL. A spatially varying change points model for monitoring glaucoma progression using visual field data. Spat Stat 2019 Apr;30:1-26 [FREE Full text] [doi: 10.1016/j.spasta.2019.02.001] [Medline: 30931247]
28. Bian Y, Xiang Y, Tong B, Feng B, Weng X. Artificial intelligence-assisted system in postoperative follow-up of orthopedic patients: exploratory quantitative and qualitative study. J Med Internet Res 2020 May 26;22(5):e16896 [FREE Full text] [doi: 10.2196/16896] [Medline: 32452807]
29. Hemelings R, Elen B, Barbosa-Breda J, Lemmens S, Meire M, Pourjavan S, et al. Accurate prediction of glaucoma from colour fundus images with a convolutional neural network that relies on active and transfer learning. Acta Ophthalmol 2020 Feb;98(1):e94-e100 [FREE Full text] [doi: 10.1111/aos.14193] [Medline: 31344328]
30. Saxena A, Vyas A, Parashar L, Singh U. A glaucoma detection using convolutional neural network. 2020 Presented at: International Conference on Electronics and Sustainable Communication Systems (ICESC); July 2-4, 2020; Coimbatore, India p. 815-820. [doi: 10.1109/icesc48915.2020.9155930]
31. Lin M, Hou B, Liu L, Gordon M, Kass M, Wang F, et al. Automated diagnosing primary open-angle glaucoma from fundus image by simulating human's grading with deep learning. Sci Rep 2022 Aug 18;12(1):14080 [FREE Full text] [doi: 10.1038/s41598-022-17753-4] [Medline: 35982106]
32. Kamal MS, Dey N, Chowdhury L, Hasan SI, Santosh K. Explainable AI for glaucoma prediction analysis to understand risk factors in treatment planning. IEEE Trans Instrum Meas 2022;71:1-9. [doi: 10.1109/tim.2022.3171613]
33. Chayan, TI, Islam, E, Rahman, Md T, Reza TS, Apon TS, Golam Rabiul Alam MD. Explainable AI based glaucoma detection using transfer learning and LIME. 2022 Presented at: IEEE Asia-Pacific Conference on Computer Science and Data Engineering (CSDE); December 18-20, 2022; Gold Coast, Australia. [doi: 10.1109/csde56538.2022.10089310]
34. Beauxis-Aussalet E, Behrisch M, Borgo R, Chau DH, Collins C, Ebert D, et al. The role of interactive visualization in fostering trust in AI. IEEE Comput Grap Appl 2021 Nov 1;41(6):7-12. [doi: 10.1109/mcg.2021.3107875]
35. Grammarly. URL: https://www.grammarly.com/ [accessed 2025-01-08]
36. ChatGPT-4o. OpenAI. URL: https://chatgpt.com/?model=gpt-4o [accessed 2025-01-08]
37. Ghaffar F, Furtado N, Ali I, Burns C. Diagnostic decision-making variability in glaucoma: comparative analysis of novice and expert optometrists to inform AI system design. JMIR Preprints Preprint posted online on Dec 1, 2024 [FREE Full text] [doi: 10.2196/preprints.63109]

Abbreviations

AI: artificial intelligence

XSL•FO
RenderX

Edited by C Lovis; submitted 10.06.24; peer-reviewed by MJ Barons, A Anderson, TK Yoo; comments to author 21.08.24; revised version received 19.09.24; accepted 01.12.24; published 29.01.25.

Please cite as:
Ghaffar F, Furtado NM, Ali I, Burns C
Diagnostic Decision-Making Variability Between Novice and Expert Optometrists for Glaucoma: Comparative Analysis to Inform AI System Design
JMIR Med Inform 2025;13:e63109
URL: https://medinform.jmir.org/2025/1/e63109
doi:10.2196/63109
PMID:39879089

©Faisal Ghaffar, Nadine M. Furtado, Imad Ali, Catherine Burns. Originally published in JMIR Medical Informatics (https://medinform.jmir.org), 29.01.2025. This is an open-access article distributed under the terms of the Creative Commons Attribution License (https://creativecommons.org/licenses/by/4.0/), which permits unrestricted use, distribution, and reproduction in any medium, provided the original work, first published in JMIR Medical Informatics, is properly cited. The complete bibliographic information, a link to the original publication on https://medinform.jmir.org/, as well as this copyright and license information must be included.

XSL•FO
RenderX

Original Paper

Improving AI-Based Clinical Decision Support Systems and Their Integration Into Care From the Perspective of Experts: Interview Study Among Different Stakeholders

Godwin Denk Giebel[1], Dr. rer. medic.; Pascal Raszke[1], MA; Hartmuth Nowak[2,3], PD, Dr. med.; Lars Palmowski[2], Dr. med.; Michael Adamzik[2], Prof Dr; Philipp Heinz[4], Dipl-Kfm; Marianne Tokic[5], MSc; Nina Timmesfeld[5], Prof Dr; Frank Martin Brunkhorst[6], Prof Dr; Jürgen Wasem[1], Prof Dr; Nikola Blase[1], Dr. med.

[1]Institute for Health Care Management and Research, University of Duisburg-Essen, Essen, Germany

[2]Department of Anesthesiology, Intensive Care and Pain Therapy, University Hospital Knappschaftskrankenhaus Bochum, Bochum, Germany

[3]Center for Artificial Intelligence, Medical Informatics and Data Science, University Hospital Knappschaftskrankenhaus Bochum, Bochum, Germany

[4]Knappschaft Kliniken GmbH, Recklinghausen, Germany

[5]Department of Medical Informatics, Biometry and Epidemiology, Ruhr University Bochum, Bochum, Germany

[6]German Sepsis Society, Berlin, Germany

Corresponding Author:
Godwin Denk Giebel, Dr. rer. medic.
Institute for Health Care Management and Research
University of Duisburg-Essen
Thea-Leymann-Str. 9
Essen, 45127
Germany
Phone: 49 201 18 33180
Email: godwin.giebel@uni-due.de

Abstract

Background: Artificial intelligence (AI)–based systems are receiving increasing attention in the health care sector. While the use of AI is well advanced in some medical applications, such as image recognition, it is still in its infancy in others, such as clinical decision support systems (CDSS). Examples of AI-based CDSS can be found in the context of sepsis prediction or antibiotic prescription. Scientific literature indicates that such systems can support physicians in their daily work and lead to improved patient outcomes. Nevertheless, there are various problems and barriers in this context that should be considered.

Objective: This study aimed to identify opportunities to optimize AI-based CDSS and their integration into care from the perspective of experts.

Methods: Semistructured web-based expert interviews were conducted. Experts representing the perspectives of patients; physicians; caregivers; developers; health insurance representatives; researchers (especially in law and IT); and experts in regulation, market admission and quality management or assurance, and ethics were included. The conversations were recorded and transcribed. Subsequently, a qualitative content analysis was performed. The different approaches to improvement were categorized into groups (“technology,” “data,” “users,” “studies,” “law,” and “general”). These also served as deductive codes. Inductive codes were determined within an internal project workshop.

Results: In total, 13 individual and 2 double interviews were conducted with 17 experts. A total of 227 expert statements were included in the analysis. Suggestions were heterogeneous and concerned improvements: (1) in the systems themselves (eg, implementing comprehensive system training involving [future] users; using a comprehensive and high-quality database; considering usability, transparency, and customizability; preventing automation bias through control mechanisms or intelligent design; conducting studies to demonstrate the benefit of the system), (2) on the user side (eg, training [future] physicians could contribute to a more positive attitude and to greater awareness and questioning decision supports suggested by the system and ensuring that the use of the system does not lead to additional work), and (3) in the environment in which the systems are used (eg, increasing the digitalization of the health care system, especially in hospitals; providing transparent public communication about the benefits and risks of AI; providing research funding; clarifying open legal issues, eg, those related to liability; and standardizing and consolidating various approval processes).

XSL•FO
RenderX

Conclusions: This study offers several possible strategies for improving AI-based CDSS and their integration into health care. These were found in the areas of "technology," "data," "users," "studies," "law," and "general." Systems, users, and the environment should be taken into account to ensure that the systems are used safely, effectively, and sustainably. Further studies should investigate both the effectiveness of strategies to improve AI-based CDSS and their integration into health care and the accuracy of their match to specific problems.

International Registered Report Identifier (IRRID): RR2-10.2196/62704

(JMIR Med Inform 2025;13:e69688) doi:10.2196/69688

KEYWORDS

artificial intelligence; AI; clinical decision support systems; CDSS; decision-making; care; interviews

Introduction

Background

The use of artificial intelligence (AI), especially machine learning, is becoming increasingly common in all areas of life. This is also evident in health care. In July 2024, the US Food and Drug Administration database included 882 AI- and machine learning–enabled devices from various medical fields such as radiology (n=671), cardiovascular medicine (n=90), neurology (n=32), hematology (n=17), gastroenterology and urology (n=13), anesthesiology (n=9), ophthalmology (n=9), clinical chemistry (n=8), general and plastic surgery (n=6), microbiology (n=6), pathology (n=6), or orthopedics (n=5) [1]. AI is believed to have tremendous potential to revolutionize patient care and outcomes [2,3]. This is especially because of its ability to support diagnosing, individualization of treatment plans, and clinical decision-making [2,4]. AI-based clinical decision support systems (CDSS) offer the potential to support physicians in their work and to optimize patient outcomes. For example, this is evident in the context of sepsis. In this context, such systems can support prediction, diagnosis, subphenotyping, prognosis, and clinical management [5]. This can lead to earlier treatment [6] and ultimately to shorter hospital stays [6,7] as well as reduced mortality [6-8].

Given these potential positive effects, it is questionable why AI-based CDSS have only been used in isolated cases in real care. One possible reason could be the barriers to establishing such systems: regulators must approve them. The systems must be integrated into electronic health record systems, and they must be standardized to the extent that similar products operate in a similar way. Clinicians must be trained to use them, they must be updated over time, and payment must be organized [4]. Furthermore, user perception is a fundamental criterion that decides acceptance [9].

The literature describes a further wide range of problems and barriers in the context of AI-based CDSS [10-12]. These relate to AI or CDSS and a combination of both, AI-based CDSS. While some of the problems relate to technical integration and operational use [10,11], others relate to the legal and ethical framework [12]. Regarding strategies for implementing AI-based CDSS in clinical practice, a study conducted by Peek et al [13] analyzed the literature and concluded that perspectives from groups other than health care professionals (eg, patients, carers, AI developers, health care managers, and leaders, and especially regulators and policy makers) should be investigated.

Objective

To investigate the perceived problems and possible improvements involved in integrating AI-based CDSS to health care and to develop a user-oriented requirements profile for the systems, we established the research project "KI@work" [14]. It was founded by the German Federal Joint Committee (01VSF22050).

As part of the project, a scoping review (Raszke P, unpublished data, April 2025) was conducted to collect fundamental evidence. On the basis of the results, we conducted interviews with experts to further investigate the following questions: (1) What problems and barriers hinder the integration of AI-based CDSS into health care? (2) What approaches might be used to enhance the quality of AI-based CDSS and their integration into care? While the first question was covered in a previous article [15], this paper especially focuses on the second. Thus, this study aims to gather expert opinions on how AI-based CDSS and their integration into care can be optimized.

Methods

Overview

Expert interviews were conducted to identify approaches to solve perceived problems in the context of AI-based CDSS. We followed the standards of O'Brien et al [16] and the 32-item COREQ (Consolidated Criteria for Reporting Qualitative Research) checklist (Multimedia Appendix 1) [17] in preparing this manuscript. Therefore, transparency is guaranteed in all aspects of our study. The underlying interviews and corresponding transcripts, have already been examined for existing problems and barriers in the context of AI-based CDSS from the perspective of experts.

Theoretical Framework

There is some evidence of problems and barriers, but as the field of AI-based CDSS is relatively new, little is known about how to optimize its use. Therefore, qualitative research in the form of expert interviews was conducted to approach the topic in an explorative way. The interviews were conducted with experts in the context of AI-based CDSS. The interviewees represented a wide range of different areas and professions. The interviews had 2 objectives, and the proceeding remained consistent: they started with open questions and topics and then addressed more specific questions. Within each topic, we first asked about different problems and barriers in the context of

XSL•FO
RenderX

AI-based CDSS. Then, we asked about ways to improve care with AI-based CDSS.

Ethical Considerations

Because patient views were collected through representatives and not from patients themselves, and no personal data were collected, the Ethics Committee of the Medical Faculty of the University of Duisburg-Essen confirmed that no application for ethics approval was required. Before the conversations, experts were informed via email about the topic and the proceeding. The email also included information about privacy and that the conversations would be recorded and transcribed for data analysis. Furthermore, the interviewees were informed that they could end the conversations on their part at any time without giving a reason and without experiencing any disadvantages. All experts provided consent to participate. The interviews were recorded and either transcribed automatically in Microsoft Teams (Microsoft) or manually for Zoom (Zoom Video Communications) interviews. Revision and pseudonymization were subsequently performed by research assistants and quality-checked, each by one of the moderators. After quality checking, the transcripts were sent to the respective experts for review to ensure the accuracy of the content. Three experts made use of this option, and their feedback was incorporated into the transcripts. The video recordings were then deleted. Therefore, it is not possible to assign individual statements to individual experts unless recalled by participants or moderators.

Participant Selection and Preliminary Information

The question “Who are the relevant stakeholders in the context of AI-based CDSS?” was discussed during a project meeting to create a list of experts to contact. The list included representatives of patients; physicians; caregivers; developers; statutory health insurance funds; researchers (especially in law and informatics); and experts in regulation, market admission, quality management or assurance, and ethical issues. On the basis of this list, appropriate institutions were sought and contacted to find eligible interview partners. If a consortium member had a connection to one of the identified institutions, they helped establish contact with a potential interview partner (n=7). Five (71%) of the 7 people contacted participated in an interview. In 2 (29%) cases, the person originally contacted arranged an interview partner within their institution. The remaining 8 interviewees were recruited independently of personal networks. In all cases except one, it was ensured that the interviewers had no prior contact with any of the interviewees.

Possible participants were contacted directly via email by the consortium. After contacting the experts, none of them declined to take part in the study. Four experts did not respond to the request. Ultimately, all target groups were represented in the interviews.

Setting and Conducting the Interviews

All interviews were conducted on the web via the conferencing platforms Microsoft Teams (Microsoft) or Zoom (Zoom Video Communications). Interviews included 1 or a maximum of 2 experts at a time. Circumstances or events which had an unintended influence on the conversations are not known. The interviews were moderated by 1 person and attended by at least 1 other person from a pool of 3 possible moderators (GDG, PR, and NB). The characteristics of the moderators are listed in Multimedia Appendix 2. Notable relationships did not exist between the researchers and the interviewees. There was no clear position for or against the use of AI-based CDSS in health care.

An interview guideline was developed (based on the preliminary results of a scoping review conducted before the interviews) by the team of the University of Duisburg-Essen and quality was assured within the consortium. The guideline included questions about both problems and barriers in the context of AI-based CDSS, as well as questions about possible improvements. It was slightly adapted with stakeholder-specific questions. The core version can be found in Multimedia Appendix 3. The interviews took place between June and August 2023.

Data Analysis

A content-structuring qualitative analysis following the study by Kuckartz [18] was conducted using MAXQDA (VERBI Software GmbH) based on the final transcripts. The analysis aimed to conduct a content- and topic-oriented evaluation, as well as the development of main topics and subtopics. The analysis was based on deductive codes to create an overarching systematization. These included six categories in which approaches for optimization were suggested: (1) “technology,” (2) “data,” (3) “user,” (4) “studies,” (5) “law,” and (6) “general.” After deductive coding, relevant expert statements were concisely summarized (GDG) and subsequently discussed in a workshop (GDG, NB, and PR). The workshop aimed to develop finer-grained groups for a more differentiated perspective. Similar statements within the 6 overarching categories were grouped into subcategories (inductive codes), which were then used for further systematization. Finally, the expert statements were coded according to the inductive codes and systematized within a matrix using Excel (Microsoft Corporation; Multimedia Appendix 4). Data analysis was finished in October 2023.

Results

Overview

In total, 17 experts were interviewed in 13 individual and 2 double interviews. The professional backgrounds of the experts are provided in Table 1. The intrinsic motivation and participation of the experts were high.

XSL•FO
RenderX

Table 1. Conducted interviews.

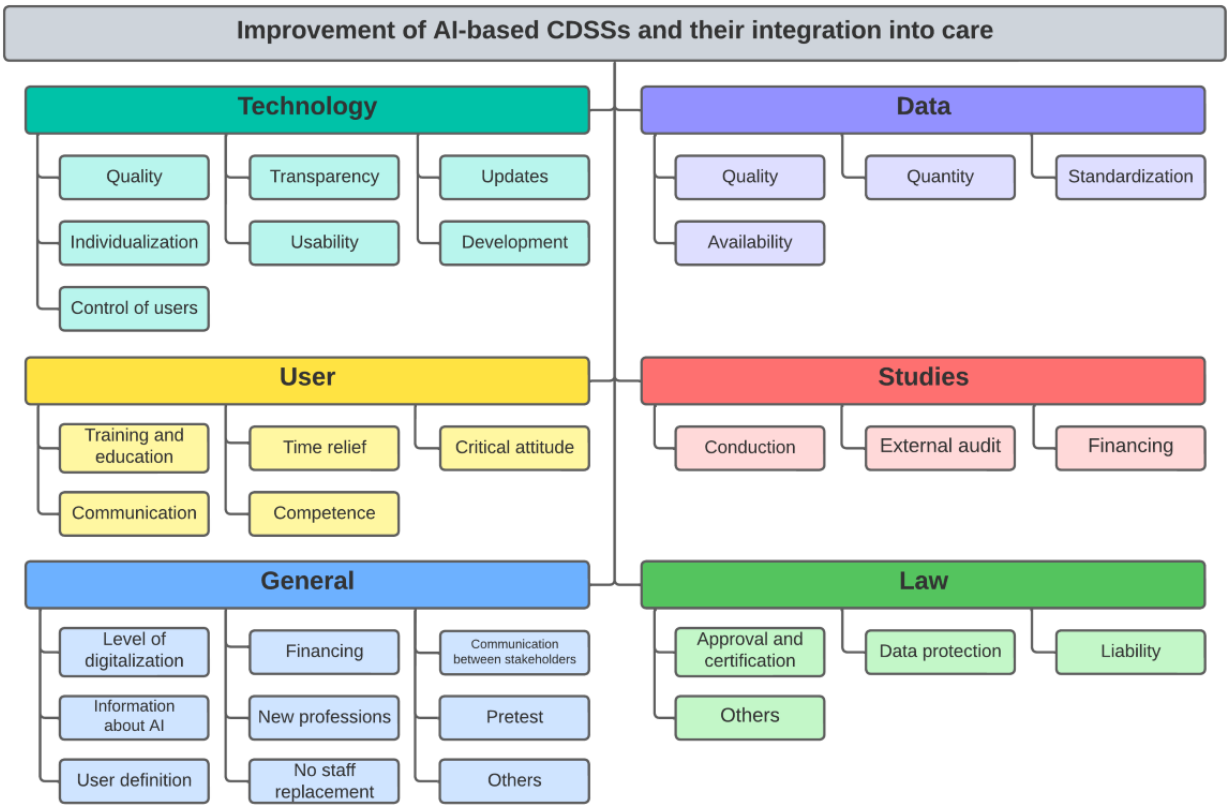
Number	Stakeholder	Setting	Date
1	Caregiver representative	Individual interview	June 5, 2023
2	Representative of quality management	Individual interview	June 5, 2023
3	Researcher—AI[a] in health care	Individual interview	June 6, 2023
4	Medical product consultant	Individual interview	June 16, 2023
5	Caregiver representative	Individual interview	June 27, 2023
6	Caregiver representative	Double interview	June 27, 2023
7	Representative of quality assurance	Double interview	July 4, 2023
8	Representative of an ethics committee	Individual interview	July 17, 2023
9	Researcher—Social and health law	Individual interview	July 19, 2023
10	Medical product consultant	Individual interview	July 27, 2023
11	Developer of AI-based CDSS[b]	Individual interview	July 27, 2023
12	Patient representative	Individual interview	July 31, 2023
13	Physician representative (Intensive care)	Individual interview	August 8, 2023
14	Developer of AI-based CDSS	Individual interview	August 11, 2023
15	Representative of health insurance fund	Individual interview	August 17, 2023

[a]AI: artificial intelligence.

[b]CDSS: clinical decision support systems.

A total of 227 expert statements included suggestions for improvement of AI-based CDSS and their integration into care. As described in the Methods section, these were categorized into 6 categories: “technology,” “data,” “user,” “studies,” “law,” and “general.” The systematization is presented in Figure 1. The complete and systematized list of summarized expert statements is presented in Multimedia Appendix 4.

Figure 1. Identified improvement approaches matched with problem categories. AI: artificial intelligence; CDSS: clinical decision support systems.



XSL•FO
RenderX

Technology

Optimization potential in the category of technology included "quality," "transparency," "updates," "individualization," "usability," "development," and "control of users." Experts explained that the "quality" of AI-based CDSS is a fundamental factor affecting trust and acceptance over time. Therefore, requirements for high-quality systems should be considered. According to the experts, such requirements include that the systems be evidence-based and reliable and meet at least the current gold standard for value. Quality and validity assessments should be conducted regularly to maintain good quality over time. This should include checking the system against a validation dataset, sampling procedures, or test loops. The quality of systems could also reduce the burden of false alerts. Therefore, on the one hand, the systems should be able to identify false-positive and false-negative results. On the other hand, an appropriate balance between sensitivity and specificity might avoid unnecessary alerts as well as associated alert fatigue. Finally, incorrect recommendations can be avoided if systems clearly stick to evidence-based or, at least, consensus-based guidelines:

> *That means, the only reasonable method to increase acceptance, is to increase the quality of products and to gain trust in this way. That we currently have very low acceptance in some areas, maybe that's a good thing and that it must increase over the next years is due to the innovative technology. A normal process.* [Medical product consultant]

"Transparency" can be guaranteed by avoiding black-box characters (incomprehensible AI). According to experts, AI-suggested decisions should be transparent, and systems should provide explanations. This could be achieved by identifying decisive parameters or using so-called heat maps to visualize data and give at least clues as to where the proposed decision stems from. Finally, it was mentioned that self-learning systems should stop evolving when they are no longer comprehensible:

> *So, the idea is actually that the decision that the AI gives me is justified by the AI in such way that I can, in a way that is so clear and comprehensible that I can perhaps also understand mistakes in the decision-making chain.* [Caregiver representative]

Experts stated that "updates" must be conducted to include new data and guidelines as well as to adapt the algorithm accordingly. Sensible implementation of user feedback should be considered during updates as well:

> *So, I demand diligence from the AI, but I also need the teacher somewhere, who must have a learning concept, the algorithm must always be continuously checked and adapted.* [Representative of quality assurance]

Experts with a more technical background saw "individualization" as a way of enhancing the quality of the systems. They explained that systems must be adapted to individual hospitals and that models from the United States should be optimized for local use in Germany. A physician representative, by contrast, stated that system standardization would be necessary to enable system use across locations:

> *I believe that you can't do it preclinically. I have to talk to the hospitals, I have to set up the project in the hospital, in the care setting. Because [...] we have 1,200 ecosystems, if I'm only talking about acute hospitals now [...]. I have to involve the doctors in each hospital individually. I have to involve IT in every hospital.* [Developer of AI-based CDSS]

A further suggested approach lies in "usability." User-friendliness should be considered to facilitate use and point users directly to relevant points. This includes the convenient use of AI-based CDSS for bedside conversations. User skills, as well as knowledge gaps, should be considered within system design. According to experts, a thorough "development phase" with a clearly determined question or target problem could contribute to the prevention of problems in the context of AI-based CDSS. The systems should be extensively and sufficiently developed and trained. False-positive and false-negative results must be checked during the training phase. The causes of identified errors must be eliminated. A balance between sensitivity, specificity, and overfitting (ie, training too specifically based on a fixed dataset) should be maintained. An interdisciplinary development, including experts and stakeholders from various fields (eg, future users, physicians, IT managers, and patient advocates) was desired. Involvement could include statements, tests of prototypes, participatory development, conceptual design, and open discourse. The development process should always be controlled by an independent process attendant:

> *I believe that it is crucial that, when you develop something AI-based like this, the people who will have to work with it later, who will have to use it, are involved as much as possible, right from the development phase.* [Caregiver representative]

Finally, "control of users" could improve the quality of AI-based CDSS and their integration into care. The intelligent design, implementation, and testing of risk control measures and their corresponding implementation in AI-based CDSS could prevent blind trust and automation bias. Furthermore, deliberately incorrectly proposed decisions by AI might be used to check the awareness of users:

> *Problems like this [such as automation bias], can be countered by designing and implementing intelligently enough, I would say.* [Caregiver representative]

Data

A further starting point for improvement is the area of "data." Approaches in this context concern the "quality," "quantity," "standardization," and "availability" of data.

First, according to the experts, high data "quality" must be guaranteed. Therefore, the quality of the training data should be improved. This can be done through data management, reflective data synthesis, or reflective filling of incomplete datasets. The validity of the primary dataset should be made transparent:

XSL•FO
RenderX

> *So that would be a very important point for me, especially at the beginning of the study protocols, from our experience, also in terms of quality assurance, to be able to make a statement about the validity of the primary data pools.* [Representative of quality assurance]

"Quantity" included the enlargement of the database as well as its completeness. According to experts, both would contribute to better results. Structured and unstructured data should be included, and longitudinal data should be used in the analysis. No data should be excluded because of the age, origin, or sex of patients. Databases should be equally weighted, sufficiently represent women as well as minority individuals, and consider age and diseases:

> *And of course it is very important that we have equally weighted data sets, that we represent minorities and so on. But that's a craft, it can be done. It has to happen, yes, but it's not inherent in the technology, it's simply a manual part of using the technology.* [Researcher—AI in health care]

A further approach was seen in "standardization." Experts asked for national-level data standardization and integration. Therefore, data could be merged and made usable. Generic data patterns should be predefined:

> *[...] yes, I like, this generic character of data sets. This is, I rather think, the field, you have to create generic data patterns that hospitals have to adhere to in order to achieve accuracy.* [Developer of AI-based CDSS]

Finally, the "availability" of data could contribute to improving the systems and their integration into care. Experts suggested the creation of a national or European data pool, as well as networks, to obtain sufficiently large datasets. Data should also be accessible for the private sector to develop AI-based CDSS. Analogous data from hospitals should be made available using machine reading, such as optical character recognition, of PDF documents such as scans or photos. During the digitization process, experts should be involved in reading out subject-specific documents:

> *And that means we should take the EU Commission's proposal with the draft regulation on the European Health Data Space seriously so that private sector companies that develop AI-based CDSS can also access such data. Because every year we have 550 million outpatient data records and 15 million inpatient data records that are not accessible for this development or not easily accessible.* [Medical product consultant]

User

Many of the identified improvements are user-oriented. These include "training/education," "time relief," "critical attitude," "communication," and "competence."

First, "training/education" might lead to more openness to AI-based CDSS. Therefore, information on AI should be a part of both medical training and further staff training. Staff training should include educational courses or workshops on the general topic of AI, its threats (eg, errors in its use, especially automation bias), its limitations, and information on its impact on existing care pathways. Courses should provide the opportunity to try out AI-based CDSS. Their application under stress should be exercised. In contrast to most of the other respondents, a developer stated that only those who modify the systems needed training but not those who just use the systems. A physician representative stated that trainings and courses should be nonmandatory. Experts pronounced that, within training, it should be clarified that AI will not replace humans:

> *And I think what would help to increase that acceptance would be just regular training. If you could also show examples of what a specific case might look like.* [Caregiver representative]
>
> *And I believe, if there are no training courses or no sensitization, then there is a risk that such recommendations for action will simply be adopted and that would be disastrous.* [Developer of AI-based CDSS]

Experts saw "time relief" of physicians and caregiving professionals as a solution for missing acceptance. They stated that the temporal valences of users should be considered and that AI should not lead to major additional work. Rather, it should make day-to-day work easier, for example, by supporting documentation. Furthermore, it was explained that clinicians should be relieved for scientific tasks in the context of AI and use their competence to assess complex cases:

> *[...] that you have a mixture of easier and more difficult cases, and AI will tend to mean that the easy cases can be checked off very quickly by the AI or with the help of the AI, and that only the very difficult cases will actually end up with the doctors. And maybe there needs to be some relief here. You have to say that somehow you have to take more breaks [...] because looking at the screen all day and then only having to differentiate between the worst cases is not easy.* [Representative of an ethics committee]

A further improvement approach was seen in the "critical attitude" of users. It was stated that decisions suggested by AI must always be scrutinized, validated, and checked for plausibility. There should be no blind reliance on AI. One expert explained that regardless of whether recommendations are made by AI or humans, they should always be questioned. A critical attitude was described as relevant to both positive and negative findings. Thus, even supposed false alarms should be taken seriously. One stakeholder wished for mutual skepticism between AI and users:

> *This means that the suggestions or recommendations for action of an AI-based CDSS must be evaluated by the doctor in the same way as a laboratory value or another parameter or a pathological ECG. It must be critically scrutinized; it must be validated [...].* [Medical product consultant]

In addition, an opposing view was taken in the context of "critical attitude": users should gain greater trust in AI and, in

XSL•FO
RenderX

some future cases, might also implement recommendations for action without checking them:

> *And at some point, we will receive recommendations for action that we can rely on 100% and then we can implement them without checking them. So, the answer to your question is: we encounter the problem by only implementing recommendations for action unchecked where we have a sufficiently high level of certainty that it will work due to the validation.* [Medical product consultant]

A last improvement approach concerning the user was seen in "competence." According to experts, users need personal and professional competence to use and deal with decisions suggested by the AI, as well as to maintain decision-making authority and avoid dependence on AI. In particular, the implicit knowledge from experience should be maintained. Finally, interviewees also explained that trust increases with competence:

> *So, who decides and who does not, I think it has something to do with education, it has something to do with personal competence and of course it also has a lot to do with professional competence.* [Caregiver representative]

Studies

Regarding "studies," improvement approaches were named within 3 areas. These were "study conduction," "external audit," and "financing."

"Study conduction" was seen as essential to prove evidence, to assess benefits, and to track side effects. Demonstrating success in studies would lead to increased public acceptance and trust. A general need for more valid (comparative) and prospective studies was pronounced. A "clean, best possible study design depending on the disease" [Representative of health insurance fund] was demanded. Orientation of studies on standards of scientific institutes and the involvement of experts was described as necessary:

> *We now need prospective randomized studies, one part gets standard care, one part gets AI and then we have to look and that has to be done on a relatively large number of patients across several sites so that we can see whether it is possible to detect organ dysfunction and sepsis in advance.* [Physician representative—intensive care]

> *In general, of course, the higher the quality of the study design - and a randomized controlled trial is of course the gold standard - the more reliable the results are.* [Representative of health insurance fund]

Experts stated that studies should also include an "external audit" to get a neutral view of the situation. Furthermore, involving patient organizations in studies can help increase acceptance among patients. Finally, in this context, an improvement approach was seen in the "financing"—specifically, the funding of studies. The federal or state governments or the European Union (EU) were seen as responsible for study funding:

> *We must now have this willingness to carry out these studies, [...] I mean we're talking about a few million euros, [...]. That is now indicated, that is the next logical step and if we were to do that, we would be very far ahead, not just in Europe, but globally.* [Physician representative—intensive care]

Law

"Approval/certification," "data protection," and "liability" were seen as possible improvement approaches within the category of "law." Further suggestions within this category were aggregated under "others."

"Approval/certification" and review of AI-based CDSS should be conducted regularly by independent bodies to increase acceptance. It was expressed that certifying bodies would need more staff with a background in science, technology, engineering, and mathematics. Approval of AI should not lead to major additional costs compared with conventional medical devices. Another approach expressed was a certification that authorizes humans to use AI:

> *I think independence is important. An established, independent institute and regular repetition, [...] and AI systems are also constantly changing, because they are - AI means a self-learning system, which means that you have to check them every now and then. So regularly, independently and in an understandable way.* [Patient representative]

Further opportunities were seen in the regulation of "data protection." Data protection standards should always be appropriate, and data integration should be standardized nationwide. Users could benefit from already certified plug and play hardware solutions to avoid data protection issues. Whether researchers are allowed to use the collected data should be decided by the patients. Furthermore, experts stated that problems in the context of data protection are often caused by data protectors and not by data protection requirements and are thus avoidable:

> *Every data protection officer has a problem with personal data that goes off campus, and I absolutely understand that. But what I always like to ask is, has anyone ever asked the patients whether they could possibly care less? [...] There are clinics that do this in Germany, they use all their patients' data for research purposes. It's not forbidden, I'm just saying opt-in, opt-out.* [Developer of AI-based CDSS]

Regarding "liability," experts have suggested that modes of action and responsibilities should be clarified. In this context, it was proposed that it should be legally anchored that diagnostic and therapeutic responsibility remains with the user, specifically the physician. Users should be informed about the legal framework. Otherwise, one expert explained that physicians should not be made liable for AI-proposed decisions that cannot be verified because of a black-box character of the systems:

> *And liability risks are also a major issue, and doctors naturally don't want to be held liable for anything, for possible treatment errors or that they have overlooked something if they can't actually assess*

XSL•FO
RenderX

> *the quality of this AI. And that's why I would say that increasing acceptance is also possible through regulation.* [Representative of an ethics committee]

A further two improvement approaches were described. These were the obligations to report and publish errors that occur in the context of the systems in general and to report and track, especially, the causes of incorrect decision recommendations.

General

Under the category "general," various suggestions for improvement were summarized that did not match one of the other categories. These include "level of digitalization," "financing," "communication between stakeholders," "information about AI," "new professions," "pretest," "user definition," "no staff replacement," and "others."

The "level of digitalization" should be expanded for IT infrastructure. There is a demand for high-performance computing to ensure fast, reliable, and failure-free operation of the systems. Digitization should be standardized to close gaps in the documentation:

> *And I remember that from before, when we had the paper curve, we really had a lot of gaps in the documentation as far as vital signs were concerned. So that's why we should have uniform digitization, which would of course be the optimum.* [Caregiver representative]

Improvement in "financing" concerned 3 aspects. First, service providers should be motivated with incentives to use AI-based CDSS. Second, incentivization could lead service providers to collect data more conscientiously. Third, experts saw the federal states and the German social policy as responsible for participation in hospital financing and the financing of digitalization infrastructure of the health care system:

> *But on the whole, people act as if this is purely a private matter. [...] My personal opinion would be that German social policy should contribute to the financing of infrastructure within the digitalization of the healthcare system in particular [...].* [Caregiver representative]

"Communication between stakeholders" could be improved by using a common language between the professions. Experts suggested appointing a chief medical IT officer to build bridges between stakeholders and drive the integration of AI:

> *It's not down to our doctors' willingness to innovate, on the contrary, it's a lot down to IT and a lot down to the data protection officer and a lack of communication within the hospital. My hospital is divided into two departments. On the one hand we have white, everything that is medicine and on the other hand it is a normal company. That's why I think one of the most important positions in a company is the CMIO, the Chief Medical IT Officer, who has a view from both sides. And he can also build a very big bridge.* [Developer of AI-based CDSS]

Another much-discussed improvement category is "information about AI." In this context, communication should include both the benefits and the limits of AI. According to experts, education and transparent information would create acceptance and trust and would avoid exaggerated expectations. Communication should be tailored to the target group. It should convey skepticism toward technology to younger people and introduce older people to the technology. Stakeholders wished for clarification on the fact that the technology can save time and does not take away expertise. Therefore, one should communicate that the outputs are basically suggestions, and the decision remains with the physician. Showrooms and practical examples should be used to convince people of the benefits and to create acceptance:

> *[...] I believe that it is very important for acceptance that you manage to make it clear that it is a system that can ultimately save time, which is then regained by the doctor for the patient.* [Representative of quality assurance]

> *We should certainly try to educate users and we do this by holding seminars, for example, where we remove the magic from AI and explain that it is machine learning. We also explain how it works and where the limits are. Because, as I always like to say, "there is no free lunch.* [Researcher—AI in health care]

"New professions" could also contribute to improvement. One expert explained the need for new professions to guarantee high data quality:

> *And I believe that if we don't have new professional fields that can actually be called data secretaries or whatever, i.e. all those who actually ensure that the quality of the data is excellent, we will just have to make do with bad data and then also with bad results.* [Representative of an ethics committee]

Before the system becomes distributed, a "pretest" should be done in predefined settings. A system running in the background should serve to identify and check discrepancies in decisions between humans and the systems. Dissemination should begin in expert institutions to achieve a certain standard of quality and should always proceed from the most to the least competent users. During this process, systems should learn from mistakes:

> *That's why there's a phase of around six months where the system runs in parallel, in the background, where a comparison is made between what the machine would have decided and what the doctor would have done. A machine also learns from this so that it can then say when the system is introduced - I would never do an untested implementation.* [Developer of AI-based CDSS]

> *[...] at some point a state will be reached, a kind of steady state, in which it is very mature, [...] and then you can go further, but I think it is very important in the first few years to work together with the competent people and not to present it as a help that those who have resource problems or qualification problems can now do things with it that they would otherwise not be able to do.* [Representative of quality assurance]

XSL•FO
RenderX

In the context of AI-based CDSS, it should always be clear who the target users are. Therefore, the developer should clearly offer a "user definition." Experts explained that systems should neither be used to "replace staff" nor to make up for a lack of specialist staff. Ideally, there should be teamwork or cooperation between the AI and users. AI-based CDSS should not undermine the expertise of physicians. While the systems should aim to support users, they should not overtake their task of decision-making:

> *Furthermore, I think it is important that we do not immediately say, yes, there is great dynamism, we can replace the missing specialist staff in a few years or save on staff now and eliminate an economic deficit.* [Representative of quality assurance]

Finally, two other possible improvements were seen in this category. First, software consulting firms should always be available as contact partners. Second, a self-fulfilling solution was seen over time. This was seen because, on the one hand, the use of good systems will automatically lead to acceptance and, on the other hand, because future generations are more open to AI.

Discussion

Principal Findings

The results of this study show that there is already a wide range of suggested improvements in the context of AI-based CDSS. These exist in 6 areas: "technology," "data," "user," "studies," "law," and "general." A structured overview of all identified solution strategies can be found in Multimedia Appendix 4. As in other studies on AI-based CDSS, improvements were found that address the technology itself, the users, and the context in which the systems are used [19-21]. Among others, the recommendations concerning the systems encompass the following aspects: a comprehensive developmental and evaluative process with the active engagement of users before the implementation; systematic training on an extensive, high-quality database; rigorous studies proving the system benefits; optimized ease of use and accessibility; customized systems tailored to specific settings, hospitals, and patient populations; and the incorporation of control mechanisms or the use of intelligent design and smart implementation to mitigate automation bias. On the user side, enhancements were suggested to the training program for (future) users. Training should include communication about the advantages as well as sensitization for critical thinking. Temporal valences of the users should be considered; systems should alleviate the burden on staff rather than augment their workload. Finally, regarding the context, experts suggested strategies such as increasing the level of digitalization of the health care system, especially hospitals; transparently communicating in public about the advantages and risks of AI; providing funding for research; clarifying open legal questions, for example, with regard to liability; and standardizing and consolidating various approval processes.

There are already some studies that investigate factors enabling or facilitating the use of AI-based CDSS. These stem from various fields such as antibiotic prescription in hospitals [19,20,22], rhythm management of atrial fibrillation [23], red blood cell transfusion [24], and aortic dissection [25]. For example, they focus on health professionals [19,23-25] or hospital managers [22]. Our study was not aimed at a special medical field or a single group of experts. Therefore, we were able to investigate indication-independent improvements from a broad range of different experts. This is especially important because several complex problems need interdisciplinary cooperation to be solved.

According to the experts interviewed in our study, a high-quality and user-friendly design of AI-based CDSS should be guaranteed. In this way, problems occurring during use could be prevented. One such problem is automation bias. To prevent this issue, systems should be designed with a well-thought-out design. This includes system outputs with fewer on-screen details, dynamic updates of the confidence levels of recommendations, and the provision of supportive information rather than orders [26]. Another example mentioned by experts and confirmed by the literature was transparency. Trust from physicians can be gained by providing as much transparency as possible [27]. An example not restricted to AI-based CDSS but relevant to digital solutions, in general, is the topic of usability. By integrating future users at every stage during the design process, ease of use can be enabled [28].

Both manufacturers and policy makers are in charge of guaranteeing a high quality of AI-based CDSS. While manufacturers should have an intrinsic motivation to develop high-quality systems, policy makers should set the framework conditions.

The EU first took the step of introducing the AI Act [29]. A prerequisite for the development of reliable AI-based CDSS is the availability of sufficient quality data. Therefore, experts stated that data should be collected in a standardized format and made available to researchers as well as private companies. One example of a large collection of physiological and clinical data is the PhysioNet platform, managed by members of the MIT Laboratory for Computational Physiology [30]. A German project funded by the EU is the SepsisDataNet.NRW [31]. One of the project's goals is to create a sepsis-related biomarker database. From a legislative perspective, the German Bundestag adopted the Act on the Improved Use of Health Data (Health Data Use Act [Gesundheitsdatennutzungsgesetz]) [32]. At the European level, it is planned to create the "European Health Data Space," an initiative to enable patients to easily control their electronic health data and to make this data available for research, innovation, and political decision-making [33].

Experts explained that the perception of users should be positively influenced. There is little experience with the new technology. In a survey conducted by Chen et al [34], only 27% of the physicians and medical students surveyed worldwide had used clinical AI. A total of 13% reported having good knowledge of AI. Furthermore, 77% expressed a high willingness to learn about the topic, and 78% agreed that training should be provided by hospitals or schools. Only 8% feared that physicians would be replaced by AI [34]. The low level of knowledge, together with a great openness [35,36] to the topic, provides an ideal basis for education. In this context, a special

XSL•FO
RenderX

focus should lie on scrutinizing proposed decisions to prevent blind trust, automation bias, and alert fatigue.

Regarding studies, interviewees demanded more prospective randomized studies. This aligns with the existing literature. In 2022, a systematic review of randomized controlled trials (RCTs) of AI in clinical practice identified only 39 eligible studies and concluded with the need for more RCTs of AI-assisted tools integrated into clinical practice [37]. To enable such studies, national or international bodies should provide funding.

According to experts, regulation in the context of AI-based CDSS has not yet been fully elaborated. Questions regarding the trade-off between data protection and patient benefit, regarding the liability and the certification of AI-based CDSS, should be the subject of further discussion and research. For example, there is no uniform opinion between physicians and patients regarding liability for AI in health care [38].

The spectrum of general improvements proposed by experts was broad. Two topics should be particularly underlined. First, in Germany, where the interviews took part, many hospitals are still not sufficiently digitally equipped to enable the use of AI-based CDSS. Given the combination of the high costs of digitalization and the financially strained situation of most hospitals in Germany, the burden cannot be borne by the hospitals alone. Therefore, more funded initiatives, such as the SmartHospital.NRW initiative are required. The aims of this initiative are, on the one hand, to develop a process model that can be transferred to hospitals with different levels of digitalization and, on the other hand, to develop and test innovative, AI-based applications for real-world use-case scenarios [39]. Second, interviewees expressed a high need for education, not only for medical professionals but also for the public. Even if the attitude toward AI is generally positive, there are also some concerns or perceptions. For example, consumers fear the dehumanization of the clinician-patient relationship, see a threat to shared decision-making involving patients, assume low trustworthiness of AI advice, and express uncertainty around fairness and equity in treatment allocation [40]. These concerns should be taken seriously and addressed through open and transparent communication about the opportunities and limitations of AI.

Implications

The suggested improvements should not be used without reflection because there is a risk that improvements will result in further problems. For example, experts suggested that information about the benefits of AI should be given. Thereby, on the one hand, acceptance could be improved, but on the other hand, there is a potential risk that users have too much confidence in the systems and are prone to blind trust, respectively automation bias. Another example is the critical attitude of users. Some experts stated that every decision proposed by the systems should be scrutinized. While, in general, this sounds comprehensible, it bears the risk that the systems might not lead to a significant reduction in workload and thus might become rejected by physicians.

Even if our research provides a variety of different improvement approaches, we did not search for an ideal match between existing problems and improvements. Even if, in some cases, the matching is obvious (eg, a lack of transparency could be reduced by providing decisive parameters), there are more complex interrelationships between some problems and solutions. For example, there is no direct solution for discrimination. Rather, various improvements should be considered here. An optimization of the system itself, the underlying database, or raising user awareness of the problem could be possible approaches. Therefore, further studies should be conducted to investigate such relationships.

The hierarchical framework from the study conducted by Kaiser et al [41] might serve as a starting point to identify the key implementation barriers and improvements that must be considered when introducing AI-based CDSS. According to this, the top level requires an effective implementation strategy (strategy level), the middle level should consider the capabilities and resources needed to successfully integrate an innovation, and finally the bottom level focuses on the implementation and change of processes and routines that are needed to accommodate the innovation.

Recommendations

On the basis of the results of this study, some actionable, solution-oriented recommendations can be proposed that could be practically implemented by stakeholders (Table 2). These recommendations are not specific to the German health care system, as they address cross-cutting challenges, such as data quality, user behavior, regulatory complexity, and clinical validation—issues that arise independently of national health care structures. Their relevance extends to many countries facing similar demands in safely and effectively integrating AI-based CDSS into routine care.

XSL•FO
RenderX

Table 2. Solution-oriented recommendations based on this study.

Number	Recommendation	Problem	Solution
1	Postmarket monitoring	AI[a]-based CDSS[b] should rely on the current state of medical knowledge. However, medical knowledge is subject to constant change, leading to concept and data drifts. Consequently, the original assumptions on which systems are based are no longer up to date, potentially reducing their accuracy or even their validity.	Regularly investigating the quality and reliability of AI-based systems might uncover drifts at an early stage. These verifications should not only be of a purely technical nature but also include actual use in care.[c]
2	Control mechanisms	A severe threat in using AI-based CDSS is automation bias.	Control mechanisms within the systems could be used to encourage users to think and avoid blindly implementing recommendations. One possible approach might be to provide system-based recommendations only after the assessment of the user.[d]
3	Comprehensive data pools	The quality and quantity of data are considered major problems. This may be particularly true for rare diseases.	Building supranational data pools can provide more data to train reliable AI-based CDSS. Common data standards, such as FHIR[e], can support standardization. However, the special characteristics of health care systems and patients, as well as other potential factors arguing against generalization, should also be considered.[f]
4	User training	The perception of AI differs greatly. The spectrum ranges from exaggerated fear to unrealistic expectations. There are problems in both directions: either the systems are rejected, or users trust them blindly.	By integrating AI into the curricula of medical faculties, future users can engage with the technology in a more informed way. This could provide the skills to critically engage with AI-based CDSS. Thus, both automation bias and irrational fear can be met at an early stage.
5	Implementation of studies	User acceptance presents a possible hurdle for the introduction of AI-based CDSS in health care. While studies could be convincing because of the proof of benefit, the implementation of studies is associated with high costs.	Studies are essential to establish the evidence of AI-based CDSS. While current studies mostly focus on the accuracy of the algorithms (eg, recall and precision), future studies should also examine the actual benefits of their use in a clinical setting. Preferably, this should be done with RCT[g] studies. However, as such studies are costly, they should be financed by national or supranational funds. Such an approach would enable universities and smaller independent institutes, in particular, to conduct research in this field.
6	Harmonization of approval procedures	The approval of medical systems is already associated with high effort, including outside Europe. This affects not only developers but also certifying bodies.	Future legislation (eg, the AI Act in Europe) should consider and harmonize existing regulations. This could significantly reduce workload and documentation burden. Possible areas include postmarket surveillance, risk assessment, safety and performance requirements, and technical documentation.

[a]AI: artificial intelligence.

[b]CDSS: clinical decision support systems.

[c]The European Union is introducing such postmarketing monitoring for high-risk products as part of the AI Act. The actual implementation is planned for February 2026.

[d]The actual design requires further research to prevent users from using "dummy inputs" to get recommendations. A cooperative process between the user and AI might be a promising approach.

[e]FHIR: Fast Healthcare Interoperability Resources.

[f]The European Union recently decided that such a data space ("the European Health Data Space") will be created for the member states.

[g]RCT: randomized controlled trial.

While these recommendations appear well-founded and may offer valuable insights for optimizing AI-based CDSS and their integration into health care, it is important to emphasize that they are derived from a qualitative, exploratory approach. Therefore, they should be considered preliminary and require further investigation and validation. This will be addressed in the context of our overarching research project "KI@work" [14]. On the basis of the results of these expert interviews, supplemented by a literature review, focus groups with physicians and nursing staff, a quantitative questionnaire survey and workshops with experts, and well-founded recommendations for action are to be developed that are more binding in nature.

Limitations

Some limitations of our research should be mentioned. First, we conducted a qualitative interview study. Therefore, the results are more exploratory than deterministic. In addition, the attitudes, values, and experiences of the interviewers may have

XSL•FO
RenderX

impacted the final results. To minimize this risk, only a structuring and no further interpretation of the results was carried out. In addition, we have presented the methodological approach as transparently as possible and provided data (eg, appropriate citations in the paper and systematization of the statements in Multimedia Appendix 4) to substantiate the results. In our study, we focused on the German health care sector. Therefore, we only interviewed German experts. This might have an impact on the results for two reasons. First, some of the improvements identified could be specific to the German health care system. While, from our view, only a few improvements are affected by this, one should always scrutinize whether the individual identified improvements are transferable to other health care systems. Second, in the context of this publication, it was necessary to translate the individual statements into English. To avoid translation errors, we conducted quality checks of the citations within the consortium to guarantee that the initial meaning was not distorted.

Rather than providing an exhaustive list of all possible improvements, the objective of this study was to offer comprehensive perspectives. Therefore, it is unlikely that data saturation was fully achieved for each expert group. More specialized research should focus on specific groups, such as caregivers, patients, medical product consultants, experts in ethics and law, or manufacturers of AI-based CDSS, to identify conclusive lists of group-specific problems and improvements. Furthermore, the present findings should be further investigated and elaborated on in more detailed studies focusing on individual improvement categories or individual starting points for improvements, as well as in quantitative studies. A further practical step would be to systematically map implementation studies from the existing literature and examine them for successful improvement strategies.

Because AI-based CDSS are relatively new, there is no conclusive knowledge about underlying problems and barriers. Consequently, new problems and barriers could occur and require further solutions. Therefore, both the problems and barriers, as well as the improvements, should be continuously investigated and developed.

Conclusions

There is evidence that AI-based CDSS have the potential to improve patient outcomes and optimize efficiency in health care. However, to fully realize these benefits and to guarantee safety for patients and a good user experience for medical staff, it is essential to urgently address the existing barriers and unresolved challenges. Possible strategies for improvement should address the systems, the users, and the environment in which they are used. Experts saw concrete points of contact in “technology,” “data,” “user,” “studies,” “law,” and “general.” These should serve as a starting point for further, detailed research.

Acknowledgments

This study is part of a larger research project (User-Oriented Requirements for Artificial Intelligence–Based Clinical Decision Support Systems [KI@work]; project 01VSF22050). The project is funded by the German Federal Joint Committee. The funders did not influence the study design, the conduct of the study, or the decision to publish or prepare the manuscript. The authors acknowledge support from the Open Access Publication Fund of the University of Duisburg-Essen.

Generative AI tools (ChatGPT and DeepL) were used exclusively to improve the linguistic clarity and comprehensibility of the manuscript.

Data Availability

With the exception of the full interview transcripts and the wording of all key statements, all relevant data can be found in the paper or in Multimedia Appendix 4. The complete transcripts, even in pseudonymized form, are not publicly available owing to data protection considerations. However, selected relevant passages are quoted verbatim in the manuscript to ensure transparency.

Authors' Contributions

All authors contributed to the conceptualization of the study and to acquiring funding. GDG, NB, and PR were responsible for data curation and investigation. GDG conducted the main data analysis. Project administration was managed by JW and NB. Methodology was developed by all authors. Resources were provided by the Institute of Health Care Management and Research at the University of Duisburg-Essen. NB supervised the project. Validation was carried out by NB and PR. GDG drafted the original manuscript, and all authors participated in the review and editing of the final version.

Conflicts of Interest

None declared.

Multimedia Appendix 1
COREQ (Consolidated Criteria for Reporting Qualitative Research) checklist.
[PDF File (Adobe PDF File), 485 KB - medinform_v13i1e69688_app1.pdf]

XSL•FO
RenderX

Multimedia Appendix 2
Characteristics of moderators.
[DOCX File , 13 KB - medinform_v13i1e69688_app2.docx]

Multimedia Appendix 3
Interview guideline.
[DOCX File , 17 KB - medinform_v13i1e69688_app3.docx]

Multimedia Appendix 4
Systematization of the expert statements.
[XLSX File (Microsoft Excel File), 41 KB - medinform_v13i1e69688_app4.xlsx]

References

1. Artificial intelligence and machine learning (AI/ML)-enabled medical devices. U.S. Food & Drug Administration. URL: https://www.fda.gov/medical-devices/software-medical-device-samd/artificial-intelligence-and-machine-learning-aiml-enabled-medical-devices [accessed 2024-07-23]
2. Alowais SA, Alghamdi SS, Alsuhebany N, Alqahtani T, Alshaya AI, Almohareb SN, et al. Revolutionizing healthcare: the role of artificial intelligence in clinical practice. BMC Med Educ 2023 Sep 22;23(1):689 [FREE Full text] [doi: 10.1186/s12909-023-04698-z] [Medline: 37740191]
3. Tang A, Tam R, Cadrin-Chênevert A, Guest W, Chong J, Barfett J, et al. Canadian Association of Radiologists white paper on artificial intelligence in radiology. Can Assoc Radiol J 2018 May;69(2):120-135 [FREE Full text] [doi: 10.1016/j.carj.2018.02.002] [Medline: 29655580]
4. Davenport T, Kalakota R. The potential for artificial intelligence in healthcare. Future Healthc J 2019 Jun 13;6(2):94-98 [FREE Full text] [doi: 10.7861/futurehosp.6-2-94] [Medline: 31363513]
5. Wu M, Du X, Gu R, Wei J. Artificial intelligence for clinical decision support in sepsis. Front Med (Lausanne) 2021;8:665464 [FREE Full text] [doi: 10.3389/fmed.2021.665464] [Medline: 34055839]
6. Adams R, Henry KE, Sridharan A, Soleimani H, Zhan A, Rawat N, et al. Prospective, multi-site study of patient outcomes after implementation of the TREWS machine learning-based early warning system for sepsis. Nat Med 2022 Jul 21;28(7):1455-1460. [doi: 10.1038/s41591-022-01894-0] [Medline: 35864252]
7. Shimabukuro DW, Barton CW, Feldman MD, Mataraso SJ, Das R. Effect of a machine learning-based severe sepsis prediction algorithm on patient survival and hospital length of stay: a randomised clinical trial. BMJ Open Respir Res 2017;4(1):e000234 [FREE Full text] [doi: 10.1136/bmjresp-2017-000234] [Medline: 29435343]
8. Bologheanu R, Kapral L, Laxar D, Maleczek M, Dibiasi C, Zeiner S, et al. Development of a reinforcement learning algorithm to optimize corticosteroid therapy in critically ill patients with sepsis. J Clin Med 2023 Feb 14;12(4):1513 [FREE Full text] [doi: 10.3390/jcm12041513] [Medline: 36836046]
9. Davis FD, Bagozzi RP, Warshaw PR. User acceptance of computer technology: a comparison of two theoretical models. Manag Sci 1989 Aug;35(8):982-1003 [FREE Full text] [doi: 10.1287/mnsc.35.8.982]
10. Sutton RT, Pincock D, Baumgart DC, Sadowski DC, Fedorak RN, Kroeker KI. An overview of clinical decision support systems: benefits, risks, and strategies for success. NPJ Digit Med 2020;3:17 [FREE Full text] [doi: 10.1038/s41746-020-0221-y] [Medline: 32047862]
11. Rajpurkar P, Chen E, Banerjee O, Topol EJ. AI in health and medicine. Nat Med 2022 Jan 20;28(1):31-38. [doi: 10.1038/s41591-021-01614-0] [Medline: 35058619]
12. Statement of the Central Ethics Committee at the German Medical Association “decision support by artificial intelligence in medical practice”. Deutsches Ärzteblatt. 2021. URL: https://www.zentrale-ethikkommission.de/fileadmin/user_upload/zentrale-ethikkommission/BAEK_Aerztliche_Taetigkeit_durch_KI_englisch.pdf [accessed 2024-07-23]
13. Peek N, Capurro D, Rozova V, van der Veer SN. Bridging the gap: challenges and strategies for the implementation of artificial intelligence-based clinical decision support systems in clinical practice. Yearb Med Inform 2024 Aug;33(1):103-114 [FREE Full text] [doi: 10.1055/s-0044-1800729] [Medline: 40199296]
14. Raszke P, Giebel GD, Abels C, Wasem J, Adamzik M, Nowak H, et al. User-oriented requirements for artificial intelligence-based clinical decision support systems in sepsis: protocol for a multimethod research project. JMIR Res Protoc 2025 Jan 30;14:e62704 [FREE Full text] [doi: 10.2196/62704] [Medline: 39883929]
15. Giebel GD, Raszke P, Nowak H, Palmowski L, Adamzik M, Heinz P, et al. Problems and barriers related to the use of AI-based clinical decision support systems: interview study. J Med Internet Res 2025 Feb 03;27:e63377 [FREE Full text] [doi: 10.2196/63377] [Medline: 39899342]
16. O'Brien BC, Harris IB, Beckman TJ, Reed DA, Cook DA. Standards for reporting qualitative research: a synthesis of recommendations. Acad Med 2014 Sep;89(9):1245-1251 [FREE Full text] [doi: 10.1097/ACM.0000000000000388] [Medline: 24979285]

XSL•FO
RenderX

17. Tong A, Sainsbury P, Craig J. Consolidated criteria for reporting qualitative research (COREQ): a 32-item checklist for interviews and focus groups. Int J Qual Health Care 2007 Dec;19(6):349-357. [doi: 10.1093/intqhc/mzm042] [Medline: 17872937]
18. Kuckartz U. Qualitative Inhaltsanalyse. Methoden, Praxis, Computerunterstützung. Weinheim, Germany: Beltz Verlagsgrupp; 2018.
19. Tokgöz P, Hafner J, Dockweiler C. [Factors influencing the implementation of AI-based decision support systems for antibiotic prescription in hospitals: a qualitative analysis from the perspective of health professionals]. Gesundheitswesen 2023 Dec 14;85(12):1220-1228 [FREE Full text] [doi: 10.1055/a-2098-3108] [Medline: 37451276]
20. Tokgöz P, Hafner J, Dockweiler C. Factors influencing the implementation of decision support systems for antibiotic prescription in hospitals: a systematic review. BMC Med Inform Decis Mak 2023 Feb 06;23(1):27 [FREE Full text] [doi: 10.1186/s12911-023-02124-4] [Medline: 36747193]
21. Knop M, Weber S, Mueller M, Niehaves B. Human factors and technological characteristics influencing the interaction of medical professionals with artificial intelligence-enabled clinical decision support systems: literature review. JMIR Hum Factors 2022 Mar 24;9(1):e28639 [FREE Full text] [doi: 10.2196/28639] [Medline: 35323118]
22. Tokgöz P, Krayter S, Hafner J, Dockweiler C. Decision support systems for antibiotic prescription in hospitals: a survey with hospital managers on factors for implementation. BMC Med Inform Decis Mak 2024 Apr 15;24(1):96 [FREE Full text] [doi: 10.1186/s12911-024-02490-7] [Medline: 38622595]
23. Stacy J, Kim R, Barrett C, Sekar B, Simon S, Banaei-Kashani F, et al. Qualitative evaluation of an artificial intelligence-based clinical decision support system to guide rhythm management of atrial fibrillation: survey study. JMIR Form Res 2022 Aug 11;6(8):e36443 [FREE Full text] [doi: 10.2196/36443] [Medline: 35969422]
24. Choudhury A. Factors influencing clinicians' willingness to use an AI-based clinical decision support system. Front Digit Health 2022 Aug 16;4:920662 [FREE Full text] [doi: 10.3389/fdgth.2022.920662] [Medline: 36339516]
25. Fujimori R, Liu K, Soeno S, Naraba H, Ogura K, Hara K, et al. Acceptance, barriers, and facilitators to implementing artificial intelligence-based decision support systems in emergency departments: quantitative and qualitative evaluation. JMIR Form Res 2022 Jun 13;6(6):e36501 [FREE Full text] [doi: 10.2196/36501] [Medline: 35699995]
26. Goddard K, Roudsari A, Wyatt JC. Automation bias: a systematic review of frequency, effect mediators, and mitigators. J Am Med Inform Assoc 2012;19(1):121-127 [FREE Full text] [doi: 10.1136/amiajnl-2011-000089] [Medline: 21685142]
27. Evans RP, Bryant LD, Russell G, Absolom K. Trust and acceptability of data-driven clinical recommendations in everyday practice: a scoping review. Int J Med Inform 2024 Mar;183:105342 [FREE Full text] [doi: 10.1016/j.ijmedinf.2024.105342] [Medline: 38266426]
28. Saffer D. Designing for Interaction: Creating Innovative Applications and Devices. Indianapolis, IN: New Riders Publishing; 2010.
29. Artificial intelligence (AI) act: council gives final green light to the first worldwide rules on AI. European Council. 2024 May 21. URL: https://www.consilium.europa.eu/en/press/press-releases/2024/05/21/artificial-intelligence-ai-act-council-gives-final-green-light-to-the-first-worldwide-rules-on-ai/ [accessed 2024-11-05]
30. Goldberger AL, Amaral LA, Glass L, Hausdorff JM, Ivanov PC, Mark RG, et al. PhysioBank, PhysioToolkit, and PhysioNet: components of a new research resource for complex physiologic signals. Circulation 2000 Jun 13;101(23):E215-E220. [doi: 10.1161/01.cir.101.23.e215] [Medline: 10851218]
31. SepsisDataNet.NRW. Bundesinstitut für Arzneimittel und Medizinprodukte. 2019. URL: https://drks.de/search/de/trial/DRKS00018871 [accessed 2025-06-26]
32. Gesundheitsdatennutzungsgesetz (GDNG). Bundesministerium für Gesundheit. URL: https://www.bundesgesundheitsministerium.de/service/gesetze-und-verordnungen/detail/gesundheitsdatennutzungsgesetz.html [accessed 2024-11-05]
33. Proposal for a regulation of the European Parliament and of the Council on the European Health Data Space. European Union. URL: https://eur-lex.europa.eu/legal-content/EN/TXT/?uri=celex:52022PC0197 [accessed 2024-11-05]
34. Chen M, Zhang B, Cai Z, Seery S, Gonzalez MJ, Ali NM, et al. Acceptance of clinical artificial intelligence among physicians and medical students: a systematic review with cross-sectional survey. Front Med (Lausanne) 2022 Aug 31;9:990604 [FREE Full text] [doi: 10.3389/fmed.2022.990604] [Medline: 36117979]
35. Vijayakumar S, Lee VV, Leong QY, Hong SJ, Blasiak A, Ho D. Physicians' perspectives on AI in clinical decision support systems: interview study of the CURATE.AI personalized dose optimization platform. JMIR Hum Factors 2023 Oct 30;10:e48476 [FREE Full text] [doi: 10.2196/48476] [Medline: 37902825]
36. van der Meijden SL, de Hond AA, Thoral PJ, Steyerberg EW, Kant IM, Cinà G, et al. Intensive care unit physicians' perspectives on artificial intelligence-based clinical decision support tools: preimplementation survey study. JMIR Hum Factors 2023 Jan 05;10:e39114 [FREE Full text] [doi: 10.2196/39114] [Medline: 36602843]
37. Lam TY, Cheung MF, Munro YL, Lim KM, Shung D, Sung JJ. Randomized controlled trials of artificial intelligence in clinical practice: systematic review. J Med Internet Res 2022 Aug 25;24(8):e37188 [FREE Full text] [doi: 10.2196/37188] [Medline: 35904087]

XSL•FO
RenderX

38. Khullar D, Casalino LP, Qian Y, Lu Y, Chang E, Aneja S. Public vs physician views of liability for artificial intelligence in health care. J Am Med Inform Assoc 2021 Jul 14;28(7):1574-1577 [FREE Full text] [doi: 10.1093/jamia/ocab055] [Medline: 33871009]
39. SmartHospital.NRW homepage. SmartHospital.NRW. URL: https://smarthospital.nrw/ [accessed 2024-11-05]
40. Scott IA, Carter SM, Coiera E. Exploring stakeholder attitudes towards AI in clinical practice. BMJ Health Care Inform 2021 Dec 09;28(1):e100450 [FREE Full text] [doi: 10.1136/bmjhci-2021-100450] [Medline: 34887331]
41. Kaiser C, Ackerhans S, Huynh T, Denzinger J, Riegler M, Dumitrescu D, et al. Challenges in the implementation of disruptive innovations in health care organizations. Stud Health Technol Inform 2023 Oct 20;309:145-149. [doi: 10.3233/SHTI230763] [Medline: 37869828]

Abbreviations

AI: artificial intelligence
CDSS: clinical decision support systems
COREQ: Consolidated Criteria for Reporting Qualitative Research
EU: European Union
RCT: randomized controlled trial

Edited by A Benis; submitted 05.12.24; peer-reviewed by O Akanji, F Quazi, VV Khanna; comments to author 25.03.25; revised version received 08.04.25; accepted 09.06.25; published 07.07.25.

Please cite as:
Giebel GD, Raszke P, Nowak H, Palmowski L, Adamzik M, Heinz P, Tokic M, Timmesfeld N, Brunkhorst FM, Wasem J, Blase N Improving AI-Based Clinical Decision Support Systems and Their Integration Into Care From the Perspective of Experts: Interview Study Among Different Stakeholders
JMIR Med Inform 2025;13:e69688
URL: https://medinform.jmir.org/2025/1/e69688
doi:10.2196/69688
PMID:

©Godwin Denk Giebel, Pascal Raszke, Hartmuth Nowak, Lars Palmowski, Michael Adamzik, Philipp Heinz, Marianne Tokic, Nina Timmesfeld, Frank Martin Brunkhorst, Jürgen Wasem, Nikola Blase. Originally published in JMIR Medical Informatics (https://medinform.jmir.org), 07.07.2025. This is an open-access article distributed under the terms of the Creative Commons Attribution License (https://creativecommons.org/licenses/by/4.0/), which permits unrestricted use, distribution, and reproduction in any medium, provided the original work, first published in JMIR Medical Informatics, is properly cited. The complete bibliographic information, a link to the original publication on https://medinform.jmir.org/, as well as this copyright and license information must be included.

XSL•FO
RenderX

Original Paper

Deep Learning and Image Generator Health Tabular Data (IGHT) for Predicting Overall Survival in Patients With Colorectal Cancer: Retrospective Study

Seo Hyun Oh[1], BS; Youngho Lee[2*], PhD; Jeong-Heum Baek[3*], MD, PhD; Woongsang Sunwoo[4], MD

[1]Department of IT Convergence, Gachon University, 1342, Seongnam-daero, Sung-nam si, Republic of Korea

[2]Department of Computer Engineering, Gachon University, Sung-nam si, Republic of Korea

[3]Division of Colon and Rectal Surgery, Department of Surgery, Gil Medical Center, 21, Namdong-daero 774beon-gil, Incheon, Republic of Korea

[4]Department of Otorhinolaryngology-Head and Neck Surgery, Gachon University College of Medicine, Gil Medical Center, 21, Namdong-daero 774beon-gil, Incheon, Republic of Korea

[*]these authors contributed equally

Corresponding Author:
Youngho Lee, PhD
Department of Computer Engineering
Gachon University
1342, Seongnam-daero
Sung-nam si, 13120
Republic of Korea
Phone: 82 31 750 5011
Fax: 82 31 750 5743
Email: lyh@gachon.ac.kr

Abstract

Background: Recent advances in artificial intelligence (AI) have contributed to improved predictive modeling in health care, particularly in oncology. Traditional methods often rely on structured tabular data, but these approaches can struggle to capture complex interactions among clinical variables. Image generator for health tabular data (IGHT) transform tabular electronic medical record (EMR) data into structured 2D image matrices, enabling the use of powerful computer vision–based deep learning models. This approach offers a novel baseline for survival prediction in colorectal cancer by leveraging spatial encoding of clinical features, potentially enhancing prognostic accuracy and interpretability.

Objective: This study aimed to develop and evaluate a deep learning model using EMR data to predict 5-year overall survival in patients with colorectal cancer and to examine the clinical interpretability of model predictions using explainable artificial intelligence (XAI) techniques.

Methods: Anonymized EMR data of 3321 patients at the Gil Medical Center were analyzed. The dataset included demographic details, tumor characteristics, laboratory values, treatment modalities, and follow-up outcomes. Clinical variables were converted into 2D image matrices using the IGHT. Patients were stratified into colon and rectal cancer groups to account for biological and prognostic differences. Three models were developed and compared: a conventional artificial neural network (ANN), a basic convolutional neural network (CNN), and a transfer learning–based Visual Geometry Group (VGG)16 model. Model performance was assessed using accuracy, sensitivity, specificity, precision, and F1-scores. To interpret model decisions, gradient-weighted class activation mapping (Grad-CAM) was applied to visualize regions of the input images that contributed most to predictions, enabling identification of key prognostic features.

Results: Among the tested models, VGG16 exhibited superior predictive performance, achieving an accuracy of 78.44% for colon cancer and 74.83% for rectal cancer. It showed notably high specificity (89.55% for colon cancer and 87.9% for rectal cancer), indicating strong reliability in correctly identifying patients likely to survive beyond 5 years. Compared to ANN and CNN models, VGG16 achieved a better balance between sensitivity and specificity, demonstrating robustness in the presence of moderate class imbalance within the dataset. Grad-CAM visualization highlighted clinically relevant features (eg, age, gender, smoking history, American Society of Anesthesiologists physical status classification (ASA) grade, liver disease, pulmonary disease, and initial carcinoembryonic antigen [CEA] levels). Conversely, the CNN model yielded lower overall accuracy and low specificity, which limits its immediate applicability in clinical settings.

XSL•FO
RenderX

Conclusions: The proposed IGHT-based deep learning model, particularly leveraging the VGG16 architecture, demonstrates promising accuracy and interpretability in predicting 5-year overall survival in patients with colorectal cancer. Its capability to effectively stratify patients into risk categories with balanced sensitivity and specificity underscores its potential utility as a clinical decision support system (CDSS) tool. Future studies incorporating external validation with multicenter cohorts and prospective designs are necessary to establish generalizability and clinical integration feasibility.

(JMIR Med Inform 2025;13:e75022) doi:10.2196/75022

KEYWORDS

colon; rectum; cancer; predict; prediction; predictions; predictive; model; models; health care; clinical informatics; electronic health record; EHR; South Korea; convolutional neural networks; VGG16; neural network; deep learning

Introduction

Artificial intelligence (AI) has evolved, becoming integral to various fields, including health care, bioscience, and medical diagnostics. In the medical field, AI applications range from disease detection to drug prescription optimization [1]. Health care providers use AI for patient disease prediction and data anonymization, addressing the growing health care costs associated with increasing chronic diseases and life expectancy [2]. Recent studies have increasingly applied advanced machine learning and explainable artificial intelligence (XAI) methods to improve disease survival prediction. For instance, Yang et al [3] and Yau et al [4] have demonstrated effective survival modeling using time-to-event algorithms and survival tree analyses, respectively. Huang et al [5] applied explainable machine learning approaches to uncover important risk factors across major cancers, including colorectal cancer. These studies highlight the growing trend and validate the clinical relevance of AI-driven survival prediction.

Recent advances in medical imaging technology have enabled sophisticated tumor image analysis using AI models [6]. In the field of medical image analysis, active research is being conducted using convolutional neural network (CNN) models to predict responses to treatment in patients with colorectal cancer. Yang et al [7] built a model to evaluate the risk of recurrence and metastasis by applying deep learning technology to the data of patients with benign breast cancer. Full hematoxylin and eosin (H&E)-stained images were obtained from surgical specimens of patients with breast cancer, and a CNN was applied to them. The model used in the study achieved an area under the curve (AUC) of 0.76 and showed the potential for evaluating the risk of recurrence and metastasis in patients with human epidermal growth factor receptor 2 (HER2)-positive breast cancer. Althammer et al [8] conducted a study on image analysis to predict the response to durvalumab therapy targeting the programmed cell death-1/programmed cell death ligand-1 (PD1/PD-L1) pathway in patients with non–small cell lung cancer. The results showed that the median overall survival in patients receiving durvalumab was 21 months for those positive for the CD8xPD-L1 signature and 7.8 months for those negative (P<.001).

In particular, the image-guided tabular data (IGTD) method proposed by Zhu et al [9] showed that arranging numerical variables into a 2D matrix format can improve model performance by enabling CNNs to capture local feature interactions. Inspired by this approach, we developed an image generator for health tabular data (IGHT) encoding method tailored to our clinical dataset, converting 25 normalized features into a 5×5 image matrix. This fixed spatial layout allows the model to process tabular information through CNN-based architectures, facilitating the use of transfer learning and potentially enhancing predictive performance. There has been growing interest in transforming structured tabular data into image representations to leverage the power of CNNs in domains traditionally dominated by machine learning. For example, Lara-Abelenda et al [10] introduced low mixed image-guided tabular data IGTD (LM-IGTD), an enhanced pipeline based on the IGTD approach. Their method applies noise-based augmentation and preserves explicit feature-to-pixel mappings, allowing for the integration of post hoc explanation techniques, such as gradient-weighted class activation mapping (Grad-CAM) and saliency maps for better interpretability. These developments reflect a broader trend toward interpretable and robust AI in clinical settings.

In this study, we built upon this direction by applying a novel tabular-to-image transformation method, IGHT, which converts structured electronic medical record (EMR) features(tabular data) into images, enabling deep CNN architectures to extract spatial patterns for survival prediction in patients with colorectal cancer.

Building upon these developments, Sharma et al [11] introduced DeepInsight, one of the pioneering frameworks that enables CNNs to process tabular data by converting them into image representations. This method uses dimensionality reduction techniques, such as t-distributed stochastic neighbor embedding (t-SNE) or principal component analysis (PCA), to spatially arrange high-dimensional features in a 2D grid, while preserving interfeature relationships. Such transformations allow CNNs to extract local and global patterns from structured data—patterns that may be overlooked by traditional machine learning approaches. This early work demonstrated the potential of tabular-to-image conversion to enhance classification performance across domains, and it has laid the foundation for subsequent advances, including this study.

AI has shown strong performance in learning from existing patient information using big data and in predicting or recommending outcomes desired by clinicians, who are key decision makers. In particular, the clinical decision support system (CDSS), an AI system that helps clinicians make decisions, has attracted considerable attention. The CDSS trains an AI model with existing medical knowledge and patient data to predict outcomes and make recommendations for clinicians

XSL•FO
RenderX

based on new patient data [12]. Watson for Oncology (WFO), a representative CDSS, was developed by IBM Corp and is a system that analyzes more than 15 million pages of medical documents, 300 medical journals, and 200 guidelines [13]. The WFO was designed to recommend treatment options to oncologists and was first introduced and used in 2016 at the Gil Medical Center in Korea [14]. Although the WFO at the Gil Medical Center helped inform treatment decisions, it could not reflect regional characteristics due to differences in insurance coverage and medical costs [15].

Lee et al [16] compared the treatment recommendations generated by the WFO with the actual treatment received by 656 patients with stage 2, 3, and 4 colon cancer between 2009 and 2016 to determine the concordance rate. The results showed that the agreement rate between the WFO and the Gil Medical Center's treatment recommendations was low, at only 48.9%. Since the WFO was trained using data from Americans patients, the prescription recommendations did not match well with those for Korean patients. In addition, it was noted that the treatment recommendations under the Korean insurance system and those under the American insurance system differed, resulting in a low concordance rate with actual treatment practices. Therefore, it is important to establish a CDSS using Korean patient data.

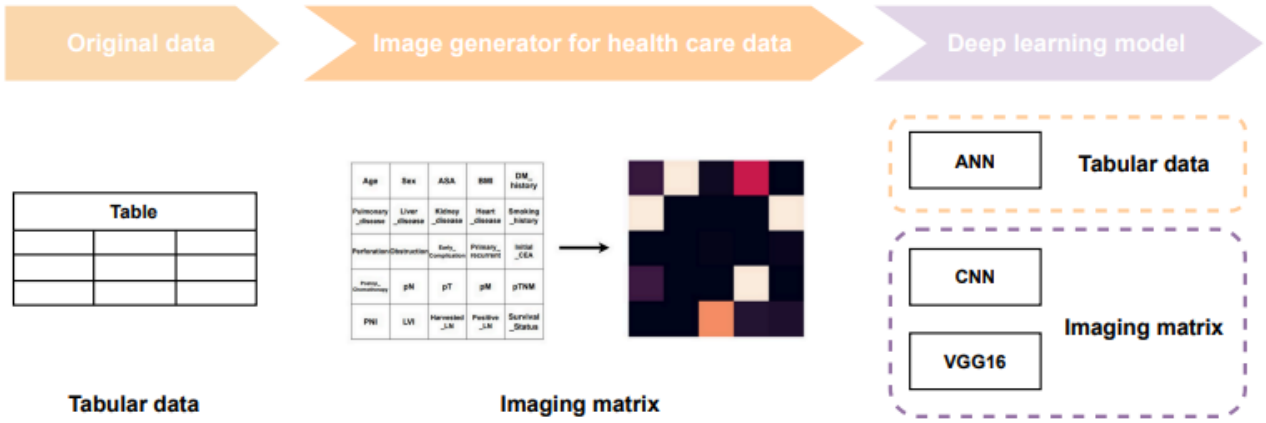
To build a CDSS, many studies have been conducted to enhance the performance of medical data–based AI models. Park et al [17] used an oversampling technique to address data imbalance and predicted colorectal cancer chemotherapy based on data from the Gil Medical Center in Korea using a deep learning model. Kwon et al [18] used machine learning models, such as the gradient boosted model, the distributed random forest, the generalized linear model, and the deep neural network, for a stacking ensemble. They diagnosed breast cancer using the best-performing model in the stacking ensemble. Oh et al [19] classified colorectal cancer chemotherapy regimens using machine learning models: k-nearest neighbor (kNN), support vector machine (SVM), decision tree, and light gradient boosting machine (LightGBM), and compared the results across multiple models.

Colorectal cancer is the second-most common malignancy in South Korea [20] and the second leading cause of cancer-related mortality worldwide [21]. Surgery is the primary treatment for colon and rectal cancer [22], but due to its high postsurgical mortality rate, ongoing prognosis management is essential. Therefore, research aimed at extending patient survival is being conducted from various perspectives, including the prediction of overall survival, disease-free survival, and recurrence. Overall survival and disease-free survival periods are key indicators for assessing a patient's prognosis, and to extend life expectancy, further research is needed to evaluate prognosis based on patient-specific factors.

Studies on predicting the survival period have mainly been conducted in the clinical field using statistical techniques, such as the Kaplan-Meier method [23] and Cox's proportional hazards model [24]. Yeom et al [25] identified prognostic factors that increase the risk of death in patients with terminal cancer and predicted the survival period according to the number of these prognostic factors. Using the Kaplan-Meier method and the log-rank test, they investigated whether there were differences in the survival period according to clinical variables. Using Cox's proportional hazards model, they identified variables that increase the risk of death among clinical variables and used them as prognostic factors, which were then incorporated into the Weibull proportional hazards function model to predict survival periods.

Figure 1 presents an overview of the pipeline of this study. In this study, we aimed to develop and evaluate deep learning–based models for predicting survival using data from patients with colorectal cancer. This study used image data by converting tabular electronic medical record (EMR) data received from the health care system into image data to enhance their utility. These deep learning models are expected to improve the performance of predicting the prognosis of patients with colorectal cancer by effectively using EMR data.

Figure 1. Overview pipeline of this study process. ANN: artificial neural network; ASA: American Society of Anesthesiologists physical status classification; CEA: carcinoembryonic antigen; CNN: convolutional neural network; DM: diabetes mellitus; LN: lymph nodes; LVI: lymphovascular invasion; pM: pathological distant metastasis; pN: pathological regional lymph node; PNI: perineural invasion; pT: pathological primary tumor; pTNM: pathological tumor, node, metastasis.



XSL•FO
RenderX

Methods

Dataset

In this study, EMR data were retrospectively collected from the Gil Medical Center, a tertiary referral hospital in Incheon, South Korea. A total of 3321 patients who underwent elective surgery with curative intent for colorectal cancer between 2004 and 2018 were included. The dataset was constructed through iterative chart review conducted by colorectal cancer clinicians.

Demographics are patient characteristics that can typically be known without the need for surgery. These included basic information, such as age, sex, BMI, and the patient status, as classified by the American Society of Anesthesiologists physical status classification (ASA): "DM_history" refers to a history of diabetes mellitus; "Pulmonary_disease," a history of lung disease; "Liver_disease," a history of liver disease; and "Kidney_disease," a history of kidney disease.

Perioperative clinical features included information about each patient gathered before and after surgery: "Initial CEA" and "Initial Hb" represent the first blood tests performed at the time of cancer diagnosis (serum carcinoembryonic antigen [CEA] and serum hemoglobin [Hb] levels, respectively), "Transfusion_op" indicates whether a blood transfusion was performed during surgery; "Early_complication" is defined as a case of complications occurring within 30 days after surgery, and "Postop_Chemotherapy" indicates whether chemotherapy was used after surgery.

Histopathologic features can be known after a biopsy of the patient's tumor following surgery. Here, "pTNM" is a variable that integrates the pathological tumor, node, metastasis (TNM) stage and is classified into stages 1, 2, 3, and 4. The TNM stage classification was based on the *AJCC Cancer Staging Manual, Eighth Edition*. "pT" (pathological primary tumor) includes Tis, T1, T2, T3, or T4 (T4a, T4b) as the T stage; "pN" (pathological regional lymph node) includes N0, N1 (N1a, N1b, N1c), or N2 (N2a, N2b) as the N stage; and "pM" (pathological distant metastasis) includes M1 as the M stage.

In the "Intraoperative_tumor_location" variable, colon cancer is classified into cecum, ascending colon, hepatic flexure, transverse colon, splenic flexure, descending colon, sigmoid colon, and rectosigmoid junction cancer according to the location of the primary tumor. In the case of rectal cancer, 0-5 cm of the anal verge (AV) is classified as the lower rectum, 6-10 cm of the AV is the midrectum, and 11-15 cm of the AV is the upper rectum. The final colon cancer dataset consisted of 2091 patients, and the rectal cancer dataset consisted of 1190 patients.

Ethical Considerations

This study was reviewed and approved by the Institutional Review Board of the Gil Medical Center (GFIRB 2023-034). EMR data from the Gil Medical Center were used. Overall, data of 3321 patients were retrospectively collected through an iterative chart review conducted by colorectal cancer specialists. Due to its retrospective nature, the study was exempt from requiring informed consent from the participants.

Data Preprocessing

The variables were selected in consultation with a clinician. To select and use clinical variables to enhance the explanatory power of the results, pretreatment was performed after discussion with the clinician. Patient exclusion, variable categorization, missing value removal, and variable selection were performed in that order. All continuous variables were normalized to a (0,1) scale using min-max normalization to standardize the color intensity across features. Categorical variables were first one-hot-encoded and then similarly mapped to the image matrix, ensuring consistent scaling across data types during the image generation process. Images were constructed by arranging features sequentially based on the column order in the original dataset. No domain-driven grouping or clustering of related variables was applied to preserve reproducibility and avoid introducing subjective bias. Although the spatial arrangement of semantically related features may potentially affect CNN performance, this aspect was not explored in the study and is left for future investigation.

Prior to variable selection, patient cases excluded from the analysis were removed. In the case of "Kidney_disease," missing values were deleted. Patients who underwent surgery for recurrent colorectal cancer were also excluded.

After excluding patients, variable categorization was performed. Age was categorized by the number 65, which is a standard used to divide age. The BMI was categorized as 18 or less and 18 or more and as 25 or less and 25 or more. In addition, "DM_history," "Pulmonary_disease," "Liver_disease," and "Heart_disease," which are variables corresponding to the patient's medical history, were categorized by the presence or absence of a medical history.

Among the perioperative clinical features, "Initial_CEA," which indicates the first CEA level after diagnosis, was categorized according to 5 criteria, and 166 missing values were replaced with the average value. Missing values were removed for "Early_Complication," which indicates complications within 30 days after surgery. In particular, "Overall_Survival" was calculated from the date of surgery until the date of death for uncensored cases or until the date of last follow-up for censored cases. In addition, patients were categorized based on 5 years (60 months), which is the criterion for cure.

Among histopathologic features, missing values were removed and categorized in "Havested_LN," which represents the number of lymph nodes removed from the patient during surgery. If more than 12 pieces were removed, the operation was considered successful, and if less than 12 pieces were removed, the operation was classified as insufficient. Missing values were also removed from "Positive_LN," which indicates the number of metastatic lymph nodes that could be recognized during surgery. The final selected variables are listed in Table S1 in Multimedia Appendix 1.

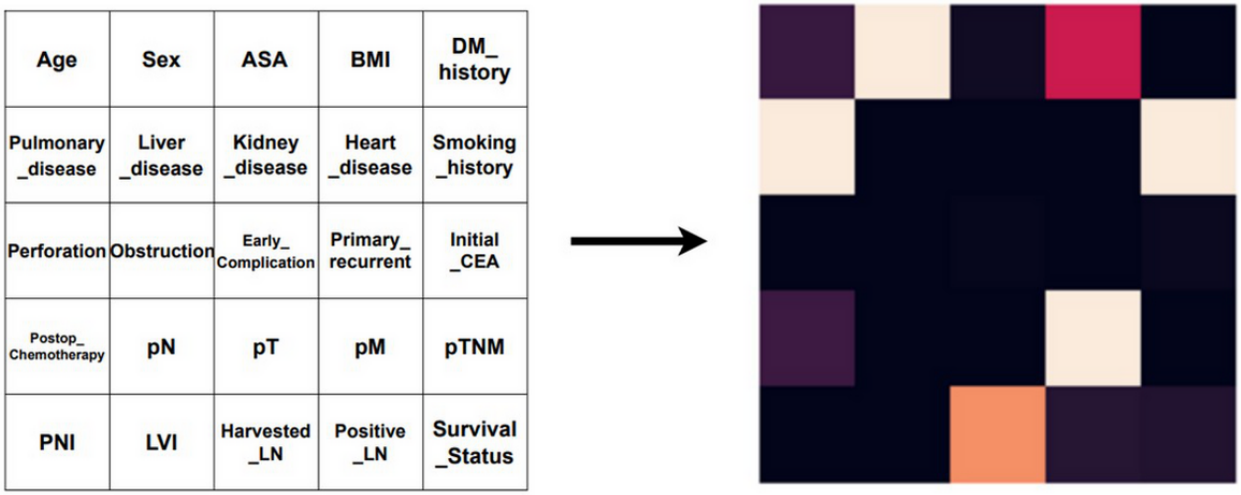
Image Generation Health Care Tabular Data Method

In this study, we aimed to convert the data from structured data into 2D unstructured image data to use as input to the deep learning model. The variables of the tabular data were visualized in matrix form and developed according to the data. Each

XSL•FO
RenderX

variable in Table S1 in Multimedia Appendix 1 was mapped to one column of the heat map and implemented in the form of an image. Figure 2 shows an example of an imaging matrix. The image is in the form of N×N, where N is 5, and the number of variables used for image conversion is 25.

Figure 2. Method of generating IGHT. ASA: American Society of Anesthesiologists physical status classification; CEA: carcinoembryonic antigen; DM: diabetes mellitus; IGHT: image generator health care tabular data; LN: lymph nodes; LVI: lymphovascular invasion; pM: pathological distant metastasis; pN: pathological regional lymph node; PNI: perineural invasion; pT: pathological primary tumor; pTNM: pathological tumor, node, metastasis.



In this study, we selected 25 clinically relevant variables and reshaped them into a 5×5 matrix to generate 2D images for input into the CNN models. Variables were categorized into three clinically meaningful groups: demographic, perioperative, and histopathologic features. These variables were mapped from left to right and top to bottom in the 5×5 matrix, following the order of these categories. This spatial configuration was carefully designed to enable the deep learning model to effectively capture interactions among clinically related variables. By organizing the input into a square-shaped matrix, the convolutional filters in the CNN architecture could exploit spatial proximities from the input layer, thereby enhancing the model's ability to learn joint patterns and improving both performance and interpretability.

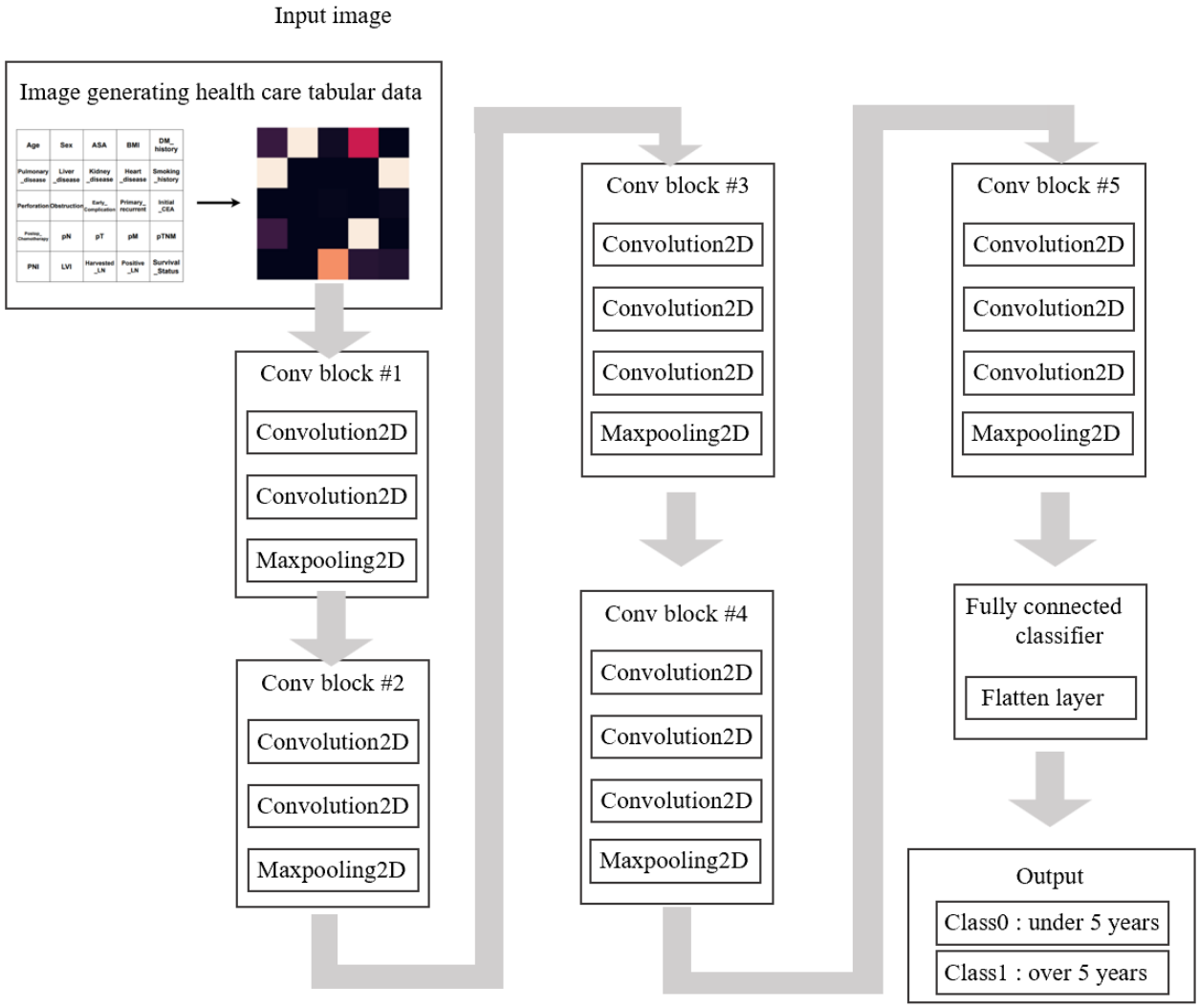
We also considered scenarios where the number of input features may not perfectly form a square matrix. In such cases, possible strategies include (1) zero-padding to fill the remaining space without introducing clinical meaning and (2) modifying the CNN input layer to accept nonsquare (rectangular) input dimensions. Although these were not necessary in this study, they remain relevant for future extensions of this framework.

Deep Learning Model Prediction

Figure 3 shows a pictorial representation of the VGG16 model, proposed by the Visual Geometry Group (VGG), used in this study. The weights of VGG16 learned using a large dataset called ImageNet were imported and used to classify the imaging matrix. All modeling and analysis were conducted using Google Colaboratory with the following software environment: Python 3.7.13, TensorFlow 2.8.0, Keras 2.8.0, pandas 1.3.5, scikit-learn 1.0.2, NumPy 1.21.5, matplotlib 3.4.3, and seaborn 0.11.2.

XSL•FO
RenderX

Figure 3. Pipeline of VGG16 using the IGHT technique. ASA: American Society of Anesthesiologists physical status classification; CEA: carcinoembryonic antigen; DM: diabetes mellitus; IGHT: image generator for health tabular data; LN: lymph nodes; LVI: lymphovascular invasion; pM: pathological distant metastasis; pN: pathological regional lymph node; PNI: perineural invasion; pT: pathological primary tumor; pTNM: pathological tumor, node, metastasis; VGG: Visual Geometry Group.



For model interpretation, Grad-CAM was implemented using custom code adapted from tf-keras-vis and compatible TensorFlow visualization utilities. We divided the dataset of 3321 patients with colorectal cancer into two cohorts—colon cancer (n=2089, 62.9%) and rectal cancer (n=1232, 37.1%)—and trained separate models for each group. For both cohorts, the data were randomly split into training and testing sets in a 7:3 ratio.

ANN and CNN models were trained using default hyperparameters. For the VGG16-based model, we adopted a transfer learning approach: the convolutional base of VGG16 pretrained on ImageNet was used (include_top=False), and all layers were set to be trainable. A flattened output was passed through a dense layer with 256 units (rectified linear unit [ReLU] activation), followed by a dropout layer (rate=0.25) and a sigmoid output layer for binary classification. The optimizer used was Adam with a learning rate of 0.01, and the loss function was binary cross-entropy. We also tested the Stochastic Gradient Descent (SGD) optimizer during model development, but it yielded inferior performance compared to Adam. Key hyperparameters, such as optimizer type, learning rate, and dropout rate, were selected based on empirical validation performance, rather than being used as default values.

Model performance was evaluated using the testing set, and the metrics reported included accuracy, sensitivity, and specificity.

ANN Model

After converting the tabular data into an imaging matrix, an ANN was constructed to compare and verify the AI model results. Instead of using the data converted to the imaging matrix (tabular data), the original dataset was used. Using the original dataset, an ANN was used to predict the survival period of patients with colorectal cancer and validate the results. Table S2 in Multimedia Appendix 1 lists the parameters of the baseline model in detail.

XSL•FO
RenderX

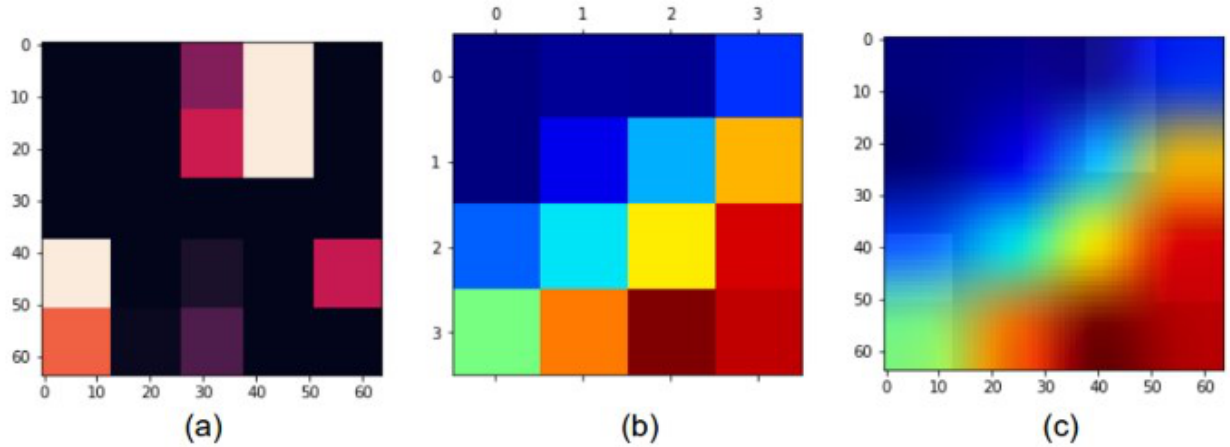
CNN Model

In this study, after transformation of data into an imaging matrix, a CNN model was applied. The model was constructed to classify the data by dividing the survival period of patients with colorectal cancer by 5 years. The classification performance of the patient survival period was confirmed using the CNN model, which showed good performance in image classification. Table S3 in Multimedia Appendix 1 lists the parameters of the CNN model.

VGG16 Model

In this study, transfer learning based on the VGG16 model created by Simonyan and Ziserman in 2014 was performed. The VGG16 model is a structure developed from the existing CNN structure, and because it is convenient to apply, studies using VGG16 are actively being conducted to improve classification performance. Table S4 in Multimedia Appendix 1 shows the structure of VGG16 used in this study. Figure 4 shows a pictorial representation of the transfer learning method used in this study. In this study, the weights of VGG16 learned using a large dataset called ImageNet were imported and used to classify the imaging matrix.

Figure 4. Example of Grad-CAM results: (a) original data from the image generator, (b) heat map produced by Grad-CAM, and (c) visualized image generated by Grad-CAM. Grad-CAM: gradient-weighted class activation mapping.



Gradient-Weighted Class Activation Mapping

To demonstrate the models' potential as a CDSS, we used Grad-CAM [26] to visualize important features for individual patient predictions. VGG16 is a CNN-based model that cannot explain the results of a model [27]. Therefore, Grad-CAM was used to increase the explanatory potential of the model results. Grad-CAM was used to generate heat maps that highlighted variables with notable influence on the models' prediction of the survival period of patients with colorectal cancer. The heat maps generated by Grad-CAM are highlighted in red and are a method of displaying the variable area that has a large influence on the prediction. Grad-CAM extracts features using weights extracted from the last convolutional layer of the models used for prediction [28].

An example of converting Grad-CAM is shown in Figure 4. In the weight of the models trained using patient data (Figure 4a), the influence of the variable that affected the prediction result was converted into a heat map of the form in Figure 4b. Next, an image was created in a form that could intuitively determine the influence, as shown in Figure 4c, overlaid on Figure 4a.

Evaluation Metrics

The predictive performance of the models was evaluated using three key metrics: accuracy, sensitivity, and specificity.

Accuracy measures the overall proportion of correctly classified instances. Sensitivity (also known as recall) quantifies the proportion of true-positive cases correctly identified by the model, while specificity measures the proportion of true negatives correctly identified.

These metrics were calculated on the test datasets to assess the generalization performance of the models.

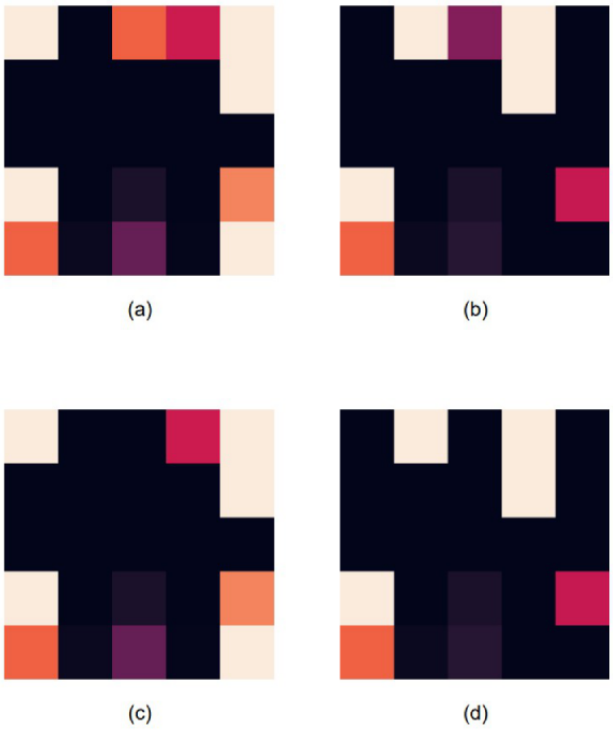
Results

Imaging Matrix Transformation

The transformation of tabular data into 5×5 imaging matrices using 25 variables from patients with colorectal cancer demonstrated distinctive visual patterns. The heat map representation, where values approaching 1 appear white and those approaching 0 appear black, provided an intuitive visualization of patient data. For survival period prediction, we established a binary classification. Figure 5 shows an example of the imaging matrix created. Class 0 represented patients with a survival period of less than 5 years, while class 1 represented patients with a survival period of more than 5 years.

XSL•FO
RenderX

Figure 5. Example of an imaging matrix: (a) class 0 image in colon cancer, (b) class 1 image in colon cancer, (c) class 0 image in rectal cancer, and (d) class 1 image in rectal cancer.



Comprehensive Model Performance Evaluation

We conducted an extensive comparative analysis across three distinct deep learning architectures, each revealing unique strengths in colorectal cancer survival prediction.

As shown in Tables 1 and 2, the accuracy and specificity of VGG16 were the best among the three models. However, the sensitivity of VGG16 was the lowest among the three models, which means that the model mistakenly thought that the actual survival period of a patient was less than 5 years but that the patient had a good prognosis. Compared to VGG16, the ANN and CNN showed higher sensitivities (84%-99%) in identifying patients with poor prognoses well. However, in terms of specificity, VGG16 showed better performance in correctly predicting patients with a 5-year survival period (89.55% for colon cancer and 87.9% for rectal cancer).

Table 1. Overall survival prediction in patients with colon and rectal cancer using ANN[a], CNN[b], and VGG16[c] models.

Model	Accuracy (%)	Sensitivity (%)	Specificity (%)	Precision (%)	F_1-score (%)
ANN	71.47	84.00	54.23	71.59	76.86
CNN	61.90	99.40	4.90	61.58	76.17
VGG16	78.23	40.79	89.55	80.55	54.33

[a]ANN: artificial neural network.

[b]CNN: convolutional neural network.

[c]VGG: Visual Geometry Group.

Table 2. Overall survival prediction in patients with rectal cancer using ANNa, CNNb, and VGG16c models.

Model	Accuracy (%)	Sensitivity (%)	Specificity (%)	Precision (%)	F_1-score (%)
ANN	74.78	87.46	55.26	74.14	80.18
CNN	61.80	97.71	4.93	61.35	75.81
VGG16	76.54	35.56	87.90	78.68	49.02

[a]ANN: artificial neural network.

[b]CNN: convolutional neural network.

[c]VGG: Visual Geometry Group.

XSL•FO
RenderX

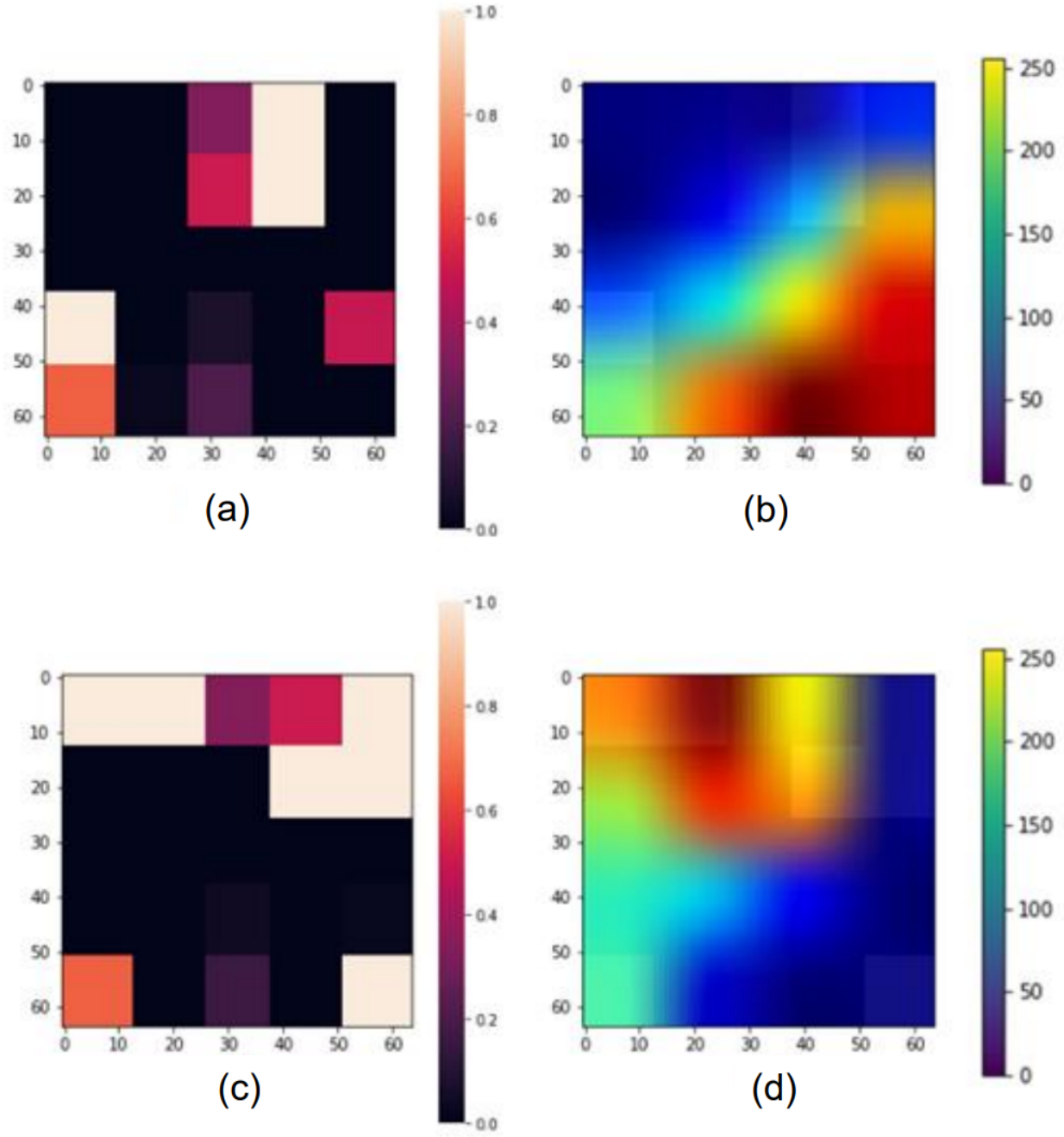
Gradient-Weighted Class Activation Mapping

Grad-CAM analysis was used to enhance the interpretability of the VGG16 model predictions. This technique generated heat maps highlighting variables that appeared most influential in the three models' survival period predictions.

Analysis of Patients With Colon Cancer

Figure 6 presents examples of heat map conversion results and Grad-CAM application results for patients with colon cancer. The patient has a survival period of more than 5 years and is a successful case of deep learning model prediction. Looking at Figure 6a, the patient was in an early pTNM stage. Considering this, it can be confirmed that the factor that played a major role in VGG16 predicting the survival of this patient was the pTNM stage. The results of Grad-CAM for patients without liver disease and a moderate ASA grade had an impact on predicting that patients would have longer survival times (Figure 6d).

Figure 6. Visualized results generated by Grad-CAM in patients with colon cancer: (a, c) original data from the image generator and (b, d) visualized image generated by Grad-CAM. Grad-CAM: gradient-weighted class activation mapping.



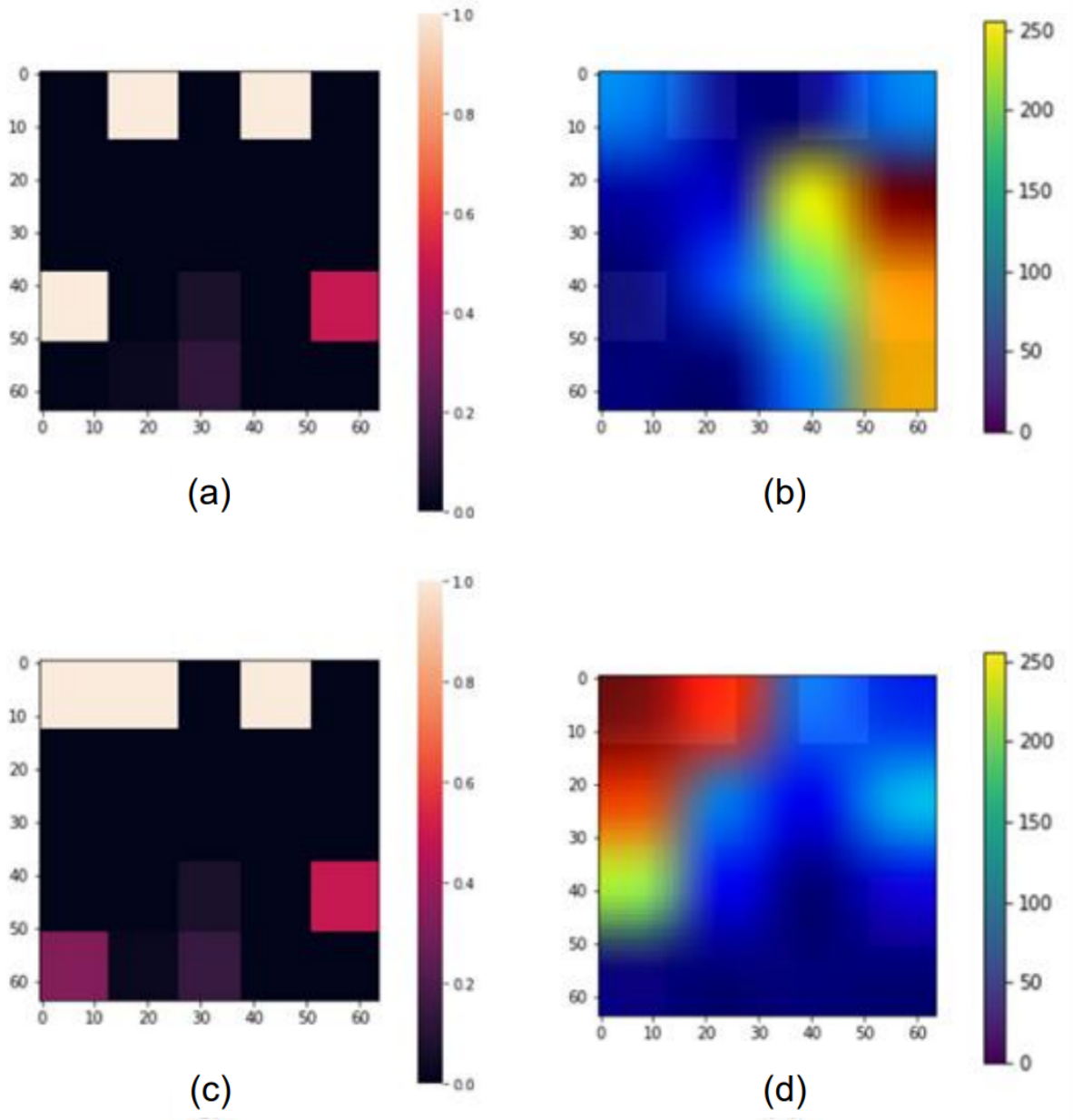
Analysis of Patients With Rectal Cancer

Figure 7 presents examples of heat map conversion results and Grad-CAM application results for patients with rectal cancer. Figures 7a and 7c are the learned images, and Figures 7b and 7d show the results of Grad-CAM as a heat map. As shown in the imaging matrix in Figure 7b, the smoking history, initial CEA level, and pTNM stage were indicated as variables that

XSL•FO
RenderX

had a major influence on the prediction of the model: there was no smoking history, the initial CEA level was moderate, and the TNM stage was early. As the patient's survival period was well predicted to be more than 5 years, it was found that the Grad-CAM analysis results were consistent with the results of existing clinical studies. As shown in Figure 7d, age, sex, the ASA grade, and pulmonary disease affected the survival time prediction results. For a patient with a high age, a low ASA grade, and no pulmonary disease, with a well-predicted survival of more than 5 years, because the ASA grade was low, the patient's physical condition was good, and there was no pulmonary disease, the survival period seemed to be predicted for a long time. As described earlier, Grad-CAM can be used to determine which variables have the most influence on the prediction of survival time for individual patients and their risk factors.

Figure 7. Visualized results generated by Grad-CAM in patients with rectal cancer: (a, c) original data from the image generator and (b, d) visualized image generated by Grad-CAM. Grad-CAM: gradient-weighted class activation mapping.



Discussion

Principal Findings

In this study, we developed a model to predict the survival period of colorectal cancer using EMR data and investigated which variables contributed to the prediction. In particular, we improved the performance of the model through an innovative approach to convert tabular medical data into image data. The results of the study showed that the VGG16 model achieves the best performance, which suggests a new methodology for developing a CDSS for patients with colorectal cancer in clinical settings.

Deep learning models performed important clinical predictions on whether the survival period of patients with colorectal cancer

XSL•FO
RenderX

who underwent surgery is more than 5 years. If the survival period of a patient with cancer is more than 5 years, it indicates that the patient's prognosis is good and the risk of cancer recurrence is low, which can provide clinically helpful information. Furthermore, it shows that doctors can use this as a reference to understand the patient's condition and support them in making better decisions.

In this study, the prediction accuracy of VGG16 was 75%, and that of the CNN was 61%, showing that the VGG16 model, which used more weights through transfer learning, performs better. The reason for the large performance difference between the CNN and VGG16, about 14%, is probably because the amount of data used in this study was less than that used in other deep learning models. However, VGG16 is a transfer learning model trained using a large ImageNET-based dataset and provides the weights obtained as a result. In this study, we used the weights of VGG16 for learning, and we were able to see that the prediction performance was improved by overcoming the limitations of quantitative data volume.

Given the class imbalance in our dataset and the differing behavior observed across models, a clear understanding of the trade-off between sensitivity and specificity is essential for clinical application. Although oversampling techniques, such as the synthetic minority oversampling technique (SMOTE), were initially considered to mitigate the imbalance, we ultimately decided not to apply them after consultation with clinical experts. It was determined that artificially augmenting the minority classes could compromise the clinical validity and real-world representativeness of colorectal cancer data. Therefore, we maintained the original class distribution and focused on evaluating model performance through sensitivity and specificity, which are more aligned with clinical priorities. To further enhance model interpretability and support clinical decision-making, we applied Grad-CAM to visualize the features contributing to model predictions.

Our best-performing model, VGG16, exhibited high specificity (88%-90%) but relatively low sensitivity (35%-40%). This indicates that when the model predicts early mortality (nonsurvival within 5 years), it is highly reliable, minimizing false positives in identifying high-risk patients. Such high specificity is valuable in clinical settings where unnecessary aggressive follow-up could impose physical, psychological, and economic burdens. Considering the class distribution (approximately 6:4 for positive to negative outcomes, where "positive" refers to patients surviving for more than 5 years), precision and F_1-scores provide further insight into model behavior. VGG16, which showed the highest specificity and precision, tended to make more conservative predictions regarding long-term survival, resulting in fewer false positives. From a CDSS perspective, its relatively high F_1-score and sensitivity suggest potential usefulness in identifying patients unlikely to survive beyond 5 years. Although the ANN and CNN also demonstrated comparable sensitivity, VGG16 maintained this without compromising specificity, indicating a more balanced performance that may help reduce false alarms in clinical practice.

The VGG16 model outperformed the ANN model by achieving an accuracy improvement of 6.76% (78.23% vs 71.47%) in colon cancer survival prediction and 1.76% (76.54% vs 74.78%) in rectal cancer survival prediction. Additionally, VGG16 demonstrated markedly higher specificity compared to the ANN (89.55% vs 54.23% for colon cancer and 87.9% vs 55.26% for rectal cancer), indicating improved ability to correctly identify patients with better survival outcomes.

In contrast, the CNN model showed substantially lower accuracy (61.9% for colon cancer and 61.8% for rectal cancer) and poor specificity (<5%), suggesting limited clinical utility in its current form. These findings highlight that although basic CNN architectures may underperform, deeper networks, such as VGG16, can capture complex patterns to improve prediction reliability.

However, the lower sensitivity implies that some patients who do die early are not identified by the model (false negatives), potentially missing individuals who could benefit from intensified monitoring or interventions. This limitation is crucial to acknowledge, as underdetection may reduce the model's effectiveness in guiding proactive clinical decision-making.

Conversely, the CNN model showed the opposite pattern, with high sensitivity but low specificity, which would result in many false alarms and potentially excessive interventions.

Therefore, the choice of model and classification threshold must be carefully tailored to the clinical context and intended use case. For example, a model prioritizing sensitivity may be preferred in screening scenarios to ensure at-risk patients are not missed, whereas one prioritizing specificity may be favored where reducing false positives is paramount.

Unlike the black-box model, the demand for a white-box model that provides a reason for the result is increasing [29]. A white-box model explains the results of an AI model and has recently been attracting attention under the name of XAI [30].

Although our model achieved an accuracy of 75%-78% in predicting 5-year survival, the existing literature indicates that this level of performance is clinically meaningful. Kos et al [31] used various machine learning models (eg, decision tree, stacking ensemble, and SVM) to predict survival rates from 1 to 10 years using large-scale data of patients with colorectal cancer in Australia. In this study, the 5-year survival prediction models showed an AUC of approximately 0.86-0.89 and an accuracy of over 70%, and the performance by cancer stage also showed an excellent predictive power of over 70%. Compared to the prediction accuracy of this study (78.4% for colon cancer and 74.8% for rectal cancer), both studies suggest that machine learning–based clinical data use is effective for survival prediction, and this study is particularly different in that it converted EMR data into images and applied them to a CNN-based model. Similarly, Gao et al [32] compared nine ML models against TNM staging alone (AUC=0.784) and found that most models only modestly outperform staging, often with overlapping CIs.

These findings suggest that our image-based deep learning model operates within a comparable performance band, while adding the benefit of interpretable Grad-CAM visualization.

XSL•FO
RenderX

Furthermore, staging-only approaches often fall short when applied to patients with stage II-III cancer, whose outcomes are less deterministic. Our model showed improved discrimination in this subgroup, indicating its potential to complement staging heuristics in borderline clinical cases.

Finally, the alignment between Grad-CAM highlighting (eg, pTNM stage, smoking history, age) and established prognostic factors enhances the model's trustworthiness and suitability for integration into explainable CDSSs. To help clinical decision-making, it is better for deep learning models to also provide reasons for their decisions. In this study, Grad-CAM was used to provide XAI in deep learning models. Grad-CAM can answer the reasons for individual patient outcomes, and the survival prediction model shows the possibility of providing tailored medicine as part of a CDSS.

Clinical Implications

Figures 6 and 7 show the results of analyzing the results for some patients with colorectal cancer using Grad-CAM. Among the patients with colon and rectal cancer, we randomly selected 2 patients and examined the heatmap from the Grad-CAM analysis results. As a result, the pTNM stage was found to be the variable that had the greatest influence on the model prediction in both cancer types. However, additional variables that affected each patient were different: age, gender, smoking history, ASA grade, liver disease, pulmonary disease, and initial CEA levels. The results of Grad-CAM analysis for patients in Figure 5d,e show that the pTNM stage has an influence on the prediction, which is consistent with existing medical knowledge [33]. Figure 6 shows that smoking history has a major influence on the prediction by the model. In existing clinical studies, smoking history has been identified as a relevant factor affecting patient survival [34]. Since various factors must be considered in order to determine the prognosis of patients with colon cancer, if we conduct an analysis that can identify the influential variables at once, such as Grad-CAM, we will be able to provide better clinical services.

Limitations and Future Work

When training a deep learning model using a small amount of data, overfitting may occur. If overfitting occurs, predictions may not work well with data other than trained data. Therefore, if we can collect more multicenter studies or data in future research, we will further increase the reliability of the study by conducting an analysis by stage.

To leverage the spatial learning capabilities of CNNs, we transformed 25 clinical variables into a 5×5 image for each patient. Each feature was min-max-normalized and assigned to a fixed position in the 5×5 matrix, ensuring consistent spatial encoding across all samples. Although clinical tabular data do not possess an inherent spatial structure, prior studies have shown that imposing a structured layout allows CNNs to effectively capture local feature interactions and complex nonlinear relationships that may be overlooked by traditional models. This image-based representation also enables the application of transfer learning using pretrained CNN architectures.

Although the variable layout was arbitrarily fixed in this study, future work may explore data-driven arrangements based on feature correlation or clinical relevance to further enhance the model's representational capacity.

The proposed model, although demonstrating strong predictive performance, must address several practical considerations to be implemented as a CDSS. Integration into existing EMR systems would require standardized data pipelines, interoperability, and real-time processing capabilities. Additionally, interpretability remains essential for clinical adoption. In this study, we used Grad-CAM to identify features contributing most to each prediction, providing visual explanations that could be embedded into future CDSS interfaces.

From a clinical perspective, prediction models for survival outcomes in colorectal cancer can serve as valuable tools, particularly in the postoperative setting. Previous studies have demonstrated the utility of machine learning for guiding surveillance and adjuvant therapy decisions [35,36]. Our deep learning–based model offers automated and objective risk stratification using routinely collected clinical data, supporting multidisciplinary teams in identifying high-risk patients. Within clinical workflows, the system could deliver actionable alerts—such as notifications flagging patients with poor predicted survival—to prompt timely follow-up or intervention. These alerts, coupled with interpretable Grad-CAM visualizations, can enhance clinical reasoning, build trust, and facilitate shared decision-making by clearly communicating risk to both clinicians and patients.

Although this study adopted a binary classification approach (predicting 5-year survival), we acknowledge that this represents a simplification of the underlying clinical reality. In oncology, the timing of events such as recurrence or mortality is often just as important as whether the events occur. Therefore, future work will explore modeling survival outcomes in a time-to-event framework using deep learning–based survival models. Methods such as DeepSurv, a Cox proportional hazards–based neural network, have shown promise in capturing complex nonlinear relationships, while preserving the structure of survival data [37]. These approaches could yield more clinically informative predictions, especially in patient-level prognostication and individualized treatment planning.

In addition, future enhancements could include the use of more advanced convolutional architectures, such as ResNet or EfficientNet, as well as ensemble learning strategies. These techniques may help improve both performance and generalizability, especially in heterogeneous clinical datasets.

The dataset used in this study was built through the EMR system of a single institution. For multi-institutional research, if a standardized medical information system for each type of medical institution in Korea is established and advanced, it will be possible to produce generalized prediction results using more patient data. Furthermore, if data construction standards for each institution are established, it is believed that the establishment of a data mart will help Korea's data ecosystem and contribute to the generalization of research results.

XSL•FO
RenderX

The dataset used in this study was limited as it was collected from a single institution. Therefore, the characteristics of the patient group in this study may not reflect the clinical features of patients in other medical institutions. In future research, we will present a generalized model that reflects the clinical features of patients in a multicenter study.

Conclusion

XAI research that enhances the interpretability of deep learning model results is actively progressing. In this study, we used the IGHT technique to convert structured data into images, which allowed us to capture relationships between variables effectively. Using this approach, we developed models to predict overall survival, a key indicator for determining the prognosis of patients with colorectal cancer after surgery.

An ANN model, a CNN model, and transfer learning with a pretrained VGG16 model were used to evaluate predictive performance. Our results suggest that image-based input leads to improved prediction compared to traditional tabular data analysis. Additionally, CNN-based models provide opportunities for enhanced interpretability through techniques such as Grad-CAM.

Acknowledgments

This work was supported by the Gachon University research fund of 2021 (GCU-202110290001).

Authors' Contributions

S-HO contributed to data cleansing, analysis, modeling, and manuscript writing. WS provided clinical direction and assisted the manuscript. J-HB was responsible for data collection, curation, interpretation, and verification. YL designed and supervised the research and critically reviewed the final manuscript. All authors had access to the data, reviewed the study results, and approved the final manuscript.

Conflicts of Interest

None declared.

Multimedia Appendix 1
Feature overview of the dataset, parameters of the artificial neural network (ANN) model, parameters of the convolutional neural network (CNN) model, and parameters of the Visual Geometry Group (VGG)16 model.
[DOCX File , 15 KB - medinform_v13i1e75022_app1.docx]

References

1. Lee Y, Park Y, Park J, Yi B. Association between electronic medical record system adoption and healthcare information technology infrastructure. Healthc Inform Res 2018 Oct;24(4):327-334 [FREE Full text] [doi: 10.4258/hir.2018.24.4.327] [Medline: 30443421]
2. Hlatky MA, Kazi DS. PCSK9 inhibitors: economics and policy. J Am Coll Cardiol 2017 Nov 28;70(21):2677-2687 [FREE Full text] [doi: 10.1016/j.jacc.2017.10.001] [Medline: 29169476]
3. Yang X, Qiu H, Wang L, Wang X. Predicting colorectal cancer survival using time-to-event machine learning: retrospective cohort study. J Med Internet Res 2023 Oct 26;25:e44417 [FREE Full text] [doi: 10.2196/44417] [Medline: 37883174]
4. Yau STY, Hung CT, Leung EYM, Lee A, Yeoh EK. Survival tree analysis of interactions among factors associated with colorectal cancer risk in patients with type 2 diabetes: retrospective cohort study. JMIR Public Health Surveill 2025 Apr 29;11:e62756 [FREE Full text] [doi: 10.2196/62756] [Medline: 40300170]
5. Huang X, Ren S, Mao X, Chen S, Chen E, He Y, et al. Association between risk factors and major cancers: explainable machine learning approach. JMIR Cancer 2025 May 02;11:e62833 [FREE Full text] [doi: 10.2196/62833] [Medline: 40315870]
6. Timp S, Varela C, Karssemeijer N. Computer-aided diagnosis with temporal analysis to improve radiologists' interpretation of mammographic mass lesions. IEEE Trans Inf Technol Biomed 2010 May;14(3):803-808. [doi: 10.1109/TITB.2010.2043296] [Medline: 20403792]
7. Yang J, Ju J, Guo L, Ji B, Shi S, Yang Z, et al. Prediction of HER2-positive breast cancer recurrence and metastasis risk from histopathological images and clinical information via multimodal deep learning. Comput Struct Biotechnol J 2022;20:333-342 [FREE Full text] [doi: 10.1016/j.csbj.2021.12.028] [Medline: 35035786]
8. Althammer S, Tan TH, Spitzmüller A, Rognoni L, Wiestler T, Herz T, et al. Automated image analysis of NSCLC biopsies to predict response to anti-PD-L1 therapy. J Immunother Cancer 2019 May 06;7(1):121 [FREE Full text] [doi: 10.1186/s40425-019-0589-x] [Medline: 31060602]
9. Zhu Y, Brettin T, Xia F, Partin A, Shukla M, Yoo H, et al. Converting tabular data into images for deep learning with convolutional neural networks. Sci Rep 2021 May 31;11(1):11325 [FREE Full text] [doi: 10.1038/s41598-021-90923-y] [Medline: 34059739]

XSL•FO
RenderX

10. Lara-Abelenda FJ, Chushig-Muzo D, Peiro-Corbacho P, Gómez-Martínez V, Wägner AM, Granja C, et al. Transfer learning for a tabular-to-image approach: a case study for cardiovascular disease prediction. J Biomed Inform 2025 May;165:104821 [FREE Full text] [doi: 10.1016/j.jbi.2025.104821] [Medline: 40209918]
11. Sharma A, Vans E, Shigemizu D, Boroevich KA, Tsunoda T. DeepInsight: a methodology to transform a non-image data to an image for convolution neural network architecture. Sci Rep 2019 Aug 06;9(1):11399 [FREE Full text] [doi: 10.1038/s41598-019-47765-6] [Medline: 31388036]
12. Lee DH, Jung HY, Kim MH, Lim ME, Kim DH, Han YW, et al. Trends of clinical decision support system (CDSS). Electron Telecommun Trends 2016;31(4):77-85 [FREE Full text]
13. Somashekhar SP, Sepúlveda MJ, Puglielli S, Norden AD, Shortliffe EH, Rohit Kumar C, et al. Watson for Oncology and breast cancer treatment recommendations: agreement with an expert multidisciplinary tumor board. Ann Oncol 2018 Feb 01;29(2):418-423 [FREE Full text] [doi: 10.1093/annonc/mdx781] [Medline: 29324970]
14. Gachon University Gil Medical Center adopts IBM Watson for Oncology trained by Memorial Sloan Kettering, marking Watson's first deployment in Korea. IBM UK Newsroom. 2016 Sep 7. URL: https://tinyurl.com/mr3bccxd [accessed 2022-08-14]
15. Lee KA, Kim CH, Baek JH, Shim SJ, Ahn SM, Ahn HK, et al. Concordance assessment and satisfaction of medical professionals for the artificial intelligence Watson. J Health Technol Assess 2019;7(2):112-118 [FREE Full text]
16. Lee W, Ahn SM, Chung J, Kim KO, Kwon KA, Kim Y, et al. Assessing concordance with Watson for Oncology, a cognitive computing decision support system for colon cancer treatment in Korea. JCO Clin Cancer Inform 2018 Dec(2):1-8 [FREE Full text] [doi: 10.1200/cci.17.00109]
17. Park J, Baek J, Sym SJ, Lee KY, Lee Y. A data-driven approach to a chemotherapy recommendation model based on deep learning for patients with colorectal cancer in Korea. BMC Med Inform Decis Mak 2020 Sep 22;20(1):241 [FREE Full text] [doi: 10.1186/s12911-020-01265-0] [Medline: 32962726]
18. Kwon H, Park J, Lee Y. Stacking ensemble technique for classifying breast cancer. Healthc Inform Res 2019 Oct;25(4):283-288 [FREE Full text] [doi: 10.4258/hir.2019.25.4.283] [Medline: 31777671]
19. Oh SH, Baek JH, Kang UG. Classification models for chemotherapy recommendation using LGBM for the patients with colorectal cancer. J Korea Soc Comput Inf 2021;26(7):9-17 [FREE Full text] [doi: 10.9708/jksci.2021.26.07.009]
20. Data visualization tools for exploring the global cancer burden in 2022. International Agency for Research on Cancer. 2019. URL: https://gco.iarc.fr/today/home [accessed 2022-09-13]
21. Sung H, Ferlay J, Siegel RL, Laversanne M, Soerjomataram I, Jemal A, et al. Global cancer statistics 2020: GLOBOCAN estimates of incidence and mortality worldwide for 36 cancers in 185 countries. CA Cancer J Clin 2021 May;71(3):209-249 [FREE Full text] [doi: 10.3322/caac.21660] [Medline: 33538338]
22. Lee EO, Eom A, Song R, Chae YR, Lam P. [Factors influencing quality of life in patients with gastrointestinal neoplasms]. J Korean Acad Nurs 2008 Oct;38(5):649-655. [doi: 10.4040/jkan.2008.38.5.649] [Medline: 19114753]
23. Goel MK, Khanna P, Kishore J. Understanding survival analysis: Kaplan-Meier estimate. Int J Ayurveda Res 2010 Oct;1(4):274-278 [FREE Full text] [doi: 10.4103/0974-7788.76794] [Medline: 21455458]
24. Cox DR. Regression models and life ‐ tables. J R Stat Soc Series B Stat Methodol 1972 Jan;34(2):187-202 [FREE Full text] [doi: 10.1111/j.2517-6161.1972.tb00899.x]
25. Yeom CH, Choi YS, Hong YS, Park YG, Lee HR. Prediction of life expectancy for terminally ill cancer patients based on clinical parameters. J Hosp Palliat Care 2002 Nov 30;5(2):111-124 [FREE Full text]
26. Selvaraju RR, Cogswell M, Das A, Vedantam R, Parikh D, Batra D. Grad-CAM: visual explanations from deep networks via gradient-based localization. 2017 Presented at: IEEE International Conference on Computer Vision (ICCV); 2017; Venice, Italy p. 618-626 URL: https://ieeexplore.ieee.org/document/8237336 [doi: 10.1109/ICCV.2017.74]
27. An J, Joe I. Attention map-guided visual explanations for deep neural networks. Appl Sci 2022 Apr 11;12(8):3846 [FREE Full text] [doi: 10.3390/app12083846]
28. Selvaraju RR, Das A, Vedantam R, Cogswell M, Parikh D, Batra D. Grad-CAM: why did you say that? arXiv. Preprint posted online 2016. [doi: 10.48550/arXiv.1611.07450] [FREE Full text] [doi: 10.48550/arXiv.1611.07450]
29. Preece A, Harborne D, Braines D, Tomsett R, Chakraborty S. Stakeholders in explainable AI. arXiv. Preprint posted online 2018. [doi: 10.48550/arXiv.1810.00184] . [doi: 10.48550/arXiv.1810.00184]
30. Gunning D. Explainable artificial intelligence (XAI). Defense Advanced Research Projects Agency (DARPA). 2017. URL: https://www.darpa.mil/research/programs/explainable-artificial-intelligence [accessed 2025-08-06]
31. Kos FT, Cecen Kaynak S, Aktürk Esen S, Arslan H, Uncu D. Comparison of different machine learning models for predicting long-term overall survival in non-metastatic colorectal cancers. Cureus 2024 Dec;16(12):e75713. [doi: 10.7759/cureus.75713] [Medline: 39811215]
32. Gao P, Zhou X, Wang Z, Song Y, Tong L, Xu Y, et al. Which is a more accurate predictor in colorectal survival analysis? Nine data mining algorithms vs. the TNM staging system. PLoS One 2012;7(7):e42015 [FREE Full text] [doi: 10.1371/journal.pone.0042015] [Medline: 22848691]
33. Weiser MR. AJCC 8th edition: colorectal cancer. Ann Surg Oncol 2018 Jun;25(6):1454-1455. [doi: 10.1245/s10434-018-6462-1] [Medline: 29616422]

XSL•FO
RenderX

34. Zhu Y, Yang SR, Wang PP, Savas S, Wish T, Zhao J, et al. Influence of pre-diagnostic cigarette smoking on colorectal cancer survival: overall and by tumour molecular phenotype. Br J Cancer 2014 Mar 04;110(5):1359-1366 [FREE Full text] [doi: 10.1038/bjc.2014.6] [Medline: 24448365]
35. Bibault JE, Giraud P, Housset M, Durdux C, Taieb J, Berger A, et al. Deep learning and radiomics predict complete response after neo-adjuvant chemoradiation for locally advanced rectal cancer. Sci Rep 2018 Aug 22;8(1):12611 [FREE Full text] [doi: 10.1038/s41598-018-30657-6] [Medline: 30135549]
36. Jiang F, Jiang Y, Zhi H, Dong Y, Li H, Ma S, et al. Artificial intelligence in healthcare: past, present and future. Stroke Vasc Neurol 2017 Dec;2(4):230-243 [FREE Full text] [doi: 10.1136/svn-2017-000101] [Medline: 29507784]
37. Katzman JL, Shaham U, Cloninger A, Bates J, Jiang T, Kluger Y. DeepSurv: personalized treatment recommender system using a Cox proportional hazards deep neural network. BMC Med Res Methodol 2018 Feb 26;18(1):24 [FREE Full text] [doi: 10.1186/s12874-018-0482-1] [Medline: 29482517]

Abbreviations

AI: artificial intelligence
ANN: artificial neural network
ASA: American Society of Anesthesiologists physical status classification
AUC: area under the curve
AV: anal verge
CDSS: clinical decision support system
CEA: carcinoembryonic antigen
CNN: convolutional neural network
DM: diabetes mellitus
EMR: electronic medical record
Grad-CAM: gradient-weighted class activation mapping
IGHT: image generator health care tabular data
IGTD: image-guided tabular data
pM: pathological distant metastasis
pN: pathological regional lymph node
pT: pathological primary tumor
pTNM: pathological tumor, node, metastasis
PNI: perineural invasion
LN: lymph nodes
LVI: lymphovascular invasion
SVM: support vector machine
TNM: tumor, node, metastasis
VGG: Visual Geometry Group
WFO: Watson for Oncology
XAI: explainable artificial intelligence

Edited by A Coristine; submitted 30.03.25; peer-reviewed by H Woo, D Chushig-Muzo, SR Polamuri, E Bai; comments to author 28.04.25; revised version received 23.06.25; accepted 31.07.25; published 19.08.25.

Please cite as:
Oh SH, Lee Y, Baek JH, Sunwoo W
Deep Learning and Image Generator Health Tabular Data (IGHT) for Predicting Overall Survival in Patients With Colorectal Cancer: Retrospective Study
JMIR Med Inform 2025;13:e75022
URL: https://medinform.jmir.org/2025/1/e75022
doi:10.2196/75022
PMID:40828572

©Seo Hyun Oh, Youngho Lee, Jeong-Heum Baek, Woongsang Sunwoo. Originally published in JMIR Medical Informatics (https://medinform.jmir.org), 19.08.2025. This is an open-access article distributed under the terms of the Creative Commons Attribution License (https://creativecommons.org/licenses/by/4.0/), which permits unrestricted use, distribution, and reproduction in any medium, provided the original work, first published in JMIR Medical Informatics, is properly cited. The complete

XSL•FO
RenderX

bibliographic information, a link to the original publication on https://medinform.jmir.org/, as well as this copyright and license information must be included.

XSL•FO
RenderX

Original Paper

Machine Learning–Based Prediction of In-Hospital Falls in Adult Inpatients: Retrospective Observational Multicenter Study

Takuya Nishino[1]; Kotone Matsuyama[1,2], BPharm; Yasuo Miyagi[3,4], MD, PhD; Nari Tanabe[5], PhD; Fumiko Yamaguchi[3]; Hiroki Ito[3]; Shizuka Soh[3]; Ayako Yano[6], MSN; Masako Mizuno[7], MSN; Katsuhito Kato[8], MD, PhD; Hiroshige Jinnouchi[8], PhD; Chol Kim[6,9], MD, PhD; Yosuke Ishii[4], MD, PhD; Hiroki Yamaguchi[3,10], MD, PhD; Yukihiro Kondo[1,11], MD, PhD

[1]Department of Health Policy and Management, Nippon Medical School, Tokyo, Japan
[2]Center for Clinical Research and Development, National Center for Child Health and Development, Tokyo, Japan
[3]Department of Medical Safety Control, Nippon Medical School Hospital, Tokyo, Japan
[4]Department of Cardiovascular Surgery, Nippon Medical School, Tokyo, Japan
[5]Faculty of Engineering, Suwa University of Science, Nagano, Japan
[6]Department of Medical Safety Control, Nippon Medical School, Chiba Hokusoh Hospital, Chiba, Japan
[7]Nursing Department, Nippon Medical School, Chiba Hokusoh Hospital, Chiba, Japan
[8]Department of Hygiene and Public Health, Nippon Medical School, Tokyo, Japan
[9]Department of Anesthesiology, Nippon Medical School, Chiba Hokusoh Hospital, Chiba, Japan
[10]Department of Hematology, Nippon Medical School, Tokyo, Japan
[11]Department of Urology, Nippon Medical School, Tokyo, Japan

Corresponding Author:
Kotone Matsuyama, BPharm
Department of Health Policy and Management
Nippon Medical School
1-1-5 Sendagi, Bunkyo-ku
Tokyo, 113-8603
Japan
Phone: 81 3 3822 2131
Email: m-kotone@nms.ac.jp

Abstract

Background: Falls among hospitalized patients are a critical issue that often leads to prolonged hospital stays and increased health care costs. Traditional fall risk assessments typically rely on standardized scoring systems; however, these may fail to capture the complex and multifactorial nature of fall risk factors.

Objective: This retrospective observational multicenter study aimed to develop and validate a machine learning–based model to predict in-hospital falls and to evaluate its performance in terms of discrimination and calibration.

Methods: We analyzed the data of 83,917 inpatients aged 65 years and older with a hospital stay of at least 3 days. Using Diagnosis Procedure Combination data and laboratory results, we extracted demographic, clinical, functional, and pharmacological variables. Following the selection of 30 key features, 4 predictive models were constructed: logistic regression, extreme gradient boosting, light gradient boosting machine (LGBM), and categorical boosting (CatBoost). The synthetic minority oversampling technique and isotonic regression calibration were applied to improve the prediction quality and address class imbalance.

Results: Falls occurred in 2173 (2.6%) patients. CatBoost achieved the highest F_1-score (0.189, 95% CI 0.162-0.215) and area under the precision-recall curve (0.112, 95% CI 0.091-0.136), whereas LGBM had the best calibration slope (0.964, 95% CI 0.858-1.070) with good discrimination (F_1-score 0.182, 95% CI 0.156-0.209; area under the precision-recall curve 0.094, 95% CI 0.078-0.113). Logistic regression had the lowest discrimination (F_1-score 0.120, 95% CI 0.100-0.143). Shapley Additive Explanations analysis consistently identified low albumin, impaired transfer ability, and the use of sedative-hypnotics or diabetes medications as major contributors to fall risk. In incident report analysis (n=435), 49.2% of falls were toileting-related, peaking between 4 and 6 AM, with bedside falls predominating in high or very high risk groups.

XSL•FO
RenderX

Conclusions: CatBoost and LGBM offer clinically valuable prediction performance, with CatBoost favored for high-risk patient identification and LGBM for probability-based intervention thresholds. Integrating such models into electronic health records could enable real-time risk scoring and trigger targeted interventions (eg, toileting assistance and mobility support). Future work should incorporate dynamic, time-varying patient data to improve real-time risk prediction.

(JMIR Med Inform 2025;13:e75958) doi:10.2196/75958

KEYWORDS

falls; machine learning; predictive model; inpatients; risk assessment; hospitals; calibration

Introduction

Falls among hospitalized patients represent a considerable concern that can adversely affect patient health outcomes and the quality of care. Falls are often associated with prolonged hospital stays and increased hospitalization costs [1]. The World Health Organization defines a fall as “an event that results in a person coming to rest inadvertently on the ground, floor, or other lower level, excluding intentional position changes to lean against furniture, walls, or other objects” [2]. Several studies have identified various risk factors associated with falls, including advanced age, a history of falls, reduced activities of daily living (ADL), the use of sleeping medications, and malnutrition [3-6]. Given the multifactorial and complex nature of fall risk, numerous guidelines for fall prevention in hospitalized patients have been established worldwide [7-9]. These guidelines recommend performing multifactorial assessments for each patient rather than relying solely on standardized fall risk scores. Similar to many other hospitals in Japan, at our institution, we adopt a scoring system based on a number of risk factors. This scoring system facilitates easy evaluation and achieves high sensitivity [10]. However, applying a uniform evaluation to all patients may limit specificity and fail to reflect varying clinical contexts; as a result, individual clinical differences and interactions among risk factors may be overlooked [11]. This limitation underscores the multifaceted and complex nature of fall-related risk.

In Japan, nurses primarily assess fall risk through bedside clinical observation. However, limited time for patient care and insufficient staffing of registered nurses are associated with higher fall rates, underscoring the need for effective prediction models [12]. To capture these complex risk factors more accurately, recent studies have increasingly focused on machine learning–based models for fall prediction models [13]. These models are capable of analyzing complex interactions among numerous variables and can identify patterns that traditional scoring systems may overlook. Previous studies conducted in Japanese university hospitals have primarily evaluated the performance of these models using the area under the receiver operating characteristic curve (ROAUC) and reported values between 0.78 and 0.90 [14-17]. However, in clinical practice, calibration accuracy is as important as discriminatory performance. Poor calibration may lead to excessive interventions for patients classified as high risk, increasing the workload of medical staff and health care costs. Conversely, insufficient care for patients classified as low risk could result in severe fall incidents, highlighting the critical need for calibration evaluation. Despite its importance, reports on the calibration performance of machine learning models remain limited.

In this study, we aimed to develop a fall prediction model for hospitalized patients and validate its performance using discriminatory and calibration metrics. Additionally, we aimed to elucidate the factors that contribute to falls to support the development and implementation of more effective fall-prevention strategies.

Methods

Study Design and Data Collection

This retrospective observational multicenter study was conducted using inpatient data from 2 affiliated hospitals of Nippon Medical School: Nippon Medical School Hospital and Chiba Hokusoh Hospital. The dataset was compiled from the Diagnosis Procedure Combination data and laboratory test results extracted from electronic medical records.

Ethical Considerations

Ethics approval for this study was obtained from the central ethics review committee of Nippon Medical School (approval M-2023-137). This study adhered to the principles of the Declaration of Helsinki. Informed consent was obtained using an opt-out approach, and the study was reported following the TRIPOD (Transparent Reporting of a Multivariable Prediction Model for Individual Prognosis or Diagnosis) guidelines [18]. No compensation was provided to the participants because this study was a retrospective observational study using de-identified data.

Patients and Outcomes

All the patients included in this study were hospitalized between April 2018 and March 2023. Patients younger than 65 years of age and those with a hospital stay of less than 3 days were excluded. Patient and feature selection were guided by a fall risk assessment sheet used at the study facility. As the assessment sheet identified individuals aged 65 years or older as a fall risk factor, patients younger than 65 years of age were excluded accordingly (Table S1 in Multimedia Appendix 1). The outcome was defined as the first occurrence of a fall within 30 days of the admission date based on incident reports. These reports are considered highly reliable due to mandatory reporting requirements, and they contain detailed information such as the time, location, trigger of the fall, and classification into mild or severe cases.

XSL•FO
RenderX

Variables

The Diagnosis Procedure Combination data contained information on all hospitalized patients, including demographic details (such as age and sex), physical metrics (height, weight, and BMI, calculated by dividing body weight in kilograms by the square of height in meters), and clinical information (comorbidities, procedures, medications, and consciousness levels at admission) [19]. Medications were defined according to those included in the hospital fall risk assessment protocol. The physical condition of the patients was assessed using the nursing care needs score on admission [19]. This score measures the level of assistance required for activities such as turning over, transferring, oral hygiene, eating, and changing clothes (0 points=no assistance, 1 point=partial assistance, and 2 points=full assistance). It also evaluated one's ability to understand medical instructions (0 points=yes and 1 point=no) and the presence of risky behaviors (0 points=no and 2 points=yes; Table S2 in Multimedia Appendix 1).

Blood test results were obtained from electronic medical records to assess known factors influencing falls, such as anemia, malnutrition, and electrolyte imbalance. The test results were defined as the closest sample collected to the admission date within 60 days prior to admission. To minimize missing values, we extracted blood test results and medication-related variables 60 days before the admission date, rather than strictly limiting extraction to the admission date. Before model development, we assessed multicollinearity among all candidate predictors by calculating the variance inflation factor (VIF). All variables had VIF values <5, indicating no concerning multicollinearity. Therefore, all variables were retained for model construction without further dimensionality reduction (Table S3 in Multimedia Appendix 1).

Imputation of Missing Data

Missing BMI values and blood test results were imputed using a single imputation in the Python *MissForest* package [20,21]. As the missing rate for all variables was below 20%, all variables were included in the analysis. A 20% threshold was used as the exclusion criterion.

Predictive Model Development

The dataset was randomly divided into 80% training and 20% test sets using stratified sampling to ensure that the end-point occurrence rates were preserved, as in the original population. We used extreme gradient boosting (XGB) to select the top 30 features based on their importance in the training data [22]. These selected features were used for subsequent modeling and analysis. The following predictive models were used: conventional logistic regression (LR), XGB, light gradient boosting machine (LGBM), and categorical boosting (CatBoost) [23,24]. To address class imbalance, we applied the synthetic minority oversampling technique algorithm to artificially increase the proportion of fall cases to 20% of the total cases in the training data [25]. Additionally, class-balanced loss functions were used during the training phase to mitigate the effects of imbalanced data. Hyperparameter optimization for each model was performed using Optuna for up to 500 trials (Table S4 in Multimedia Appendix 1) [26]. The average precision score was used as the evaluation metric. To improve model calibration, we used isotonic regression to adjust the predicted probabilities of each model [27]. Finally, all models were trained using a 10-fold stratified k-fold cross-validation.

Model Interpretation

Shapley Additive Explanations (SHAP) values were used to interpret the output of the machine learning models [28]. SHAP is a game-theoretic approach to explain individual predictions by calculating each feature's marginal contribution to the difference between the actual prediction and the average prediction across the dataset. SHAP values provide quantitative insights into the contribution (positive or negative) of each feature to the predicted fall risk for a given patient, thereby enhancing the interpretability and transparency of the decision-making process of the model.

Model Validation

The optimal threshold for each model was determined by maximizing the F_1-score to achieve the highest possible predictive performance. Then, calibration was applied to ensure that the predicted probabilities accurately reflected the true probabilities. Additionally, the bootstrap method was applied to the test set to evaluate the performance of the predictive models. A total of 3000 bootstrap resamples obtained from the test set were used to calculate 95% CIs for each performance metric. The discriminatory ability of the model was assessed using the ROAUC and area under the precision-recall curve (PRAUC), a threshold-independent metric that quantifies the average precision across all possible recall values, providing a robust measure of the ability of a model to correctly identify positive cases, particularly in imbalanced datasets. The predicted probabilities for the calibration plots were divided into 10 percentiles, and the mean predicted and observed probabilities of the outcome for each bin were plotted. Two indices were used to evaluate the calibration: the calibration slope, which indicates the agreement between the predicted probabilities and the observed outcomes; and the Brier score, which measures the accuracy of the probability predictions. A calibration slope closer to 1 and a Brier score closer to 0 indicate ideal model performance.

Statistical Analysis

All statistical analyses were performed using Python (version 3.10.10; Python Software Foundation).

Results

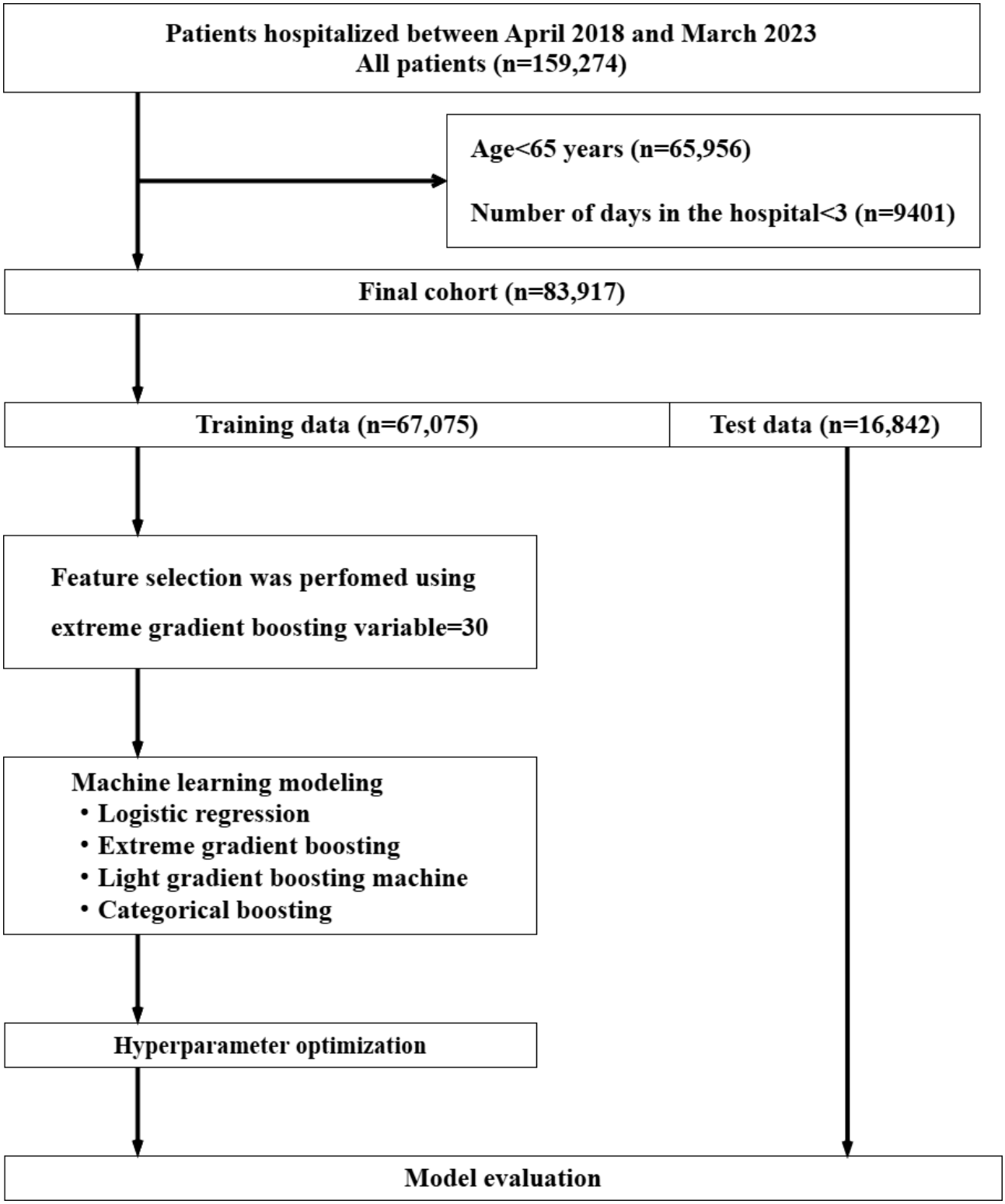
Study Population and Baseline Characteristics

Among the initial 159,274 patients, 65,956 were younger than 65 years of age, and 9401 had a hospital stay of less than 3 days. Therefore, 83,917 participants were included in the final analysis after applying the exclusion criteria. Of these, 67,705 (80%) were allocated to the training dataset and 16,842 (20%) to the validation dataset (Figure 1). Table 1 presents the key variables included in the final prediction models, along with their descriptive statistics in the overall, training, and test datasets. Complete descriptive statistics for all candidate variables prior to feature selection, including VIF values, are provided in Table

XSL•FO
RenderX

S3 in Multimedia Appendix 1. Outcomes were observed in 2173 (2.6%) patients, and the characteristics of the training and test datasets were well balanced. The 30 selected features used in the analysis are illustrated in Multimedia Appendix 2. Multimedia Appendix 2 highlights the relative importance of each variable, with risky behavior (0.148), oral hygiene (0.086), and unconsciousness (Japan Coma Scale≠0; 0.044) among the top predictors, providing context for the feature selection process.

Figure 1. Flowchart for patient assignment and model development.



XSL•FO
RenderX

Table 1. Characteristics of patients included in the predictive model.

Variable	Overall (N=83,917)	Training dataset (n=67,075)	Test dataset (n=16,842)
Outcome, n (%)	2173 (2.6)	1733 (2.6)	440 (2.6)
Demographic			
Age (years), median (IQR)	75 (71-81)	75 (71-81)	75 (71-81)
Male sex, n (%)	50,623 (60.3)	40,435 (60.3)	10,188 (60.5)
Emergency admission, n (%)	31,819 (37.9)	25,491 (38)	6328 (37.6)
Unconsciousness (JCS[a]≠0), n (%)	10,925 (13)	8796 (13.1)	2129 (12.6)
Intensive care unit on admission, n (%)	9655 (11.5)	7716 (11.5)	1939 (11.5)
Transfer, n (%)[b]			
0	61,528 (73.3)	49,135 (73.3)	12,393 (73.6)
1	16,066 (19.1)	12,884 (19.2)	3182 (18.9)
2	6323 (7.5)	5056 (7.5)	1267 (7.5)
Food intake, n (%)[b]			
0	69,759 (83.1)	55,721 (83.1)	14,038 (83.4)
1	9955 (11.9)	7973 (11.9)	1982 (11.8)
2	4203 (5)	3381 (5)	822 (4.9)
Dressing or undressing, n (%)[b]			
0	62,796 (74.8)	50,199 (74.8)	12,597 (74.8)
1	12,427 (14.8)	9947 (14.8)	2480 (14.7)
2	8694 (10.4)	6929 (10.3)	1765 (10.5)
Oral hygiene, n (%)[b]	19,923 (23.7)	15,946 (23.8)	3977 (23.6)
Ability to understand medical instructions, n (%)[b]	8604 (10.3)	6876 (10.3)	1728 (10.3)
Risky behavior, n (%)[b]	5599 (6.7)	4511 (6.7)	1088 (6.5)
Nursing care needs score, median (IQR)	0 (0-3)	0 (0-3)	0 (0-3)
Comorbidity, n (%)			
Certain infectious diseases (A00-B99)	7257 (8.6)	5814 (8.7)	1443 (8.6)
Neoplasms (C00-D48)	29,679 (35.4)	23,637 (35.2)	6042 (35.9)
Diseases of the blood (D50-D89)	13,214 (15.7)	10,583 (15.8)	2631 (15.6)
Endocrine diseases (E00-E90)	37,836 (45.1)	30,302 (45.2)	7534 (44.7)
Mental disorders (F00-F99)	5878 (7)	4721 (7)	1157 (6.9)
Nervous system diseases (G00-G99)	20,222 (24.1)	16,249 (24.2)	3973 (23.6)
Respiratory diseases (J00-J99)	15,862 (18.9)	12,705 (18.9)	3157 (18.7)
Digestive diseases (K00-K93)	46,192 (55)	36,981 (55.1)	9211 (54.7)
Skin and subcutaneous tissue diseases (L00-L99)	5741 (6.8)	4533 (6.8)	1208 (7.2)
Injury and poisoning (S00-T98)	14,297 (17)	11,471 (17.1)	2826 (16.8)
Special purpose codes (U00-U99)	1041 (1.2)	857 (1.3)	184 (1.1)
Medications at admission			
Medication score, median (IQR)	3 (2-4)	3 (2-4)	3 (2-4)
Antiparkinsonism drugs, n (%)	1579 (1.9)	1264 (1.9)	315 (1.9)
Hypnotics and sedatives, n (%)	20,146 (24)	16,048 (23.9)	4098 (24.3)
Chemotherapy agents, n (%)	10,926 (13)	8686 (12.9)	2240 (13.3)
Antiplatelet or coagulation drugs, n (%)	29,453 (35.1)	23,545 (35.1)	5908 (35.1)

XSL•FO
RenderX

Variable	Overall (N=83,917)	Training dataset (n=67,075)	Test dataset (n=16,842)
Diabetes treatments, n (%)	19,839 (23.6)	15,858 (23.6)	3981 (23.6)
Antihypertensive drugs, n (%)	46,430 (55.3)	37,075 (55.3)	9355 (55.5)
Laboratory findings at admission (g/dL), median (IQR)			
Albumin level	3.9 (3.5-4.2)	3.9 (3.5-4.2)	3.9 (3.5-4.2)

[a]JCS: Japan Coma Scale.

[b]Nursing care needs score: 0=no assistance, 1=partial assistance, and 2=full assistance.

Evaluation of Prediction Models

We evaluated the performances of 4 classification models: LR, XGB, LGBM, and CatBoost. The performance of each model was assessed using the F_1-score, PRAUC, calibration slope, and optimal threshold, with a 95% CI provided for each metric. The LR model achieved an F_1-score of 0.120 (95% CI 0.100-0.143), with an optimal threshold of 0.069. Its PRAUC was 0.066 (95% CI 0.055-0.0792), and the calibration slope was 0.838 (95% CI 0.739-0.934). In comparison, XGB showed a slightly higher F_1-score of 0.182 (95% CI 0.157-0.207), with an optimal threshold of 0.074. It achieved a PRAUC of 0.098 (95% CI 0.081-0.117) and had an improved calibration slope of 0.937 (95% CI 0.829-1.040). Similarly, the LGBM model demonstrated an F_1-score of 0.182 (95% CI 0.156-0.209) and an optimal threshold of 0.0846. Its PRAUC was 0.094 (95% CI 0.078-0.113), and it demonstrated the most accurate calibration among all models at 0.964 (95% CI 0.858-1.070). Among the 4 models, the CatBoost model achieved the highest F_1-score of 0.189 (95% CI 0.162-0.215) and an optimal threshold of 0.0724. It also recorded the higher PRAUC at 0.112 (95% CI 0.091-0.136). Although its calibration slope of 1.120 (95% CI 1.000-1.240) was slightly above 1, it was close to the ideal value. While CatBoost outperformed the other models in terms of the F_1-score and PRAUC, the LGBM model demonstrated the most accurate calibration, with a calibration slope closest to 1, indicating superior reliability in risk prediction relative to the observed outcomes (Table 2 and Figure 2). The predicted probabilities of in-hospital falls were stratified assuming actual clinical use and compared with the observed in-hospital fall rates. The observed fall rates in the 4 defined risk categories (low, medium, high, and very high) fell within the range of predicted probabilities (Table 3).

Table 2. Model evaluation index.

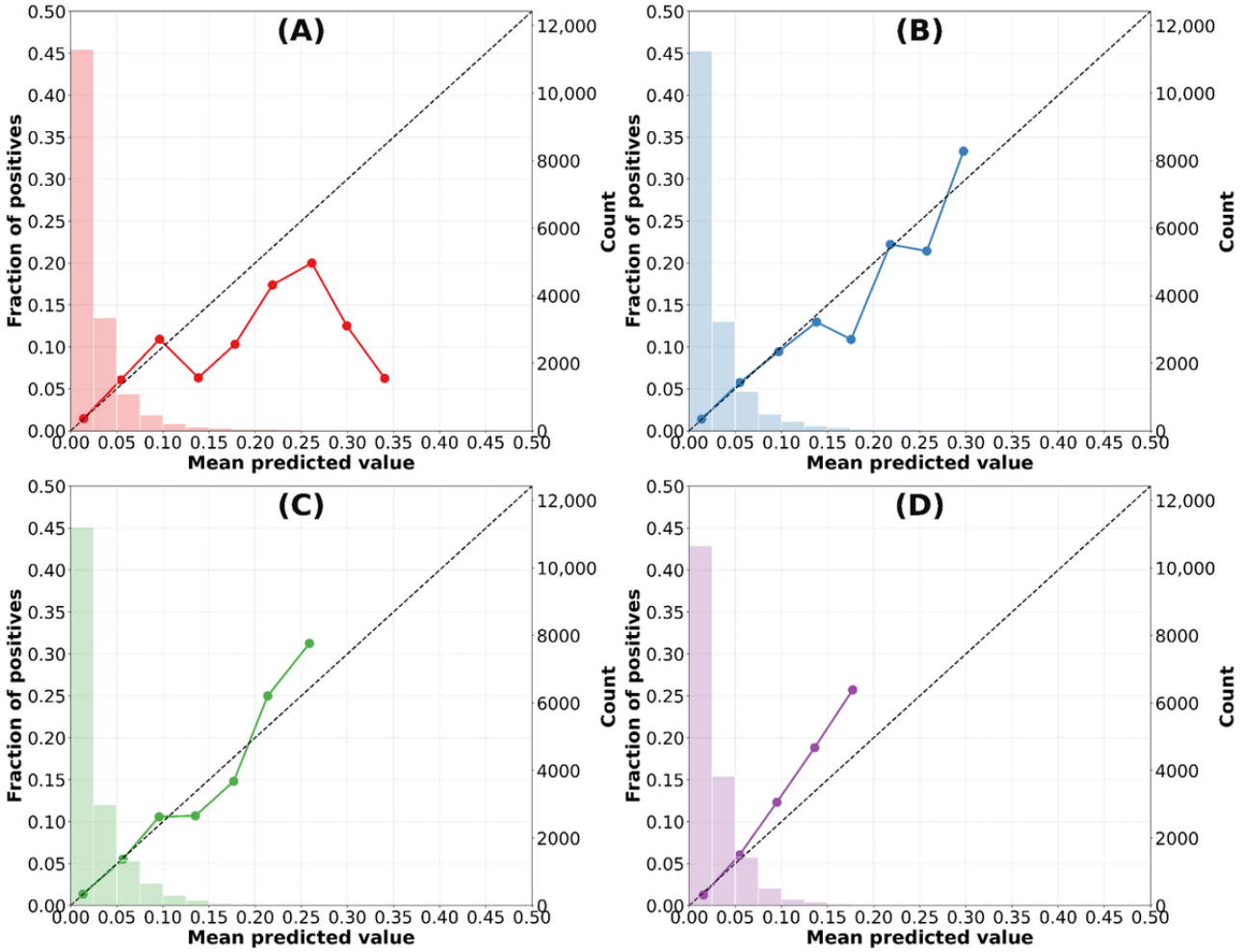
Model	F_1-score (95% CI)	Optimal threshold	ROAUC[a] (95% CI)	PRAUC[b] (95% CI)	Calibration slope (95% CI)	Brier score (95% CI)
Logistic regression	0.120 (0.100-0.143)	0.069	0.729 (0.705-0.753)	0.066 (0.055-0.0792)	0.838 (0.739-0.934)	0.025 (0.023-0.027)
Extreme gradient boosting	0.182 (0.157-0.207)	0.074	0.774 (0.751-0.798)	0.098 (0.081-0.117)	0.937 (0.829-1.040)	0.024 (0.022-0.026)
Light gradient boosting machine	0.182 (0.156-0.209)	0.085	0.774 (0.751-0.797)	0.094 (0.078-0.113)	0.964 (0.858-1.070)	0.024 (0.022-0.026)
Categorical boosting	0.189 (0.162-0.215)	0.072	0.787 (0.764-0.809)	0.112 (0.091-0.136)	1.120 (1.000-1.240)	0.024 (0.022-0.026)

[a]ROAUC: area under the receiver operating characteristic curve.

[b]PRAUC: area under the precision-recall curve.

XSL•FO
RenderX

Figure 2. Model validations. Calibration plot of the models. (A) Logistic regression, (B) extreme gradient boosting, (C) light gradient boosting machine, and (D) categorical boosting.



XSL•FO
RenderX

Table 3. Observed outcomes for each risk stratum classified by predicted probability.

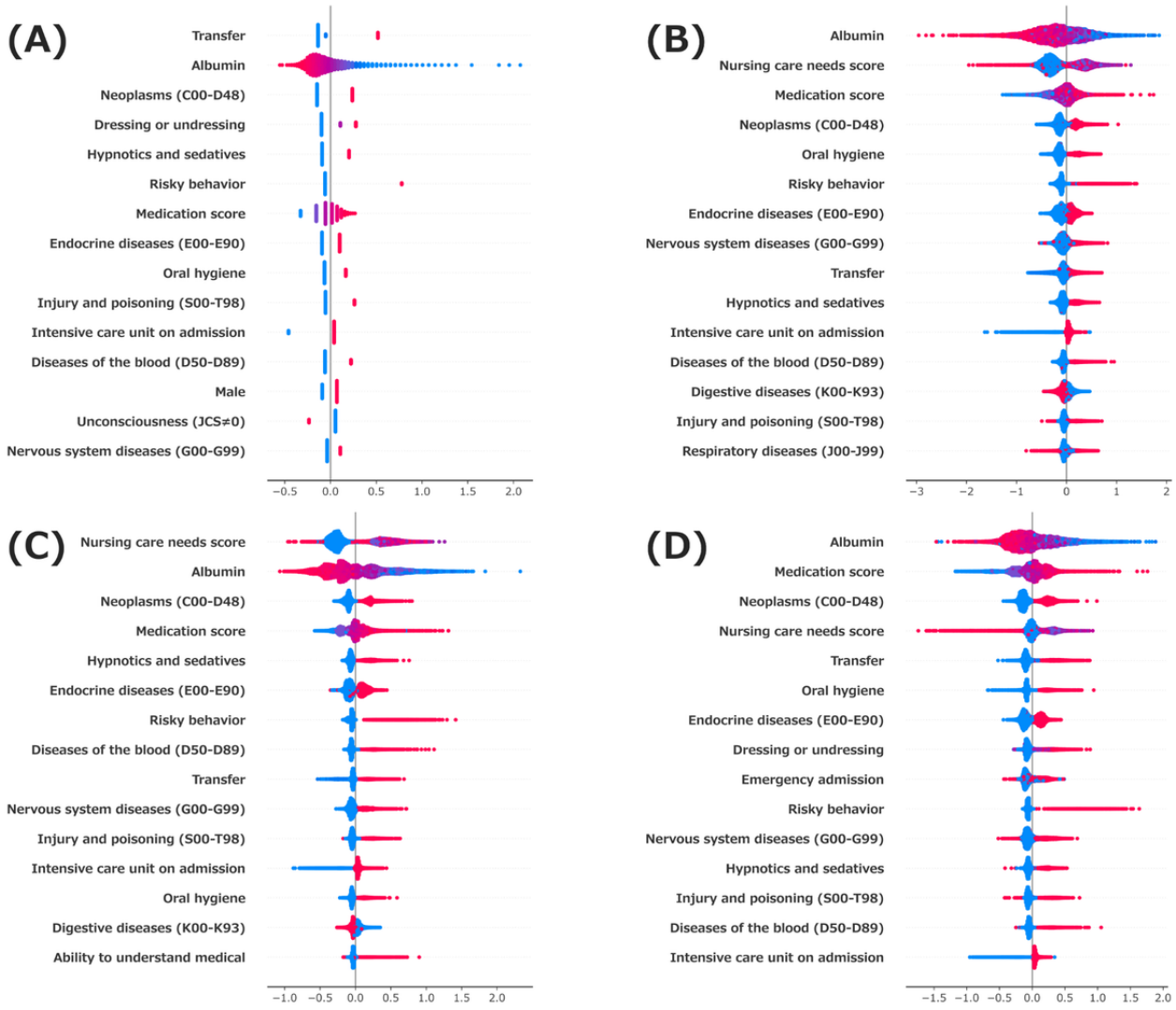
Risk stratum (range of predictive probability)	Patients (total), n (%)	Patients (outcomes), n (%)	Observed outcome rate
Logistic regression			
Low: <0.02	10,064 (59.8)	96 (1)	0.01
Middle: ≥0.02, <0.05	4570 (27.2)	146 (3.2)	0.03
High: ≥0.05, <0.10	1563 (9.3)	127 (8.1)	0.08
Very high: ≥0.10	587 (3.5)	66 (11.2)	0.11
Extreme gradient boosting			
Low: <0.02	10,255 (60.9)	97 (0.9)	0.01
Middle: ≥0.02, <0.05	4289 (25.5)	134 (3.1)	0.03
High: ≥0.05, <0.10	1588 (9.4)	117 (7.4)	0.07
Very high: ≥0.10	652 (3.9)	87 (13.3)	0.13
Light gradient boosting machine			
Low: <0.02	10,375 (53.6)	91 (0.9)	0.01
Middle: ≥0.02, <0.05	4125 (34.1)	124 (3)	0.03
High: ≥0.05, <0.10	1602 (10.2)	126 (8.3)	0.08
Very high: ≥0.10	682 (1.5)	94 (15.4)	0.14
Categorical boosting			
Low: <0.02	9045	79	0.01
Middle: ≥0.02, <0.05	5753	173	0.03
High: ≥0.05, <0.10	1727	143	0.08
Very high: ≥0.10	259	40	0.15

Model Interpretation

The contribution of each feature to the prediction of outcomes was visualized using the SHAP algorithm. The features were ranked in descending order of importance, with red indicating high influence and blue indicating low influence. All 4 models identified albumin levels, transfer, and neoplasms as key predictors, although the magnitude of their impact varied across the models (Figure 3). Additionally, medications—particularly hypnotics, sedatives, and diabetes treatments—were identified as important features in all models. These findings suggest that, in addition to medical conditions, functional abilities, such as transfer and dressing or undressing, play a significant role in predicting outcomes.

XSL•FO
RenderX

Figure 3. Shapley Additive Explanations values in the models. The top 20 variables of SHAP analysis in each model are shown with an impact of contribution to the prediction. (A) Logistic regression, (B) extreme gradient boosting, (C) light gradient boosting machine, and (D) categorical boosting. JCS: Japan Coma Scale.



Classification From Incident Reports

We presented descriptive statistics of falls during hospitalization based on 435 incidents from the test data, categorized into different risk groups (low, middle, high, and very high) according to the predicted probabilities from the LGBM model (Table 4). These findings suggest that falls occur primarily at bedside, with the urge to defecate identified as the most common trigger. Notably, the characteristics of falls vary across risk groups; the proportion of bedside falls was higher in the high and very high risk groups (76/126, 60.3% vs 54/91, 59.3%, respectively), whereas falls occurring inside the patient room are more common in the low and middle risk groups (38/105, 36.2% and 41/113, 36.3%, respectively) These findings indicate that appropriately managing toileting needs and movements around the bedside is essential to prevent falls during hospitalization.

XSL•FO
RenderX

Table 4. Location and occasion of falls by risk.

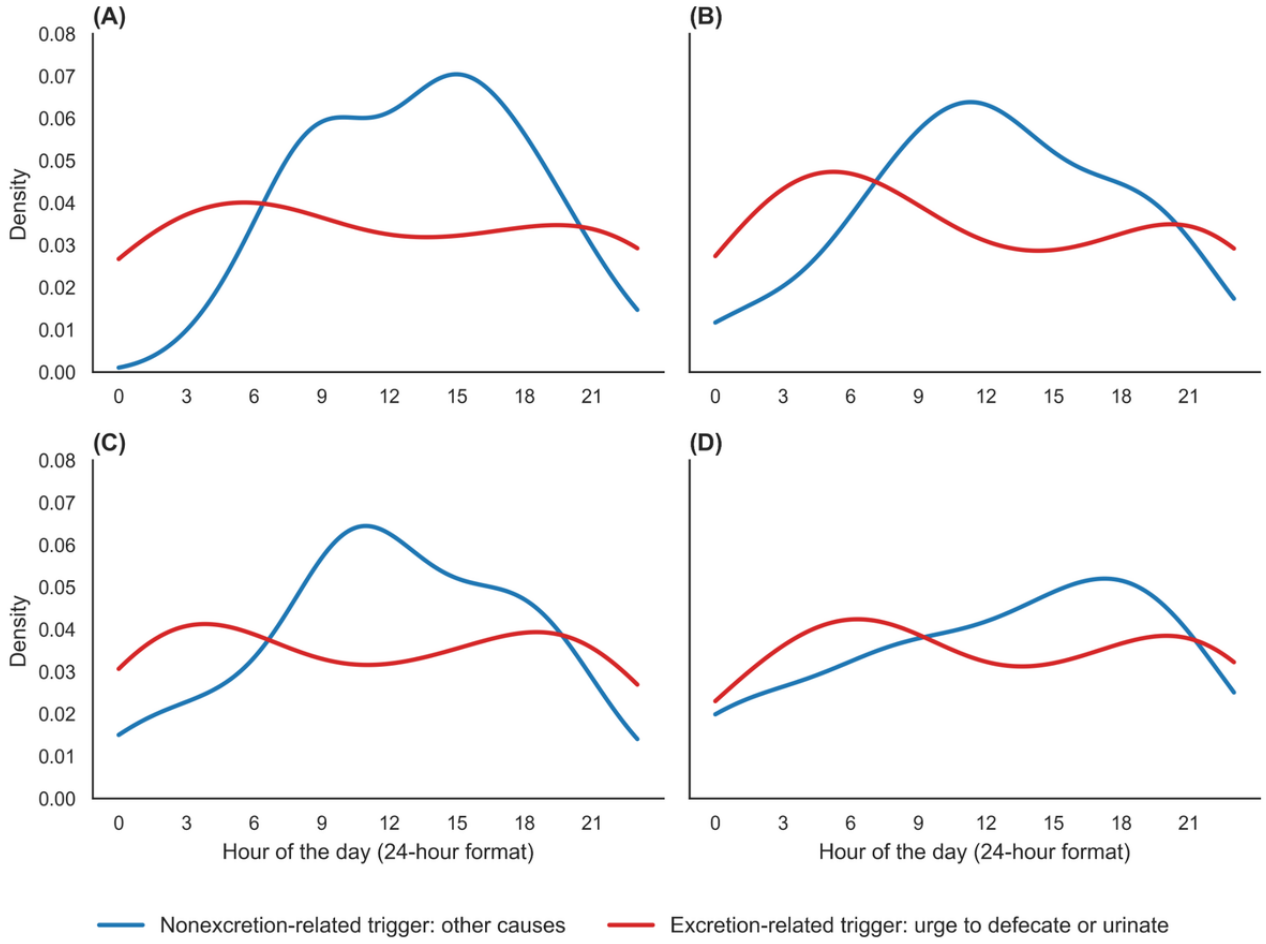
	Overall (n=435)	Low (n=91)	Middle (n=124)	High (n=126)	Very high (n=94)
Occurrence date of falls during hospitalization, median (IQR)	9 (4-17)	8 (4-14)	11 (5-16)	7 (3-15)	9 (6-18)
Location of occurrence, n (%)					
Bedside	218 (50.1)	32 (35.2)	56 (45.2)	76 (60.3)	54 (57.4)
Inside the patient room	80 (18.4)	23 (25.3)	24 (19.4)	17 (13.5)	16 (17)
Inside the toilet	57 (13.1)	10 (11)	21 (16.9)	15 (11.9)	11 (11.7)
In the bathroom or washbasin area	15 (3.4)	5 (5.5)	5 (4)	3 (2.4)	2 (2.1)
Inside the hospital	63 (14.5)	21 (23.1)	17 (13.7)	15 (11.9)	10 (10.6)
Outside the hospital	2 (0.5)	0 (0)	1 (0.8)	0 (0)	1 (1.1)
Trigger of occurrence, n (%)					
Urge to defecate	214 (49.2)	39 (42.9)	58 (46.8)	64 (50.8)	53 (56.4)
Attempting to grab something	51 (11.7)	14 (15.4)	14 (11.3)	12 (9.5)	11 (11.7)
Standing or sitting position	79 (18.2)	14 (15.4)	22 (17.7)	31 (24.6)	12 (12.8)
Changing clothes	12 (2.8)	3 (3.3)	5 (4)	3 (2.4)	1 (1.1)
While walking	46 (10.6)	15 (16.5)	16 (12.9)	5 (4)	10 (10.6)
Others	33 (7.6)	6 (6.6)	9 (7.3)	11 (8.7)	7 (7.4)

Given that excretion-related falls accounted for the largest proportion of falls (217/435, 49.9%), we conducted a more detailed analysis of their characteristics.

Figure 4 presents the kernel density estimation of fall triggers by hour of the day, distinguishing between excretion-related triggers (such as the urge to defecate or urinate) and nonexcretion-related causes. The red curve indicates that excretion-related falls peaked in the early morning, particularly between 4 and 6 AM. In contrast, the blue curve representing nonexcretion-related falls displayed a broader temporal distribution, with a higher incidence in the afternoon. Among the 217 incidents involving toileting, 132 (61%) occurred while moving to the toilet, 52 (24%) occurred inside the toilet, and 33 (15%) occurred while returning from the toilet.

XSL•FO
RenderX

Figure 4. Factors in falls related to excretion. Kernel density estimation graphs showing the hourly distribution of triggers categorized by light gradient boosting machine–predicted probabilities ((A) low, (B) middle, (C) high, and (D) very high). The blue lines represent nonexcretion-related triggers (eg, other causes), and the red lines represent excretion-related triggers (urge to defecate or urinate). Density is plotted against the hour of the day (24-hour format).



Discussion

Principal Findings

This study evaluated the predictive accuracy and interpretability of machine learning models for assessing the in-hospital fall risk. Using LR, XGB, LGBM, and CatBoost, we aimed to identify high-risk patients and categorize falls based on their backgrounds and functional abilities. Our findings revealed that CatBoost achieved the highest F_1-score and PRAUC, whereas LGBM demonstrated the best calibration slope, closely approximating the ideal for risk prediction. Notably, functional abilities, such as transfer, and clinical factors, such as albumin and neoplasms, consistently contributed to fall prediction across the models. Further analysis of incident reports revealed that fall locations and triggers varied by risk level; falls near the bedside were more frequent in higher-risk groups, whereas excretion-related falls often occurred in the early morning hours. These findings suggest that proactive management of toileting and bedside movements may effectively reduce the incidence of falls among hospitalized patients.

In previous studies on machine learning–based fall prediction models, the reported ROAUC ranged from 0.7 to 0.9 [13]. Similarly, this study demonstrated a comparable predictive performance. However, it is important to note that model performance is influenced by several factors, including algorithms used, techniques for data balancing, data augmentation, and methods for handling missing values. To address class imbalance in this study, we applied the synthetic minority oversampling technique algorithm to increase the proportion of fall cases from 2.6% to 20%. While this approach improved model training, it may have altered the underlying data distribution and could lead to overestimation of predicted probabilities for the minority class (fall incidents). Therefore, such artificial balancing should be interpreted with caution, as it may introduce inherent bias into model performance metrics and clinical applicability. In comparing the models in this study, boosting algorithms exhibited a slight advantage over LR, likely due to their ability to capture the complexity of fall predictions more effectively. Although the existing literature on calibration is limited, the event incidence observed in each risk layer fell within the predicted probability ranges (low, middle, high, and very high), suggesting that appropriate risk stratification for falls was achieved. When evaluating the model utility, poor calibration can lead to overestimation or underestimation of risk, which poses substantial concern [29]. In clinical settings, overestimating fall risk could lead to inefficient allocation of nursing resources, potentially diverting attention from patients

XSL•FO
RenderX

truly at high risk, whereas underestimating risk may delay preventive interventions and increase adverse outcomes. Therefore, calibration is particularly important when predicted probabilities are linked to intervention thresholds or staffing decisions. The LGBM model developed in this study demonstrated reasonable calibration, as shown in the calibration plot, effectively mitigating the risk of overestimation and underestimation. Among the 4 models evaluated in this study, the boosting models exhibited good performance. Specifically, CatBoost proved more effective for discrimination, whereas LGBM was most suitable for calibration. In clinical application, the choice between models should depend on the intended use. Miscalibration may result in inefficient allocation of nursing resources or delayed preventive interventions, underscoring the importance of calibration when predicted probabilities are directly linked to intervention thresholds or staffing decisions. For scenarios where intervention thresholds are defined by predicted probabilities, a well-calibrated model such as LGBM may be preferable. In contrast, when resources are limited and identifying the highest-risk patients is the priority, CatBoost may be more advantageous. Future studies could also explore ensemble approaches that combine both strengths. Practical integration of the model into the electronic health record could allow nurses to view individualized fall risk scores in real time, and predefined thresholds could trigger tailored preventive interventions (eg, increased observation, assistance with toileting, or targeted rehabilitation exercises). Future prospective studies are needed to determine the optimal threshold settings and evaluate their impact on clinical outcomes. However, research on more precise calibration algorithms that use neural networks is ongoing, and the application of these methods could offer further improvements [30].

The key features identified in this study include decreased serum albumin levels, limitations in ADL, and the use of sedative-hypnotic medications, all of which are consistent with findings of previous reports [31]. Additionally, changes in gait, impaired balance, history of falls, muscle weakness, and polypharmacy have been identified as significant factors contributing to falls. These factors overlap with certain abnormalities in locomotive frailty, highlighting the importance of comprehensive assessment of nutritional status and ADL [32]. Importantly, these high-impact features are clinically modifiable to varying degrees. For example, low albumin levels may be addressed through nutritional supplementation, protein-enriched diets, and early mobilization programs. Impaired ADL, particularly transfer ability, could be targeted with physiotherapy and environmental adjustments to reduce mobility-related hazards. For patients receiving sedative-hypnotics or antidiabetic drugs, careful medication review, dose adjustment, or substitution should be considered to minimize adverse effects (eg, dizziness or hypoglycemia). Integrating these targeted interventions into clinical workflows could help translate model outputs into personalized fall-prevention strategies. From a pharmacological perspective, sedative medications and diabetes treatments have been identified as significant contributors to fall risk. Several studies have consistently reported that antipsychotics, antidepressants, and benzodiazepines are associated with a high risk of falls across [4]. Moreover, hypoglycemia and hyperglycemia during diabetes treatment increase the risk of falls in hospitalized patients. Abnormal blood glucose levels (either <70 mg/dL or >200 mg/dL) are associated with an increased risk of falls, and treatment with insulin or oral hypoglycemic agents is considered a contributing factor [33]. Patients with diabetes often present multiple comorbidities that can increase the risk of polypharmacy, further increasing the likelihood of falls [34,35]. These findings underscore the need for a comprehensive approach to reduce the risk of falls.

Toileting-related falls accounted for a significant percentage of the incidents (49.2%), particularly during the night. Nighttime toileting has been reported to be a significant risk factor, especially when associated with intravenous fluid infusion, history of falls, visual impairment, and gait instability [36]. The high frequency of falls occurring during transfer from beds or chairs to toilets supports these findings [37]. It has also been noted that the urge to urinate can increase walking speed and stride length, thereby heightening the risk of falls. This effect is closely related to the severity of urinary incontinence, and gait is strongly associated with complex cognitive functions. As cognitive function declines, executive function is also impaired, which can lead to abnormal gait patterns [38]. Additionally, the use of sleeping medications should be considered another factor contributing to toileting-related falls. These sleeping medications can impair reaction speed upon awakening in older adults, potentially affecting balance and muscle control [39,40]. Benzodiazepines and other sedatives have been shown to cause dizziness during nighttime awakening, further increasing the risk of falling during toilet-related activities. Therefore, it is essential to assess the use of sleeping medications and consider alternative drugs or dose reductions when necessary.

Limitations

This study has some limitations. First, as a retrospective study, the explanatory variables for the machine learning models were limited to those that could be easily collected from clinical data and had minimal missing values. Consequently, data such as fall history, vital signs, social factors, and implementation of fall-prevention measures were excluded. Second, because the study was conducted solely in medical facilities in Japan, the findings may not be generalizable to patients from other regions. Differences in health care delivery systems, patient demographics, and cultural practices related to fall prevention could influence the baseline risk and the effectiveness of prediction models. Therefore, future studies should validate the machine learning models using independent external data from hospitals in diverse geographic regions and health care systems, ideally in settings with different staffing models, resource availability, and fall-prevention protocols. Third, this study used only 4 machine learning algorithms (LR, XGB, LGBM, and CatBoost), whereas other algorithms, such as neural networks and support vector machines, may demonstrate superior predictive performance. Finally, the features used were limited to those available at the time of admission, and dynamic changes during hospitalization (eg, postoperative status, new-onset infections, and medication adjustments) were not considered. The absence of time-dependent variables, including repeated assessments of vital signs, mobility, nutritional status, and

XSL•FO
RenderX

mental state, may limit the ability of the model to capture short-term fluctuations in fall risk. Incorporating such dynamic patient data and continuous risk assessment throughout hospitalization could enable the development of models that more accurately reflect real-time risk and support timely, individualized preventive interventions. Future research integrating these factors, along with advanced transformer-based model architectures capable of capturing complex temporal and contextual relationships, may lead to more accurate and clinically useful prediction models [41].

Additionally, as with any machine learning approach, there is a potential risk of algorithmic bias, which may arise if certain patient subgroups (eg, older individuals, those with cognitive impairment, or those from resource-limited backgrounds) are underrepresented or systematically differ in predictor distributions. Such biases could inadvertently lead to unequal predictive performance across subpopulations, potentially exacerbating disparities in fall prevention efforts. Thus, future studies should include fairness assessment and bias mitigation strategies to ensure that prediction models are equitable and beneficial across all patient groups.

Conclusions

We developed a machine learning–based model for predicting inpatient fall risk and assessed its performance in terms of discrimination and calibration, achieving excellent calibration. SHAP analysis identified several factors associated with an increased risk of falls, including indicators of frailty and the use of sedatives, hypnotics, and diabetes medications. A detailed analysis of fall incidents revealed that toileting-related falls—particularly those occurring near the bedside during late-night and early morning hours—were prevalent. These findings underscore the importance of implementing preventive measures tailored to individual patient conditions and behaviors, such as mitigating risk during toilet transfers and maintaining balance upon awakening. We believe that these insights contribute to the development of more precise and effective fall-prevention strategies in hospitals.

Acknowledgments

The authors sincerely thank all the medical staff, technicians, medical engineers, nurses, pharmacists, and physicians at Nippon Medical School Hospital and Nippon Medical School Chiba Hokusoh Hospital for their dedicated care of patients. This work was supported by JSPS KAKENHI (grant 25K13474 to TN).

Data Availability

The datasets generated and analyzed during this study are not publicly available due to ethical restrictions and patient confidentiality concerns, as they contain sensitive information derived from Diagnosis Procedure Combination data and electronic medical records. However, deidentified data may be available from the corresponding author upon reasonable academic request and subject to approval by the institutional ethics committee.

Authors' Contributions

TN contributed to the conceptualization, methodology, investigation, original draft writing, and project administration. YK contributed to the conceptualization, methodology, investigation, review and editing of the manuscript, project administration, and funding acquisition. KM contributed to the methodology and review and editing of the manuscript. YM and NT contributed to the methodology and supervision. FY, HI, SS, AY, and MM contributed to data curation. KK, HJ, CK, YI, and HY contributed to conceptualization and supervision. All authors reviewed and approved the final version of the manuscript.

Conflicts of Interest

None declared.

Multimedia Appendix 1
The falls assessment tool, severity and nursing care needs scoring, baseline characteristics and missing data of the study population, and hyperparameter settings for machine learning models.
[DOCX File , 42 KB - medinform_v13i1e75958_app1.docx]

Multimedia Appendix 2
Top 30 most important features selected for model development.
[DOCX File , 206 KB - medinform_v13i1e75958_app2.docx]

References

1. Morello RT, Barker AL, Watts JJ, Haines T, Zavarsek SS, Hill KD, et al. The extra resource burden of in-hospital falls: a cost of falls study. Med J Aust 2015;203(9):367. [doi: 10.5694/mja15.00296] [Medline: 26510807]
2. WHO global report on falls prevention in older age. World Health Organization. 2008. URL: https://www.who.int/publications/i/item/9789241563536 [accessed 2025-10-13]

XSL•FO
RenderX

3. Zhao YL, Kim H. Older adult inpatient falls in acute care hospitals: intrinsic, extrinsic, and environmental factors. J Gerontol Nurs 2015;41(7):29-43; quiz 44. [doi: 10.3928/00989134-20150616-05] [Medline: 26126026]
4. Seppala LJ, Wermelink AMAT, de Vries M, Ploegmakers KJ, van de Glind EMM, Daams JG, et al. Fall-risk-increasing drugs: a systematic review and meta-analysis: II. Psychotropics. J Am Med Dir Assoc 2018;19(4):371.e11-371.e17. [doi: 10.1016/j.jamda.2017.12.098] [Medline: 29402652]
5. Deandrea S, Bravi F, Turati F, Lucenteforte E, La Vecchia C, Negri E. Risk factors for falls in older people in nursing homes and hospitals. A systematic review and meta-analysis. Arch Gerontol Geriatr 2013;56(3):407-415. [doi: 10.1016/j.archger.2012.12.006] [Medline: 23294998]
6. Ishida Y, Maeda K, Nonogaki T, Shimizu A, Yamanaka Y, Matsuyama R, et al. Malnutrition at admission predicts in-hospital falls in hospitalized older adults. Nutrients 2020;12(2):541 [FREE Full text] [doi: 10.3390/nu12020541] [Medline: 32093144]
7. Falls in older people: assessing risk and prevention. Clinical guideline CG161. National Institute for Health and Care Excellence (NICE). 2013. URL: https://www.nice.org.uk/guidance/cg161 [accessed 2025-10-24]
8. Learning from patient safety: falls prevention resources. National Health Service (NHS) Improvement. 2018. URL: https://www.england.nhs.uk/patient-safety/ [accessed 2025-10-24]
9. Preventing falls in the hospital. Brown Health University. 2010. URL: https://www.brownhealth.org/patients-visitors/safety-tips-patients-and-visitors/preventing-falls-hospital [accessed 2025-10-09]
10. Kim EAN, Mordiffi SZ, Bee WH, Devi K, Evans D. Evaluation of three fall-risk assessment tools in an acute care setting. J Adv Nurs 2007;60(4):427-435. [doi: 10.1111/j.1365-2648.2007.04419.x] [Medline: 17919164]
11. Aranda-Gallardo M, Morales-Asencio JM, Canca-Sanchez JC, Barrero-Sojo S, Perez-Jimenez C, Morales-Fernandez A, et al. Instruments for assessing the risk of falls in acute hospitalized patients: a systematic review and meta-analysis. BMC Health Serv Res 2013;13:122 [FREE Full text] [doi: 10.1186/1472-6963-13-122] [Medline: 23547708]
12. Boyle DK, Cramer E, Potter C, Staggs VS. Longitudinal association of registered nurse national nursing specialty certification and patient falls in acute care hospitals. Nurs Res 2015;64(4):291-299 [FREE Full text] [doi: 10.1097/NNR.0000000000000107] [Medline: 26049719]
13. Parsons R, Blythe RD, Cramb SM, McPhail SM. Inpatient fall prediction models: a scoping review. Gerontology 2023;69(1):14-29 [FREE Full text] [doi: 10.1159/000525727] [Medline: 35977533]
14. Nakanishi T, Ikeda T, Nakamura T, Yamanouchi Y, Chikamoto A, Usuku K. Development of an algorithm for assessing fall risk in a Japanese inpatient population. Sci Rep 2021;11(1):17993 [FREE Full text] [doi: 10.1038/s41598-021-97483-1] [Medline: 34504235]
15. Kawazoe Y, Shimamoto K, Shibata D, Shinohara E, Kawaguchi H, Yamamoto T. Impact of a clinical text-based fall prediction model on preventing extended hospital stays for elderly inpatients: model development and performance evaluation. JMIR Med Inform 2022;10(7):e37913 [FREE Full text] [doi: 10.2196/37913] [Medline: 35896017]
16. Tago M, Katsuki NE, Oda Y, Nakatani E, Sugioka T, Yamashita S. New predictive models for falls among inpatients using public ADL scale in Japan: a retrospective observational study of 7,858 patients in acute care setting. PLoS One 2020;15(7):e0236130 [FREE Full text] [doi: 10.1371/journal.pone.0236130] [Medline: 32673366]
17. Hyohdoh Y, Hiyama M, Hatakeyama Y, Okuhara Y. Effect of mild hyponatremia on in-hospital falls of elderly hospitalized patients: a retrospective, cohort study. Arch Gerontol Geriatr 2024;118:105315. [doi: 10.1016/j.archger.2023.105315] [Medline: 38128267]
18. No authors listed. TRIPOD+AI statement: updated guidance for reporting clinical prediction models that use regression or machine learning methods. BMJ 2024;385:q902 [FREE Full text] [doi: 10.1136/bmj.q902] [Medline: 38636956]
19. Hayashida K, Murakami G, Matsuda S, Fushimi K. History and profile of Diagnosis Procedure Combination (DPC): development of a real data collection system for acute inpatient care in Japan. J Epidemiol 2021;31(1):1-11 [FREE Full text] [doi: 10.2188/jea.JE20200288] [Medline: 33012777]
20. Dong W, Fong DYT, Yoon J, Wan EYF, Bedford LE, Tang EHM, et al. Generative adversarial networks for imputing missing data for big data clinical research. BMC Med Res Methodol 2021;21(1):78 [FREE Full text] [doi: 10.1186/s12874-021-01272-3] [Medline: 33879090]
21. Waljee AK, Mukherjee A, Singal AG, Zhang Y, Warren J, Balis U, et al. Comparison of imputation methods for missing laboratory data in medicine. BMJ Open 2013;3(8):e002847 [FREE Full text] [doi: 10.1136/bmjopen-2013-002847] [Medline: 23906948]
22. Chen T, Guestrin C. XGBoost: a scalable tree boosting system. 2016 Presented at: KDD '16: Proceedings of the 22nd ACM SIGKDD International Conference on Knowledge Discovery and Data Mining (KDD 2016); August 13-17, 2016; San Francisco, CA, United States p. 785-794. [doi: 10.1145/2939672.2939785]
23. Ke G, Meng Q, Finley T, Wang T, Chen W, Ma W, et al. LightGBM: a highly efficient gradient boosting decision tree. 2017 Presented at: 31st Conference on Neural Information Processing Systems (NIPS 2017); December 4-9, 2017; Long Beach, CA, United States p. 3146-3154 URL: https://proceedings.neurips.cc/paper_files/paper/2017/file/6449f44a102fde848669bdd9eb6b76fa-Paper.pdf
24. Dorogush A, Eershov V, Gulin A. CatBoost: gradient boosting with categorical features support. ArXiv Preprint posted online on October 24, 2018. [doi: 10.48550/arXiv.1810.11363]

XSL•FO
RenderX

25. Chawla NV, Bowyer KW, Hall LO, Kegelmeyer WP. SMOTE: synthetic minority over-sampling technique. J Artif Intell Res 2002;16:321-357. [doi: 10.1613/jair.953]
26. Akiba T, Sano S, Yanase T. Optuna: a next-generation hyperparameter optimization framework. 2019 Presented at: KDD '19: Proceedings of the 25th ACM SIGKDD International Conference on Knowledge Discovery & Data Mining; August 4-8, 2019; Anchorage, AK, United States p. 2623-2631. [doi: 10.1145/3292500.3330701]
27. Zadrozny B, Elkan C. Transforming classifier scores into accurate multiclass probability estimates. 2002 Presented at: KDD '02: Proceedings of the Eighth ACM SIGKDD International Conference on Knowledge Discovery and Data Mining; July 23-26, 2002; Edmonton, Alberta, Canada p. 694-699. [doi: 10.1145/775047.775151]
28. Lundberg S, Lee S. A unified approach to interpreting model predictions. 2017 Presented at: NIPS'17: Proceedings of the 31st International Conference on Neural Information Processing Systems; December 4-9, 2017; Long Beach, CA, United States p. 4768-4777 URL: https://dl.acm.org/doi/10.5555/3295222.3295230 [doi: 10.5555/3295222.3295230]
29. Alba AC, Agoritsas T, Walsh M, Hanna S, Iorio A, Devereaux PJ, et al. Discrimination and calibration of clinical prediction models: users' guides to the medical literature. JAMA 2017;318(14):1377-1384. [doi: 10.1001/jama.2017.12126] [Medline: 29049590]
30. Guo C, Pleiss G, Sun Y, Weinberger KQ. On calibration of modern neural networks. 2017 Presented at: Proceedings of the 34th International Conference on Machine Learning (ICML 2017); August 6-11, 2017; Sydney, New South Wales, Australia p. 1321-1330 URL: https://dl.acm.org/doi/10.5555/3305381.3305518 [doi: 10.5555/3305381.3305518]
31. Tinetti ME, Kumar C. The patient who falls: "It's always a trade-off". JAMA 2010;303(3):258-266 [FREE Full text] [doi: 10.1001/jama.2009.2024] [Medline: 20085954]
32. Lan X, Li H, Wang Z, Chen Y. Frailty as a predictor of future falls in hospitalized patients: a systematic review and meta-analysis. Geriatr Nurs 2020;41(2):69-74. [doi: 10.1016/j.gerinurse.2019.01.004] [Medline: 30765177]
33. Berra C, De Fazio F, Azzolini E, Albini M, Zangrandi F, Mirani M, et al. Hypoglycemia and hyperglycemia are risk factors for falls in the hospital population. Acta Diabetol 2019;56(8):931-938. [doi: 10.1007/s00592-019-01323-8] [Medline: 30929079]
34. Horii T, Iwasawa M, Kabeya Y, Atuda K. Polypharmacy and oral antidiabetic treatment for type 2 diabetes characterised by drug class and patient characteristics: a Japanese database analysis. Sci Rep 2019;9(1):12992 [FREE Full text] [doi: 10.1038/s41598-019-49424-2] [Medline: 31506542]
35. Kuribayashi R, Hasebe S, Ishida D, Hirose S, Mimori S, Takizawa T, et al. An age-stratified cross-sectional study of antidiabetic and non-antidiabetic drugs prescribed to Japanese outpatients with diabetes. Glob Health Med 2023;5(5):294-300 [FREE Full text] [doi: 10.35772/ghm.2023.01059] [Medline: 37908508]
36. Decalf V, Bower W, Rose G, Petrovic M, Pieters R, Eeckloo K, et al. Prevalence and characteristics of incident falls related to nocturnal toileting in hospitalized patients. Acta Clin Belg 2021;76(2):85-90. [doi: 10.1080/17843286.2019.1660022] [Medline: 31478467]
37. Tzeng H. Understanding the prevalence of inpatient falls associated with toileting in adult acute care settings. J Nurs Care Qual 2010;25(1):22-30. [doi: 10.1097/NCQ.0b013e3181afa321] [Medline: 19553863]
38. Zou M, Lu R, Jiang Y, Liu P, Tian B, Liang Y, et al. Association between toileting and falls in older adults admitted to the emergency department and hospitalised: a cross-sectional study. BMJ Open 2023;13(6):e065544 [FREE Full text] [doi: 10.1136/bmjopen-2022-065544] [Medline: 37263694]
39. Kobayashi K, Ando K, Nakashima H, Suzuki Y, Nagao Y, Imagama S. Relationship between use of sleep medication and accidental falls during hospitalization. Nagoya J Med Sci 2021;83(4):851-860 [FREE Full text] [doi: 10.18999/nagjms.83.4.851] [Medline: 34916727]
40. Anyfanti P, Malliora A, Chionidou A, Mastrogiannis K, Lazaridis A, Gkaliagkousi E. Clinical significance of nocturnal hypertension and nighttime blood pressure dipping in hypertension. Curr Hypertens Rep 2024;26(2):69-80. [doi: 10.1007/s11906-023-01277-x] [Medline: 37906342]
41. Wen Q, Zhou T, Zhang C, Chen W, Ma Z, Yan J, et al. Transformers in time series: a survey. ArXiv Preprint posted online on May 11, 2023 [FREE Full text]

Abbreviations

ADL: activities of daily living
CatBoost: categorical boosting
LGBM: light gradient boosting machine
LR: logistic regression
PRAUC: area under the precision-recall curve
ROAUC: area under the receiver operating characteristic curve
SHAP: Shapley Additive Explanations
TRIPOD: Transparent Reporting of a Multivariable Prediction Model for Individual Prognosis or Diagnosis
VIF: variance inflation factor
XGB: extreme gradient boosting

XSL•FO
RenderX

Edited by A Benis; submitted 11.05.25; peer-reviewed by M Moon, W Wei, T Yusuff; comments to author 11.08.25; revised version received 27.08.25; accepted 06.10.25; published 04.12.25.

Please cite as:
Nishino T, Matsuyama K, Miyagi Y, Tanabe N, Yamaguchi F, Ito H, Soh S, Yano A, Mizuno M, Kato K, Jinnouchi H, Kim C, Ishii Y, Yamaguchi H, Kondo Y
Machine Learning–Based Prediction of In-Hospital Falls in Adult Inpatients: Retrospective Observational Multicenter Study
JMIR Med Inform 2025;13:e75958
URL: https://medinform.jmir.org/2025/1/e75958
doi:10.2196/75958
PMID:

©Takuya Nishino, Kotone Matsuyama, Yasuo Miyagi, Nari Tanabe, Fumiko Yamaguchi, Hiroki Ito, Shizuka Soh, Ayako Yano, Masako Mizuno, Katsuhito Kato, Hiroshige Jinnouchi, Chol Kim, Yosuke Ishii, Hiroki Yamaguchi, Yukihiro Kondo. Originally published in JMIR Medical Informatics (https://medinform.jmir.org), 04.12.2025. This is an open-access article distributed under the terms of the Creative Commons Attribution License (https://creativecommons.org/licenses/by/4.0/), which permits unrestricted use, distribution, and reproduction in any medium, provided the original work, first published in JMIR Medical Informatics, is properly cited. The complete bibliographic information, a link to the original publication on https://medinform.jmir.org/, as well as this copyright and license information must be included.

XSL•FO
RenderX

Original Paper

Online Clinical Calculator for Predicting 28-Day Mortality in Older Adult Patients With Sepsis-Associated Encephalopathy: Retrospective Study Using MIMIC-IV

Guangyong Jin[1,2*], MD; Menglu Zhou[3*], MD; Jiayi Chen[1,2*], MD; Mengyuan Diao[1*], MD, PhD; Wei Hu[1], MD

[1]Department of Critical Care Medicine, Affiliated Hangzhou First People's Hospital, School of Medicine, Westlake University, Hangzhou, China

[2]Department of Critical Care Medicine, Hangzhou Geriatric Hospital, Hangzhou, China

[3]Department of Rehabilitation, Affiliated Hangzhou First People's Hospital, School of Medicine, Westlake University, Hangzhou, China

[*]these authors contributed equally

Corresponding Author:
Wei Hu, MD
Department of Critical Care Medicine
Affiliated Hangzhou First People's Hospital, School of Medicine, Westlake University
No.261, Huansha Road, Hangzhou, Zhejiang 310006 China
Hangzhou, 310006
China
Phone: 86 13750890929
Email: huwei@hospital.westlake.edu.cn

Abstract

Background: Sepsis-associated encephalopathy (SAE) represents a critical complication of sepsis, especially among older adults. Despite its clinical relevance, there remains a lack of accessible and practical tools specifically designed to predict 28-day mortality in this vulnerable population.

Objective: We aimed to enhance the practical applicability of the model by creating a web-based tool that allows real-time, individualized mortality risk prediction, facilitating early intervention and informed decision-making in clinical practice.

Methods: Using data extracted from the MIMIC-IV (Medical Information Mart for Intensive Care IV) database, we identified older patients (≥65 years) with SAE (n=2165) and divided them into a development cohort (n=1531) and a validation cohort (n=634). Key risk factors associated with 28-day mortality were identified, and a predictive nomogram was constructed. Model performance was evaluated using the concordance index, integrated discrimination improvement, net reclassification index, and calibration curve analysis. Clinical applicability was assessed through decision curve analysis and benchmarked against traditional intensive care unit (ICU) scoring systems. Furthermore, the nomogram was deployed as a web-based application, enabling clinicians to input data and generate individualized mortality predictions.

Results: A total of 2165 older patients with SAE were included, among whom 290 (13.4%) died within 28 days of ICU admission. Multivariable logistic regression identified lower body weight (odds ratio [OR] 0.985, 95% CI 0.975-0.994; *P*=.001), lower systolic blood pressure (OR 0.972, 95% CI 0.957-0.986; *P*<.001), lower hemoglobin (OR 0.984, 95% CI 0.974-0.995; *P*=.005), lower PaO2 (OR 0.996, 95% CI 0.994-0.997; *P*<.001), and lower Glasgow Coma Scale score (OR 0.825, 95% CI 0.786-0.864; *P*<.001) as mortality risk factors. Higher respiratory rate (OR 1.083, 95% CI 1.029-1.141; *P*=.002), increased anion gap (OR 1.081, 95% CI 1.031-1.135; *P*=.001), elevated blood urea nitrogen (OR 1.045, 95% CI 1.016-1.076; *P*=.002), prolonged partial thromboplastin time (OR 1.033, 95% CI 1.016-1.050; *P*<.001), and reduced urine output (OR>0.99, 95% CI 0.999-1.000; *P*=.002) were also predictive. Patients admitted to "other" ICU types had lower mortality compared with the medical ICU reference group (OR 0.327, 95% CI 0.176-0.609; *P*<.001). The nomogram achieved concordance index values of 0.899 (development) and 0.897 (validation), outperforming sequential organ failure assessment (0.692), Acute Physiology Score III (0.804), Logistic Organ Dysfunction System (0.771), Simplified Acute Physiology Score II (0.704), and Oxford Acute Severity of Illness Score (0.753), with significant integrated discrimination improvement and net reclassification index improvements (all *P*<.001). Calibration curves confirmed good agreement between predicted and observed outcomes, while decision curve analysis supported the model's superior clinical utility.

XSL•FO
RenderX

Conclusions: This study presents a novel, validated nomogram for predicting 28-day mortality in older patients with SAE, integrating routinely available clinical data. The deployment of the model as a digital tool enhances its accessibility and usability, providing clinicians with a practical resource for risk stratification and individualized patient management.

(JMIR Med Inform 2025;13:e76417) doi:10.2196/76417

KEYWORDS

clinical prediction model; geriatrics; intensive care unit; outcome assessment; sepsis-associated encephalopathy

Introduction

Sepsis stands as a prevalent critical condition encountered within intensive care units (ICUs), presenting a formidable obstacle to global health care systems [1,2]. Characterized by diffuse cerebral dysfunction devoid of direct central nervous system infection or structural anomalies, sepsis-associated encephalopathy (SAE) emerges as a significant complication of sepsis [3]. The escalating global phenomenon of population aging has further accentuated the burden of sepsis [4-6], with a disproportionately heightened incidence observed among the older adult demographic [7]. Advanced age, in itself, emerges as an independent predictor of sepsis mortality, with older adult nonsurvivors succumbing earlier during hospitalization compared to their younger counterparts [7]. Nevertheless, older adult survivors of sepsis frequently necessitate specialized nursing or rehabilitative care post discharge [7]. Moreover, within the realm of older adult sepsis patients, the risk of developing SAE amplifies with advancing age, concomitantly exacerbating prognosis [6]. Precise prognostication of older adult patients with SAE holds paramount importance, facilitating risk stratification, fostering effective doctor-patient communication, and guiding clinical decision-making and therapeutic interventions.

The mortality prediction model, as a fundamental prognostic tool, epitomizes a distinct subset within clinical prediction models. Operating on the principle of predicting the unknown through the known, these models embody mathematical formulations wherein known variables are leveraged to compute the probability of an unforeseen outcome [8,9]. Central to the efficacy of such models lie the predictive variables, which serve as the bedrock for their construction [10]. When deliberating variable selection, considerations spanning economic feasibility, standardization, and accessibility necessitate careful scrutiny [10]. Conventional clinical parameters and hematological indices emerge as prime candidates for inclusion, owing to their cost-effectiveness, standardized measurement protocols, and ease of acquisition, thus positioning them as pivotal elements in the construction of robust clinical prediction models.

While several predictive models have been devised to anticipate mortality rates in cases of SAE [11-14], the development of such models tailored specifically for the older adult cohort remains, to the best of our knowledge, unprecedented. Therefore, this study aimed to develop and validate a clinically useful nomogram based on readily available clinical data from the MIMIC-IV (Medical Information Mart for Intensive Care IV) database. Additionally, we aimed to enhance the practical applicability of the model by creating a web-based tool that allows real-time, individualized mortality risk prediction, facilitating early intervention and informed decision-making in clinical practice.

Methods

Database

In adherence to the TRIPOD (Transparent Reporting of a Multivariable Prediction Model for Individual Prognosis or Diagnosis) guidelines [9], this retrospective investigation harnessed data derived from the MIMIC-IV database, version 2.1, for the purpose of clinical predictive model development. MIMIC-IV serves as a repository for an extensive array of clinical data sourced from tens of thousands of patients treated at the Beth Israel Deaconess Medical Center in Boston, Massachusetts, encompassing a spectrum of vital signs, hematological parameters, and therapeutic interventions [15]. The primary investigator has undergone requisite human research training (certificate number 46141344) and has executed a PhysioNet-certified health data usage agreement, thereby obtaining authorized access to the MIMIC-IV database.

Ethical Considerations

The Institutional Review Committee at Beth Israel Deaconess Medical Center meticulously scrutinized the process of patient data collection and the establishment of the MIMIC (Medical Information Mart for Intensive Care) database [16]. Subsequently, the committee accorded an exemption from the requirement of obtaining informed consent and provided explicit approval for the dissemination of data as per the predefined data sharing protocol. In adherence to stringent privacy standards, a randomized cipher was used to substitute patient identifiers, thereby generating deidentified integer codes for patients, hospitalizations, and ICU admissions [16].

In accordance with prevailing national regulations governing research involving human subjects in life sciences and medicine, studies using human information data devoid of potential harm to individuals, sensitive personal details, or commercial interests may qualify for exemption from ethical review. Specifically, such exemptions apply to research endeavors using legally acquired public data or anonymized information. Our study satisfies the stipulated criteria for exemption from ethical review. Moreover, given the retrospective nature of our investigation, the requirement for individual informed consent has been waived in accordance with prevailing national regulations. No compensation was provided to participants.

Study Participants

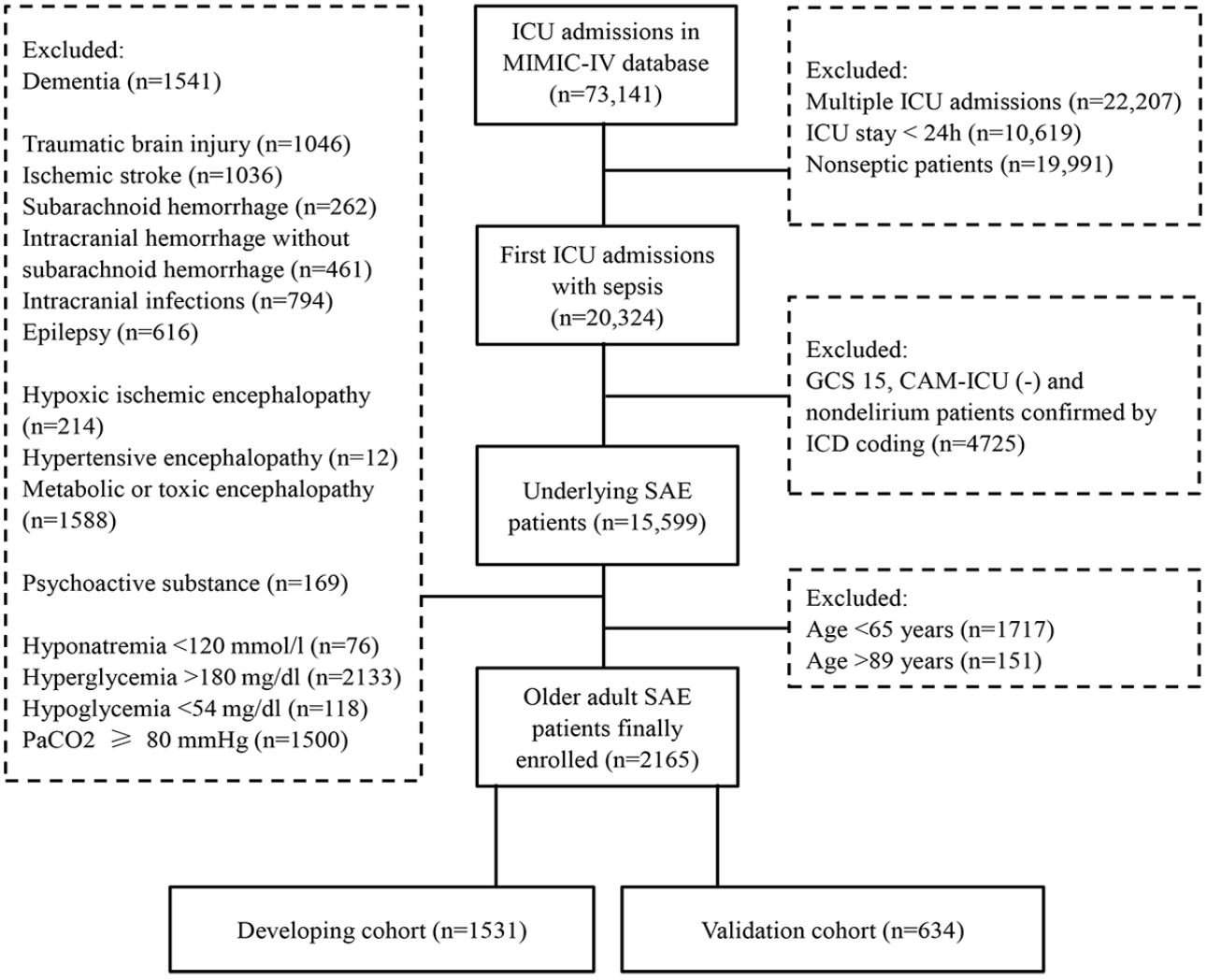
The study cohort comprises older adult patients with SAE undergoing their initial admission to the ICU. Inclusion criteria were ascertained as follows [3,6,11-14]: (1) patients classified

XSL•FO
RenderX

as sepsis 3.0, denoting those diagnosed or suspected of infection within the MIMIC database with a SOFA (sequential organ failure assessment) score of ≥2. The MIMIC code library provides comprehensive codes for sepsis determination [17]; (2) SAE identification criteria: sepsis patients were deemed to have SAE if they met any of the following conditions on the first day after ICU admission: Glasgow Coma Scale (GCS) score=15 points with delirium, or GCS score <15 points. Delirium was determined based on positive Confusion Assessment Method for the Intensive Care Unit, or confirmed *ICD* (*International Classification of Diseases*) codes (2930, 2931, F05); (3) older adult classification: patients aged between 65 and 89 years (MIMIC encodes patients older than 89 years as 91 for deidentification purposes).

Exclusion criteria were formulated based on prior investigations [11,13,14], comprising: (1) records indicating second or subsequent ICU admissions; (2) ICU duration less than 24 hours; (3) diagnosis of dementia; (4) primary brain injuries, inclusive of traumatic brain injury, ischemic stroke, subarachnoid hemorrhage, intracranial hemorrhage excluding subarachnoid hemorrhage, intracranial infections, and epilepsy; (5) hypoxic ischemic encephalopathy; (6) hypertensive encephalopathy; (7) metabolic or toxic encephalopathy; (8) mental and behavioral disorders attributed to alcohol, drug, or psychoactive substance usage, including delirium induced by opioids, cannabis, cocaine, sedatives, hallucinogens, or other psychoactive substances; (9) concurrent severe electrolyte or blood glucose disturbances, such as hyponatremia (<120 mmol/L), hyperglycemia (>180 mg/dl), or hypoglycemia (<54 mg/dl) and PaCO2 (partial pressure of CO2) ≥ 80 mm Hg. The process of cohort selection is outlined in Figure 1.

Figure 1. Diagrammatic illustration of the patient selection protocol. CAM-ICU: Confusion Assessment Method for the Intensive Care Unit; GCS: Glasgow Coma Scale; ICD: International Classification of Diseases; ICU: intensive care unit; MIMIC-IV: Medical Information Mart for Intensive Care IV; PaCO2: partial pressure of CO2; SAE: sepsis-associated encephalopathy.



Data Extraction and Preparation

Data preparation and statistical processing in this study closely mirror methodologies used in our prior investigations [15,18]. Extracted research data encompass demographic particulars such as age, gender, weight, marital status, race, underlying medical conditions, and Charlson Comorbidity Index scores. Additionally, vital signs, pivotal laboratory parameters, use of

XSL•FO
RenderX

invasive mechanical ventilation, renal replacement therapy, administration of vasoactive agents, albumin infusion, GCS scores, and other critical care scoring metrics were captured on the inaugural day of ICU admission. Vasoactive drug use encompassed the administration of norepinephrine, adrenaline, dopamine, dobutamine, vasopressin, or milrinone. For variables measured multiple times on the initial day of ICU admission, MIMIC concepts were used to derive minimum, maximum, and, if applicable, average values.

The primary end point of interest was the 28-day mortality, ascertained based on survival status 28 days post-ICU admission.

Preliminary dataset preparation entailed outlier management and handling of missing values, executed using Stata software (version 17.0, Stata Corporation LLC). As illustrated in Figure S1 of Multimedia Appendix 1, the extent of missingness for each variable was visualized using the *DataExplorer* package in R (version 4.3.2, R Foundation for Statistical Computing). Variables with more than 20% missing values were excluded from further analysis to ensure data quality. Initial outlier detection entailed histogram analysis to pinpoint anomalies within the dataset. Subsequent to identification, winsorization was used to mitigate outlier influence by replacing extreme values with thresholds established at the 0.1% and 99.9% quantiles using the Winsor2 command. Addressing missing data conundrums necessitated the application of diverse interpolation techniques to generate 5 sets of interpolated data. For variables with ≤20% missingness, multiple imputation was performed using Stata under the multivariate normal regression framework, as implemented by the command. The imputation model included all candidate predictor variables, relevant demographic characteristics, comorbidities, and severity scores to preserve associations among variables and reduce bias. Five imputed datasets were generated with 500 iterations of Markov Chain Monte Carlo data augmentation following a 100-iteration burn-in phase. Collinearity was checked before imputation, and variables causing collinearity were omitted automatically by Stata. Post imputation, 1 randomly selected dataset was extracted for subsequent analyses, following Rubin rules for ensuring consistency across imputations. Descriptive checks confirmed that imputed values were within plausible clinical ranges and maintained the overall distributional properties of the observed data.

Statistical Analysis

Statistical analyses were conducted using R software (version 4.3.2). The cohort of older adult patients with SAE was randomly partitioned into development and validation subsets at a ratio of 7:3, using a seed size of 73. Univariate analyses were performed on both the development and validation cohorts using the "gtsummary" software package. Continuous variables demonstrating nonnormal distribution were summarized using median and IQR, while categorical variables were presented as numerical counts or percentages. Statistical significance was defined as P value <.05.

In the development cohort, LASSO (least absolute shrinkage and selection operator) regression, facilitated by the "glmnet" R package, was used to identify potential variables associated with 28-day mortality in older adult patients with SAE. Subsequently, multiple-factor binary logistic regression was conducted to discern the final independent risk factors. The "car" R package was used to compute the variance inflation factor, assessing collinearity between variables. A prognostic nomogram was constructed using the "rms" R data package.

To evaluate the predictive performance of the nomogram, the "pROC" R package was used to calculate the concordance index (C-index), while the "PredictABEL" R software package facilitated computation of the integrated discrimination improvement (IDI) and net reclassification improvement (NRI). Receiver operating characteristic curves for both the development and validation datasets were generated using the "riskRegression" R package to assess model sensitivity and specificity across different probability thresholds. Calibration of the nomogram was assessed via generation of a calibration curve using the "val.prob" function within the "rms" R data package. Additionally, the Hosmer-Lemeshow goodness-of-fit test was performed using the "hoslem.test" function in the *ResourceSelection* R package to further evaluate model calibration. Subsequently, decision curve analysis was conducted using the "rmda" R data package to meticulously evaluate the clinical utility and benefits conferred by the developed nomogram. We deployed the developed predictive model as a web-based tool using the *Shiny* and *rsconnect* packages in R. This web-based application allows users to input patient-specific data and obtain an estimated probability of 28-day mortality, facilitating clinical utility and accessibility of the nomogram.

Results

Baseline Characteristics

A total of 2165 older adult patients with SAE were included, among whom 290 (13.4%) died within 28 days of ICU admission. Table S1 in Multimedia Appendix 2 offers a comprehensive summary of the baseline characteristics observed across the entire cohort of older adult patients with SAE, delineating findings from both the developmental cohort (n=1531) and the validation cohort (n=634). Following meticulous examination, no statistically significant differences (P>.05) were discerned in demographic attributes, comorbidities, indices of disease severity, vital signs, common hematological parameters, or therapeutic interventions between the development and validation cohorts. Notably, the absence of statistically significant distinctions underscores the efficacy of random allocation methodologies in ensuring comparability between cohorts, thus underscoring the robust scientific underpinnings guiding cohort allocation. Older adult patients with SAE were stratified into distinct survival and mortality groups based on their 28-day survival outcomes. Baseline comparisons between these groups within the development and validation cohorts are presented in the supplementary materials for comprehensive elucidation.

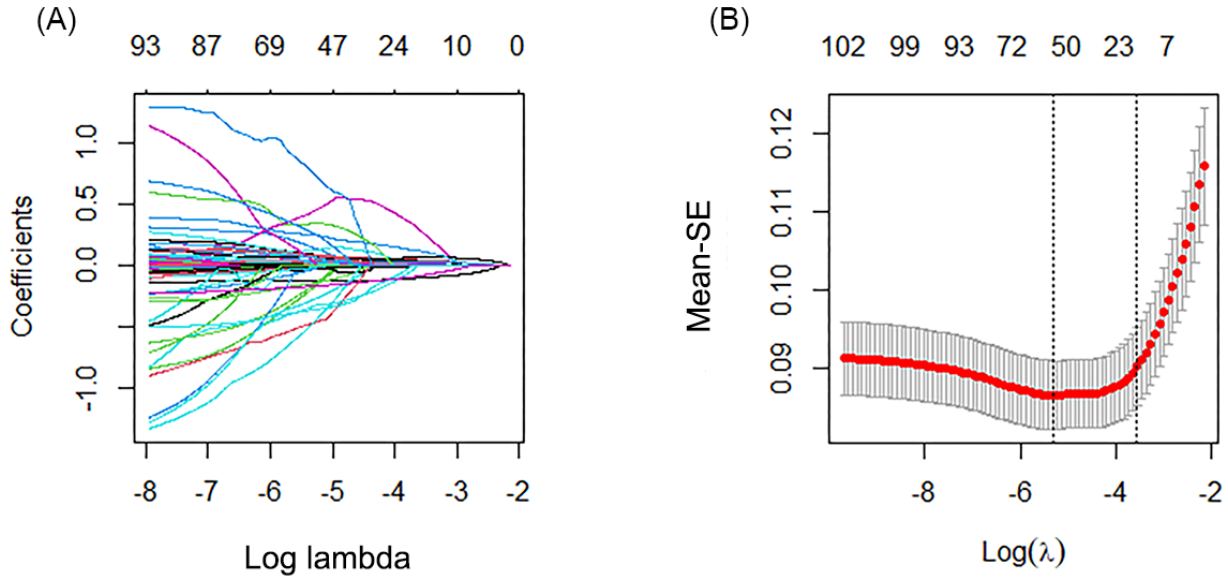
Variable Selection and Nomogram Construction

Using a hybrid approach of LASSO regression coupled with 10-fold cross-validation (Figure 2A and 2B), potential clinical determinants correlating with 28-day mortality in older adult patients with SAE were identified. Subsequent binary multivariate logistic regression analysis corroborated the

XSL•FO
RenderX

significance of 11 distinct clinical factors or hematological parameters as independent predictors of 28-day mortality within this cohort (P<.05; Table 1). All included predictors demonstrated acceptable collinearity, with variance inflation factor values presented in Multimedia Appendix 3 (Figure S1), confirming that multicollinearity did not compromise the stability of the regression model. These discerned variables were subsequently integrated to devise a prognostic nomogram (Figure 3).

Figure 2. LASSO regression-based feature selection process with tenfold cross-validation. (A) The plot illustrates the relationship between the coefficients of clinical features and lambda values within the LASSO regression framework. (B) The graph depicts the 10-fold cross-validation curve used in LASSO regression, offering insights into model selection. The left dashed vertical line indicates the optimal log (lambda) value (λ=0.004900582) corresponding to the minimum mean SE. Additionally, following the 1 SE rule, the right dashed vertical line represents the model incorporating 11 variables (λ=0.02870281). LASSO: least absolute shrinkage and selection operator regression.



XSL•FO
RenderX

Table 1. Multivariable logistic regression analysis reveals independent predictors of 28-day mortality in older adult patients with sepsis-associated encephalopathy: findings from the developmental cohort.

Variables	OR[a] (95% CI)	*P* value
Weight (kg)	0.985 (0.975-0.994)	.001
First care unit (SICU[b])	0.605 (0.305-1.177)	.14
First care unit (MICU[c]/SICU)	1.135 (0.635-2.033)	.67
First care unit (Neuro SICU[d])	0.567 (0.027-4.650)	.64
First care unit (TSICU[e])	0.683 (0.344-1.332)	.27
First care unit (Other)	0.327 (0.176-0.609)	<.001
SBP[f] (mm Hg)[g]	0.972 (0.957-0.986)	<.001
Respiratory rate (breaths/min)[g]	1.083 (1.029-1.141)	.002
First-day urine output (ml)	1.000 (0.999-1.000)	.002
Hemoglobin (g/l)[h]	0.984 (0.974-0.995)	.005
Anion gap (mmol/l)[h]	1.081 (1.031-1.135)	.001
Blood urea nitrogen (mg/dl)[i]	1.045 (1.016-1.076)	.002
PTT[j] (s)[i]	1.033 (1.016-1.050)	<.001
PaO2 (mm Hg)[h]	0.996 (0.994-0.997)	<.001
First-day GCS[i,k]	0.825 (0.786-0.864)	<.001

[a]OR: odds ratio.

[b]SICU: surgical intensive care unit.

[c]MICU: medical intensive care unit.

[d]Neuro SICU: neurosurgical intensive care unit.

[e]TSICU: trauma surgical intensive care unit.

[f]SBP: systolic blood pressure.

[g]Denotes the mean values of relevant indicators observed during the initial day of intensive care unit admission.

[h]Indicates the maximum values of clinical parameters recorded within the first day of intensive care unit admission.

[i]Represents the minimum recorded values of essential indicators observed on the initial day of admission to the intensive care unit.

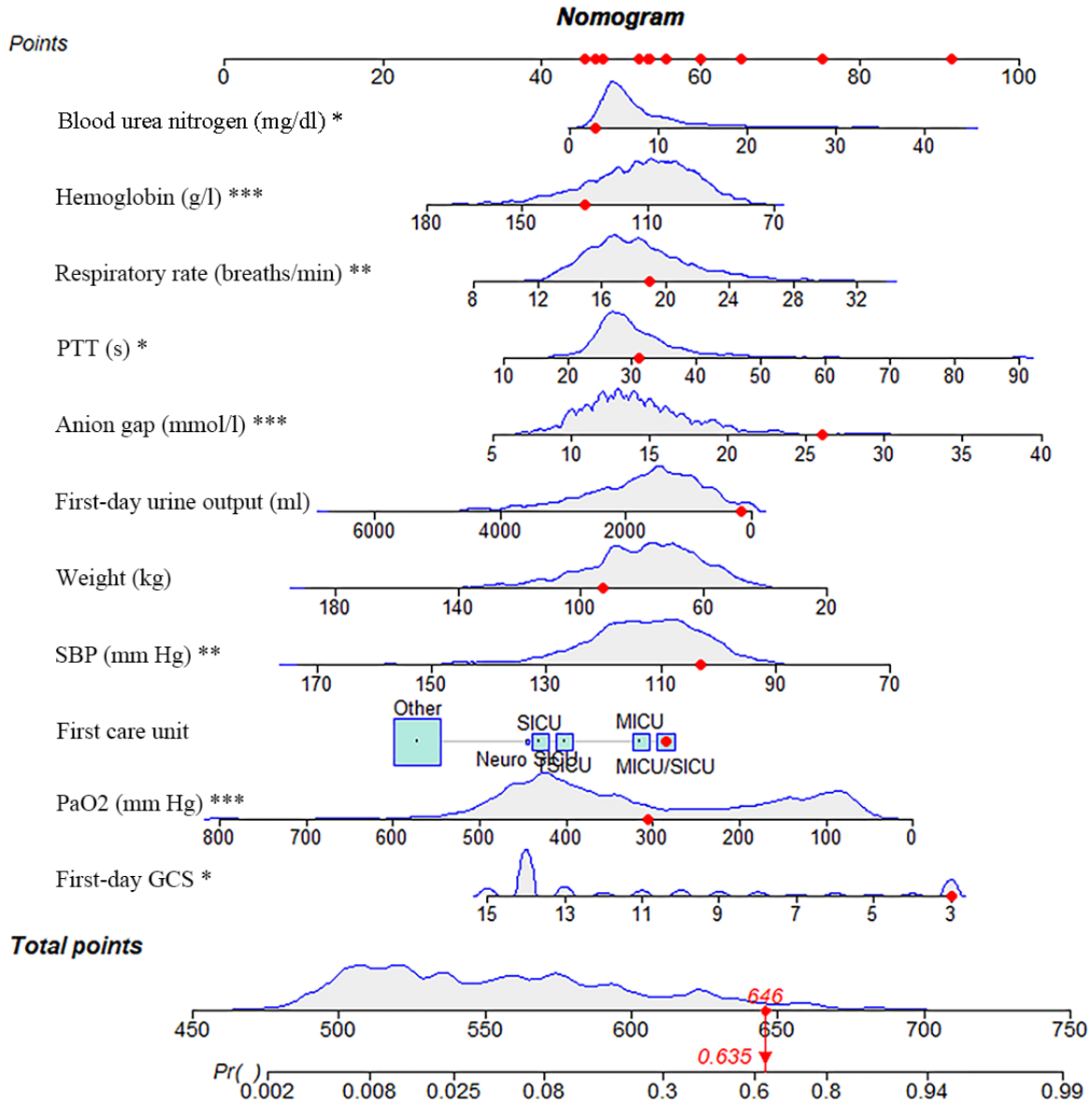
[j]PTT: partial thromboplastin time.

[k]GCS: Glasgow Coma Scale.

Figure 3 depicts a representative case: an older adult patient with SAE, weighing 93 kg, was admitted to the medical or surgical intensive care unit (SICU). On the initial day of admission, the patient exhibited the following clinical and hematological parameters: the lowest blood urea nitrogen level recorded was 2.86 mg/dl, the highest hemoglobin concentration was 130 g/l, the mean respiratory rate was 18.96 beats/min, the lowest partial thromboplastin time (PTT) was 31.1 seconds, the maximum anion gap (AG) was 26 mmol/L, the first day urine output was 185 ml, the average systolic blood pressure was 103.02 mm Hg, the highest partial pressure of arterial oxygen was 306 mm Hg, and the lowest GCS score was 3 points. Based on these findings, the cumulative score for this patient was calculated as 646 points, corresponding to a predicted 28-day mortality rate of 0.635.

XSL•FO
RenderX

Figure 3. Nomogram visualization for predicting 28-day mortality probability in geriatric patients with SAE. This graphical representation illustrates a nomogram tailored to estimate the likelihood of 28-day mortality among older adult individuals diagnosed with SAE. The nomogram operates by assigning points to specific variables based on their respective values. These points are then totaled, and the corresponding 28-day mortality rate can be determined by referencing the total points axis. This depiction elucidates the operational framework of the nomogram in forecasting personalized mortality risks for older adult patients with SAE. *Represents the minimum recorded values of essential indicators observed on the initial day of admission to the intensive care unit. **Indicates the mean values of clinical parameters recorded within the first day of intensive care unit admission. ***Denotes the maximum values of relevant indicators observed during the initial day of intensive care unit admission. GCS: Glasgow Coma Scale; MICU: medical intensive care unit; Neuro SICU: neurosurgical intensive care unit; PTT: partial thromboplastin time; SAE: sepsis-associated encephalopathy; SBP: systolic blood pressure; SICU: surgical intensive care unit; TSICU: trauma surgical intensive care unit.



Discriminative Performance and Calibration Assessment of Nomogram

The derived prognostic nomogram exhibited a calculated C-index of 0.899 (95% CI 0.877-0.921) in the development cohort and 0.897 (95% CI 0.864-0.929) in the validation cohort. Comparative analyses revealed that the discriminatory performance of the constructed nomogram surpassed conventional benchmarks, including GCS score and commonly used disease severity scoring systems (Table 2). Receiver operating characteristic curve analysis was also performed to assess model sensitivity and specificity across different thresholds, with the resulting curves for both the development and validation datasets presented in Figure S1 of Multimedia Appendix 4, further demonstrating the classification ability and clinical utility of the nomogram. Furthermore, evaluations using IDI and NRI metrics revealed substantial enhancements in the predictive accuracy of the devised nomogram for 28-day mortality (both P<.001; Table 3).

XSL•FO
RenderX

Table 2. Assessment of C-index[a] performance: nomogram versus models incorporating commonly used ICU[b] scoring systems for predicting 28-day mortality in geriatric patients with sepsis-associated encephalopathy.

Models	Development dataset, C-index (95% CI)	Validation dataset, C-index (95% CI)
Nomogram	0.899 (0.877-0.921)	0.897 (0.864-0.929)
GCS[c]	0.664 (0.626-0.702)	0.603 (0.537-0.668)
SOFA[d]	0.692 (0.652-0.732)	0.715 (0.654-0.776)
APS III[e]	0.804 (0.775-0.832)	0.783 (0.733-0.833)
LODS[f]	0.771 (0.736-0.806)	0.746 (0.686-0.806)
SAPS II[g]	0.704 (0.667-0.741)	0.718 (0.660-0.777)
OASIS[h]	0.753 (0.718-0.789)	0.741 (0.681-0.800)

[a]C-index: concordance index.
[b]ICU: intensive care unit.
[c]GCS: Glasgow Coma Scale.
[d]SOFA: sequential organ failure assessment.
[e]APS III: Acute Physiology Score III.
[f]LODS: Logistic Organ Dysfunction System.
[g]SAPS II: Simplified Acute Physiology Score II.
[h]OASIS: Oxford Acute Severity of Illness Score.

Table 3. Evaluation of NRI[a] and IDI[b] in predictive models for 28-day mortality among geriatric patients afflicted with sepsis-associated encephalopathy.

Index[c]	Development dataset		Validation dataset	
	Estimate (95% CI)	*P* value	Estimate (95% CI)	*P* value
NRI (vs GCS[d])	0.709 (0.624-0.795)	<.001	0.651 (0.531-0.771)	<.001
NRI (vs SOFA[e])	0.576 (0.487-0.666)	<.001	0.405 (0.267-0.543)	<.001
NRI (vs APS III[f])	0.398 (0.309-0.488)	<.001	0.339 (0.205-0.472)	<.001
NRI (vs LODS[g])	0.405 (0.309-0.501)	<.001	0.359 (0.213-0.506)	<.001
NRI (vs SAPS II[h])	0.585 (0.499-0.670)	<.001	0.570 (0.432-0.708)	<.001
NRI (vs OASIS[i])	0.435 (0.335-0.536)	<.001	0.346 (0.189-0.502)	<.001
IDI (vs GCS)	0.325 (0.289-0.361)	<.001	0.324 (0.268-0.379)	<.001
IDI (vs SOFA)	0.287 (0.252-0.321)	<.001	0.240 (0.191-0.288)	<.001
IDI (vs APS III)	0.183 (0.150-0.216)	<.001	0.186 (0.143-0.228)	<.001
IDI (vs LODS)	0.213 (0.178-0.247)	<.001	0.215 (0.160-0.269)	<.001
IDI (vs SAPS II)	0.293 (0.258-0.328)	<.001	0.271 (0.217-0.326)	<.001
IDI (vs OASIS)	0.240 (0.202-0.278)	<.001	0.226 (0.170-0.282)	<.001

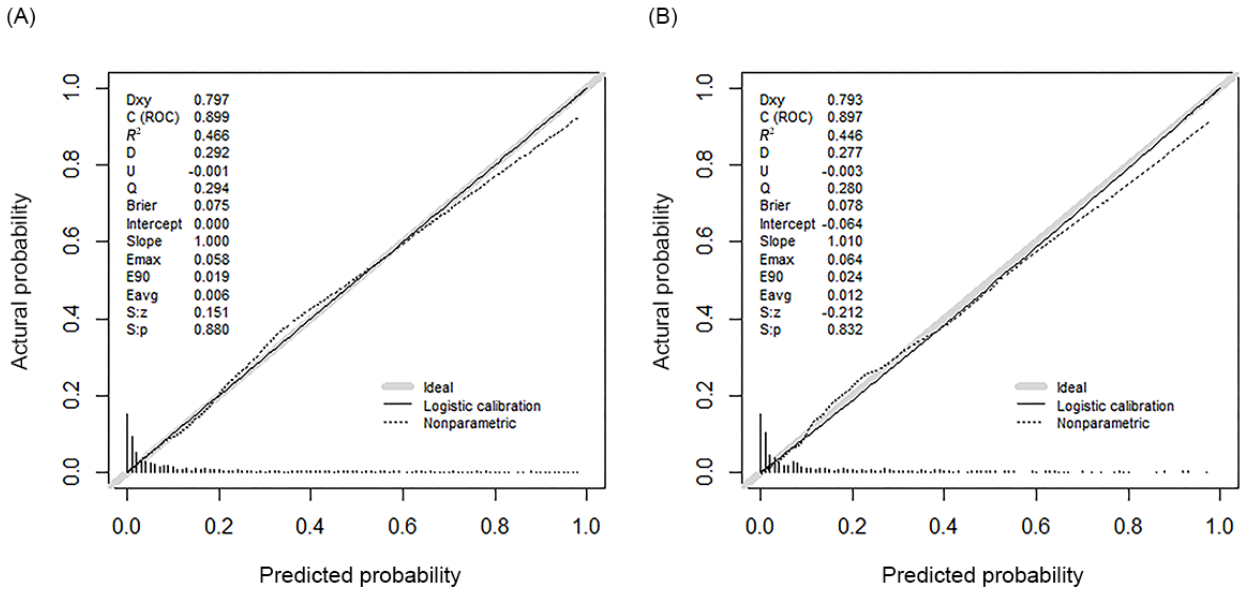
[a]NRI: net reclassification index.
[b]IDI: integrated discrimination improvement.
[c]Cutoff: 0, 0.2, 0.4, 1.
[d]GCS: Glasgow Coma Scale.
[e]SOFA: sequential organ failure assessment.
[f]APS III: Acute Physiology Score III.
[g]LODS: Logistic Organ Dysfunction System.
[h]SAPS II: Simplified Acute Physiology Score II.
[i]OASIS: Oxford Acute Severity of Illness Score.

Significantly, a striking resemblance between the anticipated and observed 28-day mortality rates was observed, with statistical analyses revealing no discernible differences within both the development and validation cohorts (Figure 4A and

XSL•FO
RenderX

4B). The Hosmer-Lemeshow goodness-of-fit test further confirmed adequate calibration of the nomogram, with nonsignificant results in both the development cohort (χ^2_8=4.6, *P*=.81) and the validation cohort (χ^2_8=8.7, *P*=.37), indicating no evidence of lack of fit.

Figure 4. Calibration curve assessing the predictive accuracy of the established nomogram for 28-day mortality. This calibration curve illustrates the alignment between predicted and observed 28-day mortality rates in both the (A) development and (B) validation sets. The lack of statistically significant differences (*P*>.05) indicates the robustness and reliability of the predictive model, affirming its accuracy in estimating mortality outcomes. C (ROC): concordance index (receiver operating characteristic curve); D: discrimination index; Dxy: rank correlation between predicted probabilities and observed values; E90: 90th percentile of the prediction error; Eavg: average error; Emax: maximum absolute error; Q: quality index; R2: Nagelkerke-Cox-Snell-Maddala-Magee R-squared index; S:p: the *P* value of Spiegelhalter z-test; S:z: The z-value of Spiegelhalter z-test; U: unreliability index.

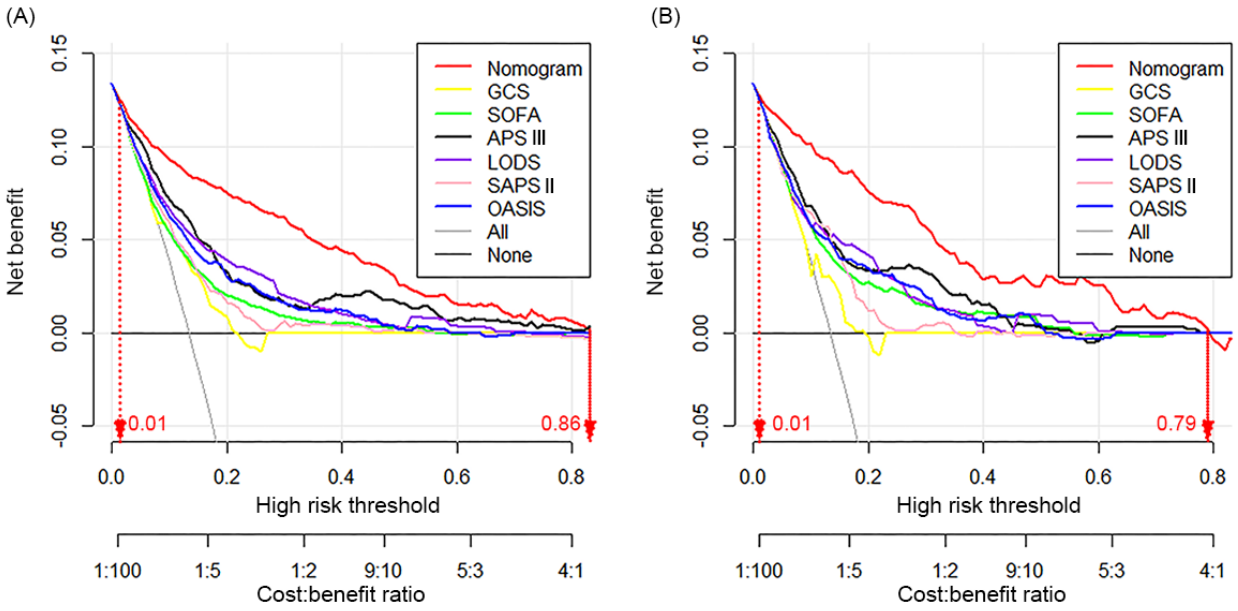


Evaluation of Nomogram Clinical Applicability in Predicting 28-Day Mortality in Older Adult Patients With SAE

As depicted in Figure 5, the graphical representation illustrates the pronounced net clinical benefit conferred by the developed nomogram, denoted by the red line, in comparison to established metrics such as the GCS score and widely used scoring systems. Across a probability threshold range of 0.01-0.86 in the development cohort and 0.01-0.79 in the validation cohort, the nomogram consistently demonstrated greater net benefit. Remarkably, our formulated nomogram demonstrates markedly heightened clinical effectiveness, underscoring its superior practical applicability and utility in prognostication relative to conventional scoring methodologies.

XSL•FO
RenderX

Figure 5. Evaluation of clinical utility through decision curve analysis: comparative assessment between the developed nomogram and established clinical scoring systems in the training and validation cohorts. Decision curve analysis is used to compare the clinical utility of the nomogram developed in this study with conventional clinical scoring systems in predicting outcomes. The red line represents the nomogram, which showed higher net benefit across the threshold ranges of 0.01-0.86 (training cohort) and 0.01-0.79 (validation cohort). APS III: Acute Physiology Score III; GCS: Glasgow Coma Score; LODS: Logistic Organ Dysfunction System; OASIS: Oxford Acute Severity of Illness Score; SAPS II: Simplified Acute Physiology Score II; SOFA: sequential organ failure assessment.



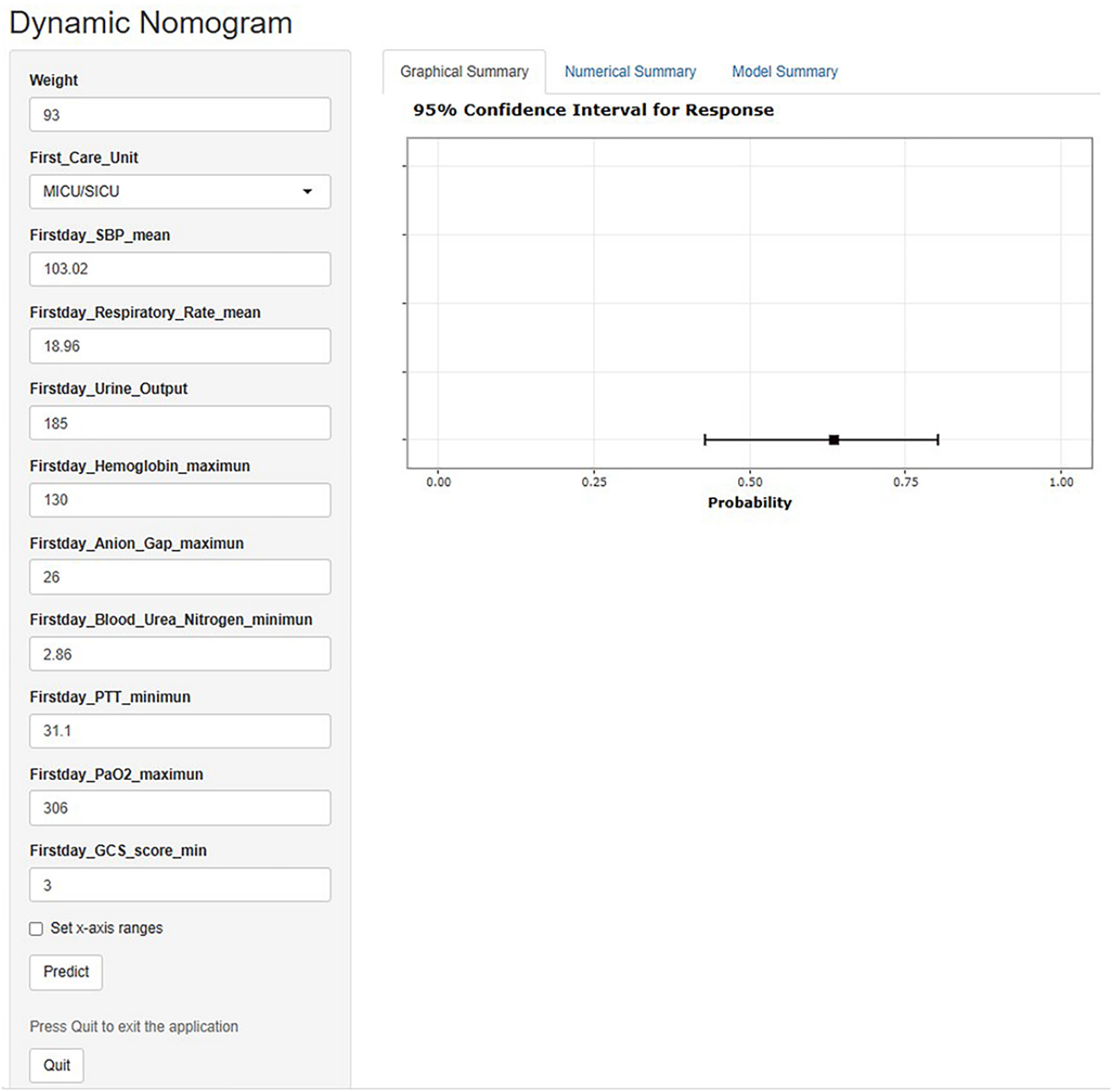
Deployment of the Web-Based Nomogram

To enhance clinical applicability, we deployed the developed nomogram as a web-based calculator using the *Shiny* and *rsconnect* packages in R. This web-based tool is accessible online [19]. Clinicians can input readily available clinical parameters to obtain an individualized estimate of 28-day mortality risk in older adult patients with SAE.

To illustrate the practical use of the web-based calculator, we applied the same patient case presented in Figure 3 to generate a predicted probability of 28-day mortality through the web interface (Figure 6). As shown in Figure 6, the model provides an intuitive visual output that complements the static nomogram, offering immediate clinical insight for bedside decision-making.

XSL•FO
RenderX

Figure 6. Web-based application demonstration using a representative patient case. GCS: Glasgow Coma Scale; MICU: medical intensive care unit; SBP: systolic blood pressure; SICU: surgical intensive care unit; PTT: partial thromboplastin time.



The web-based dynamic calculator interface for the 28-day mortality nomogram is shown. Clinical parameters from the same representative case in Figure 3 were entered into the web tool, generating an individualized prediction of 28-day mortality risk. The tool provides an intuitive output that enhances the model's accessibility and facilitates clinical application at the bedside.

Discussion

Principal Results

In the context of societal aging, precise evaluation of short-term prognosis among older adult patients with SAE becomes imperative. Regrettably, the current landscape lacks tailored clinical prediction models for this demographic subset. To our knowledge, our study marks the inaugural development and validation of a clinical prediction model meticulously crafted to forecast 28-day mortality rates in older adult patients with SAE. Moreover, the deployment of the nomogram as a web-based application enhances its accessibility and ease of use, offering real-time, individualized mortality risk assessments that can support decision-making in busy clinical settings.

Clinical prediction models for SAE have attracted increasing academic interest, with existing studies mainly focusing on 2 aspects: models predicting the occurrence of SAE and models predicting mortality among patients with SAE [11-14,20-23]. For example, a nomogram was constructed using 9 variables identified through multivariable regression analysis to predict the occurrence of SAE. However, it is noteworthy that the use of midazolam was also included as one of the predictive factors, which may be somewhat perplexing, because alterations in consciousness induced by midazolam require careful distinction

XSL•FO
RenderX

from those attributable to SAE [22]. Older adult populations have also received special attention, as SAE has been identified as an independent risk factor for in-hospital mortality among older adult ICU patients, and a nomogram has been established to predict the probability of SAE in this subgroup [21]. Machine learning methods have likewise been applied to SAE prediction, with 6 classifiers compared for their performance in predicting SAE occurrence. Among them, an Extreme Gradient Boosting–based model demonstrated superior predictive accuracy using simple clinical indicators while offering visual interpretability [23]. However, this model relied on predictors such as length of stay and ventilation duration [23]. In practice, such time-dependent indicators may only become available late in the hospitalization process, at which point SAE onset may already be apparent, thus limiting clinical utility.

Prediction models have also been developed for SAE-related mortality, using both nomograms and machine learning methods to estimate 30-day outcomes [11,13]. For instance, models using APS III (Acute Physiology Score III) and SOFA score as predictors have been reported [13], though their clinical applicability is hampered by the complexity of APS III calculation. More advanced machine learning approaches have even combined the 3 best-performing classifiers (elastic net, support vector machine, and Extreme Gradient Boosting) into a stacked ensemble model for predicting ICU mortality in patients with SAE. This model achieved an internal validation AUC of 0.807, but external validation revealed a reduced AUC of 0.671, raising concerns about generalizability and stability [20]. In comparison with extant clinical prediction models for SAE [11-14,20], our study shares a commonality in the inclusion of GCS scores and respiratory rate as key independent variables. This convergence offers novel avenues for future investigations into SAE-related prediction models. However, our investigation diverges by specifically targeting SAE mortality rates in the older adult population [11-14], leveraging the updated MIMIC-IV database. Notably, meticulous attention was devoted to refining inclusion and exclusion criteria for patients with SAE during data processing, ensuring the enrollment of cohorts with comprehensive data profiles and mitigating selection biases. Using the simplest supervised learning algorithm predicated on binary classification outcomes, our study used logistic regression, showcasing distinct advantages over alternative machine learning methodologies [8,24,25]. Notable benefits include a parsimonious model structure, robust fitting, and enhanced user-friendliness. Despite its simplicity, the nomogram devised in our study incorporates a select number of variables yet demonstrates commendable discriminative capacity. Furthermore, the nomogram's accessibility renders it amenable to integration into routine clinical practice, bolstering its utility in real-world health care settings.

Leveraging commonplace clinical data and hematological parameters sourced from the MIMIC-IV database, our model stands as a user-friendly tool poised to address this critical gap. Using LASSO regression for initial dimensionality reduction mitigates overfitting concerns and enhances model practicality and interpretability [26,27]. Logistic regression, a venerable statistical technique in clinical research, aids in identifying independent risk factors [28]. Our analysis pinpointed several variables, including type of first care unit, GCS score, weight, systolic blood pressure, respiratory rate, urine output, and hematological indices (blood urea nitrogen, hemoglobin, PTT, AG, and PaO2), as significant predictors. Evaluation metrics such as the C-index gauge predictive efficacy across development and validation cohorts [29], while NRI and IDI analyses highlight performance enhancements relative to conventional ICU scoring systems. Calibration curves attest to the alignment of predicted outcomes with actual observations. Furthermore, decision curve analysis underscores the superior practical utility and clinical decision-making benefits of our predictive model compared to existing scoring systems. Additionally, a user-friendly column chart has been devised for seamless clinical integration, thus facilitating wider adoption and dissemination of our model in clinical practice.

The GCS score stands as a pragmatic tool for clinical evaluation of consciousness impairment [30], serving as a cornerstone in defining SAE [6]. Even subtle alterations in mental status, such as GCS scores ranging from 13 to 14, independently correlate with mortality [31]. The prognosis of SAE may be intertwined with impaired brain autoregulation and inadequate cerebral perfusion. Continuous monitoring of cerebral blood oxygen levels via near-infrared spectroscopy enables delineation of the blood pressure range conducive to optimizing brain autoregulation, thereby enhancing cerebral perfusion in SAE [32]. The threshold for detrimental cerebral hypoperfusion manifests variably across individuals, and dysregulation in SAE may arise from blood pressure dipping below the optimal range [32]. Our findings align with this notion, indicating a detrimental association between lower blood pressure and poor prognosis in SAE. Additionally, respiratory rate, a fundamental vital sign, emerges as a pivotal indicator in emergency and critical care settings, exhibiting robust prognostic value in sepsis patients [33].

In terms of laboratory parameters incorporated into our model, blood urea nitrogen serves as a reflective indicator of renal function, in common with urine output. Sonneville et al [31], in a multicenter retrospective study, identified acute renal failure as a risk factor for SAE, attributing this association to biological alterations potentially impacting brain function, including severe acidosis and uremia. Additionally, diminished renal function may precipitate the accumulation of neurotoxic substances [31]. Notably, elevated blood urea nitrogen levels [13] and diminished urine output emerge as risk factors for short-term mortality in SAE, a conclusion echoed in our study among the older adult population. Hemoglobin levels, commonly used to assess the overall anemia status across diverse patient populations, and an investigation involving 8853 patients with SAE revealed that the ratio of hemoglobin to red blood cell distribution width offers enhanced prognostic value for ICU all-cause mortality in patients with SAE [34]. Moreover, activated PTT waveform analysis has been posited as an effective means to discern sepsis [35], with previous data indicating that coagulation abnormalities exacerbate mortality risk in sepsis patients [36]. Elevated activated PTT levels, indicative of coagulation dysregulation, have been closely associated with SAE mortality [14], corroborated by our findings within the older adult population. Hypoxemia presents a prevalent concern among

XSL•FO
RenderX

ICU patients, with its severity proving to be an independent predictor of mortality within this cohort [37]. Reduced oxygen saturation has emerged as a mortality risk factor in SAE [12], paralleling our assertion that diminished oxygenation index poses a risk to 28-day survival in older adult patients with SAE.

The type of initial care unit, AG, and body weight constitute 3 pivotal variables within our model. Previous studies have suggested that the introduction of specialized neurocritical care teams, including a dedicated full-time neurointensivist, is associated with significantly reduced in-hospital mortality and length of stay, although no effect was observed on readmission rates or long-term mortality [38]. Moreover, the presence of a neurointensivist has been linked to improved clinical outcomes, particularly among patients with aneurysmal subarachnoid hemorrhage, whereas patients with intracerebral hemorrhage often exhibit poor prognosis regardless of the availability of a neurointensive care unit or physician [39]. In our analysis, however, the type of ICU (including neurosurgical intensive care unit) did not appear to exert a strong influence on short-term mortality in older adult patients with SAE. However, existing mortality prediction models for SAE have not thoroughly explored the interplay between these factors, including the initial care unit type, and SAE [11-14], necessitating further inquiry in forthcoming high-quality investigations. Body weight influences lifespan, and notably, BMI exhibits a U-shaped relationship with 28-day mortality rates in severe sepsis patients [40]. Nevertheless, in prognosticating sepsis outcomes, the focus should extend beyond mere BMI-mortality associations, emphasizing the nuanced interplay with disease severity [41]. A prospective cohort study involving 862 older adult individuals aged 65 years and older in South Korea unveiled high serum AG as a potential independent predictor of overall mortality in this demographic, with elevated AG also impacting cardiovascular and infection-related mortality [42]. Lower body weight and elevated AG emerge as mortality risk factors in older adult SAE, as delineated in our investigation.

Limitations

This study is subject to several inherent limitations warranting discussion. Primarily, despite the extensive clinical dataset available within the MIMIC-IV database, the presence of missing values and outliers poses a potential challenge. To address this concern, rigorous data cleaning and processing protocols were implemented to enhance data quality and mitigate potential biases. Second, certain pertinent clinical features, such as electroencephalogram data, central imaging techniques, cerebral oxygen levels, neurofilament light chain, and cerebral blood flow measurements, were not incorporated into our analysis due to their absence within the MIMIC database. Nevertheless, our study used rigorous inclusion and exclusion criteria to ensure well-defined cohorts. Moreover, this study focused on investigating a broad array of clinical features and hematological parameters that were readily accessible. Additionally, although variables such as lactate and white blood cell count were available, they were excluded during the LASSO regression variable selection process. Other potentially relevant inflammatory markers, including procalcitonin, C-reactive protein, serum amyloid A, and heparin-binding protein, were not included due to their unavailability in the database. To enhance the clinical practicality of the model, our study focused on commonly measured and readily accessible variables as candidate predictors. Third, our study solely undertook internal validation of the predictive model. Further external validation across diverse patient cohorts is imperative to ascertain the generalizability and robustness of the established nomogram. Lastly, the retrospective nature of this investigation underscores the imperative for future prospective studies to validate the clinical applicability and effectiveness of our developed nomogram. Prospective studies would afford opportunities to confirm the predictive accuracy of the nomogram in real-time clinical settings, thus enhancing confidence in its utility and informing clinical decision-making.

Conclusions

In this study, we developed and internally validated a nomogram for predicting 28-day mortality in older adult patients with SAE using commonly available clinical data from the MIMIC-IV database. The model demonstrated satisfactory discriminative performance and calibration, with potential clinical utility as compared to traditional ICU scoring systems. Additionally, by implementing the nomogram as a web-based tool, we aimed to improve its accessibility and practical use in clinical settings. While promising, further external validation and prospective studies are necessary to confirm its broader applicability and effectiveness in diverse health care environments.

Acknowledgments

The authors wish to acknowledge the creators of the MIMIC database and ChatGPT (OpenAI) service for their invaluable contributions to this research endeavor. Furthermore, the authors express their appreciation to Home for Researchers [43] for their assistance with paper preparation and journal selection. During the preparation of this work, the authors used ChatGPT 3.5 in order to improve the readability and language of this paper. After using this tool or service, the authors reviewed and edited the content as needed and take full responsibility for the content of the publication. This study was supported by the grant from the Construction Fund of Key Medical Disciplines of Hangzhou (grant 2025HZZD04), the Traditional Chinese Medicine Science and Technology Project of Zhejiang Province (grant 2024ZL750), and the 2024 Public Welfare Research Guidance Project in the Field of Agriculture and Social Development (grant 20241029Y088).

Data Availability

The original data are available online [16].

XSL•FO
RenderX

Authors' Contributions

GJ conceptualized and visualized this study, acquired software, wrote the original draft, and acquired funding. MZ conceptualized this study, curated the data, and wrote the original draft. JC handled the methodology and formally analyzed, investigated, and validated the data. MD conceptualized this study and reviewed and edited the writing. WH conceptualized, supervised, acquired resources for, and administered this project, and reviewed and edited the writing.

Conflicts of Interest

None declared.

Multimedia Appendix 1
Visualization of the extent of missingness for each variable using the DataExplorer package in R.
[PNG File , 1189 KB - medinform_v13i1e76417_app1.png]

Multimedia Appendix 2
Baseline characteristics of geriatric patients with sepsis-associated encephalopathy: a comprehensive overview of demographic and clinical features in the study cohort.
[DOC File , 165 KB - medinform_v13i1e76417_app2.doc]

Multimedia Appendix 3
VIF values of included predictors for assessing collinearity. VIF: variance inflation factor.
[PNG File , 155 KB - medinform_v13i1e76417_app3.png]

Multimedia Appendix 4
ROC curves of the constructed nomogram versus conventional ICU scoring systems in the development and validation cohorts. ICU: intensive care unit; ROC: receiver operating characteristic.
[PNG File , 149 KB - medinform_v13i1e76417_app4.png]

References

1. Shankar-Hari M, Phillips GS, Levy ML, Seymour CW, Liu VX, Deutschman CS, Sepsis Definitions Task Force. Developing a new definition and assessing new clinical criteria for septic shock: for the third international consensus definitions for sepsis and septic shock (Sepsis-3). JAMA 2016;315(8):775-787 [FREE Full text] [doi: 10.1001/jama.2016.0289] [Medline: 26903336]
2. Bauer M, Gerlach H, Vogelmann T, Preissing F, Stiefel J, Adam D. Mortality in sepsis and septic shock in Europe, North America and Australia between 2009 and 2019- results from a systematic review and meta-analysis. Crit Care 2020;24(1):239 [FREE Full text] [doi: 10.1186/s13054-020-02950-2] [Medline: 32430052]
3. Sonneville R, Benghanem S, Jeantin L, de Montmollin E, Doman M, Gaudemer A, et al. The spectrum of sepsis-associated encephalopathy: a clinical perspective. Crit Care 2023;27(1):386 [FREE Full text] [doi: 10.1186/s13054-023-04655-8] [Medline: 37798769]
4. Petsko GA. A seat at the table. Genome Biol 2008;9(12):113 [FREE Full text] [doi: 10.1186/gb-2008-9-12-113] [Medline: 19144208]
5. Angus DC, Linde-Zwirble WT, Lidicker J, Clermont G, Carcillo J, Pinsky MR. Epidemiology of severe sepsis in the United States: analysis of incidence, outcome, and associated costs of care. Crit Care Med 2001;29(7):1303-1310. [doi: 10.1097/00003246-200107000-00002] [Medline: 11445675]
6. Jin G, Wang S, Chen J, Hu W, Zhu Y, Xi S. Identification of sepsis-associated encephalopathy risk factors in elderly patients: a retrospective observational cohort study. Turk J Med Sci 2022;52(5):1513-1522 [FREE Full text] [doi: 10.55730/1300-0144.5491] [Medline: 36422495]
7. Martin GS, Mannino DM, Moss M. The effect of age on the development and outcome of adult sepsis. Crit Care Med 2006;34(1):15-21. [doi: 10.1097/01.ccm.0000194535.82812.ba] [Medline: 16374151]
8. Zhou Z, Wang W, Li Y, Jin K, Wang X, Wang Z, et al. In-depth mining of clinical data: the construction of clinical prediction model with R. Ann Transl Med 2019;7(23):796 [FREE Full text] [doi: 10.21037/atm.2019.08.63] [Medline: 32042812]
9. Moons KGM, Altman DG, Reitsma JB, Ioannidis JPA, Macaskill P, Steyerberg EW, et al. Transparent Reporting of a Multivariable Prediction Model for Individual Prognosis or Diagnosis (TRIPOD): explanation and elaboration. Ann Intern Med 2015;162(1):W1-W73 [FREE Full text] [doi: 10.7326/M14-0698] [Medline: 25560730]
10. Han Q, Hu Z. Clinical prediction model construction and evaluation: a challenge for clinical researchers. Ann Transl Med 2020;8(4):74 [FREE Full text] [doi: 10.21037/atm.2019.11.145] [Medline: 32175367]

XSL•FO
RenderX

11. Yang Y, Liang S, Geng J, Wang Q, Wang P, Cao Y, et al. Development of a nomogram to predict 30-day mortality of patients with sepsis-associated encephalopathy: a retrospective cohort study. J Intensive Care 2020;8:45 [FREE Full text] [doi: 10.1186/s40560-020-00459-y] [Medline: 32637121]
12. Zhao L, Li Y, Wang Y, Gao Q, Ge Z, Sun X, et al. Development and validation of a nomogram for the prediction of hospital mortality of patients with encephalopathy caused by microbial infection: a retrospective cohort study. Front Microbiol 2021;12:737066 [FREE Full text] [doi: 10.3389/fmicb.2021.737066] [Medline: 34489922]
13. Peng L, Peng C, Yang F, Wang J, Zuo W, Cheng C, et al. Machine learning approach for the prediction of 30-day mortality in patients with sepsis-associated encephalopathy. BMC Med Res Methodol 2022;22(1):183 [FREE Full text] [doi: 10.1186/s12874-022-01664-z] [Medline: 35787248]
14. Guo J, Cheng H, Wang Z, Qiao M, Li J, Lyu J. Factor analysis based on Shapley Additive Explanations for sepsis-associated encephalopathy in ICU mortality prediction using XGBoost - a retrospective study based on two large database. Front Neurol 2023;14:1290117 [FREE Full text] [doi: 10.3389/fneur.2023.1290117] [Medline: 38162445]
15. Jin G, Hu W, Zeng L, Diao M, Chen H, Chen J, et al. Development and verification of a nomogram for predicting short-term mortality in elderly ischemic stroke populations. Sci Rep 2023;13(1):12580 [FREE Full text] [doi: 10.1038/s41598-023-39781-4] [Medline: 37537270]
16. MIMIC-IV (version 2.1). PhysioNet. URL: https://physionet.org/content/mimiciv/2.1/ [accessed 2025-10-09]
17. mimic-code. GitHub. URL: https://github.com/MIT-LCP/mimic-code/ [accessed 2025-10-10]
18. Jin G, Hu W, Zeng L, Ma B, Zhou M. Prediction of long-term mortality in patients with ischemic stroke based on clinical characteristics on the first day of ICU admission: an easy-to-use nomogram. Front Neurol 2023;14:1148185 [FREE Full text] [doi: 10.3389/fneur.2023.1148185] [Medline: 37122313]
19. Dynamic nomogram. URL: https://predictx.shinyapps.io/sae_28d_mortality_prediction_model [accessed 2025-10-11]
20. Liu X, Niu H, Peng J. Enhancing predictions with a stacking ensemble model for ICU mortality risk in patients with sepsis-associated encephalopathy. J Int Med Res 2024;52(3):3000605241239013 [FREE Full text] [doi: 10.1177/03000605241239013] [Medline: 38530021]
21. Zhao Q, Xiao J, Liu X, Liu H. The nomogram to predict the occurrence of sepsis-associated encephalopathy in elderly patients in the intensive care units: a retrospective cohort study. Front Neurol 2023;14:1084868 [FREE Full text] [doi: 10.3389/fneur.2023.1084868] [Medline: 36816550]
22. Jin J, Yu L, Zhou Q, Zeng M. Improved prediction of sepsis-associated encephalopathy in intensive care unit sepsis patients with an innovative nomogram tool. Front Neurol 2024;15:1344004 [FREE Full text] [doi: 10.3389/fneur.2024.1344004] [Medline: 38445262]
23. Lu X, Kang H, Zhou D, Li Q. Prediction and risk assessment of sepsis-associated encephalopathy in ICU based on interpretable machine learning. Sci Rep 2022;12(1):22621 [FREE Full text] [doi: 10.1038/s41598-022-27134-6] [Medline: 36587113]
24. Luo J, Zhao Q, Tu G. Clinical prediction models in the precision medicine era: old and new algorithms. Ann Transl Med 2020;8(6):274 [FREE Full text] [doi: 10.21037/atm.2020.02.63] [Medline: 32355718]
25. Van Calster B, Wynants L. Machine learning in medicine. N Engl J Med 2019;380(26):2588. [doi: 10.1056/NEJMc1906060] [Medline: 31242379]
26. Jaouimaa F, Do Ha I, Burke K. Penalized variable selection in multi-parameter regression survival modeling. Stat Methods Med Res 2023;32(12):2455-2471 [FREE Full text] [doi: 10.1177/09622802231203322] [Medline: 37823396]
27. Tibshirani R. The lasso method for variable selection in the Cox model. Stat Med 1997;16(4):385-395 [FREE Full text] [doi: 10.1002/(sici)1097-0258(19970228)16:4<385::aid-sim380>3.0.co;2-3] [Medline: 9044528]
28. Tripepi G, Jager K, Dekker F, Zoccali C. Linear and logistic regression analysis. Kidney Int 2008;73(7):806-810 [FREE Full text] [doi: 10.1038/sj.ki.5002787] [Medline: 18200004]
29. Su W, He B, Zhang YD, Yin G. C-index regression for recurrent event data. Contemp Clin Trials 2022;118:106787. [doi: 10.1016/j.cct.2022.106787] [Medline: 35568377]
30. Teasdale G, Maas A, Lecky F, Manley G, Stocchetti N, Murray G. The Glasgow Coma Scale at 40 years: standing the test of time. Lancet Neurol 2014;13(8):844-854. [doi: 10.1016/S1474-4422(14)70120-6] [Medline: 25030516]
31. Sonneville R, de Montmollin E, Poujade J, Garrouste-Orgeas M, Souweine B, Darmon M, et al. Potentially modifiable factors contributing to sepsis-associated encephalopathy. Intensive Care Med 2017;43(8):1075-1084. [doi: 10.1007/s00134-017-4807-z] [Medline: 28466149]
32. Rosenblatt K, Walker KA, Goodson C, Olson E, Maher D, Brown CH, et al. Cerebral autoregulation-guided optimal blood pressure in sepsis-associated encephalopathy: a case series. J Intensive Care Med 2020;35(12):1453-1464 [FREE Full text] [doi: 10.1177/0885066619828293] [Medline: 30760173]
33. Quinten VM, van Meurs M, Olgers TJ, Vonk JM, Ligtenberg JJM, Ter Maaten JC. Repeated vital sign measurements in the emergency department predict patient deterioration within 72 hours: a prospective observational study. Scand J Trauma Resusc Emerg Med 2018;26(1):57 [FREE Full text] [doi: 10.1186/s13049-018-0525-y] [Medline: 30005671]
34. Huang X, Yuan S, Ling Y, Tan S, Huang T, Cheng H, et al. The hemoglobin-to-red cell distribution width ratio to predict all-cause mortality in patients with sepsis-associated encephalopathy in the MIMIC-IV database. Int J Clin Pract 2022;2022:7141216 [FREE Full text] [doi: 10.1155/2022/7141216] [Medline: 36683597]

XSL•FO
RenderX

35. Schneider CP, Angele MK, Hartl WH. Activated partial thromboplastin time waveform analysis as specific sepsis marker in cardiopulmonary bypass surgery. Crit Care 2010;14(1):104 [FREE Full text] [doi: 10.1186/cc8226] [Medline: 20122294]
36. Guo F, Zhu X, Wu Z, Zhu L, Wu J, Zhang F. Clinical applications of machine learning in the survival prediction and classification of sepsis: coagulation and heparin usage matter. J Transl Med 2022;20(1):265 [FREE Full text] [doi: 10.1186/s12967-022-03469-6] [Medline: 35690822]
37. SRLF Trial Group. Hypoxemia in the ICU: prevalence, treatment, and outcome. Ann Intensive Care 2018;8(1):82 [FREE Full text] [doi: 10.1186/s13613-018-0424-4] [Medline: 30105416]
38. Suarez JI, Zaidat OO, Suri MF, Feen ES, Lynch G, Hickman J, et al. Length of stay and mortality in neurocritically ill patients: impact of a specialized neurocritical care team. Crit Care Med 2004;32(11):2311-2317. [doi: 10.1097/01.ccm.0000146132.29042.4c] [Medline: 15640647]
39. Knopf L, Staff I, Gomes J, McCullough L. Impact of a neurointensivist on outcomes in critically ill stroke patients. Neurocrit Care 2012;16(1):63-71 [FREE Full text] [doi: 10.1007/s12028-011-9620-x] [Medline: 21847702]
40. Lin S, Ge S, He W, Zeng M. Association between body mass index and short-term clinical outcomes in critically ill patients with sepsis: a real-world study. Biomed Res Int 2020;2020:5781913 [FREE Full text] [doi: 10.1155/2020/5781913] [Medline: 33123579]
41. Jagan N, Morrow L, Walters R, Plambeck R, Wallen T, Patel T, et al. Sepsis and the obesity paradox: size matters in more than one way. Crit Care Med 2020;48(9):e776-e782. [doi: 10.1097/CCM.0000000000004459] [Medline: 32590388]
42. Ahn SY, Ryu J, Baek SH, Han JW, Lee JH, Ahn S, et al. Serum anion gap is predictive of mortality in an elderly population. Exp Gerontol 2014;50:122-127. [doi: 10.1016/j.exger.2013.12.002] [Medline: 24333141]
43. Home for researchers. URL: https://www.home-for-researchers.com [accessed 2025-10-10]

Abbreviations

AG: anion gap
APS III: Acute Physiology Score III
C-index: concordance index
GCS: Glasgow Coma Scale
ICD: International Classification of Diseases
ICU: intensive care unit
IDI: integrated discrimination improvement
LASSO: least absolute shrinkage and selection operator regression
MIMIC: Medical Information Mart for Intensive Care
MIMIC-IV: Medical Information Mart for Intensive Care IV
NRI: net reclassification improvement
OR: odds ratio
PaCO2: partial pressure of CO2
PTT: partial thromboplastin time
SAE: sepsis-associated encephalopathy
SOFA: sequential organ failure assessment
TRIPOD: Transparent Reporting of a Multivariable Prediction Model for Individual Prognosis or Diagnosis

Edited by A Benis; submitted 23.04.25; peer-reviewed by J Jin, S Xie, B Xu; comments to author 11.08.25; revised version received 21.08.25; accepted 18.09.25; published 04.12.25.

Please cite as:
Jin G, Zhou M, Chen J, Diao M, Hu W
Online Clinical Calculator for Predicting 28-Day Mortality in Older Adult Patients With Sepsis-Associated Encephalopathy: Retrospective Study Using MIMIC-IV
JMIR Med Inform 2025;13:e76417
URL: https://medinform.jmir.org/2025/1/e76417
doi:10.2196/76417
PMID:

©Guangyong Jin, Menglu Zhou, Jiayi Chen, Mengyuan Diao, Wei Hu. Originally published in JMIR Medical Informatics (https://medinform.jmir.org), 04.12.2025. This is an open-access article distributed under the terms of the Creative Commons Attribution License (https://creativecommons.org/licenses/by/4.0/), which permits unrestricted use, distribution, and reproduction in any medium, provided the original work, first published in JMIR Medical Informatics, is properly cited. The complete

XSL•FO
RenderX

bibliographic information, a link to the original publication on https://medinform.jmir.org/, as well as this copyright and license information must be included.

XSL•FO
RenderX

Comparison of Risk Factors, Their Interaction Patterns, and Scoring Systems for Liver Cancer Between Patients With and Those Without Diabetes: Retrospective Cohort Study Using Electronic Health Records and Tree-Structured Algorithms

Sarah Tsz Yui Yau, MSc, MPH; Chi Tim Hung, MBBS; Eman Yee Man Leung, PhD; Albert Lee, MPH, MD, LLM; Eng Kiong Yeoh, MBBS

JC School of Public Health and Primary Care, The Chinese University of Hong Kong, 4/F, School of Public Health Building, Prince of Wales Hospital, Shatin, Hong Kong, China (Hong Kong)

Corresponding Author:
Eman Yee Man Leung, PhD
JC School of Public Health and Primary Care, The Chinese University of Hong Kong, 4/F, School of Public Health Building, Prince of Wales Hospital, Shatin, Hong Kong, China (Hong Kong)

Abstract

Background: Patients with diabetes are at higher risk of developing liver cancer. Nevertheless, risk factors and their interaction patterns have rarely been compared between patients with and those without diabetes, nor have their interactions been incorporated into scoring system development.

Objective: This study aims to compare risk factors, their interaction patterns, and resulting scoring systems for liver cancer risk according to diabetes and liver disease status using tree-structured algorithms.

Methods: A retrospective cohort study was conducted using electronic health records in Hong Kong. Patients who had used public health care services between 1997 and 2021 without cancer history were identified and followed up until December 31, 2021. Scoring systems were developed based on aggregate results from individual survival trees in random survival forest, and interaction patterns among factors were separately examined using conditional inference survival tree.

Results: Of the 190,971 patients included, 1275 developed liver cancer during follow-up (median 6.25 y). Across 4 scoring systems, alanine aminotransferase (ALT) levels, age, sex, and triglycerides were commonly chosen as predictors irrespective of diabetes and liver disease status. In the overall systems, liver cirrhosis was additionally selected as a predictor, with chronic viral hepatitis uniquely chosen in diabetes. In the absence of liver disease, fasting glucose and smoking were uniquely selected for diabetes and nondiabetes, respectively. Chronic viral hepatitis appeared as the strongest risk factor in diabetes but not in nondiabetes. Among people with diabetes, in the absence of chronic viral hepatitis, sex became the most important factor, followed by age, statin use, and ALT levels. Among people without diabetes, age became the most dominant risk factor. For older patients (>55 y), uncontrolled lipids and male sex became key risk factors in statin and nonstatin users, respectively, when the ALT level was higher (>43.4 U/L), while smoking became a key risk factor when the ALT level was lower (≤43.4 U/L). For younger patients (≤55 y), sex remained the most significant factor.

Conclusions: Patients with and those without diabetes exhibit distinctive interaction patterns among key factors on liver cancer risk. The resulting scoring systems reflect interaction patterns among predictors in individual survival trees. This study may help identify targets for public health interventions and provide clinical cancer risk prediction according to diabetes status.

(JMIR Med Inform 2025;13:e72239) doi:10.2196/72239

KEYWORDS

liver cancer; diabetes; risk factor; interaction; risk prediction; risk score; risk stratification; decision tree; random forest; survival analysis

Introduction

Liver cancer is the third leading cause of cancer death worldwide [1]. Previous research has shown that diabetes is associated with an increased risk of cancer at several sites, including the liver [2,3]. Nevertheless, there is a lack of systematic comparison on the interaction patterns among key factors between patients with and those without diabetes. Nor have scoring systems been developed separately according to diabetes status.

While most risk prediction models for liver cancer focus on patients with known risk factors such as liver cirrhosis, chronic viral hepatitis, hepatic steatosis, and heavy alcohol use [4,5],

XSL•FO
RenderX

several risk scoring systems developed among patients with [6,7] and those without known risk factors [8] have incorporated diabetes as a predictor. Nevertheless, only a few risk scoring systems have been developed specifically for diabetes population [9,10]. Si et al [9] has developed a scoring system for liver cancer prediction among people with diabetes without chronic viral hepatitis or alcoholic cirrhosis from South Korea with only 3 predictors, namely age, triglycerides, and gamma-glutamyl transferase (GGT), where lower triglyceride levels were found to be predictive of an elevated risk of liver cancer. On the other hand, Li et al [10] have incorporated a number of predictors, including age, sex, smoking, alanine aminotransferase (ALT) levels, glycated hemoglobin, liver cirrhosis, chronic viral hepatitis, and lipid profile into a scoring system for liver cancer prediction developed among people with diabetes from Taiwan. However, these diabetes-specific scoring systems lack comparison with people without diabetes, nor were interaction patterns among covariates examined.

Existing scoring systems rarely incorporate interaction patterns into variable selection. Nevertheless, previous research suggests that factors associated with liver cancer are often interrelated. For example, while both chronic hepatitis B or C [11] and diabetes [3] are independent risk factors for liver cancer, previous studies have also shown that hepatitis B or C infection could be linked to an elevated risk of type 2 diabetes development [12,13]. Also, while sex-specific elevated ALT thresholds are available [8], the potential age dependence of ALT [14-16] has rarely been incorporated. Furthermore, despite the common coconsumption of alcohol and smoking, and heavy alcohol use as known cause for liver damage [11], the role of smoking in liver injury is less clear [17,18].

While Cox proportional hazards regression is conventionally applied to examine a time-to-event outcome, tree-structured (or recursive partitioning) algorithms are more suitable to handle interactions among covariates and nonlinearity between a set of covariates and an outcome. On one hand, single tree-structured algorithms are intuitively interpretable and could be visually illustrated to demonstrate the interaction patterns [19,20] among split variables. Unlike traditional tree-structured algorithms which often lack a theoretical foundation, conditional inference survival tree [21] is embedded with statistical theory of conditional inference. On the other hand, tree-structured ensemble algorithms tend to be more stable and their aggregate results have lower variance than results from individual trees. Recently, Xie et al [22] have proposed a framework to develop clinical scoring system by integrating random survival forest in variable selection and retaining the use of beta coefficients from Cox regression in generating a final scoring system, where interaction patterns among covariates are taken into account in scoring system development, and clinical interpretability is ensured in the final scoring system.

The objective of the study is to compare risk factors, their interaction patterns, and resulting scoring systems for liver cancer risk according to diabetes and liver disease status using tree-structured algorithms.

Methods

Study Design and Study Population

This is a retrospective cohort study performed using territory-wide electronic health records in Hong Kong. The Hospital Authority (HA) is a statutory body responsible for managing public health care services and maintains a centralized clinical data repository, which stores information on patient demographics (sex and year of birth), disease diagnoses, prescription records, laboratory measurements, clinical notes, and radiology reports. Data used in this study were linked to death records from the Immigration Department. Individual-level data across datasets were linked via pseudonymous identifiers. Disease diagnoses were coded according to the *ICD-10* (*International Statistical Classification of Diseases, Tenth Revision*), or the International Classification of Primary Care, 2nd Edition (ICPC-2). Data were accessed via HA Data Collaboration Lab.

Patients

Patients who had used public health care services between 1997 and 2021 were initially identified. Laboratory records on (1) ALT levels, (2) fasting glucose, (3) low-density lipoprotein (LDL) cholesterol, (4) high-density lipoprotein (HDL) cholesterol, and (5) triglycerides were extracted. Patients with at least one record on each of the above laboratory measurements were selected. Prescription records on antidiabetic drugs were extracted to determine diabetes status of patients. Those who were prescribed any antidiabetic drugs during the study period were identified as patients with diabetes, while those who did not receive any antidiabetic drugs during the study period were identified as patients without diabetes. Patients with diabetes who had at least 2 records on each selected laboratory measurement within 1 year of initiation of antidiabetic drugs or diabetes onset were further selected (n=161,790). Patients without diabetes who had at least 2 records on each selected laboratory measurement within 1 year of the earliest record of the above measurement were further selected (n=67,777). For each laboratory measurement, the mean value of at least 2 records closest to the baseline within 1 year was taken as baseline measurement. The index dates for patients with and those without diabetes were initiation of antidiabetic drugs and earliest selected laboratory record, respectively. For both patients with and those without diabetes, those with a cancer history at baseline were excluded. To exclude possible cases of type 1 diabetes, patients who were diagnosed with diabetes younger than 30 years [23], or those diagnosed with diabetes younger than 60 years and received insulin treatment within 1 year of diabetes onset [23] (but did not receive any other antidiabetic drugs during the study period) were excluded. In addition, exclusion of early insulin users may help remove more severe diabetes cases, since we intend to capture an incident diabetes cohort. Patients without diabetes younger than 30 years at baseline were also excluded. For both patients with and those without diabetes, to minimize reverse causality, those with less than 6 months of follow-up were excluded [24]. In addition, since the diagnosis of one cancer may influence the diagnosis of another cancer [24], those who were diagnosed with cancer types other than liver cancer during follow-up were

XSL•FO
RenderX

also excluded. In other words, only patients who developed liver cancer or remained cancer-free during follow-up were included. Finally, a total of 132,221 patients with diabetes and 58,750 patients without diabetes were included.

Outcome

The outcome of interest was diagnosis of liver cancer (ICD-10: C22) during follow-up.

Input Variables

The set of input variables included demographics (sex and age at baseline), disease history, lifestyle behavior (smoking), laboratory measurements, and medication use. Disease history included liver cirrhosis [11], chronic viral hepatitis [11], fatty liver [11], and common comorbidities (ischemic heart disease, cerebrovascular disease, heart failure, chronic obstructive pulmonary disease, pneumonia, tuberculosis, hematuria, and cystitis). Disease diagnoses were extracted from both inpatient and outpatient diagnosis codes. The presence of fatty liver was determined from diagnosis codes or radiology reports (ultrasonography, computed tomography, and magnetic resonance imaging). Smoking habits were extracted from clinical notes, and patients were categorized as ever versus never smokers. Laboratory measurements included fasting glucose, LDL cholesterol, HDL cholesterol, triglycerides, and ALT levels. Medication included antidiabetic drugs (metformin, sulfonylurea, insulin, dipeptidyl peptidase-4 inhibitors, acarbose, meglitinide, glitazone, sodium-glucose cotransporter-2 inhibitors, and glucagon-like peptide-1 receptor agonists), aspirin, nonsteroidal anti-inflammatory drugs, anticoagulants, antiplatelets, statins, antihypertensive drugs (alpha-blockers, angiotensin-converting enzyme inhibitors, angiotensin receptor blockers, beta-blockers, calcium channel blockers, and diuretics). Medication use was defined as whether patients had taken a drug at baseline.

Data Analysis

Conditional Inference Survival Tree

Conditional inference survival tree [21] was applied to examine the interaction patterns among the set of candidate predictors. At each split, a global null hypothesis of independence between a set of covariates and an outcome is tested at a prespecified α level. If rejected, a set of partial null hypotheses of independence between each covariate and an outcome is then tested at the same α level. The covariate with the minimum Bonferroni-corrected *P* value smaller than α is then selected as the split variable. Partitioning is recursively conducted until the global null hypothesis cannot be rejected. For continuous variables, the cutoff point is the optimal value to maximize the between-group differences in survival probability. Each path from the root node to a terminal node represents an interaction pattern [20]. Two separate survival trees, which are independent of the random survival forest used in scoring, were generated according to diabetes status. The α and maximum depth of the survival trees were set at .01 and 4 respectively.

Advantages of this algorithm include (1) incorporating conditional inference framework into the partitioning procedures, (2) avoiding overfitting, (3) minimizing bias toward selecting covariates with many possible values, and (4) not requiring explicit pruning.

Scoring System Guided by Random Survival Forest

The scoring system development followed a previously proposed framework [22]. For each scoring system, patients were first split into 70% train, 10% validation, and 20% test sets by default. Variable importance was first ranked by random survival forest using the train set. Random survival forest is a tree-structured ensemble algorithm to produce aggregated results from a predetermined number of decorrelated individual survival trees. There are 2 random components in random survival forest, namely bootstrapping in sampling and random selection in feature selection. To build each tree, a bootstrapped train set is selected. At each split, a set of *k* number of predictors is selected from a full set of *m* number of predictors, where *k* is equal to the square root of *m* by convention. Considering computing time, the number of trees in the survival forest was set at 10. Each variable was then added to a Cox regression model sequentially according to their ranking in variable importance in the random survival forest. The performance of the model was then evaluated on the validation set using area under the curve as a metric. Variables for the final scoring system were then selected using model improvement and parsimony as criteria. For continuous variables, the cutoff points were determined by default quantiles. Fine-tuning of variable selection and cutoff points was conducted according to domain knowledge and existing literature. The chosen set of variables was then added into a final scoring system, where score assignment was based on beta coefficients in the Cox regression model and model performance was evaluated on the unseen test set using Harrell's concordance index (C-index) and integrated Brier score as metrics. In total, 4 scoring systems were separately developed according to diabetes and liver disease (presence or absence of liver cirrhosis or chronic viral hepatitis) status.

Advantages of this approach include (1) tree-structured algorithms have higher interpretability than other machine learning algorithms, (2) aggregate results from a tree ensemble may have lower variance than results from individual trees, (3) interactions among covariates on an outcome in single trees are taken into account in a tree ensemble, (4) adopting a more objective way to incorporating less established risk factors as predictors in variable selection process, (5) categorizing continuous variables in deriving scoring systems may help address nonlinearity, and (6) converting risk prediction models into point-based scores could be more clinically useful.

Ethical Considerations

Ethics approval for secondary data analysis was provided by the Chinese University of Hong Kong – Survey and Behavioral Research Ethics Committee (reference number: SBRE-22 - 0386). Patient consent was waived since individuals were not identifiable in this study.

XSL•FO
RenderX

Results

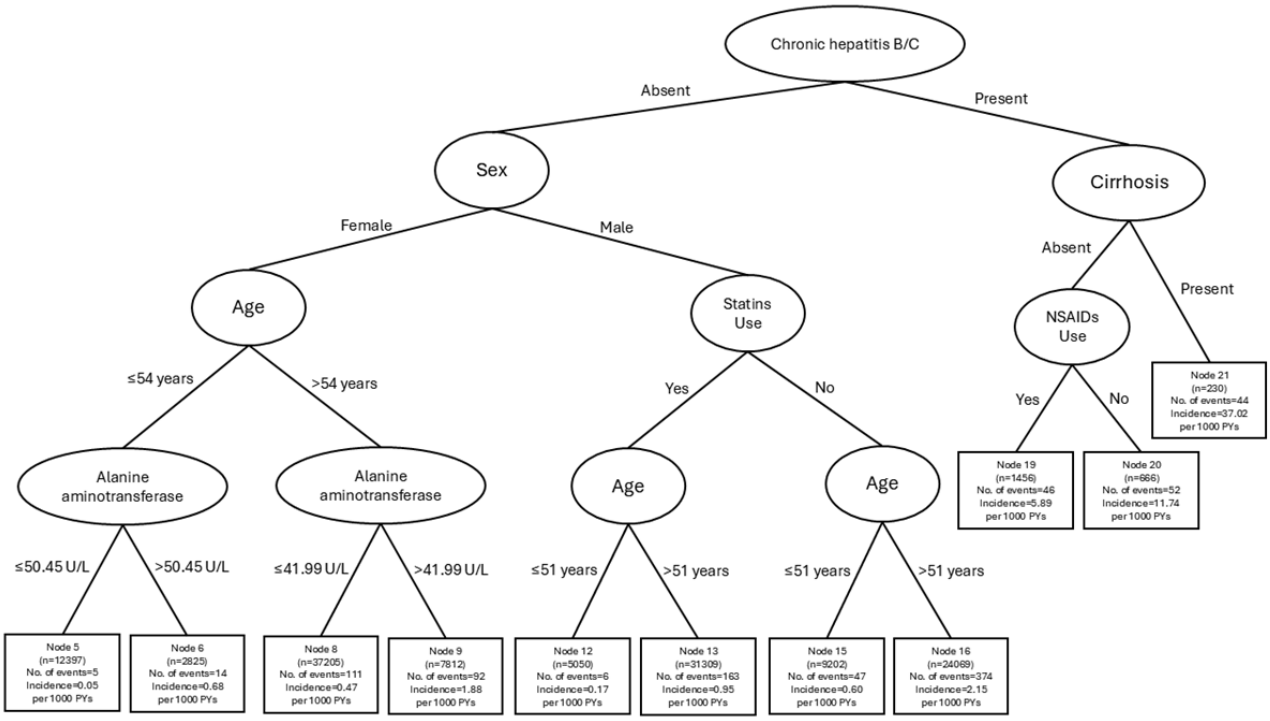
Overview

A total of 190,971 patients were included. Among patients with (n=132,221) and those without (n=58,750) diabetes, 954 and 321 developed liver cancer during follow-up (median 6.25 y), respectively. The corresponding incidence rates were 1.04 and 0.61 per 1000 person-years. Among 129,609 patients with diabetes and 58,635 patients without diabetes in the absence of liver disease, 792 and 310 developed liver cancer during follow-up, respectively.

Interaction Patterns–Diabetes

Chronic hepatitis B or C status emerged as primary factor in differentiating the risk of liver cancer. In the presence of chronic viral hepatitis, the most dominant risk factor was liver cirrhosis. On the other hand, in the absence of chronic viral hepatitis, sex became the most significant factor. In males, statin use and age were key factors. In females, age and ALT levels became key factors (Figure 1).

Figure 1. Conditional inference survival tree illustrating the interaction patterns among factors associated with the risk of liver cancer among patients with diabetes. NSAID: nonsteroidal anti-inflammatory drugs; PYs: person-years; U/L: unit per liter.



Absence of Chronic Viral Hepatitis, Male Sex, Statin Use, and Age

Among males in the absence of chronic viral hepatitis, statin use became the dominant factor in differentiating the risk of liver cancer. Across statin users and nonstatin users, an age of 51 years was symmetrically identified as optimal cutoff for differentiating liver cancer risk (Figure 1).

Absence of Chronic Viral Hepatitis, Female Sex, Age, and ALT Levels

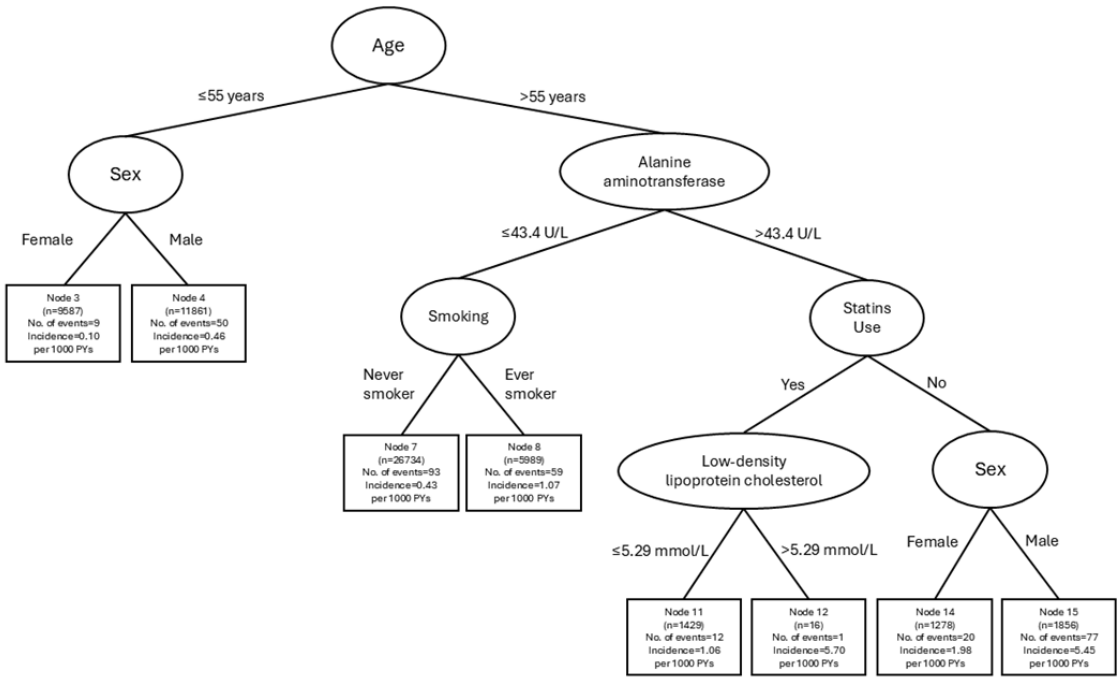
Among females in the absence of chronic viral hepatitis, age became the subsequent dominant factor in differentiating the risk of liver cancer. Among older (>54 y) and younger (≤54 y) females, elevated ALT was identified as the most important risk factor at differential optimal cutoffs (41.99 and 50.45 U/L for older and younger females, respectively; Figure 1).

Interaction Patterns—No Diabetes

Age emerged as the primary factor in differentiating the risk of liver cancer. Among older patients (>55 y), ALT level became the dominant factor. For those with higher ALT levels, statin use, LDL cholesterol, and sex became key factors. For those with lower ALT levels, smoking became the dominant risk factor. Among younger patients (≤55 y), male sex became the most significant risk factor (Figure 2).

XSL•FO
RenderX

Figure 2. Conditional inference survival tree illustrating the interaction patterns among factors associated with the risk of liver cancer among patients without diabetes. PYs: person-years.



Older Age, Higher ALT Levels, Statin Use, and LDL Cholesterol or Sex

Among older patients (>55 y) with higher ALT levels (>43.4 U/L), uncontrolled LDL cholesterol (>5.29 mmol/L) and male sex became dominant risk factors in statin users and nonstatin users respectively (Figure 2).

Older Age, Lower ALT, and Smoking

Among older patients (>55 y) with lower ALT levels (≤43.4 U/L), smoking became the most important risk factor.

Overall Scoring Systems by Diabetes Status

In the overall scoring systems, liver cirrhosis, ALT levels, age, sex, and serum triglycerides were commonly included as predictors regardless of diabetes status. Chronic hepatitis B or C status was uniquely included in diabetes but not in nondiabetes (Table 1). Comparing to the overall scoring system for diabetes-only (D_0), generally, there was an increase in relative contribution of liver cirrhosis and triglycerides in the overall scoring system for nondiabetes-only (N_0). Nevertheless, triglycerides exhibited an inverse association with the risk of liver cancer across diabetes (D_0) and nondiabetes (N_0) models (Table 2).

Table . Variable selection in scoring systems for liver cancer prediction among patients with and those without diabetes.

	Overall		No liver disease	
Variable	DM[a] (D_0)	Non-DM (N_0)	DM (D_1)	Non-DM (N_1)
Chronic hepatitis B or C	✓			
Liver cirrhosis	✓	✓		
Alanine aminotransferase	✓	✓	✓	✓
Age	✓	✓	✓	✓
Sex	✓	✓	✓	✓
Triglycerides	✓	✓	✓	✓
Fasting glucose			✓	
Smoking				✓

[a]DM: diabetes mellitus.

XSL•FO
RenderX

Table . Scoring systems for liver cancer prediction among patients with and those without diabetes.

	DM[a] (D_0)		Non-DM (N_0)	
Variable	Value	Point	Value	Point
Chronic hepatitis B or C				
	None	0	—[b]	—
	Chronic hepatitis B-only	13	—	—
	Chronic hepatitis C-only	19	—	—
	Coinfection of chronic hepatitis B and C	9	—	—
Alanine aminotransferase (U/L)				
	<11.5	0	<11	2
	[11.5, 17)	3	[11, 15.5)	0
	[17, 44.1)	9	[15.5, 38)	4
	[44.1, 83.1)	19	[38, 76)	16
	≥83.1	21	≥76	20
Age (years)				
	<42	0	<40	0
	[42, 51)	12	[40, 50)	14
	[51, 72)	24	[50, 71)	22
	≥72	27	≥71	30
Liver cirrhosis				
	Absent	0	Absent	0
	Present	16	Present	24
Sex				
	Female	0	Female	0
	Male	7	Male	8
Triglycerides (mmol/L)				
	<0.73	11	<0.875	18
	[0.73, 1.02)	9	[0.875, 1.88)	16
	[1.02, 2.26)	5	[1.88, 2.82)	14
	[2.26, 3.58)	0	≥2.82	0
	≥3.58	1	—	—

[a]DM: diabetes mellitus.

[b]Not applicable.

Scoring Systems by Diabetes Status in the Absence of Liver Disease

In the absence of liver disease, ALT levels, age, sex, and triglycerides were commonly included as predictors irrespective of diabetes status. Baseline fasting glucose and smoking status were unique predictors in the scoring systems for diabetes (D_1) and nondiabetes (N_1), respectively (Table 1). The relative contributions of common predictors appeared comparable across 2 models (D_1 and N_1). In addition, triglycerides consistently demonstrated a negative relationship with the risk of liver cancer across diabetes (D_1) and nondiabetes (N_1) models (Table 3).

XSL•FO
RenderX

Table . Scoring systems for liver cancer prediction among patients with and those without diabetes in the absence of liver disease.

	DM[a] (D_1)		Non-DM (N_1)	
Variable	Value	Point	Value	Point
Alanine aminotransferase (U/L)				
	<11.5	0	<11	0
	[11.5, 17)	2	[11, 15.5)	3
	[17, 44.4)	9	[15.5, 38)	6
	[44.4, 82.5)	24	[38, 76.3)	23
	≥82.5	29	≥76.3	29
Age (years)				
	<42	0	<39	0
	[42, 52)	12	[39, 50)	19
	[52, 72)	28	[50, 71)	29
	≥72	34	≥71	39
Sex				
	Female	0	Female	0
	Male	10	Male	6
Triglycerides (mmol/L)				
	0.735	18	<0.875	19
	[0.735, 1.03)	13	[0.875, 1.87)	13
	[1.03, 2.28)	6	[1.87, 2.83)	10
	≥2.28	0	≥2.83	0
Fasting glucose (mmol/L)				
	<6.4	0	—[b]	—
	[6.4, 9.55)	1	—	—
	[9.55, 12.8)	3	—	—
	≥12.8	8	—	—
Smoking				
	—	—	Never smoker	0
	—	—	Ever smoker	6

[a]DM: diabetes mellitus.

[b]Not applicable.

Model Performance

The C-indexes of D_0, N_0, D_1, and N_1 on unseen test sets were 0.80 (95% CI 0.76 - 0.83), 0.80 (95% CI 0.74 - 0.86), 0.75 (95% CI 0.71 - 0.79), and 0.82 (95% CI 0.77 - 0.88), respectively. The corresponding integrated Brier scores were 0.011, 0.006, 0.011, and 0.006, respectively.

Discussion

Principal Findings

This study compared risk factors, their interactions, and resulting scoring systems for liver cancer risk between patients with and those without diabetes. The resulting scoring systems took into account interaction patterns among the set of candidate predictors. Across four scoring systems stratified by diabetes and liver disease status, ALT levels, age, sex, and triglycerides were commonly chosen as predictors. Chronic viral hepatitis was uniquely selected in the overall system for diabetes. On the other hand, in the absence of liver disease, fasting glucose and smoking were uniquely chosen for diabetes and nondiabetes, respectively. Across all systems, triglycerides uniformly exhibited an inverse association with the risk of liver cancer. Among people with diabetes, chronic viral hepatitis remained the dominant risk factor for liver cancer. In the absence of chronic viral hepatitis, sex was identified as a subsequent key factor, followed by age, statin use, and ALT levels. Among people without diabetes, age became the primary factor. For older patients, statin use, LDL cholesterol, and sex became key factors when the ALT level was higher. On the other hand,

XSL•FO
RenderX

smoking became a key risk factor when the ALT level was lower.

Comparison to Previous Work

Overall scoring systems developed in this study included liver cirrhosis, ALT levels, age, and sex as common predictors across the diabetes-only and nondiabetes-only models. These variables have been commonly used as predictors of liver cancer [4,5]. Nevertheless, chronic hepatitis B or C status was uniquely chosen as a predictor for diabetes but not for nondiabetes. In the individual trees, chronic viral hepatitis only emerged as a primary factor for differentiating the risk of liver cancer in diabetes, but not in nondiabetes. Previous research suggests that hepatitis B or C infection [12,13] or hepatitis B virus (HBV)–induced cirrhosis [25] could be potentially associated with an increased risk of type 2 diabetes. Possible mechanisms include disturbances of insulin signaling pathways [12,13], alterations in glucose [12,13] and lipid metabolism [26], as well as induction of inflammation in promoting type 2 diabetes development [27]. These provide possible explanations for the more important role of chronic viral hepatitis in liver cancer development in diabetes found in this study.

In the absence of chronic viral hepatitis in diabetes, elevated ALT appeared as a key risk factor for liver cancer in females, with a higher cutoff for the younger group but a lower cutoff for the older group. While ALT is a marker for liver function [28] and a common predictor of liver cancer risk [4,5], a number of previous studies have found that ALT tends to decline with aging [14,15,29], possibly with stronger effects in males than females [16,30]. However, in this study, statin use was observed to be a more important factor in influencing the risk of liver cancer in their male counterparts. There are several possible explanations for the potential association between aging and reduced ALT thresholds for elevated liver cancer risk. In animal studies, the liver demonstrates slower and weakened regenerative ability, as well as reduced inflammatory response during aging [31]. Furthermore, in human studies, the liver appears to shrink its volume and have less blood flow during aging [32].

Moreover, in the absence of chronic viral hepatitis in diabetes, statin use emerged as a subsequent key factor in differentiating the risk of liver cancer in males, followed by age (with 51 y being symmetrically identified as optimal cutoff across statin users and non–statin users). Past observational studies have shown that statin use is potentially associated with a lower risk of liver disease [33] and liver cancer [33-35], particularly in Asian populations [34,35]. However, no effects of statin use on cancer risk have been demonstrated in randomized controlled trials [36].

Furthermore, in the presence of elevated ALT among older patients without diabetes, statin use emerged as a subsequent key factor in differentiating the risk of liver cancer, where uncontrolled LDL cholesterol and male sex were identified as dominant risk factors in statin users and nonstatin users, respectively. Previous research suggests altered lipid metabolism in carcinogenesis of the liver [26]. It is possible that under a state of potential liver dysfunction, as indicated by elevated ALT, statin use may confer protective effects against liver cancer development. Possible mechanisms of statins use against liver cancer include inhibition of tumor growth via downregulating the mevalonate pathway [37]. It has also been suggested that statins may exercise antagonistic effects against carcinogenic effects of HBV [34], potentially via suppressing cholesterol synthesis and HBV replication [38].

On the other hand, circulating triglycerides were selected as predictors and exhibited an inverse association with the risk of liver cancer across the 4 scoring systems regardless of diabetes and liver disease status. Epidemiological studies on the associations between circulating lipids and liver cancer risk remain conflicting [26,39]. Several studies found that lower levels of triglycerides [9] or total cholesterol [8,40,41] are predictive of elevated liver cancer risk in the presence [40-42] or absence [8,9] of chronic viral hepatitis. While lipids were not directly identified as a key factor in the diabetes-only individual tree, statin use emerged as a dominant factor among subgroups of patients across diabetes and nondiabetes subpopulations. Possible mechanisms linking low lipids to elevated liver cancer risk include higher lipids as indicator of preserved liver function [43], suppression of liver tumor growth via activating effector functions in natural killer cells [44], as well as uptake of circulating lipids by underlying liver tumor cells to meet their demand for lipids [39].

In addition, fasting glucose and smoking were chosen as unique predictors of liver cancer risk among patients with and those without diabetes in the absence of liver disease, respectively. The variation in baseline fasting glucose at the time of initiation of antidiabetic drugs among patients with diabetes may reflect their differential levels of diabetes severity. Previous studies have shown that fasting glucose could be individually associated with the risk of liver cancer [45]. The exact mechanism remains unknown. Possible mechanisms include upregulation of insulin-like growth factor-1 (which has a higher mitogenic and antiapoptotic potency than insulin) via hyperglycemia and hyperinsulinemia, as well as higher levels of proinflammatory factors under chronic inflammation [2,45]. On the other hand, smoking has been shown to be a carcinogenic agent to the liver in humans [46]. Several previously developed scoring systems for liver cancer risk [8,10] have also incorporated smoking as predictors. Possible mechanisms include conversion of chemicals in tobacco smoke into reactive carcinogenic metabolites in the liver, concurrent consumption of alcohol along with tobacco smoking, chronic inflammation, immunosuppression, and accelerated telomere dysfunction [47,48].

Furthermore, in the absence of diabetes, smoking emerged as a dominant risk factor for liver cancer among older patients with lower ALT. Previous research [17,18,49] suggests that smoking exposure does not directly induce liver damage, but may exacerbate liver injury caused by heavy alcohol use. Smoking was only shown to be positively associated with GGT in heavy alcohol users [17,18]. On the other hand, smoking was inversely linked to ALT and aspartate aminotransferase [17,49]. One possible explanation for elevated specific liver enzyme is that concurrent consumption of smoking and alcohol intensifies oxidative stress [50], since GGT is an oxidative stress marker [51]. In addition, previous research [52] has shown that smoking

XSL•FO
RenderX

is only associated with increased ALT levels in patients who are seropositive for hepatitis C virus, but not in those who are seropositive for HBV. This may help partially explain the dominance of smoking as a risk factor among older nondiabetes patients with lower ALT from a HBV-endemic region.

Implications

There are several public health and clinical implications of this study. First, chronic viral hepatitis appears to be a more dominant risk factor for liver cancer among patients with diabetes than those without diabetes. Second, while elevated triglycerides are one of the components of metabolic syndrome [53] and associated with adverse cardiovascular outcomes, they appear to be inversely associated with the risk of liver cancer in this study cohort. Third, in the absence of liver disease, several modifiable factors such as fasting glucose and smoking become more dominant in liver cancer risk prediction. Fourth, lipid control appears to be important to liver cancer prevention across diabetes and nondiabetes subpopulations. Fifth, the resulting linear scoring systems developed from ensemble tree-structured models reflect the interaction patterns among the set of candidate predictors in individual tree-structured models. Sixth, the risk scoring systems may help predict the risk of liver cancer in the presence or absence of liver disease across people with and those without diabetes. Further studies are needed to establish clinical thresholds to stratify patients into different levels of risk to potentially provide prioritization for public health strategies and guide clinical decision-making.

Limitations and Future Directions

Several limitations are potentially present in this study. First, diabetes status was defined by use of antidiabetic medication. Undiagnosed diabetes or nonuse of antidiabetic medications for diagnosed diabetes is potentially present. Fasting glucose or hemoglobin A_{1c} records were not checked for potential undiagnosed diabetes cases since it was not feasible. Second, while we intend to capture an incident diabetes cohort, some patients may have received a diagnosis of diabetes before the available prescription records period. Nevertheless, delayed diagnosis and treatment initiation is likely to be partially reflected in the presence of liver disease and levels of liver enzyme and fasting glucose in the risk scoring systems. Third, the possibility of reverse causality cannot be fully eliminated. Some risk factors such as fasting glucose and triglycerides could be influenced by subclinical liver dysfunction. Altered lipid and glucose metabolism may occur under liver dysfunction [26,54]. Fourth, some potential confounders such as adiposity indicators or alcohol use were not available in this study. Fifth, current and former smoking status was not differentiated since smokers may report inconsistent status between clinical visits. Differentiating current and former smokers may further subcategorize ever smokers into 2 different risk levels in the risk scoring system for patients without diabetes in the absence of liver disease (N_1). Sixth, information on serological tests for hepatitis virus was not available in this study. Seventh, further studies are warranted to evaluate generalizability to hepatitis C virus-endemic regions. Eighth, different populations may vary in prevalence [55], screening, diagnosis, and treatment of diabetes. Future research is warranted to examine generalizability to other populations with different diabetes management practices. Ninth, medication use and laboratory measurements were taken at baseline. However, these may change during follow-up. Tenth, the number of liver cancer cases in certain terminal nodes in the individual trees was low and may restrict generalizability of the identified optimal cutoffs beyond the study population. Eleventh, the optimal cutoffs in the scoring systems were defined by quantiles, and the values may vary across populations. Nevertheless, the optimal cutoffs could be fine-tuned [22] according to domain knowledge. Lastly, while variable selection in scoring development involves fine-tuning processes based on domain knowledge, split variable selection in separately built individual trees is automatic. Future research may consider undiagnosed diabetes, incorporate a broader list of candidate variables such as adiposity indicators and alcohol use, subcategorize current and former smoking status, evaluate serological status for hepatitis virus if available, establish clinical thresholds for risk scoring systems, and examine generalizability to other populations.

Conclusions

This study compared risk factors, their interaction patterns, and resulting scoring systems for liver cancer risk according to diabetes and liver disease status using tree-structured algorithms. Patients with and those without diabetes demonstrate distinctive interaction patterns among key factors on liver cancer risk. The resulting scoring systems reflect interaction patterns among the set of candidate predictors. Findings of the study may help identify targets for public health interventions and provide clinical cancer risk prediction for patients with and those without diabetes.

Acknowledgments

This study was supported by Hong Kong SAR government - Strategic Public Policy Research Funding Scheme (S2019.A4.015.19S).

Data Availability

Data access is restricted to authorized users. Requests for data access should be made to the Hospital Authority.

Authors' Contributions

Conceptualization and methodology: STYY, CTH, EYML, and EKY;
Data curation and formal analysis: STYY;
Writing – Original Draft Preparation: STYY;

XSL•FO
RenderX

Writing – Review and Editing: CTH, EYML, AL, and EKY;
Supervision: CTH and EKY;
Funding Acquisition: AL.

Conflicts of Interest

None declared.

References

1. Bray F, Laversanne M, Sung H, et al. Global cancer statistics 2022: GLOBOCAN estimates of incidence and mortality worldwide for 36 cancers in 185 countries. CA Cancer J Clin 2024;74(3):229-263. [doi: 10.3322/caac.21834] [Medline: 38572751]
2. Giovannucci E, Harlan DM, Archer MC, et al. Diabetes and cancer: a consensus report. Diabetes Care 2010 Jul;33(7):1674-1685. [doi: 10.2337/dc10-0666] [Medline: 20587728]
3. El-Serag HB, Hampel H, Javadi F. The association between diabetes and hepatocellular carcinoma: a systematic review of epidemiologic evidence. Clin Gastroenterol Hepatol 2006 Mar;4(3):369-380. [doi: 10.1016/j.cgh.2005.12.007] [Medline: 16527702]
4. Wu S, Zeng N, Sun F, et al. Hepatocellular carcinoma prediction models in chronic hepatitis b: A systematic review of 14 models and external validation. Clin Gastroenterol Hepatol 2021 Dec;19(12):2499-2513. [doi: 10.1016/j.cgh.2021.02.040] [Medline: 33667678]
5. Kubota N, Fujiwara N, Hoshida Y. Clinical and molecular prediction of hepatocellular carcinoma risk. J Clin Med 2020 Nov 26;9(12):3843. [doi: 10.3390/jcm9123843] [Medline: 33256232]
6. Flemming JA, Yang JD, Vittinghoff E, Kim WR, Terrault NA. Risk prediction of hepatocellular carcinoma in patients with cirrhosis: the ADRESS-HCC risk model. Cancer 2014 Nov 15;120(22):3485-3493. [doi: 10.1002/cncr.28832] [Medline: 25042049]
7. Hsu YC, Yip TCF, Ho HJ, et al. Development of a scoring system to predict hepatocellular carcinoma in Asians on antivirals for chronic hepatitis B. J Hepatol 2018 Aug;69(2):278-285. [doi: 10.1016/j.jhep.2018.02.032] [Medline: 29551708]
8. Sinn DH, Kang D, Cho SJ, et al. Risk of hepatocellular carcinoma in individuals without traditional risk factors: development and validation of a novel risk score. Int J Epidemiol 2020 Oct 1;49(5):1562-1571. [doi: 10.1093/ije/dyaa089] [Medline: 32725117]
9. Si WK, Chung JW, Cho J, et al. Predictors of increased risk of hepatocellular carcinoma in patients with type 2 diabetes. PLoS ONE 2016;11(6):e0158066. [doi: 10.1371/journal.pone.0158066] [Medline: 27359325]
10. Li TC, Li CI, Liu CS, et al. Risk score system for the prediction of hepatocellular carcinoma in patients with type 2 diabetes: Taiwan Diabetes Study. Semin Oncol 2018 Oct;45(5-6):264-274. [doi: 10.1053/j.seminoncol.2018.07.006] [Medline: 30342872]
11. Llovet JM, Kelley RK, Villanueva A, et al. Hepatocellular carcinoma. Nat Rev Dis Primers 2021 Jan 21;7(1):6. [doi: 10.1038/s41572-020-00240-3] [Medline: 33479224]
12. White DL, Ratziu V, El-Serag HB. Hepatitis C infection and risk of diabetes: a systematic review and meta-analysis. J Hepatol 2008 Nov;49(5):831-844. [doi: 10.1016/j.jhep.2008.08.006] [Medline: 18814931]
13. Hong YS, Chang Y, Ryu S, et al. Hepatitis B and C virus infection and diabetes mellitus: A cohort study. Sci Rep 2017 Jul 4;7(1):4606. [doi: 10.1038/s41598-017-04206-6] [Medline: 28676706]
14. Preuss HG, Kaats GR, Mrvichin N, Bagchi D, Preuss JM. Circulating ALT levels in healthy volunteers over life-span: Assessing aging paradox and nutritional implications. J Am Coll Nutr 2019;38(8):661-669. [doi: 10.1080/07315724.2019.1580169] [Medline: 31075051]
15. Dong MH, Bettencourt R, Brenner DA, Barrett-Connor E, Loomba R. Serum levels of alanine aminotransferase decrease with age in longitudinal analysis. Clin Gastroenterol Hepatol 2012 Mar;10(3):285-290. [doi: 10.1016/j.cgh.2011.10.014] [Medline: 22020064]
16. Petroff D, Bätz O, Jedrysiak K, Kramer J, Berg T, Wiegand J. Age dependence of liver enzymes: An analysis of over 1,300,000 consecutive blood samples. Clin Gastroenterol Hepatol 2022 Mar;20(3):641-650. [doi: 10.1016/j.cgh.2021.01.039] [Medline: 33524594]
17. Wannamethee SG, Shaper AG. Cigarette smoking and serum liver enzymes: the role of alcohol and inflammation. Ann Clin Biochem 2010 Jul;47(Pt 4):321-326. [doi: 10.1258/acb.2010.009303] [Medline: 20511375]
18. Breitling LP, Arndt V, Drath C, Rothenbacher D, Brenner H. Smoking and γ-glutamyltransferase: opposite interactions with alcohol consumption and body mass index. PLoS One 2010 Sep 30;5(9):e13116. [doi: 10.1371/journal.pone.0013116] [Medline: 20927196]
19. Parizadeh D, Ramezankhani A, Momenan AA, Azizi F, Hadaegh F. Exploring risk patterns for incident ischemic stroke during more than a decade of follow-up: A survival tree analysis. Comput Methods Programs Biomed 2017 Aug;147:29-36. [doi: 10.1016/j.cmpb.2017.06.006] [Medline: 28734528]

XSL•FO
RenderX

20. Ramezankhani A, Tohidi M, Azizi F, Hadaegh F. Application of survival tree analysis for exploration of potential interactions between predictors of incident chronic kidney disease: a 15-year follow-up study. J Transl Med 2017 Nov 28;15(1):240. [doi: 10.1186/s12967-017-1346-x] [Medline: 29183386]
21. Hothorn T, Hornik K, Zeileis A. Unbiased recursive partitioning: a conditional inference framework. J Comput Graph Stat 2012;15(3):651-674. [doi: 10.1198/106186006X133933]
22. Xie F, Ning Y, Yuan H, et al. AutoScore-Survival: Developing interpretable machine learning-based time-to-event scores with right-censored survival data. J Biomed Inform 2022 Jan;125:103959. [doi: 10.1016/j.jbi.2021.103959] [Medline: 34826628]
23. Thomas NJ, Jones SE, Weedon MN, Shields BM, Oram RA, Hattersley AT. Frequency and phenotype of type 1 diabetes in the first six decades of life: a cross-sectional, genetically stratified survival analysis from UK Biobank. Lancet Diabetes Endocrinol 2018 Feb;6(2):122-129. [doi: 10.1016/S2213-8587(17)30362-5] [Medline: 29199115]
24. Johnson JA, Carstensen B, Witte D, et al. Diabetes and cancer (1): evaluating the temporal relationship between type 2 diabetes and cancer incidence. Diabetologia 2012 Jun;55(6):1607-1618. [doi: 10.1007/s00125-012-2525-1] [Medline: 22476947]
25. Zhang J, Shen Y, Cai H, Liu YM, Qin G. Hepatitis B virus infection status and risk of type 2 diabetes mellitus: A meta-analysis. Hepatol Res 2015 Nov;45(11):1100-1109. [doi: 10.1111/hepr.12481] [Medline: 25601609]
26. Paul B, Lewinska M, Andersen JB. Lipid alterations in chronic liver disease and liver cancer. JHEP Rep 2022 Jun;4(6):100479. [doi: 10.1016/j.jhepr.2022.100479] [Medline: 35469167]
27. Shintani Y, Fujie H, Miyoshi H, et al. Hepatitis C virus infection and diabetes: direct involvement of the virus in the development of insulin resistance. Gastroenterology 2004 Mar;126(3):840-848. [doi: 10.1053/j.gastro.2003.11.056] [Medline: 14988838]
28. Green RM, Flamm S. AGA technical review on the evaluation of liver chemistry tests. Gastroenterology 2002 Oct;123(4):1367-1384. [doi: 10.1053/gast.2002.36061] [Medline: 12360498]
29. Dong MH, Bettencourt R, Barrett-Connor E, Loomba R. Alanine aminotransferase decreases with age: the Rancho Bernardo Study. PLoS ONE 2010 Dec 8;5(12):e14254. [doi: 10.1371/journal.pone.0014254] [Medline: 21170382]
30. Hill TA, Crooks CJ, West J, Morling JR. Trends in indirect liver function marker testing in Wales from 2000 to 2017 and their association with age and sex: an observational study. BMJ Open Gastroenterol 2022 Apr;9(1):e000885. [doi: 10.1136/bmjgast-2022-000885] [Medline: 35487590]
31. Gagliano N, Grizzi F, Annoni G. Mechanisms of aging and liver functions. Dig Dis 2007;25(2):118-123. [doi: 10.1159/000099475] [Medline: 17468546]
32. Schmucker DL. Aging and the liver: an update. J Gerontol A Biol Sci Med Sci 1998 Sep;53(5):B315-B320. [doi: 10.1093/gerona/53a.5.b315] [Medline: 9754128]
33. Vell MS, Loomba R, Krishnan A, et al. Association of statin use with risk of liver disease, hepatocellular carcinoma, and liver-related mortality. JAMA Netw Open 2023 Jun 1;6(6):e2320222. [doi: 10.1001/jamanetworkopen.2023.20222] [Medline: 37358849]
34. Singh S, Singh PP, Singh AG, Murad MH, Sanchez W. Statins are associated with a reduced risk of hepatocellular cancer: a systematic review and meta-analysis. Gastroenterology 2013 Feb;144(2):323-332. [doi: 10.1053/j.gastro.2012.10.005] [Medline: 23063971]
35. Kim G, Jang SY, Nam CM, Kang ES. Statin use and the risk of hepatocellular carcinoma in patients at high risk: A nationwide nested case-control study. J Hepatol 2018 Mar;68(3):476-484. [doi: 10.1016/j.jhep.2017.10.018] [Medline: 29107150]
36. Dale KM, Coleman CI, Henyan NN, Kluger J, White CM. Statins and cancer risk: a meta-analysis. JAMA 2006 Jan 4;295(1):74-80. [doi: 10.1001/jama.295.1.74] [Medline: 16391219]
37. Jiang P, Mukthavaram R, Chao Y, et al. In vitro and in vivo anticancer effects of mevalonate pathway modulation on human cancer cells. Br J Cancer 2014 Oct 14;111(8):1562-1571. [doi: 10.1038/bjc.2014.431] [Medline: 25093497]
38. Sinn DH, Kang D, Park Y, et al. Statin use and the risk of hepatocellular carcinoma among patients with chronic hepatitis B: an emulated target trial using longitudinal nationwide population cohort data. BMC Gastroenterol 2023 Oct 25;23(1):366. [doi: 10.1186/s12876-023-02996-w] [Medline: 37880589]
39. Zhou F, Sun X. Cholesterol metabolism: A double-edged sword in hepatocellular carcinoma. Front Cell Dev Biol 2021;9:762828. [doi: 10.3389/fcell.2021.762828] [Medline: 34869352]
40. An C, Choi JW, Lee HS, et al. Prediction of the risk of developing hepatocellular carcinoma in health screening examinees: a Korean cohort study. BMC Cancer 2021 Jun 29;21(1):755. [doi: 10.1186/s12885-021-08498-w] [Medline: 34187409]
41. Yi SW, Kim SH, Han KJ, Yi JJ, Ohrr H. Higher cholesterol levels, not statin use, are associated with a lower risk of hepatocellular carcinoma. Br J Cancer 2020 Mar;122(5):630-633. [doi: 10.1038/s41416-019-0691-3] [Medline: 31857717]
42. Kitahara CM, Berrington de González A, Freedman ND, et al. Total cholesterol and cancer risk in a large prospective study in Korea. J Clin Oncol 2011 Apr 20;29(12):1592-1598. [doi: 10.1200/JCO.2010.31.5200] [Medline: 21422422]
43. Kaplan DE, Serper MA, Mehta R, et al. Effects of hypercholesterolemia and statin exposure on survival in a large national cohort of patients with cirrhosis. Gastroenterology 2019 May;156(6):1693-1706. [doi: 10.1053/j.gastro.2019.01.026] [Medline: 30660733]

XSL•FO
RenderX

44. Qin WH, Yang ZS, Li M, et al. High serum levels of cholesterol increase antitumor functions of nature killer cells and reduce growth of liver tumors in mice. Gastroenterology 2020 May;158(6):1713-1727. [doi: 10.1053/j.gastro.2020.01.028] [Medline: 31972238]
45. Han H, Zhang T, Jin Z, et al. Blood glucose concentration and risk of liver cancer: systematic review and meta-analysis of prospective studies. Oncotarget 2017 Jul 25;8(30):50164-50173. [doi: 10.18632/oncotarget.16816] [Medline: 28432278]
46. IARC monographs on the identification of carcinogenic hazards to humans. International Agency for Research on Cance.: World Health Organization; 2025. URL: https://monographs.iarc.who.int/agents-classified-by-the-iarc/ [accessed 2025-10-16]
47. Marti-Aguado D, Clemente-Sanchez A, Bataller R. Cigarette smoking and liver diseases. J Hepatol 2022 Jul;77(1):191-205. [doi: 10.1016/j.jhep.2022.01.016] [Medline: 35131406]
48. Rossiello F, Jurk D, Passos JF, d'Adda di Fagagna F. Telomere dysfunction in ageing and age-related diseases. Nat Cell Biol 2022 Feb;24(2):135-147. [doi: 10.1038/s41556-022-00842-x] [Medline: 35165420]
49. Breitling LP, Arndt V, Drath C, Brenner H. Liver enzymes: interaction analysis of smoking with alcohol consumption or BMI, comparing AST and ALT to γ-GT. PLoS ONE 2011;6(11):e27951. [doi: 10.1371/journal.pone.0027951] [Medline: 22132177]
50. Breitling LP, Raum E, Müller H, Rothenbacher D, Brenner H. Synergism between smoking and alcohol consumption with respect to serum gamma-glutamyltransferase. Hepatology 2009 Mar;49(3):802-808. [doi: 10.1002/hep.22727] [Medline: 19152425]
51. Lee DH, Blomhoff R, Jacobs DR Jr. Is serum gamma glutamyltransferase a marker of oxidative stress? Free Radic Res 2004 Jun;38(6):535-539. [doi: 10.1080/10715760410001694026] [Medline: 15346644]
52. Wang CS, Wang ST, Chang TT, Yao WJ, Chou P. Smoking and alanine aminotransferase levels in hepatitis C virus infection: implications for prevention of hepatitis C virus progression. Arch Intern Med 2002 Apr 8;162(7):811-815. [doi: 10.1001/archinte.162.7.811] [Medline: 11926856]
53. Alberti K, Eckel RH, Grundy SM, et al. Harmonizing the metabolic syndrome: a joint interim statement of the International Diabetes Federation Task Force on Epidemiology and Prevention; National Heart, Lung, and Blood Institute; American Heart Association; World Heart Federation; International Atherosclerosis Society; and International Association for the Study of Obesity. Circulation 2009 Oct 20;120(16):1640-1645. [doi: 10.1161/CIRCULATIONAHA.109.192644] [Medline: 19805654]
54. Satriano L, Lewinska M, Rodrigues PM, Banales JM, Andersen JB. Metabolic rearrangements in primary liver cancers: cause and consequences. Nat Rev Gastroenterol Hepatol 2019 Dec;16(12):748-766. [doi: 10.1038/s41575-019-0217-8] [Medline: 31666728]
55. Sun H, Saeedi P, Karuranga S, et al. IDF Diabetes Atlas: Global, regional and country-level diabetes prevalence estimates for 2021 and projections for 2045. Diabetes Res Clin Pract 2022 Jan;183:109119. [doi: 10.1016/j.diabres.2021.109119] [Medline: 34879977]

Abbreviations:

ALT: alanine aminotransferase
C-index: concordance index
GGT: gamma-glutamyl transferase
HA: Hospital Authority
HBV: hepatitis B virus
HDL: high-density lipoprotein
***ICD-10*:** *International Statistical Classification of Diseases, Tenth Revision*
ICPC-2: International Classification of Primary Care 2nd edition
LDL: low-density lipoprotein

Edited by A Coristine; submitted 06.02.25; peer-reviewed by C Sun, D Khanna; revised version received 29.08.25; accepted 29.08.25; published 27.10.25.

Please cite as:
Yau STY, Hung CT, Leung EYM, Lee A, Yeoh EK
Comparison of Risk Factors, Their Interaction Patterns, and Scoring Systems for Liver Cancer Between Patients With and Those Without Diabetes: Retrospective Cohort Study Using Electronic Health Records and Tree-Structured Algorithms
JMIR Med Inform 2025;13:e72239
URL: https://medinform.jmir.org/2025/1/e72239
doi:10.2196/72239

XSL•FO
RenderX

© Sarah Tsz Yui Yau, Chi Tim Hung, Eman Yee Man Leung, Albert Lee, Eng Kiong Yeoh. Originally published in JMIR Medical Informatics (https://medinform.jmir.org), 27.10.2025. This is an open-access article distributed under the terms of the Creative Commons Attribution License (https://creativecommons.org/licenses/by/4.0/), which permits unrestricted use, distribution, and reproduction in any medium, provided the original work, first published in JMIR Medical Informatics, is properly cited. The complete bibliographic information, a link to the original publication on https://medinform.jmir.org/, as well as this copyright and license information must be included.

XSL•FO
RenderX

Named Entity Recognition for Chinese Cancer Electronic Health Records—Development and Evaluation of a Domain-Specific BERT Model: Quantitative Study

Junbai Chen[1,2], MA; Butian Zhao[1], PhD; Xiaohan Tian[1], BA; Zhengkai Zou[1], BA; Ruojia Wang[1], PhD; Jiarui Wu[1], PhD; Songxing Du[3], BA; Fengying Guo[1], MS

[1]School of Management, Beijing University of Chinese Medicine, No. 11, North Third Ring Road East, Chaoyang District, Beijing, China

[2]Department of Information Management, Peking University, Beijing, China

[3]Information Center, Dongfang Hospital, Beijing, China

Corresponding Author:
Fengying Guo, MS
School of Management, Beijing University of Chinese Medicine, No. 11, North Third Ring Road East, Chaoyang District, Beijing, China

Abstract

Background: The unstructured data of Chinese cancer electronic health records (EHRs) contains valuable medical expertise. Accurate medical entity recognition is crucial for building a medical-assisted decision system. Named entity recognition (NER) in cancer EHRs typically uses general models designed for English medical records. There is a lack of specialized handling for cancer-specific records and limited application to Chinese medical records.

Objective: This study aims to propose a specific NER model to enhance the recognition of medical entities in Chinese cancer EHRs.

Methods: Desensitized inpatient EHRs related to breast cancer were collected from a leading hospital in Beijing. Building upon the MC Bidirectional Encoder Representations from Transformers (BERT) foundation, the study further incorporated a Chinese cancer corpus for pretraining, resulting in the construction of the ChCancerBERT pretrained model. In conjunction with dilated-gated convolutional neural networks, bidirectional long short-term memory, multihead attention mechanism, and a conditional random field, this model forms a multimodel, multilevel integrated NER approach.

Results: This approach effectively extracts medical entity features related to symptoms, signs, tests, treatments, and time in Chinese breast cancer EHRs. The entity recognition performance of the proposed model surpasses that of the baseline model and other models compared in the experiment. The F_1-score reached 86.93%, precision reached 87.24%, and recall reached 86.61%. The model introduced in this study demonstrates exceptional performance on the CCKS2019 dataset, attaining a precision rate of 87.26%, a recall rate of 87.27%, and an impressive F_1-score of 87.26%, surpassing that of existing models.

Conclusions: The experiments demonstrate that the approach proposed in this study exhibits excellent performance in NER within breast cancer EHRs. This advancement will further contribute to clinical decision support for cancer treatment and research. In addition, the study reveals that incorporating domain-specific corpora in clinical NER tasks can further enhance the performance of BERT models in specialized domains.

(JMIR Med Inform 2025;13:e76912) doi:10.2196/76912

KEYWORDS

BERT; named entity recognition; cancer; electronic health records; deep learning

Introduction

Background

Cancer is one of the leading causes of mortality [1], imposing a significant psychological burden on patients and potentially triggering mental health disorders such as anxiety and depression [2]. The proliferation of electronic health records (EHRs) has provided a crucial source of demographic information, medical history, diagnostic tests, and clinical treatment data for cancer research, aiding in better diagnosis, prognosis, and treatment of the disease [3]. However, the large amount of unstructured text in EHRs presents significant challenges for clinical research and analysis. Structuring this unstructured information is essential for subsequent data analysis and mining to support clinical decision-making. Named entity recognition (NER) is a critical component of natural language processing (NLP), plays a key role in this process by identifying and classifying entities, allowing for transforming raw clinical texts into structured data,

XSL•FO
RenderX

thereby enabling large-scale data mining and supporting intelligent health care applications [4].

In recent years, many studies have explored different NER methods to structure EHRs. The widespread application of pretrained models such as Bidirectional Encoder Representations from Transformers (BERT) has significantly enhanced NER performance in the medical field [5,6]. These improvements are especially valuable in the medical domain, where precise recognition of specialized entities directly impacts the reliability of downstream analyses including cohort selection, clinical decision support, and the construction of medical knowledge bases [7,8]. However, most of these studies focus on English texts, and the differences between English and Chinese in terms of language expression may limit the generalizability of English medical NER methods when directly applied to Chinese medical texts.

Compared to medical texts in common diseases, cancer EHRs contain richer and more complex information. These records span multiple fields, including medicine, biology, and pharmacology, and encompass specific medical terminologies such as cancer staging, treatment plans, and drug names. They also include diagnostic and treatment records like surgical notes and pathology results, with a prevalent occurrence of nested entities. In current NER tasks for the cancer domain, models such as BERT and other deep learning approaches based on general corpora are often used without fine-tuning for the numerous specialized terms and specific expressions in this field, which may result in errors or omissions. In addition, there is no publicly available dataset benchmark for the cancer domain. Therefore, NER tasks for Chinese cancer EHRs remain both challenging and necessary.

To address the aforementioned issues, this study contributes the following:

1. We retrained the MC-BERT model using a corpus specific to the Chinese cancer domain, resulting in the ChCancerBERT pretrained model tailored for NER tasks in the Chinese cancer field. This approach effectively enhances the semantic representation capabilities of pretrained models in a specialized domain.
2. In the Chinese medical domain, we built a hybrid model to capture temporal features and bidirectional semantic information. This combination enhances the model's ability to perform multidimensional feature modeling.
3. To validate the model's effectiveness, we created a Chinese breast cancer EHR corpus with manual annotations. We applied various models to this corpus, and the experimental results demonstrated that our proposed model outperforms existing models, achieving superior performance. We also applied the model proposed in this study to the CCKS2019 dataset and compared the results with those from existing studies for evaluation.

Related Work

In the medical field, prior research has developed various NER methods for extracting information from unstructured data such as EHRs. Table 1 summarizes related studies and methods for clinical NER in the medical field.

NER techniques can be categorized into 3 main types: dictionary and rule-based methods, machine learning–based methods, and deep learning–based methods. Dictionary and rule-based NER methods rely primarily on researchers analyzing textual writing rules and establishing dictionaries, then using regular expression matching to achieve entity recognition and information extraction. For instance, Najafabadipour et al [9] extracted multiple cancer concepts such as tumor staging, mutation status, and patient presentation from lung cancer clinical records using regular expressions and the UMLS8 dictionary. Yim et al [10] used rule-based extraction to identify 3 liver cancer entities: tumor size, staging level, and percentage of tumors invading the liver. These methods are straightforward and efficient but lack generalizability and require significant human effort to build dictionaries [10]. Machine learning–based methods use sequence labeling and train models such as hidden Markov model, conditional random fields (CRFs), and maximum entropy Markov model on large manually annotated feature corpora to achieve NER. For example, Savova et al [11] developed the DeepPhe software, which uses a combination of rules, domain knowledge bases, and machine learning to extract cancer phenotypes from clinical records. Weegar et al [12] used a CRF model to extract cervical cancer symptom information.

In recent years, deep learning methods have made significant progress in medical NER tasks, demonstrating substantial advantages in NLP compared to traditional feature-based machine learning methods. These approaches typically predict the boundaries and types of entities by labeling each word, thereby capturing deeper and more abstract features. For instance, An et al [13] used a bidirectional long short-term memory (BiLSTM)-CRF model with a multihead attention (MHA) mechanism to perform Chinese clinical EHR NER. Kong et al [14] combined multilayer convolutional neural networks (CNNs) with an attention mechanism to improve NER in Chinese EHRs. The emergence of pretrained models like BERT has further enhanced the performance of NER. In the medical domain, existing research shows that BERT-based models can be effectively applied to medical information extraction tasks. Li et al [5] achieved excellent results using a BERT-BiLSTM-CRF model on the CCKS2018 and CCKS2019 datasets. Li et al [15] proposed an A Lite Bidirectional Encoder Representations from Transformers (ALBERT)-based model with a MHA mechanism for Chinese medical NER, validated on the CCKS2019 dataset. Chen et al [6] constructed a hybrid model combining MC-BERT, BiLSTM, CNN, MHA, and CRF to achieve NER in Chinese EHRs. Most of these studies primarily applied their deep learning models to publicly available datasets such as CCKS2017 and CCKS2019, without further testing them on specific medical departments or diseases.

Existing research indicates that using domain-specific text as training data, as opposed to general language models, can yield better performance. For the cancer field, Zhou et al [7] proposed CancerBERT, a pretrained model specifically designed for the English language in the cancer domain. Currently, there is no similar model for the Chinese cancer domain. Given the differences between Chinese and English in terms of vocabulary, sentence structure, grammatical rules, and semantic expression,

XSL•FO
RenderX

directly applying models trained on English corpora may lead to suboptimal results.

Table . Summary of related work on clinical named entity recognition methods in the medical and cancer domains.

Proposal	Approach	Method	Domain	Domain model	Benchmark	Language
Najabadipour et al 2018 [9]	Rules	Rule-based methods	Cancer	Yes	No	Spanish
Yim et al.2016 [10]	Rules	Rule-based methods	Cancer	Yes	No	English
Savova et al 2017 [11]	Rules and machine learning	Rule-based methods	Cancer	Yes	No	English
Weegar et al 2015 [12]	Machine learning	CRF[a]	Cancer	No	No	English
An et al 2022 [13]	Deep learning	BiLSTM[b]-MHA[c]-CRF	Medical	No	Yes	Chinese
Kong et al [14]	Deep learning	CNN[d]	Medical	No	Yes	Chinese
Li et al 2022 [5]	Deep learning	ALBERT[e]-IDCNN[f]-MHA-CRF	Medical	No	Yes	Chinese
Li et al 2020 [5]	Deep learning	BERT[g]-BiLSTM-CRF	Medical	No	Yes	Chinese
Chen et al 2022 [6]	Deep learning	MC-BERT-BiLSTM-CNN-MHA-CRF	Medical	Yes	Yes	Chinese
Li et al 2023 [16]	Deep learning	• MC-BERT • GCN[h]-CRF	Medical	Yes	Yes	Chinese
Zhou et al 2022,2023 [7,8]	Deep learning	CancerBERT	Cancer	Yes	No	English

[a]CRF: conditional random field.

[b]BiLSTM: bidirectional long short-term memory.

[c]MHA: multihead attention

[d]CNN: convolutional neural network.

[e]ALBERT: A Lite Bidirectional Encoder Representations from Transformers.

[f]IDCNN: iterated dilated convolutional neural network.

[g]BERT: Bidirectional Encoder Representations from Transformers.

[h]GCN: graph convolutional network.

Methods

Ethical Considerations

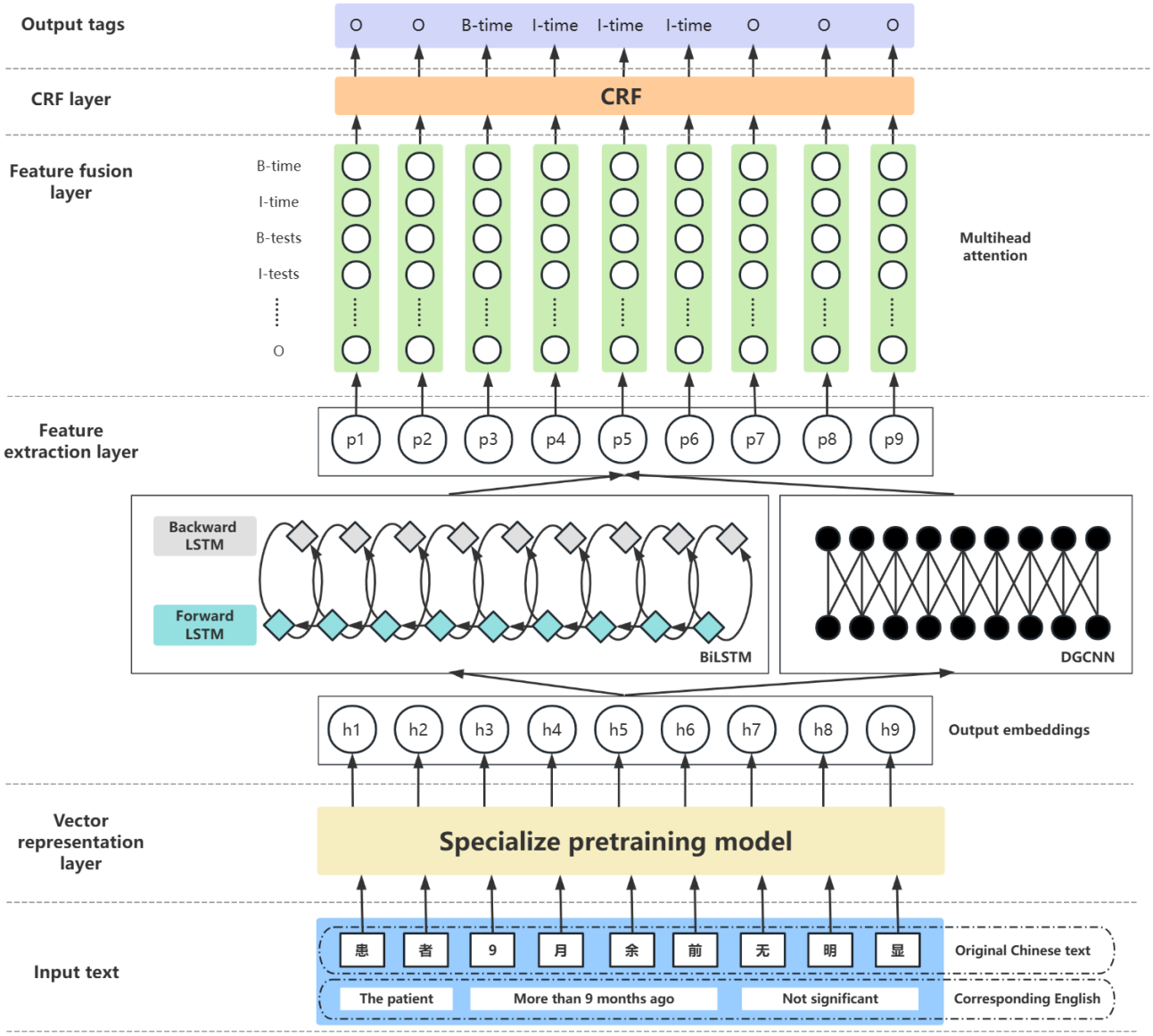
Based on Article 32 of the *Measures for Ethical Review of Life Sciences and Medical Research Involving Human Subjects* [17] research using human data or biological samples that does not cause harm to the human body, does not involve sensitive personal information or commercial interests, is eligible for exemption from ethical review. This exemption is intended to reduce unnecessary burdens on researchers and to facilitate the progress of life sciences and medical research. In our study, the dataset used has undergone thorough anonymization, with all personal patient information removed. In addition, the patients involved in the clinical activities at the hospital have already signed the relevant informed consent forms, confirming their agreement to the use of their data for research purposes. Therefore, as per the national regulations, our study did not require ethical review. The data were granted permission to be accessed by SD, who is the director of the Information Center of Dongfang Hospital Beijing University of Chinese Medicine, responsible for managing all the hospital's data, and he is listed as a contributing author.

Model Construction

The proposed model architecture in this study is illustrated in Figure 1.

XSL•FO
RenderX

Figure 1. The architecture of the proposed model, for ease of viewing and understanding, the input text examples in the figure are accompanied by corresponding English translations. BiLSTM: bidirectional long short-term memory; CRF: conditional random field; DGCNN: dilated-gated convolutional neural network; LSTM: long short-term memory.



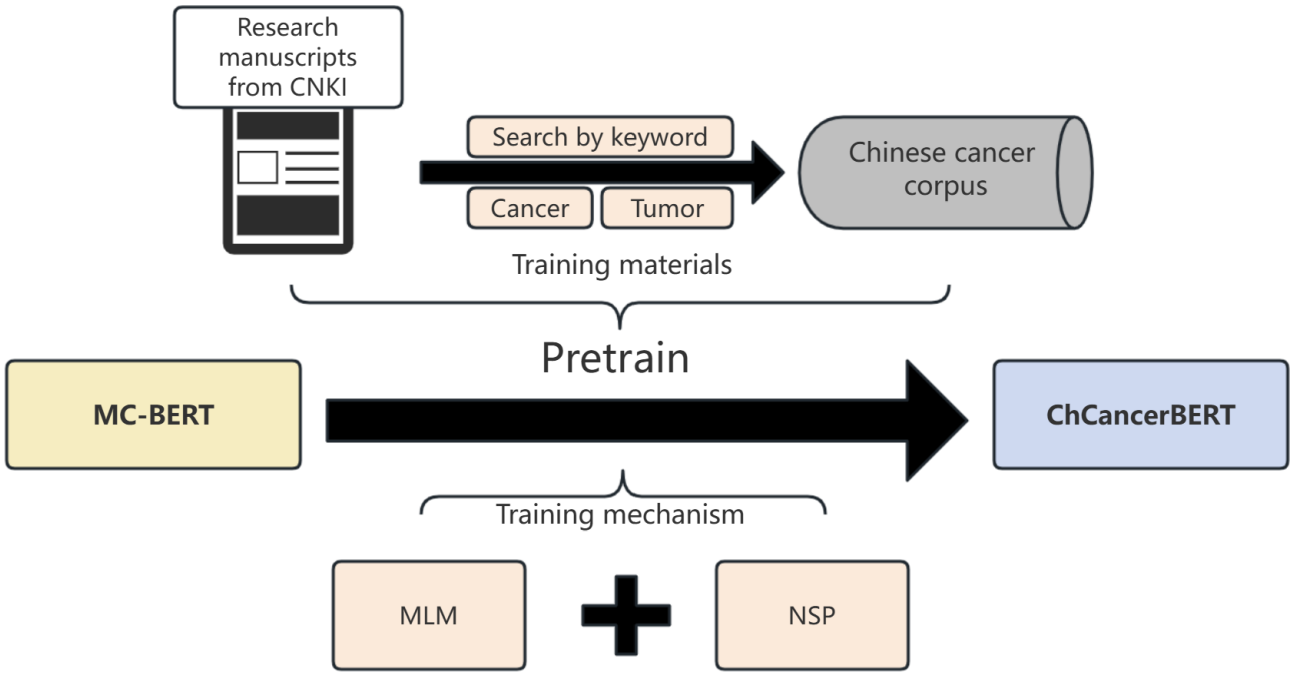
The model comprises 4 parts: the vector representation layer, feature extraction layer, feature fusion layer, and CRF layer. The Chinese cancer EHR texts are input into the model, where the input text is segmented into individual characters to form the basic sequence X={x1,x2,…,xi}, where xi is the *i*-th character. Initially, in the vector representation layer, the input sequences X={x1,x2,…,xi} are represented as semantically rich character-level embedding vectors hi using the autonomously trained BERT model tailored to the Chinese cancer domain (ChCancerBERT), forming the embedding sequence H={h1,h,…,hi}. Subsequently, the sequence H={h1,h,…,hi} is fed into the BiLSTM and dilated-gated convolutional neural network (DGCNN) models within the feature extraction layer. The feature extraction layer uses BiLSTM to extract long-distance dependency associations and temporal features from the sequences, while DGCNN captures spatial features. In the feature fusion layer, a MHA mechanism with enhanced generalization capability dynamically fuses the features extracted by BiLSTM and DGCNN to enhance the model's feature representation capability. The CRF layer imposes constraints on the output to obtain the optimal labeling results. Finally, the model outputs a set of label sequences Y={y1,y,…,yi}, where each label yi corresponds to a character in the input text. For instance, "B-TIME" denotes the beginning of a TIME entity, while "I-TIME" denotes the inside of a TIME entity, with the label sequence indicating the model's classification results for each character.

Chinese Cancer Specialized BERT

To better capture semantics in cancer electronic medical records, this study trained a specialized BERT model tailored for the Chinese cancer domain (ChCancerBERT) to enhance the performance of extracting cancer-related phenotypes. Figure 2 illustrates the training process of the ChCancerBERT model.

XSL•FO
RenderX

Figure 2. The training process of ChCancerBERT models. BERT: Bidirectional Encoder Representations from Transformers; CNKI: China National Knowledge Infrastructure; MC: ;MLM: masked language model; NSP: next sentence prediction



Pretrained models are typically based on large-scale general corpora for data pre-training. Depending on the specific needs, they can also incorporate domain-specific vocabulary to calculate the probability P(S) of all possible language sequences.

$$(1)P(S)=p(\omega 1,\omega 2,\ldots,\omega n)=\prod i=1np(\omega|\omega 1,\omega 2,\ldots,\omega i-1)$$

The most commonly used pretrained model is the BERT model, a deep bidirectional language representation model that offers significant advantages in capturing textual semantic information and entity extraction [18-20]. Although BERT achieves good results in most domains, its generic nature may limit its ability to fully capture the specialized terminology and semantic nuances of the medical field [15]. MC-BERT fine-tuned on BERT by using different pretraining strategies to incorporate medical-specific and related vocabulary, enabling superior performance in medical NER tasks [6].

The ChCancerBERT model proposed in this study is further pretrained based on the MC-BERT model. The specific steps are as follows: firstly, a Chinese cancer corpus was constructed. Using keywords “cancer” and “tumor,” a search strategy retrieved relevant Chinese-language literature from the China National Knowledge Infrastructure (CNKI) database. The corpus included abstracts from the first 6000 articles, organized chronologically, resulting in a comprehensive dataset of 3,268,570 tokens. This dataset ensures that ChCancerBERT is exposed to terminology and context unique to the cancer domain, thus improving its capacity for semantic understanding. Second, the pretraining of ChCancerBERT used both masked language model and next sentence prediction tasks to enhance semantic representation. Based on the masked language model, the approach involves randomly masking certain characters within a sentence to learn the semantic information of each character in context. This encourages ChCancerBERT to learn nuanced semantic relationships, particularly for specialized terminology within cancer-specific contexts. In addition, the next sentence prediction model is used to learn the association between 2 consecutive sentences, enabling it to capture long-distance dependencies and contextual flows frequently present in medical records. This step is particularly beneficial for understanding the multisentence descriptions often found in medical documents.

BiLSTM Model

Long short-term memory (LSTM) is a specialized form of recurrent neural network that can capture larger and longer-distance information. By using a set of gate controllers, LSTM effectively addresses the gradient vanishing and exploding problems inherent in traditional recurrent neural networks [21]. An LSTM, the input gate it controls information into the current cell, the forget gate ft manages the forgetting of information, and the output gate ot controls the information output. ht records the output at the current time step, while ct preserves the current cell state and serves as input for the next cell. The sigmoid activation function is denoted by σ, the weight matrix by W, the bias term by b, and the current cell input by xt. st represents the updated state at the current time step, and the hyperbolic tangent activation function is denoted by tanh:

$$(2)ft=\sigma(Wf\cdot[ht-1,xt]+bf)it=\sigma(Wi\cdot[ht-1,xt]+bi)ot=\sigma(Wo\cdot[ht-1,xt]+bo)\tilde{c}t=\tanh(Wc\cdot[ht-1,xt]+bc)ct=ft\ast ct-1+it\ast\tilde{c}tht=ot\ast\tanh(ct)$$

BiLSTM consists of a forward LSTM and a backward LSTM, which respectively capture forward and backward information from the text sequence [22]. These are then concatenated to obtain the final hidden layer feature representation. Compared to a single LSTM model, BiLSTM provides a more nuanced understanding of bidirectional semantic dependencies and allows for more precise semantic discrimination [23].

In our model, BiLSTM is applied immediately after the vector representation layer, where ChCancerBERT generates the character-level embeddings tailored to the cancer domain. These embeddings are then fed into the BiLSTM, which consists of a forward and backward LSTMs, capturing both forward and

XSL•FO
RenderX

backward contextual information. By leveraging BiLSTM, the model can retain bidirectional semantic dependencies that are crucial in understanding complex medical texts.

DGCNN Model

DGCNN is a neural network model with residual connections that uses gated dilated convolutions to gather more information through stacked convolutional layers [4]. Its convolutional structure, which enables the model to analyze sequences in segments, examining local patterns that are essential to textual spatial characteristics, which are usually referred to the arrangement and relationships of words and phrases that form meaningful units [4]. These units include nearby dependencies and longer-range relationships, like multiword medical entities in EHRs. DGCNN's use of dilated convolutions allows it to capture these features at different scales or distances, enabling it to handle both close and distant relationships within the text [14]. The convolution operations proceed as follows:

(3)ct=Wc k=0rxt±k

In the model, Wc denotes a filter with window size *r*, and ct represents the output after convolution transformation. The symbol ⊕ indicates vector concatenation. Building on this, dilation is introduced for interval sampling of data, enabling the coverage of longer sentences. The calculation method for dilated convolution is as follows:

(4)ct=Wc k=0rxt±kδ

δ represents the dilation rate, and Wc is a filter with window size r. ct denotes the output, while ⊕ signifies vector concatenation. A gating mechanism is also incorporated to control data flow and reduce the risk of gradient vanishing. The operations within each convolutional gated unit are as follows:

(5)Y=X+Conv1D1(X)⊗σ(Conv2D2(X))

X represents the input. Conv1D1 and Conv2D2 are dilated convolutions with the same parameter structure but without sharing weights. σ denotes the sigmoid function, and ⊗ represents the Hadamard product of vectors.

After the ChCancerBERT model generates the character-level embeddings, these embeddings are input independently into the DGCNN model, extracting spatial dependencies and local features, which are essential for identifying nested entities and capturing complex structures within cancer-related records.

MHA Mechanism

The attention mechanism simulates human attention by scoring and weighting important content to highlight significant features [24]. The calculation formula is as follows:

(6)Attention(Q,K,V)=Softmax(QKTdk)V

The AttentionQ,K,Vvalue represents the attention score, where Qs the query vector matrix, K is the key vector matrix, and V is the value vector matrix. dk is the word vector dimension which normalizes the similarity between the query and key vectors calculated via QKT to prevent overly large results. Softmax normalization is then applied, followed by multiplication with the value vector to obtain the final attention value. When vector dimensions are high, a single attention calculation may not capture all features of a word. Thus, the MHA mechanism is used, linearly mapping Q,K,V into multiple subspaces and combining the calculated results:

This study uses an MHA mechanism to dynamically fuse the BiLSTM and DGCNN models. First, the outputs of both models are mapped to separate feature spaces, generating 2 sets of Q,K,V matrices. Next, the attention values for each model are calculated, resulting in 2 attention representation matrices. Finally, these matrices are combined into a single matrix through matrix multiplication.

CRF Model

CRF is a sequence modeling framework that incorporates constraints between labels to assign higher probabilities to reasonable label sequences [20]. This approach effectively addresses the issue of label bias.

The probability formula for obtaining the predicted label sequence X=(x1,x2,…,xn)given the input sequence Y=(y1,y2,…,yn) is as follows:

(8)P(Y|X)=eT(X,Y)∑Y′∈ YXT(X,Y′)

Given the true label sequence Y`, and all possible label sequences YX, the likelihood function for predicting the label sequence Y is as follows:

(9)ln (P(Y|X))=T(X,Y)−ln (∑Y′∈ YXT(X,Y′))

By maximizing the likelihood function, the most probable and reasonable label sequence is determined and output. The specific formula is as follows:

(10)Y∗=argy~∈ YXmaxs(X,y~)

Experiment Setups

Dataset Construction

The study's data were sourced from the inpatient EHRs at a renowned hospital in Beijing, China, spanning from 2013 to 2022. After excluding patients with unrelated admission reasons (ie, those who have previously had breast cancer but whose current reason for admission is not breast cancer), the illness histories from all patients' admission records within this time period were included. Each patient had 1 record per visit, and we ultimately obtained 876 records of patients with breast cancer (total tokens: 528,925, average length: 659.67, SD 354.23). The data received full approval from the hospital. All procedures in this research adhere to ethical standards. Patient privacy data were deidentified before manipulation, ensuring anonymity and confidentiality of personal information.

Annotation Procedure for the Dataset

The annotation of data from 876 admission records of patients with breast cancer was a collaborative effort involving 7 annotators. All of these annotators were the students of the Management School of Beijing University of Chinese Medicine and possessed relevant medical and computer expertise. To enhance the precision of the labeling outcomes, 2 oncology clinicians from the Beijing University of Chinese Medicine were enlisted to train the annotators. They also facilitated content segmentation and offered guidance throughout the labeling process. Based on information extracted from the

XSL•FO
RenderX

collected data, in conjunction with insights from pertinent clinical studies [25,26] and guided by categorizations and classifications in clinical literature, as well as referencing indicators present in public medical databases such as SEER, CCKS2017, CCKS2019, along with existing study labeling protocols [27], an index system (Table 2) and labeling criteria (Table 3) were formulated for this research. These encompassed symptoms, tests, treatments, and time.

Table . Index system of the annotated dataset for Chinese breast cancer electrical health records (EHRs).

Class	Entity
Symptoms	Nodule
Tests	• Vascular tumor thrombus and nerve aggress • Incisal edge • Lymph node dissection • Birads • TNM[a] • ER[b] • PR[c] • HER2[d] • Ki67
Treatments	• Surgery name • Chemotherapy • Radiotherapy • Targeted therapy • Endocrine therapy
Time	Time

[a]TNM: TNM classification of malignant tumors.

[b]ER: Estrogen receptor.

[c]PR: progesterone receptor.

[d]HER2: human epidermal growth factor receptor-2.

XSL•FO
RenderX

Table . Entity labeling standards with examples[a].

Entity	Standard	Example	Example in English
Time	Date and time in various formats	2011年	2011
Surgery name	Name of a patient undergoing surgery	左侧乳腺癌根治术	Left breast cancer radical surgery
Nodule	Examination results and location of breast nodules	右乳腺肿物	Right breast mass
Chemotherapy	Patient chemotherapy regimen, medication, cycle	术后行辅助化疗6周期 (紫杉醇+环磷酰胺，具体剂量不详）	After surgery, undergo adjuvant chemotherapy for 6 cycles (paclitaxel+ cyclophosphamide, specific dosages not specified)
Radiotherapy	The patient's radiotherapy regimen and frequency	放疗25次，具体剂量不详	Undergo 25 sessions of radiation therapy, specific dosage not specified
Targeted therapy	Targeted therapy, drugs	后续贯赫赛汀靶向治疗18次	Followed by 18 sessions of trastuzumab targeted therapy
Endocrine therapy	Endocrine treatment options, drugs	阿那曲唑1mgQd口服内分泌治疗	Anastrozole 1mg once daily, oral administration for endocrine therapy
Incisal edge	Whether the incisal edge of the patient is cancerous	各皮肤切缘未见癌侵润	No cancer infiltration is observed at the margins of the skin
Vascular tumor thrombus and nerve aggression	Results of examination of vascular tumor thrombus and nerve aggression	侵及周围脂肪组织及神经纤维束，脉管中见癌栓	Involvement of surrounding adipose tissue and nerve fiber bundles, with cancer emboli seen in blood vessels
Lymph node dissection	The patient's lymph node dissection results	淋巴结未见转移癌 (0/21），腋窝淋巴结 (0/18），(右腋窝淋巴结）0/3	No metastatic cancer detected in lymph nodes (0/21), axillary lymph nodes (0/18), (right axillary lymph nodes) 0/3
Bi-RADS[b]	Bi-RADS classification of breast nodules	BI_RADS4b类[b]	BI-RADS4b[b]
TNM[c]	The patients' TNM stages	pT2N0M0, IIa期	pT2N0M0,IIa
ER[d]	Patient pathology reported ER results	ER (+++)	ER (+++)
PR[e]	Patient pathology reported PR results	PR (+++)	PR (+++)
HER2[f]	HER2 results were reported pathologically	HER2 (–)	HER2 (–)
Ki67	Patient pathology reported KI67 results	ki-67index约20%	Ki-67 index is approximately 20%

[a]All texts to be annotated are in Chinese; for ease of viewing and understanding, the annotated examples in the table are accompanied by corresponding English translations, the patient information presented is simulated.

[b]Bi-RADS: breast imaging reporting and data system.

[c]TNM: TNM classification of malignant tumors.

[d]ER: estrogen receptor.

[e]PR: progesterone receptor.

[f]HER2: human epidermal growth factor receptor-2.

The "symptom" labels serve to indicate pathophysiological alterations and breast cancer symptoms, including details about breast nodules such as their location and dimensions. The "tests" label designates the array of tests undergone by patients with breast cancer during diagnosis and treatment, aiding physicians in precise assessments. These encompass parameters like resection margins, vascular thrombosis, nerve invasion, lymph node dissection, Bi-RADS grading, TNM staging, and immunohistochemical markers (ER, PR, HER2, and Ki-67). The "treatments" label encompasses therapies previously administered to patients with breast cancer, comprising chemotherapy, radiation, targeted therapy, endocrine therapy, and surgery. The "time" label incorporates details regarding each temporal point within the admission record of a patient with breast cancer.

Data annotation was performed using Label Studio software (Human Signal). A total of 7 trained annotators, each responsible for a distinct portion of the dataset, performed the initial labeling

XSL•FO
RenderX

in strict accordance with the predefined annotation guidelines. The annotated corpus was then independently reviewed and revised by 2 experienced clinical oncologists, resulting in 2 expert-annotated versions. To assess interannotator agreement between the 2 experts, Cohen κ coefficient was calculated, which indicated almost perfect agreement (κ=0.82). Any discrepancies between the 2 expert versions were subsequently identified and resolved through discussion, leading to the final consensus gold-standard dataset. This finalized version was used for training and validation of the entity recognition model.

Data Partitioning

For evaluation, we use the hold-out method, partitioning the dataset randomly into training, validation, and test sets, distributed at a ratio of 6:2:2. Diverging from typical NER tasks, this model primarily deals with medical nouns or statements as named entities, with a particular focus on breast cancer–related terms. Table 4 illustrates the count of entities corresponding to each label within the training, validation, and test sets. Concurrently, the length of labels within each category was tabulated, and the outcomes are presented in Table 4.

Table . Distribution and length statistics of entities in training, validation, and test sets.

Class and entity	Train set, n (%)	Development set, n (%)	Test set, n (%)	Entities length		
				Minimum	Maximum	Mean (SD)
Symptoms						
Nodule	600 (61.66)	192 (19.73)	181 (18.60)	3	123	15.49 (17.84)
Tests						
Vascular tumor thrombus and nerve aggress	208 (56.68)	76 (20.71)	83 (22.62)	4	42	13.93 (7.79)
Incisal edge	155 (58.49)	53 (20)	57 (21.51)	4	75	24.15 (17.06)
Lymph node dissection	558 (62.21)	137 (15.27)	202 (22.52)	4	139	27.92 (24.67)
Bi-RADS[a]	161 (54.39)	58 (19.59)	77 (26.01)	8	82	48.59 (22.54)
TNM[b]	55 (57.89)	15 (15.79)	25 (26.32)	5	17	10.97 (3.76)
ER[c]	438 (61.78)	132 (18.62)	139 (19.61)	3	45	9.7 (5.52)
PR[d]	430 (61.69)	131 (18.79)	136 (19.51)	2	33	5.61 (4.88)
HER2[e]	393 (61.50)	117 (18.31)	129 (20.19)	5	82	13.64 (10.36)
Ki67	420 (62.22)	132 (19.56)	123 (18.22)	7	59	14.66 (7.06)
Treatments						
Surgery name	985 (60.39)	304 (18.64)	342 (20.97)	3	74	18.91 (9.06)
Chemotherapy	1027 (61.72)	319 (19.17)	318 (19.11)	2	940	101.43 (107.68)
Radiotherapy	177 (62.32)	56 (19.72)	51 (17.96)	2	141	21.32 (21.42)
Targeted therapy	155 (65.96)	30 (12.77)	50 (21.28)	5	352	68.83 (68.16)
Endocrine therapy	229 (61.89)	71 (19.19)	70 (18.92)	5	202	32.55 (26.9)
Time						
Time	2765 (59.54)	892 (19.21)	987 (21.25)	2	395	56.41 (55.25)

[a]Bi-RADS: breast imaging reporting and data system.

[b]TNM: TNM classification of malignant tumors.

[c]ER: estrogen receptor.

[d]PR: progesterone receptor.

[e]HER2: human epidermal growth factor receptor-2.

Evaluation Metrics

During the experiment, the evaluation of the NER model used 3 metrics: precision (P), recall (R), and F_1-score (F_1). The formulas for calculating precision, recall, and F_1-score are as follows:

$$(11)\{P=TPTP+FP\times100\%R=TPTP+FN\times100\%F1=2PRP+R\times100\%$$

where TP represents the number of true positive entities, FP indicates the number of false positive entities, and FN denotes the number of false negative entities.

XSL•FO
RenderX

Implementation Details

The experiments were conducted using the PyTorch 1.6 framework in a Python (version 3.7; Python Software Foundation) environment. The CPU used is Intel(R) Core i5-12500H, and the GPU used is NVIDIA T4 GPU. The ChCancerBERT model parameters were configured identically to the BERT model, with 12 transformer layers, 12 attention heads, and 768 hidden units. The hyperparameters for the NER experiment are detailed in Table 5.

Table . Hyperparameter settings.

Hyperparameters	Value
Batch size	8
Dropout	0.5
Learning rate	0.00003
Epoch	64
Maximum length	128
Embedding	768

Results

Using the partitioned dataset, we devised comparative experiments, ablation experiments, and separate pretrained model comparative experiments to facilitate a comprehensive assessment of the recognition efficacy across various mechanisms and models.

Results of the Comparative Experiment for NER Models

We applied our proposed model and the NER models mentioned in Table 1, which have been developed for medical and cancer fields in recent years, to our dataset to compare performance. Detailed results can be found in Table 6. We did not include Zhou et al CancerBERT model [7] in the comparison because it is not yet publicly available. Our results demonstrate that, for the Chinese breast cancer EHR dataset we constructed, our proposed model outperformed existing models, with F_1-scores increasing by 1.40%, 2.57%, and 1.13%, respectively.

Table . Comparative performance of baseline and proposed models on the breast cancer dataset.

Model	Precision (%)	Recall (%)	F_1-score (%)
BERT[a]- BiLSTM[b] -CRF [5]	85.77	85.38	85.58
ALBERT[c]-IDCNN[d]-MHA-CRF [15]	87.78	81.28	84.41
MC-BERT-BiLSTM-CNN[e]-MHA[f]-CRF[g] [6]	85.64	86.07	85.85
Our proposed model	87.63	86.34	86.98

[a]BERT: Bidirectional Encoder Representations from Transformers.

[b]BiLSTM: bidirectional long short-term memory.

[c]ALBERT: A Lite Bidirectional Encoder Representations from Transformers.

[d]IDCNN: iterated dilated convolutional neural network.

[e]CNN: convolutional neural network.

[f]MHA: multihead attention.

[g]CRF: conditional random field.

Results of the Ablation Experiment

We employ the fundamental BERT-BiLSTM-CRF model as a baseline to assess the impact of distinct mechanisms on the recognition of named entities within Chinese EHRs pertaining to breast cancer. Subsequently, BERT-DGCNN-CRF replaces the BiLSTM model within the baseline, while the baseline+DGCNN model merges the BiLSTM and DGCNN models. In addition, the baseline+DGCNN+MHA model introduces a MHA mechanism to the BERT-BiLSTM-DGCNN-CRF foundation. The corresponding experimental outcomes are detailed in Table 7.

Analysis of the ablation outcomes reveals that the substitution of the BiLSTM model with the DGCNN model results in a reduction of the precision and F_1-score on the dataset of this study by 0.37% and 0.14%. However, the amalgamation of the DGCNN model and the BILSTM model yields F_1-score increments of 0.35% and 0.49% compared to both the baseline and BERT-DGCNN-CRF models. This amalgamation also improves precision by 0.02% and 0.29%, and recall by 0.69%,

XSL•FO
RenderX

compared to the baseline and BERT-DGCNN-CRF models, respectively. This observation underscores that, within the context of feature extraction, the standalone DGCNN model presents no notable superiority over the BiLSTM model. Conversely, the combined application of these 2 models augments recognition effectiveness. Building upon this foundation, the incorporation of the MHA serves to enhance the extraction of pertinent information within the data, thereby mitigating the impact of irrelevant data. Consequently, the F_1-score experiences a supplementary enhancement of 0.17%, with a precision decrease of 0.46% offset by a substantial recall increase of 0.82%. This suggests that although the addition of the MHA slightly reduces precision, it compensates for this by capturing a broader range of relevant information, ultimately enhancing overall recognition effectiveness. Thus, based on the insights garnered from ablation experiments, it is ascertained that the optimal approach for this study involves the incorporation of the BiLSTM-DGCNN fusion model as the feature extraction layer, accompanied by the integration of the MHA mechanism.

Table . Results of ablation studies and pretrained model comparisons.

Model	Precision (%)	Recall (%)	F_1-score (%)
BERT[a]-BiLSTM[b]-CRF[c] (baseline)	85.77	85.38	85.58
BERT-DGCNN[d]-CRF	85.50	85.38	85.44
BERT-DGCNN-BiLSTM-CRF	85.79	86.07	85.93
BERT-DGCNN-BiLSTM-MHA[e]-CRF	85.33	86.89	86.10
ALBERT[f]-BiLSTM-CRF	87.50	77.32	82.10
ALBERT-DGCNN-BiLSTM-MHA-CRF	86.61	84.98	85.78
RoBERTa[g]-BiLSTM-CRF	86.14	82.51	84.29
RoBERTa-DGCNN-BiLSTM-MHA-CRF	86.86	85.79	86.32
XLNet[h]-BiLSTM-CRF	86.66	78.55	82.40
XLNet-DGCNN-BiLSTM-MHA-CRF	87.52	85.93	86.72
MC-BERT-BiLSTM-CRF	85.36	85.25	85.30
MC-BERT-DGCNN-BiLSTM-MHA-CRF	86.98	86.48	86.73
ChCancerBERT-BiLSTM-CRF	85.75	86.61	86.18
Our proposed model	87.63	86.34	86.98

[a]BERT: Bidirectional Encoder Representations from Transformers.

[b]BiLSTM: bidirectional long short-term memory.

[c]CRF: conditional random field.

[d]DGCNN: dilated gated convolutional neural network.

[e]MHA: multihead attention.

[f]ALBERT: A Lite Bidirectional Encoder Representations from Transformers.

[g]RoBERTa: robustly optimized Bidirectional Encoder Representations from Transformers pretraining approach.

[h]XLNet: generalized autoregressive pretraining.

Results of the Comparative Experiment for the Pretrained Models

Leveraging the model exhibiting the highest F_1-score from the aforementioned experiments, we proceeded to perform comparative experiments by substituting various pretrained models. Comparison experiments were conducted by integrating different pretrained models with both BiLSTM+CRF and DGCNN-BiLSTM-MHA-CRF architectures. All used pretrained models are available for download from the “Models-Hugging Face” website. The corresponding outcomes are presented in Table 7.

The results indicate that using the proposed pretraining model, ChCancerBERT, for character-level embedding outperforms various pretrained models compared in the experiment. Specifically, in the comparison experiment combined with BiLSTM+CRF, the F_1-scores of the ChCancerBERT model increased by 0.6%, 4.08%, 1.89%, 3.78%, and 0.88% compared to BERT, ALBERT, RoBERTa, XLNet, and MC-BERT, respectively. In the comparison experiment with the DGCNN-BiLSTM-MHA-CRF architecture, it achieved F_1-score

XSL•FO
RenderX

improvements of 0.88%, 1.20%, 0.66%, 0.26%, and 0.25% over BERT, ALBERT, RoBERTa, XLNet, and MC-BERT, respectively. In addition, regardless of the pretraining model used, the F_1-scores obtained with the DGCNN-BiLSTM-MHA-CRF architecture were consistently higher than those obtained with the BiLSTM+CRF model alone, further demonstrating that the DGCNN-BiLSTM-MHA model, by integrating multidimensional text features, possesses a stronger semantic representation capability than the BiLSTM model alone.

After using ChCancerBERT for character-level embedding and integrating it with the DGCNN-BILSTM-MHA-CRF model to fuse multidimensional text features, the semantic representation capability is further enhanced, and the F_1-score had a 1.4% improvement compared to the current mainstream BERT-BiLSTM-CRF (baseline) model. In addition, our model achieves a precision of 87.63% and a recall of 86.34%, which represents increases of 1.86% in precision and 0.96% in recall compared to the baseline BERT-BiLSTM-CRF model. This reflects both high detection accuracy and robustness in capturing target entities.

Error Analysis

We conducted a comprehensive analysis of the 4 main entity categories in this study, including their quantity, average length, as well as precision, recall, and F_1-scores. The specific results are presented in Table 8.

The results presented in Table 8 indicate that TIME entities are the most frequently occurring, totaling 4644 instances. The model demonstrates the highest recognition effectiveness for these entities, achieving an F_1-score of 92.79%. In contrast, although the treatments category also has a high number of entities, it shows the lowest recognition performance with an F_1-score of 74.24%. This lower performance can be attributed to the complexity and variability of treatment-related terms, which is further compounded by the fact that the average length of treatment entities is 17.27 characters, significantly longer than other entity categories. Treatment entities often contain multiple details, including various drugs, dosages, treatment methods, and frequencies, such as in the example: “Chemotherapy: Cyclophosphamide 1000 mg on day 1, Epirubicin 50 mg on day 1, 21 days per cycle, 4 cycles.” However, the model only identifies the drugs and their dosages used in chemotherapy, while ignoring the subsequent frequency information. The increased length and complexity of these entities make it more challenging for the model to accurately identify and classify them, resulting in a decrease in overall recognition accuracy.

Table . Performance obtained for each entity.

Class	Entity number	Average length	Precision (%)	Recall (%)	F_1-score (%)
Symptoms	973	7.62	82.86	84.89	83.86
Tests	640	7.82	82.61	81.40	81.02
Treatments	4184	17.27	76.90	72.30	74.24
Time	4644	8.01	92.62	92.96	92.79

Experiment on CCKS2019

In order to comprehensively validate the efficacy of the model proposed in this study, we applied it to the CCKS2019 dataset and conducted a performance comparison with models recently introduced in the literature. The CCKS2019 dataset, publicly accessible and broadly used within China’s medical NLP research community, offers a standardized evaluation platform for diverse NER models (CCKS2019 [28]). In total, we compared 8 models, including 3 models in 5.1, and the other 5 models are as follows:

- Embeddings from language models (ELMo)-lattice-LSTM-CRF model: this model uses the lattice LSTM-CRF architecture and integrates variant contextual character representations (Chinese Embeddings from Language Models [ELMo]) to enhance the use of character and word information in Chinese EHRs [29].
- ELMo-encoder from transformer–CRF model: this model fine-tunes the ELMo model using domain-specific clinical records and uses transformer (encoder from transformer) as an encoder to address long-context dependencies [30].
- All CNN model: this model incorporates Chinese radical characters to enhance the morphosemantic representation of Chinese characters [14].
- Graph attention network–BiLSTM-CRF model: this model uses a graph neural network to model lexical dependency inertia as syntactic semantics and integrates semantic information at various levels to enhance contextual representation [31].
- Chinese medical–NER model: this model enhances the MC-BERT model by incorporating graph convolutional networks and CRFs [16].

Table 9 presents a comparison of the performance of our proposed model on the CCKS2019 dataset with that of models introduced in recent literature. Our model achieves an F_1-score of 87.26%, surpassing recent models by margins of 2.64%, 2.24%, 2.13%, 1.67%, 1.63%, 1.34%, 0.99%, and 0.97%. These results strongly affirm the effectiveness of our model. The experimental findings clearly demonstrate that our cancer-specific named NER model outperforms existing models on the CCKS2019 dataset, highlighting its potential for effectively handling larger medical datasets.

XSL•FO
RenderX

Table . Performance comparison of the proposed model and recent models on the CCKS2019 dataset.

Model	Precision (%)	Recall (%)	F_1-score (%)
BERT[a]- BiLSTM[b] -CRF[c] [5]	82.09	87.32	84.62
ELMo[d]-lattice-LSTM[e]-CRF [29]	85.35	84.69	85.02
ACNN[f] [14]	87.29	83.07	85.13
ELMo-ET[g]-CRF model [30]	87.61	83.65	85.59
ALBERT[h]-IDCNN[i]-MHA[j]-CRF [15]	84.82	86.46	85.63
GAT[k]-BiLSTM-CRF [31]	86.74	85.11	85.92
MC-BERT-BiLSTM-CNN[l]-MHA-CRF [6]	84.90	87.67	86.27
CM[m]-NER[n] [16]	86.45	86.13	86.29
Our proposed model	87.26	87.27	87.26

[a]BERT: Bidirectional Encoder Representations from Transformers.

[b]BiLSTM: bidirectional long short-term memory.

[c]CRF: conditional random field.

[d]ELMo: embeddings from language models.

[e]LSTM: long short-term memory.

[f]ACNN: all convolutional neural network.

[g]ET: encoder from transformer.

[h]ALBERT: A Lite Bidirectional Encoder Representations from Transformers.

[i]IDCNN: iterated dilated convolutional neural network.

[j]MHA: multihead attention.

[k]GAT: graph attention network.

[l]CNN: convolutional neural network.

[m]CM: Chinese medical.

[n]NER: named entity recognition.

Discussion

Principal Findings

Unstructured EHR data contains valuable patient information that can be used for clinical decision support and research [32]. In the Chinese breast cancer EHR corpus constructed in this study, there are 876 admission records, comprising a total of 528,925 tokens. Annotations were performed for 4 major categories and 17 subcategories of named entities, with each subcategory having more than 100 annotated instances. In the NER task, the model we propose outperforms other models currently applied in medical-related fields. The results of ablation experiments revealed that the fusion of the pretrained model with the DGCNN-BILSTM-MHA-CRF model effectively enhances entity recognition performance. Specifically, the introduction of the DGCNN structure on top of the baseline results in the maximum improvement of 0.35%. This enhancement is attributed to the structure's ability to mitigate the risk of gradient vanishing and facilitate information transmission across multiple channels, capturing a wealth of feature information. In addition, the incorporation of the MHA mechanism on this foundation not only enhances the model's generalization capability but also enables parallel attention computation, strengthening feature fusion capability [24]. This leads to improved use of valid information and reduced impact of irrelevant information, resulting in a further F_1-score improvement of 0.17%.

Comparing the results of the pretrained model experiments, it is evident that the proposed ChCancerBERT pretrained model outperforms various state-of-the-art BERT models, with the medical domain-specific MC-BERT model ranking second. This is attributed to MC-BERT incorporating more medical corpus training into BERT, and ChCancerBERT further including the Chinese cancer corpus on top of MC-BERT. This augmentation effectively enhances the model's semantic representation capability in the Chinese cancer domain, yielding superior results in the Chinese breast cancer corpus in this study. In addition, the study's results indicate that pretrained BERT models based on specific domains can lead to improved performance in downstream tasks [7].

Among the 4 categories extracted in this study, the performance in extracting time entities stood out, with an impressive F_1-score of 92.79%. This result can be attributed to the relatively high quantity of time entities in this dataset, amounting to 4644, and the fact that time entities exhibit a more standardized writing format compared to other entities, which, to some extent,

XSL•FO
RenderX

reduces the difficulty of recognition and enhances recognition accuracy [33].

We scrutinize the entity recognition outcomes of the most proficient fusion model derived from our experiments. Categories with infrequent occurrences in the dataset, such as TNM, Bi-RADS, and some other entities in class "tests," are prone to omission errors. These errors manifest as instances where entities that should have been identified remain undetected, suggesting a propensity of the model used in this study to overlook less common entity categories [34]. Such omissions may result in incomplete information extraction, which is crucial for disease diagnosis and the formulation of treatment plans. Therefore, downstream applications should incorporate clinician verification mechanisms or error correction modules to ensure safety in clinical use.

In this study, entities characterized by considerable length, such as chemotherapy, radiotherapy, and other in-class "treatments," are typically classified correctly by the model. However, the model is susceptible to boundary recognition errors [7], leading to either the exclusion of words at the sentence's periphery or the inclusion of extraneous words beyond the sentence, which may cause confusion in clinical documentation. Furthermore, on one hand, Chinese words frequently exhibit polysemy and ambiguity [33]; on the other hand, the dataset for this study contains instances where statements are nested within the entity categories of other entities. Such intricacies heighten the risk of erroneous entity category determinations.

Concurrently, we apply the model introduced in this research to the publicly accessible CCKS2019 dataset, and the findings illustrate its superior performance compared to prior research efforts, suggesting the ChCancerBERT framework has the potential to be extended to other cancer types and even broader clinical domains. Nevertheless, differences in documentation style and terminology across hospitals may affect generalization. Domain adaptation strategies such as continual pretraining on local EHR corpora and transfer learning can be explored to improve portability to other institutions.

Using our proposed model, vital clinical data encompassing timestamps, examination details, symptoms, and treatment modalities can be readily extracted from the EHRs of patients with cancer. The extracted entities provide important value for both clinical and research applications. Time, symptom, test, and treatment information can be structured into patient timelines to support disease monitoring, clinical decision support, population health analysis, and trial recruitment. These entities can also be mapped to standards such as International Classification of Diseases, 10th Revision, enabling interoperability and secondary use of structured cancer data.

Conclusions

This study designed and developed a pretrained model specifically tailored to the Chinese cancer domain, named ChCancerBERT. The model was then integrated with various NER models proposed in the field of computer science, resulting in the ChCancerBERT-DGCNN-BILSTM-MHA-CRF model. This integrated model was used to extract 4 major types of entities related to cancer from admission records in the oncology department of hospitals. We applied the model proposed in this study to Chinese breast cancer EHR data and CCKS2019 for experimentation and validation. The proposed model achieved an F_1-score of 86.98%, surpassing other models compared in the experiment.

The primary limitation of this study is the restricted data accessibility and relatively small sample size. This limited sample size may affect the statistical power and robustness of the findings. Moreover, potential variations in clinical documentation practices across different regions or institutions in China could pose challenges to the generalizability of the model. Despite these limitations, it is worth noting that the model demonstrated promising transferable capability by achieving competitive performance on the CCKS2019 medical dataset, which suggests its potential applicability beyond breast cancer data. Therefore, future research should aim to acquire EHR data for other types of cancer to further validate the generalizability of the proposed model. Furthermore, a NER system tailored for clinical application is envisaged to be constructed based on this model. This system aims to assist clinical researchers in data organization and extraction. In addition, plans encompass the establishment of a clinical decision support system to facilitate more effective treatment for patients.

Acknowledgments

This work is supported by Beijing University of Chinese Medicine Independent Topic Selection Young Faculty Project (grant: 040201004002011), 2024 Independent Research Projects for Postgraduate Students of Beijing University of Chinese Medicine (grant: ZJKT2024033), 2022 Basic Research Business Fund 'Top-Down Leadership' Project (grant: 2022JYBJBRW012), the Fundamental Research Funds for the Central Universities (grant: 2025JYBXJSJJ022), Beijing University of Chinese Medicine Educational and Teaching Reform Special Project (grant: XJYZ25010), Beijing Social Science Fund (grant: 24XCC022), Research Funding on TCM Monitoring and Statistics for 2025 of the Monitoring and Statistics Center of the National Administration of Traditional Chinese Medicine (grant: 2025JCTJE50), 'Top-Down Leadership' Educational Reform Project of Beijing University of Chinese Medicine (grant: JXJBGS2501005), and the 2025 Basic Research Business Fund 'Top-Down Leadership' Project (grant: 2025JYBJBGS009).

XSL•FO
RenderX

Data Availability

The annotated datasets generated and analyzed during the current study are not publicly available due to hospital policy and regulation, but the ChCancerBERT model is available from the corresponding author on reasonable request.

Authors' Contributions

JC and SD participated in data collection and collation. JC, BZ, XT, and ZZ participated in the method design, analyzed data, and drafted the initial manuscript. JC, BZ, XT, ZZ, and JW participated in text checking correction and helped to draft the manuscript. FG and RW oversaw and provided input on all aspects of manuscript writing and the final analytical plan. All the authors read and approved the final manuscript.

Conflicts of Interest

None declared.

References

1. Deimazar G, Sheikhtaheri A. Machine learning models to detect and predict patient safety events using electronic health records: a systematic review. Int J Med Inform 2023 Dec;180:105246. [doi: 10.1016/j.ijmedinf.2023.105246] [Medline: 37837710]
2. Chen PE, Hung HH, Huang WT, et al. Chinese herbal medicine improved survival in stage IV breast cancer patients: data mining of the Incorporated Taiwan Cancer Registry Database and hospital database. Integr Cancer Ther 2023;22:15347354231178898. [doi: 10.1177/15347354231178898] [Medline: 37278256]
3. Zhao X, Tong Z, Sun L, et al. Clinical characteristics, treatment patterns, and effectiveness in Chinese patients with angina pectoris using electronic patient-reported outcomes: protocol for a multicenter, prospective, cohort study (GREAT). Adv Ther 2023 Apr;40(4):1899-1912. [doi: 10.1007/s12325-023-02425-0] [Medline: 36737594]
4. Abdullah MHA, Aziz N, Abdulkadir SJ, Alhussian HSA, Talpur N. Systematic literature review of information extraction from textual data: recent methods, applications, trends, and challenges. IEEE Access 2023;11:10535-10562. [doi: 10.1109/ACCESS.2023.3240898]
5. Li X, Zhang H, Zhou XH. Chinese clinical named entity recognition with variant neural structures based on BERT methods. J Biomed Inform 2020 Jul;107:103422. [doi: 10.1016/j.jbi.2020.103422] [Medline: 32353595]
6. Chen P, Zhang M, Yu X, Li S. Named entity recognition of Chinese electronic medical records based on a hybrid neural network and medical MC-BERT. BMC Med Inform Decis Mak 2022 Dec 1;22(1):315. [doi: 10.1186/s12911-022-02059-2] [Medline: 36457119]
7. Zhou S, Wang N, Wang L, Liu H, Zhang R. CancerBERT: a cancer domain-specific language model for extracting breast cancer phenotypes from electronic health records. J Am Med Inform Assoc 2022 Jun 14;29(7):1208-1216. [doi: 10.1093/jamia/ocac040] [Medline: 35333345]
8. Zhou S, Wang N, Wang L, et al. A cross-institutional evaluation on breast cancer phenotyping NLP algorithms on electronic health records. Comput Struct Biotechnol J 2023;22:32-40. [doi: 10.1016/j.csbj.2023.08.018] [Medline: 37680211]
9. Najafabadipour M, Tunas JM, Rodriguez-Gonzalez A. Lung cancer concept annotation from Spanish clinical narratives. Presented at: 13th International Conference on Data Integration in the Life Sciences 2018 (DILS2018); Nov 20-21, 2018. [doi: 10.1007/978-3-030-06016-9_15]
10. Yim WW, Kwan SW, Yetisgen M. Tumor reference resolution and characteristic extraction in radiology reports for liver cancer stage prediction. J Biomed Inform 2016 Dec;64:179-191. [doi: 10.1016/j.jbi.2016.10.005] [Medline: 27729234]
11. Savova GK, Tseytlin E, Finan S, et al. DeepPhe: A natural language processing system for extracting cancer phenotypes from clinical records. Cancer Res 2017 Nov 1;77(21):e115-e118. [doi: 10.1158/0008-5472.CAN-17-0615] [Medline: 29092954]
12. Weegar R, Kvist M, Sundström K, Brunak S, Dalianis H. Finding cervical cancer symptoms in Swedish clinical text using a machine learning approach and NegEx. AMIA Annu Symp Proc 2015;2015:1296-1305 [FREE Full text] [Medline: 26958270]
13. An Y, Xia X, Chen X, Wu FX, Wang J. Chinese clinical named entity recognition via multi-head self-attention based BiLSTM-CRF. Artif Intell Med 2022 May;127:102282. [doi: 10.1016/j.artmed.2022.102282] [Medline: 35430042]
14. Kong J, Zhang L, Jiang M, Liu T. Incorporating multi-level CNN and attention mechanism for Chinese clinical named entity recognition. J Biomed Inform 2021 Apr;116:103737. [doi: 10.1016/j.jbi.2021.103737] [Medline: 33737207]
15. Li D, Long J, Qu J, Zhang X. Chinese clinical named entity recognition with ALBERT and MHA mechanism. Evid Based Complement Alternat Med 2022;2022(2056039):2056039. [doi: 10.1155/2022/2056039] [Medline: 35656458]
16. Li M, Gao CR, Zhang K, Zhou HJ, Ying J. A weakly supervised method for named entity recognition of Chinese electronic medical records. Med Biol Eng Comput 2023 Oct;61(10):2733-2743. [doi: 10.1007/s11517-023-02871-6] [Medline: 37453978]

XSL•FO
RenderX

17. Measures for ethical review of life sciences and medical research involving human subjects [Website in Chinese]. National Health Commission. 2023. URL: https://www.gov.cn/zhengce/zhengceku/2023-02/28/content_5743658.htm [accessed 2025-10-30]
18. Khan MA, Huang Y, Feng J, et al. A multi-attention approach using BERT and stacked bidirectional LSTM for improved dialogue state tracking. Appl Sci (Basel) 2023;13(3):1775. [doi: 10.3390/app13031775]
19. Sun J, Liu Y, Cui J, He H. Deep learning–based methods for natural hazard named entity recognition. Sci Rep 2022 Mar 17;12(1):4598. [doi: 10.1038/s41598-022-08667-2] [Medline: 35301387]
20. Li D, Yan L, Yang J, Ma Z. Dependency syntax guided BERT-BiLSTM-GAM-CRF for Chinese NER. Expert Syst Appl 2022 Jun;196:116682. [doi: 10.1016/j.eswa.2022.116682]
21. Runmei Z, Lulu L, Lei Y, et al. Chinese named entity recognition method combining ALBERT and a local adversarial training and adding attention mechanism. Int J Semant Web Inf Syst 2022 Jan;18(1):1-20 [FREE Full text] [doi: 10.4018/IJSWIS.313946]
22. Zhou F, Wang C, Wang J, Zhang J. Named entity recognition of ancient poems based on Albert - BiLSTM - MHA - CRF model. Wirel Commun Mob Comput 2022 Jan;2022(1):1-11 [FREE Full text] [doi: 10.1155/2022/6507719]
23. Xu K, Yang Z, Kang P, Wang Q, Liu W. Document-level attention-based BiLSTM-CRF incorporating disease dictionary for disease named entity recognition. Comput Biol Med 2019 May;108:122-132. [doi: 10.1016/j.compbiomed.2019.04.002] [Medline: 31003175]
24. Zhu ZC, Li JQ, Zhao Q, Akhtar F. A dictionary-guided attention network for biomedical named entity recognition in Chinese electronic medical records. Expert Syst Appl 2023 Nov;231:120709. [doi: 10.1016/j.eswa.2023.120709]
25. Frei J, Kramer F. Annotated dataset creation through large language models for non-English medical NLP. J Biomed Inform 2023 Sep;145:104478. [doi: 10.1016/j.jbi.2023.104478] [Medline: 37625508]
26. Lingren T, Deleger L, Molnar K, et al. Evaluating the impact of pre-annotation on annotation speed and potential bias: natural language processing gold standard development for clinical named entity recognition in clinical trial announcements. J Am Med Inform Assoc 2014;21(3):406-413. [doi: 10.1136/amiajnl-2013-001837] [Medline: 24001514]
27. Uzuner O, Solti I, Xia F, Cadag E. Community annotation experiment for ground truth generation for the i2b2 medication challenge. J Am Med Inform Assoc 2010;17(5):519-523. [doi: 10.1136/jamia.2010.004200] [Medline: 20819855]
28. China conference on knowledge graph and semantic computing. URL: https://www.sigkg.cn/ccks2019/ [accessed 2025-11-14]
29. Li Y, Wang X, Hui L, et al. Chinese clinical named entity recognition in electronic medical records: development of a lattice long short-term memory model with contextualized character representations. JMIR Med Inform 2020 Sep 4;8(9):e19848. [doi: 10.2196/19848] [Medline: 32885786]
30. Wan Q, Liu J, Wei LN, Ji B. A self-attention based neural architecture for Chinese medical named entity recognition. Math Biosci Eng 2020 May 9;17(4):3498-3511. [doi: 10.3934/mbe.2020197] [Medline: 32987540]
31. Shi J, Sun M, Sun Z, Li M, Gu Y, Zhang W. Multi-level semantic fusion network for Chinese medical named entity recognition. J Biomed Inform 2022 Sep;133:104144. [doi: 10.1016/j.jbi.2022.104144] [Medline: 35878823]
32. Landolsi MY, Hlaoua L, Ben Romdhane L. Information extraction from electronic medical documents: state of the art and future research directions. Knowl Inf Syst 2023;65(2):463-516. [doi: 10.1007/s10115-022-01779-1] [Medline: 36405956]
33. Qiu Q, Tian M, Huang Z, et al. Chinese engineering geological named entity recognition by fusing multi-features and data enhancement using deep learning. Expert Syst Appl 2024 Mar;238:121925. [doi: 10.1016/j.eswa.2023.121925]
34. Yu Y, Wang Y, Mu J, et al. Chinese mineral named entity recognition based on BERT model. Expert Syst Appl 2022 Nov;206:117727. [doi: 10.1016/j.eswa.2022.117727]

Abbreviations

BiLSTM: bidirectional long short-term memory.
DGCNN: dilated-gated convolutional neural network
EHR: electronic health record
ELMo: embeddings from language models
LSTM: long short-term memory
MHA: multihead attention
NER: named entity recognition
NLP: natural language processing

XSL•FO
RenderX

Edited by A Benis; submitted 04.05.25; peer-reviewed by C Cheligeer, D Chrimes, P Tekkali; revised version received 08.10.25; accepted 13.10.25; published 14.11.25.

Please cite as:
Chen J, Zhao B, Tian X, Zou Z, Wang R, Wu J, Du S, Guo F
Named Entity Recognition for Chinese Cancer Electronic Health Records—Development and Evaluation of a Domain-Specific BERT Model: Quantitative Study
JMIR Med Inform 2025;13:e76912
URL: https://medinform.jmir.org/2025/1/e76912
doi:10.2196/76912

© Junbai Chen, Butian Zhao, Xiaohan Tian, Zhengkai Zou, Ruojia Wang, Jiarui Wu, Songxing Du, Fengying Guo. Originally published in JMIR Medical Informatics (https://medinform.jmir.org), 14.11.2025. This is an open-access article distributed under the terms of the Creative Commons Attribution License (https://creativecommons.org/licenses/by/4.0/), which permits unrestricted use, distribution, and reproduction in any medium, provided the original work, first published in JMIR Medical Informatics, is properly cited. The complete bibliographic information, a link to the original publication on https://medinform.jmir.org/, as well as this copyright and license information must be included.

XSL•FO
RenderX

Unsupervised Coverage Sampling to Enhance Clinical Chart Review Coverage for Computable Phenotype Development: Simulation and Empirical Study

Zigui Wang[1], BS; Jillian H Hurst[2], PhD; Chuan Hong[1], PhD; Benjamin Alan Goldstein[1,2], PhD

[1]Department of Biostatistics and Bioinformatics, Duke University School of Medicine, Duke University, 2424 Erwin Road, 9023 Hock Plaza, Durham, NC, United States

[2]Department of Pediatrics, Duke University School of Medicine, Duke University, Durham, NC, United States

Corresponding Author:
Benjamin Alan Goldstein, PhD
Department of Biostatistics and Bioinformatics, Duke University School of Medicine, Duke University, 2424 Erwin Road, 9023 Hock Plaza, Durham, NC, United States

Abstract

Background: Developing computable phenotypes (CP) based on electronic health records (EHR) data requires "gold-standard" labels for the outcome of interest. To generate these labels, clinicians typically chart-review a subset of patient charts. Charts to be reviewed are most often randomly sampled from the larger set of patients of interest. However, random sampling may fail to capture the diversity of the patient population, particularly if smaller subpopulations exist among those with the condition of interest. This can lead to poorly performing and biased CPs.

Objective: This study aimed to propose an unsupervised sampling approach designed to better capture a diverse patient cohort and improve the information coverage of chart review samples.

Methods: Our coverage sampling method starts by clustering by the patient population of interest. We then perform a stratified sampling from each cluster to ensure even representation for the chart review sample. We introduce a novel metric, nearest neighbor distance, to evaluate the coverage of the generated sample. To evaluate our method, we first conducted a simulation study to model and compare the performance of random versus our proposed coverage sampling. We varied the size and number of subpopulations within the larger cohort. Finally, we apply our approach to a real-world data set to develop a CP for hospitalization due to COVID-19. We evaluate the different sampling strategies based on the information coverage as well as the performance of the learned CP, using the area under the receiver operator characteristic curve.

Results: Our simulation studies show that the unsupervised coverage sampling approach provides broader coverage of patient populations compared to random sampling. When there are no underlying subpopulations, both random and coverage perform equally well for CP development. When there are subgroups, coverage sampling achieves area under the receiver operating characteristic curve gains of approximately 0.03 - 0.05 over random sampling. In the real-world application, the approach also outperformed random sampling, generating both a more representative sample and an area under the receiver operating characteristic curve improvement of 0.02 (95% CI −0.08 to 0.04).

Conclusions: The proposed coverage sampling method is an easy-to-implement approach that produces a chart review sample that is more representative of the source population. This allows one to learn a CP that has better performance both for subpopulations and the overall cohort. Studies that aim to develop CPs should consider alternative strategies other than randomly sampling patient charts.

(JMIR Med Inform 2025;13:e72068) doi:10.2196/72068

KEYWORDS

electronic health records; EHR; chart review sampling; coverage metric; computable phenotypes

Introduction

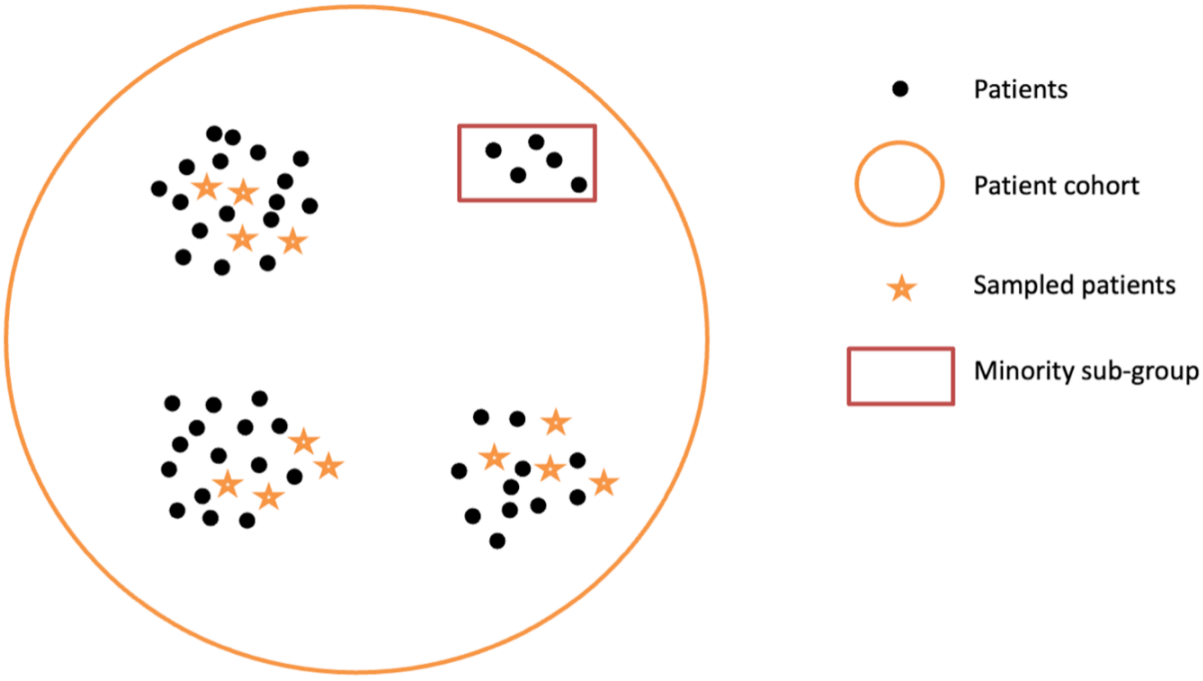
Electronic health records (EHR) data are widely used in clinical research. While they contain dense, often granular information on a patient's health status, they also pose challenges for clinical studies since they lack explicit documentation for the reason for the health care encounter (eg, admission due to infection). In principle, the problem list, which provides a historical listing of previous health problems, can be used to identify chronic conditions, though it is often unreliable [1,2]. Similarly, fields such as discharge diagnosis may not accurately represent the reason a patient had a visit. Instead, information from diagnosis codes, laboratory test results, and prescriptions or administered medications is used to indicate the presence of a specific clinical

XSL•FO
RenderX

condition [3-5]. This is a well-known challenge in working with EHR data and has led to the growth of computable phenotypes (CPs). CPs are algorithms, typically Boolean, though sometimes probabilistic, that use multiple sources of clinical data—such as diagnoses, laboratory results, and medication records—to infer the clinical condition of a patient or the reason for a visit [6-8].

Creating CPs is a multiphase process that often requires significant collaborative effort from clinicians and informaticians [5,9]. One of the key components in CP development is the creation of a set of "gold standard" outcome labels. The outcome labels are typically generated based on manual review of a subset of eligible patient charts, which can require significant time [6-8,10]. The set of charts that are used to develop these gold-standard labels is usually sampled randomly [11]. While random sampling will, on average, produce a representative view of the population of interest, since one usually wants to review only a small number of charts, random sampling may not adequately represent the complete range of disease presentations or patient demographics. In the scenario shown in Figure 1, subgroups that have a rarer presentation within the larger data set (eg, rarer presentations of the disease of interest and disease presentation in minority subgroups) are less likely to be adequately covered based on random sampling. In this case, much larger sample sets are necessary to find a meaningful number of charts from people from these subgroups [12]. In such scenarios, random sampling strategies might not be effective in generating a sample covering all subgroups for chart review purposes and result in a CP that does not accurately capture the heterogeneity of the condition of interest. This can lead to a CP that performs worse for those subpopulations.

Figure 1. Example of the impact of random sampling on the representation of patient subgroups. The black dots represent unsampled patients; stars represent the sampled patients. The red box represents a subgroup that was missed by random sampling.



In recent years, various methods have been developed to enhance the coverage of labeled data [13-16]. However, these methods either rely on external population resources or focus solely on maximizing demographic coverage, which do not fully align with the chart review objective. Among these methods, active learning is one such approach that iteratively selects the most informative samples for labeling, aiming to optimize model performance with a minimal amount of data [17,18]. However, active learning typically requires an initial set of labeled data to train the model and guide the selection process [19]. Moreover, active learning methods are typically focused on identifying the samples that will provide the most leverage on the final model, as opposed to the ones that would best capture the diversity of the patient cohort [18-21].

In this paper, we propose a process for selecting medical charts for review to generate gold standard labeling when constructing CPs. The goal of this method is to ensure that our selection captures the diversity of the full patient cohort. To achieve this, we propose a clustering-based process to generate potential samples. We then introduce a novel metric to identify the most representative sample that should be used for label generation. By enhancing the information coverage of the training sample, our approach is expected to yield a better performing CP for both subgroups and the full patient cohort. To illustrate this approach, we use simulation methods coupled with a real-world data example to demonstrate how this novel sampling approach can match or even surpass the performance of random sampling.

Methods

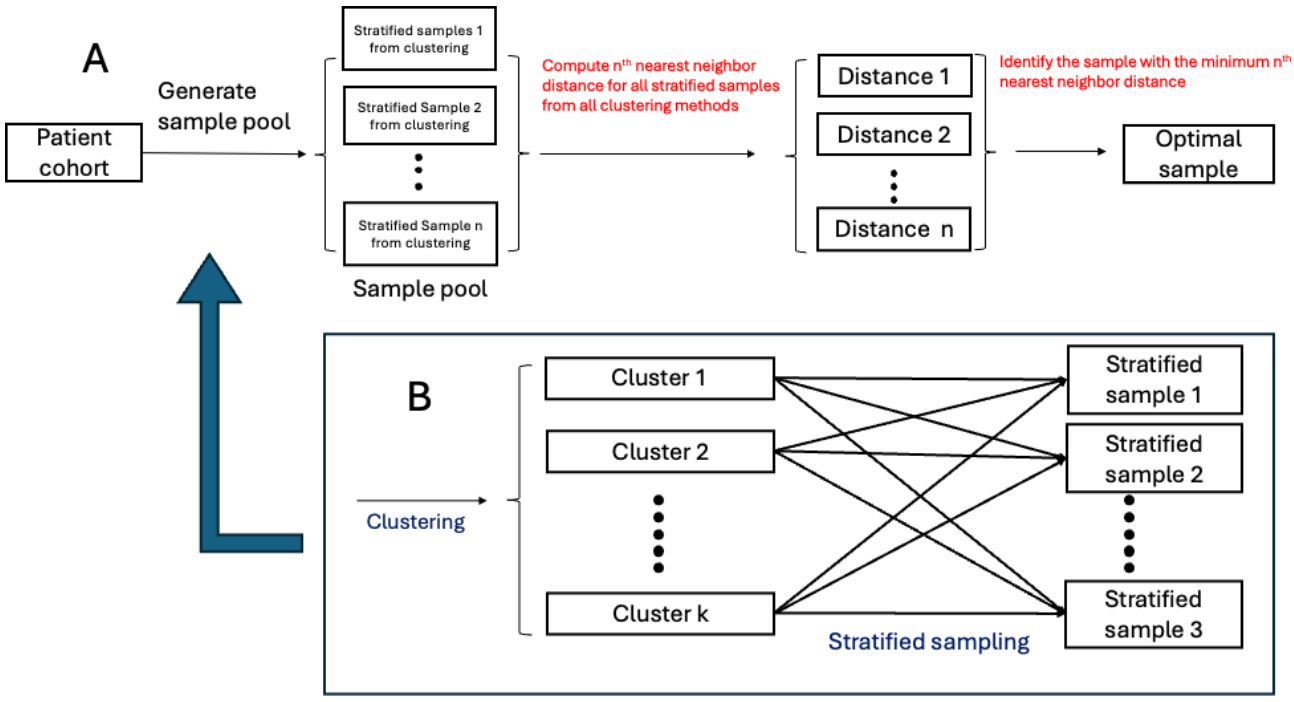
Sampling Approach

The overall methodological approach is illustrated in Figure 2. We start by considering a study cohort for whom we want to create labels for the presence or absence of a condition of interest (eg, diabetes, cause-specific admission). We presume that our study cohort is large enough that we do not want to

XSL•FO
RenderX

review and label all patient charts. Instead, we want to generate an optimal chart review sample, from which we will develop or "learn" a CP. In this paper, our analytic task is to determine how to best identify that sample. We propose that the best sample is one that maximizes coverage of the cohort, providing information about all of the subgroups that compose the cohort (Figure 2A). In other words, the sample should be equally representative of each subgroup, rather than merely reflecting the source population distribution. To assess coverage, we define a novel metric, described below. A variety of methods can be used to generate the sample pool. In this study, we propose using a stratified sampling framework, in other words, clustering the data and then sampling from these clusters (Figure 2B). By identifying and then sampling from clusters, we hypothesize that we will be able to represent different patient subgroups, making the chart review sample more reflective of the entire patient cohort.

Figure 2. Diagram illustrating our sampling approach. (A) procedures for general coverage sampling; (B) procedures for generating the sample pool.



Optimal Sample Generation

After defining a cohort of interest, we start by clustering the individual patient records. As illustrated in our real data example, our groupings are driven by clinical factors, so we only use clinical features (ie, not demographic factors) to conduct the clustering. We then sample records randomly from each of the clusters. For example, if we prespecify that we want to review 100 charts, and we generate 4 clusters, we would sample 25 records from each cluster. While a variety of clustering algorithms can be used, we suggest hierarchical clustering. The nested cluster structure provided by hierarchical clustering is reflective of our proposed interpretation that the cohort consists of patient subgroups. For comparison, we also present results from K-means clustering. Notably, with a sufficiently large number of replications, we expect different clustering methods to generate similar optimal samples, resulting in comparable representative samples.

Coverage Assessment

A primary step is assessing data coverage. To do so, we propose a novel metric that measures the coverage of the sample for the full data cohort. We define the n^{th} nearest neighbor distance as:

$$\text{nth nearest neighbor distance} = \sum_{i=1}^{N} d_{in}$$

For each person, *i*, in the study cohort of size N, we calculate the Euclidean distance, *d*, to each person from the sampled set. din is the distance between the ith person in the cohort, to the nth nearest sampled person. For example, the 5th nearest neighbor distance refers to the sum of the distance between every patient *i* and its 5th closest sampled person. After generating the sample pool, we calculate the distance for each individual in the patient cohort to the nth nearest sampled person. We choose the chart review sample with the lowest nth nearest neighbor distance. The intuition for the nth nearest neighbor distance is to ensure that for each person in the full cohort, there is someone in the chart review sample that is "near" or representative of them. This should result in greater coverage for underrepresented subgroups and phenotypes compared to random sampling. For example, for a disease that can present clinically in a variety of ways (eg, diabetes), if a rarer presentation is not represented in the chart sample, then for a person i from this minority group, the closest sampled individuals will be in other subgroups, resulting in a larger nth nearest neighbor distance. Moreover, sampling to minimize the nth nearest neighbor distance will not adversely impact the majority presentation since group members will still have representative samples.

Our coverage sampling process can be summarized as follows:

1. Cluster the dataset based on clinical factors across a range of k clusters.

XSL•FO
RenderX

2. Conduct stratified sampling with a specified sample size across the clusters multiple times to generate the sample pool.
3. Calculate the nth nearest neighbor distance for each sample set in the sample pool and identify the sample with the minimal nth nearest neighbor distance.

The primary tuning parameter is n. This can be prespecified by the user, or *n* can be assessed over a range of values, and taking the mean distance. As we show below, the approach is not very sensitive to the choice of n. Although the results presented are based on Euclidean distance, given the mixed data types of the EHR data, we also assessed Manhattan and Gower distances and found that they had minimal impact on the final results.

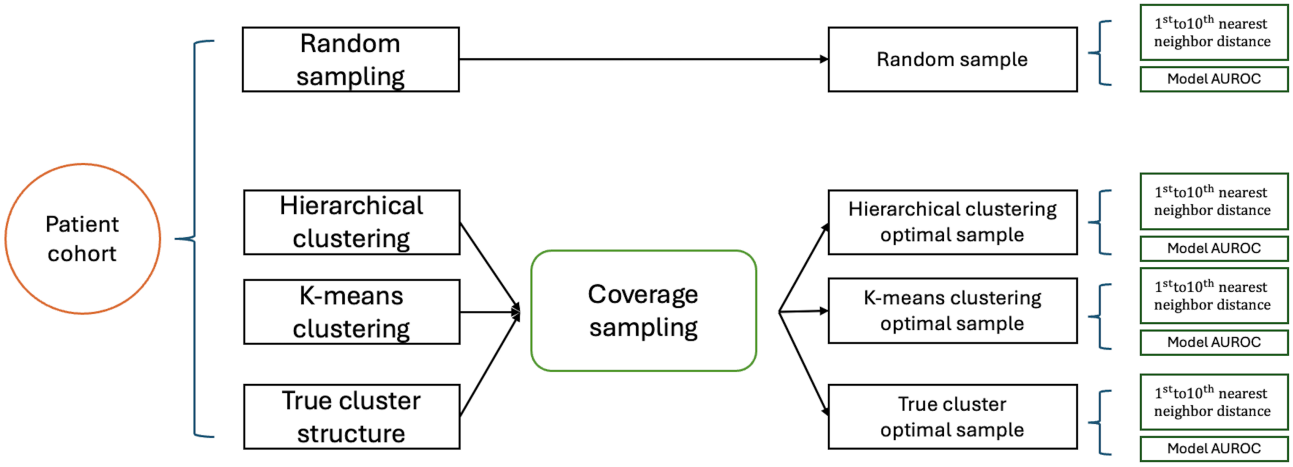
Assumptions

The primary assumption of this procedure is that we have a broad cohort from which to sample that fully captures all individuals with the condition from which we wish to define a CP. Meaning, our identified patient cohort (ie, our denominator) has perfect sensitivity for the outcome of interest, and the analytic challenge is improving the specificity of the CP.

Evaluation Criteria

As shown in Figure 3, we assess the quality of a selected sample for chart review in 2 ways: cohort coverage and CP performance. For cohort coverage, we compare the nth nearest neighbor distance, with samples exhibiting smaller distances considered more representative of the study cohort. For CP performance, we train a classification model using a sample derived from either our proposed coverage sampling or random sampling methods. All the unsampled patients are regarded as the test dataset. We evaluate the efficacy of these models by comparing the area under the receiver operating characteristic curve (AUROC) using the test dataset. Samples that yield models with higher AUROC values are considered to be better.

Figure 3. Diagram to show the evaluation criteria of sample quality. The coverage sampling refers to the sampling procedure outlined in Figure 2. AUROC: area under the receiver operating characteristic curve.



Simulation Study

We conduct a simulation study to evaluate the efficacy of coverage sampling outlined above. We sample 120 patients from 250 simulated datasets with a size of 10,000 and 10 characteristic variables by both random sampling and coverage sampling. Across the datasets, we generate 4 clusters and create a sample with different proportions of each cluster: (simulation set 0: 1.0,0,0,0; simulation set 1: 0.25, 0.25, 0.25, 0.25; simulation set 2: 0.1, 0.3, 0.3, 0.3; simulation set 3: 0.1, 0.1, 0.4, 0.4 and simulation set 4: 0.1, 0.1, 0.1, 0.7). These samples can be interpreted as: no underlying cluster structure, equally distributed subgroups, 1 minority subgroup, 2 minority subgroups, and one majority group. The initial 2 simulation sets (sets 0 - 1) serve as baselines, where either no underlying cluster exists or all clusters are of equal size. The subsequent simulations (sets 2 - 4) delve into more complex scenarios, incorporating minority subgroups to assess their impact on the representation of subgroups within the samples.

To generate the clustered data, we used the R package fungible [13], which uses the following model:

$$X=DjB+e$$

Where X is the matrix of simulated observations, where each row representing an observation and each column representing a variable; Dj is a matrix of indicator for cluster j, identifying the membership of observation within this cluster; B is a matrix that represents the correlation between the cluster membership and observation scores), and e represents the deviations that generated from a mixture distribution.

To generate outcomes (ie, phenotypes to be derived), we apply the following model:

$$\text{logit}(P(\text{event}=1))=\alpha 0+\sum_{j=1}^{k} I(\text{clusteri}=j)\alpha j+\sum_{l=1}^{p} X il\beta l$$

Where Pevent=1 represents the probability of ith encounter outcome equal to 1. I(clusteri=j) is the indicator of whether the ith encounter belongs to jth cluster or not. *X* is the design matrix where each row represents one encounter, and each column represents one explanatory variable. $\alpha 0$, αi, and βl are the intercept and main effects corresponding to I(clusteri=j) and *X*. To more accurately reflect real-world conditions, only half of the explanatory variables were incorporated into the generation of the outcome variables, treating the remaining variables as noise (with respect to the outcome).

For each simulated dataset, we assessed information coverage and model performance across 3 samples. First, using the

XSL•FO
RenderX

procedure described in the optimal sample generation section, we averaged the 1st to 10th nearest neighbor distances to obtain a hierarchical-cluster-based sample of size 120 and a k-means-cluster-based sample of size 120. For comparison, we selected 120 random samples and 120 that were sampled from the true underlying clusters. In this manuscript, we refer to the 4 samples as hierarchical, k-means, random, and truth. All data not included in these samples were retained as test data for further analysis. For the model performance comparison, we used each of the 4 derived samples (hierarchical cluster coverage, k-means cluster coverage, random, truth) to fit a logistic regression model to learn a probabilistic CP. For the scenario without an underlying cluster structure, only hierarchical cluster coverage, k-means coverage, and random sampling results are presented, as there is no true cluster structure to compare against. We computed the AUROC to evaluate the model's performance and averaged the performance over 50 iterations.

Real-World Data Application

Our application is motivated by our previous work to develop a CP for a hospital admission due to COVID-19. During the height of the COVID-19 pandemic, hospitals tested all patients for SARS-CoV-2. Work by us [14] and others [15] has indicated that up to 38% of patients who tested positive for SARS-CoV-2 upon admission were admitted for reasons other than COVID-19. Therefore, a CP for admission due to COVID-19 would need to be more complex than simply a positive SARS-CoV-2 test. Our goal then is to define a sample of patients for chart review, in aid of learning a CP for admission due to COVID-19. Since COVID-19 patients could have different presentations, we hypothesize that our coverage sampling approach would be better for learning a CP.

Data Source

We abstracted data from the Duke University Health System EHR system. Duke University Health System consists of 3 hospitals on a common, EPIC-based EHR system. The clinical data are organized into a research-ready datamart, based on the PCORnet Common Data Model [16].

Source Cohort

Our study cohort consisted of all patients with an inpatient admission and a positive test for SARS-CoV-2 from March 2020 to March 2023 (when routine testing stopped). This definition has perfect sensitivity, but poor specificity, for capturing admissions due to COVID-19. Following our previous work, we split this cohort into training and testing data. The testing data consisted of 441 patients admitted from January 16 to 22, 2022 and were already chart reviewed for operational purposes. Additional information regarding the testing data can be found in [14]. The training data consisted of the other 7743 unlabeled patients with positive SARS-CoV-2 tests from 2020 - 2023.

Features Used

For coverage sampling and CP generation, we used 46 clinically relevant features such as encounter characteristics (encounter type, admitting source, and discharge disposition), diagnoses, laboratory tests conducted, and medications administered. Table S1 in Multimedia Appendix 1 provides full details on features used. While we extracted demographic characteristics, we did not include these in the sampling or CP development steps.

Sampling and Outcome Labeling

We generated 2 samples of 100 using coverage and random sampling from the training dataset of 7743 patients. For the coverage sampling, we used hierarchical clustering and identified the cluster structure that minimized the *1st* nearest neighbor distance. An infectious disease specialist (JHH) chart reviewed and labeled the encounter as due to COVID-19 or related sequela, or not.

Method Evaluation

We compare the patient characteristics for the samples that were selected from each sampling approach. Then, using the criteria defined above, we evaluate the coverage of the sample of the full cohort. Finally, we used each sample to learn a probabilistic CP based on a least absolute shrinkage and selection operator logistic regression. We evaluated each version on the independent test data.

All analyses were conducted in R version 4.3.2. The source code used in these experiments is available at GitHub [22].

Ethical Considerations

This study was approved and declared exempt by the Duke School of Medicine IRB, protocol Pro00109397 (9/14/2021). We used a limited analytical dataset within a secure computing environment, and patients did not receive any compensation.

Results

Evaluation of Sampling Methods Using Simulated Data

Figure 4 presents the mean 1st to 10th nearest neighbor distances for both random and coverage sampling methods across 4 distinct scenarios. Figure 4A illustrates a baseline scenario where all clusters are of equal size, while Figure 4B-D depict scenarios with 1, 2, and 3 minority subgroups, respectively. In each scenario, the coverage samples consistently exhibit smaller nearest neighbor distances compared to those from random samples. As minority subgroups are incorporated into the simulated cohort, the advantage of the coverage sample over a random sample increases. Notably, the distances in the hierarchical and k-means-clustered coverage samples are closely aligned with those observed in true cluster configurations, indicating similar coverage of the cohort.

XSL•FO
RenderX

Figure 4. From 1st to 10th nearest neighbor distance mean across 200 simulated data samples for 4 cluster ratios. The red line represents the random sample; the blue line represents the coverage sampling based on hierarchical cluster; the orange line represents the coverage sampling based on k-means clustering; the green line represents the coverage sampling based on the true cluster. (A) All simulated data follows the baseline cluster ratio (0.25,0.25,0.25,0.25). (B) All simulated data follows cluster ratio (0.1,0.3,0.3,0.3). (C) All simulated data follows cluster ratio (0.2,0.2,0.4,0.4). (D) All simulated data follows cluster ratio (0.1,0.1,0.1,0.7).

XSL•FO
RenderX

After generating the samples, we used the data to learn a probabilistic CP and tested its performance. Table 1 presents the mean 1st to 10th nearest neighbor distance and the mean logistic model's AUROC between a random sample and coverage samples generated using hierarchical clustering, k-means clustering, and a true cluster structure of size 120 across 250 simulated datasets. Values highlighted in asterisk (Table 1) indicate AUROCs that are significantly higher than those of the random sample at the 0.05 significance level. The visualization of the AUROC results is shown in Figure S1 in Multimedia Appendix 1. Consistent with coverage results, in the baseline scenario without any minority subgroup or any underlying cluster structure, coverage samples exhibit similar AUROC compared to random samples. However, with the introduction of a minority subgroup, the coverage samples based on hierarchical, k-means, and true cluster structures all produced significantly higher AUROC values compared to random samples. Additionally, we observed that the coverage samples using hierarchical clustering and k-means clustering exhibited similar performance, suggesting that the choice of clustering method has minimal impacts on coverage sampling, provided there are sufficient repetitions.

XSL•FO
RenderX

Table . Comparison of mean distance and area under the curve between random sample, sample based on coverage samples based on hierarchical clustering, k-means clustering, and true cluster.

Cluster ratio and sample type	Mean of 1st-10th nearest neighbor Distance	Overall AUROC[a] (95% CI)	Subgroup 1 AUROC (95% CI)	Subgroup 2 AUROC (95% CI)	Subgroup 3 AUROC (95% CI)	Subgroup 4 AUROC (95% CI)
(1.0,0,0,0)						
Random	3877.728	0.806 (0.803-0.809)	N/A[b]	N/A	N/A	N/A
Hierarchical	3802.404	0.805 (0.801-0.808)	N/A	N/A	N/A	N/A
K-means	3823.452	0.805 (0.802-0.809)	N/A	N/A	N/A	N/A
(0.25,0.25,0.25,0.25)						
Random	3257.498	0.751 (0.747-0.755)	0.735 (0.732-0.738)	0.739 (0.735-0.743)	0.731 (0.728-0.735)	0.733 (0.730-0.736)
Hierarchical	3170.708	0.751 (0.747-0.756)	0.734 (0.731-0.738)	0.739 (0.735-0.742)	0.731 (0.727-0.734)	0.732 (0.729-0.735)
K-means	3163.75	0.752 (0.748-0.757)	0.735 (0.732-0.738)	0.738 (0.734-0.742)	0.731 (0.727-0.734)	0.732 (0.729-0.735)
Truth	3173.694	0.748 (0.744-0.753)	0.731 (0.727-0.735)	0.735 (0.731-0.738)	0.727 (0.724-0.731)	0.729 (0.725-0.732)
(0.1,0.3,0.3,0.3)						
Random	2293.954	0.691 (0.678-0.703)	0.706 (0.694-0.717)	0.607 (0.596-0.618)	0.609 (0.599, 0.618)	0.601 (0.593-0.610)
Hierarchical	2192.928	0.742[c] (0.731-0.753)	0.750[c] (0.741-0.760)	0.633[c] (0.623-0.643)	0.638[c] (0.630-0.647)	0.629[c] (0.620-0.638)
K-means	2183.826	0.740[c] (0.729-0.752)	0.746[c] (0.737-0.755)	0.632[c] (0.623-0.642)	0.636[c] (0.628-0.644)	0.628[c] (0.620-0.636)
Truth	2197.208	0.739[c] (0.727-0.751)	0.747[c] (0.736-0.757)	0.631[c] (0.621-0.642)	0.634 (0.625-0.643[c])	0.622[c] (0.613-0.632)
(0.1,0.1,0.4,0.4)						
Random	2478.755	0.747 (0.737-0.757)	0.746 (0.737-0.756)	0.743 (0.734-0.753)	0.619 (0.612-0.626)	0.617 (0.609-0.626)
Hierarchical	2286.317	0.778[c] (0.769-0.788)	0.774[c] (0.767-0.781)	0.769[c] (0.762-0.776)	0.636[c] (0.630-0.641)	0.635[c] (0.628-0.642)
K-means	2276.429	0.775[c] (0.764-0.786)	0.774[c] (0.767-0.781)	0.771[c] (0.764-0.778)	0.633[c] (0.628-0.639)	0.634[c] (0.627-0.640)
Truth	2292.119	0.782[c] (0.773-0.791)	0.778[c] (0.772-0.784)	0.773[c] (0.767-0.779)	0.639[c] (0.633-0.644)	0.637[c] (0.630-0.644)
(0.1,0.1,0.1,0.7)						
Random	2584.656	0.731 (0.718-0.745)	0.740 (0.730-0.750)	0.743 (0.735-0.752)	0.739 (0.730-0.747)	0.586 (0.580-0.592)
Hierarchical	2287.864	0.769[c] (0.756-0.782)	0.776[c] (0.771-0.782)	0.776[c] (0.770-0.781)	0.772[c] (0.767-0.777)	0.601[c] (0.595-0.607)
K-means	2276.252	0.775[c] (0.762-0.788)	0.777[c] (0.771-0.783)	0.774[c] (0.769-0.780)	0.771[c] (0.765-0.776)	0.600[c] (0.594-0.606)
Truth	2290.974	0.772[c] (0.759-0.785)	0.780[c] (0.774-0.786)	0.778[c] (0.773-0.783)	0.774[c] (0.769-0.780)	0.601[c] (0.596-0.607)

[a]AUROC: area under the receiver operating characteristic curve.

[b]N/A: not applicable.

[c]indicates that the AUROC is significantly higher than that of random sampling method at the .05 significance level.

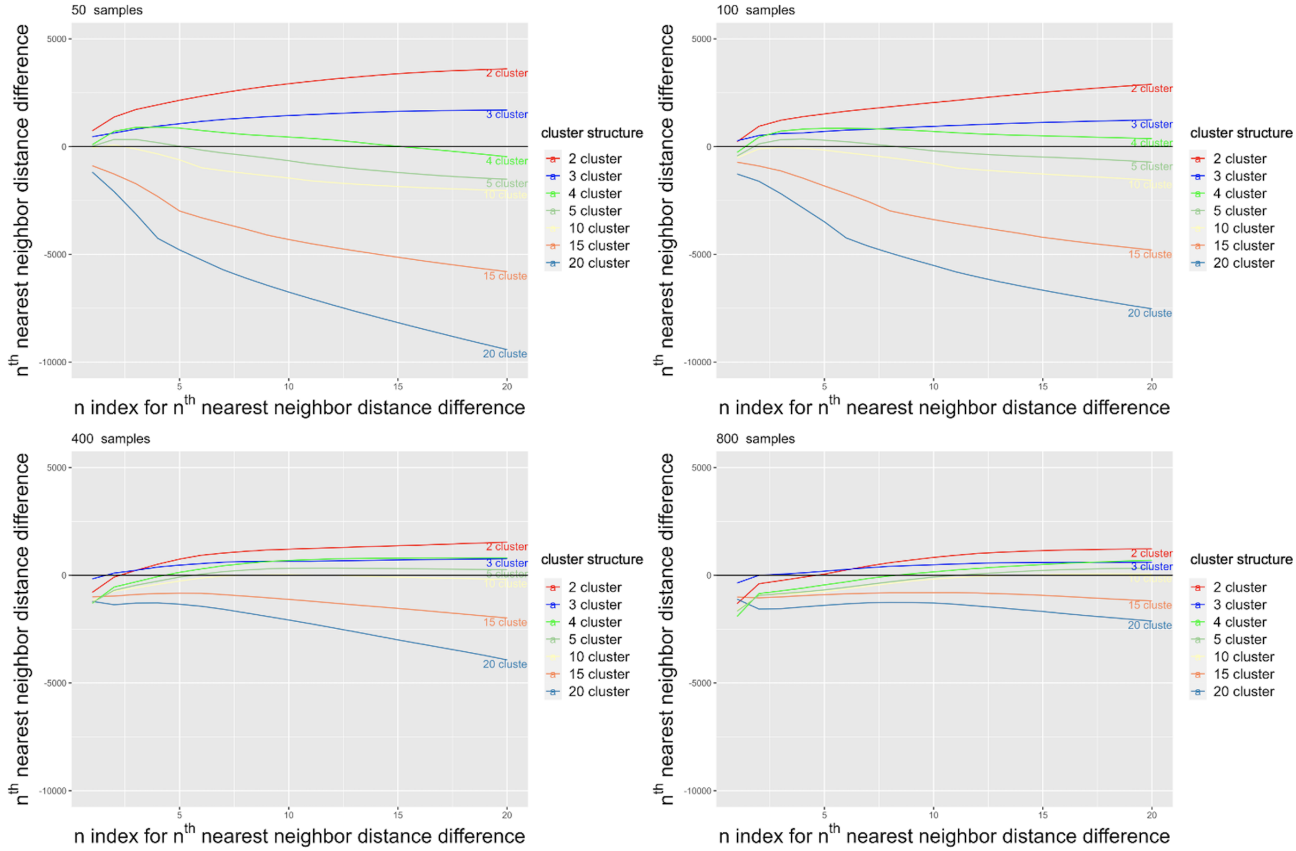
Evaluation of Sampling Methods Using Real-World Data

In real-world data, the true number of clusters or patient subgroups is unknown. We therefore explored a range of potential cluster structures, including 2, 3, 4, 5, 10, 15, and 20 cluster structures. Based on simulated data results, with enough replications, the choice of clustering method does not impact our sampling approach; thus, we only evaluated hierarchical clustering in the real-world data analysis. Figure 5 shows the difference in the mean 1st to 20th nearest neighbor distances in samples generated using the coverage and random samples (ie, coverage sample nth nearest neighbor distance subtracted from random sample nthnearest neighbor distance). The results

XSL•FO
RenderX

demonstrate that for smaller sample sizes (50 and 100), samples drawn from structures with 2, 3, and 4 clusters provide a more accurate representation than their random counterparts. However, as the chart review sample size increases from 400 to 800, the nth nearest neighbor distance of the coverage samples aligns more closely with that of random samples. It is noteworthy that samples derived from 10, 15, and 20 cluster structures perform less effectively across all sample sizes.

Figure 5. Mean n^{th} nearest neighbor distance difference (random sample distance–coverage sample distance) over 100 replications for real-world data.



We conducted a chart review of the 100 random samples and 100 coverage samples. Our coverage sampling approach selected a sample based on 1st nearest neighbor distance. Assessing the clusters using nearest neighbor distance indicated that 2 clusters were the optimal cluster structure. Major clinical differences between the 2 clusters included the C-Reactive protein test, D-dimer test, and BMI (Table S1 in Multimedia Appendix 1). Moreover, while clustering was performed using only clinical variables, the resulting clusters also exhibited meaningful demographic differences, with cluster 1 consisting of an older population compared to cluster 2 (50% vs 25% individuals older than 65 y old). Additional details regarding the cluster characteristics are provided in Table S1 in Multimedia Appendix 1. Table 2 presents the demographic characteristics of the full 7743 patient cohort, as well as the demographics of the coverage and random samples. The standardized mean differences of the random sample and coverage sample are also shown. Notably, the coverage sample includes a higher percentage of young adults (24/100) compared to the random sample (11/100), with other demographic variables showing similar prevalence patterns in both samples.

XSL•FO
RenderX

Table . Demographic characteristics of real-world data, full sample, coverage sample, and random sample.

Characteristics	Full sample	Test dataset	Coverage sample	Random sample	Random versus cluster SMD[a]
Sample size	7743	441	100	100	
Male sex, n (%)	3737 (48.3)	221 (50.1)	43 (43.0)	47 (47.0)	0.080
Age (years), n (%)					0.391
Children (0 - 18)	307 (4.0)	11 (2.5)	3 (3.0)	2 (2.0)	
Young adult (18-35)	995 (12.9)	63 (14.3)	24 (24.0)	11 (11.0)	
Middle adult (35-65)	3015 (38.9)	177 (40.1)	38 (38.0)	38 (38.0)	
Older adult (>65)	3426 (44.2)	190 (43.1)	35 (35.0)	49 (49.0)	
Race and Ethnicity, n (%)					0.131
Hispanic	833 (10.8)	30 (6.8)	13 (13.0)	15 (15.0)	
Non-Hispanic Black	2999 (38.7)	211 (47.8)	44 (44.0)	39 (39.0)	
Non-Hispanic white	3572 (46.1)	187 (42.4)	36 (36.0)	40 (40.0)	
Non-Hispanic Asian	110 (1.4)	1 (0.2)	3 (3.0)	2 (2.0)	
Other races	229 (3.0)	12 (2.7)	4 (4.0)	4 (4.0)	
Group primary payment					0.239
Private	3564 (46.0)	216 (49.0)	48 (48.0)	50 (50.0)	
Public	3215 (41.5)	176 (39.9)	42 (42.0)	35 (34.0)	
Self-pay	307 (4.0)	22 (5.0)	4 (4.0)	3 (3.0)	
Others	657 (8.5)	27 (6.1)	6 (6.0)	12 (12.0)	

[a]SMD: standardized mean differences.

After generating labels, we fit a least absolute shrinkage and selection operator logistic regression model to learn and test a CP. Table 3 presents the *1st* nearest neighbor distance for both the coverage sample and random sample, as well as the AUROC for the learned CP. Additionally, we plot the 1st to 20th nearest neighbor distances of coverage and random sample in Figure S2 in Multimedia Appendix 1.

Given that the true cluster structure is unknown, we report the AUROC at the demographic variable level. The 1st nearest neighbor distance and the AUROC results indicate that the coverage sample slightly outperforms the random sample. This pattern is also observed at the demographic feature level; however, these differences did not reach statistical significance. Nonetheless, in terms of magnitude, coverage samples demonstrate a notable improvement in the coverage of young adults compared to random samples. Of note, we found that increased coverage of demographic groups is not directly correlated with model performance. For example, the coverage and random samples both have similar proportions of males and females. However, the coverage sampling performs nominally better within each sex group. This supports not including demographics in the clustering step and relying on clinical drivers of differentiation. We further evaluated the performance of coverage sampling using additional model architectures, including random forest and XGBoost, for real-world data. Across all models, the coverage sampling approach consistently performed as well as, or better than, random sampling. More details can be found in Table S2 in Multimedia Appendix 1.

For very small subgroups, the performance of the coverage sample may vary. For instance, in the “Other race” group (n=12), the coverage sample shows a substantial AUROC improvement over random sampling (0.611 vs 0.925). In contrast, for the “Other payment” group (n=27), the coverage sample performs slightly worse than random sampling (0.805 vs 0.820).

XSL•FO
RenderX

Table . Mean area under the curve comparison between the coverage sample and the random sample on real-world data.

Characteristics (n)	Random sample AUROC[a] (95% CI)	Cluster sample AUROC (95% CI)
First nearest neighbor distance	57777.82	54213.58
Overall	0.726 (0.680-0.772)	0.747 (0.701-0.793)
Sex		
Female (n=220)	0.724 (0.659-0.784)	0.763 (0.695-0.824)
Male (n=221)	0.725 (0.656-0.789)	0.730 (0.663-0.797)
Age (years), n (%)		
Children (0 - 18; n=2)	0.609 (0.312-0.875)	0.656 (0.312-0.937)
Young adult (18 – 35; n=65)	0.789 (0.685-0.886)	0.867 (0.774-0.947)
Middle adult (35 – 65; n=179)	0.723 (0.652-0.793)	0.727 (0.647-0.797)
Older adult (>65; n=185)	0.669 (0.587-0.749)	0.673 (0.588-0.754)
Race and ethnicity, n (%)		
Hispanic (n=30)	0.828 (0.674-0.963)	0.850 (0.692-0.973)
Non-Hispanic Black (n=211)	0.730 (0.660,0.791)	0.736 (0.664-0.802)
Non-Hispanic white (n=187)	0.703 (0.629,0.778)	0.725 (0.658-0.798)
Non-Hispanic Asian (n=1)	N/A[b]	N/A
Other races (n=12)	0.611 (0.222-0.944)	0.925 (0.778-1)
Group primary payment		
Private (n=216)	0.698 (0.626-0.764)	0.737 (0.667-0.805)
Public (n=176)	0.743 (0.672-0.811)	0.736 (0.661-0.809)
Self-pay (n=22)	0.642 (0.423-0.857)	0.733 (0.485-0.923)
Others (n=27)	0.820 (0.641-0.961)	0.805 (0.623-0.950)

[a]AUROC: area under the receiver operating characteristic curve.

[b]N/A: Not applicable.

Discussion

Principal Findings

CPs are a key component of secondary research with EHR data [23,24]. A required step in CP development is conducting a manual chart review to establish a set of "gold-standard" labels to identify patients with and without the condition or outcome of interest. This manual review can be highly time-consuming [25,26]. Little work has been conducted on how to optimally select charts for review, with investigators most often using random chart selection [11]. This can lead to inefficiencies as potentially informative or edge cases can be missed. To address this concern, we have proposed a sampling strategy to select charts for review that captures the diversity of a population of interest. The key aspect of our method is identifying the optimal sample using a new metric that we have termed the nth nearest neighbor distance. We assessed our method using both simulated and real-world data, evaluating both the information coverage and CP performance. Our findings indicate that coverage sampling performs as well as, if not better than, random sampling. We recommend using a representative sample when developing a computable phenotype. Alternatively, if the phenotype has already been developed, it should be recalibrated using a representative sample of the population before deployment.

One of the motivations for this approach is the presumption that within any group of patients with a particular condition, there are patient subgroups that may have a different presentation of that condition. For example, while many patients with diabetes will have glycosylated hemoglobin test values >6.5% there will be some individuals with controlled diabetes and normal glycosylated hemoglobin values; however, these patients still have diabetes [27]. Such scenarios require the creation of complex CPs that can identify patients with diabetes who have a variety of disease presentations [28]. If these patient subgroups are small enough, a random selection of charts may not provide sufficient coverage of these subgroups to ensure that the CP performs equitably for all patient subgroups. As our results demonstrate, coverage sampling has its greatest impact in CP performance when minority subgroups are present. However, the presence of such minority subgroups is not a requirement for the method to perform well. In scenarios without minority subgroups, our method performs comparably to random sampling, highlighting the robustness of the approach. Moreover, even when there is no underlying cluster structure at all, coverage sampling performs as well as random sampling.

XSL•FO
RenderX

A novel aspect of our approach is the development of a metric, the nth nearest neighbor distance, to measure the coverage of a given sample. While previous methods have used nearest neighbor distances to detect and quantify spatial randomness, they have primarily focused on analyzing spatial patterns in populations [29]. Existing representativeness metrics, such as Simpson's Diversity Index and Shannon's Entropy, quantify overall variability across multiple demographic features [30]. Simpson's Diversity Index measures the probability that 2 individuals randomly selected from a sample will belong to different categories, thereby emphasizing the dominance or evenness of group representation [31]. Shannon's Entropy quantifies diversity by accounting for both the abundance and the evenness of the categories present, using information theory to assess the uncertainty in predicting the category of a randomly chosen individual [32]. While these metrics effectively address general diversity measurement goals, they do not directly align with our specific goal of evaluating the representation and coverage of minority subgroups. The nth nearest neighbor distance explicitly evaluates the distance between records in the unsampled group to those in the sampled group. This targeted focus enables a more precise assessment of the extent to which minority subgroups are included in study samples, thereby avoiding underrepresentation in the set of records used for CP development. As our real data analysis results showed, we can use the nth nearest neighbor distance to choose an optimal number of cluster k from which to sample. In particular, choosing too large of k leads to suboptimal performance.

Although the construction and generation of a chart review sample has not been widely discussed in the CP literature, parallel work exists in the active learning literature. Current active learning methods can be categorized as query-acquiring (pool-based) or query-synthesizing [20,33]. We focus on query-acquiring active learning, as query-synthesizing methods are not directly analogous to our work. Query-acquiring active learning uses various sampling strategies, including uncertainty sampling or information-theoretic measures, to identify which sampling strategies would be most impactful for continued labeling [18,34]. Therefore, the underlying burden for query-acquiring active learning is the same as in our method: an efficient need for labeling [35,36]. Most existing methods, including uncertainty sampling or information-theoretic measures, focus on identifying the most influential records to enhance the performance of a given prediction task [20,21,37-40]. In contrast, our method is not based on a supervised objective. Further, our method seeks to select records that best capture diversity, rather than records that are most representative. While representativeness and diversity may be related, they are not necessarily equivalent.

To illustrate our approach, we tested our method with the real-world task of identifying hospital encounters due to COVID-19. During the height of the COVID-19 pandemic (2020 - 2023), all patients admitted to our health system's hospitals were tested for SARS-CoV-2. As we and others have noted, approximately 38.2% of patients with a positive SARS-CoV-2 test were admitted for reasons other than COVID-19 [14,15]. Therefore, if one wanted to identify patients admitted due to COVID-19, a positive SARS-CoV-2 test would not be a sufficient CP because of its poor specificity. We compared the performance of the chart review sample based on a random selection of charts and our coverage sampling method. Overall, the coverage sample yielded a comparable performing CP. So, while coverage sampling did not yield better performance, the results conform to the simulation findings, which indicate that coverage is robust even when there is no underlying cluster structure or minority group.

While we selected charts based solely on clinical data elements, there were meaningful demographic differences between samples derived from randomly selected charts and through coverage sampling. For example, cluster 1 includes a much older patient population, with 50.2% (2959/5897) over the age of 65, compared to 25.3% (467/1846) in cluster 2. Patients in cluster 1 also have longer hospital stays (9.42 d on average) than those in cluster 2 (3.52 d). Additional details on cluster characteristics are provided in Table S1 in Multimedia Appendix 1. Consequently, the coverage sample exhibits a different distribution than the random sample. Specifically, the coverage sample included younger patients, a greater number of non-Hispanic Black patients (though fewer Hispanic patients), and more individuals with public insurance compared to the cohort derived from random sampling. This result highlights one of the key opportunities in this approach: deriving a less biased sample on which to build a CP. As others have described, one of the mechanisms of algorithmic bias is having unrepresentative samples used to develop the algorithm [41]. For instance, in the context of rare diseases, the typical ratio of patients with a given rare condition to those without the condition is approximately 100:1 [42,43]. In such scenarios, using random sampling may result in underrepresentation of minority subgroups in the chart review sample. When the review sample does not accurately reflect the patient population, the resulting CPs can produce biased results. For example, if certain demographic groups are underrepresented in the dataset, the CP may not learn to make accurate predictions for these groups, leading to disparities in performance [44]. To account for this, algorithmic solutions have been proposed, including data augmentation [45,46], resampling techniques [47,48], and algorithmic adjustments [49]. However, instead of addressing this problem algorithmically, we propose addressing it via design. As such, by clustering the data and sampling equally from the obtained clusters, we aim for the chart review sample to better represent the patient population. An advantage of our method is that it does not require the researcher to prespecify groups. Moreover, as our empirical results show, we are able to capture demographic diversity with just clinical data.

Limitations

While our approach shows promise, there are some limitations. First, while our simulation results illustrate the potential improvement for coverage sampling, our real-world data example only showed nominal improvement. Further work should be conducted in other contexts. Second, the performance of our method is related to the quality of the cluster analysis. As others have noted, clustering methods can be highly variable [50]. This variability may be more obvious in EHR data, which often experience data quality issues. Because the clustering step is a means of obtaining a representative sample, we address this

XSL•FO
RenderX

by generating multiple samples from multiple cluster structures and selecting the one with the best coverage. In principle, it is possible to skip the clustering step and directly choose an optimal sample, leading to more robust results. While such an approach is worthy of further exploration, it would be more computationally expensive and would not necessarily yield meaningfully better results. Third, while our study suggests that coverage sampling is not very sensitive to the choice of *n*, its robustness warrants further evaluation. Future researchers are encouraged to test a small range of *n* values (eg, n=1, 5, 10), as different choices of *n* may yield different samples. Another potential limitation is that the coverage sample (intentionally) generates a sample that will likely have a different event rate than the true event rate within the full patient population. While this does not present a problem for rank-based metrics like AUROC, it may affect the calibration of other metrics, such as Kullback-Leibler divergence [51]. When calibration is a priority, recalibration methods can be used [52].

Conclusions

Overall, our results show that our coverage sampling method can provide a more representative sample than random sampling, especially when the source cohort contains minority subgroups. This approach can lead to the generation of a CP that has better performance in the overall study population as well as within subgroups. While CP development is a key part of secondary research with EHR data, little work has been done on how best to derive samples for learning CPs. This work addresses this gap and seeks to spur more investigation in this area. Ultimately, this sampling method has the potential to improve future clinical research by making gold-standard chart review labeling a more efficient process.

Acknowledgments

This work was supported by Food and Drug Administration Broad Agency Announcement (FDA BAA) 75F40121C00158 (principal investigator: BAG).

During the preparation of this work, the authors used ChatGPT in order to improve the language and readability of the manuscript. After using this tool or service, the authors reviewed and edited the content as needed and take full responsibility for the content of the publication.

Funding

This work was supported by Food and Drug Administration Broad Agency Announcement (FDA BAA) 75F40121C00158 (principal investigator: BAG).

Data Availability

The code for the simulated dataset used in this study is available at GitHub [22]; the real-world datasets analyzed during this study are not publicly available due to Duke University policies but are available from the corresponding author on reasonable request.

Authors' Contributions

ZW: Conceptualization; Data Curation; Formal analysis; Methodology; Writing-original draft; Writing-review and editing.
JH: Data Curation; Writing-review and editing.
CH: Writing-review and editing.
BG: Conceptualization; Funding Acquisition; Methodology; Supervision; Writing-review and editing.

Conflicts of Interest

None declared.

Multimedia Appendix 1
Supplemental materials regarding study results.
[DOCX File, 407 KB - medinform_v13i1e72068_app1.docx]

References

1. Wang ECH, Wright A. Characterizing outpatient problem list completeness and duplications in the electronic health record. J Am Med Inform Assoc 2020 Aug 1;27(8):1190-1197. [doi: 10.1093/jamia/ocaa125] [Medline: 32620950]
2. Grauer A, Kneifati-Hayek J, Reuland B, et al. Indication alerts to improve problem list documentation. J Am Med Inform Assoc 2022 Apr 13;29(5):909-917. [doi: 10.1093/jamia/ocab285] [Medline: 34957491]
3. Ghirardello S, Garrè ML, Rossi A, Maghnie M. The diagnosis of children with central diabetes insipidus. J Pediatr Endocrinol Metab 2007 Mar;20(3):359-375. [doi: 10.1515/jpem.2007.20.3.359] [Medline: 17451074]

XSL•FO
RenderX

4. Miller RL, Grayson MH, Strothman K. Advances in asthma: New understandings of asthma's natural history, risk factors, underlying mechanisms, and clinical management. J Allergy Clin Immunol 2021 Dec;148(6):1430-1441. [doi: 10.1016/j.jaci.2021.10.001] [Medline: 34655640]
5. Wang L, Olson JE, Bielinski SJ, et al. Impact of diverse data sources on computational phenotyping. Front Genet 2020 Jun;11. [doi: 10.3389/fgene.2020.00556]
6. Gearing RE, Mian IA, Barber J, Ickowicz A. A methodology for conducting retrospective chart review research in child and adolescent psychiatry. J Can Acad Child Adolesc Psychiatry 2006 Aug;15(3):126-134. [Medline: 18392182]
7. Panacek EA. Performing chart review studies. In: Panacek EA, editor. Air Med J 2007;26(5):206-210. [doi: 10.1016/j.amj.2007.06.007] [Medline: 17765825]
8. McKenzie J, Rajapakshe R, Shen H, Rajapakshe S, Lin A. A semiautomated chart review for assessing the development of radiation pneumonitis using natural language processing: diagnostic accuracy and feasibility study. JMIR Med Inform 2021 Nov 12;9(11):e29241. [doi: 10.2196/29241] [Medline: 34766919]
9. Ho JC, Ghosh J, Steinhubl SR, et al. Limestone: high-throughput candidate phenotype generation via tensor factorization. J Biomed Inform 2014 Dec;52:199-211. [doi: 10.1016/j.jbi.2014.07.001] [Medline: 25038555]
10. Carrell DS, Floyd JS, Gruber S, et al. A general framework for developing computable clinical phenotype algorithms. J Am Med Inform Assoc 2024 Aug 1;31(8):1785-1796. [doi: 10.1093/jamia/ocae121] [Medline: 38748991]
11. Vassar M, Holzmann M. The retrospective chart review: important methodological considerations. J Educ Eval Health Prof 2013;10:12. [doi: 10.3352/jeehp.2013.10.12] [Medline: 24324853]
12. Elfil M, Negida A. Sampling methods in clinical research; an educational review. Emerg (Tehran) 2017;5(1):e52. [Medline: 28286859]
13. Waller NG, Underhill JM, Kaiser HA. A method for generating simulated plasmodes and artificial test clusters with user-defined shape, size, and orientation. Multivariate Behav Res 1999 Apr 1;34(2):123-142. [doi: 10.1207/S15327906Mb340201] [Medline: 26753933]
14. Chang F, Krishnan J, Hurst JH, et al. Comparing natural language processing and structured medical data to develop a computable phenotype for patients hospitalized due to COVID-19: retrospective analysis. JMIR Med Inform 2023 Aug 22;11:e46267. [doi: 10.2196/46267] [Medline: 37621195]
15. Klann JG, Strasser ZH, Hutch MR, et al. Distinguishing admissions specifically for COVID-19 from incidental SARS-CoV-2 admissions: National Retrospective Electronic Health Record Study. J Med Internet Res 2022 May 18;24(5):e37931. [doi: 10.2196/37931] [Medline: 35476727]
16. Hurst JH, Liu Y, Maxson PJ, Permar SR, Boulware LE, Goldstein BA. Development of an electronic health records datamart to support clinical and population health research. J Clin Trans Sci 2021;5(1):1. [doi: 10.1017/cts.2020.499]
17. Miller B, Linder F, Mebane WR. Active learning approaches for labeling text: review and assessment of the performance of active learning approaches. Polit Anal 2020 Oct;28(4):532-551. [doi: 10.1017/pan.2020.4]
18. Cohn DA, Ghahramani Z, Jordan MI. Active learning with statistical models [abstract]. 1996 Presented at: Advances in Neural Information Processing Systems 7 (NIPS 1994); Nov 28 to Dec 1, 1994 URL: https://papers.nips.cc/paper_files/paper/1994/hash/7f975a56c761db6506eca0b37ce6ec87-Abstract.html [accessed 2025-11-11]
19. Huang SJ, Jin R, Zhou ZH. Active learning by querying informative and representative examples. IEEE Trans Pattern Anal Mach Intell 2014 Oct;36(10):1936-1949. [doi: 10.1109/TPAMI.2014.2307881] [Medline: 26352626]
20. Sinha S, Ebrahimi S, Darrell T. Variational adversarial active learning. 2019 Mar 31 Presented at: 2019 IEEE/CVF International Conference on Computer Vision (ICCV). [doi: 10.1109/ICCV.2019.00607]
21. Li X, Guo Y. Adaptive active learning for image classification. 2013 Presented at: IEEE Conference on Computer Vision and Pattern Recognition; Jun 23-28, 2013; Portland, OR, USA p. 859-866. [doi: 10.1109/CVPR.2013.116]
22. Wang Z. phenotype-sampling. URL: https://github.com/justinwang97/phenotype-sampling [accessed 2025-07-19]
23. Pfaff ER, Crosskey M, Morton K, Krishnamurthy A. Clinical Annotation Research Kit (CLARK): computable phenotyping using machine learning. JMIR Med Inform 2020 Jan 24;8(1):e16042. [doi: 10.2196/16042] [Medline: 32012059]
24. Tayefi M, Ngo P, Chomutare T, et al. Challenges and opportunities beyond structured data in analysis of electronic health records. WIREs Computational Stats 2021 Nov;13(6). [doi: 10.1002/wics.1549]
25. Johnston KM, Lakzadeh P, Donato BMK, Szabo SM. Methods of sample size calculation in descriptive retrospective burden of illness studies. BMC Med Res Methodol 2019 Jan 9;19(1):9. [doi: 10.1186/s12874-018-0657-9] [Medline: 30626343]
26. Connolly A, Kirwan M, Matthews A. A scoping review of the methodological approaches used in retrospective chart reviews to validate adverse event rates in administrative data. Int J Qual Health Care 2024 May 10;36(2):mzae037. [doi: 10.1093/intqhc/mzae037] [Medline: 38662407]
27. Richesson RL, Rusincovitch SA, Wixted D, et al. A comparison of phenotype definitions for diabetes mellitus. J Am Med Inform Assoc 2013 Dec;20(e2):e319-e326. [doi: 10.1136/amiajnl-2013-001952] [Medline: 24026307]
28. Spratt SE, Pereira K, Granger BB, et al. Assessing electronic health record phenotypes against gold-standard diagnostic criteria for diabetes mellitus. J Am Med Inform Assoc 2017 Apr 1;24(e1):e121-e128. [doi: 10.1093/jamia/ocw123] [Medline: 27616701]
29. Thompson HR. Distribution of distance to Nth neighbour in a population of randomly distributed individuals. Ecology 1956 Apr;37(2):391-394. [doi: 10.2307/1933159]

XSL•FO
RenderX

30. Peet RK. The measurement of species diversity. Annu Rev Ecol Syst 1974;5:285-307 [FREE Full text]
31. Simpson EH. Measurement of diversity. Nature New Biol 1949 Apr 30;163(4148):688-688. [doi: 10.1038/163688a0]
32. Shannon CE. A mathematical theory of communication. Bell System Technical Journal 1948 Jul;27(3):379-423. [doi: 10.1002/j.1538-7305.1948.tb01338.x]
33. Settles B. Active learning literature survey. : Minds@UW; 2009 URL: https://minds.wisconsin.edu/handle/1793/60660 [accessed 2025-11-24]
34. Freund Y, Seung HS, Shamir E, Tishby N. Selective sampling using the query by committee algorithm. Mach Learn 1997 Aug;28(2):133-168. [doi: 10.1023/A:1007330508534]
35. Muslea I, Minton S, Knoblock C. Active semi-supervised learning = robust multi-view learning. ICML '02: Proceedings of the Nineteenth International Conference on Machine Learning 2002;2:435-442. [doi: 10.5555/645531.655845]
36. McCallum A, Nigam K. Employing EM and pool-based active learning for text classification. 1998 Presented at: Proceedings of the 15th International Conference on Machine Learning; Jul 24-27, 1998; Madison, WI, USA p. 350-358. [doi: 10.5555/645527.757765]
37. Jain P, Kapoor A. Active learning for large multi-class problems. 2009 Presented at: 2009 IEEE Computer Society Conference on Computer Vision and Pattern Recognition Workshops (CVPR Workshops); Jun 20-25, 2009; Miami, FL, USA p. 762-769. [doi: 10.1109/CVPR.2009.5206651]
38. Kapoor A, Grauman K, Urtasun R, Darrell T. Active learning with gaussian processes for object categorization. 2007 Presented at: 2007 IEEE 11th International Conference on Computer Vision p. 1-8. [doi: 10.1109/ICCV.2007.4408844]
39. MacKay DJC. Information-based objective functions for active data selection. Neural Comput 1992 Jul;4(4):590-604. [doi: 10.1162/neco.1992.4.4.590]
40. Tong S, Koller D. Support vector machine active learning with applications to text classification. J Mach Learn Res 2002 Mar;2:45-66. [doi: 10.1162/153244302760185243]
41. Suresh H, Guttag J. A framework for understanding sources of harm throughout the machine learning life cycle. 2021 Oct 5 Presented at: 1st ACM Conference on Equity and Access in Algorithms, Mechanisms, and Optimization (EAAMO '21); Oct 5-9, 2021. [doi: 10.1145/3465416.3483305]
42. Mealy MA, Wingerchuk DM, Greenberg BM, Levy M. Epidemiology of neuromyelitis optica in the United States: a multicenter analysis. Arch Neurol 2012 Sep;69(9):1176-1180. [doi: 10.1001/archneurol.2012.314] [Medline: 22733096]
43. Stoller JK. The challenge of rare diseases. Chest 2018 Jun;153(6):1309-1314. [doi: 10.1016/j.chest.2017.12.018] [Medline: 29325986]
44. Buolamwini J, Gebru T. Gender shades: intersectional accuracy disparities in commercial gender classification. In: Friedler SA, Wilson C, editors. 2018 May Presented at: Proceedings of the 1st Conference on Fairness, Accountability and Transparency; New York, NY, USA p. 77-91 URL: https://proceedings.mlr.press/v81/buolamwini18a.html [accessed 2025-11-19]
45. Kennedy G, Dras M, Gallego B. Augmentation of electronic medical record data for deep learning. In: In Studies in Health Technology and Informatics: IOS Press BV; 2022:582-586. [doi: 10.3233/SHTI220144]
46. Shorten C, Khoshgoftaar TM. A survey on image data augmentation for deep learning. J Big Data 2019 Dec;6(1):1. [doi: 10.1186/s40537-019-0197-0]
47. Chawla NV, Bowyer KW, Hall LO, Kegelmeyer WP. SMOTE: synthetic minority over-sampling technique. jair 2002;16:321-357. [doi: 10.1613/jair.953]
48. Kim YT, Kim DK, Kim H, Kim DJ. A comparison of oversampling methods for constructing a prognostic model in the patient with heart failure. Presented at: 2020 International Conference on Information and Communication Technology Convergence (ICTC); Oct 21-23, 2020. [doi: 10.1109/ICTC49870.2020.9289522]
49. Hino H. Active learning: problem settings and recent developments. arXiv. Preprint posted online on Dec 8, 2020. [doi: 10.48550/arXiv.2012.04225]
50. Jain AK. Data clustering: 50 years beyond K-means. Pattern Recognit Lett 2010 Jun;31(8):651-666. [doi: 10.1016/j.patrec.2009.09.011]
51. Hershey JR, Olsen PA. Approximating the kullback leibler divergence between Gaussian mixture models. 2007 Presented at: 2007 IEEE International Conference on Acoustics, Speech and Signal Processing - ICASSP '07; Honolulu, HI, USA p. IV-317. [doi: 10.1109/ICASSP.2007.366913]
52. King G, Zeng L. Logistic regression in rare events data. Polit anal 2001;9(2):137-163. [doi: 10.1093/oxfordjournals.pan.a004868]

Abbreviations

AUROC: area under the receiver operator characteristic curve
CP: computable phenotypes
EHR: electronic health record

XSL•FO
RenderX

Edited by A Coristine; submitted 03.02.25; peer-reviewed by F Chang, V Borza; revised version received 09.10.25; accepted 09.10.25; published 27.11.25.

Please cite as:
Wang Z, Hurst JH, Hong C, Goldstein BA
Unsupervised Coverage Sampling to Enhance Clinical Chart Review Coverage for Computable Phenotype Development: Simulation and Empirical Study
JMIR Med Inform 2025;13:e72068
URL: https://medinform.jmir.org/2025/1/e72068
doi:10.2196/72068

© Zigui Wang, Jillian H Hurst, Chuan Hong, Benjamin Alan Goldstein. Originally published in JMIR Medical Informatics (https://medinform.jmir.org), 27.11.2025. This is an open-access article distributed under the terms of the Creative Commons Attribution License (https://creativecommons.org/licenses/by/4.0/), which permits unrestricted use, distribution, and reproduction in any medium, provided the original work, first published in JMIR Medical Informatics, is properly cited. The complete bibliographic information, a link to the original publication on https://medinform.jmir.org/, as well as this copyright and license information must be included.

XSL•FO
RenderX

Leveraging Machine Learning and Robotic Process Automation to Identify and Convert Unstructured Colonoscopy Results Into Actionable Data: Proof-of-Concept Study

Elizabeth R Stevens[1,2], MPH, PhD; Jager Hartman[2], MS; Paul Testa[2], MD, MPH; Ajay Mansukhani[3], BA; Casey Monina[3], RN; Amelia Shunk[1,4], MMCi; David Ranson[3], BS; Yana Imberg[3], MHI; Ann Cote[3], MIS; Dinesha Prabhu[3], BS; Adam Szerencsy[2], DO

[1]Department of Population Health, Grossman School of Medicine, New York University, 227 E30th Street, Rm 636, New York, United States

[2]Department of Health Informatics, Medical Center Information Technology, NYU Langone Health, New York, NY, United States

[3]MCIT Clinical Systems NYU Langone, New York, NY, United States

[4]School of Medicine, Tulane University, New Orleans, LA, United States

Corresponding Author:
Elizabeth R Stevens, MPH, PhD
Department of Population Health, Grossman School of Medicine, New York University, 227 E30th Street, Rm 636, New York, United States

Abstract

Background: With rising patient volumes and a focus on quality, our health system had the objective to create a more efficient way to ensure accurate documentation of colorectal cancer (CRC) screening intervals from inbound colonoscopy reports to ensure timely follow-up. We developed an integrated end-to-end workflow solution using machine learning (ML) and robotic process automation (RPA) to extract and update electronic health record (EHR) follow-up dates from unstructured data.

Objective: This study aimed to automate data extraction from external, free-text colonoscopy reports to identify and document recommended follow-up dates for CRC screening in structured EHR fields.

Methods: As proof of concept, we outline the process development, validity, and implementation of an approach that integrates available tools to automate data retrieval and entry within the EHR of a large academic health system. The health system uses Epic Systems as its EHR platform, and the ML model used was trained on health system patient colonoscopy reports. This proof-of-concept process study consisted of six stages: (1) identification of gaps in documenting recommendations for follow-up CRC screening from external colonoscopy reports, (2) defining process objectives, (3) identification of technologies, (4) creation of process architecture, (5) process validation, and (6) health system–wide implementation. A chart review was performed to validate process outcomes and estimate impact.

Results: We developed an automated process with 3 primary steps leveraging ML and RPA to create a fully orchestrated workflow to update CRC screening recall dates based on colonoscopy reports received from external sources. Process validity was assessed with 690 scanned colonoscopy reports. During process validation, the overall automated process achieved an accuracy of 80.7% (557/690, 95% CI 77.8%-83.7%) for correctly identifying the presence or absence of a valid follow-up date and a follow-up date false negative identification rate of 32.9% (130/395, 95% CI 29.4%-36.4%). From the organization-wide implementation to go-live until December 31, 2024, the system processed 16,563 external colonoscopy reports. Of these, 35.3% (5841/16,563) had a follow-up date meeting the relevant ML model threshold and thus were identified as ready for RPA processing.

Conclusions: Implementation of an automated workflow to extract and update CRC screening follow-up dates from colonoscopy reports is feasible and has the potential to improve accuracy in patient recall while reducing documentation burden. By standardizing data ingestion, extending this approach to various unstructured data types can address deficiencies in structured EHR documentation and solve for a lack of data integration and reporting for quality measures. Automated workflows leveraging ML and RPA offer practical solutions to overcome interoperability challenges and the use of unstructured data within health care systems.

(JMIR Med Inform 2025;13:e73504) doi:10.2196/73504

KEYWORDS

colorectal cancer; RPA; automation; colonoscopy; machine learning; artificial intelligence; robotic process automation

XSL•FO
RenderX

Introduction

Colorectal cancer (CRC) is the second most common cause of cancer-related death in the United States [1] and has a growing incidence rate, particularly among younger individuals [2]. Effective CRC screening is a cornerstone of preventive health care, significantly reducing both the incidence and mortality rates associated with CRC [3]. To realize the full benefit of CRC screening, an accurate and timely recall of patients for follow-up screening is needed.

Despite the availability of electronic health record (EHR) tools to facilitate reminders for CRC screening follow-up, these tools often fail to address clinician needs [4,5]. The limited interoperability of health information exchanges between health care systems and reliance on unstructured data to convey recommendations for follow-up place a high documentation burden on clinicians, leading to substantial missed opportunities for improved CRC follow-up screening and surveillance [6-8].

EHR tools are rarely responsive to patient-specific factors or colonoscopy and pathology findings. Consequently, recalling a patient for more frequent follow-up screening requires a manual update [9]. To enhance CRC screening follow-up accuracy, while minimizing documentation burden, solutions that automate the retrieval and processing of colonoscopy results are needed. An automated process for updating CRC screening follow-up–based colonoscopy findings is likely to increase the number of patients with a documented guideline-concordant CRC follow-up screening interval [10,11].

As with nearly 80% of EHR data [12], colonoscopy and pathology findings are frequently documented within the EHR as free text [13]. Further complexity arises when colonoscopy results are received as inbound medical records from external sources. These records, often received via fax, mail, or email, require additional steps to document the relevant data into the EHR, posing a significant administrative burden for documenting CRC screening due dates [14].

Natural language processing (NLP) models have the potential to address barriers associated with leveraging unstructured data and accurately extract relevant data from free-text colonoscopy and pathology reports [15]. However, NLP alone cannot address all workflow steps required to convert text-based reports into structured fields in the EHR. It is essential to pair the model with supplemental tools for data entry. A solution is needed that orchestrates multiple technologies to address each step in the workflow necessary to update the appropriate CRC follow-up dates.

With rising patient volumes and a focus on quality, our health system needed a more efficient way to ensure accurate documentation of CRC screening follow-up intervals from inbound colonoscopy reports. To address this, we developed an integrated workflow using machine learning (ML) and robotic process automation (RPA) to extract and update follow-up dates from unstructured data. With the objective of demonstrating a proof of concept, in this paper, we outline the process and validity of an approach to process inbound colonoscopy reports that integrates available tools to automate data retrieval and entry within the EHR. We hypothesize that this framework can be adapted to other clinical information to improve reporting, data accuracy, and workflow efficiency.

Methods

Overview

This proof-of-concept study was part of an institutional initiative to improve the accuracy of documented CRC screening follow-up recommendations extracted from unstructured colonoscopy reports from external organizations. The study developed an integrated workflow using existing technologies to address this care gap and assessed its validity. This study consisted of six stages: (1) identification of gaps in operationalizing recommendations for follow-up CRC screening from external colonoscopy reports, (2) defining process objectives, (3) identification of available technological tools, (4) creation of process architecture, (5) process validation and refinement, and (6) health system–wide process implementation.

Study Setting and Participants

The New York University Langone Health (NYULH) system is a private, nonprofit hospital system serving the greater New York area and Florida with over 9 million patients. The NYULH system uses Epic Systems as its EHR platform. For the process validation component of this study, EHR data were extracted prospectively for a series of 4 sequential simple random samples of scanned colonoscopy reports from adult patients aged 45 to 75 years from external sources between August 2023 and September 2023.

Health Informatics Care Gap

Ensuring timely follow-up for CRC screening was identified as an important quality measure for the health system. Accurately tracking patients due for CRC screening is facilitated by having the next colonoscopy follow-up date documented discretely in the EHR's health maintenance (HM) activity.

Gaps in this process frequently occur when colonoscopy reports from external organizations are scanned into the health system's EHR. Since these documents contain unstructured data, critical information remains inaccessible unless manually transcribed into the EHR [12,13]. If this information is not updated manually, the HM follow-up screening interval defaults to 10 years, which may not be appropriate for many patients [8]. As a result, the HM activity often fails to reflect the recommended follow-up intervals indicated in the colonoscopy report unless users manually update it. Factors such as procedural findings, pathology results, and patient-specific risk factors may necessitate more frequent surveillance. To ensure transparency and awareness for both patients and clinicians, as well as for accurate reporting, this information should be documented discretely in the appropriate fields within the EHR.

Manually updating the HM follow-up intervals is time-consuming, often leading to unchanged follow-up dates in the EHR and failing to reflect the appropriate recall time frame. This documentation gap can result in missed or delayed surveillance, potentially impacting patient outcomes. To address this challenge, an efficient and effective process is needed to

XSL•FO
RenderX

extract and process unstructured text from colonoscopy reports to automatically update HM follow-up intervals.

Defining the Process Objective

After identifying the care gap, the objective was to develop a process to automate updating the HM based on the external colonoscopy reports. We sought to leverage ML to identify follow-up recommendations within the reports and RPA to automate the entry of recommended recall dates into the HM activity.

It was also determined that the process must operate within the following constraints: (1) use existing technologies within the health system, (2) not override any recommendations that have been manually entered by a clinician, (3) ML engine identifies follow-up date above a technical performance threshold of >70% confidence; and (4) No human intervention after the colonoscopy report has been scanned into the EHR.

Although pathology results should ideally serve as the gold standard for assessing follow-up intervals, due to limited availability, the recommendation listed within the colonoscopy report was deemed a sufficiently accurate alternative for the purpose of updating HM.

Orchestrated Workflow Development

To develop the orchestrated workflow, the team first broke the process into concrete steps. We then mapped out existing technological components within the healthy IT ecosystem needed for each action. The steps included: (1) daily extraction of scanned external colonoscopy reports, (2) a mechanism for an ML model to receive and analyze those reports to identify the next follow-up date, and (3) an automated process that updates the HM activity when appropriate.

The team established care assumptions to guide when the process updates would take precedence over existing HM follow-up frequencies. These assumptions included: (1) all updates must be associated with a colonoscopy order; (2) the bot should only update HM if the scanned report is more recent than the last documented colonoscopy; (3) the scanned report would not override manual entry; (4) the bot should not update a follow-up date if the patient has an existing earlier follow-up date; (5) if the ML engine's determination of follow-up date is below the performance threshold, the report should be queued for manual review; (6) if an outstanding colonoscopy order exists and the procedure date is after the order date, the report should be scanned to that order; and (7) if there is a range of follow-up dates (eg, return in 3 - 5 y) the bot will use the earlier date. Based on these assumptions, business exceptions within the decision rules were defined to establish scenarios in which it would be inappropriate for the bot to update the HM.

Identified Technological Tools

Overview

Existing technologies were evaluated for their applicability to each workflow step, resulting in a process comprising six key components, including: (1) an internally developed ML model, (2) fax management software, (3) a document management platform, (4) input spreadsheets, (5) RPA, and (6) Epic's HM activity.

Fax Management Software

RightFax (OpenText) is an enterprise fax server software that allows the organization to send and receive faxes. It also transforms faxes for easier management and integration into other digital systems, including the EHR [16]. RightFax was used to receive colonoscopy reports from external sources.

ML Techniques

ML techniques, including optical character recognition and NLP, enable systems to "read" documents and extract relevant information [17,18]. ML is a subset of artificial intelligence (AI) that enables systems to learn patterns from data and make predictions or classifications without explicit programming. These classifier algorithms can identify patterns, structures, and key data within various document formats, automating the extraction process and reducing the need for manual intervention. This capability is widely used in data entry, document analysis, and information retrieval. A proprietary model was internally developed to identify the follow-up dates for the next screening. The model was trained on 7021 unique documents, 90.6% (6358/7021) of which were colonoscopy reports, 6.7% (473/7021) were pathology reports, and 2.7% (190/7021) were other types of documents. Details of the ML model training data set can be found in Multimedia Appendix 1. This process required model training by a clinical subject matter expert.

The ML was validated using a 4:1 patient-based split with manual review of a sample of 1758 documents and associated RPA actions in the EHR. The validation documents included 90.8% (1597/1758) colonoscopy reports, 6.5% (114/1758) pathology reports, and 2.7% (47/1758) other types of documents. Details of the ML model validation data set can be found in Multimedia Appendix 1.

RPA Technology

UiPath RPA is a technology that uses software robots, or "bots," to automate repetitive and rule-based tasks typically performed by humans. These RPA bots can work across platforms and mimic human actions such as data entry, processing transactions, and managing records, thereby increasing efficiency and reducing errors. Unlike AI, RPA follows predefined workflows and does not learn or adapt on its own [19]. In this case, the RPA tool "read" the output of the ML engine, updated the HM activity date if applicable, and documented the actions taken. If any business exceptions existed, they were similarly documented. Finally, the RPA sent a summary of the completed process to operational leadership for review.

Document Management Platform

OnBase is an enterprise content management platform developed by Hyland Software. It helps organizations manage documents in a unified system, acting as a digital filing cabinet with advanced automation capabilities. OnBase supports document storage, quick retrieval, and task automation, enhancing efficiency and compliance [20]. In this process, OnBase is used as the underlying application where the reports were scanned

XSL•FO
RenderX

into the EHR. A specific directory was created to process incoming colonoscopy reports so that they can be processed by the ML model.

Input Spreadsheet

The input spreadsheet was a Microsoft Excel document that was used as a working tool to list the findings and follow-up dates of the colonoscopy reports as identified by the ML model. Any findings with low confidence were indicated as such. The RPA solution reviewed the spreadsheet, "read" the follow-up dates, and documented what actions it took.

HM EHR Feature

Epic Systems' HM activity is an EHR feature designed to help providers manage and track preventive care and chronic disease management for patients. It allows health care organizations to set up and monitor recommended screenings, vaccinations, and follow-up care based on clinical guidelines, patient demographics, and medical history. It serves as a designated location in the EHR to document completed colonoscopies and the recommended follow-up date. However, it is not linked to clinical notes and must be manually updated to reflect changes due to pathology findings or patient-specific conditions [6].

Process Validation

Overview

Prior to systemwide activation, outcome validation was performed via manual review of a sample of colonoscopy reports and associated RPA actions in the EHR. The measures of outcome validity were the number of reports with a missed follow-up date, and the number of reports with a correctly updated HM. Each colonoscopy report was reviewed by trained clinical analysts (DR and CM) for accuracy. Discrepancies were reviewed with the physician informaticist lead (AS). The validation outcomes were divided into two phases: (1) ML evaluation, determining whether a follow-up date was identified within the colonoscopy report and ready for bot processing; and (2) RPA bot action documented in the EHR. Reports not ready for the bot were categorized as (1) correct, with no follow-up date specified; (2) incorrect, having a follow-up date listed that was not picked up by the ML; or (3) an inaccurate follow-up date was identified. Outcomes for reports processed by the RPA update were categorized as: (1) a correct HM update; (2) correct business exception assignment; or (3) incorrect HM update. Four rounds of validation testing were performed with a prospective sample of 690 reports manually reviewed until a saturation of automated outcomes was observed.

Process Refinement

A protocol was established to modify and refine the ML algorithm and bot activities if error patterns were identified during validation. After each round of validation testing, if an error was addressable, the team adjusted either the ML model or RPA based on the error source.

Governance Approval

Validation study findings were presented at leadership committee meetings to obtain governance approval for system-wide implementation. Besides confirming the process's validity, the approval process emphasized potential improvements in HM follow-up date accuracy compared to the current reliance on a default 10-year interval and limited manual updates by clinicians.

Process Implementation

After validation, refinement, and all necessary approvals, the process was implemented in the live environment. The implementation was performed for received documents labeled as colonoscopy reports only, not all document types used in the training and validation of the ML model. This began with a period of careful monitoring of the process known as hypercare [21]. The automated process was first implemented in the live environment as small batches, where 10 reports were run through the process and assessed for validity before proceeding to the next 10. This procedure was performed until it was determined that the process performed appropriately in the live environment. After the initial phase, the process was expanded to analyze all prospectively received external colonoscopy reports.

Ethical Considerations

As an operational quality improvement project, the NYULH institutional review board waived the need for approval for the study procedures. A waiver of Health Insurance Portability and Accountability Act (HIPAA) authorization and consent was included to access patient medical records. All study procedures complied with institutional ethical and privacy standards. Informed consent was waived and no compensation was provided.

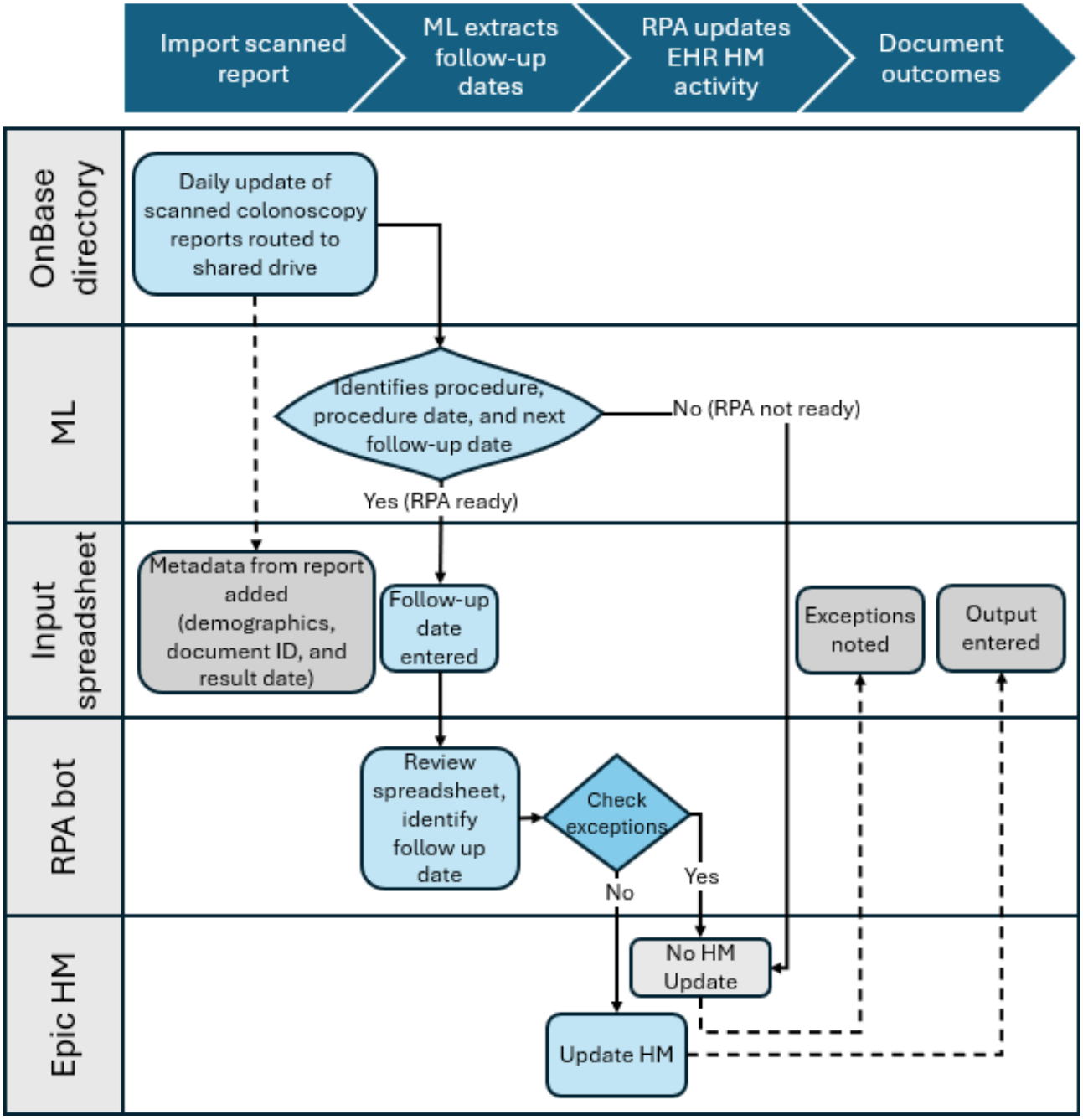
Results

Overview

Our system established a streamlined, 3-step process integrating preexisting technologies to automate updates to the CRC screening follow-up date based on external colonoscopy results. The process steps, the workflow, and technology resources used for each function are presented in Figure 1.

XSL•FO
RenderX

Figure 1. Automation process and technology tools used in each process step for the automation proof of concept to identify and convert unstructured colonoscopy results into actionable data note: HM: health maintenance; ML: machine learning; RPA: robotic process automation;



The three steps are as follows:

1. Documentation identification and routing: scanned colonoscopy reports are identified and sent to a designated work queue in the OnBase shared drive.
2. ML processing: an ML model verifies that the document is a colonoscopy report, then extracts key data, including patient ID, report date, and follow-up recommendations. If data meets predefined accuracy thresholds, it is added to an input spreadsheet and labeled "RPA ready." If below thresholds, the document is marked "RPA not ready" and sent to a work queue for human validation. ML model details, including model parameters, training processes, and performance are reported in Multimedia Appendix 1.
3. RPA execution: the bot processes "RPA ready" entries by accessing the patient's EHR, comparing the extracted follow-up date with existing HM follow-up frequency, and updating the recall date if no business exceptions are detected. All processed data, including business exceptions, are documented in the input spreadsheet.

Business Exceptions

Nine business exceptions were defined such that if any criteria were met, the bot would not update HM. These criteria included: (1) the follow-up date in the scanned document is longer than existing HM follow-up frequency, (2) a patient has a HM frequency modifier that sets a patient-specific screening frequency, (3) the next HM due date has been manually assigned after the scanned procedure date and these exceptions ensure

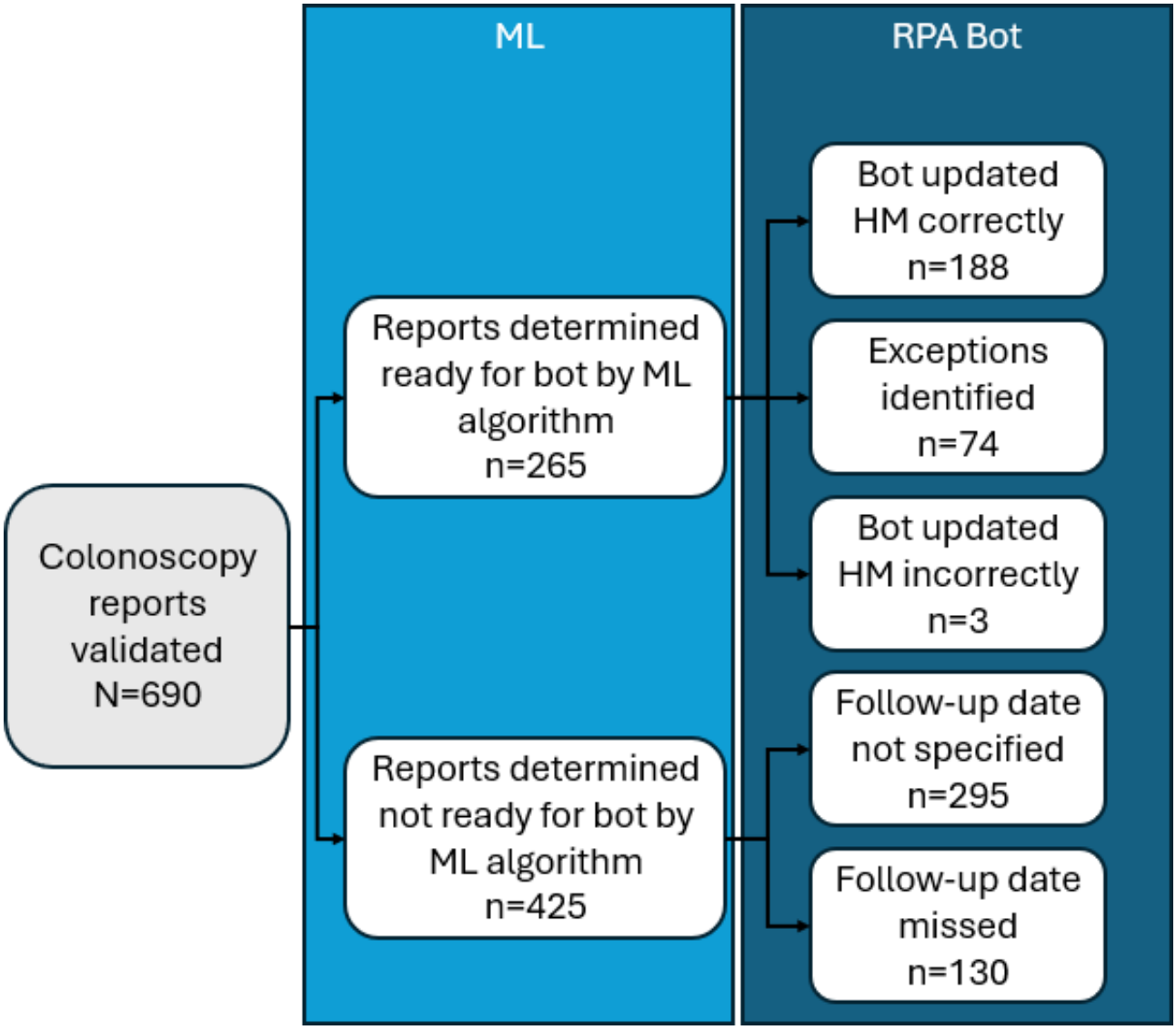
XSL•FO
RenderX

the bot never takes precedence over a provider-set screening frequency or patient-specific factors, (4) the report has a follow-up date over 10 years, (5) the input spreadsheet cannot assess follow-up date, (6) the procedure date linked to that document does not match the scanned document date, (7) the patient does not have the colonoscopy screening topic assigned in Epic due to age criteria, (8) the patient is not found, or (9) an order for the scanned colonoscopy report is not found. This exception ensures that the HM updates are associated with an appropriate colonoscopy order.

Process Validation Outcomes

Figure 2 presents the validation outcome findings. Process validity was assessed for 690 scanned colonoscopy reports. Of these, 61.6% (425/690) were categorized by the ML algorithm as not ready for the bot. Of those, 30.6% (130/425) listed a follow-up date not detected by the ML algorithm and 69.4% (295/425) did not specify a follow-up date. Among the reports identified as ready for the bot, 70.9% (188/265) HM were correctly updated, 27.9% (74/265) were flagged with an update exception, and 1% (3/265) HM were incorrectly updated. During the process validation, the final document processing overall automated process had an accuracy of 80.7% (557/690, 95% CI 77.8%-83.7%) for correctly identifying the presence or absence of a valid follow-up date (a measure that requires both the identification of the follow-up interval and the result date), determining the absence of a follow-up date, or recognizing a business exception that precluded updating the follow-up date. The process demonstrated a false negative identification rate of 32.9% (130/395, 95% CI 29.4%-36.4%) for follow-up date identification. Based on validation data, we estimate that this process correctly identified and updated 27.2% (188/690) of cases, either correcting instances that would have otherwise defaulted to an incorrect interval or confirming a 10-year follow-up interval was appropriate. Validation outcomes for the ML model specifically can be found in Multimedia Appendix 1.

Figure 2. Process validation outcomes for the automation proof of concept used to identify and convert unstructured colonoscopy results into actionable data note: HM: health maintenance; ML: machine learning; RPA: robotic process automation.



XSL•FO
RenderX

Process Refinements

During validation, the three incorrectly updated HM were due to (1) the bot creating an update based on an older report and (2) overriding a provider modification. These errors led to process refinement by updating the RPA steps to validate clinical information. The process error rate of 32.9% (130/395, 95% CI 29.4%-36.4%) for missing an available follow-up date was deemed acceptable, as refining the model to be more sensitive led to the extraction of incorrect dates, seen as a greater issue than missing a date.

System-Wide Implementation

The solution was implemented system-wide on October 4, 2023. From go-live until December 31, 2024, the system processed 16,563 external colonoscopy reports. Of these, 35.3% (5841/16,563) had a follow-up date meeting the ML model threshold and thus identified as "RPA Ready." Of the "RPA Ready" documents, the HM topic was successfully updated in 77.2% (4512/5841) of patient records. Among all processed reports, 72.8% (12,051/16,563) were not updated; this included 22.8% (1329/5841) that were "RPA Ready," but had business exceptions. Of the "RPA Ready" documents, 3.9% (225/5841) had a patient-specific follow-up date modifier, 3.2% (189/5841) had a more recent procedure, 6.8% (398/5841) were manually updated by a provider, 8.3% (485/5841) were outside standard screening age and did not have a colonoscopy HM topic assigned, and 0.6% (32/5841) had a discrepancy where the procedure result date did not match the scanned document.

Discussion

Principal Findings

This proof of concept demonstrated the feasibility of using ML and RPA to develop an automated process capable of extracting key clinical information from unstructured documents and converting it into discrete, accessible data. The system improved the accuracy of CRC screening follow-up dates while reducing the documentation burden on clinical staff. This pragmatic and innovative approach represents one of the first end-to-end solutions to address the challenges of processing faxed, text-based results by converting free text into structured data. This work provides a template for health care systems to reduce documentation burden, improve follow-up date accuracy, and address care gaps arising from a lack of system integration.

The process automates all workflow stages from the initial receipt of the free-text report to the entry of the follow-up date into the EHR. The use of ML combined with RPA allows for the process to function across workflow stages and software that would not be possible without human intervention if using existing NLP- and rule-based methods alone. Traditionally, this information would be difficult to locate within existing workflows, limiting its influence on patient recall processes. By structuring and integrating this data, the system ensures timely follow-ups and supports downstream workflows to recall patients within recommended timeframes, ultimately improving preventive care management.

Many important data elements are not updated in the EHR because updating them is time-consuming [11]. This strategy reduces documentation burden while minimizing data entry errors. As demonstrated in the process validation study, this process improved the accuracy of HM CRC screening dates by nearly 30% by updating records that would have otherwise remained unchanged. This has the potential to substantially impact downstream patient outcomes. The process was designed to err on the side of being clinically conservative (eg, selecting earlier recall dates if a range was present in the colonoscopy report). While selecting the earlier date in the recall range is a clinical guideline-concordant decision, this conservative approach may increase the rate of colonoscopy compared to selecting the mid- or end-range recall date [22]. During process validation, the accuracy for finding a valid follow-up date was slightly lower than the recall found in the ML model testing (Multimedia Appendix 1). This was anticipated, as a follow-up date is a measure that requires both the identification of the follow-up interval (recall 99.9%) and the result date (recall 86.7%) as well as the recall of other document features; however, this decline in performance from the ML model to the complete process should be considered during process development. Future research should examine whether the increase in screening date accuracy and conservative follow-up date selection translates into improved CRC clinical outcomes.

Beyond improving follow-up date accuracy, this workflow reduces the administrative burden on clinical staff, ensuring timely and appropriate care. By automating the update of recall dates for nearly 30% of scanned colonoscopy reports, health systems can save significant labor time. Even if each report requires just a few minutes of manual processing, the time savings can add up to hundreds of hours—especially in large health systems like NYULH, which may order upwards of 80,000 colonoscopies annually. Transforming unstructured text into structured data also has significant implications for quality reporting. By automating data extraction and integration into the EHR, health care systems can more effectively track completed screenings and tests, ensuring comprehensive reporting on quality measures, closing care gaps, and improving population health management.

Comparison With Prior Work

The use of automation, including RPA, has previously been proposed as a theoretical solution to address limitations in the EHR and other elements of data-driven health care [23-27]. However, prior literature has not presented a fully integrated end-to-end automated workflow. Prior research has primarily focused on data automation in structured formats [27], such as health care claims [25,26] and the extraction and processing of EHR data for research [27-32]. A few studies present cases for using ML and AI for other data types [30,32], but their full integration into health system operations remains hypothetical. Our work builds upon previous research to demonstrate the feasibility and validity of implementing a pragmatic, automated workflow within the EHR to address real-world challenges. While we developed a proprietary model to extract follow-up dates from colonoscopy reports, we anticipate advancements in generative AI will enable multimodal large language models to achieve similar outcomes. However, validation testing is needed to determine large language model accuracy in these use cases. These models can support this use case and be scaled

XSL•FO
RenderX

to extract other critical clinical data from unstructured text, reducing documentation burden and enhancing automation in health care systems.

This process framework can address inefficiencies from the lack of EHR interoperability or discordant information within various areas of the EHR. Despite the progress of EHR interoperability, health care organizations still rely on electronic fax transmissions of clinical information containing important yet unstructured data. Our institution has adapted the described process to automate the documentation of follow-up dates for internally performed colonoscopies documented within ancillary systems and interfaced back as free text reports. Before a recent 2023 institutional effort to code colonoscopy pathology findings [11], all colonoscopy reports were stored as unstructured text. Using a modified version of this automated process, the institution has retrospectively processed 80,864 internal reports from May 2020 to April 2023, updating 71.8% (58,060) CRC screening HM follow-up dates. This successful application of ML combined with RPA highlights their potential to address other high-burden, low-complexity tasks in the EHR and could address deficiencies in structured EHR documentation. By standardizing data ingestion, extending this approach to various unstructured data types can address deficiencies in structured EHR documentation for tests performed at outside organizations and solve for a lack of data integration and reporting for quality measures. Moreover, scaling similar processes to other report types with discrete values, such as cholesterol or HbA_{1c}, may demonstrate an even greater success.

Incorporating ML into the workflow was critical to the automated process's utility. Nearly 80% of EHR data [12], including colonoscopy reports and pathology findings, are documented as free text [13]. Therefore, the critical information within the reports remains inaccessible in the EHR unless manually transcribed [12,13]. Most proposed automations cannot use free-text data and rely on discretely stored data, such as laboratory result values [27], which is unavailable for many EHR data sources unless data entry systems and clinician behaviors are modified. By documenting discrete data without requiring behavior change or system structure modifications, these tools may facilitate broader data capture automation. As AI advances, integrating more sophisticated large language models may further refine and scale these efforts. Future work should evaluate the long-term impact, scalability across different health care systems, and additional opportunities for automation to support clinical workflows, quality reporting, and patient care.

Limitations

This study had several limitations. First, as this workflow integrates multiple disparate technologies to create an automated process, it is susceptible to technical issues from changes to any of the individual components. For example, system updates can change the user interface, causing the bot to no longer recognize its inputs. To address this, the process requires consistent monitoring and maintenance that may incur long-term maintenance costs.

Second, using colonoscopy reports rather than pathology results as the source for follow-up interval means some dates may require updating after pathology results are available. However, as colonoscopy reports are more commonly transmitted from external sources, this decision was pragmatic and provided a sufficiently accurate representation to process the greatest number of results. Future iterations may consider incorporating logic based on the pathology results if included along with the colonoscopy report.

In addition, the ML model used as a component of this intelligent document processing pipeline was not validated on an external dataset and was only validated within 1 health system. While training and internal validation included multiple data sources (ie, Cologuard and colonoscopy, pathology results, documents received from various external clinics), validation in only 1 health system may limit the generalizability of this tool, and adaptation may be needed for other health care environments, particularly those with different EHR systems. While efforts were iteratively made to improve the model as more types of report formats are received, regular refinements including larger data training sets are needed to increase model recall. However, due to finite resources and available backup manual processes, the accuracy was deemed sufficient for operational purposes and our model is not regularly refined. The percentage of follow-up dates updated by the process, however, was lower than would be expected based solely on estimated model performance. While approximately 31% (130/425) of not identified follow-up dates were due to the ML model's technical limitations, the limited update rate was primarily due to clinical factors as well as purposeful operational decision-making. Clinically, the process's effectiveness was limited by the high rate of missing elements in the received colonoscopy reports [33,34]. From an operational perspective, this process was likely to remain largely unsupervised once deployed. While automation outperforms existing human-only workflows for updating HM, the automation of clinical documentation can pose ethical and safety concerns if errors occur. To ensure accountability and trust, governance safeguards are essential, and taking a more cautious approach is advisable when designing automated systems intended to fully replace manual oversight. To mitigate potential risks, we institute a number of business exceptions designed to function as safeguards, thereby erring on the side of caution. These business exceptions included limiting overwrites of prior clinician input, allowing clinician overrides, reviewing records with high uncertainty, and clearly assigning responsibility to prevent overreliance on automation. Therefore, a substantial number of records were not updated by the automation process due to available prior clinician input, even if the model correctly identified a follow-up date. If no clinician actions were taken prior to the process being executed, the rate of update would be expected to be higher than what was seen in a real clinical setting.

Conclusions

This study demonstrates the feasibility of developing a high-validity, automated process to update CRC screening follow-up recommendations within the EHR using scanned colonoscopy reports. By leveraging ML and RPA, we successfully extracted key clinical information from unstructured documents and converted it into structured, actionable data. The

XSL•FO
RenderX

success of this approach highlights the potential for similar automation strategies in other high-volume, low-complexity documentation tasks in healthcare, enhancing efficiency, reducing manual errors, and improving patient outcomes.

Acknowledgments

Artificial intelligence was not used in the writing of this manuscript.

Funding

This work was funded by operational funds from New York University Langone Health.

Data Availability

The datasets generated or analyzed during this study are not publicly available due to privacy of clinical data used in the study and as an operational initiative, the code underlying the machine learning model falls under the purview of intellectual property and confidential business information, but is available from the corresponding author on reasonable request.

Authors' Contributions

All authors meet the criteria for authorship stated in the *Uniform Requirements for Manuscripts Submitted to Biomedical Journals*. The specific areas of contributions are as follows: study concept and design (ERS, PT, AM, and A Szerencsy); data acquisition (CM, DR, YI, AC, and DP); analysis and interpretation of data (all authors); drafting of the manuscript (ERS, AS, and AS); and critical revision of the manuscript for important intellectual content (all authors).

Conflicts of Interest

None declared.

Multimedia Appendix 1
Technical Summary of natural language processing (NLP) model development for colonoscopy report extraction.
[PDF File, 240 KB - medinform_v13i1e73504_app1.pdf]

References

1. Dharwadkar P, Zaki TA, Murphy CC. Colorectal cancer in younger adults. Hematol Oncol Clin North Am 2022 Jun;36(3):449-470. [doi: 10.1016/j.hoc.2022.02.005] [Medline: 35577711]
2. Siegel RL, Wagle NS, Cercek A, Smith RA, Jemal A. Colorectal cancer statistics, 2023. CA A Cancer J Clinicians 2023 May;73(3):233-254. [doi: 10.3322/caac.21772]
3. Ladabaum U, Dominitz JA, Kahi C, Schoen RE. Strategies for colorectal cancer screening. Gastroenterology 2020 Jan;158(2):418-432. [doi: 10.1053/j.gastro.2019.06.043] [Medline: 31394083]
4. Atlas SJ, Tosteson ANA, Burdick TE, et al. Primary care practitioner perceptions on the follow-up of abnormal cancer screening test results. JAMA Netw Open 2022 Sep 1;5(9):e2234194. [doi: 10.1001/jamanetworkopen.2022.34194] [Medline: 36173627]
5. Makam AN, Lanham HJ, Batchelor K, et al. Use and satisfaction with key functions of a common commercial electronic health record: a survey of primary care providers. BMC Med Inform Decis Mak 2013 Aug 9;13(1):86. [doi: 10.1186/1472-6947-13-86] [Medline: 24070335]
6. Gaffney A, Woolhandler S, Cai C, et al. Medical documentation burden among US office-based physicians in 2019: a national study. JAMA Intern Med 2022 May 1;182(5):564. [doi: 10.1001/jamainternmed.2022.0372] [Medline: 35344006]
7. Johnson KB, Stead WW. Making electronic health records both SAFER and SMARTER. JAMA 2022 Aug 9;328(6):523. [doi: 10.1001/jama.2022.12243] [Medline: 35834286]
8. Øines M, Helsingen LM, Bretthauer M, Emilsson L. Epidemiology and risk factors of colorectal polyps. Best Pract Res Clin Gastroenterol 2017 Aug;31(4):419-424. [doi: 10.1016/j.bpg.2017.06.004]
9. Coronado GD, Burdick T, Petrik A, Kapka T, Retecki S, Green B. Using an automated data-driven, EHR-embedded program for mailing FIT kits: lessons from the STOP CRC pilot study. J Gen Pract (Los Angel) 2014 Jan 5;2(1):1000141. [doi: 10.4172/2329-9126.1000141] [Medline: 25411657]
10. Schrembs TR. Use of Electronic Health Record Reminders to Improve Primary Care Providers' Colorectal Cancer Screening Recommendations [Dissertation]. : Doctor of Nursing Practice Papers; 2023 URL: https://ir.library.louisville.edu/dnp/130 [accessed 2025-11-08]
11. Stevens ER, Nagler A, Monina C, et al. Pathology-driven automation to improve updating documented follow-up recommendations in the electronic health record after colonoscopy. Clin Transl Gastroenterol 2024 Dec 1;15(12):e00785. [doi: 10.14309/ctg.0000000000000785] [Medline: 39665587]

XSL•FO
RenderX

12. Murdoch TB, Detsky AS. The inevitable application of big data to health care. JAMA 2013 Apr 3;309(13):1351-1352. [doi: 10.1001/jama.2013.393] [Medline: 23549579]
13. Millares Martin P. Consultation analysis: Use of free text versus coded text. Health Technol (Berl) 2021;11(2):349-357. [doi: 10.1007/s12553-020-00517-3] [Medline: 33520588]
14. Ford B. Colonoscopy follow-up: U.S. multi-society task force on colorectal cancer updates recommendations. Am Fam Physician 2021 Mar 1;103(5):314-316. [Medline: 33630559]
15. Imler TD, Morea J, Kahi C, Imperiale TF. Natural language processing accurately categorizes findings from colonoscopy and pathology reports. Clin Gastroenterol Hepatol 2013 Jun;11(6):689-694. [doi: 10.1016/j.cgh.2012.11.035] [Medline: 23313839]
16. OpenText Fax (RightFax). OpenText. 2024. URL: https://www.opentext.com/products/fax [accessed 2024-12-19]
17. OCR—Optical Character Recognition. Microsoft. 2024. URL: https://learn.microsoft.com/en-us/azure/ai-services/computer-vision/overview-ocr [accessed 2025-11-08]
18. Fanni SC, Febi M, Aghakhanyan G, Neri E. Natural language processing. In: Klontzas ME, Fanni SC, Neri E, editors. Introduction to Artificial Intelligence: Springer International Publishing; 2023:87-99. [doi: 10.1007/978-3-031-25928-9_5]
19. What is robotic process automation (RPA)? IBM. 2024. URL: https://www.ibm.com/topics/rpa [accessed 2024-10-01]
20. What can you do with OnBase? Hyland. URL: https://www.hyland.com/en/resources/articles/what-can-you-do-with-onbase [accessed 2024-10-01]
21. Wren H. Hypercare: What it means and why it matters in CX. Zendesk. URL: https://www.zendesk.com/blog/hypercare [accessed 2024-10-19]
22. Gupta S, Lieberman D, Anderson JC, et al. Recommendations for follow-up after colonoscopy and polypectomy: a consensus update by the US Multi-Society Task Force on Colorectal Cancer. Gastroenterology 2020 Mar;158(4):1131-1153. [doi: 10.1053/j.gastro.2019.10.026] [Medline: 32044092]
23. Dagli MM, Ghenbot Y, Ahmad HS, et al. Development and validation of a novel AI framework using NLP with LLM integration for relevant clinical data extraction through automated chart review. Sci Rep 2024 Nov 5;14(1):26783. [doi: 10.1038/s41598-024-77535-y] [Medline: 39500759]
24. Venigandla K. Integrating RPA with AI and ML for enhanced diagnostic accuracy in healthcare. Power Syst Technol 2022;46(4). [doi: 10.52783/pst.251]
25. Deepak V, Prabhu K, Srinivasan R. AI-powered data integration in healthcare claims processing: enhancing workflow efficiency and reducing processing errors. J Artif Intell Res 2024 Feb;4(1):395-438 [FREE Full text]
26. Prabhu K, Ravi Kumar B, Bhavani K. Automating data integration for healthcare claims processing: enhancing accuracy and speed with cloud-based solutions. J Mach Learn Healthc Decis Support 2024 Feb;4(1):247-290 [FREE Full text]
27. Tiase VL, Hull W, McFarland MM, et al. Patient-generated health data and electronic health record integration: a scoping review. JAMIA Open 2020 Dec;3(4):619-627. [doi: 10.1093/jamiaopen/ooaa052] [Medline: 33758798]
28. Cheng AC, Banasiewicz MK, Johnson JD, et al. Evaluating automated electronic case report form data entry from electronic health records. J Clin Transl Sci 2023;7(1):e29. [doi: 10.1017/cts.2022.514] [Medline: 36845316]
29. Parciak M, Suhr M, Schmidt C, et al. FAIRness through automation: Development of an automated medical data integration infrastructure for FAIR health data in a maximum care university hospital. BMC Med Inform Decis Mak 2023 May 15;23(1):94. [doi: 10.1186/s12911-023-02195-3] [Medline: 37189148]
30. Ahmed Salamkar M. Data integration: AI-driven approaches to streamline data integration from various sources. Int J Sci Res 2023 Mar 27;12(3):1855-1863. [doi: 10.21275/SR230311115337]
31. Kaspar M, Fette G, Hanke M, Ertl M, Puppe F, Störk S. Automated provision of clinical routine data for a complex clinical follow-up study: a data warehouse solution. Health Informatics J 2022;28(1):14604582211058081. [doi: 10.1177/14604582211058081] [Medline: 34986681]
32. Pulivarthy P. Enhancing data integration in Oracle databases: leveraging machine learning for automated data cleansing, transformation, and enrichment. Int J Holist Manag Perspect 2023 Jun;4(4):1-18 [FREE Full text]
33. Sharma RS, Rossos PG. A review on the quality of colonoscopy reporting. Can J Gastroenterol Hepatol 2016;2016:9423142. [doi: 10.1155/2016/9423142] [Medline: 27446877]
34. Keswani RN, Crockett SD, Calderwood AH. AGA Clinical Practice Update on strategies to improve quality of screening and surveillance colonoscopy: expert review. Gastroenterology 2021 Aug;161(2):701-711. [doi: 10.1053/j.gastro.2021.05.041] [Medline: 34334168]

Abbreviations

CRC: colorectal cancer
EHR: electronic health record
HIPAA: Health Insurance Portability and Accountability Act
HM: health maintenance
ML: machine learning
NLP: natural language processing

XSL•FO
RenderX

NYULH: New York University Langone Health
RPA: robotic process automation

Edited by A Coristine; submitted 05.03.25; peer-reviewed by SM Shaffi, X Xiao; accepted 29.10.25; published 20.11.25.

Please cite as:
Stevens ER, Hartman J, Testa P, Mansukhani A, Monina C, Shunk A, Ranson D, Imberg Y, Cote A, Prabhu D, Szerencsy A
Leveraging Machine Learning and Robotic Process Automation to Identify and Convert Unstructured Colonoscopy Results Into Actionable Data: Proof-of-Concept Study
JMIR Med Inform 2025;13:e73504
URL: https://medinform.jmir.org/2025/1/e73504
doi:10.2196/73504

© Elizabeth R Stevens, Jager Hartman, Paul Testa, Ajay Mansukhani, Casey Monina, Amelia Shunk, David Ranson, Yana Imberg, Ann Cote, Dinesha Prabhu, Adam Szerencsy. Originally published in JMIR Medical Informatics (https://medinform.jmir.org), 20.11.2025. This is an open-access article distributed under the terms of the Creative Commons Attribution License (https://creativecommons.org/licenses/by/4.0/), which permits unrestricted use, distribution, and reproduction in any medium, provided the original work, first published in JMIR Medical Informatics, is properly cited. The complete bibliographic information, a link to the original publication on https://medinform.jmir.org/, as well as this copyright and license information must be included.

XSL•FO
RenderX

Label Accuracy in Electronic Health Records and Its Impact on Machine Learning Models for Early Prediction of Gestational Diabetes: 3-Step Retrospective Validation Study

Mark Germaine[1,2], PhD; Amy C O'Higgins[3], PhD; Brendan Egan[2], PhD; Graham Healy[1], PhD

[1]School of Computing, Dublin City University, Glasnevin, Dublin, Ireland

[2]School of Health and Human Performance, Dublin City University, Dublin, Ireland

[3]UCD (University College Dublin) Centre for Human Reproduction, Coombe Women & Infants University Hospital, Dublin, Ireland

Corresponding Author:
Mark Germaine, PhD
School of Computing, Dublin City University, Glasnevin, Dublin, Ireland

Abstract

Background: Several studies have used electronic health records (EHRs) to build machine learning models predicting the likelihood of developing gestational diabetes mellitus (GDM) later in pregnancy, but none have described validation of the GDM "label" within the EHRs.

Objective: This study examines the accuracy of GDM diagnoses in EHRs compared with a clinical team database (CTD) and their impact on machine learning models.

Methods: EHRs from 2018 to 2022 were validated against CTD data to identify true positives (TP), false positives (FP), true negatives (TN), and false negatives (FN). Logistic regression models were trained and tested using both EHR and validated labels, whereafter simulated label noise was introduced to increase FP and FN rates. Model performance was assessed using the area under the receiver operating characteristic curve (ROC AUC) and average precision (AP).

Results: Among 3952 patients, 3388 (85.7%) were correctly identified with GDM in both databases, while 564 cases lacked a GDM label in EHRs, and 771 were missing a corresponding CTD label. Overall, 32,928 (87.5%) of cases were TN, 3388 (9%) TP, 771 (2%) FP, and 564 (1.5%) FN. The model trained and tested with validated labels achieved an ROC AUC of 0.817 and an AP of 0.450, whereas the same model tested using EHR labels achieved 0.814 and 0.395, respectively. Increased label noise during training led to gradual declines in ROC AUC and AP, while noise in the test set, especially elevated FP rates, resulted in marked performance drops.

Conclusions: Discrepancies between EHR and CTD diagnoses had a limited impact on model training but significantly affected performance evaluation when present in the test set, emphasizing the importance of accurate data validation.

(JMIR Med Inform 2025;13:e72938) doi:10.2196/72938

KEYWORDS

electronic health records; gestational diabetes; label noise; pregnancy; validation; machine learning

Introduction

Electronic health records (EHRs) are an important source of real-world data, offering detailed, longitudinal patient information historically stored in medical charts, and forming the basis of real-world evidence [1,2]. Together with advancements in artificial intelligence and machine learning (ML), EHRs are increasingly being used to develop models that improve the prediction of health and disease outcomes [3].

Integration of EHRs into clinical research offers numerous opportunities for advancing health care delivery and patient outcomes. However, EHR data is often stored in unstructured formats such as free text, requiring information extraction algorithms to enable ML applications [4]. This extraction process can introduce data quality concerns due to various issues such as data entry errors and cut-and-paste errors [5]. The quality and consistency of EHR data are particularly critical when the target variable, that is, the variable being predicted, is used in ML models.

Inaccuracies in EHRs present challenges for developing and applying ML algorithms in health care, primarily due to the dependency on data quality and accuracy of target labels [6]. This "label noise," which refers to inaccuracies or inconsistencies in the data labels (eg, diagnosis codes) extracted from EHRs, can significantly impact model performance by introducing errors in the target variable, leading to potentially misleading conclusions [7]. Training ML models on unvalidated EHRs may lead to systematic errors in the model output with

XSL•FO
RenderX

the potential for the model to miss, underestimate, or overestimate clinically significant relationships [8,9].

Accurate diagnosis and recording of gestational diabetes mellitus (GDM) in EHRs is important not only for effective patient management but also for informing public health strategies and economic forecasting in national health care planning [10,11]. EHRs are often used to train ML approaches that support clinical decision-making and care pathways that improve pregnancy outcomes [12]. However, the utility of EHRs remains a concern due to potential discrepancies in data recording practices [8]. When using ML in GDM prediction [13], the accuracy of input data is paramount because inaccuracies can lead to flawed prediction models and ineffective or adverse clinical decisions [14].

Several studies have used EHRs to build ML models predicting the likelihood of developing GDM later in pregnancy [15], but none have described validation of the GDM "label" within the EHRs. This study has 3 primary aims: first, to assess the accuracy of reporting of GDM diagnoses in EHRs by comparing them to a database maintained in real-time by the hospital's clinical team; second, to evaluate how discrepancies in GDM reporting impact ML models; and third, to examine ML model performance using varying levels of simulated label noise in the dataset. By identifying discrepancies between these data sources, we aim to highlight the importance of data validation for advancing digital health and ML-driven health care.

Methods

Study Design

A retrospective validation design was used to assess the accuracy of GDM diagnoses recorded in the EHRs of a national maternity hospital (The Coombe Hospital, Dublin). We matched patient ID between the EHR system and a reference standard established by a real-time clinical team database (CTD) of those formally diagnosed with and managed for GDM, which served as a ground truth. This approach allowed for direct comparison between the recorded GDM status in the EHRs and the validated GDM status from the CTD, enabling identification of true positives (TP), false positives (FP), true negatives (TN), and false negatives (FN) in the EHRs. Further, the effect of label noise on ML model performance in predicting the development of GDM (binary classification) was evaluated by first examining its impact in our current EHR dataset, and then second, simulating progressively increasing levels of label noise to understand its effect on ML model performance both in terms of training and testing.

Data Source and Validation

The EHR system serves as the repository for patient medical histories, including diagnoses, family history, and outcomes for pregnant women receiving care at the institution. The data are collected routinely from all women by trained midwives using standardized questions and are then computerized onto the electronic system of the hospital, "Euroking K2." EHRs were collected from 2018 to 2022 and consisted of over 35,000 pregnancies during this time. The dataset from the CTD spanned from 2018 to 2022; thus, the timeframe for this analysis spanned from 2018 to 2022 (inclusive). Women aged 18 years or older with complete information on GDM status were included in the analysis. Pregnancies with missing or incomplete data for critical variables, women without a recorded GDM status, and pregnancies with pre-existing diabetes were excluded. ML models were trained and tested on pregnancies with complete EHR data up to the 12th week of gestation.

GDM diagnoses were extracted from the EHRs based on information recorded in a column titled "medical problems during pregnancy." When this column contained the entry "diabetes developed during pregnancy," the patient was coded as having GDM in a newly created column designated for this study's analysis, referred to hereafter as "EHR-GDM." Patient records not meeting this criterion were coded as not having GDM. The legacy EHR has a single structured problem field; it does not store *ICD* (*International Statistical Classification of Diseases and Related Health Problems*) or SNOMED (Systematized Nomenclature of Medicine) codes. GDM is recorded exclusively by selecting "diabetes developed during pregnancy" from that field's drop-down list. No alternative structured or coded location exists.

Patient IDs from the EHRs were then matched with a separate database maintained in real-time by the clinical team responsible for diabetes care, with patient details entered each day upon confirmation from the hospital laboratory of a diagnosis of GDM from an oral glucose tolerance test following the IADPSG (International Association of the Diabetes and Pregnancy Study Groups) guidelines. The CTD was considered the definitive ground truth for GDM diagnoses, given its real-time, clinician-entered, laboratory-confirmed data recording process. This matching process produced a merged dataset for validating EHR-recorded GDM diagnoses against the CTD database, leading to the creation of 2 comparison columns: "EHR-GDM" for EHR-identified cases of GDM and "CTD-GDM" for cases of GDM recorded by the CTD.

The validation process involved comparing the GDM diagnosis status in the EHR ("EHR-GDM") with that in the CTD ("CTD-GDM") to examine the agreement between the 2 datasets. This comparison allowed for the identification of TPs (positive in EHRs and present in CTD), FPs (positive in EHRs and not present in CTD), TNs (negative in EHRs and not present in CTD), and FNs (negative in EHRs and present in CTD), and thereby enabled evaluation of the accuracy of the reporting of GDM diagnosis in the EHRs. An additional column, validated gestational diabetes mellitus label (only in cases where electronic health record and clinical team database labels matched; VAL-GDM), was created indicating a positive or negative diagnosis of GDM for cases where the EHR-GDM and CTD-GDM labels matched, that is, for TPs and TNs, excluding records with FPs and FNs. Thus, for the purpose of the following stage of ML modeling, only records that matched between EHR-GDM and CTD-GDM were used, reducing the risk of bias from either dataset. The TPR, FPR, TNR, and FNR were calculated for the dataset [16].

Evaluation of Label Noise on ML Modeling

To evaluate the impact of label noise on the performance of ML models in predicting GDM, we used logistic regression (LR),

XSL•FO
RenderX

where the dataset was split into 70% training and 30% test sets to ensure robust evaluation. Default model hyperparameters were used, as the primary objective was to compare performance across different training datasets rather than optimizing hyperparameter settings. The training and testing data comprised EHR data that was available during the first booking visit, typically the 12th week of gestation, and included 79 training features. The target label was GDM. The dataset contained both categorical and numerical features. Categorical features were processed using OneHotEncoder with the "first" category dropped, and numerical features were standardized using StandardScaler. While the goal of this paper is not to produce an end point AI model, a self-assessment checklist for reporting was followed to ensure that adequate information about the ML model was present [17].

We trained 2 ML models: one with the EHR-GDM labels and the other with the VAL-GDM labels. Both models were evaluated using the same test set, which used VAL-GDM labels, to facilitate a direct comparison of the effects of label noise during training on a consistent test set. The year 2020 was excluded from these analyses due to emerging research demonstrating reduced detection of diseases during this period [18], something that we confirm in our results below. By using both the "raw" and "validated" datasets, the study aimed to demonstrate the impact of label noise on model performance in the prediction of GDM, providing insights into the importance of accurate label validation in developing reliable predictive models using ML. In addition to the LR model, we replicated this process with other ML models to ensure any effects were not model specific. External validation datasets were sought, but this was not successful, as documented [19].

Additionally, varying levels of label noise were introduced to determine the threshold at which label noise significantly affects model performance. This simulation was performed by progressively increasing the number of FPs and FNs in the VAL-GDM training set from 0% to 90%, that is, changing a percentage of the positive labels to negative labels (creating FNs) and changing a percentage of negative labels to positive labels (creating FPs). This approach resulted in the training of 100 different models. Next, in a separate analysis, we applied this progressive noise insertion to the VAL-GDM test set to specifically assess the impact of test set label noise on model evaluation, that is, evaluating these test sets using a model trained with the "clean" VAL-GDM labels. For reproducibility, the code used to perform the label noise simulation is made available in the Simulated Label Noise section.

Statistical Analysis

The validation findings were quantitatively assessed using accuracy, precision, recall, F_1-score, and overall agreement measured by Cohen κ, between the EHR-recorded GDM (EHR-GDM) and the CTD (CTD-GDM) diagnoses. The performance of the LR ML models was evaluated using the area under the receiver operating characteristic curve (ROC AUC) and the average precision (AP) score. Additionally, the calibration of the model's predictions will be examined visually by calibration curves and quantitatively by the slope and intercept. The statistical and ML analyses were performed using Python (version 3.8.8; Python Software Foundation) with libraries including NumPy 1.23.5, pandas 1.2.4, and scikit-learn 1.2.1.

Ethical Considerations

Ethical approval was granted by The Coombe Hospital Research Ethics Committee (Study No. 06–2023; Exploring the Utility of Machine Learning for the Classification of Gestational Diabetes Risk During the First Antenatal Visit).

Results

Population Characteristics

The dataset comprised 37,651 EHRs from 31,100 unique patients. The mean patient age was 32 (SD 5) years, and BMI was 26.2 (SD 5.5) kg/m^2, with 20.7% exhibiting a BMI greater than 30.0 kg/m^2. The prevalence of GDM according to the EHRs was 11%, whereas the prevalence according to the CTD was 10.5%. Patient characteristics for the most important features in the ML models are presented in Table 1.

XSL•FO
RenderX

Table . Patient characteristics for the most important features in the machine learning models, according to the validated dataset (n=27,561). The validated dataset represents a dataset where both the EHRs[a] andCTDs[b] agree.

Characteristics	Values
Age (years), mean (SD)	32 (5)
BMI (kg/m^2), mean (SD)	26.2 (5.3)
Systolic blood pressure (mm Hg), mean (SD)	111 (11)
Diastolic blood pressure (mm Hg), mean (SD)	67 (8)
Parity, mean (SD)	0.9 (1.1)
Ethnic origin, n (%)	
Caucasian	24,180 (87.8)
South East Asian	1360 (4.9)
Black African	554 (2.0)
Asian	489 (1.8)
Middle Eastern	154 (0.6)
Latin American	26 (0.1)
Mixed	10 (0.1)
Other	788 (3)
Occupation skill level (ISCO[c]), n (%)	
Level 0 (unemployed)	5254 (19)
Level 1 (elementary occupations)	369 (1.3)
Level 2 (clerical and service)	4404 (15.9)
Level 3 (technicians and associates)	2389 (8.6)
Level 4 (professionals and managers)	15,145 (55.1)
Family history of diabetes mellitus, n (%)	6407 (23.3)
History of GDM[d], n (%)	1078 (3.9)
Other endocrine problems, n (%)	5854 (21.4)
Prevalence of GDM, n (%)	3188 (11.7)

[a]EHR: electronic health record.

[b]CTD: clinical team database.

[c]ISCO: International Standard Classification of Occupations.

[d]GDM: gestational diabetes mellitus.

Diagnosis Discrepancies

Of 3952 patients with matching IDs in both databases, 3388 were correctly identified with GDM in both EHR-GDM and CTD-GDM (9% TP and 85.7% true positive rate [TPR]), while 564 lacked a corresponding GDM label in EHR-GDM (1.5% FN and 14.3% false negative rate [FNR]). Additionally, 771 patients were incorrectly identified with GDM in EHR-GDM without matching IDs in CTD-GDM (2% FP and 2.3% false positive rate [FPR]). In EHRs, there were 32,928 (87.5%) TN cases (97.7% true negative rate [TNR]). The accuracy, precision, F_1-score, and Cohen κ are reported in Table 2.

XSL•FO
RenderX

Table . Performance metrics for the comparison of GDM[a] diagnoses in EHRs[b] with the real-time CTD[c].

Year	Cohen κ	Accuracy	Precision	Recall	F_1-score
All years	0.82	0.96	0.81	0.86	0.84
2018	0.80	0.96	0.78	0.86	0.82
2019	0.82	0.96	0.86	0.82	0.84
2020	0.77	0.96	0.70	0.90	0.79
2021	0.86	0.97	0.89	0.87	0.88
2022	0.82	0.97	0.82	0.86	0.84
All minus 2020	0.82	0.97	0.84	0.85	0.84

[a]GDM: gestational diabetes mellitus.

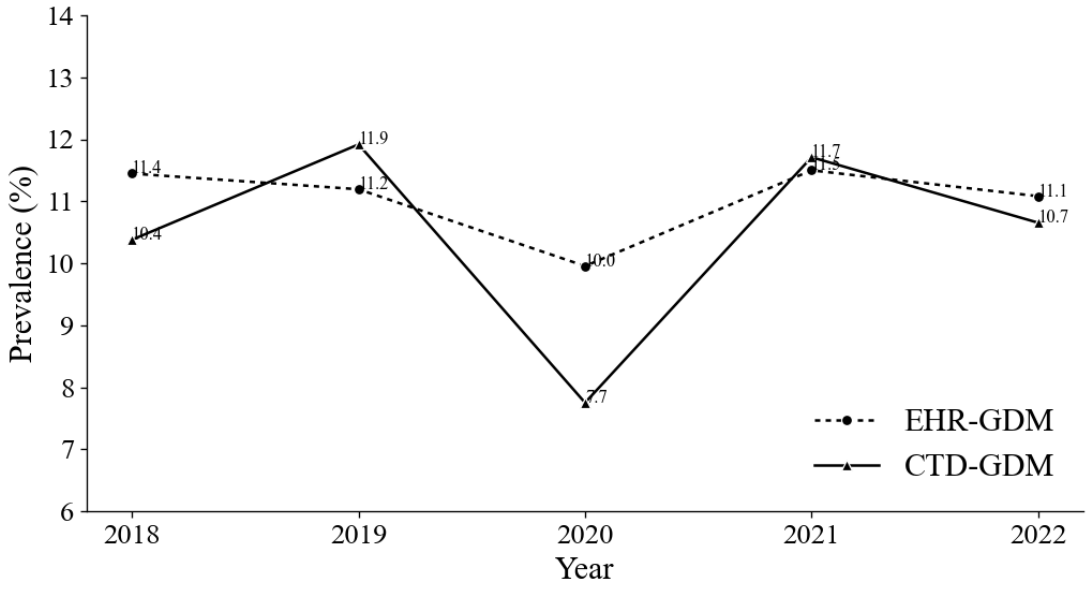
[b]EHR: electronic health record.

[c]CTD: clinical team database.

Yearly Data Comparison

Ninety-eight patients identified in CTD lacked corresponding entries in EHRs. In total, 67 (68%) of these discrepancies were observed in 2020. Furthermore, GDM prevalence for both EHRs and CTD datasets revealed a notable reduction in 2020 (recorded at 10% in EHRs and 7.7% in CTD), indicating a deviation from the trend observed in other years (Figure 1). These discrepancies align with COVID-19–related disruptions to screening practices within the hospital between March 2020 and September 2020.

Figure 1. Comparison of prevalence rates of EHR-GDM data and CTD-GDM data from 2018 to 2022. The solid line represents the CTD data, and the dashed line represents the EHR data. CTD: clinical team database; CTD-GDM: gestational diabetes mellitus label as recorded in the clinical team database (reference standard label); EHR: electronic health record; EHR-GDM: gestational diabetes mellitus label as recorded in the EHR.



Label Noise in EHRs

The performance of LR models trained using the raw (EHR-GDM) and validated (VAL-GDM) labels was evaluated using a test set with VAL-GDM labels only. The model trained using the EHR-GDM labels achieved an ROC AUC of 0.817 (95% CI 0.802 - 0.833) and an AP score of 0.451. The calibration curve is shown in Figure 2, with an intercept of 0.093 and a slope of 0.984. In comparison, the model trained using the VAL-GDM labels showed an ROC AUC of 0.817 (95% CI 0.803 - 0.832) and an AP score of 0.450 (Figure 3), indicating a minor impact of label noise in training the model for this dataset (intercept −0.027 and slope 0.955). However, when the performance of the LR ML model trained using VAL-GDM labels was evaluated on a test set with EHR-GDM labels, an ROC AUC of 0.814 and an AP score of 0.395 was achieved, which demonstrates a greater impact of label noise when it is present in the test set.

XSL•FO
RenderX

Figure 2. (Left) Calibration curve for the EHR (electronic health record)-GDM model, which was trained on EHR-GDM labels. (Right) Calibration curve for the VAL-GDM model, which was trained on the subset of cases where electronic health record and clinical team database labels agree. Both are evaluated against the identical standard reference labels. EHR-GDM: gestational diabetes mellitus label as recorded in the EHR; GDM: gestational diabetes mellitus; VAL-GDM: validated gestational diabetes mellitus label (only in cases where the EHR and clinical team database labels matched).

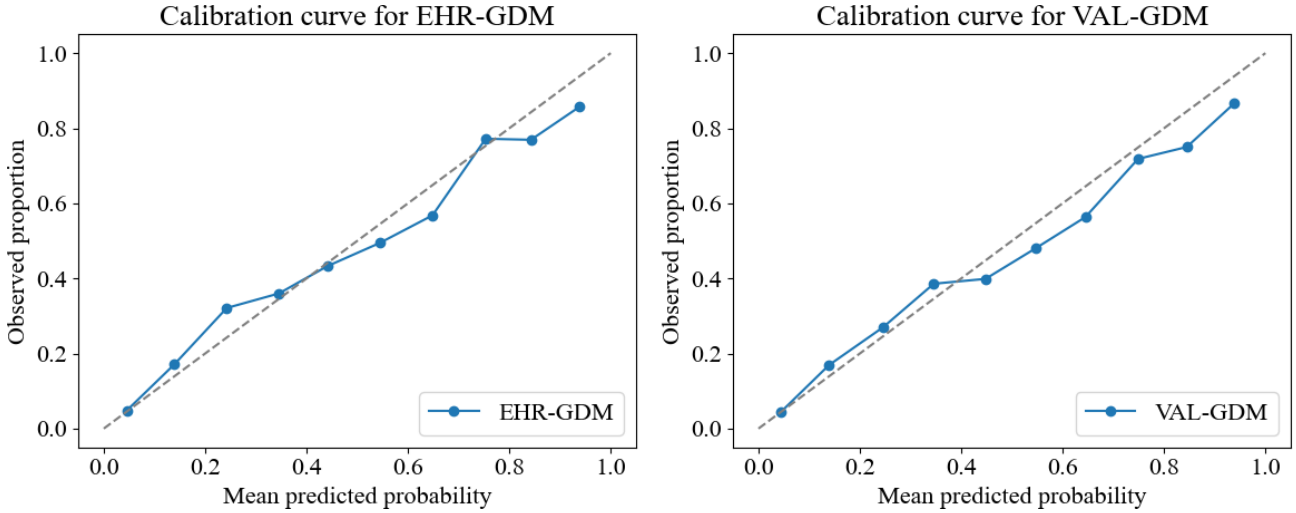
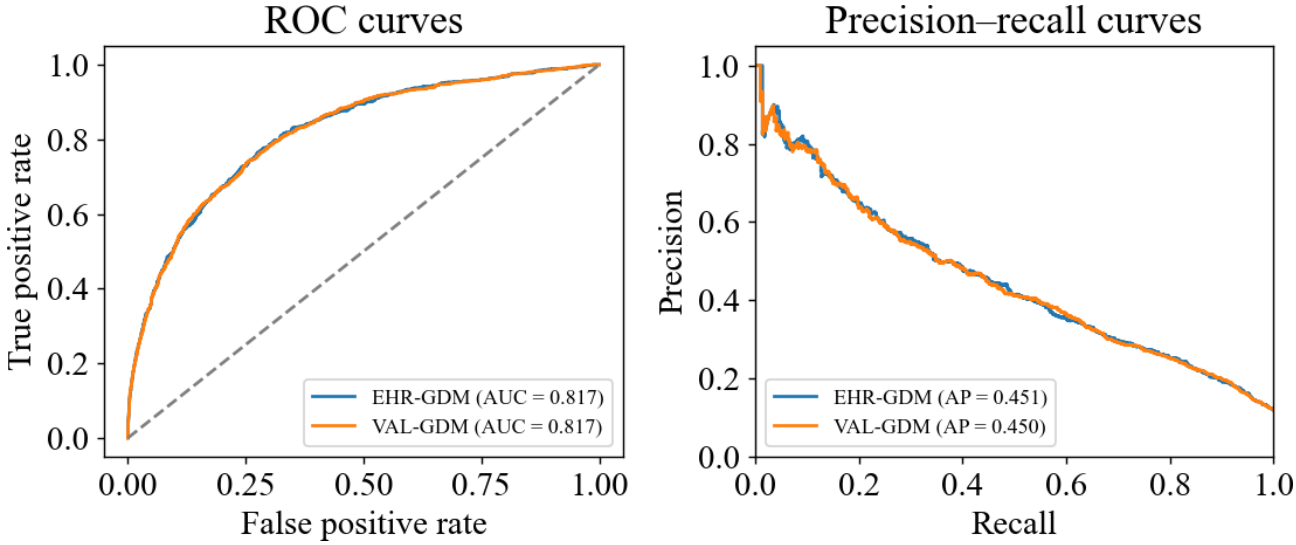


Figure 3. (Left) ROC curves and (right) precision - recall curves showing the performance of 2 logistic - regression models for predicting GDM. "EHR-GDM" refers to the model trained on electronic health record (EHR)–GDM labels, and "VAL-GDM" refers to the model trained on the subset of cases where the EHR and clinical team database labels agree. Both models are evaluated against the same reference labels (VAL-GDM). EHR: electronic health record; EHR-GDM: gestational diabetes mellitus label as recorded in the EHR; GDM: gestational diabetes mellitus; ROC: receiver operating characteristic; VAL-GDM: validated gestational diabetes mellitus label (only in cases where EHR and clinical team database labels matched).



In addition to LR, random forest, XGBoost (Extreme Gradient Boosting), and an Explainable Boosting Machine were assessed to compare their performance and robustness to label noise. As shown in Table 3, all 3 models achieved performance metrics in a similar range to the LR model, with none of the models demonstrating large changes in evaluation metrics regardless of the validation data used.

XSL•FO
RenderX

Table . Comparison of ROC AUC[a] and average precision for machine learning models predicting GDM[b] trained on the EHR[c] data and VAL[d] data, and validated against the VAL data.

Model	ROC AUC		Average precision		Intercept		Slope	
	EHR-GDM	VAL-GDM	EHR-GDM	VAL-GDM	EHR-GDM	VAL-GDM	EHR-GDM	VAL-GDM
Logistic regression	0.817	0.817	0.451	0.450	0.093	−0.027	0.984	0.955
Random forest	0.797	0.801	0.418	0.419	−0.747	−0.618	0.553	0.638
XGBoost[e]	0.780	0.782	0.389	0.393	−0.427	−0.507	0.619	0.608
EBM[f]	0.818	0.816	0.456	0.450	0.078	−0.047	0.975	0.940

[a]ROC AUC: area under the receiver operating characteristic curve.

[b]GDM: gestational diabetes mellitus.

[c]EHR: electronic health record.

[d]VAL: validated.

[e]XGBoost: Extreme Gradient Boosting.

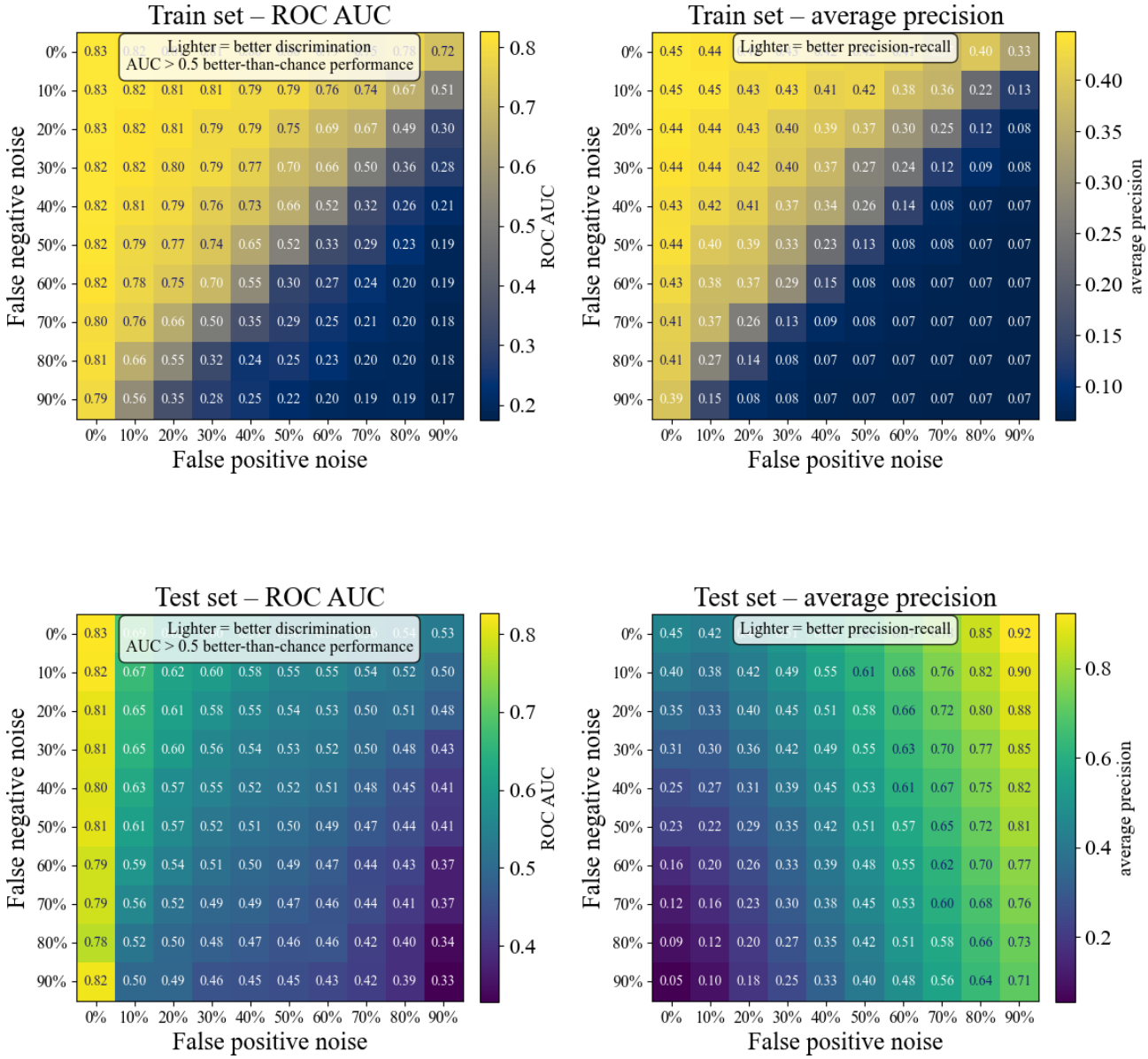
[f]EBM: Explainable Boosting Machine.

Simulated Label Noise

The impact of simulated label noise on model performance was assessed by progressively increasing the number of FNs (FN noise) and FPs (FP noise) in the training set (where 0% noise equates to the original VAL-GDM labels) without modifying the testing set. The results demonstrate a decline in model performance as the level of label noise increases (Figure 4).

XSL•FO
RenderX

Figure 4. Heatmaps illustrating how gradually introducing random label noise (NAR) degrades model performance. In each panel, the x-axis denotes the percentage of true negatives flipped to false positives, and the y-axis denotes the percentage of true positives flipped to false negatives. In the top-left heatmap, the ROC AUC on the training set is plotted; lighter cells signify stronger discrimination, and values above 0.5 represent performance better than random chance. The top-right heatmap presents the corresponding average precision on the same noisy training data, with lighter colors indicating a more favorable precision-recall trade-off. The bottom-left and bottom-right heatmaps repeat these experiments on the held-out test set, showing ROC AUC and average precision, respectively, under increasing label noise in the test data. The unusual behavior of average precision is discussed in this paper. Each cell is annotated with the exact metric value for that combination of false positive and false negative noise levels. AUC: area under the curve; NAR: noise at random; ROC AUC: area under the receiver operating characteristic curve.



Further analysis of noise in the test set showed that model performance metrics, particularly ROC AUC and AP scores, were sensitive to increasing levels of noise, especially FP noise. As the FP rate was increased, the ROC AUC consistently decreased, while the AP score initially decreased before increasing. The introduction of FN into the test set had a less pronounced effect on performance compared to FP, unless both types of noise were combined, which led to a more substantial impact (Figure 4).

Discussion

This study highlights significant discrepancies between GDM diagnoses recorded in EHRs and those validated by the CTD. Correcting label noise in the training set had a negligible impact on the performance of an LR-based ML model developed from EHRs to predict GDM from early pregnancy data. However, correcting label noise in the test set improved the model's AP, underscoring the importance of accurate labeling for evaluating model performance accurately. This study also found that increasing label noise in the training set led to a gradual decline in model performance, while increasing FPs in the test set had a particularly strong negative impact on ROC AUC, but counterintuitively increased AP scores. FNs had a less pronounced impact on ROC AUC unless combined with FP, which then caused a decline in model performance.

Approximately 14% (564/3952) of GDM cases were not recorded in the EHRs, while 18.5% (771/4,159) of positive GDM diagnoses in EHRs did not align with CTD records.

XSL•FO
RenderX

Overall, there were 32,928 (87.5%) TN, 3388 (9%) TP, 771 (2%) FP, and 564 (1.5%) FN. The FPR (2.3%) remained low in comparison to the FNR (14.3%). Similar discrepancies in accuracy of EHRs have been reported in previous studies within Irish maternal hospitals, though with higher agreement in other contexts, such as miscarriage measurements (k=0.92) [20]. More widely across Europe, wide variations exist in the accuracy of reporting in EHRs as it relates to acute cardiovascular outcomes, with sensitivity reported at <66% for heart failure diagnoses in particular [21]. A key challenge in these studies is the absence of a recommended reference standard for validating EHR data, leading to the use of various data sources [8].

The impact of COVID-19 on screening and diagnostic practices, especially in 2020, manifested in a relative reduction of 31% in GDM diagnoses, that is, 11.2% across 2018, 2019, 2021, and 2022 compared to 7.7% in 2020. These observations align with research indicating reduced diagnosis rates for various medical conditions during the first year of the pandemic [18], and suggest caution is warranted when using EHRs during this year for the purpose of health care modeling. The decrease in recorded GDM cases in 2020 was likely driven by changes in clinical protocols at the onset of the COVID-19 pandemic. The Irish Health Service Executive adopted procedures recommended by the Royal College of Obstetrics and Gynecologists in the United Kingdom, which recommended alternative testing strategies for screening pregnant women for GDM that focused on replacing the 2-h oral glucose tolerance test with other tests of shorter duration [22].

Correcting label noise has been shown to mitigate its adverse effects on model performance, underscoring the importance of "clean" and accurate datasets for training and validating ML algorithms to ensure their efficacy in clinical decision support systems [23]. For example, training a model on a "clean" dataset resulted in an accuracy of 73.6%, whereas with 30% label noise the accuracy fell to 64.1% (−9.5%) [23]. However, the current analysis demonstrated that training an LR model using EHR-GDM labels versus VAL-GDM yielded negligible differences in performance metrics, with ROC AUCs of 0.817 and 0.817, respectively (Figure 3), a performance in line with previous research using EHRs to predict GDM [13,15]. This is presumably due to the low overall representation of FN and FP in the dataset of 3.5% combined, which limited the impact of label noise on the training process.

Previous work has simulated noisy labels with artificial introduction of different levels of label noise (10%, 20%, and 40%) into the training set and demonstrated a gradual decline in the accuracy of all models (mean AUC of all models at 80.3, SD 3.3, 10%; 79.3, SD 3.4, 20%; and 77.6, SD 3.0, 40%) as label noise increased [24]. The approach taken in the present study differs in that it introduces systematic label noise using noise at random [25], increasing both the FP and FN rates linearly. Introducing noise into the training set resulted in a gradual decline in model performance, with both ROC AUC and AP scores decreasing as the level of noise increased. The model was particularly sensitive to FP, which caused a more pronounced decline in performance compared to FN. Introducing noise into the test set also impacted model performance, but the effects were more complex. The ROC AUC consistently decreased as FP rates increased, indicating that the model's ability to distinguish between classes was compromised. However, the AP score showed a different pattern, with an initial decline followed by an increase as noise levels were increased. The introduction of FN in the test set had a less pronounced effect on performance compared to FP, unless FP and FN were combined, which led to a more marked decline in the model's overall performance.

The counterintuitive increase in the AP score as the FP rate in the test set increased can be attributed to the method of calculating AP. AP evaluates the precision-recall trade-off across different thresholds, specifically calculating the proportion of TP to the sum of (TP + FP). When most of the negative class in the test set is artificially converted to positive, the opportunity for FP to occur is significantly reduced. This reduction in potential FP leads to an increase in precision, which in turn increases the AP score. Additionally, this manipulation dramatically alters the (eg, class balance from 90% negative to 90% positive), further influencing the precision-recall dynamics and contributing to the observed ostensible increase in AP. In practical terms, this finding emphasizes that certain performance metrics such as AP can behave unexpectedly in the presence of extensive label noise or class imbalance, underscoring the importance of using multiple evaluation metrics that are robust to changes in classes (discrimination and calibration) to fully understand model performance. These results reinforce that deploying predictive models trained on unvalidated EHR data can amplify false-positive and false-negative risks.

This study has several limitations that may affect the generalizability of these findings. First, the analysis was conducted using data from a single hospital and did not perform any external validation with data from other hospitals or a formal temporal validation using a future period. Therefore, it is uncertain whether the findings would directly generalize to different clinical settings, particularly those with different screening practices, disease encoding, and EHR systems. Second, the CTD, which is treated as the ground truth, is manually maintained by the clinical team. While it is likely more accurate than the EHR, it is not immune to possible human errors or omissions. Any such errors in the CTD would affect the data validation results by erroneously labeling some EHR entries as false positives or false negatives. However, this should minimally impact ML modeling as only data that had agreement across both databases were included. Third, there is potential for model overfitting due to the lack of an external validation set and default parameters, which we attempted to mitigate with the use of k-fold cross-validation, a relatively simple linear model, and a hold-out test set. Finally, noise at random linearly increases the FP and FN rate in the dataset, which may not accurately reflect how errors in EHRs typically occur.

In conclusion, the identified discrepancies in EHR-recorded GDM diagnoses compared to "true" GDM diagnoses reflect broader concerns about the accuracy of EHRs for public health and ML applications. Further, the magnitude of inaccuracies may play an important role in maximizing the utility of EHRs in enhancing health care outcomes, particularly for conditions such as GDM. However, when these discrepancies remain a small percentage (eg, <5%) of the dataset, such as in the case

XSL•FO
RenderX

of this study, there was no noticeable impact on model training performance. Conversely, the risk of incorrect model evaluation increases when the test set labels are impacted by noise, as this has a more pronounced effect on performance metrics. These observations emphasize the importance of incorporating robust data cleaning, preprocessing, and validation methodologies in the development of ML models for health care. Future efforts should aim at developing standardized validation protocols for EHRs to ensure high data quality for training and evaluating ML algorithms. Such protocols could include harmonizing how GDM diagnoses are recorded across different sites, implementing automated consistency checks (for instance, prompting for a GDM diagnosis entry in the EHR when a laboratory result confirming GDM is received), and performing regular audits comparing EHR records with reference databases or laboratory results. By improving the integrity of data entry and maintenance in EHR systems, these measures could reduce discrepancies and enhance the utility of EHR data for both clinical care and ML applications.

Acknowledgments

The authors are grateful to The Coombe Hospital for their collaboration, without whom this analysis would not be possible. This work has emanated from research supported in part by a grant from Science Foundation Ireland (18/CRT/6183).

Data Availability

The datasets analyzed in this study are not publicly available because patient IDs were used to match the corresponding databases. The code has been made available online [26].

Conflicts of Interest

None declared.

References

1. Garrison LP, Neumann PJ, Erickson P, Marshall D, Mullins CD. Using real-world data for coverage and payment decisions: the ISPOR real-world data task force report. Value Health 2007 Sep;10(5):326-335. [doi: 10.1111/j.1524-4733.2007.00186.x]
2. Berger ML, Sox H, Willke RJ, et al. Good practices for real-world data studies of treatment and/or comparative effectiveness: recommendations from the joint ISPOR-ISPE Special Task Force on real-world evidence in health care decision making. Pharmacoepidemiol Drug Saf 2017 Sep;26(9):1033-1039. [doi: 10.1002/pds.4297] [Medline: 28913966]
3. Wong J, Horwitz MM, Zhou L, Toh S. Using machine learning to identify health outcomes from electronic health record data. Curr Epidemiol Rep 2018 Dec;5(4):331-342. [doi: 10.1007/s40471-018-0165-9] [Medline: 30555773]
4. Ford E, Carroll JA, Smith HE, Scott D, Cassell JA. Extracting information from the text of electronic medical records to improve case detection: a systematic review. J Am Med Inform Assoc 2016 Sep;23(5):1007-1015. [doi: 10.1093/jamia/ocv180] [Medline: 26911811]
5. Bowman S. Impact of electronic health record systems on information integrity: quality and safety implications. Perspect Health Inf Manag 2013;10(Fall):1c. [Medline: 24159271]
6. Frénay B, Kaban A. A comprehensive introduction to label noise. 2014. URL: http://hdl.handle.net/2078.1/156597 [accessed 2025-08-09]
7. Yang J, Triendl H, Soltan AAS, Prakash M, Clifton DA. Addressing label noise for electronic health records: insights from computer vision for tabular data. BMC Med Inform Decis Mak 2024 Jun 27;24(1):183. [doi: 10.1186/s12911-024-02581-5] [Medline: 38937744]
8. Nissen F, Quint JK, Morales DR, Douglas IJ. How to validate a diagnosis recorded in electronic health records. Breathe (Sheff) 2019 Mar;15(1):64-68. [doi: 10.1183/20734735.0344-2018]
9. Zhang C, Bengio S, Hardt M, Recht B, Vinyals O. Understanding deep learning (still) requires rethinking generalization. Commun ACM 2021 Mar;64(3):107-115. [doi: 10.1145/3446776]
10. Cebul RD, Love TE, Jain AK, Hebert CJ. Electronic health records and quality of diabetes care. N Engl J Med 2011 Sep;365(9):825-833. [doi: 10.1056/NEJMsa1102519]
11. Veinot TC, Zheng K, Lowery JC, Souden M, Keith R. Using electronic health record systems in diabetes care. 2010 Nov 11 Presented at: IHI '10; Nov 11-12, 2010; Arlington, VA p. 240-249. [doi: 10.1145/1882992.1883026]
12. Gianfrancesco MA, Tamang S, Yazdany J, Schmajuk G. Potential biases in machine learning algorithms using electronic health record data. JAMA Intern Med 2018 Nov 1;178(11):1544-1547. [doi: 10.1001/jamainternmed.2018.3763] [Medline: 30128552]
13. Mennickent D, Rodríguez A, Farías-Jofré M, Araya J, Guzmán-Gutiérrez E. Machine learning-based models for gestational diabetes mellitus prediction before 24–28 weeks of pregnancy: a review. Artif Intell Med 2022 Oct;132:102378. [doi: 10.1016/j.artmed.2022.102378]
14. de Hond AAH, Leeuwenberg AM, Hooft L, et al. Guidelines and quality criteria for artificial intelligence-based prediction models in healthcare: a scoping review. NPJ Digit Med 2022 Jan 10;5(1):1-13. [doi: 10.1038/s41746-021-00549-7]

XSL•FO
RenderX

15. Zhang Z, Yang L, Han W, et al. Machine learning prediction models for gestational diabetes mellitus: meta-analysis. J Med Internet Res 2022 Mar 16;24(3):e26634. [doi: 10.2196/26634] [Medline: 35294369]
16. Fawcett T. An introduction to ROC analysis. Pattern Recognit Lett 2006 Jun;27(8):861-874. [doi: 10.1016/j.patrec.2005.10.010]
17. Cabitza F, Campagner A. The need to separate the wheat from the chaff in medical informatics: introducing a comprehensive checklist for the (self)-assessment of medical AI studies. Int J Med Inform 2021 Sep;153:104510. [doi: 10.1016/j.ijmedinf.2021.104510] [Medline: 34108105]
18. Burus T, Lei F, Huang B, et al. Undiagnosed cancer cases in the US during the first 10 months of the COVID-19 pandemic. JAMA Oncol 2024 Apr 1;10(4):500-507. [doi: 10.1001/jamaoncol.2023.6969] [Medline: 38386344]
19. Germaine M, Healy G, Egan B. Lack of data sharing despite data availability statements in studies using machine learning models for prediction of gestational diabetes mellitus. Diabetes Care 2024 Oct 1;47(10):e78-e79. [doi: 10.2337/dc24-1483] [Medline: 39159281]
20. San Lazaro Campillo I, Meaney S, Harrington M, et al. Assessing the concordance and accuracy between hospital discharge data, electronic health records, and register books for diagnosis of inpatient admissions of miscarriage: a retrospective linked data study. J Obstet Gynaecol Res 2021 Jun;47(6):1987-1996. [doi: 10.1111/jog.14785] [Medline: 33932071]
21. Davidson J, Banerjee A, Muzambi R, Smeeth L, Warren-Gash C. Validity of acute cardiovascular outcome diagnoses recorded in European electronic health records: a systematic review. Clin Epidemiol 2020;12:1095-1111. [doi: 10.2147/CLEP.S265619] [Medline: 33116903]
22. Neville J, Foley K, Lacey S, et al. Impact of changes in gestational diabetes mellitus diagnostic criteria during the COVID-19 pandemic. Ir J Med Sci 2025 Jun;194(3):1097-1104. [doi: 10.1007/s11845-025-03926-3] [Medline: 40072817]
23. Bernhardt M, Castro DC, Tanno R, et al. Active label cleaning for improved dataset quality under resource constraints. Nat Commun 2022 Mar 4;13(1):1161. [doi: 10.1038/s41467-022-28818-3]
24. Ju L, Wang X, Wang L, et al. Improving medical images classification with label noise using dual-uncertainty estimation. IEEE Trans Med Imaging 2022 Jun;41(6):1533-1546. [doi: 10.1109/TMI.2022.3141425] [Medline: 34995185]
25. Sáez JA. Noise models in classification: unified nomenclature, extended taxonomy and pragmatic categorization. Mathematics 2022 Jan;10(20):3736. [doi: 10.3390/math10203736]
26. Gestational ‐ Diabetes label noise study. GitHub. URL: https://github.com/MarkGermaine/Label_Noise [accessed 2025-07-25]

Abbreviations:

AP: average precision
CTD: clinical team database
CTD-GDM: gestational diabetes mellitus label as recorded in the clinical team database (reference standard label)
EHR: electronic health record
EHR-GDM: gestational diabetes mellitus label as recorded in the electronic health record
FN: false negative
FP: false positive
GDM: gestational diabetes mellitus
IADPSG: International Association of the Diabetes and Pregnancy Study Groups
***ICD*:** *International Statistical Classification of Diseases and Related Health Problems*
LR: logistic regression
ML: machine learning
ROC AUC: area under the receiver operating characteristic curve
SNOMED: Systematized Nomenclature of Medicine
TN: true negative
TP: true positive
VAL-GDM: validated gestational diabetes mellitus label (only in cases where electronic health record and clinical team database labels matched)
XGBoost: Extreme Gradient Boosting

XSL•FO
RenderX

Edited by A Castonguay; submitted 21.02.25; peer-reviewed by A Adeoye, O Kehinde, P Tekkali, S Sivarajkumar; revised version received 09.05.25; accepted 17.06.25; published 21.08.25.

Please cite as:
Germaine M, O'Higgins AC, Egan B, Healy G
Label Accuracy in Electronic Health Records and Its Impact on Machine Learning Models for Early Prediction of Gestational Diabetes: 3-Step Retrospective Validation Study
JMIR Med Inform 2025;13:e72938
URL: https://medinform.jmir.org/2025/1/e72938
doi:10.2196/72938

© Mark Germaine, Amy C O'Higgins, Brendan Egan, Graham Healy. Originally published in JMIR Medical Informatics (https://medinform.jmir.org), 21.8.2025. This is an open-access article distributed under the terms of the Creative Commons Attribution License (https://creativecommons.org/licenses/by/4.0/), which permits unrestricted use, distribution, and reproduction in any medium, provided the original work, first published in JMIR Medical Informatics, is properly cited. The complete bibliographic information, a link to the original publication on https://medinform.jmir.org/, as well as this copyright and license information must be included.

XSL•FO
RenderX

Co-Opetition Strategies of Superior and Subordinate Hospitals for Integration of Electronic Health Records Within the Medical Consortiums in China Based on Two-Party Evolutionary Game Theory: Mixed Methods Study

Shenghu Tian[1,2], PhD; Rong Jiang[2,3], PhD; Jianfeng Yao[4], PhD; Yu Chen[5], PhD

[1]Business School, Yunnan University of Finance and Economics, Kunming, China

[2]Yunnan Provincial Key Laboratory of Service Computing, Kunming, China

[3]Information School, Yunnan University of Finance and Economics, Kunming, China

[4]Continuing Education School, Yunnan University of Finance and Economics, Kunming, China

[5]Management and Economics School, Kunming University of Science and Technology, No. 68 Wenchang Road, Wuhua District, Kunming, China

Corresponding Author:
Yu Chen, PhD
Management and Economics School, Kunming University of Science and Technology, No. 68 Wenchang Road, Wuhua District, Kunming, China

Abstract

Background: Medical consortiums take the integration of electronic health records (EHR) as a breakthrough point and the construction of an integrated medical service system as the ultimate goal. However, their establishment has disrupted the balance between the original medical order and interest patterns. While promoting active cooperation among hospitals, it has also intensified active competition between them.

Objective: This study aimed to explore the internal evolution mechanism of the co-opetition strategies adopted by the superior and subordinate hospitals in the medical consortiums, providing a theoretical foundation and policy reference for achieving EHR integration.

Methods: On the basis of analyzing the structure of the main players in the co-opetition game and their game motivations, we established an evolutionary game model, analyzed the impact mechanism of key parameters, simulated the dynamic evolution process of the co-opetition strategies using MATLAB (MathWorks), and finally proposed actionable policy recommendations.

Results: The results indicate that three factors positively promote EHR integration: (1) EHR complementarity, (2) hospitals' willingness and ability to use EHR, and (3) the average revenue per unit of EHR. Conversely, the investment cost per unit of resources hinders EHR integration. Neither the original income of hospitals nor the stock of EHR significantly affects the evolution direction of the game system.

Conclusions: Medical consortiums should actively involve all levels and different types of medical institutions, and continuously improve hospitals' willingness and ability to use EHR through training, assistance, support, and sinking of medical resources, etc. The government should establish a reward and punishment system, optimize the operation and supervision mechanism of medical consortiums, and monitor and punish opportunism behaviors such as "free-riding." It is also crucial to strengthen the construction of hospital informatization infrastructure and improve the technical, content, and sharing standards for EHR construction. In addition, designing reward and punishment mechanisms as well as cost accounting based on "unit EHR resources" is also of great significance for promoting the EHR integration.

(JMIR Med Inform 2025;13:e70866) doi:10.2196/70866

KEYWORDS

electronic health records; EHR; medical consortiums; evolutionary game; co-opetition strategy

Introduction

In the traditional health care delivery system, medical institutions were fragmented and scattered, and hospitals competed for access to patients in order to achieve the goal of maximizing their own interests, but active cooperation in medical care was basically nonexistent. To address this fragmentation and scattering of health care services and achieve an integrated health care delivery pattern of services, responsibilities, benefits, and management [1]. Medical consortium building has become a major strategic choice for

XSL•FO
RenderX

countries around the world. Medical consortiums are a type of health care alliance that has gained attention in China in recent years. In China, medical consortiums, a form of health care alliance that has gained significant attention in recent years, primarily manifest in 4 organizational models: urban medical groups, county-level medical communities, cross-regional specialty alliances, and telemedicine collaboration networks [2]. Medical consortiums typically use electronic health records (EHR) integration as a foundational strategy to realize the objectives of "primary diagnosis at grassroots institutions, two-way referrals, tiered treatment for acute and chronic cases, and coordinated care across different levels of healthcare providers," and ultimately building an integrated medical service system. However, the development of medical consortiums has broken the balance of the original medical order and interest pattern, and has intensified active competition among hospitals while promoting active cooperation among them. Consequently, in the process of promoting the EHR integration within medical consortiums, hospitals inevitably adopt co-opetition strategies to safeguard and maximize their own interests.

Brandenburger and Nalebuff [3], who developed the concept of co-opetition, believe that the organization's operating activities are not all zero-sum games, but also win-win nonzero-sum games, and that the strategy to achieve this win-win outcome is "co-opetition strategy." In fact, competition and cooperation are the driving force for sustainable economic and social development [4]. The social value of medical consortiums predominantly stems from the co-opetition relationship among member. Regarding EHR integration, hospitals at all levels are characterized by imperfect rationality and imperfect information. Evolutionary game can be used to reveal the competition and cooperation relationship between players and the law of their strategy selection. Existing studies have primarily examined: (1) individual hospitals' data-sharing willingness [5], (2) access control models [6], and (3) the game between the government and the hospital [7]. However, these studies have inadequately analyzed the competition and cooperation relationship between the superior and subordinate hospitals in depth from the perspective of medical consortiums, and also failed to reveal the evolution mechanism of competition and cooperation strategies choices, which has limited the practical reference value of research results for policy optimization.

As far as the related research is concerned, evolutionary game theory is favored because its finite rationality assumption is more realistic, and has wide applications in the fields of multivariate governance, organizational synergy, and information behavior [8]. For instance, evolutionary game models have been used to analyze interest equilibria in open data ecosystems [9], revealing the impact of the changing psychology of individuals on group behavior [10]. In health care applications, evolutionary game theory has been principally applied to investigate: (1) privacy disclosure behaviors in "online health communities" [11], (2) quality assurance strategies for emergency medical supplies [12], (3) selection behaviors regarding internet hospitals [13], (4) models of epidemic information dissemination [14], and (5) hierarchical diagnosis and treatment strategy and 2-way referral mechanism [15,16]. The related research reasonably explains the evolution mechanism of relevant strategy selection behavior, and establishes a solid methodological foundation for our study.

China's EHR development has progressed through 3 evolutionary phases, namely independent construction, system integration, and shared usage. In the initial phase, EHR was built separately by each hospital, realizing a breakthrough from scratch, and the construction is effective and widely applied within the hospital. The EHR integration is the premise and foundation of crossinstitutional "sharing and utilization," which is the key link in releasing the EHR application, and also the bottleneck in the EHR development at present. There exists an urgent need to elucidate the co-opetition strategies between superior and subordinate hospitals facilitating EHR integration within medical consortiums, thereby establishing a theoretical foundation for policy optimization. Previous studies suggested that evolutionary games provide a valuable framework for elucidating the emergence and maintenance of cooperative behavior [17]. Accordingly, this study uses evolutionary game theory to uncover the intrinsic mechanisms governing co-opetition strategy evolution between superior and subordinate hospitals during EHR integration within medical consortiums. The study comprises three key components: (1) from the perspective of the evolution of co-opetition strategies, analyzing the structure of competition and cooperation game subjects and their game motivations; (2) establishing a game model for the evolution of the competition of the superior and subordinate hospitals; and (3) simulating the dynamic evolution process of the co-opetition strategy using MATLAB (MathWorks). This study bridges the previous gap of focusing only on superficial policy recommendations and neglecting to reveal the game mechanism of multiple subjects behind the policies. The findings provide both theoretical foundations and policy-relevant insights for achieving EHR integration objectives.

Methods

Research Design

This study followed the research approach of "basic assumptions - model construction - result analysis - numerical simulation." First, for the convenience of modeling and analysis, combined with the actual situation of EHR integration in China, the superior hospital A and its subordinate hospital B were randomly set as research objects within the medical consortiums. Referring to related studies on cooperative competitive games in the big data innovation alliance and information ecosystem [18,19], the basic assumptions were put forward from 6 aspects: game players, co-opetition relationships, value-added benefits, synergistic effects, co-operation costs, and reward-punishment system. Second, an evolutionary game model of the competitive and cooperative behaviors between the superior and subordinate hospitals was constructed. Then, we analyzed the influence mechanisms of key factors on the selection of competition and cooperation strategies, and MATLAB was used to conduct simulation experiments on the model operation. Finally, targeted policy recommendations were proposed to highlight the practical reference value of the research conclusions.

XSL•FO
RenderX

Underlying Assumptions

Game Players and Co-Opetition Relationships

In China, medical consortiums consist of dozens or even hundreds of hospitals at different levels and scales, including tertiary hospitals, secondary hospitals, county hospitals, community hospitals, and rural hospitals. These hospitals belong to different levels of administrative divisions. In the existing medical order designed by the "hierarchical diagnosis and treatment" system, these hospitals present an unstructured hierarchical relationship with each other. When a patient is transferred from a county hospital to a tertiary hospital for treatment, the county hospital becomes a subordinate hospital to the tertiary hospital; when a patient is transferred from a community hospital to a county hospital for treatment, the county hospital is again a superior hospital to the community hospital. Obviously, "superior and subordinate hospitals" is a relative concept, but it can accurately portray the main structure of the co-opetition game among hospitals at each level in medical consortiums. Therefore, we classify the players participating in the co-opetition evolutionary game into superior hospitals and subordinate hospitals.

The superior and subordinate hospitals have not only formed a cooperative relationship based on policy requirements and integration goals but also formed a competitive relationship due to risk avoidance and interest maximization. They continuously create and add value through both competition and cooperation. In summary, the co-opetition relationship between superior and subordinate hospitals manifests in the following four situations [20]: (1) Creation of integrated medical value (cooperation): improves health care service quality and alleviates the social contradictions of difficult and expensive access to health care; (2) pursuit of patient volume (competition): the number of patients directly determines the hospital's financial gains; (3) policy and contractual regulation (cooperation): hospitals must comply with the requirements of the hierarchical diagnosis and treatment system, share EHR and implement referral regulations; and (4) opportunistic behavior (competition): may include cost-input bargaining, income concealment, inaction, and "free-riding" situations.

Hospitals are profit-seeking entities that aim to maximize their own interests in the co-opetition process [21]. Hospitals compare their benefits and strategies with reference hospitals and adjust their strategies accordingly, resulting in various game behaviors. Influenced by changes in external factors and constrained by imperfect rationality and incomplete information, hospitals can only continuously adjust their strategies according to a certain probability to maximize income, which forms an evolutionary game. Assume both hospitals *A* and *B* have 2 optional strategies in EHR integration, namely competition and cooperation. The probability of hospital *A* choosing cooperation is *x*, then the probability of hospital *A* choosing competition is 1-*x*; similarly, hospital *B*'s g cooperation probability is *y*, making its competition probability 1-*y*. where x,y∈[0,1] and *x* and *y* are both functions of time *t*.

Value-Added Benefits and Synergistic Effects

The EHR integration can easily realize "two-way referral," enabling *A* and *B* to gain value-added benefits. The value-added benefits include not only economic benefits, but also noneconomic benefits, such as social reputation, brand image, collective honor, hospital responsibility, superior praise, promotion, and public praise. The benefits that hospitals were able to obtain before EHR integration can be referred to as the original benefits and are denoted by Ri. Whether EHR integration can generate value-added and the magnitude of the value-added depends on the hospital's willingness to use EHR ρi)(0≤ρi≤1,i=A,B), the ability to use EHR (μi)(0≤μi≤1,i=A,B), and the number of the other's health records shared (ri)(0≤μi,i=A,B). It is assumed that the average benefit per unit resource is *I* (*I*≥0).

A hospital's willingness to use EHR is fundamentally determined by the decision makers' cognition, which includes both the decision makers' awareness of realizing the social value of the medical consortium and their perceived future expected use. Therefore, a higher ρi indicates that the decision makers perceive greater value and future utility of EHR integration, while a smaller value of ρi represents that the decision makers pay more attention to immediate and local interests. The ability to use EHR reflects the level of medical care in the hospital, and it includes both the ability of physicians to use the EHR and the medical equipment conditions that the hospital has to use the external EHR. The number of EHRs shared is proportional to the value-added benefit of the other party. The more EHRs shared by the sharing party, the greater value-added benefit the user may gain. Therefore, the value-added benefits received by hospital *A* and *B* are ρAμArBI and ρBμBrAI, respectively.

Usefulness, the ultimate goal of the game, refers to the material or spiritual benefits players obtain through the game [22]. Synergistic effects refer to the enhanced profitability from mutual EHR sharing among hospitals, representing the core objective of medical consortia in promoting EHR integration When both *A* and *B* choose the "cooperation" strategy, synergy will occur, which depends on the hospital's willingness to use EHR (ρi), the ability to use EHR (μi) and the EHR resources complementarity (β). Then the synergy benefits of *A* and *B* are βρAμArAI and βρBμBrBI respectively.

Cooperation Cost and Reward-Punishment Mechanism

EHR integration can impose additional costs on hospitals, such as direct costs (IT infrastructure modification and file formatting), risk costs (data privacy/security issues), opportunity costs (potential patient attrition), and indirect costs (reduced revenue from test information reuse) [23]. Existing research suggests that high fines can not only prevent free riding but they also demotivate some of the most generous altruists [24]. To promote the smooth integration of EHRs in medical consortiums, local governments often establish reward and punishment systems to achieve cost compensation while reducing opportunism. The reward and punishment system are the most easily regulated and more frequently adjusted factor, and its changes are more likely to cause changes in the competing strategies of the superior and subordinate hospitals, which in

XSL•FO
RenderX

turn affects the evolutionary game direction. Assuming that the average input cost in terms of human, financial, and other resources required to integrate unit resources is *C*, the input costs of *A* and *B* are rAC and rBC, respectively. When hospitals actively share and use EHRs for integration purposes, the government grants a unit resource subsidy of *H*, otherwise a unit resource penalty of *H* is granted.

According to the game motives of the players and the above assumptions, the co-opetition relationship between the 2 sides of the game can be portrayed by the following scenarios. First, when both players choose "cooperation," the benefits obtained by both players include the original benefit (Ri), value-added benefit (riI), and government incentive (riH). The synergy benefits generated by *A* and *B* are βρAμArAI andρBμBrBI. Also considering the costs rAC and rBC due to the inputs in the cooperation, we can derive the benefit functions of *A* and *B* as RA+ρAμA(rBI+βrAI)+rAH-rAC and RB+ρBμB(rAI+βrBI)+rBH-rBC. Second, when 1 player chooses "cooperation" and the other chooses "competition." When *A* chooses "cooperation" and *B* chooses "competition," *A*'s benefits include the original benefit R_A and financial subsidy rAH, and *A* incurs investment costs rAC due to the choice of cooperation. At this time, *A* cannot use *B*'s EHR, and *A*'s value-added benefits are 0. Therefore, *A*'s benefit function is RA+rAH-rAC. The benefit of *B* includes both the original benefit R_B and the value-added benefit RB+ρBμBrAI-rBH from free-riding. At this point, *B* has no input cost but receives a penalty rBH from the government. Therefore, the benefit function of *B* is RB+ρBμBrAI-rBH. Similarly, when *B* chooses "cooperation" and *A* chooses "competition," the benefit function of *A* is RA+ρAμArBI-rAH, and the benefit function of *B* is RB+rBH-rBC. Finally, when both players choose "competition," both players gain only the original benefits R_A and R_B, and the penalties for both players are rAH and rBH.

When 1 player chooses "cooperation" and the other chooses "competition." When *A* chooses "cooperation" and *B* chooses "competition," *A*'s benefits include the original benefit R_A and financial subsidy rAH, and *A* incurs investment costs rAC due to the choice of cooperation. At this time, *A* cannot use *B*'s EHR, and *A*'s value-added benefits are 0. Therefore, *A*'s benefit function is RA+rAH-rAC. The benefit of *B* includes both the original benefit R_B and the value-added benefit RB+ρBμBrAI-rBH from free-riding. At this point, *B* has no input cost but receives a penalty rBH from the government. Therefore, the benefit function of *B* is RB+ρBμBrAI-rBH. Similarly, when *B* chooses "cooperation" and *A* chooses "competition," the benefit function of *A* is RA+ρAμArBI-rAH, and the benefit function of *B* isRB+rBH-rBC.

When both players choose "competition." Both players gain only the original benefits R_A and R_B, and the penalties for both players are rAH and rBH.

Model Construction

As a result, an evolutionary game payment matrix can be constructed for hospitals *A* and *B*, as shown in Table 1.

Table . Evolutionary game payment matrix.

Players and optional strategies	Subordinate hospital *B*	
Superior hospital *A*	Cooperation (*y*)	Competition (1-*y*)
Cooperation (*x*)	RA+ρAμA(rBI+βrAI)+rAH-rAC	RA+rAH-rAC
	RB+ρBμB(rAI+βrBI)+rBH-rBC	RB+ρBμBrAI-rBH
Competition (1-*x*)	RA+ρAμArBI-rAH	RA-rAH
	RB+rBH-rBC	RB-rBH

According to Table 1, the expected benefit EA1 of the cooperation strategy chosen by *A* is:

(1)EA1=y[RA+ρAμA(rBI+βrAI)+rAH−rAC]+(1−y)(RA+rAH−rAC)

The expected benefit of the competitive strategy chosen by *A* is EA2:

(2)EA2=y[RA+ρAμArBI−rAH]+(1−y)(RA−rAH)

Then the average expected benefit E−A of superior hospital *A* is:

(3)E−A=xEA1+(1−x)EA2=RA+xrA(2H−C)+y(xβrA+rB)ρAμAI−rAH

Therefore, the replication dynamic equation of the cooperation strategy chosen by the superior hospital *A* can be derived as follows:

F(x)=dxdt=x(EA1−E¯A)

(4)=x(1−x)[rA(2H−C)+yβρAμArAI]

Similarly, the expected benefit EB1 of the cooperation strategy chosen by *B* is:

(5)EB1=x[RB+ρBμB(rAI+βrBI)+rBH−rBC]+(1−x)(RB+rBH−rBC)

The expected benefit of the competitive strategy chosen by *B* is EB2：

(6)EB2=x[RB+ρBμBrAI−rBH]+(1−x)(RB−rBH)

Then the average expected benefit E-B of subordinate hospital *B* is:

(7)E−B=yEB1+(1−y)EB2=RB+yrB(2H−C)+x(rA+yβrB)ρBμBI−rBH

Therefore, the replication dynamic equation of the cooperation strategy chosen by the subordinate hospital *B* can be derived as follows:

(8)F(y)=dydt=y(EB1−E−B)=y(1−y)[rB(2H−C)+xβρBμBrBI]

Ethical Considerations

No formal ethical approvement was necessary for the study according to the China Science and Technology Ethics Committee.

XSL•FO
RenderX

Results

Stability of Equilibrium Points and Their Evolutionary Path Analysis

In the evolutionary game process, hospitals *A* and *B* participate in the game through repeated trial and error, learning and imitation, constantly adjusting their own strategies, so that the dynamic system will eventually reach a stable state. According to the stability theorem of differential equations, let:

(9)F(x)=dxdt=0F(y)=dydt=0

By solving equation (9), 5 local equilibrium points of the dynamic evolutionary game system can be obtained, which are *O* (0,0), *F* (0,1), *G* (1,0), *K* (1,1), *and T* (C−2HβρBμBI, C−2HβρAμAI). These 5 equilibrium points together constitute the boundary (x,y)0≤x≤1;0≤y≤1of the evolutionary game system solution domain of superior and subordinate hospitals in EHR integration.

The Jacobi matrix can be obtained by solving the partial derivatives of (4) and (8) with respect to x and y, respectively.

J=[∂F(x)∂x∂F(x)∂y∂F(y)∂y∂F(y)∂x]

(10)[1−2y(C−H)+βρAμAAI(1−2x)βρAμAAI(1−x)βρBμBBI(1−2y)βρBμBBI(1−y)]

For a 2-party behavior dynamic system described by differential equations, whether the above 5 local equilibrium points are evolutionary stable strategies of the dynamic system can be determined by the sign of the det(J) and tr(J) of the Jacobi matrix [8,25]. When 2H>C, the stability of the 5 equilibrium points can be obtained as shown in Table 2. This situation is theoretically valid but difficult to realize in reality. When 2H<C, Since 0<C−2HβρBμBI<1 and 0<C−2HβρAμAI<1, we can obtain βρBμBI>C−2H and βρAμAI>C−2H, and then obtain the stability of the 5 equilibrium points as shown in Table 3 and Figure 1 (2H>C). This situation is more realistic and has a solid practical basis. Therefore, we chose this situation to carry out an in-depth analysis in order to clarify the influence mechanism and influence effect of key factors on the evolutionary game system. The evolutionary path of the dynamic system is shown in Figure 1, where 1 denotes the cooperative strategy and 0 denotes the competitive strategy.

Table . Equilibrium points of evolutionary game system and their stability (2H>C).

Equilibrium points	Sign of det (J)	Sign of tr (J)	Attribute
O (0,0)	+	+	Unstable point
F (0,1)	−-	NO	Saddle point
G (1,0)	−-	NO	Saddle point
K (1,1)	+	−-	ESS[a]
T (x^*, y^*)	−-	0	Saddle point

[a] ESS: evolutionary stable strategies.

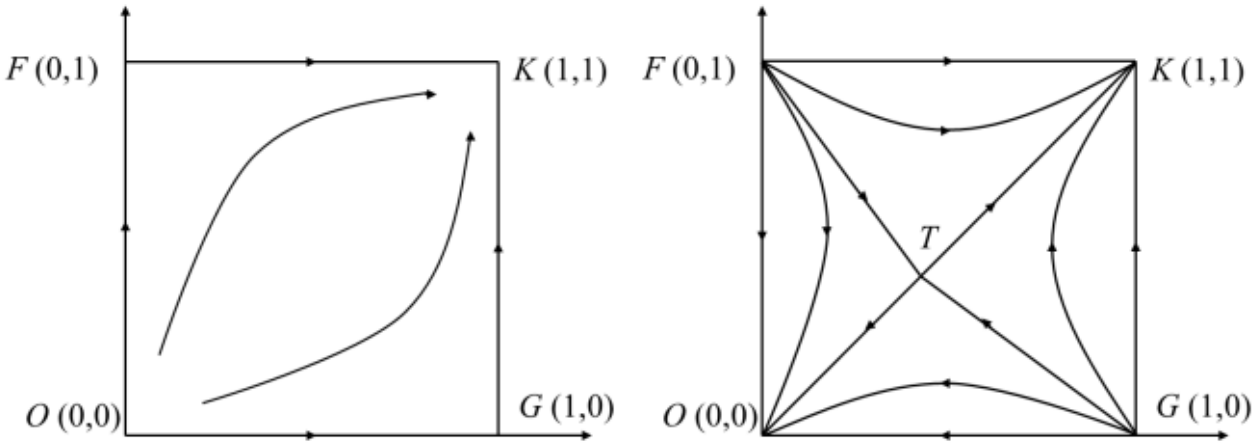
Table . Equilibrium points and their stability (2H>C).

Equilibrium points	Sign of det (J)	Sign of tr (J)	Attribute
O (0,0)	+	−-	ESS[a]
F (0,1)	+	NO	Unstable point
G (1,0)	+	NO	Unstable point
K (1,1)	+	−-	ESS
T (x^*, y^*)	−-	0	Saddle point

[a]ESS: evolutionary stable strategies.

XSL•FO
RenderX

Figure 1. Evolutionary path phase diagram.



It can be seen from Table 2 and Figure 1 (2H<C), the evolutionary game system has 2 stable points, *O* (0, 0) and *K* (1, 1). The game strategies corresponding to the stable points are {competition, competition} and {cooperation, cooperation}. *F* (0, 1) and *G* (1, 0) are the unstable points, and their corresponding game strategies are {competition, cooperation} and {cooperation, competition}, respectively. The equilibrium points *T* (x*, y*) is a saddle point located in the plane(x,y)0≤x≤1;0≤y≤1. When the initial state of the dynamic system is within the FTGK region, the evolutionary result will converge to the stability point *K* (1, 1), that is, both the hospitals *A* and *B* choose the cooperation strategy to actively promote the EHR integration. When the initial state of the dynamic system is within the FTGO region, the evolutionary result will converge to the stability point *O* (0, 0), that is, both A and B choose the competition strategy. The final convergence of the evolutionary game system to that stable point depends on the prediction and judgment of both sides of the game on their own ability and the other side's strategy choice. The willingness and ability of hospitals to use EHR, the number of EHR shared by the other party, and the complementarity of EHR have positive effects on the integration.

Analysis of the Influence Mechanism of Key Factors

It can be seen from Figure 1 that the size of FTGK area depends on the location of saddle point *T* (C-2HβρBμBI,C-2HβρAμAI). The location of *T* point is influenced by the complementarity of EHR resources (β), hospital's willingness (ρi) and ability to use HER (μi), the average income of unit EHR resources (*I*), unit EHR resource sharing cost (*C*), and unit resource reward and punishment (*H*). The influence mechanism of the relevant parameters is analyzed below. Where the area of the FTGK region can be expressed as follows [26]:

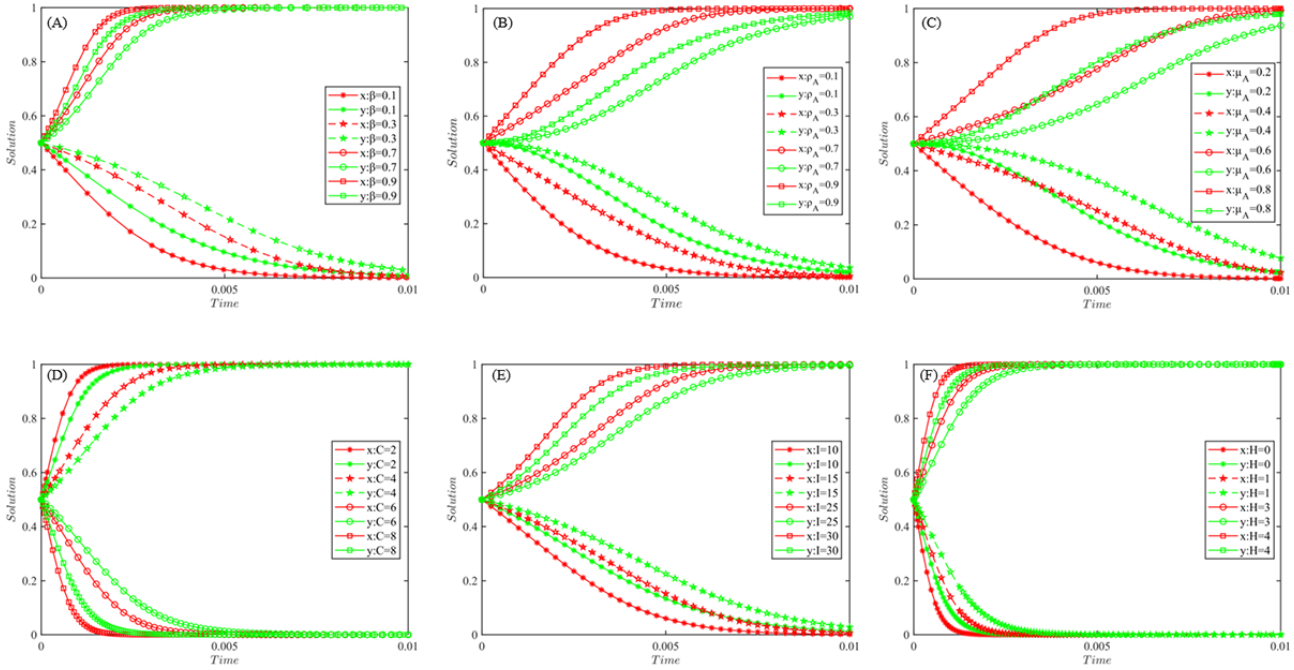
$$S_{FTGK}=1-\frac{1}{2}(x^*+y^*)=1-\frac{1}{2}\left(\frac{C-2H}{\beta\rho B\mu BI}+\frac{C-2H}{\beta\rho A\mu AI}\right) \quad (11)$$

The Influencing Mechanism of Original Revenue Ri and EHR Stock ri

The location of the saddle point T in Figure 2 determines the likelihood of the evolutionary direction of the game system. The position of saddle point T depends on the combined effect of multiple factors. However, according to the model solution results equation (11), it can be seen that these factors do not include the original revenue Ri and the stock of EHRs ri. This indicates that hospitals' original revenue and EHR stock have no substantial effect on the evolutionary direction of the gaming system. One reason is that the superior hospitals we conceptualize are not equivalent to large hospitals, and subordinate hospitals are not equivalent to small hospitals either. More importantly, incentives, penalties, and costs are calculated on the basis of "EHR resources per unit," not on the basis of the hospital's original revenue and total EHR.

XSL•FO
RenderX

Figure 2. Simulation results of influence effects based on MATLAB. (A) Effect of β on the evolutionary game system, (B) effect of ρi on the evolutionary game system, (C) effect of μi on the evolutionary game system, (D) effect of C on the evolutionary game system, (E) effect of I on the evolutionary game system, and (F) effect of *H* on the evolutionary game system.



The Influencing Mechanism of EHR Resource Complementarity (β)

Let SFTGKtake the derivative of β, we can get

∂SFTGK∂β=12C-2Hβ2ρBμBI+C-2Hβ2ρAμAI(12)

Since equation (12) is always greater than zero, it means that SFTGK is an increasing function of the EHR resource complementarity (β). The area of the region SFTGK in the upper right of the polyline ETG increases with β. With the increase of resource complementarity, the willingness of participating institutions of medical consortiums to use EHR will increase, which will help promote close cooperation between superior and subordinate hospitals, and thus promote the creation of integrated medical value by medical consortiums. On the contrary, if the EHR complementarity is low, then hospitals at all levels will be more willing to use their own generated EHR. Even if it is mandatory under the policy, hospitals are likely to only share their own EHR and will not take the initiative to use the EHR shared by other hospitals. This would go against the original intention and social expectations of EHR integration. The impact path of the EHR complementarity (β) on the co-opetition strategy of the superior and subordinate hospitals is reflected in the phase diagram, that is, as β increases, the saddle point T will keep moving toward the *O* (0, 0), which makes the upper right area of ETG keep increasing, which keeps increasing the probability of the superior and subordinate hospitals choosing the {cooperation, cooperation} strategy.

It is important to note that because β, ρi, μiand*I* have similar mathematical properties, meaning that these 4 parameters have the same mechanism of action on the influence of the co-opetition strategies of the superior and subordinate hospitals. That is to say, with the increase of the value of the 4 parameters of EHR resource complementarity (β), hospital's willingness (ρi) and ability (μi) to use EHR, the average income of unit EHR resources (*I*), the probability of the superior and subordinate hospitals choosing the {cooperation, cooperation} strategy will increase, and then the game system will evolve to the {1, 1} stable point.

The Influencing Mechanism of Unit EHR Resource Sharing Cost (C)

Let SFTGKtake the derivative of C, we can get

∂SFTGK∂β=-121βρBμBI+1βρAμAI(13)

Because equation (3) is constantly less than 0, meaning that SFTGK is a decreasing function of the unit resource sharing cost *C*, the area of the region SFTGK at the top right of the polyline ETG decreases with the increase of *C*. With the increase of unit resource sharing cost, the willingness of participating institutions of medical consortiums to use EHR will diminish, indicating that the higher the unit resource sharing cost *C*, the lower the willingness and probability of hospitals to participate in the EHR integration. On the contrary, if the unit resource sharing cost *C* is low, the motivation of hospitals at all levels to share and use EHRs will increase, which is a strong impetus to achieve the goal of EHR integration. The impact path of unit resource sharing cost *C* is reflected in the phase diagram, that is, with the increase of *C*, the saddle point *T* will continue to move to the point *K*, making the area of the upper right of the ETG continue to decrease, weakening the motivation of the superior and subordinate hospitals' choice of {cooperation, cooperation} strategy; With the decrease of *C*, the saddle point *T* will keep moving toward the point *O*, making the upper right area of ETG keep increasing, keep increasing the probability of the superior and subordinate hospitals choosing the {cooperation, cooperation} strategy.

XSL•FO
RenderX

The Influencing Mechanism of Unit EHR Resource Reward and Punishment Intensity (H)

Let SFTGKtake the derivative of H, we can get

$$\partial SFTGK\partial\beta=1\beta\rho B\mu BI+1\beta\rho A\mu AI \quad (14)$$

Since equation (14) is strictly positive, SFTGK becomes a monotonically increasing function of H, indicating that the area of region SFTGK located in the upper-right quadrant relative to the polyline ETG grows with H. With the increase of the unit resource reward and punishment, the probability of using EHR in participating institutions of medical consortiums will keep increasing, indicating that the greater the unit resource reward and punishment intensity *H* the greater the motivation of hospitals at all levels to participate in the EHR integration. On the contrary, if the reward and punishment of unit resources intensity *H* is low, the enthusiasm of hospitals at all levels to share and use EHR will be weakened, which will hinder the realization of the goal of EHR integration to a certain extent. The impact path of *H* on the co-opetition relationship between the superior and subordinate hospitals is reflected in the phase diagram, that is, with the increase of *H*, the saddle point *T* will continue to move toward the point *O*, making the upper right area of the ETG continue to increase, thus increasing the probability of the superior and subordinate hospitals to choose the {cooperation, cooperation} strategy; with the decrease of *H*, the saddle point *T* will continue to move toward the point *K*, making the upper right area of the ETG continue to decrease, and the probability of hospitals choosing the {competition, competition} strategy will increase.

MATLAB-Based Simulation of Influence Effects

In order to more intuitively describe the influence effect, and to verify the reasonableness and reliability of the analysis of the influence mechanism of the key factors, MATLAB R2018b was used to carry out numerical simulation and analysis of the differential equation (equation 9). When a parameter was simulated, other parameters ware taken as fixed values. The initial values of each parameter are set as follows: $rA=800, rB=500, \beta=0.4, \rho i=0.5, \mu i=0.5, I=20, H=2, C=5$, x and y are taken as 0.5. The simulation results are shown in Figure 2.

Effect of EHR Resource Complementarity (β)

From Figure 2A, the lower the EHR resource complementarity (β), the more hospitals tend to choose the competitive strategy. With the increasing complementarity of EHR resources, the strategy choice of superior and subordinate hospitals gradually shifts from competition to cooperation. And after the critical state, the evolutionary game system converges to {cooperative, cooperative} stable strategy at a faster speed. Complementarity refers to the nonoverlapping content of EHRs owned by each of the superior and subordinate hospitals. The more frequent the “up and down referrals” are, the greater the nonoverlap of EHR contents. Therefore, the medical consortiums should actively involve different types of hospitals in the region, and continuously improve the complementarity of EHR resources between superior and subordinate hospitals, while expanding the patient’s right to choose medical treatment.

Effect of Hospitals’ Willingness (ρi) and Ability (μi) to Use EHR

From Figure 2B and (C), it can be seen that the willingness and ability to use EHR of superior and subordinate hospitals have similar effects on the evolution of the evolutionary game system. With the increase of hospitals’ willingness or ability to use EHR, the probability of dynamic game system tending to {cooperation, cooperation} state will keep increasing, and vice versa. Both the willingness and ability to use the EHR are prerequisites for creating benefits after EHR integration. The stronger the willingness and ability, the stronger the hospital’s perception of use, the more confident it will be in the expected benefits, and the more motivated it will be to participate in EHR integration.

Effect of Unit EHR Shared Cost (*C*)

As can be seen from Figure 2D, when the other parameters are taken as fixed values, the probability of choosing the cooperation strategy for superior and subordinate hospitals gradually decreases as the unit EHR sharing cost *C* keeps increasing. When the unit EHR sharing cost *C* is less than the critical value, the probability of the superior and subordinate hospitals chooses to actively cooperate increases continuously with the decrease of *C*. At present, the technical standards and content formats of EHR, EMR and other systems used by different hospitals are likely to be different. To achieve EHR integration, hospitals may need to revamp system interfaces, format content, optimize management practices, and even staff more technical personnel. The increased difficulty of integration will lead to higher integration costs, which will objectively reduce the enthusiasm of hospitals to implement the integration of EHR, and ultimately lead to the evolution of the game system towards a stable strategy of competition.

Effect of Average Revenue of Unit EHR (*I*)

From Figure 2E, it can be seen that the evolutionary game system gradually converges to the {cooperative, cooperative} state as the average revenue of unit EHR (*I*) keeps increasing, when the other parameters are taken constant. When the average revenue of unit EHR (*I*) is below a critical value, both superior and subordinate hospitals choose a competitive strategy to ensure that their respective interests are maximized. Both the unit EHR sharing cost (*C*) and the unit EHR average benefit (*I*) are crucial to ensure the sustainable development and usage of EHR, and they have a decisive impact on the hospital’s revenue as well as rewards and penalties. Therefore, while promoting the EHR integration, medical consortiums must continuously develop and expand the channels for creating value and revenue, and adopt advanced technologies and measures to gradually reduce sharing costs.

Effect of Rewards and Punishments of Unit EHR (*H*)

It can be seen from Figure 2F that when the other parameters take fixed values, the probability that both sides of the game choose to cooperate gradually increases with the increase of the unit EHR rewards and punishments (*H*). In order to promote hospitals to actively share and use EHR, and to avoid opportunistic behaviors such as “free-riding,” reward and punishment mechanisms are often established to protect the

XSL•FO
RenderX

legitimate benefits of superior and subordinate hospitals. Compared with the unit EHR resource sharing cost (*C*) and the average benefit of unit EHR (*I*), the reward and punishment intensity (*H*) is the easiest to regulate and control. The evolutionary game system is more sensitive to *H*. It means that the strength of rewards and punishments will play a more obvious role in promoting the medical consortiums to achieve the goal of EHR integration.

Discussion

Principal Findings

To make both the superior and subordinate hospitals *A* and *B* choose the cooperation strategy and promote the smooth implementation of EHR integration in the medical consortiums, it is necessary to ensure that the initial probability of both sides of the game to choose the cooperation strategy is within the FTGK region (as shown in Figure 2). At this time, the probability requirements for the superior and subordinate hospitals *A* and *B* to choose cooperation are as follows:

$$x>x^{*}=C-2H\beta\rho B\mu BI;\ y>y^{*}=C-2H\beta\rho A\mu AI \quad (15)$$

The complementarity of EHR resources, hospitals' willingness and ability to use EHRs, and the average benefit of unit EHRs have a positive effect on the realization of EHR integration in medical consortiums. The input cost of unit EHR resource has a negative hindering effect on achieving EHR integration. The original revenue of the superior and subordinate hospitals *A* and *B*, and the stock of EHRs have no effect on the evolutionary direction of the game system. In other words, whether it is a superior hospital or a subordinate hospital, no matter how much or how little EHR that can be shared and used, there is no substantial impact on achieving the goal of the EHR integration in medical consortiums.

Designing a reasonable reward and punishment mechanism is great significance to promote medical consortiums to realize the EHR integration, especially in the initial stage. The integration progress can be accelerated if the rewards and punishments are more than half of the sharing cost. In the initial stage, rewards and punishments can be appropriately increased to speed up the progress of EHR integration. The goal of EHR integration can also be achieved when the rewards and punishments are less than half the sharing cost under the condition of $\beta\rho i\mu iI>C-2H$. Therefore, with the deepening of the EHR integration, the increasing willingness and ability of hospitals to use EHR, and the increasing efficiency of sharing EHR, government subsidies can be appropriately reduced or even eliminated according to the actual situation, thus reducing financial pressure.

Management Insights

To promote the enthusiasm of superior and subordinate hospitals to share and use EHR, and increase the probability of choosing cooperation strategies, the following aspects need to be emphasized. First, the medical consortiums should actively involve different levels and various types of medical institutions (general hospitals, maternal and child health care centers, specialized hospitals, rehabilitation hospitals, etc.) to improve the complementarity of EHR resources. Second, we should continuously improve the subjective willingness and ability of hospitals to use EHR through training, assistance, support, medical resources sinking and other ways. Third, the government should establish a reward and punishment system, optimize the operation mechanism and supervision mechanism of the medical consortiums, supervise and punish opportunistic behaviors such as "free-riding," and ensure that the goals of the hospital are consistent with those of the medical consortiums. Fourth, hospitals should continuously strengthen the construction of information infrastructure, actively improve the technical standards, content standards and sharing standards for the EHR construction [27], further improve the benefits of EHR, and reduce the investment cost of EHR sharing and use.

The decision-making groups are the actual game players of the hospital. The hospital's willingness to use EHR is fundamentally determined by the cognitive level of the decision-making groups. Therefore, the choice of hospital decision makers also has an important influence on the promotion of EHR integration. In the appointment of hospital decision makers, especially the head of the appointment, the cognitive pattern, medical values, social responsibility, dedication and commitment of the appointment candidate should be fully considered. At the same time, medical consortiums should adopt a wide publicity and mobilization, design and announce a reward and punishment system at the early stage of embarking on the integration of EHR to improve the motivation of hospital decision makers to adopt the cooperation strategy. Ensure that the policies and measures can receive positive response and support from the hospital's decision-making collective, to lay a solid foundation for the realization of the EHR integration.

Hospitals participating in the same consortium should have the same institutional constraints, both at superior hospitals and subordinate hospitals. There should be no differentiation in the system based on the size of the hospital. More importantly, in order to promote the active participation of both superior hospitals and subordinate hospitals in the integration of EHR, the design of incentive and penalty mechanisms and cost accounting should be based on the "unit EHR resources," rather than on the original revenue of the hospital and the total amount of EHR.

Research Limitations

In this paper, we take superior and subordinate hospitals within the medical consortium as the research object to explore the evolution mechanism of co-opetition strategies in the EHR integration. Therefore, we adopted a 2-party evolutionary game without considering the game scenario involving more stakeholders, such as the government, integrators, and patients. In addition, due to the lack of real data in practice, only the MATLAB simulation method was used to verify the model rationality, while failing to use empirical methods to test the accuracy of the model. With the continuous deepening of practice, it is necessary to continuously collect relevant data in the future and use empirical methods to further test the scientific validity of research findings.

XSL•FO
RenderX

Acknowledgments

This work was funded by National Natural Science Foundation of China [72164037] and Fundamental Research Program of Yunnan Province [202301AT070419], and Supported by the Foundation of Yunnan Key Laboratory of Service Computing [YNSC23105].

Data Availability

All data generated or analyzed during this study are included in this published article.

Authors' Contributions

ST contributed to model construction and writing-original draft. RJ managed formal analysis and writing-original draft. JY handled writing-review and editing. YC contributed to methodology, supervision, writing-review and editing.

Conflicts of Interest

None declared.

References

1. Qinling X, Min S, Pengqian F, et al. Key issues and pathway of the incentive and constraint mechanism of medical alliances in China. Chinese Journal of Hospital Administration 2017;33(12):889-892. [doi: 10.3760/cma.j.issn.1000-6672.2017.12.003]
2. National Health Commission of China, National Administration of Traditional Chinese Medicine of China. Notice on the administrative measures for medical consortium (for trial implementation) [EB/OL]. 2020 Jul 9. URL: http://www.gov.cn/zhengce/zhengceku/2020-07/18/content_5528009.htm [accessed 2025-02-03]
3. Brandenburger AM, Nalebuff BJ. Co-Opetition: Doubleday; 1996.
4. Yanyu F, Yunya X. Research on the competition and cooperation process between network-connected enterprises under business model innovation. Management and Administration 2022;8:57-64. [doi: 10.16517/j.cnki.cn12-1034/f.2022.08.007]
5. Pu H, Liang G, Jiaming Z. Research on willingness to share medical data from perspective of privacy protection——based on tripartite evolutionary game analysis. Journal of Modern Information 2021;41(3):148-158. [doi: 10.3969/j.issn.1008-0821.2021.03.015]
6. Jiang R, Han S, Yu Y, Ding W. An access control model for medical big data based on clustering and risk. Inf Sci (Ny) 2023 Apr;621:691-707. [doi: 10.1016/j.ins.2022.11.102]
7. Zhibin J, Na G, Na L, Liping Z, Rui M. Industrial Engineering-Based Systematic Management of Healthcare: Science Press; 2021.
8. Tian S, Chen Y. Vertical integration of electronic health records in medical consortiums: dynamic modeling approach based on the evolutionary game theory. JMIR Serious Games 2023 Mar 6;11:e41528. [doi: 10.2196/41528] [Medline: 36877574]
9. Li Q, Pi B, Feng M, Kurths J. Open data in the digital economy: an evolutionary game theory perspective. IEEE Trans Comput Soc Syst 2024;11(3):3780-3791. [doi: 10.1109/TCSS.2023.3324087]
10. Feng M, Pi B, Deng LJ, Kurths J. An evolutionary game with the game transitions based on the Markov process. IEEE Trans Syst Man Cybern, Syst 2024;54(1):609-621. [doi: 10.1109/TSMC.2023.3315963]
11. Junping Q, Zhongyang X, Xihui C. Research on user privacy disclosure behavior in online health communities based on tripartite evolutionary game. Information Studies: Theory & Application 2023;46(1):24-36. [doi: 10.16353/j.cnki.1000-7490.2023.01.004]
12. Yinghua S, Xiaoyan S, Zhe W, Hongqian X. Research on quality assurance strategy of emergency medical materials based on evolutionary game. Journal of Safety Science and Technology 2022;18(5). [doi: 10.11731/j.issn.1673-193x.2022.05.005]
13. Benhai J. Evolutionary game analysis of Internet hospital choice behavior of hospitals of different sizes from the perspective of medical consortium. Med Soc (Berkeley) 2022;35(3):1-5. [doi: 10.13723/j.yxysh.2022.03.001]
14. Fengjiao C, Dehai L. Evolutionary path analysis of multi-channel epidemic information release of major infectious diseases. Chinese Journal of Management Science 2024;32(4):237-249. [doi: 10.16381/j.cnki.issn1003-207x.2021.0793]
15. Shuhui S, Qiang S. Evolutionary game analysis of graded diagnosis and treatment strategies affected by patients' emotions under Regional Medical Association. Chinese Journal of Management Science 2023;31(11):288-299. [doi: 10.16381/j.cnki.issn1003-207x.2020.1886]
16. Feng L, Limeng Y, Yajie W, Zexin J, Qian W. Evolutionary game and simulation analysis of two-way referral mechanism based on DRGs medical insurance payment method. Industrial Engineering and Management 2022;27(4):159-169. [doi: 10.19495/j.cnki.1007-5429.2022.04.019]
17. Pi B, Feng M, Deng LJ. A memory-based spatial evolutionary game with the dynamic interaction between learners and profiteers. Chaos 2024 Jun 1;34(6):12. [doi: 10.1063/5.0215761] [Medline: 38848270]
18. Anfeng X, Yu C, Yue L. Research on failed knowledge sharing mechanism of big data industry alliance members based on evolutionary game. Frontiers of Science and Technology of Engineering Management 2022;41(2):77-83. [doi: 10.11847/fj.41.2.77]

XSL•FO
RenderX

19. Haitao Z, Siyang S, Liang R, Zezhong L. Evolutionary game on business network information ecology chain based on co-optition. Information Studies: Theory & Application 2018;41(10):60-65. [doi: 10.16353/j.cnki.1000-7490.2018.10.010]
20. Shenghu T. Research on the dynamic mechanism of vertical integration of electronic health records within a medical association. : Kunming University of Science and Technology, Doctoral Dissertation; 2023. [doi: 10.27200/d.cnki.gkmlu.2023.002498]
21. LeTourneau B. Co-opetition: an alternative to competition. J Healthc Manag 2004;49(2):81-83. [doi: 10.1097/00115514-200403000-00003] [Medline: 15074116]
22. Dengbing Z. Analysis of game elements based on agents. Mathematics in Practice and Theory 2013;43(14):252-257.
23. Qiang Z, Liya W, Na G, Zhibin J. Evolutionary game analysis of medical information sharing based on the government regulation. Operations Research and Management Science 2020;29(1):23-31. [doi: 10.12005/orms.2020.0004]
24. Jiang LL, Chen Z, Perc M, Wang Z, Kurths J, Moreno Y. Deterrence through punishment can resolve collective risk dilemmas in carbon emission games. Chaos 2023 Apr 1;33(4):043127. [doi: 10.1063/5.0147226] [Medline: 37097939]
25. Friedman D. Evolutionary games in economics. Econometrica 1991 May;59(3):637. [doi: 10.2307/2938222]
26. Kai S, Wen G. Research on the stability of high-tech enterprise innovation alliance from the perspective of co-opetition. Chinese Journal of Management Science 2021;29(3):219-229. [doi: 10.16381/j.cnki.issn1003-207x.2018.1674]
27. Tian SH, Chen Y, Bai TZ. Key influencing factors of vertical integration of electronic health records in medical consortiums. Int J Med Inform 2023 Feb;170:104959. [doi: 10.1016/j.ijmedinf.2022.104959] [Medline: 36542900]

Abbreviations

EHR: electronic health record

Edited by A Benis; submitted 03.01.25; peer-reviewed by M Feng, YL Sun; revised version received 26.05.25; accepted 27.05.25; published 14.08.25.

Please cite as:
Tian S, Jiang R, Yao J, Chen Y
Co-Opetition Strategies of Superior and Subordinate Hospitals for Integration of Electronic Health Records Within the Medical Consortiums in China Based on Two-Party Evolutionary Game Theory: Mixed Methods Study
JMIR Med Inform 2025;13:e70866
URL: https://medinform.jmir.org/2025/1/e70866
doi:10.2196/70866

© Shenghu Tian, Rong Jiang, Jianfeng Yao, Yu Chen. Originally published in JMIR Medical Informatics (https://medinform.jmir.org), 14.8.2025. This is an open-access article distributed under the terms of the Creative Commons Attribution License (https://creativecommons.org/licenses/by/4.0/), which permits unrestricted use, distribution, and reproduction in any medium, provided the original work, first published in JMIR Medical Informatics, is properly cited. The complete bibliographic information, a link to the original publication on https://medinform.jmir.org/, as well as this copyright and license information must be included.

XSL•FO
RenderX

Bridging Global Frameworks and Local Practice: Quantitative Evaluation of Electronic Health Record Safety in Kuwait's Public Hospitals

Anwar AlHussainan[1]; Dari Alhuwail[1,2], PhD

[1]Information Science Department, College of Life Sciences, Kuwait University, Sabah AlSalem University City, P.O. Box 5969, Kuwait City, Kuwait
[2]Health Informatics Unit, Dasman Diabetes Institute, Kuwait City, Kuwait

Corresponding Author:
Dari Alhuwail, PhD
Information Science Department, College of Life Sciences, Kuwait University, Sabah AlSalem University City, P.O. Box 5969, Kuwait City, Kuwait

Abstract

Background: Electronic health records (EHRs) play a critical role in today's health care by enhancing data management, improving workflows, and supporting clinical decision-making. However, EHR implementation introduces technical and clinical challenges that can compromise patient safety. The Safety Assurance Factors for Electronic Health Record Resilience guides, developed by the Office of the National Coordinator for Health Information Technology, provide a structured framework for evaluating and optimizing EHR safety practices. Despite extensive research on EHR safety in developed countries, little is known about its implementation in regions with differing health care systems, such as Kuwait.

Objective: This study aims to examine the EHR safety across hospitals in the State of Kuwait via (1) conducting a proactive risk assessment examining current safety practices and (2) proposing recommendations to improve EHR safety practices.

Methods: A quantitative approach was used to evaluate EHR safety practices in 6 public hospitals. Multidisciplinary teams completed the Safety Assurance Factors for Electronic Health Record Resilience self-assessment questionnaire, scoring their implementation status of 165 recommended practices as "fully," "partially," or "not" implemented across 9 Safety Assurance Factors for Electronic Health Record Resilience guides. Data were analyzed to calculate the percentage of "fully implemented" recommended practices for each hospital, guide, and EHR safety domain. Standard deviations were calculated to assess data variability, and comparative analysis was conducted to identify implementation patterns.

Results: The findings revealed significant variability in the implementation of recommended safety practices, with an average of 53% rated as "fully implemented" across hospitals. Infrastructure-focused guides, such as system configuration (77%) and system interfaces (80%), had the highest implementation rates, while clinical process guides, such as clinician communication (25%), scored the lowest. Among the 9 guides, 16 recommended practices were unanimously rated as "fully implemented," while 8 were predominantly rated as "not implemented." The high-priority guide showed notable variability, with implementation rates ranging from 17% to 89% across hospitals. Hospitals with longer EHR adoption periods tended to perform better, though hospital size and implementation type showed inconsistent effects on safety practices scores.

Conclusions: The study highlights variability in EHR safety practice implementation across Kuwait's public hospitals, with stronger performance in technical domains and gaps in clinical processes. By applying the Safety Assurance Factors for EHR Resilience guides in a non-US context, the study offers a foundational understanding of EHR safety implementation in Kuwait's public health care system. Given the study's limited scope and reliance on self-reported data, findings should be interpreted with caution. Future research should adopt broader sampling and mixed methods approaches to validate these results and inform the development of context-specific strategies to enhance EHR safety and patient outcomes.

(JMIR Med Inform 2025;13:e70782) doi:10.2196/70782

KEYWORDS

electronic health records; safety assurance factors for electronic health record resilience; patient safety; risk assessment; electronic health record safety practices; public hospitals

Introduction

Health IT is defined as "the application of information processing involving both computer hardware and software that deals with the storage, retrieval, sharing, and use of healthcare information, data, and knowledge for communication and decision making" to improve and maintain health care quality and patient safety [1,2]. Today, many hospitals rely on robust

XSL•FO
RenderX

health IT solutions in their clinical practice, one of which is electronic health records (EHRs) [1,3].

In the United States, 78% of office-based physicians use EHRs in their medical practice [4-6]. EHRs include a set of documented information related to patient health care, such as demographics, progress notes, problems, medications, vital signs, medical history, immunizations, laboratory data, and imaging reports [7,8]. EHRs can also integrate with other advanced systems and features like clinical decision support (DS) systems, computerized physician order entry, health information exchange, and safety alerts [8,9].

With all these data, systems, and features, EHRs can support physicians in collecting medical history easily, providing better health care, and maintaining patient safety compared to relying on paper-based records [8]. Thus, EHRs contribute to improved data tracking and follow-up over time, which in turn helps guide health care providers (HCPs) in decision-making [8,10]. Moreover, the secondary utilization of EHRs offers the potential to transform existing data into actionable insights through health research, public health surveillance, quality improvement initiatives, and safety monitoring [11-13]. These applications are critical for identifying and addressing patient safety challenges within health care processes and for improving the quality of patient care [11,14].

The World Health Organization estimates that 1 in every 10 patients in developed countries is harmed while receiving health care in hospitals. Medical errors, often associated with diagnosis, prescription, and medication use [15], can be broadly categorized into two types: (1) adverse events that directly affect the patient, resulting in minor or severe injury or death, and (2) near misses that are intercepted before reaching the patient in unsafe conditions that elevate the risk of a future safety incident. These errors can lead to significant consequences, including fatalities, disabilities, poor health outcomes, increased health care costs, and legal complications [16-19].

A recent study in Kuwait found that approximately 60% of the frequency of medical errors ranged from incidences of prolonged hospital stays, adverse events, life-threatening complications, and fatalities. The causes of these medical errors included high workload, the lack of EHRs, HCPs' non-compliance with safety guidelines, untrained or inexperienced administrative staff, and poor communication with patients and between HCPs [20]. While EHRs are designed to reduce the workload of HCPs and improve practice efficiency, cost, and error reduction, some studies reveal that implementing and using EHRs increases the work burden on HCPs [8,16,21,22].

In the United States, many physicians reported spending twice their working hours on EHR-related tasks, with some dedicating an additional 1-2 hours after work [8,23]. Consequently, this increased workload may elevate the risk of medical errors, ultimately compromising health care quality and patient safety [8,16,20,24]. Achieving the safe and effective use of EHRs presents several challenges, including usability issues, concerns about data integrity, safety risks, and the need for proper and ongoing system maintenance [10,25-29].

Evidence suggests that EHRs have demonstrated potential in reducing medication errors and adverse events and improving care quality [30-32]. In Kuwait, while health care professionals have shown acceptance of EHR adoption and expressed positive expectations, most hospitals remain in the early stages of implementation [33,34]. However, the adoption of EHRs introduces new risks that can adversely impact patient safety. These risks often stem from challenges related to system design, implementation, and usage. Specific issues include system downtime, poor usability, data entry errors, inadequate implementation processes, weak security measures, and malpractice by EHR users [35-37]. Addressing these risks is crucial to ensuring the safe and effective utilization of EHRs in health care settings [3,35].

Given that many health care organizations and HCPs prioritize patient safety, conducting regular assessments of EHR safety becomes essential [38]. EHR safety refers to the strategies and practices that ensure EHRs are used safely, securely, and effectively. These measures protect patients by preventing errors, harm, or any compromise to the quality of care [3,39-41]. The Office of the National Coordinator for Health Information Technology published a report highlighting key issues related to EHR safety and called for the development of proactive risk assessment tools [42].

One such tool is the Safety Assurance Factors for EHR Resilience (SAFER) guides, which provide a proactive risk evaluation framework that contributes to ensuring EHR safety, thereby supporting overall patient safety [42,43]. Furthermore, it is imperative to note that ensuring EHR safety requires a collaborative approach, with shared responsibilities between clinical and technical experts to optimize the use of EHRs [44].

In the State of Kuwait, the health care system is comprised of 2 main sectors: public and private. The public sector provides about 70% of health care services for citizens and residents, offering primary, secondary, and tertiary care within 6 health regions under the Ministry of Health [45,46]. Primary health care services are provided by polyclinics and health care centers located in residential areas. Notably, these centers and polyclinics offer initial diagnosis and treatment for patients, coordinating referrals to specialists in secondary and tertiary care if necessary. In contrast, secondary health care services are provided by 6 general hospitals distributed across the 6 governorates in Kuwait, while specialized health care services are offered by various specialized hospitals and centers [46-48].

This empirical study aims to conduct a proactive risk assessment examining the current EHR safety practices across public hospitals in Kuwait, with the goal of helping optimize EHR safety practices. To our knowledge, no prior studies have explored this topic in Kuwait or in comparable health care systems.

Methods

Ethical Considerations

This study was conducted in accordance with the Declaration of Helsinki, and the protocol was approved by the Standing Committee for Coordination of Health and Medical Research

XSL•FO
RenderX

in the Ministry of Health in the State of Kuwait (1615/2021). All participants voluntarily signed the informed consent form before participating in the study procedures (Multimedia Appendix 1). Participants in the study were not paid for their participation. To maintain confidentiality and protect privacy, the names of the participating hospitals and health care staff have been anonymized throughout the study.

Data Collection

This study used a quantitative approach to evaluate the current EHR safety practices among public hospitals in the State of Kuwait using the SAFER guides. [43,49,50]. Hospitals were selected based on the presence of EHR systems, whether fully or partially implemented. Initially, 6 public secondary care hospitals were targeted; however, 1 was excluded due to the absence of an EHR system. To maintain the sample size and ensure data relevance, a tertiary care hospital from the same health region was included as a substitute. The participating hospitals were targeted to complete the SAFER self-assessment questionnaire, rating their implementation status as "fully," "partially," or "not" implemented (Multimedia Appendix 2).

Each participating hospital was required to assemble a multidisciplinary team of health care staff, following a similar approach to a previous study [49]. A letter was sent to the hospital administration requesting the formation of a multidisciplinary team to complete the questionnaire or to designate an authorized and experienced individual who could assemble an appropriate team to evaluate the recommended practices using the SAFER guides, ensuring a comprehensive approach to patient care. This team typically included physicians, nurses, allied health professionals, and other specialists relevant to the study objectives.

Prior to data collection, the researchers conducted training sessions on the SAFER guides for the hospital teams, providing guidance and support to facilitate the completion of the questionnaires. During these sessions, a PowerPoint presentation was used to explain the purpose of the SAFER guides and the mechanism for completing the assessment. Additionally, researchers provided their contact information for assistance and distributed QR codes linking to instructional videos, the official SAFER guides website, a demographic information collection form for participating hospitals, and an Excel spreadsheet template of the SAFER questionnaire for data entry to ensure ease of use and consistency [49].

The SAFER guides, introduced in 2014 by the Office of the National Coordinator for Health Information Technology, were designed to support health care organizations in conducting proactive risk assessments of their EHR practices, with the goal of enhancing and advancing EHR safety. The SAFER guides include 165 recommended practices related to EHR safety, distributed across 9 guides [50]. Of these, 8 guides comprise 147 unique recommended practices, while the ninth, the high priority guide, consolidates 18 of the most critical recommended practices from the other guides.

In previous studies [49,51], the total number of recommendations was reported as 140 because the high priority guide was excluded from the count. Additionally, an audit and comparison of the official SAFER guides website with prior studies concluded that 7 recommendations were omitted due to thematic similarity with those already included in the high priority guide, which did not significantly impact SAFER guide scores. However, this study considers all 165 recommendations [50] to provide a more comprehensive assessment of EHR safety practices.

Overall, the SAFER guides are organized into three primary areas: (1) foundational guides, (2) infrastructure guides, and (3) clinical process guides. Foundational guides focus on high-priority practices and organizational responsibilities. Infrastructure guides involve contingency planning, system configuration, and system interfaces. Clinical process guides focus on areas such as patient identification, computerized provider order entry (CPOE) with DS, test results reporting and follow-up, and clinician communication. Each guide includes between 12 and 29 recommended practices, structured into 3 domains: Safe Health IT, Using Health IT Safely, and Using Health IT to Monitor and Improve Safety [42,43,49,52].

Data Analysis

Following a similar analysis conducted in a previous study [49], the collected data were analyzed as follows: (1) calculated the percentage of "fully implemented" recommended practices across all 9 guides for each hospital, along with the standard deviation to measure data dispersion; (2) determined the mean percentage of "fully implemented" recommended practices across all participating hospitals for each guide; (3) assessed the percentage of "fully implemented" recommended practices across all participating hospitals for each EHR safety-related domain; and (4) evaluated the percentage of "partially implemented" and "not implemented" recommended practices in the high priority guide for each participating hospital.

Results

Demographic Attributes of Participating Hospitals

In total, 6 public hospitals participated in the study by completing the SAFER self-assessment questionnaire: 5 hospitals providing secondary health care services and 1 hospital providing specialized tertiary health care services. The participating hospitals had varied characteristics with respect to size, EHR adoption experience, and EHR implementation type (hospital demographic information is shown in Table 1).

XSL•FO
RenderX

Table . Demographics of participating hospitals.

Participated hospitals (N=6)	Numbers of hospitals
Hospital type	
Secondary health care	5
Tertiary health care	1
Hospital size	
Small	1
Medium	3
Large	2
EHR adoption year	
2006	1
2008	1
2015	2
2018	1
2019	1
EHR implementation type	
Outsourced developed	5
In-house developed	1

Hospitals were classified by size based on the number of beds and the total number of health care staff, including clinical, technical, and administrative staff. Small hospitals had less than 200 beds and fewer than 3000 employees (n=1), medium hospitals had 200-799 beds and 3000-6500 employees (n=3), while large hospitals had 800 or more beds and over 6500 employees (n=2) [45].

The participating hospitals also differed in their EHR adoption experience, ranging from 3 to 16 years, with initial implementations occurring between 2006 and 2019. Their approaches to EHR implementation varied, with 5 hospitals outsourcing the process through contracts with private companies for system deployment and support. Of these, 3 hospitals used the same vendor, while the other 2 engaged different vendors. In contrast, 1 hospital implemented its EHR system in-house, relying on local support from Ministry of Health developers.

A total of 38 health care staff members, forming multidisciplinary teams, participated in completing the SAFER guides questionnaire. Of the participants, 20 were female and 18 were male. While 2 hospitals assembled multidisciplinary teams of 6 members each, the remaining 4 hospitals formed teams of 7 members each (participant demographic information is shown in Table 2).

XSL•FO
RenderX

Table . Demographics of health care staff participants across the 6 hospitals.

Health care staff (N=38)	H1 (n=7)	H2 (n=7)	H3 (n=6)	H4 (n=6)	H5 (n=6)	H6 (n=6)
Age group						
24 - 34	—[a]	2	—	1	2	4
35 - 45	4	5	3	4	3	2
46 - 56	3	—	2	1	1	—
57 - 67	—	—	1	—	—	—
Health care staff sections						
Information systems	1	3	1	1	1	1
Medical records andstatisticsc	1	1	1	1	2	2
Pharmacy	1	1	1	—	1	1
Nursing	2	—	—	—	—	—
Physicians	2	1	1	2	1	2
Laboratory	—	1	1	1	1	—
Radiology	—	—	1	1	—	—
Years of experience						
1 - 11	1	5	1	1	2	4
12 - 23	5	2	2	5	3	2
24 - 35	1	—	3	—	1	—
Gender						
Female (n=20)	4	4	3	3	3	3
Male (n=18)	3	3	3	3	3	3

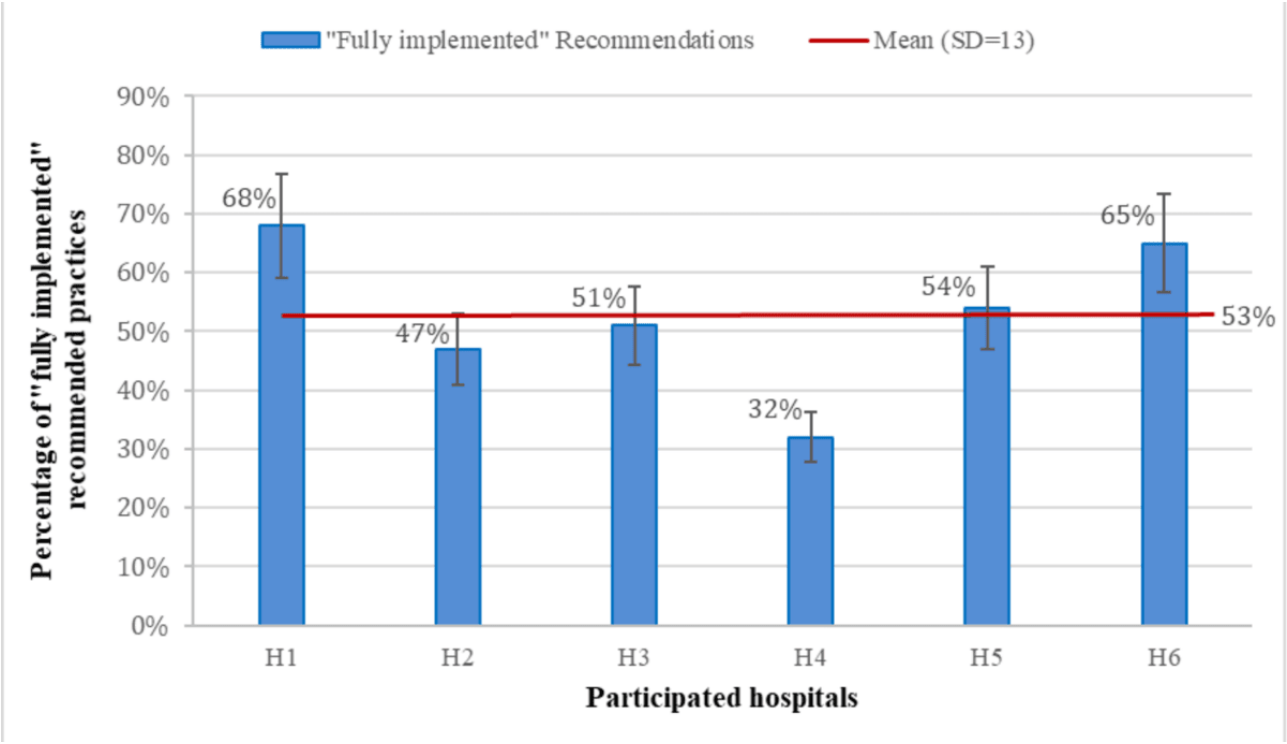
[a]Not applicable.

SAFER Guide's Responses

The percentage of "fully implemented" recommended practices across the 9 guides for each hospital, with a mean of 53% (SD 13), is shown in Figure 1. The highest percentage was 68% achieved by H1, while the lowest percentage was 32% achieved by H4.

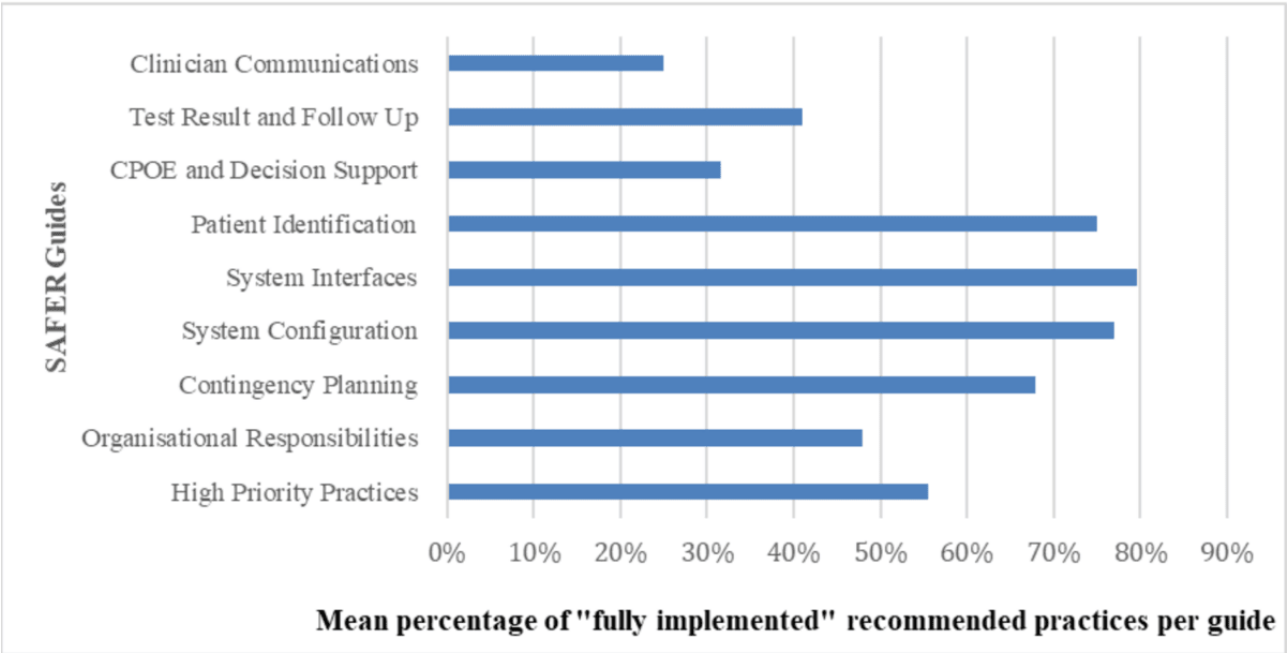
XSL•FO
RenderX

Figure 1. Percentage of "fully implemented" recommended practices across the 9 SAFER (Safety Assurance Factors for Electronic Health Record Resilience) guides for each hospital.



The mean percentage of "fully implemented" recommended practices of SAFER guides across the 6 hospitals is shown in Figure 2. The system interfaces guide, with 18 recommended practices, achieved 80% and ranked the highest, while the clinician communication guide, with 12 recommended practices, reached 25% and ranked the lowest. Among the 3 SAFER guides broad classifications, infrastructure guides (contingency planning [68%], system configuration [77%], and system interfaces [80%]) achieved the highest mean percentage of "fully implemented" recommended practices. Hence, foundational guides ranked second with an average of 52%, while clinical process guides ranked third with an average of 43%.

Figure 2. Mean percentage of "fully implemented" recommended practices of SAFER (Safety Assurance Factors for Electronic Health Record Resilience) guides across the 6 hospitals.



Furthermore, the safe Health IT domain, which comprised 54 recommended practices, achieved 66% of "fully implemented" recommended practices across the 6 hospitals, exceeding the Using Health IT to Monitor and Improve Safety domain, which comprised 23 recommended practices (54%), and Using Health IT Safely domain, which included 88 recommended practices (45%).

XSL•FO
RenderX

Regarding high-priority guide recommended practices, the percentage of implementation status for each hospital is shown in Table 3. The percentage of "fully implemented" recommended practices ranged from 17 to 89%, with H6 achieving the highest and H2 the lowest. While the percentage of "partially implemented" recommended practices ranged from 11 to 83%, only 2 hospitals had recommended practices rated as "not implemented": H3 (22%) and H5 (11%).

Table . Percentage of implementation status for the high priority guide recommended practices for each hospital.

Implementation status	H1	H2	H3	H4	H5	H6
"Fully implemented"	78%	17%	67%	39%	44%	89%
"Partially implemented"	22%	83%	11%	61%	44%	11%
"Not implemented"	0%	0%	22%	0%	11%	0%

Examining hospital responses revealed that 16 recommended practices were unanimously rated as "fully implemented." These recommended practices were distributed across 6 SAFER guides: high priority; contingency planning; system configuration; system interfaces; patient identification; and test results and follow-up. The system interfaces guide contained the highest number of recommended practices (n=5). On the other hand, 8 recommended practices were predominantly rated as "not implemented" by most hospitals. These "not implemented" recommended practices were drawn from 3 SAFER guides: CPOE/DS; test results and follow-up; and clinical communications, with the CPOE/DS and test results and follow-up guides each containing the highest number (3 recommended practices). Both "fully implemented" and "not implemented" recommended practices are provided in Tables 4 and 5.

XSL•FO
RenderX

Table . SAFER (Safety Assurance Factors for EHR[a] Resilience) guide recommended practices were rated "fully implemented" by all 6 hospitals.

SAFER guide	SAFER recommendation
Total of 16 "fully implemented" recommended practices	
High priority	• "Information required to accurately identify the patient is clearly displayed on screens and printouts."
Contingency planning	• "Paper forms are available to replace key EHR functions during downtimes." • "Patient data and software application configurations critical to the organization's operations are backed up." • "Policies and procedures are in place to ensure accurate patient identification when preparing for, during, and after downtimes."
System configuration	• "There are an adequate number of EHR access points in all clinical areas." • "The EHR is hosted safely in a physically and electronically secure manner." • "System hardware and software required to run the EHR (eg, operating system) and their modifications are tested individually and as-installed before go-live and are closely monitored after go-live."
System interfaces	• "System-to-system interfaces are properly configured and tested to ensure that both coded and free-text data elements are transmitted without loss of or changes to information content." • "Changes to hardware or software on either side of the interface are tested before and monitored after go-live." • "The operational status of the system interface is clear to its users with regard to clinical use, such as knowing when the interface cannot transmit or receive messages, alerts, or crucial information." • "The organization monitors the performance and use of system interfaces regularly, including monitoring the interface error log and the volume of transactions over the interface." • "When interface errors are detected, they are reported, fixed, and used to construct new test cases to improve the interface testing."
Patient identification	• "Patient names on adjacent lines in the EHR display are visually distinct." • "Medical record numbers incorporate a "check digit" to help prevent data entry errors." • "Patients are registered using a centralized, common database using standardized procedures."
Test result and follow-up	• "After system changes in components or applications related to CPOE and diagnostic services, the data and data presentation are reviewed to ensure accuracy and completeness."

[a]EHR: electronic health record.

XSL•FO
RenderX

Table . SAFER (Safety Assurance Factors for EHR[a] Resilience) guides recommended practices were most likely rated "not implemented" at the 6 hospitals.

SAFER guide	SAFER recommendation
Total of 8 "not implemented" recommended practices	
CPOE and DS[b]	• "Clinicians are required to re-enter their password, or a unique PIN, to "sign" (authenticate) an order." • "Users can access authoritative clinical reference materials directly from the EHR, including organization-specific information when available." • "Additional safeguards, such as double check by a second specialist, are implemented in the EHR before high-risk medications are prescribed."
Test result and follow-up	• "There is an EHR-based process for clinicians to either assign surrogates for reviewing notifications or enable surrogates to look at the principal clinicians' inboxes." • "There are mechanisms to forward results and results notifications from one clinician to another." • "The EHR has the capability for the clinician to set reminders for themselves and other responsible clinical staff for future tasks to facilitate test result follow-up."
Clinician communications	• "Electronic message systems include the capability to indicate the urgency of messages." • "The EHR displays time-sensitive and time-critical information more prominently than less urgent information."

[a]EHR: electronic health record.

[b]CPOE and DS: computerized provider order entry with decision support.

Discussion

Principal Findings

EHR implementation provides a valuable opportunity to optimize health care safety, services, procedures, processes, and outcomes [53]. The conducted assessment helps health care staff engage appropriately across various specialties and tasks to deliver better EHR safety, considering all relevant aspects. Data from the 6 hospitals were analyzed to evaluate the extent to which they have implemented the best recommended safety practices related to EHR adoption and usage, using the SAFER guides.

SAFER Scores Variability

The percentage of "fully implemented" recommended practices from the SAFER guides across participating hospitals showed significant variability, with an average implementation rate of 53%, as illustrated in Figure 1. For instance, the implementation rates ranged from 4% to 92% for the organizational responsibilities guide, 23% to 100% for the system configuration, and 0% to 58% for the clinician communication guide. While previous studies mention that hospital size, years of EHR adoption, and type of EHR implementation affect EHR safety [54,55], the findings indicate an imperfect relationship between these factors (hospital demographics; Table 1) and the scores of "fully implemented" SAFER-recommended practices, with no clear and consistent direct or inverse relationship.

Hospitals with longer EHR adoption periods generally perform better, but variations in safety outcomes suggest that experience alone does not fully determine EHR safety. Similarly, in this study, hospital size showed no clear correlation with SAFER scores, as medium and large hospitals exhibit differing results likely influenced by other factors. The type of EHR implementation (in-house or outsourced) also did not directly predict SAFER scores, as both types displayed wide variations in implementation levels.

Accordingly, this variability highlights the significance of hospital-specific factors in determining EHR safety effectiveness. More influential than demographic characteristics alone, these factors include available resources (human and financial), safety culture, technical capabilities, workflow integration, quality of staff training, implementation strategies, and leadership commitment. These critical elements significantly impact EHR safety outcomes and the extent to which EHR safety measures and recommended practices are implemented [54,56,57].

Infrastructure and Technical Focus

Out of the 165 recommended practices in the SAFER guides, only 16 (10%) were "fully implemented" by the participating hospitals. The researchers observed that all participating hospitals focus more on infrastructure and technical aspects across guides or domains. The implementation rate for infrastructure guides gets a higher mean percentage (75%), specifically system configuration (77%) and system interfaces (80%). In contrast, the clinical process guides had a much lower implementation rate of only 43%.

Additionally, the percentage of implemented recommended practices varied considerably across each different EHR-related patient safety domain. Domain 2—Using Health IT Safely,

XSL•FO
RenderX

which focuses on ensuring the effective and safe utilization of EHRs by health care staff and patients—had an implementation rate of only 45%. Meanwhile, Domain 1—Safe Health IT, which emphasizes the technical protection aspects of EHR structure and functionality, reached 66%. Hospitals tend to be technically oriented for several reasons. Technical aspects, such as systems configuration, interface management, and interoperability, are fundamental to EHR functionality [58-60]. A secure, reliable, and robust technical setup is essential for the health care system to prevent failures and errors that could disrupt clinical care. Studies have emphasized the importance of solid testing environments in determining safety and usability issues during the system implementation phases [61-63].

Furthermore, EHR vendors can influence the hospitals' technical orientation. Many hospitals rely on external technology vendors to implement, develop, and support their EHR systems [64,65]. However, these vendors often lack a deep understanding of the clinical intricacies of specific hospitals [66]. Instead, they prioritize technical capabilities and compliance standards—such as security, databases, interoperability, and system function and updates—that are directly manageable and required for system credentials and regulatory compliance with governmental regulations [67-69].

Moreover, hospitals may find that technical issues (eg, data security, usability, and privacy) are easier to address than clinical process issues (eg, clinician communication and workflow integration), particularly in the early test cases [70,71]. Technical adjustments are generally more straightforward to standardize, implement, measure, and audit, whereas clinical workflows are inherently more complex [72,73].

Lastly, there is a common misconception that technical stability, including a well-functioning EHR, guarantees health care safety [27,68]. Many hospitals assume that if their EHR system is secure, interoperable, and compliant, it will inherently be safe for health care staff use and patients [23,61,74,75]. Thus, hospitals prioritize technical improvements to avoid system failures and mitigate risks. However, these efforts alone cannot address other critical issues such as health care staff acceptance issues, communication breakdowns, and workflow discrepancies, which often pose more significant risks to patient safety [76-79]. Therefore, achieving EHR safety requires a comprehensive approach that addresses both technical and clinical process factors [80].

These factors contribute to the hospital's tendency toward technical over clinical processes for EHR safety, which can lead to neglecting the significant effects on clinical practices and patient care. Addressing both aspects of the health care system is necessary for a robust and effective safety setting [80,81].

Clinician Communication Challenges

Communication between health care staff, particularly clinicians, is a fundamental aspect of clinical processes encompassing critical tasks and decisions. Communication breakdowns can directly affect patient safety, leading to medical errors and patient harm [50,82]. The implementation rate for the clinician communication guide's recommended practices was the lowest across the hospitals, ranging from 0% to 58%. This guide often receives the lowest scores in EHR safety evaluations due to several factors. First, there is a lack of robust integration features for communication tools. For instance, disjointed messaging systems lead clinicians to rely on multiple platforms or external solutions, and fragmented data through EHR's various sections make it difficult to reach, particularly during clinical discussion communications [83].

Additionally, usability challenges, such as poorly designed interfaces and alert fatigue, impact the efficiency of clinician communication. Interfaces may include many steps or unclear options, making it difficult for clinicians to follow. An overabundance of notifications or irrelevant alerts may lead to ignored or missed important communications [25,84]. Moreover, inconsistent communication and time constraints lead to workflow misalignment, creating barriers to facilitating clinical workflows. EHRs are mostly designed for individual duties, prioritizing their development (eg, data or order entry and individual decision-making) rather than promoting collaborative communications between health care team members. EHR communication tools can increase clinicians' burden, conflicting with their time-sensitive workflow [85,86].

Furthermore, health care staff attitudes and knowledge gaps, such as a lack of awareness and resistance to change, contribute to communication challenges. Clinicians may not have adequate awareness of using EHRs due to insufficient onboarding or training in EHR communication features. Many clinicians find that the traditional methods (eg, phone calls and face-to-face discussions) are easier and more effective than using EHRs [85,87]. Lastly, interdepartmental and interdisciplinary communication processes face significant obstacles. The lack of communication tools that meet various requirements for multidisciplinary teams hinders effective communication, especially among nonphysician or specialist staff. Besides, data may not be easily accessible or shareable across systems or roles within the same hospital [87]. These challenges should be considered, addressed, and improved to integrate seamlessly and effectively into clinical workflows. Developing clinician communications within EHRs requires simplified interfaces, adequate integration of collaborative tools, practical training, and adjustable workflow regulations [85,87].

Comparison With Prior Work

Previous studies have applied SAFER guides as a methodology. A study evaluating 8 health care organizations in the United States found that, on average, only 18% of the 140 unique safety recommendations were fully implemented [49]. Adherence was higher in the Safe Health IT domain (82.1%) compared to Using Health IT Safely (72.5%) and Monitoring Health IT (67%). This aligns with our study's findings, where technical infrastructure showed higher adherence, emphasizing a common trend of prioritizing technical domains over clinical processes and communication.

On the other hand, another study introduced a self-assessment focused on the Computerized Provider Entry system, using 2 SAFER guides—the CPOE with DS guide and clinician communication guide—which were filled out by nursing students [43]. The study demonstrated that such a tool could effectively uncover usability and safety issues, particularly

XSL•FO
RenderX

medication ordering and visual display issues. It explored nursing students' experiences with EHR safety, highlighting the importance of education and training in promoting safe EHR use. This underscores the need for comprehensive training programs to enhance EHR safety practices, a factor that may contribute to variability in adherence observed in our study. While our study did not focus on CPOE systems, the emphasis on self-assessment tools aligns with our study approach of using SAFER guides to proactively identify and address EHR-related safety concerns.

Several factors may be considered for the observed differences between our study and previous studies. The stage of experience with the system and EHR adoption can influence the implementation of safety recommendations [23,88]. Likewise, organizational commitment to implementing safety practices and the diversity of cultural attitudes toward patient safety can lead to variability in adherence levels [89]. Additionally, health care system differences between the State of Kuwait and other countries, such as variations in health care priorities, infrastructure, and policies, can impact the implementation of SAFER-recommended practices [90]. Furthermore, resource availability can influence the capacity to effectively implement EHR safety practices, including differences in technical, human, and financial resources [91,92].

Recommendations

EHR safety encompasses organizational, clinical, technical, and behavioral dimensions, all of which are essential and interdependent in ensuring health care quality and patient safety [56]. Achieving EHR safety requires shared responsibility among interdisciplinary health care teams, fostering collaboration to enhance safety practices and integrate clinical and technical workflows seamlessly [44,87,93]. Additionally, promoting awareness of EHR safety through comprehensive and ongoing training for health care staff can improve their proficiency and confidence in using EHR systems [63].

Hospitals must also commit to regularly conducting proactive risk assessments, such as those outlined in the SAFER guides, to identify potential vulnerabilities in EHR safety practices. These assessments allow for the implementation of preventive measures, mitigating risks before adverse events occur and improving health care outcomes and patient safety. Proactive assessments can further foster interdisciplinary collaboration among HCPs by bringing together diverse expertise, supported by strong leadership to establish organizational priorities, promote workflow adaptability, and actively involve EHR vendors in optimization initiatives [51,78,94].

EHR vendors should gain a comprehensive understanding of clinicians' workflows and the broader operations of health care teams to design systems that integrate effectively into clinical processes [86]. Actively involving health care staff as EHR users is critical, as they can provide valuable feedback to identify areas for improvement, emphasizing the need for established channels for user input [95].

Although not widely available at the time the SAFER guides were first introduced, advanced technologies such as artificial intelligence (AI) and machine learning (ML) now offer significant potential to enhance EHR safety [96,97]. Early evidence suggests that these technologies can improve DS, streamline workflows, and reduce clinician burden, particularly through advanced data entry automation and error detection mechanisms [98]. However, their impact on EHR safety remains in the early stages of evaluation, and further research is required to comprehensively understand their effectiveness.

Integrating AI and ML into the SAFER guides could provide a proactive framework for assessing and mitigating risks associated with these technologies while optimizing their benefits for EHR safety. This integration would support health care organizations in identifying best practices for leveraging AI and ML to address safety challenges, such as improving data integrity, detecting potential errors, and enhancing user experience. Future studies should focus on the long-term impact of AI and ML in real-world clinical settings and provide evidence-based recommendations for their inclusion in SAFER guides, thereby advancing EHR safety and patient care.

Study Strengths and Limitations

As with any research, this study has both strengths and limitations. First, it represents the first empirical investigation into EHR safety practices in public hospitals outside the United States using the SAFER guides. The lack of similar international studies restricts opportunities for benchmarking and cross-context comparisons, limiting the ability to generalize findings beyond Kuwait.

Second, although the study included only 6 public hospitals, it effectively captured nearly the entire population of secondary care facilities in Kuwait, providing a comprehensive snapshot of this health care segment. One secondary hospital was excluded due to the absence of an EHR system and was replaced with a tertiary care hospital from the same region. While this maintained the sample size and focus on EHR-active facilities, it may have introduced variability, as tertiary hospitals typically differ in patient complexity, resource availability, and EHR usage. Future studies should stratify by care level and include tertiary and private hospitals to enhance generalizability.

Third, a significant limitation of the SAFER guides is the reliance on self-assessment, which may not always yield objective evaluations of EHR safety practices. Because the tool depends on health care staff to assess their own systems and processes, the accuracy of the results is influenced by participants' understanding, perceptions, and interpretations of the recommended practices. This self-reporting approach introduces potential biases, as participants may overestimate adherence to best practices or fail to identify existing deficiencies. Lastly, the differences in health care system regulations and policies between Kuwait and the United States may affect how SAFER scores are interpreted and applied.

Nonetheless, the SAFER guides offer a valuable framework for health care staff and hospitals to identify gaps, enhance EHR safety practices, improve workflow efficiencies, and achieve better health care outcomes. To address these limitations, future studies should consider incorporating complementary methodologies, such as external audits, qualitative interviews, and observational studies. These approaches can validate

XSL•FO
RenderX

findings from SAFER self-assessments, provide more objective evaluations, and yield deeper insights into the practical challenges and successes of implementing the recommended practices across diverse health care contexts. Additionally, studies focusing on the long-term impact of SAFER-guided interventions could assess improvements in patient safety and organizational efficiency, contributing valuable knowledge to the global discourse on EHR safety and optimization.

Conclusions

This study used the SAFER guides as a structured framework to conduct a proactive risk assessment of EHR safety practices in Kuwait's public hospitals. The findings reveal considerable variability in the implementation of recommended safety practices, with stronger adherence observed in technical and infrastructure-related domains compared to clinical processes and clinician communication. These results underscore the importance of addressing both technical and clinical dimensions to achieve a balanced and effective approach to EHR safety.

The study contributes to the growing body of literature on EHR safety by demonstrating the applicability of the SAFER framework in a non-US context. While the SAFER guides proved useful in identifying gaps and strengths in current practices, the results do not establish causal relationships between hospital characteristics and safety outcomes. Instead, they offer a foundational understanding of EHR safety implementation in Kuwait's public health care sector. The unique regulatory and operational characteristics of Kuwait's health care system necessitate tailored strategies for effective implementation. Future research should build on these findings through broader sampling, mixed methods approaches, and longitudinal assessments to evaluate the impact of targeted interventions on EHR safety and patient outcomes.

Acknowledgments

We would like to acknowledge the support of the Ministry of Health in facilitating the project and sincerely thank all study participants for their dedication to patient safety and their support in participating in the study. Grammarly Premium was used to review, edit, and improve the manuscript's language structure. This work encompasses a subset of the work originally submitted in partial fulfillment of the requirements for the Master's degree in Computing Information Systems at Kuwait University.

Data Availability

All data generated and analyzed during this study are included in this published article. However, some datasets are not publicly available due to privacy and confidentiality protections but may be obtained from the corresponding author upon reasonable request.

Authors' Contributions

AH acquired the data and played a played a pivotal role in coordinating the study activities. DA supervised the project, and designed and conceptualized the study. All authors analyzed and interpreted the results of the data. AH drafted the manuscript, and DA provided critical feedback. All authors reviewed and approved the final version of the manuscript.

Conflicts of Interest

None declared.

Multimedia Appendix 1
Informed consent form used for the survey.
[PDF File, 119 KB - medinform_v13i1e70782_app1.pdf]

Multimedia Appendix 2
SAFER (Safety Assurance Factors for EHR [Electronic Health Record] Resilience) guides (Self-evaluation Questionnaire).
[XLSX File, 61 KB - medinform_v13i1e70782_app2.xlsx]

References

1. Yen PY, McAlearney AS, Sieck CJ, Hefner JL, Huerta TR. Health information technology (HIT) adaptation: refocusing on the journey to successful HIT implementation. JMIR Med Inform 2017 Sep 7;5(3):e28. [doi: 10.2196/medinform.7476] [Medline: 28882812]
2. Mengestie ND, Yeneneh A, Baymot AB, et al. Health information technologies in a resource-limited setting: knowledge, attitude, and practice of health professionals. Biomed Res Int 2023;2023(4980391):4980391. [doi: 10.1155/2023/4980391] [Medline: 36778058]
3. Keshta I, Odeh A. Security and privacy of electronic health records: concerns and challenges. Egypt Inform J 2021 Jul;22(2):177-183. [doi: 10.1016/j.eij.2020.07.003]
4. Sinsky CA, Rule A, Cohen G, et al. Metrics for assessing physician activity using electronic health record log data. J Am Med Inform Assoc 2020 Apr 1;27(4):639-643. [doi: 10.1093/jamia/ocz223]

XSL•FO
RenderX

5. Hansen S, Baroody AJ. Beyond the boundaries of care: electronic health records and the changing practices of healthcare. Inform Organ 2023 Sep;33(3):100477. [doi: 10.1016/j.infoandorg.2023.100477]
6. Office-based physician electronic health record adoption. HealthIT.gov. URL: https://www.healthit.gov/data/quickstats/office-based-physician-electronic-health-record-adoption [accessed 2025-07-24]
7. The impact of electronic health records on patient care and outcomes: a comprehensive review. World J Adv Res Rev 2024;21(2):1446-1455. [doi: 10.30574/wjarr.2024.21.2.0592]
8. Aldosari B. Patients' safety in the era of EMR/EHR automation. Inform Med Unlocked 2017;9:230-233. [doi: 10.1016/j.imu.2017.10.001]
9. Chen Z, Liang N, Zhang H, et al. Harnessing the power of clinical decision support systems: challenges and opportunities. Open Heart 2023 Nov 28;10(2):e002432. [doi: 10.1136/openhrt-2023-002432] [Medline: 38016787]
10. Ratwani RM, Savage E, Will A, et al. Identifying electronic health record usability and safety challenges in pediatric settings. Health Aff (Millwood) 2018 Nov;37(11):1752-1759. [doi: 10.1377/hlthaff.2018.0699] [Medline: 30395517]
11. Russo E, Sittig DF, Murphy DR, Singh H. Challenges in patient safety improvement research in the era of electronic health records. Healthcare (Basel) 2016 Dec;4(4):285-290. [doi: 10.1016/j.hjdsi.2016.06.005]
12. Colquhoun DA, Shanks AM, Kapeles SR, et al. Considerations for integration of perioperative electronic health records across institutions for research and quality improvement: the approach taken by the multicenter perioperative outcomes group. Anesth Analg 2020;130(5):1133-1146. [doi: 10.1213/ANE.0000000000004489]
13. Sarkar IN. Transforming health data to actionable information: recent progress and future opportunities in health information exchange: Yearbook of Medical Informatics Georg Thieme Verlag KG; 2022, Vol. 31:203-214. [doi: 10.1055/s-0042-1742519]
14. Neves AL, Poovendran D, Freise L, et al. Health care professionals' perspectives on the secondary use of health records to improve quality and safety of care in England: qualitative study. J Med Internet Res 2019 Sep 26;21(9):e14135. [doi: 10.2196/14135] [Medline: 31573898]
15. 10 facts on patient safety. World Health Organization. 2019. URL: http://www.who.int/features/factfiles/patient_safety/en/ [accessed 2025-07-24]
16. Palojoki S, Mäkelä M, Lehtonen L, Saranto K. An analysis of electronic health record-related patient safety incidents. Health Informatics J 2017 Jun;23(2):134-145. [doi: 10.1177/1460458216631072] [Medline: 26951568]
17. Kohn LT, Corrigan JM, Donaldson MS, editors. Committee on Quality of Health Care in America To Err is Human: Building a Safer Health System: National Academies Press (US); 2000. [Medline: 25077248]
18. Averill P, Vincent C, Reen G, Henderson C, Sevdalis N. Conceptual and practical challenges associated with understanding patient safety within community-based mental health services. Health Expect 2023 Feb;26(1):51-63. [doi: 10.1111/hex.13660] [Medline: 36370458]
19. Marra AR, Algwizani A, Alzunitan M, Brennan TMH, Edmond MB. Descriptive epidemiology of safety events at an academic medical center. Int J Environ Res Public Health 2020 Jan 4;17(1):353. [doi: 10.3390/ijerph17010353] [Medline: 31947963]
20. Ahmed Z, Saada M, Jones AM, Al-Hamid AM. Medical errors: healthcare professionals' perspective at a tertiary hospital in Kuwait. PLoS ONE 2019;14(5):e0217023. [doi: 10.1371/journal.pone.0217023] [Medline: 31116773]
21. Asgari E, Kaur J, Nuredini G, et al. Impact of electronic health record use on cognitive load and burnout among clinicians: narrative review. JMIR Med Inform 2024 Apr 12;12(1):e55499. [doi: 10.2196/55499] [Medline: 38607672]
22. Entzeridou E, Markopoulou E, Mollaki V. Public and physician's expectations and ethical concerns about electronic health record: benefits outweigh risks except for information security. Int J Med Inform 2018 Feb;110:98-107. [doi: 10.1016/j.ijmedinf.2017.12.004] [Medline: 29331259]
23. Colicchio TK, Cimino JJ, Del Fiol G. Unintended consequences of nationwide electronic health record adoption: challenges and opportunities in the post-meaningful use era. J Med Internet Res 2019 Jun 3;21(6):e13313. [doi: 10.2196/13313] [Medline: 31162125]
24. Baumann LA, Baker J, Elshaug AG. The impact of electronic health record systems on clinical documentation times: a systematic review. Health Policy 2018 Aug;122(8):827-836. [doi: 10.1016/j.healthpol.2018.05.014] [Medline: 29895467]
25. Nijor S, Rallis G, Lad N, Gokcen E. Patient safety issues from information overload in electronic medical records. J Patient Saf 2022 Sep 1;18(6):e999-e1003. [doi: 10.1097/PTS.0000000000001002] [Medline: 35985047]
26. Bani Issa W, Al Akour I, Ibrahim A, et al. Privacy, confidentiality, security and patient safety concerns about electronic health records. Int Nurs Rev 2020 Jun;67(2):218-230. [doi: 10.1111/inr.12585] [Medline: 32314398]
27. Wijayanti D, Ujianto EIH, Rianto R. Uncovering security vulnerabilities in electronic medical record systems: a comprehensive review of threats and recommendations for enhancement. J Ilm Tek Elektro Komput Dan Inform 2024;10(1):73. [doi: 10.26555/jiteki.v10i1.28192]
28. Shah SM, Khan RA. Secondary use of electronic health record: opportunities and challenges. IEEE Access 2020;8:136947-136965. [doi: 10.1109/ACCESS.2020.3011099]
29. Janett RS, Yeracaris PP. Electronic medical records in the American Health System: challenges and lessons learned. Ciênc saúde coletiva 2020;25(4):1293-1304. [doi: 10.1590/1413-81232020254.28922019]

XSL•FO
RenderX

30. Alanazi B, Butler-Henderson K, Alanazi M. Perceptions of healthcare professionals about the adoption and use of EHR in Gulf Cooperation Council countries: a systematic review. BMJ Health Care Inform 2020 Jan;27(1):31924667. [doi: 10.1136/bmjhci-2019-100099] [Medline: 31924667]
31. Campanella P, Lovato E, Marone C, et al. The impact of electronic health records on healthcare quality: a systematic review and meta-analysis. Eur J Public Health 2016 Feb;26(1):60-64. [doi: 10.1093/eurpub/ckv122] [Medline: 26136462]
32. Murthi S, Martini N, Falconer N, Scahill S. Evaluating EHR-integrated digital technologies for medication-related outcomes and health equity in hospitalised adults: a scoping review. J Med Syst 2024 Aug 23;48(1):79. [doi: 10.1007/s10916-024-02097-5] [Medline: 39174723]
33. Bazzaz NA, Paget T. Hospital staff have positive attitudes towards EHR and optimistic expectations towards EHR implementation: a quantitative survey on one hospital in Kuwait. Nurs Primary Care 2019;3(5):1-6. [doi: 10.33425/2639-9474.1119]
34. Al-Otaibi J, Tolma E, Alali W, Alhuwail D, Aljunid SM. The factors contributing to physicians' current use of and satisfaction with electronic health records in Kuwait's public health care: cross-sectional questionnaire study. JMIR Med Inform 2022 Oct 7;10(10):e36313. [doi: 10.2196/36313] [Medline: 36206039]
35. Graber ML, Siegal D, Riah H, Johnston D, Kenyon K. Electronic health record-related events in medical malpractice claims. J Patient Saf 2019 Jun;15(2):77-85. [doi: 10.1097/PTS.0000000000000240] [Medline: 26558652]
36. Palabindala V, Pamarthy A, Jonnalagadda NR. Adoption of electronic health records and barriers. J Community Hosp Intern Med Perspect 2016;6(5):32643. [doi: 10.3402/jchimp.v6.32643] [Medline: 27802857]
37. Wang Y, Coiera E, Gallego B, et al. Measuring the effects of computer downtime on hospital pathology processes. J Biomed Inform 2016 Feb;59:308-315. [doi: 10.1016/j.jbi.2015.12.016] [Medline: 26732996]
38. Mistri IU, Badge A, Shahu S. Enhancing patient safety culture in hospitals. Cureus 2023 Dec;15(12):e51159. [doi: 10.7759/cureus.51159] [Medline: 38283419]
39. Sittig DF, Yackel EE, Singh H. Five strategies for a safer EHR modernization journey. J Gen Intern Med 2023 Oct;38(Suppl 4):940-942. [doi: 10.1007/s11606-023-08331-z] [Medline: 37798588]
40. Walker JM, Carayon P, Leveson N, et al. EHR safety: the way forward to safe and effective systems. J Am Med Inform Assoc 2008;15(3):272-277. [doi: 10.1197/jamia.M2618] [Medline: 18308981]
41. Singh H, Sittig DF. Measuring and improving patient safety through health information technology: The Health IT Safety Framework. BMJ Qual Saf 2016 Apr;25(4):226-232. [doi: 10.1136/bmjqs-2015-004486] [Medline: 26369894]
42. Wright A, Aaron S, Sittig DF. Testing electronic health records in the "production" environment: an essential step in the journey to a safe and effective health care system. J Am Med Inform Assoc 2017 Jan;24(1):188-192. [doi: 10.1093/jamia/ocw039] [Medline: 27107450]
43. Whitt KJ, Eden L, Merrill KC, Hughes M. Nursing student experiences regarding safe use of electronic health records: a pilot study of the safety and assurance factors for EHR resilience guides. Comput Inform Nurs 2017 Jan;35(1):45-53. [doi: 10.1097/CIN.0000000000000291] [Medline: 27575967]
44. Sittig DF, Belmont E, Singh H. Improving the safety of health information technology requires shared responsibility: It is time we all step up. Healthcare (Basel) 2018 Mar;6(1):7-12. [doi: 10.1016/j.hjdsi.2017.06.004]
45. Alhuwail D. Understanding health information management practices in public hospitals in Kuwait. Helth Inf Manage J 2020 May;49(2-3):127-136. [doi: 10.1177/1833358319837247]
46. AlHussainan AF, Jasem ZA, Alhuwail D. Evaluating the presence of hospitals on social media: an analytical study of private and public hospital Instagram accounts in the State of Kuwait. Int J Healthc Inf Syst Inform 2022 Jan;17(2):1-17. [doi: 10.4018/IJHISI.299954]
47. Katoue MG, Somerville SG, Barake R, Scott M. The perceptions of healthcare professionals about accreditation and its impact on quality of healthcare in Kuwait: a qualitative study. J Eval Clin Pract 2021 Dec;27(6):1310-1320. [doi: 10.1111/jep.13557] [Medline: 33749091]
48. Albassam A, Almohammed H, Alhujaili M, Koshy S, Awad A. Perspectives of Primary Care Physicians and Pharmacists on Interprofessional Collaboration in Kuwait: A Quantitative Study: PLOS ONE Public Library of Science; 2020, Vol. 15. [doi: 10.1371/journal.pone.0236114]
49. Sittig DF, Salimi M, Aiyagari R, et al. Adherence to recommended electronic health record safety practices across eight health care organizations. J Am Med Inform Assoc 2018 Jul 1;25(7):913-918. [doi: 10.1093/jamia/ocy033] [Medline: 29701854]
50. SAFER Guides. Office of the National Coordinator for Health Information Technology (ONC).: HealthIT.gov URL: https://www.healthit.gov/topic/safety/safer-guides [accessed 2020-02-01]
51. Alhajeri M, Alhuwail D, Alfeeli M, Marafi F. Assessing the adherence to recommended health information technology safety practices: a case study of a nuclear medicine and molecular imaging center. J Nucl Med Soc Nucl Med. 2020 May 1. URL: https://jnm.snmjournals.org/content/61/supplement_1/3025 [accessed 2025-07-24]
52. Sittig DF, Ash JS, Singh H. The SAFER guides: empowering organizations to improve the safety and effectiveness of electronic health records. Am J Manag Care 2014 May;20(5):418-423. [Medline: 25181570]
53. Tubaishat A. The effect of electronic health records on patient safety: a qualitative exploratory study. Inform Health Soc Care 2019 Jan;44(1):79-91. [doi: 10.1080/17538157.2017.1398753] [Medline: 29239662]

XSL•FO
RenderX

54. Campione J, Liu H. Perceptions of hospital electronic health record (EHR) training, support, and patient safety by staff position and tenure. BMC Health Serv Res 2024 Aug 20;24(1):955. [doi: 10.1186/s12913-024-11322-3] [Medline: 39164672]
55. Opoku-Agyeman W. Levels of electronic health records (EHR) implementation and their influence on quality and safety (preprint). JMIR Infodemiol. Preprint posted online on 2023. [doi: 10.2196/preprints.46199]
56. Azyabi A, Karwowski W, Davahli MR. Assessing patient safety culture in hospital settings. Int J Environ Res Public Health 2021 Mar 3;18(5):2466. [doi: 10.3390/ijerph18052466] [Medline: 33802265]
57. Holmgren AJ, McBride S, Gale B, Mossburg S. Technology as a tool for improving patient safety technology as a tool for improving patient safety. PSNet. 2023. URL: https://psnet.ahrq.gov/perspective/technology-tool-improving-patient-safety [accessed 2024-11-07]
58. Chacko AM. 2 - interoperability issues in EHR systems: research directions. In: Data Analytics in Biomedical Engineering and Healthcare: Academic Press; 2021:13-28. [doi: 10.1016/B978-0-12-819314-3.00002-1]
59. Priestman W, Sridharan S, Vigne H, Collins R, Seamer L, Sebire NJ. What to expect from electronic patient record system implementation; lessons learned from published evidence. J Innov Health Inform 2018 Jun 15;25(2):92-104. [doi: 10.14236/jhi.v25i2.1007] [Medline: 30398452]
60. Reegu FA, Abas H, Gulzar Y, et al. Blockchain-based framework for interoperable electronic health records for an improved healthcare system. Sustainability 2023 Jan;15(8):6337. [doi: 10.3390/su15086337]
61. Basil NN, Ambe S, Ekhator C, Fonkem E. Health records database and inherent security concerns: a review of the literature. Cureus 2022 Oct;14(10):e30168. [doi: 10.7759/cureus.30168] [Medline: 36397924]
62. Kariotis TC, Prictor M, Chang S, Gray K. Impact of electronic health records on information practices in mental health contexts: scoping review. J Med Internet Res 2022 May 4;24(5):e30405. [doi: 10.2196/30405] [Medline: 35507393]
63. Sittig DF, Wright A, Coiera E, et al. Current challenges in health information technology-related patient safety. Health Informatics J 2020 Mar;26(1):181-189. [doi: 10.1177/1460458218814893] [Medline: 30537881]
64. Fennelly O, Cunningham C, Grogan L, et al. Successfully implementing a national electronic health record: a rapid umbrella review. Int J Med Inform 2020 Dec;144:104281. [doi: 10.1016/j.ijmedinf.2020.104281] [Medline: 33017724]
65. Moncho V, Marco-Simo JM, Cobarsi J. EHR implementation: a literature review. In: Rocha Á, Ferrás C, López-López PC, Guarda T, editors. Information Technology and Systems: Springer International Publishing; 2021:3-12. [doi: 10.1007/978-3-030-68418-1_1]
66. Hong Mershon B, Vannucci A, Bryson T, et al. A collaborative partnership between the multicenter handoff collaborative and an electronic health record vendor. Appl Clin Inform 2021 May;12(3):647-654. [doi: 10.1055/s-0041-1731714] [Medline: 34320682]
67. Alnashmi M, Salman A, AlHumaidi H, Yunis M, Al-Enezi N. Exploring the health information management system of Kuwait: lessons and opportunities. ASI 2022 Feb;5(1):25. [doi: 10.3390/asi5010025]
68. Carlos Ferreira J, Elvas LB, Correia R, Mascarenhas M. Enhancing EHR interoperability and security through distributed ledger technology: a review. Healthcare (Basel) 2024 Oct 2;12(19):1967. [doi: 10.3390/healthcare12191967] [Medline: 39408147]
69. de Mello BH, Rigo SJ, da Costa CA, et al. Semantic interoperability in health records standards: a systematic literature review. Health Technol 2022 Mar;12(2):255-272. [doi: 10.1007/s12553-022-00639-w]
70. Greenes RA, Bates DW, Kawamoto K, Middleton B, Osheroff J, Shahar Y. Clinical decision support models and frameworks: seeking to address research issues underlying implementation successes and failures. J Biomed Inform 2018 Feb;78:134-143. [doi: 10.1016/j.jbi.2017.12.005] [Medline: 29246790]
71. Mackey TK, Kuo TT, Gummadi B, et al. "Fit-for-purpose?" - challenges and opportunities for applications of blockchain technology in the future of healthcare. BMC Med 2019 Mar 27;17(1):68. [doi: 10.1186/s12916-019-1296-7] [Medline: 30914045]
72. Maier-Hein L, Eisenmann M, Sarikaya D, et al. Surgical data science - from concepts toward clinical translation. Med Image Anal 2022 Feb;76:102306. [doi: 10.1016/j.media.2021.102306] [Medline: 34879287]
73. Mathews SC, McShea MJ, Hanley CL, Ravitz A, Labrique AB, Cohen AB. Digital health: a path to validation. npj Digit Med 2019 May 13;2(1):1-9. [doi: 10.1038/s41746-019-0111-3]
74. Brady AP, Allen B, Chong J, Kotter E, Kottler N, Mongan J. Implementing and monitoring AI tools in radiology: practical considerations. In: A Multi-Society Statement From the ACR, CAR, ESR, RANZCR & RSNA: Can Assoc Radiol J SAGE Publications Inc; 2024, Vol. 75:226-244. [doi: 10.1177/08465371231222229]
75. Rehman A, Naz S, Razzak I. Leveraging big data analytics in healthcare enhancement: trends, challenges and opportunities. Multimedia Syst 2022 Aug;28(4):1339-1371. [doi: 10.1007/s00530-020-00736-8]
76. Argaw ST, Troncoso-Pastoriza JR, Lacey D, et al. Cybersecurity of Hospitals: discussing the challenges and working towards mitigating the risks. BMC Med Inform Decis Mak 2020 Jul 3;20(1):146. [doi: 10.1186/s12911-020-01161-7] [Medline: 32620167]
77. Cohen TN, Wiegmann DA, Kanji FF, Alfred M, Anger JT, Catchpole KR. Using flow disruptions to understand healthcare system safety: a systematic review of observational studies. Appl Ergon 2022 Jan;98:103559. [doi: 10.1016/j.apergo.2021.103559] [Medline: 34488190]

XSL•FO
RenderX

78. Liu HC, Zhang LJ, Ping YJ, Wang L. Failure mode and effects analysis for proactive healthcare risk evaluation: a systematic literature review. J Eval Clin Pract 2020 Aug;26(4):1320-1337. [doi: 10.1111/jep.13317] [Medline: 31849153]
79. Wright B, Lennox A, Graber ML, Bragge P. Closing the loop on test results to reduce communication failures: a rapid review of evidence, practice and patient perspectives. BMC Health Serv Res 2020 Sep 23;20(1):897. [doi: 10.1186/s12913-020-05737-x] [Medline: 32967682]
80. Singh H, Sittig DF. A sociotechnical framework for safety-related electronic health record research reporting: The SAFER reporting framework. Ann Intern Med 2020 Jun 2;172(11 Suppl):S92-S100. [doi: 10.7326/M19-0879] [Medline: 32479184]
81. Canfell OJ, Woods L, Meshkat Y, et al. The impact of digital hospitals on patient and clinician experience: systematic review and qualitative evidence synthesis. J Med Internet Res 2024 Mar 11;26(1):e47715. [doi: 10.2196/47715]
82. Guttman OT, Lazzara EH, Keebler JR, Webster KLW, Gisick LM, Baker AL. Dissecting communication barriers in healthcare: a path to enhancing communication resiliency, reliability, and patient safety. J Patient Saf 2021 Dec 1;17(8):e1465-e1471. [doi: 10.1097/PTS.0000000000000541] [Medline: 30418425]
83. Quinn M, Forman J, Harrod M, et al. Electronic health records, communication, and data sharing: challenges and opportunities for improving the diagnostic process. Diagnosis (Berl) 2019 Aug 27;6(3):241-248. [doi: 10.1515/dx-2018-0036] [Medline: 30485175]
84. Alobayli F, O'Connor S, Holloway A, Cresswell K. Electronic health record stress and burnout among clinicians in hospital settings: a systematic review. Digit Health 2023;9(20552076231220241):20552076231220241. [doi: 10.1177/20552076231220241] [Medline: 38130797]
85. Amano A, Brown-Johnson CG, Winget M, et al. Perspectives on the intersection of electronic health records and health care team communication, function, and well-being. JAMA Netw Open 2023 May 1;6(5):e2313178. [doi: 10.1001/jamanetworkopen.2023.13178] [Medline: 37171816]
86. Carayon P, Salwei ME. Moving toward a sociotechnical systems approach to continuous health information technology design: the path forward for improving electronic health record usability and reducing clinician burnout. J Am Med Inform Assoc 2021 Apr 23;28(5):1026-1028. [doi: 10.1093/jamia/ocab002] [Medline: 33537756]
87. Murphy DR, Giardina TD, Satterly T, Sittig DF, Singh H. An exploration of barriers, facilitators, and suggestions for improving electronic health record inbox-related usability: a qualitative analysis. JAMA Netw Open 2019 Oct 2;2(10):e1912638. [doi: 10.1001/jamanetworkopen.2019.12638] [Medline: 31584683]
88. Tsai CH, Eghdam A, Davoody N, Wright G, Flowerday S, Koch S. Effects of electronic health record implementation and barriers to adoption and use: a scoping review and qualitative analysis of the content. Life (Basel) 2020 Dec 4;10(12):327. [doi: 10.3390/life10120327] [Medline: 33291615]
89. Ali H, Ibrahem SZ, Al Mudaf B, Al Fadalah T, Jamal D, El-Jardali F. Baseline assessment of patient safety culture in public hospitals in Kuwait. BMC Health Serv Res 2018 Mar 6;18(1):158. [doi: 10.1186/s12913-018-2960-x] [Medline: 29510705]
90. Tzenios N. The determinants of access to healthcare: a review of individual, structural, and systemic factors. J Humanities Appl Sci Res 2019 Dec 9 [FREE Full text]
91. Upadhyay S, Opoku-Agyeman W. Factors that determine comprehensive categorical classification of EHR implementation levels. Health Serv Insights 2021;14(11786329211024788):11786329211024788. [doi: 10.1177/11786329211024788] [Medline: 34188485]
92. O'Donnell A, Kaner E, Shaw C, Haighton C. Primary care physicians' attitudes to the adoption of electronic medical records: a systematic review and evidence synthesis using the clinical adoption framework. BMC Med Inform Decis Mak 2018 Nov 13;18(1):101. [doi: 10.1186/s12911-018-0703-x] [Medline: 30424758]
93. Gluck P. Patient Safety in Obstetrics and Gynecology, An Issue of Obstetrics and Gynecology Clinics: Elsevier Health Sciences; 2019.
94. Sittig DF, Lakhani P, Singh H. Applying requisite imagination to safeguard electronic health record transitions. J Am Med Inform Assoc 2022 Apr 13;29(5):1014-1018. [doi: 10.1093/jamia/ocab291] [Medline: 35022741]
95. Kiepek W, Sengstack PP. An Evaluation of System End-User Support During Implementation of an Electronic Health Record Using the Model for Improvement Framework: Applied Clinical Informatics Georg Thieme Verlag KG; 2019, Vol. 10:964-971. [doi: 10.1055/s-0039-3402450]
96. Tighe P, Mossburg S, Gale B. Artificial intelligence and patient safety: promise and challenges. Artificial Intelligence and Patient Safety: Promise and Challenges. 2024. URL: https://psnet.ahrq.gov/perspective/artificial-intelligence-and-patient-safety-promise-and-challenges [accessed 2025-01-01]
97. Bates DW, Levine D, Syrowatka A, et al. The potential of artificial intelligence to improve patient safety: a scoping review. npj Digit Med 2021 Mar 19;4(1):1-8. [doi: 10.1038/s41746-021-00423-6]
98. Choudhury A, Asan O. Role of artificial intelligence in patient safety outcomes: systematic literature review. JMIR Med Inform 2020 Jul 24;8(7):e18599. [doi: 10.2196/18599] [Medline: 32706688]

Abbreviations

AI: artificial intelligence
CPOE: computerized provider order entry

XSL•FO
RenderX

DS: decision support
EHR: electronic health record
HCP: health care provider
ML: machine learning
SAFER: Safety Assurance Factors for EHR Resilience

Edited by A Coristine; submitted 02.01.25; peer-reviewed by H Elamir, J Walsh; revised version received 12.06.25; accepted 12.06.25; published 14.08.25.

Please cite as:
AlHussainan A, Alhuwail D
Bridging Global Frameworks and Local Practice: Quantitative Evaluation of Electronic Health Record Safety in Kuwait's Public Hospitals
JMIR Med Inform 2025;13:e70782
URL: https://medinform.jmir.org/2025/1/e70782
doi:10.2196/70782

© Anwar AlHussainan, Dari Alhuwail. Originally published in JMIR Medical Informatics (https://medinform.jmir.org), 14.8.2025. This is an open-access article distributed under the terms of the Creative Commons Attribution License (https://creativecommons.org/licenses/by/4.0/), which permits unrestricted use, distribution, and reproduction in any medium, provided the original work, first published in JMIR Medical Informatics, is properly cited. The complete bibliographic information, a link to the original publication on https://medinform.jmir.org/, as well as this copyright and license information must be included.

XSL•FO
RenderX

Relationship Between Stroke Knowledge, Health Information Literacy, and Health Self- Management Among Patients with Stroke: Multicenter Cross-Sectional Study

Mengxue Zeng[1,2*], MNS; Yanhua Liu[2*], MNS; Ying He[2*], MNS; Wenxia Huang[1], MD

[1]Health Management Center, General Practice Medical Center, West China Hospital, Sichuan University, 37 Guoxue Lane, Wuhou District, Chengdu, China

[2]West China School of Nursing, Sichuan University, Chengdu, China

[*]these authors contributed equally

Corresponding Author:
Wenxia Huang, MD
Health Management Center, General Practice Medical Center, West China Hospital, Sichuan University, 37 Guoxue Lane, Wuhou District, Chengdu, China

Related Article:

This is a corrected version. See correction statement: https://medinform.jmir.org/2025/1/e80547

Abstract

Background: The World Health Organization highlights the essential role of effective self-management in the prevention and control of chronic diseases, noting that proper self-management can significantly slow disease progression. Stroke, which ranks as the third leading cause of death worldwide, is often accompanied by inadequate self-management among patients. While health information literacy (HIL) has been shown to influence self-management in conditions such as diabetes and hypertension, its role as a mediating factor linking disease perception and health behavior in patients with stroke remains insufficiently explored. Addressing this research gap is vital for developing targeted interventions.

Objective: The aim of this study was to investigate the current status of HIL, stroke knowledge, and self-management abilities among patients with stroke in Southwest China. Additionally, the study analyzed the relationships among these three factors and their mechanisms of action, providing evidence to inform the development of effective health education strategies for enhancing self-management in patients with stroke.

Methods: A multicenter cross-sectional design was employed, enrolling 514 patients with stroke from the neurology departments of three tertiary general hospitals in Chengdu between September 2022 and March 2023. Data collection used a standardized set of scales: the health information literacy questionnaire for stroke assessed HIL, the stroke prevention questionnaire evaluated knowledge levels, and the stroke self-management assessment scale measured self-management abilities. Regression analysis and bootstrap mediation effect testing were conducted using SPSS software (version 26.0).

Results: Patients with stroke had a mean (SD) score of 17.61 (6.46) for stroke knowledge, 61.17 (13.58) for HIL, and 158.70 (19.07) for self-management skills. Correlation analysis indicated a positive correlation of stroke knowledge with both self-management (r=0.668; P<.001) and HIL (r=0.138; P<.001). The mediation test showed a significant mediating effect of HIL between stroke knowledge and self-management (β=0.543; 95% CI: 0.431 - 0.663), with an effect share of 82.77%.

Conclusion: There is a correlation between HIL and self-management; the higher the HIL, the better is the self-management behavior. Furthermore, HIL partially mediates the effect of stroke knowledge on self-management.

(JMIR Med Inform 2025;13:e63956) doi:10.2196/63956

KEYWORDS

stroke; health information literacy; self-management; stroke knowledge; mediating effect

Introduction

Stroke is the leading cause of adult mortality worldwide, particularly among Chinese adults, with a rapidly increasing incidence, poor prognosis, mortality, and varying degrees of disability among survivors. This imposes a significant economic burden on patients' families and society [1,2]. Inadequate health information about stroke leads to delayed consultation and suboptimal prevention and control due to the lack of timely

XSL•FO
RenderX

disease-related relief [3]. Therefore, increasing the awareness of patients with stroke has a positive impact on the prevention and management of stroke. In particular for the population with poststroke dysfunction, low health information literacy (HIL) affects treatment and recovery and significantly reduces their quality of life. Research has shown that improving HIL in patients with stroke is crucial to promoting overall well-being, as it improves public understanding of health and disease and positively influences patients' self-management practices [4,5]. Effective self-management can motivate patients to improve unhealthy lifestyles, increase their ability to monitor their disease, improve adherence to treatment, and consequently improve their quality of life [6]. HIL combines the concepts of health literacy and information literacy; it focuses on an individual's ability to obtain, understand, and use health information and services, and to make appropriate judgments and decisions to maintain and improve their health [7,8]. Existing studies have primarily investigated the current status of HIL in patients with stroke, with less investigation into the possible mediating effect of HIL on knowledge levels and self-management skills [9-11]. Therefore, the aims of this study were to analyze the relationship between stroke knowledge, HIL, and self-management in patients with stroke, to examine the mediating effect of HIL, to provide new ideas for interventions to improve patients' self-management ability, and to target the implementation of health education for patients with stroke.

Methods

Setting and Samples

This was an observational, multicentere, cross-sectional study, which included hospitalized patients with stroke from September 2022 to March 2023 in the emergency and critical care center of tertiary hospitals in three stroke centers: West China Hospital of Sichuan University, West China Tianfu Hospital of Sichuan University, and West China Shangjin Hospital of Sichuan University. The patient recruitment process of this study strictly adhered to the ethical review requirements as follows: physicians initially screened eligible patients with stroke according to the inclusion and exclusion criteria of the study, and after obtaining preliminary consent from the patients, the research team conducted extensive face-to-face communication with the patients. The survey consisted of three main questionnaires, and each participant took approximately 15 - 20 minutes to complete all the questionnaires; all the participants' questionnaires were collected at once. Quality control measures were implemented during the data collection process, with researchers receiving uniform language training and participants being interviewed face-to-face and asked to complete the questionnaires independently. For patients who were unable to complete the questionnaire, the investigators asked the items neutrally and objectively to ensure the accuracy of the questionnaire.

The inclusion criteria were (1) stroke diagnosis based on computed tomography or magnetic resonance imaging results, (2) mental and physical fitness to participate, and (3) willingness to participate and cooperate. The exclusion criteria were (1) severe complications and loss of self-management, (2) associated with psychiatric disease or intellectual disability, (3) unwillingness to participate in the survey, or (4) participation in other research projects at the same time.

Variables and Instruments

Sociodemographic and Clinical Characteristics

Based on the characteristics of stroke and relevant studies [12,13], the general information form included socio-demographic and disease-related information. The socio-demographic information included age, gender, residence, marriage, living conditions (primary caregiver), education level, occupation, history of tobacco and alcohol consumption, and type of health insurance. Disease-related data included age at onset and first symptoms. All variables above were categorical, and complete data were obtained.

The Stroke Prevention Questionnaire

The Stroke Prevention Questionnairewas developed by Zhang [14] to assess stroke knowledge of patients with stroke and contains 36 items with 8 dimensions (Cronbach α=.791), including lifestyle, diet, exercise, knowledge of risk factors, medication, blood pressure monitoring, knowledge of stroke signs and stroke management. Each item was scored on a scale of 0 and 1, where 0 indicated "wrong answer" or "don't know" and 1 indicated a "correct answer." The total score ranged from 0 to 36; the higher the score, the better was the stroke outcome.

The HIL Questionnaire for Stroke

The HIL questionnairewas a specific HIL assessment tool developed by Yao [15] and included 5 dimensions of health information with 21 items, such as health information awareness (4 items), acquisition (4 items), comprehension (4 items), evaluation (6 items), and application (3 items). The scale followed a Likert-5 scale, with each item having a minimum score of 1 and a maximum score of 5. The total score ranged from 21 to 105, with higher scores indicating higher levels of HIL. The instrument showed good reliability. The overall Cronbach α of the scale was 0.915, and the Cronbach α of each dimension ranged from 0.745 to 0.878, indicating a better model fit index and high structural validity.

The Stroke Self-Management Assessment Scale

The stroke self-management assessment scale was developed by Wang [16] and consisted of 50 items in 7 dimensions, including disease management, medication management, diet management, daily life management, emotional management, social and interpersonal management, and rehabilitation management. The options were mostly "no," "occasionally," "sometimes," "often," and "always," with total scale scores ranging from 50 to 255. Higher scores indicated better self-management. The scale had a Cronbach α of 0.835, content validity of 0.95, and structural validity of 0.594 - 0.771. The scores of the different dimensions were compared using the standard score index. The formula for the standard score index = (the actual score of this dimension/the highest score of the dimension) × 100%. The standard score index of <60% indicated poor self-management, 60% - 80% indicated moderate self-management, and >80% indicated good self-management.

XSL•FO
RenderX

Data Analysis

SPSS software (version 26.0; IBM Corp) was used for data analysis, and Microsoft Excel spreadsheets were used for data entry. Quantitative data were expressed as mean (standard deviation), and comparisons between groups were made using *t* tests or one-way analysis of variance. Categorical data were expressed as proportions (%), and comparisons between groups were made using the χ^2 test. Regression analysis was performed to determine the relationship between HIL, stroke knowledge, and self-management. Regression analysis was also used to test whether HIL in patients with stroke mediated the relationship between stroke knowledge and self-management based on relevant analysis results. A *P* value <.05 was considered statistically significant.

Ethical Considerations

Prior to data collection, the study was approved by the Ethics Committee on Biomedical Research, West China Hospital, Sichuan University (2023 Review (688)). All participants provided consent to participate in the study on a voluntary basis, and the data were anonymized. No benefits or compensation were offered or given to any participant.

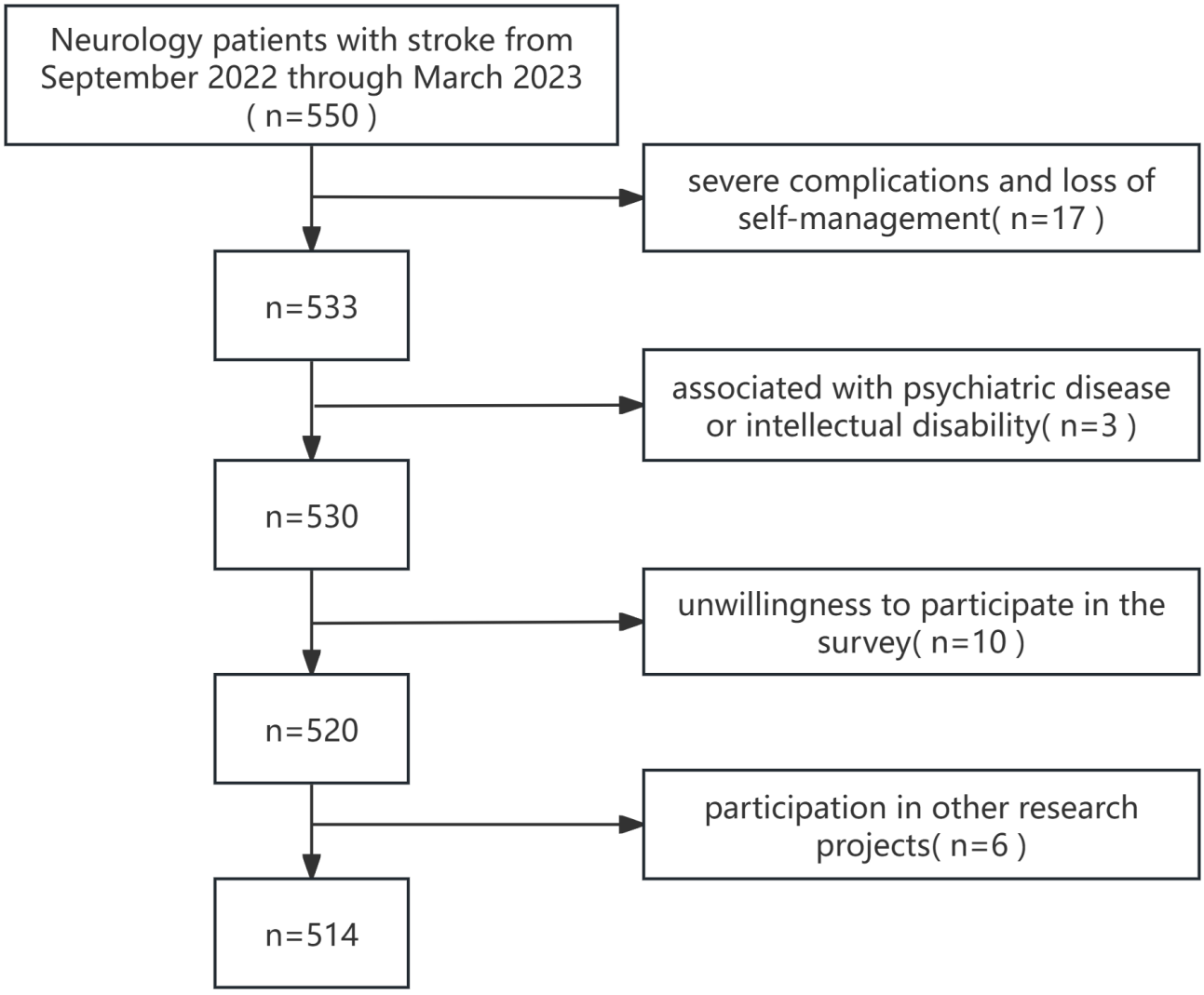
Results

Characteristics of Participants

A total of 550 stroke survivors were recruited and 514 valid questionnaires were recovered, with a valid recovery rate of 93.45%. The flowchart showing the inclusion and exclusion of patients is shown in Figure 1.

The general characteristics of the study participants are given in Table 1. Of the 514 participants, 338 (65.8%) were male and had a mean (SD) self-management ability score of 157.05 (18.78) points. Of the 514 participants, 465 (90.4%) of the participants were aged 50 - 85 years, among whom the minimum age of first stroke was 20 years. Furthermore, the distribution of residence locations revealed that the majority of the participants, 331/514 (64.4%), resided in urban areas, with a substantial proportion having completed middle school as their highest level of education (185/514, 36%). The initial incidence of stroke was predominantly observed among individuals aged 60 years and older.

Figure 1. Flowchart for including and excluding study participants.



XSL•FO
RenderX

Table . General information of patient participants.

Variable	n (%)	Self-management ability score, mean (SD)	*t* test or *F* test *(df)*	*P* value
Gender			*t*=2.754 (512)	.006
Male	338 (65.8)	157.05 (18.78)		
Female	176 (34.2)	161.90 (19.26)		
Age years			*t*=-2.461 (512)	.014
<50	49 (9.5)	152.37 (18.45)		
50-85	465 (90.5)	159.38 (19.03)		
Residence			*t*=6.328 (398.95)	<.001
Urban	331 (64.4)	162.46 (18.87)		
Rural	183 (35.6)	151.95 (17.55)		
Education			*F*=10.981 (3, 510)	<.001
Elementary school	154 (30)	153.10 (18.07)		
Middle school	185 (36)	157.73 (17.47)		
High school or secondary school	81 (15.8)	164.36 (21.20)		
College and above	94 (18.3)	164.99 (18.89)		
Previous occupation			*F*=26.771 (3, 510)	<.001
Manual workers	216 (42)	154.87 (18.23)		
Commercial or service workers	153 (29.8)	153.70 (15.72)		
Professional and technical workers	143 (27.8)	169.48 (19.16)		
Freelance or unemployed	2 (0.4)	188.50 (3.54)		
Marriage			*F*=2.42 (3, 510)	.065
Unmarried	14 (2.7)	154.36 (19.38)		
Married	67 (13)	164.31 (21.17)		
Divorces	7 (1.4)	156.14 (16.93)		
Widowed	426 (82.9)	158.02 (18.65)		
Living conditions			*F*=1.239 (2, 511)	.290
Alone	38 (7.4)	160.95 (23.43)		
Cohabitation with family	471 (91.6)	158.66 (18.56)		
Nursing home	5 (1)	146.80 (29.55)		
Smoking status			*t*=4.036 (512)	<.001
No	243 (47.3)	162.25 (18.36)		
Yes	271 (52.7)	155.55 (19.17)		
Alcohol consumption			*t*=1.244 (489.50)	.214
No	260 (50.6)	159.75 (17.16)		
Yes	254 (49.4)	157.65 (20.83)		
Age at first incidence of stroke (years)			*F*=5.516 (3, 510)	.001
<40	15 (2.9)	146.73 (19.59)		
40-50	39 (7.6)	156.69 (16.50)		
50-60	151 (29.4)	155.38 (19.13)		
≥60	309 (60.1)	161.18 (18.91)		

XSL•FO
RenderX

Stroke Knowledge, HIL, and Self-Management Scores

The mean (SD) estimated stroke knowledge score of 514 patients with stroke was 17.61 (6.46) points, the mean (SD) total score on the HIL scale was 61.17 (13.58) points, and the mean (SD) total score on the stroke self-management assessment scale was 158.70 (19.07) points. The scores for each dimension are shown in Table 2.

Table . The scores of stroke knowledge, health information literacy (HIL), and self-management ($x \pm s$).

Variable and dimension	Dimension score, mean (SD)	Total score, mean (SD)
Stroke knowledge[a]		17.61 (6.46)
Lifestyle	4.14 (2.00)	
Exercise	1.74 (1.21)	
Diet	2.64 (1.30)	
Risk factors	1.76 (1.26)	
Medication	2.76 (1.14)	
Blood pressure monitoring	1.33 (0.70)	
Stroke signs	2.69 (1.45)	
Management	0.54 (0.75)	
HIL[b]		61.17 (13.58)
Awareness	12.76 (3.30)	
Acquisition	7.92 (2.95)	
Comprehension	10.64 (3.52)	
Evaluation	16.44 (4.79)	
Application	13.42 (1.94)	
Self-management[c]		158.70 (19.07)
Disease	20.54 (8.24)	
Medication	20.20 (2.97)	
Diet	30.53 (4.67)	
Daily life	31.61 (3.48)	
Emotion	18.98 (4.10)	
Social and interpersonal	19.98 (2.97)	
Rehabilitation	16.89 (5.63)	

[a]Stroke knowledge: actual score ranged from 4 to 35.

[b]HIL: actual score ranged from 26 to 97.

[c]Self-management: actual score scores ranged from 111 to 216.

Correlation Analysis (Stroke Knowledge, HIL, and Self-Management)

Table 3 shows the correlations between stroke knowledge, HIL, and self-management. Stroke knowledge was positively correlated with self-management (r=0.668, P<.001) and the HIL score (r=0.138, P<.001), while HIL was positively correlated with self-management (r=0.155, P<.001).

Table . Association between stroke knowledge, health information literacy (HIL), and self-management.

Variable	Self-management	HIL	Stroke knowledge
Self-management	1		
HIL	0.155[a]	1	
Stroke Knowledge	0.668[a]	0.138[a]	1

[a]P<.001

XSL•FO
RenderX

The Mediating Effect of HIL (Between Stroke Knowledge and Self-Management)

Based on the mediation effect testing process proposed by Wen and Ye [17], the theoretical model and rationale based on the construction by Tang and Wang [18] and Mao [19], a mediation model was established with self-management as the dependent variable, stroke knowledge as the independent variable, and HIL as the mediating variable. In the first step, regression analysis was performed, where stroke knowledge was the independent variable and self-management was the dependent variable, and the coefficient c was tested. In the second step, regression analysis was performed using stroke knowledge as the independent variable and HIL as the dependent variable, and the coefficient a was tested. In the third step, regression analysis was performed with stroke knowledge and HIL as the independent variables and self-management as the dependent variable, with coefficients b and c. The results showed that coefficients a, b, and c were significant, indicating a partial mediating effect of HIL between stroke knowledge and stroke self-management behaviors. Details are shown in Table 4.

Table . Mediating effect of health information literacy (HIL) on stroke knowledge and self-management.

Step	Dependent variable	Independent variable	Coefficient	Standardized β coefficient	*t* test[a] *(df)*	*P* value	Adjusted R^2
1	Self-management	Stroke knowledge	c	1.199	16.87 (1)	<.001	0.356
2	HIL	Stroke knowledge	a	1.957	14.622 (1)	<.001	0.293
3	Self-management	HIL	b	0.277	13.849 (2)	<.001	0.531
		Stroke knowledge	c	0.656	9.084 (2)	<.001	

[a] The t test was 2-tailed

Testing the Mediating Effects of HIL

The bootstrap mediation test was conducted using SPSS software (version 26.0). The bootstrap method is a repeated sampling method that treats the original sample as a whole, extracts a large number of new subsamples by repeated sampling with replacement, and obtains statistics. The 95% CI was calculated by repeating the sample 5000 times. The bootstrapped 95% CI for the overall effect of the model did not include a value of 0 (β=1.199, 95% CI 1.059, 1.339). The direct effect of stroke knowledge on self-management in terms of bootstrap 95% CI did not include a value of 0 (β=.656, 95% CI 0.514, 0.798). The mediated effect path was stroke knowledge, followed by HIL, and finally self-management, and the bootstrap 95% CI for its indirect effect did not include a 0 value (β=.543, 95% CI 0.431, 0.663), indicating a significant mediating effect of HIL between stroke knowledge and self-management (Table 5). The mediation pathway is detailed in Figure 2.

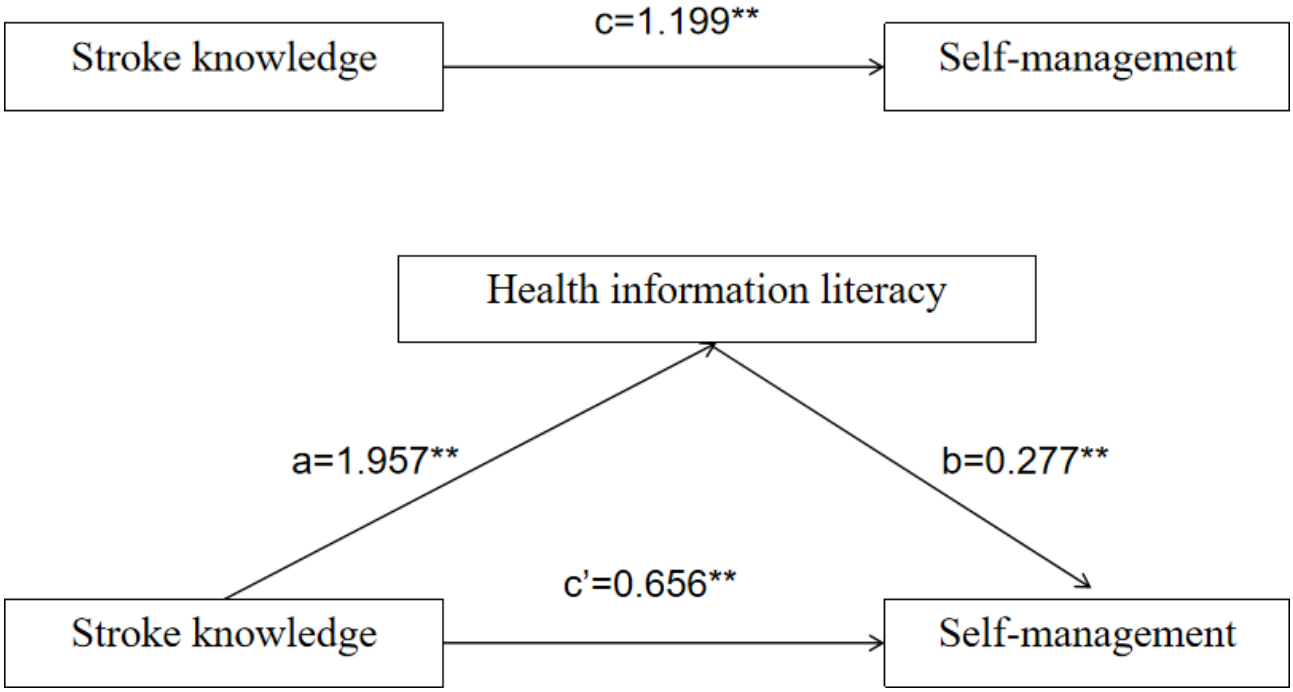
Table . Significance test of the mediating effect of health information literacy (HIL) on stroke knowledge and self-management.

Effect size	Effect	SE	*t* test *(df)*	*P* value	95% confidence limits
Overall effect	1.199	0.071	*t*=16.870 (512)	＜.001	1.059, 1.339
Direct effect	0.656	0.072	*t*=9.085 (511)	＜.001	0.514, 0.798
Indirect effect	0.543	0.058	—[a]	—	0.431, 0.663

[a]not applicable.

XSL•FO
RenderX

Figure 2. The mediating pathway of health information literacy (HIL) between stroke knowledge and self-management. “a” and “b” are mediating effects of the mediating variable HIL; “c” is a direct effect; **P<.001.



Discussion

Principal Findings and Comparison With Previous Works

There was a positive correlation between stroke knowledge, HIL and self-management. Using the Bootstrap test, the total effect, indirect effect, and direct effect of stroke knowledge on self-management were estimated to be 1.199, 0.543, and 0.656, respectively. The 95% CI did not include 0, indicating the significance of the total effect, indirect effect, and direct effect. This indicates that HIL partially mediates the relationship between stroke knowledge and self-management behavior; stroke knowledge and HIL can directly influence the level of self-management in patients with stroke. Stroke knowledge may also indirectly affect the self-management in patients with stroke through the partial mediating effect of HIL; the direct effect was larger than the indirect effect in this study.

The mean (SD) total knowledge level score of patients with stroke was 17.61(6.457), with the highest score in the dimension of lifestyle, and the lowest score in the knowledge of emergency measures for stroke, which was overall moderate. This result was slightly lower than that reported in other studies [20,21], which was related to factors such as differences in the patients' educational level and residence in the western region. This study mainly focused on elderly patients with primary and junior high school education, who have relatively weak learning and adaptation abilities [22]. The mean (SD) HIL score of the patients with stroke was 61.17 (13.58), with the highest health information evaluation score and the lowest health information access score among the dimensions, a result consistent with the findings by Wang et al [23]. Although patients with stroke had moderate levels of HIL, they lacked the ability to access high-quality health information. The mean (SD) total self-management score of patients with stroke was 158.7 (19.07) points, which was moderately low, lower than the survey results obtained by Zhou et al [21] but higher than that obtained by Huang et al [24], with the highest score for daily life management and the lowest score for rehabilitation and exercise management among the dimensions. This may be due to a general lack of knowledge about stroke and self-management skills among first-time patients with stroke and their families. Previous studies have shown substantial enhancements in self-efficacy, activities of daily living, and health-related quality of life in patients with stroke following the implementation of self-management interventions [25-27]. Consequently, it is imperative to enhance the self-management competencies of patients with stroke.

A positive correlation was identified between stroke knowledge, HIL, and stroke self-management behaviors. Sufficient knowledge about stroke is a necessary but not sufficient condition for establishing self-management behaviors. In this study, stroke knowledge had a direct effect on self-management, suggesting that the accumulation of more relevant knowledge about stroke disease or treatment and care may directly encourage such patients to adopt healthy coping behaviors and develop good habits. This was also observed by Fisher et al [28], who suggested that information may have a direct impact on behaviors in situations where novel behavioral skills or complex transformation processes are not required in prevention or self-care processes. Self-management is the process of translating professional knowledge guidelines into daily life [29,30]. The ability to obtain health information in HIL directly affects the level of stroke knowledge of an individual. Patients with lower levels of education have restricted access to information due to their limited reading and comprehension skills [18,31]. Health educators can provide more direct knowledge about stroke management through effective health education, such as hospital education, community health lectures, and health manuals. In community education, as shown

XSL•FO
RenderX

in the study by Yang et al [32] and Singh et al [33], community-based group rehabilitation and culturally relevant education are effective in improving patients' quality of life, HIL, and self-management.

HIL is the influencing factor of self-management behaviors. The higher the level of HIL, the more health information is sought, thus promoting more active self-management behaviors [18,22]. However, simple accumulation of knowledge does not necessarily lead to changes in self-management behaviors [34,35], that is, knowledge is not necessarily successfully translated into self-management behaviors. With the COM-B model [36], we can see that the translation of knowledge into behaviors also depends on the ability of patients to recognize the importance of this knowledge. This also depends on their ability to appropriately evaluate the applicability of the knowledge and apply it to health behaviors decisions, and involves a distinction between "knowing knowledge" and "whether to do it." Stroke self-management is a process that is highly dependent on individual health decision-making, and a weak ability to evaluate information may lead patients to engage in unhealthy behaviors [37,38], in line with the health empowerment theory model. For example, patients who are aware of stroke warning signals may not necessarily respond quickly and take appropriate coping measures, thereby missing the best time for rescue and treatment of the condition. Patients with varying degrees of HIL have unique needs regarding self-management educational content [4,39]. Health professionals must direct their focus towards the older population and those with low literacy levels within their clinical practice, using the HIL scale dimension score to identify patients' deficiencies and take the individual circumstances of patients into account when formulating a rehabilitation, exercise, and follow-up program as well as self-management education content that is both realistic and patient-centred.

Good HIL means that individuals are aware of the importance of health information and their performance in evaluation and applicability is more pronounced. Good HIL also helps patients to accumulate knowledge about stroke and to make full use of self-management knowledge in health decision-making. As posited by Alzayer et al [40], concerted efforts must be made to enhance awareness and educate the public. These measures ought to be initiated at the outset in order to enhance the HIL level of patients with stroke, facilitate the transformation of knowledge pertaining to stroke into self-management behaviors, and improve the self-management effect of affected patients to ensure optimal treatment outcomes.

Limitations

Some limitations of this study include the lack of control trials in healthy individuals. Only a population from three hospitals was included, and patients with stroke in the community were not included. The self-report instrument and convenience sampling method may have potential response bias. In addition, this study was a cross-sectional study and could not explore possible causal relationships. Further research should be performed in other regions to confirm and explore intervention studies.

Conclusions

The self-management of patients with stroke was found to be at a moderate to low level and needs further improvement. There is a correlation between HIL and self-management in various items; the higher the HIL, the better were the self-management behaviors. In addition, HIL is a mediating factor between stroke knowledge and self-management behaviors and can effectively promote the translation of knowledge into behaviors.

Acknowledgments

Funding for this study was provided by the Project of Science and Technology Department of Sichuan Province (No. 2023NSFSC0518) and West China School of Nursing, Sichuan University (No. HXHL21004).

Authors' Contributions

Study design: MZ, YL
Data collection: MZ, YL, YH
Data analysis and interpretation: MZ, YL, YH
Manuscript writing: MZ, YL
Critical revision of the article: WH, MZ

Conflicts of Interest

None declared.

References

1. Ye Y, Zhu YT, Zhang JC, et al. Burden and attributable risk factors of ischemic stroke in China from 1990 to 2019: an analysis from the global burden of disease study 2019. Front Neurol 2023;14:1216777. [doi: 10.3389/fneur.2023.1216777] [Medline: 37564738]
2. Martin SS, Aday AW, Allen NB, et al. 2025 Heart disease and stroke statistics: a report of US and global data from the American heart association. Circulation 2025 Feb 25;151(8):e41-e660. [doi: 10.1161/CIR.0000000000001303] [Medline: 39866113]

XSL•FO
RenderX

3. Bisaillon S, Douen A, Neabel B, Pageau N, Selchen D. Saving costs using an ounce of prevention: introduction of a regional stroke prevention clinic. Axone 2006;27(3):29-33. [Medline: 16764405]
4. Eke R, Jannat KT, Yang XT, Parton JM. Disparity and factors associated with internet health information seeking among US adults living with diabetes mellitus: cross-sectional study. J Med Internet Res 2022 May 30;24(5):e32723. [doi: 10.2196/32723] [Medline: 35635741]
5. Trutner ZD, Furlough K, Martinez A, et al. Is health literacy associated with surgical outcomes? a systematic review. J Surg Res 2023 Nov;291:720-733. [doi: 10.1016/j.jss.2023.06.044] [Medline: 37572516]
6. Reed RL, Roeger L, Howard S, et al. A self-management support program for older Australians with multiple chronic conditions: a randomised controlled trial. Med J Aust 2018 Feb 5;208(2):69-74. [doi: 10.5694/mja17.00127] [Medline: 29385967]
7. Wang Y, Wen X, Liang W, Lin X. Capital endowment, health information literacy and healthy dietary behaviors: Evidence from a survey of Chinese rural residents. Food Qual Prefer 2023 Jan;105:104766. [doi: 10.1016/j.foodqual.2022.104766]
8. Pagán CR, Schmitter-Edgecombe M. Health literacy in older adults: the newest vital sign and its relation to cognition and healthy lifestyle behaviors. Appl Neuropsychol Adult 2024 Mar 29;29(1-8):1-8. [doi: 10.1080/23279095.2024.2334348] [Medline: 38552259]
9. He Y, Guo L, Zauszniewski JA, et al. A reliability and validity study of the electronic health literacy scale among stroke patients in China. Top Stroke Rehabil 2023 Apr;30(3):272-280. [doi: 10.1080/10749357.2021.2016100] [Medline: 34927574]
10. Ouyang W, Wang R, He Y, Song Y, Mo L, Feng L. Status and influential factors of health literacy in patients with ischemic stroke: a cross-sectional study. PLoS ONE 2024;19(7):e0307928. [doi: 10.1371/journal.pone.0307928] [Medline: 39074119]
11. Xue M, Wang Q, Wang J, Ge S, Zhang Z, Mei Y. E-health literacy in stroke patients: latent profile analysis and influencing factors. J Adv Nurs 2025 Mar;81(3):1388-1398. [doi: 10.1111/jan.16351] [Medline: 39058032]
12. Ben-Shabat I, Darehed D, Eriksson M, Salzer J. Characteristics of in-hospital stroke patients in Sweden: a nationwide register-based study. Eur Stroke J 2023 Sep;8(3):777-783. [doi: 10.1177/23969873231182761] [Medline: 37329299]
13. Li S, Wang L, Liu B, et al. Clinical and prognostic characteristics of acute BAD-related stroke: a multicenter MRI-based prospective study. Stroke 2024 Oct;55(10):2431-2438. [doi: 10.1161/STROKEAHA.124.047688] [Medline: 39315825]
14. Zhang XP. Study on relativity between health behavior and quality of life of cerebral apoplexy patients after discharging from hospital [Dissertation]. : Sun Yat-sen University; 2009 URL: https://kns.cnki.net/kcms/detail/detail.aspx?dbname=CJFD2011&filename=SXHZ201106009&dbcode=CJFD [accessed 2025-06-12]
15. Yao ZZ. Development of health information literacy questionnaire for stroke [dissertation]. : Naval Medical University; 2019 URL: https://kns.cnki.net/kcms/detail/detail.aspx?dbname=CMFD202301&filename=1023414944.NH&dbcode=CMFD [accessed 2025-06-12]
16. Wang YQ. Construction and application of self-management intervention project for patients after stroke [dissertation]. : Chengdu University of TCM; 2012 URL: https://kns.cnki.net/kcms/detail/detail.aspx?dbname=CMFD2013&filename=1013111761.nh&dbcode=CMFD [accessed 2025-06-12]
17. Wen Z, Ye B. Analyses of mediating effects: the development of methods and models. Advances in Psychological Science 2014;22(5):731. [doi: 10.3724/SP.J.1042.2014.00731]
18. Tang L, Wang J. Exploring the relationship between health information literacy and health behaviors of the elderly. Iran J Public Health 2023 Jul;52(7):1439-1446. [doi: 10.18502/ijph.v52i7.13245] [Medline: 37593515]
19. Mao XE, Guo XJ, Shi Y. Moderating effect of health information literacy on diabetic knowledge reserve and self-management behavior of patients with type 2 diabetes. Journal of Clinical Medicine in Practice 2021;25(16):90-94. [doi: 10.7619/jcmp.20210646]
20. Liu QH, Tan JX, Hu CX, Hu DL, Wan LH. A decade-long comparison of prestroke health behaviors among hypertensive stroke patients in mainland China. J Neurosci Nurs 2022 Feb 1;54(1):42-47. [doi: 10.1097/JNN.0000000000000628] [Medline: 34775393]
21. Zhou J, He CY, Yang H, et al. Correlation between disease knowledge, self-efficacy and self-management behavior in patients with first-episode stroke. Journal of Chengdu Medical College 2023;18(1):91-96.
22. Vemuri AK, Hejazian SS, Vafaei Sadr A, et al. Self-management among stroke survivors in the United States, 2016 to 2021. J Clin Med 2024 Jul 25;13(15):4338. [doi: 10.3390/jcm13154338] [Medline: 39124605]
23. Wang Z, Fan Y, Lv H, et al. The gap between self-rated health information literacy and internet health information-seeking ability for patients with chronic diseases in rural communities: cross-sectional study. J Med Internet Res 2022 Jan 31;24(1):e26308. [doi: 10.2196/26308] [Medline: 35099401]
24. Huang SQ, Li SQ, Wu XY, Yang R, Zhao LH. The risk factors of self-management behavior among Chinese stroke patients. Int J Clin Pract 2023;2023:4308517. [doi: 10.1155/2023/4308517] [Medline: 36941873]
25. Lo SHS, Chau JPC, Choi KC, Wong RYM, Kwan JCY, Iu IHL. Health professional- and volunteer-partnered self-management support (COMBO-KEY) to promote self-efficacy and self-management behaviors in people with stroke: a randomized controlled trial. Ann Behav Med 2023 Sep 13;57(10):866-876. [doi: 10.1093/abm/kaad028] [Medline: 37260291]
26. Sexton E, Fowler K, Hickey A, et al. Priorities for developing stroke care in Ireland from the perspectives of stroke survivors, family carers and professionals involved in stroke care: A mixed methods study. PLoS ONE 2024;19(1):e0297072. [doi: 10.1371/journal.pone.0297072] [Medline: 38241235]

XSL•FO
RenderX

27. Mendes Pereira C, Matos M, Carvalho D, et al. Building bridges between people with stroke, families, and health professionals: development of a blended care program for self-management. J Clin Med 2024 Jan 4;13(1):300. [doi: 10.3390/jcm13010300] [Medline: 38202307]
28. Fisher JD, Fisher WA, Williams SS, Malloy TE. Empirical tests of an information-motivation-behavioral skills model of AIDS-preventive behavior with gay men and heterosexual university students. Health Psychol 1994 May;13(3):238-250. [doi: 10.1037//0278-6133.13.3.238] [Medline: 8055859]
29. Al Sayah F, Majumdar SR, Williams B, Robertson S, Johnson JA. Health literacy and health outcomes in diabetes: a systematic review. J Gen Intern Med 2013 Mar;28(3):444-452. [doi: 10.1007/s11606-012-2241-z] [Medline: 23065575]
30. Butayeva J, Ratan ZA, Downie S, Hosseinzadeh H. The impact of health literacy interventions on glycemic control and self-management outcomes among type 2 diabetes mellitus: A systematic review. J Diabetes 2023 Sep;15(9):724-735. [doi: 10.1111/1753-0407.13436] [Medline: 37407516]
31. Li S, Cui G, Yin Y, Wang S, Liu X, Chen L. Health-promoting behaviors mediate the relationship between eHealth literacy and health-related quality of life among Chinese older adults: a cross-sectional study. Qual Life Res 2021 Aug;30(8):2235-2243. [doi: 10.1007/s11136-021-02797-2] [Medline: 33661455]
32. Yang C, Zhao F, Xie C, Zhang Y, Dou Z, Wei X. Community-based group rehabilitation program for stroke patients with dysphagia on quality of life, depression symptoms, and swallowing function: a randomized controlled trial. BMC Geriatr 2023 Dec 20;23(1):876. [doi: 10.1186/s12877-023-04555-0] [Medline: 38124046]
33. Singh H, Fulton J 4th, Mirzazada S, Saragosa M, Uleryk EM, Nelson MLA. Community-based culturally tailored education programs for black communities with cardiovascular disease, diabetes, hypertension, and stroke: systematic review findings. J Racial Ethn Health Disparities 2023 Dec;10(6):2986-3006. [doi: 10.1007/s40615-022-01474-5] [Medline: 36508135]
34. Glasgow RE, Toobert DJ, Hampson SE, Brown JE, Lewinsohn PM, Donnelly J. Improving self-care among older patients with type II diabetes: the “Sixty Something...” Study. Patient Educ Couns 1992 Feb;19(1):61-74. [doi: 10.1016/0738-3991(92)90102-o] [Medline: 1298950]
35. Zhong X, Li S, Luo M, Ma X, Fisher EB. Peer support self-management intervention for individuals with type 2 diabetes in rural primary care settings: protocol for a mixed methods study. JMIR Res Protoc 2023 Sep 4;12:e47822. [doi: 10.2196/47822] [Medline: 37665619]
36. Paterson S, Dawes H, Winward C, et al. Use of the capability, opportunity and motivation behaviour model (COM-B) to understand interventions to support physical activity behaviour in people with stroke: an overview of reviews. Clin Rehabil 2024 Apr;38(4):543-557. [doi: 10.1177/02692155231224365] [Medline: 38192225]
37. Svendsen SJ, Grov EK, Staats K. Patients’ experiences with shared decision-making in home-based palliative care - navigation through major life decisions. BMC Palliat Care 2024 Apr 17;23(1):101. [doi: 10.1186/s12904-024-01434-2] [Medline: 38627710]
38. Paakkari L, Balch-Crystal E, Manu M, et al. Health-literacy education drives empowerment and agency. The Lancet 2023 Feb;401(10374):343-344. [doi: 10.1016/S0140-6736(23)00107-1]
39. Kim S, Song Y, Park J, Utz S. Patients’ experiences of diabetes self-management education according to health-literacy levels. Clin Nurs Res 2020 Jun;29(5):285-292. [doi: 10.1177/1054773819865879] [Medline: 31394916]
40. Alzayer R, Barakat M, Jirjees F, et al. Knowledge and awareness of stroke and associated factors in the Saudi general population: a cross-sectional study. Front Neurol 2023;14:1225980. [doi: 10.3389/fneur.2023.1225980] [Medline: 37808501]

Abbreviations

HIL: health information literacy

Edited by A Coristine; submitted 03.07.24; peer-reviewed by K Tsakpounidou, X Ding; revised version received 26.05.25; accepted 27.05.25; published 23.06.25.

Please cite as:
Zeng M, Liu Y, He Y, Huang W
Relationship Between Stroke Knowledge, Health Information Literacy, and Health Self- Management Among Patients with Stroke: Multicenter Cross-Sectional Study
JMIR Med Inform 2025;13:e63956
URL: https://medinform.jmir.org/2025/1/e63956
doi:10.2196/63956

© Mengxue Zeng, Yanhua Liu, Ying He, Wenxia Huang. Originally published in JMIR Medical Informatics (https://medinform.jmir.org), 23.6.2025. This is an open-access article distributed under the terms of the Creative Commons Attribution License (https://creativecommons.org/licenses/by/4.0/), which permits unrestricted use, distribution, and reproduction

XSL•FO
RenderX

in any medium, provided the original work, first published in JMIR Medical Informatics, is properly cited. The complete bibliographic information, a link to the original publication on https://medinform.jmir.org/, as well as this copyright and license information must be included.

XSL•FO
RenderX

Implementation of an Integrated, Clinical Decision Support Tool at the Point of Antihypertensive Medication Refill Request to Improve Hypertension Management: Controlled Pre-Post Study

John Charles Matulis 3rd[1], DO, MPH; Jason Greenwood[1], MD; Michele Eberle[2], MBA; Benjamin Anderson[3], PharmD, RPh; David Blair[2], MD; Rajeev Chaudhry[1], MBBS, MPH

[1]Division of Community Internal Medicine, Geriatrics and Palliative Care, Mayo Clinic, 200 1st St. SW, Rochester, MN, United States

[2]Department of Family Medicine, Mayo Clinic Health System, Eau Claire, WI, United States

[3]Department of Pharmacy, Mayo Clinic, Rochester, MN, United States

Corresponding Author:
John Charles Matulis 3rd, DO, MPH
Division of Community Internal Medicine, Geriatrics and Palliative Care, Mayo Clinic, 200 1st St. SW, Rochester, MN, United States

Abstract

Background: Improving processes regarding the management of electronic health record (EHR) requests for chronic antihypertensive medication renewals may represent an opportunity to enhance blood pressure (BP) management at the individual and population level.

Objective: This study aimed to evaluate the effectiveness of the eRx HTN Chart Check, an integrated clinical decision support tool available at the point of antihypertensive medication refill request, in facilitating enhanced provider management of chronic hypertension.

Methods: The study was conducted at two Mayo Clinic sites—Northwest Wisconsin Family Medicine and Rochester Community Internal Medicine practices—with control groups in comparable Mayo Clinic practices. The intervention integrated structured clinical data, including recent BP readings, laboratory results, and visit dates, into the electronic prescription renewal interface to facilitate prescriber decision-making regarding hypertension management. A difference-in-differences (DID) design compared pre- and postintervention hypertension control rates between the intervention and control groups. Data were collected from the Epic EHR system and analyzed using linear regression models.

Results: The baseline BP control rates were slightly higher in intervention clinics. Postimplementation, no significant improvement in population-level hypertension control was observed (DID estimate: 0.07%, 95% CI −4.0% to 4.1%; *P*=.97). Of the 19,968 refill requests processed, 46% met all monitoring criteria. However, clinician approval rates remained high (90%), indicating minimal impact on prescribing behavior.

Conclusions: Despite successful implementation, the tool did not significantly improve hypertension control, possibly due to competing quality initiatives and high in-basket volumes. Future iterations should focus on enhanced integration with other decision support tools and strategies to improve clinician engagement and patient outcomes. Further research is needed to optimize chronic disease management through EHR-integrated decision support systems.

(JMIR Med Inform 2025;13:e70752) doi:10.2196/70752

KEYWORDS

clinical decision support systems; population health; hypertension; electronic health records

Introduction

The contemporary electronic health record (EHR) enables patients and pharmacies to request chronic medication renewals, which comprise significant in-basket volumes that primary care teams must address. Typical EHR renewal request interfaces provide clinicians with limited information when addressing the refill request [1]. For patients not seen recently, it takes time for conscientious clinicians to review relevant electronic data to ensure that the requested renewal is appropriate for that patient's care plan. Ideally, physicians or a staff member would always review relevant data, including the date of the last clinician visit, presence of up-to-date laboratory monitoring, and prior documentation, to confirm that the medication is appropriately addressing important outcomes such as blood pressure, blood glucose, or cholesterol control [2]. However, in the context of rapidly increasing in-basket volumes, such diligence is unlikely in the absence of a supportive system, as

XSL•FO
RenderX

primary care providers (PCP) struggle to "get through one's in-basket" [3].

The EHRs have long been recognized as powerful tools that can provide real-time decision support to assist clinicians in cognitively demanding and tedious tasks. Examples of clinical decision support integrated into EHR medication prescription platforms include alerts when prescribing medications to which a patient may be allergic, medications that may have an unsafe interaction with another prescribed medication, and medications that would generate significant out-of-pocket costs for the patient [4-6]. Hypertension, the most common chronic condition treated in primary care [7], has shown that EHR-integrated applications, as described by Funes et al [8], can improve clinician workflows in chronic disease management. In addition, the American Heart Association and the American Medical Association have called upon primary care teams to better leverage protocols and team-based care to improve hypertension control [9]. This study is particularly timely, as the management of hypertension when patients are not in the office is becoming increasingly relevant for quality reporting and reimbursement [10]. As more health care systems transition to value-based payment [11], the management of uncontrolled hypertension will become a higher priority in clinical practice. Given this context, prescription renewal requests provide a valuable opportunity for the primary care team to ensure safe prescribing practices and improved management of this difficult-to-treat condition.

In this study, we describe the implementation and evaluation of an EHR-integrated clinical decision support tool, eRx HTN Chart Check, which incorporates relevant structured data necessary for monitoring hypertension management into the prescription renewal request interface. We aimed for this tool to improve care provided to both individual patients with hypertension and population-level control of hypertension.

Methods

Study Setting: Mayo Clinic Health System, Northwest Wisconsin and Mayo Clinic, Rochester, MN

The division of Family Medicine, Mayo Clinic Health System (MCHS)-Northwest Wisconsin (NWWI) employs 108 providers, including 80 physicians and 28 advanced practice providers (APPs), caring for approximately 96,000 patients in 11 primary care clinics across a five-county area centered around Eau Claire, Wisconsin. The Mayo Clinic division of Community Internal Medicine (CIM) in Rochester Minnesota, employs 75 PCPs (60 physicians, 15 APPS) caring for 35,000 patients at 5 primary care sites within a 40-mile radius of the community of Rochester, MN. Both sites are part of Mayo Clinic, a not-for-profit health care system providing both "destination" care for serious and complex issues and primary care for local communities.

The control groups consisted of the Department of Family Medicine in Southeast Minnesota, which employs 57 physicians and 88 APPs who care for 115,000 patients, and the Department of Internal Medicine in MCHS-Southwest Wisconsin, which employs 7 physicians and 3 APPs who care for 7,000 patients. All primary care practices included in this study have designated the management of uncontrolled hypertension as a quality management priority during the intervention period.

eRx HTN Chart Check Project and Team

Before the eRx HTN chart check project, automated prescription renewal requests were sent directly to PCPs through the EHR in-basket without additional clinical information. Specifically, refill requests did not include relevant clinical information such as the patient's most recent blood pressure, most recent office visit, or relevant laboratory results.

In January 2022, a multidisciplinary team representing Mayo Clinic campuses in Rochester, MN, and Mayo Clinic Health System-NWWI was assembled. The project team aimed to integrate clinical decision support into the electronic prescription renewal process to improve clinical efficiency, provider experience, and the quality of care provided. The project team included a project manager, 3 physician leaders from the two participating sites, nursing leaders, a pharmacist informaticist, and a practice administrator.

Hypertension Chart Check Protocol Development

Internal EHR user data showed that PCPs spent significant in-basket time reviewing and approving chronic prescription medications. Antihypertensive medication renewals were selected as the initial target for integrated clinical decision support, given the importance of hypertension management in population health and the need for an interface to facilitate an efficient review of relevant clinical information. This included hypertension control, the date of the most recent office visit or blood pressure reading on file, and appropriate laboratory monitoring for specific medications.

The eRx HTN Chart Check integrated key clinical data (BP readings, visit dates, and laboratory results) directly into the prescription renewal interface. A pass/fail grading system flagged values based on predefined thresholds: BP readings from the past 24 months and laboratory results from the past 12 months. A detailed view, available to the clinician via hyperlink, displayed up to three recent values, with standing laboratory orders and future laboratory orders. For patients without an active hypertension diagnosis, the system excluded recent BP readings, and for those of childbearing age, it ensured no positive pregnancy test within the past 12 months.

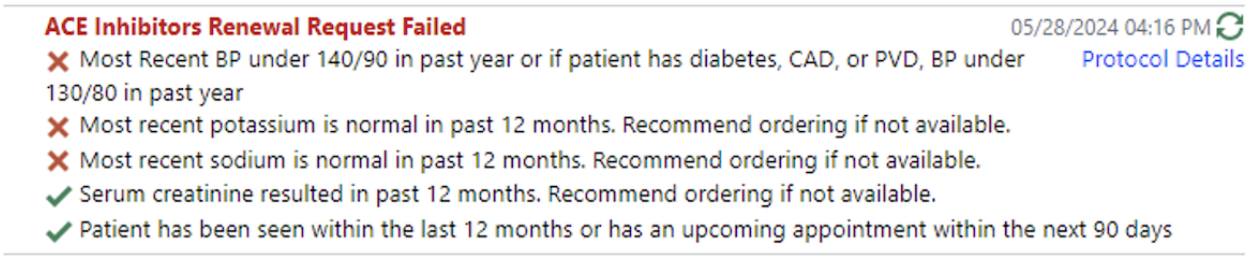
The team, with selective input from Mayo Clinic experts and practice resources, determined appropriate monitoring and developed protocols for commonly prescribed classes of antihypertensive medications (Multimedia Appendix 1). The pass/fail criteria were determined through an iterative process involving a multidisciplinary team of physician leaders, pharmacists, nursing informaticists, and EHR specialists. Criteria were based on established clinical guidelines for hypertension management, including recommended monitoring intervals for BP measurements and laboratory assessments for antihypertensive medication safety. Adjustments were made based on Mayo Clinic expertise coupled with historical prescribing patterns to balance clinical rigor with practical usability. While no formal external validation was conducted, the criteria were aligned with national guidelines and vetted

XSL•FO
RenderX

through internal stakeholder feedback to ensure clinical appropriateness.

After completion of medication selection and protocol development, relevant discrete data for the medication renewal protocol were converted into a visual pass/fail display, which would appear directly below the renewal request message (Figure 1).

Figure 1. Pass/fail display in renewal requests. This figure illustrates how the eRx HTN Chart Check tool presents structured clinical data within the prescription renewal interface. Green checkmarks (✔) indicate that the required clinical data (e.g., recent BP reading, appropriate laboratory monitoring) meet predefined thresholds; red marks ( ) flag missing or outdated data, prompting clinician review before approving renewal.



Preimplementation efforts (April 2022) included clinician presentations and educational materials. The tool was launched at MCHS-NWWI on July 15, 2022, and at Rochester CIM on August 1, 2022. No modifications were made postimplementation, but periodic clinician meetings reinforced tool usage.

The eRX HTN Chart Check tool was adopted across both practice environments with minimal levels to workflows. Some physicians raised concerns about whether the eRx HTN Chart Check failure implied an expectation that the physician was responsible for addressing outstanding items. Clarification was provided to clinician teams that this was not the intent; rather, the information was presented only for the prescribing physician's awareness. In our subjective experience, most clinicians impacted by the change found the additional information available to be helpful in efficiently completing these renewal requests, although this finding was not quantitatively evaluated.

Study Design and Sample

We evaluated our eRx HTN Chart Check intervention using a DID design. The outcomes in the intervention group were collected through monthly hypertension control metrics, spanning 6.5 months before and 5.5 months after the intervention's implementation period, which occurred between June and August 2022. The specific dates of the intervention timelines are outlined in Table 1. The DID design allows estimation of the intervention effect by comparing the change in outcomes over time between the intervention group relative to the control group, accounting for secular trends. Visual inspection of these trends indicated similar trajectories, supporting the validity of the parallel trend's assumption. Additionally, no significant interaction between time and group was observed in the preintervention period when tested using regression analysis, further reinforcing this assumption. No patients or prescribers at either intervention or control sites were excluded.

Table . Timelines for baseline data collection, intervention implementation, and postimplementation data collection. The intervention was implemented sequentially at different sites, with clinician education provided before each launch. Postimplementation surveillance included monitoring clinician engagement and assessing hypertension control trends.

Study phase	Timelines for data collection	Intervention group	Control group	Activities
Preintervention	January-June 2022	NWWI[a] FM+[b]RST[c] CIM[d]	MCHS[e] CIM+RST FM	Intervention design, iterative feedback
Implementation	July 15, 2022	NWWI FM	FM RST	Education, real-time support
Implementation	August 1, 2022	RST CIM	SWWI CIM	Education, real-time support
Post Implementation	August 2022-December 2022	NWWI FM + RST CIM	MCHS CIM+ RST FM	Surveillance

[a]NWWI: Northwest Wisconsin.

[b]FM: Family Medicine.

[c]RST: Rochester.

[d]CIM: Community Internal Medicine.

[e]MCHS: Mayo Clinic Health System.

Ethical Considerations

The Mayo Clinic Institutional Review Board deemed this project as a quality improvement initiative and exempted it from formal review. All data were maintained on encrypted, password-protected systems behind the organization's firewall, with access limited to authorized project team members only. No patient identifiers were retained in the final analysis or manuscript, and all reporting is based on deidentified, aggregate

XSL•FO
RenderX

information to ensure confidentiality and compliance with institutional privacy standards.

Primary Outcomes

The primary outcome was the average percentage of patients with a recorded BP reading of <140/90 before and after the study period. This BP target of <140/90 was selected in accordance with the Minnesota Community Measurement program and National Quality Foundation standards [12,13]. The 6-month follow-up period for outcome assessment was chosen to allow the prescriber to evaluate the possible impact of subsequent BP management after an antihypertensive prescription refill request.

Secondary Outcomes

Secondary outcomes reflect measures related to antihypertensive refill volumes and the rates of clinician approval for medications prepared via the eRx HTN Chart Check protocol.

Data Sources and Analysis

The unit of analysis for the primary outcome was all eligible patients within each practice who had a formal diagnosis of hypertension in the EHR, compatible with definitions of the Minnesota Community Measurement program's definitions [12]. For secondary outcomes, the unit of analysis included patients whose eRx HTN Chart Check renewals were completed during the study period. We ascertained patient-level data on hypertension control through an internal EHR data platform used for quality improvement. We extracted eligible prescription renewal encounter data from the Epic EHR Cogito resources [14] (Workbench, SlicerDicer, and direct data queries with either internal or external visualization tools) to determine clinician response rates to eligible chart check encounters.

Statistical Methods

To assess changes in BP control across practices, we calculated the proportion of all eligible patients with a recorded BP at treatment goal (<140/90) within the preceding 12 months, consistent with National Quality Foundation guidelines [13]. We calculated these proportions by both study period and group and conducted a DID analysis using aggregated clinic-level proportions as the dependent variable and exposure to the intervention as the independent variable. We calculated the between-group differences using a linear regression model to adjust for the clustering of data within clinics. The model included fixed effects for time and group to control for baseline differences and time trends. The intervention effect was reported as the mean difference in proportions, with 95% CIs and *P* values. Statistical significance was defined as $P<.05$, and analyses were performed using Blue Sky Statistics (version 10.3.4; BlueSky Statistics LLC). Secondary outcomes were analyzed using descriptive statistics.

Results

Baseline Characteristics of Intervention Patients

We identified 15,591 patients in the NWWI division of Family Medicine and 11,766 patients in the Rochester CIM cohort in our baseline dataset. Relevant study characteristics are included in Table 2.

Table . Baseline preintervention patient characteristics.

Clinical site	Patients with essential hypertension (n)	Average number of total medications	Eligible patients taking antihypertension medication (N=15,591), n (%)	Average number of antihypertension medications (n)	Average age (years)	White patients, n (%)	English-speaking patients, n (%)	Smoker patients, n (%)
NWWI-FM[a]	15,591	11.6	14,439 (93)	2.1	66	15,159 (97)	15,441 (99)	1766 (11.3)
RST-CIM[b]	11,766	13.1	10,709 (91)	1.7	69	15,314 (88)	16,393 (94)	1096 (9.3)
SWWI-CIM[c]	3368	14.1	3154 (94)	2.1	70.9	3267 (97)	3354 (99)	242 (7.2)
RST-FM[d]	24,782	11.8	22,166 (89)	1.8	61.2	22,303 (90)	24,073 (97)	1437 (5.8)

[a]NWWI: Northwest Wisconsin-Family Medicine.

[b]RST-CIM: Community Internal Medicine.

[c]SWWI: Southwest Wisconsin-Family Medicine.

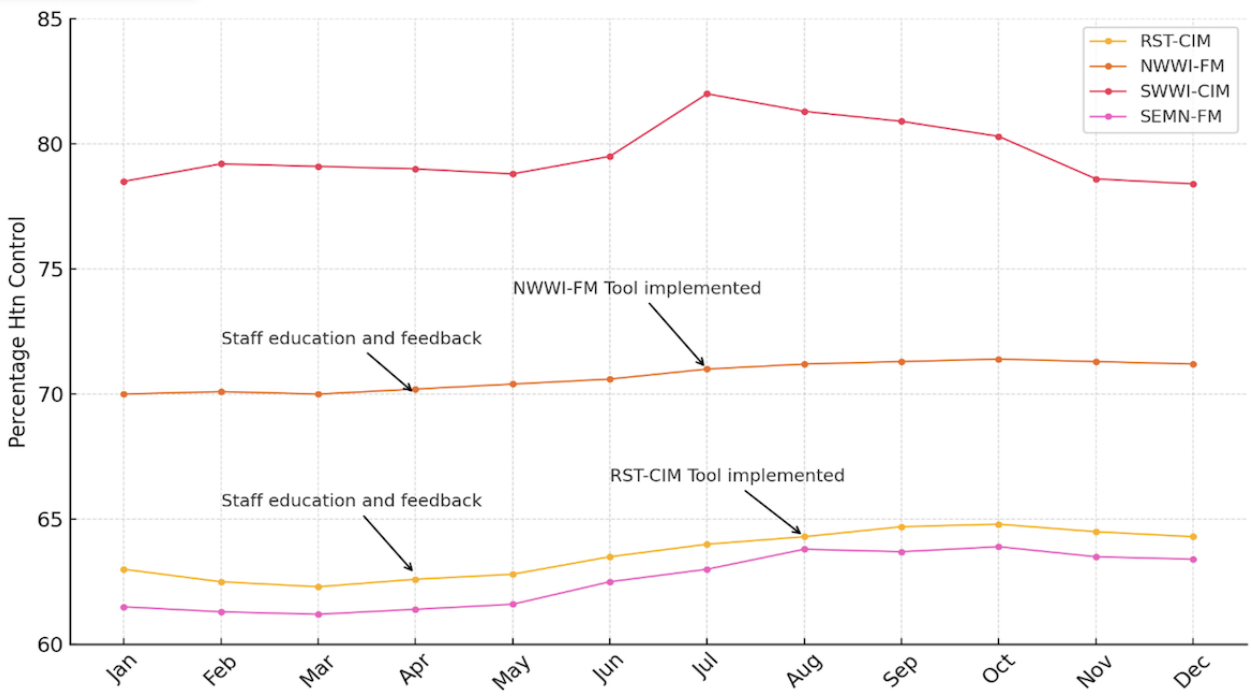
[d]RST-FM: Family Medicine.

We then performed a DID analysis to evaluate the impact of eRx HTN Chart Check implementation on clinic-level compliance proportions. The baseline compliance proportion was higher in the intervention clinics compared to the control clinics (difference: 3.32%, 95% CI 0.5%-6.2%; *P*=.02). Across all clinics, there was no significant change in compliance proportions from the baseline to the intervention period (difference: 1.29%, 95% CI: −1.6% to 4.2%; *P*=.37). The DID estimate, reflecting the interaction between intervention group and time period, was not statistically significant (difference: 0.07%, 95% CI −4.0% to 4.1%; *P*=.97). These findings suggest that the intervention did not result in a significant additional improvement in compliance proportions compared to the control group.

Figure 2 presents a line chart depicting BP changes before, during, and after the intervention across all analyzed patient cohorts. No significant DID was observed in compliance proportion changes between groups over the study period.

XSL•FO
RenderX

Figure 2. Hypertension control by site. Htn: hypertension; RST-CIM: Rochester-Community Internal Medicine; NWWI-FM: Northwest Wisconsin-Family Medicine; SWWI: Southwest Wisconsin-Community Internal Medicine; SEMN-FM: Southeast Minnesota-Family Medicine.



Secondary Outcomes: Chart Check Completion Rates and Subsequent Blood Pressure Re-Measurement

Secondary outcomes are displayed in Table 3. A total of 19,968 refills for antihypertensive medications were completed through the eRx HTN Chart Check process during the study period. Among these, 9,256 (46%) prescriptions "passed" or had all current monitoring information (Figure 2) available at the time of renewal.

Table . Secondary outcomes.

Clinical site	Refills submitted via chart check (n)	Number of refills "passed protocol", n (%)	Refills approved by clinician, n (%)
NWWI-FM[a]	10,771	5018 (47)	9225 (86)
RST-CIM[b]	9197	4238 (46)	8748 (95)
Combined intervention group	19,968	9256 (46.4)	17,973 (90)

[a]NWWI: Northwest Wisconsin-Family Medicine.

[b]RST-CIM: Rochester-Community Internal Medicine.

Discussion

Principal Findings

In this evaluation of the implementation of the eRx HTN Chart Check tool, we found that its use was not associated with significant improvements in population-level hypertension control when compared with practices in the same health care system that were unexposed to the intervention. While the eRx HTN chart check tool identified that approximately 50% of patients requesting prescription renewals had incomplete hypertension management parameters, most prescriptions were still filled, suggesting that this tool may not have significantly changed prescriber behavior.

There are several possible explanations that may account for why the eRx HTN Chart Check intervention did not result in improved population-level hypertension control compared with unexposed practices, as hypothesized. First, the management of hypertension was a concurrent quality priority across all health care system sites at the time of this intervention, and several ongoing efforts for patient outreach and enhanced office care and blood pressure rechecks. These efforts were already underway, including efforts to better capture home BP readings in the EHR and proactive follow-up for patients with hypertension, among others. Given the heightened awareness of hypertension management, clinicians may have relied on other interventions to address hypertension management rather than the eRx HTN Chart Check tool, which may have been used primarily to ensure appropriate medication monitoring. Additionally, changes in clinical guidelines, medication costs, insurer coverage, increasing telehealth utilization, and health care consumerism could have played a role in shaping hypertension outcomes independent of our intervention. While the DID analysis adjusted for baseline differences and time trends, the presence of multiple simultaneous initiatives limited our ability to isolate the specific impact of the eRx HTN Chart

XSL•FO
RenderX

Check intervention. Second, in the post-COVID period, primary care in-basket volumes increased substantially across our practice and other clinics nationwide [15]. This increased workload may have resulted in less clinician attention being allocated to prescription renewal requests. This premise is supported by the remarkably prescription approval rates reported in our secondary outcomes, suggesting that time constraints may have led clinicians to prioritize efficiency over detailed clinical review when addressing these requests. Third, the eRx HTN Chart Check intervention only appeared for refill requests that originated from the pharmacy, meaning it may not have effectively captured or been applied to all prescription renewal requests, including those sent directly from patients, thereby limiting the overall reach of this intervention.

This study applies a novel EHR clinical decision support (CDS) tool aimed at promoting chronic disease management through extant processes of routine medication renewals. The successful implementation of the eRx HTN Chart Check tool demonstrates that routine care processes such as chronic disease medication renewals can present opportunities for the integration of clinical decision support and current clinical workflows, as well as standardizing the information gathered across sites in a group practice. The eRx HTN Chart Check tool can be enhanced, adapted, and combined with other interventions to address important population health priorities such as control of hypertension. Additionally, other important outcomes, such as prescribing safety, appropriate monitoring, care escalation, patient engagement, provider satisfaction, and cognitive load should be explored in subsequent assessments of integrated CDS in the contemporary primary care setting.

This study is subject to the typical limitations of this study design, including the possibility of selection bias due to lack of randomization, regression to the mean, the Hawthorne effect, and time-related biases such as misattribution. These limitations were significantly mitigated by the inclusion of similar control groups practicing in comparable environments and with similar quality priorities. However, it is important to note that the findings may have limited generalizability due to the geographic, health care system, and patient population characteristics of the included sites. In health care systems with fewer resources, different clinician workflows, or alternative staffing models, the adaptation of this tool may vary. Additionally, patient populations served by community health centers or safety-net institutions may have different levels of medication adherence and follow-up needs. Therefore, future research should evaluate how this tool functions in other nonintegrated health care settings. Moreover, while our primary outcome focused on population-level hypertension control, we did not examine patient-level variables that could influence blood pressure outcomes, such as medication adherence, follow-up visit rates, or patient-reported measures of disease burden. These factors are critical in understanding hypertension management but were not captured in our dataset, which was limited to structured EHR-derived clinical data. Future research should incorporate patient-centered metrics—including follow-up care, medication adherence, and qualitative assessments of patient and provider experiences—to provide a more comprehensive evaluation of CDS interventions in chronic disease management.

Future efforts should be closely tied with other team-based efforts to maximize efficiency and leverage important patient touchpoints, such as prescription renewals, to improve care delivery and standardize practices enabling cross-clinic site support. Machine learning and artificial learning may serve as valuable future enhancements in potentially aiding clinicians in targeted interventions [16]. Additional efforts are needed to understand how organizations can optimally support PCPs in using valuable tools such as the eRx HTN Chart Check. Additionally, further alignment between add-on tools such as the eRx HTN Chart Check and other CDS tools such as Practice Advisories, Health Maintenance Navigators, and outreach platforms should be encouraged. This alignment would ensure a uniform approach, easier maintenance, and facilitate seamless updates as guidelines and protocols change.

Conclusion

In this controlled pre-post study evaluating the implementation of a CDS tool for antihypertensive medication refill requests, we found that implementation of this tool into existing workflows did not improve population-level BP control compared with groups unexposed to the intervention. Despite the lack of significant improvements in hypertension control, this study highlights the potential for EHR-based decision support tools to impact chronic disease management. Aligning the eRx HTN Chart Check with other EHR-based interventions such as automated patient outreach, remote BP monitoring integration, and machine learning may improve its utility and adoption. Future research should explore multimodal decision support strategies, clinician education initiatives, and the impact of interoperability with broader population health tools to optimize hypertension management in diverse clinical settings. Future research should focus on optimizing these interventions, exploring alternative implementation strategies, and expanding their application to other chronic conditions.

Conflicts of Interest

None declared.

Multimedia Appendix 1
Hypertension chart check protocol.
[DOCX File, 32 KB - medinform_v13i1e70752_app1.docx]

References

XSL•FO
RenderX

1. Grossman JM, Cross DA, Boukus ER, Cohen GR. Transmitting and processing electronic prescriptions: experiences of physician practices and pharmacies. J Am Med Inform Assoc 2012;19(3):353-359. [doi: 10.1136/amiajnl-2011-000515] [Medline: 22101907]
2. Pattin AJ, Devore N, Fowler J, Weldy D. An examination of the prescription renewal process and implications for primary care physicians and community pharmacists. J Pharm Pract 2020 Apr;33(2):187-191. [doi: 10.1177/0897190018799217] [Medline: 30222033]
3. Steckowych K, Smith M. Workflow process mapping to characterize office-based primary care medication use and safety: a conceptual approach. Res Social Adm Pharm 2019 Apr;15(4):378-386. [doi: 10.1016/j.sapharm.2018.06.003] [Medline: 30025884]
4. Sutton RT, Pincock D, Baumgart DC, Sadowski DC, Fedorak RN, Kroeker KI. An overview of clinical decision support systems: benefits, risks, and strategies for success. NPJ Digit Med 2020;3:17. [doi: 10.1038/s41746-020-0221-y] [Medline: 32047862]
5. Légat L, Van Laere S, Nyssen M, Steurbaut S, Dupont AG, Cornu P. Clinical decision support systems for drug allergy checking: systematic review. J Med Internet Res 2018 Sep 7;20(9):e258. [doi: 10.2196/jmir.8206] [Medline: 30194058]
6. McMullin ST, Lonergan TP, Rynearson CS, Doerr TD, Veregge PA, Scanlan ES. Impact of an evidence-based computerized decision support system on primary care prescription costs. Ann Fam Med 2004;2(5):494-498. [doi: 10.1370/afm.233] [Medline: 15506587]
7. Finley CR, Chan DS, Garrison S, et al. What are the most common conditions in primary care? Systematic review. Can Fam Physician 2018 Nov;64(11):832-840. [Medline: 30429181]
8. Funes Hernandez M, Babakhanian M, Chen TP, et al. Design and implementation of an electronic health record-integrated hypertension management application. J Am Heart Assoc 2024 Jan 16;13(2):e030884. [doi: 10.1161/JAHA.123.030884] [Medline: 38226516]
9. Abdalla M, Bolen SD, Brettler J, et al. Implementation strategies to improve blood pressure control in the United States: a scientific statement from the American Heart Association and American Medical Association. Hypertension 2023 Oct;80(10):e143-e157. [doi: 10.1161/HYP.0000000000000232] [Medline: 37650292]
10. Dzau VJ, Balatbat CA. Future of hypertension: The need for transformation. Hypertension 2019;74:450-457. [doi: 10.1161/HYPERTENSIONAHA.119.13437] [Medline: 31352827]
11. Muhlestein D, Bleser WK, Saunders RS, McClellan M. All‐payer spread of acos and value‐based payment models in 2021: the crossroads and future of value‐based care. RAMAONHEALTHCARE. 2021. URL: https://ramaonhealthcare.com/all-payer-spread-of-acos-and-value-based-payment-models-in-2021-the-crossroads-and-future-of-value-based-care/ [accessed 2024-09-26]
12. Measure: controlling high blood pressure. Minnesota Department of Health. 2024. URL: https://www.health.state.mn.us/diseases/cardiovascular/cardio-dashboard/hbpcont.html [accessed 2024-09-26]
13. Controlling high blood pressure. National Quality Forum. 2024. URL: https://www.qualityforum.org/Projects/c-d/Cardiovascular_Endorsement_and_Maintenance_2010/0018_Controlling_high_blood_pressure.aspx [accessed 2024-09-26]
14. Data & Analytics. Epic Systems Corporation. 2024. URL: https://www.epic.com/software/analytics-insights-discovery/ [accessed 2024-09-26]
15. Nath B, Williams B, Jeffery MM, et al. Trends in electronic health record inbox messaging during the COVID-19 pandemic in an ambulatory practice network in New England. JAMA Netw Open 2021 Oct 1;4(10):e2131490. [doi: 10.1001/jamanetworkopen.2021.31490] [Medline: 34636917]
16. Huang AA, Huang SY. Shapely additive values can effectively visualize pertinent covariates in machine learning when predicting hypertension. J Clin Hypertens (Greenwich) 2023 Dec;25(12):1135-1144. [doi: 10.1111/jch.14745] [Medline: 37971610]

Abbreviations

APP: advanced practice provider
BP: blood pressure
CDS: clinical decision support
CIM: Community Internal Medicine
DID: difference-in-differences
EHR: electronic health record
MCHS: Mayo Clinic Health System
NWWI: Northwest Wisconsin
PCP: primary care provider

XSL•FO
RenderX

Edited by C Lovis; submitted 01.01.25; peer-reviewed by O Kehinde, S Huang; revised version received 10.03.25; accepted 15.03.25; published 11.04.25.

Please cite as:
Matulis 3rd JC, Greenwood J, Eberle M, Anderson B, Blair D, Chaudhry R
Implementation of an Integrated, Clinical Decision Support Tool at the Point of Antihypertensive Medication Refill Request to Improve Hypertension Management: Controlled Pre-Post Study
JMIR Med Inform 2025;13:e70752
URL: https://medinform.jmir.org/2025/1/e70752
doi:10.2196/70752

© John Charles Matulis 3rd, Jason Greenwood, Michele Eberle, Benjamin Anderson, David Blair, Rajeev Chaudhry. Originally published in JMIR Medical Informatics (https://medinform.jmir.org), 11.4.2025. This is an open-access article distributed under the terms of the Creative Commons Attribution License (https://creativecommons.org/licenses/by/4.0/), which permits unrestricted use, distribution, and reproduction in any medium, provided the original work, first published in JMIR Medical Informatics, is properly cited. The complete bibliographic information, a link to the original publication on https://medinform.jmir.org/, as well as this copyright and license information must be included.

XSL•FO
RenderX

Biases in Race and Ethnicity Introduced by Filtering Electronic Health Records for "Complete Data": Observational Clinical Data Analysis

Jose Miguel Acitores Cortina[1,2*], MSc; Yasaman Fatapour[1,2*], PhD; Kathleen LaRow Brown[3,4], MA; Undina Gisladottir[3,4], PhD; Michael Zietz[1], PhD; Oliver John Bear Don't Walk IV[5], PhD; Danner Peter[5], MPH; Jacob S Berkowitz[1,2], BSc; Nadine A Friedrich[1,2], MD; Sophia Kivelson[1,2], MSc; Aditi Kuchi[1,2], MSc; Hongyu Liu[1,2], PhD, MD; Apoorva Srinivasan[1,2], MSc; Kevin K Tsang[1,2], MSc; Nicholas P Tatonetti[1,2,3,4], PhD

[1]Department of Computational Biomedicine, Cedars-Sinai Medical Center, 700 North San Vicente Boulevard, Pacific Design Center Suite G540, Los Angeles, CA, United States

[2]Cedars-Sinai Cancer, Cedars-Sinai Medical Center, Los Angeles, CA, United States

[3]Department of Systems Biology, Columbia University, New York, NY, United States

[4]Department of Biomedical Informatics, Columbia University, New York, NY, United States

[5]Department of Biomedical Informatics and Medical Education, University of Washington, Seattle, WA, United States

[*]these authors contributed equally

Corresponding Author:
Nicholas P Tatonetti, PhD
Department of Computational Biomedicine, Cedars-Sinai Medical Center, 700 North San Vicente Boulevard, Pacific Design Center Suite G540, Los Angeles, CA, United States

Abstract

Background: Integrated clinical databases from national biobanks have advanced the capacity for disease research. Data quality and completeness filters are used when building clinical cohorts to address limitations of data missingness. However, these filters may unintentionally introduce systemic biases when they are correlated with race and ethnicity.

Objective: In this study, we examined the race and ethnicity biases introduced by applying common filters to 4 clinical records databases. Specifically, we evaluated whether these filters introduce biases that disproportionately exclude minoritized groups.

Methods: We applied 19 commonly used data filters to electronic health record datasets from 4 geographically varied locations comprising close to 12 million patients to understand how using these filters introduces sample bias along racial and ethnic groupings. These filters covered a range of information, including demographics, medication records, visit details, and observation periods. We observed the variation in sample drop-off between self-reported ethnic and racial groups for each site as we applied each filter individually.

Results: Applying the observation period filter substantially reduced data availability across all races and ethnicities in all 4 datasets. However, among those examined, the availability of data in the white group remained consistently higher compared to other racial groups after applying each filter. Conversely, the Black or African American group was the most impacted by each filter on these 3 datasets: Cedars-Sinai dataset, UK Biobank, and Columbia University dataset. Among the 4 distinct datasets, only applying the filters to the All of Us dataset resulted in minimal deviation from the baseline, with most racial and ethnic groups following a similar pattern.

Conclusions: Our findings underscore the importance of using only necessary filters, as they might disproportionally affect data availability of minoritized racial and ethnic populations. Researchers must consider these unintentional biases when performing data-driven research and explore techniques to minimize the impact of these filters, such as probabilistic methods or adjusted cohort selection methods. Additionally, we recommend disclosing sample sizes for racial and ethnic groups both before and after data filters are applied to aid the reader in understanding the generalizability of the results. Future work should focus on exploring the effects of filters on downstream analyses.

(JMIR Med Inform 2025;13:e67591) doi:10.2196/67591

KEYWORDS

health disparities; data quality; observational research; electronic health records; racial and ethnic biases

XSL•FO
RenderX

Introduction

The rapid adoption of electronic health records (EHRs) in the past decade has greatly expanded the availability and accessibility of clinical data. This advancement enables health care professionals to harness vast amounts of information, driving medical research, personalized medicine, and overall improvements in health care delivery [1,2]. Additionally, it helps to build big data in health care, providing a foundation for advanced analytics and informed decision-making on a large scale. This supports the training and validation of artificial intelligence methodologies and models, leading to improved diagnostic accuracy, personalized treatment plans, and more efficient health care delivery. Therefore, the collected data significantly influence the results and hypotheses derived from these methods.

To improve diversity in health care, studies must include populations underrepresented in the biomedical, clinical, behavioral, and social sciences, such as individuals from racial and ethnic minority groups, those with disabilities, and people from disadvantaged backgrounds [3]. Fostering diversity is vital for producing more accurate, inclusive research outcomes that reflect the needs of all populations, ultimately leading to more equitable health care and improved patient outcomes [4,5].

However, the usefulness of available clinical data is limited if it does not reliably reflect the diversity of the underlying population. Bias in health care research refers to systematic errors or deviations that lead to inaccurate or skewed results, interpretations, or decisions. It usually occurs when certain factors, whether intentional or unintentional, disproportionately influence the research process, leading to outcomes that do not accurately represent the truth. Thus, scientific progress is delayed, flawed conclusions perpetuated, and disparities in health care outcomes are reinforced [6].

Lack of diversity, which may be due to systemic biases and discrimination against individuals and groups from minoritized populations, can lead to biased research outcomes that exacerbate health disparities [7-10]. This can lead to inaccurate conclusions about treatment or interventions that may not apply equally across different populations. In addition, there are still not enough big clinical longitudinal datasets, which are essential for understanding long-term health trends, progression of diseases over time, and evaluating treatment outcomes.

When conducting observational clinical data analysis, it is often preferable to aim for a dataset that is as complete as possible. However, well-meaning filters that improve completeness may introduce unintended biases in the target population [11].

Data completeness can be defined as the extent to which EHRs or other data sources capture all necessary and relevant information to accurately represent a patient's medical history, care processes, or outcomes. It includes both the presence and accuracy of essential data elements, such as diagnoses, treatments, laboratory results, and preventive care measures, ensuring a comprehensive and reliable foundation for clinical care, research, and quality assessment [12-14].

In this study, we aim to evaluate the effect of data completeness filters originally used by Weber et al [11] on different datasets and how various filters impact the patient cohort. This work extends the analysis to 4 large datasets, including the All of Us (AoU) dataset, UK Biobank (UKBB), and 2 geographically distinct academic medical centers. Specifically, we focus on identifying race and ethnicity biases introduced by commonly used filters [15].

Methods

We examined 4 distinct data sources, AoU, UKBB, Columbia University dataset, and Cedars-Sinai dataset comprising approximately 12 million patients. By analyzing the available data and applying each filter, we aimed to investigate the potential biases these filters may introduce.

All of Us

The AoU study, sponsored by the National Institutes of Health, has enrolled more than 814,000 participants as of June 18, 2024, with 80% of them coming from underrepresented populations [16]. These groups include racial and ethnic minorities, people with disabilities, those in rural or underserved areas, and individuals from lower socioeconomic backgrounds. Figure S1 in Multimedia Appendix 1 (provided by the AoU study) showcases the self-reported races and ethnicities of the participants who have completed the initial steps of the program, providing a diverse representation. The recruitment process spans all regions of the United States.

The AoU workbench encompasses a wealth of information gathered from EHRs, including data from Fitbit devices, survey responses, and socioeconomic factors. Notably, a recent release of data in April 2023 included approximately 245,400 whole genome sequencing records and 312,940 genotyping microarrays, further enhancing the dataset's depth and potential for analysis.

UK Biobank

The UKBB is a large-scale, population-based study that aims to improve the prevention, diagnosis, and treatment of various diseases. It involves the collection of extensive health-related data, including genetic information, from over 500,000 participants in the United Kingdom. Participants in the UKBB, recruited at ages 40 - 69 years, were registered with the National Health Service. Researchers can download the data through the UKBB's Data Showcase, which collaborates closely with the European Genome Archive.

Cedars-Sinai

Cedars-Sinai Medical Center (CSMC) is one of the largest hospitals in California, based in Los Angeles, and serves up to 1 million diverse patients every year across its 40 locations in Southern California. CSMC also serves as a large research center. The studied database comprises over 4 million patients.

Columbia University

Columbia University Irving Medical Center (CUIMC) is a clinical, research, and educational enterprise located on a campus in Northern Manhattan. They are home to 4 colleges

XSL•FO
RenderX

and schools that work on scientific research, education, and patient care. The studied database comprises over 5 million patients.

The self-reported race and ethnicity distributions of each dataset, along with the number of participants in each dataset, are presented in Table 1. In addition to those self-reported categories for race and ethnicity, we defined an all group, which includes every patient in that specific dataset. This group serves as a baseline for comparison within the dataset.

Table . Self-reported race and ethnicity percentages of each dataset, along with the total number of participants in each dataset.

Dataset	CSMC[a]	CUIMC[b]	All of Us	UKBB[c]
Total patients, n	4,031,307	7,121,848	287,012	502,364
Race, n (%)				
American Indian and/or Alaska Native	5695 (0.14)	8275 (0.12)	—[d]	—
Asian	205,978 (5.11)	100,046 (1.40)	8294 (2.89)	11,472 (2.28)
Black or African	373,130 (9.26)	445,623 (6.26)	58,264 (20.30)	3552 (0.71)
Native Hawaiian or Pacific Islanders	7082 (0.18)	6693 (0.09)	344 (0.12)	—
White	1,992,336 (49.42)	1,252,219 (17.58)	154,678 (53.89)	473,353 (94.22)
Mixed	—	—	5000 (1.74)	1731 (0.34)
Other	—	1,037,027 (14.56)	4727 (1.65)	10,394 (2.07)
Unknown	1,447,086 (35.89)	4,271,965 (59.99)	55,705 (19.40)	1931 (0.38)
Ethnicity, n (%)				
Hispanic or Latino	344,708 (8.55)	657,288 (9.23)	54,054 (18.83)	—
Non-Hispanic or non-Latino	1,691,775 (41.97)	1,298,181 (18.23)	221,935 (77.32)	—
Unknown	1,994,824 (49.48)	5,166,379 (72.54)	11,023 (3.84)	—

[a]CSMC: Cedars-Sinai Medical Center.

[b]CUIMC: Columbia University Irving Medical Center.

[c]UKBB: UK Biobank.

[d]Not available.

A straightforward approach to identifying subsets of patients whose data are suitable for research studies is to use heuristic computational filters [11] that exclude patients lacking various types of data in their records. For this study, we evaluated 19 different filters, which can be grouped into 3 categories. The first category is based on patient demographics. This includes filters that check whether the patient has both age and sex recorded (AgeSex), if the patient is alive at the time of the search (Alive), if the patient has a known address or zip code (Address or zip), and a set of age filters. The age filters have been applied to age at the time of any diagnosis, for example, the age filter≥65 selects patients who are 65 years or older than 65 years at the time of any of their recorded diagnoses.

The second category is a record-based filter, which checks whether patients have at least 1 recorded instance of various medical data. These filters are the presence of at least 1 diagnosis, the presence of medication records, and records for outpatient visits.

The last category is the time span or observational period filter, which selects patients who have had multiple interactions with the health care system during a specific period of time. The maximum time window for this category was the 6-year follow-up.

We used 19 filters, originally defined by Weiskopf et al [17] as a metric for evaluating the completeness of EHRs, to build patient cohorts within each dataset. These filters helped identify the types of data available after their application. To maintain consistency across datasets, we applied these filters to the patient populations with EHR data in each dataset. Detailed descriptions of each filter, along with their categories, are presented in Table 2.

XSL•FO
RenderX

Table . Filters used in our analysis, grouped by category and descriptions of each filter.

Group and filter		Description
Demographics		
	Alive	Patient is alive at the time of the query
	AgeSex	Patient has both sex and age recorded
	Age filter ≥18	Patient has a diagnosis at an age included in the filter
	Age filter ≤21	Patient has a diagnosis at an age included in the filter
	Age filter ≤40	Patient has a diagnosis at an age included in the filter
	Age filter ≤65	Patient has a diagnosis at an age included in the filter
	Age filter ≥65	Patient has a diagnosis at an age included in the filter
	Age filter ≤80	Patient has a diagnosis at an age included in the filter
	Address or zip code	Patient has an address or zip code recorded
Medical interactions		
	Diagnosis	Patient has at least 1 diagnosis recorded
	Medication	Patient has at least 1 medication prescribed and recorded
	Outpatient visit	Patient has at least 1 outpatient visit recorded
Observation period		
	1 week	Patient has a recorded observation period equal or longer than the filter span
	2 weeks	Patient has a recorded observation period equal or longer than the filter span
	1 month	Patient has a recorded observation period equal or longer than the filter span
	6 months	Patient has a recorded observation period equal or longer than the filter span
	1 year	Patient has a recorded observation period equal or longer than the filter span
	2 years	Patient has a recorded observation period equal or longer than the filter span
	6 years	Patient has a recorded observation period equal or longer than the filter span

First, we queried our databases to get a count of all the patients, grouping them by self-reported race and ethnicity. After establishing the initial groups, we applied each filter one at a time to see the effect of that filter on sample availability.

This study aimed to identify the biases of different types of filters that are used by researchers to evaluate data completeness in electronic EHR datasets. Our focus is biases that may be introduced upon applying these filters to races and ethnicities.

We then assessed the statistical significance of the filters' impact on different racial and ethnic subgroups through binomial testing. Comparing the expected sample to the observed filtered sample. For each group, we calculated the *P* values by comparing the observed proportion relative to the sum of that group and the white baseline group against an expected baseline.

$$\text{Observed proportion} = \frac{\text{filtered group n}}{\text{filtered group n} + \text{filtered White n}}$$

$$\text{Expected proportion} = \frac{\text{group total n}}{\text{group total n} + \text{White total n}}$$

Subsequently, we adjusted the *P* values for multiple hypothesis correction using the Bonferroni method.

Ethical Considerations

The research performed complies with all relevant ethical regulations; the institutional review boards (IRBs) that approved the study protocol are Columbia (IRB AAAL0601) and CSMC (IRB STUDY00003395). Patients were enrolled under a waiver of consent in CSMC and CUIMC. Consent in AoU and UKBB

XSL•FO
RenderX

is managed by each platform, respectively. During the study, we only accessed nonprotected health information and total counts, maintaining the confidentiality of every patient.

Results

Overview

We applied the filters to each dataset separately to assess their individual effects. Table 3 indicates the percentage of patients remaining after applying each filter for each dataset.

Table . Percentage of population remaining on each dataset after applying the different filters.

Filter	Cedars-Sinai, n (%)	Columbia, n (%)	All of Us, n (%)	UKBB[a], n (%)
Alive	3,852,435 (95.56)	6,774,829 (95.12)	283,806 (98.88)	467,333 (93.02)
AgeSex	4,026,072 (99.87)	6,002,422 (84.28)	28,701 (100)	502,364 (100)
Age filter ≥18	1,624,951 (40.30)	4,286,839 (60.19)	253,948 (88.48)	229,960 (45.77)
Age filter ≤21	127,771 (3.16)	1,328,385 (18.65)	21,881 (7.62)	82,953 (16.51)
Age filter ≤40	733,191 (18.18)	2,814,216 (39.51)	103,431 (36.04)	178,503 (35.53)
Age filter ≤65	1,348,000 (33.43)	4,393,121 (61.98)	227,072 (79.12)	225,790 (44.49)
Age filter ≥65	424,790 (10.53)	1,170,388 (16.43)	81,938 (28.55)	122,327 (24.35)
Age filter ≤80	1,584,518 (39.30)	4,992,410 (70.09)	252,875 (88.10)	229,961 (45.77)
Has address or zip	1,829,303 (45.37)	4,024,099 (56.50)	287,007 (99.99)	148,261 (29.51)
Has medications	1,316,735 (32.66)	2,513,715 (35.29)	239,691 (83.51)	368,599 (77.37)
Has diagnoses	1,663,429 (41.26)	5,158,066 (72.42)	254,449 (88.66)	466,982 (92.95)
Has outpatient visits	2,963,959 (73.25)	2,893,964 (40.63)	286,214 (99.72)	230,078 (45.79)
Observation period 1 week	2,242,853 (55.63)	4,993,424 (70.11)	5254 (1.83)	223,398 (44.46)
Observation period 2 weeks	2,190,443 (54.33)	4,937,814 (69.33)	4916 (1.71)	223,203 (44.43)
Observation period 1 month	2,121,948 (52.63)	4,855,922 (68.18)	4398 (1.53)	222,915 (44.37)
Observation period 6 months	1,889,240 (46.86)	4,240,529 (59.54)	2938 (1.02)	222,006 (44.19)
Observation period 1 year	1,734,906 (43.03)	4,082,843 (57.32)	2602 (1)	221,321 (44.05)
Observation period 2 years	1,541,480 (38.23)	3,880,143 (54.48)	2241 (1)	220,300 (43.85)
Observation period 6 years	733,203 (18.18)	3,151,463 (44.25)	2007 (1)	217,257 (43.24)

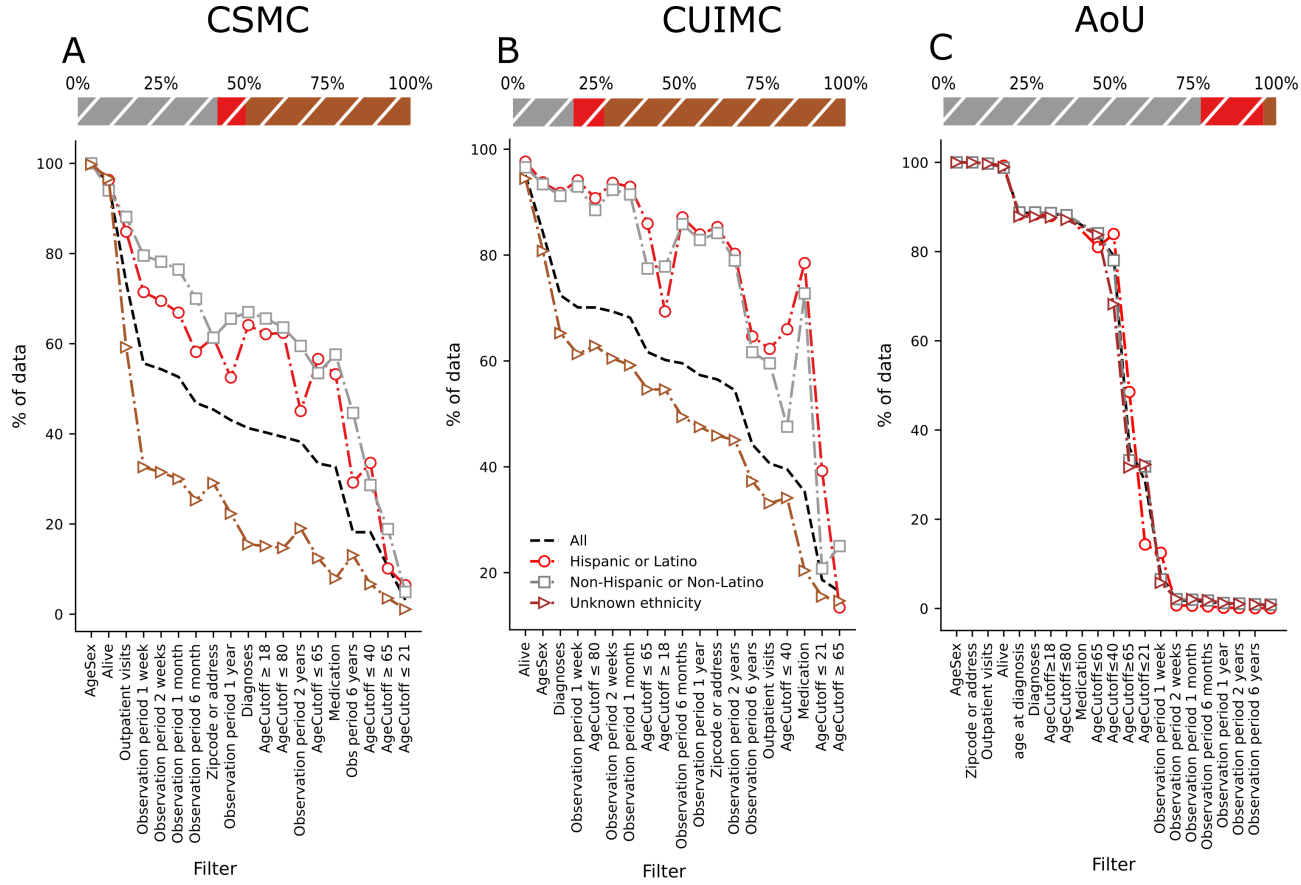
[a]UKBB: UK Biobank.

Cedars-Sinai

Figures 1A and 2A show the percentage of available patients in the CSMC after applying each filter. The results show that both unknown race and unknown ethnicity are the most affected groups when applying the filters. This causes the values for the group all to decrease too, and it is shown across every cohort.

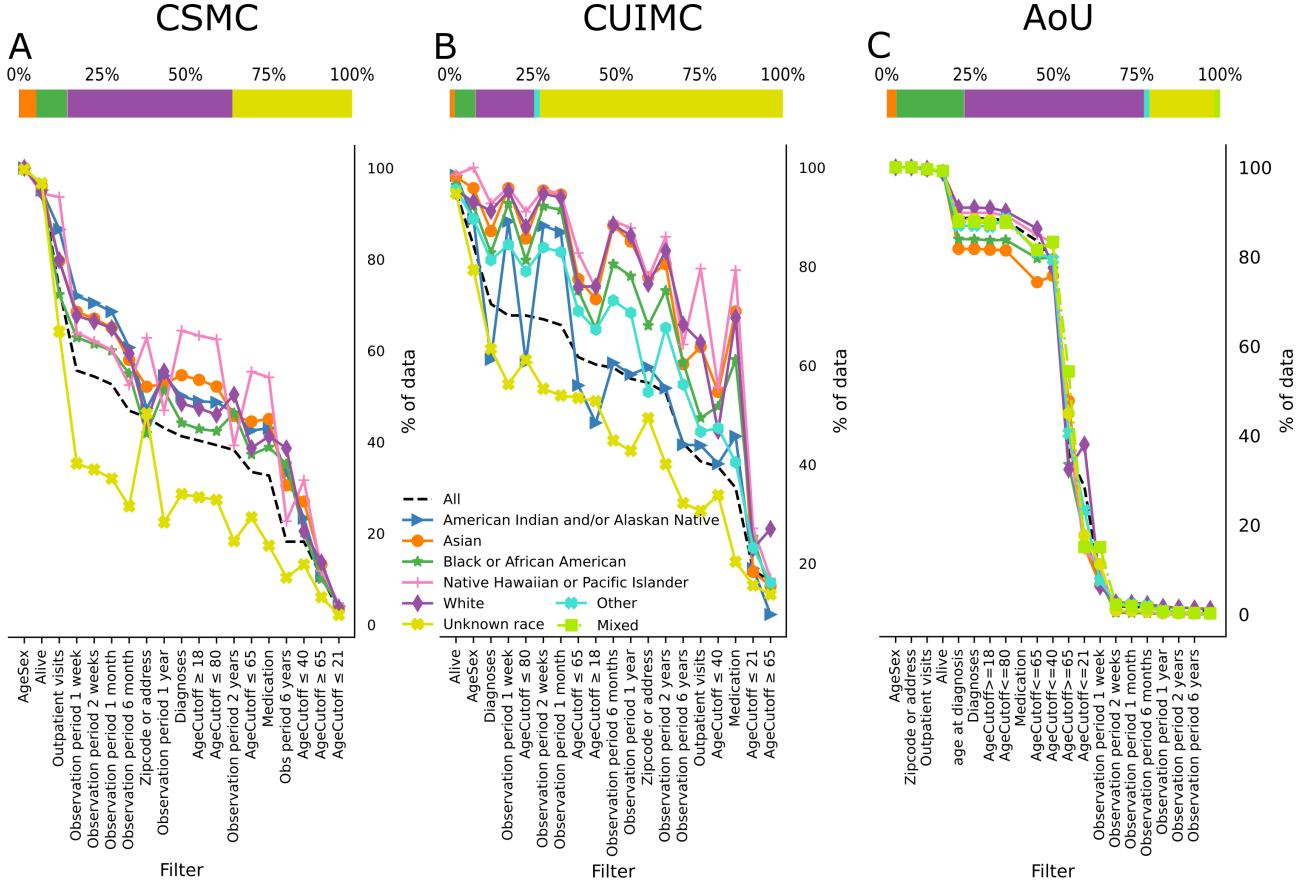
XSL•FO
RenderX

Figure 1. Available percentage of patients' data upon individually applying all 19 filters in different ethnic subgroups in (A) the Cedars-Sinai dataset, (B) the CUIMC dataset, and (C) the AoU dataset. The filters are in descending order following the available percentage of the category, all. The points are connected to ease the visualization, but the filters are not cumulative. Stacked bar plots show the ethnicity distribution of the datasets in percentages. Stacked bar plot from CSMC has 8.55% (n=344,708) of Hispanic or Latino, 41.97% (n=1,691,775) of non-Hispanic or non-Latino, and 49.48% (n=1,994,824) of unknown ethnicity. Stacked bar plot from CUIMC has 9.23% (n=657,288) of Hispanic or Latino, 18.23% (n=1,298,181) of non-Hispanic or non-Latino, and 72.54% (n=5,166,379) of unknown ethnicity. Stacked bar plot from AoU has 18.83% (n=54,054) of Hispanic or Latino, 77.32% (n=221,935) of non-Hispanic or non-Latino, and 3.84% (n=11,023) of unknown ethnicity. The available percentage values can be found in Tables S2-S4 in Multimedia Appendix 1. AoU: All of Us; CSMC: Cedars-Sinai Medical Center; CUIMC: Columbia University Irving Medical Center.



XSL•FO
RenderX

Figure 2. Available percentage of patients' data upon individually applying all 19 filters in different racial subgroups in (A) the Cedars-Sinai dataset, (B) the CUIMC dataset, (C) and the AoU dataset. The filters are in descending order following the available percentage of the category, all. The points are connected to ease the visualization, but the filters are not cumulative. Stacked bar plots show the race distribution of the datasets in percentages. Stacked bar plot from CSMC has 0.14% (n=5695) of American Indian and/or Alaska Native, 5.11% (n=205,978) of Asian, 9.26% (n=373,130) of Black or African, 0.18% (n=7082) of Hawaiian Native or Pacific Islander, 49.42% (n=1,992,336) of white, and 35.89% (n=1,447,086) of unknown race. Stacked bar plot from CUIMC has 0.12% (n=8275) of American Indian and/or Alaska Native, 1.40% (n=100,046) of Asian, 6.26% (n=445,623) of Black or African, 0.09% (n=6693) of Hawaiian Native or Pacific Islander, 17.58% (n=1,252,219) of white, 14.56% (n=1,037,027) of another race, and 59.99% (n=4,271,965) of unknown race. Stacked bar plot from AoU has 2.89% (n=8294) of Asian, 20.30% (n=58,264) of Black or African, 0.12% (n=344) of Hawaiian Native or Pacific Islander, 53.89% (n=154,678) of white, 1.74% (n=5000) of mixed race, 1.65% (n=4727) of another race, and 19.40% (n=55,705) of unknown race. The available percentage values can be found in Tables S2-S4 in Multimedia Appendix 1. AoU: All of Us; CSMC: Cedars-Sinai Medical Center; CUIMC: Columbia University Irving Medical Center.



The results of the CSMC cohort show that every known race or ethnicity group is above "all" in almost every filter. However, both unknown race and unknown ethnicity are the most affected groups when applying the filters. This causes the values for the group all to decrease too, and it is shown across every cohort.

Nevertheless, it is important to note that in this dataset, the Black or African American population is the most affected group by the filters, being significantly more affected than the white population in 16 of 19 filters, as seen in Table S6 in Multimedia Appendix 1. Additionally, as the observation period filter increases, every race group becomes more affected than the white population.

All of Us

For the AoU dataset, we applied the filters to the cohort of patients in the controlled tier 7 who had EHR records. This process reduced the number of patients from 410,235 to 287,012. Upon applying age or sex, medication, zip code or address (in this dataset, we have state of residence, so we used that instead of zip code), alive status, and outpatient visits, the initial cohort remained largely unchanged. However, as more stringent age filters were applied and the observational period was extended, the cohort population significantly decreased. Among all the races, the Asian group was most noticeably impacted, particularly when the observation period filter was applied, as shown in Figure 2A. Within this dataset, unlike at CSMC, the majority of racial and ethnic groups follow the same pattern when each filter is applied. It is remarkable that most of the groups experience significant data loss compared to the White group on the same filters, as shown in Table S7 in Multimedia Appendix 1.

Columbia University Irving Medical Center

Similarly to the cohort from CSMC, the unknown race or ethnicity and other values decrease the most when applying the filters, bringing down the overall percentage. The known races or ethnicities are again above the all group's percentage in almost every category. It is important to note that unknown race and ethnicity represent close to 60%(n=4,271,965) and 72%(n=5,166,379) of Columbia University Medical Center's cohort, respectively, contributing to the low baseline percentage for the all group.

XSL•FO
RenderX

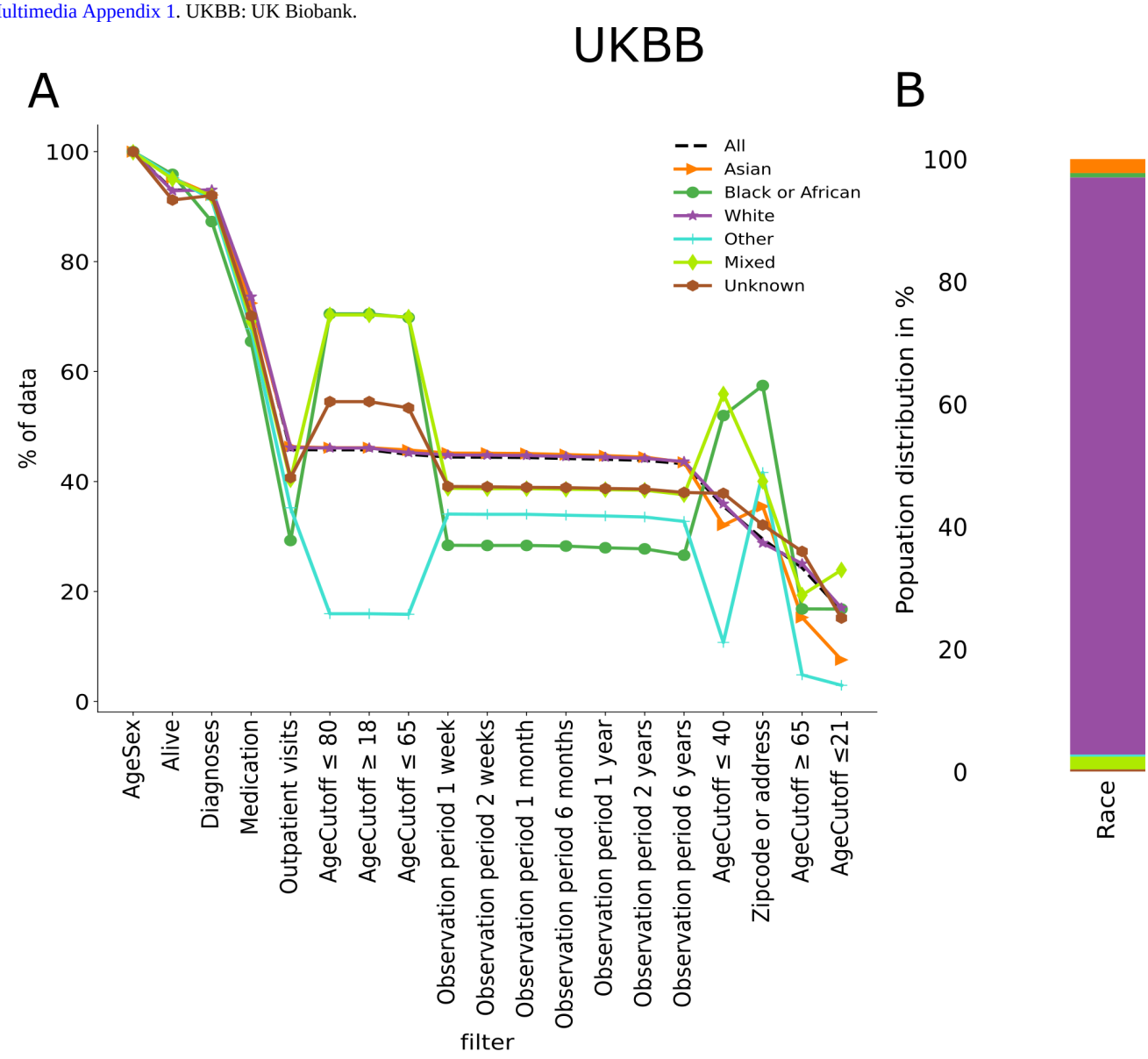
Of the known races and ethnicities, we can see in Figures 1B and 2B that the American Indian and/or Alaska Native population is the most significantly affected by the filters, 18 of 19, even crossing the all line. This is followed by Black or African American, which takes the second place in 16 of 19. However, contrary to the CSMC cohort, the non-Hispanic or non-Latino ethnicity is the most affected by the filters, 10 of 19 filters.

UK Biobank

In the UKBB, race and ethnicity classifications differ from those used in American institutions. To ensure consistency in data presentation, we applied the UK government's recommended grouping strategy [18], aligning it with the US classification system for comparability. We included any other Black background, African, Black or Black British, and Caribbean under the category Black or African origin; any other Asian background, Asian or Asian British, Bangladeshi, Chinese, Indian, and Pakistani under the category Asian; any other white background, British, Irish, and white under the category white; do not know and prefer not to answer under unknown; any other mixed background, mixed, white and Asian, white and Black African, and white and Black Caribbean under mixed; and finally, other ethnic group under other.

After this grouping, there are some aspects to remark on from this dataset, white population represents close to 94%(n=473,353) of the group, which biases completely the all results. Having that in mind, we can see in Figure 3 how every other race was impacted more than the baseline, especially the Black or African origin group.

Figure 3. Available percentage of patients' data upon individually applying all 19 filters in different racial subgroups (**A**) in the UKBB dataset. The filters are in descending order following the available percentage of the category, all. The points are connected to ease the visualization, but the filters are not cumulative. Stacked bar plots show the race distribution of the datasets in percentages. (B) Stacked bar plot shows the racial distribution of the dataset in percentages, showing 2.28% (n=11,472) of Asian, 0.71% (n=3552) of Black or African, 94.22% (n=473,353) of white, 0.34% (n=1731) of mixed race, 2.07% (n=10,394) of another race, and 0.38% (n=1931) of unknown race. The available percentage values can be found in Table S5 in Multimedia Appendix 1. UKBB: UK Biobank.



XSL•FO
RenderX

We then analyzed the differences within the most prevalent groups in this dataset, evaluating only the 5 most common categories. We found that the British group accounts for 91%(n=442,973) of the total, only counting the top 5 groups. This approach yielded results similar to those of the complete one. The first 5 categories, in order of percentage, were the following: British (91.7%, n=442,973), ny other white background (3.4%, n=16,455), Irish (2.8%,n=13,346), Indian (1.2%, n=5,955), and other ethnic group (1%, n=4,609). These percentages account for the addition of the population of the top 5 groups and not the total.

A low adjusted *P* value (eg, <.001) suggests that the subgroup is significantly more affected by the specific filter than the white group used as a baseline. We see across every dataset that most of the groups are significantly more affected by the filter than our baseline, but it is particularly notable in groups like Black or African American and American Indian and/or Alaska Native. The Hispanic or Latino ethnic group also shows more significant data loss than non-Hispanic or non-Latino across every dataset. The *P* values can be found in Tables S6-S8 in Multimedia Appendix 1.

Discussion

Overview

Our study investigates the potential racial and ethnic biases introduced by applying common data quality and completeness filters in clinical research databases, including AoU, UKBB, and 2 academic medical centers. We analyzed 19 filters across approximately 12 million patients and discovered that certain filters significantly reduce data availability and have a differential effect on racial and ethnic groups.

The challenge with these filters lies in distinguishing between patients with missing data who could be relatively healthy, have not recently sought medical care, or have limited access to health care systems. Each group will have a low number of data entries in their records. Consequently, these filters might bias the resulting cohort by selecting sicker patients who interact with the health care system more frequently and/or those who have more access to health care systems. For example, in a cohort of 10,000 patients, those with poorer health status had more laboratory tests and medication orders, resulting in more comprehensive data in their records [19]. On the other hand, minoritized populations usually have less access to health care [20], which affects the data's completeness and reduces their data points when we apply different types of filters. We focused on bringing attention to the second point.

Principal Findings

Throughout the analysis of the 4 different cohorts, a consistent pattern emerged: applied filters disproportionately affected minoritized groups, particularly the Black or African American group, which consistently has one of the lowest data availabilities across all datasets, and the American Indian and/or Alaska Native group. These filters significantly reduced the already limited data points for minoritized groups, further diminishing the completeness and usability of their data compared to white or non-Latino patients. We observe a similar pattern in the Hispanic or Latino group, where data availability is consistently lower in every cohort compared to the non-Hispanic or non-Latino group.

In the self-reported race groups, we observe that almost every group has less data availability than the white group, which is the largest within the known self-reported races across all datasets except at CSMC. At CSMC, the most complete group varies by filter, alternating between Asian, Native Hawaiian or Pacific Islander, American Indian and/or Alaska Native, and white. In contrast, in the CUIMC dataset, the American Indian and/or Alaska Native group has the lowest data availability.

Among the 4 distinct datasets, only the AoU dataset closely reflects the diversity of the US population, with approximately 50%(n=132,334) of the data representing populations other than white. Upon applying different filters on this dataset, as shown in Figures 1C and 2C, most groups follow the same original pattern prior to applying the filters and deviate from the baseline to a lesser extent, demonstrating that it is possible to achieve a diverse and complete dataset.

Dataset diversity is essential for enhancing the generalizability and inclusivity of clinical research, addressing disparities, and improving health care outcomes for underrepresented populations. The AoU dataset, designed as a nationwide research program, aims to collect health data from a diverse population and succeeds at creating an equitable framework for research where most of the groups share the same data availability percentage. In contrast, the CUIMC and CSMC datasets reflect the specific patient populations of their respective regions, leading to localized diversity compared to the national scope of the AoU dataset. However, both are based in highly racially and ethnically diverse US cities, giving them a unique advantage over other institutional-level datasets. The information for the different populations and distributions of the locations for the 4 datasets can be found in Table S1 in Multimedia Appendix 1.

Both in the United States and the United Kingdom, the white population constitutes the majority. Minorities, as defined by the US Office of Management and Budget, include racial and ethnic groups such as American Indian, Alaska Native, Asian, Black or African American, and Native Hawaiian or Pacific Islander. These groups often face health disparities, which can result in reduced access to health care and underrepresentation in research cohorts [21]. This underrepresentation may lead to inaccurate clinical care decisions, skewed genetic associations, and suboptimal treatment strategies.

Limitations

Our findings highlight the importance of carefully selecting filters to ensure equitable research outcomes, particularly for minority populations. While we do not claim these are the most frequently used filters by researchers, nor the optimal ones for selecting patients with complete data, it is essential to investigate any potential biases that may be introduced upon applying each filter before conducting research on these populations.

Additionally, methods to mitigate bias must be used when possible. One example is artificial intelligence–driven synthetic data generation for bias mitigation, which can be done using

XSL•FO
RenderX

different methodologies such as generative adversarial networks, synthetic minority oversampling, or Bayesian networks [22]. Other techniques include reweighting, suppression, or multiple imputation [23]. Advanced statistical techniques like inverse probability weighting can also help address these challenges and enhance dataset diversity [24].

Future Directions

Future work should focus on understanding how the application of these filters affects the results of common downstream analyses, such as disease risk prediction tasks and genome-wide association studies, and how to improve existing techniques for bias mitigation. We also recommend that researchers begin including sample sizes for relevant racial and ethnic groups both before and after any used filters are applied so that readers can better contextualize the results of the study.

Addressing disparities in representation is critical to creating research cohorts that accurately reflect the target population. This work underscores the challenges of achieving data completeness and proper representation of racial and ethnic populations and other minoritized groups in clinical research. Strategies to mitigate these disparities, along with careful consideration of filters, are crucial for ensuring equitable research outcomes and enhancing the inclusivity of health datasets.

Conclusions

Our findings underscore the importance of using only necessary filters, as they may affect the diversity and completeness of sample data, which particularly affects underrepresented populations. Upon applying different filters to the 4 distinct datasets, we observed that only the AoU dataset maintained the original sample distribution along racial and ethnic groupings, with minimal deviation from the baseline, demonstrating the potential to achieve a diverse and complete dataset.

Researchers must consider their target population when conducting studies and proactively address unintentional biases that may arise in data-driven research as well as the impact of these biases on downstream analyses. While sample filters are often necessary, we recommend that researchers implement techniques to mitigate biases and provide sample size information across racial and ethnic groupings both before and after the filters are applied, so readers can better understand the generalizability of the study.

Future work should characterize how the application of these filters affects downstream analyses and improve on existing techniques to minimize their impact. We strive to achieve a state where the datasets accurately represent the target population of the studies and where research studies are performed on the same population that institutions serve.

Acknowledgments

NAF was supported by NIH T32 HL116273.

Conflicts of Interest

None declared.

Multimedia Appendix 1
Additional information and detailed information of the results.
[DOCX File, 193 KB - medinform_v13i1e67591_app1.docx]

References

1. Toh CP, Brody J. Applications of machine learning in healthcare. In: Yen Kheng T, editor. Smart Manufacturing—When Artificial Intelligence Meets the Internet of Things: IntechOpen; 2021. [doi: 10.5772/intechopen.92297]
2. Javaid M, Haleem A, Pratap Singh R, Suman R, Rab S. Significance of machine learning in healthcare: features, pillars and applications. International Journal of Intelligent Networks 2022;3:58-73. [doi: 10.1016/j.ijin.2022.05.002]
3. Togioka B, Duvivier D, Young E. Diversity and Discrimination in Health Care: StatPearls; 2024.
4. National Academies of Sciences, Engineering, and Medicine, Policy and Global Affairs, Committee on Women in Science, Engineering, and Medicine. Improving Representation in Clinical Trials and Research: Building Research Equity for Women and Underrepresented Groups Why Diverse Representation in Clinical Research Matters and the Current State of Representation within the Clinical Research Ecosystem: National Academies Press (US); 2022.
5. Sharma A, Palaniappan L. Improving diversity in medical research. Nat Rev Dis Primers 2021 Oct 14;7(1):74. [doi: 10.1038/s41572-021-00316-8] [Medline: 34650078]
6. Hammond MEH, Stehlik J, Drakos SG, Kfoury AG. Bias in medicine. JACC: Basic to Translational Science 2021 Jan;6(1):78-85. [doi: 10.1016/j.jacbts.2020.07.012]
7. Adan C. The importance of diversity in clinical research. Br J Nurs 2023 Oct 12;32(18):898-901. [doi: 10.12968/bjon.2023.32.18.898] [Medline: 37830855]
8. Landry LG, Ali N, Williams DR, Rehm HL, Bonham VL. Lack of diversity in genomic databases is a barrier to translating precision medicine research into practice. Health Aff (Millwood) 2018 May;37(5):780-785. [doi: 10.1377/hlthaff.2017.1595] [Medline: 29733732]

XSL•FO
RenderX

9. Ramamoorthy A, Pacanowski MA, Bull J, Zhang L. Racial/ethnic differences in drug disposition and response: review of recently approved drugs. Clin Pharmacol Ther 2015 Mar;97(3):263-273. [doi: 10.1002/cpt.61] [Medline: 25669658]
10. Clark LT, Watkins L, Piña IL, et al. Increasing diversity in clinical trials: overcoming critical barriers. Curr Probl Cardiol 2019 May;44(5):148-172. [doi: 10.1016/j.cpcardiol.2018.11.002] [Medline: 30545650]
11. Weber GM, Adams WG, Bernstam EV, et al. Biases introduced by filtering electronic health records for patients with "complete data". J Am Med Inform Assoc 2017 Nov 1;24(6):1134-1141. [doi: 10.1093/jamia/ocx071] [Medline: 29016972]
12. Heintzman J, Bailey SR, Hoopes MJ, et al. Agreement of Medicaid claims and electronic health records for assessing preventive care quality among adults. J Am Med Inform Assoc 2014 Jul 1;21(4):720-724. [doi: 10.1136/amiajnl-2013-002333]
13. Devoe JE, Gold R, McIntire P, Puro J, Chauvie S, Gallia CA. Electronic health records vs Medicaid claims: completeness of diabetes preventive care data in community health centers. Ann Fam Med 2011;9(4):351-358. [doi: 10.1370/afm.1279] [Medline: 21747107]
14. Hersh WR, Weiner MG, Embi PJ, et al. Caveats for the use of operational electronic health record data in comparative effectiveness research. Med Care 2013 Aug;51(8 Suppl 3):S30-S37. [doi: 10.1097/MLR.0b013e31829b1dbd] [Medline: 23774517]
15. Gopal DP, Chetty U, O'Donnell P, Gajria C, Blackadder-Weinstein J. Implicit bias in healthcare: clinical practice, research and decision making. Future Healthc J 2021 Mar;8(1):40-48. [doi: 10.7861/fhj.2020-0233] [Medline: 33791459]
16. Data snapshots (public data). All of Us Research Program. URL: https://www.researchallofus.org/data-tools/data%20snapshots/ [accessed 2025-02-01]
17. Weiskopf NG, Hripcsak G, Swaminathan S, Weng C. Defining and measuring completeness of electronic health records for secondary use. J Biomed Inform 2013 Oct;46(5):830-836. [doi: 10.1016/j.jbi.2013.06.010] [Medline: 23820016]
18. List of ethnic groups. National Health System of UK. URL: https://www.ethnicity-facts-figures.service.gov.uk/style-guide/ethnic-groups/ [accessed 2025-02-01]
19. Rusanov A, Weiskopf NG, Wang S, Weng C. Hidden in plain sight: bias towards sick patients when sampling patients with sufficient electronic health record data for research. BMC Med Inform Decis Mak 2014 Jun 11;14(1):51. [doi: 10.1186/1472-6947-14-51] [Medline: 24916006]
20. National Academies of Sciences, Engineering, and Medicine, Health and Medicine Division, Board on Population Health and Public Health Practice, Committee on Community-Based Solutions to Promote Health Equity in the United States. The state of health disparities in the United States. In: Baciu A, Geller A, editors. Communities in Action: Pathways to Health Equity: National Academies Press (US); 2017.
21. Minority health and health disparities definitions. National Institute of Minority Health and Health Disparities. URL: https://www.nimhd.nih.gov/resources/understanding-health-disparities/minority-health-and-health-disparities-definitions.html [accessed 2025-02-01]
22. Shahul Hameed MA, Qureshi AM, Kaushik A. Bias mitigation via synthetic data generation: a review. Electronics (Basel) 2024 Oct 2;13(19):3909. [doi: 10.3390/electronics13193909]
23. Nazer LH, Zatarah R, Waldrip S, et al. Bias in artificial intelligence algorithms and recommendations for mitigation. PLOS Digit Health 2023 Jun;2(6):e0000278. [doi: 10.1371/journal.pdig.0000278] [Medline: 37347721]
24. Seaman SR, White IR. Review of inverse probability weighting for dealing with missing data. Stat Methods Med Res 2013 Jun;22(3):278-295. [doi: 10.1177/0962280210395740]

Abbreviations

AoU: All of Us
CSMC: Cedars-Sinai Medical Center
CUIMC: Columbia University Irving Medical Center
EHR: electronic health record
IRB: institutional review board
UKBB: UK Biobank

Edited by C Lovis; submitted 15.10.24; peer-reviewed by G Weber, O Evbuomwan; revised version received 06.01.25; accepted 12.01.25; published 27.03.25.

Please cite as:
Acitores Cortina JM, Fatapour Y, Brown KL, Gisladottir U, Zietz M, Bear Don't Walk IV OJ, Peter D, Berkowitz JS, Friedrich NA, Kivelson S, Kuchi A, Liu H, Srinivasan A, Tsang KK, Tatonetti NP
Biases in Race and Ethnicity Introduced by Filtering Electronic Health Records for "Complete Data": Observational Clinical Data Analysis
JMIR Med Inform 2025;13:e67591
URL: https://medinform.jmir.org/2025/1/e67591
doi:10.2196/67591

XSL•FO
RenderX

© Jose Miguel Acitores Cortina, Yasaman Fatapour, Kathleen LaRow Brown, Undina Gisladottir, Michael Zietz, Oliver John Bear Don't Walk IV, Danner Peter, Jacob S Berkowitz, Nadine A Friedrich, Sophia Kivelson, Aditi Kuchi, Hongyu Liu, Apoorva Srinivasan, Kevin K Tsang, Nicholas P Tatonetti. Originally published in JMIR Medical Informatics (https://medinform.jmir.org), 27.3.2025. This is an open-access article distributed under the terms of the Creative Commons Attribution License (https://creativecommons.org/licenses/by/4.0/), which permits unrestricted use, distribution, and reproduction in any medium, provided the original work, first published in JMIR Medical Informatics, is properly cited. The complete bibliographic information, a link to the original publication on https://medinform.jmir.org/, as well as this copyright and license information must be included.

XSL•FO
RenderX

Electronic Health Record Use Patterns Among Well-Being Survey Responders and Nonresponders: Longitudinal Observational Study

Daniel Tawfik[1], MS, MD; Tait D Shanafelt[2,3], MD; Mohsen Bayati[4], PhD; Jochen Profit[1], MPH, MD

[1]Department of Pediatrics, Stanford University School of Medicine, Palo Alto, CA, United States

[2]Department of Medicine, Stanford University School of Medicine, Stanford, CA, United States

[3]Stanford Medicine WellMD & WellPhD Center, Stanford, CA, United States

[4]Department of Operations, Information and Technology, Stanford Graduate School of Business, Stanford, CA, United States

Corresponding Author:
Daniel Tawfik, MS, MD
Department of Pediatrics, Stanford University School of Medicine, Palo Alto, CA, United States

Abstract

Background: Physician surveys provide indispensable insights into physician experience, but the question of whether responders are representative can limit confidence in conclusions. Ubiquitously collected electronic health record (EHR) use data may improve understanding of the experiences of survey nonresponders in relation to responders, providing clues regarding their well-being.

Objective: The aim of the study was to identify EHR use measures corresponding with physician survey responses and examine methods to estimate population-level survey results among physicians.

Methods: This longitudinal observational study was conducted from 2019 through 2020 among academic and community primary care physicians. We quantified EHR use using vendor-derived and investigator-derived measures, quantified burnout symptoms using emotional exhaustion and interpersonal disengagement subscales of the Stanford Professional Fulfillment Index, and used an ensemble of response propensity-weighted penalized linear regressions to develop a burnout symptom prediction model.

Results: Among 697 surveys from 477 physicians with a response rate of 80.5% (697/866), always responders were similar to nonresponders in gender (204/340, 60% vs 38/66, 58% women; P=.78) and age (median 50, IQR 40 - 60 years vs median 50, IQR 37.5 - 57.5 years; P=.88) but with higher clinical workload (median 121.5, IQR 58.5 - 184 vs median 34.5, IQR 0 - 115 appointments; P<.001), efficiency (median 5.2, IQR 4.0-6.2 vs median 4.3, IQR 0 - 5.6; P<.001), and proficiency (median 7.0, IQR 5.4 - 8.5 vs median 3.1, IQR 0 - 6.3; P<.001). Survey response status prediction showed an out-of-sample area under the receiver operating characteristics curve of 0.88 (95% CI 0.77-0.91). Burnout symptom prediction showed an out-of-sample area under the receiver operating characteristics curve of 0.63 (95% CI 0.57-0.70). The predicted burnout prevalence among nonresponders was 52%, higher than the observed prevalence of 28% among responders, resulting in an estimated population burnout prevalence of 31%.

Conclusions: EHR use measures showed limited utility for predicting burnout symptoms but allowed discrimination between responders and nonresponders. These measures may enable qualitative interpretations of the effects of nonresponders and may inform survey response maximization efforts.

(JMIR Med Inform 2025;13:e64722) doi:10.2196/64722

KEYWORDS

electronic health record metadata; electronic health record; EHR; electronic medical record; patient record; health records; personal health record; use; response bias; well-being; burnout; physicians; experiences; surveys; longitudinal studies; observational studies

Introduction

Symptoms of burnout among physicians have risen sharply in recent years [1], but burnout symptoms and other markers of physician well-being are currently identified by voluntary responses to surveys [2]. Such intermittent surveys often have low response rates and carry the risk of response bias, as physicians with burnout or other symptoms of poor well-being may have systematically different likelihood of responding [3]. Although prior analyses have shown few significant differences between early and late responders or between initial responders and those who respond to incentivized secondary surveys of nonresponders [1,4], in many studies, information about

XSL•FO
RenderX

nonresponders is limited to standard demographics. Evaluating survey results in relation to EHR use measures reflecting the work environment and experiences of each physician may allow a more detailed analysis of the differences between responders and nonresponders, thereby enabling extrapolations relevant to the well-being of nonresponders.

Symptoms of burnout affect primary care physicians disproportionately [1,4,5] and pose a threat to quality of care and patient safety [6,7]. Almost 50% of primary care physicians believe that the amount of time spent on clerical tasks is unreasonable [8], those with a high electronic health record (EHR) task load have a higher likelihood of burnout [9-11], and up to 75% believe that the EHR contributes to burnout [12,13]. Although these findings may suggest that EHR-based measures could be used to predict burnout symptoms, the performances of EHR-based measures in prediction models have been limited [14,15]. This combination of findings suggests that a more complex interplay exists among EHR use, physician well-being, and survey response.

This study sought (1) to identify systematic differences in EHR use measures between physician survey responders and nonresponders and (2) to provide a prediction modeling approach for estimating symptom burden among survey nonresponders using physician burnout as a use case.

Methods

Overview and Study Design

We used a repeated cross-sectional observational design to assess a wide range of EHR use characteristics in relation to burnout symptoms. EHR measures were compiled by the institution's EHR vendor (Epic Systems) or calculated from the local EHR data repository. Burnout measures relevant to this study were part of larger routine surveys on professional fulfillment at Stanford University School of Medicine.

Ethical Considerations

This study was approved by the institutional review board at Stanford University School of Medicine (IRB-49374) with deidentification processes enabling the waiver of informed consent. Data were deidentified prior to analysis. Incentives previously provided for survey completion are detailed below, but no further compensation was provided for inclusion in this study.

Study Participants

All primary care physicians at a large US academic medical center and its community affiliates were surveyed as part of routine quality improvement efforts and professional fulfillment benchmarking. Participants were invited via email, followed by 4 reminder email requests over the following 6 weeks at 2 time points (2019 and 2020). Participation was voluntary, with local department chairs, division chiefs, and well-being champions allowed to encourage participation at their discretion. At the academic medical center, a department-level financial incentive of US $50 per respondent was offered to the 3 departments with the highest response rates. At the community affiliate, survey completion was a prerequisite for individuals to receive their annual clinical bonuses. The primary stated purpose of the survey was to "help inform our efforts to make operational improvements to make Stanford University a better place for all to practice, educate, and conduct research." The survey was administered by a third party (SullivanLuallin Group), and all responses were deidentified to preserve confidentiality.

Each physician was categorized as a "never responder" if they did not provide survey responses at either time point, "always responder" if they responded to each yearly invitation received, or "partial responder" if they were invited both years but only responded once.

Burnout Measures

Surveys were distributed at the academic medical center in May 2019 and October 2020 and distributed at the community affiliate in March 2019 and March 2020. We used the Stanford Professional Fulfillment Index, which includes 10 prompts assessing burnout symptoms, 4 related to work exhaustion and 6 related to interpersonal disengagement. Details of this index and full burnout prompts are provided in prior publications [16,17]. In line with prior research [17], we calculated the mean score for these 10 burnout items, which are scored 0 - 4 on a Likert scale, then transposed to a 0 - 10 scale by multiplying by 2.5. Although all analyses were conducted on continuous scores, for ease of reporting, we dichotomized such that a score of ≥3.325 was considered indicative of burnout symptoms, in line with the validation results for this instrument [17].

EHR Use Measures

For each physician, we compiled EHR use measures for the 3-month period leading up to survey administration. We used Signal data compiled by Epic Systems to approximate key measures of workload, use, and efficiency, as defined in Epic's UserWeb. We calculated additional measures of workload from the institution's EHR data repository, including number of unique patients with appointments, number of patients with multiple appointments in a given month, sentiment scores of progress notes (range −1 to +1 for maximally negative to maximally positive sentiment), and principal components. We reduced this large feature set of 1677 overlapping predictors to a smaller set of 214 candidate predictors by manually curating to measures with low collinearity, high cardinality, and known or potential associations with physician well-being from published literature [8-11,18-27]. Introducing this manual curation step, compared to relying solely on automated machine learning methods, aligns with prior literature demonstrating that incorporating clinician expertise into feature generation can improve model performance [28]. We also extracted physician gender and birth year (binned in 5-year increments) from the EHR database as well as practice type and clinic (both hashed to preserve confidentiality).

Statistical Analysis

We used descriptive statistics including frequencies, means, and SDs to compare EHR use measures and demographics between survey responders and nonresponders using nonparametric methods to assess statistical significance, including Fisher exact test for categorical variables,

XSL•FO
RenderX

Kruskal-Wallis test for continuous variables with unpaired observations, and Wilcoxon signed rank for continuous variables with paired observations. Reference values were set at the modal value (categorical variables) or the lowest value (ordinal variables).

Because the population of interest (nonresponders) may differ from the population available for model training (responders), we developed a weighting schema to tune the model for predictions more heavily weighted toward individuals less likely to respond. To develop these weights for our prediction model, we developed propensity scores quantifying the likelihood of survey response (vs nonresponse) in any given year based on EHR use measures. We used penalized logistic regression with 10-fold cross-validation to generate these propensity scores for survey response, using the full dataset of survey invitations, with the binary outcome of survey response defined as answering ≥4 out of 10 burnout prompts. We then used these propensity scores, denoted by p, to inform 3 approaches to weighting in our predictive models for burnout score, lending varying levels of higher weight to observations more similar to nonresponders (unweighted, $1/p$ weighting, and $1-p$ weighting). Unweighted predictions approximate the population of responders by ascribing equal weight to all observations in the training set. $1/p$-Weighted predictions approximate the full population of responders and nonresponders by ascribing proportionately higher weight to responses with the lowest likelihood of response, with the lower limit of propensity scores truncated at 0.1 to prevent extreme weights. $1-p$-Weighted predictions approximate the nonresponders by ascribing lower weight to responses with a higher likelihood of response.

To create our ensemble prediction model, we used a sample of always responders to train 3 separate prediction models, then used the remainder of always responders to calculate bias-correction coefficients governing the weight of each of the 3 models in the final ensemble model. To accomplish this task, we trained penalized linear regression models to predict burnout scores using a random 272 (80% sample) of the 340 always responders, grouped by physician. We generated 3 burnout predictions (1 for each weighting schema) for the remaining 68 (20% sample) of the 340 always responders. On this held-out test set, we then applied a bias-correction step in which we regressed actual burnout scores on the 3 predictions (1 from each weighting schema), then extracted the resultant β coefficients for each weighting schema as bias-correction coefficients, such that predictions consistently over- or underestimating burnout scores would be adjusted accordingly in the ensemble (bias-corrected) prediction.

Because nonresponders may represent a systematically different population than our training set of always responders, we chose to test predictive performance using the held-out test set of partial responders (physicians who responded to the survey in 1 year but declined to respond in the other year). We chose the partial responders as the test set because this group of physicians may most closely approximate nonresponders while still providing usable survey data in 1 year. Using the models generated in the training step and the coefficients generated in the bias-correction step, the performance of the ensemble model was tested to predict burnout scores for these partial responders. For ease of interpretation, we converted burnout predictions to the likelihood of burnout score ≥3.325 using a sigmoid distribution.

Because the partial responders may provide the most relevant data for predicting burnout among nonresponders, we then retrained the model using all responses (from always responders and the response years of partial responders) and used this final model to predict burnout scores among nonresponders. We combined these predicted burnout scores with the observed burnout scores from survey responses to estimate the population-level burnout burden.

Recognizing that we cannot directly assess the performance of our final predictions of nonresponders but that our sample contained a strong response rate, we also performed additional validation in which we synthetically reduced our response rate by pseudorandomly selecting a subset of physicians to be synthetic nonresponders. This approach allowed us to estimate applicability to institutions or years with lower response rates. For this synthetic survey response reduction, each person's response propensity was jittered using a triangularly distributed random jitter from −0.5 to 0.5, centered at 0. Then we selected out the 20% of physicians with the lowest average response propensity as "candidate synthetic nonresponders." We repeated this process 100 times, then chose any physician who was a candidate synthetic nonresponder in at least 50 cycles as a final synthetic nonresponder, to be added to the actual nonresponders. We retrained the model using only the limited set of responses, and then predicted burnout scores among the larger set of nonresponses.

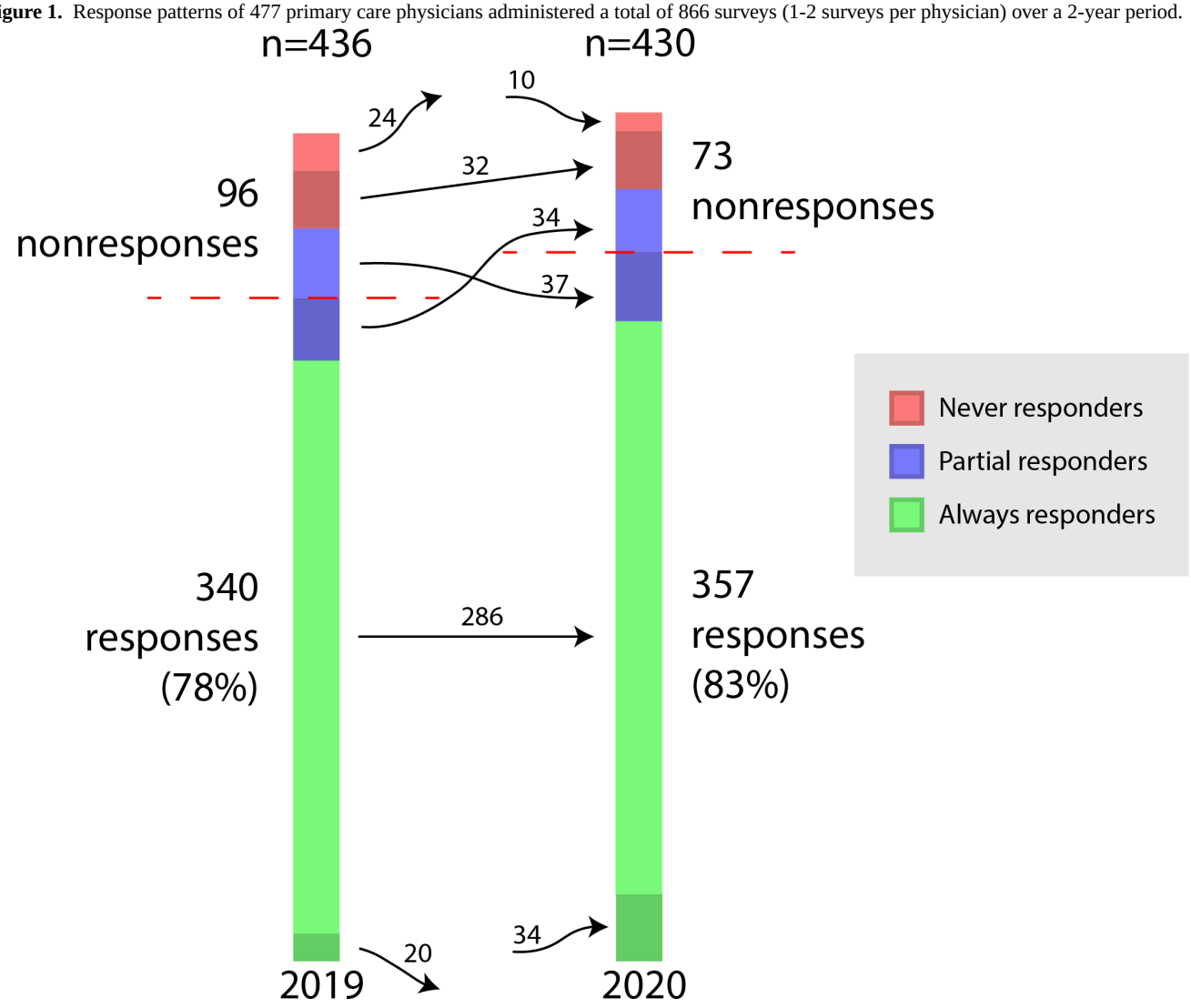
Due to the hypothesis-generating nature of these analyses, no corrections were made for multiple testing. Statistical analyses were performed in Stata (version 17.0; StataCorp) and Python (version 3.3; Python Software Foundation) with modules scipy and sklearn.

Results

A total of 477 unique physicians received 866 survey invitations (in 2019 alone: n=44, in 2020 alone: n=44, and in both years: n=389). The overall response rate was that 697 of 866 (80.5%) surveys were completed (in 2019: n=340, 78% and in 2020: n=357, 83%), with 66 never responders, 71 partial responders, and 340 always responders (Figure 1). Baseline demographics of the 3 groups of physicians are shown in Table 1.

XSL•FO
RenderX

Figure 1. Response patterns of 477 primary care physicians administered a total of 866 surveys (1-2 surveys per physician) over a 2-year period.



XSL•FO
RenderX

Table . Baseline characteristics of never responders, partial responders, and always responders[a].

	Responder group			*P* value[b]
	Always responders	Partial responders	Never responders	
Physicians, n	340	71	66	—[c]
Surveys administered[d], n	626	142	98	—
Surveys completed, n	626	71	0	—
Demographics				
Women, n (%)	204 (60)	53 (75)	38 (58)	.048
Age (years), median (IQR)	50 (40-60)	50 (40-60)	50 (35-60)	.88
Workload and patient complexity measures, median (IQR)				
Appointments	121.5 (58.5-184.0)	107.0 (45.0-161.0)	34.5 (0.0-115.0)	<.001
Appointments per work day	9.2 (6.2-11.7)	8.8 (6.9-11.7)	5.9 (0.0-9.6)	<.001
Laboratory orders	69.0 (15.0-173.5)	65.0 (11.0-156.0)	12.0 (0.0-71.0)	<.001
Mean number of patient conditions	167.9 (96.7-348.1)	275.9 (144.9-399.2)	206.8 (48.0-374.1)	.001
Number of messages	567.0 (277.0-953.5)	435.0 (86.0-891.0)	69.5 (0.0-279.0)	<.001
Number of notes written	187.0 (95.0-300.0)	149.0 (45.0-234.0)	33.0 (0.0-150.0)	<.001
Number of patients touched	212.0 (106.5-331.0)	148.0 (68.0-285.0)	48.5 (7.0-151.0)	<.001
EHR[e] efficiency measures, median (IQR)				
Epic efficiency score	5.2 (4.0-6.2)	4.9 (3.6-5.8)	4.3 (0.0-5.6)	<.001
Minutes in Work Outside of Work per 8 hours of appointments	24.5 (11.5-47.6)	21.2 (4.5-47.2)	3.0 (0.0-20.7)	<.001
Minutes during pajama time	180.3 (21.3-599.5)	95.3 (22.7-389.9)	15.1 (0.0-132.3)	<.001
Minutes per off day	31.8 (13.5-66.0)	29.3 (5.1-59.1)	0.2 (0.0-19.0)	<.001
Minutes per 8 hours of appointments	173.1 (114.3-247.1)	189.6 (119.2-242.1)	120.8 (0.0-181.0)	<.001
Minutes in chart review per appointment	2.0 (1.1-3.7)	2.5 (1.3-3.7)	1.0 (0.0-3.8)	.003
Minutes in inbasket per 8 hours of appointments	31.7 (15.4-48.1)	29.1 (9.2-48.1)	9.6 (0.0-27.9)	<.001
Minutes in notes per 8 hours of appointments	60.9 (32.8-97.3)	60.2 (34.9-93.9)	42.8 (0.0-68.6)	<.001
Minutes in prescriptions per 8 hours of appointments	24.8 (14.5-38.2)	27.2 (14.5-36.4)	12.0 (0.0-30.4)	<.001
Average typos per note	1.2 (1.1-1.3)	1.1 (1.0-1.4)	1.0 (0.0-1.3)	<.001
Average words per note	396.2 (259.4-575.5)	402.6 (246.4-623.4)	264.5 (77.1-481.1)	<.001
Undivided attention (estimated)	0.7 (0.5-0.8)	0.6 (0.4-0.7)	0.5 (0.0-0.7)	.002
EHR proficiency measures				
Epic proficiency score, median (IQR)	7.0 (5.4-8.5)	6.5 (3.8-8.0)	3.1 (0.0-6.3)	<.001
Chart search, n (%)	325 (95.6)	64 (90)	46 (70)	<.001
Number of shared smartphrases, median (IQR)	140.0 (60.0-288.5)	184.0 (66.0-381.0)	40.5 (0.0-191.0)	<.001

[a]Data shown represent the month leading up to the most recent survey administration within the study period for each physician.

[b]*P* values obtained using the Fisher exact test (categorical variables) or the Kruskal-Wallis test (continuous variables).

XSL•FO
RenderX

[c]Not applicable.

[d]Physicians who joined or left the organization between survey administrations were only eligible to receive 1 survey. They were categorized with "always responders" if they responded or "never responders" if they did not respond. Full details are illustrated in Figure 1.

[e]EHR: electronic health record.

EHR use patterns for the 3 groups of physicians are also shown in Table 1, with never responders showing generally lower clinical workload and overall EHR proficiency, always responders showing generally higher clinical workload and EHR proficiency, and partial responders with intermediate values. In particular, never responders had a median of 5.9 (IQR 0.0-9.6) appointments per work day compared to 8.8 (IQR 6.9-11.7) for partial responders and 9.2 (IQR 6.2-11.7) for always responders. Although never responders exhibited the lowest summary EHR efficiency scores (partial responders: median 4.3, IQR 0.0-5.6 vs median 4.9, IQR 3.6-5.8 and always responders: median 5.2, IQR 4.0-6.2), they also showed the lowest minutes in notes per 8 hours of appointments (partial responders: median 42.8, IQR 0.0-68.6 vs median 60.2, IQR 34.9-93.9 and always responders: median 60.9, IQR 32.8-97.3), lowest minutes in EHR in basket per 8 hours of appointments (partial responders: median 9.6, IQR 0.0-27.9 vs median 29.1, IQR 9.2-48.1 and always responders: median 31.7, IQR 15.4-48.1), and lowest minutes in chart review per appointment (partial responders: median 1.0, IQR 0.0-3.8 vs median 2.5, IQR 1.3-37 and always responders: median 2.0, IQR 1.1-3.7).

Among the 71 partial responders, the year in which a response was given showed several differences in comparison to the nonresponse year as shown in Table 2. In particular, physicians responded in years in which they had higher clinical workload (eg, more appointments per work day: median 10.1, IQR 8.0-12.2 vs median 8.3, IQR 6.2-12.3; P=.03) but relatively similar EHR efficiency measures (eg, similar Epic efficiency score: median 5.0, IQR 4.1-5.9 vs median 4.7, IQR 3.4-5.8; P=.14). The results were similar when stratified by physicians who responded the first year and failed to respond the second year versus those with the reverse chronology.

XSL•FO
RenderX

Table . Electronic health record (EHR) use measures for the 71 partial responders, during nonresponse years and response years[a].

	Nonresponse year	Response year	*P* value
Physicians, n	71	71	N/A[b]
Workload and patient complexity measures, median (IQR)			
Appointments	97.0 (41.5-151.0)	138.0 (65.0-192.0)	.001
Appointments per work day	8.3 (6.2-12.3)	10.1 (8.0-12.2)	.03
Laboratory orders	80.0 (2.0-139.0)	92.0 (14.0-203.0)	.001
Mean number of patient conditions	253.1 (131.1-408.6)	275.9 (125.6-375.7)	.51
Number of messages	309.0 (91.5-839.0)	462.0 (138.0-957.5)	.002
Number of notes written	145.0 (36.0-234.0)	184.0 (85.0-325.5)	.001
Number of patients touched	134.0 (57.0-250.0)	175.0 (82.5-313.0)	<.001
EHR efficiency measures, median (IQR)			
Epic efficiency score	4.7 (3.4-5.8)	5.0 (4.1-5.9)	.14
Minutes in work outside of work per 8 hours of appointments	17.7 (1.8-42.1)	22.3 (7.5-54.1)	.04
Minutes during pajama time	54.4 (0.0-321.7)	42.0 (0.0-201.0)	.51
Minutes per off day	32.3 (0.0-51.8)	34.6 (11.0-63.6)	.15
Minutes per 8 hours of appointments	184.3 (93.4-237.1)	183.8 (121.5-263.9)	.52
Minutes in chart review per appointment	2.4 (1.0-4.0)	2.3 (1.4-3.5)	.64
Minutes in inbasket per 8 hours of appointments	26.6 (8.6-48.3)	24.6 (11.0-45.4)	.71
Minutes in notes per 8 hours of appointments	59.6 (22.2-87.4)	60.2 (40.6-100.2)	.22
Minutes in prescriptions per 8 hours of appointments	25.5 (10.4-35.3)	28.0 (16.5-44.4)	.12
Average typos per note	1.1 (1.0-1.3)	1.1 (1.0-1.4)	.37
Average words per note	394.7 (257.2-593.7)	417.8 (274.4-625.4)	.61
Undivided attention (estimated)	0.6 (0.4-0.7)	0.7 (0.5-0.8)	.03
EHR proficiency measures			
Epic proficiency score, median (IQR)	5.8 (2.5-7.7)	6.4 (3.8-8.0)	.13
Chart search, n (%)	61 (86)	67 (94)	.16
Number of shared smartphrases, median (IQR)	122.0 (46.5-353.0)	225.0 (62.0-375.5)	.04

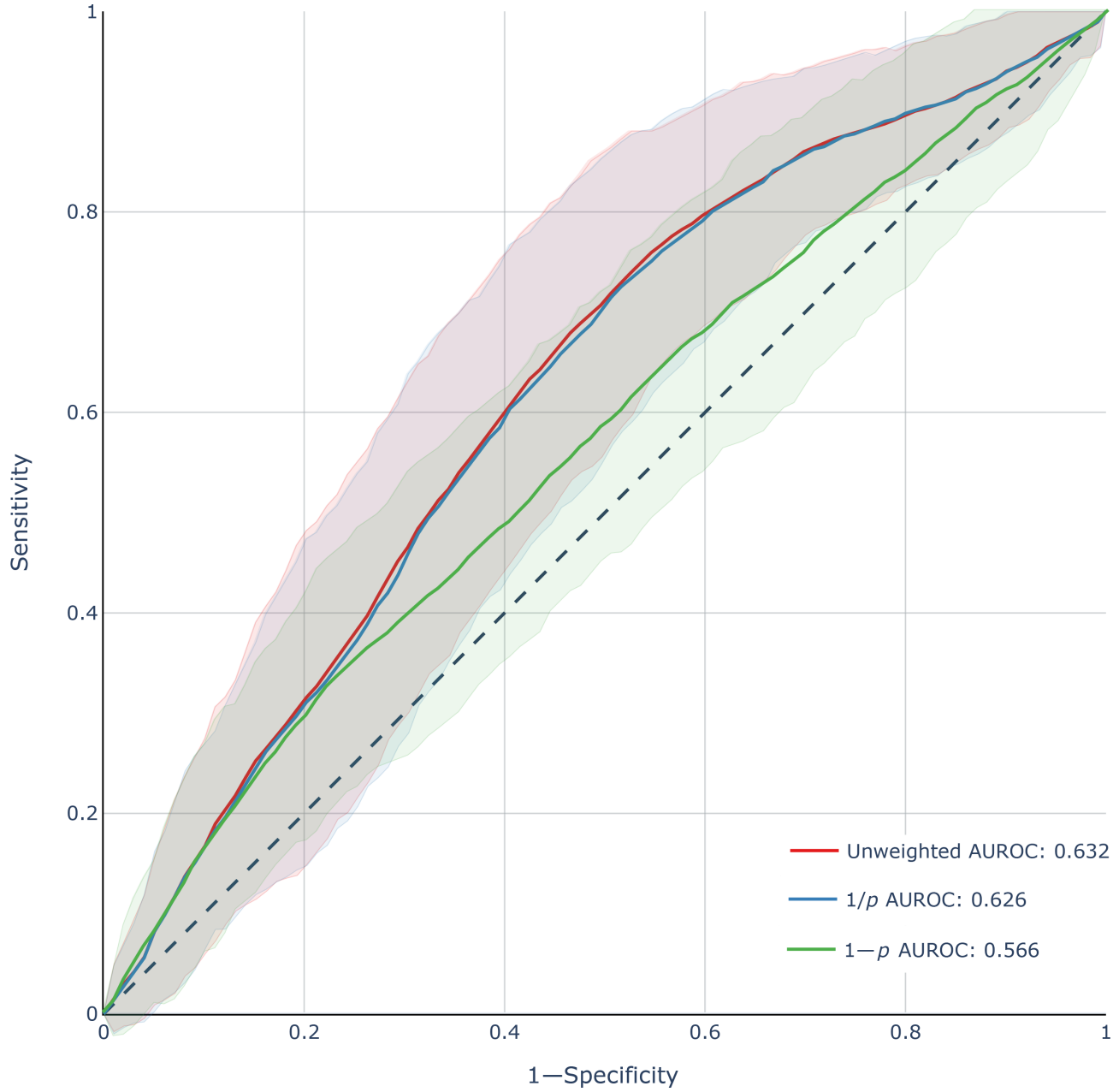
[a]*P* values obtained via Wilcoxon signed rank test.

[b]N/A: not applicable.

Prediction models for survey response using multivariable logistic regression achieved an area under the receiver operating characteristic curve (AUROC) of 0.88 (95% CI 0.77 - 0.91) as determined by 10-fold cross-validation grouped by physician. Prediction models for burnout score using multivariable linear regression with subsequent sigmoid transformation to probability of burnout achieved an out-of-sample AUROC of 0.63 (95% CI 0.57 - 0.69) on the unweighted model, 0.62 (95% CI 0.57 - 0.69) on the 1/*p* weighted model, and 0.57 (95% CI 0.50 - 0.62) on the 1–p weighted model as shown in Figure 2. The ensemble model achieved an out-of-sample AUROC of 0.63 (95% CI 0.57 - 0.70), sensitivity of 62%, specificity of 64%, and area under the precision-recall curve of 0.39 (95% CI 0.33 - 0.48) for predicting burnout symptoms as shown in Figure 3.

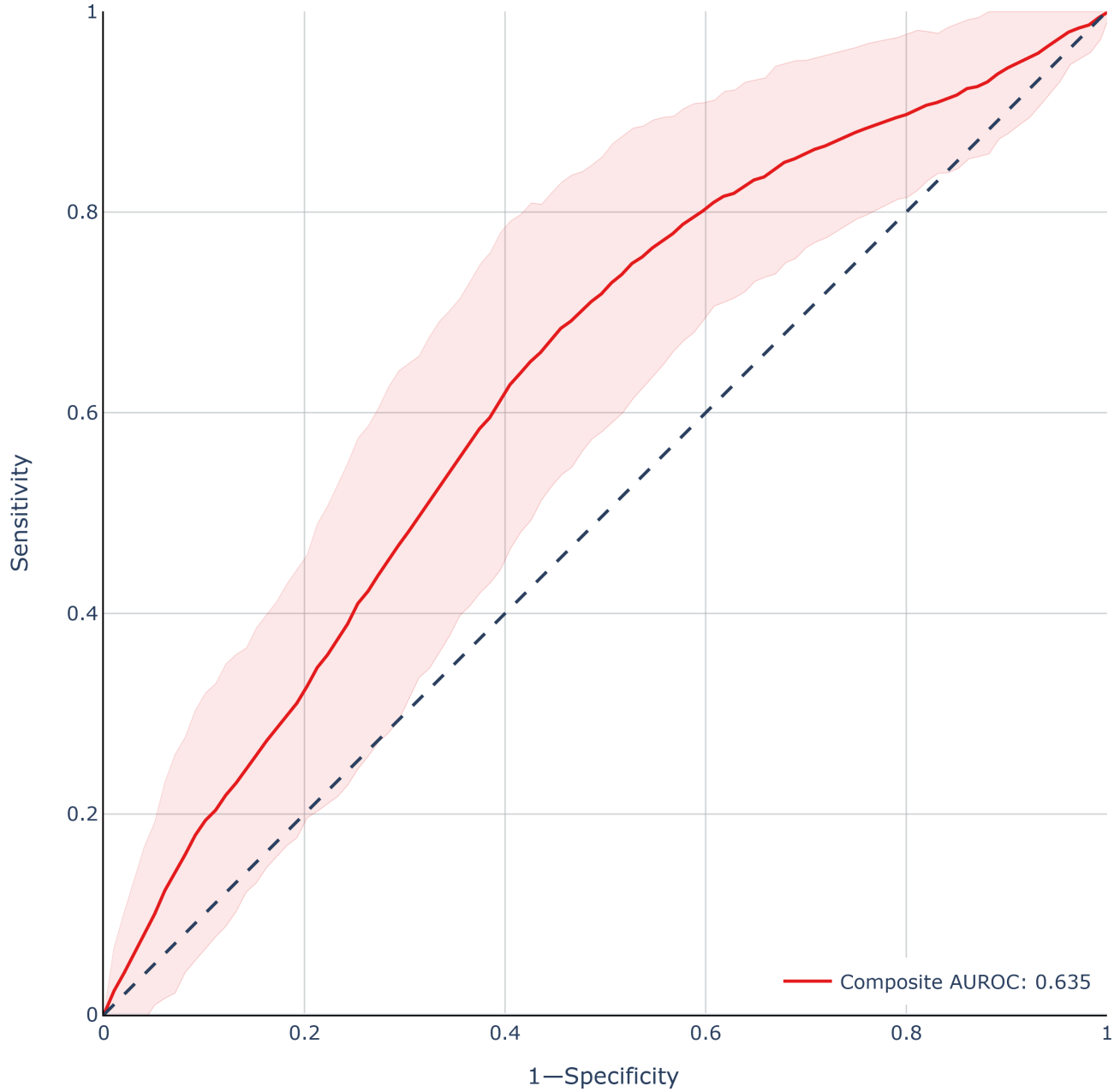
XSL•FO
RenderX

Figure 2. Receiver operating characteristics curves for 3 burnout prediction models: unweighted, weighted by inverse probability of survey response (1/p), and weighted by reversed probability of survey response (1−*p*). Results for the held-out test set of partial responders shown. Shaded areas represent 95% CIs obtained using bootstrap resampling methods. AUROC: area under the receiver operating characteristic curve.



XSL•FO
RenderX

Figure 3. Receiver operating characteristics curve for the bias-corrected ensemble burnout prediction model. Results for the held-out test set of partial responders shown. Shaded area represents 95% CI obtained using bootstrap resampling methods. AUROC: area under the receiver operating characteristic curve.



After final training on all available data (see Multimedia Appendix 1 for coefficients from the top-performing model), the ensemble model predicted 52% (95% CI 41% - 63%) burnout prevalence among the nonresponders, higher than the 28% rate observed in responders. These predictions suggest a population-level estimated 31% (95% CI 30% - 33%) burnout prevalence, after incorporating the observed 28% burnout prevalence among responders.

In secondary analysis with synthetic response rate reduction, the observed burnout prevalence was 26% (excluding the synthetic nonresponders—individuals whose responses were concealed for the purposes of this secondary analysis), while the predicted burnout prevalence was 46% (including predictions for true nonresponders and synthetic nonresponders). The resultant population-level estimate of 33% burnout prevalence represented a 2% increase in estimated burnout compared to the fully informed model.

Discussion

Principal Findings

In this study, we found well-being survey responses to be more common among physicians with higher clinical workload and higher EHR proficiency measures, with a strong ability to predict survey response status using routinely collected EHR measures. However, we achieved lower predictive performance to predict burnout scores, which were better (AUROC 0.63, 95% CI 0.57-0.70) than chance (AUROC 0.5), but below the threshold for clinical actionability when predicting outcomes in an individual (typically AUROC of at least 0.8). The ability of EHR measures to predict burnout was not markedly improved

XSL•FO
RenderX

by including propensity weighting schemas, though it remains possible that predictions on true nonresponders are more accurate as a result or that this approach may inform survey analysis strategies for other applications. Although we found predicted burnout scores among nonresponders to be higher than observed burnout scores among responders, there remains uncertainty regarding the magnitude of difference.

Comparison to Prior Work

Previous studies looking for systematic differences between well-being survey responders and nonresponders have consistently failed to show meaningful differences. Using a large national sample of physicians, Shanafelt et al [29] reported no substantial differences between early responders and late responders nor between responders to the initial survey versus an incentivized, multimodality survey of nonresponders (2 standard approaches to evaluate for response bias) [1,4]. Ortega et al [30] reported no differences in burnout prevalence among responders to 3 consecutive surveys versus those who provided only 1 or 2 responses. Cardell et al [31] also reported no differences in burnout among responders who fully completed a survey and those with selective responses. These findings are in line with other studies of physician surveys in ambulatory practice or oncology care [32-34]. Studies that identified demographic differences by response status primarily note small differences in age, gender, specialty, and urbanicity [35-38].

Our study largely confirms these findings, with similar demographics among all responder groups, but extends these findings by evaluating highly granular EHR measures related to the work environment of physicians, providing much greater detail than has previously been available for nonresponders. Although we are unable to directly evaluate the predictive accuracy of our model on nonresponders, our findings suggest that in this sample of physicians, nonresponders have EHR use measures more similar to physicians who reported higher symptoms of burnout. Notably, these nonresponders tended to exhibit a lower volume of clinical workload, but many of the predictive features in our model related rather to the composition of the clinical workload (ie, the proportion of appointments that are level 5 rather than the raw number of appointments). However, the relatively weak predictive performance of this model to predict burnout (when evaluated against the surrogate group of partial responders) suggests caution in interpreting the magnitude of any such effect. In addition, the 1-year interval between the survey time points and response or nonresponse years of the partial responders may reflect important differences in burnout symptoms or work experiences, further distancing their relevance as a surrogate test population.

Strengths and Limitations

Although burnout prediction accuracy falls below the threshold of actionability consistent with prior studies [14,15], the directionality of the difference between observed and predicted burnout may be valuable as a qualitative measure. Our findings suggest that institutions could leverage population-level EHR measures to identify if their nonresponders are expected to have better, worse, or similar symptoms to those measured among responders. In this way, comparisons may be better informed, particularly across years with different survey response rates. Although burnout was evaluated as a use case in this study, it remains possible that this approach may be more effective for predicting response to other survey instruments, particularly those with more direct conceptual connections with EHR use metadata (eg, EHR experience, control over schedule, or sleep-related impairment).

This study should be viewed in light of its design. As an observational study, we cannot infer any causality of the observed associations between EHR measures and burnout symptoms. Additionally, the nonresponders have survey results that are by definition not observable, and it remains possible that additional differences exist between nonresponders and our surrogate populations of partial responders and low-propensity responders. While this study population represents a large sample of academic and community primary care physicians, the results may not generalize to other specialties or institutions, and the necessary deidentification process prevented us from knowing the practice setting or clinic names of individual respondents. The response rates among this sample of physicians were relatively high due to strong institutional efforts to maximize responses, which may limit generalizability to institutions with lower response rates. The survey time points occurred both prior to and during the early phase of the COVID-19 response, which provided an exogenous shock to the health care delivery system including fluctuating visit volumes and a transition toward telehealth that may have unmasked relevant associations. However, changes in physician's work and personal lives since that time may affect future results. Although we evaluated burnout prediction as a use case, this framework applied to other survey measures may provide better or worse predictive performance.

Future Directions

We achieved moderate to strong performance in predicting survey response versus nonresponse. This finding highlights an opportunity to improve response rates by better targeting or incentivizing individuals predicted as less likely to respond. In general, the nonresponders appeared to exhibit a less clinically engaged phenotype with a lower workload and fewer EHR customizations. This phenotype may be reflective of reduced clinical load due to exhaustion, other academic or nonclinical responsibilities, vacation or sabbatical, or competing responsibilities in personal life. Decreased EHR proficiency as defined by EHR customizations may occur for many reasons, including lower clinical workload that may provide a lower payoff to an individual's efforts toward customization, perceptions of helplessness or reduced motivation to engage in available tools, or unfamiliarity with available customizations.

Allowing physicians to self-select their survey delivery format or providing protected time for survey completion [30,39-42] may improve response rates. In particular, evaluating phenotypes associated with nonresponse may further inform survey timing, delivery modes, or incentive structures to maximize response rates. For example, an institution that predicates a year-end clinical bonus on survey completion may inadvertently oversample those with high clinical loads, as their incentive will carry relatively more value. Alternatively, an institution that provides survey invitations and reminders during daytime

XSL•FO
RenderX

hours or posted only in clinical locations may inadvertently reduce engagement by physicians with infrequent or off-hours clinical work.

Conclusions

In this sample of primary care physicians in a large academic medical center and its community affiliates, we found that differences in EHR use measures may enable the prediction of physician survey response with moderate to strong accuracy, but that EHR use measures have limited ability to predict burnout symptoms. Our finding that nonresponders had EHR use measures more similar to responders with symptoms of burnout suggested that, if anything, nonresponders may have higher rates of burnout than responders. Further studies are needed to validate these findings in other settings and over a longer time horizon.

Acknowledgments

This research was supported by research grants from the Agency for Healthcare Research and Quality (K08 HS027837, PI: DT) and the Eunice Kennedy Shriver National Institute of Child Health and Human Development (R01 HD084679, PI: JP). All funders had no role in the design and conduct of the study; collection, management, analysis, and interpretation of the data; preparation, review, or approval of the manuscript; nor the decision to submit the manuscript for publication.

Data Availability

The datasets generated and analyzed during this study are not publicly available due to the sensitive nature of the data and are not available to be distributed by the corresponding author in accordance with data use agreements.

Authors' Contributions

DT made substantial contributions to study design, interpretation of data, and drafting the manuscript; had full access to all the data in the study and takes responsibility for the integrity of the data and the accuracy of the data analysis; and approved the submitted version. TDS, MB, and JP made substantial contributions to study design, interpretation of data, critically reviewing the manuscript, and approval of the submitted version.

Conflicts of Interest

TDS is coinventor of the Well-Being Index instruments (Physician Well-Being Index, Nurse Well-Being Index, Medical Student Well-Being Index, and the Well-Being Index) and the Mayo Leadership Index. Mayo Clinic holds the copyright for these instruments and has licensed them for use outside of Mayo Clinic. TDS receives a portion of any royalties received. As an expert on the well-being of health care professionals, TDS frequently gives grand rounds or key note lecture presentations and provides advising for health care organizations. He receives honoraria for some of these activities.

Multimedia Appendix 1

Standardized coefficients from top-performing model for features selected via penalized linear regression. Features are ordered by coefficient value, with the highest listed features associating with higher burnout scores and the lowest listed features associating with lower burnout scores.

[DOCX File, 15 KB - medinform_v13i1e64722_app1.docx]

References

1. Shanafelt TD, West CP, Sinsky C, et al. Changes in burnout and satisfaction with work-life integration in physicians and the general US working population between 2011 and 2020. Mayo Clin Proc 2022 Mar;97(3):491-506. [doi: 10.1016/j.mayocp.2021.11.021] [Medline: 35246286]
2. Maslach C, Jackson SE. Maslach Burnout Inventory: Consulting Psychologists Press, Inc; 1981.
3. Rotenstein LS, Torre M, Ramos MA, et al. Prevalence of burnout among physicians: a systematic review. JAMA 2018 Sep 18;320(11):1131-1150. [doi: 10.1001/jama.2018.12777] [Medline: 30326495]
4. Shanafelt TD, West CP, Sinsky C, et al. Changes in burnout and satisfaction with work-life integration in physicians and the general US working population between 2011 and 2017. Mayo Clin Proc 2019 Sep;94(9):1681-1694. [doi: 10.1016/j.mayocp.2018.10.023] [Medline: 30803733]
5. Han S, Shanafelt TD, Sinsky CA, et al. Estimating the attributable cost of physician burnout in the United States. Ann Intern Med 2019 Jun 4;170(11):784-790. [doi: 10.7326/M18-1422] [Medline: 31132791]
6. Tawfik DS, Scheid A, Profit J, et al. Evidence relating health care provider burnout and quality of care: a systematic review and meta-analysis. Ann Intern Med 2019 Oct 15;171(8):555-567. [doi: 10.7326/M19-1152] [Medline: 31590181]
7. Tawfik DS, Profit J, Morgenthaler TI, et al. Physician burnout, well-being, and work unit safety grades in relationship to reported medical errors. Mayo Clin Proc 2018 Nov;93(11):1571-1580. [doi: 10.1016/j.mayocp.2018.05.014] [Medline: 30001832]

XSL•FO
RenderX

8. Tran B, Lenhart A, Ross R, Dorr DA. Burnout and EHR use among academic primary care physicians with varied clinical workloads. AMIA Jt Summits Transl Sci Proc 2019;2019:136-144. [Medline: 31258965]
9. Shanafelt TD, Dyrbye LN, Sinsky C, et al. Relationship between clerical burden and characteristics of the electronic environment with physician burnout and professional satisfaction. Mayo Clin Proc 2016 Jul;91(7):836-848. [doi: 10.1016/j.mayocp.2016.05.007] [Medline: 27313121]
10. Babbott S, Manwell LB, Brown R, et al. Electronic medical records and physician stress in primary care: results from the MEMO Study. J Am Med Inform Assoc 2014 Feb;21(e1):e100-e106. [doi: 10.1136/amiajnl-2013-001875] [Medline: 24005796]
11. Tawfik DS, Phibbs CS, Sexton JB, et al. Factors associated with provider burnout in the NICU. Pediatrics 2017 May;139(5):e20164134. [doi: 10.1542/peds.2016-4134] [Medline: 28557756]
12. Robertson SL, Robinson MD, Reid A. Electronic health record effects on work-life balance and burnout within the I3 population collaborative. J Grad Med Educ 2017 Aug;9(4):479-484. [doi: 10.4300/JGME-D-16-00123.1] [Medline: 28824762]
13. Poll TH. How doctors feel about electronic health records. : Stanford Medicine; 2018 URL: http://med.stanford.edu/content/dam/sm/ehr/documents/EHR-Poll-Presentation.pdf [accessed 2025-01-11]
14. Tawfik D, Bayati M, Liu J, et al. Predicting primary care physician burnout from electronic health record use measures. Mayo Clin Proc 2024 Sep;99(9):1411-1421. [doi: 10.1016/j.mayocp.2024.01.005] [Medline: 38573301]
15. Lou SS, Liu H, Warner BC, Harford D, Lu C, Kannampallil T. Predicting physician burnout using clinical activity logs: model performance and lessons learned. J Biomed Inform 2022 Mar;127:104015. [doi: 10.1016/j.jbi.2022.104015] [Medline: 35134568]
16. Brady KJS, Ni P, Carlasare L, et al. Establishing crosswalks between common measures of burnout in US physicians. J Gen Intern Med 2022 Mar;37(4):777-784. [doi: 10.1007/s11606-021-06661-4] [Medline: 33791938]
17. Trockel M, Bohman B, Lesure E, et al. A brief instrument to assess both burnout and professional fulfillment in physicians: reliability and validity, including correlation with self-reported medical errors, in a sample of resident and practicing physicians. Acad Psychiatry 2018 Feb;42(1):11-24. [doi: 10.1007/s40596-017-0849-3] [Medline: 29196982]
18. Melnick ER, Dyrbye LN, Sinsky CA, et al. The association between perceived electronic health record usability and professional burnout among US physicians. Mayo Clin Proc 2020 Mar;95(3):476-487. [doi: 10.1016/j.mayocp.2019.09.024] [Medline: 31735343]
19. Eschenroeder HC, Manzione LC, Adler-Milstein J, et al. Associations of physician burnout with organizational electronic health record support and after-hours charting. J Am Med Inform Assoc 2021 Apr 23;28(5):960-966. [doi: 10.1093/jamia/ocab053] [Medline: 33880534]
20. Perez HR, Beyrouty M, Bennett K, et al. Chaos in the clinic: characteristics and consequences of practices perceived as chaotic. J Healthc Qual 2017;39(1):43-53. [doi: 10.1097/JHQ.0000000000000016] [Medline: 26566238]
21. Linzer M, Poplau S, Grossman E, et al. A cluster randomized trial of interventions to improve work conditions and clinician burnout in primary care: results from the healthy work place (HWP) study. J Gen Intern Med 2015 Aug;30(8):1105-1111. [doi: 10.1007/s11606-015-3235-4] [Medline: 25724571]
22. Linzer M, Poplau S, Babbott S, et al. Worklife and wellness in academic general internal medicine: results from a national survey. J Gen Intern Med 2016 Sep;31(9):1004-1010. [doi: 10.1007/s11606-016-3720-4] [Medline: 27138425]
23. Gardner RL, Cooper E, Haskell J, et al. Physician stress and burnout: the impact of health information technology. J Am Med Inform Assoc 2019 Feb 1;26(2):106-114. [doi: 10.1093/jamia/ocy145] [Medline: 30517663]
24. Kroth PJ, Morioka-Douglas N, Veres S, et al. Association of electronic health record design and use factors with clinician stress and burnout. JAMA Netw Open 2019 Aug 2;2(8):e199609. [doi: 10.1001/jamanetworkopen.2019.9609] [Medline: 31418810]
25. Adler-Milstein J, Zhao W, Willard-Grace R, Knox M, Grumbach K. Electronic health records and burnout: time spent on the electronic health record after hours and message volume associated with exhaustion but not with cynicism among primary care clinicians. J Am Med Inform Assoc 2020 Apr 1;27(4):531-538. [doi: 10.1093/jamia/ocz220] [Medline: 32016375]
26. Hilliard RW, Haskell J, Gardner RL. Are specific elements of electronic health record use associated with clinician burnout more than others? J Am Med Inform Assoc 2020 Jul 1;27(9):1401-1410. [doi: 10.1093/jamia/ocaa092] [Medline: 32719859]
27. Marckini DN, Samuel BP, Parker JL, Cook SC. Electronic health record associated stress: a survey study of adult congenital heart disease specialists. Congenit Heart Dis 2019 May;14(3):356-361. [doi: 10.1111/chd.12745] [Medline: 30825270]
28. Vallon JJ, Panjwani N, Ling X, et al. Patient-level clinical expertise enhances prostate cancer recurrence predictions with machine learning. medRxiv. Preprint posted online on Mar 25, 2022. [doi: 10.1101/2022.03.22.22272635]
29. Shanafelt TD, Hasan O, Dyrbye LN, et al. Changes in burnout and satisfaction with work-life balance in physicians and the general US working population between 2011 and 2014. Mayo Clin Proc 2015 Dec;90(12):1600-1613. [doi: 10.1016/j.mayocp.2015.08.023] [Medline: 26653297]
30. Ortega MV, Hidrue MK, Lehrhoff SR, et al. Patterns in physician burnout in a stable-linked cohort. JAMA Netw Open 2023 Oct 2;6(10):e2336745. [doi: 10.1001/jamanetworkopen.2023.36745]

XSL•FO
RenderX

31. Cardell CF, Yuce TK, Zhan T, et al. What they are not telling us: analysis of nonresponders on a national survey of resident well-being. Ann Surg Open 2022 Dec;3(4):e228. [doi: 10.1097/AS9.0000000000000228] [Medline: 36590893]
32. Hing E, Shimizu IM, Talwalkar A. Nonresponse bias in estimates from the 2012 National Ambulatory Medical Care Survey. Vital Health Stat 2 2016 Feb(171):1-42. [Medline: 27301078]
33. Robertson J, Walkom EJ, McGettigan P. Response rates and representativeness: a lottery incentive improves physician survey return rates. Pharmacoepidemiol Drug Saf 2005 Aug;14(8):571-577. [doi: 10.1002/pds.1126] [Medline: 15937989]
34. Willis GB, Smith T, Lee HJ. Do additional recontacts to increase response rate improve physician survey data quality? Med Care 2013;51(10):945-948. [doi: 10.1097/MLR.0b013e3182a5023d]
35. McFarlane E, Olmsted MG, Murphy J, Hill CA. Nonresponse bias in a mail survey of physicians. Eval Health Prof 2007 Jun;30(2):170-185. [doi: 10.1177/0163278707300632] [Medline: 17476029]
36. Cull WL, O'Connor KG, Sharp S, Tang SFS. Response rates and response bias for 50 surveys of pediatricians. Health Serv Res 2005 Feb;40(1):213-226. [doi: 10.1111/j.1475-6773.2005.00350.x] [Medline: 15663710]
37. Kellerman SE, Herold J. Physician response to surveys. A review of the literature. Am J Prev Med 2001 Jan;20(1):61-67. [doi: 10.1016/s0749-3797(00)00258-0] [Medline: 11137777]
38. Li A, Cronin S, Bai YQ, et al. Assessing the representativeness of physician and patient respondents to a primary care survey using administrative data. BMC Fam Pract 2018 May 30;19(1):77. [doi: 10.1186/s12875-018-0767-9] [Medline: 29848292]
39. Barnhart BJ, Reddy SG, Arnold GK. Remind me again: physician response to web surveys: the effect of email reminders across 11 opinion survey efforts at the American Board of Internal Medicine from 2017 to 2019. Eval Health Prof 2021 Sep;44(3):245-259. [doi: 10.1177/01632787211019445] [Medline: 34008437]
40. James KM, Ziegenfuss JY, Tilburt JC, Harris AM, Beebe TJ. Getting physicians to respond: the impact of incentive type and timing on physician survey response rates. Health Serv Res 2011 Feb;46(1 Pt 1):232-242. [doi: 10.1111/j.1475-6773.2010.01181.x] [Medline: 20880042]
41. Brtnikova M, Crane LA, Allison MA, Hurley LP, Beaty BL, Kempe A. A method for achieving high response rates in national surveys of U.S. primary care physicians. PLoS One 2018;13(8):e0202755. [doi: 10.1371/journal.pone.0202755] [Medline: 30138406]
42. Cunningham CT, Quan H, Hemmelgarn B, et al. Exploring physician specialist response rates to web-based surveys. BMC Med Res Methodol 2015 Apr 9;15:32. [doi: 10.1186/s12874-015-0016-z] [Medline: 25888346]

Abbreviations

AUROC: area under the receiver operating characteristic curve
EHR: electronic health record

Edited by C Lovis; submitted 31.07.24; peer-reviewed by S Zeng, S Lou; revised version received 26.11.24; accepted 25.12.24; published 04.02.25.

Please cite as:
Tawfik D, Shanafelt TD, Bayati M, Profit J
Electronic Health Record Use Patterns Among Well-Being Survey Responders and Nonresponders: Longitudinal Observational Study
JMIR Med Inform 2025;13:e64722
URL: https://medinform.jmir.org/2025/1/e64722
doi:10.2196/64722

© Daniel Tawfik, Tait D Shanafelt, Mohsen Bayati, Jochen Profit. Originally published in JMIR Medical Informatics (https://medinform.jmir.org), 4.2.2025. This is an open-access article distributed under the terms of the Creative Commons Attribution License (https://creativecommons.org/licenses/by/4.0/), which permits unrestricted use, distribution, and reproduction in any medium, provided the original work, first published in JMIR Medical Informatics, is properly cited. The complete bibliographic information, a link to the original publication on https://medinform.jmir.org/, as well as this copyright and license information must be included.

XSL•FO
RenderX

Linking Electronic Health Record Prescribing Data and Pharmacy Dispensing Records to Identify Patient-Level Factors Associated With Psychotropic Medication Receipt: Retrospective Study

Peng Wu[1], MS; Jillian H Hurst[2], PhD; Alexis French[3], PhD; Michael Chrestensen[4], BA; Benjamin A Goldstein[1,2], PhD

[1]Department of Biostatistics and Bioinformatics, School of Medicine, Duke University, 2424 Erwin Road Suite 902, 9023 Hock Plaza, Durham, NC, United States

[2]Department of Pediatrics, School of Medicine, Duke University, Durham, NC, United States

[3]Department of Psychiatry and Behavioral Sciences, School of Medicine, Duke University, Durham, NC, United States

[4]Duke Health Technology Solution, Duke University Health System, Durham, NC, United States

Corresponding Author:
Benjamin A Goldstein, PhD
Department of Biostatistics and Bioinformatics, School of Medicine, Duke University, 2424 Erwin Road Suite 902, 9023 Hock Plaza, Durham, NC, United States

Abstract

Background: Pharmacoepidemiology studies using electronic health record (EHR) data typically rely on medication prescriptions to determine which patients have received a medication. However, such data do not affirmatively indicate whether these prescriptions have been filled. External dispensing databases can bridge this information gap; however, few established methods exist for linking EHR data and pharmacy dispensing records.

Objective: We described a process for linking EHR prescribing data with pharmacy dispensing records from Surescripts. As a use case, we considered the prescriptions and resulting fills for psychotropic medications among pediatric patients. We evaluated how dispensing information affects identifying patients receiving prescribed medications and assessing the association between filling prescriptions and subsequent health behaviors.

Methods: This retrospective study identified all new psychotropic prescriptions to patients younger than 18 years of age at Duke University Health System in 2021. We linked dispensing to prescribing data using proximate dates and matching codes between RxNorm concept unique identifiers and National Drug Codes. We described demographic, clinical, and service use characteristics to assess differences between patients who did versus did not fill prescriptions. We fit a least absolute shrinkage and selection operator (LASSO) regression model to evaluate the predictability of a fill. We then fit time-to-event models to assess the association between whether a patient filled a prescription and a future provider visit.

Results: We identified 1254 pediatric patients with a new psychotropic prescription. In total, 976 (77.8%) patients filled their prescriptions within 30 days of their prescribing encounters. Thus, we set 30 days as a cut point for defining a valid prescription fill. Patients who filled prescriptions differed from those who did not in several key factors. Those who did not fill had slightly higher BMIs, lived in more disadvantaged neighborhoods, were more likely to have public insurance or self-pay, and included a higher proportion of male patients. Patients with prior well-child visits or prescriptions from primary care providers were more likely to fill. Additionally, patients with anxiety diagnoses and those prescribed selective serotonin reuptake inhibitors were more likely to fill prescriptions. The LASSO model achieved an area under the receiver operator characteristic curve of 0.816. The time to the follow-up visit with the same provider was censored at 90 days after the initial encounter. Patients who filled prescriptions showed higher levels of follow-up visits. The marginal hazard ratio of a follow-up visit with the same provider was 1.673 (95% CI 1.463 - 1.913) for patients who filled their prescriptions. Using the LASSO model as a propensity-based weight, we calculated the weighted hazard ratio as 1.447 (95% CI 1.257 - 1.665).

Conclusions: Systematic differences existed between patients who did versus did not fill prescriptions. Incorporating external dispensing databases into EHR-based studies informs medication receipt and associated health outcomes.

(JMIR Med Inform 2025;13:e63740) doi:10.2196/63740

KEYWORDS

electronic health records; pharmacy dispensing; psychotropic medications; prescriptions; predictive modeling

XSL•FO
RenderX

Introduction

Electronic health record (EHR) data have become a vital data resource for health outcomes and health services research [1]. These data provide detailed patient information, including demographics, diagnoses, prescriptions, and procedures, which can facilitate comprehensive studies that reflect real-world clinical practice [2]. EHR data are increasingly being used to support clinical decision-making with prediction models [3,4] and assess population health [5]. Additionally, EHR data facilitate clinical trial simulation by assessing assumptions and guiding study design of the actual trials [6,7]. They have also emerged as a key resource for the observation of long-term drug safety and effectiveness [8,9], providing insights into drug benefits, interactions, and side effects [10]. Beyond this, EHR data provide valuable opportunities for uncovering disease phenotypes, mapping treatment pathways, and informing drug repurposing and safety studies [11,12]. The use of EHR data in pharmacoepidemiology research can further our understanding of drug impacts and access, driving advancements in care [13].

Despite the utility of EHR data, a significant limitation arises for research focused on medication use. While EHRs contain granular information on medication prescriptions, commercial pharmacy data are typically held in a separate database that must be connected to the EHR. Because these databases are separate, prescription fill data may not be readily available and are often not directly connected to a specific encounter [14,15]. This discrepancy can lead to inaccuracies in understanding which patients have actually received medication and how medication receipt may influence patient outcomes [16]. This challenge can be thought of as a missing data or observability problem, which can ultimately bias the analysis and interpretation of EHR-based health outcomes research [17,18]. External pharmacy dispensing databases present a potential solution to bridge the information gap regarding prescription fills [19-21], thereby improving our ability to identify patients who have received a specific medication [22].

While commercial pharmacy databases such as Surescripts have begun to be integrated into EHR databases, there have been few studies that have directly linked Surescripts to EHR data for research purposes. Such linkages can be challenging due to the differences in how these various data streams are accessed and updated, and the different ontologies used for medications across systems. In this study, we present a process to link Surescripts and EHR data. To evaluate the utility of this linkage and the impact of evaluating prescriptions versus pharmacy fill data, we conducted an analysis of prescription fills among children and adolescents who were prescribed psychotropic medication. Identification of psychotropic medication receipt is of particular importance in pediatric populations [23-26]. The management of these conditions requires medication adherence and regular follow-up with a provider to ensure that the patient is being adequately treated and that the side effects of these medications are minimal and acceptable to the patient and their family. Notably, access to these medications can vary significantly based on social drivers of health, patient and family attitudes, insurance, and national and global supply chains [26,27]. Given the need for continued evaluation once a psychoactive medication is prescribed, we specifically evaluated patient and prescriber characteristics and the association between a pharmacy fill for a psychoactive medication and subsequent follow-up with the prescribing provider.

Methods

Study Environment and Data

This study included retrospective data from pediatric patients less than 18 years of age who received new psychotropic medication prescriptions within the Duke University Health System (DUHS). DUHS is a medium-sized health system in Durham, North Carolina. DUHS contains over 100 pediatric-serving clinics and is the primary health care provider for approximately 86% of children living in Durham county [28]. All EHR data were extracted from the Duke Clinical Research Datamart, an extract of structured DUHS EHR data that are curated using the standards of the PCORnet common data model [29]. The datamart additionally includes Surescripts prescription fill data, which are reconciled with patient charts within the Epic System. Surescripts facilitates the electronic transmission of prescriptions from EHR to pharmacies and also receives prescription dispense data from most major US pharmacies and pharmacy benefit managers; as of 2020, 96.5% of pharmacies in North Carolina are Surescripts-enabled [30,31]. Data are provided daily based on pharmacy reports and integrated into the EHR system for patient record matching. Pharmacy data for a given patient are updated within the DUHS EHR only upon scheduling of a clinical encounter within the health system.

Study Population

We identified children younger than 18 years of age with new psychotropic medication prescriptions written at an outpatient visit in 2021. Throughout this paper, the term “prescriptions” refers to psychotropic medication prescriptions. All prescriptions were identified using RxNorm concept unique identifiers (RxCUIs; Table S1 in Multimedia Appendix 1). RxNorm is a normalized naming system, and RxCUIs serve as an identifier assigned to an individual drug entity in RxNorm. A new prescription was defined as a prescription made to a patient who did not have a record of a psychotropic medication prescription or pharmacy fill in the 12 months prior to the date of the index prescription. Because Surescripts data are only incorporated for patients with a subsequent health care encounter, the patient cohort was limited to patients who had any DUHS encounter in 2022.

Medication Identification and Matching

A primary challenge in working with Surescripts data is the lack of a direct linkage between EHR prescriptions and pharmacy dispensing records. Moreover, the EHR and Surescripts data use 2 different ontologies for medications: RxCUIs and National Drug Codes (NDCs). NDCs provide package-level information about specific drugs, while RxCUIs can correspond to multiple NDCs for similar drug products with the same active ingredient, strength, and dose form but different package sizes or manufacturers. We first mapped the RxCUIs from the EHR to NDCs in the Surescripts data, incorporating

XSL•FO
RenderX

the drug name to ensure a correct match between RxCUIs and NDCs [32,33]. Second, using data from 2021 through 2022, we matched prescriptions with dispensing records by identifying the nearest fill date that occurred after the prescription date. Thus, prescriptions with matching NDCs and a fill closest to the prescribing date were considered potential matches. A cutoff of days was ultimately applied to define a valid prescription fill, as this interval aligned with an observed inflection point in the Kaplan-Meier curve of filling prescriptions (see Results section).

Contextual Variables

We assessed differences between patients who did versus did not fill their prescriptions on 22 contextual variables, including demographic information, clinical characteristics, encounter characteristics, and service use history (Table S2 in Multimedia Appendix 1). Variables included age, sex, race or ethnicity, BMI, the Area of Deprivation Index (ADI) state rank [34], diagnosis (one or more) at the prescribing encounter, prescription of a selective serotonin reuptake inhibitor (the predominant medication class for depression and certain anxiety disorders) versus other type of psychotropic medication [35], the presence or absence of a completed Patient Health Questionnaire-9 (PHQ-9), the PHQ-9 score (categorized as 0‐4=nonminimal, 5-9=mild, 10-14=moderate, 15-19=moderately severe, and 20-27=severe for patients who had a PHQ-9 in the 2 weeks prior to the index prescription) [36], the number of psychotropic medication prescriptions at the index encounter, the number of psychotropic medication prescriptions in 2021, insurance type at the index encounter [37], characteristics of the prescribing provider and clinic, including provider specialty, and health system service use history in 2020 or 2021, including outpatient, inpatient, and well-child visits [38].

Data Analysis

We initially fit a Kaplan-Meier curve to assess the time from the encounter at which the prescription was created to when the prescription was filled. We then described the demographic and clinical characteristics of patients who did versus did not fill their prescriptions. Continuous variables were summarized using median and IQR. Categorical variables were presented as the number (percentage) for each group. The standardized mean difference was used to measure the magnitude of differences between patients who did versus did not fill their prescriptions, with a standardized mean difference greater than 0.10 indicating an imbalance between groups [39].

To further assess systematic differences between patients who filled their prescriptions and those who did not, we developed a predictive model to identify patients who filled their prescriptions. We applied the least absolute shrinkage and selection operator (LASSO) regression [40] to evaluate the predictability of prescription fills. Data were split into training and testing sets in a 9:1 ratio, with a 5-fold cross-validation conducted to optimize the regularization parameter using the training data and applied the final model to the test data. We evaluated the model performance via the area under the receiver operator characteristic curve (AUROC).

Finally, we evaluated subsequent health care use for patients who did versus did not fill their prescriptions. Using data through 2022, we conducted a time-to-event analysis to identify associations between whether a psychotropic medication prescription was filled and the time until a follow-up encounter with the prescribing provider. We limited eligible follow-up encounters to occur within 90 days of the encounter with the prescription. The period was chosen to provide a sufficient window for capturing relevant follow-up care, as this time frame allows patients to schedule appointments around potential barriers, such as availability or transportation issues, and aligns with common clinical practices for monitoring initial medication responses within 6‐8 weeks [41]. We estimated the marginal hazard ratio (HR) using the Cox proportional hazards model. We derived propensity scores (PSs) using predicted probabilities from the LASSO regression model (described in the Data Analysis section). Inverse probability weighting of PSs was used to adjust for potential confounders (ie, the contextual variables described earlier) by balancing the distribution of covariates between groups. This corrected for the bias that might arise from systematic differences between those who filled their prescriptions and those who did not. All analyses were conducted in R (version 4.1.3; R Foundation for Statistical Computing).

Ethical Considerations

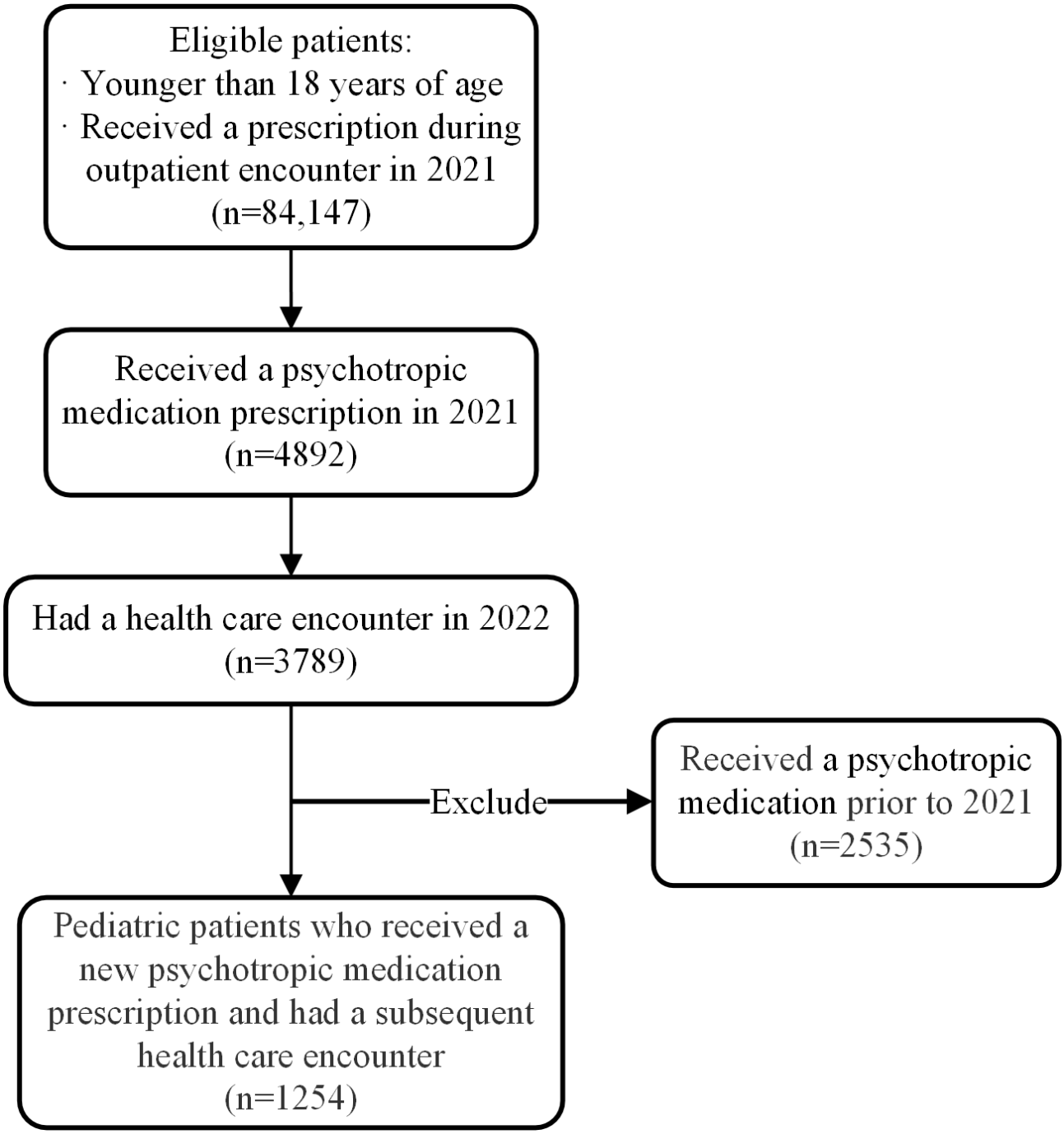
This study was declared exempt by the DUHS institutional review board (PRO00091342). The institutional review board determined that the study posed minimal risk to participants, as it involved retrospective analysis of deidentified EHRs and pharmacy dispensing data. Patient privacy and data confidentiality were maintained by using deidentified datasets, and access to sensitive information was restricted to authorized study personnel.

Results

We identified 1254 pediatric patients with new psychotropic medication prescriptions in 2021 (Figure 1). In total, 976 (77.8%) patients had a fill within 30 days of the prescribing encounter, with only 64 prescription fills occurring more than 1 month after the prescribing encounter (Figure 2). Among a total of 1040 patients who filled their prescription, 950 (91.3%) filled it within 7 days, with 844 (81.2%) filling the prescription on the day of the encounter. We then set 30 days as the cutoff for a valid prescription fill. We found that 278 (22.2%) patients did not fill their prescriptions. These patients would have been misclassified as receiving psychotropic medication if only prescriptions were used to identify recipients of these medications.

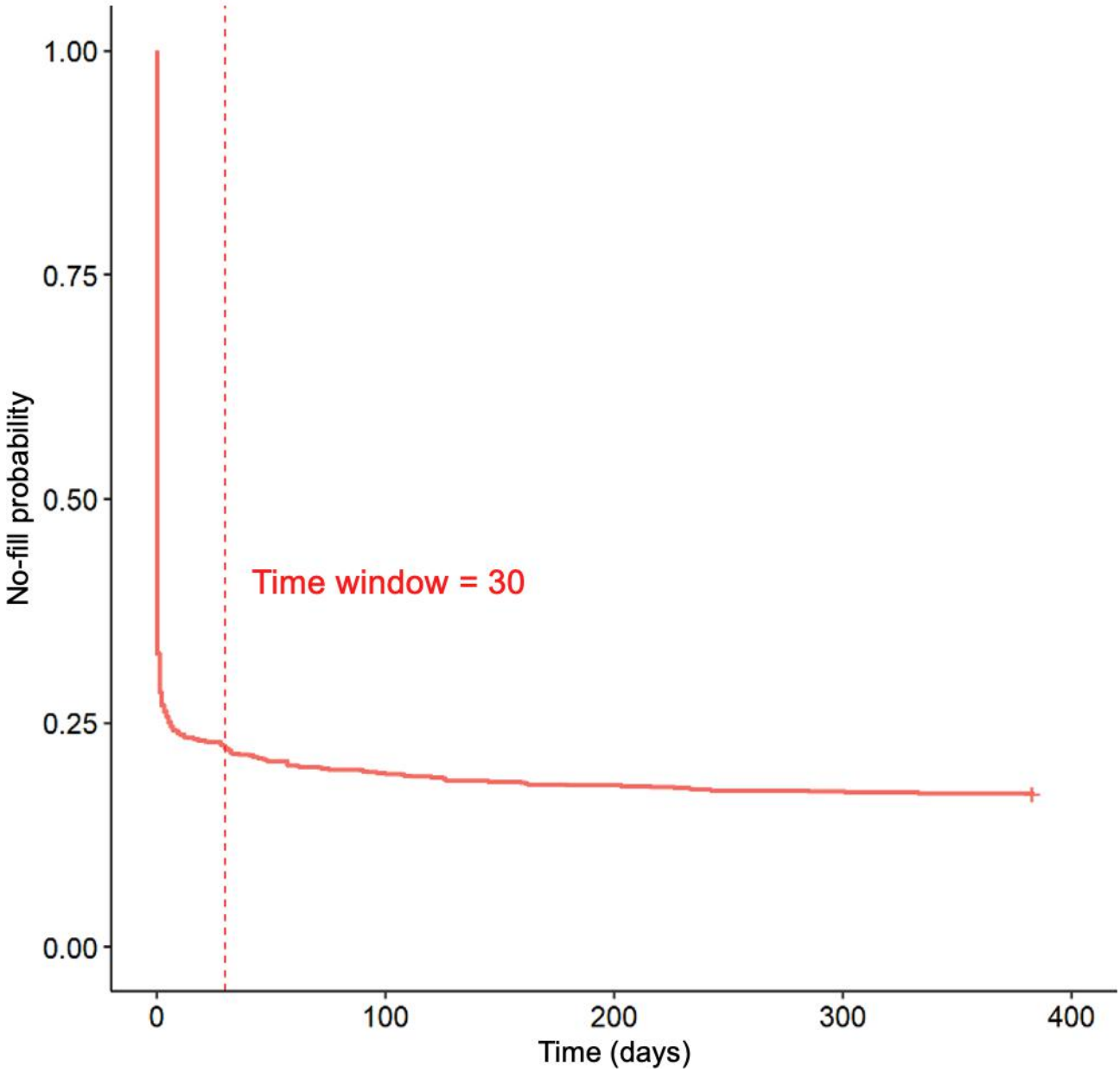
XSL•FO
RenderX

Figure 1. CONSORT (Consolidated Standards of Reporting Trials) diagram.



XSL•FO
RenderX

Figure 2. Kaplan-Meier curve depicting time from prescription receipt to prescription fill.



We evaluated the demographic and clinical characteristics of patients who filled versus did not fill their prescriptions (Table 1). Notably, the 2 groups were similar in terms of race or ethnicity, age, and rates of inpatient and emergency department encounters. We observed a slight difference in sex, with more female patients receiving prescriptions and also a slightly greater proportion of female patients among those who filled their prescriptions. We additionally observed differences in patient BMI, ADI rank, outpatient health care use, and insurance type. Among patients who did not fill their prescriptions, we observed slightly higher BMIs, higher ADI ranks (indicating that patients lived in a more disadvantaged neighborhood), and a greater proportion of patients with public insurance or who were self-pay. Completion of a well-child visit, a marker of health care engagement and receipt of preventive care, was less common among patients who did not fill their prescriptions, but well-child visit rates did not differ significantly in the year after prescription receipt. We additionally observed differences related to the visit type and prescribing provider among patients who did versus did not fill their prescriptions, with a greater proportion of primary care prescribers among patients who ultimately filled their prescriptions. We found that patients diagnosed with anxiety and those who received a prescription for a selective serotonin reuptake inhibitor were more likely to be among those who filled their prescriptions. Patients who had not taken a PHQ-9 recently or who had a PHQ-9 score less than 5 were less likely to fill their prescriptions. Half of the patients (n=635, 50.6%) did not have a recent PHQ-9 score recorded, though some patients may have received the PHQ-9 modified for Adolescents, which was not extracted for this study. There was a slightly higher median number of psychotropic medication prescriptions throughout the year among patients who filled their initial prescription compared to those who did not (median 2, IQR 1-3 vs median 1, IQR 1-2).

XSL•FO
RenderX

Table . Demographic and clinical characteristics of patients stratified by prescription fill status.

Patient and prescriber characteristics	Overall (N=1254)	Prescription filled (n=976)	Prescription not filled (n=278)	SMD[a]
Age (years), median (IQR)	14 (12-16)	14 (12-16)	14 (12-15)	0.035
Sex, n (%)				0.115
Female	838 (66.8)	664 (68)	174 (62.6)	
Male	416 (33.2)	312 (32)	104 (37.4)	
Race or ethnicity, n (%)				0.102
Hispanic	137 (10.9)	106 (10.9)	31 (11.2)	
Non-Hispanic Asian	35 (2.8)	25 (2.6)	10 (3.6)	
Non-Hispanic Black	242 (19.3)	195 (20)	47 (16.9)	
Non-Hispanic White	700 (55.8)	544 (55.7)	156 (56.1)	
Other	140 (11.2)	106 (10.9)	34 (12.2)	
BMI, median (IQR)	21.90 (18.89-26.78)	21.62 (18.89-26.10)	22.86 (18.94-28.04)	0.164
ADI[b] state rank, median (IQR)	3 (2-5)	3 (2-5)	3 (2-6)	0.193
Well-child visit in 2020, n (%)	541 (43.1)	448 (45.9)	93 (33.5)	0.257
Well-child visit in 2021, n (%)	725 (57.8)	571 (58.5)	154 (55.4)	0.063
Outpatient visit in 2020, n (%)	960 (76.6)	764 (78.3)	196 (70.5)	0.179
Inpatient visit in 2020, n (%)	10 (0.8)	6 (0.6)	4 (1.4)	0.082
Emergency department visit 2020, n (%)	55 (4.4)	42 (4.3)	13 (4.7)	0.018
Primary payer, n (%)				0.305
Public	558 (44.5)	404 (41.4)	154 (55.4)	
Private	670 (53.4)	554 (56.8)	116 (41.7)	
Self-pay	26 (2.1)	18 (1.8)	8 (2.9)	
Provider type, n (%)				0.103
Physician	931 (72.8)	715 (73.3)	216 (77.7)	
Other provider type	323 (25.8)	261 (26.7)	62 (22.3)	
Prescribing provider specialty, n (%)				0.384
Primary care	1037 (82.7)	833 (85.3)	204 (73.4)	
Psychiatry	56 (4.5)	47 (4.8)	9 (3.2)	
Other specialty	151 (12)	88 (9)	63 (22.7)	
Unknown specialty	10 (0.8)	8 (0.8)	2 (0.7)	
Prescribing clinic type, n (%)				0.655
Primary care	913 (72.8)	760 (77.9)	153 (55)	
Behavioral health	100 (8)	87 (8.9)	13 (4.7)	
Other clinic type	140 (11.2)	82 (8.4)	58 (20.9)	
Unknown	101 (8.1)	47 (4.8)	54 (19.4)	
Diagnosis at prescribing visit, n (%)				
Depression	327 (26.1)	262 (26.8)	65 (23.4)	0.080
Anxiety	670 (53.4)	572 (58.6)	98 (35.3)	0.481
ADHD[c]	175 (14)	138 (14.1)	37 (13.3)	0.024

XSL•FO
RenderX

Patient and prescriber characteristics	Overall (N=1254)	Prescription filled (n=976)	Prescription not filled (n=278)	SMD[a]
Headache	185 (14.8)	149 (15.3)	36 (12.9)	0.067
Number of prescriptions[d] at the prescribing encounter, median (IQR)	1 (1-1)	1 (1-1)	1 (1-1)	0.153
Number of prescriptions[d] in 2021, median (IQR)	1 (1-2)	2 (1-3)	1 (1-2)	0.31
SSRI[e] received, n (%)	1074 (85.6)	858 (87.9)	216 (77.7)	0.273
PHQ-9[f] score severity, n (%)				0.39
Nonminimal	133 (10.6)	94 (9.6)	39 (14)	
Mild	126 (10)	100 (10.2)	26 (9.4)	
Moderate	132 (10.5)	117 (12)	15 (5.4)	
Moderately severe	125 (10)	108 (11.1)	17 (6.1)	
Severe	103 (8.2)	89 (9.1)	14 (5)	
Not taken	635 (50.6)	468 (48)	167 (60.1)	

[a]SMD: standardized mean difference.

[b]ADI: Area Deprivation Index.

[c]ADHD: attention-deficit/hyperactivity disorder.

[d]It refers to psychotropic medication prescriptions.

[e]SSRI: selective serotonin reuptake inhibitor.

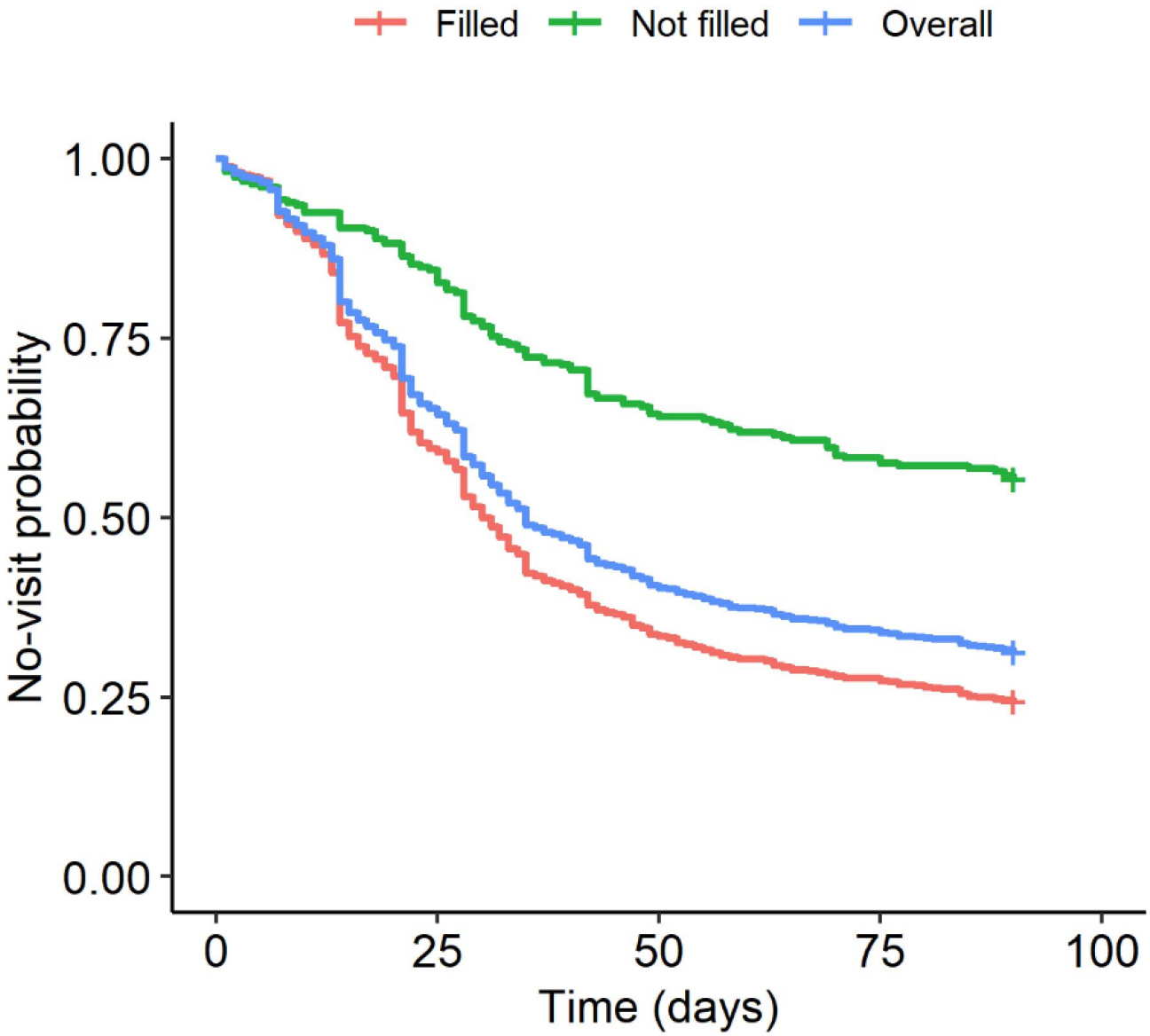
[f]PHQ-9: Patient Health Questionnaire-9.

Using these patient-level variables, we fit a LASSO regression model to discriminate between patients who did versus did not fill their prescriptions. The model achieved an AUROC of 0.816, demonstrating good discriminative ability, and further indicating that clinical and demographic variables differ significantly between patients who did versus did not fill their prescriptions.

We next evaluated the time to follow-up visit with the prescribing provider between patients who did versus did not fill their psychotropic medication prescriptions (Figure 3). Among patients who filled their prescriptions, 737 (75.5%) had a follow-up visit compared to 123 (44.3%) of those who did not. Patients who filled their prescriptions were more likely to have a subsequent appointment with their prescribing provider than patients who did not fill their prescriptions (marginal HR 1.673, 95% CI 1.463 - 1.913). To account for potential systematic differences between these 2 groups, we derived PSs using predicted probabilities from the LASSO regression model. Inverse probability weighting of PSs was used to adjust for potential confounders. After weighting, we calculated the propensity-weighted HR as 1.447 (95% CI 1.257 - 1.665).

XSL•FO
RenderX

Figure 3. Kaplan-Meier curve depicting days until follow-up visit for patients who did versus did not fill their psychotropic medication prescriptions.



Discussion

Principal Findings

While EHRs contain data on prescriptions, they often lack information on whether these prescriptions are subsequently filled. We sought to evaluate how prescription fill information influenced our understanding of which patients actually receive a prescribed medication and whether a prescription is filled is associated with subsequent health behaviors. We evaluated prescription fill rates among a cohort of pediatric patients who had received prescriptions for psychotropic medications and found that approximately 22.2% (n=278) did not fill their prescriptions. Moreover, there were systematic differences between patients who did versus did not fill their prescriptions. We additionally found that whether a prescription was filled was associated with the likelihood of having a follow-up visit with the prescribing provider. These findings demonstrate that pharmacy dispensing data provide important insights into medication use and contextual information about which populations receive medications and how medication receipt may influence health system interactions and patient outcomes. Importantly, the inclusion of prescription fill data was required to understand how medication receipt may influence subsequent health behavior.

Most prescriptions were filled within 1 week of prescription receipt, with 844 (81.2%) of those who filled doing so on the day of the prescribing encounter. Because these were all new prescriptions, it is likely that patients or their caregivers were motivated to fill the prescriptions to address an acute concern. We found that a greater proportion of female patients filled their psychotropic medication prescriptions compared to male patients. Our finding is consistent with the study by Chua et al [42], which found that female adolescents had a substantially higher monthly antidepressant dispensing rate compared to male adolescents between March 2020 and December 2022. We also found that non-Hispanic White patients and publicly insured patients were more prevalent among the group of patients who did not fill their prescriptions. Children and families with public insurance, such as Medicaid, are more likely to experience adverse social drivers of health [43], which may make it more challenging to follow up with treatment recommendations, including filling a prescription. Our finding that private

XSL•FO
RenderX

insurance is associated with higher prescription fill rates is consistent with trends observed in other populations, such as adults on antihypertension medications [44]. We found that a greater proportion of patients filled their prescriptions from a primary care or psychiatry provider compared to those who did not fill. Patients and families may have felt more confident in a course of treatment from a provider with behavioral health expertise than from providers practicing in other specialties. Results indicated that patients with an anxiety disorder were more likely to fill their prescriptions. Prior research has shown that almost three-quarters of pediatric patients who were newly diagnosed with an anxiety disorder received a psychotropic medication order within 5 years of their anxiety diagnosis [45]. Our findings revealed that patients who filled their initial psychotropic prescription had a higher median number of psychotropic prescriptions throughout the year. This suggests that patients who engage with their initial treatment might be more likely to continue with psychotropic medication management. Such findings align with literature emphasizing the importance of initial adherence as a predictor of sustained engagement in mental health care [46]. These findings support previous research that highlights the complex factors contributing to medication nonadherence [47].

The pronounced differences between children and adolescents who did versus did not fill initial psychotropic medication prescriptions underscore the potential risk of differential misclassification. This is particularly noteworthy, as differential misclassification can introduce bias in estimating associations [15,48]. For instance, if we rely only on prescription records, we may misclassify some patients who did not pick up their prescriptions as medication users. By incorporating dispensing records, however, we can more accurately identify actual medication users, as only those who filled their prescriptions would be classified as having received the drug. In our analysis, we found that patients who filled their prescriptions were more likely to have a follow-up visit than those who did not. This demonstrates how including dispensing records changes our understanding of patient behavior, providing a clearer picture of which patients are truly receiving the prescribed treatment.

Our LASSO regression model, which achieved an AUROC of 0.816, indicated that patient demographic and clinical factors were useful predictors of whether prescriptions were filled. This signifies the potential for developing a clinical decision support tool to indicate which patients are more likely to fill versus not to fill a prescription. Such a tool could guide providers in either tailoring additional follow-up or adjusting treatment modalities. It is also important to understand the factors underlying the reasons that patients do not fill a prescription, such as social drivers that may present barriers to filling a prescription, lack of education provided about the rationale for the medication and possible side effects, or not feeling comfortable telling a provider that they do not want to start a psychotropic medication. The LASSO model identified characteristics that may influence both prescription filling and follow-up visits. By using these predicted probabilities as PSs in our analyses on the association between filling and follow-up visits, we reduced potential confounding, strengthening the robustness of our findings.

We identified a significant association between filling prescriptions and follow-up visits with the prescribing provider. This result indicates that prescription filling behavior likely influences subsequent health care engagement and also highlights the importance of including prescription fill data in EHR analyses that account for medication receipt. It is recommended that youths who receive a prescription for a psychotropic medication have weekly to biweekly follow-up visits with their prescribing provider for the first 6 to 8 weeks after initiating a psychotropic medication to monitor treatment response and side effects [41]. We found that patients who filled their prescriptions were more likely to have a follow-up visit with their prescribing provider. Conversely, patients who did not fill prescriptions were less likely to have a follow-up visit. While this analysis is not able to establish whether medication adherence drives health care engagement or health care engagement drives medication adherence, this association nonetheless highlights the relationship between adherence to medication and health care interactions. At the very least, a lack of prescription fills could serve as an early marker of a lack of health care engagement. It is possible that patients did not return to care due to access challenges, reluctance to discuss not filling prescriptions with providers, or a perceived lack of necessity for medical monitoring. Future research should aim to understand patient outcomes when recommended treatment is not followed, especially if moderate to severe mental health symptoms are present.

Strength and Limitations

This study has some limitations. Of the 4892 patients prescribed psychotropic medication in 2021, a total of 1103 (22.5%) were excluded due to the absence of a follow-up appointment in 2022. While this criterion was applied to ensure complete capture of Surescripts data, it may limit the generalizability of our findings to patients with more consistent health care engagement. Additionally, 635 (50.6%) patients lacked a recent PHQ-9 score, and categorizing PHQ-9 modified for Adolescent scores as “not taken” for consistency limits our ability to interpret associations between PHQ-9 scores and prescription fills. Additionally, we focused on prescription filling behavior for a single prescription per patient; consequently, in instances involving multiple prescriptions on different dates, our matching methodology may require refinement to avoid matching the same dispensing record to more than 1 prescription and ensure each medication dispensing record corresponds to a specific prescription. It is challenging to determine whether prescriptions that lacked a corresponding dispensing record were indeed not filled or simply did not align with a dispensation entry. It is also possible that patients filled their prescriptions at non-Surescripts participating pharmacies, such as digital pharmacies or paid for their prescription out of pocket. Nonetheless, the dispensing rates observed align with prior studies [49]. Furthermore, we restricted our analysis to patients who received health care exclusively within the DUHS and focused only on the prescriptions for psychotropic medications rather than examining multiple health systems or a broader range of medication classes. Future work should investigate prescription filling behavior more broadly across different clinical and geographic populations. Finally, our sample size did not allow us to assess

XSL•FO
RenderX

differences in clinical outcomes between those who did and did not fill their medications.

Conclusions

Overall, our study established a process to link EHR prescription data and pharmacy dispensing databases and shows that the inclusion of dispensing data helps identify patients who have received a medication. This approach enhances our understanding of how medication receipt is associated with health care behaviors, such as follow-up visits. Our findings can potentially inform tools to improve patient medication receipt. The inclusion of dispensing data can be used to reduce potential biases in future pharmacoepidemiology studies.

Acknowledgments

This work was supported in part by National Institutes of Health (grant K01-AI173398 awarded to JHH) and the National Center for Advancing Translational Sciences Clinical and Translational Science Award (grant UL1TR002553).

Conflicts of Interest

None declared.

Multimedia Appendix 1
RxNorm concept unique identifiers for psychotropic medications and descriptions of the contextual variables used to compare patients who did and did not fill their prescriptions.
[DOCX File, 25 KB - medinform_v13i1e63740_app1.docx]

References

1. Bérard A. Pharmacoepidemiology research-real-world evidence for decision making. Front Pharmacol 2021;12:723427. [doi: 10.3389/fphar.2021.723427] [Medline: 34557096]
2. Blonde L, Khunti K, Harris SB, Meizinger C, Skolnik NS. Interpretation and impact of real-world clinical data for the practicing clinician. Adv Ther 2018 Nov;35(11):1763-1774. [doi: 10.1007/s12325-018-0805-y] [Medline: 30357570]
3. Goldstein BA, Mohottige D, Bessias S, Cary MP Jr. Enhancing clinical decision support in nephrology: addressing algorithmic bias through artificial intelligence governance. Am J Kidney Dis 2024 Dec;84(6):780-786. [doi: 10.1053/j.ajkd.2024.04.008] [Medline: 38851444]
4. Goldstein BA, Navar AM, Pencina MJ, Ioannidis JPA. Opportunities and challenges in developing risk prediction models with electronic health records data: a systematic review. J Am Med Inform Assoc 2017 Jan;24(1):198-208. [doi: 10.1093/jamia/ocw042] [Medline: 27189013]
5. Casey JA, Schwartz BS, Stewart WF, Adler NE. Using electronic health records for population health research: a review of methods and applications. Annu Rev Public Health 2016;37:61-81. [doi: 10.1146/annurev-publhealth-032315-021353] [Medline: 26667605]
6. Tannen RL, Weiner MG, Marcus SM. Simulation of the Syst-Eur randomized control trial using a primary care electronic medical record was feasible. J Clin Epidemiol 2006 Mar;59(3):254-264. [doi: 10.1016/j.jclinepi.2005.08.008] [Medline: 16488356]
7. Danaei G, Rodríguez LAG, Cantero OF, Logan R, Hernán MA. Observational data for comparative effectiveness research: an emulation of randomised trials of statins and primary prevention of coronary heart disease. Stat Methods Med Res 2013 Feb;22(1):70-96. [doi: 10.1177/0962280211403603] [Medline: 22016461]
8. Holmgren AJ, Co Z, Newmark L, Danforth M, Classen D, Bates D. Assessing the safety of electronic health records: a national longitudinal study of medication-related decision support. BMJ Qual Saf 2020 Jan;29(1):52-59. [doi: 10.1136/bmjqs-2019-009609] [Medline: 31320497]
9. Hughes RG, editor. Advances in patient safety. In: Patient Safety and Quality: An Evidence-Based Handbook for Nurses: Agency for Healthcare Research and Quality (US); 2008. [Medline: 21328752]
10. Campanella P, Lovato E, Marone C, et al. The impact of electronic health records on healthcare quality: a systematic review and meta-analysis. Eur J Public Health 2016 Feb;26(1):60-64. [doi: 10.1093/eurpub/ckv122] [Medline: 26136462]
11. Tang AS, Woldemariam SR, Miramontes S, Norgeot B, Oskotsky TT, Sirota M. Harnessing EHR data for health research. Nat Med 2024 Jul;30(7):1847-1855. [doi: 10.1038/s41591-024-03074-8]
12. Xu H, Li J, Jiang X, Chen Q. Electronic health records for drug repurposing: current status, challenges, and future directions. Clin Pharmacol Ther 2020 Apr;107(4):712-714. [doi: 10.1002/cpt.1769] [Medline: 32012237]
13. Abul-Husn NS, Kenny EE. Personalized medicine and the power of electronic health records. Cell 2019 Mar 21;177(1):58-69. [doi: 10.1016/j.cell.2019.02.039] [Medline: 30901549]
14. Kim MK, Rouphael C, McMichael J, Welch N, Dasarathy S. Challenges in and opportunities for electronic health record-based data analysis and interpretation. Gut Liver 2024 Mar 15;18(2):201-208. [doi: 10.5009/gnl230272] [Medline: 37905424]
15. Young JC, Conover MM, Funk MJ. Measurement error and misclassification in electronic medical records: methods to mitigate bias. Curr Epidemiol Rep 2018 Dec;5(4):343-356. [doi: 10.1007/s40471-018-0164-x] [Medline: 35633879]

XSL•FO
RenderX

16. Mabotuwana T, Warren J, Harrison J, Kenealy T. What can primary care prescribing data tell us about individual adherence to long-term medication?—Comparison to pharmacy dispensing data. Pharmacoepidemiol Drug Saf 2009 Oct;18(10):956-964. [doi: 10.1002/pds.1803] [Medline: 19609958]
17. Gianfrancesco MA, Goldstein ND. A narrative review on the validity of electronic health record-based research in epidemiology. BMC Med Res Methodol 2021 Oct 27;21(1):234. [doi: 10.1186/s12874-021-01416-5] [Medline: 34706667]
18. Haneuse S, Arterburn D, Daniels MJ. Assessing missing data assumptions in EHR-based studies: a complex and underappreciated task. JAMA Netw Open 2021 Feb 1;4(2):e210184. [doi: 10.1001/jamanetworkopen.2021.0184] [Medline: 33635321]
19. Hoopes M, Angier H, Raynor LA, et al. Development of an algorithm to link electronic health record prescriptions with pharmacy dispense claims. J Am Med Inform Assoc 2018 Oct 1;25(10):1322-1330. [doi: 10.1093/jamia/ocy095] [Medline: 30113681]
20. Gabriel MH, Smith JY, Sow M, Charles D, Joseph S, Wilkins TL. Dispatch from the non-HITECH-incented Health IT world: electronic medication history adoption and utilization. J Am Med Inform Assoc 2016 May;23(3):562-569. [doi: 10.1093/jamia/ocv151] [Medline: 26554429]
21. Pevnick JM, Palmer KA, Shane R, et al. Potential benefit of electronic pharmacy claims data to prevent medication history errors and resultant inpatient order errors. J Am Med Inform Assoc 2016 Sep;23(5):942-950. [doi: 10.1093/jamia/ocv171] [Medline: 26911817]
22. Blecker S, Adhikari S, Zhang H, et al. Validation of EHR medication fill data obtained through electronic linkage with pharmacies. J Manag Care Spec Pharm 2021 Oct;27(10):1482-1487. [doi: 10.18553/jmcp.2021.27.10.1482] [Medline: 34595945]
23. Bitsko RH, Claussen AH, Lichstein J, et al. Mental health surveillance among children—United States, 2013-2019. MMWR Suppl 2022 Feb 25;71(2):1-42. [doi: 10.15585/mmwr.su7102a1] [Medline: 35202359]
24. Merikangas KR, He JP, Burstein M, et al. Lifetime prevalence of mental disorders in U.S. adolescents: results from the National Comorbidity Survey Replication—Adolescent Supplement (NCS-A). J Am Acad Child Adolesc Psychiatry 2010 Oct;49(10):980-989. [doi: 10.1016/j.jaac.2010.05.017] [Medline: 20855043]
25. Visser SN, Danielson ML, Bitsko RH, et al. Trends in the parent-report of health care provider-diagnosed and medicated attention-deficit/hyperactivity disorder: United States, 2003-2011. J Am Acad Child Adolesc Psychiatry 2014 Jan;53(1):34-46. [doi: 10.1016/j.jaac.2013.09.001] [Medline: 24342384]
26. Whitney DG, Peterson MD. US national and state-level prevalence of mental health disorders and disparities of mental health care use in children. JAMA Pediatr 2019 Apr 1;173(4):389-391. [doi: 10.1001/jamapediatrics.2018.5399] [Medline: 30742204]
27. Bornheimer LA, Acri MC, Gopalan G, McKay MM. Barriers to service utilization and child mental health treatment attendance among poverty-affected families. Psychiatr Serv 2018 Oct 1;69(10):1101-1104. [doi: 10.1176/appi.ps.201700317] [Medline: 29983111]
28. Stolte A, Merli MG, Hurst JH, Liu Y, Wood CT, Goldstein BA. Using electronic health records to understand the population of local children captured in a large health system in Durham County, NC, USA, and implications for population health research. Soc Sci Med 2022 Mar;296:114759. [doi: 10.1016/j.socscimed.2022.114759] [Medline: 35180593]
29. Hurst JH, Liu Y, Maxson PJ, Permar SR, Boulware LE, Goldstein BA. Development of an electronic health records datamart to support clinical and population health research. J Clin Transl Sci 2020 Jun 23;5(1):e13. [doi: 10.1017/cts.2020.499] [Medline: 33948239]
30. 2020 National progress report. Surescripts. URL: https://surescripts.com/news-center/national-progress-report-2020 [accessed 2024-10-15]
31. Why it matters: prescribers can now access accurate medication history data for virtually every American. Surescripts. URL: https://surescripts.com/news-center/intelligence-in-action/interoperability/why-it-matters-prescribers-can-now-access-accurate-medication-history-data-for-virtually-every-american [accessed 2024-10-15]
32. Mapping NDC, RXCUI, and drug names in the RxNorm files. National Library of Medicine. 2022. URL: https://www.nlm.nih.gov/research/umls/user_education/quick_tours/RxNorm/ndc_rxcui/NDC_RXCUI_DrugName.html [accessed 2023-04-02]
33. Lester CA, Flynn AJ, Marshall VD, Rochowiak S, Rowell B, Bagian JP. Comparing the variability of ingredient, strength, and dose form information from electronic prescriptions with RxNorm drug product descriptions. J Am Med Inform Assoc 2022 Aug 16;29(9):1471-1479. [doi: 10.1093/jamia/ocac096] [Medline: 35773948]
34. Kind AJH, Buckingham WR. Making neighborhood-disadvantage metrics accessible—the neighborhood atlas. N Engl J Med 2018 Jun 28;378(26):2456-2458. [doi: 10.1056/NEJMp1802313] [Medline: 29949490]
35. Sharp T, Collins H. Mechanisms of SSRI therapy and discontinuation. Curr Top Behav Neurosci 2024;66:21-47. [doi: 10.1007/7854_2023_452] [Medline: 37955823]
36. Kroenke K, Spitzer RL, Williams JB. The PHQ-9: validity of a brief depression severity measure. J Gen Intern Med 2001 Sep;16(9):606-613. [doi: 10.1046/j.1525-1497.2001.016009606.x] [Medline: 11556941]

XSL•FO
RenderX

37. Kesselheim AS, Huybrechts KF, Choudhry NK, et al. Prescription drug insurance coverage and patient health outcomes: a systematic review. Am J Public Health 2015 Feb;105(2):e17-e30. [doi: 10.2105/AJPH.2014.302240] [Medline: 25521879]
38. Schor EL, Bergman D. Pediatric preventive care: population health and individualized care. Pediatrics 2021 Sep;148(3):e2020049877. [doi: 10.1542/peds.2020-049877] [Medline: 34433687]
39. Nguyen TL, Collins GS, Spence J, et al. Double-adjustment in propensity score matching analysis: choosing a threshold for considering residual imbalance. BMC Med Res Methodol 2017 Apr 28;17(1):78. [doi: 10.1186/s12874-017-0338-0] [Medline: 28454568]
40. Tibshirani R. Regression shrinkage and selection via the Lasso. J R Stat Soc Series B Stat Methodol 1996 Jan 1;58(1):267-288. [doi: 10.1111/j.2517-6161.1996.tb02080.x]
41. Cheung AH, Zuckerbrot RA, Jensen PS, Laraque D, Stein REK, GLAD-PC STEERING GROUP. Guidelines for Adolescent Depression in Primary Care (GLAD-PC): Part II. Treatment and ongoing management. Pediatrics 2018 Mar;141(3):e20174082. [doi: 10.1542/peds.2017-4082] [Medline: 29483201]
42. Chua KP, Volerman A, Zhang J, Hua J, Conti RM. Antidepressant dispensing to US adolescents and young adults: 2016-2022. Pediatrics 2024 Mar 1;153(3):e2023064245. [doi: 10.1542/peds.2023-064245] [Medline: 38404197]
43. Medicaid's role in addressing social determinants of health. Robert Wood Johnson Foundation. URL: https://www.rwjf.org/en/insights/our-research/2019/02/medicaid-s-role-in-addressing-social-determinants-of-health.html [accessed 2024-04-28]
44. Chang TE, Ritchey MD, Park S, et al. National rates of nonadherence to antihypertensive medications among insured adults with hypertension, 2015. Hypertension 2019 Dec;74(6):1324-1332. [doi: 10.1161/HYPERTENSIONAHA.119.13616] [Medline: 31679429]
45. Whiteside SP, Sim LA, Olsen MW, Hord MK. The 5-year course of medication treatment in childhood anxiety disorders. J Clin Psychiatry 2019 May 14;80(3):18m12318. [doi: 10.4088/JCP.18m12318] [Medline: 31091028]
46. Chen M, Zhou L, Ye L, et al. Initial adherence by psychiatric outpatients in a general hospital and relevant personal factors. BMC Psychiatry 2022 Feb 21;22(1):137. [doi: 10.1186/s12888-022-03797-3] [Medline: 35193529]
47. Brown MT, Bussell JK. Medication adherence: WHO cares? Mayo Clin Proc 2011 Apr;86(4):304-314. [doi: 10.4065/mcp.2010.0575]
48. Hempenius M, Groenwold RHH, de Boer A, Klungel OH, Gardarsdottir H. Drug exposure misclassification in pharmacoepidemiology: sources and relative impact. Pharmacoepidemiol Drug Saf 2021 Dec;30(12):1703-1715. [doi: 10.1002/pds.5346] [Medline: 34396634]
49. Xing S, Dipaula BA, Lee HY, Cooke CE. Failure to fill electronically prescribed antidepressant medications: a retrospective study. Prim Care Companion CNS Disord 2011;13(1):PCC.10m00998. [doi: 10.4088/PCC.10m00998blu] [Medline: 21731832]

Abbreviations

ADI: Area of Deprivation Index
AUROC: area under the receiver operator characteristic curve
DUHS: Duke University Health System
EHR: electronic health record
HR: hazard ratio
LASSO: least absolute shrinkage and selection operator
NDC: National Drug Code
PHQ-9: Patient Health Questionnaire-9
PS: propensity score
RxCUI: RxNorm concept unique identifier

Edited by C Lovis; submitted 28.06.24; peer-reviewed by J Pevnick, M Gabriel; revised version received 05.02.25; accepted 06.02.25; published 04.03.25.

Please cite as:
Wu P, Hurst JH, French A, Chrestensen M, Goldstein BA
Linking Electronic Health Record Prescribing Data and Pharmacy Dispensing Records to Identify Patient-Level Factors Associated With Psychotropic Medication Receipt: Retrospective Study
JMIR Med Inform 2025;13:e63740
URL: https://medinform.jmir.org/2025/1/e63740
doi:10.2196/63740

XSL•FO
RenderX

© Peng Wu, Jillian H Hurst, Alexis French, Michael Chrestensen, Benjamin A Goldstein. Originally published in JMIR Medical Informatics (https://medinform.jmir.org), 4.3.2025. This is an open-access article distributed under the terms of the Creative Commons Attribution License (https://creativecommons.org/licenses/by/4.0/), which permits unrestricted use, distribution, and reproduction in any medium, provided the original work, first published in JMIR Medical Informatics, is properly cited. The complete bibliographic information, a link to the original publication on https://medinform.jmir.org/, as well as this copyright and license information must be included.

XSL•FO
RenderX

Original Paper

Large-Scale Evaluation and Liver Disease Risk Prediction in Finland's National Electronic Health Record System: Feasibility Study Using Real-World Data

Viljami Männikkö[1,2], MSc; Janne Tommola[1], MSc; Emmi Tikkanen[3], PhD; Olli-Pekka Hätinen[3], PhD; Fredrik Åberg[4], MD, PhD

[1]Atostek Oy, Tampere, Finland

[2]Faculty of Medicine and Health Technology, Tampere University (TUNI), Tampere, Finland

[3]Pfizer Oy, Helsinki, Finland

[4]Transplantation and Liver Surgery Unit, Helsinki University Hospital and University of Helsinki, Helsinki, Finland

Corresponding Author:
Viljami Männikkö, MSc
Atostek Oy
Hermiankatu 3 A
Tampere, 33720
Finland
Phone: 358 45 7834 70
Email: viljami.mannikko@tuni.fi

Abstract

Background: Globally, the incidence and mortality of chronic liver disease are escalating. Early detection of liver disease remains a challenge, often occurring at symptomatic stages when preventative measures are less effective. The Chronic Liver Disease score (CLivD) is a predictive risk model developed using Finnish health care data, aiming to forecast an individual's risk of developing chronic liver disease in subsequent years. The Kanta Service is a national electronic health record system in Finland that stores comprehensive health care data including patient medical histories, prescriptions, and laboratory results, to facilitate health care delivery and research.

Objective: This study aimed to evaluate the feasibility of implementing an automatic CLivD score with the current Kanta platform and identify and suggest improvements for Kanta that would enable accurate automatic risk detection.

Methods: In this study, a real-world data repository (Kanta) was used as a data source for "The ClivD score" risk calculation model. Our dataset consisted of 96,200 individuals' whole medical history from Kanta. For real-world data use, we designed processes to handle missing input in the calculation process.

Results: We found that Kanta currently lacks many CLivD risk model input parameters in the structured format required to calculate precise risk scores. However, the risk scores can be improved by using the unstructured text in patient reports and by approximating variables by using other health data–like diagnosis information. Using structured data, we were able to identify only 33 out of 51,275 individuals in the "low risk" category and 308 out of 51,275 individuals (<1%) in the "moderate risk" category. By adding diagnosis information approximation and free text use, we were able to identify 18,895 out of 51,275 (37%) individuals in the "low risk" category and 2125 out of 51,275 (4%) individuals in the "moderate risk" category. In both cases, we were not able to identify any individuals in the "high-risk" category because of the missing waist-hip ratio measurement. We evaluated 3 scenarios to improve the coverage of waist-hip ratio data in Kanta and these yielded the most substantial improvement in prediction accuracy.

Conclusions: We conclude that the current structured Kanta data is not enough for precise risk calculation for CLivD or other diseases where obesity, smoking, and alcohol use are important risk factors. Our simulations show up to 14% improvement in risk detection when adding support for missing input variables. Kanta shows the potential for implementing nationwide automated risk detection models that could result in improved disease prevention and public health.

(JMIR Med Inform 2025;13:e62978) doi:10.2196/62978

XSL•FO
RenderX

KEYWORDS

Kanta archive; national patient data repository; real world data; risk prediction; chronic liver disease; mortality; risk detection; alcoholic liver; prediction; obesity; overweight; electronic health record; wearables; smartwatch

Introduction

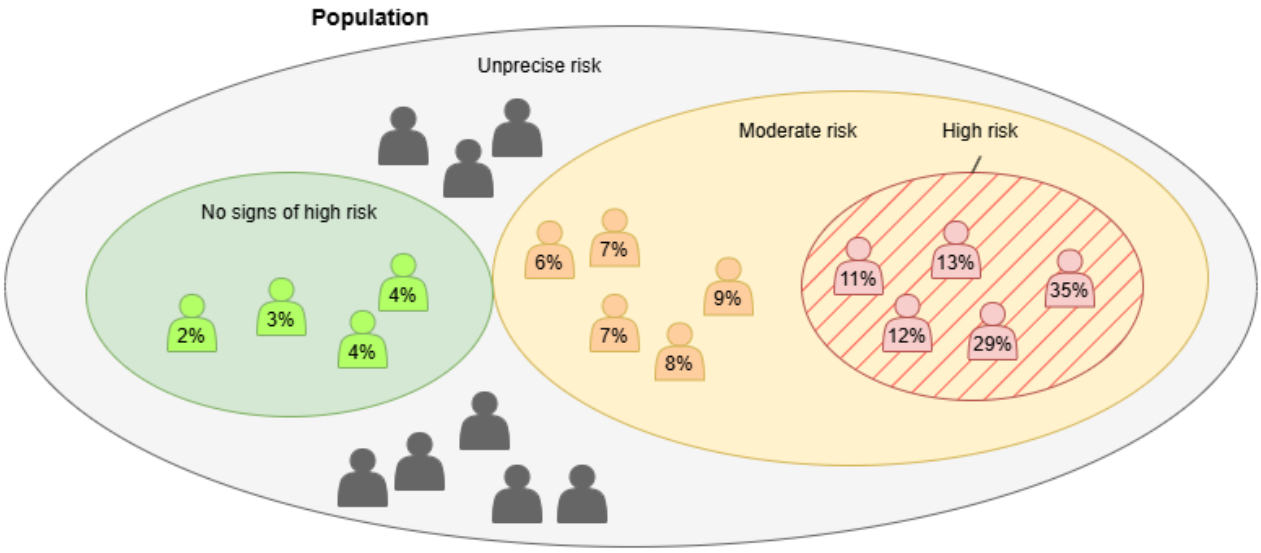
Background

Even though health care risk models have been developed for a very long time and have been implemented to be available for individuals, health care still lacks automated health-risk analysis because of limited real-world data (RWD). The burden of liver disease increases yearly in Finland because the Finnish population age average grows, and obesity and overweight are more common problems in the Finnish population [1]. On average, there are 1000 deaths caused by alcoholic liver disease every year [2]. For the early detection of individuals from the general population at high risk for future severe liver disease, the CLivD (Chronic Liver Disease score) score was developed. It can be used to predict severe liver disease incidence in 10 years. The model itself was developed by linking data from Finnish population–based health examination surveys "FINRISK" and "Health 2000" with Finnish health care registries. The model has been validated using data from the United Kingdom, Denmark, the United States, and China [1,3-5].

Risk Model Application to RWD

The missing input data pose a challenge for the large-scale implementation of established risk models in real life [1]. To be able to calculate the exact risk value in many cases, we would not only require additional RWD sources but also changes in health care professionals' practices to ensure they regularly measure the correct parameters from patients. One problem is the negation of information, particularly in cases where data on behaviors, such as a person not smoking or not consuming alcohol, is missing. This leads to a problem where we cannot determine whether a person, for example, is a nonsmoker if there is no record of it. Despite the challenges, health care RWD enables early identification of individuals at high risk by analyzing their current characteristics, which is crucial for health care professionals in planning treatments. The exact risk value would be easy for everyday people to understand, but for health care professionals in preventive work and treatment planning, it is also important to detect potential high-risk cases as early as possible and identify if the person is a high-risk patient. For this kind of usage, we introduce a process that helps to detect high-risk and potential high-risk individuals. Figure 1 describes that kind of division at the population level.

Figure 1. Case example of population risk categorization based on a personal risk value.



The Finnish National Electronic Health Record System

Kanta Services is the Finnish National Electronic health record system where data are recorded from almost all Finnish health care providers including the public and private sectors and primary and special care [6]. Kanta Services entered production in Finland in 2010 and it has been used for more than 10 years in Finland overall [6]. However, Kanta has been developed in stages, resulting in different data types having different levels of availability. Kanta Services in general consists of four different parts: (1) the social health care part, (2) the prescription center, (3) the patient data repository (PDR), and (4) personal health records [7]. In this study, we only use data from the Kanta PDR.

In Finland, the 2019 Act on Secondary Law made it possible to use health care data for research purposes [8]. Before that, the data were available only for their primary use, which is patient care. Kanta is an exceptional RWD source because it covers almost the whole Finnish population and has recordings from more than 90% of all Finnish health care service providers. [6] This makes it possible to analyze previously developed health care risk models and develop new risk models by using large data sources that represent the entire national population.

XSL•FO
RenderX

Since data are continuously generated in Finnish day-to-day health care and all Finnish health care systems are integrated into Kanta, developed and tested risk models can also be applied in actual patient care. Popular well-being service providers have implemented automated health risk analysis based on data collected from the person regularly or data obtained from wearable devices like smartwatches [9]. These types of data still lack validation from health care professionals. Validation is a key element for incorporating automated risk analysis results in everyday patient care and using them as a diagnostic tool. The Kanta PDR contains only data validated by health care professionals, as only they are authorized to record information in the system [10]. Kanta Services also has a personal health records data repository containing data recorded by the people themselves. However, it is not used in this research as it is still under development. In this study, we aim to analyze data validated by health care professionals [11].

Methods

Overview

In this study, we aim to research the CLivD score risk model automation possibilities with Kanta PDR. We use Kanta PDR as the only data source for the risk model to have an overall picture of the data availability status. We consider four different scenarios of data usage possibilities: (1) first, we test the risk model results with the available structured data; (2) next, we aim to use other structured health care information to approximate missing information; (3) after that, we analyze the possibilities of using free text; and (4) finally, we analyze completely missing input variables. For this research, we have 2 main objectives:

1. To evaluate the feasibility of implementing an automatic CLivD score with the current Kanta platform.
2. To identify and suggest improvements for Kanta that would enable accurate automatic risk detection.

Dataset

In this study, we used the dataset consisting of the medical documents of 192,400 individuals archived in the Kanta PDR between 2014 and mid-2022. Data in Kanta are recorded using the Clinical Document Architecture Release 2 (CDA R2) format, as defined by Health Level 7 (HL7) [12]. CDA R2 documents are XML documents that follow a defined format [13]. In the Finnish health care environment, the local Finnish version of the global HL7 CDA R2 is defined by Health Level 7 Finland, Kela, and the Finnish Institute for Health and Welfare (THL) [12].

The dataset was chosen by Kela from Kanta and the study cohort was randomly selected across the whole Finnish population without any limitations to specific health care providers or locations. The dataset included all documents that were recorded in Kanta PDR after an individual turned 18 years old. Documents were pseudonymized by Findata and delivered in the original CDA R2 XML format to the secure Kapseli environment. Before the analysis was done, the dataset was split randomly into development and validation datasets. Data were evenly divided, with both development and validation datasets containing 96,200 patients. The data were split to accommodate future plans for using machine learning and other methods requiring validation in subsequent projects; however, in this project, only the first half of the data were used. After the data are split, CDA R2 XML documents must be processed so that all relevant data are parsed for analysis. For data processing, a separate data process library and data model were designed. Data parsing consisted of structured laboratory measurements, structured diagnosis data, structured physiological measurements, free-text sections of patients' ongoing treatment reports, and some basic information about the document and patient. We did not obtain access to death records because they are not recorded in Kanta and would have required separate permission and retrieval from the Digital and Population Data Services agency. A more detailed analysis of the dataset can be found in the study by Männikkö et al [14].

Risk Model Implementation

The original research on the CLivD score introduced 2 risk calculation models: $Model_{lab}$ and $Model_{nonlab}$. Both models predict the risk of chronic liver disease in people aged 40 years or older. The difference between models is that $Model_{lab}$ also considers the person's gamma glutamyl transferase (GGT) laboratory test result. Both risk calculators have 4 different exclusion criteria [1]. If a person meets even 1 of the exclusion criteria, there is a possibility that the risk calculator may not function as expected. Exclusion criteria are listed in Textbox 1.

For these risk models and use cases, we introduce a model for categorizing patients to 4 different categories: "low risk," "moderate risk," "high risk," and "not specified risk." Categorization is based on 2 risk values: "minimum risk" and "maximum risk." The risk calculation process itself was introduced slightly later. This approach is good from the Kanta development point of view, as future developments and the addition of more information to Kanta will allow risk categorization to be easily applied to the new data. The more data we collect from the person, the more reliable the model becomes, resulting in a significant reduction in the "Not Specified" category. Table 1 presents the cutoff values for each category.

XSL•FO
RenderX

Textbox 1. Chronic liver disease score risk model exclusion criteria.

Exclusion criteria

- Age: above 40 and under 71 years.
- Liver disease diagnosis: *ICD-10* (*International Statistical Classification of Diseases and Related Health Problems, 10th Revision*): K70-K77, C22.0; *ICD-8* (*The International Classification of Diseases, 8th Revision*) and *ICD-9* (*International Classification of Diseases, 9th Revision*): 570-573, 155.0.
- Chronic viral hepatitis diagnosis: *ICD-10*: B18.
- Current alcohol abstainer: previous alcohol use. Can be identified with *ICD-10* codes: F10.20 and other F10.2X.

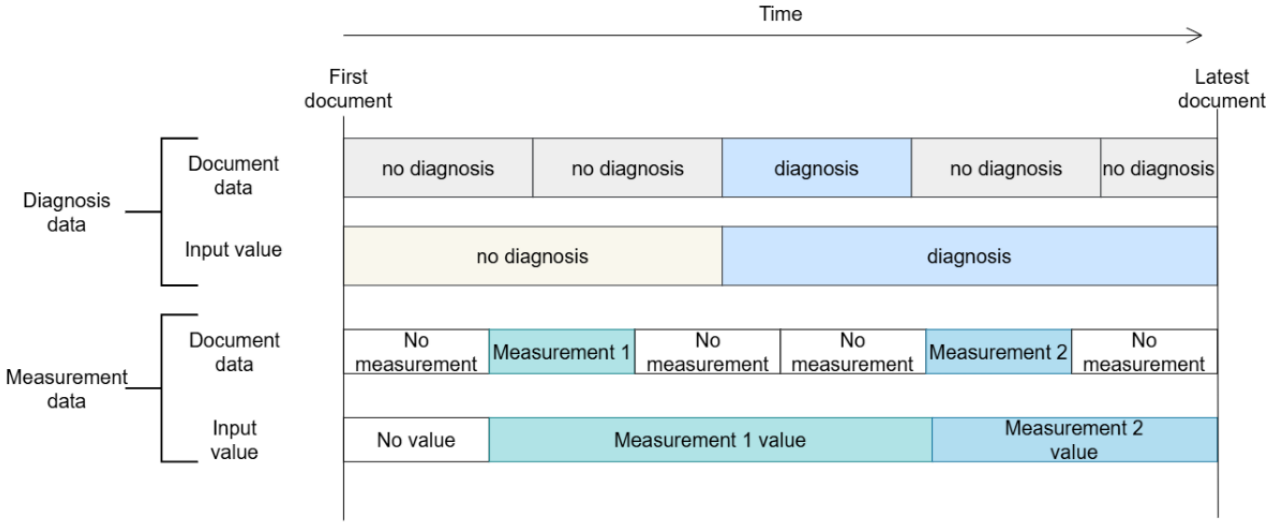
Table 1. Risk categories' cutoff values for minimum and maximum risk.

Risk	Low risk	Moderate risk	High risk	Not specified risk
Minimum risk	≤5%	>5% and <10%	≥10%	<5%
Maximum risk	<5%	>5%	≥10%	>10%

The CLivD score risk function was developed and validated using cohort studies, where the population is sampled, assessed at a certain time, and then followed for outcomes [1]. Kanta patient data are distributed over time, with measurements conducted at different points in time.

We use parameter lifecycles or lifetimes to do this, where we specify the length of time a measurement or diagnosis is valid, both before and after it appears in the medical record. In this work, we used 2 different lifecycles: 1-year lifecycles where measurements are valid for 1 year after measurement, and infinite lifecycles where they stay valid until the next measurement, or until the end of document history. For both lifecycle types, we used an infinite validity time for diagnoses. An example of parameter lifecycles is shown in Figure 2 with a finite (eg, 1 year) lifetime for measurements and an infinite lifetime for diagnoses.

Figure 2. In real-world data, the validity period of input parameters must be defined, as different measurements remain valid for varying durations both before and after the measurement.



We implemented the CLivD risk function in Kapseli using Python (Python Software Foundation). The implementation flow diagram is described in Figure 3. The timeline is formed by using all known relevant patient data and applying the previously discussed parameter lifecycles to it. Due to missing input variables, we calculate 2 risk values: the minimum and maximum risk. The minimum risk is obtained by substituting the missing variables with their lowest values, while the maximum risk is determined by using their highest value. The complete list of default values can be found in Table 2. Values are used in the case where the input value is not available from an individual's medical history.

By calculating the minimum risk and maximum risk, we obtain a risk range. A smaller risk range directly implies a more accurate risk value. Missing input parameters increase the risk value range. The goal is to narrow the risk value range toward the actual risk value in the long term. Possible ways to narrow the risk range are, for example, getting the exact missing value from other data sources, asking for information from the patient, or determining the magnitude of the missing information from free-text evaluation.

XSL•FO
RenderX

Figure 3. Risk categorization process flow. CLivD: Chronic Liver Disease; GGT: gamma glutamyl transference.

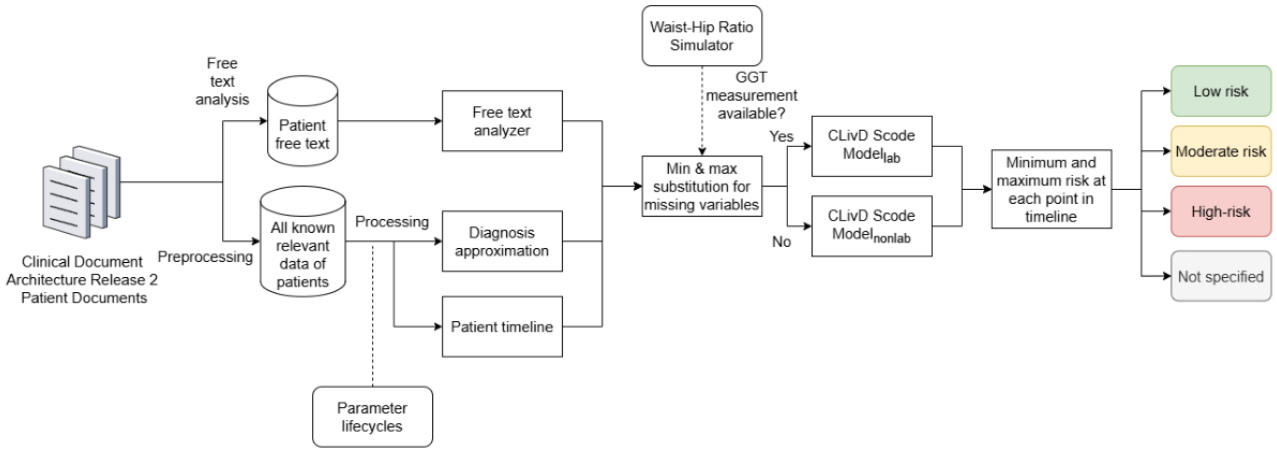


Table 2. Default values for risk calculation when an input parameter is missing.

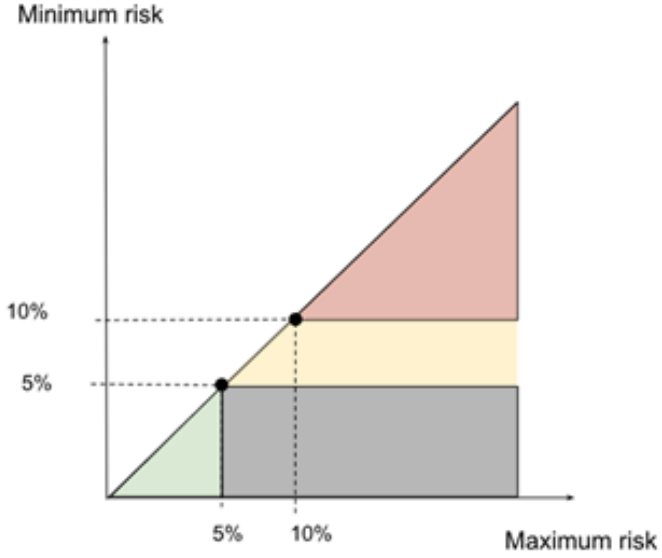
Input parameter	Default minimum value	Default maximum value
Gender	Always available	Always available
Age (years)	40 (basically, always available)	70 (basically, always available)
GGT[a]	Use non-GGT model	Use non-GGT model
WHR[b]	0.7	1.3
Smoking	False	True
Alcohol usage	0	49
Diabetes	False	True

[a]GGT: gamma glutamyl transferase.

[b]WHR: waist-hip ratio.

In Figure 4, an illustration and example goal for the risk value ranges are shown. The line represents an ideal case where all input variables are known, and an exact risk value with equal minimum and maximum risk can be calculated. The lower turquoise triangle represents an area where the maximum risk is below 5%, and the patient can be considered low risk. The upper red triangle represents an area where the minimum risk is above 10%, and the patient is at high risk. The yellow area is the moderate risk area where patients' risk value is higher than 5% but not high enough to determine the person as a high-risk patient. The gray-colored area represents the "not specified risk" category, where the risk range between the minimum risk and maximum risk is too wide to identify the correct category.

Figure 4. Risk categories in minimum and maximum risk plane.



XSL•FO
RenderX

In this study, we target these colored areas as a goal, as an exact risk value is not feasible with the missing data, but a risk range is still helpful for determining the course of action. The risk thresholds can be configured for different use cases. The complete risk calculation formula can be found in Multimedia Appendix 1.

Ethical Considerations

This study involved pseudonymized health care data produced in health care services in Finland. Data were collected, delivered, and pseudonymized under the legislation on secondary use of health care data in Finland. Finnish authority Findata validates data requests and project plans before granting permission to access data (THL/1851/14.02.00/2021). Findata also has the responsibility to create the data pseudonymization before delivery. Data were processed and analyzed in an audited secure computing environment known as "Kapseli" with restricted access to it. All the results presented in this paper have gone through the Findata anonymization validation process where Findata ensures that results taken out of a secure environment are anonymized. Ethical aspects of the project have been evaluated by Findata during the data request process.

Results

Overview

Analysis was made in 4 iterations. At first, we analyzed the structural data and its occurrences. After that, we tried to improve the model with the diagnosis use to determine the magnitude of missing input variables. After that, we used free-text for tobacco and alcohol information, and at last, we simulated waist-hip ratio (WHR) in cases where it would have been available from different data sources.

The study initially included 96,200 participants. After applying the exclusion criteria, only 51,275 eligible individuals remained for the risk model. A total of 44,925 individuals were left out of this analysis because they did not match the original criteria. Almost 50% of the individuals were excluded, with the age-related criteria being the most common reason for exclusion.

Structural Data

We can analyze the CLivD score risk calculation results using Kanta PDR structured data as a precise input parameter, without approximating the parameter magnitude. In Table 3, we describe the frequency of relevant variables appearing in a patient's medical history in a structured format. The occurrence of 1 means that the variable has been measured just once during the patient's medical history according to the Kanta data. Age and gender are registered in every document and are always available. The table shows that 0 measurements are the most common, and more than 5 measurements are a very rare case among risk model input variables.

WHR and alcohol use are not shown in this table as they are not present in a structured format in the Kanta data. Besides age and gender, the only input variables with at least 1% availability are GGT and fasting glucose, with approximately 5% and 13% total occurrence, respectively. As fasting glucose (7 mmol/L) is only used as an alternative to a diabetes diagnosis, it is not a required input variable. We interpret a missing measurement to mean that the patient does not have diabetes, provided the other criteria are not met. BMI and waist circumference are not input variables for the risk model but were investigated as possible alternatives to the missing WHR. Waist circumference measurements are very rare and will not considered further, whereas BMI has moderate availability and will be discussed later.

Table 3. Parameter occurrences in the Kanta patient data repository between 2014 and 2022 (N=96,200).

Occurrence during patient history, n	Fasting glucose, n (%)	Height, n (%)	Weight, n (%)	BMI, n (%)	Waist circumference, n (%)	Gamma glutamyl transferase, n (%)	Smoking, n (%)
0	84,521 (87)	76,815 (79)	78,003 (81)	80,651 (83)	95,812 (99)	91,891 (95)	96,193 (99)
1	9141 (10)	10923 (11)	9007 (9)	8482 (9)	349 (<1)	3144 (3)	7 (<1)
2-5	2460 (2)	7752 (8)	7311 (8)	6393 (6)	39 (<1)	1067 (1)	0 (0)
6-10	64 (<1)	608 (1)	1364 (1)	567 (1)	0 (0)	77 (<1)	0 (0)
11-15	8 (<1)	82 (<1)	329 (<1)	85 (<1)	0 (0)	12 (<1)	0 (0)
>15	6 (<1)	20 (<1)	186 (<1)	22 (<1)	0 (0)	9 (<1)	0 (0)

Diagnosis Use

Because the Kanta PDR is missing WHR data, and alcohol usage data and tobacco usage information are quite rarely found in a structured format, we need to use other health care information found in the Kanta PDR. For alcohol and tobacco usage, there are some *ICD-10* (International Statistical Classification of Diseases and Related Health Problems, 10th Revision) and ICPC-2 (International Classification of Primary Care version 2) diagnosis codes that can be used for risk calculation. With the smoking diagnosis codes, we get the information that an individual smokes. This serves as the exact value for the CLivD score model, as it does not consider the number of cigarettes a person smokes per week.

For alcohol usage, the CLivD score model uses the number of servings as an input. Consequently, by using diagnosis codes, we aim to estimate the magnitude of alcohol usage and narrow the risk range. For alcohol usage, we use diagnosis codes that relate to heavy consumption of alcohol. Based on those diagnosis codes, we can say that the person has consumed alcohol at above-average levels for some time before getting the diagnosis. The largest *ICD-10* group that will be used is F10 "Mental and behavioral disorders due to the use of alcohol" and from the ICPC-2 codes we will use P15 "Chronic alcohol abuse"

XSL•FO
RenderX

and P16 “Acute alcohol abuse.” For high-risk alcohol users, we use the “23 alcohol servings per week” approximation for men and the “12 alcohol servings per week” approximation for women [15]. The complete list of diagnosis code mappings to risk model input parameters can be found in Multimedia Appendix 2. Table 4 shows the statistics from diagnosis occurrences in our dataset.

Table 4. Alcohol and smoking-related diagnosis occurrences in the Kanta patient data repository between 2014 and 2022 (N=96,200).

Diagnosis code	Display name	Number of diagnoses, n
Alcohol-related		
F10.09	Unspecified alcohol intoxication	2158
F10.1	Alcohol abuse	18,141
F10.20	Alcohol dependence uncomplicated	3697
F10.24	Alcohol dependence with alcohol-induced mood disorder	3251
F10.25	Alcohol dependence with alcohol-induced psychotic disorder	3921
F10.26	Alcohol dependence with alcohol-induced persisting amnestic disorder	3328
F10.29	Alcohol dependence with unspecified alcohol-induced disorder	3268
F10.39	Alcohol withdrawal symptoms unspecified	1690
P15	Alcohol abuse (chronic)	4494
P16	Alcohol abuse (acute)	2417
Smoking-related		
Z72.0	Tobacco use	1102
P17	Tobacco abuse	465

Free-Text Analysis

Kanta PDR contains a lot of free text in patients’ ongoing treatment reports that describe the patient’s overall health status and living habits. As a result, the free text can be used to find information concerning alcohol usage habits and tobacco use. Due to the limitations on available resources, such as the lack of a graphics card in a secure “Kapseli” environment, we had limited options for free-text analysis. We were not able to use advanced machine learning models or any generic artificial intelligence for text analysis. Instead of those methods, we used a simple regex-based keyword search and converted found text phrases into usage categories. With this analysis, we aimed to understand how often tobacco- or alcohol-related texts appear in ongoing treatment reports and how it would improve the CLivD score model. For more precise free-text analysis, more advanced tools should be used to gain more reliable results.

Tobacco usage is simpler because we can find texts that indicate whether a person is a smoker or a nonsmoker. There are cases where the texts might state, “person has smoked 10 years ago,” making it difficult to determine whether the person currently smokes without additional context. However, in most cases, we can get quite good results by finding sentences related to smoking status.

Alcohol usage is different than tobacco use. Because alcohol servings are defined in a weekly servings format in the CLivD Score model, we must define alcohol usage categories also for free-text analysis. Based on the analysis, we converted phrases into alcohol usage categories. Category mappings are defined in Multimedia Appendix 3 and are based on the THL alcohol risk table [15]. We noticed that alcohol usage was described in free text using various ways and words. We also noticed that the amount descriptions were, in many cases, abstract, and the conversion to the alcohol usage category was not reliable. However, we managed to find clear and reliable cases of alcohol usage from the free text and managed to use them. For the text finding, we used keywords like “käytä alkohol,” “ei\s*\w*\s*alkohol,” “runsa\w*\s*alcohol,” and “vieroitus|vierotus|päihtymys|putki|katkaisu.” Multimedia Appendix 3 defines the alcohol usage categories used in free-text analysis. The categories are based on THL definitions for alcohol usage risk groups defined as alcohol servings per week. In each category, there is minimum and maximum alcohol usage. In the risk model when calculating the minimum risk, the alcohol usage category minimum value is used and vice versa. A complete list of alcohol usage and tobacco use text analysis keywords and mappings can be found in Multimedia Appendix 4.

Risk Calculation Results

We apply the risk function to the patient’s timelines and attempt to assign their risks to the colored areas shown in Figure 4. These risk areas would be enough to classify patients into low- and high-risk groups, with the uncolored area representing gray area where no definite conclusions can be made.

The average risk difference from our test runs is presented in Figures 5 and 6, with Figure 5 representing cases where an infinite timeline was used and Figure 6 representing cases where a 1-year lifetime was used. Risk difference is calculated by subtracting the minimum risk value from the maximum risk value. Smaller differences imply a more precise risk value. As we can see from the figures, the average risk difference has decreased as the data have been developed in Kanta. If we look

XSL•FO
RenderX

at the case where structural data, diagnosis, and free text all have been used, the risk difference has been reduced by almost 20% points. We can also see that the free text use and the high availability simulation of WHR have had the largest impact on the risk difference.

In the test run, we calculated the most precise risk value for each person throughout their history in Kanta and categorized them by that risk value. Results can be seen in Multimedia Appendix 5.

Figure 5. Average risk difference development between 2014 and 2021 with eternal parameter lifetime. WHR: waist-hip ratio.

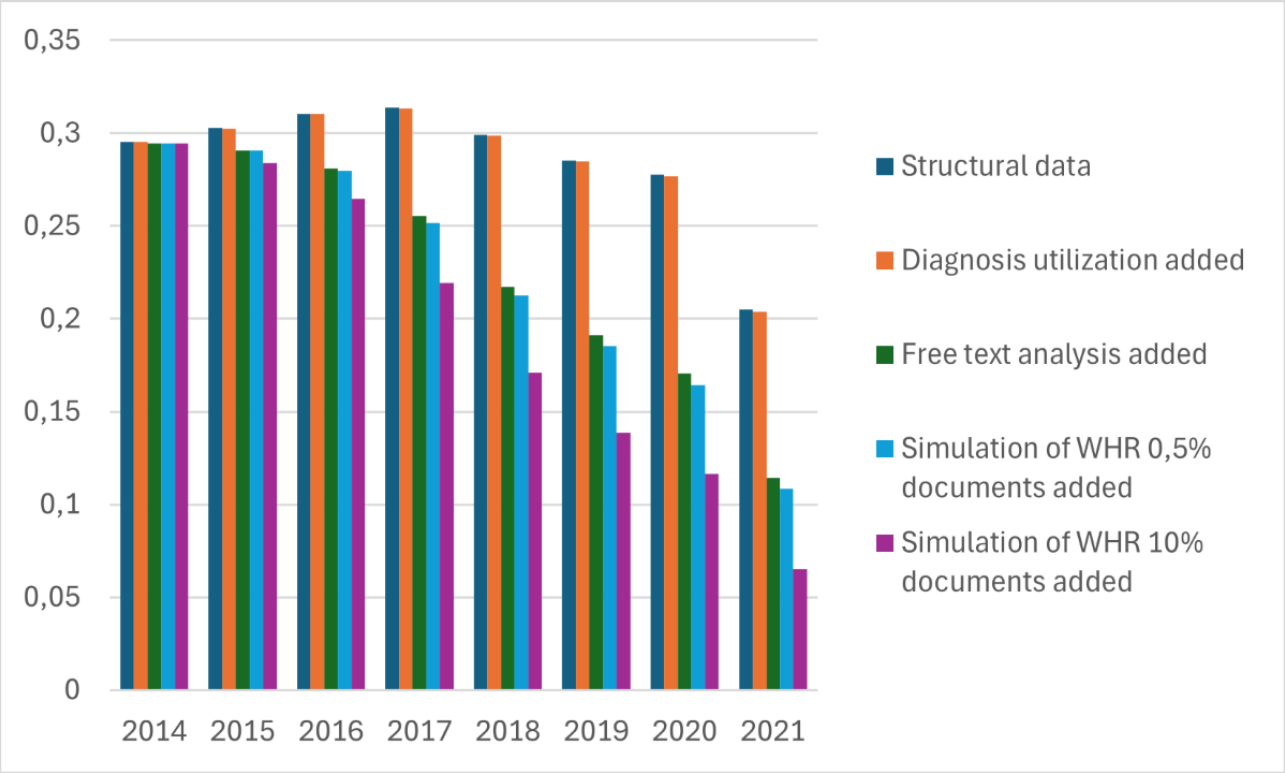
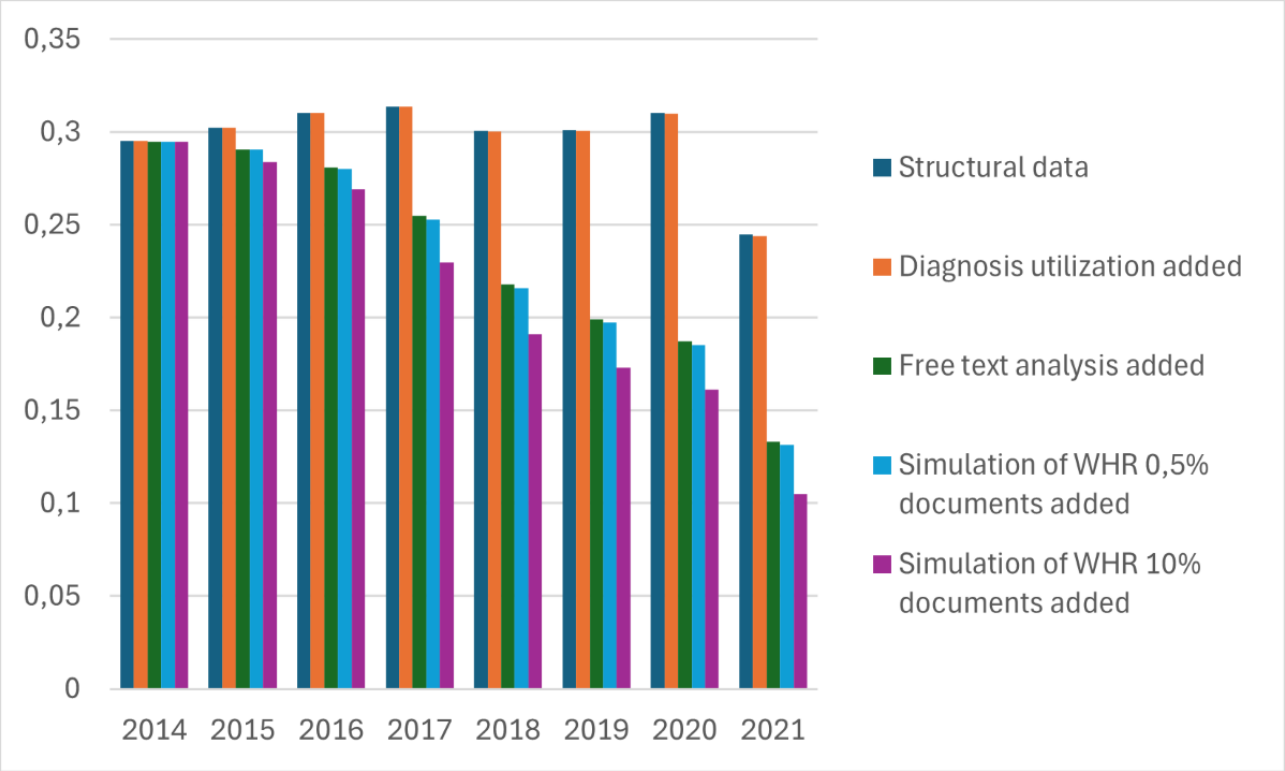


Figure 6. Average risk difference development between 2014 and 2021 with one year parameter lifetime. WHR: waist-hip ratio.



XSL•FO
RenderX

As we can see, based on the results with only structural data, we can only categorize 341 out of 51,275 (<1%) individuals into any category. By adding diagnosis use for approximation, we did not achieve notable improvement in categorization. When adding the free-text analysis, we were able to categorize 21,020 out of 51,275 people (41%). Even though we did not manage to categorize any person into the high-risk category, we managed to identify individuals who were not at high risk. Due to the high availability of WHR information, we can categorize 38,279 out of 51,275 people (75%). A small number of individuals may be incorrectly placed in the high-risk category in the WHR simulation due to an inaccurate WHR value relative to their overall health status. However, this does not affect the overall categorization percentage, as it represents the proportion of individuals successfully categorized rather than the distribution across specific categories. At the original CLivD score research, fewer than 2% of individuals were identified as high-risk from a cohort of 25,760 individuals. Approximately 3% were identified as being at moderate risk in the original research. In our categorization, 2125 out of 51,275 individuals (4%) were classified into that category [8]. Based on these results, we can say that the results match because the CLivD score development dataset was from before 2012, while our dataset was from after 2014, and the risk for chronic liver disease has increased in the overall population in Finland.

WHR Data

The WHR is among the most important variables for the CLivD risk score. Unfortunately, it cannot currently be obtained from Kanta data, as it is not supported in a structured format, and we were also unable to find it in the texts as well. As an alternative, we considered BMI, waist circumference, or hip circumference to predict the WHR. Of these, only BMI has meaningful availability in Kanta, so waist and hip circumferences were not considered further. BMI has been measured for 15,359 out of 51,275 (17%) individuals.

While associations between BMI and WHR can be found in the literature [16,17], the suitability of BMI as a predictor for severe liver disease has recently been disputed [18-21], with its suitability affected by gender and potentially other factors. Due to the seemingly complex and unclear nature of BMI and WHR interaction, we decided not to pursue WHR prediction for now.

For the analysis purpose, we simulated WHR data effect on the CLivD score risk model results in a few different scenarios. The first scenario involved obtaining the exact WHR data from the Kanta PDR, the second scenario involved the individual requesting their WHR data using the WHR groups, and the last scenario involved the individual measuring their exact WHR. These 3 scenarios were created because they serve as use case scenarios of the risk model differently.

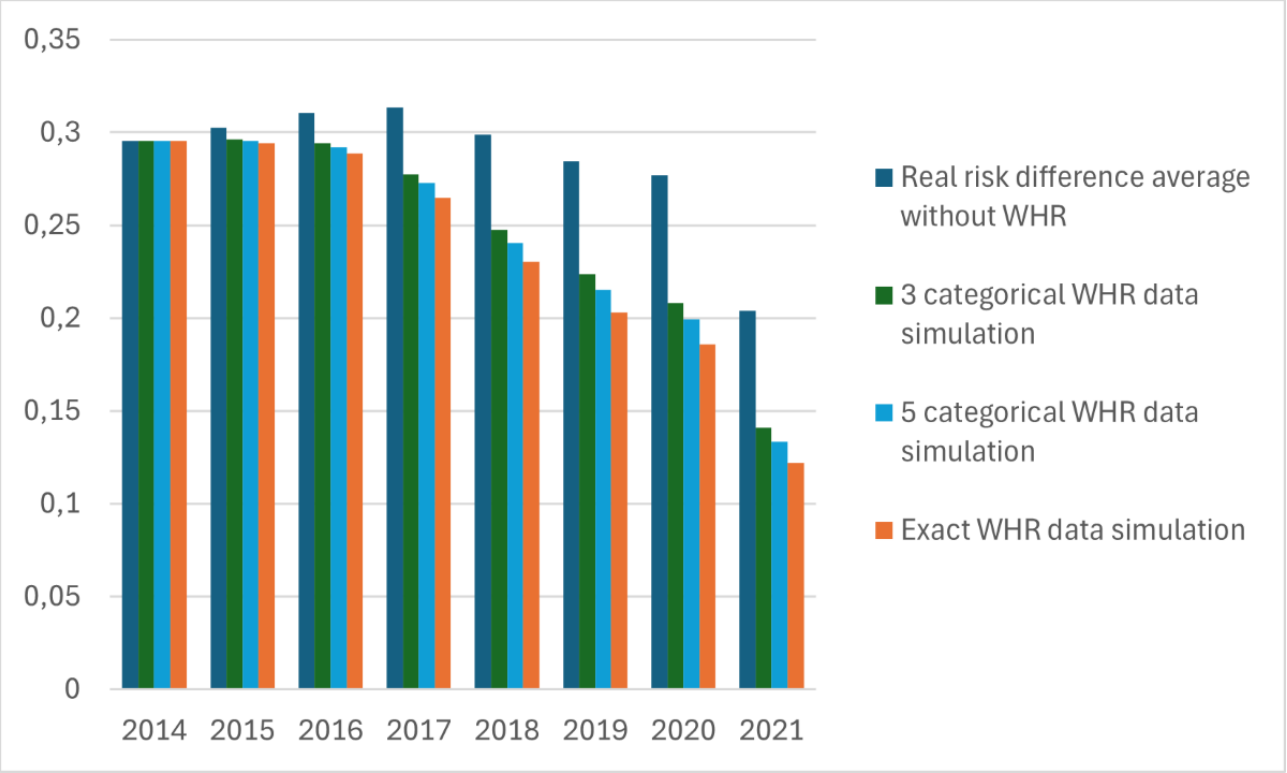
The simulation was done by populating the timelines with WHR data. In the first case, 0.5% of all documents recorded in Kanta contained the WHR data, while in the second case, 10% of documents recorded in Kanta would have contained the WHR data. The first case represents the condition where WHR data would have the same kind of availability as all other basic physiological measurements currently in Kanta. The second case represents the condition where the WHR data would be highly available for individuals, for example, from other data sources. For the simulation, WHR values were generated using a normal distribution, with a mean of 0.96 for men, a mean of 0.84 for women, and a variance of 0.07. These values are found to be representative of the Finnish population based on research [22].

WHR as a measurement is slightly complicated for individuals to assess on their own, which raises the bar for using it in the CLivD score risk model. Because of this, we tested the cases to see if the simpler WHR categorization would give good results for risk categorization. The WHR categorization for a person could be easily implemented by displaying images of different body types and using these types to represent a WHR range. For the person, it would be easy to answer which image matches their own body. In this simulation, the exact WHR values were changed to the corresponding WHR category. After that, the average risk differences for the population were calculated for the cases, using 3 categories and 5 categories. WHR categorization definitions can be seen in Multimedia Appendix 3.

The results of the test run with the WHR simulation can be found in Figure 7. As we can see from the graph, there is no big change between the 3 categorical WHR data simulations and the exact WHR data simulation. If the WHR were requested by the individual, it would be simpler to assess body type using 3 categorical questionnaires rather than obtaining the exact WHR value.

XSL•FO
RenderX

Figure 7. Waist-hip ratio (WHR) categorization impact to risk difference development between 2014 and 2021.



Discussion

Principal Findings

We conclude that the current Kanta PDR data are not enough for precise risk calculation for the CLivD score or other risk models where obesity, smoking, and alcohol information are important risk factors. Our simulations show up to 14% improvement in risk detection when additional data sources are considered for obesity. Kanta shows excellent potential for implementing nationwide automated risk detection models that could result in improved disease prevention and public health.

Based on the results of this study, it is not possible to calculate precise risk scores using the CLivD risk model with the current data in Kanta PDR. However, risk categorization enables the possibility to use the CLivD risk model with Kanta PDR data so that it considers missing input parameters and enables future data development in Kanta. We noticed that risk categorization improved when the magnitude of input parameters was approximated using diagnosis information, and free text from the patient's ongoing treatment report was used for input parameter parsing. When using the structured data from Kanta PDR as an input, we were able to identify only 33 out of 51,275 (<1%) individuals in the "low-risk" category and 308 out of 51,275 (<1%) individuals in "moderate-risk" category. When diagnosis use and free-text analysis were added to the model, we were able to identify 18,895 out of 51,275 (37%) individuals in the "low risk" category and 2125 out of 51,275 (4%) individuals in the "moderate risk" category. In both cases, we were not able to identify any individuals in the "high-risk" category, because of the missing WHR data. When we added the WHR simulation to the risk model, we started to identify "high-risk" individuals. We evaluated 3 scenarios to improve the coverage of WHR data in Kanta and these yielded the most substantial improvement in prediction accuracy.

Comparison With Previous Work

In Finland, there is no systematic screening or automated risk assessment for chronic liver disease implemented in everyday health care. Diagnostics are quite random, and, in many cases, incidents are noticed during the treatment of other symptoms. Based on studies in Great Britain and Denmark, 70%-75% of cases of cirrhosis are only diagnosed when the patient ends up in the hospital's emergency room with a serious complication of cirrhosis. In this case, the mortality rate is very high. Although similar research has not been conducted in Finland, the situation is presumed to be equally concerning.

There are automated methodologies implemented to diagnose liver fibrosis, but large-scale systematic analysis and screening are still yet to be implemented because of missing nationwide data. One randomized controlled study developed a care pathway for identifying advanced liver disease in patients with type 2 diabetes in Hong Kong and Malaysia. In that study, the results show that automation can lead to an increase in the number of referrals for patients with type 2 diabetes and abnormal fibrosis scores [23]. Another study showed that nationwide screening helps the early detection of liver cirrhosis [24]. Both of these studies have shown that screening and automated risk assessment can improve liver disease detection and it would be beneficial to implement nationwide health care analysis.

Strengths and Limitations

The applied risk model used in this study has built-in flexibility for different availabilities of input data. This supports data quality development and enables flexible adaptation of different formats of input data. With this approach to risk assessment,

XSL•FO
RenderX

we do not obtain the exact risk value from the model. However, this provides flexibility, as the risk categories offer valuable information as the exact risk value.

Approximation of smoking status and alcohol usage can be extracted using free text or various *ICD-10* or ICPC-2 diagnosis codes. These are still approximations and have the possibility for errors. In particular, it is unusual to have exact values from free text for alcohol usage, as it can be described using various words. As we were not able to use modern models for text analysis, such as generative large language models, we were still able to identify texts that refer to alcohol usage and smoking status. This means that although multiple texts refer to that information in free text, a consistent model is needed to analyze the data and achieve more reliable results. For that, the modern and more developed models would be a better option. To mitigate the analysis risk, we should target to convert alcohol usage free text into predefined categories, which would decrease the magnitude of errors in the analysis results.

Defining the new measurement type in the Kanta structural data does not require much work, but transferring the measurement results to Kanta can be time-consuming since the changes need to be implemented across all patient management systems that record actual data. In addition to changes to the actual systems to support the new measurements, changes in health care professional's everyday patient care practices are also necessary to perform the actual measurement.

Future Directions

To enhance the accuracy of risk model results, WHR data would be required. There are several possible ways to obtain WHR information, and their effectiveness depends on the use case. For example, Kanta PDR could have a new measurement type and WHR measurement could be added to general measurements in health care visits. It would take several years for Kanta to achieve broader population coverage since data are recorded only from individuals who use health care services. The other possible way would be to ask for information from the individual and use that in the risk model. There are a few ways to request a value from an individual; an exact value, a categorical question, or a camera measurement. The exact value asking is beneficial for the risk model because it will give the best results, but the measurement is quite difficult for individuals to perform on their own. Categorical questioning is easier to answer for the individual and can be implemented by showing photos of different body types, allowing the person to select the one that resembles them the most. This method would have the most errors, but it would be the easiest way for individuals. The last option would be to use a smartphone to measure WHR through the camera. The body can be identified using artificial intelligence, and the ratio can be calculated accurately based on an image. This requires a little bit of effort from the person but gives a precise risk value as a result.

As an alternative, we could show the WHR ranges assigning a patient to the low- or high-risk category, or we may consider developing a new risk function using BMI instead of WHR. As a potential future development, we may consider using Kanta PHR where patients themselves could record their WHR or ask categorized questions from the patient about the WHR.

Even though the risk model could not identify any high-risk patients with current Kanta data, it would still be important to implement this kind of risk model to use in everyday health care, because it would give real-time feedback about Kanta data quality development and guide health care professionals to make correct measurements for the patient. Patient management systems could inform health care professionals during patient visits about the exact measurements missing from the Kanta, preventing the calculation of the risk.

One option for finding missing data is using local data sources or mobile wellness apps. Both cases have their strengths and weaknesses. Local data sources for each patient management system may contain richer data than what is stored in Kanta, but integrating them into each local system requires a lot of work and maintenance. The National Electronic Health Record system in this case offers greater flexibility and simplifies data use. Changes should be made so that local data sources record all key values to Kanta. On the other hand, mobile wellness apps like Apple Health, Google Fit, and so on, store a lot of valuable data from personal health perspectives. The problem is that with the current legislation, nonmedical device data cannot be used in health care. This means that this offers possibilities only for personal health risk assessments and not for health care professional use cases.

In future work, the time dimension could be further used to track a patient's risk over their whole patient history by plotting a graph of their minimum and maximum risk at each point in their timeline. This could help determine, for example, whether a change in their risk warrants an intervention or highlight a period of missing data in their history where the risk value is more uncertain.

In conclusion, the Finnish national electronic health record system has the potential to support automated risk detection models across the nation. However, capturing key chronic disease risk factors such as obesity, smoking, and alcohol use requires improvement.

Acknowledgments

The authors would like to thank Klaus Förger and Mika Torhola for helping in planning the initial project and revising the idea and MSc Esa Harju for helping with the analysis implementation. This study was funded by Pfizer.

Data Availability

Data were used under the secondary use of health care data law. The Finnish data permit authority Findata gave permission to use the data. The data were collected by Kela, the owner of Kanta Services. Data were processed in an audited secure environment

XSL•FO
RenderX

with limited access. To have access to similar data, you must apply to Kanta Services data through Findata and define the collected data types. After the permission has been granted, the secure environment can be ordered, and the data will be delivered to it. The generative AI model ChatGPT was used only for clarifying the language.

Authors' Contributions

VM contributed to writing the original draft. JT conducted formal analysis. ET contributed to conceptualization. O-PH managed supervision. FÅ handled review and editing of the manuscript.

Conflicts of Interest

ET and O-PH work for Pfizer Oy and own Pfizer stocks. VM and JT work for Atostek Oy. Atostek Oy provides an eHealth application programming interface gateway service that enables health care and social welfare providers a fast and easy connection to Finland's national Kanta services. The publication is related to the quality of data stored in the Kanta archive and improving the quality of the data could have a positive impact on Atostek's services. We do not consider this to be a conflict of interest as improving the quality of the data in the national Kanta archive is possible only through constructive criticism of the current situation.

Multimedia Appendix 1
Risk calculation formula.
[DOCX File , 16 KB - medinform_v13i1e62978_app1.docx]

Multimedia Appendix 2
Diagnosis mappings.
[DOCX File , 15 KB - medinform_v13i1e62978_app2.docx]

Multimedia Appendix 3
Category definitions.
[DOCX File , 21 KB - medinform_v13i1e62978_app3.docx]

Multimedia Appendix 4
Free text search keywords.
[DOCX File , 16 KB - medinform_v13i1e62978_app4.docx]

Multimedia Appendix 5
Risk categorization results.
[DOCX File , 16 KB - medinform_v13i1e62978_app5.docx]

References

1. Åberg F, Luukkonen PK, But A, Salomaa V, Britton A, Petersen KM, et al. Development and validation of a model to predict incident chronic liver disease in the general population: the CLivD score. J Hepatol 2022;77(2):302-311 [FREE Full text] [doi: 10.1016/j.jhep.2022.02.021] [Medline: 35271949]
2. Kuolemansyyt - Kuolleet tilaston peruskuolemansyyn (ICD-10, 3-merkkitaso). Fin Stat. 2024. URL: https://pxdata.stat.fi/PxWeb/pxweb/fi/StatFin/StatFin__ksyyt/statfin_ksyyt_pxt_11be.px/table/tableViewLayout1/ [accessed 2024-01-29]
3. Pang Y, Åberg F, Chen Z, Li L, Kartsonaki C, China Kadoorie Biobank Collaborative Group. Predicting risk of chronic liver disease in Chinese adults: external validation of the CLivD score. J Hepatol 2024;80(6):e264-e266. [doi: 10.1016/j.jhep.2023.12.022] [Medline: 38181826]
4. Åberg F, Asteljoki J, Männistö V, Luukkonen PK. Combined use of the CLivD score and FIB-4 for prediction of liver-related outcomes in the population. Hepatology 2024;80(1):163-172 [FREE Full text] [doi: 10.1097/HEP.0000000000000707] [Medline: 38112489]
5. Song J, Jiang ZG. A good step toward low-cost prognostication of liver-related outcome awaits more validation. J Hepatol 2022;77(3):887-889. [doi: 10.1016/j.jhep.2022.04.008] [Medline: 35460724]
6. Kanta Statistics. Kela. 2024. URL: https://www.kanta.fi/en/statistics [accessed 2025-03-11]
7. What are the Kanta services? Kela. 2024. URL: https://www.kanta.fi/en/professionals/what-are-kanta-services [accessed 2025-03-11]
8. Act on the secondary use of social and health information. Finlex. 2019. URL: https://www.finlex.fi/fi/laki/alkup/2019/20190552 [accessed 2025-03-11]

XSL•FO
RenderX

9. Himi ST, Monalisa NT, Whaiduzzaman M, Barros A, Uddin MS. MedAi: a smartwatch-based application framework for the prediction of common diseases using machine learning. IEEE Access 2023;11:12342-12359. [doi: 10.1109/access.2023.3236002]
10. The data saved in Kanta are shown in MyKanta. Kela. 2024. URL: https://www.kanta.fi/en/data-in-kanta [accessed 2025-03-11]
11. Kanta PHR. Kela. URL: https://www.kanta.fi/en/system-developers/kanta-phr [accessed 2025-03-11]
12. Kanta patient data archive report and forms CDA R2 structure. HL7 Finland. URL: https://www.hl7.fi/hl7-rajapintakartta/kanta-earkiston-kertomus-ja-lomakkeet-cda-r2/ [accessed 2025-03-11]
13. Dolin RH, Alschuler L, Boyer S, Beebe C, Behlen FM, Biron PV, et al. HL7 clinical document architecture, release 2. Journal of the American Medical Informatics Association 2006;13(1):30-39. [doi: 10.1197/jamia.m1888]
14. Männikkö V, Förger K, Urhonen H, Tikkanen J, Antikainen S, Munukka J. Overview of finnish national patient data repository for research on medical risk assessment. FinJeHeW 2024;16(3):254-268. [doi: 10.23996/fjhw.146124]
15. Addressing alcohol use and mini-intervention. Finnish institute for Health and Welfare. URL: https://thl.fi/aiheet/alkoholi-tupakka-ja-riippuvuudet/ehkaiseva-paihdetyo/puheeksiotto-ja-mini-interventio/alkoholin-kayton-puheeksiotto-ja-mini-interventio [accessed 2025-03-11]
16. Lahti-Koski M, Pietinen P, Männistö S, Vartiainen E. Trends in waist-to-hip ratio and its determinants in adults in finland from 1987 to 1997. Am J Clin Nutr 2000;72(6):1436-1444. [doi: 10.1093/ajcn/72.6.1436] [Medline: 11101468]
17. Waist circumference and waist-hip ratio: report of a WHO expert consultation. World Health Organization. URL: https://www.who.int/publications/i/item/9789241501491 [accessed 2025-03-11]
18. Andreasson A, Carlsson AC, Önnerhag K, Hagström H. Waist/Hip ratio better predicts development of severe liver disease within 20 years than body mass index: a population-based cohort study. Clin Gastroenterol Hepatol 2017;15(8):1294-1301.e2. [doi: 10.1016/j.cgh.2017.02.040] [Medline: 28342948]
19. Schult A, Mehlig K, Björkelund C, Wallerstedt S, Kaczynski J. Waist-to-hip ratio but not body mass index predicts liver cirrhosis in women. Scand J Gastroenterol 2018;53(2):212-217. [doi: 10.1080/00365521.2017.1420219] [Medline: 29276897]
20. Åberg F, Jula A. The sagittal abdominal diameter: role in predicting severe liver disease in the general population. Obes Res Clin Pract 2018;12(4):394-396. [doi: 10.1016/j.orcp.2018.06.007] [Medline: 30078405]
21. Sahlman P, Nissinen M, Puukka P, Jula A, Salomaa V, Männistö S, et al. Genetic and lifestyle risk factors for advanced liver disease among men and women. J Gastroenterol Hepatol 2020;35(2):291-298. [doi: 10.1111/jgh.14770] [Medline: 31260143]
22. Åberg F, Färkkilä M, Salomaa V, Jula A, Männistö S, Perola M, et al. Waist-hip ratio is superior to BMI in predicting liver-related outcomes and synergizes with harmful alcohol use. Commun Med (Lond) 2023;3(1):119 [FREE Full text] [doi: 10.1038/s43856-023-00353-2] [Medline: 37674006]
23. Zhang X, Yip TC, Wong GL, Leow W, Liang LY, Lim L, et al. Clinical care pathway to detect advanced liver disease in patients with type 2 diabetes through automated fibrosis score calculation and electronic reminder messages: a randomised controlled trial. Gut 2023;72(12):2364-2371 [FREE Full text] [doi: 10.1136/gutjnl-2023-330269] [Medline: 37549979]
24. Labenz C, Arslanow A, Nguyen-Tat M, Nagel M, Wörns MA, Reichert MC, et al. Structured early detection of asymptomatic liver cirrhosis: results of the population-based liver screening program SEAL. Journal of Hepatology 2022;77(3):695-701. [doi: 10.1016/j.jhep.2022.04.009] [Medline: 35472313]

Abbreviations

CDA R2: Clinical Document Architecture Release 2
CLivD score: Chronic Liver Disease score
GGT: gamma glutamyl transferase
HL7: Health Level 7
ICD-10: International Statistical Classification of Diseases and Related Health Problems 10th Revision
ICPC-2: International Classification of Primary Care version 2
Kanta PDR: Kanta Patient Data Repository
RWD: real-world data
THL: Finnish Institute for Health and Welfare
WHR: waist-hip ratio

XSL•FO
RenderX

Edited by A Coristine; submitted 07.06.24; peer-reviewed by S Dalal, C Sun; comments to author 31.10.24; revised version received 20.12.24; accepted 13.02.25; published 02.04.25.

Please cite as:
Männikkö V, Tommola J, Tikkanen E, Hätinen OP, Åberg F
Large-Scale Evaluation and Liver Disease Risk Prediction in Finland's National Electronic Health Record System: Feasibility Study Using Real-World Data
JMIR Med Inform 2025;13:e62978
URL: https://medinform.jmir.org/2025/1/e62978
doi:10.2196/62978
PMID:40172947

©Viljami Männikkö, Janne Tommola, Emmi Tikkanen, Olli-Pekka Hätinen, Fredrik Åberg. Originally published in JMIR Medical Informatics (https://medinform.jmir.org), 02.04.2025. This is an open-access article distributed under the terms of the Creative Commons Attribution License (https://creativecommons.org/licenses/by/4.0/), which permits unrestricted use, distribution, and reproduction in any medium, provided the original work, first published in JMIR Medical Informatics, is properly cited. The complete bibliographic information, a link to the original publication on https://medinform.jmir.org/, as well as this copyright and license information must be included.

XSL•FO
RenderX

Original Paper

Clinician Attitudes and Perceptions of Point-of-Care Information Resources and Their Integration Into Electronic Health Records: Qualitative Interview Study

Marlika Marceau[1], BA; Sevan Dulgarian[2], BA, BS; Jacob Cambre[2], BS; Pamela M Garabedian[1], MS; Mary G Amato[2,3], BCPS, MPH, PharmD; Diane L Seger[1], RPh; Lynn A Volk[1], MHS; Gretchen Purcell Jackson[4,5], MD, PhD; David W Bates[1,2,6,7], MS, MD; Ronen Rozenblum[2,6*], MPH, PhD; Ania Syrowatka[2,6*], PhD

[1]Clinical and Quality Analysis, Mass General Brigham, Somerville, MA, United States

[2]Division of General Internal Medicine, Brigham and Women's Hospital, Boston, MA, United States

[3]Massachusetts College of Pharmacy and Health Sciences (MCPHS), Boston, MA, United States

[4]Vanderbilt University Medical Center, Nashville, TN, United States

[5]Intuitive Surgical, Sunnyvale, CA, United States

[6]Harvard Medical School, Boston, MA, United States

[7]Harvard TH Chan School of Public Health, Boston, MA, United States

[*]these authors contributed equally

Corresponding Author:
Marlika Marceau, BA
Clinical and Quality Analysis
Mass General Brigham
399 Revolution Drive
Somerville, MA, 02145
United States
Phone: 1 8572827001
Email: mmarceau@mgb.org

Abstract

Background: Electronic health records (EHRs) are widely used in health care systems across the United States to help clinicians access patient medical histories in one central location. As medical knowledge expands, clinicians are increasingly using evidence-based point-of-care information (POCI) resources to facilitate clinical decision-making in medical practices. While these tools can improve clinical outcomes, few studies have assessed clinicians' opinions on integrating them with EHRs.

Objective: This study aims to assess clinicians' attitudes and the perceived value of POCI resources for finding medication- and disease-related information in clinical practice and their integration with EHRs.

Methods: Semistructured interviews were conducted with 10 clinicians from various roles and specialties between December 2021 and January 2022 at Brigham and Women's Hospital in Boston, Massachusetts. A content analysis approach was used to examine participants' responses and feedback on their current use of POCI resources, barriers and facilitators, mobile app use, and recommendations for improved integration.

Results: Of the 10 participants, 6 (60%) were female, 9 (90%) were aged <40 years, and 8 (80%) had ≤10 years of experience in clinical practice. While UpToDate was the most preferred disease-related information resource (n=9, 90%), preferences for medication-related resources varied, with 2 (20%) participants favoring Micromedex, 2 (20%) favoring Lexicomp, 2 (20%) favoring Brigham and Women's Hospital–specific drug administration guidelines, 2 (20%) favoring UpToDate, and 1 (10%) favoring Medscape. Most participants used their preferred tools weekly. Most clinicians preferred comprehensive POCI tools with clear, navigable layouts that eased and quickened the search for information. Features such as heavy text density, the lack of citations, and frequent log-ins to access the tool were viewed as barriers that limited content legibility, credibility, and accessibility. Access-related, tool-specific, and integration-related barriers were reported to negatively impact clinical workflow. Most (n=8, 80%) of the participants reported currently using mobile apps, reasoning that they facilitated quick and convenient searches for information; however, frequent updates, time-consuming log-ins, and high text density on smaller screens posed challenges. Most participants favored further integration of POCI resources with EHRs, with all reporting them being currently

XSL•FO
RenderX

available as embedded links that launch externally. Some recommended that further integration would allow us to leverage existing POCI tool features, such as chatbots and knowledge links, as well as aspects of artificial intelligence and machine learning, such as predictive algorithms and personalized alert systems, to enhance EHR functionality.

Conclusions: Participants favored integration to improve usability and optimize workplace efficiency by reducing the amount of time spent seeking answers to their medication- and disease-related questions. Recommendations on integration highlighted the need for stakeholder input in developing clinical decision support tools and interfaces that leverage advancements in artificial intelligence and machine learning while not compromising user experience or increasing time spent on tasks.

(JMIR Med Inform 2025;13:e60191) doi:10.2196/60191

KEYWORDS

point-of-care tools; clinical decision support; artificial intelligence; point-of-care information; online databases; efficiency; quality of care; electronic health records; health information system interoperability; machine learning

Introduction

Background

Being a practicing clinician requires navigating and retaining an immense and evolving breadth of knowledge as the field of medicine progresses and standards of care change. To address the knowledge gaps that arise during a busy workday, clinicians use a variety of methods to support their clinical decision-making [1]. To be effective, clinical resources must be accurate, reliable, helpful, and quickly accessible in addressing clinicians' questions on various medical topics [1-3].

While it is common to use search engines, such as Google, clinicians have increasingly come to rely on evidence-based online information resources, such as point-of-care information (POCI) tools, to help answer medication- and disease-related questions that arise during patient care [1]. POCI tools are evidence-based online information websites and databases that support clinical decision-making by providing quick and reliable responses to clinical questions [1,4]. Clinicians can use these types of clinical decision support systems to find peer-reviewed literature and clinical practice guidelines to inform standards and practices used during patient care delivery [1,4]. BMJ Best Practice, DynaMed, Micromedex, and UpToDate are some examples of POCI tools that have different content areas of focus with a wide range of features, layouts, and modes of access [1,4]. Health care organizations often offer access to a variety of online resources via institutional subscriptions, including collections of electronic textbooks and journals, search tools for bibliographies and abstracts of primary literature (eg, PubMed or Embase), and more focused resources, such as the Natural Medicines Comprehensive Database [4].

Online information resources often include barriers that challenge their users at the point of care. For example, clinicians have reported that some POCI tools are difficult to navigate, thereby prolonging their search time, lack depth in their explanations, and provide unsatisfactory answers, all of which might affect their acceptance and use [2,5]. However, these resources have been proven to enhance the delivery of care and clinical outcomes when properly implemented by improving diagnostic accuracy and treatment plans [6,7]. Therefore, a need exists for innovative methods to address these barriers and optimize POCI tools to best meet clinical needs.

There have been increasing efforts to integrate POCI tools with electronic health records (EHRs) to improve usability and clinical workflow [8]. Examples include the ability to access a resource directly from the EHR without having to launch it via an external browser and the option to download apps to access the tools via mobile devices. If effectively implemented, integrating these tools may help optimize the speed of information retrieval and reduce clinician burden during searches for information to inform clinical practice [8]. Furthermore, clinicians' input on the integration of these tools can help identify potential areas for improvement due to their experience with using these tools in the clinical setting [2,5,8].

Objectives

This study aimed to assess clinicians' attitudes, current use, and the perceived value of POCI tools for finding medication- and disease-related information. In addition, this study examined the attitudes of clinicians toward the integration of POCI tools with EHRs, identified barriers and facilitators, and solicited recommendations for improved integration.

Methods

Study Design and Setting

We conducted semistructured interviews with clinicians (30-45 min) employed at the Brigham and Women's Hospital (BWH) in Boston, Massachusetts, from December 2021 to January 2022.

Study Participants, Sampling, and Recruitment

Our targeted recruitment method sought to engage clinicians from a diverse range of specialties and experiences. Physicians, physician assistants (PAs), pharmacists, and registered nurses providing patient care in internal medicine, infectious diseases, neurology, and critical care were included. We used purposive sampling to recruit from a pool of participants who completed a usability study on the combined DynaMed and Micromedex with Watson tool (DynaMedex, hereafter referred to as the combined tool), given their experience with this POCI tool [2,9,10]. Participants involved in the usability study were asked if they would be interested in taking part in a subsequent study; thereafter, all interested individuals were invited to participate in this study. The combined tool was selected for evaluation as it represented typical medication- and disease-related information resources that clinicians commonly use. It also

XSL•FO
RenderX

incorporated artificial intelligence (AI)–powered features, such as a conversational interface to facilitate search.

Interview Guide

A semistructured interview guide was developed in collaboration with subject matter experts (MGA, DLS, and DWB), a human factors expert (PMG), and an experienced qualitative researcher with expertise in the topic investigated in the study (RR; Multimedia Appendix 1). We added preliminary questions to better understand participants' clinical backgrounds and their previous use of the POCI resources to gather feedback on their experiences using these resources in their particular practice. The guide was then piloted with 1 clinician and the internal research team to identify areas for improvement and ensure perspectives could be shared without input from the interviewer. We integrated the feedback received from the pilot by revising the guide to address gaps and concerns.

The revised and final guide contained 15 open-ended questions divided into 4 parts. Part 1 comprised questions about participants' demographics and clinical backgrounds. Part 2 addressed their use of current clinical tools, part 3 inquired about Micromedex and DynaMed use, and part 4 explored their experiences with the combined tool and recommendations for integrating it with the EHR. The combined tool was deployed as a use case to assess participants' perceptions of the value of integrating the information resources.

Ethical Considerations

The study was exempted by the Mass General Brigham Institutional Review Board (protocol #2021P001813). All participants provided verbal informed consent to be interviewed and recorded before starting the interview. Participants could opt out and stop the interview at any time without providing a reason. All interview data were deidentified to protect participants' privacy and confidentiality and stored on password-protected computers behind the firewall at Mass General Brigham. Each participant received a US $50 Amazon gift card as compensation for their time participating in the study.

Data Collection and Analysis

All interviews were conducted on Zoom (Zoom Communications, Inc) by SD. The video recordings were transcribed by a professional transcription company. Using a content analysis approach, 2 reviewers (SD and MM) independently abstracted data from the transcripts and entered it into a Microsoft Excel document organized according to the sections of the interview guide. Similar ideas were grouped together to identify and summarize a set of concepts for each interview topic [11]. The reviewers cross validated each other's groupings to ensure that the data analysis was consistent and replicable [12]. To further validate their findings and ensure transparency in the review process, the reviewers met with the experienced researchers (RR and AS) to discuss discrepancies and achieve consensus [12]. The results were structured according to the concepts derived from each section of the interview guide and were titled as follows: participant demographics and clinical backgrounds, overview of current practices, use of preferred web-based tools in current practice, barriers to using web-based information resources in current practice, preferred mobile apps, and attitudes on integrating web-based information resources into the EHR. We subsequently report the study findings using the terms *a few* (30% or fewer participants), *some* (>30% and <70% of the participants), or *most* (>70% of the participants) to describe the frequency of perspectives shared and specific patterns in participant responses. Data saturation was reached after 10 interviews, as no new significant themes emerged, with key themes consistently repeated across participants, indicating that further interviews would not provide substantially different insights [13].

Results

Participant Demographics and Clinical Backgrounds

We contacted 12 clinicians from BWH and interviewed 10 with diverse clinical backgrounds and experiences (Table 1). Of these 10 participants, 3 (30%) physicians, 3 (30%) pharmacists, 2 (20%) PAs, and 2 (20%) nurses were interviewed. Most clinicians identified as female (n=6, 60%), were aged <40 years (n=9, 90%), and had ≤10 years of experience practicing (n=8, 80%). Half (5/10, 50%) of the participants self-reported being in leadership roles in their practice, and there were equal numbers working in inpatient and outpatient settings.

XSL•FO
RenderX

Table 1. Demographic characteristics and clinical backgrounds of study participants (N=10).

Characteristics	Participants, n (%)
Sex	
Female	6 (60)
Male	4 (40)
Age group (y)	
21-30	2 (20)
31-40	7 (70)
41-50	1 (10)
Clinical role	
Physician	3 (30)
Physician assistant	2 (20)
Pharmacist	3 (30)
Registered nurse	2 (20)
Specialty	
Critical care	3 (30)
Infectious diseases	1 (10)
Internal medicine	4 (40)
Neurology	2 (20)
Duration of practice (y)	
<1-5	3 (30)
6-10	5 (50)
11-20	1 (10)
21-30	1 (10)
Duration of practice at BWH [a] (y)	
<1	1 (10)
2-5	5 (50)
6-10	4 (40)
Clinical setting	
Inpatient	5 (50)
Outpatient	5 (50)
Leadership role	
Yes	5 (50)
No	5 (50)

[a]BWH: Brigham and Women's Hospital.

Overview of Current Practices

All interviewed clinicians reported using various web-based resources to look up information in clinical settings (Table 2). There was substantial overlap in the resources used to find medication- and disease-related information. Participants favored web-based tools that were available within the EHR as links from a pull-down resource menu. Most participants used POCI tools, such as Micromedex (6/10, 60%), UpToDate (5/10, 50%), or Lexicomp (3/10, 30%), to find medication-related information. UpToDate (9/10, 90%) or primary literature databases (4/10, 40%), such as PubMed and Google Scholar, were used most often to find disease-related information. A few participants reported accessing web-based content resources, such as hospital-based policies or clinical practice guidelines, before using POCI tools because they provided more specialty-specific information. A few participants relied on direct communication with others, such as calling a pharmacy or consulting with colleagues for medication-related questions.

XSL•FO
RenderX

Table 2. Reported use of web-based medication–related and disease-related information resources by study participants (N=10)[a].

Name of resource	Brief description[b]	Type of resource	Participants who reported using the medication-related resource, n (%)	Participants who reported using the disease-related resource, n (%)
Clinical practice guidelines[c]	Clinical practice guidelines provide best practice recommendations based on evidence-based research on how to identify and treat medical conditions [14].	Content resource	2 (20)	2 (20)
DynaMed	DynaMed is a clinical decision support tool that provides clinicians with evidence-based information for quick answers at the point of care [15].	POCI[d] tool	N/A[e]	1 (10)
Hospital-based policies[f]	Hospital-based policies are the rules and guidelines adopted by hospitals that guide decisions and standards of practice [16].	Content resource	1 (10)	1 (10)
Lexicomp (through UpToDate)	Lexicomp is a drug reference database that provides evidence-based recommendations to help clinicians treat and counsel patients on their conditions and medical histories [17].	POCI tool	3 (30)	N/A
Medscape	Medscape is an online platform that provides access to medical news, expert feedback, and medical and disease information while supporting clinicians with professional education opportunities, including continuing medical education [18].	POCI tool	1 (10)	1 (10)
Micromedex	Micromedex is a comprehensive database that provides information on medications, diseases, and toxicology to support diagnostic and treatment decision-making in clinical practice [19].	POCI tool	6 (60)	N/A
Primary literature databases[g]	Primary literature databases are platforms that provide access to journal articles on health and medical sciences and other related content [20].	Content resource	2 (20)	4 (40)
UpToDate	UpToDate is a subscription-based clinical decision support resource that helps clinicians access evidence-based medical information while facilitating patient care [21].	POCI tool	5 (50)	9 (90)

[a]Percentages added to >100% because participants reported using multiple tools.

[b]The descriptions were taken from the official websites of the products and tools.

[c]Examples are Johns Hopkins Antibiotic Guide, Fast Facts, drug administration guidelines, and the Centers for Disease Control and Prevention Opioid Guideline.

[d]POCI: point-of-care information.

[e]N/A: not applicable.

[f]Examples are Brigham and Women's Hospital policies, such as the empiric antibiotic guide.

[g]Examples are PubMed, Embase, and Google Scholar.

Use of Preferred Web-Based Tools in Current Practice

Overview

All participants expressed a preference for specific web-based resources. A few participants preferred Micromedex (2/10, 20%) or Lexicomp (2/10, 20%) to find medication-related information, and 10% (1/10) of the participants used both tools interchangeably. Other preferred medication resources included clinical practice guidelines (ie, BWH-specific drug administration guidelines; 2/10, 20%), UpToDate (2/10, 20%), and Medscape (1/10, 10%). UpToDate (9/10, 90%) was the most favored resource for finding disease-related information. Moreover, 10% (1/10) of the participants preferred using Medscape.

Reasons for Selection

The reasons for selecting preferred tools were similar for medication- and disease-related resources. Most participants preferred their tool due to its targeted information, function, and capabilities, while some favored their tool for its

XSL•FO
RenderX

comprehensiveness in combining both disease- and medication-related information into one place.

Most participants found it convenient to use tools that they were familiar with and were quickly accessible, often through the EHR. For example, one physician stated the following:

[I will] probably go to UpToDate because it is easily accessible, and I [am] familiar with that. UpToDate is my go-to...because of the familiarity and ease of access. [Internist]

Most participants also acknowledged that content and layout influenced the selection of their preferred tool, especially when the tool's design made it easy to find information quickly:

> *[It is] designed with the clinician in mind in the sense that you can search through it, you can click by topic, you can click within subtopics...You can narrow in on what it is that you need help with.* [Neurologist]

Given their reliance on evidence-based information, most participants selected tools based on their assessments of whether the information provided was reliable and credible. For instance, some participants favored evidence-based disease-related resources because they helped them learn about unfamiliar topics and clinically reason through possibilities while generating differential diagnoses for a medical case:

> *It's a good start for me to go to something like UpToDate for a disease state that I'm not familiar with, just because it does give you a general recommendation, but it also ties in a lot of the most recent guidelines of literature.* [Critical care pharmacist]

Finally, a few participants were encouraged to use their tool because it offered continuing medical education (CME) credits:

> *Because it also provides CME, I want to make sure that I have my information passed through because I can collect some CME through my searches.* [Internist]

Experience With Preferred Tool

Most participants reported positive experiences using their preferred information resource, finding it useful, usable, and informative. Some participants expressed their appreciation for clear layouts, bulleted formats, in-depth explanations, and embedded links to supporting literature, which helped provide evidence-based recommendations:

> *I think both are...usable. I appreciate that Micromedex has both the short version of things, but then you can also look at an in-depth version that expands beyond the monograph and to citing more data and the reason behind certain recommendations.* [Infectious disease pharmacist]
>
> *I think [it is] comprehensive. I think...[it is] accurate. I like that [there are] links to references so you can choose to read the primary research.* [Neurologist]

One participant felt it was important that their tool provided details on when the information was updated, and another mentioned the positives of being able to access information that is specific to their institution's policies through their tool on the EHR system.

While most participants reported positive experiences using their information resources, they also expressed shortcomings, such as a lack of depth in certain areas and longer times spent looking for information. These caveats are further explained as follows:

> *Sometimes [there are] specific questions that are a little bit more in depth that [are not] really covered by some of these resources, but [that is] expected...Resources [cannot] cover everything.* [Critical care pharmacist]
>
> *I think [in] UpToDate...you need to scroll a little bit more and the way [it is] laid out, I find it just takes me longer to read it.* [Neurologist]

In addition, a recurrent theme mentioned was high text density and large paragraphs, which made navigation difficult, especially when trying to quickly skim through the text. Some participants did not feel that the navigation bars helped to reduce the time spent looking for information, as mentioned in the following statements:

> *What I think [it is] missing is...sometimes the paragraph format is too long...I find that [it is] a little bit too much information. Sometimes, when [you are] reading something new or when [you are] not sure what [you are] looking for, [it is] harder to zone into exactly the point that you want.* [Neurologist]

It was also noted that it was more time consuming to find specific answers regarding disease-related questions as opposed to medication-related ones because disease-based sections were more text dense. For example, one participant stated the following:

> *You pretty much know, no matter what medicine you look at, how much content, and how is it laid out, and [that is] very predictable. I think for diseases, it can be a little bit more vast. Sometimes, you might need to narrow your search a little bit more or figure out which section you want to jump to because you really do not have time to read the whole thing, nor are the sections always finite because [they] can sometimes be super-long depending on the disease.* [Internist]

Accessing Resources

Most participants accessed their preferred resource through their institutional EHR system. Once in the EHR, some participants described a variety of pathways to their preferred resource, which all involved clicking an embedded link to launch an external web browser that redirected to the resource website. Information resources could be accessed through the resources drop-down in the EHR, the KnowledgeLink portal of the EHR, or the institution's handbook containing electronic references for clinical use. Resources were also located in the hospital employee intranet through Citrix Workspace. These pathways were discussed in the following statement:

> *For at least me, specifically, within Epic [there are] tabs that they have embedded links for clicking on*

XSL•FO
RenderX

> *access to UpToDate, Micromedex, so [that is] the easiest way for me to do so.* [Critical care pharmacist]

A few participants accessed the resources directly through a web browser because they found this to be a quicker and easier method. They expressed dislike for Internet Explorer (Microsoft Corporation) as a default browser, stating that it is not user-friendly. One pharmacist explained as follows:

> *I honestly generally just pull up a web browser tab and do it that way, because [that is] through Chrome, which is much quicker than if you click on it through Epic. It goes through Internet Explorer, which is an awful browser.* [Infectious disease pharmacist]

Frequency of Use

Half (5/10, 50%) of the participants estimated using their preferred medication-related resource either once or a couple of times a week. Conversely, 30% (3/10) of the clinicians used it daily, and a few used it monthly, depending on their clinical needs. Regarding preferred tools for disease-related queries, 60% (6/10) of the participants used them on a weekly basis, 30% (3/10) used them monthly, and 10% (1/10) used them on a daily basis.

Timing of Use

Most participants gave a broad range of answers for when they used their preferred resource in the context of patient care, regardless of their clinical background. All participants accessed their tool at different times throughout the patient care journey. Approximately 70% (7/10) of the clinicians used their tool before a patient encounter, often to learn more about the patient's condition; 70% (7/10) of the clinicians used the resources during encounters, and 60% (6/10) of the clinicians used them after an encounter while writing notes or looking up additional information. Moreover, 60% (3/5) of the inpatient clinicians also reported using their preferred resource during rounds. Most participants said they would be most likely to use a combination of the aforementioned time points, depending on their needs, as noted in the following response:

> *If I [have not] heard of a disease, then I would obviously want to learn about it just before going to see the patient...so I can understand what [we are] doing a little bit better if it impacts why [they are] in the hospital. Then, maybe after, if they have the new diagnosis on the differential, I would look into it just to make sure I totally understand what [they are] thinking is going on for a patient.* [Critical care nurse]

Page Utility

Most participants were on a specific page of the EHR when they decided to seek medication- or disease-related information in their tool. For instance, most participants reported using the clinical notes page when looking for disease-related information from their tool, while the medications list page was most frequently used when looking for medication-related guidance in their tool, as described in the following statements:

> *[There are] medication searches and disease searches, and those definitely have different views. The medication searches would happen on the medication tab, versus disease searches would probably be more likely in the Notes or the Past Medical History section.* [Infectious disease pharmacist]

> *I would most likely be on the medication administration page just because that [is] where the medication order is, and I have that in front of me. [That is] what I need to access to look up the information.* [Internal medicine nurse]

Notably, one pharmacist mentioned being on the results page of the EHR when they launched their medication-related resource, as articulated in the following statement:

> *If I'm looking to see about an adverse event, I might be on the Results tab to see how labs are trending compared to what might be published.* [Infectious disease pharmacist]

Another pharmacist reported using their tool for disease-related questions while navigating the medications list page to better understand how medications may impact a patient's condition.

Barriers to Using Web-Based Information Resources in Current Practice

Most participants reported a range of access-related, tool-specific, and integration-related barriers that negatively impacted clinical workflow (Multimedia Appendix 2). Specifically, some users found it challenging to rely on institutional permissions to access resources, efficiently navigate to their preferred tools from the EHR, and find information in the resources when the pages were too wordy.

Preferred Mobile Apps

Details about the use of preferred mobile apps and barriers to use in current practice are described subsequently. The use of mobile apps to access POCI resources reported by the study participants is given in the subsequent sections.

In total, 8 (80%) of the 10 participants reported currently using mobile apps to access POCI resources (Table 3). These participants accessed these apps on phones or tablets when a desktop computer was not available:

> *Folks that are running around and seeing dozens and dozens of patients, and only might have phone access between seeing patients.* [Infectious disease pharmacist]

XSL•FO
RenderX

Table 3. The current use of mobile apps reported by study participants to access point-of-care information resources.

Characteristic	Participants, n (%)[a]	Clinical roles
Name of mobile app (n=8)		
Lexicomp	1 (12)	1 pharmacist
Medscape	1 (12)	1 nurse
Micromedex	2 (25)	1 MD[b] and 1 pharmacist
UpToDate	6 (75)	2 MDs, 1 pharmacist, and 2 PAs[c]
Other[d]	6 (75)	2 MDs, 2 pharmacists, 1 PA, and 1 nurse
Frequency of use (n=8)		
Daily	3 (38)	2 PAs and 1 nurse
Once a week	1 (12)	1 pharmacist
Once a month	2 (25)	1 MD and 1 pharmacist
A few times per year	2 (25)	2 MDs
At what point in the patient encounter were the apps used? (n=8)		
Before	6 (75)	3 MDs, 1 PA, 1 pharmacist, and 1 nurse
During	3 (38)	1 PA and 2 pharmacists
After	6 (75)	3 MDs, 1 PA, 1 pharmacist, and 1 nurse
Other (pages, off shift, etc)	1 (13)	1 pharmacist
Patient rounds (inpatient clinicians only; n=5)	1 (20)	1 MD

[a]Centers for Disease Control Opioid Guideline, Fast Facts, Johns Hopkins Antimicrobial Guide, Sanford Guide, University of California–San Francisco Outpatient Medicine Handbook.

[b]MD: physician.

[c]PA: physician assistant.

[d]Frequency reflects the number of participants who mentioned using these mobile apps.

Most participants used UpToDate, Micromedex, and specialty-specific mobile apps that were also available as web-based versions. Most of the participants cited the ease of access, enhanced portability, the speed of information retrieval, and familiarity with the resources as reasons for using these apps. They found that these mobile apps were a convenient way to pull up specific resources quickly, with 38% (3/8) of the participants using these tools daily (Table 3). For example, one PA expressed the following:

> *UpToDate is certainly the thing I'm the most comfortable [with]. I think especially when [you are using a mobile device, I feel like your ability to navigate it quickly is a key to success actually, depending on what you're looking for. Also, when I'm looking something up on my phone [it is] not like [I am] looking to spend a long time reading something of interest. [It is] usually like, "I need to know something right now."* [Internal medicine PA]

Some participants used mobile apps to avoid barriers related to using desktop tools:

> *On my phone, I can just click on the app. I [do not] have to worry about logging in and [it is] faster. Going to the computer, you have to log in, load and all that stuff...I only use the app.* [Internal medicine nurse]

One physician appreciated that the mobile versions of the tools promised the same standards as the web versions. Most clinicians used the apps before and after patient encounters, and of the 5 inpatient clinicians, only 1 (20%) used an app during rounds. Physicians avoided using the tool during patient encounters, considering it would be inappropriate to be on a mobile phone in front of patients.

Barriers to mobile app use included challenges navigating copious amounts of text on smaller screens, updates, and log-ins. Some participants reported needing the content to be made app friendly:

> *[There is] usually either lots of text, if [you are] talking about disease state management, or lots of information, if [you are] talking about a drug monograph...you do a lot of scrolling on your phone to find what you need. It takes a little bit longer, versus on the larger screen.* [Infectious disease pharmacist]

One pharmacist described finding the log-in process time consuming:

XSL•FO
RenderX

> *Some of the barriers, like I mentioned, any Apple application having updates or login maybe if [they are] retyping a login and stuff like that that either cost time, or...[if] it was a hospital code [and] I forgot it [then] I [would not] have access.* [Critical care pharmacist]

Participants who no longer used the apps cited various barriers that affected their user experience. One physician reported no longer using a mobile app because the subscription renewal process and logging in were challenging and time consuming.

Attitudes on Integrating Web-Based Information Resources Into the EHR

Current Status of Integration With EHR

All participants reported that their preferred web-based resources were not fully integrated but were generally available as embedded links that launched external web pages:

> *[It is] a completely separate link. [It is] not like if you have atrial fibrillation in your note and [there is] a link [to] UpToDate. No, you have to open it as a resource.* [Neurologist]

A few participants described partial integration for medication orders, such as direct hyperlinks to medication information through an external browser:

> *In certain medication orders, there are hyperlinks directly so that it goes straight to the medication [information] from order in Epic.* [Infectious disease pharmacist]

One participant commented on the customizability of the EHR, noting that they were able to ease their access to their preferred tool by personalizing it to meet their needs:

You can set your settings. I had an Epic person...set that up for me. Epic modified my toolbar in [the] Epic menu and rearranged things...It tells you what you use the most. There [are] different ways to arrange things the way you want. [Neurology PA]

Participants considered full integration to provide quick and direct access to medication- and disease-related information within the EHR:

> *I honestly think the less there is clicking and the more something is going to directly take you to what you want the more it's going to get used.* [Internal medicine PA]

Preferences Regarding Integration

Most respondents favored accessing the resources via embedded links to external pages:

> *Probably better if it launches separately because when in [the] EHR, you [do not] want [what is] in front of your face to be hijacked by your search, necessarily.* [Internist]

A few preferred the information to be presented within the EHR. They reasoned that this would provide faster access to information by avoiding browser-related interruptions. For example, 20% (2/10) of the participants stated the following:

> *If it can be further integrated into EHR, it would definitely be useful. I think everybody benefits from getting quicker information.* [Internal medicine nurse]
>
> *I think in EHR. The only reason I say that is because of consistent browser issues.* [Neurology PA]

Suggestions for Improving Integration

Participants proposed a variety of solutions to improve integration with the EHR. To facilitate the quick retrieval of information resources, a couple of participants suggested the following:

> *You need to have it kind of like in a panel approach, so like, our EHR, Epic, has a side bar and then the main page, and the only way I can see it working well is if it was somehow integrated into that side bar, or in some sort of pop-up that you could still [see] the chart behind it.* [Infectious disease pharmacist]
>
> *You could even put it under the chart search bar so that [you are] really specifying are you searching the chart or are you searching information. You could also integrate it into the search so when you search the chart, [it is] like,"'[Here is] the patient information' or '[Here is] information about it.' What are you searching?" I think that it might be cool to put it where alerts pop up so if the contraindications pop-up comes up, it could have a link [to the resource].* [Neurologist]
>
> *[It would] be nice if there was either a dedicated activity within the EHR or a window or a corner or an icon where, when you click into it, it expands, and then [you will] see [the information resource], and then a search box opens up. Then, when you click enter, then [it is] okay if it opens up a new browser or window. Up to that point, it would feel a lot more integrated because you [are] able to type in your search string while [you are] still within your EHR.* [Internist]

It was also important to maintain a simple and user-friendly display with direct pathways to the resources embedded throughout the EHR, especially to make it easier for users to find the most relevant resource for their questions, as described in the following statement:

> *If I have a question and am not sure which part of the software I should be using, that is problematic, so there should be a way to guide you to the most appropriate application based off [the] question. The pathway needs to be really streamlined—it has to be really clear this is where I need to go.* [Internist]

Some participants identified existing features of the EHR that could be leveraged for integrating resources, given their current usefulness. For example, one participant discussed the potential use of KnowledgeLinks:

> *I can see a world in which you put diverticulitis down as a visit diagnosis and there [is] a little ⓘ next to diverticulitis and you click it, and it takes you to that*

XSL•FO
RenderX

> *page. That would be sweet for me.* [Internal medicine PA]

A chatbot was another feature favored by a few clinicians that could assist in finding information:

> *You know the little chat box at some websites, like [you are] on [a] travel [website] and [it] is like, "I can help?" Maybe if it was there and it was either just available as a search bar or if it had little suggestions based on what [you are] typing or what page [you are] on or stuff like that.* [Neurologist]

Some suggestions for integration involved using currently evolving capabilities to optimize the usability of the EHR. A few participants noted that AI could be used to identify critical information from patient charts, such as potential contraindications based on the medication list. They added that AI features could even evolve to provide alerts based on information from the resource for specific patient charts. This is expressed in the following comment:

> *You could incorporate [AI] to alert to contraindications. We get a bunch of alerts like, "Your patient is due for vaccines" or "Your patient needs the flu vaccine." I work [in] the inpatient [setting], but primary care, they also get a lot of alerts about guidelines around screening, stuff like that.* [Neurologist]

Concerns About Integration

Despite the widespread support for integration, some participants expressed reservations. They argued that integration must center on functionality, with a few citing concerns that it could interrupt their workflow by altering the current view of the EHR. For example, one participant stated the following:

> *A little bit of me is like if this is going to mess up how Epic looks, I'd rather have it be an external page that pins because then [it is] not in any way altering your view of [the] Epic screen.* [Internal medicine PA]

Similarly, most participants preferred that their resources existed as embedded, externally launched links, emphasizing that a poorly designed integration could lead to launching windows that obscure their view of patient information:

> *[It is] nice for me to be able to control whether or not I want to move that pop-up window or browser to the side or if I want to spend a moment and read all of it. This is where it sounds a little bit like [it is] paradoxical in a way. I want to integrate it, but I [do not] necessarily need it to take over the screen that [I am] working at.* [Internist]

> *The link right now that we have for UpToDate opens up a clunky Internet Explorer browser within the EHR, and [it is] not that user-friendly overall. I [do not] suggest that. Then, also, if it opens up in a new tab in your EHR in the first place, that kind of negates the point because then you [cannot] see patient [information] at the same time because [it is] covering it up.* [Infectious diseases pharmacist]

Discussion

Principal Findings

As medical knowledge rapidly evolves, web-based POCI resources have become common tools used to support complex decision-making in clinical practice. Although these tools have the potential to improve workplace efficiency, diagnostic accuracy, and treatment plans, few studies have examined clinician attitudes toward integrating them with EHRs [6,7]. This qualitative study examines clinician attitudes, current use, and perceived utility of POCI tools for answering medication- and disease-related questions during patient care delivery. Attitudes, barriers, and facilities regarding the integration of POCI tools with EHRs were also evaluated, in addition to recommendations for enhancing integration. Most participants preferred POCI tools and mobile apps with clear layouts that allowed for quick and easy access to medication- and disease-related information. Most participants supported the integration of POCI tools with EHRs, while some provided recommendations to improve the usefulness of the EHR, which included the addition of existing POCI tool features, such as chatbots and knowledge links, as well as AI and machine learning functions, such as predictive algorithms.

We conducted semistructured interviews with various clinicians to understand the current uses of POCI tools, barriers to and facilitators of use, and recommendations for integrating these tools with EHRs. We found that there were a variety of POCI tools used, most of which were large information databases that provided medication- or disease-related information, such as UpToDate and Micromedex, allowing users to access a wide breadth and depth of answers in a central location. In addition to an appreciation for comprehensiveness, there was a strong preference for POCI tools that eased the search for evidence-based information via clear, user-friendly layouts consisting of features such as bullets and embedded links that directed users to relevant information. The absence of such layouts in existing tools made it challenging for most users, who found disease-related pages to be text heavy, rendering navigation difficult and prolonging their search for information.

Comparison to Prior Work

These reported barriers and facilitators are consistent with previous studies where clinicians favored tools with minimalistic designs because they valued finding information easily and quickly [2,22]. The participants reasoned that complex layouts that are either too text dense or require multiple steps to locate relevant information reduced content visibility and tool accessibility, respectively [2,22]. They also emphasized that it was important for tools to cite sources supporting clinical information because it improved clinicians' understanding of the evidence for standards of care, which can enable adherence to clinical guidelines [6,22].

Participants also reported positive experiences using mobile web apps of their preferred POCI resources, reasoning that their portability, accessibility, and speed allowed them to find information quickly. In addition to frequent log-ins, participants reported that high levels of text density were still a barrier they experienced while using these apps. A previous study reported

XSL•FO
RenderX

similar findings, recommending that improvements to text and content clarity as well as offline access can support better participant experiences using mobile web app versions of POCI resources [23].

Regarding integration, participants had positive attitudes toward integrating these tools into the EHR, with most preferring that they be launched through embedded links while a few favored that they display directly within the EHR. It was important to most clinicians that integration leverage features that exist in both POCI tools and the EHR, including chatbots, knowledge links, and search functions, to improve resource navigability and usability. Recent studies reported positive experiences with integrating tool features into the EHR, including automatic calculations and assistance in treatment planning that improved clinician workflow and heightened quality care delivery [7,24].

Given the recent focus on AI and machine learning in medicine, a few participants proposed the use of AI predictive features to alert clinicians to relevant medical information, such as medication contraindications and patients in need of more individualized care. In recent studies, AI, natural language processing, and machine learning algorithms were found to increase the accuracy of clinical decision support systems in areas ranging from identifying at-risk patients requiring regular ophthalmology visits to facilitating laboratory diagnostics that account for patients' medical histories [25-27]. If implemented, some studies emphasized that alert systems apply customizable alert filtration schemes that tailor to the specific, clinically relevant needs of the clinician to limit the number of low-value alerts that contribute to alert fatigue [6-8,28,29]. These predictive features may also reduce clinicians' cognitive load and increase clinical task efficiency by reducing time spent searching for medically relevant information [27]. Effectively implementing predictive features could help detect clinicians' latent needs and improve patient safety through increases in diagnostic accuracy [30,31]. This will undoubtedly play an important role in the future. Overall, improvements to POCI resources and their integration with the EHR may have positive downstream effects on task efficiency by decreasing the number of actions performed to reach a desired outcome, resulting in enhancements to the clinician work experience by reducing time spent seeking information and increasing time delivering quality care [8,32].

Limitations

First, this study was limited to a small sample of clinicians with previous experience using POCI resources at the same academic medical institution. However, we were able to recruit a range of clinician types with a variety of experiences in the clinical setting to provide perspectives on the use of POCI resources and their integration with EHRs. Second, the insights and recommendations provided may not be generalizable to all clinical settings and clinicians' experiences, which may differ according to several factors, including the availability of health IT, geographic location, access to resources, and clinical experience. It is important that future studies account for a wide range of clinicians' perspectives on updates to POCI resources and EHRs to identify opportunities for improvement and workflow considerations that benefit clinicians' experiences in clinical settings and their ability to effectively care for their patients. Future research must also be conducted across a wider range of clinical settings and geographic locations to account for differences in access to and experience with health IT.

Conclusions

We evaluated the preferred features and uses of POCI resources of clinicians as well as their attitudes toward integration with the EHR. Clinicians had strong preferences for POCI resources that were comprehensive, user-friendly, and allowed them quick access to medication- and disease-related information. Suggestions for integration included optimizing EHR usability to improve workflow efficiency by reducing time spent navigating resources and searching for relevant clinical information. Novel advancements in AI and machine learning could also be incorporated into the EHR to assist clinicians with identifying risk factors, including adverse events, which could impact patient health outcomes. This study demonstrated that including clinician input in the development of clinical decision support and health IT is key to ensuring that clinical workflow needs can be met to improve both the clinician and patient experience in medical settings.

Acknowledgments

This work has been supported by International Business Machines (IBM) Watson Health, now known as Merative (Cambridge, Massachusetts, the United States), which was not involved in any of the interviews, data analysis, data interpretation, or manuscript preparation. Generative artificial intelligence was not used for any part of this study.

Data Availability

The datasets generated or analyzed during this study are available from the corresponding authors on reasonable request.

Authors' Contributions

MM was responsible for data curation, formal analysis, visualization, writing the original draft, and reviewing and editing the manuscript. SD was responsible for investigation, data curation, formal analysis, visualization, writing the original draft, and reviewing and editing the manuscript. JC was responsible for conceptualization and reviewing and editing the manuscript. PMG was responsible for the methodology and reviewing and editing the manuscript. MGA was responsible for conceptualization and reviewing and editing the manuscript. DLS was responsible for conceptualization and reviewing and editing the manuscript. LAV

XSL•FO
RenderX

was responsible for project administration and reviewing and editing the manuscript. GPJ was responsible for conceptualization and reviewing and editing the manuscript. DWB was responsible for funding acquisition, supervision, and reviewing and editing the manuscript. RR was responsible for methodology, supervision, writing the original draft, and reviewing and editing the manuscript. AS was responsible for methodology, supervision, writing the original draft, and reviewing and editing the manuscript.

Conflicts of Interest

MM, SD, PMG, MGA, DLS, LAV, DWB, RR, and AS received salary support from grants funded by International Business Machines (IBM) Watson Health. GPJ was employed by IBM Watson Health and is employed by Intuitive Surgical; her compensation from both IBM and Intuitive Surgical includes salary and equity. DWB also reports, outside the submitted work, grants and personal fees from EarlySense, personal fees from Center for Digital Innovation (CDI) Negev, equity from Valera Health, equity from Clew, equity from MDClone, personal fees and equity from AESOP Technology, personal fees and equity from Feelbetter, and equity from Guided Clinical Solutions. RR reports holding equity in Hospitech Respiration, Tri.o Medical, AEYE Health, RxE2, OtheReality, and Medyx.ai, all of which are unrelated to this project. He is also receiving research funding from Telem, Calosense Health, Breath of Health, and BriefCam; these are unrelated to this project. All other authors declare no conflicts of interest.

Multimedia Appendix 1
Semistructured interview guide.
[DOCX File , 38 KB - medinform_v13i1e60191_app1.docx]

Multimedia Appendix 2
Barriers to using web-based information resources in current practice with frequencies (number of participants who mentioned these barriers) and examples reported by study participants (N=10).
[DOCX File , 21 KB - medinform_v13i1e60191_app2.docx]

References

1. Bradley-Ridout G, Nekolaichuk E, Jamieson T, Jones C, Morson N, Chuang R, et al. UpToDate versus DynaMed: a cross-sectional study comparing the speed and accuracy of two point-of-care information tools. J Med Libr Assoc 2021 Jul 01;109(3):382-387 [FREE Full text] [doi: 10.5195/jmla.2021.1176] [Medline: 34629966]
2. Rui A, Garabedian PM, Marceau M, Syrowatka A, Volk LA, Edrees HH, et al. Performance of a web-based reference database with natural language searching capabilities: usability evaluation of DynaMed and Micromedex with Watson. JMIR Hum Factors 2023 Apr 17;10:e43960 [FREE Full text] [doi: 10.2196/43960] [Medline: 37067858]
3. Wasserman RL, Seger DL, Amato MG, Co Z, Mugal A, Rui A, et al. Straight to the point: evaluation of a Point of Care Information (POCI) resource in answering disease-related questions. J Med Libr Assoc 2024 Jan 16;112(1):13-21 [FREE Full text] [doi: 10.5195/jmla.2024.1770] [Medline: 38911524]
4. Kwag KH, González-Lorenzo M, Banzi R, Bonovas S, Moja L. Providing doctors with high-quality information: an updated evaluation of web-based point-of-care information summaries. J Med Internet Res 2016 Jan 19;18(1):e15 [FREE Full text] [doi: 10.2196/jmir.5234] [Medline: 26786976]
5. Green ML, Ruff TR. Why do residents fail to answer their clinical questions? A qualitative study of barriers to practicing evidence-based medicine. Acad Med 2005 Feb;80(2):176-182. [doi: 10.1097/00001888-200502000-00016] [Medline: 15671325]
6. Sutton RT, Pincock D, Baumgart DC, Sadowski DC, Fedorak RN, Kroeker KI. An overview of clinical decision support systems: benefits, risks, and strategies for success. NPJ Digit Med 2020;3:17 [FREE Full text] [doi: 10.1038/s41746-020-0221-y] [Medline: 32047862]
7. Alexiuk M, Elgubtan H, Tangri N. Clinical decision support tools in the electronic medical record. Kidney Int Rep 2024 Jan;9(1):29-38 [FREE Full text] [doi: 10.1016/j.ekir.2023.10.019] [Medline: 38312784]
8. Laing S, Mercer J. Improved preventive care clinical decision-making efficiency: leveraging a point-of-care clinical decision support system. BMC Med Inform Decis Mak 2021 Nov 11;21(1):315 [FREE Full text] [doi: 10.1186/s12911-021-01675-8] [Medline: 34763691]
9. DynaMed® and Micromedex® with Watson™ is now DynaMedex™. EBSCO Information Services. URL: https://www.ebsco.com/news-center/press-releases/dynamed-and-micromedex-watson-now-dynamedex [accessed 2024-04-30]
10. Jensen K. Three ways DynaMed® and Micromedex® with Watson™ - supports value-based care. EBSCO Information Services. URL: https://www.ebsco.com/blogs/health-notes/three-ways-dynamed-and-micromedex-with-watson-supports-value-based-care [accessed 2024-04-30]
11. Hsieh HF, Shannon SE. Three approaches to qualitative content analysis. Qual Health Res 2005 Nov;15(9):1277-1288. [doi: 10.1177/1049732305276687] [Medline: 16204405]
12. Braun V, Clarke V. Toward good practice in thematic analysis: avoiding common problems and be(com)ing a researcher. Int J Transgend Health 2023;24(1):1-6 [FREE Full text] [doi: 10.1080/26895269.2022.2129597] [Medline: 36713144]

XSL•FO
RenderX

13. Hennink M, Kaiser BN. Sample sizes for saturation in qualitative research: a systematic review of empirical tests. Soc Sci Med 2022 Jan;292:114523 [FREE Full text] [doi: 10.1016/j.socscimed.2021.114523] [Medline: 34785096]
14. Panteli D, Legido-Quigley H, Reichebner C, Ollenschläger G, Schäfer C, Busse R. Clinical practice guidelines as a quality strategy: characteristics, effectiveness and implementation of different strategies. National Library of Medicine. 2019. URL: https://www.ncbi.nlm.nih.gov/books/NBK549283/ [accessed 2024-04-30]
15. DynaMed. EBSCO Information System. URL: https://www.ebsco.com/clinical-decisions/dynamed-solutions/dynamed [accessed 2024-04-30]
16. O'Donnell J, Vogenberg FR. Policies and procedures: enhancing pharmacy practice and limiting risk. P T 2012 Jun;37(6):341-344 [FREE Full text] [Medline: 22876095]
17. Lexicomp is now UpToDate lexidrug. Wolters Kluwer. URL: https://www.wolterskluwer.com/en/solutions/uptodate/enterprise/lexidrug [accessed 2024-04-30]
18. Tell me about Medscape. Medscape. URL: https://help.medscape.com/hc/en-us/articles/360001482192-Tell-me-about-Medscape [accessed 2024-04-30]
19. Comprehensive clinical decision support. Merative. URL: https://www.merative.com/clinical-decision-support [accessed 2024-04-30]
20. Khare R, Leaman R, Lu Z. Accessing biomedical literature in the current information landscape. Methods Mol Biol 2014;1159:11-31 [FREE Full text] [doi: 10.1007/978-1-4939-0709-0_2] [Medline: 24788259]
21. UpToDate: trusted, evidence-based solutions for modern healthcare. Wolters Kluwer. URL: https://www.wolterskluwer.com/en/solutions/uptodate [accessed 2024-04-30]
22. Jones EK, Banks A, Melton GB, Porta CM, Tignanelli CJ. Barriers to and facilitators for acceptance of comprehensive clinical decision support system-driven care maps for patients with thoracic trauma: interview study among health care providers and nurses. JMIR Hum Factors 2022 Mar 16;9(1):e29019 [FREE Full text] [doi: 10.2196/29019] [Medline: 35293873]
23. Lee M, Lin X, Chai JZ, Lee ES, Smith H, Tudor Car L. Smartphone apps for point-of-care information summaries: systematic assessment of the quality and content. BMJ Evid Based Med 2023 Oct;28(5):320-327. [doi: 10.1136/bmjebm-2022-112146] [Medline: 36922021]
24. Patel DM, Churilla BM, Thiessen-Philbrook H, Sang Y, Grams ME, Parikh CR, et al. Implementation of the kidney failure risk equation in a United States nephrology clinic. Kidney Int Rep 2023 Dec;8(12):2665-2676 [FREE Full text] [doi: 10.1016/j.ekir.2023.09.001] [Medline: 38106577]
25. Young JA, Chang CW, Scales CW, Menon SV, Holy CE, Blackie CA. Machine learning methods using artificial intelligence deployed on electronic health record data for identification and referral of at-risk patients from primary care physicians to eye care specialists: retrospective, case-controlled study. JMIR AI 2024 Mar 12;3:e48295 [FREE Full text] [doi: 10.2196/48295] [Medline: 38875582]
26. Szumilas D, Ochmann A, Zięba K, Bartoszewicz B, Kubrak A, Makuch S, et al. Evaluation of AI-driven labtest checker for diagnostic accuracy and safety: prospective cohort study. JMIR Med Inform 2024 Aug 14;12:e57162 [FREE Full text] [doi: 10.2196/57162] [Medline: 39149851]
27. Park EH, Watson HI, Mehendale FV, O'Neil AQ, Clinical Evaluators. Evaluating the impact on clinical task efficiency of a natural language processing algorithm for searching medical documents: prospective crossover study. JMIR Med Inform 2022 Oct 26;10(10):e39616 [FREE Full text] [doi: 10.2196/39616] [Medline: 36287591]
28. Lee EK, Mejia AF, Senior T, Jose J. Improving patient safety through medical alert management: an automated decision tool to reduce alert fatigue. AMIA Annu Symp Proc 2010 Nov 13;2010:417-421 [FREE Full text] [Medline: 21347012]
29. Krall MA, Sittig DF. Clinician's assessments of outpatient electronic medical record alert and reminder usability and usefulness requirements. Proc AMIA Symp 2002:400-404 [FREE Full text] [Medline: 12463855]
30. Bates DW, Kuperman GJ, Wang S, Gandhi T, Kittler A, Volk L, et al. Ten commandments for effective clinical decision support: making the practice of evidence-based medicine a reality. J Am Med Inform Assoc 2003;10(6):523-530 [FREE Full text] [doi: 10.1197/jamia.M1370] [Medline: 12925543]
31. Tao L, Zhang C, Zeng L, Zhu S, Li N, Li W, et al. Accuracy and effects of clinical decision support systems integrated with BMJ best practice-aided diagnosis: interrupted time series study. JMIR Med Inform 2020 Jan 20;8(1):e16912 [FREE Full text] [doi: 10.2196/16912] [Medline: 31958069]
32. Gardner RL, Cooper E, Haskell J, Harris DA, Poplau S, Kroth PJ, et al. Physician stress and burnout: the impact of health information technology. J Am Med Inform Assoc 2019 Feb 01;26(2):106-114 [FREE Full text] [doi: 10.1093/jamia/ocy145] [Medline: 30517663]

Abbreviations

AI: artificial intelligence
BWH: Brigham and Women's Hospital
CME: continuing medical education
EHR: electronic health record

XSL•FO
RenderX

PA: physician assistant
POCI: point-of-care information

Edited by A Coristine; submitted 06.05.24; peer-reviewed by M Popovic, S Markham, UM Kinnunen; comments to author 08.09.24; revised version received 22.01.25; accepted 18.04.25; published 26.05.25.

Please cite as:
Marceau M, Dulgarian S, Cambre J, Garabedian PM, Amato MG, Seger DL, Volk LA, Jackson GP, Bates DW, Rozenblum R, Syrowatka A
Clinician Attitudes and Perceptions of Point-of-Care Information Resources and Their Integration Into Electronic Health Records: Qualitative Interview Study
JMIR Med Inform 2025;13:e60191
URL: https://medinform.jmir.org/2025/1/e60191
doi:10.2196/60191
PMID:

©Marlika Marceau, Sevan Dulgarian, Jacob Cambre, Pamela M Garabedian, Mary G Amato, Diane L Seger, Lynn A Volk, Gretchen Purcell Jackson, David W Bates, Ronen Rozenblum, Ania Syrowatka. Originally published in JMIR Medical Informatics (https://medinform.jmir.org), 26.05.2025. This is an open-access article distributed under the terms of the Creative Commons Attribution License (https://creativecommons.org/licenses/by/4.0/), which permits unrestricted use, distribution, and reproduction in any medium, provided the original work, first published in JMIR Medical Informatics, is properly cited. The complete bibliographic information, a link to the original publication on https://medinform.jmir.org/, as well as this copyright and license information must be included.

XSL•FO
RenderX

Original Paper

Service Users' Perspectives on an Integrated Electronic Care Record in Mental Health Care: Qualitative Vignette and Interview Study

Timothy Kariotis[1,2], BA, BNutrSc, BSocSc, MPH, MBA, MHCM; Megan Prictor[2,3], LLB, PhD; Kathleen Gray[3], MLibSc, MEnvSc, PhD; Shanton Chang[1], BCom, PhD

[1]Faculty of Engineering and Information Technology, University of Melbourne, Carlton, Australia

[2]Melbourne Law School, University of Melbourne, Carlton, Australia

[3]Centre for Digital Transformation of Health, University of Melbourne, Parkville, Australia

Corresponding Author:
Timothy Kariotis, BA, BNutrSc, BSocSc, MPH, MBA, MHCM
Faculty of Engineering and Information Technology, University of Melbourne
700 Swanston St
Carlton, 3053
Australia
Phone: 61 488300223
Email: tkariotis@student.unimelb.edu.au

Abstract

Background: There have been suggestions that electronic health records (EHRs) should be expanded beyond clinical mental health care services to a broader array of care services that support mental health service users, which we call an integrated electronic care record (IECR). Previous research has considered service users' general views on information being stored and shared via an EHR. However, little consideration has been given to service users' attitudes toward how EHRs should be used in the provision of care or the concept of an IECR.

Objective: This study aimed to understand mental health care service users' perspectives on an IECR and how it should be used in practice when receiving care.

Methods: Ten people with lived experience of accessing multiple services in Australia's mental health care system were provided with 2 vignettes that depicted fictional service users making decisions about an IECR. Participants were asked to respond to several scenarios that the fictional service users might experience in their journey through the mental health care system with an IECR. Participants provided written responses and took part in a semistructured interview to discuss their responses. An interpretative phenomenological analysis was undertaken, which led to 5 major themes and 15 subthemes being developed.

Results: Service users wanted an IECR that they had control over, supported them as equal partners in their care, and contributed toward more collaborative and proactive mental health care. However, participants were concerned that care professionals' perspectives would be privileged in the IECR and overshadow service users' needs. Participants also had concerns that stigmatizing and discriminatory information documented in their IECR would negatively impact their interactions with the mental health care system and their access to care. Participants saw value in an IECR bringing together information to support collaborative and proactive care. However, participants thought that the benefits of the IECR had to be balanced with potential risks to their privacy. Participants thought that the IECR should contain only information relevant to their care and should be shared only with relevant care professionals. There were concerns that service users might lack the skills, resources, and information required to manage their IECR.

Conclusions: An IECR has the potential to fill the gaps in an increasingly complex and fragmented mental health care system but risks entrenching service users' experiences of stigma and discrimination unless service users are meaningfully involved in their IECR.

(JMIR Med Inform 2025;13:e64162) doi:10.2196/64162

XSL•FO
RenderX

KEYWORDS

electronic health record; mental health care; qualitative vignettes; mental health; social care; qualitative study; user perspectives; health care; Australia; semistructured interview; service user; stigma; health record; patient portal

Introduction

Background

Electronic health records (EHRs) are increasingly adopted in mental health care services to improve information collection, sharing, and use [1]. EHRs promise more integrated and connected care [2-4], especially when they enable information sharing across different care services. EHRs may be especially promising in the mental health care system due to the complex array of services that service users access [5]. Recent attention has turned to how EHRs may enable information to be shared beyond clinical services to include the various social and community care services that people with mental health conditions access [1,6,7]. However, care professionals have raised numerous concerns about the adoption of EHRs in mental health care contexts, including how sensitive information should be documented and the impact of EHRs on the therapeutic relationship [2]. Most of the available research involving service users has focused on their general attitudes toward the electronic storage and sharing of their health data [3], especially secondary uses of EHR data [4]. There has been limited research on service users' attitudes toward how EHRs should be used in the provision of mental health care, especially EHRs accessible by multiple types of care professionals. We sought to explore service users' perspectives on how an integrated EHR, which would include clinical and social and community care services, could be used in their care.

Information and how it is managed is critical to modern health care, with the health record being central to providing quality care [5]. Information is managed through a range of information practices of both service users and care professionals, including disclosing, documenting, seeking, and sharing information [8]. The health record plays a key role in these information practices, including enabling communication among care professionals, providing a central source of information about a service user, and acting as an informal workspace [9]. Increasingly, health records are being replaced by EHRs, many of which can be accessed by multiple care professionals and service users [10,11]. Because EHRs are used mainly by care professionals, their experience and needs have been the primary focus of research in the design of EHRs [12-14]. However, there is increasing recognition of how EHRs shape service users' experiences of care and the need to design EHRs that contribute toward person-centered care [13,15].

Integrated Electronic Care Record

EHR is a broad umbrella term that captures a range of technologies used to collect, manage, and share information about service users [16,17]. Generally, an EHR is an electronic record of patient information that is accessible by care professionals within or across health services. Some EHRs provide service users with access via a patient portal. An increasing number of EHRs seek to collate information from all treating care professionals rather than from a specific service or type of service [18,19]. For example, Australia's My Health Record is a national summary record that allows any treating clinician to access and contribute information. However, EHRs tend to be limited to health care services and exclude many other social and community care services that play a critical role in mental health care [20].

There is increasing recognition of the need to improve information sharing between all the services that contribute to people's care, not just those in the health care system [21,22]. In Australia, a recent Royal Commission into Victoria's mental health care system recommended establishing a state-wide Electronic Mental Health and Wellbeing Record and a Mental Health Information and Data Exchange to facilitate information sharing between all services that contribute to people's mental health and well-being [23]. This is similar to a recommendation made by the Australian National Mental Health Commission [24] in 2014 that there was a need for an EHR accessible by services beyond the health care system. In this study, the term *integrated electronic care record* (IECR) is used to capture this concept of a digital record that all care services can contribute to and access regardless of whether they are within or outside the traditional health care system.

Experiences of EHRs in Mental Health Contexts

Care professionals have raised concerns that EHRs will impact the therapeutic relationship and how sensitive information is documented [25]. The concerns regarding the therapeutic relationship relate to how an EHR might impact communication between service users and care professionals [13]. For example, studies exploring the adoption of EHRs have found that they can act as a barrier to communication in clinical encounters [26]. The issue of documenting sensitive information is related to whether such information is appropriate for other health care professionals to view, the perceived risk of sensitive information being shared too widely, and the risk of service users experiencing an adverse reaction when accessing their EHR [2,27].

There is limited research on mental health service users' attitudes toward EHRs. A recent scoping review of EHRs in mental health contexts found that 10% (4/40) of the studies included a service user perspective. A service user perspective is important because they have different views compared to care professionals regarding how EHRs should be used in mental health care [28]. Previous research has focused on mental health service users' general attitudes toward the storage and sharing of mental health information via an EHR and electronic health information exchange more generally [3,4,29]. In comparison, research with care professionals has focused on how an EHR is used in practice [25]. Because mental health care involves various sensitive information practices, such as people sharing a range of sensitive and potentially stigmatizing information [30,31], and service users may experience stigma from health professionals [32], the increased availability of information via an EHR may be concerning for service users. There is evidence

XSL•FO
RenderX

suggesting that EHRs may affect service users' decisions to disclose information to care professionals due to privacy and security concerns [33]. However, at the same time, service users may be more likely to want their information shared if they see a practical benefit for their care [3].

We aimed to understand mental health care service users' perspectives regarding an IECR and how it should be used in practice when receiving care and to answer the following questions: (1) on the basis of service users' experience of the mental health care system, how do they think an IECR would be used in their care? (2) If an IECR were implemented in mental health care contexts, how would service users want it used in their care?

Note on Terminology

In this paper, we use the term *care professional* to capture everyone who provides care across the health, mental health, and social and community care systems.

We specifically chose to use the term *service user* rather than terms such as *patient*, *consumer*, or *person*. We acknowledge that each of these terms comes with certain assumptions. For this study, *service users* best captured our intention to focus on people actively engaging with the mental health care system.

Methods

We used qualitative vignettes and semistructured interviews to answer the research questions by exploring service users' attitudes toward an IECR. We were informed by the Critical Appraisal Skills Programme's checklist [34] for qualitative research.

Context

Australia's mental health care system is split across several systems and levels of government [35]. Primary health care, including general practitioners and psychologists, are private services that service users receive rebates to access through the federally funded Medicare system. Secondary mental health services, including community mental health care, are funded by state and territory governments. Another critical source of care is the National Disability Insurance Scheme (NDIS), which provides funding for disability support services, including psychosocial support, and sits separately from the health and mental health care system. Other support services such as housing and homelessness services, drug and alcohol services, and community support are provided by the state, territory, and local governments.

Study Design

We used a qualitative vignette method to answer the research questions. Vignettes are short stories or scenarios involving a fictional individual, which can be used to explore participants' perspectives on specific scenarios [36,37]. Qualitative vignettes include concrete examples of people, behaviors, and systems and can provide the opportunity to explore people's interpretation of specific scenarios and sensitive issues or cases in which subjective judgment is required [36,37]. There are various approaches to how participants respond to vignettes [36]. In this study, participants were asked to consider the advice that they would provide to a fictional character in the vignette based on their own lived experience. Vignettes have been used in other studies to explore service users' attitudes toward and perceptions of EHRs [38].

Ethical Considerations

The University of Melbourne Human Research Ethics Committee approved this study under application 13697. Participants were emailed details of the study, including a plain-language statement and consent form. Participants were compensated for their time with an AUD $80 (US $51.51) gift card. Written responses, interview recordings, and transcripts were assigned a number, and all identifying information was removed.

Study Instruments

Two vignettes were developed involving fictional characters and situations designed to reflect common experiences identified in the literature and our previous research on service users' experience of the mental health care system. Central to the vignettes was the concept of an IECR, with the vignettes including a 1-paragraph description of the IECR (Textbox 1). The description of the IECR was purposefully short to encourage participants to ask questions and identify issues that they would need to consider if an IECR was implemented. A similar approach is taken in the use of technology probes in human-computer interaction research, which are minimally designed to explore how participants see this technology fitting into their lives [39]. Two narratives presented different contextual factors that may resonate more with certain participants. The vignettes and questions are provided in Multimedia Appendix 1, with the key differences outlined in Textbox 2. Participants were provided with a written and audio version of the vignettes and questions that they were asked to provide written responses to before taking part in a semistructured interview. The written responses and interviews were used as a form of triangulation to support the credibility of the results. Participants who struggled to provide written responses to the vignettes were invited to read and respond to the vignettes and questions during the interview.

The interview schedule included 3 sections. First, participants were asked to give their general reflections on the vignettes. Second, specific follow-up questions were asked based on their written responses. The follow-up questions focused on answers in which participants had made assumptions, asked questions, or provided limited detail. Third, general questions were asked about some of the themes identified in the previous literature and in the introduction to this paper regarding how stigma and the retelling of their story should be managed in the context of an IECR.

XSL•FO
RenderX

Textbox 1. Description of the integrated electronic care record in the vignettes.

Jona

Recently, Jona's general practitioner told him that they had adopted an "Integrated Electronic Care Record (IECR)." This IECR would allow all the services Jona accesses—the GP, homelessness service, psychiatrist, and pharmacist—to access and share information online through a secure internet site. Jona would also be able to access his IECR and the information on it, as well as being able to record information on his record and upload information from personal devices. Services would only need verbal consent from Jona to upload or access information in the record. The GP says that the record could include Jona's medication record, housing history, consultation notes, test results, and referral letters. Jona's GP asks him if he would be happy to agree to have an IECR.

Riley

Recently, Riley was told by her psychiatrist that an "Integrated Electronic Care Record" (IECR) was being implemented and that she would receive one unless she chose to "opt-out." The record would allow all her service providers to view her health record and share information electronically. It would also allow Riley to access her IECR and the information on it. Riley would also be able to record information on her record and upload information from personal devices. The psychiatrist says that the record could include Riley's medication record, consultation notes, test results, and referral letters.

Textbox 2. Summary of the vignettes.

Story 1: Jona

- Opt-in integrated electronic care record (IECR)
- Lives in an urban area
- History of living interstate
- Diagnosed first with schizophrenia and then with borderline personality disorder (BPD)
- Experience of homelessness
- Accesses welfare payments
- No family support and limited social network
- Involuntarily admitted to an inpatient psychiatric ward
- Accesses the National Disability Insurance Scheme

Story 2: Riley

- Opt-out IECR
- Lives in a rural area
- Diagnosis of BPD
- Close family support
- Comorbidity of type 1 diabetes
- Voluntarily admitted to an inpatient psychiatric ward
- Experience of substance use issues

Recruitment and Participants

Our primary population of interest was people with mental health conditions that require them to access a range of health care, mental health care, and social and community care services. This framing may appear broad, but we wanted to avoid specifying a set of diagnoses that we may assume correlate with complexity (eg, so-called severe mental illness) but that people may not identify with and may risk alienating participants. Instead, we chose to focus on the experience of accessing multiple services as it is this experience that an IECR would seek to improve.

Participants were recruited through 2 approaches. First, service users who had participated in our previous research and had consented to be contacted about future research were emailed with details of the study. Second, the study details were circulated to mental health care organizations that included service user advisory groups. The reason for inviting previous participants and service users with experience in advisory roles was due to the effort required to read and respond to the vignettes and to minimize the risk of distress among participants sharing their experiences.

We planned to recruit and analyze data iteratively until we reached data saturation, where similar concepts were reoccurring in the data analysis. We expected that we would reach saturation with fewer participants using the chosen methodology than using other qualitative methods given that all participants responded to the same vignettes. Through our iterative analysis of the interviews, we used an online whiteboard to cluster the codes and concepts from each interview. We determined that

XSL•FO
RenderX

saturation had been reached when no new unique clusters of codes were identified.

Ten participants expressed an interest in taking part in this study, and all were recruited to participate. Of those 10 participants, 7 provided written answers to the vignettes before taking part in an interview, whereas 3 provided verbal answers to the vignettes during their interviews. The interviews with the participants who did not complete the prewritten activity were generally longer as the interviewer had to explain the scenarios and the questions. We chose not to collect demographic details of our participants given that our research did not intend to consider how demographics might relate to the qualitative themes. The participants all had a mental health condition and experience accessing a range of care services.

Analysis

All interviews were transcribed with the support of automated transcription software [40]. We used the inductive interpretative phenomenological analysis methodology from Smith et al [41] to analyze the data from the interviews and written responses. Interpretative phenomenological analysis is a methodology useful in understanding how people's lived experience shapes their experiences of situations [42]. The first author read each transcript and the associated written response and performed in-line coding using the comment function within a word processor. The research team each coded a subset of the transcripts and discussed their coding decisions to determine the breadth of potential codes. These codes were compiled and organized to identify common clusters of codes within each transcript. Codes and clusters from each participant were uploaded to an online whiteboard and clustered into common groups. These groups were compared with the coding and clusters developed for each participant and discussed among the research team to ensure that each participant's data were appropriately reflected in the groupings. The research team discussed these clusters until they reached a consensus on how to determine the appropriate delineation and naming of themes and subthemes.

Results

Thematic Results

The analysis led to the development of 5 major themes and 15 subthemes, which are outlined in Table 1. These themes were framed based on the participants' attitudes toward how an IECR *should* be used in their care. However, at the same time, the substance of each theme also reflects how participants expected an IECR *would* be used, based on their experience within the mental health care system. Further illustrative quotes are provided in Multimedia Appendix 2.

Table 1. Outline of themes and subthemes.

Theme	Subthemes
Service users have agency and control over their IECR[a] (theme 1).	• Care professionals minimize the use of the IECR during inpatient stays (subtheme 1.1). • Service users can establish a trusting relationship with care professionals before their IECR is used (subtheme 1.2). • Service users can see how their IECR is accessed and used (subtheme 1.3). • Service users have control, through informed consent, over who can access their IECR (subtheme 1.4). • Service users have control over what information in the IECR is available to different care professionals (subtheme 1.5).
Service users' perspectives, needs, and voice are included in what is documented in the IECR (theme 2).	• Stigmatizing or discriminatory information is not documented in the IECR (subtheme 2.1). • Information in the IECR supports rather than overrides the service user's needs (subtheme 2.2). • Service users can contribute and shape the information in their IECR (subtheme 2.3).
The IECR brings together an accurate record of relevant information about the service user (theme 3).	• Care professionals document information in the IECR that balances the need for care and the risk to service users' privacy (subtheme 3.1). • The IECR is a reliable and accurate record according to the service user (subtheme 3.2).
Service users are empowered to confidently use their IECR (theme 4).	• Service users receive detailed information about their IECR (subtheme 4.1). • Service users are supported to use their IECR (subtheme 4.2).
Care professionals use the IECR to proactively support and coordinate care across all services (theme 5).	• The IECR supports collaborative and integrated care across all services (subtheme 5.1). • The IECR supports more proactive care and feedback loops between services (subtheme 5.2). • The IECR supports service users in retelling their story (subtheme 5.3).

[a]IECR: integrated electronic care record.

XSL•FO
RenderX

Theme 1: Service Users Have Agency and Control Over Their IECR

Overview

Participants thought that service users should be able to manage who can access their IECR and what information they can view and that this required well-designed consent options that provided service users with explicit control over their IECR. The issue of consent was complicated when considering inpatient admissions and the level of agency that service users maintained during periods of acute symptoms. Participants thought that access to the IECR should be based on a trusting relationship between the service user and the care professional. However, in a time- and resource-limited care system, there may be limited opportunities to develop this trust before care professionals need access to a service user's IECR. In reflecting on how service user autonomy could already be circumvented in the mental health care system, some participants were concerned with how an IECR may be used in such situations. For example, one participant reflected on the fact that, in some circumstances, people with a diagnosis of schizophrenia could lose agency over their finances.

Subtheme 1.1: Care Professionals Minimize the Use of the IECR During Inpatient Stays

A question in both vignettes prompted participants to consider how the IECR should be managed in voluntary and involuntary inpatient care scenarios. Five participants thought that access to the IECR should be limited during inpatient care to reduce any distress that service users may experience knowing that their IECR is being accessed, especially without their consent. Participants acknowledged that the information in the IECR could benefit service users' inpatient care. However, they thought that it should only be accessed with informed consent from the service user or a trusted family member or carer.

> *Because they were involuntarily hospitalised, because they did not have access to their records, so they couldn't check their record and see that they were happy with it, that there was right information on there. If they're not allowed to access their own information, no one should be because that's just—it feels like a human rights violation to me. Like they should be able to access their record whether they're well or not. Either with or without a family member present. But that's their own record and for doctors to be accessing and adding things while that person can't even see what's going on, on that record, that's a big no-no. Talk about trust issues, that's...you can imagine being unwell, having schizophrenia. Having your voices screaming at you from outside of you. Like "they're putting down the wrong medications, they're trying to kill you."...Yeah, like I couldn't imagine how I'd be feeling when other people...could access my records but I was not allowed to. That just—just seems really wrong.* [P3011]

Some participants assumed that, during a voluntary admission, the service user would have access to their IECR, whereas in an involuntary admission, they would not. Participants thought that, if the service user cannot access and manage their IECR during an inpatient stay, which participants assumed would be the case, then no information should be uploaded to their IECR until after they are discharged and with their consent. Some participants considered that information could still be uploaded to the IECR during an inpatient stay but flagged for review by the service user before being made available for other care professionals to view after the admission.

Two participants thought that the record should be accessed and kept up-to-date during inpatient stays to inform the service user's treatment.

Subtheme 1.2: Service Users Can Establish a Trusting Relationship With Care Professionals Before Their IECR Is Used

All participants discussed the role of trust in shaping how service users share information with care professionals, which would also shape service users' perceptions of the IECR. Participants thought that service users would need to meet the care professionals first to ensure that they can establish a rapport and trust before providing them with access to their IECR. An element of building trust related to theme 2 was that care professionals should get to know the service user rather than just making assumptions about them based on their IECR. The need to establish a trusting relationship was contextualized with comments that Jona and Riley from the vignettes might feel frightened and isolated if they moved locations and saw a new care professional. Participants also questioned whether access to the IECR could be revoked if Jona or Riley found that they could not establish trust or rapport with the care professional.

> *It depends who you let see it. I'd really have to trust someone...for instance if you go to a psychologist or psychiatrist, I'd have to have a couple of session with them before I knew that I could trust them. Because you have to build that rapport with them before you can let them and trust them with your information.* [P3030]

Five participants raised the broader issue that service users might not trust the mental health care system or might have developed trust issues from previous life experiences, which may factor into whether they trust the use of an IECR.

Subtheme 1.3: Service Users Can See How Their IECR Is Accessed and Used

Five participants discussed the need for transparency over who accessed their IECR, what organization they were from, and what information they accessed or uploaded. Some participants discussed the current lack of transparency over what information is shared between care professionals. Transparency was also viewed as important for managing their symptoms, such as paranoia over who might be accessing their record. Some participants also thought that there needed to be transparency within care encounters as to whether the care professional had read the record and sensitivity regarding how information in the IECR was raised with the service user.

> *Without them absolutely blurting out, "well I know da-da-da," maybe...their introduction to you should*

XSL•FO
RenderX

be, "I have read your record, is there anything you'd like to talk about?" [P3090]

Subtheme 1.4: Service Users Have Control, Through Informed Consent, Over Who Can Access Their IECR

All participants thought that service users should have control over who can access the IECR and that providing access should be based on informed consent. Participants also questioned whether consent should be continuous (consent is provided for each care professional until the service user revokes it) or episodic (care professionals would have to seek consent each time they wanted to access a service user's IECR). Participants outlined how Jona and Riley should only consider providing consent to care professionals with whom they have a current and ongoing trusting relationship. One participant recommended that the default IECR setting should be to remove access for care professionals whom they have not seen in a while. There were also questions about how nuanced the consent options would be and whether service users could reveal only parts of their record to certain care professionals. The vignettes explicitly stated that verbal consent would be sought from service users for a care professional to access their record. Two participants questioned how their consent would be documented so they had evidence that they had given it. Some participants questioned whether care professionals could share information in the IECR with other care professionals without service user consent.

> *...how could we show whether or not I provided consent if I'm not signing anything?...my concerns are around, like Jona has a couple of diagnoses and experiences that are really quite stigmatised and wanting to make sure that Jona is able to protect himself around—like if he wants to access a service but doesn't want to reveal parts of that...like can I say, my pharmacist can access my scripts, and my mediations, but not my housing information.* [P3020]

In addition to having a thorough and informed consent process, participants thought that consent preferences should be visible to service users so that they can be confident that they are being followed. Participants identified that a potential barrier to informed consent is when service users are unwell or experiencing symptoms that may impact their ability to consider the benefits and risks of providing care professionals with access to their IECR.

Five participants raised queries about family involvement in the IECR, including how much control service users had over family members accessing their IECR. One participant identified that there may be circumstances in which a family member or another support person might need to access Riley's record to support them. Conversely, another participant, in reflecting on Riley's story, considered that, if Riley had a negative relationship with her parents, she might not want to provide access to her family members.

> *If Riley later has children or a violent partner or a toxic employer or family carer or workers compensation claim, how will you ensure her legal rights, privacy, + confidentiality are protected?* [P2050]

Subtheme 1.5: Service Users Have Control Over What Information in the IECR Is Available to Different Care Professionals

In addition to deciding who can access the IECR, 6 participants thought that service users should have control over what information different care professionals can view. One participant outlined how the onus should be on the care professional to justify to the service users the information they need to access in the IECR. Some participants framed this as ensuring that care professionals can only access what is relevant to their care and information that they will use in providing care. Participants also identified factors that service users might consider when determining what information to allow care professionals to access, including whether the information is accurate and up-to-date, whether they are comfortable sharing it with a new care professional, whether it is relevant for that care professional, and the current reason they are accessing care. Some participants also acknowledged that the IECR may include information from difficult periods in a service user's life, which they may not want current care professionals to access.

> *...is there a way for me to block that information...from another service, if I've just had a bad day and yelled at someone because I've been sleeping on the street for three weeks?...if I move out of this difficult period of my life to where I'm flourishing more, does my new pharmacist need to know that I was also accessing homelessness services?* [P3020]

The concept of "relevance" was pervasive across several answers that participants provided as to who should be able to access their IECR and what information they should be able to view. These 2 issues intersected in that relevant information may depend on who is accessing it and in what circumstances. For example, one participant thought that, if Jona gave the NDIS access to their IECR, it should only be for information relevant to supporting their application. This issue of relevance is further explored in theme 3.

Theme 2: Service Users' Perspectives, Needs, and Voice Are Included in What Is Documented in the IECR

Overview

Seven participants were concerned that the IECR would be used as the key source of information in providing care and would override service users' voice and needs. Underlying this concern was the risk that the IECR may only reflect care professionals' view of the service user, which may be outdated, include only negative information, and possibly include stigmatizing or judgmental information. However, 2 participants thought that it would be valuable for their care professional to review the IECR before a session so that they have the most up-to-date information. The risk that the information in the IECR will be prioritized over service users' voice could be managed by including service users' views and needs in the record (subtheme 2.2) and by ensuring the relevance, accuracy, and quality of the information in the IECR (theme 3).

XSL•FO
RenderX

Subtheme 2.1: Stigmatizing or Discriminatory Information Is Not Documented in the IECR

Nine participants raised the risk that an IECR might entrench service users' experiences of stigma, judgment, and discrimination both inside and outside the mental health care system. Participants were concerned that an IECR would allow for a greater reach and permanency of information that might negatively impact the care they receive, including their ability to access care. Several participants were concerned that information in the IECR might "leak" outside the health care system, such as to employers, and would lead to stigma and discrimination in other areas of life. There were also concerns about how certain information in the IECR could lead to the experience of stigma and discrimination within the health care system. For example, some participants were concerned that certain diagnoses being stigmatized, such as borderline personality disorder and also the label "mentally ill," may automatically lead to someone being treated differently by certain care professionals. Some participants discussed how they had opted out of My Health Record due to the risk of their diagnosiare.

> *I purposely was, in some of my answers, pushing the boundaries back of, well, really...why would this be good for Jona or whoever, you know, the person with the condition who's got disadvantage and discrimination happening? Why would this be good for them? I guess I got a flavour from...the scenarios that perhaps certain people and agencies would think an electronic record is a really good idea and that it wouldn't disadvantage...the service user at all. As long as we can maintain security, privacy, confidentiality...they won't be disadvantaged and I think it's a really strong underpinning for me about power and language and, you know...the electronic record is just neutral, right, it could be good or it could be bad for somebody but unless we address the actual disadvantage of Jona having a mental health diagnosis and all the other issues that he was facing...I suspect that an electronic record will disadvantage him...because of the underlying inequity he is facing.* [P3050]

Four participants were concerned that historical information from previous admissions, such as diagnoses and treatments irrelevant to their current care, might lead care professionals to prejudge or overlook their current issues or might impact their access to care. For example, one participant outlined how much of the information documented about them was from when they were at their worst, so future clinicians who access the IECR will only see the negative information that has followed them. This situation may inform a deficit-based rather than a strengths-based approach to care—especially if their strengths and achievements are not documented in the IECR. Another participant shared how their previous eating disorder diagnosis still impacted the care they received today even though they had recovered and no longer met the criteria for an eating disorder diagnosis.

> *Yeah, so I chose not to opt into the My Health Record, because of my history of BPD...after I stopped meeting criteria for borderline disorder, I just straight up don't have that issue anymore, I went to ED because of some intense anxiety...they read borderline, and then I was treated that way, instead of treated for what I was actually presenting for, and that was just in my hospital record. I didn't need other services, like, I don't think my pharmacist needs to know that I used to have a history of borderline.* [P2020]

Participants were also concerned that information relevant in one care context could be perceived negatively or be stigmatizing in another context, especially by care professionals with less knowledge of mental health. For example, one participant discussed how their previous drug use may negatively affect their access to mental health care even though it was a historical issue that they had overcome. This issue relates to whether information is relevant to care professionals, as discussed previously and further in theme 3. Participants suggested that care professionals needed to document information in their IECR in a way that was respectful and balanced, with consideration to how the service user may view the information.

Subtheme 2.2: Information in the IECR Supports Rather Than Overrides the Service User's Needs

Six participants were concerned that care professionals who accessed the IECR would focus on information from other care professionals and not on the service user's perspective. The risk of having information precede service users and shape their care before they can discuss their needs was viewed as entrenching a biomedical model of care in which service users' individual needs are not recognized or are viewed through a diagnostic lens. Furthermore, participants identified a risk that care professionals may not capture the service users' perspectives or voice in the IECR, further amplifying the care professionals' perceptions, ideas, and judgments. Even if the service user could contribute to the IECR, participants were concerned that clinical knowledge would be privileged in the IECR and in how the IECR is used. There were also concerns that the IECR may lead to some health issues, especially physical health issues, being overshadowed by the mental health issues documented in the IECR. Some participants thought that it was important for the service user to be able to tell their story before the care professional accessed their IECR as what is written in the IECR may be framed differently.

> *He would have the very real problem of clinicians not listening to where he is at and what is happening for him, because they are only going on what others have put in his record.* [P3011]

Subtheme 2.3 Service Users Can Contribute and Shape the Information in Their IECR

Although a number of participants thought that it was important for a service user perspective to be included in the IECR, there was less consideration of whether service users should directly add information to their IECR. One participant, when initially asked about the potential for a service user to contribute to their

XSL•FO
RenderX

IECR, thought that it was not necessary or valuable. However, later in the interview, they revisited their response and suggested that it could be valuable to have a service user write up their story. There was also consideration given to the potential for service users to add notes to care professionals' records that put information in their own words or to identify areas in which they disagreed with their care professionals. One participant thought that there was a risk that service users might change their IECR when unwell, which could negatively impact their care.

> *Yeah, because then you've got more input into it. You could say whether you disagree or agree with the doctor. Yeah, I think it'd be good actually. Sometimes doctors are not—like I just said, they don't understand [laughs] that they've said the wrong thing. So, yeah. If you could put little notes there to say I do not understand—I don't agree with the way he's described me, or this was—I don't see it this way or something. That'll be good.* [P3030]

Theme 3: The IECR Brings Together an Accurate Record of Relevant Information About the Service User

Beyond wanting the IECR to recognize service users' perspectives and needs, participants also discussed what information care professionals should include in the IECR. The concept of relevance was central to participants' views on what information an IECR should contain, and it appeared to capture both the need for privacy over certain information and the recognition that information could contribute positively to the care that service users receive.

Subtheme 3.1: Care Professionals Document Information in the IECR That Balances the Need for Care and the Risk to Service Users' Privacy

There was an assumption in the vignettes that the IECR would collate all information about a service user. However, participants were generally supportive of a summary of information being included in the IECR and thought that there should be a standard template or guidance for what should be documented. Participants thought that the information documented in the IECR should be relevant to their care and support future treatment, such as their diagnosis, medication, care plan, evaluation of previous treatment, family medical history, presenting problems, the types of services being accessed, and what participants do to manage their condition. One participant thought that the IECR should not include the personal "chit chat" that might also be shared during the clinical encounter. Participants also discussed that service users would need to determine what to disclose to care professionals that might be uploaded to an IECR and the risks posed by this information being shared. One participant outlined the balance of providing enough information to receive appropriate care but not so much as to create a risk of that information being used against them. For example, it may be appropriate to have information about alcohol and drug counseling in their IECR, but depending on how that information is presented, it could be interpreted in a certain way that does not represent their current needs or presentation.

> *I think it is important to have things like the diagnosis and the types of medication. Maybe just a little bit of what they do outside that helps them with their condition, especially if they have chronic pain and stuff, is there anything they do to help that. Keep it relatively minimal but succinct at the same time, because I just think that clinicians are honestly just—they're so overworked that they don't have time to look through everything. So just keeping it short and sweet and relevant.* [P3080]

Some participants were concerned that incomplete information could create an inaccurate picture of the service user. These participants were not necessarily in favor of everything being documented in the IECR, with one participant, who had concerns with gaps in their IECR, also stating that only relevant information to support treatment and not personal information should be uploaded. Participants also had questions about what would happen to their information if they opted out of the IECR for a period and then opted back in. In general, participants did not consider that the IECR should be a comprehensive record of all the information from the various services they accessed but that the IECR needed to present an accurate picture of the person's needs.

> *...there was another question that I answered stating that if a person opts out and then after six months opts back in, will that record that he had previous be put back on? (Interviewer: Is that important), Oh, yeah, I think so. I think any record is important.* [P2010]

The issue of sensitive information was only explicitly raised by 3 participants and, generally, was considered as not appropriate to document in an IECR. One participant classed their sexuality as potentially sensitive information, whereas another classed their experiences of hallucinations and delusions as sensitive information.

Subtheme 3.2: The IECR Is a Reliable and Accurate Record According to the Service User

One of the scenarios in the case studies was of a care professional watering down information uploaded to the IECR. Three participants were concerned that such a scenario may negatively impact the service user if the IECR does not reflect their care and condition. It was acknowledged that watering down information might be done for a valid reason, such as where information may be triggering for the service user. Participants considered that reducing the level of detail documented should be done in conversation with the service user and for their benefit and that information could be reframed to be shared on the IECR. Watering down information may also impact service users' ability to access other services, such as the NDIS, if those services rely on the IECR to assess eligibility for access to care. One participant outlined that, in such cases, service users should be able to annotate their IECR if information has been omitted, or the care professional should identify when information has been diluted.

XSL•FO
RenderX

> *So, something like that, watering that down...no history of being suicidal there, is there? So that automatically puts my life at risk. Just that one scenario...and there can be a gazillion things that watered down, is a safety hazard for the person in question...* [P3011]

Six participants raised concerns and questions about the management of inaccurate information in the IECR, with some sharing experiences of having inaccurate information recorded in their health record. Participants asked how Jona and Riley could receive support if inaccurate information was uploaded to the IECR and who would be responsible for ensuring that the information was accurate. There were also questions about whether service users could edit inaccurate information or whether care professionals would be required to confirm the accuracy of the IECR with the service user. One participant contrasted the IECR with a referral letter, asking "what's wrong with a referral letter that you give to the patient, and they read and say, oh, yeah, that sounds right but you missed this, or could you write it like this?" (P3050). Participants were also concerned with care professionals introducing their own subjective judgment into the IECR.

> *Also, because...it's done quick and rapid, the chances of an inaccuracy occurring can be high...obviously it impacts their health, it could damage—it could do harm to the client.* [P3010]

Participants thought that the accuracy and relevance of the IECR should be reviewed to ensure that historical information that is not directly relevant to their current care is not available on the IECR. Participants also thought that care professionals should discuss the accuracy and veracity of the record with the service user to identify information from previous encounters that may not present the service user's perspective or needs (theme 3). One participant who had a challenging experience of seeking to have incorrect information in their health record updated thought that service users would lack the time and resources to engage with their IECR to address such issues.

Theme 4: Service Users Are Empowered to Confidently Use Their IECR

Overview

Most participants had limited experience with EHRs. During the interviews, 8 participants identified that they had heard of an EHR, mainly Australia's My Health Record. Of these 8 participants, 1 opted out due to the risk of stigma, 1 noted that they had limited knowledge of My Health Record, and 1 shared that their general practitioner did not upload information to their My Health Record.

Four participants noted that being able to view the IECR could benefit service users by acting as a reference point for their condition, supporting their memory, and facilitating discussions with care professionals. Participants thought that seeing what their care professionals had written would help them engage in conversations about things that they agreed with and areas where they disagreed. There was also an acknowledgment that the digital nature of the IECR could benefit some service users, especially those experiencing homelessness, as they would not have to carry paper documents with them. Some participants thought that the IECR provided an opportunity to check that what was being uploaded to the IECR was correct and would allow them to have conversations with their care professionals about issues that they may not be focusing on or to see what their care professionals thought about them.

> *...if Jona is sleeping rough...Having something electronically, means that you—if it is cloud based, I don't have to keep it with me. So, I don't have to be worried about if it is stolen, and I don't have to be worried about if my bag gets wet when it rains. Like my scripts aren't potentially going to be destroyed, or even if a paper script is destroyed, I can be like, no, really, I have been diagnosed—like I have been prescribed these things and pointing to an electronic option.* [P3020]

Four participants thought that service users might require support when reading their IECR as the content could be distressing and the clinical terminology might be perceived negatively. For example, one participant thought that service users may have an experience of thinking, "is that how they really see me" (P3030).

> *...before the service provider jots information on the record, knowing that the patient will read it, it's important that whatever he jots down as a record, he notifies the patient of, if it's something that may cause fright. For example, a diagnosis of cancer, right, you don't just put it on someone's record unless you've had discussion with that person about it and is informed about it.* [P3010]

Subtheme 4.1: Service Users Receive Detailed Information About Their IECR

Participants actively engaged with the vignettes and spent time considering the benefits and risks of each scenario. Many of the written answers were framed as questions about the IECR. Participants actively considered the trade-offs of different decisions that the vignettes posed, such as whether to opt in or opt out of the IECR. Although some participants were more supportive of or more against the IECR, most saw reasons why someone might opt in or out.

> *Can he trust the benefits outweigh his fears and mistrust? Does he feel more confident to tell medical staff himself or would this be easier? Why can't I or a family member simply tell the doctors? What makes this a better option?* [P3011]

One way in which the case studies differed was whether the IECR had an opt-in or opt-out model. Six participants thought that it was important that service users be actively supported to make an informed choice as to whether to have an IECR. Some participants considered that service users may not have the opportunity to make an informed choice under an opt-out model, especially if they are unwell when they are required to decide whether to opt out. Participants questioned whether service users can opt in or out whenever they want and what happens to their records during periods in which they opt out.

XSL•FO
RenderX

> *Yeah, so one of my questions would be, can I opt out, after I've opted in? Can I—how do I withdraw consent for someone to access it? Those two things would be pretty key for me.* [P2020]

Participants raised broad concerns regarding the privacy, confidentiality, and security of the IECR. Some participants considered that there were many unknown risks of adopting an IECR because it is hard to foresee risks that may arise in the future. Participants raised various comments and questions about the security of the IECR and what would happen in the event of a security breach, referencing that there has been a lot of online information theft recently in Australia. Participants wanted to know what support would be available to service users in the case of a security breach. There were also concerns, which were identified in other themes, of potential breaches of privacy and confidentiality through inappropriate use of and access to the IECR by care professionals. Participants considered that service users would need assurances as to the privacy and security of their IECR so that they can confidently use it without worrying about the potential risks of their data being inappropriately accessed.

> *A breach in the security of IECR could mean serious harm to Riley's health or current employment or her perspective employment.* [P2011]

Some participants thought that service users would require someone such as an advocate to explain the IECR and help them make an informed choice about how it is used. A verbal explanation was considered important as written information could be overwhelming. However, such conversations may not be appropriate for care professionals to provide given the time constraints placed on them to provide such information.

Subtheme 4.2: Service Users Are Supported to Use Their IECR

All participants identified barriers that service users might face when using their IECR. These barriers included the skills needed to manage IECR settings, the resources needed to access the IECR, and the knowledge needed to understand the IECR and the information documented in it. The lack of access to appropriate information technology may limit services users' ability to use their IECR. Participants questioned whether training would be provided to support service users to utilise their IECR. Participants also suggested that the IECR should be easy to use. For example, password management should be simple because service users may struggle to remember passwords. Several participants questioned what support would be provided alongside the IECR to ensure that service users can use it and manage any issues arising from the IECR, such as inappropriate use by care professionals.

> *Firstly the "patient log-in password" should be one easy to remember by the patient and hard to decipher by anyone else foreign to the patient...It should not be shared by anyone.* [P3010]

A couple of participants considered that service users' symptoms may act as a barrier to using and making informed decisions about their IECR and that this would need to be considered in the design of the IECR and the support available to service users. A couple of participants considered that service users may negatively react to what is written in their IECR but that this should be managed by the care professional notifying the service user before uploading information to the IECR.

Although participants considered privacy settings an important component of the IECR, 3 questioned whether all service users would have the skills and knowledge required to use these settings. Participants thought that in-depth information and support would be required to ensure that Jona and Riley could use and understand the implications of the privacy settings of their IECR. There were questions about who Jona and Riley could contact for support and whether they could access free legal advice if there were issues or breaches with their IECR. Participants acknowledged that, in the vignette, Jona used a public computer to access his IECR, which could raise privacy risks for him.

> *I would be very selective with my...privacy...whereas in this situation of the two people in the stories, I don't know if they had enough knowledge and ability to perhaps do that, to work out what amount of privacy they would need.* [P3090]

Theme 5: Care Professionals Use the IECR to Proactively Support and Coordinate Care Across All Services

Overview

Participants discussed how the IECR could support more collaborative and integrated care across various services. Integrating various sources of information in the IECR may also enable more proactive care by providing care professionals with a more holistic picture of service users' needs. One participant thought that the IECR might help them prove their eligibility for other services. However, some participants questioned whether care professionals would use the record or whether they would still have to repeat their information when accessing a service.

Subtheme 5.1: The IECR Supports Collaborative and Integrated Care Across Relevant Services

Six participants considered that the IECR may support more collaborative care by linking the different care professionals supporting service users. It was acknowledged that the IECR may benefit services that are not usually kept informed, such as pharmacists and the NDIS.

> *Having One Record...One File...Electronically kept...and shared by everyone Jona agrees to doing with...is better than having many records scattered everywhere among service providers...better collaboration can occur...an easier / more precise healthcare can be administered.* [P3010]

Although some participants saw benefits in integrating their information via the IECR, 8 were also concerned about the IECR being accessed or information in the IECR being shared with too broad a range of organizations. This concern included whether noncare services such as employers, other government agencies, and the police could access the IECR. Participants also raised the concern that, depending on the policies of

XSL•FO
RenderX

different organizations, providing consent for an individual might allow others within that organization to view their IECR. Different participants usually identified a different list of organizations that they were concerned would access their IECR. One participant framed organizations that should not have access as those that did not have the service user's health as their primary focus. However, one participant considered the NDIS as an inappropriate service to be provided with access to their IECR.

Subtheme 5.2: The IECR Supports More Proactive Care and Feedback Loops Between Services

Four participants thought that care professionals might be more informed about the current needs of service users, including their social needs, by having more services involved in the IECR. For example, one participant thought that, in Jona's story, the IECR may help care professionals identify a risk of social isolation when he moved to a new suburb. Identifying this risk to Jona could prompt care professionals to support Jona in settling into his new community. Including social and community care services was viewed as important by participants because these services tend to have a long-term recovery focus and might see more of the service user over their recovery journey. Participants also identified that bringing together different services on the IECR could support the identification of inconsistencies, inadequacies, or overlaps in care that could, in turn, improve the effectiveness and adequacy of care. Some participants also thought that the IECR might help care professionals link the dots between different pieces of information to identify patterns or other factors, such as socioeconomic factors, that might contribute to their mental health.

> *IECR also might pick up on Jonas "pattern of unwellness," noting that Jona tends to have particular problems at certain times of the year so preventative measures and extra supports could be put in place ahead of time.* [P3011]

Providing a broader range of care professionals with access to the IECR was also viewed as supporting holistic care. For example, one participant thought that having their housing risk assessment and diabetes information in the IECR could better inform other care professionals of their needs.

Subtheme 5.3: The IECR Supports Service Users in Retelling Their Story

Nine participants discussed how the IECR could help bring service users' story together in one place to minimize the need to unnecessarily retell it when accessing new services. Participants thought that the IECR may also make transitions between services easier and provide care professionals with a picture of service users' current needs. Some participants noted that service users need to share a lot of information just to be prioritized when accessing a service, but at the same time, some of this information can be challenging to share. With the appropriate controls in place, the IECR could support service users in sharing their story, and as one participant put it, make sure that it is "translated to clinical speak." The IECR could also act as proof for the service user when sharing information with new care professionals. Participants discussed that, when they are acutely unwell, it can be challenging to remember information and put it in words that care professionals will understand. However, as was outlined in previous themes, there is a balance between the benefits of not having to retell the story and having the IECR override the service user's voice. Some participants were also concerned that care professionals would not read the IECR and they would still be required to retell their story.

> *Yeah, it can get depressive, it can get frustrating, it can get upsetting because you're talking about the past and no one wants to go to the past particularly when it's been related to an unfortunate experience.* [P3010]

Discussion

Principal Findings

Overview

This study sought to explore mental health service users' perspectives on an IECR. The results suggest that service users want to feel empowered to shape the content of their IECR and how it is used. However, participants were concerned that the IECR would likely be used to privilege the perspectives of care professionals, especially if service users were not supported to use their IECR. Participants thought that an IECR could bring together a comprehensive picture of their needs and support more collaborative and proactive care. However, there was also the risk that inaccurate and out-of-date information would overshadow the actual needs of service users or that care professionals would prejudge them based on the information in their IECR. The concept of relevance, including relevant care professionals accessing the IECR and relevant information being uploaded to the IECR, was central to participants' views on how the IECR should be used. The findings of this study provide insights into how IECRs and EHRs should be designed for use in the mental health care context.

There were some contradictions in the findings of this study. For example, participants wanted the IECR to minimize the need for them to retell their story while also not wanting to lose control of how their story is told. Similarly, participants only wanted relevant information in the IECR but were concerned about gaps in their record. One way to understand these contradictions is in the context of Australia's mental health care system, where there is an entrenched power imbalance between service users and the mental health care system that contributes to the disadvantage and marginalization of people with mental health conditions [43,44]. Our findings suggest that participants are concerned that an IECR might entrench many of these existing issues in the mental health care system. In the ideal care system, service users might feel confident relying on an IECR as a complete record of their story. However, in the current mental health care system, the risk of judgment, stigma, poor treatment, and a lack of service user control over their care may underpin a lack of trust in how an IECR would be used.

XSL•FO
RenderX

Risk of Care Professionals Prejudging Service Users Based on Their IECR

Participants were concerned that the IECR would entrench experiences of stigma and discrimination. This finding is not unexpected given the evidence that people with mental health diagnoses experience stigma and discrimination across various health care settings [45,46]. Stigma operates at different levels in the mental health care system, including the structural (eg, discriminatory policy and social structures), interpersonal (eg, prejudice and misinformation), and intrapersonal (eg, negative beliefs about the self) levels [45,47]. Henderson et al [45], in reviewing the evidence on stigma in mental health care settings, found that research has focused on interpersonal stigma, with less consideration being given to how structural stigma may shape interpersonal stigma. There could be an opportunity in the design of EHRs to manage structural stigma by shaping how organizations collect and manage stigmatizing information, which contributes to interpersonal stigma. Addressing stigma is important as it can act as a barrier to help seeking [48]. Grando et al [49] found that stigma was a key reason mental health service users might not consent for care professionals to access their EHR. Service users also anticipate stigma based on their past experiences, which may shape how they interact with care professionals and the information they disclose [46,50]. Some participants in this study anticipated, based on their previous experiences, that the IECR could further entrench stigma and discrimination and that stigmatizing information may follow them via their IECR.

Relevant and Sensitive Information

Participants did not support the IECR being a comprehensive record but rather valued a record that could provide relevant information to relevant care professionals to support their current care needs. This focus on relevance was framed as ensuring that the information available could be used by care professionals to improve their care. This finding supports previous research by Shen et al [3], who, in interviewing mental health service users about their privacy perspectives, found that they were supportive of health information exchange when it would contribute to better care. This finding also reflects modern theories of privacy, such as the theory of privacy as contextual integrity by Nissenbaum [51], which situates people's experiences of privacy within specific contexts. Nissenbaum [51] frames privacy as the *appropriate flow of information in a specific context*. Thus, some information may not raise privacy concerns when shared in some care contexts, but in others, it may be seen as inappropriate. Thus, the context in which the IECR is used will shape what service users may define as relevant to be shared.

These findings also challenge the purpose of the health record. Historically, the health record was a record of the care that someone received, usually within one specific health care setting [9]. Although EHRs are regularly framed as "digitizing" the health care record [52], EHRs introduce fundamentally different information-sharing practices compared to paper health records [25,53]. Currently, if information is shared between services, it is done via a letter, phone call, specific shared care plan, or the service user. In all these cases, the information shared is curated for a specific point in time, for a specific receiver, and usually as an outcome of the service user engaging with a service [53]. This approach to information sharing has been described as "pushing information" to other services [53,54]. In the case of the IECR or Australia's My Health Record, information is "pulled" out of a repository with limited curation by another care professional or the service user for that specific receiver [53,54]. There is a risk that an IECR would become unwieldy due to the amount of information stored in it, which risks becoming quickly out-of-date or irrelevant. It may be more appropriate for an IECR to operate similarly to a shared care plan, which is designed to be used in team-based care for a particular condition and include information relevant to the team and the care they are providing [55].

A comprehensive IECR may also breach modern privacy principles such as data minimization and privacy by design. Privacy by design asserts that the minimum necessary information should be collected for a specific purpose [56]. The challenge with IECRs, as articulated in this study, is defining what is useful or relevant at the point of collection in a complex care system in which the next step in someone's care journey is not always clear. The risk of an IECR is that it goes in the opposite direction of data minimization toward data maximization, which poses practical issues for care professionals trying to find relevant information and privacy issues for service users. Even when EHRs allow service users to place access controls on parts of their record, this may not be feasible when there are large amounts of content in the record.

Managing Sensitive Information

Only some participants in this study raised the issue of how sensitive information is managed. Other studies have found more explicit views on the management of sensitive information. Soni et al [57], in a mixed methods study with behavioral health patients, found that most (76%) participants considered mental health information sensitive and 24% feared stigma and discrimination in relation to their mental health. Participants also reported wanting to restrict the sharing of mental health information in the EHR. Similarly, a survey study by Soni et al [58] found that participants were less willing to share information that they perceived as sensitive. Mental health information was considered the most sensitive, and many participants wanted to restrict access to some or all of this information by care professionals. This study does highlight that service users consider information collected about them during involuntary inpatient treatment as requiring careful consideration before it is made available to other care professionals.

Service User Control and Consent

Consent was a key issue raised by participants, who thought it was important for informed consent to be required before care professionals can access their IECR. However, there are questions as to how consent is managed in cases of involuntary treatment, where service users are deemed to lack the capacity to make decisions about their care. Participants were concerned with how an IECR would be used in such cases and generally were against the IECR being used in involuntary inpatient care. There is growing research on the use of dynamic consent

XSL•FO
RenderX

mechanisms and psychiatric advance care plans that would provide service users with the ability to predetermine their preferences for care when they may be assessed to lack capacity [59]. However, research on psychiatric advance care plans has found low completion rates due to barriers such as service users not understanding the advance care plan, the complexity of completing the forms, and skepticism about their benefit [60,61]. Similarly, care professionals report barriers to using advance care plans due to a lack of access to and time to review documents in a crisis and a lack of training [61]. Research on advance care planning has questioned their ability to improve care when the processes required to establish and use an advance care plan rarely align with the realities of clinical practice [62]. There is a broader question as to whether service users should lose their ability to make decisions about their IECR in inpatient settings. There is recent evidence suggesting that most service users with psychiatric conditions in inpatient care have the capacity to make complex and important decisions about their care [63].

Participants also wanted control over what information certain care professionals could access. Given the findings of this study and others [64], it appears that service users would likely want to hide information that they perceive as sensitive or irrelevant to their care. However, Schwartz et al [65], in a study of how service users manage the privacy functions of their EHR, found that most service users who chose to limit access to their EHR chose to limit access to the entire EHR. This finding may be due to the effort required to restrict access to certain types of information [65]. Further research is required to understand how service users make decisions to use privacy controls and approaches to supporting them in managing their IECR. One approach to addressing this issue is through identifying sensitive information upfront when information is documented and allowing service users to preset conditions for when sensitive information can be accessed. For example, Chivilgina et al [66] found in a qualitative study with psychiatric service users that they wanted care professionals to obtain purpose-related informed consent when documenting sensitive information in their EHR.

Service User Contributions to the IECR

Participants thought that it was important that service users' perspectives were captured in the IECR. However, there were concerns that service users may not have the resources and time to independently add information to their IECR. Approaches such as collaborative documentation may facilitate care professionals working with service users to agree on what should be documented in the IECR [67]. However, the design of EHRs may also actively limit care professionals' ability to capture service users' stories and perspectives. One of the proposed benefits of EHRs is that they improve data quality and enable the collection of structured and standardized data that can be used for other purposes, such as research. Our previous research [25] and that by Varpio et al [68] have found that EHRs that require structured data entry can limit the capturing of narrative information, which may include service user perspectives. Furthermore, Rathert et al [26], in reviewing the literature on EHRs, found that they may limit the documentation of psychosocial and emotional information. Finding ways to capture, share, and use narrative data appears key to ensuring that service users' voices are considered in care encounters when using an IECR.

Participants questioned the level of support that service users would be provided with to access and manage their IECR. There were concerns that service users, including the fictional characters in the vignettes, would lack the skills and knowledge to make informed choices about their IECR. Ensuring the usability of EHRs is an ongoing issue in Australia, with research identifying gaps in the usability of My Health Record, including the educational resources available for service users, which may negatively impact those with low health literacy [69-71]. A notable finding in this study was the importance that participants placed on having support to engage with the privacy functions of the IECR. While existing literature has focused on the availability of privacy functions in EHRs [58,72], participants in this study highlighted the importance of having skills and capabilities to manage these functions, as well as support pathways outside the IECR to address privacy issues.

Inclusion of Social and Community Services

In presenting participants with the concept of an IECR, we purposefully expanded the potential array of care services that could contribute to the health record, which in turn may expand the types of information available. There is growing research on the inclusion of social and behavioral data in health records, with some researchers positing that such information provides broader context to tailor interventions and clinical decisions [73,74]. One of the challenges that has been identified in collecting such information is that service users may perceive it as sensitive and, therefore, not disclose it [75]. Where care professionals record this information, there is a risk that service users may perceive this negatively, especially if the information is viewed as a pejorative assessment of them, such as assessments of their income. What this study found is that service users perceive such information as enabling more proactive care but are concerned as to how broadly their IECR might be shared. This aligns with suggestions in the literature that service users should be engaged as partners in the process of collecting such information, with transparency over how it will be collected and shared [75].

Use of Qualitative Vignettes

The findings suggest that qualitative vignettes are a feasible approach to exploring service users' perspectives on digital health technologies that they have not yet experienced. One potential avenue for future research using this methodology includes exploring story completion methods alongside vignettes to encourage participants to explore ways in which the vignettes might evolve based on different responses to the scenarios [76].

Limitations

This study is limited by the breadth of our recruitment strategy. Due to the novel nature of the research topic, we determined that our recruitment strategy would focus on people with a specific experience (accessing multiple services for their mental health) rather than a targeted demographic of service users. Future research could include specific groups of service users, such as those with certain diagnoses, to determine how

XSL•FO
RenderX

perspectives on an IECR differ across various groups of service users. The sample is also not representative of all people who access the mental health care system. Those with the most acute presentations were likely not represented in this study due to the approach to recruitment and the resources required to participate. However, some participants did share that they had previous experiences of acute illness, including inpatient admissions.

Conclusions

This study found that mental health service users see two alternative ways in which an IECR might impact their care. The first is one in which the IECR entrenches issues that service users experience in the mental health care system and adds a new, burdensome system for care professionals to try to use. The alternative is an IECR that contributes to care professionals having access to relevant information that supports collaborative and proactive care and service users having control over and being able to see how their information is managed. Although an IECR will not solve the systemic issues present in Australia's mental health care system, it could help improve the coordination and proactiveness of care, amplifying service users' needs and supporting service users as active participants in their care. For an IECR to have a positive contribution to broader mental health care reforms, the design and implementation of such a record should consider how service users and care professionals will be supported in using the record, issues of service user consent, what information is necessary to support coordinated and proactive care, and how service users' self-defined needs can be captured and acted upon in an IECR.

Acknowledgments

TK was supported by an Australian Government Research Training Program stipend and a Research Training Program Scholarship (Fee Offset) through the University of Melbourne. Generative artificial intelligence was not used in the research, preparation, writing, or editing of this manuscript.

Authors' Contributions

TK was involved in conceptualization, writing the original draft, and investigation. TK, MP, KG, and SC were involved in reviewing and editing the draft and study supervision.

Conflicts of Interest

None declared.

Multimedia Appendix 1
Qualitative vignettes.
[DOCX File , 25 KB - medinform_v13i1e64162_app1.docx]

Multimedia Appendix 2
Illustrative quotes.
[DOCX File , 34 KB - medinform_v13i1e64162_app2.docx]

References

1. Callahan CM, Carter A, Carty HS, Clark DO, Grain T, Grant SL, et al. Building the infrastructure to integrate social care in a safety net health system. Am J Public Health 2024 Jun;114(6):619-625. [doi: 10.2105/AJPH.2024.307602] [Medline: 38574317]
2. Triplett P. Psychiatry and the meaningful use of electronic health records. Perspect Biol Med 2013 Jun;56(3):407-421. [doi: 10.1353/pbm.2013.0028] [Medline: 24375121]
3. Shen N, Sequeira L, Silver MP, Carter-Langford A, Strauss J, Wiljer D. Patient privacy perspectives on health information exchange in a mental health context: qualitative study. JMIR Ment Health 2019 Nov 13;6(11):e13306 [FREE Full text] [doi: 10.2196/13306] [Medline: 31719029]
4. Bakken V, Koposov R, Røst TB, Clausen C, Nytrø Ø, Leventhal B, et al. Attitudes of mental health service users toward storage and use of electronic health records. Psychiatr Serv 2022 Sep 01;73(9):1013-1018. [doi: 10.1176/appi.ps.202100477] [Medline: 35291817]
5. Haux R. Health information systems - past, present, future. Int J Med Inform 2006 Mar;75(3-4):268-281. [doi: 10.1016/j.ijmedinf.2005.08.002] [Medline: 16169771]
6. Hoghton M, Harris S, Oughtibridge N, Sharma V. Pathways to interoperable electronic patient records in health and social care, Part 2: introduction for commissioners, chief clinical information officers and senior medical and social care leaders involved in health IT commissioning and strategy. Future Healthc J 2023 Nov;10(3):238-243 [FREE Full text] [doi: 10.7861/fhj.2023-0072] [Medline: 38162211]

XSL•FO
RenderX

7. Lombardi BM, Zerden LD, Richman EL, Guan T. When the note doesn't fit: social workers documenting in the electronic health record on integrated health teams. J Technol Hum Serv 2023 Jun 21;41(2):164-181. [doi: 10.1080/15228835.2023.2224402]
8. Fourie I. Learning from research on the information behaviour of healthcare professionals: a review of the literature 2004-2008 with a focus on emotion. Health Info Libr J 2009 Sep 25;26(3):171-186 [FREE Full text] [doi: 10.1111/j.1471-1842.2009.00860.x] [Medline: 19712210]
9. Coiera E. Guide to Health Informatics. Boca Raton, FL: CRC Press; 2015.
10. Fragidis LL, Chatzoglou PD. Development of nationwide electronic health record (NEHR): an international survey. Health Policy Technol 2017 Jun;6(2):124-133. [doi: 10.1016/j.hlpt.2017.04.004]
11. Lee J, Park Y, Park YR, Lee J. Review of national-level personal health records in advanced countries. Healthc Inform Res 2021 Apr;27(2):102-109 [FREE Full text] [doi: 10.4258/hir.2021.27.2.102] [Medline: 34015875]
12. Busse TS, Jux C, Laser J, Rasche P, Vollmar HC, Ehlers JP, et al. Involving health care professionals in the development of electronic health records: scoping review. JMIR Hum Factors 2023 Jul 10;10:e45598 [FREE Full text] [doi: 10.2196/45598] [Medline: 37428524]
13. Matthews EB. Whose system is it anyway? How clients and providers evaluate the impact of session EHR use on communication in mental health treatment. Community Ment Health J 2020 Apr 04;56(3):540-548. [doi: 10.1007/s10597-019-00511-8] [Medline: 31802323]
14. Windle JR, Windle TA, Shamavu KY, Nelson QM, Clarke MA, Fruhling AL, et al. Roadmap to a more useful and usable electronic health record. Cardiovasc Digit Health J 2021 Dec;2(6):301-311 [FREE Full text] [doi: 10.1016/j.cvdhj.2021.09.007] [Medline: 35265926]
15. Asan O, Tyszka J, Fletcher KE. Capturing the patients' voices: planning for patient-centered electronic health record use. Int J Med Inform 2016 Nov;95:1-7 [FREE Full text] [doi: 10.1016/j.ijmedinf.2016.08.002] [Medline: 27697228]
16. Häyrinen K, Saranto K, Nykänen P. Definition, structure, content, use and impacts of electronic health records: a review of the research literature. Int J Med Inform 2008 May;77(5):291-304. [doi: 10.1016/j.ijmedinf.2007.09.001] [Medline: 17951106]
17. Honeyford K, Expert P, Mendelsohn E, Post B, Faisal A, Glampson B, et al. Challenges and recommendations for high quality research using electronic health records. Front Digit Health 2022 Aug 19;4:940330 [FREE Full text] [doi: 10.3389/fdgth.2022.940330] [Medline: 36060540]
18. Evans RS. Electronic health records: then, now, and in the future. Yearb Med Inform 2016 May 20;Suppl 1(Suppl 1):S48-S61 [FREE Full text] [doi: 10.15265/IYS-2016-s006] [Medline: 27199197]
19. Progress on implementing and using electronic health record systems. Organization for Economic Cooperation and Development (OECD). URL: https://www.oecd.org/en/publications/progress-on-implementing-and-using-electronic-health-record-systems_4f4ce846-en.html [accessed 2025-05-29]
20. Ser G, Robertson A, Sheikh A. A qualitative exploration of workarounds related to the implementation of national electronic health records in early adopter mental health hospitals. PLoS One 2014 Jan 16;9(1):e77669 [FREE Full text] [doi: 10.1371/journal.pone.0077669] [Medline: 24454678]
21. Fernández Ò, Pérez CG, García-Cuyàs F, Giménez NA, Gallego MB, Font AG, et al. Shared medical record, personal health folder and health and social integrated care in Catalonia: ICT services for integrated care. In: Rinaldi G, editor. New Perspectives in Medical Records: Meeting the Needs of Patients and Practitioners. Cham, Switzerland: Springer; 2017:49-64.
22. King G, O'Donnell C, Boddy D, Smith F, Heaney D, Mair FS. Boundaries and e-health implementation in health and social care. BMC Med Inform Decis Mak 2012 Sep 07;12(1):100 [FREE Full text] [doi: 10.1186/1472-6947-12-100] [Medline: 22958223]
23. Royal commission into Victoria's mental health system - final report: volume 1 a new approach to mental health and wellbeing in Victoria. State Government of Victoria. 2024. URL: https://www.vic.gov.au/royal-commission-victorias-mental-health-system-final-report [accessed 2025-05-29]
24. Contributing lives, thriving communities: report of the national review of mental health programmes and services. Analysis & Policy Observatory. 2014. URL: https://apo.org.au/node/56413 [accessed 2025-05-29]
25. Kariotis TC, Prictor M, Chang S, Gray K. Impact of electronic health records on information practices in mental health contexts: scoping review. J Med Internet Res 2022 May 04;24(5):e30405 [FREE Full text] [doi: 10.2196/30405] [Medline: 35507393]
26. Rathert C, Mittler JN, Banerjee S, McDaniel J. Patient-centered communication in the era of electronic health records: what does the evidence say? Patient Educ Couns 2017 Jan;100(1):50-64. [doi: 10.1016/j.pec.2016.07.031] [Medline: 27477917]
27. Blease C, Torous J, Kharko A, DesRoches CM, Harcourt K, O'Neill S, et al. Preparing patients and clinicians for open notes in mental health: qualitative inquiry of international experts. JMIR Ment Health 2021 Apr 16;8(4):e27397 [FREE Full text] [doi: 10.2196/27397] [Medline: 33861202]
28. Pisciotta M, Denneson LM, Williams HB, Woods S, Tuepker A, Dobscha SK. Providing mental health care in the context of online mental health notes: advice from patients and mental health clinicians. J Ment Health 2019 Feb 23;28(1):64-70. [doi: 10.1080/09638237.2018.1521924] [Medline: 30468100]

XSL•FO
RenderX

29. Adanijo A, McWilliams C, Wykes T, Jilka S. Investigating mental health service user opinions on clinical data sharing: qualitative focus group study. JMIR Ment Health 2021 Sep 03;8(9):e30596 [FREE Full text] [doi: 10.2196/30596] [Medline: 34477558]
30. Kampf A, McSherry B, Ogloff J, Rothschild A. Confidentiality for Mental Health Professionals: A Guide to Ethical and Legal Principles. Sydney, Australia: Australian Academic Press; 2009.
31. Kariotis TC, Harris KM. Clinician perceptions of My Health Record in mental health care: medication management and sharing mental health information. Aust J Prim Health 2019 Mar;25(1):66-71. [doi: 10.1071/PY17181] [Medline: 30636668]
32. Aviram RB, Brodsky BS, Stanley B. Borderline personality disorder, stigma, and treatment implications. Harv Rev Psychiatry 2006;14(5):249-256. [doi: 10.1080/10673220600975121] [Medline: 16990170]
33. Campos-Castillo C, Anthony DL. The double-edged sword of electronic health records: implications for patient disclosure. J Am Med Inform Assoc 2015 Apr;22(e1):e130-e140. [doi: 10.1136/amiajnl-2014-002804] [Medline: 25059953]
34. CASP checklist: CASP qualitative studies checklist. Critical Appraisal Skills Programme. URL: https://casp-uk.net/casp-tools-checklists/qualitative-studies-checklist/ [accessed 2024-05-29]
35. Duckett SJ, Willcox S. The Australian Health Care System. 5th edition. Sydney, Australia: OUP Australia & New Zealand; 2015.
36. Barter C, Renold E. The use of vignettes in qualitative research. Soc Res Update 1999;25(9):1-6 [FREE Full text]
37. Braun V, Clarke V, Hayfield N, Moller N, Tischner I. Qualitative story completion: a method with exciting promise. In: Liamputtong P, editor. Handbook of Research Methods in Health Social Sciences. Cham, Switzerland: Springer; 2020:1-18.
38. Moerenhout T, Devisch I, Cooreman L, Bernaerdt J, De Sutter A, Provoost V. Patients' moral attitudes toward electronic health records: survey study with vignettes and statements. Health Informatics J 2021 Jan 14;27(1):1460458220980039 [FREE Full text] [doi: 10.1177/1460458220980039] [Medline: 33446034]
39. Graham C, Rouncefield M. Probes and participation. In: Proceedings of the 10th Anniversary Conference on Participatory Design. 2008 Presented at: PDC '08; October 1-4, 2008; Bloomington, IN p. 194-197 URL: https://dl.acm.org/doi/10.5555/1795234.1795272 [doi: 10.5555/1795234.1795272]
40. Transcribe create collaborate. TRINT. URL: https://trint.com/ [accessed 2025-05-29]
41. Smith JA, Flowers P, Larkin M. Interpretative Phenomenological Analysis: Theory, Method and Research. Thousand Oaks, CA: Sage Publication; 2009.
42. Smith JA. Evaluating the contribution of interpretative phenomenological analysis. Health Psychol Rev 2011 Mar;5(1):9-27. [doi: 10.1080/17437199.2010.510659]
43. Griffiths KM, Mendoza J, Carron-Arthur B. Whereto mental health reform in Australia: is anyone listening to our independent auditors? Med J Aust 2015 Mar 02;202(4):172-174. [doi: 10.5694/mja14.01034] [Medline: 25716589]
44. Royal commission into Victoria's mental health system - final report. State Government of Victoria. 2020. URL: https://www.vic.gov.au/royal-commission-victorias-mental-health-system-final-report [accessed 2025-05-29]
45. Henderson C, Noblett J, Parke H, Clement S, Caffrey A, Gale-Grant O, et al. Mental health-related stigma in health care and mental health-care settings. Lancet Psychiatry 2014 Nov;1(6):467-482. [doi: 10.1016/S2215-0366(14)00023-6] [Medline: 26361202]
46. Mestdagh A, Hansen B. Stigma in patients with schizophrenia receiving community mental health care: a review of qualitative studies. Soc Psychiatry Psychiatr Epidemiol 2014 Jan 9;49(1):79-87. [doi: 10.1007/s00127-013-0729-4] [Medline: 23835576]
47. Cook JE, Purdie-Vaughns V, Meyer IH, Busch JT. Intervening within and across levels: a multilevel approach to stigma and public health. Soc Sci Med 2014 Feb;103:101-109. [doi: 10.1016/j.socscimed.2013.09.023] [Medline: 24513229]
48. Clement S, Schauman O, Graham T, Maggioni F, Evans-Lacko S, Bezborodovs N, et al. What is the impact of mental health-related stigma on help-seeking? A systematic review of quantitative and qualitative studies. Psychol Med 2015 Jan 21;45(1):11-27. [doi: 10.1017/S0033291714000129] [Medline: 24569086]
49. Grando MA, Murcko A, Mahankali S, Saks M, Zent M, Chern D, et al. A study to elicit behavioral health patients' and providers' opinions on health records consent. J Law Med Ethics 2017 Jun 14;45(2):238-259 [FREE Full text] [doi: 10.1177/1073110517720653] [Medline: 30976154]
50. Huggett C, Birtel MD, Awenat YF, Fleming P, Wilkes S, Williams S, et al. A qualitative study: experiences of stigma by people with mental health problems. Psychol Psychother 2018 Sep 18;91(3):380-397. [doi: 10.1111/papt.12167] [Medline: 29345416]
51. Nissenbaum H. Privacy in Context: Technology, Policy, and the Integrity of Social Life. Stanford, UK: Stanford University Press; 2009.
52. Cáceres SB. Electronic health records: beyond the digitization of medical files. Clinics (Sao Paulo) 2013 Aug;68(8):1077-1078 [FREE Full text] [doi: 10.6061/clinics/2013(08)02] [Medline: 24037000]
53. Kariotis T, Prictor M, Chang S, Gray K. Evaluating the contextual integrity of Australia's my health record. Stud Health Technol Inform 2019 Aug 09;265:213-218. [doi: 10.3233/SHTI190166] [Medline: 31431601]
54. Zwaanswijk M, Ploem MC, Wiesman FJ, Verheij RA, Friele RD, Gevers JK. Understanding health care providers' reluctance to adopt a national electronic patient record: an empirical and legal analysis. Med Law 2013 Mar;32(1):13-31. [Medline: 23781762]

XSL•FO
RenderX

55. Wilkinson S, Borycki EM. Designing an electronic shared care plan to enable person-centred, team-based home care. Stud Health Technol Inform 2022 Jan 14;289:102-105. [doi: 10.3233/SHTI210869] [Medline: 35062102]
56. Koops BJ, Leenes R. Privacy regulation cannot be hardcoded. A critical comment on the 'privacy by design' provision in data-protection law. Int Rev Law Comput Technol 2013 Jul 27;28(2):159-171. [doi: 10.1080/13600869.2013.801589]
57. Soni H, Grando A, Murcko A, Diaz S, Mukundan M, Idouraine N, et al. State of the art and a mixed-method personalized approach to assess patient perceptions on medical record sharing and sensitivity. J Biomed Inform 2020 Jan;101:103338 [FREE Full text] [doi: 10.1016/j.jbi.2019.103338] [Medline: 31726102]
58. Soni H, Grando A, Aliste MP, Murcko A, Todd M, Mukundan M, et al. Perceptions and preferences about granular data sharing and privacy of behavioral health patients. Stud Health Technol Inform 2019 Aug 21;264:1361-1365. [doi: 10.3233/SHTI190449] [Medline: 31438148]
59. Gaillard AS, Braun E, Vollmann J, Gather J, Scholten M. The content of psychiatric advance directives: a systematic review. Psychiatr Serv 2023 Jan 01;74(1):44-55. [doi: 10.1176/appi.ps.202200002] [Medline: 36039553]
60. Swanson JW, Swartz MS, Elbogen EB, Van Dorn RA, Ferron J, Wagner HR, et al. Facilitated psychiatric advance directives: a randomized trial of an intervention to foster advance treatment planning among persons with severe mental illness. Am J Psychiatry 2006 Nov;163(11):1943-1951 [FREE Full text] [doi: 10.1176/ajp.2006.163.11.1943] [Medline: 17074946]
61. Swanson J, Swartz M, Hannon M, Elbogen E, Wagner H, McCauley B, et al. Psychiatric advance directives: a survey of persons with schizophrenia, family members, and treatment providers. Int J Forensic Ment Health 2003 Apr 01;2(1):73-86. [doi: 10.1080/14999013.2003.10471180]
62. Morrison RS, Meier DE, Arnold RM. What's wrong with advance care planning? JAMA 2021 Oct 26;326(16):1575-1576 [FREE Full text] [doi: 10.1001/jama.2021.16430] [Medline: 34623373]
63. Calcedo-Barba A, Fructuoso A, Martinez-Raga J, Paz S, Sánchez de Carmona M, Vicens E. A meta-review of literature reviews assessing the capacity of patients with severe mental disorders to make decisions about their healthcare. BMC Psychiatry 2020 Jun 30;20(1):339 [FREE Full text] [doi: 10.1186/s12888-020-02756-0] [Medline: 32605645]
64. Whiddett R, Hunter I, Engelbrecht J, Handy J. Patients' attitudes towards sharing their health information. Int J Med Inform 2006 Jul;75(7):530-541. [doi: 10.1016/j.ijmedinf.2005.08.009] [Medline: 16198142]
65. Schwartz PH, Caine K, Alpert SA, Meslin EM, Carroll AE, Tierney WM. Patient preferences in controlling access to their electronic health records: a prospective cohort study in primary care. J Gen Intern Med 2015 Jan 6;30 Suppl 1(Suppl 1):S25-S30 [FREE Full text] [doi: 10.1007/s11606-014-3054-z] [Medline: 25480721]
66. Chivilgina O, Elger BS, Benichou MM, Jotterand F. "What's the best way to document information concerning psychiatric patients? I just don't know"-A qualitative study about recording psychiatric patients notes in the era of electronic health records. PLoS One 2022 Mar 3;17(3):e0264255 [FREE Full text] [doi: 10.1371/journal.pone.0264255] [Medline: 35239698]
67. Maniss SM, Pruit AG. Collaborative documentation for behavioral healthcare providers: an emerging practice. J Hum Serv Train Res Pract 2018;3(1):22 [FREE Full text]
68. Varpio L, Rashotte J, Day K, King J, Kuziemsky C, Parush A. The EHR and building the patient's story: a qualitative investigation of how EHR use obstructs a vital clinical activity. Int J Med Inform 2015 Dec;84(12):1019-1028. [doi: 10.1016/j.ijmedinf.2015.09.004] [Medline: 26432683]
69. Walsh L, Hemsley B, Allan M, Adams N, Balandin S, Georgiou A, et al. The e-health literacy demands of Australia's my health record: a heuristic evaluation of usability. Perspect Health Inf Manag 2017;14(Fall):1f [FREE Full text] [Medline: 29118683]
70. Walsh L, Hemsley B, Allan M, Dahm MR, Balandin S, Georgiou A, et al. Assessing the information quality and usability of within a health literacy framework: what's changed since 2016? Health Inf Manag 2021 Aug 01;50(1-2):13-25 [FREE Full text] [doi: 10.1177/1833358319864734] [Medline: 31370712]
71. Walsh L, Hill S, Allan M, Balandin S, Georgiou A, Higgins I, et al. A content analysis of the consumer-facing online information about My Health Record: implications for increasing knowledge and awareness to facilitate uptake and use. Health Inf Manag 2018 Sep 07;47(3):106-115 [FREE Full text] [doi: 10.1177/1833358317712200] [Medline: 28589741]
72. Fernández-Alemán JL, Señor IC, Lozoya P, Toval A. Security and privacy in electronic health records: a systematic literature review. J Biomed Inform 2013 Jun;46(3):541-562 [FREE Full text] [doi: 10.1016/j.jbi.2012.12.003] [Medline: 23305810]
73. Chen M, Tan X, Padman R. Social determinants of health in electronic health records and their impact on analysis and risk prediction: a systematic review. J Am Med Inform Assoc 2020 Nov 01;27(11):1764-1773 [FREE Full text] [doi: 10.1093/jamia/ocaa143] [Medline: 33202021]
74. Goodday SM, Kormilitzin A, Vaci N, Liu Q, Cipriani A, Smith T, et al. Maximizing the use of social and behavioural information from secondary care mental health electronic health records. J Biomed Inform 2020 Jul;107:103429 [FREE Full text] [doi: 10.1016/j.jbi.2020.103429] [Medline: 32387393]
75. Hollister B, Bonham VL. Should electronic health record-derived social and behavioral data be used in precision medicine research? AMA J Ethics 2018 Sep 01;20(9):E873-E880 [FREE Full text] [doi: 10.1001/amajethics.2018.873] [Medline: 30242819]
76. Gravett K. Story completion: storying as a method of meaning-making and discursive discovery. Int J Qual Methods 2019 Dec 08;18:155. [doi: 10.1177/1609406919893155]

XSL•FO
RenderX

Abbreviations

EHR: electronic health record
IECR: integrated electronic care record
NDIS: National Disability Insurance Scheme

Edited by A Schwartz; submitted 11.07.24; peer-reviewed by J Schwarz, E Matthews; comments to author 09.12.24; revised version received 30.01.25; accepted 11.03.25; published 03.06.25.

Please cite as:
Kariotis T, Prictor M, Gray K, Chang S
Service Users' Perspectives on an Integrated Electronic Care Record in Mental Health Care: Qualitative Vignette and Interview Study
JMIR Med Inform 2025;13:e64162
URL: https://medinform.jmir.org/2025/1/e64162
doi:10.2196/64162
PMID:

©Timothy Kariotis, Megan Prictor, Kathleen Gray, Shanton Chang. Originally published in JMIR Medical Informatics (https://medinform.jmir.org), 03.06.2025. This is an open-access article distributed under the terms of the Creative Commons Attribution License (https://creativecommons.org/licenses/by/4.0/), which permits unrestricted use, distribution, and reproduction in any medium, provided the original work, first published in JMIR Medical Informatics, is properly cited. The complete bibliographic information, a link to the original publication on https://medinform.jmir.org/, as well as this copyright and license information must be included.

XSL•FO
RenderX

Original Paper

Identifying People Living With or Those at Risk for HIV in a Nationally Sampled Electronic Health Record Repository Called the National Clinical Cohort Collaborative: Computational Phenotyping Study

Eric Hurwitz[1*], PhD; Cara D Varley[2*], MPH, MD; A Jerrod Anzolone[3], PhD; Vithal Madhira[4], MS; Amy L Olex[5], PhD; Jing Sun[6], MPH, MD, PhD; Dimple Vaidya[7], MS; Nada Fadul[8], MD; Jessica Y Islam[9,10], MPH, PhD; Lesley E Jackson[11], MD; Kenneth J Wilkins[12], PhD; Zachary Butzin-Dozier[13], MPH, PhD; Dongmei Li[14], PhD; Sandra E Safo[15], PhD; Julie A McMurry[1], MPH; Pooja Maheria[11], MS; Tommy Williams[11]; Shukri A Hassan[7], BS; Melissa A Haendel[1], PhD; Rena C Patel[11], MPH, MPhil, MD; The National Clinical Cohort Collaborative (N3C) Consortium[16*]

[1]Department of Genetics, University of North Carolina at Chapel Hill, Chapel Hill, NC, United States

[2]School of Medicine, Oregon Health & Science University, Portland, OR, United States

[3]Department of Biostatistics, University of Nebraska Medical Center, Omaha, NE, United States

[4]Palila Software, Reno, NV, United States

[5]Wright Center for Clinical and Translational Research, Virginia Commonwealth University, Richmond, VA, United States

[6]Department of Epidemiology, Johns Hopkins Bloomberg School of Public Health, Baltimore, MD, United States

[7]Department of Medicine, University of Washington, Seattle, WA, United States

[8]Department of Internal Medicine, University of Nebraska Medical Center, Omaha, NE, United States

[9]Department of Cancer Epidemiology, H. Lee Moffitt Cancer Center and Research Institute, Tampa, FL, United States

[10]Department of Oncologic Sciences, University of South Florida, Tampa, FL, United States

[11]Department of Medicine, University of Alabama at Birmingham, Birmingham, AL, United States

[12]Biostatistics Program Office of the Director, National Institute of Diabetes and Digestive and Kidney Diseases, National Institutes of Health, Bethesda, MD, United States

[13]Division of Biostatistics, University of California Berkeley School of Public Health, Berkeley, CA, United States

[14]Department of Clinical and Translational Research, University of Rochester Medical Center, Rochester, NY, United States

[15]Department of Biostatistics, School of Public Health, University of Minnesota, Minneapolis, MN, United States

[16]See Acknowledgments

[*]these authors contributed equally

Corresponding Author:
Eric Hurwitz, PhD
Department of Genetics
University of North Carolina at Chapel Hill
120 Mason Farm Road
Chapel Hill, NC 27514
United States
Phone: 1 919 843 8724
Email: eric_hurwitz@med.unc.edu

Abstract

Background: Electronic health records (EHRs) provide valuable insights to address clinical and epidemiological research concerning HIV, including the disproportionate impact of the COVID-19 pandemic on people living with HIV. To identify this population, most studies using EHR or claims databases start with diagnostic codes, which can result in misclassification without further refinement using drug or laboratory data. Furthermore, given that antiretrovirals now have indications for both HIV and COVID-19 (ie, ritonavir in nirmatrelvir/ritonavir), new phenotyping methods are needed to better capture people living with HIV. Therefore, we created a generalizable and innovative method to robustly identify people living with HIV, preexposure prophylaxis

XSL•FO
RenderX

(PrEP) users, postexposure prophylaxis (PEP) users, and people not living with HIV using granular clinical data after the emergence of COVID-19.

Objective: The primary aim of this study was to use computational phenotyping in EHR data to identify people living with HIV (cohort 1), PrEP users (cohort 2), PEP users (cohort 3), or "none of the above" (people not living with HIV; cohort 4) and describe COVID-19–related characteristics among these cohorts.

Methods: We used diagnostic and laboratory measurements and drug concepts in the National Clinical Cohort Collaborative to create a computational phenotype for the 4 cohorts with confidence levels. For robustness, we conducted a randomly sampled, blinded clinician annotation to assess precision. We calculated the distribution of demographics, comorbidities, and COVID-19 variables among the 4 cohorts.

Results: We identified 132,664 people living with HIV with a high level of confidence, 36,088 PrEP users, 4120 PEP users, and 20,639,675 people not living with HIV. Most people living with HIV were identified by a combination of medical conditions, laboratory measurements, and drug exposures (74,809/132,664, 56.4%), followed by laboratory measurements and drug exposures (15,241/132,664, 11.5%) and then by medical conditions and drug exposures (14,595/132,664, 11%). A higher proportion of people living with HIV experienced COVID-19–related hospitalization (4650,132,664, 3.5%) or mortality (828/132,664, 0.6%) and all-cause mortality (2083/132,664, 1.6%) compared to other cohorts.

Conclusions: Using an extensive phenotyping algorithm leveraging granular data in an EHR repository, we have identified people living with HIV, people not living with HIV, PrEP users, and PEP users. Our findings offer transferable lessons to optimize future EHR phenotyping for these cohorts.

(JMIR Med Inform 2025;13:e68143) doi:10.2196/68143

KEYWORDS

HIV; electronic health records phenotype; epidemiologic methods; COVID-19; preexposure prophylaxis; postexposure prophylaxis

Introduction

Background

In the United States, there are an estimated 1.2 million people living with HIV, with 32,100 new cases diagnosed in 2021 [1]. The COVID-19 pandemic has disproportionately impacted people living with HIV, who have a 4-fold higher likelihood of contracting COVID-19 and experiencing severe outcomes, such as increased disease severity, higher hospitalization rates, and elevated mortality [2-4]. Initially, the COVID-19 pandemic introduced challenges to optimal HIV management, including a substantial reduction in HIV testing, resulting in underdiagnosis and barriers to necessary treatment [5-8]. Beyond its effects on people living with HIV, the COVID-19 pandemic also disrupted preexposure prophylaxis (PrEP) use and availability, potentially increasing the vulnerability of those at risk of acquiring HIV [9]. For example, PrEP users experienced a 6% to 11.5% decline in medication coverage early in the pandemic [5,9,10]. Disparities related to social determinants of health that have historically affected minoritized (ie, racial, ethnic, gender, rural, and socioeconomic) communities with HIV became more apparent since the onset of the COVID-19 pandemic [11-15]. The pronounced impact of COVID-19 on people living with HIV and those at risk for HIV underscores the urgent need for focused research within this population for better preparedness for the next public health crisis that may affect an already vulnerable population.

Electronic health records (EHRs) provide valuable insights to address specific clinical and epidemiological research concerning HIV, including the disproportionate impact of the COVID-19 pandemic on this population [2,13-15]. The National Clinical Cohort Collaborative (N3C) is a nationally sampled EHR repository in the United States with granular, individual-level clinical data from >98 data partner sites and houses >32 billion rows of data for >22 million individuals [16]. These rich EHR data have allowed investigation of questions related to the COVID-19 pandemic and HIV, including identification of an elevated risk of poor COVID-19 outcomes in people living with HIV with a low cluster of differentiation 4 (CD4) count (<200 cells/µL) and racial disparities with COVID-19 positivity among people living with HIV, in addition to both individual and area-level social determinants of health with COVID-19 outcomes [2,13-15]. The N3C Enclave not only provides a large sample size for answering research questions but also contains granular individual-level information, such as social determinants of health [17], visit and prescription frequencies, and geographic information to better identify health disparities during the COVID-19 pandemic [18,19].

Nonetheless, identifying potential people living with HIV, PrEP users, or postexposure prophylaxis (PEP) users in any EHR dataset necessitates indirectly inferring data from source information. Most studies using EHR or claims databases start with diagnostic codes, which can result in misclassification without further refinement using drug or laboratory data [20-22]. While these previous studies have performed computational phenotyping of HIV on smaller cohorts, with data or validation often limited to a single institution or health system, one study [23], conducted with All of Us data, has included additional complexity such as self-reporting of medical conditions, which is not always feasible with large datasets [22-26]. While each approach has strengths, they also suffer from limitations, such as (1) variation in the availability of EHR data among individuals that potentially leads to differential misclassification, (2) use of nonstandardized codes specific to a single health system preventing interoperability across health systems, (3) inability to distinguish between individuals with high- or low-confidence designations, (4) additional misclassification

XSL•FO
RenderX

with increased uptake of PrEP or PEP, and (5) the use of antiretrovirals that now have indications for both HIV and COVID-19 treatment (ie, ritonavir in nirmatrelvir/ritonavir) resulting in misclassification.

Objectives

Our objective was to use an innovative approach after the emergence of COVID-19 to robustly identify people living with HIV, PrEP users, PEP users, and people not living with HIV using granular clinical data in N3C, augmented by clinician annotation without chart abstraction of source data. We used the standardized Observational Medical Outcomes Partnership (OMOP) Common Data Model to create 4 cohorts or "phenotypes," including people living with HIV (cohort 1), PrEP users (cohort 2), PEP users (cohort 3), and people not living with HIV (cohort 4), based on medical conditions, laboratory measurements, and drug data available in N3C. We conducted a clinician-curated annotation to reduce and describe misclassification. In addition, we introduced confidence levels to classify individuals into categories of low, medium, or high confidence in their status as people living with HIV, allowing researchers to tailor the cohorts to their specific research needs. These cohorts will serve as a framework for future research to address questions related to HIV within N3C, and our methods inform more generalizable approaches to phenotyping HIV in EHR data.

Methods

Study Population

The N3C Enclave contains EHR data from clinical sites and represents the largest limited dataset of COVID-19 cases and controls in the United States. N3C contains harmonized EHR data for individuals who tested positive and negative for COVID-19 from January 1, 2020, to present through routine weekly updates to incorporate near real-time clinical encounters and procedures, in addition to historical data dating back to January 1, 2018. Data include individuals who tested positive for COVID-19 matched with 2 controls who tested negative for COVID-19 based on a maximum of 4 sociodemographic variables (age, sex, race, and ethnicity) whenever available by data partner site. Our cohorts of people living with HIV, PrEP users, PEP users, and people not living with HIV were defined based on the N3C Enclave data release as of November 2, 2023 (version 148; from 93 data partner sites) using a limited dataset.

Procedures

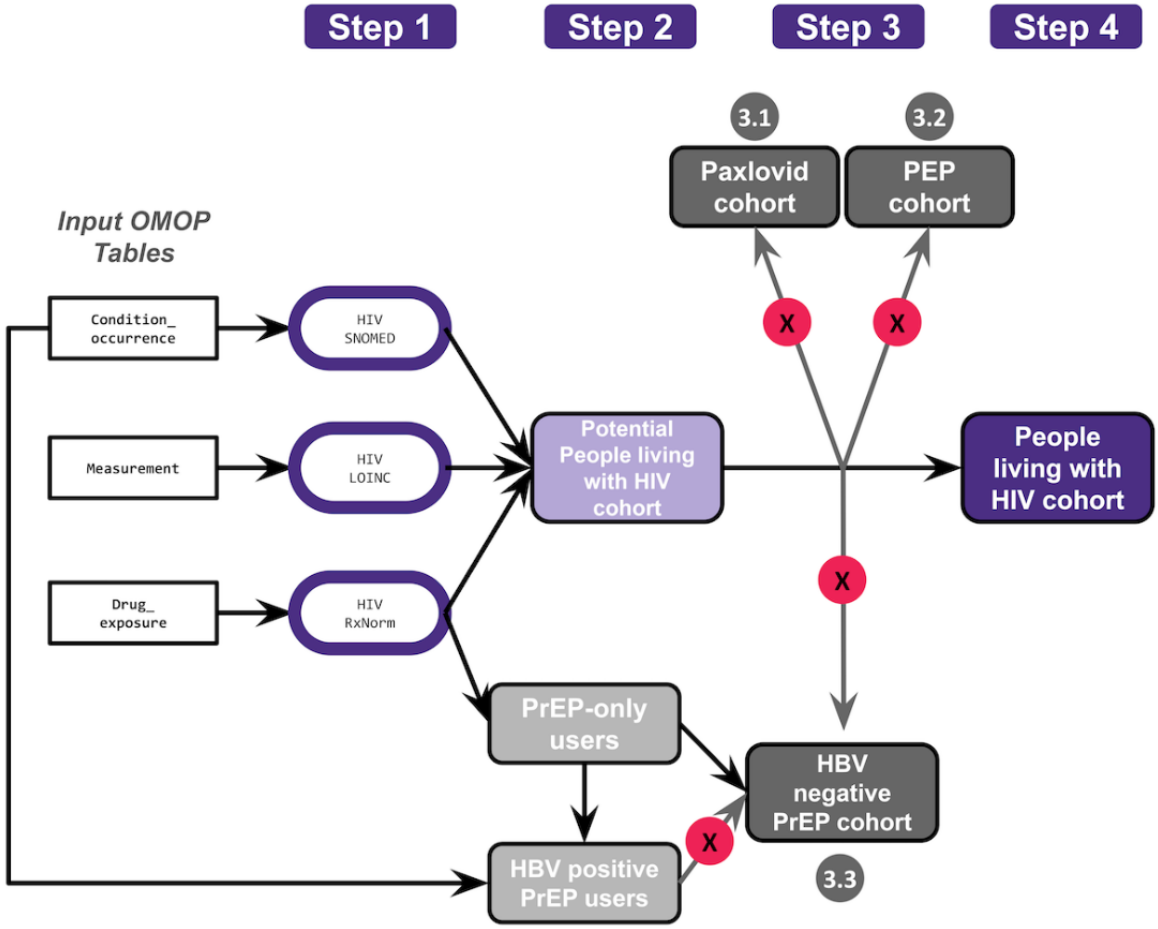
HIV Phenotyping Overview Scheme

Our cohorts were identified in the N3C Enclave through the use of OMOP concepts, where concept IDs, concept set names, and our phenotyping pipeline can be searched in our public-facing GitHub repository for transferable methods in and out of N3C [27]. These standardized concepts correspond to three major sources of data: (1) Systematized Medical Nomenclature for Medicine Clinical Terminology (SNOMED CT) codes and *International Classification of Diseases, Tenth Revision* (*ICD-10*) mapped to SNOMED CT codes for HIV diagnosis from the HIV-related condition occurrence table; (2) Logical Observation Identifiers Names and Codes for HIV measurements from the measurement table; and (3) HIV medication exposures from the drug exposure table in RxNorm [28]. The selection of OMOP concepts across these 3 domains was carried out using the Observational Health Data Sciences and Informatics Atlas tool [29,30], in collaboration with HIV clinicians, to identify and include all relevant HIV-related OMOP concept IDs.

Conceptually, our approach identified possible people living with HIV, followed by subtyping PrEP and PEP users and removing people using HIV drugs for only chronic hepatitis B virus (HBV) or COVID-19 infection (Figure 1). From the potential cohort of people living with HIV, using the table of individuals prescribed HIV-related drugs, we phenotyped PrEP users using concept IDs in the *(immunosuppressed or compromised) PrEP concept set* and excluding individuals with an HIV diagnostic code or positive laboratory measurement (eg, antibody and antigen, viral load [VL] ≥50 copies/mL, or CD4 ≤200 cells/μL) [27]. The final cohort of PrEP users was created by excluding individuals with HBV infection to avoid potential misclassification (as tenofovir disoproxil fumarate [TDF] alone is often used for HBV treatment and avoided for PrEP to reduce the risk of acute hepatitis flare upon discontinuation of TDF for PrEP). From the potential cohort of people living with HIV, identified earlier by drug exposures (after excluding PrEP users), PEP users were identified using the concepts in the *PEP concept set* [27]. Individuals with ritonavir-only exposure (ie, those with no other antiretroviral exposure for HIV treatment, no medical conditions, and no laboratory measurements), were categorized as "uncertain classification," given the overlap of ritonavir use for COVID-19 treatment in nirmatrelvir/ritonavir using concepts listed in *Ritonavir concept set* and *Paxlovid concept set* [27]. In addition to our "ritonavir only" group, we identified those with uncertain classification status for whom, despite our best efforts, we could not adjudicate with precision which cohort they belonged to and therefore excluded these individuals from all cohorts. For instance, some individuals had repeat HIV VL testing without any results or other HIV-related laboratory measurements, drug exposures, or medical conditions, where the repeat testing could represent monitoring not only HIV treatment but also HIV screening. We considered this uncertain classification to be of low confidence, with high concern for misclassification. Given the risk of additional misclassification that assigning such individuals to one of the 4 specific cohorts would cause, we chose to remove them from the 4 specific cohorts altogether. Thus, the final cohort of people living with HIV was created by including individuals positive for HIV by medical conditions, laboratory measurements, or drug exposures and excluding any individuals listed in the final PrEP, PEP, and "ritonavir-only" cohorts (Figure 1).

XSL•FO
RenderX

Figure 1. A schematic detailing the process of creating our people living with HIV cohort. Individuals were included in the HIV cohort by a combination of medical conditions, laboratory measurements, or drug exposures (step 1) to create a potential cohort of people living with HIV (step 2). Individuals taking nirmatrelvir/ritonavir (step 3.1), postexposure prophylaxis (PEP) users (step 3.2), and pre-exposure prophylaxis (PrEP) users (step 3.3) were excluded from the intermediate cohort (step 3), which is depicted by "X" in the red circle, to create a final cohort of people living with HIV (step 4). HBV: hepatitis B virus; LOINC: Logical Observation Identifiers Names and Codes; OMOP: Observational Medical Outcomes Partnership; SNOMED: Systematized Medical Nomenclature for Medicine.



Data Preprocessing

Laboratory measurements, such as absolute CD4 cell count and percentage and VL measures, are crucial to research among people living with HIV. To extract meaningful data related to CD4 and VL measurements, we first identified concept IDs for CD4 and VL measurements seen in the *CD4 Cell Count (Absolute)* and the *HIV Viral Load (version 3) concept sets* [27]. CD4 and VL phenotyping were performed on all individuals in N3C using the measurement table.

Applying Levels of Confidence to the Cohort of People Living With HIV

To determine, with varying levels of confidence, who within the cohort were people living with HIV, we assigned a confidence level between 1 and 3 (with 1 indicating the highest confidence) per individual to reflect the degree of certainty in their status as someone living with HIV. Briefly, confidence level 1 included individuals with positive HIV laboratory results; confidence level 2 comprised individuals identified through a combination of medical conditions, the presence of laboratory measurements, and HIV medication exposures but without available laboratory results; and confidence level 3 consisted of individuals identified solely based on HIV drug exposures or only 1 record of an HIV diagnosis. More details are provided in the applying levels of confidence to the cohort of people living with HIV section in Multimedia Appendix 1 [16,31-33].

PrEP Phenotyping

In order to identify PrEP users, we first identified those using PrEP drugs (emtricitabine and tenofovir) from the possible HIV cohort who were identified by drug exposures only (ie, excluding individuals with an HIV diagnostic code or positive laboratory measurement, such as antibody and antigen, VL ≥50 copies/mL, or CD4 ≤200 cells/μL). Due to low numbers, cabotegravir for PrEP was not included. Among these, as noted earlier, individuals with likely chronic HBV infection were excluded based on concept IDs listed in the *HBV concept set* [27]. Further details about PrEP phenotyping and assigning confidence levels for PrEP users are provided in Multimedia Appendix 1.

PEP Phenotyping

PEP phenotyping was performed using the potential cohort of people living with HIV identified by drug exposures after excluding those in the PrEP cohort. We then filtered individuals based on the following criteria: (1) had a record of emtricitabine/TDF and dolutegravir or emtricitabine/TDF and

XSL•FO
RenderX

raltegravir use on the same date, (2) had a supply of <30 days (or the supply information was null), and (3) only had one row of data (indicating they were not receiving an HIV treatment regimen repeatedly, which would otherwise be more indicative of an HIV-infection–related treatment). Given that our phenotyping approach was dependent on accounting for all data available over time, it was not possible to distinguish, with confidence, PEP users who later acquired HIV. Concepts used in this workflow are available in the *PEP concept set* [27]. Given the overall small size of the PEP cohort, we chose not to pursue confidence level typing of this group.

Ritonavir-Only Phenotyping

We recognized that several individuals may have been prescribed ritonavir as part of nirmatrelvir/ritonavir (ie, Paxlovid) or another off-label regimen as a COVID-19 therapeutic. Therefore, those entering our cohort of people living with HIV by drug exposures only and who had only been prescribed ritonavir (without any other antiretrovirals used for HIV treatment documented) after January 1, 2020, were categorized separately for further evaluation using concepts described earlier [27]. We then identified those taking ritonavir as part of nirmatrelvir/ritonavir via concepts and drug source values. Individuals who only used ritonavir as part of nirmatrelvir/ritonavir were subsequently excluded. Given that there were no other laboratory tests, medical conditions, or drug exposures consistent with HIV, we suspected this group reflected people not living with HIV; however, due to the uncertainty of the indication for the ritonavir prescription, we categorized them in an uncertain classification.

Clinician Annotation Activity

To ensure the robustness of our cohorts of people living with HIV, PrEP users, and PEP users, clinicians experienced in treating HIV conducted a blinded annotation activity. Briefly, clinician annotation involving 120 randomly selected individuals (n=90, 75% people living with HIV; n=10, 8.3% PrEP users; n=10, 8.3% PEP users; and n=10, 8.3% individuals not living with HIV) was performed. Three clinicians with experience of treating HIV, blinded to the study procedures, reviewed row-level HIV EHR data (including medical conditions, laboratory measurements, and drug exposures) and classified each individual as person living with HIV, PrEP user, PEP user, or person not living with HIV based on the available data for each individual. For each clinician, we generated a confusion matrix and calculated sensitivity, specificity, positive predictive value, negative predictive value, precision, recall, and F_1-score. Multimedia Appendix 1 provides further details about this process.

Demographics and Comorbidity Definitions

Demographics and comorbidities of individuals were defined using standardized N3C-wide definitions. The set of comorbidities selected included those in the Charlson Comorbidity Index. Concept sets were created for each medical condition listed using the primary conditions listed in the SNOMED CT hierarchy, including all descendants. Specific details for each concept set can be found in the N3C concept set browser and are described in the data dictionary [16,34].

COVID-19 Outcome Definitions

The COVID-19 severity and outcomes for individuals were defined using N3C-wide definitions. In this analysis, COVID-19 positivity was defined by (1) a set of a priori–defined SARS-CoV-2 laboratory tests (that included polymerase chain reaction or antigen positivity but not antibody positivity) or (2) a "strong positive" diagnostic code (this cohort code is available on GitHub) [35,36].

Ethical Considerations

Direct patient consent was not obtained for this repository of deidentified data per N3C policies. The N3C received a waiver of consent from the National Institutes of Health (NIH) Institutional Review Board (IRB), and NIH takes care to ensure the highest privacy and security requirements are met and adhered to for housing and protecting these data in the NIH-managed N3C Enclave. More details can be found in N3C resources [37].

The N3C Enclave is approved through the NIH IRB. Each individual data partner site maintains its own IRB-approved data transfer agreement or joins under a Johns Hopkins University Reliance Protocol (IRB00249128). Each investigator accessing the N3C Enclave receives local IRB approval from their respective institutions. The N3C Data Access Committee approved this project (RP-CA3365).

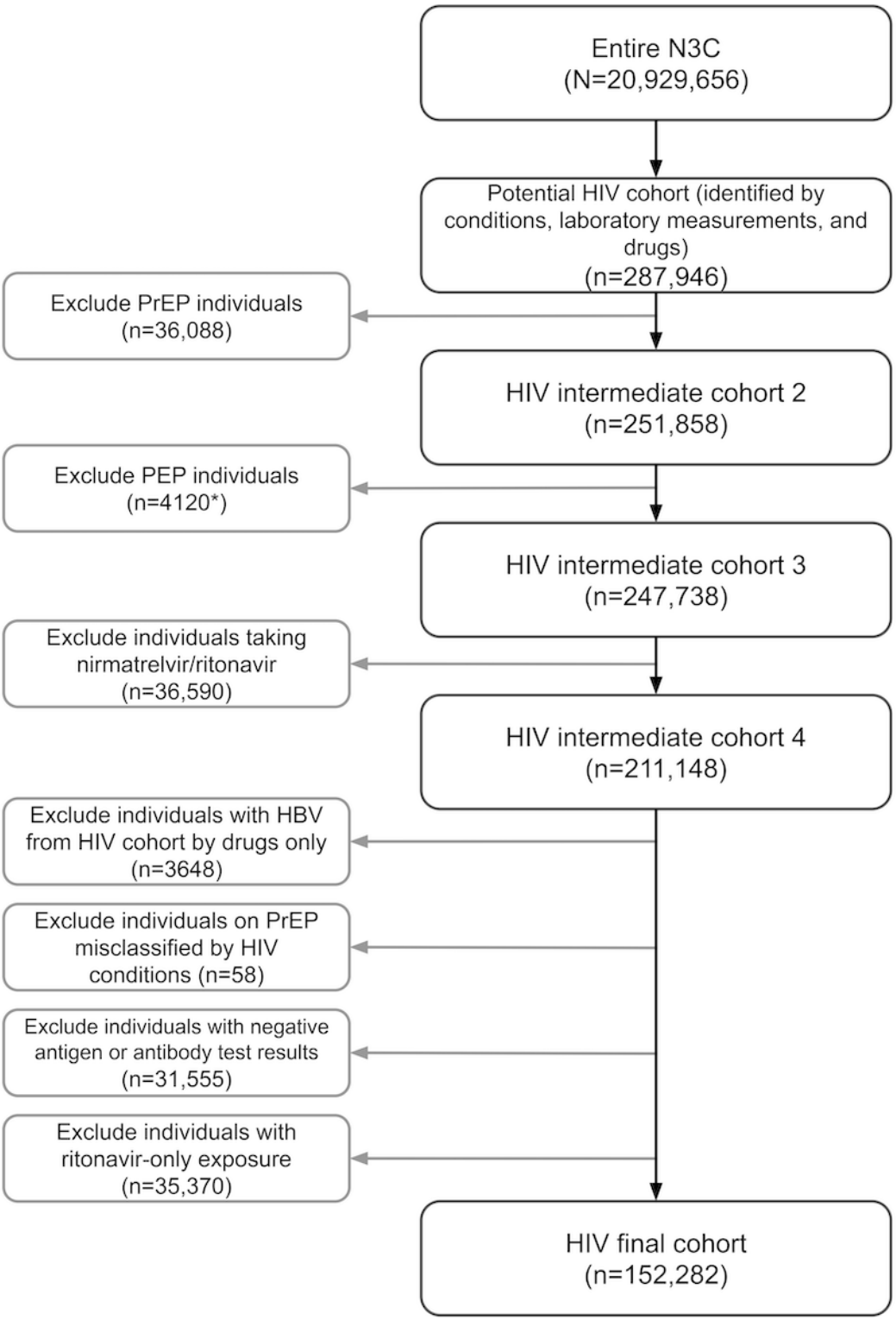
Results

Identifying People Living With HIV, PrEP Users, and PEP Users in N3C

Using a computational phenotype through a combination of medical conditions, laboratory measurements, and medication data, we identified 152,282 (0.7%) individuals as people living with HIV from a total population of 20,928,656 (Figure 2). Among these cases, many were recognized through the combination of medical conditions, laboratory measurements, and drug exposures (n=74,809, 49.1%), followed by medical conditions alone (n=15,617, 10.3%), and then by laboratory measurements and drug exposures (n=15,241, 10%; Figure 3). When categorizing people living with HIV based on confidence levels, we found that most individuals fell into confidence level 1 (n=108,068, 71%), followed by level 2 (n=24,596, 16.2%), and then level 3 (n=19,618, 12.9%; Table 1). Our phenotyping process also identified 36,088 PrEP users (after excluding 303 individuals for HBV monoinfection), 4120 PEP users (the total number of PEP users is presented as an estimate due to N3C governance rules to obfuscate counts <20), and 96,491 individuals with uncertain classification (Table 2). In terms of our confidence levels for each PrEP user, most individuals were categorized as level 1 (20,742/36,088, 57.5%), followed by level 3 (11,560/36,088, 32%) and then level 2 (3786/36,088, 10.5%; Table 3). We did observe a small number of individuals from the people living with HIV cohort (24/152,282, 0%) with possible PrEP exposure before a diagnosis of HIV.

XSL•FO
RenderX

Figure 2. Flow diagram describing the inclusion and exclusion criteria of the HIV cohort. *Total number of postexposure prophylaxis (PEP) users is presented as an estimate due to National Clinical Cohort Collaborative (N3C) governance rules to obfuscate counts <20. HBV: hepatitis B virus; PrEP: pre-exposure prophylaxis.



XSL•FO
RenderX

Figure 3. A Venn diagram displaying the number of individuals in the HIV cohort identified by medical conditions, laboratory measurements, and drug exposures (n=152,282). Top numbers represents the count (and percentage) of individuals in specific categories (eg, 14,595 individuals identified by the combination of medications and medical conditions), while bottom numbers display the number of individuals broadly identified by medical conditions, laboratory measurements, and medications (eg, 116,155 individuals in the HIV cohort have an HIV-related condition).

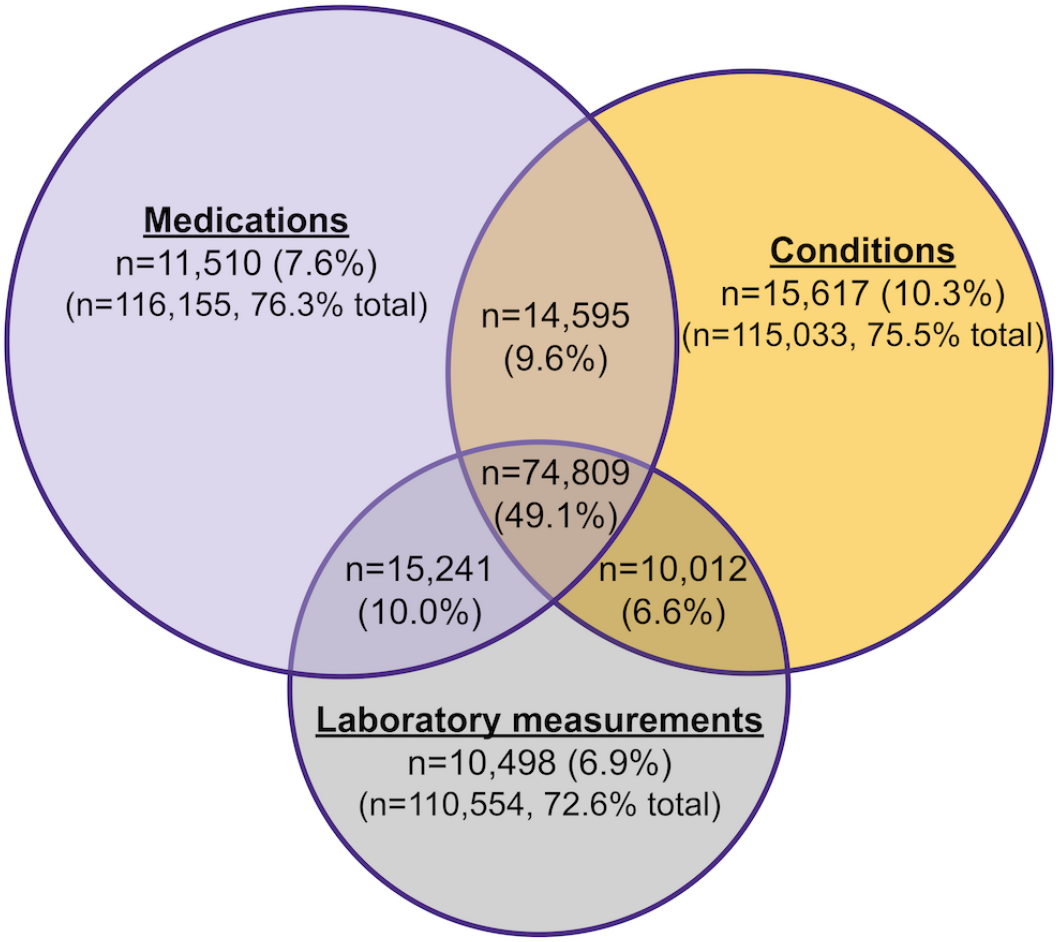


Table 1. Counts and percentages of people living with HIV in each confidence level by criterion (n=152,282).

Confidence level	Count, n (%)
Level 1 total	108,068 (71)
Criterion 1	41,923 (27.5)
Criterion 2	28,512 (18.7)
Criterion 3	1379 (0.9)
Criterion 4	5606 (3.7)
Criterion 5	18,499 (12.1)
Criterion 6	12,495 (8.2)
Level 2 total	24,596 (16.2)
Criterion 7	264 (0.2)
Criterion 8	13,061 (8.6)
Criterion 9	7509 (4.9)
Level 3 total	19,618 (12.9)
Criterion 10	7078 (4.6)
Criterion 11	4432 (2.9)
Criterion 12	8108 (5.3)

XSL•FO
RenderX

Table 2. Counts and percentages of individuals in each cohort (N=20,928,656)[a].

Cohort	Count, n (%)
People living with HIV (confidence levels 1-3)	152,282 (0.7)
People not living with HIV	20,639,675 (98.6)
PrEP[b] users	36,088 (0.2)
PEP[c] users	4120 (0)
Uncertain classification	96,491 (0.5)

[a]Count for the entire National Clinical Cohort Collaborative.

[b]PrEP: preexposure prophylaxis.

[c]PEP: postexposure prophylaxis.

Table 3. Counts and percentages of preexposure prophylaxis (PrEP) users in each confidence level (n=36,088).

Confidence level	Count, n (%)
Level 1	20,742 (57.5)
Level 2	3786 (10.5)
Level 3	11,560 (32)

Verification of Cohort of People Living With HIV, PrEP Users, and PEP Users via a Clinician Annotation Activity

To enhance the reliability of our methods, we conducted a clinician annotation process aimed at assessing the accuracy of our phenotyping methods for people living with HIV, PrEP users, and PEP users. Our results demonstrated excellent sensitivity (range 0.90-1), specificity (range 0.97-1), positive predictive value (range 0.77-1), negative predictive value (range 0.88-1), precision (range 0.77-1), recall (range 0.90-1), and F_1-score (range 0.87-1; Multimedia Appendix 2). Similarly, the κ values exhibited high levels of interrater reliability (range 0.91-0.98; Multimedia Appendix 2).

Characteristics of People Living With HIV, PrEP Users, and PEP Users in N3C

To obtain a more comprehensive understanding of the individuals within our various cohorts, we described their sociodemographic characteristics. Within the cohort of people living with HIV in the highest 2 confidence levels (132,664/152,282, 87.1% of all potential people living with HIV identified), the highest proportion of non-Hispanic Black individuals is in the people living with HIV cohort (49,769/132,664, 37.5%), followed by PEP users (784/4120, 19%), people not living with HIV (2,909,443/20,639,675, 14.1%), and finally among PrEP users (4534/36,088, 12.6%; Table 4). Notably, PrEP users contained the highest proportion of Hispanic or Latinx individuals (5829/36,088, 16.2%) of any race and ethnicity compared to other cohorts (people living with HIV: 20,925/132,664, 15.8%; PEP users: 403/4120, 9.8%; people not living with HIV: 2,628,308/20,639,675, 12.7%; Table 4). Male individuals constituted a higher proportion of people living with HIV (90,496/132,664, 68.2%) and PrEP users (31,722/36,088, 87.9%), which was notably higher than the proportion of male individuals among PEP cohorts (1399/4120, 34%) and people not living with HIV (9,044,853/20,639,675, 43.8%; Table 4). The median ages of people living with HIV, PrEP users, PEP users, and people not living with HIV were 51 (IQR 38-61), 36 (IQR 30-46), 35 (IQR 28-44), and 44 (IQR 26-63) years, respectively, demonstrating that PrEP and PEP users were generally younger than people living with HIV and people living without HIV (Table 4). We also examined comorbidities among people living with HIV compared to other cohorts and found that people living with HIV experienced chronic lung disease, liver disease, hypertension, kidney disease, and diabetes more often compared to PrEP users, PEP users, and people not living with HIV (Table 4).

XSL•FO
RenderX

Table 4. Descriptive statistics of people living with HIV, preexposure prophylaxis (PrEP) users, postexposure prophylaxis (PEP) users, and people not living with HIV cohorts.

Characteristics	People living with HIV (n=132,664; confidence level 1-2)	People living with HIV (n=152,282; confidence level 1-3)	PrEP users (n=36,088)	PEP users (n=4120)[a]	People not living with HIV (n=20,639,675)
Race or ethnicity, n (%)					
Hispanic or Latinx, any race	20,925 (15.8)	23,346 (15.3)	5829 (16.2)	403 (9.8)	2,628,308 (12.7)
Non-Hispanic American Indian or Alaska Native	615 (0.5)	684 (0.4)	163 (0.5)	<20 (0.5)	85,524 (0.4)
Non-Hispanic Asian	2753 (2.1)	3517 (2.3)	1726 (4.8)	222 (5.4)	729,491 (3.5)
Non-Hispanic Black or African American	49,769 (37.5)	55,144 (36.2)	4534 (12.6)	784 (19)	2,909,443 (14.1)
Non-Hispanic combined[b]	903 (0.7)	1150 (0.8)	505 (1.4)	40 (1)	281,450 (1.4)
Non-Hispanic Native Hawaiian or Pacific Islander	247 (0.2)	300 (0.2)	88 (0.2)	<20 (0.5)	67,808 (0.3)
Non-Hispanic White	48,604 (36.6)	57,479 (37.7)	19,663 (54.5)	2119 (51.4)	11,966,553 (58)
Unknown	8848 (6.7)	10,662 (7)	3580 (9.9)	512 (12.4)	1,971,098 (9.6)
Age (y), median (IQR)	51 (38-61)	51 (37-61)	36 (30-46)	35 (28-44)	44 (26-63)
Sex, n (%)					
Female	42,093 (31.7)	49,846 (32.7)	4253 (11.8)	2693 (65.4)	11,579,223 (56.1)
Male	90,496 (68.2)	102,332 (67.2)	31,722 (87.9)	1399 (34)	9,044,853 (43.8)
Combined or unknown[c]	75 (0.1)	104 (0.1)	113 (0.3)	<20 (0.5)	15,599 (0.1)
Comorbidity, n (%)					
Myocardial infarction	9265 (7)	10,349 (6.8)	482 (1.3)	57 (1.4)	795,829 (3.9)
Congestive heart failure	10,926 (8.2)	12,106 (7.9)	406 (1.1)	42 (1)	998,313 (4.8)
Peripheral vascular disease	8002 (6)	8971 (5.9)	352 (1)	52 (1.3)	787,932 (3.8)
Cerebrovascular disease	9082 (6.8)	10,123 (6.6)	492 (1.4)	76 (1.9)	977,070 (4.7)
Dementia	3177 (2.4)	3638 (2.4)	225 (0.6)	63 (1.5)	475,742 (2.3)
Chronic lung disease	40,080 (30.2)	44,328 (29.1)	5617 (15.6)	716 (17.5)	3,562,138 (17.3)
Rheumatologic disease	10,245 (7.7)	11,502 (7.6)	1280 (3.5)	139 (3.4)	1,097,753 (5.3)
Peptic ulcer	4445 (3.4)	4919 (3.2)	466 (1.3)	61 (1.5)	335,672 (1.6)
Liver disease	32,690 (24.6)	35,536 (23.3)	2965 (8.2)	320 (7.8)	1,314,849 (6.4)
Diabetes	28,307 (21.3)	31,731 (20.8)	2631 (7.3)	321 (7.8)	2,750,693 (13.3)
Hemiplegia or paraplegia	3751 (2.8)	4124 (2.7)	121 (0.3)	32 (0.8)	281,201 (1.4)
Kidney disease	26,015 (19.6)	28,288 (18.6)	1142 (3.2)	157 (3.8)	1,681,615 (8.1)
Cancer	20,035 (15.1)	22,447 (14.7)	1399 (3.9)	143 (3.5)	1,866,452 (9)
Hypertension	63,025 (47.5)	69,487 (45.6)	7464 (20.7)	691 (16.9)	5,904,993 (28.6)
Tobacco smoking	34,189 (25.8)	37,120 (24.4)	5830 (16.2)	550 (13.4)	1,844,538 (8.9)
BMI, n (%)					
Underweight	2280 (1.7)	2931 (1.9)	378 (1)	90 (2.2)	1,156,445 (5.6)
Healthy weight	20,789 (15.7)	23,743 (15.6)	6684 (18.5)	710 (17.3)	2,837,262 (13.7)
Overweight	35,471 (26.7)	39,718 (26.1)	10,600 (29.4)	864 (21.1)	3,565,102 (17.3)
Obese	52,872 (39.9)	59,238 (38.9)	12,240 (33.9)	1369 (33.4)	6,260,259 (30.3)
Missing	21,252 (16)	26,652 (17.5)	6186 (17.1)	1066 (26)	6,820,607 (33)

XSL•FO
RenderX

[a]The PEP cohort is estimated to obfuscate any groups with counts <20 to follow National Clinical Cohort Collaborative governance rules. This will also cause percentages not to sum to 100 in this group.

[b]Includes individuals with race and ethnicity variable values that do not include Hispanic, White, Black or African American, Asian, American Indian or Alaska Native, and Native Hawaiian or Other Pacific Islander.

[c]Includes individuals with sex variable values that do not include male or female.

HIV-Related Characteristics Among People Living With HIV in N3C

Of the 132,664 people living with HIV in the highest 2 confidence levels, 86,148 (64.9%) had at least 1 VL measurement, and 69,704 (52.5%) had at least 1 CD4 count recorded. The median number of VL and CD4 count laboratory tests was 5 (IQR 2-9) and 4 (IQR 2-8), respectively, per individual (Table 5). Of those with recorded VL and CD4 count measurements, 76,456 (57.6%) had VL and 69,254 (52.2%) had CD4 count results available for analysis (Table 5). Of those who had results, 41,923 (31.6%) had ≥1 detectable VLs (defined as VL >50 copies/mL) and 51,707 (39%) had ≥1 CD4 count <200 cells/µL (Table 5).

Table 5. HIV-related characteristics of people living with HIV, preexposure prophylaxis (PrEP) user, postexposure prophylaxis (PEP) user, and people not living with HIV cohorts.

Characteristics	People living with HIV (n=132,664; confidence level 1-2)	People living with HIV (n=152,282; confidence level 1-3)	PrEP users (n=36,088)	PEP users (n=4120)[a]	People not living with HIV (n=20,639,675)
Individuals with VL[b] and CD4[c] measurements, n (%)					
≥1 VL measurement	86,148 (64.9)	86,148 (56.6)	3983 (11)	0 (0)	11,390 (0.1)
≥1 CD4 measurement	69,704 (52.5)	69,704 (45.8)	259 (0.7)	0 (0)	36,528 (0.2)
VL measurements for analysis	76,456 (57.6)	76,456 (50.2)	3483 (9.7)	0 (0)	7599 (0)
CD4 measurement for analysis	69,254 (52.2)	69,254 (45.5)	238 (0.7)	0 (0)	36,121 (0.2)
VL and CD4 measurements per person (n), median (IQR)					
VL measurement count	5 (2-9)	5 (2-9)	1 (1-2)	0 (0-0)	1 (1-1)
CD4 measurement count	4 (2-8)	4 (2-8)	1 (1-1)	0 (0-0)	1 (1-3)
Individuals per VL category (copies/mL), n (%)					
VL ≥50	41,923 (31.6)	41,923 (27.5)	0 (0)	0 (0)	0 (0)
VL <50	34,533 (26)	34,533 (22.7)	3483 (9.7)	0 (0)	7599 (0)
VL unknown	9692 (7.3)	9692 (6.4)	500 (1.4)	4120[a] (100)	3792 (0)
VL null	46,516 (35.1)	66,134 (43.4)	32,105 (89)	0 (0)	20,628,284 (99.9)
Individuals per CD4 category (cells/µL), n (%)					
CD4 >200	51,707 (39)	51,707 (34)	238 (0.7)	0 (0)	27,718 (0.1)
CD4 ≤200	17,547 (13.2)	17,547 (11.5)	0 (0)	0 (0)	8403 (0)
CD4 unknown	450 (0.3)	450 (0.3)	21 (0.1)	4120[a] (100)	407 (0)
CD4 null	62,960 (47.5)	82,578 (54.2)	35,829 (99.3)	0 (0)	20,603,147 (99.8)
Individuals with HIV-related conditions and negative laboratory results, n (%)	11,048 (8.3)	11,048 (7.3)	0 (0)	0 (0)	0 (0)

[a]The PEP cohort is estimated to obfuscate any groups with counts <20 to follow National Clinical Cohort Collaborative governance rules.

[b]VL: viral load.

[c]CD4: cluster of differentiation 4.

COVID-19 Outcomes in People Living With HIV, PrEP Users, and PEP Users in N3C

We examined the distribution of COVID-19–related variables within the cohorts of people living with HIV, PrEP users, and PEP users in comparison to people not living with HIV. The number of individuals who were tested for COVID-19, regardless of the results, was 104,903 (79.1%) among 132,664 people living with HIV (confidence levels 1 and 2), 30,799 (85.3%) for 36,008 PrEP users, 3704 (89.9%) for 4120 PEP users, and 17,756,497 (86%) in 20,639,675 people not living with HIV (Table 6). The proportions who tested positive for COVID-19 were similar between the cohorts; there were 34.4% (45,609/132,664) people living with HIV, 33.6% (12,121/36,088) PrEP users, 37% (1525/4120) PEP users, and 38.6% (7,970,336/20,639,675) people not living with HIV who tested positive for COVID-19 (Table 6). When categorizing individuals based on the severity of COVID-19, a higher

XSL•FO
RenderX

proportion of people living with HIV experienced a COVID-19–related hospitalization (4650/132,664, 3.5%), COVID-19–related mortality (828/132,664, 0.6%), and all-cause mortality (2083/132,664, 1.6%) outcomes compared to people not living with HIV who had a lower proportion of COVID-19–related hospitalization (407,894/20,639,675, 2%), COVID-19–related mortality (95,421/20,639,675, 0.5%), and all-cause mortality (192,519/20,639,675, 0.9%; Table 6). With regard to receipt of COVID-19 vaccinations, people living with HIV exhibited a lower proportion of full primary (ie, completing 2 doses when applicable) vaccination documentation (15,387/132,664, 11.6%) compared to PrEP users (5414/36,088, 15%), although it was higher compared to PEP users (441/4120, 10.7%) and similar to people not living with HIV (2,327,522/20,639,675, 11.3%; Table 6). The booster vaccination documentation displayed a lower proportion of people living with HIV receiving any booster vaccination (28,520/132,664, 21.5%) compared to PrEP users (12,547/36,088, 34.8%) but higher than PEP users (559/4120, 13.6%) and people not living with HIV (2,521,638/20,639,675, 12.2%; Table 6).

Table 6. COVID-19–related characteristics of the people living with HIV, preexposure prophylaxis (PrEP) user, postexposure prophylaxis (PEP) user, and people not living with HIV cohorts.

Characteristics	People living with HIV (n=132,664; confidence level 1-2), n (%)	People living with HIV (n=152,282; confidence level 1-3), n (%)	PrEP users (n=36,088), n (%)	PEP users (n=4120)[a], n (%)	People not living with HIV (n=20,639,675), n (%)
COVID-19 testing and outcomes					
COVID-19 screening	104,903 (79.1)	121,130 (79.5)	30,799 (85.3)	3704 (90.4)	17,756,497 (86)
COVID-19 positivity	45,609 (34.4)	52,223 (34.3)	12,121 (33.6)	1525 (37.2)	7,970,336 (38.6)
COVID-19–associated hospitalization	4650 (3.5)	5259 (3.5)	226 (0.6)	51 (1.2)	407,894 (2)
COVID-19–associated mortality	828 (0.6)	1027 (0.7)	<20 (0.1)	<20 (0.5)	95,421 (0.5)
All-cause mortality among individuals with COVID-19	2083 (1.6)	2412 (1.6)	40 (0.1)	<20 (0.5)	192,519 (0.9)
Had ≥1 COVID-19 reinfection	2864 (2.2)	3204 (2.1)	612 (1.7)	118 (2.9)	353,177 (1.7)
COVID-19 vaccination					
No vaccination documented	81,096 (61.1)	95,300 (62.6)	15,855 (43.9)	2922 (71.3)	15,087,131 (73.1)
Partial primary vaccination series documented	7661 (5.8)	8464 (5.6)	2272 (6.3)	177 (4.3)	703,384 (3.4)
Full primary vaccination series documented	15,387 (11.6)	17,301 (11.4)	5414 (15)	441 (10.7)	2,327,522 (11.3)
Booster vaccination documented	28,520 (21.5)	31,217 (20.5)	12,547 (34.8)	559 (13.6)	2,521,638 (12.2)

[a]The PEP cohort is estimated to obfuscate any groups with counts <20 to follow National Clinical Cohort Collaborative governance rules.

Discussion

Principal Findings

Using an extensive phenotyping algorithm that leverages granular data for medical conditions, laboratory measurements, and drug exposures available in an EHR repository, we have identified people living with HIV, PrEP users, and PEP users, augmented by confidence levels to provide flexibility in cohort selection to address potential misclassification. Our algorithm was refined using an iterative process with multiple reviews by clinicians with HIV experience to reduce misclassification. Our work allows for rapid identification of people living with HIV in large datasets originating from multiple health systems, with reduced misclassification among PrEP or PEP users, those with HBV infection only, or those prescribed ritonavir only for COVID-19 treatment. Our computational phenotyping approach allows for greater transferability to other EHR data sources, accounts for nuances after the emergence of COVID-19, and is applicable for optimizing future research. Our approach lays the groundwork for large epidemiological investigations among people living with HIV and those at risk of acquiring HIV [13,14,38-41], noting that analyses to date that use this phenotyping have influenced guidance for COVID-19 vaccination prioritization for people living with HIV and can inform interventions, ranging from addressing clinical to social needs.

We have identified one of the largest cohorts of people living with HIV in the United States, leveraging a nationally sampled EHR repository. The overall distribution of sociodemographic, comorbidity, and COVID-19 findings of our cohorts is consistent with available literature. We identified a higher proportion of diabetes, hypertension, and chronic lung disease in people living with HIV than in people not living with HIV, which reflects the epidemiology of comorbidity burden for HIV in the United States [1,42]. Similarly, where laboratory results were available, our proportion of people living with HIV with undetectable VL

XSL•FO
RenderX

(34,533/132,664, 26%) reflects the HIV care continuum for the United States [1]. In addition, the demographics for PrEP users are also consistent with what has been previously reported in the United States. Similarly, with regard to COVID-19, we saw increased COVID-19–related hospitalizations, mortality, and all-cause mortality in people living with HIV than in people not living with HIV, which has been previously reported in other cohorts of people living with HIV [43-46]. Nonetheless, appreciating the nuanced similarities and differences between our N3C cohorts and others helps articulate places of generalizability to the HIV or PrEP populations in the United States.

One key element of our computational phenotype, with clinician annotation, aimed to minimize potential misclassification. For instance, in the entire N3C, we identified 121,099 individuals with a condition for HIV, but 16,185 (13.4%) of them had tested negative for HIV, suggesting these individuals may be misclassified if we used medical conditions alone. In our experience, it also appeared that medical conditions were occasionally applied inappropriately for those who were being screened for HIV or receiving prescriptions for PrEP or PEP. Many of the published HIV case-finding algorithms, with specificity frequently >90%, were validated before approval of and more expanded access to PrEP or nonoccupational PEP [47,48]. Thus, the potential for misclassification is greater now than ever.

Our computational phenotyping approach parallels other recent work, although arguably, it adds nuances that help reduce potential misclassification. Yang et al [23] conducted a study involving computational phenotyping of people living with HIV and PrEP users within the All of Us research program. They used a hybrid approach, with both EHR and self-reported survey data, to identify people living with HIV. Notably, their findings indicated that the identification of people living with HIV was most prevalent through a combination of drug exposures and medical conditions (n=3324 individuals, constituting 43.4% as opposed to our study with 14,595/152,282, 9.6%) as well as drug exposure alone (n=2191 individuals, accounting for 28.6% as opposed to our study with 11,510/152,282, 7.6%), with 19.9% (43,419/216,971) of the individuals with drug exposure only to ritonavir [23]. Similarly, in the HIV-Phen algorithm, May et al [24] identified misclassification with *ICD-10* codes alone, including roughly 6.5% of individuals who only had a screening test. Within the Veterans Health Administration, using a single *ICD-10* code alone provided a positive predictive value of only 69% [25]. Notably, among our cohort of people not living with HIV, 6065 individuals had inappropriate HIV-related conditions assigned despite their data suggesting they are not living with HIV, and 4159 (68.6%) of them had only a single medical condition; 58 of the PrEP users in our PrEP cohort had a condition for HIV inappropriately assigned. This misclassification was relatively small for the people not living with HIV cohort (6065/20,639,675, 0.03%); however, it would make up 4% of our people living with HIV cohort if they were included. This underscores the fallibility of relying on diagnostic codes alone, and our work can provide estimates of misclassification for researchers who may not have access to additional clinical data (ie, those limited to claims data). To help address the low specificity of medical conditions alone, we used a comprehensive approach evaluating not only positive or negative laboratory results to identify our cohorts but also repeated laboratory measurements over time. For example, an instance of an individual with one row of medical condition data followed by multiple negative HIV antigen or antibody tests is more consistent with an HIV-related condition assigned incorrectly. In contrast, an instance of an individual with one row of medical condition data followed by repeated VL and CD4 laboratory measurements is more consistent with an HIV-related condition being assigned correctly. We estimate that using medical conditions alone in other published algorithms, approximately 13.4% of probable people living with HIV were potentially misclassified according to the methods developed by Yang et al [23]. Adding an algorithm to identify PEP users also allows for reduced misclassification, as these individuals were identified by drug exposures only and would be classified as people living with HIV if not properly removed.

Another novel element of our computational phenotyping is the ability to identify individuals at risk for HIV through both PrEP and PEP exposures. Unfortunately, due to low numbers of people with exposure to long-acting injectables (cabotegravir and lenacapavir) in N3C, these were not included in our phenotyping; however, this work is currently in progress as the use of these agents expands. Among the aforementioned studies, only one [23] conducts computational phenotyping to identify PrEP or PEP users, with the latter being a group of people exposed to HIV drugs but only for a short time and, thus, embodying an element of temporality that is only available in longitudinal datasets. This provides the benefit of reducing potential misclassification between these 3 cohorts with antiretroviral drug exposure for differing reasons and provides additional comparator groups at risk of acquiring HIV for analyses. Nonetheless, readers should consider that our overall approach lacks source validation, as N3C prohibits reidentification of individuals with site data. While our clinician annotation provided measures of high consistency, we are unable to assess accuracy. Thus, we are limited in adjudicating further these reductions in potential misclassification without source validation.

With the emergence of COVID-19 and one of its primary treatments (ie, oral nirmatrelvir/ritonavir), which includes an antiretroviral also used for HIV treatment, using a single antiretroviral alone after COVID-19 can result in misclassification. Out of the entire N3C population, we identified 0.21% (43,149/20,832,144) of the individuals with only ritonavir exposure and 0.03% (6586/20,832,144) with ritonavir exposure and an HIV laboratory measurement. From this point forward, in the post–COVID-19 era, additional steps need to be implemented to reduce misclassification of people not living with HIV as people living with HIV when isolated ritonavir exposures exist. Yang et al [23] identified 2191 individuals (accounting for 28.6% of people living with HIV) by drug exposure alone; 19.9% (43,149/216,971) of our study's drug-only population had ritonavir-only exposures, underscoring the point that, after the emergence of COVID-19, potential misclassification based on drug alone may be a significant issue [23].

XSL•FO
RenderX

A clinician-annotated approach to computational phenotyping of a cohort involving individuals with HIV is desirable from several points of view, engendering, for example, the use of clinically relevant data and insights. However, such efforts are less reproducible and repeatable over time. Thus, future work in automation, for example, through machine learning, could provide unique insights into how such a cohort can more readily be derived in any EHR dataset. Future research can assess various performance characteristics of clinician-annotated or curated approaches to automation approaches, as we acknowledge that our clinician-annotated approach was time consuming and may face challenges in transferability to other EHR repositories, despite our best efforts in making our phenotyping approach and code as transparent as possible.

Strengths and Limitations

While our work has several strengths, including identifying one of the largest cohorts of people living with HIV in the United States, demonstrating high consistency with our phenotyping using clinician annotation, and identifying PrEP and PEP users, it also faces several challenges. First, as already noted, the lack of source validation or any external validation limits our ability to assess the accuracy of the phenotypes. That being said, given our use of highly specific HIV laboratory data and repeated measures over time, we are extremely confident in our identification of people living with HIV in our confidence levels 1 and 2. Second, our dataset contains a significant amount of noninformative data. For example, there are instances where we can ascertain that an HIV screening test was performed, but the result is not available in an interpretable form, or a CD4 count is available, but the units are missing. This is likely a by-product of data ingestion and harmonization across multiple different health systems; while major strides have been made in EHR interoperability, more work needs to be done to meaningfully use all available data in the various EHRs and improve the quality of data ingestion processes. Third, while the N3C Enclave cohort is inclusive of multiple health systems across the United States, it is still only inclusive of individuals with encounters with the health care system, hence various characteristics, including COVID-19 outcomes, may not be fully generalizable to those affected by HIV with limited or no access to care, who are often the most vulnerable of the vulnerable.

Conclusions

Using an extensive phenotyping algorithm leveraging granular data in an EHR repository for medical conditions, laboratory measurements, and drug exposures, we have identified people living with HIV, PrEP users, and PEP users with high precision in the post–COVID-19 era. Our approach offers flexibility to select cohorts with confidence levels that best fit the needs of the research question under investigation, with regard to potential misclassification. We offer transferable lessons to optimize future EHR phenotyping for these cohorts. Our approach lays the groundwork for large epidemiological investigations among people living with HIV and those at risk for acquiring HIV and can inform interventions addressing clinical and social needs.

Acknowledgments

The authors would like to especially thank patients whose data are used in this analysis and the various National Clinical Cohort Collaborative (N3C) team members, whose work enables this and other research.

ChatGPT (GPT-3.5; OpenAI) and Claude (Anthropic) were used to edit pieces of the manuscript, including language, grammar, and synonyms. All edits by ChatGPT and Claude were reviewed by the authors and were not used for idea or content creation.

The analyses described in this paper were conducted with data or tools accessed through the National Center for Advancing Translational Sciences (NCATS) N3C Data Enclave [49] and N3C Attribution and Publication Policy (version 1.2-2020-08-25b) supported by NCATS U24 TR002306 and Axle Informatics subcontract (NCATS-P00438-B). Individual authors were supported by the following funding sources: National Institute of Mental Health (NIMH; R01131542; principal investigator [PI] RCP). The funding sources or study sponsors had no role in study design; in the collection, analysis, and interpretation of data; in the writing of the report; and in the decision to submit the paper for publication. This research was possible because of the patients whose information is included within the data and the organizations [50] and the scientists who have contributed to the ongoing development of this community resource [51].

The authors gratefully acknowledge the following core contributors to N3C: Adam B Wilcox, Adam M Lee, Alexis Graves, Alfred (Jerrod) Anzalone, Amin Manna, Amit Saha, Andrea Zhou, Andrew E Williams, Andrew Southerland, Andrew T Girvin, Anita Walden, Anjali A Sharathkumar, Benjamin Amor, Benjamin Bates, Brian Hendricks, Brijesh Patel, Caleb Alexander, Carolyn Bramante, Cavin Ward-Caviness, Charisse Madlock-Brown, Christine Suver, Christopher Chute, Christopher Dillon, Chunlei Wu, Clare Schmitt, Cliff Takemoto, Dan Housman, Davera Gabriel, David A Eichmann, Diego Mazzotti, Don Brown, Eilis Boudreau, Elaine Hill, Elizabeth Zampino, Emily Carlson Marti, Emily R Pfaff, Evan French, Farrukh M Koraishy, Federico Mariona, Fred Prior, George Sokos, Greg Martin, Harold Lehmann, Heidi Spratt, Hemalkumar Mehta, Hongfang Liu, Hythem Sidky, JW Awori Hayanga, Jami Pincavitch, Jaylyn Clark, Jeremy Richard Harper, Jin Ge, Joel Gagnier, Joel H Saltz, Joel Saltz, Johanna Loomba, John Buse, Jomol Mathew, Joni L Rutter, Justin Guinney, Justin Starren, Karen Crowley, Katie Rebecca Bradwell, Kellie M Walters, Kenneth R Gersing, Kenrick Dwain Cato, Kimberly Murray, Kristin Kostka, Lavance Northington, Lee Allan Pyles, Leonie Misquitta, Lesley Cottrell, Lili Portilla, Mariam Deacy, Mark M Bissell, Marshall Clark, Mary Emmett, Mary Morrison Saltz, Matvey B Palchuk, Melissa A Haendel, Meredith Adams, Meredith Temple-O'Connor, Michael G. Kurilla, Michele Morris, Nabeel Qureshi, Nasia Safdar, Nicole Garbarini, Noha Sharafeldin, Ofer Sadan, Patricia A Francis, Penny Wung

XSL•FO
RenderX

Burgoon, Peter Robinson, Philip RO Payne, Rafael Fuentes, Randeep Jawa, Rebecca Erwin-Cohen, Richard A Moffitt, Richard L Zhu, Rishi Kamaleswaran, Robert Hurley, Robert T Miller, Saiju Pyarajan, Sam G Michael, Samuel Bozzette, Sandeep Mallipattu, Satyanarayana Vedula, Scott Chapman, Shawn T O'Neil, Soko Setoguchi, Stephanie S Hong, Steve Johnson, Tellen D Bennett, Tiffany Callahan, Umit Topaloglu, Usman Sheikh, Valery Gordon, Vignesh Subbian, Warren A Kibbe, Wenndy Hernandez, Will Beasley, Will Cooper, William Hillegass, and Xiaohan Tanner Zhang.

Details of contributions are available at the N3C Data Enclave website [52].

Additional collaborators were Jasvinder A Singh, Alfred Anzalone, Christopher G Chute, Alyssa Columbus, Mary Emmett, and Evguenia Malaia.

The following include data partner institutions, whose data are released or pending:

Available: Advocate Health Care Network—UL1TR002389: The Institute for Translational Medicine); Aurora Health Care Inc—UL1TR002373: Wisconsin Network For Health Research; Boston University Medical Campus—UL1TR001430: Boston University Clinical and Translational Science Institute; Brown University—U54GM115677: Advance Clinical Translational Research; Carilion Clinic—UL1TR003015: Integrated Translational Health Research Institute of Virginia; Case Western Reserve University—UL1TR002548: The Clinical and Translational Science Collaborative of Cleveland; Charleston Area Medical Center—U54GM104942: West Virginia Clinical and Translational Science Institute; Children's Hospital Colorado—UL1TR002535: Colorado Clinical and Translational Sciences Institute; Columbia University Irving Medical Center—UL1TR001873: Irving Institute for Clinical and Translational Research; Dartmouth College—None (Voluntary) Duke University—UL1TR002553: Duke Clinical and Translational Science Institute; George Washington Children's Research Institute—UL1TR001876: Clinical and Translational Science Institute at Children's National; George Washington University—UL1TR001876: Clinical and Translational Science Institute at Children's National; Harvard Medical School—UL1TR002541: Harvard Catalyst; Indiana University School of Medicine—UL1TR002529: Indiana Clinical and Translational Science Institute; Johns Hopkins University—UL1TR003098: Johns Hopkins Institute for Clinical and Translational Research; Louisiana Public Health Institute—None (Voluntary); Loyola Medicine—Loyola University Medical Center; Loyola University Medical Center—UL1TR002389: The Institute for Translational Medicine; Maine Medical Center—U54GM115516: Northern New England Clinical and Translational Research Network; Mary Hitchcock Memorial Hospital and Dartmouth Hitchcock Clinic—None (Voluntary);Massachusetts General Brigham—UL1TR002541: Harvard Catalyst; Mayo Clinic Rochester—UL1TR002377: Mayo Clinic Center for Clinical and Translational Science; Medical University of South Carolina—UL1TR001450: South Carolina Clinical and Translational Research Institute; MITRE Corporation—None (Voluntary); Montefiore Medical Center—UL1TR002556: Institute for Clinical and Translational Research at Einstein and Montefiore; Nemours—U54GM104941: Delaware Clinical and Translational Research, Accelerating Clinical and Translational Research Program; NorthShore University Health System—UL1TR002389: The Institute for Translational Medicine; Northwestern University at Chicago—UL1TR001422: Northwestern University Clinical and Translational Science Institute; Oregon Community Health Information Network—INV-018455: Bill and Melinda Gates Foundation grant to Sage Bionetworks; Oregon Health and Science University—UL1TR002369: Oregon Clinical and Translational Research Institute; Penn State Health Milton S Hershey Medical Center—UL1TR002014: Penn State Clinical and Translational Science Institute; Rush University Medical Center—UL1TR002389: The Institute for Translational Medicine; Rutgers, The State University of New Jersey—UL1TR003017: New Jersey Alliance for Clinical and Translational Science;Stony Brook University—U24TR002306; The Alliance at the University of Puerto Rico, Medical Sciences Campus—U54GM133807: Hispanic Alliance for Clinical and Translational Research (The Alliance); The Ohio State University—UL1TR002733: Center for Clinical and Translational Science; The State University of New York at Buffalo—UL1TR001412: Clinical and Translational Science Institute; The University of Chicago—UL1TR002389: The Institute for Translational Medicine; The University of Iowa—UL1TR002537: Institute for Clinical and Translational Science; The University of Miami Leonard M. Miller School of Medicine—UL1TR002736: University of Miami Clinical and Translational Science Institute; The University of Michigan at Ann Arbor—UL1TR002240: Michigan Institute for Clinical and Health Research; The University of Texas Health Science Center at Houston—UL1TR003167: Center for Clinical and Translational Sciences; The University of Texas Medical Branch at Galveston—UL1TR001439: The Institute for Translational Sciences; The University of Utah—UL1TR002538: Uhealth Center for Clinical and Translational Science; Tufts Medical Center—UL1TR002544: Tufts Clinical and Translational Science Institute; Tulane University—UL1TR003096: Center for Clinical and Translational Science; The Queens Medical Center—None (Voluntary); University Medical Center New Orleans—U54GM104940: Louisiana Clinical and Translational Science Center; University of Alabama at Birmingham—UL1TR003096: Center for Clinical and Translational Science; University of Arkansas for Medical Sciences—UL1TR003107: UAMS Translational Research Institute; University of Cincinnati—UL1TR001425: Center for Clinical and Translational Science and Training; University of Colorado Denver, Anschutz Medical Campus—UL1TR002535: Colorado Clinical and Translational Sciences Institute; University of Illinois at Chicago—UL1TR002003: University of Illinois Center for Clinical and Translational Science; University of Kansas Medical Center—UL1TR002366: Frontiers: University of Kansas Clinical and Translational Science Institute; University of Kentucky—UL1TR001998: UK Center for Clinical and Translational Science; University of Massachusetts Medical School Worcester—UL1TR001453: The UMass Center for Clinical and Translational Science; University Medical Center of Southern Nevada—None (voluntary); University of Minnesota—UL1TR002494: Clinical and Translational Science Institute; University

XSL•FO
RenderX

of Mississippi Medical Center—U54GM115428: Mississippi Center for Clinical and Translational Research; University of Nebraska Medical Center—U54GM115458: Great Plains IDeA-Clinical and Translational Research; University of North Carolina at Chapel Hill—UL1TR002489: North Carolina Translational and Clinical Science Institute; University of Oklahoma Health Sciences Center—U54GM104938: Oklahoma Clinical and Translational Science Institute; University of Pittsburgh—UL1TR001857: The Clinical and Translational Science Institute; University of Pennsylvania—UL1TR001878: Institute for Translational Medicine and Therapeutics; University of Rochester—UL1TR002001: UR Clinical and Translational Science Institute; University of Southern California—UL1TR001855: The Southern California Clinical and Translational Science Institute; University of Vermont—U54GM115516: Northern New England Clinical and Translational Research Network; University of Virginia—UL1TR003015: Integrated Translational Health Research Institute of Virginia; University of Washington—UL1TR002319: Institute of Translational Health Sciences; University of Wisconsin-Madison—UL1TR002373: UW Institute for Clinical and Translational Research; Vanderbilt University Medical Center—UL1TR002243: Vanderbilt Institute for Clinical and Translational Research; Virginia Commonwealth University—UL1TR002649: C. Kenneth and Dianne Wright Center for Clinical and Translational Research; Wake Forest University Health Sciences—UL1TR001420: Wake Forest Clinical and Translational Science Institute; Washington University in St Louis—UL1TR002345: Institute of Clinical and Translational Sciences; Weill Medical College of Cornell University—UL1TR002384: Weill Cornell Medicine Clinical and Translational Science Center; West Virginia University—U54GM104942: West Virginia Clinical and Translational Science Institute.

Submitted: Icahn School of Medicine at Mount Sinai—UL1TR001433: ConduITS Institute for Translational Sciences; The University of Texas Health Science Center at Tyler—UL1TR003167: Center for Clinical and Translational Sciences; University of California, Davis—UL1TR001860: UCDavis Health Clinical and Translational Science Center; University of California, Irvine—UL1TR001414: The UC Irvine Institute for Clinical and Translational Science; University of California, Los Angeles—UL1TR001881: UCLA Clinical Translational Science Institute; University of California, San Diego—UL1TR001442: Altman Clinical and Translational Research Institute; University of California, San Francisco—UL1TR001872: UCSF Clinical and Translational Science Institute.

Pending: Arkansas Children's Hospital—UL1TR003107: University of Arkansas for Medical Sciences Translational Research Institute; Baylor College of Medicine—None (Voluntary); Children's Hospital of Philadelphia—UL1TR001878: Institute for Translational Medicine and Therapeutics; Cincinnati Children's Hospital Medical Center—UL1TR001425: Center for Clinical and Translational Science and Training; Emory University—UL1TR002378: Georgia Clinical and Translational Science Alliance; HonorHealth—None (Voluntary); Loyola University Chicago—UL1TR002389: The Institute for Translational Medicine; Medical College of Wisconsin—UL1TR001436: Clinical and Translational Science Institute of Southeast Wisconsin; MedStar Health Research Institute—None (Voluntary); Georgetown University—UL1TR001409: The Georgetown-Howard Universities Center for Clinical and Translational Science; MetroHealth—None (Voluntary); Montana State University—U54GM115371: American Indian/Alaska Native CTR; New York University Langone Medical Center—UL1TR001445: Langone Health's Clinical and Translational Science Institute; Ochsner Medical Center—U54GM104940: Louisiana Clinical and Translational Science Center; Regenstrief Institute—UL1TR002529: Indiana Clinical and Translational Science Institute; Sanford Research—None (Voluntary); Stanford University—UL1TR003142: Spectrum: The Stanford Center for Clinical and Translational Research and Education; The Rockefeller University—UL1TR001866: Center for Clinical and Translational Science; The Scripps Research Institute—UL1TR002550: Scripps Research Translational Institute; University of Florida—UL1TR001427: University of Florida Clinical and Translational Science Institute; University of New Mexico Health Sciences Center—UL1TR001449: University of New Mexico Clinical and Translational Science Center; University of Texas Health Science Center at San Antonio—UL1TR002645: Institute for Integration of Medicine and Science; Yale New Haven Hospital—UL1TR001863: Yale Center for Clinical Investigation

The overall work was supported by the National Institutes of Health (NIH; National Institute of Mental Health [NIMH]) R01131542; PI RCP and the National Institute of Diabetes and Digestive and Kidney Diseases Office of the Director; KJW). The funding sources or study sponsors had no role in study design; in the collection, analysis, and interpretation of data; in the writing of the report; and in the decision to submit the paper for publication.

The N3C Publication committee confirmed that this manuscript (MSID:2139.561) is in accordance with N3C data use and attribution policies; however, this content is solely the responsibility of the authors and does not necessarily represent the official views of the NIH or the N3C program.

The N3C data transfer to NCATS is performed under a Johns Hopkins University Reliance Protocol (IRB00249128) or individual site agreements with NIH. The N3C Data Enclave is managed under the authority of the NIH; information can be found at the NCATS website [53].

Data Availability

The National Clinical Cohort Collaborative (N3C) data transfer to the National Center for Advancing Translational Sciences is performed under a Johns Hopkins University Reliance Protocol (IRB00249128) or individual site agreements with the National Institutes of Health (NIH). The N3C Data Enclave is managed under the authority of the NIH; information can be found [54]. N3C Enclave data are protected and can be accessed for COVID-19–related research with an NIH-approved (1) IRB protocol

XSL•FO
RenderX

and (2) institutional Data Use Request (DUR ID: RP-CA3365). A detailed accounting of data protections and access tiers is found at the NCATS website [54]. N3C Enclave and data access instructions can be found at the N3C website [55]; all codes used to produce the analyses in this manuscript are available within the N3C Enclave to users with valid log-in credentials to support reproducibility.

Authors' Contributions

EH and CDV take responsibility for the whole manuscript. RCP, EH, CDV, VM, and ALO were responsible for conceptualization. RCP, CDV, EH, KJW, and AJA were responsible for methodology. RCP, CDV, EH, AJA, VM, and ALO were responsible for phenotype development. RCP, CDV, EH, NF, JS, LEJ, and DV were responsible for phenotype validation. EH was responsible for software validation and data curation. Formal analysis was conducted by EH, KJW, DL, and SES. Investigation was performed by RCP, CDV, and EH. RCP and MAH were responsible for resources. CDV, EH, and RCP were responsible for the original manuscript draft preparation. AJA, VM, ALO, JS, DV, NF, JYI, LEJ, KJW, ZB-D, DL, SES, JAM, PM, TW, SAH, and MAH were responsible for reviewing and editing the manuscript. EH and JAM were responsible for visualization. RCP was responsible for supervision. RCP, SAH, TW, and PM were involved in project administration. RCP and MAH were responsible for funding acquisition.

Conflicts of Interest

None declared.

Multimedia Appendix 1
Supplementary methods for applying confidence levels to people living with HIV, pre-exposure prophylaxis users, the clinician annotation activity, demographic and comorbidity definitions, and COVID-19 outcomes definitions.
[DOC File , 1236 KB - medinform_v13i1e68143_app1.doc]

Multimedia Appendix 2
Performance of our clinician annotation activity in people living with HIV, pre-exposure prophylaxis, postexposure prophylaxis, and people not living with HIV cohorts.
[DOC File , 78 KB - medinform_v13i1e68143_app2.doc]

References

1. Fast facts: HIV in the United States. Centers for Disease Control and Prevention. 2024 Apr 22. URL: https://www.cdc.gov/hiv/data-research/facts-stats/index.html [accessed 2025-05-28]
2. Sun J, Patel RC, Zheng Q, Madhira V, Olex AL, Islam JY, et al. COVID-19 disease severity among people with HIV infection or solid organ transplant in the United States: a nationally-representative, multicenter, observational cohort study. medRxiv Preprint posted online on July 28, 2021 [FREE Full text] [doi: 10.1101/2021.07.26.21261028] [Medline: 34341798]
3. Kouhpayeh H, Ansari H. HIV infection and increased risk of COVID-19 mortality: a meta-analysis. Eur J Transl Myol 2021 Dec 21;31(4):10107 [FREE Full text] [doi: 10.4081/ejtm.2021.10107] [Medline: 34962366]
4. Tesoriero JM, Swain CA, Pierce JL, Zamboni L, Wu M, Holtgrave DR, et al. COVID-19 outcomes among persons living with or without diagnosed HIV infection in New York State. JAMA Netw Open 2021 Feb 01;4(2):e2037069 [FREE Full text] [doi: 10.1001/jamanetworkopen.2020.37069] [Medline: 33533933]
5. Hoover KW, Zhu W, Gant ZC, Delaney KP, Wiener J, Carnes N, et al. HIV services and outcomes during the COVID-19 pandemic - United States, 2019-2021. MMWR Morb Mortal Wkly Rep 2022 Dec 02;71(48):1505-1510 [FREE Full text] [doi: 10.15585/mmwr.mm7148a1] [Medline: 36454696]
6. Menza TW, Zlot A, Gonzalez-Pena Y, Capizzi J, Bush L, Humphrey S, et al. The ongoing impact of COVID-19 on testing for and diagnoses of HIV and bacterial sexually transmitted infections in Oregon. Sex Transm Dis 2023 Aug 01;50(8):543-549 [FREE Full text] [doi: 10.1097/OLQ.0000000000001817] [Medline: 37074311]
7. Moitra E, Tao J, Olsen J, Shearer RD, Wood BR, Busch AM, et al. Impact of the COVID-19 pandemic on HIV testing rates across four geographically diverse urban centres in the United States: an observational study. Lancet Reg Health Am 2022 Mar;7:100159 [FREE Full text] [doi: 10.1016/j.lana.2021.100159] [Medline: 34961858]
8. Meyer D, Slone SE, Ogungbe O, Duroseau B, Farley J. Impact of the COVID-19 pandemic on HIV healthcare service engagement, treatment adherence, and viral suppression in the United States: a systematic literature review. AIDS Behav 2023 Jan;27(1):344-357 [FREE Full text] [doi: 10.1007/s10461-022-03771-w] [Medline: 35916951]
9. Tao L, Hojilla J, Shvachko V, Yang J, Carter CC, Das M. Increase in new HIV diagnoses following decrease in use of pre-exposure prophylaxis (PrEP) during the COVID-19 pandemic. Open Forum Infect Dis 2023;10(Supplement_2):ofad500.1391 [FREE Full text] [doi: 10.1093/ofid/ofad500.1391]

XSL•FO
RenderX

10. Fallahi M, Guadamuz JS, Shooshtari A, Qato DM. Changes in HIV pre-exposure prophylaxis (PrEP) coverage at state and county level during the COVID-19 pandemic in the United States. AIDS Behav 2024 Mar;28(3):799-804 [FREE Full text] [doi: 10.1007/s10461-023-04180-3] [Medline: 37751110]
11. Millett G. New pathogen, same disparities: why COVID-19 and HIV remain prevalent in U.S. communities of colour and implications for ending the HIV epidemic. J Int AIDS Soc 2020 Nov;23(11):e25639 [FREE Full text] [doi: 10.1002/jia2.25639] [Medline: 33222424]
12. Beltran RM, Holloway IW, Hong C, Miyashita A, Cordero L, Wu E, et al. Social determinants of disease: HIV and COVID-19 experiences. Curr HIV/AIDS Rep 2022 Feb;19(1):101-112 [FREE Full text] [doi: 10.1007/s11904-021-00595-6] [Medline: 35107810]
13. Islam J, Madhira V, Sun J, Olex A, Franceschini N, Kirk G, et al. Racial disparities in COVID-19 test positivity among people living with HIV in the United States. Int J STD AIDS 2022 Apr;33(5):462-466 [FREE Full text] [doi: 10.1177/09564624221074468] [Medline: 35306931]
14. Vaidya D, Wilkins KJ, Hurwitz E, Islam JY, Li D, Sun J, et al. Assessing associations between individual-level social determinants of health and COVID-19 hospitalizations: investigating racial/ethnic disparities among people living with human immunodeficiency virus (HIV) in the U.S. National COVID Cohort Collaborative (N3C). J Clin Transl Sci 2024;8(1):e107 [FREE Full text] [doi: 10.1017/cts.2024.550] [Medline: 39296577]
15. Islam JY, Hurwitz E, Li D, Camacho-Rivera M, Sun J, Safo S, et al. Associations of county-level social determinants of health with COVID-19 related hospitalization among people with HIV: a retrospective analysis of the U.S. National COVID Cohort Collaborative (N3C). AIDS Behav 2024 Oct;28(Suppl 1):136-148. [doi: 10.1007/s10461-024-04466-0] [Medline: 39292319]
16. National COVID cohort collaborative. GitHub. URL: https://github.com/National-COVID-Cohort-Collaborative [accessed 2024-05-23]
17. Phuong J, Hong S, Palchuk MB, Espinoza J, Meeker D, Dorr DA, et al. Advancing interoperability of patient-level social determinants of health data to support COVID-19 research. AMIA Jt Summits Transl Sci Proc 2022;2022:396-405 [FREE Full text] [Medline: 35854720]
18. Anzalone AJ, Horswell R, Hendricks BM, Chu S, Hillegass WB, Beasley WH, et al. Higher hospitalization and mortality rates among SARS-CoV-2-infected persons in rural America. J Rural Health 2023 Jan;39(1):39-54 [FREE Full text] [doi: 10.1111/jrh.12689] [Medline: 35758856]
19. Yoo YJ, Wilkins KJ, Alakwaa F, Liu F, Torre-Healy LA, Krichevsky S, et al. Geographic and temporal trends in COVID-associated acute kidney injury in the National COVID Cohort Collaborative. Clin J Am Soc Nephrol 2023 Aug 01;18(8):1006-1018 [FREE Full text] [doi: 10.2215/CJN.0000000000000192] [Medline: 37131278]
20. O'Malley KJ, Cook KF, Price MD, Wildes K, Hurdle JF, Ashton CM. Measuring diagnoses: ICD code accuracy. Health Serv Res 2005 Oct;40(5 Pt 2):1620-1639 [FREE Full text] [doi: 10.1111/j.1475-6773.2005.00444.x] [Medline: 16178999]
21. van Walraven C, Bennett C, Forster AJ. Administrative database research infrequently used validated diagnostic or procedural codes. J Clin Epidemiol 2011 Oct;64(10):1054-1059 [FREE Full text] [doi: 10.1016/j.jclinepi.2011.01.001] [Medline: 21474278]
22. Pocobelli G, Oliver M, Albertson-Junkans L, Gundersen G, Kamineni A. Validation of human immunodeficiency virus diagnosis codes among women enrollees of a U.S. health plan. BMC Health Serv Res 2024 Feb 22;24(1):234 [FREE Full text] [doi: 10.1186/s12913-024-10685-x] [Medline: 38389066]
23. Yang X, Zhang J, Cai R, Liang C, Olatosi B, Weissman S, et al. Computational phenotyping with the All of Us Research Program: identifying underrepresented people with HIV or at risk of HIV. JAMIA Open 2023 Oct;6(3):ooad071 [FREE Full text] [doi: 10.1093/jamiaopen/ooad071] [Medline: 37614566]
24. May SB, Giordano TP, Gottlieb A. A phenotyping algorithm to identify people with HIV in electronic health record data (HIV-Phen): development and evaluation study. JMIR Form Res 2021 Nov 25;5(11):e28620 [FREE Full text] [doi: 10.2196/28620] [Medline: 34842532]
25. Fultz SL, Skanderson M, Mole LA, Gandhi N, Bryant K, Crystal S, et al. Development and verification of a "virtual" cohort using the National VA Health Information System. Med Care 2006 Aug;44(8 Suppl 2):S25-S30 [FREE Full text] [doi: 10.1097/01.mlr.0000223670.00890.74] [Medline: 16849965]
26. Paul DW, Neely NB, Clement M, Riley I, Al-Hegelan M, Phelan M, et al. Development and validation of an electronic medical record (EMR)-based computed phenotype of HIV-1 infection. J Am Med Inform Assoc 2018 Feb 01;25(2):150-157 [FREE Full text] [doi: 10.1093/jamia/ocx061] [Medline: 28645207]
27. National-Clinical-Cohort-Collaborative / CS-ISC. GitHub. URL: https://github.com/National-COVID-Cohort-Collaborative/CS-ISC/tree/main/HIV-Phenotyping [accessed 2024-09-27]
28. RxNorm. National Institutes of Health National Library of Medicine. URL: https://www.nlm.nih.gov/research/umls/rxnorm/index.html [accessed 2025-06-06]
29. OHDSI / Atlas. GitHub. URL: https://github.com/OHDSI/Atlas [accessed 2025-06-06]
30. ATLAS homepage. ATLAS. URL: https://atlas-demo.ohdsi.org/#/home [accessed 2025-06-06]

XSL•FO
RenderX

31. Jones S, Bradwell KR, Chan LE, Olson-Chen C, Tarleton J, Wilkins KJ, et al. Who is pregnant? Defining real-world data-based pregnancy episodes in the National COVID Cohort Collaborative (N3C). medRxiv Preprint posted online on August 6, 2022 [FREE Full text] [doi: 10.1101/2022.08.04.22278439] [Medline: 35982668]
32. Binswanger IA, Narwaney KJ, Gardner EM, Gabella BA, Calcaterra SL, Glanz JM. Development and evaluation of a standardized research definition for opioid overdose outcomes. Subst Abus 2019;40(1):71-79 [FREE Full text] [doi: 10.1080/08897077.2018.1546263] [Medline: 30875477]
33. Adult BMI categories. Centers for Disease Control and Prevention. URL: https://www.cdc.gov/bmi/adult-calculator/bmi-categories.html [accessed 2025-06-05]
34. National-Clinical-Cohort-Collaborative / Logic-Liaison-Confirmed-COVID-Positive-Template. GitHub. URL: https://github.com/National-Clinical-Cohort-Collaborative/Logic-Liaison-Confirmed-COVID-Positive-Template/blob/main/pyspark%20version/README%20for%20Logic%20Liaison%20Confirmed%20Covid%20Positive%20Template.pdf [accessed 2024-09-20]
35. Haendel MA, Chute CG, Bennett TD, Eichmann DA, Guinney J, Kibbe WA, et al. The National COVID Cohort Collaborative (N3C): rationale, design, infrastructure, and deployment. J Am Med Inform Assoc 2021 Mar 01;28(3):427-443 [FREE Full text] [doi: 10.1093/jamia/ocaa196] [Medline: 32805036]
36. Bennett TD, Moffitt RA, Hajagos JG, Amor B, Anand A, Bissell MM, et al. Clinical characterization and prediction of clinical severity of SARS-CoV-2 infection among US adults using data from the US National COVID Cohort Collaborative. JAMA Netw Open 2021 Jul 01;4(7):e2116901 [FREE Full text] [doi: 10.1001/jamanetworkopen.2021.16901] [Medline: 34255046]
37. N3C COVID enclave forms and resources. National Institutes of Health National Center for Advancing Translational Sciences. URL: https://ncats.nih.gov/research/research-activities/n3c/covid-enclave/resources [accessed 2025-05-12]
38. Nkodo EN, Maheria P, Hurwitz EG, Anzalone J, Li D, Islam J, et al. 1097 – Disparities in COVID-19 therapeutics access among people with and without HIV: an N3C analysis. In: Proceedings of the Conference on Retroviruses and Opportunistic Infections. 2025 Presented at: CROI 2025; March 9-12, 2025; San Francisco, CA URL: https://www.croiconference.org/abstract/2826-2025/
39. Vaidya D, Wilkins K, Hurwitz EG, Butzin-Dozier Z, Hill E, Maheria P, et al. 1100 – Differential impact of social determinants of health by sex in HIV for COVID-19 hospitalizations. In: Proceedings of the Conference on Retroviruses and Opportunistic Infections. 2025 Presented at: CROI 2025; March 9-12, 2025; San Francisco, CA URL: https://www.croiconference.org/abstract/666-2025/
40. Yang H, Anzalone J, Hurwitz EG, Nosyk B, Patel RC, Xiao Z. 1120 – Racial/ethnic and regional disparities in HIV testing before, during, and after COVID-19 in the US. In: Proceedings of the Conference on Retroviruses and Opportunistic Infections. 2025 Presented at: CROI 2025; March 9-12, 2025; San Francisco, CA URL: https://www.croiconference.org/abstract/1683-2025/
41. Kunz M, Rott KW, Hurwitz E, Kunisaki K, Sun J, Wilkins KJ, et al. The intersections of COVID-19, HIV, and race/ethnicity: machine learning methods to identify and model risk factors for severe COVID-19 in a large U.S. national dataset. AIDS Behav 2024 Oct;28(Suppl 1):5-21 [FREE Full text] [doi: 10.1007/s10461-024-04266-6] [Medline: 38326668]
42. Gallant J, Hsue PY, Shreay S, Meyer N. Comorbidities among US patients with prevalent HIV infection-a trend analysis. J Infect Dis 2017 Dec 19;216(12):1525-1533 [FREE Full text] [doi: 10.1093/infdis/jix518] [Medline: 29253205]
43. Coburn SB, Humes E, Lang R, Stewart C, Hogan BC, Gebo KA, et al. COVID-19 infections post-vaccination by HIV status in the United States. medRxiv Preprint posted online on December 05, 2021 [FREE Full text] [doi: 10.1101/2021.12.02.21267182] [Medline: 34909791]
44. Coburn SB, Humes E, Lang R, Stewart C, Hogan BC, Gebo KA, et al. Analysis of postvaccination breakthrough COVID-19 infections among adults with HIV in the United States. JAMA Netw Open 2022 Jun 01;5(6):e2215934 [FREE Full text] [doi: 10.1001/jamanetworkopen.2022.15934] [Medline: 35671054]
45. Jefferson C, Watson E, Certa JM, Gordon KS, Park LS, D'Souza G, et al. Differences in COVID-19 testing and adverse outcomes by race, ethnicity, sex, and health system setting in a large diverse US cohort. PLoS One 2022;17(11):e0276742 [FREE Full text] [doi: 10.1371/journal.pone.0276742] [Medline: 36417366]
46. Park LS, McGinnis KA, Gordon KS, Justice AC, Leyden W, Silverberg MJ, et al. SARS-CoV-2 testing and positivity among persons with and without HIV in 6 US cohorts. J Acquir Immune Defic Syndr 2022 Jul 01;90(3):249-255 [FREE Full text] [doi: 10.1097/QAI.0000000000002943] [Medline: 35195574]
47. Antoniou T, Zagorski B, Loutfy MR, Strike C, Glazier RH. Validation of case-finding algorithms derived from administrative data for identifying adults living with human immunodeficiency virus infection. PLoS One 2011;6(6):e21748 [FREE Full text] [doi: 10.1371/journal.pone.0021748] [Medline: 21738786]
48. Goetz MB, Hoang T, Kan VL, Rimland D, Rodriguez-Barradas M. Development and validation of an algorithm to identify patients newly diagnosed with HIV infection from electronic health records. AIDS Res Hum Retroviruses 2014 Jul;30(7):626-633 [FREE Full text] [doi: 10.1089/aid.2013.0287]
49. National COVID Cohort Collaborative homepage. National COVID Cohort Collaborative. URL: https://covid.cd2h.org [accessed 2025-06-06]

XSL•FO
RenderX

50. Data transfer agreement signatories. National Institutes of Health National Center for Advancing Translational Sciences. URL: https://ncats.nih.gov/n3c/resources/data-contribution/data-transfer-agreement-signatories [accessed 2025-06-06]
51. Haendel MA, Chute CG, Bennett TD, Eichmann DA, Guinney J, Kibbe WA, et al. The National COVID Cohort Collaborative (N3C): rationale, design, infrastructure, and deployment. J Am Med Inform Assoc 2021 Mar 01;28(3):427-443 [FREE Full text] [doi: 10.1093/jamia/ocaa196] [Medline: 32805036]
52. N3C core contributors. National COVID Cohort Collaborative. URL: https://covid.cd2h.org/contributors/ [accessed 2025-06-06]
53. N3C COVID enclave forms and resources. National Institutes of Health National Center for Advancing Translational Sciences. URL: https://ncats.nih.gov/research/research-activities/n3c/covid-enclave/resources [accessed 2025-06-06]
54. N3C data access forms and resources. National Institutes of Health National Center for Advancing Translational Sciences. URL: https://ncats.nih.gov/n3c/resources/data-access [accessed 2025-06-06]
55. Researcher essentials. National COVID Cohort Collaborative. URL: https://covid.cd2h.org/for-researchers/ [accessed 2025-06-06]

Abbreviations

CD4: cluster of differentiation 4
EHR: electronic health record
HBV: hepatitis B virus
ICD-10: International Classification of Diseases, Tenth Revision
IRB: Institutional Review Board
N3C: National Clinical Cohort Collaborative
NIH: National Institutes of Health
OMOP: Observational Medical Outcomes Partnership
PEP: postexposure prophylaxis
PrEP: preexposure prophylaxis
SNOMED CT: Systemized Medical Nomenclature for Medical Clinical Terminology
TDF: tenofovir disoproxil fumarate
VL: viral load

Edited by A Coristine; submitted 29.10.24; peer-reviewed by Y Liu, P Ebrahimi; comments to author 14.04.25; revised version received 13.05.25; accepted 15.05.25; published 11.07.25.

Please cite as:
Hurwitz E, Varley CD, Anzolone AJ, Madhira V, Olex AL, Sun J, Vaidya D, Fadul N, Islam JY, Jackson LE, Wilkins KJ, Butzin-Dozier Z, Li D, Safo SE, McMurry JA, Maheria P, Williams T, Hassan SA, Haendel MA, Patel RC, The National Clinical Cohort Collaborative (N3C) Consortium
Identifying People Living With or Those at Risk for HIV in a Nationally Sampled Electronic Health Record Repository Called the National Clinical Cohort Collaborative: Computational Phenotyping Study
JMIR Med Inform 2025;13:e68143
URL: https://medinform.jmir.org/2025/1/e68143
doi:10.2196/68143
PMID:

©Eric Hurwitz, Cara D Varley, A Jerrod Anzolone, Vithal Madhira, Amy L Olex, Jing Sun, Dimple Vaidya, Nada Fadul, Jessica Y Islam, Lesley E Jackson, Kenneth J Wilkins, Zachary Butzin-Dozier, Dongmei Li, Sandra E Safo, Julie A McMurry, Pooja Maheria, Tommy Williams, Shukri A Hassan, Melissa A Haendel, Rena C Patel, The National Clinical Cohort Collaborative (N3C) Consortium. Originally published in JMIR Medical Informatics (https://medinform.jmir.org), 11.07.2025. This is an open-access article distributed under the terms of the Creative Commons Attribution License (https://creativecommons.org/licenses/by/4.0/), which permits unrestricted use, distribution, and reproduction in any medium, provided the original work, first published in JMIR Medical Informatics, is properly cited. The complete bibliographic information, a link to the original publication on https://medinform.jmir.org/, as well as this copyright and license information must be included.

XSL•FO
RenderX

Genotype Distribution and Migration Patterns of Hepatitis C Virus in Shandong Province, China: Molecular Epidemiology and Phylogenetic Study

Lin Lin[1], MD; Guoyong Wang[1], MSc; Lianzheng Hao[1]; Tingbin Yan[2], PhD, MD

[1]HIV/AIDS Control and Prevention, Key Laboratory of Infectious Disease Control and Prevention, Shandong Center for Disease Control and Prevention, Jinan, China

[2]Department of Orthopedic Surgery, School of Basic Medical Sciences, Qilu Hospital of Shandong University, No. 107 Wenhua West Road, Jinan, Shandong Province, China

Corresponding Author:
Tingbin Yan, PhD, MD
Department of Orthopedic Surgery, School of Basic Medical Sciences, Qilu Hospital of Shandong University, No. 107 Wenhua West Road, Jinan, Shandong Province, China

Abstract

Background: Hepatitis C virus (HCV) remains a significant public health concern in China, particularly in Shandong Province, where detailed molecular epidemiological data are limited. HCV exhibits substantial genetic diversity, and understanding its genotype distribution and transmission dynamics is critical for developing effective control strategies.

Objective: This study aimed to investigate the genetic diversity, geographic dissemination, and evolutionary history of HCV genotypes in Shandong Province, China, using molecular techniques and phylogenetic methods.

Methods: A total of 320 HCV-positive serum samples were collected from multiple hospitals across Shandong Province between 2013 and 2021. HCV RNA was extracted and amplified targeting the 5′ untranslated region (UTR), Core, and NS5B regions. Sequencing was conducted, and genotypes were determined using the National Center for Biotechnology Information's Basic Local Alignment Search Tool (NCBI BLAST). Phylogenetic trees were constructed using maximum likelihood methods with the general time reversible with Gamma-distributed rate variation among sites [(GTR)+Gamma model]. The temporal and geographic evolution of the major subtypes (1b and 2a) was analyzed using Bayesian Markov chain Monte Carlo (MCMC) methods implemented in Bayesian Evolutionary Analysis Sampling Trees (BEAST). The Bayesian skyline plot (BSP) was used to infer population dynamics and estimate the time to the most recent common ancestor (tMRCA).

Results: Genotypes 1b (n=165) and 2a (n=131) were identified as the predominant subtypes, with a small number of genotypes 3b, 6a, 6k, and potential recombinant strains also detected. Phylogenetic analysis revealed distinct evolutionary clustering of 1b and 2a strains, suggesting multiple diffusion events within the province. The tMRCA of subtypes 1b and 2a were estimated to be 1957 and 1979, respectively. Bayesian skyline analysis showed that both subtypes experienced long-term population stability, followed by a rapid expansion period between 2014 and 2019 (1b) and 2014 to 2016 (2a), respectively. The analysis also identified key transmission hubs such as Jinan, Liaocheng, Tai'an, and Dezhou, indicating city-level variations in HCV spread.

Conclusions: This study provides data-supported insights into the genotypic landscape and evolutionary patterns of HCV in Shandong Province. The identification of dominant subtypes, potential recombinant strains, and regional transmission pathways enhances our understanding of local HCV epidemiology. These findings have implications for public health policy, resource allocation, and targeted treatment strategies. The integration of molecular epidemiology and phylogenetics offers a valuable model for infectious disease surveillance and control in similar settings.

(JMIR Med Inform 2025;13:e60207) doi:10.2196/60207

KEYWORDS

hepatitis C virus; genotypic diversity; phylogenetic analysis; migration patterns; Shandong Province; Bayesian skyline plot; migration; genotype; prevention; disease control; phylogenetic; HCV; genotypic diversity; migration pattern; epidemiological; China

Introduction

Hepatitis C virus (HCV) is an enveloped virus containing a single-stranded positive RNA genome approximately 9.6 kilobases in length, belonging to the Flaviviridae family, *Hepacivirus* genus [1]. It can lead to acute and chronic hepatitis, and if not treated promptly and effectively, may progress to cirrhosis and hepatocellular carcinoma [2]. HCV infection

XSL•FO
RenderX

remains a global health burden, with an estimated 58 million chronic cases, 1.5 million new infections, and 290,000 deaths annually [3]. China is one of the most severely affected countries, with the highest number of HCV infections globally [4].

In recent years, the global epidemic trend of HCV has garnered significant attention [5]. Hepatitis C is primarily transmitted through blood contact and is associated with severe complications, including cirrhosis and liver cancer [6]. The prevalence and distribution of various HCV genotypes vary across different regions [7]. These disparities are influenced by factors such as geography, population mobility, and sanitation conditions [8].

Molecular epidemiological research is a critical tool for comprehending the dynamics of virus dissemination, transmission, and evolution [9]. The sequencing of viral RNA offers a more precise understanding of the viral genotype and its genetic variations [10]. Moreover, conducting phylogenetic tree analysis using viral sequence data can yield valuable insights into the virus's origins, transmission routes, and evolutionary pathways [11]. The 5′ untranslated region (UTR), NS5B region, and C region are recognized as core components of HCV, and variations in their sequences are closely linked to the virus's biological characteristics and epidemiological attributes [12]. Yang et al [13], found that HCV in Guizhou Province is mainly divided into six subtypes: 1a, 1b, 3a, 3b, 6a, and 6n, with subtype 6a being the dominant strain. In the coastal area of Putian, China, subtype 1b dominates, followed by 2a and 1a [4], while in Yunnan Province, subtype 3b is predominant, followed by 3a and 6n [14]. However, the prevalence of HCV in Shandong Province remains insufficiently studied, leaving a significant research gap in this field.

With the rapid advancements in modern bioinformatics technology, machine learning algorithms have found extensive applications in various biomedical domains [15]. In the context of HCV research, machine learning can expedite the classification of extensive viral sequence data and enhance the ability to predict epidemic trends and migration patterns of the virus [16,17]. For example, the Phylogenetic Maximum Likelihood (PhyML) method calculates branch probabilities based on the general time reversible (GTR)+Gamma model and determines the optimal topological structure, which is used to classify the evolutionary relationships of viral subtypes. The Bayesian Markov chain Monte Carlo (MCMC; Bayesian Evolutionary Analysis Sampling Trees [BEAST]) method reconstructs population history using the skyline model and generates posterior distribution trees (maximum clade credibility [MCC] trees) through MCMC sampling to infer the origins and transmission paths of viral subtypes. The exponential clock model uses sample collection time to calibrate the evolutionary tree and estimates the time to the most recent common ancestor (tMRCA) using Bayesian inference, providing estimates of viral divergence times. Although this study did not use traditional supervised learning models (eg, random forests and SVM), it integrates Bayesian statistical inference and maximum likelihood estimation to solve the evolutionary classification, spatiotemporal transmission inference, and divergence time estimation issues of HCV subtypes. These methods enable dynamic analysis of viral evolutionary history through probabilistic modeling and parameter optimization.

Given its economic significance and large population, Shandong Province holds a pivotal role in China. Therefore, conducting comprehensive research on the prevalence of HCV in the province carries significant public health importance [18]. Understanding the trends in prevalence, distribution of primary genotypes, and patterns of HCV transmission in Shandong Province can provide a scientific foundation for disease prevention and control in the region. Furthermore, it can serve as a valuable reference for comprehending the HCV epidemic in other areas of China and globally [19]. Therefore, the goal of this study is to conduct a molecular epidemiology and systematic geography crossover study of HCV isolates from various cities in Shandong using machine learning algorithms. It integrates viral genomics, bioinformatics modeling, and public health policy analysis, aiming to reveal the evolutionary history, transmission networks, and interactions with socioeconomic factors of HCV within the region. This multidimensional integrated analysis provides a scientific basis for regional infectious disease prevention and control.

Methods

Subjects

This study collected a total of 320 plasma samples from patients with hepatitis C. The samples were obtained from outpatient and inpatient settings in various hospitals in Shandong Province between 2013 and 2021. The main hospitals include Xintai People's Hospital, Tai'an Central Hospital, and Dongping People's Hospital, among others. A total of 38 hospitals participated in sample collection, with further details available in Table S1 in Multimedia Appendix 1. After centrifugation at 3000 rpm for 10 minutes, the obtained plasma samples are divided into 2 tubes and stored at −80 °C. All patients tested positive for anti-HCV antibodies and HCV RNA, with HCV RNA quantification ranging from 1.62×10^3 to 7.22×10^7 copies/mL. Serum samples were collected from healthy individuals who tested negative for anti-HCV and were allocated to the negative control group. Serum samples were collected from individuals in the positive control group who were confirmed to have HCV genotypes through sequencing and HCV RNA quantification of $\geq10^5$ copies/mL.

Furthermore, the researchers collected baseline demographic information from all participants and evaluated risk factors for HCV infection using a thorough epidemiological questionnaire. The questionnaire covered aspects such as age at diagnosis, gender, occupation, and place of residence. The diagnostic criteria for HCV infection are established according to the 2022 edition of the Chinese Guidelines for the Prevention and Control of Hepatitis C. The study follows the Helsinki Declaration [13].

Exclusion Criteria

Patients who tested positive for antibodies against the hepatitis B virus, hepatitis D virus (HDV), and HIV were excluded from this study. In addition, patients with known alcohol abuse, drug issues, pregnancy, and those with Child-Pugh grade B or C liver function were not included in this study.

XSL•FO
RenderX

Patients with high-risk factors, such as a history of blood selling, blood transfusion, blood product usage, hemodialysis, intravenous injections, needlestick injuries, maternal infection, high-risk behaviors, or a history of dental treatments, were also excluded [13].

HCV RNA Extraction and Polymerase Chain Reaction Amplification

Quantitative Polymerase Chain Reaction (qPCR) was performed using the Artus HCV QS-RGQ kit (Qiagen) and the Quant Studio 5 system (Thermo Fisher Scientific). In brief, following the manufacturer's protocol, viral RNA was reverse transcribed into complementary DNA (cDNA) using the RT-master mixture. A 4-µL aliquot of cDNA was used as a template in a 50-µL PCR reaction mixture. The PCR conditions included an initial incubation at 95 °C for 15 minutes, followed by 50 amplification cycles: denaturation at 95 °C for 30 seconds, annealing at 50 °C for 1 minute, extension at 72 °C for 30 seconds, and a final extension of 5 minutes at 72 °C, followed by a holding step at 37 °C for 1 minute and storage at 4 °C [20]. The primer sequences for the 5′ UTR, Core region, and NS5B region can be found in Table S2 in Multimedia Appendix 1, while specific primer sets for each region are detailed in Tables S3-S5 in Multimedia Appendix 1.

The 5′ UTR, Core region, and NS5B region are helpful in distinguishing different subtypes of HCV [21]. The 5′ UTR refers to the nontranslated region of the viral genome. This region may contain specific sequence variations that can be used for differentiating genotypes. The Core region is the gene region encoding the viral core protein, and its sequence analysis can reveal differences between genotypes and subtypes. The NS5B region encodes the RNA-dependent RNA polymerase of HCV, which plays a critical role in the virus replication process. Sequence analysis of the NS5B region can aid in identifying different genotypes and subtypes [21].

Sequencing and Phylogenetic Tree Analysis

After separation and amplification of the products through agarose gel electrophoresis, the amplified products of joyous bands (approximately 311 bp in the 5′UTR, 392 bp in the NS5B region [22], and approximately 503 bp in the C region; Figure S1 in Multimedia Appendix 1) were sent to Qinko Biotechnology Co, Ltd for sequencing. The sequencing data were used for genotyping analysis with National Center for Biotechnology Information's Basic Local Alignment Search Tool (NCBI BLAST). The sequences obtained from the different primers were renamed based on the sequence information, integrating the original sequence name, sequencing primers, and subtyping information. For instance, the sequence derived from the PV01 primer in the 5′ UTR was renamed P283uPV01-1b. P283u is the original sequence name, PV01 represents the sequencing primer name, and 1b signifies the subtype information.

Subsequently, all sequences from each region were combined with 10 reference strain sequences and were used for evolutionary analysis. The reference strains of HCV include: HCV genotype 1a (M62321), HCV genotype 1b (D90208), HCV genotype 1c (D14853), HCV genotype 2a (D00944), HCV genotype 2b (D10988), HCV genotype 2c (D50409), HCV genotype 2k (AB031663), HCV genotype 3a (D17763), HCV genotype 3b (D49374), and HCV genotype 3k (D63821).

MUSCLE software (Multiple Sequence Comparison by Log-Expectation; version 5.1.linux64; Robert C Edgar) was used for sequence alignment of the 5′ UTR, NS5B, and C regions, applying default parameters. Conserved sequence positions were extracted using Gblocks software (version 0.91b) for further evolutionary analysis. To construct the phylogenetic tree, we applied the GTR+Gamma model and used PhyML software (Phylogenetic Maximum Likelihood; version PhyML 3.3.20190909) to create the maximum likelihood phylogenetic tree. A bootstrap test with 1000 replicates was conducted to validate the results. The tree diagram was visualized and enhanced using EvolView software [23].

Bayesian Markov Chain Monte Carlo Evolutionary Analysis

This study is based on classifying the major subtypes (1b and 2a) into 2 datasets, each representing a specific HCV subtype. We constructed a maximum likelihood tree using PhyML and imported it into TempEst (Temporal Signal Estimation; v1.5.3), using sample collection year as a covariate. A linear regression analysis was performed between the root-to-tip distance and sample collection time. We observed a correlation coefficient (R^2) >0.2, with a positive slope, indicating the presence of a temporal signal in the data that can be used for molecular clock analysis. Therefore, we used the BEAST software package [24]. In this study, we used the Bayesian MCMC algorithm to investigate the ancestral relationships and migration patterns of various HCV subtypes among patients in Shandong Province.

According to research, exponential models perform better than log-normal and strict molecular clock models in HCV sequence analysis [25]. The population model incorporates the Bayesian skyline coalescent model, which surpasses constant size, exponential growth, logistic growth, and expansive growth models [26]. To analyze different HCV genotypes, we used the exponential clock model in combination with the GTR+Gamma+I substitution model and the Bayesian skyline model. The MCMC chain iterates a total of the number of sequences squared multiplied by 3000 times. A tree is generated at intervals of 25,000 iterations.

Each dataset underwent 2 independent MCMC runs, and the effective sample size for each parameter was evaluated using Tracer v1.7.2 software to confirm convergence between chains. The initial generated tree should be aged by 10%, and an MCC tree should be created using TreeAnnotator v1.10.4 software. The resultant posterior tree could be viewed using FigTree v1.4.4 software. Furthermore, this study used the Tracer v1.7.2 software to reconstruct the Bayesian Skyline Plot (BSP) to trace the growth history of HCV in patients with hepatitis C from Shandong province. It also estimated the evolutionary rate and the time of the most recent common ancestor. The BSP is a general skyline graph derived from the target sequence dataset. The distribution of the general skyline graph is then sampled, and these skyline graphs are combined to obtain the posterior distribution of the effective population size over time. Software

XSL•FO
RenderX

packages are exclusively obtained from the official BEAST website [13].

Ethical Considerations

This study was reviewed and approved by the Ethics Committee of Shandong Center for Disease Control and Prevention (institutional review board approval number: SDJK-2021-93-01). All study procedures involving human participants were performed in accordance with the ethical standards of the institutional and national research committees and with the principles of the Declaration of Helsinki (2013 version).

Written informed consent was obtained from all participants prior to the collection of blood samples and epidemiological data. For patients included through secondary data analysis, informed consent had been obtained during the original data collection. The protocol for secondary analysis was separately reviewed and approved by the same ethics committee, and a waiver of reconsent was granted in accordance with institutional policy and relevant regulations.

All data used in the study were fully deidentified prior to analysis to protect participant privacy and confidentiality. No identifiable personal information was collected, recorded, or stored. Data were managed and stored in compliance with institutional data protection policies, and access was restricted to authorized research personnel only.

Participants did not receive monetary or material compensation for participation. All samples and data were collected during routine clinical visits, and no additional interventions or burdens were imposed. The study did not involve vulnerable populations. No identifiable individual images or information are included in the manuscript or supplementary materials. All figures and data are anonymized, and individual identities cannot be inferred in any way.

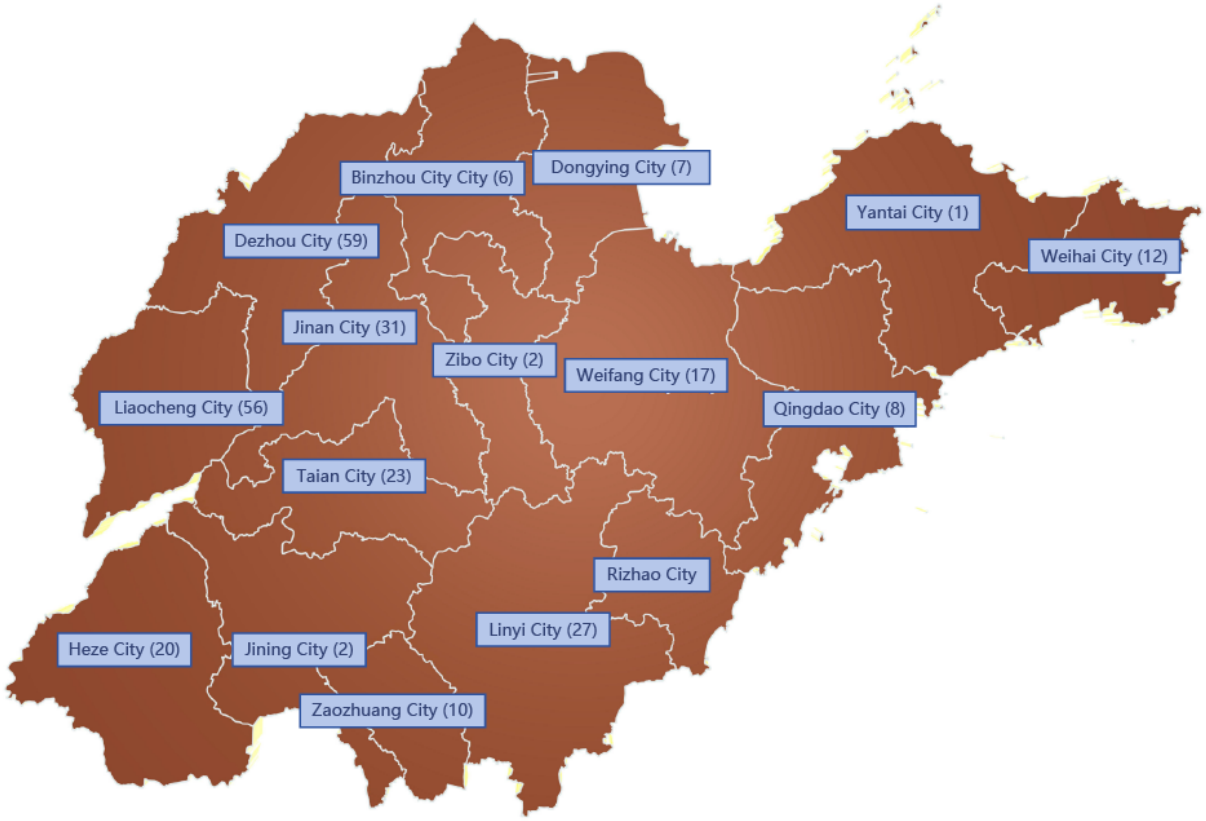
Results

Demographic Characteristics and Age-Occupation Correlation of HCV Infections in the Shandong Region

A total of 320 blood samples from patients infected with HCV in different regions of Shandong, collected from 2013 to 2021, were included based on the established exclusion criteria. Excluding the few patients with incomplete identity information, the population's demographic characteristics are displayed in Figure 1 and Table 1. The data reveal 161 (50.3%) males and 121 (37.8%) females in the sample. The patients included in this study were HCV positive; their ages ranged from 7 to 80 years, with a mean age of 54.3 (14.3) years. The prevalence of HCV infection is approximately 7.8% in the age group under 30 years, 23.8% in the age group between 30 and 49 years, 54.9% in the age group between 50 and 69 years, and 13.5% in the age group 70 years and older. Analysis of the age-specific data clearly shows a higher frequency of HCV infection in the 50 - 69 years age group. Furthermore, when excluding patients who have not yet received a clinical diagnosis, it is observed that 97.6% of patients infected with HCV suffer from chronic hepatitis. This condition is particularly prevalent among farmers (75.2%), with homemakers and unemployed individuals at home exhibiting the next highest prevalence rates.

XSL•FO
RenderX

Figure 1. Population distribution of patients with hepatitis C in different regions of Shandong Province.



XSL•FO
RenderX

Table . Demographic characteristics of hepatitis C virus-positive patients, 2013-2021, Shandong, China.

Characteristics	Total patients (N=320), n (%)
Sex	
Male	161 (50.31)
Female	121 (37.81)
Unknown	38 (11.88)
Age (years)	
<30	22 (7.8)
30 - 39	23 (8.2)
40 - 49	44 (15.6)
50 - 59	86 (30.5)
60 - 69	69 (24.4)
≥70	38 (13.5)
Unknown	38 (11.88)
Disease type	
Chronic	245 (97.6)
Acute	6 (2.4)
Unknown	69 (21.56)
Occupation	
Farmer	212 (75.2)
Nonfarmers	70 (24.8)
Unknown	38 (11.88)

Methodology and Success Rates of HCV Genotyping in the 5′ UTR, Core Region, and NS5B Region With Sequence Variability Analysis

The genome of HCV comprises a 5′ UTR, which contains a highly conserved RNA structure. This region also includes a single open reading frame responsible for encoding structural proteins (Core, E1, and E2) and nonstructural proteins (p7, NS2, NS3, NS4A, NS4B, NS5A, and NS5B). A 3′ UTR is also present within the genome [27]. HCV's 5′ UTR is highly conserved, exhibiting minimal sequence variability. Hence, it is well-suited for the development of specific primers for amplification purposes. This region exhibits a high detection rate and is crucial in HCV RNA quantification and genotyping. However, several studies have identified limitations in using the 5′ UTR for distinguishing HCV genotypes, as the misclassification of 1a as 1b is quite prevalent [28]. Types 1, 2, 3, and 4 cannot be fully differentiated solely by their subtypes [29]. Certain 6-type sequences in the Southeast Asian region closely resemble the 1a and 1b sequences. As a result, it is not uncommon for 6-type sequences to be mistakenly classified as 1a and 1b [17]. In the species-specific region of the HCV genome, such as the C, E1, and NS5B regions, there is a high degree of heterogeneity between genotypes and subtypes, with gene sequences containing valuable information for genotyping. Therefore, sequence analysis based on this region can accurately differentiate HCV subtypes and even different isolates within the same subtype. Given the situation above, scholars have proposed a combined approach that uses 5′ UTR genotyping methods along with genotyping of the Core or NS5B region in recent years. This approach improves the detection rate and accurately distinguishes between HCV genotypes [30].

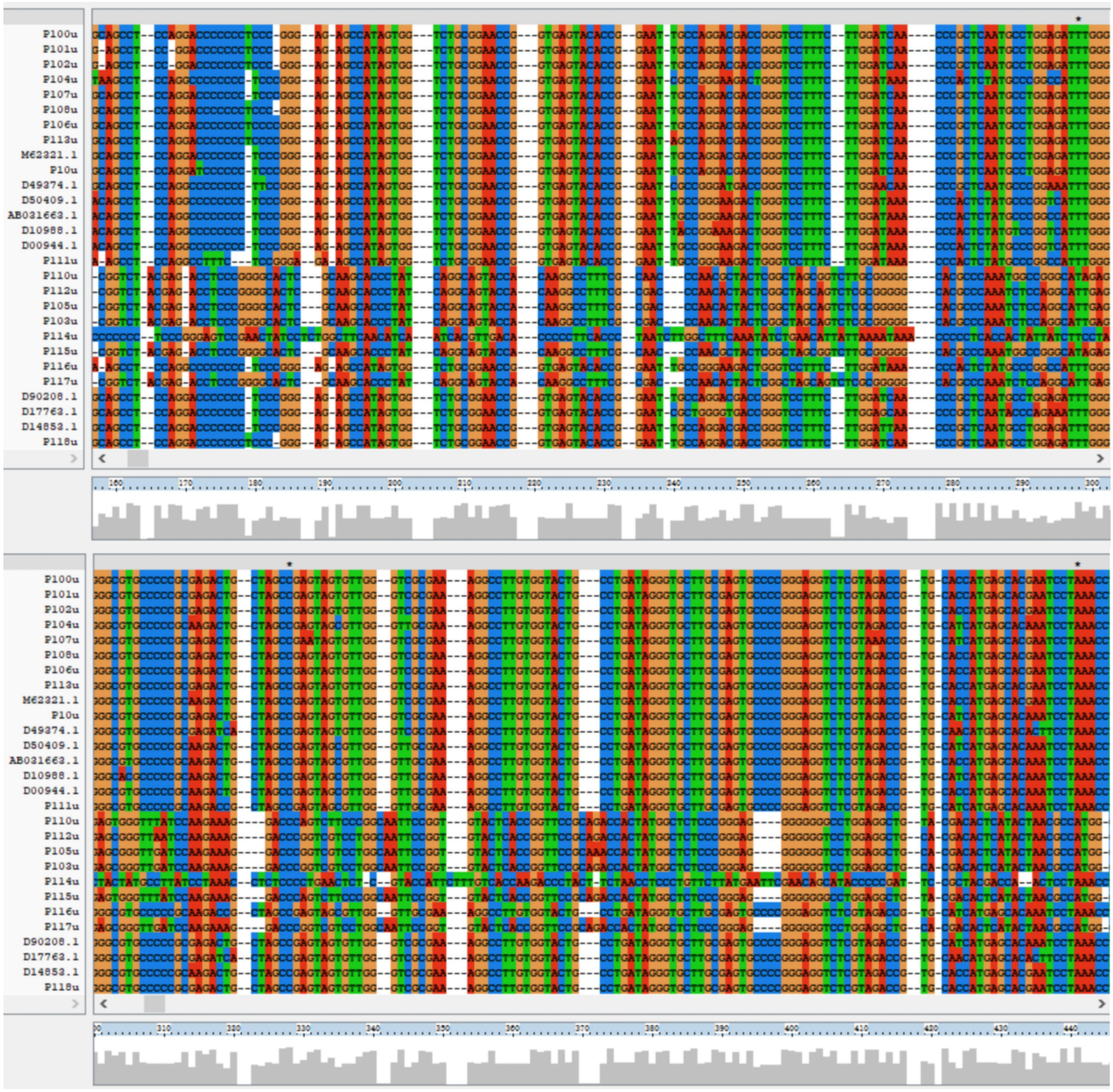
We primarily focused on sequencing the 5′ UTR. In addition, we used sequencing of the NS5B and Core regions as supplementary methods for genotyping analysis of 320 patients. A total of 320 gene fragments from the 5′ UTR were successfully amplified and sequenced, yielding a success rate of 98.8% (320/324). Similarly, 282 gene fragments from the Core region were successfully amplified and sequenced, resulting in a success rate of 89.5% (282/315). Furthermore, 233 gene fragments from the NS5B region were successfully amplified and sequenced, with a success rate of 77.7% (233/300). Consistent with previous studies, the amplification frequencies vary among the three regions, with the highest frequency observed in the 5′ UTR, followed by the Core region, and the lowest frequency observed in the NS5B region. A total of 104 cases of amplification failure may be attributed to low viral load and weak primer specificity.

After successful amplification, the resulting sequences were used as input for NCBI BLAST to search for the most likely similar sequences, thus determining the genotype of each region. Taking the P4u sequence from the 5′ UTR as an example, the BLAST analysis results (Table S6 in Multimedia Appendix 1) showed that the nucleotide homology (PNI) of the P4u sequence was 100%, with the highest score of 414. This 280 bp fragment showed 100% similarity to the HCV isolate QC156 (Accession: KJ439771.1) from nt32 to nt311, 100% similarity to the HCV

XSL•FO
RenderX

subtype 1b strain MD29 (Accession: AF207770.1) from nt85 to nt364, and 99.29% similarity to the HCV open reading frame gene (Accession: D90208.1) from nt85 to nt364. A multiple sequence alignment was performed on 307 partial gene sequences from the 5′ UTR using ClustalX2 software and compared to 10 reference strain sequences from the GenBank database. The nucleotide sequences of the 5′ UTR are considered highly conserved; however, as shown in Figure 2, there were some mutations and variations in the 5′ UTR of different HCV genotypes.

Figure 2. Comparison of 307 cases' 5' untranslated region nucleotide sequences with reference sequences in the GenBank database.



Distribution of HCV Genotypes, Potential Recombinants, and Correlation With Gender and Age

A total of 307 cases were genotyped for the 5′ UTR of the gene, 280 cases for the Core region, and 233 cases for the NS5B region. The typing results are presented in Table 2. It is evident that the 5′ UTR exhibits a high amplification frequency; however, distinguishing between many gene segments is challenging in the typing comparison. Conversely, while the amplification frequencies of the Core region and NS5B region are relatively low, they demonstrate superior capability in analyzing gene subtypes. The detection sensitivity was improved after conducting a combined analysis of the three. Four samples that did not amplify in the 5′ UTR could differentiate genotypes through successful amplification in the Core and NS5B regions. Moreover, gene fragments with ambiguous genotyping in the 5′ UTR could be further classified into subtypes.

XSL•FO
RenderX

Table . Results of Hepatitis C virus segmentalization and combined analysis in patients with hepatitis C.

Genotype	HCV[a] genotype											
	Genotype 1[b]				Genotype 2[b]			Genotype 33b	Genotype 6[b]			Total
	1a	1b	1a/1b	1b/2k,2a	2*[c]	2a	2a,2k/1b		6a	6k	6u	
5’ UTR[d]	2	170	5	1	50	75	1	1	1		0	307
Core	1	160	0	0	0	117	0	0	1	1	1	280
NS5B	1	134	0	0	0	96	0	0	1		1	233
Joint analysis	312											

[a]HCV: Hepatitis C virus.

[b]Types 1, 2, and 6 all contain different numbers of recombinant cases, totaling 13 cases.

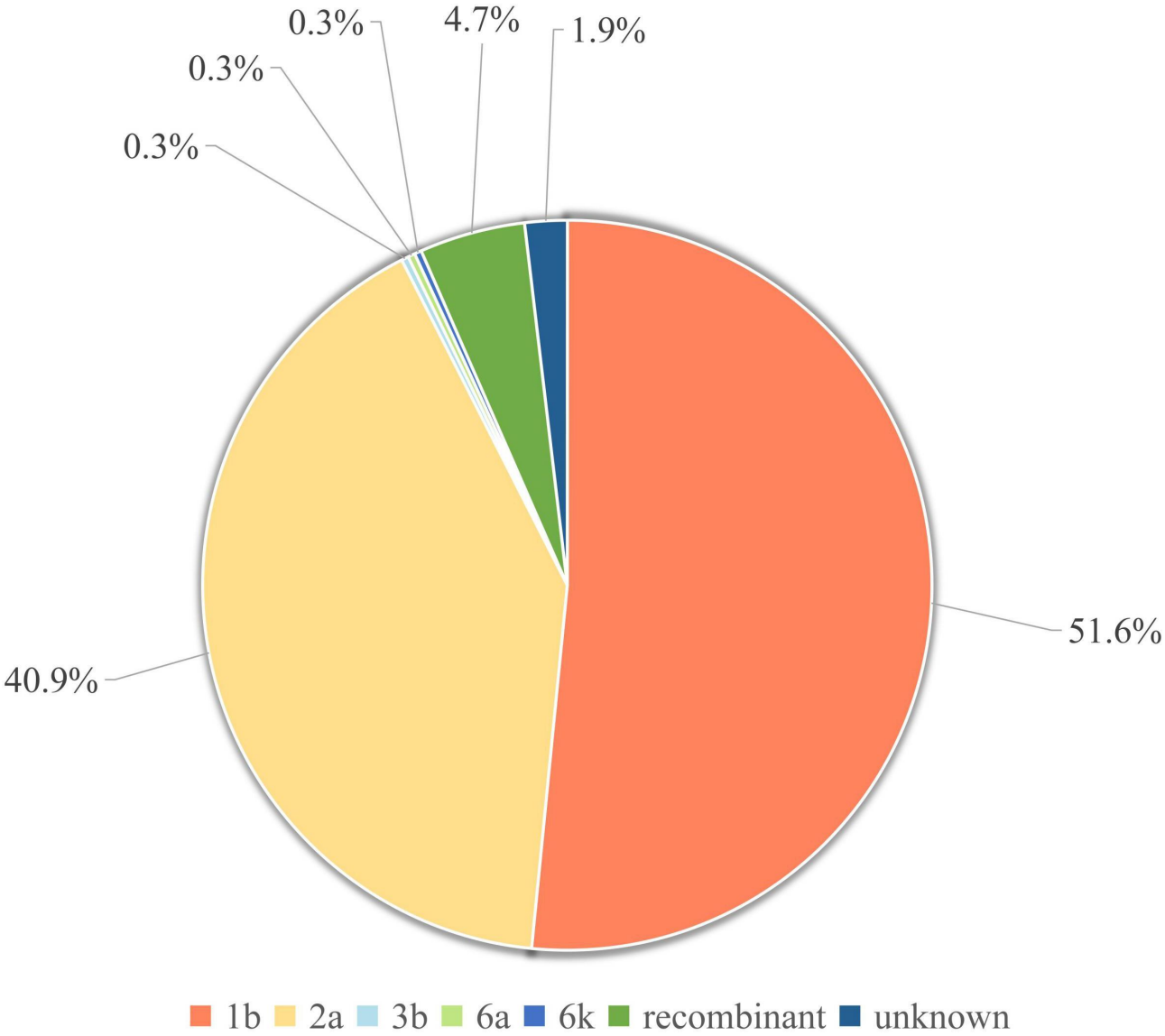
[c] *The number of cases indicates that this type cannot further differentiate subtypes.

[d]5′ UTR: 5′ untranslated region.

The main genotypes of HCV prevalent in most regions of our country are genotype 1b, followed by genotype 2a. These results are confirmed by our typing analysis (Figure 3). Among the 320 patients with hepatitis C analyzed, the most common HCV subtypes include 1b, 2a, 3b, 6a, and 6k. Of these subtypes, 1b (n=165) is the most dominant, followed by 2a (n=131), 3b (n=1), 6a (n=1), and 6k (n=1). Since 2002, Kalinina et al [31] reported the first case of the HCV natural recombinant 2k/1b in 2002, and several researchers have identified different recombinant strains through multiregion genotyping. This study found 13 cases with inconsistent genotyping in the 5′ UTR, Core region, and NS5B region, which are preliminarily considered potential recombinant strains of HCV, pending further confirmation in subsequent studies. In addition, there are 8 cases whose genotypes remain unclear.

XSL•FO
RenderX

Figure 3. Distribution of HCV genotypes in 320 hepatitis C patients with hepatitis C.



As demonstrated in Table 3, with the exclusion of a few patients with incomplete identity information, the HCV genotype ratio is higher in females compared to males. Out of the 148 patients diagnosed with genotype 1b, the average age was 54.7 (14.0) years. Among them, 86 were males (58.1%) and 62 were females (41.0%). One hundred eleven patients with genotype 2a were included in the study, with an average age of 54.9 (14.4) years. The patient population comprised 57 males (51.4%) and 54 females (48.6%). Based on statistical analysis, there was no difference in the average age of patients infected with genotypes 1b and 2a of HCV (P>.05).

XSL•FO
RenderX

Table . Correlation between clinicopathological features and hepatitis C virus genotype frequencies among 282 patients with hepatitis C.

Clinicopathological feature	HCV[a] genotype					
	Genotype 11b	Genotype 22a	Genotype 33b	Genotype 6		Recombinant
				6a	6k	
Sex, mean (SD)						
Male	86 (58.1)	57 (51.4)	0	0	1	3
Female	62 (41.0)	54 (48.6)	1	1	0	9
Age (years), mean (SD)						0
<30	10 (6.8)	7 (6.3)	0	0	0	1
30 - 39	10 (6.8)	13 (11.7)	0	0	0	0
40 - 49	24 (16.1)	14 (12.6)	1	1	0	2
50 - 59	46 (31.1)	34 (30.6)	0	0	1	4
60 - 69	38 (25.7)	26 (23.4)	0	0	0	4
≥70	20 (13.5)	17 (15.3)	0	0	0	1
Age (years), mean (SD)	54.7 (14.0)	54.9 (14.4)				55.3 (12.8)
Total, mean (SD)	148 (54.0)	111 (40.5)	1 (0.4)	1 (0.4)	1 (0.4)	12 (5.8)

[a]HCV: hepatitis C virus.

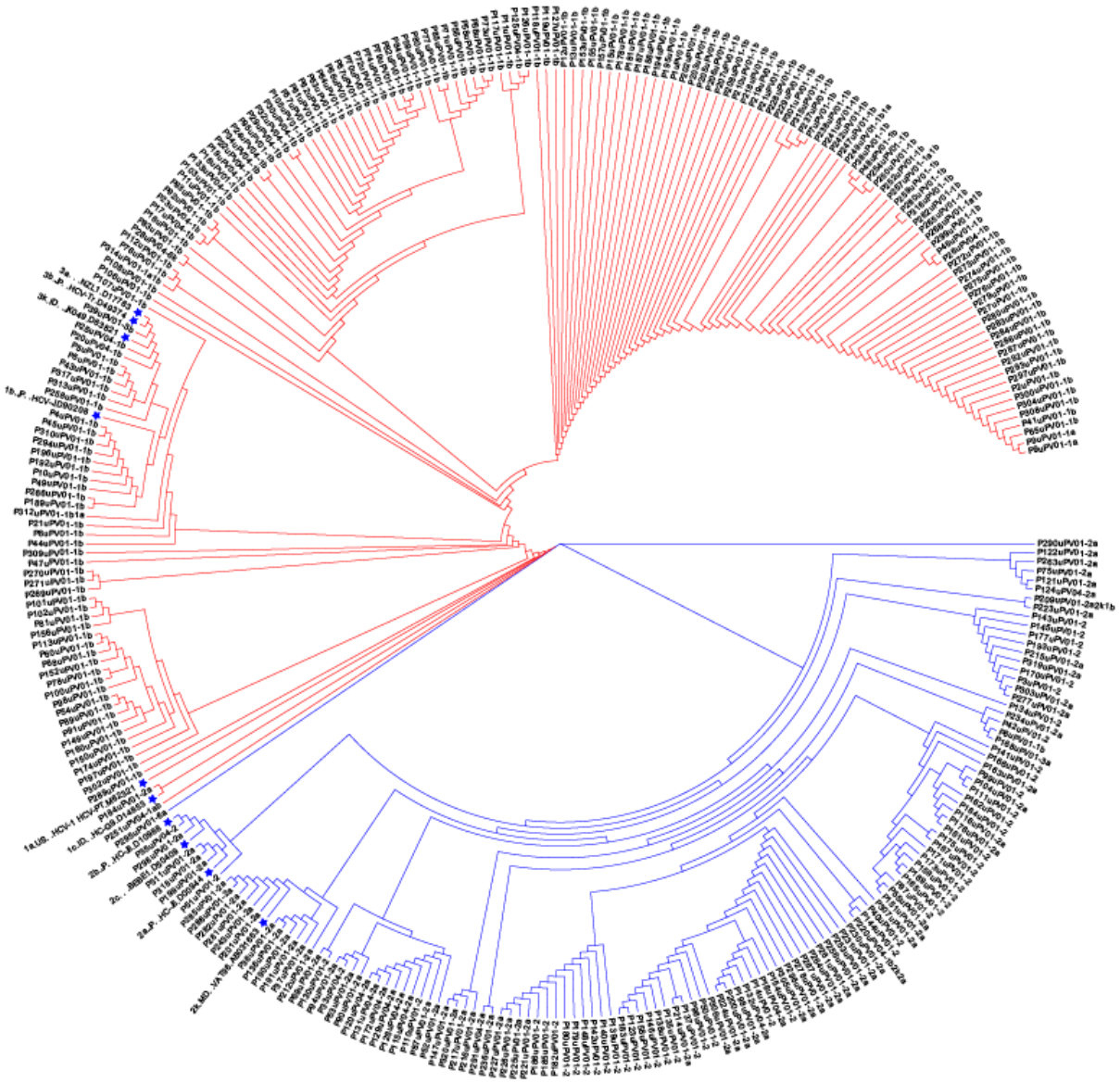
The youngest patient diagnosed with hepatitis C is a 7-year-old girl with HCV genotype 1b, while the oldest patient is an 87-year-old woman with HCV genotype 1b. No deviation was observed in the age-specific incidence rates of the main HCV genotypes (1b, 2a) in this study. Most patients with hepatitis C are older than 50 years, with genotype 1b accounting for 70.3% and genotype 2a accounting for 69.3%. There is a lower prevalence in patients younger than 50 years, with 29.7% having genotype 1b and 30.7% having genotype 2a.

Phylogenetic Analysis of HCV Sequences Using Maximum Likelihood and Genotype Clustering Validation

We merged the 10 reference strain sequences obtained from the GenBank database with 307 5′ UTR sequences, 280 Core region sequences, and 233 NS5B region sequences. We selected the GTR+Gamma model and used the PhyML software to construct a maximum likelihood phylogenetic tree based on these sequences. We repeated the sequence alignment 1000 times using Bootstrap. The phylogenetic analysis of the 5′ UTR, Core region, and NS5B region circular system revealed substantial diversity among HCV isolates belonging to different genotypes, as demonstrated by Figure 4 and Figure S2-S3 in Multimedia Appendix 1. Furthermore, the clustering of genotypes 1b and 2a provided additional validation for the accuracy of the NCBI Blast results.

XSL•FO
RenderX

Figure 4. Evolutionary tree analysis of nucleotide sequences in the 5′ untranslated region. Sequences marked with asterisks represent reference strain sequences; branch lengths are proportional to the evolutionary distance and scale between sequences.



Geographical Dissemination, Estimation of the Most Recent Common Ancestor, and Population Dynamics of HCV Subtypes 1b and 2a in Shandong Province

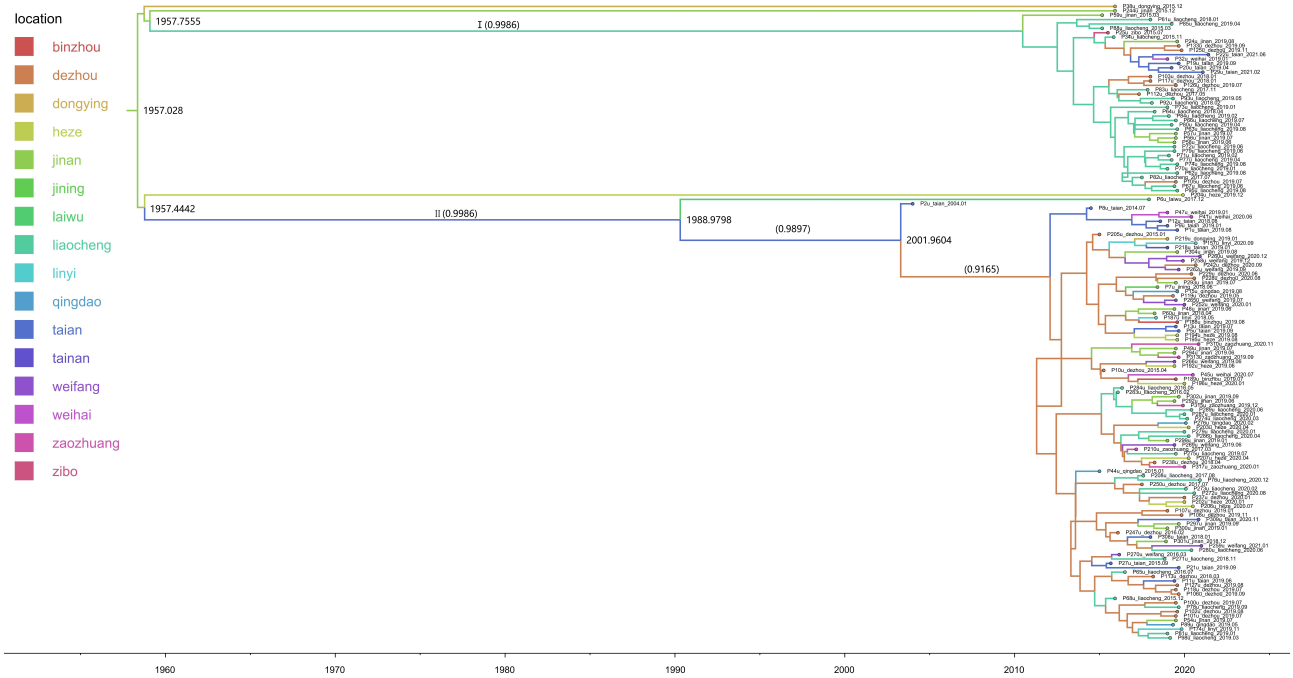
To estimate the evolutionary relationship and emergence time of the 2 major HCV genotypes (1b and 2a) among patients with hepatitis C in different cities of Shandong Province, we conducted an evolutionary analysis using the highly conserved 5′ UTR sequences, taking into account their conservation in the region.

A systematic geographical analysis of the 1b subtype revealed a pronounced genetic relationship among 1b isolates from various cities in Shandong Province. Jinan may be the origin of the 1b subtype in Shandong, dating its divergence back to 1957 (Figure 5). The MCC tree of sequence 1b is roughly divided into 2 clusters, exhibiting a high posterior probability. The 2a subtypes of Cluster I primarily spread in the Licheng region, with a few cases extending to other urban areas. Regarding the transmission of the 2a subtypes in Cluster II, Taian and Dezhou have acted as conduits, enabling the successive spread of the 2a subtypes to surrounding cities.

In the phylogenetic analysis of subgenotype 2a (Figure 6), we divided the MCC tree of 2a sequences into two clusters, both exhibiting a high posterior probability. Both clusters suggest that Jinan and Liaocheng could have been bridge points in transmitting the 2a variant. The dissemination of the 2a variant to neighboring cities could be traced back to 1979.

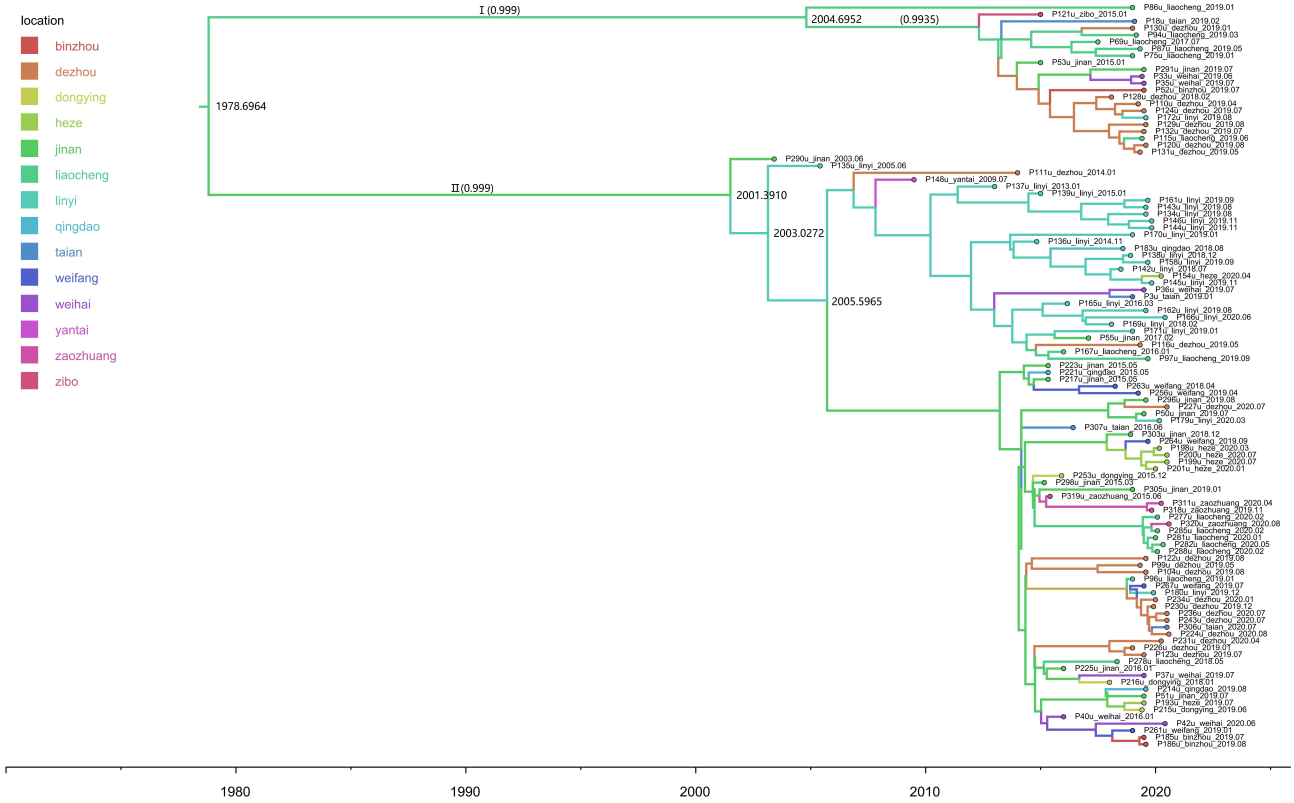
XSL•FO
RenderX

Figure 5. Maximum clade credibility tree based on the 5' untranslated region of subtype 1b. The time scale on the x-axis represents years (1960 - 2020). The branches of the tree are colored based on the sampling city in Shandong Province (as shown in the legend). Only nodes with Bayesian posterior probabilities > 0.9 are shown, with posterior support values in parentheses. The phylogenetic tree can be roughly divided into two major clusters (Cluster I and Cluster II), each showing high geographic clustering and clear transmission paths. In Cluster I, the viral strains from the Liaocheng region show strong clustering, with a relatively limited transmission range. In Cluster II, viral strains from Tai'an and Dezhou are radially distributed, potentially playing a "bridge" role in the transmission of the 1b subtype. There is a noticeable temporal structure between the viral strains from multiple cities, reflecting the long-term dynamics of HCV transmission.



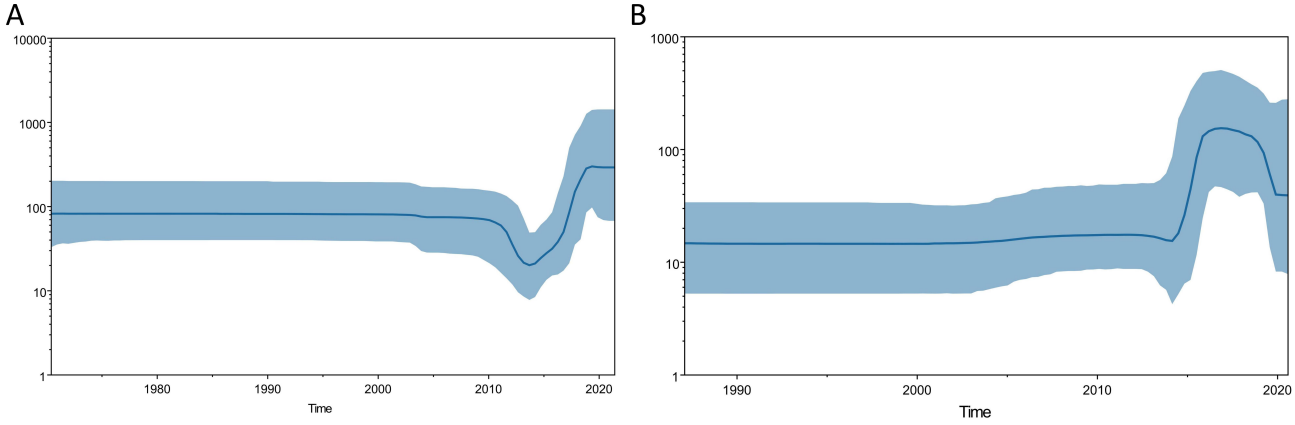
XSL•FO
RenderX

Figure 6. Maximum clade credibility tree based on the 5' untranslated region of subtype 2a. The time scale on the x-axis represents years (1980 - 2020), and the branches of the tree are colored based on the sampling cities in Shandong Province (as indicated in the legend). Only nodes with Bayesian posterior probabilities >0.9 are displayed, with posterior support values in parentheses. The tree structure can be roughly divided into two major clusters (Cluster I and Cluster II), each showing high confidence (posterior probability of 0.999). This suggests that the HCV subtypes in Shandong may have undergone at least 2 major diffusion events: Cluster I: Centered around the Liaocheng region, showing a certain degree of local transmission clustering. Cluster II: Exhibiting a multi-region mixed distribution, with Tai'an and Dezhou positioned as key nodes in the transmission network, potentially acting as "bridges" in the spread of the 2a subtype.



Subsequently, we performed a Bayesian skyline analysis to estimate the most recent common ancestor (tMRCA) time and the growth dynamics for these 2 prominent HCV subtypes (Figure 7). tMRCA for subtype 1b is estimated to be 1957 (95% CI 1943 - 1973), and for subtype 2a, it is estimated to be 1979 (95% CI 1967 - 1989). We used the Tracer software to generate a BSP to investigate the rapid expansion stage in the viral population. The rapid growth of phases 1b and 2a occurred from 2014 to 2019 and from 2014 to 2016, respectively. Before these rapid phases, the population sizes of 1b and 2a had remained relatively stable for the past 40 and 30 years. Furthermore, both population groups 1b and 2a underwent a decrease in size. The rapid decline stage of 1b (2010 - 2014) preceded the rapid growth stage, whereas the rapid decline stage of 2a (2018 - 2020) followed the rapid growth stage. Until now, there has been a relatively stable trend in the population sizes of 1b and 2a.

Figure 7. Bayesian skyline plot of the 2 major hepatitis C virus subtypes in Shandong. Graphs A and B represent HCV genotypes 1b and 2a, respectively. The horizontal ruler (x-axis) at the bottom displays years, while the vertical ruler (y-axis) on the left displays effective population size on a logarithmic scale. The black curve represents the median estimate of the changing effective population size over time. The blue curve with upper and lower areas defines the 95% highest posterior density confidence interval.



XSL•FO
RenderX

Discussion

Principal Findings

This study uses advanced phylogenetic and machine learning algorithms to perform genotype classification and evolutionary analysis of HCV isolates [32]. Previous research primarily relied on traditional molecular biology techniques, including nested PCR and gene sequencing [33]. By integrating machine learning algorithms, we enhance analysis accuracy, processing speed, and efficiency when dealing with complex data [34]. This technological innovation facilitates more precise migration and evolution tracking, providing robust data support for future disease control strategies [35].

We collected serum samples from 320 patients with hepatitis C in Shandong Province and successfully sequenced the 5 UTR from all 320 cases, the Core region from 282 cases, and the NS5B region from 233 cases. The predominant HCV subtypes in Shandong were 1b and 2a. The early spread of HCV 1b and 2a in Shandong occurred primarily in Jinan and Liaocheng, with population trends exhibiting stability, growth, and decline over time. Although the 1b subtype is globally widespread, other subtypes may be more common in regions such as Europe and North America [36]. This finding suggests that different geographical locations may have unique viral epidemic patterns, which is crucial for developing localized disease prevention strategies.

Comparison to Previous Work

While subtype 1b is widely distributed worldwide, certain regions, such as Europe and North America, may exhibit a higher prevalence of other subtypes [36]. This discovery underscores the significance of recognizing distinct geographical patterns in viral outbreaks, which is essential for developing localized disease prevention and control strategies. Using Bayesian phylogenetic inference, we estimated the tMRCA (time to the most recent common ancestor) for the 1b and 2a subtypes in Shandong Province to be 1957 and 1979, respectively. The spread of HCV 1b and 2a subtypes closely correlates with the socioeconomic development of Shandong. The origin of the 1b subtype in 1957 likely corresponds with the first systemic public health interventions post-1949 in China, during the “golden age” of public health system construction. During the late 1950s, China implemented large-scale vaccination, patriotic health campaigns, and grassroots health care network development, which increased the frequency of contact between medical institutions and populations, potentially elevating the risk of bloodborne pathogen transmission [37]. Conversely, the 1979 spread of the 2a subtype reflects the consequences of medical resource imbalance during China’s market-oriented reforms. The rapid urbanization and frequent population movement in Shandong, coupled with the concentration of medical resources in cities and limited rural health care facilities, may have increased the occurrence of high-risk behaviors, such as paid blood donations and unsafe injections, contributing to the spread of the virus [37]. Both Jinan and Liaocheng played pivotal roles in these diffusion events, highlighting the central role of major cities in pathogen transmission.

Limitations

First, the time span is limited, while the study covers samples collected from 2013 to 2021, this timeframe may not be sufficient to fully capture the long-term evolution of a chronic viral disease like HCV, which has a prolonged latency period and complex evolutionary history. Certain subtype introductions may have occurred earlier than the period observed, which could introduce uncertainty in the tMRCA estimation.

Second, there is a potential bias in the sample source: all samples were collected from patients attending medical institutions, which may introduce biases as individuals with mild symptoms, asymptomatic infections, or high-risk but undiagnosed individuals were likely excluded, potentially limiting the representativeness of the sample in terms of age, sex, and transmission route.

Third, there are limitations in the technical methods: although this study uses the BEAST Bayesian MCMC method and Bayesian skyline plots, these methods rely on certain assumptions (such as molecular clock assumptions, substitution model settings, and sample representativeness) and may introduce biases when facing uneven sequence distributions, weak time signals, or recombination events. In addition, machine learning and maximum likelihood methods for genotyping and phylogenetic tree construction may be limited by input data quality.

Fourth, the identification of recombinant strains remains uncertain: some samples identified as potential recombinants have not been validated by whole-genome sequencing or recombination detection algorithms, so the current conclusions should be interpreted cautiously.

Future Directions

Future research should aim to address several limitations identified in this study. First, expanding the temporal scope to include earlier samples would improve estimates of long-term viral evolution and help clarify the historical introduction of HCV subtypes in the region. In addition, community-based sampling—including asymptomatic individuals and high-risk populations not captured in hospital-based studies—would enhance the representativeness and generalizability of findings.

Incorporating whole-genome sequencing and advanced recombination detection tools would also enable more accurate identification of recombinant strains, particularly those with inconsistent genotyping results across genomic regions. Applying and comparing a broader range of machine learning algorithms may further enhance the efficiency and precision of genotypic classification and transmission modeling.

Moreover, future studies could explore the application of these approaches at a national scale by including data from other provinces in China. Such expansion would provide a more comprehensive understanding of HCV’s genetic and geographic diversity across the country. Finally, interdisciplinary collaboration among experts in virology, public health, clinical medicine, and bioinformatics will be essential to translate molecular epidemiological insights into targeted intervention

XSL•FO
RenderX

strategies, such as genotype-specific treatments and vaccine development.

Conclusions

This study investigated the genetic diversity and dissemination patterns of HCV in Shandong Province through sequencing and phylogenetic analysis. Genotypes 1b and 2a were identified as the predominant subtypes, with evidence of localized transmission and multiple diffusion events. Temporal and geographic reconstructions suggest distinct expansion phases for these subtypes, particularly between 2014 and 2019. The findings offer insights into regional HCV epidemiology that may support public health strategies in Shandong and similar settings. However, interpretations should be made in light of the study's methodological and temporal limitations.

Acknowledgments

This study was supported by Shandong Province Medical and Health Science and Technology Development Program Project (2018WS305).

Data Availability

The data underlying this article will be shared with the corresponding author at a reasonable request.

Authors' Contributions

LL contributed to conceptualization, methodology, data curation, and formal analysis. LL also wrote the original draft, participated in writing – review and editing, and performed supervision. TY contributed to conceptualization, participated in writing – review and editing, and performed supervision. GW contributed to data curation and formal analysis and wrote the original draft. LH contributed to data curation and formal analysis and wrote the original draft. All authors have read and approved the final version of the manuscript.

Conflicts of Interest

None declared.

Multimedia Appendix 1
Additional figures and tables.
[DOCX File, 1399 KB - medinform_v13i1e60207_app1.docx]

References

1. Reed KE, Rice CM. Overview of hepatitis C virus genome structure, polyprotein processing, and protein properties. Curr Top Microbiol Immunol 2000;242:55-84. [doi: 10.1007/978-3-642-59605-6_4] [Medline: 10592656]
2. Gupta E, Samal J, Pandey A, et al. Treatment response and drug resistance profiling of genotype 6 of hepatitis C virus in HCV/HIV co-infected patients: a pilot study from INDIA. Viruses 2022 Apr 30;14(5):944. [doi: 10.3390/v14050944] [Medline: 35632686]
3. Zitha T, Chen CY, Mudawi H, et al. Molecular characterization and genotyping of hepatitis C virus from Sudanese end-stage renal disease patients on haemodialysis. BMC Infect Dis 2022 Nov 14;22(1):848. [doi: 10.1186/s12879-022-07833-1] [Medline: 36376846]
4. Li XM, Qiu RX, Song CH, et al. Genotype and genetic variation of HCV infections with low-risk factors in Putian coastal regions, China. Epidemiol Infect 2017 Dec;145(16):3385-3397. [doi: 10.1017/S0950268817002357] [Medline: 29081304]
5. Bawazir A, AlGusheri F, Jradi H, AlBalwi M, Abdel-Gader AG. Hepatitis C virus genotypes in Saudi Arabia: a future prediction and laboratory profile. Virol J 2017 Nov 2;14(1):208. [doi: 10.1186/s12985-017-0873-7] [Medline: 29096662]
6. Basit H, Tyagi I, Koirala J, Hepatitis C. StatPearls: StatPearls Publishing; 2023.
7. Dickey BL, Coghill AE, Rathwell JA, et al. Hepatitis C virus (HCV) seroprevalence, RNA detection, and genotype distribution across Florida, 2015-2018. Prev Med 2022 Aug;161:107136. [doi: 10.1016/j.ypmed.2022.107136] [Medline: 35803347]
8. Alhazzani AA, Mahfouz AA, Abolyazid AY, et al. In hospital stroke mortality: rates and determinants in Southwestern Saudi Arabia. Int J Environ Res Public Health 2018 May 7;15(5):927. [doi: 10.3390/ijerph15050927] [Medline: 29735898]
9. Langedijk AC, Harding ER, Konya B, et al. A systematic review on global RSV genetic data: Identification of knowledge gaps. Rev Med Virol 2022 May;32(3):e2284. [doi: 10.1002/rmv.2284] [Medline: 34543489]
10. Kim D, Lee JY, Yang JS, Kim JW, Kim VN, Chang H. The architecture of SARS-CoV-2 transcriptome. Cell 2020 May 14;181(4):914-921. [doi: 10.1016/j.cell.2020.04.011] [Medline: 32330414]
11. Roder A, Johnson K, Knoll M, et al. Optimized quantification of intrahost viral diversity in SARS-cov-2 and influenza virus sequence data. Microbiology. Preprint posted online on 2021. [doi: 10.1101/2021.05.05.442873]

XSL•FO
RenderX

12. de Oliveira PSB, Silva Júnior JVJ, Weiblen R, Flores EF. Subtyping bovine viral diarrhea virus (BVDV): Which viral gene to choose? Infect Genet Evol 2021 Aug;92:104891. [doi: 10.1016/j.meegid.2021.104891] [Medline: 33945882]
13. Yang XC, Hong ZP, Wang Y, et al. Growth history of hepatitis C virus among HIV/HCV co-infected patients in Guizhou Province. Front Genet 2023;14:1171892. [doi: 10.3389/fgene.2023.1171892] [Medline: 37347053]
14. Jia Y, Yue W, Gao Q, et al. Characterization of a novel hepatitis C subtype, 6xj, and its consequences for direct-acting antiviral treatment in Yunnan, China. Microbiol Spectr 2021 Sep 3;9(1):e0029721. [doi: 10.1128/spectrum.00297-21] [Medline: 34479413]
15. Ndumia JN, Kang M, Gbenontin BV, Lin J, Nyambura SM. A review on the wear, corrosion and high-temperature resistant properties of wire arc-sprayed fe-based coatings. Nanomaterials (Basel) 2021 Sep 27;11(10):2527. [doi: 10.3390/nano11102527] [Medline: 34684967]
16. Haga H, Sato H, Koseki A, et al. A machine learning-based treatment prediction model using whole genome variants of hepatitis C virus. PLoS ONE 2020;15(11):e0242028. [doi: 10.1371/journal.pone.0242028] [Medline: 33152046]
17. Hraber PT, Fischer W, Bruno WJ, Leitner T, Kuiken C. Comparative analysis of hepatitis C virus phylogenies from coding and non-coding regions: the 5' untranslated region (UTR) fails to classify subtypes. Virol J 2006 Dec 14;3(1):103. [doi: 10.1186/1743-422X-3-103] [Medline: 17169155]
18. Zhu Y, Liu J, Guo K, et al. Outbreak of a novel disease caused by Staphylococcus pseudintermedius in raccoon dogs (Nyctereutes procyonoides). Transbound Emerg Dis 2021 Jul;68(4):1995-2004. [doi: 10.1111/tbed.13847] [Medline: 32966709]
19. Hu HH, Zhang C, Xie CB, et al. Prevalence and genotype distribution of hepatitis C virus from 1,668 individuals of Sichuan Area in China. Clin Lab 2021 Jan 1;67(1). [doi: 10.7754/Clin.Lab.2020.200335] [Medline: 33491428]
20. Sah UK, Sah AK, Ansari M, et al. HCV co-infection and its genotypic distribution in HIV-infected patients in Nepalese population. Trop Med Infect Dis 2023 Jul 13;8(7):361. [doi: 10.3390/tropicalmed8070361] [Medline: 37505657]
21. Mallory MA, Lucic DX, Sears MT, Cloherty GA, Hillyard DR. Evaluation of the Abbott realtime HCV genotype II RUO (GT II) assay with reference to 5'UTR, core and NS5B sequencing. J Clin Virol 2014 May;60(1):22-26. [doi: 10.1016/j.jcv.2014.02.006] [Medline: 24656214]
22. Daniel HDJ, David J, Raghuraman S, et al. Comparison of three different hepatitis C virus genotyping methods: 5'NCR PCR-RFLP, Core type-specific PCR, and NS5b sequencing in a tertiary care hospital in South India. J Clin Lab Anal 2017 May;31(3):e22045. [doi: 10.1002/jcla.22045] [Medline: 27580956]
23. Paraschiv S, Foley B, Otelea D. Diversity of HIV-1 subtype C strains isolated in Romania. Infect Genet Evol 2011 Mar;11(2):270-275. [doi: 10.1016/j.meegid.2010.07.002] [Medline: 20620240]
24. Drummond AJ, Rambaut A. BEAST: Bayesian evolutionary analysis by sampling trees. BMC Evol Biol 2007 Nov 8;7(1):214. [doi: 10.1186/1471-2148-7-214] [Medline: 17996036]
25. Chen M, Ma Y, Chen H, et al. Multiple introduction and naturally occuring drug resistance of HCV among HIV-infected intravenous drug users in Yunnan: an origin of China's HIV/HCV epidemics. PLoS ONE 2015;10(11):e0142543. [doi: 10.1371/journal.pone.0142543]
26. Huang K, Chen J, Xu R, et al. Molecular evolution of hepatitis C virus in China: A nationwide study. Virology (Auckl) 2018 Mar;516:210-218. [doi: 10.1016/j.virol.2018.01.015] [Medline: 29407379]
27. Moradpour D, Penin F, Rice CM. Replication of hepatitis C virus. Nat Rev Microbiol 2007 Jun;5(6):453-463. [doi: 10.1038/nrmicro1645] [Medline: 17487147]
28. Chen Z, Weck KE. Hepatitis C virus genotyping: interrogation of the 5' untranslated region cannot accurately distinguish genotypes 1a and 1b. J Clin Microbiol 2002 Sep;40(9):3127-3134. [doi: 10.1128/JCM.40.9.3127-3134.2002] [Medline: 12202542]
29. Simmonds P. 2000 Fleming Lecture. The origin and evolution of hepatitis viruses in humans. J Gen Virol 2001 Apr 1;82(4):693-712. [doi: 10.1099/0022-1317-82-4-693]
30. Bouchardeau F, Cantaloube JF, Chevaliez S, et al. Improvement of hepatitis C virus (HCV) genotype determination with the new version of the INNO-LiPA HCV assay. J Clin Microbiol 2007 Apr;45(4):1140-1145. [doi: 10.1128/JCM.01982-06] [Medline: 17251399]
31. Kalinina O, Norder H, Mukomolov S, Magnius LO. A natural intergenotypic recombinant of hepatitis C virus identified in St. Petersburg. J Virol 2002 Apr;76(8):4034-4043. [doi: 10.1128/jvi.76.8.4034-4043.2002] [Medline: 11907242]
32. Li G, Panday SK, Alexov E. SAAFEC-SEQ: a sequence-based method for predicting the effect of single point mutations on protein thermodynamic stability. Int J Mol Sci 2021 Jan 9;22(2):606. [doi: 10.3390/ijms22020606] [Medline: 33435356]
33. Ge Y, Chen Z, Fu Y, et al. Identification and validation of hub genes of synovial tissue for patients with osteoarthritis and rheumatoid arthritis. Hereditas 2021 Sep 28;158(1):37. [doi: 10.1186/s41065-021-00201-0] [Medline: 34583778]
34. Schaffter T, Buist DSM, Lee CI, et al. Evaluation of combined artificial intelligence and radiologist assessment to interpret screening mammograms. JAMA Netw Open 2020 Mar 2;3(3):e200265. [doi: 10.1001/jamanetworkopen.2020.0265] [Medline: 32119094]
35. Kamali N, Abbas F, Lehane M, Griew M, Furey A. A review of in situ methods-Solid Phase Adsorption Toxin Tracking (SPATT) and Polar Organic Chemical Integrative Sampler (POCIS) for the collection and concentration of marine biotoxins

XSL•FO
RenderX

and pharmaceuticals in environmental waters. Molecules 2022 Nov 15;27(22):7898. [doi: 10.3390/molecules27227898] [Medline: 36431996]
36. Chan CP, Uemura H, Kwan TH, et al. Review on the molecular epidemiology of sexually acquired hepatitis C virus infection in the Asia-Pacific region. J Int AIDS Soc 2020 Sep;23(9):e25618. [doi: 10.1002/jia2.25618] [Medline: 32969173]
37. Kamboj S, Kumar M. Global origin and spatiotemporal spread of hepatitis C virus epidemic genotypes/subtypes: a complete genome-based phylodynamic and phylogeographic analyses. J Med Virol 2024 Dec;96(12):e70123. [doi: 10.1002/jmv.70123] [Medline: 39697008]

Abbreviations list

BEAST: Bayesian Evolutionary Analysis Sampling Trees
BSP: Bayesian skyline plot
GTR: general time reversible
HCV: hepatitis C virus
HDV: hepatitis D virus
MCC: maximum clade credibility
MCMC: Markov chain Monte Carlo
MUSCLE: Multiple Sequence Comparison by Log-Expectation
NCBI BLAST: National Center for Biotechnology Information Basic Local Alignment Search Tool
PhyML: Phylogenetic Maximum Likelihood
qPCR: quantitative polymerase chain reaction
tMRCA: time to the most recent common ancestor
UTR: untranslated region

Edited by A Coristine; submitted 07.05.24; peer-reviewed by S Laguna-Meraz, Y Yazdani; revised version received 29.05.25; accepted 29.05.25; published 18.08.25.

Please cite as:
Lin L, Wang G, Hao L, Yan T
Genotype Distribution and Migration Patterns of Hepatitis C Virus in Shandong Province, China: Molecular Epidemiology and Phylogenetic Study
JMIR Med Inform 2025;13:e60207
URL: https://medinform.jmir.org/2025/1/e60207
doi:10.2196/60207

© Lin Lin, Guoyong Wang, Lianzheng Hao, Tingbin Yan. Originally published in JMIR Medical Informatics (https://medinform.jmir.org), 18.8.2025. This is an open-access article distributed under the terms of the Creative Commons Attribution License (https://creativecommons.org/licenses/by/4.0/), which permits unrestricted use, distribution, and reproduction in any medium, provided the original work, first published in JMIR Medical Informatics, is properly cited. The complete bibliographic information, a link to the original publication on https://medinform.jmir.org/, as well as this copyright and license information must be included.

XSL•FO
RenderX

Effectiveness of the Facility for Elderly Surveillance System (FESSy) in Two Public Health Center Jurisdictions in Japan: Prospective Observational Study

Junko Kurita[1,2], MSN; Motomi Hori[3], MD; Sumiyo Yamaguchi[4]; Aiko Ogiwara[3]; Yurina Saito[4]; Minako Sugiyama[3], MD, PhD; Asami Sunadori[3]; Tomoko Hayashi[3], MSN; Akane Hara[3]; Yukari Kawana[3]; Youichi Itoi[3]; Tamie Sugawara[5], PhD; Yoshiyuki Sugishita[3], MD, PhD; Fujiko Irie[4], MD, PhD; Naomi Sakurai[6], PhD

[1]Department of Nursing, Faculty of Sports & Health Science, Daito Bunka University, Higashimatsuyama-shi, Japan

[2]Graduate School of Health Sciences (Nursing), Ibaraki Prefectural University of Health Sciences, Ami-machi, Japan

[3]Sumida City Public Health Center, Sumida City, Japan

[4]Tsuchiura Public Health Center, Tsuchiura City, Japan

[5]National Institute of Infectious Diseases, Shinjuku City, Japan

[6]Center for Medical Sciences, Ibaraki Prefectural University of Health Sciences, Ami-machi, Japan

Corresponding Author:
Junko Kurita, MSN
Department of Nursing, Faculty of Sports & Health Science, Daito Bunka University, Higashimatsuyama-shi, Japan

Abstract

Background: Residents of facilities for older people are vulnerable to COVID-19 outbreaks. Nevertheless, timely recognition of outbreaks at facilities for older people at public health centers has been impossible in Japan since May 8, 2023, when the Japanese government discontinued aggressive countermeasures against COVID-19 because of the waning severity of the dominant Omicron strain. The Facility for Elderly Surveillance System (FESSy) has been developed to improve information collection.

Objective: This study examined FESSy experiences and effectiveness in two public health center jurisdictions in Japan.

Methods: This study assessed the use by public health centers of the detection mode of an automated AI detection system (ie, FESSy AI), as well as manual detection by the public health centers' staff (ie, FESSy staff) and direct reporting by facilities to the public health centers. We considered the following aspects: (1) diagnoses or symptoms, (2) numbers of patients as of their detection date, and (3) ultimate numbers of patients involved in incidents. Subsequently, effectiveness was assessed and compared based on detection modes. The study lasted from June 1, 2023, through January 2024.

Results: In both areas, this study examined 31 facilities at which 87 incidents were detected. FESSy (AI or staff) detected significantly fewer patients than non-FESSy methods, that is, direct reporting to the public health center of the detection date and ultimate number of patients.

Conclusions: FESSy was superior to direct reporting from facilities for the number of patients as of the detection date and for the ultimate outbreak size.

(JMIR Med Inform 2025;13:e58509) doi:10.2196/58509

KEYWORDS

early detection; facility for older people; outbreak; public health center; syndromic surveillance; Japan; older adults

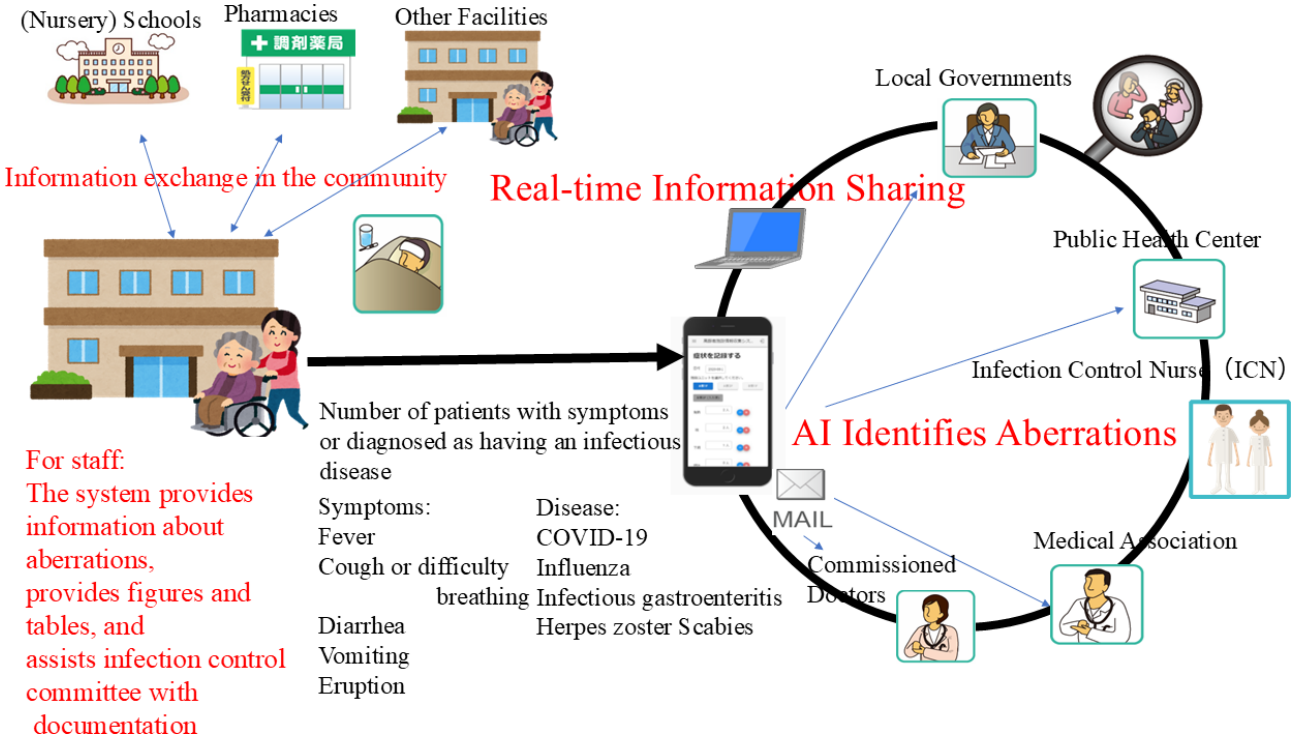
Introduction

Residents at facilities for older people have remained remarkably vulnerable to COVID-19 outbreaks [1]. Infection control at such facilities is expected to be the most important method to reduce the disease burden attributable to COVID-19 [2]. However, on May 8, 2023, infection control policies for COVID-19 in Japan were relaxed. For that reason, public health centers have become unable to recognize outbreak situations at facilities for older people unless the outbreak grows to include more than 10 cases [3]. To fill this information gap, the Facility for Elderly Surveillance System (FESSy) has been used [4] as a mode of syndromic surveillance that monitors symptoms and infectious diseases among facility residents. This web data exchange system transmits data entered from a smartphone or PC. Each facility inputs data on the number of residents or staff members with certain symptoms or who have been diagnosed as having infectious diseases in units where residents cohabitate and unit staff members manage them. Figure 1 presents the system concept. The targeted symptoms include fever, cough or difficulty breathing, vomiting, diarrhea, and eruption. The diagnosed infectious diseases include COVID-19, influenza,

XSL•FO
RenderX

infectious gastroenteritis, herpes zoster, and scabies. Data aberrations can be detected by the unit at each facility using artificial intelligence (AI). If an aberration is detected, this information is then delivered to the commissioned doctors, public health centers, medical associations, infection control nurses in the community, and local governments, who are allowed access to data entered at the facility, as shown on the right-hand side of Figure 1.

Figure 1. Concept of the Facility for Elderly Surveillance System (FESSy). Facilities enter data (shown on the left) on the number of patients with certain symptoms or infectious diseases; this is shared with stakeholders that include public health centers, local governments, infection control nurses, commissioned doctors, and the medical association (shown in the circle on the right). Moreover, the FESSy AI monitors the entered data to identify aberrations through comparison with past aberration data and patterns, as judged by the public health center staff or developers. When the AI finds an aberration, it sends an email to the stakeholders and FESSy facility correspondents.



Development of FESSy was begun in 2008 by a research group headed by Dr Yasushi Ohkusa of the National Institute of Infectious Diseases, with trials conducted at a few facilities. However, use of FESSy and the related research were then suspended for an extended period. Recently, an author of this study (JK) developed a smartphone version of FESSy and has renewed use of the system and related research. Currently, its copyright is held by a nonprofit organization that took over the project from the original research group and a private company (Milabo Co Ltd). It has been functioning in Ibaraki prefecture and Sumida City in Tokyo as part of research group activities headed by author NS.

Two public health centers operating FESSy in Sumida City in Tokyo and Tsuchiura in Ibaraki prefecture cooperated in this study. Sumida City, which is located in the center of metropolitan Tokyo, has approximately 280,000 residents. The Tsuchiura Public Health Center jurisdiction comprises 3 cities with a total population of 250,000. In Japan, most medical services are financed by national public health insurance. The same policies for older persons apply in all areas in Japan. In this sense, Sumida City and Tsuchiura present similar situations in terms of health care and welfare. Sumida City is a somewhat more urban area when compared with Tsuchiura. FESSy was activated in March 2023 in Sumida City. It was activated in September 2023 in Tsuchiura based on a request from the Ibaraki Prefectural University of Health Sciences. The Tsuchiura Public Health Center jurisdiction includes 31 long-term care facilities (special nursing homes for older people). There are 10 long-term care facilities in Sumida City.

Soon, FESSy is expected to be activated nationwide, where it can contribute to timely detection and rapid infection control at facilities. This study was conducted to summarize experiences of FESSy and to evaluate its effectiveness.

A system similar to FESSy has reportedly been operational in the Netherlands since April 2017 [5]. The Meldpunt voor Uitbraken van Infectieziekten en Bijzonder Resistente Micro-organismen (MUIZ) is a system for recording outbreaks at facilities and for the timely sharing of information, although it does not clearly define outbreaks for diseases other than COVID-19. All COVID-19 cases since March 2020 should have been recorded through the system, as it operated during the pandemic. However, it remains unknown how it has operated after the pandemic. It is noteworthy that the system does not function until an outbreak emerges. Therefore, unlike FESSy, MUIZ might not be suitable for early intervention and outbreak prevention for diseases other than COVID-19.

In Australia, the Aged Care National Antimicrobial Prescribing Survey and Victorian Healthcare Associated Infection Surveillance System operate at some facilities [6]. However, these facilities join voluntarily; like FESSy, participation is not

XSL•FO
RenderX

enforced by law. The Australian system is aimed at saving time used for data entry, which must also be considered in Japan [7].

Methods

Overview

This study was conducted at the Sumida City Public Health Center in Tokyo and at the Tsuchiura Public Health Center in Ibaraki prefecture. Study participants were limited to patients at facilities for older people in the jurisdictions of the 2 public health centers, as we particularly wanted to study long-term care facilities, specifically, special nursing homes for older people. The study period was from June 2023 to the end of January 2024. If a facility joined FESSy during the study period, data that the facility had accumulated before joining FESSy were ignored.

In each unit of the facility, FESSy detects aberrations using AI, based on the "C1-MILD" method of the Early Aberration Reporting System (EARS) [8], which includes symptoms and diagnoses. In EARS, C1-MILD defines a data aberration as being 3 times the standard deviation during the prior 7 days and higher than average in the same period. If the AI finds an aberration, then emails are sent automatically to facility managers or staff, public health centers, local governments, commissioned doctors, infection control nurses in the community, and medical associations. Hereafter, we refer to this AI detection mode in FESSy as "FESSy AI." Based on email notifications from FESSy AI, a public health center can activate a public health intervention at a facility. Of course, public health center staff can always monitor the situation at facilities using FESSy, even if they have not yet received an alert email from FESSy AI. Sometimes a very early-stage outbreak is identifiable by staff, facilitating a rapid public health response. We refer to this detection mode as "FESSy staff." Aside from FESSy AI and FESSy staff, a public health center sometimes receives a report from a facility directly, rather than via FESSy. We refer to that as a "direct report."

First, public health center operations can be generalized into 3 dimensions for all detection modes (FESSy AI, FESSy staff, and direct report): (1) diseases or symptoms, (2) number of patients as of the detection date, and (3) ultimate number of patients involved in the incident. Regarding (1), examination of diseases or symptoms can engender multiple answers.

We tested the overall FESSy effectiveness (sum of results for FESSy AI and FESSy staff) compared to the non-FESSy method, which can only operate based on direct reports from facilities. Moreover, we sought to ascertain, by testing, which was the more effective of the 2 FESSy communication modes: FESSy AI or FESSy staff. The effectiveness of each detection mode was measured as the number of patients as of the detection date or as of the end of the outbreak. The Wilcoxon rank-sum test was used to compare FESSy versus non-FESSy methods, as well as FESSy AI versus FESSy staff. We adopted 5% as the significance level and used software (Stata SE version 17.0; Stata Corp) for all statistical analyses.

Ethical Considerations

This study was approved by the Ethics Committee of Ibaraki Prefectural University of Health Sciences on August 21, 2023 (1103); the applicant was the corresponding author (JK). We obtained written informed consent from the two public health centers.

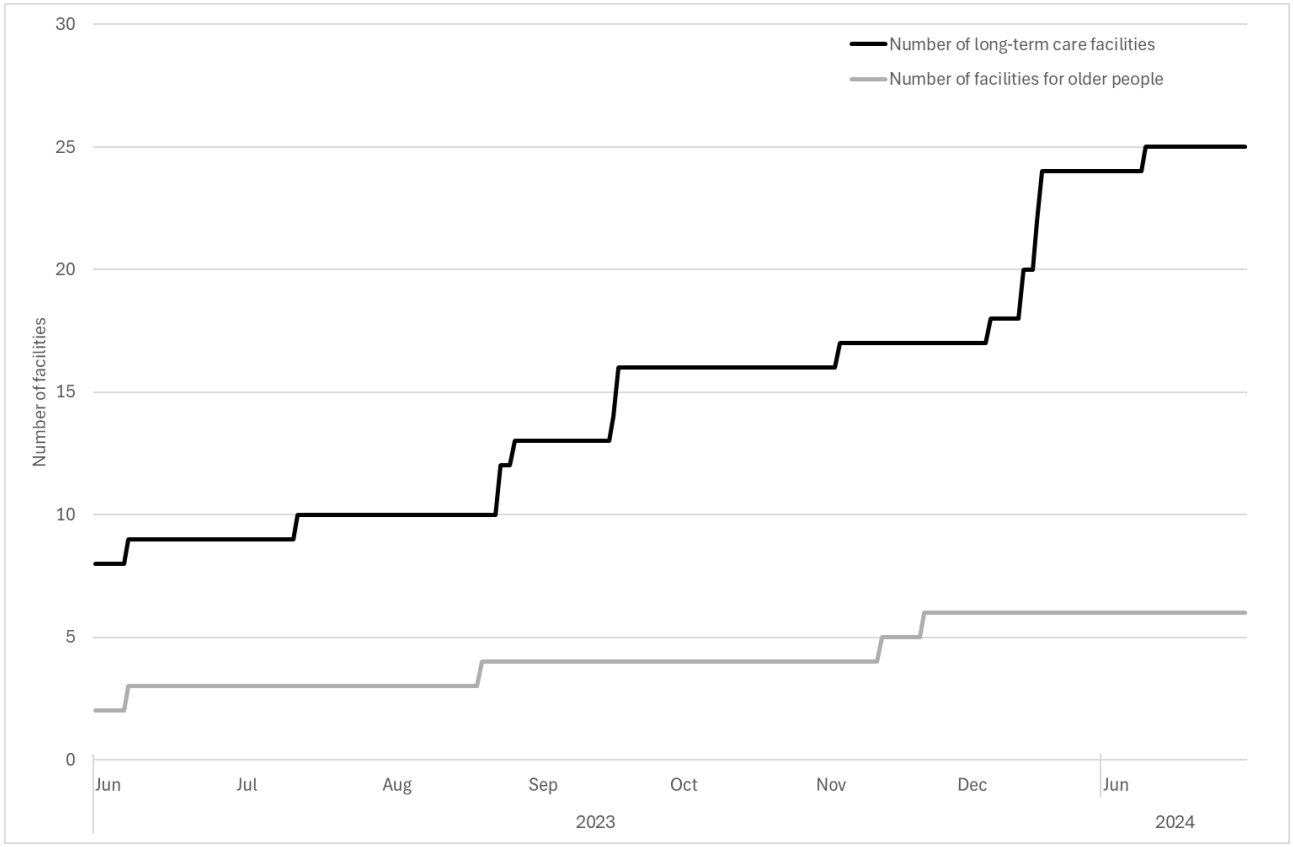
Results

As of the end of January 2024, 17 facilities had joined FESSy that were under the jurisdiction of the Tsuchiura Public Health Center: 16 were long-term care facilities (special nursing homes for older people) and 1 was a geriatric health services facility. In Sumida City, 14 facilities joined FESSy, of which 9 were long-term care facilities; others included geriatric health services facilities, low-cost homes for older people, and fee-based facilities. The proportion of long-term care facilities that joined FESSy was 53% (16/30 facilities) in the Tsuchiura Public Health Center and approximately 90% (9/10 facilities) in the Sumida City Public Health Center as of the end of January 2024. The increases in the number of facilities joining in the two areas are shown in Figure 2.

Figure 3 presents the proportion of data entry at FESSy facilities, which fluctuated between 50% and 80%. However, the average was almost 65%. In fact, some facilities that had joined never entered data into the FESSy system. In addition, facilities that immediately started to enter data into FESSy continued to enter data every day.

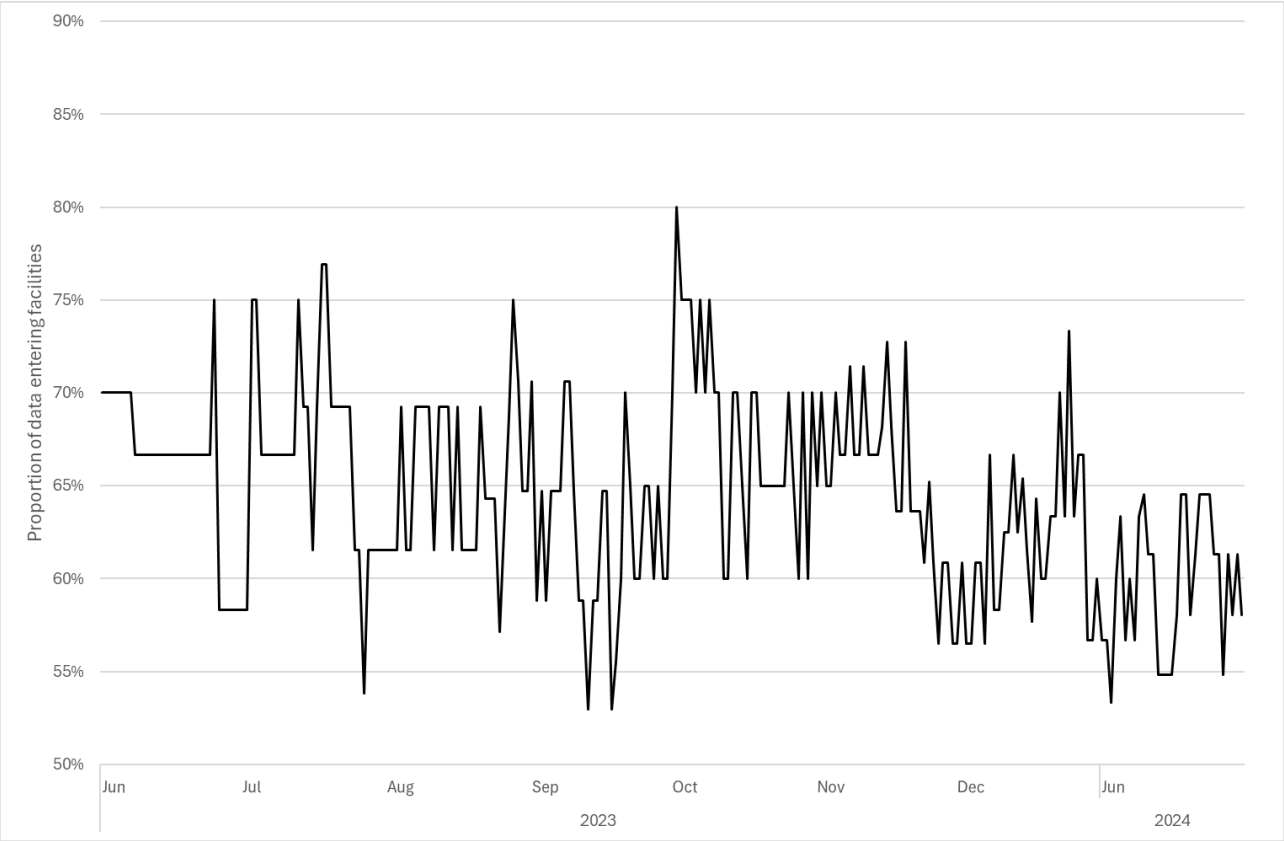
XSL•FO
RenderX

Figure 2. Number of facilities joining the Facility for Elderly Surveillance System (FESSy) in the Sumida City Public Health Center and the Tsuchiura Public Health Center from June 1, 2023, to January 31, 2024. The black line represents the number of long-term care facilities joining FESSy. The gray line represents the number of facilities for older people joining FESSy, other than long-term care facilities. In the Tsuchiura Public Health Center jurisdiction, FESSy started operation on September 1, 2023. Finally, 14 facilities had joined FESSy in the Sumida Public Health Center jurisdiction and 17 facilities had joined FESSy in the Tsuchiura Public Health Center jurisdiction as of the end of January 2024.



XSL•FO
RenderX

Figure 3. Proportion of facilities that entered data into the Facility for Elderly Surveillance System (FESSy) in the jurisdictions of the Sumida City Public Health Center and Tsuchiura Public Health Center from June 1, 2023, to January 31, 2024. Proportions for data entry were defined as the number of facilities that entered data in a day divided by the number of facilities that had joined FESSy as of the dates shown in Figure 2. A facility was defined as having entered data if it had entered information on symptoms, including an absence of patients with a certain symptom. Twelve facilities entered data every day, while another 10%-30% of facilities entered data but did not do so every day.



During the study period, 87 incidents were detected in both jurisdictions. Figure 4 presents the number of incidents by week and by detection mode. More than half of all incidents were detected through FESSy AI (n=21 incidents) and FESSy staff (n=26 incidents). Aside from those, 40 incidents were reported directly to the public health centers.

XSL•FO
RenderX

Figure 4. Number of incidents per week by detection mode for the Facility for Elderly Surveillance System (FESSy) at Sumida City Public Health Center and Tsuchiura Public Health Center from June 1, 2023, to January 31, 2024.

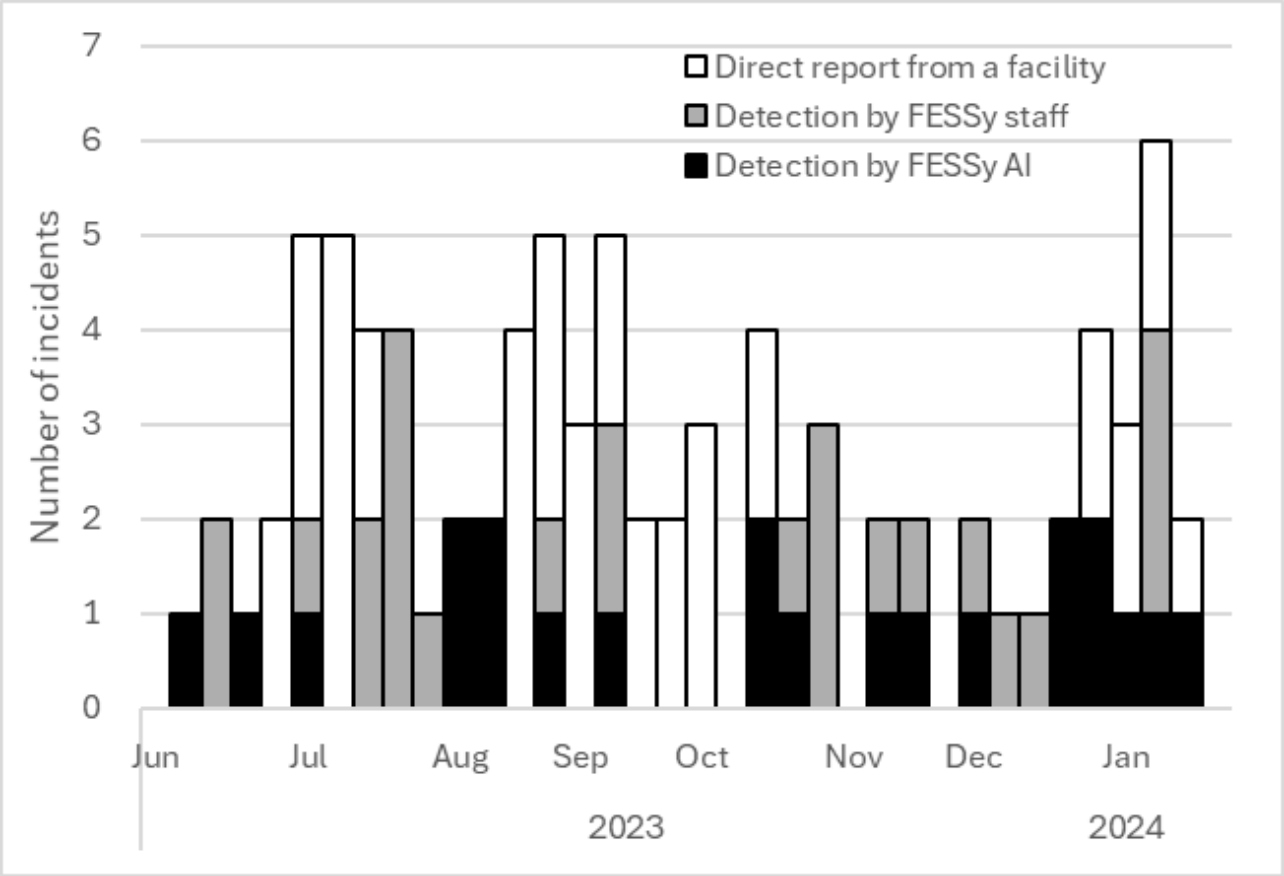


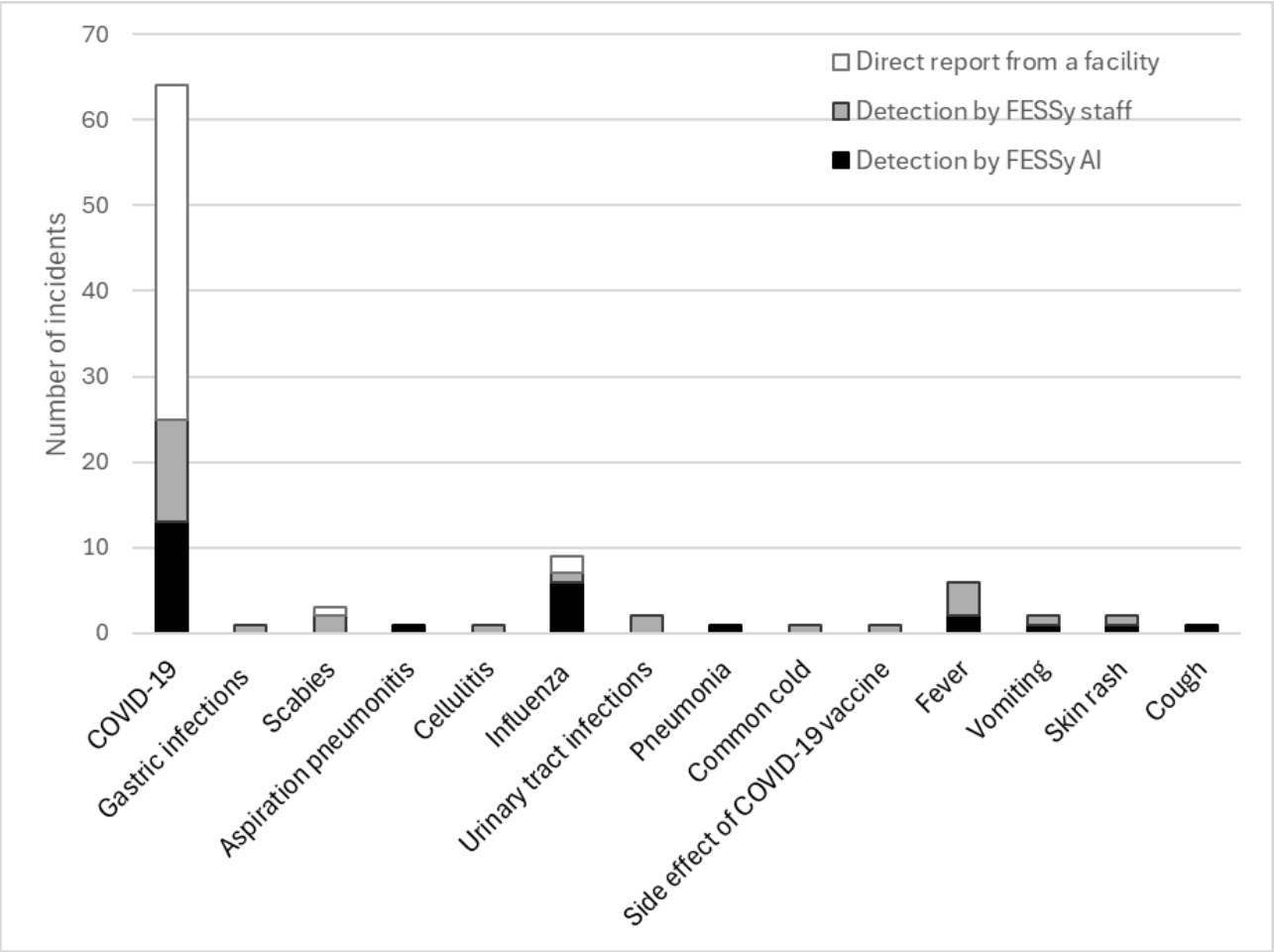
Figure 5 shows the distribution of diseases and symptoms by detection mode. The incidents caused by COVID-19 were the most numerous at 63. The next most frequent incidents were caused by influenza, with 8 incidents. Incidents detected by direct reports were limited mainly to COVID-19, with 2 incidents of influenza and 1 incident of scabies. Conversely, FESSy AI and FESSy staff found aberrations for diseases other than COVID-19, including symptoms such as fever, vomiting, and rash.

Figure 6 presents the distribution of the number of patients as of the detection date by detection mode. One reported incident did not include the number of patients. The mode for number of patients was 2. The largest number of patients was 26, which was attributable to a COVID-19 outbreak. Incidents with more than 11 patients were limited to detection by direct report. By detection mode, the average number of patients detected by FESSy AI was 4.29 (SD 2.80) for 21 incidents. For FESSy staff, the average number was 1.83 (SD 1.09) for 26 incidents. For direct reports, it was 6.55 (SD 6.18) for 40 incidents. The estimated *P* value of a rank-sum test comparison between FESSy and non-FESSy methods was .004. The *P* value was <.001 for a comparison of FESSy AI and FESSy staff.

Figure 7 shows a distribution of the ultimate number of patients involved in incidents by detection mode. Three incidents did not include this information because of the outbreak was ongoing at the end of the study period. The mode for number of patients was 1. The largest number of patients was 82, which was attributable to a COVID-19 outbreak. Incidents with more than 19 patients were limited to detection by direct report. By detection mode, the average number of patients detected by FESSy AI was 7.00(SD 3.60) for 21 incidents. For FESSy staff, the average number was 2.52 (SD 3.25) for 26 incidents. For direct report, it was 16.5 (SD 15.4 for 37 incidents. The estimated *P* value of a rank-sum test comparison of FESSy and non-FESSy methods was <.001. The P value was .001 for a comparison of FESSy AI and FESSy staff.

XSL•FO
RenderX

Figure 5. Numbers of incidents by disease or symptom and by detection and notification modes of the Facility for Elderly Surveillance System (FESSy) in Sumida City Public Health Center and Tsuchiura Public Health Center from June 1, 2023, to January 31, 2024. Terms from "COVID-19" through "side effect of COVID-19 vaccine" are diseases. Terms from "fever" through "cough" are symptoms. There were a total of 95 incidents with disease or symptoms (some incidents were caused by more than 1 disease or symptom).



XSL•FO
RenderX

Figure 6. Numbers of incidents by the number of patients as of the detection date and by detection mode of the Facility for Elderly Surveillance System (FESSy) in Sumida City Public Health Center and Tsuchiura Public Health Center from June 1, 2023, to January 31, 2024. One detected incident did not include the number of patients detected. The total number of incidents was 87.

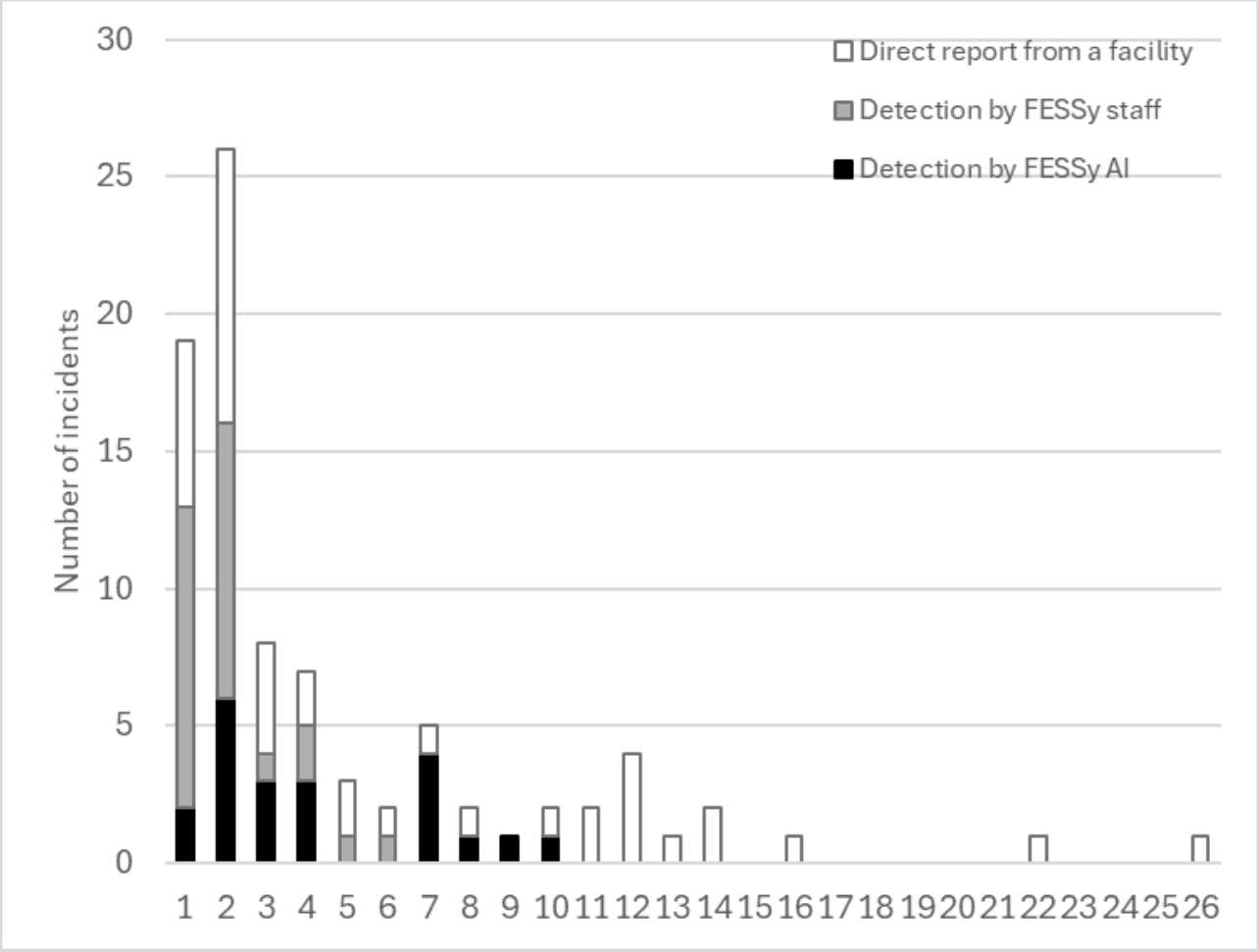
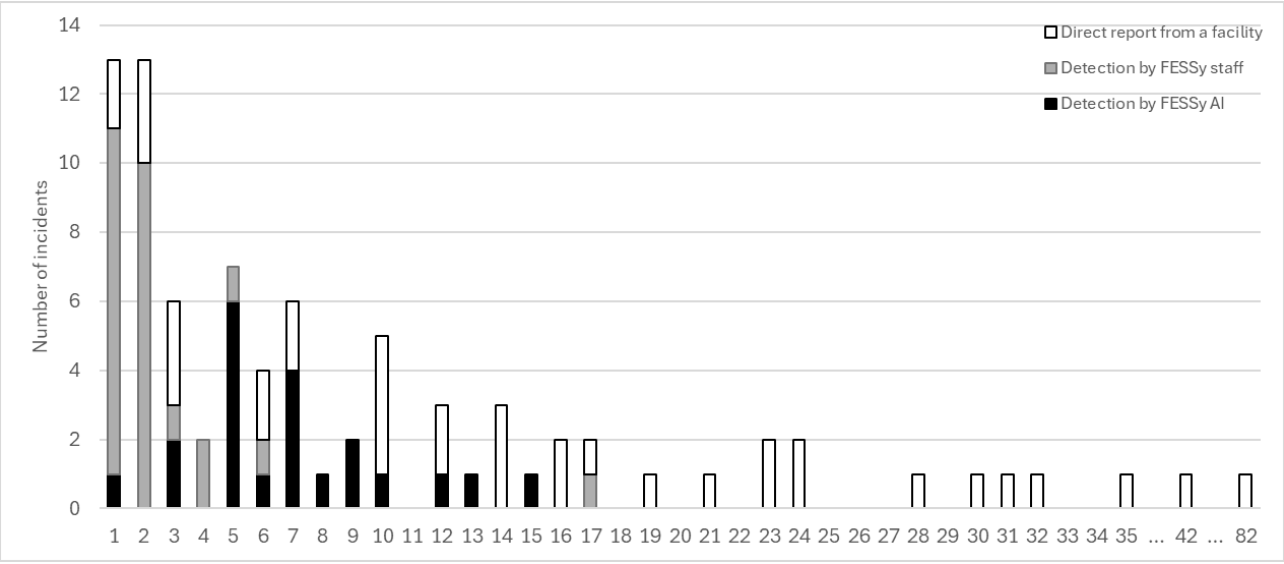


Figure 7. Number of incidents by ultimate number of patients and by detection mode of the Facility for Elderly Surveillance System (FESSy) in Sumida City and Tsuchiura from June 1, 2023, to January 31, 2024. The total number of incidents was 84. Three incidents were ongoing at the end of the study period; the ultimate number of patients was thus not available.



XSL•FO
RenderX

Discussion

Principal Findings

Findings from statistical analysis indicate that FESSy detected outbreaks earlier than non-FESSy methods (eg, direct reporting). Notably, FESSy staff could detect an outbreak earlier than FESSy AI. Similarly, the ultimate number of patients was smaller for incidents detected by FESSy than by non-FESSy methods. Figure 5 shows that FESSy AI and FESSy staff detected aberrations for diseases other than COVID-19 and for certain symptoms. This finding suggests the usefulness of FESSy, for which detection is not limited to a particular disease, in contrast to MUIZ in the Netherlands, which is limited to COVID-19.

Comparison of the FESSy detection modes, FESSy AI and FESSy staff, showed that the latter was more timely than the former. FESSy staff sometimes detected an aberration with only 1 person. In this situation, AI usually inferred a nonaberration. In fact, the C1-MILD method was too sensitive: it produced many false positive results because it referred only to the prior 7 days. The use of AI reduced false positives by incorporating information from a longer period or that was obtained with other methods for aberration inference, including FESSy staff. Particularly, Figure 6 shows that, with few exceptions, AI did not recognize the initiation of an outbreak if the number of patients was merely 1. Therefore, a FESSy AI notification might be sent later than a FESSy staff notification. Regarding outcomes, the number of patients at the time of detection might be appropriate to evaluate timeliness. However, that measure does not include information about final outcomes, such as the outbreak size or whether mortality cases are included. In other words, the number of patients as of the time of detection can reflect timeliness or sensitivity, but might not reflect specificity for an aberration.

Evaluation of specificity not only for FESSy but also for syndromic surveillance in general was quite difficult because, unlike laboratory tests, no gold standard exists for surveillance. In the case of FESSy, specificity was defined as not detecting aberrations that would not develop into large outbreaks. Thus, to determine specificity for FESSy, one would have to know the proportion of aberrations found by FESSy that would not develop into a large outbreak if countermeasures were not taken. However, in the real world, FESSy immediately found aberrations, after which countermeasures at the facility or public health center were activated to reduce the probability of these aberrations developing into large outbreaks. Because FESSy was so effective, the high probability of an outbreak was removed. In other words, we could not observe a situation at a FESSy-affiliated facility in which FESSy detected no aberration. Moreover, at non-FESSy facilities, it was difficult to find aberrations that occurred with the same timing according to which FESSy usually detects an aberration. Public health centers sometimes recognize a situation at such facilities after an outbreak has already expanded. Because of these difficulties and paradoxical comparisons, we anticipate that evaluation of specificity will be a future challenge for the evaluation of FESSy.

On May 8, 2023, the government changed the criterion for reporting COVID-19 infections at facilities to a public health center: instead of reporting all cases, reporting was relaxed to the reporting of only clusters involving more than 10 cases. However, the modes for the number of patients detected by direct reports in this study were 2 and 1 at the two centers. This finding might indicate that the earlier criterion for reporting to a public health center (all cases) continued in facilities even after May 8, 2023, depending on spontaneous decisions at facilities, even though public health centers were never required to report all cases after May 8, 2023.

Before FESSy initiation in both areas, we were concerned about burdens imposed by data entry at the facilities. Nevertheless, no complaints have been made by facility staff members about data entry burdens. The data were entered regularly every day. To reduce the data entry burden at facilities joining FESSy, we developed a method for automatic data transfer from electronic care records at facilities [7], as suggested by the results of a study in Australia [6]. However, because the share of electronic care records including symptoms and diagnoses that could be transferred automatically as data was not very high, use of the method has been limited to a small number of facilities. We expect that other ideas to reduce the data entry burden will be necessary.

Moreover, information from FESSy has been shared with public health centers. That information has contributed to the detection of outbreaks of COVID-19 and other infectious diseases in a timely manner. Developing situations are followed up without additional effort. Infection control nurses in communities or at affiliated hospitals and public health nurses at public health centers in particular highly regarded its effectiveness at controlling outbreaks.

In Tsuchiura, the proportion of facilities joining FESSy remained at 51% (n=16 facilities), much lower than the corresponding proportion in Sumida City of 90% (n=9 facilities). However, the number of facilities joining FESSy was larger in Tsuchiura than in Sumida City. Therefore, this difference might reflect only the number of facilities covered by the public health center, irrespective of those participating in FESSy. We consider that there is no fundamental difference between them. Moreover, the program was introduced in Tsuchiura 3 months later than in Sumida City. Thus, we expect that the proportion of participating facilities in Tsuchiura will increase in the coming months. We will examine whether there are any difficulties associated with FESSy in Tsuchiura through surveys of facilities. If some particular difficulty is found, then a challenge for future research will be to solve it.

Study periods were insufficiently long: 8 months for Sumida City and 5 months for Tsuchiura. However, we found that FESSY had some degree of effectiveness. Earlier publication of this fact might have contributed to a more rapid spread of FESSy participation, even though we expect that ongoing verification of the robustness of our results will be necessary.

Finally, we used an AI system to detect aberrations. In FESSy, AI support for public health center staff awareness of situations can contribute to a reduced burden of monitoring the system. When the AI detects an aberration, the decision-making about

XSL•FO
RenderX

what actions to take as countermeasures and how to respond to the outbreak are made by public health center staff. Therefore, the AI itself can take no action after detecting an aberration other than sending email messages to an established list of recipients. Because the AI in our system only monitors data in FESSy, including the number of patients with certain symptoms and diagnoses, the AI never refers to the general internet outside of FESSy. Therefore, no ethical issues arose in relation to using AI in FESSy [9]. Moreover, the AI in FESSy has been learning about the criteria used for aberration detection by humans, public health center staff, facilities, and others to improve its own criteria. Therefore, the AI criteria will not deviate from the human criteria. If the number of participating facilities increases rapidly, then the AI criteria might converge to the human criteria in the near future.

Limitations

First, this study was an evaluation conducted at only 2 public health centers. The results might depend on the characteristics of the facilities or the public health centers. The findings' robustness must be verified through similar evaluations of FESSy conducted in other cities with other public health centers.

Second, the sample size of this study was too small for the AI to study and learn aberration patterns, especially those found by the FESSy staff. A longer period and a wider area can be expected to alleviate this limitation. In this sense, the results obtained from this study must be regarded as tentative, not final.

Third, data entry at participating FESSy facilities was based on free decisions made by the facility management. Therefore, facility participation in FESSy and data entry in FESSy might have been biased, reflecting especially strong concerns about infectious disease. That bias might have led to overestimation of FESSy's effectiveness. This is particularly the case in Tsuchiura because the proportion of facilities participating in FESSy was much smaller than in Sumida City, so the potential bias might be stronger. We cannot randomly assign participation in FESSy or data entry in FESSy, but an average treatment effect model might be able to resolve these issues. That is left as a challenge for a future study.

Conclusion

Our results show that FESSy was superior to direct reporting from facilities, which was the only method available in areas where FESSy had not been activated, not only for the number of patients as of the detection date but also the ultimate outbreak size. As a useful tool for public health centers, FESSy clearly improved the public health situations in both areas it was used.

Recently, special cities in Tokyo, including Sumida City, have been obligated to construct infection prevention plans based on a Japanese law, the Act on the Prevention of Infectious Diseases and Medical Care for Patients with Infectious Diseases. If FESSy were incorporated into the plan, it would support stable infection control measures before the emergence of outbreaks.

Acknowledgments

We acknowledge all staff and residents of the older-adult facilities in both areas. We received support from Project Research at the Ibaraki Prefectural University of Health Sciences in 2023 as part of a project titled "Construction of training course for infection control professional care givers" headed by NS, who is a professor at Ibaraki Prefectural University of Health Sciences.

Authors' Contributions

JK was responsible for the coordination of the study and developed FESSy. TS performed statistical analysis. MH, SY, Y Saito, AO, MS, AS, TH, AH, YK, YI, FI, and Y Sugishita jointly monitored FESSy and summarized activities at the public health centers. NS provided research funds and set the requirements for operating FESSy at the Sumida and Tsuchiura public health centers. All authors contributed to the writing of the final manuscript.

Conflicts of Interest

None declared.

References

1. Shimizu K, Maeda H, Sando E, et al. Epidemiology of SARS-CoV-2 infection in nursing facilities and the impact of their clusters in a Japanese core city. J Infect Chemother 2022 Jul;28(7):955-961. [doi: 10.1016/j.jiac.2022.04.010] [Medline: 35461770]
2. Vijh R, Ng CH, Shirmaleki M, Bharmal A. Factors associated with transmission of COVID-19 in long-term care facility outbreaks. J Hosp Infect 2022 Jan;119:118-125. [doi: 10.1016/j.jhin.2021.11.008] [Medline: 34808312]
3. The reporting of infectious disease outbreaks in social welfare facilities (revised on April 28, 2023). Ministry of Health, Labour and Welfare. URL: https://www.pref.ibaraki.jp/hokenfukushi/tsuho/hoken/kansensyou/hasseitodokede/documents/syakaihukusisisetsu-hokoku.pdf [accessed 2023-11-13]
4. Kurita J, Sugawara T, Ohkusa Y, Sakurai N. Experiment of surveillance for long-term care facilities for elderly people. Bull of Daito Bunka Univ 2023;61:9-14 [FREE Full text] [doi: 10.51094/jxiv.79]
5. Meima A, Whelan J, Dijks J, van der Hagen N, van Duuren M, Tjon-A-Tsien A. Introducing a novel "real-time" outbreak alert and notification system to monitor SARS-CoV-2 outbreaks and case fatality in elderly care facilities, the Netherlands,

XSL•FO
RenderX

2020-2022. J Public Health Res 2023 Jan;12(1):22799036231160634. [doi: 10.1177/22799036231160634] [Medline: 36998971]
6. Watson E, Dowson L, Dunt D, et al. Identifying barriers and enablers to participation in infection surveillance in Australian residential aged care facilities. BMC Public Health 2023;23(1):2160. [doi: 10.1186/s12889-023-16891-2] [Medline: 37924023]
7. Kurita J, Sakurai N. An examination for automatic upload function in elderly facility surveillance system from electronical care record [in Japanese]. Jpn J Med Inform 2024;44(1):39-46.
8. Hutwagner L, Thompson W, Seeman GM, Treadwell T. The bioterrorism preparedness and response Early Aberration Reporting System (EARS). J Urban Health 2003 Jun;80(2 Suppl 1):i89-i96. [doi: 10.1007/pl00022319] [Medline: 12791783]
9. Ethics of artificial intelligence. United Nations Educational, Scientific and Cultural Organization (UNESCO). URL: https://www.unesco.org/en/artificial-intelligence/recommendation-ethics [accessed 2024-04-26]

Abbreviations

EARS: Early Aberration Reporting System
MUIZ: Meldpunt voor Uitbraken van Infectieziekten en Bijzonder Resistente Micro-organismen

Edited by C Lovis; submitted 18.03.24; peer-reviewed by H Kitamura, Y Ohkusa; revised version received 02.11.24; accepted 15.11.24; published 10.01.25.

Please cite as:
Kurita J, Hori M, Yamaguchi S, Ogiwara A, Saito Y, Sugiyama M, Sunadori A, Hayashi T, Hara A, Kawana Y, Itoi Y, Sugawara T, Sugishita Y, Irie F, Sakurai N
Effectiveness of the Facility for Elderly Surveillance System (FESSy) in Two Public Health Center Jurisdictions in Japan: Prospective Observational Study
JMIR Med Inform 2025;13:e58509
URL: https://medinform.jmir.org/2025/1/e58509
doi:10.2196/58509

© Junko Kurita, Motomi Hori, Sumiyo Yamaguchi, Aiko Ogiwara, Yurina Saito, Minako Sugiyama, Asami Sunadori, Tomoko Hayashi, Akane Hara, Yukari Kawana, Youichi Itoi, Tamie Sugawara, Yoshiyuki Sugishita, Fujiko Irie, Naomi Sakurai. Originally published in JMIR Medical Informatics (https://medinform.jmir.org), 10.1.2025. This is an open-access article distributed under the terms of the Creative Commons Attribution License (https://creativecommons.org/licenses/by/4.0/), which permits unrestricted use, distribution, and reproduction in any medium, provided the original work, first published in JMIR Medical Informatics, is properly cited. The complete bibliographic information, a link to the original publication on https://medinform.jmir.org/, as well as this copyright and license information must be included.

XSL•FO
RenderX

Health Information Exchange Usage in Japan: Content Analysis of Audit Logs

Jun Suzumoto[1,2*], Dr med; Yukiko Mori[1,3,4*], PhD; Tomohiro Kuroda[1,3,4*], PhD

[1]Graduate School of Medicine, Kyoto University, 43 Shogoin-kawahara-cho, Sakyo-ku, Kyoto, Japan

[2]Health Policy Bureau, Ministry of Health, Labour and Welfare, Tokyo, Japan

[3]Division of Medical Information Technology and Administration Planning, Kyoto University Hospital, Kyoto, Japan

[4]Graduate School of Informatics, Kyoto University, Kyoto, Japan

[*]all authors contributed equally

Corresponding Author:
Jun Suzumoto, Dr med
Graduate School of Medicine, Kyoto University, 43 Shogoin-kawahara-cho, Sakyo-ku, Kyoto, Japan

Abstract

Background: In Japan, research on the types of medical data requested by health care workers in health information exchanges (HIEs) is limited. Examining the number of views for each data type is important to quantify its benefits.

Objective: This study aimed to identify the types of medical data that are frequently viewed on demand using HIEs in Japan.

Methods: We analyzed audit log data from two HIEs, Choukai Net and PicaPicaLink, covering the period from April 1, 2017, to March 31, 2022. First, we calculated the cumulative monthly usage days of the HIEs by each institution for the financial year (FY) 2021/22. Second, we calculated the cumulative annual usage days of the HIEs by each user type for FY 2021/22. Third, we calculated the view rate for each output field and content within each HIE, using institution type or year as the aggregation unit. Fourth, we calculated the cumulative annual usage days of the HIEs for days with and without progress note viewing, and for days without any content viewing. Fifth, we calculated the cumulative number of viewed days for content scheduled to be included in the national HIE compared to that which was not.

Results: In 32.6% (47/144) of hospitals connected to Choukai Net and 2.3% (20/875) of hospitals connected to PicaPicaLink, cumulative monthly usage days exceeded 101. Additionally, in 32.4% (56/173) of visiting nursing stations connected to Choukai Net, cumulative monthly usage days were over 51. User types viewing HIEs were heavily biased toward institution types other than hospitals. The overall view rate for progress notes was highest among all content types, at 67.4% (83,476/123,915) for Choukai Net and 32.9% (26,159/79,612) for PicaPicaLink. In both HIEs, when comparing by institution type, the view rate for progress notes was highest for visiting nursing stations, reaching 91.8% (5553/6052) for Choukai Net and 65.3% (126/193) for PicaPicaLink. We also found that 17% (5417/31,944) of Choukai Net usage and 9.6% (1802/18,862) of PicaPicaLink usage involved referencing only progress notes in FY 2021/22. The view rate of content scheduled to be included in the national HIE was 45.6% (56,499/123,791) for Choukai Net and 47.7% (37,972/79,612) for PicaPicaLink. Conversely, the view rate for content not scheduled to be included in the national HIE was higher, at 80.2% (99,234/123,791) for Choukai Net and 56.6% (45,052/79,612) for PicaPicaLink.

Conclusions: In both HIEs analyzed in this study, progress notes were the most viewed content. As more health care organizations disclose the progress notes they manage to their HIEs, progress notes are likely to be viewed more frequently. The cost-benefit of disclosing progress notes to HIEs remains unclear, and both health care providers and patients have concerns about privacy risks. Future research is needed to quantify and maximize the benefits of disclosure while mitigating the associated privacy risks.

(JMIR Med Inform 2025;13:e65575) doi:10.2196/65575

KEYWORDS

health information exchange; query-based exchange; audit log; Japan; ID-Link; PicaPicaLink; Choukai Net; Asia; health information; audit; content analysis; medical data; audit logs; use; HIE; nursing

Introduction

Recently, health care delivery systems have undergone a profound global transformation catalyzed by advancements in information technology. Among the numerous innovations, the health information exchange (HIE) stands out as a remarkable tool for revolutionizing the health care sector by facilitating electronic data sharing among health care providers [1]. Currently, at least 200 HIEs are operating in Japan [2]. The most common feature of an HIE in Japan is on-demand viewing

XSL•FO
RenderX

or searching for medical data from other institutions [3,4], also known as a query-based exchange or query-based HIE [1,5,6]. In addition to already established regional HIEs, the Ministry of Health, Labour and Welfare (MHLW) is considering the establishment of a nationwide HIE. The MHLW intends to share 3 types of documents and 6 types of information (3D6I) [7] across this nationwide HIE, which is referred to as Clinical Information Sharing (CLINS) [8].

It is crucial to investigate the types of medical data required by health care workers using the HIE, as medical data, which are in high demand, may not always be disclosed to Japanese HIEs. In Japan, the types of medical data disclosed to HIEs vary among HIEs. For example, a 2023 questionnaire survey targeting 48 HIEs revealed that while prescription data and laboratory test data were disclosed in all HIEs, the disclosure rate of progress notes written by doctors was only 41% [9]. This variation in data disclosure is further complicated by the differences in the data types provided by each institution to the HIE. Sharing data incurs costs, making it crucial to assess the demand and value of each data type and share it selectively.

In Japan, research on the types of medical data in demand for HIEs is limited. The MHLW conducted at least 2 studies on the types of data that should be included in the CLINS [10,11]. However, both surveys were based on interviews or questionnaires with medical workers and did not incorporate data from regional HIEs. As noted above, not all data types are available in existing HIEs; however, analyzing the audit logs of HIEs to clarify the data types can provide valuable quantitative data.

To address these data type clarity limitations, this study aimed to determine the types of data frequently viewed on query-based exchanges in Japan by analyzing HIE audit logs. Considering our internal analysis of audit logs in a previous study [4], we suspected that there may be a large demand for progress notes written by doctors. Therefore, we analyzed audit logs of HIEs that share progress notes in this study.

Methods

HIE for Data Analysis

Selection of HIEs

We collected data on HIEs that met the following inclusion criteria: (1) they were included in the survey report "About the current situation of regional healthcare network" published by the MHLW, (2) the HIE was connected to more than 100 institutions and had more than 10,000 patients according to the report, and (3) progress notes from at least some of the connected institutions were shared in the HIE as of March 2022. The first two criteria were included in previous studies, while the third criterion was new to this study. We approached operators of HIEs that met these criteria to participate in the study and obtained consent from the operators of 2 HIEs, as described below.

Overview of Regions and HIEs

The first HIE, Choukai Net, operates in the Shonai medical area of Yamagata Prefecture [12]. The second HIE, PicaPicaLink, operates in Saga Prefecture [13].

These HIEs are operated by different regional health information organizations—the Shonai Medical Information Network Council and the Saga Prefecture Medical Information Regional Collaboration System Council, respectively. Both HIEs use the same commercial HIE, ID-Link [14], developed by SEC Co Ltd, with NEC Corporation as the service contact. ID-Link is a computer system that enables viewing patient data stored in other institutions using a query-based exchange. Institutions using ID-Link are categorized as either data disclosure institutions (DDIs), which disclose their patient data to the HIE, or data viewing institutions (DVIs), which only view the patient data. The DDIs can also view the patient data disclosed to the HIE. Table 1 presents the basic statistics for both HIEs and the regions in which they operate. Choukai Net collaborates with medical institutions from other HIEs; however, these institutions are not included in this analysis. The population in both regions is declining, with both regions experiencing a stronger trend of population decline than the national average and aging populations. In addition, the Shonai medical area, where Choukai Net operates, has a population density about one-third of the national average.

The type of disclosed patient data differed by DDI. Tables S1 and S2 in Multimedia Appendix 1 list the DDIs and the types of disclosed patient data. Additionally, there are restrictions on the types of jobs that use HIE. Choukai Net is available only to medical personnel and nursing care support specialists who are required by law or contracts (or labor contracts among DVI employees) to maintain confidentiality [15]. For employees who belong to DVIs other than nursing care institutions, occupations that can use PicaPicaLink are determined by the respective institution's manager. For DVI employees in nursing care institutions, the occupations that can use PicaPicaLink are limited to those with national qualifications that are legally required to maintain confidentiality [16].

XSL•FO
RenderX

Table . Basic information on regions and health information exchanges.

Characteristics	Choukai Net	PicaPicaLink
Estimated area population, n[a]	257,122	800,668
Population density of the area, people/km^2[b]	109.50	332.50
Proportion of population aged ≥65 years in the region[c], %	36.10	30.60
Regional population growth rate from 2015 to 2020[d], %	−5.76	−2.57
Number of participating patients, n[a]	55,131	559,650
Number of data viewing institutions, n [a]		
Hospital	12[e]	73
Medical clinic	78	154
Dental clinic	22	8
Pharmacy	25	125
Visiting nursing station	14	10
Nursing facilities	83	22
Number of data disclosure institutions, n[a]	7	15
Year in which the health information exchange started operation	2011	2010

[a]Aggregated values as of the end of March 2022.

[b]Census data from the Ministry of Internal Affairs and Communications in 2020. The national average is 338.2 people/km^2.

[c]Census data from the Ministry of Internal Affairs and Communications in 2020. The national average is 28.6%.

[d]Census data from the Ministry of Internal Affairs and Communications in 2015 and 2020. The national average is –0.75%.

[e]Yamagata University Hospital, Yamagata Prefectural Central Hospital, Yamagata Prefectural Shinjo Hospital, Okitama Public General Hospital, and Sanyudo Hospital are excluded from the tally.

Patient Consent

Both HIEs require explicit patient consent before health care workers can use the HIE to view a patient's medical data [17,18]. If a DVI medical worker wants to use the HIE to refer to a certain patient's medical data stored in the DDI (eg, for treatment purposes), the medical worker must first explain the HIE to the patient. If the patient agrees to participate, they must complete a written consent form providing their demographic data, such as their name and date of birth. The DVI health care worker then adds the name of the DDI requesting disclosure of the patient's medical data and faxes the consent form. For Choukai Net, the consent form is sent to the HIE secretariat, and for PicaPicaLink, it is sent to the DDI requesting the disclosure. At the institution receiving the fax, an administrative worker releases the patient's medical data, as specified in the consent form, from the designated DDI to the fax sender's DVI. This process allows medical workers at the DVI to view the patient's medical data stored in the DDI using the HIE. Other DVIs cannot view the patient's medical data stored in the DDI. Once a patient consents to the disclosure of their medical data from the DDI to the DVI and the process is completed, the patient does not need to complete the consent form again for the same institution. When disclosing patient medical data from another DDI or to a new DVI, the patients must fill out an additional consent form.

However, there are some exceptions to the above operation. The first exception is when medical workers use the "emergency medical service" (EMS) [19]. The EMS is the default feature of ID-Link. Typically, DVI health care workers cannot view a patient's medical data unless the DDI actively discloses the patient's data. However, this feature allows DVI health care workers to view patient data without waiting for the DDI to take action. When DVI health care workers urgently need to view a patient's medical data stored in a DDI, they can do so by entering the patient's ID from the DDI into the HIE in a certain way. Medical workers can use the EMS in 2 main situations. The first situation is when emergency medical care is required, and the patient is unable to fill out a consent form. The second case is when medical data need to be accessed, but the DDI or HIE office is unable to perform operations for data disclosure.

The second exception is the "patient demographic data synchronization feature" (PDDSF) [20] and "name matching feature" (NMF) [21]. These features are available only in PicaPicaLink and are not available in Choukai Net. PDDSF allows for all basic patient data stored in DDIs to be uploaded to the ID-Link Data Center. These basic data include the name, date of birth, gender, address, telephone number, and insurance number of a patient. The NMF enumerates the IDs of the same patient in each DDI by comparing patient data collected using the PDDSF, thus enabling name matching. These features are used when DVI medical workers need to access a patient's medical data stored in a specific DDI using the EMS function but do not know the patient's ID in the DDI.

XSL•FO
RenderX

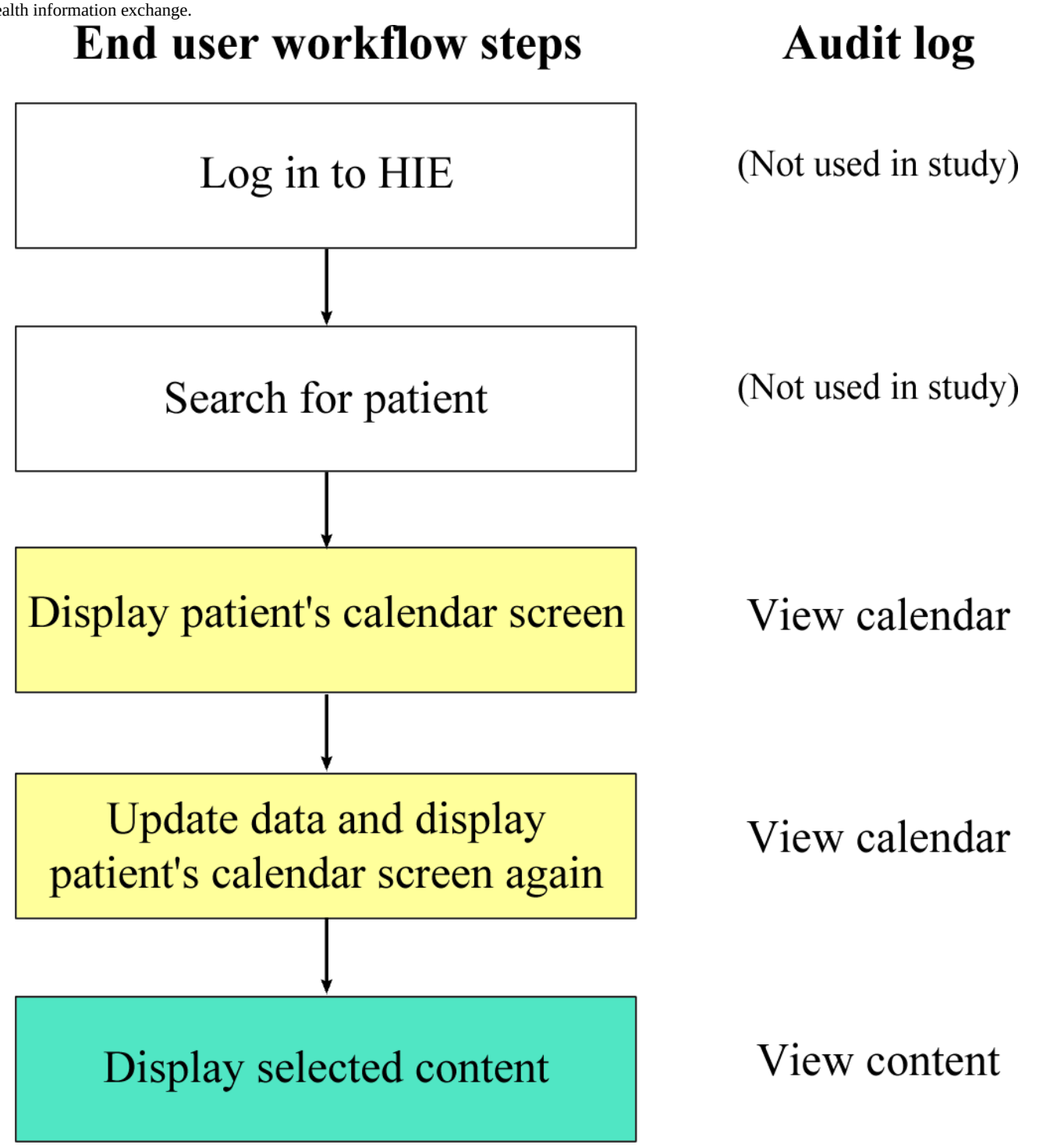
The third exception is an interagency data-sharing feature called "Sagan-Path Net" [22]. This feature is also available on PicaPicaLink and allows facilities to share summary data of stroke patients transferred from acute care hospitals to rehabilitation hospitals. To use this feature for a patient, the patient must also fill out a consent form, but they cannot specify the DVI details for each DDI. Instead, all DVIs with access to the patient's data through PicaPicaLink can view the shared summary data using Sagan-Path Net.

Flow of HIE Use

As explained in the previous section, both HIEs require explicit patient consent to view their data, except in emergencies by using the EMS functionality. A user logs in to the HIE with their ID and password. Subsequently, the user enters the name or registration ID of the patient whose information they want to view in the search field. Patients viewed within the past 14 days are displayed in a list, allowing the user to select from the list. When the desired patient appears in the list, the user clicks to select the patient option. The selected patient's medical information is then displayed in chronological order by item, known as the patient's calendar screen. When the user first opens the patient's calendar screen, the data remain unchanged from the last time they viewed the patient's page. Therefore, it is necessary to press the data-update button to obtain the most recent patient data. Once the data are updated, users can review the patient's calendar screen and select the contents displayed. This series of steps is illustrated in Figure 1.

XSL•FO
RenderX

Figure 1. Workflow when end users use ID-Link. We analyzed the usage data of users who had at least accessed the patient's calendar screen. HIE: health information exchange.



Ethical Considerations

This study was approved by the ethics committee of Kyoto University Graduate School and Faculty of Medicine (accession number R3266-7). The disclosure document outlining the research plan and data to be extracted were published on the Kyoto University Hospital website [23], ensuring that research subjects had the opportunity to opt out. Personal data obtained in the study were pseudonymized by the HIEs that provided the data. Research subjects did not receive compensation.

Data Collection

We collected profile and audit log data from health care workers enrolled in the 2 HIEs. The type of data collected was consistent with that from our previous study [4]. The data that were collected are presented in Textbox 1.

The data extraction period was from April 1, 2017, to March 31, 2022. We also obtained data on the number of participating institutions and patients per month for each HIE. The IDs of the patients accessed by medical workers were not extracted in this study.

XSL•FO
RenderX

Textbox 1. Health information exchange user data collected in this study.

- Occupation Institution
- Anonymous identifier
- Date of account registration and account deletion in health information exchange
- Date and time of access to health information exchange
- Type of data accessed by the user
- Access details: calendar access or content access? If content access, what content?

Measures and Data Analyses

Overview

For each user, we counted records of "View calendar" or "View content" in the audit log, as shown in Figure 1, as a measure of HIE use. The aggregation unit used was days. When counting the number of views for a specific type of output field or content, we extracted only the relevant audit logs and counted them in the same way. As a unit for counting HIE use by group, 1 man-day was defined as HIE use on 1 day with 1 user account. The cumulative number of accesses to an institution was calculated as the total number of days of HIE use by each user associated with that institution.

We classified the institutions enrolled in HIE into 6 categories: hospitals, medical clinics, dental clinics, pharmacies, visiting nursing stations, and nursing facilities. Institutions that could not be classified into any of these categories were excluded from the analysis. For example, this study did not analyze public institutions, such as fire departments, public health centers, local medical associations, or HIE development vendors.

The financial year (FY) ran from April 1 of one year to March 31 of the following year. For example, FY 2021/22 started on April 1, 2021, and ended on March 31, 2022. R software (version 4.3.1; R Foundation for Statistical Computing) was used for the analysis.

Man-Days for Monthly HIE Use by Each Institution in FY 2021/22

We calculated the man-days for monthly HIE use by each institution and aggregated them by institution type. For each institution enrolled in both HIEs, the man-days for monthly HIE use in FY 2021/22 were aggregated. Subsequently, for each institution type, we tallied the number of months for each man-day group, which was divided into 5- or 10-day increments. Finally, the percentage of each man-day group was calculated for each institution type. This analytical method is consistent with that used in our previous study [4].

Man-Days for Annual HIE Use by User Type and Institution Type in FY 2021/22

We classified all user occupation data into 8 user types: "doctor," "nurse," "rehabilitation staff," "pharmacist," "dental profession," "nursing care staff," "other medical professions," and "type unknown." For each institution category, we aggregated the total number of man-days of HIE use by user type in FY 2021/22.

Man-Days and View Rate for Each Output Field and Content

For each HIE, we calculated the man-days and view rate for each output field and content. The aggregation units were FY and institution type. In the analysis using FY as the aggregation unit, all log data from the 5-year period were analyzed. In the analysis using institution type as the aggregation unit, only audit log data for FY 2021/22 were analyzed. The viewed output fields and content were listed for each man-day of HIE use. We then tallied the total number of man-days for HIE use, the number of man-days for views of each output field, and the content in each aggregation unit. Finally, we calculated the view rate for each output field and content in each aggregation unit. The view rates of the output field and content are defined as follows:

(Number of man-days viewing the output field and content in each aggregation unit / Total number of man-days of HIE use in each aggregation unit) × 100

In the analysis using FY as the aggregation unit, we presented the top 5 content views by man-days over the total data analysis period in bar graphs. In the analysis using institution type as the aggregation unit, we listed the man-days and view rates for each output field and content.

As a supplementary analysis, we divided all man-days into 2 categories: those that included audit logs of viewing any content and those that only included audit logs of viewing the patient's calendar screen (Figure 1). Man-days that included audit logs of viewing any content were further categorized as follows: man-days where (1) the only viewed content was progress notes, (2) the viewed content included both progress notes and other content, and (3) the viewed content did not include progress notes. This analysis was conducted to evaluate the impact of the disclosure of progress notes on usage man-days.

Man-Days of Views of Content That Corresponds to 3D6I and Content That Does Not Correspond to 3D6I

For each HIE and FY, we calculated the number of man-days spent viewing content that corresponded to 3D6I as well as content that did not correspond to 3D6I. The 3 types of documents in 3D6I were patient referral documents, discharge summaries, and health examination documents. The 6 data types in 3D6I are as follows: the name of the illness or injury; infectious disease; drug contraindications; allergies; laboratory test results and prescriptions written in the patient referral document; and discharge summary.

First, the total number of man-days for each HIE used in each FY was tallied. Subsequently, we sorted all content into categories corresponding to 3D6I and those that did not. The

XSL•FO
RenderX

results for each content type are listed in Table S3 in Multimedia Appendix 2. We then tallied the number of man-days during which any content corresponding to 3D6I was viewed for each FY or HIE. We also tallied the number of man-days spent viewing content that did not correspond to 3D6I for both FY and HIE. Finally, we calculated the percentage of man-days in which any content corresponding to 3D6I was viewed, as well as the percentage of man-days in which any content not corresponding to 3D6I was viewed.

Results

Man-Days for Monthly HIE Use by Each Institution in FY 2021/22

Table 2 presents man-days of monthly HIE use in hospitals. For hospitals, the percentage of man-days with monthly HIE use of 0 was 9% in this study, which is less than one-fifth of that of our previous study [4]. Similarly, the percentage of man-days with monthly HIE use of 101 or more was 32.6%, which is more than 10 times that in our previous study. PicaPicaLink usage closely aligned with that reported in our previous study.

Table 3 presents man-days of monthly HIE use in other institution types. Choukai Net was actively used in some visiting nursing stations. The percentage of man-days with monthly HIE use of 26 or more was 42.2%, which is approximately 6 times that of our previous study [4]. Such high frequency of usage by visiting nursing stations was not observed on PicaPicaLink. Overall, HIE use by dental clinics was low, consistent with our previous findings [4].

Table . Distribution of man-days for monthly health information exchange, use of hospitals in financial year 2021/22.

Man-days for monthly health information exchange, use per institution, n	Choukai Net, n (%)	PicaPicaLink, n (%)
0	13 (9)	430 (49.1)
1 - 10	31 (21.5)	217 (24.8)
11 - 20	19 (13.2)	99 (11.3)
21 - 30	9 (6.3)	50 (5.7)
31 - 40	1 (0.7)	25 (2.9)
41 - 50	3 (2.1)	15 (1.7)
51 - 60	4 (2.8)	13 (1.5)
61 - 70	4 (2.8)	3 (0.3)
71 - 80	5 (3.5)	0 (0)
81 - 90	6 (4.2)	0 (0)
91 - 100	2 (1.4)	3 (0.3)
≥101	47 (32.6)	20 (2.3)
Total	144 (100)	875 (100)

XSL•FO
RenderX

Table . Distribution of man-days for monthly health information exchange use in other institution types in financial year 2021/22.

Man-days for monthly health information exchange use, n		Medical clinic, number of months (%)	Dental clinic, number of months (%)	Pharmacy, number of months (%)	Visiting nursing station, number of months (%)	Nursing facility, number of months (%)
Choukai Net						
	0	418 (44.3)	251 (95.1)	216 (72)	43 (24.9)	612 (62.6)
	1 - 5	246 (26.1)	13 (4.9)	54 (18)	12 (6.9)	117 (12)
	6 - 10	66 (7)	0 (0)	10 (3.3)	9 (5.2)	59 (6)
	11 - 15	37 (3.9)	0 (0)	5 (1.7)	16 (9.2)	45 (4.6)
	16 - 20	30 (3.2)	0 (0)	12 (4)	17 (9.8)	40 (4.1)
	21 - 25	74 (7.8)	0 (0)	3 (1)	3 (1.7)	45 (4.6)
	26 - 30	37 (3.9)	0 (0)	0 (0)	1 (0.6)	20 (2)
	31 - 35	14 (1.5)	0 (0)	0 (0)	2 (1.2)	12 (1.2)
	36 - 40	9 (1)	0 (0)	0 (0)	2 (1.2)	13 (1.3)
	41 - 45	3 (0.3)	0 (0)	0 (0)	4 (2.3)	4 (0.4)
	46 - 50	1 (0.1)	0 (0)	0 (0)	8 (4.6)	4 (0.4)
	≥51	9 (1)	0 (0)	0 (0)	56 (32.4)	7 (0.7)
	Total	944 (100)	264 (100)	300 (100)	173 (100)	978 (100)
PicaPicaLink						
	0	1303 (71)	96 (100)	1284 (85.1)	93 (77.5)	154 (60.9)
	15	219 (11.9)	0 (0)	120 (8)	11 (9.2)	33 (13)
	6 - 10	85 (4.6)	0 (0)	38 (2.5)	8 (6.7)	12 (4.7)
	11 - 15	80 (4.4)	0 (0)	16 (1.1)	8 (6.7)	7 (2.8)
	16 - 20	77 (4.2)	0 (0)	23 (1.5)	0 (0)	5 (2)
	21 - 25	47 (2.6)	0 (0)	7 (0.5)	0 (0)	5 (2)
	26 - 30	10 (0.5)	0 (0)	8 (0.5)	0 (0)	8 (3.2)
	31 - 35	5 (0.3)	0 (0)	9 (0.6)	0 (0)	5 (2)
	36 - 40	3 (0.2)	0 (0)	2 (0.1)	0 (0)	6 (2.4)
	41 - 45	3 (0.2)	0 (0)	1 (0.1)	0 (0)	4 (1.6)
	46 - 50	2 (0.1)	0 (0)	0 (0)	0 (0)	2 (0.8)
	≥51	0 (0)	0 (0)	0 (0)	0 (0)	12 (4.7)
	Total	1834 (100)	96 (100)	1508 (100)	120 (100)	253 (100)

Man-Days for Annual HIE Use by User Type and Institution Type in FY 2021/22

Table 4 presents man-days of annual HIE use by user type and institution type in both HIEs in FY 2021/22. In both HIEs, there are significant differences in the proportion of user types depending on the institution type. For hospitals, no single occupation accounts for half of the man-days. On the other hand, doctors at medical clinics, dentists at dental clinics, pharmacists at pharmacies, nurses at visiting nursing stations, and nursing care staff at nursing homes each account for more than half of the total man-days for their respective institution type. These distributions reflect the characteristics of each institution type.

XSL•FO
RenderX

Table . Man-days of annual health information exchange use by user type and institution type in financial year 2021/22.

Health information exchange and user type		Hospital, n (%)	Medical clinic, n (%)	Dental clinic, n (%)	Pharmacy, n (%)	Visiting nursing station, n (%)	Nursing facility, n (%)
Choukai Net							
	Doctor	5906 (42.6)	5054 (80.1)	0 (0)	0 (0)	0 (0)	516 (9.8)
	Nurse	2357 (17)	845 (13.4)	0 (0)	0 (0)	5644 (93.3)	680 (12.9)
	Rehabilitation staff	860 (6.2)	0 (0)	0 (0)	0 (0)	144 (2.4)	1 (0)
	Pharmacist	906 (6.5)	0 (0)	0 (0)	555 (97.7)	0 (0)	0 (0)
	Dental professional	4 (0)	0 (0)	13 (68.4)	0 (0)	0 (0)	0 (0)
	Nursing care staff	219 (1.6)	0 (0)	0 (0)	0 (0)	20 (0.3)	3929 (74.5)
	Other medical professionals	3263 (23.5)	335 (5.3)	6 (31.6)	13 (2.3)	60 (1)	100 (1.9)
	Type unknown	344 (2.5)	75 (1.2)	0 (0)	0 (0)	184 (3)	51 (1)
	Total	13,859 (100)	6309 (100)	19 (100)	568 (100)	6052 (100)	5277 (100)
PicaPicaLink							
	Doctor	2416 (27.2)	3812 (70.2)	0 (0)	254 (13.1)	0 (0)	92 (4.1)
	Nurse	640 (7.2)	400 (7.4)	0 (0)	0 (0)	192 (99.5)	602 (26.9)
	Rehabilitation staff	202 (2.3)	9 (0.2)	0 (0)	0 (0)	0 (0)	71 (3.2)
	Pharmacist	146 (1.6)	0 (0)	0 (0)	1641 (84.5)	0 (0)	0 (0)
	Dental professional	7 (0.1)	0 (0)	0 (0)	0 (0)	0 (0)	5 (0.2)
	Nursing care staff	1191 (13.4)	0 (0)	0 (0)	0 (0)	0 (0)	1152 (51.6)
	Other medical professionals	3686 (41.5)	839 (15.4)	0 (0)	35 (1.8)	0 (0)	308 (13.8)
	Type unknown	590 (6.6)	374 (6.9)	0 (0)	11 (0.6)	1 (0.5)	4 (0.2)
	Total	8878 (100)	5434 (1000)	0 (0)	1941 (100)	193 (100)	2234 (100)

Man-Days and View Rate for Each Output Field and Content

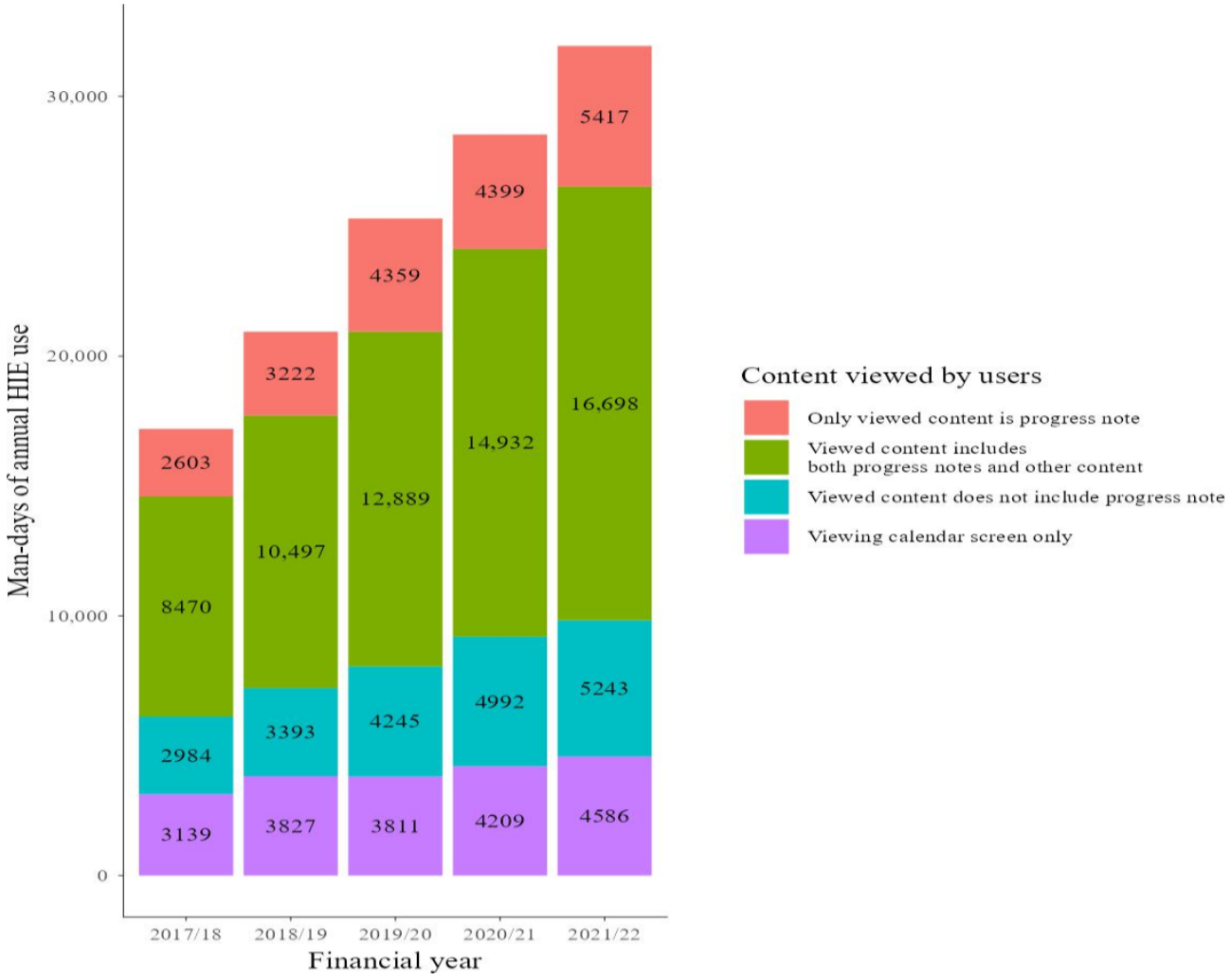
Man-Days for Content View

In both HIEs analyzed, the most viewed data were progress notes. On Choukai Net, the overall number of man-days for progress notes was 83,476 and the overall view rate for progress notes was 67.4% (83,476/123,915). This was nearly 3 times higher than the overall man-days for patient summary, which was the second most viewed content. On PicaPicaLink, the number of overall man-days for progress notes was 26,159, and the overall view rate for progress notes was 32.9% (26,159/79,612).

We present the top 5 content views by man-days over the total data analysis period in Figures 2 and 3. Figure 2 presents the man-days on Choukai Net, and Figure 3 presents the man-days for PicaPicaLink. Man-days and the view rates including other types of content views, not just the top 5, are listed in Tables S4 and S5 in Multimedia Appendix 3. These supplementary tables include content with a total view rate of 1% or more.

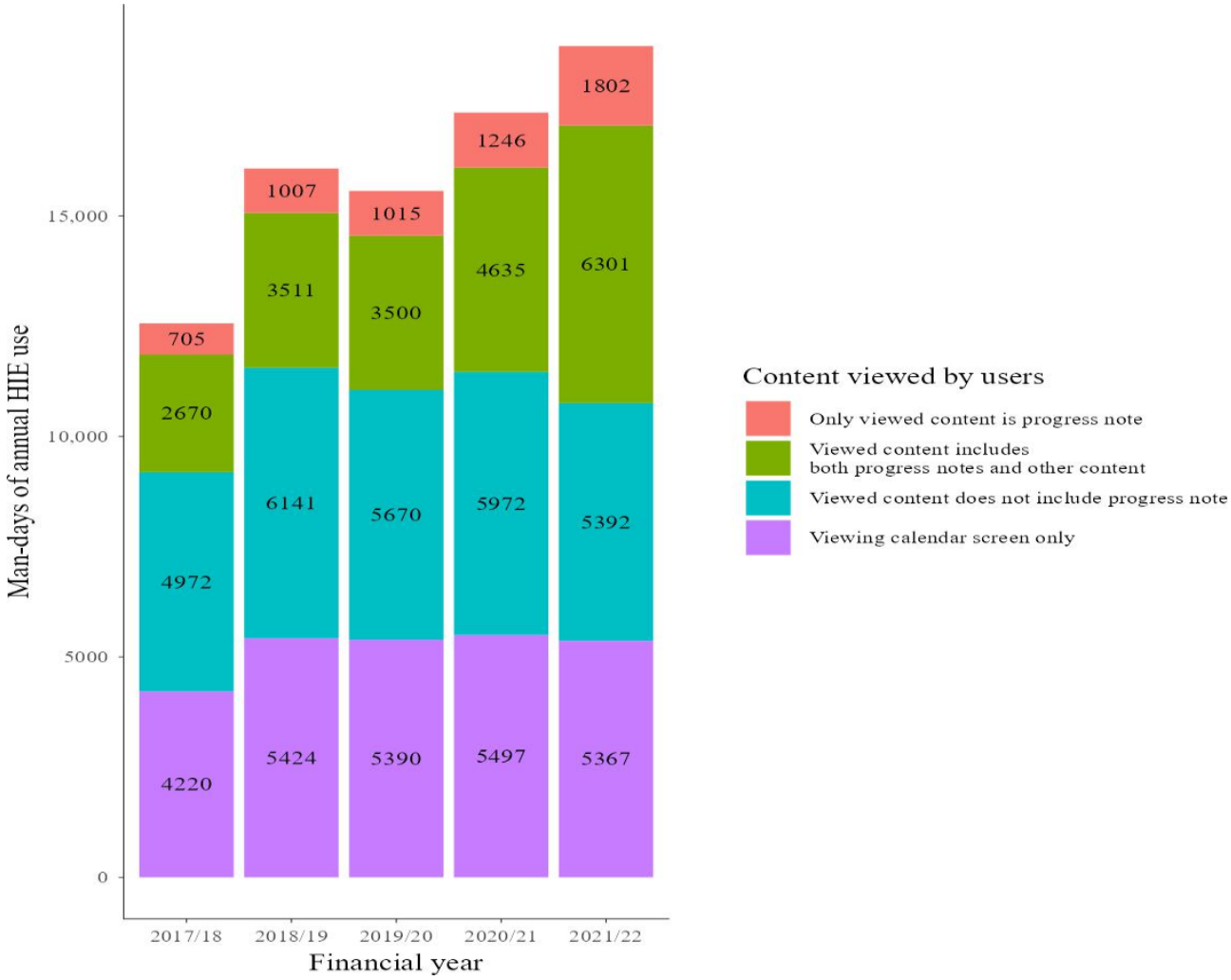
XSL•FO
RenderX

Figure 2. Top 5 content views by man-days on Choukai Net. HIE: health information exchange.



XSL•FO
RenderX

Figure 3. Top 5 content views by man-days on PicaPicaLink. HIE: health information exchange.



Man-Days and View Rate for Content and Output Field by Institution Type in FY 2021/22

The view rates for each output field and content by institution type are listed in Tables 5 and 6. Table 5 presents the view rate for Choukai Net, and Table 6 presents the view rate for PicaPicaLink. These tables include content with a total view rate of 1% or more in FY 2021/22.

XSL•FO
RenderX

Table . Man-days and view rate for each output field and content by institution type in financial year 2021/22 on Choukai Net.

Output field and content		Hospital (total man-days=18,356), n (%)	Medical clinic (total man-days=6309), n (%)	Dental clinic (total man-days=19), n (%)	Pharmacy (total man-days=568), n (%)	Visiting nursing station (total man-days=6052), n (%)	Nursing facility (total man-days=5277), n (%)	Total, n (%)
Note								
	Total contents	7187 (51.9)	4824 (76.5)	6 (31.6)	463 (81.5)	5601 (92.5)	4857 (92)	22,933 (71.8)
	Progress note	6598 (47.6)	4715 (74.7)	6 (31.6)	457 (80.5)	5553 (91.8)	4784 (90.7)	22,108 (69.3)
	Patient summary	3743 (27)	2132 (33.8)	3 (15.8)	121 (21.3)	1015 (16.8)	1162 (22)	8173 (25.6)
	Disease name	279 (2)	123 (1.9)	0 (0)	0 (0)	87 (1.4)	519 (9.8)	1008 (3.2)
	Allergy	183 (1.3)	56 (0.9)	0 (0)	0 (0)	164 (2.7)	596 (11.3)	999 (3.1)
	Nursing record	156 (1.1)	150 (2.4)	0 (0)	0 (0)	130 (2.1)	185 (3.5)	621 (1.9)
Reports								
	Total contents	2969 (21.4)	3269 (51.8)	1 (5.3)	107 (18.8)	1399 (23.1)	934 (17.7)	8676 (27.2)
	Patient referral document	2091 (15.1)	1976 (31.3)	0 (0)	51 (9)	668 (11)	472 (8.9)	5256 (16.5)
	Radiology report	1275 (9.2)	2051 (32.5)	1 (5.3)	46 (8.1)	476 (7.9)	365 (6.9)	4213 (13.2)
	Discharge summary	514 (3.7)	589 (9.3)	0 (0)	40 (7)	270 (4.5)	156 (3)	1569 (4.9)
	Nursing summary	468 (3.4)	268 (4.2)	0 (0)	25 (4.4)	518 (8.6)	169 (3.2)	1448 (4.5)
Prescription		1901 (13.7)	1596 (25.3)	3 (15.8)	318 (56)	2071 (34.2)	1297 (24.6)	7186 (22.5)
Test results								
	Total content	1403 (10.1)	2113 (33.5)	1 (5.3)	174 (30.6)	1376 (22.7)	1018 (19.3)	6085 (19.1)
	Laboratory test result	1329 (9.6)	2095 (33.2)	1 (5.3)	173 (30.5)	1342 (22.2)	981 (18.6)	5921 (18.6)
	Bacterial examination test result	280 (2)	218 (3.5)	0 (0)	12 (2.1)	118 (1.9)	105 (2)	733 (2.3)
DICOM[a] image list		2712 (19.6)	1239 (19.6)	2 (10.5)	0 (0)	294 (4.9)	159 (3)	4406 (13.8)
Image test order								
	Total content	1500 (10.8)	1149 (18.2)	1 (5.3)	56 (9.9)	661 (10.9)	685 (13)	4051 (12.7)
	Radiology imaging order	1335 (9.6)	936 (14.8)	1 (5.3)	46 (8.1)	600 (9.9)	571 (10.8)	3489 (10.9)
	Physiological test order	437 (3.2)	431 (6.8)	0 (0)	11 (1.9)	89 (1.5)	184 (3.5)	1152 (3.6)
	Endoscopy order	84 (0.6)	159 (2.5)	0 (0)	2 (0.4)	33 (0.5)	49 (0.9)	327 (1)
Injection		601 (4.3)	456 (7.2)	1 (5.3)	72 (12.7)	976 (16.1)	617 (11.7)	2723 (8.5)
Summary view		298 (2.2)	230 (3.6)	1 (5.3)	21 (3.7)	70 (1.2)	110 (2.1)	730 (2.3)
Chart display		174 (1.3)	107 (1.7)	0 (0)	1 (0.2)	192 (3.2)	96 (1.8)	568 (1.8)
File list		237 (1.7)	70 (1.1)	0 (0)	0 (0)	5 (0.1)	1 (0)	313 (1)

[a]DICOM: Digital Imaging and Communications in Medicine.

XSL•FO
RenderX

Table . Man-days and view rate for each output field and content by institution type in financial year 2021/22 on PicaPicaLink.

Output field and content		Hospital (total man-days=8878), n (%)	Medical clinic (total man-days=5434), n (%)	Pharmacy (total man-days=1941), n (%)	Visiting nursing station (total man-days=193), n (%)	Nursing facility (total man-days=2234), n (%)	Total, n (%)
Note							
	Total content	2417 (27.2)	3336 (61.4)	1064 (54.8)	128 (66.3)	1208 (54.1)	8153 (43.6)
	Progress note	2340 (26.4)	3301 (60.7)	1064 (54.8)	126 (65.3)	1201 (53.8)	8032 (43)
	Nursing record	287 (3.2)	197 (3.6)	0 (0)	43 (22.3)	112 (5)	639 (3.4)
	Disease name	187 (2.1)	246 (4.5)	6 (0.3)	0 (0)	49 (2.2)	488 (2.6)
Reports							
	Total content	1751 (19.7)	2896 (53.3)	308 (15.9)	39 (20.2)	1011 (45.3)	6005 (32.1)
	Radiology report	1007 (11.3)	1939 (35.7)	104 (5.4)	25 (13)	621 (27.8)	3696 (19.8)
	Patient referral document	848 (9.6)	1495 (27.5)	173 (8.9)	9 (4.7)	447 (20)	2972 (15.9)
	Discharge summary	243 (2.7)	468 (8.6)	113 (5.8)	7 (3.6)	211 (9.4)	1042 (5.6)
	Nursing summary	242 (2.7)	261 (4.8)	19 (1)	5 (2.6)	281 (12.6)	808 (4.3)
	Surgical record	122 (1.4)	143 (2.6)	2 (0.1)	0 (0)	0 (0)	267 (1.4)
	Other documents	114 (1.3)	88 (1.6)	0 (0)	0 (0)	3 (0.1)	205 (1.1)
Test results							
	Total content	1397 (15.7)	2342 (43.1)	1041 (53.6)	90 (46.6)	827 (37)	5697 (30.5)
	Laboratory test result	1383 (15.6)	2327 (42.8)	1038 (53.5)	90 (46.6)	826 (37)	5664 (30.3)
	Bacterial examination test result	161 (1.8)	105 (1.9)	26 (1.3)	0 (0)	9 (0.4)	301 (1.6)
Prescription		1115 (12.6)	1466 (27)	728 (37.5)	113 (58.5)	926 (41.5)	4348 (23.3)
Image test order							
	Total content	718 (8.1)	1226 (22.6)	274 (14.1)	6 (3.1)	406 (18.2)	2630 (14.1)
	Radiology imaging order	686 (7.7)	1193 (22)	267 (13.8)	6 (3.1)	368 (16.5)	2520 (13.5)
	Physiological test order	110 (1.2)	146 (2.7)	36 (1.9)	1 (0.5)	111 (5)	404 (2.2)
Injection							
	Total content	611 (6.9)	791 (14.6)	623 (32.1)	55 (28.5)	406 (18.2)	2486 (13.3)
	Injection order	536 (6)	582 (10.7)	543 (28)	49 (25.4)	405 (18.1)	2115 (11.3)
	Injection	127 (1.4)	314 (5.8)	145 (7.5)	18 (9.3)	14 (0.6)	618 (3.3)
DICOM[a] image list		1196 (13.5)	1133 (20.9)	0 (0)	2 (1)	91 (4.1)	2422 (13)
Summary view							
	Total content	221 (2.5)	169 (3.1)	237 (12.2)	21 (10.9)	41 (1.8)	689 (3.7)
	Examination summary view	158 (1.8)	137 (2.5)	180 (9.3)	18 (9.3)	12 (0.5)	505 (2.7)
	Medication summary view	87 (1)	51 (0.9)	92 (4.7)	6 (3.1)	33 (1.5)	269 (1.4)
Chart display		34 (0.4)	3 (0.1)	7 (0.4)	0 (0)	136 (6.1)	180 (1)

[a]DICOM: Digital Imaging and Communications in Medicine.

XSL•FO
RenderX

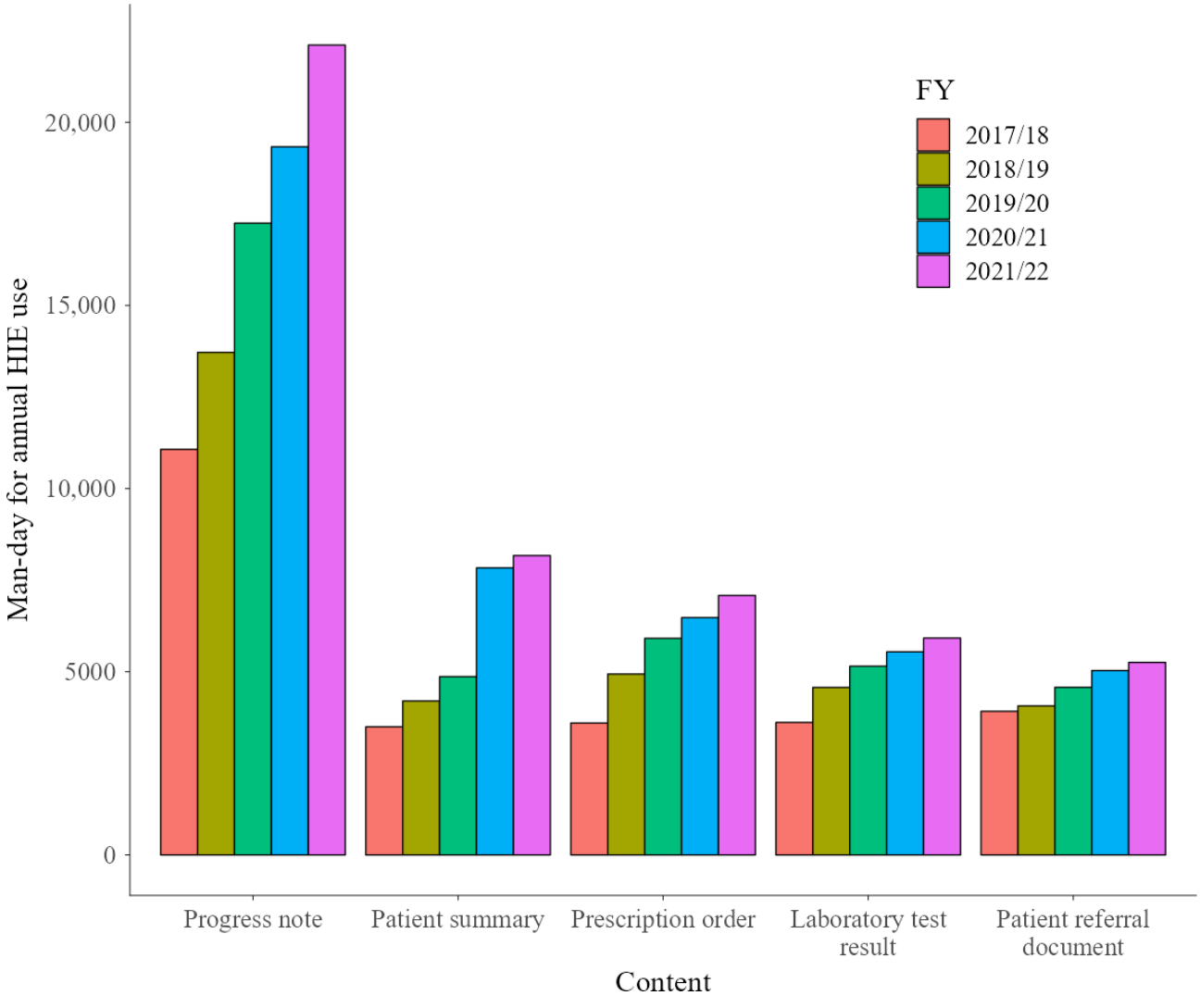
Progress notes are the most frequently viewed content at every institution type on both HIEs. When comparing the view rate of progress notes by institution type, visiting nursing stations had the highest rates, with 91.8% for Choukai Net and 65.3% for PicaPicaLink. On the other hand, the view rate of the Digital Imaging and Communications in Medicine (DICOM) image list was relatively low for most institution types. In both HIEs, the view rate of the DICOM image list was less than 5% in pharmacies, visiting nursing stations, and nursing facilities. The view rate for radiology reports was higher than for DICOM image lists in all these institution types. Even in medical clinics, the view rate for DICOM image lists was lower than the view ratio for radiology reports, indicating that many medical workers view the radiology reports written by radiologists rather than viewing the DICOM images. Hospitals were the only institution category where the view rate for DICOM image lists was higher than for radiology reports.

Man-Days of Viewing Content Out of the Total Man-Days of Viewing the Calendar and the Breakdown of Progress Note Views

The following presents the results of an analysis of content views and calendar views, and the percentage of progress note views among content views. The aggregated results are shown as bar graphs, with Choukai Net illustrated in Figure 4 and PicaPicaLink in Figure 5. On Choukai Net, the number of man-days in which progress notes were the only content viewed accounted for 17% (5417/31,944) of the total in FY 2021/22, a rate not significantly different from 15.1% (2603/17,196) in FY 2017/18. This may be because the medical institutions that disclose progress notes have remained unchanged from FY 2017/18 to FY 2021/22 (Table S1 in Multimedia Appendix 1).

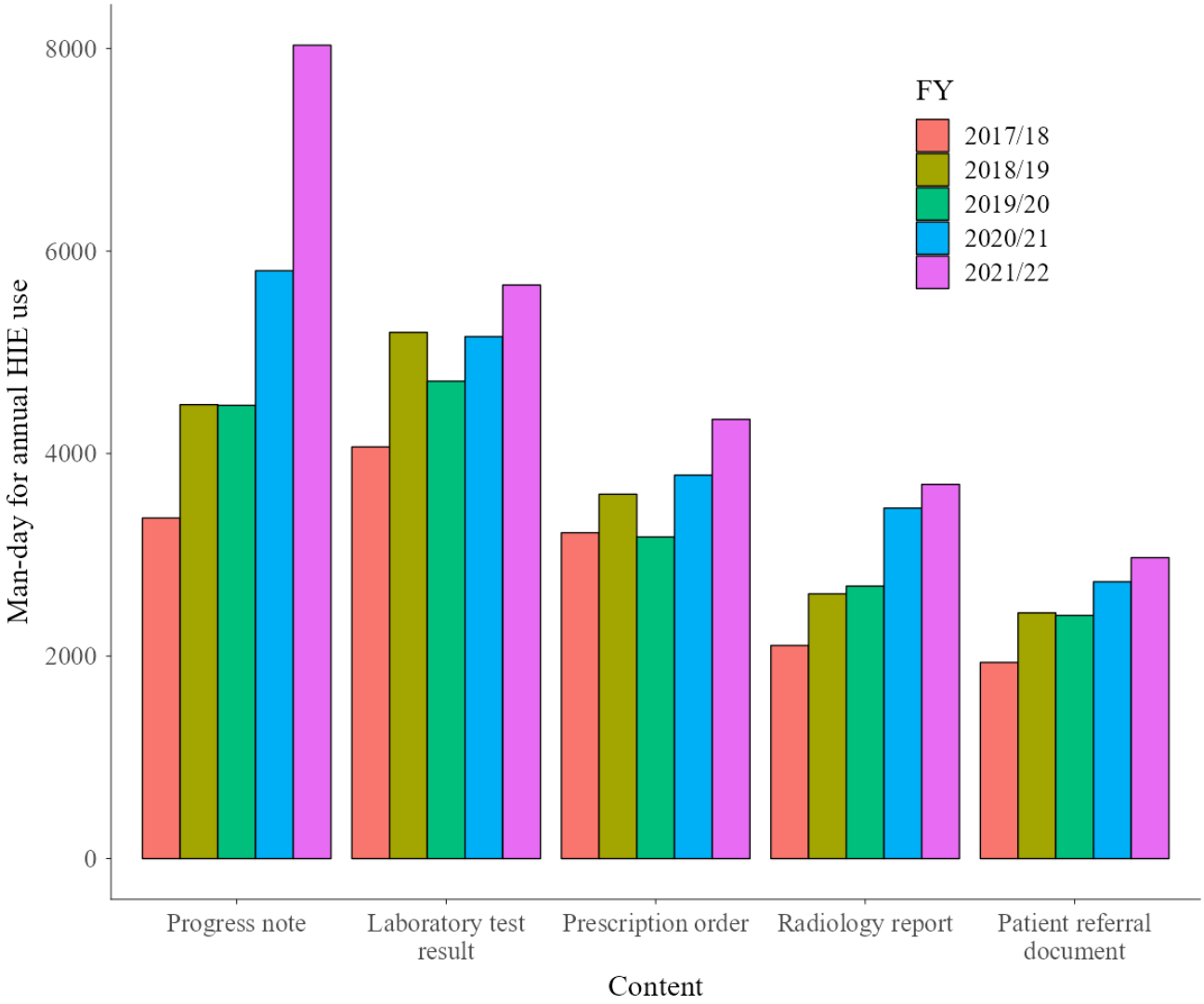
In contrast, on PicaPicaLink, the disclosure of progress notes was implemented in stages over 5 years (Table S2 in Multimedia Appendix 1). At the beginning of FY 2017/18, only 2 of the 13 DDIs were disclosing progress notes. Over the 5 years analyzed, the DDIs of PicaPicaLink proceeded to disclose progress notes, and by March 2022, 8 of 15 DDIs had done so. Therefore, the proportion of viewing only progress notes on PicaPicaLink also increased from 5.6% (705/12,567) in FY 2017/18 to 9.6% (1802/18,862) in FY 2021/22.

Figure 4. Content viewed by users when using Choukai Net. FY: financial year; HIE: health information exchange.



XSL•FO
RenderX

Figure 5. Content viewed by users when using PicaPicaLink. Views of Sagan-Path Net are not included in the statistics. FY: financial year; HIE: health information exchange.



Man-Days of Views of Content Corresponding to 3D6I and Non-3D6I Content

In Table 7, we present the man-days of total views, views of content corresponding to 3D6I, and views of content not corresponding to 3D6I by FY. The view rate of content corresponding to 3D6I was below 50%. On the other hand, the view rate of content not included in the 3D6I consistently exceeded 50%.

XSL•FO
RenderX

Table . Man-days of total views, views of content corresponding to 3D6I, and views of content not corresponding to 3D6I by financial year.[a]

Health information exchange and financial year		Total number of man-days	3D6I, number of man-days (%)	Other information, number of man-days (%)
Choukai Net				
	2017/18	17,187	7806 (45.4)	13,351 (77.7)
	2018/19	20,910	9666 (46.2)	16,252 (77.7)
	2019/20	25,262	11,784 (46.6)	20,394 (80.7)
	2020/21	28,514	13,022 (45.7)	23,117 (81.1)
	2021/22	31,918	14,221 (44.6)	26,120 (81.8)
	Total	123,791	56,499 (45.6)	99,234 (80.2)
PicaPicaLink				
	2017/18	12,447	6138 (49.3)	6561 (52.7)
	2018/19	15,953	7722 (48.4)	8504 (53.3)
	2019/20	15,396	7093 (46)	8286 (53.8)
	2020/21	17,136	7998 (46.7)	9975 (58.2)
	2021/22	18,680	9021 (48.3)	11,726 (62.8)
	Total	79,612	37,972 (47.7)	45,052 (56.6)

[a]3D6I: 3 documents and 6 types of information.

Discussion

Principal Findings

As mentioned in the Results section, the use of Choukai Net in hospitals and visiting nursing stations is more active than in previous studies (Tables 2 and 3). These findings suggest that the frequency of HIE use in Japan is not necessarily low and that certain factors may contribute to increased usage. To clarify these reasons, a survey of individual facilities using HIEs is needed rather than a survey of overall HIE usage. Although it is difficult to attribute the cause of active use to general statistical indicators of the region, low population density may have increased the need for medical coordination between institutions (Table 1). On the other hand, the population density of Saga Prefecture, where PicaPicaLink is operated, is roughly the same as the national average.

In both HIEs analyzed, the most viewed data were progress notes (Figures 2 and 3). In FY 2021/22, 17% of Choukai Net usage and 9.6% of PicaPicaLink usage involved referencing only progress notes (Figures 4 and 5). The overall view rate for progress notes was 67.4% for Choukai Net and 32.9% for PicaPicaLink. One reason for the more than 2-fold difference in view rate between the 2 HIEs is that each DDI has different progress note disclosure policies. On Choukai Net, 5 of the 7 DDIs had been disclosing progress notes since April 2017, and none changed their disclosure policies until March 2022 (Table S1 in Multimedia Appendix 1). In contrast, only 2 of the 13 DDIs of PicaPicaLink had disclosed progress notes as of April 2017 (Table S2 in Multimedia Appendix 1). As a result, the view rate of progress notes in FY 2017/18 was only 27%. However, in FY 2021/22, when 8 of 15 DDIs were disclosing progress notes, the view rate increased to 43%. The differences between the 2 HIEs and increase in progress note viewing rate on PicaPicaLink suggest that DDI data disclosure policies influence health care workers' data viewing behavior in HIEs. Previous studies have not necessarily examined the specific types of data disclosed by each DDI in HIEs, but this aspect is crucial for understanding HIE usage.

The results of these analyses do not necessarily align with those of previous studies. Laboratory results, medication data, and radiology data have been reported as the most frequently accessed types of data in HIEs [24-26]. This difference is partly because the number of views for progress notes was not aggregated in previous research. A recent study conducted in 2024 on Mame-Net, one of Japan's HIEs, found that medical records were the most frequently viewed, which is consistent with the findings of this study [27].

When comparing the view rate of progress notes by institution type, visiting nursing stations had the highest rates, with 91.8% for Choukai Net and 65.3% for PicaPicaLink (Tables 4 and 5). The distribution of occupations using HIEs is strongly influenced by institution type, and most users of HIE at visiting nursing stations are nurses (Table 4). It is understandable that the progress notes written by doctors are important for nurses who work based on doctors' instructions [28]. A similar trend has been observed in pharmacies, where pharmacies dispense medicines based on a doctor's prescription and therefore must check the doctor's notes to validate the prescription. However, the viewing rate of patient summaries, which are also written by physicians, is low across all institution types. Patient summaries or patient referral documents do not necessarily include detailed medical histories. Additionally, information is generally updated more frequently in progress notes. These factors may explain why progress notes are viewed more frequently. Further research, including qualitative studies, is needed to explore the benefits of disclosing progress notes and how they can be used in DVI.

XSL•FO
RenderX

Despite relatively high demand compared to other types of data, progress note disclosure is uncommon in Japanese HIEs. A survey conducted on HIEs in 2023 found that the disclosure rate of progress notes written by doctors was only 38.6% (81/210) [29]. The most common reason for not disclosing progress notes, cited by 48.6% (35/72) of HIEs, was the "lack of consent from DDIs to share progress notes." The fourth most common reason, cited by 15.3% (11/72) of HIEs, was that "it may limit doctors' entries in progress notes." These results suggest that concerns about violating patient and doctor privacy, owing to the sensitive information contained in progress notes, prevent their disclosure. On the other hand, the second most common reason, cited by 41.7% (30/72) of HIEs, was that "the system did not have a progress note sharing function". The third most common reason, given by 16.7% (12/72) of HIEs, was that "management organizations consider it unnecessary to disclose progress notes." These results indicate that the system would need modification to enable progress note sharing and this is not currently considered worth the cost in these HIEs. Past surveys have shown that the benefits of disclosing progress notes and reports include the ability to quickly share detailed medical information and improvements in the quality of progress notes [29]. However, these descriptions remain abstract, and the benefits are not quantified. Further research is needed to quantify the benefits of disclosure and evaluate whether they justify the additional costs and privacy risks. Moreover, efforts must be made to maximize the benefits relative to the costs of disclosure while minimizing privacy concerns.

The results of this study raise questions about the effectiveness of CLINS. Progress notes and radiology reports are not included in the 3D6I that CLINS plans to share. The discharge summary, a physician's record written in natural language, is included in 3D6I, but its view rate was less than 10% in this analysis. In the HIEs analyzed in this study, the view rate of 3D6I was less than 50%, which is lower than the view rate of data not included in 3D6I (Table 7). However, except for patient referral documents and discharge summaries, data shared via CLINS can be accessed by both patients and medical professionals. In contrast, most regional HIEs in Japan, including the 2 HIEs studied here, do not allow patients to view shared data using the HIE. Past surveys have shown that only 6.3% (14/224) of HIEs in Japan offer personal health record functionality [29]. Future evaluations of CLINS and regional HIEs should assess not only the types of data shared but also whether or not it is shared with patients.

It is necessary to consider whether the usefulness of the HIE analyzed in this study is worth the cost. There was no publicly available data on the costs of PicaPicaLink, making it difficult to estimate the cost-benefits. Regarding Choukai Net, some basic operational figures were presented at an academic conference in 2018 [30]. Excluding implementation cost, the annual maintenance costs are 3.89 million yen (US $27,020) for total data center usage, and 1.03 million yen (US $7020) for the HIE Management Council. The cost of replacing the systems at the 3 hospitals is 12.1 million yen (US $83,180). Assuming that the average system replacement cost for 1 facility is one-third of this amount, the cost of replacing the systems at all 7 DDI facilities can be roughly estimated to be 28.2 million yen (US $193,850). Assuming that system replacement occurs once every 5 years, the annual reserve required for system replacement of all DDIs of Choukai Net is 5.64 million yen (US $38,760). Therefore, the annual cost of data center usage fees, council operating fees, and annual reverse funds for system replacement of DDIs is about 10.6 million yen (US $72,850) per year. If we divide these annual costs by the number of man-days of Choukai Net usage in FY 2021/22, 31,918 person-days, we get an approximate cost of 331 yen (US $2.28) per 1 man-day of HIE use. Further research is needed to determine whether the health care workers' benefits per man-day of use are commensurate with these costs. On the other hand, from the perspective of benefits to patients, a randomized controlled trial on the benefits of HIEs to patients has been conducted in Japan [31]. However, the results were not necessarily clear, and analysis of HIE use or viewed data was not included. Further research is also needed to assess the benefits of HIEs for patients, including the associated costs and actual utilization.

As detailed in the "Patient consent" section under "Methods," patients must fill out a paper consent form each time to increase the number of sources or recipients of the patient medical information shared. This method takes privacy into consideration as patients have some control over whether or not their medical data are disclosed to specific medical institutions. This consent method is common in Japanese HIEs. Previous studies have shown that 87.8% (195/222) of HIEs in Japan require patients to complete a consent form when they first join the HIE. In addition, 58.5% (103/176) of HIEs require patients to complete additional consent forms when transferring patient medical information between new facilities [3]. However, the MHLW has notified that patient completion of a consent form is not necessarily required for them to participate in an HIE [32]. In addition, previous studies and reports have pointed out that opt-in consent policies not only impose an administrative burden on hospital medical staff, but also have the potential to lower consent rates and hinder the use of HIEs [33-35]. A future challenge for regional HIEs in Japan is how to reduce the effort of medical workers to obtain the consent required to use HIEs while respecting patient privacy. Recent research suggests that a hybrid combination of opt-in and opt-out policies can balance privacy considerations with the quality of consent [35]. As another approach, previous systematic reviews have noted that patients' perceptions of the benefits of HIEs may alleviate privacy concerns [36]. Another study also suggested that when patients are aware of an HIE's privacy policy and sharing procedures, and have trust in the HIE, they may be more likely to disclose their health information [37]. As we continue to study the benefits of HIEs and share these findings, it is possible that patients become less wary of HIEs and require simpler consent.

Limitations

This study had some limitations. The most significant limitation was that we analyzed data from only 2 HIEs. For example, the view rate of each item in HIEs that do not publish progress notes may differ significantly from the results of this study. As we have not been able to obtain audit log data, the detailed usage status of Sagan-Pass Net is unknown. In addition, because this

XSL•FO
RenderX

study was a quantitative analysis of audit logs, no questionnaires or interview surveys were conducted to directly ask medical workers about the factors influencing differences in utilization and content-viewing rates. A combination of audit log analysis and qualitative research will be necessary to identify in what situations medical data are being accessed during daily work and for what purposes.

Conclusions

In both HIEs analyzed in this study, progress notes were the most viewed content. As more health care organizations disclose the progress notes they manage to HIEs, their view rates are likely to increase. The cost-benefit of disclosing progress notes to HIEs remains unclear, and both health care providers and patients are concerned about privacy risks. Future research is needed to quantify and maximize the benefits of disclosure while minimizing privacy risks.

Acknowledgments

This work was supported by JST, CREST, and grant number JPMJCR21M1 from Japan. We would like to thank Tetsuya Otsubo, Naoki Ishizuka, Taichi Hatta, and Hiroshi Yamazaki for their helpful discussions. We also thank Editage for the English language editing.

Conflicts of Interest

None declared.

Multimedia Appendix 1
List of institutions that disclose electronic medical record data to health information exchanges and the disclosed data.
[XLSX File, 14 KB - medinform_v13i1e65575_app1.xlsx]

Multimedia Appendix 2
Results of the content sort.
[DOCX File, 20 KB - medinform_v13i1e65575_app2.docx]

Multimedia Appendix 3
Man-days and view rate of each output field and content by financial year.
[XLSX File, 14 KB - medinform_v13i1e65575_app3.xlsx]

References

1. What is HIE? HealthIT.gov. URL: https://www.healthit.gov/topic/health-it-and-health-information-exchange-basics/what-hie [accessed 2023-07-28]
2. [About the current situation of regional healthcare network] chiki iryou zyoho renkei nettowaku no genzyo ni tuite [Website in Japanese]. Ministry of Health, Labour and Welfare. URL: https://www.mhlw.go.jp/content/10800000/000683765.pdf [accessed 2023-07-24]
3. [Overview of the national regional medical information collaboration network using ICT (2021 edition) and urgent survey on the continuation of the regional medical information collaboration network] ICT wo riyou sita zenkoku chiki iryou zyoho nettowa-ku no gaikyou (2021 nendo ban) oyobi chiki iryo renkei nettowa-ku sonzoku ni kannsuru kinkyu chosa [Website in Japanese]. Japan Medical Association Research Institute. URL: https://www.jmari.med.or.jp/result/working/post-3560/ [accessed 2023-07-28]
4. Suzumoto J, Mori Y, Kuroda T. Health care worker usage of large-scale health information exchanges in Japan: user-level audit log analysis study. JMIR Med Inform 2024 Oct 9;12(1):e56263. [doi: 10.2196/56263] [Medline: 39382566]
5. Vest JR, Hilts KE, Ancker JS, Unruh MA, Jung HY. Usage of query-based health information exchange after event notifications. JAMIA Open 2019 Oct;2(3):291-295. [doi: 10.1093/jamiaopen/ooz028] [Medline: 31984363]
6. Vest JR, Unruh MA, Casalino LP, Shapiro JS. The complementary nature of query-based and directed health information exchange in primary care practice. J Am Med Inform Assoc 2020 Jan 1;27(1):73-80. [doi: 10.1093/jamia/ocz134] [Medline: 31592529]
7. [Regarding the handling of document information (3 documents) and electronic medical record information (6 information)] bunsyo joho oyobi denshikarute joho no toriatsukai ni tsuite [Website in Japanese]. Ministry of Health, Labour and Welfare. URL: https://www.mhlw.go.jp/content/10808000/001016921.pdf [accessed 2024-07-08]
8. [Health, medical, and nursing information utilization review committee medical information utilization working group] kenko iryo kaigo joho rikatsuyo kentokai iryo tou joho rikatsuyo wa-kingu guru-pu [Website in Japanese]. Ministry of Health, Labour and Welfare. 2024. URL: https://www.mhlw.go.jp/stf/shingi/other-isei_210261.html [accessed 2024-07-08]
9. The 11th Nationwide ID-Link Study Group. [Questionnaire survey result] anke-to chosa kekka [Website in Japanese]. Mykarte.org. 2023. URL: https://www.mykarte.org/11th_ID-Link_workshop/QuestionnaireResults.pdf [accessed 2024-07-08]

XSL•FO
RenderX

10. [Research project on a system that allows health and medical information to be checked at nationwide medical institutions] hoken iryo joho wo zenkoku no iryokikan tou de kakunin dekiru shikumi no chosa jigyo [Website in Japanese]. Ministry of Health, Labour and Welfare. 2020. URL: https://www.mhlw.go.jp/content/10808000/000613009.pdf [accessed 2024-07-08]
11. [Survey on network-based collaboration between medical institutions and insurers] nottowa-ku wo katsuyo shita iryokikan hokennsya kan renkei ni kansuru chosa [Website in Japanese]. Ministry of Health, Labour and Welfare. 2020. URL: https://www.mhlw.go.jp/content/10808000/000613010.pdf [accessed 2024-07-08]
12. Choukai Net. Shonai Medical Information Network Council. URL: https://www.nihonkai-hos.jp/choukai-net [accessed 2025-05-16]
13. PicaPicaLink [Website in Japanese]. Saga Prefecture Medical Information Regional Collaboration System Council. URL: https://pica2.link/ [accessed 2024-07-08]
14. ID-Link Web [Website in Japanese]. Mykarte.org. URL: https://www.mykarte.org/ [accessed 2024-04-19]
15. [Shonai medical information network operation and management regulations] shonai iryo joho nettowa-ku unyo kanri kitei [Website in Japanese]. Shonai Medical Information Network Council. URL: https://www.nihonkai-hos.jp/choukai-net/pdf/kitei.pdf [accessed 2024-07-08]
16. [List of restrictions on participation and use of picapicalink] picapicalink ni okeru sanka, riyo tou ni kansuru seigen [Website in Japanese]. Saga Prefecture Medical Information Regional Collaboration System Council. URL: https://pica2.link/wp-content/uploads/2018/03/180312riyoseigen.pdf [accessed 2024-07-08]
17. Patient consent flow [Website in Japanese]. Saga Prefecture Medical Information Regional Collaboration System Council. URL: https://pica2.link/wp-content/uploads/2023/08/doui-Flow.pdf [accessed 2024-07-08]
18. [About choukai net] choukai net toha [Website in Japanese]. Shonai Medical Information Network Council. URL: https://www.nihonkai-hos.jp/choukai-net/about/about.html [accessed 2024-07-08]
19. [EMS feature usage manual] EMS kinou riyou tezyunsho [Website in Japanese]. Saga Prefecture Medical Information Regional Collaboration System Council. URL: https://pica2.link/wp-content/uploads/2018/12/EMS_manual_Ver1.3.pdf [accessed 2024-07-08]
20. [Patient demographic data synchronization feature] kanzya demographic joho douki kinou [Website in Japanese]. Mykarte.org. URL: https://www.mykarte.org/idlink/file/download/PtSync.pdf [accessed 2024-07-08]
21. [Name matching feature] nayose kinou [Website in Japanese]. Picapicalink. 2024. URL: https://pica2.link/wp-content/uploads/2019/05/ysk5-1.pdf [accessed 2024-07-08]
22. [Sagan-path net registration instructions and agreement] sagan-pas.net touroku setumeisyo ken douisho [Website in Japanese]. Picapicalink. URL: https://pica2.link/wp-content/uploads/2019/05/ysk5-1.pdf [accessed 2024-07-08]
23. [Disclosure of information regarding medical research involving human subjects] hito wo taisho to suru igakukei kenkyu ni kansuru joho kokai [Website in Japanese]. Kyoto University Hospital. URL: https://kyoto.bvits.com/rinri/publish.aspx [accessed 2024-09-19]
24. Taylor HL, Apathy NC, Vest JR. Health information exchange use during dental visits. AMIA Annu Symp Proc 2020;2020(1210–1219):1210-1219. [Medline: 33936497]
25. Campion TR Jr, Edwards AM, Johnson SB, Kaushal R, HITEC investigators. Health information exchange system usage patterns in three communities: practice sites, users, patients, and data. Int J Med Inform 2013 Sep;82(9):810-820. [doi: 10.1016/j.ijmedinf.2013.05.001] [Medline: 23743323]
26. Adler-Milstein J, McAfee AP, Bates DW, Jha AK. The state of regional health information organizations: current activities and financing. Health Aff (Millwood) 2008;27(1):w60-w69. [doi: 10.1377/hlthaff.27.1.w60] [Medline: 18073225]
27. Nagoshi K, Tamura T, Matsumoto S, Sugiura H, Matsumoto T, Kosaka S. Visualization of usage status of healthcare information exchange activity. Shimane J Med Sci 2024;41(2):23-28. [doi: 10.51010/sjms.41.2_23]
28. [Visiting nursing] houmon kango [Website in Japanese]. Ministry of Health, Labour and Welfare. URL: https://www.mhlw.go.jp/content/12300000/001123919.pdf [accessed 2024-07-11]
29. [Overview of the nationwide regional healthcare network using ICT (2023 edition)] ICT wo riyou sita zenkoku chiki iryou zyoho nettowa-ku no gaikyou (2023 nendo ban) [Website in Japanese]. Japan Medical Association Research Institute. URL: https://www.jmari.med.or.jp/result/working/post-4511/ [accessed 2025-03-01]
30. Takao S. [Consideration of operational costs and utilization indicators for the continued operation of choukai net] choukai net keizoku unyo no tameno unei kosuto to katuyo shihyo kara mita kosatsu [Website in Japanese]. Japan Association for Medical Informatics. URL: https://confit.atlas.jp/guide/organizer/jcmi/jcmi2018f/subject/2-E-2-2/search [accessed 2025-01-19]
31. Nakayama M, Inoue R, Miyata S, Shimizu H. Health information exchange between specialists and general practitioners benefits rural patients. Appl Clin Inform 2021 May;12(3):564-572. [doi: 10.1055/s-0041-1731287] [Medline: 34107543]
32. [Examples of methods for obtaining consent in regional health information exchanges] chiki iryo zyoho renkei nettowaku ni okeru doi shutoku hoho no rei ni tuite [Website in Japanese]. Ministry of Health, Labor and Welfare. 2020. URL: https://www.mhlw.go.jp/content/000621515.pdf [accessed 2025-02-11]
33. Apathy NC, Holmgren AJ. Opt-in consent policies: potential barriers to hospital health information exchange. Am J Manag Care 2020 Jan 1;26(1):e14-e20. [doi: 10.37765/ajmc.2020.42148] [Medline: 31951362]
34. Satoshi S. [Current status and challenges of medical information network operation for hospital community liaison departments] byoin chiki renkei bumon karamita iryo joho renkei nettowa-ku unyo no genjo to kadai [Website in Japanese].

XSL•FO
RenderX

2022. URL: https://www8.cao.go.jp/kisei-kaikaku/kisei/meeting/wg/2201_03medical/220922/medical09_0101.pdf [accessed 2025-05-16]
35. Ito A, Nakamura F. Consent mechanisms and default effects in health information exchange in Japan. Front Digit Health 2025;7:1498072. [doi: 10.3389/fdgth.2025.1498072] [Medline: 40094152]
36. Shen N, Bernier T, Sequeira L, et al. Understanding the patient privacy perspective on health information exchange: a systematic review. Int J Med Inform 2019 May;125:1-12. [doi: 10.1016/j.ijmedinf.2019.01.014] [Medline: 30914173]
37. Esmaeilzadeh P. The effect of the privacy policy of health information exchange (HIE) on patients' information disclosure intention. Computers & Security 2020 Aug;95:101819. [doi: 10.1016/j.cose.2020.101819]

Abbreviations

3D6I: 3 documents and 6 types of information
CLINS: Clinical Information Sharing
DDI: data disclosure institution
DICOM: Digital Imaging and Communications in Medicine
DVI: data viewing institution
EMS: emergency medical service
FY: financial year
HIE: health information exchange
MHLW: Ministry of Health, Labour and Welfare
NMF: name matching feature
PDDSF: patient demographic data synchronization feature

Edited by A Coristine; submitted 19.08.24; peer-reviewed by M Nakayama, N Ihana-Sugiyama; revised version received 11.04.25; accepted 14.04.25; published 27.05.25.

Please cite as:
Suzumoto J, Mori Y, Kuroda T
Health Information Exchange Usage in Japan: Content Analysis of Audit Logs
JMIR Med Inform 2025;13:e65575
URL: https://medinform.jmir.org/2025/1/e65575
doi:10.2196/65575

© Jun Suzumoto, Yukiko Mori, Tomohiro Kuroda. Originally published in JMIR Medical Informatics (https://medinform.jmir.org), 27.5.2025. This is an open-access article distributed under the terms of the Creative Commons Attribution License (https://creativecommons.org/licenses/by/4.0/), which permits unrestricted use, distribution, and reproduction in any medium, provided the original work, first published in JMIR Medical Informatics, is properly cited. The complete bibliographic information, a link to the original publication on https://medinform.jmir.org/, as well as this copyright and license information must be included.

XSL•FO
RenderX

The Impact of Data Control and Delayed Discounting on the Public's Willingness to Share Different Types of Health Care Data: Empirical Study

Dongle Wei, MD; Pan Gao, MD; Yunkai Zhai, MD, PhD

School of Management, Zhengzhou University, Zhengzhou, China

Corresponding Author:
Yunkai Zhai, MD, PhD
School of Management, Zhengzhou University, Zhengzhou, China

Abstract

Background: Health data typically include patient-generated data and clinical medical data. Different types of data contribute to disease prevention, precision medicine, and the overall improvement of health care. With the introduction of regulations such as the Health Insurance Portability and Accountability Act (HIPAA), individuals play a key role in the sharing and application of personal health data.

Objective: This study aims to explore the impact of different types of health data on users' willingness to share. Additionally, it analyzes the effect of data control and delay discounting rate on this process.

Methods: The results of a web-based survey were analyzed to examine individuals' perceptions of sharing different types of health data and how data control and delay discounting rates influenced their decisions. We recruited participants for our study through the web-based platform "Wenjuanxing." After screening, we obtained 257 valid responses. Regression analysis was used to investigate the impact of data control, delayed discounting, and mental accounting on the public's willingness to share different types of health care data.

Results: Our findings indicate that the type of health data does not significantly affect the perceived benefits of data sharing. Instead, it negatively influences willingness to share by indirectly affecting data acquisition costs and perceived risks. Our results also show that data control reduces the perceived risks associated with sharing, while higher delay discounting rates lead to an overestimation of data acquisition costs and perceived risks.

Conclusions: Individuals' willingness to share data is primarily influenced by costs. To promote the acquisition and development of personal health data, stakeholders should strengthen individuals' control over their data or provide direct short-term incentives.

(JMIR Med Inform 2025;13:e66444) doi:10.2196/66444

KEYWORDS

health data control; delay discounting rate; mental accounting; health data; data sharing; willingness; patient-generated data; clinical medical data; disease prevention; precision medicine; health care; portability; accountability; app; web-based survey; data security; data privacy; mobile phone

Introduction

Background

Health data encompass information related to medical diagnosis, treatment, prevention, and health risks [1,2]. This includes patient-generated data (PGD) and clinical medical data. PGD refer to health-related data created, recorded, or collected by patients [3,4] often through automatic tracking devices like smartphones and wearables as well as manual logs and surveys. Conversely, clinical medical data are derived from clinical research, medical diagnostic records, and health insurance company records. Using public health data can significantly reduce operational costs for health care providers and enhance the quality of services provided [5,6]. Sharing health data allows physicians to gain detailed insights into patients' conditions, facilitating the development of personalized treatment plans and enabling the exploration of new treatments for diseases such as cancer [7]. For the public, health data sharing and interaction offer substantial benefits, including the reduction of unnecessary hospitalizations, the avoidance of duplicate medical tests, and the prevention of adverse drug events [8,9]. Furthermore, the application of public health data aids policy makers in formulating equitable health care policies and improving public health management at a societal level [1,10]. The National Institutes of Health recently announced the "All of Us" initiative, aiming to collect data from 1 million or more patients, including electronic health records, medical imaging, sociobehavioral data, and environmental data.

XSL•FO
RenderX

Despite the potential advantages of data use, public willingness to share health data is shifting [11]. Sharing health data involves intertemporal decision-making, where individuals must balance benefits and costs over time [12,13]. The costs may include psychological, financial, or other nonfinancial costs, while the benefits relate to potential future advantages such as reduced disease incidence and improved personal health management. The public's delay discounting rate significantly impacts these intertemporal decisions. Individuals with a high delay discounting rate prefer immediate rewards, whereas those with a low rate prioritize long-term benefits [14,15]. Unlike other health behaviors, sharing health data involves both health benefits and the risk of privacy breaches. Different types of health data carry varying levels of benefits and risks. Clinical medical data, for example, present higher privacy concerns and greater application value compared to PGD. Health data contain vast amounts of sensitive personal information, and any breach can lead to significant social and economic losses for individuals, thus decreasing their willingness to share such data [16,17]. Additionally, social stigmatization is a significant barrier to sharing sensitive health data with numerous health care organizations [18-20]. For instance, a data breach in a health information exchange (HIE) could reveal genetic diseases, causing distress for affected families.

Simultaneously, the unique nature of health data has made the issue of related rights a significant topic of discussion within the health care industry and academia. A key factor contributing to the public's reluctance to share health data is their lack of control over it [19,21]. The public cannot ascertain how other organizations or individuals will use their health data once it is acquired nor can they know whether their data will be transmitted to third parties [20]. Many people fear that their personal medical information could be used for marketing purposes without their authorization, posing a significant privacy risk [20]. Reports indicate that many American adults are highly anxious about how their health information is accessed and used [22]. Currently, it is widely accepted that other institutions or individuals must obtain the data owner's consent before acquiring and using health data in accordance with relevant laws. For instance, the health care industry has established policies and regulations such as the Health Insurance Portability and Accountability Act (HIPAA) and the General Data Protection Regulation. Therefore, understanding public willingness to share health data is crucial for the future development of public health initiatives. Our study, based on the theory of mental accounting, explores how different types of health data impact the public's willingness to share their data through perceived benefits and costs. Additionally, it analyzes the mechanisms by which the public's delay discounting rate and health data control influence their willingness to share health data.

Related Work

With the increasing prevalence of patient-centered design (PCD), the role and authority of the public in the sharing and interaction of health data have garnered significant attention. Existing research has analyzed the factors influencing health data sharing from various perspectives. For example, van Panhuis et al [23] conducted a systematic review of potential barriers to public health data sharing, identifying 20 potential barriers and categorizing them into 6 types: technical, motivational, economic, political, legal, and ethical. Sun et al [24], from the perspective of satisfaction, analyzed the factors influencing users of web-based health communities in disclosing their health information. Demographic characteristics such as participant age, region of residence, country or region of residence, and education level have a certain impact on the willingness to share personal health data [11]. Additionally, the public's ability to access, understand, and use health data directly influences their willingness to share health data [7].

Moreover, the privacy of health data is a crucial concern for patients, and preferences vary depending on the type of health data and the characteristics of the patients involved [21,25]. Watson et al [19], through semistructured interviews with patients, identified data type as a significant factor influencing patients' willingness to share personal health data. Patients' preferences for sharing PGD vary: some consistently share their data to keep their clinicians informed [3], while others refuse to share due to privacy concerns or fear of judgment [18,26]. Some public limit sharing their PGD to only trusted clinicians [27]. Moreover, research indicates that the public tends to avoid sharing sensitive health data [28]. Kim et al [29] collected participants' exercise and sleep data through experiments and used questionnaires to analyze their views on sharing daily health data. Kirkham et al [18] used ordinal logistic regression to study the impact of demographic factors, clinical service experience, and primary mental illness on the willingness to share mental health data, comparing it with physical health data. Seltzer et al [30] analyzed patients' willingness to share different types of data. The results showed that 50% of patients agreed to share at least 1 type of digital data, and 78% agreed to donate at least 1 type of data posthumously, with the highest percentages for electronic medical record, wearable device data, and Google search histories. Kim et al [31] and Mello et al [32], respectively, analyzed the types of institutions to which participants are more inclined to share their medical records and biospecimens. However, there is limited research that focuses on the impact of both PGD and clinical medical data on the public's willingness to share data as well as the underlying mechanisms of these effects.

Existing research increasingly emphasizes the rights of patients regarding their health data. Scholars have studied patients' control over health data from ethical [33], legal [34,35], managerial [36], and other perspectives. Currently, the entire process of HIE is managed by health care institutions for the interaction. In this process, patients, as the owners and beneficiaries of health information, often have their rights overlooked [37]. According to Hunter [38], as the quantity and scope of collected personal health data increase, the greatest demand is for transparency in their use. Kish and Topol [39] point out that to fully realize the benefits of digital health care, we need not only to find a shared home for personal health data but also to empower individuals to own them. PCD increases patients' willingness to share health data with others [40]. Esmaeilzadeh [41], drawing on utility theory, explores the factors influencing patients' adoption of HIE from the perspectives of perceived value and perceived risk. The public

XSL•FO
RenderX

expects to know the purpose of sharing their health data and desires control over data circulation [28]. Karway et al [42] found in their research that patients prefer to share their health data when they can control it themselves. The majority (87%) also reported feeling more comfortable sharing their data when they know its purpose. Sanderson et al [43] examined the public's willingness to share their biological data under different consent scenarios. In contrast, our study focuses on the public's evaluation of the current situation and examines the interaction effect between delay discounting and data control.

While existing research has extensively studied the factors influencing the public's willingness to share health data, much of it has been conducted through structured interviews, literature analysis, and similar methods. The mechanisms through which types of health data and the public's control over data affect their willingness to share remain unclear. Additionally, as intertemporal decisions, the public's preference for delay discounting rate directly impacts their data-sharing behavior, but there has been no research analyzing its underlying mechanisms. Therefore, our study poses the following research questions: How do different types of health data affect the public's willingness to share through benefits and costs? What is the role of the public's control over their health data and delay discounting rate in health data sharing?

Research Model and Hypotheses

The benefits and costs inherent in different types of health data vary. Our study categorizes health data into PGD and clinical medical data. Compared to clinical medical data, PGD entail lower sensitivity and fewer legal compliance requirements. Clinical medical data, comprising medical diagnostic records, clinical research data, and health insurance company records, are highly sensitive and private, necessitating strict adherence to regulations such as HIPAA. Consequently, patients are more inclined to share PGD rather than clinical medical data due to the relatively less sensitive nature of PGD information. In contrast, clinical medical data involve highly sensitive personal health information, raising concerns about privacy breaches and data misuse. Furthermore, PGD acquisition costs are lower, as it is obtained through various wearable smart devices and the internet. However, the self-reporting nature and lower accuracy of PGD may diminish its value in medical research and clinical applications. In contrast, clinical medical data possess high precision and professional recording, making it directly applicable to medical research, clinical trials, and precision medicine, thus yielding higher sharing benefits. However, acquiring clinical medical data requires involvement from medical institutions or insurance companies, necessitating strict permission management and incurring potential costs and time expenses. Hence, we hypothesize the following:

- Hypothesis 1: The public exhibits a higher willingness to share PGD compared to clinical medical data.
- Hypothesis 2: The relationship between the type of health data and willingness to share data is mediated by perceived benefits (hypothesis 2a), perceived risks (hypothesis 2b), and data acquisition costs (hypothesis 2c).

The concept of mental accounting, introduced by Thaler [44], is a key area in behavioral decision-making. Tversky and Kahneman [45] further defined it as the cognitive processes of categorizing, encoding, evaluating, and budgeting outcomes. It essentially involves assessing gains and losses during decision-making [46]. Since its introduction, mental accounting theory has found extensive applications in behavioral economics, consumer behavior, and decision-making [47-49]. Additionally, Hossain [50] explored how individual cognition influences mental accounting and its application to different product types.

Moreover, mental accounting influences individuals' engagement in health data-sharing behavior. In the context of health data sharing, individuals tend to view the potential benefits of sharing as part of the "benefit account." The greater the perceived benefits, the more likely they are to share health data. Meanwhile, the potential risks of privacy leakage are classified under the "loss account." The stronger the perception of risk, the lower the individual's willingness to share data. Furthermore, the theory of mental accounting also highlights the impact of sunk costs—time and effort already invested are seen as irrecoverable losses, which, in turn, reduce the individual's willingness to continue sharing data. Hence, we propose the following hypotheses:

- Hypothesis 3: Perceived benefits positively affect the willingness to share health data.
- Hypothesis 4: Perceived risks negatively affect the willingness to share health data.
- Hypothesis 5: Data acquisition costs negatively affect the willingness to share health data.

The notion of health data control pertains to individuals' rights to manage their health care information. Drawing from the theory of psychological ownership, individuals tend to perceive objects they own as extensions of themselves, influencing their attitudes, motivations, and behaviors [51]. Psychological ownership refers to the feeling individuals have that an object belongs to them, emphasizing their sense of possession [52]. In our study, health data serve as the focus of psychological ownership. Belanger and James [53] discovered that users prefer direct control over personal privacy compared to corporate control. Direct control enhances users' self-efficacy and willingness to disclose personal information.

Moreover, PCD significantly impacts patients' adoption of electronic health record systems. PCD ensures that all users within health care institutions can access patient health information with patient confirmation [54]. PCD increases patients' willingness to share health data [40] and empowers them to manage their information. Greater public control over health data reduces perceived privacy risks and enhances awareness of data-sharing benefits while downplaying associated costs. Thus, we propose the following hypothesis:

- Hypothesis 6: Health data control increases the perceived benefits (hypothesis 6a) and reduces the perceived risks (hypothesis 6b) in data sharing.

Intertemporal decision-making involves balancing and judging between time and gains or losses [55]. It includes choices like immediate gratification versus future enjoyment or the immediate pleasure of smoking versus future health concerns. This process, known as intertemporal choice, reflects the value

XSL•FO
RenderX

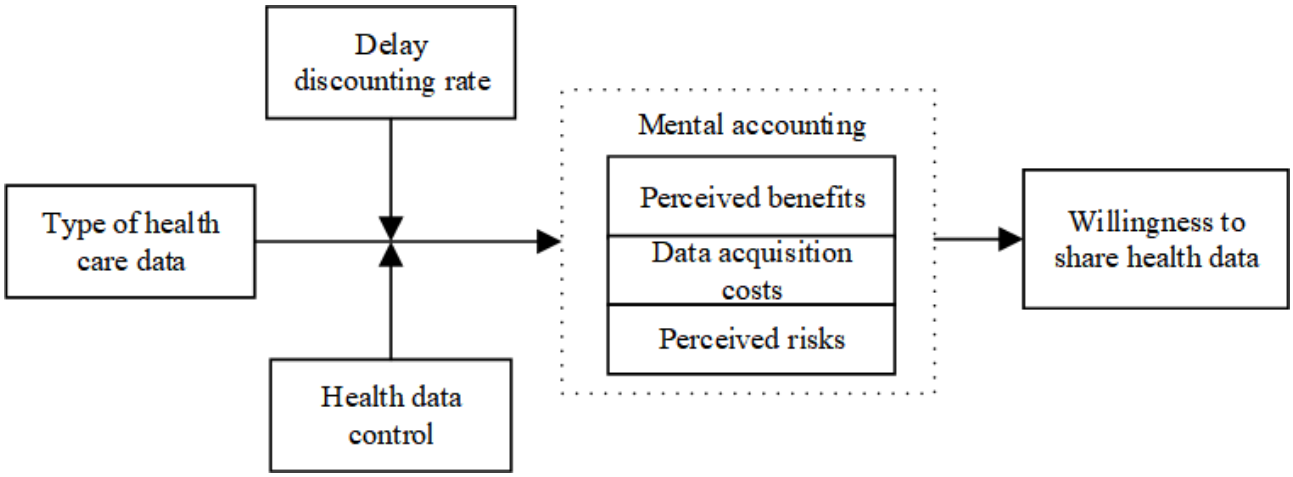
people assign to payoffs at different times [56]. Most decisions require trading off costs and benefits over time. Delay discounting rate and subjective value are key indicators of intertemporal choice; a higher discounting rate or lower subjective value suggests greater impulsivity and preference for immediate rewards over larger future gains [14,15].

Research has examined intertemporal decision-making in health care. Snider et al [57] studied how intertemporal preferences affect adverse health and financial behaviors using delay discounting rates. Tian et al [58] investigated the role of delay discounting rate in adolescent internet gaming addiction. Studies also show that altering intertemporal preferences can improve health behaviors. Interventions that reduce delay discounting rate or enhance future time orientation have been shown to promote better health behaviors [59]. Individuals with high delay discounting rates prioritize immediate gratification, undervaluing health data-sharing benefits and focusing on privacy risks. Conversely, those with lower rates prioritize long-term benefits, emphasizing data-sharing benefits and overlooking privacy risks and data acquisition costs. Therefore, we hypothesize the following:

- Hypothesis 7: Delay discounting rate reduces perceived benefit (hypothesis 7a), increasing perceived risk (hypothesis 7b) and data acquisition costs (hypothesis 7c).

Consequently, we propose a moderated mediation model (Figure 1) that is mediated by 3 factors in mental accounting, using health data control and delay discounting rate as moderators.

Figure 1. Theoretical model.



Methods

Participants and Procedure

This study was conducted through the web-based questionnaire platform "Wenjuanxing." After excluding invalid and incomplete questionnaires, a total of 257 valid responses were collected. To ensure the diversity and representativeness of the sample, recruitment information was posted on the platform. The recruitment notice clearly stated that participants must be between the ages of 20 and 69 years, with no specific educational background requirements, aiming to include individuals from various educational backgrounds. Prior to completing the questionnaire, participants were required to confirm their voluntary participation and understanding of all relevant research information, including the research objectives, expected time commitment, and potential risks involved.

At the beginning of the questionnaire, all participants were presented with a detailed informed consent form, which included a statement of voluntary participation, an explanation of data collection and use, a commitment to protecting personal privacy, and assurances of data anonymity. Participants were required to read this consent form carefully and check a consent box before proceeding with the questionnaire. All data collected were strictly for academic research purposes. Upon completion of the questionnaire, participants were rewarded with US $0.7 - $1.4 based on the completeness and quality of their responses. This incentive was designed to encourage careful and thoughtful participation. To ensure the reliability of the research results, all data were anonymized to prevent any personal identifying information (eg, names, contact information, and IP addresses) from being recorded.

The ages of participants ranged from 20 to 69 years. The majority of participants held undergraduate degrees (n=122, 47.5%), followed by master degree holders (n=70, 27.2%), individuals with college degrees or below (n=55, 21.4%), and doctoral students (n=10, 3.9%).

Ethical Considerations

This study has obtained ethics approval from the institutional review board of the School of Management, Zhengzhou University. In accordance with the regulations of the institutional review board, this research is deemed to meet ethical standards, and a series of measures have been implemented to ensure ethical compliance throughout the study process. Specifically, all participants' data have been anonymized to ensure the strict protection of their privacy. Throughout the research, no personal identifying information will be linked to the data, and all raw data will be restricted to use by the research team only. Furthermore, participants were fully informed of the research purpose, the manner in which their data would be used, and the commitment to privacy protection, and they voluntarily consented to participate.

XSL•FO
RenderX

Overview of the Scenarios

In our study, health data sharing refers to sharing one's own data with health care providers. Health care providers include hospitals, health insurance companies, and medical device companies. The questionnaire consisted of 3 parts. The first part used nominal scales to collect demographic information, including sex, age, and educational level. The second and third parts focused on variables related to the willingness to share PGD and clinical medical data, respectively. Participants respond using a 5-point Likert scale (1=strongly disagree and 5=strongly agree).

For data types, we classify them as PGD and clinical medical data. PGD include, but are not limited to, the following parts: data measured by wearable smart devices or home medical and health devices, data generated by daily activities, and internet health data. Clinical medical data are mainly electronic medical record data, medical image data, laboratory test data, etc. We divide mental accounts into perceived benefits, perceived risks, and data acquisition costs. Perceived benefits are people's self-perception of the benefits of sharing health care data based on their own expertise and experience. Perceived risk measures people's assessment of the risk of data leakage in the process of data sharing and the negative impact of data leakage on them. Data acquisition cost, on the other hand, refers to the effort people put into obtaining relevant health care before sharing health care data. The moderating variables in the paper are data control and delay discount, while data control refers to the degree of control people have over their own health care data. Delay discount rates were calculated using the 27-item Monetary Choice Questionnaire [14]. Each question contained an immediate reward option (eg, US $1.5 today) and a delayed reward option (eg, US $3 in 7 days). We simply replace the US dollar ($) with the Chinese yuan (¥) based on World Bank data. We still use Kirby's method to calculate the discount rate. In the Kirby task, the 27 trails were divided into 3 groups according to the magnitude of the delay reward, and the discount rates corresponding to the 9 trails in each group were ranked from smallest to largest (0.00016-0.250).

Results

Demographics

This study includes several demographic factors, such as sex (male and female) and education level among adolescents. Among the 257 participants, 40.9% (n=105) were male, and 59.1% (n=152) were female. Furthermore, among the respondents, 3.1% (n=8) were aged 20 years and younger, 48.6% (n=125) were aged 21 - 29 years, 16% (n=41) were aged 30 - 39 years, 13.6% (n=35) were aged 40 - 49 years, and 18.7% (n=48) were aged 49 years and older. Additionally, 21.4% (n=22) of individuals had education levels below an undergraduate degree, 47.5% (n=122) had undergraduate degrees, 27.2% (n=70) had master's degrees, and 3.9% (n=10) had doctoral degrees (Table 1).

Table . Demographic characteristics.

Variable	Values, n (%)
Sex	
Male	105 (40.9)
Female	152 (59.1)
Age (years)	
<20	8 (3.1)
21 - 29	125 (48.6)
30 - 39	41 (16)
40 - 49	35 (13.6)
>50	48 (18.7)
Education	
Below an undergraduate degree	22 (21.4)
Undergraduate degree	122 (47.5)
Master's degree	70 (27.2)
Doctoral degree	10 (3.9)

Preliminary Analyses

Table 2 presents the Pearson and point-biserial correlation coefficients of the variables. Data acquisition cost positively correlates with the data type. Perceived risk positively correlates with sex and data type. The delay discounting rate positively correlates with sex and negatively correlates with education. Health data control positively correlates with education and data type. Willingness to share health data negatively correlates with data type, data acquisition cost, perceived risk, and health data control and positively correlates with perceived benefits.

XSL•FO
RenderX

Table . Pearson and point-biserial correlation coefficients.

Variable	Sex	Age	Education	DT[a]	DC[b]	PB[c]	PR[d]	DR[e]	HC[f]	HS[g]
Sex										
r	1	0.038	0.083	0.000	0.009	−0.013	0.105	0.104	0.068	−0.037
P value	—[h]	.42	.08	>.99	.85	.78	.03	.03	.15	.43
Age										
r	0.038	1	−0.468	0.000	−0.064	0.038	0.003	0.048	−0.009	0.008
P value	.42	—	<.001	>.99	.17	.42	.96	.31	.84	.86
Education										
r	0.083	−0.468	1	0.000	0.038	0.049	0.010	−0.146	0.100	0.063
P value	.08	<.001	—	>.99	.41	.30	.83	.002	.03	.18
DT										
r	0.000	0.000	0.000	1	0.485	−0.043	0.482	0.000	0.213	−0.354
P value	>.99	>.99	>.99	—	<.001	.36	<.001	>.99	<.001	<.001
DC										
r	0.009	−0.064	0.038	0.485	1	−0.001	0.435	−0.025	0.085	−0.374
P value	.85	.17	.41	<.001	—	.98	<.001	.59	.07	<.001
PB										
r	−0.013	0.038	0.049	−0.043	−0.001	1	0.023	0.065	−0.112	0.306
P value	.78	.42	.30	.36	.98	—	.63	.17	.02	<.001
PR										
r	0.105	0.003	0.010	0.482	0.435	0.023	1	−0.078	0.328	−0.342
P value	.03	.96	.83	<.001	<.001	.63	—	.10	<.001	<.001
DR										
r	0.104	0.048	−0.146	0.000	−0.025	0.065	−0.078	1	−0.035	−0.010
P value	.03	.31	.002	>.99	.59	.17	.010	—	.46	.83
HC										
r	0.068	−0.009	0.100	0.213	0.085	−0.112	0.328	−0.035	1	−0.109
P value	.15	.84	.03	<.001	.07	.01	<.001	.46	—	.02
HS										
r	−0.037	0.008	0.063	−0.354	−0.374	0.306	−0.342	−0.010	−0.109	1
P value	.43	.86	.18	<.001	<.001	<.001	<.001	.83	.02	—

[a]DT: type of health care data.

[b]DC: data acquisition cost.

[c]PB: perceived benefit.

[d]PR: perceived risk.

[e]DR: delay discounting rate.

[f]HC: health data control.

[g]HS: willingness to share health data.

[h]Not available.

Hypotheses Testing

Table 3 shows the direct effects of each variable on the impact of health data sharing. The type of health data has a significant and direct effect on willingness to share (β=−0.28, SE=0.10; *P*<.001), supporting hypothesis 1. Perceived benefits positively influence the willingness to share (Table 2) health data (β=0.40, SE=0.06; *P*<.001), supporting hypothesis 3. Additionally, the data acquisition cost and perceived risk have significant negative direct effects on types of health data, supporting hypothesis 4 and hypothesis 5.

XSL•FO
RenderX

Table . The direct effect of the variable on health data sharing.

Paths	β (SE)	LLCI[a]	ULCI[b]
DT[c]	−0.28 (0.10)	−0.47	−0.10
DC[d]	−0.27 (0.06)	−0.38	−0.16
PR[e]	−0.18 (0.05)	−0.27	−0.08
PB[f]	0.40 (0.06)	0.29	0.51

[a]LLCI: lower level of confidence interval.

[b]ULCI: upper level of confidence interval.

[c]DT: type of health care data.

[d]DC: data acquisition cost.

[e]PR: perceived risk.

[f]PB: perceived benefit.

The results, as summarized in Table 4, indicate that there is no significant relationship between types of health data and perceived benefit (β=−0.06; P=.68; t_{249}=−0.92), suggesting that types of health data do not directly impact perceived benefit. However, it is noteworthy that in the moderated mediation model, participants' education level has a positive influence on perceived benefit (β=0.11; P=.02; t_{249}=2.24).

XSL•FO
RenderX

Table . Regression coefficients in the mediation model and moderated mediation model.

	Data acquisition cost				Perceived risk				Perceived benefit			
	Model (1)		Model (2)		Model (1)		Model (2)		Model (1)		Model (2)	
	β value	*t* test (*df*=249)	β value	*t* test (*df*=249)	β value	*t* test (*df*=249)	β value	*t* test (*df*=249)	β value	*t* test (*df*=249)	β value	*t* test (*df*=249)
DT[a]	0.82[b]	11.78	0.27	1.10	0.97[b]	11.73	1.20[b]	4.53	−0.06	−0.92	0.25	1.12
DR[c]	—[d]	—	−0.06[e]	−2.38	—	—	−0.08[f]	−3.05	—	—	0.03	1.17
DT×DR	—	—	0.09[e]	2.65	—	—	0.09[e]	2.10	—	—	0.00	0.17
HC[g]	—	—	−0.08	−1.58	—	—	0.33[b]	5.62	—	—	−0.02	−0.39
DT×HC	—	—	0.10	1.37	—	—	−0.22[e]	−2.57	—	—	−0.11	−1.72
DC[h]	—	—	—	—	—	—	—	—	—	—	—	—
PR[i]	—	—	—	—	—	—	—	—	—	—	—	—
PB[j]	—	—	—	—	—	—	—	—	—	—	—	—
Sex (male=0; female=1)	0.08	0.25	0.30	0.42	0.22[e]	0.08	0.20[e]	2.48	−0.03	−0.50	−0.04	−0.62
Age	−0.04	−1.28	−0.04	−1.27	−0.00	−0.02	−0.01	−0.31	0.05	1.49	0.05	1.65
Education	0.01	0.20	0.00	0.91	0.00	0.02	0.04	−0.70	0.08	1.65	0.11[f]	2.24
Constant	2.88	14.16	3.27	12.86	2.47	10.13	2.05	7.04	3.36	16.66	3.23	12.87
R^2	0.49	0.49	0.50	0.50	0.49	0.49	0.56	0.56	0.09	0.09	0.18	0.18

[a]DT: type of health care data.

[b]*P*<.001.

[c]DR: delay discounting rate.

[d]Not available.

[e]*P*<.05.

[f]*P*<.01.

[g]HC: health data control.

[h]DC: data acquisition cost.

[i]PR: perceived risk.

[j]PB: perceived benefit.

Furthermore, the results demonstrate that types of health data positively influence data acquisition costs (β=0.82; *P*<.001; t_{249}=11.78) and perceived risk (β=0.97; *P*<.001; t_{249}=11.73). Interestingly, sex also has a significant influence on perceived risk, with female participants perceiving higher risk in data sharing compared to male participants.

These findings suggest that while the types of health data themselves may not directly impact perceived benefit, they do influence both data acquisition cost and perceived risk. Additionally, participants' education level plays a role in shaping their perceptions of the benefits associated with sharing health data.

Table 5 shows the indirect effects of types of health data on the impact of health data sharing. Both data acquisition cost and perceived risk have significant mediating effects on the relationship between types of health data and willingness to share health data (β=−0.22, SE=0.05; odds ratio [OR] 0.80, 95% CI −0.33 to −0.12 and β=−0.17, SE=0.06; OR 0.84, 95% CI −0.28 to −0.07), supporting hypothesis 2b and hypothesis 2c. However, the mediating effect of perceived benefits on the relationship between types of health data and willingness to share health data is not significant (β=−0.03, SE=0.03; OR 0.97, 95% CI −0.08 to 0.03), hypothesis 2a was not supported.

XSL•FO
RenderX

Table . The indirect effect of the variable on health data sharing.

Paths	β (SE)	LLCI[a]	ULCI[b]
DT[c]→DC[d]→HS[e]	−0.22 (0.05)	−0.33	−0.12
DT→PR[f]→HS	−0.17 (0.05)	−0.28	−0.07
DT→PB[g]→HS	−0.03 (0.04)	−0.08	0.03

[a]LLCI: lower level of confidence interval.
[b]ULCI: upper level of confidence interval.
[c]DT: type of health care data.
[d]DC: data acquisition cost.
[e]HS: willingness to share health data.
[f]PR: perceived risk.
[g]PB: perceived benefit.

Meanwhile, the relationship between types of health care and perceived benefits is not moderated by health data control and delay discount rate (β=−0.11; *P*=.13; t_{249}=−1.72 and β=0.01; *P*=.97; t_{249}=0.17), hypothesis 6a and hypothesis 7a were not supported. Additionally, Table 6 indicates that the relationship between types of health data and willingness to share health data through the cost of data acquisition and perceived risk is influenced by delay discounting (β=0.09, SE=0.03; *P*=.01 and β=0.09, SE=0.04; *P*=.03), supporting hypothesis 7b and hypothesis 7c. Health data control moderates the relationship between types of health data and willingness to share health data through perceived risk (β=−0.23, SE=0.08; *P*=.004), supporting hypothesis 6b.

Table . Moderating effect of delay discounting rate and health data control.

Paths	β (SE)	LLCI[a]	ULCI[b]
DT[c]→DC[d]→HS [e] (DR[f])			
DR=mean−1SD	0.65 (0.09)	0.46	0.83
DR=mean	0.81 (0.06)	0.68	0.95
DR=mean＋1SD	0.98 (0.10)	0.79	1.17
DT→PR[g]→HS (DR)			
DR=mean−1SD	0.80 (0.11)	0.58	1.02
DR=mean	0.96 (0.08)	0.80	1.12
DR=mean＋1SD	1.14 (0.11)	0.91	1.36
DT→PR→HS (HC[h])			
HC=mean−1SD	1.10 (0.11)	0.88	1.33
HC=mean	0.87 (0.08)	0.71	1.03
HC=mean＋1SD	0.63 (0.12)	0.40	0.86

[a]LLCI: lower level of confidence interval.
[b]ULCI: upper level of confidence interval.
[c]DT: type of health care data.
[d]DC: data acquisition cost.
[e]HS: willingness to share health data.
[f]DR: delay discounting rate.
[g]PR: perceived risk.
[h]HC: health data control.

Discussion

Overview

With the advent of the digital age, the application and sharing of health data have garnered significant attention. However, issues such as privacy breaches and ambiguous ownership have emerged, resulting in individuals' reluctance to share their health care information. Scholars have increasingly focused on strategies to enhance public willingness to share or disclose their health data with institutions. Nonetheless, the influence of different data types on individuals and the moderating effects of delay discounting and health data control remain

XSL•FO
RenderX

underexplored. This study aims to analyze the impact of different types of health data on individual data sharing through the lens of psychological ownership theory and examine the moderating effects of delay discounting and health data control.

Principal Findings

Consistent with other studies, our study demonstrates that higher perceived benefits and lower perceived risks are associated with an increased willingness to share health data [24,41]. Building on this foundation, the study also explores the impact of the effort individuals invest in obtaining data on their willingness to share it. The findings indicate a correlation between lower data acquisition costs and a greater willingness to share data. When individuals expend considerable effort to obtain data, they develop a sense of psychological ownership, perceiving the data as something they have acquired at a cost and therefore value more highly. Due to this psychological ownership effect, they become more cautious and conservative about sharing the data, showing reluctance to share it easily with others. As indicated by Karway et al [42], the public is more inclined to share their health data when they can exercise control over it.

Types of health data may not only directly influence the willingness to share data but also indirectly affect it through mental accounting. Our mediation model revealed that types of health data negatively impact individuals' willingness to share data by increasing data acquisition costs and perceived risks. Obtaining clinical medical data requires more effort compared to everyday health data due to its complexity and sensitivity, which involves more permissions and privacy protection measures during the acquisition process. Additionally, clinical medical data contain more sensitive information, and its leakage may result in more severe consequences [28,30]. Consequently, the public perceives higher risks associated with sharing such data, resulting in a greater reluctance to share it.

However, contrary to our hypothesis, types of health data do not influence the public's perception of data-sharing benefits. Whether it is PGD or clinical medical data, the public may prioritize whether data sharing can improve the quality of health care services and enhance health management. However, the public cannot ascertain how their data will be used after sharing nor can they accurately perceive the benefits to themselves after data sharing [22,23]. For different types of health data, the differences in the perceived benefits of data sharing by the public may not be significant.

In the moderated mediation model, participants' educational level has a positive influence on perceived benefits. This indicates that individuals with higher education levels are more inclined to perceive higher benefits from data sharing. Individuals with higher education levels typically possess greater information literacy and understanding, enabling them to recognize better the potential benefits of data sharing in health management, disease prevention, and medical research. Therefore, they have a more positive perception of the benefits of data sharing. Similarly, sex has a positive influence on participants' perception of data-sharing risks, with female participants perceiving higher risks compared to male participants. This finding is consistent with existing literature, where female participants typically demonstrate higher sensitivity and caution regarding data privacy and security [60,61]. Female participants may exhibit greater sensitivity to data privacy issues due to societal processes emphasizing security concerns or experiences of insecurity in the use and management of health data.

The delay discounting rate has a positive moderating effect on the relationship between types of health data and the effort participants expend in obtaining data as well as their perceived risks. Individuals with a higher delay discounting rate tend to be more impulsive, with a lower valuation of future rewards. This leads them to rely more on immediate costs and benefits rather than long-term gains in decision-making [14,15]. This psychological characteristic may lead them to perceive the effort required to obtain data as part of the decision-making process. Additionally, compared to long-term health management and potential benefits, individuals with a higher delay discounting rate may prioritize immediate security and privacy protection. Consequently, they may overly focus on the immediate risks associated with sharing medical data, such as privacy breaches and data misuse, while overlooking the potential long-term health benefits and medical advancements that data sharing could bring about.

The relationship between types of health data and perceived data-sharing risks is negatively moderated by health data control rights. Individuals with higher health data control rights typically have more resources and means to simplify the data acquisition process, reduce the complexity and difficulty of obtaining data, and enhance their data protection capabilities, thereby mitigating the perceived risks associated with data sharing [42]. Additionally, granting the public more control over their health data increases their engagement in data sharing, thereby promoting it [40]. Enhancing transparency in the data-sharing process can further empower the public with greater control over their health data [38].

The following insights were gained: to enhance participation in data sharing, health care institutions and policy makers should simplify the data authorization and acquisition processes. By reducing complex authorization steps and clarifying the permissions involved in the sharing process, individuals' psychological burden and practical operational costs during data sharing can be significantly reduced. For example, adopting a unified user authorization platform or a "single consent" mechanism can simplify the public's decision-making process regarding data sharing. Additionally, users should be clearly informed about the context and purpose of data use, and options for data modification, deletion, and revocation of consent should be provided. During the data sharing process, a "transparent data use statement" should be made available to ensure that the public has a clearer understanding of the data's destination, use, and potential impact. Furthermore, the moderating role of delayed discounting on data-sharing decisions offers new perspectives for research. For individuals with a high delayed discounting rate, the immediate risks associated with data sharing may be overemphasized, potentially overshadowing the long-term health benefits. To address this issue, future data-sharing initiatives could focus on increasing public awareness of the long-term benefits of data sharing, emphasizing its potential in health management, disease prevention, and

XSL•FO
RenderX

medical research. This approach could help individuals balance short-term privacy protection with long-term benefits.

Limitations

There are some limitations in our study. First, we classified health data only into PGD and clinical medical data. Future research could categorize them in more detail. Second, although we included variables such as sex, age, and education in our questionnaire, we did not analyze other personal characteristics, such as history of illness. Additionally, our study did not provide a detailed categorization of the recipients of data sharing. Future studies could specify recipients more precisely, categorizing them as hospitals, insurance agencies, medical device companies, and so on.

Conclusions

Our study has revealed the multifaceted impacts of different types of health data on public willingness to data sharing and highlighted the significant roles of data acquisition costs, delay discounting rates, and health data control rights in this process. These findings not only contribute to a deeper understanding of public attitudes and behaviors regarding data sharing but also provide valuable insights for the development of effective data-sharing policies and privacy protection measures.

Acknowledgments

This work was supported by the Postdoctoral Fellowship Program (grade C; GZC20232414), the Henan Province Science and Technology Research Project (242102310140), and the joint construction project of Henan Medical Science and Technology Research Program (LHGJ20240274).

Conflicts of Interest

None declared.

References

1. Ibrahim H, Liu X, Zariffa N, Morris AD, Denniston AK. Health data poverty: an assailable barrier to equitable digital health care. Lancet Digit Health 2021 Apr;3(4):e260-e265. [doi: 10.1016/S2589-7500(20)30317-4] [Medline: 33678589]
2. Schneble CO, Elger BS, Shaw DM. All our data will be health data one day: the need for universal data protection and comprehensive consent. J Med Internet Res 2020 May 28;22(5):e16879. [doi: 10.2196/16879] [Medline: 32463372]
3. Zhu H, Colgan J, Reddy M, Choe EK. Sharing patient-generated data in clinical practices: an interview study. AMIA Annu Symp Proc 2016;2016:1303-1312. [Medline: 28269928]
4. Choe EK, Lee B, Andersen TO, Wilcox L, Fitzpatrick G. Harnessing the power of patient-generated data. IEEE Pervasive Comput 2018;17(2):50-56. [doi: 10.1109/MPRV.2018.022511243]
5. Wang Y, Kung L, Wang WYC, Cegielski CG. An integrated big data analytics-enabled transformation model: application to health care. Inf Manag 2018 Jan;55(1):64-79. [doi: 10.1016/j.im.2017.04.001]
6. Esfandiari N, Babavalian MR, Moghadam AME, Tabar VK. Knowledge discovery in medicine: current issue and future trend. Expert Syst Appl 2014 Jul;41(9):4434-4463. [doi: 10.1016/j.eswa.2014.01.011]
7. Luo Y, Oh CY, Jean BS, Choe EK. Interrelationships between patients' data tracking practices, data sharing practices, and health literacy: onsite survey study. J Med Internet Res 2020 Dec 22;22(12):e18937. [doi: 10.2196/18937] [Medline: 33350960]
8. Davoody N, Koch S, Krakau I, Hägglund M. Accessing and sharing health information for post-discharge stroke care through a national health information exchange platform—a case study. BMC Med Inform Decis Mak 2019 May 3;19(1):95. [doi: 10.1186/s12911-019-0816-x] [Medline: 31053141]
9. Yaraghi N. An empirical analysis of the financial benefits of health information exchange in emergency departments. J Am Med Inform Assoc 2015 Nov;22(6):1169-1172. [doi: 10.1093/jamia/ocv068] [Medline: 26117143]
10. Heijlen R, Crompvoets J. Open health data: mapping the ecosystem. Digit Health 2021;7:20552076211050167. [doi: 10.1177/20552076211050167] [Medline: 34777853]
11. Karampela M, Ouhbi S, Isomursu M. Connected health user willingness to share personal health data: questionnaire study. J Med Internet Res 2019 Nov 27;21(11):e14537. [doi: 10.2196/14537] [Medline: 31774410]
12. Chapman GB. Temporal discounting and utility for health and money. J Exp Psychol Learn Mem Cogn 1996;22(3):771-791. [doi: 10.1037//0278-7393.22.3.771]
13. Ortendahl M, Fries JF. Framing health messages based on anomalies in time preference. Med Sci Monit 2005 Aug;11(8):RA253-RA256. [Medline: 16049392]
14. Kirby KN, Petry NM, Bickel WK. Heroin addicts have higher discount rates for delayed rewards than non-drug-using controls. J Exp Psychol Gen 1999 Mar;128(1):78-87. [doi: 10.1037//0096-3445.128.1.78] [Medline: 10100392]
15. Li H, Guo Y, Yu Q. Self-control makes the difference: the psychological mechanism of dual processing model on internet addicts' unusual behavior in intertemporal choice. Comput Human Behav 2019 Dec;101:95-103. [doi: 10.1016/j.chb.2019.07.010]
16. Kim HL, Kim YG, Yoon SH, Ryu S. Effect of media context on avoidance of skippable pre-roll ads in online video platform: a mental accounting of time perspective. J Bus Res 2023 Sep;164:113966. [doi: 10.1016/j.jbusres.2023.113966]

XSL•FO
RenderX

17. Park YJ, Shin DD. Contextualizing privacy on health-related use of information technology. Comput Human Behav 2020 Apr;105:106204. [doi: 10.1016/j.chb.2019.106204]
18. Kirkham EJ, Lawrie SM, Crompton CJ, et al. Experience of clinical services shapes attitudes to mental health data sharing: findings from a UK-wide survey. BMC Public Health 2022 Feb 19;22(1):357. [doi: 10.1186/s12889-022-12694-z] [Medline: 35183146]
19. Watson E, Fletcher-Watson S, Kirkham EJ. Views on sharing mental health data for research purposes: qualitative analysis of interviews with people with mental illness. BMC Med Ethics 2023 Nov 14;24(1):99. [doi: 10.1186/s12910-023-00961-6] [Medline: 37964278]
20. Grande D, Mitra N, Shah A, Wan F, Asch DA. Public preferences about secondary uses of electronic health information. JAMA Intern Med 2013 Oct 28;173(19):1798-1806. [doi: 10.1001/jamainternmed.2013.9166] [Medline: 23958803]
21. Hajian A, Prybutok VR, Chang HC. An empirical study for blockchain-based information sharing systems in electronic health records: a mediation perspective. Comput Human Behav 2023 Jan;138:107471. [doi: 10.1016/j.chb.2022.107471]
22. Zhang X, Liu S, Chen X, Wang L, Gao B, Zhu Q. Health information privacy concerns, antecedents, and information disclosure intention in online health communities. Inf Manag 2018 Jun;55(4):482-493. [doi: 10.1016/j.im.2017.11.003]
23. van Panhuis WG, Paul P, Emerson C, et al. A systematic review of barriers to data sharing in public health. BMC Public Health 2014 Nov 5;14(1):1-9. [doi: 10.1186/1471-2458-14-1144] [Medline: 25377061]
24. Sun S, Zhang J, Zhu Y, Jiang M, Chen S. Exploring users' willingness to disclose personal information in online healthcare communities: the role of satisfaction. Technol Forecast Soc Change 2022 May;178:121596. [doi: 10.1016/j.techfore.2022.121596]
25. Lafky DB, Horan TA. Personal health records: consumer attitudes toward privacy and security of their personal health information. Health Inform J 2011;17(1):63-71. [doi: 10.1177/1460458211399403]
26. Ostherr K, Borodina S, Bracken RC, Lotterman C, Storer E, Williams B. Trust and privacy in the context of user-generated health data. Big Data Soc 2017 Jun;4(1):2053951717704673. [doi: 10.1177/2053951717704673]
27. Halamka JD, Mandl KD, Tang PC. Early experiences with personal health records. J Am Med Inform Assoc 2008;15(1):1-7. [doi: 10.1197/jamia.M2562] [Medline: 17947615]
28. Ivanova J, Grando A, Murcko A, et al. Mental health professionals' perceptions on patients control of data sharing. Health Informatics J 2020 Sep;26(3):2011-2029. [doi: 10.1177/1460458219893845]
29. Kim J, Im E, Kim H. From intention to action: the factors affecting health data sharing intention and action. Int J Med Inform 2023 Jul;175:105071. [doi: 10.1016/j.ijmedinf.2023.105071] [Medline: 37099875]
30. Seltzer E, Goldshear J, Guntuku SC, et al. Patients' willingness to share digital health and non-health data for research: a cross-sectional study. BMC Med Inform Decis Mak 2019 Aug 8;19(1):157. [doi: 10.1186/s12911-019-0886-9] [Medline: 31395102]
31. Kim J, Kim H, Bell E, et al. Patient perspectives about decisions to share medical data and biospecimens for research. JAMA Netw Open 2019 Aug 2;2(8):e199550. [doi: 10.1001/jamanetworkopen.2019.9550] [Medline: 31433479]
32. Mello MM, Lieou V, Goodman SN. Clinical trial participants' views of the risks and benefits of data sharing. N Engl J Med 2018 Jun 7;378(23):2202-2211. [doi: 10.1056/NEJMsa1713258] [Medline: 29874542]
33. Kulynych J, Greely HT. Clinical genomics, big data, and electronic medical records: reconciling patient rights with research when privacy and science collide. J Law Biosci 2017 Apr;4(1):94-132. [doi: 10.1093/jlb/lsw061] [Medline: 28852559]
34. Mikk KA, Sleeper HA, Topol EJ. The pathway to patient data ownership and better health. JAMA 2017 Oct 17;318(15):1433-1434. [doi: 10.1001/jama.2017.12145] [Medline: 28973063]
35. Bietz MJ, Bloss CS, Calvert S, et al. Opportunities and challenges in the use of personal health data for health research. J Am Med Inform Assoc 2016 Apr;23(e1):e42-e48. [doi: 10.1093/jamia/ocv118] [Medline: 26335984]
36. Kruse CS, Goswamy R, Raval YJ, Marawi S. Challenges and opportunities of big data in health care: a systematic review. JMIR Med Inform 2016 Nov 21;4(4):e38. [doi: 10.2196/medinform.5359] [Medline: 27872036]
37. Shachar C, Cadario R, Cohen IG, Morewedge CK. HIPAA is a misunderstood and inadequate tool for protecting medical data. Nat Med 2023 Aug;29(8):1900-1902. [doi: 10.1038/s41591-023-02355-y] [Medline: 37237047]
38. Hunter P. The big health data sale: as the trade of personal health and medical data expands, it becomes necessary to improve legal frameworks for protecting patient anonymity, handling consent and ensuring the quality of data. EMBO Rep 2016 Aug;17(8):1103-1105. [doi: 10.15252/embr.201642917] [Medline: 27402546]
39. Kish LJ, Topol EJ. Unpatients—why patients should own their medical data. Nat Biotechnol 2015 Sep;33(9):921-924. [doi: 10.1038/nbt.3340] [Medline: 26348958]
40. Ozok AA, Wu H, Gurses AP. Exploring patients' use intention of personal health record systems: implications for design. Int J Hum-Comput Interact 2017 Apr 3;33(4):265-279. [doi: 10.1080/10447318.2016.1277637]
41. Esmaeilzadeh P. Healthcare consumers' opt-in intentions to Health Information Exchanges (HIEs): an empirical study. Comput Human Behav 2018 Jul;84:114-129. [doi: 10.1016/j.chb.2018.02.029]
42. Karway G, Ivanova J, Kaing T, et al. My Data Choices: pilot evaluation of patient-controlled medical record sharing technology. Health Informatics J 2022 Oct;28(4):14604582221143893. [doi: 10.1177/14604582221143893]

XSL•FO
RenderX

43. Sanderson SC, Brothers KB, Mercaldo ND, et al. Public attitudes toward consent and data sharing in biobank research: a large multi-site experimental survey in the US. Am J Hum Genet 2017 Mar 2;100(3):414-427. [doi: 10.1016/j.ajhg.2017.01.021] [Medline: 28190457]
44. Thaler R. Mental accounting and consumer choice. Mktg Sci 1985 Aug;4(3):199-214. [doi: 10.1287/mksc.4.3.199]
45. Tversky A, Kahneman D. The framing of decisions and the psychology of choice. Science 1981 Jan 30;211(4481):453-458. [doi: 10.1126/science.7455683] [Medline: 7455683]
46. Thaler RH. Mental accounting and consumer choice. Mark Sci 2008 Jan;27(1):15-25. [doi: 10.1287/mksc.1070.0330]
47. Skwara F. Effects of mental accounting on purchase decision processes: a systematic review and research agenda. J Consum Behav 2023 Sep;22(5):1265-1281. [doi: 10.1002/cb.2193]
48. Reinholtz N, Bartels DM, Parker JR. On the mental accounting of restricted-use funds: how gift cards change what people purchase. J Consum Res 2015;42(4):596-614. [doi: 10.1093/jcr/ucv045]
49. Lee CY, Morewedge CK. Mental accounting of product returns. J Consum Psychol 2023 Jul;33(3):583-590. [doi: 10.1002/jcpy.1354]
50. Hossain MT. How cognitive style influences the mental accounting system: role of analytic versus holistic thinking. J Consum Res 2018;45(3):615-632. [doi: 10.1093/jcr/ucy020]
51. Belk RW. Possessions and the extended self. J Consum Res 1988 Sep 1;15(2):139-168. [doi: 10.1086/209154]
52. Pierce JL, Rubenfeld SA, Morgan S. Employee ownership: a conceptual model of process and effects. Acad Manag Rev 1991 Jan;16(1):121-144. [doi: 10.5465/amr.1991.4279000]
53. Bélanger F, James TL. A theory of multilevel information privacy management for the digital era. Inf Syst Res 2020 Jun;31(2):510-536. [doi: 10.1287/isre.2019.0900]
54. Haux R, Ammenwerth E, Herzog W, Knaup P. Health care in the information society. A prognosis for the year 2013. Int J Med Inform 2002 Nov 20;66(1-3):3-21. [doi: 10.1016/s1386-5056(02)00030-8] [Medline: 12453552]
55. Loewenstein G, Prelec D. Anomalies in intertemporal choice: evidence and an interpretation. Q J Econ 1992 May 1;107(2):573-597. [doi: 10.2307/2118482]
56. Prelec D, Loewenstein G. Decision making over time and under uncertainty: a common approach. Manage Sci 1991 Jul;37(7):770-786. [doi: 10.1287/mnsc.37.7.770]
57. Snider SE, DeHart WB, Epstein LH, Bickel WK. Does delay discounting predict maladaptive health and financial behaviors in smokers? Health Psychol 2019 Jan;38(1):21-28. [doi: 10.1037/hea0000695] [Medline: 30474996]
58. Tian M, Tao R, Zheng Y, et al. Internet gaming disorder in adolescents is linked to delay discounting but not probability discounting. Comput Human Behav 2018 Mar;80:59-66. [doi: 10.1016/j.chb.2017.10.018]
59. Rung JM, Madden GJ. Demand characteristics in episodic future thinking: delay discounting and healthy eating. Exp Clin Psychopharmacol 2018 Feb;26(1):77-84. [doi: 10.1037/pha0000171] [Medline: 29323506]
60. Schomakers EM, Lidynia C, Müllmann D, Ziefle M. Internet users' perceptions of information sensitivity—insights from Germany. Int J Inf Manage 2019 Jun;46:142-150. [doi: 10.1016/j.ijinfomgt.2018.11.018]
61. Smith HJ, Dinev T, Xu H. Information privacy research: an interdisciplinary review. MIS Q 2011;35(4):989. [doi: 10.2307/41409970]

Abbreviations

HIE: health information exchange
HIPAA: Health Insurance Portability and Accountability Act
OR: odds ratio
PCD: patient-centered design
PGD: patient-generated data

Edited by M Focsa; submitted 12.09.24; peer-reviewed by L Bonomi, W Lu; revised version received 30.11.24; accepted 05.12.24; published 22.01.25.

Please cite as:
Wei D, Gao P, Zhai Y
The Impact of Data Control and Delayed Discounting on the Public's Willingness to Share Different Types of Health Care Data: Empirical Study
JMIR Med Inform 2025;13:e66444
URL: https://medinform.jmir.org/2025/1/e66444
doi:10.2196/66444

XSL•FO
RenderX

© Dongle Wei, Pan Gao, Yunkai Zhai. Originally published in JMIR Medical Informatics (https://medinform.jmir.org), 22.1.2025. This is an open-access article distributed under the terms of the Creative Commons Attribution License (https://creativecommons.org/licenses/by/4.0/), which permits unrestricted use, distribution, and reproduction in any medium, provided the original work, first published in JMIR Medical Informatics, is properly cited. The complete bibliographic information, a link to the original publication on https://medinform.jmir.org/, as well as this copyright and license information must be included.

XSL•FO
RenderX

Original Paper

Influences on Emergency Clinician Use of Health Information Exchange: Interview Study

Brian E Dixon[1,2], MPA, PhD; Umesh Ghimire[1], MS, MPH; Benjamin Richter[3,4], MD; Corinne Bowditch[2], BS; Saurabh Rahurkar[1,5], DDS, DrPH; John T Finnell[3], MD, MS; Joshua R Vest[1,2], MPH, PhD

[1]Department of Health Policy & Management, Fairbanks School of Public Health, Indiana University Indianapolis, Indianapolis, IN, United States

[2]Center for Biomedical Informatics, Regenstrief Institute, Indianapolis, IN, United States

[3]School of Medicine, Indiana University, Indianapolis, IN, United States

[4]Department of Internal Medicine, Thomas Jefferson University, Philadelphia, PA, United States

[5]Department of Biomedical Informatics, College of Medicine, The Ohio State University, Columbus, United States

Corresponding Author:
Brian E Dixon, MPA, PhD
Department of Health Policy & Management
Fairbanks School of Public Health
Indiana University Indianapolis
1050 Wishard Blvd
Indianapolis, IN, 46202
United States
Phone: 1 3172783072
Email: bedixon@regenstrief.org

Abstract

Background: Health information exchange (HIE) supports clinical decision-making in emergency medicine settings. Despite evidence and policies that encourage the adoption of HIE, use by clinicians is limited. Moreover, few studies examine HIE use years after adoption by hospitals or clinics.

Objective: This study aims to examine the perceptions and use of a mature, operational HIE system by emergency department clinicians years after its implementation.

Methods: We interviewed 21 clinicians in various roles (eg, attending physician and nurse practitioner) across multiple health systems that participate in a statewide HIE network. We asked questions about their use of the HIE system and the factors that facilitate or inhibit use. Analysis of interview transcripts was guided by a theoretical framework derived from information systems theories describing individual perception of, and use behavior toward, HIE systems.

Results: A total of 26 factors across 6 domains were identified by respondents. All respondents recognized the value of HIE for medical decision-making in the emergency department, and access to information via the HIE system was preferred over traditional methods of telephoning other facilities or waiting for faxed records. Ease of use, particularly single sign-on functionality, was recognized as a key facilitator of routine use, enabling clinicians to access a patient's HIE record with a single click from within their electronic health record system. Access to integrated data and advanced search features supported clinical decision-making. Limited training and poor system usability were identified as barriers to use.

Conclusions: Achieving widespread adoption and use of HIE systems globally will require a focused effort to address multiple individual perception and behavioral factors. Researchers, leaders of HIE organizations, and policymakers alike should leverage these factors to achieve the goals of HIE and interoperability.

(JMIR Med Inform 2025;13:e75865) doi:10.2196/75865

KEYWORDS

health information exchange; medical informatics applications; qualitative research; information systems; information seeking; information needs; viewpoints on and experiences with digital technologies in health; emergency medicine

XSL•FO
RenderX

Introduction

Background

The adoption and use of health information exchange (HIE)—the electronic transfer of patient-level data or information across diverse and often competing health-related organizations [1]—offers a number of benefits, including reductions in inpatient readmissions, reduced duplicate laboratory and imaging studies, and decreased inpatient length of stay [2]. Multiple studies have demonstrated benefits especially to emergency department (ED) care [3-8]. Moreover, HIE facilitates intelligent communication, including clinical decision support [9], remote monitoring [2], and automated data integration [10]. As HIE is linked to better outcomes and efficiencies in care delivery processes, US health policies, including the Health Information Technology for Economic and Clinical Health Act [11] and the 21st Century Cures Act [12], have systematically encouraged adoption and use across myriad clinical settings [13].

As a result of multiple federal- and state-level policies, HIE availability—as well as the types of HIE systems available (eg, community based and vendor based)—has increased in many communities across the United States [13,14]. In 2021, according to the Office of the National Coordinator for Health Information Technology (ONC), 61% of hospitals reported using an HIE system to electronically query or find patient health information from external sources, suggesting that most clinicians use HIE routinely in care delivery [15]. Moreover, the ONC reported that in 2021, four out of 10 hospitals participated in more than one type of HIE, and most of these hospitals reported exchanging data with a community-based HIE network [15].

However, despite clear policy incentives, robust literature demonstrating impact, increasing organizational adoption, and evidence of more widespread availability, the actual state of individual HIE use in clinical practice seems to be limited; for example, using log data from a community-based HIE in operation for >15 years, we observed low rates of use among health care providers across inpatient, emergency, and outpatient settings despite overall increased adoption and use over time [16]. Other studies and reviews have reported relatively low use by clinicians [17]. As a further complication, much of the existing evidence on clinician use and perceptions was generated when HIE was a novel intervention or in the period shortly after implementation. These studies documented multiple barriers to implementation and use, including HIE system conflicts with workflow as well as usability challenges [18]. Clinicians may also be frustrated by the lack of information available (eg, in terms of breadth and depth) from smaller-scale exchange efforts [19]. While these earlier studies are critical, HIE has since evolved, electronic health record (EHR) systems and workflows have continued to change, and modern HIE is no longer an innovation but rather a routine capability.

A better understanding of actual use would support system improvements and identify additional, and potentially valuable, use cases. This is particularly true in the ED setting, where clinicians may not have a longitudinal relationship with patients, and access to prior information may be difficult [20]. Prior research involving ED clinicians before the implementation of technologies for accessing past medical history found that these clinicians desired better access to prior medical information [19,20]. Despite the value of HIE in the ED, reviews suggest that the ED is becoming a less-studied setting [21]. This study sought to elucidate ED users' perceptions and use of a mature and robust HIE system.

Purpose

As knowledge of HIE use by health care providers is limited, we conducted a qualitative study of ED clinicians to capture their perceptions and use of an operational HIE system many years after its introduction in the community. Our goal was to better understand when HIE is useful and the context of HIE use in ED care. We hypothesized that clinicians would perceive HIE to be useful and effective; yet, HIE would not be used for every patient, given the availability of information from a broad array of sources, including the patient, family, and intraorganizational EHR data.

Methods

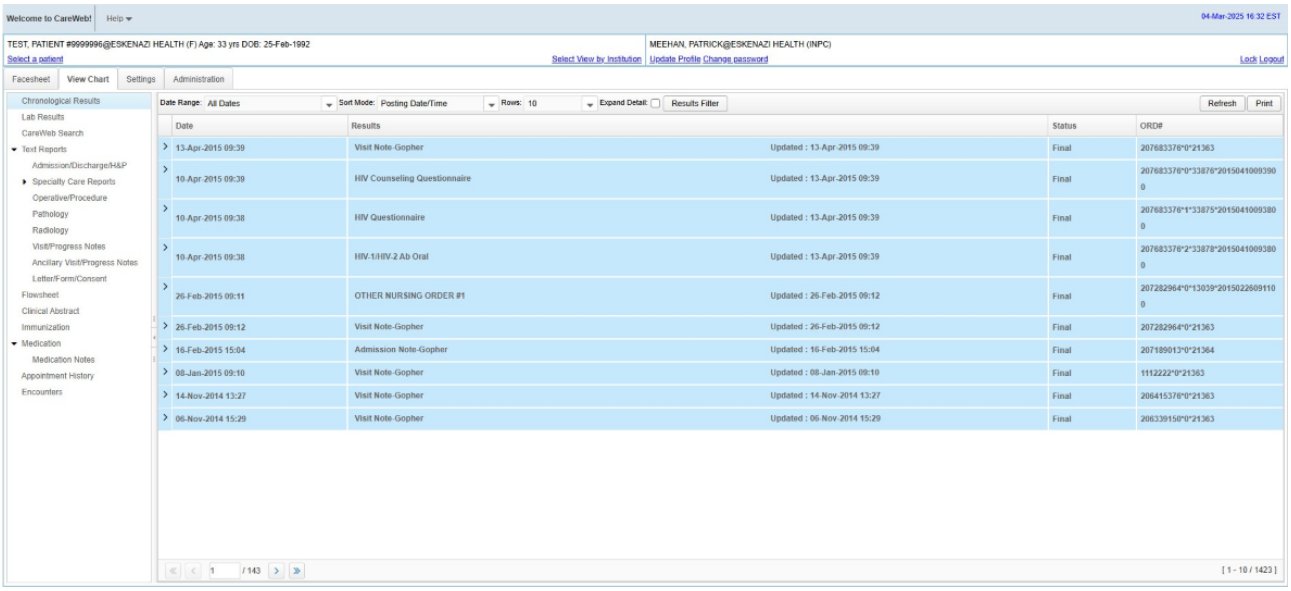
Study Design and Setting

This study used qualitative methods to explore the antecedents of HIE use factors that act as facilitators or barriers to its adoption within ED settings. We recruited ED clinicians with access to the Indiana Network for Patient Care (INPC), a community-based HIE network operational since the late 1990s [22]. The INPC is managed by the Indiana Health Information Exchange, which has systematically expanded the service area and capabilities of the INPC, integrating longitudinal data from 38 health systems that encompass >100 hospitals with EDs [23,24]. The INPC is routinely used as a platform for research [25], including innovations in HIE [26-29] and interoperability [30,31].

Clinicians with access to the INPC interact with patient medical records via a web-based intelligent communication system known as CareWeb. Originally, CareWeb was developed using Java. The current version was redesigned in 2009 using ZK, an open-source Ajax web application framework written in Java for mobile and web apps. Users are managed by the Indiana Health Information Exchange, and updated user lists are provided regularly by each INPC organization. As depicted in Figure 1, the CareWeb system provides access to patients' integrated, longitudinal medical records. By default, recent notes and results are displayed in reverse chronological order. The left-hand menu provides access to specific types of information (eg, immunizations, radiology, and discharge summaries) as well as CareWeb Search, an intelligent search that enables clinicians to query patients' medical records. In the past, clinicians logged into CareWeb using an internet browser—outside of their EHR system (Multimedia Appendix 1). Currently, clinicians access CareWeb primarily via a button in their EHR system that launches a web browser and opens the same patient record that they have open in the EHR.

XSL•FO
RenderX

Figure 1. Screenshot of the CareWeb application that clinicians use to access patient medical records available in the Indiana Network for Patient Care.



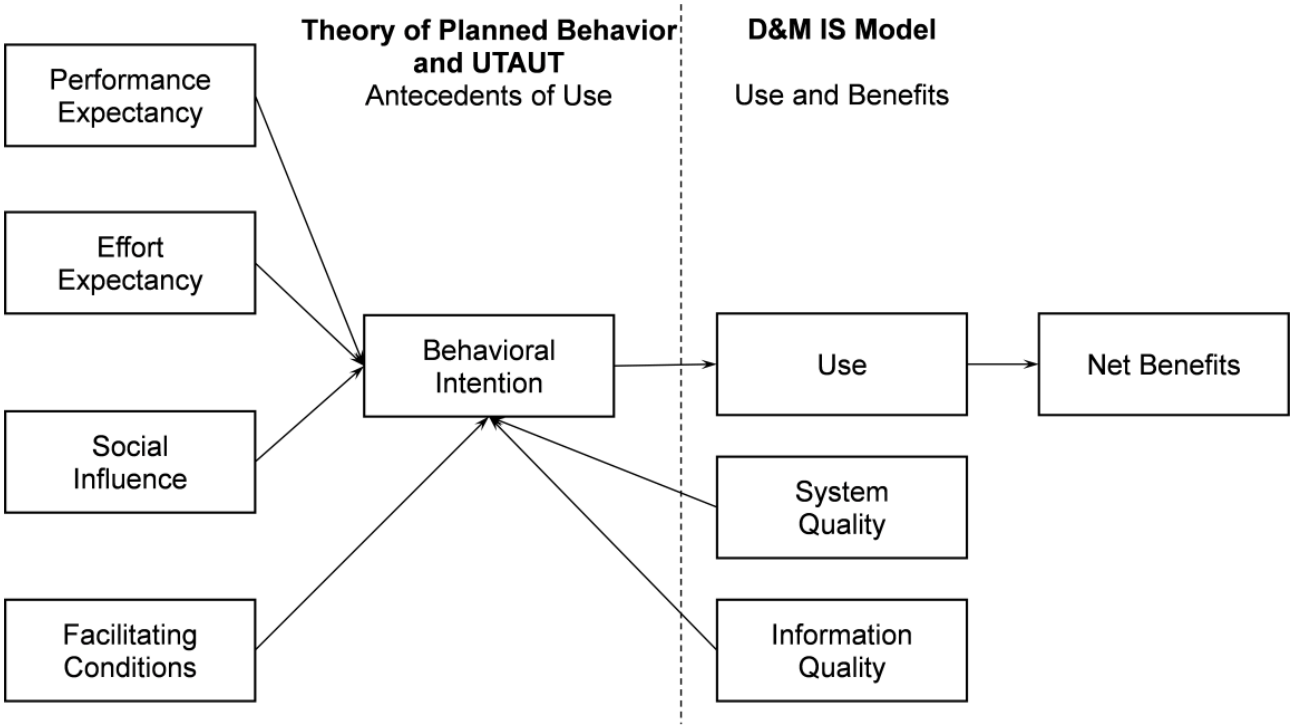
Our target participants were ED clinicians practicing in central Indiana, a region with the longest-established use of the INPC that includes urban, suburban, and rural communities. We purposely sampled clinicians with a goal of 30 users, stratified by clinical role (eg, physician, nurse practitioner or physician assistant, and registered nurse). The target sample was further stratified by level of HIE use, observed from INPC log files that measure the number of log-ins to CareWeb. We purposely sought to include low users (eg, approximately 1-2 log-ins per mo or up to 26 log-ins per y), medium users (eg, approximately 1 log-in per wk or 27-51 log-ins per y), and high users (eg, ≥52 log-ins per y, representing an average of ≥1 log-in per wk). We recruited clinicians across these strata until thematic saturation was achieved after 21 interviews [32,33].

Theoretical Framework

Our research is grounded in a novel integration of 3 conceptual frameworks from the information sciences (Figure 2). These frameworks are compatible and complementary, given that each theory centers on the concept of information systems (IS) use and its antecedents. The combined model allows for an examination of the factors that influence behavioral intention (BI) and use, which in turn influence net benefits. In the context of HIE use within ED settings, which manage a substantial proportion of clinical conditions, the integrated theoretical model facilitates a comprehensive exploration of the factors influencing ED clinicians' intentions to use HIE as part of patient care. This exploration extends to understanding how these factors influence decision-making processes regarding individual care delivery and impact patient care outcomes. We hypothesized that a variety of factors, including system quality (eg, ease of use) and information quality (eg, data available in the INPC for patient care), would influence clinicians' engagement with the HIE platform.

XSL•FO
RenderX

Figure 2. Theoretical framework used to guide the research. The framework integrates concepts from the theory of planned behavior, the unified theory of acceptance and use of technology (UTAUT), and the DeLone and McLean information systems (D&M IS) success model.



The theory of planned behavior posits that human behavior follows BI, which is influenced by a number of factors, including subjective norms [34]. This theory has been widely used in many fields, including health care, to explain behaviors as well as the factors that influence behaviors, such as vaccination uptake [35] or the adoption of EHR systems [36,37].

The unified theory of acceptance and use of technology (UTAUT) is a model that enables the measurement and study of the acceptance and use of technology and has been used to examine the adoption and use of EHR systems [38-40]. The UTAUT identifies 3 primary constructs that influence BI: performance expectancy, effort expectancy, and social influence [38,41]. Performance expectancy refers to the degree to which an individual believes that using the system will improve their performance. Effort expectancy denotes the perceived ease of using the system. Social influence refers to the degree to which an individual perceives that important others (eg, a supervisor or an influential colleague) believe that they should use the new system. The UTAUT posits an additional construct—facilitating conditions—defined as the individual's belief that sufficient organizational and technical infrastructure is available to support the use of the system.

The DeLone and McLean IS success model is a multidimensional, interrelated framework for conceptualizing IS success [42,43]. The model involves 3 distinct but interrelated levels of success: technical, referring to system quality (eg, does the system perform as intended?); semantic, referring to information quality (eg, does the information convey the intended meaning?); and effectiveness, referring to the impact of the IS on the receiver (eg, user behavior, individual impact, and organizational impact). Success is defined in terms of net benefits to the user or the organization. The choice of "net benefits" is purposeful because there are always costs to implementing and using an IS. Furthermore, the model allows for an examination of the complex interrelationships between use and impact (eg, system use influences the products that in turn influence the individual user, which may in turn impact organizational outputs).

Data Collection

Semistructured interviews with ED providers were conducted from February 2019 through January 2020 via Zoom (Zoom Video Communications, Inc), Skype (Microsoft Corporation), or telephone. Several respondents preferred to participate from home on their day off. Each interview lasted approximately 45 minutes.

During each interview, one researcher facilitated discussion while another took detailed notes. The questions aimed to elicit clinicians' experiences of seeking information on patients from outside facilities; awareness and use of the INPC during ED encounters; perceptions of INPC tools, including the interface; and use of any other HIE tools, such as Care Everywhere. Probing questions were asked to dig deeper into clinicians' experiences with HIE, particularly when responses were vague or involved specific use cases. All interviews were audio recorded and transcribed verbatim. The interview guide is presented in Multimedia Appendix 2.

Data Analysis

We analyzed the interviews using a deductive approach. The initial codebook was developed by BED based on the theoretical framework and iteratively refined with input from the broader study team, including CB. Two coders (BR and MF) then analyzed the transcripts independently, meeting weekly throughout the process to review each other's coding, discuss and refine codes and subcodes, and draw codes into broader themes. Any disagreements between the coders were resolved

XSL•FO
RenderX

through discussion with BED. UG later independently reviewed and summarized these codes to ensure accuracy. Data were coded and analyzed using NVivo 12 (Lumivero) [44].

Ethical Considerations

This study was approved by the institutional review board of Indiana University (protocol number 1710653338). All interviews were anonymized to protect participant confidentiality. Participants received a $50 gift card as remuneration.

Results

Participant Characteristics

We interviewed 21 ED clinicians drawn from 7 distinct health systems (Table 1). Of these 21 clinicians, 11 (52%) were physicians, 5 (24%) were registered nurses, 3 (14%) were nurse practitioners, and 2 (10%) were physician assistants. Most of the respondents (14/21, 67%) reported being in practice for 5 years, while 7 (33%) of the 21 respondents reported being in practice for ≤2 years (average 11, SD 8 y; range: 1-23 y). Nearly one-third of the respondents (6/21, 29%) reported dedicating between 80% and 100% of their work time to clinical activities, while others balanced patient care and administrative roles such as division chief, medical director, or manager. Participants were drawn from both large health systems (11/21, 52%) and community hospitals (10/21, 48%).

Table 1. Participants by clinical role and site (N=21).

Participant role	Large health system (n=11), n (%)	Community hospital (n=10), n (%)
Physician	6 (55)	5 (50)
Registered nurse	1 (9)	4 (40)
Nurse practitioner	2 (18)	1 (10)
Physician assistant	2 (18)	0 (0)

Factors That Influence HIE Use

Overview

As summarized in Table 2, respondents identified an array of factors that influence their HIE use. A more complete synthesis of responses and example quotes from respondents is presented in Multimedia Appendix 1. In this subsection, we summarize some of the major themes from clinicians relevant to their use of HIE.

XSL•FO
RenderX

Table 2. Key factors, summarized by theoretical framework domain, that influence the use of health information exchange (HIE) by clinicians in emergency department (ED) settings.

Domains and factors	Illustrative quote
Performance expectancy	
Changes to decision-making	"I was able to pull up their imaging studies from a week ago which helped guide my decision." [R7; y in practice: 10]
Continuity of care	"The ability to see that they were just at the hospital twelve hours ago...keeps us from doing unnecessary tests." [R16; y in practice: 21]
Frequency of use	"I probably use it every day for a few of my patients to confirm what happened at other hospitals." [R5; y in practice: 15]
Information retrieval in workflow	"Right after the patient left, I went back to CareWeb to double-check and then it changed the approach we were taking." [R4; y in practice: 23]
Patient characterization	"By pulling in all their previous admissions, I had a clearer picture of their frequent ED visits and issues." [R9; y in practice: 7]
Efficient retrieval	"It takes a few minutes to get through all the records, but it's worth it when you're avoiding duplication." [R6; y in practice: 11]
Motivation for information retrieval	"Patients come from all over, and to give them the best care, we need to know what's been done at other hospitals." [R10; y in practice: 5]
Effort expectancy	
Desired features for ease of use	"I just think if I could make it so that I can stay logged in longer. So not constantly having to log in and log out." [R2; y in practice: 14]
Ease of use	"CareWeb is fairly self-explanatory, especially for information gathering rather than charting or placing orders." [R1; y in practice: 21]
Effort to retrieve information	"It took us a few minutes just to kind of read through, and they were all fairly much the same story." [R1; y in practice: 23]
Features that facilitate ease of use	"I like Care[Web]. I can often go into documents and copy and paste data directly into my notes." [R2; y in practice: 14]
Information display	"I think it may be organizing it differently...you can primarily organize by dates or something with tabs for labs, et cetera." [R3; y in practice: 1]
Speed of information retrieval	"It's fast compared to a lot of our systems." [R21; y in practice: 22]
Social influence	
Discussion of use	"I first learned about using CareWeb when my colleague mentioned it as a helpful tool during our shift." [R12; y in practice: 2]
Expectation of use	"It's pretty much expected now that we check the HIE before making any big decisions." [R14; y in practice: 4]
Resident use	"We always ask the residents to check CareWeb as part of their evaluation process." [R11; y in practice: 13]
Facilitating conditions	
Organizational support	"[A] patient came in saying they were just seen and had a test done...I asked the provider if I should contact the facility." [R17; y in practice: 2]
Team support	"Whenever someone has trouble accessing information, we work together to figure it out." [R19; y in practice: 1]
Training	"[A] colleague mentioned it as being useful. So that's kind of how I found out about it just working with coworkers." [R4; y in practice: 23]
Technical support	"We always reach out to IT if the system is slow or down, and they respond quickly." [R13; y in practice: 9]
Information quality	
Desired information	"I need to make sure that they haven't had seven CT scans already in 2020." [R2; y in practice: 14]
Missing information	"I've had this before where a patient was recently discharged but the actual discharge summary is not in the system yet." [R8; y in practice: 13]
Missing institutions	"The VA has no records online that I know of anywhere, so you always have to call and get records from there." [R1; y in practice: 21]

XSL•FO
RenderX

Domains and factors	Illustrative quote
Usability of information	"As long as we can get to it, that's super helpful." [R17; y in practice: 2]
System quality	
Network reliability	"[H]ospitals created that VPN connection, so I don't have a problem with that anymore." [R8; y in practice: 13]
System reliability	"If that link works...it's so much more useful and quicker." [R1; y in practice: 23]

Performance Expectancy

All respondents indicated that they knew about CareWeb and used it at least sometimes to look up information. Respondents reported that, overall, CareWeb enhances the retrieval of information for clinical decision-making. First, the HIE system provided access within "five to ten minutes" (R15; y in practice: 13), which was an improvement over waiting "fifteen to twenty minutes" (R19; y in practice: 1) or "up to an hour" (R13; y in practice: 4) to retrieve information from outside facilities. Moreover, one physician stated as follows:

> *A lot of times patients seem to fall apart in the evenings or at night when there's no office staff, and the on-call person doesn't want to or doesn't have the capabilities to fax or email me the patient information.* [R12; y in practice: 2]

Second, most respondents reported that accessing CareWeb fits well into clinical workflow. Respondents generally accessed CareWeb either before they went into the examination room to see the patient or right after examining the patient to "double-check" information they obtained from their conversation with the patient.

Clinicians further viewed accessing the HIE system as critical to making good clinical decisions, with most respondents reporting that information from CareWeb had changed a clinical decision. Providers noted as follows:

> *Looking at that information can change what needs to be done in the immediate emergent future.* [R2; y in practice: 14]

> *The ability to see that they were just at the hospital twelve hours ago across town and got whatever treatment plan was there...keeps us from doing unnecessary tests.* [R16; y in practice: 21]

Reduction in duplicate procedures and tests, especially imaging, was frequently cited by clinicians as a major reason for looking up information in the HIE system. Some also reported experiences where information in the HIE system likely saved their patient's life:

> *Had I not known how big it [tumor] had been before, he might have been discharged, and that could have had a poor outcome for him.* [R12; y in practice: 2]

Respondents also reported instances where the HIE system is unlikely to impact their performance as clinicians and therefore cases in which they do not feel that they need to use it. First, for patients whose care is immediate in nature, where past history might not make a difference in the care provided, some respondents indicated that using the HIE system would not be fruitful. Second, some clinicians were less likely to use it if patients reported that their prior care was delivered in the same health system. In these cases, health care providers used only the EHR to look up prior medical records.

Effort Expectancy

Respondents identified several effort expectancy factors that influence their use of HIE. With respect to factors that encouraged use, respondents highlighted ease of use, speed of access, comprehensiveness of data, SSO integration with the EHR, search capabilities, and features that allow information to be copied and pasted into their local notes. Factors that discouraged use included feeling overwhelmed by the volume of data in the HIE system and the system frequently logging out users.

Several aspects of the HIE system facilitated ease of use and supported clinicians' effort. Several respondents reported that the system is intuitive to use or "fairly self-explanatory" and requires minimal training for basic functions such as accessing patient information, which encourages them to use it during clinical encounters. A frequently cited feature was SSO, which allows clinicians to click a single button in their home EHR to easily bring up the same patient's records in CareWeb. Multiple respondents mentioned SSO as a key effort expectancy factor that encouraged HIE use. Clinicians who mentioned SSO functionality were generally those who had practiced for several years and compared accessing the HIE currently to a previous time when accessing it required a separate username and password:

> *Being able to click the button in Cerner that opens and goes directly to the patient's chart without me having to remember and enter another password...has dramatically increased how often I use CareWeb compared to the way it was ten years ago.* [R15; y in practice: 13]

Respondents who did not report SSO as a feature were practicing in smaller community hospitals that had not yet implemented this feature, and these respondents often suggested that a more efficient log-in process would encourage their use of the HIE system.

Similarly, a few respondents reported that the search capability, which enables clinicians to conduct a Google-like search of the records in the HIE system, was a major enabling factor for wading through the comprehensive data available:

> *If you want to look up someone's renal function or a CBC, you can just type in CBC in the box, and it'll pull up the most recent ones. These little things are*

XSL•FO
RenderX

> *helpful to the clinician on the front lines.* [R8; y in practice: 13]

Respondents who did not mention the search feature reported that they did not know about it and that it would be a useful, desired feature:

> *Especially the lab results, it can get tedious clicking through [multiple pages].* [R19; y in practice: 1]

Finally, some clinicians reported that easily copying and pasting information from the HIE system into their notes within their EHR system was an important factor encouraging their use of CareWeb:

> *I can often go into documents and see if they've had a CT scan or MRI, then copy and paste that directly into my note. So, I find it the easiest to use.* [R2; y in practice: 14]

A few clinicians mentioned challenges with the volume and organization of data within the HIE system. While the respondents noted that comprehensive data were available to them, they felt overwhelmed by the volume of data and the fact that, by default, it is organized in reverse chronological order. These clinicians expressed a desire for tools that allow users to better sort and organize or filter the data to enable streamlined views that facilitate clinical decision-making. Similarly, some clinicians reported getting logged out of the HIE system when interrupted or during an encounter:

> *I just think if I could make it so that I can stay logged in longer. So not constantly having to log in and log out.* [R2; y in practice: 14]

Clinicians suggested that longer log-out times or ways to prevent involuntary log out would be an improvement. Such features would encourage clinicians' use of the HIE system.

Social Influence

Respondents discussed several social influences on HIE use. Many respondents credited colleagues with introducing them to CareWeb:

> *A colleague mentioned it as being useful, so that's how I found out about it.* [R3; y in practice: 1]

Most respondents who trained in Indiana were introduced to it during residency. A clinician who supervises trainees stated as follows:

> *I often have to prompt my learners to look in CareWeb.* [R18; y in practice: 6]

Other clinicians made the following observations:

> *The residents encourage us to use CareWeb more than we encourage them.* [R19; y in practice: 1]

> *We all use it. It's extremely helpful.* [R1; y in practice: 21]

All these responses suggest that for most clinicians, at least those in training hospitals, there is broad use and a social contract to use it regularly.

Social influences were less clear in community hospital settings. A clinician practicing in a community hospital stated as follows:

> *I think some of [my colleagues] are still requesting records from the coordinator...not knowing what that kind of information exchange is.* [R7; y in practice: 10]

Therefore, social influence is not ubiquitous across Indiana despite the fact that the HIE system has existed for >25 years.

Facilitating Conditions

Health care providers discussed several organizational and technical factors that acted either as facilitators or barriers to use. Some respondents worked in organizations that actively promoted HIE use through experienced colleagues who encouraged their peers to use the system. A nurse practitioner stated as follows:

> *[A] patient came in saying they were just seen and had a test done...I asked the provider if I should contact the facility for records, and he showed me the CareWeb log-in.* [R17; y in practice: 2]

However, few respondents indicated that their organization embraced the HIE system. Rather, their colleagues showed them how to use it or encouraged their use:

> *It's never been encouraged, and I've worked at three different hospitals here in [city].* [R20; y in practice: 21]

> *[I] don't know if it's a cost issue or utilization, um, but I think not having an auto enrollment, um, especially for providers is a disadvantage just because it's not available.* [R17; y in practice: 2]

Therefore, organizational processes may not be set up to encourage HIE use.

A lack of organizational support for HIE was also evidenced in comments from multiple respondents who indicated that they learned how to access and use the HIE system from colleagues or on their own:

> *I just sort of started using it and figured it out myself.* [R11; y in practice: 13]

Another respondent stated as follows:

> *We don't really include it in our formal onboarding or training of physicians.* [R1: y in practice: 21]

Moreover, none of the respondents indicated that the HIE system or anyone from the clinical organization provided updated, refresher training on the system:

> *There was never like, um, information session on how it can be used in a different, different ways that you can navigate through it that might be more beneficial.* [R3; y in practice: 1]

However, respondents did suggest that they perceived sufficient technical support to use the system when things did not seem to work:

> *I don't feel as frustrated now because I know I can rely on 24/7 technical support—there's always someone available.* [R14; y in practice: 4]

XSL•FO
RenderX

Other respondents similarly stated that they could contact the HIE organization directly or their hospital IT team and receive technical assistance with access or use.

Information Quality

All respondents emphasized the critical importance of information quality in the ED. The dimensions of quality mentioned often included completeness and information timeliness. The respondents expressed a strong desire for access to detailed past medical records, specifically laboratory results, imaging reports, encounter notes, and discharge summaries:

> *I need to make sure that they haven't had seven CT scans already in 2020.* [R2; y in practice: 14]

Many respondents noted that the availability of timely information, such as recent diagnostic tests, was critical for swift decision-making in the ED.

Although most respondents said that the INPC generally possessed needed information, they also identified gaps. Some respondents reported incomplete access to records from specialized care settings, such as psychiatric facilities or smaller independent health care providers:

> *Most patients get cardiology care at XYZ, and I almost never find an EKG from them.* [R11; y in practice: 13]

A frequently mentioned institution was the Veterans Health Administration, from which clinicians strongly desired information on encounters but perceived it as obtainable only after first making a telephone call to request details by fax. In addition, respondents highlighted difficulty in accessing raw imaging data, with some relying solely on reports due to the time constraints inherent in ED workflows.

System Quality

Nearly all respondents indicated that the INPC was reliable, especially when accessed through the virtual private network (VPN) connection that most were using for their EHR system. Few clinicians reported technical challenges, apart from a provider who had difficulty with their VPN connection from home. An experienced provider who has accessed the INPC in multiple ways over the years noted that VPNs and other modern networking solutions have reduced technical barriers to accessing the INPC, thus motivating increased HIE use. System upgrades and downtime, when they occurred, were noted by clinicians as challenging. However, most respondents noted that these events occurred infrequently and were no more bothersome than when their EHR systems experienced downtime.

Summary of Findings

Most ED clinicians had practiced in Indiana for >10 years (11/21, 52%) and reported being frequent users of the Indiana HIE, although several were categorized as low users based on system log-in events (eg, approximately 1-2 log-ins per mo). Knowledge of HIE was generally acquired during residency or through informal peer support on the job. Some clinicians received information about the CareWeb system when joining Indiana-based health systems from out of state. Clinicians unanimously emphasized the critical role of CareWeb in accessing patient information for informed decision-making and improving continuity of care.

Most clinicians recognized the utility of the HIE system while identifying areas for improvement, particularly in accessing the most relevant subset of information for clinical decision-making. HIE use was constrained by data availability, with most clinicians estimating its use for approximately 20% of their patient population. Ease of use, particularly the SSO functionality, was recognized as a key facilitator, allowing access with a single click from the EHR system directly into the patient's CareWeb record. Although clinicians noted the usability of CareWeb for retrieving data from multiple institutions where their patients received care, they identified gaps in institutional participation within the HIE network.

The clinicians reported that the system was reliable and fast, and they appreciated the availability of support for troubleshooting when needed. Nevertheless, many were unfamiliar with advanced features such as the intelligent search function, which could enhance efficiency by streamlining information retrieval compared to manually scrolling through multiple encounter records. Persistent gaps in training and limitations in system usability were identified as significant barriers to HIE use.

Discussion

Principal Findings

This study of ED clinicians working in various health systems with access to a mature, statewide intelligent communications system highlights the complex, interrelated, and multifaceted factors influencing HIE use. Although purposely sampled to include clinicians who rarely used the HIE system and those who use it regularly (based on log data), respondents generally reported using CareWeb regularly. The HIE system was overwhelmingly viewed favorably by the clinicians, who unanimously preferred accessing information from other hospitals via the system rather than relying on telephone calls or waiting for faxed records. Multiple effort, performance, social, and organizational factors encouraged HIE use. These included the level of integration with their EHR (eg, SSO and an "easy button"), access to comprehensive information that influenced decision-making, and peers who encouraged and demonstrated HIE use. Nevertheless, several clinicians reported multiple effort, performance, and organizational factors that discouraged use. These included information missing from specific sources, information overload, and lack of training. The findings have implications for the advancement and adoption of HIE networks, including policies to encourage HIE use and strategies to enhance HIE operations.

Importance of Research on HIE Use and Study Contributions

This study makes several important contributions to existing literature on HIE. First, the study used theoretical frameworks from the information sciences. A recent scoping review by Lum et al [17] identified gaps in HIE implementation studies and specifically encouraged researchers to "employ theoretical

XSL•FO
RenderX

frameworks." Second, most existing HIE literature focuses on organizational adoption of HIE systems and technologies (eg, whether a hospital reports having the capability to exchange information with outside hospitals [45,46]). Other studies have surveyed or interviewed clinicians before or just after HIE implementation [47,48], with virtually no research examining clinician perceptions years after implementation [19]. Moreover, few studies have assessed the level of use by clinicians, and while the annual American Hospital Association IT Survey asks organizations to report how "frequently do providers" use health information received electronically "from outside providers or sources," it is unclear how hospitals distinguish responses such as "often," "sometimes," or "rarely" [49]. In this study, respondents characterized their frequency of use, with most reporting regular use and estimating HIE use for approximately 20% of their patient population. Third, respondent comments provide valuable context to prior work that examined the benefits of HIE [2,50], underscoring that data available through HIE networks indeed influence clinical decision-making, have benefited patient outcomes, and are perceived as highly valuable to clinicians. In other words, HIE systems are critical components of intelligent communications in health care, as evidenced by respondents reporting that HIE information enhanced their diagnostic reasoning, improved continuity of care, and led to a reduction in duplicate procedures and tests, often influencing clinical decisions and potentially improving patient outcomes.

Implications for Advancing Adoption and Use of HIE

Interoperability and HIE remain key areas of focus for the Assistant Secretary of Technology and Policy and a global priority as specified in many nations' digital health strategies. Achieving greater adoption and use of HIE will require attention to the factors described in this study; for example, existing studies suggest that hospitals with strong adoption of HIE functionality report higher levels of HIE use [51,52]. Therefore, many states and nations will need to continue to focus on performance expectancy factors, improving clinician perceptions of the value of HIE [46,53], enabling clinicians to apply HIE knowledge to clinical decision-making, and making the right thing to do the easy thing to do [54]. Approaches to support performance expectancy include asking clinicians to share why they use HIE, conducting quantitative assessments of HIE benefits, and performing mixed methods studies of clinician use cases. One example is a statewide survey of clinicians in Virginia [55]. Addressing challenges, such as the usability of HIE systems [56], seamless log-in mechanisms [57], and other effort expectancy factors, will also be critical to securing routine adoption and use. Seamless integration with EHR systems, search functionalities, and ways to optimize interaction with comprehensive patient data are additional effort expectancy strategies implied by this study to support clinician use.

Social and organizational factors are also critical to HIE adoption and use. A weakness of the INPC is the lack of training for newly hired clinicians. None of the respondents could recall learning about the HIE during onboarding or training by staff from the HIE organization. While training is often part of HIE implementation, ongoing training for both new and existing users years after implementation is important to sustain and expand use. HIE networks should help health systems incorporate training into onboarding of new clinicians, or the HIE organization should offer regular in situ training opportunities for new employees. Online, on-demand training might also be a strategy to deliver information to existing users about new features (eg, search functionality) or new data sources added to the HIE. Moreover, HIE networks should work with their health care facilities to establish a culture in which regular HIE use is expected, fostering resiliency that ensures use well beyond the implementation phase.

Finally, the findings from this study call into question existing metrics [58] of clinician HIE use. Respondents reported using the HIE system for between 5% and 30% of their patients. These data might help refine expectations around what constitutes frequent versus "sometimes" use. Moreover, they imply that there is a theoretical maximum proportion of patients for whom accessing the HIE yields value. Given that this study focused solely on the ED setting, a ballpark figure of 20% of patients might not be appropriate for every HIE use case. Still, these data suggest that work is necessary to refine metrics for clinician use, which may be lower than some stakeholders expect or promote. Regardless of the proportion, it is clear that clinicians value having information from HIE networks for those patients whose care and outcomes can be meaningfully impacted.

Limitations and Future Directions for HIE Research

This study has several limitations. First, the study involved perspectives from clinicians on a single HIE network that has been operational for many years, and the participants primarily worked in health systems with established EHR use. Therefore, the results may not generalize to all HIE networks despite our efforts to purposely sample clinicians in different roles and practicing at hospitals of varied sizes and in diverse locations. Second, respondents worked in the ED, and perspectives from other specialties may differ. Third, despite our best attempts to interview clinicians who do not use the HIE system regularly, all respondents indicated that they use it on a regular basis. This might bias the findings because clinicians who purposely avoid using or have never used the HIE system were not interviewed.

While this study provides meaningful insights into HIE use in the ED setting, more research is needed to measure HIE use in various clinical settings and establish better indices for clinician use. Longitudinal studies on HIE use in relation to clinical outcomes could more firmly establish the evidence base needed to guide policy and practice. Cost-effectiveness studies involving clinician use data from logs could better demonstrate the value and return on investment of HIE infrastructure. Future research should examine the role of emerging technologies in enhancing HIE functionality, such as artificial intelligence summaries of clinical documents or comprehensive records, and their impact on clinician use. In addition, future research could explore potential differences in HIE use and perceptions across clinical roles (eg, physicians, nurses, and advanced practice providers) using a larger sample size and a mixed methods analysis approach.

XSL•FO
RenderX

Conclusions

This study of ED clinicians' perspectives illuminated several factors that facilitate or inhibit HIE use. As policymakers and health systems develop strategies to implement nationwide HIE, noting and leveraging these factors could be useful in achieving the goals of universal HIE adoption and use. Supporting clinicians' performance and effort through advanced HIE technologies will be critical for adoption and for impacting care outcomes and costs.

Acknowledgments

This work was supported by the US Agency for Healthcare Research and Quality (grant 1R21HS025502). The funder was not involved in drafting or editing the manuscript. This paper is solely the responsibility of the authors and does not necessarily represent the official views of the Agency for Healthcare Research and Quality or the US government.

The authors thank Ashley Wiensch, MPH, program manager at the Regenstrief Institute, for her assistance with logistics for the study and review of publication and presentation materials. We further thank Dr. Matthew Ferguson, who helped with the coding of data while serving as an a summer intern in the Indiana University Medical Student Program for Research and Scholarship (IMPRS).

Conflicts of Interest

None declared.

Multimedia Appendix 1
Screenshot of the CareWeb log-in page and complete qualitative results of interviews.
[DOCX File , 141 KB - medinform_v13i1e75865_app1.docx]

Multimedia Appendix 2
Interview guide.
[DOCX File , 24 KB - medinform_v13i1e75865_app2.docx]

References

1. Dixon BE. Introduction to health information exchange. In: Dixon BE, editor. Health Information Exchange: Navigating and Managing a Network of Health Information Systems. 2nd edition. San Diego, CA: Academic Press; 2023:3-20.
2. Menachemi N, Rahurkar S, Harle CA, Vest JR. The benefits of health information exchange: an updated systematic review. J Am Med Inform Assoc 2018 Sep 01;25(9):1259-1265 [FREE Full text] [doi: 10.1093/jamia/ocy035] [Medline: 29718258]
3. Slovis BH, Lowry T, Delman BN, Beitia AO, Kuperman G, DiMaggio C, et al. Patient crossover and potentially avoidable repeat computed tomography exams across a health information exchange. J Am Med Inform Assoc 2017 Jan;24(1):30-38 [FREE Full text] [doi: 10.1093/jamia/ocw035] [Medline: 27178985]
4. Shapiro JS, Crowley D, Hoxhaj S, Langabeer 2nd J, Panik B, Taylor TB, et al. Health information exchange in emergency medicine. Ann Emerg Med 2016 Feb;67(2):216-226. [doi: 10.1016/j.annemergmed.2015.06.018] [Medline: 26233924]
5. Politi L, Codish S, Sagy I, Fink L. Use patterns of health information exchange systems and admission decisions: reductionistic and configurational approaches. Int J Med Inform 2015 Dec;84(12):1029-1038. [doi: 10.1016/j.ijmedinf.2015.06.012] [Medline: 26212125]
6. Lammers EJ, Adler-Milstein J, Kocher KE. Does health information exchange reduce redundant imaging? evidence from emergency departments. Med Care 2014 Mar;52(3):227-234. [doi: 10.1097/MLR.0000000000000067] [Medline: 24374414]
7. Shapiro JS, Johnson SA, Angiollilo J, Fleischman W, Onyile A, Kuperman G. Health information exchange improves identification of frequent emergency department users. Health Aff (Millwood) 2013 Dec;32(12):2193-2198. [doi: 10.1377/hlthaff.2013.0167] [Medline: 24301405]
8. Johnson KB, Unertl KM, Chen Q, Lorenzi NM, Nian H, Bailey J, et al. Health information exchange usage in emergency departments and clinics: the who, what, and why. J Am Med Inform Assoc 2011;18(5):690-697 [FREE Full text] [doi: 10.1136/amiajnl-2011-000308] [Medline: 21846788]
9. Dixon BE, Schwartzkopf AL, Guerrero VM, May J, Koufacos NS, Bean AM, et al. Regional data exchange to improve care for veterans after non-VA hospitalization: a randomized controlled trial. BMC Med Inform Decis Mak 2019 Jul 04;19(1):125 [FREE Full text] [doi: 10.1186/s12911-019-0849-1] [Medline: 31272427]
10. Downing NL, Adler-Milstein J, Palma JP, Lane S, Eisenberg M, Sharp C, Northern California HIE Collaborative, et al. Health information exchange policies of 11 diverse health systems and the associated impact on volume of exchange. J Am Med Inform Assoc 2017 Jan;24(1):113-122 [FREE Full text] [doi: 10.1093/jamia/ocw063] [Medline: 27301748]
11. Devine EB, Totten AM, Gorman P, Eden KB, Kassakian S, Woods S, et al. Health information exchange use (1990-2015): a systematic review. EGEMS (Wash DC) 2017 Dec 07;5(1):27 [FREE Full text] [doi: 10.5334/egems.249] [Medline: 29881743]

XSL•FO
RenderX

12. 21st century cures act: interoperability, information blocking, and the ONC health IT certification program. Department of Health and Human Services. URL: https://www.federalregister.gov/documents/2020/05/01/2020-07419/21st-century-cures-act-interoperability-information-blocking-and-the-onc-health-it-certification [accessed 2025-05-29]
13. Rahurkar S, Jonnalagadda P, Tutt JK, Dixon BE, Menachemi N. Policies and incentives for adoption: toward broader use. In: Dixon BE, editor. Health Information Exchange: Navigating and Managing a Network of Health Information Systems. San Diego, CA: Academic Press; 2023:57-86.
14. Swain M, Charles D, Patel V, Searcy T. Health information exchange among U.S. non-federal acute care hospitals: 2008-2013. National Coordinator for Health Information Technology. 2015. URL: https://www.ncbi.nlm.nih.gov/books/NBK612963/pdf/Bookshelf_NBK612963.pdf [accessed 2025-05-29]
15. Interoperability and methods of exchange among hospitals in 2021. Office of the National Coordinator for Health Information Technology. URL: https://www.healthit.gov/data/data-briefs/interoperability-and-methods-exchange-among-hospitals-2021 [accessed 2025-05-29]
16. Rahurkar S, Vest JR, Finnell JT, Dixon BE. Trends in user-initiated health information exchange in the inpatient, outpatient, and emergency settings. J Am Med Inform Assoc 2021 Mar 01;28(3):622-627 [FREE Full text] [doi: 10.1093/jamia/ocaa226] [Medline: 33067617]
17. Lum B, Weerasinghe N, Chu CH, Perri D, Cranley L. Examining implementation outcomes in health information exchange systems: a scoping review. J Biomed Inform 2025 Mar;163:104782 [FREE Full text] [doi: 10.1016/j.jbi.2025.104782] [Medline: 39842684]
18. Franzosa E, Traylor M, Judon KM, Guerrero Aquino V, Schwartzkopf AL, Boockvar KS, et al. Perceptions of event notification following discharge to improve geriatric care: qualitative interviews of care team members from a 2-site cluster randomized trial. J Am Med Inform Assoc 2021 Jul 30;28(8):1728-1735 [FREE Full text] [doi: 10.1093/jamia/ocab074] [Medline: 33997903]
19. Bowden TC, Lyell D, Coiera E. Emergency department and urgent care clinician perspectives on digital access to past medical histories. BMJ Health Care Inform 2022 May;29(1):e390 [FREE Full text] [doi: 10.1136/bmjhci-2022-100567] [Medline: 35618316]
20. Klapman S, Sher E, Adler-Milstein J. A snapshot of health information exchange across five nations: an investigation of frontline clinician experiences in emergency care. J Am Med Inform Assoc 2018 Jun 01;25(6):686-693 [FREE Full text] [doi: 10.1093/jamia/ocx153] [Medline: 29409028]
21. Tarver WL, Jonnalagadda P, Rahurkar S. Evidence base for health information exchange. In: Dixon BE, editor. Health Information Exchange: Navigating and Managing a Network of Health Information Systems. 2nd edition. New York, NY: Academic Press; 2023:359-377.
22. McDonald CJ, Overhage JM, Barnes M, Schadow G, Blevins L, Dexter PR, INPC Management Committee. The Indiana network for patient care: a working local health information infrastructure. An example of a working infrastructure collaboration that links data from five health systems and hundreds of millions of entries. Health Aff (Millwood) 2005;24(5):1214-1220. [doi: 10.1377/hlthaff.24.5.1214] [Medline: 16162565]
23. Overhage JM, Kansky JP. The Indiana health information exchange. In: Dixon BE, editor. Health Information Exchange: Navigating and Managing a Network of Health Information Systems. 2nd edition. New York, NY: Academic Press; 2023:471-487.
24. Williams KS, Rahurkar S, Grannis SJ, Schleyer TK, Dixon BE. Evolution of clinical health information exchanges to population health resources: a case study of the Indiana network for patient care. BMC Med Inform Decis Mak 2025 Feb 24;25(1):97 [FREE Full text] [doi: 10.1186/s12911-025-02933-9] [Medline: 39994604]
25. Dixon BE, Whipple EC, Lajiness JM, Murray MD. Utilizing an integrated infrastructure for outcomes research: a systematic review. Health Info Libr J 2016 Mar;33(1):7-32 [FREE Full text] [doi: 10.1111/hir.12127] [Medline: 26639793]
26. Schleyer TK, Rahurkar S, Baublet AM, Kochmann M, Ning X, Martin DK, FHIR Development Team, et al. Preliminary evaluation of the Chest Pain Dashboard, a FHIR-based approach for integrating health information exchange information directly into the clinical workflow. AMIA Jt Summits Transl Sci Proc 2019;2019:656-664 [FREE Full text] [Medline: 31259021]
27. Hosseini M, Faiola A, Jones J, Vreeman DJ, Wu H, Dixon BE. Impact of document consolidation on healthcare providers' perceived workload and information reconciliation tasks: a mixed methods study. J Am Med Inform Assoc 2019 Feb 01;26(2):134-142 [FREE Full text] [doi: 10.1093/jamia/ocy158] [Medline: 30566630]
28. Dixon BE, Zhang Z, Arno JN, Revere D, Joseph Gibson P, Grannis SJ. Improving notifiable disease case reporting through electronic information exchange-facilitated decision support: a controlled before-and-after trial. Public Health Rep 2020 Apr 06;135(3):401-410 [FREE Full text] [doi: 10.1177/0033354920914318] [Medline: 32250707]
29. Dixon BE, Grannis SJ, McAndrews C, Broyles AA, Mikels-Carrasco W, Wiensch A, et al. Leveraging data visualization and a statewide health information exchange to support COVID-19 surveillance and response: application of public health informatics. J Am Med Inform Assoc 2021 Jul 14;28(7):1363-1373 [FREE Full text] [doi: 10.1093/jamia/ocab004] [Medline: 33480419]
30. Dixon BE, Hook J, Vreeman DJ. Learning from the crowd in terminology mapping: the LOINC experience. Lab Med 2015;46(2):168-174 [FREE Full text] [doi: 10.1309/LMWJ730SVKTUBAOJ] [Medline: 25918199]

XSL•FO
RenderX

31. Grannis SJ, Xu H, Vest JR, Kasthurirathne S, Bo N, Moscovitch B, et al. Evaluating the effect of data standardization and validation on patient matching accuracy. J Am Med Inform Assoc 2019 May 01;26(5):447-456 [FREE Full text] [doi: 10.1093/jamia/ocy191] [Medline: 30848796]
32. Guest G, Bunce A, Johnson L. How many interviews are enough? an experiment with data saturation and variability. Field Methods 2006 Feb 01;18(1):59-82. [doi: 10.1177/1525822x05279903]
33. Hennink MM, Kaiser BN, Marconi VC. Code saturation versus meaning saturation: how many interviews are enough? Qual Health Res 2017 Mar 26;27(4):591-608 [FREE Full text] [doi: 10.1177/1049732316665344] [Medline: 27670770]
34. Armitage CJ, Conner M. Efficacy of the theory of planned behaviour: a meta-analytic review. Br J Soc Psychol 2001 Dec;40(Pt 4):471-499. [doi: 10.1348/014466601164939] [Medline: 11795063]
35. Kasting ML, Shapiro GK, Rosberger Z, Kahn JA, Zimet GD. Tempest in a teapot: a systematic review of HPV vaccination and risk compensation research. Hum Vaccin Immunother 2016 Jun 02;12(6):1435-1450 [FREE Full text] [doi: 10.1080/21645515.2016.1141158] [Medline: 26864126]
36. Leblanc G, Gagnon MP, Sanderson D. Determinants of primary care nurses' intention to adopt an electronic health record in their clinical practice. Comput Inform Nurs 2012 Sep;30(9):496-502. [doi: 10.1097/NXN.0b013e318257db17] [Medline: 22592453]
37. Holden RJ. Physicians' beliefs about using EMR and CPOE: in pursuit of a contextualized understanding of health IT use behavior. Int J Med Inform 2010 Feb;79(2):71-80 [FREE Full text] [doi: 10.1016/j.ijmedinf.2009.12.003] [Medline: 20071219]
38. Venkatesh V, Sykes TA, Xiaojun Z. 'Just what the doctor ordered': a revised UTAUT for EMR system adoption and use by doctors. In: Proceedings of the 44th Hawaii International Conference on System Sciences. 2011 Presented at: HICSS '11; January 4-7, 2011; Kauai, HI p. 1-10 URL: https://ieeexplore.ieee.org/document/5718549 [doi: 10.1109/hicss.2011.1]
39. Seeman E, Gibson S. Predicting acceptance of electronic medical records: is the technology acceptance model enough? SAM Adv Manag J 2009;74(4):21-26 [FREE Full text]
40. Hu PJ, Chau PY, Sheng OR, Tam KY. Examining the technology acceptance model using physician acceptance of telemedicine technology. J Manag Inf Syst 2015 Dec 02;16(2):91-112. [doi: 10.1080/07421222.1999.11518247]
41. Venkatesh V, Morris MG, Davis GB, Davis FD. User acceptance of information technology: toward a unified view. MIS Q 2003;27(3):425. [doi: 10.2307/30036540]
42. Delone WH, McLean ER. The DeLone and McLean model of information systems success: a ten-year update. J Manag Inf Syst 2014 Dec 23;19(4):9-30. [doi: 10.1080/07421222.2003.11045748]
43. DeLone WH, McLean ER. Information systems success: the quest for the dependent variable. Inf Syst Res 1992 Mar;3(1):60-95. [doi: 10.1287/isre.3.1.60]
44. NVivo 12.0. Lumivero. URL: https://lumivero.com/resources/free-trial/nvivo/ [accessed 2025-05-29]
45. Everson J, Patel V. Hospital's adoption of multiple methods of obtaining outside information and use of that information. J Am Med Inform Assoc 2022 Aug 16;29(9):1489-1496 [FREE Full text] [doi: 10.1093/jamia/ocac079] [Medline: 35652172]
46. Holmgren AJ, Patel V, Adler-Milstein J. Progress in interoperability: measuring US hospitals' engagement in sharing patient data. Health Aff (Millwood) 2017 Oct 01;36(10):1820-1827. [doi: 10.1377/hlthaff.2017.0546] [Medline: 28971929]
47. Martin TR, Gasoyan H, Pirrotta G, Mathew R. A national survey assessing health information exchange: readiness for changes to veterans affairs access standards. Perspect Health Inf Manag 2021;18(3):1i [FREE Full text] [Medline: 34858121]
48. Altman R, Shapiro JS, Moore T, Kuperman GJ. Notifications of hospital events to outpatient clinicians using health information exchange: a post-implementation survey. Inform Prim Care 2012;20(4):249-255 [FREE Full text] [doi: 10.14236/jhi.v20i4.14] [Medline: 23890336]
49. The American Hospital Association information technology supplement survey. American Hospital Association. URL: https://www.aha.org/american-hospital-association-information-technology-supplement-survey [accessed 2025-09-02]
50. Nakayama M, Inoue R, Miyata S, Shimizu H. Health information exchange between specialists and general practitioners benefits rural patients. Appl Clin Inform 2021 May 09;12(3):564-572 [FREE Full text] [doi: 10.1055/s-0041-1731287] [Medline: 34107543]
51. Furukawa MF, Patel V, Charles D, Swain M, Mostashari F. Hospital electronic health information exchange grew substantially in 2008-12. Health Aff (Millwood) 2013 Aug;32(8):1346-1354. [doi: 10.1377/hlthaff.2013.0010] [Medline: 23918477]
52. Miller AR, Tucker C. Health information exchange, system size and information silos. J Health Econ 2014 Jan;33:28-42. [doi: 10.1016/j.jhealeco.2013.10.004] [Medline: 24246484]
53. Vest JR, Gamm LD. Health information exchange: persistent challenges and new strategies. J Am Med Inform Assoc 2010;17(3):288-294 [FREE Full text] [doi: 10.1136/jamia.2010.003673] [Medline: 20442146]
54. Patel V, Abramson EL, Edwards A, Malhotra S, Kaushal R. Physicians' potential use and preferences related to health information exchange. Int J Med Inform 2011 Mar;80(3):171-180. [doi: 10.1016/j.ijmedinf.2010.11.008] [Medline: 21156351]
55. Feldman SS, Hikmet N, Modi S, Schooley B. Impact of provider prior use of HIE on system complexity, performance, patient care, quality and system concerns. Inf Syst Front 2022 Sep 23;24(1):121-131 [FREE Full text] [doi: 10.1007/s10796-020-10064-x] [Medline: 32982572]

XSL•FO
RenderX

56. Adler-Milstein J, Worzala C, Dixon BE. Future directions for health information exchange. In: Dixon BE, editor. Health Information Exchange: Navigating and Managing a Network of Health Information Systems. 2nd edition. New York, NY: Academic Press; 2023:447-468.
57. Rudin R, Volk L, Simon S, Bates D. What affects clinicians' usage of health information exchange? Appl Clin Inform 2011 Jan 01;2(3):250-262 [FREE Full text] [doi: 10.4338/ACI-2011-03-RA-0021] [Medline: 22180762]
58. Strawley CE, Adler-Milstein J, Holmgren AJ, Everson J. New indices to track interoperability among US hospitals. J Am Med Inform Assoc 2025 Feb 01;32(2):318-327. [doi: 10.1093/jamia/ocae289] [Medline: 39724921]

Abbreviations

BI: behavioral intention
ED: emergency department
EHR: electronic health record
HIE: health information exchange
INPC: Indiana Network for Patient Care
IS: information systems
ONC: Office of the National Coordinator for Health Information Technology
SSO: single sign-on
UTAUT: unified theory of acceptance and use of technology
VPN: virtual private network

Edited by A Benis; submitted 11.04.25; peer-reviewed by M Chomali, S Thawillarp; comments to author 29.05.25; revised version received 23.07.25; accepted 15.08.25; published 20.10.25.

Please cite as:
Dixon BE, Ghimire U, Richter B, Bowditch C, Rahurkar S, Finnell JT, Vest JR
Influences on Emergency Clinician Use of Health Information Exchange: Interview Study
JMIR Med Inform 2025;13:e75865
URL: https://medinform.jmir.org/2025/1/e75865
doi:10.2196/75865
PMID:

©Brian E Dixon, Umesh Ghimire, Benjamin Richter, Corinne Bowditch, Saurabh Rahurkar, John T Finnell, Joshua R Vest. Originally published in JMIR Medical Informatics (https://medinform.jmir.org), 20.10.2025. This is an open-access article distributed under the terms of the Creative Commons Attribution License (https://creativecommons.org/licenses/by/4.0/), which permits unrestricted use, distribution, and reproduction in any medium, provided the original work, first published in JMIR Medical Informatics, is properly cited. The complete bibliographic information, a link to the original publication on https://medinform.jmir.org/, as well as this copyright and license information must be included.

XSL•FO
RenderX

Predicting Metabolic Dysfunction–Associated Fatty Liver Disease Phenotypes Among Adults: 2-Stage Contrastive Learning Method

Sizhe Jasmine Chen[1], MSc; Da Xu[2], PhD; Derek K Hu[3], PhD; Paul Jen-Hwa Hu[1], PhD; Ting-Shuo Huang[4,5,6], PhD

[1]Department of Operations and Information Systems, David Eccles School of Business, University of Utah, 1655 East Campus Center Drive, Salt Lake City, UT, United States

[2]Department of Marketing, Analytics, and Professional Sales, School of Business Administration, University of Mississippi, University, MS, United States

[3]Department of Biomedical Engineering and Department of Computer Engineering and Computer Science, California State University, Long Beach, Long Beach, CA, United States

[4]Division of General Surgery, Department of Surgery, Jen-Ai Hospital, Taichung, Taiwan

[5]Department of Surgery, Chang Gung Memorial Hospital, Keelung Branch, Keelung, Taiwan

[6]Department of Chinese Medicine, College of Medicine, Chang Gung University, Taoyuan, Taiwan

Corresponding Author:
Paul Jen-Hwa Hu, PhD
Department of Operations and Information Systems, David Eccles School of Business, University of Utah, 1655 East Campus Center Drive, Salt Lake City, UT, United States

Abstract

Background: Metabolic dysfunction–associated fatty liver disease (MAFLD) is a leading cause of chronic disease and can progress to liver fibrosis or hepatocellular carcinoma. Its subtypes—obese, diabetic, and lean—are associated with varying degrees of fibrotic burden and different complications, yet the existing analytics methods often overlook its multisystem nature, intraphenotype variability, and disease dynamics. These limitations hinder accurate risk stratification and restrict personalized intervention planning.

Objective: This study developed a novel, 2-stage, contrastive learning–based method to predict the phenotype of MAFLD among adults. This method leverages multiview contrastive learning; it models individual heterogeneities and important relationships in clinical and survey-based data to predict phenotypes among adults, thus supporting clinical decision-making and personalized care.

Methods: Demographic, clinical, lifestyle, and genetic family history data of 4408 adults revealed how capturing essential relationships in patient data from different sources can transform individual-level representations into multiple, complementary views. Evaluation of the predictive efficacy of the proposed method in comparison with 8 prevalent methods relied on recall, precision, F_1-score, and area under the curve values. Moreover, a Shapley additive explanation analysis was performed for interpretability.

Results: The proposed method consistently and significantly outperformed all benchmark methods. It attained the highest F_1-score, showing a 32.8% improvement for nondiabetic MAFLD (0.531 vs 0.400) and 30.4% improvement for diabetic MAFLD (0.519 vs 0.398) over the respective best-performing benchmark. The results underscore the clinical value and utility of integrating clinical and survey-based data in the prediction of MAFLD phenotypes among adults.

Conclusions: The proposed method is a viable approach for MAFLD phenotype prediction. It is more effective in identifying at-risk adults than many prevalent data-driven analytics methods and thereby can enhance clinical decision-making and support patient-centric care and management.

(JMIR Med Inform 2025;13:e75747) doi:10.2196/75747

KEYWORDS

metabolic dysfunction–associated fatty liver disease; phenotype; graph representation learning; multiview contrastive learning; predictive analytics

XSL•FO
RenderX

Introduction

Background

Metabolic dysfunction–associated fatty liver disease (MAFLD) is a leading cause of chronic liver disease, affecting more than one-third of the global population [1,2] and resulting in annual, direct medical costs of US $103 billion in the United States and €35 billion (US $40 billion) in Europe [3]. The relabeling of nonalcoholic fatty liver disease as MAFLD reflects a deeper understanding of fatty liver disease [4]. It also helps identify adults at risk of serious prognoses [5] such as liver cirrhosis and hepatocellular carcinoma, which account for most liver-related deaths [6,7]. The exacerbation of comorbid conditions due to MAFLD amplifies its clinical significance; patients with chronic liver diseases often develop severe infections, chronic cardiovascular or kidney disease, cancer, and death [8]. Yet, therapeutic options for devastating MAFLD-induced liver diseases are limited. Liver transplantation is the optimal treatment [9,10] but is greatly restricted by organ availability and financial costs [11].

A diagnosis of MAFLD requires hepatic steatosis in the presence of excessive weight, type 2 diabetes mellitus, or metabolic dysregulation, manifested in the obese, diabetic, and lean phenotypes (subtypes) of MAFLD, respectively [12]. These phenotypes have distinct prognostic values [5], fibrotic burden [13,14], and complications [15,16]. For example, the diabetic phenotype is characterized by severe insulin resistance and is associated with the highest risk of any-cause and disease-specific mortality [17]. The obese phenotype is related to lifestyle factors (eg, diet and physical inactivity) and can lead to systemic inflammation and metabolic dysfunction. The lean phenotype involves ectopic fat deposition and genetic predispositions to MAFLD, although without obesity [18]. Because of the differences between the MAFLD phenotypes, accurate phenotype prediction is crucial for clinical decision-making, personalized care planning, and efficient resource allocation [19]. With relevant insights into the underlying etiology and pathology [20], effective phenotype prediction can facilitate patient stratification and treatment planning for streamlining diagnostic procedures, optimizing the use of laboratory tests or imaging, and specifying necessary lifestyle changes, all of which have cost-containment implications [21-23].

Physicians usually rely on liver biopsies [24,25] or score-based methods [26,27] that require contemporaneous clinical data, impose substantial costs, and misidentify at-risk adults. These constraints favor the potential of data-driven analytics for supporting timely identification of at-risk adults such that clinicians can formulate actionable risk reduction measures and effective patient stratification and researchers can design more appropriate clinical trials and treatment plans [28]. Despite the promise, data-driven analytics for MAFLD phenotyping face several challenges. First, MAFLD is a multisystem disease [29] because clinical, family genetics, lifestyle, and socioeconomic factors can influence fatty liver development and progression [30]. Incorporating such heterogeneous data in analytics methods, which typically are gathered from different sources, is difficult. For example, surveys designed to gather genetic family history data or lifestyle data tend to have small samples and often suffer from data incompleteness. Second, due to the complex nature of MAFLD, people with the same MAFLD phenotype may exhibit intraphenotype variability in etiology or pathology, which also should be considered for phenotype predictions. Third, both disease classification hierarchy and manifestations of MAFLD involve temporal complexity at the individual level.

Objective

In an effort to design a data-driven method to predict MAFLD phenotypes more accurately, we developed a novel, 2-stage, contrastive learning–based method. This method leverages graph representation learning, in combination with interindividual similarity, to process integrated individual-level data pertaining to genetic family history or lifestyle, which then can inform downstream predictions by complementing (incomplete) survey-based data with clinical data or vice versa. In addition, the proposed method incorporates multiview, contrastive pretraining that captures intraphenotype variability on the basis of clinical, genetic family history, and lifestyle data. By linking important data from different sources, it constructs individual-level representations for downstream tasks and predictions. Finally, its 2-stage estimation design accounts for disease hierarchy and temporal complexity, such that the proposed method can predict phenotypes among adults more accurately and explicitly than the existing analytics methods.

To demonstrate the predictive efficacy of the proposed method, we used clinical and survey-based data of 4408 adults in Taiwan [31] and included 8 prevalent methods as benchmarks. The results indicated that the proposed method consistently and significantly outperformed all the benchmarks in both F_1-score and area under the curve (AUC). This novel method can predict phenotypes accurately and can potentially contribute to medical informatics research and support personalized care for at-risk adults.

Related Work

MAFLD and Its Phenotypes

Clinically, MAFLD involves metabolic abnormalities [32], and its diagnosis requires hepatic steatosis, which can be determined by imaging, blood biomarker scores, or liver biopsies [20]. Adults diagnosed with MAFLD often differ in their phenotypes, prognoses, and complications [5], leading to distinct clinical manifestations and metabolic characteristics. For example, diabetic MAFLD is characterized by diabetes mellitus, independent of BMI, and exhibits a higher fibrotic burden than other phenotypes, with substantial risks of hepatocellular carcinoma [33] and cardiovascular disease (CVD) [15]. Both obese MAFLD and lean MAFLD are determined on the basis of BMI: ≥23 kg/m² and <23 kg/m², respectively. The former condition involves excess adiposity and is associated with insulin resistance, systemic inflammation, and increased risk of cardiovascular complications [34]. The latter, also known as metabolic dysregulation, is characterized by metabolic abnormalities, and individuals with this phenotype are at a greater risk of liver-related complications and mortality [21]. Because both obese MAFLD and lean MAFLD are determined

XSL•FO
RenderX

on the basis of BMI, they can be considered in combination for phenotype predictions. Phenotypic heterogeneity reflects the significant complexity of MAFLD and its varied pathophysiological mechanisms [35], which stem from demographic characteristics, clinical variables, lifestyle factors, and genetic predisposition [36].

In turn, the heterogeneity and complexity of MAFLD make timely, accurate phenotype prediction important but difficult. Notably, MAFLD is reversible in its early stages, with appropriate lifestyle changes and clinical interventions [35]. On the other hand, advanced stages can induce liver diseases and are associated with poor prognoses [37]. In general, accurate phenotype predictions are needed within a 1-year timeframe [38] because MAFLD often exhibits few or no directly observable symptoms until liver damage has occurred. By identifying at-risk adults in a timely manner, physicians can encourage lifestyle changes such as dietary alterations or reduced alcohol consumption [39,40] and plan for laboratory tests or imaging examinations (eg, abdominal ultrasound) [36].

Data-Driven Analytics Methods for Patient Risk and Outcome Predictions

Existing data-driven analytics for MAFLD phenotype predictions rely on regression-based [41-43], tree-based [44-46], neural network (NN)–based [47-49], or graph-based [50-52] methods. Regression-based methods, such as Cox regression–based risk estimation [42] and logistic regression models [43], use statistical modeling to predict patient risk and outcomes, support patient risk predictions, and identify important factors. However, these methods cannot deal with high-dimensional data or nonlinear relationships and often make strong data property assumptions. A tree-based method can model nonlinear relationships and derive predictions by applying variable values to split the data recursively, as exemplified by decision tree (DT) [44], random forest (RF) [45], and extreme gradient boosting (XGBoost) [46] methods. While intuitive and interpretable, tree-based methods struggle with overfitting in the presence of noise or data sparsity, and they cannot handle missing data or individual heterogeneity effectively [53]. The deep learning, NN-based methods are able to model complex relationships and nonlinear interactions [54]. For example, deep autoencoders [49] and multilayer perceptron (MLP) [48] methods are advantageous for representing multisource data with high-dimensional features. But they can be difficult to train and are prone to overfitting, especially with insufficient, incomplete, or low-quality data [55]. Finally, graph-based methods represent data as nodes and edges in a graph; they are designed to capture complex relationships and interactions among entities (eg, patients and medications) to inform downstream predictions. Representative methods include graph convolutional networks (GCNs) [56], graph attention networks (GATs) [57], and GraphSAGE [58]. Despite their general effectiveness, graph-based methods rely on predefined graph structures, which can restrict their ability to account for complex, multifaceted, individual feature interactions.

As summarized in Table 1, the existing analytics methods seem generally effective for estimating patient risk and outcome, but their direct use for MAFLD phenotype prediction is insufficient for several reasons. First, many methods depend on clinical data available in electronic health records, which prevents them from accounting for the multifactorial nature of MAFLD. For example, effective phenotype prediction needs to consider genetic family history and lifestyle data, but the incorporation of such data complicates the modeling and obscures patterns essential for accurate prediction, in addition to sample size and data incompleteness issues. Second, most of the prevalent methods do not capture intraphenotype variability, which is critical for downstream predictions. For example, semisupervised (eg, contrastive) learning can deal with complex representations [59-61], but its use requires data augmentation [62-65] and complementary views [66], in addition to the tabular data common in healthcare settings. Third, MAFLD phenotype prediction involves disease classification hierarchy and temporal dynamics. For instance, individuals are classified as those with and without MAFLD (MAFLD and non-MAFLD, respectively), and those with MAFLD need to be further classified into distinct phenotypes by a selective layer, which implies a priori knowledge to inform appropriate feature selection.

XSL•FO
RenderX

Table . Comparison of this study with representative previous studies.

Study	Method	Multisource data integration	Data heterogeneity	Intraphenotype variability	Disease dynamics
Jia et al (2019) [42]	Regression-based	No	No	No	No
Yang et al (2024) [67]	Regression-based	Yes	No	No	No
Książek et al (2021) [43]	Regression-based	No	No	No	No
Pasadana et al (2021) [68]	Tree-based	No	No	No	No
Wang et al (2019) [69]	Tree-based	No	No	No	Yes
Hashem et al (2012) [70]	NN-based[a]	No	No	No	Yes
Franco et al (2021) [49]	NN-based	Yes	No	No	No
Chowdhury et al (2024) [51]	Graph-based	No	No	Yes	No
Zhang et al (2022) [52]	Graph-based	Yes	No	No	No
Zheng et al (2022) [71]	Graph-based	Yes	No	No	Yes
This study	2-Stage, contrastive learning–based	Yes	Yes	Yes	Yes

[a]NN: neural network.

Methods

Materials

We used 2-year longitudinal data of 4408 adults, obtained from a major healthcare organization in Taiwan, to evaluate the proposed method in comparison with 8 prevalent methods. No adults in the sample had MAFLD in year 1. For each person, the data include 2 demographic variables, 36 clinical variables, 32 lifestyle variables, and 42 genetic family history–related variables. Multimedia Appendix 1 provides the description and coding of variables. With these data, we evaluated the ability of each method to predict whether a person would develop MAFLD in year 2 and, if so, of which phenotype.

Of the 4408 individuals in our sample, 2999 (68.1%) were women, and 1409 (31.9%) were men, with an average age of 58.18 (SD 12.94) years. The outcome class distribution was imbalanced: 85.0% non-MAFLD (3747/4408), 11.5% nondiabetic MAFLD (507/4408), and 3.5% diabetic MAFLD (154/4408). We used class weights during model training to address the imbalance issue. Prior to making phenotype predictions, we applied z score standardization to numeric variables and one-hot encoding to categorical variables to prepare the data.

Ethical Considerations

This study was approved by the Chang Gung Medical Foundation Institutional Review Board (201800270B0). All procedures were performed in accordance with relevant guidelines and regulations. Written informed consent was obtained from all participants. All patient information was anonymized prior to analysis, and the study complied with ethical standards for research involving deidentified healthcare data. Participants were informed that their involvement was voluntary and that they could withdraw from the study at any time without penalty. No financial compensation was provided.

Proposed Method

Problem Definition

Let D be individual demographics, C represent clinical variables, S denote genetic family history–related and lifestyle data, and Y indicate distinct MAFLD outcomes. Phenotype prediction represents a multiclass classification task: given D, C, and S, the objective is to effectively process S based on the observed values, then integrate with D and C to predict whether an individual is likely to develop a specific MAFLD phenotype within a 1-year timeframe. By effectively processing S, it is possible to extract useful information from S, to better cope with the missingness that often arises among self-reported genetic family history data and lifestyle data for improved predictive efficacy. We considered 3 outcome classes for the multiclass classification task, Y=Y1,Y2,Y3, which correspond to the non-MAFLD, nondiabetic MAFLD, and diabetic MAFLD phenotypes, respectively. The combination of obese MAFLD and lean MAFLD phenotypes into a single outcome class (nondiabetic MAFLD) is justified because both phenotypes rely solely on BMI. It also simplifies the outcome class classification and allows for meaningful, accurate predictions, in that physicians can readily separate obese and lean MAFLD according to BMI values, which offers clinical practicality [33,72] and facilitates predictions [73,74].

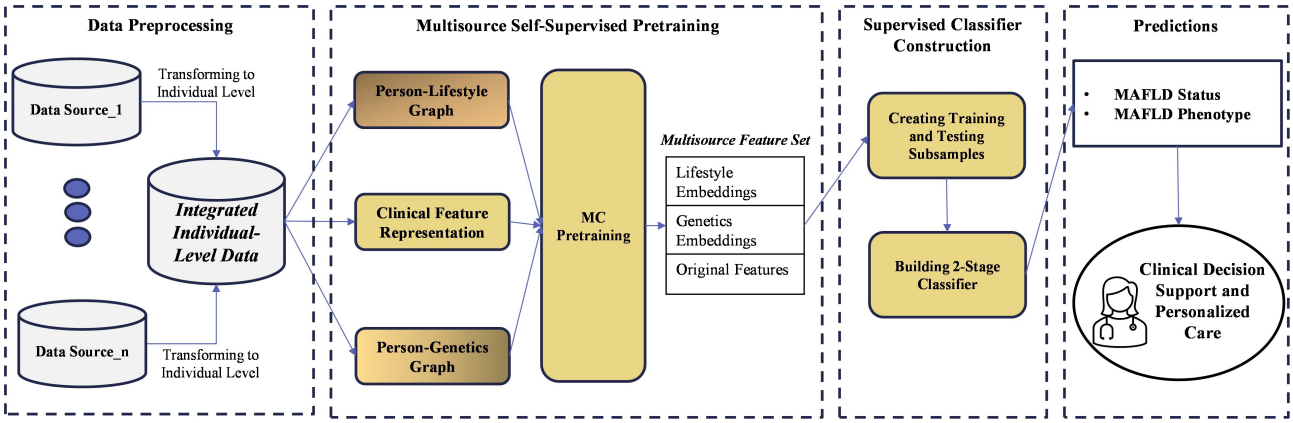
Architectural Framework

Figure 1 depicts the proposed method's architectural framework and highlights its 3 important components: graph representation learning, multiview contrastive pretraining, and 2-stage risk

XSL•FO
RenderX

estimation. With graph representation learning, the method uses sparse, incomplete survey data to build 2 individual-feature bipartite networks, a person-lifestyle graph and a person-genetics graph, which are used to learn graph representations. The multiview contrastive pretraining component then uses the individual graph representations as inputs to capture intraphenotype variability and create lifestyle and genetics embeddings. Finally, these embeddings are combined with demographic and clinical data in the 2-stage risk estimation process to predict the likelihood of each outcome class for an individual.

Figure 1. Architectural framework of the proposed method. MAFLD: metabolic dysfunction–associated fatty liver disease; MC: multiview contrastive.



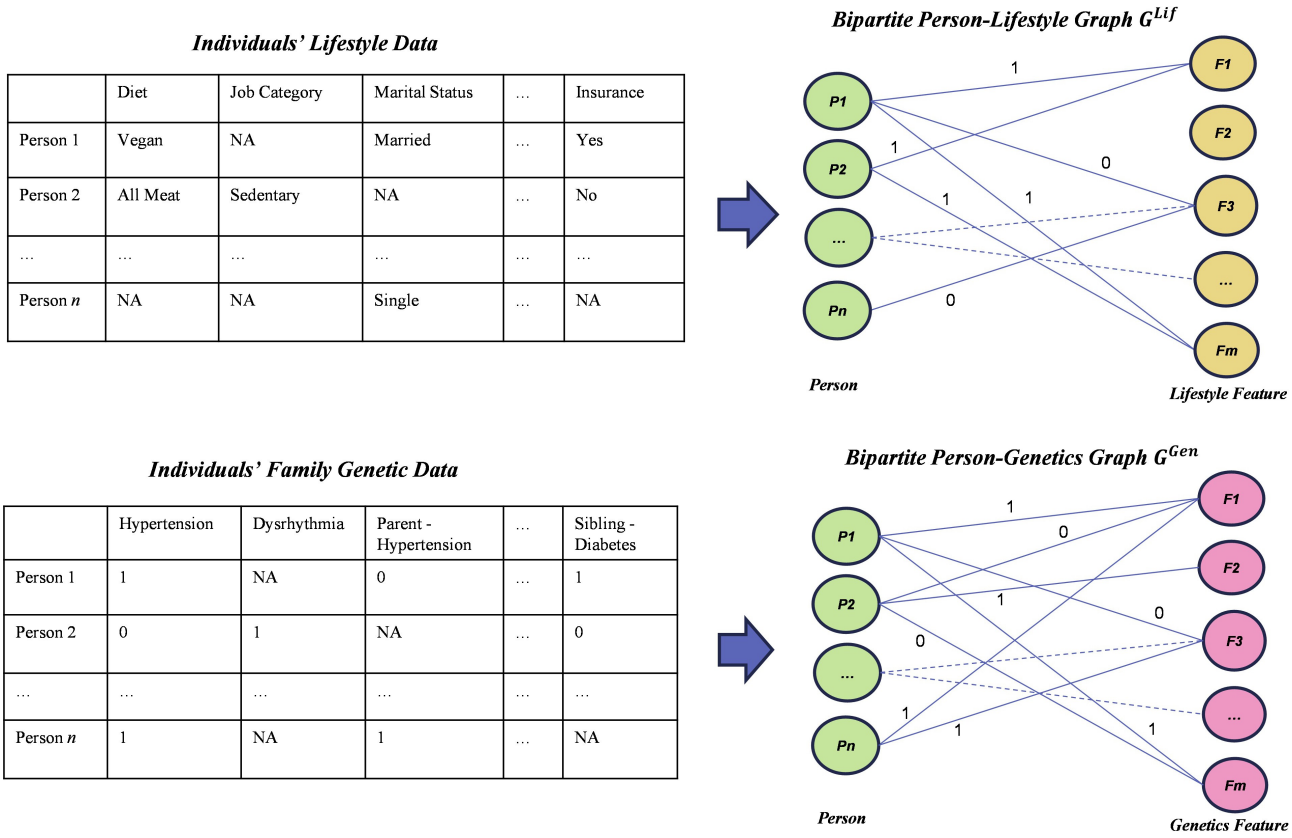
Graph Representation Learning

We used lifestyle and genetic family history data to perform the novel graph representation learning and construct both person-lifestyle and person-genetics networks. The former captures relationships among individuals according to their lifestyle predispositions (eg, shared dietary habits and physical activities). The latter leverages genetic family history–related variables (eg, shared alleles and single nucleotide polymorphisms) that can influence individuals' biological or genetic predispositions. These 2 networks were constructed separately to enable the graph representation learning component to concentrate on unique structures and relationships intrinsic to each type of data, thereby capturing the interplay of lifestyle and family genetic variables.

Figure 2 illustrates the construction of 2 bipartite networks. For the person-lifestyle bipartite network, GLif={VPLif,VFLif,ELif}, VPLif={P1,P2,…,PN} refers to a set of individuals, VFLif={F11,F12,…Fij,…,FMJ} represents lifestyle features, and ELif denotes an edge set that links VPLif and VFLif. N and M denote the total number of individuals and lifestyle feature values, respectively. For each lifestyle feature, multiple nodes are used to indicate its plausible (coded) values. J denotes the number of distinct values or categories of FM; thus, Fij denotes the jth category of feature Fi. If person Pu has a value on lifestyle feature Fv of the jth category, there exists an undirected link eu,vj between nodes Pu and Fvj, and the edge weight reflects Pu's value on feature Fvj.

XSL•FO
RenderX

Figure 2. Graph representation learning component of the proposed method. NA: not applicable.



	Diet	Job Category	Marital Status	…	Insurance
Person 1	Vegan	NA	Married	…	Yes
Person 2	All Meat	Sedentary	NA	…	No
…	…	…	…	…	…
Person *n*	NA	NA	Single	…	NA

	Hypertension	Dysrhythmia	Parent - Hypertension	…	Sibling - Diabetes
Person 1	1	NA	0	…	1
Person 2	0	1	NA	…	0
…	…	…	…	…	…
Person *n*	1	NA	1	…	NA

For the person-lifestyle bipartite network, we used GraphSAGE [58] to learn representations for the nodes and edges. We relied on triplet loss to train the graph representation model, which involved an anchor node, a positive sample (neighboring nodes or the node itself if no neighbors existed), and a negative sample:

$$(1)L=\max(0,d(f(a),f(p)-f(a),f(n))+\alpha)$$

where a is the anchor node, p is the positive node, n is the negative sample, d(·) is the distance function, f(·) is the embedding function, and α is a margin parameter. APiLif represents the learned node embedding for each person Pi. Similarly, we built the person-genetics bipartite network, GGen={VPGen,VFGen,EGen}, to learn the genetic representation APiGen. The representations learned from these 2 networks provided the input for the contrastive pretraining component.

Multiview Contrastive Pretraining

Originally developed for computer vision tasks, contrastive learning leverages data augmentation and complementary views for effective representation learning [66]. Conventional, supervised learning faces multifaceted challenges, especially when dealing with high intraclass variance and imbalanced outcome class distribution. Contrastive learning offers a viable solution by learning data representations through instance discrimination. The core idea is intuitive: instead of solely relying on labeled examples, contrastive learning learns to distinguish among different patients while ensuring that similar patients have similar representations in the learned feature space. This self-supervised approach can learn robust features, particularly in scenarios involving limited or imbalanced labeled data. However, existing contrastive learning methods, such as MoCo [63] and SimCLR [65], rely heavily on data augmentation techniques such as cropping and rotation in images, which are not directly applicable to structured patient data.

We designed a novel multiview contrastive pretraining component that leverages multiple context-specific representations to capture intraphenotype variability. In the proposed method, multiview contrastive learning examines patients' clinical profiles from multiple perspectives and learns discriminative representations that better predict infrequent but important MAFLD subtypes while maintaining performance across different categories. For this task, an intuitive learning objective can be defined by the cosine similarity among individuals, according to the person-lifestyle representation APiLif, person-genetic representation APiGen, and clinical data C. The intent is to capture intraphenotype variability. We applied guided, collaborative training to steer the training process, for which we used clinical variables for the teacher view and survey-based, context-specific representations (APiLif and APiGen) for the learner views. The resulting model can integrate and align critical information from clinical and survey-based data.

Figure 3 depicts the contrastive pretraining component, in which 3 encoders (Enca, Encb, and Encc) process the representations of lifestyle data, clinical data, and genetic family history data, respectively. Thus, Encb is pretrained with an autoencoder to produce the teacher view that anchors the learning process. As learner views, Enca and Encc are trained according to Encb during the contrastive learning process. Both Enca and Encc adopt the same 3-layer MLP with nonlinear activation functions. The outputs of Enca, Encb, and Encc are represented by za, zb, and zc, which denote the embeddings of lifestyle, clinical, and

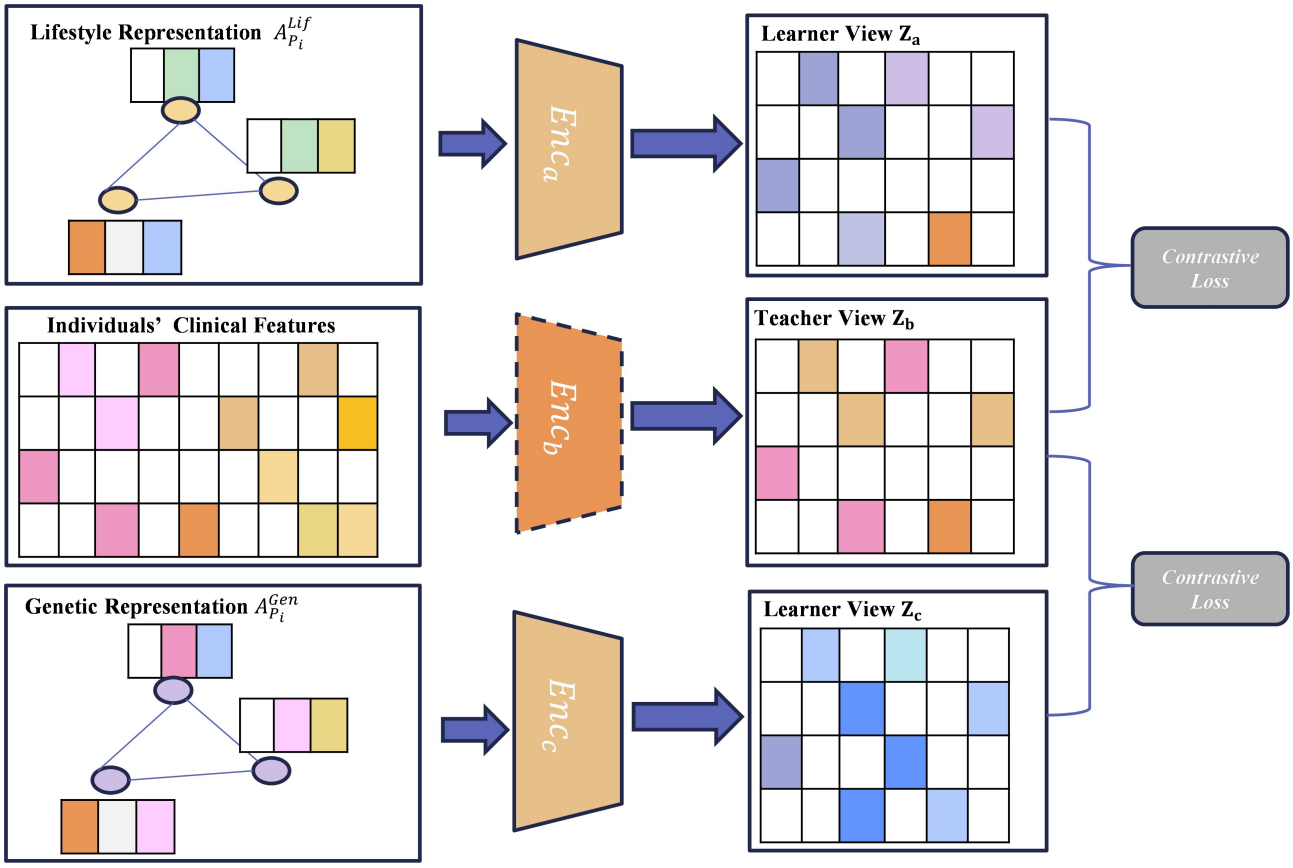
XSL•FO
RenderX

genetic family history data, respectively. For a person Pi, the objective is to align the cosine similarity of the embeddings of positive pairs {za(i),zb(i)} and {zc(i),zb(i)}, according to the infoNCEloss:

(2)Lcontrastive(za,zb)=−log⁡exp⁡(sim(za(i),zb(i))/τbatch)∑k=1nexp⁡(sim(za(i),zb(k))/τbatch)

where sim(·,·) is the similarity function, and τbatch is the temperature parameter.

Figure 3. Multiview contrastive learning component of the proposed method.



In contrastive learning, fixed temperature settings are generally ineffective for heterogeneous data distributions [75]. Therefore, we designed an adaptive temperature network (ATN) to adjust the temperature, τbatch, dynamically. As a lightweight NN, the ATN uses batch-level aggregated statistics as input and generates a single temperature value:

(3)Vbatch=1n∑inzb(i)

and

(4)τbatch=W·Relu(Vbatch)

where n is the batch size; Vbatch is the aggregated feature representation, calculated as the batch average of clinical representations {Zb(i)}; and τbatch is the temperature value for each data batch.

Both Enca and Encc are trained with a cross-entropy loss:

(5)Ltotal=Lcontrastive(za,zb)+Lcontrastive(zc,zb)

where Lcontrastive(za,zb) and Lcontrastive(zc,zb) reflect the contrastive loss between za and zb and zb and zc, respectively.

Multiview contrastive learning ensures that the learned lifestyle and family genetics embeddings (learner view) align with the clinical embeddings (teacher view), which enhances representation quality.

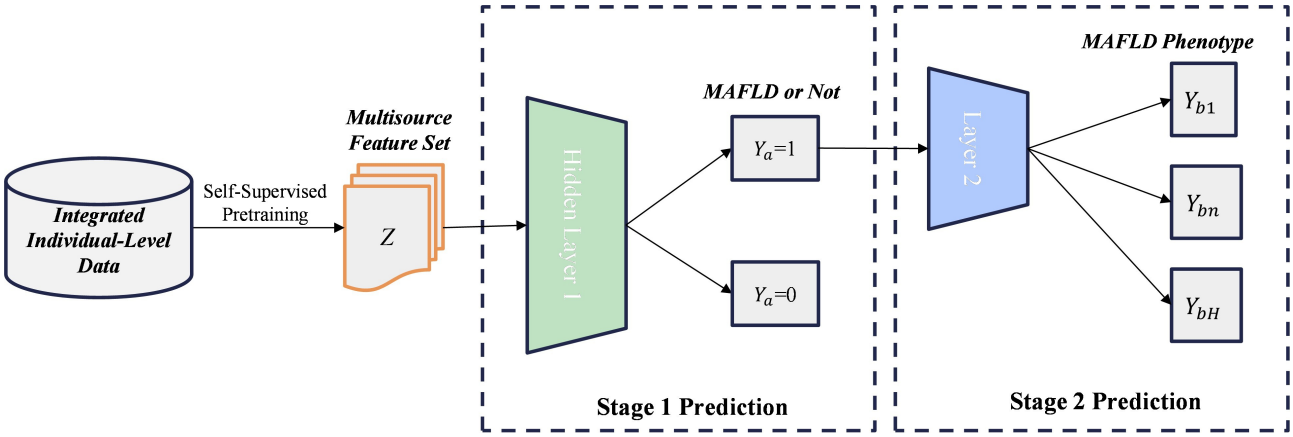
Two-Stage Risk Estimation

Finally, the 2-stage deep NN component for MAFLD phenotype prediction targets important interphenotype relationships. As depicted in Figure 4, this component estimates whether a person is likely to develop MAFLD (Y^i,a=[Y^i,a1,Y^i,a2]), such that Y^i,a1=1 if there is an indication of any MAFLD phenotype and Y^i,a1=0 otherwise. In the former case, the component then estimates the likelihood of a specific phenotype and produces the probability distribution Y^i,b=[Y^i,b1,…,Y^i,bH], corresponding to distinct phenotypes, where H is the total number of phenotypes. This hierarchical estimation design enables the proposed method to capture general characteristics of MAFLD and distinct phenotypes for predictions. The overall probability distribution Y^i can be calculated as follows:

(6)Y^i=[1−Y^i,a1,Y^i,b1·Y^i,a1,Y^i,b2·Y^i,a1,Y^i,b3·Y^i,a1,…,Y^i,bH·Y^i,a1]

XSL•FO
RenderX

Figure 4. Two-stage phenotype prediction component of the proposed method, where Y_a represents the first-stage binary prediction, indicating the presence (Y_a=1) or absence (Y_a=0) of any MAFLD phenotype. Y_b represents the second-stage probability distribution over the H specific phenotypes, which is subsequently estimated if Y_a=1. Y_{b1}, Y_{bn}, and Y_{bH} denote the estimated probabilities for the first, -th, and -th (final) specific MAFLD phenotypes, respectively. MAFLD: metabolic dysfunction–associated fatty liver disease.



In the 2-stage estimation process, we also designed a loss function to train the proposed method:

(7)Ltotal=−∑i=1Nyi(n)log(y^i(n))+γ(−∑i=1Kyi,a(k)log(y^i,a(k)))+λ(−∑i=1Mbi(m)log(y^i,b(m)))

The first term of Ltotal is the negative log-likelihood loss, calculated according to the actual and predicted MAFLD phenotype. The second and third terms denote the losses in the first and second stages, respectively, and γ and are hyperparameters that control the trade-offs among these 3 terms. Specifically, y^i(n) indicates the overall predicted probability of the nth class for person i, y^i,a(k) is the estimated probability of MAFLD (binary, k=2), and y^i,b(m) denotes the estimated probability of the mth phenotype for individuals predicted to have MAFLD in stage 2. With Ltotal, our method learns interphenotype relationships for phenotype prediction.

Evaluations

Eight prevalent methods were included as benchmarks: DT [44], RF [45], XGBoost [46], MLP [48], autoencoder [49], GAT [57], GCN [56], and GraphSAGE [58]. These methods represent different analytics approaches and are frequently used for clinical prediction tasks; therefore, they are suitable for performance comparisons. Many of these benchmark methods are not designed to deal with incomplete data. Because the sample had missing values, we applied k-nearest neighbor (k=5) imputation [76-78] to the dataset and used one-hot encoding for categorical variables during data preprocessing to ensure consistency and comparability in the evaluations, that is, all methods used the same preprocessed data for fair comparisons. The only difference was that the proposed method also used the raw, nonimputed survey data (genetic family history and lifestyle data) as input for graph representation learning and contrastive learning, which are components capable of handling missing values. Moreover, we conducted an ablation study to examine the relative contribution of each key component to the proposed method's overall performance.

To examine the prediction performance of each method, we randomly split the sample 10 times, using different random seeds to ensure robustness. In each trial, we used 80% of the data for model training and the remaining 20% for testing [76]. We also conducted 5-fold cross-validation on the training data prior to the evaluations and performed a series of analyses to fine-tune the key parameters of each method. Multimedia Appendix 2 summarizes important parameter values of the respective methods. Performance assessments relied on precision, recall, F_1-score, and AUC values. We did not consider accuracy, as it could not reflect prediction performance due to the imbalanced distribution of the outcome classes [79]. Compared with precision or recall, the F_1-score and AUC are arguably better indicators of a method's efficacy of predicting MAFLD phenotypes. As reported by Docherty et al [80], we adopted a one-versus-rest strategy to assess each outcome class and compared the respective AUC values of all methods, which supports a fair, holistic analysis of their ability to predict MAFLD phenotypes.

Results

Overall Prediction Performance

Table 2 presents each method's prediction performance across 10 trials. The proposed method has a 2-stage estimation design—stage 1 estimates whether an individual will develop MAFLD, and stage 2 predicts the likelihood of each MAFLD phenotype. Therefore, we report the results for each stage separately. As Table 2 shows, the proposed method attained higher AUC values in both stages, indicating its ability to distinguish patients with different outcomes. In stage 1, it accurately identified adults likely to develop MAFLD, with few false alarms, as signified by the relatively high precision and recall values. In stage 2, the proposed method generated effective predictions by consolidating the stage 1 results. The multiclass prediction results in stage 2 also allowed for direct comparisons with the benchmark methods. As seen in Table 2, the proposed method outperformed all benchmarks on both F_1-score and AUC. It exhibited a 7.2% improvement in AUC over the best-performing benchmark (0.898 vs 0.838) and had a 16.6% higher F_1-score than the best-performing benchmark (0.652 vs 0.559). Paired two-tailed *t* tests performed to examine differences in AUC indicated that the observed improvements were statistically significant (P<.001).

XSL•FO
RenderX

Figure 5 presents the respective receiver operating characteristic curves of all methods. The proposed method's AUC curve was notably better than that of any benchmark method. This result further affirms its superior efficacy in estimating MAFLD phenotypes among adults compared with many prevalent methods.

Table . Overall performance of each investigated method.

Method	Performance metric, mean (SE)			
	Precision	Recall	F_1-score	AUC[a]
DT[b]	0.549 (0.012)	0.468 (0.007)	0.493 (0.007)	0.765 (0.007)
RF[c]	0.576 (0.021)	0.542 (0.019)	0.541 (0.016)	0.819 (0.007)
XGBoost[d]	0.598 (0.019)	0.490 (0.015)	0.525 (0.019)	0.812 (0.019)
MLP[e]	0.567 (0.008)	0.570 (0.019)	0.557 (0.008)	0.831 (0.002)
Autoencoder	0.537 (0.011)	0.566 (0.023)	0.528 (0.010)	0.832 (0.003)
GAT[f]	0.528 (0.014)	0.542 (0.022)	0.512 (0.010)	0.823 (0.004)
GCN[g]	0.505 (0.011)	0.554 (0.012)	0.512 (0.014)	0.824 (0.005)
GraphSAGE	0.540 (0.010)	0.598 (0.011)	0.559 (0.009)	0.838 (0.004)
Proposed method (stage 1)	0.713 (0.016)	0.745 (0.008)	0.726 (0.011)	0.859 (0.004)
Proposed method (stage 2)	0.644 (0.022)	0.678 (0.027)	0.652 (0.013)	0.898 (0.003)

[a]AUC: area under the curve.

[b]DT: decision tree.

[c]RF: random forest.

[d]XGBoost: extreme gradient boosting.

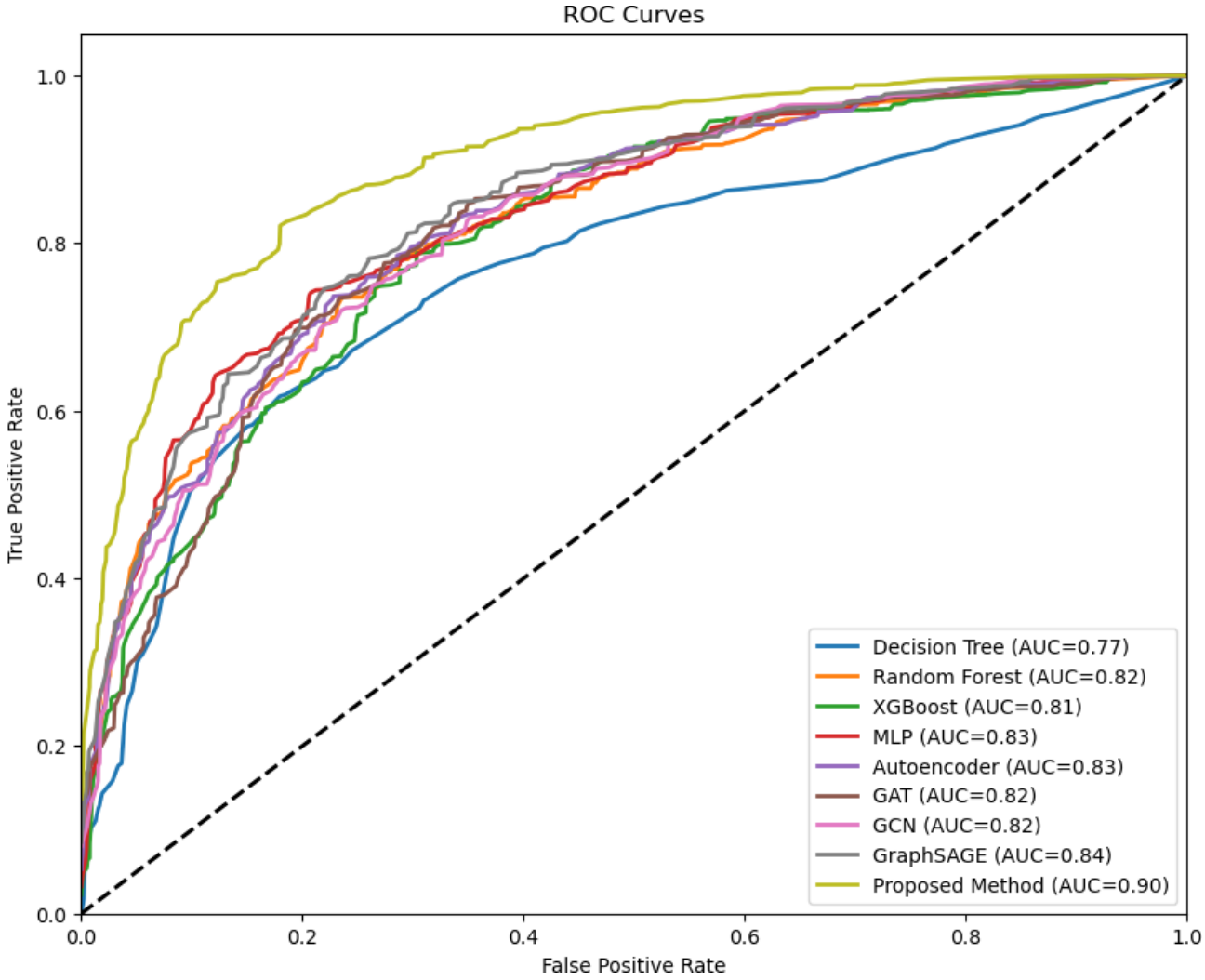
[e]MLP: multilayer perceptron.

[f]GAT: graph attention network.

[g]GCN: graph convolutional network.

XSL•FO
RenderX

Figure 5. Area under the curve (AUC) values for the investigated methods. GAT: graph attention network; GCN: graph convolutional network; MLP: multilayer perceptron; ROC: receiver operating characteristic.



Prediction Performance for Each Outcome Class

In addition to overall performance, we examined the respective methods' performance for each outcome class. As shown in Table 3, the proposed method achieved the highest F_1-score and AUC values for each outcome class, reaffirming its superior prediction ability. It attained a higher F_1-score (0.913) and AUC (0.859) for non-MAFLD than the respective best-performing benchmarks (DT: F_1-score=0.908; GraphSAGE: AUC=0.801). The performance improvements were especially prominent for the MAFLD phenotypes. For nondiabetic MAFLD, our method achieved an F_1-score of 0.531, much higher than that of the best-performing benchmark (MLP: F_1-score=0.400), exhibiting a 32.8% improvement. It also attained the highest AUC (0.878), higher than that of the best-performing benchmark (GraphSAGE: AUC=0.804). For diabetic MAFLD, the proposed method's F_1-score (0.519) was 30.4% higher than that of the best-performing benchmark (GraphSAGE: F_1-score=0.398). Moreover, its precision value was superior to that of other methods, suggesting that it can identify adults who are likely to develop diabetic MAFLD with fewer false alarms.

XSL•FO
RenderX

Table . Prediction performance of each method for 3 outcome classes.

Outcome class and method	Performance metric, mean (SE)			
	Precision	Recall	F_1-score	AUC
Non-MAFLD[a]				
Decision tree	0.879 (0.002)	0.941 (0.004)	0.908 (0.002)	0.746 (0.007)
Random forest	0.892 (0.004)	0.938 (0.003)	0.901 (0.004)	0.781 (0.006)
XGBoost[b]	0.881 (0.002)	0.954 (0.003)	0.895 (0.004)	0.798 (0.006)
MLP[c]	0.899 (0.004)	0.898 (0.010)	0.897 (0.003)	0.788 (0.005)
Autoencoder	0.905 (0.004)	0.878 (0.011)	0.892 (0.004)	0.800 (0.005)
GAT[d]	0.899 (0.006)	0.845 (0.023)	0.870 (0.012)	0.777 (0.008)
GCN[e]	0.913 (0.004)	0.825 (0.032)	0.861 (0.018)	0.799 (0.005)
GraphSAGE	0.907 (0.003)	0.875 (0.011)	0.890 (0.005)	0.801 (0.004)
Proposed method	0.925 (0.005)	0.899 (0.017)	0.913 (0.008)	0.859 (0.011)
Nondiabetic MAFLD				
Decision tree	0.436 (0.016)	0.253 (0.021)	0.316 (0.019)	0.781 (0.010)
Random forest	0.444 (0.021)	0.334 (0.031)	0.359 (0.028)	0.787 (0.009)
XGBoost	0.495 (0.020)	0.251 (0.016)	0.329 (0.015)	0.803 (0.005)
MLP	0.423 (0.016)	0.392 (0.026)	0.400 (0.017)	0.800 (0.006)
Autoencoder	0.347 (0.026)	0.344 (0.020)	0.337 (0.014)	0.777 (0.008)
GAT	0.301 (0.022)	0.387 (0.045)	0.323 (0.014)	0.777 (0.007)
GCN	0.280 (0.014)	0.421 (0.055)	0.317 (0.016)	0.765 (0.007)
GraphSAGE	0.384 (0.018)	0.405 (0.023)	0.388 (0.014)	0.804 (0.008)
Proposed method	0.506 (0.016)	0.563 (0.021)	0.531 (0.019)	0.878 (0.003)
Diabetic MAFLD				
Decision tree	0.331 (0.022)	0.210 (0.013)	0.255 (0.015)	0.769 (0.018)
Random forest	0.392 (0.023)	0.381 (0.035)	0.363 (0.024)	0.891 (0.012)
XGBoost	0.450 (0.027)	0.255 (0.010)	0.323 (0.012)	0.848 (0.018)
MLP	0.376 (0.020)	0.421 (0.053)	0.371 (0.020)	0.905 (0.008)
Autoencoder	0.358 (0.045)	0.480 (0.071)	0.354 (0.023)	0.920 (0.003)
GAT	0.378 (0.043)	0.395 (0.061)	0.344 (0.022)	0.915 (0.006)
GCN	0.322 (0.025)	0.417 (0.046)	0.353 (0.025)	0.907 (0.007)
GraphSAGE	0.330 (0.024)	0.519 (0.033)	0.398 (0.023)	0.917 (0.005)
Proposed method	0.500 (0.016)	0.570 (0.042)	0.519 (0.019)	0.957 (0.009)

[a]MAFLD: metabolic dysfunction–associated fatty liver disease.

[b]XGBoost: extreme gradient boosting.

[c]MLP: multilayer perceptron.

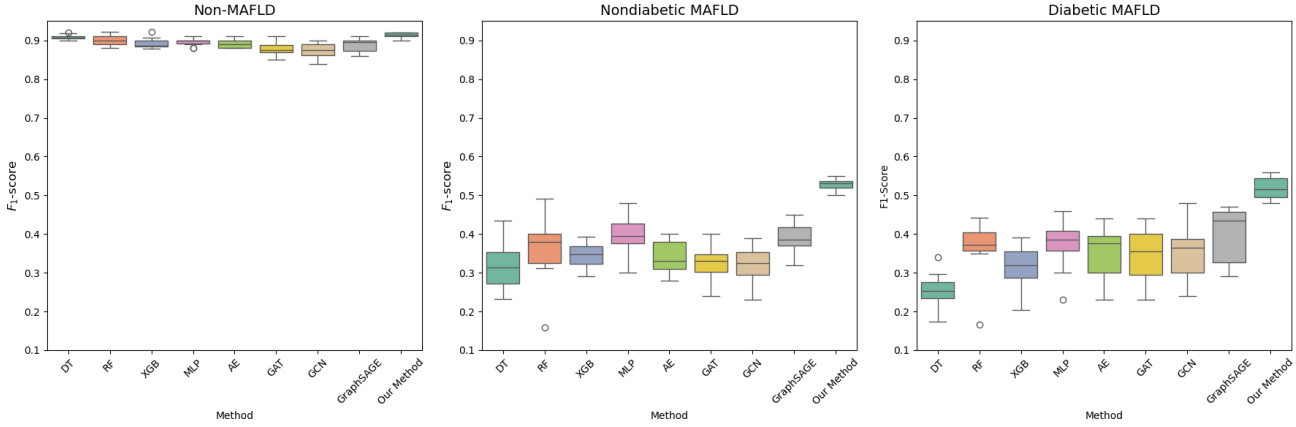
[d]GAT: graph attention network.

[e]GCN: graph convolutional network.

The box plots in Figure 6 indicate the proposed method's robust performance for each outcome class across 10 trials. It attained high F_1-scores for each outcome class, especially nondiabetic MAFLD and diabetic MAFLD, while the benchmark methods exhibited notably greater variance and occasional outliers. Together, these plots provide further evidence of the proposed method's efficacy and value for clinical decision-making and patient management.

XSL•FO
RenderX

Figure 6. Box plots showing F_1-scores (median and IQR) of each method for different outcome classes. AE: autoencoder; DT: decision tree; GAT: graph attention network; GCN: graph convolutional network; MAFLD: metabolic dysfunction–associated fatty liver disease; MLP: multilayer perceptron; RF: random forest; XGBoost: extreme gradient boosting.



Ablation Study

We also performed an ablation study to examine the relative contribution of each key component of the proposed method. We considered MLP, Graph, Graph + contrastive learning, and the (complete) proposed method. In essence, MLP serves as a baseline because it only uses the preprocessed data, without any key components of the proposed method. Graph builds on MLP and includes the graph representation learning of genetic family history and lifestyle data, together with the learned embeddings concatenated to the preprocessed dataset to train the MLP classifier. Graph + contrastive learning further extends Graph by incorporating contrastive learning after graph representation learning. The complete proposed method included all 3 key components. The results of the ablation study (Table 4) revealed how each component contributed to the method's performance. They jointly produced the best predictions, indicating that MAFLD phenotype prediction can benefit from graph representation, multiview contrastive pretraining, and 2-stage estimation design.

Table . Results of the ablation study.

Model	AUC[a]
MLP[b]	0.831 (0.002)
Graph	0.847 (0.004)
Graph + CL[c]	0.881 (0.001)
Complete proposed method	0.898 (0.003)

[a]AUC: area under the curve.

[b]MLP: multilayer perceptron.

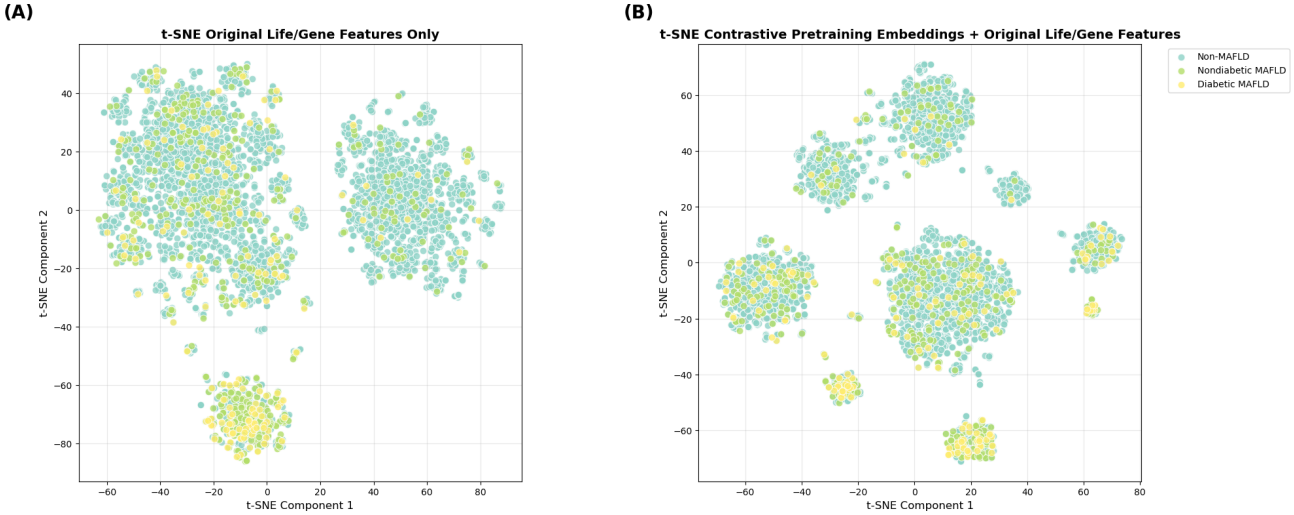
[c]CL: contrastive learning.

Interpretability Analysis

To gain clinical insights into the proposed method's learned representations, we examined its interpretability by depicting the embeddings visually. Specifically, we applied t-distributed stochastic neighbor embedding (t-SNE) [81] to visualize the contrastive pretraining embeddings and performed a Shapley additive explanation (SHAP) analysis [82] to reveal feature importance. Figure 7A presents a visualization of the original lifestyle and genetic features, and Figure 7B provides a visualization of the features obtained by concatenating the contrastive pretraining embeddings with the original lifestyle and genetic features. The original lifestyle and genetic features exhibited a scattered distribution, without any clear patterns. With contrastive pretraining embeddings, more distinctive clusters emerged, suggesting that patients with similar characteristics tend to cluster more closely than those with dissimilar characteristics. While these visual plots are exploratory without formal proof of class separability, they still illustrate that incorporating contrastive pretraining embeddings can potentially create a more structured, distinguishable representation of patient outcomes for effective MAFLD phenotype prediction.

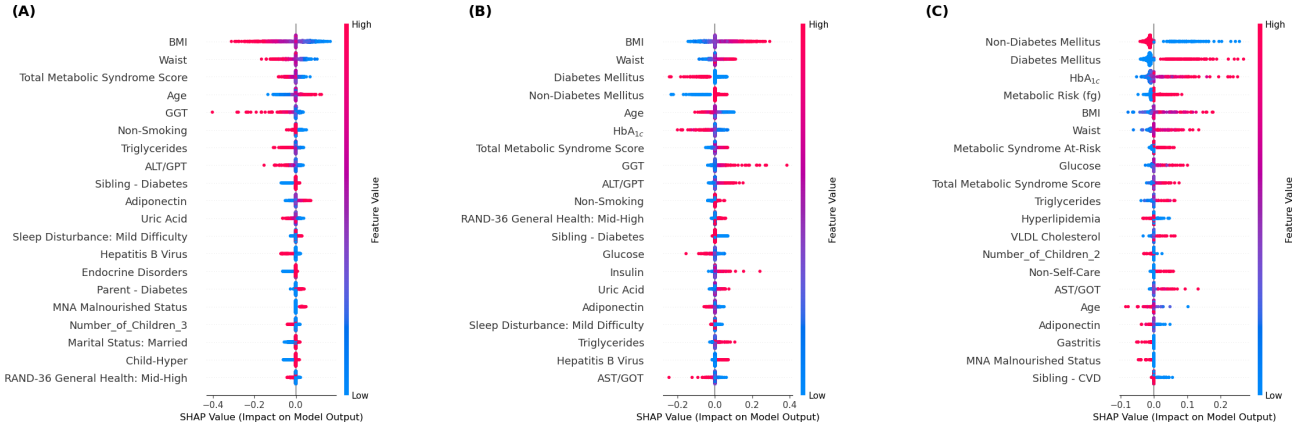
XSL•FO
RenderX

Figure 7. T-distributed stochastic neighbor embedding (t-SNE) visualization of (A) original lifestyle and genetic (life/gene) features and (B) contrastive pretraining embeddings with lifestyle and genetic features. MAFLD: metabolic dysfunction–associated fatty liver disease.



We further examined the feature importance for each outcome class, as depicted by the SHAP summary plots in Figure 8. Because the proposed method adopted a 2-stage estimation (architecture) design, the model-agnostic explainer KernelSHAP was used with a background dataset of 100 training instances. For all test instances, SHAP values were computed on a representative model instance (ie, median test AUC across 10 trials). As seen in Figure 8, several metabolic indicators were important predictors consistently across different outcome classes. For example, BMI and waist circumference were highly influential. As Figure 8A shows, high BMI values (marked as red points) greatly reduced the likelihood of non-MAFLD predictions; particularly, high BMI and waist circumference values were associated with a greater likelihood of nondiabetic MAFLD or diabetic MAFLD, as shown in Figure 8B and C. Predictions of nondiabetic MAFLD were influenced by a combination of general metabolic indicators (eg, BMI and waist circumference) and lifestyle factors (eg, smoking and sleep disturbance). For diabetic MAFLD, definitive disease markers and factors related to disease consequence and management, such as self-care status and nutritional status (Mini Nutritional Assessment), appeared to be essential auxiliary predictors. These results align with clinical knowledge and reveal the proposed method's ability to capture phenotype-specific patterns from patient data, with desirable interpretability.

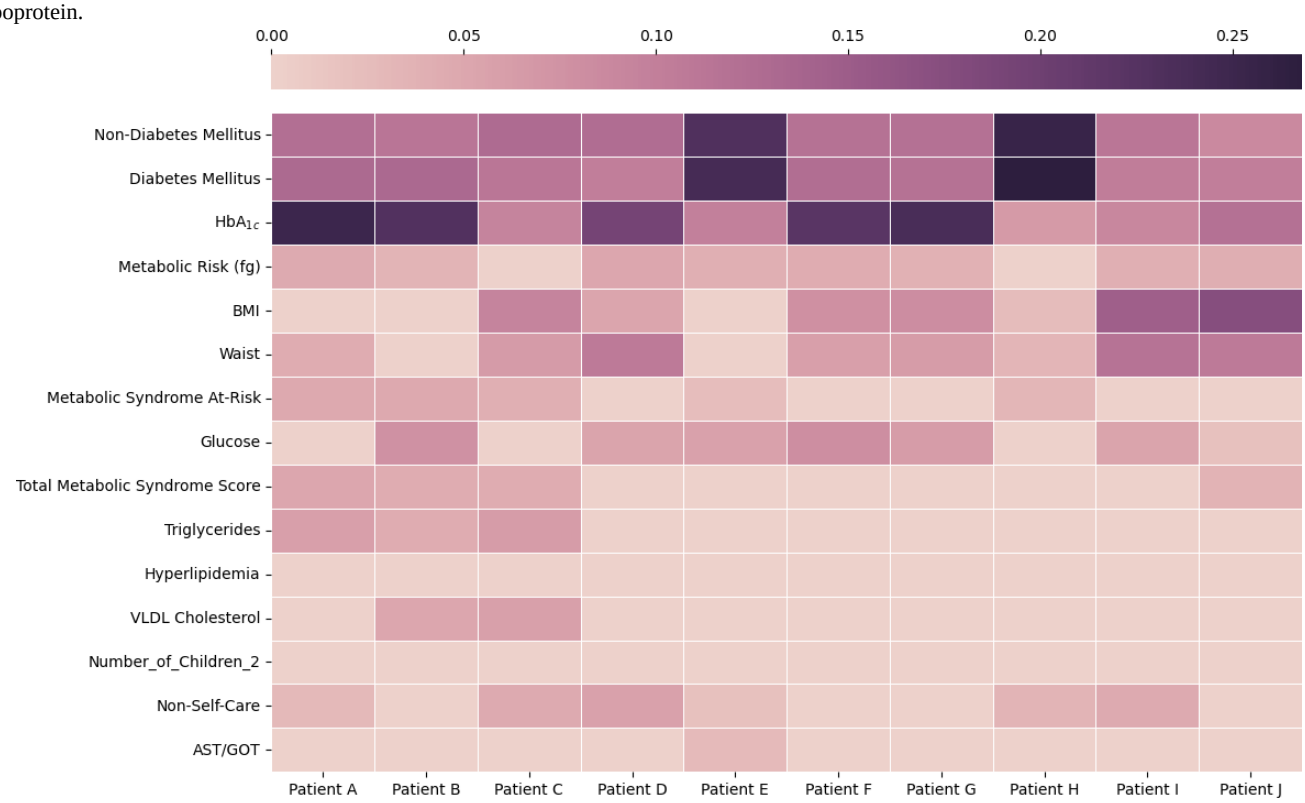
Figure 8. Summary plots of Shapley additive explanation (SHAP) values for (A) non–metabolic dysfunction–associated fatty liver disease (non-MAFLD), (B) nondiabetic MAFLD, and (C) diabetic MAFLD. ALT/GPT: alanine aminotransferase/glutamic-pyruvic transaminase; AST/GOT: aspartate aminotransferase/glutamic-oxaloacetic transaminase; CVD: cardiovascular disease; GGT: gamma-glutamyl transferase; HbA_{1c}: hemoglobin A_{1c}; MNA: Mini Nutritional Assessment.



Additionally, SHAP analyses allow for reasoning at the individual level. Figure 9 provides a visualization of SHAP values for 10 patients who were predicted to develop diabetic MAFLD. The heat map shows that diabetes mellitus and high hemoglobin A_{1c} diagnoses were consistently important predictors for most patients in this group, including patients B, G, and H. We also observed significant intraphenotype variability among patients. For example, the prediction for patient J was also significantly influenced by BMI and waist circumference, whereas triglycerides were a more important factor for patient C. The interpatient variability can help physicians better understand the impact of different factors at the individual level and thereby support personalized care and treatment planning.

XSL•FO
RenderX

Figure 9. Heat map of sample patients with the predicted phenotype diabetic metabolic dysfunction–associated fatty liver disease (diabetic MAFLD) and top 15 features. AST/GOT: aspartate aminotransferase/glutamic oxaloacetic transaminase; HbA_{1c}: hemoglobin A_{1c}; VLDL, very-low-density lipoprotein.



Discussion

Principal Findings

The proposed method leverages deep learning to estimate MAFLD phenotypes among adults, using graph representation learning and contrastive learning. It provides several methodological novelties that can advance medical informatics research and enhance clinical decision-making for improved patient management. The evaluation results establish its predictive efficacy, demonstrate the value of combining clinical and survey-based data, and underscore the importance of intraphenotype variability and disease dynamics for MAFLD phenotype prediction. Furthermore, this method is generalizable and can be applied to other prediction tasks in similar clinical scenarios (eg, gauging the risk of diabetes or CVD) that feature multisource data, individual heterogeneities, intraclass variance, and intervariable relationships.

Using the proposed method, physicians will be able to identify individuals at higher risk of fibrosis and generate timely alerts for effective patient-centric care [83], which can mitigate the likelihood of significant disease progression and serious patient outcomes. Accurate prediction of MAFLD phenotypes also helps reduce hepatic complications such as CVD, chronic kidney disease [16], hepatocellular carcinoma [6], osteoporosis, endocrine disorders, and cognitive impairment [84]. The proposed method is capable of distinguishing high-risk versus low-risk adults on the basis of pathogenesis, spanning lifestyle, genetic, and metabolic factors; as a result, the likelihood of fibrosis or cirrhosis can be reduced, with broad implications for precision medicine and drug development [85]. In a related sense, its ability to predict phenotypes in an accurate and timely manner also enables personalized surveillance, treatment choice assessments, lifestyle changes, and treatment planning.

Although the proposed method does not achieve an objectively high F_1-score for MAFLD phenotypes, it still offers meaningful improvements over prevalent methods, even in the presence of the inherent challenges created by highly imbalanced patient clinical data. In our sample, most adults were in the non-MAFLD category, and few had MAFLD phenotypes, which made model training difficult for every method we investigated. This challenge is common to many clinical settings and has been documented across different patient outcome or risk prediction tasks. For example, recent related studies report F_1-scores in the range between 0.10 and 0.51 for minority classes [86,87]. Despite this persistent difficulty, the proposed method consistently outperformed all the benchmarks on MAFLD phenotypes (minority classes), which are clinically important. Hence, the observed improvements with our method represent valuable advances [22,88].

We illustrate the clinical use of the proposed method as a proactive risk stratification approach for clinical decision support and patient management. In stage 1, it estimates the probability of a person developing MAFLD within 1 year. To flag individuals as high risk, a physician can use the probability to select a decision threshold for balancing the trade-off between precision (the proportion of flagged individuals who are truly at high risk) and recall (the proportion of all true positive individuals who are truly flagged as high risk). If the physician prefers high certainty, they can choose a high threshold value. For example, our post hoc analysis showed that by setting the

XSL•FO
RenderX

threshold to 0.60, the proposed method's precision increased to 0.777, that is, approximately 78% of flagged patients indeed developed MAFLD. By choosing an even higher threshold value of 0.70, its precision further increased to 0.820, although at the cost of reduced sensitivity (0.59 in recall). As a result, the physician can identify adults who should be monitored more closely (for example, a semiannual follow-up instead of an annual follow-up), need immediate lifestyle counseling, or require proactive baseline liver function tests to track changes over time.

Furthermore, the proposed method provides additional insights based on the stage 2 estimate, which can support personalized planning and care. In general, obtaining clinically meaningful precision requires a higher threshold value. For example, with a threshold value of 0.50, the proposed method's precision reached 0.506 for nondiabetic MAFLD and 0.500 for diabetic MAFLD. Emphasizing high-probability instances with a threshold value of 0.70 increased the precision to 0.762 and 0.778, respectively, which would allow physicians to tailor management strategies for adults whose phenotype can be predicted with higher confidence. Additionally, physicians can leverage the instance-level SHAP analysis, as depicted in Figure 9, to identify the specific factors that drive patient risk. While these insights do not directly indicate a definitive diagnosis, they can still guide physicians to engage in preventive care through patient risk stratification, while coping with the challenge of precise phenotype classification. Overall, physicians can adopt an appropriate threshold value to balance precision and recall while minimizing the likelihood of missing at-risk individuals for proactive stratification.

In summary, a multiview architecture leverages complementary information from lifestyle, genetic, and clinical data perspectives for richer representations that help distinguish infrequent yet clinically important MAFLD phenotypes, without sacrificing interpretability. The 2-stage design offers flexibility and additional utility. Accurate and robust estimates in stage 1 help physicians assess whether or not an individual is likely to develop MAFLD for initial screening purposes. In addition to that determination, even a moderate improvement in the F_1-score in stage 2 can facilitate physicians' decision-making by providing additional information and clinical insights. These valuable risk stratification capabilities enable physicians to identify high-risk adults who may need close monitoring or alternative treatments. The 2-stage design also offers beneficial flexibility. Physicians can adjust their focus across the first or second stage, depending on their objective (eg, early screening, risk stratification, or intervention planning). According to 2 experienced hepatologists (who wish to remain anonymous), "Early, better estimates of individuals' likelihood of MAFLD is valuable clinically," and "The use of data-driven analytics methods to predict MAFLD phenotypes can enhance clinical decision-making and personalized patient management" (September 2, 2025). These expert inputs affirm the clinical value and practicality of our proposed method.

Limitations and Research Directions

This study has several limitations, and it can be extended by further research. First, we used a sample from a single healthcare organization, which offered relatively limited diversity in terms of data sources and patient populations. In a related sense, our sample was imbalanced in the outcome class distribution, which constrained the prediction performance for minority classes, as reflected by the relatively low F_1-scores, which is in line with previous research [87]. Future studies should consider additional data sources and types such as image and text [89] to extend the proposed method, use different patient cohorts to affirm its efficacy, and apply synthetic data augmentation or multimodal foundation models to better address the issue of imbalanced outcome class distribution with cross-modal learning capabilities [62]. Second, because intraphenotype variability introduces complexity with regard to achieving compact clusters in the embedding space, a trade-off arises between variability and compactness, which could restrict the predictive utility for large datasets or different diseases. Therefore, we call for efforts to explore an optimal balance of variability and compactness for both accuracy and generalizability, such as clustering-based contrastive learning [90]. Third, the proposed 2-stage method provides some limited interpretability, through a feature attribution–based approach (ie, SHAP); its contrastive pretraining component deserves further exploration for greater transferability and interpretability. Ongoing efforts could facilitate and interpret embeddings in focal clinical contexts. Fourth, an international, multisociety Delphi process led to the proposal of metabolic dysfunction–associated steatotic liver disease (MASLD) in 2023 [91]. Although our findings might be extrapolated to adults with MASLD [92], the proposed method should be extended with research that tests for differences between MAFLD and MASLD and refines the proposed method to ensure robustness and prediction performance.

Conclusion

Predicting MAFLD phenotypes among adults is crucial, but existing analytic methods overlook its multisystem nature and phenotypic heterogeneity. As a solution, we developed a novel method that leverages graph representation learning, multiview contrastive pretraining, and a 2-stage estimation design to produce effective predictions that reflect phenotypic heterogeneity, complex relationships, and disease dynamics. It is effective in identifying at-risk adults and thus offers support for clinical decision-making and personalized care. This study reveals a promising pathway to advance health informatics research and clinical practice by leveraging rich, detailed clinical data in electronic health records and survey-based data to predict MAFLD phenotypes.

Acknowledgments

This work was partially supported by the Chang Gung Memorial Hospital Research Project (CRRPG2H0061-5).

XSL•FO
RenderX

Data Availability

The data used in this study cannot be made publicly accessible, because the patient consensus that we obtained does not articulate data access by other institutions and individuals.

The authors can arrange data access upon request.

Conflicts of Interest

None declared.

Multimedia Appendix 1
Description and coding of variables.
[DOCX File, 32 KB - medinform_v13i1e75747_app1.docx]

Multimedia Appendix 2
Key hyperparameters of the investigated methods.
[DOCX File, 15 KB - medinform_v13i1e75747_app2.docx]

References

1. Kim D, Konyn P, Sandhu KK, Dennis BB, Cheung AC, Ahmed A. Metabolic dysfunction-associated fatty liver disease is associated with increased all-cause mortality in the United States. J Hepatol 2021 Dec;75(6):1284-1291. [doi: 10.1016/j.jhep.2021.07.035] [Medline: 34380057]
2. Devarbhavi H, Asrani SK, Arab JP, Nartey YA, Pose E, Kamath PS. Global burden of liver disease: 2023 update. J Hepatol 2023 Aug;79(2):516-537. [doi: 10.1016/j.jhep.2023.03.017] [Medline: 36990226]
3. Younossi ZM, Blissett D, Blissett R, et al. The economic and clinical burden of nonalcoholic fatty liver disease in the United States and Europe. Hepatology 2016 Nov;64(5):1577-1586. [doi: 10.1002/hep.28785] [Medline: 27543837]
4. Gofton C, Upendran Y, Zheng MH, George J. MAFLD: How is it different from NAFLD? Clin Mol Hepatol 2023 Feb;29(Suppl):S17-S31. [doi: 10.3350/cmh.2022.0367] [Medline: 36443926]
5. De A, Ahmad N, Mehta M, Singh P, Duseja A. NAFLD vs. MAFLD - it is not the name but the disease that decides the outcome in fatty liver. J Hepatol 2022 Feb;76(2):475-477. [doi: 10.1016/j.jhep.2021.09.002] [Medline: 34530064]
6. Huang DQ, El-Serag HB, Loomba R. Global epidemiology of NAFLD-related HCC: trends, predictions, risk factors and prevention. Nat Rev Gastroenterol Hepatol 2021 Apr;18(4):223-238. [doi: 10.1038/s41575-020-00381-6] [Medline: 33349658]
7. Yamamura S, Eslam M, Kawaguchi T, et al. MAFLD identifies patients with significant hepatic fibrosis better than NAFLD. Liver Int 2020 Dec;40(12):3018-3030. [doi: 10.1111/liv.14675] [Medline: 32997882]
8. Stefan N, Yki-Järvinen H, Neuschwander-Tetri BA. Metabolic dysfunction-associated steatotic liver disease: heterogeneous pathomechanisms and effectiveness of metabolism-based treatment. Lancet Diabetes Endocrinol 2025 Feb;13(2):134-148. [doi: 10.1016/S2213-8587(24)00318-8] [Medline: 39681121]
9. Tampaki M, Papatheodoridis GV, Cholongitas E. Management of hepatocellular carcinoma in decompensated cirrhotic patients: a comprehensive overview. Cancers (Basel) 2023 Feb 18;15(4):1310. [doi: 10.3390/cancers15041310] [Medline: 36831651]
10. Dowman JK, Armstrong MJ, Tomlinson JW, Newsome PN. Current therapeutic strategies in non-alcoholic fatty liver disease. Diabetes Obes Metab 2011 Aug;13(8):692-702. [doi: 10.1111/j.1463-1326.2011.01403.x] [Medline: 21449949]
11. Moriwaki H. Prevention of liver cancer: basic and clinical aspects. Exp Mol Med 2002 Nov 30;34(5):319-325. [doi: 10.1038/emm.2002.45] [Medline: 12526094]
12. Eslam M, Newsome PN, Sarin SK, et al. A new definition for metabolic dysfunction-associated fatty liver disease: an international expert consensus statement. J Hepatol 2020 Jul;73(1):202-209. [doi: 10.1016/j.jhep.2020.03.039] [Medline: 32278004]
13. Sohn W, Kwon HJ, Chang Y, Ryu S, Cho YK. Liver fibrosis in Asians with metabolic dysfunction-associated fatty liver disease. Clin Gastroenterol Hepatol 2022 May;20(5):e1135-e1148. [doi: 10.1016/j.cgh.2021.06.042] [Medline: 34224877]
14. Lim TS, Chun HS, Kim SS, et al. Fibrotic burden in the liver differs across metabolic dysfunction-associated fatty liver disease subtypes. Gut Liver 2023 Jul 15;17(4):610-619. [doi: 10.5009/gnl220400] [Medline: 36799062]
15. Santos RD, Valenti L, Romeo S. Does nonalcoholic fatty liver disease cause cardiovascular disease? Current knowledge and gaps. Atherosclerosis 2019 Mar;282:110-120. [doi: 10.1016/j.atherosclerosis.2019.01.029] [Medline: 30731283]
16. Wang TY, Wang RF, Bu ZY, et al. Association of metabolic dysfunction-associated fatty liver disease with kidney disease. Nat Rev Nephrol 2022 Apr;18(4):259-268. [doi: 10.1038/s41581-021-00519-y] [Medline: 35013596]
17. Sakurai Y, Kubota N, Yamauchi T, Kadowaki T. Role of insulin resistance in MAFLD. Int J Mol Sci 2021 Apr 16;22(8):4156. [doi: 10.3390/ijms22084156] [Medline: 33923817]

XSL•FO
RenderX

18. Fukunaga S, Nakano D, Kawaguchi T, et al. Non-obese MAFLD is associated with colorectal adenoma in health check examinees: a multicenter retrospective study. Int J Mol Sci 2021 May 22;22(11):5462. [doi: 10.3390/ijms22115462] [Medline: 34067258]
19. Huang J, Ou W, Wang M, et al. MAFLD criteria guide the subtyping of patients with fatty liver disease. Risk Manag Healthc Policy 2021;Volume 14:491-501. [doi: 10.2147/RMHP.S285880]
20. Eslam M, Sanyal AJ, George J, International Consensus Panel. MAFLD: a consensus-driven proposed nomenclature for metabolic associated fatty liver disease. Gastroenterology 2020 May;158(7):1999-2014. [doi: 10.1053/j.gastro.2019.11.312] [Medline: 32044314]
21. Chung GE, Yu SJ, Yoo JJ, et al. Lean or diabetic subtypes predict increased all-cause and disease-specific mortality in metabolic-associated fatty liver disease. BMC Med 2023 Jan 4;21(1):4. [doi: 10.1186/s12916-022-02716-3] [Medline: 36600263]
22. Chen S, Xue H, Huang R, Chen K, Zhang H, Chen X. Associations of MAFLD and MAFLD subtypes with the risk of the incident myocardial infarction and stroke. Diabetes Metab 2023 Sep;49(5):101468. [doi: 10.1016/j.diabet.2023.101468] [Medline: 37586479]
23. Kwon OY, Choi JY, Jang Y. The effectiveness of eHealth interventions on lifestyle modification in patients with nonalcoholic fatty liver disease: systematic review and meta-analysis. J Med Internet Res 2023 Jan 23;25:e37487. [doi: 10.2196/37487] [Medline: 36689264]
24. Kleiner DE. Hepatocellular carcinoma: liver biopsy in the balance. Hepatology 2018 Jul;68(1):13-15. [doi: 10.1002/hep.29831] [Medline: 29405373]
25. Ronot M, Bahrami S, Calderaro J, et al. Hepatocellular adenomas: accuracy of magnetic resonance imaging and liver biopsy in subtype classification. Hepatology 2011 Apr;53(4):1182-1191. [doi: 10.1002/hep.24147] [Medline: 21480324]
26. Kantartzis K, Rettig I, Staiger H, et al. An extended fatty liver index to predict non-alcoholic fatty liver disease. Diabetes Metab 2017 Jun;43(3):229-239. [doi: 10.1016/j.diabet.2016.11.006]
27. Ben-Assuli O, Jacobi A, Goldman O, et al. Stratifying individuals into non-alcoholic fatty liver disease risk levels using time series machine learning models. J Biomed Inform 2022 Feb;126:103986. [doi: 10.1016/j.jbi.2022.103986] [Medline: 35007752]
28. Cheng KL, Wang SW, Cheng YM, Hsieh TH, Wang CC, Kao JH. Prevalence and clinical outcomes in subtypes of metabolic associated fatty liver disease. J Formos Med Assoc 2024 Jan;123(1):36-44. [doi: 10.1016/j.jfma.2023.07.010] [Medline: 37491179]
29. Byrne CD, Targher G. NAFLD: a multisystem disease. J Hepatol 2015 Apr;62(1 Suppl):S47-S64. [doi: 10.1016/j.jhep.2014.12.012] [Medline: 25920090]
30. Ghazanfar H, Javed N, Qasim A, et al. Metabolic dysfunction-associated steatohepatitis and progression to hepatocellular carcinoma: a literature review. Cancers (Basel) 2024 Mar 20;16(6):1214. [doi: 10.3390/cancers16061214] [Medline: 38539547]
31. Huang TS, Wu IW, Lin CL, Shyu YC, Chen YC, Chien RN. Prognosis of chronic kidney disease in patients with non-alcoholic fatty liver disease: a northeastern Taiwan community medicine research cohort. Biomed J 2023 Apr;46(2):100532. [doi: 10.1016/j.bj.2022.04.003] [Medline: 35460926]
32. Lin S, Huang J, Wang M, et al. Comparison of MAFLD and NAFLD diagnostic criteria in real world. Liver Int 2020 Sep;40(9):2082-2089. [doi: 10.1111/liv.14548] [Medline: 32478487]
33. Kim MN, Han K, Yoo J, Hwang SG, Zhang X, Ahn SH. Diabetic MAFLD is associated with increased risk of hepatocellular carcinoma and mortality in chronic viral hepatitis patients. Intl Journal of Cancer 2023 Oct 15;153(8):1448-1458. [doi: 10.1002/ijc.34637]
34. Wu H, Ballantyne CM. Metabolic inflammation and insulin resistance in obesity. Circ Res 2020 May 22;126(11):1549-1564. [doi: 10.1161/CIRCRESAHA.119.315896] [Medline: 32437299]
35. Kuchay MS, Choudhary NS, Mishra SK. Pathophysiological mechanisms underlying MAFLD. Diabetes Metab Syndr: Clin Res Rev 2020 Nov;14(6):1875-1887. [doi: 10.1016/j.dsx.2020.09.026]
36. Stefano JT, Duarte SMB, Ribeiro Leite Altikes RG, Oliveira CP. Non-pharmacological management options for MAFLD: a practical guide. Ther Adv Endocrinol Metab 2023;14:20420188231160394. [doi: 10.1177/20420188231160394] [Medline: 36968655]
37. Lencioni R. Loco-regional treatment of hepatocellular carcinoma. Hepatology 2010 Aug;52(2):762-773. [doi: 10.1002/hep.23725] [Medline: 20564355]
38. Wu CT, Chu TW, Jang JSR. Current-visit and next-visit prediction for fatty liver disease with a large-scale dataset: model development and performance comparison. JMIR Med Inform 2021 Aug 12;9(8):e26398. [doi: 10.2196/26398] [Medline: 34387552]
39. Wong VWS, Wong GLH, Chan RSM, et al. Beneficial effects of lifestyle intervention in non-obese patients with non-alcoholic fatty liver disease. J Hepatol 2018 Dec;69(6):1349-1356. [doi: 10.1016/j.jhep.2018.08.011] [Medline: 30142427]
40. Montemayor S, Bouzas C, Mascaró CM, et al. Effect of dietary and lifestyle interventions on the amelioration of NAFLD in patients with metabolic syndrome: the FLIPAN study. Nutrients 2022 May 26;14(11):2223. [doi: 10.3390/nu14112223] [Medline: 35684022]

XSL•FO
RenderX

41. Wu Y, Yang X, Morris HL, et al. Noninvasive diagnosis of nonalcoholic steatohepatitis and advanced liver fibrosis using machine learning methods: comparative study with existing quantitative risk scores. JMIR Med Inform 2022 Jun 6;10(6):e36997. [doi: 10.2196/36997] [Medline: 35666557]
42. Jia X, Baig MM, Mirza F, GholamHosseini H. A Cox-based risk prediction model for early detection of cardiovascular disease: identification of key risk factors for the development of a 10-year CVD risk prediction. Adv Prev Med 2019;2019:8392348. [doi: 10.1155/2019/8392348] [Medline: 31093375]
43. Książek W, Gandor M, Pławiak P. Comparison of various approaches to combine logistic regression with genetic algorithms in survival prediction of hepatocellular carcinoma. Comput Biol Med 2021 Jul;134:104431. [doi: 10.1016/j.compbiomed.2021.104431] [Medline: 34015670]
44. Yu CS, Lin YJ, Lin CH, et al. Predicting metabolic syndrome with machine learning models using a decision tree algorithm: retrospective cohort study. JMIR Med Inform 2020 Mar 23;8(3):e17110. [doi: 10.2196/17110] [Medline: 32202504]
45. Zhang L, Huang Y, Huang M, Zhao CH, Zhang YJ, Wang Y. Development of cost-effective fatty liver disease prediction models in a Chinese population: statistical and machine learning approaches. JMIR Form Res 2024 Feb 16;8:e53654. [doi: 10.2196/53654] [Medline: 38363597]
46. Huang G, Jin Q, Mao Y. Predicting the 5-year risk of nonalcoholic fatty liver disease using machine learning models: prospective cohort study. J Med Internet Res 2023 Sep 12;25:e46891. [doi: 10.2196/46891] [Medline: 37698911]
47. Chen YS, Chen D, Shen C, et al. A novel model for predicting fatty liver disease by means of an artificial neural network. Gastroenterol Rep (Oxf) 2020 Aug;9(1):31-37. [doi: 10.1093/gastro/goaa035] [Medline: 33747524]
48. Edelson M, Kuo TT. Generalizable prediction of COVID-19 mortality on worldwide patient data. JAMIA Open 2022 Jul;5(2):ooac036. [doi: 10.1093/jamiaopen/ooac036] [Medline: 35663116]
49. Franco EF, Rana P, Cruz A, et al. Performance comparison of deep learning autoencoders for cancer subtype detection using multi-omics data. Cancers (Basel) 2021 Apr 22;13(9):2013. [doi: 10.3390/cancers13092013] [Medline: 33921978]
50. Ruan X, Jiang C, Lin P, et al. MSGCL: inferring miRNA-disease associations based on multi-view self-supervised graph structure contrastive learning. Brief Bioinform 2023 Mar 19;24(2):bbac623. [doi: 10.1093/bib/bbac623] [Medline: 36790856]
51. Chowdhury S, Chen Y, Li P, et al. Stratifying heart failure patients with graph neural network and transformer using electronic health records to optimize drug response prediction. J Am Med Inform Assoc 2024 Aug 1;31(8):1671-1681. [doi: 10.1093/jamia/ocae137] [Medline: 38926131]
52. Zhang G, Peng Z, Yan C, Wang J, Luo J, Luo H. A novel liver cancer diagnosis method based on patient similarity network and DenseGCN. Sci Rep 2022;12(1):6797. [doi: 10.1038/s41598-022-10441-3]
53. Hashem S, Esmat G, Elakel W, et al. Comparison of machine learning approaches for prediction of advanced liver fibrosis in chronic hepatitis C patients. IEEE/ACM Trans Comput Biol Bioinform 2018 May 1;15(3):861-868. [doi: 10.1109/TCBB.2017.2690848]
54. Wu CC, Yeh WC, Hsu WD, et al. Prediction of fatty liver disease using machine learning algorithms. Comput Methods Programs Biomed 2019 Mar;170:23-29. [doi: 10.1016/j.cmpb.2018.12.032] [Medline: 30712601]
55. Liu M, Li S, Yuan H, et al. Handling missing values in healthcare data: a systematic review of deep learning-based imputation techniques. Artif Intell Med 2023 Aug;142:102587. [doi: 10.1016/j.artmed.2023.102587] [Medline: 37316097]
56. Kipf TN, Welling M. Semi-supervised classification with graph convolutional networks. Presented at: International Conference on Learning Representations (ICLR); Apr 24-26, 2017 URL: https://openreview.net/pdf?id=SJU4ayYgl [accessed 2025-09-16]
57. Veličković P, Cucurull G, Casanova A, Romero A, Liò P, Bengio Y. Graph attention networks. Presented at: International Conference on Learning Representations (ICLR); Apr 30 to May 3, 2018 URL: https://openreview.net/pdf?id=rJXMpikCZ [accessed 2025-09-16]
58. Hamilton W, Ying Z, Leskovec J. Inductive representation learning on large graphs. In: NIPS'17: Proceedings of the 31st International Conference on Neural Information Processing Systems: Curran Associates Inc; 2017. [doi: 10.5555/3294771.3294869]
59. Sangha V, Khunte A, Holste G, et al. Biometric contrastive learning for data-efficient deep learning from electrocardiographic images. J Am Med Inform Assoc 2024 Apr 3;31(4):855-865. [doi: 10.1093/jamia/ocae002] [Medline: 38269618]
60. Feng W, Wu H, Ma H, et al. Applying contrastive pre-training for depression and anxiety risk prediction in type 2 diabetes patients based on heterogeneous electronic health records: a primary healthcare case study. J Am Med Inform Assoc 2024 Jan 18;31(2):445-455. [doi: 10.1093/jamia/ocad228] [Medline: 38062850]
61. Uçar T, Hajiramezanali E, Edwards L. Subtab: subsetting features of tabular data for self-supervised representation learning. In: NIPS '21: Proceedings of the 35th International Conference on Neural Information Processing Systems: Curran Associates Inc; 2021:18853-18865.
62. Radford A, Kim JW, Hallacy C, et al. Learning transferable visual models from natural language supervision. arXiv. Preprint posted online on Feb 26, 2021. [doi: 10.48550/arXiv.2103.00020]
63. He K, Fan H, Wu Y, Xie S, Girshick R. Momentum contrast for unsupervised visual representation learning. Presented at: 2020 IEEE/CVF Conference on Computer Vision and Pattern Recognition (CVPR); Jun 13-19, 2020; Seattle, WA p. 9729-9738. [doi: 10.1109/CVPR42600.2020.00975]

XSL•FO
RenderX

64. Gao T, Yao X, Chen D. SimCSE: simple contrastive learning of sentence embeddings. Presented at: Proceedings of the 2021 Conference on Empirical Methods in Natural Language Processing; Nov 7-11, 2021 URL: https://aclanthology.org/2021.emnlp-main [accessed 2025-09-16] [doi: 10.18653/v1/2021.emnlp-main.552]
65. Chen T, Kornblith S, Norouzi M, Hinton G. A simple framework for contrastive learning of visual representations. arXiv. Preprint posted online on Feb 13, 2020. [doi: 10.48550/arXiv.2002.05709]
66. Tian Y, Krishnan D, Isola P. Contrastive multiview coding. arXiv. Preprint posted online on Jun 13, 2019. [doi: 10.48550/arXiv.1906.05849]
67. Yang H, Zhou S, Rao Z, et al. Multi-modality risk prediction of cardiovascular diseases for breast cancer cohort in the All of Us Research Program. J Am Med Inform Assoc 2024 Dec 1;31(12):2800-2810. [doi: 10.1093/jamia/ocae199] [Medline: 39058572]
68. Pasadana IA, Hartama D, Zarlis M, et al. Chronic kidney disease prediction by using different decision tree techniques. J Phys Conf Ser 2019 Aug 1;1255(1):012024. [doi: 10.1088/1742-6596/1255/1/012024]
69. Wang Y, Wang D, Ye X, Wang Y, Yin Y, Jin Y. A tree ensemble-based two-stage model for advanced-stage colorectal cancer survival prediction. Inf Sci 2019 Feb;474:106-124. [doi: 10.1016/j.ins.2018.09.046]
70. Hashem AM, Rasmy MEM, Wahba KM, Shaker OG. Single stage and multistage classification models for the prediction of liver fibrosis degree in patients with chronic hepatitis C infection. Comput Methods Programs Biomed 2012 Mar;105(3):194-209. [doi: 10.1016/j.cmpb.2011.10.005] [Medline: 22070853]
71. Zheng S, Zhu Z, Liu Z, et al. Multi-modal graph learning for disease prediction. IEEE Trans Med Imaging 2022 Sep;41(9):2207-2216. [doi: 10.1109/TMI.2022.3159264] [Medline: 35286257]
72. Bugianesi E, Gastaldelli A, Vanni E, et al. Insulin resistance in non-diabetic patients with non-alcoholic fatty liver disease: sites and mechanisms. Diabetologia 2005 Apr;48(4):634-642. [doi: 10.1007/s00125-005-1682-x] [Medline: 15747110]
73. Pan Y, Li X, Huang W. Increase statistical reliability without losing predictive power by merging classes and adding variables. BDIA 2016 Oct;1(4):341-348. [doi: 10.3934/bdia.2016014]
74. Nicodemus KK, Malley JD. Predictor correlation impacts machine learning algorithms: implications for genomic studies. Bioinformatics 2009 Aug 1;25(15):1884-1890. [doi: 10.1093/bioinformatics/btp331] [Medline: 19460890]
75. Zhang O, Wu M, Bayrooti J, Goodman N. Temperature as uncertainty in contrastive learning. arXiv. Preprint posted online on Oct 8, 2021. [doi: 10.48550/arXiv.2110.04403]
76. Amrollahi F, Shashikumar SP, Meier A, Ohno-Machado L, Nemati S, Wardi G. Inclusion of social determinants of health improves sepsis readmission prediction models. J Am Med Inform Assoc 2022 Jun 14;29(7):1263-1270. [doi: 10.1093/jamia/ocac060] [Medline: 35511233]
77. Ibrahim ZM, Wu H, Hamoud A, Stappen L, Dobson RJB, Agarossi A. On classifying sepsis heterogeneity in the ICU: insight using machine learning. J Am Med Inform Assoc 2020 Mar 1;27(3):437-443. [doi: 10.1093/jamia/ocz211] [Medline: 31951005]
78. Faghri F, Brunn F, Dadu A, et al. Identifying and predicting amyotrophic lateral sclerosis clinical subgroups: a population-based machine-learning study. Lancet Digit Health 2022 May;4(5):e359-e369. [doi: 10.1016/S2589-7500(21)00274-0] [Medline: 35341712]
79. Thabtah F, Hammoud S, Kamalov F, Gonsalves A. Data imbalance in classification: experimental evaluation. Inf Sci 2020 Mar;513:429-441. [doi: 10.1016/j.ins.2019.11.004]
80. Docherty M, Regnier SA, Capkun G, et al. Development of a novel machine learning model to predict presence of nonalcoholic steatohepatitis. J Am Med Inform Assoc 2021 Jun 12;28(6):1235-1241. [doi: 10.1093/jamia/ocab003] [Medline: 33684933]
81. van der Maaten L, Hinton G. Visualizing data using t-SNE. J Mach Learn Res 2008;9(86):2579-2605 [FREE Full text]
82. Lundberg SM, Lee SI. A unified approach to interpreting model predictions. arXiv. Preprint posted online on May 22, 2017. [doi: 10.48550/arXiv.1705.07874]
83. Bouayad L, Padmanabhan B, Chari K. Can recommender systems reduce healthcare costs? The role of time pressure and cost transparency in prescription choice. Manag Inf Syst Q 2020 Dec 1;44(4):1859-1903. [doi: 10.25300/MISQ/2020/14435/]
84. Colognesi M, Gabbia D, De Martin S. Depression and cognitive impairment-extrahepatic manifestations of NAFLD and NASH. Biomedicines 2020 Jul 21;8(7):229. [doi: 10.3390/biomedicines8070229] [Medline: 32708059]
85. Fouad Y, Palmer M, Chen M, et al. Redefinition of fatty liver disease from NAFLD to MAFLD through the lens of drug development and regulatory science. J Clin Transl Hepatol 2022 Apr 28;10(2):374-382. [doi: 10.14218/JCTH.2021.00408] [Medline: 35528969]
86. Lin WC, Chen A, Song X, Weiskopf NG, Chiang MF, Hribar MR. Prediction of multiclass surgical outcomes in glaucoma using multimodal deep learning based on free-text operative notes and structured EHR data. J Am Med Inform Assoc 2024 Jan 18;31(2):456-464. [doi: 10.1093/jamia/ocad213] [Medline: 37964658]
87. Masayoshi K, Hashimoto M, Toda N, et al. Training language models for estimating priority levels in ultrasound examination waitlists: algorithm development and validation. JMIR AI 2025 Jul 22;4:e68020. [doi: 10.2196/68020] [Medline: 40694843]
88. Chen X, Chen S, Pang J, Tang Y, Ling W. Are the different MAFLD subtypes based on the inclusion criteria correlated with all-cause mortality? J Hepatol 2021 Oct;75(4):987-989. [doi: 10.1016/j.jhep.2021.06.013] [Medline: 34153396]

XSL•FO
RenderX

89. AlSaad R, Abd-Alrazaq A, Boughorbel S, et al. Multimodal large language models in health care: applications, challenges, and future outlook. J Med Internet Res 2024 Sep 25;26:e59505. [doi: 10.2196/59505] [Medline: 39321458]
90. Caron M, Misra I, Mairal J, Goyal P, Bojanowski P, Joulin A. Unsupervised learning of visual features by contrasting cluster assignments. arXiv. Preprint posted online on Jun 17, 2020. [doi: 10.48550/arXiv.2006.09882]
91. Rinella ME, Lazarus JV, Ratziu V, et al. A multisociety Delphi consensus statement on new fatty liver disease nomenclature. Hepatology 2023 Dec 1;78(6):1966-1986. [doi: 10.1097/HEP.0000000000000520] [Medline: 37363821]
92. Younossi ZM, Paik JM, Stepanova M, Ong J, Alqahtani S, Henry L. Clinical profiles and mortality rates are similar for metabolic dysfunction-associated steatotic liver disease and non-alcoholic fatty liver disease. J Hepatol 2024 May;80(5):694-701. [doi: 10.1016/j.jhep.2024.01.014] [Medline: 38286339]

Abbreviations

ATN: adaptive temperature network
AUC: area under the curve
CVD: cardiovascular disease
DT: decision tree
GAT: graph attention network
GCN: graph convolutional network
MAFLD: metabolic dysfunction–associated fatty liver disease
MASLD: metabolic dysfunction–associated steatotic liver disease
MLP: multilayer perceptron
NN: neural network
RF: random forest
SHAP: Shapley additive explanation
t-SNE: t-distributed stochastic neighbor embedding
XGBoost: extreme gradient boosting

Edited by A Benis; submitted 09.04.25; peer-reviewed by G Lim, J Song; accepted 23.10.25; published 12.12.25.

Please cite as:
Chen SJ, Xu D, Hu DK, Hu PJH, Huang TS
Predicting Metabolic Dysfunction–Associated Fatty Liver Disease Phenotypes Among Adults: 2-Stage Contrastive Learning Method
JMIR Med Inform 2025;13:e75747
URL: https://medinform.jmir.org/2025/1/e75747
doi:10.2196/75747

© Sizhe Jasmine Chen, Da Xu, Derek K Hu, Paul Jen-Hwa Hu, Ting-Shuo Huang. Originally published in JMIR Medical Informatics (https://medinform.jmir.org), 12.12.2025. This is an open-access article distributed under the terms of the Creative Commons Attribution License (https://creativecommons.org/licenses/by/4.0/), which permits unrestricted use, distribution, and reproduction in any medium, provided the original work, first published in JMIR Medical Informatics, is properly cited. The complete bibliographic information, a link to the original publication on https://medinform.jmir.org/, as well as this copyright and license information must be included.

XSL•FO
RenderX

Methods for Addressing Missingness in Electronic Health Record Data for Clinical Prediction Models: Comparative Evaluation

Jean Digitale[1,2], PhD, MPH, BSN; Deborah Franzon[3], MD; Mark J Pletcher[2], MD, MPH; Charles E McCulloch[2], PhD; Efstathios D Gennatas[2], MBBS, PhD

[1]National Clinician Scholars Program, University of California, San Francisco, San Francisco, CA, United States

[2]Department of Epidemiology and Biostatistics, University of California, San Francisco, 550 16th St, 2nd Floor, San Francisco, CA, United States

[3]Department of Pediatrics, Benioff Children's Hospital, University of California, San Francisco, San Francisco, CA, United States

Corresponding Author:
Jean Digitale, PhD, MPH, BSN
National Clinician Scholars Program, University of California, San Francisco, San Francisco, CA, United States

Abstract

Background: Missing data are a common challenge in electronic health record (EHR)–based prediction modeling. Traditional imputation methods may not suit prediction or machine learning models, and real-world use requires workflows that are implementable for both model development and real-time prediction.

Objective: We evaluated methods for handling missing data when using EHR data to build clinical prediction models for patients admitted to the pediatric intensive care unit (PICU).

Methods: Using EHR data containing missing values from an academic medical center PICU, we generated a synthetic complete dataset. From this, we created 300 datasets with missing data under varying mechanisms and proportions of missingness for the outcomes of (1) successful extubation (binary) and (2) blood pressure (continuous). We assessed strategies to address missing data including simple methods (eg, last observation carried forward [LOCF]), complex methods (eg, random forest multiple imputation), and native support for missing values in outcome prediction models.

Results: Across 886 patients and 1220 intubation events, 18.2% of original data were missing. LOCF had the lowest imputation error, followed by random forest imputation (average mean squared error [MSE] improvement over mean imputation: 0.41 [range: 0.30, 0.50] and 0.33 [0.21, 0.43], respectively). LOCF generally outperformed other imputation methods across outcome metrics and models (mean improvement: 1.28% [range: −0.07%, 7.2%]). Imputation methods showed more performance variability for the binary outcome (balanced accuracy coefficient of variation: 0.042) than the continuous outcome (mean squared error coefficient of variation: 0.001).

Conclusions: Traditional imputation methods for inferential statistics, such as multiple imputation, may not be optimal for prediction models. The amount of missingness influenced performance more than the missingness mechanism. In datasets with frequent measurements, LOCF and native support for missing values in machine learning models offer reasonable performance for handling missingness at minimal computational cost in predictive analyses.

(JMIR Med Inform 2025;13:e79307) doi:10.2196/79307

KEYWORDS

clinical prediction models; imputation; machine learning; missing data; electronic health record

Introduction

Background and Significance

Addressing missing data is necessary for developing a clinical prediction model. Electronic health record (EHR) data are a rich data source but present particular challenges. Missing data may result from lack of documentation or measurement [1]. EHR data are generated via clinical care, with values measured at irregular intervals.

Raw EHR data are often transformed into an analytic dataset by binning variables by time. Missing data arise if a variable is not measured within a time window [2]. Measurement frequency (and resultant missingness) is often linked to how abnormal the value is or is expected to be, such that missingness itself may be informative. Given many algorithms require complete data, a principled approach to address missingness is required.

Techniques for handling missing data for inferential models that seek to describe or causally explain are well established. Missingness is traditionally categorized into three mechanisms [3,4]:

1. Missing completely at random (MCAR)—probability of missingness does not depend on variables in the dataset or

XSL•FO
RenderX

depends only on observed values of covariates included in the model; for example, a laboratory technician forgets to record results for a patient, unrelated to any characteristics of that patient or their health [5].

2. Missing at random (MAR)—probability of missingness depends on observed values in the data, including the outcome; for example, height is not recorded for a patient but is related to weight and sex of the patient, which are present in the EHR.
3. Missing not at random (MNAR)—probability of missingness depends on unobserved values; for example, no lactate is measured on a patient because the clinician expects it to be normal.

Bias from MNAR can be intractable for inferential models [4]. Given EHR data are likely MNAR, this could be problematic if also true for clinical prediction models. For inferential models, simple strategies, such as complete case analysis, mean imputation, and last observation carried forward, are known to produce biased results [6,7]. Preferred strategies, such as multiple imputation, incorporate uncertainty into imputed values, thereby accurately characterizing uncertainty in parameter estimates.

Literature on handling missing data in prediction modeling is less developed. Unlike inferential models, which focus on bias and precision in parameter estimates, prediction models prioritize improving predictive accuracy and interpretability [4]. Classic statistical imputation methods may be complex to implement for prediction models [8] or less relevant, particularly as medicine advances toward ever more complex machine learning algorithms [4,9,10]. There is little guidance on best practices to address missing data for clinical prediction models [11]. Methods for handling missing data are rarely reported, and complete case analysis is the most common approach [11,12]. This may not only result in bias but also risk significant loss of data in high-dimensional EHR datasets [9]. Machine learning is increasingly being used to address missing data, both as imputation models (eg, random forests) [13] and by natively handling missing data in prediction models themselves, bypassing the need for imputation altogether. Tree-based methods [14] are particularly suited for this task [9]. Yet, few studies have compared classic imputation methods with such built-in strategies in EHR data [9,12].

Real-world application of clinical prediction models presents additional challenges. Many risk models currently in practice require complete data or use imputation methods that may be overly simplistic, limiting their usefulness [15,16]. Implementing models prospectively requires data workflows that can be applied in the same way to both retrospective data to build the model and new data for real-time prediction for individuals [4,10,11,15]. There are no established techniques for managing missing data post-model development. Studies assessing methods for handling missing data in prospective applications on individual patients often used datasets containing only a few predictors [16,17]. These findings may not translate to datasets with more variables because some imputation methods may struggle to handle large numbers of correlated features and binary variables are more likely to be perfectly predicted, leading to overfitting. Furthermore, outcome prediction models after addressing missing data were often standard statistical methods such as logistic regression [15,17] or Cox proportional hazard models [16], when different methods for addressing missingness may be preferable for predictive machine learning models.

Objective

We used EHR data from a live use case (predicting extubation readiness of children in the pediatric intensive care unit [PICU]) to generate a synthetic complete dataset to evaluate multiple methods for imputation and their effects on predictive performance. We included methods that learn from training data and apply to new data. As the relative performance of methods varies by type of missingness (MAR, MCAR, and MNAR) and proportion of missing values [18], we varied both in our assessment.

Methods

Study Population

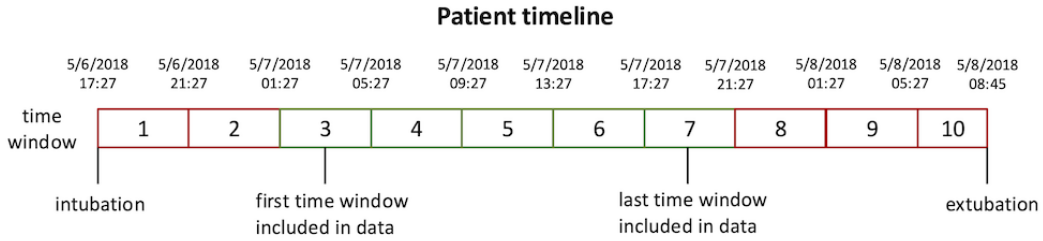
The study population was patients aged >30 days and <18 years old from the PICU at the University of California, San Francisco (UCSF) Benioff Children's Hospital intubated between January 1, 2013, and March 31, 2023. Patient encounters were eligible for the sample if the child was intubated for more than 24 hours. We excluded patients intubated for less than 24 hours as they were likely intubated for surgeries, procedures, or other indications and extubated quickly without complications. Children with repeated intubations were eligible for inclusion for each intubation event.

Data

We used EHR data extracted from the UCSF Clinical Data Warehouse (updated daily from the real-time EHR). Based on expert opinion, peer-reviewed literature, and group consensus of the UCSF Pediatric Critical Care Research Group, we selected a broad range of clinical, physiologic, and laboratory variables in the EHR that could be relevant to extubation readiness including: vital signs, ventilator settings, laboratory values, medications, neurological status, fluid balance, and other patient characteristics (Table S1 in Multimedia Appendix 1). Raw data were collapsed into 4-hour time windows [1] containing the mean of each numeric or binary variable and mode of each multi-level categorical variable, resulting in 99 variables. Collapsing variables into time windows made imputation more tractable as it increased the probability of at least 1 nonmissing value per time window and more computationally feasible by decreasing the number of observations on which we needed to impute. In practice, nursing assessments are completed at least every 4 hours (with some assessments in the ICU performed hourly); thus, the 4-hour interval is clinically meaningful. The first time window included in the model ended 12 hours after intubation (Figure 1).

XSL•FO
RenderX

Figure 1. Example patient timeline and resultant data. The example patient timeline depicts 4-hour time windows beginning at intubation and ending at extubation. The table in the figure demonstrates the data resulting from this patient that would be included in the model. This patient was intubated at 17:27 on 5/6/2018 and extubated at 08:45 on 5/8/2018. The first time window included as an observation in the model ended 12 hours after intubation at 05:27 on 5/7/2018. Time-varying data from the prior 2 time windows were included for each observation as lagged variables to capture the trajectory of the patient. The final time window included in the model for this patient is from 17:27 to 21:27 on 5/7/2018. The extubation outcome for each time window was the status 12 hours (or 3 time windows) later. The blood pressure outcome for each time window was the value 4 hours (or 1 time window) later.



Patient data

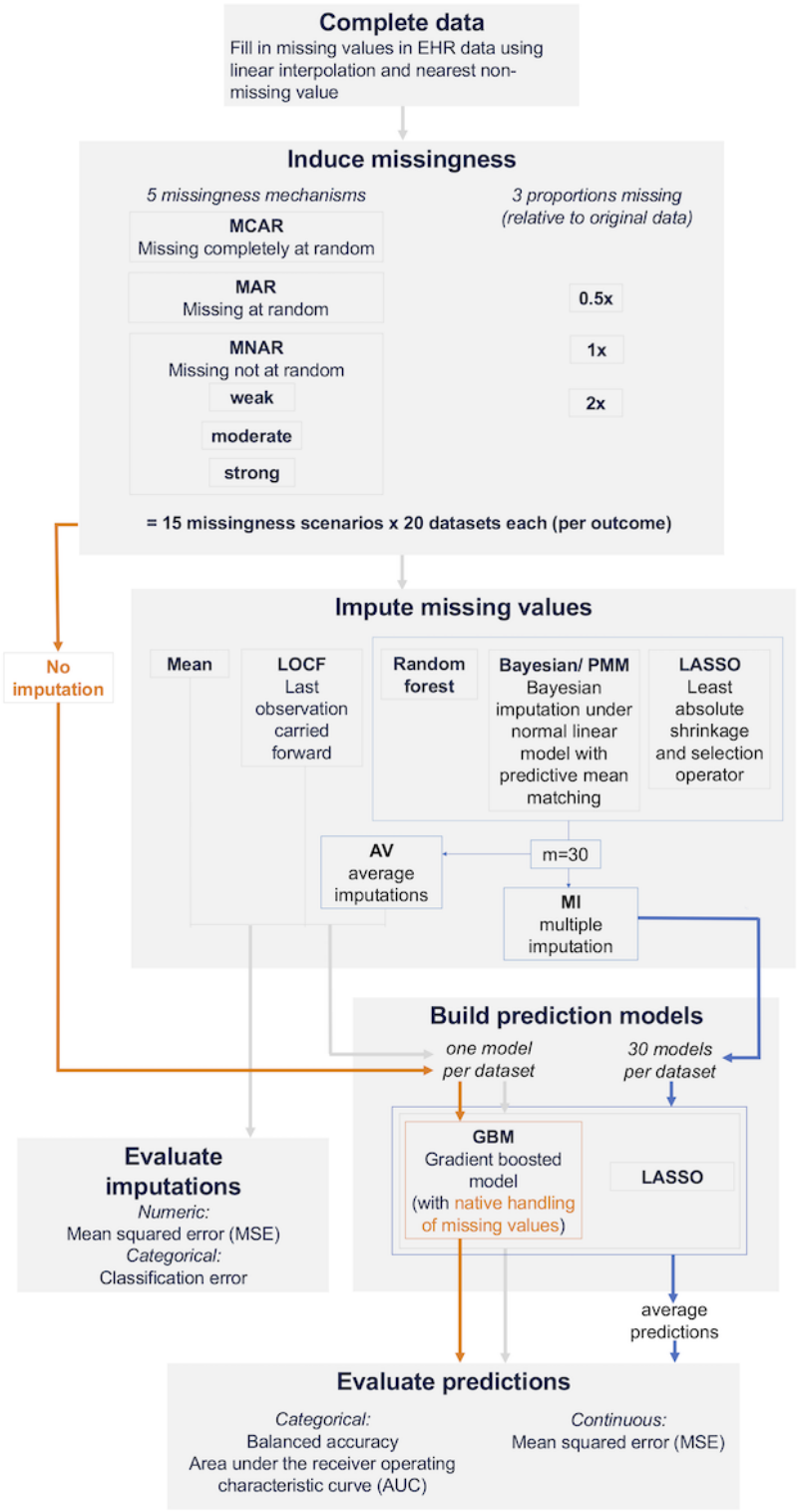
Row	Start time	End time	Time window	Lagged variables: Time windows	Outcome		Extubation status time
					Extubation status: Time window	Blood pressure: Time window	
1	5/6/2018 01:27	5/6/2018 05:27	3	1 and 2	6	4	5/7/2018 17:27
2	5/6/2018 05:27	5/7/2018 09:27	4	2 and 3	7	5	5/7/2018 21:27
3	5/7/2018 09:27	5/7/2018 13:27	5	3 and 4	8	6	5/8/2018 01:27
4	5/7/2018 13:27	5/7/2018 17:27	6	4 and 5	9	7	5/8/2018 05:27
5	5/7/2018 17:27	5/7/2018 21:27	7	5 and 6	10	8	5/8/2018 08:45

The binary outcome of successful extubation was defined as extubation that did not result in reintubation within 48 hours. The extubation outcome assigned to each time window indicated status 12 hours after the end of the time window (Figure 1; Multimedia Appendix 1), as we aimed to predict successful extubation prior to clinician actions indicating they already decided to extubate a patient. A secondary outcome of age-adjusted systolic blood pressure percentile [19] was added to ascertain whether findings were similar for a continuous outcome. The blood pressure outcome assigned to each time window was the value 4 hours after the end of the time window.

To generate a synthetic dataset with no missing values (Figure 2), we filled in missing numeric values with linear interpolation between last value observed and next value observed [20]. We filled in all remaining missing values with the nearest nonmissing value. For never observed variables (1.4% of cells), we made reasonable assumptions (eg, we used the standard endotracheal tube [ETT] size formula [age in years/4+4] for pediatrics to fill in missing ETT sizes [21]) and then filled in remaining missingness using the *missRanger* package [22], which implements random forest imputation with predictive mean matching and is optimized for speed and memory efficiency. Analyses were conducted in R version 4.3.2 [23].

XSL•FO
RenderX

Figure 2. Experimental methods flowchart. EHR: electronic health record.



Missingness Mechanisms

We induced missingness in the complete, synthetic dataset to simulate 5 missing data mechanisms:

1. MCAR
2. MAR
3. weak MNAR (twice as much weight given to observed compared with missing variables to determine missingness)
4. moderate MNAR (equal weight given to observed compared with missing variables to determine missingness)
5. strong MNAR (missingness solely based on missing variables)

For each, we created 3 scenarios varying the amount of missingness: approximately 0.5x, 1x, and 2x the percentage of missing cells in the original data, generating 15 total missingness scenarios. We divided variables into 5 groups (Table S1 in Multimedia Appendix 1) to create patterns of missing data. The

XSL•FO
RenderX

outcome was allowed to influence missingness in MAR and MNAR scenarios (Multimedia Appendix 1). Using the ampute command in the *mice* package [24], we induced missingness in 20 unique datasets (enough to have a distribution of results, but not exceed our computing power) for each of the 15 scenarios, resulting in 300 datasets per outcome. All datasets for both outcomes contained the same predictor variables.

Imputation Methods

To incorporate temporal patterns in the predictors, we added values of time-varying variables from the prior 2 lagged time windows to each row for a total of 265 features. These data were structured in wide format, such that each row included the current value and its 2 lags as separate variables. This allowed the imputation models to use all 3 time points to inform each other's missing values. For simplicity, we treated these repeated measurements as distinct variables in imputation models (rather than using a multilevel model). While some studies suggest this approach yields comparable performance [25], others have reported advantages of multilevel models [26]. Data were split into training (75% of intubations) and test (25% of intubations) sets ordered by date, with earlier intubations included in training and later ones in test. We ensured each patient was only in either the training or test set.

To simulate a real-time prediction workflow, imputation models were built using only training data and excluded the outcome [15]. In total, 6 methods to handle missingness were applied to each amputed dataset (Table 1, Multimedia Appendix 1):

1. Mean: Mean imputation is frequently used in practice [27]. We imputed test set values using the unconditional mean (numeric and binary) or mode (factor) in the training set.
2. Last observation carried forward (LOCF): This simple approach is recommended for imputation in time series data where data are available only before the missing value [20] (true in prospective implementation of clinical decision support). We allowed values to be carried forward indefinitely across time windows.
3. Random forest: Traditional statistical imputation relies on parametric assumptions. However, nonparametric methods, such as this, have been shown to outperform established methods (especially in settings with complex interactions and nonlinear relationships) [28]. *Mice* [29] imputes missing values by building a random forest for each variable, identifying observations in the same terminal node, and sampling a donor value from one of these observations.
4. Bayesian imputation under the normal linear model with predictive mean matching (Bayesian/PMM): PMM is a hot deck method where missing values are imputed from cases with observed values matched according to predictions of the imputation model (here, Bayesian imputation under the normal linear model in *mice* [29]). PMM is robust against model misspecification and ensures imputed values are constrained to the range of observed data [7].
5. Least absolute shrinkage and selection operator (LASSO): Regularized models, such as LASSO, are beneficial to handle multicollinearity and prevent overfitting in high-dimensional data. We used *mice* [29] to fit LASSO-penalized regression models on bootstrap samples of observed data and drew imputed values from the resulting distributions.
6. Native support for missing data in prediction model (no imputation required): Some machine learning algorithms can handle missing values directly, without dropping cases or requiring separate imputation. We used gradient boosted trees for our primary prediction model [30]. The LightGBM package [31] allocates missing values to the bins that optimally minimize loss.

XSL•FO
RenderX

Table . Methods for handling missing data.

Method	Assumptions	Computational complexity	Limitations	Benefits
Mean imputation	• Assumes missing values are similar to the mean	Negligible	• Artificially reduces variance • Disturbs relationships between variables	• Simple to implement • Constant imputation creates patterns that machine learning can exploit
Last observation carried forward	• Assumes stability over time	Negligible	• Data remain missing if no prior measurement exists • May not reflect true patient progression • Can introduce bias if trends are not stable over time	• Simple to implement • Reflects how clinicians practice for many variables (assume no changes or re-measure if important)
Random forest	• MCAR[a] or MAR[b]	High computational cost	• Requires significant computational resources • May not perform well in small datasets • Dearth of packages that allow models to impute on new data	• Nonparametric method handles complex interactions and nonlinear relationships well • Works with mixed data types (categorical and continuous)
Bayesian imputation under the normal linear model with predictive mean matching (Bayesian/PMM)	• MCAR or MAR • Assumes normality for underlying distribution	High computational cost	• Works best with large samples • Dearth of packages that allow models to impute on new data	• Robust against model misspecification • Ensures imputed values are within the range of observed data
Least absolute shrinkage and selection operator (LASSO)	• MCAR or MAR	High computational cost	• May not capture nonlinear relationships well • Dearth of packages that allow models to impute on new data	• Handles multicollinearity well • Prevents overfitting in high-dimensional data
Native support for missing data in prediction models	• Varies by model • Methods [12] include surrogate splits and allocating missing values to bins that optimally minimize loss	None for imputation	• This capability is not available in all machine learning algorithms • Performance depends on algorithm's internal handling of missing values	• No need for explicit imputation

[a]MCAR: missing completely at random.

[b]MAR: missing at random.

We used available software for imputation to avoid the need to develop custom software and enable our findings to be more readily applicable to practitioners. We did not include deep-learning methods in our experiment as they were impractical with our relatively small sample size. We generated 30 imputations per dataset using the *mice* package [29] for methods 3 - 5. Models built with the training data were then used to impute on the test set. We tested the imputations 2 ways. *Mice* purposefully incorporates uncertainty into imputations because it is advantageous for inferential analysis. First, we averaged the imputations to get a more stable estimate of each missing value to use in a single outcome model. Second, we implemented multiple imputation by estimating 30 outcome models and averaging the predicted probabilities for a final prediction.

Prediction Model

For the outcome prediction model, we used gradient boosted trees [30]. It is one of the best-performing algorithms in structured data in general and within biomedical datasets [32] and uses all cases in training data, even if they are incomplete. To assess whether imputation method performance was consistent across outcome models, we also compared a LASSO outcome model. However, linear models like LASSO cannot accommodate missing values, so this was only performed on imputed datasets. Outcome models were implemented using the rtemis package [33] with LightGBM [34] and glmnet [35].

XSL•FO
RenderX

We used 5-fold cross-validation in the training set to tune hyperparameters and inverse frequency weighting to upweight the minority class given the data were unbalanced.

Analysis of Imputation Accuracy

It is established that in imputation for statistical inference, focusing on improving accuracy of the imputations at the cost of correctly incorporating true uncertainty leads to biased and invalid results [7]. However, the relationship between imputation accuracy and prediction model performance is less well-studied. We compared the accuracy of imputations by calculating mean squared error (MSE) for numeric variables and classification error for categorical variables in each dataset and creating box plots. Before calculating MSE, we standardized the variables by dividing by their standard deviations in the complete dataset. To calculate MSE for random forest, Bayesian/PMM, and LASSO, we compared the average of the 30 imputations to the true value. We also assessed whether temporal autocorrelation of each variable was associated with imputation performance across all methods descriptively using scatterplots and quantified using correlation coefficients (Multimedia Appendix 1). In addition, we conducted a sensitivity analysis stratifying imputation error by whether a variable's values had been missing in the original data (and filled in to create the synthetic complete dataset) versus not originally missing, to evaluate whether this initial filling step influenced the apparent performance of the imputation methods.

To assess the accuracy of imputation for different categories of variables, we built linear models for MSE and classification error. Each observation's outcome was the error value for a given variable in a given dataset. Each model included imputation type, missingness type, proportion missing data (0.5x, 1x, and 2x original), and variable group (Multimedia Appendix 1). We included all 3-way and 2-way interactions and completed a backward stepwise elimination procedure based on *P* values (included $P<.05$) to determine the final models.

Analysis of Outcome Model Performance

We assessed the performance of outcome prediction models for extubation with 2 primary metrics: balanced accuracy [36] and area under the receiver operating characteristic curve (AUC) [37]. We present secondary results for sensitivity, specificity, positive predictive value, negative predictive value, and F1 [38]. We assessed the performance of the outcome prediction models for blood pressure with the primary metric of MSE. Secondary results are presented for mean absolute error, root MSE, and R^2 [39]. We compared these graphically to the performance of a model built with the complete data and calculated the coefficient of variation (CV) to assess variability.

Ethical Considerations

We received ethical approval from the University of California, San Francisco Institutional Review Board (study #17 - 23751), which granted a waiver of informed consent. No financial incentives were provided to patients. Patient privacy and confidentiality were protected through secure data storage, restricted access to authorized study personnel, and compliance with institutional and regulatory requirements.

Results

Data

The data contained 886 patients and 1220 intubations, 929 (76.1%) of which ended in successful extubation (Table 2). The median duration of intubation in the PICU was 4.4 (IQR 2.2-8.5) days, leading to 50,187 four-hour time windows in the analytic dataset.

XSL•FO
RenderX

Table . Description of sample[a].

Variable	Value
Patients	
Total, n	886
Female patients, n (%)	405 (45.7)
Race or ethnicity, n (%)	
Asian	117 (13.9)
Black	67 (8)
Latinx	340 (40.4)
Other	88 (10.5)
White	229 (27.2)
Intubations	
Total, n	1220
Age at intubation (years), median (IQR)	4.3 (1-12.1)
Outcome, n (%)	
Extubation success	929 (76.1)
Extubation failure	100 (8.2)
Death	96 (7.9)
Tracheostomy	36 (3)
Transfer to another unit	25 (2)
ETT[b] change	34 (2.8)
Duration of intubation (days), median (IQR)	4.4 (2.2-8.5)

[a]Patients intubated multiple times during the study period may have multiple intubation events included in the sample. The binary outcome of successful extubation for the model collapsed all other outcome categories. Here, extubation failure is defined as reintubation within 48 hours, death is death before or within 48 hours of extubation, and ETT change is an extubation that was immediately and purposefully replaced by another ETT (eg, to change the size).

[b]ETT: endotracheal tube.

Missingness for each variable in the original data (collapsed into 4 h time windows) varied from 0% (0/56,287; eg, sex, age) to 77% (43,077/56,287; white blood cells) (Table 3; Table S2 in Multimedia Appendix 1). Overall, 18.2% of cells (1,012,668/5,561,767) were missing (Table S3 in Multimedia Appendix 1). After simulating missingness, datasets approximating 0.5x, 1x, and 2x missingness of the original data averaged 9.6%, 18.1%, and 35.9% missing cells, respectively.

XSL•FO
RenderX

Table . Missingness in original data[a].

Variable	Number of 4-hour time windows missing variable	Percent of 4-hour time windows missing variable
Age at time of intubation (in days)	0	0.0
Medication: total oral morphine equivalents (mg kg^{-1})	0	0.0
Sex	0	0.0
Intake or output total milliliter over the prior 12 hours kg^{-1}	167	0.3
Pulse	420	0.7
Respiratory rate (recorded in vital signs)	1179	2.1
ETT[b] size	6179	11.0
Respiratory pattern: tachypneic	7290	13.0
PEEP[d]	8975	15.9
Exhaled tidal volume kg^{-1}	10,274	18.3
State behavioral scale	15,888	28.2
Secretion amount (categories: none, scant, small, moderate, large, copious)	16,325	29.0
Glasgow coma scale score	25,751	45.7
pH	25,804	45.8
Upper extremity motor response	28,839	51.2
Cough: present	35,254	62.6
White blood cell count	43,077	76.5

[a]Example variables display the range of proportion of missingness in the original data (N=56,287 4-h time windows; these data include more time windows than the final analytic dataset because they were compiled before excluding time windows that were constructed solely for creating lagged variables). Detailed data for all variables are available in Table S2 in Multimedia Appendix 1.

[b]EET: endotracheal tube.

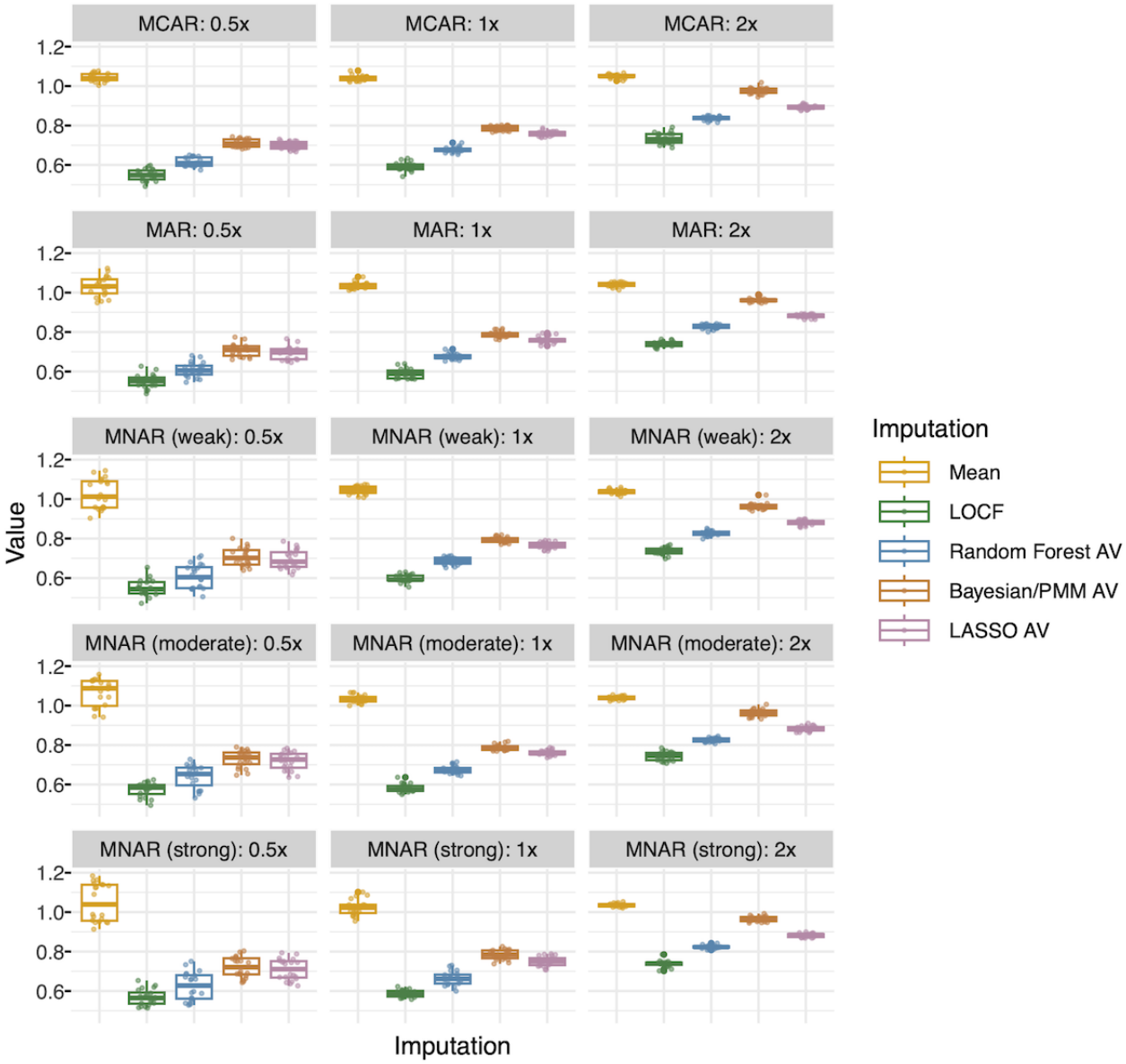
[c]PEEP: positive end-expiratory pressure.

Imputation Performance

Across 300 datasets with induced missingness per outcome, the same 176 numeric and 6 categorical variables were imputed. Figure 3 presents MSE for datasets for the outcome of extubation.

XSL•FO
RenderX

Figure 3. Imputation test performance metrics (extubation): mean squared error. Each point represents mean squared error calculated for 176 numeric variables for 1 of 300 datasets created for the outcome of extubation. There are 20 datasets per missingness scenario and imputation type represented in each box plot. AV: average (average of 30 imputations); Bayesian/PMM: Bayesian imputation under the normal linear model with predictive mean matching; LASSO: least absolute shrinkage and selection operator; LOCF: last observation carried forward; MAR: missing at random; MCAR: missing completely at random; MNAR: missing not at random.



The results for the outcome of blood pressure (which imputed the same variables) were virtually identical (Multimedia Appendix 2). Performance in the test sets showed that LOCF had the lowest MSE on average in all missingness scenarios for numeric variables (average improvement of MSE compared with mean imputation was 0.41 for the outcome of extubation [range: 0.30, 0.50]). Random forest imputation was consistently second best (0.33 [0.21, 0.43]), followed by LASSO (0.26 [0.15, 0.35]), Bayesian/PMM (0.22 [0.07, 0.34]), and finally, mean imputation (Reference). Performance overall degraded as the proportion of missing data increased, with proportion missing having a greater effect than missingness mechanism. Classification error displayed similar patterns overall for categorical variables (Multimedia Appendix 3). While LOCF and mean imputation did not generally overfit in the training data compared with the test set, all model-based imputation methods overfit the training data, with random forest doing so the least (Multimedia Appendices 4 and 5). Temporal autocorrelation was negatively associated with imputation error for all methods except mean imputation, which showed little association (r=–0.13; Multimedia Appendix 6). The association was strongest for LOCF (r=–0.92), followed by random forest (r=–0.74). For these, error decreased almost monotonically with increasing autocorrelation, indicating substantially better accuracy for more temporally stable variables.

In a sensitivity analysis, we examined whether the initial filling of originally missing values influenced subsequent comparisons of imputation performance. Overall, MSE was lower for values that were missing in the original data and filled in to create the synthetic complete dataset, especially for LOCF and random forest imputation (2 methods used to fill in the original missingness). Still, both LOCF and random forest continued to

XSL•FO
RenderX

achieve the best performance when imputing values not missing in the original data (Multimedia Appendix 7).

In models for mean squared error, a significant 3-way interaction existed between imputation method, proportion missing, and variable group (Tables S4 and S5 in Multimedia Appendix 1) due to the fact that (1) all methods except mean imputation degraded with increased missingness and (2) variables with a response of "select all that apply" were more poorly predicted (Multimedia Appendix 8). There was no interaction between missingness mechanism and (1) imputation method or (2) variable group.

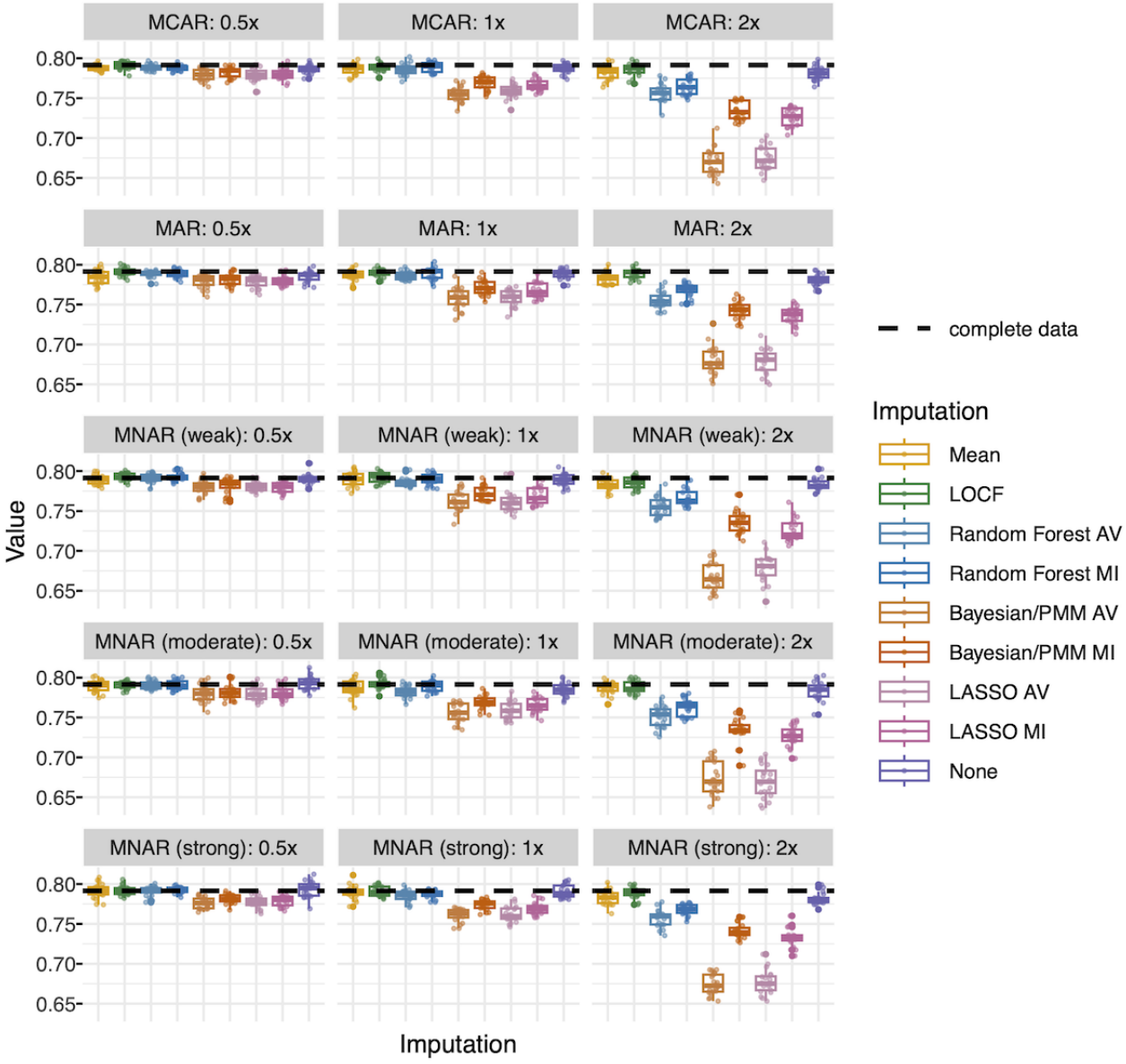
Prediction Model Performance

Gradient Boosted Models

Extubation: Balanced accuracy

For the outcome of extubation using gradient boosted models, balanced accuracy was the highest for LOCF (Figure 4). Mean imputation and no imputation (native support for missing values) performed almost as well. Random forest (both averaged and multiple imputation) also performed well at 0.5x and 1x missingness, but its performance degraded at 2x missingness. The amount of missingness was more influential than the missingness mechanism (Table S6 in Multimedia Appendix 1).

Figure 4. Gradient boosted model test performance (extubation): balanced accuracy. Each point represents balanced accuracy for 1 dataset. There are 20 datasets per missingness scenario and imputation type represented in each box plot. Balanced accuracy in the complete dataset is represented by a dashed line. AV, average (average of 30 imputations); Bayesian/PMM: Bayesian imputation under the normal linear model with predictive mean matching; LASSO: least absolute shrinkage and selection operator; LOCF: last observation carried forward; MAR, missing at random; MCAR: missing completely at random; MI: multiple imputation; MNAR: missing not at random.



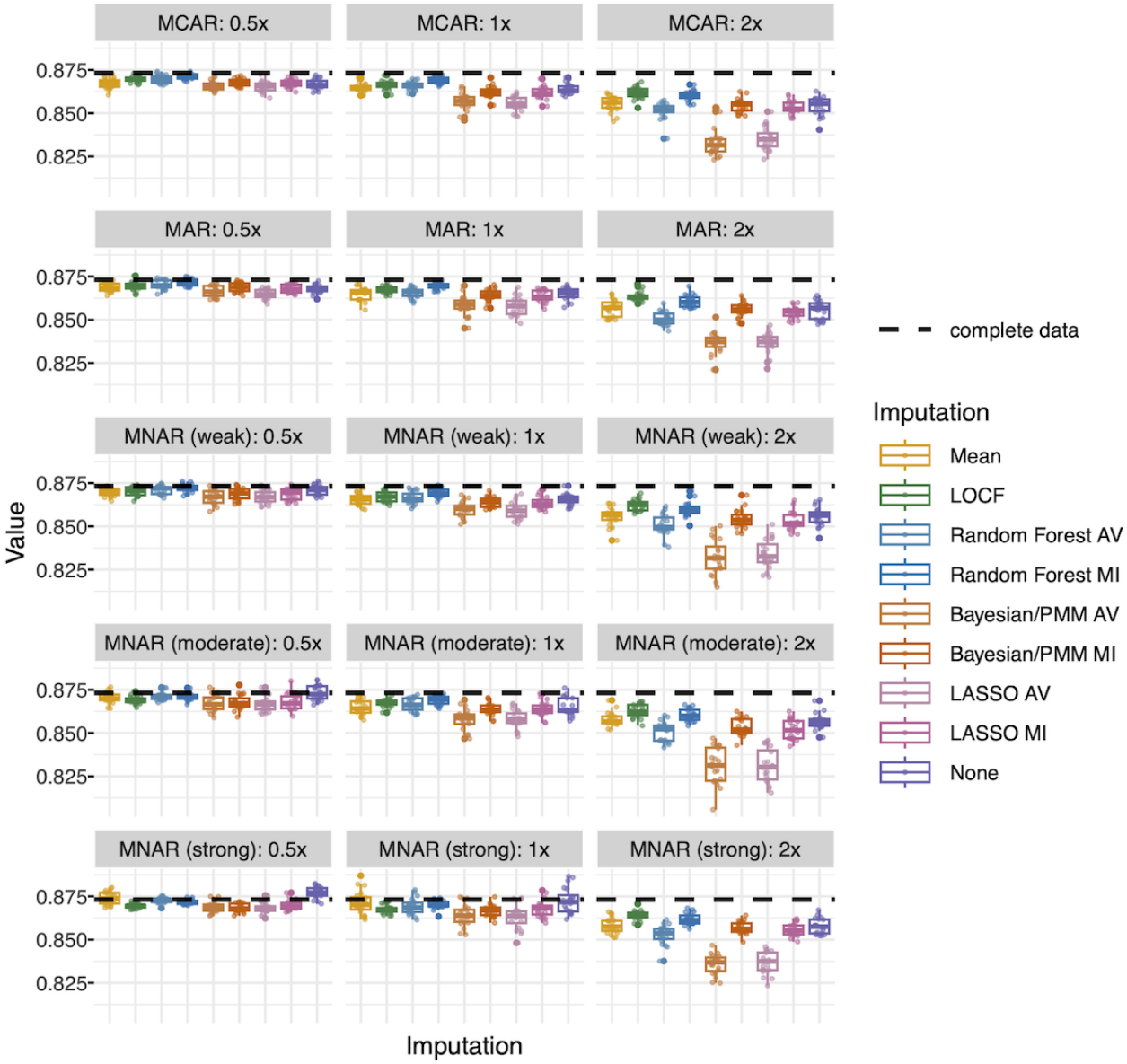
Extubation: AUC

Random forest multiple imputation had the highest AUC for gradient boosted models for 0.5x and 1x missingness, while LOCF did for 2x missingness (Figure 5). Random forest averaged, mean imputation, and no imputation had reasonable performance but degraded at 2x missingness. The amount of

XSL•FO
RenderX

missingness continued to have a greater effect on performance than the missingness mechanism.

Figure 5. Gradient boosted model test performance (extubation): AUC. Each point represents AUC for 1 dataset. There are 20 datasets per missingness scenario and imputation type represented in each box plot. AUC in the complete dataset is represented by a dashed line. Other performance outcome metrics (sensitivity, specificity, positive predictive value [PPV], negative predictive value [NPV], and F1) are presented in Multimedia Appendix 9. AV, average (average of 30 imputations); Bayesian/PMM: Bayesian imputation under the normal linear model with predictive mean matching; LASSO: least absolute shrinkage and selection operator; LOCF: last observation carried forward; MAR, missing at random; MCAR: missing completely at random; MI: multiple imputation; MNAR: missing not at random.

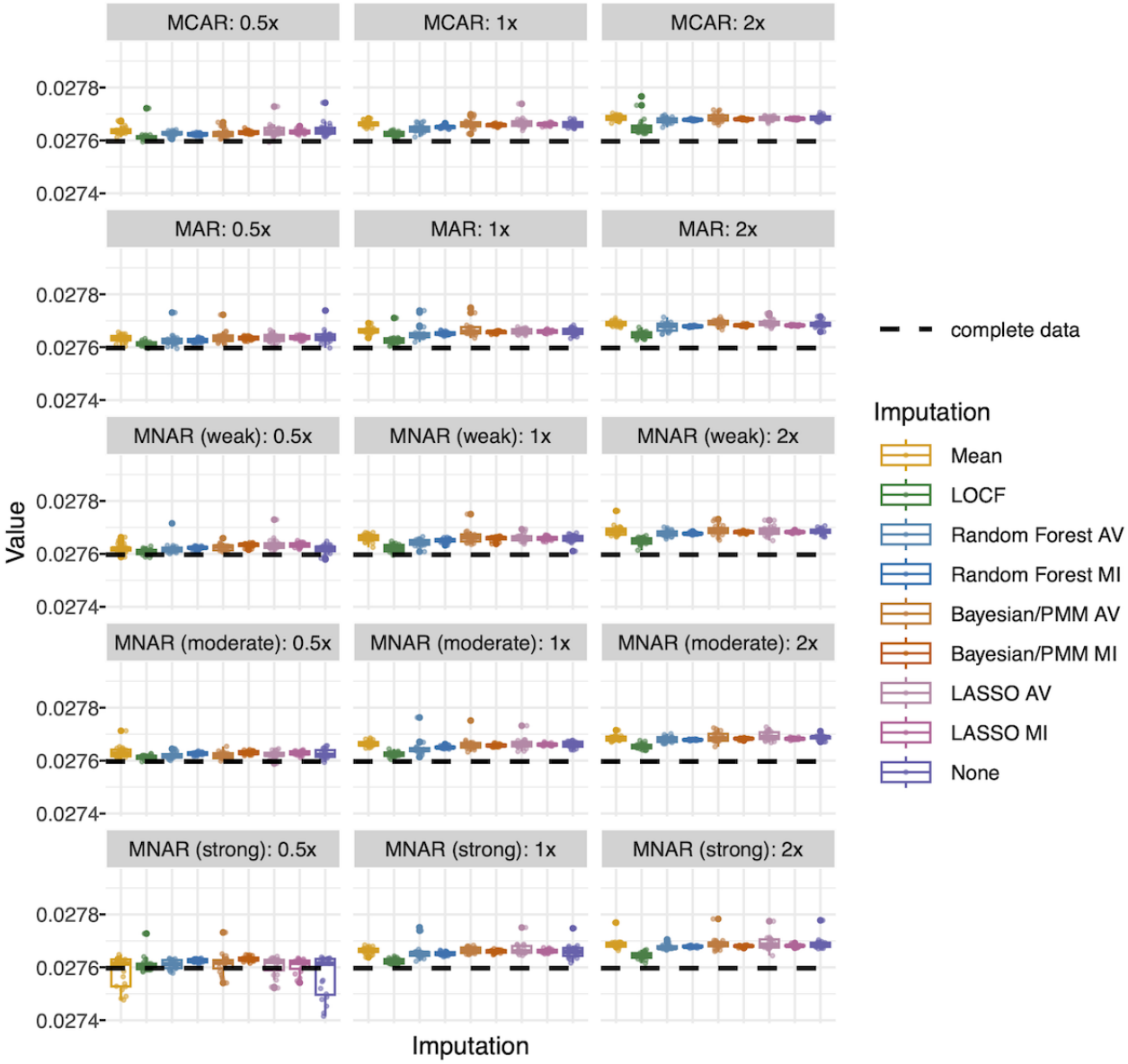


Blood Pressure: MSE

LOCF had the lowest overall MSE (Figure 6). Random forest (both averaged and multiple imputation) generally had the next lowest MSE. Unlike in extubation models, mean imputation and no imputation did not perform substantially better than other methods. Performance was again more sensitive to amount of missingness than to missingness mechanism; overall, MSE increased in a stepwise fashion as missingness increased. However, there was less overall variability (CV=0.001) between models than for balanced accuracy (CV=0.042) and AUC (CV=0.012).

XSL•FO
RenderX

Figure 6. Gradient boosted model test performance (blood pressure): mean squared error (MSE). Each point represents MSE for 1 dataset. There are 20 datasets per missingness scenario and imputation type represented in each box plot. MSE in the complete dataset is represented by a dashed line. Other performance outcome metrics (mean absolute error [MAE], root MSE, and R^2) are presented in Multimedia Appendix 10. AV, average (average of 30 imputations); Bayesian/PMM: Bayesian imputation under the normal linear model with predictive mean matching; LASSO: least absolute shrinkage and selection operator; LOCF: last observation carried forward; MAR, missing at random; MCAR: missing completely at random; MI: multiple imputation; MNAR: missing not at random.



LASSO Models

Extubation: Balanced Accuracy

For the LASSO outcome model, performance and patterns were similar to the gradient boosted model for balanced accuracy, with LOCF demonstrating top performance (Table S7 in Multimedia Appendix 1; Multimedia Appendix 11). Mean imputation did not perform as well in LASSO models. Interestingly, imputation methods that performed worst—Bayesian/PMM and LASSO—yielded better results in LASSO models than in gradient boosted models, with less variation in performance across methods (CV=0.029).

Extubation: AUC

AUC followed similar patterns to balanced accuracy for LASSO. LOCF had the best performance. Mean imputation again performed worse comparatively, and there was a smaller performance gap between the best and worst imputation methods relative to gradient boosted models (CV=0.011; Table S7 in Multimedia Appendix 1; Multimedia Appendix 11).

Blood Pressure: MSE

LOCF had the lowest overall MSE (Multimedia Appendix 12). MSE again increased as missingness increased. MSE of LASSO models for all imputation methods was higher than gradient boosted models, although LASSO MSE was consistently closer to the MSE for complete data. The range between the best and

XSL•FO
RenderX

worst imputation methods was narrower than for gradient boosted models (CV=0.0008).

Overfitting to training data: Both models

Extubation: Balanced Accuracy and AUC

Overfitting to the training data (Multimedia Appendices 13 and 14) increased as proportion of missingness increased. It was greatest for the worst-performing imputation methods (Bayesian/PMM and LASSO) in both gradient-boosted and LASSO outcome models. It was higher overall for gradient boosted models than for LASSO outcome models.

Blood Pressure: MSE

Gradient boosted models exhibited more overfitting overall and higher variability in overfitting than LASSO models (Multimedia Appendices 15 and 16).

Discussion

Overview

EHR data present challenges in how to handle missing data when developing clinical prediction models. It is critical to use methods that are transferable to new data when generating real-time predictions for use cases like clinical decision support tools. In a realistic EHR dataset, we compared imputation methods based on (1) imputation accuracy and (2) outcome prediction.

Imputation Performance

LOCF and random forest multiple imputation consistently had the lowest MSE and classification error. LOCF has performed well in health survey and cohort datasets [18,20]. In our data, per-variable LOCF imputation error decreased monotonically with first-order autocorrelation, indicating better performance for more temporally stable variables. Random forest, while not explicitly designed for longitudinal data, was informed by lagged variables in our implementation and therefore also showed some gains for more temporally stable variables, though the association was weaker than for LOCF. By contrast, mean imputation does not account for correlation across repeated measures, and accordingly showed no relationship between autocorrelation and error. In the PICU, where many measurements are recorded frequently and less frequent measurements often indicate presumed stability over time, LOCF may be particularly suitable, while random forest may provide added value when temporal patterns are weaker.

As expected, imputation performance degraded as the proportion of missingness increased. Jäger et al [13] also found imputation performance generally worsened when difficulty (eg, higher missingness fraction and MNAR) increased. We found that missingness proportion affected imputation quality more than missingness mechanism. Although the imputation methods we employed are only theoretically valid in MCAR and MAR settings, performance in MNAR data was fairly similar, possibly due to the availability of repeated measurements over time, which may have captured underlying patterns. This is fortunate, given that EHR data are often likely MNAR [9].

Prediction Model Performance

Many studies do not report imputation performance [9,15,16], focusing instead on prediction performance. In our experiment, LOCF generally yielded the highest prediction performance across outcome types and models. We evaluated whether LOCF's strong performance was influenced by how we constructed the synthetic, complete dataset. Although it may have been somewhat inflated, sensitivity analyses confirmed that LOCF remained a top performer. Its accuracy was greatest for variables with higher first-order autocorrelation, which may help explain its strong performance in this setting. While criticized in inferential statistics for causing bias and low standard errors [6,40], here it outperformed many multiple imputation methods.

Random forest multiple imputation was the best performing multiple imputation model. Jaeger et al [27] also found it led to the best predictive performance across 12 imputation strategies with 2 different outcome models in a registry dataset. Perez-Lebel et al [9] attributed multiple imputation's improved performance to ensembling (averaging multiple predictors) rather than accurately capturing the distribution of the missing values (the theoretical basis for its use in inferential statistics).

Native support for missing values (no imputation) yielded high balanced accuracy for gradient boosted models and reasonable performance for other metrics. Perez-Lebel et al [9] concluded that it had the best predictive performance in real-world EHR data, with the lowest computational cost. LOCF (which they did not test) also has very little computational cost but may be less broadly applicable.

As with imputation performance, missingness mechanism had less impact on prediction performance than proportion of missingness. Performance degraded substantially as missingness fraction increased, consistent with prior findings [13]. Interestingly, performance was similar across MAR, MCAR, and MNAR scenarios. Some studies suggest explicitly adding indicator variables for missingness to outcome models improves prediction in MNAR settings [9,10,41]. However, others argue against them because they are fragile to operational and practice changes and may not generalize well to other settings [11,12,42]. We therefore did not include such indicators, and performance in MNAR scenarios was comparable to MAR and MCAR scenarios. Machine learning models with native support for missing data may exploit missingness patterns for prediction. If no imputation is employed, missingness patterns should be closely monitored for drift and its effect on predictive performance [42].

Variability between imputation methods differed by model type and performance metric. LASSO outcome models showed less variability than gradient boosted models. In our experiment, imputation method appeared to have a greater impact on the binary outcome than the continuous outcome. Balanced accuracy had the highest variability between methods, followed by AUC; MSE exhibited substantially less variability than either. All imputation methods had lower MSE for gradient boosted models than LASSO models, indicating choice of outcome model mattered more than choice of imputation method.

XSL•FO
RenderX

Relationship Between Imputation and Prediction Performance

The best performing methods for imputation—LOCF and random forest multiple imputation—also performed well in prediction. Thus, our main results for imputation and prediction performance were largely concordant. Mean imputation had the worst MSE but performed relatively well in gradient boosted models, possibly because constant imputation creates patterns that machine learning can exploit [9,43]. Its performance dropped in LASSO models. Others have noted that more accurate imputation methods do not always yield better predictions [9,27], especially when features are weakly correlated [9].

Overfitting in imputation models reduced imputation accuracy, which subsequently impacted the accuracy of outcome models. Outcome metrics that overfit more (eg, balanced accuracy in gradient boosted models) also showed greater variability between imputation methods in patterns that reflected differences in imputation accuracy.

Imputation and Interpretability

For clinical decision support, it is important to assess how missing data handling affects interpretability. The full promise of artificial intelligence will not be realized if it is not deemed trustworthy and transparent by humans [44,45]. Mean imputation, the most common method of imputation in machine learning clinical prediction models [12], may reduce interpretability for clinicians trying to understand predictions for individual patients, as the mean is not meaningful at the individual level. Native support by algorithms may improve interpretability by relying only on recorded values. LOCF is simple to implement and aligns with clinical reasoning—if a measurement is expected to change and that change is important, it will be remeasured if possible. Finally, if complex methods like random forests (while less interpretable themselves) generate accurate imputations that reflect a biological or clinical relationship between the predictor and outcome, this could lead to more interpretable outcome models that are also more robust over time and across populations [9].

Limitations

The primary limitation of this experiment is its reliance on both a single dataset and a single method for generating the complete dataset on which the analysis is based. However, a key strength is the high fidelity of the data, with detailed, frequent measurements typical of the intensive care unit. This contrasts with EHR data from settings like primary care, where visits may be months or years apart. Although we predicted both a binary and continuous outcome, our dataset was limited to a single PICU at one academic medical center. Raw data were transformed into a structured format with time windows and summary variables, a common approach for EHR data [2,46]. Thus, our findings may not generalize to other settings or data structures.

We restricted imputation methods in our experiment to those with readily available packages in R that allowed model training on 1 dataset and subsequent imputation in new data. Deep learning methods were not included, nor were novel approaches [47-49] that may outperform tested methods but are more complex to implement for applied practitioners. Performance could also theoretically be improved by combining imputation approaches (eg, a SuperLearner [50]).

Most existing imputation packages do not allow users to save model parameters to apply on new data, limiting the methods available [15]. Some have proposed workarounds, such as stacking data from a new patient with all training data and rerunning multiple imputation models [15,17]. However, this was computationally infeasible in a dataset of our size. Privacy concerns may also prevent access to training data in deployment. Even packages like *mice* that allow imputation on single new cases have limitations—each call refits an iteration of the model, making real-time imputation for new patients infeasible due to speed. The lack of scalable imputation tools remains a barrier to progress to deploying real-time clinical prediction models.

Conclusion

When using EHR data with frequent measurements to build a prediction model, LOCF offers reasonable performance with simple implementation. Native support for missing data in machine learning models, such as gradient boosted trees, is the least computationally intensive approach, with decent performance and potentially broader applicability than LOCF. While multiple imputation is the gold standard for inferential models, it is extremely computationally intensive, may not be optimal for prediction models, and may not be feasible in real time. As clinical prediction models continue to integrate into real-time patient care, addressing missing data appropriately remains essential.

Acknowledgments

ChatGPT was used for assistance in writing R code and to make minor copyedits to the manuscript for conciseness and clarity.

Funding

This work was supported by NIH F31HL156498 (National Heart, Lung, and Blood Institute, Digitale).

Data Availability

The data underlying this article cannot be shared publicly because they contain protected health information.

XSL•FO
RenderX

Authors' Contributions

Conceptualization: CEM (equal), DF (equal), EDG (equal), JD (lead), MJP (equal),
Data curation: DF (supporting), JD (lead)
Formal analysis: JD (lead)
Funding acquisition: CEM (supporting), DF (supporting), EDG (supporting), JD (lead), MJP (supporting)
Methodology: CEM (equal), DF (equal), EDG (equal), JD (lead), MJP (equal)
Resources: JD (lead), MJP (supporting)
Software: EDG (supporting), JD (lead)
Supervision: CEM (equal), DF (equal), EDG (equal), MJP (equal)
Validation: JD (lead)
Visualization: JD (lead)
Writing – original draft: JD (lead)
Writing – review & editing: CEM (supporting), DF (supporting), EDG (supporting), JD (lead), MJP (supporting)

Conflicts of Interest

None declared.

Multimedia Appendix 1
Supplementary methods and tables.
[PDF File, 727 KB - medinform_v13i1e79307_app1.pdf]

Multimedia Appendix 2
Imputation test performance metrics (blood pressure): mean squared error. Each point represents mean squared error calculated for 176 numeric variables for 1 of 300 datasets created for the outcome of blood pressure. There are 20 datasets per missingness scenario and imputation type represented in each box plot. AV: average (average of 30 imputations); Bayesian/PMM: Bayesian imputation under the normal linear model with predictive mean matching; LASSO: least absolute shrinkage and selection operator; LOCF: last observation carried forward.
[PDF File, 126 KB - medinform_v13i1e79307_app2.pdf]

Multimedia Appendix 3
Imputation test performance metrics (extubation and blood pressure): classification error. Each point represents classification error calculated for 6 categorical variables for 1 dataset (of 300 created for the outcome of extubation and 300 created for the outcome of blood pressure). There are 20 datasets per missingness scenario and imputation type represented in each box plot. The mice implementation of LASSO cannot accommodate multiclass categorical outcomes; thus, we used a simple classification tree. AV: average (average of 30 imputations); Bayesian/PMM: Bayesian imputation under the normal linear model with predictive mean matching; LASSO: least absolute shrinkage and selection operator; LOCF: last observation carried forward.
[PDF File, 249 KB - medinform_v13i1e79307_app3.pdf]

Multimedia Appendix 4
Imputation performance difference between train and test (extubation and blood pressure): mean squared error. Each point represents the difference in mean squared error between training and test sets calculated for 176 numeric variables for 1 dataset (of 300 created for the outcome of extubation and 300 created for the outcome of blood pressure). There are 20 datasets per missingness scenario and imputation type represented in each box plot. AV: average (average of 30 imputations); Bayesian/PMM: Bayesian imputation under the normal linear model with predictive mean matching; LASSO: least absolute shrinkage and selection operator; LOCF: last observation carried forward.
[PDF File, 256 KB - medinform_v13i1e79307_app4.pdf]

Multimedia Appendix 5
Imputation performance difference between train and test (extubation and blood pressure): classification error. Each point represents the difference in mean squared error between training and test sets calculated for 6 categorical variables for 1 dataset (of 300 created for the outcome of extubation and 300 created for the outcome of blood pressure). There are 20 datasets per missingness scenario and imputation type represented in each box plot. The mice implementation of LASSO cannot accommodate multiclass categorical outcomes; thus, we used a simple classification tree. AV: average (average of 30 imputations); Bayesian/PMM: Bayesian imputation under the normal linear model with predictive mean matching; LASSO: least absolute shrinkage and selection operator; LOCF: last observation carried forward.
[PDF File, 255 KB - medinform_v13i1e79307_app5.pdf]

XSL•FO
RenderX

Multimedia Appendix 6
Autocorrelation versus imputation error by method (extubation). Scatterplot of per-variable temporal autocorrelation (AR(1) coefficient, *x*-axis) versus imputation error (*y*-axis; mean squared error (MSE) for numeric variables, classification error for categorical) using 4-hour windows. Each point represents 1 predictor; higher persistence corresponds to lower error for last observation carried forward (LOCF).
[PDF File, 22 KB - medinform_v13i1e79307_app6.pdf]

Multimedia Appendix 7
Imputation test performance metrics by missingness in original data (extubation and blood pressure): mean squared error. Each point represents mean squared error calculated for 176 numeric variables for 1 dataset stratified by whether the value was missing in the original data (of 300 created for the outcome of extubation and 300 created for the outcome of blood pressure). There are 20 datasets per missingness scenario and imputation type represented in each box plot. AV: average (average of 30 imputations); Bayesian/PMM: Bayesian imputation under the normal linear model with predictive mean matching; LASSO: least absolute shrinkage and selection operator; LOCF: last observation carried forward.
[PDF File, 768 KB - medinform_v13i1e79307_app7.pdf]

Multimedia Appendix 8
Marginal means for interaction between imputation method, proportion missing, and variable group (extubation and blood pressure). We calculated marginal means for interaction from linear models of mean squared error comparing imputed values to complete dataset (for each outcome: 1 observation [n=264,000] per 176 variables per 300 datasets per 5 imputation methods). We calculated marginal means for interaction from linear models of classification error comparing imputed values to complete dataset (for each outcome: 1 observation [n=9000] per 6 variables per 300 datasets per 5 imputation methods) with random intercepts for each of the 1500 datasets. We included all 3-way and 2-way interactions and completed a backward stepwise elimination procedure (included $P<.05$) to determine the final model. Variable group 4, unlike other variable groups, included mostly indicator variables constructed from “select all that apply” responses in the electronic health record (EHR) (see Table S1). Bayesian/PMM: Bayesian imputation under the normal linear model with predictive mean matching; LASSO: least absolute shrinkage and selection operator; LOCF: last observation carried forward.
[PDF File, 76 KB - medinform_v13i1e79307_app8.pdf]

Multimedia Appendix 9
Gradient-boosted model test performance (extubation): other metrics. Each point represents performance for 1 dataset. There are 20 datasets per missingness scenario and imputation type represented in each box plot. Performance in the complete dataset is represented by a dashed line. AV: average (average of 30 imputations); Bayesian/PMM: Bayesian imputation under the normal linear model with predictive mean matching; LASSO: least absolute shrinkage and selection operator; LOCF: last observation carried forward; MI: multiple imputation; NPV: negative predictive value; PPV: positive predictive value.
[PDF File, 1010 KB - medinform_v13i1e79307_app9.pdf]

Multimedia Appendix 10
Gradient boosted model test performance (blood pressure): other metrics. Each point represents performance for 1 dataset. There are 20 datasets per missingness scenario and imputation type represented in each box plot. Performance in the complete dataset is represented by a dashed line. AV: average (average of 30 imputations); Bayesian/PMM: Bayesian imputation under the normal linear model with predictive mean matching; LASSO: least absolute shrinkage and selection operator; LOCF: last observation carried forward; MAE: mean absolute error; MI: multiple imputation; NPV: negative predictive value; PPV: positive predictive value; RMSE: root mean squared error.
[PDF File, 617 KB - medinform_v13i1e79307_app10.pdf]

Multimedia Appendix 11
LASSO test performance (extubation): all metrics. Each point represents performance for 1 dataset. There are 20 datasets per missingness scenario and imputation type represented in each box plot. Performance in the complete dataset is represented by a dashed line. AV: average (average of 30 imputations); Bayesian/PMM: Bayesian imputation under the normal linear model with predictive mean matching; LASSO: least absolute shrinkage and selection operator; LOCF: last observation carried forward; MAE: mean absolute error; MI: multiple imputation; NPV: negative predictive value; PPV: positive predictive value; RMSE: root mean squared error.
[PDF File, 1232 KB - medinform_v13i1e79307_app11.pdf]

Multimedia Appendix 12

XSL•FO
RenderX

LASSO test performance (blood pressure): all metrics. Each point represents performance for 1 dataset. There are 20 datasets per missingness scenario and imputation type represented in each box plot. Performance in the complete dataset is represented by a dashed line. AV: average (average of 30 imputations); Bayesian/PMM: Bayesian imputation under the normal linear model with predictive mean matching; LASSO: least absolute shrinkage and selection operator; LOCF: last observation carried forward; MAE: mean absolute error; MI: multiple imputation; MSE: mean squared error; NPV: negative predictive value; PPV: positive predictive value; RMSE: root mean squared error.
[PDF File, 719 KB - medinform_v13i1e79307_app12.pdf]

Multimedia Appendix 13
Gradient-boosted model difference between train and test (extubation): All performance metrics. Each point represents a difference in performance between train and test sets for 1 dataset. There are 20 datasets per missingness scenario and imputation type represented in each box plot. The difference in the complete dataset is represented by a dashed line. AV: average (average of 30 imputations); Bayesian/PMM: Bayesian imputation under the normal linear model with predictive mean matching; LASSO: least absolute shrinkage and selection operator; LOCF: last observation carried forward; MAE: mean absolute error; MI: multiple imputation; MSE: mean squared error; NPV: negative predictive value; PPV: positive predictive value; RMSE: root mean squared error.
[PDF File, 1428 KB - medinform_v13i1e79307_app13.pdf]

Multimedia Appendix 14
LASSO model difference between train and test (extubation): all performance metrics. Each point represents a difference in performance between train and test sets for 1 dataset. There are 20 datasets per missingness scenario and imputation type represented in each box plot. The difference in the complete dataset is represented by a dashed line. AUC: area under the receiver operating characteristic curve; AV: average (average of 30 imputations); Bayesian/PMM: Bayesian imputation under the normal linear model with predictive mean matching; LASSO: least absolute shrinkage and selection operator; LOCF: last observation carried forward; MAE: mean absolute error; MI: multiple imputation; MSE: mean squared error; NPV: negative predictive value; PPV: positive predictive value; RMSE: root mean squared error.
[PDF File, 1247 KB - medinform_v13i1e79307_app14.pdf]

Multimedia Appendix 15
Gradient boosted model difference between train and test (blood pressure): all performance metrics. Each point represents a difference in performance between train and test sets for 1 dataset. There are 20 datasets per missingness scenario and imputation type represented in each box plot. The difference in the complete dataset is represented by a dashed line. AV: average (average of 30 imputations); Bayesian/PMM: Bayesian imputation under the normal linear model with predictive mean matching; LASSO: least absolute shrinkage and selection operator; LOCF: last observation carried forward; MAE: mean absolute error; MI: multiple imputation; MSE: mean squared error; NPV: negative predictive value; PPV: positive predictive value; RMSE: root mean squared error.
[PDF File, 819 KB - medinform_v13i1e79307_app15.pdf]

Multimedia Appendix 16
LASSO model difference between train and test (blood pressure): all performance metrics. Each point represents a difference in performance between train and test sets for 1 dataset. There are 20 datasets per missingness scenario and imputation type represented in each box plot. The difference in the complete dataset is represented by a dashed line. AV: average (average of 30 imputations); Bayesian/PMM: Bayesian imputation under the normal linear model with predictive mean matching; LASSO: least absolute shrinkage and selection operator; LOCF: last observation carried forward; MAE: mean absolute error; MI: multiple imputation; MSE: mean squared error; NPV: negative predictive value; PPV: positive predictive value; RMSE: root mean squared error.
[PDF File, 711 KB - medinform_v13i1e79307_app16.pdf]

References

1. Wells BJ, Chagin KM, Li L, Hu B, Yu C, Kattan MW. Using the landmark method for creating prediction models in large datasets derived from electronic health records. Health Care Manag Sci 2015 Mar;18(1):86-92. [doi: 10.1007/s10729-014-9281-3] [Medline: 24752545]
2. Tang S, Davarmanesh P, Song Y, Koutra D, Sjoding MW, Wiens J. Democratizing EHR analyses with FIDDLE: a flexible data-driven preprocessing pipeline for structured clinical data. J Am Med Inform Assoc 2020 Dec 9;27(12):1921-1934. [doi: 10.1093/jamia/ocaa139] [Medline: 33040151]
3. Rubin DB. Inference and missing data. Biometrika 1976;63(3):581-592. [doi: 10.1093/biomet/63.3.581]
4. Sperrin M, Martin GP, Sisk R, Peek N. Missing data should be handled differently for prediction than for description or causal explanation. J Clin Epidemiol 2020 Sep;125:183-187. [doi: 10.1016/j.jclinepi.2020.03.028] [Medline: 32540389]

XSL•FO
RenderX

5. Getzen E, Ungar L, Mowery D, Jiang X, Long Q. Mining for equitable health: assessing the impact of missing data in electronic health records. J Biomed Inform 2023 Mar;139:104269. [doi: 10.1016/j.jbi.2022.104269] [Medline: 36621750]
6. Lachin JM. Fallacies of last observation carried forward analyses. Clin Trials 2016 Apr;13(2):161-168. [doi: 10.1177/1740774515602688]
7. Buuren S. Flexible Imputation of Missing Data, 2nd edition: CRC Press; 2018. URL: https://stefvanbuuren.name/fimd/sec-pmm.html [accessed 2022-11-04]
8. Wood AM, Royston P, White IR. The estimation and use of predictions for the assessment of model performance using large samples with multiply imputed data. Biom J 2015 Jul;57(4):614-632. [doi: 10.1002/bimj.201400004] [Medline: 25630926]
9. Perez-Lebel A, Varoquaux G, Le Morvan M, Josse J, Poline JB. Benchmarking missing-values approaches for predictive models on health databases. GigaScience 2022 Apr 15;11:giac013. [doi: 10.1093/gigascience/giac013] [Medline: 35426912]
10. Sisk R, Sperrin M, Peek N, van Smeden M, Martin GP. Imputation and missing indicators for handling missing data in the development and deployment of clinical prediction models: a simulation study. Stat Methods Med Res 2023 Aug;32(8):1461-1477. [doi: 10.1177/09622802231165001]
11. Tsvetanova A, Sperrin M, Peek N, Buchan I, Hyland S, Martin GP. Missing data was handled inconsistently in UK prediction models: a review of method used. J Clin Epidemiol 2021 Dec;140:149-158. [doi: 10.1016/j.jclinepi.2021.09.008] [Medline: 34520847]
12. Nijman S, Leeuwenberg AM, Beekers I, et al. Missing data is poorly handled and reported in prediction model studies using machine learning: a literature review. J Clin Epidemiol 2022 Feb;142:218-229. [doi: 10.1016/j.jclinepi.2021.11.023] [Medline: 34798287]
13. Jäger S, Allhorn A, Bießmann F. A benchmark for data imputation methods. Front Big Data 2021;4:693674. [doi: 10.3389/fdata.2021.693674] [Medline: 34308343]
14. Breiman L, Friedman J, Stone C, Olshen R. Classification and Regression Trees: Wadsworth & Brooks; 1984. URL: https://www.taylorfrancis.com/books/mono/10.1201/9781315139470/classification-regression-trees-leo-breiman-jerome-friedman-olshen-charles-stone [accessed 2025-11-10]
15. Hoogland J, van Barreveld M, Debray TPA, et al. Handling missing predictor values when validating and applying a prediction model to new patients. Stat Med 2020 Nov 10;39(25):3591-3607. [doi: 10.1002/sim.8682] [Medline: 32687233]
16. Nijman SWJ, Hoogland J, Groenhof TKJ, et al. On behalf of the UCC-CVRM and UCC-SMART study groups. Real-time imputation of missing predictor values in clinical practice. Eur Heart J - Digit Health 2021 Mar 1;2(1):154-164. [doi: 10.1093/ehjdh/ztaa016]
17. Janssen KJM, Vergouwe Y, Donders ART, et al. Dealing with missing predictor values when applying clinical prediction models. Clin Chem 2009 May;55(5):994-1001. [doi: 10.1373/clinchem.2008.115345] [Medline: 19282357]
18. Ribeiro C, Freitas AA. A data-driven missing value imputation approach for longitudinal datasets. Artif Intell Rev 2021 Dec;54(8):6277-6307. [doi: 10.1007/s10462-021-09963-5]
19. Rosner B, Cook N, Portman R, Daniels S, Falkner B. Determination of blood pressure percentiles in normal-weight children: some methodological issues. Am J Epidemiol 2008 Mar 15;167(6):653-666. [doi: 10.1093/aje/kwm348] [Medline: 18230679]
20. Engels JM, Diehr P. Imputation of missing longitudinal data: a comparison of methods. J Clin Epidemiol 2003 Oct;56(10):968-976. [doi: 10.1016/s0895-4356(03)00170-7] [Medline: 14568628]
21. Ahmed RA, Tube B. Endotracheal Tube: StatPearls Publishing; 2023. [Medline: 30969569]
22. Mayer M. missRanger: fast imputation of missing values. 2023. URL: https://CRAN.R-project.org/package=missRanger [accessed 2025-10-25]
23. A language and environment for statistical computing. R Core Team. URL: https://www.R-project.org [accessed 2025-11-04]
24. Schouten RM, Lugtig P, Vink G. Generating missing values for simulation purposes: a multivariate amputation procedure. J Stat Comput Simul 2018 Oct 13;88(15):2909-2930. [doi: 10.1080/00949655.2018.1491577]
25. Huque MH, Carlin JB, Simpson JA, Lee KJ. A comparison of multiple imputation methods for missing data in longitudinal studies. BMC Med Res Methodol 2018 Dec 12;18(1):168. [doi: 10.1186/s12874-018-0615-6] [Medline: 30541455]
26. Li J, Yan XS, Chaudhary D, et al. Imputation of missing values for electronic health record laboratory data. NPJ Digit Med 2021 Oct 11;4(1):1-14. [doi: 10.1038/s41746-021-00518-0]
27. Jaeger BC, Cantor R, Sthanam V, Xie R, Kirklin JK, Rudraraju R. Improving outcome predictions for patients receiving mechanical circulatory support by optimizing imputation of missing values. Circ Cardiovasc Qual Outcomes 2021 Sep;14(9):e007071. [doi: 10.1161/CIRCOUTCOMES.120.007071] [Medline: 34517728]
28. Shah AD, Bartlett JW, Carpenter J, Nicholas O, Hemingway H. Comparison of random forest and parametric imputation models for imputing missing data using MICE: a CALIBER study. Am J Epidemiol 2014 Mar 15;179(6):764-774. [doi: 10.1093/aje/kwt312] [Medline: 24589914]
29. Buuren SV, Groothuis-Oudshoorn K. mice: multivariate imputation by chained equations in R. J Stat Softw 2011;45(3). [doi: 10.18637/jss.v045.i03]
30. Friedman JH. Greedy function approximation: a gradient boosting machine. Ann Statist 2001;29(5):1180-1232. [doi: 10.1214/aos/1013203451]

XSL•FO
RenderX

31. Shi Y, Ke G, Soukhavong D, et al. Lightgbm: light gradient boosting machine. 2023. URL: https://CRAN.R-project.org/package=lightgbm [accessed 2025-10-25]
32. Olson RS, Cava WL, Mustahsan Z, Varik A, Moore JH. Data-driven advice for applying machine learning to bioinformatics problems. In: Biocomput 2018 World Scientific 2018:192-203. [doi: 10.1142/9789813235533_0018]
33. Gennatas ED. Towards precision psychiatry: gray matter development and cognition in adolescence. : University of Pennsylvania; 2017 URL: https://repository.upenn.edu/entities/person/8f68097c-4130-40bd-9e6d-453632bbfe1e [accessed 2025-11-04]
34. Ke G, Meng Q, Finley T, et al. LightGBM: a highly efficient gradient boosting decision tree.: Adv Neural Inf Process Syst Curran Associates, Inc; 2017. URL: https://papers.nips.cc/paper_files/paper/2017/hash/6449f44a102fde848669bdd9eb6b76fa-Abstract.html [accessed 2023-12-22]
35. Friedman J, Hastie T, Tibshirani R. Regularization paths for generalized linear models via coordinate descent. J Stat Softw 2010;33(1):1-22. [Medline: 20808728]
36. Brodersen KH, Ong CS, Stephan KE, Buhmann JM. The balanced accuracy and its posterior distribution. 2010 Presented at: 2010 20th Int Conf Pattern Recognit p. 3121-3124. [doi: 10.1109/ICPR.2010.764]
37. Binuya MAE, Engelhardt EG, Schats W, Schmidt MK, Steyerberg EW. Methodological guidance for the evaluation and updating of clinical prediction models: a systematic review. BMC Med Res Methodol 2022 Dec 12;22(1):316. [doi: 10.1186/s12874-022-01801-8] [Medline: 36510134]
38. Hicks SA, Strümke I, Thambawita V, et al. On evaluation metrics for medical applications of artificial intelligence. Sci Rep 2022 Aug;12(1):5979. [doi: 10.1038/s41598-022-09954-8]
39. Efthimiou O, Seo M, Chalkou K, Debray T, Egger M, Salanti G. Developing clinical prediction models: a step-by-step guide. BMJ 2024 Sep 3:e078276. [doi: 10.1136/bmj-2023-078276]
40. Little RJ, D'Agostino R, Cohen ML, et al. The prevention and treatment of missing data in clinical trials. N Engl J Med 2012 Oct 4;367(14):1355-1360. [doi: 10.1056/NEJMsr1203730] [Medline: 23034025]
41. Sharafoddini A, Dubin JA, Maslove DM, Lee J. A new insight into missing data in intensive care unit patient profiles: observational study. JMIR Med Inform 2019 Jan 8;7(1):e11605. [doi: 10.2196/11605] [Medline: 30622091]
42. van Smeden M, Groenwold RHH, Moons KG. A cautionary note on the use of the missing indicator method for handling missing data in prediction research. J Clin Epidemiol 2020 Sep;125:188-190. [doi: 10.1016/j.jclinepi.2020.06.007] [Medline: 32565213]
43. Josse J, Prost N, Scornet E, Varoquaux G. On the consistency of supervised learning with missing values. arXiv. Preprint posted online on 2020. [doi: 10.48550/arXiv.1902.06931]
44. Payrovnaziri SN, Chen Z, Rengifo-Moreno P, et al. Explainable artificial intelligence models using real-world electronic health record data: a systematic scoping review. J Am Med Inform Assoc 2020 Jul 1;27(7):1173-1185. [doi: 10.1093/jamia/ocaa053] [Medline: 32417928]
45. Shortliffe EH, Sepúlveda MJ. Clinical decision support in the era of artificial intelligence. JAMA 2018 Dec 4;320(21):2199-2200. [doi: 10.1001/jama.2018.17163] [Medline: 30398550]
46. Gupta M, Gallamoza B, Cutrona N, Dhakal P, Poulain R, Beheshti R. An extensive data processing pipeline for MIMIC-IV. Proc Mach Learn Res 2022 Nov;193:311-325. [Medline: 36686986]
47. Luo Y. Evaluating the state of the art in missing data imputation for clinical data. Brief Bioinform 2022 Jan 17;23(1):bbab489. [doi: 10.1093/bib/bbab489] [Medline: 34882223]
48. Kazijevs M, Samad MD. Deep imputation of missing values in time series health data: a review with benchmarking. J Biomed Inform 2023 Aug;144:104440. [doi: 10.1016/j.jbi.2023.104440] [Medline: 37429511]
49. Liu M, Li S, Yuan H, et al. Handling missing values in healthcare data: a systematic review of deep learning-based imputation techniques. Artif Intell Med 2023 Aug;142:102587. [doi: 10.1016/j.artmed.2023.102587]
50. van der Laan MJ, Polley EC, Hubbard AE. Super learner. Stat Appl Genet Mol Biol 2007;6(1). [doi: 10.2202/1544-6115.1309]

Abbreviations

AUC: area under the receiver operating characteristic curve
CV: coefficient of variation
EHR: electronic health record
ETT: endotracheal tube
LASSO: least absolute shrinkage and selection operator
LOCF: last observation carried forward
MAR: missing at random
MCAR: missing completely at random
MI: multiple imputation
MNAR: missing not at random
MSE: mean squared error
PICU: pediatric intensive care unit

XSL•FO
RenderX

PMM: predictive mean matching

Edited by A Benis; submitted 18.06.25; peer-reviewed by J Speiser, Z Kern; revised version received 25.09.25; accepted 13.10.25; published 14.11.25.

Please cite as:
Digitale J, Franzon D, Pletcher MJ, McCulloch CE, Gennatas ED
Methods for Addressing Missingness in Electronic Health Record Data for Clinical Prediction Models: Comparative Evaluation
JMIR Med Inform 2025;13:e79307
URL: https://medinform.jmir.org/2025/1/e79307
doi:10.2196/79307

© Jean Digitale, Deborah Franzon, Mark J Pletcher, Charles E McCulloch, Efstathios D Gennatas. Originally published in JMIR Medical Informatics (https://medinform.jmir.org), 14.11.2025. This is an open-access article distributed under the terms of the Creative Commons Attribution License (https://creativecommons.org/licenses/by/4.0/), which permits unrestricted use, distribution, and reproduction in any medium, provided the original work, first published in JMIR Medical Informatics, is properly cited. The complete bibliographic information, a link to the original publication on https://medinform.jmir.org/, as well as this copyright and license information must be included.

XSL•FO
RenderX

Number of Publications on New Clinical Prediction Models: A Bibliometric Review

Banafsheh Arshi[1,2], PhD; Laure Wynants[1,3,4], PhD; Eline Rijnhart[1], MD, MSc; Kelly Reeve[5], PhD; Laura Elizabeth Cowley[6], PhD; Luc J Smits[1], PhD

[1]Department of Epidemiology, CAPHRI Care and Public Health Research Institute, Faculty of Health, Medicine and Life Sciences, Maastricht University, Peter Debyeplein 1, P.O. Box 616, Maastricht, The Netherlands

[2]Institute for Risk Assessment Sciences (IRAS), Utrecht University, Utrecht, The Netherlands

[3]Department of Development and Regeneration, KU Leuven, Leuven, Belgium

[4]Leuven Unit for Health Technology Assessment Research (LUHTAR), KU Leuven, Leuven, Belgium

[5]Epidemiology, Biostatistics and Prevention Institute, University of Zürich, Zurich, Switzerland

[6]Population Data Science, Swansea University Medical School, Wales, United Kingdom

Corresponding Author:
Luc J Smits, PhD
Department of Epidemiology, CAPHRI Care and Public Health Research Institute, Faculty of Health, Medicine and Life Sciences, Maastricht University, Peter Debyeplein 1, P.O. Box 616, Maastricht, The Netherlands

Abstract

Background: Concerns have been expressed about the abundance of new clinical prediction models (CPMs) proposed in the literature. However, the extent of this proliferation in prediction research remains unclear.

Objective: This study aimed to estimate the total and annual number of CPM development-related publications available across all medical fields.

Methods: Using a validated search strategy, we conducted a systematic search of literature for prediction model studies published in Pubmed and Embase between 1995 and the end of 2020. By taking random samples for each year, we identified eligible studies that developed a multivariable model (ie, diagnostic or prognostic) for individual-level prediction of a health outcome across all medical fields. Exclusion criteria included development of models with a single predictor, studies not involving humans, methodological studies, conference abstracts, articles with unavailable full text, and those not available in English. We estimated the total and annual number of published regression-based multivariable CPM development articles, based on the total number of publications, proportion of included articles, and the search sensitivity. Furthermore, we used an adjusted Poisson regression to extrapolate our results to the period 1950 - 2024. Additionally, we estimated the number of articles that developed CPMs using techniques other than regression (eg, machine learning).

Results: From a random sample of 10,660 articles published between 1995 and 2020, 109 regression-based CPM development articles were included. We estimated that 82,772 (95% CI 65,313 - 100,231) CPM development articles using regression were published, with an acceleration in model development from 2010 onward. With the addition of articles that developed non-regression-based CPMs, the number increased to 147,714 (95% CI 125,201-170,226). After extrapolation to the years 1950 - 2024, the number of articles increased to 156,673 and 248,431 for regression-based models and total CPMs, respectively.

Conclusions: Based on a representative sample of publications from the literature, we estimated that nearly 250,000 articles reporting the development of CPMs across all medical fields were published until 2024. CPM development–related publications continue to increase in number. To prevent research waste and close the gap between research and clinical practice, focus should shift away from developing new CPMs to facilitating model validation and impact assessment of the plethora of existing CPMs. Limitations of this study include restriction of search to articles available in English and development of the validated search strategy prior to the popularity of artificial intelligence and machine learning models.

International Registered Report Identifier (IRRID): RR2-10.1136/bmjopen-2023-073174

(JMIR Med Inform 2025;13:e62710) doi:10.2196/62710

KEYWORDS

prediction modeling; model development; external validation; public health; research waste; clinical prediction; clinical practice; online databases; health outcomes; publication records; publication

XSL•FO
RenderX

Introduction

Concerns have been expressed about the abundance of new clinical prediction models (CPMs) proposed in the literature and their limited application in clinical practice, pointing to a high level of research waste [1,2]. Despite efforts to regulate model development and shift focus to model evaluation and implementation, new models appear to be developed at an ever increasing rate [3-5]. Although the number of published CPMs has been reported for specific medical fields or target groups [6-8], a comprehensive overview of the publication of CPM development studies across the spectrum of health care practice does not currently exist. In this study, we estimated the total and annual number of CPM development articles available across all medical fields.

Methods

Study design

This study is a bibliometric analysis of a previously published protocol [9], registered on the Open Science Framework Registries platform [10]. We conducted a systematic search of prediction model articles published between January 1, 1995, and December 31, 2020, in PubMed and Embase, using a validated search strategy for retrieval of clinical prediction modeling studies [sensitivity: 98.2% (91.5% - 99.9%) and specificity: 86.1% (85.4% - 86.7%)] (see Textbox 1) [11-15]. Publication records including titles and abstracts from the searched online databases were stored separately based on each publication year.

Textbox 1. Search terms for prediction models developed and validated by Ingui and Rogers

‘(Validat$ OR Predict$.ti. OR Rule$) OR (Predict$ AND (Outcome$ OR Risk$ OR Model$)) OR ((History OR Variable$ OR Criteria OR Scor$ OR Characteristic$ OR Finding$ OR Factor$) AND (Predict$ OR Model$ OR Decision$ OR Identif$ OR Prognos$)) OR (Decision$ AND (Model$ OR Clinical$ OR Logistic Models/)) OR (Prognostic AND (History OR Variable$ OR Criteria OR Scor$ OR Characteristic$ OR Finding$ OR Factor$ OR Model$))’

This study has been prepared in accordance with the reporting bibliometric reviews of the biomedical literature (BIBLIO) guideline [16]. The PRISMA (Preferred Reporting Items for Systematic reviews and Meta-Analyses) [17] elements have been incorporated into the description of the systematic search.

Random Sampling

We aimed to obtain an unbiased stratified sample of at least 100 published CPM articles. Based on published search string metrics, positive predictive value 3.5% (95% CI 2.7% - 4.6%), we calculated that 2860 records needed screening; therefore, 110 records were randomly selected per publication year. As the target sample size of 100 articles—with a minimum of one development article per year— was not reached after the screening process, we increased the sample size in increments of 30 articles per year until at least 100 articles were included. Details about the sample size calculation and random selection of records are provided in Multimedia Appendix 1 and the published protocol [9].

Eligibility, Screening Process and Data Extraction

Articles were eligible for inclusion in this study if they described the development or external validation of a multivariable model [18]. Studies that described development of a regression-based multivariable prediction model for a health outcome were the focus of the current analysis. Studies that reported development of a prediction model without using logistic, proportional hazards, or linear regression were designated as non-regression–based development articles (eg, machine learning models or scoring rules based on multiple unadjusted bivariate associations). Studies updating existing models were also categorized as development articles.

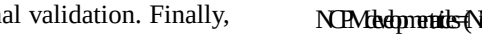
Articles that externally validated a CPM in a different population or in a different time period were designated as validation articles. Of note, an article could be of more than one type (eg, CPM development and external validation article). A random train-test split was not considered external validation. Finally, decision curve analysis (net benefit) was regarded as a method of validation.

We excluded articles that did not present any developed prediction models or external validation in the main results sections (eg, etiologic studies, risk factor assessments, reviews). Articles were also excluded if they were based on a single predictor; reported development or validation of a diagnostic questionnaire (eg, for diagnosis of depression); presented models that were neither diagnostic nor prognostic; did not yield individual-level predictions; did not involve humans; or if they were methodological studies. Articles that were not available in English; conference abstracts; and those without available full texts were also excluded.

Six reviewers (BA, ER, KR, LC, LS, and LW) independently screened titles and abstracts, in pairs. After selection of potential eligible articles, two independent researchers (BA and ER) reviewed the full text articles for eligibility and extracted data. Disagreements were discussed among the reviewers and unresolved conflicts were solved during team consensus meetings. Extracted data included medical domain (based on outcome or target population, or both); publishing journal; publication year; country; study design; study setting; data sources; study population; sample size; outcomes; number of models; model type (diagnostic or prognostic); internal or external validation; performance measures (eg, discrimination, calibration); and model presentation (model equation, nomogram, sum score, etc.).

Data Analysis

Characteristics of eligible regression-based CPM development articles were described using frequencies (n) and percentages (%) for categorical data. We categorized articles by medical field, geographical origin, model type (diagnostic or prognostic), and other characteristics. Next, we estimated the annual number of CPM development articles using the following formula:



XSL•FO
RenderX

To estimate the overall number of articles, we used the weighted average of year-specific proportions of CPM development articles, weighted by the number of hits per year using a conventional estimator of proportion based on a stratified sample [19]. Further details, including calculation of 95% CI is shown in Multimedia Appendix 1. As the search string was developed for identification of regression-based CPMs, we focused primarily on these models for our primary analysis. Additionally, we extrapolated our estimates to 1950 - 2024 using Poisson regression adjusted for publication year. We compared the fit of models with a quadratic term and a linear term for publication year, which showed no apparent difference between the two models (P=.82). Therefore, a linear term was used for the publication year.

In additional analyses, we estimated the total and annual number of articles that reported development of non-regression–based CPMs and external validation articles using the above-mentioned formula, and calculated their respective 95% CIs. For sensitivity analyses, we recalculated our estimations using search sensitivity reported in a validation study by Geersing et al [15].

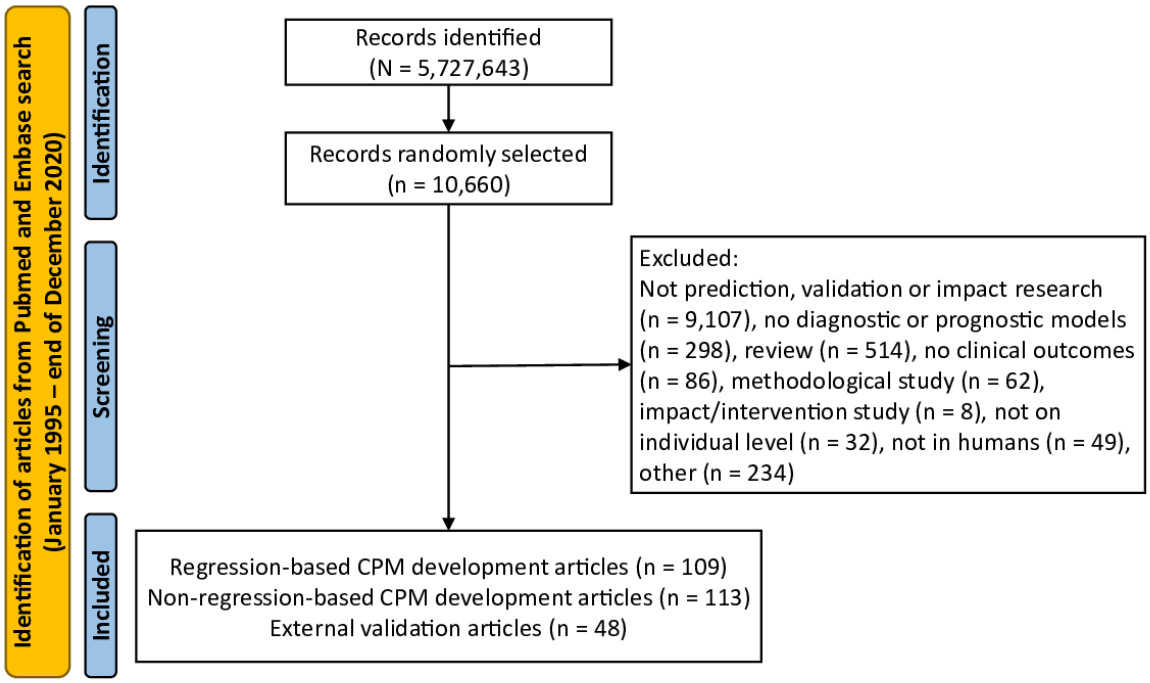
Ethical Considerations

This study was deemed as conforming to the ethics standards of Maastricht University by the ethics committee (case number: FHML-REC/2023/066).

Results

Our search yielded 5,727,643 publications, from which a random sample of 10,660 (410 articles per year) were screened. A total of 222 CPM development articles were identified. including 109 reporting on regression-based models and 113 on non-regression–based models (Figure 1). Characteristics of the regression-based articles are shown in Table 1. Most articles were from North America 41 (37.6%), Europe 37 (33.9%), and Asia 25 (22.9%). The most common medical fields for models development were cardiovascular medicine 22 (20.1%), gynecology and obstetrics 16 (14.7%), and gastroenterology 14 (12.8%). Across all medical fields, 38 (34.9%) of the articles were related to oncology (Table S1 in Multimedia Appendix 1). In addition, 67 (61.5%) of articles described prognostic models while 42 (38.5%) described diagnostic models. Model calibration and discrimination were reported in 31 (28%) and 87 (80%) of the articles, respectively; only 37 (33.9%) of the articles presented their final model.

Figure 1. PRISMA chart for screening and selection of eligible articles. CPM: clinical prediction model.



XSL•FO
RenderX

Table . Characteristics of included regression-based CPM development articles.

Study characteristics	Articles (N=109), n (%)
Continent	
North America	41 (37.6)
Europe	37 (33.9)
Asia	25 (22.9)
South America	1 (0.9)
Australia	1 (0.9)
Africa	1 (0.9)
North America-Europe	3 (2.8)
Medical field	
Cardiovascular disease	22 (20.1)
Gynecology and Obstetrics	16 (14.7)
Gastroenterology	14 (12.8)
Neurology	13 (11.9)
Urology	8 (7.3)
Pulmonology	7 (6.4)
Pediatrics	6 (5.5)
Psychiatry	5 (4.6)
Other fields[a]	18 (16.5)
Type of model	
Prognostic	67 (61.5)
Diagnostic	42 (38.5)
Calibration information given	31 (28.0)
Calibration plot reported	15 (13.8)
Discriminative performance reported	87 (80.0)
C-statistic reported	65 (59.6)
Validation of developed models	
Internal validation	27 (24.8)
External validation	14 (12.8)
Internal validation technique	
Random split of dataset into development and testing sets	8 (7.3)
Cross-validation	7 (6.4)
Bootstrapping	9 (8.3)
Temporal split of dataset into development and testing sets	1 (0.9)
Unclear	3 (2.8)
Final model presented	37 (33.9)

[a]Other fields: Infectious disease: 4 (3.7%); Endocrinology: 3 (2.7%); Hematology: 3 (2.7%); Dermatology: 2 (1.8%); Critical care: 2 (1.8%); Orthopedic surgery: 2 (1.8); Ophthalmology: 1 (0.9%); Emergency medicine: 1 (0.9%).

The estimated number of published regression-based CPM development articles from 1995 to 2020 was 82,772 (95% CI 65,313 - 100,231), with the number of these articles rapidly increasing from 2010 onward (Figure 2, darker area). The number of regression-based CPM development articles that were published increased to 156,673 after extrapolating the findings to 1950 - 2024 (Figure 2, lighter area). Furthermore, an estimated 64,942 (95% CI 50,484 - 79,400) non-regression–based development articles were published between 1995 and 2020 (Figure 3, darker area), increasing the estimated total number of CPM development articles during this period to 147,714 (95% CI 125,201 - 170,226). When

XSL•FO
RenderX

expanded to 1950 - 2024, this number increased to 248,431 (Figure 3, lighter area).

In additional analysis, the estimated number of CPM external validation articles (n=48) published between 1995 and 2020 was 36,394 (95% CI 24,837 - 47,952) (Figure S1 in Multimedia Appendix 1). The estimated number of articles based on search sensitivity reported by Geersing et al [15] are presented in Multimedia Appendix 1.

Figure 2. Cumulative estimated number of regression-based CPM development articles published between 1950 and 2024.

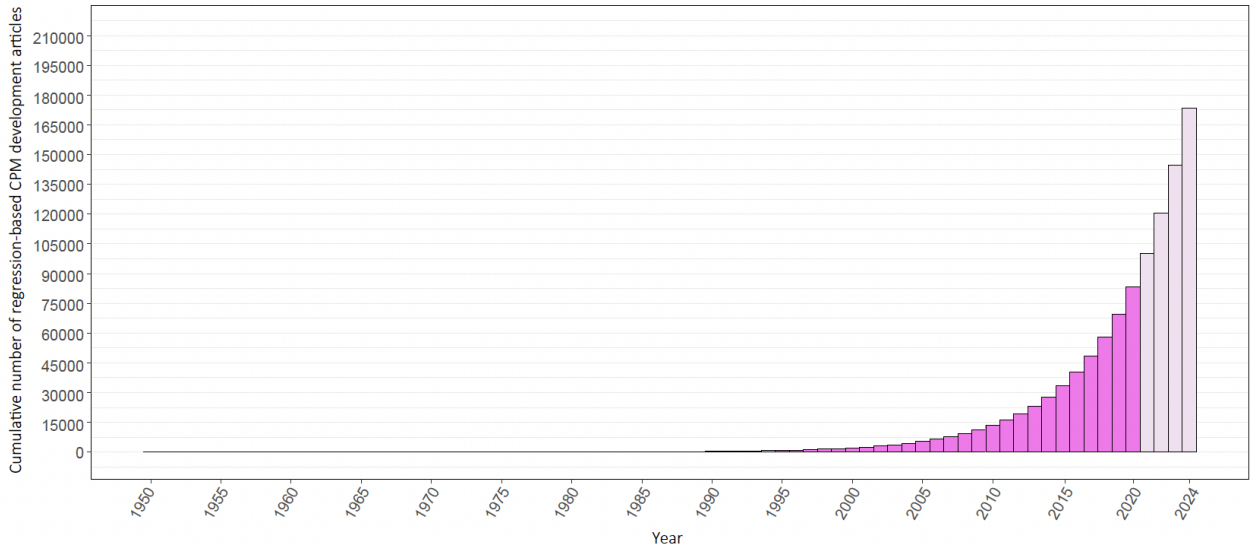
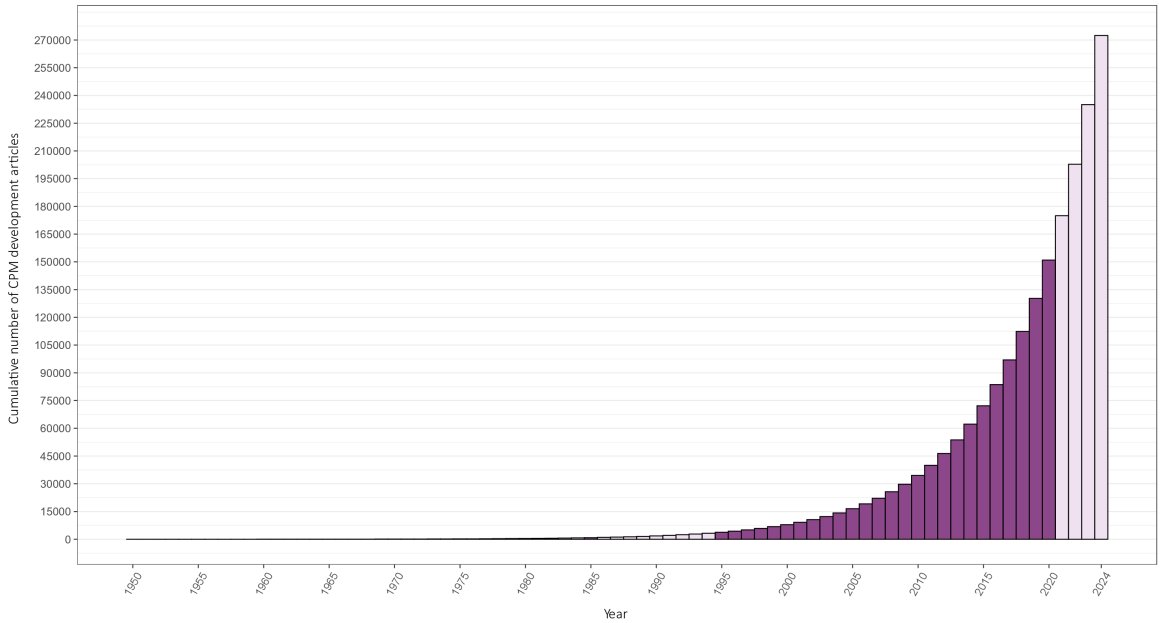


Figure 3. Cumulative estimated number of regression and non-regression–based CPM development articles between 1950 and 2024.



Discussion

Summary

More than 150,000 articles reporting new regression-based CPMs have been published in the medical literature up to 2024, with the number increasing rapidly in recent years—about 10,000 per year. After the addition of non-regression models, the current total approaches 250,000 articles.

Trends in the numbers of model development studies had not been systematically assessed across different medical fields to date. Previously, CPM development for cardiovascular outcomes showed a three-fold increase between 2005-2014, compared to 1995 - 2004 [5]. Further, a sharp increase was observed in the number of models developed using electronic health record data between 2009 - 2019 [3]. Our study shows that despite all regulatory efforts, the growth in model development is ever increasing and is not limited to a specific field [11]. This surge in model development publication has been attributed to the growing accessibility to data and analytical tools [12,20]. However, the excessive model development may obscure decent models and hinder their evaluation [2]. Without further

XSL•FO
RenderX

evaluation such as external validation, these models are unlikely to be fit for adoption in clinical practice.

The proportion of CPMs that undergo external validation remains the topic of ongoing research [9,21]. Among 127 selected CPMs developed before 2010, the probability of external validation within 5 years was only 16% [21]. At such rates, the current surge in model development is bound to produce excess research waste. Adequate methodology and transparent reporting may increase the chances of validation [5,22]. In our study, two-thirds of the development articles did not report the final model. With such an omission, the likelihood that a model will be further evaluated is limited.

Our study benefits from a long time span across more than two decades, assessment of a random sample, and a validated search strategy. However, certain limitations should be acknowledged. Our search was restricted to articles available in English. In addition, the validated strategy that we used was developed prior to the rise in popularity of machine learning and artificial intelligence models. Therefore, our estimates may be considered a lower bound of the actual abundance of CPM development. Despite this, our findings underscore the implications for the current enthusiasm and rapid growth of machine learning and artificial intelligence models. Given the emphasis on retraining, we reiterate that these models also need to undergo rigorous evaluation [7,23,24]. The lack of interpretability of these complex models poses additional challenges; when it is difficult to understand how a model arrives at its predictions, rigorous validation is all the more important.

Implication for Researchers and Stakeholders

To enhance efficiency, prediction research must shift from developing new CPMs to evaluating existing ones [1]. Targeted validation and impact assessment of current CPMs, along with active dissemination and implementation of prediction model-based innovations are crucial steps in minimizing research waste and bridging the gap between research and clinical practice [25]. The responsibility for advancing model evaluation beyond development falls on researchers, clinicians, funding agencies, and other stakeholders. Future validation efforts may depend on both pre-development factors (eg, a clearly defined clinical need, clinician, or public demand) and post-development considerations (eg, model complexity, feasibility of use or the absence of a dissemination or implementation plan) [5]. Additionally, the emphasis on novelty by funding agencies may inadvertently discourage evaluation of existing models. We also advocate for greater transparency in reporting (including presentation of model equations), alongside adherence to contemporary methodological standards by researchers.

Conclusion

Based on a random sample of publications from a validated search strategy, we estimate that nearly 250,000 articles reporting the development of clinical prediction models were published in the literature until 2024. The proliferation of model development, regardless of medical field has accelerated at an unprecedented rate in recent years. It is critical to shift focus from model development to model validation and assessing impact on health care.

Data Availability

The datasets generated or analyzed during this study are available from the corresponding author on reasonable request.

Authors' Contributions

Conceptualization: BA, LJS, LW
Data curation: BA, ER, KR, LEC, LJS, LW
Formal analysis: BA, LW
Methodology: BA, LJS, LW
Project administration: BA, LJS, LW
Resources: LJS, LW
Writing – original draft: BA, LJS, LW
Writing – review & editing: BA, ER, KR, LEC, LJS, LW

Conflicts of Interest

None declared.

Multimedia Appendix 1
Description of methods and data analysis.
[DOCX File, 259 KB - medinform_v13i1e62710_app1.docx]

Checklist 1
PRISMA (Preferred Reporting Items for Systematic reviews and Meta-Analyses) checklist.
[DOCX File, 32 KB - medinform_v13i1e62710_app2.docx]

References

XSL•FO
RenderX

1. Moons KGM, Kengne AP, Grobbee DE, et al. Risk prediction models: II. External validation, model updating, and impact assessment. Heart 2012 May;98(9):691-698. [doi: 10.1136/heartjnl-2011-301247] [Medline: 22397946]
2. Bonnett LJ, Snell KIE, Collins GS, Riley RD. Guide to presenting clinical prediction models for use in clinical settings. BMJ 2019 Apr 17;365:l737. [doi: 10.1136/bmj.l737] [Medline: 30995987]
3. Yang C, Kors JA, Ioannou S, et al. Trends in the conduct and reporting of clinical prediction model development and validation: a systematic review. J Am Med Inform Assoc 2022 Apr 13;29(5):983-989. [doi: 10.1093/jamia/ocac002] [Medline: 35045179]
4. Steyerberg EW, Moons KGM, van der Windt DA, et al. Prognosis Research Strategy (PROGRESS) 3: prognostic model research. PLoS Med 2013;10(2):e1001381. [doi: 10.1371/journal.pmed.1001381] [Medline: 23393430]
5. Wessler BS, Paulus J, Lundquist CM, et al. Tufts PACE Clinical Predictive Model Registry: update 1990 through 2015. Diagn Progn Res 2017;1(1-8):20. [doi: 10.1186/s41512-017-0021-2] [Medline: 31093549]
6. Wessler BS, Lai Yh L, Kramer W, et al. Clinical prediction models for cardiovascular disease: Tufts predictive analytics and comparative effectiveness clinical prediction model database. Circ Cardiovasc Qual Outcomes 2015 Jul;8(4):368-375. [doi: 10.1161/CIRCOUTCOMES.115.001693] [Medline: 26152680]
7. Collins GS, Moons KGM. Reporting of artificial intelligence prediction models. Lancet 2019 Apr;393(10181):1577-1579. [doi: 10.1016/S0140-6736(19)30037-6]
8. Canturk TC, Czikk D, Wai EK, et al. A scoping review of complication prediction models in spinal surgery: an analysis of model development, validation and impact. N Am Spine Soc J 2022 Sep;11(100142):100142. [doi: 10.1016/j.xnsj.2022.100142] [Medline: 35983028]
9. Arshi B, Wynants L, Rijnhart E, Reeve K, Cowley LE, Smits LJ. What proportion of clinical prediction models make it to clinical practice? Protocol for a two-track follow-up study of prediction model development publications. BMJ Open 2023 May 17;13(5):e073174. [doi: 10.1136/bmjopen-2023-073174] [Medline: 37197813]
10. Arshi B, Wynants L, Rijnhart E, Reeve K, Cowley LE, Smits LJ. What proportion of clinical prediction models make it to clinical practice? protocol for a two-track follow-up study. OSF Registries. 2023 Feb 16. URL: https://osf.io/nj8s9/ [accessed 2025-06-18]
11. Ingui BJ, Rogers MAM. Searching for clinical prediction rules in MEDLINE. J Am Med Inform Assoc 2001;8(4):391-397. [doi: 10.1136/jamia.2001.0080391] [Medline: 11418546]
12. Collins GS, Reitsma JB, Altman DG, Moons KGM, TRIPOD Group. Transparent reporting of a multivariable prediction model for individual prognosis or diagnosis (TRIPOD): the TRIPOD statement. Circulation 2015 Jan 13;131(2):211-219. [doi: 10.1161/CIRCULATIONAHA.114.014508] [Medline: 25561516]
13. Moons KGM, de Groot JAH, Bouwmeester W, et al. Critical appraisal and data extraction for systematic reviews of prediction modelling studies: the CHARMS checklist. PLoS Med 2014 Oct;11(10):e1001744. [doi: 10.1371/journal.pmed.1001744] [Medline: 25314315]
14. Moons KGM, Wolff RF, Riley RD, et al. PROBAST: a tool to assess risk of bias and applicability of prediction model studies: explanation and elaboration. Ann Intern Med 2019 Jan 1;170(1):W1-W33. [doi: 10.7326/M18-1377] [Medline: 30596876]
15. Geersing GJ, Bouwmeester W, Zuithoff P, Spijker R, Leeflang M, Moons KGM. Search filters for finding prognostic and diagnostic prediction studies in Medline to enhance systematic reviews. PLoS One 2012;7(2):e32844. [doi: 10.1371/journal.pone.0032844] [Medline: 22393453]
16. Montazeri A, Mohammadi S, M Hesari P, Ghaemi M, Riazi H, Sheikhi-Mobarakeh Z. Preliminary guideline for reporting bibliometric reviews of the biomedical literature (BIBLIO): a minimum requirements. Syst Rev 2023 Dec 15;12(1):239. [doi: 10.1186/s13643-023-02410-2] [Medline: 38102710]
17. Page MJ, McKenzie JE, Bossuyt PM, et al. The PRISMA 2020 statement: an updated guideline for reporting systematic reviews. Syst Rev 2021 Mar 29;10(1):89. [doi: 10.1186/s13643-021-01626-4] [Medline: 33781348]
18. Kleinrouweler CE, Cheong-See FM, Collins GS, et al. Prognostic models in obstetrics: available, but far from applicable. Am J Obstet Gynecol 2016 Jan;214(1):79-90. [doi: 10.1016/j.ajog.2015.06.013] [Medline: 26070707]
19. Lohr SL. Sampling: Design and Analysis: CRC press; 2021.
20. Liao WL, Tsai FJ. Personalized medicine: a paradigm shift in healthcare. Biomedicine (Taipei) 2013 Jun;3(2):66-72. [doi: 10.1016/j.biomed.2012.12.005]
21. Siontis GCM, Tzoulaki I, Castaldi PJ, Ioannidis JPA. External validation of new risk prediction models is infrequent and reveals worse prognostic discrimination. J Clin Epidemiol 2015 Jan;68(1):25-34. [doi: 10.1016/j.jclinepi.2014.09.007] [Medline: 25441703]
22. Wessler BS, Nelson J, Park JG, et al. External validations of cardiovascular clinical prediction models: a large-scale review of the literature. medRxiv. Preprint posted online on 2021. [Medline: 34340529]
23. Mathur P, Srivastava S, Xu X, Mehta JL. Artificial intelligence, machine learning, and cardiovascular disease. Clin Med Insights Cardiol 2020;14:1179546820927404. [doi: 10.1177/1179546820927404] [Medline: 32952403]
24. Carrasco Ramírez. D, Islam M, Even AIH. Machine learning applications in healthcare: current trends and future prospects. J Artif Intell Gen Sci 2024;1(1). [doi: 10.60087/jaigs.v1i1.33]

XSL•FO
RenderX

25. Cowley LE, Farewell DM, Maguire S, Kemp AM. Methodological standards for the development and evaluation of clinical prediction rules: a review of the literature. Diagn Progn Res 2019;3(1):16. [doi: 10.1186/s41512-019-0060-y] [Medline: 31463368]

Abbreviations

CPM: clinical prediction model

Edited by A Coristine; submitted 29.05.24; peer-reviewed by A Atashi, K Miyata, ST Moghadam; revised version received 31.03.25; accepted 31.03.25; published 04.07.25.

Please cite as:
Arshi B, Wynants L, Rijnhart E, Reeve K, Cowley LE, Smits LJ
Number of Publications on New Clinical Prediction Models: A Bibliometric Review
JMIR Med Inform 2025;13:e62710
URL: https://medinform.jmir.org/2025/1/e62710
doi:10.2196/62710

© Banafsheh Arshi, Laure Wynants, Eline Rijnhart, Kelly Reeve, Laura Elizabeth Cowley, Luc J Smits. Originally published in JMIR Medical Informatics (https://medinform.jmir.org), 4.7.2025. This is an open-access article distributed under the terms of the Creative Commons Attribution License (https://creativecommons.org/licenses/by/4.0/), which permits unrestricted use, distribution, and reproduction in any medium, provided the original work, first published in JMIR Medical Informatics, is properly cited. The complete bibliographic information, a link to the original publication on https://medinform.jmir.org/, as well as this copyright and license information must be included.

XSL•FO
RenderX

Patients' Experienced Usability and Satisfaction With Digital Health Solutions in a Home Setting: Instrument Validation Study

Susan J Oudbier[1,2,3,4], MD; Ellen M A Smets[2,4,5], PhD; Pythia T Nieuwkerk[2,6], PhD; David P Neal[3,7], PhD; S Azam Nurmohamed[8], MD, PhD; Hans J Meij[1,9], PhD; Linda W Dusseljee-Peute[7], PhD

[1]Outpatient Division, Amsterdam University Medical Center, Meibergdreef 9, Amsterdam, The Netherlands
[2]Department of Medical Psychology, Amsterdam University Medical Center, University of Amsterdam, Amsterdam, The Netherlands
[3]Digital Health, Amsterdam Public Health Research Institute, Amsterdam, The Netherlands
[4]Quality of Care, Amsterdam Public Health Research Institute, Amsterdam, The Netherlands
[5]Personalized Medicine, Amsterdam Public Health Research Institute, Amsterdam, The Netherlands
[6]Amsterdam Institute for Infection and Immunity, Amsterdam, The Netherlands
[7]Department of Medical Informatics, Amsterdam University Medical Center, University of Amsterdam, Amsterdam, The Netherlands
[8]Department of Nephrology, Amsterdam University Medical Center, Amsterdam, The Netherlands
[9]Yong Loo Lin School of Medicine, National University of Singapore, Singapore, Singapore

Corresponding Author:
Susan J Oudbier, MD
Outpatient Division, Amsterdam University Medical Center, Meibergdreef 9, Amsterdam, The Netherlands

Related Article:

This is a corrected version. See correction statement: https://medinform.jmir.org/2025/1/e73416

Abstract

Background: The field of digital health solutions (DHS) has grown tremendously over the past years. DHS include tools for self-management, which support individuals to take charge of their own health. The usability of DHS, as experienced by patients, is pivotal to adoption. However, well-known questionnaires that evaluate usability and satisfaction use complex terminology derived from human-computer interaction and are therefore not well suited to assess experienced usability of patients using DHS in a home setting.

Objective: This study aimed to develop, validate, and assess an instrument that measures experienced usability and satisfaction of patients using DHS in a home setting.

Methods: The development of the "Experienced Usability and Satisfaction with Self-monitoring in the Home Setting" (GEMS) questionnaire followed several steps. Step I consisted of assessing the content validity, by conducting a literature review on current usability and satisfaction questionnaires, collecting statements and discussing these in an expert meeting, and translating each statement and adjusting it to the language level of the general population. This phase resulted in a draft version of the GEMS. Step II comprised assessing its face validity by pilot testing with Amsterdam University Medical Center's patient panel. In step III, psychometric analysis was conducted and the GEMS was assessed for reliability.

Results: A total of 14 items were included for psychometric analysis and resulted in 4 reliable scales: convenience of use, perceived value, efficiency of use, and satisfaction.

Conclusions: Overall, the GEMS questionnaire demonstrated its reliability and validity in assessing experienced usability and satisfaction of DHS in a home setting. Further refinement of the instrument is necessary to confirm its applicability in other patient populations in order to promote the development of a steering mechanism that can be applied longitudinally throughout implementation, and can be used as a benchmarking instrument.

(JMIR Med Inform 2025;13:e63703) doi:10.2196/63703

KEYWORDS

digital health solutions; questionnaire development; usability instruments; self-management; home setting; validation; reliability

XSL•FO
RenderX

Introduction

The number of digital health solutions (DHS) has increased rapidly, with the potential to significantly enhance the way health care is delivered [1]. DHS include, among others, tools for self-management of clinical data such as blood pressure measurements, for medication adherence, and for education on health-related behaviours such as diet, smoking, and exercise [2]. These tools present the opportunity to increase access to health care and optimize disease management, and they ultimately aim to alleviate health care expenditure [3]. Self-management, as per the World Health Organization, encompasses the capacity of individuals to support and sustain their own health, prevent diseases, and cope with illness and disability, whether independently or with the assistance of a health care professional (HCP) [4,5]. The use of DHS serves a dual purpose in patient self-management: (1) facilitating proactive engagement of individuals in their health journey to optimize treatment outcomes and (2) enhancing prevention of negative health outcomes [6,7]. Consequently, ensuring accessibility and adoption of DHS among target users is crucial for effective implementation [8]. The experienced usability of DHS is pivotal to their adoption, especially for individuals with disabilities or those living with chronic diseases who need to make frequent use of a DHS within their care journey [9-11]. Measuring DHS usability and patient satisfaction is crucial to understand and improve accessibility and use of DHS, thereby fostering patient engagement.

The international organization for standardization defines usability, as comprising effectiveness, efficiency, and satisfaction, given a specific user in a context [12]. In the context of DHS, effectiveness refers to the capacity for thorough and accurate task completion, such as logging into a patient portal or setting personal preferences for medication reminders. Efficiency, on the other hand, involves accomplishing these tasks with minimal effort. Finally, satisfaction is expressed as the comfort and acceptability experienced by patients when using a DHS tool. Usability is often measured by (validated) usability and satisfaction questionnaires, as they allow efficient collection and structured assessment of data from a large number of individual users [13,14]. Usability questionnaires originate from the field of human-computer interaction and user-centered design and have emerged as a means to evaluate the effectiveness, efficiency, and satisfaction of interactive systems, particularly software and digital interfaces from the perspective of end users [15]. Therefore, existing well-known and applied usability questionnaires, such as the System Usability Scale (SUS) and mHealth App Usability Questionnaire (MAUQ) apply software terminology such as the "*various functions* in this system," or "*navigation* between screens" [16-18]. These statements are difficult to interpret for individuals lacking familiarity with software terminology, particularly for patients with low levels of digital literacy [19]. These statements are therefore not suited to measure the usability of self-management tools in healthcare practice by all users.

In addition, introducing DHS in a self-management care journey may increase disparities, as it requires particular skills to use it that comprise both health and digital literacy [20]. In terms of patient characteristics, patients with high health literacy, a higher educational level, and patients who are familiar with DHS find it easier to use these tools [21]. Variability in digital literacy skills among patients are well-recognized, posing challenges in its utilization [22]. Comprehensive research on the specific patient groups for which DHS is relevant, and our understanding of usability in this domain are still in the nascent stages. Disparities arising within groups due to the utilization of technology might lead to one group adopting the technology, while the other group opts not to use it. With the increasing availability and reliance on DHS [26], these tools should be usable for the majority of the patient population. Evaluations of patient experiences with DHS should therefore also be accessible to diverse groups of patients. Thus, to optimize health outcomes and to deliver high quality care, evaluating patients' experienced DHS usability and satisfaction in a home setting is imperative for health care organizations and HCPs [1,23]. In order to ensure patient inclusivity, a general and accessible instrument is needed, which can be applied as a steering mechanism, deployed at multiple points in time to measure usability and satisfaction of DHS in a home setting.

The aim of this study is to develop, validate, and assess the reliability of an instrument that measures experienced usability of and satisfaction with DHS use, taking digital (language) literacy into account. When developing the Experienced Usability and Satisfaction with Self-monitoring in the Home Setting (GEMS) questionnaire, our goal is to find a middle ground between innovation and familiarity, drawing from established statements and questionnaires while tailoring them to be able to evaluate patients experiences with DHS from an inclusive perspective. In doing so, we aim to advance DHS implementation and expand our understanding of end users' needs, for efficient, effective and satisfied DHS use.

Methods

Ethical Considerations

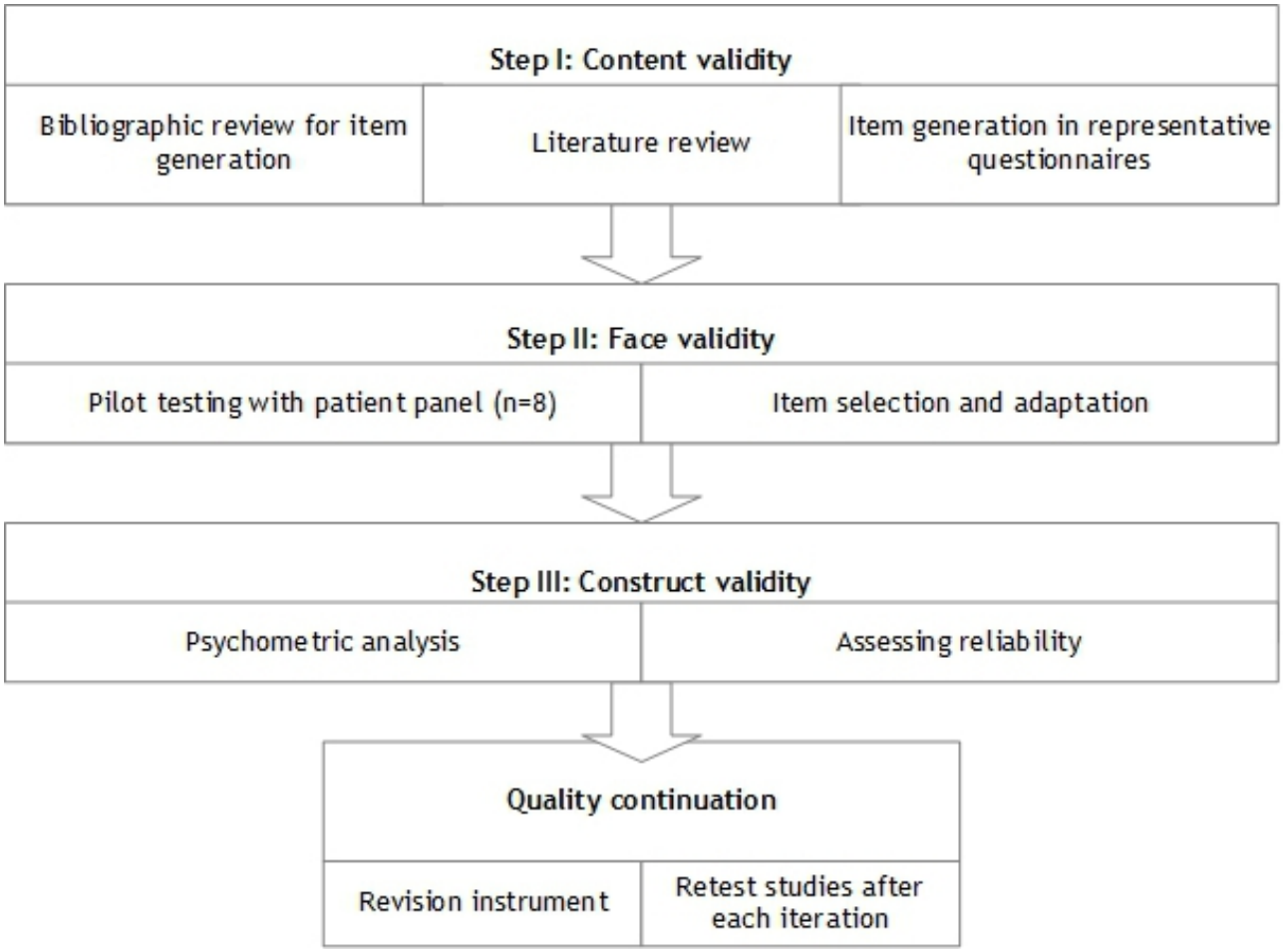
The Medical Ethical Committee of Amsterdam University Medical Center (Academic Medical Center) declared that this study was not subject to the Medical Research Involving Human Subject Act and that further approval was not required (W22 291 # 22.352).

GEMS Questionnaire Development

To develop and validate the questionnaire "Gebruiksvriendelijkheid en Ervaring met Monitoren in de ThuisSetting," translated as Experienced Usability and Satisfaction with self-monitoring in the Home Setting, we followed several steps, as depicted in Figure 1.

XSL•FO
RenderX

Figure 1. Flowchart of the development of experienced usability and satisfaction with digital health solutions in a home setting.



Step I: Content Validity - Collecting User Experience Statements

To design the GEMS questionnaire, we first searched for published literature on user experience questionnaires in the context of DHS in PubMed using the keywords “Digital Health Solutions,” “Digital Health Technologies,” “Self-Management tools,” “Digital health apps,” “mHealth apps,” AND (“Usability” OR “Satisfaction”) [24]. We searched for questionnaires that measured end-user experiences, and restricted our search to studies published in the last 5 years due to the rapidly evolving nature of the field.

After the literature review, an expert meeting was held, for which we invited several usability experts in the field. We went through the domains and statements from the validated questionnaires retrieved from the literature search. The outcome of this meeting was a list of requirements for domains with items that should be included in the GEMS questionnaire. This is in line with the 6 domains of usability, according to the general guidelines for usability assessment [12,25]: “Effectiveness,” “Efficiency,” “Satisfaction,” “Learnability,” “Perceived value,” and “Privacy and Security Issues.”

After the selection of the items during the expert meeting, we translated the items that were only available in English into Dutch. We applied a forward-backward translation (English to Dutch) procedure for each item. This procedure was executed by 2 people who were native proficiency speakers of both Dutch and English (DPN and Stephanie Medlock). A formal assessment of each item’s linguistic complexity using the Common European Framework of Reference for Language was conducted, including translating items as required to B1 level, by an expert that had experience in making patient instructions accessible (Marieke van Maanen) [26,27]. Items from 6 individual (validated) questionnaires were collected (Table S1 in Multimedia Appendix 1). In addition, insights from the article of the authors Berkman and Karahoca [28] were integrated into the process, as they describe that the change in sensitivity of a scale varies due to the responses, while in human-computer interaction, a scale is expected to be sensitive to the differences between systems instead of people. This insight enriched the questionnaire development with current research findings and best practices in usability metrics. We therefore maintained the item scores consistent with the current scoring methodology across responses. This has resulted in sufficient differentiation at the system level; however, further refinement is required to optimize the scoring of the GEMS.

Step II: Face Validity - Pilot Testing, Item Selection, and Adaptation

We recruited participants to take part in the evaluation of (1) the questionnaire itself, and (2) the evaluation of DHS using the draft GEMS instrument (Figure S1 in Multimedia Appendix 1). Round I consisted of an appreciative inquiry, to get feedback from stakeholders, to ensure that the instrument reflected their perspectives and values and that questions were understandable

XSL•FO
RenderX

[29]. We presented the questionnaire to the patient panel from the Amsterdam University Medical Center (n=8; Table S2 in Multimedia Appendix 1). After this round, an expert meeting including all authors (and Thomas Engelsma) was held to make adjustments to the language and wording of the questions.

Step III: Construct Validity - Psychometric Analysis

Round II consisted of the validation of the questionnaire by applying it with users of two self-management tools within the Amsterdam University Medical Center patient portal, which are available from the electronic health record for patients under the nephrology department: (1) entering home measurements of kidney transplant patients' vital statistics such as blood pressure, pulse, and temperature and (2) medication reminders. Patients were included when they participated in home measurements, or in the use of medication reminders, could read and understand the Dutch language, and downloaded the app from the patient portal in order to use one of these functionalities. Patients were invited to participate in this study by their HCP (physician or nurse practitioner). Informed consent of the participants was provided online (e-consent). Patients who agreed to participate were contacted by a researcher (SJO or a supportive researcher) to administer the GEMS questionnaire by email. Data were collected using Castor EDC [30]. Patients who did not return the questionnaire or did not fully complete the questionnaire received a reminder after 2 weeks, and, if necessary, a phone call after 4 weeks. After psychometric analysis, an expert meeting was held to discuss the findings, and if necessary, adjustments were made to the instrument.

Assessing Acceptability

The data from the questionnaire were analyzed using SPSS statistics (version 28.0.1.1, IBM) [31]. Respondents who missed more than one item of the GEMS were removed from the data set. Records missing other data, such as demographics, that were not part of the core of the GEMS questionnaire were not excluded. All items were recoded so that "1" was the most negative value on the Likert scale. In order to be able to perform factor analysis, the questions with scales ranging from "1-10" were recoded to "1 - 5" (1 and 2 were recoded to 1, 3 and 4 recoded to 2, and so on). The question with a Likert scale from "1-7" was recoded to "1 - 5," where the extremes are taken together (1 and 2 were recoded to 1; 6 and 7 were recoded to 5).

The Single Ease Questions (SEQ) is a single-item measure that assesses the complexity of a task for a user, such as entering home blood pressure measurements into the patient portal [32,33]. The SEQ aligns with the main features available in the system [33]. The different tasks that patients have to fulfil for the two separate DHS are difficult to compare, as logging into the system is the only task that is consistent across our analyses. Consequently, in psychometric evaluations, only the question regarding the ease or difficulty of "logging into the system" was included for both DHS assessments. For items where the nonresponse rate reached or exceeded 90%, it was inferred that patients chose not to answer the respective question. Consequently, the item in question was deemed unnecessary and was subsequently removed from the GEMS questionnaire [34]. With regard to the distribution of item scores, a skewness of 90% was considered to indicate redundancy for inclusion of the item in the GEMS questionnaire [34].

Assessing Construct Validity

An item correlation analysis was performed using the Spearman rank-order correlation coefficient. All items were compared with each other to find inter-item overlap, with a score of r_s>0.70 meaning that there could be singularity. Prior to performing a factor analysis, we tested whether the data set was suitable by assessing the Kaiser-Meyer-Olkin test of sampling adequacy (>0.60), and Bartlett test of sphericity (α<.05) [35,36]. A principal component analysis (PCA) with direct Oblimin rotation was used for factor analysis (FA). In addition, a scree plot was made of the PCA results. The number of values above the scree plateau were taken as the number of factors the items contributed to. In case of no clear scree plateau, a threshold of 1.0 was used.

Assessing Reliability and Internal Consistency

For all factors, extracted with PCA, the reliability and internal consistency were assessed by using the Cronbach α (>0.70) and item-total correlations (>0.40). Per factor, the items were dropped one by one to see whether items had to be removed to increase the Cronbach α to the threshold of 0.70. Finally, the items were scrutinised in an expert meeting (SJO, LWDP, DPN, SAN, HJM, and EMAS) using the results of the aforementioned analyses to determine which items were to be dropped and which should remain. In addition, we assigned labels to the constructs.

Results

Step I: Content Validity

In evaluations of DHS, researchers readily access numerous validated questionnaires from the literature, using them as tools for assessing usability and satisfaction in order to improve the product or system. Drawing from our literature review, the SUS is the most widely used usability evaluation instrument in the digital health industry [10,11]. For a long time, it has been a standard procedure to evaluate the usability of digital technology using general benchmarking tools, which has led to the adoption of generic tools like the SUS [11]. However, this questionnaire was developed in the early stages of the human-computer interaction field, at a time when digital health did not yet exist [16,37]. Newer questionnaires in the field such as the MAUQ and eHealth UsaBility Benchmarking Instrument try to be more specific within their domain; however, these questionnaires are still extensive, not easy to deploy, and using terminology derived from human-computer interaction [11,18]. In addition, as questionnaires such as SUS and Usability Metric for User Experience (UMUX) are primarily designed for software development, they use complex software-related terminology, such as functionalities of a system, that is often not understood by the general population [11].

We excluded statements regarding software interaction due to their complexity, which could potentially hinder understanding. We collected 14 unique statements from the identified questionnaires [12,25]. We chose to incorporate the 4-item UMUX (with Likert scale 1 - 5), along with SEQ (Likert scale 1 - 7). To include learnability, we added a question from the

XSL•FO
RenderX

SUS on whether patients had to learn a lot about the specific DHS before they could use it (Likert scale 1 - 5). Regarding perceived value, we added 2 questions from the MAUQ on whether the DHS contributed to the patient's health, and whether patients had the feeling that the DHS improved health care (both Likert scale 1 - 7). Finally, for perceived value, we added a question from Timmermans et al [38] on whether using the DHS reminded patients of being sick (Likert scale 1 - 5). To assess privacy and security, we added a question from Timmermans et al [38] (Likert scale 1 - 5). Regarding satisfaction, we opted to include the Net Promoter Score (NPS; Likert scale 1 - 10), the Customer Satisfaction Score (CSAT; Likert scale 1 - 5), and continued use, as we aimed to investigate whether satisfaction had an influence on continued use and vice versa (Likert scale 1 - 10). We added demographics such as gender, age, educational level, and health literacy [39,40]. At a later stage, we also added one question on digital literacy. The final GEMS questionnaire for validation consisted of 14 items (Table S4 in Multimedia Appendix 1).

Step II: Face Validity

In total, 92 patients participated in the validation: 65.2% (n=58) were male, 38% (n=35) were aged between 40 and 59 years, and 32.6% (n=30) had a higher professional education (Table S3 in Multimedia Appendix 1). A total of 92 patients were included for the psychometric analysis. All items presented to patients had a response rate of over 95%. For item skewness, no score was answered more than 90% for any of the answered questions. In the distribution of scores, we noticed that the highest value not applicable was entered with 10.9% on Q5 (question 5; "Q#" represents the questions involved in this study). The highest missing value with 17.4% was on Q13. No items of the GEMS were removed. Not all patients completed the question about digital literacy as this question was added to the demographics later (n=43). Patients' remarks and suggestions for improvement mainly focused on Q5, with some patients being unfamiliar with the nondigital method of filling in home measurements on paper. Therefore, some patients were unable to fill in this question. In addition, with Q8, patients indicated that the disease process is much more intense for some people than others, and that this question is difficult to answer in the home setting (Table 1).

XSL•FO
RenderX

Table . Description of each measurement instrument found in explorative literature search.

Measurement instrument	Abbreviation	Author	Items, n	Population validated	Scale	Reference where questionnaire has been used in health care context
Usability						
Questionnaire for User Interaction Satisfaction	QUIS	Chin et al [41]	27	150 users	1 - 9	[42,43]
System Usability Scale	SUS	Brooke [16]	10	184, aimed to include a diverse range of participants	1 - 5	[44-46]
mHealth App Usability Questionnaire	MAUQ	Zhou et al [18]	20	128, majority included were students with a bachelor's degree	1 - 7	[47,48]
The Usability Metric for User Experience	UMUX	Finstad [49]	4	255, not extensively described	1 - 7	[50]
Poststudy System Usability Questionnaire	PSSUQ	Lewis [37] Lewis [51]	16	48, and 210 in second validation study	1 - 7	[44,52]
Technology Acceptance Model questionnaire	TAM	Davis [53]	12	107 users	1 - 7	[54]
User version of the Mobile App Rating Scale	uMARS	Stoyanov et al [55]	20	164 young people	1 - 5	[56,57]
Mobile app rating scale	MARS	Terhorst et al [58]	23	1299 mobile health apps	1 - 5	[59]
eHealth Usability Benchmarking Instrument	HUBBI	Broekhuis et al [11]	18	148 persons	1 - 5	[60]
Satisfaction						
Net Promoter Score	NPS	Reichheld [61] Mekonnen [62]	1	Not described	1 - 10	[63,64]
Client Satisfaction Questionnaire	CSQ-8	Larsen et al [65]	8	Different populations, also in health care setting	1 - 4	[66]
Patient satisfaction questionnaire III	PSQ-III	Ware et al [67]	50	Various populations, in individuals with various medical conditions	1 - 5	[68]
Other						
Single Ease Questionnaire	SEQ	Nielsen and Molich [25]	1	Not described	1 - 7	[69]

Step III: Construct Validity

Spearman's rank correlation coefficient indicated Q8 as redundant as it showed a negative correlation on almost all items. The calculated UMUX score was also taken into consideration but did not show a significant correlation with items other than its own questions (Q1-Q4). None of the items was extremely skewed. Since none of the items were completed by less than 95% of the respondents, all items were included for psychometric analyses. The data set consisted of 14 items that were used for psychometric analysis (Table S4 in Multimedia Appendix 1 presents the Dutch original items). Kaiser-Meyer-Olkin was 0.72, and Bartlett Test of Sphericity was $P<.01$. PCA suggested a 5-factor solution. However, the fifth factor had an eigenvalue of 1.05, and we, therefore, decided to not include this factor. Q1 did not load to any factor. Common factor analysis using 4 factors with a factor loading threshold of 0.40 resulted in Q1 and Q5 not loading to any factors. Q7 cross loaded into factors 3 and 4. Q7 was dropped from factor 4 because this lowered the Cronbach α. Q8, Q10, and Q13 were

XSL•FO
RenderX

also dropped because these items lowered the Cronbach α for the respective factor. As shown in Table 2, item-total correlation was considered sufficient (>0.40) for all items. Factors 1 and 3 had the lowest Cronbach α (0.66 and 0.67, respectively) and factors 2 and 4 the highest (0.77 and 0.78, respectively).

XSL•FO
RenderX

Table . Results of the GEMS validation.

Item description	NA[a]≥25%	r_s[b]>0.70	CFA[c] loading	ITC[d]	Cronbach α[e]
Factor 1: Convenience of use (Cronbach α of scale=0.66; 95% CI[f] 0.49 - 0.78)					
Q2: "Using [this DHS][g]is a frustrating experience."[h]	—[i]	—	0.85	0.52	—
Het is vervelend om [digitale tool] te gebruiken.					
Q6: "I needed to learn a lot of things before I could get going with [this DHS]."[h]	—	—	0.85	0.52	—
Ik moest veel over [digitale tool] leren voordat ik het goed kon gebruiken.					
Factor 2: Satisfaction (Cronbach α of scale=0.77; 95% CI 0.67 - 0.84)					
Q11: "Overall, how satisfied were you with [DHS]?"[h]	—	—	−0.61	0.60	0.70
Hoe tevreden bent u over digitale tool?					
Q12: "How likely is it that you would recommend [DHS] to a friend or colleague?"[h]	—	—	−0.59	0.63	0.67
Hoe waarschijnlijk is het dat u [digitale tool] aan iemand anders die deze zorg nodig heeft aanraadt?					
Q14: "I would use [this DHS] again."[h]	—	—	−0.44	0.62	0.70
Hoe waarschijnlijk is het dat u de [digitale tool] blijft gebruiken?					
Factor 3: Perceived value (Cronbach α of scale=0.67; 95% CI 0.51 - 0.79)					
Q7: "The [DHS] would be useful for my health and well-being."[h]	—	—	0.50	0.53	—
Het gebruik van [digitale tool] draagt bij aan mijn gezondheid.					
Q9: "The [DHS] improved my access to health care services."	—	—	0.53	0.53	—
Ik denk dat [digitale tool] de zorg verbetert.					
Factor 4: Efficiency in use (Cronbach α of scale=0.78; 95% CI 0.67 - 0.86)					
Q3: "[This DHS] is easy to use."[h]	—	—	−0.62	0.65	—
[Digitale tool] is makkelijk te gebruiken.					
Q4: "I have to spend too much time correcting things with [this DHS]."[h]	—	—	−0.43	0.65	—
Ik ben te veel tijd kwijt aan het gebruik [van digitale tool].					

[a]NA: "I do not know or not applicable" responses ≥25%.

[b]r_s:Spearman rank correlation coefficient between items >0.70.

[c]CFA: confirmatory factor analysis

[d]ITC: item-total correlation.

[e]Cronbach α of scale if item is deleted.

[f]See Baumgartner and Chung [29].

XSL•FO
RenderX

[g]DHS: Digital Health Solution.

[h]Original English item from questionnaire.

[i]Not applicable.

After PCA, a collaborate expert meeting was held to determine the most appropriate labels for these factors based on existing usability terminology: convenience of use, perceived value, efficiency of use, and satisfaction. These constructs are known in the field of human-computer interaction. A more complete definition of the 4 factors applied to the home setting are shown in Textbox 1. The final constructs of the GEMS are outlined in Figure 2.

Textbox 1. Textbox 1. Description of the constructs of the GEMS questionnaire.

Constructs and their explanations

Convenience of use

This highlights the ease and comfort with which users can interact with the digital health solutions at home. Convenience of use is a component of usability, emphasizing aspects that contribute to making the user experience more convenient, pleasant, and smooth [70]. This means tailoring it to fit to patient preferences and expectations for self-management at home.

Perceived value

Perceived value refers to the extent to which a system or product fulfills users' needs and goals, addressing the pragmatic utility it offers to its intended users [70]. It encompasses the relevance and value of the digital health solutions features and functionalities in addressing user requirements in a home setting. In a health care setting, perceived value ultimately determines the practical utility and adoption of the digital health solutions by patients [71,72].

Efficiency of use

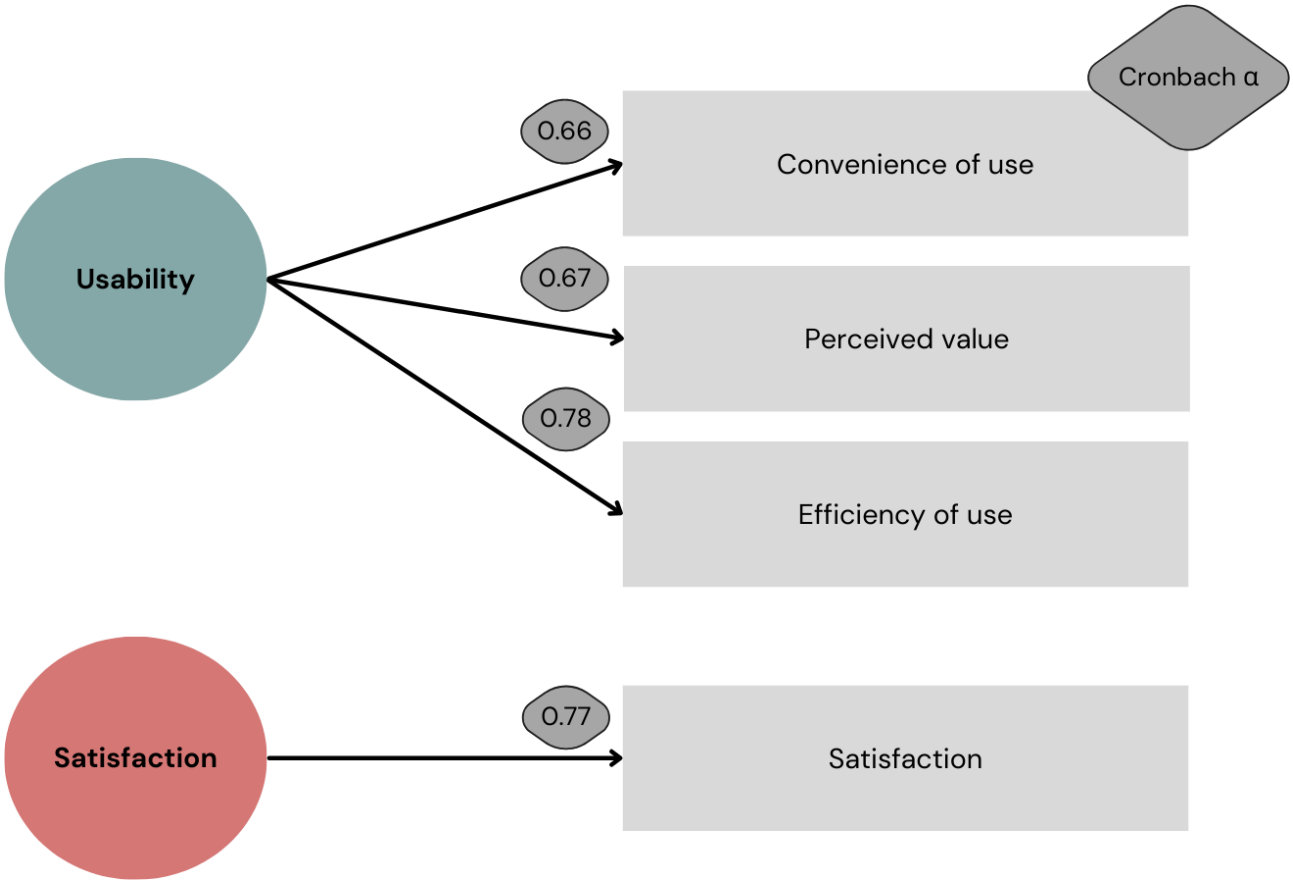
In a home setting, efficiency of use highlights how quickly users can perform tasks in a digital health solutions once they are familiar with it. Efficiency of use is influenced by factors such as learnability, memorability, and error prevention, as it pertains to how quickly and effortlessly users can achieve their goals when using a self-management tool in a home setting [12].

Satisfaction

According to International Organization for Standardization 9241, satisfaction is referred to as the degree to which users experience comfort and have positive attitudes toward using the product [12]. For self-management tools, satisfaction goes beyond mere functionality and usability, extending to factors such as efficacy, empowerment, and emotional well-being [73].

XSL•FO
RenderX

Figure 2. Visual abstract of final results and named constructs of Experienced Usability and Satisfaction With Self-Monitoring in the Home Setting Questionnaire.



Discussion

Principal Findings

Our aim, was to develop a steering instrument that enables the measurement of usability and satisfaction at various stages of adoption, with constructs that are relevant for a home setting, adapted to the language proficiency of the general population, and which might serve as a benchmarking instrument for usability and satisfaction with DHS. Following the initial translation phase of this study, it became evident that the items of the GEMS were easy to understand for patients. Although we designed the questionnaire for a broad population, our evaluation revealed that the majority of study participants had a higher level of education. In research, it is a known challenge to reach those with lower health and digital literacy levels for evaluation [74]. The applicability of the DHS varies depending on the specific needs and characteristics of different users. The GEMS questionnaire has been tailored to a B1 language proficiency level, which enhances its accessibility. However, there is a risk of obtaining biased outcomes of the GEMS depending on the demographic profile (eg, age, education, digital literacy, and health literacy) of the respondents. Therefore, collecting these demographic data are essential to understand if DHS users with different profiles assess the experienced usability and satisfaction differently. Gaining these insights may help in ensuring tailorization of the DHS to the user needs based on GEMS outcomes. This necessitates further refinement of the DHS to ensure its suitability across diverse populations.

Internal consistency of the GEMS was sufficient and factor analysis confirmed 4 factors, to which we have assigned the following labels: convenience of use, perceived value, efficiency of use, and satisfaction. Internal consistency of the GEMS, as measured with the Cronbach α, was slightly lower compared with the minimum value of 0.7 [75]. A possible explanation could lie, in our sample characteristics, as several participants also used similar applications, such as smartwatches that provided reminders. This dual usage could have influenced their responses, leading to expressed preferences or aversions towards the usage of medication reminders.

Given that the NPS was integrated into our satisfaction metric within the GEMS questionnaire, we opted to use the raw NPS as a component within our scoring scale. This approach involves incorporating the absolute values of promoters, passives, and detractors, rather than calculating the traditional NPS by subtracting the percentage of detractors from the percentage of promoters [76]. In a manner similar to the SUS questionnaire, we reversed the scales in our questionnaire to enhance reliability and validity. This approach serves several key purposes: (1) mitigating response bias, (2) maintaining participant attention and engagement, (3) ensuring balance and consistency within the questionnaire, and (4) detecting random responses on the questions by participants [16]. For the factors and questions derived from the factor analysis, we carefully examined whether reversed scaling was still present in the questionnaire. We concluded that reversed scaling was still present in 2 out of the 4 constructs.

XSL•FO
RenderX

For the statements in the GEMS questionnaire, we decided to adopt, translate, and adapt the statements from the UMUX and adjust them to using DHS in a home setting. However, in some cases, we have labeled the factors differently from those in the UMUX. Specifically, the statement "It is frustrating to use this digital tool" is classified under "Convenience of use" in the GEMS questionnaire, while it is categorized under "Satisfaction" in the UMUX. The interrelationship with the other questions in GEMS aligns more closely with the definition of convenience. We decided to address the experiences related to the context in which the DHS are used, specifically the deployment of DHS in a home setting. First, the difficulty in using the technology due to lack of digital literacy or misunderstanding of terminology. Second, ease of use, as the primary concern in a home setting is how conveniently the DHS can be integrated into daily routines. In addition, we translated and modified the UMUX question "I spend too much time correcting things with this system" to make it applicable at a higher conceptual level. The revised question no longer concerns the correction of things (errors), but instead evaluates whether the DHS is usable within its intended context [28].

Closing the feedback loop between patients and HCP through the utilization of DHS represents a pivotal strategy in enhancing health care delivery with DHS. By enabling self-management of patients through communication and data exchange, digital tools foster a collaborative environment where patients can actively participate in their care and providers can make informed decisions [77]. Incorporating the GEMS questionnaire as part of a comprehensive evaluation of DHS may enhance usability and satisfaction, contributing to adoption and the overall effectiveness of the DHS in improving health outcomes. The GEMS is therefore of relevance and value to HCPs, decision makers, health insurance companies, and public health institutions. The outcomes of the GEMS can assist these stakeholders to identify important issues as perceived by patients, and to develop strategies to address these issues and improve the quality of their DHS.

Strengths and Limitations

The strength of the GEMS questionnaire lies in the convergence of the four factors: convenience of use, perceived value, efficiency of use, and satisfaction, its concise questionnaire format, its adaptation to the language proficiency of the general population, and its utility as a steering tool as it can be used longitudinally in DHS implementation. The main strength of this study is that we applied a 4-step structured methodology to develop the GEMS questionnaire, consisting of both qualitative and quantitative evaluation phases. We also included 2 functionalities of our electronic health records in our evaluation in order to assure that the GEMS is applicable to a range of self-management tools. One of the limitations of this study is that a subset of patients may have been unable to participate in these (digital) evaluations due to requirements such as internet access, concentration, self-confidence, and proficient reading skills. We recognize that these evaluations cannot be used without considering potential issues of inequality [78]. According to the literature, this can be due to several reasons. First, the DHS may currently not be usable enough, for instance, by not involving the users during the design phase [79]. Second, health care professionals might be unfamiliar with the technology and not offering these tools to all patients [80]. Third, patients may feel having inadequate knowledge to use these tools [81], or have low (digital) literacy and therefore unable to use the tool [82]. Hence, we recommend further evaluating and refining the GEMS questionnaire in populations characterized by low (digital) literacy. Currently, we are conducting such a validation study within a demographic comprising individuals with low socioeconomic status and chronic obstructive pulmonary disease using a self-management tool. For these groups, we will conduct the evaluation on paper, using concept cards and translating the questions to graphics that visually support the questions [83]. By adopting this method, we aim to facilitate a comprehensive understanding of usability and satisfaction tailored to the needs and preferences of this specific population.

Because we used statements from various questionnaires, during the initial validation phase of the GEMS, some questions had different Likert scales. In order to ensure consistency in the analysis, the scales were converted. As a result, this might impact the interpretation of results, as the participants may interpret and respond to the items differently due to an expanded or contracted range of options [84,85]. Literature supports rescaling of 5- and 7-point scales for comparison, although it is noted that these scales may produce higher mean scores compared with a 10-point scale [84]. Finally, If the GEMS is used in another cultural setting, correct linguistic and cultural translation is needed to ensure content validity [86]. In order to facilitate this, an ongoing study is being conducted to assess a German translation of the GEMS questionnaire.

Conclusion

The GEMS questionnaire, comprising 9 items, has demonstrated its reliability and validity in assessing the usability and satisfaction of DHS within a home environment. It offers valuable insights into patient experiences with self-management tools, covering aspects of convenience of use, perceived value, efficiency of use and satisfaction. This development and validation study has been conducted with patient populations using medication reminders and home measurements. Further refinement is necessary in order to confirm the efficacy and applicability of the GEMS questionnaire in patient populations with low digital literacy. Using the GEMS questionnaire as a steering metric reflects a dedication to improving usability and satisfaction within DHS. In conclusion, the GEMS may promote development of a robust DHS , which enriches experienced usability and satisfaction and augments the efficacy of the DHS, thereby fostering positive health outcomes.

XSL•FO
RenderX

Acknowledgments

The authors would like to thank all experts who participated in the development rounds of the GEMS; Marieke van Maanen for her expertise on the adjustment of the items to the language proficiency of patients; Dr. Stephanie Medlock for contributing to the translation of the items; Hugo van Mens for his expertise on the Usability Metric for User Experience; Thomas Engelsma for the final expert meeting and questionnaire development process; and Ro Glasius for questionnaire support.

Conflicts of Interest

None declared.

Multimedia Appendix 1
Flowchart of the inclusion process, original English or Dutch items and final version of translated Dutch version of GEMS, original GEMS, and demographics of included sample for validation (n=92).
[PDF File, 221 KB - medinform_v13i1e63703_app1.pdf]

References

1. Marwaha JS, Landman AB, Brat GA, Dunn T, Gordon WJ. Deploying digital health tools within large, complex health systems: key considerations for adoption and implementation. NPJ Digit Med 2022 Jan 27;5(1):13. [doi: 10.1038/s41746-022-00557-1] [Medline: 35087160]
2. Li R, Liang N, Bu F, Hesketh T. The effectiveness of self-management of hypertension in adults using mobile health: systematic review and meta-analysis. JMIR Mhealth Uhealth 2020 Mar 27;8(3):e17776. [doi: 10.2196/17776] [Medline: 32217503]
3. van de Vijver S, Tensen P, Asiki G, et al. Digital health for all: how digital health could reduce inequality and increase universal health coverage. Digit Health 2023;9:20552076231185434. [doi: 10.1177/20552076231185434] [Medline: 37434727]
4. WHO guideline on self-care interventions for health and well-being, 2022 revision. World Health Organization. 2022. URL: https://www.who.int/publications/i/item/9789240052192 [accessed 2024-12-16]
5. Global strategy on digital health 2020-2025. : World Health Organization; 2021. URL: https://www.who.int/docs/default-source/documents/gs4dhdaa2a9f352b0445bafbc79ca799dce4d.pdf [accessed 2024-12-16]
6. Kraus S, Jones P, Kailer N, Weinmann A, Chaparro-Banegas N, Roig-Tierno N. Digital transformation: an overview of the current state of the art of research. Sage Open 2021 Jul;11(3):21582440211047576. [doi: 10.1177/21582440211047576]
7. Moqri M, Herzog C, Poganik JR, et al. Biomarkers of aging for the identification and evaluation of longevity interventions. Cell 2023 Aug;186(18):3758-3775. [doi: 10.1016/j.cell.2023.08.003]
8. Maqbool B, Herold S. Potential effectiveness and efficiency issues in usability evaluation within digital health: a systematic literature review. J Syst Softw 2024 Feb;208:111881. [doi: 10.1016/j.jss.2023.111881]
9. Jaspers MWM. A comparison of usability methods for testing interactive health technologies: methodological aspects and empirical evidence. Int J Med Inform 2009 May;78(5):340-353. [doi: 10.1016/j.ijmedinf.2008.10.002]
10. Maramba I, Chatterjee A, Newman C. Methods of usability testing in the development of eHealth applications: a scoping review. Int J Med Inform 2019 Jun;126:95-104. [doi: 10.1016/j.ijmedinf.2019.03.018] [Medline: 31029270]
11. Broekhuis M, van Velsen L, Hermens H. Assessing usability of eHealth technology: a comparison of usability benchmarking instruments. Int J Med Inform 2019 Aug;128:24-31. [doi: 10.1016/j.ijmedinf.2019.05.001] [Medline: 31160008]
12. ISO 9241-11:20:2018 ergonomics of human-system interaction - part 11: usability: definitions and concepts. International Organization for Standardization. 2018. URL: https://www.iso.org/standard/63500.html [accessed 2024-12-16]
13. Albert B, Tullis T. Measuring the User Experience: Collecting, Analyzing, and Presenting UX Metrics: Morgan Kaufmann; 2022.
14. Simola S, Hörhammer I, Xu Y, et al. Patients' experiences of a national patient portal and its usability: cross-sectional survey study. J Med Internet Res 2023 Jun 30;25:e45974. [doi: 10.2196/45974] [Medline: 37389909]
15. ISO/IEC 25002:2024: systems and software engineering — systems and software quality requirements and evaluation (square) — quality model overview and usage. International Organization for Standardization. 2024. URL: https://www.iso.org/standard/78175.html [accessed 2024-12-16]
16. Brooke J. SUS-a quick and dirty usability scale. In: Usability Evaluation In Industry: Taylor & Francis; 1996:189-194.
17. Soltanzadeh L, Babazadeh Sangar A, Majidzadeh K. The review of usability evaluation methods on tele health or telemedicine systems. Front Health Inform 2022;11(1):112. [doi: 10.30699/fhi.v11i1.357]
18. Zhou L, Bao J, Setiawan IMA, Saptono A, Parmanto B. The mHealth App Usability Questionnaire (MAUQ): development and validation study. JMIR Mhealth Uhealth 2019 Apr 11;7(4):e11500. [doi: 10.2196/11500] [Medline: 30973342]
19. Keogh A, Brennan C, Johnston W, et al. Six-month pilot testing of a digital health tool to support effective self-care in people with heart failure: mixed methods study. JMIR Form Res 2024 Mar 1;8:e52442. [doi: 10.2196/52442] [Medline: 38427410]

XSL•FO
RenderX

20. Smith B, Magnani JW. New technologies, new disparities: the intersection of electronic health and digital health literacy. Int J Cardiol 2019 Oct 1;292:280-282. [doi: 10.1016/j.ijcard.2019.05.066] [Medline: 31171391]
21. Albert NM, Dinesen B, Spindler H, et al. Factors associated with telemonitoring use among patients with chronic heart failure. J Telemed Telecare 2017 Feb;23(2):283-291. [doi: 10.1177/1357633X16630444] [Medline: 26869144]
22. Fitzpatrick PJ. Improving health literacy using the power of digital communications to achieve better health outcomes for patients and practitioners. Front Dig Health 2023;5:1264780. [doi: 10.3389/fdgth.2023.1264780] [Medline: 38046643]
23. Mathews SC, McShea MJ, Hanley CL, Ravitz A, Labrique AB, Cohen AB. Digital health: a path to validation. NPJ Digit Med 2019;2(1):38. [doi: 10.1038/s41746-019-0111-3] [Medline: 31304384]
24. White J. PubMed 2.0. Med Ref Serv Q 2020;39(4):382-387. [doi: 10.1080/02763869.2020.1826228] [Medline: 33085945]
25. Nielsen J, Molich R. Heuristic evaluation of user interfaces. Presented at: CHI '90: Proceedings of the SIGCHI Conference on Human Factors in Computing Systems; Apr 1-5, 1990; Seattle, WA. [doi: 10.1145/97243.97281]
26. Council of Europe. Common European Framework of Reference for Languages: Learning, Teaching, Assessment: Cambridge University Press; 2001.
27. Figueras N. The CEFR, a lever for the improvement of language professionals in Europe. The Mod Lang J 2007 Dec;91(4):673-675. [doi: 10.1111/j.1540-4781.2007.00627_8.x]
28. Berkman MI, Karahoca D. Re-assessing the Usability Metric for User Experience (UMUX) scale. J Usability Stud 2016;11(3) [FREE Full text]
29. Baumgartner TA, Chung H. Confidence Limits for Intraclass Reliability Coefficients. Meas Phys Educ Exerc Sci 2001 Sep;5(3):179-188. [doi: 10.1207/S15327841MPEE0503_4]
30. Castor electronic data capture. Castor EDC. 2019. URL: https://castoredc.com [accessed 2024-11-17]
31. SPSS Statistics 28.0.0 - IBM documentation. IBM. URL: https://www.ibm.com/docs/en/spss-statistics/28.0.0 [accessed 2024-12-16]
32. Sauro J, Dumas JS. Comparison of three one-question, post-task usability questionnaires. Presented at: CHI '09: Proceedings of the SIGCHI Conference on Human Factors in Computing Systems; Apr 4-9, 2009; Boston, MA. [doi: 10.1145/1518701.1518946]
33. Sauro J, Lewis JR. Quantifying the User Experience: Practical Statistics for User Research: Morgan Kaufmann; 2016. [doi: 10.1016/B978-0-12-802308-2.00002-3]
34. de Vet HCW, Terwee CB, Mokkink LB, Knol DL. Measurement in Medicine: A Practical Guide: Cambridge University Press; 2011.
35. Bartlett MS. Tests of significance in factor analysis. Br J Stat Psychol 1950 Jun;3(2):77-85. [doi: 10.1111/j.2044-8317.1950.tb00285.x]
36. Kaiser HF, Michael WB. Little Jiffy factor scores and domain validities. Educ Psychol Meas 1977 Jul;37(2):363-365. [doi: 10.1177/001316447703700210]
37. Lewis JR. Psychometric evaluation of the post-study system usability questionnaire: the PSSUQ. Proc Hum Factors Soc Annu Meet 1992 Oct;36(16):1259-1260. [doi: 10.1177/154193129203601617]
38. Timmermans I, Meine M, Szendey I, et al. Remote monitoring of implantable cardioverter defibrillators: patient experiences and preferences for follow-up. Pacing Clin Electrophysiol 2019 Feb;42(2):120-129. [doi: 10.1111/pace.13574] [Medline: 30536931]
39. Chew LD, Griffin JM, Partin MR, et al. Validation of screening questions for limited health literacy in a large VA outpatient population. J Gen Intern Med 2008 May;23(5):561-566. [doi: 10.1007/s11606-008-0520-5] [Medline: 18335281]
40. Fransen MP, Van Schaik TM, Twickler TB, Essink-Bot ML. Applicability of internationally available health literacy measures in the Netherlands. J Health Commun 2011;16 Suppl 3:134-149. [doi: 10.1080/10810730.2011.604383] [Medline: 21951248]
41. Chin JP, Diehl VA, Norman LK. Development of an instrument measuring user satisfaction of the human-computer interface. Presented at: CHI '88: Proceedings of the SIGCHI Conference on Human Factors in Computing Systems; May 15-19, 1988; Washington, DC. [doi: 10.1145/57167.57203]
42. Salmani H, Nahvijou A, Sheikhtaheri A. Smartphone-based application for self-management of patients with colorectal cancer: development and usability evaluation. Support Care Cancer 2022 Apr;30(4):3249-3258. [doi: 10.1007/s00520-021-06754-0] [Medline: 34984548]
43. Dinari F, Bahaadinbeigy K, Moulaei K, Nemati A, Ershad Sarabi R. Designing and evaluating a mobile-based self-care application for patients with gastrointestinal cancer to manage chemotherapy side effects. Med J Islam Repub Iran 2022;36:14. [doi: 10.47176/mjiri.36.14] [Medline: 35991156]
44. Bhanvadia SB, Brar MS, Delavar A, et al. Assessing usability of smartwatch digital health devices for home blood pressure monitoring among glaucoma patients. Informatics (MDPI) 2022 Dec;9(4):79. [doi: 10.3390/informatics9040079] [Medline: 36873830]
45. Stamm-Balderjahn S, Bernert S, Rossek S. Promoting patient self-management following cardiac rehabilitation using a web-based application: a pilot study. D Health 2023;9:20552076231211546. [doi: 10.1177/20552076231211546] [Medline: 37954686]

XSL•FO
RenderX

46. Bostrøm K, Børøsund E, Varsi C, et al. Digital self-management in support of patients living with chronic pain: feasibility pilot study. JMIR Form Res 2020 Oct 23;4(10):e23893. [doi: 10.2196/23893] [Medline: 33094734]
47. Moorthy P, Weinert L, Harms BC, Anders C, Siegel F. German version of the mHealth app usability questionnaire in a cohort of patients with cancer: translation and validation study. JMIR Hum Factors 2023 Nov 1;10:e51090. [doi: 10.2196/51090] [Medline: 37910144]
48. Fedkov D, Berghofen A, Weiss C, et al. Efficacy and safety of a mobile app intervention in patients with inflammatory arthritis: a prospective pilot study. Rheumatol Int 2022 Dec;42(12):2177-2190. [doi: 10.1007/s00296-022-05175-4] [Medline: 36112186]
49. Finstad K. The usability metric for user experience. Interact Comput 2010 Sep;22(5):323-327. [doi: 10.1016/j.intcom.2010.04.004]
50. Sobnath D, Philip N, Kayyali R, Nabhani-Gebara S, Pierscionek B, Raptopoulos A. Mobile self-management application for COPD patients with comorbidities: ausability study. Presented at: 2016 IEEE 18th International Conference on e-Health Networking, Applications and Services (Healthcom); Sep 14-16, 2016; Munich, Germany. [doi: 10.1109/HealthCom.2016.7749502]
51. Lewis JR. Psychometric evaluation of the PSSUQ using data from five years of usability studies. Int J Hum Comput Interact 2002 Sep;14(3-4):463-488. [doi: 10.1080/10447318.2002.9669130]
52. Bakogiannis C, Tsarouchas A, Mouselimis D, et al. A patient-oriented app (ThessHF) to improve self-care quality in heart failure: from evidence-based design to pilot study. JMIR Mhealth Uhealth 2021 Apr 13;9(4):e24271. [doi: 10.2196/24271] [Medline: 33847599]
53. Davis FD. Perceived usefulness, perceived ease of use, and user acceptance of information technology. MIS Q 1989 Sep;13(3):319. [doi: 10.2307/249008]
54. Greer DB, Abel WM. Exploring feasibility of mHealth to manage hypertension in rural black older adults: a convergent parallel mixed method study. Pat Prefer Adherence 2022;16:2135-2148. [doi: 10.2147/PPA.S361032] [Medline: 35999840]
55. Stoyanov SR, Hides L, Kavanagh DJ, Wilson H. Development and validation of the user version of the Mobile Application Rating Scale (uMARS). JMIR Mhealth Uhealth 2016 Jun 10;4(2):e72. [doi: 10.2196/mhealth.5849] [Medline: 27287964]
56. Agher D, Sedki K, Despres S, Albinet JP, Jaulent MC, Tsopra R. Encouraging behavior changes and preventing cardiovascular diseases using the prevent connect mobile health app: conception and evaluation of app quality. J Med Internet Res 2022 Jan 20;24(1):e25384. [doi: 10.2196/25384] [Medline: 35049508]
57. Wong W, Ming D, Pateras S, et al. Outcomes of end-user testing of a care coordination mobile app with families of children with special health care needs: simulation study. JMIR Form Res 2023 Aug 28;7:e43993. [doi: 10.2196/43993] [Medline: 37639303]
58. Terhorst Y, Philippi P, Sander LB, et al. Validation of the Mobile Application Rating Scale (MARS). PLoS ONE 2020;15(11):e0241480. [doi: 10.1371/journal.pone.0241480]
59. Oakley-Girvan I, Yunis R, Fonda SJ, et al. Usability evaluation of mobile phone technologies for capturing cancer patient-reported outcomes and physical functions. Dig Health 2023;9:20552076231186515. [doi: 10.1177/20552076231186515] [Medline: 37456127]
60. Barbarossa F, Amabili G, Margaritini A, et al. Design, development, and usability evaluation of a dashboard for supporting formal caregivers in managing people with dementia. Presented at: PETRA '23: Proceedings of the 16th International Conference on PErvasive Technologies Related to Assistive Environments; Jul 5-7, 2023; Corfu, Greece. [doi: 10.1145/3594806.3594820]
61. Reichheld FF. The one number you need to grow. Harv Bus Rev 2003 Dec;81(12):46-54. [Medline: 14712543]
62. Mekonnen A. The ultimate question: driving good profits and true growth. J Target Meas Anal Mark 2006 Jul;14(4):369-370. [doi: 10.1057/palgrave.jt.5740195]
63. Jonker LT, Plas M, de Bock GH, Buskens E, van Leeuwen BL, Lahr MMH. Remote home monitoring of older surgical cancer patients: perspective on study implementation and feasibility. Ann Surg Oncol 2021 Jan;28(1):67-78. [doi: 10.1245/s10434-020-08705-1] [Medline: 32602060]
64. Gelbman BD, Reed CR. An integrated, multimodal, digital health solution for chronic obstructive pulmonary disease: prospective observational pilot study. JMIR Form Res 2022 Mar 17;6(3):e34758. [doi: 10.2196/34758] [Medline: 35142291]
65. Larsen DL, Attkisson CC, Hargreaves WA, Nguyen TD. Assessment of client/patient satisfaction: development of a general scale. Eval Program Plann 1979;2(3). [doi: 10.1016/0149-7189(79)90094-6]
66. Shiraishi M, Kamo T, Kumazawa R, et al. A multicenter, prospective, observational study to assess the satisfaction of an integrated digital platform of online medical care and remote patient monitoring in Parkinson's disease. Neurology & Clinical Neurosc 2023 May;11(3):152-163. [doi: 10.1111/ncn3.12709]
67. Ware JE, Snyder MK, Wright WR, Davies AR. Defining and measuring patient satisfaction with medical care. Eval Program Plann 1983;6(3-4):247-263. [doi: 10.1016/0149-7189(83)90005-8] [Medline: 10267253]
68. Temple-Oberle C, Yakaback S, Webb C, Assadzadeh GE, Nelson G. Effect of smartphone app postoperative home monitoring after oncologic surgery on quality of recovery: a randomized clinical trial. JAMA Surg 2023 Jul 1;158(7):693-699. [doi: 10.1001/jamasurg.2023.0616] [Medline: 37043216]

XSL•FO
RenderX

69. Nautiyal S, Shrivastava A. Designing a WhatsApp inspired healthcare application for older adults: a focus on ease of use. Comp Hum Interact Res Appl 2023. [doi: 10.1007/978-3-031-49368-3_9]
70. Shaw N, Sergueeva K. Convenient or useful? consumer adoption of smartphones for mobile commerce. 2016 Presented at: DIGIT 2016 Proceedings; Dec 11, 2016; Dublin, Ireland.
71. Jo HS, Jung SM. Factors influencing use of smartphone applications for healthcare self-management: an extended technology acceptance model. Korean J Health Educ Promot 2014 Oct 1;31(4):25-36. [doi: 10.14367/kjhep.2014.31.4.25]
72. Cho H, Porras T, Flynn G, Schnall R. Usability of a consumer health informatics tool following completion of a clinical trial: focus group study. J Med Internet Res 2020 Jun 15;22(6):e17708. [doi: 10.2196/17708] [Medline: 32538796]
73. Peters D, Calvo RA, Ryan RM. Designing for motivation, engagement and wellbeing in digital experience. Front Psychol 2018;9:797. [doi: 10.3389/fpsyg.2018.00797] [Medline: 29892246]
74. Arias López MDP, Ong BA, Borrat Frigola X, et al. Digital literacy as a new determinant of health: a scoping review. PLOS Dig Health 2023 Oct;2(10):e0000279. [doi: 10.1371/journal.pdig.0000279] [Medline: 37824584]
75. Gliem JA, Gliem RR. Calculating, interpreting, and reporting cronbach's alpha reliability coefficient for likert-type scales. Presented at: Midwest Research-to-Practice Conference in Adult, Continuing, and Community Education; Mar 27-29, 2003; Columbus, OH URL: https://scholarworks.indianapolis.iu.edu/items/63734e75-1604-45b6-aed8-40dddd7036ee [accessed 2024-12-16]
76. Adams C, Walpola R, Schembri AM, Harrison R. The ultimate question? Evaluating the use of Net Promoter Score in healthcare: a systematic review. Health Expect 2022 Oct;25(5):2328-2339. [doi: 10.1111/hex.13577] [Medline: 35985676]
77. Weinhold I, Gastaldi L. From shared decision making to patient engagement in health care processes: the role of digital technologies. In: Challenges and Opportunities in Health Care Management: Springer; 2014:185-196. [doi: 10.1007/978-3-319-12178-9_15]
78. Goedhart NS, Verdonk P, Dedding C. "Never good enough." A situated understanding of the impact of digitalization on citizens living in a low socioeconomic position. Pol & Int 2022 Dec;14(4):824-844. [doi: 10.1002/poi3.315]
79. Reynoldson C, Stones C, Allsop M, et al. Assessing the quality and usability of smartphone apps for pain self-management. Pain Med 2014 Jun;15(6):898-909. [doi: 10.1111/pme.12327] [Medline: 24422990]
80. Cher BP, Kembhavi G, Toh KY, et al. Understanding the attitudes of clinicians and patients toward a self-management eHealth tool for atrial fibrillation: qualitative study. JMIR Hum Factors 2020 Sep 17;7(3):e15492. [doi: 10.2196/15492] [Medline: 32940611]
81. Halim NAA, Sopri NHA, Wong YY, Mustafa QM, Lean QY. Patients' perception towards chronic disease self-management and its program: a cross-sectional survey. Chron Illn 2023 Jul 4:17423953231185385. [doi: 10.1177/17423953231185385] [Medline: 37403449]
82. Marklund S, Tistad M, Lundell S, et al. Experiences and factors affecting usage of an ehealth tool for self-management among people with chronic obstructive pulmonary disease: qualitative study. J Med Internet Res 2021 Apr 30;23(4):e25672. [doi: 10.2196/25672] [Medline: 33929327]
83. Agúndez Del Castillo R, Ferro L, Silva E. The use of digital technologies in the co-creation process of photo elicitation. QRJ 2024. [doi: 10.1108/QRJ-06-2023-0101]
84. Dawes J. Do data characteristics change according to the number of scale points used? An experiment using 5-point, 7-point and 10-point scales. Int J Market Res 2008 Jan;50(1):61-104. [doi: 10.1177/147078530805000106]
85. Oylum K, Arslan F. Impact of the number of scale points on data characteristics and respondents' evaluations: an experimental design approach using 5-point'and 7-point Likert type scales. J Fac Pol Sci 2016;55:1-20. [doi: 10.2196/17708]
86. Beaton DE, Bombardier C, Guillemin F, Ferraz MB. Guidelines for the process of cross-cultural adaptation of self-report measures. Spine (Phila Pa 1976) 2000 Dec 15;25(24):3186-3191. [doi: 10.1097/00007632-200012150-00014] [Medline: 11124735]

Abbreviations

DHS: digital health solutions
HCP: health care professional
MAUQ: mHealth App Usability Questionnaire
PCA: principal component analysis
SEQ: Single Ease Questions
SUS: System Usability Scale
UMUX: Usability Metric for User Experience

XSL•FO
RenderX

Edited by J Hefner; submitted 27.06.24; peer-reviewed by G Parmar, M Wright; revised version received 04.10.24; accepted 06.10.24; published 08.01.25.

Please cite as:
Oudbier SJ, Smets EMA, Nieuwkerk PT, Neal DP, Nurmohamed SA, Meij HJ, Dusseljee-Peute LW
Patients' Experienced Usability and Satisfaction With Digital Health Solutions in a Home Setting: Instrument Validation Study
JMIR Med Inform 2025;13:e63703
URL: https://medinform.jmir.org/2025/1/e63703
doi:10.2196/63703

© Susan J Oudbier, Ellen M A Smets, Pythia T Nieuwkerk, David P Neal, S Azam Nurmohamed, Hans J Meij, Linda W Dusseljee-Peute. Originally published in JMIR Medical Informatics (https://medinform.jmir.org), 8.1.2025. This is an open-access article distributed under the terms of the Creative Commons Attribution License (https://creativecommons.org/licenses/by/4.0/), which permits unrestricted use, distribution, and reproduction in any medium, provided the original work, first published in JMIR Medical Informatics, is properly cited. The complete bibliographic information, a link to the original publication on https://medinform.jmir.org/, as well as this copyright and license information must be included.

XSL•FO
RenderX

Imputation and Missing Indicators for Handling Missing Longitudinal Data: Data Simulation Analysis Based on Electronic Health Record Data

Molly Ehrig, MS; Garrett S Bullock, PhD, DPT; Xiaoyan Iris Leng, MD, PhD; Nicholas M Pajewski, PhD; Jaime Lynn Speiser, MS, PhD

Department of Biostatistics and Data Science, Wake Forest University School of Medicine, Medical Center Blvd, Winston Salem, NC, United States

Corresponding Author:
Jaime Lynn Speiser, MS, PhD
Department of Biostatistics and Data Science, Wake Forest University School of Medicine, Medical Center Blvd, Winston Salem, NC, United States

Abstract

Background: Missing data in electronic health records are highly prevalent and result in analytical concerns such as heterogeneous sources of bias and loss of statistical power. One simple analytic method for addressing missing or unknown covariate values is to treat missingness for a particular variable as a category onto itself, which we refer to as the missing indicator method. For cross-sectional analyses, recent work suggested that there was minimal benefit to the missing indicator method; however, it is unclear how this approach performs in the setting of longitudinal data, in which correlation among clustered repeated measures may be leveraged for potentially improved model performance.

Objectives: This study aims to conduct a simulation study to evaluate whether the missing indicator method improved model performance and imputation accuracy for longitudinal data mimicking an application of developing a clinical prediction model for falls in older adults based on electronic health record data.

Methods: We simulated a longitudinal binary outcome using mixed effects logistic regression that emulated a falls assessment at annual follow-up visits. Using multivariate imputation by chained equations, we simulated time-invariant predictors such as sex and medical history, as well as dynamic predictors such as physical function, BMI, and medication use. We induced missing data in predictors under scenarios that had both random (missing at random) and dependent missingness (missing not at random). We evaluated aggregate performance using the area under the receiver operating characteristic curve (AUROC) for models with and with no missing indicators as predictors, as well as complete case analysis, across simulation replicates. We evaluated imputation quality using normalized root-mean-square error for continuous variables and percent falsely classified for categorical variables.

Results: Independent of the mechanism used to simulate missing data (missing at random or missing not at random), overall model performance via AUROC was similar regardless of whether missing indicators were included in the model. The root-mean-square error and percent falsely classified measures were similar for models including missing indicators versus those with no missing indicators. Model performance and imputation quality were similar regardless of whether the outcome was related to missingness. Imputation with or with no missing indicators had similar mean values of AUROC compared with complete case analysis, although complete case analysis had the largest range of values.

Conclusions: The results of this study suggest that the inclusion of missing indicators in longitudinal data modeling neither improves nor worsens overall performance or imputation accuracy. Future research is needed to address whether the inclusion of missing indicators is useful in prediction modeling with longitudinal data in different settings, such as high dimensional data analysis.

(JMIR Med Inform 2025;13:e64354) doi:10.2196/64354

KEYWORDS

missing indicator method; missing data; imputation; longitudinal data; electronic health record data; electronic health records; EHR; simulation study; clinical prediction model; prediction model; older adults; falls; logistic regression; prediction modeling

Introduction

Electronic health record (EHR) data have many analytic uses, including patient monitoring, clinical decision support, quality improvement projects, and research initiatives [1]. However, missing data are pervasive in EHRs because these systems were largely designed for the purposes of billing and because of the fragmented nature of health care in the United States where

XSL•FO
RenderX

patients often use multiple health systems with disparate EHR systems. The incomplete nature of the EHR creates significant potential for bias for research studies leveraging real-world data [2]. Statistically, missing data may be considered ignorable when they are missing completely at random (MCAR) or missing at random (MAR). A recent study illustrated that more than 1 missing mechanism may be present for EHR data, and the assumption that all missing data are MAR is generally not plausible [3]. Recent work by Hu et al [4] indicated that clinical EHR data were consistent with a mixture of random and nonrandom mechanisms. For example, a white blood cell count test was less likely to be ordered for patients who were clinically doing well (eg, lack of collection).

Current approaches to handle missing data include complete case analysis, imputation, and nonimputation approaches such as the use of missing indicators. These approaches vary in terms of their appropriateness depending on untestable assumptions about the mechanisms generating missing values. A detailed discussion of statistical approaches to handling missing data can be found in the TRIPOD (Transparent Reporting of a Multivariable Prediction Model for Individual Prognosis or Diagnosis) checklist [5,6]. Complete case analysis is a common method in which observations with missing values in any of the analysis variables are listwise deleted. If data are MCAR, complete case analysis may be appropriate, but if data are MAR or missing not at random (MNAR), complete case analysis can result in biased estimates. Independent of the missingness mechanism, complete case analysis results in a loss of statistical power by reducing the number of available observations [7,8].

Imputation is another commonly used method for handling missing data and involves using observed data to estimate and fill in values that are missing, typically through regression approaches that model the variable with missingness as the outcome with the other variables in the dataset as predictors. While this method retains all observations in the dataset and reduces bias when data are MAR, regression imputation underestimates the SE of the model parameters and therefore overestimates precision [8,9]. Multiple imputation overcomes the limitations of regression imputation by generating multiple imputed values for each missing value. By separately analyzing each dataset and combining the outputs to obtain an overall point estimate and corresponding SE, variability estimates are more accurate and the analysis accounts for the uncertainty caused by missingness [9,10]. However, the appropriate imputation strategy may depend on both the type of missingness and the objective of the analysis. One recent study has shown that regression imputation performs as well as multiple imputation when the ultimate goal is prediction rather than statistical inference or model interpretation [11]. Another study found that for logistic regression, regression imputation was comparable with multiple imputation in terms of model performance with a low percentage of missingness [12]. However, none of the imputation methods are unbiased or recommended for nonignorable missing data.

A third approach is the missing indicator method, which adds a binary predictor to the model that takes the value of 1 if the value of a certain variable is missing and zero if the value is not missing, therefore, taking advantage of the information contained in missingness itself [13]. The use of missing indicators has been introduced as a method when missingness in informative, or when the presence or absence of missingness adds prognostic information to a model. Although this is a simple method for potentially leveraging information about missingness, it increases the number of predictor variables to be included, which may not be ideal for high-dimensional datasets, datasets with many predictors, or situations where significant model flexibility is desired (ie, semiparametric models that use basis functions or splines to flexibly model continuous predictors such as vital signs or laboratory values).

There is still a lack of consensus on the appropriateness of the missing indicator method for handling missing data for clinical prediction modeling [14]. One concern is the creation of a negative feedback loop between the model and the providers using the model for decision support. When an individual knows that taking or not taking a certain measurement is informative, their decision to take the measurement could hypothetically be impacted [13,15], or the model may simply reiterate a clinical suspicion or decision that has already occurred, such as a recent prediction model for the early detection of sepsis [16]. An example for this is the decision to order certain specialized laboratory tests. In addition, prediction models that use the missing indicator method must be consistently monitored and revised due to how quickly patient medical data and factors that affect physician decision-making change [15]. However, other work has found that the missing indicator method could improve predictive performance [14,17]. One study found that the addition of missing indicators, which signaled the presence or absence of a laboratory test result, to observed measurements improved area under the receiver operating characteristic curve (AUROC) when predicting clinical outcomes [17]. Missing indicators have been shown to increase predictive performance when missingness is informative, with the effectiveness of the method increasing as the informativeness of missingness increased [14]. The same study found that the missing indicator method did not harm predictive performance when missingness was uninformative. This is an important distinction, as it is not possible to empirically test whether missingness is informative [18].

There is currently a gap in knowledge regarding the effectiveness of including missing indicators in longitudinal data modeling, specifically whether missing indicators improve model performance and the quality of model-based imputations. The setting of longitudinal repeated measures and clustered data is an important context for the missing indicator method because the correlation within clusters may be leveraged to increase the imputation accuracy and model performance, particularly in the case of data that are MNAR. However, we are not aware of work that has investigated the missing indicator method in this setting.

We aimed to assess the missing indicator method for longitudinal, repeated-measures data using a simulation study mimicking real-world EHR data. In section 2, we detail the methods we used to generate the synthetic longitudinal data, including fixed and repeated measures of predictors for MAR and MNAR missing data patterns, and we define outcome metrics used to assess performance and imputation quality. In

XSL•FO
RenderX

section 3, we present results aggregated across the simulation runs for models with and with no missing indicator variables. In section 4, we discuss the results and implications of the study, compare our study with prior studies, and consider the strengths and limitations of this work.

Methods

Study Design

This study is a simulation study in which missing indicator variables in imputation and modeling were evaluated under different missing data mechanisms (MAR and MNAR). We follow the simulation study guidelines suggested by Morris and colleagues [19]. Analyses were performed with R (version 4.2.1; The R Project for Statistical Computing). All code is available on our GitHub repository [20]. We use the following R packages in our analysis: *bindata* [21], *MASS* [22], *tidyverse* [23], *lme4* [24], *lmerTest* [25], *naniar* [26], *mice* [27], *broom.mixed* [28], *pROC* [29], *DescTools* [30], *missForest* [31], *table1* [32], *flextable* [32], *skimr* [32], *sjPlot* [33], *gridExtra* [34], *grid* [35], and *car* [36].

Data-Generating Mechanisms

This study focuses on a mixed effects logistic regression model that uses a binary outcome simulated to represent whether or not patients experienced a fall since their last visit. A total of 250 patients were simulated, each with 5 visits. Medical history variables, demographic variables, fall-specific variables, and variables intended to add noise to the model were simulated. We simulated the data to represent EHR data that may be used to develop models for falls in older adults. Predictors of falls were simulated based on previous research [37] and represent a combination of fixed, patient-level variables and visit-level variables that are collected repeatedly. The fixed variables included sex and comorbidities (diabetes, dementia, hypertension, and urinary incontinence), all of which may be related to falls in older adults. The visit-level variables included BMI, gait speed, single-leg balance, and use of medications (pain or depression), again representing variables that could be associated will falls in older adults. Table 1 lists all variables in the dataset and describes how they were simulated. We include summaries of the variables for one of the simulated datasets in Multimedia Appendix 1. For more details, including parameter values, see the code on GitHub.

XSL•FO
RenderX

Table . Variable list and description.

Variables	Data generation and description
Patient-level variables	
Birth sex, diabetes, dementia, hypertension, and urinary incontinence	Binary random variables simulated with the bindata R package
Age	Continuous with mean dependent on number of chronic conditions (ie, number of the following conditions: diabetes, dementia, hypertension, and urinary incontinence)
Visit-level variables	
Visit	Discrete, 5 visits for each patient.
BMI	Continuous, simulated with a linear mixed effects model with age, diabetes, hypertension, and birth sex as predictors. Random intercept for patient ID and random error included.
Gait speed	Continuous, simulated with a linear mixed effects model with age, BMI, diabetes, and birth sex as predictors. Random intercept for patient ID and random error included.
Single-leg balance	Continuous, simulated with a linear mixed effects model with age, BMI, diabetes, dementia, and birth sex as predictors. Random intercept for patient ID and random error included.
Pain medication	Binary, probability simulated with expit function with age, sex, and diabetes as predictors in the model. A random intercept for patient was included in the model. The probability was then used to simulate a Bernoulli random variable where: 0=did not take pain medication since last visit 1=took pain medication since last visit
Depression medication	Binary, probability simulated with expit function with age, sex, and dementia as predictors in the model. A random intercept for patient ID was included in the model. The probability was then used to simulate a Bernoulli random variable where: 0 = did not take depression medication since last visit 1 = took depression medication since last visit
Junk 1 - 5	Continuous random variables with means and SDs chosen at random.
Y	Binary outcome variable, probability simulated with expit function with all variables except the junk variables and visit as predictors. A random intercept for patient ID was also included in the model. The probability was simulated with and with no missing indicators included in the model. The probability was then used to simulate a Bernoulli random variable where: 0 = did not fall since last visit 1 = fall since last visit

The probability of the binary outcome was simulated in 2 different ways using the expit function. For both versions, the model included a random intercept for patient, and all variables except the junk variables, patient ID, and visit were included as predictors. The first version included missing indicator variables as predictors in the model, while the second did not. The outcome was a random Bernoulli variable with the probability of being one equal to the calculated probability for each visit. A total of 250 iterations were run, so 250 different datasets were created.

Missingness was induced for the visit-level continuous variables gait speed and single-leg balance, and for the binary variables pain medication and depression medication. Overall missing data percentages of 20% and 50% were simulated. Under the assumption of MAR, the probability that gait speed, single-leg balance, pain medication, and depression medication were missing for a specific visit was dependent on age, BMI, diabetes, and urinary incontinence. Specifically, the probability each variable was missing was simulated with the expit function where age, BMI, diabetes, and urinary incontinence were included as predictors. The intercept was changed to achieve different percentages of missing data. The probability was higher for older patients, patients with a larger BMI, and patients with diabetes or urinary incontinence. Missing indicators were created by defining Bernoulli random variables with the probability of being one equal to the probability of being missing, and indicator variables were created for each of the 4 variables. If the missing indicator was 1, the value of the corresponding variable was set to missing. Therefore, although all 4 variables had the same probability of being missing for each visit, different combinations of variables could be missing at each visit.

XSL•FO
RenderX

Under the MNAR missingness mechanism, the probability that gait speed, single-leg balance, pain medication, and depression medication were missing for a specific visit was dependent on the value of the variable itself. For gait speed and single-leg balance, if the value of the variable at a visit was less than the 25th percentile, the probability of the value being set to missing was .7 to target an overall missing percentage of 50% and .3 to target an overall missing percentage of 20%. Otherwise, the probability was zero. For pain medication and depression medication, if the value of the variable was 1 at a visit (indicating that the patient was taking the medication), the probability the value was set to missing was .4 to target an overall missing percentage of 50% and .1 to target an overall missing percentage of 20%. Otherwise, the probability was zero. Therefore, lower values of gait speed and single-leg balance were more likely to be missing. Similarly, if patients were taking pain medication or depression medication, these values were more likely to be missing. For all of the simulated scenarios, the outcome, all patient-level variables, and the remaining visit-level variable (BMI) were fully observed.

Missing Data-Handling Strategies

Multivariate imputation via chained equations was performed using the *mice* package in R [27]. Regression imputation was performed using single imputation (ie, multiple imputation was not used because the purpose of the model is prediction). All variables in the dataset were included in the imputation model, including the outcome variable. The 2-level structure of the dataset was specified in the imputation model by denoting patient as the clustering variable. To impute gait speed and single-leg balance, a 2-level normal model was used. Values below zero were capped at zero. To impute pain and depression medication, a 2-level logistic model was used. When imputing a variable, the indicator for that variable was not included in the imputation model because in imputation only present data are used and the value of the indicator is 1 for all present data. The indicators for the other variables were included in the imputation model.

The outcome was calculated with a mixed effects logistic regression for both analyses that included and did not include missing indicator variables. All variables except visit were included in the model as predictors, and a random intercept for patient was also included in the model. Missing indicators were included in the model when they had also been included in the imputation model. The junk variables were included with the expectation that they would not be significant in the model. Complete case analysis was performed by deleting all observations with missing values prior to running the model. A summary of the different scenarios and models run is shown in Table 2.

XSL•FO
RenderX

Table . Summary of Modeling.

Outcome simulation and missing data mechanism	Target missing percentage	Imputation and modeling strategy
Missing indicators included in model for outcome simulation		
MAR[a]	20	• Missing indicators included in imputation and modeling • No missing indicators included in imputation and modeling • Complete case analysis
MAR	50	• Missing indicators included in imputation and modeling • No missing indicators included in imputation and modeling • Complete case analysis
MNAR[b]	20	• Missing indicators included in imputation and modeling • No missing indicators included in imputation and modeling • Complete case analysis
MNAR	50	• Missing indicators included in imputation and modeling • No missing indicators included in imputation and modeling • Complete case analysis
No missing indicators included in model for outcome simulation		
MAR	20	• Missing indicators included in imputation and modeling • No missing indicators included in imputation and modeling • Complete case analysis
MAR	50	• Missing indicators included in imputation and modeling • No missing indicators included in imputation and modeling • Complete case analysis
MNAR	20	• Missing indicators included in imputation and modeling • No missing indicators included in imputation and modeling • Complete case analysis
MNAR	50	• Missing indicators included in imputation and modeling • No missing indicators included in imputation and modeling • Complete case analysis

[a]MAR: missing at random.

[b]MNAR: missing not at random.

Performance Metrics

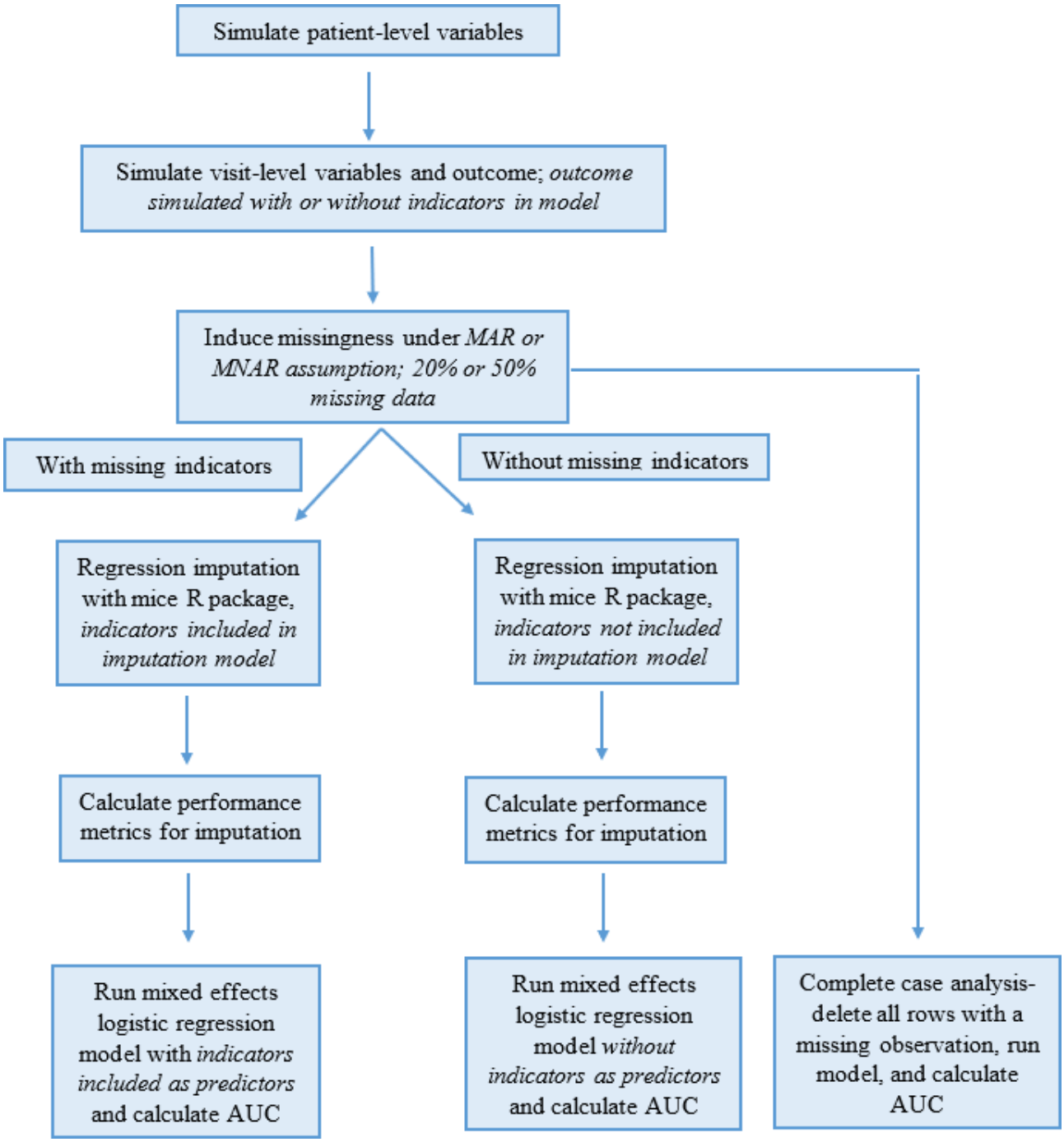
We assessed models in terms of performance and imputation quality. To assess model performance, AUROC was calculated. To assess imputation quality for binary variables, the proportion of falsely classified imputations (PFC) was calculated [38], defined as the number of incorrect binary imputed values divided by the total number of imputed values. Lower proportions indicate better quality of imputations. To assess imputation quality for continuous variables, the normalized root-mean-square error (NRMSE) between the imputed values and the observed values was calculated. The root-mean-square error is normalized by dividing by the SD of the observed values (from the study by Stekhoven and Bühlmann [38]). Lower NRSME indicates better imputation quality. For each iteration and scenario, the PFC, NRMSE, and AUROC were stored and the average values were calculated across the simulation runs.

XSL•FO
RenderX

Simulation Study Analysis Pipeline

Figure 1 provides an overview of the simulation and analysis performed in this study. The first key step is data generation, with patient-level variables generated first, then visit-level variables, and finally the outcome under the 2 underlined scenarios. Missingness is then induced under different mechanisms and at different percentages, and imputation occurs with and without the missing indicators in the imputation model. After the calculation of evaluation metrics, models were run with and without the missing indicators as predictors in the model—along with complete-case analysis—and the AUROC of each model was extracted. For models using imputation, NRMSE was calculated for continuous variables and PFC was calculated for binary variables. Results for each run of the simulation were aggregated, and averages of the performance metrics are presented.

Figure 1. Data pipeline flowchart. AUC: area under the receiver operating characteristic curve; MAR: missing at random; MNAR: missing not at random.



Results

Table 3 shows the average overall percentage of missing data and the SD for each scenario under the different missing mechanisms and data-generating mechanisms. For all scenarios, the actual missing percentage of data was slightly higher than the targeted amount.

XSL•FO
RenderX

Table . Missingness Percentages.

Outcome simulation and missing data mechanism	Target missing percentage	Actual missing percentage, mean (SD)
Indicators included in model for outcome simulation		
MAR[a]	20	22.53 (1.09)
MAR	50	52.18 (1.33)
MNAR[b]	20	22.20 (1.08)
MNAR	50	54.28 (1.33)
Indicators not included in model for outcome simulation		
MAR	20	22.50 (1.06)
MAR	50	52.34 (1.27)
MNAR	20	22.35 (1.07)
MNAR	50	54.29 (1.33)

[a]MAR: missing at random.

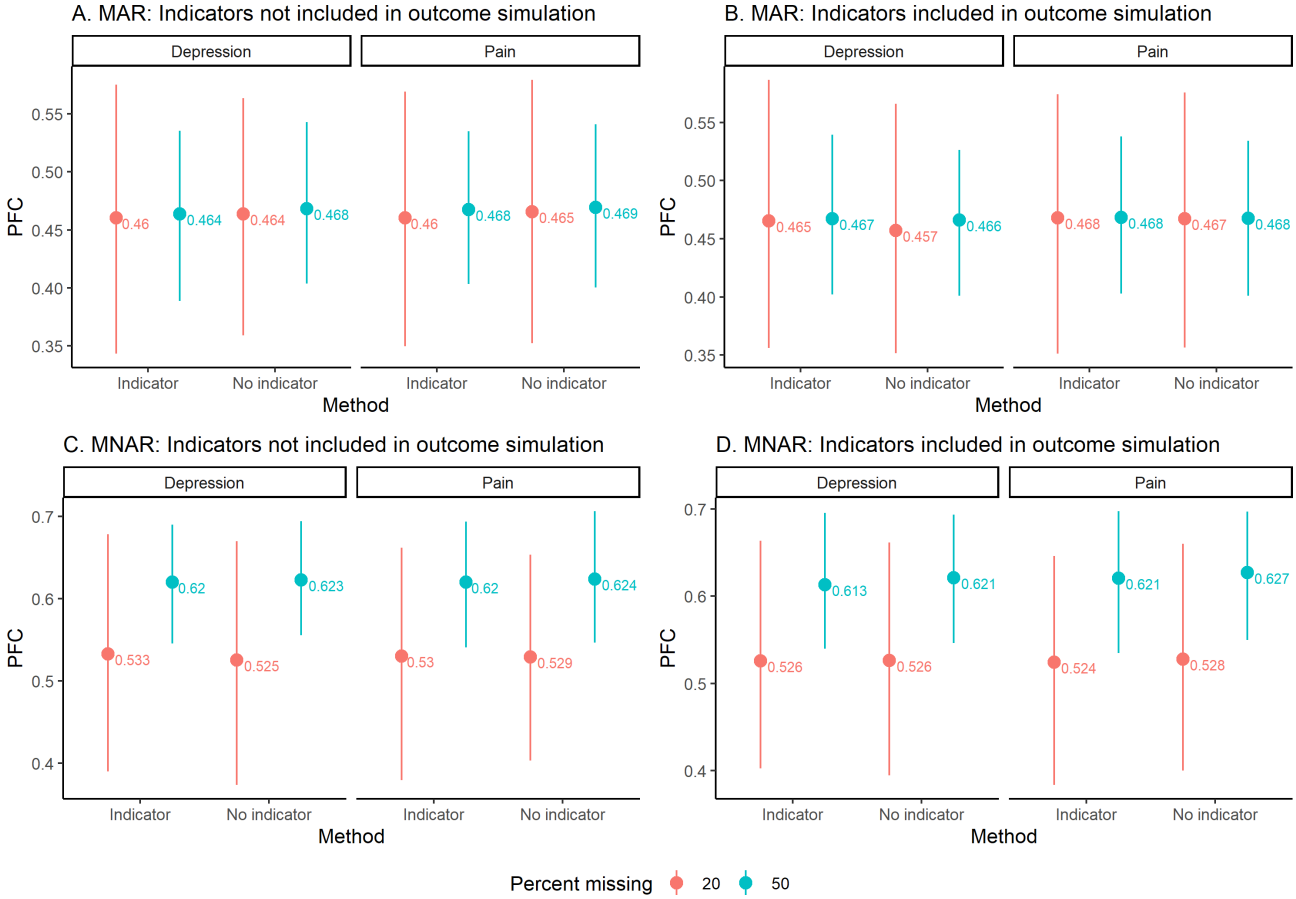
[b]MNAR: missing not at random.

Imputation Quality

First, we present results related to imputation quality. We begin by assessing the PFC for the binary variables (Figure 2), in which higher PFC indicates a higher misclassification rate and therefore worse imputation quality. For MAR scenarios (Figure 2A and B), the PFC was about 46% - 47% for both pain and depression medication, regardless of whether indicators were used to simulate the outcome. There was little difference between the PFC at 20% of missing data compared with 50% of missing data. For MNAR scenarios (Figure 2C and D), the PFC was about 61% - 63% for both pain and depression medication at 50% of missing data and about 52% - 53% for 20% of missing data. PFCs comparing including missing indicators versus not including missing indicators were similar. The PFCs were higher for MNAR data than for MAR data.

XSL•FO
RenderX

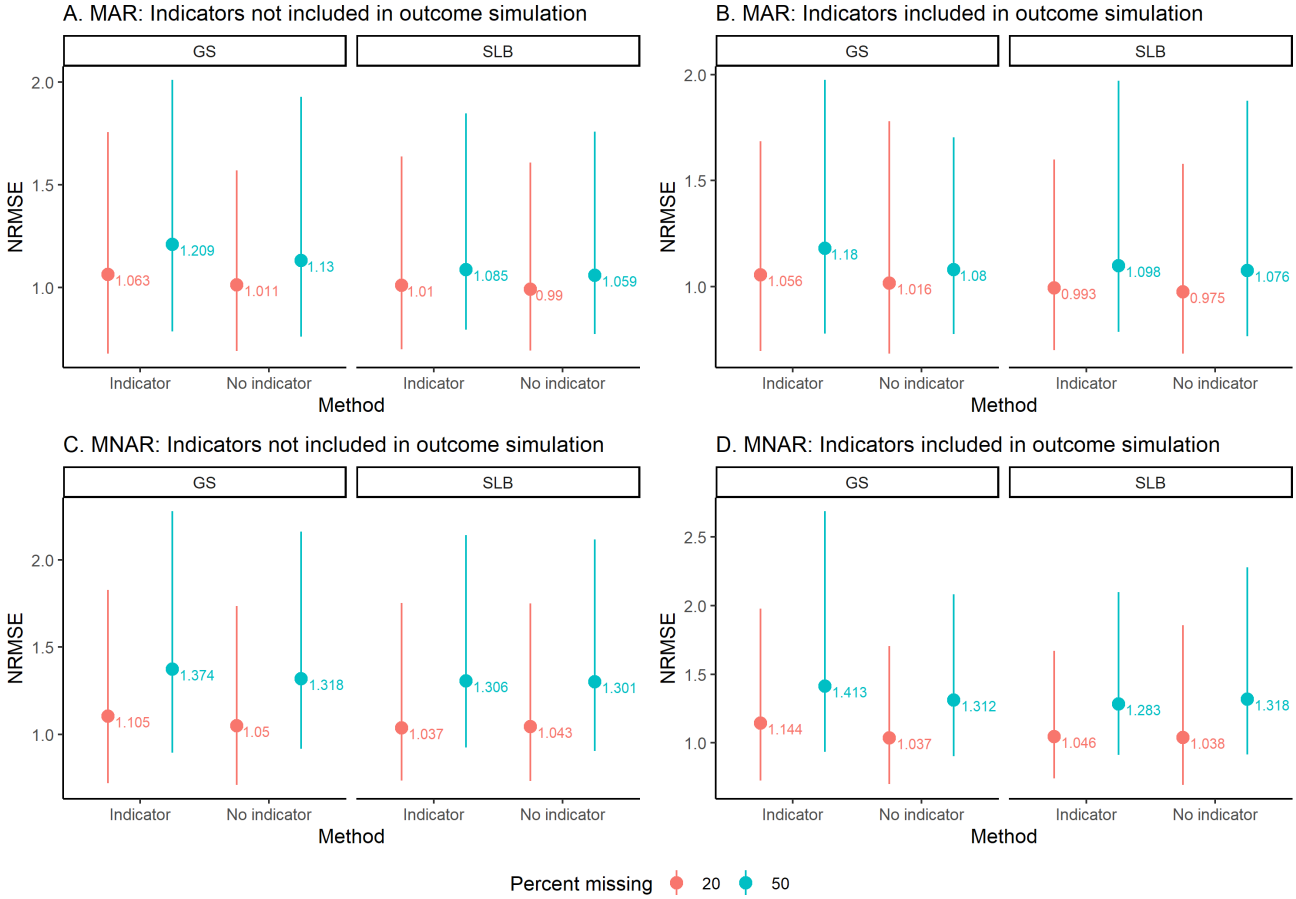
Figure 2. Average proportion of falsely classified imputations (PFC) for binary variables across iterations. The average value is indicated with a point, and the lines go to the 2.5th percentile and 97.5th quantiles. Panels A and B are for MAR data, when indicators are not included in the outcome simulation and when indicators are included in the outcome simulation. Panels C and D are for MNAR data, when indicators are not included in the outcome simulation and when indicators are included in the outcome simulation. MAR: missing at random; MNAR: missing not at random.



Next, we assess NRMSE for continuous variables (Figure 3A-D), in which higher NRMSE indicates worse imputation quality. In general, the NRMSE of single-leg balance was lower than that of gait speed. For the variables gait speed and single-leg balance, NRMSE was higher when there was 50% of missing data compared with 20% of missing. NRMSE was higher in MNAR scenarios compared with MAR scenarios. Whether or not indicators were included when simulating the outcome resulted in similar NRMSE for the variables. The NRMSE for the imputation of gait speed was slightly larger when indicators were included for all scenarios, but for single-leg balance there was no clear pattern.

XSL•FO
RenderX

Figure 3. Average normalized root-mean-square error (NRMSE) for continuous variables across iterations. The average value is indicated with a point, and the lines go to the 2.5th percentile and 97.5th quantiles. Panels A and B are for MAR data, when indicators are not included in the outcome simulation and when indicators are included in the outcome simulation. Panels C and D are for MNAR data, when indicators are not included in the outcome simulation and when indicators are included in the outcome simulation. GS: gait speed; MAR: missing at random; MNAR: missing not at random.

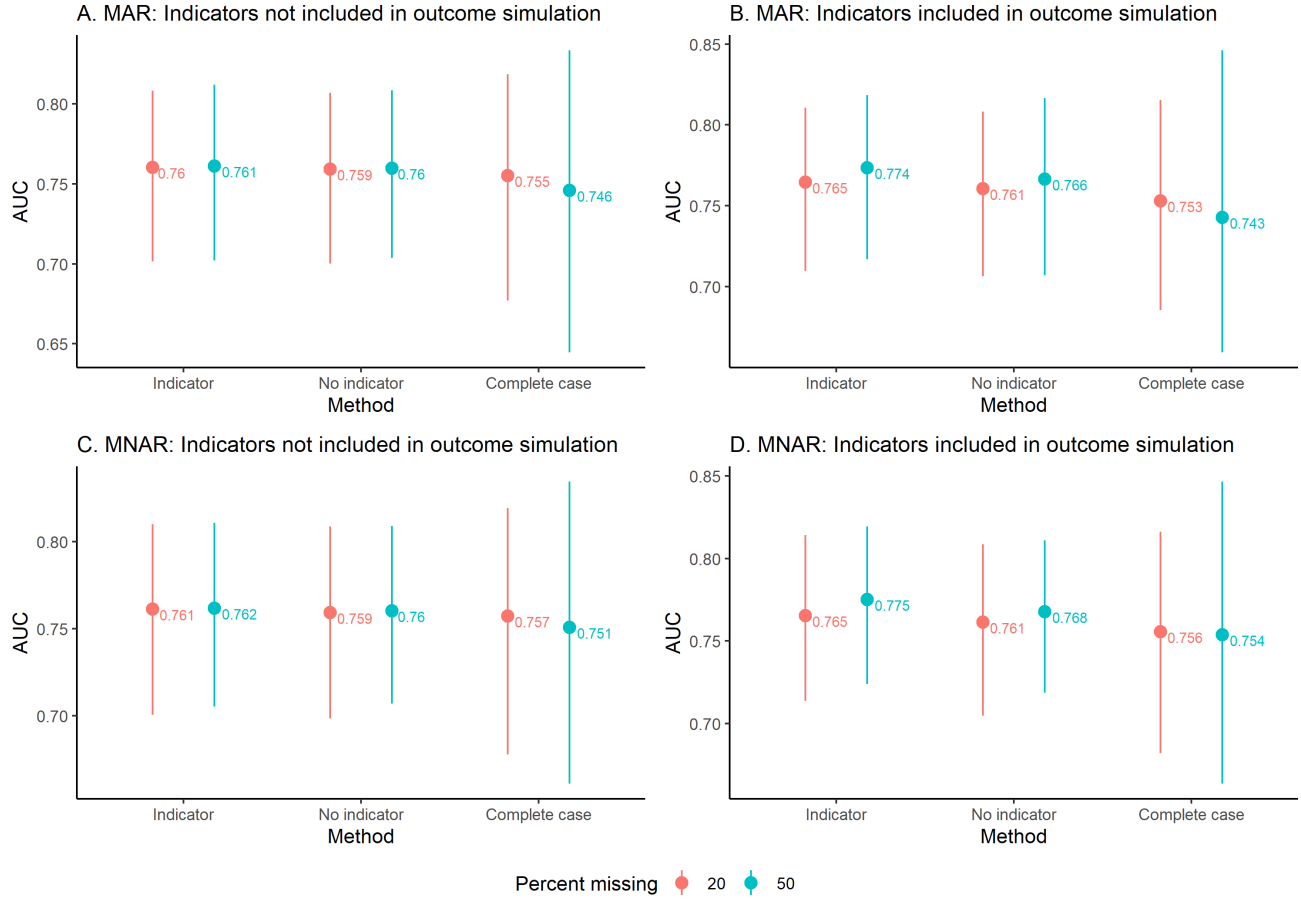


Performance Evaluation

We compare AUROC values for complete case analysis with the imputation methods (indicators included vs not included) in Figure 4A-D. AUROCs for the methods within a simulated scenario were generally similar and close to 0.75. The complete case analysis had the largest spread of AUROC values, whereas imputation with or with no missing indicators had similar spread of AUROC values. The amount of missing data (20% or 50%) and the missing data assumption (MAR and MNAR) did not substantially impact the AUROC values, which were similar across these groups. Comparing models using missing indicators with those with no missing indicators, we observed overlap in the AUROC intervals.

XSL•FO
RenderX

Figure 4. Average AUC comparison across iterations. The average value is indicated with a point, and the lines go to the 2.5th percentile and 97.5th quantiles. Panels A and B are for MAR data, when indicators are not included in the outcome simulation and when indicators are included in the outcome simulation. Panels C and D are for MNAR data, when indicators are not included in the outcome simulation and when indicators are included in the outcome simulation. AUC: area under the receiver operating characteristic curve; MAR: missing at random; MNAR: missing not at random.



Discussion

This study investigated the performance of the missing indicator method in terms of imputation quality and model performance for longitudinal data under MAR and MNAR mechanisms and different amounts of missing data. The imputation quality was worse under MNAR, as the PFC was about 15% higher under MNAR and the NRMSE for continuous values were higher under MNAR. When data were MAR and MNAR, the inclusion of missing indicators in the imputation and outcome models had a minimal effect on AUROC, regardless of whether the indicators were included as inputs when simulating the outcome. Therefore, the results from our simulation of longitudinal data mimicking data from the EHR suggest that the missing indicator method may not improve imputation quality or model performance, even when data are MNAR. However, it does not seem that including missing indicators harms imputation quality or model performance either.

In all scenarios, AUROC from complete case analysis was similar to AUROC from the other models, but the range of values was largest. While complete case analysis had similar AUROC values to imputation, we would not generally advocate for the use of complete case analysis. The increased variability associated with complete case analysis compared with imputation approaches can result in loss of power. In addition, while this study is focused on prediction and does not report model parameter estimates, complete case analysis may result in biased model coefficient estimates when data are MAR or MNAR. If model interpretation is of interest, complete case analysis will likely result in bias in settings such as EHR data, where missingness is often informative.

It was somewhat surprising that the imputations for the simulated binary variables were poor, as demonstrated by the high rates of PFC in Figure 2. We were not expecting such high errors in the imputed values. We hypothesize that some of the error may be attributed to rounding to force the imputed values to be binary, as many imputation methods provide a probability for binary variables which then must be handled in the analysis. Although the accuracy of the binary variable imputations was poor in our simulations, our main focus was on whether or not missing indicators may be beneficial for imputation and modeling. Future work may investigate the accuracy of imputation methods for multilevel data, especially when the predictors contain a mix of binary and continuous variables.

Previous studies on the missing indicator method have shown conflicting results. Van Ness et al [14] found that when missingness is informative, the missing indicator method increases predictive performance of linear models and neural networks with mean imputation and other imputation methods. The authors simulated data using an informativeness parameter, which differs from our study. The only situation where the method harmed predictive performance was in high-dimensional

XSL•FO
RenderX

data, where the addition of uninformative indicators led to overfitting. Sperrin and Martin [39] found that the method improves causal effect estimation when missingness is informative when combined with multiple imputation. Sisk et al [11] investigated the use of the missing indicator method in addition to both regression and multiple imputation to deal with nonignorable missing data in prediction modeling. Similar to Van Ness et al [14], Sisk et al [11] showed that the missing indicator method corrected bias but requires the assumption that the missing mechanism remains constant throughout the clinical prediction model pipeline, which may not be plausible because of how the likelihood of collection differs across providers.

The results of our study contribute to the growing body of literature aiming to provide guidance regarding the missing indicator method. Our simulation based on EHR data of falls in older adults using a longitudinal, repeated-measures setup suggested that the missing indicator method may not be beneficial in terms of imputation quality or model performance, but it also did not seem to cause harm. None of the previously described papers used longitudinal data when investigating the missing indicator method with a focus on prediction modeling, which may be a reason why the results of this paper differ from findings of the other papers mentioned. There is clearly debate as to the potential benefit and harm of the missing indicator method, and this paper provides guidance for longitudinal, repeated-measures data.

Our study should be considered within the context of its strengths and limitations. We used a simulation framework, which has multiple advantages that allow for the evaluation of statistical methods. A major strength of this study is the ability to define and control the missing mechanism. In practice, investigators can make assumptions regarding why data are missing, but there is no statistical test to decide whether data are MAR or MNAR. In this study, because the truth regarding the missing mechanism for each variable is known, no assumptions are made. The effectiveness of the missing indicator method can be evaluated and compared between the 2 mechanisms. In addition, because the true value of all variables is known, the imputations themselves can be evaluated for quality.

Despite the many strengths of our study, there are some limitations. One limitation of this study was the quality of imputations for the binary variables. With 45% - 60% of values being incorrectly classified, the imputation performed only slightly better than random guessing. This may have impacted how beneficial the missing indicators were in modeling. A future study could investigate how to boost imputation performance in longitudinal data, perhaps using machine learning imputation methods. Another limitation of the study is that time-dependent covariates were not considered. Future work may investigate the missing indicator method in this setting. Other limitations are related to the nature of simulation studies. Assumptions about the relationships between variables must be made, and these relationships are often oversimplified. The results may be sensitive to the parameter values chosen for the study; however, we completed a rigorous study based on a real-world scenario of falls in older adults. Future studies could evaluate how the addition of more visits, missed visits, dropout, and other missing patterns common in EHR data impacts results. In addition, a future simulation study could use an informativeness missing parameter such as that imposed in Van Ness' analysis for MNAR scenarios.

The results of this study suggest that the inclusion of missing indicators in longitudinal data modeling does not seem to be beneficial for overall performance or imputation accuracy, as neither metric improved. However, inclusion of missing indicators does not appear to cause harm in terms of performance or imputation accuracy, as neither metric worsened. Future research may address whether the inclusion of missing indicators is useful in prediction modeling with longitudinal data in different settings, such as high-dimensional data analysis.

Acknowledgments

This project was supported in part by the National Institutes of Health/National Library of Medicine (R25 LM014214) in the Department of Biomedical Engineering and Center for Biomedical Informatics at Wake Forest University School of Medicine. JLS is supported by the National Institute on Aging of the National Institutes of Health under award number K25AG068253. This study was supported in part by the Wake Forest Claude D. Pepper Older Americans Independence Centers (P30 AG021332). The content is solely the responsibility of the authors and does not necessarily represent the official views of the National Institutes of Health.

Conflicts of Interest

None declared.

Multimedia Appendix 1
Data simulation for one run of the simulation study.
[DOCX File, 35 KB - medinform_v13i1e64354_app1.docx]

References

XSL•FO
RenderX

1. Ehrenstein V, Kharrazi H, Lehmann H, Taylor CO. Obtaining data from electronic health records. In: Tools and Technologies for Registry Interoperability, Registries for Evaluating Patient Outcomes: A User's Guide, 3rd edition: Agency for Healthcare Research and Quality; 2019.
2. Wells BJ, Chagin KM, Nowacki AS, Kattan MW. Strategies for handling missing data in electronic health record derived data. EGEMS (Wash DC) 2013;1(3):1035. [doi: 10.13063/2327-9214.1035] [Medline: 25848578]
3. Haneuse S, Arterburn D, Daniels MJ. Assessing missing data assumptions in EHR-based studies: a complex and underappreciated task. JAMA Netw Open 2021 Feb 1;4(2):e210184. [doi: 10.1001/jamanetworkopen.2021.0184] [Medline: 33635321]
4. Hu Z, Melton GB, Arsoniadis EG, Wang Y, Kwaan MR, Simon GJ. Strategies for handling missing clinical data for automated surgical site infection detection from the electronic health record. J Biomed Inform 2017 Apr;68:112-120. [doi: 10.1016/j.jbi.2017.03.009] [Medline: 28323112]
5. Collins GS, Moons KGM, Dhiman P, et al. TRIPOD+AI statement: updated guidance for reporting clinical prediction models that use regression or machine learning methods. BMJ 2024 Apr 16;385:e078378. [doi: 10.1136/bmj-2023-078378] [Medline: 38626948]
6. Collins GS, Reitsma JB, Altman DG, Moons KGM. Transparent Reporting of a multivariable prediction model for Individual Prognosis Or Diagnosis (TRIPOD): the TRIPOD Statement. Br J Surg 2015 Feb;102(3):148-158. [doi: 10.1002/bjs.9736] [Medline: 25627261]
7. Papageorgiou G, Grant SW, Takkenberg JJM, Mokhles MM. Statistical primer: how to deal with missing data in scientific research? Interact Cardiovasc Thorac Surg 2018 Aug 1;27(2):153-158. [doi: 10.1093/icvts/ivy102] [Medline: 29757374]
8. Zhang Z. Missing data imputation: focusing on single imputation. Ann Transl Med 2016 Jan;4(1):9. [doi: 10.3978/j.issn.2305-5839.2015.12.38] [Medline: 26855945]
9. Emmanuel T, Maupong T, Mpoeleng D, Semong T, Mphago B, Tabona O. A survey on missing data in machine learning. J Big Data 2021;8(1):140. [doi: 10.1186/s40537-021-00516-9] [Medline: 34722113]
10. Li P, Stuart EA, Allison DB. Multiple imputation: a flexible tool for handling missing data. JAMA 2015 Nov 10;314(18):1966-1967. [doi: 10.1001/jama.2015.15281] [Medline: 26547468]
11. Sisk R, Sperrin M, Peek N, van Smeden M, Martin GP. Imputation and missing indicators for handling missing data in the development and deployment of clinical prediction models: a simulation study. Stat Methods Med Res 2023 Aug;32(8):1461-1477. [doi: 10.1177/09622802231165001] [Medline: 37105540]
12. Javanbakht M, Lin J, Ragsdale A, Kim S, Siminski S, Gorbach P. Comparing single and multiple imputation strategies for harmonizing substance use data across HIV-related cohort studies. BMC Med Res Methodol 2022 Apr 3;22(1):90. [doi: 10.1186/s12874-022-01554-4] [Medline: 35369872]
13. Groenwold RHH, White IR, Donders ART, Carpenter JR, Altman DG, Moons KGM. Missing covariate data in clinical research: when and when not to use the missing-indicator method for analysis. CMAJ 2012 Aug 7;184(11):1265-1269. [doi: 10.1503/cmaj.110977] [Medline: 22371511]
14. Van Ness M, Bosschieter TM, Halpin-Gregorio R, Udell M. The missing indicator method: from low to high dimensions. Presented at: KDD '23: Proceedings of the 29th ACM SIGKDD Conference on Knowledge Discovery and Data Mining; Aug 6-10, 2023; Long Beach, CA. [doi: 10.1145/3580305.3599911]
15. van Smeden M, Reitsma JB, Riley RD, Collins GS, Moons KG. Clinical prediction models: diagnosis versus prognosis. J Clin Epidemiol 2021 Apr;132:142-145. [doi: 10.1016/j.jclinepi.2021.01.009] [Medline: 33775387]
16. Wong A, Otles E, Donnelly JP, et al. External validation of a widely implemented proprietary sepsis prediction model in hospitalized patients. JAMA Intern Med 2021 Aug 1;181(8):1065-1070. [doi: 10.1001/jamainternmed.2021.2626] [Medline: 34152373]
17. Sharafoddini A, Dubin JA, Maslove DM, Lee J. A new insight into missing data in intensive care unit patient profiles: observational study. JMIR Med Inform 2019 Jan 8;7(1):e11605. [doi: 10.2196/11605] [Medline: 30622091]
18. Heymans MW, Twisk JWR. Handling missing data in clinical research. J Clin Epidemiol 2022 Nov;151:185-188. [doi: 10.1016/j.jclinepi.2022.08.016] [Medline: 36150546]
19. Morris TP, White IR, Crowther MJ. Using simulation studies to evaluate statistical methods. Stat Med 2019 May 20;38(11):2074-2102. [doi: 10.1002/sim.8086] [Medline: 30652356]
20. Ehrig M. Missing indicator paper. GitHub. 2024. URL: https://github.com/mehrig1/Missing-Indicator-Paper [accessed 2025-03-01]
21. Leisch F, Weingessel A, Leisch MF. Package bindata. The Comprehensive R Archive Network. 2006. URL: https://cran.r-project.org/web/packages/bindata/ [accessed 2024-07-01]
22. Ripley B, Venables B, Bates DM, Hornik K, Gebhardt A, Firth D, et al. Package mass. The Comprehensive R Archive Network. 2013. URL: https://cran.r-project.org/web/packages/MASS/index.html [accessed 2024-07-01]
23. Wickham H, Wickham MH. Package tidyverse. The Comprehensive R Archive Network. 2017. URL: https://cran.r-project.org/web/packages/tidyverse/index.html [accessed 2024-07-01]
24. Bates D, Maechler M, Bolker B, Walker S, Christensen RHB, Singmann H, et al. Package lme4. The Comprehensive R Archive Network. 2015. URL: https://cran.r-project.org/web/packages/lme4/index.html [accessed 2024-07-01]

XSL•FO
RenderX

25. Kuznetsova A, Brockhoff PB, Christensen RHB. LmerTest: tests in linear mixed effects models. J Stat Softw 2015;2(13):734. [doi: 10.18637/jss.v082.i13]
26. Tierney NJ, Cook DH. Expanding tidy data principles to facilitate missing data exploration, visualization and assessment of imputations. arXiv. Preprint posted online on Sep 7, 2018. [doi: 10.48550/arXiv.1809.02264]
27. Buuren S, Groothuis-Oudshoorn K, Robitzsch A, Vink G, Doove L, Jolani S. Package mice. The Comprehensive R Archive Network. 2015. URL: https://cran.r-project.org/web/packages/mice/index.html [accessed 2024-07-01]
28. Bolker B, Robinson D, Menne D, Gabry J, Buerkner P. Package broom.mixed. The Comprehensive R Archive Network. 2019. URL: https://cran.r-project.org/web/packages/broom.mixed/index.html [accessed 2024-07-01]
29. Robin X, Turck N, Hainard A, et al. pROC: an open-source package for R and S+ to analyze and compare ROC curves. BMC Bioinformatics 2011 Mar 17;12:1-8. [doi: 10.1186/1471-2105-12-77] [Medline: 21414208]
30. Signorell A, Aho K, Alfons A, Anderegg N, Aragon T, Arachchige C, et al. Package DescTools. The Comprehensive R Archive Network. 2021. URL: https://cran.r-project.org/web//packages/DescTools/index.html [accessed 2024-07-01]
31. Stekhoven DJ. Package missForest. The Comprehensive R Archive Network. 2013. URL: https://cran.r-project.org/web//packages//missForest/index.html [accessed 2024-07-01]
32. Arel-Bundock V. Data and model summaries in R. J Stat Softw 2022;103(1):1-23. [doi: 10.18637/jss.v103.i01]
33. Lüdecke D, Lüdecke MD. Package sjPlot. The Comprehensive R Archive Network. 2015. URL: https://cran.r-project.org/web/packages/sjPlot/index.html [accessed 2024-07-01]
34. Auguie B, Antonov A, Auguie MB. Package gridextra. The Comprehensive R Archive Network. 2017. URL: https://cran.r-project.org/web/packages/gridExtra/index.html [accessed 2024-07-01]
35. Zhou L, Braun WJ. Fun with the R Grid Package. J Stat Educ 2010 Nov;18(3):1-35. [doi: 10.1080/10691898.2010.11889587]
36. Fox J, Weisberg S, Adler D, Bates D, Baud-Bovy G, Ellison S, et al. Package car. The Comprehensive R Archive Network. 2012. URL: https://cran.r-project.org/web/packages/car/index.html [accessed 2024-07-01]
37. Hsieh KL, Speiser JL, Neiberg RH, Marsh AP, Tooze JA, Houston DK. Factors associated with falls in older adults: a secondary analysis of a 12-month randomized controlled trial. Arch Gerontol Geriatr 2023 May;108:104940. [doi: 10.1016/j.archger.2023.104940] [Medline: 36709562]
38. Stekhoven DJ, Bühlmann P. MissForest--non-parametric missing value imputation for mixed-type data. Bioinformatics 2012 Jan 1;28(1):112-118. [doi: 10.1093/bioinformatics/btr597] [Medline: 22039212]
39. Sperrin M, Martin GP. Multiple imputation with missing indicators as proxies for unmeasured variables: simulation study. BMC Med Res Methodol 2020 Jul 8;20(1):185. [doi: 10.1186/s12874-020-01068-x] [Medline: 32640992]

Abbreviations

AUROC: area under the receiver operating characteristic curve
EHR: electronic health record
MAR: missing at random
MCAR: missing completely at random
MNAR: missing not at random
NRMSE: normalized root-mean-square error
PFC: proportion of falsely classified imputations
TRIPOD: Transparent Reporting of a Multivariable Prediction Model for Individual Prognosis or Diagnosis

Edited by C Lovis; submitted 15.07.24; peer-reviewed by A Snavely, M Stein; revised version received 07.02.25; accepted 08.02.25; published 13.03.25.

Please cite as:
Ehrig M, Bullock GS, Leng XI, Pajewski NM, Speiser JL
Imputation and Missing Indicators for Handling Missing Longitudinal Data: Data Simulation Analysis Based on Electronic Health Record Data
JMIR Med Inform 2025;13:e64354
URL: https://medinform.jmir.org/2025/1/e64354
doi:10.2196/64354

© Molly Ehrig, Garrett S Bullock, Xiaoyan Iris Leng, Nicholas M Pajewski, Jaime Lynn Speiser. Originally published in JMIR Medical Informatics (https://medinform.jmir.org), 13.3.2025. This is an open-access article distributed under the terms of the Creative Commons Attribution License (https://creativecommons.org/licenses/by/4.0/), which permits unrestricted use, distribution, and reproduction in any medium, provided the original work, first published in JMIR Medical Informatics, is properly cited. The

XSL•FO
RenderX

complete bibliographic information, a link to the original publication on https://medinform.jmir.org/, as well as this copyright and license information must be included.

XSL•FO
RenderX

Use of the FHTHWA Index as a Novel Approach for Predicting the Incidence of Diabetes in a Japanese Population Without Diabetes: Data Analysis Study

Jiao Wang[1,2,3], MD, PhD; Jianrong Chen[1,2,3], MD, PhD; Ying Liu[1,2,3], MD, PhD; Jixiong Xu[1,2,3], MD, PhD

[1]Department of Endocrinology and Metabolism, The First Affiliated Hospital, Jiangxi Medical College, Nanchang University, Nanchang, China

[2]Jiangxi Clinical Research Center for Endocrine and Metabolic Disease, Nanchang, China

[3]Jiangxi Branch of National Clinical Research Center for Metabolic Disease, Nanchang, China

Corresponding Author:
Jixiong Xu, MD, PhD
Department of Endocrinology and Metabolism, The First Affiliated Hospital, Jiangxi Medical College, Nanchang University, Nanchang, China

Abstract

Background: Many tools have been developed to predict the risk of diabetes in a population without diabetes; however, these tools have shortcomings that include the omission of race, inclusion of variables that are not readily available to patients, and low sensitivity or specificity.

Objective: We aimed to develop and validate an easy, systematic index for predicting diabetes risk in the Asian population.

Methods: We collected the data from the NAGALA (NAfld [nonalcoholic fatty liver disease] in the Gifu Area, Longitudinal Analysis) database. The least absolute shrinkage and selection operator model was used to select potentially relevant features. Multiple Cox proportional hazard analysis was used to develop a model based on the training set.

Results: The final study population of 15464 participants had a mean age of 42 (range 18-79) years; 54.5% (8430) were men. The mean follow-up duration was 6.05 (SD 3.78) years. A total of 373 (2.41%) participants showed progression to diabetes during the follow-up period. Then, we established a novel parameter (the FHTHWA index), to evaluate the incidence of diabetes in a population without diabetes, comprising 6 parameters based on the training set. After multivariable adjustment, individuals in tertile 3 had a significantly higher rate of diabetes compared with those in tertile 1 (hazard ratio 32.141, 95% CI 11.545 - 89.476). Time receiver operating characteristic curve analyses showed that the FHTHWA index had high accuracy, with the area under the curve value being around 0.9 during the more than 12 years of follow-up.

Conclusions: This research successfully developed a diabetes risk assessment index tailored for the Japanese population by utilizing an extensive dataset and a wide range of indices. By categorizing the diabetes risk levels among Japanese individuals, this study offers a novel predictive tool for identifying potential patients, while also delivering valuable insights into diabetes prevention strategies for the healthy Japanese populace.

(JMIR Med Inform 2025;13:e64992) doi:10.2196/64992

KEYWORDS

prediction; diabetes; risk; index; population without diabetes

Introduction

The increasing number of patients with diabetes mellitus represents an escalating challenge worldwide [1,2]. Based on the recently published International Diabetes Federation (IDF) Diabetes Atlas, the recorded worldwide incidence of diabetes among the adult population (20 - 79 years) in 2021 was 10.5%, while the prevalence in Southeast Asia was 8.7% [3]. It is estimated that by the year 2045, the global prevalence of individuals living with diabetes will increase to an estimated 783 million, corresponding to a prevalence rate of approximately 12.2% [3], which indicates the urgent need for global diabetes prevention and control. Given the significant prevalence of patients with impaired fasting glucose or undiagnosed diabetes, it is imperative to prioritize the early screening and detection in these patients to mitigate the morbidity associated with diabetes, minimize healthcare expenditures, and prevent a decline in the quality of life [2,4].

Diabetes mellitus is a metabolic disorder, affecting both glucose and lipid metabolism [5,6]. Recent studies have investigated the correlation between glucose and lipid-related indexes and the prevalence of diabetes, including the triglyceride-glucose (TyG) index, metabolic score for insulin resistance (METS-IR), triglyceride to high-density lipoprotein cholesterol ratio

XSL•FO
RenderX

(TG/HDL-C), and total cholesterol to high-density lipoprotein cholesterol ratio (TC/HDL-C) [7-9]. However, the accuracy of these indexes remains limited, and better prognostication indexes need to be found. Meanwhile, certain researchers have redirected their attention towards employing computational methods in order to predict diabetes at an early stage with greater precision [10-14]. The diabetes risk test created by the American Diabetes Association (ADA) serves as a screening tool designed to categorize individuals at a heightened risk within the community to enhance awareness regarding modifiable risk factors and promote the adoption of a healthy lifestyle [15]. Bang et al [16] developed a new screening score using the National Health and Nutrition Examination Survey (NHANES) and a combined cohort of two community studies However, the utilization of diabetes prediction and risk assessment models has been limited due to their predominantly designed focus on White populations. Specifically, there is a scarcity of scoring systems tailored to Japanese populations.

Therefore, in this study, we aimed to develop and validate an easy, systematic index for predicting the diabetes risk in the Asian population using glucose and lipid metabolism parameters and anthropometric parameters, which will enable the clinician or lay persons to assess their own risk of undiagnosed diabetes.

Methods

Study Population

The study participants were selected from the NAGALA (NAfld [nonalcoholic fatty liver disease] in the Gifu Area, Longitudinal Analysis) database—a human dock that serves as a repository for detecting chronic diseases and their linked risk factors, with the aim of advancing public health initiatives. The cohort has been comprehensively delineated in a prior investigation undertaken by Okamura et al [17]. The NAGALA cohort was initiated in 1994, encompassing individuals who underwent health examinations at Murakami Memorial Hospital. As a significant portion of the hospital's screening participants, approximately 60%, return for annual or biennial check-ups, the NAGALA team implemented an extended follow-up study to monitor the emergence of diabetes and nonalcoholic fatty liver disease in this population over time. Furthermore, the available dataset relevant to the investigation cohort has been made accessible on the Dryad public database [18] to facilitate the sharing of data.

The present study incorporated the data of 20,944 individuals who were enrolled in the NAGALA cohort between 1994 and 2016. After the further exclusion of participants who were diagnosed with diabetes, impaired fasting glucose, liver disease, excessive drinking, missing data on potential covariates, baseline medication, and unexplained withdrawal from the survey, a total of 15,464 participants were included as the analytical sample.

Ethical Considerations

The data used in this study were obtained from publicly available online databases. As these databases consist of deidentified and aggregated data, they do not involve human subjects or animals. All data were collected from publicly available sources; therefore, ethical approval was not required. Therefore, ethical review and approval were not required for this study in accordance with the ethical standards of the institutional and national research committees, as well as with the 1964 Helsinki Declaration and its later amendments or comparable ethical standards.

Measurement

Demographic data, examination and laboratory test results, medical history, and prescription medication information were used from the NAGALA data. The laboratory test levels included alanine aminotransferase (ALT), aspartate aminotransferase (AST), gamma-glutamyl transferase (GGT), total cholesterol (TC), triglyceride (TG), fasting plasma glucose (FPG), high-density lipoprotein cholesterol (HDL-C), and low-density lipoprotein cholesterol (LDL-C). The examination and laboratory tests included the evaluation of the BMI, systolic blood pressure (SBP), diastolic blood pressure (DBP), and waist circumference (WC). Regarding exercise behaviors, the participants' frequency of engaging in physical exercise per week was evaluated, with the criterion for the habit of exercise being defined as more than once per week. Alcohol consumption was categorized as heavy, moderate, light, and none, in line with the quantity and nature of participants' weekly alcohol intake over the course of the preceding month [19]. Smoking status was categorized as current smoker, past smoker, and never smoker.

TyG index was calculated as follows: TyG index = Ln [fasting TGs (mg/dL) × fasting glucose (mg/dL) / 2] [20].

TG/HDL-C was calculated as follows: TG/HDL-C ratio = TG/HDL-C [21].

METS-IR was calculated as follows: METS-IR = Ln ((2 × FPG) + TG) × BMI) / (Ln (HDL-C)) [22].

Gastroenterologists made a diagnosis of fatty liver by evaluating specific characteristics observed on abdominal Doppler ultrasonography; these characteristics included vascular blurring, deep attenuation, liver brightness, and hepatorenal echo contrast [23].

The diagnosis of diabetes mellitus was established using the criteria set forth by the ADA. Participants were deemed to have diabetes if their HbA_{1c} measurements were ≥6.5% or if their FPG levels were ≥7 mmol/L during the follow-up period. Furthermore, the analysis incorporated the participant's self-reported diabetes diagnosis during the follow-up period.

Statistical Analysis

If the continuous variables followed a normal distribution, they were represented as the mean and the standard deviation. The variables exhibiting nonnormal distribution were presented as medians accompanied by their respective minimum and maximum values. To evaluate variations between the two groups, the statistical analysis employed the Pearson chi-square test for categorical variables, while the Mann-Whitney *U* test or Student *t*-test was utilized for continuous variables. One-way ANOVA was used to compare several groups of data that followed a normal distribution, while the Kruskal-Wallis test

XSL•FO
RenderX

was used to analyze data that did not conform to a normal distribution.

A total of 15464 participants were randomly assigned to the training (n=9280, 60%) and internal validation (n=6184, 40%) sets. To establish the index for predicting the incidence of diabetes, univariate Cox regression was applied to detect the variables related to diabetes in the training set. Subsequently, the Cox regression model incorporating the least absolute shrinkage and selection operator (LASSO) was employed to ascertain the coefficients for constructing the model by utilizing an optimal log λ value. The index was established with the following formula: risk score = value of factor 1 × β1+ value of factor 2 × β2+…value of factor n × βn (β was the weighted coefficient of each factor).

Furthermore, an analysis of the receiver operating characteristic (ROC) curve was conducted, and areas under the curve (AUCs) were carried out to assess the predictive value of fasting stress hyperglycemia ratio, FPG, and HbA_{1c} in relation to the risk of diabetes.

The patients were divided into three groups (tertile 1: <33rd percentile, tertile 2: ≥33rd to 67th percentile, and tertile 3: ≥67th percentile) according to the novel index tertiles. Cox proportional hazards regression models were employed to assess the link between the index and the incidence of diabetes. The models included several covariates, namely sex, alcohol consumption, smoking status, habit of exercise, BMI, fatty liver, ALT, AST, GGT, TC, SBP, DBP, TyG, TG/HDL-C ratio, and METS-IR.

The statistical analyses were conducted using SPSS version 23.0 (SPSS Inc.) and R version 3.6.0 (R Foundation for Statistical Computing). A two-sided *P*-value <.05 was deemed to be statistically significant.

Results

Study Population

The current investigation encompassed 15,464 diabetes-free participants, with a mean age of 42 (range 18-79) years, 8430 (54.5%) men and 7034 (45.5%) women, and a mean follow-up of 6.05 (SD 3.7) years. A 6-to-4 ratio was used to randomly allocate patients into the training (n=9280) and validation (n=6184) sets. Table S1 in Multimedia Appendix 1 displays the variations in baseline characteristics of the study population in both the training set and validation set.

Establishment of the Diabetes Incidence Index

A univariate analysis was conducted on the training dataset in order to ascertain the variables that were correlated with the occurrence of diabetes. Eight significant variables, namely age, BMI, WC, HDL-C, TC, TG, HbA_{1c}, and FPG, were employed as predictive factors for progressing diabetes (*P*<.05; see Table S2 in Multimedia Appendix 1). The 8 clinical features were subsequently included in the LASSO regression analysis, which was performed for 1000 bootstrap iterations. From this analysis, 4 features were identified with nonzero coefficients and a minimum lambda value (Figure S1 in Multimedia Appendix 1). The findings of multivariate Cox regression analysis indicate that age, WC, HDL-C, TG, HbA_{1c}, and FPG were identified as independent risk factors (Table S3 in Multimedia Appendix 1).

To develop a risk index, we constructed a clinical feature-based risk signature derived from the results of a multivariate Cox regression analysis. The risk score was calculated as follows:

$$[(FPG) \times 1.525] - [(HDL\text{-}C) \times 0.454] + [(TG) \times 0.216] + [(HbA_{1c}) \times 3.298] + [(WC) \times 0.044] + [(age) \times 0.016].$$

We defined this new parameter combined with FPG, HDL-C, TG, HbA_{1c}, WC, and age as the FHTHWA index based on the initial letter of each variable.

Baseline Characteristics

The baseline characteristics of participants were examined based on the FHTHWA index in both the training and validation sets.

For the training set, patients with increased FHTHWA index levels tended to be of advanced age and displayed characteristics indicative of fatty liver, with higher BMI, WC, ALT, AST, body weight, GGT, TC, TG, HbA_{1c}, FPG, SBP, DBP, alcohol consumption, smoking, TG/HDLC ratio, TyG index, and METS-IR, as well as low HDL-C levels (Table 1; all *P*<.01).

XSL•FO
RenderX

Table . Baseline characteristics of the study population by tertiles of the FHTHWA index in the training set.

Characteristics	Tertile 1 (n=3093)	Tertile 2 (n=3093)	Tertile 3 (n=3094)	*P* value
Sex, n (%)				<.001
Male	1106 (11.92)	1808 (19.48)	2174 (23.43)	<.001
Female	1987 (21.41)	1285 (13.85)	920 (9.91)	<.001
Age, years, mean (range)	40 (18-69)	43 (21-74)	47 (19-79)	<.001
BMI, kg/m^2, mean (SD)	20.52 (2.36)	21.88 (2.70)	23.93 (3.28)	<.001
Waist circumference, cm, mean (SD)	70.94 (7.21)	76.36 (7.61)	82.21 (8.59)	<.001
Alanine aminotransferase, IU/L, mean (range)	15 (4-141)	16 (4-129)	21 (4-149)	<.001
Aspartate aminotransferase, IU/L, mean (range)	16 (7-98)	17 (3-150)	19 (6-94)	<.001
Body weight, kg, mean (SD)	54.70 (9.03)	60.31 (10.29)	66.77 (11.98)	<.001
Gamma-glutamyl transferase, IU/L, mean (range)	12 (4-248)	15 (5-399)	19 (3-259)	<.001
High-density lipoprotein cholesterol, mmol/L, mean (range)	1.58 (0.55-3.49)	1.42 (0-3.21)	1.24 (0-3.05)	<.001
Total cholesterol, mmol/L, mean (SD)	4.86 (0.80)	5.11 (0.83)	5.38 (0.87)	<.001
Triglyceride, mmol/L, mean (range)	0.55 (0.07-3.67)	0.73 (0.11-6.75)	1.03 (0.12-7.69)	<.001
Hemoglobin A1C, %, mean (SD)	4.89 (0.23)	5.15 (0.21)	5.46 (0.24)	<.001
Fasting plasma glucose, mmol/L, mean (SD)	4.83 (0.32)	5.15 (0.31)	5.49 (0.32)	<.001
Systolic blood pressure, mmHg, mean (SD)	108.47 (13.36)	114.51 (14.25)	120.71 (14.80)	<.001
Diastolic blood pressure, mmHg, mean SD	67.60 (9.42)	71.41 (10.14)	75.94 (10.28)	<.001
Fatty liver, n (%)				<.001
Yes	118 (1.27)	394 (4.25)	1134 (12.22)	
No	2975 (32.06)	2699 (29.08)	1960 (21.12)	
Habit of exercise, n (%)				.570
Yes	529 (5.70)	547 (5.89)	561 (6.05)	
No	2564 (27.63)	2546 (27.44)	2533 (27.30)	
Alcohol consumption, n (%)				<.001
Heavy	69 (0.74)	115 (1.24)	126 (1.36)	
Moderate	220 (2.37)	301 (3.24)	305 (3.29)	
Light	318 (3.43)	366 (3.94)	367 (3.95)	
None	2486 (26.79)	2311 (24.90)	2296 (24.7)	
Smoking status, n (%)				<.001
Current	536 (5.78)	736 (7.93)	816 (8.79)	
Past	393 (4.23)	627 (6.76)	765 (8.24)	
Never	2164 (23.32)	1730 (18.64)	1513 (16.30)	
TG/HDL-C[a] ratio, n (range)	0.79 (0.11-11.35)	1.16 (0.13-15.48)	1.89 (0.19-26.73)	<.001

XSL•FO
RenderX

Characteristics	Tertile 1 (n=3093)	Tertile 2 (n=3093)	Tertile 3 (n=3094)	*P* value
Triglyceride-glucose index, mean (SD)	7.68 (0.56)	8.02 (0.57)	8.42 (0.60)	<.001
Metabolic score for insulin resistance, mean (SD)	27.45 (4.55)	30.63 (5.47)	35.52 (6.75)	<.001
FHTHWA index, mean (SD)	0.20 (0.12)	1.01 (0.43)	12.60 (24.44)	<.001
Follow-up duration, years, mean (SD)	6.79 (3.86)	5.88 (3.79)	5.47 (3.57)	<.001
Progressed to diabetes, n (%)				<.001
Yes	4 (0.04)	19 (0.20)	190 (2.05)	
No	3089 (33.29)	3074 (33.13)	2904 (31.29)	

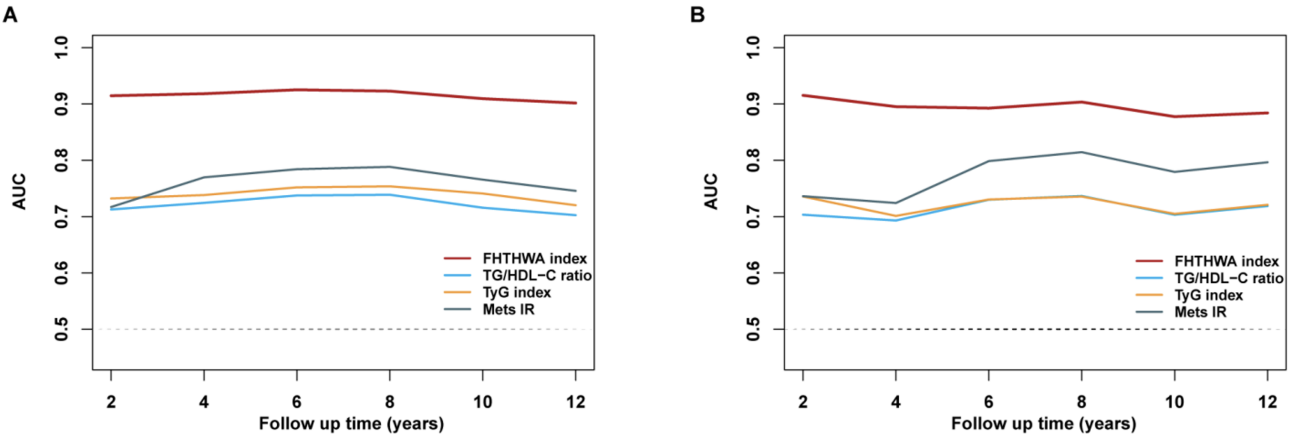
[a]TG/HDL-C: triglyceride to high-density lipoprotein cholesterol.

For the validation set, patients with increased FHTHWA index levels tended to be of advanced age and displayed characteristics indicative of fatty liver, with higher BMI, WC, ALT, AST, body weight, GGT, TC, TG, HbA_{1c}, FPG, SBP, DBP, alcohol consumption, smoking, TG/HDLC ratio, TyG index, and METS-IR, as well as low HDL-C levels (Table S4 in Multimedia Appendix 1; all $P<.05$).

Predictive Value of the FHTHWA Index

Time-dependent ROC curves were utilized in order to assess the predictive efficacy of the FHTHWA index, as well as other newly proposed predictive parameters such as TG/HDL-C, the TyG index, and METS-IR, in relation to the risk of developing diabetes in the future. Figure 1A shows the AUC of the FHTHWA index and other novel predictive parameters over time for the training set. Overall, the baseline FHTHWA index demonstrated strong predictive capabilities for future diabetes occurrence at various time intervals. The AUCs of the FHTHWA index were higher compared with the AUCs of the TG/HDL-C, TyG index, and METS-IR during the 12-year follow-up. Figure 1B shows the AUC of the FHTHWA index and other novel predictive parameters over time for the validation set. Overall, the baseline FHTHWA index demonstrated strong predictive capability for future diabetes occurrence at various time intervals. Furthermore, the FHTHWA index exhibited greater AUC values compared to the TG/HDL-C, TyG index, and METS-IR at all time points.

Figure 1. Time-dependent receiver operator characteristic curves of the FHTHWA index vary with time to predict the future risk of diabetes. (**A**) Area under the curve (AUC) comparison of the FHTHWA index, TG/HDL-C ratio, TyG index, and METS-IR in the training set. (**B**) AUC comparison of the FHTHWA index, TG/HDL-C ratio, TyG index, and METS-IR in the validation set. METS-IR: metabolic score for insulin resistance; TG/HDL-C: triglyceride to high-density lipoprotein cholesterol ratio; TyG index: triglyceride-glucose index.



Relationship of the FHTHWA Index With Diabetes Risk

In the training set, 213 (1.38%) cases progressed to diabetes during the follow-up period. From quartile 1 to quartile 3 of the FHTHWA index, the diabetes rate increased gradually from 0.04% to 2.05% (Table 1). After multivariate adjustment, including sex, consumption of alcohol, smoking status, habit of exercise, BMI, fatty liver, ALT, AST, and GGT, an elevated FHTHWA index was markedly correlated with diabetes risk (Table 2). Multivariate adjusted hazard ratios and 95% CIs from the lowest to the highest FHTHWA index categories (tertile 1, tertile 2, and tertile 3) were 1.00 (reference), 4.509 (1.520 - 13.373), and 32.141 (11.545 - 89.476), respectively, for the incidence of diabetes ($P<.001$). The analysis of weighted Kaplan-Meier curves demonstrated significant dose-response patterns within the FHTHWA index strata in relation to the incidence of diabetes. These trends persisted even after a 12-year follow-up period. Furthermore, the risk of developing diabetes across the FHTHWA index strata displayed a noticeable divergence over time (Figure 2A).

XSL•FO
RenderX

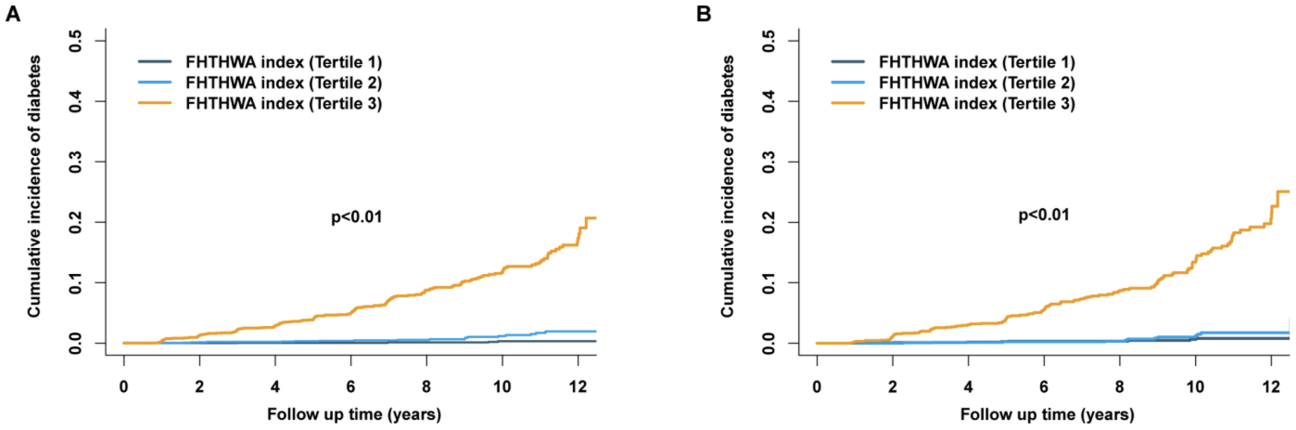
Table . Hazard ratios and corresponding 95% CIs for diabetes incidence according to the FHTHWA index among the population without diabetes in the training set.

	FHTHWA index			*P* trend	Per unit increment in the FHTHWA index
	Tertile 1	Tertile 2	Tertile 3		
Number of cases of diabetes mellitus/total	4/3093	19/3093	190/3094		
Crude	1.000 (ref.)	5.846 (1.988 - 17.158)	66.098 (24.542 - 178.020)	<.001	1.019 (1.018 - 1.021)
Model 1[a]	1.000 (ref.)	5.720 (1.914 - 16.856)	64.129 (23.679 - 173.677)	<.001	1.020 (1.018 - 1.022)
Model 2[b]	1.000 (ref.)	4.975 (1.684 - 14.695)	39.714 (14.459 - 109.084)	<.001	1.017 (1.015 - 1.019)

[a]Model 1: adjusted for sex, alcohol consumption, smoking status, and habit of exercise.

[b]Model 2: further adjusted (from Model 1) for BMI, fatty liver, ALT, AST, and GGT.

Figure 2. Weighted Kaplan-Meier curves for diabetes incidence by the baseline FHTHWA index strata. (**A**) Diabetes risk across the FHTHWA index strata in the training set exhibited divergence over time. (**B**) Diabetes risk across the FHTHWA index strata in the validation set exhibited divergence over time.



In the validation set, 160 (2.59%) cases progressed to diabetes during the follow-up period. From quartile 1 to quartile 3 of the FHTHWA index, the diabetes rate increased gradually from 0.16% to 2.25% (Table S4 in Multimedia Appendix 1). After multivariate adjustment, including sex, consumption of alcohol, smoking status, habit of exercise, BMI, fatty liver, ALT, AST, GGT, TC, TG, SBP, DBP, TyG, TG/HDL-C ratio, and METS-IR, an elevated FHTHWA index was markedly correlated with diabetes risk (Table S5 in Multimedia Appendix 1). Multivariate adjusted hazard ratios and 95% CIs from the lowest to the highest FHTHWA index categories (tertile 1, tertile 2, and tertile 3) were 1.00 (reference), 1.010 (0.419 - 2.435), and 9.924 (4.830 - 20.392), respectively, for the incidence of diabetes (*P*<.001). The utilization of weighted Kaplan-Meier curves demonstrated significant dose-response patterns across different strata of the FHTHWA index in relation to the incidence of diabetes, even after a follow-up period of 12 years. Moreover, the risk of developing diabetes across the FHTHWA index strata exhibited a noticeable divergence over time (Figure 2B).

Stratification Analyses

In the stratified analyses of the dose-response association between FHTHWA index levels and diabetes risk, participants were stratified by sex (male or female), habit of exercise (yes or no), BMI (<25 kg/m^2 or ≥25 kg/m^2), current smoker (yes or no), and current alcohol use (yes or no). In the training set, we discovered that a high FHTHWA index was linked with a higher diabetes risk, contrasted with the reference group in all subgroups (Table 3). In the validation set, the results were the same as our main results (Table S6 in Multimedia Appendix 1).

XSL•FO
RenderX

Table . Stratified analyses of the associations (hazard ratios, 95% CIs) between the FHTHWA index and diabetes incidence at the end of follow-up among people with diabetes in the training set.

Variables		Hazard ratio (95% CI)[a]	
	Event, n/N	Unadjusted model	Multivariable-adjusted model[a]
Sex			
Male	157/5088	1.019 (1.017 - 1.021)	1.020 (1.017 - 1.023)
Female	56/4192	1.019 (1.017 - 1.022)	1.013 (1.009 - 1.017)
Habit of exercise			
Yes	35/1637	1.036 (1.030 - 1.042)	1.028 (1.019 - 1.037)
No	178/7643	1.019 (1.017 - 1.020)	1.015 (1.013 - 1.018)
BMI, kg/m^2			
<25	113/7752	1.020 (1.018 - 1.023)	1.020 (1.015 - 1.025)
≥25	100/1528	1.016 (1.013 - 1.018)	1.015 (1.012 - 1.017)
Current smoker			
Yes	88/2088	1.032 (1.027 - 1.036)	1.030 (1.024 - 1.036)
No	125/7192	1.019 (1.017 - 1.020)	1.015 (1.012 - 1.017)
Current alcohol use			
Yes	56/2187	1.017 (1.014 - 1.020)	1.024 (1.018 - 1.030)
No	157/7093	1.020 (1.018 - 1.022)	1.014 (1.012 - 1.017)

[a]Hazard ratios (95% CIs) were assessed using weighted Cox proportional regression that was fully adjusted except for the stratification factor.

Discussion

Study Findings and Comparison With Previous Works

Diabetes mellitus can lead to a range of complications that result in significant psychological and physical distress for individuals who carry the disease. Moreover, this places a substantial strain on the healthcare systems [24,25]. Nevertheless, the early detection of this condition is often hindered due to the absence of distinct symptoms and a limited focus on public healthcare. Early identification of the population with high risk for diabetes might help prevent the onset of diabetes or delay its progression [26]. In this study, we developed and validated a robust parameter, named the FHTHWA index, to forecast the development of the future diabetes likelihood depending on a comprehensive longitudinal cohort study of the Japanese physical examination population. Our results revealed that the higher the FHTHWA index, the higher the risk of developing diabetes. The correlation exhibited independence from conventional risk factors, such as sex, alcohol consumption, smoking status, habit of exercise, BMI, fatty liver, SBP, DBP, TyG, TG/HDL-C ratio, and laboratory parameters.

The early identification of individuals at high risk for diabetes is crucial for implementing preventive strategies and mitigating the burden of this disease. A growth of risk assessment tools for type 2 diabetes mellitus has been observed on a global scale, such as the ADA risk score [16], the Canadian Diabetes Risk Score (CANRISK) [27], the Finnish Diabetes Risk Score (FINDRISC) [15], the Indian Diabetes Risk Score (IDRS) [28], and Indonesian Undiagnosed Diabetes Mellitus (UDDM) scoring system [29]. Both the ADA and CANRISK tools have demonstrated efficacy in identifying individuals at risk within their respective communities; nevertheless, these products were specifically created to cater to the diverse populations residing in the United States and Canada, respectively. The validation of the IDRS took place in a low- to middle-income country. The IDRS is a valuable screening tool specifically for the mono-ethnic Indian population [28]. The scoring system originated in Indonesia. However, its accuracy has not been assessed through prospective evaluation [29]. Most of the predictive indices are genetic, demographic characteristics, and clinical parameters. With the intensive study of the pathogenesis of diabetes, many studies have begun to identify the genetic associations associated with the onset of diabetes. These studies not only reveal the genetic basis of diabetes but also provide new perspectives for understanding its pathogenesis. For example, recent genome-wide association studies identified multiple genetic variants associated with type 2 diabetes that may affect insulin secretion and islet β-cell function [30]. Furthermore, studies show that certain genetic variants are strongly associated with the age of onset of diabetes, and younger patients with the onset of diabetes often face a higher risk of cardiovascular disease and all-cause mortality [31]. The effects of genetic variation also vary in different populations. For example, studies in East Asian populations found that certain genetic variants associated with type 2 diabetes mellitus showed different effects in this population, underscoring the importance of genetic studies in different ethnic groups [32]. Moreover, studies targeting monogenic diabetes have also revealed genetic mechanisms associated with autoimmunity that may play an important role in polygenic diabetes [33]. It is very important to consider incorporating genes into predictors in future studies.

XSL•FO
RenderX

Moreover, most tools are based on the general population in defined regions and may not be generalizable to populations from different regions [34,35]. Currently, there is still a lack of widely used diabetes risk tools for the Japanese population [36]. The participants in this study were selected from a longitudinal cohort study that specifically targeted those undergoing health check-ups. This study commenced in 1994 and involved the continuous recruitment of individuals who underwent health examinations at Murakami Memorial Hospital. Thus, the study population typically included Japanese or Eastern Asian populations. The genetic constitution and lifestyle of Asian populations are different from those of European or American populations. Thus, the FHTHWA index might be suitable for the Japanese general population and other East Asian populations.

Insulin resistance (IR) is a medical condition characterized by reduced cellular responsiveness to insulin, independent of hyperinsulinemia [37]. IR serves as the primary pathophysiological mechanism underlying the developing type 2 diabetes mellitus, and it has the potential to manifest in individuals up to 2 decades prior to the diagnosis [38]. IR serves as a pivotal indicator of the imminent onset of diabetes. Evidence indicates that visceral adiposity indexes, such as BMI and WC, possess the capacity to effectively detect IR [39,40]. Moreover, evidence supports the effectiveness of classic lipid indices, including TC, TG, HDL-C, and LDL-C, in diagnosing IR [41,42]. However, the predictive capacities of these factors are limited [8]. Recently, the TyG index and TG/HDL-C have been recommended as diabetes risk indicators, both of which have better performance than traditional indicators (BMI, WC, TC, TG, HDL-C, and LDL-C) [43,44]. In this study, we performed a comparison of AUC values by time-dependent ROC analyses between the FHTHWA index, TyG index, TG/HDL-C, and METS-IR. It was found that the FHTHWA index had high accuracy, with the AUC value greater than 0.9 during the more than 12 years of follow-up. However, the AUC values of the TyG index, TG/HDL-C, and METS-IR mostly ranged from 0.7 to 0.8. Thus, the novel index has a higher prediction accuracy than the traditional parameters.

Study Strengths

This study's primary strengths include the large sample size of 15464 individuals ranging from 18 - 79 years of age, who underwent thorough examination and were subsequently monitored over an extended duration of up to 13 years. This sample was representative of the entire nation, enabling the findings to be extrapolated to the broader Japanese or East Asian populations.

Study Limitations

The present study has certain limitations. First, the primary focus of this study was the onset of diabetes as the outcome of interest. Nevertheless, it is important to acknowledge that the diagnostic criteria utilized in this investigation did not include the participants' 2-hour postprandial blood glucose level. This has the potential to result in an underestimation of the incidence of diabetes. Second, due to the utilization of the NAGALA database, it was impossible to eliminate self-reported characteristics, resulting in a potential reporting bias. Consequently, the findings of this study can only be generalized to the Japanese or East Asian population. It is crucial to determine the degree to which these findings can be extrapolated to heterogeneous populations. Third, it is important to note that the primary outcome measure of this study is the occurrence of new-onset diabetes events. However, it is noteworthy to emphasize that the dataset utilized in this study does not include information on death events that may have occurred during the follow-up period. This limitation introduces a potential competing risk that could impact the findings of the current research.

Conclusion

The research has successfully developed the FHTHWA index, which demonstrates a high degree of accuracy in predicting the future risk of diabetes within the Japanese population without diabetes. This index is particularly valuable for clinical practitioners in Japan, as it is recommended for regular use in assessing the risk of diabetes and monitoring therapeutic progress among the Japanese population.

Acknowledgments

We would like to thank Prof. Okamura Takuro and his team at Kyoto Prefectural University of Medicine for sharing their data. This study was supported by grants from the Jiangxi Provincial Key R&D Plan (no. 20201BBG71006), the Natural Science Foundation of Jiangxi Province (no. 20224BAB216009), and Technology Plan of Jiangxi Health Planning Committee (no. 202210484).

Data Availability

All the data used in this study were obtained from the Dryad Digital Repository database (https://datadryad.org/stash/dataset/doi:10.5061/dryad.8q0p192).

Authors' Contributions

Conceptualization: WJ
Writing – original draft: WJ
Writing – review & editing: JC, YL, JX

XSL•FO
RenderX

Multimedia Appendix 1
Supplementary files.
[DOCX File, 148 KB - medinform_v13i1e64992_app1.docx]

References

1. Fang M, Selvin E. Cost-related insulin rationing in US adults younger than 65 years with diabetes. JAMA 2023 May 16;329(19):1700-1702. [doi: 10.1001/jama.2023.5747] [Medline: 36988971]
2. Weinstock RS, Trief PM, Burke BK, et al. Antihypertensive and lipid-lowering medication adherence in young adults with youth-onset type 2 diabetes. JAMA Netw Open 2023 Oct 2;6(10):e2336964. [doi: 10.1001/jamanetworkopen.2023.36964] [Medline: 37792373]
3. Cho NH, Shaw JE, Karuranga S, et al. IDF diabetes atlas: global estimates of diabetes prevalence for 2017 and projections for 2045. Diabetes Res Clin Pract 2018 Apr;138:271-281. [doi: 10.1016/j.diabres.2018.02.023] [Medline: 29496507]
4. Cioana M, Deng J, Nadarajah A, et al. Global prevalence of diabetic retinopathy in pediatric type 2 diabetes: a systematic review and meta-analysis. JAMA Netw Open 2023 Mar 1;6(3):e231887. [doi: 10.1001/jamanetworkopen.2023.1887] [Medline: 36930156]
5. Huckfeldt PJ, Yu JC, O'Leary PK, et al. Association of intensive lifestyle intervention for type 2 diabetes with labor market outcomes. JAMA Intern Med 2023 Oct 1;183(10):1071-1079. [doi: 10.1001/jamainternmed.2023.3283] [Medline: 37578773]
6. Ostrominski JW, Arnold SV, Butler J, et al. Prevalence and overlap of cardiac, renal, and metabolic conditions in US adults, 1999-2020. JAMA Cardiol 2023 Nov 1;8(11):1050-1060. [doi: 10.1001/jamacardio.2023.3241] [Medline: 37755728]
7. Kuang M, Yang R, Huang X, et al. Assessing temporal differences in the predictive power of baseline TyG-related parameters for future diabetes: an analysis using time-dependent receiver operating characteristics. J Transl Med 2023 May 4;21(1):299. [doi: 10.1186/s12967-023-04159-7] [Medline: 37138277]
8. Sheng G, Kuang M, Yang R, Zhong Y, Zhang S, Zou Y. Evaluation of the value of conventional and unconventional lipid parameters for predicting the risk of diabetes in a non-diabetic population. J Transl Med 2022 Jun 11;20(1):266. [doi: 10.1186/s12967-022-03470-z] [Medline: 35690771]
9. White J, Swerdlow DI, Preiss D, et al. Association of lipid fractions with risks for coronary artery disease and diabetes. JAMA Cardiol 2016 Sep 1;1(6):692-699. [doi: 10.1001/jamacardio.2016.1884] [Medline: 27487401]
10. Xiong XL, Zhang RX, Bi Y, Zhou WH, Yu Y, Zhu DL. Machine learning models in type 2 diabetes risk prediction: results from a cross-sectional retrospective study in Chinese adults. Curr Med Sci 2019 Aug;39(4):582-588. [doi: 10.1007/s11596-019-2077-4] [Medline: 31346994]
11. Cahn A, Shoshan A, Sagiv T, et al. Prediction of progression from pre-diabetes to diabetes: development and validation of a machine learning model. Diabetes Metab Res Rev 2020 Feb;36(2):e3252. [doi: 10.1002/dmrr.3252] [Medline: 31943669]
12. Boutilier JJ, Chan TCY, Ranjan M, Deo S. Risk stratification for early detection of diabetes and hypertension in resource-limited settings: machine learning analysis. J Med Internet Res 2021 Jan 21;23(1):e20123. [doi: 10.2196/20123] [Medline: 33475518]
13. Goel M, Sharma A, Chilwal AS, Kumari S, Kumar A, Bagler G. Machine learning models to predict sweetness of molecules. Comput Biol Med 2023 Jan;152:106441. [doi: 10.1016/j.compbiomed.2022.106441] [Medline: 36543004]
14. Yang H, Luo Y, Ren X, et al. Risk prediction of diabetes: big data mining with fusion of multifarious physical examination indicators. Inf Fus 2021 Nov;75:140-149. [doi: 10.1016/j.inffus.2021.02.015] [Medline: 33658909]
15. Lindström J, Tuomilehto J. The diabetes risk score: a practical tool to predict type 2 diabetes risk. Diabetes Care 2003 Mar;26(3):725-731. [doi: 10.2337/diacare.26.3.725] [Medline: 12610029]
16. Bang H, Edwards AM, Bomback AS, et al. Development and validation of a patient self-assessment score for diabetes risk. Ann Intern Med 2009 Dec 1;151(11):775-783. [doi: 10.7326/0003-4819-151-11-200912010-00005] [Medline: 19949143]
17. Okamura T, Hashimoto Y, Hamaguchi M, Obora A, Kojima T, Fukui M. Ectopic fat obesity presents the greatest risk for incident type 2 diabetes: a population-based longitudinal study. Int J Obes 2019 Jan;43(1):139-148. [doi: 10.1038/s41366-018-0076-3]
18. Takuro O, Yoshitaka H, Masahide H, Akihiro O, Takao K, Michiaki F. Dryad. Data from: ectopic fat obesity presents the greatest risk for incident type 2 diabetes: a population-based longitudinal study. 2019. URL: https://doi.org/10.5061/dryad.8q0p192 [accessed 2024-12-16]
19. Hashimoto Y, Hamaguchi M, Kojima T, et al. The modest alcohol consumption reduces the incidence of fatty liver in men: a population ‐ based large ‐ scale cohort study. J of Gastro and Hepatol 2015 Mar;30(3):546-552 [FREE Full text] [doi: 10.1111/jgh.12786]
20. Lee SB, Kim MK, Kang S, et al. Triglyceride glucose index is superior to the homeostasis model assessment of insulin resistance for predicting nonalcoholic fatty liver disease in Korean adults. Endocrinol Metab (Seoul) 2019 Jun;34(2):179-186. [doi: 10.3803/EnM.2019.34.2.179] [Medline: 31257745]
21. Khaloo P, Hasheminia M, Tohidi M, et al. Impact of 3-year changes in lipid parameters and their ratios on incident type 2 diabetes: Tehran lipid and glucose study. Nutr Metab (Lond) 2018;15(1):50. [doi: 10.1186/s12986-018-0287-6] [Medline: 30008790]

XSL•FO
RenderX

22. Bello-Chavolla OY, Almeda-Valdes P, Gomez-Velasco D, et al. METS-IR, a novel score to evaluate insulin sensitivity, is predictive of visceral adiposity and incident type 2 diabetes. Eur J Endocrinol 2018 May;178(5):533-544. [doi: 10.1530/EJE-17-0883] [Medline: 29535168]
23. Hamaguchi M, Kojima T, Itoh Y, et al. The severity of ultrasonographic findings in nonalcoholic fatty liver disease reflects the metabolic syndrome and visceral fat accumulation. Am J Gastroenterol 2007 Dec;102(12):2708-2715. [doi: 10.1111/j.1572-0241.2007.01526.x] [Medline: 17894848]
24. Chan JCN, Malik V, Jia W, et al. Diabetes in Asia: epidemiology, risk factors, and pathophysiology. JAMA 2009 May 27;301(20):2129-2140. [doi: 10.1001/jama.2009.726] [Medline: 19470990]
25. Nathan DM. Diabetes: advances in diagnosis and treatment. JAMA 2015 Sep 8;314(10):1052-1062. [doi: 10.1001/jama.2015.9536] [Medline: 26348754]
26. US Preventive Services Task Force, Mangione CM, Barry MJ, et al. Screening for prediabetes and type 2 diabetes in children and adolescents: US preventive services task force recommendation statement. JAMA 2022 Sep 13;328(10):963-967. [doi: 10.1001/jama.2022.14543] [Medline: 36098719]
27. Robinson CA, Agarwal G, Nerenberg K. Validating the CANRISK prognostic model for assessing diabetes risk in Canada's multi-ethnic population. Chronic Dis Inj Can 2011 Dec;32(1):19-31. [Medline: 22153173]
28. Mohan V, Deepa R, Deepa M, Somannavar S, Datta M. A simplified Indian diabetes risk score for screening for undiagnosed diabetic subjects. J Assoc Physicians India 2005 Sep;53:759-763. [Medline: 16334618]
29. Pramono LA, Setiati S, Soewondo P, et al. Prevalence and predictors of undiagnosed diabetes mellitus in Indonesia. Acta Med Indones 2010 Oct;42(4):216-223. [Medline: 21063043]
30. Schäfer SA, Machicao F, Fritsche A, Häring HU, Kantartzis K. New type 2 diabetes risk genes provide new insights in insulin secretion mechanisms. Diabetes Res Clin Pract 2011 Aug;93 Suppl 1:S9-24. [doi: 10.1016/S0168-8227(11)70008-0] [Medline: 21864758]
31. Zhao M, Song L, Sun L, et al. Associations of type 2 diabetes onset age with cardiovascular disease and mortality: The Kailuan study. Diabetes Care 2021 Jun 1;44(6):1426-1432. [doi: 10.2337/dc20-2375] [Medline: 35239970]
32. Taurbekova B, Mukhtarova K, Salpynov Z, Almazan J, Atageldiyeva K, Sarria-Santamera A. Genome-wide association studies of diabetic kidney disease in East Asians with type 2 diabetes: achievements and future perspectives. Curr Med Chem 2024 Oct 31. [doi: 10.2174/0109298673328801241015165257] [Medline: 39484772]
33. Roizen JD, Bradfield JP, Hakonarson H. Progress in understanding type 1 diabetes through its genetic overlap with other autoimmune diseases. Curr Diab Rep 2015 Nov;15(11):102. [doi: 10.1007/s11892-015-0668-4] [Medline: 26454449]
34. Agarwal G, Guingona MM, Gaber J, Angeles R, Rao S, Cristobal F. Choosing the most appropriate existing type 2 diabetes risk assessment tool for use in the Philippines: a case-control study with an urban Filipino population. BMC Public Health 2019 Aug 27;19(1):1169. [doi: 10.1186/s12889-019-7402-0] [Medline: 31455247]
35. Tanamas SK, Magliano DJ, Balkau B, et al. The performance of diabetes risk prediction models in new populations: the role of ethnicity of the development cohort. Acta Diabetol 2015 Feb;52(1):91-101. [doi: 10.1007/s00592-014-0607-x] [Medline: 24996544]
36. Lotta LA, Abbasi A, Sharp SJ, et al. Definitions of metabolic health and risk of future type 2 diabetes in BMI categories: a systematic review and network meta-analysis. Diabetes Care 2015 Nov;38(11):2177-2187. [doi: 10.2337/dc15-1218] [Medline: 26494809]
37. Parks BW, Sallam T, Mehrabian M, et al. Genetic architecture of insulin resistance in the mouse. Cell Metab 2015 Feb 3;21(2):334-347. [doi: 10.1016/j.cmet.2015.01.002] [Medline: 25651185]
38. Hulman A, Simmons RK, Brunner EJ, et al. Trajectories of glycaemia, insulin sensitivity and insulin secretion in South Asian and white individuals before diagnosis of type 2 diabetes: a longitudinal analysis from the Whitehall II cohort study. Diabetologia 2017 Jul;60(7):1252-1260. [doi: 10.1007/s00125-017-4275-6] [Medline: 28409212]
39. Sanz CM, Ruidavets JB, Bongard V, et al. Relationship between markers of insulin resistance, markers of adiposity, HbA1c, and cognitive functions in a middle-aged population-based sample: the MONA LISA study. Diabetes Care 2013 Jun;36(6):1512-1521. [doi: 10.2337/dc12-1017] [Medline: 23275371]
40. Wolfgram PM, Connor EL, Rehm JL, et al. In nonobese girls, waist circumference as a predictor of insulin resistance is comparable to MRI fat measures and superior to BMI. Horm Res Paediatr 2015;84(4):258-265. [doi: 10.1159/000439130] [Medline: 26352642]
41. Boyer BB, Wiener HW, Hopkins SE, et al. Obesity-associated dyslipidemia is moderated by habitual intake of marine-derived n-3 polyunsaturated fatty acids in Yup'ik Alaska native people: a cross-sectional mediation-moderation analysis. J Nutr 2023 Jan;153(1):279-292. [doi: 10.1016/j.tjnut.2022.10.009] [Medline: 36913463]
42. Glass CK, Olefsky JM. Inflammation and lipid signaling in the etiology of insulin resistance. Cell Metab 2012 May 2;15(5):635-645. [doi: 10.1016/j.cmet.2012.04.001] [Medline: 22560216]
43. Muhammad IF, Bao X, Nilsson PM, Zaigham S. Triglyceride-glucose (TyG) index is A predictor of arterial stiffness, incidence of diabetes, cardiovascular disease, and all-cause and cardiovascular mortality: A longitudinal two-cohort analysis. Front Cardiovasc Med 2022;9:1035105. [doi: 10.3389/fcvm.2022.1035105] [Medline: 36684574]

XSL•FO
RenderX

44. Maturu A, DeWitt P, Kern PA, Rasouli N. The triglyceride to high-density lipoprotein cholesterol (TG/HDL-C) ratio as a predictor of β-cell function in African American women. Metab Clin Exp 2015 May;64(5):561-565. [doi: 10.1016/j.metabol.2015.01.004] [Medline: 25687124]

Abbreviations

ADA: American Diabetes Association
ALT: alanine aminotransferase
AST: aspartate aminotransferase
AUC: area under the curve
CANRISK: Canadian Diabetes Risk Score
DBP: diastolic blood pressure
FINDRISC: Finnish Diabetes Risk Score
FPG: fasting plasma glucose
GGT: gamma-glutamyl transferase
HDL-C: high-density lipoprotein cholesterol
IDF: International Diabetes Federation
IDRS: Indian diabetes risk score
IR: insulin resistance
LASSO: least absolute shrinkage and selection operator
LDL-C: low-density lipoprotein cholesterol
METS-IR: metabolic score for insulin resistance
NAGALA: NAfld [nonalcoholic fatty liver disease] in the Gifu Area, Longitudinal Analysis
NHANES: National Health and Nutrition Examination Survey
ROC: receiver operating characteristic
SBP: systolic blood pressure
TC: total cholesterol
TC/HDL-C: total cholesterol to high-density lipoprotein cholesterol ratio
TG: triglyceride
TG/HDL-C: triglyceride to high-density lipoprotein cholesterol ratio
TyG index: triglyceride-glucose index
UDDM: Indonesian Undiagnosed Diabetes Mellitus
WC: waist circumference

Edited by C Lovis; submitted 01.08.24; peer-reviewed by F Song, V Mohan; revised version received 14.11.24; accepted 17.11.24; published 28.01.25.

Please cite as:
Wang J, Chen J, Liu Y, Xu J
Use of the FHTHWA Index as a Novel Approach for Predicting the Incidence of Diabetes in a Japanese Population Without Diabetes: Data Analysis Study
JMIR Med Inform 2025;13:e64992
URL: https://medinform.jmir.org/2025/1/e64992
doi:10.2196/64992

© Jiao Wang, Jianrong Chen, Ying Liu, Jixiong Xu. Originally published in JMIR Medical Informatics (https://medinform.jmir.org), 28.1.2025. This is an open-access article distributed under the terms of the Creative Commons Attribution License (https://creativecommons.org/licenses/by/4.0/), which permits unrestricted use, distribution, and reproduction in any medium, provided the original work, first published in JMIR Medical Informatics, is properly cited. The complete bibliographic information, a link to the original publication on https://medinform.jmir.org/, as well as this copyright and license information must be included.

XSL•FO
RenderX

Leveraging GPT-4o for Automated Extraction and Categorization of CAD-RADS Features From Free-Text Coronary CT Angiography Reports: Diagnostic Study

Youmei Chen*, MS; Mengshi Dong*, MD; Jie Sun*, MS; Zhanao Meng, BS; Yiqing Yang, MS; Abudushalamu Muhetaier, MS; Chao Li, MD; Jie Qin, MD

Departments of Radiology, The Third Affiliated Hospital, Sun Yat-Sen University, 600 Tianhe Road, Guangzhou, Guangdong, China

*these authors contributed equally

Corresponding Author:
Jie Qin, MD
Departments of Radiology, The Third Affiliated Hospital, Sun Yat-Sen University, 600 Tianhe Road, Guangzhou, Guangdong, China

Abstract

Background: Despite the Coronary Artery Reporting and Data System (CAD-RADS) providing a standardized approach, radiologists continue to favor free-text reports. This preference creates significant challenges for data extraction and analysis in longitudinal studies, potentially limiting large-scale research and quality assessment initiatives.

Objective: To evaluate the ability of the generative pre-trained transformer (GPT)-4o model to convert real-world coronary computed tomography angiography (CCTA) free-text reports into structured data and automatically identify CAD-RADS categories and P categories.

Methods: This retrospective study analyzed CCTA reports from January 2024 and July 2024. A subset of 25 reports was used for prompt engineering to instruct the large language models (LLMs) in extracting CAD-RADS categories, P categories, and the presence of myocardial bridges and noncalcified plaques. Reports were processed using the GPT-4o API (application programming interface) and custom Python scripts. The ground truth was established by radiologists based on the CAD-RADS 2.0 guidelines. Model performance was assessed using accuracy, sensitivity, specificity, and F_1-score. Intrarater reliability was assessed using Cohen κ coefficient.

Results: Among 999 patients (median age 66 y, range 58 - 74; 650 males), CAD-RADS categorization showed accuracy of 0.98 - 1.00 (95% CI 0.9730 - 1.0000), sensitivity of 0.95 - 1.00 (95% CI 0.9191 - 1.0000), specificity of 0.98 - 1.00 (95% CI 0.9669 - 1.0000), and F_1-score of 0.96 - 1.00 (95% CI 0.9253 - 1.0000). P categories demonstrated accuracy of 0.97 - 1.00 (95% CI 0.9569 - 0.9990), sensitivity from 0.90 to 1.00 (95% CI 0.8085 - 1.0000), specificity from 0.97 to 1.00 (95% CI 0.9533 - 1.0000), and F_1-score from 0.91 to 0.99 (95% CI 0.8377 - 0.9967). Myocardial bridge detection achieved an accuracy of 0.98 (95% CI 0.9680 - 0.9870), and noncalcified coronary plaques detection showed an accuracy of 0.98 (95% CI 0.9680 - 0.9870). Cohen κ values for all classifications exceeded 0.98.

Conclusions: The GPT-4o model efficiently and accurately converts CCTA free-text reports into structured data, excelling in CAD-RADS classification, plaque burden assessment, and detection of myocardial bridges and calcified plaques.

(JMIR Med Inform 2025;13:e70967) doi:10.2196/70967

KEYWORDS

GPT-4o; radiology report; CAD-RADS; coronary computed tomography angiography (CCTA); free-text reports

Introduction

The Coronary Artery Reporting and Data System (CAD-RADS), developed with support from the American College of Radiology and the American College of Cardiology, provides a standardized imaging approach for the screening, diagnosis, and treatment evaluation of coronary artery disease. CAD-RADS has been widely adopted and has had a significant impact on coronary artery disease management [1-5]. Despite the standardized approach of CAD-RADS, radiologists continue to favor free-text reports in practice. These reports often vary in style and structure, which can result in the omission of critical clinical information. This inconsistency complicates data extraction for longitudinal studies on coronary artery disease [6,7]. The issue is further exacerbated by the rapid advancements in medical technology and the increasing volume of coronary computed tomography angiography (CCTA) exams. Hospitals are now overwhelmed with unstructured reports, and manual

XSL•FO
RenderX

data extraction is both time-consuming and prone to errors. Therefore, there is an urgent need for automated methods to process these reports and enhance the efficiency and accuracy of information extraction.

Traditionally, medical natural language processing (NLP) techniques have been used to extract structured data elements from medical records, particularly in the field of radiology reports [8,9]. For instance, to bridge the gap between unstructured coronary artery reports and structured data, studies have successfully used deep learning and NLP techniques to predict coronary CAD-RADS scores [10]. However, a key challenge of traditional NLP algorithms is the scarcity of high-quality annotated datasets and the high cost associated with acquiring new annotated data [11]. Even with meticulously labeled ground truth data, the relatively small size of the corpus often leads to poor model generalization or makes generalization assessments impossible. For decades, traditional artificial intelligence (AI) systems (both symbolic and neural networks) have lacked general knowledge and common-sense reasoning.

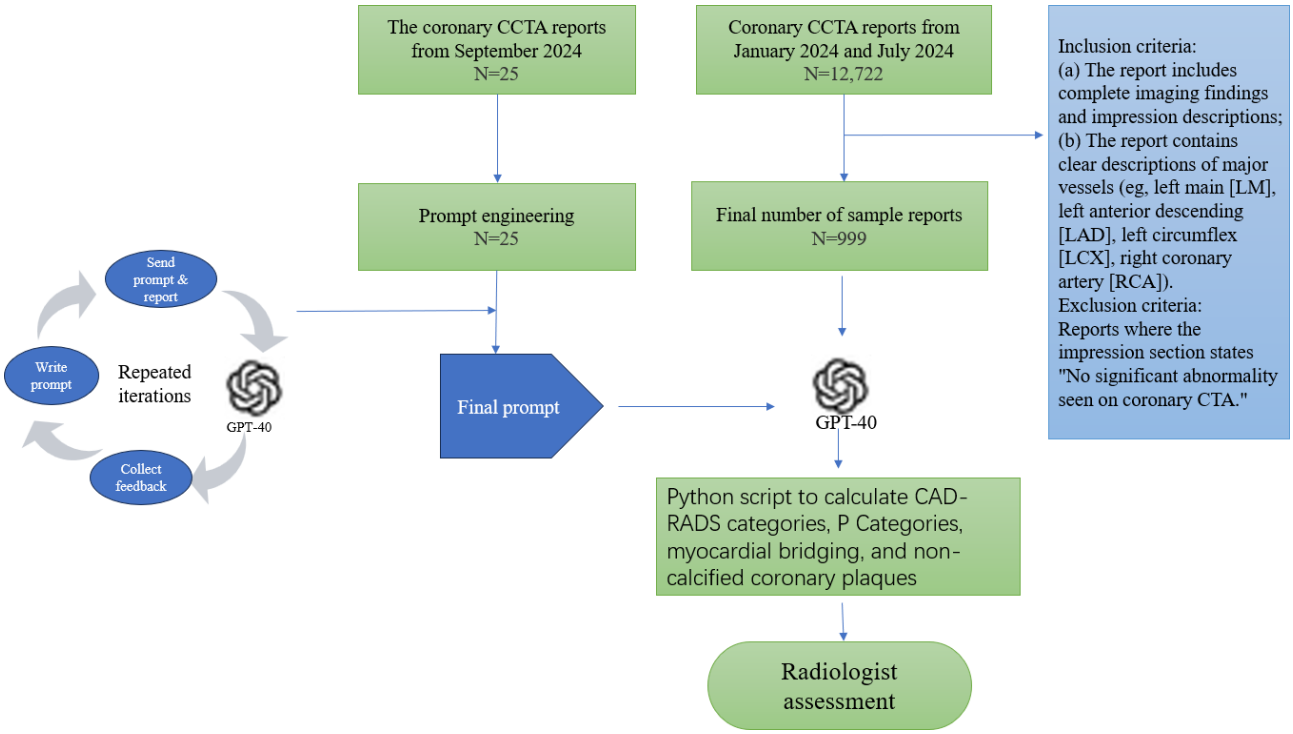
With the development of large language models (LLMs) [12,13], especially generative pre-trained transformer (GPT) models like ChatGPT, these models exhibit unique capabilities such as zero-shot and few-shot learning. Such abilities enable them to learn from prompt-based examples and perform diverse tasks [14-16]. As a result, LLMs show significant potential across multiple industries. In healthcare, LLMs, with their powerful NLP capabilities, have been used to facilitate communication between patients and clinicians [17]. In the past year, there has been a surge in the exploration of LLMs in the field of radiology reports, which has garnered increasing attention. Research has shown that LLMs can assist radiologists in tasks such as diagnosis, generating radiology reports, data extraction, error detection, incidental findings, classifying reports and data systems for various diseases, and converting unstructured free-text reports into structured formats [18-23]. Some studies have also demonstrated that LLMs excel at extracting realistic, complex, and multilingual clinical information from radiology reports, such as LI-RADS features [22,24]. However, current studies mostly rely on web-based reports and texts, with small sample sizes. Prompt engineering often involves manually created virtual reports. As a result, research on how to leverage LLMs to automatically extract structured data from vast, real-world unstructured reports and build high-quality radiology medical databases remains scarce.

This study aims to evaluate the ability of the GPT-4o model to convert real-world free-text CCTA reports into structured data and automatically identify CAD-RADS categories and Plaque Burden categories (P categories). We hypothesize that the GPT-4o model, when applied through a systematic prompt engineering approach, will demonstrate robust performance in extracting and categorizing data from CCTA reports with accuracy comparable to human experts.

Methods

The overall study workflow is shown in Figure 1. The reports used for prompt engineering and the study cohort are authentic radiological reports with all sensitive information removed. This retrospective study was approved by the ethics committee of the Third Affiliated Hospital of Sun Yat-sen University (2023-042-01). All source code used in this study is publicly available in GitHub [25].

Figure 1. Research design flowchart. CAD-RADS: Coronary Artery Reporting and Data System; CCTA: coronary computed tomography angiography.



XSL•FO
RenderX

LLM Selection

The GPT-4o model used in this study is based on the GPT-4o model released by OpenAI in May 2024 and is implemented through official API interface calls. This model is based on general domain pre-training and does not undergo institution-specific fine-tuning. The "o" in "GPT-4o" stands for "omni," a step towards more natural human-computer interaction. It accepts any combination of text, audio, images, and video as input and generates any combination of text, audio, and image output. Compared with previous LLMs such as GPT-4, it has significant improvements on text in non-English languages and is also faster in the API and 50% cheaper. Compared with existing models, GPT-4o is particularly good at visual and auditory understanding.

Study Sample

Reports from CCTA examinations conducted between January 2024 and July 2024 were retrieved from the Picture Archiving and Communication System (PACS) database of the Third Affiliated Hospital of Sun Yat-sen University. A total of 12,722 CCTA reports from this period were initially included. All reports were written by committee-certified radiologists and were in Chinese. Inclusion criteria were as follows: (1) reports containing complete imaging findings and impression descriptions, and (2) clear descriptions of major coronary vessels such as the left main, left anterior descending, left circumflex (LCX), and right coronary artery. Exclusion criteria involved reports where the impression stated, "no significant abnormalities detected in coronary CTA." After applying the inclusion and exclusion criteria, 999 reports remained for analysis (sample 1). In addition, 25 CCTA reports from September 2024 (sample 2) were included for prompt engineering.

Data Processing

The selected reports were exported to an Excel spreadsheet (Microsoft), and the author, YC, evaluated these reports, removing sensitive information such as registration numbers and names while retaining relevant details such as gender, age, imaging findings, impression descriptions, and examination dates. Except for minor typographical errors, no changes were made to the content of the reports.

Creation of the Ground Truth

The ground truth labels for each report were established by a radiologist (YC with 3 y of experience) who evaluated all reports according to the CAD-RADS (version 2.0) guidelines [1] published in 2022, with data manually extracted into CSV format. The labeling process incorporated CAD-RADS categories, P categories, as well as the identification of myocardial bridging and noncalcified coronary plaques. In instances where YC encountered challenges in labeling, expert consultations were sought from JQ, who possesses 24 years of professional experience. To assess intrarater reliability, 200 reports were randomly selected and re-evaluated after a 15-day washout period, with agreement measured using Cohen κ coefficient.

Prompt Engineering

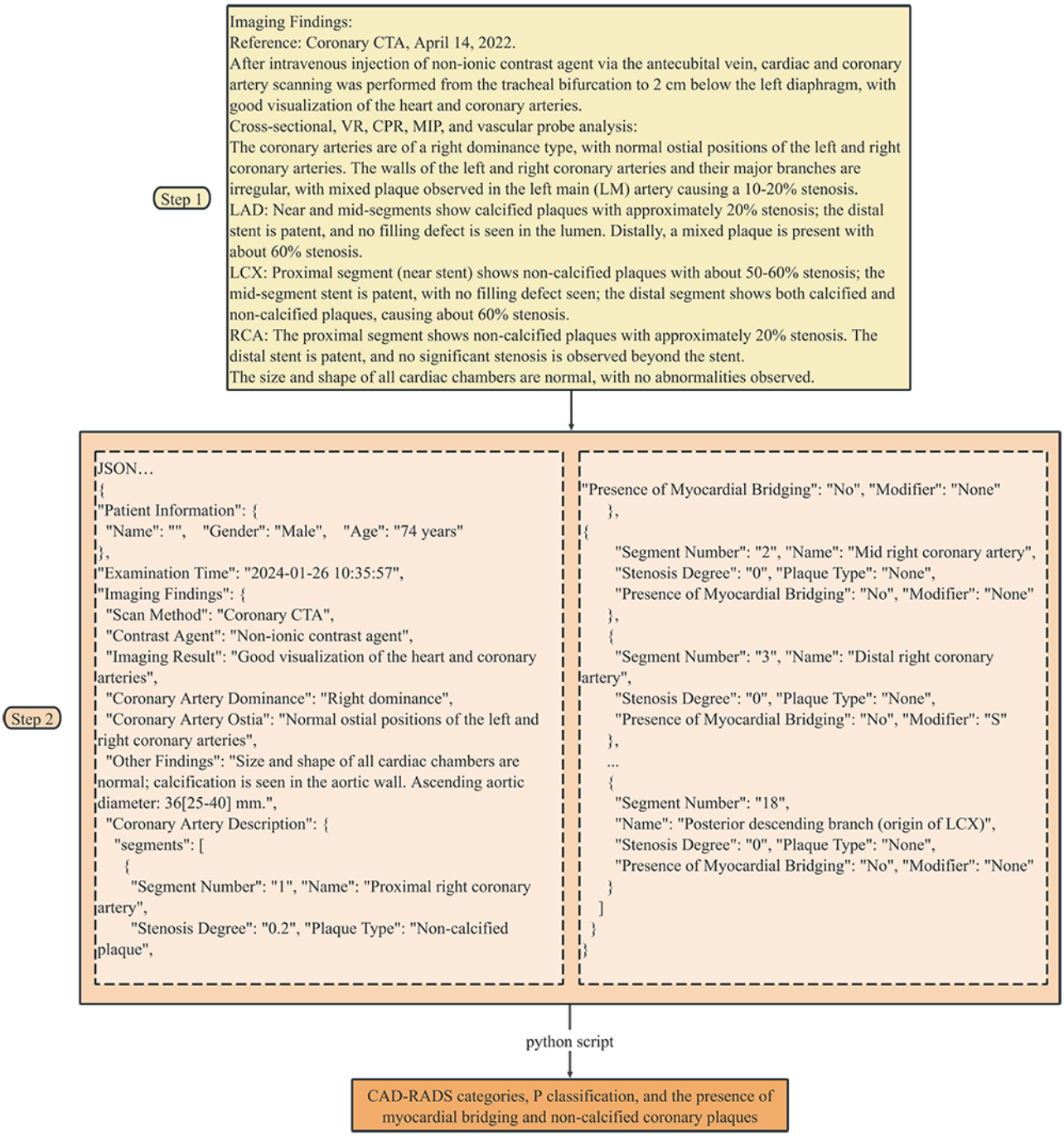
The creation of prompts strictly follows the CAD-RADS 2.0 guidelines and the 18-segment coronary artery method, aiming to extract coronary artery disease-related data through simplified steps. The task of GPT-4o is to convert the free-text CCTA report into a structured format and output the data in JSON format. The initial prompt used simple instructions, such as: "Please construct the following coronary artery CTA report and output it in JSON format." Sample 2 was used for prompt engineering, and corresponding feedback was collected. When it was found that the model output was not good or errors occurred, the instructions were modified again, such as "Please read the following report carefully, summarize it according to the CAD-RADS 2.0 guidelines, and output it in a structured form, in JSON format." The prompt was optimized through multiple iterations until the model output the best results, and the final prompt was obtained and no longer changed. The final prompt consisted of a single step: generating structured data in JSON format based on the original report, containing the current examination date, examination technique, coronary origin, dominant vessel, and key features of each coronary artery (such as stenosis degree, plaque type, presence of myocardial bridges, presence of stents, etc.). The Chinese version of the prompt is provided in Multimedia Appendix 1. GPT-4o was instructed to generate a CSV file with process details for each report.

Batch Feature Extraction and Classification

The final prompt was used to process the reports from the study cohort (Sample 1). A Python script containing the final prompt was written for batch processing of all reports. This script interacted with the GPT-4o API, sending prompts to the model one by one, with the model automatically processing the reports and converting them into CSV tables with relevant details. The characteristics of myocardial bridging and noncalcified coronary plaques were directly extracted from the model's responses, while the CAD-RADS and P categories were programmatically determined using custom Python functions based on the CAD-RADS and P categories algorithms. An example of a report and its downstream processing is depicted in Figure 2.

XSL•FO
RenderX

Figure 2. A representative example showing how GPT-4o processes and structures a coronary computed tomography angiography radiology report. The system uses a specialized prompt to transform the free-text report into a standardized JSON format, comprising 18 distinct sections (sections 1 - 18, with intermediate sections abbreviated for brevity). The structured output is subsequently analyzed by a Python script to identify the Coronary Artery Reporting and Data System categories, P categories, myocardial bridge, and noncalcified plaque.



The detailed calculation process of CAD-RADS and P categories algorithms can be viewed in GitHub [25].

Error Analysis

YC conducted a review of cases with errors in the extraction of key features, specifically the CAD-RADS category and P categories. The original report, the outputs from the structured reporting process, and the final results computed using Python were jointly examined to identify the source of the errors.

Model Performance Evaluation

The accuracy, specificity, sensitivity, and F_1-score are used to evaluate the performance of the model in extracting and classifying the 4 features. The formula is as follows:

Accuracy=TP+TNTP+TN+FP+FN

Sensitivity=TPTP+FN

Specificity=TNTN+FP

F1=2×Precision×SensitivityPrecision+Sensitivity,Precision=TPTP+FP

XSL•FO
RenderX

Statistical Analysis

In this study, baseline characteristics of the sample were described using the median and interquartile range (Q1, Q3) for continuous variables (eg, age) and frequency (n) and percentage (%) for categorical variables (eg, gender, CAD-RADS categories, P categories, and the presence of myocardial bridging and noncalcified coronary plaques). Intrarater agreement was assessed using Cohen κ statistics.

For the model-extracted features (eg, presence of myocardial bridges) and the CAD-RADS 0 - 5 classification and P 0 - 4 Categories, accuracy, specificity, sensitivity, and F_1-score were calculated. According to the CAD-RADS 2.0 guidelines, CAD-RADS 0 indicates the absence of plaque or stenosis, and P0 is not included in the Categories. However, to evaluate the performance of the LLM in patients without plaque or stenosis, patients without plaque or stenosis were treated as P0 level in the statistical analysis.

This study was conducted using Python (version 3.8.16) as the primary programming environment and the OpenAI API (version 1.33.0) for LLM interactions. The temperature parameter mainly affects the diversity and randomness of the output of the LLM. Generally speaking, the higher the temperature, the greater the diversity and randomness of the model output, and the more unpredictable the results. To minimize model variability and ensure reproducibility, the temperature parameter was consistently set to 1E-10 across all model configurations [26,27]. Statistical analyses were performed using Python's scikit-learn library (version 1.3.2) and SPSS statistical software (version 27; IBM Corporation).

Results

Study Sample

Figure 1 shows the inclusion and exclusion process for patients, while Table 1 summarizes the baseline characteristics of patients based on CAD-RADS categories and Plaque Burden categories (P categories), among other features. Initially, 12,722 coronary CTA free-text reports were screened, with 8465 reports excluded due to "no significant abnormality detected in coronary CTA," as these patients showed no obvious coronary artery disease. An additional 3258 reports were excluded due to missing comprehensive imaging results, insufficient descriptions of findings, and the absence of clear identification of the major coronary arteries. Ultimately, 999 reports were included for analysis (median age 66 y; age range 57 - 73, of whom 650 were male). All reports were successfully processed into structured data using GPT-4o, and the corresponding CAD-RADS and P categories were generated for each report.

Table . Characteristics of included patients. Unless otherwise indicated, data are numerators and data in parentheses are percentages.

Characteristics	Patients (N=999)
Gender, n (%)	
Male	650 (65.1)
Female	349 (34.9)
Age (years), median (IQR)	66 (57 - 73)
CAD-RADS[a] categories, n (%)	
0	64 (6.4)
1	236 (23.6)
2	231 (23.1)
3	224 (22.4)
4a	197 (19.7)
4b	39 (3.9)
5	8 (0.8)
Plaque Burden categories, n (%)	
0	64 (6.4)
1	310 (31.0)
2	282 (28.2)
3	294 (29.4)
4	49 (4.9)
Myocardial bridge, n (%)	438 (43.8)
Noncalcified coronary plaques, n (%)	561 (54.8)

[a]CAD-RADS: Coronary Artery Reporting and Data System.

XSL•FO
RenderX

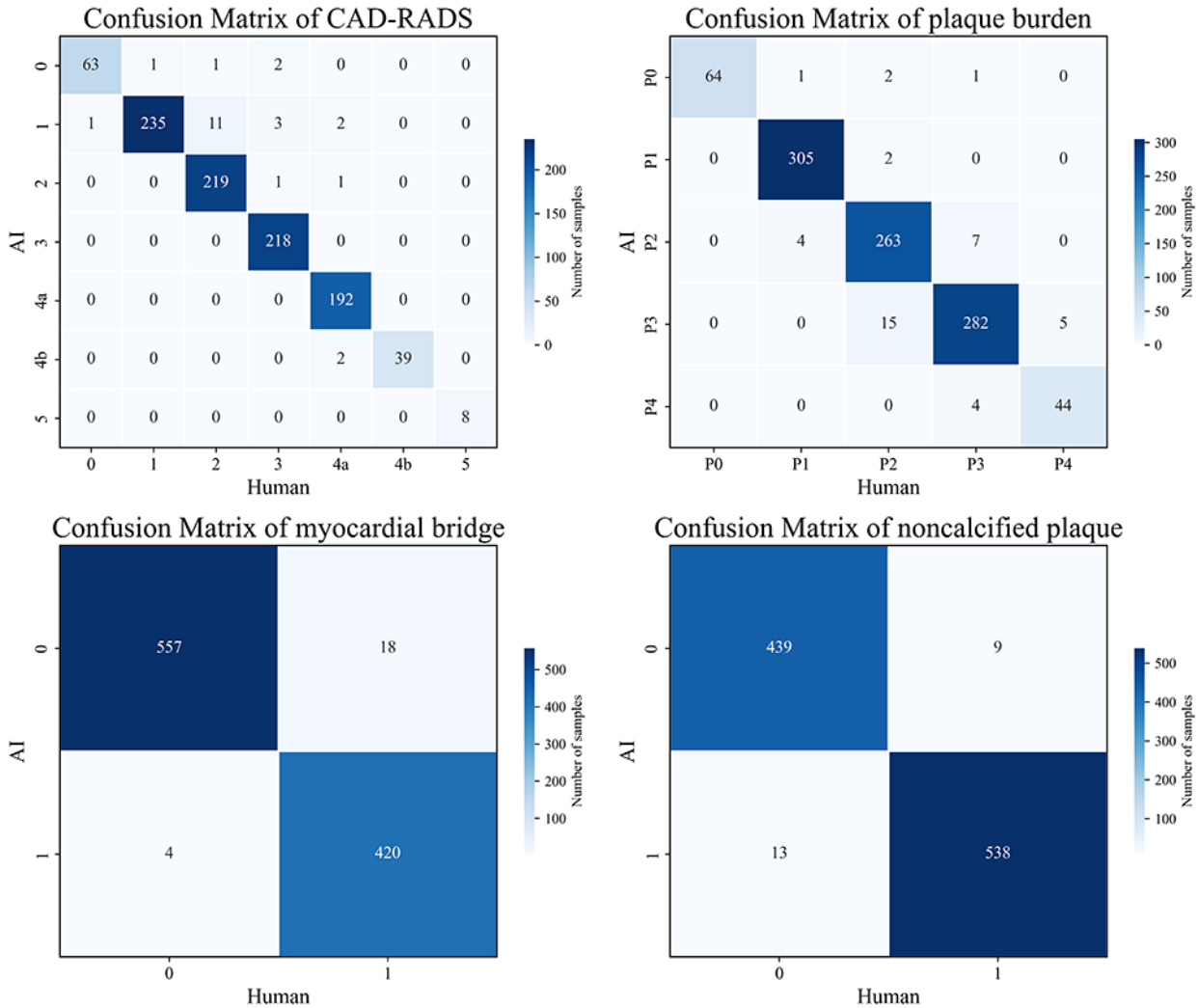
Intrarater Reliability

The κ values were 0.99 for CAD-RADS categories, 0.98 for P categories, 0.99 for myocardial bridging, and 0.98 for noncalcified plaque, indicating excellent intrarater reliability.

Model Performance Evaluation

The confusion matrix for each CAD-RADS category, P categories, and related features from the study cohort is shown in Figure 3. The X-axis represents the number calculated by human doctors (gold standard), and the Y-axis represents the number predicted by GPT-4o. Table 2 lists the accuracy, specificity, sensitivity, and F_1-score for each feature. For CAD-RADS classification (from class 0 to 5), the accuracy ranged from 0.98 to 1.00 (0.9730 - 1.0000), sensitivity from 0.95 to 1.00 (0.9191 - 1.0000), specificity from 0.98 to 1.00 (0.9669 - 1.0000), and F_1-score from 0.96 to 1.00 (95% CI 0.9253 - 1.0000). For Plaque Burden P categories (P0 to P4), the accuracy ranged from 0.97 to 1.00 (95% CI 0.9569 - 0.9990), sensitivity from 0.90 to 1.00 (95% CI 0.8085 - 1.0000), specificity from 0.97 to 1.00 (95% CI 0.9533 - 1.0000), and F_1-score from 0.91 to 0.99 (95% CI 0.8377 - 0.9967). For the presence of myocardial bridges in the coronary arteries, the accuracy was 0.98 (95% CI 0.9680 - 0.9870), sensitivity 0.96 (95% CI 0.9376 - 0.9764), specificity 0.99 (95% CI 0.9852 - 0.9983), and F_1-score 0.97 (95% CI 0.9630 - 0.9844). For the presence of noncalcified coronary plaques, the accuracy was 0.98 (95% CI 0.9680 - 0.9870), sensitivity 0.98 (95% CI 0.9710 - 0.9929), specificity 0.97 (95% CI 0.9533 - 0.9862), and F_1-score of 0.98 (95% CI 0.9709 - 0.9880). See details in Figures 4 and 5.

Figure 3. Confusion matrix of GPT-4o performance in Coronary Artery Reporting and Data System (CAD-RADS) categories and Plaque Burden categories. The confusion matrix can intuitively show the number of correct or incorrect model outputs. For example, in CAD-RADS 3 categories, the model has 218 correct answers and 6 incorrect answers.



XSL•FO
RenderX

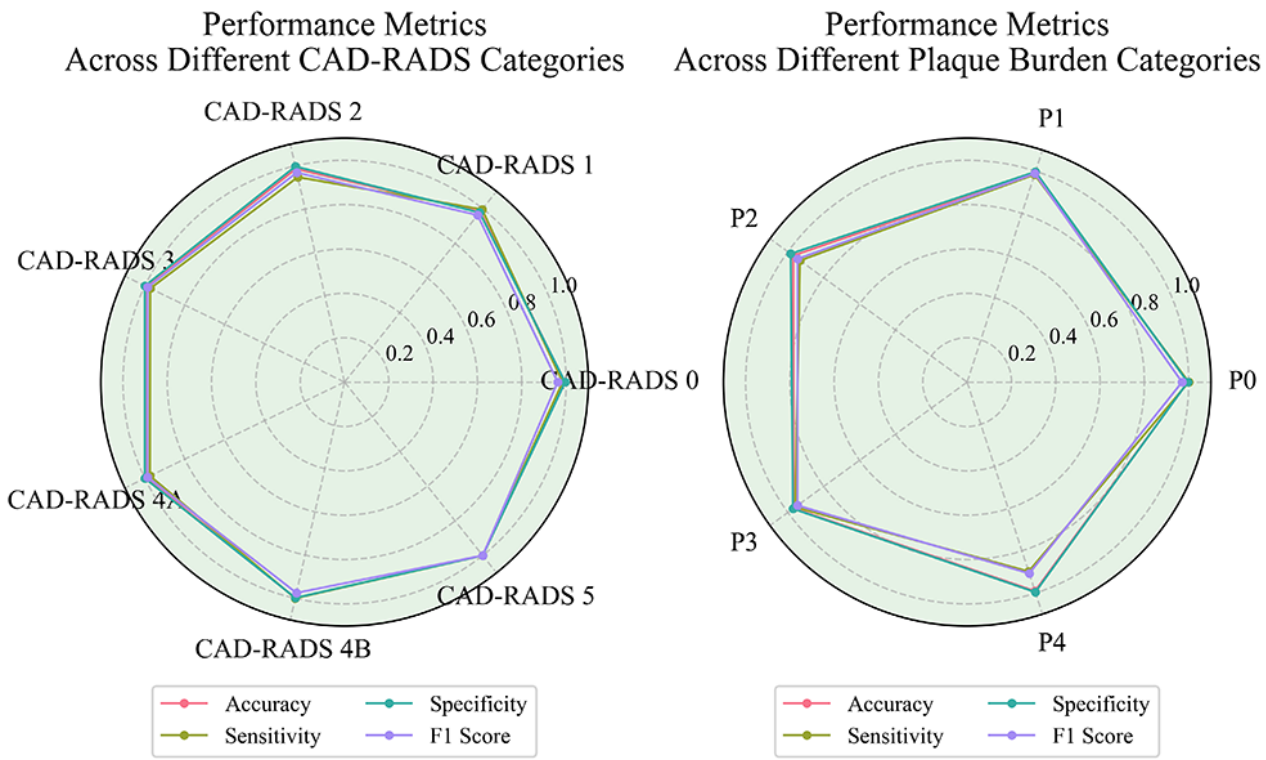
Table . Performance metrics of GPT-4o in coronary CT[a] angiography analysis.

Classifications	Accuracy (95% CI)	Sensitivity (95% CI)	Specificity (95% CI)	F_1-score (95% CI)
CAD-RADS[b] categories				
0	0.99 (0.9900 - 0.9990)	0.98 (0.9492 - 1.0000)	1.00 (0.9914 - 0.9989)	0.96 (0.9253 - 0.9916)
1	0.98 (0.9730 - 0.9900)	1.00 (0.9864 - 1.0000)	0.98 (0.9669 - 0.9881)	0.96 (0.9450 - 0.9799)
2	0.99 (0.9790 - 0.9930)	0.95 (0.9191 - 0.9750)	1.00 (0.9934 - 1.0000)	0.97 (0.9530 - 0.9845)
3	0.99 (0.9890 - 0.9980)	0.97 (0.9507 - 0.9912)	1.00 (1.0000 - 1.0000)	0.99 (0.9747 - 0.9956)
4a	0.99 (0.9900 - 0.9990)	0.97 (0.9511 - 0.9949)	1.00 (1.0000 - 1.0000)	0.99 (0.9749 - 0.9975)
4b	1.00 (0.9950 - 1.0000)	1.00 (1.0000 - 1.0000)	1.00 (0.9948 - 1.0000)	0.97 (0.9315 - 1.0000)
5	1.00 (1.0000 - 1.0000)	1.00 (1.0000 - 1.0000)	1.00 (1.0000 - 1.0000)	1.00 (1.0000 - 1.0000)
Plaque Burden categories				
0	1.00 (0.9920 - 0.9990)	1.00 (1.0000 - 1.0000)	1.00 (0.9914 - 0.9989)	0.97 (0.9362 - 0.9935)
1	0.99 (0.9870 - 0.9980)	0.98 (0.9685 - 0.9968)	1.00 (0.9927 - 1.0000)	0.99 (0.9795 - 0.9967)
2	0.97 (0.9589 - 0.9800)	0.93 (0.8985 - 0.9609)	0.98 (0.9754 - 0.9932)	0.95 (0.9247 - 0.9641)
3	0.97 (0.9569 - 0.9790)	0.96 (0.9356 - 0.9807)	0.97 (0.9576 - 0.9831)	0.95 (0.9272 - 0.9645)
4	0.99 (0.9840 - 0.9970)	0.90 (0.8085 - 0.9778)	1.00 (0.9916 - 0.9990)	0.91 (0.8377 - 0.9636)
Myocardial bridge	0.98 (0.9680 - 0.9870)	0.96 (0.9376 - 0.9764)	0.99 (0.9852 - 0.9983)	0.99 (0.9630 - 0.9844)
Noncalcified plaque	0.98 (0.9680 - 0.9870)	0.98 (0.9710 - 0.9929)	0.97 (0.9533 - 0.9862)	0.98 (0.9709 - 0.9880)

[a]CT: computed tomography.

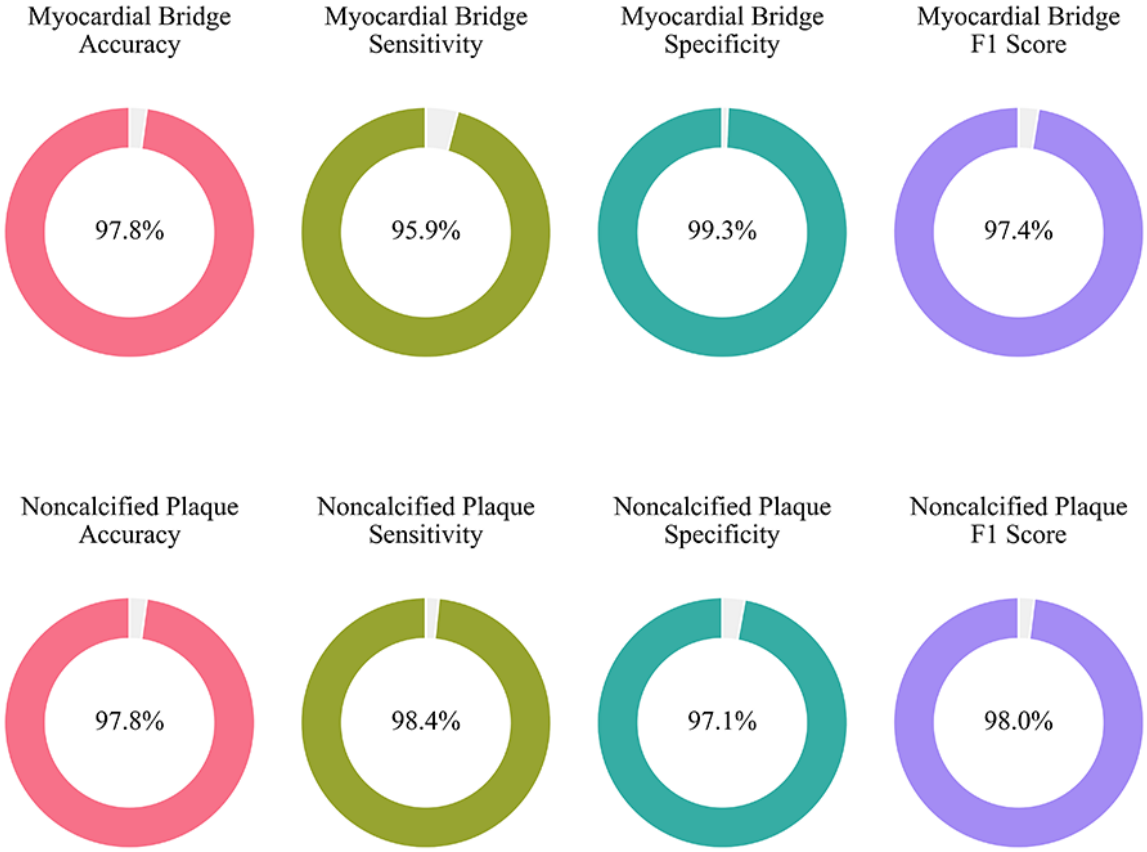
[b]CAD-RADS: Coronary Artery Disease-Reporting and Data System.

Figure 4. Performance metrics of generative pre-trained transformer (GPT)-4o in identifying Coronary Artery Reporting and Data System (CAD-RADS) categories and Plaque Burden categories (P categories). The radar chart can intuitively show that the model has a very high accuracy in various tasks in the CAD-RADS categories and P categories.



XSL•FO
RenderX

Figure 5. Performance metrics of generative pre-trained transformer (GPT)-4o in identifying myocardial bridge and noncalcified plaque.



Error Analysis

This study performed an error analysis for CAD-RADS categories and P categories, involving 1998 features, with 57 errors identified, resulting in an overall error rate of 2.9%. The errors were classified into 3 main types: model output termination errors, feature extraction errors, and ambiguities in the original report descriptions, as shown in Table 3.

XSL•FO
RenderX

Table . Error analysis. In the 18-segment coronary artery model, the left circumflex is divided into proximal and distal segments with no midsegment. When "midsegment" is mentioned in the report, it is defined as the proximal segment in our system settings for the prompt engineering.

Error type	Frequency	Explanation
CAD-RADS[a] categories		
Model output termination error	2	The model failed to output complete structured data due to unknown reasons, resulting in classification errors (n=2).
Feature extraction error	20	Although the model output the report completely, errors occurred during the feature extraction phase when converting free text to structured data, leading to classification errors (n=20). For example, in the original report, the coronary arteries had no plaques or stenosis, and the most severe stenosis was 0%. However, the model output a 10% - 20% stenosis level, misclassifying it from class 0 to class 1.
Ambiguity i then original report	0	The original report contained ambiguous or unclear descriptions, leading to erroneous structured outputs, which impacted the final classification (n=0).
Plaque Burden categories		
Model output termination error	4	The model failed to output complete structured data due to unknown reasons, resulting in classification errors (n=4).
Feature extraction error	25	Although the model output the report completely, errors occurred during the structured data conversion, particularly in recognizing coronary segment involvement, leading to classification errors (n=25). This included incorrectly identifying one or more segments as affected (n=13) or missing one or more segments (n=12), ultimately causing misclassification.
Ambiguity i then original report	6	The original report contained ambiguous or unclear descriptions, leading to erroneous structured outputs and affecting final classification (n=6). For instance, the report contained an ambiguous description of the mid-proximal segment, which was incorrectly identified as 2 separate segments during the structured output phase (n=6), resulting in misclassification.

[a]CAD-RADS: Coronary Artery Disease Reporting and Data System.

For CAD-RADS categories, there were 2 instances of model output termination errors, 20 instances of feature extraction errors, and no instances of ambiguities in the original report descriptions.

For overall plaque burden subclassification, there were 4 instances of model output termination errors, 25 instances of feature extraction errors, and 6 instances of ambiguities in the original report descriptions.

Discussion

This study aimed to evaluate the capability of GPT-4o in converting unstructured coronary CTA reports into standardized formats and automatically identifying CAD-RADS categories and P categories. Our results demonstrated exceptional performance, with accuracy rates exceeding 0.97 for CAD-RADS classification and P classification. These findings suggest that LLMs could not only automate the structuring of free-text reports to enhance radiological workflow efficiency but also facilitate the extraction of valuable structured information for database construction and subsequent clinical research.

Our findings align with previous studies showing that LLMs can effectively extract structured information from medical reports. Recent research has demonstrated similar success in extracting features for various standardized reporting systems, including LI-RADS and BI-RADS [24,28]. However, our study extends beyond previous work by using a larger dataset of real-world clinical reports rather than simulated data, providing more robust evidence of GPT-4o's clinical applicability. The model's high performance across different classification tasks suggests its potential for broader implementation in clinical radiology workflows, particularly in standardizing reporting practices and facilitating data collection for research.

XSL•FO
RenderX

Our study further confirms LLMs' exceptional performance in extracting clinically relevant data. For instance, GPT-4 demonstrated a 96% accuracy rate in extracting lesion information from lung cancer CT reports [29], and also showed high accuracy in emergency department CT reports [30]. In our study, GPT-4o successfully identified and classified coronary artery disease, particularly in the CAD-RADS and P classification tasks, with remarkable accuracy. These findings further support LLMs' efficiency in handling complex medical tasks, especially where traditional manual extraction methods may be prone to errors due to task complexity [31].

While LLM models have shown strong capabilities in medical data extraction, hallucinations and randomness remain inherent challenges [27,32]. To reduce accuracy loss caused by hallucinations, we implemented 2 key measures. First, we set the model's temperature to 1E-10 [27], which helps reduce variability in the model's outputs, thus controlling randomness. Second, for the CAD-RADS and P classification tasks, we did not rely solely on the model's output; instead, we used custom Python scripts to perform further calculations based on its structured responses. This approach ensured accuracy and validated the feasibility of our study through high performance.

Although we achieved promising results, our study still contained a small number of erroneous cases, with an overall error rate of 2.9%. Most of these errors occurred during the feature extraction phase, particularly in the CAD-RADS classification (20 out of 22 errors occurred in this phase) and P classification (25 out of 35 errors were related to segment involvement scoring). Among them, 6 errors were due to ambiguity in the original report. This error was caused by the fact that when radiologists wrote coronary CTA reports, they referred to inconsistent literature on the segmentation of coronary arteries. The descriptions of the LCX segment included the proximal LCX segment, the middle LCX segment, and the distal LCX segment. However, this study adopted the internationally accepted segmentation method of 18 coronary arteries, and the LCX only had the proximal and distal segments. For the handling of ambiguous reports, we provided the large model with relevant literature knowledge when prompt engineering and clearly informed the model that ambiguous reports generally needed to be carefully identified. After manual review and repeated iterations, the accuracy of the model for ambiguous reports was greatly improved. This shows that by giving the model specific knowledge and rules, the model can adapt to the complex clinical environment in the real world.

Due to the black-box nature of LLMs [33], we cannot directly explore the root causes of errors, but we can reasonably speculate on their sources. First, the model's inherent hallucinations [32] may cause misleading outputs during the reasoning process of structured data. Although the temperature adjustment reduced randomness to some extent, hallucinations still influenced the reasoning process. Second, external factors such as API stability, network conditions, or computational resource limitations could also impact the model's output. Additionally, ambiguities or inconsistencies in the original reports contributed to the occurrence of errors.

These issues highlight the need for professional oversight and intervention when using LLMs for large-scale data extraction [34] to ensure the accuracy and consistency of the extracted results. Regarding hallucinations, while we have taken measures to mitigate their impact, future research should further explore strategies to reduce hallucination phenomena, especially in clinical data extraction tasks. Furthermore, ambiguities in the original reports may arise from subtle differences in guidelines referenced by medical professionals when writing reports. To minimize this impact, radiologists should strive to adhere to internationally accepted segmentation methods, and the model should be further trained to enhance its understanding of medical knowledge, particularly the differences between various guidelines for the same disease. With these improvements, the accuracy and reliability of the model could be further enhanced.

The implementation of GPT-4o in clinical practice appears feasible given its high accuracy and efficiency. In addition, in terms of operating costs, based on OpenAI's official pricing, the input and output of a single report in this study is approximately 2052 (SD 15) tokens, with a cost of approximately US $0.03. Batch processing of 1000 reports a day only costs US $30.80, which has the potential to be applied in clinical practice. In the RIS (Radiology Information System) of the radiology department, there is a port that can be connected to the GPT-4o API. This may require the government, hospitals, and other relevant departments to sign a patient data privacy confidentiality agreement with OpenAI. In the future, GPT-4o will have the opportunity to be applied in the radiology workflow. However, several critical considerations must be addressed before widespread adoption. Patient privacy protection remains the foremost ethical priority, requiring robust safeguards implemented in our study through a multilayered approach: beyond foundational IRB compliance, all coronary CTA reports underwent rigorous deidentification (removing Health Insurance Portability and Accountability Act–defined Protected Health Information) prior to LLM API interaction; data transmission was secured via TLS 1.2+ encryption with explicit configuration to disable third-party data retention; and access was restricted to authorized personnel through institutional role-based controls. Crucially, future clinical deployments must enforce equally stringent, auditable protocols within existing health care IT infrastructure (eg, RIS or PACS or EHR (electronic health record). Additionally, model outputs necessitate validation by qualified radiologists—particularly for high-risk cases—to ensure clinical accountability, while regular updates to the model's knowledge base are essential to maintain alignment with evolving guidelines.

Our study has several limitations. First, all reports came from a single institution, potentially limiting the generalizability of our findings. Second, the retrospective nature of this study may have introduced selection bias, and this study used Chinese as the research subjects, mainly middle-aged and older males, so the research data may be biased, and the performance of groups in other countries may be different. Third, we only evaluated one version of GPT-4o, and performance may vary with different model versions or other LLMs. Finally, the study period was relatively short, and longer-term evaluation would be valuable for assessing the model's consistency over time.

XSL•FO
RenderX

In conclusion, GPT-4o demonstrates remarkable capability in converting unstructured coronary CTA reports from our institution into standardized formats, suggesting significant potential for LLMs to improve radiological workflow efficiency and data standardization. If integrated with clinical decision support systems in the future, it will greatly improve the accuracy of radiologists' diagnosis of coronary artery disease, facilitate the management of coronary artery disease, and reduce the time required to generate reports on coronary artery findings. However, the limitations outlined earlier, particularly concerning generalizability across diverse health care settings and report formats, must be rigorously addressed. Future research should prioritize multicenter validation to rigorously assess robustness and adaptability, investigate seamless integration with existing health care systems (RIS or PACS or EHR), and critically evaluate the model's impact on downstream clinical outcomes and decision-making.

Acknowledgments

I would like to express my sincere gratitude to my supervisor, Professor Qin Jie, and Dr. Li Chao for their invaluable guidance and support throughout this research. This research was supported by the Hospital National Natural Science Foundation Cultivation Project (2021GZRPYM06), the Five-Five Project of the Third Affiliated Hospital of Sun Yat-sen University (2023WW605), and the National Natural Science Foundation of China grant (82202129, to CL).

Authors' Contributions

Jie Qin and Chao Li are co-corresponding authors who contributed equally.

Conflicts of Interest

None declared.

Multimedia Appendix 1
Chinese prompt words.
[DOCX File, 18 KB - medinform_v13i1e70967_app1.docx]

References

1. Cury RC, Leipsic J, Abbara S, et al. CAD-RADS™ 2.0 – 2022 Coronary Artery Disease – Reporting and Data System: An Expert Consensus Document of the Society of Cardiovascular Computed Tomography (SCCT), the American College of Cardiology (ACC), the American College of Radiology (ACR) and the North America Society of Cardiovascular Imaging (NASCI). Radiol Cardiothorac Imaging 2022 Oct;4(5):e220183. [doi: 10.1148/ryct.220183] [Medline: 36339062]
2. Foldyna B, Szilveszter B, Scholtz JE, Banerji D, Maurovich-Horvat P, Hoffmann U. CAD-RADS - a new clinical decision support tool for coronary computed tomography angiography. Eur Radiol 2018 Apr;28(4):1365-1372. [doi: 10.1007/s00330-017-5105-4] [Medline: 29116390]
3. Basha MAA, Aly SA, Ismail AAA, Bahaaeldin HA, Shehata SM. The validity and applicability of CAD-RADS in the management of patients with coronary artery disease. Insights Imaging 2019 Dec 4;10(1):117. [doi: 10.1186/s13244-019-0806-7] [Medline: 31802266]
4. Xie JX, Cury RC, Leipsic J, et al. The Coronary Artery Disease-Reporting and Data System (CAD-RADS): prognostic and clinical implications associated with standardized coronary computed tomography angiography reporting. JACC Cardiovasc Imaging 2018 Jan;11(1):78-89. [doi: 10.1016/j.jcmg.2017.08.026] [Medline: 29301713]
5. Lee JW, Kim JY, Han K, et al. Coronary CT angiography CAD-RADS versus coronary artery calcium score in patients with acute chest pain. Radiology 2021 Oct;301(1):81-90. [doi: 10.1148/radiol.2021204704] [Medline: 34282972]
6. Bosmans JML, Weyler JJ, De Schepper AM, Parizel PM. The radiology report as seen by radiologists and referring clinicians: results of the COVER and ROVER surveys. Radiology 2011 Apr;259(1):184-195. [doi: 10.1148/radiol.10101045] [Medline: 21224423]
7. Wallis A, McCoubrie P. The radiology report--are we getting the message across? Clin Radiol 2011 Nov;66(11):1015-1022. [doi: 10.1016/j.crad.2011.05.013] [Medline: 21788016]
8. Hao T, Huang Z, Liang L, Weng H, Tang B. Health natural language processing: methodology development and applications. JMIR Med Inform 2021 Oct 21;9(10):e23898. [doi: 10.2196/23898] [Medline: 34673533]
9. Pathak J, Kho AN, Denny JC. Electronic health records-driven phenotyping: challenges, recent advances, and perspectives. J Am Med Inform Assoc 2013 Dec;20(e2):e206-e211. [doi: 10.1136/amiajnl-2013-002428] [Medline: 24302669]
10. Tariq A, Van Assen M, De Cecco CN, Banerjee I. Bridging the gap between structured and free-form radiology reporting: a case-study on coronary CT angiography. ACM Trans Comput Healthcare 2022 Jan 31;3(1):1-20. [doi: 10.1145/3474831]
11. Wu H, Wang M, Wu J, et al. A survey on clinical natural language processing in the United Kingdom from 2007 to 2022. NPJ Digit Med 2022 Dec 21;5(1):186. [doi: 10.1038/s41746-022-00730-6] [Medline: 36544046]

XSL•FO
RenderX

12. Touvron H, Lavril T, Izacard G, et al. Open and efficient foundation language models. arXiv. Preprint posted online on Feb 27, 2023. [doi: 10.48550/arXiv.2302.13971]
13. Achiam J, Adler S, Agarwal S, et al. Gpt-4 technical report. arXiv. Preprint posted online on Mar 15, 2023. [doi: 10.48550/arXiv.2303.08774]
14. Lyu Q, Tan J, Zapadka ME, et al. Translating radiology reports into plain language using ChatGPT and GPT-4 with prompt learning: results, limitations, and potential. Vis Comput Ind Biomed Art 2023 May 18;6(1):9. [doi: 10.1186/s42492-023-00136-5] [Medline: 37198498]
15. Sun Y, Zheng Y, Hao C, Qiu H. NSP-BERT: a prompt-based few-shot learner through an original pre-training task--next sentence prediction. arXiv. Preprint posted online on Sep 18, 2021. [doi: 10.48550/arXiv.2109.03564]
16. Wei J, Bosma M, Zhao VY, et al. Finetuned language models are zero-shot learners. arXiv. Preprint posted online on Sep 8, 2021. [doi: 10.48550/arXiv.2109.03564]
17. Lai X, Chen J, Lai Y, et al. Using large language models to enhance exercise recommendations and physical activity in clinical and healthy populations: scoping review. JMIR Med Inform 2025 May 27;13:e59309. [doi: 10.2196/59309] [Medline: 40424584]
18. Adams LC, Truhn D, Busch F, et al. Leveraging GPT-4 for post hoc transformation of free-text radiology reports into structured reporting: a multilingual feasibility study. Radiology 2023 May;307(4):e230725. [doi: 10.1148/radiol.230725] [Medline: 37014240]
19. Nakaura T, Yoshida N, Kobayashi N, et al. Preliminary assessment of automated radiology report generation with generative pre-trained transformers: comparing results to radiologist-generated reports. Jpn J Radiol 2024 Feb;42(2):190-200. [doi: 10.1007/s11604-023-01487-y] [Medline: 37713022]
20. Biswas S, Khan S, Awal SS. Can ChatGPT write radiology reports? Chin J Acad Radiol 2024 Mar;7(1):102-106. [doi: 10.1007/s42058-023-00132-x]
21. Cao JJ, Kwon DH, Ghaziani TT, et al. Accuracy of information provided by ChatGPT regarding liver cancer surveillance and diagnosis. AJR Am J Roentgenol 2023 Oct;221(4):556-559. [doi: 10.2214/AJR.23.29493] [Medline: 37222278]
22. Sievert M, Conrad O, Mueller SK, et al. Risk stratification of thyroid nodules: assessing the suitability of ChatGPT for text-based analysis. Am J Otolaryngol 2024;45(2):104144. [doi: 10.1016/j.amjoto.2023.104144] [Medline: 38113774]
23. Shan G, Chen X, Wang C, et al. Comparing diagnostic accuracy of clinical professionals and large language models: systematic review and meta-analysis. JMIR Med Inform 2025 Apr 25;13(1):e64963. [doi: 10.2196/64963] [Medline: 40279517]
24. Gu K, Lee JH, Shin J, et al. Using GPT-4 for LI-RADS feature extraction and categorization with multilingual free-text reports. Liver Int 2024 Jul;44(7):1578-1587. [doi: 10.1111/liv.15891] [Medline: 38651924]
25. Lichao312214129/code_for_cad-RADS. GitHub. URL: https://github.com/lichao312214129/code_for_CAD-RADS [accessed 2025-08-26]
26. Bhayana R, Nanda B, Dehkharghanian T, et al. Large language models for automated synoptic reports and resectability categorization in pancreatic cancer. Radiology 2024 Jun;311(3):e233117. [doi: 10.1148/radiol.233117] [Medline: 38888478]
27. Holtzman A, Buys J, Du L, Forbes M, Choi Y. The curious case of neural text degeneration. arXiv. Preprint posted online on 2019. [doi: 10.48550/arXiv.1904.09751]
28. Cozzi A, Pinker K, Hidber A, et al. BI-RADS category assignments by GPT-3.5, GPT-4, and Google Bard: a multilanguage study. Radiology 2024 Apr;311(1):e232133. [doi: 10.1148/radiol.232133] [Medline: 38687216]
29. Fink MA, Bischoff A, Fink CA, et al. Potential of ChatGPT and GPT-4 for data mining of free-text CT reports on lung cancer. Radiology 2023 Sep;308(3):e231362. [doi: 10.1148/radiol.231362] [Medline: 37724963]
30. Infante A, Gaudino S, Orsini F, et al. Large language models (LLMs) in the evaluation of emergency radiology reports: performance of ChatGPT-4, perplexity, and Bard. Clin Radiol 2024 Jul;79(7):e974. [doi: 10.1016/j.crad.2024.02.019] [Medline: 38719688]
31. Abu-Ashour W, Emil S, Poenaru D. Using artificial intelligence to label free-text operative and ultrasound reports for grading pediatric appendicitis. J Pediatr Surg 2024 Sep;59(9):783-790. [doi: 10.1016/j.jpedsurg.2024.04.005] [Medline: 38724428]
32. Ji Z, Lee N, Frieske R, et al. Survey of hallucination in natural language generation. ACM Comput Surv 2023 Dec 31;55(12):1-38. [doi: 10.1145/3571730]
33. Ehsan U, Riedl M. Explainable AI reloaded: challenging the XAI status quo in the era of large language models. Presented at: HTTF '24: Halfway to the Future; Oct 21-23, 2024; Santa Cruz CA USA. [doi: 10.1145/3686169.3686185]
34. Parillo M, Vaccarino F, Beomonte Zobel B, Mallio CA. ChatGPT and radiology report: potential applications and limitations. Radiol Med 2024 Dec;129(12):1849-1863. [doi: 10.1007/s11547-024-01915-7] [Medline: 39508933]

Abbreviations

AI: artificial intelligence
CAD-RADS: Coronary Artery Reporting and Data System
CCTA: coronary computed tomography angiography

XSL•FO
RenderX

EHR: electronic health record
GPT: generative pre-trained transformer
LCX: left circumflex
LLM: large language model
NLP: natural language processing
P categories: Plaque Burden categories
PACS: Picture Archiving and Communication System
RIS: Radiology Information System

Edited by A Castonguay; submitted 08.01.25; peer-reviewed by D Mu, N Mungoli, R Tripathi; revised version received 12.06.25; accepted 17.06.25; published 10.09.25.

Please cite as:
Chen Y, Dong M, Sun J, Meng Z, Yang Y, Muhetaier A, Li C, Qin J
Leveraging GPT-4o for Automated Extraction and Categorization of CAD-RADS Features From Free-Text Coronary CT Angiography Reports: Diagnostic Study
JMIR Med Inform 2025;13:e70967
URL: https://medinform.jmir.org/2025/1/e70967
doi:10.2196/70967

© Youmei Chen, Mengshi Dong, Jie Sun, Zhanao Meng, Yiqing Yang, Abudushalamu Muhetaier, Chao Li, Jie Qin. Originally published in JMIR Medical Informatics (https://medinform.jmir.org), 10.9.2025. This is an open-access article distributed under the terms of the Creative Commons Attribution License (https://creativecommons.org/licenses/by/4.0/), which permits unrestricted use, distribution, and reproduction in any medium, provided the original work, first published in JMIR Medical Informatics, is properly cited. The complete bibliographic information, a link to the original publication on https://medinform.jmir.org/, as well as this copyright and license information must be included.

XSL•FO
RenderX

Original Paper

Extracting Symptoms of Complex Conditions From Online Discourse (Subreddit to Symptomatology): Lexicon-Based Approach

Bushra Hossain[1], MSc; Sarah M Preum[2,3], PhD; Md Fazle Rabbi[4], MSc; Rifat Ara[5], MS; Mohammed Eunus Ali[6], PhD

[1]Department of Computer Science and Engineering, Bangladesh University of Engineering and Technology, Dhaka, Bangladesh

[2]Department of Computer Science, Dartmouth College, Hanover, NH, United States

[3]Department of Biomedical Data Science, Geisel School of Medicine, Hanover, NH, United States

[4]Department of Computer Science and Engineering, Bangladesh University of Professionals, Dhaka, Bangladesh

[5]Department of Obstetrics & Gynecology, Bangladesh College of Physicians and Surgeons, Dhaka, Bangladesh

[6]Faculty of Information Technology, Monash University, Clayton, Australia

Corresponding Author:
Mohammed Eunus Ali, PhD
Faculty of Information Technology
Monash University
20 Exhibition Walk (Woodside Building)
Clayton, VIC 3168
Australia
Phone: 61 3 9905 1741
Email: eunus.ali@monash.edu

Abstract

Background: Millions of people affected with complex medical conditions with diverse symptoms often turn to online discourse to share their experiences. While some studies have explored natural language processing methods and medical information extraction tools, these typically focus on generic symptoms in clinical notes and struggle to identify patient-reported, disease-specific, subtle symptoms from online health discourse.

Objective: We aimed to extract patient-reported, disease-specific symptoms shared on social media reflecting the lived experiences of thousands of affected individuals and explore the characteristics, prevalence, and occurrence patterns of the symptoms.

Methods: We propose a lexicon-based symptom extraction (LSE) method to identify a diverse list of disease-specific, patient-reported symptoms. We initially used a large language model to accelerate the extraction of symptom-related key phrases that formed the lexicon. We evaluated the effectiveness of lexicon extraction against human annotation using a Jaccard index score. We then leveraged BERT-Base, BioBERT, and Phrase-BERT–based embeddings to learn representations of these symptom-related key phrases and cluster similar symptoms using k-means and hierarchical density-based spatial clustering of applications with noise (HDBSCAN). Among the different options explored in our experiments, BioBERT-based k-means clustering was found to be the most effective. Finally, we applied symptom normalization to eliminate duplicate and redundant entries in the comprehensive symptom list.

Results: In a real-world polycystic ovary syndrome (PCOS) subreddit dataset, we found that LSE significantly outperformed state-of-the-art baselines, achieving at least 41% and 20% higher F_1-scores (mean 86.10) than automatic medical extraction tools and large language models, respectively. Notably, the comprehensive list of 64 PCOS symptoms generated via LSE ensured extensive coverage of symptoms reported in 7 reputable eHealth forums. Analyzing PCOS symptomatology revealed 28 potentially emerging symptoms and 8 self-reported comorbidities co-occurring with PCOS.

Conclusions: The comprehensive patient-reported, disease-specific symptom list can help patients and health practitioners resolve uncertainties surrounding the disease, eliminating the variability of PCOS symptoms prevailing in the community. Analyzing PCOS symptomatology across varied dimensions provides valuable insights for public health research.

(JMIR Med Inform 2025;13:e70940) doi:10.2196/70940

XSL•FO
RenderX

KEYWORDS

complex medical condition; polycystic ovary syndrome; online discourse; large language models; natural language processing; disease-specific symptoms; health information extraction; symptomatology

Introduction

Background

The rise of health 2.0 has significantly increased the consumption of health-related information on social media in recent years. Worldwide, 34.7% of adult internet users frequently search for health-related information online, with approximately 58.5% of adults in the United States specifically engaging in such searches as of 2023 [1,2]. Analyzing online discourse on health-related topics offers valuable insights into the lived experiences and perspectives of affected individuals [3-5]. The critical findings of these analyses are particularly significant for understanding complex medical conditions, such as different types of cancer, cognitive and mental health conditions, autoimmune disorders, and metabolic and endocrinological conditions. These medical conditions often manifest with diverse symptoms that vary significantly among patients [6-8]. Furthermore, there is often no consensus among established medical sources regarding the full range of possible symptoms for such conditions [9,10]. This variability poses challenges for patients, health care providers, and researchers seeking a comprehensive understanding of these symptoms and their characteristics. Thus, the study and analysis of symptoms associated with a disease, referred to as *symptomatology*, is crucial for understanding complex diseases [11]. We argue that a robust approach to extracting disease-specific symptoms from individuals' lived experiences shared on social media can address uncertainties surrounding complex medical conditions. This approach would also allow for the identification of symptoms that patients associate with a condition (eg, brain fog with post–COVID-19 condition), prevalence of symptom co-occurrence (eg, unexplained weight loss and pain with cancer), and how symptoms vary based on patients' comorbidities and preexisting conditions.

Recent advancements in natural language processing (NLP) have enabled public health researchers to explore medical information extraction tools [12-15] and develop novel techniques [16-18] for analyzing online health discourse, including patient-reported data from social media. However, off-the-shelf medical information extraction tools primarily excel in extracting well-known medical entities (eg, diseases, drugs, and basic symptoms). Their limitations become evident with granular, patient-centric details (eg, unusual symptom descriptions, implicit context, or subtle adverse events), which often require specialized rules or retrained models for accurate detection [19-22]. Modern transformer-based models used with medical named entity recognition have shown promising results in symptom extraction [23,24]. However, these models typically require large amounts of domain-specific data and are mostly trained on clinical notes (electronic health records), which limits their effectiveness when dealing with colloquial health discourse generated by patients [7,23-25]. A family of bidirectional encoder representations from transformers (BERT)–based models fine-tuned on colloquial data markedly improves symptom recognition in informal texts; nevertheless, their error analysis indicates that the best-trained models still capture only approximately 25% to 50% of lengthy, figurative symptom phrases and continue to misclassify many subtle or previously unseen expressions (eg, "mild difficulty taking deep breaths" or "chest again felt a little tight") [26]. A recent NLP pipeline [27] used to extract symptoms from patient narratives on social media proposed a dual-corpus symptom lexicon containing keywords (eg, *fever* and *cough*) and related modifiers (eg, *mild* or *severe*) followed by applying a rule-based postprocessing step to merge the 2. However, this fixed rule-based approach may struggle to report symptoms whenever people describe them implicitly, with spelling noise, or in new phrasing that never entered the seed lists (eg, "can't breathe properly" or "my lungs felt on fire").

While the existing lexicon-based approaches have successfully used predefined resources and deep learning frameworks for broad public health surveillance, their reliance on explicit wording limits their ability to capture the full range of informal expressions. On the other hand, large language models (LLMs) have significantly accelerated medical NLP research, especially in the field of information extraction [16,17,21,28]. While some studies have demonstrated the potential of LLMs for health information extraction from social media [29,30], they face challenges when extracting specific contexts such as health advice and disease-specific treatment [12,16].

Objectives

To overcome the aforementioned limitations of symptom extraction from social media discourse, we propose a novel NLP pipeline that systematically combines the capabilities of LLMs and other NLP methods with feedback from domain experts, resulting in a scalable and practical solution to the problem of symptom extraction from patient-reported social media discourse.

While the proposed pipeline can be applied to explore a plethora of medical conditions for which there is an abundance of patient-reported online discourse, we focused on a common chronic condition with significant uncertainty, namely, polycystic ovary syndrome (PCOS), as a use case in this paper. According to the World Health Organization [31], an estimated 116 million women (3.4% of reproductive-age women) worldwide are affected by PCOS, and its prevalence is on the rise. Despite its widespread impact, the full spectrum of PCOS remains insufficiently explored [32]. Patients report a diverse range of symptoms that vary in severity depending on previous medical history and their effect on daily life. The combination of varied symptoms, insufficient treatment guidelines, and instances of medical gaslighting often leads to psychological distress, prompting many individuals to seek support and share experiences on social media platforms [33], including Reddit. Existing research leveraging social media data to study PCOS is still underdeveloped [4,34-36]. This creates a unique opportunity to systematically identify self-reported symptoms

XSL•FO
RenderX

and related symptomatology based on the lived experiences of thousands of individuals and, thereby, inform the clinical understanding of this complex medical condition. We make 3 primary contributions. First, we developed a novel lexicon-based symptom extraction (LSE) method to identify diverse disease-specific symptoms from individuals' experiences shared on social media. This method can effectively detect even subtle symptoms mentioned in user discourse. We applied our LSE method to a novel PCOS subreddit dataset, achieving statistically significant improvements over state-of-the-art medical NLP baselines.

Second, we conducted an in-depth analysis of peer discussion threads on the extracted PCOS symptoms to reveal a set of lesser-known yet prevalent symptoms that individuals associate with PCOS and associated co-occurring symptoms and comorbidities. These findings can contribute to clinical research and public health research in a community-informed way.

Third, we curated a novel Reddit dataset containing 59,962 and 641,441 relevant posts and comments, respectively. This dataset captures self-reported PCOS symptoms and their context from 68,010 affected individuals. In addition, we curated a human-annotated, labeled dataset of 1000 posts of patient-reported symptoms related to PCOS based on guidance from domain experts and patient input. We release these resources in a public domain. These unique, rich resources can enable medical NLP and computational health researchers to further investigate the symptomatology of complex medical conditions identified and analyzed online.

Methods

Data Collection and Preprocessing

We selected Reddit as a source of data because of its anonymous nature. It encourages users to share personal experiences on stigmatized topics [4,37]. The data collection process began with the identification of the r/PCOS subreddit by considering the group posts' availability and popularity among 153,000 members engaging in discussions on PCOS. We systematically collected data from this subreddit using the *Python Reddit API Wrapper* package (Python Software Foundation) and the Pushshift application programming interface (API) [38,39]. We obtained all the posts and comments from the r/PCOS subreddit from August 4, 2010, to December 31, 2022. This timeline was chosen to ensure a comprehensive capture of recent as well as previous discussions. For each post, we retained the date, flair name, unique post ID, post title, post content, score, upvotes, and comments due to their utility and relevance.

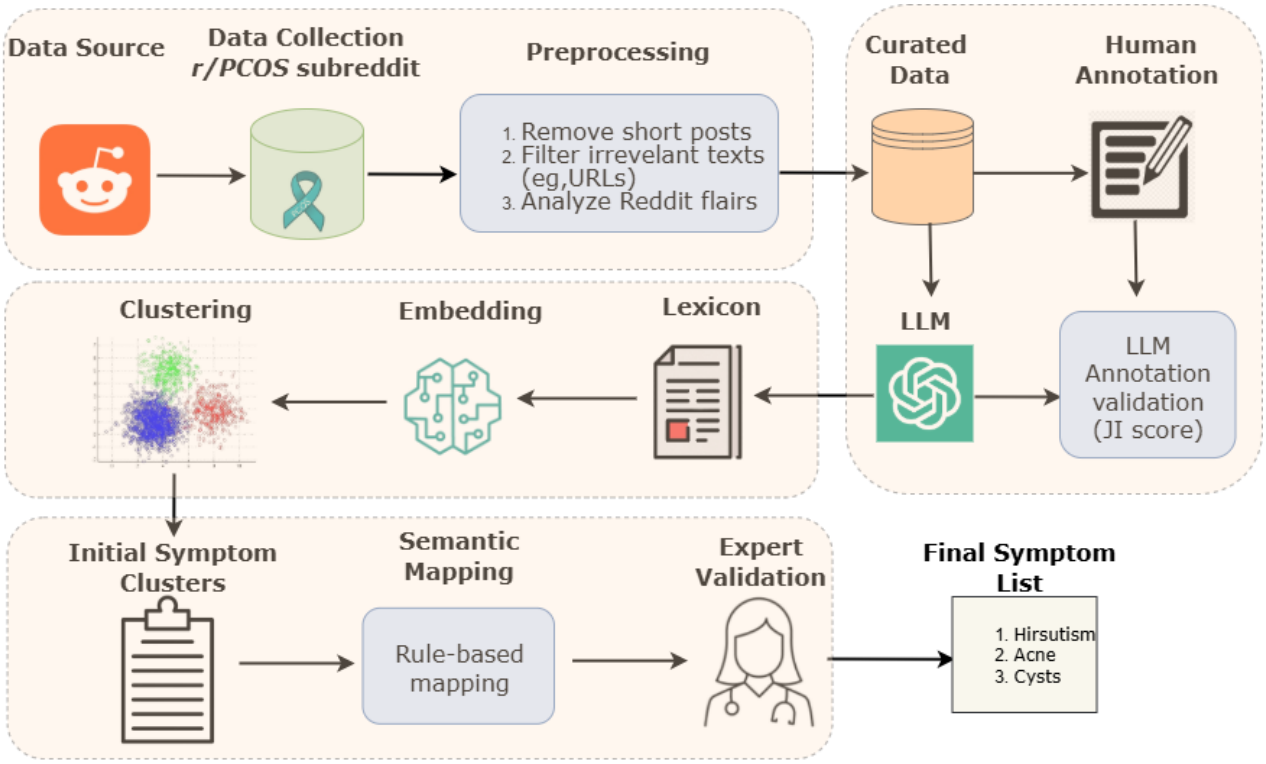
During preprocessing, we discarded entries with deleted posts or those in which the post content had <5 words as the brevity poses challenges to deriving meaningful insights from posts. We also removed posts containing irrelevant text (eg, polls, survey links only, or URLs). The URL-heavy posts were classified using a rule-based heuristic combining personal pronoun frequency and URL-to-text ratio. We provide a summary of the steps to remove irrelevant text from social media data in Table S1 in Multimedia Appendix 1. This filtering process enabled us to focus on patient-authored, experience-rich discussions. Finally, we obtained a primary dataset comprising 59,962 posts and 641,441 comments by 68,010 active unique users. Identifying task-relevant data is crucial for data-driven approaches [12] as it significantly impacts the efficiency of downstream tasks. We leveraged Reddit's post "flair" option to filter relevant data. On Reddit, a post flair is a customizable text or icon that appears next to a post title to provide additional context or categorization, similar to hashtags available on other platforms. We reviewed 30 randomly selected posts from several flairs of the PCOS subreddit. We identified that, among all the flairs, posts in the "General/Advice" flair were more likely to share knowledge and seek advice on symptoms. Further investigation on the most frequent unigrams of these flairs supported our qualitative analysis, where the presence of symptom-related unigrams such as "period," "symptom," "doctor," "birth," "control," and "diagnosed" was predominantly observed in the "General/Advice" flair. The distribution of frequent unigrams in the "General/Advice" flair is shown in Figure S1 in Multimedia Appendix 1. On the basis of these findings, we chose the "General/Advice" flair for extracting a wide range of symptoms. In addition, the "General/Advice" flair is more popular in the community as it contains the highest number of posts, as shown in Table S2 in Multimedia Appendix 1. This selection ensured a broad range of symptoms and valuable insights. Finally, we developed a corpus of 10,500 posts for the symptom identification task, randomly selected from the posts with the "General/Advice" flair.

Our Method: LSE

We propose an LSE method to analyze self-reported symptoms of a complex medical condition using social media discourse. Our proposed method consists of three main steps: (1) symptom-related lexicon extraction, (2) symptom identification, and (3) symptom normalization, as illustrated in Figure 1.

XSL•FO
RenderX

Figure 1. Steps of the lexicon-based symptom extraction method. JI: Jaccard index; LLM: large language model.



Symptom-Related Lexicon Extraction

We leveraged symptom-related key phrases for lexicon extraction as it helped distill the most relevant terms and phrases associated with physical manifestations from user narratives. We focused on extracting the key symptom-related phrases instead of the symptoms as the latter results in extracting (1) phrases that are not relevant and (2) repetitive mentions of the same symptoms, rendering the subsequent analysis challenging. Compared to the tedious and time-intensive task of manual extraction, LLMs emerge as a more economical choice, offering consistency in their responses, especially when the temperature setting is near 0 [40,41]. We used the OpenAI API *gpt-3.5-turbo-16k* [42] to annotate 10,500 user posts. To ensure precision in identifying the physical manifestation of the condition, we emphasized physical symptoms while excluding psychological aspects in our base prompt using a zero-shot prompting strategy (Figure S2 in Multimedia Appendix 1). The API responses were stored in a JSON line format containing key phrases and corresponding posts. This process yielded a lexicon of 30,370 symptom-related key phrases that we used in the subsequent steps.

We resorted to human annotation to validate the extraction conducted by ChatGPT (OpenAI). We employed 2 graduate students in the science, technology, engineering, and mathematics field particularly active in women's health–related social media forums. Before annotation, they underwent multiple training sessions led by a domain expert specializing in computational health. These sessions were designed to refine their understanding on key phrase extraction and promote annotation consistency. On a sample set of 30 posts, the interannotator agreement reached 92% in a relaxed match. Finally, we randomly selected 500 entries from 10,500 user posts. We recognize that many social media and health NLP studies use larger annotated sets, often containing 2000 to 4000 messages, and few drop below 1000 annotations [12,43-45]. However, those datasets are typically used to validate end-to-end model performance, whereas our 500-post sample supported a specific component of our pipeline. We deliberately divided tasks between the LLM and human experts to balance coverage and precision while remaining practical as (1) the cost in terms of time and resources was significant (eg, annotating just 500 entries required 4 training sessions × 3 hours = 12 hours, 35 hours for literature study and documentation, and 208.3 hours approximately for annotation per post; 500 posts × 25 minutes), making larger samples prohibitively expensive; (2) we observed a significant drop in new symptom-related key phrase discoveries after the first 200 posts, mirroring the classic "diminishing returns" shown in Table S3 in Multimedia Appendix 1, also evident in social media symptom mining and related tasks [46]; and (3) during manual inspection, we observed minimal disagreement as the annotation task was primarily syntactic rather than interpretive. Taking into consideration the above 3 points, we assigned 250 unique posts to each annotator to minimize bias and enhance the quality of our annotated set.

We choose the Jaccard index (JI) to measure the similarity between key phrases extracted by ChatGPT and the human annotators [12]. This required normalizing the extracted key phrases (eg, changing "pressure in pelvic area" to "pelvic pressure") to maintain homogeneity in both lists. We computed the JI similarity for each post in the sample using exact key phrase match. Table 1 shows 3 posts from our sample set with extracted key phrases and their corresponding JI scores. The average JI score was 74%, indicating moderate lexical similarity between the key phrases extracted by ChatGPT and the human

XSL•FO
RenderX

annotators considering the complexity of the task [47]. Our manual investigation of all missed or incorrectly extracted key phrases by the LLM revealed 5 distinct error categories, as outlined in Table S4 in Multimedia Appendix 1. For instance, in row 1 of Table 1, the LLM missed "absence of period" as it was implicitly mentioned in the post as "haven't had a period since December." Similarly, in row 3, "insulin resistance" is an ambiguous expression to be accepted as a symptom. However, a deeper analysis revealed 3 findings supporting the acceptability of the lexicon.

First, post-level JI analysis; our manual investigation showed that 12.6% (63/500) of the posts had a JI score of 0, which substantially affected the average JI. We found that most of these JIs with a value of 0 resulted from very short posts (eg, "Does anyone know if weightloss in PCOS helps or throws off hormones?") and were annotated as *no symptom* by humans, whereas the LLM incorrectly extracted the key phrases *weightloss* and *hormones*. The median JI score across all posts was 1.0 (IQR 0.5-1.0), indicating strong agreement between the LLM and human annotations in most cases.

Second, lexicon-level robustness; we observed that the LLM missed a key phrase in a post, resulting in a mismatch, but extracted the same key phrase in another post. Similar cases were found for human annotation, resulting in incorrect extraction for the LLM. We identified such cases for 61% (104/172) of the total missed or incorrectly extracted key phrases, which affected the average JI. As the final lexicon aggregates key phrases across all posts, these disagreements at the post level did not propagate to the lexicon level. When comparing the LLM-derived lexicon with the human-annotated lexicon, we observed a JI of 0.89, demonstrating strong alignment between the 2. This high agreement confirmed that discrepancies in per-post extraction had minimal impact on the final lexicon's accuracy and coverage.

Third, downstream impact on symptom list; the frequency of unique incorrectly extracted key phrases in the lexicon was very low (maximum of 3). Consequently, their influence on the cluster centroids was negligible. Because our symptom list was derived by selecting the most frequent phrases within each cluster, the effect of noisy or rare phrases was minimized. Such key phrases either formed microclusters (eg, *ultrasound*) that were discarded during the normalization step or were absorbed into broader, validated symptom cluster categories.

Table 1. Sample excerpts of human and ChatGPT annotations of posts. The Jaccard index (JI) was calculated for the similarity between the 2 annotations based on the extracted key phrases.

Post	Human annotation	ChatGPT annotation	JI score
"I haven't had a period since December, however in the past week I keep getting really bad cramping with sharp pains (almost feels like my ovaries), but no period...has anyone else experienced this? Is this normal?"	"Absence of period," "cramping," and "sharp pains"	"Cramping" and "sharp pains"	0.67
"I'm 22, F and over the years, I have gained 50 pounds. Recently, my acne is getting worse and I feel pressure in my pelvic area. I am trying to lose weight and thereby started working out but the scale is still not budging."	"Weight gain," "acne," and "pelvic pressure"	"Weight gain," "acne," and "pelvic pressure"	1.0
"Due to PCOS and insulin resistance, Does anyone else get symptoms like they're getting their period (sore breasts, crampy feeling) and just overall malaise when you're 'due' for your period you don't actually get?"	"Insulin resistance," "sore breasts," and "crampy feeling"	"Sore breasts," "crampy feeling," and "malaise"	0.5

In summary, while there were post-level discrepancies, the high lexicon-level JI (0.89) and the robustness of frequency-based clustering ensured that the final symptom list remained accurate and representative of human annotation without prohibitive annotation burden.

Symptom Identification

Overview

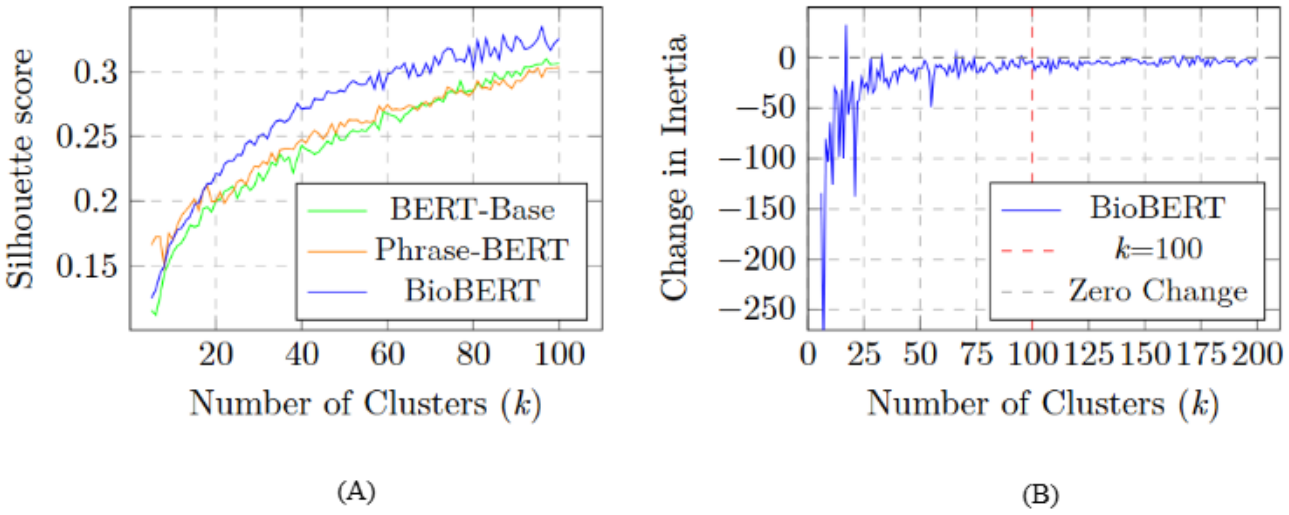
In this step, we identified a distinct set of disease symptoms using the symptom-related lexicon. As the key phrases in the lexicon were captured exactly as mentioned in users' posts, many were semantically similar with different phrasing. For example, key phrases such as *cystic ovary*, *ovarian cysts*, and *multiple cysts in ovaries* have the same semantic meaning with different surface forms. Thus, we used clustering to categorize the semantically similar key phrases and identify such categories as unique symptoms. To ensure accurate clustering, it is crucial to generate meaningful representations of symptom-related key phrases that effectively capture their semantic meaning. To achieve this, we used embeddings, which convert words into numeric representations in lower dimensions that preserve their contexts. The process of embedding and clustering the key phrases is described in the following sections.

Choosing the Right Embedding

We explored and evaluated widely used transformer models such as BERT-Base [48], Phrase-BERT [49], and BioBERT [50] to generate embeddings of symptom-related key phrases. We observed the performance of these embeddings by applying various clustering methods. For k-means clustering, we analyzed the silhouette score for each BERT-based embedding. The silhouette score considers both within-cluster and intercluster variances to determine cluster quality [51]. We plotted silhouette scores of different embedding approaches, shown in Figure 2A. The curves for BERT-Base and Phrase-BERT show a general increase but noticeable fluctuation, representing inconsistency in the results. In contrast, BioBERT shows a consistent and uniform ascent compared to the other 2 in the silhouette curve. Furthermore, applying L2 normalization during embedding improved the uniqueness of the clusters [48]. The consistent superiority of BioBERT across all clustering approaches steered our decision to adopt BioBERT as our embedding method.

XSL•FO
RenderX

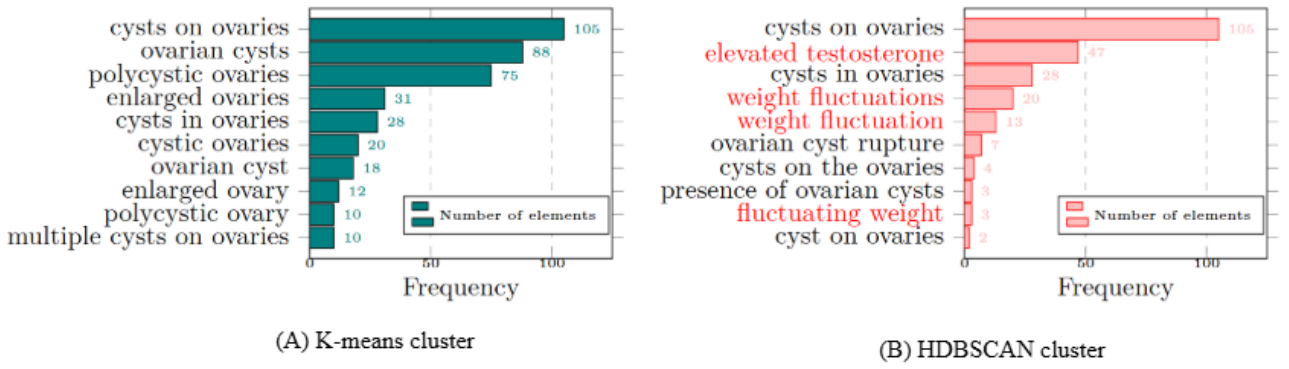
Figure 2. Characteristic analysis of embedding methods for selecting optimal clustering methods—(A) silhouette score analysis of different embeddings on k-means and (B) rate of change in inertia (within-cluster sum of the squares) decreasing as the number of clusters increases. BERT: bidirectional encoder representations from transformers.



Selecting the Optimal Clustering Method

We exploited k-means and hierarchical density-based spatial clustering of applications with noise (HDBSCAN) with BioBERT embeddings for clustering symptom-related key phrases. Comparing k-means and HDBSCAN is fairly tricky as their hyperparameters (number of clusters vs density thresholds) are fundamentally different. Although it is widely known that HDBSCAN performs better for noisy social media data as it filters out “low-density” points as noise, the choice of clustering method depends on the downstream task and the performance on specific data. In Table S5 in Multimedia Appendix 1, we report the performance of HDBSCAN under a grid of *min_cluster_size* and *min_samples* settings with the observations of cluster numbers, density-based clustering validation (DBCV) score, and noise. The DBCV score measures how dense and well separated core clusters are in a density-based clustering method [52]. Thus, HDBSCAN with lower *minimum_cluster_size* increases in DBCV scores indicates compactness of the clusters but may generate spurious microclusters. Manual observation shows that HDBSCAN with lower *minimum_cluster_size* provides better intracluster coherence but reduce intercluster separation and generate more semantically similar clusters, such as *increased testosterone* and *elevated level of testosterone*. In contrast, an increasing *minimum_cluster_size* results in lower DBCV scores. As a result, the number of clusters decreases, which may contribute to losing meaningful clusters by being too strict on cluster size. For such instances, elements of the *cysts on ovaries* cluster represents less coherence and semantic similarity in HDBSCAN compared to k-means shown in (Figure 3). In our use case, HDBSCAN labeled 31% to 56% of the points as noise across settings. This affected the downstream task as our goal was to maximize symptom coverage. On the other hand, k-means has no noise filtering, which ensures maximum coverage of symptoms. In addition, we implemented k-means using the cosine distance to improve the cluster uniqueness with fewer duplicates compared to using the Euclidean distance [53].

Figure 3. Comparison of elements within the cluster "cysts on ovaries" between 2 clustering methods: (A) k-means, containing semantically similar key phrases that are evenly distributed, and (B) hierarchical density-based spatial clustering of applications with noise, containing key phrases conflicting with the cluster name, highlighted in red, and showing more uneven distribution.



XSL•FO
RenderX

Sensitivity and Stability Analysis in Choosing the *k* Value

We varied the number of clusters (*k*) to determine the optimal number based on the silhouette score (in Figure 2A) and rate of change in inertia (in Figure 2B). In our PCOS use case, we identified that, after *k*=100, the change in inertia became flat and the rate of increment in silhouette score was also negligible. Therefore, we set *k* to range from 10 to 100, and at *k*=96, we observed an optimal silhouette score. In addition, we explored a –10 to +10 window for *k*=96 to verify the sensitivity of the resulting clusters. Across *k*=86 to 106, the silhouette score remained within approximately –0.01 to +0.01 of its value at *k*=96, and the inertia curve showed minimal change, confirming that the choice of *k* sat in the middle of a stable region. In addition, we report the bootstrap stability results for 3 representative choices between *k*=86 and 96. All 3 settings yielded high median Adjusted Rand Index (ARI) values (≥0.75) and narrow 95% CIs, demonstrating that cluster assignments are largely consistent when up to 20% of the data are held out. We provide a summary of the sensitivity and stability analysis of the choice of *k* in k-means in Table S6 in Multimedia Appendix 1.

Symptom Normalization

Overview

Each of the obtained clusters represented a symptom as the elements of the clusters were semantically similar. We considered the most frequent element of the cluster as the key symptom. The justification for selecting the most frequent element as the key symptom was 2-fold. First, its occurrences were significantly higher than those of other elements within the cluster. For instance, occurrences of *cysts on ovaries* compared to other elements within the cluster in Figure 3A were negligible. Second, all elements within a cluster consistently pointed toward the same physical condition as the key symptom. In the k-means cluster in Figure 3A, all the cluster elements referred to ovarian cysts. However, there were repetitions of symptoms in the obtained list. Therefore, we conducted symptom normalization by applying semantic mapping and validation by experts, as outlined in the following sections.

Applying Semantic Mapping

We applied semantic mapping of clusters, a manual process that involves merging symptoms with similar meanings and concepts using Unified Medical Language System Metathesaurus synonyms to avoid repetition. Through progressive discussions with our medical specialist, we formalized 4 semantic mapping rules suitable for this task. For instance, *irregular bleeding*, *irregular menstrual cycles*, and *irregular cycles* were mapped to *irregular periods* using rule 1, “synonym merging.” Applying these rules, we consolidated 11 such mappings from the initial 96 PCOS symptoms to 68 unique symptoms. The complete rule set is provided in Table S7 in Multimedia Appendix 1 to ensure reproducibility.

Validation by an Expert

We further refined the symptom list by validating the relevance of the lived experiences of patients to the disease. One of our coauthors, a gynecologist with >10 years of experience in treating PCOS, conducted this validation step. The expert’s role was to discard symptoms that were not related to the disease and resolve ambiguities between similar symptoms. For instance, the medical specialist discarded 4 irrelevant symptoms—*ultrasound*, *birth control*, *low-carb diet*, and *neck*—by manually investigating the cluster elements, resulting in a comprehensive list of 64 unique PCOS symptoms.

Ethical Considerations

We acknowledge that the research on symptom extraction from social media has multifaceted ethical concerns and requires careful attention to privacy, consent, and the responsible use of data and technology. The research was approved by Bangladesh University of Engineering and Technology's Institutional Review Board. Although Reddit is an anonymous platform, we ensured that no personally identifiable information was inadvertently revealed during data collection, analysis, or publication. All Reddit posts and comments cited as examples in this paper were paraphrased to protect user privacy. We also recognize that the demographic composition of Reddit users might not be fully representative of the broader population with PCOS, potentially limiting generalizability. Therefore, findings derived from Reddit discourse should be generalized cautiously to other populations or settings. In addition, we recognize that any biases in the dataset and the proposed model are unintentional. As the outcomes of this work are based on social media content, we emphasize the superiority of medical evidence–based facts in cases of conflict, particularly concerning direct clinical practice and medical diagnosis. We strongly encourage the use of the model for research and exploratory purposes, serving as a foundation for further developments in computational health research.

Results

Test Data Curation and Ground Truth Annotation

We initially separated 1000 sample posts of various lengths from our dataset for results evaluation. Considering the influence of post length on symptom identification, we categorized the posts into three groups: (1) short posts of <100 words, (2) medium-length posts of between 100 and 300 words, and (3) long posts of >300 words. Post length distribution in the dataset revealed that 45% (450/1000) of the posts belonged to the medium-length category (Table S8 in Multimedia Appendix 1). To ensure a balance across all categories, we selected 500 posts from the medium-length category and 250 posts from each of the short and long post categories for curating test data.

We recruited a medical graduate with domain knowledge and a patient with PCOS lived experience to perform annotation. Before annotation, both annotators participated in progressive training sessions and interactive discussions with medical specialists to refine their understanding and improve annotation consistency. During this phase, the medical specialist primarily identified 3 potential disagreements between the annotators. These observed disagreements were instances in which (1) the medical graduate often used clinical terminology (eg, “amenorrhea”) whereas the patient used informal language (eg, “no period for months”); (2) the patient included self-reported experiences (eg, “hypothyroidism”) that lacked clinical validation whereas the clinician strictly adhered to established

XSL•FO
RenderX

PCOS diagnostic criteria; and (3) the medical graduate inferred implicit symptoms (eg, laboratory test results) from domain knowledge, which was lacking in the patient annotation. Given our goal to prioritize the capture of patient-experienced symptoms, medical specialists suggested resolving these discrepancies by (1) avoiding overly technical clinical terms unless they were explicitly mentioned, (2) retaining self-reported experiences unless they were clinically invalid, and (3) including implicit symptoms as long as they were related to PCOS. Following these guidelines, both annotators extracted symptoms independently. We adopted the combination of both annotators' symptom lists per post to maximize coverage and ensure the consistency and reliability of the ground truth dataset.

In our ground truth annotation, annotators were not restricted to predefined symptom lists. They identified any symptoms that they perceived as PCOS related, resulting in free-text labels. Moreover, each post included multiple symptoms, making the traditional Cohen κ not suitable. Instead, we evaluated interannotator agreement using relaxed-match F_1-score due to the generative nature of our annotation [16,54,55]. We used BioBERT-based semantic similarity with the medical graduate's annotation as a reference. We achieved an F_1-score of 0.82, with a recall of 0.84 at a similarity threshold of 0.6, indicating substantial agreement considering the realistic complexity inherent in patient-derived, generative-nature symptom annotation.

Symptom Comparison: LSE With eHealth Forums

LSE resulted in a comprehensive list of 64 unique PCOS symptoms (Table 2) from 10,500 user posts. We also determined the unique users reporting each symptom in our primary dataset, with counts ranging from 31 to 16,001. This confirmed that LSE captures widely experienced symptoms, whereas less common symptoms are not ignored. In addition, this list provides a wide range of coverage as we cross-checked it with 7 evidence-based consumer health websites: the World Health Organization [31]; the Mayo Clinic [56]; WebMD [57]; the *International Classification of Diseases, 10th Revision* [58]; Johns Hopkins Medicine [59]; the National Health Service [60]; and the Centers for Disease Control and Prevention [61]. All symptoms mentioned in these sources were included in our list except for 4: sleep apnea, high blood pressure, low progesterone, and dandruff. Upon examining the clusters, we found that these 4 symptoms were represented within their respective key clusters—*insomnia*, *high cholesterol*, *low estrogen*, and *high DHEA*—due to their close medical relevance. Furthermore, all the forums recognized the 10 most frequently reported symptoms in our dataset (Table S9 in Multimedia Appendix 1). On the other hand, we identified 28 symptoms not acknowledged by any of the eHealth forums that we mention as potentially emerging symptoms in the Discussion section. Thus, our comprehensive symptom list reflects the diversity of self-reported PCOS lived experience symptoms and aligns closely with authoritative medical sources, helping standardize the variability in the symptom descriptions.

XSL•FO
RenderX

Table 2. Comprehensive list of 64 polycystic ovary syndrome symptoms extracted via lexicon-based symptom extraction. The counts represent the number of unique users reporting each symptom across the primary dataset. The symptoms in italics represent potentially emerging symptoms.

Symptom	Unique users reporting the symptom, n
Hirsutism	16,001
Acne	14,256
Cysts on ovaries	13,781
Pain	13,495
Weight gain	13,150
Mood swings	11,523
Insulin resistance	9859
Irregular period	9702
Infertility	7558
Cramps	7043
Diabetes	6690
Spotting	6469
Hypothyroidism	5366
No period	4846
Anovulation	4755
Nausea	4600
Cravings	4566
Fatigue	4342
Bloating	4048
Headaches	4028
Heavy period	3846
Hair loss	3517
High testosterone	2794
Skin issues	2695
Hormone imbalance	2648
Inflammation	2457
Endometriosis	2303
High DHEA [a]	2231
Loss of appetite	2013
Painful periods	1906
Insomnia	1513
Dizziness	1471
Night sweats	1457
Stomach pain	1374
Blood clots	1187
Anemia	1162
Brain fog	1158
Vomiting	1134
High androgen	1121
Oily skin	912
Back pain	843

XSL•FO
RenderX

Symptom	Unique users reporting the symptom, n
Digestive issues	826
Constipation	813
Pelvic pain	742
Belly fat	731
Acanthosis nigricans	616
High cholesterol	613
High insulin	575
Low libido	575
Abdominal pain	564
Ovary pain	496
Dry skin	480
High estrogen	480
Stretch marks	439
Low estrogen	436
Brown discharge	426
Skin tags	399
Breast tenderness	376
High prolactin	331
Pain during sex	261
Frequent urination	160
Redness	108
Weight loss	45
High LH[b] level	31

[a]DHEA: dehydroepiandrosterone.

[b]LH: luteinizing hormone.

Baseline Comparisons

Overview

We compared the performance of LSE with leading baselines, including 2 popular off-the-shelf models—Amazon Comprehend Medical (ACM) [62] and Google Healthcare Natural Language API (GHNLP) [63]—in their default configuration. In addition, we evaluated both open-source and closed-source LLMs, namely, Llama 3.1 (8B) and GPT-4o in a zero-shot, near-0 temperature (0.25) setting. We identified symptoms in each post of the test dataset using all the baselines for comparison with the ground truth. For LSE, we used GPT-4o to identify symptoms guided by the comprehensive symptom list obtained through our method. Therefore, it was not strictly zero-shot but, rather, a form of lexicon-guided prompting. The model's task was to match symptoms in the text against the LSE-provided symptom lexicon. To ensure reproducibility, we included the LLM prompt templates used for the baseline comparisons (GPT-4o and Llama 3.1), shown in Figure S3 in Multimedia Appendix 1, and LSE evaluation using GPT-4o, as detailed in Figure S4 in Multimedia Appendix 1. We evaluated competitive models using standard performance metrics—precision, recall, and F_1-score. To measure the similarity between symptoms, we used BioBERT-based semantic similarity as it performs optimally with medical data. Given the nuanced nature of symptom expressions, we set the different semantic similarity thresholds at 0.4, 0.6, and 0.8 for match acceptance, and the corresponding performance results are reported in Table 3. Experimental results show that LSE outperformed all baselines significantly across all metrics at every threshold level. As expected, increasing the similarity threshold imposed stricter matching criteria, resulting in fewer accepted symptom matches. Consequently, the performance of all baseline models dropped significantly with higher thresholds. In contrast, the performance of LSE decreased only marginally, highlighting the stability and robustness of our framework. For all subsequent analyses in this study, we adopted a semantic similarity threshold of 0.6 as the default setting. Several additional useful insights from the results are discussed in the following sections.

XSL•FO
RenderX

Table 3. Comparing lexicon-based symptom extraction (LSE) with off-the-shelf medical information extraction tools and large language models in terms of precision, recall, and F1-score across different post lengths.

Model	Post length									
	≤100 words			>100 to 300 words			>300 words			For all length, mean F_1-score
	Precision	Recall	F_1-score	Precision	Recall	F_1-score	Precision	Recall	F_1-score	
Similarity threshold of 0.4										
ACM[a]	55.27	79.85	61.21[b]	39.28	89.50	51.30	31.77	91.21	45.36	52.30
GHNLP[c]	59.96	63.41	58.69[b]	49.39	65.79	51.76	45.29	68.30	51.25	53.37
Llama 3.1 (8B)	53.26	73.00	57.38	62.49	79.11	65.91[b]	63.07	74.00	64.66	63.47
GPT-4o	64.15	60.25	60.77	79.61	74.72	74.81	84.21	71.62	75.33[b]	71.41
LSE	86.09	85.02	84.60	87.85	88.54	86.89	92.09	90.76	90.33[b]	87.17[d]
Similarity threshold of 0.6										
ACM	48.63	68.61	53.45[b]	33.47	76.29	43.85	28.85	81.14	40.30	45.37
GHNLP	47.82	49.54	46.64[b]	35.52	46.78	37.31	35.24	53.00	40.02	40.32
Llama 3.1 (8B)	48.20	63.42	51.60	56.47	71.48	59.64[b]	55.86	64.96	57.27	57.04
GPT-4o	59.05	55.63	56.02	72.11	68.86	68.57	77.97	66.86	70.14[b]	65.80
LSE	84.89	83.82	83.40	86.64	87.42	85.78	91.20	89.57	89.42[b]	86.10[d]
Similarity threshold of 0.8										
ACM	37.66	51.10	41.13[b]	20.68	46.07	26.87	18.58	52.81	26.63	30.38
GHNLP	37.85	40.01	37.62[b]	24.45	33.15	26.18	25.83	39.23	29.54	29.88
Llama 3.1 (8B)	41.12	52.23	43.60[b]	40.81	51.59	43.13	40.39	45.41	40.96	42.71
GPT-4o	49.76	47.88	43.60	55.17	52.12	52.21	60.49	51.07	54.18[b]	51.60
LSE	80.00	79.33	78.81	83.04	83.29	82.02	86.78	85.33	85.12[b]	81.99[d]

[a]ACM: Amazon Comprehend Medical.

[b]For these values, the highest value obtained by a model among the 3-length range.

[c]GHNLP: Google Healthcare Natural Language Application Programming Interface.

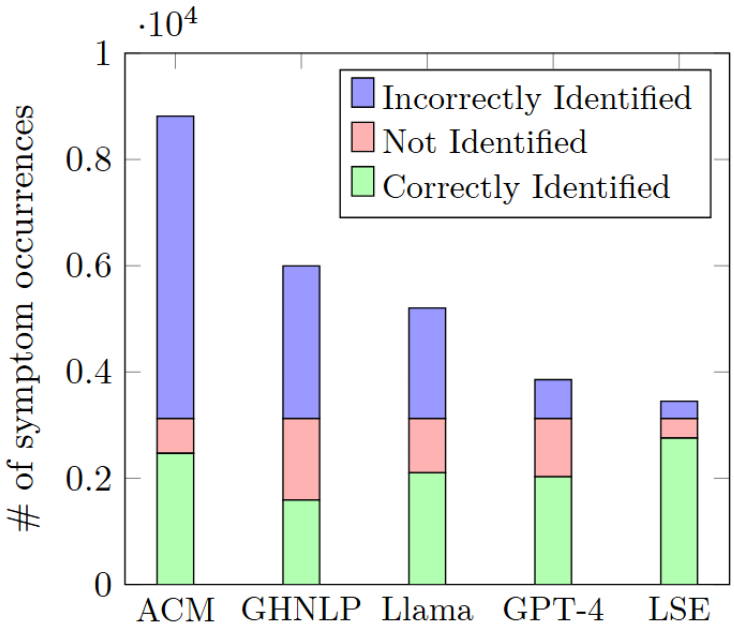
[d]For these values, the LSE obtained the highest F_1-scores among all models in all the threshold-settings.

Off-the-Shelf Models Tend to Overpredict

The GHNLP and ACM models largely extracted generic symptoms that were not disease specific, such as *pregnancy*, *cold*, *sick*, *illness*, and *discomfort*. In addition, they extracted mental conditions such as *anxiety*, *overwhelmed*, and *feeling bad* as PCOS symptoms. As a result, they identified more symptoms (4.84 and 9.05 per post by GHNLP and ACM on average, respectively) compared to the ground truth (mean 2.76, SD 1.90 per post). Moreover, they struggled to comprehend the context of the post content, often extracting medical jargon such as *side effect*, *lab report*, and *medication* as symptoms. Substantially, GHNLP and ACM extracted 64% (2874/4463) and 70% (5691/8161) incorrect symptoms, respectively, of the total symptoms identified (Figure 4). Longer posts aggravated these issues as the presence of more jargon further reduced the precision and F_1-scores of these models (Table 3). However, both models achieved better recall than precision due to overprediction.

XSL•FO
RenderX

Figure 4. Performance comparison of different models in identifying symptom occurrences from 1000 sample posts. Each bar represents the number of correctly identified, not identified, and incorrectly identified symptoms stacked on top of each other. ACM: Amazon Comprehend Medical; GHNLP: Google Healthcare Natural Language Application Programming Interface; LSE: lexicon-based symptom extraction.



Baselines Struggle to Capture Nuanced Symptoms

All the baselines struggled to detect subtle symptoms, specifically when they were stated in informal language. As a result, GHNLP correctly identified only 50% (1589/3124) of the ground truth symptoms, whereas the LLMs showed better performance with approximately 65% (4133/6248) correct matches (Figure 4). Although ACM achieved a 79% (2470/3124) match with the ground truth, its overall performance was hindered by significant overpredictions. For instance, a PCOS symptom, *high testosterone*, was mentioned informally in the following post, but only LSE and none of the baselines could identify it:

> *I had two sets of blood tests taken last year, which showed that my hormones (especially testosterone) were all over the place. My GP said that my test results were enough to confirm PCOS diagnosis.*

LSE Outperformed State-of-the-Art LLMs

Figure 4 shows that, while LLMs significantly reduced the number of incorrectly identified symptoms, they still missed a notable number of symptoms. Leveraging the symptom list generated by LSE in the base prompt for generative pretrained transformers increased the number of correctly identified symptoms, enhancing overall performance. The high values for LSE across all metrics in Table 3 indicate that the comprehensive symptom list effectively covered all PCOS lived experience symptoms while filtering out generic ones.

Statistical Significance

We also compared the F_1-score of LSE with those of the baselines using the approximated randomization test [28] with a similarity threshold of 0.6 to determine whether the results were statistically significant. As this test does not require specific distributional assumptions, it is particularly suitable for complex metrics such as the F_1-score [64]. We conducted pairwise comparisons between symptoms extracted from a post via LSE and each of the baselines. The number of occurrences in the sample set of 1000 posts in which LSE significantly outperformed the baselines at 95% (P<.05) and 90% (P<.10) confidence levels. The observed results suggest that, in terms of the F_1-score, LSE significantly outperformed all the other baselines shown in Table S10 in Multimedia Appendix 1.

Discussion

Analysis of PCOS Symptomatology

Overview

Our study was motivated by the limitations of existing information extraction methods in identifying symptom expressions from colloquial patient narratives. We propose an LSE method incorporating LLMs into the pipeline to capture disease-specific symptoms from social media discourse. We focused on PCOS as a representative case given its highly variable and often underdocumented symptomatology. We evaluated LSE against multiple strong baselines across a manually annotated Reddit dataset, and it demonstrated substantial improvements in precision, recall, and F_1-score.

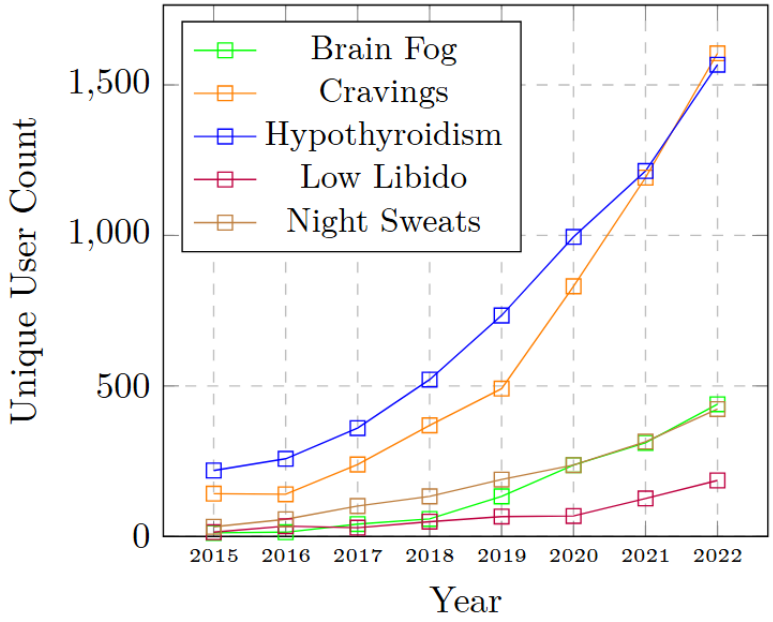
We conducted an in-depth study of PCOS symptomatology to evaluate the characteristics, prevalence, and occurrence patterns of the symptoms, capturing implicit insights from patient-generated data. We also highlighted how capturing symptoms in patient-centric language can bridge gaps between patient experiences and clinical practice, potentially enhancing health care provider communication and guiding clinical decision-making.

XSL•FO
RenderX

Potentially Emerging Symptoms

We identified 28 distinct symptoms from our comprehensive symptom list prominently reported by patients yet currently underrepresented or insufficiently explored in established medical literature and not acknowledged by existing eHealth sources (highlighted in italics in Table 2). Although many of these symptoms currently lack robust clinical evidence linking them directly to PCOS, their frequent occurrence in patient-generated data suggests that patients often experience and associate these symptoms with PCOS. As illustrated in Figure 5, the number of unique users reporting some of these symptoms, such as hypothyroidism and brain fog, demonstrate a consistent upward reporting trend over time. Moreover, some recent studies have provided medical evidence supporting the connection between some of these symptoms and PCOS, such as brain fog, thyroid disorder, low libido, digestive issues, and cravings [65-69]. Therefore, we marked them as potentially emerging symptoms. However, while frequently reported by patients, it is important to recognize that these symptoms might not represent entirely novel manifestations of PCOS. Instead, they may reflect less common but known clinical symptoms, secondary manifestations of the primary disease, or symptoms associated with frequently co-occurring conditions. For example, hypothyroidism, reported by 5366 users, reflects a well-established thyroid-PCOS comorbidity [66], underscoring potential shared pathophysiological mechanisms rather than indicating a novel PCOS symptom. In addition, nausea and cravings, although frequently reported by patients, advocate for a broader and patient-inclusive diagnostic perspective rather than confirming direct causality. These emerging findings reinforce the credibility of patient-reported underdocumented symptoms and underscore the necessity for rigorous clinical investigation to determine their prevalence, pathophysiological connections, and implications for diagnosis and treatment protocols.

Figure 5. Instances of potentially emerging symptoms mentioned by users in the primary dataset, showing notable upward trends over time.



Capturing Symptoms in Patient-Centric Language

LSE captured the lived experience symptoms as expressed by the patients. This approach makes the symptoms more accessible to laypersons compared to clinical terminology and jargon. Some symptoms with unorthodox clinical terms require complex medical tests to diagnose, whereas their effects are often evident in lived experiences, and hence, these symptoms are included in the symptom list. For instance, hyperandrogenism is a symptom that may not be familiar to all users and requires laboratory tests, whereas hirsutism, acne, or hair loss are visible outcomes of the condition that are easily recognized and commonly reported by users, as shown in Table 2.

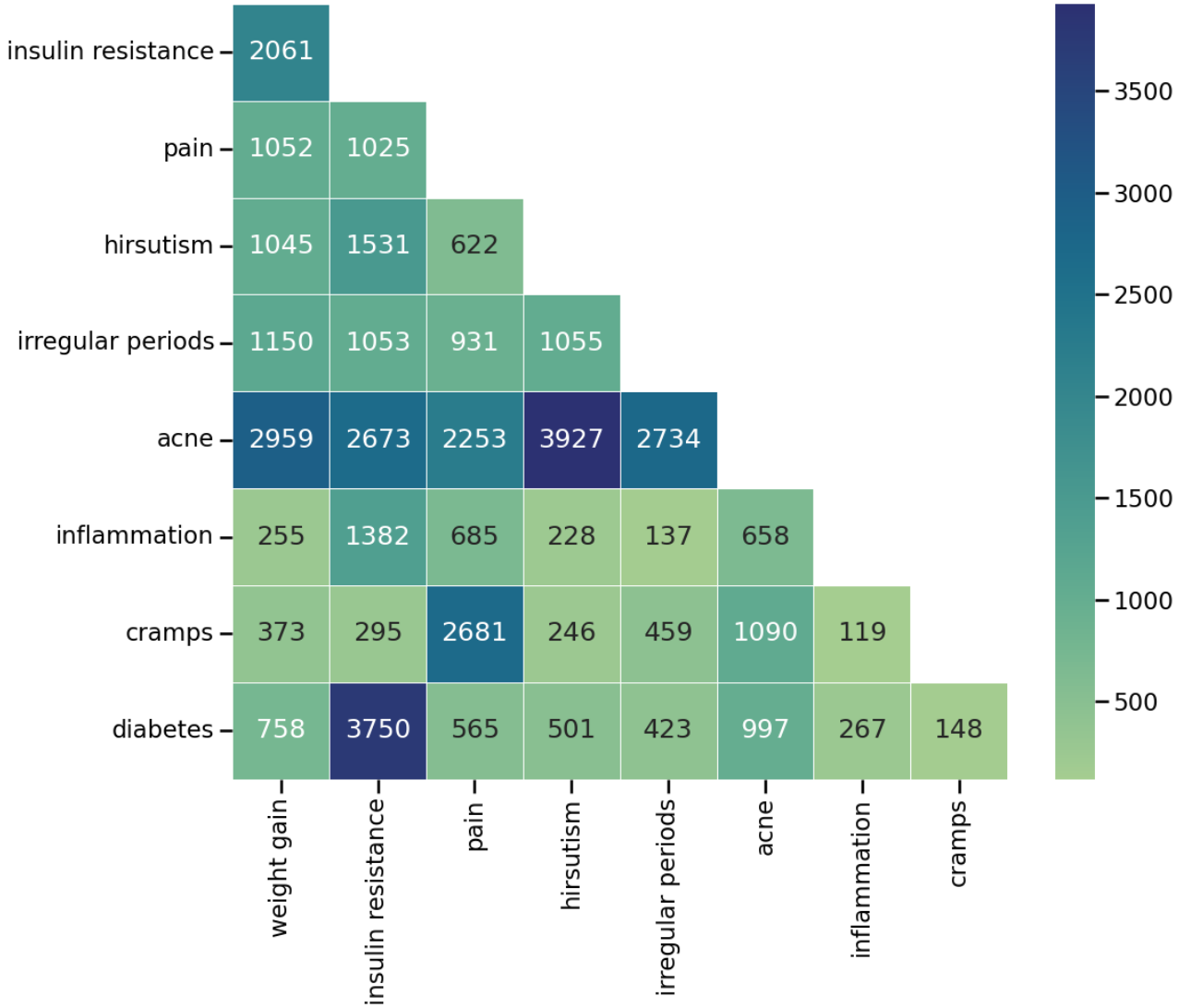
Identifying Co-Occurrence of Symptoms

We constructed a symptom co-occurrence matrix in which multiple symptoms mentioned by an individual in a single post or comment were considered as co-occurring. Figure 6 illustrates a segment of the matrix highlighting the most frequently mentioned symptom pairs with their number of co-occurrences. The eHealth forums further complemented these co-occurrences. Understanding these co-occurring symptoms raises awareness among the community and helps individuals better cope with their condition. In addition, such analysis can assist health care providers and patients in proactively diagnosing and managing symptoms such as hirsutism, oily skin, and acne, as observed in the following comment:

> *The best natural remedy I've tried is spearmint supplement. I'm a thin cysterbut have most of the other symptoms and it has been the only thing I've foundso far that helps with hirsutism, oily skin, acne.*

XSL•FO
RenderX

Figure 6. A segment of the symptom co-occurrence matrix, where hirsutism and acne appear as one of the most frequently mentioned symptom pairs.



Association With Chronic Diseases and Comorbidity

We identified 8 chronic diseases from the list of PCOS symptoms that were distinct medical conditions in their own right. For example, chronic conditions such as hypothyroidism and endometriosis were mentioned by 5366 and 2303 unique users, respectively (Table 2). The association with chronic diseases and comorbidity increases the complexity of the disease and its management and significantly impacts social determinants of health, as shown in the following example:

> *I went to the ER...but they found cysts on my ovaries and mentioned PCOS with possibly Endometriosis. Now, I have no insurance and I'm struggling to find the care. My husband and I want to start a family, but I feel like our chances are slipping away because I can't afford the help I need. Any advice on where to get financial or medical support would be greatly appreciated.*

The financial strain from frequent physician visits and prolonged medications impacts patients' overall health outcomes. This emphasizes the need for clinical and public health research to find ways to reduce the burden on patients, such as overprescription and cost. This may also involve policy reforms to ensure comprehensive coverage for chronic conditions associated with PCOS.

Enhancing Patient–Health Care Provider Communication

The comprehensive symptom list generated by our lexicon-based approach, encompassing both widely recognized and emerging patient-reported symptoms, provides clinicians with a deeper insight into how patients perceive and articulate their condition. For example, terms such as *brain fog*, *pelvic pressure*, and *fatigue* are not only clinically relevant but also capture the nuanced ways in which patients describe their daily experiences with PCOS. Studies also show that using patient-generated health-related terminology during visits deepens shared understanding and decision-making [70]. Therefore, clinicians can leverage this enriched vocabulary to enhance patient–health care provider communication, promoting empathy, validating patient experiences, and facilitating more targeted and personalized clinical interviews.

XSL•FO
RenderX

Guide to Clinical Decision-Making

The patient-derived symptom list (Table 2) can serve as a preliminary checklist during consultations to identify overlooked or underdiscussed symptoms that patients might hesitate to share spontaneously due to stigma or uncertainty. Documenting co-occurrence patterns further empowers clinicians to anticipate linked symptoms. A patient presenting with hirsutism, for instance, could be screened for insulin resistance or acne, enabling early intervention and holistic management. To scale these benefits, the symptom list can be integrated into electronic health record systems. This integration allows for auto-completion prompts that reflect patient language while supporting consistent clinical documentation. Such structured integration enhances clinical decision-making through automated reminders and promotes interoperability for population-level research. Acknowledging patient-reported symptoms does not undermine established clinical evidence; rather, it complements traditional clinical frameworks by incorporating patient perspectives into evidence-based medicine.

Limitations

Despite the promising results, this study has several limitations. First, our study focused on a single health condition and a single social media platform, which may introduce platform-specific biases and limit generalizability. Second, both the lexicon and the evaluation sample sizes are relatively small for broader conclusions. Third, our findings are exploratory and hypothesis generating and not yet clinically validated.

We also acknowledge specific implementation limitations. Although the LSE pipeline is designed for modularity and adaptability, applying it to other complex health conditions may require empirical adjustments. Determining optimal clusters for symptom identification and establishing semantic mapping rules for symptom normalization would require condition-specific customization. In this study, we used silhouette scores and inertia analysis to determine the optimal cluster metrics, such as the number of clusters (k). However, we recognize the limitation of distance-based metrics due to the curse of dimensionality, which may not fully capture cluster shape or density nuances. Despite this, our bootstrap stability analysis demonstrated consistently high Adjusted Rand Index (ARI) values across various k settings, indicating that our symptom clusters were robust to moderate changes in the number of clusters and to the random removal of data points. The performance of this framework may vary depending on the extracted lexicon due to linguistic variability and the nature of symptom discourse. Future work should focus on validating this method across diverse conditions, platforms, and languages. In addition, we plan to conduct online surveys and focus groups involving both patients and practitioners to assess the clinical relevance of our findings.

Conclusions

This work focused on extracting and analyzing disease-specific symptoms from individuals' lived experiences with an application to the PCOS use case. The uniqueness of our work lies in several key aspects. The extraction of a symptom-related lexicon ensures the capture of subtle mentions without overlooking informal expressions on social media. We generated disease-specific symptoms by integrating LLMs into the NLP pipeline rather than relying on traditional NLP methods, which often obtain generic symptoms. In addition, analyzing PCOS symptomatology across varied dimensions revealed unique findings, such as emerging new symptoms expressed in patient-centric language, symptom co-occurrence patterns, and associated comorbidities. The outcomes of this work may help eliminate uncertainties surrounding complex medical conditions and contribute to clinical research and public health policies in a community-informed way.

Acknowledgments

This work was partially supported by the Information and Communication Technology Division of Bangladesh under a postgraduate research fellowship grant. The funding body had no involvement in the study design; data collection, analysis, or experimentation; writing of the report; or decision to submit the paper for publication.

Data Availability

We have publicly released our curated Reddit dataset and human-annotated labeled dataset. To support reproducibility, all source code and resources used in this study have also been made available. The datasets and related materials can be accessed through our GitHub repository [71].

Authors' Contributions

BH conceptualized the study, curated the data, designed the methodology, and organized this study; analyzed the results; and wrote, reviewed, and revised the manuscript. SMP and MEA contributed to conceptualization; supervision; validation of the results; and writing, review, and revision of the manuscript. MFR analyzed the results and contributed to writing, reviewing, and revising the manuscript. RA conceptualized the study, validated the results, and reviewed and revised the manuscript.

Conflicts of Interest

None declared.

Multimedia Appendix 1

XSL•FO
RenderX

Supplementary tables, prompts, and results.
[DOC File , 797 KB - medinform_v13i1e70940_app1.doc]

References

1. Kemp S. Digital 2023: global overview report. DataReportal. 2023 Jan 26. URL: https://datareportal.com/reports/digital-2023-global-overview-report [accessed 2025-05-25]
2. National health interview survey. Centers for Disease Control and Prevention. URL: https://www.cdc.gov/nchs/nhis/2022nhis.htm [accessed 2025-05-25]
3. Jelodar H, Wang Y, Orji R, Huang S. Deep sentiment classification and topic discovery on novel coronavirus or COVID-19 online discussions: NLP using LSTM recurrent neural network approach. IEEE J Biomed Health Inform 2020 Oct;24(10):2733-2742. [doi: 10.1109/JBHI.2020.3001216] [Medline: 32750931]
4. Chopra S, Zehrung R, Shanmugam TA, Choe EK. Living with uncertainty and stigma: self-experimentation and support-seeking around polycystic ovary syndrome. In: Proceedings of the 2021 CHI Conference on Human Factors in Computing Systems. 2021 Presented at: CHI '21; May 8-13, 2021; Yokohama, Japan. [doi: 10.1145/3411764.3445706]
5. Chen LL, Wilson SR, Lohmann S, Negraia DV. What are you anxious about? examining subjects of anxiety during the COVID-19 pandemic. Proceedings of the Int AAAI Conf Web Soc Media 2023 Jun 02;17(1):137-148. [doi: 10.1609/icwsm.v17i1.22133]
6. Attai DJ, Cowher MS, Al-Hamadani M, Schoger JM, Staley AC, Landercasper J. Twitter social media is an effective tool for breast cancer patient education and support: patient-reported outcomes by survey. J Med Internet Res 2015 Jul 30;17(7):e188 [FREE Full text] [doi: 10.2196/jmir.4721] [Medline: 26228234]
7. Jeon J, Baruah G, Sarabadani S, Palanica A. Identification of risk factors and symptoms of COVID-19: analysis of biomedical literature and social media data. J Med Internet Res 2020 Oct 02;22(10):e20509 [FREE Full text] [doi: 10.2196/20509] [Medline: 32936770]
8. Sendra A, Farré J, Vaagan RW. Seeking, sharing and co-creating: a systematic review of the relation between social support theory, social media use and chronic diseases. Soc Theory Health 2019 May 27;18:317-339. [doi: 10.1057/s41285-019-00106-z]
9. McKillop M, Mamykina L, Elhadad N. Designing in the dark: eliciting self-tracking dimensions for understanding enigmatic disease. In: Proceedings of the 2018 CHI Conference on Human Factors in Computing Systems. 2018 Presented at: CHI '18; April 21-26, 2018; Montreal, QC. [doi: 10.1145/3173574.3174139]
10. Lentscher JA, Decherney AH. Clinical presentation and diagnosis of polycystic ovarian syndrome. Clin Obstet Gynecol 2021 Mar 01;64(1):3-11 [FREE Full text] [doi: 10.1097/GRF.0000000000000563] [Medline: 32701517]
11. Porta M, Greenland S, Hernán M, dos Santos Silva I, Last JM. A Dictionary of Epidemiology. Oxford, UK: Oxford University Press; 2014.
12. Romano W, Sharif O, Basak M, Gatto J, Preum SM. Theme-driven keyphrase extraction to analyze social media discourse. Proc Int AAAI Conf Web Soc Media 2024 May 28;18(1):1315-1327. [doi: 10.1609/icwsm.v18i1.31391]
13. Ohno Y, Aomori T, Nishiyama T, Kato R, Fujiki R, Ishikawa H, et al. Performance improvement of a natural language processing tool for extracting patient narratives related to medical states from Japanese pharmaceutical care records by increasing the amount of training data: natural language processing analysis and validation study. JMIR Med Inform 2025 Mar 04;13:e68863 [FREE Full text] [doi: 10.2196/68863] [Medline: 40053805]
14. Molenaar A, Lukose D, Brennan L, Jenkins EL, McCaffrey TA. Using natural language processing to explore social media opinions on food security: sentiment analysis and topic modeling study. J Med Internet Res 2024 Mar 21;26:e47826 [FREE Full text] [doi: 10.2196/47826] [Medline: 38512326]
15. Zhang T, Schoene AM, Ji S, Ananiadou S. Natural language processing applied to mental illness detection: a narrative review. NPJ Digit Med 2022 Apr 08;5(1):46 [FREE Full text] [doi: 10.1038/s41746-022-00589-7] [Medline: 35396451]
16. Sharif O, Gatto J, Basak M, Preum SM. Explicit, implicit, and scattered: revisiting event extraction to capture complex arguments. In: Proceedings of the 2024 Conference on Empirical Methods in Natural Language Processing. 2024 Presented at: EMNLP 2024; November 12-16, 2024; Miami, FL. [doi: 10.18653/v1/2024.emnlp-main.673]
17. Guo Y, Ovadje A, Al-Garadi MA, Sarker A. Evaluating large language models for health-related text classification tasks with public social media data. J Am Med Inform Assoc 2024 Oct 01;31(10):2181-2189. [doi: 10.1093/jamia/ocae210] [Medline: 39121174]
18. Agarwal S, Searle T, Ratas M, Shek A, Teo J, Dobson R. Improving extraction of clinical event contextual properties from electronic health records: a comparative study. ArXiv Preprint posted online on August 30, 2024. [doi: 10.48550/arXiv.2408.17181]
19. Bai L, Mulvenna MD, Wang Z, Bond R. Clinical entity extraction: comparison between MetaMap, cTAKES, CLAMP and Amazon comprehend medical. In: Proceedings of the 32nd Irish Signals and Systems Conference. 2021 Presented at: ISSC 2021; June 10-11, 2021; Athlone, Ireland URL: https://doi.org/10.1109/ISSC52156.2021.9467856 [doi: 10.1109/issc52156.2021.9467856]

XSL•FO
RenderX

20. Peng J, Zhao M, Havrilla J, Liu C, Weng C, Guthrie W, et al. Natural language processing (NLP) tools in extracting biomedical concepts from research articles: a case study on autism spectrum disorder. BMC Med Inform Decis Mak 2020 Dec 30;20(Suppl 11):322 [FREE Full text] [doi: 10.1186/s12911-020-01352-2] [Medline: 33380331]
21. Agrawal M, Hegselmann S, Lang H, Kim Y, Sontag D. Large language models are few-shot clinical information extractors. ArXiv Preprint posted online on May 25, 2022 [FREE Full text] [doi: 10.48550/arXiv.2205.12689]
22. Sorbello A, Haque SA, Hasan R, Jermyn R, Hussein A, Vega A, et al. Artificial intelligence-enabled software prototype to inform opioid pharmacovigilance from electronic health records: development and usability study. JMIR AI 2023;2:e45000 [FREE Full text] [doi: 10.2196/45000] [Medline: 37771410]
23. Luo X, Gandhi P, Storey S, Huang K. A deep language model for symptom extraction from clinical text and its application to extract COVID-19 symptoms from social media. IEEE J Biomed Health Inform 2022 Apr;26(4):1737-1748 [FREE Full text] [doi: 10.1109/JBHI.2021.3123192] [Medline: 34705659]
24. Dolatabadi E, Moyano D, Bales M, Spasojevic S, Bhambhoria R, Bhatti J, et al. Using social media to help understand patient-reported health outcomes of post-COVID-19 condition: natural language processing approach. J Med Internet Res 2023 Sep 19;25:e45767 [FREE Full text] [doi: 10.2196/45767] [Medline: 37725432]
25. Ding Q, Massey D, Huang C, Grady CB, Lu Y, Cohen A, et al. Tracking self-reported symptoms and medical conditions on social media during the COVID-19 pandemic: infodemiological study. JMIR Public Health Surveill 2021 Sep 28;7(9):e29413 [FREE Full text] [doi: 10.2196/29413] [Medline: 34517338]
26. Babaian T, Xu J. Entity recognition from colloquial text. Decis Support Syst 2024 Apr;179:114172 [FREE Full text] [doi: 10.1016/j.dss.2024.114172]
27. Guo M, Ma Y, Eworuke E, Khashei M, Song J, Zhao Y, et al. Identifying COVID-19 cases and extracting patient reported symptoms from Reddit using natural language processing. Sci Rep 2023 Aug 22;13(1):13721 [FREE Full text] [doi: 10.1038/s41598-023-39986-7] [Medline: 37607963]
28. Goel A, Gueta A, Gilon O, Liu C, Erell S, Nguyen LH, et al. LLMs accelerate annotation for medical information extraction. ArXiv Preprint posted online on December 4, 2023. [doi: 10.48550/arXiv.2312.02296]
29. Wei WI, Leung CL, Tang A, McNeil EB, Wong SY, Kwok KO. Extracting symptoms from free-text responses using ChatGPT among COVID-19 cases in Hong Kong. Clin Microbiol Infect 2024 Jan;30(1):142.e1-142.e3 [FREE Full text] [doi: 10.1016/j.cmi.2023.11.002] [Medline: 37949111]
30. Li Y, Viswaroopan D, He W, Li J, Zuo X, Xu H, et al. Improving entity recognition using ensembles of deep learning and fine-tuned large language models: a case study on adverse event extraction from VAERS and social media. J Biomed Inform 2025 Mar;163:104789 [FREE Full text] [doi: 10.1016/j.jbi.2025.104789] [Medline: 39923968]
31. Polycystic ovary syndrome. World Health Organization. 2025 Feb 07. URL: https://www.who.int/news-room/fact-sheets/detail/polycystic-ovary-syndrome [accessed 2025-05-25]
32. Escobar-Morreale HF. Polycystic ovary syndrome: definition, aetiology, diagnosis and treatment. Nat Rev Endocrinol 2018 May;14(5):270-284. [doi: 10.1038/nrendo.2018.24] [Medline: 29569621]
33. Rowlands IJ, Teede H, Lucke J, Dobson AJ, Mishra GD. Young women's psychological distress after a diagnosis of polycystic ovary syndrome or endometriosis. Hum Reprod 2016 Sep 13;31(9):2072-2081. [doi: 10.1093/humrep/dew174] [Medline: 27412249]
34. Malhotra K, Kempegowda P. Appraising unmet needs and misinformation spread about polycystic ovary syndrome in 85,872 YouTube comments over 12 years: big data infodemiology study. J Med Internet Res 2023 Sep 11;25:e49220 [FREE Full text] [doi: 10.2196/49220] [Medline: 37695666]
35. Naroji S, John J, Gomez-Lobo V. Understanding PCOS-related content across social media platforms-a cross-sectional analysis. J Pediatr Adolesc Gynecol 2024 Apr;37(2):142-148. [doi: 10.1016/j.jpag.2023.10.007] [Medline: 37992985]
36. Cruz J, Qazi Z, Vasireddy AM, Vilchez-Russell KA, Stuparich MA, Nahas S, et al. Instagram cysters: what's available on polycystic ovarian syndrome? Fertil Steril 2022 Oct;118(4):e323 [FREE Full text]
37. Proferes N, Jones N, Gilbert S, Fiesler C, Zimmer M. Studying Reddit: a systematic overview of disciplines, approaches, methods, and ethics. Soc Media Soc 2021 May 26;7(2). [doi: 10.1177/20563051211019004]
38. Boe B. PRAW: the python Reddit API wrapper. GitHub. 2020. URL: https://github.com/praw-dev/praw/ [accessed 2025-08-13]
39. Baumgartner J. Pushshift Reddit API Documentation. 2018. URL: https://reddit-api.readthedocs.io/ [accessed 2025-08-27]
40. Patel D, Timsina P, Raut G, Freeman R, Levin MA, Nadkarni GN, et al. Exploring temperature effects on large language models across various clinical tasks. medRxiv Preprint posted online on July 22, 2024 [FREE Full text] [doi: 10.1101/2024.07.22.24310824]
41. Hu Y, Chen Q, Du J, Peng X, Keloth VK, Zuo X, et al. Improving large language models for clinical named entity recognition via prompt engineering. J Am Med Inform Assoc 2024 Sep 01;31(9):1812-1820. [doi: 10.1093/jamia/ocad259] [Medline: 38281112]
42. Ouyang L, Wu J, Jiang X, Almeida D, Wainwright CL, Mishkin P, et al. Training language models to follow instructions with human feedback. In: Proceedings of the 36th International Conference on Neural Information Processing Systems. 2022 Presented at: NIPS'22; November 28-December 9, 2022; New Orleans, LA URL: https://dl.acm.org/doi/10.5555/3600270.3602281 [doi: 10.5860/choice.189890]

XSL•FO
RenderX

43. Leas EC, Ayers JW, Desai N, Dredze M, Hogarth M, Smith DM. Using large language models to support content analysis: a case study of ChatGPT for adverse event detection. J Med Internet Res 2024 May 02;26:e52499 [FREE Full text] [doi: 10.2196/52499] [Medline: 38696245]
44. Kuo HY, Chen SY. Predicting user engagement in health misinformation correction on social media platforms in Taiwan: content analysis and text mining study. J Med Internet Res 2025 Jan 23;27:e65631 [FREE Full text] [doi: 10.2196/65631] [Medline: 39847418]
45. Mohr I, Wuhrl A, Klinger R. CoVERT: a corpus of fact-checked biomedical COVID-19 tweets. In: Proceedings of the 13th Conference on Language Resources and Evaluation. 2022 Presented at: LREC 2022; June 20-25, 2022; Marseille, France URL: https://aclanthology.org/2022.lrec-1.26.pdf
46. Herman Bernardim Andrade G, Nishiyama T, Fujimaki T, Yada S, Wakamiya S, Takagi M, et al. Assessing domain adaptation in adverse drug event extraction on real-world breast cancer records. Int J Med Inform 2024 Nov;191:105539 [FREE Full text] [doi: 10.1016/j.ijmedinf.2024.105539] [Medline: 39084086]
47. Sarwar TB, Noor NM, Saef Ullah Miah M. Evaluating keyphrase extraction algorithms for finding similar news articles using lexical similarity calculation and semantic relatedness measurement by word embedding. PeerJ Comput Sci 2022;8:e1024 [FREE Full text] [doi: 10.7717/peerj-cs.1024] [Medline: 35875631]
48. Devlin J, Chang MW, Lee K, Toutanova K. Bert: pre-training of deep bidirectional transformers for language understanding. ArXiv Preprint posted online on October 11, 2018 [FREE Full text] [doi: 10.18653/v1/N19-1423]
49. Wang S, Thompson L, Iyyer M. Phrase-BERT: improved phrase embeddings from BERT with an application to corpus exploration. ArXiv Preprint posted online on September 13, 2021 [FREE Full text] [doi: 10.18653/v1/2021.emnlp-main.846]
50. Lee J, Yoon W, Kim S, Kim D, Kim S, So CH, et al. BioBERT: a pre-trained biomedical language representation model for biomedical text mining. Bioinformatics 2020 Feb 15;36(4):1234-1240 [FREE Full text] [doi: 10.1093/bioinformatics/btz682] [Medline: 31501885]
51. Shahapure KR, Nicholas C. Cluster quality analysis using silhouette score. In: Proceedings of the IEEE 7th International Conference on Data Science and Advanced Analytics. 2020 Presented at: DSAA 2020; October 6-9, 2020; Sydney, Australia. [doi: 10.1109/dsaa49011.2020.00096]
52. Moulavi D, Jaskowiak PA, Campello RJ, Zimek A, Sander J. Density-based clustering validation. In: Proceedings of the 2014 SIAM International Conference on Data Mining. 2014 Presented at: SIAM 2014; April 24-26, 2014; Philadelphia, PA. [doi: 10.1137/1.9781611973440.96]
53. Meng Y, Huang J, Wang G, Zhang C, Zhuang H, Kaplan L, et al. Spherical text embedding. In: Proceedings of the 33rd International Conference on Neural Information Processing Systems. 2019 Presented at: NIPS'19; December 8-14, 2019; Vancouver, BC.
54. Risch J, Möller T, Gutsch J, Pietsch M. Semantic answer similarity for evaluating question answering models. In: Proceedings of the 3rd Workshop on Machine Reading for Question Answering. 2021 Presented at: MRQA 2021; November 10, 2021; Online. [doi: 10.18653/v1/2021.mrqa-1.15]
55. Liu J, Gupta S, Chen A, Wang CK, Mishra P, Dai HJ, et al. OpenDeID pipeline for unstructured electronic health record text notes based on rules and transformers: deidentification algorithm development and validation study. J Med Internet Res 2023 Dec 06;25:e48145 [FREE Full text] [doi: 10.2196/48145] [Medline: 38055317]
56. Mayo clinic. Mayo Foundation for Medical Education and Research. URL: https://www.mayoclinic.org/ [accessed 2025-05-25]
57. A Visual Guide to PCOS. WebMD. 2025 Jun 24. URL: https://www.webmd.com/women/ss/slideshow-pcos-overview [accessed 2025-08-27]
58. Free ICD-10-CM data. ICD10Data.com. URL: https://www.icd10data.com/ICD10CM [accessed 2025-05-25]
59. Polycystic ovary syndrome (PCOS). Johns Hopkins University. URL: https://www.hopkinsmedicine.org/health/conditions-and-diseases/polycystic-ovary-syndrome-pcos [accessed 2025-05-25]
60. Polycystic ovary syndrome. National Health Service. URL: https://www.nhs.uk/conditions/polycystic-ovary-syndrome-pcos/ [accessed 2025-05-25]
61. Diabetes and polycystic ovary syndrome (PCOS). Centers for Disease Control and Prevention. 2024 May 15. URL: https://www.cdc.gov/diabetes/risk-factors/pcos-polycystic-ovary-syndrome.html [accessed 2025-05-25]
62. Amazon comprehend medical. Amazon Web Services. URL: https://aws.amazon.com/comprehend/medical/ [accessed 2025-05-25]
63. Cloud healthcare API. Google Cloud. URL: https://cloud.google.com/healthcare-api?hl=en [accessed 2025-05-25]
64. Yeh A. More accurate tests for the statistical significance of result differences. In: Proceedings of the COLING 2000 Volume 2: The 18th International Conference on Computational Linguistics. 2000 Presented at: COLING 2000; July 31-August 4, 2000; Saarbrücken, Germany. [doi: 10.3115/992730.992783]
65. Huddleston HG, Jaswa EG, Casaletto KB, Neuhaus J, Kim C, Wellons M, et al. Associations of polycystic ovary syndrome with indicators of brain health at midlife in the CARDIA cohort. Neurology 2024 Feb 27;102(4). [doi: 10.1212/wnl.0000000000208104]
66. Singla R, Gupta Y, Khemani M, Aggarwal S. Thyroid disorders and polycystic ovary syndrome: an emerging relationship. Indian J Endocrinol Metab 2015;19(1):25-29 [FREE Full text] [doi: 10.4103/2230-8210.146860] [Medline: 25593822]

XSL•FO
RenderX

67. Eftekhar T, Sohrabvand F, Zabandan N, Shariat M, Haghollahi F, Ghahghaei-Nezamabadi A. Sexual dysfunction in patients with polycystic ovary syndrome and its affected domains. Iran J Reprod Med 2014 Aug;12(8):539-546 [FREE Full text] [Medline: 25408703]
68. Kałużna M, Kompf P, Wachowiak-Ochmańska K, Moczko J, Królczyk A, Janicki A, et al. Are patients with polycystic ovary syndrome more prone to irritable bowel syndrome? Endocr Connect 2022;11(4):e210309 [FREE Full text] [doi: 10.1530/ec-21-0309]
69. Jeanes YM, Reeves S, Gibson EL, Piggott C, May VA, Hart KH. Binge eating behaviours and food cravings in women with polycystic ovary syndrome. Appetite 2017 Feb 01;109:24-32. [doi: 10.1016/j.appet.2016.11.010] [Medline: 27825940]
70. Staehelin D, Dolata M, Stöckli L, Schwabe G. How patient-generated data enhance patient-provider communication in chronic care: field study in design science research. JMIR Med Inform 2024 Sep 10;12:e57406 [FREE Full text] [doi: 10.2196/57406] [Medline: 39255481]
71. Subreddit to symptomatology data and code. GitHib. URL: https://github.com/bush1987/LSE-Symptomatology [accessed 2025-08-02]

Abbreviations

ACM: Amazon Comprehend Medical
API: application programming interface
BERT: bidirectional encoder representations from transformers
DBCV: density-based clustering validation
GHNLP: Google Healthcare Natural Language Application Programming Interface
HDBSCAN: hierarchical density-based spatial clustering of applications with noise
JI: Jaccard index
LLM: large language model
LSE: lexicon-based symptom extraction
NLP: natural language processing
PCOS: polycystic ovary syndrome

Edited by A Castonguay; submitted 06.01.25; peer-reviewed by S Hwang, R Sauvayre, S Sivarajkumar; comments to author 26.04.25; revised version received 25.05.25; accepted 09.07.25; published 12.09.25.

Please cite as:
Hossain B, Preum SM, Rabbi MF, Ara R, Ali ME
Extracting Symptoms of Complex Conditions From Online Discourse (Subreddit to Symptomatology): Lexicon-Based Approach
JMIR Med Inform 2025;13:e70940
URL: https://medinform.jmir.org/2025/1/e70940
doi:10.2196/70940
PMID:

©Bushra Hossain, Sarah M Preum, Md Fazle Rabbi, Rifat Ara, Mohammed Eunus Ali. Originally published in JMIR Medical Informatics (https://medinform.jmir.org), 12.09.2025. This is an open-access article distributed under the terms of the Creative Commons Attribution License (https://creativecommons.org/licenses/by/4.0/), which permits unrestricted use, distribution, and reproduction in any medium, provided the original work, first published in JMIR Medical Informatics, is properly cited. The complete bibliographic information, a link to the original publication on https://medinform.jmir.org/, as well as this copyright and license information must be included.

XSL•FO
RenderX

Interpretable Machine Learning Model for Predicting and Assessing the Risk of Diabetic Nephropathy: Prediction Model Study

Yili Wen[1], MM; Zhiqiang Wan[2], MEng; Huiling Ren[1], MM; Xu Wang[1], MM; Weijie Wang[1], MM

[1]Institute of Medical Information/Medical Library, Chinese Academy of Medical Sciences & Peking Union Medical College, 3 Yabao Road, Chaoyang District, Beijing, China

[2]Peking Union Medical College Hospital, Chinese Academy of Medical Science & Peking Union Medical College, Beijing, China

Corresponding Author:
Huiling Ren, MM
Institute of Medical Information/Medical Library, Chinese Academy of Medical Sciences & Peking Union Medical College, 3 Yabao Road, Chaoyang District, Beijing, China

Abstract

Background: Diabetic nephropathy (DN), a severe complication of diabetes, is characterized by proteinuria, hypertension, and progressive renal function decline, potentially leading to end-stage renal disease. The International Diabetes Federation projects that by 2045, 783 million people will have diabetes, with 30% - 40% of them developing DN. Current diagnostic approaches lack sufficient sensitivity and specificity for early detection and diagnosis, underscoring the need for an accurate, interpretable predictive model to enable timely intervention, reduce cardiovascular risks, and optimize health care costs.

Objective: This study aimed to develop and validate a machine learning–based predictive model for DN in patients with type 2 diabetes, with a focus on achieving high predictive accuracy while ensuring transparency and interpretability through explainable artificial intelligence techniques, thereby supporting early diagnosis, risk assessment, and personalized clinical decision-making.

Methods: Our retrospective cohort study investigated 1000 patients with type 2 diabetes using data from electronic medical records collected between 2015 and 2020. The study design incorporated a sample of 444 patients with DN and 556 without, focusing on demographics, clinical metrics such as blood pressure and glucose levels, and renal function markers. Data collection relied on electronic records, with missing values handled via multiple imputation and dataset balance achieved using Synthetic Minority Oversampling Technique (SMOTE). In this study, advanced machine learning algorithms, namely Extreme Gradient Boosting (XGBoost), CatBoost, and Light Gradient-Boosting Machine (LightGBM), were used due to their robustness in handling complex datasets. Key metrics, including accuracy, precision, recall, F_1-score, specificity, and area under the curve, were used to provide a comprehensive assessment of model performance. In addition, explainable machine learning techniques, such as Local Interpretable Model-Agnostic Explanations (LIME) and Shapley Additive Explanations (SHAP), were applied to enhance the transparency and interpretability of the models, offering valuable insights into their decision-making processes.

Results: XGBoost and LightGBM demonstrated superior performance, with XGBoost achieving the highest accuracy of 86.87%, a precision of 88.90%, a recall of 84.40%, an F_1-score of 86.44%, and a specificity of 89.12%. LIME and SHAP analyses provided insights into the contribution of individual features to elucidate the decision-making processes of these models, identifying serum creatinine, albumin, and lipoproteins as significant predictors.

Conclusions: The developed machine learning model not only provides a robust predictive tool for early diagnosis and risk assessment of DN but also ensures transparency and interpretability, crucial for clinical integration. By enabling early intervention and personalized treatment strategies, this model has the potential to improve patient outcomes and optimize health care resource usage.

(JMIR Med Inform 2025;13:e64979) doi:10.2196/64979

KEYWORDS

type 2 diabetes; machine learning; interpretability analysis; ML; diabetes; risk assessment; diabetic nephropathy; hypertension; renal disease; renal function; glucose; oxidative stress; inflammation; fibrosis; kidney; quality of life; ML model; predictive tool; early diagnosis; patient outcomes

XSL•FO
RenderX

Introduction

Background

Diabetic nephropathy (DN), severe microvascular complications of diabetes, primarily manifests as proteinuria, hypertension, and a progressive decline in renal function, potentially leading to end-stage renal disease. The pathogenesis of DN is attributed to a high-glucose milieu, oxidative stress, inflammation, and fibrosis, collectively contributing to substantial morphological changes in kidneys including thickening of glomerular basement membrane, glomerulosclerosis, tubular atrophy, interstitial inflammation, and renal fibrosis [1]. The prevalence of diabetes and diabetic kidney disease has been increasing, and the International Diabetes Federation projected that the number of patients with diabetes would rise to 783 million by 2045. Notably, approximately 30%‐40% of these patients are expected to develop DN [2], with a mortality rate 30 times higher than that of diabetic patients without kidney disease [3]. Hence, the importance of early detection cannot be overstated in managing DN. Early diagnosis not only significantly reduces the reliance on costly medical resources such as dialysis and transplantation but also alleviates the economic burden on patients [4]. By intervening in the early stages of DN, clinicians can effectively preserve renal function and slow disease progression, thereby enhancing the quality of life and reducing the risk of cardiovascular complications, a major cause of death among patients with diabetes. Moreover, from a perspective of health economics, early detection is crucial as it reduces the need for intensive later-stage treatments, allowing for the reallocation of medical resources to other pressing needs [5]. Consequently, investing in the early detection of DN not only benefits patients but also enhances the efficiency of health care resource usage across society.

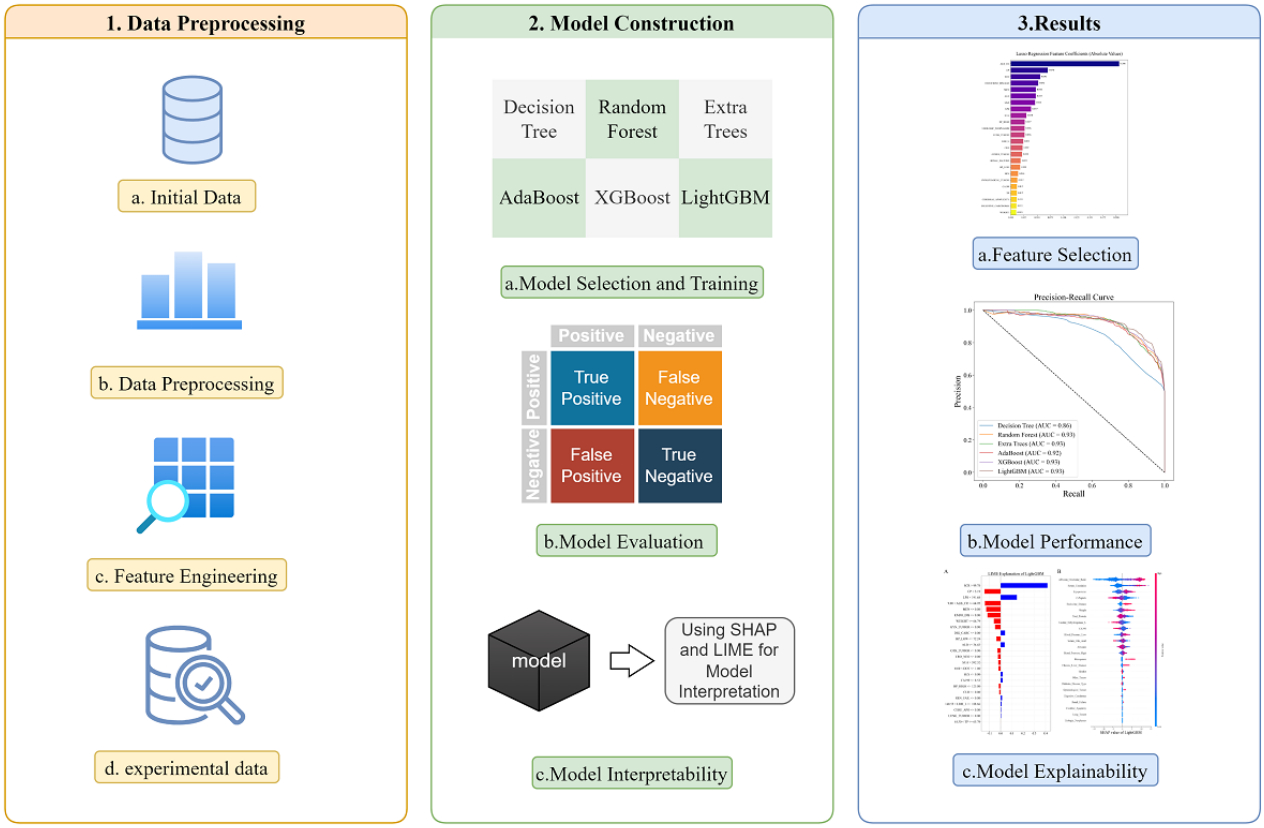
Machine learning (ML), as a significant branch of artificial intelligence (AI), has revolutionized the field of medical research by analyzing complex datasets to discover models and make predictions. Particularly in disease prediction and classification, ML algorithms can handle vast amounts of clinical and biological data, identify risk factors, predict disease onset, and accurately classify disease subtypes [6]. In contrast, traditional statistical methods often perform poorly when dealing with the high dimensionality and nonlinearity of biomedical data, whereas ML algorithms, such as decision trees, random forests, support vector machines, and neural networks, exhibit advantages that traditional statistical methods cannot match [7]. ML algorithms have been widely applied in clinical research and shown outstanding performance in various fields. For example, they have achieved significant results in the early prediction of acute kidney injury [8], malaria prediction [9], and cervical cancer survival prediction [10]. Despite the tremendous potential of ML models in predictive analysis, their application in clinical environments is often hindered by the "black box" nature of many algorithms. This opacity limits clinicians' understanding, trust, and effective use of ML predictions. To address this issue, explainable machine learning (XML) techniques have emerged, aiming to enhance the transparency and interpretability of models [11]. By using techniques such as Shapley Additive Explanations (SHAP) and Local Interpretable Model-Agnostic Explanations (LIME), XML can elucidate the contribution of individual features to prediction outcomes, thereby increasing the model's transparency and interpretability [12]. This interpretability is crucial for integrating ML into clinical workflows, as it allows health care providers to validate model outputs based on clinical knowledge, explain decisions to patients, and comply with regulatory standards [13]. Ultimately, XML holds the promise of bridging the gap between advanced analytics and clinical applications, fostering more informed and more confident decision-making in patient care.

Objective

In the clinical management of DN, early diagnosis and precise treatment are crucial for improving patient outcomes. However, traditional diagnostic methods often fall short in predicting the complex progression of the disease, necessitating new tools to enhance predictive accuracy and reliability. This study aims to develop and validate an ML-based model for predicting DN, emphasizing both high predictive accuracy and model interpretability to meet clinicians' needs for transparency. By addressing the gap in both predictive performance and interpretability, this model provides a more holistic approach to managing DN. By creating a new predictive tool, we aim to provide clinicians with a deep understanding of the model's predictive logic, thereby enhancing trust and application of the predictions. We meticulously designed and integrated various ML algorithms, including decision trees, random forests, extra trees, Adaptive Boosting (AdaBoost), Extreme Gradient Boosting (XGBoost), and Light Gradient-Boosting Machine (LightGBM), to build a model with significant predictive accuracy. Concurrently, we used LIME and SHAP methods for in-depth analysis of the model's interpretability, ensuring transparency and fairness in the prediction process. The core contribution of this study lies in enhancing model interpretability, thereby increasing its credibility and practicality in real medical applications. This model not only provides a scientifically transparent decision support system for early diagnosis, risk assessment, and personalized treatment of DN but also aids doctors in devising more precise intervention strategies to improve patient outcomes. We believe that the generalizability and effectiveness of these methods will lay a solid foundation for the broader application of ML technologies in various medical scenarios and open new avenues for medical research. We outline the overall approach of our study as shown in Figure 1.

XSL•FO
RenderX

Figure 1. Overview of the research framework. This diagram illustrates the complete workflow from data preprocessing to model interpretability, where the orange module represents the data processing stage, the green module denotes the model construction phase, and the blue module signifies the result analysis stage. The directional arrows indicate the sequential order of processes. AdaBoost: Adaptive Boosting; AUC: area under the curve; LightGBM: Light Gradient-Boosting Machine; LIME: Local Interpretable Model-Agnostic Explanations; SHAP: Shapley Additive Explanations; XGBoost: Extreme Gradient Boosting.



Related Work

XML has been introduced to enhance model transparency and reliability, helping clinicians better understand the predictions made by these models. Several studies have successfully demonstrated how interpretability techniques can improve the transparency of clinical decision-making. Chadaga et al [14] used SHAP and LIME to predict COVID-19 prognosis using clinical markers, aiming to identify high-risk patients early and provide appropriate treatments to prevent severe outcomes, while also making AI predictions interpretable and trustworthy for medical professionals. Khanna et al [15] built a decision support system using SHAP and LIME to predict osteoporosis risk, aiming to enhance early diagnosis and treatment while making ML models interpretable and reliable for medical professionals. Guan et al [16] used SHAP to interpret venous thromboembolism risks in patients who are critically ill, with the goal of improving early risk identification, enabling timely interventions, and fostering transparency and trust in the decision-making process. Zhong et al [17] introduced SHAP to significantly improve the accuracy of blood oxygen saturation estimation based on neck photoplethysmography, thereby enhancing the reliability of noninvasive oxygen monitoring. Suh et al [18] used LIME to analyze a deep learning model for osteoporosis risk screening, identifying and ranking critical features that contribute to risk prediction. This approach enhances the interpretability of ML models, facilitating personalized health care and aiding clinicians in understanding the decision-making process. In the domain of XML, SHAP and LIME are among the most commonly used methods; however, other approaches, such as partial dependence plot (PDP), are also available. Bernard et al [19] used PDP to visualize the influence of individual features on the model's output by isolating their effects while averaging over all other features. Zhang et al [20] used PDP to analyze the marginal effect of individual features on the model's predictions by averaging their impacts while keeping other features constant. This method helps reveal how changes in a particular feature influence the predicted outcomes, providing clinicians with interpretable insights into feature significance and supporting informed decision-making in personalized health care.

Methods

Data Source

The dataset for this study originated from the National Population Health Data Center's "Diabetes Complications Dataset" and comprised detailed records of 1000 patients with type 2 diabetes. The complete dataset of 1000 patients was used for our analysis without applying any additional inclusion or exclusion criteria, as the dataset had already undergone an initial selection and screening process before public release by the data provider. The dataset covers 87 features, including patients' basic demographic information such as age, gender, ethnicity, and marital status, biochemical test results such as blood glucose

XSL•FO
RenderX

levels, lipid analysis, renal function indicators, and other relevant hematological parameters, and comorbidities such as kidney disease, cardiovascular diseases, fatty liver, and many other chronic conditions. The dataset contained information on 444 patients with DN and 556 patients without nephropathy, providing a rich empirical basis for the study of DN risk prediction.

Data Preprocessing

In this study, features with a data missing proportion exceeding 75% (750/1000) were excluded due to their severely limited informational content and minimal impact on the research outcomes. For features with a data missing proportion less than 75% (750/1000), multiple imputation was used. This method, based on multivariate regression models and iterative algorithms, is well-suited for handling clinical data with diverse feature types due to its ability to preserve interfeature correlations and prevent the disruption of internal data relationships, which is typical for singular imputation methods. The fundamental approach involves initially filling each feature containing missing values with simple methods such as the mean to provide initial values, followed by the use of current filled values from other features to predict and update missing values through regression models. This process iterates until the imputation converges or the predefined maximum number of iterations is reached. In addition, we noted that the ratio of patients with DN to those without is 444:556, close to 4:5. Although this imbalance is not particularly severe, we used the Synthetic Minority Oversampling Technique (SMOTE) to enhance the accuracy and reliability of our model predictions. SMOTE generates new synthetic samples by randomly interpolating between minority class samples and their nearest neighbors. This method not only increases the number of minority class samples but also maintains intraclass diversity, thereby avoiding the potential overfitting issues associated with simple sample replication. Through this approach, SMOTE has effectively addressed the issue of data imbalance, laying a solid foundation for the development of a more robust and more accurate predictive model.

Statistical Analysis

This study used Python version 3.9.5, originally developed by Guido van Rossum and currently maintained by the Python Software Foundation, for data analysis. In the statistical data analysis, the Shapiro-Wilk test was first conducted on continuous variables to determine whether they follow a normal distribution. If these variables did not follow a normal distribution, the Mann-Whitney *U* test was used to explore their associations with DN. The Mann-Whitney *U* test helped examine whether there are significant statistical differences between the patient and nonpatient groups, making it an effective nonparametric testing method. If these variables followed a normal distribution, the Student *t* test was used to analyze their associations with DN. This parametric testing method assessed the significance of differences in the means of 2 samples, aiding in the identification of key indicators related to the risk of DN. For categorical variables, chi-square tests were used to analyze their associations with DN, detecting distribution differences of categorical variables across different disease states. Through these tests, we gained a more comprehensive understanding of how different types of data characteristics influence the risk of DN. Statistical significance was defined as $P<.001$.

Feature Selection

Given the limited sample size and large number of features in the data involved in this study, we adopted the least absolute shrinkage and selection operator (lasso) method for feature selection to ensure the efficiency of the analysis and the accuracy of the results. Lasso introduces the L1 paradigm as a penalty term in regression analysis, making it widely used in high-dimensional data processing [21]. Its objective function is:

$$\min\beta\{12n\sum i=0n(yi-\sum j=1pxij\beta j)2+\lambda\sum j=0p\beta j\}$$

where, yi is the response variable of the ith observation, xij is the jth feature of the ith observation, βj is the regression coefficient of the jth feature, λ is the regularization parameter used to control the complexity of the model, n is the number of samples, and p is the number of features.

By adjusting the regularization parameter λ, lasso achieves a balance between model complexity and fitting accuracy. The core mechanism is to drive some of the regression coefficients to zero through the L1 paradigm penalty, enabling variable selection and feature downscaling. This capability gives lasso a significant advantage when dealing with clinical data, as it is able to automatically screen out important variables and eliminate redundant or irrelevant features, making it particularly suitable for high-dimensional data with a large number of features. Through this regularization, lasso enhances the stability and predictive power of the model, preventing overfitting and ensuring more robust model performance on test sets. In addition, by retaining only the most predictive features, lasso significantly improves the accuracy of the model's predictions.

Model Construction

In this study, we used a series of powerful ensemble learning algorithms, including random forests, extra trees, AdaBoost, XGBoost, and LightGBM. These algorithms are widely used in a variety of ML applications due to their excellent predictive performance and efficient processing speed.

Decision tree is a fundamental ML algorithm used for classification and regression [22]. The data are split into different subsets based on a series of conditions, ultimately forming a tree structure. Each node represents a feature, each branch represents one possible value of the feature, and each leaf node represents a category or regression value.

Random forest is an ensemble learning method that enhances prediction accuracy and stability by constructing multiple decision trees [23]. The core idea is to train multiple decision trees using different subsets of data and features, and obtain the final result by voting or averaging the predictions of all trees. This approach effectively reduces overfitting and improves the model's generalization ability.

Extra trees, or extremely randomized trees, is an improved random forest method that constructs decision trees by randomly selecting features and split points [24]. Unlike random forests, extra trees randomly selects multiple split points at each node,

XSL•FO
RenderX

from which the best split point is chosen. This completely random strategy reduces the variance of the model and improves generalization while retaining the interpretability and training speed of the decision tree model.

AdaBoost is a boosting method based on an additive model that improves overall classification performance by progressively weighting the training of multiple weak classifiers [25]. In each round of training, misclassified samples are given higher weights, prompting subsequent classifiers to focus more on these difficult-to-classify samples. The final model is a weighted sum of multiple weak classifiers, which gradually reduces error and significantly enhances performance.

XGBoost is an efficient gradient-boosting decision tree algorithm that combines parallel processing and regularization techniques to improve the speed and performance of the model [26]. Key features include the use of second-order derivative information, the ability to handle missing values, and pruning operations on the decision tree. These features enable XGBoost to perform well when dealing with large-scale and high-dimensional data.

LightGBM is an efficient gradient-boosting framework that improves training speed and memory usage through a histogram-based decision tree learning algorithm [27]. Its features include support for categorical features, a depth-first strategy using leaf-count limitation, and efficient parallel processing. These characteristics allow LightGBM to have a significant advantage in handling large-scale data.

Model Evaluation

To comprehensively evaluate the model's performance, this study used multiple evaluation metrics, including accuracy, precision, recall, F_1-score, specificity, and area under the curve (AUC). These metrics reflect various aspects of the model's performance, ensuring an objective and thorough assessment.

Accuracy refers to the ratio of correctly predicted samples to the total number of samples and reflects the overall prediction accuracy of the model. The formula for accuracy is:

$$\text{Accuracy}=\frac{TP+TN}{TP+TN+FP+FN}$$

where, TP is true positives, TN is true negatives, FP is false positives, and FN is false negatives.

A higher accuracy indicates that the model makes correct predictions in most cases.

Precision represents the proportion of true positives among all samples predicted as positive. It primarily measures the accuracy of the model's positive predictions. The formula for precision is:

$$\text{Precision}=\frac{TP}{TP+FP}$$

Recall, also known as sensitivity, is the proportion of true positives among all actual positive samples. A higher recall indicates fewer false negatives and a better ability of the model to identify positive samples. The formula for recall is:

$$\text{Recall}=\frac{TP}{TP+FN}$$

F_1-score means the harmonic mean of precision and recall, and is used to evaluate the balance between these 2 metrics. It is suitable for datasets with class imbalance. The formula for F_1-score is:

$$\text{F1Score}=2\times\frac{\text{Precision}\times\text{Recall}}{\text{Precision}+\text{Recall}}$$

A higher F_1-score indicates better performance in both precision and recall.

Specificity represents the proportion of true negatives among all actual negative samples. It measures the model's ability to identify negative samples. The formula for specificity is:

$$\text{Specificity}=\frac{TN}{TN+FP}$$

The AUC of the receiver operating characteristic (ROC) curve is used to evaluate the overall performance of the model. The ROC curve reflects the trade-off between the true-positive rate and false-positive rate at different thresholds. A higher AUC indicates better discrimination ability of the model, balancing the true-positive rate and false-positive rate more effectively. AUC is especially useful for comparing the performance of different models, providing a global perspective on evaluation.

By comprehensively assessing these metrics, we can understand the models' performance in various aspects, identify their strengths and weaknesses, and provide a solid basis for further optimization and improvement. This multiangle, multidimensional evaluation approach ensures a more accurate and comprehensive evaluation of the model's performance, enhancing its reliability and effectiveness in practical applications.

Model Interpretability

For the interpretability of ML models, we primarily used 2 widely recognized methods, LIME [28] and SHAP [29]. LIME approximates complex ML models by fitting an interpretable linear model within a local neighborhood of the target prediction point. This approach provides individualized feature importance interpretations for each instance, thus elucidating the logic behind specific model predictions. Unlike LIME, which focuses on local interpretation, SHAP quantifies the global contribution of each feature to the model prediction based on the Shapley value from game theory. The SHAP value ensures that the contribution of each feature is consistent and fair across all possible feature combinations. By calculating the SHAP value for each feature, SHAP reveals the interactions and dependencies between features and model predictions. Both methods have their respective strengths. SHAP offers a more comprehensive and in-depth interpretation, while LIME is more intuitive and flexible for instance-specific explanations. Combining the local interpretability of LIME with the global analysis of SHAP provides a more thorough and detailed interpretative support for ML models in clinical data. This combination is crucial for enhancing the transparency of the models, increasing the trust of health care professionals, and optimizing the clinical decision-making process.

Ethical Considerations

This study conducted a secondary analysis using the publicly available Diabetes Complications Dataset [30] from the National Population Health Data Center. As this study exclusively used anonymized secondary data without direct human participant involvement, it is exempt from additional institutional ethics

XSL•FO
RenderX

review. The original data collection by the National Population Health Data Center complies with the "Regulations on the Management of Human Genetic Resources of the People's Republic of China" and relevant ethical guidelines. All data are completely deidentified with no personally identifiable information included, and formal data access approval was obtained from the data provider following their established protocols. The original informed consent permits secondary analysis of the deidentified data for research purposes.

Results

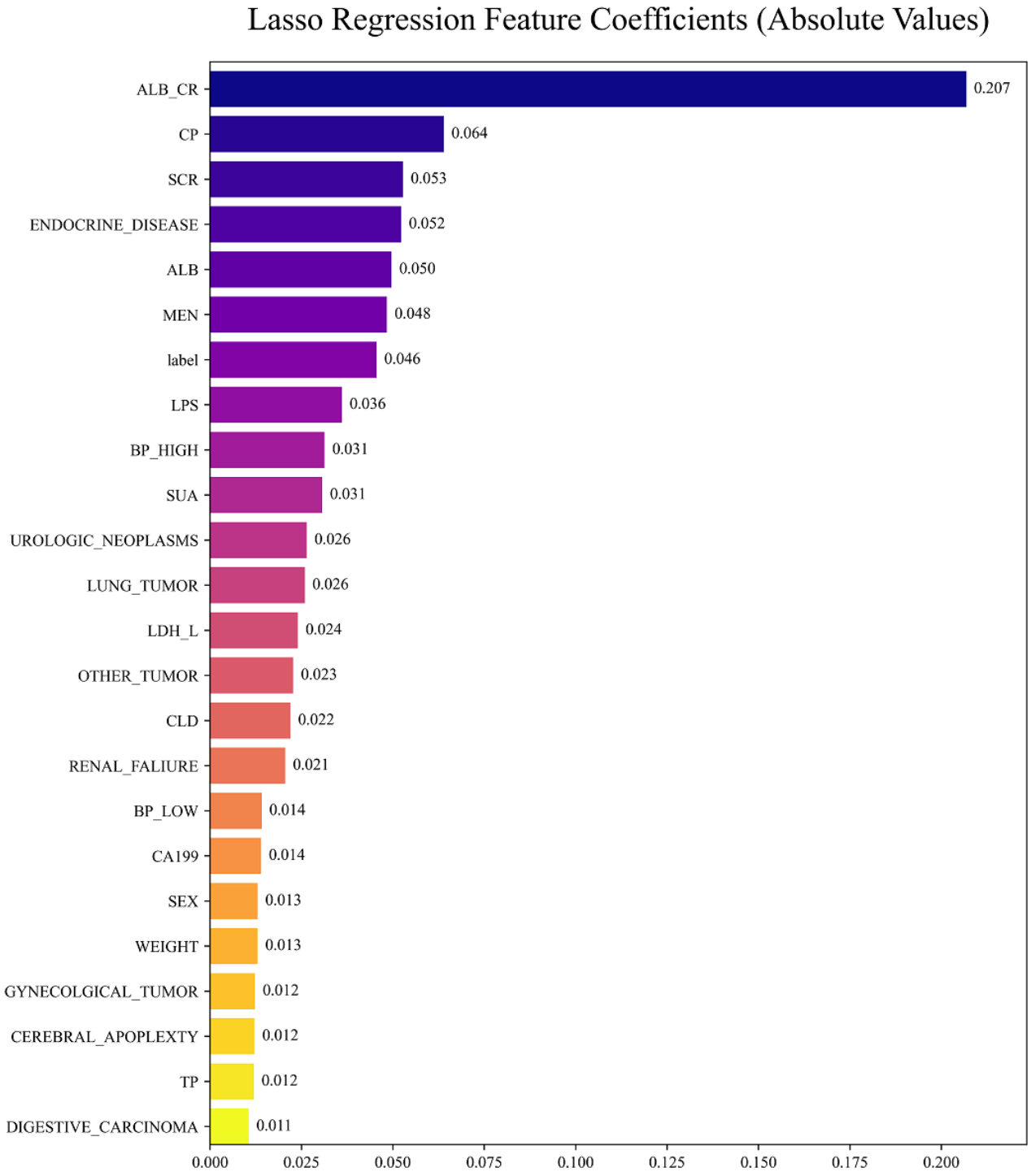
Feature Selection

As illustrated in Figures 2 and 3, lasso regression effectively filters and optimizes the variables in the model by adjusting the regularization parameter λ (Log Lambda). Each curve represents the coefficients of a feature. It can be observed that as λ increases, most coefficients gradually approach zero (Figure 3A). This phenomenon demonstrates the unique feature selection capability of lasso regression, to reduce the coefficients of unimportant features by increasing λ, and thereby simplify the model. Simultaneously, it can be seen that the mean squared error remains low when λ is small (Figure 3B), indicating that the model has a good fitting performance. However, as λ continues to increase, the mean squared error value starts to rise significantly after a relatively stable period. This trend indicates that excessive regularization will result in an overly simplified model, impairing its predictive ability. Through lasso regression, we eventually selected the 24 features, including 14 numerical features and 10 categorical ones.

Table 1 summarizes the differences in features between the DN group and the non-DN group. The statistical data reveal significant disparities between the two groups across various biochemical indicators and health conditions. Specifically, the albumin level is significantly higher in the non-DN group (mean 41.9, range 39.7-44.3) than that in the DN group (mean 38.2, range 32.4-41.4), with a *P* value of less than .001. Similar trends are observed for albumin creatinine ratio, blood pressure high, and blood pressure low. For instance, the albumin creatinine ratio is significantly lower in the non-DN group (mean 12.0, range 4.0-60.2) than that in the DN group (mean 272.7, range 79.0-472.1), with a *P* value of less than .001. Blood pressure high and blood pressure low are also lower in the non-DN group with means of 130.0 (range 120.0-142.0) and 80.0 (range 70.0-86.0) compared to the DN group with means of 142.0 (range 130.0-160.0) and 80.0 (range 75.0-90.0), respectively, both with *P* values less than .001. The levels of CA199, lactate dehydrogenase L, and lipoproteins indicate more severe renal impairment in the DN group compared to the non-DN group. For example, the CA199 level is significantly higher in the DN group (mean 16.5, range 9.5-26.3) than that in the non-DN group (mean 13.0, range 7.8-21.9), with a *P* value of less than .001. Similarly, the lactate dehydrogenase L level is higher in the DN group (mean 169.8, range 142.5-203.2) than that in the non-DN group (mean 153.2, range 135.6-176.6), with a *P* value of less than .001. Furthermore, patients with DN exhibit a higher incidence of certain clinical conditions compared to those without DN. For instance, the incidence of digestive carcinoma in the DN group is 18.33%, whereas it is 46.06% in the non-DN group, with a *P* value of less than .001. Similar significant differences are observed for other conditions such as rheumatic immunity disease, other tumors, cerebral apoplexy, and hypertension. Table 1 provides a detailed comparison of these features between the DN and non-DN groups, highlighting significant health disparities and emphasizing the need for targeted clinical interventions. Table 2 lists the variables and their corresponding abbreviations used throughout the analysis, providing a clear reference for understanding the various health indicators assessed in this study.

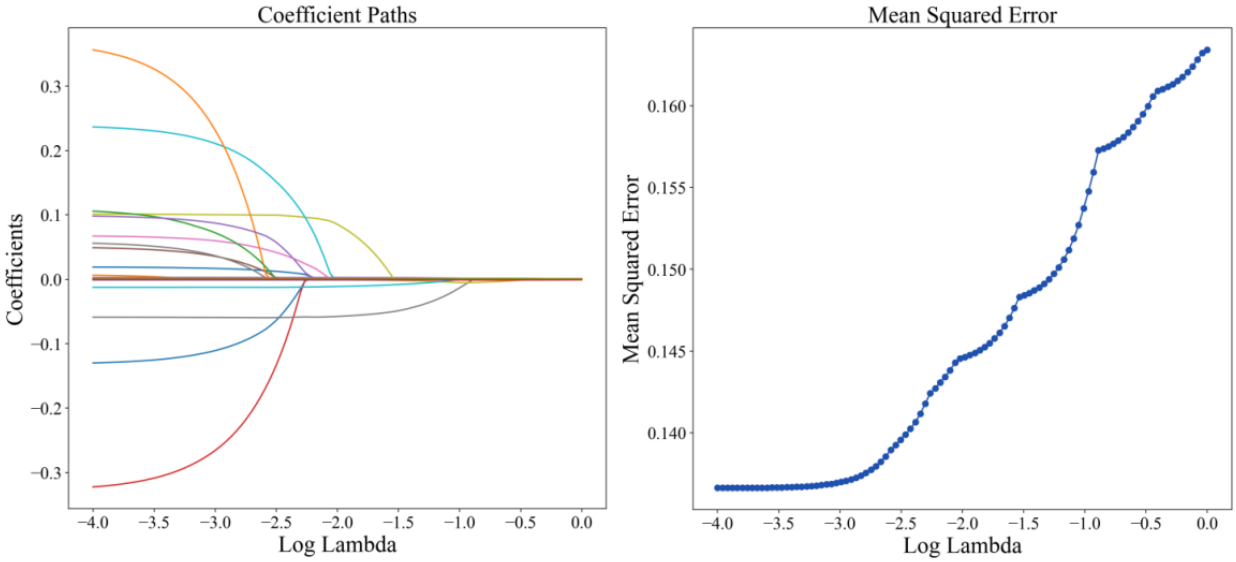
XSL•FO
RenderX

Figure 2. Absolute values of feature coefficients in lasso regression. The color gradient reflects the magnitude of coefficients, with darker shades indicating higher absolute values. Key features (ALB_CR, CP, SCR, ENDOCRINE_DISEASE, ALB) are highlighted as dominant contributors to model performance. ALB: albumin; ALB_CR: albumin creatinine ratio; BP_HIGH: blood pressure high; BP_low: blood pressure low; CLD: chronic liver disease; CP: C-reactive protein; LDH_L: lactate dehydrogenase L; LPS: lipoproteins; MEN: endocrine gland tumors; SCR: serum creatinine; SUA: serum uric acid; TP: total protein.



XSL•FO
RenderX

Figure 3. Variable selection via lasso regression. (A) Coefficient paths illustrate the trajectory of feature coefficients as a function of log(λ), demonstrating variable shrinkage and exclusion. (B) The mean-squared error curve identifies the optimal λ value at its minimum, balancing model complexity and predictive accuracy.



XSL•FO
RenderX

Table . Feature differences between diabetic nephropathy (DN) and non-DN groups.

Variable name	DN (n=444), median (IQR)	Non-DN (n=556), median (IQR)	*P* value
Albumin	38.2 (32.4-41.4)	41.9 (39.7-44.3)	<.001
Albumin_Creatinine_Ratio	272.7 (79.0-472.1)	12.0 (4.0-60.2)	<.001
Blood_Pressure_High	142.0 (130.0-160.0)	130.0 (120.0-142.0)	<.001
Blood_Pressure_Low	80.0 (75.0-90.0)	80.0 (70.0-86.0)	<.001
CA199	16.5 (9.5-26.3)	13.0 (7.8-21.9)	<.001
C-Peptide	2.4 (1.5-3.5)	2.4 (1.5-3.1)	.25
Lactate_Dehydrogenase_L	169.8 (142.5-203.2)	153.2 (135.6-176.6)	<.001
Lipoproteins	134.8 (78.6-212.7)	100.2 (48.8-163.1)	<.001
Serum_Creatinine	95.8 (68.7-161.0)	67.5 (55.2-78.7)	<.001
Serum_Uric_Acid	352.6 (292.1-416.1)	302.8 (242.6-363.2)	<.001
Total_Protein	63.3 (58.2-68.1)	67.2 (63.9-70.9)	<.001
Weight	74.0 (66.0-83.0)	72.9 (66.0-79.0)	.10
Other_Tumor, n (%)			.36
No	46 (50.55)	510 (56.11)	
Yes	45 (49.45)	399 (43.89)	
Endocrine_Disease, n (%)			<.001
No	169 (47.08)	387 (60.37)	
Yes	190 (52.92)	254 (39.63)	
Gynecological_Tumor, n (%)			>.99
No	16 (55.17)	540 (55.61)	
Yes	13 (44.83)	431 (44.39)	
Cerebral_Apoplexy, n (%)			.09
No	29 (44.62)	527 (56.36)	
Yes	36 (55.38)	408 (43.64)	
Endocrine_Gland_Tumors, n (%)			<.001
No	9 (21.95)	547 (57.04)	
Yes	32 (78.05)	412 (42.96)	
Renal_Failure, n (%)			<.001
No	0 (0.00)	556 (59.15)	
Yes	60 (100.00)	384 (40.85)	
Lung_Tumor, n (%)			.08
No	18 (75.00)	538 (55.12)	
Yes	6 (25.00)	438 (44.88)	
Urologic_Neoplasms, n (%)			.04
No	1 (12.50)	555 (59.15)	
Yes	7 (87.50)	437 (44.05)	
Gender, n (%)			.06
Male	347 (53.38)	209 (59.71)	
Female	303 (46.62)	141 (40.29)	
Chronic_Liver_Disease, n (%)			.002
No	67 (43.79)	489 (57.73)	
Yes	86 (56.21)	358 (42.27)	

XSL•FO
RenderX

Variable name	DN (n=444), median (IQR)	Non-DN (n=556), median (IQR)	*P* value
Digestive_Carcinoma, n (%)			<.001
No	49 (81.67)	507 (53.94)	
Yes	11 (18.33)	433 (46.06)	
Diabetes_Disease_Type, n (%)			<.001
Type 2 diabetes	182 (36.4)	374 (74.8)	
Diabetic retinopathy	318 (63.6)	126 (25.2)	

Table . Variable names and their abbreviations.

Variable name	Abbreviation
Albumin	ALB
Albumin creatinine ratio	BU
Blood pressure high	BP_HIGH
Blood pressure low	BP_LOW
CA199	CA199
C-reactive protein	CP
Lactate dehydrogenase L	LDH_L
Lipoproteins	LPS
Serum creatinine	SCR
Serum uric acid	SUA
Total protein	TP
Weight	WEIGHT
Other tumor	OTHER_TUMOR
Other endocrine diseases	ENDOCRINE_DISEASE
Gynecological tumor	GYNECOLOGICAL_TUMOR
Cerebral apoplexy	CEREBRAL_APOPLEXTY
Endocrine gland tumors	MEN
Renal failure	RENAL_FAILURE
Lung tumor	LUNG_TUMOR
Urologic neoplasms	UROLOGIC_NEOPLASMS
Gender	SEX
Chronic liver disease	CHRONIC_LIVER_DISEASE
Digestive carcinoma	DIGESTIVE_CARCINOMA
Diabetes disease type	DIABETES_DISEASE_TYPE

Model Performance

In this study, we used various ML algorithms to construct predictive models, including decision tree, random forest, extra trees, AdaBoost, XGBoost, and LightGBM. In order to determine the optimal model parameters, we used ten-fold cross-validation and grid search strategies, ensuring thorough and accurate model tuning. The final results, presented in Table 3, show that XGBoost and LightGBM exhibited superior performance across multiple evaluation metrics, including accuracy, precision, recall, F_1-score, and specificity. In particular, XGBoost achieved the highest accuracy of 86.87%, with a precision of 88.90%, a recall of 84.40%, an F_1-score of 86.44%, and a specificity of 89.12%. LightGBM followed closely with an accuracy of 86.78%, a precision of 88.72%, a recall of 84.37%, an F_1-score of 86.35%, and a specificity of 88.88%. These results highlight the exceptional capability of both XGBoost and LightGBM in handling complex datasets, making them ideal for predictive modeling in this context. The other effective models, however, did not match the overall performance of XGBoost and LightGBM.

XSL•FO
RenderX

Table . Performance comparison of different machine learning models.

Model	Accuracy (%)	Precision (%)	Recall (%)	F_1-score (%)	Specificity (%)
Decision tree	78.24	85.02	69.88	76.07	86.26
Random forest	85.07	88.25	80.72	84.22	89.16
Extra trees	84.26	89.06	78.32	83.16	89.98
AdaBoost[a]	83.10	85.44	79.77	82.29	86.31
XGBoost[b]	86.87	88.90	84.40	86.44	89.12
LightGBM[c]	86.78	88.72	84.37	86.35	88.88

[a]AdaBoost: Adaptive Boosting.

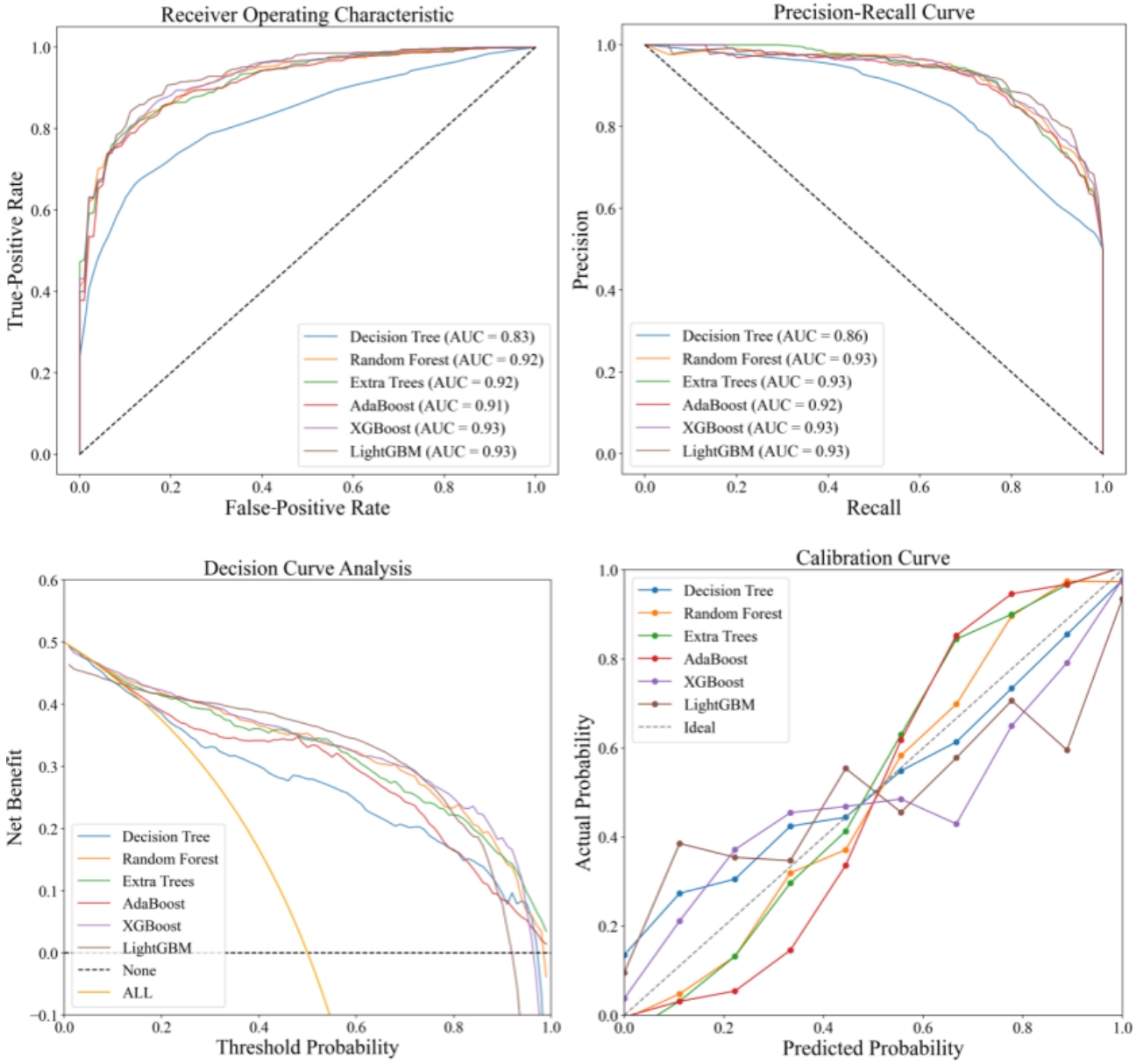
[b]XGBoost: Extreme Gradient Boosting.

[c]LightGBM: Light Gradient-Boosting Machine.

As shown in Figure 4, through a comprehensive performance evaluation that included ROC curves, precision-recall curves, decision curve analysis, and calibration curves, we found that LightGBM and XGBoost performed exceptionally well. Both models demonstrated strong discriminative abilities with an AUC of 0.93, indicating their effectiveness at distinguishing between positive and negative classes. The precision-recall curves, particularly valuable for imbalanced datasets, also showed an AUC of 0.93 for both models, reflecting their capability to maintain high precision and recall, which minimizes false positives and negatives. In the decision curve analysis, XGBoost provided the highest net benefit, highlighting its robustness and wide applicability across various clinical decision thresholds. This indicates that XGBoost can be particularly useful in diverse clinical scenarios, offering reliable support for decision-making processes. The calibration curves further confirmed the reliability of the predicted probabilities from both models, showing that their predictions closely matched the actual outcomes, especially in the high probability prediction range. This means that when the models predict a high probability for an event, the prediction is likely to be accurate, which is essential for building trust in model predictions. In summary, LightGBM and XGBoost excelled across all evaluated metrics, demonstrating superior performance and robustness. Their high AUC values, significant net benefit, and accurate probability predictions collectively underscore their effectiveness in handling complex clinical datasets, making them highly suitable for predictive modeling in health care where accurate and reliable predictions are critical for effective patient management and treatment planning.

XSL•FO
RenderX

Figure 4. Comprehensive evaluation of model performance. (A) Receiver operating characteristic (ROC) curves demonstrate discriminative ability, with LightGBM achieving the highest AUC (0.93) [6,10]. (B) Precision-recall curves highlight performance in imbalanced datasets, where XGBoost and LightGBM maintain high precision across recall ranges. (C) Decision curve analysis reveals net clinical benefit, indicating LightGBM's superiority over alternative models at most threshold probabilities. (D) Calibration curves assess predictive accuracy, showing LightGBM aligns closest to the ideal calibration line. AdaBoost: Adaptive Boosting; AUC: area under the curve; LightGBM: Light Gradient-Boosting Machine; XGBoost: Extreme Gradient Boosting.



Model Explainability

In the analysis of the LIME diagram, we identified a series of key biomarkers and clinical indicators closely associated with the occurrence and progression of DN. As depicted in Figure 5A, the values next to each feature represent the contribution of that feature to the model's prediction outcomes, denoted as the importance score. Blue indicates a positive correlation between the feature value and the model's prediction outcomes, meaning that as the feature value increases, the likelihood of the model predicting the positive class also increases. Conversely, red indicates a negative correlation, suggesting that as the feature value increases, the likelihood of the model predicting the negative class increases. LIME technology provides an intuitive explanation of the factors influencing model predictions by constructing local surrogate models around the model's predictions in the form of linear models, approximating the original complex model. Specifically, the level of serum creatinine was identified as a significant positive predictive factor, with a threshold exceeding 99.78 µmol/L associated with an increased risk of DN. This finding aligns with the clinical understanding that elevated creatinine levels typically indicate decreased kidney filtration capacity. Albumin levels within the range of 9.00 to 64.95 g/L were also associated with the risk of DN. As the main protein in plasma, abnormal albumin levels may indicate malnutrition or an inflammatory state, both of which can impact kidney health. The lipopolysaccharide level exceeding 191.68 mg/dL was identified as another positive predictive factor. As an inflammatory mediator, elevated lipopolysaccharide levels may be linked to the inflammatory processes in DN. The level of serum uric acid

XSL•FO
RenderX

exceeding 392.32 µmol/L was also identified as a positive predictive factor. Hyperuricemia is associated with various kidney diseases and may increase the risk of DN through mechanisms such as promoting inflammation and oxidative stress. Blood pressure indicators, including diastolic blood pressure (BP_LOW) at 72.24 mmHg and systolic blood pressure (BP_HIGH) not exceeding 125.00 mmHg, were also considered to be significant in the LIME analysis. Effective blood pressure control is crucial for slowing the progression of DN. In addition, the levels of total protein within the range of 61.30 to 65.70 g/L and lactate dehydrogenase within the range of 160.55 to 188.66 U/L played a role in the model's predictions. Abnormalities in these indicators may reflect systemic metabolic disorders or tissue damage, both of which are related to the risk of DN. The presence of other medical conditions such as gynecological tumors, endocrine diseases, and lung tumors also showed a negative correlation with the risk of DN, suggesting that these factors may have a protective or neutralizing effect in this specific dataset. Through this detailed analysis, LIME technology provided a comprehensive and intuitive explanation of the key factors influencing model predictions, thereby enhancing our understanding of the biomarkers and clinical indicators associated with DN.

Figure 5. Feature importance analysis of the LightGBM model. (A) LIME explanation highlights individual feature contributions, where blue/red bars indicate positive/negative impacts on predictions. (B) SHAP values reveal global feature influence, with ALB_CR and SCR exhibiting the strongest associations (purple/blue gradient reflects feature magnitude). ALB: albumin; ALB_CR: albumin creatinine ratio; BP_HIGH: blood pressure high; BP_LOW: blood pressure low; CLD: chronic liver disease; CP: C-reactive protein; LDL_L: lactate dehydrogenase L; LightGBM: Light Gradient-Boosting Machine; LIME: Local Interpretable Model-Agnostic Explanations; LPS: lipoproteins; MEN: endocrine gland tumors; SCR: serum creatinine; SHAP: Shapley Additive Explanations; SUA: serum uric acid; TP: total protein.

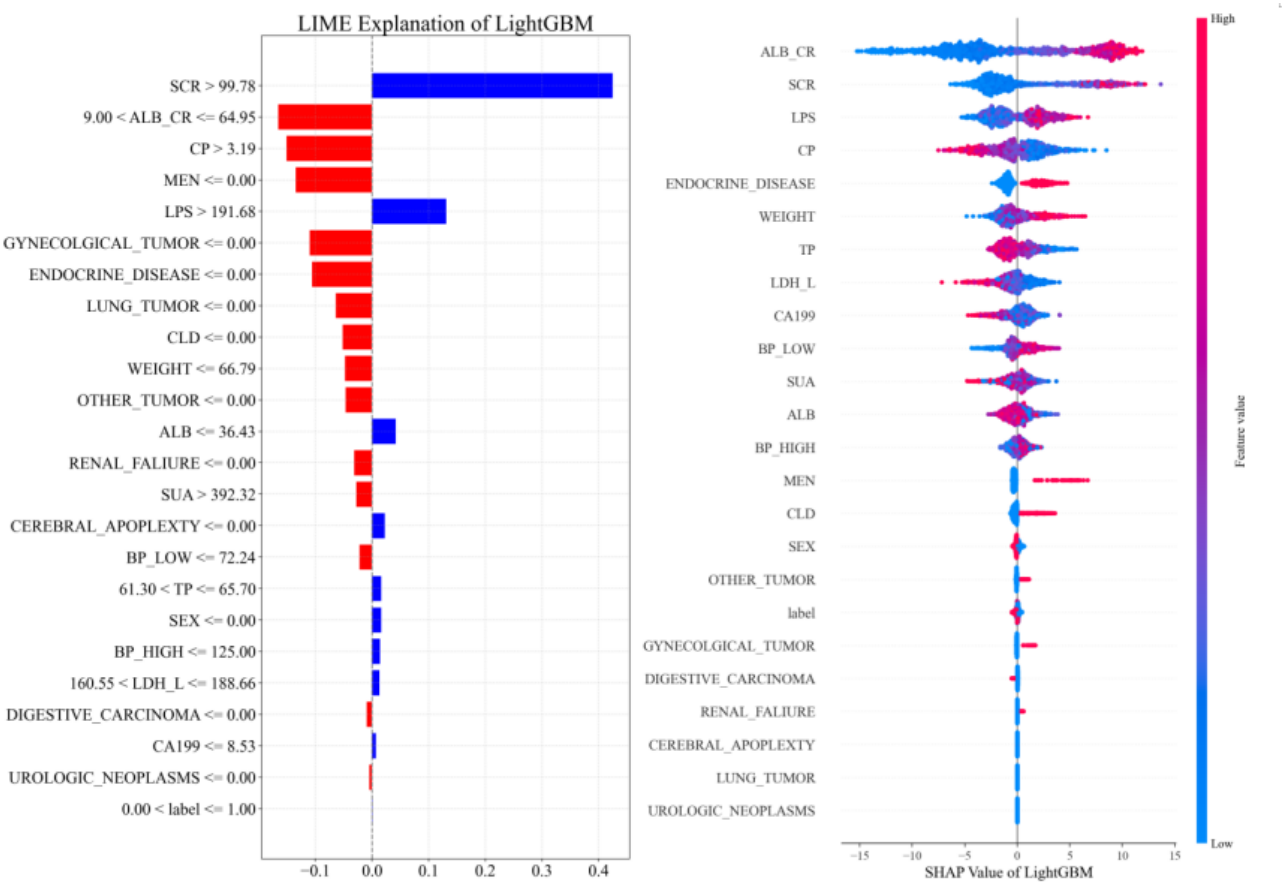


Figure 5B illustrates the SHAP importance of features within the LightGBM model, identifying primary factors such as lipoprotein A, serum creatinine, C-reactive protein, albumin, and blood pressure high as crucial ones in evaluating DN. These features are pivotal across models, underscoring their integral role in disease assessment. Lipoprotein_A and other lipoproteins serve as critical lipid markers, essential for gauging the cardiovascular risks and progression of kidney disease in patients with diabetes. Abnormal lipid metabolism is intimately linked with the onset of DN, highlighting a potential need for enhanced lipid management strategies to thwart disease advancement. Furthermore, Serum_Creatinine and Blood_Urea nitrogen are paramount biochemical indicators for renal function assessment. Elevated concentrations of these markers generally denote diminished kidney filtration ability, serving as significant indicators of DN progression. Regular monitoring of these parameters is vital for the early detection of renal impairment and timely medical intervention. Albumin serves as a sensitive biomarker for early DN. The abnormal rate of urinary albumin excretion reflects the extent of renal damage. Early detection and continual monitoring of urinary albumin levels enable physicians to assess disease progression and the efficacy of their treatment protocols, thereby facilitating the development of customized therapeutic strategies aimed at decelerating disease progression. Hypertension significantly accelerates DN development; thus, effective blood pressure management is

XSL•FO
RenderX

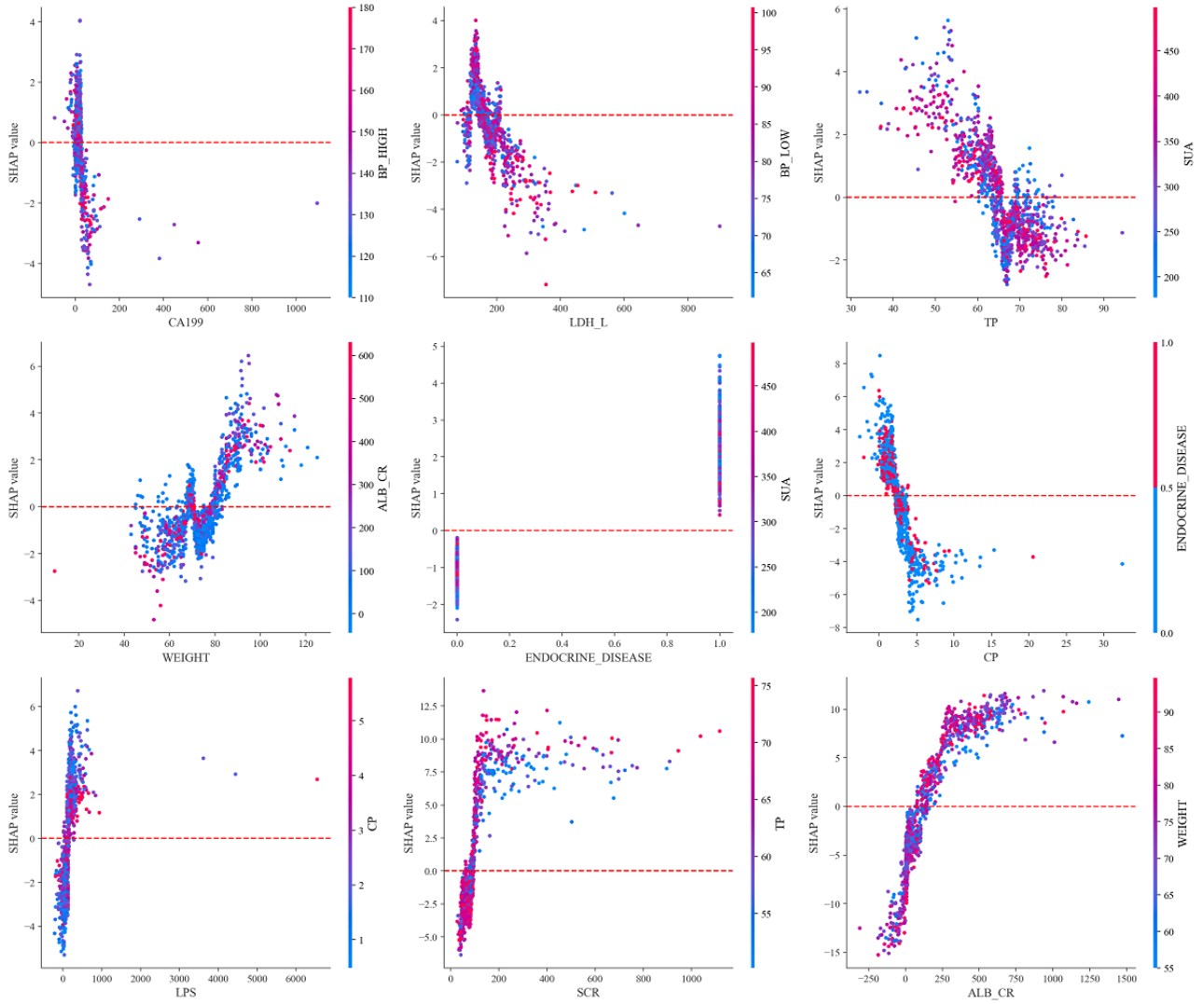
imperative for delaying or preventing disease progression. Optimal control of hypertension not only preserves renal function but also mitigates the risk of cardiovascular incidents. The collective significance of these features underscores their pivotal role in DN assessment. Through a comprehensive analysis of these factors, physicians can obtain a deeper understanding of the disease's complexity, and develop more effective monitoring and treatment modalities that enhance patients' management and prognosis.

Figure 6 delineates the correlation between various biochemical indicators and their SHAP values in interpretable ML models designed for predicting and evaluating the risk of DN. An in-depth analysis of these biochemical markers furnishes critical scientific insights into their influence on DN risk predictions, thereby informing clinical intervention strategies. The analysis reveals a pronounced negative correlation between the levels of blood urea nitrogen (blood urea) and the model's predictive accuracy. As blood urea nitrogen levels increase, the associated SHAP values decline markedly, signifying an augmented risk of DN. This trend underscores the prognostic importance of blood urea nitrogen in the early detection of renal dysfunction, establishing it as an essential indicator for kidney disease risk assessments. Similarly, fluctuations in albumin levels are critical for forecasting DN. The presented data indicate that rising albumin levels correlate with decreasing SHAP values, underscoring albumin's predictive utility, particularly in detecting microalbuminuria—an early manifestation of kidney damage. Elevated levels of C-reactive protein, a marker of systemic inflammation, also correspond with reduced SHAP values, suggesting that high concentrations of this protein are linked to an increased risk of DN. This relationship may stem from chronic inflammatory states that foster the progression of DN. The findings concerning serum creatinine demonstrate that increased creatinine levels are indicative of reduced kidney filtration capabilities, mirrored by a decline in SHAP values. This reinforces the value of serum creatinine as a crucial indicator of renal insufficiency and a metric for assessing the risk of DN. The analysis also highlights the significant negative impact of elevated lipoprotein markers on the model's predictions, emphasizing the imperative role of lipid management in the prevention and treatment of DN. The perturbations in these indicators not only relate to cardiovascular diseases but also pose a substantial risk factor for DN. Furthermore, the notable SHAP values for endocrine disease and diabetes type underscore the critical role of these conditions in assessing DN risk, indicating that they are significant contributors to the disease's development. By synthesizing these data, we can enhance our comprehension of the risk factors associated with DN. This integration aids medical professionals in more accurately identifying patients at high risk, thereby facilitating the development of more effective treatment strategies and management practices to improve the renal health of patients with diabetes.

For the purpose of evaluating the predictive models for DN, the SHAP value plots for three distinct samples (Figure 7) offer a nuanced understanding of the contribution of various biochemical and physiological indicators to disease risks prediction. These comprehensive data enable insights into how different indicators, either individually or synergistically, influence disease risk assessment, thereby furnishing a scientific foundation for clinical decision-making. The analysis of the first sample elucidates that elevated levels of serum creatinine and C-reactive protein markedly enhance disease risks. Serum creatinine, a key marker of renal function impairment, signals a significant reduction in kidney function, which is particularly crucial in DN where renal lesions often correlate with prolonged suboptimal diabetes control. C-reactive protein, indicative of the body's inflammatory response, suggests the presence of an inflammatory state that is instrumental in accelerating renal damage. Furthermore, hypertension is a significant risk factor for DN, and the notably increased low blood pressure might suggest inadequate blood pressure management in this sample, exacerbating the renal burden. Conversely, higher levels of serum uric acid and albumin are generally viewed as protective in the first sample. Although elevated serum uric acid levels are linked to other conditions like gout, they may indicate preserved renal excretion function to a degree. Albumin, a crucial component of plasma proteins, with maintained levels suggests a favorable nutritional state and some preservation of kidney filtration function. The analysis of the second sample, with its positive prediction value indicating disease absence, highlights the critical role of lipoprotein A in increasing disease risks. Lipoprotein A, an independent risk factor for cardiovascular diseases, underscores a possible link between cardiovascular and renal health in the context of DN. Moreover, an elevated level of serum lipase (lipopolysaccharides) contributes to lowering disease risks in this sample, possibly due to its role in modulating immune responses and inflammation. The third sample's negative prediction value signals a heightened disease risk. In this context, increased serum creatinine and high blood pressure significantly elevate disease risks, emphasizing the importance of vigilant monitoring and control of these indicators. Although blood urea contributes less significantly to the prediction value, its elevation is typically associated with renal insufficiency and warrants clinical attention. Through this meticulous SHAP value–based analysis, we unveil not only the specific contributions of each biochemical indicator to disease risks but also the intricate interplay and connections among these indicators. This profound understanding provides invaluable information for medical professionals in the early diagnosis, risk assessment, and therapeutic decision-making of DN, facilitating personalized medicine and enhancing treatment outcomes of patients.

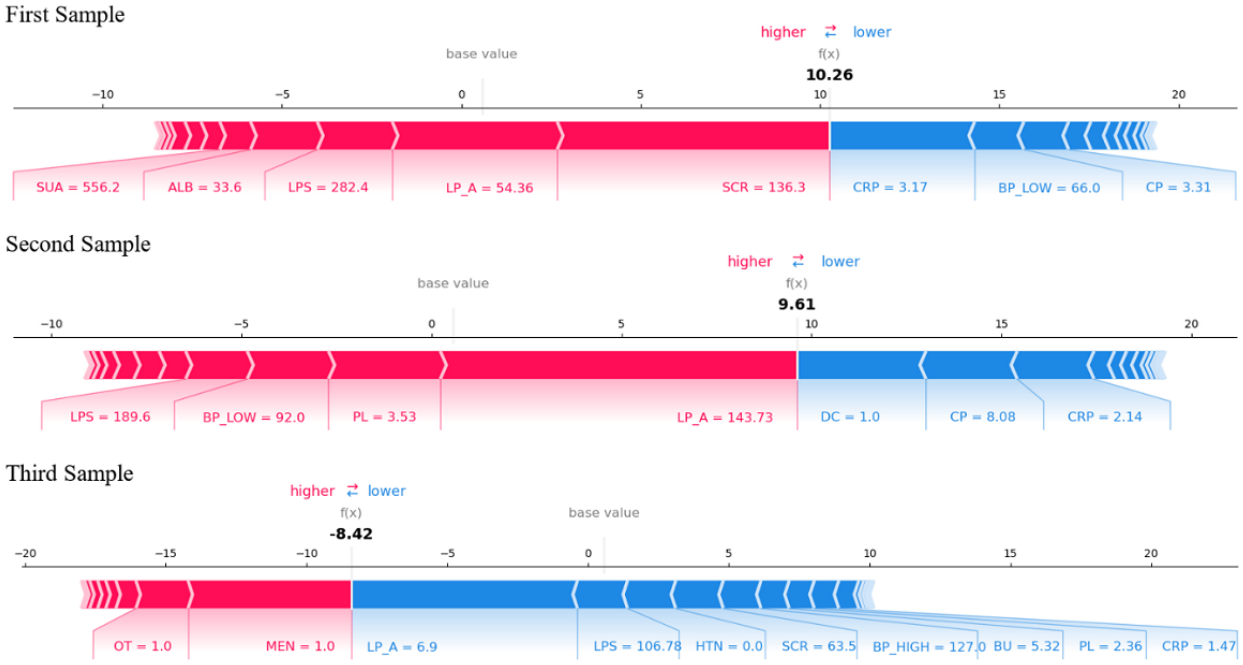
XSL•FO
RenderX

Figure 6. SHAP value distributions for key biochemical indicators in nephropathy risk prediction. Each subplot illustrates the relationship between feature values (x-axis) and SHAP values (y-axis), with color gradients indicating feature magnitude. Red dashed lines denote baseline thresholds, where features above/below these thresholds significantly influence model predictions. Notably, ALB_CR and SCR exhibit the strongest associations with nephropathy risk due to their wide SHAP value ranges and distinct clustering patterns. Detailed subfigures are available in Multimedia Appendices 1-9. ALB_CR: albumin creatinine ratio; BP_HIGH: blood pressure high; CP: C-reactive protein; LDL_L: lactate dehydrogenase L; SCR: serum creatinine; SHAP: Shapley Additive Explanations; SUA: serum uric acid; TP: total protein.



XSL•FO
RenderX

Figure 7. Comparative analysis of Shapley Additive Explanations (SHAP) values across three patient samples for diabetic nephropathy prediction. Each waterfall plot illustrates individual feature contributions to the final prediction score, where red/blue segments indicate positive/negative impacts on diabetic nephropathy risk. The base value represents the average model output without feature effects, while the final f(x) reflects personalized risk assessment. Notably, SUA and ALB exhibit consistent positive associations in high-risk samples (first/second), whereas MEN and HTN dominate negative contributions in low-risk cases (third). ALB: albumin; BP_HIGH: blood pressure high; BP_LOW: blood pressure low; BU: albumin creatinine ratio; CP: C-peptide; CRP: C-reactive protein; LP_A: lysophosphatidic acid; LPS: lipoproteins; DC: digestive carcinoma; HTN: hypertension; LPS: lipoproteins; MEN: endocrine gland tumors; OT: other tumor; PL: phospholipid; SCR: serum creatinine; SUA: serum uric acid.



Discussion

Principal Findings

In this study, we focused on developing a predictive model for DN risks and conducted an extensive feature analysis, aiming to identify patients at risk of progressing to severe kidney disease in a clinical setting. To achieve this goal, we thoroughly analyzed a range of biomarkers and clinical indicators and evaluated several popular ML algorithms. Among these various algorithms tested, we found that the gradient-boosting–based algorithms, XGBoost and LightGBM, performed exceptionally well on our dataset. The models not only demonstrated significant advantages in training speed and handling large datasets but also exhibited superior predictive performance across key metrics such as accuracy, precision, recall, and AUC, showcasing their outstanding predictive capabilities. Our study also found that serum creatinine, the albumin-creatinine ratio (ACR), abnormal levels of lipoproteins, C-peptide, and hypertension were the most relevant factors associated with DN, aligning with findings from clinical research on the key risk factors for DN progression.

Comparison With Prior Work

Serum creatinine is a key biomarker for evaluating DN and core indicator of kidney function, and its elevated levels are often closely associated with kidney damage. In patients with diabetes, even a slight increase in serum creatinine levels is sufficient to indicate early kidney function impairment [31]. As serum creatinine levels rise, the risk of kidney damage also increases; thus, it is recommended to closely monitor serum creatinine levels in diabetes management [32]. Serum creatinine levels have independent predictive value in the progression of DN. Regular monitoring of serum creatinine levels helps the early identification of potential kidney disease risks and the taking of appropriate preventive measures [33]. By optimizing medical management for patients with diabetes and regularly assessing serum creatinine levels, clinicians can detect and address kidney function damage earlier, thereby reducing the progression risk of DN.

The ACR is an important method for detecting microalbuminuria, used to evaluate early changes in kidney disease in patients with diabetes. An increase in ACR is closely related to the progression of DN, and even a slight elevation in ACR should be considered as a warning signal for the development of DN [34]. Elevated ACR is an independent predictor for the progression of DN, and regular monitoring of ACR levels helps the early identification of potential kidney disease risks, aiding clinicians in assessing disease progression and treatment response [35]. Moreover, a reduction in ACR is associated with a slowdown in the progression of DN and a decrease in cardiovascular event rates. By optimizing medical management for patients with diabetes and regularly monitoring ACR levels, clinicians can detect and address kidney function damage earlier, thus reducing the risk of progression of DN [36].

Abnormal levels of lipoproteins, particularly elevated low-density lipoprotein (LDL) and very low–density lipoprotein (VLDL), are significant risk factors in the development of diabetic kidney disease. These lipid particles damage vascular

XSL•FO
RenderX

endothelium, thereby accelerating the progression of diabetic kidney disease. Research indicates that changes in the size and number of LDL particles in patients with diabetes are significantly correlated with renal function impairment [37]. Elevated LDL levels not only lead to atherosclerosis but also directly harm renal function by promoting inflammation and oxidative stress. This damage mechanism is primarily manifested by the thickening of the glomerular basement membrane and glomerulosclerosis, which may ultimately result in renal failure [38]. Similarly, elevated VLDL levels are closely associated with the progression of kidney disease. VLDL carries a large amount of triglycerides and can be absorbed by renal tubular cells, causing cytotoxic reactions that further exacerbate tubular damage and accelerate the progression of kidney disease [39]. Even after other comorbid factors are controlled, high LDL levels remain significantly associated with the progression of kidney disease. Multiple studies have also shown that high LDL levels are closely related to increased urinary protein excretion and decreased renal function [40,41]. Therefore, managing lipoprotein levels is crucial to slowing the progression of diabetic kidney disease. Dietary adjustments, medication treatments such as statins, and lifestyle changes can effectively lower LDL and VLDL levels, thus protecting renal function.

C-peptide is an important marker for evaluating β-cell function in the pancreas, with its levels closely associated with metabolic control in diabetes. Low C-peptide levels are linked to an increased risk of DN, possibly due to metabolic disorders caused by insufficient insulin secretion. In contrast, high C-peptide levels are associated with a reduced risk of renal function deterioration in patients with type 2 diabetes. Research indicates that patients with higher C-peptide levels would experience slower declines in renal function and less increase in albuminuria [42]. Moreover, C-peptide shows potential in the treatment of DN. C-peptide replacement therapy can reduce glomerular hyperfiltration, decrease albumin excretion, and prevent glomerular and renal hypertrophy [43]. Supporting this view, another study demonstrates that C-peptide at physiological concentrations can improve glomerular filtration rate and increase renal plasma flow, and effect further validation in clinical trials [44]. C-peptide levels play a crucial role in the progression and management of DN. Monitoring and potentially modulating these levels through therapeutic interventions can provide significant benefits for the prevention and treatment of DN.

Hypertension is a major risk factor for the development and progression of DN. Persistent hypertension can lead to structural and functional changes in the renal vasculature, accelerating the decline in renal function. Patients with hypertension experience faster progression of kidney damage and thus require earlier intervention to prevent further deterioration of renal function [45]. In the context of hypertension, a sustained high pressure load on the renal blood vessels results in the thickening and hardening of the vessel walls. These structural changes weaken the kidney's filtration function and accelerate glomerulosclerosis and renal fibrosis [34]. Effective hypertension management typically includes the use of angiotensin-converting enzyme inhibitors and angiotensin receptor blockers, which not only lower blood pressure but also provide renal protection [46]. On the other hand, although hypotension is less common in patients with diabetes, it can have negative effects on renal function in certain situations. In severe circulatory failure or shock, hypotension can lead to inadequate renal perfusion, reducing blood flow to the kidneys and exacerbating renal damage. In clinical practice, the management strategies for hypertension and hypotension need to be individualized. For patients with hypertension, the goal is to reduce blood pressure to recommended levels while avoiding excessive hypotension. For patients at risk of hypotension, particularly older adults, close monitoring of blood pressure fluctuations is essential to prevent inadequate renal perfusion. Overall, blood pressure management plays a crucial role in the prevention and treatment of DN. Appropriate pharmacological treatment and lifestyle interventions can control blood pressure effectively, protect renal function, and delay the progression of DN.

Limitations

This study has made notable progress in predicting DN; however, certain limitations remain. First, the data used in the study were sourced from a single medical institution. Although the model performed well on this dataset, validation with data from other institutions is needed to assess its effectiveness and generalizability. Additionally, the model has not yet undergone comprehensive clinical validation, and some features selected by the algorithm may lack diagnostic significance, while commonly used clinical indicators might not have been included.

Future Directions

Future research should focus on the following improvements: collecting data from multiple institutions to validate the model's robustness, strengthening collaboration with clinical experts to optimize feature selection based on clinical knowledge, and investigating potential nonlinear relationships among features. Developing a user-friendly online platform and a simplified scoring system would make the model more intuitive and accessible for clinical use. Furthermore, incorporating multimodal data, such as imaging and genomic information, could enhance the model's predictive performance and clinical value, providing robust support for the early diagnosis and personalized treatment of DN.

Conclusion

In this study, we developed a robust predictive model for DN using various ML techniques. Among the models tested, XGBoost and LightGBM demonstrated superior performance, achieving notable metrics across other performance indicators. The integration of XML techniques, such as LIME and SHAP, provided valuable insights into the contribution of individual features, enhancing the model's transparency and interpretability, which is crucial for clinical application. Our analysis identified several significant risk factors for DN, including serum creatinine, C-peptide, albumin, and lipoproteins. These findings are well-supported by extensive literature, reinforcing the reliability and relevance of our predictive model. The ability to accurately predict DN and understand the underlying risk factors allows for early intervention and

XSL•FO
RenderX

personalized treatment strategies, ultimately improving patients' outcomes and optimizing health care resource usage.

Acknowledgments

The authors would like to thank the Population Health Data Archive for providing the Diabetes Complications Dataset, which was instrumental in this research. This work is supported by the Innovation Engineering project "Construction of a Digital Resource System for Biomedical Literature" (grant 24C0001-1).

Data Availability

The data used in this study are publicly available from the National Population Health Data Center under the title "Diabetes Complications Dataset" (DOI: 10.12213/11.A0005.201905.000282). The dataset can be accessed at [46]. This study was conducted with formal approval from the data provider following submission of a data access request through the National Population Health Data Center platform. All data have been deidentified and privacy-protected by the data provider, with assurance that no personally identifiable information or other sensitive data are included in the deposited dataset. Researchers interested in accessing this dataset should submit a formal request through the National Population Health Data Center platform according to their data-sharing policies. Further details regarding the dataset and its structure are provided in Multimedia Appendix 10.

Conflicts of Interest

None declared.

Multimedia Appendix 1
Shapley Additive Explanations (SHAP) scatter plot for CA199.
[PNG File, 104 KB - medinform_v13i1e64979_app1.png]

Multimedia Appendix 2
Shapley Additive Explanations (SHAP) scatter plot for lactate dehydrogenase L.
[PNG File, 131 KB - medinform_v13i1e64979_app2.png]

Multimedia Appendix 3
Shapley Additive Explanations (SHAP) scatter plot for total protein.
[PNG File, 187 KB - medinform_v13i1e64979_app3.png]

Multimedia Appendix 4
Shapley Additive Explanations (SHAP) scatter plot for weight.
[PNG File, 164 KB - medinform_v13i1e64979_app4.png]

Multimedia Appendix 5
Shapley Additive Explanations (SHAP) scatter plot for endocrine disease.
[PNG File, 80 KB - medinform_v13i1e64979_app5.png]

Multimedia Appendix 6
Shapley Additive Explanations (SHAP) scatter plot for C-reactive protein.
[PNG File, 106 KB - medinform_v13i1e64979_app6.png]

Multimedia Appendix 7
Shapley Additive Explanations (SHAP) scatter plot for lipoproteins.
[PNG File, 107 KB - medinform_v13i1e64979_app7.png]

Multimedia Appendix 8
Shapley Additive Explanations (SHAP) scatter plot for serum creatinine.
[PNG File, 128 KB - medinform_v13i1e64979_app8.png]

Multimedia Appendix 9
Shapley Additive Explanations (SHAP) scatter plot for albumin creatinine ratio.
[PNG File, 158 KB - medinform_v13i1e64979_app9.png]

XSL•FO
RenderX

Multimedia Appendix 10
Diabetes Complications Dataset.
[XLSX File, 439 KB - medinform_v13i1e64979_app10.xlsx]

References

1. Agarwal R. Pathogenesis of diabetic nephropathy. Compendia 2021 Jun;2021(1):2-7. [doi: 10.2337/db20211-2]
2. Umanath K, Lewis JB. Update on diabetic nephropathy: core curriculum 2018. Am J Kidney Dis 2018 Jun;71(6):884-895. [doi: 10.1053/j.ajkd.2017.10.026] [Medline: 29398179]
3. Zhang L, Wang Z, Zhang X, et al. Alterations of the gut microbiota in patients with diabetic nephropathy. Microbiol Spectr 2022 Aug 31;10(4):e0032422. [doi: 10.1128/spectrum.00324-22]
4. Pereira PR, Carrageta DF, Oliveira PF, Rodrigues A, Alves MG, Monteiro MP. Metabolomics as a tool for the early diagnosis and prognosis of diabetic kidney disease. Med Res Rev 2022 Jul;42(4):1518-1544. [doi: 10.1002/med.21883] [Medline: 35274315]
5. Naaman SC, Bakris GL. Diabetic nephropathy: update on pillars of therapy slowing progression. Diabetes Care 2023 Sep 1;46(9):1574-1586. [doi: 10.2337/dci23-0030] [Medline: 37625003]
6. Richens JG, Lee CM, Johri S. Improving the accuracy of medical diagnosis with causal machine learning. Nat Commun 2020 Aug 11;11(1):3923. [doi: 10.1038/s41467-020-17419-7] [Medline: 32782264]
7. Rajula HSR, Verlato G, Manchia M, Antonucci N, Fanos V. Comparison of conventional statistical methods with machine learning in medicine: diagnosis, drug development, and treatment. Med Bogota Colomb 2020;56(9):455. [doi: 10.3390/medicina56090455]
8. Dong J, Feng T, Thapa-Chhetry B, et al. Machine learning model for early prediction of acute kidney injury (AKI) in pediatric critical care. Crit Care 2021 Dec;25(1):288. [doi: 10.1186/s13054-021-03724-0]
9. Lee YW, Choi JW, Shin EH. Machine learning model for predicting malaria using clinical information. Comput Biol Med 2021 Feb;129:104151. [doi: 10.1016/j.compbiomed.2020.104151] [Medline: 33290932]
10. Rahimi M, Akbari A, Asadi F, Emami H. Cervical cancer survival prediction by machine learning algorithms: a systematic review. BMC Cancer 2023 Apr 13;23(1):341. [doi: 10.1186/s12885-023-10808-3] [Medline: 37055741]
11. Farah L, Murris JM, Borget I, Guilloux A, Martelli NM, Katsahian SIM. Assessment of performance, interpretability, and explainability in artificial intelligence-based health technologies: what healthcare stakeholders need to know. Mayo Clin Proc Digit Health 2023 Jun;1(2):120-138. [doi: 10.1016/j.mcpdig.2023.02.004] [Medline: 40206724]
12. Li Z, Bouazizi M, Ohtsuki T, Ishii M, Nakahara E. Toward building trust in machine learning models: quantifying the explainability by SHAP and references to human strategy. IEEE Access 2024;12:11010-11023. [doi: 10.1109/ACCESS.2023.3347796]
13. El Shawi R, Sherif Y, Al-Mallah M, Sakr S. Interpretability in healthcare a comparative study of local machine learning interpretability techniques. Presented at: 2019 IEEE 32nd International Symposium on Computer-Based Medical Systems (CBMS); Jun 5-7, 2019; Cordoba, Spain p. 275-280. [doi: 10.1109/CBMS.2019.00065]
14. Chadaga K, Prabhu S, Sampathila N, et al. Explainable artificial intelligence approaches for COVID-19 prognosis prediction using clinical markers. Sci Rep 2024 Jan 20;14(1):1783. [doi: 10.1038/s41598-024-52428-2] [Medline: 38245638]
15. Khanna VV, Chadaga K, Sampathila N, et al. A decision support system for osteoporosis risk prediction using machine learning and explainable artificial intelligence. Heliyon 2023 Dec;9(12):e22456. [doi: 10.1016/j.heliyon.2023.e22456]
16. Guan C, Ma F, Chang S, Zhang J. Interpretable machine learning models for predicting venous thromboembolism in the intensive care unit: an analysis based on data from 207 centers. Crit Care 2023;27(1):406. [doi: 10.1186/s13054-023-04683-4]
17. Zhong Y, Jatav A, Afrin K, Shivaram T, Bukkapatnam STS. Enhanced SpO2 estimation using explainable machine learning and neck photoplethysmography. Artif Intell Med 2023 Nov;145:102685. [doi: 10.1016/j.artmed.2023.102685] [Medline: 37925216]
18. Suh B, Yu H, Kim H, et al. Interpretable deep-learning approaches for osteoporosis risk screening and individualized feature analysis using large population-based data: model development and performance evaluation. J Med Internet Res 2023 Jan 13;25:e40179. [doi: 10.2196/40179] [Medline: 36482780]
19. Bernard D, Doumard E, Ader I, et al. Explainable machine learning framework to predict personalized physiological aging. Aging Cell 2023 Aug;22(8):e13872. [doi: 10.1111/acel.13872] [Medline: 37300327]
20. Zhang J, Cui X, Yang C, et al. A deep learning‐based interpretable decision tool for predicting high risk of chemotherapy‐induced nausea and vomiting in cancer patients prescribed highly emetogenic chemotherapy. Cancer Med 2023 Sep;12(17):18306-18316. [doi: 10.1002/cam4.6428]
21. Tibshirani R. Regression shrinkage and selection via the lasso. J R Stat Soc Series B Stat Methodol 1996 Jan 1;58(1):267-288. [doi: 10.1111/j.2517-6161.1996.tb02080.x]
22. Quinlan JR. Induction of decision trees. Mach Learn 1986 Mar;1(1):81-106. [doi: 10.1007/BF00116251]
23. Breiman L. Random forests. Mach Learn 2001 Oct;45(1):5-32. [doi: 10.1023/A:1010933404324]
24. Geurts P, Ernst D, Wehenkel L. Extremely randomized trees. Mach Learn 2006 Apr;63(1):3-42. [doi: 10.1007/s10994-006-6226-1]

XSL•FO
RenderX

25. Freund Y, Schapire RE. A decision-theoretic generalization of on-line learning and an application to boosting. J Comput Syst Sci 1997 Aug;55(1):119-139. [doi: 10.1006/jcss.1997.1504]
26. Chen T, Guestrin C. XGBoost: a scalable tree boosting system. Presented at: Proceedings of the 22nd ACM SIGKDD International Conference on Knowledge Discovery and Data Mini; Aug 13-17, 2016; San Francisco, CA p. 785-794. [doi: 10.1145/2939672.2939785]
27. Ke G, Meng Q, Finley T, et al. LightGBM: a highly efficient gradient boosting decision tree. In: Guyon I, Von Luxburg U, Bengio S, Wallach H, Fergus R, Vishwanathan S, et al, editors. Advances in Neural Information Processing Systems 30 (NIPS 2017) 2017:3149-3157.
28. Ribeiro MT, Singh S, Guestrin C. "Why Should I Trust You?": explaining the predictions of any classifier. arXiv. Preprint posted online on Aug 9, 2016. [doi: 10.48550/arXiv.1602.04938]
29. Lundberg S, Lee SI. A unified approach to interpreting model predictions. . Preprint posted online on Nov 24, 2017. [doi: 10.48550/arXiv.1705.07874]
30. Diabetes Complications Data Set. Population Health Data Archive. URL: https://www.ncmi.cn/phda/dataDetails.do?id=CSTR:A0006.11.A0005.201905.000282-V1.0 [accessed 2025-10-20]
31. Narva AS, Bilous RW. Laboratory assessment of diabetic kidney disease. Diabetes Spectr 2015 Aug;28(3):162-166. [doi: 10.2337/diaspect.28.3.162] [Medline: 26300608]
32. Neumiller JJ, Alicic RZ, Tuttle KR. Optimization of guideline-directed medical therapies in patients with diabetes and chronic kidney disease. Clin Kidney J 2024 Jan;17(1):sfad285. [doi: 10.1093/ckj/sfad285] [Medline: 38213492]
33. American Diabetes Association Professional Practice Committee. 11. Chronic kidney disease and risk management: standards of care in diabetes—2024. Diabetes Care 2023;47(Supplement_1):S219-S230. [doi: 10.2337/dc24-S011]
34. Davis KN, Hines AE, Schaefer MC, Naseman KW. Protecting the kidneys: update on therapies to treat diabetic nephropathy. Clin Diabetes 2022;40(3):305-311. [doi: 10.2337/cd21-0090] [Medline: 35983418]
35. Li B, Wang J, Ye W. A meta-analysis of urinary transferrin for early diagnosis of diabetic nephropathy. Lab Med 2024 Jul 3;55(4):413-419. [doi: 10.1093/labmed/lmad115] [Medline: 38335130]
36. Sulaiman MK. Diabetic nephropathy: recent advances in pathophysiology and challenges in dietary management. Diabetol Metab Syndr 2019;11(1):7. [doi: 10.1186/s13098-019-0403-4] [Medline: 30679960]
37. Barbagallo CM, Cefalù AB, Giammanco A, et al. Lipoprotein abnormalities in chronic kidney disease and renal transplantation. Life (Basel) 2021 Apr 5;11(4):315. [doi: 10.3390/life11040315] [Medline: 33916487]
38. Gupta A, Gupta R. Current understanding of diabetic dyslipidemia: a review. J Indian Inst Sci 2023 Jan;103(1):287-307. [doi: 10.1007/s41745-022-00346-5]
39. Chen J, Fang Z, Luo Q, et al. Unlocking the mysteries of VLDL: exploring its production, intracellular trafficking, and metabolism as therapeutic targets. Lipids Health Dis 2024 Jan 12;23(1):14. [doi: 10.1186/s12944-023-01993-y] [Medline: 38216994]
40. Weldegiorgis M, Woodward M. Elevated triglycerides and reduced high-density lipoprotein cholesterol are independently associated with the onset of advanced chronic kidney disease: a cohort study of 911,360 individuals from the United Kingdom. BMC Nephrol 2022 Sep 15;23(1):312. [doi: 10.1186/s12882-022-02932-2] [Medline: 36109725]
41. Bauer F, Seibert FS, Rohn B, Babel N, Westhoff TH. Estimation of LDL cholesterol in chronic kidney disease. Eur J Prev Cardiol 2021 Oct 13;28(12):1402-1408. [doi: 10.1093/eurjpc/zwaa003] [Medline: 33624033]
42. Yang Q, Liu Y, Peng J, et al. High levels of serum C-peptide are associated with a decreased risk for incident renal progression in patients with type 2 diabetes: a retrospective cohort study. BMJ Open Diabetes Res Care 2023 Mar;11(2):e003201. [doi: 10.1136/bmjdrc-2022-003201] [Medline: 36958752]
43. Wahren J, Ekberg K, Samnegård B, Johansson BL. C-peptide: a new potential in the treatment of diabetic nephropathy. Curr Diab Rep 2001 Dec;1(3):261-266. [doi: 10.1007/s11892-001-0044-4] [Medline: 12643208]
44. Hills CE, Brunskill NJ, Squires PE. C-peptide as a therapeutic tool in diabetic nephropathy. Am J Nephrol 2010;31(5):389-397. [doi: 10.1159/000289864] [Medline: 20357430]
45. Colbert GB, Elrggal ME, Gaddy A, Madariaga HM, Lerma EV. Management of hypertension in diabetic kidney disease. J Clin Med 2023 Oct 31;12(21):6868. [doi: 10.3390/jcm12216868] [Medline: 37959333]
46. Steigerwalt S. Management of hypertension in diabetic patients with chronic kidney disease. Diabetes Spectr 2008 Jan 1;21(1):30-36. [doi: 10.2337/diaspect.21.1.30]

Abbreviations

ACR: albumin-creatinine ratio
AdaBoost: Adaptive Boosting
AI: artificial intelligence
AUC: area under the curve
DN: diabetic nephropathy
lasso: least absolute shrinkage and selection operator
LDL: low-density lipoprotein

XSL•FO
RenderX

LightGBM: Light Gradient-Boosting Machine
LIME: Local Interpretable Model-Agnostic Explanations
ML: machine learning
PDP: partial dependence plot
ROC: receiver operating characteristic
SHAP: Shapley Additive Explanations
SMOTE: Synthetic Minority Oversampling Technique
VLDL: very low–density lipoprotein
XGBoost: Extreme Gradient Boosting
XML: explainable machine learning

Edited by A Coristine; submitted 01.08.24; peer-reviewed by K Chadaga, VR Yella; revised version received 09.09.25; accepted 09.09.25; published 22.10.25.

Please cite as:
Wen Y, Wan Z, Ren H, Wang X, Wang W
Interpretable Machine Learning Model for Predicting and Assessing the Risk of Diabetic Nephropathy: Prediction Model Study
JMIR Med Inform 2025;13:e64979
URL: https://medinform.jmir.org/2025/1/e64979
doi:10.2196/64979

© Yili Wen, Zhiqiang Wan, Huiling Ren, Xu Wang, Weijie Wang. Originally published in JMIR Medical Informatics (https://medinform.jmir.org), 22.10.2025. This is an open-access article distributed under the terms of the Creative Commons Attribution License (https://creativecommons.org/licenses/by/4.0/), which permits unrestricted use, distribution, and reproduction in any medium, provided the original work, first published in JMIR Medical Informatics, is properly cited. The complete bibliographic information, a link to the original publication on https://medinform.jmir.org/, as well as this copyright and license information must be included.

XSL•FO
RenderX

Original Paper

Holistic Influence of Multimodal Medical Crowdfunding Affordances on Charitable Crowdfunding Outcome: Systematic Multimodel Analysis Study

Yuxuan Du[1], PhD; Yujin Yang[2], MA; Zihe Li[3], PhD; Jiaolong Xue[4], PhD

[1]Department of Marketing, School of Economics and Management, Tsinghua University, Beijing, China

[2]Department of Marketing, Booth School of Business, University of Chicago, Chicago, IL, United States

[3]Graduate School of Economics and Management, Tohoku University, Sendai, Japan

[4]Department of Marketing, Business School, Sichuan University, Chengdu, China

Corresponding Author:
Jiaolong Xue, PhD
Department of Marketing
Business School
Sichuan University
No. 24, South Section 1, Yihuan Road
Wuhou Distract
Chengdu, 610065
China
Phone: 86 15708468050
Email: jiaolongxue@scu.edu.cn

Abstract

Background: Medical crowdfunding has emerged as a critical tool to alleviate the financial burden of health care costs, particularly in regions where economic disparities limit access to medical treatment. Despite its potential, the success rates of medical crowdfunding projects remain low, with only 9% achieving their fundraising goals in China. Previous research has examined isolated factors influencing success, but a holistic understanding of how multimodal affordances—narrativity, visibility, and progress—collectively impact donor behavior and project outcomes is lacking.

Objective: This study aims to investigate how medical crowdfunding affordances, as an integrated system, influence the success of charitable crowdfunding projects. Specifically, it explores the roles of narrativity (textual elements), visibility (visual elements), and progress (dynamic updates) affordances, and how these interact with patient demographics to shape donor engagement and fundraising outcomes.

Methods: A multimodal analysis was conducted using 1261 medical crowdfunding projects from the Shuidichou platform in China. Machine learning techniques (eg, sentiment analysis via SnowNLP) and regression models were used to examine textual content, visual elements, and progress updates. Control variables included patient age, gender, and beneficiary type. Hypotheses were tested using both continuous (success ratio) and binary (success indicator) measures of project success. In total, 6 models were constructed to examine the influences of affordances.

Results: The study found that narrativity affordances—longer titles (model 1a: P=.04; model 3a: P=.03) and detailed surplus fund descriptions (P=.03)—boosted success, while overly lengthy surplus fund explanations had diminishing returns (P=.005). Disease mentions in titles increased donations (model 1a: P=.01; model 3a: P=.003). A neutral tone in the project plan also improved success (P<.001). For visibility affordances, a moderate number of progress photos maximized project success, while excessive visuals reduced impact (P<.001). Progress affordances followed a similar pattern, with a moderate number of updates enhancing success (P<.001). Critically, when all affordances were considered, only progress update frequency retained a strong inverted U-shaped effect on success (P<.001). Demographics, particularly age, also influenced donations: patients at both ends of the age spectrum received greater support , while middle-aged individuals received less (model 1b: P=.02; model 2b: P=.005; model 3b: P=.02).

Conclusions: This study advances medical crowdfunding affordance theory by demonstrating the interconnected effects of narrativity, visibility, and progress affordances on project success. Practically, results highlight the importance of strategically crafted titles, targeted demographic disclosures, and balanced progress updates—with moderate update frequency being crucial

XSL•FO
RenderX

when controlling all affordances—to enhance donor engagement. Platform designers and project organizers can apply these insights to optimize fundraising outcomes and effectively address health care inequalities. Future research should further investigate visual content analysis and donor psychology to refine engagement strategies.

(JMIR Med Inform 2025;13:e75563) doi:10.2196/75563

KEYWORDS

medical crowdfunding; multimodal approach; information affordance; donor behavior; machine learning

Introduction

Background and Research Aim

By 2030, the economic burden of chronic diseases is projected to reach approximately 343 trillion CNY (US $47 trillion) [1]. In China, the average direct medical expenditure for a case of lung cancer was 39,015 CNY (US $6041) in 2011, with an annual growth rate of 7.55% [2]. Meanwhile, Statista's 2024 data reported that the average annual disposable income per capita in 2015 was just 21,966 CNY (US $3404)—showing how severe illnesses could push average-income families into poverty.

In light of these financial challenges, crowdfunding has emerged as a key charitable tool, enabling widespread, low-cost support for individuals facing medical expenses without expectation of reciprocation [3]. In China, platforms such as Shuidichou (also called Waterdrop) and Qingsongchou have been developed and supported more than 5 million patients from September 2014 to the end of 2021, raising more than 80 billion CNY (US $12.03 billion) [4]. However, medical crowdfunding projects on these platforms have low success rates: Only 9% of the projects reach their fundraising goals, while 70% achieve just 10% of their target [5]. This underscores the urgent need for research to improve crowdfunding success.

Previous medical crowdfunding research has largely examined success factors in isolation. These factors include cultural proximity [6], social media outreach [7], gender dynamics [8], socioeconomic status [9], linguistic style and structure [10,11], and donor-recipient relationships [3]. More recently, research has begun to explore the properties of information, extending to textual [12-17], visual [12,14,15,18,19], and progress-related [12,13,15,17,20] features of crowdfunding projects.

Most previous studies have focused on GoFundMe [13,14,16,21], which hosts a wide range of projects and primarily serves Western populations, leaving donor behavior in Asian contexts less understood. The majority of Chinese relevant research in China has been conducted using data from Qingsongchou [12,19,22,23] and Tencent Charity platform [15,20]. In contrast, Shuidichou, China's largest medical crowdfunding platform, is dedicated exclusively to health care projects and remains understudied despite its relevance to Chinese users. While prior research has examined individual informational features, few studies have explored how different cues interact to shape outcomes. To address these gaps, this study applies Gibson's affordance theory [24], which emphasizes how environments provide actionable information that guides behavior. In the context of medical crowdfunding platforms, the platform serves as the environment, and crowdfunding projects act as information offered to potential donors. Overall, this study aims to address key gaps in prior research [12-17,19,25-29], which has often focused on Western populations and overlooked the interplay among affordances.

Guided by this framework, our study explores: (1) how narrativity affordances (text length, patient demographics, sentiment) influence project success; (2) how visibility affordances (number and type of images) shape donor engagement; (3) how progress affordances (update frequency and sentiment) impact project outcomes; (4) how different types of information—narrativity, visibility, and progress affordances—shape success when controlling for other affordances within the same environment; and 5) how these affordances interact with demographic and contextual factors to shape crowdfunding success.

Building on prior studies, this research responds to Zhang et al [11] by extending the analysis of narrativity affordances beyond project titles to include project descriptions and all textual content. It expands visibility affordances by drawing on Karahanna et al [30] and Zhang et al [31] to examine the number of images across projects. Inspired by Thies et al [32], it investigates progress affordances—particularly update frequency—and incorporates update sentiment, following Zhang et al [3], for a more nuanced content analysis. Additionally, building on findings by Zhou [33], it includes demographic and project characteristics as control variables to assess how affordance effects vary across contexts. By synthesizing insights across modalities, this study constructs a comprehensive multimodal framework encompassing narrativity, visibility, and progress affordances.

Literature Review

Affordance, as an ecological and psychological concept, has been developed and extended for decades. It was initially proposed by Gibson [24], defining it as the information offered by the environment with references to the abilities of animals to act, mainly in the field of visual perception. Post-Gibson stream researchers [34-36] extend Gibson's theories and summarize affordance as the property of the environment. Debates and discussions led to further development of Gibson's theories. Norman [37] was among the earliest to link affordance with human-computer interaction, laying the groundwork for a future extended definition of interaction-oriented affordance. He stresses that users are important because they can perceive and interpret affordances that are built into the design of computers and systems. Later, Jiao et al [38] apply affordances to technologies. He denies and criticizes technological determinism and stresses that affordances are embedded in interactions among users, objects, and technologies. Through

XSL•FO
RenderX

perceiving and understanding technologies, users can achieve different goals and outcomes. Heft [34] emphasizes that users can take corresponding actions based on the provided information. Meanwhile, these actions influence information effectiveness.

The rapid rise of the internet and digital technologies has made social media platforms an integral part of daily life, supporting a wide range of activities such as self-promotion, marketing, entertainment, political engagement, and crowdfunding. In recent years, a growing body of academic research has explored the influence of platform affordances on user behavior. For instance, Karahanna et al [30] proposed that individuals use social media to fulfill both psychological and emotional needs, with platform affordances—particularly IT-enabled ones—helping to meet these objectives. Several studies further highlight how platform affordances shape web-based behavior. Zhou [33] finds that changes in social media affordances can causally affect communication among users. Theocharis et al [39] examine how platform features and user interaction reshape political participation. Scharlach and Hallinan [40] argue that IT-enabled affordances transform abstract social values into measurable actions on the web, guiding users' decisions. In the context of medical crowdfunding, Choy and Schlagwein [41] used the Earthship Kapita case to illustrate how IT affordances on crowdfunding platforms satisfy donors' psychological needs and motivations, making web-based charity models more effective than traditional offline approaches. Jiao et al [38] deliver a web-based survey and prove that IT affordances effectively influence donors' perceptions and, therefore, donors' donation decisions. Collectively, these studies emphasize the central role of affordances in shaping user behavior on the web.

Medical crowdfunding has emerged as a trending method for financing high-cost medical treatments. Severe diseases, exemplified by the far-reaching impact of the COVID-19 pandemic over the past few years, typically put significant economic pressures on patients and their families. Consequently, many resort to medical crowdfunding as a source of economic assistance. To better understand the mechanism of the practice and to optimize the chances of the success of crowdfunding projects, we frame medical crowdfunding as a multimodal information system facilitating the complex interaction between the three central stakeholders: (1) project initiator (organizer or patient), (2) the platform's technology and information infrastructure, and (3) prospective donors. We maintain that when information relevant to the project is properly presented and creates interaction between these actors, the chances of project success can be greatly improved.

Table 1 [12-17,19,20,22,23,42] displays related works and research data of medical crowdfunding platforms over the past several years. Based on the table, the primary studied medical crowdfunding platform includes GoFundMe, Tencent Charity, and Qingsongchou, while the primary methodologies used in related works are text analysis and linear regression. Independent and dependent variables are also acquired as seen in Table 2 [12-17,19,20,22,23,42]. Although various variables are chosen, related works only analyze the impact of the chosen variables on the project success in isolation.

Our study uses data from the Shuidichou platform, which serves a Chinese demographic, to examine both the individual effects of variables and the interaction. In contrast to prior research mentioned that has predominantly relied on data from GoFundMe—a platform primarily used in the United States—our approach expands the demographic scope by focusing on the Chinese context. As the largest crowdfunding platform in China, Shuidichou specializes in health care–related projects, offering a reliable and relevant data source for studying medical crowdfunding. While Qingsongchou is another Chinese platform with comparable functions, it presents a critical limitation: project organizers can alter fundraising goals during a project, potentially introducing bias and compromising data consistency. Therefore, Shuidichou provides a more targeted and stable foundation for our research. In addition to these, while each affordance may individually influence project success, their interactions must also be considered. Beyond studies using field data from platforms like GoFundMe that analyze affordances in isolation, previous experimental research—such as Jiao et al [38]—has used surveys to manipulate specific features and examine their effects. In contrast, our study uses objective field data from Shuidichou and considers affordances simultaneously, capturing how they function together in real-world settings. This integrated approach provides a more realistic and comprehensive understanding of crowdfunding dynamics and offers actionable insights on optimizing information presentation to enhance project effectiveness. In addition, clear explanations on how information presentation can be managed to enhance crowdfunding success are provided, along with examples.

XSL•FO
RenderX

Table 1. Medical crowdfunding affordance-related literature in the past 5 years.

Platform	Obs number	Method	Findings	Source
GoFundMe	997	Visual analytics approach	Social media plays a crucial role in boosting medical crowdfunding success.	Ren et al [14]
Qingsongchou	1010	Convolutional neural networks	Emotional-related and credible-related photos increase the donation amount, while rational-related ones decrease it.	Wang et al [19]
Tencent Charity	1891	Linear regression	Project with health-related and disease-related keywords are more likely to succeed	Ba et al [20]
Tencent Le Donation	29,700	Textual analysis	Persuasive language significantly influences donor willingness and trust.	Wu et al [15]
Shuidichou	50,000	Linear regression	Projects with positive expressions achieve higher success rates.	Zheng and Jiang [17]
Qingsongchou	754	Linear regression	Funding goals and project duration can help to predict crowdfunding project performances.	Chen et al [12]
GoFundMe	1830	Univariate, multivariate analysis	The success rate of the project heavily depends on the cancer type and the donor's social networks.	Holler et al [13]
GoFundMe	92,753	Textual analysis	Hard-to-treat, high-mortality cancers attract more donors. Projects with strong sentiment words and female beneficiaries are more likely to succeed.	Zhang et al [16]
GoFundMe	243,795	Topic model	Images featuring younger individuals, more people, and more smiles significantly improve the success of projects.	Wang et al [42]
Qinsongchou	116,282	Linear regression	Air pollution negatively impacts donations for critical illness, increasing negative emotions.	Hua et al [22]
Qingsongchou	84,712	Linear regression	Key factors such as patient age, disease type, geographical location, and donation target, influence the success of projects.	Zhang et al [23]

Table 2. Affordance indicators chosen by the works in Table 1.

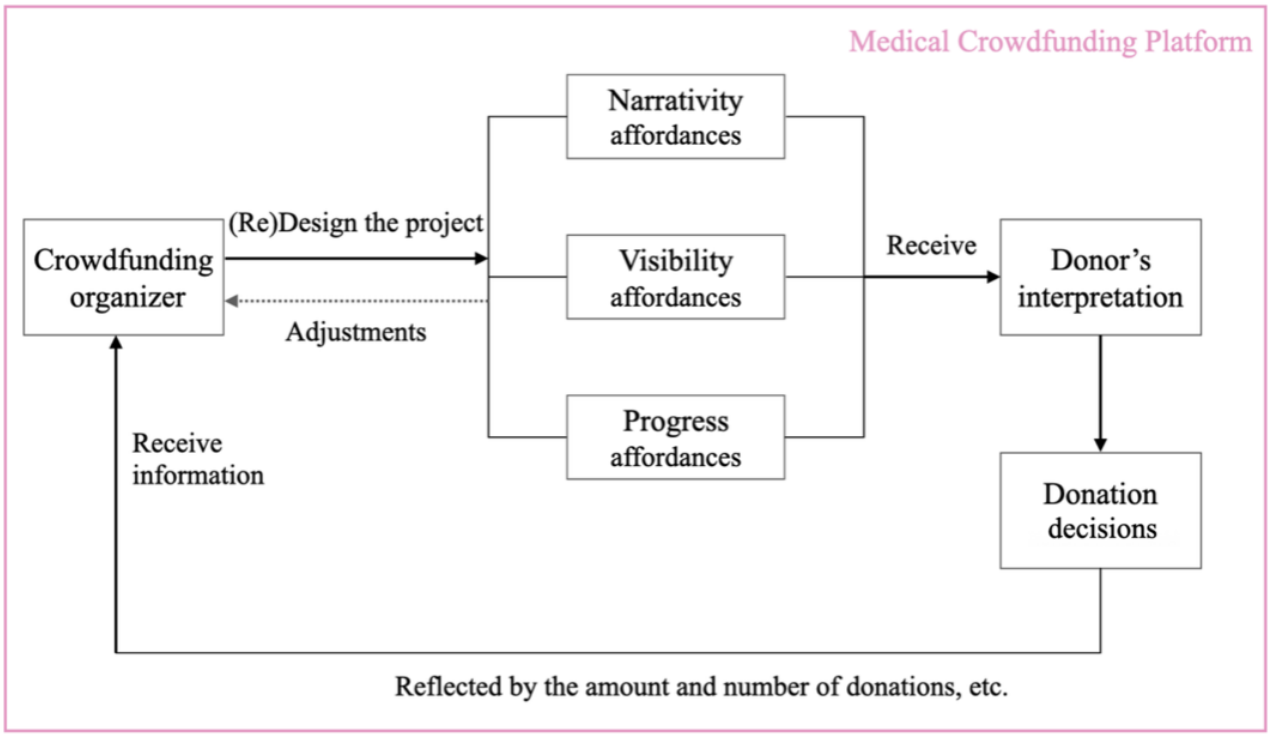
Authors	Independent variable			Dependent variable			
	Textual	Visual	Progress	Success rate	Raised amount	Donation number	Willingness
Ren et al [14]	✓	✓		✓			
Wang et al [19]		✓			✓		
Ba et al [20]	✓		✓	✓			
Wu et al [15]	✓	✓	✓				
Zheng and Jiang [17]	✓		✓	✓			✓
Chen et al [12]	✓	✓	✓		✓		
Holler et al [13]	✓		✓		✓	✓	
Zhang et al [16]	✓			✓			
Wang et al [42]	✓	✓		✓			
Hua et al [22]	✓			✓			
Zhang et al [23]	✓			✓	✓		

Hypothesis Development

Drawing on affordance theory [24], we conceptualize the crowdfunding platform as an environment in which textual, visual, and progress-related elements function as informational affordances. Similarly, signaling theory states the presence of information asymmetry between sender and receiver [43]. In web-based medical crowdfunding (Figure 1), we have the sender as the crowdfunding project organizer, while the receivers are potential donors online. Senders use affordances to make information signals efficiently to influence receivers, and receivers make informed decisions based on the signals. All interactions among receivers and senders and the information presented on the platform exert a significant influence on donor behavior, ultimately shaping the success rate of crowdfunding projects.

XSL•FO
RenderX

Figure 1. Interaction between project organizers or patients, potential donors, and the platform.



To quantitatively evaluate a project's success, the most frequently applied metric is the project's success rate, although its definition is not uniform across earlier studies. For example, Ba et al [20] use a variable termed *Goal_Pro*, where the percentage of raised funds compared with the target donation is used. Likewise, Zhang et al [44] follow the same benchmark. By way of contrast, Zheng and Jiang [17] gauge success by measuring the number of donations received and the donation amount. A lesser-used measure is binary success—whether a project is a success. For example, Parhankangas and Renko [45] create a dummy variable where 1 represents a goal achieved and 0 represents failure. Both continuous and binary measures are used by our study for the dependent variables, providing a richer assessment of project results. Based on these theoretical underpinnings and earlier results (Tables 1 and 2), the following hypotheses are proposed.

We define narrativity affordance as the action possibilities offered by textual elements written by project organizers. On Shuidichou, these include the project title, project description, fundraising purpose, donation plans, and surplus fund use (Figure 2). To capture donor attention, patients and platform managers must craft descriptions using effective language. Multiple indicators, including text length and sentiment analysis, are selected to evaluate narrativity affordance.

The text lengths of titles and project descriptions have been widely studied, yet findings remain inconsistent. Hou et al [18] and Chen et al [12] claim that a longer text length, especially the length of the story, can attract more attention. However, Zhang et al [44] conclude that there is an inverted U-shaped relationship between story length and the success of a project, meaning that a project with a medium-length description is more likely to succeed. Similarly, Ren et al [14] conclude that the optimal length of a successful project title should be 6 to 11 words. Zhang et al [44] claim that statistically, the length of the title is not significant, and a shorter project description positively influences the success of the project. We develop our first hypothesis as follows.

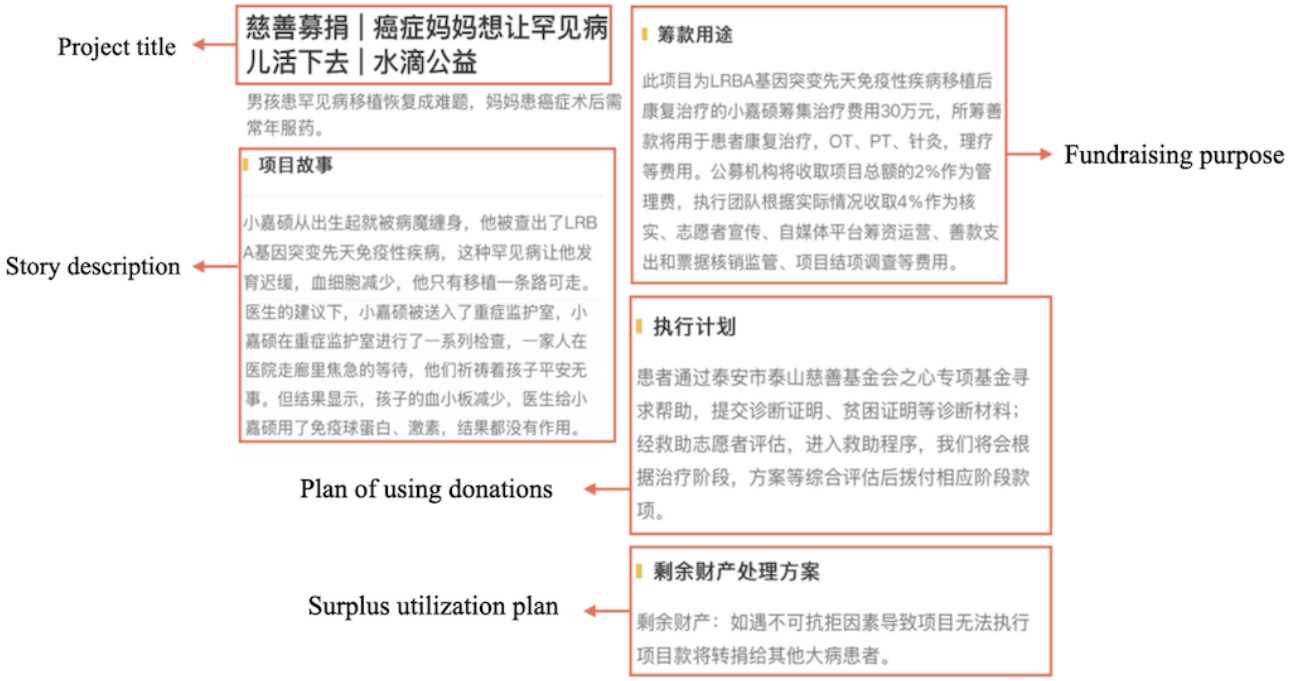
> *Text length has an inverted U-shaped relationship with the success of a project.* [H1a]

Studies also discussed whether project titles or project descriptions should contain disease type, gender, and age in order to improve the success of the project. Chen et al [12], Hou et al [18], and Peng et al [46] all conclude that projects for younger patients, especially children, are more likely to succeed. Zhang et al [44] confirm that if the project title includes disease type, the success rate of the project increases. No past research has directly proved that gender information included in the title and description can impact the success rate of a project. However, Holler et al [13] conclude that female patients are more willing to initiate crowdfunding projects. We develop our second hypothesis as follows.

> *Disease type, gender, and age in the project title and the project description positively influence the success of a project.* [H1b]

XSL•FO
RenderX

Figure 2. Screenshots of narrativity affordances.



The sentiments in the title and the project description also influence the success of a project. Researchers apply various methods to capture sentiments. Kim et al [47] designed questionnaires and divided project sentiments into 3 types: responsibility, guilt, and urgency. In the experiment of Wang et al [48], sentiments are measured using scales that include pride and guilt. Although questionnaires and experiments can measure sentiments more precisely, their limitation lies in the need for fully qualified participants; otherwise, accuracy may be compromised. Current techniques can be divided into 2 groups: Lexicon-based and machine learning methods. Agarwal et al [49] construct a domain-specific ontology with ConceptNet and WordNet, extract wordings with natural language processing (NLP), and convert them into a contextual polarity lexicon, classifying sentiments into positive, negative, and neutral ones. Similar lexicon-based methods are used by multiple research works [50-53]. Machine learning techniques are commonly used by extracting and crawling keywords, followed by classification. With such techniques, it is possible to analyze a relatively larger volume of texts and quantify the sentiments in them [54-56].

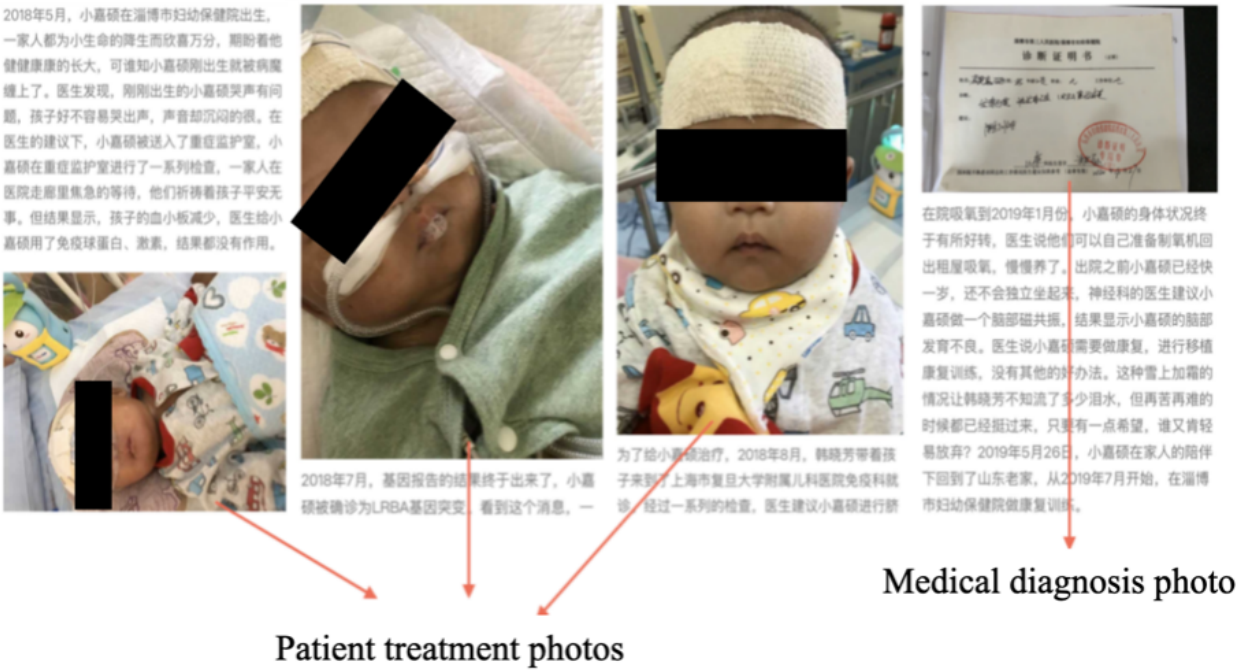
Previous studies report various findings on sentiments in titles and project descriptions. Zhang et al [57] conclude that the negative sentiments in project titles decrease the success rate, but if these words are in project descriptions, the success rate increases. Hou et al [18] and Zheng and Jiang [17] confirm that if the project description narratives are more positive, the project tends to succeed. We propose a hypothesis as follows.

> *Positive or negative sentiments of the project title and project descriptions significantly influence the success of a project.* [H1c]

We define visibility affordance (Figure 3) as the action possibilities through design and graphical elements, specifically referring to the number of photos in different sections (main page and progress updates). Studies have proven that photos and videos on social media are effective tools for establishing web-based identification and attracting the attention of online users [58,59]. Similarly, posting photos for medical crowdfunding projects can provide potential donors with more direct information, and photo types, such as the current status of patients and ID verification, can influence donor motivation and donor trust [14]. Wang et al [19] list the influence of different types of photos on the success of a project. They point out that photos related to the current health status and treatment status positively influence the success of a project, while those presenting treatment expenses negatively influence the success of a project. Thies et al [32] and Wu et al [15] conclude that the number of photos included positively influences the success of a project. Therefore, our hypothesis is as follows.

XSL•FO
RenderX

Figure 3. Screenshots of visibility affordances.



The number of photos included in a project positively influences the success of a project. [H2]

We define progress visibility (Figure 4) as the action possibilities offered by progress updates, including elements such as patient treatments, donation cash flows, etc. The progress updates of a project can be crucial for the following reasons. First, regularly posting updates establishes the credibility of the project organizer [15], because this shows that the project is transparent and that donors can track their donations. Second, platform managers can structure textual descriptions and use words that convey positive or negative sentiments to evoke donor empathy. Some prior academic research has already highlighted the impact of progress updates. Parhankangas and Renko [45] claim that a higher frequency of progress updates improves donor engagement, thereby enhancing the project's success. Ren et al [14] and Wu and Peng [60] have similar conclusions. Zhang et al [44] conclude that a high frequency of progress updates with negative sentiment words can significantly increase the success rate of a project. Wu and Peng [60] propose that sentiments in progress updates significantly influence donation amounts. Previous studies also suggest an inverted U-shaped relationship between progress update frequencies and project success. Thies et al [32] and Wu et al [15] mention that when the frequency is too high, donors can be negatively influenced by information overload. We develop 2 hypotheses as follows.

The frequency of progress updates has an inverted U-shaped relationship with the success of a project. [H3a]

Positive or negative sentiments in progress updates significantly influence the success of a project. [H3b]

XSL•FO
RenderX

Figure 4. Screenshots of progress affordances.



Methods

Ethical Considerations

This study did not require ethics board review because it did not involve direct interaction with human participants nor the collection of any private or identifiable information. All analyses were conducted on aggregated, anonymized data from public sources. This rationale is consistent with prevailing ethical research standards and common institutional practices for studies of this nature.

Overview

All data were extracted from disease-related crowdfunding projects on the Shuidichou platform. This study did not involve any surveys or experimental interventions; thus, no RCT registration number is applicable. Launched in July 2016, Shuidichou is China's leading platform for medical crowdfunding. By the end of 2020, the Shuidichou platform had facilitated over 37 billion RMB (approximately US $5.1 billion) in donations from more than 340 million contributors across 1.7 million medical aid projects, according to its publicly reported data.

According to company profile summaries on Tracxn.com, while GoFundMe remains the leading crowdfunding platform [31], Shuidichou specializes in health care, making it China's top platform and the world's third-largest. Backed by US $251 million from major investors like Tencent and IDG Capital, its scale and user base offer a strong basis for analyzing information affordances in crowdfunding success.

On Shuidichou, project pages follow a standardized format. Information—such as the project title, target amount, funds raised, timeline, beneficiary, initiating organization, project leader, and donation recipient—is shown on the right side. On the left, donors can navigate three sections: (1) Project Details, which outlines the patient's story, fundraising purpose, fund allocation, execution plan, and surplus handling; (2) Project Progress, which provides updates on the patient's condition and fund use; and (3) Donation Status, which tracks contributions from donors.

To ensure representative results, this study uses a sample of 1261 crowdfunding projects initiated between May 11, 2018, and September 5, 2024. Due to platform restrictions requiring additional authorization for long-expired projects, we extracted data from all publicly available projects as of November 11, 2024, without applying additional selection criteria. As such, we consider the dataset broadly representative of various disease types, while acknowledging that its demographic scope is limited to the Chinese population and that some projects may have been overlooked due to limitations in platform visibility. Among these projects, 1228 out of 1261 (97.38%) have already closed. Given that this study aims to understand how the platform's information management capabilities influence whether a project reaches its funding goal, and recognizing that projects may meet their objectives before the intended end dates, we chose not to exclude any projects based on their completion status.

Data Extraction

The Shuidichou platform restricts the direct extraction of comprehensive project data. To address this, research assistants manually collected project links to include all available projects for individuals with various diseases. Software engineers then used Python to scrape donor-visible data. Since patient gender,

XSL•FO
RenderX

age, and name are not explicitly displayed in a dedicated section, these variables were manually coded.

After removing duplicates, we conducted a comprehensive textual analysis to examine how affordances influence donation behavior across project titles, project descriptions, progress updates, fund purposes, fund use plans, and surplus fund use. All text elements were evaluated for length and sentiment using SnowNLP. Titles and project descriptions were the primary focus, as they conveyed crucial information to donors. We measured text length excluding spaces and punctuation to assess information density and generated dummy variables for age, gender, and disease presence using Python-based text-matching methods.

For sentiment analysis, we preprocessed text using the Jieba Chinese segmentation tool and generated sentiment scores with SnowNLP, which assigns values from 0 (negative) to 1 (positive). SnowNLP is a widely used tool for Chinese sentiment analysis, particularly effective for processing user-generated content such as social media and crowdfunding texts. Prior studies have successfully applied SnowNLP for sentiment analysis in Chinese platforms, demonstrating its suitability for this context [61]. We further analyzed the frequency of positive, negative, and degree words using the Hownet Chinese dictionary [62].

Variables and Models

Dependent Variables

The success of crowdfunding projects is measured in two ways: (1) success ratio: the ratio of the donations received to the funding goal. (2) success indicator: a binary indicator of whether the project met or exceeded its goal. Only 39 projects have fully reached their funding targets. Given the limited number of successful cases, we conducted bootstrap robustness tests for each model using *success_ind* as the dependent variable. Only models that passed the robustness test—indicating low bias and stable results—were considered.

Independent Variables

The main independent variable in this study is information affordance, comprising three components: (1) narrativity affordance, which examines how textual elements influence donation behavior through factors such as text length, word frequency, and sentiment scores; (2) visibility affordance, which explores the role of visual information, particularly the number of images in project descriptions and progress updates, in shaping donor engagement; and (3) progress affordance, which analyzes how the frequency and content of patient progress update impact donation patterns over time.

Control Variables

The control variables in this study are patient age, patient gender, and an indicator of whether the beneficiary is an individual or a group of recipients.

The multivariable models assess how narrativity, visibility, and progress affordances influence crowdfunding success. Each model is tested with both the success indicator and success ratio using regression analysis and U-tests. Given that each affordance includes distinct elements—such as textual length, which may be reflected in title length, story length, or other components—that may influence donor decisions differently, we analyze them separately to test for differential effects. Models 1-5 assess the individual impact of specific affordance elements on the success ratio, while model 6 takes a holistic approach to examine how narrativity, visibility, and progress affordances collectively influence success.

Models 1 to 3 focus on narrativity affordance, leveraging the textual richness of titles and project descriptions. Model 1 examines titles, model 2 analyzes project stories, and model 3 combines both, along with additional elements such as purpose statements, plans, and surplus fund use, to assess the impact of narrative elements on donation behavior. Model 4 captures visibility affordance by measuring the effect of image counts in project descriptions and progress updates. Model 5 addresses progress affordance by incorporating patient progress updates' frequency, length, and sentiment to explore how updates shape donation behavior.

Model 6 integrates the 3 affordances into a comprehensive framework. To assess the effect of each affordance type while controlling for the others, we aggregated related variables within each category. Narrative length is calculated by summing all relevant text fields. Demographic information—patient age, gender, and disease type—is combined into a composite index, with higher values indicating more demographic content. Wording valence is derived by subtracting total negative word counts from total positive word counts. Additionally, degree words and their intensity scores from both the title and project descriptions are summed to capture overall linguistic intensity.

Results

Descriptive Statistics

Overview

Only 39 out of 1261 projects (3%) successfully reached their funding goals. On average, the projects achieved only 18% of their target. To validate our success measures, we examined their correlations with key outcomes. Both the number of donations (R=0.5512 and 0.2359) and the amount received (R=0.5455 and 0.2167) show strong, significant correlations with success ratio and success indicator (all P<.001). Descriptive statistics are provided in Tables S2 and S3 in Multimedia Appendix 1.

Robustness Test

To ensure the statistical validity of our results, we conducted robustness tests for both the success ratio and success indicator models. Given the small number of fully successful projects, these tests help confirm that our findings are stable and not driven by random variation. Specifically, we used nonparametric bootstrapping with 1000 replications for models 1 to 6 using both dependent variables.

For the success ratio models, bootstrap analyses demonstrated generally stable coefficient estimates across models 1 to 6, with low bias (< ±0.05) and moderate standard errors (<0.10). However, in model 2, the sentiment score calculated using the

XSL•FO
RenderX

SnowNLP algorithm exhibited substantially inflated standard errors (up to 30) and high bias, indicating instability for this predictor. Similarly, in model 3, the indicator for whether the project beneficiary is an individual showed large standard errors (up to 1464.41) and considerable bias, likely due to model complexity and multicollinearity among narrative-related features. These unstable predictors were excluded from interpretation, while the remaining estimates across models 1 to 6 demonstrate solid robustness in explaining the success ratio.

In the success indicator models, bootstrapping with 1000 resamples for models 1 to 3 (focused on narrative affordances) revealed substantial statistical instability. Several predictors showed significant bias (eg, exceeding ±1.0 in model 1 and reaching up to $\pm 1.78\times10^{13}$ in model 3) and substantial standard errors (up to 4.65×10^{14}). Consequently, estimates from these models are excluded from further interpretation. In contrast, bootstrap analyses for models 4 to 6, which examine visual, progress, and combined affordances, produced substantially more stable results. Most key predictors in these models exhibited minimal bias (< ±0.05) and moderate standard errors (<0.10), supporting the reliability of these estimates. Therefore, models 4 to 6 are retained for interpretation, given their demonstrated stability.

Collectively, these analyses demonstrate that the majority of models in this study produce stable and reliable estimates, with specific unstable predictors identified and excluded from interpretation. To further assess the robustness of the success ratio models, we conducted a sensitivity analysis by re-estimating the models after excluding projects that fully met or exceeded their fundraising goals. This approach tested whether these extreme cases disproportionately influenced the results. The findings remained consistent, with similar coefficient magnitudes and significance levels, and only minor fluctuations were observed. All results based on the filtered dataset are reported for transparency (Tables S4-S6 in Multimedia Appendix 1). Together, the bootstrap and sensitivity analyses provide a comprehensive assessment of model reliability, while acknowledged limitations ensure cautious, evidence-based interpretation.

Regression Results

Overall, we present 6 models using the success ratio (Tables 3-5) and success indicator (Tables 5 and 6). U-shaped relationships are visualized in Figures 5-7.

XSL•FO
RenderX

Table 3. Regression results for success ratio (models 1-3). This table presents regression results for narrative affordance models (models 1-3) with success ratio as the dependent variable. Model (a) shows main effects; model (b) adds U-tests for significant predictors.

	Model 1a		Model 1b		Model 2a		Model 2b		Model 3a		Model 3b	
	T-value	*P* value	T-value	*P* value	T-value	*P* value	T-value	*P* value	T-value	*P* value	T-value	*P* value
Title length	2.112	.04	0.611	.54	__[a]	—	—	—	2.252	.03	0.000	>.99
I(title length)^2	N/A[b]	N/A	–0.448	.65	—	—	—	—	—	—	0.144	.89
Title age	–1.652	.10	–1.818	.07	—	—	—	—	–0.343	.73	–0.342	.73
Title gender	–0.776	.44	–0.734	.46	—	—	—	—	–0.784	.43	–0.730	.47
Title disease	2.583	.01	2.517	.01	—	—	—	—	2.940	.003	2.806	.005
Title negative words	–0.190	.85	–0.297	.77	—	—	—	—	–0.504	.62	–0.382	.70
Title positive words	–1.452	.15	–1.304	.19	—	—	—	—	–1.788	.07	–1.757	.08
Title sentiment	–2.286	.02	0.173	.86	—	—	—	—	0.401	.69	0.623	.53
I(title sentiment)^2	—		–0.624	.53	—	—	—	—	—	—	—	—
Title degree words	1.767	.08	1.723	.09	—	—	—	—	1.422	.16	1.360	.17
Title degree score	1.113	.27	1.071	.28	—	—	—	—	–0.961	.34	–0.860	.39
Story length	—	—	—	—	1.116	.27	1.131	.26	0.319	.75	0.626	.53
Story age	—	—	—	—	0.817	.41	1.273	.20	0.554	.58	0.897	.37
Story gender	—	—	—	—	1.288	.20	1.263	.21	1.764	.08	1.483	.14
Story negative words	—	—	—	—	0.384	.70	0.220	.83	–0.493	.62	–0.473	.64
Story positive words	—	—	—	—	–0.202	.84	–0.044	.97	–0.317	.75	–0.225	.82
Story sentiment	—	—	—	—	—	—	—	—	–0.657	.51	–0.650	.52
Story degree words	—	—	—	—	–0.683	.50	–0.805	.42	1.154	.25	–1.336	.18
Story degree score	—	—	—	—	0.299	.77	0.414	.68	1.139	.26	1.257	.21
Purpose length	—	—	—	—	—	—	—	—	–2.754	.006	0.130	.90
I(purpose length)^2	—	—	—	—	—	—	—	—	—		–0.840	.40
Purpose sentiment	—	—	—	—	—	—	—	—	0.568	.57	1.175	.24
Plan length	—	—	—	—	—	—	—	—	–1.303	.19	–1.626	.10
Plan sentiment	—	—	—	—	—	—	—	—	2.160	.03	3.990	<.001
I(plan sentiment)^2	—	—	—	—	—	—	—	—	—	—	–3.717	<.001
Surplus length	—	—	—	—	—		—	—	2.139	.03	3.335	.001
I(surplus length)^2	—	—	—	—	—		—	—	—	—	–2.838	.005
Surplus sentiment	—	—	—	—	—		—	—	–0.252	.80	–2.153	.03
Patient age (years)	–3.701	<.001	–3.456	.001	–3.119	.002	–3.604	<.001	–2.699	.007	–3.138	.002
I(patient age)^2	—	—	2.420	.02	—	—	2.791	.005	—	—	2.409	.02
Patient gender	–1.499	.13	–1.484	.14	–0.764	.45	–0.796	.43	–1.061	.30	–1.300	.19

XSL•FO
RenderX

	Model 1a		Model 1b		Model 2a		Model 2b		Model 3a		Model 3b	
	T-value	*P* value	T-value	*P* value	T-value	*P* value	T-value	*P* value	T-value	*P* value	T-value	*P* value
Beneficiary indicator	–3.831	<.001	–3.827	<.001	–2.816	.005	–2.770	.006	—	—	—	

[a]Variable was not available and therefore not included in the model.

[b]N/A: not applicable, but included in the model under every table.

Table 4. Regression results for success ratio (models 4 and 5). presents regression results for visual and progress affordance models (models 4 and 5) with success ratio as the dependent variable. Model (a) shows main effects; model (b) adds U-tests for significant predictors.

	Model 4a		Model 4b		Model 5a		Model 5b	
	T-value	*P* value	T-value	*P* value	T-value	*P* value	T-value	*P* value
Project description picture number	–1.304	.19	–1.834	.07	__[a]	—	—	—
Progress picture number	9.494	<.001	17.741	<.001	—	—	—	—
I(progress picture number)^2	—	—	–14.734	<.001	—	—	—	—
Progress number	—	—	—	—	6.288	<.001	10.960	<.001
I(progress number)^2	—	—	—	—	—	—	–8.787	<.001
Progress length	—	—	—	—	–0.496	.62	–2.438	.02
Progress sentiment	—	—	—	—	–0.667	.51	–1.049	.29
Patient age (years)	–3.506	<.001	–2.431	.02	–3.138	.002	–2.135	.03
I(patient age)^2	—	—	1.946	.06	—	—	1.536	.13
Patient gender	–1.667	.10	–1.776	.08	–1.921	.06	–1.827	.07
Beneficiary indicator	–0.330	.74	1.857	.06	–1.188	.24	–1.970	.049

[a]Not applicable.

Table 3 presents the regression analyses for the narrativity affordance models (models 1-3), using success ratio as the dependent variable. T-values are reported with *P* values in parentheses. Story sentiment (model 2) and the beneficiary indicator (model 3) are marked as "N/A" to reflect their exclusion from interpretation due to substantial bias found in robustness tests. Model (a) shows the main effects, while model (b) includes U-tests for variables significant in model (a). U-tests (quadratic terms) are only estimated for continuous predictors. For binary variables, quadratic terms are perfectly collinear with the original variable and therefore omitted from the models.

For H1a, our findings reveal that the impact of text length on success varies by text type, providing partial support for H1a. Surplus use length shows a significant inverted U-shaped impact on the success ratio (*P*=.005), but not for other texts (Figure 5). The main effects suggest that longer text generally leads to greater success. Longer titles (model 1a: *P*=.04; model 3a: *P*=.03) and more detailed surplus fund explanations (*P*=.03) improve the success ratio, while longer fund purpose descriptions (*P*=.006) reduce it.

XSL•FO
RenderX

Table 5. Regression results for the overall model. This table presents regression analyses for overall model 6. Model (a) shows main effects; model (b) adds U-tests for significant predictors.

	Success ratio				Success indicator			
	Model 6a		Model 6b		Model 6a		Model 6b	
	T-value	*P* value	T-value	*P* value	T-value	*P* value	T-value	*P* value
Narrative length	–0.288	.77	–0.389	.70	1.856	.06	1.851	.06
Narrative demographic	1.695	.09	–1.397	.16	1.233	.22	0.989	.32
Narrative valence word	–0.185	.85	–0.234	.82	–1.919	.06	–2.076	.04
Narrative degree words	0.224	.82	–0.407	.68	–0.022	.98	–0.198	.84
Narrative degree score	0.088	.93	0.780	.44	0.137	.89	0.311	.76
Project description picture number	–1.594	.11	–1.726	.09	–2.104	.04	–0.661	.51
I(project description picture number)	__[a]	—	—	—	—	—	–0.165	.87
Progress picture number	–0.109	.91	9.079	<.001	–2.848	.004	2.063	.04
I(progress picture number^2)	—	—	—	—	—	—	–1.562	.12
Progress number	4.144	<.001	8.046	<.001	4.009	<.001	3.747	<.001
I(progress number^2)	—	—	–13.008	<.001	—	—	–2.244	.03
Progress length	–0.399	.69	–4.026	<.001	–0.435	.66	–1.890	.06
Progress sentiment	–0.551	.58	–0.718	.47	–0.467	.64	–0.454	.65
Patient age (years)	–3.029	.003	–1.902	.06	–0.881	.38	–0.149	.88
I(patient age^2)	—	—	1.470	.14	—	—	—	—
Patient gender	–1.612	.11	–1.331	.18	–0.359	.72	–0.201	.84
Beneficiary indicator	–1.174	.24	0.148	.88	1.019	.31	1.771	.08

[a]Variable was not available and therefore not included in the model.

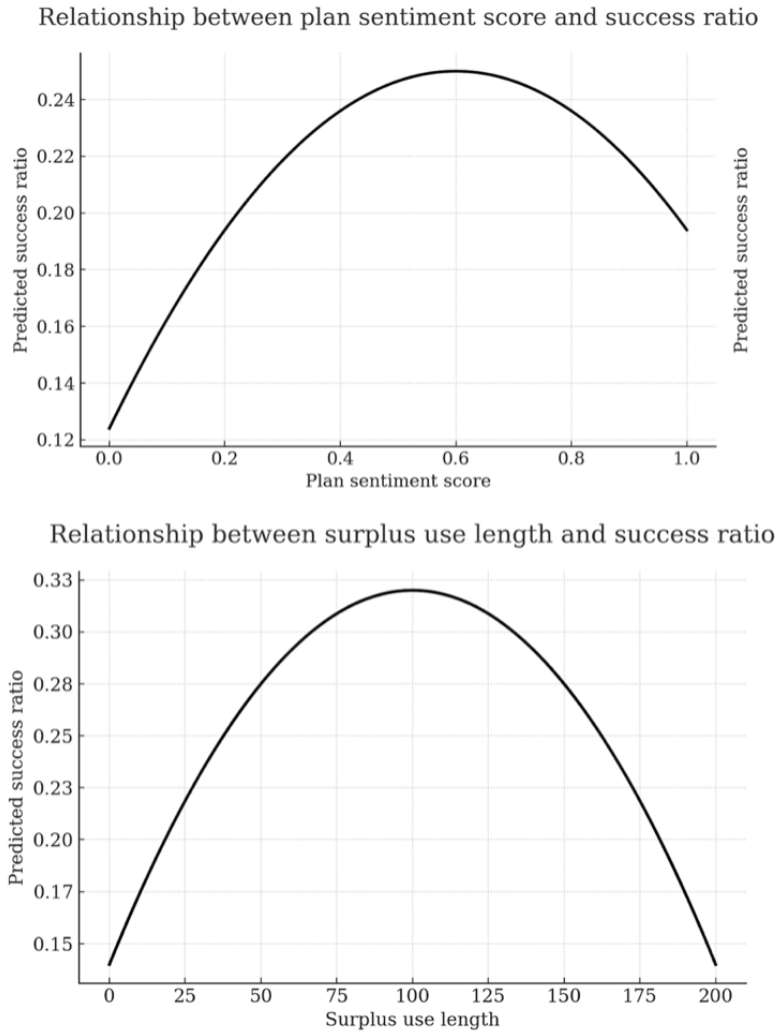
Table 6. Regression results for the success indicator (models 4 and 5). This table presents regression analyses for visual and progress affordance models (models 4 and 5), using the success indicator as the dependent variable. Model (a) shows main effects; model (b) adds U-tests for significant predictors.

	Model 4a		Model 4b		Model 5a		Model 5b	
	Z-value	*P* value	Z-value	*P* value	Z-value	*P* value	Z-value	*P* value
Project description picture number	–0.095	.92	–0.742	.46	__[a]	—	—	—
Progress picture number	2.289	.02	5.415	<.001	—	—	—	—
I(progress picture number)^2	—	—	–3.298	.001	—	—	—	—
Progress number	—	—	—	—	1.981	.048	3.854	<.001
I(progress number)^2	—	—	—	—	—	—	–2.588	.01
Progress length	—	—	—	—	–0.015	.99	–1.096	.27
Progress sentiment	—	—	—	—	–0.177	.86	–0.416	.68
Patient age (years)	–1.839	.07	–0.444	.66	–1.769	.08	–1.084	.28
Patient gender	–0.569	.57	–0.547	.58	–0.521	.60	–0.418	.68
Beneficiary indicator	0.918	.36	1.290	.20	1.246	.21	0.478	.63

[a]Variable was not available and therefore not included in the model.

XSL•FO
RenderX

Figure 5. U-test results for model 3.



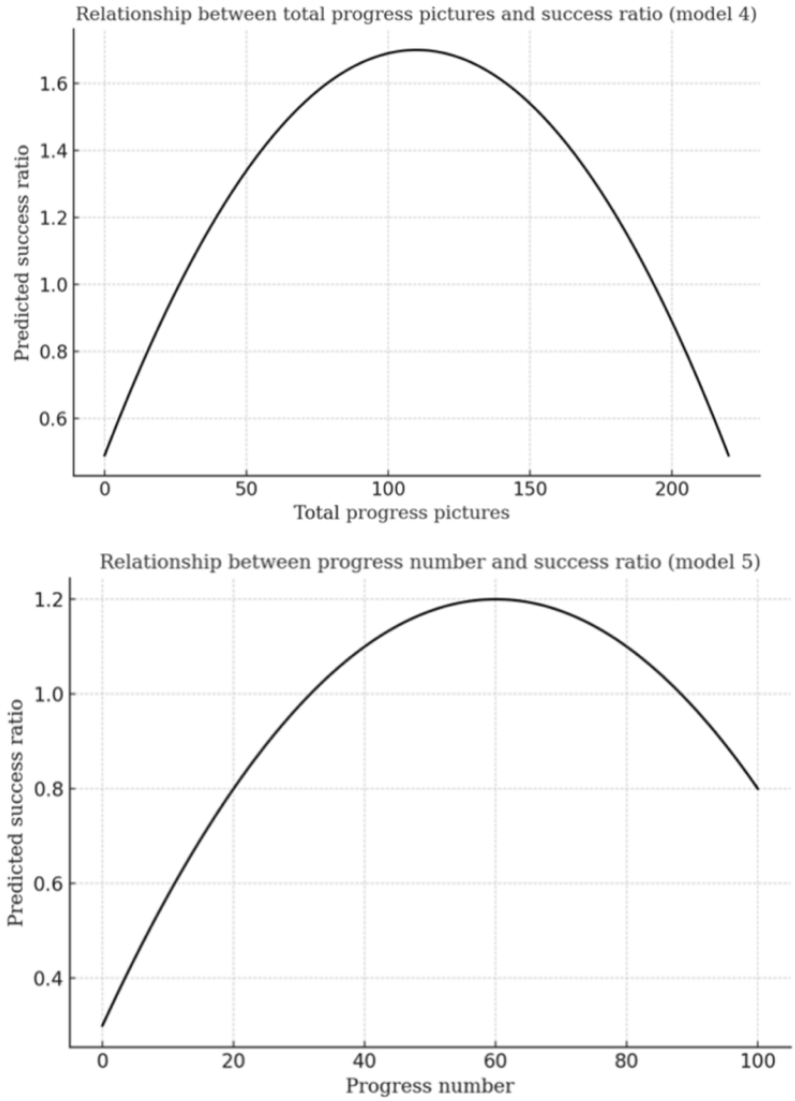
Including demographic information does not consistently enhance project success; only when the title includes a disease (model 1a: *P*=.01; model 3a: *P*=.003) does it show a significant positive effect, offering partial support for H1b. H1c is largely supported. A more positive-phrased fund use plan (*P*<.001) significantly improves the success ratio, with a U-shaped pattern (*P*<.001) suggesting moderate sentiment is more effective than extremes (Figure 5). In contrast, greater positivity in titles (*P*=.02) reduces the success ratio.

The results support H2, showing that a higher number of progress update images (*P*<.001) is associated with greater success across both outcome measures, though this relationship follows an inverted U-shaped pattern. Progress-related models confirm an inverted U-shaped relationship between update frequency (*P*<.001) and project success, supporting H3a (Figure 6). Although frequent updates enhance both the success ratio and the likelihood of success, the effect diminishes at higher frequencies. H3b is not supported, as progress update sentiment shows no significant effect on project success.

We conducted interaction analyses only when the corresponding main effects were significant to avoid testing interactions without meaningful baseline effects (Tables S7 and S8 in Multimedia Appendix 1). The success ratio, including gender in the title (*P*=.03), positively affects success, but this effect weakens when the patient is male (*P*=.01). The positive effect of story length is reduced when age is mentioned in the title (*P*=.01), and the negative effect of negative words in the story also diminishes under the same condition (*P*=.02). Moreover, positive sentiment in the story description (*P*=.04) amplifies the positive effect of story length and mitigates the negative effect of negative words. Degree words in the story (*P*=.03) also moderate the impact of negative language, reducing its negative effect when more degree words are present, but enhancing it when the intensity of degree words is higher (*P*=.03).

XSL•FO
RenderX

Figure 6. U-test results for models 4 and 5.



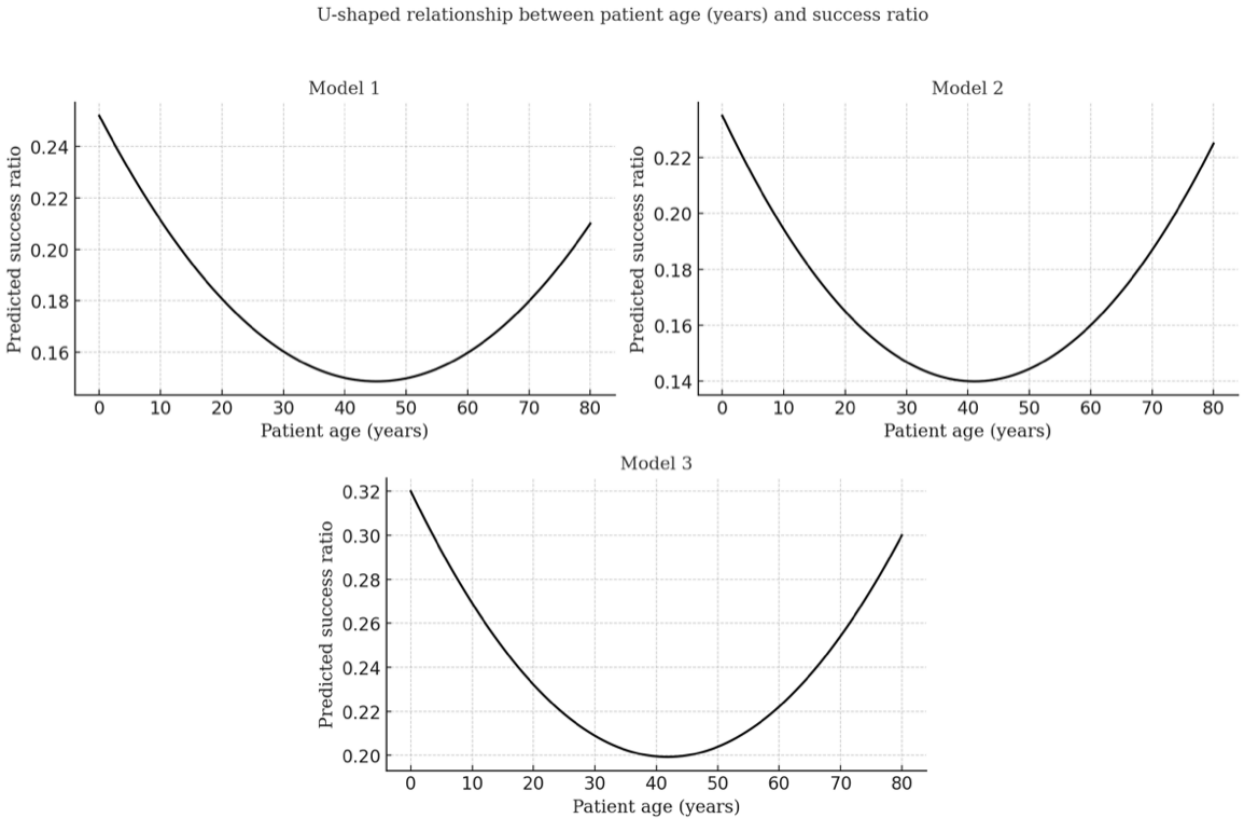
Additionally, for success ratio, interaction analysis for model 4 reveals a marginally significant positive effect of total progress pictures (P=.05). This positive effect weakens for older patients (P=.045) but strengthens when the project supports multiple beneficiaries compared with a single patient (P<.001). Model 5, focusing on progress updates, shows no significant effect on the success ratio but does influence the likelihood of success. Negative sentiment in progress updates (P=.01) reduces success likelihood, especially in single-beneficiary projects (P=.03) though more updates mitigate this effect (P<.001).

Beyond hypothesis testing and interaction analysis, control variables show consistent effects. Projects with older patients (models 1-6) and individual beneficiaries (models 1 and 2) tend to have lower success ratios. Quadratic tests reveal a U-shaped relationship for patient age across affordances (models 1-3), indicating that both younger and older patients see higher success than middle-aged ones (Figure 7).

The final model integrates all affordances into a cohesive framework. When controlling for all factors, the inclusion of demographic information in narrative text marginally improves the success ratio (P=.09). A higher number of progress updates (P<.001) significantly enhances both the success ratio and the likelihood of success, with an inverted U-shaped pattern indicating diminishing returns at higher frequencies—consistent with earlier models. Patient age remains significant (P=.003), with younger patients more likely to succeed. The success indicator further suggests that more project description images are associated with lower success.

XSL•FO
RenderX

Figure 7. U-test results for age.



Additional Analysis

The XGBoost (extreme gradient boosting) models were implemented for both dependent variables to capture complex relationships between predictors. The regression model demonstrated strong predictive performance, with a root mean square error of 0.00083, indicating a close alignment between predicted and actual donation outcomes. The classification model achieved 91% accuracy, effectively distinguishing successful projects from unsuccessful ones.

To interpret the contributions of individual features to success predictions, we conducted SHAP (Shapley additive explanations) analysis for the success ratio. The analysis identified donation frequency and donation amounts as the most influential predictors, with mean absolute SHAP values of 0.287 and 0.025, respectively. This aligns with expectations, as a higher number of contributions and greater total donations naturally increase the likelihood of success. Beyond these factors, patient age emerged as the second most significant predictor (0.084) (Table 7), highlighting a demographic bias where younger patients tend to receive stronger donor support.

Table 7. Shapley additive explanations (SHAP) analysis results.

Variable	Mean absolute
Patient age	0.0841
Title gender	0.0180
Title length	0.0092
Patient gender	0.0007
Progress picture numbers	0.0006
All other variables	0

Discussion

Primary Findings

Key findings reveal nuanced effects of textual content: longer, informative titles boost success, while the impact of story length varies by context. Moderate detail in surplus fund explanations and explicit demographic cues, particularly disease and gender (female), enhance appeal. This finding directly contradicts the finding of Wang et al [42] regarding the negative impact of female gender on the success of crowdfunding projects. Emotional framing with negative titles and moderately positive fund use plans engages donors effectively. Visual and progress updates predict success through positive inverted U-shaped relationships. Critically, when controlling for all affordances simultaneously, only the frequency of progress updates

XSL•FO
RenderX

maintains a robust, inverted U-shaped positive effect. Finally, patient demographics, especially age extremes, significantly improve success, underscoring the importance of multimodal analysis in understanding crowdfunding outcomes.

This study analyzes 1261 health-related crowdfunding projects from Shuidichou to examine how narrativity, visibility, and progress affordances collectively influence project success. After removing models 1 to 3 for the success indicator due to failed robustness tests, we found highly consistent outcomes between the 2 success measures for the visual, progress, and combined affordance models.

Narrativity plays a critical role in crowdfunding outcomes. While prior research suggests an inverted U-shaped relationship between text length and success [14,16,44], our findings show no such pattern for title or story length, instead indicating a more nuanced effect. Specifically, longer titles consistently improve project success, suggesting that donors favor more informative titles. Given their generally short length (max 13 characters), even small increases may have a noticeable impact. The influence of story length appears context-dependent. Its positive effect weakens when age appears in the title, suggesting informational redundancy may lessen effectiveness. Conversely, a more positive tone in the story strengthens the effect, implying that longer narratives are more impactful when framed optimistically. This may be because a positive tone helps sustain engagement in longer texts by reducing emotional fatigue. In emotionally charged contexts like medical crowdfunding, optimistic framing can also convey resilience and hope, making the project appear more credible and worth supporting.

Beyond the title and main description, the length of surplus fund explanations matters—donors appear to value how extra funds will be used. Moderate detail can build trust and encourage donations [63]. Extending prior research, we find that overly long fund purpose descriptions negatively impact success, possibly because donors assume funds will support severe cases or due to reduced patience with lengthy text [64]. Regarding demographic information in textual content, our findings partially align with prior research. Titles mentioning disease positively influence success [44], likely because they clearly communicate the medical issue, drawing attention and encouraging users to click and engage with the project. However, the inclusion of other demographic details showed no significant effect, failing to replicate findings from previous studies [12,13,18,44,46].

The emotional tone of textual content significantly shapes project success [17,18,57]. Consistent with prior research, a negative tone in titles is effective in increasing donations [44], while positive sentiment in fund use plans enhances success. A U-shaped relationship between plan sentiment and success further suggests that moderate emotional tone may be more persuasive than extreme positivity or negativity. This may indicate that overly cheerful language in serious medical funding explanations may come across as insincere or discordant, whereas a moderately positive tone can convey hope and resilience without downplaying the gravity of the situation. Striking this balance may foster empathy and trust, highlighting the importance of context-appropriate emotional framing. Although overall story sentiment was removed from the robustness test due to potential bias, a higher number of negative words still reduces success. This effect is mitigated by age references in titles or the presence of positive and intensifying language in the story, though a stronger degree of intensity slightly amplifies it. Interestingly, while donors may respond to a negatively framed title, they seem less receptive to a high concentration of negative words in the story. This contrast may stem from donors being drawn in by urgency in titles but feeling overwhelmed by negative narratives in the main story.

Although prior research suggests images may have a stronger impact than text [18], we find no such effect for project description images. In contrast, more images in progress updates enhance project success, though their effectiveness declines when used excessively. The relationship also varies by context, with stronger effects in projects for individual beneficiaries and weaker effects when the patient is older. This may suggest that while donors value helping more people, moderate image use is effective when focused on a single recipient, as it may evoke stronger, individually oriented empathy. In contrast, for older patients, donor preferences may favor younger individuals, making additional images less impactful. Similarly, the number of progress updates supports project success, with an inverted U-shaped pattern—while frequent updates generally encourage greater donations [65], excessive updates may reduce their effectiveness. This highlights the importance of both visual and textual progress affordances, though their impact diminishes when overused.

Departing from prior work that isolates individual factors, our study provides a multimodal analysis of how narrativity, visibility, and progress affordances jointly influence crowdfunding success, capturing the complex dynamics of donor behavior. Although a large body of prior work highlights the significant role of narrativity affordances [12-17,20], our findings differ. After accounting for visual and progress-related cues, most narrative effects become insignificant. Only the inclusion of demographic information shows a marginal positive impact. Similarly, we find no significant effect from visual elements. Notably, progress cues remain strong predictors of project success, with an inverted U-shaped relationship observed. This suggests that in the context of similarly structured crowdfunding projects, donors may rely most on progress updates to guide their decisions. Frequent updates likely signal transparency and build trust, enhancing donor motivation, while excessive updates may lead to fatigue or reduced engagement.

The final research question integrates patient demographic characteristics into the discussion. Building on prior research, this study validates and extends the findings of Ba et al [20] and Zhang et al [23], which found that projects featuring younger patients attract more donations and better meet funding goals across affordance types. Similar to Zhang et al [23], we find that older patients also receive higher donations than middle-aged ones. This pattern underscores the preference for supporting beneficiaries at the extremes of the age spectrum. Furthermore, this study builds on Ba et al's findings [20] by using advanced techniques, including XGBoost and SHAP models, to examine the nuanced role of patient age. These models consistently identify age as a key predictor of success

XSL•FO
RenderX

across all 3 affordance dimensions, reinforcing the importance of demographics in crowdfunding outcomes. Additionally, projects supporting individual beneficiaries appear to weaken the influence of narrative and visual features, suggesting these affordances are more effective in projects aiding multiple recipients.

Practical Implications

Our findings provide practical guidance for patients and platform managers on structuring crowdfunding projects to maximize donations and funding success. First, our multimodal analysis shows that projects featuring younger or older patients and those supporting multiple beneficiaries attract more donations. Therefore, project descriptions should emphasize these demographic factors. For example, a project supporting patients with blood-related diseases shares the story of both a child and a 29-year-old mother. Focusing on the child's story could attract more donations, so the project might prioritize highlighting children over detailing the mother's story, thereby maximizing benefits for all beneficiaries.

Then, for projects benefiting individual patients, platform managers might consider grouping similar cases to improve visibility and broaden appeal. For example, a patient aged 53 years with Parkinson disease may struggle individually but could gain enhanced visibility and attract more donors by being grouped with other Parkinson patients, increasing the likelihood of meeting fundraising targets.

Beyond demographic insights, projects should use longer titles that specify the disease and convey urgency in a negative tone, omitting age details. Generic titles like "Partnering with the Very Sick to Get Through Difficult Times" lack specificity and urgency. Instead, platforms could guide projects to include the specific disease, rather than vague terms such as "very sick." Moreover, replacing optimistic wording, such as "partnering," with more urgent language can emphasize the severity. For example, titles such as "A Female with Cancer Needs Urgent Help," which reached its funding goal of 80,154 CNY (US $11,694), or "Boy's Leukemia relapsed twice, restarting the fight of survival," which achieved its funding goal with 800,000 CNY (US $114,555). Well-framed titles can more effectively emphasize the urgency of the need and drive greater engagement.

The interaction suggests that the effectiveness of a title depends on demographic factors such as gender and beneficiary type. Titles with gender details generally have a positive impact, but are less effective for male patients or individual beneficiary projects. To compensate, these projects could emphasize visual updates or progress-related details to enhance engagement. Similarly, including patient age in titles weakens the positive effect of narrative length, especially for male patients. To maintain donor interest, projects should omit age details and focus on emotionally compelling or progress-oriented narratives. Platforms should also ensure surplus fund use plans are clear, while avoiding overly lengthy or repetitive explanations. Tailoring strategies to patient characteristics and optimizing key narrative elements can maximize donor response and crowdfunding success. Importantly, active and transparent treatment updates are crucial, but should not be overly frequent. Our findings show that, when all types of information are available, donors rely most on progress updates. Project managers should therefore encourage patients to maintain regular updates while avoiding excess that could dilute donor attention.

Our findings are meaningful and applicable across diverse crowdfunding platforms. Although some might argue that Shuidichou's results are limited to a Chinese context, we emphasize that the types of information examined (textual narratives, visual elements, and progress updates) are universally present across platforms. Crucially, our analysis demonstrates that when all affordances are considered simultaneously, the impact of narrative elements diminishes, while the strong positive effect of progress updates persists. This result underscores the importance of examining information integratively, as donors typically encounter all these elements together. Unlike previous studies, our findings distinctly show that dynamic elements (eg, update frequency) have a stronger influence on donor decisions compared with static narrative elements, highlighting a vital direction for future crowdfunding research.

Overall, all findings offer practical guidance for both patients and platform managers. In general, patients should openly share details to build trust, while platform managers should be informed about new research related to crowdfunding practices. Our findings highlight the importance of collaboration between these 2 parties in improving the effectiveness of crowdfunding. The strategic application of affordances can help projects optimize donor engagement and increase the probability of success.

Limitations and Future Research

While this study provides valuable information on the multimodal impact of information affordance on donations, several limitations should be noted. Due to time constraints and limited access to the data of the Shuidichou platform, we could not extract all health-related projects automatically. Instead, project selection required manual link extraction, potentially leading to omissions within the selected timeframe. To mitigate this, multiple research assistants manually extracted links by navigating from the top to the bottom of the platform pages. Nonetheless, we acknowledge the possibility of omitted cases. Additionally, during extraction, we observed that the platform predominantly features severe illnesses such as cancer or trauma from events like fires, while chronic conditions (eg, vision impairment) are rarely represented. This suggests our results may not fully generalize to chronic disease projects.

Although the initial aim was to extract patients' names and their relationship with the project creators, these details were not accessible through Python-based methods, limiting our analysis of these personal connections. Additionally, we retained model 2 and model 3 despite each containing one variable with moderate bias to preserve the integrity of the simultaneous information environment that donors encounter on crowdfunding platforms. These variables were excluded from interpretation to mitigate potential bias, and an additional sensitivity analysis was conducted to verify the overall stability of the results. Nonetheless, we acknowledge this as a potential limitation.

XSL•FO
RenderX

Beyond these limitations, this study opens several avenues for future research. While our multimodal approach incorporates visual information through numeric counts, deeper analysis of image content—such as facial expressions or the number of people—could provide richer insights. Further investigation is also needed to understand why donors respond to specific cues, such as disease references in titles or gender mentions in descriptions. Survey-based or scenario-driven experiments may help identify psychological mechanisms that mediate these effects. Importantly, we find that progress updates exert the most consistent influence on project success, even after controlling for other affordances. Future research could explore which types of progress updates (eg, medical and emotional) are most effective in engaging donors.

This study highlights the complexity of crowdfunding dynamics, showing that text length and emotional tone can have contrasting effects depending on context. Studying elements in isolation is insufficient. Future work should adopt a holistic approach, examining how donors interact with the overall platform environment to understand what drives donations and how platform design shapes donor behavior.

Acknowledgments

The work described in this paper was supported by grants from the National Natural Science Foundation of China (grants 72102238, 72302168, and 72172100), and the China Postdoctoral Science Foundation (grant 2021M702319).

Data Availability

The datasets analyzed during this study are available from the corresponding author on reasonable request.

Conflicts of Interest

None declared.

Multimedia Appendix 1
Supporting data in Supplementary Tables S1-S8.
[DOCX File , 40 KB - medinform_v13i1e75563_app1.docx]

References

1. Hacker K. The burden of chronic disease. Mayo Clin Proc Innov Qual Outcomes 2024;8(1):112-119 [FREE Full text] [doi: 10.1016/j.mayocpiqo.2023.08.005] [Medline: 38304166]
2. Zhang X, Shi J, Liu G, Ren J, Guo L, Huang W, et al. Medical expenditure for lung cancer in China: a multicenter, hospital-based retrospective survey. Cost Eff Resour Alloc 2021;19(1):53 [FREE Full text] [doi: 10.1186/s12962-021-00306-3] [Medline: 34404418]
3. Zhang Y, Zhou Y, Gao Y. A study on the influence of donor-recipient relation- ship on donation amount in online donation crowdfunding. J Northeast Univ 2020;22(1):49 [FREE Full text]
4. New center to financially help families battling serious illnesses. China Daily. URL: https://www.chinadaily.com.cn/a/202009/16/WS5f617c66a31024ad0ba79dc6.html [accessed 2025-08-25]
5. Jin P. Medical crowdfunding in China: empirics and ethics. J Med Ethics 2019;45(8):538-544. [doi: 10.1136/medethics-2018-105054] [Medline: 31217228]
6. Burtch G, Ghose A, Wattal S. Cultural differences and geography as determinants of online prosocial lending. MISQ 2014;38(3):773-794 [FREE Full text] [doi: 10.25300/misq/2014/38.3.07]
7. Ortiz RA, Witte S, Gouw A, Sanfilippo A, Tsai R, Fumagalli D, et al. Engaging a community for rare genetic disease: best practices and education from individual crowdfunding campaigns. Interact J Med Res 2018;7(1):e3 [FREE Full text] [doi: 10.2196/ijmr.7176] [Medline: 29402763]
8. Greenberg J, Mollick E. "Leaning in or leaning on" gender, homophily, and activism in crowdfunding. Acad Manag Proc 2015;2015(1):18365. [doi: 10.5465/ambpp.2015.18365abstract]
9. van Duynhoven A, Lee A, Michel R, Snyder J, Crooks V, Chow-White P, et al. Spatially exploring the intersection of socioeconomic status and Canadian cancer-related medical crowdfunding campaigns. BMJ Open 2019;9(6):e026365 [FREE Full text] [doi: 10.1136/bmjopen-2018-026365] [Medline: 31227531]
10. Su L, Sengupta J, Li Y. “Want” versus “Need”: how linguistic framing influences responses to crowdfunding appeals. J Consum Res 2024;50(5):923-944. [doi: 10.1093/jcr/ucad033]
11. Zhang X, Wang X, Wang D, Xiao Q, Deng Z. How the linguistic style of medical crowdfunding charitable appeal influences individuals' donations. Technol Forecast Soc Change 2024;203:123394. [doi: 10.1016/j.techfore.2024.123394]
12. Chen Y, Zhou S, Jin W, Chen S. Investigating the determinants of medical crowdfunding performance: a signaling theory perspective. INTR 2022;33(3):1134-1156. [doi: 10.1108/intr-09-2021-0652]
13. Holler J, Sadighian M, Ghaffar U. Online medical crowdfunding in the United States: a cross-sectional analysis of gendered cancer campaign outcomes. J Mens Health 2023;19(3):29-37. [doi: 10.22514/jomh.2023.022]

XSL•FO
RenderX

14. Ren J, Raghupathi V, Raghupathi W. Understanding the dimensions of medical crowdfunding: a visual analytics approach. J Med Internet Res 2020;22(7):e18813 [FREE Full text] [doi: 10.2196/18813] [Medline: 32618573]
15. Wu Y, Zhang X, Xiao Q. Appeal to the head and heart: the persuasive effects of medical crowdfunding charitable appeals on willingness to donate. Inf Process Manage 2022;59(1):102792. [doi: 10.1016/j.ipm.2021.102792]
16. Zhang X, Tao X, Ji B, Wang R, Sörensen S. The success of cancer crowdfunding campaigns: project and text analysis. J Med Internet Res 2023;25:e44197 [FREE Full text] [doi: 10.2196/44197] [Medline: 36692283]
17. Zheng L, Jiang L. Influence of narrative strategies on fundraising outcome: an exploratory study of online medical crowdfunding. J Soc Comput 2022;3(4):303-321. [doi: 10.23919/jsc.2022.0015]
18. Hou J, Zhang J, Zhang K. Pictures that are worth a thousand donations: how emotions in project images drive the success of online charity fundraising campaigns? an image design perspective. MISQ 2023;47(2):535-584. [doi: 10.25300/misq/2022/17164]
19. Wang X, Wu Y, Guo J. Says what in your photos? the impacts of photographic narratives on medical crowdfunding performance. 2020 Presented at: PACIS; 2020 June 20-24; Dubai p. 231 URL: https://aisel.aisnet.org/pacis2020/231
20. Ba Z, Zhao Y, Song S, Zhu Q. Understanding the determinants of online medical crowdfunding project success in China. Inf Process Manag 2021;58(2):102465. [doi: 10.1016/j.ipm.2020.102465]
21. Stratopoulos TC, Ye H. Engagement and crowding-out effects of leaderboard gamification on medical crowdfunding. J Manag Inf Syst 2024;41(3):866-891 [FREE Full text] [doi: 10.1080/07421222.2024.2376379]
22. Hua S, Liu H, Ji Z, Liang H. The impact of air pollution on crowdfunding donations for critical illnesses: evidence from China. China Econ Rev 2025;91:102391. [doi: 10.1016/j.chieco.2025.102391]
23. Zhang S, Zhang Q, Wang M, Tang X, Lu X, Huang W. Key drivers of medical crowdfunding success: a comprehensive analysis of 84,712 projects. Humanit Soc Sci Commun 2025;12(1):1-17. [doi: 10.1057/s41599-024-04160-5]
24. Gibson J. The theory of affordances. In: Perceiving, Acting and Knowing: Towards an Ecological Psychology. New Jersey: Erlbaum; 1977:83.
25. Wu Y, Zhang M, Shen Y, Liu N, Li Y. How do project updates influence fundraising on online medical crowdfunding platforms? examining the dynamics of content updates. IEEE Trans Eng Manage 2024;71:9135-9149. [doi: 10.1109/tem.2023.3321664]
26. Wu Y, Ye H, Jensen ML, Liu L. Impact of project updates and their social endorsement in online medical crowdfunding. J Manag Inf Syst 2024;41(1):73-110. [doi: 10.1080/07421222.2023.2301173]
27. Xiao S, Ho Y, Che H. Building the momentum: information disclosure and herding in online crowdfunding. Prod Oper Manag 2021;30(9):3213-3230. [doi: 10.1111/poms.13425]
28. Xu K, Wang X. "Kindhearted People, Please Save My Family": narrative strategies for new media medical crowdfunding. Health Commun 2020;35(13):1605-1613. [doi: 10.1080/10410236.2019.1654173] [Medline: 31455114]
29. Yazdani E, Chakravarty A, Inman J. (Mis)alignment between facial and textual emotions and its effects on donors engagement behavior in online crowdsourcing platforms. J Acad Mark Sci 2024. [doi: 10.1007/s11747-024-01002-3]
30. Karahanna E, Xin Xu S, Xu Y, Zhang N. The needs–affordances–features perspective for the use of social media. MISQ 2018;42(3):737-756 [FREE Full text] [doi: 10.25300/misq/2018/11492]
31. Zhang X, Lyu H, Luo J. What contributes to a crowdfunding campaign's success? evidence and analyses from goFundMe data. J Soc Comput 2021;2(2):183-192. [doi: 10.23919/jsc.2021.0010]
32. Thies F, Wessel M, Benlian A. Effects of social interaction dynamics on platforms. J Manag Inf Syst 2016;33(3):843-873. [doi: 10.1080/07421222.2016.1243967]
33. Zhou A. Causal effects of affordance change on communication behavior: empirical evidence from organizational and leadership social media use. Telemat Inform 2021;59:101549. [doi: 10.1016/j.tele.2020.101549]
34. Heft H. Affordances and the body: an intentional analysis of Gibson's ecological approach to visual perception. J Theory Soc Behav 2007;19(1):1-30. [doi: 10.1111/j.1468-5914.1989.tb00133.x]
35. Hutchby I. Technologies, texts and affordances. SOC 2001;35(2):441-456. [doi: 10.1017/s0038038501000219]
36. Turvey M. Affordances and prospective control: an outline of the ontology. Ecol Psychol 1992;4(3):173-187. [doi: 10.1207/s15326969eco0403_3]
37. Norman D. The psychopathology of everyday thing. In: Readings in Human-Computer Interaction. Burlington, Massachusetts: Morgan Kaufmann; 1995:5-21.
38. Jiao H, Tang W, Liu T, Wang X, Ma L. How do IT affordances support behavioral intention in charitable crowdfunding? the mediating effects of donor perceptions and motivations. Kybernetes 2021;51(11):3172-3200 [FREE Full text] [doi: 10.1108/k-09-2020-0575]
39. Theocharis Y, Boulianne S, Koc-Michalska K, Bimber B. Platform affordances and political participation: how social media reshape political engagement. West Eur Politics 2022;46(4):788-811. [doi: 10.1080/01402382.2022.2087410]
40. Scharlach R, Hallinan B. The value affordances of social media engagement features. J Comput Mediat Commun 2023;28(6):zmad040. [doi: 10.1093/jcmc/zmad040]
41. Choy K, Schlagwein D. IT affordances and donor motivations in charitable crowdfunding: the “Earthship Kapita” case. 2015 Presented at: European Conference on Information Systems (ECIS); 2025 Feb 18; Amman, Jordan.

XSL•FO
RenderX

42. Wang R, Xu H, Zhang X. Impact of image content on medical crowdfunding success: a machine learning approach. J Med Internet Res 2024;26:e58617 [FREE Full text] [doi: 10.2196/58617] [Medline: 39546798]
43. Spence M. Signaling in retrospect and the informational structure of markets. Am Econ Rev 2002;92(3):434-459 [FREE Full text] [doi: 10.1257/00028280260136200]
44. Zhang F, Xue B, Li Y, Li H, Liu Q. Effect of textual features on the success of medical crowdfunding: model development and econometric analysis from the tencent charity platform. J Med Internet Res 2021;23(6):e22395 [FREE Full text] [doi: 10.2196/22395] [Medline: 34114959]
45. Parhankangas A, Renko M. Linguistic style and crowdfunding success among social and commercial entrepreneurs. J Bus Ventur 2017;32(2):215-236. [doi: 10.1016/j.jbusvent.2016.11.001]
46. Peng N, Feng Y, Song X, Niu B, Yu J. Configurational paths to medical crowdfunding success and failure based on a crisp-set qualitative comparative analysis. IMDS 2022;122(5):1306-1332. [doi: 10.1108/imds-03-2021-0184]
47. Kim JG, Kraut RE, Karahalios K. Designing a medical crowdfunding website from sense of community theory. Proc ACM Hum Comput Interact 2022;6(CSCW2):1-25. [doi: 10.1145/3555181]
48. Wang X, Zhang X, Tong A. The impact of linguistic style of medical crowdfunding philanthropic appeals on individual giving. Procedia Comput Sci 2022;199:293-300. [doi: 10.1016/j.procs.2022.01.036]
49. Agarwal B, Mittal N, Bansal P, Garg S. Sentiment analysis using common-sense and context information. Comput Intell Neurosci 2015;2015:715730 [FREE Full text] [doi: 10.1155/2015/715730] [Medline: 25866505]
50. Catelli R, Pelosi S, Comito C, Pizzuti C, Esposito M. Lexicon-based sentiment analysis to detect opinions and attitude towards COVID-19 vaccines on Twitter in Italy. Comput Biol Med 2023;158:106876 [FREE Full text] [doi: 10.1016/j.compbiomed.2023.106876] [Medline: 37030266]
51. Hao J, Dai H. Social media content and sentiment analysis on consumer security breaches. JFC 2016;23(4):855-869. [doi: 10.1108/jfc-01-2016-0001]
52. Hossen MS, Dev NR. An improved lexicon based model for efficient sentiment analysis on movie review data. Wireless Pers Commun 2021;120(1):535-544. [doi: 10.1007/s11277-021-08474-4]
53. Mansour S. Social media analysis of user's responses to terrorism using sentiment analysis and text mining. Procedia Comput Sci 2018;140:95-103. [doi: 10.1016/j.procs.2018.10.297]
54. Aslan S. A deep learning-based sentiment analysis approach (MF-CNN-BILSTM) and topic modeling of tweets related to the Ukraine–Russia conflict. Appl Soft Comput 2023;143:110404. [doi: 10.1016/j.asoc.2023.110404]
55. Kaur H, Ahsaan SU, Alankar B, Chang V. A proposed sentiment analysis deep learning algorithm for analyzing COVID-19 tweets. Inf Syst Front 2021;23(6):1417-1429 [FREE Full text] [doi: 10.1007/s10796-021-10135-7] [Medline: 33897274]
56. Martin-Domingo L, Martín JC, Mandsberg G. Social media as a resource for sentiment analysis of airport service quality (ASQ). J Air Transp Manage 2019;78:106-115. [doi: 10.1016/j.jairtraman.2019.01.004]
57. Zhang X, Hu W, Xiao Q. Influences of medical crowdfunding website design features on trust and intention to donate: controlled laboratory experiment. J Med Internet Res 2021;23(5):e25554 [FREE Full text] [doi: 10.2196/25554] [Medline: 33944787]
58. Stsiampkouskaya K, Joinson A, Piwek L, Stevens L. Imagined audiences, emotions, and feedback expectations in social media photo sharing. Soc Media Soc 2021;7(3):20563051211035692. [doi: 10.1177/20563051211035692]
59. Zappavigna M. Social media photography: construing subjectivity in instagram images. Vis Commun 2016;15(3):271-292. [doi: 10.1177/1470357216643220]
60. Wu J, Peng Y. Understanding unmet medical needs through medical crowdfunding in China. Public Health 2023;223:202-208. [doi: 10.1016/j.puhe.2023.07.030] [Medline: 37672833]
61. Lu S, Liu Q, Zhang Z. Sentiment analysis of Weibo platform based on LDA-SnowNLP Model. : IEEE; 2023 Presented at: 2023 2nd International Conference on Machine Learning, Cloud Computing and Intelligent Mining (MLCCIM); 2023 July 25-29; Jiuzhaigou, China p. 505-510 URL: https://doi.org/10.1109/MLCCIM60412.2023.00081 [doi: 10.1109/mlccim60412.2023.00081]
62. Dong Z, Dong Q. Hownet and the computation of meaning (with CD-ROM). Singapore: World Scientific; 2006:302.
63. Nan L, Tang C, Wang X, Zhang G. The real effects of transparency in crowdfunding. Contemp Account Res 2023;41(1):39-68. [doi: 10.1111/1911-3846.12903]
64. Hanish SJ, Cherian N, Baumann J, Gieg SD, DeFroda S. Reducing the use of complex words and reducing sentence length to 15 words improves readability of patient education materials regarding sports medicine knee injuries. Arthrosc Sports Med Rehabil 2023;5(1):e1-e9 [FREE Full text] [doi: 10.1016/j.asmr.2022.10.004] [Medline: 36866291]
65. Mejia J, Urrea G, Pedraza‐Martinez AJ. Operational transparency on crowdfunding platforms: effect on donations for emergency response. Prod Oper Manag 2019;28(7):1773-1791. [doi: 10.1111/poms.13014]

Abbreviations

NLP: natural language processing
SHAP: Shapley additive explanations
XGBoost: extreme gradient boosting

XSL•FO
RenderX

Edited by A Castonguay; submitted 06.04.25; peer-reviewed by X Xu, LZ Xu; comments to author 23.05.25; revised version received 16.07.25; accepted 25.07.25; published 16.09.25.

Please cite as:
Du Y, Yang Y, Li Z, Xue J
Holistic Influence of Multimodal Medical Crowdfunding Affordances on Charitable Crowdfunding Outcome: Systematic Multimodel Analysis Study
JMIR Med Inform 2025;13:e75563
URL: https://medinform.jmir.org/2025/1/e75563
doi:10.2196/75563
PMID:

©Yuxuan Du, Yujin Yang, Zihe Li, Jiaolong Xue. Originally published in JMIR Medical Informatics (https://medinform.jmir.org), 16.09.2025. This is an open-access article distributed under the terms of the Creative Commons Attribution License (https://creativecommons.org/licenses/by/4.0/), which permits unrestricted use, distribution, and reproduction in any medium, provided the original work, first published in JMIR Medical Informatics, is properly cited. The complete bibliographic information, a link to the original publication on https://medinform.jmir.org/, as well as this copyright and license information must be included.

XSL•FO
RenderX

Original Paper

Multisource Coherence Analysis of the First European Multicenter Cohort Study for Cancer Prevention in People Experiencing Homelessness: Data Quality Study

Antonio Blasco-Calafat[1], MSc; Vicent Blanes-Selva[1], PhD; Tobias Fragner[2], MSc; Ascensión Doñate-Martínez[1], PhD; Tamara Alhambra-Borrás[3], PhD; Julia Gawronska[4], PhD; Lee Smith[4], PhD; Juan M Garcia-Gomez[1], Prof Dr; Igor Grabovac[2], PhD; Carlos Sáez[1], PhD

[1]Biomedical Data Science Laboratory, Institute of Information and Communication Technologies, Universitat Politècnica de València, Valencia, Spain
[2]Department of Social and Preventive Medicine, Center for Public Health, Medical University of Vienna, Vienna, Austria
[3]Instituto de Investigación en Políticas de Bienestar Social, Department of Social and Preventive Medicine, Universitat de València, Valencia, Spain
[4]Center for Health, Performance and Wellbeing, Anglia Ruskin University, Cambridge, United Kingdom

Corresponding Author:
Antonio Blasco-Calafat, MSc
Biomedical Data Science Laboratory
Institute of Information and Communication Technologies
Universitat Politècnica de València
Building 8G, 1st Floor, Camino de vera, sn
Valencia, 46022
Spain
Phone: 34 963877000 ext 75278
Email: anblaca@upv.es

Abstract

Background: Coherence across sites in multicenter datasets is one substantial data quality dimension for reliable health data reuse, as unexpected heterogeneity in data can lead to biases in data analyses and suboptimal generalization of results.

Objective: This work aims to characterize and label the data coherence across sites in the first European multicenter dataset for cancer prevention in people and early detection among the homeless population in Europe: coadapting and implementing the health navigator model. This dataset emerged to enable research to address disparities in health challenges and health care access due to barriers such as unstable housing, limited resources, and social stigma in people experiencing homelessness.

Methods: The dataset comprises 652 cases: 142 from Austria, 158 from Greece, 197 from Spain, and 155 from the United Kingdom. All participants fit classifications from the European Typology of Homelessness and Housing Exclusion. This longitudinal study collected questionnaires at baseline, after 4 weeks, and at the end of the intervention. The 180-question survey covered sociodemographic data, overall health, mental health, empowerment, and interpersonal communication. Data variability was assessed using information theory and geometric methods to analyze discrepancies in distributions and completeness across the dataset.

Results: Substantial variability was observed among the 4 pilot countries, both in the overall analysis and within specific domains. In particular, measures of health care empowerment, quality of life, and interpersonal communication demonstrated the greatest discrepancies among pilot sites, with the exception of the health domain. Notably, Spain exhibited the most pronounced differences, characterized by a high number of missing values related to interpersonal communication and the use of health care services.

Conclusions: Health data may be comparable across the 4 countries; however, substantial differences were observed in the other questionnaires, requiring independent, country-specific analyses. This study underscores the heterogeneity among people experiencing homelessness and the critical need for data quality assessments to inform future research and policymaking in this field.

(JMIR Med Inform 2025;13:e73596) doi:10.2196/73596

XSL•FO
RenderX

KEYWORDS

homelessness; data quality; data variability; public health; data analysis; curated dataset; multisource

Introduction

Homelessness is a complex and multifaceted phenomenon, encompassing more than the mere absence of a physical dwelling. It signifies a state of profound vulnerability and social exclusion, characterized by a lack of stable, safe, or adequate housing [1-3]. The experience of homelessness is deeply intertwined with a range of social, economic, and individual factors, including poverty, unemployment, mental health challenges, substance use, and domestic violence. People experiencing homelessness constitute a highly heterogeneous group with varying backgrounds, needs, and challenges, encompassing socioeconomic, cultural, physical, and mental health aspects, as well as historical and geographical contexts [4,5]. This inherent diversity within the group of people experiencing homelessness, coupled with inconsistent definitions and methodological variations in data collection across countries, makes it exceedingly challenging to accurately estimate the true prevalence of homelessness. Despite these complexities, it is estimated that at least 895,000 individuals in Europe are experiencing homelessness on any given night, living rough or in temporary or emergency accommodations [6].

Research consistently demonstrates substantial health disparities between people experiencing homelessness and the housed population. Homelessness is associated with poorer health outcomes, including premature mortality, partly due to barriers to accessing health care [7-9]. Furthermore, people experiencing homelessness experience higher cancer morbidity, lower cancer screening rates, later-stage cancer diagnoses, and poorer cancer-specific health outcomes compared to the housed population [10], with cancer being the second most common cause of death among people experiencing homelessness [11]. Among the most relevant factors, people experiencing homelessness usually report low health literacy, especially regarding cancer [12], and they tend to experience barriers to accessing fragmented cancer prevention and community health services [13].

Research interest in improving the health status and cancer prevention efforts for people experiencing homelessness is growing, leading to the implementation and piloting of innovative health care strategies, such as the patient navigation model and the patient empowerment model [14,15]. In the patient navigation model, patient navigators, defined as health care professionals or peers specializing in care coordination, case management, and reducing barriers to care, play a crucial role in guiding individuals to overcome obstacles and access health care services in a timely manner [16]. This includes facilitating access to preventive care and health promotion programs, which have been shown to improve their users' health outcomes and care satisfaction [17]. The patient empowerment model focuses on equipping individuals with the knowledge, skills, and confidence to take an active role in managing their health and navigating the health care system [18,19]. This approach emphasizes self-efficacy and shared decision-making, empowering patients to make informed choices about their health care and advocate for their needs.

Within the CANCERLESS project, a multicenter study funded by the European Union, critical components of the patient navigation and patient empowerment models have converged into the novel health navigator model. This model was co-designed with input from both people experiencing homelessness and health and social care professionals working with them as well as those working in primary care settings. The project piloted this model in 4 European countries to assess its effectiveness in connecting people experiencing homelessness with cancer prevention services. To the authors' knowledge, CANCERLESS is the first multicenter study involving people experiencing homelessness from different countries, marking substantial progress in research within this field. However, challenges such as data variability, missing data (missing completely at random and missing not at random), and fragmented in care may introduce biases in the results [20,21].

Building on the premise that various studies have highlighted the inherent heterogeneity within this population [22,23], this diversity becomes even more pronounced when research conducted in different geographical and cultural contexts is considered. While such variability is evident, it should not be regarded solely as an intrinsic characteristic of the data but must be systematically quantified. This necessity arises because a portion of this heterogeneity may stem from biases introduced either by differences among the population subgroups studied or by external factors unrelated to the participants, such as variations in the conditions under which the interventions were conducted. If left unaddressed, this heterogeneity could lead to erroneous interpretations of the results and, consequently, to inaccurate conclusions that undermine the validity of the analysis [24-26]. Several techniques aim to detect variability among samples and approach the data quality (DQ) of datasets [27]. Among them, spatial DQ techniques [28] have been developed to evaluate the differences between the probability distribution function from multiple sources, and these techniques have been demonstrated to deal with sets of heterogeneous data, including multivariate and multitype. Additionally, these are valuable tools for dealing with DQ issues, such as missing values among the datasets, which provide metrics that quantify this heterogeneity and outliers.

Given the above considerations, an exhaustive DQ analysis is needed for several reasons. First, this is key to extracting information about the participants' characteristic distribution for each pilot site. Second, to examine the differences between these distributions and obtain knowledge about the status of homelessness in different European countries. Finally, these analyses allow us to understand if the information gathered can be used as a different pilot-specific dataset. Thus, this work aims to examine the heterogeneity between the people experiencing homelessness data in 4 different European countries and provide quality metadata while delivering a

XSL•FO
RenderX

curated CANCERLESS dataset to extract common knowledge and conclusions.

Methods

Dataset Conformation

Data collection was carried out between June 2022 and November 2023. A total sample of 652 people experiencing homelessness was collected: 142 from Austria, 158 from Greece, 197 from Spain, and 155 from the United Kingdom. Participants were included if they were at least 18 years of age and experiencing homelessness, fitting any classification of the European Typology of Homelessness and Housing Exclusion [29]. Participants were excluded if they could not provide informed consent, had difficulties interpreting the aim of the research, did not accept to participate in the study, if they had a known cancer diagnosis or have had cancer previously, and the intervention or study would harm them.

Data used in this study were collected as part of the CANCERLESS project. The study followed a pre- and postdesign, but in this specific analysis, we present only data collected at baseline (T0), that is, before each individual started the intervention. This approach allows us to see the characteristics of each pilot at the beginning of the intervention and, subsequently, to observe the initial differences that will serve to perform a correct analysis of the data.

The questionnaires included in the database were the following: EQ-5D-5L to measure self-reported health-related quality of life [30], Health Care Empowerment Questionnaire (HCEQ) to assess users' empowerment related to health care [31], Brief Symptom Inventory-18 to measure psychological distress [32], and the Person-Centered Coordinated Care Experience Questionnaire to evaluate several domains of person-centered coordinated care from the perspective of the user [33]. Additionally, specific-purpose questions were included regarding the following information: sociodemographics, health literacy, active diagnosis, medication taken, risk behaviors, healthy lifestyles, and previous use of health care services. Multimedia Appendix 1 provides the complete list of the T0 questionnaires.

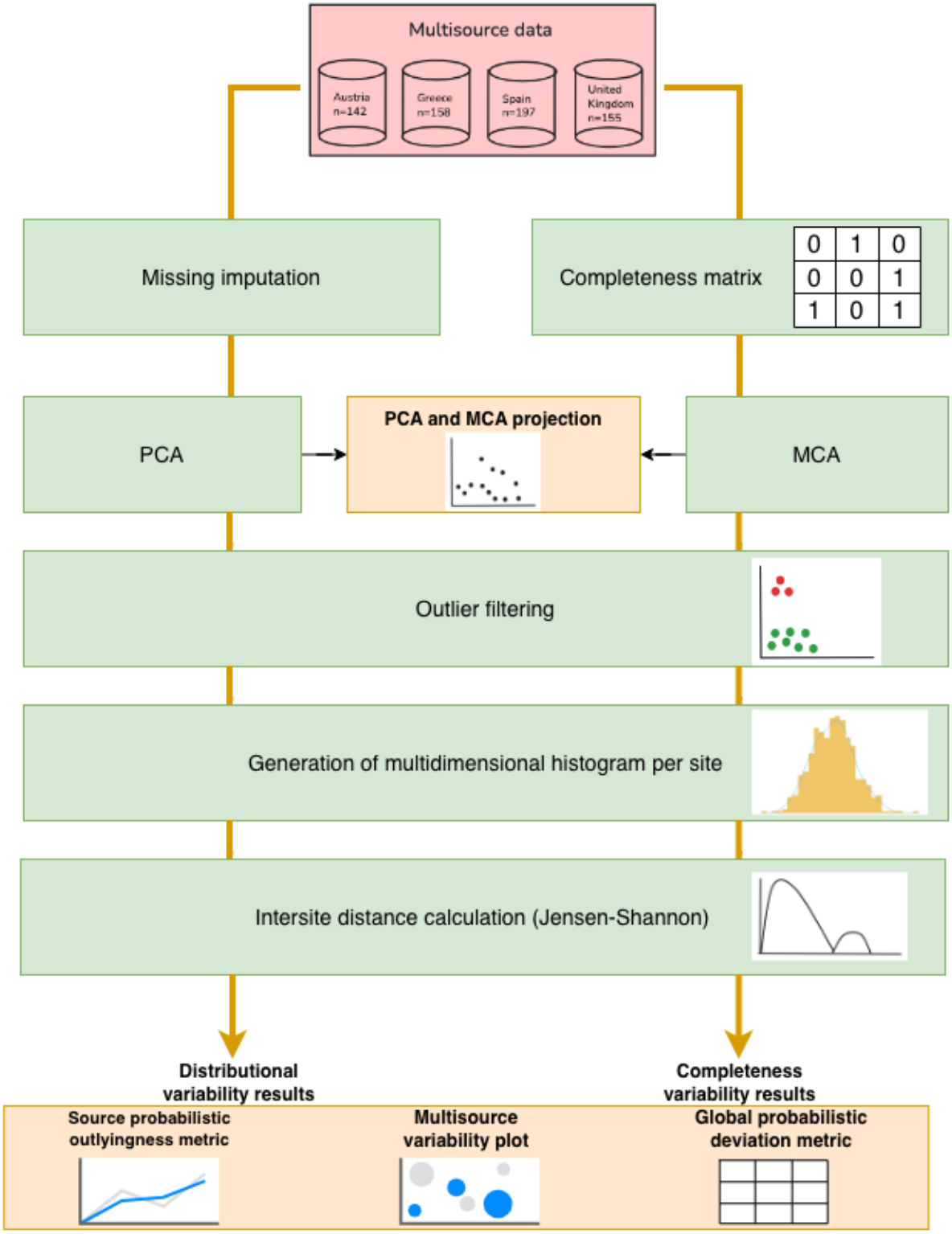
The T0 questionnaire was administered to all pilot participants. A coordinator at each pilot site recorded the responses. Later, the information was uploaded by the research team of each pilot to a digital platform created by this research consortium called CANCERLESS Interventions Data Management Application, which stores the data in a digital format. This platform also provides feedback to the coordinator through metrics and aggregated information.

Methods—Data Quality Workflow

Figure 1 shows the methodology followed in this study. The workflow is divided into 2 blocks for assessing the intersite coherence, one across the information captured in the questionnaires and the other across their completeness patterns. The main difference lies in the preprocessing step: for the questionnaire, imputation is performed, whereas for completeness, a matrix of fault categories is used. Subsequently, a dimensional reduction technique was applied according to the analysis performed—see the specific details in the following subsections. The following steps were common to both analyses: calculating outlier filtering, histogram application to represent the probability density function of the dataset, followed by flattening, normalization, and column stacking, to be used as input for the information theory–based DQ metrics. The technique for evaluating DQ and response variability across the pilot studies involved transforming each dataset into a probability distribution, then applying comparative metrics to measure similarity and identify missing information and therefore the level of nonoverlapping between them. The technique relies on the calculus of a simplex, multidimensional generalization of a triangle, conserving the intersite dissimilarity where the centroid represents an informed average distribution of the sources. Subsequently, 2 metrics were computed, constrained to the Jensen-Shannon distance: the source probabilistic outlyingness (SPO), measuring the dissimilarity of each source to the average distribution; and the global probabilistic deviation (GPD), gauging the degree of global variability among the sources [34,35]. The derived metrics, that is, GPD and SPO, are bounded between 0 and 1, so 0 means equal distributions and 1 means nonoverlapping. For the SPO, a value of 0 denotes the closest possible approach to the centroid, while for the GPD, it indicates the least data variability. Finally, visual plots of these metrics are shown to compare the variability results in a visual form between the different pilots. All these steps were later used to extract GPD, SPO, and multisource variability (MSV) for the global dataset and each section inside the questionnaire.

XSL•FO
RenderX

Figure 1. Overview of the methodology to obtain data quality metrics for the CANCERLESS dataset. Two types of analysis are conducted, with shared steps. For the complete dataset, missing values are imputed using iterative imputation techniques. In the missing data analysis, a matrix is built with values indicating 0=ordinary, 1=dependent, or 2=nonmissing. Dimensionality reduction is applied: PCA for complete data and MCA for missing data. After preprocessing, histograms for each country are normalized and combined to calculate distances from the centroid, yielding global probabilistic deviation, source probabilistic outlyingness, and multisource variability values. For specific dataset sections, the same process is applied to each subset. MCA: multiple correspondence analysis; PCA: principal component analysis.



Questionnaire Information

This approach has been used following a top-down methodology analyzing multivariate to univariate data, that is, to compare the whole T0 questionnaire and its sections. We excluded textual and multiple-choice options from the analysis since there was a high number of missing data and a much smaller number of category selections per question than the total number of choices, implying minimal variability with no final effect on the analysis. First, we preprocessed the data to transform

XSL•FO
RenderX

categorical text into numerical variables along with an iterative imputation method [36,37]. This method performs multivariate imputation through chained equations. Initially, all missing values are filled with simple univariate estimates (eg, the feature's mean). Thereafter, each incomplete variable is regressed on the other features using a Bayesian ridge estimator to predict its missing entries. Predicted values replace the initial estimates, and this process cycles through all variables for a predefined number of iterations or until convergence of the imputed values is reached.

Subsequently, to obtain a multivariate representation, we applied principal component analysis (PCA) [38] to reduce the dimensionality of the original 130-variable space to 3 dimensions and select the top 20 variables with the highest explained variance. Following this, we segregated the data by pilot source and conducted outlier filtering using the local outlier factor method [39], removing outliers specific to each pilot site. Finally, we computed a 3D histogram for each pilot, using 10 bins for each dimension, which were then used as the input in the method.

Completeness Patterns

Regarding the comparison of patterns related to blank responses or missing data, the T0 questionnaire comprises questions with varying levels of branching—specific queries are intended to be answered only if certain conditions from prior responses are met (eg, the question about the number of cigarettes smoked daily is only relevant if the participant declares themselves as a smoker in the preceding questions). Consequently, we distinguished between "not applicable missing" and ordinary missing data, which was applied using a predefined rule set. Once the rule was defined, it was applied to the dataset, obtaining a missing matrix and transforming the values into one of these categories. After the transformation, we applied the multiple correspondence analysis (MCA) [40] technique to reduce the dimensionality of the data and select the top 20 variables with the highest explained variance, thus identifying the most influential questionnaires since MCA is a specific technique to reduce dimensionality for categorical values. Next, the local outlier factor methodology was applied to remove outliers over the data on the reduced space. Finally, the multidimensional histogram that was flattened and normalized to be used as GPD's input was created.

Exploratory Analyses

The exploratory analyses of the study are presented using the following methods. First, biplots with 2 dimensions are generated after the original data undergo dimensionality reduction either using PCA or MCA. Additionally, the GDP methodology incorporates the MSV plot [35], where the 2 or 3 components with the highest variances are projected using multidimensional scaling. In the MSV plot, sources are represented as circles or spheres, and the distance between them indicates the distance between their distributions, based on the Jensen-Shannon distance, with the circle's radius representing the number of cases.

To conduct this analysis, we used the Python 3 programming language [41] and the NumPy, pandas, scikit-learn, and prince libraries [42-45]. The experimentation notebooks, including a Python version of the MSV metrics and visualizations, are available on GitHub [46].

Ethical Considerations

The study was approved by the ethics committee of the Medical University of Vienna (1702/2021), which served as the lead ethics committee for the project. Additionally, each pilot site in the 4 countries secured approval from their respective ethical review boards or institutions before commencing data collection, and Universitat Politècnica de València also obtained approval from an ethics committee, specifically for the management of participants' personal data. Prior to conducting any data collection, participants were given an information leaflet detailing the study's purpose and were allowed to ask questions to help them decide on their participation. It was emphasized to all participants that their involvement was entirely voluntary, and they could opt out of answering any questions that made them uncomfortable. Participants were explicitly reassured that declining participation would not negatively impact their access to health and social care services. Informed consent was obtained from all participants through signed forms, which were also verbally confirmed at the beginning of the data collection sessions. All collected data have been securely stored in accordance with data protection regulations. CANCERLESS Interventions Data Management Application platform securely stores data in agreement with the General Data Protection Regulation, following strict guidelines for collecting, processing, storing, and transferring personal data in the European Union and the European Economic Area. Participants did not receive any financial compensation for taking part in the project.

Results

Overview

Data used in this study comprehend the whole T0 set of responses, whose demographic distribution is presented in Table 1.

Table 1. Demographic distribution among the different pilots.

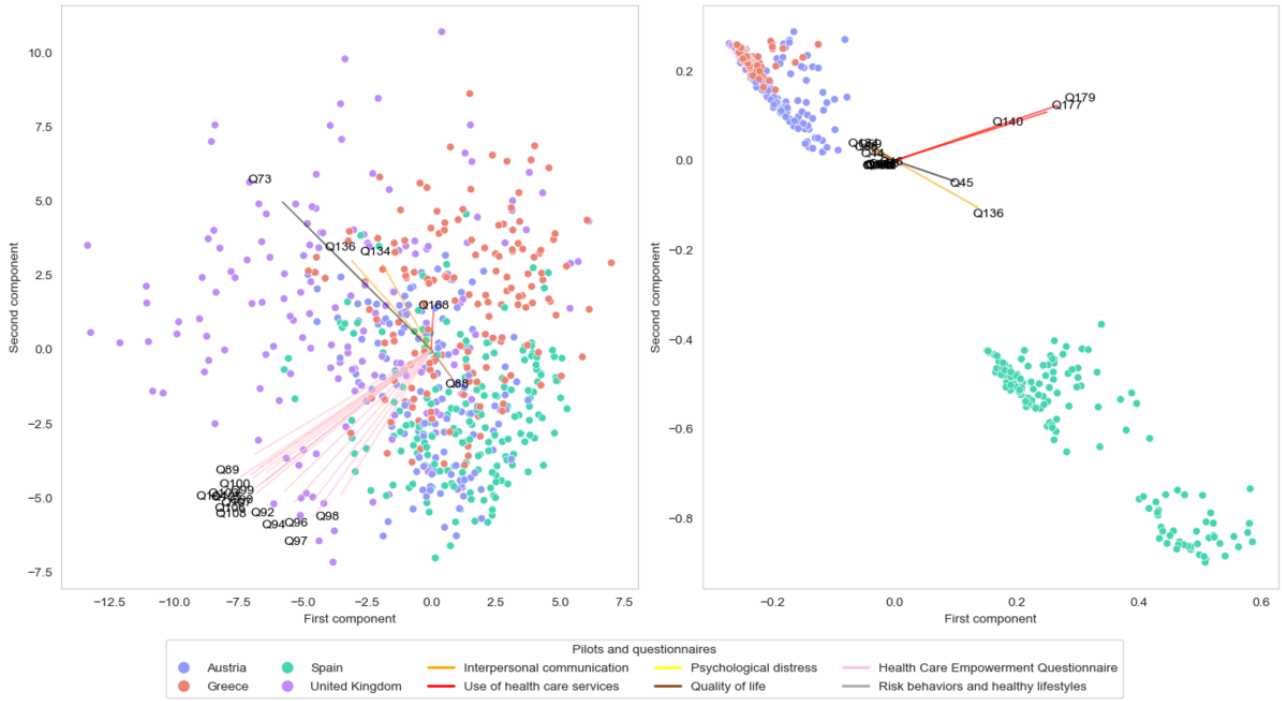
Pilot	Values, n (%)	Age (years), mean (SD)	Male, n (%)	Female, n (%)	Nonbinary, n (%)	Other, n (%)	Do not want to disclose sex, n (%)
Austria	142 (21.8)	45.28 (12.83)	60 (42.3)	82 (57.7)	0 (0)	0 (0)	0 (0)
Greece	158 (24.2)	51.57 (13.53)	121 (76.6)	34 (21.5)	0 (0)	2 (1.3)	1 (0.6)
Spain	198 (30.3)	48.94 (14.82)	110 (55.6)	87 (43.9)	0 (0)	0 (0)	0 (0)
United Kingdom	155 (23.8)	42.91 (12.04)	127 (81.9)	27 (17.4)	1 (0.6)	0 (0)	0 (0)
Total	652 (100)	47.87 (13.06)	418 (64.1)	230 (35.3)	1 (0.2)	2 (0.3)	1 (0.2)

XSL•FO
RenderX

Questionnaire Data Analysis

The left side of Figure 2 shows the scatter plot of the 2 first PCA components of the complete dataset for the entire questionnaire. The UK pilot shows a larger variance in comparison to the others. In addition, substantial differences in position and sparsity can be appreciated between the different pilot sites. The PCA loadings in the figure show the most critical variables that have influenced the PCA, which are divided into sections. The HCEQ, which is the one with the greatest dispersion, is also the most influential, as it is the questionnaire with the highest contribution to the PCA with questions Q89, Q90, Q92, Q94, Q96, Q97, Q98, Q99, Q100, Q103, Q104, Q105, Q106, Q107, and Q10, followed by the interpersonal communication questionnaire with Q134 and Q136, afterward use of health care services with Q168, quality of life with Q88, and psychological distress with Q73. Table S1 in Multimedia Appendix 2 provides detailed information regarding the questions corresponding to the selected numbering.

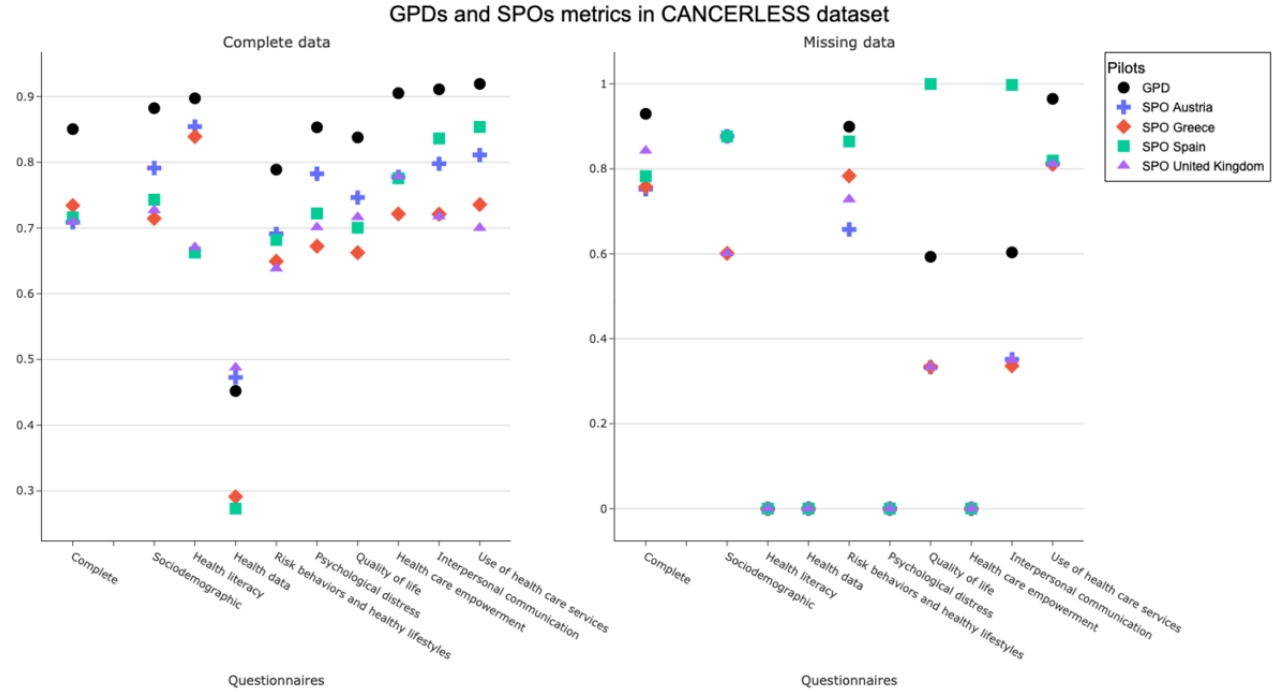
Figure 2. Scatter plot of data along the 2 principal components elicited from the principal component analysis and the multiple correspondence analysis, respectively. Each point is colorized depending on its pilot precedence. Most contributed questions for the principal component analysis calculation have been shown with arrows, depending on the questionnaire they belong to. Tables S1 and S2 in Multimedia Appendix 2 present a detailed table of both, indicating the specific questions and their associated questionnaires. For the global analysis, the principal component analysis indicates a central point where most of the samples are concentrated, with the UK pilot showing the greatest dispersion relative to the others. There is a substantial difference between the UK and Spanish pilot samples. In contrast, Austria and Greece pilots show a wider distribution of their samples. In the completeness case, the figure clearly shows 2 different parts, being the pilots from the United Kingdom, Greece, and Austria quite similar compared to Spain, where it presents an entirely different type of missing from the other pilots, being interpersonal communication and use of health care services sections the most relevant in the calculation of the multiple correspondence analysis. Q: question.



The left side of Figure 3 shows the resultant DQ metrics, which generally present a wide dispersion between pilots for the overall questionnaire and most of the questionnaires. Noteworthy, the health data questionnaire shows metrics less than 0.5 observed, in contrast to those in the other questionnaires with values exceeding 0.8, indicating a clear difference for each pilot. For health care services, interpersonal communication, and health care empowerment, the GPD value exceeds 0.9, highlighting the divergence shown in Figure 2. However, several imputations have been performed for the case of Spain in the interpersonal communication and use of health care services sections.

XSL•FO
RenderX

Figure 3. Results from the GDP and SPO multicentric analysis were applied to both the complete dataset (left side) and the completeness (right side) from the dataset composed of the T0 interviews in Austria, Greece, Spain, and the United Kingdom. The SPO indicates the distance of that pilot from the latent central tendency; the GPD can be understood as the mean of the variability of each pilot; a value close to 0 means less variability. In our case, a value of 0 indicates no missings for these questionnaires. Generally, a large variability is observed, especially in the Spanish pilot. GPD: global probabilistic deviation; SPO: source probabilistic outlyingness.



The overall analysis of the questionnaire reveals 3 types of variability patterns. First, we found questionnaires with very different distributions between pilots. Still, there are no decisive questions within the questionnaire, as they do not appear on the left side of Figure 2 as the most relevant in the PCA, such as sociodemographic data, health literacy, and risk behaviors and healthy lifestyles. Second, questions related to health data showed fewer differences concerning the pilots compared to the other questionnaires, which had a GPD of 0.452. Finally, questionnaires such as psychological distress, quality of life, HCEQ, interpersonal communication (Person-Centered Coordinated Care Experience Questionnaire), and the items related to the use of health care services, apart from diverging between the different pilots according to the metrics applied, present some questions that are determinant and differentiable by country.

Missing Patterns Analysis

From the 652 participants analyzed and the 130 questions collected at T0, a total of 84,760 values were obtained. Of these, 70,384 of 84,760 (83%) values are complete and valid, 6260 of 84,760 (7.4%) values are not applicable missing, and 8116 of 84,760 (9.6%) values are ordinary missing.

The right side of Figure 2 shows the MCA projection of the missing profiles to 2 dimensions, where a cluster of Austria, Greece, and the United Kingdom can be observed at the top-left side of the plot. Mainly, Spain samples can be observed at the bottom-right of the figure, denoting that Spain is very different from the other sites in terms of the missing pattern. In this instance, the questionnaire with the highest number of questions was the use of health care services, comprising Q155, Q158, Q167, Q161, Q152, Q180, Q176, Q179, and Q178. This was followed by the interpersonal communication questionnaire, which included Q138, Q142, Q140, Q136, and Q134. Next was risk behaviors and healthy lifestyle, encompassing Q45, Q46, Q44, and Q59, and quality of life with Q88. Table S2 in Multimedia Appendix 2 provides detailed information regarding the questions corresponding to the selected numbering.

The right side of Figure 3 offers both a global and section-by-section view of missing-data behavior after applying the GPD and SPO metrics. Overall variability is high; yet, 3 distinct patterns emerge. First, several sections—health literacy, health data, psychological distress, and health care empowerment—show virtually no disparity across pilots because they contain no missing values, so their GPD and SPO scores sit near 0. Second, marked differences appear in sociodemographic data, risk behaviors, healthy lifestyles, and use of health care services, where some pilots contribute many missings, while others contribute few. Third, a distinct Spain-specific pattern emerges. Spain is the only pilot exhibiting substantial variability that elevates the mean GPD in sections where the remaining pilots show minimal variability—particularly in quality of life (Spain: 100/1576, 6.3% missing; others combined: 10/3640, 0.3% missing) and in interpersonal communication, where the SPO profile departs markedly from the consistently low missingness observed elsewhere.

XSL•FO
RenderX

Discussion

Summary of Main Findings

This study investigated heterogeneity among people experiencing homelessness in 4 European countries and evaluated the quality of data collected in a multicenter cohort. Understanding variability in demographics, health status, and service use is essential for designing interventions tailored to this population's needs. The analysis showed pronounced between-pilot differences: for most questionnaires, the GPD exceeded 0.7 at both pilot and aggregate levels (Figures S1 and S2 in Multimedia Appendix 3), indicating substantial heterogeneity. The sole exception was the health questionnaire, whose lower GPD likely reflects that only a single quantitative item remained after discarding multichoice and free-text responses. Missing-data diagnostics revealed further site-specific discrepancies, with the Spanish cohort diverging most markedly, particularly in the use of health services, quality of life, and interpersonal communication (Figures 2 and 3).

Participants' responses reveal notable differences in the experiences of people experiencing homelessness across the various countries. While the heterogeneity observed within the homeless population can, in part, be attributed to country-specific factors, such as distinct socioeconomic and health care contexts, variations in responses may also stem from differences in the implementation of interventions and the subjective perceptions of individual participants. These discrepancies are particularly evident in key areas assessed by the PCA, including health-related domains, where divergent patterns emerge based on both contextual and personal factors. In the case of Q136: "Do you have a care plan (or a single plan of care) that takes into account all your health and wellbeing needs?" Spain stands out as the only country, where more individuals have health plans than those without. Additionally, Austria is unique in having no instances of "I don't know" responses to this question. For Q134: "Do you have a single professional (or several professionals) who takes responsibility for coordinating your care across the services that you use?" Spain and the United Kingdom are distinguished by having more positive responses than negative ones. Notably, the United Kingdom records the highest number of participants uncertain about their answers. Furthermore, Spain shows a substantially higher number of blank responses for both Q136 and Q134. Meanwhile, concerning 3 questions belonging to the HCEQ subquestionnaire: Q104: "During the last 6 months, how important is it that you obtained all the information you wanted?" Q106: "During the last 6 months, how important is it that you and your loved ones decide the need for the health care and services?" and Q108: "During the last 6 months, how important is it that you and your loved ones decide the amount of health care and services?" In general terms, both in the United Kingdom and Austria, the response rate is higher than in Spain and Greece. Meanwhile, the United Kingdom and Austria maintain the same number of answers for these questions, with the UK participants being the most important for all 3 questions and the Austrian participants the second most important. We see how, in the case of Greek cities and Spain, the difference lies in the type of question; in the case of Q106, the Greek cities considered it very unimportant, while the participants in the Spanish pilot considered it the most important of the 3. However, the opposite effect was observed in the case of Q104 and Q108. Finally, for Q88: "We would like to know how good or bad your health is today. 100 means the best health you can imagine. 0 means the worst health you can imagine." being the perceived health status is a major patient-reported experience measure of the study.

Significance

This study, as far as the authors know, is the first study confirming the heterogeneity within the group of people experiencing homelessness in a European multicenter study, as most of the previous studies have been primarily focused on the US-American context [22,23,47]. The study's results enable quantifying this heterogeneity between the different pilots that conform to the database through various factors that should be considered in a posteriori analysis. First, despite heterogeneity, the only set of items that can be assumed to be the most appropriate if a global analysis is desired is the health data questions since they do not present any missings, as are the ones with the least variability between pilots. Second, in the case of interpersonal communication and use of health care services, the global result could not be correctly determined since most of the data were imputed in the case of Spain, which does not make the analysis at a global level appropriate. Finally, the analyses at the section level should be done separately for each pilot, with the HCEQ being the most relevant since it presents greater variability between pilots and does not contain missing values. Therefore, the analysis of the pilots must be carried out independently, and the conclusions of one pilot cannot be extrapolated to the others, given the great divergence found between them. The disparities in the global dataset are more pronounced for Spain. In contrast to the other pilots, the methodology shows that ordinary missing values constitute the majority, especially within the interpersonal communication and health care utilization questionnaires.

In this context, it is important to recognize that eliciting such variation, whether through the proposed methodology or other approaches, is not necessarily a DQ issue. Rather, it is an expected step for adapting the interventions to the specific socioeconomic and health care contexts. However, the nature and source of this variation should be carefully considered, as concerns may arise if the variation is driven by systematic measurement error or bias, which could influence the validity of the findings and the effectiveness of the interventions. This proposed methodology can help to find such variation prior to any analysis and therefore approach it, considering the characteristics of the dataset under study.

Strengths and Limitations

Including this methodology to analyze the data enables us to demonstrate 3 objectives that help ensure DQ for improved analysis. First, our approach allows us to evaluate the variability existing in the data, especially the differences between the data from different sources from a more visual perspective and with a single iteration, considering all types of variables for the analysis, without going into detail in classical tests that are more sensitive to the analysis. The technique used for DQ of the

XSL•FO
RenderX

responses in the different pilots and to evaluate their quality in terms of missing information makes use of the comparative datasets, transforming them into probability distributions that allow using comparative metrics of similarity and, therefore, the level of nonoverlapping between them. Thus, it is necessary to know the boundaries regarding the exploitation capacity of the dataset for prospective uses, especially with the scarcity of homelessness quantitative information. Second, this hierarchical approach allows for monitoring the pilots' progress and comparing them as a whole and by different sections. As data become available, we can promptly detect and correct deviations from the established methodology or protocol. This approach also enables the systematic identification of patterns and causes of missing data, supports the implementation of targeted corrective measures, and—by embedding these methods in a control framework—drives continuous improvement in information quality. Third, further analyses of DQ with new data or batches can be applied thanks to the replicability of the methodology, given that the source code has been made public.

The analysis of the overall results is affected by the large number of missing values in the Spain dataset. Since there are many questions with missing data, an imputation had to be performed, which negatively influenced the results. In addition, the number of samples is not very high for our applied method, which may also impact the results. This is because the methodology used is sensitive and requires a large amount of data to generalize results more accurately. Missing values were imputed with reference to the pooled empirical distribution of all pilot sites. While this cross-site approach may introduce some location-specific bias, it enhances methodological robustness by preserving the overall variance structure; this was exemplified in the Spanish cohort, where the 2-part analysis coupled with the imputation procedure successfully pinpointed the sources of variability.

Future Perspectives

For all of those reasons, the results of this study will facilitate prospective dataset DQ labeling for prospective publication in related health data access bodies in the framework of the European Union's European Health Data Space (EHDS) initiative [48] in compliance with Article 78 on DQ that will allow secondary use of health data for research, innovation, and policymaking under conditions of security and privacy by ensuring a certain level of DQ that will enable users to know in advance the characteristics of the CANCERLESS dataset thanks to the applied methodology.

Following current best-practice guidance on dataset curation, other DQ dimensions not covered in this study—such as temporal coherence, consistency, or correctness—will be assessed as part of the mid-scale pilot of the EHDS project QUANTUM ("Quality, Utility and Maturity Measured"). QUANTUM will pilot an European Union–wide framework for rating both the intrinsic quality of health datasets and the maturity of their curation processes; CANCERLESS database will conform to one of these analyses, supporting our analysis and getting externally validated, a multidimensional appraisal that complements this analysis.

Conclusions

The analysis of this multicenter sample of people experiencing homelessness from 4 different European countries revealed substantial heterogeneity between sites of special importance for health care empowerment, quality of life, and interpersonal communication values, which showed the most differences between pilots. Particularly, differences in missingness patterns in data were larger than the ones found on the raw data, especially for the Spain pilot, highlighting that the interpersonal communication, health care empowerment, and use of health services data present a high number of nulls and should not be used for analysis. Further qualitative techniques are needed to understand the cause of this deviation from the other pilots. This methodology should be applied to multicentric data to monitor a pilot as the data become available and, therefore, amend possible protocol deviations. In summary, as quantitative data about homelessness are scarce, using a DQ-validated dataset in the context of the EHDS is crucial to ensure the reliable use of data to facilitate research on vulnerable populations such as people experiencing homelessness.

Acknowledgments

The CANCERLESS project has been funded by the European Commission's Programme Horizon 2020 (grant agreement 965351). This publication reflects the author's views. The European Commission is not responsible for any use that may be made of the information it contains. The study is partly funded through the QUANTUM project HORIZON-HLTH-2023-TOOL-05-09—Developing a Data Quality and Utility Label for the European Health Data Space (grant agreement 101137057).

Conflicts of Interest

None declared.

Multimedia Appendix 1
T0 questionnaire.
[DOCX File , 171 KB - medinform_v13i1e73596_app1.docx]

Multimedia Appendix 2
Most principal component analysis and multiple correspondence analysis relevant questions.

XSL•FO
RenderX

[DOCX File , 115 KB - medinform_v13i1e73596_app2.docx]

Multimedia Appendix 3
Multiple correspondence analysis metrics for CANCERLESS dataset.
[DOCX File , 247 KB - medinform_v13i1e73596_app3.docx]

References

1. Fragner T, Belogianni K, Grabovac I. Cancer care in people experiencing homelessness: identifying key issues, challenges, and facilitators. Br J Gen Pract 2024;74(745):342-343 [FREE Full text] [doi: 10.3399/bjgp24X738801] [Medline: 39054087]
2. Somerville P. Understanding homelessness. Hous Theory Soc 2013;30(4):384-415 [FREE Full text] [doi: 10.1080/14036096.2012.756096]
3. Toro P. Toward an international understanding of homelessness. J Soc Issues 2007;63(3):461-481 [FREE Full text] [doi: 10.1111/j.1540-4560.2007.00519.x]
4. Nilsson SF, Nordentoft M, Hjorthøj C. Individual-level predictors for becoming homeless and exiting homelessness: a systematic review and meta-analysis. J Urban Health 2019;96(5):741-750 [FREE Full text] [doi: 10.1007/s11524-019-00377-x] [Medline: 31388823]
5. Warburton WA, Papic M, Whittaker E. Heterogeneity among homeless Australian women and their reasons for homelessness entry. Int J Environ Res Public Health 2022;19(15):8909 [FREE Full text] [doi: 10.3390/ijerph19158909] [Medline: 35897280]
6. Alexiev V. Eighth overview of housing exclusion in Europe. Florent Houdmon (City of Marseille, France). 2023. URL: https://www.feantsa.org/public/user/Resources/reports/2023/OVERVIEW/Rapport_EN.pdf [accessed 2025-10-08]
7. Funk AM, Greene RN, Dill K, Valvassori P. The impact of homelessness on mortality of individuals living in the United States: a systematic review of the literature. J Health Care Poor Underserved 2022;33(1):457-477. [doi: 10.1353/hpu.2022.0035] [Medline: 35153234]
8. Jones CA, Perera A, Chow M, Ho I, Nguyen J, Davachi S. Cardiovascular disease risk among the poor and homeless—what we know so far. Curr Cardiol Rev 2009;5(1):69-77 [FREE Full text] [doi: 10.2174/157340309787048086] [Medline: 20066152]
9. Carmichael C, Schiffler T, Smith L, Moudatsou M, Tabaki I, Doñate-Martínez A, et al. Barriers and facilitators to health care access for people experiencing homelessness in four European countries: an exploratory qualitative study. Int J Equity Health 2023;22(1):206 [FREE Full text] [doi: 10.1186/s12939-023-02011-4] [Medline: 37803317]
10. Jeleff M, Haider S, Schiffler T, Gil-Salmerón A, Yang L, Barreto Schuch F, et al. Cancer risk factors and access to cancer prevention services for people experiencing homelessness. Lancet Public Health 2024;9(2):e128-e146 [FREE Full text] [doi: 10.1016/S2468-2667(23)00298-0] [Medline: 38307679]
11. Aldridge RW, Menezes D, Lewer D, Cornes M, Evans H, Blackburn RM, et al. Causes of death among homeless people: a population-based cross-sectional study of linked hospitalisation and mortality data in England. Wellcome Open Res 2019;4:49 [FREE Full text] [doi: 10.12688/wellcomeopenres.15151.1] [Medline: 30984881]
12. Lawrie K, Charow R, Giuliani M, Papadakos J. Homelessness, cancer and health literacy: a scoping review. J Health Care Poor Underserved 2020;31(1):81-104. [doi: 10.1353/hpu.2020.0010] [Medline: 32037319]
13. Schiffler T, Carmichael C, Smith L, Doñate-Martínez A, Alhambra-Borrás T, Varadé MR, et al. Access to cancer preventive care and program considerations for people experiencing homelessness across four European countries: an exploratory qualitative study. EClinicalMedicine 2023;62:102095 [FREE Full text] [doi: 10.1016/j.eclinm.2023.102095] [Medline: 37533422]
14. Carmichael C, Smith L, Aldasoro E, Gil Salmerón A, Alhambra-Borrás T, Doñate-Martínez A, et al. Exploring the application of the navigation model with people experiencing homelessness: a scoping review. J Soc Distress Homeless 2022;32(2):352-366 [FREE Full text] [doi: 10.1080/10530789.2021.2021363]
15. Baggett TP, Barbosa Teixeira J, Rodriguez EC, Anandakugan N, Sporn N, Chang Y, et al. Patient navigation to promote lung cancer screening in a community health center for people experiencing homelessness: protocol for a pragmatic randomized controlled trial. Contemp Clin Trials 2022;113:106666. [doi: 10.1016/j.cct.2021.106666] [Medline: 34971796]
16. Robinson L, Trevors Babici L, Tedesco A, Spaner D, Morey T, Dosani N. Assessing the impact of a health navigator on improving access to care and addressing the social needs of palliative care patients experiencing homelessness: a service evaluation. Palliat Med 2023;37(4):646-651 [FREE Full text] [doi: 10.1177/02692163221146812] [Medline: 36576315]
17. Kline RM, Rocque GB, Rohan EA, Blackley KA, Cantril CA, Pratt-Chapman ML, et al. Patient navigation in cancer: the business case to support clinical needs. J Oncol Pract 2019;15(11):585-590 [FREE Full text] [doi: 10.1200/JOP.19.00230] [Medline: 31509483]
18. WHO guidelines on hand hygiene in health care. World Health Organization. 2010. URL: https://www.who.int/publications/i/item/9789241597906 [accessed 2025-10-08]

XSL•FO
RenderX

19. Te Boveldt N, Vernooij-Dassen M, Leppink I, Samwel H, Vissers K, Engels Y. Patient empowerment in cancer pain management: an integrative literature review. Psychooncology 2014;23(11):1203-1211. [doi: 10.1002/pon.3573] [Medline: 24816749]
20. Gianfrancesco MA, Tamang S, Yazdany J, Schmajuk G. Potential biases in machine learning algorithms using electronic health record data. JAMA Intern Med 2018;178(11):1544-1547 [FREE Full text] [doi: 10.1001/jamainternmed.2018.3763] [Medline: 30128552]
21. Sáez C, Robles M, García-Gómez JM. Comparative study of probability distribution distances to define a metric for the stability of multi-source biomedical research data. 2013 Presented at: 35th Annual International Conference of the IEEE Engineering in Medicine and Biology Society (EMBC); July 3-7, 2013; Osaka, Japan p. 3226-3229 URL: https://doi.org/10.1109/EMBC.2013.6610228 [doi: 10.1109/embc.2013.6610228]
22. Peressini T. Pathways into homelessness: testing the heterogeneity hypothesis. In: Finding Home Policy Options for Addressing Homelessness in Canada. Toronto, Ontario: University of Toronto; 2009:1-17.
23. Rosenheck R, Bassuk E, Salomon A. Special populations of homeless Americans. In: Practical Lessons from the 1998 National Symposium on Homeless Research. Washington, DC: US Department of Health and Human Services; 1999:1-27.
24. Rajkomar A, Dean J, Kohane I. Machine learning in medicine. N Engl J Med 2019;380(14):1347-1358. [doi: 10.1056/NEJMra1814259] [Medline: 30943338]
25. Kelly CJ, Karthikesalingam A, Suleyman M, Corrado G, King D. Key challenges for delivering clinical impact with artificial intelligence. BMC Med 2019;17(1):195 [FREE Full text] [doi: 10.1186/s12916-019-1426-2] [Medline: 31665002]
26. Sáez C, Romero N, Conejero JA, García-Gómez JM. Potential limitations in COVID-19 machine learning due to data source variability: a case study in the nCov2019 dataset. J Am Med Inform Assoc 2021;28(2):360-364 [FREE Full text] [doi: 10.1093/jamia/ocaa258] [Medline: 33027509]
27. Souza J, Johnata C, Ismael S, João L, Mariana P, Andreia V, et al. Measuring variability in acute myocardial infarction coding using a statistical process control and probabilistic temporal data quality control approaches. 2021 Presented at: Trends and Applications in Information Systems and Technologies (WorldCIST 2021); April 30, 2021; Azores, Portugal p. 193-202. [doi: 10.1007/978-3-030-72651-5_19]
28. Sáez C, Martínez-Miranda J, Robles M, García-Gómez JM. Organizing data quality assessment of shifting biomedical data. Stud Health Technol Inform 2012 Aug;180:721-725 [FREE Full text] [doi: 10.3233/978-1-61499-101-4-721]
29. Edgar B. The ETHOS definition and classification of homelessness and housing exclusion. Eur J Homelessness 2012;6(2):219-225 [FREE Full text]
30. EuroQol Group. EuroQol—a new facility for the measurement of health-related quality of life. Health Policy 1990;16(3):199-208. [doi: 10.1016/0168-8510(90)90421-9] [Medline: 10109801]
31. Gagnon M, Hibert R, Dubé M, Dubois M. Development and validation of an instrument measuring individual empowerment in relation to personal health care: the Health Care Empowerment Questionnaire (HCEQ). Am J Health Promot 2006;20(6):429-435. [doi: 10.4278/0890-1171-20.6.429] [Medline: 16871823]
32. Derogatis LR. Brief Symptom Inventory 18. Baltimore, MD: Johns Hopkins University; 2001.
33. Lloyd H, Fosh B, Whalley B, Byng R, Close J. Validation of the person-centred coordinated care experience questionnaire (P3CEQ). Int J Qual Health Care 2019;31(7):506-512 [FREE Full text] [doi: 10.1093/intqhc/mzy212] [Medline: 30508089]
34. Sáez C, Robles M, García-Gómez JM. Stability metrics for multi-source biomedical data based on simplicial projections from probability distribution distances. Stat Methods Med Res 2017;26(1):312-336. [doi: 10.1177/0962280214545122] [Medline: 25091808]
35. Sáez C, Zurriaga O, Pérez-Panadés J, Melchor I, Robles M, García-Gómez JM. Applying probabilistic temporal and multisite data quality control methods to a public health mortality registry in Spain: a systematic approach to quality control of repositories. J Am Med Inform Assoc 2016;23(6):1085-1095 [FREE Full text] [doi: 10.1093/jamia/ocw010] [Medline: 27107447]
36. Van Buuren S, Groothuis-Oudshoorn K. mice: multivariate imputation by chained equations in R. J Stat Softw 2011;45:1-67. [doi: 10.32614/cran.package.mice]
37. Ferri P, Romero-Garcia N, Badenes R, Lora-Pablos D, Morales TG, Gómez de la Cámara A, et al. Extremely missing numerical data in electronic health records for machine learning can be managed through simple imputation methods considering informative missingness: a comparative of solutions in a COVID-19 mortality case study. Comput Methods Programs Biomed 2023;242:107803 [FREE Full text] [doi: 10.1016/j.cmpb.2023.107803] [Medline: 37703700]
38. Abdi H, Williams LJ. Principal component analysis. WIREs Comput Stat 2010;2(4):433-459 [FREE Full text] [doi: 10.1002/wics.101]
39. Breunig MM, Kriegel HP, Ng RT, Sander J. LOF: identifying density-based local outliers. 2000 Presented at: SIGMOD/PODS00: ACM International Conference on Management of Data and Symposium on Principles of Database Systems; May 15-18, 2000; Dallas, TX, United States p. 93-104. [doi: 10.1145/342009.335388]
40. Greenacre M, Blasius J. Multiple Correspondence Analysis and Related Methods. 1st Edition. Boca Raton, FL: Chapman and Hall/CRC; 2006.
41. Van Rossum G, Drake FL. Python reference manual. Centrum voor Wiskunde en Informatica. 1995. URL: https://ir.cwi.nl/pub/5008 [accessed 2025-10-08]

XSL•FO
RenderX

42. Harris CR, Millman KJ, van der Walt SJ, Gommers R, Virtanen P, Cournapeau D, et al. Array programming with NumPy. Nature 2020;585(7825):357-362 [FREE Full text] [doi: 10.1038/s41586-020-2649-2] [Medline: 32939066]
43. McKinney W. Data structures for statistical computing in Python. 2010 Presented at: Proceedings of the 9th Python in Science Conference (Vol 445); June 28-July 3, 2010; Austin, TX, United States p. 51-56 URL: https://proceedings.scipy.org/articles/Majora-92bf1922-00a [doi: 10.25080/majora-92bf1922-00a]
44. Pedregosa, E F, Varoquaux G, Gramfort A, Michel V, Thirion B, Grisel O, et al. Scikit-learn: machine learning in Python. J Mach Learn Res 2011;12:2825-2830 [FREE Full text] [doi: 10.3389/fninf.2014.00014]
45. Halford M. prince. GitHub. 2025. URL: https://github.com/MaxHalford/prince [accessed 2025-10-08]
46. Blasco A, Blanes V. bdslab-upv/dq_cancerless_analysis. GitHub. URL: https://github.com/bdslab-upv/dq_cancerless_analysis [accessed 2025-10-08]
47. Toro PA, Dworsky A, Fowler PJ. Homeless youth in the United States: recent research findings and intervention approaches. 2007 Presented at: National Symposium on Homelessness Research (Vol 6); March 1-2, 2007; Washington DC URL: https://www.researchgate.net/publication/237287723_6-_Homeless_Youth_in_the_United_States_Recent_Research_Findings_and_Intervention_Approaches
48. European Health Data Space Regulation. European Commission. 2024. URL: https://health.ec.europa.eu/ehealth-digital-health-and-care/european-health-data-space_en [accessed 2024-10-07]

Abbreviations

DQ: data quality
EHDS: European Health Data Space
GPD: global probabilistic deviation
HCEQ: Health Care Empowerment Questionnaire
MCA: multiple correspondence analysis
MSV: multisource variability
PCA: principal component analysis
SPO: source probabilistic outlyingness

Edited by A Benis; submitted 07.03.25; peer-reviewed by F Estupiñán-Romero, V Gejjegondanahalli Yogeshappa; comments to author 20.04.25; revised version received 12.06.25; accepted 04.08.25; published 14.11.25.

Please cite as:
Blasco-Calafat A, Blanes-Selva V, Fragner T, Doñate-Martínez A, Alhambra-Borrás T, Gawronska J, Smith L, Garcia-Gomez JM, Grabovac I, Sáez C
Multisource Coherence Analysis of the First European Multicenter Cohort Study for Cancer Prevention in People Experiencing Homelessness: Data Quality Study
JMIR Med Inform 2025;13:e73596
URL: https://medinform.jmir.org/2025/1/e73596
doi:10.2196/73596
PMID:41236789

©Antonio Blasco-Calafat, Vicent Blanes-Selva, Tobias Fragner, Ascensión Doñate-Martínez, Tamara Alhambra-Borrás, Julia Gawronska, Lee Smith, Juan M Garcia-Gomez, Igor Grabovac, Carlos Sáez. Originally published in JMIR Medical Informatics (https://medinform.jmir.org), 14.11.2025. This is an open-access article distributed under the terms of the Creative Commons Attribution License (https://creativecommons.org/licenses/by/4.0/), which permits unrestricted use, distribution, and reproduction in any medium, provided the original work, first published in JMIR Medical Informatics, is properly cited. The complete bibliographic information, a link to the original publication on https://medinform.jmir.org/, as well as this copyright and license information must be included.

XSL•FO
RenderX

The State of Practice About Security in Telemedicine Systems in Chile: Exploratory Study

Gaston Marquez[1,2*], PhD; Michelle Pacheco[2*], RN; Priscilla Vergara[3*], BEng; Felix Liberona[3*], MS; May Chomali[3*], MD; Eric Rojas[3,4,5*], PhD

[1]Departamento de Ciencias de la Computación y Tecnologías de la Información, Universidad del Bío-Bío, Av. Andrés Bello 720, Chillán, Chile

[2]Transferencia Gestión Colaborativa en Salud Pública (Polo de Salud) para la región de Ñuble, Chillán, Chile

[3]Centro Nacional de Sistemas de Información en Salud (CENS), Santiago, Chile

[4]Institute for Biological and Medical Engineering, Pontificia Universidad Católica de Chile, Santiago, Chile

[5]Department of Clinical Laboratories, School of Medicine, Pontificia Universidad Católica de Chile, Santiago, Chile

[*]all authors contributed equally

Corresponding Author:
Gaston Marquez, PhD
Departamento de Ciencias de la Computación y Tecnologías de la Información, Universidad del Bío-Bío, Av. Andrés Bello 720, Chillán, Chile

Abstract

Background: Information security within telemedicine systems is essential to advancing the digital transformation of health care. Telemedicine encompasses diverse modalities, including teleconsultation, telehealth, and remote patient monitoring, all of which depend on digital platforms, secured communication networks, and internet-connected devices. Although these systems have progressed in aligning with information security standards and regulations, there remains a shortage of comprehensive, practice-oriented studies evaluating which aspects of security are effectively addressed and which remain insufficiently managed, particularly within the Chilean context.

Objective: This study aims to examine how effectively telemedicine systems in Chile address the core security attributes of confidentiality, availability, and integrity.

Methods: Data were analyzed from an evaluation tool designed to assess the quality of telemedicine systems in Chile. Over a 6-year period, 25 telemedicine systems from different providers were assessed, and an in-depth examination of how companies manage key information security subcharacteristics within their systems was undertaken.

Results: The findings indicate that 52% (n=13) of telemedicine systems optimally implement cryptographic techniques to protect confidentiality. In contrast, 44% (n=11) lack robust strategies for adapting to, recovering from, and mitigating security-related incidents. Fault tolerance mechanisms are frequently integrated to minimize service disruption caused by system failures. However, the prioritization of data integrity varies: while some companies treat it as a critical requirement, others assign it limited importance.

Conclusions: This study offers an understanding of the security priorities and practices adopted by telemedicine providers. It highlights a prevailing tendency to prioritize security measures over usability, underscoring the need for a balanced approach that safeguards patient information while supporting efficient clinical workflows.

(JMIR Med Inform 2025;13:e77395) doi:10.2196/77395

KEYWORDS

assessment; quality; security; telemedicine systems; usability

Introduction

Security within telemedicine systems constitutes a critical component of the digital transformation in the health care sector [1]. The rapid expansion in the utilization of these technologies, significantly accelerated by the COVID-19 pandemic, necessitates the enhancement of mechanisms to safeguard medical information, thereby ensuring the confidentiality, integrity, and availability of patient data [2]. Telemedicine encompasses a range of modalities, including teleconsultation, telehealth, and remote patient monitoring, all of which depend on digital platforms, secured communication networks, and internet-connected devices [3]. Nevertheless, the deployment of these systems presents substantial risks, such as vulnerabilities in data transmission, unauthorized access, cybersecurity threats, and interoperability challenges among diverse health information systems. Countries generally establish guidelines for the storage and processing of personal data, which also affect telemedicine services [4]. However, despite these advancements, security in telemedicine continues to pose a global challenge due to the

XSL•FO
RenderX

diversity of regulations, the rapid evolution of cyber threats, and the necessity for digital security awareness among health care professionals [5,6]. In this context, as reported by Nobili et al [7], hospitals and their information systems, including telemedicine systems, were the principal targets of cyberattacks, accounting for 42% of all computer-related incidents from 2022 to 2023.

In Chile, the regulation of personal data storage and processing is governed by law. Within the realm of telemedicine, the Chilean public health care systems have initiated efforts to enhance the digitalization of health care services among companies offering telemedicine services to their patients [8,9]. Specific guidelines have been established to safeguard patient data privacy and ensure the security of clinical information. Despite the notable advancements made by telemedicine companies in adhering to Chile's information security guidelines and regulations, there is a paucity of systematic research that practically examines the aspects of information security that telemedicine companies effectively address and those they do not. Furthermore, there is limited information regarding the trade-offs that telemedicine companies undertake to fulfill the information security requirements of their systems.

This study presents a study examining the success levels associated with information security subcharacteristics within telemedicine companies in Chile. This study aims to identify which subcharacteristics of information security are adequately addressed and which remain insufficiently addressed by current telemedicine systems from a practical perspective. Information security was characterized through the properties of confidentiality, availability, and integrity, utilizing 7 specific subcharacteristics. The study involved an analysis of data collected from an instrument designed to assess the quality of telemedicine systems in Chile. Over a period of 6 years, the success levels of 25 telemedicine systems from different companies were evaluated, and an in-depth discussion was conducted on how these systems address the information security subcharacteristics within their telemedicine systems. The study contributes a pragmatic analysis of the priorities and actions undertaken by telemedicine companies to address subcharacteristics related to information security, as well as the trade-offs these companies encounter in ensuring security in Chile. The findings of this study offer practical insights for professionals and researchers concerned with the security of telemedicine systems.

Methods

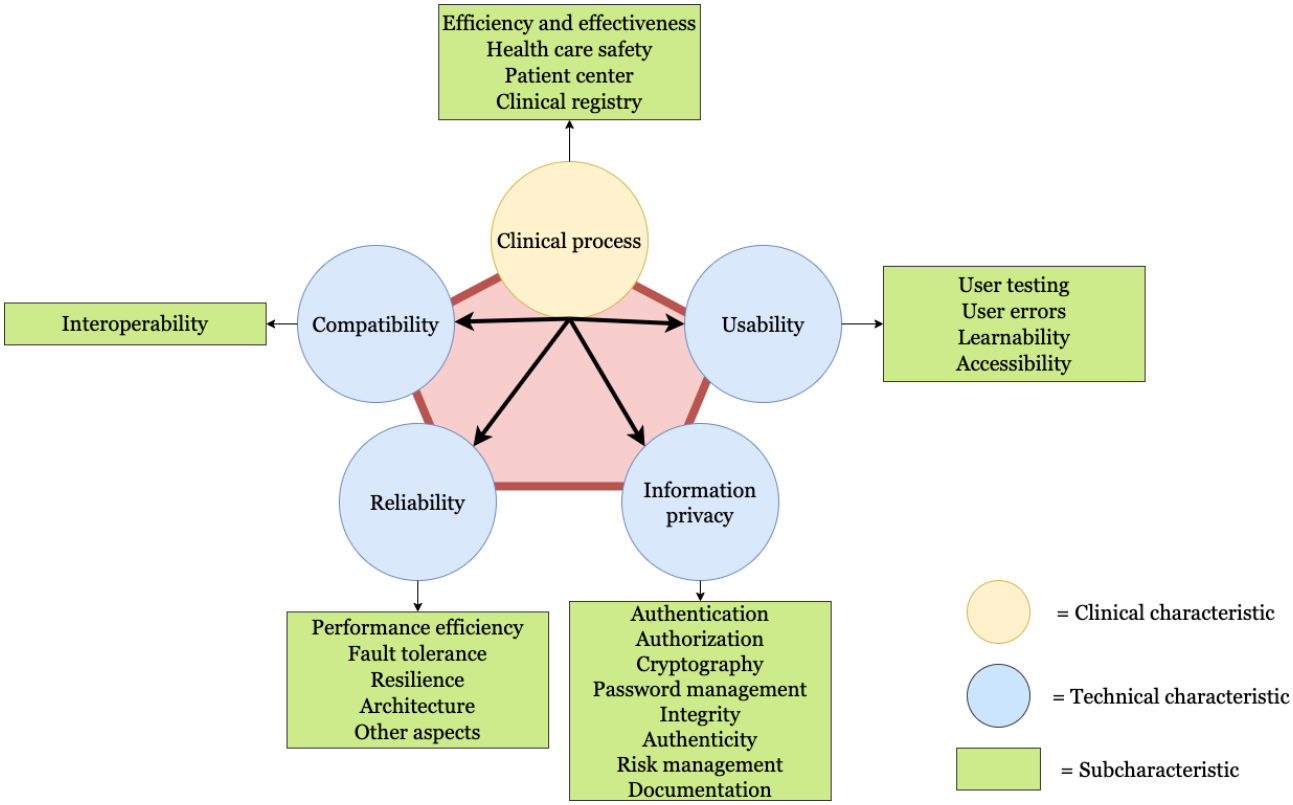
Instrument

The utilization of information technologies in health care delivery through telemedicine necessitates adherence to quality criteria typically mandated by public and private health organizations. Consequently, it is imperative to assess multiple technical and clinical aspects to ensure that the telemedicine tools employed meet the requisite minimum standards. In response to this scenario, we developed an instrument (see Multimedia Appendix 1) that evaluates the quality of telemedicine systems through an assessment process with the objective of verifying that the desired minimum requirements required by health care stakeholders are fulfilled (see Figure 1).

To validate the instrument, we conducted a comprehensive literature review to determine the elements used in the evaluation of telemedicine systems, particularly in the context of information privacy [5]. This preliminary research enabled us to identify the key security subcharacteristics considered in the assessment of telemedicine systems, as well as to derive and pinpoint additional characteristics and subcharacteristics, as illustrated in Figure 1. Subsequently, we conducted 3 pilot studies of the instrument in collaboration with (1) telemedicine experts, (2) clinical professionals, and (3) health care decision-makers. In each pilot study, we evaluated the instrument's usefulness in assessing Chilean public telemedicine systems. At the conclusion of each pilot, we collected feedback from participants and revised the instrument accordingly. Thereafter, we engaged 3 telemedicine companies, partners of our research group, to apply the revised instrument to their telemedicine systems. Upon the completion of the system evaluations, we considered the observations made by each company's teams and further refined the instrument.

XSL•FO
RenderX

Figure 1. Instrument for assessing the quality of telemedicine systems, including their corresponding technical and clinical characteristics as well as their subcharacteristics.



The evaluation process focuses on 2 characteristics: clinical and technical. Each characteristic evaluates multiple aspects. In the clinical characteristic, the context, description of the telemedicine solution, and role of the patient in the clinical process are evaluated. For this reason, we evaluated the following subcharacteristics: (1) efficiency and effectiveness, (2) health care safety, (3) patient center, and (4) clinical registry. These subcharacteristics represent the most relevant concerns regarding telemedicine in Chile. In the technical characteristic, 4 properties are evaluated: compatibility, usability, reliability, and information privacy. In turn, each characteristic has 18 subcharacteristics representing different concerns. The decision to evaluate the clinical and technical dimensions is based on the priorities faced by health decision-makers in Chile. These priorities aim to address laws that have been enacted in the country, which are oriented toward cybersecurity, data privacy, interoperability, and patient protection.

Each subcharacteristic evaluates the telemedicine company's adherence to both technical and legal standards. Consequently, the instrument requires the telemedicine company to provide pertinent information and documentation from the telemedicine system to confirm the accuracy of the responses recorded in the instrument. Given the complexity of evaluating telemedicine systems, our instrument employs a simplified scale for stakeholder comprehension. The scale considers a score of 3 points for optimal, 2 points for acceptable, 1 point for risky, and 0 points for unsatisfied.

An optimal score is defined when the telemedicine company proposes novel mechanisms or methodologies that exceed the baseline expectations defined by the instrument in each subcharacteristic; that is, when the telemedicine company implements additional or more advanced security techniques to provide a higher degree of patient trust. Some of these techniques include hash encryption algorithms, role and access management through identifiers, zero trust architecture, intrusion detection, multifactor authentication, and network micro-segmentation, among others. Similarly, an acceptable score is defined when the telemedicine company provides the explicit evidence required by the instrument and complies with the legal regulations associated with each subcharacteristic. A company receives a risk score when it does not explicitly describe the required evidence and does not fully comply with the legal regulations associated with each subcharacteristic. Finally, an unsuccessful score corresponds to a company that neither provides evidence nor complies with regulations.

Research Objectives

In this study, we focused on examining subcharacteristics related to security. Therefore, the conceptualization of security is structured into 3 fundamental properties: confidentiality, availability, and integrity. Confidentiality pertains to the protection of information, ensuring that access is restricted to authorized individuals by preventing unauthorized access, improper disclosure, or data breaches [10]. Availability guarantees that information is accessible and usable when needed by authorized users [11]. Integrity ensures that information remains accurate and reliable, without unauthorized modifications [11].

Correspondingly, as elucidated by the instrument presented in Figure 1, we established that the confidentiality characteristic encompasses 4 subcharacteristics: authentication, authorization, cryptography, and authenticity. Authentication refers to the

XSL•FO
RenderX

process of verifying the identity of a user, system, or device prior to granting access to a resource or service [12]. Authorization involves determining the actions or resources that an authenticated user is permitted to access [12]. Cryptography is the study of techniques for safeguarding information by converting data into an encrypted format, which can only be read or modified by authorized individuals or systems [13]. Information authenticity ensures that data originate from a legitimate source and have not been altered during transmission or storage [12].

Concurrently, the availability characteristic is composed of 2 subcharacteristics: fault tolerance and resilience. Fault tolerance refers to a system's capacity to maintain proper functionality despite the failure of 1 or more of its components [14]. Resilience, on the other hand, denotes a system's ability to adapt, recover, and continue operations following an adverse event, such as a cyberattack, hardware malfunction, or natural disaster [15].

Therefore, we define the following objectives:

1. Identify security-related subcharacteristics that telemedicine companies successfully address. This objective is oriented toward analyzing the subcharacteristics of the instrument that perform optimally in the context of security, demonstrating telemedicine companies' ability to meet information security requirements.
2. Investigate the factors enabling telemedicine companies to achieve optimal and acceptable scores in security-related subcharacteristics. This objective aims to explore the key elements that contribute to successful performance in the security subcharacteristics.
3. Determine the security-related subcharacteristics that telemedicine companies fail to effectively address. This objective focuses on identifying subcharacteristics that exhibit low scores and understanding their implications for information security.
4. Analyze the reasons telemedicine companies fail to achieve favorable scores in security-related subcharacteristics. This objective aims to uncover the underlying challenges or limitations that prevent companies from meeting their security requirements.
5. Examine the trade-offs telemedicine companies create between usability and security in their systems. Usability and security frequently exhibit conflicting objectives [11]. While usability aims to simplify access and enhance user experience, security focuses on safeguarding data and systems, which typically necessitates the implementation of restrictions or additional measures to ensure such protection. Therefore, this objective is oriented toward understanding how usability considerations influence security decisions and how companies balance these 2 critical aspects within their systems.

Although there are regulations and security standards, such as the Health Insurance Portability and Accountability Act (HIPAA) [16], ISO/IEC 27001 [17], Control Objectives for Information and Related Technologies [18], and the NIST Cybersecurity Framework [19], not all can be fully applied to the reality of telemedicine in Chile owing to work culture, institutional organization, and the level of maturity of telemedicine systems. For this reason, our instrument draws on these regulations and standards to adapt security assessments to the Chilean context, with the aim of establishing an initial security baseline for telemedicine systems in Chile.

Research Questions

We defined the following research question:

RQ1: Which subcharacteristics of telemedicine systems address security concerns? Rationale: The objective of this research question is to elucidate the subcharacteristics of our instrument that performs optimally in the context of security. While the instrument employs a multidimensional approach, this research question aims to demonstrate the capacity of telemedicine companies to meet information security requirements.

RQ2: Which subcharacteristics of telemedicine systems do not address security concerns? Rationale: In contrast to RQ1, this research question aims to identify the subcharacteristics that exhibit low scores within the security context. In addition, this research question is intended to describe the reasons telemedicine companies are unable to achieve favorable security scores.

RQ3: In the context of usability, which trade-offs do telemedicine companies make to ensure security within their systems? Rationale: Addressing security necessitates a balance between the properties and quality of telemedicine systems. This research question aims to elucidate the trade-offs that our instrument identifies when addressing information security in telemedicine systems.

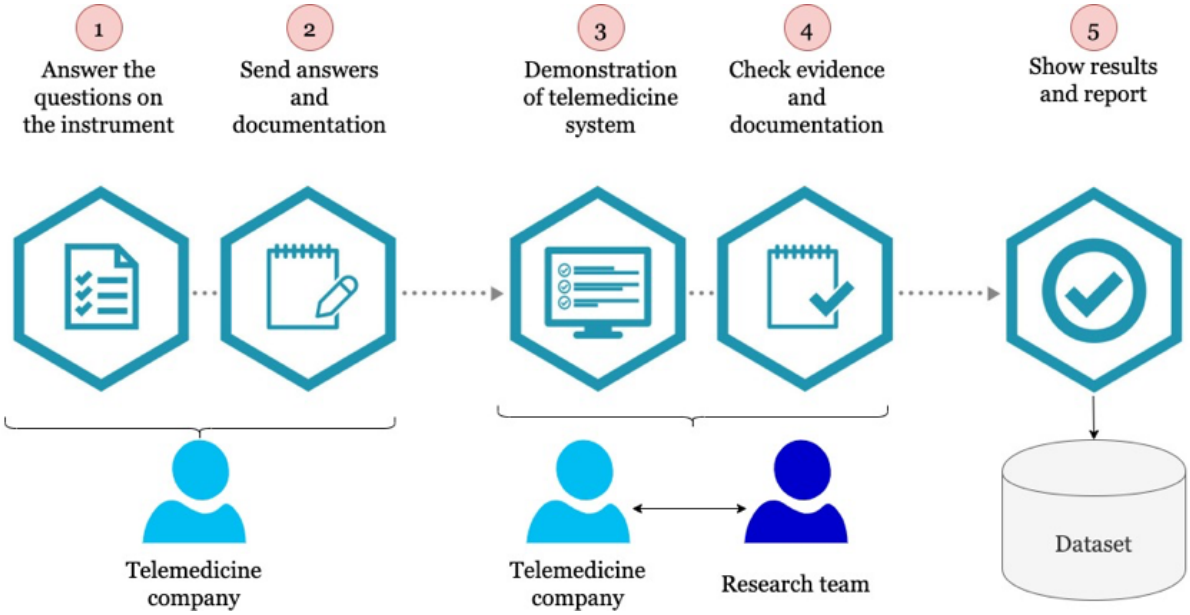
Data Collection

The data collection process is illustrated in Figure 2.

The data collection process is characterized by 2 distinct perspectives. First, it involves a self-assessment process conducted by the telemedicine company, wherein the company's technical and clinical representatives utilize our instrument to respond to key inquiries and provide corresponding documentation to substantiate their responses. Second, our research team performs a cross-validation of the documentation and responses obtained from the instrument through a demonstration of the telemedicine system, focusing on corroborating the answers provided in the instrument. The selection of the 25 telemedicine companies was based on a technical analysis of the telemedicine system each company offered, the number of clients, and the volume of telemedicine services provided to both public and private health care services in Chile. In addition, the quality agreements held by the companies were reviewed, as these had been granted by public health institutions, given that this sector serves the largest number of patients in Chile. We used a nonprobabilistic, convenience-based sampling approach. Specifically, we engaged companies willing to participate in order to provide them with reports on the security and quality of their systems, thereby supporting the continuous improvement of their security mechanisms.

XSL•FO
RenderX

Figure 2. Process for collecting data from telemedicine companies as well as from their telemedicine systems.



In the initial phase, the telemedicine company is tasked with assembling clinical and technical experts to address all inquiries associated with our instrument. The instrument was developed within a web-based system that facilitates the upload of documentation in various formats. Upon the compilation of all information and the completion of the instrument's inquiries by the telemedicine company, the subsequent phase involves transmitting the information to our research team. Upon receiving notification from the company and verifying that no information was pending, we informed the telemedicine company of the assessment's initiation. The third phase aims to mitigate subjectivism and bias in the company's responses by demonstrating the functionalities associated with the inquiries evaluated by the instrument. For this phase, our research team convenes with the stakeholders of the telemedicine company to discuss pertinent aspects of the instrument. Subsequently, in the fourth phase, the research team organizes to evaluate the telemedicine company's documentation and demonstration to assign a score to each subcharacteristic that our instrument assesses. The assessment is conducted by 3 members of the research team and subsequently validated by a senior researcher. The 3 investigators independently evaluated the responses and documentation submitted by the telemedicine company, ultimately determining the final score through consensus. Following score assignment, a preliminary report is generated, which must be approved or rejected by a senior researcher on the team. The company initiates an improvement process in which the aspects to be improved are addressed until the necessary score for approval is reached. The number of interactions depends on how the company presents corresponding evidence and documentation. If the report is approved, the fifth phase consists of creating a formal instance to present the results of our analysis and inform the company of its qualification. Additionally, the entire analysis and its results are stored in a dataset utilized for research purposes.

Data Analysis

We used descriptive statistics and manual analysis of documentation to address the research questions. About RQ1 and RQ2, we analyzed the frequency of scores to categorize the number of companies that achieved optimal, acceptable, risky, and unsuccessful scores.

Regarding RQ1 and RQ2, we conducted a comprehensive review of all documents and software artifacts that our instrument mandates companies to submit for the evaluation of their telemedicine systems, in addition to responding to the questions within the instrument. For each assessed security subcharacteristic, companies are required to furnish evidence demonstrating their compliance with the subcharacteristic, thereby substantiating the responses provided in the instrument. In our study, we requested explicit evidence from companies to ensure the objectivity of the evaluation. For instance, when companies submit evidence of authentication, they typically provide documentation on the authentication mechanisms implemented in the telemedicine system, along with source code packages. This procedure is similarly applied to other security subcharacteristics. Finally, a team of researchers independently assessed the evidence and provided a review, which was subsequently verified by a senior researcher on the team.

Concerning RQ3, the subcharacteristics related to security are classified into 2 categories: successful and not successful. The subcharacteristics categorized as "successful" are those that obtained optimal (score 3) and acceptable (score 2) scores. Conversely, subcharacteristics categorized as "not successful" are those that received risky (score 1) and unsatisfied (score 0) scores. Subsequently, we compared the percentages of usability and security. The percentage of successful corresponds to the ratio of subcharacteristics that are categorized as "successful" compared to the total (subcharacteristics with "successful" and "not successful" categories).

Ethical Considerations

According to the applicable ethical and legal framework in Chile, including Law No. 19.628 on the Protection of Private Life, research ethics review is required for studies involving human participants, biological samples, or personal data [20].

XSL•FO
RenderX

As this study did not involve the collection, processing, or analysis of any personal, sensitive, or health-related data, it was not subject to review by an institutional ethical research board.

Results

In relation to RQ1, Table 1 shows that telemedicine systems prioritize cryptography as principal subcharacteristic to ensure security.

A total of 13 companies, representing 52% of the total, obtained the optimal score as they considered cryptographic methods to be pertinent to ensuring the protection of sensitive patient data as well as the security of patient-physician communication. With the exception of the subcharacteristic of authenticity, where the distribution of scores is more equitable, in the subcharacteristics of authorization and fault tolerance, the acceptable score leads to the preferences (15 companies representing 60% are inclined toward this score in these 2 subcharacteristics). In the same context, authentication and integrity also share the same preferences for this score (10 companies representing 40% favor these 2 subcharacteristics). Table 2 summarizes the main reasons identified in the documentation provided by the companies for which telemedicine companies achieve favorable scores in security-related subcharacteristics.

Table . Frequency of scores obtained by telemedicine companies.

		Subcharacteristic	Optimal	Acceptable	Risky	Unsatisfied
Security	Confidentiality	Authentication	3	10	10	2
		Authorization	6	15	2	2
		Cryptography	13	8	1	3
		Authenticity	7	8	7	3
	Availability	Fault tolerance	6	15	3	1
		Resilience	4	7	3	11
	Integrity	Integrity	2	10	10	3

XSL•FO
RenderX

Table . Summary of the main reasons telemedicine companies achieve optimal and acceptable scores.

Subcharacteristic	Reason
Cryptography	Most telemedicine systems use AWS Cognito, SHA[a] 256, or HTTPS[b] as cryptographic tools. This means that the data encryption acts over the TLS[c]. In addition, most telemedicine systems have their infrastructure hosted in the cloud, mainly in AWS[d]. All telemedicine systems use cryptographic mechanisms for video encryption. DTLS[e] 1.2 or SRTP[f] is the most commonly used method for encrypting transmitted data.
Authentication	Most telemedicine systems employ username and password authentication. Furthermore, these systems utilize 2-factor access to enhance security mechanisms. Nevertheless, we observed that although the instrument requires explicit information regarding access to sensitive data, not all companies provide evidence of role-based access control within their telemedicine systems.
Authorization	Telemedicine companies have access control mechanisms that use specific permission profiles for each type of user. Nevertheless, not all companies explicitly describe whether they have validation from the Chilean Registry of Individual Health Care Providers to access data.
Authenticity	Telemedicine systems use unique and random login identifiers. This identifier changes when the user is authenticated. However, we note that some companies do not describe evidence that a single sign-on is implemented in the telemedicine system.
Fault tolerance	Most telemedicine systems have implemented functionalities that offer patients the possibility of resuming consultations in case of failure through a link and code provided by email. Although companies are able to identify failure scenarios and implement prevention and mitigation measures, not all companies are able to guarantee response times to allow users to continue using the services in case of failure.
Integrity	Telemedicine companies manage sensitive data through security protocols that classify information into public, proprietary, client, and privileged categories. They recognize the confidentiality of patients' clinical information, applying stringent protection measures.

[a]SHA: Secure Hash Algorithm.

[b]HTTPS: Hypertext Transfer Protocol Secure.

[c]TLS: Transport Layer Security.

[d]AWS: Amazon Web Services.

[e]DTLS: Datagram Transport Layer Security.

[f]SRTP: Secure Real-time Transport Protocol.

Regarding RQ2, Table 3 describes that the subcharacteristic with the lowest score corresponds to resilience. A total of 11 companies (44% of the total number of companies analyzed) did not address methodologies to adapt, recover, and overcome security-related situations effectively. As in RQ1, authentication and integrity exhibit equivalent frequencies of scores, but in this instance with respect to the risk score.

Regarding RQ3, Figure 3 compares the results of the security and usability subcharacteristics with their corresponding successful-related percentages for each company. The results reveal variations in success levels, ranging from significant to subtle.

For system 1, the system satisfied 75% of the usability subcharacteristics. However, in terms of security, the system only satisfies 43% of the subcharacteristics, with all availability and integrity subcharacteristics remaining unaddressed. For systems 2 and 3, both address a greater proportion of security subcharacteristics compared to usability subcharacteristics, with system 2 addressing 100% of the subcharacteristics. However, system 3 demonstrated inadequate performance in cryptography, despite exhibiting a higher successful percentage in security. System 4 focuses exclusively on usability but only successfully addresses 1 security subcharacteristic. It is noteworthy that this company does not address fundamental security standards such as cryptography and authorization.

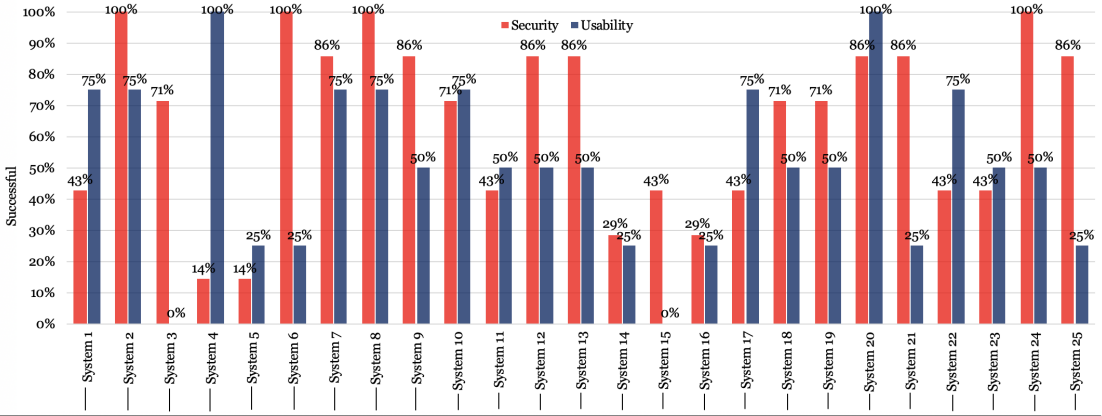
Although system 5 demonstrates no significant difference between the successful-related percentages for usability and security, the overall percentage remains low. This indicates that the company maintains equilibrium between both properties, albeit at a substantially low level of success. Systems 6-9 have successfully addressed security concerns, but with varying levels of usability success: company 6 addressed only 25% of usability criteria, while systems 7-9 exceeded 50%.

XSL•FO
RenderX

Table . Summary of the main reasons telemedicine companies achieve risky and unsuccessful scores.

Subcharacteristic	Reason
Resilience	Documentation submitted by telemedicine companies indicates that they use a resilient mechanism in their telemedicine systems. However, when analyzing the documentation submitted to the instrument, companies do not necessarily explicitly describe a recovery plan.
Authentication	Table 2 indicates that the companies do not provide precise information regarding their roles. In these instances, companies attempt to elucidate role-based authentication mechanisms but omit pertinent information. However, certain companies, despite mentioning the utilization of roles for authentication, merely attach screenshots or provide no information whatsoever.
Integrity	Companies often lack explicit methods for eliminating unnecessary data and inadequately address error detection in data entry within telemedicine systems.

Figure 3. Distribution of percentages of success with security and usability.



		Subdomain	Score																								
Security	Confidentiality	Authentication	0	3	2	1	1	2	2	3	2	3	1	2	2	0	1	1	1	2	1	1	2	1	1	2	2
		Authorization	2	3	2	0	1	2	3	3	3	3	2	2	2	0	2	2	2	2	2	2	2	1	2	2	3
		Cryptography	3	3	1	0	0	3	2	3	0	3	2	2	2	3	3	2	3	3	3	3	3	2	2	2	3
		Authenticity	3	3	3	1	3	2	1	3	2	2	1	2	2	0	0	0	1	3	1	2	2	1	1	2	3
	Availability	Fault Tolerance	0	2	3	2	1	2	3	3	2	2	2	2	2	2	3	1	2	2	2	3	2	2	1	2	3
		Resilience	0	2	3	1	0	3	3	2	2	1	0	0	1	0	0	0	0	2	2	0	2	2	3	0	
	Integrity	Integrity	0	2	1	0	1	2	2	2	2	1	1	2	2	0	1	1	1	1	3	2	2	1	1	2	3
		Successful	3	7	5	1	1	7	6	7	6	5	3	6	6	2	3	2	3	5	5	6	6	3	3	7	6
		Not successful	4	0	2	6	6	0	1	0	1	2	4	1	1	5	4	5	4	2	2	1	1	4	4	0	1
		% Successful	**43%**	**100%**	**71%**	**14%**	**14%**	**100%**	**86%**	**100%**	**86%**	**71%**	**43%**	**86%**	**86%**	**29%**	**43%**	**29%**	**43%**	**71%**	**71%**	**86%**	**86%**	**43%**	**43%**	**100%**	**86%**
Usability		User testing	2	2	1	2	1	0	1	3	0	1	0	1	1	0	0	0	2	1	2	2	0	2	2	3	1
		User errors	2	3	0	2	1	2	2	1	3	2	3	1	3	3	1	3	3	3	2	2	2	3	2	1	1
		Learnability	2	3	1	2	1	0	2	3	2	2	2	2	1	1	1	1	2	3	1	2	1	2	1	2	2
		Accessibility	0	0	1	2	3	0	3	3	0	2	0	3	2	0	0	0	0	1	0	3	0	0	0	1	0
		Successful	3	3	0	4	1	1	3	3	2	3	2	2	2	1	0	1	3	2	2	4	1	3	2	2	1
		Not successful	1	1	4	0	3	3	1	1	2	1	2	2	2	3	4	3	1	2	2	0	3	1	2	2	3
		% Successful	**75%**	**75%**	**0%**	**100%**	**25%**	**25%**	**75%**	**75%**	**50%**	**75%**	**50%**	**50%**	**50%**	**25%**	**0%**	**25%**	**75%**	**50%**	**50%**	**100%**	**25%**	**75%**	**50%**	**50%**	**25%**

Systems 10 and 11 exhibit a situation analogous to system 4, wherein they maintain a balance in addressing security and usability. However, system 10 demonstrates higher successful-related percentages compared to system 11. Systems 12 and 13 yielded identical results, significantly favoring security measures. System 14 maintains equilibrium in satisfying usability and security requirements, albeit at notably low percentages. In this regard, the company focuses exclusively on cryptography and fault tolerance as security mechanisms. Concerning usability, they have successfully addressed only user error control measures.

System 15 prioritized security over usability; however, it exhibited a notably low successful percentage. Similar to system 14, system 16 achieved equivalent percentages of success in both usability and security. System 17 placed greater emphasis on usability compared to security, specifically focusing on user error control in terms of usability. Systems 18 and 19 demonstrated identical results regarding success with security versus usability. Nevertheless, system 18 made a concerted effort to develop a user-accessible system.

System 20 distinguishes itself through high successful levels in both security and usability. In this regard, the company surpassed others in terms of usability and security success. System 21 addresses security to a greater extent than usability. However, this company does not delineate any process to address the resilience of telemedicine systems. System 22 satisfied more usability subcharacteristics than security subcharacteristics. System 23 demonstrates a balanced, albeit low, successful percentage. Systems 24 and 25 exhibited a trend of addressing more security subcharacteristics than usability subcharacteristics.

XSL•FO
RenderX

Discussion

Overview of the Findings

The instrument proposed in this study delineates the state of practice of characteristics that define the structure of telemedicine systems. The objective of this study is to elucidate the state of security from 3 perspectives: confidentiality, availability, and integrity.

From a confidentiality perspective, the results elucidate significant findings for the analysis. Regarding authentication, organizations balance acceptable and risky outcomes in the authentication mechanisms implemented in their telemedicine systems. As authentication verifies the identity of the user attempting access by validating credentials, 10 companies achieve acceptable results, while 10 companies exhibit risky outcomes. Among the acceptable results, organizations have adopted mechanisms that extend beyond basic username and password management. For instance, these companies utilize multifactor authentication to provide an additional security layer. Conversely, companies with risk scores limit themselves to the minimum requirements in user and password management. Analyzing the extreme scores, 3 companies achieved optimal results by not only implementing multifactor authentication but also incorporating biometric authentication features for users. Regarding unsuccessful scores, these companies demonstrated no evidence of documentation pertaining to authentication.

From the perspective of authorization, 15 companies adhere to acceptable mechanisms for authorizing access to sensitive data. It is deemed acceptable for a company to not only utilize basic authorization mechanisms but also to adapt to governmental regulations regarding access to clinical data. In Chile, specifically, there are legally mandated regulations governing access to sensitive information. In total, 4 companies that received risky or unsuccessful scores did not fully comply with these regulations. Conversely, 6 companies achieved an optimal score in authorization due to their implementation of internal processes and protocols for data authorization. This scenario is advantageous for security as it systematizes activities related to authorization, thereby facilitating traceability and auditing.

Cryptography is the preferred subcharacteristic for telemedicine companies. It was observed that 13 companies focused their efforts on providing adequate levels of cryptography using tools or algorithms specifically designed for this purpose. Similarly, 8 companies implemented cryptographic levels using libraries from development frameworks (eg, OAuth) but did not extend their efforts beyond those companies with an optimal score. Conversely, 1 company received a risk score because although it claimed to use cryptographic mechanisms, it provided no supporting evidence. Finally, 3 companies failed to meet cryptographic standards. This deficiency is primarily attributed to a lack of knowledge among telemedicine system developers regarding the implementation of cryptographic methods in their systems.

With regard to authenticity, ensuring that data, messages, or transactions originate from legitimate and reliable sources and have not been altered during transmission or storage is a primary concern for telemedicine companies. Although 8 companies adequately met the fundamental requirements for authenticity, 7 companies distinguished themselves by implementing nonrepudiation methods in their authentication processes. Specifically, these companies ensure that the data cannot be modified and that the sender cannot deny having generated the data. However, 7 companies failed to adequately describe the authenticity mechanisms in their systems. Furthermore, it was observed that some companies conflated the concept of authenticity with networking.

About availability, the results demonstrated disparities between fault tolerance and resilience. In terms of fault tolerance, 15 companies with acceptable scores implemented cluster strategies and load balancing. These companies opted for these techniques due to the availability of various technology stacks in the market that support their implementation. Furthermore, 6 companies employed additional mechanisms related to fault tolerance, specifically failover mechanisms. This technique ensures that in the event of a component or service failure, the system automatically transitions to an alternative resource capable of performing the same function. Conversely, it is imperative to note that the results presented in Table 1 elucidate a substantial disparity between resilience mechanisms.

A total of 11 companies failed to delineate the methodologies employed in their systems to address resilience, and 3 companies provided ambiguous indications of resilience, lacking sufficient clarity. The research team found that explicit references to resilience were uncommon among telemedicine companies, suggesting that further understanding of the related techniques and technologies could be beneficial. Among the companies that address resilience, 7 adhere to the recommendations from the Chilean Ministry of Health concerning the application of resilience in health information systems. In total, 4 companies implemented additional techniques specifically related to server redundancy.

Regarding integrity, the results in Table 1 are analogous to those of the authentication. The highest scores are concentrated in the acceptable and risky categories. The 10 companies that achieve an acceptable score primarily focus their efforts on delineating processes and mechanisms involving encryption protocols, such as Transport Layer Security [21], to safeguard data from tampering during transmission. Furthermore, 2 companies distinguished themselves in integrity by implementing hashing algorithms to verify data integrity.

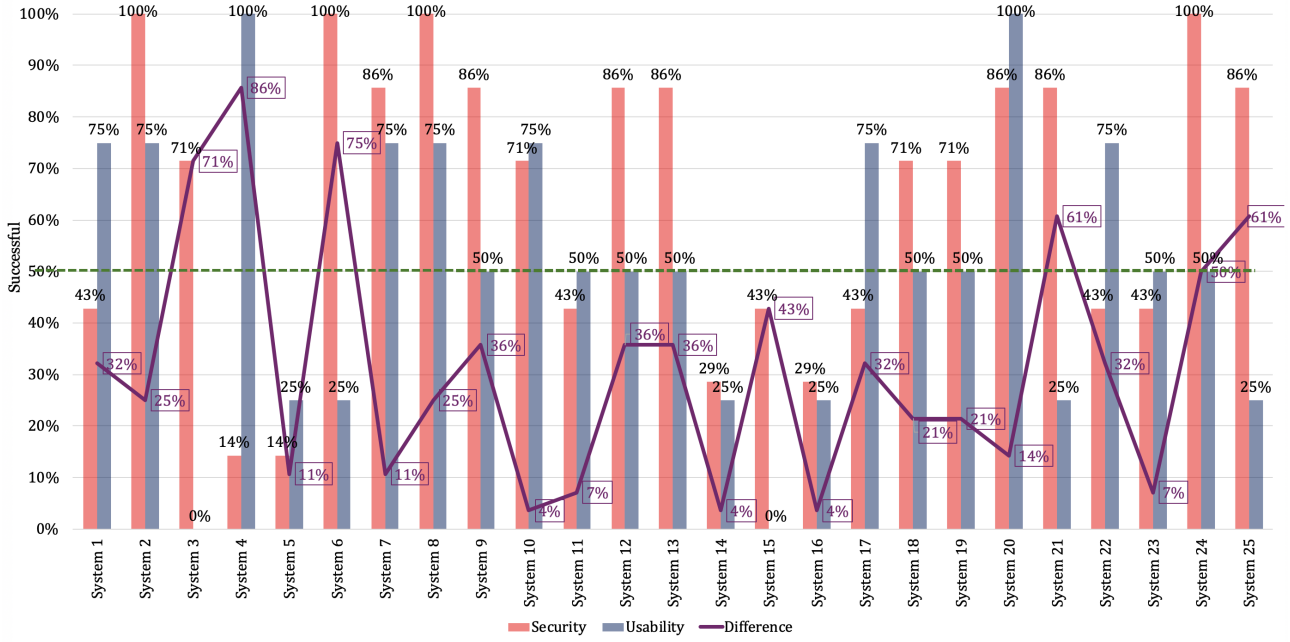
Conversely, 10 companies attain risky results as they inadequately meet the minimum requirements for information integrity. In this regard, these companies have made insufficient efforts to address data integrity in teleconsultations. Figure 4 describes that telemedicine companies generally prioritize security over usability, although the disparity in successful-related percentages exhibits volatility.

Utilizing 50% as a threshold to differentiate successful levels, certain companies, specifically companies 3, 4, 6, 20, 21, and 25, described a difference in percentages exceeding 50%. In these instances, the trends are distinct, favoring either usability or security. Conversely, in the remaining companies, the difference between the percentages was less than 50%. While

XSL•FO
RenderX

this indicator does not comprehensively reflect the actual situation of companies, it serves as a parameter to determine the nature of trade-offs they make. Among the 6 companies with a difference greater than 50%, 5 exhibited a tendency to prioritize security in their telemedicine systems over usability, while 1 company demonstrated an inclination in the opposite direction.

Figure 4. Distribution of the difference in percentages of success concerning security and usability. The dashed line represents the upper and lower 50% threshold.



Principal Results

Cryptography is the subcharacteristic in which we observed the highest proportion of organizations that attained the maximum score. This phenomenon may be attributed to the prevalent perception that cryptography constitutes the most efficacious and widely utilized method for data protection and security. Of the 25 companies evaluated, 13 achieved an optimal score in cryptography, while 8 companies attained an acceptable score.

Another aspect in which the organizations demonstrated positive performance is fault tolerance. Although the majority of organizations performed adequately in this characteristic, most did not attain the highest scores. This can be attributed to limitations in infrastructure, scalability, dependence on third-party services, and integration with other systems. Most organizations are likely capable of managing basic faults, such as implementing backup mechanisms or addressing minor interruptions, but lack robust solutions to mitigate major failures such as complete system crashes, loss of critical data, or failures during high-demand situations.

In contrast, a significant negative aspect is recovery capability. The suboptimal results in this characteristic can be attributed to various factors, one of which is successful fault-tolerance scores. Both aspects are closely related as they address how systems manage failures. The recovery capability focuses on how the system restores itself after failure. Many organizations may prioritize developing fault-tolerant systems while neglecting the implementation of postfailure recovery measures. This situation can be problematic because although fault tolerance results are generally positive, most organizations did not achieve the highest scores, suggesting that their systems may not be resilient to severe errors. By not prioritizing recovery capability, a significant failure could render it extremely challenging to restore the system to its normal state.

Another subcharacteristic in which the majority of companies demonstrated suboptimal results is accessibility. The inadequacy of accessible systems impedes the utilization of these platforms by individuals with special needs as well as the elderly population, who frequently experience visual or auditory impairments. This deficiency represents a missed commercial opportunity, as a substantial number of elderly individuals and persons with disabilities could potentially derive significant benefits from telemedicine. Due to the absence of adequate accessibility options, these companies have restricted access to a crucial demographic segment, resulting in biased systems that can only be effectively utilized by young and middle-aged adults.

The findings identified critical areas with direct practical implications for the development of telemedicine systems. The high scores in cryptography indicate a strong emphasis on data protection; however, organizations must continue updating these measures to counter evolving threats. The moderate level of fault tolerance suggests basic resilience but also highlights vulnerabilities during significant system failures, necessitating investment in scalable and robust infrastructure. The poor performance in recovery capability is particularly concerning, as it may result in extended service downtime and compromise patient safety, underscoring the need for formal disaster recovery plans.

XSL•FO
RenderX

Limitations

First, the assessment of security in telemedicine systems frequently presents numerous challenges due to the complex and sensitive nature of clinical data and the system itself. Consequently, the development of an instrument to evaluate the current state of a telemedicine system across various characteristics may inadvertently omit aspects that are fundamental to telemedicine. From a systemic perspective, system evaluation encompasses diverse complexities and details, ranging from requirement identification to software architecture. Nevertheless, international regulations such as the HIPAA [16], the European Union's General Data Protection Regulation [22], and the Fast Healthcare Interoperability Resources or Health Level Seven standard [23], among others, establish various levels and concerns that must be addressed by telemedicine systems. Furthermore, the policies and regulations of individual countries constitute perspectives that must be considered in any instrument designed to evaluate telemedicine systems.

Second, the instrument proposed in this study to evaluate telemedicine systems has limitations in encompassing all variants and scenarios that should be considered in telemedicine. It is conceivable that this instrument may require adaptation to the diverse regulatory frameworks for telemedicine across different countries. Nevertheless, this instrument represents the first endeavor inspired by international telemedicine regulations and is focused on the Chilean context. This initial approach has been refined and endorsed by public and foreign health decision-makers in Chile, resulting in the participation of 25 companies in this study to determine the preliminary status of their telemedicine systems' quality. Regarding security, the results of this study enable the determination of the current status of fundamental aspects of confidentiality and privacy in telemedicine systems. While a comprehensive security assessment should consider multiple levels of abstraction, such as infrastructure, networks, and providers, this study represents an initial step in the pragmatic discussion of security in telemedicine systems within the Chilean context.

Third, the instrument described in this study does not evaluate the security techniques and mechanisms employed by telemedicine companies. Specifically, the instrument is not designed to empirically analyze cryptographic techniques or compare software architecture styles, components, or technological infrastructure. The scale assessed the level of evidence provided by the company regarding the implementation of security subcharacteristics in telemedicine systems. A more comprehensive and empirical analysis of the quality and efficacy of the techniques, processes, mechanisms, and methods utilized by telemedicine companies to implement security-related subcharacteristics should be conducted in a separate study. Additionally, in our study, we primarily focused on identifying the security mechanisms employed by telemedicine systems, rather than conducting an in-depth analysis of which techniques are more significant than others. This level of detail would require examining the source code of the systems and applying more advanced comparative methods to determine the degree of importance. Therefore, our intention was to illustrate to the reader what telemedicine systems are currently implementing in terms of security, rather than analyzing the complexity of the security mechanisms themselves.

Fourth, the 6-year span of our study may not fully capture the evolution of security threats related to telemedicine systems. The field of information security and cybersecurity in telemedicine is continuously evolving in terms of vulnerability techniques and methods. In this context, our study focuses on the responses provided by telemedicine system developers, without delving into whether the techniques implemented in these systems remain adequate in light of emerging security scenarios. Nevertheless, Chilean regulations require telemedicine companies to demonstrate, through a series of processes and software artifacts, that they comply with governmental information-security standards. Consequently, companies providing telemedicine services are obliged to stay up to date with new types of security incidents. Therefore, during the 6 years covered by the study, the information provided by the telemedicine companies at least meets Chilean regulations on information security in telemedicine.

While the limitations outlined in this section may affect the generalizability of our study's findings, the instrument we developed is adaptable to a range of contexts and security environments. At present, the instrument is tailored to the Chilean context. Nevertheless, as telemedicine regulations in Chile are largely based on international standards, the instrument can be adapted to suit different scenarios in other countries. Furthermore, although adverse security scenarios in telemedicine continue to evolve, our instrument enables a cross-sectional analysis of security, which may subsequently inform more in-depth analyses of each subcharacteristic. In this regard, our study focuses on the evidence provided by telemedicine companies concerning how they address the various aspects of security; however, it does not consider how these companies adapt to different security scenarios.

Future Work

Future research will concentrate on the systematic refinement and validation of the assessment instrument employed in this study, ensuring its alignment with the evolving landscape of telemedicine technologies and emerging regulatory requirements. While the current version offers a practical evaluation of key dimensions, such as security, interoperability, and usability, the rapid advancement of digital health tools, particularly those incorporating artificial intelligence, introduces new challenges in risk management, data governance, and ethical compliance.

In the Chilean context, recent legislative developments concerning cybersecurity, personal data protection, and artificial intelligence–driven clinical decision support systems underscore the urgency of equipping telemedicine providers with tools that not only evaluate but also anticipate compliance gaps and technological vulnerabilities. This calls for a research agenda oriented toward the codesign of adaptive, evidence-based instruments that integrate technical, clinical, and legal perspectives, thereby supporting secure and more trustworthy digital health services.

XSL•FO
RenderX

Comparison With Prior Work

Poleto et al [24] addressed the increasing adoption of telemedicine systems in Brazil, driven by the necessity for health care access in remote areas and expedited implementation during the COVID-19 pandemic. The authors proposed the utilization of fuzzy cognitive maps to analyze the complexity of cybersecurity, translating expert knowledge into maps that represent causal relationships between security concepts, facilitating scenario creation, and enhancing cybersecurity strategies. For security assessment, 15 variables influencing cyberattacks were identified and validated by an information technology manager, and a fuzzy cognitive map diagram was constructed. This study demonstrates how changes and incorrect configurations can overburden servers and how insufficient investment can generate inefficiencies, emphasizing the significance of controlling information technology services.

Vidanagamachchi et al [25] conducted an analysis of the privacy and security challenges in telemedicine systems in Sri Lanka, emphasizing their significance due to the rapid adoption precipitated by the COVID-19 pandemic. Despite technological advancements and the implementation of government policies for digitalization, deficiencies in patient data protection persist due to the lack of specificity in the regulations. The authors propose a self-assessment mechanism for patients to evaluate the security of telemedicine apps. To this end, a questionnaire was developed encompassing 7 critical characteristics related to telemedicine and cybersecurity, considering the demographic and ethnic diversity of Sri Lanka. The evaluation involved collecting responses from 100 users utilizing an online questionnaire. The results indicated that the majority of participants do not peruse privacy and security policies and are unaware of storage capabilities and backup policies.

Poleto et al [26] emphasized the significance of managing cyber risks in telemedicine, particularly in the exchange of medical images, due to the susceptibility of systems to cyberattacks. They proposed a cybersecurity risk management framework for telemedicine utilizing a bowtie analysis approach that integrates fault tree analysis and event tree analysis. To assess security, the framework identifies risk factors and potential risk events, prioritizes actions to mitigate the impact of cyberattacks, and provides recommendations for establishing effective security policies. This framework is predicated on the ISO/TS 13131:2014 standard, which delineates recommendations for developing quality objectives and guidelines for telehealth services. The study also elucidates the importance of control measures to ensure the confidentiality, integrity, and availability of medical information.

Zhou et al [27] addressed concerns regarding privacy and security in telemedicine services within the context of increased utilization driven by the necessity to enhance health care access in rural areas. They proposed the development and validation of a self-assessment questionnaire for telemedicine providers to evaluate their privacy and security measures. This questionnaire was constructed based on a systematic review of security practices and the HIPAA audit protocol. The study encompassed 31 telemedicine providers who responded to 49 questions in the questionnaire. The results demonstrated that the questionnaire exhibits high reliability for assessing privacy and security practices in telemedicine systems and identified key vulnerabilities in areas such as data storage, secure networks, encryption, data backup, and informed consent.

Kim et al [1] examined the necessity of managing security risks in telemedicine systems due to the increased utilization of these technologies for remote diagnosis and prescription, particularly in the context of infectious diseases such as COVID-19, SARS-CoV, and MERS-CoV. This investigation proposes the development of a security risk assessment model for telemedicine systems utilizing an attack tree approach with attack occurrence probability and attack success probability as variables. Security threats were analyzed across 7 characteristics of telemedicine services using data collected through surveys conducted at a medical institution. The model was implemented to identify system vulnerabilities.

The studies analyzed offer diverse perspectives on security within telemedicine systems and the approaches to addressing these concerns. Several of these perspectives are reflected in the security subcharacteristics examined in our study, as they are broadly applicable to telemedicine systems. Furthermore, these studies align with the cross-sectional analysis of security policies and practices in telemedicine systems in Chile, allowing us to adapt our study to different national contexts. However, most existing studies rely primarily on theoretical frameworks, high-level risk assessment models, or self-assessment questionnaires that provide general guidance but lack direct application to operational telemedicine environments. In contrast, our study adopts a practice-oriented approach that examines how security is effectively implemented and perceived in real telemedicine systems used in Chile. This approach contributes to a contextualized understanding of how security measures are operationalized in Chile with evolving telehealth regulation, thereby complementing and extending the insights offered by previous international frameworks.

Conclusions

This study presents an investigation into the security status of telemedicine systems. Utilizing an instrument developed by the research team, the study analyzed 25 telemedicine companies and their respective systems based on 3 critical security attributes: confidentiality, availability, and integrity. The analysis aims to identify the subcharacteristics of confidentiality, availability, and integrity that telemedicine companies effectively address and the underlying reasons for their success. Conversely, the study also aims to identify the primary reasons for telemedicine companies' failure to adequately address security and the factors contributing to these shortcomings. Furthermore, the study explores the trade-offs involved in ensuring security in telemedicine, particularly concerning the usability of telemedicine systems.

We investigated 3 research questions relating to the security subcharacteristics addressed by telemedicine systems (RQ1), those that are not addressed (RQ2), and the trade-offs telemedicine companies make to ensure security (RQ3). With regard to RQ1, the findings revealed that cryptography is the principal subcharacteristic of interest in telemedicine systems in relation to confidentiality. In terms of availability, fault

XSL•FO
RenderX

tolerance is consistently addressed to prevent disruptions in medical care caused by system failures. Data integrity emerges as a variable concern among telemedicine providers; some consider it highly important, while others do not regard integrity as a particularly relevant characteristic. Concerning RQ2, the subcharacteristic receiving the least attention is resilience. The findings for RQ3 indicated that telemedicine companies generally prioritize security over usability.

The findings of this study highlight critical areas with direct practical implications for the advancement of telemedicine systems. Strong performance in cryptography reflects a clear commitment to secure data; however, organizations must ensure these measures are continuously updated to address emerging cyber threats. The moderate level of fault tolerance indicates some degree of system resilience but also exposes vulnerabilities during major failures, emphasizing the need for investment in scalable and robust infrastructure. Of particular concern is the weak performance in recovery capability, which could lead to prolonged service interruptions.

Acknowledgments

We thank José Fuentes and Sebastián Jouannet for their significant contribution to the study.

Funding

This study was funded by the National Centre on Health Information Systems (ANID-CTI230006 CENS) and the Fondo Nacional de Desarrollo Científico y Tecnológico (No. 11230708).

Data Availability

The data can be consulted at [27].

Authors' Contributions

Funding acquisition: MC
Investigation: ER, GM, MP
Methodology: FL, PV
Project administration: MC
Validation: ER, FL, MC, MP, PV
Visualization: GM
Writing – original draft: GM
Writing – review & editing: GM

Conflicts of Interest

None declared.

Multimedia Appendix 1
Instrument used in our research and its corresponding questions by characteristic.
[XLSX File, 12 KB - medinform_v13i1e77395_app1.xlsx]

References

1. Kim DW, Choi JY, Han KH. Risk management-based security evaluation model for telemedicine systems. BMC Med Inform Decis Mak 2020 Jun 10;20(1):106. [doi: 10.1186/s12911-020-01145-7] [Medline: 32522216]
2. Portnoy J, Waller M, Elliott T. Telemedicine in the era of COVID-19. J Allergy Clin Immunol Pract 2020 May;8(5):1489-1491. [doi: 10.1016/j.jaip.2020.03.008] [Medline: 32220575]
3. Yellowlees PM. Successfully developing a telemedicine system. J Telemed Telecare 2005 Oct;11(7):331-335. [doi: 10.1177/1357633X0501100707]
4. Ivanova J, Cummins MR, Ong T, et al. Regulation and compliance in telemedicine: viewpoint. J Med Internet Res 2025 Jan 23;27:e53558. [doi: 10.2196/53558] [Medline: 39847413]
5. Marquez G, Astudillo H, Taramasco C. Security in telehealth systems from a software engineering viewpoint: a systematic mapping study. IEEE Access 2020;8:10933-10950. [doi: 10.1109/ACCESS.2020.2964988]
6. Katz C, Ruiz JM, Saigí-Rubió F, Novillo-Ortiz D. The state of the art of telemedicine implementation architecture: rapid umbrella review of systematic reviews. J Med Internet Res 2025;27:e70276. [doi: 10.2196/70276]
7. Nobili M, Raguseo D, Setola R. Cybersecuity analysis of a telemedicine platform. Healthcare (Basel) 2025;13(2):184. [doi: 10.3390/healthcare13020184]

XSL•FO
RenderX

8. Garcia-Huidobro D, Rivera DS, Valderrama Chang S, Bravo P, Capurro D. System-wide accelerated implementation of telemedicine in response to COVID-19: mixed methods evaluation. J Med Internet Res 2020 Oct 6;22(10):e22146. [doi: 10.2196/22146] [Medline: 32903195]
9. Vidal-Silva C, Sánchez-Ortiz A, Serrano-Malebrán J, et al. Social influence, performance expectancy, and price value as determinants of telemedicine services acceptance in Chile. Heliyon 2024 Mar 15;10(5):e27067. [doi: 10.1016/j.heliyon.2024.e27067] [Medline: 38562504]
10. Smith HJ, Dinev T, Xu H. Information privacy research: an interdisciplinary review. MIS Q 2011;35(4):989. [doi: 10.2307/41409970]
11. Bass L, Clements P, Kazman K. Software Architecture in Practice: Addison-Wesley Professional; 2021.
12. Fernandez-Buglioni E. Security Patterns in Practice: Designing Secure Architectures Using Software Patterns: Wiley; 2013.
13. Buchmann JA. Introduction to Cryptography: Springer; 2004. [doi: 10.1007/978-1-4419-9003-7]
14. Shah MA, Hellerstein JM, Brewer E. Highly available, fault-tolerant, parallel dataflows. Presented at: SIGMOD '04: Proceedings of the 2004 ACM SIGMOD International Conference on Management of Data; Jun 13-18, 2004; Paris France p. 827-838. [doi: 10.1145/1007568.1007662]
15. Uday P, Marais K. Designing resilient systems‐of‐systems: a survey of metrics, methods, and challenges. Syst Eng 2015 Oct;18(5):491-510. [doi: 10.1002/sys.21325]
16. Adashi EY, O'Mahony DP, Cohen IG. The privacy of reproductive health care data: a critical Health Insurance Portability and Accountability Act of 1996 Update. J Womens Health (Larchmt) 2025 Sep;34(9):1061-1063. [doi: 10.1089/jwh.2025.0036] [Medline: 39916505]
17. Podrecca M, Culot G, Nassimbeni G, Sartor M. Information security and value creation: the performance implications of ISO/IEC 27001. Comput Ind 2022 Nov;142:103744. [doi: 10.1016/j.compind.2022.103744]
18. Khan NE, Rudman RJ. IoT medical device risks: data security, privacy, confidentiality and compliance with HIPAA and COBIT 2019. S Afr J Bus Manag 2025;56(1):4796. [doi: 10.4102/sajbm.v56i1.4796]
19. Möller DP. NIST cybersecurity framework and MITRE cybersecurity criteria. In: Möller DP, editor. Guide to Cybersecurity in Digital Transformation: Trends, Methods, Technologies, Applications and Best Practices: Springer; 2023:231-271. [doi: 10.1007/978-3-031-26845-8_5]
20. Ley 19628: sobre proteccion de la vida privada. Biblioteca del Congreso Nacional de Chile. URL: https://www.bcn.cl/leychile/navegar?idNorma=141599 [accessed 2025-11-17]
21. Turner S. Transport layer security. IEEE Internet Comput 2014;18(6):60-63. [doi: 10.1109/MIC.2014.126]
22. Macrin S. The General Data Protection Regulation (GDPR): a landmark in privacy law. SSRN Journal 2025. [doi: 10.2139/ssrn.5078893]
23. Saripalle R, Runyan C, Russell M. Using HL7 FHIR to achieve interoperability in patient health record. J Biomed Inform 2019 Jun;94:103188. [doi: 10.1016/j.jbi.2019.103188] [Medline: 31063828]
24. Poleto T, Oliveira RCP, Silva ALB, Carvalho VDH. Using fuzzy cognitive map approach for assessing cybersecurity for telehealth scenario. In: Trends and Innovations in Information Systems and Technologies: Springer Cham; 2020:828-837. [doi: 10.1007/978-3-030-45691-7_78]
25. Vidanagamachchi S, Mallikarachchi S. Exploring privacy and security concerns in Sri Lankan telemedicine systems: a patient-centric self-assessment. Sri Lankan J Appl Stat 2024;3(1):15-22 [FREE Full text]
26. Poleto T, Silva MM, Clemente TRN, de Gusmão APH, Araújo APDB, Costa APCS. A risk assessment framework proposal based on bow-tie analysis for medical image diagnosis sharing within telemedicine. Sensors (Basel) 2021 Apr 1;21(7):2426. [doi: 10.3390/s21072426] [Medline: 33915932]
27. Zhou L, Thieret R, Watzlaf V, Dealmeida D, Parmanto B. A telehealth privacy and security self-assessment questionnaire for telehealth providers: development and validation. Int J Telerehabil 2019;11(1):3-14. [doi: 10.5195/ijt.2019.6276] [Medline: 31341542]

Abbreviations

HIPAA: Health Insurance Portability and Accountability Act

Edited by A Coristine; submitted 13.05.25; peer-reviewed by KF Rafat, M Dieguez-Rebolledo; revised version received 18.10.25; accepted 21.10.25; published 21.11.25.

Please cite as:
Marquez G, Pacheco M, Vergara P, Liberona F, Chomalí M, Rojas E
The State of Practice About Security in Telemedicine Systems in Chile: Exploratory Study
JMIR Med Inform 2025;13:e77395
URL: https://medinform.jmir.org/2025/1/e77395
doi:10.2196/77395

XSL•FO
RenderX

© Gaston Marquez, Michelle Pacheco, Priscilla Vergara, Felix Liberona, May Chomalí, Eric Rojas. Originally published in JMIR Medical Informatics (https://medinform.jmir.org), 21.11.2025. This is an open-access article distributed under the terms of the Creative Commons Attribution License (https://creativecommons.org/licenses/by/4.0/), which permits unrestricted use, distribution, and reproduction in any medium, provided the original work, first published in JMIR Medical Informatics, is properly cited. The complete bibliographic information, a link to the original publication on https://medinform.jmir.org/, as well as this copyright and license information must be included.

XSL•FO
RenderX

Medical Science Data Value Evaluation Model: Mixed Methods Study

Dandan Wang[1*], BE, MM, PhD; Yaning Liu[2*], BM, MM

[1]Business School, Henan University of Science and Technology, Luoyang, China

[2]School of Economics and Management, Guangzhou University of Applied Science and Technology, 20 Fengle Road, Lianhua Town, Dinghu District, Zhaoqing, Guangdong Province, China

[*]all authors contributed equally

Corresponding Author:
Yaning Liu, BM, MM
School of Economics and Management, Guangzhou University of Applied Science and Technology, 20 Fengle Road, Lianhua Town, Dinghu District, Zhaoqing, Guangdong Province, China

Abstract

Background: Medical science data hold significant value, and open platforms play a crucial role in unlocking this potential. While relevant platforms are being developed, the overall usage of these data values remains limited.

Objective: This study aims to propose a set of practical and effective data value evaluation processes and methods for medical science data open platforms, enabling them to manage and unlock the value of these data.

Methods: Integrating the information system success model, technology acceptance model, and consumer perceived value theory, a set of medical science data value assessment index systems was developed by adopting the literature review and expert survey methods. Data from 10 domestic and international open platforms were collected and empirically analyzed using the entropy-weighted Technique for Order Preference by Similarity to Ideal Solution technique.

Results: Based on the scores of each indicator, the intragroup correlation coefficient was calculated to be 0.489, indicating consistency in the evaluation. The highest information entropy values and weights determined using the entropy weighting method were the number of datasets (0.70, 17.68%), data timeliness (0.77, 13.44%), search comprehensiveness (0.78, 12.92%), and system responsiveness (0.80, 11.55%), respectively. Based on the weighted analysis, the platform with the highest overall score was the National Population Health Sciences Data Center, with a score of 62.32.

Conclusions: The evaluation index system and model developed can be used not only to optimize the platform's data value evaluation processes, but also to enhance the platform's overall data value and encourage users to reuse data.

(JMIR Med Inform 2025;13:e63544) doi:10.2196/63544

KEYWORDS

value evaluation model; medical informatics; open platform; health medicine; scientific data

Introduction

Background

Medical science data refer to data generated through basic and applied research, experimental development, as well as raw and derived data obtained through observation, monitoring, inspection, and testing [1]. These data include electronic health records, long-term treatment outcome data, experimental drug performance data, and wearable device data. Medical science data are considered a strategic resource, offering significant scientific benefits such as reducing research costs, accelerating the research process, improving research quality, and increasing the impact of data [2]. For example, electronic health records can not only help doctors make diagnostic and treatment decisions more accurately and quickly, but also assist patients in understanding their own health status and promoting self-management.

According to investigations, approximately 469 and 750 medical science data platforms have been registered on FAIRsharing and Re3data, respectively [3,4]. Despite such widespread availability, user survey reports indicate that the usage and downloads of many platforms are far lower than expected. This gap stems from users' insufficient awareness of the research field and potential benefits. For example, clinicians still rely heavily on experience and traditional methods for clinical decision-making rather than using data-driven analytical tools. The public perceives medical data as overly specialized, thus overlooking its importance. Platforms often fail to demonstrate the value of data in an understandable and user-friendly way, making it difficult for users to grasp its practical applications.

XSL•FO
RenderX

Existing open health care platforms have challenges such as limited open sharing of data, low standardization, poor data quality, insufficient value mining, insufficient privacy protection, and low usage. The main reason behind these challenges is the inability of both platforms and users to objectively quantify the potential value of data. Platforms suggest identifying the key factors in the formation of data value and allocating resources effectively, while users are unable to carry out data activities based on the true value of data.

Prior Work

In the past, scholars have assessed the value of data in different scenarios, including the assessment of enterprise data value in business contexts [5,6], the evaluation of government data [7,8], and social media data [9] in nontransactional scenarios. Given that platform data are more readily accessible, research has increasingly focused on assessing the value of data from platforms. In terms of assessment theories and perspectives, assessment is usually conducted from the accounting perspective, stakeholder perspective [10], data life cycle or data value chain perspective [11], data traceability perspective [12], and seldom adopts a comprehensive perspective or innovative theories. In terms of evaluation content and methods, the valuation of intangible assets [13,14] typically uses approaches such as the cost method, market method, and income method, with a focus on data value components such as cost and income. In recent years, scholars have introduced revenue monetization, impact-based approaches, experimental and survey techniques, comprehensive multiattribute evaluation, and intelligent methods, which emphasize evaluation from multiple value dimensions and factors affecting data value [15-17].

Medical science data are rich and sensitive enough to generate valuable scientific insights, but the assessment of their value remains fragmented. Initially, Wang and Strong [18] proposed one of the most widely used frameworks for assessing data quality, but due to the complexity of the data quality concept, there is still no consensus on its measurement. Given that different types of data apply to different contexts, they cannot be assessed with a one-size-fits-all approach [19]. Scholars have made significant efforts to assess the value of research data. For example, Schmidt et al [20] developed a framework for assessing the quality of research data. Uribe et al [21] assessed the quality of research data based on the FAIR (Findable, Accessible, Interoperable, and Reusable) principle. Regarding the quality of health care data or information, Feder [22] summarized the dimensions and methods for assessing the quality of EHR data. Kim et al [23] proposed a conceptual model for the quality of health care data. Zhang and Trace [24] explored the quality of self-tracking data. Lasim et al [25] identified accuracy, timeliness, completeness, and consistency as key dimensions for assessing the quality of health care data. Wu et al [26] described the quality of health data in terms of dataset quality, descriptive data quality, and metadata quality.

This study assesses the value of medical science data on open platforms based on an integrated perspective and using a combination of qualitative and quantitative methods, aiming to fill the gaps in existing research.

Objective

This study aims to construct the index system and model of medical science data value assessment from the perspective of the platform and propose the optimization process of data value assessment and data value enhancement strategy. Specifically, the medical science data open platform includes a medical science data resource base and a knowledge base. The platform perspective refers to analyzing and understanding the role, value, and function of the platform in a specific ecosystem from the perspectives of the platform's overall architecture, functional design, and interaction with users, data, and other stakeholders.

The questions to be addressed are as follows: (1) How to construct the medical science data value assessment index system and assessment model? (2) How much do different assessment dimensions and indicators contribute to the value of medical science data? (3) How scientific and usable are the constructed assessment models?

Methods

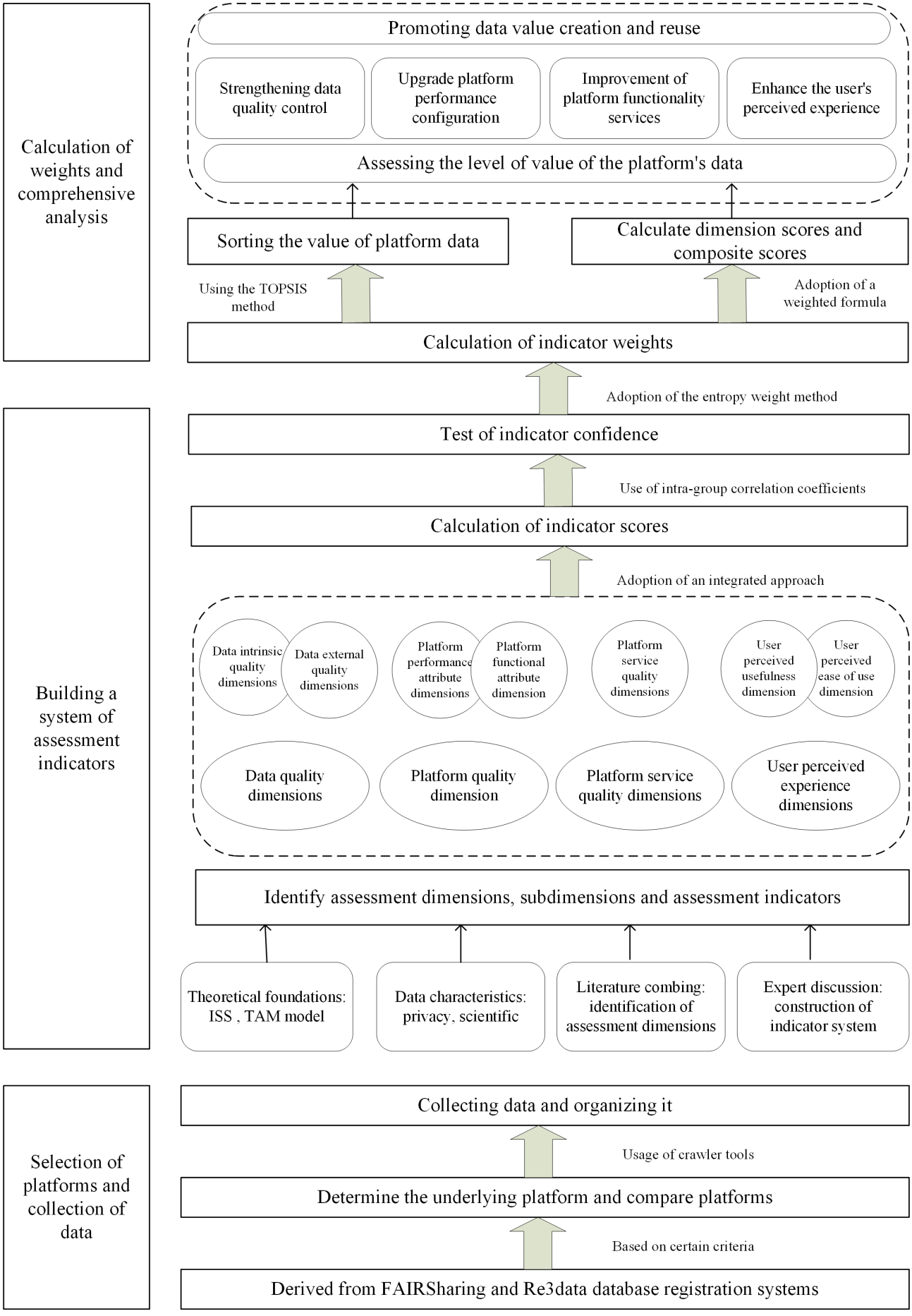
Study Design

The key steps in this process include developing an assessment index system, calculating weights, and conducting comprehensive analyses, which are as follows:

1. Determination of the assessment subject: a selection of domestic and international platforms was chosen as subjects for comparison, using FAIRsharing and Re3data as primary sources, with large datasets serving as standards. These data resources were mined using web scraping tools to provide the foundation for calculating indicator weights.
2. Development of the assessment indicator system: drawing on the theoretical model, a review of the literature, and the characteristics of the data, the initial set of assessment indicators was identified. The indicator system was refined through expert evaluation, with manual verification and other methods used to assess indicator scores and validate their reliability using the intraclass correlation coefficient (ICC).
3. Collection of indicator weights: the entropy weight method was used to determine the weights of the indicators. For a comprehensive evaluation, the Technique for Order Preference by Similarity to Ideal Solution method was applied. The weighted scores were then used to calculate the overall data value of each platform. This model aids platforms in quantifying the potential value of their data, assessing data quality, and enhancing control mechanisms. The study design is presented in Figure 1.

XSL•FO
RenderX

Figure 1. Model for assessing the value of medical science data. TOPSIS: Technique for Order Preference by Similarity to Ideal Solution.

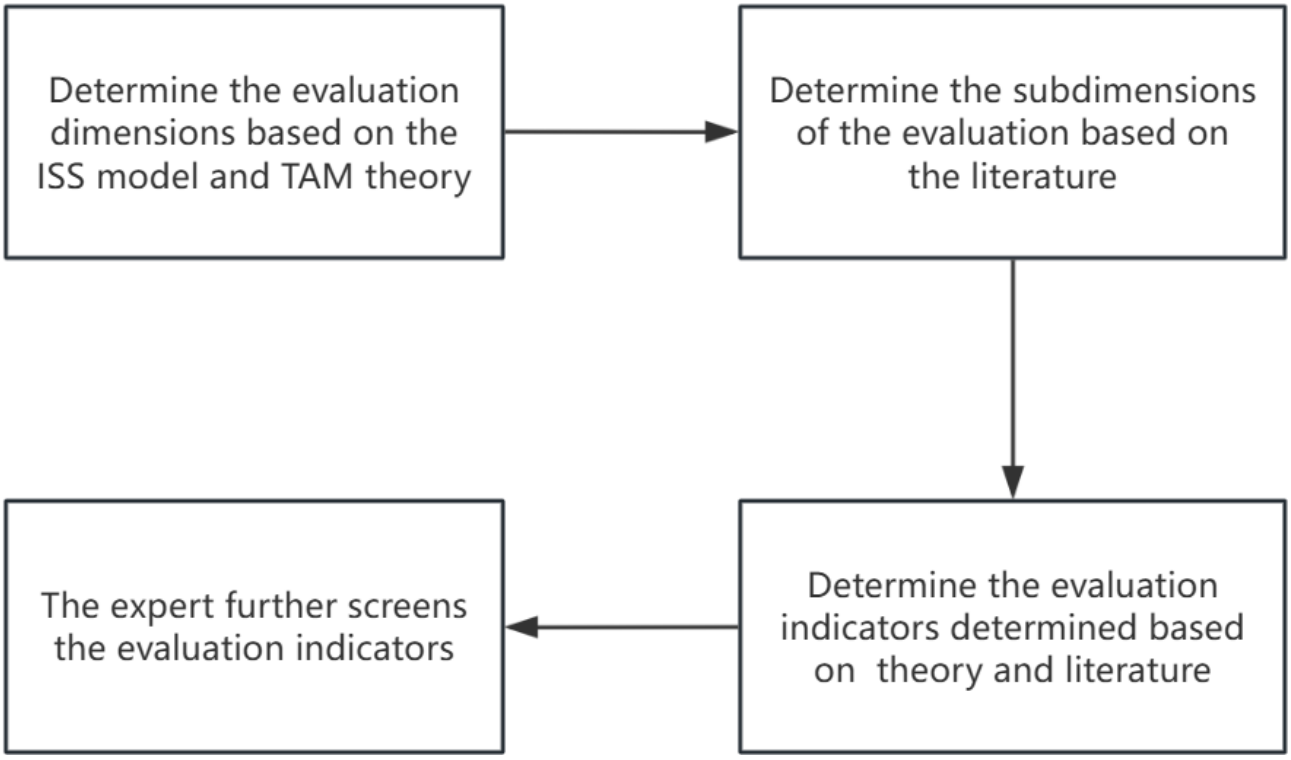


XSL•FO
RenderX

Construction of the Indicator System

Figure 2 shows the steps to build the evaluation index system.

Figure 2. Steps to construct an evaluation value indicator system. ISS: information systems success; TAM; technology acceptance model.



Assessment Framework Construction

The formation of the potential value of the data mainly relies on the platform, and the user is the platform experiencer and data user, who will develop specific subjective cognitions while using the platform data and will give an overall evaluation of the platform's data value. As a result, medical science data value can be defined as the perceived value generated by users in the process of discovering, acquiring, manipulating, and reusing medical science data captured and organized by the platform, involving data, platform, and user dimensions. The data dimension directly assesses data value, while the platform and user dimensions indirectly assess data value.

This study constructs an evaluation theoretical framework based on the information systems success model (ISSM), the technology acceptance model (TAM), and the theory of perceived value of users. An open platform can be regarded as an information system, so the influence factors of data value realization can be analyzed using ISSM. However, because ISSM focuses on analyzing the influence of the data and platform dimensions on the user's net benefit (perceived value), it is integrated with TAM to supplement the influence of the user dimension on the user's net benefit.

As shown in Figures 3 and 4, in ISSM, 3 factors—information quality, system quality, and service quality—affect users' willingness to use. In TAM, the user's perceived usefulness and perceived ease of use will also affect the user's attitude. Therefore, the dimensions of information quality, system quality, service quality, perceived usefulness, and perceived ease of use were selected to evaluate the value of data.

XSL•FO
RenderX

Figure 3. Information systems success model.

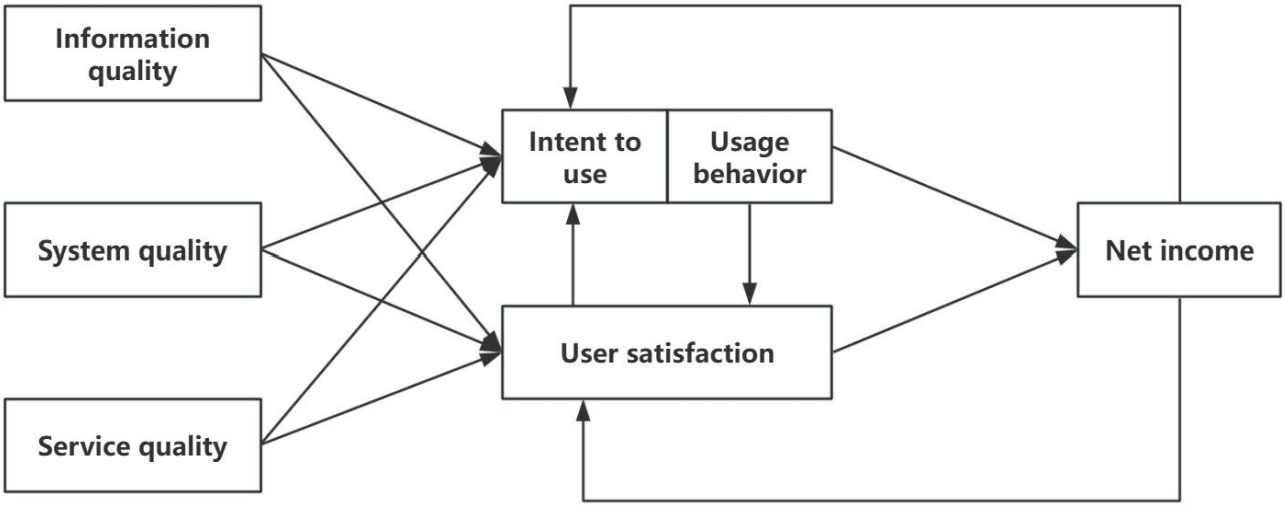


Figure 4. Technology acceptance model.

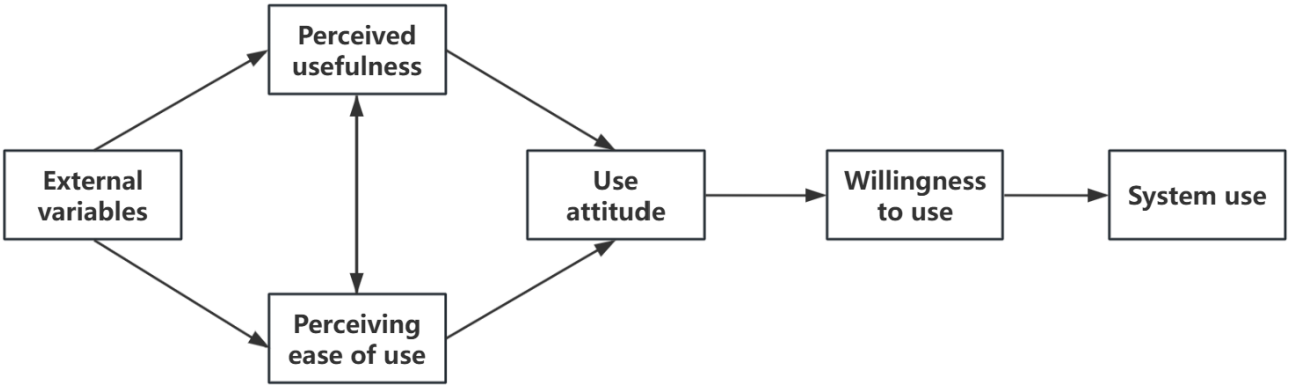


Table 1 illustrates the dimensions of each theory and their unique role in the model.

In this framework, good data quality ensures that users have access to high-quality data resources; good platform quality and platform service quality ensure access to perfect infrastructure and services; and perceived usefulness and ease of use ensure motivation to use the data. All 5 dimensions influence users' willingness to use the system and their behaviors, which stimulates the formation of data value.

Table . Theoretical dimension action table.

Theoretical model	Assessment dimensions	Unique role
ISSM[a]	• Information quality: data quality • System quality: platform quality • Quality of service: platform service quality	Evaluate the objective attributes of the data (eg, accuracy and completeness), stability of the technology platform, and effectiveness of support services.
TAM[b]	• User-perceived usefulness • User-perceived ease of use	Measure the user's subjective perception of the value of the data for their research or practice, and the impact of the platform's ease of use on willingness to use.
Consumer-perceived value theory	• Final value assessment	Integrate objective quality and subjective perception to form the user's overall judgment of the value of the data (eg, willingness to pay and willingness to recommend).

[a]ISSM: information systems success model.

[b]TAM: technology acceptance model.

Selection of Assessment Indicators

Based on the principles of objectivity, systematicity, and scientific rigor, this study identifies 5 dimensions: data quality, platform quality, platform service quality, user-perceived usefulness, and ease of use. The data quality dimension is subdivided into the quality of intrinsic data attributes and extrinsic attributes, while platform quality is subdivided into platform performance and functional attributes. Combined with

XSL•FO
RenderX

the literature research, specific assessment indicators were identified under each dimension.

Screening of Assessment Indicators

The Delphi method was used to construct the medical data assessment system. Thirteen cross-disciplinary experts (5 data assessment experts, 4 medical informaticians, and 4 clinicians) were invited to conduct 3 rounds of iterative review to screen the indicators based on a 5-level Likert scale (retention thresholds: mean ≥3.0 and SD <1.0). The data accuracy indicator was removed due to overlap with data integrity, and new indicators related to service confidentiality, assurance, and other medical-specific characteristics were added, resulting in a 5D, 35-indicator system, with complete definitions provided in Table 2 and Multimedia Appendix 1.

Table . Indicator framework for assessing the value of medical science data.

Dimension and source	Subdimension	Indicators
Data quality		
Saxena [8]	Quality of intrinsic data attributes	• Number of datasets • Data integrity • Data comprehensiveness • Data timeliness • Data authenticity
Zhang and Trace [24]	Quality of data external attributes	• Data consistency • Machine readability • Format openness • Data understandability
Platform quality		
Wu et al [26]	Quality of platform performance attributes	• System stability • System security • System responsiveness • System compatibility • Interface friendliness • Linguistic diversity
Martin et al [27]	Platform functional attributes	• Platform infrastructure • Platform overview function • Platform guidance function • Data access function • Results display function • Comprehensiveness of functions
Platform service quality		
Azeroual et al [28]	Quality of platform services	• Service interactivity • Service personalization • Service accessibility • Service confidentiality • Service assurance • Search comprehensiveness
User-perceived usefulness		
Imran and Ahmad [29]	User-perceived usefulness	• Relevance • Usefulness • Uniqueness • Novelty
User perceived ease of use		
Imran and Ahmad [29]	User perceived ease of use	• Findable • Accessible • Interoperable • Reusable

XSL•FO
RenderX

Empirical Analysis

Sample Platform Selection

China's open platforms for medical and scientific data boast several advantages, including "large data volume, diverse data sources, and high data quality." However, they also face challenges such as "an overemphasis on data security, limited data sharing, and reliance on a single data-providing organization." The sample platforms were screened from authoritative websites such as Re3data.org and FAIRsharing. The selection criteria required that the platforms be open and stable, provide basic data, regularly update content, offer comprehensive functionality, and demonstrate mature construction. The selection process for the sample platform is shown in the Multimedia Appendix 2. Table 3 lists the selected platforms, and data collection was conducted using Octopus (Shenzhen Digital Broad Information Technology Co).

Table . Overview of the 10 sample platforms selected for this study.

Nation	Name of platform	Developer	Data resource
China	National Population Health Sciences Data Center (NCMI)	Institute of Medical Information, Chinese Academy of Medical Sciences	Population health science data
China	GigaDB Database	Beijing Institute of Genomics, Chinese Academy of Sciences	Biological and biomedical field data
China	GSA[a] for Human	National Genomics Data Center (NGDC)	Raw data on human genetic resources genomics
United States	National Addiction and HIV Data Archive Program (NAHDAP)	Inter-University Consortium for Political and Social Research (ICPSR)	Data from research related to drug addiction and HIV
United States	PhysioNet	Massachusetts Institute of Technology (MIT)	Physiological and clinical data
Multinational	MGnify	European Bioinformatics Institute (EMBL-EBI)	Microbiome data and macrogenomic data
United States	OpenNeuro	Stanford University	Brain imaging datasets
United States	Immunology Database and Analysis Portal (ImmPort)	National Institute of Allergy and Infectious Diseases (NIAID)	Clinical and basic research data
Multinational	BioImage Archive	European Bioinformatics Institute (EMBL-EBI)	Bioimaging data
Multinational	EBRAINS	Human Brain Project (HBP)	Brain research data

[a]GSA: Genome Sequence Archive.

Calculation of Indicator Scores

The indicators can be divided into three categories: (1) simple indicators, such as the number of datasets and data completeness, can be determined by simple calculations and are suitable for manual checking, 0 - 1 assignment, and mathematical statistics; (2) text-based indicators, such as data comprehensiveness and comprehensibility, necessitate the processing of textual information, such as data categories and data summaries, and are suited for data crawling and text analysis; (3) subjective indicators, such as interface friendliness and relevance, are based on users' subjective feelings and can be calculated using the illumination interview approach. The formulas and results of each indicator are shown in the Multimedia Appendix 3.

Indicator Reliability Tests

The ICC can be used to determine consistency. In this paper, both the differences between different assessment indicators and the differences between different platforms are considered, while systematic errors are not considered. The output results from the Statistical Product and Service Solutions Automatically Using Software are shown in Table 4.

Because the evaluation index scores are processed in advance, the "average measure ICC(C,K)" is used, with an ICC value ranging from 0 to 1. ICC values of more than 0.40 typically indicate good consistency. Table 4 reveals that the final ICC value is 0.489, which is greater than 0.4, indicating that the evaluation's consistency is good and the indicator is reasonable.

XSL•FO
RenderX

Table . Results of correlation coefficients within intraclass correlation coefficient groups.

Bidirectional mixing and randomization consistency	ICC[a] (95% CI)
Single metric ICC(C[b],1[c])	0.027 (−0.003 to 0.137)
Average metric ICC(C,K)[d]	0.489 (−0.101 to 0.848)

[a]ICC: intraclass correlation coefficient.

[b]C denotes consistency.

[c]1 denotes a single measure.

[d]K denotes an average measure.

Calculation of Indicator Weights

The entropy weight approach is appropriate for dealing with the problem of multi-indicator empowerment because it can handle the interplay between various elements while also considering the correlation between different indicators. Its specific steps include (1) data standardization, (2) calculation of the ratio of each indicator in each scheme, (3) calculation of the information entropy of each indicator, (4) calculation of the weight of each indicator through the information entropy value, and (5) calculation of the comprehensive score of each scheme. Multimedia Appendix 4 shows the weights of the complete indicators derived from the entropy weight method.

Ethical Considerations

This study did not require formal ethics committee review, as it exclusively analyzed publicly accessible platform interfaces, technical documentation, and aggregated system-level characteristics, without the collection of identifiable human data. This exemption aligns with the National Health Commission of China Regulations, Article 24, which states: "Ethics review may be waived for studies using publicly available data or records where individuals cannot be identified, and the research does not interact with human participants." It also aligns with the JMIR policy on nonhuman participants research, which states: "Ethics approval is not required for studies evaluating technology systems, public documentation, or organizational practices where human participants are neither involved nor identifiable."

Results

Comprehensive Analysis

To determine the optimal and worst solutions, the positive and negative ideal solution distances and relative proximity were calculated, as shown in Table 5. From Table 5, it can be seen that the National Population Health Sciences Data Center (NCMI; Institute of Medical Information, Chinese Academy of Medical Sciences) has the highest data value, which is close to the ideal level and serves as a valuable benchmark for other platforms.

Table . Technique for Order Preference by Similarity to Ideal Solution (TOPSIS) evaluation calculations.

Platform	Distance to positive ideal solution, D^+ (unit:fraction)	Distance to negative ideal solution, D^- (unit:fraction)	Relative proximity, C (dimensionless)	Sort result
NCMI[a]	17.384	22.253	0.561	1
GigaDB	25.848	5.021	0.163	8
GSA[b] for Human	22.135	14.685	0.399	3
NAHDAP[c]	27.571	3.289	0.107	10
PhysioNet	25.939	6.400	0.198	7
MGnify	18.945	15.405	0.448	2
OpenNeuro	24.785	12.671	0.338	5
ImmPort	24.143	9.990	0.293	6
BioImage Archive	26.479	4.795	0.153	9
EBRAINS	23.127	14.120	0.379	4

[a]NCMI: National Population Health Sciences Data Center.

[b]GSA: Genome Sequence Archive.

[c]NAHDAP: National Addiction and HIV Data Archive Program.

The weighted formula was used to calculate the scores and composite scores for the different dimensions of data value for each platform:

$$(1)\text{Score}(Pij)=\sum wkXk$$

$$(2)\text{Score}(Pi)=\sum j=17wj\text{Score}(Pij)$$

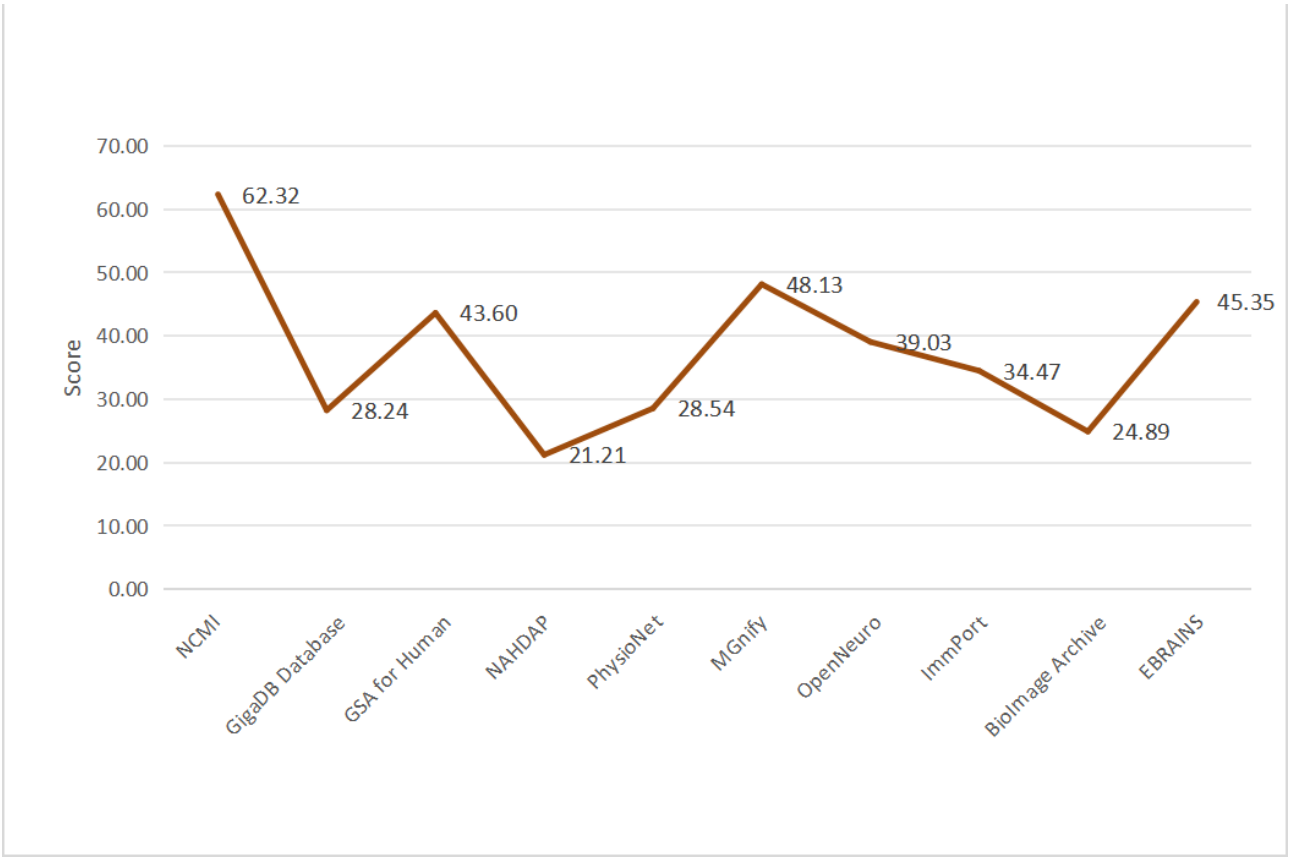
Where i denotes the ith platform, j the jth dimension, and k the kth indication. Score (P) reflects the data value score of the jth dimension of the ith platform, as well as the platform's

XSL•FO
RenderX

overall data value score. Figures 5 and 6 show the differences between each platform's data value by dimension and their comprehensive scores.

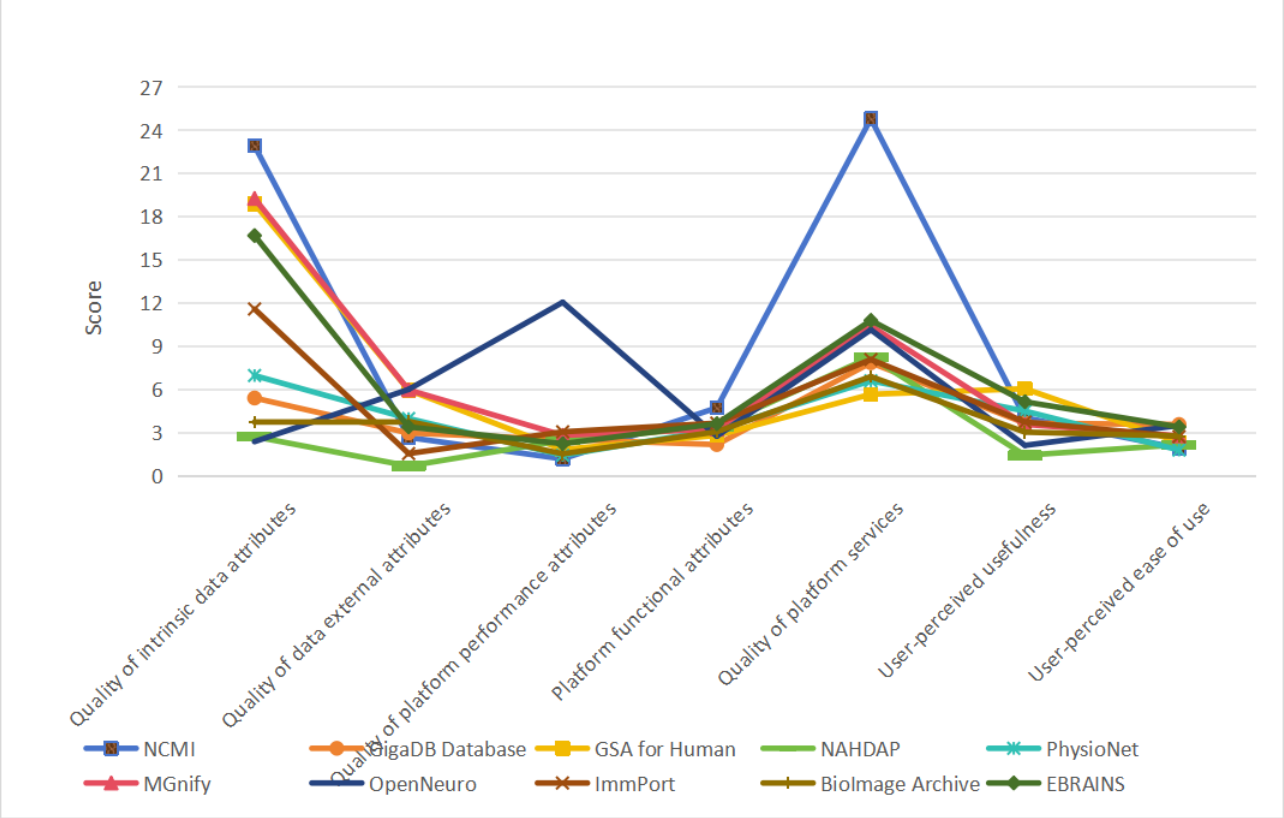
As shown in Figures 5 and 6, there are large differences in data value across the dimensions of intrinsic attribute quality, extrinsic attribute quality, platform service quality, and perceived usefulness. The average score of the platforms is 37.579, with NCMI, MGnify (European Bioinformatics Institute), EBRAINS (Human Brain Project), GSA for Human (National Genomics Data Center), and OpenNeuro (Stanford University) scoring higher than the average, reflecting good overall performance.

Figure 5. Line graph of data value dimension scores for each platform. GSA: Genome Sequence Archive; NAHDAP: National Addiction and HIV Data Archive Program; NCMI: National Population Health Sciences Data Center.



XSL•FO
RenderX

Figure 6. Line graph of the composite data value score of each platform. GSA: Genome Sequence Archive; NAHDAP: National Addiction and HIV Data Archive Program; NCMI: National Population Health Sciences Data Center.



Model Validation

The evaluation reveals that (1) Chinese platforms demonstrate data quality strengths but require improvements (eg, NCMI shows slow updates and low availability of machine-readable format; GSA lacks completeness in data attributes/types), (2) platform functionality favors NCMI for comprehensiveness, while OpenNeuro leads in responsiveness, (3) service quality analysis shows NCMI's advantages in personalization and search capability; however, all platforms need enhancements in service assurance and confidentiality, (4) GSA excels in content novelty/relevance despite overall low data utility across platforms, and (5) GiagDB demonstrates strong usability despite partial FAIR compliance. The model successfully identifies critical gaps in China's platform data management and proposes targeted optimization pathways, thereby validating its scientific rigor.

Discussion

Principal Findings

This study establishes a novel medical data valuation framework through a 3D (data-platform-user) analysis, integrating service privacy metrics. By combining qualitative and quantitative methods, the hybrid approach reduces subjectivity bias, generating an evaluation model that enables data value quantification and personalized management strategies.

Comparing the results of government data value assessment, the following conclusions can be drawn: (1) indicators related to the data itself, such as the number of datasets, data timeliness, and machine readability, as well as indicators such as system responsiveness and service interactivity, are considered very important, (2) compared with government data, medical science data is private and scientific, so the weight of indicators such as service security, service confidentiality, accessibility, and reusability are more prominent, and (3) in the process of data value realization, the data itself have potential value, but their actual realization requires further development, so indicators related to platform quality and platform service quality, such as search comprehensiveness and service personalization, are also crucial.

Model Application

Optimize the Process of Assessing the Value of Platform Data

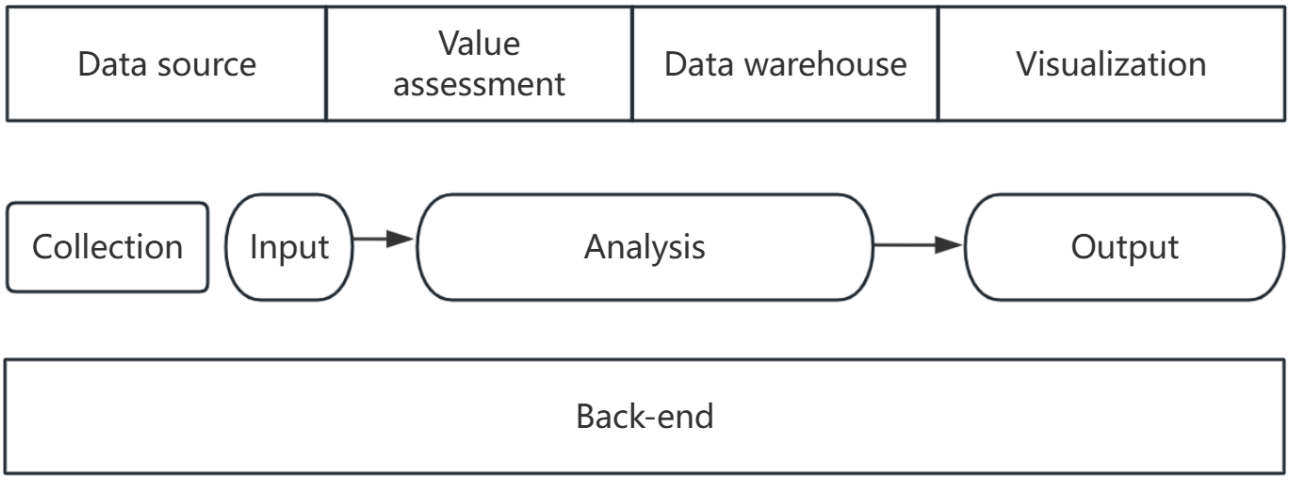
1. To assist platforms in efficiently assessing data value and formulating management strategies, this study proposes two practical solutions based on the established evaluation index system: (1) designing a universal self-assessment tool, leveraging the international Confederation of Open Access Repositories (COAR) community framework to enable convenient self-evaluation; and (2) developing an intelligent assessment system that enhances evaluation efficiency by integrating automation technologies with human intervention. These solutions synergistically advance data value assessment from theoretical frameworks to practical implementation.
2. Design of a generic self-assessment tool: the COAR, an international association that brings together repositories from around the world to build a global network of

XSL•FO
RenderX

knowledge repositories, has developed a global COAR Community of Good Practice for Repositories framework designed to help repositories in different regions and of different types evaluate and improve their practices [30]. In November 2023, the COAR Asia OA Webinar, based on the COAR community framework, proposed the survey toolkit—a self-assessment tool for repository development that asks repositories to answer 60 questions to assess their practices and identify areas for improvement. Repositories that provide affirmative responses to all "Essential" questions are awarded a digital badge, which can be displayed on their websites [31]. Drawing inspiration from these examples, this study can also propose a data value self-assessment tool, which will undergo iterative updates and refinements based on feedback and usage.

3. Development of an automated assessment system: creating automated and semiautomated assessment tools can improve the accuracy and efficiency of assessments. Blacketer et al [32] created the data quality dashboard, an open-source R package to evaluate the quality of observational health care data and indicate potential data quality issues by merging the Data General Model with established data quality assessment methodologies. The architecture of the automated data value assessment system (Figure 7) should cover the modules of input, analysis, output, and back-end, and the assessment of the implementation process should include several aspects: the data source, data quality assessment model, and data warehouse. Therefore, analyzing the data value of the platform should be done systematically and configured with automated assessment procedures and methods, tools, and software.

Figure 7. Architecture of the data value assessment system.



The automated assessment of data value faces a double challenge: at the technical level, it needs to break through data dependency, cross-domain generalization bottlenecks, and algorithmic interpretability defects; at the ethical level, it must construct a privacy-informed dynamic balancing mechanism that controls leakage risk through differential privacy and federated learning, and embeds fairness checking modules to eliminate group bias.

Multidimensional Improvement of the Data Value of the Platform

To advance medical data platforms holistically, this study proposes a multifaceted enhancement strategy spanning four critical dimensions: implementing dual-track data quality control (source integration and FAIR-aligned standardization), upgrading platform performance functionality through technical optimization and value-visualization tools, establishing a tripartite privacy governance framework (organizational-management-technical), and constructing user-centric service ecosystems with demand-driven customization and collaborative training.

A dual strategy is needed to improve data quality. First, a mechanism should be established for data aggregation from multiple sources, including integration of data resources from research institutions, development of unified classification standards, and implementation of update cycles to maintain data currency. Second, data presentation format should be standardized by mandating the use of machine-readable formats, ensuring metadata completeness, and aligning attribute descriptions with the FAIR principles. Technically, intelligent quality control tools can be integrated, such as an RNA-Seq data cleaning algorithm [33], to automatically filter contaminated data.

The quality of the platform must be improved in both directions through performance and functionality: the technical side adopts resource compression algorithms and multilevel content delivery network caching to ensure that page loading time is reasonable; the functional side builds a data value visualization system (dynamic leaderboards/timing trend charts) and integrates data challenges and health apps to improve the usage rate. The platform needs to expand higher-order functional modules (eg, thematic data aggregation, blockchain traceability verification, and knowledge graph mining), build a full-cycle service system (training-consultation-feedback closed-loop), and improve the effectiveness of data usage through intelligent operation and maintenance optimization.

In terms of data services, the platform can draw on the Tencent Foraging Open Experimental Platform (jointly developed by Tencent Cloud and a team from Tencent's Medical AI Lab) to build a comprehensive intelligent service system for medical imaging research application scenarios. This includes data

XSL•FO
RenderX

management and labeling, algorithm training, testing, and application. In addition, medical data privacy protection needs to build an organization-management-technology synergistic system: set up an ethical review committee at the organizational level and formulate a GDPR (General Data Protection Regulation)-compatible privacy agreement, implement k-anonymization and homomorphic encryption technology at the management level, and deploy a federal learning framework at the technical level to achieve data availability and invisibility. Given the existing problems, such as the disconnection between privacy algorithms and scenarios, and the shortcomings of a single level of protection, it is recommended that we borrow the concept of the United Kingdom's "five safe" to build a trinity of protection systems for "data-people-environment," and synchronize the development of a multilayered architectural platform similar to the MNSSp3, so that we can balance the value of medical research with individual privacy rights and interests [34]. The platform needs to build a user-centered service system. First, it should build a demand portrait based on collaborative filtering algorithms, collect user feedback on time, dynamically adjust the data opening strategy, realize the accurate push of high-value data, establish a grading model of user capabilities, and provide differentiated data service interfaces. Second, the platform should unite with academic institutions to create a modular training system, integrate multidimensional education scenarios such as workshops, internet-based communities, and data competitions, break through the traditional one-way training model, and improve users' data reuse capabilities. It can draw on the World Health Organization (WHO) to create automated tools and regional customized training experiences [35].

Limitations

This study acknowledges three principal methodological constraints that warrant consideration when interpreting the findings:

1. Indicator subjectivity: the construction of the indicator system and the scoring of certain indicators are more subjective, which may introduce assessment bias. The expert survey method was used to discuss and screen the indicators, and the ICC method was used to test the consistency of the assessment; the ICC value is 0.489, indicating that the consistency is at a medium level. This may be due to the differences among evaluators, overly complex measurement dimensions, or a small sample size. This issue can be improved by clarifying the scoring criteria, revising the scale, and increasing the sample size.
2. Sample coverage: the current empirical evidence covers 10 platforms. Although the number of sample platforms selected is relatively limited, it covers mainstream medical data types and has a certain selection basis (refer to Multimedia Appendix 2 for details). A follow-up study is planned to expand the number of sample platforms and include European medical science data platforms.
3. Limitations of value dimension: data value assessment is carried out along the mechanism of "value perception and identification→value realization→value assessment→data governance." However, this paper focuses on the assessment of perceived value and does not involve the mechanism of value realization. The next step is to construct a data trust assessment framework, develop value stream analysis tools, and explore collaborative governance models.

Comparison With Prior Work

At the theoretical level, this study broadens the perspectives, objects, and methods of data value assessment research and refines the strategies for value enhancement of medical science data on open platforms. At the practical level, the assessment model developed in this study can not only help platforms reasonably quantify the potential value of data, identify key factors in the formation of data value, discover deficiencies in data collection and organization, formulate data investment decisions and openness plans, and promote the effective allocation of data resources; it can also help users recognize the potential benefits of the data on the platforms and better use the data resources in their data activities, and help countries to understand the benefits of open medical science data to optimize data regulations and systems.

Conclusions

This study focuses on assessing the value of medical science data from the perspective of platforms, and the results of the study include (1) a data value assessment index system with 5 dimensions and 35 indicators was created by using ISSM, TAM, and the theory of perceived value of consumers, which is scientific, (2) 10 open platforms were selected, data were collected through Octopus and empirically examined using the entropy weight Technique for Order Preference by Similarity to Ideal Solution method, and the assessment model was established and scientifically verified, and (3) the practical application of the proposed model can not only optimize the data value assessment process, but also enhance the data value of the platform from multiple dimensions.

Acknowledgments

With the emphasis on the value of medical science data and the development of related platforms in full swing, it is critical to assess the value of medical science data from a platform viewpoint, which may assist platforms in managing data and unlocking data value. As a result, this research has emerged. The author would like to extend gratitude to every expert who took part in our research, since their insights substantially improved our findings.

Conflicts of Interest

None declared.

XSL•FO
RenderX

Multimedia Appendix 1
Indicator framework for assessing the value of medical science data.
[DOCX File, 21 KB - medinform_v13i1e63544_app1.docx]

Multimedia Appendix 2
The selection process for the sample platform.
[DOCX File, 148 KB - medinform_v13i1e63544_app2.docx]

Multimedia Appendix 3
The calculation methods and results of the 35 evaluation indicators.
[DOCX File, 28 KB - medinform_v13i1e63544_app3.docx]

Multimedia Appendix 4
Summary of the results of the entropy method of calculating weights.
[DOCX File, 20 KB - medinform_v13i1e63544_app4.docx]

References

1. NIH Data sharing policy and implementation guidance. National Institute of Health. 2022. URL: https://grants.nih.gov/grants/policy/data_sharing/data_sharing_guidance.htm. [accessed 2024-04-06]
2. Soleimani A, Fahim Nia F, Naghshineh N, Soleimani Nejad A. Providing a framework for the reuse of research data based on the development dynamic framework of United Nations Development Program (UNDP). Library Hi Tech 2023 Jun 1;41(2):642-665. [doi: 10.1108/LHT-01-2021-0007]
3. Databases. FAIRsharing.org. 2023. URL: https://fairsharing.org/search?fairsharingRegistry=Database [accessed 2023-05-07]
4. Browse by subject. Re3data.org. 2023. URL: https://www.re3data.org/search?query=&countries%5B0%5D=CHN&page=4 [accessed 2023-05-07]
5. Yonghong L, Kexin Q. Value evaluation on data assets of P2P net loan platform. J Phys Conf Ser 2019 Mar 1;1168(3):032001. [doi: 10.1088/1742-6596/1168/3/032001]
6. Holst L, Stich V, Schuh G, et al. Towards a comparative data value assessment framework for smart product service systems. Presented at: Towards Smart and Digital Manufacturing: IFIP WG 57 International Conference; Aug 30 to Sep 3, 2020; Novi Sad, Serbia. [doi: 10.1007/978-3-030-57997-5_39]
7. Vetrò A, Canova L, Torchiano M, Minotas CO, Iemma R, Morando F. Open data quality measurement framework: definition and application to open government data. Gov Inf Q 2016 Apr;33(2):325-337. [doi: 10.1016/j.giq.2016.02.001]
8. Saxena S. Open government data (OGD) in six Middle East countries: an evaluation of the national open data portals. DPRG 2018 Jul 4;20(4):310-322. [doi: 10.1108/DPRG-10-2017-0055]
9. Shan S, Liu X, Wei Y, Xu L, Zhang B, Yu L. A new emergency management dynamic value assessment model based on social media data: a multiphase decision-making perspective. Enterp Inf Syst 2020 May 27;14(5):680-709. [doi: 10.1080/17517575.2020.1722251]
10. Buteau S, Rao P, Mehta AK, Kadirvell V. Developing a framework to assess socio-economic value of open data in india. 2018 Aug 22 Presented at: OpenSym '18; Aug 22-24, 2018; Paris, France URL: https://dl.acm.org/doi/proceedings/10.1145/3233391 [accessed 2025-07-30] [doi: 10.1145/3233391.3233532]
11. Serhani MA, El Kassabi HT, Taleb I, Nujum A. An hybrid approach to quality evaluation across big data value chain. Presented at: 2016 IEEE International Congress on Big Data (BigData Congress); Jun 27 to Jul 2, 2016; San Francisco, CA URL: https://ieeexplore.ieee.org/xpl/mostRecentIssue.jsp?punumber=7584314 [accessed 2025-07-27] [doi: 10.1109/BigDataCongress.2016.65]
12. Li Z, Ni Y, Gao X, Cai G. Value evaluation of data assets: progress and enlightenment. Presented at: 2019 IEEE 4th International Conference on Big Data Analytics (ICBDA); Mar 15-18, 2019; Suzhou, China. [doi: 10.1109/ICBDA.2019.8713240]
13. Lin Z, Wu Y. Research on the method of evaluating the value of data assets. 2016 Presented at: 2016 International Conference on Education, E-learning and Management Technology; 2016; Xi'an, China. [doi: 10.2991/iceemt-16.2016.95]
14. Rogers WP, Kahraman MM, Dessureault S. Formal assessment and measurement of data utilization and value for mines. Min Metall Explor 2019 Apr;36(2):257-268. [doi: 10.1007/s42461-018-0044-4]
15. What Do We Know About the Value of Data. Global Partnership for Sustainable Development Data. 2018. URL: http://www.data4sdgs.org/news/what-do-we-know-about-value-data [accessed 2023-02-20]
16. What is the value of data? A review of empirical methods. Bennett Institute for Public Policy. 2022. URL: https://www.bennettinstitute.cam.ac.uk/publications/value-of-data [accessed 2023-02-20]
17. Coyle D, Manley A. Potential social value from data: an application of discrete choice analysis. : Bennett Institute for Public Policy, University of Cambridge; 2021 URL: https://www.bennettinstitute.cam.ac.uk/wp-content/uploads/2020/12/Working_paper_Potential_social_value_from_data.pdf [accessed 2025-07-30]

XSL•FO
RenderX

18. Wang RY, Strong DM. Beyond accuracy: what data quality means to data consumers. J Manag Inf Syst 1996 Mar;12(4):5-33. [doi: 10.1080/07421222.1996.11518099]
19. Poeppelmann D, Schultewolter C. Towards a data quality framework for decision support in a multidimensional context. Int J Bus Intell Res 2012 Jan;3(1):17-29 [FREE Full text] [doi: 10.4018/jbir.2012010102]
20. Schmidt CO, Struckmann S, Enzenbach C, et al. Facilitating harmonized data quality assessments. A data quality framework for observational health research data collections with software implementations in R. BMC Med Res Methodol 2021 Apr 2;21(1):63. [doi: 10.1186/s12874-021-01252-7] [Medline: 33810787]
21. Uribe SE, Sofi-Mahmudi A, Raittio E, Maldupa I, Vilne B. Dental research data availability and quality according to the FAIR principles. J Dent Res 2022 Oct;101(11):1307-1313. [doi: 10.1177/00220345221101321] [Medline: 35656591]
22. Feder SL. Data quality in electronic health records research: quality domains and assessment methods. West J Nurs Res 2018 May;40(5):753-766. [doi: 10.1177/0193945916689084] [Medline: 28322657]
23. Kim KH, Choi W, Ko SJ, et al. Multi-center healthcare data quality measurement model and assessment using OMOP CDM. Appl Sci (Basel) 2021;11(19):9188. [doi: 10.3390/app11199188]
24. Zhang Y, Trace CB. The quality of health and wellness self‐tracking data: a consumer perspective. Asso for Info Science & Tech 2022 Jun;73(6):879-891 [FREE Full text] [doi: 10.1002/asi.24591]
25. Lasim OU, Ansah EW, Apaak D. Maternal and child health data quality in health care facilities at the Cape Coast Metropolis, Ghana. BMC Health Serv Res 2022 Aug 30;22(1):1102. [doi: 10.1186/s12913-022-08449-6] [Medline: 36042447]
26. Wu D, Xu H, Yongyi W, Zhu H. Quality of government health data in COVID-19: definition and testing of an open government health data quality evaluation framework. Library Hi Tech 2022 Mar 29;40(2):516-534. [doi: 10.1108/LHT-04-2021-0126]
27. Martin EG, Law J, Ran W, Helbig N, Birkhead GS. Evaluating the quality and usability of open data for public health research: a systematic review of data offerings on 3 open data platforms. J Public Health Manag Pract 2017;23(4):e5-e13. [doi: 10.1097/PHH.0000000000000388] [Medline: 26910872]
28. Azeroual O, Saake G, Wastl J. Data measurement in research information systems: metrics for the evaluation of data quality. Scientometrics 2018 Jun;115(3):1271-1290. [doi: 10.1007/s11192-018-2735-5]
29. Imran M, Ahmad A. Enhancing data quality to mine credible patterns. J Inf Sci 2023 Apr;49(2):544-564. [doi: 10.1177/01655515211013693]
30. COAR community framework for good practices in repositories. COAR. 2022. URL: https://www.coar-repositories.org/coar-community-framework-for-good-practices-in-repositories [accessed 2024-04-01]
31. COAR community framework version 2 - self-assessment. Suvery Tookit. 2023. URL: https://surveytoolkit.ir.rcos.nii.ac.jp/#/enquetes/beef69edb6032b1fd907e3e2e991300b [accessed 2024-04-01]
32. Blacketer C, Defalco FJ, Ryan PB, Rijnbeek PR. Increasing trust in real-world evidence through evaluation of observational data quality. J Am Med Inform Assoc 2021 Sep 18;28(10):2251-2257. [doi: 10.1093/jamia/ocab132] [Medline: 34313749]
33. Zhou Q, Su X, Jing G, Chen S, Ning K. RNA-QC-chain: comprehensive and fast quality control for RNA-Seq data. BMC Genomics 2018 Feb 14;19(1):144. [doi: 10.1186/s12864-018-4503-6] [Medline: 29444661]
34. Wu X, Zhang Y, Wang A, Shi M, Wang H, Liu L. MNSSp3: Medical big data privacy protection platform based on Internet of things. Neural Comput & Applic 2022 Jul;34(14):11491-11505. [doi: 10.1007/s00521-020-04873-z]
35. District data quality assurance: a training package for monthly use of DHIS2 data quality dashboards at district and health facility levels. World Health Organization. URL: https://iris.who.int/handle/10665/365745 [accessed 2024-04-02]

Abbreviations

COAR: Confederation of Open Access Repositories
FAIR: Findable, Accessible, Interoperable, and Reusable
GDPR: General Data Protection Regulation
ICC: intraclass correlation coefficient
ISSM: information systems success model
NCMI: National Population Health Sciences Data Center
TAM: technology acceptance model
WHO: World Health Organization

XSL•FO
RenderX

Edited by C Perrin; submitted 23.06.24; peer-reviewed by H Lehmann, VG Yogeshappa; revised version received 26.05.25; accepted 08.06.25; published 21.08.25.

Please cite as:
Wang D, Liu Y
Medical Science Data Value Evaluation Model: Mixed Methods Study
JMIR Med Inform 2025;13:e63544
URL: https://medinform.jmir.org/2025/1/e63544
doi:10.2196/63544

© Dandan Wang, Yaning Liu. Originally published in JMIR Medical Informatics (https://medinform.jmir.org), 21.8.2025. This is an open-access article distributed under the terms of the Creative Commons Attribution License (https://creativecommons.org/licenses/by/4.0/), which permits unrestricted use, distribution, and reproduction in any medium, provided the original work, first published in JMIR Medical Informatics, is properly cited. The complete bibliographic information, a link to the original publication on https://medinform.jmir.org/, as well as this copyright and license information must be included.

XSL•FO
RenderX

Assessing Internet Quality Across Public Health Centers in Indonesia: Cross-Sectional Evaluation Study

Dewi Nur Aisyah[1,2,3], PhD; Agus Heri Setiawan[2], MPH; Alfiano Fawwaz Lokopessy[2], BSc; Chyntia Aryanti Mayadewi[2,4], MSc; M Thoriqul Aziz Endryantoro[2], BSc; Viktor Wibowo[2], BSc; Sarah Disviana[2], BSc; Indra Laksana[2], BEc; Mohammad Aviandito[2], MSc; Zisis Kozlakidis[5], PhD; Logan Manikam[1,6], PhD

[1]Department of Epidemiology and Public Health, Institute of Epidemiology and Health Care, University College London, 1-19 Torrington Place, London, United Kingdom

[2]Digital Transformation Office, Ministry of Health Republic of Indonesia, Jakarta, Indonesia

[3]Monash University Indonesia, Banten, Indonesia

[4]Faculty of Medicine, Universitas Indonesia, Jakarta, Indonesia

[5]International Agency for Research on Cancer, World Health Organization, Lyon, France

[6]Aceso Global Health Consultants Pte Limited, Singapore, Singapore

Corresponding Author:
Logan Manikam, PhD
Department of Epidemiology and Public Health, Institute of Epidemiology and Health Care, University College London, 1-19 Torrington Place, London, United Kingdom

Abstract

Background: Primary health care centers (Puskesmas) serve as the cornerstone of Indonesia's health care system, providing integrated services aimed at improving individual health through prevention, treatment, and health promotion. To fulfill these roles effectively, robust technological infrastructure, particularly reliable internet connectivity, is increasingly essential. Assessing the availability and quality of internet access in Puskesmas is therefore a critical step in understanding their readiness to implement digital health initiatives and fulfill their responsibilities in delivering accessible and effective healthcare services.

Objective: This study provides a national baseline assessment of internet quality and its relevant IT infrastructure in more than 10,000 Puskesmas across Indonesia.

Methods: A cross-sectional survey was conducted throughout all Puskesmas (10,382) in 34 provinces in Indonesia, using an online questionnaire. Categorization was done to analyze internet quality level results.

Results: A total of 10,378 out of 10,382 public health centers (99.96%) participated in this study. Overall, 745 of 10,382 (7.18%) did not have internet access, 1487 (14.33%) had limited internet access, 5567 (53.64%) had sufficient internet access, and 2579 (24.85%) had sufficient and fast internet access. Moreover, 832 of 10,382 Puskesmas (8.02%) did not have 24-hour electricity, 44,196 (43.7%) had a central processing unit (CPU) with i3 specifications, 43,044 (42.56%) had 512 GB hard disk capacity, and 67,272 (66.5%) used antivirus.

Conclusions: Although 79% (8201/10,382) of Puskesmas in Indonesia already had sufficient internet access, 21% (2180/10,382) still have limited and insufficient access. To ensure universal internet availability, it is essential to build collaborative support among internet providers and government to foster the availability and use of internet satellites, high-quality computers, and electrical power to support internet connectivity.

(JMIR Med Inform 2025;13:e65940) doi:10.2196/65940

KEYWORDS

public health centres; public health; Puskesmas; primary care; primary health care; family physicians; primary care physicians; internet; web; internet connection; internet connectivity; internet access; infrastructure; community healthcare; technology; healthcare technology; digital health; medical informatics; evaluation studies

Introduction

Primary health care (Puskesmas) is a core component of health systems [1]. Based on the Alma Ata Declaration in 1978, Puskesmas is defined as essential health care that meets the needs of communities, is easy to access, acceptable, and affordable [2]. The declaration combined 3 elements considered core to delivering sustainable and equitable health services: multisectoral public policy, empowered communities, and primary public health care [2,3].

XSL•FO
RenderX

In 2022, the Ministry of Health (MoH) of the Republic of Indonesia launched its health system transformation strategy. There are 6 pillars of the transformation strategy, and one of them is primary health care (PHC) transformation, which in its implementation focuses on strengthening promotive and preventive activities to create more healthy people, improve health screening, and increase primary service capacity. The number of Puskesmas has increased since 2017, from 9825 units to 10,374 Puskesmas in 2022. The ratio of Puskesmas in Indonesia to subdistricts in 2022 is 1.4. This illustrates that the ideal ratio of Puskesmas to subdistricts, namely a minimum of 1 Puskesmas in 1 subdistrict, has been fulfilled nationally. In terms of an average ratio, each Puskesmas serves 27,000 - 30,000 residents in 2023. What needs to be considered is the distribution of the Puskesmas in all subdistricts, especially in remote, frontier, and outermost areas to provide public health services to households with a focus on maternal and child health services, elderly health, communicable disease, and noncommunicable disease prevention [4].

Puskesmas in Indonesia spread across all types of characteristic regions such as urban, rural, remote, and very remote in Indonesia within all 38 provinces and 514 districts or cities. In Indonesia, there are two main functions of Puskesmas: (1) provide an integrated individual health care that includes the activity and a series of basic individual medical services to improve the individual health, preventing and curing disease, and (2) provide essential public health services to the community, including health promotion, maternal and child health, nutrition, disease prevention and control, and environmental health. Puskesmas in Indonesia also has a responsibility to carry out technical guidance to clinics and other community health services as the Puskesmas networking partner institutions in the area. Other tasks of Puskesmas are to provide continuous and comprehensive care, to refer to specialists and hospital services, to coordinate health services, to guide the patient within the network of public health services, and to provide the best possible health services [5].

One of the elements that support health care services is IT. In the era of digital, Internet of Things, and artificial intelligence (AI), the digital transformation in health care also increases expectations of the quality of care [6]. Since the COVID-19 pandemic, digital information from the internet has gained importance in all areas of life. This trend was already evident before the COVID-19 pandemic. However, it accelerated this development and is also reflected in the health care sector [7]. With the widespread use of smartphones, downloadable or internet-based apps will play a major role in the diagnosis of diseases and monitoring and management of patients.

Technology and internet connection have played a significant role in bridging the gaps of health access and equity toward all individuals amid the geographic and socioeconomic challenges. In Indonesia's decentralized health care system, Puskesmas are mandated to deliver not only curative services but also promotive, preventive, and administrative functions, particularly within the framework of the national health insurance program (Jaminan Kesehatan Nasional). Achieving these responsibilities requires functional coordination across various health system components, many of which increasingly depend on stable internet connectivity.

Internet access supports critical digital infrastructure for public health surveillance, insurance claims, medicine supply chain management, and national health program reporting. For example, real-time reporting through the Sistem Kewaspadaan Dini dan Respon and Sistem Informasi Malaria enables early detection and response to disease outbreaks—a crucial function in archipelagic and remote regions where delayed reporting can lead to localized epidemics [8]. Similarly, routine reporting on immunization services and noncommunicable disease screenings is now conducted through the Aplikasi Sehat IndonesiaKu, a digital platform mandated by the MoH for primary care reporting and national dashboard integration [9].

In addition, internet connectivity is required to operate pharmaceutical inventory management tools, such as e-Logistik, which help prevent medicine stockouts—one of the persistent challenges in rural and remote areas [10]. The national Cek Kesehatan Gratis campaign, a government-initiated free screening program for all Indonesian population, also requires digital reporting systems for real-time coverage tracking and participant data documentation [11]. Administrative functions, particularly processing health care claims via Indonesia Case-Based Groups under Badan Penyelenggara Jaminan Sosial Kesehatan, are highly dependent on reliable internet access to ensure service reimbursement and continuity [12]. Moreover, in the absence of specialist doctors in many rural settings, internet-based coordination with referral hospitals has become a crucial alternative for maintaining continuity of care. More recently, the implementation of the SATUSEHAT (ie, Satu Data Kesehatan) platform by the Ministry of Health requires Puskesmas to connect their electronic medical record (EMR) systems to a national health data exchange ecosystem, making stable internet access a prerequisite for full participation in Indonesia's digital health integration efforts [13].

At the PHC level, internet connection has been a very critical infrastructure to support health data recording and reporting through a health information system, which is rooted from a routine data collection and serves as health indicators for government evaluations. These health data are critical to be disseminated to the health officials as evidence for program planning, and also to inform the patients related to immunization schedule, visit reminder, laboratory referrals, and other activities related to patients' follow-up [14].

Indonesia is the world's fourth most populous country with more than 270 million people residing across more than 17,000 islands [15,16]. As an archipelagic country, this condition results in disadvantages in terms of information and communication technology (ICT) infrastructure [17]. In addition, almost all internet users in Indonesia connect through mobile devices. Although mobile broadband (3G, but now increasingly 4G/LTE) is the most widely used internet service in Indonesia, it is not at par with fixed broadband with respect to capacity, quality of service, high bandwidth performance, and cost-efficiency. Such limited access to high-quality internet prevents the population from unlocking its productive capabilities to fully reap the benefits of a digital economy and points to two key challenges:

XSL•FO
RenderX

how to make fixed broadband internet access universal and increase internet quality. Increased optical fiber network coverage is a necessary but insufficient solution to meeting the key challenges. While investment by private service providers, along with government projects such as Palapa Ring, has steadily increased connectivity and service availability across Indonesian districts, internet subscriptions have not increased in parallel. Only 26% of homes with access to a fixed broadband provider subscribe to this service [18].

Several studies on IT infrastructure supporting health information systems in health care facilities have been conducted in Indonesia and other countries [19-21]. However, there is no detailed information available that can describe the accessibility and quality of the internet at Public Health Centers (Puskesmas) in Indonesia. This paper aims to provide, for the first time, a comprehensive overview of internet availability and connection reliability, as well as supporting IT infrastructure across Puskesmas throughout the country. While reliable internet connectivity is increasingly recognized as a foundational enabler for digital health transformation—including telemedicine, electronic health records, digital logistics, and surveillance systems—this study does not assess the direct impact of internet infrastructure on health care delivery or patient outcomes. Instead, it offers a baseline mapping of digital connectivity conditions to identify geographic disparities and inform future investments needed to enhance digital readiness in Indonesia's primary care system.

Methods

Data Collection

A cross-sectional approach was conducted, using a survey conducted between November 15, 2022, and March 16, 2023. The population study covered 10,378 Puskesmas in 34 provinces in Indonesia. A questionnaire was used to collect data from participants. To ensure the validity and reliability of the questionnaire, a pilot survey was conducted with a total of 20 participants from Puskesmas across 5 major islands in Indonesia. This sample size aligns with established methodological guidance, which recommends 10 - 30 participants for pilot testing to identify potential issues with instrument design and administration [22,23]. The pilot yielded a Cronbach α value of 0.76, indicating acceptable internal consistency [24] and supporting the reliability of the questionnaire items. These results provide a sound empirical and methodological basis for proceeding with the full-scale implementation of the instrument.

A standardized questionnaire survey was created using KoboToolbox (Kobo), an online application that allows users to create survey forms and collect data in real time. This tool was chosen because it can be accessed online or in offline mode (with automatic synchronization), even when the internet connectivity is poor. The tool also allows users to save drafts as they complete the surveys, giving them the flexibility to participate in surveys and carry out their daily tasks at Puskesmas. This is well suited to the uneven internet conditions in Indonesia.

The questionnaire was developed based on existing framework and literature, identifying aspects that may affect the internet quality. We adapted components from established internet quality assessment frameworks, primarily based on Quality of Service (QoS) and Quality of Experience (QoE) metrics, tailored to the infrastructure and operational context of Puskesmas in Indonesia [25-27]. The framework integrates both technical indicators (network performance) and infrastructure readiness (device and power availability). Network quality indicators (based on QoS) included type of internet connection (Wi-Fi, LAN, and routing), frequency and duration of internet disconnections, and bandwidth speed measured by Ookla speed test tool. In addition, we included device and environment indicators (infrastructure readiness): specifications and number of computers (CPU, RAM, and storage), availability of antivirus software, and electricity availability (uninterrupted power supply). To finalize the indicators, a series of discussions were carried out with experts from the infrastructure team at the Digital Transformation Office Ministry of Health Republic of Indonesia, IT specialists, public health professionals, and Public Health Governance team MoH. The final questionnaire (Multimedia Appendix 1) consisted of four sections, including (1) result of bandwidth speed test measured using Ookla speedtest tool in the morning and afternoon. Speedtest measures the speed between the device and the test server, using the Puskesmas device's internet connection. (2) Type and quality of internet network such as Wi-Fi, LAN, routing, and so on, This section also provides qualitative information such as the condition of frequent internet disconnections and how the internet speed in Puskesmas. (3) Specification and quantity of computers or laptops in Puskesmas. This section collects information such as the capacity of CPU, memory, RAM, the total number of computers or laptops, antivirus installation, and the ownership of the computer or laptop. (4) Availability of electricity in Puskesmas. This section collects information on 24-hour electricity availability and any backup electricity used in Puskesmas.

Univariate analysis was conducted by open-source tools, using Python (Python Software Foundation) and R languages (R Core Team) version 3.10.0, to examine the internet quality in Puskesmas across Indonesia. Scoring was performed to determine the categories of internet quality. There were 11 principal component indicators used for scoring the quality of internet, including: (1) result of morning upload speed test; (2) result of afternoon upload speed test; (3) result of morning download speed test; (4) result of afternoon download speed test; (5) type of internet connection; (6) the quality of internet connection; (7) computer or laptop RAM specification used; (8) computer or laptop CPU specification used; (9) 24-hour electricity availability; (10) presence of backup or alternative electricity power supply; and (11) the number of laptops or computers with installed antivirus. Each indicator was assigned a maximum score and relative weight based on its potential contribution to the internet performance in PHC services. A weighted scoring table was used to rank the overall internet quality per facility. Indicators were given weights based on literature evidence and expert consensus. The detailed scoring calculation and weighting can be seen in Multimedia Appendix 1.

XSL•FO
RenderX

Final scores were divided into 4 categories, namely levels 1, 2, 3, and 4. Level 1 is for Puskesmas that have fast and reliable internet connection with 24-hour electricity and backup, as well as high specification of computer or laptop. Level 2 is for Puskesmas with normal and sufficient internet connection, standard specification of computer or laptop, and 24-hour electricity availability. Level 3 is for Puskesmas that have unreliable or insufficient internet connection, computer or laptop below standard, and lack of 24-hour electricity. The lowest level, level 4, is for Puskesmas with no internet connection, computer, or laptop below standard, minimum quantity, and lack of 24-hour electricity.

The major islands of Indonesia were classified into five categories: (1) Java Island, which includes provinces such as Banten, DKI Jakarta (Special Capital Region of Jakarta), West Java, Central Java, Yogyakarta Special Region, and East Java; (2) Bali and Nusa Tenggara, comprising Bali, East Nusa Tenggara, and West Nusa Tenggara provinces; (3) Sumatra, encompassing Aceh, North Sumatra, West Sumatra, Riau, Riau Kepulauan, Jambi, South Sumatra, Bengkulu, Bangka Belitung, and Lampung provinces; (4) Kalimantan, which includes West Kalimantan, Central Kalimantan, South Kalimantan, East Kalimantan, and North Kalimantan provinces; and (5) Maluku and Papua, consisting of Maluku, North Maluku, Papua, and West Papua provinces. After weighting each performance category of Puskesmas and understanding the demographic landscape of Indonesia, we used descriptive analysis, a statistical method used to summarize and describe the characteristics of a dataset to depict the condition of the internet in Indonesia.

The data cleaning procedure was carried out to ensure the accuracy and consistency of responses prior to analysis. First, all survey responses were screened for completeness; records with more than 20% missing values across key indicators were excluded. For records with limited missing values, we chose to analyze only complete cases (complete case analysis) for each variable to maintain transparency and avoid introducing assumptions about missing values. Given that the proportion of missing data was low and appeared to be randomly distributed, the risk of bias was minimal. While complete case analysis may reduce the sample size slightly, it ensures that the results are based solely on observed data, preserving the integrity of variable-level relationships and simplifying interpretation [28,29]. After calculating individual facility-level scores based on weighted indicators, we summarized the results at the provincial level by aggregating the total number of facilities in each internet quality category or selected indicators. The findings are presented descriptively to illustrate provincial-level distribution and variation. This approach allows for transparent comparison across provinces while preserving the granularity of facility-level scoring.

To minimize the risk of selection bias due to online survey assessment, we collaborated with the MoH Public Health Governance team working together with provincial and district health offices to ensure the survey completeness from Puskesmas. We allowed a 3-month period for survey submission for provincial and district health offices to have offline coordination with local Puskesmas, especially those located in remote and limited internet connectivity areas. We also conducted biweekly monitoring to ensure Puskesmas participation and completeness of the survey with provincial and district health offices.

Ethical Considerations

We confirm that the data collected for this study did not require ethical approval, as no identifiable individual-level information was obtained or presented. Written informed consent was obtained from all participants prior to the commencement of the survey. The consent form explicitly stated that no personal or sensitive data would be collected and that all responses would be stored and analyzed in anonymized form. Participants were also provided with an information sheet outlining the study objectives and duration. No incentives or compensation were provided to participants.

Results

Internet Quality Across Puskesmas

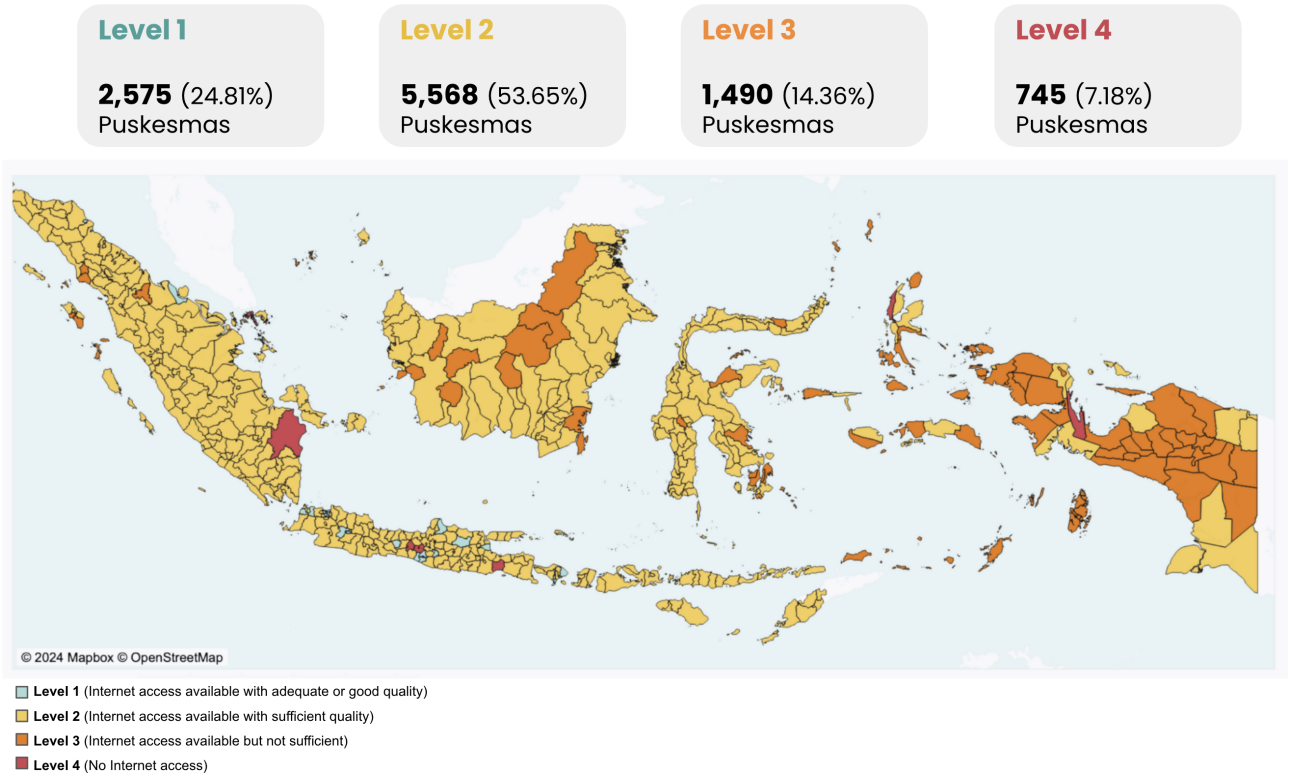
A total of 99.96% Puskesmas (10,378/10,382 Puskesmas in Indonesia), spread across 514 districts or cities from 34 provinces, participated in the survey. Among the 34 provinces, all Puskesmas in 30 provinces (88%) successfully participated in this survey. Based on the location of Puskesmas, 29.2% (3034/10,378) were located in urban areas, 45.3% (4700/10,378) in rural areas, 13.9% (1446/10,378) in remote areas, and 11.5% (1198/10,378) in very remote areas. The detailed participation rate across Puskesmas in 34 provinces can be accessed from Multimedia Appendix 2

Based on the study results, 7.18% Puskesmas in Indonesia (745/10,378) had no internet access (level 4), 14.33% Puskesmas (1,487/10,378) had insufficient internet access (level 3), 53.64% Puskesmas (5,567/10,378) had sufficient internet access (level 2), and 24.85% Puskesmas (2,579/10,378) had sufficient and fast internet connection (level 1). Given this condition, 78% (8,097/10,378) Puskesmas in Indonesia, categorized under levels 1 and 2, exhibited sufficient internet access, whereas 22% (2,235/10,378) of Puskesmas in levels 3 and 4 experienced inadequate internet connectivity.

After obtaining data on each Puskesmas, we calculated the level of internet quality at the provincial level by averaging the scores of all Puskesmas in each province (Figure 1). Provinces with the highest proportion of Puskesmas having level 1 internet access were DI Yogyakarta (86/121, 71%), followed by DKI Jakarta (206/315, 65.4%), and Bali (51/120, 42.5%). In contrast, 48.9% (222/454) Puskesmas in Papua, 48.9% (81/227) Puskesmas in Maluku, and 25.7% (42/163) Puskesmas in West Papua had the highest number of Puskesmas with no internet access in the province. Out of 745 Puskesmas without internet, the provinces with the highest number of Puskesmas with no internet access were Papua (222/745, 29.79%), Maluku (81/745, 10.87%), North Sumatra (45/745, 6.04%), West Papua (42/745, 5.63%), and North Maluku (35/745, 4.69%). Further details are available in Multimedia Appendix 3.

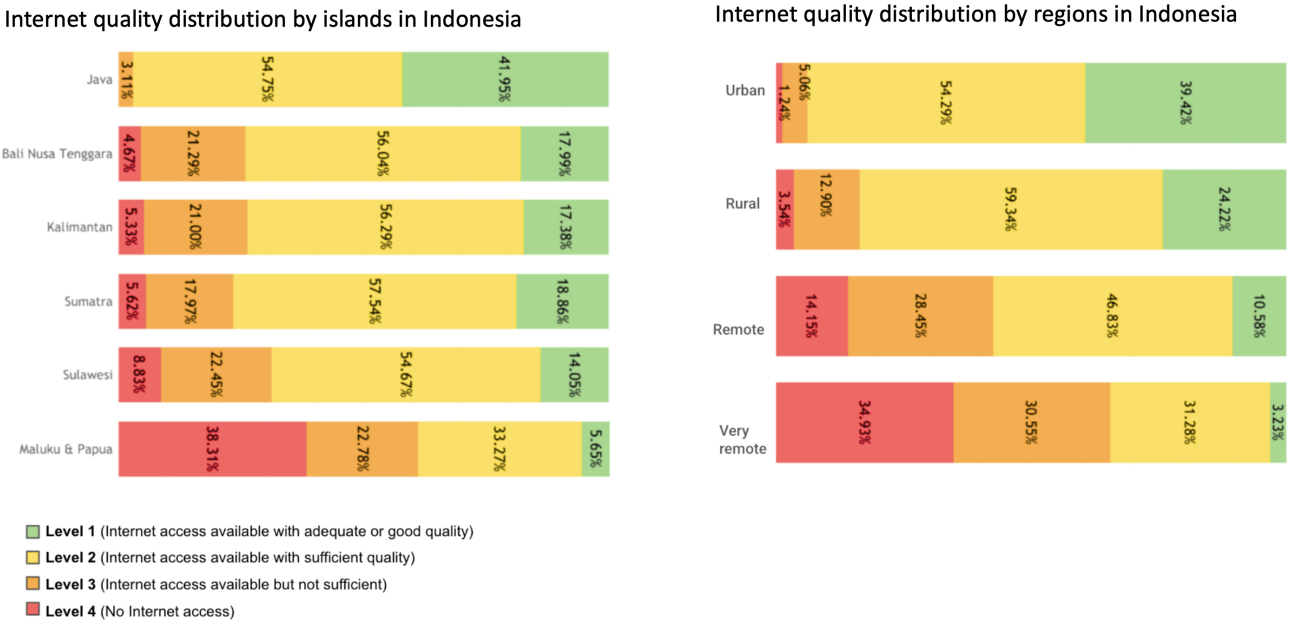
XSL•FO
RenderX

Figure 1. Distribution of Puskesmas internet quality across provinces in Indonesia.



The disparities in the distribution of Puskesmas with different levels of internet quality across the islands of Indonesia were identified. Java Island led with a large number of Puskesmas having level 1 internet access (1525/3635, 41.95%), marking a stark contrast to other islands, such as Sumatra Island, Sulawesi, Kalimantan, Bali, and Nusa Tenggara, where the proportion of Puskesmas with fast internet access did not exceed more than 20%. Nationally, the level 2 internet category is the most common, with 53.64% (5,567/10,378) Puskesmas having sufficient internet access, and Sumatra Island having the highest proportion within this category (1,556/2,704, 57.54%). In sharp contrast, the Maluku and Papua Islands have the highest distribution of level 4 internet quality with 38.31% (380/992) Puskesmas having no internet access, which is significantly higher than other islands (Figure 2).

Figure 2. Distribution of Puskesmas internet quality based on islands and locations in Indonesia.



The distribution of Puskesmas with varying levels of internet quality is also significant across different locations in Indonesia. Puskesmas located in urban areas were more likely to have better internet quality, with 39.42% (1177/2986) Puskesmas having sufficient and fast internet access. Puskesmas located in rural areas were more likely to have sufficient quality internet with 59.34% (3004/5062) Puskesmas in level 2. Puskesmas in very remote areas were disproportionately affected by lower

XSL•FO
RenderX

internet quality, with the highest occurrences of level 4 and level 3 internet quality (335/959, 34.93% and 293/959, 30.55%, respectively) (Figure 2).

Based on computer connection, majority type connections in Indonesian Puskesmas were Wi-Fi (5179/10,378, 49.9%), followed by Wi-Fi and LAN (2288/10,378, 22.05%), and tethering from mobile data (772/10,378, 7.44%). Referring to participants' perspective, 38.83% (4030/10,378) Puskesmas had robust internet access, 31.83% (3303/10,378) had slow internet connection, 22.16% (2300/10,378) had very slow internet connection, and lastly 7.18% (745/10,378) had no access to internet at all (Multimedia Appendix 4). Type of internet connection and internet connection quality in public health centers have a weight of 8% each of the total assessment.

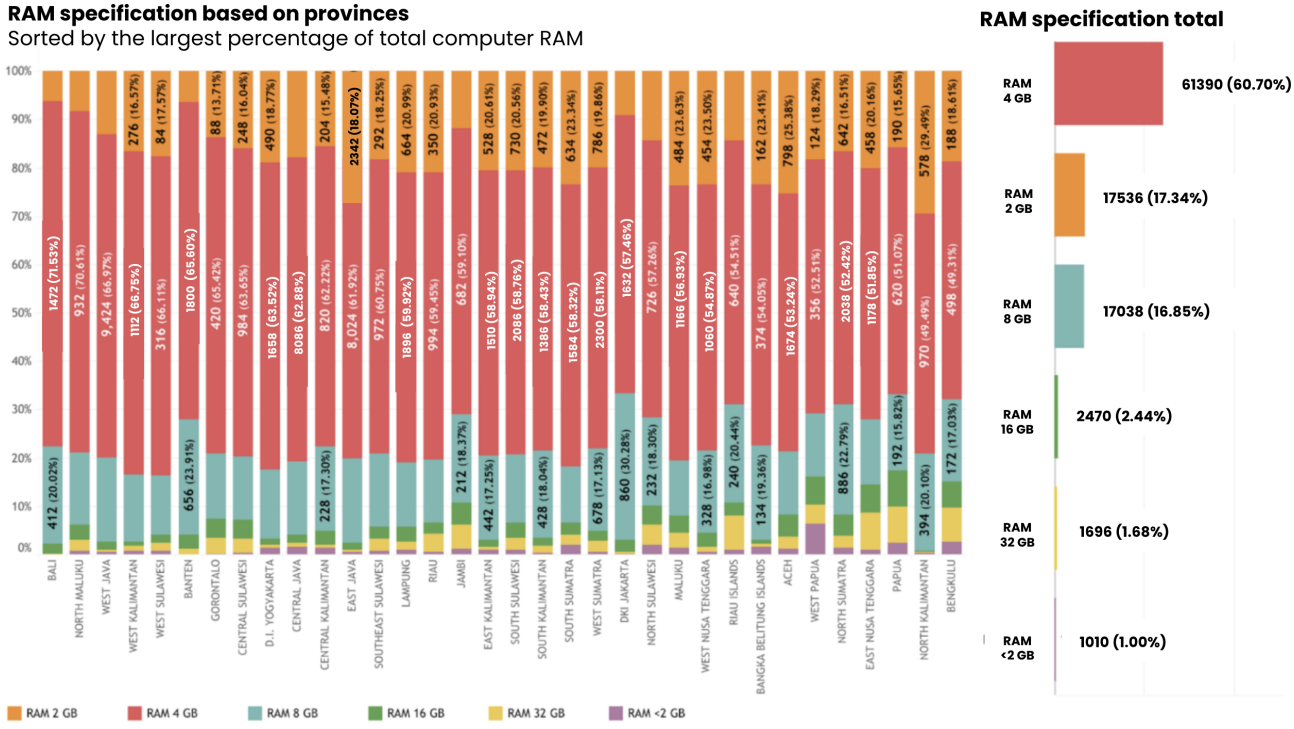
Factors Influencing Internet Quality Across Public Health Centers

Computer Specification

A separate analysis was conducted to determine other factors that affect internet quality, including RAM specifications, CPU, hard disk capacity, and antivirus updates on the hardware used. Based on the study, the most common RAM specification used in Puskesmas was 4 GB RAM (61,390/101,140, 60.7%), followed by 2 GB RAM (17,536/101,140, 17.34%), and 8 GB RAM (17,038/101,140, 16.85%).

Based on regional distribution, the provinces with the largest proportion of 4 GB RAM were Bali (1472/2058, 71.53%), followed by North Maluku (932/1320, 70.61%) and West Java (9942/14,072, 66.97%). In addition, East Nusa Tenggara had the highest proportion of Puskesmas with 23 GB RAM computer specification (174/2272, 7.66%), followed by Papua (90/1214, 7.41%), Riau Islands (84/1174, 7.16%), and Bengkulu (70/1010, 6.93%). On the other hand, West Papua Province was the province with the highest proportion of hardware with a low specification less than 2 GB RAM (44/678, 6.49%), followed by Bengkulu (28/1010, 2.77%), Papua (30/1214, 2.47%), and North Sulawesi (26/1268, 2.05%) (Figure 3).

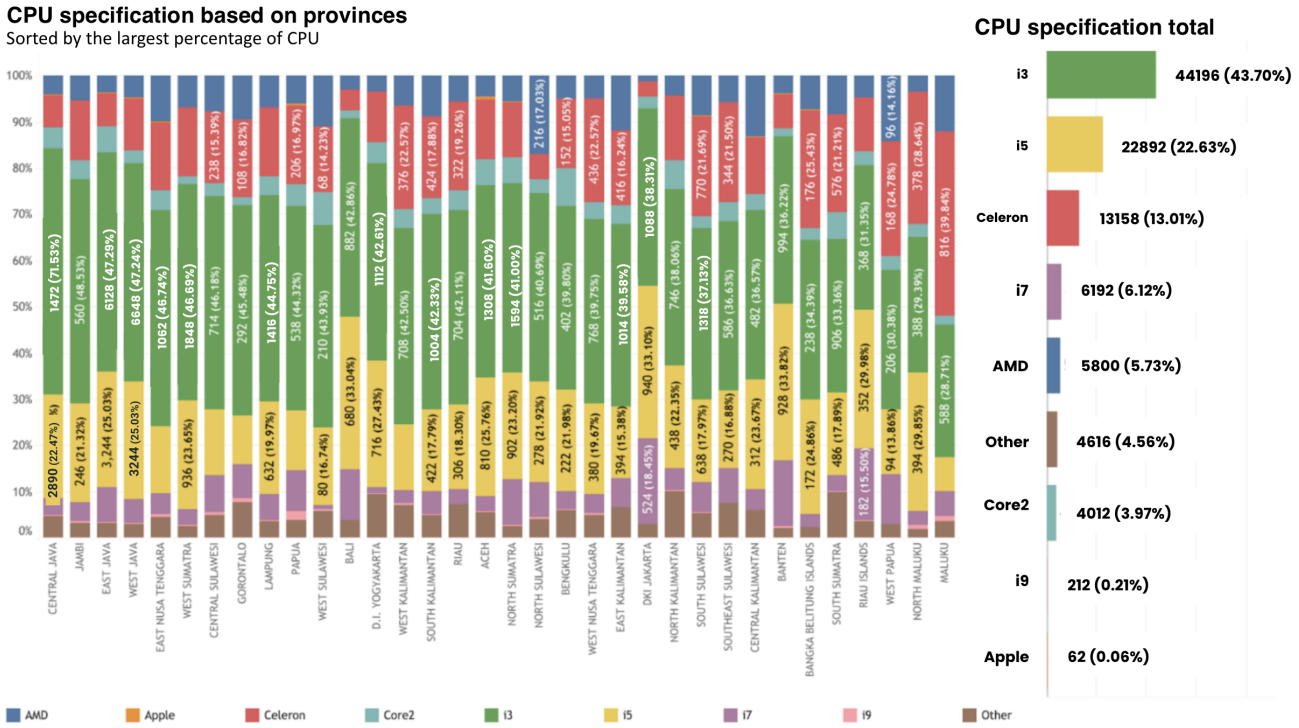
Figure 3. RAM specification based on provinces and total values.



By region, the provinces with the highest proportion of hardware with CPU type i3 were Central Java (6860/12,860, 53.34%), followed by Jambi (560/1154, 48.53%), and East Java (6128/12,958, 47.29%). In addition, provinces with the highest CPU specification of i7 type were DKI Jakarta (5242/2840, 18.45%), Riau Islands (182/1174, 15.5%), and Banten (390/2744, 14.21%). In contrast, the provinces that had below-average CPU type distribution with Celeron type were Maluku (816/2048, 39.84%), followed by North Maluku (378/1320, 28.64%) and Bangka Belitung (176/692, 25.43%) (Figure 4). Based on CPU specifications, nationally, hardware with i3 specifications dominated at 43.7% (44,196/101,140), followed by i5 at 22.63% (22,892/101,140), and Celeron at 13.01% (13,158/101,140) (Figure 4).

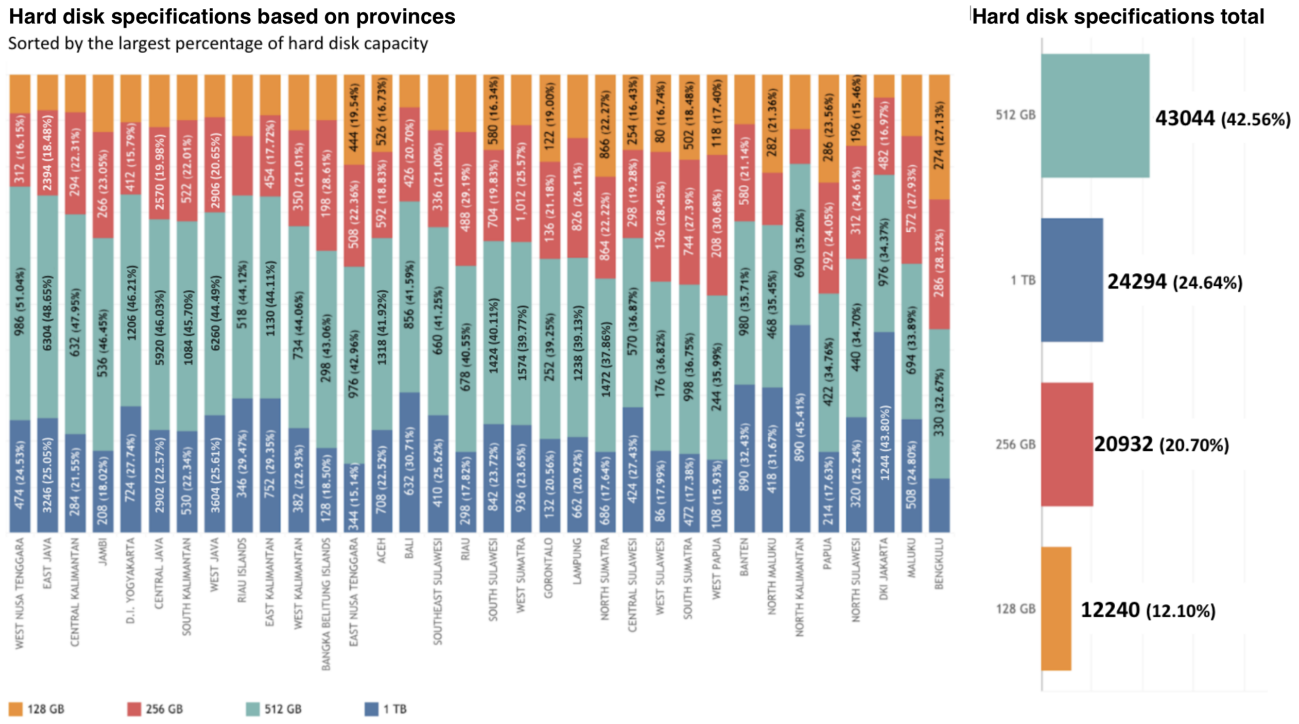
XSL•FO
RenderX

Figure 4. CPU specification based on provinces and at the national level.



At the province level, the provinces with highest distribution of 512 GB hard disk capacity were West Nusa Tenggara (986/1932, 51.04%), followed by East Java (6304/12,958, 48.65%), Central Kalimantan (632/1318, 47.95%), and Jambi (536/1154, 46.45%). In addition, provinces with the highest proportion of highest hard disk capacity of 1 TB were North Kalimantan (890/1960, 45.41%), followed by DKI Jakarta (1244/2840, 43.8%), Banten (890/2744, 32.43%), and North Maluku (418/1320, 31.67%). In contrast, the province with the highest distribution of lowest hard disk specification of 128 GB was Bengkulu (274/1010, 27.13%), followed by Papua (286/1214, 23.56%), North Sumatra (866/3888, 22.27%), and North Maluku (282/1320, 21.36%). The details can be seen in Figure 5; it shows that nationally, the most hard disk capacity used in Puskesmas was 512 GB (43,044/101,140, 42.56%), followed by 1 TB (24,924/101,140, 24.64%), 256 GB (20,932/101,140, 20.7%), and 128 GB (12,240/101,140, 12.1%).

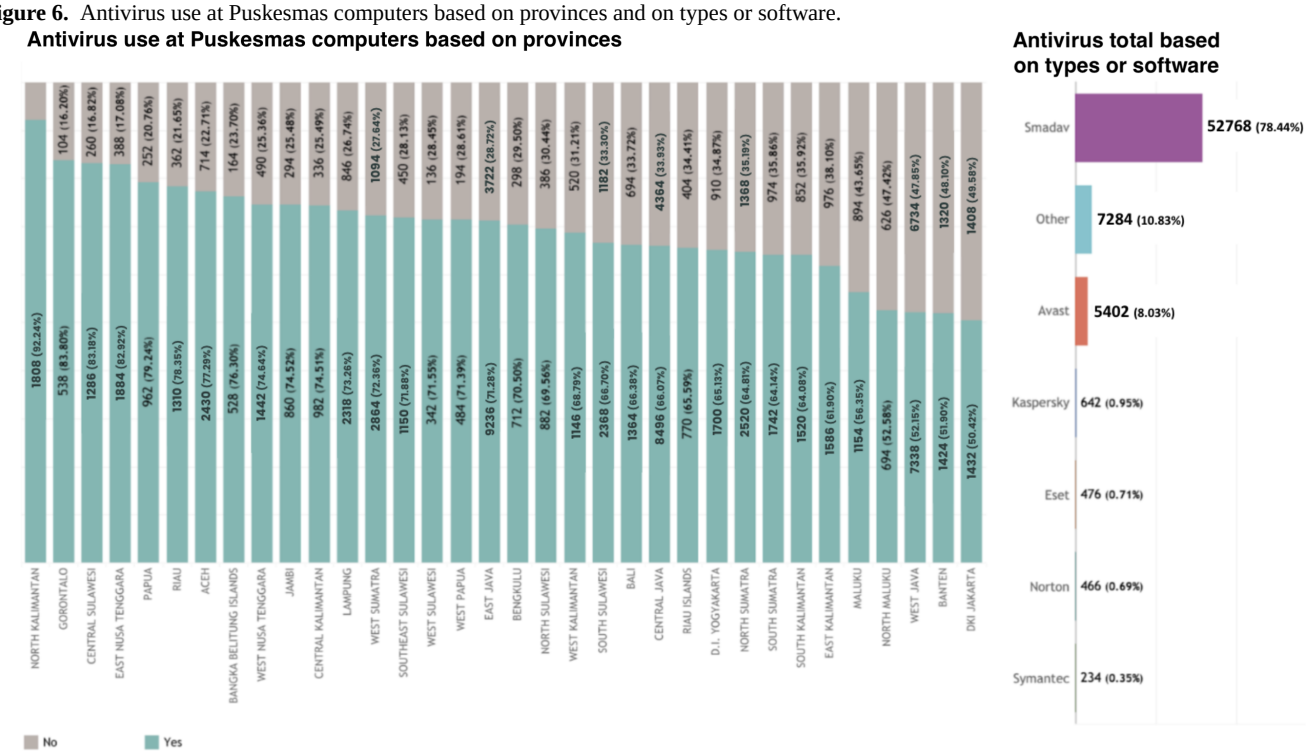
Figure 5. Hard disk specification based on provinces and at the national level.



XSL•FO
RenderX

The province with the highest proportion of computers with installed antivirus was North Kalimantan (1808/1960, 92.24%), followed by Gorontalo (538/642, 83.8%), Central Sulawesi (1286/1546, 83.18%), and East Nusa Tenggara (1884/2272, 82.92%). In contrast, DKI Jakarta, with 49.58% (1408/2840) of their computers, did not install antivirus, followed by Banten at 48.1% (1320/2744), West Java at 47.85% (6734/14,072), and North Maluku at 47.42% (626/1320) (Figure 6). Based on the study, 33.5% (33.868/101,140) of computers in Puskesmas did not install antivirus. Among the computers with installed antivirus, the most antivirus used was Smadav (52,768/67,272, 78.44%), followed by Avast (5402/67,272, 8.03%), and others (7284/67,272, 10.83%) (Figure 6).

Figure 6. Antivirus use at Puskesmas computers based on provinces and on types or software.

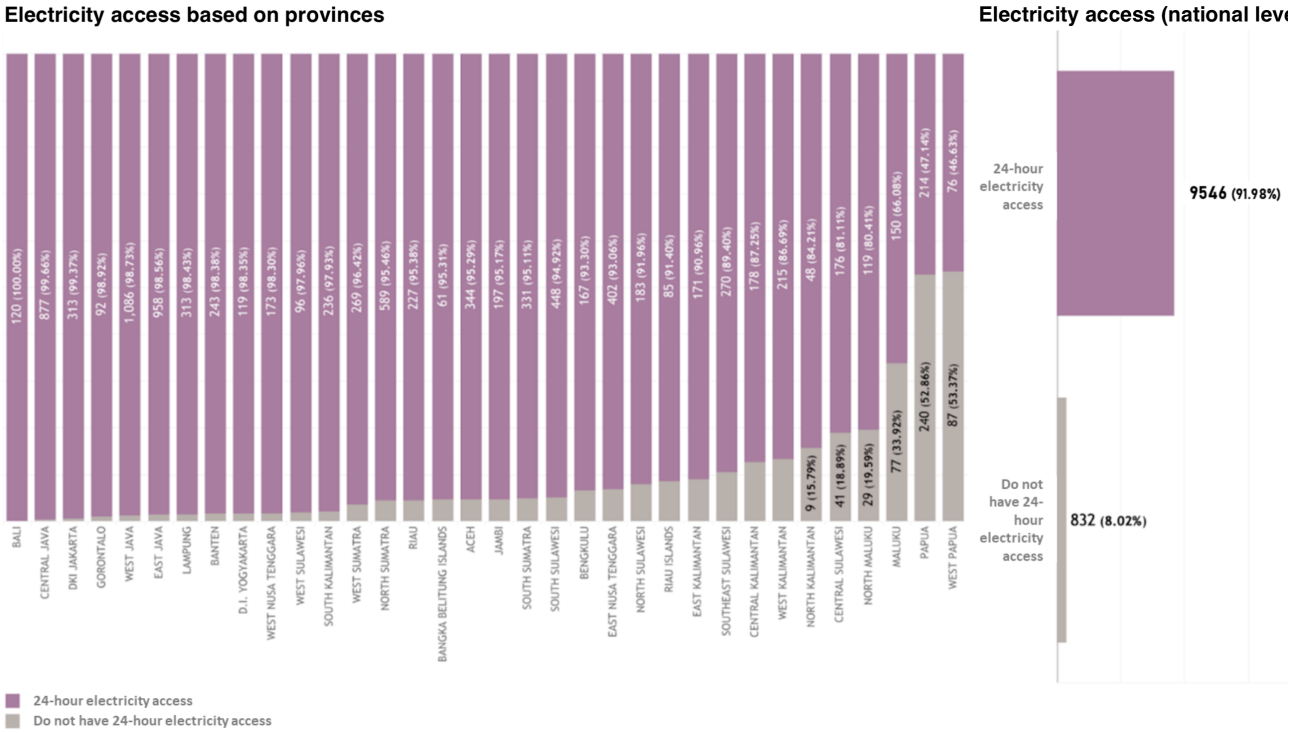


Electricity Access

In terms of province distribution, 100% (120/120) Puskesmas in Bali have access to 24-hour electricity, followed by Central Java (99.66%, 877/880), DKI Jakarta (313/315, 99.37%), and Gorontalo (92/93, 98.92%). In contrast, provinces with the highest number of Puskesmas that do not have access to 24-hour electricity were West Papua (87/143, 53.37%), followed by Papua (240/454, 52.86%), Maluku (77/227, 33.92%), and North Maluku (29/148, 19.59%) (Figure 7A). At the national level, 91.98% (9546/10,378) Puskesmas in Indonesia have electricity access for 24 hours, whereas 8.02% (832/10,378) Puskesmas do not have access to 24-hour electricity (Figure 7B).

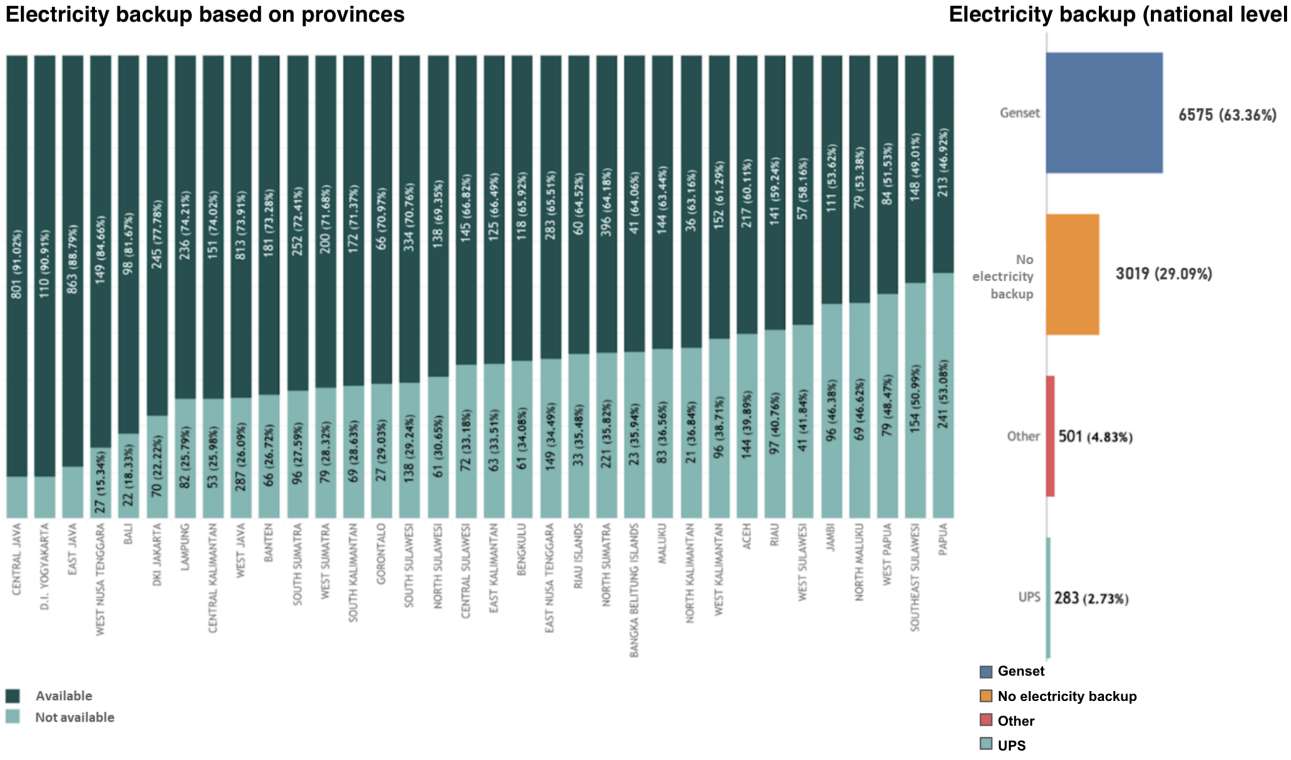
XSL•FO
RenderX

Figure 7. Electricity access based on (A) provinces and (B) at the national level.



The provision of electricity backup is also an important point in the operational process of public health centers. Based on the study, 29.09% (3019/10,378) of Puskesmas did not have electricity backup (Figure 8). Among the Puskesmas who had electricity backup, the most common type of electricity backup owned by Puskesmas was a generator (6575/10,378, 63.36%), followed by other backups (501/10,378, 4.83%), and UPS (uninterrupted power supply; 283/10,378, 2.73%). At the provincial level, the provinces with the highest number of Puskesmas having electricity backup were Central Java (801/880, 91.02%), followed by DI Yogyakarta (110/121, 90.91%), East Java (863/972, 88.79%), and West Nusa Tenggara (149/176, 84.66%). In contrast, 53.08% (241/454) Puskesmas in Papua did not have any electricity backup, followed by South East Sulawesi (154/302, 50.99%), West Papua (79/163, 48.47%), and North Maluku (69/168, 46.62%).

Figure 8. Electricity backup based on (**A**) provinces and (**B**) at the national level.



XSL•FO
RenderX

Discussion

The internet's significant role in aiding public health services is undeniable. This paper marks the first comprehensive depiction of the accessibility and quality of internet connections and computer systems across Indonesia's Puskesmas, providing crucial insights into the information technology infrastructure. The internet availability in the health facility is highly crucial to foster the delivery of healthcare among communities [28,29]. By presenting baseline data on internet quality across Puskesmas, this study contributes foundational insights to support future efforts aimed at strengthening health information systems and expanding the digital infrastructure needed for more equitable and efficient PHC delivery in Indonesia.

Indonesia presents a particularly interesting case when it comes to internet connectivity and accessibility to health care services, especially in the context of health care digitization [30]. In numerous instances, technological advancements have the potential to significantly reduce health care inequalities. Furthermore, digital health is recognized as a valuable technological approach that can effectively bridge the significant gap between urban and rural populations [31] and between high-income and low- and middle-income countries (LMIC) [32].

One way of improving health care service delivery is through adoption of broadband Internet access [33]. In the health system, service delivery refers to where patients receive the treatment as well as supplies entitled. Broadband internet access helps to reshape many health-related processes and supports effective treatment of patients [33]. It helps medics to provide patients with faster diagnosis to their respective health conditions, the development of treatment plans, making patient records as well as test results accessible by patients from the examination room, facilitates faster consultation electronically on treatment plans, helps patients and their attendants access practice guidelines faster [15,34,35], and led to the adoption of telehealth technologies which has contributed to easy access to health services [36]. The availability of Internet access, coupled with the accelerated adoption of eHealth and mHealth platforms and the rapid evolution of digital technology access, has generated a significant opportunity to enhance the reach, quality, and efficiency of PHC service delivery, thereby facilitating the achievement of universal health coverage [37].

According to this study, it was found that 78.4% (8,143/10,378) of Puskesmas have good and sufficient internet quality, 14.4% (1,490/10,378) Puskesmas have insufficient internet connection, and 7.2% (745/10,378) of the Puskesmas do not have internet access at all. The study depicts that the eastern part of Indonesia had the least internet connection in Puskesmas compared to other parts of Indonesia, which includes Maluku and Papua regions. This is aligned with previous findings related to the limited internet access in the eastern part of Indonesia and low ICT development index in 2020 - 2021 throughout the areas [38-41]. The ICT Development Index, published by the United Nations International Telecommunication Union, serves as a crucial benchmarking tool for measuring the information society by utilizing internationally agreed ICT indicators, assisting governments, operators, development agencies, researchers, and others in assessing the digital divide and comparing ICT performance globally [42]. Poor internet connectivity is one of the barriers to implementing telehealth [43]. Studies reveal varying rates of internet connection across different countries affect the adoption and implementation of telehealth and eHealth [44,45]; and digital health initiatives, especially in rural areas [46]. The underlying causes of limited internet access in the eastern part of Indonesia may be due to several aspects, including challenging geography, archipelagic region, size of territory to cover, limited infrastructure, which should be taken into account as barriers that limit the accesses [47-49]. High service costs to provide IT infrastructure (including tower, fiber optic, etc) have become the challenge to evenly provide internet access across the country, especially in remote areas [50]. While at the same time, the user also finds it a burden to subscribe to the certain internet monthly fee [51-53]. Some studies also showed that sociobehavioral values and perceptions toward digitalization also influence enhancing or limiting the internet availability, including unwillingness of the local people to allow the internet infrastructure development, lower education attainment, and low adult literacy [52,54].

For completing administrative tasks in Puskesmas, such as browsing, data input, upload and download files, or to support any other health service tasks, according to information and technology literatures, it requires a minimum specification of 4 GB RAM and CPU i3 or above for computer or laptop to perform basic data management (input/edit/delete data or simple online browsing) [55,56]. These findings show that the majority (60.70%, 61,390/101,140) of the Puskesmas in Indonesia already had 4 GB RAM or above in their computers, while 18.34% (18,546/101,140) of them were lower (2 GB and 1 GB). As for the CPU specification, 83% (83,970/101,140) of the Puskesmas had the sufficient CPU specification (i3 type or above), while 17% (17,170/101,140) of them had insufficient, which were Celeron and Core2. It is understood higher RAM capacity and newest CPU specifications are linked with better computer performance, which is highly important to be provided in Puskesmas to ensure smooth operation of critical health care software, efficient management of electronic health records, and reliable services, ultimately supporting effective patient care delivery in the health care facilities [57,58].

Although CPU, RAM, and memory do not directly control bandwidth or download speeds, they significantly influence the user's ability to use the internet efficiently for digital health service. The CPU determines how quickly a computer can process incoming data from the internet, execute scripts, and render web pages. A slower CPU may lead to delays in page loading, application responsiveness, and user interaction, particularly with web-based health information systems. Goel et al [59] demonstrated that lowering CPU performance (eg, through power-saving modes on Android devices) results in slower page loading and degraded user experience in accessing online resources. Similarly, another study notes that a slow processor can act as a bottleneck when decoding or rendering content received over the internet, making the browsing experience sluggish [60]. RAM enables systems to temporarily store and quickly access active data. Systems with insufficient

XSL•FO
RenderX

RAM often struggle when running multiple applications or browser tabs, leading to frequent slowdowns or crashes. This affects the usability of internet-dependent applications, especially in environments such as health centers where simultaneous tasks are common. While RAM does not increase raw internet speed, having adequate memory ensures smoother browser and application performance [61]. Another report supports this by showing that memory capacity and technology trends directly influence web system performance and throughput [62].

Similarly, with RAM capacity and processors, hard disk was also found to affect the computer's capacity to process [58]. This study reveals that the majority of Puskesmas have a sufficient hard disk of 256 GB or above (88%, 20,932/100,510), and 12% (12,240/100,510) of them have an insufficient one (128 GB). Literature findings show that 128 GB internal storage is able to undergo basic operations; however, it will demand higher capacity for extensive computer use [63]. The hard disk is crucial for computer performance as it stores and retrieves data, including the operating system and applications, facilitating efficient multitasking and overall system responsiveness [57,58].

Across various low- and middle-income countries, the results consistently highlight significant disparities in hardware infrastructure at the PHC level, which directly impact the implementation of digital health systems [64]. In Nigeria, many PHC centers still rely on desktop computers with only 512 MB to 2 GB of RAM and outdated Pentium IV processors, limiting their ability to run modern eHealth applications [65]. Similarly, in Uganda, facilities were found using laptops with 1 GB RAM and low-speed CPUs, which caused frequent delays and hindered real-time data entry and synchronization [66]. In Kenya, a study revealed that more than half of the PHC sites were equipped with low-specification devices using Intel Atom processors and 2 GB RAM, often unable to handle multiple web-based platforms simultaneously [67]. In parts of Latin America, such as Peru and Bolivia, rural clinics were reported to operate with refurbished computers having less than 2 GB RAM, rendering them incompatible with many EMR systems [68]. These findings underscore the urgent need for targeted investment in basic digital infrastructure to ensure the successful adoption of health information systems in resource-constrained settings [69].

As for the antivirus, this finding shows that the coverage of antivirus installation in Puskesmas' computers is still incomplete, especially in DKI Jakarta, Banten, and West Java provinces, which leave almost half of its Puskesmas unprotected with the antivirus. In health care facilities, malware protection is critical for computer performance as it safeguards sensitive patient data, prevents potential cyberattacks, and ensures the uninterrupted operation of vital medical software, maintaining the integrity and security of patient care services [70,71]. Several studies have highlighted the limited implementation of antivirus software and weak cybersecurity practices in PHC facilities across LMICs. Hasegawa et al [72] conducted a scoping review and found that antivirus installation in PHC settings was often inconsistent or absent due to limited funding, lack of technical support, and absence of standardized cybersecurity policies. Similarly, the World Health Organization (2021) reported that many LMIC PHCs do not regularly update or install antivirus software, making them vulnerable to malware and data breaches [73]. A scoping review study by He et al [74] found that one of the major challenges of healthcare cybersecurity is the lack of security awareness. Collectively, these findings underscore the urgent need for national digital health policies that mandate and support sustainable cybersecurity infrastructure, including antivirus software, within PHC systems across LMICs.

This study found that 8.02% (832/10,378) of Puskesmas in Indonesia have no access to electricity for 24 hours. Most provinces that did not have access to 24-hour electricity were located in the eastern part of Indonesia, such as Maluku and Papua island. Modern energy enables health service delivery. Access to electricity is, however, unreliable in many health facilities in developing countries [75]. Reliable basic infrastructure, particularly electricity, is a critical enabling factor in improving health systems [76]. Previous literature showed that the availability of electricity is an important determinant of receiving health information and use of health services [77,78]. Based on a literature study conducted in developing countries [65,], there are many barriers that can occur during the electricity provision across the nation, this includes the lack of IT infrastructure, especially electricity supply. Indonesia started the rural electrification program in the late 1950s, but how to provide electricity in a sustainable way both organizationally and institutionally still becomes a big challenge [79]. According to the World Health Organization (2023), nearly 1 billion people globally are served by health care facilities that either lack electricity altogether or rely on highly unreliable sources, with PHC centers being especially affected [78]. A systematic review by Ibrahim et al [80] found that fewer than 30% of PHC facilities in LMICs had consistent electricity access, which severely undermines the ability to store vaccines, operate diagnostic equipment, and provide emergency care [80]. In a multicountry study of surgical hospitals across 21 LMICs, continuous electricity availability was reported in less than two-thirds of facilities, with countries such as Sierra Leone and Malawi experiencing 0% reliable power supply [81]. These power gaps directly limit the deployment of digital health technologies, vaccine cold chains, and essential services. According to the Electricity Power Supply Business Plan 2019 - 2028, Indonesia's average electricity growth is at 6.42%. Indonesia successfully surpassed its electrification ratio target at the end of the year 2018 [81]. However, there are still 2510 villages across Indonesia that are not yet electrified [82]. Increasing the electrification ratio always becomes a challenging task because Indonesia has many islands, and many communities are isolated from one another [79]. This geographical situation also worsens with poor infrastructure access, making the area hard to reach [83]. There are several fundamental requirements that need to be implemented in order to cope with the rural electrification challenges [84-86]. The lessons learned from other countries that have successfully achieved universal electricity access were summarized in several studies [87]. Committed governance and supportive regulations and policies are one of the most often stated in the literature [87]. Moreover, a collaboration of appropriate policies and government will increase the private sector's participation in the rural electrification program [88].

XSL•FO
RenderX

Based on this study and consultation with experts, it is recommended that Puskesmas facilities in Indonesia require a minimum internet bandwidth of 10 to 20 Mbps. This range is deemed as a minimum essential requirement to ensure reliable access to digital resources and the efficient input of patient EMR data. In addition, PHC services should be equipped with at least Intel Core i3 processors, 8 GB RAM, and 256 GB solid-state drive storage to enable smooth operation of digital applications and web-based platforms [69]. Optimal performance, especially in urban or high-volume facilities, may require upgrading to Intel Core i5 processors and 16 GB RAM, which align with the performance needs of multitasking systems and real-time data entry [67,68]. This study provides a structured and evidence-based framework for assessing internet quality in PHC facilities, which is especially relevant for benchmarking across comparable middle-income countries. Many countries with similar socioeconomic and infrastructural conditions face shared challenges in ensuring reliable digital connectivity in remote or underserved health centers [89,90]. By developing and validating a weighted, multi-indicator scoring system, grounded in technical, infrastructural, and operational factors, this study offers a replicable model that can inform digital health readiness assessments beyond Indonesia. Such benchmarking tools are essential as countries pursue universal health coverage and integrate eHealth systems in alignment with the World Health Organization's Global Strategy on Digital Health 2020 - 2025. Additionally, initiatives like the International Telecommunication Union and the World Bank's Digital Economy for Africa and Asia programs emphasize the need for context-sensitive indicators to guide investments in health ICT infrastructure [91,92]. Therefore, this study not only addresses a national implementation gap but also contributes to the global evidence base supporting digital health infrastructure development in resource-constrained settings.

Successful implementation, rollout, and use of the digital system require PHC facilities to be equipped with appropriate digital and data infrastructure. In Tanzania, as part of the National PHC Rolling Digital Transformation Roadmap, service delivery points for in-facility continuity of care are using a LAN that is installed within facilities [93]. While interfacility referrals and integration with public domain systems. While in China, in order to guide the development of internet health care, the Chinese government has issued a series of regulations and guidelines. The State Council of the People's Republic of China has issued the Guidance on Actively Promoting the Action of "Internet Plus." It proposed to develop internet-based health care services, encourage internet enterprises to cooperate with medical institutions for establishing medical network information platforms, reinforce the integration of regional health care resources, and actively apply the mobile internet to explore and provide health services [94]. Depending on the different initiators, there are 3 main modes of internet health care service provision in mainland China: hospital-led, government-led, and enterprise-led internet healthcare platforms [95].

This research exhibits several strengths that contribute to its significance in the field. The study at hand is a groundbreaking research effort that has comprehensively assessed a wide range of internet components in PHC facilities, including device availability, access, and internet quality in nearly all public health centers across Indonesia. The findings of this study provide valuable insights into various supporting factors that can facilitate the implementation of IT transformation. The study highlights the significance of the availability, quality, barriers of computer systems, hardware, and software devices, which can serve as instrumental inputs for the government in their decision-making processes regarding the implementation of such transformations.

However, certain limitations must be acknowledged: (1) Bandwidth checks to assess the quality of internet access were only carried out in the morning and evening, which depends on local conditions and the respondent's honesty; (2) the completeness of filling out the questionnaire was influenced by the capacity of the assigned respondents; (3) validation of CPU, RAM, and antivirus could not be done directly; (4) potential selection bias may occur as we performed the assessment using an online survey, although we have minimized this bias by having coordination with the designated Public Health Governance team MoH and district or Provincial Health Offices allowing them to complete the survey within a 2-month period, having offline coordination to ensure we obtained survey feedback from Puskesmas. Nevertheless, this study provides a deeper overview of the access and barriers of internet access and other supporting IT infrastructure in 10,378 public health centers throughout Indonesia.

Conclusions

The internet plays a vital role in health care services, facilitating communication, information exchange, and access to medical resources. Despite the fact that 78% of health care centers in Indonesia have sufficient internet connectivity, challenges persist, with some areas experiencing limited access or complete absence of internet connectivity. To ensure universal availability of the internet across primary care services in Indonesia, additional measures are imperative. This study demonstrates the need for collaborative actions among government, health care workers, and telecom providers to allocate a supportive budget for sustainable internet infrastructure, including satellite-based internet services that enable strong internet connection in remote, underserved, and digitally excluded regions. Technology infrastructure should also follow, including high-quality computer systems with adequate specifications to handle health care–related tasks efficiently, as well as ensuring uninterrupted 24-hour access to electrical power to support continuous internet connectivity and operational efficiency in health care facilities. Future studies are encouraged to explore the relationship between internet quality and health care service delivery outcomes to better understand its operational impact. Additionally, longitudinal assessments could help monitor improvements over time and guide digital infrastructure investments in public health systems. Although this study does not assess clinical performance or health care outcomes, it provides crucial baseline evidence on digital infrastructure status. These insights can help guide targeted investments and future evaluations as Indonesia advances toward nationwide digital health integration.

XSL•FO
RenderX

Acknowledgments

The authors would like to thank the Digital Transformation Office Ministry of Health Republic of Indonesia for supporting the study implementation; the Public Health Centers, Districts, and Provincial Health Offices across Indonesia who have participated in the study; and MoH Data and Information Centre (Pusdatin), Directorate General of Public Health, Directorate General of Health Care Services who have supported the study implementation. All authors did not receive funding for the creation of this manuscript. This work was supported in part by the IARC/WHO, through training by the Biobanking and Population Cohort Network (BCNet; CRDF Global, Award No. 66415). The company does not have a role in the study design, data collection and analysis, decision to publish, or preparation of the manuscript. Where authors are identified as personnel of the International Agency for Research on Cancer or World Health Organization, the authors alone are responsible for the views expressed in this article and they do not necessarily represent the decisions, policy or views of the International Agency for Research on Cancer or World Health Organization.

Disclaimer

The company does not have a role in the study design, data collection and analysis, decision to publish, or preparation of the manuscript. Where authors are identified as personnel of the International Agency for Research on Cancer/World Health Organization, the authors alone are responsible for the views expressed in this article and they do not necessarily represent the decisions, policy or views of the International Agency for Research on Cancer/World Health Organization.

Data Availability

The data sets generated during and/or analyzed during this study are available from the corresponding author on reasonable request.

Authors' Contributions

DNA led the study design, built the paper concept, main structure and methodology. AHS, CAM, and AFL carried out the study. MTAE, VW, SD, IL, and MA accessed and analyzed the data. DNA, AHS, CAM, AFL, MTAE, VW, SD, and IL wrote the first draft of the paper. ZK and LM validated the study and critically revised the manuscript content. DNA and AHS had primary responsibility for the final content.

Conflicts of Interest

While two authors (LM and DNA) are affiliated with Aceso Global Health Consultants Pte Limited, which is a private company, we declare that this research project does not receive funding from Aceso Global Health Consultants. LM is the director of the company, and DNA is a consultant of the company. However, both of them contributed to this paper on a pro-bono basis.

Multimedia Appendix 1
Scoring and weighting for internet quality data analysis.
[DOCX File, 12 KB - medinform_v13i1e65940_app1.docx]

Multimedia Appendix 2
Number of Puskesmas without internet by province.
[DOCX File, 150 KB - medinform_v13i1e65940_app2.docx]

Multimedia Appendix 3
Participation rate of Puskesmas in “internet quality assessment across public health center (Puskesmas) in Indonesia.”
[DOCX File, 9 KB - medinform_v13i1e65940_app3.docx]

Multimedia Appendix 4
Distribution based on types of internet use and internet quality based on participants’ perspectives. LAN: local area network; VSAT: very small aperture terminal.
[DOCX File, 289 KB - medinform_v13i1e65940_app4.docx]

References

1. The world health report 2008 — primary health care (now more than ever). : World Health Organization; 2008 URL: https://iris.who.int/handle/10665/43949 [accessed 2025-09-08]

XSL•FO
RenderX

2. Rifkin SB. Alma ata after 40 years: primary health care and health for all-from consensus to complexity. BMJ Glob Health 2018;3(Suppl 3):e001188. [doi: 10.1136/bmjgh-2018-001188] [Medline: 30622747]
3. The declaration of Alma-Ata. World Health Organization. 1988. URL: https://www.who.int/publications/i/item/declaration-of-alma-ata [accessed 2025-08-25]
4. Profil Kesehatan Indonesia 2022. : Kementerian Kesehatan RI; 2023 URL: https://kemkes.go.id/id/profil-kesehatan-indonesia-2022 [accessed 2025-09-08]
5. Peraturan Menteri Kesehatan Republik Indonesia Nomor 43 Tahun 2019 Tentang Pusat Kesehatan Masyarakat [Article in Indonesian]. Kementerian Kesehatan RI. 2019. URL: https://repository.kemkes.go.id/book/515 [accessed 2025-09-11]
6. Hertling S, Hertling D, Schleußner E, Loos F, Graul I. E-health – The importance of the internet as an informative digital health application for gynecological patients in times of SARs-CoV2: a national cross-sectional survey. Informatics in Medicine Unlocked 2022;30:100942. [doi: 10.1016/j.imu.2022.100942]
7. Hertling S, Hertling D, Loos F, Martin D, Graul I. Digitization in gynecology and obstetrics in times of COVID-19: Results of a national survey. Internet Interv 2021 Dec;26:100478. [doi: 10.1016/j.invent.2021.100478] [Medline: 34786351]
8. Manurung MK, Reo SE, Pardosi JF, Muscatello DJ. Evaluation of the Indonesian Early Warning Alert and Response System (EWARS) in West Papua, Indonesia. WHO South East Asia J Public Health 2020 Sep;9(2):111-117. [doi: 10.4103/2224-3151.294304] [Medline: 32978343]
9. Aisyah DN, Utami A, Rahman FM, et al. Using an electronic immunization registry (Aplikasi Sehat IndonesiaKu) in Indonesia: cross-sectional study. Interact J Med Res 2025 Mar 27;14:e53849. [doi: 10.2196/53849] [Medline: 40146988]
10. Putri UA, Prasetijo AB, Purnami CT. Drug Logistics Management Information System in Puskesmas Pharmacy Services: Literature Review. MPPKI ;6(6) [FREE Full text]
11. Pemeriksaan kesehatan gratis (PKG) [Article in Indonesian]. Kemenkes RI. 2025. URL: https://ayosehat.kemkes.go.id/diet-sehat/pemeriksaan-kesehatan-gratis [accessed 2025-07-16]
12. Herni D, Lestari S, Supadiyasa IW. Implementation Of The National Health Insurance Policy Within The Banggai District Health Office. Public Policy Journal 2025;6(1) [FREE Full text]
13. Pemeriksaan kesehatan gratis (PKG) [Article in Indonesian]. Kemenkas.: Jakarta: Direktorat Jenderal Pelayanan Kesehatan; 2023. URL: https://ayosehat.kemkes.go.id/diet-sehat/pemeriksaan-kesehatan-gratis [accessed 2025-08-01]
14. Siyam A, Ir P, York D, et al. The burden of recording and reporting health data in primary health care facilities in five low- and lower-middle income countries. BMC Health Serv Res 2021 Sep 13;21(Suppl 1):691. [doi: 10.1186/s12913-021-06652-5] [Medline: 34511083]
15. Martha S. The analysis of geospatial information for validating some numbers of islands in Indonesia. IJG 2017 Dec 27;49(2):204. [doi: 10.22146/ijg.12792]
16. Population, total. World Bank Group. 2022. URL: https://data.worldbank.org/indicator/SP.POP.TOTL [accessed 2023-08-02]
17. Djawwad Y, Suhaeb S, Mustakim R, Jaya H, Ronge S, Sakka S. The Development of an intelligent e-health Mobile Application in Indonesia: A Preliminary Study. INSIST 2019 Oct(2):240-245. [doi: 10.23960/ins.v4i2.240]
18. How can Indonesia improve the quality of its internet services and universalize access? World Bank blogs. URL: https://blogs.worldbank.org/eastasiapacific/how-can-indonesia-improve-quality-its-internet-services-and-universalize-access [accessed 2025-08-01]
19. Afrizal SH, Handayani PW, Hidayanto AN, Eryando T, Budiharsana M, Martha E. Barriers and challenges to Primary Health Care Information System (PHCIS) adoption from health management perspective: a qualitative study. Inform Med Unlocked 2019;17:100198. [doi: 10.1016/j.imu.2019.100198]
20. Odekunle FF, Odekunle RO, Shankar S. Why sub-Saharan Africa lags in electronic health record adoption and possible strategies to increase its adoption in this region. Int J Health Sci (Qassim) 2017;11(4):59-64. [Medline: 29085270]
21. deRiel E, Puttkammer N, Hyppolite N, et al. Success factors for implementing and sustaining a mature electronic medical record in a low-resource setting: a case study of iSanté in Haiti. Health Policy Plan 2018 Mar 1;33(2):237-246. [doi: 10.1093/heapol/czx171] [Medline: 29253138]
22. Johanson GA, Brooks GP. Initial scale development: sample size for pilot studies. Educ Psychol Meas 2010 Jun;70(3):394-400. [doi: 10.1177/0013164409355692]
23. van Teijlingen E, Hundley V. The importance of pilot studies. Nurs Stand 2002;16(40):33-36. [doi: 10.7748/ns2002.06.16.40.33.c3214] [Medline: 12216297]
24. Thorndike RM. Book Review: psychometric theory (3rd ed.) by Jum Nunnally and Ira Bernstein New York: McGraw-Hill, 1994, xxiv + 752 pp. Appl Psychol Meas 1995 Sep;19(3):303-305. [doi: 10.1177/014662169501900308]
25. Mazhar T, Malik MA, Mohsan SAH, et al. Quality of service (QoS) performance analysis in a traffic engineering model for next-generation wireless sensor networks. Symmetry (Basel) 2023;15(2):513. [doi: 10.3390/sym15020513]
26. Alkenani J, Nassar KA. Network monitoring measurements for quality of service: a review. IJEEE 2022 Dec 15;18(2):33-42. [doi: 10.37917/ijeee.18.2.5]
27. Panahi PHS, Jalilvand AH, Diyanat D. Machine learning-driven open-source framework for assessing qoe in multimedia networks. arXiv. Preprint posted online on Sep 10, 2024. [doi: 10.48550/arXiv.2406.08564]
28. Yu J, Meng S. Impacts of the internet on health inequality and healthcare access: a cross-country study. Front Public Health 2022;10:935608. [doi: 10.3389/fpubh.2022.935608] [Medline: 35757602]

XSL•FO
RenderX

29. Van Parys J, Brown ZY. Broadband internet access and health outcomes: patient and provider responses in Medicare. Int J Ind Organ 2024 Jul;95:103072. [doi: 10.1016/j.ijindorg.2024.103072]
30. Biga R, Nottebaum S, Kozlakidis Z, Psomiadis S. Digitalization of healthcare in LMICS: digital health and the digital divide based on technological availability and development. In: Kozlakidis Z, Muradyan A, Sargsyan K, editors. Digitalization of Medicine in Low- and Middle-Income Countries. Sustainable Development Goals Series: Springer; 2024. [doi: 10.1007/978-3-031-62332-5_18]
31. Marcin JP, Shaikh U, Steinhorn RH. Addressing health disparities in rural communities using telehealth. Pediatr Res 2016 Jan;79(1-2):169-176. [doi: 10.1038/pr.2015.192] [Medline: 26466080]
32. Labrique AB, Wadhwani C, Williams KA, et al. Best practices in scaling digital health in low and middle income countries. Global Health 2018 Nov 3;14(1):103. [doi: 10.1186/s12992-018-0424-z] [Medline: 30390686]
33. Eze SC, Awa HO, Okoye JC, Emecheta BC, Anazodo RO. Determinant factors of information communication technology (ICT) adoption by government‐owned universities in Nigeria. Journal of Ent Info Management 2013 Jul 19;26(4):427-443. [doi: 10.1108/JEIM-05-2013-0024]
34. Georgiou A, Li J, Thomas J, Dahm MR, Westbrook JI. The impact of health information technology on the management and follow-up of test results - a systematic review. J Am Med Inform Assoc 2019 Jul 1;26(7):678-688. [doi: 10.1093/jamia/ocz032] [Medline: 31192362]
35. Nimgaonkar V, Aggarwal C, Berman AT, et al. Impact of telemedicine adoption on accessibility and time to treatment in patients with thoracic malignancies during the COVID-19 pandemic. BMC Cancer 2021 Oct 11;21(1):1094. [doi: 10.1186/s12885-021-08819-z] [Medline: 34635061]
36. Puplampu KP, Hanson KT, Shaw TM. From MDGS to SDGS: African development challenges and prospects. In: From Millennium Development Goals to Sustainable Development Goals, 1st edition: Routledge; 2017. [doi: 10.4324/9781315228068-1]
37. Erku D, Khatri R, Endalamaw A, et al. Digital health interventions to improve access to and quality of primary health care services: a scoping review. Int J Environ Res Public Health 2023 Sep 28;20(19):6854. [doi: 10.3390/ijerph20196854] [Medline: 37835125]
38. Badan Pusat Statistik (BPS). Indeks Pembangunan Teknologi Informasi Dan Komunikasi [Book in Indonesian]: Badan Pusat Statistik; 2022. URL: https://tinyurl.com/4wdmnftr [accessed 2025-09-11]
39. UNICEF, ITU, BCG. Indonesia case study (giga in collaboration with boston consulting group). 2021 URL: https://www.itu.int/en/ITU-D/Regional-Presence/AsiaPacific/Documents/Indonesia%20case%20study%5B1%5D.pdf [accessed 2025-09-11]
40. Husna A, Budiman L. Lessons for enhancing fast and reliable internet from southwest sumba district. Center for Indonesian Policy Studies Indonesia. 2023. URL: https://repository.cips-indonesia.org/media/publications/566907-connecting-the-unconnected-lessons-for-e-8357258b.pdf [accessed 2025-09-11]
41. Harmadi SAB, Adji A. A. REGIONAL INEQUALITY IN INDONESIA: PRE AND POST REGIONAL AUTONOMY ANALYSIS. WORKING PAPER 50-e - 2020. TNP2K. 2020 URL: https://kms.kemenkopm.go.id/index.php?p=show_detail&id=71&keywords=
42. The ICT development index. The telecommunication development sector (ITU-d). URL: https://www.itu.int/en/ITU-D/Statistics/Pages/IDI/default.aspx [accessed 2025-08-01]
43. Centers for Disease Control and Prevention. Using Telehealth to Expand Access to Essential Health Services During the COVID-19 Pandemic. 2020. URL: https://web.archive.org/web/20220105100151/https://www.cdc.gov/coronavirus/2019-ncov/hcp/telehealth.html
44. Ghia CJ, Patil AS, Ved JK, Jha RK. Benefits of telemedicine and barriers to its effective implementation in rural India: a multicentric E-survey. Ind Med Gaz 2013;146:1-7 [FREE Full text]
45. Martínez A, Villarroel V, Seoane J, del Pozo F. A study of a rural telemedicine system in the Amazon region of Peru. J Telemed Telecare 2004;10(4):219-225. [doi: 10.1258/1357633041424412] [Medline: 15273032]
46. Kaboré SS, Ngangue P, Soubeiga D, et al. Barriers and facilitators for the sustainability of digital health interventions in low and middle-income countries: a systematic review. Front Digit Health 2022;4:1014375. [doi: 10.3389/fdgth.2022.1014375] [Medline: 36518563]
47. Mossberger K, Tolbert CJ, Franko W. 7 the geography of barriers to broadband adoption. In: Digital Cities: The Internet and the Geography of Opportunity, Oxford Studies in Digital Politics: Oxford Academic; 2012. [doi: 10.1093/acprof:oso/9780199812936.001.0001]
48. Weltevreden JWJ, Atzema O, Frenken K, de Kruif K, van Oort FG. The geography of internet adoption by independent retailers in the Netherlands. Environ Plann B Plann Des 2008 Jun;35(3):443-460. [doi: 10.1068/b33032]
49. Jing-hao S. The effect of AS's geographic locations on internet's stability. Presented at: Proceedings of the 2nd International Conference On Systems Engineering and Modeling (ICSEM 2013); Apr 19-20, 2013; Beijing, China p. 347-353. [doi: 10.2991/icsem.2013.65]
50. Rajagukguk W. The demographic and economic features: the nexus with internet use. Heliyon 2022 Sep;8(9):e10686. [doi: 10.1016/j.heliyon.2022.e10686] [Medline: 36177234]

XSL•FO
RenderX

51. Greenstein S. The basic economics of internet infrastructure. Journal of Economic Perspectives 2020 May 1;34(2):192-214. [doi: 10.1257/jep.34.2.192]
52. Korkmaz Ö, Erer E, Erer D. Internet access and its role on educational inequality during the COVID-19 pandemic. Telecomm Policy 2022 Jun;46(5):102353. [doi: 10.1016/j.telpol.2022.102353] [Medline: 35437338]
53. Afzal A, Khan S, Daud S, Ahmad Z, Butt A. Addressing the digital divide: access and use of technology in education. JSSR 2023 Apr 8;3(2):883-895. [doi: 10.54183/jssr.v3i2.326]
54. Pratama A, Al-Shaikh M. Relation and growth of internet penetration rate with human development level from 2000 to 2010. CIBIMA 2012:1-8. [doi: 10.5171/2012.778309]
55. Makoviy KA, Proskurin DK, Khitskova YV, Metelkin YV. A comparison of linear programming and the genetic algorithm approaches to the problem of optimizing the server hardware resources for hosting virtual desktops. J Phys: Conf Ser 2018 Sep 1;1096:012171. [doi: 10.1088/1742-6596/1096/1/012171]
56. Gupta N, Batra M, Khosla A. Optimizing greedy algorithm to balance the server load in cloud simulated environment. 2021 Presented at: 2021 Third International Conference on Inventive Research in Computing Applications (ICIRCA); Sep 2-4, 2021; Coimbatore, India p. 351-356. [doi: 10.1109/ICIRCA51532.2021.9544107]
57. Gbedawo VW, Agyeman GO, Ankah CK, Daabo MI. An overview of computer memory systems and emerging trends. American Journal of Electrical and Computer Engineering 2023;7:19-26. [doi: 10.11648/j.ajece.20230702.11]
58. Wang L. Analysis of factors affecting computer data processing speed. J Phys: Conf Ser 2020 Oct 1;1648(2):022136. [doi: 10.1088/1742-6596/1648/2/022136]
59. Goel U, Ludin S, Steiner M. Web performance with android's battery-saver mode. arXiV. Preprint posted online on Mar 13, 2020. [doi: 10.48550/arXiv.2003.06477]
60. Internet speeds guide. MCSnet. URL: https://mcsnet.ca/support/understanding-speeds/ [accessed 2025-05-25]
61. What is RAM (random access memory)? Lifewire. URL: https://www.lifewire.com/what-is-random-access-memory-ram-2618159 [accessed 2025-05-25]
62. Andreolini M, Colajanni M, Lancellotti R. Impact of memory technology trends on performance of web systems. 2005 Presented at: International Conference on Next Generation Web Services Practices (NWeSP'05), Seoul, Korea (South); Aug 22-26, 2005. [doi: 10.1109/IEEECONF11129.2005]
63. Drew S. Apple Macos and IOS System Administration: Integrating and Supporting Iphones, Ipads, and Macbooks: United States, Apress; 2020. [doi: 10.1007/978-1-4842-5820-0]
64. Global Strategy on Digital Health 2020–2025: Regional Implementation Progress: Geneva: WHO; 2003. URL: https://www.who.int/publications/i/item/9789240020924 [accessed 2025-09-11]
65. Odekunle FF, Odekunle RO, Shankar S. Why sub-Saharan Africa lags in electronic health record adoption and possible strategies to increase its adoption. Int J Health Sci (Qassim) 2017;11(4):59-64. [Medline: 29085270]
66. Were MC, Sutherland JM, Bwana M, Ssali J, Emenyonu N, Tierney WM. Using computer decision support systems to improve HIV care in resource-constrained settings: lessons from the field. Journal of the American Medical Informatics Association (JAMIA) 2019;26(9):1099-1103. [doi: 10.1093/jamia/ocz076]
67. Nyangena J, Rajgopal R, Ombech EA, et al. Maturity assessment of Kenya's health information system interoperability readiness. BMJ Health Care Inform 2021 Jun;28(1):e100241. [doi: 10.1136/bmjhci-2020-100241] [Medline: 34210718]
68. Luna D, Almerares A, Mayan JC III, González Bernaldo de Quirós F, Otero C. Health informatics in developing countries: going beyond pilot practices to sustainable implementations: a review of the current challenges. Healthc Inform Res 2014 Jan;20(1):3-10. [doi: 10.4258/hir.2014.20.1.3] [Medline: 24627813]
69. Fraser HSF, Blaya J, et al. Implementing medical information systems in developing countries, what works and what doesn't. BMJ Health & Care Informatics 2018;25(1):66-71 [FREE Full text] [Medline: 21346975]
70. Bhat WA. Capacity barriers in hard disks: problems, solutions and lessons. Int j inf tecnol 2020 Mar;12(1):155-163. [doi: 10.1007/s41870-018-0144-x]
71. Wood R. Future hard disk drive systems. J Magn Magn Mater 2009 Mar;321(6):555-561. [doi: 10.1016/j.jmmm.2008.07.027]
72. Hasegawa K, O'Brien N, Prendergast M, Ajah CA, Neves AL, Ghafur S. Cybersecurity interventions in health care organizations in low- and middle-income countries: scoping review. J Med Internet Res 2024 Nov 20;26:e47311. [doi: 10.2196/47311] [Medline: 39566062]
73. Global strategy on digital health 2020–2025: regional implementation progress. World Health Organization. 2021. URL: https://www.who.int/publications/i/item/9789240020924 [accessed 2025-09-11]
74. He Y, Aliyu A, Evans M, Luo C. Health care cybersecurity challenges and solutions under the climate of COVID-19: scoping review. J Med Internet Res 2021 Apr 20;23(4):e21747. [doi: 10.2196/21747] [Medline: 33764885]
75. Suhlrie L, Bartram J, Burns J, Joca L, Tomaro J, Rehfuess E. The role of energy in health facilities: a conceptual framework and complementary data assessment in Malawi. PLoS ONE 2018;13(7):e0200261. [doi: 10.1371/journal.pone.0200261] [Medline: 30028861]
76. Chen YJ, Chindarkar N, Xiao Y. Effect of reliable electricity on health facilities, health information, and child and maternal health services utilization: evidence from rural Gujarat, India. J Health Popul Nutr 2019 Feb 19;38(1):7. [doi: 10.1186/s41043-019-0164-6] [Medline: 30782203]

XSL•FO
RenderX

77. Bhandari L, Dutta S. Health infrastructure in rural india. In: Kalra P, Rastogi A, editors. India Infrastructure Report 2007 2007. URL: https://www.academia.edu/40176448/Health_Infrastructure_in_Rural_India [accessed 2025-09-11]
78. Close to one billion people globally are served by health-care facilities with no electricity access or with unreliable electricity. WHO. 2003. URL: https://tinyurl.com/2fzb4ntm [accessed 2025-08-01]
79. Sambodo MT. Rural Electrification Program in Indonesia: Comparing SEHEN and SHS Program. Econ Financ Indones 2015;61(2):107. [doi: 10.7454/efi.v61i2.505]
80. Khogali A, et al. Building power-ful health systems: the impacts of electrification on health outcomes in LMICs. Psychol Health Med 2022;27(9):1836-1850. [doi: 10.1080/13548506.2022.2109049] [Medline: 35929975]
81. Chawla S, Kurani S, Wren SM, et al. Electricity and generator availability in LMIC hospitals: improving access to safe surgery. J Surg Res 2018 Mar;223(1):136-141. [doi: 10.1016/j.jss.2017.10.016] [Medline: 29433865]
82. Lestari H, Arentsen M, Bressers H, Gunawan B, Iskandar J, Parikesit P. Sustainability of renewable off-grid technology for rural electrification: a comparative study using the IAD framework. Sustainability 2018;10(12):4512. [doi: 10.3390/su10124512]
83. Kanagawa M, Nakata T. Assessment of access to electricity and the socio-economic impacts in rural areas of developing countries. Energy Policy 2008 Jun;36(6):2016-2029. [doi: 10.1016/j.enpol.2008.01.041]
84. McCawley P. Rural electrification in Indonesia–is it time? Bull Indones Econ Stud 1978 Jul;14(2):34-69. [doi: 10.1080/00074917812331333311]
85. Indah RN, Rarasati AD. Enabling electricity access to rural areas in Indonesia: challenges and opportunities. IOP Conf Ser: Mater Sci Eng 2020 Apr 1;830(2):022069. [doi: 10.1088/1757-899X/830/2/022069]
86. Rencana Usaha Penyediaan Tenaga Listrik 2019-2028 [Report in Indonesian]. : Perusahaan Listrik Negara PT. PLN (PERSERO); 2018 URL: https://web.pln.co.id/statics/uploads/2021/08/5b16d-kepmen-esdm-no-39-k-20-mem-2019-tentang-pengesahan-ruptl-pt-pln-2019-2028.pdf
87. Haanyika CM. Rural electrification policy and institutional linkages. Energy Policy 2006 Nov;34(17):2977-2993. [doi: 10.1016/j.enpol.2005.05.008]
88. Urmee T, Harries D, Schlapfer A. Issues related to rural electrification using renewable energy in developing countries of Asia and Pacific. Renewable Energy 2009 Feb;34(2):354-357. [doi: 10.1016/j.renene.2008.05.004]
89. Measuring digital development: facts and figures 2022. International telecommunication union (ITU). URL: https://www.itu.int/en/ITU-D/Statistics/Pages/facts/default.aspx [accessed 2025-08-01]
90. Global strategy on digital health 2020–2025. World Health Organization (WHO). 2020. URL: https://www.who.int/publications/i/item/9789240020924 [accessed 2025-08-01]
91. The digital economy for africa initiative (DE4A). World Bank Group. 2021. URL: https://www.worldbank.org/en/programs/all-africa-digital-transformation [accessed 2025-08-01]
92. Global benchmarking report: measuring digital health transformation. ITU. 2023. URL: https://www.itu.int/dms_pub/itu-d/opb/ind/D-IND-SDDT_AFR-2025-PDF-E.pdf [accessed 2025-09-11]
93. Digital transformation roadmap (2023 – 2028). Ministry Of Information, Communication and Information Technology, The United Republic of Tanzania. URL: https://ict.go.ug/site/documents/Digital%20Transformation%20Roadmap.pdf [accessed 2025-09-11]
94. Wang L, Liang D, HuangFu H, Ke C, Wu S, Lai Y. Enterprise-led internet healthcare provision in China: insights from a leading platform. Front Digit Health 2025;7:1491183. [doi: 10.3389/fdgth.2025.1491183] [Medline: 40099033]
95. Han Y, Lie RK, Guo R. The internet hospital as a telehealth model in China: systematic search and content analysis. J Med Internet Res 2020 Jul 29;22(7):e17995. [doi: 10.2196/17995] [Medline: 32723721]

Abbreviations

CPU: central processing unit
DTO: Digital Transformation Office
EMR: electronic medical record
ICT: information and communication technology
LAN: local area network
LMIC: low- and middle-income countries
MoH: Ministry of Health
PHC: primary health care
Puskesmas: public health centers
QoE: Quality of Experience
QoS: Quality of Service
SISMAL: Sistem Informasi Malaria

XSL•FO
RenderX

Edited by C Perrin; submitted 30.08.24; peer-reviewed by M Arief, MA Bahar; revised version received 16.07.25; accepted 17.07.25; published 15.09.25.

Please cite as:
Aisyah DN, Setiawan AH, Lokopessy AF, Mayadewi CA, Endryantoro MTA, Wibowo V, Disviana S, Laksana I, Aviandito M, Kozlakidis Z, Manikam L
Assessing Internet Quality Across Public Health Centers in Indonesia: Cross-Sectional Evaluation Study
JMIR Med Inform 2025;13:e65940
URL: https://medinform.jmir.org/2025/1/e65940
doi:10.2196/65940

© Dewi Nur Aisyah, Agus Heri Setiawan, Alfiano Fawwaz Lokopessy, Chyntia Aryanti Mayadewi, M Thoriqul Aziz Endryantoro, Viktor Wibowo, Sarah Disviana, Indra Laksana, Mohammad Aviandito, Zisis Kozlakidis, Logan Manikam. Originally published in JMIR Medical Informatics (https://medinform.jmir.org), 15.9.2025. This is an open-access article distributed under the terms of the Creative Commons Attribution License (https://creativecommons.org/licenses/by/4.0/), which permits unrestricted use, distribution, and reproduction in any medium, provided the original work, first published in JMIR Medical Informatics, is properly cited. The complete bibliographic information, a link to the original publication on https://medinform.jmir.org/, as well as this copyright and license information must be included.

XSL•FO
RenderX

Original Paper

Toward Interoperable Digital Medication Records on Fast Healthcare Interoperability Resources: Development and Technical Validation of a Minimal Core Dataset

Eduardo Salgado-Baez[1,2], MD, Dr med; Raphael Heidepriem[1,2]; Renate Delucchi Danhier[3], Dr phil; Eugenia Rinaldi[2], MSc; Vishnu Ravi[4], MD; Akira-Sebastian Poncette[5], Prof Dr; Iris Dahlhaus[5], Dr phil nat; Daniel Fürstenau[5,6], Prof Dr; Felix Balzer[5], Prof Dr; Sylvia Thun[2], Prof Dr; Julian Sass[2], MSc

[1]Department of Anesthesiology and Intensive Care Medicine (CVK/CCM), Charité - Universitätsmedizin Berlin, Berlin, Germany

[2]Core Unit Digital Medicine and Interoperability, Berlin Institute of Health, Charité - Universitätsmedizin Berlin, Berlin, Germany

[3]Institute for Diversity Studies, TU Dortmund University, Dortmund, Germany

[4]Stanford Mussallem Center for Biodesign, Stanford University, Stanford, United States

[5]Institute of Medical Informatics, Charité - Universitätsmedizin Berlin, Berlin, Germany

[6]School of Business & Economics, Freie Universität Berlin, Berlin, Germany

Corresponding Author:
Eduardo Salgado-Baez, MD, Dr med
Core Unit Digital Medicine and Interoperability
Berlin Institute of Health
Charité - Universitätsmedizin Berlin
Charitéplatz 1
Berlin, 10117
Germany
Phone: 49 030450631167
Email: eduardo.salgado@charite.de

Abstract

Background: Medication errors represent a widespread, hazardous, and costly challenge in health care settings. The lack of interoperable medication data within and across hospitals not only creates an administrative burden through redundant data entry but also increases the risk of errors due to human mistakes, imprecise data transformations, and misinterpretations. While digital solutions exist, fragmented systems and nonstandardized data hinder effective medication management.

Objective: This study aimed to assess medication data available across the multiple systems of a large university hospital, identify a minimum dataset with the most relevant information, and propose a standard interoperable FHIR-based solution that can import and transfer information from a standardized drug master database to various target systems.

Methods: Medication data from all relevant departments of a large German hospital were thoroughly analyzed. To ensure interoperability, data elements for developing a minimum dataset were defined based on relevant medication identifiers, the Health Level 7 Fast Health Interoperability Resources (HL7 FHIR) standard, and the German Medical Informatics Initiative (MII) specifications. To enhance medication identification accuracy, the dataset was further enriched with information from Germany's most comprehensive drug database and European Standard Drug Terms (EDQM) to further enrich medication identification accuracy. Finally, data on 60 frequently used medications in the institution were systematically extracted from multiple medication systems used in the institution and integrated into a new structured, dedicated database.

Results: The analysis of all the available medication datasets within the institution identified 7964 drugs. However, limited interoperability was observed due to a fragmented local IT infrastructure and challenges in medication data standardization. Data integrated and available in the new structured medication dataset with key elements to ensure data identification accuracy and interoperability, successfully enabled the generation of medication order messages, ensuring medication interoperability, and standardized data exchange.

Conclusions: Our approach addresses the lack of interoperability in medication data and the need for standardized data exchange. We propose a minimum set of data elements aligned with German and international coding systems to be used in combination

XSL•FO
RenderX

with the FHIR standard for processes such as the digital transfer of discharge medication prescriptions from intensive care units to general wards, which can help to reduce medication errors and enhance patient safety.

(JMIR Med Inform 2025;13:e64099) doi:10.2196/64099

KEYWORDS

FHIR; FAIR; standardization; dataset; electronic health records; digital; medication records; technical; validation; medication error; Fast Healthcare Interoperability Resources; Findability, Accessibility, Interoperability, and Reusability; software

Introduction

Medication Errors

In 2022, approximately seventeen million patients were treated in German hospitals, of which more than 2 million were admitted to an intensive care unit (ICU) for the treatment of life-threatening conditions due to the dysfunction of one or more organs [1], which inevitably requires the administration of multiple medicaments [2]. As a result of the complexity of the medication process, medication errors have been a frequent and safety-relevant problem in medical care [3]. The first major groundbreaking study that quantified this situation was the "To Err is Human: Building a Safer Health Care System" report conducted by the Institute of Medicine in the United States [4]. In recent years, as reported by the Joint Commission in 2020 [5], medication errors are involved in 5.4% of all severe injuries or patient deaths, with a total annual cost of USD 42 billion according to estimates of the World Health Organization (WHO) [6,7].

This situation is caused, among other factors, by a lack of interoperable pharmaceutical documentation systems [8] as well as because many steps of the process (ie, prescription, transmission of the information, and documentation) are still highly dependent on manual input and prevent the implementation of medication reconciliation systems (MedRec). As a result, medication errors and adverse drug events related to unintended medication discrepancies in electronic health records (EHR) are still a major public health problem and are listed unsurprisingly among the top 10 health technology hazards for 2020 by the Emergency Care Research Institute [9-11].

Interoperability, Standardization, and Data Access

There is evidence that interoperable IT systems and the use of international standards can help to mitigate medication errors and facilitate the exchange of information across different platforms and software used for drug prescription and administration [12].

The Healthcare Information and Management Systems Society defines interoperability as the capacity of at least 2 IT systems to communicate by exchanging standardized data, allowing the use of the exchanged information [13]. Its implementation in the medication field is critical for the digital transformation of drug prescription, administration, and research [14], and relies on the employment of internationally standardized data and terminologies.

For the health care industry, Health Level 7 (HL7) has provided a comprehensive set of international standards for clinical and administrative data transfer across software that numerous health care providers employ to promote data exchange and interoperability, including our hospital and its EHR. It remains the most popular and widespread health care framework, improving diagnostics, therapy, and patient safety and outcomes. [15,16].

In 2011, due to the rapidly growing amount of health data, HL7 started developing the Fast Interoperability Resources (FHIR), a standard that addresses the need for faster and better methods for interoperable data exchange.

FHIR was designed to be flexible and adaptable, making this standard easy to implement and suitable for a wide range of clinical processes. It uses a modern web-based application programming interface (API) [17].

For global standardization and interoperability of medication data, the International Organization for Standardization (ISO) has been developing the Identification of Medicinal Products (IDMP) since 2012, providing a suite of 5 standards (ISO 11615, ISO 11616, ISO 11238, ISO 11239, and ISO 11240) for identifying and exchanging the information of each medicinal product for human use throughout the world [18-23].

Although these standards were created for pharmacovigilance purposes, over the years, the ISO IDMP standards have come to support various other activities, including those related to the norms for the unique identification and exchange of regulated information about medicinal and pharmaceutical products.

In Europe, the European Medicines Agency (EMA) is the institution responsible for gradually implementing ISO IDMP standards through a plan and services based on four domains of master data in pharmaceutical regulatory processes (Substance, Product, Organization, and Referential [SPOR]), which are crucial to ensuring interoperability [24,25].

In cooperation with the EMA, the European Directorate for the Quality of Medicines and HealthCare (EDQM) promotes the development of a common pharmacopoeia in Europe. In this context and as part of the implementation of quality standards for medicines, the EDQM [26] released the EDQM standard terms, comprising terms and definitions to describe (among others) pharmaceutical dose forms, routes and methods of administration, administration devices, and units of presentation [27], providing a legal and scientific basis for quality control of medications from development to marketing as well as a framework for the safe use of medicines on patients [28].

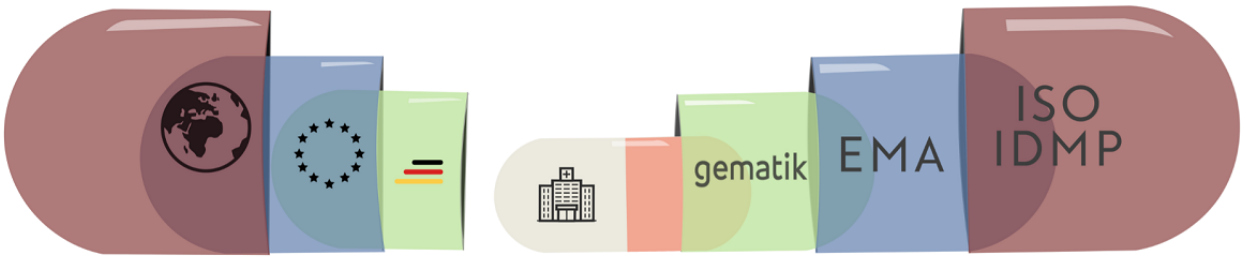
According to the EMA, the standards and services mentioned above enable operational benefits, especially considering their positive impact on the regulation of medicines and the simplification of medication information exchange in Europe and internationally. This higher degree of standardization and

XSL•FO
RenderX

regulation aims to provide a framework to improve data transfer, patient safety, and public health [29].

At the national level, the German Medical Informatics Initiative (MII) is a federal effort dedicated to digitizing the German health care system. As a part of this initiative, a medication task force group has been established to leverage standardized frameworks for different medication processes [30]. In addition, the gematik [31] is the current organization responsible for the federal telematics infrastructure (TI), a central platform for digital applications. One central function of the gematik is the definition and enforcement by law of binding standards for services, components, and applications for the TI and the implementation of standards' specifications like FHIR, SNOMED CT (Systematized Nomenclature of Medicine Clinical Terms), and LOINC (Logical Observation Identifiers Names and Codes). In the case of medication, the gematik is developing the ISiK-Modules (Informationstechnische Systeme in Krankenhäusern; English: Information technology systems in hospitals) based on FHIR resources for exchanging medication data [32]. An overview of the different standardization levels is presented in Figure 1.

Figure 1. Visualization of the standardization levels of medicinal products. EDQM: European Directorate for the Quality of Medicines; EMA: European Medicines Agency; IDMP: Identification of Medicinal Products; ISO: International Standardization Organization.



Responding to the need to make digital data assets and their associated metadata more usable by machines and reusable by humans, Wilkinson et al [33], developed a set of 15 guiding principles for scientific data management and stewardship, which are grouped into the four higher principles of Findability, Accessibility, Interoperability, and Reusability (FAIR). Implementing the FAIR Principles is relevant to improving efficiency and access to research and health care data. Since their publication, many authors have highlighted the benefits of its adoption [34-36].

In contrast, the most comprehensive medication records in Germany, such as the ABDA (Federal Union of German Associations of Pharmacists) or ABDA-MED (ABDA Medication Database) and MMI Pharmaindex Plus, are commercial, proprietary databases that can only be accessed under license, limiting public availability, and requiring authorized usage for comprehensive pharmaceutical data retrieval [37,38].

Objective

As our institution is not immune to the risk of medication errors, and modern IT solutions for medication management are set to be gradually implemented in the coming years, this paper aims to (1) assess the extent to which medication systems in our hospital use standardized medication data and comply with established standards and (2) propose a proof-of-concept FHIR-based interoperable solution with noncommercial, standardized, minimal, and FAIR medication data to enhance medication interoperability.

Methods

Departments Involved

The key units involved in the medication process were identified by the Chief Medical Informatics Officer (CMIO) team before the start of the study. Therefore, no additional partners were required for this project. The study included the IT department, the pharmacy, the PDMS used throughout the institution's ICUs, and selected general wards. It examined their databases, focusing on data quality, standardization, storage, governance, and both semantic and technical interoperability. The medication data provided and extracted from these datasets were systematically structured and classified to develop a standardized database.

Selection of Drugs and Data Components for the Standardized Database

As medication datasets are not freely accessible by default for safety and commercial reasons, governance staff responsible for managing medication records on a particular stakeholder's software provided access to the data. They provided the authors with access to the medication databases, detailed information about the software communication protocols for exchanging data, and the methods used to keep the information up to date. The selection criteria for drugs included in this study's novel and standardized database were based on the 60 most frequently administered medications in an anesthesiology ICU. These drugs are documented using quick-access buttons in the medication section of the ICU Patient Data Management System (PDMS), designed for recording commonly used medications. For this study, data related to these drugs were extracted from the datasets of the units participating in the study, which used different systems, and were integrated into our database.

We searched and selected data components from multiple datasets used in the institution to develop a minimal, FAIR, and

XSL•FO
RenderX

standardized dataset capable of accurately identifying every single drug with the least possible amount of data. Our selection was based on the Medication and Medication Request resources of the HL7 FHIR standard, given a future modernization of medication software. The following data elements for each drug were included: drug name, institution-specific product number, Pharmacy Central Number (PZN), Pharmacy Product Number (PPN), Anatomical Therapeutic Chemical (ATC), and the German Drug Substance Catalog (ASK) code.

Data provided from institutional databases was complemented with records drawn from the most comprehensive German medication register, the ABDA or ABDA-MED proprietary database [39]. To ensure compatibility with European standards [40], we added information available on the EDQM standard terms [41], incorporating standardized data on administration methods, intended site, and routes of administration. Ultimately, all data was compiled into a single medication core dataset [42], used to generate FHIR order message prototypes.

As summarized in Figure 2, the different pieces of information were gathered according to their availability to the different stakeholders as well as national and international databases.

Figure 2. Source of specific medication data and included data elements in the standardized database. ABDA: Federal Union of German Associations of Pharmacists; ABDA-MED: ABDA Medication Database; ASK: German drug substance catalog; ATC: Anatomical Therapeutic Chemical; EDQM: European Directorate for the Quality of Medicines and HealthCare; PPN: Pharmacy Product Number; PZN: Pharmacy Central Number.

	Pharmacy	IT department ABDA/ABDAMED	ICU's PDMS	General ward	EDQM
Drug name	x		x	x	
Product number	x				
Hospital's pharmacy code	x				
PPN	x	x			
PZN		x		x	
ATC		x	x	x	
ASK		x			
Administration method					x
Intended site					x
Basic dose form			x		x

Ethical Considerations

This work was conceived as part of an operative medication project at Charité - Universitätsmedizin Berlin and the Berlin Institute of Health (BIH) to assess the status quo and modernize medication software and management across the institution. The study did not gather patient data and focused solely on general medication records that included drug information for the analysis. Consequently, the authors did not pursue approval from the institutional ethics committee.

Results

Overview

Multiple medication software and datasets were used throughout the hospital. Medication software was provided by different companies with limited data compatibility and transfer capabilities between them. Different departments maintained medication records separately. For these reasons, it was necessary to contact the hospital staff responsible for each medication software and dataset used to analyze medication.

The EHR maintained the relevant medication master data by using the commercial medication database ABDA or ABDA-MED as the basis for the internal medication data managed by the IT department. A critical unit relying on this information was the pharmacy. The pharmacy information system (PIS) could exchange data directly with the ABDA-MED database, demonstrating interoperability through the shared use of the same database.

However, we found that the PIS lacked an interface to share data directly with other systems, such as the ICU PDMS or medication software in the general wards. Its working database was a spreadsheet listing 3146 medications available in the hospital's drug storage, containing four data attributes: institution-specific material number, PZN, drug name, and manufacturer. In other words, apart from communicating with the main database, the pharmacy was isolated and unable to exchange information in an interoperable manner with any other system involved in the medication process.

The assessment of the study ICU showed that medications were always prescribed and documented in digital form using the ICU's PDMS. Nonetheless, the digital user interface (UI) was founded on a spreadsheet-based database containing information about 4818 drugs, which was compiled and imported manually by a senior physician and an employee from the division of clinical procedures.

The PDMS database contained nonstandardized information, including drug ID, PDMS name, trade name, generic name, active ingredient, medication family, main administration method, application form, calories, weight, dosage, and incomplete administrative data. The PDMS was also isolated

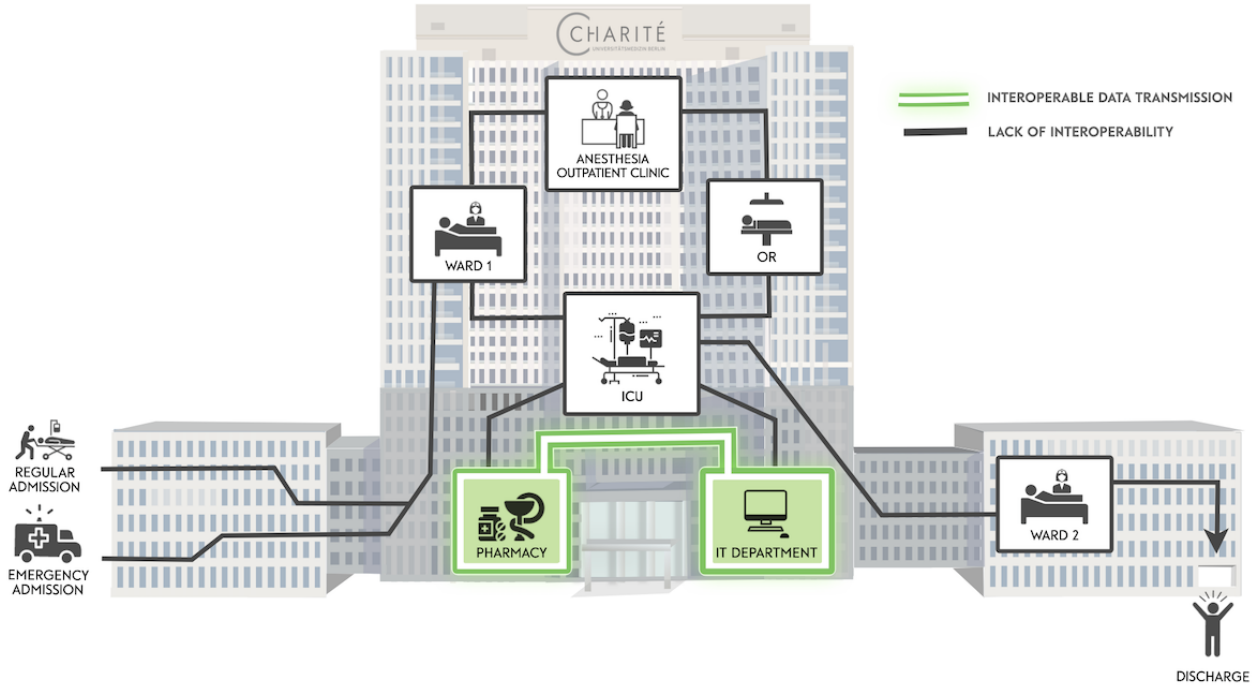
XSL•FO
RenderX

and noninteroperable, as it lacked an IT interface to transfer data to the EHR, PIS, or general wards.

The medication workflow in the examined general wards required a medication application to digitalize the medications prescribed to a particular patient. This system used data stored in another proprietary dataset, the MMI Pharmaindex, comprising the following information: ATC and *ICD-10* (*International Statistical Classification of Diseases, Tenth Revision*) codes, company type, country of production, molecule type, pharmaceutical form, molecule unit, molecule nature, and package unit. This software was incompatible with the other medication applications mentioned earlier due to the absence of an interface, and its data access was highly restricted.

In summary, we examined communication flow concerning medication in a large hospital. This process spans across several phases and departments, such as admission, ward, anesthesia, ICU, pharmacy, inpatient stay, and discharge as shown in Figure 3. Little interoperability was found across the examined systems; medication information was isolated and needed human intervention to be exchanged. The absence of a central database with uniform medication standards led to the maintenance of a wide range of isolated, noninteroperable datasets by different stakeholders, except for PIS and the IT Department, which used the ABDA-MED database.

Figure 3. Visualization of pharmaceutical data flow within the assessed organization: Green lines represent departments where interoperable data transmission has been successfully implemented, while black lines highlight areas where interoperability is still lacking. The visualization emphasizes the significant work that remains to be done.



After analyzing various databases and identifying a minimum dataset of the most relevant medication-related information, we developed a standardized medication database. This novel database incorporates a minimal set of FAIR-compliant data for 60 drugs frequently used in our hospital's ICUs, enabling accurate identification of each drug. The final database includes the following data: drug name, institution-specific product number, PZN, PPN, ATC, ASK, and EDQM codes for administration method, intended site of use, and routes of administration. Examples of 10 drugs are shown in Figure 4. A full version of the database is accessible on Figshare [43].

XSL•FO
RenderX

Figure 4. Extract of 10 drugs and their standardized identification codes. ASK: German drug substance catalog; ATC: Anatomical Therapeutic Chemical; EDQM: European Directorate for the Quality of Medicines and HealthCare; MN: Material Number; PPN: Pharmacy Product Number; PZN: Pharmacy Central Number.

Drug	EHR MN	NAME	PZN	PPN	ATC	ASK	EDQM (Basic dose form)	EDQM (Administration method)	EDQM (Intended site)
Propofol 1% 20ml	112279	Propofol-Lipuro 10mg/ml	1116443	111116444325	N01AX10	22898	BDF-080	AME-011	ISI-0033
Rocuronium 50mg	108808	Esmeron 10mg/ml	4793434	110479343486	M03AC09	25794	BDF-0083	AME-011	ISI-0033
Norardrenalin 1mg	107978	Artenerol 1mg/ml	3870227	110387022754	C01CA03	229	BDF-0083	AME-011	ISI-0033
Fentanyl 500µg	108915	Fentanyl Panpharma 50µg/ml	16200014	111620001424	N01AH01	6904	BDF-0083	AME-011	ISI-0033
Meropenem 1g	109742	Meropenem F. Eberth1g P.z.H.Inj.-/Inf.-L.	12472431	111247243107	J01DH02	27630	BDF-0066	AME-011	ISI-0033
Amiodaron 150mg	108460	Cordarex Injektionslösung Amp.	4590382	110459938244	C01BD01	21609	BDF-0083	AME-011	ISI-0033
Metamizol 1g	110132	Novaminsulfon-Ratiopharm 1g/2ml Inj.- Lsg. Amp.	6882768	110688276891	N02BB02	258	BDF-0083	AME-011	ISI-0033
Ibuprofen 600mg	115595	Ibuhexal 600mg Filmtabletten	245227	110024522722	M01AE01	5682	BDF-0069	AME-0019	ISI-0107
Clopidogrel 75mg	113490	Plavix 75mg Filmtabletten	51055	110005105572	B01AC04	29200	BDF-0069	AME-0019	ISI-0107
Midazolam 5mg	108672	Dormicum i.v. 5 mg/1 ml 5 Amp.	3085793	110308579327	N05CD08	22661	BDF-0083	AME-011	ISI-0033

Technical Validation and Proof-of-Concept Development

By using the developed database together with HL7 FHIR specifications, we generated order messages for communication within medication software (Multimedia Appendices 1 and 2). These messages incorporated drug-specific, standardized data essential for the exchange of information between various software and applications. These are the messages that each source node in the network would generate to be validated and forwarded to its destination by the FHIR server.

Another essential aspect identified during the analysis of medication prescriptions in the ICU was the standardization of custom formulations, where a composition of 2 or more drugs must be represented. These are frequently used in an ICU setting and thus have high therapeutic relevance. In this regard, an agreement between the IT and pharmacy departments was established, introducing a new material number for identifying compounded medications to comply with the proposed standardization (Multimedia Appendices 3 and 4).

Discussion

Principal Results

This study assessed pharmaceutical records in a large university hospital and proposes a standardized solution for digitalization and interoperability across various medication systems and datasets. Leveraging the HL7 FHIR standard, it outlines the development of a proof-of-concept solution to enhance seamless data exchange and integration.

As described by Lehne et al [44], noninteroperable systems lead to undesired outcomes, such as redundant data storage, manual data maintenance, data discrepancies, difficulty in drug tracking, billing problems, inefficiency, and resource waste due to the high costs and time demands on trained personnel. Manual entry and transmission of medication information can contribute to clinical staff dissatisfaction and pose risks of patient harm, including errors that could result in injuries or death [45]. In addition, these practices hinder extensive medication research and artificial intelligence (AI) adoption [46-48], making large-scale studies nearly unfeasible. They also impede the implementation of closed-loop medication administration (CLMA) and MedRec systems, which could significantly reduce medication administration errors [49-51].

Integrating documentation software across different clinical departments (eg, emergency room, normal ward, operating room, and ICU) and including nonclinical areas (eg, pharmacy or IT department) in data management remains an open challenge. Therefore, a standardized central database and an interoperable interface enabling seamless communication among various software systems in hospital settings are needed.

At the time of analysis, our clinic lacked a central medication database that considered all stakeholders in the prescription process or the scientific reuse of data across departments, leading to data isolation and lack of interoperability. This issue is a crucial obstacle to enhancing patient safety and quality of care. Consequently, the institution is undergoing a significant overhaul of medication processes with FHIR standards playing a significant role.

These challenges are not unique to our institution but represent a global issue stemming from the general lack of standardization [52]. Efforts such as ISO IDMP standards, EMA medication guidelines, and local initiatives like MII and gematik [53] in Germany are crucial and should be considered when developing any IT medication solution. Overcoming obstacles such as the absence of public medication databases is a significant public health concern, as it directly affects data accessibility, exchange, transparency, management [54], and reuse.

To tackle these issues, we propose a FHIR R4–based solution designed to seamlessly import and transfer information from a standardized drug master database to various target systems in a configurable manner. Developed with an international perspective, this approach aims to enhance interoperability and standardization in medication data exchange.

The FHIR profiles used derive from the German MII, which is currently only used for secondary purposes by our large hospital. We rely on MII assets for terminology services, validation, and profile conformance.

To implement this solution, we propose creating a FHIR server, built upon an open-source FHIR implementation such as HAPI FHIR. The server would facilitate the interoperable exchange of medication data between existing hospital systems.

XSL•FO
RenderX

In a messaging-based approach, the server could act as a middleware between systems using FHIR messaging operations for real-time bidirectional communication, with clients publishing medication-related events that the server transforms and forwards. Either of these solutions will use the MII terminology service to validate medication codes. In the next stage of our project, we will validate this approach in our environment by developing an application for medication management.

Its primary objective is to address and solve local challenges while optimizing workflows for health care stakeholders both nationally and internationally in the context of health data management. By providing a nonproprietary, FAIR medication core dataset, our solution has the potential to be integrated into broader initiatives such as the European Health Data Space (EHDS) [55]. This integration would promote secure, efficient, and timely communication, as well as seamless use of electronic medication data across the EU.

Furthermore, it is designed to meet the needs of physicians, pharmacists, computer scientists, researchers, and administration personnel while adhering to national and international IT standards and guidelines, such as Germany's Interop Council for Digital Health [56] and the WHO's 2020 global strategy on digital health [57]. It aligns with the widely accepted perspective that standardization and interoperability are crucial for enhancing patient care and safety [58], improving workforce satisfaction and productivity, and fostering research and innovation. To the best of our knowledge, no comparable proposal has been presented in the literature.

Limitations

This investigation has several limitations. Due to our institution's large size, we did not consider medication data transfer and documentation of each general ward or ICU, potentially overlooking an already interoperable solution that could serve as a model for further development. However, given the widespread use of diverse medication software standards, an institution-wide analysis would likely reveal more interoperability conflicts when implementing any IT solution.

In addition, although HL7 version 2.3 is the most popular and widely used health care framework, we focused on FHIR due to its efficiency, flexibility, and suitability for mobile applications, her, and cloud communications [59,60]. Nonetheless, the database presented here could also be adapted for HL7 v.2.3 thanks to its standardized structure.

Code Availability

All FHIR order messages were developed using Microsoft Visual Studio Code Version 1.90.2 and are available without restrictions on Figshare [61].

Conclusions

Our results show that it is very challenging to achieve standardization and interoperability of medication records across the different IT platforms used in a hospital ecosystem.

To address this situation, we propose a solution that facilitates seamless data exchange among stakeholders using medication software, leveraging FHIR standards to overcome system disparities and data silos based on a noncommercial minimal, and FAIR medication dataset. This approach seeks to streamline digitization efforts across hospital departments, in key processes like patient discharge from the ICU to general wards. Beyond improving operational efficiency, our interoperable medication solution can help to reduce errors, enhance patient safety, and elevate the quality of care by enabling standardized data exchange and seamless stakeholder communication across the hospital ecosystem. Our study represents a conceptual proposal for a future solution at this stage, with no specific application or API interactions developed yet.

Acknowledgments

The authors would like to thank Josef Schepers, Moritz Lehne, and Prof Marcus Friedrich, for providing a valubale overview of this complex topic. Our gratitude to Muazzez Weiss and Jan Fahrenkrog-Petersen for their support in gathering data for standardization, and to Thomas Ocker for his remarks on the standardization of custom drug mixtures.

This project was financed with special funds from the Berlin Institute of Health (BIH).

Authors' Contributions

JS performed supervision. ESB, RH, ID, and ER performed the investigation. ESB, ST, and FB contributed to the methodology. ESB, RH, ID, and ER performed data curation, supported by VR and JS. ESB performed formal analysis, supported by RH, DF, ASP, RDD, and JS. ST and FB acquired funding. JS handled project administration. VR and JS managed resources. JS, ESB, and ST managed software, including code creation for communication within IT medication platforms. JS and all authors conducted validation. RDD performed visualization. ESB wrote the original draft. All authors contributed to the conceptualization, writing—review and editing, and approval of the submitted manuscript and will be accountable for its contents.

Conflicts of Interest

None declared.

Multimedia Appendix 1

XSL•FO
RenderX

FHIR (Fast Healthcare Interoperability Resources) order message prototype with instructions for requesting a single medication (Propofol 1%) for a patient.
[PNG File , 33 KB - medinform_v13i1e64099_app1.png]

Multimedia Appendix 2
FHIR (Fast Healthcare Interoperability Resources) order message prototype with instructions for administration of a single medication (Propofol 1%) to a patient.
[PNG File , 96 KB - medinform_v13i1e64099_app2.png]

Multimedia Appendix 3
FHIR (Fast Healthcare Interoperability Resources) order message prototype with instructions for the request of a mixed medication (Noradrenaline and Sodium chloride [NaCl]) for a patient.
[PNG File , 103 KB - medinform_v13i1e64099_app3.png]

Multimedia Appendix 4
FHIR (Fast Healthcare Interoperability Resources) order message prototype with instructions for the administration of a mixed medication (Noradrenaline and Sodium chloride [NaCl]) to a patient.
[PNG File , 176 KB - medinform_v13i1e64099_app4.png]

References

1. Medical facilities, hospital beds and movement of patients. Destatis Statistisches Bundesamt. 2020. URL: https://www.destatis.de/EN/Themes/Society-Environment/Health/Hospitals/Tables/gd-hospitals-years.html [accessed 2022-04-10]
2. Biswal S, Mishra P, Malhotra S, Puri GD, Pandhi P. Drug utilization pattern in the intensive care unit of a tertiary care hospital. J Clin Pharmacol 2006;46(8):945-951. [doi: 10.1177/0091270006289845] [Medline: 16855079]
3. Valentin A, Capuzzo M, Guidet B, Moreno R, Metnitz B, Bauer P, Research Group on Quality Improvement of the European Society of Intensive Care Medicine (ESICM), Sentinel Events Evaluation (SEE) Study Investigators. Errors in administration of parenteral drugs in intensive care units: multinational prospective study. BMJ 2009;338:b814 [FREE Full text] [doi: 10.1136/bmj.b814] [Medline: 19282436]
4. Institute of Medicine (US) Committee on Quality of Health Care in America, Kohn LT, Corrigan JM, Donaldson MS. To Err is Human: Building a Safer Health System. Washington (DC): National Academies Press; 2000.
5. Sentinel event data summary. Joint Commission. 2020. URL: https://www.jointcommission.org/sentinel_event_statistics_quarterly [accessed 2021-05-14]
6. Sanduende-Otero Y, Villalón-Coca J, Romero-García E, Díaz-Cambronero Ó, Barach P, Arnal-Velasco D. Patterns in medication incidents: a 10-yr experience of a cross-national anaesthesia incident reporting system. Br J Anaesth 2020;124(2):197-205 [FREE Full text] [doi: 10.1016/j.bja.2019.10.013] [Medline: 31780140]
7. Medication without harm. World Health Organisation. 2017. URL: https://www.who.int/initiatives/medication-without-harm [accessed 2023-01-03]
8. Nelson SD, Parker J, Lario R, Winnenburg R, Erlbaum MS, Lincoln MJ, et al. Interoperability of medication classification systems: lessons learned mapping established pharmacologic classes (EPCs) to SNOMED CT. Stud Health Technol Inform 2017;245:920-924 [FREE Full text] [Medline: 29295234]
9. ECRI thought leadership. ECRI. 2020. URL: https://www.ecri.org/landing-2020-top-ten-health-technology-hazards [accessed 2021-10-21]
10. Moges TA, Akalu TY, Sema FD. Unintended medication discrepancies and associated factors upon patient admission to the internal medicine wards: identified through medication reconciliation. BMC Health Serv Res 2022;22(1):1251 [FREE Full text] [doi: 10.1186/s12913-022-08628-5] [Medline: 36243696]
11. Rahmawati HK, Adisasmito WBB. The benefits of interoperability to prevent medication error in hospital. 2019 Presented at: The 6th International Conference on Public Health; 2019 October 23-24; Surakarta, Indonesia p. 379-387. [doi: 10.26911/the6thicph-fp.04.21]
12. Agrawal A. Medication errors: prevention using information technology systems. Br J Clin Pharmacol 2009;67(6):681-686 [FREE Full text] [doi: 10.1111/j.1365-2125.2009.03427.x] [Medline: 19594538]
13. Zeng ML. Interoperability. Knowl Org 2019;46(2):122-146. [doi: 10.5771/0943-7444-2019-2-122]
14. Benson T, Grieve G. Snomed CT. In: Principles of Health Interoperability. Cham: Springer; 2016.
15. Noumeir R. Active learning of the HL7 medical standard. J Digit Imaging 2019;32(3):354-361 [FREE Full text] [doi: 10.1007/s10278-018-0134-3] [Medline: 30353411]
16. About HL7. HL7 International. 2021. URL: http://www.hl7.org/about/index.cfm?ref=nav [accessed 2021-08-20]
17. Ayaz M, Pasha MF, Alzahrani MY, Budiarto R, Stiawan D. The fast health interoperability resources (FHIR) standard: systematic literature review of implementations, applications, challenges and opportunities. JMIR Med Inform 2021;9(7):e21929 [FREE Full text] [doi: 10.2196/21929] [Medline: 34328424]

XSL•FO
RenderX

18. Revised IDMP standards to improve description of medicinal products worldwide. International Organization for Standardization (ISO). 2020. URL: https://www.iso.org/news/ref2234.html [accessed 2021-01-20]
19. FDA Data Standards Advisory Board. FDA. 2022. URL: https://www.fda.gov/industry/fda-data-standards-advisory-board [accessed 2023-12-20]
20. Health informatics — identification of medicinal products — data elements and structures for the unique identification and exchange of regulated medicinal product information. International Organization for Standardization (ISO). 2020. URL: https://www.iso.org/standard/70150.html [accessed 2020-01-20]
21. Health informatics — identification of medicinal products — data elements and structures for unique identification and exchange of regulated pharmaceutical product information. International Organization for Standardization (ISO). 2020. URL: https://www.iso.org/standard/70044.html [accessed 2021-01-20]
22. Health informatics — identification of medicinal products — data elements and structures for the unique identification and exchange of regulated information on substances. International Organization for Standardization (ISO). 2020. URL: https://www.iso.org/standard/69697.html [accessed 2021-01-20]
23. Health informatics — identification of medicinal products — data elements and structures for the unique identification and exchange of regulated information on pharmaceutical dose forms, units of presentation, routes of administration and packaging. International Organization for Standardization (ISO). 2020. URL: https://www.iso.org/obp/ui/#iso:std:iso:11239:ed-1:v1:en [accessed 2021-01-20]
24. Data on medicines (ISO IDMP standards): overview. European Medicines Agency (EMA). 2020. URL: https://www.ema.europa.eu/en/human-regulatory/overview/data-medicines-iso-idmp-standards-overview [accessed 2021-03-23]
25. Substance, product, organisation and referential (SPOR) master data. European Medicines Agency (EMA). 2020. URL: https://www.ema.europa.eu/en/human-regulatory/research-development/data-medicines-iso-idmp-standards/substance-product-organisation-referential-spor-master-data [accessed 2021-03-26]
26. European directorate for the quality of medicines and healthCare (EDQM) of the council of Europe. European Medicines Agency (EMA). 2020. URL: https://www.ema.europa.eu/en/partners-networks/international-activities/multilateral-organisations-initiatives/european-directorate-quality-medicines-healthcare-edqm-council-europe [accessed 2021-03-26]
27. Ph eur reference standards: orders and catalogue. European Directorate for the Quality of Medicines and HealthCare (EDQM). 2020. URL: https://www.edqm.eu/en/ph-eur-reference-standards-orders-catalogue [accessed 2021-03-23]
28. European pharmacopoeia - background and mission. European Directorate for the Quality of Medicines and HealthCare (EDQM). 2020. URL: https://www.edqm.eu/en/European-Pharmacopoeia-Background-Mission [accessed 2021-04-14]
29. Data on medicines (ISO IDMP standards): overview. European Medicines Agency. 2016. URL: https://www.ema.europa.eu/en/human-regulatory-overview/research-and-development/data-medicines-iso-idmp-standards-overview [accessed 2023-12-14]
30. Zabka S, Ammon D, Ganslandt T, Gewehr J, Haverkamp C, Kiefer S, et al. Towards a medication core data set for the medical informatics initiative (MII): initial mapping experience between the German procedure classification (OPS) and the identification of medicinal products (IDMP). In: Proceedings of the Joint Ontology Workshops. 2019 Presented at: Proceedings of the Joint Ontology Workshops 2019: Episode V: The Styrian Autumn of Ontology; 2019 September 23-25; Graz, Austria p. 23-25. [doi: 10.3233/shti210074]
31. Drees D. The Introduction of Health Telematics in Germany. In: ISSE/SECURE 2007 Securing Electronic Business Processes. Cham: Springer Vieweg; 2007:396-400.
32. Interoperability thanks to ISiK. gematik Fachportal. 2022. URL: https://fachportal.gematik.de/informationen-fuer/isik [accessed 2024-02-15]
33. Wilkinson M, Dumontier M, Aalbersberg IJJ, Appleton G, Axton M, Baak A, et al. The FAIR guiding principles for scientific data management and stewardship. Sci Data 2016;3:160018 [FREE Full text] [doi: 10.1038/sdata.2016.18] [Medline: 26978244]
34. Queralt-Rosinach N, Kaliyaperumal R, Bernabé CH, Long Q, Joosten SA, van der Wijk HJ, BEAT-COVID Group, COVID-19 LUMC Group. Applying the FAIR principles to data in a hospital: challenges and opportunities in a pandemic. J Biomed Semantics 2022;13(1):12 [FREE Full text] [doi: 10.1186/s13326-022-00263-7] [Medline: 35468846]
35. Barker M, Chue Hong NP, Katz DS, Lamprecht AL, Martinez-Ortiz C, Psomopoulos F, et al. Introducing the FAIR principles for research software. Sci Data 2022;9(1):622 [FREE Full text] [doi: 10.1038/s41597-022-01710-x] [Medline: 36241754]
36. Du X, Dastmalchi F, Ye H, Garrett TJ, Diller MA, Liu M, et al. Evaluating LC-HRMS metabolomics data processing software using FAIR principles for research software. Metabolomics 2023;19(2):11. [doi: 10.1007/s11306-023-01974-3] [Medline: 36745241]
37. ABDAmed2: the complete package for hospitals and doctor's offices. ABDATA Pharma-Daten-Service. 2023. URL: https://abdata.de/produkte/abdamed2/ [accessed 2023-08-12]
38. MMI pharmindex products. ViDAL mmi Germany. 2023. URL: https://www.mmi.de/mmi-pharmindex [accessed 2023-08-15]
39. Expert knowledge for secure drug data. ABDATA Pharma-Daten-Service. 2020. URL: https://abdata.de [accessed 2022-11-17]
40. Bouin AS, Wierer M. Quality standards of the European pharmacopoeia. J Ethnopharmacol 2014;158 Pt B:454-457. [doi: 10.1016/j.jep.2014.07.020] [Medline: 25043777]

XSL•FO
RenderX

41. Standard terms. European Directorate for the Quality of Medicines and HealthCare (EDQM). 2020. URL: https://standardterms.edqm.eu [accessed 2023-04-29]
42. Resource medication. HL7 FHIR. 2023. URL: https://build.fhir.org/medication.html [accessed 2023-12-04]
43. Salgado-Baez E, Heidepriem R, Danhier RD, Rinaldi E, Poncette AS, Dahlhaus I, et al. FAIR IOP medication database. figshare. 2024. URL: https://doi.org/10.6084/m9.figshare.26142688 [accessed 2025-03-01]
44. Lehne M, Sass J, Essenwanger A, Schepers J, Thun S. Why digital medicine depends on interoperability. NPJ Digit Med 2019;2:79 [FREE Full text] [doi: 10.1038/s41746-019-0158-1] [Medline: 31453374]
45. Bauer JC, John E, Wood C, Plass D, Richardson D. Data entry automation improves cost, quality, performance, and job satisfaction in a hospital nursing unit. J Nurs Adm 2020;50(1):34-39. [doi: 10.1097/NNA.0000000000000836] [Medline: 31804410]
46. Tripathi N, Goshisht MK, Sahu SK, Arora C. Applications of artificial intelligence to drug design and discovery in the big data era: a comprehensive review. Mol Divers 2021;25(3):1643-1664. [doi: 10.1007/s11030-021-10237-z] [Medline: 34110579]
47. Yang X, Wang Y, Byrne R, Schneider G, Yang S. Concepts of artificial intelligence for computer-assisted drug discovery. Chem Rev 2019;119(18):10520-10594. [doi: 10.1021/acs.chemrev.8b00728] [Medline: 31294972]
48. Liu C, Hogan AM, Sturm H, Khan MW, Islam MM, Rahman ASMZ, et al. Deep learning-driven prediction of drug mechanism of action from large-scale chemical-genetic interaction profiles. J Cheminform 2022;14(1):12 [FREE Full text] [doi: 10.1186/s13321-022-00596-6] [Medline: 35279211]
49. Austin JA, Smith IR, Tariq A. The impact of closed-loop electronic medication management on time to first dose: a comparative study between paper and digital hospital environments. Int J Pharm Pract 2018;26(6):526-533. [doi: 10.1111/ijpp.12432] [Medline: 29356171]
50. Burkoski V, Yoon J, Solomon S, Hall TNT, Karas AB, Jarrett SR, et al. Closed-loop medication system: leveraging technology to elevate safety. Nurs Leadersh (Tor Ont) 2019;32(SP):16-28. [doi: 10.12927/cjnl.2019.25817] [Medline: 31099744]
51. Ciapponi A, Fernandez Nievas SE, Seijo M, Rodríguez MB, Vietto V, García-Perdomo HA, et al. Reducing medication errors for adults in hospital settings. Cochrane Database Syst Rev 2021;11(11):CD009985 [FREE Full text] [doi: 10.1002/14651858.CD009985.pub2] [Medline: 34822165]
52. Parrish RH, Gilak L, Bohannon D, Emrick SP, Serumaga B, Guharoy R. Minimizing medication errors from electronic prescription transmission-digitizing compounded drug preparations. Pharmacy (Basel) 2019;7(4):149 [FREE Full text] [doi: 10.3390/pharmacy7040149] [Medline: 31703306]
53. e-prescription: The fast way to the right medication. gematik. 2022. URL: https://www.gematik.de/anwendungen/e-rezept [accessed 2023-11-10]
54. Salgado-Baez E, Näher AF, Friedrich M, Kremser G, Braune K, Balzer F. Health data management im krankenhaus umsetzen. In: Henke V, Hülsken G, Schneider H, Varghese J, editors. Health Data Management: Schlüsselfaktor für erfolgreiche Krankenhäuser. Wiesbaden: Springer Gabler; 2024:363-377.
55. European health data space regulation (EHDS). European Comission. 2023. URL: https://health.ec.europa.eu/ehealth-digital-health-and-care/european-health-data-space_en [accessed 2024-04-01]
56. INTEROP COUNCIL for digital health in Germany. 2023. URL: https://www.ina.gematik.de/en/interoperability-governance/interop-council [accessed 2024-01-29]
57. NA. Global Strategy on Digital Health 2020-2025. Geneva: Wolrd Health Organization; 2022. URL: https://www.who.int/docs/default-source/documents/gs4dhdaa2a9f352b0445bafbc79ca799dce4d.pdf [accessed 2024-05-05]
58. Biltoft J, Finneman L. Clinical and financial effects of smart pump-electronic medical record interoperability at a hospital in a regional health system. Am J Health Syst Pharm 2018;75(14):1064-1068. [doi: 10.2146/ajhp161058] [Medline: 29987060]
59. Enabling health interoperability through FHIR. HL7 FHIR Foundation. 2020. URL: http://fhir.org [accessed 2021-10-17]
60. Braunstein ML. Health care in the age of interoperability part 6: the future of FHIR. IEEE Pulse 2019;10(4):25-27. [doi: 10.1109/MPULS.2019.2922575] [Medline: 31395530]
61. Salgado E, Heidepriem R, Danhier RD, Rinaldi E, Poncette AS, Dahlhaus I, et al. FHIR medication order messages prototypes. figshare. 2024. URL: https://doi.org/10.6084/m9.figshare.26142685 [accessed 2025-03-01]

Abbreviations

ABDA: Federal Union of German Associations of Pharmacists
ABDA-MED: ABDA Medication Database
AI: artificial intelligence
API: application programming interface
ASK: German Drug Substance Catalog
ATC: Anatomical Therapeutic Chemical
BIH: Berlin Institute of Health

XSL•FO
RenderX

CLMA: closed-loop medication administration
CMIO: Chief Medical Informatics Officer
EDQM: European Directorate for the Quality of Medicines and HealthCare
EHDS: European Health Data Space
EHR: electronic health record
EMA: European Medicines Agency
FAIR: Findability, Accessibility, Interoperability, and Reusability
FHIR: Fast Healthcare Interoperability Resources
HL7: Health Level 7
ICD-10: *International Statistical Classification of Diseases, Tenth Revision*
ICU: intensive care unit
IDMP: Identification of Medical Products
ISO: International Organization for Standardization
LOINC: Logical Observation Identifiers Names and Codes
MedRec: Medication Reconciliation
MII: Medical Informatics Initiative
PDMS: patient data management system
PIS: pharmacy information system
PPN: Pharmacy Product Number
PZN: Pharmacy Central Number
SNOMED CT: Systematized Nomenclature of Medicine Clinical Terms
SPOR: Substance, Product, Organization, and Referential
TI: telematics infrastructure
UI: user interface
WHO: World Health Organization

Edited by C Lovis; submitted 11.07.24; peer-reviewed by S Leitch, R Campbell; comments to author 30.10.24; revised version received 29.01.25; accepted 31.01.25; published 09.05.25.

Please cite as:
Salgado-Baez E, Heidepriem R, Delucchi Danhier R, Rinaldi E, Ravi V, Poncette AS, Dahlhaus I, Fürstenau D, Balzer F, Thun S, Sass J
Toward Interoperable Digital Medication Records on Fast Healthcare Interoperability Resources: Development and Technical Validation of a Minimal Core Dataset
JMIR Med Inform 2025;13:e64099
URL: https://medinform.jmir.org/2025/1/e64099
doi:10.2196/64099
PMID:

©Eduardo Salgado-Baez, Raphael Heidepriem, Renate Delucchi Danhier, Eugenia Rinaldi, Vishnu Ravi, Akira-Sebastian Poncette, Iris Dahlhaus, Daniel Fürstenau, Felix Balzer, Sylvia Thun, Julian Sass. Originally published in JMIR Medical Informatics (https://medinform.jmir.org), 09.05.2025. This is an open-access article distributed under the terms of the Creative Commons Attribution License (https://creativecommons.org/licenses/by/4.0/), which permits unrestricted use, distribution, and reproduction in any medium, provided the original work, first published in JMIR Medical Informatics, is properly cited. The complete bibliographic information, a link to the original publication on https://medinform.jmir.org/, as well as this copyright and license information must be included.

XSL•FO
RenderX

Predicting Unplanned Readmission Risk in Patients With Cirrhosis: Complication-Aware Dynamic Classifier Selection Approach

Zixin Shi[1], MS; Linjun Huang[1], BE; Xiaomei Xu[2], MD; Kexue Pu[1], PhD; Qingpeng Zhang[3,4], PhD; Haolin Wang[1], PhD

[1]College of Medical Informatics, Chongqing Medical University, 1 Yixueyuan Road, Yuzhong District, Chongqing, China

[2]Department of Infectious Diseases, Chengdu Fifth People's Hospital, Chengdu, China

[3]Musketeers Foundation Institute of Data Science, University of Hong Kong, Hong Kong, China (Hong Kong)

[4]Department of Pharmacology and Pharmacy, University of Hong Kong, Hong Kong, China (Hong Kong)

Corresponding Author:
Haolin Wang, PhD
College of Medical Informatics, Chongqing Medical University, 1 Yixueyuan Road, Yuzhong District, Chongqing, China

Abstract

Background: Cirrhosis is a leading cause of noncancer deaths in gastrointestinal diseases, resulting in high hospitalization and readmission rates. Early identification of high-risk patients is vital for proactive interventions and improving health care outcomes. However, the quality and integrity of real-world electronic health records (EHRs) limit their utility in developing risk assessment tools.

Objective: Despite the widespread application of classical and ensemble machine learning for EHR-based predictive tasks, the diversity of health conditions among patients and the inherent limitations of the data, such as incompleteness, sparsity, and temporal dynamics, have not been fully addressed. To tackle those challenges, we explored a framework that characterizes patient subgroups and adaptively selects optimal predictive models for each patient on the fly to enable individualized decision support.

Methods: The proposed framework uniquely addresses patient heterogeneity by aligning diverse subgroups with dynamically selected classifiers. First, patient subgroups are generated and characterized using rules indicating medical diagnosis patterns. Next, a meta-learning framework trains a meta-classifier for optimal dynamic model selection, which identifies suitable models for individual patients. Notably, we incorporated a tailored region of competence to refine model selection, specifically accounting for cirrhosis complications. This approach not only enhances predictive performance but also elucidates why individualized predictions are better supported by selected classifiers trained on specific data subsets.

Results: The proposed framework was evaluated for predicting 14-day and 30-day readmission in patients with cirrhosis using multicenter data obtained from 6 hospitals. The final dataset comprised 3307 patients with at least 2 admission records, along with a range of factors including demographic information, complications, and laboratory test results. The proposed framework achieved an average AUC (area under the curve) improvement of 5% and 4% compared to the best baseline models, respectively.

Conclusions: By leveraging the expertise of the most competent classifiers for each patient subgroup, our approach enables interpretable training and dynamic selection of heterogeneous predictive models. This advancement not only improves prediction accuracy but also highlights its considerable potential for clinical applications, facilitating the alignment of diverse patient subgroups with tailored decision-support algorithms.

(JMIR Med Inform 2025;13:e63581) doi:10.2196/63581

KEYWORDS

data mining; electronic health records; multiple classifier systems; predictive models; readmission risk; EHR; cirrhosis; gastrointestinal disease; decision-making; framework

Introduction

Cirrhosis, a chronic condition caused by hepatocyte injury and liver fibrosis [1], is often accompanied by complications [2] such as ascites and hepatic encephalopathy, posing severe risks to patients' health and survival. Patients with cirrhosis typically have high hospitalization rates, prolonged hospital stays, and frequent readmissions [3]. Notably, patients with decompensated cirrhosis are particularly vulnerable, with a 5-year survival rate of merely 14% - 35% [4] and a readmission rate ranging from 10% to 50% within 7-90 days postdischarge [5]. These challenges not only disrupt the continuity of care and degrade patients' quality of life but also impose a substantial economic and societal burden on hospitals and health care systems [6]. Statistics indicate that the annual economic expenditure attributable to unplanned readmissions from cirrhosis amounts

XSL•FO
RenderX

to approximately US $17.4 billion [7]. Given the significant impact of the readmission issue on health care resource allocation [8], the Patient Protection and Affordable Care Act (2010) established reducing hospital readmission rates as a pivotal objective in the reforming of fee-for-service hospital reimbursement policies [9]. Even though the readmission rate is not commonly used as an evaluation metric by hospitals, the global significance of the readmission problem cannot be ignored [10,11].

Research has demonstrated that a substantial proportion, up to 27.1% [12], of readmissions are potentially preventable, highlighting a substantial opportunity for the development of predictive models aimed at identifying high-risk patients. In recent years, electronic health records (EHRs) have gained widespread adoption in both clinical practice and research endeavors, providing a vast and diverse dataset for machine learning algorithms [13]. By harnessing clinical indicators embedded within EHRs, such as laboratory test results and vital signs, researchers have developed numerous predictive models to precisely evaluate patients' risk of readmission. For instance, Berman et al [14] used comprehensive EHR data sourced from 2 prominent academic medical centers to identify variables predictive of 30-day readmission among patients with liver disease. Similarly, Hu and colleagues [15] conducted an analysis of 30-day and 90-day readmission rates for patients with end-stage liver disease, leveraging EHR data in conjunction with models such as logistic regression, support vector machines, and random forests. These models hold significant potential to enhance our ability to anticipate and mitigate the risk of readmission in vulnerable patient populations [15].

However, the diverse patient population and the inherent challenges of EHR data [16], including high dimensionality, incompleteness, sparsity, and temporal dynamics, pose substantial obstacles for model development. While individual machine learning models have demonstrated effectiveness on specific datasets, they frequently face difficulties in comprehensively addressing these complexities [17]. Multiple classifier systems [18] with dynamic ensemble selection (DES) [19] emerge as a promising approach to address those challenges. DES typically surpasses single models in predictive performance by selecting and integrating diverse classifiers tailored to unknown test instances during the inference process, thereby enhancing predictive accuracy.

The META-DES (dynamic ensemble selection using meta-learning) framework [20] transforms the task of classifier selection into a meta-problem. This approach entails extracting meta-features pertinent to the base classifiers and training a meta-classifier to assess their classification prowess. Nonetheless, when applied to tabular data classification, particularly in predicting readmissions for patients with cirrhosis, the existing DES algorithms do not always outperform state-of-the-art ensemble models. This performance gap seems to stem from 2 challenges. First, the development of predictive models needs to be deeply integrated with the characteristics of specific clinical problems, such as the complexity and diversity of inpatient care. Second, the quality issues of EHR data, such as incompleteness, sparsity, and temporal dynamics, further exacerbate the difficulties in model development.

To address these challenges, this study aims to develop an interpretable framework that dynamically aligns patient subgroups with optimized classifier selection. Specifically, the aim of this study is threefold: (1) to generate and characterize patient subgroups through clinically meaningful rules based on complication and comorbidity patterns; (2) to design a tailored region of competence incorporating medical diagnoses, enabling optimized dynamic selection of patient-specific predictive models; and (3) to establish a paradigm shift from conventional one-size-fits-all approaches to an adaptive methodology that accounts for heterogeneous patient profiles. By integrating medical knowledge with DES, this approach not only improves predictive performance but also provides interpretable insights into the classifier selection rationale for diverse clinical subgroups.

Methods

Ethical Considerations

The study received ethics review and approval from the institutional review board of Chongqing Medical University (approval no. 2023098). Due to its retrospective nature, this study required no informed consent. All collected data were fully anonymized with no personally identifiable information included. No financial or material incentives were provided to participants.

Data Collection

This retrospective prognostic study focused on decompensated liver cirrhosis data sourced from 6 tertiary hospitals in Chongqing, China. The initial cohort encompassed 13,476 patient records from January 2011 to June 2020, identified using cirrhosis diagnostic codes according to the ICD-9 (*International Classification of Diseases*, 9th Revision) or ICD-10 (*International Classification of Diseases*, 10th Revision) systems. We followed the TRIPOD (Transparent Reporting of a Multivariable Prediction Model for Individual Prognosis or Diagnosis) [21] guidelines for reporting cohort studies. To refine our cohort, we applied the following exclusion criteria: (1) patients hospitalized for cancer, malignant tumors, tuberculosis, or HIV (n=1906); (2) patients lost to follow-up or who died during their initial hospitalization (n=151); (3) patients with no recorded readmissions (n=7150); and (4) patients with missing data exceeding 10% (n=1113).

Variable Description

The refined cohort consisted of 3307 patients, each with at least 1 readmission record. The dataset covered a wide range of variables, including 3 demographic factors, 5 etiological variables, 35 comorbidities and complications, 38 clinical test indicators, 10 surgical variables, 7 medication-related factors, 1 composite scoring variable, and 1 outcome variable. All included indicators were thoroughly reviewed by clinical experts. Demographic data included age, gender, and the number of hospitalizations. The list of complications featured hepatic encephalopathy, acute-on-chronic liver failure, ascites, and esophageal or gastric varices. The laboratory test indicators included prothrombin time, international normalized ratio, hemoglobin concentration, creatinine, and several other critical

XSL•FO
RenderX

measurements. A comprehensive list is provided in Multimedia Appendix 1.

Statistical Methods

For descriptive analyses, continuous variables, such as laboratory indices, were summarized using medians and IQRs, while categorical variables were presented with frequencies and proportions. A 2-step variable selection process was used.

Univariate Analysis

Potential predictors of 14-day and 30-day readmissions were evaluated. Quantitative predictors were assessed using the Mann-Whitney *U* test, and binary predictors were analyzed with the chi-square test or the Fisher exact test. Considering the high dimensionality of the data and the complexity of the model, predictors with a *P* value less than .05 were retained for further analysis.

Automated Feature Selection

The selected predictors from the univariate analysis were then incorporated into an automatic variable selection process within the DES framework to identify the optimal subset of predictors. The final set of variables included in the model was determined based on a careful balance between accuracy and simplicity.

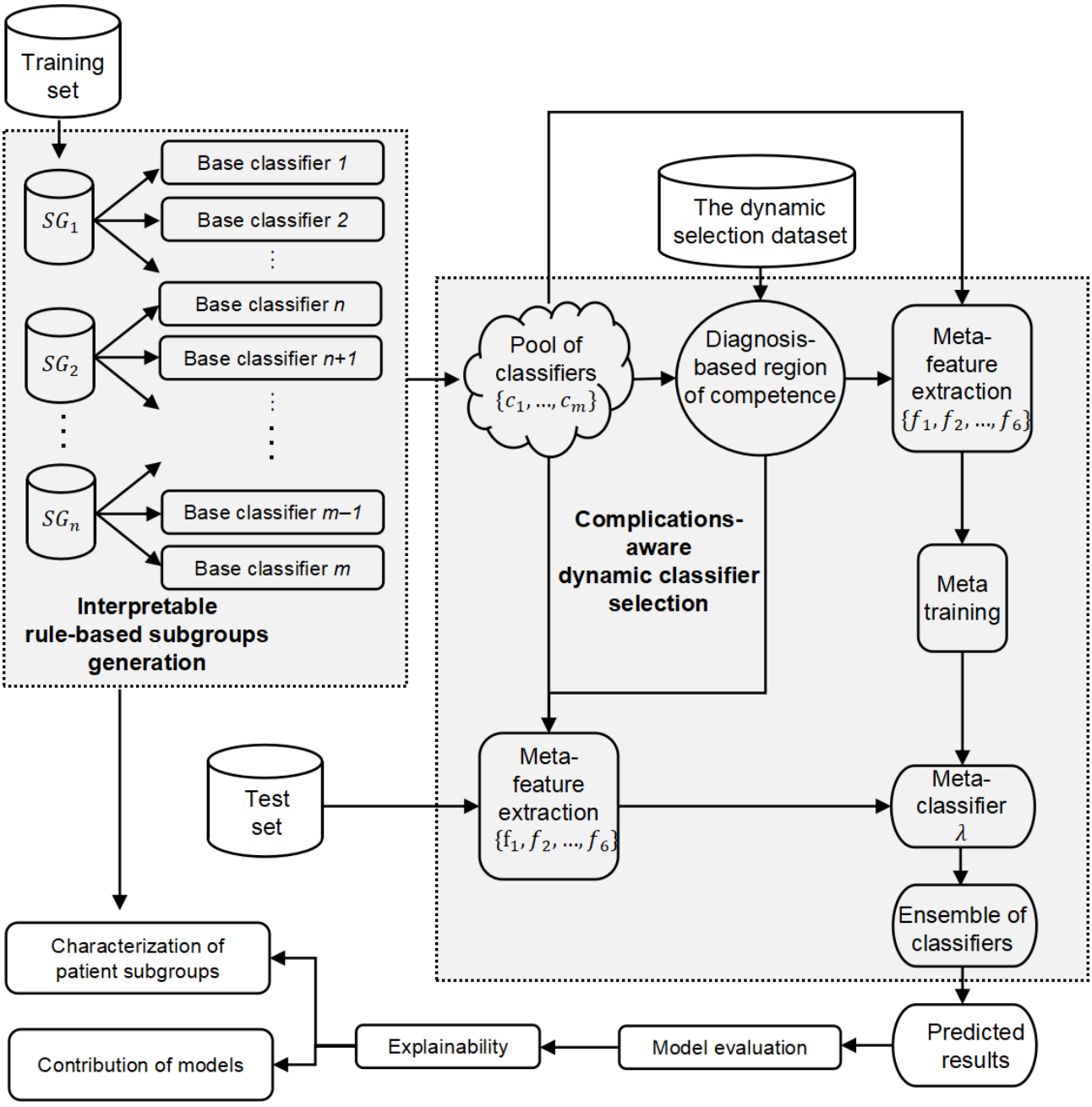
The DES Framework

Key Features of the Framework

The proposed framework highlights 2 critical components: the generation of the classifier pool and the dynamic selection of classifiers. The classifiers trained with different training subsets play a pivotal role in tackling issues such as the incompleteness and sparsity of EHR data by capitalizing on the diverse feature selection capabilities across the heterogeneous classifiers. This approach enables the framework to maximize data utility even with fragmented or scarce data. Moreover, as patients' health status evolves over time, the dynamic classifier selection process enables the framework to adapt more effectively to these fluctuations, enhancing its overall adaptability and relevance in real-world clinical scenarios. Notably, medical expert knowledge can be seamlessly integrated into both classifier pool generation and dynamic selection processes. This integration ensures that the framework is not only data-driven but also informed by the expertise and insights of medical professionals, adding a layer of clinical validity and practicality. An overview of the framework is graphically presented in Figure 1, providing a clear visual representation of its core components and interrelationships.

XSL•FO
RenderX

Figure 1. Overview of the proposed framework.



Classifier Pool Generation

Traditional DES systems typically generate diverse classifier pools through strategies such as altering initialization parameters, hyperparameter configurations, classifier models, training datasets, and feature subsets. In this study, to ensure the diversity of the base classifiers, we introduced a rule-based method to generate data subsets to support the training of classifiers. Given that complications are major causes of readmission in patients with cirrhosis as reported in existing studies, the descriptions of complications and comorbidities associated with liver cirrhosis are presented in Table 1. Based on this, we extracted rule sets that consist of binary variables representing medical diagnoses from real-world datasets. These rule sets allow us to characterize patient subgroups (SG_1, SG_2,..., SG_n) based on distinct combinations of these complications and comorbidities. For example, a rule might be

(Electrolyte metabolic disorders=TRUE) AND (Hepatic encephalopathy=FALSE)

This rule-based method, grounded in medical diagnosis patterns, represents an innovative approach to integrating medical knowledge into the classifier generation process. By examining these subgroups, researchers and clinicians can gain deeper insights into the underlying reasons why individualized predictions are supported by classifiers trained on certain subsets of the data. By leveraging diverse data subsets and training heterogeneous classifiers, the classifier pool can capture a wide range of patterns within the EHR data to enhance the overall predictive performance. In this phase, a classifier pool C={c1,c2,...,cm} was generated with *m* classifiers.

Besides diverse patient subgroups, a variety of machine learning algorithms can be integrated into the framework to create the classifier pool.

XSL•FO
RenderX

Table . Definition of complications and comorbidities.

Category	Complications	Comorbidities
Definition	Diseases or pathological conditions directly caused by liver cirrhosis	Other independent diseases or pathological conditions coexisting with the patient
Cause	Caused by liver cirrhosis (eg, portal hypertension and liver failure)	Caused by factors other than liver cirrhosis
Common stage	Most common in the decompensated stage	Can occur at any stage of the disease

Meta-Feature Extraction and Meta-Training

The DES problem involves selecting an optimal subset of base classifiers C′⊂C to classify a given test sample x_j. To train a meta-classifier λ that acts as a classifier selector, the key challenge is to define the criteria to evaluate the competence of base classifiers as meta-features. In this study, 2 sets of meta-features are used. The first set of meta-features includes the criteria to measure the local accuracy in the region of competence (f_1), extent of consensus in the region of competence (f_2), overall accuracy in the region of competence (f_3), accuracy in the decision space (f_4), and degree of confidence for the input sample (f_5). To extract those meta-features, a region of competence θ_j is defined, for instance, x_j, using the *k*-nearest neighbors clustering of the entire feature space of each data subset.

To effectively incorporate complications and comorbidities into the characterization of patients with cirrhosis and refine dynamic classifier selection, a novel competence region θj′ is defined. This region, grounded in medical diagnoses, emphasizes complications and comorbidities as binary indicators of their presence or absence. Notably, the competence region θj′ consists of an equal number of positive and negative data samples to ensure a balanced evaluation of the base classifiers' performance. The new set of meta-features (f_6) was defined as the local accuracy within the region of competence θj′ to be aware of patients' subgroup with specific complications or comorbidities. Thus, a meta-feature vector is extracted as vij={f1,f2,f3,f4,f5,f6} for classifier c_i and instance x_j. To construct the training set for the meta-classifier, labels are assigned to each meta-feature vector: for each meta-feature vector, its label αij=1 if classifier c_i correctly classifies instance x_j, otherwise αij=0. By embedding patients' medical diagnoses, this framework proficiently captures the impact of complications and comorbidities during the dynamic selection of suitable classifiers. This approach represents an improvement over traditional methods, as it explicitly incorporates the unique characteristics of patients with cirrhosis. The critical role of this redefinition lies in its ability to determine model applicability for specific patient subgroups. Technical details of the implementation can be found in the GitHub repository [22]. This dynamic framework not only improves the predictive performance but also enhances the model's adaptability to real-world clinical scenarios.

Dynamic Classifier Ensemble

In traditional machine learning workflows, a single model is typically used for both the training and testing datasets. Nevertheless, different models display diverse strengths and weaknesses in terms of accuracy, interpretability, and other aspects. The fundamental theory of dynamic classifier selection postulates that not every classifier in a pool is an expert for all unseen samples. On the contrary, each base classifier is proficient in distinct regions of the feature space. When we apply this concept to our study, it becomes clear that no single classifier can yield optimal prediction results for the entire test set. However, by using the dynamic classifier selection strategy, we are able to extract diverse meta-features for different data subsets and choose the base classifier that provides the most accurate prediction for each subset. This method guarantees the achievement of the optimal prediction results.

Given an instance xj,test, the dynamic selection dataset, and the classifier pool, the set of meta-features {f1,f2,f3,f4,f5} is extracted using the region of competence θ_j, and the meta-feature f_6 is extracted using the region of competence θj′ based on the diagnosis of patients. Once the meta-features are extracted, the meta-classifier λ is used to calculate competence scores for each classifier in the pool. These competence scores, typically expressed as probabilities estimated by the meta-classifier, indicate the capability of each classifier. The classifiers with the highest competence score are selected as the pool of ensemble of classifiers *C**. If multiple classifiers have equal competence scores, the predictions of those classifiers are aggregated using the majority vote rule.

Results

Data Analysis

The final dataset comprises 3307 patients with readmission records in this study. Among these patients, 1121 (33.9%) are female and 2186 (66.1%) are male, with an average age of 55 years. Within a 14-day period, 423 (12.8%) patients were readmitted, while within 30 days, 879 (26.6%) patients experienced readmission. Tables 2 and 3 present detailed descriptive statistics for the entire dataset. Taking total bilirubin levels (normal range of 1.7 - 21 μmol/L) as an example, it was observed that patients fulfilling the discharge criteria exhibited heightened total bilirubin levels. Upon admission, the percentages of patients with total bilirubin levels exceeding the normal range were 71.9% (304/423) for the 14-day period and 60.4% (531/879) for the 30-day period. However, at discharge, these percentages declined to 65.9% (279/423) and 54.7% (481/879), respectively. Both admission and discharge laboratory indicators aligned with the anticipated clinical outcomes for cirrhotic patients. The missing rates for all selected features are below 10%, and missing data were imputed using the mean of *k*-nearest neighbors.

XSL•FO
RenderX

Table . Characteristics of patients experiencing 14-day readmission.

Characteristics	Readmission (n=423)	Nonreadmission (n=2884)	*P* value
Demographics, n (%)			.006
Female	118 (27.9)	1003 (34.8)	
Male	305 (72.1)	1881 (65.2)	
Complications, n (%)			
Peritonitis	111 (26.2)	470 (16.3)	<.001
Hepatic encephalopathy	55 (13.0)	199 (6.9)	<.001
Abdominal fluid	55 (13.0)	232 (8.0)	.001
Liver failure	55 (13.0)	252 (8.7)	<.001
EMD[a]	49 (11.6)	230 (8.0)	.02
Ruptured esophagogastric varices	178 (42.1)	1603 (55.6)	<.001
Comorbidities, n (%)			
Autoimmune diseases	34 (8.0)	329 (11.4)	.07
Gastritis	28 (6.6)	316 (11.0)	.008
Neuropathy	22 (5.5)	75 (2.6)	.005
Ulcers	26 (6.2)	297 (10.3)	.009
Surgery, n (%)			
Bilirubin adsorption-plasma exchange	13 (3.1)	13 (0.5)	<.001
Bone marrow puncture biopsy	60 (14.2)	252 (8.7)	<.001
Autologous ascites concentration and reinfusion	48 (11.4)	88 (3.1)	<.001
Laboratory tests, median (IQR)			
Albumin	29.6 (26.50 - 33.23)	31.7 (27.80 - 36.20)	<.001
Erythrocyte count	3.13 (2.58 - 3.62)	3.35 (2.80 - 3.87)	<.001
Leukocyte count	4.59 (3.10 - 6.89)	3.86 (2.74 - 5.32)	<.001
Hemoglobin concentration	93 (74.00 - 112.00)	100 (81.00 - 119.00)	<.001
Total platelets	73 (46.00 - 117.50)	63 (43.00 - 100.00)	<.001
Total bilirubin	35.7 (17.55 - 82.65)	24.75 (15.90 - 41.50)	<.001
INR[b]	1.48 (1.28 - 1.87)	1.34 (1.20 - 1.55)	<.001
Prothrombin time	17.75 (15.70 - 21.40)	16.4 (14.90 - 18.60)	<.001
Creatinine	69.3 (57.10 - 89.75)	65.7 (55.20 - 0.40)	.002
Serum sodium	137.5 (132.90 - 140.50)	139.3 (136.40 - 141.80)	<.001
Serum potassium	4 (3.62 - 4.40)	3.87 (3.57 - 4.20)	<.001
Neutrophil count	3.14 (1.98 - 5.23)	2.46 (1.64 - 3.66)	<.001
Fibrinogen concentration	1.77 (1.27 - 2.46)	2 (1.55 - 2.62)	<.001
Urea nitrogen	6.02 (4.49 - 9.38)	5.38 (4.17 - 7.41)	<.001
Total protein	66.8 (56.75 - 69.95)	66.2 (59.42 - 72.57)	<.001
Prealbumin	65 (44.00 - 95.50)	83 (54.00 - 122.00)	<.001
Direct bilirubin	17.2 (8.70 - 47.10)	11.5 (7.20 - 21.60)	<.001
Indirect bilirubin	14.9 (8.30 - 30.60)	11.8 (7.90 - 18.70)	<.001
Total bile acids	39.1 (15.15 - 94.30)	29.15 (12.30 - 60.80)	<.001
Discharge laboratory tests, median (IQR)			

XSL•FO
RenderX

Characteristics	Readmission (n=423)	Nonreadmission (n=2884)	*P* value
Albumin	30.1 (27.80 - 33.00)	32.2 (29.40 - 36.00)	<.001
Serum sodium	137.7 (134.00 - 140.45)	139.2 (136.70 - 141.45)	<.001
Total bilirubin	31.5 (16.25 - 71.70)	23.5 (15.30 - 38.30)	<.001
Total white blood cells	3.74 (2.42 - 5.28)	3.4 (2.43 - 4.63)	.006
INR	1.5 (1.29 - 1.87)	1.34 (1.20 - 1.57)	<.001
Creatinine	71.2 (56.35 - 91.75)	68 (56.30 - 83.80)	.02
Scoring variables, median (IQR)			
MELD[c]	13 (10.00 - 18.00)	11 (8.00 - 14.00)	<.001

[a]EMD: electrolyte metabolism disorder. It is an imbalance in the balance of electrolytes (eg, sodium, potassium, calcium, and chloride) in the body, usually caused by levels of electrolytes in the body that are outside of normal ranges.

[b]INR: international normalized ratio. INR = $(PTpatient/PTcontrol)^{ISI}$, where PTpatient is the patient's prothrombin time, PTcontrol is the average normal prothrombin time, and ISI is the international sensitivity. The normal range of INR varies among hospitals, laboratories, and patient,s and ranges from 0.8 to 1.2.

[c]MELD: Model for End-Stage Liver Disease [23]. MELD = 9.57*ln(creatinine) + 3.78*ln(bilirubin) + 11.20*ln(INR) + 6.43. The patient's serum creatinine value is in milligrams per deciliter (mg/dL), the patient's total bilirubin value is in milligrams per deciliter (mg/dL), and the INR is the patient's international normalized ratio for coagulation. The higher the value, the higher the risk level.

XSL•FO
RenderX

Table . Characteristics of patients experiencing 30-day readmission.

Characteristics	Readmission (n=879)	Non-readmission (n=2428)	*P* value
Demographics, n (%)			.003
Female	262 (29.8)	859 (35.4)	
Male	617 (70.2)	1569 (64.6)	
Complications, n (%)			
Peritonitis	209 (23.8)	372 (15.3)	<.001
Hepatic encephalopathy	87 (9.9)	167 (6.9)	.005
Abdominal fluid	109 (12.4)	178 (7.3)	<.001
Liver failure	140 (15.9)	198 (8.2)	<.001
EMD[a]	90 (10.2)	189 (7.8)	.03
Ruptured esophagogastric varices	445 (50.6)	1336 (55.0)	.03
Comorbidities, n (%)			
Autoimmune diseases	70 (8.0)	293 (12.1)	<.001
Gastritis	67 (7.6)	277 (11.4)	.002
Neuropathy	35 (4.0)	62 (2.6)	.04
Ulcers	67 (7.6)	256 (10.5)	.02
Surgery, n (%)			
Bilirubin adsorption-plasma exchange	18 (2.1)	8 (0.3)	<.001
Bone marrow puncture biopsy	104 (11.8)	208 (8.6)	.006
Autologous ascites concentration and reinfusion	77 (8.8)	59 (2.4)	<.001
Laboratory tests, median (IQR)			
Albumin	30.1 (26.70 - 33.70)	31.9 (27.90 - 36.40)	<.001
Erythrocyte count	3.11 (2.60 - 3.63)	3.38 (2.83 - 3.89)	<.001
Leukocyte count	4.36 (3.02 - 6.40)	3.8 (2.71 - 5.28)	<.001
Hemoglobin concentration	93 (74.00 - 113.00)	101 (82.00 - 119.00)	<.001
Total platelets	71 (46.00 - 115.00)	63 (43.00 - 97.00)	<.001
Total bilirubin	29.1 (15.90 - 64.25)	24.6 (16.10 - 40.20)	<.001
INR[b]	1.42 (1.24 - 1.72)	1.33 (1.20 - 1.54)	<.001
Prothrombin time	17.2 (15.40 - 20.20)	16.3 (14.90 - 18.40)	<.001
Creatinine	68.9 (57.25 - 87.10)	63.3 (55.00 - 79.17)	<.001
Serum sodium	138 (134.00 - 140.90)	139.4 (136.60 - 141.90)	<.001
Serum potassium	3.92 (3.58 - 4.34)	3.87 (3.57 - 4.20)	<.001
Neutrophil count	2.93 (1.92 - 4.71)	2.41 (1.59 - 3.60)	<.001
Fibrinogen concentration	1.88 (1.40 - 2.56)	2.02 (1.56 - 2.61)	<.001
Urea nitrogen	5.96 (4.35 - 9.04)	5.32 (4.14 - 7.25)	<.001
Total protein	63.8 (58.00 - 70.30)	66.3 (59.70 - 72.88)	<.001
Prealbumin	70 (46.00 - 109.00)	84 (55.00 - 122.00)	<.001
Direct bilirubin	14.1 (7.70 - 35.80)	11.4 (7.20 - 21.10)	<.001
Indirect bilirubin	12.8 (7.70 - 25.70)	11.8 (7.95 - 18.30)	<.001
Total bile acids	32.3 (11.99 - 79.16)	29.45 (12.80 - 59.79)	.01
Discharge laboratory tests, median (IQR)			

XSL•FO
RenderX

Characteristics	Readmission (n=879)	Non-readmission (n=2428)	*P* value
Albumin	30.6 (28.40 - 33.70)	32.4 (29.50 - 36.10)	<.001
Serum sodium	138.1 (135.00 - 140.78)	139.4 (137.00 - 141.60)	<.001
Total bilirubin	27.4 (15.60 - 54.80)	23.6 (15.40 - 37.40)	<.001
Total white blood cells	3.66 (2.47 - 5.06)	3.39 (2.41 - 4.60)	.001
INR	1.42 (1.25 - 1.75)	1.34 (1.20 - 1.56)	<.001
Creatinine	70.85 (57.10 - 90.10)	67.7 (56.00 - 82.40)	<.001
Scoring variables, median (IQR)			
MELD[c]	12 (10.00 - 17.00)	11 (8.00 - 14.00)	<.001

[a]EMD: electrolyte metabolism disorder. It is an imbalance in the balance of electrolytes (eg, sodium, potassium, calcium, and chloride) in the body, usually caused by levels of electrolytes in the body that are outside of normal ranges.

[b]INR: international normalized ratio. INR = $(PTpatient/PTcontrol)^{ISI}$, where PTpatient is the patient's prothrombin time, PTcontrol is the average normal prothrombin time, and ISI is the international sensitivity. The normal range of INR varies among hospitals, laboratories, and patients, and ranges from 0.8 to 1.2.

[c]MELD: Model for End-Stage Liver Disease [23]. MELD = 9.57*ln(creatinine) + 3.78*ln(bilirubin) + 11.20*ln(INR) + 6.43. The patient's serum creatinine value is in milligrams per deciliter (mg/dL), the patient's total bilirubin value is in milligrams per deciliter (mg/dL), and the INR is the patient's international normalized ratio for coagulation. The higher the value, the higher the risk level.

Feature Selection and Statistical Analysis

A 2-step variable selection procedure was applied to the 14-day and 30-day readmission datasets, using tailored statistical methods for both quantitative and binary predictive factors. The application of these methods resulted in slightly different sets of included predictors for the 2 datasets. The *P* values for each variable are presented in Tables 2 and 3. Predictive factors with *P* values less than .05 were subsequently considered in the automatic variable selection process within the DES framework, aimed at pinpointing the optimal subset of predictors. Selected variables for both datasets are detailed in Multimedia Appendices 2 and 3.

The DES Framework Development

In the proposed DES framework, the classifier pool generation phase used an ensemble of 11 machine learning algorithms, each trained on different subsets and feature sets, to enhance the diversity and accuracy of trained models. During this phase, an interpretable set of rules was derived from each training dataset. Notably, these rules exhibited considerable overlap, suggesting the existence of common features across different rules. Across all training datasets, a total of 80 rules were extracted, with each rule covering at least 500 instances. These rules served as patterns for identifying specific characteristics or conditions within patient records. Using these rules, tailored data subsets were generated for experiments. Subsequently, during the meta-feature extraction and meta-training phase, 2 groups of meta-features were defined and extracted. Specifically, a customized competence region was designed to leverage the complications and comorbidities of cirrhotic patients, to extract meta-feature vectors for training the meta-classifier. Finally, in the dynamic classifier ensemble phase, the meta-classifier calculated the competence score of each classifier. Either the classifier with the highest score was selected, or a majority voting rule was applied to make predictions, ensuring optimal predictive performance in local regions for each patient.

The machine learning algorithms used to train the base classifiers include Naïve Bayes, *k*-nearest neighbors, logistic regression, linear discriminant analysis, quadratic discriminant analysis, and ensemble models such as random forest, extra trees, AdaBoost (adaptive boosting), gradient boosting classifier, LightGBM (light gradient boosting machine), and XGBoost (extreme gradient boosting). The hyperparameter tuning in this study comprised 2 components. First, the PyCaret library was used to automate machine learning workflows, including feature selection, model training, and hyperparameter optimization. Each model required tailored tuning metrics, such as the selection of the optimal *k*-value and distance metrics for *k*-nearest neighbors, tuning the *C* and γ parameters for the support vector machine, and adjusting the number and depth of trees for the random forest. Second, for the DES framework, hyperparameters such as the type of meta-classifier and the number of neighbors in local regions were optimized via grid search.

Furthermore, a 5-fold cross-validation approach was applied to maximize the use of a limited dataset, achieve stable predictions, and mitigate overfitting concerns. Building on the established framework of the DESlib library [24], the implementation of the proposed framework is accessible for online reference [22].

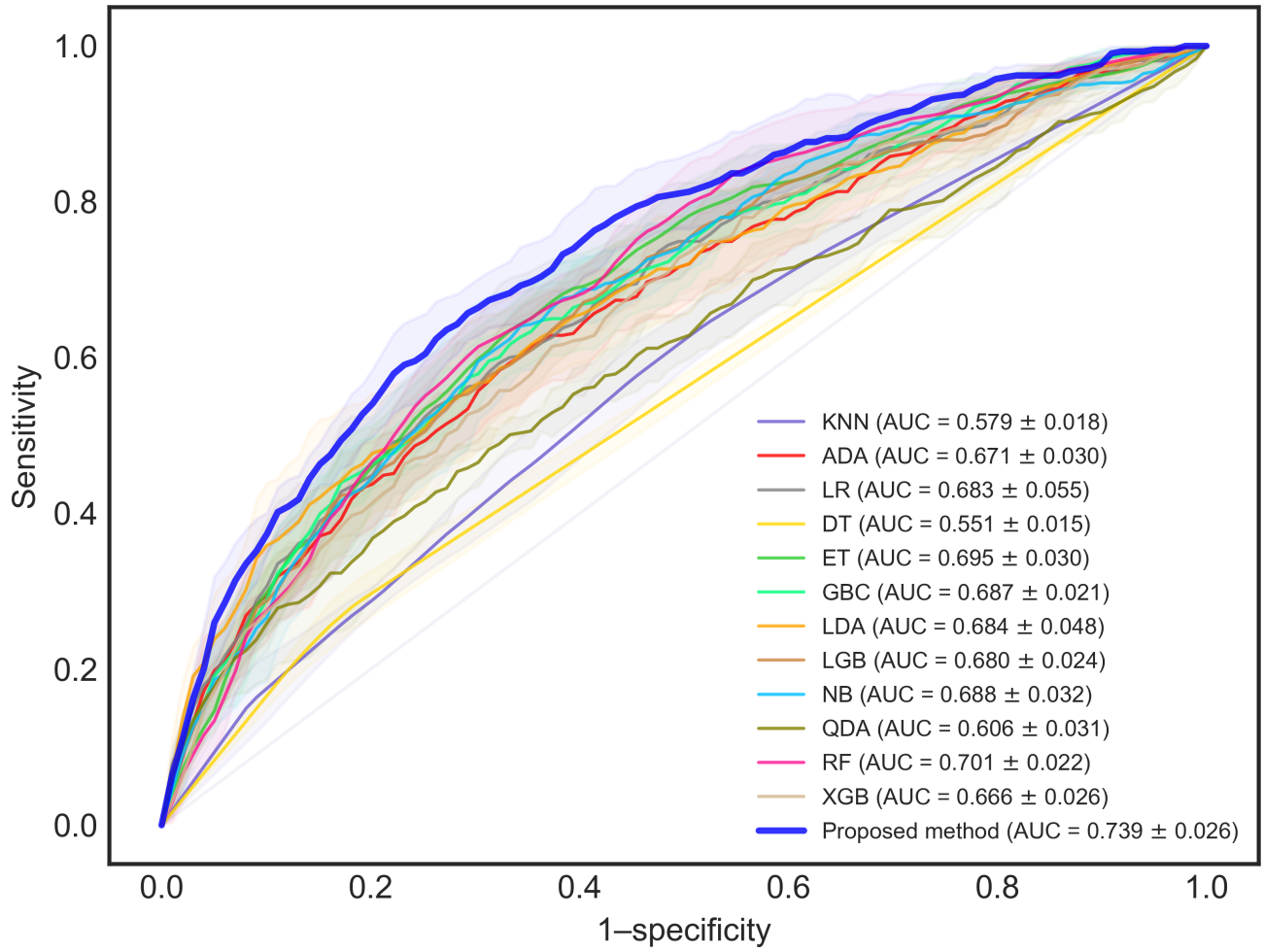
Evaluation Results

The evaluation focused on assessing unplanned readmissions within 14 days and 30 days. To address the challenge of imbalanced classification, where the model might tend to predict the majority class, we implemented a sensitivity-focused threshold adjustment. The threshold used for calculating the accuracy score was chosen to ensure a sensitivity greater than 0.5, indicating a focus on correctly identifying positive cases. The AUROC metric quantifies the area under the receiver operating characteristic curve, which illustrates the relationship between the true positive rate and the false positive rate at various thresholds. Visual representations of these metrics are presented in Figures 2 and 3. Table 4 summarizes the average scores obtained during cross-validation, alongside the maximum

XSL•FO
RenderX

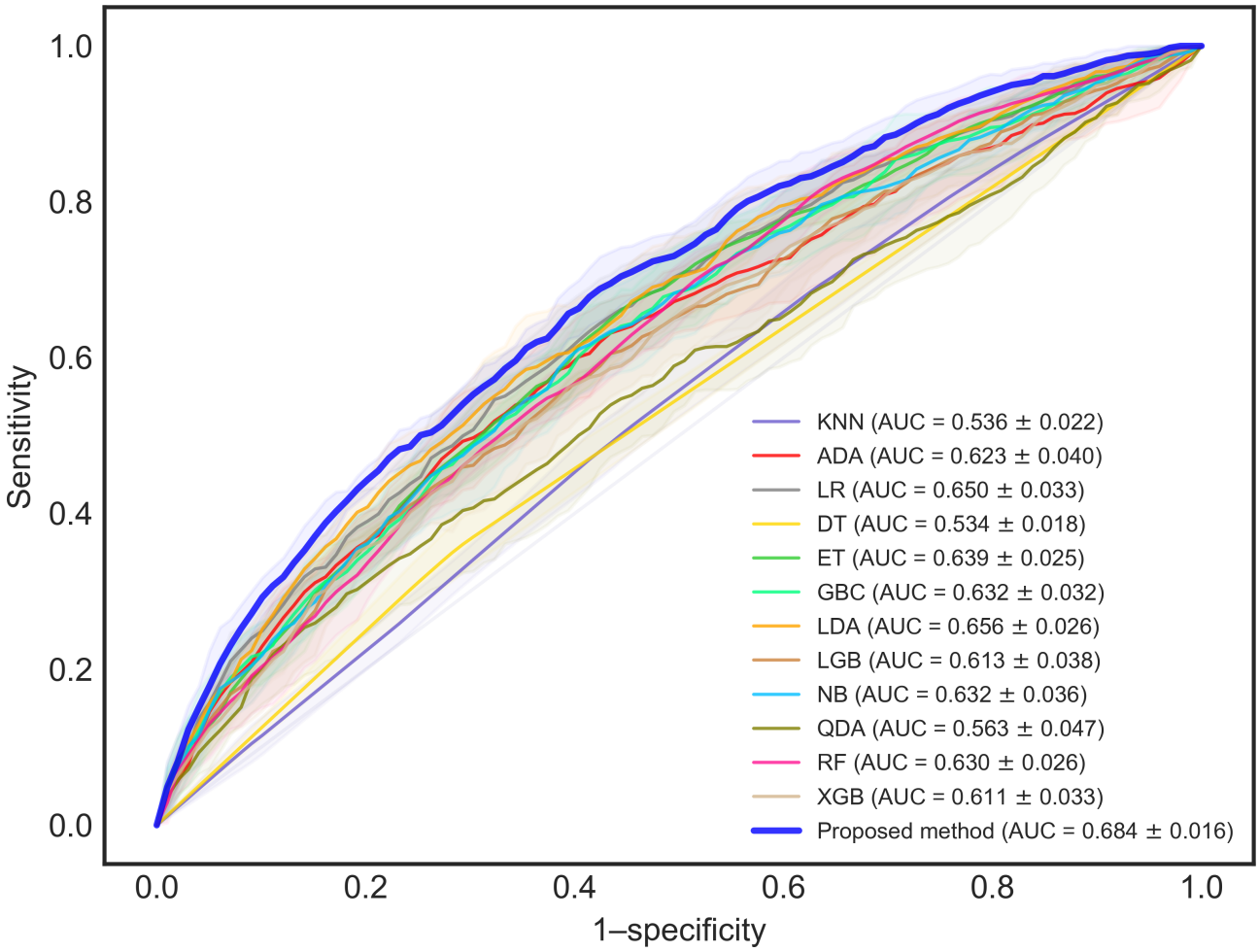
and minimum values observed. For 14-day readmission prediction, the DES framework achieved the highest accuracy of 0.783 and the peak AUC (area under the curve) of 0.739. For 30-day readmission prediction, it attained the best accuracy of 0.683 and the highest AUC of 0.684. In both accuracy and AUROC, the proposed method demonstrated superiority over the baseline models. This performance improvement can be attributed to the innovative features of our framework, such as the dynamic classifier selection based on patient subgroups.

Figure 2. ROC (receiver operating characteristic) curves for the prediction of 14-day readmission. ADA: adaptive boosting; AUC: area under the receiver operating characteristic curve; DT: decision tree; ET: extra trees; GBC: gradient boosting classifier; KNN: *k*-nearest neighbors; LDA: linear discriminant analysis; LGB: light gradient boosting machine; LR: logistic regression; NB: Naive Bayes; QDA: quadratic discriminant analysis; RF: random forest; XGB: extreme gradient boosting.



XSL•FO
RenderX

Figure 3. ROC (receiver operating characteristic) curves for the prediction of 30-day readmission. ADA: adaptive boosting; AUC: area under the receiver operating characteristic curve; DT: decision tree; ET: extra trees; GBC: gradient boosting classifier; KNN: *k*-nearest neighbors; LDA: linear discriminant analysis; LGB: light gradient boosting machine; LR: logistic regression; NB: Naive Bayes; QDA: quadratic discriminant analysis; RF: random forest; XGB: extreme gradient boosting.



XSL•FO
RenderX

Table . Performance comparison of different prediction models.

Classifier	14-day readmission		30-day readmission	
	AUROC[a]	Accuracy	AUROC	Accuracy
AdaBoost[b]	0.671 (0.619 - 0.706)	0.717 (0.635 - 0.736)	0.623 (0.548 - 0.659)	0.644 (0.590 - 0.675)
Extra trees	0.695 (0.642 - 0.727)	0.733 (0.682 - 0.779)	0.639 (0.593 - 0.662)	0.636 (0.581 - 0.658)
Gradient boosting classifier	0.687 (0.648 - 0.710)	0.729 (0.685 - 0.791)	0.632 (0.579 - 0.670)	0.635 (0.593 - 0.657)
K-nearest neighbors	0.579 (0.558 - 0.605)	0.557 (0.504 - 0.589)	0.536 (0.502 - 0.557)	0.507 (0.424 - 0.569)
Linear discriminant analysis	0.684 (0.624 - 0.761)	0.732 (0.657 - 0.835)	0.656 (0.606 - 0.681)	0.659 (0.578 - 0.699)
LightGBM[c]	0.680 (0.644 - 0.711)	0.718 (0.658 - 0.772)	0.613 (0.546 - 0.653)	0.623 (0.570 - 0.679)
Logistic regression	0.683 (0.618 - 0.763)	0.721 (0.604 - 0.790)	0.650 (0.591 - 0.681)	0.653 (0.584 - 0.685)
Naïve Bayes	0.688 (0.641 - 0.742)	0.735 (0.657 - 0.802)	0.632 (0.560 - 0.658)	0.642 (0.576 - 0.676)
Quadratic discriminant analysis	0.606 (0.548 - 0.631)	0.647 (0.623 - 0.672)	0.563 (0.492 - 0.628)	0.580 (0.501 - 0.672)
Random forest	0.701 (0.668 - 0.726)	0.728 (0.711 - 0.748)	0.630 (0.586 - 0.655)	0.620 (0.606 - 0.634)
XGBoost[d]	0.666 (0.624 - 0.702)	0.694 (0.622 - 0.739)	0.611 (0.561 - 0.660)	0.616 (0.563 - 0.678)
Proposed method	0.739 (0.697 - 0.775)	0.783 (0.766 - 0.803)	0.684 (0.664 - 0.709)	0.683 (0.658 - 0.701)

[a]AUROC: area under the receiver operating characteristic curve.

[b]AdaBoost: adaptive boosting.

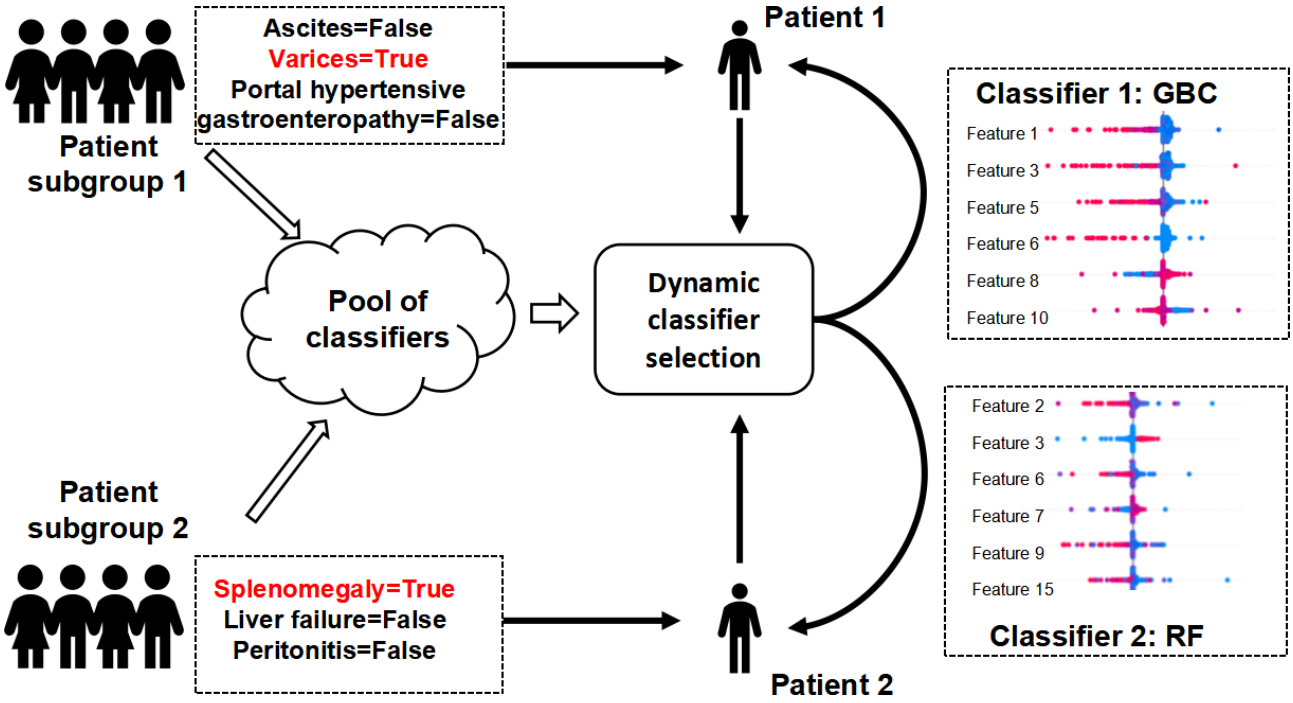
[c]LightGBM: light gradient boosting machine.

[d]XGBoost: extreme gradient boosting.

Although the accuracy of the model is not particularly high, a result similar to those reported in comparable literature, it was found that in some patient subgroups, the framework we used can exhibit more promising application prospects. This also constitutes one of the significant values of our research. Data-driven models are challenging to implement in real-world clinical applications due to their potential lack of generalizability across all patient populations. Within our framework, during the process of dynamic classifier selection, we can initially ascertain whether a model is suitable for a specific patient. This is accomplished by evaluating the performance of models with respect to the corresponding patient subgroups. As illustrated in Figure 4, patient subgroup 1 consists of patients with liver cirrhosis who have varices but no ascites or portal hypertensive gastroenteropathy. Patient subgroup 2 comprises patients with liver cirrhosis who have splenomegaly but no liver failure or peritonitis. Multiple heterogeneous classifiers were trained using multiple data subsets that meet these criteria to form the classifier pool. For patients 1 and 2, a gradient boosting classifier and a random forest classifier were selected, respectively. We evaluated the performance of the aforementioned subgroups. For the patients (n=152) in the test set who fit the criteria of subgroup 1, the accuracy, precision, recall, and F_1-score were 0.881, 0.862, 0.881, and 0.870, respectively. For the patients (n=195) in the test set who met the criteria of subgroup 2, the accuracy, precision, recall, and F_1-score were 0.891, 0.872, 0.891, and 0.879, respectively.

XSL•FO
RenderX

Figure 4. Illustration of characterization of patient subgroups and dynamic model selection for different patients. GBC: gradient boosting classifier; RF: random forest.



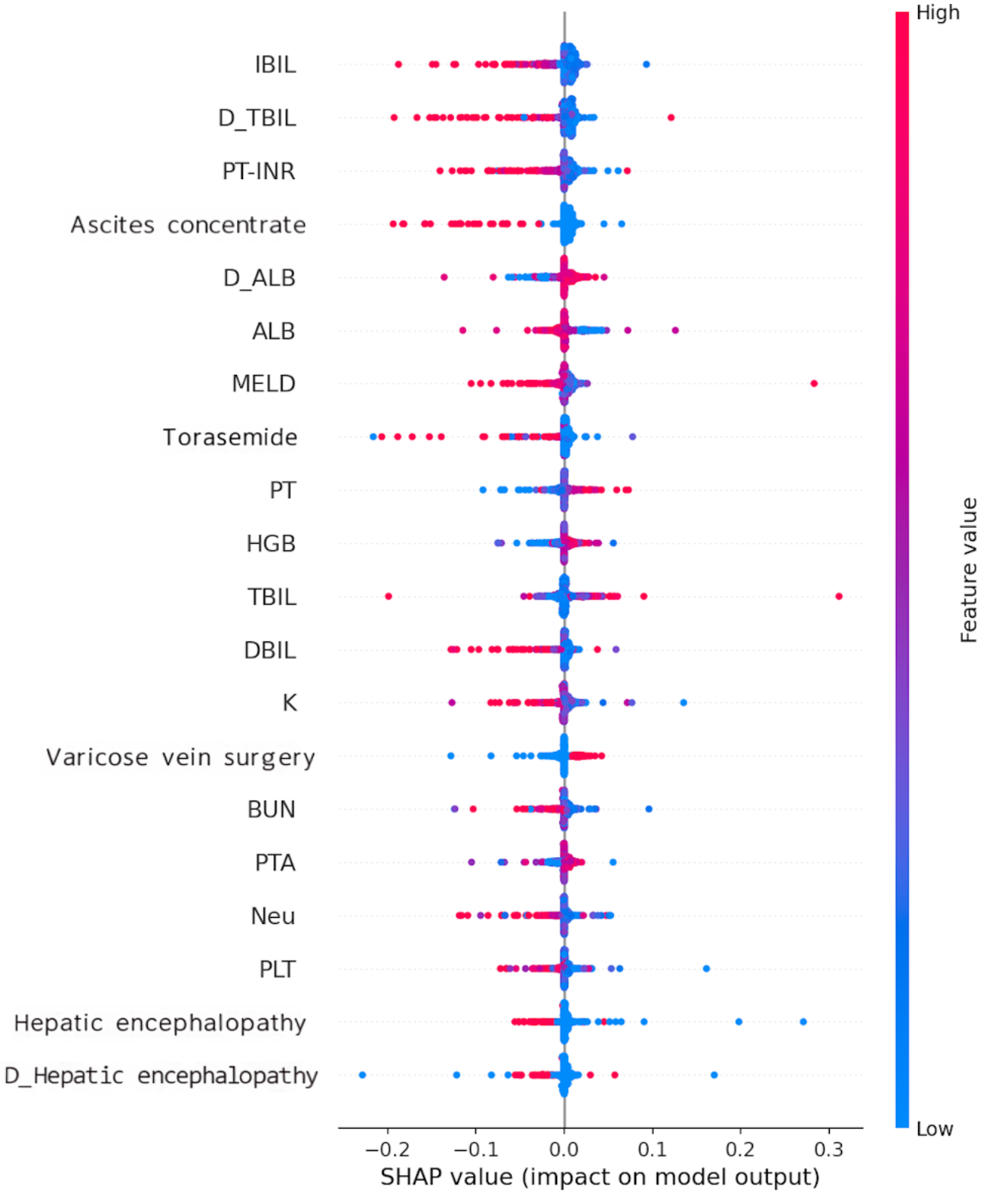
Interpretability

In addition to improving accuracy, the proposed method offers the capability to generate a classifier pool and facilitate dynamic selection of classifiers in a highly interpretable manner [25]. The interpretable rules used to generate the training subset for this classifier can describe clinical characteristics of patient subgroups. These rules provide insights into the specific features or conditions that contribute to the prediction, thereby assisting clinicians in making informed decisions and tailoring interventions for different patient subgroups. In cases where multiple classifiers are selected for prediction, analyzing the intersection of elements across these rules can provide additional insights for characterizing patient subgroups.

During the dynamic classifier selection phase, the proposed method selects classifiers with the highest competence scores for prediction. Our experiments revealed that, in most instances, a single optimal classifier was chosen for each individual to predict the risk of readmission. When the selected classifier is inherently intelligible and explainable, its predictions can be directly interpreted and understood. If multiple classifiers or black box models are selected for prediction, interpretability techniques such as SHAP (Shapley Additive Explanations) can be used to interpret the model's predictions. For instance, Figure 5 demonstrates that higher indirect bilirubin, total bilirubin at discharge, prothrombin time – international normalized ratio, ascites concentrate, and lower albumin at discharge were associated with higher predicted outcomes for a patient subgroup. Figure 6 presents individual SHAP force diagrams for non-readmitted and readmitted patients, with predicted probabilities of 0.41 and 0.80 for patients 1 and 2, respectively. For the first patient, total bile acid, platelet count, glutathione, aspartate aminotransferase, and peritonitis contributed negatively to the predicted outcome, while calcium and hemoglobin contributed positively. Conversely, for the second patient, calcium, hemoglobin, sex, electrolyte metabolism disorder, autoimmune diseases, total bilirubin at discharge, and sodium at discharge contributed positively to the prediction, while glutathione contributed negatively.

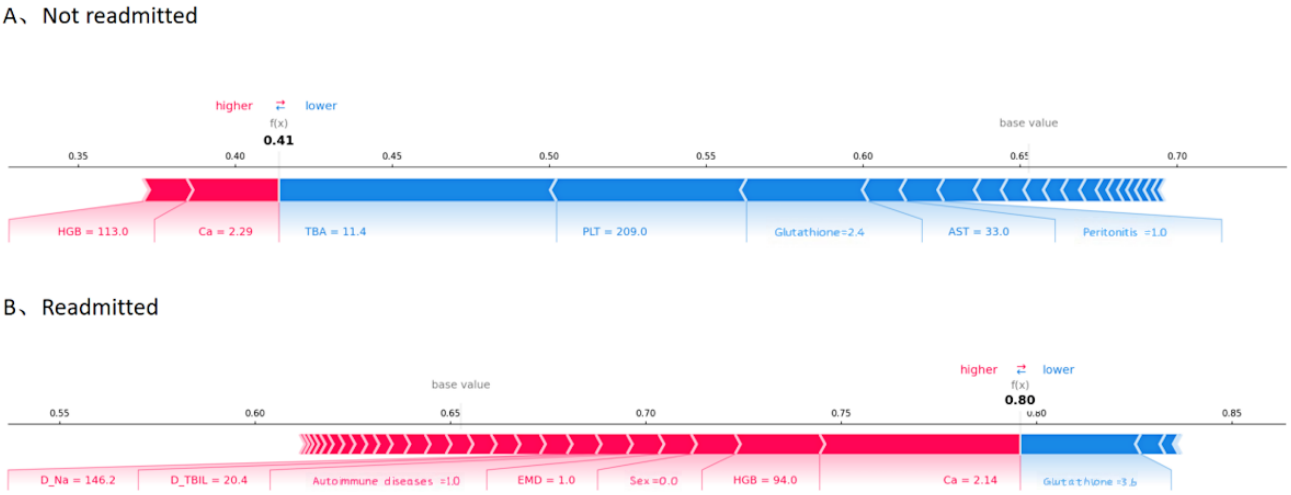
XSL•FO
RenderX

Figure 5. SHAP summary plot of the effect of input variables for 14-day readmission. ALB: albumin; BUN: blood urea nitrogen; D_ALB: albumin at discharge; D_Hepatic encephalopathy: hepatic encephalopathy at discharge; D_TBIL: total bilirubin at discharge; DBIL: bilirubin at discharge; HGB: hemoglobin; IBIL: indirect bilirubin; K: potassium; MELD: Model for End-Stage Liver Disease; Neu: neutrophils; PLT: platelet count; PT: prothrombin time; PTA: prothrombin activity; PT-INR: prothrombin time – international normalized ratio; SHAP: Shapley Additive Explanations; TBIL: total bilirubin.



XSL•FO
RenderX

Figure 6. SHAP (Shapley Additive Explanations) force plot showing (A) not readmitted and (B) readmitted. AST: aspartate aminotransferase; Ca: calcium; D_Na: sodium at discharge; D_TBIL: total bilirubin at discharge; EMD: electrolyte metabolism disorder; HGB: hemoglobin; PLT: platelet count; TBA: total bile acid.



Discussion

In this study, we developed a DES framework that comprises 3 components: classifier pool generation, meta-feature extraction and meta-training, and dynamic classifier ensemble. Initially, the classifier pool was formed by generating data subsets using a rule-based method to characterize patient subgroups and train heterogeneous machine learning models. Subsequently, by defining competence regions that encompass both complications and comorbidities, meta-features were extracted, and a meta-classifier was trained. Finally, a dynamic classifier ensemble was used to select the optimal classifier based on competent scores calculated by the meta-classifier, while a majority voting strategy was used when deemed necessary. This framework demonstrates its potential for application in EHR-based predictive tasks, by adaptively selecting models for individuals, enhanced by the medical knowledge integrated into the DES framework. The dynamic alignment of classifier selection with diverse patient subgroups, identified as the core contribution of this research, significantly enhances the clinical applicability and reliability of the model. By capturing heterogeneous health profiles and treatment responses across patient populations, the framework accommodates the complexity of real-world clinical care, thereby facilitating clinical experts' comprehension and trust in model predictions.

Readmission, a critical indicator of hospital quality [26], performance [27], and patient care standards [12], imposes significant burdens on health care systems and costs, with nationwide readmission expenses surpassing US $4.45 billion annually [28] and posing substantial survival challenges for low-income families [29]. Accurate prediction of readmission is increasingly essential for the effectiveness of interventions aimed at reducing readmissions. While bed availability may influence the timing of readmissions, it is not a determinant of readmission occurrence itself. In China's highly efficient health care system, most patients requiring treatment can access timely care, and bed availability variations (eg, overcrowding vs idleness in specialized units) were not major factors in the hospitals included in this study. To address potential timing biases, this research reports predictions for 2 discrete time intervals (14-day and 30-day readmission), providing comprehensive coverage of readmission dynamics [30]. Although bed availability could theoretically be a confounding factor, its impact was minimized in our analysis.

Over the past decade, numerous studies have modeled readmission risks using diverse methods, typically reporting AUC scores within the range of 0.60 to 0.78 [10,14,15]. The majority of studies have focused on developing and validating a single machine learning model. In contrast, within our study, the proposed DES method demonstrated superiority over other approaches. Notably, the framework implicitly addressed class imbalance through subgroup-specific undersampling during classifier pool generation, whereas explicit techniques such as SMOTE (Synthetic Minority Oversampling Technique) did not improve performance in our experiments.

Our study revealed that the 14-day unplanned readmission rate for patients with cirrhosis was 12.8% (423/3307), while the 30-day readmission rate stood at 26.6% (879/3307). In contrast, the 30-day readmission rates among insurance-covered populations in 2014 and 2019 were 22.6% and 21%, respectively [7]. The slightly elevated readmission rates observed in our study may be attributed to the higher average patient age of 55 years, which is associated with increased disease severity and a greater propensity for comorbidities. These patients are also more susceptible to developing complications and infections during hospitalization [2]. According to weighted analyses of readmission databases, complications [31], MELD (Model for End-Stage Liver Disease) scores [7], and infections [28] are crucial predictors of readmission in patients with cirrhosis. Our study echoed these findings, with prevalent complications including ascites (14-day data: 368 cases vs 55 controls; 30-day data: 770 cases vs 106 controls), variceal bleeding (14-day: 245 vs 178; 30-day: 434 vs 445), hepatic encephalopathy (reference 21; 14-day: 368 vs 55; 30-day: 792 vs 87), spontaneous bacterial peritonitis (14-day: 312 vs 111; 30-day: 670 vs 209), and acute-on-chronic liver failure (14-day: 337 vs 86; 30-day: 739 vs 140). These results are largely in alignment with previous studies [32]. Our study further revealed a gender disparity in liver disease prevalence, with male patients comprising the

XSL•FO
RenderX

majority of readmissions (14-day: 305 vs 118; 30-day: 617 vs 262). This may be linked to unhealthy lifestyle behaviors, including a higher prevalence of alcohol-related cirrhosis in males [33] and increased susceptibility to infections, both of which contribute to elevated readmission rates. Smoking, another established risk factor for cirrhosis, underscores the need for early intervention targeting smoking and alcohol cessation in cirrhotic patients. However, the asymptomatic nature of early-stage cirrhosis often delays diagnosis, exacerbating disease severity and readmission risks in males.

The advantages of this study can be summarized as follows. First, by leveraging heterogeneous classifiers' diverse feature selection capabilities and integrating temporal dynamics of patient health status into the DES framework, the model's robustness and clinical applicability are enhanced to address real-world EHR data limitations. Second, medical expert knowledge is seamlessly integrated into both classifier pool generation and dynamic selection processes. Specifically, medical diagnosis-based rules are used to define patient subgroups and competence regions, ensuring the framework is not purely data-driven but also informed by clinical expertise. This integration adds clinical validity—for example, incorporating complications and comorbidities (critical factors in clinical assessments)—to enhance model relevance and interpretability in real-world practice. Third, the framework enables dynamic updates of classifier pools and meta-classifiers with incoming data, demonstrating flexibility and scalability that hold promise for extending its application to prediction and management of a broad spectrum of diseases.

This study acknowledges several limitations. First, the dataset used in this study does not include patients readmitted from other hospitals. Although previous research suggests that the majority of readmissions occur within the same institution, this limitation may potentially affect the comprehensiveness of the study. Additionally, the study only encompasses patients who have had at least 2 readmissions. Future research should strive to expand the dataset and the scope of the sample to improve the reliability and generalizability of the findings. Second, the risk of readmission is affected by a multitude of factors, including socioeconomic status, educational level, and health insurance. This complexity poses a certain constraint on the model's discriminatory power. In future research, the goal is to incorporate these indicators through prospective and follow-up studies, thereby enhancing the model's predictive accuracy. Third, the practical implementation of the model requires continuous monitoring and calibration in line with local medical environments. Future studies should give priority to developing methods to enhance data interoperability across different sites, which will facilitate a wider application of the model.

Acknowledgments

This work was supported by the National Natural Science Foundation of China (grant 72101040) and the Intelligent Medicine Research Project of Chongqing Medical University (grant ZHYXQNRC202201).

Data Availability

The datasets generated or analyzed during the study are not publicly available due to institutional review board regulations and patient privacy policies but are available from the corresponding author upon reasonable request, subject to institutional or regulatory approvals.

Authors' Contributions

Conceptualization: XX, KP, QZ, HW
Data curation: XX
Formal analysis: ZS, LH
Funding acquisition: HW
Investigation: ZS, LH, XX
Methodology: ZS, HW
Software: ZS, LH, HW
Supervision: HW
Validation: ZS, HW
Writing – original draft: ZS
Writing – review & editing: KP, QZ, HW

Conflicts of Interest

None declared.

Multimedia Appendix 1
All variables in the dataset collected in the study.
[XLS File, 23 KB - medinform_v13i1e63581_app1.xls]

XSL•FO
RenderX

Multimedia Appendix 2
All variables in the 14-day readmission prediction dataset.
[XLS File, 21 KB - medinform_v13i1e63581_app2.xls]

Multimedia Appendix 3
All variables in the 30-day readmission prediction dataset.
[XLS File, 20 KB - medinform_v13i1e63581_app3.xls]

References

1. Arroyo V, Moreau R, Kamath PS, et al. Acute-on-chronic liver failure in cirrhosis. Nat Rev Dis Primers 2016 Jun 9;2:16041. [doi: 10.1038/nrdp.2016.41] [Medline: 27277335]
2. D'Amico G, Morabito A, D'Amico M, et al. Clinical states of cirrhosis and competing risks. J Hepatol 2018 Mar;68(3):563-576. [doi: 10.1016/j.jhep.2017.10.020] [Medline: 29111320]
3. Gajendran M, Umapathy C, Perisetti A, et al. Nationwide analysis of incidence and predictors of 30-day readmissions in patients with decompensated cirrhosis. Frontline Gastroenterol 2022;13(4):295-302. [doi: 10.1136/flgastro-2021-101850] [Medline: 35722599]
4. D'Amico G, Pasta L, Morabito A, et al. Competing risks and prognostic stages of cirrhosis: a 25-year inception cohort study of 494 patients. Aliment Pharmacol Ther 2014 May;39(10):1180-1193. [doi: 10.1111/apt.12721] [Medline: 24654740]
5. Tapper EB, Halbert B, Mellinger J. Rates of and reasons for hospital readmissions in patients with cirrhosis: a multistate population-based cohort study. Clin Gastroenterol Hepatol 2016 Aug;14(8):1181-1188. [doi: 10.1016/j.cgh.2016.04.009] [Medline: 27085758]
6. Morales BP, Planas R, Bartoli R, et al. HEPACONTROL. A program that reduces early readmissions, mortality at 60 days, and healthcare costs in decompensated cirrhosis. Dig Liver Dis 2018 Jan;50(1):76-83. [doi: 10.1016/j.dld.2017.08.024] [Medline: 28870446]
7. Orman ES, Ghabril M, Emmett TW, Chalasani N. Hospital readmissions in patients with cirrhosis: a systematic review. J Hosp Med 2018 Jul;13(7):490-495. [doi: 10.12788/jhm.2967] [Medline: 29694458]
8. Moon AM, Singal AG, Tapper EB. Contemporary epidemiology of chronic liver disease and cirrhosis. Clin Gastroenterol Hepatol 2020 Nov;18(12):2650-2666. [doi: 10.1016/j.cgh.2019.07.060] [Medline: 31401364]
9. Donzé J, Aujesky D, Williams D, Schnipper JL. Potentially avoidable 30-day hospital readmissions in medical patients: derivation and validation of a prediction model. JAMA Intern Med 2013 Apr 22;173(8):632-638. [doi: 10.1001/jamainternmed.2013.3023] [Medline: 23529115]
10. Mahmoudi E, Kamdar N, Kim N, Gonzales G, Singh K, Waljee AK. Use of electronic medical records in development and validation of risk prediction models of hospital readmission: systematic review. BMJ 2020 Apr 8;369:m958. [doi: 10.1136/bmj.m958] [Medline: 32269037]
11. Kansagara D, Englander H, Salanitro A, et al. Risk prediction models for hospital readmission: a systematic review. JAMA 2011 Oct 19;306(15):1688-1698. [doi: 10.1001/jama.2011.1515] [Medline: 22009101]
12. van Walraven C, Bennett C, Jennings A, Austin PC, Forster AJ. Proportion of hospital readmissions deemed avoidable: a systematic review. Can Med Assoc J 2011 Apr 19;183(7):E391-E402. [doi: 10.1503/cmaj.101860]
13. Matheny ME, Ricket I, Goodrich CA, et al. Development of electronic health record-based prediction models for 30-day readmission risk among patients hospitalized for acute myocardial infarction. JAMA Netw Open 2021 Jan 4;4(1):e2035782. [doi: 10.1001/jamanetworkopen.2020.35782] [Medline: 33512518]
14. Berman K, Tandra S, Forssell K, et al. Incidence and predictors of 30-day readmission among patients hospitalized for advanced liver disease. Clin Gastroenterol Hepatol 2011 Mar;9(3):254-259. [doi: 10.1016/j.cgh.2010.10.035] [Medline: 21092762]
15. Hu C, Anjur V, Saboo K, et al. Low predictability of readmissions and death using machine learning in cirrhosis. Am J Gastroenterol 2021 Feb 1;116(2):336-346. [doi: 10.14309/ajg.0000000000000971] [Medline: 33038139]
16. Sarwar T, Seifollahi S, Chan J, et al. The secondary use of electronic health records for data mining: data characteristics and challenges. ACM Comput Surv 2023 Feb 28;55(2):1-40. [doi: 10.1145/3490234]
17. Xu C, Fu C, Liu W, Sheng S, Yang S. Data-driven decision model based on dynamical classifier selection. Knowl Based Syst 2021 Jan;212:106590. [doi: 10.1016/j.knosys.2020.106590]
18. Cruz RMO, Sabourin R, Cavalcanti GDC. Dynamic classifier selection: recent advances and perspectives. Information Fusion 2018 May;41:195-216. [doi: 10.1016/j.inffus.2017.09.010]
19. Britto AS, Sabourin R, Oliveira LES. Dynamic selection of classifiers—a comprehensive review. Pattern Recognit DAGM 2014 Nov;47(11):3665-3680. [doi: 10.1016/j.patcog.2014.05.003]
20. Cruz RMO, Sabourin R, Cavalcanti GDC, Ing Ren T. META-DES: a dynamic ensemble selection framework using META-learning. Pattern Recognit DAGM 2015 May;48(5):1925-1935. [doi: 10.1016/j.patcog.2014.12.003]

XSL•FO
RenderX

21. Collins GS, Reitsma JB, Altman DG, Moons KGM. Transparent reporting of a multivariable prediction model for individual prognosis or diagnosis (TRIPOD): the TRIPOD statement. Ann Intern Med 2015 Jan 6;162(1):55-63. [doi: 10.7326/M14-0697] [Medline: 25560714]
22. Cirrhosis readmission. GitHub. URL: https://github.com/wanghaolin/metades-cirrhosis-readmission [accessed 2025-08-07]
23. Kim WR, Mannalithara A, Heimbach JK, et al. MELD 3.0: the model for end-stage liver disease updated for the modern era. Gastroenterology 2021 Dec;161(6):1887-1895. [doi: 10.1053/j.gastro.2021.08.050] [Medline: 34481845]
24. Cruz RMO, Hafemann LG, Sabourin R, Cavalcanti GDC. DESlib: a dynamic ensemble selection library in Python. J Mach Learn Res 2020;21(8):1-5 [FREE Full text]
25. Murdoch WJ, Singh C, Kumbier K, Abbasi-Asl R, Yu B. Definitions, methods, and applications in interpretable machine learning. Proc Natl Acad Sci USA 2019 Oct 29;116(44):22071-22080. [doi: 10.1073/pnas.1900654116]
26. Gaspar R, Rodrigues S, Silva M, et al. Predictive models of mortality and hospital readmission of patients with decompensated liver cirrhosis. Dig Liver Dis 2019 Oct;51(10):1423-1429. [doi: 10.1016/j.dld.2019.03.016] [Medline: 31113738]
27. Chirapongsathorn S, Poovorawan K, Soonthornworasiri N, Pan-Ngum W, Phaosawasdi K, Treeprasertsuk S. Thirty-day readmission and cost analysis in patients with cirrhosis: a nationwide population-based data. Hepatol Commun 2020 Mar;4(3):453-460. [doi: 10.1002/hep4.1472] [Medline: 32140661]
28. Chirapongsathorn S, Krittanawong C, Enders FT, et al. Incidence and cost analysis of hospital admission and 30-day readmission among patients with cirrhosis. Hepatol Commun 2018 Feb;2(2):188-198. [doi: 10.1002/hep4.1137] [Medline: 29404526]
29. Brahmania M, Wiskar K, Walley KR, Celi LA, Rush B. Lower household income is associated with an increased risk of hospital readmission in patients with decompensated cirrhosis. J Gastroenterol Hepatol 2021 Apr;36(4):1088-1094. [doi: 10.1111/jgh.15153] [Medline: 32562577]
30. Zhang M, Liu S, Bi Y, Liu J. Comparison of 30-day planned and unplanned readmissions in a tertiary teaching hospital in China. BMC Health Serv Res 2023 Mar 6;23(1):213. [doi: 10.1186/s12913-023-09193-1] [Medline: 36879245]
31. Volk ML, Tocco RS, Bazick J, Rakoski MO, Lok AS. Hospital readmissions among patients with decompensated cirrhosis. Am J Gastroenterol 2012 Feb;107(2):247-252. [doi: 10.1038/ajg.2011.314] [Medline: 21931378]
32. Bajaj JS, Reddy KR, Tandon P, et al. The 3‐month readmission rate remains unacceptably high in a large North American cohort of patients with cirrhosis. Hepatology 2016;64(1):200-208. [doi: 10.1002/hep.28414]
33. Singal AK, DiMartini A, Leggio L, Arab JP, Kuo YF, Shah VH. Identifying alcohol use disorder in patients with cirrhosis reduces 30-days readmission rate. Alcohol Alcohol 2022 Sep 10;57(5):576-580. [doi: 10.1093/alcalc/agac015] [Medline: 35544033]

Abbreviations

AdaBoost: adaptive boosting
AUC: area under the curve
AUROC: area under the receiver operating characteristic curve
DES: dynamic ensemble selection
EHR: electronic health record
ICD-10: *International Classification of Diseases*, 10th Revision
ICD-9: *International Classification of Diseases*, 9th Revision
LightGBM: light gradient boosting machine
MELD: Model for End-Stage Liver Disease
META-DES: dynamic ensemble selection using meta-learning
SHAP: Shapley Additive Explanations
SMOTE: Synthetic Minority Oversampling Technique
TRIPOD: Transparent Reporting of a Multivariable Prediction Model for Individual Prognosis or Diagnosis
XGBoost: extreme gradient boosting

Edited by A Benis; submitted 24.06.24; peer-reviewed by J Zhang, Y Liu; revised version received 13.07.25; accepted 15.07.25; published 10.09.25.

Please cite as:
Shi Z, Huang L, Xu X, Pu K, Zhang Q, Wang H
Predicting Unplanned Readmission Risk in Patients With Cirrhosis: Complication-Aware Dynamic Classifier Selection Approach
JMIR Med Inform 2025;13:e63581
URL: https://medinform.jmir.org/2025/1/e63581
doi:10.2196/63581

XSL•FO
RenderX

© Zixin Shi, Linjun Huang, Xiaomei Xu, Kexue Pu, Qingpeng Zhang, Haolin Wang. Originally published in JMIR Medical Informatics (https://medinform.jmir.org), 10.9.2025. This is an open-access article distributed under the terms of the Creative Commons Attribution License (https://creativecommons.org/licenses/by/4.0/), which permits unrestricted use, distribution, and reproduction in any medium, provided the original work, first published in JMIR Medical Informatics, is properly cited. The complete bibliographic information, a link to the original publication on https://medinform.jmir.org/, as well as this copyright and license information must be included.

XSL•FO
RenderX

A Validation Tool (VaPCE) for Postcoordinated SNOMED CT Expressions: Development and Usability Study

Tessa Ohlsen[1,2], MSc; Viola Hofer[3], Dr rer nat; Josef Ingenerf[1], Prof Dr, Dr rer nat

[1]Section for Clinical Research IT, Institute of Medical Biometry and Statistics, University of Luebeck and University Hospital Schleswig-Holstein, Luebeck, Germany

[2]Institute of Medical Informatics, University of Luebeck, Lübeck, Germany

[3]Thieme Compliance GmbH, Erlangen, Germany

Corresponding Author:
Tessa Ohlsen, MSc
Section for Clinical Research IT, Institute of Medical Biometry and Statistics, University of Luebeck and University Hospital Schleswig-Holstein, Luebeck, Germany

Abstract

Background: The digitalization of health care has increased the demand for efficient data exchange, emphasizing semantic interoperability. SNOMED Clinical Terms (SNOMED CT), a comprehensive terminology with over 360,000 medical concepts, supports this need. However, it cannot cover all medical scenarios, particularly in complex cases. To address this, SNOMED CT allows postcoordination, where users combine precoordinated concepts with new expressions. Despite SNOMED CT's potential, the creation and validation of postcoordinated expressions (PCEs) remain challenging due to complex syntactic and semantic rules.

Objective: This work aims to develop a tool that validates postcoordinated SNOMED CT expressions, focusing on providing users with detailed, automated correction instructions for syntactic and semantic errors. The goal is not just validation, but also offering user-friendly, actionable suggestions for improving PCEs.

Methods: A tool was created using the Fast Healthcare Interoperability Resource (FHIR) service $validate-code and the terminology server Ontoserver to check the correctness of PCEs. When errors are detected, the tool processes the SNOMED CT Concept Model in JSON format and applies predefined error categories. For each error type, specific correction suggestions are generated and displayed to users. The key added value of the tool is in generating specific correction suggestions for each identified error, which are displayed to the users. The tool was integrated into a web application, where users can validate individual PCEs or bulk-upload files. The tool was tested with real existing PCEs, which were used as input and validated. In the event of errors, appropriate error messages were generated as output.

Results: In the validation of 136 PCEs from 304 FHIR Questionnaires, 18 (13.2%) PCEs were invalid, with the most common errors being invalid attribute values. Additionally, 868 OncoTree codes were evaluated, resulting in 161 (20.9%) PCEs containing inactive concepts, which were successfully replaced with valid alternatives. A user survey reflects a favorable evaluation of the tool's functionality. Participants found the error categorization and correction suggestions to be precise, offering clear guidance for addressing issues. However, there is potential for enhancement, particularly regarding the level of detail in the error messages.

Conclusions: The validation tool significantly improves the accuracy of postcoordinated SNOMED CT expressions by not only identifying errors but also offering detailed correction instructions. This approach supports health care professionals in ensuring that their PCEs are syntactically and semantically valid, enhancing data quality and interoperability across systems.

(JMIR Med Inform 2025;13:e67984) doi:10.2196/67984

KEYWORDS

SNOMED CT; PCE; postcoordination; FHIR; validation; postcoordinated expression; Fast Healthcare Interoperability Resource

Introduction

Background

The ongoing digitalization in medicine has significantly increased the amount of available medical data in the health care sector. To optimize medical care, it is crucial to use this data efficiently. For this, it is essential that the data can be exchanged and processed automatically across different systems. This requires not only technical compatibility but also semantic interoperability. Semantic interoperability ensures that the meaning of the data is maintained when it is transferred to another system. A key aspect of semantic interoperability is the sophisticated use of suitable coding systems and medical standards for medical terms [1]. One example is the terminology SNOMED Clinical Terms (SNOMED CT). With over 360,000

XSL•FO
RenderX

concepts, SNOMED CT is considered the most comprehensive terminology in medicine. SNOMED CT facilitates machine-readable data exchange and reduces issues related to country-specific and domain-specific coding, as well as difficult versioning issues. However, despite its comprehensiveness, SNOMED CT cannot cover every possible medical circumstance by precoordinated concepts alone due to the complexity of natural language [2]. For instance, an allergy to metals: The SNOMED CT International Edition, version 2024-09-01, lists a total of 1575 different metals. However, only 43 specific allergies to metals are included in this edition and version of SNOMED CT. This indicates that not every allergy-relevant metal or substance can be expressed through a precoordinated concept, such as an allergy to Cobalt-chromium alloy. To address such gaps, SNOMED CT offers postcoordination in contrast to many other vocabularies. Here, existing precoordinated concepts are combined into new expressions using formal grammar. This avoids the well-known problem of combinatorial explosion [2]. An example postcoordinated expression (PCE) for an allergy to a Cobalt-chromium alloy based on Compositional Grammar [3] is as follows:

1155942004 |Allergy to metal and/or metal compound|:

{719722006 |Has realization| = 472964009 |Allergic process|,

246075003 |Causative agent| = 256526003 |Cobalt-chromium alloy|}.

Here, the focus concept Allergy to metal and/or metal compound is refined by combining attributes (eg, Causative agent) with corresponding attribute values (eg, Cobalt-chromium alloy) as attribute relations.

Creating PCEs improves the detailed recording of medical facts and enhances patient record quality and automated processing. PCEs are complex due to the syntactic requirements of the Compositional Grammar [3] and the semantic rules of the Concept Model [4]. The syntactic requirements ensure that PCEs are correctly structured, while the semantic rules ensure that they accurately represent medical concepts and their relationships. This complexity makes it challenging to create valid accurate PCEs [2].

Since Germany acquired a license for SNOMED CT in January 2021, the interest in using SNOMED CT has grown. SNOMED CT is increasingly being used in various national projects [5,6]. Despite this, postcoordinated SNOMED CT expressions are still used hesitantly. Nevertheless, PCEs are used in the Medical Information Objects of the National Association of Statutory Health Insurance Physicians [7] or in anamnesis forms from Thieme Compliance [8]. Nonetheless, some do not fully comply with the rules of the Compositional Grammar or the Concept Model. To address these issues, this work aims to develop a tool for the validation of PCEs. The focus is not only on determining whether a PCE is correct but also on providing detailed information and concrete suggestions for correcting a PCE (Figure 1). These suggestions are based on the analyzed errors and provide targeted recommendations for correcting specific PCEs.

Figure 1. For every invalid PCE, a correction suggestion should be made automatically using the developed tool. PCE: postcoordinated expression.



Related Work

Currently, SNOMED International provides a tool called "SNOMED International APG Parser: SNOMED CT Compositional Grammar" which validates PCEs based on syntactic rules of Compositional Grammar [9]. Nevertheless, this tool only assesses syntactic correctness and does not consider the semantic rules of the Concept Model, which are essential for ensuring contextually accurate PCEs. This work aims to supplement this by adding semantic validation, which should provide better feedback for the user.

An alternative method for the syntactic and semantic validation of PCEs is using the commercial terminology server Ontoserver [10] of Commonwealth Scientific and Industrial Research Organization. Ontoserver is currently the only Fast Healthcare Interoperability Resource (FHIR) terminology server that supports postcoordination at all. Ontoserver is used to validate the PCEs in combination with the FHIR service $validate-code [11]. This checks a PCE against specific coding systems, such as SNOMED CT. This method provides a validation result through a Representational State Transfer (REST) request that returns a JSON object [11]. Although this service indicates errors, it presents them in a technical manner that requires a solid understanding of SNOMED CT. This work's tool will build upon the FHIR service $validate-code based on Ontoserver to offer more comprehensive validation and suggestions. Hence, the difference between this work and the Ontoserver is that the focus is on the individual correction instructions for each PCE.

Methods

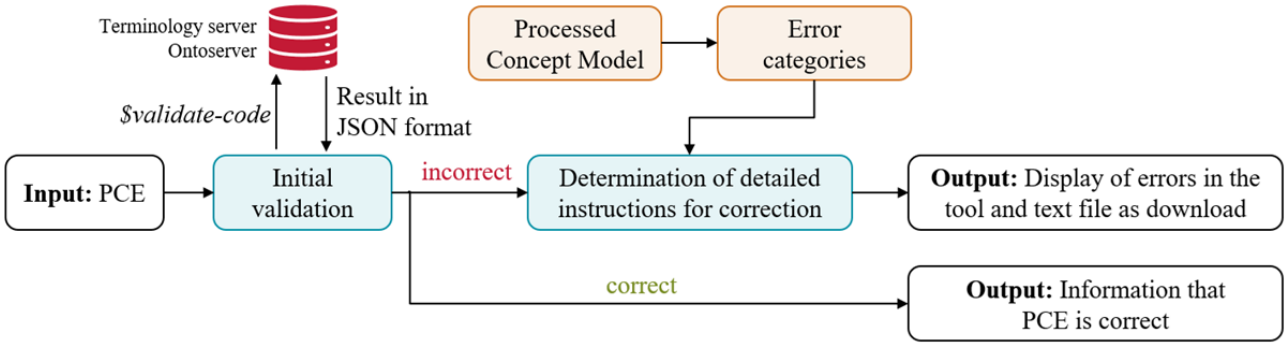
Overview

This work aims to develop a user-friendly tool for validating postcoordinated SNOMED CT expressions. The focus is on the automated provision of detailed correction instructions if a PCE contains syntactic or semantic errors. The tool's pipeline is illustrated in Figure 2. First, a PCE is validated using the FHIR service $validate-code [11] and the terminology server Ontoserver [10]. If the entered PCE is correct, this is communicated to the user, and the algorithm terminates. For incorrect PCEs, the tool generates detailed correction instructions in the next step, based on the results of the FHIR service. A processed Concept Model in JSON format and custom error categories are also used for this purpose. The correction

XSL•FO
RenderX

instructions are presented to the user. The individual components of the pipeline are explained in more detail below.

Figure 2. Pipeline for the validation of a PCE. PCE: postcoordinated expression.

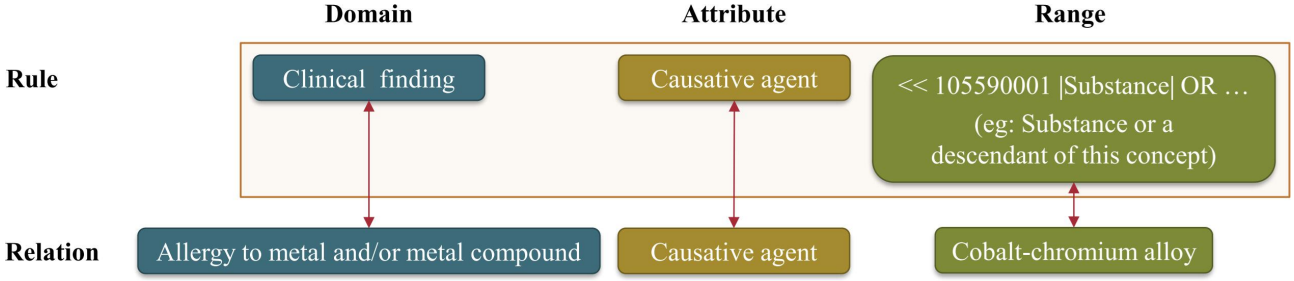


Initial Validation

FHIR, an interoperable data standard developed by Health Level 7 [1], is gaining increasing importance both nationally [12] and internationally [13,14]. In addition to the exchange of patient-related health information, FHIR also offers a terminology module with various services [1]. In this project, the FHIR service $validate-code [11] combined with Ontoserver [10] plays a central role. This is used to verify the syntactic and semantic correctness of a postcoordinated SNOMED CT expression, in combination with a terminology server. The $validate-code service operates via an HTTP POST request. The response is a JSON object that contains the results of the validation. Figure 3 shows an excerpt from this JSON object for an invalid PCE. The error messages indicate that the concept 472964009 |Allergic process| is not a valid attribute. This detailed output is attributed to the commercial Ontoserver, which possesses extensive knowledge of SNOMED CT, enabling precise analysis of PCEs.

Although the output is focused on automatic processing rather than human readability, it remains particularly valuable due to this specialization. This output provides a crucial basis for the next stages of the tool's pipeline.

Figure 3. Domain and range example for the SNOMED CT attribute Causative agent.



Determination of Detailed Instructions for Correction

Processed Concept Model

The Concept Model defines rules for how SNOMED CT concepts and PCEs are structured using formal logic and specific guidelines. These rules ensure that medical expressions are meaningful and consistent. For each SNOMED CT attribute, the Concept Model specifies a domain and a range (Figure 4):

- Domain: This includes concepts (eg, Allergy to metal and/or metal compound) from at least one of the 19 Top-Level Hierarchies (eg, Clinical finding).
- Range: This specifies a subset of SNOMED CT concepts that are valid values for an attribute. For the attribute Causative agent, for instance, only certain substances, such as Cobalt-chromium alloy, are included in the range.

XSL•FO
RenderX

Figure 4. Extract of an error message for an invalid PCE based on an Ontoserver request. PCE: postcoordinated expression.

Invalid PCE:

1155942004 |Allergy to metal and/or metal compound|:
{719722006 |Has realization| = 472964009 |Allergic process|,
472964009 |Allergic process| = 256526003 |Cobalt-chromium alloy|}

Error message:

{"name": "reason",
"valueString": "MRCM: 256526003 is not in range for attribute 472964009"},
{"name": "reason",
"valueString": "MRCM: 472964009 IS NOT a valid attribute for 1155942004"},
{"name": "reason",
"valueString": "MRCM: Total 1 occurrence of attribute 472964009 is not allowed for 1155942004; expected []"}
…

Additionally, the Concept Model specifies the cardinality of the attributes and whether attributes must be grouped [2,4].

To facilitate the tool, a machine-readable Concept Model (MRCM) is included in the RF2 files for each SNOMED CT edition and version [15]. For our purposes, the MRCM Domain Reference Set (International Edition, 2024-05-01) is used. The MRCM Domain Reference Set is provided as a text file, with each domain represented by a detailed entry. Each entry includes all essential information about the respective domain, including a so-called template that is particularly significant for this work [15,16]. An excerpt from one of these templates is shown on the left side of Figure 5. The syntax of the templates is based on Compositional Grammar and includes the relevant attributes, as well as the cardinalities and value ranges for each domain. To further enhance usability, we developed an algorithm that decomposes the template into its individual components and presents this information in JSON format. This allows for a structured and efficient processing of the template components in the next step. All relevant information is already available in the appropriate format, enabling subsequent processes to use it directly without any further conversions. An extract of the JSON is displayed on the right side of Figure 5. The JSON is available on GitHub [17].

Figure 5. Extract from the processed machine-readable Concept Model in JSON format which proves to be advantageous for further processing.

Template:

```
[[+id(<< 404684003 |Clinical finding (finding)|)]]:
[[0..*]] {
    [[0..1]] 246075003 |Causative agent| =
                [[+id(<< 105590001 |Substance (substance)| OR ...]],
    …
}
```

Processed template:

```
{ "domainConstraint": "<< 404684003 |Clinical finding (finding)|",
  …
  "domainTemplate": [
    { "init": "...",
      "focusConcept": "<<404684003",
      "withRoleGroups": [
        { "roleGroupCardinalityMin": "0",
          "roleGroupCardinalityMax": "*",
          "attribute": [
            { "attributeNameCode": "246075003",
              "attributeNameDisplay": "Causative agent",
              "constraint": "<<105590001OR…",
              "attributeCardinalityMin": "0",
              "attributeCardinalityMax": "1"
            }, …
          ]
        }
      ]
    }
  ]
}
```

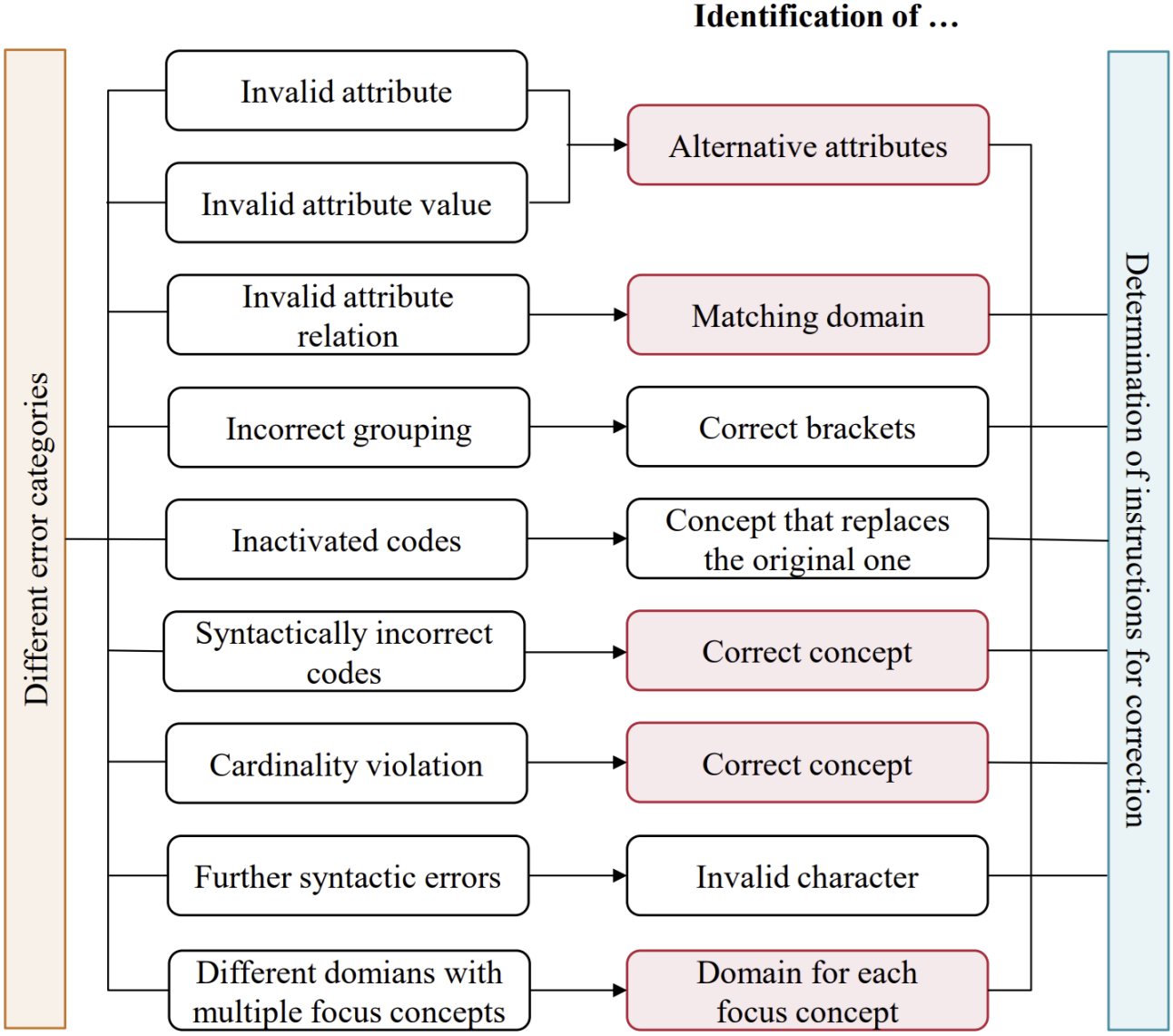
Error Categories

Overview

Based on the authors' expertise in SNOMED CT postcoordination [2,18-20], a total of nine error categories have been identified. For each error category, specific guidelines have been developed and are provided for an individual PCE. A general overview of the error categories and the focus of the guidelines is shown in Figure 6. The following sections provide a detailed description of each error category. Examples of the individual error categories are available on GitHub [21].

XSL•FO
RenderX

Figure 6. An overview of the various error categories (left side) and the corresponding correction focus (right side). For all categories, the processed Concept Model in JSON format plays a certain role. For the correction instructions highlighted in red, a terminology server and FHIR services are also used.



Invalid Attribute

If a SNOMED CT concept is used that does not belong to the valid 126 attributes or is not valid in a specific domain, it is categorized under this category.

Correction Instruction

The solution involves identifying a valid SNOMED CT attribute. Users are provided with information about the domain of the focus concept, along with definitions and value ranges for alternative attributes. This helps to replace the invalid attribute with a suitable one. If no appropriate alternative is found, or if no attributes exist within the domain, the user must either modify the attribute value or create a new PCE with a different focus concept. For the invalid PCE shown in Figure 2, this error category is identified. The algorithm would also determine that the incorrect attribute Allergic process should be replaced with Causative agent or Associated with.

Technical Implementation

To implement this, the FHIR service $expand is used in combination with a terminology server and the Expression Constraint Language (ECL) of SNOMED CT [22]. The ECL in this case defines the value range of an attribute, such as << 105590001 |Substance| OR .... This allows for verifying whether the current attribute value is included in the provided list. If an alternative attribute is identified, the PCE is revalidated to check for any additional errors.

Invalid Attribute Value

In this case, the chosen attribute value is not in the value range for the attribute.

Correction Instruction

For manually created PCEs, the attribute value is typically chosen correctly as it directly relates to a specific medical circumstance. However, the chosen value might not be within the valid range. The focus is on identifying appropriate alternative attribute values. Users will receive similar guidance

XSL•FO
RenderX

as in the "Invalid Attribute" error category, including details on the acceptable value range and potential alternatives.

Technical Implementation

The process adheres to the same principle outlined in the "Invalid Attribute" section.

Invalid Domain

In this error category, the attribute relation (comprising an attribute and its value) is semantically correct but does not match the domain of the focus concept.

Correction Instruction

Achieving a semantically correct relation requires a different domain of the focus concept. Users are provided with a list of domains where the current attribute relation is valid, enabling them to modify the focus concept accordingly.

Technical Implementation

The appropriate domain is determined using the FHIR service $expand and a terminology server. The request is based on an ECL that specifies the domain constraint from the Concept Model. For instance, an expression might be << 404684003 |Clinical finding|. If the focus concept appears in the results returned by this query, it belongs to the corresponding domain.

Different Domains With Multiple Focus Concepts

Overview

According to the Compositional Grammar, it is valid to use multiple focus concepts connected by "+" (AND). If multiple focus concepts from different domains are used—such as Clinical finding and Procedure—this results in a semantic error. In such cases, the PCE is categorized under this error category.

Correction Instruction

The domains of the focus concepts used are displayed.

Technical Implementation

We determined the Concept Model Domain performed as described in the "Incorrect attribute relation" category.

Incorrect Grouping

Overview

This category includes errors related to the bracketing of RoleGroups, which are crucial for the syntactic and semantic integrity of PCEs. Common issues involve missing or incorrect brackets, as well as imbalances between open and closed brackets.

Correction Instruction

Users are provided with detailed information on which attributes are incorrectly grouped and where bracket corrections are necessary. Specific guidance is given on how to fix incorrectly placed brackets.

Technical Implementation

A straightforward analysis of the error message and the PCE is conducted to provide targeted correction instructions. The error message shows the position and the concept before which the error occurs. For example, it may indicate that the character "{" is missing, suggesting that a RoleGroup is missing and should be started at the specified location. In this case, the tool would also determine the position where the RoleGroup should be closed again. Technically, this is done through simple processing of the strings for the error message, as well as the JSON object of the PCE.

Inactivated Codes

This error category pertains to PCEs that include codes that are no longer valid or active in the current version and have been replaced by others.

Correction Instruction

Users are provided with an alternative concept that is semantically equivalent to the inactivated concept.

Technical Implementation

Identifying active concepts for inactivated codes is part of version management. SNOMED International offers Historical Association Reference Sets (RefSets) for this purpose. In this work, the following two RefSets are used:

- 900000000000527005 | SAME AS association reference set|: For identifying semantically equivalent active concepts.
- 900000000000526001 | REPLACED BY association reference set|: For linking deactivated concepts that have been replaced by new concepts.

These RefSets can be integrated into ECL. Additionally, ECL provides member filters that can be used in combination with respective RefSets, for example:

^ [targetComponentId] 900000000000526001 | REPLACED BY association reference set|

{{ M referencedComponentId = 224799004 |Unfamiliar environment (environment)| }}.

This ECL queries the REPLACED BY association reference set to identify the concept that has replaced the inactivated concept 224799004 |Unfamiliar environment (environment)|. In this case, the result would be 1186687002 |Unfamiliar environment (finding)|.

Syntactically Incorrect Codes

Overview

This error category refers to SNOMED CT Identifiers that cannot be linked to any valid SNOMED CT concept. The issue is not that the concept is inactive, but rather that the identifier is missing characters.

Correction Instruction

Identifying a valid SNOMED CT concept that corresponds to the numerical sequence of the incorrect identifier is necessary for correcting a PCE. The user will then be provided with this concept.

Technical Implementation

For this category, the FHIR service $expand, a terminology server, and ECL are also used. The ECL expression << 138875005 |SNOMED CT Concept| is used to return all

XSL•FO
RenderX

SNOMED CT concepts. Subsequently, all concepts containing the specified numeric sequence are identified. These concepts are then validated using the FHIR service $validate-code to determine which one fits both syntactically and semantically with the original identifier.

Cardinality Violation

Overview

As previously mentioned, the Concept Model defines cardinalities that specify the minimum and maximum occurrences of an attribute. A PCE is categorized in this category if it does not adhere to these cardinality constraints.

Correction Instruction

Initially, the user is shown the attribute that violates the cardinality constraints, along with the cardinalities defined for this attribute in the Concept Model. If there is a violation of the minimum cardinality, the attribute must be added. In case of a violation of the maximum cardinality, either a grouped attribute should be moved to an additional RoleGroup or ungrouped attributes should be deleted.

Technical Implementation

A basic analysis of the error message and the PCE is performed using the processed Concept Model in JSON format. The error message precisely indicates which attribute violates a cardinality (minimum or maximum) constraint. This information is automatically extracted from the JSON. Using the JSON object, an appropriate error correction can be easily determined.

Further Syntactic Errors

Overview

If a PCE contains characters that do not conform to the Compositional Grammar rules, it falls into this category. For instance, using the symbol ":@" instead of ":" before refinement would trigger an error indicating that the symbol "@" is not allowed.

Correction Instruction

The instructions specify which character needs to be replaced and the exact position where the replacement should occur.

Technical Implementation

A fundamental analysis of the error message and the PCE is conducted to provide accurate correction instructions. Through string processing and parsing, the position and the incorrect character are also extracted here.

Results

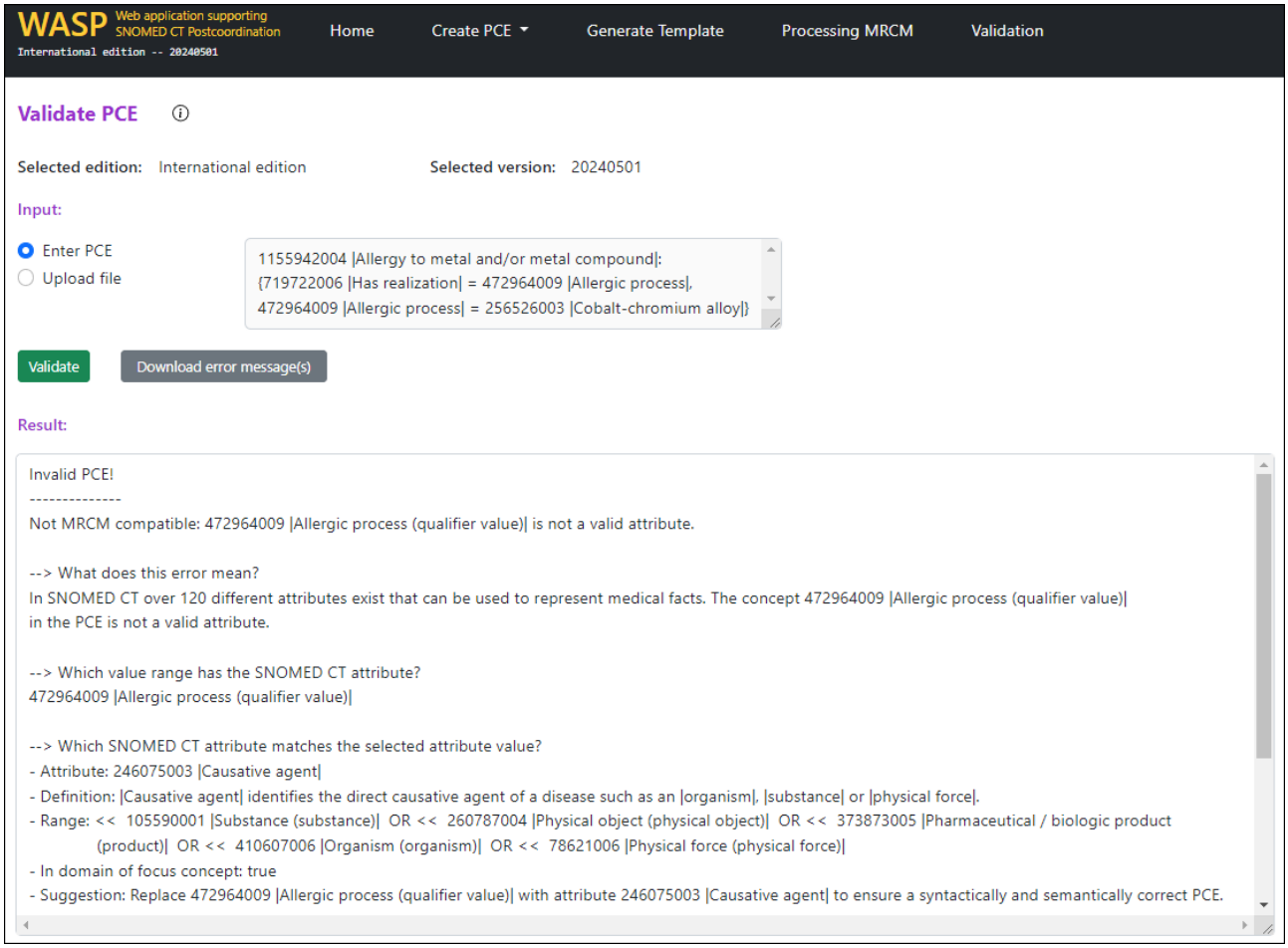
Validation Tool

The validation tool has been seamlessly integrated into the existing web application WASP [18], which was developed in a previous project. Accessible to the public via [23], the application enables users to use the new tool through the "Validation" option in the main menu. Users can choose to validate a single PCE directly or upload a file for validation. The tool supports various formats, including FHIR Questionnaires [24] and FHIR ValueSets [25] in JSON format, as well as CSV files, offering a flexible and versatile approach for validating different types of data.

Upon completing the validation, users receive a comprehensive overview of any errors detected during the process. These errors are clearly displayed on the user interface, ensuring easy traceability and resolution. Additionally, users have the option to download the error reports as a text file, enabling further analysis or optimization when needed. A screenshot of the web application, highlighting the user interface and layout, is shown in Figure 7.

XSL•FO
RenderX

Figure 7. Extract from the tool for validating the postcoordinated SNOMED CT expressions.



Use Case 1: Existing PCEs in FHIR Questionnaires

For the validation of the tool, real existing postcoordinated SNOMED CT expressions were used to establish a practical and reliable testing environment. These PCEs were incorporated into the FHIR Questionnaires developed by Thieme Compliance, which are designed for modeling anamnesis forms. Thieme Compliance offers these anamnesis forms in multiple languages to enhance usability for both patients and medical professionals. For machine processing and analysis, on the other hand, language-independent codes are used, ensuring precise and efficient data evaluation regardless of the language used [8]. This validation specifically focused on the German-language anamnesis forms as FHIR Questionnaires [24].

In total, 1122 postcoordinated SNOMED CT expressions were identified across 303 FHIR Questionnaires. Since many of these PCEs were repeated, 136 unique PCEs were distinguished. The validation results using the developed tool were as follows:

- 118 (86.8%) correct PCEs
- 18 (13.2%) invalid PCEs

In addition to identifying the correct and invalid PCEs, the developed algorithm carried out a detailed error categorization, uncovering six distinct error categories as shown in Table 1. These errors were analyzed in collaboration with the coders from Thieme Compliance. It was confirmed that all errors were correctly identified, and the correction suggestions were content-wise accurate.

Table . Various error categories and their frequency in the 18 invalid PCEs[a].

Error categories	Frequency
Invalid attribute value	9
Invalid grouping	2
Inactivated codes (International Edition, 2024-05-01)	3
Syntactically incorrect codes	1
Cardinality violation	2
Further syntactic error	1

[a]PCE: postcoordinated expression.

XSL•FO
RenderX

Use Case 2: Existing PCEs in FHIR ConceptMaps

In a previous project, ICD-O tuples were mapped to the OncoTree, using SNOMED CT as an intermediary step [20]. All 868 OncoTree codes were represented as postcoordinated SNOMED CT expressions based on the International Edition, 2021-01-31 in a FHIR ConceptMap [26]. The developed tool is now being used to validate all PCEs. Since the ConceptMap is from 2021, it was expected to contain inactive concepts. If this is the case, they will be replaced by active concepts from the International Edition, dated May 1, 2024 [20]. Any other errors will also be corrected accordingly.

Using the tool, 161 (20.9%) out of 868 PCEs were identified, each containing a concept that is no longer present in the International Edition, 2024-01-05. Some of these inactive concepts occurred multiple times, leading to the identification of 79 distinct inactive concepts. For all inactive concepts, an equivalent active SNOMED CT concept was found and was manually validated by an SNOMED CT expert, ensuring that the PCEs in the newer version are once again both semantically and syntactically correct. In addition, no other causes of error could be identified in the data.

Usability Survey

For the user survey, the participants received four real existing invalid PCEs along with the corresponding error messages. It was ensured that each was assigned to a different error category (Multimedia Appendix 1). The following error categories were used:

- Syntactically incorrect code
- Inactivated code
- Invalid attribute
- Invalid attribute value

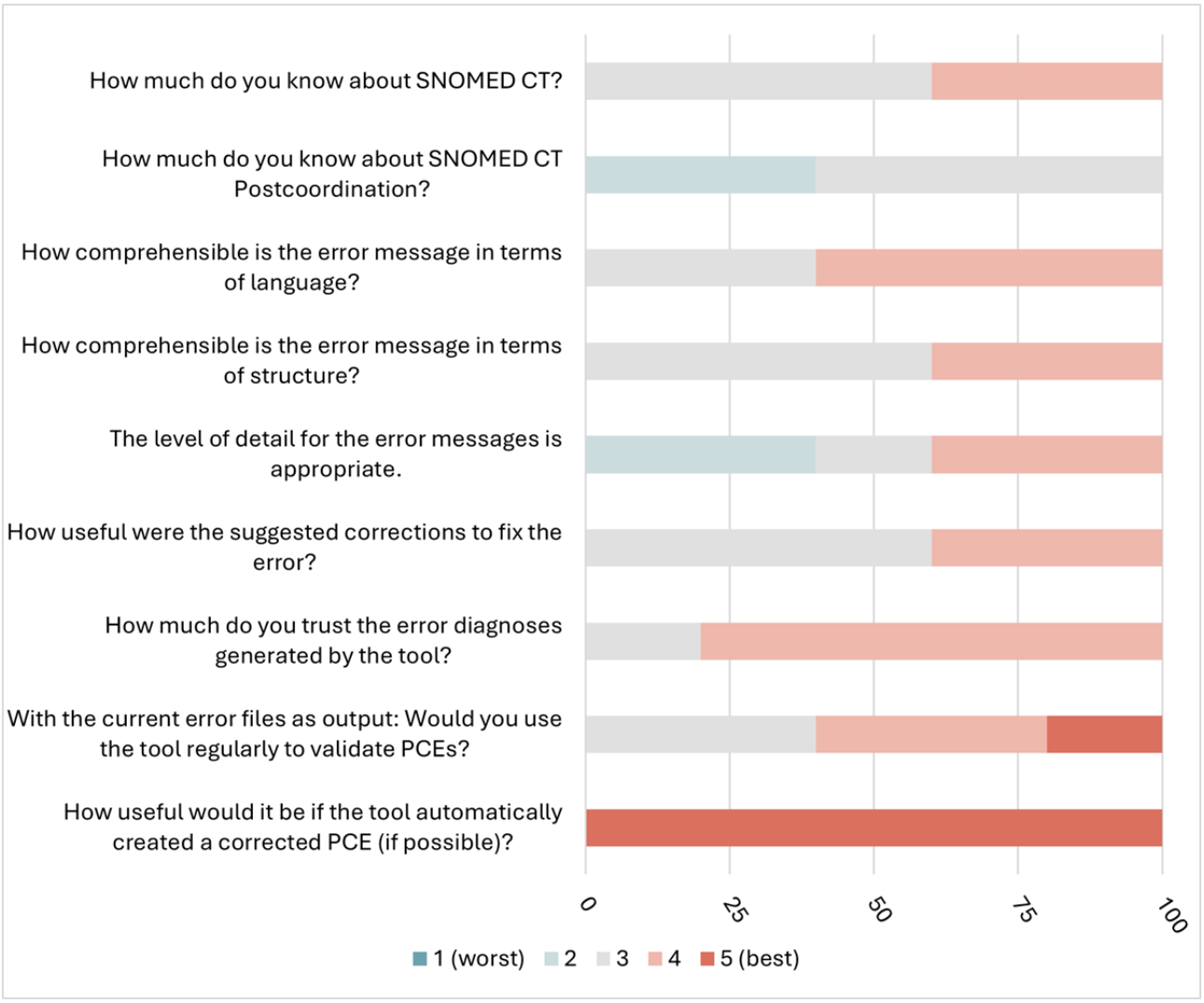
To select these categories, PCEs from the literature were reviewed and analyzed. Additionally, discussions were held with professionals actively involved in coding PCEs. This allows us to identify the error categories most commonly causing issues in practice.

In addition, the authors developed a customized questionnaire with ten questions that assessed both the self-evaluation of SNOMED CT knowledge and the overall user experience with the error messages. For nine of the questions, an ordinal scale with five levels ranging from 1=worst to 5=best rating was used, while the last question was open-ended. None of the questions were mandatory, and no answer options were preselected. The complete questionnaire with the answer options is displayed in Multimedia Appendix 1. The survey was conducted with five employees of Thieme Compliance, all of whom have basic knowledge of SNOMED CT postcoordination. Each participant was given the four invalid PCEs along with the corresponding error messages. Subsequently, the participants completed the questionnaire anonymously.

The chart in Figure 8 summarizes the survey results on various aspects of the tool's functionality. Overall, the tool received predominantly positive feedback, as indicated by the fact that only one question garnered slightly negative ratings from two participants. The comprehensibility of the error messages—both in terms of language and structure—was rated with high or neutral scores, with the structure being assessed somewhat more critically than the language. Opinions were divided regarding the level of detail in the error messages: two participants found the level appropriate, another participant gave a neutral rating, and two participants provided less favorable feedback. These were also documented in the free-text comments. Despite these criticisms, trust in the tool and the readiness to use it regularly for PCE validation remain high, as reflected in the overall positive ratings. Additionally, all participants rated the tool's potential expansion to include automatic PCE correction functionality with the highest score of 5. In summary, the chart demonstrates a positive assessment of the tool's functionality, though there is room for improvement in areas such as the level of detail in the error messages.

XSL•FO
RenderX

Figure 8. Results of the usability survey. PCE: postcoordinated expression.



Discussion

Principal Findings

In this work, a tool for validating postcoordinated SNOMED CT expressions was developed that detects both syntactic and semantic errors. Incorrect PCEs are classified into one of the nine developed error categories, enabling the user to receive targeted feedback. The key added value and focus of the tool lies in generating specific correction suggestions for each identified error.

The successful integration of this tool into the existing web application WASP [23] was confirmed through tests with real existing PCEs in FHIR Questionnaires [24] and an FHIR ConceptMap [26]. The use of these PCEs, provided in the FHIR Questionnaires from Thieme Compliance [8], demonstrated that the tool can reliably verify the correctness and validity of expressions. This is particularly relevant for accurate modeling of medical data and its integration into electronic health records. Additionally, the error files of the 18 PCEs were provided to Thieme Compliance for correction. Another use case, the validation of PCEs in the context of a mapping between ICD-O and OncoTree [20], highlights the tool's flexibility and usefulness in identifying and replacing inactive concepts. The ability to replace outdated concepts with current ones is crucial for the quality and relevance of medical data. The tool contributes to enabling cross-version analyses. It offers a solution for legacy data coded with earlier versions of SNOMED CT, where certain concepts may no longer exist. In such cases, the developed tool can assist in replacing these concepts with current equivalents.

A user survey has indicated that there is both interest and trust in the application. The results show a generally positive evaluation of the tool's functionality, although there is some potential for improvement regarding the level of detail in the error messages. In fact, 50% of participants rated the messages as too complex. Considering this, the development of the tool will place a special emphasis on revision. The plan is to allow users to choose between a newly developed, concise error message, and a more detailed version.

A comparison with existing methods, such as the SNOMED International APG Parser [9] and the FHIR service $validate-code [11] combined with the terminology server Ontoserver [10], shows that the developed tool adopts a more comprehensive validation approach, placing particular emphasis on providing correction suggestions. While the APG Parser primarily checks syntactic correctness and the $validate-code

XSL•FO
RenderX

service is limited to technical errors, the developed tool goes a step further: it enables in-depth error analysis, allowing for more precise corrections. This ensures that PCEs are created not only with correct syntax but also with accurate semantics. As a result, the quality and applicability of these expressions in practice are significantly improved.

A key aspect of this work is that the tool should not be understood as an automatic system for improving PCEs; rather, it provides targeted suggestions for the manual optimization of expressions. As the results of the user survey indicate, this would be a worthwhile feature. Automated corrections are often difficult to implement, as there is rarely a single correct solution. For instance, the tool suggests alternative attributes for the example PCE of Figure 1:

1155942004 |Allergy to metal and/or metal compound|:

{719722006 |Has realization| = 472964009 |Allergic process|,

472964009 |Allergic process| = 256526003 |Cobalt-chromium alloy|} such as:

- Causative agent
- Associated with

In this case, the attribute Causative agent should be used because this attribute is typically used in combination with allergies. A system that autonomously selects the appropriate attributes by analyzing attribute relations would indeed be an advancement, yet, manual validation by users remains essential. This ensures that no invalid PCEs are generated, which could negatively affect subsequent processes.

It should also be noted that the output of error messages is always dependent on the input PCE. If very complex PCEs with numerous errors are created, it may not be possible to correct them immediately. In such cases, the user must refine the PCE and validate it again, repeating the process until all errors are resolved iteratively. Users should be encouraged to construct manageable PCEs rather than attempting to encapsulate an entire medical history within a single PCE.

Conclusions

In conclusion, this work demonstrates that the development of a comprehensive validation tool for postcoordinated SNOMED CT expressions can significantly enhance data quality and interoperability in health care, while also addressing and resolving versioning issues. The successful integration of the tool into existing systems highlights that it provides both syntactic and semantic support at a high level.

The creation of postcoordinated SNOMED CT expressions (PCEs) is not straightforward, as it requires adherence to the complex rules of the Compositional Grammar and the Concept Model. As seen in validations with real-world PCEs, ensuring syntactic and semantic accuracy can be challenging. The development of a validation tool for postcoordinated SNOMED CT expressions represents a significant advancement in addressing these challenges. In addition to technical validation, the tool provides helpful correction guidance, enabling the iterative improvement of PCEs. Users receive error reports and correction suggestions based on nine identified error categories. While the level of detail in the error messages can still be further optimized, the tool already offers valuable support for targeted and effective error resolution. The tool leverages state-of-the-art technologies such as the FHIR $validate-code service, the terminology server Ontoserver, and the SNOMED CT Concept Model. Ontoserver is indeed commercial, which poses a minor limitation. However, it was chosen because it is currently the only terminology server that supports postcoordination—a crucial criterion for the requirements of this project. The methodological approach combines intelligent error detection with tailored correction suggestions, making it easier for users to independently optimize their expressions. In this way, the tool makes a significant contribution to improving data quality in health care.

Acknowledgments

This work is funded by the German Federal Ministry of Education and Research (BMBF) as part of the Medical Informatics Initiative Germany, grant 01ZZ2312A.

Conflicts of Interest

None declared.

Multimedia Appendix 1
Usability survey.
[DOCX File, 36 KB - medinform_v13i1e67984_app1.docx]

References

1. Benson T, Grieve G. Principles of Health Interoperability: FHIR, HL7 and SNOMED CT, 4th edition: Springer; 2021.
2. Ingenerf J, Drenkhahn C. REFERENZTERMINOLOGIE SNOMED CT: Interlingua Zur Gewährleistung Semantischer Interoperabilität in Der Medizin [REFERENCE TERMINOLOGY SNOMED CT: Interlingua To Ensure Semantic Interoperability in Medicine]: Springer; 2024. [doi: 10.1007/978-3-658-35562-3]
3. International Health Terminology Standards Development Organisation. SNOMED CT compositional grammar specification and guide. 2020. URL: https://confluence.ihtsdotools.org/display/DOCSCG?preview=/33496020/115880553/doc_CompositionalGrammar_v2.4-en-US_INT_20201116.pdf [accessed 2024-09-12]

XSL•FO
RenderX

4. International Health Terminology Standards Development Organisation. SNOMED CT starter guide. 2019. URL: https://confluence.ihtsdotools.org/display/DOCSTARTDE/SNOMED+CT+Starter+Guide?preview=/61153991/87039892/doc_StarterGuide_de_INT_20190611.pdf [accessed 2024-09-12]
5. Rinaldi E, Saas J, Thun S. Use of LOINC and SNOMED CT with FHIR for microbiology data. In: Röhrig R, Beißbarth T, Brannath W, editors. Studies in Health Technology and Informatics: IOS Press; 2021. [doi: 10.3233/SHTI210064]
6. Thun S, Stellmach C, Saß J, Bartschke A. Der GECCO datensatz für die COVID-19-forschung. In: Henke V, Hülsken G, Meier PM, Beß A, editors. Digitalstrategie Im Krankenhaus: Springer Fachmedien Wiesbaden; 2022:505-516. [doi: 10.1007/978-3-658-36226-3_36]
7. Kassenärztliche Bundesvereinigung. Medizinische Informationsobjekte (MIO) [Medical Information Objects (MIO)]. URL: https://www.kbv.de/html/mio.php [accessed 2024-09-02]
8. Thieme Compliance. Simplifier: Thieme Compliance Anamnese. URL: https://simplifier.net/thiemecomplianceanamnese [accessed 2024-09-03]
9. SNOMED International. SNOMED International APG Parser (for PCEs) oD. URL: https://apg.ihtsdotools.org/SCT-cg.html [accessed 2022-04-27]
10. Metke-Jimenez A, Steel J, Hansen D, Lawley M. Ontoserver: a syndicated terminology server. J Biomed Semantics 2018 Sep 17;9(1):24. [doi: 10.1186/s13326-018-0191-z] [Medline: 30223897]
11. HL7 International. Operation $validate-code on codesystem—FHIR v4.0.0. URL: https://hl7.org/fhir/R4/codesystem-operation-validate-code.html [accessed 2024-09-04]
12. Lau T. Gesundheitsdaten: FHIR wird europaweiter standard. : Ärzteblatt URL: https://www.aerzteblatt.de/nachrichten/142159/Gesundheitsdaten-FHIR-wird-europaweiter-Standard [accessed 2024-01-04]
13. Vorisek CN, Lehne M, Klopfenstein SAI, et al. Fast Healthcare Interoperability Resources (FHIR) for interoperability in health research: systematic review. JMIR Med Inform 2022 Jul 19;10(7):e35724. [doi: 10.2196/35724] [Medline: 35852842]
14. Ayaz M, Pasha MF, Alzahrani MY, Budiarto R, Stiawan D. The Fast Health Interoperability Resources (FHIR) standard: systematic literature review of implementations, applications, challenges and opportunities. JMIR Med Inform 2021;9(7):e21929. [doi: 10.2196/21929]
15. SNOMED International. SNOMED CT MRCM (machine readable concept model) maintenance tool. URL: https://browser.ihtsdotools.org/mrcm/ [accessed 2021-04-08]
16. International Health Terminology Standards Development Organisation. Template syntax DRAFT specification. 2020. URL: https://confluence.ihtsdotools.org/display/DOCSTS?preview=/45529301/115875508/doc_TemplateSyntax_v1.1.1-en-US_INT_20201020.pdf [accessed 2024-09-12]
17. Ohlsen T. Processed MRCM as JSON. URL: https://gitlab.com/tessa00/wasp-data/-/blob/main/wasp/mrcm.json [accessed 2024-09-04]
18. Drenkhahn C, Ohlsen T, Wiedekopf J, Ingenerf J. WASP—a web application to support syntactically and semantically correct SNOMED CT postcoordination. Appl Sci (Basel) 2023;13(10):6114. [doi: 10.3390/app13106114]
19. Ohlsen T, Ingenerf J, Essenwanger A, Drenkhahn C. PCEtoFHIR: decomposition of postcoordinated SNOMED CT expressions for storage as HL7 FHIR resources. JMIR Med Inform 2024 Sep 17;12:e57853. [doi: 10.2196/57853] [Medline: 39287966]
20. Ohlsen T, Kruse V, Krupar R, Banach A, Ingenerf J, Drenkhahn C. Mapping of ICD-O tuples to OncoTree codes using SNOMED CT post-coordination. Stud Health Technol Inform 2022 May 25;294:307-311. [doi: 10.3233/SHTI220464] [Medline: 35612082]
21. Ohlsen T. Examples of error categories. URL: https://gitlab.com/tessa00/wasp-supporting-snomed-ct-postcoordination/-/tree/main/SpringBoot/src/main/resources/validation-pce-examples?ref_type=heads [accessed 2024-10-15]
22. SNOMED International. Expression constraint language—specification and guide. URL: https://confluence.ihtsdotools.org/display/DOCECL [accessed 2024-09-17]
23. Ohlsen T. Web application “WASP.”. URL: https://wasp.imi.uni-luebeck.de [accessed 2024-09-12]
24. HL7 International Resource Questionnaire—FHIR v4.0.0. URL: https://hl7.org/fhir/R4/questionnaire.html [accessed 2024-09-12]
25. HL7 International Resource ValueSet—FHIR v4.0.0. URL: https://hl7.org/fhir/R4/valueset.html [accessed 2024-09-12]
26. HL7 International Resource ConceptMap—FHIR v4.0.0. URL: https://hl7.org/fhir/R4/conceptmap.html [accessed 2024-09-25]

Abbreviations

ECL: Expression Constraint Language
FHIR: Fast Healthcare Interoperability Resource
MRCM: machine-readable Concept Model
PCE: postcoordinated expression
SNOMED CT: SNOMED clinical terms

XSL•FO
RenderX

Edited by C Lovis; submitted 25.10.24; peer-reviewed by J Ehrsam, T Karen; revised version received 11.12.24; accepted 25.12.24; published 28.02.25.

Please cite as:
Ohlsen T, Hofer V, Ingenerf J
A Validation Tool (VaPCE) for Postcoordinated SNOMED CT Expressions: Development and Usability Study
JMIR Med Inform 2025;13:e67984
URL: https://medinform.jmir.org/2025/1/e67984
doi:10.2196/67984

© Tessa Ohlsen, Viola Hofer, Josef Ingenerf. Originally published in JMIR Medical Informatics (https://medinform.jmir.org), 28.2.2025. This is an open-access article distributed under the terms of the Creative Commons Attribution License (https://creativecommons.org/licenses/by/4.0/), which permits unrestricted use, distribution, and reproduction in any medium, provided the original work, first published in JMIR Medical Informatics, is properly cited. The complete bibliographic information, a link to the original publication on https://medinform.jmir.org/, as well as this copyright and license information must be included.

XSL•FO
RenderX

Taxonomy Portraits: Deciphering the Hierarchical Relationships of Medical Large Language Models

Radha Nagarajan[1], PhD; Vanessa Klotzman[1], MS; Midori Kondo[2], PharmD; Sandip Godambe[1], MBA, PhD, MD; Adam Gold[1], MBA; John Henderson[1], MBA; Steven Martel[1], MD

[1]Rady Children's Health, 1201 W La Veta Ave, Orange, CA, United States

[2]Fred Hutch Cancer Center, Seattle, WA, United States

Corresponding Author:
Radha Nagarajan, PhD
Rady Children's Health, 1201 W La Veta Ave, Orange, CA, United States

Abstract

Background: Large language models (LLMs) continue to enjoy enterprise-wide adoption in health care while evolving in number, size, complexity, cost, and most importantly performance. Performance benchmarks play a critical role in their ranking across community leaderboards and subsequent adoption.

Objective: Given the small operating margins of health care organizations and growing interest in LLMs and conversational artificial intelligence (AI), there is an urgent need for objective approaches that can assist in identifying viable LLMs without compromising their performance. The objective of the present study is to generate taxonomy portraits of medical LLMs (n=33) whose domain-specific and domain non-specific multivariate performance benchmarks were available from Open-Medical LLM and Open LLM leaderboards on Hugging Face.

Methods: Hierarchical clustering of multivariate performance benchmarks is used to generate taxonomy portraits revealing inherent partitioning of the medical LLMs across diverse tasks. While domain-specific taxonomy is generated using nine performance benchmarks related to medicine from the Hugging Face Open-Medical LLM initiative, domain non-specific taxonomy is presented in tandem to assess their performance on a set of six benchmarks and generic tasks from the Hugging Face Open LLM initiative. Subsequently, non-parametric Wilcoxon rank-sum test and linear correlation are used to assess differential changes in the performance benchmarks between two broad groups of LLMs and potential redundancies between the benchmarks.

Results: Two broad families of LLMs with statistically significant differences (α=.05) in performance benchmarks are identified for each of the taxonomies. Consensus in their performance on the domain-specific and domain non-specific tasks revealed robustness of these LLMs across diverse tasks. Subsequently, statistically significant correlations between performance benchmarks revealed redundancies, indicating that a subset of these benchmarks may be sufficient in assessing the domain-specific performance of medical LLMs.

Conclusions: Understanding medical LLM taxonomies is an important step in identifying LLMs with similar performance while aligning with the needs, economics, and other demands of health care organizations. While the focus of the present study is on a subset of medical LLMs from the Hugging Face initiative, enhanced transparency of performance benchmarks and economics across a larger family of medical LLMs is needed to generate more comprehensive taxonomy portraits for accelerating their strategic and equitable adoption in health care.

(JMIR Med Inform 2025;13:e72918) doi:10.2196/72918

KEYWORDS

large language models; health care; performance benchmark; taxonomy; redundancy

Introduction

Large language models (LLMs) continue to show considerable promise and growth in health care [1]. Popular health care LLM applications fall under three broad task categories, namely clinical tasks, documentation tasks, and medical research and education tasks [2]. Specific LLM health care applications include (1) virtual health assistants and language translation [3], (2) summarization of clinical narratives and ambient listening [4,5], (3) patient education [6], and (4) clinical trial matching [7]. More importantly, LLMs have continued to evolve in numbers, size, complexity, costs, and performance, impacting their adoption [8]. A recent perspective discussed three broad LLM implementation pathways (Training from Scratch, Fine-Tuned Pathway, and Out of the Box Pathway) along with the risks, benefits, and economics across four major cloud service providers for their equitable and strategic adoption in health care [9]. The study also elucidated the essential

XSL•FO
RenderX

ingredients such as digital data, infrastructure, workforce, ethics, and regulatory aspects that can significantly impact LLM implementations. While helpful, these three pathways represent broad categorizations of LLM implementations and do not necessarily provide insights into their similarities. Similarities between LLMs can be based on a number of characteristics including architecture, size, cost, and their performance across diverse tasks [10]. Understanding the similarities in LLM performance can assist in strategically selecting those with comparable performance while aligning with the budgeting and needs of health care organizations.

The present study focuses on standardized and objective performance benchmarks that interrogate the ability of LLMs across diverse tasks. Their weighted average, is often used to rank LLMs across leaderboards [11], impacting their adoption. These aggregated benchmarks implicitly map the multivariate benchmark profiles onto a univariate score, diminishing their usefulness, as each benchmark interrogates unique capabilities of the LLMs. Therefore, it should not be surprising to note that similarity in ranks may not necessarily imply similarity in performance benchmark profiles. The present study generates LLM taxonomies elucidating their similarities and hierarchical associations from multivariate performance benchmarks. The taxonomy is shown to reveal inherent partitioning of the LLMs into sub-groups with varying performance. LLMs can be either open-source or closed source. While these implementations have distinct advantages [12], proprietary aspects and lack of transparency in the performance of closed-source LLMs prevent their inclusion in the present study. In the case of open-source LLMs, domain-specific (DS) as well as domain non-specific (DN) multivariate performance benchmarks were available publicly from Open LLM [13] and Open Medical LLM [14] leaderboards at Hugging Face [15,16]. While DS benchmarks interrogate task-specific abilities of the LLMs, DN benchmarks assess their generic capabilities. Hugging Face has witnessed increasing visibility, growth, and adoption by the Generative AI and LLM communities over the years. Its structured and transparent approach enables enhanced reproducibility of the reported metrics and implementation; widespread collaboration between experts; unbiased comparison of the different models; and the selection of the LLMs based on the performance, needs, and affordability. The DS benchmarks considered include those that assess the medical question and answering capabilities and reasoning skills related to medical licensing examinations, a series of subject and DS evaluations broadly under massive multitask language understanding, and the ability of LLMs to comprehend and reason biomedical literature. The DN benchmarks were also retrieved for the medical LLMs through the Open LLM initiative to assess their ability to answer questions that are not specifically related to medical tasks. These benchmarks included (1) those that assess the LLMs ability to follow verifiable instructions, (2) chain of thought prompting, (3) mathematical problem-solving skills, (4) graduate level reasoning capabilities across diverse subjects, (5) multistep reasoning abilities, and (6) multitask language understanding on challenging reasoning-based questions. A detailed description of the DS and DN benchmarks along with the references and their abbreviations is included in Table 1. The taxonomies were generated by hierarchical clustering of the DS and DN multivariate performance benchmarks that assess the task-specific and generic capabilities of these LLMs. Subsequently, two broad groups of medical LLMs with markedly different performance benchmark profiles is discussed. Potential redundancies between the performance benchmarks across the DS and DN taxonomies are also elucidated. Given the low-operating margins [17] of health care organizations, understanding the taxonomy and potential redundancies between the performance benchmarks is expected to assist in objectively justifying the choice of LLMs while controlling costs [18].

XSL•FO
RenderX

Table . Description and abbreviations of domain-specific (DS) and domain non-specific (DN) performance benchmarks with references.

Type	Benchmark description	Abbreviation
DS	MedQA [Medical Question and Answer]: Consists of multiple-choice questions (11,450 questions in the development set and 1273 questions in the test set) from the United States Medical License Exam for benchmarking the LLMs general medical knowledge and reasoning skills on United States Medical Licensure.	MQA [19]
DS	MedMCQA [Medical Multiple-Choice Question and Answer]: Consists of multiple-choice questions (187,000 questions in the development set and 6100 questions in the test set) related to the Indian Medical Entrance Exam (AIIMS/NEET). As with MedQA, MedMCQA is used to benchmark the LLMs general medical knowledge and reasoning ability as it pertains to the Indian medical entrance exam.	MCQA [20]
DS	MMLU Anatomy: [Massive Multitask Language Understanding, Anatomy]: MMLU subset consists of multiple-choice questions (135 questions) for benchmarking the knowledge of the LLM[a] on human anatomy.	ANAT [21]
DS	MMLU Clinical Knowledge [Massive Multitask Language Understanding, Clinical Knowledge]: MMLU subset consists of multiple-choice questions (265 questions) for benchmarking the clinical knowledge and decision-making skills.	CLIN [21]
DS	MMLU College Biology [Massive Multitask Language Understanding, College Biology]: MMLU subset with multiple-choice questions (144 questions) for benchmarking the knowledge on college biology.	BIOL [21]
DS	MMLU College Medicine [Massive Multitask Language Understanding, College Medicine] MMLU subset with multiple-choice questions (173 questions) for benchmarking the college-level medical knowledge.	CMED [21]
DS	MMLU Medical Genetics [Massive Multitask Language Understanding, Medical Genetics] MMLU subset consists of 100 questions related to medical genetics.	GEN [21]
DS	MMLU Professional Medicine [Massive Multitask Language Understanding, Professional Medicine] MMLU subset consists of multiple-choice questions (272 questions) for benchmarking the LLM on knowledge required for medical professionals.	PMED [21]
DS	PUBMEDQA [PUBMED Question & Answer] Closed-domain dataset comprising expert-labeled question-answer pairs (500 questions in the development set and 500 questions in the test set) for benchmarking the LLMs ability to comprehend and reason biomedical literature.	PUBM [22]
DN	IFEval [Instruction Following Evaluation]: Benchmarks LLMs ability to follow verifiable instructions using 25 distinct types of verifiable instructions and 500 prompts, with each prompt containing at least one verifiable instruction.	IFEV [23]

XSL•FO
RenderX

Type	Benchmark description	Abbreviation
DN	BBH [Big Bench Hard]: Benchmarks the performance of LLMs on 23 challenging Big Bench tasks (BBH) where prior LLMs failed to outperform an average-human rater. Emphasized the importance of chain-of-thought prompting.	BBH [24]
DN	MATH [Math]: Benchmarks the mathematical problem-solving ability of the LLM using 12,500 mathematics competition problems.	MATH [25]
DN	GPQA [Graduate Level Google Proof Q & A]: Benchmarks LLMs using 448 multiple choice questions generated by experts in areas such as biology, physics, and chemistry.	GPQA [26]
DN	MuSR [Multistep Soft Reasoning]: Benchmarks LLMs ability on complex multistep reasoning instances and long-range (~1000 words) free text narratives from real-world domains.	MUSR [27]
DN	MMLU Pro [Multitask Language Understanding Pro]: Benchmarks the reasoning and language comprehension abilities of LLMs across diverse domains by incorporating challenging, reasoning-focused question, and expanding the choice of the original MMLU from four to ten.	MPRO [28]

[a]LLM: large language model.

Methods

Medical LLMs with DS and DN benchmarks were retrieved from Hugging Face Open Medical LLM [14] and Open LLM [13] leaderboards on January 2025. While Hugging Face features several contributions from the AI open-source community, it is important to note that these are voluntary efforts. Since there were instances of sparse documentation across LLMs by individual contributors, the present study excluded LLMs by individual contributors, resulting in 33 medical LLMs whose DS and DN performance benchmarks were available. Abbreviations and size of the 33 LLMs are enclosed in Table 2. LLM taxonomies were generated using hierarchical clustering [29] of the DS and DN multivariate performance benchmarks. As each performance benchmark interrogates specific characteristic of the LLM, they were scaled to zero-mean and unit variance prior to clustering to minimize the impact of potential variations in the magnitude across the different benchmarks. Subsequently, the Manhattan distance was used to assess the similarity between the LLMs, as it is robust to outliers. Other measures of similarity such as cosine distance can also be used as alternatives [29]. This study uses complete linkage that merges clusters based on the distance between the most dissimilar members (ie, farthest distance) [29]. While complete linkage is robust to outliers resulting in stable and well-formed clusters, other linkage approaches for merging the clusters can also be explored [29].

The DS taxonomy was based on the nine performance benchmarks, whereas the DN taxonomy was generated based on the six performance benchmarks, as shown in Table 1. Color-coded dendrograms were subsequently used to generate visualizations of the performance benchmark profiles of the respective taxonomies. Statistically significant differential changes in performance benchmark profiles between clusters for the DS and DN taxonomy were investigated using the Wilcoxon rank-sum test (α=.01), a non-parametric statistical test that does not impose normality assumptions on their distribution. Subsequently, Pearson correlation and scatter plots were used to elucidate potential redundancies between the performance benchmarks for the DS and DN taxonomies. Pearson correlation can provide insights into linear dependency (a=0.01) between variables. However, its estimates can be deceptive under sparse distribution of data points about the linear trend. Therefore, scatter plots of the pair-wise performance benchmarks are provided in addition to the statistical test for visualization. As differential changes in the performance benchmarks and the test for correlation involved multiple statistical tests, multiple testing correction (Bonferroni correction) [30] was used to control for the family-wise error rate, with the adjusted significance level α^* given by $\alpha^* = \alpha/M$, where M represents the total number of statistical tests.

XSL•FO
RenderX

Table . Open-source large language models (LLMs; n=33) from Hugging Face with their abbreviations.

Open-source LLM (Hugging Face)	Abbreviation	Open-source LLM (contd.)	Abbreviation (contd.)
mistralai/Mistral-7B-Instruct-v0.1	MISI-7B[a]	VAGOsolutions/SauerkrautLM-Gemma-7b	GEMS-7B
mistralai/Mistral-7B-v0.1	MIS-7B	VAGOsolutions/Llama-3-SauerkrautLM-8b-Instruct	LM3SI-8B
EleutherAI/pythia-2.8b	PYT-2.8B	openai-community/gpt2-xl	GPTL-1.5B
EleutherAI/gpt-neo-2.7B	GPTN-2.7B	openai-community/gpt2	GPT2-1.5B
lmsys/vicuna-7b-v1.5	VIC-7B	HuggingFaceH4/zephyr-7b-beta	ZEP-7B
abacusai/Llama-3-Smaug-8B	LM3S-8B	tiiuae/falcon-7b-instruct	FALI-7B
abacusai/Liberated-Qwen1.5-14B	QWN-14B	tiiuae/falcon-7b	FAL-7B
HPAI-BSC/Llama3-Aloe-8B-Alpha	LM3A-8B	NousResearch/Nous-Hermes-2-Mistral-7B-DPO	MISD-7B
google/gemma-2b	GEM-2B	NousResearch/Hermes-2-Pro-Mistral-7B	MISH-7B
google/gemma-1.1-7b-it	GEMI-7B	CohereForAI/aya-23-8B	AYA-8B
google/recurrentgemma-2b	GEMR-2B	upstage/SOLAR-10.7B-Instruct-v1.0	SL-10.7B
google/gemma-7b	GEM-7B	01-ai/Yi-1.5-9B-32K	YIK-9B
microsoft/phi-1_5	PHI-1.3B	01-ai/Yi-1.5-9B	YI-9B
TinyLlama/TinyLlama-1.1B-intermediate-step-1431k-3T	TLM-1.1B	lightblue/suzume-llama-3-8B-multilingual	LM3Z-8B
Qwen/Qwen1.5-7B	QWN-7B	meta-llama/Meta-Llama-3-8B-Instruct	LMMI-8B
Qwen/Qwen1.5-7B-Chat	QWNC-7B	meta-llama/Meta-Llama-3-8B	LMM-8B
stabilityai/stablelm-2 - 1_6b	STA-6B		

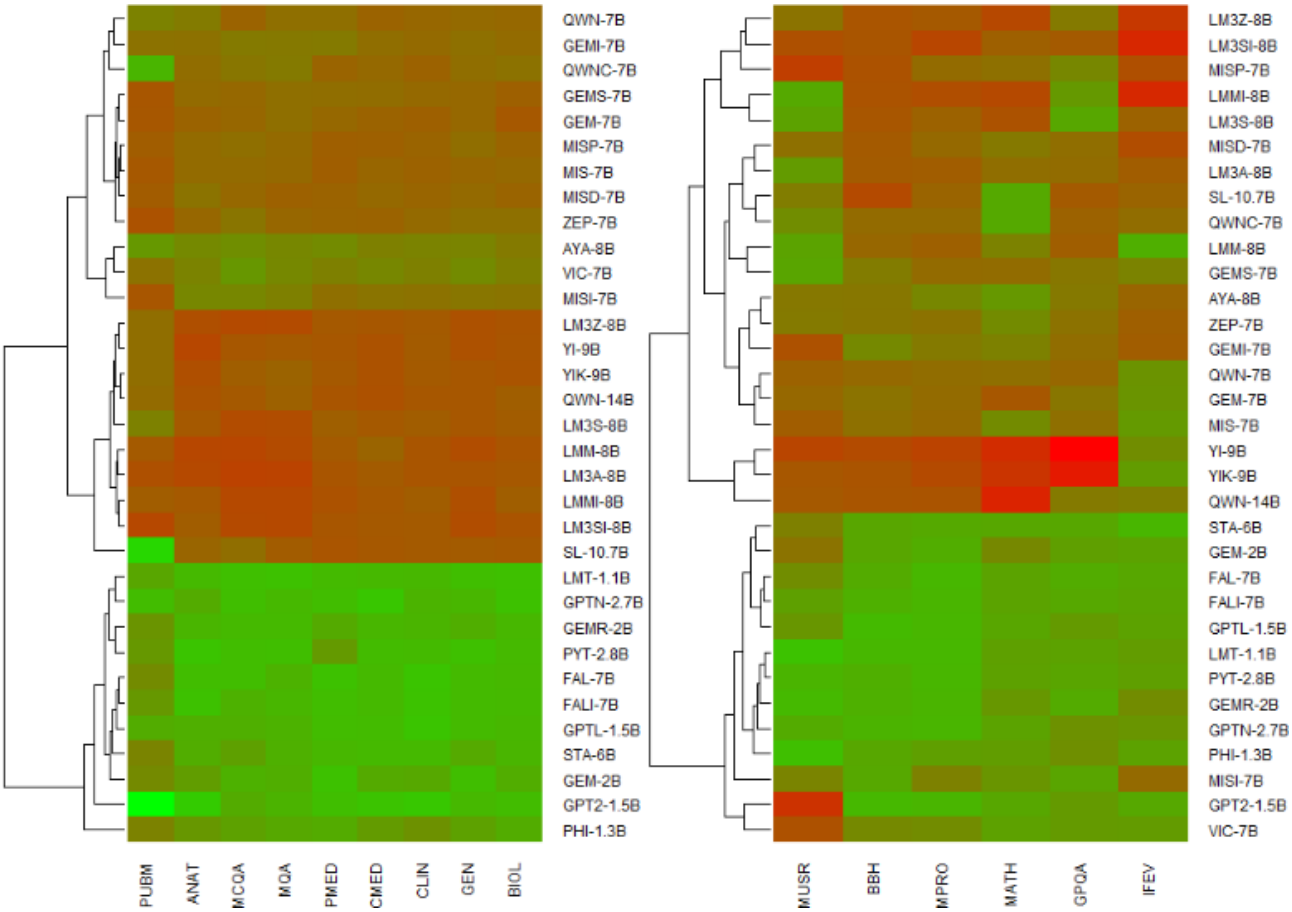
[a]The suffix (B) represents billions of parameters.

Results

The DS and DN taxonomies of the 33 medical LLMs generated by hierarchical clustering (Figure 1) revealed two well-separated clusters of high (H) and low (L) with markedly different median benchmark profiles (Figure 2). For the DS taxonomy, the H cluster comprised 22 LLMs, whereas the L cluster had 11 LLMs. The Wilcoxon rank-sum tests were used to assess statistically significant differences between these clusters across the nine benchmarks at the adjusted significance level controlling for family-wise error rate ($\alpha^*=\alpha/M=.01/9\sim.001$). The corresponding *P* values were MCQA (*P*<.001), MQA (*P*<.001), ANAT (*P*<.001), CLIN (*P*<.001), BIOL (*P*<.001), CMED (*P*<.001), GEN (*P*<.001), PMED (*P*<.001), and PUBM (*P*<.001), revealing statistically significant differential changes in the nine benchmarks between the H and L clusters. LLMs in the H cluster were MISI-7B, MIS-7B, VIC-7B, LM3S-8B, QWN-14B, LM3A-8B, GEMI-7B, GEM-7B, QWN-7B, QWNC-7B, GEMS-7B, LM3SI-8B, ZEP-7B, MISD-7B, MISP-7B, AYA-8B, SL-10.7B, YIK-9B, YI-9B, LM3Z-8B, LMMI-8B, and LMM-8B, whereas those in the L cluster were PYT-2.8B, GPTN-2.7B, GEM-2B, GEMR-2B, PHI-1.3B, LMT-1.1B, STA-6B, GPTL-1.5B, GPT2-1.5B, FALI-7B, and FAL-7B. The L cluster with a relatively lower median performance profile consisted primarily of LLMs with relatively smaller numbers of parameters. While earlier studies [31,32] emphasized the impact of parameters on LLM performance, the present findings reiterated these empirical findings from a DS standpoint.

XSL•FO
RenderX

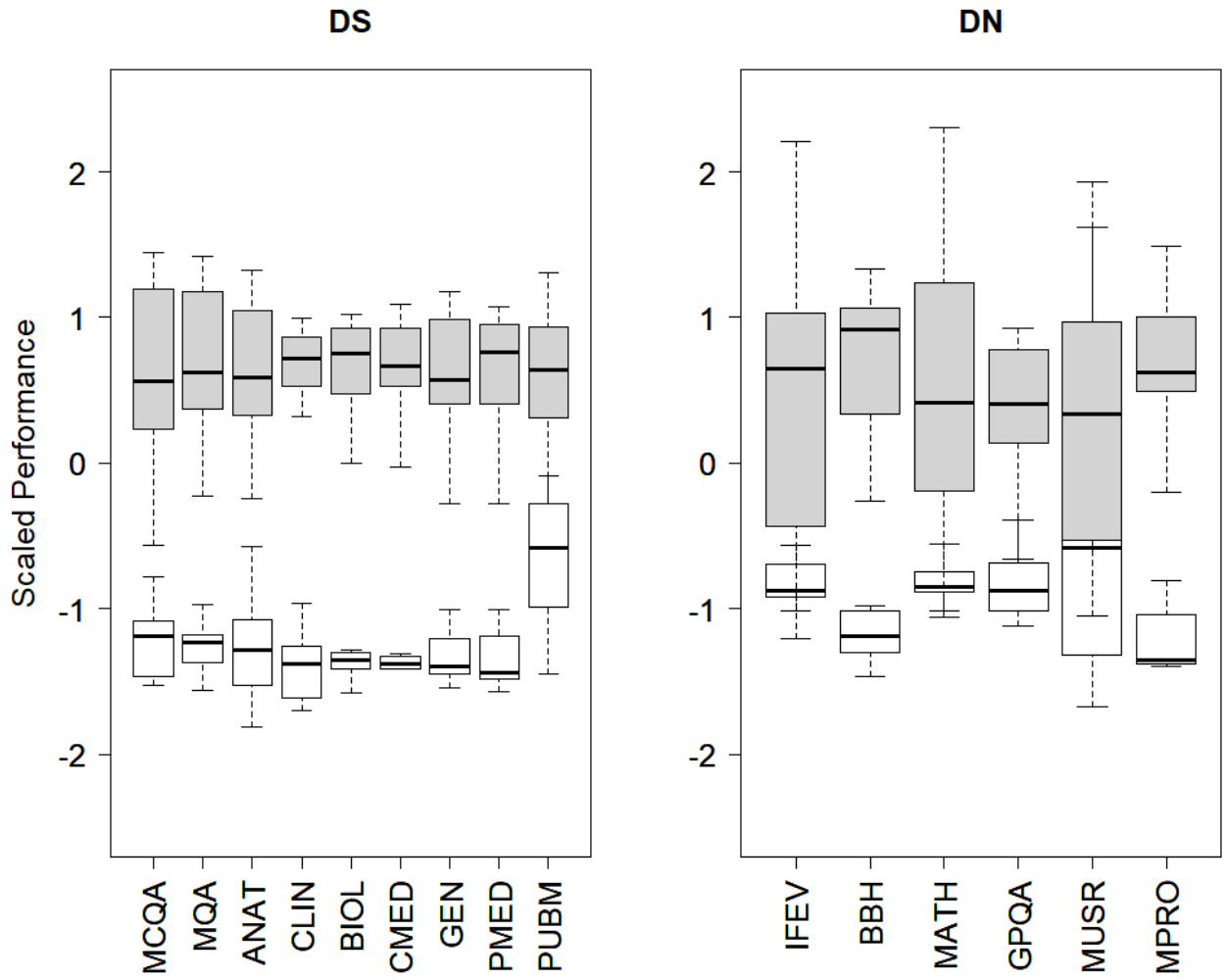
Figure 1. Dendrogram representing the domain-specific (DS; left) and domain non-specific (DN; right) taxonomy portraits from hierarchical clustering of scaled multivariate performance benchmark profiles of 33 medical LLMs. The magnitude of the scaled performance benchmark profiles increases from green (low) to red (high).



For the DN taxonomy, the H and the L clusters comprised 20 LLMs and 13 LLMs, respectively (Figure 1). The Wilcoxon rank-sum tests of differential change between the H and L clusters across the six benchmarks at the adjusted significance level controlling for family-wise error rate ($\alpha^*=\alpha/M=0.01/6\sim0.002$) resulted in IFEV ($P<.001$), BBH ($P<.001$), MATH ($P<.001$), GPQA ($P<.001$), and MPRO ($P<.001$), indicating significant differential change across these benchmarks. However, the differential change for MUSR ($P=.036$) was not statistically significant. The corresponding boxplots are shown in Figure 2. LLMs in the H cluster were MIS-7B, LM3S-8B, QWN-14B, LM3A-8B, GEMI-7B, GEM-7B, QWN-7B, QWNC-7B, GEMS-7B, LM3SI-8B, ZEP-7B, MISD-7B, MISP-7B, AYA-8B, SL-10.7B, YIK-9B, YI-9B, LM3Z-8B, LMMI-8B, and LMM-8B, whereas those in the L cluster were MISI-7B, PYT-2.8B, GPTN-2.7B, VIC-7B, GEM-2B, GEMR-2B, PHI-1.3B, LMT-1.1B, STA-6B, GPTL-1.5B, GPT2-1.5B, FALI-7B, and FAL-7B. In line with earlier empirical observations, LLMs in the L cluster with relatively lower median performance benchmarks were predominantly smaller in size. There were also marked consensus in the distribution of the LLMs between the L (11 LLMs) and H (20 LLMs) clusters of the DS and DN taxonomies, revealing the robustness of the LLMs across generic as well as domain-specific tasks. The variance for a majority of the performance benchmarks was markedly higher for the H cluster as opposed to the L cluster across DS and DN taxonomies, indicating considerable heterogeneity in the performance of the LLMs in the H cluster (Figure 2).

XSL•FO
RenderX

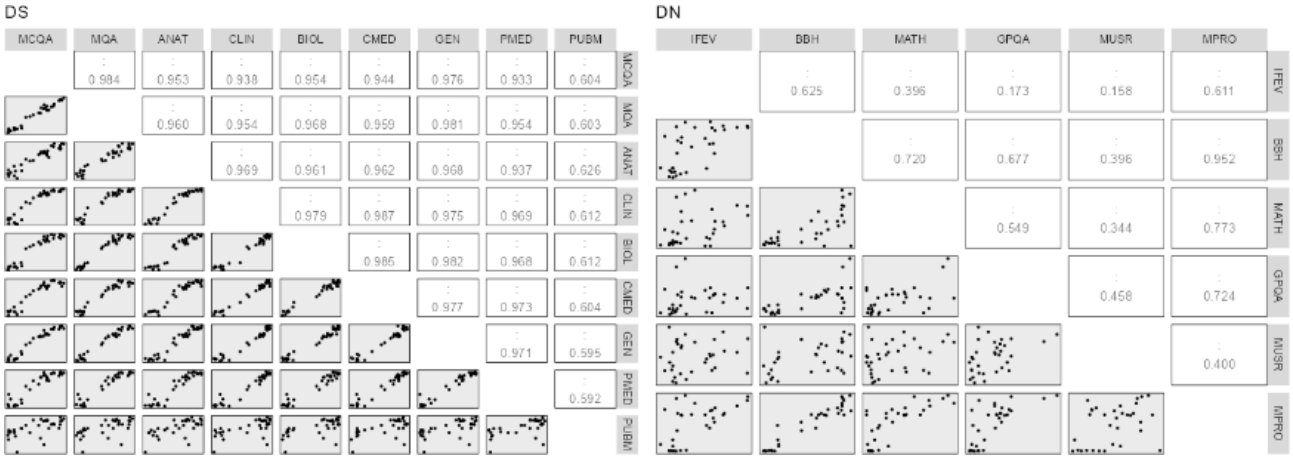
Figure 2. Box-whisker plots of the scaled performance benchmark profiles corresponding to high (H; gray) and low (L; white) clusters of the domain-specific (DS; left) and the domain non-specific (DN; right) taxonomies. Outliers are not shown for clarity.



The Pearson correlation was used to assess statistically significant correlations between pair-wise performance benchmarks of the DS and DN taxonomies (Figure 3). The nine DS performance benchmarks resulted in 9(9 - 1)/2=36 independent tests for correlation. Therefore, the adjusted significance level was chosen as (α^*=0.01/36~0.0002) to control for the family-wise error rate. The correlation for all pairs other than PMED-PUBM (P=.00028>α^*) were statistically significant (ie, $P<\alpha^*$). The linear trend was especially pronounced between MCQA, MQA, and MMLU for various subjects. A possible explanation is LLMs that perform well on the different medically related MMLU subject-wise benchmarks (ANAT, CLIN, BIOL, CMED, GEN, and PMED) may also perform well on comprehensive medical exams (MCQA and MQA). While the linear correlation between the MMLU subject-wise benchmarks was statistically significant, the scatter plots revealed instances of sparse distribution of points along the linear trend line for some of these pairs (eg, BIOL and PMED), challenging reliable correlation estimates (Figure 3). The clustering of points about the linear trend line may in fact align with earlier observations of statistical differences (Figure 2) between two broad groups of LLMs within the DS taxonomy (Figures 1 and 2). The magnitude of performance benchmark (PUBM), which assesses the LLMs ability to comprehend and reason biomedical literature, did not exhibit a strong correlation with others, as reflected by lack of a clear linear trend in the scatter plots (Figure 3). In contrast to DS taxonomy, the correlation structures between the performance benchmarks was noisy in the case of DN taxonomy, as reflected by the scatter plots in Figure 3. The six DS performance benchmarks resulted in 6(6 - 1)/2=15 independent tests for correlation. Therefore, the adjusted significance level was chosen as (α^*=0.01/15~0.0007) to control for the family-wise error rate. While there were instances of DN performance benchmark pairs with significant correlation, the redundancy was markedly lower than that observed in the case of DS taxonomy. Pairs that did not exhibit significant correlation ($P<\alpha^*$) included IFEV-MATH (P=.022), IFEV-GPQA (P=.336), IFEV-MUSR (P=.379), BBH-MUSR (P=.022), MATH-MUSR (P=0.049), GPQA-MUSR (P=.007), and MUSR-MPRO (P=.021). Since the correlation structure across DN performance benchmarks was much lower than that of DS performance benchmarks, DN performance benchmarks may assess the LLMs complementary characteristics of the LLM.

XSL•FO
RenderX

Figure 3. Scatter plots (gray panels) of the correlation structure between the performance benchmarks corresponding to domain-specific (DS; left) and domain non-specific (DN; right) taxonomies are shown. The pair-wise linear correlation (white panels) of the corresponding (row, column) pairs of performance benchmarks are shown in the upper triangle. The diagonals represent auto-correlation, and are hence not presented.



Discussion

The present study investigated taxonomies of LLMs whose DS and DN performance benchmarks were available from Open MedLLM and Open LLM initiatives at Hugging Face. As noted, LLM ranks estimated from aggregated benchmarks have been featured by leaderboards, impacting their adoption. However, similarity in these aggregated univariate scores and ranks may not necessarily imply similarity in the underlying multivariate performance profiles, making the study relevant. The DS and DN taxonomies revealed inherent subgroups and two broad clusters with statistically significant differences in performance. Overlap of the cluster members between the DS and DN taxonomies also indicated robustness of these LLMs across diverse tasks. As with some of the earlier empirical studies on LLM scaling laws, clusters with lower performance consisted predominantly of LLMs with relatively smaller size. The results also revealed redundancies in the performance benchmarks that was especially pronounced in the case of DS performance benchmarks.

Practical relevance of these taxonomies include their ability to assist in selecting LLMs with comparable performance while controlling costs. This is especially critical in low-profit margins industry such as health care that is in its initial phases of adopting AI tools for improved efficiency and outcomes. Taxonomies can also assist in choosing a combination of LLMs, perhaps across distinct clusters with diverse performance characteristics [33,34] as opposed to a single LLM. However, unlike performance benchmarks, the lack of transparency with regards to costs and LLM economics [35] discourages concerted analysis of costs and performance benchmarks. Moreover, several factors can impact LLM economics including digital readiness, infrastructure, workforce, and cloud-based implementations [9]. While faithful cost estimation can be challenging, economics of LLM training, fine-tuning, and inference is generally agreed to be proportional to the LLM size. Thus, the size of the LLM can serve as a surrogate for costs. The DS and DN taxonomies revealed considerable consensus and two broad clusters (H, L). For the H cluster, LLMs QWN-14B and YIK-9B were proximal across the DS and DN taxonomy. However, the size of QWN-14B (~14 billion parameters) was considerably larger than that of YIK-9B (~9 billion parameters). Based on the DS and DN taxonomies, YIK-9B is preferred over QWN-14B. On a related note, the L cluster also comprised LLMs of markedly different sizes with comparable performance. For instance, FALI-7B (~7 billion parameters) was proximal to GPTL-1.5B (~2.8 billion parameters) recommending GPTL-1.5B over FALI-7B. Pair-wise correlation profiles revealed marked association between the DS performance benchmarks. While performance benchmarks are expected to ideally interrogate complementary characteristics of an LLM, the presence of correlations indicated inherent redundancies between the DS benchmarks. As LLM ranks are generally estimated as the weighted average of the performance benchmarks, eliminating redundancies may be critical for generating unbiased rank estimates. Eliminating redundant benchmarks can also assist in minimizing the overall evaluation cost [36].

There are several limitations of the present study. The study focused primarily on medium-sized LLMs (n=33) with around tens of billions of parameters. Generating comprehensive taxonomy portraits with a larger pool of LLMs spanning a wider range of sizes (large, ~100 billion parameters; medium, ~10 billion parameters; and small, ~millions of parameters) can reveal universal patterns characteristic of medical LLMs. Such an analysis may also assist in selecting LLM ensembles with varying sizes and complementary performance benchmark profiles, as opposed to the popular practice of selecting a single LLM. While the present study focused on standardized performance benchmarks, it may have limited usefulness in assessing capabilities [37] such as summarization, used routinely by health care conversational AI agents (eg, Chatbots and Ambient Listening Tools). The non-deterministic nature of the LLM response can also pose challenges in assessing such summaries, especially when these tools are deployed in clinical workflows [38]. While performance benchmarks used in generating the DS and DN taxonomies interrogate certain unique characteristics of the LLMs, they are by no means exhaustive. The rapid evolution of LLMs and their health care applications might demand incorporating novel benchmarks. Assessment may also explore relative benchmarking strategies, where characteristics, such as factual accuracy of information, time to

XSL•FO
RenderX

retrieve information, and ease of use, are compared to tools that are currently in place using randomized controlled designs. While the size of the LLMs were used as surrogates for costs in the present study, e enhanced transparency on LLM economics across training, fine-tuning, and inference could assist in tailored recommendations for strategic decision making in health care settings. As noted earlier, several factors can dictate the economics of implementation, deployment, and operationalization of LLMs in health care workflows. This includes digital and analytics maturity, infrastructure, workforce across a spectrum of areas, choice of the LLM onboarding pathways, and the needs of the health system. While the focus of the present study has been primarily on open-source LLMs, enhanced transparency of closed-source LLMs can facilitate unbiased comparisons for equitable and strategic adoption of these tools across health care enterprises.

Authors' Contributions

RN conceived the presented idea and carried out the analysis. All authors contributed to the writing and review of the manuscript.

Conflicts of Interest

None declared.

References

1. Shah NH, Entwistle D, Pfeffer MA. Creation and adoption of large language models in medicine. JAMA 2023 Sep 5;330(9):866-869. [doi: 10.1001/jama.2023.14217] [Medline: 37548965]
2. Denecke K, May R, LLM Health Group, Rivera Romero O. Potential of large language models in health care: Delphi study. J Med Internet Res 2024 May 13;26:e52399. [doi: 10.2196/52399] [Medline: 38739445]
3. Sezgin E. Redefining virtual assistants in health care: the future with large language models. J Med Internet Res 2024 Jan 19;26:e53225. [doi: 10.2196/53225] [Medline: 38241074]
4. Van Veen D, Van Uden C, Blankemeier L, et al. Adapted large language models can outperform medical experts in clinical text summarization. Nat Med 2024 Apr;30(4):1134-1142. [doi: 10.1038/s41591-024-02855-5] [Medline: 38413730]
5. Duggan MJ, Gervase J, Schoenbaum A, et al. Clinician experiences with ambient scribe technology to assist with documentation burden and efficiency. JAMA Netw Open 2025 Feb 3;8(2):e2460637. [doi: 10.1001/jamanetworkopen.2024.60637] [Medline: 39969880]
6. Zaretsky J, Kim JM, Baskharoun S, et al. Generative artificial intelligence to transform inpatient discharge summaries to patient-friendly language and format. JAMA Netw Open 2024 Mar 4;7(3):e240357. [doi: 10.1001/jamanetworkopen.2024.0357] [Medline: 38466307]
7. Wornow M, Lozano A, Dash D, Jindal J, Mahaffey KW, Shah NH. Zero-shot clinical trial patient matching with LLMs. NEJM AI 2025 Jan;2(1):AIcs2400360. [doi: 10.1056/AIcs2400360]
8. Klang E, Apakama D, Abbott EE, et al. A strategy for cost-effective large language model use at health system-scale. NPJ Digit Med 2024 Nov 18;7(1):320. [doi: 10.1038/s41746-024-01315-1] [Medline: 39558090]
9. Nagarajan R, Kondo M, Salas F, et al. Economics and equity of large language models: health care perspective. J Med Internet Res 2024 Nov 14;26:e64226. [doi: 10.2196/64226] [Medline: 39541580]
10. Cao Y, et al. Toward generalizable evaluation in the llm era: a survey beyond benchmarks. arXiv. Preprint posted online on Apr 26, 2025 URL: https://doi.org/10.48550/arXiv.2504.18838
11. Hu T, Zhou XH. Unveiling LLM evaluation focused on metrics: challenges and solutions. arXiv. Preprint posted online on Apr 14, 2024 URL: https://doi.org/10.48550/arXiv.2404.09135
12. Dennstädt F, Hastings J, Putora PM, Schmerder M, Cihoric N. Implementing large language models in healthcare while balancing control, collaboration, costs and security. NPJ Digit Med 2025 Mar 6;8(1):143. [doi: 10.1038/s41746-025-01476-7] [Medline: 40050366]
13. Face H. Open LLM Leaderboard: Performance Evaluation. 2024. URL: https://huggingface.co/docs/leaderboards/en/open_llm_leaderboard/about [accessed 2025-09-19]
14. Face H. Hugging Face Open Medical LLM Leaderboard. 2024. URL: https://huggingface.co/blog/leaderboard-medicalllm [accessed 2025-09-19]
15. Riedemann L, Labonne M, Gilbert S. The path forward for large language models in medicine is open. NPJ Digit Med 2024 Nov 27;7(1):339. [doi: 10.1038/s41746-024-01344-w] [Medline: 39604549]
16. Face H. Hugging Face: Evaluate Documentation: A Quick Tour. 2025. URL: https://huggingface.co/docs/evaluate/main/en/a_quick_tour [accessed 2025-09-19]
17. Ly DP, Jha AK, Epstein AM. The association between hospital margins, quality of care, and closure or other change in operating status. J Gen Intern Med 2011 Nov;26(11):1291-1296. [doi: 10.1007/s11606-011-1815-5] [Medline: 21837374]
18. Jindal JA, Lungren MP, Shah NH. Ensuring useful adoption of generative artificial intelligence in healthcare. J Am Med Inform Assoc 2024 May 20;31(6):1441-1444. [doi: 10.1093/jamia/ocae043] [Medline: 38452298]
19. Shekar S, et al. People over trust AI-generated medical responses and view them to be as valid as doctors, despite low accuracy. arXiv. Preprint posted online on Aug 11, 2024. [doi: 10.1056/AIoa2300015]

XSL•FO
RenderX

20. Pal A, Umapathi LK, Sankarasubbu M. Medmcqa: a large-scale multi-subject multi-choice dataset for medical domain question answering. arXiv. Preprint posted online on Mar 27, 2022 URL: https://doi.org/10.48550/arXiv.2203.14371
21. Hendrycks D, et al. Measuring massive multitask language understanding. arXiv. Preprint posted online on Sep 7, 2020 URL: https://doi.org/10.48550/arXiv.2009.03300
22. Jin Q, Dhingra B, Liu Z, Cohen W, Lu X. PubMedQA: a dataset for biomedical research question answering. 2019 Presented at: Proceedings of the 2019 Conference on Empirical Methods in Natural Language Processing and the 9th International Joint Conference on Natural Language Processing (EMNLP-IJCNLP); Hong Kong, China URL: https://www.aclweb.org/anthology/D19-1 [doi: 10.18653/v1/D19-1259]
23. Zhou J, et al. Instruction-following evaluation for large language models. arXiv. Preprint posted online on Nov 14, 2023 URL: https://doi.org/10.48550/arXiv.2311.07911
24. Suzgun M, et al. Challenging big-bench tasks and whether chain-of-thought can solve them. arXiv. Preprint posted online on Oct 17, 2022 URL: https://doi.org/10.48550/arXiv.2210.09261
25. Hendrycks D, et al. Measuring mathematical problem solving with the MATH dataset. arXiv. Preprint posted online on Mar 5, 2021 URL: https://doi.org/10.48550/arXiv.2103.03874
26. Rein D, et al. GPQA: a graduate-level google-proof q&a benchmark. arXiv. Preprint posted online on Nov 20, 2023 URL: https://doi.org/10.48550/arXiv.2311.12022
27. Sprague Z, et al. MuSR: testing the limits of chain-of-thought with multistep soft reasoning. arXiv. Preprint posted online on Oct 24, 2023 URL: https://doi.org/10.48550/arXiv.2310.16049
28. Wang Y, et al. MMLU-pro: a more robust and challenging multi-task language understanding benchmark. arXiv. Preprint posted online on Jun 3, 2024 URL: https://doi.org/10.48550/arXiv.2406.01574
29. Manning CR, Schütze H. Introduction to Information Retrieval: Cambridge University Press; 2008. URL: https://nlp.stanford.edu/IR-book/pdf/irbookonlinereading.pdf [accessed 2025-09-19]
30. Hastie T, Tibshirani R, Friedman JH. The Elements of Statistical Learning: Data Mining, Inference, and Prediction: Springer; 2009, Vol. 2. URL: https://link.springer.com/book/10.1007/978-0-387-84858-7 [accessed 2025-09-19]
31. Kaplan J, et al. Scaling laws for neural language models. arXiv. Preprint posted online on Jan 23, 2020 URL: https://doi.org/10.48550/arXiv.2001.08361
32. Thirunavukarasu AJ, Ting DSJ, Elangovan K, Gutierrez L, Tan TF, Ting DSW. Large language models in medicine. Nat Med 2023 Aug;29(8):1930-1940. [doi: 10.1038/s41591-023-02448-8] [Medline: 37460753]
33. Chen L, Zaharia M, Zou J. Less is more: using multiple llms for applications with lower costs. 2023 Presented at: Workshop on Efficient Systems for Foundation Models@ ICML2023 URL: https://openreview.net/forum?id=TkXjqcwQ4s [accessed 2025-09-22]
34. Chen L, Zaharia M, Zou J. Frugalgpt: how to use large language models while reducing cost and improving performance. arXiv. Preprint posted online on May 9, 2023 URL: https://doi.org/10.48550/arXiv.2305.05176
35. Velasco AA, et al. Is your LLM overcharging you? tokenization, transparency, and incentives. arXiv. Preprint posted online on May 27, 2025 URL: https://doi.org/10.48550/arXiv.2505.21627
36. Li Y, et al. Active evaluation acquisition for efficient LLM benchmarking. arXiv. Preprint posted online on Oct 8, 2024 URL: https://doi.org/10.48550/arXiv.2410.05952
37. McIntosh TR, Susnjak T, Arachchilage N, et al. Inadequacies of large language model benchmarks in the era of generative artificial intelligence. IEEE Trans Artif Intell 2025:1-18. [doi: 10.1109/TAI.2025.3569516]
38. Cohen IG, Ritzman J, Cahill RF. Ambient listening-legal and ethical issues. JAMA Netw Open 2025 Feb 3;8(2):e2460642. [doi: 10.1001/jamanetworkopen.2024.60642] [Medline: 39969887]

Abbreviations

DN: domain non-specific
DS: domain-specific
H: high
L: low
LLM: large language model

Edited by A Benis; submitted 26.02.25; peer-reviewed by JM Immanuvel Arockiasamy, MB Patel, PM Naliyatthaliyazchayil; revised version received 31.07.25; accepted 01.09.25; published 07.10.25.

Please cite as:
Nagarajan R, Klotzman V, Kondo M, Godambe S, Gold A, Henderson J, Martel S
Taxonomy Portraits: Deciphering the Hierarchical Relationships of Medical Large Language Models
JMIR Med Inform 2025;13:e72918
URL: https://medinform.jmir.org/2025/1/e72918
doi:10.2196/72918

XSL•FO
RenderX

© Radha Nagarajan, Vanessa Klotzman, Midori Kondo, Sandip Godambe, Adam Gold, John Henderson, Steven Martel. Originally published in JMIR Medical Informatics (https://medinform.jmir.org), 7.10.2025. This is an open-access article distributed under the terms of the Creative Commons Attribution License (https://creativecommons.org/licenses/by/4.0/), which permits unrestricted use, distribution, and reproduction in any medium, provided the original work, first published in JMIR Medical Informatics, is properly cited. The complete bibliographic information, a link to the original publication on https://medinform.jmir.org/, as well as this copyright and license information must be included.

XSL•FO
RenderX

Original Paper

An Ontology for Digital Medicine Outcomes: Development of the Digital Medicine Outcomes Value Set (DOVeS)

Benjamin Rosner[1,2], MD, PhD; Matthew Horridge[3], PhD; Guillen Austria[4], BA; Tiffany Lee[2], BA; Andrew Auerbach[2], MD, MPH

[1]Division of Clinical Informatics and Digital Transformation, University of California San Francisco, San Francisco, CA, United States

[2]Division of Hospital Medicine, University of California San Francisco, San Francisco, CA, United States

[3]Stanford Center for Biomedical Informatics Research, Stanford University, Stanford, CA, United States

[4]School of Public Health, University of California Berkeley, Berkeley, CA, United States

Corresponding Author:
Benjamin Rosner, MD, PhD
Division of Clinical Informatics and Digital Transformation
University of California San Francisco
10 Koret Way, Room K-301
UCSF DOM CLIIR Box 0737
San Francisco, CA, 94143
United States
Phone: 1 415 502 1371
Email: benjamin.rosner@ucsf.edu

Abstract

Background: Over the last 10-15 years, US health care and the practice of medicine itself have been transformed by a proliferation of digital medicine and digital therapeutic products (collectively, digital health tools [DHTs]). While a number of DHT classifications have been proposed to help organize these tools for discovery, retrieval, and comparison by health care organizations seeking to potentially implement them, none have specifically addressed that organizations considering their implementation approach the DHT discovery process with one or more specific outcomes in mind. An outcomes-based DHT ontology could therefore be valuable not only for health systems seeking to evaluate tools that influence certain outcomes, but also for regulators and vendors seeking to ascertain potential substantial equivalence to predicate devices.

Objective: This study aimed to develop, with inputs from industry, health care providers, payers, regulatory bodies, and patients through the Accelerated Digital Clinical Ecosystem (ADviCE) consortium, an ontology specific to DHT outcomes, the Digital medicine Outcomes Value Set (DOVeS), and to make this ontology publicly available and free to use.

Methods: From a starting point of a 4-generation–deep hierarchical taxonomy developed by ADviCE, we developed DOVeS using the Web Ontology Language through the open-source ontology editor Protégé, and data from 185 vendors who had submitted structured product information to ADviCE. We used a custom, decentralized, collaborative ontology engineering methodology, and were guided by Open Biological and Biomedical Ontologies (OBO) Foundry principles. We incorporated the Mondo Disease Ontology (MONDO) and the Ontology of Adverse Events. After development, DOVeS was field-tested between December 2022 and May 2023 with 40 additional independent vendors previously unfamiliar with ADviCE or DOVeS. As a proof of concept, we subsequently developed a prototype DHT Application Finder leveraging DOVeS to enable a user to query for DHT products based on specific outcomes of interest.

Results: In its current state, DOVeS contains 42,320 and 9481 native axioms and distinct classes, respectively. These numbers are enhanced when taking into account the axioms and classes contributed by MONDO and the Ontology of Adverse Events.

Conclusions: DOVeS is publicly available on BioPortal and GitHub, and has a Creative Commons license CC-BY-SA that is intended to encourage stakeholders to modify, adapt, build upon, and distribute it. While no ontology is complete, DOVeS will benefit from a strong and engaged user base to help it grow and evolve in a way that best serves DHT stakeholders and the patients they serve.

(JMIR Med Inform 2025;13:e67589) doi:10.2196/67589

XSL•FO
RenderX

KEYWORDS

digital health; digital medicine; digital therapeutics; ontology; medical informatics; value set; ontology; development; digital health tool; DHT; health systems; digital medicine outcomes value set; prototype; users

Introduction

Over the last 10-15 years, the US health care industry and the practice of medicine itself have been transformed by a proliferation of digital health software applications. It has been estimated, for example, that more than 350,000 health and wellness apps are available in mainstream app stores [1], and that more than 300 million people have used them in one form or another [2]. Along with this breadth of applications comes a variety of terminology describing them. The colloquially used umbrella term "digital health," for example, encapsulates many concepts including wellness apps, consumer grade mobile health apps, personal health tracking devices, remote patient monitoring applications, telemedicine platforms, and software as a medical device [3].

Driven in part by regulatory agencies and industry advocacy groups in the United States and abroad, efforts have been undertaken to more clearly delineate the boundaries between these types of applications. For example, "digital health" has been defined as technologies, platforms, and systems that engage consumers for lifestyle, wellness, and health-related purposes; capture, store, or transmit health data; and/or support life science and clinical operations [4]. As such, digital health products typically do not require clinical evidence, and do not meet the regulatory definition of a medical device. Digital *medicine* products, on the other hand, include evidence-based software and/or hardware products that measure and/or intervene in the service of human health. These products require clinical evidence and may (or may not) be classified as medical devices. At the most regulated end of this spectrum, digital *therapeutics* are health software intended to treat or alleviate a disease, disorder, condition, or injury by generating and delivering a medical intervention that has a demonstrable positive therapeutic impact on patient health and produce real-world outcomes [5]. Digital therapeutics typically do fall under regulatory oversight, with prescription digital therapeutics as those that are prescribed by a licensed health care professional.

While these definitions organize digital health tools (DHTs), a term we use here for convenience to encapsulate digital medicine and digital therapeutic products into regulatory and potentially clinical versus nonclinical categories, they do not necessarily enable the side-by-side outcomes-based comparison of similar products for the purpose of understanding relative efficacy or safety, nor do they facilitate establishing, for regulators and for vendors filing 510(k) applications, whether certain products may be "substantially equivalent" to predicate devices [6,7]. This need to evaluate evidence of health technologies and compare them with predicate devices partially overlaps with the purpose of Health Technology Assessment (HTA) frameworks, formal, systematic processes for synthesizing and evaluating existing evidence for health technologies, often for the use of policy and decision makers [8]. Users of HTA frameworks (whether federal bodies abroad or individual stakeholders in the United States where no centralized federal HTA body exists [9]) might also benefit from a means to readily identify similar or related devices, particularly in a domain as complex and rapidly evolving as digital medicine. Furthermore, most DHT end users (eg, clinicians and patients) or decision makers (eg, health system leaders making subscription or purchasing decisions, digital pharmacy and therapeutic committees making formulary decisions, or payers making coverage decisions), have one or more *outcomes* in mind that they are hoping the digital application can be used to influence.

While a few taxonomies do exist that categorize DHTs on a limited set of functional categories and characteristics [10,11], these are narrow in scope, and lack the interrelationships of an ontology. Establishing DHT organizational frameworks as ontologies provides a solution to heterogeneity problems like this, thereby defining the concepts and relationships that make interoperability possible [12]. It is common, for example, for ontologies to have "off the shelf" tooling; logic-based, precisely defined semantics; modeling languages to describe complex relationships; machine processing capability allowing for the computation of relationships; rigorous relationship structures, and in many cases the ability to be incorporated into other ontologies. In these respects, a system to organize DHTs according to the outcomes they intend to influence, and a common set of outcome metrics, would be valuable.

The purpose of this work is to describe the development of an *outcomes-based* ontology, the Digital medicine Outcomes Value Set (DOVeS). This ontology came into being as part of the Accelerated Digital Clinical Ecosystem (ADviCE) consortium, a group of health systems, vendors, payers, policymakers, and patient advocacy groups whose mission is to enable and scale the safe and effective adoption of DHTs in clinical practice [13].

Methods

Phase 0: Defining Scope and Purpose

DOVeS emanated from needs of the University of California San Francisco-Stanford-FDA (Food and Drug Administration) Center of Excellence in Regulatory Science and Innovation-funded ADviCE consortium to identify real-world performance metrics with which the safety and efficacy of DHTs could be characterized, whether for health care system leaders seeking to comparatively assess and implement DHTs, or for regulators seeking to classify them into similar outcomes-based groupings [14]. The purpose of DOVeS was to establish common sets of DHT real-world performance measure (RWPM) outcomes to facilitate more straightforward comparison between DHT products. The scope of DOVeS was to capture a body of outcomes with the potential to be influenced by DHTs, preferably but not exclusively by products capable of integrating into the electronic health record (EHR). DOVeS was intended to satisfy questions posed to vendors in a Digital Health Common Application (DHCA, refer to "Phase 1: PreDOVeS Development [Background Context and Knowledge Capture]" section), and to address competency questions for use cases

XSL•FO
RenderX

such as: what DHT applications influence (specific outcome) pertaining to disease X, what DHT applications satisfy health care administrative outcome Y, what DHT applications potentially mitigate adverse event Z?

Phase 1: PreDOVeS Development (Background Context and Knowledge Capture)

DOVeS emanated from ADviCE, about which background context will be helpful. Briefly, in order to inform a RWPM framework, leaders from 5 health systems participating in ADviCE formulated a strategy to learn from the DHT marketplace and collaboratively developed a Digital Health Common Application. The purpose of the DHCA was to collect from vendors a standardized set of intake and discovery information about their products and the populations and disease areas these products serve. Information collected through the DHCA across many vendors could then empower health system decision makers with a variety of common metrics in 1 place as their health systems, or any other, embark upon initial DHT vendor discovery for implementation decisions. Fields captured in the DHCA included, for example: whether the DHT integrates with the EHR (and if so, which ones); mechanisms of integration (eg, application programming interfaces, flat files, and data warehouses); current or planned regulatory status of the DHT product; stage of company development (eg, conceptual, proof of concept, beta, or commercial deployment); security, privacy, and data sharing policies; disease indications; intended patient populations; device integration; safety and efficacy evidence; accessibility, equity, feature types; and the outcomes that the product seeks to improve.

Between April 2019 and June 2020, a total of 185 vendors voluntarily completed and submitted DHCA data to ADviCE. Based on these data, on the FDA's Developing Software Precertification Program: A Working Model [15], and on consensus-building work carried out by the ADviCE consortium, a RWPM taxonomical hierarchy was initially developed, with 3 top-level DHT classes: "Healthcare outcomes," "Non-clinical product performance outcomes," and "User experience outcomes." Beneath these top-level classes were 3 levels of descendant outcome classes. The taxonomy resided in a spreadsheet, but without the functionalities of an ontology.

Phase 2: Development of DOVeS Ontology

Ontology Engineering Methodology

A number of Ontology Engineering Methodologies (OEMs) exist to guide and structure ontology development from a state of informal knowledge to formal representation [16]. Many OEMs have been organized into different classes, including, for example, collaborative, noncollaborative, and custom OEMs [17]. Our approach, a custom, decentralized, collaborative OEM, emanated from the asynchronous nature of information acquisition and stakeholder input that spanned the course of the ADviCE project (a portion of which preceded DOVeS in which DHT vendors supplied data that would later inform the top-level classes of the ontology) and the DOVeS project itself (in which domain experts and engineers collaborated synchronously and iteratively with a consortium of stakeholders).

Specifically, our custom approach resembles aspects of the Human-Centered Ontology Engineering Methodology framework, emphasizing agile, collaborative, and community-driven ontology development, involving both "knowledge engineers" and "knowledge workers" (eg, DHT vendors) empowering the latter to participate iteratively in the ontology lifecycle leveraging their experience and their work setting-specific domain expertise [18]. This is consistent with recent trends in ontology engineering, and avoids rigidly defined workflows and phases, instead focusing on iterative development and leveraging tools like GitHub and Protégé to facilitate decentralized collaboration. Our synchronous, active collaboration with communities of practice included the ADviCE consortium consisting of partners from academic medical centers; community health systems; policy makers; patient advocacy groups; industry members including DHT vendors, pharma, and payers; and domain experts, an ontology engineer, and an additional round of DHT vendors during field testing (refer to Phase 3 below). Asynchronous collaboration included input from the 185 DHT vendors who completed and submitted DHCAs before formal DOVeS development began. Supported by GitHub for versioning and issue tracking, the open-source ontology editor Protégé for editing [19], and BioPortal for publishing [20], DOVES reflects principles of liveness, evolution, and reusability.

Content Addition

Beginning with the 3 top-level classes and the collection of descendant outcomes described above, we used the web ontology language (OWL) through the open-source ontology editor Protégé to create an ontology, and to populate subclasses, definitions, and axioms related to DHTs. Based on data supplied by the 185 vendors, input from members of the ADviCE consortium, 1 investigator's first-hand knowledge of the digital health space [BR], and 2 investigators' involvement in the University of California San Francisco's Digital Diagnostics and Therapeutics Committee, a digital Pharmacy and Therapeutics committee [21] [BR and AA], we added more structure including subclasses, definitions, relationships, and refining values.

Technical Considerations

The DOVeS ontology was developed specifically using the OWL2EL fragment. This fragment is commonly used in many biomedical ontologies due to its balance between expressivity and computational efficiency [22]. Throughout the development process, we aimed to follow the Open Biological and Biomedical Ontologies (OBO) Foundry principles [23]. While these principles do not themselves constitute a methodology, they represent well-established community standards that when used in conjunction with a methodology, help ensure that the processes for creating and maintaining DOVeS would be robust, scalable, interoperable, and aligned with widely accepted ontology development best practices [23]. Since DOVeS is specific to digital medicine and therapeutic applications, and not a general-purpose biomedical domain ontology, there are no plans to submit it to the OBO Foundry Library.

Of the OBO Foundry's 15 principles, the following 6 directly influenced our development environment and setup (Table 1),

XSL•FO
RenderX

while other principles such as P8: documentation, P10: commitment to collaboration, and several others were used for management and maintenance, and are accommodated through our use of GitHub and BioPortal.

Table 1. Open Biological and Biomedical Ontologies Foundry principles directly influencing Digital medicine Outcomes Value Set development environment and setup.

OBO[a] Foundry principle	Description
P1: Open	DOVeS[b] ontology sources and releases are publicly available on GitHub under the open and permissive CC-BY-SA Creative Commons license.
P2: Common Format	We represented DOVeS using OWL[c]. OWL supports serialization into several accepted concrete syntaxes, including the OBO syntax, allowing interoperability with various ontology tools. This choice aligns with the OBO principle of adhering to a common format across ontologies.
P3: URI[d]/Identifier Space	Uniform naming conventions were applied to the DOVeS ontology Resource Identifier and all associated terms. Each term is assigned a universally unique alphanumeric identifier, prefixed by "https://w3id.org/doves/." This approach follows the OBO Foundry recommendation to use a meaningless alpha-numeric identifier for ontology terms, with human-readable labels encoded separately, as noted above.
P4: Versioning	GitHub served as the primary platform for ontology development, providing out-of-the-box versioning and release functionality. Our development approach closely followed the established ontology engineering practices popularized by the Gene Ontology Consortium [24,25]. Released versions of DOVeS are made publicly available on BioPortal to support accessibility and dissemination [20].
P6: Textual Definitions	Terms within DOVeS are accompanied by textual definitions, which follow the Aristotelian genus-differentia descriptive format. This format defines a term by specifying its broader category (genus) and its distinguishing characteristics (differentia). These definitions are provided using the IAO:0000115 (definition) annotation property.
P12: Naming Conventions	We applied consistent naming conventions across all DOVeS terms. Specifically, terms are named in lowercase unless they are proper nouns, and each term has exactly 1 primary label specified by an "rdfs:label" annotation. In addition, synonyms and alternative labels are provided using "skos:altLabel" annotations.

[a]OBO: Open Biological and Biomedical Ontologies.

[b]DOVeS: Digital medicine Outcomes Value Set.

[c]OWL: Web Ontology Language.

[d]URI: Unique Resource Identifier.

Secondary Ontology Integrations

Because many DHTs are meant to influence diseases or disease trajectories, we incorporated the Mondo Disease Ontology (MONDO), an OWL ontology unifying multiple disease ontologies and terminologies. MONDO is a publicly available ontology with an active maintenance userbase that harmonizes multiple disease resources [26]. It consists of 54,000 classes of which the human disease branch has 22,500 classes. We extracted the human disease branch (MONDO:0700096) using the *minimum information to reference an external ontology term* (MIREOT) method [27] provided by the ROBOT command line tool [28]. We chose MONDO over the *ICD-10* (*International Classification of Diseases, Tenth Revision*), for example, because MONDO is a richly axiomatized OWL ontology whereas *ICD-10* is a structured taxonomy that is optimized for health care reporting and billing. Using MONDO, therefore, allowed us to leverage the built-in semantics of OWL and an OWL reasoner to infer relationships between disease terms and for runtime querying. Furthermore, terms in MONDO are, to a greater degree than *ICD-10*, richly annotated with synonyms and definitions, including synonyms from *ICD-10*. This makes MONDO more useful for DOVeS at runtime where applications may need to search for DHTs by synonyms. Finally, MONDO worked well with our build tools. We used the ODK (Ontology Development Kit), which works best with OBO-style ontologies, like MONDO.

Because many DHTs influence or improve outcomes by mitigating adverse events, feedback from collaborators strongly emphasized the importance of addressing adverse events in a manner that would be both scalable and interoperable. We therefore incorporated the Ontology of Adverse Events (OAE) [29]. The OAE is an OBO Foundry ontology available in OWL, which ensures compatibility with and facilitates seamless integration into DOVeS. This allows DHTs to be described in terms of outcomes that correspond to mitigation of certain types of adverse events such as the number or rate of diabetic hypoglycemic events (OAE:0001057).

Phase 3: Testing and Refinement

After initial ontology development based on input from the ADviCE consortium, internal expertise, and DHCA data of vendors in the ADviCE database, the DOVeS ontology was then externally field tested with an independent sample of DHT vendors who had not been through the DHCA intake process and were not otherwise familiar with it. Lists of potential vendors for outreach were provided by ADviCE collaborators, the Digital Therapeutics Alliance, and ORCHA (Organization for the Review and Care of Health Apps). Inclusion criteria consisted of vendors serving the US market with digital medicine or digital therapeutic products that in some way served patients, clinicians, or both, for clinical care and were not purely administrative in nature.

XSL•FO
RenderX

To carry out this field testing, we reached out by email to 206 new DHT vendors from the above lists between December 2022 and May 2023. Nonresponses were followed up with an additional 2 outreach emails of varying invitation language. A total of 40 vendors replied, expressing interest (19.4% response rate), and were subsequently invited to one-on-one semistructured interviews (Multimedia Appendix 1) by web meetings to allow them to visually inspect the ontology in a dynamic manner in Protégé, and to suggest additions and modifications. Thirty-seven of these vendors (92.5%), 17 of which were manufacturers of FDA-listed Artificial Intelligence/Machine Learning Medical Devices, accepted this invitation and participated in the web meetings. To plan for these meetings and to facilitate quickly honing in on the areas within the ontology of greatest relevance to each of the vendors during the limited time of the 1 hour web meetings, vendors were sent REDCap (Research Electronic Data Capture; Vanderbilt University) surveys in advance (Multimedia Appendix 2), asking them to describe the areas in which their products operated and the types of outcomes their products aimed to influence, including: clinical outcomes, educational outcomes (eg, patient comprehension), engagement and adherence outcomes (eg, user engagement), health economic outcomes, health care operations outcomes (eg, operational efficiency), health care utilization outcomes (eg, hospital readmission), patient reported outcomes (eg, patient reported outcome response rates), process of care outcomes (eg, adherence to HEDIS [Healthcare Effectiveness Data and Information Set] measures), cybersecurity (eg, security and privacy certifications), interoperability, EHR integration, user experience (eg, Net Promoter Score), product uptime or downtime outcomes, and any peer reviewed manuscripts describing outcomes. Vendors could respond to 1 or more of these areas, or to none of them, thereby providing investigators insight as to where within the ontology to begin the semistructured interview. Of the 40 vendors sent REDCap surveys, 26 (65%) completed them before meeting with us. Those that did not complete them, but that nevertheless participated in one-on-one web meetings (11), had opportunities to describe their outcomes and areas of focus verbally. Information gleaned from the web meetings were captured in a database for potential DOVeS modifications.

Before new ontology information was to be captured through these meetings, we preidentified a stopping point for the one-on-one vendor meetings, as the point in time at which a "steady state" had been achieved in the top-level classes and their 3 descendent generations (ie, the original hierarchy from ADviCE plus any updates from the Phase 2 development process). This steady state was defined as the absence of additional suggestions for modification to these classes in the top 4 generations from no less than 5 sequential vendors. Any single vendor suggestion to modify one of these high-level classes constituted a signal to continue to interview vendors, record their suggestions, and make modifications as indicated. The stopping point of 5 vendors in a row without modification suggestions to these top classes was achieved by the 35th one-on-one meeting, but we nevertheless completed the remaining vendor meetings that had already been scheduled. Although some vendors late in the process had no ontology modification suggestions at all (suggesting some degree of ontology maturity even at deeper generation levels), many had highly use-case specific outcomes suggestions particular to their products at generations greater than 3 descendants deep from the top class. Although no ontology can be considered "complete," we took this trend in modification suggestions as a sign of reasonable high-level class content and structural stability.

Phase 4: Prototype Development for Real-World Application Demonstration

To demonstrate the potential use of DOVeS for practical application, we built a prototype DHT Application Finder that allows a user to search for DHTs based on filter settings, outcomes-based search terms, conditions, specialties, procedures, types of technology, regulatory status, and EHR integration capabilities. The backend of the DHT Application Finder used OWL reasoning in particular standard subsumption tests, to compute answers to queries from the frontend. To identify specific DHTs, the DHT Application Finder referenced the ADviCE database of 185 vendors' products. The records in the database were annotated with ontology terms from DOVeS that described the conditions treated by the application, outcomes of relevance, and other product parameters that were available in the original data collected by the DHCA. At runtime we constructed an OWL class expression that ontologically described each DHT application. When a user submits a search request, the criteria in the search request are translated to a complex OWL class expression that describes a general class of DHT applications. Then OWL reasoning is used to classify and retrieve the DHT applications that are entailed to be subclasses of the general class.

Results

Phases 0-3 Scope, Background, Development, Refinement, and Testing (Principal Results)

Despite the large set of classes pertaining directly to health care outcomes, "Non-clinical product performance outcomes" and "User experience outcomes" were nevertheless felt to be important not only to health systems and regulators, but to DHT vendors themselves. These classes consisted respectively of (1) technical outcomes associated with the product (cybersecurity and privacy certification outcomes), interoperability, technical certification, and system availability outcomes to name a few, and (2) a variety of outcomes associated with user satisfaction and usability.

In its current state, DOVeS contains 42,320 and 9481 native axioms and distinct classes respectively (Table 2). These numbers are enhanced when taking into account the axioms and classes contributed by MONDO and the OAE. A static view of a selected portion of the ontology hierarchy is shown in Figure 1. Dynamic views of the full ontology can be explored at BioPortal [30].

XSL•FO
RenderX

Table 2. Digital medicine Outcomes Value Set summary metrics.

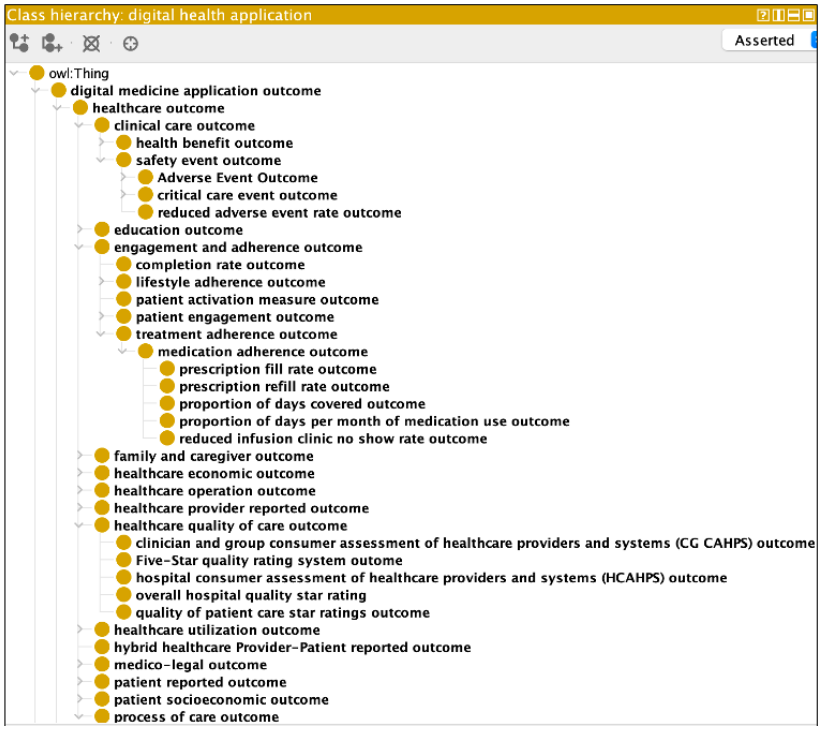
Metric	Count native to DOVeS[a]	Count including MONDO[b] and OAE[c]
Axioms	42,320	286,097
Number of distinct, named classes	9481	36,412
Object properties	12	32

[a]DOVeS: Digital medicine Outcomes Value Set.

[b]MONDO: Mondo Disease Ontology.

[c]OAE: Ontology of Adverse Events.

Figure 1. A selected hierarchical segment of Digital medicine Outcomes Value Set from the Protégé development environment.



Phase 4 Prototype Development (Principal Results)

The prototype DHT Application Finder front end and sample search results are shown in Figure 2. The DHT Application Finder's functionality is best illustrated with an example. Because of the availability of multiple DHTs in the ADviCE database pertaining to diabetes, we describe a use case in which a health system decision maker seeks to find candidate DHTs to help patients with diabetes in their health system achieve glycemic control (ie, glycemic control is the outcome of interest). The example is most informative by illustrating an end user seeking to identify DHTs first without, and then with outcomes-based search terms. In this example, the end user initially searches for DHTs based only on "diabetes" in the Conditions field. (Figure 3A) The user selects "diabetes mellitus" from the type-ahead list that appears, and presses "Search." The search results show a list of DHTs associated with diabetes mellitus including those for "type 2 diabetes mellitus" as well as "diabetic retinopathy." However, neither of these provides a list of DHTs exclusively related to the outcome of glycemic control.

Therefore, the user, in addition, (or could have done so as the first step) enters the term "Glyc" into the "Outcomes to be influenced" entry field (Figure 3B), and the type-ahead offers 2 choices: "Glycemic Control" and "Reduction in Glycemic Events." Choosing "Glycemic Control Outcome" and performing the search again, the user obtains a list now of only those DHTs specific to achieving glycemic control (eg, this time not including DHTs associated specifically with diabetic retinopathy). In the case of the ADviCE database, this outcomes-based search reduced the field of products that the user might otherwise have needed to explore further by 33%.

XSL•FO
RenderX

Figure 2. Prototype Digital Health Tool Application Finder with underlying DOVeS (Digital medicine Outcomes Value Set) ontology. (A) Search for outcome "glycemic control." (B) A set of search results. (Company and product names redacted).

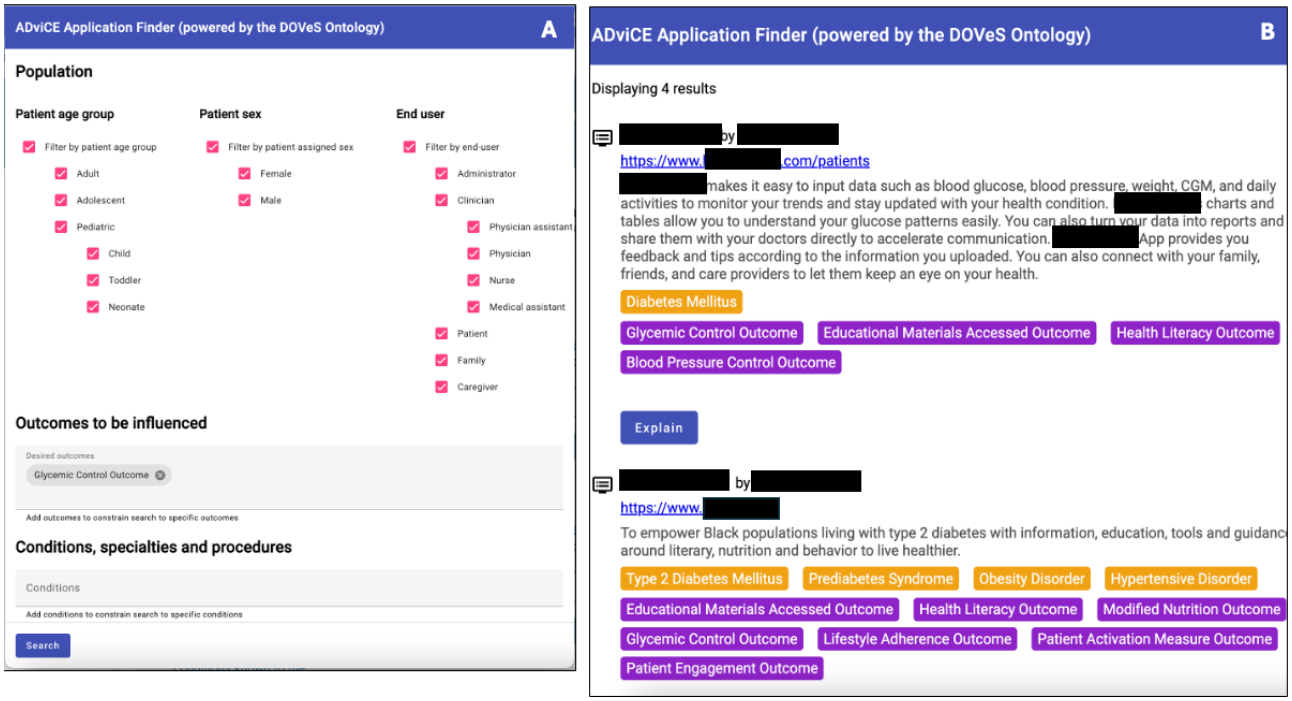
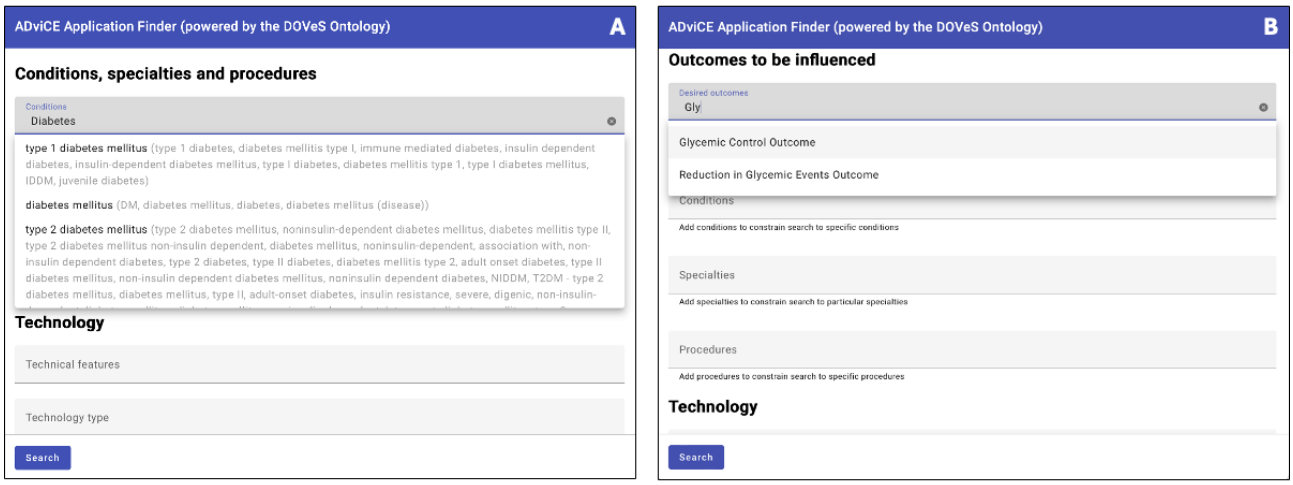


Figure 3. Entry fields in the Digital Health Tool Application Finder for (A) conditions, specialties, and procedures, and (B) outcomes to be influenced. The fields show type-ahead completion options for conditions known to the system, along with their synonyms that are drawn directly from Mondo Disease Ontology (MONDO).



Discussion

Principal Results

In developing DOVeS, we describe an ontology framed by outcomes specific to DHTs, rather than technical or implementation features. Because our goal was to address products that would potentially be used in clinical practice that might fall under regulatory oversight, we focused on digital medicine and digital therapeutic products, and did not intend to capture outcomes associated with the much broader category of digital health.

The 3 top-level classes of DOVeS, derived from the background work done by the ADviCE consortium, consisted of "Healthcare outcomes," "Non-clinical product performance outcomes," and "User experience outcomes." The top-level class "Healthcare outcomes" is central to DHTs, as most such products intend to influence something in this class. It is composed of descendent classes including, for example, clinical care outcomes (eg, health benefits and mitigation of adverse events), health care utilization outcomes, health care operational outcomes, process of care outcomes, medico-legal outcomes, education outcomes, health care economic outcomes, socioeconomic outcomes, family and caregiver outcomes, and engagement and adherence outcomes (Figure 1).

Related Works

Efforts to organize DHTs to date have been described in part based on the specialties they serve, disease areas, user types,

XSL•FO
RenderX

and certain functionalities [31], but this can limit the way in which DHTs that are platforms, serving functions across multiple specialties, or that span diseases of multiple organ systems (eg, diabetes) are organized. The World Health Organization developed the Classifications of Digital Health Interventions as a nonontological framework according to different user types (persons, health care providers, health management, and support personnel), data services, and services and application types, but not on outcomes, and not in a computable format [32].

Although some limited outcomes-based taxonomies [33] and classifications exist [34], to our knowledge, none are specific to digital medicine or digital therapeutics applications. Organizing DHTs into common categories based on the outcomes they influence then gives the marketplace an opportunity to compare different DHTs side by side for their impacts on common outcomes, and with the appropriate outcomes results, may make regulatory, purchasing, formulary, and coverage decisions more efficient and objective.

Limitations

Several limitations to this work exist. First, by design, DOVeS was informed by DHTs excluding those in the "digital health" class (that class of products focused on wellness that does not fall under regulatory oversight). Second, while it would be methodologically satisfying after DOVeS development to return to the original 185 DHT vendor products and quantitatively describe the degree of concept mapping achieved, doing so could be misleading because the only data available to us from these vendors were high-level concepts captured in the DHCAs before DOVeS was built. Therefore, a future and important direction for the DHT Application Finder will be a guided intake module through which the vendor can submit a product for automated annotation based on the dynamic class content of the ontology at the time of submission. Another limitation is that, while the classes for the ontology were developed with academic, regulatory, community health, payer, and patient advocacy stakeholders, and included field testing with an independent set of DHT vendors, DOVeS, like most ontologies, is not complete, but will rely and depend on an active base of engaged supporters to continue to build and maintain it. In addition, outcomes and the metrics to measure those outcomes are not necessarily universal in the DHT industry. In the process of outcome and metrics discovery, we attempted to select outcomes through both internal and external consensus. However, these outcomes and metrics may need modification in the future as the ontology grows and is further informed by the broader community of stakeholders and the evolving industry.

Conclusions

An ontology for organizing DHTs into outcomes-based groupings is an important step as the digital medicine and digital therapeutics industry matures. While the DOVeS ontology provides an open-source framework as a starting point to do this, real-world value from the ontology will be achieved through the development of robust tools similar to the prototype DHT Application Finder that will leverage the ontology for specific use cases. These may include, for example, use by regulators to streamline the process for determining substantial equivalence to predicate devices, and use by health system decision makers to identify products that influence the same or related outcomes so that the universe of potential DHT products being considered for implementation can be rapidly narrowed to only those that are most relevant. While it is not known whether the 33% reduction in products that were more specifically identified with an outcomes-based search relative to a disease-based search described in the example from the ADviCE database above will necessarily translate if the entire marketplace of DHT products were to be indexed, any reasonable reduction would nevertheless offer savings in time and effort by decision makers attempting to identify DHTs for deeper discovery for potential clinical use.

DOVeS is publicly available on BioPortal [30] and GitHub [35], and has a Creative Commons license CC-BY-SA that is intended to encourage stakeholders to modify, adapt, build upon, and distribute it. Only with an engaged userbase will the ontology continue to grow and evolve, and when applied to the marketplace help organize DHTs in a way that is beneficial to stakeholders and ultimately to the patients they serve.

Acknowledgments

We thank Leeda Rashid and Vinay Pai of the FDA for thoughtful project feedback. We acknowledge the Digital Therapeutics Alliance, and ORCHA for assistance in identifying potential vendors to review the ontology. This project was supported by the Food and Drug Administration of the US Department of Health and Human Services as part of The Center for Radiological Health Digital Health Center of Excellence and The Center of Excellence in Regulatory Science and Innovation grant to University of California, San Francisco (U01FD005978). The contents are those of the author(s) and do not necessarily represent the official views of, nor an endorsement, by FDA/HHS, or the US Government.

Conflicts of Interest

BR and AA report equity in Kuretic.

Multimedia Appendix 1
Semi-structured interview questions for web meetings with Digital Health Tool vendors.
[DOCX File , 15 KB - medinform_v13i1e67589_app1.docx]

XSL•FO
RenderX

Multimedia Appendix 2
REDCap survey sent to vendors in advance of web meetings in order to help investigators focus on the most relevant parts of the ontology for the web meeting.
[PDF File (Adobe PDF File), 39 KB - medinform_v13i1e67589_app2.pdf]

References

1. Olsen E. Digital health apps balloon to more than 350,000 available on the market, according to IQVIA report. mobihealthnews. 2021. URL: https://www.mobihealthnews.com/news/digital-health-apps-balloon-more-350000-available-market-according-iqvia-report [accessed 2024-04-08]
2. Wylie L. Health app revenue and usage statistics (2024). Business of Apps. URL: https://web.archive.org/web/20240412105511/https://www.businessofapps.com/data/health-app-market/ [accessed 2024-04-08]
3. Software as a medical device (SaMD). International Medical Device Regulators Forum. 2014. URL: https://www.imdrf.org/working-groups/software-medical-device-samd [accessed 2019-11-30]
4. Digital Health, Digital Medicine, Digital Therapeutics (DTx): What's the difference? Digital Medicine Society. 2019. URL: https://dimesociety.org/digital-health-digital-medicine-digital-therapeutics-dtx-whats-the-difference/ [accessed 2025-02-05]
5. ISO/TR 11147:2023-Health informatics — Personalized digital health — Digital therapeutics health software systems. 2023. URL: https://www.iso.org/standard/83767.html [accessed 2024-04-09]
6. The 510(k) program: evaluating substantial equivalence in premarket notifications [510(k)] guidance for industry and food and drug administration staff. US Food and Drug Administration. 2014. URL: https://www.fda.gov/media/82395/download?attachment [accessed 2024-12-04]
7. Wreh E. Premarket notification [510(k)]. In: Medical Device Regulation. Netherlands: Elsevier; 2023:57-89. [doi: 10.1016/B978-0-323-95354-2.00006-2]
8. Sullivan SD, Watkins J, Sweet B, Ramsey SD. Health technology assessment in health-care decisions in the United States. Value Health 2009;12 Suppl 2:S39-S44 [FREE Full text] [doi: 10.1111/j.1524-4733.2009.00557.x] [Medline: 19523183]
9. Fontrier AM, Visintin E, Kanavos P. Similarities and differences in health technology assessment systems and implications for coverage decisions: evidence from 32 countries. Pharmacoecon Open 2022;6(3):315-328 [FREE Full text] [doi: 10.1007/s41669-021-00311-5] [Medline: 34845671]
10. Glöggler M, Ammenwerth E. Development and validation of a useful taxonomy of patient portals based on characteristics of patient engagement. Methods Inf Med 2021;60(S 01):e44-e55 [FREE Full text] [doi: 10.1055/s-0041-1730284] [Medline: 34243191]
11. Ritchie J, Welch B. Categorization of third-party apps in electronic health record app marketplaces: systematic search and analysis. JMIR Med Inform 2020;8(5):e16980. [doi: 10.2196/16980] [Medline: 32469324]
12. Abbes H, Gargouri F. MongoDB-based modular ontology building for big data integration. J Data Semant 2017;7(1):1-27. [doi: 10.1007/s13740-017-0081-z]
13. Curated health apps for health systems. ADVICE (Accelerated Digital Clinical Ecosystem). URL: https://www.advicehealth.org [accessed 2024-04-09]
14. Developing frameworks and tools for integration of digital health tools into clinical practice. U.S. Food and Drug Administration. URL: https://www.fda.gov/science-research/advancing-regulatory-science/developing-frameworks-and-tools-integration-digital-health-tools-clinical-practice [accessed 2024-10-01]
15. Developing software precertification program: a working model (v0.2-June 2018). U.S. Food and Drug Administration. 2018. URL: https://www.fda.gov/media/113802/download?attachment [accessed 2019-04-06]
16. Spoladore D, Pessot E, Trombetta A. A novel agile ontology engineering methodology for supporting organizations in collaborative ontology development. Computers in Industry 2023;151:103979. [doi: 10.1016/j.compind.2023.103979]
17. Kotis KI, Vouros GA, Spiliotopoulos D. Ontology engineering methodologies for the evolution of living and reused ontologies: status, trends, findings and recommendations. The Knowledge Engineering Review 2020;35. [doi: 10.1017/s0269888920000065]
18. Kotis K, Vouros GA. Human-centered ontology engineering: the HCOME methodology. Knowl Inf Syst 2005;10(1):109-131. [doi: 10.1007/s10115-005-0227-4]
19. Musen MA, Protégé Team. The protégé project: a look back and a look forward. AI Matters 2015;1(4):4-12 [FREE Full text] [doi: 10.1145/2757001.2757003] [Medline: 27239556]
20. Whetzel PL, Noy NF, Shah NH, Alexander PR, Nyulas C, Tudorache T, et al. BioPortal: enhanced functionality via new web services from the national center for biomedical ontology to access and use ontologies in software applications. Nucleic Acids Res 2011;39(Web Server issue):W541-W545 [FREE Full text] [doi: 10.1093/nar/gkr469] [Medline: 21672956]
21. Auerbach AD, Neinstein A, Khanna R. Balancing innovation and safety when integrating digital tools into health care. Ann Intern Med 2018;168(10):733-734 [FREE Full text] [doi: 10.7326/M17-3108] [Medline: 29582072]
22. Baader F, Brandt S, Lutz C. Institut für Theoretische Informatik TU Dresden. Pushing the EL Envelope. Dresden: Technsiche Universität Dresden; 2005.
23. Principles: overview. OBO Foundry. URL: https://obofoundry.org/principles/fp-000-summary.html [accessed 2024-09-13]

XSL•FO
RenderX

24. Gene Ontology Consortium, Aleksander SA, Balhoff J, Carbon S, Cherry JM, Drabkin HJ, et al. The gene ontology knowledgebase in 2023. Genetics 2023;224(1) [FREE Full text] [doi: 10.1093/genetics/iyad031] [Medline: 36866529]
25. Ashburner M, Ball CA, Blake JA, Botstein D, Butler H, Cherry JM, et al. Gene ontology: tool for the unification of biology. The gene ontology consortium. Nat Genet 2000;25(1):25-29 [FREE Full text] [doi: 10.1038/75556] [Medline: 10802651]
26. Vasilevsky NA, Matentzoglu NA, Toro S, Flack JE, Hegde H, Unni DR, et al. Mondo: unifying diseases for the world, by the world. medRxiv 2022. [doi: 10.1101/2022.04.13.22273750]
27. Courtot M, Gibson F, Lister A, Malone J, Schober D, Brinkman R, et al. MIREOT: the minimum information to reference an external ontology term. Appl Ontol 2011;6(1):23-33. [doi: 10.3233/ao-2011-0087]
28. Jackson RC, Balhoff JP, Douglass E, Harris NL, Mungall CJ, Overton JA. ROBOT: a tool for automating ontology workflows. BMC Bioinformatics 2019;20(1):407 [FREE Full text] [doi: 10.1186/s12859-019-3002-3] [Medline: 31357927]
29. He Y, Sarntivijai S, Lin Y, Xiang Z, Guo A, Zhang S, et al. OAE: the ontology of adverse events. J Biomed Semantics 2014;5:29 [FREE Full text] [doi: 10.1186/2041-1480-5-29] [Medline: 25093068]
30. Rosner B. Digital medicine outcomes value set (DOVeS) ontology. NCBO BioPortal. URL: https://bioportal.bioontology.org/ontologies/DOVES [accessed 2024-09-27]
31. Digital health technology gallery. Digital.Health. URL: https://digital.health/new-products [accessed 2024-04-09]
32. World Health Organization. Classification of Digital Interventions, Services, and Applications in Health. A Shared Language to Describe the Uses of Digital Technology for Health. Geneva: World Health Organization; 2023.
33. Dodd S, Clarke M, Becker L, Mavergames C, Fish R, Williamson PR. A taxonomy has been developed for outcomes in medical research to help improve knowledge discovery. J Clin Epidemiol 2018;96:84-92 [FREE Full text] [doi: 10.1016/j.jclinepi.2017.12.020] [Medline: 29288712]
34. Library of digital endpoints. Digital Medicine Society (DiMe). URL: https://dimesociety.org/get-involved/library-of-digital-endpoints/ [accessed 2024-09-04]
35. Horridge M. dovesproject. Github. URL: https://github.com/dovesproject [accessed 2024-09-27]

Abbreviations

ADviCE: Accelerated Digital Clinical Ecosystem
DHCA: Digital Health Common Application
DHT: digital health tool
DOVeS: Digital medicine Outcomes Value Set
EHR: electronic health record
FDA: Food and Drug Administration
HEDIS: Healthcare Effectiveness Data and Information Set
HTA: Health Technology Assessment
ICD-10: International Classification of Diseases, Tenth Revision
MIREOT: minimum information to reference an external ontology term
MONDO: Mondo Disease Ontology
OAE: Ontology of Adverse Events
OBO: Open Biological and Biomedical Ontologies
ODK: Ontology Development Kit
OEM: Ontology Engineering Methodology
ORCHA: Organization for the Review and Care of Health Apps
OWL: Web Ontology Language
REDCap: Research Electronic Data Capture
RWPM: Real World Performance Metrics

Edited by C Lovis; submitted 16.10.24; peer-reviewed by C Gaudet-Blavignac, D Spoladore; comments to author 16.11.24; revised version received 25.12.24; accepted 12.01.25; published 06.02.25.

Please cite as:
Rosner B, Horridge M, Austria G, Lee T, Auerbach A
An Ontology for Digital Medicine Outcomes: Development of the Digital Medicine Outcomes Value Set (DOVeS)
JMIR Med Inform 2025;13:e67589
URL: https://medinform.jmir.org/2025/1/e67589
doi:10.2196/67589
PMID:

XSL•FO
RenderX

©Benjamin Rosner, Matthew Horridge, Guillen Austria, Tiffany Lee, Andrew Auerbach. Originally published in JMIR Medical Informatics (https://medinform.jmir.org), 06.02.2025. This is an open-access article distributed under the terms of the Creative Commons Attribution License (https://creativecommons.org/licenses/by/4.0/), which permits unrestricted use, distribution, and reproduction in any medium, provided the original work, first published in JMIR Medical Informatics, is properly cited. The complete bibliographic information, a link to the original publication on https://medinform.jmir.org/, as well as this copyright and license information must be included.

XSL•FO
RenderX

Original Paper

Assessing Data Quality in Heterogeneous Health Care Integration: Simulation Study of the AIDAVA Framework

Jens Declerck[1,2], MSc; Ömer Durukan Kılıç[3], MSc; Ensar Emir Erol[3], MSc; Shervin Mehryar[3], MSc; Dipak Kalra[1,2], Prof Dr; Isabelle de Zegher[4], Dr med; Remzi Celebi[3], Dr

[1]The European Institute for Innovation Through Health Data, Oosterzele, Belgium

[2]Department of Public Health and Primary Care, Unit of Medical Informatics and Statistics, Ghent University, Ghent, Belgium

[3]Department of Advanced Computing Sciences, Institute of Data Science, Maastricht University, Maastricht, The Netherlands

[4]B!lboa, Tervuren, Belgium

Corresponding Author:
Jens Declerck, MSc
The European Institute for Innovation Through Health Data
Merebaaistraat 10
Oosterzele, 9860
Belgium
Phone: 32 093323421
Email: jens.declerck@i-hd.eu

Abstract

Background: Integrated health data are foundational for secondary use, research, and policymaking. However, data quality issues—such as missing values and inconsistencies—are common due to the heterogeneity of health data sources. Existing frameworks often use static, 1-time assessments, which limit their ability to address quality issues across evolving data pipelines.

Objective: This study evaluates the AIDAVA (artificial intelligence–powered data curation and validation) data quality framework, which introduces dynamic, life cycle–based validation of health data using knowledge graph technologies and SHACL (Shapes Constraint Language)–based rules. The framework is assessed for its ability to detect and manage data quality issues—specifically, completeness and consistency—during integration.

Methods: Using the MIMIC-III (Medical Information Mart for Intensive Care-III) dataset, we simulated real-world data quality challenges by introducing structured noise, including missing values and logical inconsistencies. The data was transformed into source knowledge graphs and integrated into a unified personal health knowledge graph. SHACL validation rules were applied iteratively during the integration process, and data quality was assessed under varying noise levels and integration orders.

Results: The AIDAVA framework effectively detected completeness and consistency issues across all scenarios. Completeness was shown to influence the interpretability of consistency scores, and domain-specific attributes (eg, diagnoses and procedures) were more sensitive to integration order and data gaps.

Conclusions: AIDAVA supports dynamic, rule-based validation throughout the data life cycle. By addressing both dimension-specific vulnerabilities and cross-dimensional effects, it lays the groundwork for scalable, high-quality health data integration. Future work should explore deployment in live clinical settings and expand to additional quality dimensions.

(JMIR Med Inform 2025;13:e75275) doi:10.2196/75275

KEYWORDS

data quality; knowledge graph; ontology; health data; data quality dimensions; data quality assessment; secondary use; data quality framework; fit for purpose

Introduction

Background

The integration of high-quality, complete, and interoperable patient health records is essential to modern health care and medical research [1-4]. Accurate and well-structured data enhance research reproducibility [5-7], which in turn drives more effective clinical decision-making and improved patient outcomes. However, as health data is collected across diverse and heterogeneous sources [8,9], its quality can be compromised by fragmentation [10,11], variability [12,13], and incomplete

XSL•FO
RenderX

information [14-16]. These challenges compromise data usability and hinder the development of unified, clinically meaningful datasets suitable for both primary and secondary uses [17,18].

Existing efforts on health data quality often focus on defining standardized quality dimensions and organizing these into structured frameworks [19-23]. However, many current approaches rely on static, 1-time evaluations that do not reflect the dynamic and iterative nature of the entire data life cycle [24,25]. This limits their effectiveness in identifying evolving quality issues that emerge across stages of data transformation—such as extraction [26,27], harmonization [28,29], or final validation [21]—as they do not provide continuous, iterative assessment.

To address this gap, the AIDAVA (artificial intelligence–powered data curation and validation) project [30], launched in 2022 as part of a Horizon Europe initiative, proposes a dynamic data quality framework that enables continuous assessment throughout the data life cycle. At its core is the personal health knowledge graph (PHKG), a patient-centered, interoperable data model built using knowledge graph (KG) technologies and validated with SHACL (Shapes Constraint Language)–based rules. This approach allows for the assessment of data quality constraints across multiple integration stages. For instance, if a patient record includes a diagnosis of prostate cancer but the patient is listed as a female, or if a discharge date appears earlier than the admission date, AIDAVA's rule-based validation will automatically detect and flag these inconsistencies during the integration process.

This paper also demonstrates how completeness directly influences the interpretability of consistency scores.

This paper evaluates the AIDAVA framework's effectiveness in detecting and improving data quality issues, with a particular focus on completeness and consistency. The framework's ability to validate data dynamically across stages of integration is essential for supporting artificial intelligence–driven, automated curation workflows, a central goal of the AIDAVA project. As health care systems increasingly rely on semantic technologies and automation to manage large-scale, heterogeneous data, life cycle–based quality monitoring becomes a requirement. By situating this work within that broader vision, we aim to demonstrate how dynamic rule-based validation can enhance the reliability and scalability of next-generation health data integration pipelines. It also investigates how these dimensions evolve across the data transformation pipeline, highlighting their interdependencies and implications for integrated health data (Textbox 1).

Textbox 1. Main contributions of this paper.

- Introduces the AIDAVA (artificial intelligence–powered data curation and validation) framework for dynamic health data quality validation using SHACL (Shapes Constraint Language) and knowledge graphs.
- Defines and applies completeness and consistency rules across the integration pipeline.
- Simulates realistic data quality issues using controlled noise in the MIMIC-III (Medical Information Mart for Intensive Care-III) dataset.
- Evaluates SHACL validation across different integration sequences and noise levels.

Related Work

Ensuring the quality of integrated health care data, particularly for the secondary use of electronic health records, has been the subject of extensive research [31]. Prior efforts generally focus on defining and measuring data quality along dimensions such as completeness, consistency, conformance, and plausibility [20-24]. These dimensions serve as the foundation for several frameworks and tools developed to detect anomalies and enforce standards across clinical datasets [15,22,32].

Framework-based approaches have sought to structure and formalize the assessment of health data quality. Notably, Kahn et al [21] introduced a widely adopted framework that groups quality concerns into 3 core dimensions—completeness, conformance, and plausibility—further divided into verification and validation contexts. This framework laid the groundwork for systematic quality checks but remains limited to static evaluations that do not adapt to the changing nature of data pipelines.

Dimension-specific studies have also provided deeper insights. Issa et al [33] conducted a comprehensive review of completeness in KGs, identifying 7 distinct subtypes, including 3 previously unclassified forms. Their findings emphasized the interplay between completeness and other quality dimensions such as consistency and correctness—further highlighting the need for more context-aware, dynamic quality assessments.

Tool-based solutions, such as Achilles Heel [34], offer practical mechanisms for identifying data quality issues. As part of the Observational Health Data Sciences and Informatics (OHDSI) ecosystem, Achilles Heel applies 70 predefined validation rules to detect anomalies in large-scale clinical datasets. While effective in identifying static inconsistencies, these tools typically evaluate data quality at a single point in time and cannot accommodate the iterative transformations that occur during integration workflows.

In contrast to these prior approaches, the AIDAVA framework introduces a life cycle–based, dynamic model of data quality validation. By embedding SHACL-based validation rules directly into a KG pipeline, AIDAVA allows for continuous monitoring and enforcement of constraints during data ingestion, transformation, and integration. It extends existing methodologies by addressing data quality not as a 1-time task, but as an ongoing process—ensuring that completeness and consistency are maintained across evolving data structures.

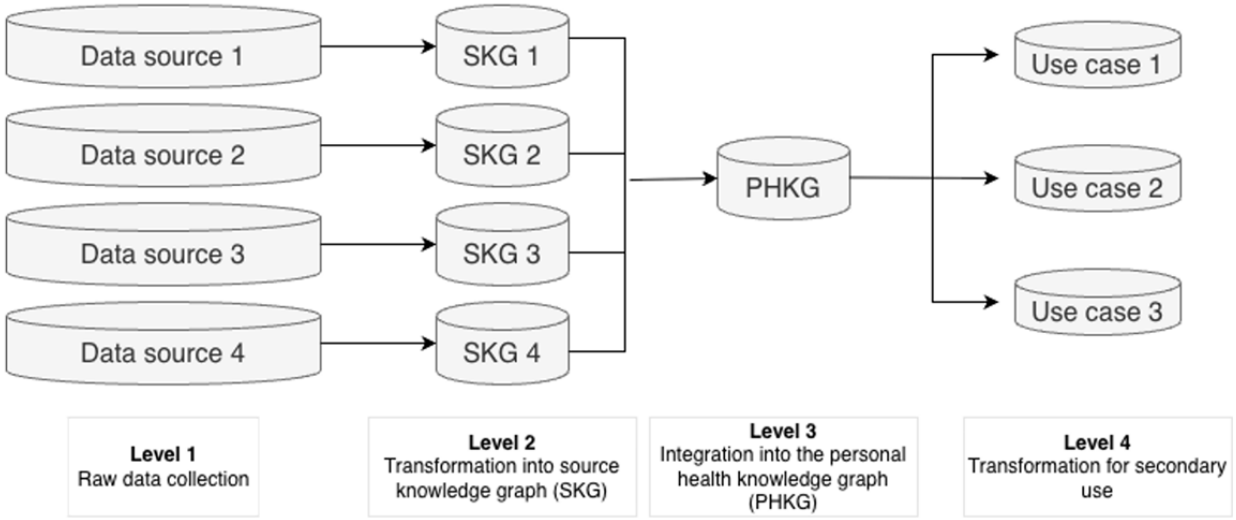
AIDAVA Data Quality Framework

The AIDAVA data quality framework is designed to ensure semantic and structural standardization across the entire health

XSL•FO
RenderX

data life cycle, addressing the complexities of integrating heterogeneous health data sources. The framework operates across 4 levels, each targeting specific points in the health data integration process. These 4 levels of the framework are illustrated in Figure 1.

Figure 1. The 4 levels of the AIDAVA data quality framework. AIDAVA: artificial intelligence–powered data curation and validation; PHKG: personal health knowledge graph; SKG: source knowledge graph.



Level 1: Raw Data Collection

At the initial level, the framework relies on data providers to provide data that meets baseline standards. Given the variability of data sources, direct transformations or validations at this stage are limited. Instead, the framework ensures compliance with transfer specifications, verifying that incoming data adheres to structural and format requirements before progressing to the next level.

Level 2: Transformation Into Source Knowledge Graphs

In this stage, raw data are transformed into source knowledge graphs (SKG) by executing a data curation tool from the library of tools available in AIDAVA and delivering data sources in a KG format aligned with the AIDAVA Reference Ontology. The AIDAVA Reference Ontology plays a dual role in enabling semantic interoperability and systematic quality evaluation. It provides a formal semantic layer that aligns PHKGs with standards such as Health Level Seven International Fast Healthcare Interoperability Resources (FHIR), SNOMED CT (Systematized Nomenclature of Medicine–Clinical Terms), and Clinical Data Interchange Standards Consortium. This process ensures semantic and structural standardization of each data source, which is critical for interoperability. Standardizing the data at this level minimizes inconsistencies and enables proper integration with multiple sources.

Level 3: Integration Into the PHKG

In this phase, multiple SKGs are integrated into a unified PHKG, creating a longitudinal representation of an individual's health history. This step consolidates fragmented patient data sources while maintaining consistency and logical coherence in the integrated patient record. The integration process ensures that patient data is well-structured, complete, and free of inconsistent and redundant information to support clinical decision-making and research applications. For example, during PHKG integration, a birth year recorded as 1875, implying an implausible age of over 140 years, would be flagged by age-consistency rules. This type of anomaly is automatically detected through SHACL-based validation during the integration process.

Level 4: Transformation for Secondary Use

In the final stage, the PHKG is transformed into formats tailored for secondary use. This step adapts integrated data to align with specific output formats, enabling accurate analysis (eg, Breast Cancer registry in Observational Medical Outcomes Partnership [OMOP] compliant format), improved patient care (eg, patient International Patient Summary in FHIR format), and effective reuse across clinical and research settings.

This study focuses on levels 2 and 3, as they are the earliest feasible and scalable stages for enforcing semantic standardization and integrating fragmented, heterogeneous data sources. Performing this at level 1 is not practical due to diverse formats and limited control over data provider systems. Level 4 is only partially addressed, as downstream transformation is performed, but full data quality assessment from the perspective of a specific use case lies outside the scope of this paper.

Data Quality Dimensions and Categories

To evaluate data quality, the AIDAVA framework adopts a structured approach based on dimensions and categories. Dimensions provide a high-level perspective on data quality, grouping related categories to help identify systemic issues. Recent research underscores the increasing need to evaluate diverse data quality dimensions, especially when repurposing health data for secondary use [19]. While multiple dimensions contribute to ensuring high-quality health data, the AIDAVA

XSL•FO
RenderX

framework currently focuses on 2 data quality dimensions: completeness and consistency. Completeness ensures that all necessary data elements are present, preventing critical information gaps. Consistency verifies that data adheres to defined constraints and logical relationships, such as ensuring that diagnoses and procedures align with a patient's demographic details. Within these dimensions, categories provide a more granular level of assessment, as outlined in Table 1.

The decision to focus on completeness and consistency is driven by their widespread use in data quality research [35-37] and their suitability for automated assessment [23]. Unlike other dimensions, which often require subjective interpretation or manual validation, completeness and consistency can be systematically measured using predefined rules and automated validation techniques. By prioritizing completeness and consistency, the AIDAVA framework establishes a scalable approach to data quality assessment. These dimensions not only support automated validation but also provide a foundation for expanding the framework to address more complex data quality dimensions.

Table 1. Overview of data quality dimensions and categories in the AIDAVA[a] framework.

Dimension and category	Description	Example
Completeness		
Essential variable completeness	Identifies when critical data elements are missing	Missing patient date of birth
Conditional variable completeness	Detects cases where missing variables prevent consistency checks	Diagnosis present, but no recorded gender
Consistency		
Data type for property	Ensures values conform to expected data types	Text found in a numeric age field
Time sequence consistency	Identifies implausible event sequences	Discharge date before admission date
Diagnosis for gender consistency	Detects diagnoses incompatible with a patient's gender	Prostate cancer assigned to a female patient
Diagnosis for age consistency	Flags diagnoses that are incompatible with a patient's age	Lung cancer diagnosed in an infant
Procedure for gender consistency	Detects gender-incompatible procedures	Hysterectomy assigned to a male patient
Procedure for age consistency	Flags procedures that are inappropriate for the patient's age	Radiotherapy procedure in a toddler

[a]AIDAVA: artificial intelligence–powered data curation and validation.

Data Quality Instruments

The AIDAVA framework relies on a robust instrument for scalable and automated data quality assessment: the SHACL. As a World Wide Web Consortium standard, SHACL defines and enforces semantic and structural constraints on Resource Description Framework (RDF) KGs, enabling rule-based validation to detect inconsistencies, missing elements, and structural misalignments.

Within the AIDAVA framework, SHACL validation rules are categorized into 2 types, as outlined in Table 2: ontology-based and domain-specific rules. Each category includes several validation rules, technically known as SHACL shapes—an SHACL term referring to rule templates that define how data should conform to expected structures or values. The number of rules differs between categories due to the nature of the information being encoded. For instance, completeness checks such as "essential variable" rely on the fully connected structure of the admission node to validate the presence of key attributes (eg, admission date and discharge status) across sources. In contrast, rules such as "diagnosis for gender" require a distinct SHACL shape for each valid gender related pairing (eg, "prostate cancer – male" and "ovarian cancer – female"), increasing the number of shapes. Table 2 shows the number of SHACL shapes associated with each rule category, reflecting the complexity and granularity of the validations.

To enable meaningful evaluation of data quality across different rule categories, we use normalized data quality scores rather than raw violation counts. This is necessary because the number of rules (SHACL shapes) and corresponding checked nodes varies significantly by category (Table 2). Violation counts alone would disproportionately reflect rule volume rather than actual quality trends. We calculate a category-specific quality score using the formula:

$$\textit{Quality score} = 1 - e$$

Where e represents the error rate, calculated as the violation count divided by the total number of checked nodes. This provides a relative measure of how well the data conforms to the specified rules within each category.

XSL•FO
RenderX

Table 2. Categories and counts of SHACL[a] validation rules in the AIDAVA[b] framework.

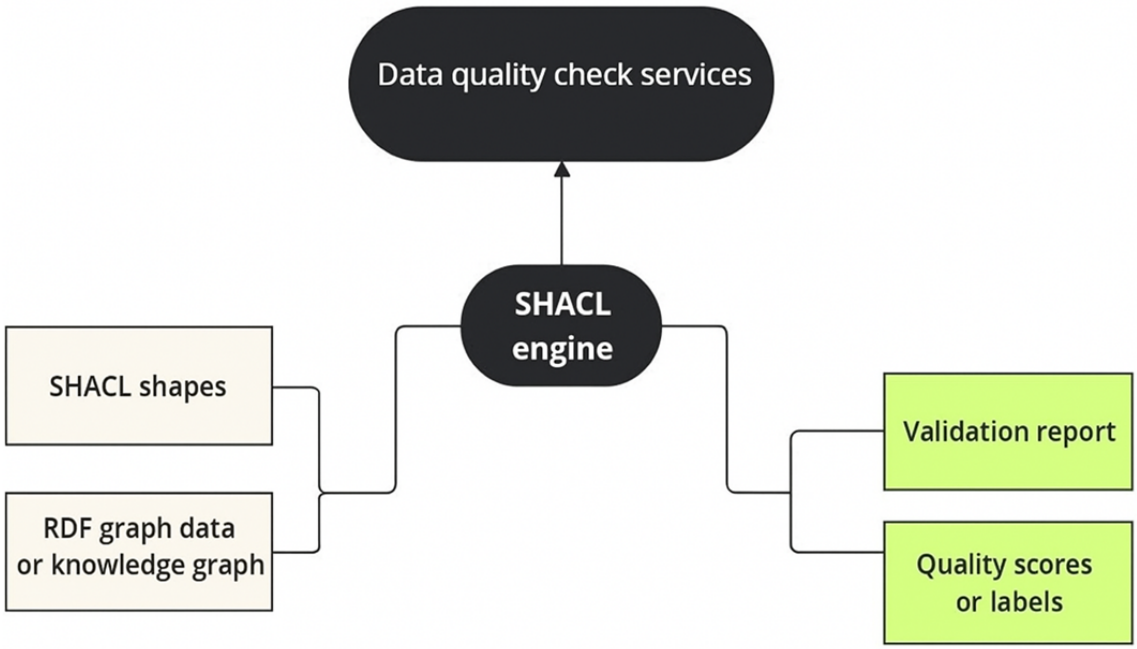
Type and category	SHACL shape count
Ontology-based checks	
Essential variable completeness (eg, admission date must be present)	14
Conditional variable completeness (eg, discharge status cannot be validated without discharge time)	1
Data type for property (eg, age must be a number, not text)	6
Medical and common-sense checks	
Time sequence consistency (eg, admission after discharge flagged as invalid)	6
Diagnosis for gender consistency (eg, female patient assigned prostate cancer code)	5208
Diagnosis for age consistency (eg, infant patient assigned prostate cancer code)	130
Procedure for gender consistency (eg, male patient assigned hysterectomy code)	640
Procedure for age consistency (eg, infant patient assigned colonoscopy procedure)	79

[a]SHACL: Shapes Constraint Language.

Ontology-based rules in the AIDAVA framework are derived from the AIDAVA reference ontology [38], which builds on established standards such as Health Level Seven International FHIR, SNOMED (Systematized Nomenclature of Medicine), and LOINC (Logical Observation Identifiers Names and Codes) to ensure interoperability and support automated curation. These rules ensure conformance with predefined semantic standards, such as verifying data types, relationships, and the presence of mandatory variables. Domain-specific rules are informed by health care–specific knowledge. These rules address real-world data quality challenges, including validating gender-appropriate procedures and ensuring consistency in clinical attributes. The definition and validation of domain-specific rules require expert consensus. However, data quality research has established a variety of validated domain-specific rules over time [39]. The AIDAVA framework leverages these existing, literature-validated rules, allowing it to build upon proven methodologies while avoiding redundancy, ensuring alignment with best practices in health data quality management.

These SHACL shapes are applied within SKGs (intrasource consistency and completeness) and PHKGs (across data source consistency and completeness), ensuring semantic and structural standardization at each stage. Figure 2 illustrates this validation process, applied at both the SHKG and PHKG levels.

Figure 2. SHACL-based data quality check pipeline. RDF: Resource Description Framework; SHACL: Shapes Constraint Language.



The SHACL engine processes health data represented as an RDF graph—a structured format used to build KGs—by applying predefined constraints (SHACL shapes). These rules define the expected structure and content of the data, including semantic relationships and required elements. As the engine executes these rules, it produces an SHACL validation report that highlights data quality violations, such as missing values, incorrect data types, or inconsistent relationships. This validation step is critical for identifying and addressing quality issues before integration into the PHKG.

XSL•FO
RenderX

Methods

Study Design

To evaluate the robustness and effectiveness of the AIDAVA framework in detecting and managing data quality issues, we conducted a controlled experiment using the MIMIC-III (Medical Information Mart for Intensive Care-III) dataset, a publicly available and well-structured critical care database. While MIMIC-III offers a rich and diverse set of clinical variables, it does not contain the types of data quality issues typically encountered in real-world health information systems. As such, this study introduced artificial noise to simulate common completeness and consistency problems found in heterogeneous clinical data. This approach allows us to systematically assess how well the AIDAVA framework, particularly its SHACL-based validation rules, can identify quality issues under different conditions and at multiple stages of data integration. The following subsections describe the dataset, noise injection methodology, and the process of KG construction and validation.

Data Source and Data Preparation

We used the MIMIC-III dataset due to its structured format and breadth of clinical variables, offering an optimal foundation for simulating real-world integration scenarios. The dataset includes deidentified health records from over 58,000 admissions. For this study, hospital admissions lacking relevant diagnosis or procedure codes (as required for SHACL validation) were excluded, resulting in a final cohort of 13,607 admissions. A total of 4 tables were used: PATIENTS, ADMISSIONS, DIAGNOSES_ICD, and CPTEVENTS.

Data cleaning was performed using OpenRefine [40], with date fields standardized to ISO 8601 format (YYYY-MM-DDThh:mm:ss+zz:zz) and gender values mapped to SNOMED CT codes to support interoperability and nonbinary classifications. These steps ensured alignment with the AIDAVA reference ontology and interoperability across sources.

Adding Noise to the Dataset

To simulate real-world data quality challenges [41-43], artificial noise was introduced into the dataset based on 2 parameters: noise level and completeness ratio. Noise level ($\in$ [0,1]) defines the proportion of KG statements impacted by errors. The completeness ratio specifies the share of this noise that results in missing values (as opposed to logically inconsistent entries). For example, a noise level of 0.50 and a completeness ratio of 0.25 imply that 50% of selected statements are altered, with 25% of them made incomplete and the remainder made inconsistent. Noise was introduced across 2 categories: consistency noise, reflecting logical contradictions, and completeness noise simulating missing information. All injections were performed in a reproducible manner using a fixed randomization seed.

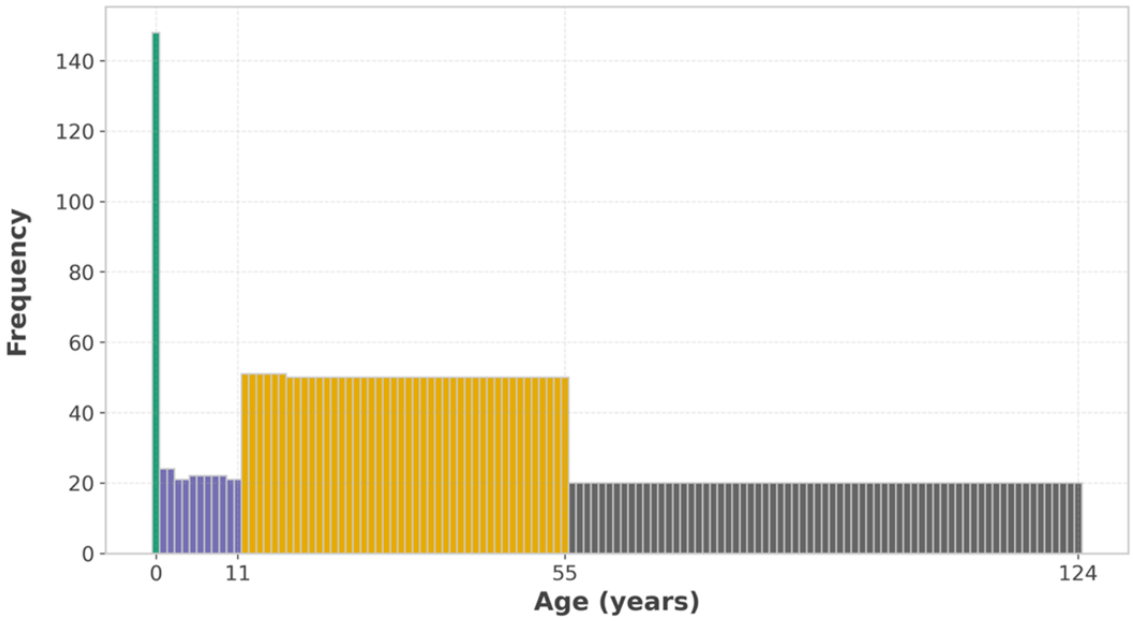
Consistency Noise

We targeted error types that frequently occur in clinical data entry or integration processes [41-43]. These methods included:

1. Gender swapping: male and female values in the PATIENTS table were randomly exchanged. This modification introduced inconsistencies in gender-specific diagnoses and procedures, affecting validation rules such as diagnosis for gender consistency and procedure for gender consistency. Gender values are sampled from a binomial distribution with 2 trials and success probability, P=.5, ensuring a balanced distribution of changes.
2. Age alteration: instead of randomly changing a patient's age, we introduced interval-based errors by defining plausible age groups. These age groups were determined based on clustering patterns observed in diagnosis for age consistency and procedure for age consistency rules (Figure 3). In this implementation, age groups were defined as [0,1] for infants, [1,12] for children, [12,56] for teens and adults, and [56,124] for seniors. Birth years in the PATIENTS table were altered so that a new age was randomly selected from another age group, triggering violations in age-dependent diagnosis and procedure rules. To ensure realistic distribution, the selection of a new age group was sampled using a multinomial distribution with 4 trials, where the event probabilities were weighted based on the frequency of each age group in the dataset.
3. Swapping admission and discharge dates: in the ADMISSIONS table, admission, and discharge dates were swapped. This modification introduced inconsistencies relevant to time-sequence validation rules and triggered errors in age calculations that depended on the admission date.
4. Day-month swapping in dates: day and month values in date fields across PATIENTS, ADMISSIONS, and CPTEVENTS were randomly swapped, leading to invalid date formats where month values exceeded 12, or sequences where the chronological order of events became disrupted. These errors mirrored common data entry mistakes in hospital settings, where clinicians or administrative staff may mistakenly invert date components.
5. Inconsistencies in medical coding: we randomly changed diagnosis and procedure codes in the DIAGNOSES_ICD and CPTEVENTS tables. *ICD-9* (*International Classification of Diseases, Ninth Revision*) diagnosis codes and Current Procedural Terminology procedure codes were replaced with alternative codes randomly drawn from their respective rulesets. This change indirectly caused invalid gender and age violations in both diagnoses and procedures because certain codes are only applicable to specific demographic groups. To implement this, each affected record had its original code excluded and replaced with another randomly sampled value from the remaining choices, ensuring a uniform distribution of errors across the dataset.

XSL•FO
RenderX

Figure 3. Age distribution histogram.



Completeness Noise

Missing data, based on real-world completeness issues, was introduced to replicate the effects of incomplete records on validation outcomes [41-43]. The affected tables and fields were:

1. Patient demographic records: missing values were introduced by randomly removing gender (GENDER) or date of birth fields in the PATIENTS table with equal probabilities of being chosen. This noise is intended to represent missing or deidentified patient information.
2. Hospital admission records: missing values were introduced by deleting admission or discharge timestamps (ADMITTIME, DISCHTIME) as well as admission or discharge locations (ADMISSION_LOCATION, DISCHARGE_LOCATION) from the ADMISSIONS table. As with demographic records, the field to be deleted is chosen with equal percentages of 25%. The selection of omitted records was performed randomly yet consistently across the experiment, preserving the dataset's structural integrity while reflecting real-world gaps in clinical administrative case documentation.
3. Procedure records: missing values were introduced by removing procedure chart dates (CHARTDATE) or procedural codes (CPT_CD) in the CPTEVENTS table. Same with the others, equal probabilities of 0.5 decided which cell type should be deleted. The omission process was randomized across the experiment, replicating common record-keeping errors that lead to incomplete procedural documentation.
4. Diagnosis records: missing values were introduced by deleting *ICD-9* diagnosis codes (ICD9_CODE) from the DIAGNOSES_ICD table. As there is only 1 column type able to be deleted, it is chosen with the probability of 1, dissimilar to other categories of introducing completeness noise. This modification simulates errors observed by not typing *ICD* (*International Classification of Diseases*) codes for billing purposes.

While these noise injection scenarios may overlap in their effects, the incompleteness was introduced independently at this stage. The combined effects of the above, as they relate to triage and patient data acquisition progressions, are further elaborated and investigated in the following section. To account for the randomness in choosing the cell types to be deleted, this process was carried out in a reproducible manner using a fixed randomization seed.

Data Integration and Data Quality Assessment

After noise injection, the dataset was mapped into SKGs using RDFCraft [44], aligning data elements to the AIDAVA reference ontology. These SKGs were then integrated into a unified PHKG, following a typical data ingestion workflow. We began with demographic information from the PATIENTS table, which provided key patient attributes. Next, temporal data from the ADMISSIONS table was incorporated, establishing admission and discharge events. This was followed by procedural details from the CPTEVENTS table, and finally, diagnostic information from the DIAGNOSES_ICD table. This stepwise integration reflects a typical hospital workflow, where patient registration occurs first, followed by admissions, treatments, and recorded diagnoses. At each step, SHACL validation rules were applied to assess data quality in terms of completeness and consistency. As each patient is modeled as an independent SKG, SHACL validation can be parallelized across patients, supporting scalable execution on large datasets. This staged validation aligns with levels 2 and 3 of the AIDAVA framework and reflects both intrasource and cross-source quality checks.

To evaluate the effect of the order of data addition on data quality, alternative sequences were also tested by changing the ingestion order (eg, loading procedures or diagnoses before demographics). This allows us to observe how quality issues propagate or get masked depending on integration order.

XSL•FO
RenderX

Results

Overview

The integration process followed a sequential order, beginning with the PATIENTS table, followed by ADMISSIONS, CPTEVENTS, and DIAGNOSES_ICD tables. The framework assessed completeness and consistency at each stage, tracking how data quality changed throughout the process. To evaluate the robustness of the framework, we also conducted an alternative integration sequence, starting with CPTEVENTS, followed by DIAGNOSES_ICD, ADMISSIONS, and finally PATIENTS.

In the following section, we first present the baseline data quality assessment without noise, establishing a reference for comparison. We then provide the final data quality scores after full integration across varying noise levels for both integration orders, highlighting key trends. A detailed breakdown of progressive changes at specific noise levels is available in Multimedia Appendix 1.

Data Quality Assessment Without Noise

The baseline analysis, presented in Table 3, was conducted without artificial noise to establish a reference for data quality. The results showed that most dimensions and categories achieved nearly perfect quality scores, indicating that the integration process preserved data integrity and did not amplify errors. “Essential variable” completeness remained at 100% (13,607 of 13,607 admissions), confirming that all mandatory data elements were present in the KG. The domain consistency checks for diagnosis and gender, as well as diagnosis and age, yielded perfect quality scores. Similarly, data type adherence at all integration stages is achieved with no errors.

Table 3. Baseline data quality analysis results.

Dimension and category	PATIENTS	ADMISSIONS	CPTEVENTS	DIAGNOSES_ICD
Completeness				
Essential variable (%)	100	100	100	100
Conditional variable (%)	N/A[a]	N/A	N/A	100
Consistency				
Time sequence (%)	100	99.9	99.9	99.9
Diagnosis for gender (%)	100	100	100	100
Procedure for gender (%)	100	100	100	100
Diagnosis for age (%)	100	100	100	100
Procedure for age (%)	100	100	99.89	99.89
Data type for property (%)	100	100	100	100

[a]N/A: not applicable.

Although overall data quality is high, minor discrepancies were observed in specific categories. “Conditional variable” completeness category assesses whether all necessary concepts from different sources are properly integrated and complete. As SHACL rules evaluate conditional variables across every table, an incomplete graph would return 0% (0 of 13,607 admissions) quality score until the last stage of integration. To reflect this dependency, the “conditional variable” completeness scores for PATIENTS, ADMISSIONS, AND CPTEVENTS were marked as “N/A” because these values would not be meaningful to assess. Only at the DIAGNOSES_ICD stage could this category be properly evaluated, where all variable nodes will be reachable.

The procedure for gender and age categories received near-perfect scores of 99.99% (13,606 of 13,607 admissions) and 99.89% (13,593 of 13,607 admissions), respectively. These errors were not due to integration issues, but rather pre-existing errors in the MIMIC-III dataset. The errors in the “procedure for age” category originated from the dataset’s deidentification process, which assigned a few birth dates to years in the 1800s, resulting in implausible patient ages exceeding 300 years—a violation of age-related consistency rules. Similarly, errors in the “procedure for gender” category were traced to a data entry mistake in MIMIC-III, where a laparoscopic procedure on the oviduct or ovary (Current Procedural Terminology 58660) was attributed to a male patient. Additionally, time sequence consistency scored 99.9% (13,594 of 13,607 admissions), with errors primarily linked to discharge times recorded earlier than admission times. This discrepancy is a known artifact of the MIMIC-III data collection process, likely caused by inconsistent timestamp recording practices [45].

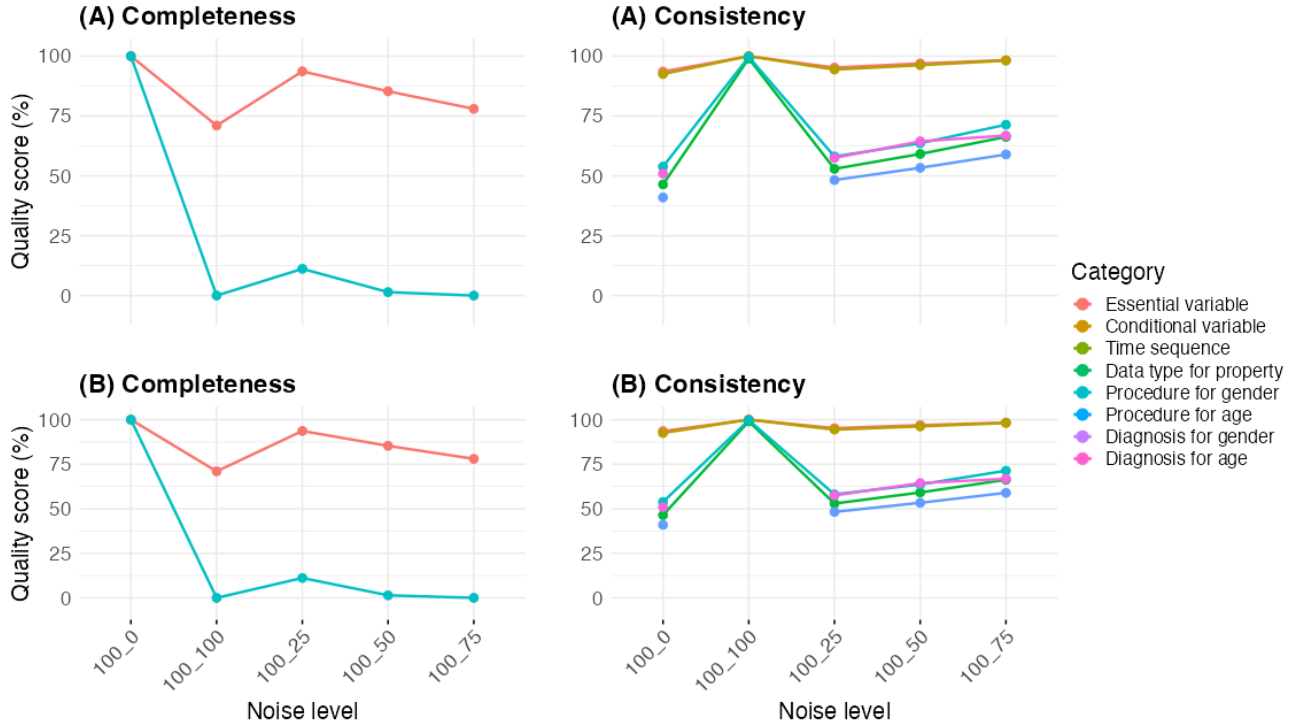
Data Quality Assessment With Noise

Overall Trends Across All Noise Levels

To simulate real-world data quality challenges, we introduced artificial noise and repeated the integration process under 2 different orders. Figure 4 presents the final data quality scores after full integration for both orders. The results confirm that data quality scores remained consistent regardless of integration sequence, indicating that the order of data source integration does not alter overall data quality scores. While intermediate values may vary slightly, the progression of completeness and consistency follows the same overall patterns.

XSL•FO
RenderX

Figure 4. Final data quality scores after full integration.



"Essential variable" completeness declined gradually from 100% to 71% (9661 of 13,607 admissions), with the largest drop occurring between 100_0 (100%) and 100_25 (93.65%), continuing to decrease at higher noise levels. "Conditional variable" completeness dropped sharply from 100% to 11.17% (1521 of 13,607 admissions) at 100_25, reaching near zero at higher noise levels, reflecting its strong dependence on cross-source relationships.

Time sequence and data type consistency improved throughout the integration, rising from 93.57% (12,732 of 13,607 admissions) and 92.51% (12,588 of 13,607 admissions) at 100_0 to 100% at 100_100. Procedure consistency for gender and age increased, starting at 46.43% (6136 of 13,607 admissions) and 53.86% (7329 of 13,607 admissions), respectively, and reaching 99.01% (13,472 of 13,607 admissions) and 99.68% (13,563 of 13,607 admissions) at 100_100. Diagnosis consistency for gender and age followed a different pattern, increasing steadily from 40.98% (5576 of 13,607 admissions) and 50.91% (6927 of 13,607 admissions) at 100_0 to 58.94% (8021 of 13,607 admissions) and 66.82% (9089 of 13,607 admissions) at 100_75, but both became unmeasurable at 100_100.

Detailed Analysis at 100% Consistency and 50% Completeness Noise (100_50)

To gain deeper insights into how data quality changes during data integration under specific noise levels, this section provides a detailed analysis of the 100_50 noise level. Figure 5 presents the data quality scores at each step of the integration process, illustrating how completeness and consistency evolve as new data sources are incorporated.

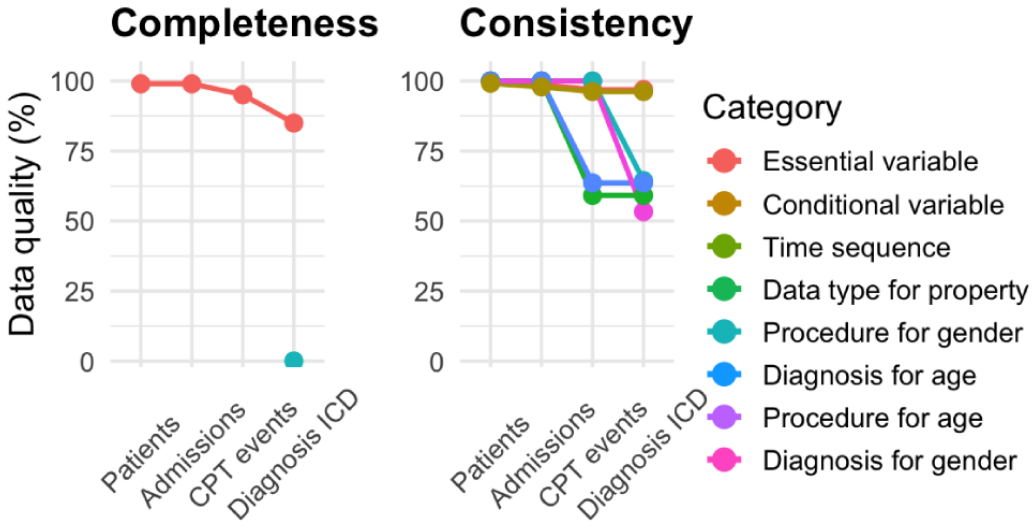
At this noise level, where consistency noise is set to 100% and completeness noise to 50%, all relevant KG statements (100%) are modified, with 50% of them containing missing data. The introduction of ADMISSIONS caused time sequence consistency to decrease slightly to 98.64% (13,422 of 13,607 admissions). With CPTEVENTS added, this metric dropped to 96.94% (13,191 of 13,607 admissions), where it remained stable after DIAGNOSES_ICD. Procedure consistency for gender declined to 59.14% (8047 of 13,607 admissions), while procedure consistency for age dropped to 63.63% (8658 of 13,607 admissions).

As expected, missing data impacted completeness measures. "Essential variable" completeness declined sharply, reaching 85% after DIAGNOSES_ICD. "Conditional variable" completeness remained "N/A" for PATIENTS, ADMISSIONS, and CPTEVENTS. Once DIAGNOSES_ICD was incorporated, "conditional variable" completeness increased slightly to 1.45% (195 of 13,607 admissions), reflecting a minimal recovery of required data.

An analysis of data quality trends across other noise levels is provided in Multimedia Appendix 1, detailing variations in completeness and consistency scores under different conditions.

XSL•FO
RenderX

Figure 5. Data quality scores at each step of the integration process. CPT: Current Procedural Terminology; ICD: International Classification of Diseases.



Discussion

Principal Findings

Our findings demonstrate consistent patterns in data quality dynamics across all noise levels, characterized by a progressive degradation in consistency scores and a steady decline in completeness as noise levels increase. The category of "essential variable" completeness deteriorates gradually as noise accumulates, while "conditional variable" completeness declines more sharply due to its dependence on relationships across data sources. Meanwhile, "time sequence" and "data type consistency" remain relatively stable, whereas procedure and diagnosis consistency degrade significantly based on integration order, underscoring the importance of cross-source attribute alignment.

These trends confirm the adaptability of the AIDAVA data quality framework, which maintains stability in core structural checks (eg, time and data type validation) even as data volume and disorder increase. AIDAVA's patient-level modularity enables SHACL validation to be performed independently per patient, supporting parallel processing and scalability. This design allows for incremental integration of new patient data without reprocessing the full dataset, making the framework suitable for real-time or batch-based deployments. However, the results also revealed that procedure and diagnosis consistency were more sensitive to integration order, emphasizing the need for targeted, domain-specific validation strategies during data merging.

To more explicitly frame these insights, the AIDAVA framework not only detects data quality issues with high granularity but also enables their continuous assessment throughout the integration pipeline. By embedding SHACL-based rules directly into the SKG and PHKG construction process, AIDAVA captures completeness and consistency violations both within and across data sources. This staged, rule-based validation empowers the framework to not only detect anomalies but also manage them by pinpointing their origin and timing—enabling early intervention and downstream reliability.

Completeness and Conditional Dependencies in Data Integration

When examining the completeness dimension, the results reveal distinct patterns of degradation across our 2 categories: "essential variable" and "conditional variable" completeness. As expected, both categories are increasingly affected as the completeness ratio level rises. However, their rates of decline differ, highlighting important nuances in their behavior during the integration process. "Essential variable" completeness steadily declines, suggesting that core patient attributes are progressively impacted by noise—particularly those embedded in the PATIENTS table. In contrast, "conditional variable" completeness cannot be meaningfully assessed until the final integration step, as it depends on the availability of interconnected variables across all datasets. This explains why intermediate scores are marked as "N/A" and only become valuable after the final source (DIAGNOSES_ICD) is added.

These findings emphasize that "conditional variable" completeness is inherently linked to the integration process itself rather than noise alone. Unlike "essential variable" completeness, which is primarily affected by missing values within a single dataset, "conditional variable" completeness is more directly influenced by the presence or absence of cross-source relationships. As a result, its behavior differs from other completeness measures, demonstrating that missing values alone do not dictate "conditional variable" completeness trends—rather, it is the sequence and completeness of integrated sources that determine its final value.

Consistency Challenges in Stepwise Data Integration

The consistency results reveal that step-by-step integration of data sources introduces challenges related to compliance with data type and time sequence consistency. However, these declines are relatively minor, suggesting that the overall format

XSL•FO
RenderX

of the ontology remains stable and that temporal relationships are preserved throughout the integration process. Notably, time sequence consistency exhibits only minor fluctuations, reinforcing its resilience to integration steps. In contrast, the categories related to procedure consistency and diagnosis consistency show more pronounced declines, highlighting the critical role of integration order in determining data quality outcomes. The results indicate that integrating the CPTEVENTS table first has a substantial impact on procedure consistency, causing notable drops in gender and age consistency. Similarly, the integration of DIAGNOSES_ICD exacerbates diagnosis-related inconsistencies, suggesting that diagnostic data is particularly vulnerable to integration-induced errors. This trend highlights that procedure and diagnosis consistency are more reliant on cross-source relationships and attribute alignment than on other categories, such as data type and time sequence consistency.

The findings suggest that a case-specific data quality strategy is essential when integrating different types of health data. This underscores the need for tailored validation approaches that consider the vulnerabilities of various clinical data types during integration. This need for targeted strategies is evident both within and across data quality dimensions. For instance, within consistency, procedure, and diagnosis categories exhibit greater instability, highlighting that medical domain-specific content is more sensitive to inconsistencies than general data attributes such as timestamps or data types.

Interdependencies Between Data Quality Dimensions

Beyond individual dimensions, these findings offer an in-depth perspective on the interrelationships between data quality dimensions, reinforcing the complex and dynamic nature of data quality in health data integration. While previous research has suggested that data quality dimensions are interrelated [42,46], our results offer a unique demonstration of how these interdependencies manifest in real-world integration scenarios. A key finding from the results is that consistency measures alone cannot be fully trusted without ensuring adequate completeness. The results reveal that missing data directly impacts the interpretability of consistency scores, making it difficult to determine whether the observed consistency is genuine or merely an artifact of incomplete data. When key information is missing, certain contradictions—such as conflicts between diagnoses and procedures—may go undetected, creating a false impression of data reliability.

These insights highlight the critical need for health data integration strategies that not only address individual data quality dimensions but also account for their interdependencies. Overlooking these relationships can lead to misleading assessments, where high consistency scores mask underlying data gaps, or missing values distort the true extent of consistencies. To ensure reliable data quality assessment, integration of data must prioritize completeness validation before consistency assessment, ensuring that inconsistencies are accurately detected rather than artificially hidden. By adopting an approach that considers both dimension-specific vulnerabilities and their cross-dimensional effects, we can enhance the integrity of downstream analyses, clinical decision-making, and secondary research applications—ultimately improving the reliability of integrated health data. Overall, our findings demonstrate that ontology-constrained SHACL validation enables interpretable, dynamic assessment of health data quality, with robustness across integration orders and degradation levels. This paper also extends prior research [47] (REF) by embedding semantic and clinical context into the data validation process. While existing tools such as OHDSI's Data Quality Dashboard provide valuable population-level data quality checks after extract, transform, load into the OMOP common data model (eg, conformance, completeness, and plausibility), AIDAVA complements these approaches by offering patient-level validation throughout the integration pipeline. This facilitates early detection and localized resolution of issues that might otherwise remain hidden in aggregate-level analyses.

Limitations

Several limitations must be acknowledged to contextualize the findings and guide future research directions. First, this study was conducted using the MIMIC-III dataset, a structured and deidentified critical care database. While this dataset provides a controlled environment for testing data integration, it does not fully capture the heterogeneity and complexity of live health care data environments. Relying on a single dataset also limits the generalizability of our findings, as results may differ across other institutions, coding practices, and patient populations. Although MIMIC-III was chosen for its structured format and public availability, access to additional well-curated benchmark datasets remains restricted due to privacy, licensing, and interoperability constraints. Future research should evaluate the framework on diverse, nondeidentified hospital datasets that better reflect real-world conditions. Second, this study simulated real-world data quality issues by introducing structured artificial noise, allowing for a systematic evaluation of the framework under different levels of data inconsistencies. However, artificial noise does not fully replicate the unpredictability of errors found in operational health data. Health datasets often contain context-dependent inconsistencies, undocumented missingness patterns, and human-introduced biases that cannot be easily simulated. Future research should explore how the framework performs when applied in a real-world scenario. Third, the AIDAVA framework evaluated consistency and completeness as the core data quality dimensions. However, other important dimensions, such as timeliness and uniqueness, were not explicitly assessed in this study. Future work should extend the framework to incorporate a broader range of quality dimensions, ensuring a more complete evaluation of integrated health data. Last, this study demonstrated the effectiveness of the AIDAVA framework in a controlled dataset; its scalability for large-scale, high-velocity health data integration was not examined in depth. Future research should investigate the framework's performance in large-scale deployments. Finally, while AIDAVA was tested using structured simulations, adapting the framework for use with unstructured or semistructured real-world data (eg, electronic health records or clinical registries) remains a future challenge. These sources often include free text, heterogeneous coding, and loosely structured formats that require preprocessing steps (eg, terminology mapping). Investigating these adaptations

XSL•FO
RenderX

is part of the ongoing research agenda within the AIDAVA project.

Conclusions

This study evaluated the AIDAVA data quality framework for its effectiveness in detecting and managing data quality issues—specifically completeness and consistency—during the integration of heterogeneous health data. Using the MIMIC-III dataset, we simulated real-world challenges by introducing structured noise and systematically assessed how the framework performed across different integration sequences and noise levels. The staged SHACL-based validation enabled fine-grained analysis of data quality at multiple points along the integration pipeline. Our findings show that the AIDAVA framework successfully identifies both missing and inconsistent data elements and provides interpretable feedback at each stage of transformation. Together, these findings support the AIDAVA framework's suitability for dynamic, life cycle–based data quality assessment. By enabling validation at each transformation step, the framework allows early detection, interpretable tracking, and strategic mitigation of data quality issues. Importantly, it encourages a holistic view of data quality—one that considers not only dimension-specific weaknesses but also how dimensions influence each other across the pipeline. As health systems increasingly rely on integrated datasets for clinical and research applications, frameworks such as AIDAVA provide essential infrastructure for building trust in secondary health data use.

Future Research

Future work should focus on improving the AIDAVA data quality framework by aligning SHACL shapes with the OMOP common data model [41] and comparing multiple integration orders to assess their impact on data quality. Developing an OMOP-based RDF schema and implementing SHACL constraints would also support interoperability with OHDSI tools and promote the broader adoption of semantic, constraint-driven approaches to data quality. Expanding SHACL validation to laboratory results, prescriptions, and other hospital records will enhance its clinical applicability. Additionally, developing more realistic noise introduction methods will better simulate real-world inconsistencies, strengthening the framework's robustness.

Acknowledgments

The authors are grateful to all the members of the AIDAVA consortium who diligently support the project with their expertise. A special thanks goes to the team at the Department of Advanced Computing Sciences, Institute of Data Science at Maastricht University, for their invaluable contributions in setting up the experiment and developing the mechanism for noise addition, which was essential for this study. The authors declare that financial support was received for the research, authorship, or publication of this paper. This work was supported by the European Union's Horizon Europe research and innovation program under grant agreements No. 101057062 (AIDAVA). Supported by a license waiver from SNOMED (Systematized Nomenclature of Medicine) International for a period of 2 years (2024-2025), on condition that SNOMED CT (Systematized Nomenclature of Medicine – Clinical Tems) is not used or deployed commercially. The work of the Swiss Partner (MIDATA) received funding by the Swiss State Secretariat for Education, Research and Innovation (SBFI), subvention contract 22.00093, REF-1131-52104.

Conflicts of Interest

None declared.

Multimedia Appendix 1
A detailed breakdown of progressive changes at specific noise levels and analysis of data quality trends across other noise levels.
[DOCX File , 439 KB - medinform_v13i1e75275_app1.docx]

References

1. Beresniak A, Schmidt A, Proeve J, Bolanos E, Patel N, Ammour N, et al. Cost-benefit assessment of using electronic health records data for clinical research versus current practices: contribution of the electronic health records for clinical research (EHR4CR) European Project. Contemp Clin Trials 2016;46:85-91. [doi: 10.1016/j.cct.2015.11.011] [Medline: 26600286]
2. van Drumpt S, Chawla K, Barbereau T, Spagnuelo D, van de Burgwal L. Secondary use under the European Health Data Space: setting the scene and towards a research agenda on privacy-enhancing technologies. Front Digit Health 2025;7:1602101 [FREE Full text] [doi: 10.3389/fdgth.2025.1602101] [Medline: 40613075]
3. De Moor G, Sundgren M, Kalra D, Schmidt A, Dugas M, Claerhout B, et al. Using electronic health records for clinical research: the case of the EHR4CR project. J Biomed Inf 2015;53:162-173 [FREE Full text] [doi: 10.1016/j.jbi.2014.10.006] [Medline: 25463966]
4. Saelaert M, Mathieu L, Van Hoof W, Devleesschauwer B. Expanding citizen engagement in the secondary use of health data: an opportunity for national health data access bodies to realise the intentions of the European Health Data Space. Arch Public Health 2023;81(1):168 [FREE Full text] [doi: 10.1186/s13690-023-01182-4] [Medline: 37700330]

XSL•FO
RenderX

5. Krusche P, Trigg L, Boutros PC, Mason CE, De La Vega FM, Moore BL, Global Alliance for GenomicsHealth Benchmarking Team. Best practices for benchmarking germline small-variant calls in human genomes. Nat Biotechnol 2019;37(5):555-560 [FREE Full text] [doi: 10.1038/s41587-019-0054-x] [Medline: 30858580]
6. Alonzo TA. Clinical prediction models: a practical approach to development, validation, and updating: by Ewout W. Steyerberg. Am J Epidemiol 2009 May 28;170(4):528. [doi: 10.1093/aje/kwp129] [Medline: 15583369]
7. Rajkomar A, Oren E, Chen K, Dai AM, Hajaj N, Hardt M, et al. Scalable and accurate deep learning with electronic health records. npj Digit Med 2018;1:18 [FREE Full text] [doi: 10.1038/s41746-018-0029-1] [Medline: 31304302]
8. Bernardi FA, Alves D, Crepaldi N, Yamada DB, Lima VC, Rijo R. Data quality in health research: integrative literature review. J Med Internet Res 2023;25:e41446 [FREE Full text] [doi: 10.2196/41446] [Medline: 37906223]
9. Shara N, Anderson KM, Falah N, Ahmad MF, Tavazoei D, Hughes JM, et al. Early identification of maternal cardiovascular risk through sourcing and preparing electronic health record data: machine learning study. JMIR Med Inf 2022;10(2):e34932 [FREE Full text] [doi: 10.2196/34932] [Medline: 35142637]
10. Wei W, Leibson CL, Ransom JE, Kho AN, Caraballo PJ, Chai HS, et al. Impact of data fragmentation across healthcare centers on the accuracy of a high-throughput clinical phenotyping algorithm for specifying subjects with type 2 diabetes mellitus. J Am Med Inf Assoc 2012;19(2):219-224 [FREE Full text] [doi: 10.1136/amiajnl-2011-000597] [Medline: 22249968]
11. Turbow SD, Ali MK, Culler SD, Rask KJ, Perkins MM, Clevenger CK, et al. Association of fragmented readmissions and electronic information sharing with discharge destination among older adults. JAMA Netw Open 2023;6(5):e2313592 [FREE Full text] [doi: 10.1001/jamanetworkopen.2023.13592] [Medline: 37191959]
12. Razzaghi H, Greenberg J, Bailey LC. Developing a systematic approach to assessing data quality in secondary use of clinical data based on intended use. Learn Health Syst 2022;6(1):e10264 [FREE Full text] [doi: 10.1002/lrh2.10264] [Medline: 35036548]
13. Huang Y, Guo J, Chen Z, Xu J, Donahoo WT, Carasquillo O. The impact of electronic health records (EHR) data continuity on prediction model fairness and racial-ethnic disparities. arXiv Preprint posted online on September 5, 2023. [doi: 10.48550/arXiv.2309.01935]
14. Li Y, Sperrin M, Martin G, Ashcroft D, van Staa TP. Examining the impact of data quality and completeness of electronic health records on predictions of patients' risks of cardiovascular disease. Int J Med Inf 2020;133:104033. [doi: 10.1016/j.ijmedinf.2019.104033] [Medline: 31785526]
15. Declerck J, Vandenberk B, Deschepper M, Colpaert K, Cool L, Goemaere J, et al. Building a foundation for high-quality health data: multihospital case study in Belgium. JMIR Med Inf 2024;12:e60244 [FREE Full text] [doi: 10.2196/60244] [Medline: 39727158]
16. Deng Y, Jiang X, Long Q. Privacy-preserving methods for vertically partitioned incomplete data. AMIA Annu Symp Proc 2020;2020:348-357 [FREE Full text] [Medline: 33936407]
17. Verheij RA, Curcin V, Delaney BC, McGilchrist MM. Possible sources of bias in primary care electronic health record data use and reuse. J Med Internet Res 2018;20(5):e185 [FREE Full text] [doi: 10.2196/jmir.9134] [Medline: 29844010]
18. Lucero RJ, Kearney J, Cortes Y, Arcia A, Appelbaum P, Fernández RL, et al. Benefits and risks in secondary use of digitized clinical data: views of community members living in a predominantly ethnic minority urban neighborhood. AJOB Empir Bioeth 2015;6(2):12-22 [FREE Full text] [doi: 10.1080/23294515.2014.949906] [Medline: 26101782]
19. Declerck J, Kalra D, Vander Stichele R, Coorevits P. Frameworks, dimensions, definitions of aspects, and assessment methods for the appraisal of quality of health data for secondary use: comprehensive overview of reviews. JMIR Med Inf 2024;12:e51560 [FREE Full text] [doi: 10.2196/51560] [Medline: 38446534]
20. Bian J, Lyu T, Loiacono A, Viramontes TM, Lipori G, Guo Y, et al. Assessing the practice of data quality evaluation in a national clinical data research network through a systematic scoping review in the era of real-world data. J Am Med Inf Assoc 2020;27(12):1999-2010 [FREE Full text] [doi: 10.1093/jamia/ocaa245] [Medline: 33166397]
21. Kahn MG, Callahan TJ, Barnard J, Bauck AE, Brown J, Davidson BN, et al. A harmonized data quality assessment terminology and framework for the secondary use of electronic health record data. EGEMS (Wash DC) 2016;4(1):1244 [FREE Full text] [doi: 10.13063/2327-9214.1244] [Medline: 27713905]
22. Liaw S, Guo JGN, Ansari S, Jonnagaddala J, Godinho MA, Borelli AJ, et al. Quality assessment of real-world data repositories across the data life cycle: a literature review. J Am Med Inf Assoc 2021;28(7):1591-1599 [FREE Full text] [doi: 10.1093/jamia/ocaa340] [Medline: 33496785]
23. Ozonze O, Scott PJ, Hopgood AA. Automating electronic health record data quality assessment. J Med Syst 2023;47(1):23 [FREE Full text] [doi: 10.1007/s10916-022-01892-2] [Medline: 36781551]
24. Weiskopf NG, Bakken S, Hripcsak G, Weng C. A data quality assessment guideline for electronic health record data reuse. EGEMS (Wash DC) 2017;5(1):14 [FREE Full text] [doi: 10.5334/egems.218] [Medline: 29881734]
25. Sendak M, Sirdeshmukh G, Ochoa T, Premo H, Tang L, Niederhoffer K. Development and validation of ML-DQA – a machine learning data quality assurance framework for healthcare. Proceedings of the 7th Machine Learning for Healthcare Conference; Proceedings of Machine Learning Research: PMLR 2022;182:741-759.
26. Seitl F, Kovárík T, Mirshahi S, Krystufek J, Dujava R, Ondreicka M. Assessing the quality of information extraction. arXiv Preprint posted online on May 22, 2024. [doi: 10.48550/arXiv.2404.04068]

XSL•FO
RenderX

27. Azeroual O, Saake G, Abuosba M, Schöpfel J. Text data mining and data quality management for research information systems in the context of open data and open science. arXiv Preprint posted online on December 11, 2018. [doi: 10.48550/arXiv.1812.04298]
28. Palojoki S, Lehtonen L, Vuokko R. Semantic interoperability of electronic health records: systematic review of alternative approaches for enhancing patient information availability. JMIR Med Inf 2024;12:e53535 [FREE Full text] [doi: 10.2196/53535] [Medline: 38686541]
29. Hendler J. Data integration for heterogenous datasets. Big Data 2014;2(4):205-215 [FREE Full text] [doi: 10.1089/big.2014.0068] [Medline: 25553272]
30. AIDAVA. 2025. URL: https://www.aidava.eu/ [accessed 2025-10-24]
31. Juran JM, Gryna FM, Bingham RS. Quality Control Handbook. New York: McGraw-Hill; 1974.
32. Liaw S, Rahimi A, Ray P, Taggart J, Dennis S, de Lusignan S, et al. Towards an ontology for data quality in integrated chronic disease management: a realist review of the literature. Int J Med Inf 2013;82(1):10-24. [doi: 10.1016/j.ijmedinf.2012.10.001] [Medline: 23122633]
33. Issa S, Adekunle O, Hamdi F, Cherfi SS, Dumontier M, Zaveri A. Knowledge graph completeness: a systematic literature review. IEEE Access 2021;9:31322-31339. [doi: 10.1109/access.2021.3056622]
34. Huser V, DeFalco FJ, Schuemie M, Ryan PB, Shang N, Velez M, et al. Multisite evaluation of a data quality tool for patient-level clinical data sets. EGEMS (Wash DC) 2016;4(1):1239 [FREE Full text] [doi: 10.13063/2327-9214.1239] [Medline: 28154833]
35. Ghalavand H, Shirshahi S, Rahimi A, Zarrinabadi Z, Amani F. Common data quality elements for health information systems: a systematic review. BMC Med Inf Decis Mak 2024;24(1):243 [FREE Full text] [doi: 10.1186/s12911-024-02644-7] [Medline: 39223578]
36. Schmidt L, Finnerty Mutlu AN, Elmore R, Olorisade BK, Thomas J, Higgins JPT. Data extraction methods for systematic review (semi)automation: update of a living systematic review. F1000Res 2021;10:401 [FREE Full text] [doi: 10.12688/f1000research.51117.3] [Medline: 34408850]
37. Schmidt CO, Struckmann S, Enzenbach C, Reineke A, Stausberg J, Damerow S, et al. Facilitating harmonized data quality assessments. A data quality framework for observational health research data collections with software implementations in R. BMC Med Res Methodol 2021;21(1):63 [FREE Full text] [doi: 10.1186/s12874-021-01252-7] [Medline: 33810787]
38. de Zegher I, Norak K, Steiger D, Müller H, Kalra D, Scheenstra B, et al. Artificial intelligence based data curation: enabling a patient-centric European health data space. Front Med (Lausanne) 2024;11:1365501 [FREE Full text] [doi: 10.3389/fmed.2024.1365501] [Medline: 38813389]
39. Mohamed Y, Song X, McMahon TM, Sahil S, Zozus M, Wang Z, Greater Plains Collaborative, et al. Electronic health record data quality variability across a multistate clinical research network. J Clin Transl Sci 2023;7(1):e130 [FREE Full text] [doi: 10.1017/cts.2023.548] [Medline: 37396818]
40. Ham K. OpenRefine (version 2.5). http://openrefine.org. Free, open-source tool for cleaning and transforming data. J Med Libr Assoc 2013;101(3):233-234 [FREE Full text] [doi: 10.3163/1536-5050.101.3.020]
41. Lewis AE, Weiskopf N, Abrams ZB, Foraker R, Lai AM, Payne PRO, et al. Electronic health record data quality assessment and tools: a systematic review. J Am Med Inf Assoc 2023;30(10):1730-1740 [FREE Full text] [doi: 10.1093/jamia/ocad120] [Medline: 37390812]
42. Syed R, Eden R, Makasi T, Chukwudi I, Mamudu A, Kamalpour M, et al. Digital health data quality issues: systematic review. J Med Internet Res 2023;25:e42615 [FREE Full text] [doi: 10.2196/42615] [Medline: 37000497]
43. Fraser HSF, Mugisha M, Bacher I, Ngenzi JL, Seebregts C, Umubyeyi A, et al. Factors influencing data quality in electronic health record systems in 50 health facilities in Rwanda and the role of clinical alerts: cross-sectional observational study. JMIR Public Health Surveill 2024;10:e49127 [FREE Full text] [doi: 10.2196/49127] [Medline: 38959048]
44. MaastrichtU-IDS / RDFCraft. 2025. URL: https://github.com/MaastrichtU-IDS/RDFCraft [accessed 2025-10-24]
45. Khaled A, Sabir M, Qureshi R, Camillo M, Caruso, Guarrasi V. Leveraging MIMIC datasets for better digital health: a review on open problems, progress highlights, and future promises. arXiv Preprint posted online on June 15, 2025. [doi: 10.48550/arXiv.2506.12808]
46. Badr N. Guidelines for health IT addressing the quality of data in EHR information systems. 2019 Presented at: Proceedings of the 12th International Joint Conference on Biomedical Engineering Systems and Technologies (BIOSTEC 2019); February 22-24, 2019; Prague, Czech Republic p. 169-181. [doi: 10.5220/0006941001690181]
47. Touré V, Krauss P, Gnodtke K, Buchhorn J, Unni D, Horki P, et al. FAIRification of health-related data using semantic web technologies in the Swiss personalized health network. Sci Data 2023;10(1):127 [FREE Full text] [doi: 10.1038/s41597-023-02028-y] [Medline: 36899064]

Abbreviations

AIDAVA: artificial intelligence–powered data curation and validation
FHIR: Fast Healthcare Interoperability Resources
ICD: International Classification of Diseases

XSL•FO
RenderX

ICD-9: International Classification of Diseases, Ninth Revision
KG: knowledge graph
LOINC: Logical Observation Identifiers Names and Codes
MIMIC-III: Medical Information Mart for Intensive Care-III
OHDSI: Observational Health Data Sciences and Informatics
OMOP: Observational Medical Outcomes Partnership
PHKG: personal health knowledge graph
RDF: Resource Description Framework
SHACL: Shapes Constraint Language
SKG: source knowledge graph
SNOMED: Systematized Nomenclature of Medicine
SNOMED CT: Systematized Nomenclature of Medicine–Clinical Terms

Edited by A Benis; submitted 31.03.25; peer-reviewed by M Yaqub, Y Wang, H Kim; comments to author 16.06.25; revised version received 07.08.25; accepted 06.10.25; published 12.11.25.

Please cite as:
Declerck J, Kılıç ÖD, Emir Erol E, Mehryar S, Kalra D, de Zegher I, Celebi R
Assessing Data Quality in Heterogeneous Health Care Integration: Simulation Study of the AIDAVA Framework
JMIR Med Inform 2025;13:e75275
URL: https://medinform.jmir.org/2025/1/e75275
doi:10.2196/75275
PMID:

©Jens Declerck, Ömer Durukan Kılıç, Ensar Emir Erol, Shervin Mehryar, Dipak Kalra, Isabelle de Zegher, Remzi Celebi. Originally published in JMIR Medical Informatics (https://medinform.jmir.org), 12.11.2025. This is an open-access article distributed under the terms of the Creative Commons Attribution License (https://creativecommons.org/licenses/by/4.0/), which permits unrestricted use, distribution, and reproduction in any medium, provided the original work, first published in JMIR Medical Informatics, is properly cited. The complete bibliographic information, a link to the original publication on https://medinform.jmir.org/, as well as this copyright and license information must be included.

XSL•FO
RenderX

Effects of the National Institutes of Health Stroke Scale and Modified Rankin Scale on Predictive Models of 30-Day Nonelective Readmission and Mortality After Ischemic Stroke: Cohort Study

Mai N Nguyen-Huynh[1,2], MAS, MD; Janet Alexander[1], MSPH; Zheng Zhu[1], MS; Melissa Meighan[3], RN, MS, DNP; Gabriel Escobar[1], MD

[1]Division of Research, Kaiser Permanente, Pleasanton, CA, United States

[2]Department of Neurology, Kaiser Permanente Walnut Creek Medical Center, 1515 Newell Avenue, Walnut Creek, CA, United States

[3]Regional Quality, Accreditation, Regulation & Licensing Department, Kaiser Permanente Foundation Hospitals, Oakland, CA, United States

Corresponding Author:
Mai N Nguyen-Huynh, MAS, MD
Division of Research, Kaiser Permanente, Pleasanton, CA, United States

Abstract

Background: Patients with stroke have high rates of all-cause readmission and case fatality. Limited information is available on how to predict these outcomes.

Objective: We aimed to assess whether adding the initial National Institutes of Health Stroke Scale (NIHSS) score or modified Rankin scale (mRS) score at discharge improved predictive models of 30-day nonelective readmission or 30-day mortality poststroke.

Methods: Using a cohort of patients with ischemic stroke in a large multiethnic integrated health care system from June 15, 2018, to April 29, 2020, we tested 2 predictive models for a composite outcome (30-day nonelective readmission or death). The models were based on administrative data (Length of Stay, Acuity, Charlson Comorbidities, Emergency Department Use score; LACE) as well as a comprehensive model (Transition Support Level; TSL). The models, initial NIHSS score, and mRS scores at discharge, were tested independently and in combination with age and sex. We assessed model performance using the area under the receiver operator characteristic (c-statistic), Nagelkerke pseudo-R^2, and Brier score.

Results: The study cohort included 4843 patients with 5014 stroke hospitalizations. Average age was 71.9 (SD 14) years, 50.6% (2537/5014) were female, and 52.1% (2614/5014) were White. Median initial NIHSS score was 4 (IQR 2-8). There were 538 (10.7%) nonelective readmissions and 150 (3.9%) deaths within 30 days. The logistic models revealed that the best performing models were TSL (c-statistic=0.69) and TSL plus mRS score at discharge (c-statistic=0.69).

Conclusions: We found that neither the initial NIHSS score nor the mRS score at discharge significantly enhanced the predictive ability of the LACE or TSL models. Future efforts at prediction of short-term stroke outcomes will need to incorporate new data elements.

(JMIR Med Inform 2025;13:e69102) doi:10.2196/69102

KEYWORDS

ischemic stroke; readmission; predictive modeling; mortality; National Institutes of Health Stroke Scale; NIHSS; modified Rankin scale; mRS

Introduction

Stroke has a massive impact on patients, their caregivers, and the health system. Approximately 795,000 stroke cases occur annually in the United States. It is the fifth leading cause of death and the leading cause of long-term disability, with nearly 7 million stroke survivors in the United States. With an increasing aging population, it is estimated that nearly 4% of the US adult population would have had a stroke by 2030 [1]. It is all the more tragic that a substantial proportion of stroke survivors will be readmitted to the hospital: current 30-day all-cause readmission rates range from 6.5% - 24.3% and these rates increase to 30% - 62.2% within a year [2]. Mortality following the initial hospitalization is also substantial: the case fatality rate in the hospital is 5% - 7%, increasing to 13% - 15% at 30 days, and 25% - 30% by 1 year [3].

Nearly one-fifth of Medicare beneficiaries discharged from a hospital get readmitted within 30 days [4]. Spurred by a landmark paper by Jencks et al [5] hospitals across the United States have begun implementing strategies to identify and reduce avoidable readmissions. Furthermore, beginning in 2013, 30-day readmission rates for a hospital's Medicare patients with acute

XSL•FO
RenderX

myocardial infarction, heart failure, and pneumonia have been compared with the expected rate of readmissions, using risk adjustment to account for age, gender, medical diagnosis, and selected medical history. Under the Hospital Readmissions Reduction Program, Medicare penalizes hospitals for higher-than-expected rates of readmissions among patients with these diagnoses [6,7]. Additional conditions are likely to be added in the future.

Given the clinical and policy significance of stroke, identifying factors that influence readmission risk is important to assist clinicians and hospitals in the care of patients with stroke and to prevent the preventable. Many factors may contribute to a hospital's readmission rate after stroke, including patient preferences, demographics, socioeconomic status, comorbidities, stroke severity, health system, clinical care or process, and health outcome. It is important that the risk adjustment mechanisms account for these factors so that hospitals caring for a more complex patient mix are not unduly penalized for readmissions.

The purpose of our investigation was to determine whether we could develop predictive models, specific to patients with stroke, for nonelective readmission or death within 30 days after hospital discharge. In these models, we assessed the ability of commonly used administrative data, newer predictors from the electronic health record (EHR), and 2 manually assigned stroke-specific scales (National Institutes of Health Stroke Scale [NIHSS] and modified Rankin scale [mRS]).

Methods

Study Setting

Kaiser Permanente Northern California (KPNC) provides care at 21 Joint Commission certified stroke centers serving 4.5+ million members, who are highly representative of the ethnic and socioeconomic diversity of the surrounding and statewide population [8]. There are approximately 1.3 million ED visits and 3500 ischemic stroke discharges per year. Patients are cared for by a single provider group of 9600 physicians (including approximately 100 neurologists) of The Permanente Medical Group, Inc. In 2016, KPNC implemented the Stroke EXPRESS (Expediting the Process of Evaluating and Stopping Stroke) program [9]. The program included immediate evaluation by a teleneurologist, expedited intravenous thrombolytic treatment, rapid computed tomography angiographic study, and expedited transfer and treatment for patients with large vessel occlusion. Deployment of the Epic EHR [10] was completed in mid-2010.

Study Cohort

The study cohort included patients meeting the following criteria: (1) admitted to a KPNC hospital between June 15, 2018, and April 29, 2020, (2) at least 18 years of age, (c) diagnosis of incident ischemic stroke (*ICD-10* codes: I63.xx, see Multimedia Appendix 1), and (4) for patients who experienced interhospital transport, the first hospital stay was at a KPNC hospital. Patients with in-hospital deaths were excluded from the final analysis of the study cohort.

The dependent variable for our analyses was a composite outcome (nonelective readmission or death within 30 days of discharge from index event). We defined nonelective readmission as one that began in the emergency department. These were captured from KPNC databases using methods we have recently described [11].

Data Collection

We obtained the following data elements for all patients directly from the EHR: demographic data; traditional claims (administrative) data (admission and discharge dates, diagnosis and procedure codes, and discharge disposition); newer clinical data such as laboratory test results; vital signs; neurological examinations as recorded in nursing flow sheets; admission and discharge care directives (code status) [12]; bed histories [13]; and length of stay. We assigned all patients a Charlson Comorbidity Index score [14].

As a measure of stroke severity, we captured the initial NIHSS score [15] electronically from the EHR. NIHSS score ranged from 0 to 42, with higher score indicated higher severity and poorer prognosis. Preferences were given to NIHSS performed by neurologists, then by emergency department physicians, then by hospitalists, and finally by nursing. As a measure of functional status at the time of discharge which may influence the patient's ability to care for self at home and subsequently contribute to readmission, we captured the modified mRS at discharge, which has been mandated for all patients with stroke. The mRS score ranged from 0 to 6, with 0 being no disability and 6 being dead. On a daily basis, the study team identified all patients with stroke admitted in KPNC hospitals. This list was reviewed by 2 research assistants who communicated daily with the local stroke coordinators to ensure that the mRS score has been completed before discharge. If unable to complete before discharge, the research team contacted the patients and their caregivers to complete the equivalent mRS-9Q [16] through phone within 7 days of discharge. The mRS-9Q has been validated for use in person or by telephone.

We also evaluated the following in-hospital data elements as potential predictors: presence of a foley catheter, feeding tube, tracheostomy, peg tube, whether an interpreter was needed, and Functional Independence Measurement (FIM) [17,18] score components. However, the rate of missing data was high without full individual chart reviews (for example, the FIM was only found in 11% of hospitalizations). We did not include these variables in our analyses. Validation of these variables was beyond the scope of our project at this time.

We also captured patients' longitudinal comorbidity burden and severity of illness at admission. At KPNC, all adults with a medical record number are assigned a Comorbidity Point Score monthly, version 2 (COPS2), which is based on CMS Hierarchical Condition Categories (score range, 0 - 1014 [scores above 300 are rare], with higher scores indicating increased mortality risk) [12]. The score is assigned based on all diagnoses a patient has accrued in the preceding 12 months. Patients are also assigned a Laboratory-based Acute Physiology Score, version 2 (LAPS2; range 0 - 414 [scores above 200 are uncommon] on admission and every hour after hospitalization, with higher scores indicating worsening instability). The LAPS2 incorporates patients' vital signs, neurological status checks, pulse oximetry, and 16 laboratory tests. For example, in July

XSL•FO
RenderX

2018, the median hourly LAPS2 among all patients in the intensive care unit was 110, whereas the median ward score was 52. It is not possible to admit a patient to KPNC hospitals without specifying code status, which can be subsequently updated. We classified each patient's care directive as full code or not (which included partial code, do not resuscitate, and comfort care only).

For our outcomes, we examined readmission within 30 days or mortality within 30 days postdischarge. For readmission and mortality within 30 days, there were no missing data. For those who were readmitted to a non-Kaiser hospital, we identified their readmission through claim data. The study was limited to health plan members only, for whom we had full data on mortality.

Using the above data elements, we assigned all patients a LACE (Length of Stay, Acuity, Charlson Comorbidities, Emergency Department Use) score [19], which is commonly employed in some Kaiser Permanente regions as well as in other hospital systems. The LACE is widely used to predict a 30-day readmission or mortality composite outcome. We also assigned patients a Transition Support Level (TSL) score [20]. The TSL, an automated score that was developed in KPNC included the LAPS2, COPS2, recent use, and a patient's care directive on the day of discharge, was assigned in real time daily to all KPNC hospitalized adults.

The paper adheres to recommended reporting guidelines for observational studies, and the STROBE (Strengthening the Reporting of Observational Studies in Epidemiology) guidelines (Checklist 1) were followed.

Statistical Analysis

We performed bivariate comparisons using chi-square and *t* tests. We fit logistic regression models to predict the composite outcome. We tested the following as independent predictors: NIHSS, mRS, LACE, and TSL; the individual components of the LACE and TSL; and combinations of these (NIHSS+age+sex; MRS+age+set; LACE+NIHSS, LACE+MRS; TSL+NIHSS, TSL+MRS). To establish the probable maximum performance of these predictors, we also tested a random forest model that included age, sex, NIHSS, mRS, and all of the individual predictors included in the LACE and TSL.

We evaluated model performance using the area under the receiver operator characteristic curve (c statistic, the Nagelkerke pseudo-R^2, and the Brier score) [21-23]. All models were assessed using 5-fold cross validation, and the models' performance metrics are those based on 5-fold cross validation. All analyses were done in SAS (version 9.3; SAS Institute).

Ethical Considerations

All KPNC facilities are under the jurisdiction of one institutional review board for the protection of human participants. This study was approved by the KPNC Institutional Review Board, which waived the requirement for written informed consent (IRB number: 1279378). Only aggregate data is provided here. Participants received no compenstation from the study.

Results

Between June 15, 2018, and April 29, 2020, there were 5808 hospitalizations for adult patients with ischemic stroke. Of these 5808 hospitalizations, 794 (13.7%) were excluded from the study analysis because the patient died during the index hospitalization (n=198, 3.4%), the hospitalization originated at a non-KPNC facility (n=504, 8.7%), or follow-up data was incomplete (n=92, 1.6%). The final study population included 5014 hospitalizations. The average age of the study population was 71.9 (SD 13.99) years and 49.4% (2477/5014) of patients were male. The racial and ethnic distribution was 52.1% (2614/5014) White, 15.6% (782/5014) Hispanic, 15% (751/5014) Asian, and 14.3% (718/5014) Black. The median initial NIHSS score was 4 (IQR 2-8). The average mRS score at discharge was 2.8 (SD 1.64). Mean length of stay was 6.5 days (SD 7.71), and 55% (2756/5014) were discharged home. Table 1 presents the other characteristics of the study population.

Out of 5014 hospitalizations, 688 (13.7%) had a nonelective readmission within 30 days or died within 30 days postdischarge (composite outcome). Out of 5014 hospitalizations, 492 (9.8%) had a readmission only within 30 days, 150 (3.0%) died with no readmission within 30 days, and 46 (0.9%) had both a readmission within 30 days and died within 30 days (see Figure 1 and Table 1). Patients who died but had no readmission within 30 days, had an elevated history of atrial fibrillation (47/150, 31.3%). Patients who had no readmission or death within 30 days tended to be more likely to have received alteplase during the index hospital stay (639/4326, 14.8%). The proportion of patients with full code orders at discharge varied across patient groups (range 8.7%-80.4%). The proportion of patients who were discharged home after the index event varied by outcome group. Of those who were both readmitted and died, 28% (13/46) had been released to home, compared with 40.7% (200/492) of those who were readmitted and alive, and 56.2% (2433/4326) of those who were alive and had no readmission. In total, 50% of patients (23/46) who died within 30 days but had no readmission within 30 days, had been released to a regular (noncustodial) skilled nursing facility. Furthermore, 4% (6/150) of patients with death but no readmission, were originally discharged to a custodial skilled nursing facility (Table 1).

For hospitalizations that resulted in readmission within 30 days or death within 30 days post-discharge, the patients tended to be older (median age 78, IQR 68-86 years vs 72, IQR 62-82 years), were less likely to be male (290/688, 42.2% vs 2187/4326, 50.6%; $P<.001$), and more likely to have a Charlson comorbidity score greater than or equal to 4 (387/688, 56.3% vs 1584/4326, 36.6%; $P<.001$). More patients without the composite outcome had full code care directive at discharge (3476/4326, 80.4% vs 402/688, 58.4%; $P<.001$; see Table 2).

Table 3 shows results from performance testing of several multivariable predictive models of the composite outcome. The best performing models were TSL (c-statistic=0.685) and TSL plus mRS score at discharge (c-statistic=0.694). The model with TSL+NIHSS performed similarly (c-statistic=0.684) to the model with TSL alone (Table 3).

XSL•FO
RenderX

Table . Cohort characteristics. Study composite outcome is nonelective readmission and/or death within 30 days of discharge.

Variable	No readmission or death within 30 days	Readmission only within 30 days	Readmission within 30 days and died within 30 days	Death within 30 days only	Composite outcome	All patients
Hospitalizations, n	4326	492	46	150	688	5014
All patients, n	4250	481	46	150	669	4843
Age (years), mean (SD)	71.2 (13.99)	73.9 (13.08)	78.4 (11.63)	83.2 (11.48)	76.2 (13.21)	71.9 (13.99)
Male, n (%)	2187 (50.6)	219 (44.5)	21 (45.7)	50 (33.3)	290 (42.2)	2477 (49.4)
Race and ethnicity, n (%)						
Asian	654 (15.1)	74 (15)	5 (10.9)	18 (12)	97 (14.1)	751 (15)
Black	620 (14.3)	77 (15.7)	6 (13)	15 (10)	98 (14.2)	718 (14.3)
Hispanic	674 (15.6)	79 (16.1)	6 (13)	23 (15.3)	108 (15.7)	782 (15.6)
Other or multiracial	134 (3.1)	10 (2.0)	1 (2.2)	4 (2.7)	15 (2.2)	149 (3.0)
White	2244 (51.9)	252 (51.2)	28 (60.9)	90 (60)	370 (53.8)	2614 (52.1)
KFHP[a] membership, n (%)	3634 (84)	452 (91.9)	44 (95.7)	135 (90)	631 (91.7)	4265 (85.1)
Inpatient incident stroke, n (%)	397 (9.2)	38 (7.7)	1 (2.2)	14 (9.3)	53 (7.7)	450 (9)
Medical history, n (%)						
Previous stroke	199 (4.6)	34 (6.9)	3 (6.5)	10 (6.7)	47 (6.8)	247 (4.9)
Atrial fibrillation	636 (14.7)	96 (19.5)	8 (17.4)	47 (31.3)	151 (21.9)	789 (15.5)
Myocardial infarction	109 (2.5)	24 (4.9)	3 (6.5)	4 (2.7)	31 (4.5)	140 (2.7)
COPS2[b], mean (SD)	35.4 (35.74)	49.4 (43.95)	69.8 (52.12)	64.6 (47.71)	54.1 (45.92)	38.0 (37.85)
≥65[c], n (%)	755 (17.5)	141 (28.7)	22 (47.8)	68 (45.3)	231 (33.6)	986 (19.7)
LAPS2[d] at admission, mean (SD)	58.1 (29.63)	69.0 (33.05)	83.9 (24.81)	87.0 (30.95)	74.0 (33.01)	60.3 (30.60)
≥110[e], n (%)	252 (5.8)	61 (12.4)	7 (15.2)	37 (24.7)	105 (15.3)	357 (7.1)
Received alteplase, n (%)	639 (14.8)	52 (10.6)	4 (8.7)	13 (8.7)	69 (10)	708 (14.1)
mRS[f] score at discharge, mean (SD)	2.7 (1.63)	3.1 (1.57)	3.7 (1.37)	3.7 (1.78)	3.3 (1.62)	2.8 (1.64)
Initial NIHSS[g] score, median (IQR)	4 (2-8)	4 (2-9)	5 (3-8)	15 (6-22)	6 (2-13)	4 (2-8)
Full code at discharge, n (%)	3476 (80.4)	366 (74.4)	23 (50)	13 (8.7)	402 (58.4)	3878 (77.3)
LOS[h] in days, mean (SD)	6.4 (7.91)	6.7 (6.37)	7.7 (7.19)	7.3 (5.74)	6.9 (6.30)	6.5 (7.71)
Discharge disposition, n (%)						
CSNF[i]	13 (0.3)	0 (0)	0 (0)	6 (4)	6 (0.9)	19 (0.4)
Home health	1067 (24.7)	121 (24.6)	10 (21.7)	8 (5.3)	139 (20.2)	1206 (24.1)
Home	2433 (56.2)	200 (40.7)	13 (28.3)	110 (73.3)	323 (46.9)	2756 (55)

XSL•FO
RenderX

Variable	No readmission or death within 30 days	Readmission only within 30 days	Readmission within 30 days and died within 30 days	Death within 30 days only	Composite outcome	All patients
RSNF[j]	813 (18.8)	171 (34.8)	23 (50)	26 (17.3)	220 (32)	1033 (20.6)

[a]KFHP: Kaiser Foundation Health Plan.

[b]COPS2: Comorbidity Point Score, version 2.

[c]COPS2 (range: 0 to 1010; higher scores indicate increasing comorbidity burden) is assigned based on all diagnoses incurred by a patient in the 12 months preceding the index hospitalization. The univariate relationship of COPS2 with 30-day mortality is as follows: 0-39, 1.7%; 40-64, 5.2%; 65+,9.0%. See Escobar et al [12] for details.

[d]LAPS2: Laboratory-based Acute Physiology Score, version 2.

[e]LAPS2 (range: 0 to 414; higher scores indicating increasing physiologic derangement) is assigned based on a patient's worst vital signs, pulseoximetry, neurological status, and 16 laboratory test results in the 72 hours preceding hospitalization. The univariate relationship of an admission LAPS2 with 30-day mortality is as follows: 0-59, 1.0%; 60-109, 5.0%; 110+, 13.7%. See text and Escobar et al [12] for details.

[f]mRS: modified Rankin Scale.

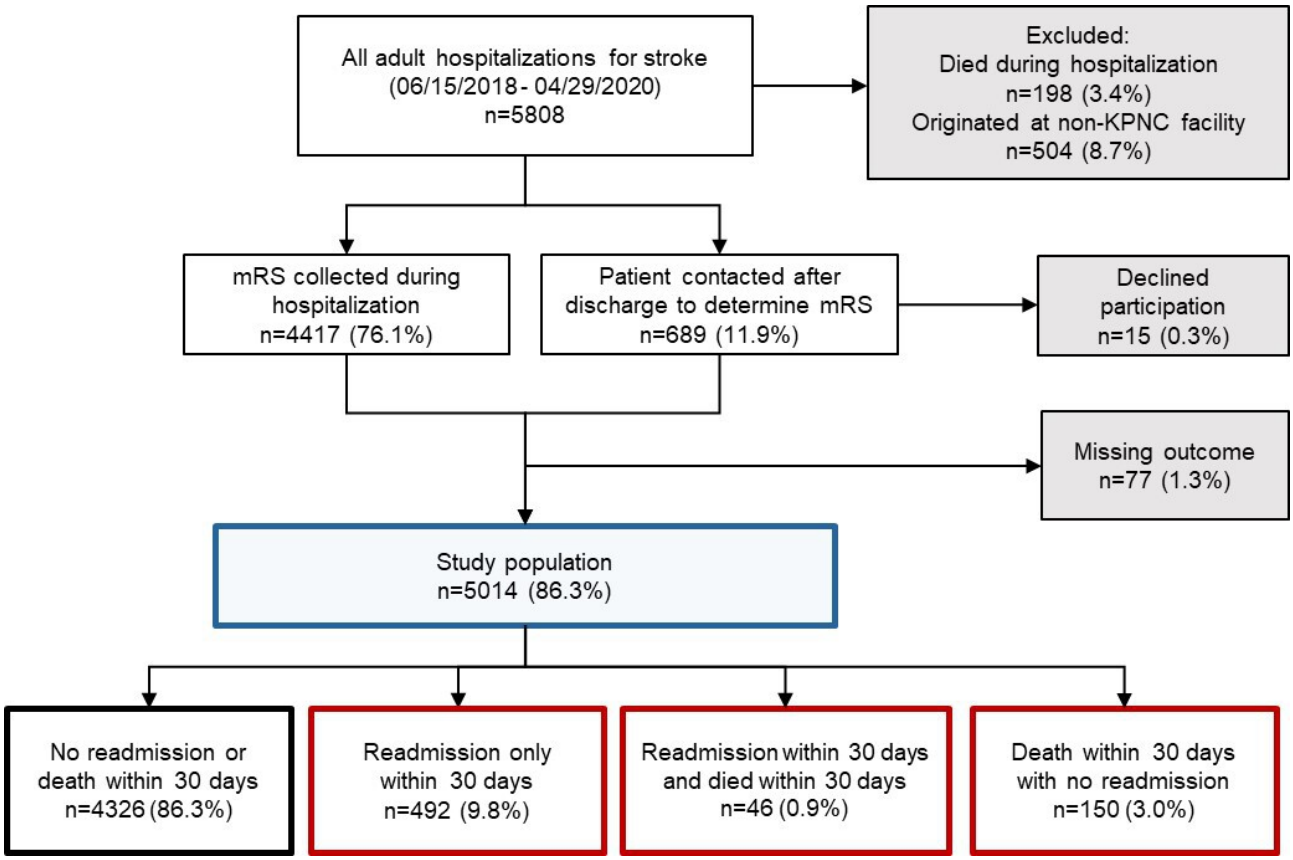
[g]NIHSS: National Institutes of Health Stroke Scale.

[h]LOS: length of stay.

[i]CSNF: custodial skilled nursing facility.

[j]RSNF: regular skilled nursing facility.

Figure 1. Definition of study cohort. Eligible patients are those patients meeting the following criteria: (1) admitted to a KPNC hospital between June 15, 2018, and April 29, 2020; (2) age ≥18 years; (3) diagnosis of incident ischemic stroke; and (4) for patients who experience interhospital transport, the first hospital stay was at a KPNC hospital. KPNC: Kaiser Permanente Northern California; mRS: modified Rankin Scale.



XSL•FO
RenderX

Table . Distribution of key predictors in the study cohort.

	Patients without study composite outcome	Patients with study composite outcome	*P* value
Age (years), median (IQR)	72 (6282)	78 (68-86)	—[a]
Sex (male), n (%)	2187 (50.6)	290 (42.2)	<.001
Admitted via ED[b], n (%)	3929 (90.8)	635 (92.3)	.21
CCI[c] score, median (IQR)[d]	2 (0-5)	4 (2-6)	—
CCI ≥4, n (%)	1584 (36.6)	387 (56.3)	<.001
Length of stay, median (IQR)[e]	4 (3-6)	5 (3-6)	—
mRS[f] score, median (IQR)[g]	3 (1-4)	4 (2-4)	—
mRS >2, n (%)	2119 (60.1)	425 (73.9)	<.001
NIHSS[h] score, median (IQR)[i]	4 (2-7)	5 (2-13)	—
NIHSS >5, n (%)	1270 (35)	272 (50.1)	<.001
Full code at discharge, n (%)[j]	3476 (80.4)	402 (58.4)	<.001
LACE[o], median (IQR)[l]	7 (4-10)	9 (6-12)	—
COPS2[m], median (IQR)[n]	21 (10-50)	42 (13-81.5)	—
LAPS2[k], median (IQR)[p]	55 (36-75)	72.5 (50-94)	—
Prior hospitalizations, n (%)[q]	168 (3.9)	56 (8.1)	<.001
TSL[r] score, median (IQR)[s]	10.7 (7.5-17.6)	18.2 (10.7-29.1)	—

[a]Not available.

[b] ED: emergency department.

[c] CCI: Charlson Comorbidity Index.

[d]CCI score (range 0-40; higher scores indicate greater comorbidity burden) was calculated using the methodology of Deyo et al [14].

[e]Length of stay is extracted in hours and reported in days, rounded to the nearest 0.1 day.

[f]mRS: modified Rankin Scale.

[g]mRS score range is 0-6 (0=no symptoms at all,1=no significant disability despite symptoms, 2=slight disability, 3=moderate disability, 4=moderately severe disability 5=severe disability/bedridden, 6=dead). See text and van Swieten et al [24] for details.

[h] NIHSS: National Institutes of Health Stroke Scale.

[i]NIHSS score range is 0-42 (0-5 typically indicates minor stroke; higher scores indicate more severe stroke). See text and Brott et al [25] for details.

[j]Assignment is based on patient's last care directive before discharge.

[k]LACE: Length of Stay, Acuity, Charlson Comorbidities, Emergency Department Use.

[l]LACE score range is 0 to 19, with higher scores indicating increased risk of the composite outcome. See text and van Walraven et al [19] for details.

[m]COPS2: Comorbidity Point Score, version 2.

[n]COPS2 (range: 0 to 1010; higher scores indicate increasing comorbidity burden) is assigned based on all diagnoses incurred by a patient in the 12 months preceding the index hospitalization. The univariate relationship of COPS2 with 30-day mortality is as follows: 0-39, 1.7%; 40-64, 5.2%; 65+, 9.0%. See Escobar et al [12] for details.

[o]LAPS2: Laboratory-based Acute Physiology Score, version 2.

[p]LAPS2 (range: 0 to 414; higher scores indicating increasing physiologic derangement) is assigned based on a patient's worst vital signs, pulse oximetry, neurological status, and 16 laboratory test results in the 72 hours preceding hospitalization. The univariate relationship of an admission LAPS2 with 30-day mortality is as follows: 0-59, 1.0%; 60-109, 5.0%; 110+, 13.7%. See text and Escobar et al [12] for details.

[q]Number with any hospitalizations in the 30 days preceding the index hospitalization.

[r] TSL: transition support level.

[s]This is expressed as a % risk of the composite outcome within 30 days of hospital discharge. The score incorporates the LAPS2, COPS2, discharge care directive, and previous hospitalizations in the 30 days preceding the index hospitalization. Patients with TSL scores ≥25% are enrolled in Kaiser Permanente Northern California readmission prevention program. See text and Escobar et al [20] for details.

XSL•FO
RenderX

Table . Multivariate model performance[a].

Model	c-statistic	Nagelkerke pseudo-R^2	Brier score
NIHSS[b]	0.60	0.03	0.11
NIHSS+age+sex	0.64	0.05	0.11
mRS[c]	0.61	0.03	0.12
mRS+age+sex	0.62	0.04	0.12
LACE[d]	0.63	0.04	0.12
LACE+NIHSS	0.66	0.06	0.11
LACE+mRS	0.67	0.07	0.12
TSL[e]	0.69	0.08	0.11
TSL+NIHSS	0.68	0.09	0.11
TSL+mRS	0.69	0.10	0.11
Random forest[f]	0.66	0.04	0.11

[a]All models except the random forest model employed logistic regression. Metrics reported: c-statistic (area under the receiver operator characteristic curve); Nagelkerke pseudo-R^2 (Nagelkerke [22] and Brier score [23].

[b]NIHSS: National Institutes of Health Stroke Score (range 0-42; higher scores indicate more severe stroke). See text and Brott et al [25] for details.

[c]mRS: modified Rankin Scale, (range 0-6; higher scores indicate severe disability or death). See text and van Swieten et al [24] for details.

[d]LACE: Length of Stay, Acuity, Charlson Comorbidities, Emergency Department Use. Score range is 0 to 19, with higher scores indicating increased risk of the composite outcome. See text and van Walraven et al [19] for details.

[e]TSL: Transition Support Level. This score is expressed as a % risk of the composite outcome within 30 days of hospital discharge. The score incorporates the Laboratory-based Acute Physiology Score, version 2; Comorbidity Point Score, version 2; discharge care directive; and previous hospitalizations in the 30 days preceding the index hospitalization. Patients with TSL scores ≥25% are enrolled in Kaiser Permanente Northern California readmission prevention program. See text and Escobar et al [20] for details.

[f]For the random forest model, we included age, sex, NIHSS, mRS, and all subcomponents of the LACE and TSL scores.

Discussion

We have completed a study where we developed an adult patient stroke-specific predictive model for a composite outcome of readmission within 30 days and mortality within 30 days postdischarge. Among the models that were tested, the TSL model performed the best. Adding manually assigned stroke scales such as initial NIHSS (as a measure of stroke severity) and mRS at discharge (as a measure of functional status) to clinical data from a comprehensive EHR did not improve the performance of the TSL model significantly. The previously published TSL model [20] included an extensive amount of data for each patient including the LAPS2, COPS2, discharge care directive, and previous hospitalizations in the 30 days preceding the index hospitalization. Some of these data (such diagnoses in the previous 12 months before hospitalization, vital signs, laboratory data, and code status) were unique to our dataset and were never examined in previously published studies on 30-day readmission or mortality poststroke.

Readmissions after stroke are associated with worse disability, higher mortality, and higher costs of care [26,27]. Reduction of 30-day readmission is a quality metric set by the Centers for Medicare & Medicaid Services. Publications on readmission have been more focused on reported global performance and other conditions, and less so on stroke. In addition, most previous studies excluded patients aged <65 years. Being able to predict readmission after stroke may help to identify high-risk patients for targeted interventions and postdischarge programs, limit preventable readmissions, and improve long-term outcomes.

Previously published studies on readmissions after stroke provided only limited data on patient-level factors in their risk analysis. A systematic review of stroke readmission in 2010 identified only 16 published studies that reported risk-adjustment models at the patient level [2]. Considerable variation in reported outcomes was identified: 30-day all-cause readmission rates ranged from 6.5% to 24.3%, 1-year all-cause readmission rates from 30% to 62.2%, 30-day stroke-related readmission from 7.4% to 9.4%, and 1-year stroke-related readmission from 10.5% to 31.1%. Patient characteristics that were found to be associated with stroke readmissions included age, longer index hospital length of stay, worse physical functioning after stroke, and increased number of hospitalizations before stroke. Although some of these included stroke severity measures, no consistency existed across the models. A statement from the American Heart Association on risk adjustment of ischemic stroke outcomes for comparing hospital performance emphasized a minimum list of patient-level variables including age, sex, stroke severity, comorbid conditions, and risk factors [3]. However, in order to improve the usability of risk-adjusted models, the statement recommended that researchers should try to identify other factors, especially those not typically measured in administrative databases. To our knowledge, no previously published models on 30-day readmission or 30-day mortality included the mRS at discharge (a functional status assessment).

XSL•FO
RenderX

A number of studies on readmission and mortality poststroke used Medicare database therefore restricting their cohorts by older age and limited the generalizability of their results [28,29]. Our 30-day readmission rate of 9.7% was lower than rates (12% - 14%) reported from those studies using Medicare data. However, advanced age is associated with increased readmission after ischemic stroke [29]. On the other hand, a recent analysis of 30-day readmission after ischemic stroke for adults 18 years and older using the 2019 Nationwide Readmission Database reported a rate of 9.7%, which was nearly identical to ours [30].

For our cohort, the rate for 30-day mortality postdischarge was 3%, and the inpatient mortality rate was 3.4%, totaling 6.4% for 30 days from admission. Studies from Canada and the United Kingdom reported a 30-day mortality rate from admission of about 12% [31,32]. A US study using Medicare data reported a 30-day mortality rate of 13.6% [33]. Our lower 30-day mortality rate may be a reflection of a cohort of patients with insurance and access to care, inclusion of younger patients (ages 18 years and older), and an excellent performance of acute stroke treatment time as previously published [9].

The current state of predictive analytics for hospital readmission has not evolved enough to guide effective prevention efforts [4,5,34,35]. In addition, medical record technology, along with other aspects of health care in the United States is both fragmented and—from an informatics perspective—heterogeneous. Some institutions, such as university medical centers and KPNC, have sophisticated EHRs, while others still use paper charts. Similarly, the ability of institutions to retrieve electronic data varies considerably, as does the timeliness of such retrieval. Given this heterogeneous information environment, it is important to (1) highlight desirable characteristics of future readmission predictive models for patients with stroke, and (2) develop models that can be instantiated in different settings (ie, ranging from those using only claims data to those that use comprehensive EHRs). This would permit the development of modular approaches that individual institutions could adapt to their specific circumstances.

It was not surprising that models using only administrative data (LACE) did not perform well. However, it was disappointing that the TSL model with inclusion of detailed EHR data (longitudinal comorbidity in the 12 months preceding index hospitalization, COPS2; and LAPS2) did not result in great discrimination. Adding the initial NIHSS score and the mRS score at discharge to the model did not improve its performance, perhaps because the TSL model at baseline already contained other data elements relating to patient status and severity of their condition while hospitalized. NIHSS and mRS were moderately correlated to LAPS2 score, LACE, and TSL. We did not have other potential measures of stroke severity such as infarct size from neuroimaging study, or change in mRS at discharge compared with baseline prehospital mRS, or mRS postdischarge.

Our study had several strengths. Our approach synthesizes two types of expertise: deep understanding of the clinical aspects of stroke (including intimate familiarity with the current state of the art in assessment of its severity and prognosis) combined with sophistication in the area of predictive analytics. Tools developed by our experienced predictive analytics team have entered routine operations in one of the most advanced integrated health care delivery systems in the United States. We were able to characterize the study cohort better than has been done previously. The TSL model included detailed data from index hospitalization not in previous studies on readmission poststroke, including vital signs, laboratory data, patient's care directive and mRS score at discharge. This study was embedded in a community setting with comprehensive longitudinal information infrastructure. The study cohort was diverse in race-ethnicity and included all ages, not just Medicare-eligible patients. We used prospective validation. All analyses were based on two basic data standards: claims data (functionally, the lowest common denominator) and modern EHR data. This study started from the premise that prediction of a patient with stroke's risk for readmission should be automated, presented through a comprehensive EHR, and occur in real time.

There were also limitations with our study. We relied on data collected in the course of routine clinical operations rather than strict research protocols. While our hospitals treat patients with stroke regardless of insurance, our study cohort and analysis were limited to an insured population with access to care to one of the most highly integrated health care delivery systems in the world. The study results may not be applicable to the uninsured population. All of our centers are Joint Commission certified stroke centers with the highest awards from the Get With the Guidelines program. More than 50% of acute ischemic stroke cases qualifying for intravenous thrombolytic were treated within 30 minutes [9]. Therefore, our study results may not be representative of all hospitals caring for patients with ischemic stroke. We did not have baseline functional status and, therefore, could not include a change in functional status to the models. We also did not have indicators for postdischarge functional status. We were unable to include other in-hospital data such as placement of feeding tube or trach due to a high rate of missing data perhaps due to difficulty with pulling correct data electronically. We did not have data on social support or a cognitive function measure at discharge, which may play a significant role in readmission. Our study results are generalizable to an adult population with ischemic stroke who have insurance and access to care who survive the index hospitalization and are treated in certified stroke centers.

In summary, we have tested a more comprehensive predictive model (TSL) for readmission and death within 30 days post ischemic stroke. Having a comprehensive look at the important factors that may influence that decision-making process (socioeconomic status, living arrangement or social support, functional status, code status, cognitive status, etc) would go a long way at improving the performance of a predictive model. Future studies should seek to improve upon our study and evaluate other factors not included here, such as changes from baseline functional status, the volume of brain infarcted, social support, and cognitive status at the time of discharge.

XSL•FO
RenderX

Acknowledgments

This research was funded by the National Institute of Neurological Disorders and Stroke. The funders had no role in study design, data collection and analysis, the decision to publish, or preparation of the paper.

Data Availability

The datasets generated or analyzed during this study are not publicly available due to the patient data being owned by the Kaiser Foundation Health Plan, Inc; Kaiser Foundation Hospitals, Inc; and The Permanente Medical Group, Inc. Because of their third-party rights, it is not possible to make the data publicly available without restriction but they may be available from the corresponding author on reasonable request.

Authors' Contributions

MNNH and GE contributed to conceptualization. MNNH, GE, ZZ, and JA contributed to methodology. MNNH and GE contributed to writing the original draft. All authors contributed to writing, review, and editing. MNNH and GE contributed to funding acquisition. MNNH and GE contributed to supervision. All authors contributed to data curation.

Conflicts of Interest

None declared.

Multimedia Appendix 1
ICD-10 codes for diagnosis of ischemic stroke. *ICD-10*: *International Classification of Diseases, Tenth Revision*.
[DOCX File, 12 KB - medinform_v13i1e69102_app1.docx]

Checklist 1
STROBE (Strengthening the Reporting of Observational Studies in Epidemiology) checklist.
[DOCX File, 40 KB - medinform_v13i1e69102_app2.docx]

References

1. Ovbiagele B, Goldstein LB, Higashida RT, et al. Forecasting the future of stroke in the United States: a policy statement from the American Heart Association and American Stroke Association. Stroke 2013 Aug;44(8):2361-2375. [doi: 10.1161/STR.0b013e31829734f2] [Medline: 23697546]
2. Lichtman JH, Leifheit-Limson EC, Jones SB, et al. Predictors of hospital readmission after stroke: a systematic review. Stroke 2010 Nov;41(11):2525-2533. [doi: 10.1161/STROKEAHA.110.599159] [Medline: 20930150]
3. Katzan IL, Spertus J, Bettger JP, et al. Risk adjustment of ischemic stroke outcomes for comparing hospital performance: a statement for healthcare professionals from the American Heart Association/American Stroke Association. Stroke 2014 Mar;45(3):918-944. [doi: 10.1161/01.str.0000441948.35804.77] [Medline: 24457296]
4. Report to the Congress: promoting greater efficiency in Medicare. : Medicare Payment Advisory Commission; 2007 URL: https://www.medpac.gov/wp-content/uploads/2022/08/Jun07_EntireReport_SEC.pdf [accessed 2023-05-20]
5. Jencks SF, Williams MV, Coleman EA. Rehospitalizations among patients in the Medicare fee-for-service program. N Engl J Med 2009 Apr 2;360(14):1418-1428. [doi: 10.1056/NEJMsa0803563] [Medline: 19339721]
6. Patient Protection and Affordable Care Act. Congress.gov. 2010. URL: https://www.congress.gov/111/plaws/publ148/PLAW-111publ148.pdf [accessed 2025-05-05]
7. Examining the drivers of readmissions and reducing unnecessary readmissions for better patient care. American Hospital Association. 2011. URL: https://www.aha.org/system/files/2018-02/11sep-tw-readmissions.pdf [accessed 2025-05-05]
8. Gordon NP. Similarity of adult Kaiser Permanente members to the adult population in Kaiser Permanente's Northern California service area: comparisons based on the 2017/2018 cycle of the California Health Interview Survey. Division of Research. 2020. URL: https://divisionofresearch.kaiserpermanente.org/projects/memberhealthsurvey/SiteCollectionDocuments/compare_kp_ncal_chis2017-18.pdf [accessed 2023-05-20]
9. Nguyen-Huynh MN, Klingman JG, Avins AL, et al. Novel telestroke program improves thrombolysis for acute stroke across 21 hospitals of an integrated healthcare system. Stroke 2018 Jan;49(1):133-139. [doi: 10.1161/STROKEAHA.117.018413] [Medline: 29247142]
10. EPIC. URL: www.epicsystems.com [accessed 2023-05-22]
11. Escobar GJ, Plimier C, Greene JD, Liu V, Kipnis P. Multiyear rehospitalization rates and hospital putcomes in an integrated health care system. JAMA Netw Open 2019 Dec 2;2(12):e1916769. [doi: 10.1001/jamanetworkopen.2019.16769] [Medline: 31800072]

XSL•FO
RenderX

12. Escobar GJ, Gardner MN, Greene JD, Draper D, Kipnis P. Risk-adjusting hospital mortality using a comprehensive electronic record in an integrated health care delivery system. Med Care 2013 May;51(5):446-453. [doi: 10.1097/MLR.0b013e3182881c8e] [Medline: 23579354]
13. Escobar GJ, Greene JD, Gardner MN, Marelich GP, Quick B, Kipnis P. Intra-hospital transfers to a higher level of care: contribution to total hospital and intensive care unit (ICU) mortality and length of stay (LOS). J Hosp Med 2011 Feb;6(2):74-80. [doi: 10.1002/jhm.817] [Medline: 21290579]
14. Deyo RA, Cherkin DC, Ciol MA. Adapting a clinical comorbidity index for use with ICD-9-CM administrative databases. J Clin Epidemiol 1992 Jun;45(6):613-619. [doi: 10.1016/0895-4356(92)90133-8] [Medline: 1607900]
15. Beardslee WR, Keller MB, Lavori PW, Staley J, Sacks N. The impact of parental affective disorder on depression in offspring: a longitudinal follow-up in a nonreferred sample. J Am Acad Child Adolesc Psychiatry 1993 Jul;32(4):723-730. [doi: 10.1097/00004583-199307000-00004] [Medline: 8340291]
16. Patel N, Rao VA, Heilman-Espinoza ER, Lai R, Quesada RA, Flint AC. Simple and reliable determination of the modified rankin scale score in neurosurgical and neurological patients: the mRS-9Q. Neurosurgery 2012 Nov;71(5):971-975. [doi: 10.1227/NEU.0b013e31826a8a56] [Medline: 22843133]
17. Dodds TA, Martin DP, Stolov WC, Deyo RA. A validation of the functional independence measurement and its performance among rehabilitation inpatients. Arch Phys Med Rehabil 1993 May;74(5):531-536. [doi: 10.1016/0003-9993(93)90119-u] [Medline: 8489365]
18. Bottemiller KL, Bieber PL, Basford JR, Harris M. FIM scores, FIM efficiency, and discharge disposition following inpatient stroke rehabilitation. Rehabil Nurs 2006;31(1):22-25. [doi: 10.1002/j.2048-7940.2006.tb00006.x] [Medline: 16422041]
19. van Walraven C, Dhalla IA, Bell C, et al. Derivation and validation of an index to predict early death or unplanned readmission after discharge from hospital to the community. CMAJ 2010 Apr 6;182(6):551-557. [doi: 10.1503/cmaj.091117] [Medline: 20194559]
20. Escobar GJ, Ragins A, Scheirer P, Liu V, Robles J, Kipnis P. Nonelective rehospitalizations and postdischarge mortality: predictive models suitable for use in real time. Med Care 2015 Nov;53(11):916-923. [doi: 10.1097/MLR.0000000000000435] [Medline: 26465120]
21. Cook NR. Use and misuse of the receiver operating characteristic curve in risk prediction. Circulation 2007 Feb 20;115(7):928-935. [doi: 10.1161/CIRCULATIONAHA.106.672402] [Medline: 17309939]
22. Nagelkerke NJD. A note on A general definition of the coefficient of determination. Biometrika 1991;78(3):691-692. [doi: 10.1093/biomet/78.3.691]
23. Brier GW. Verification of forecasts expressed in terms of probability. Mon Wea Rev 1950 Jan;78(1):1-3. [doi: 10.1175/1520-0493(1950)078<0001:VOFEIT>2.0.CO;2]
24. van Swieten JC, Koudstaal PJ, Visser MC, Schouten HJ, van Gijn J. Interobserver agreement for the assessment of handicap in stroke patients. Stroke 1988 May;19(5):604-607. [doi: 10.1161/01.str.19.5.604] [Medline: 3363593]
25. Brott T, Adams HP Jr, Olinger CP, et al. Measurements of acute cerebral infarction: a clinical examination scale. Stroke 1989 Jul;20(7):864-870. [doi: 10.1161/01.STR.20.7.864]
26. Kind AJH, Smith MA, Liou JI, Pandhi N, Frytak JR, Finch MD. The price of bouncing back: one-year mortality and payments for acute stroke patients with 30-day bounce-backs. J Am Geriatr Soc 2008 Jun;56(6):999-1005. [doi: 10.1111/j.1532-5415.2008.01693.x] [Medline: 18422948]
27. Bjerkreim AT, Thomassen L, Brøgger J, Waje-Andreassen U, Næss H. Causes and predictors for hospital readmission after ischemic stroke. J Stroke Cerebrovasc Dis 2015 Sep;24(9):2095-2101. [doi: 10.1016/j.jstrokecerebrovasdis.2015.05.019] [Medline: 26142260]
28. Lichtman JH, Allen NB, Wang Y, Watanabe E, Jones SB, Goldstein LB. Stroke patient outcomes in US hospitals before the start of the Joint Commission Primary Stroke Center certification program. Stroke 2009 Nov;40(11):3574-3579. [doi: 10.1161/STROKEAHA.109.561472] [Medline: 19797179]
29. Bambhroliya AB, Donnelly JP, Thomas EJ, et al. Estimates and temporal trend for US nationwide 30-day hospital readmission among patients with ischemic and hemorrhagic stroke. JAMA Netw Open 2018 Aug 3;1(4):e181190. [doi: 10.1001/jamanetworkopen.2018.1190] [Medline: 30646112]
30. Zhou LW, Lansberg MG, de Havenon A. Rates and reasons for hospital readmission after acute ischemic stroke in a US population-based cohort. PLoS One 2023;18(8):e0289640. [doi: 10.1371/journal.pone.0289640] [Medline: 37535655]
31. Saposnik G, Hill MD, O'Donnell M, et al. Variables associated with 7-day, 30-day, and 1-year fatality after ischemic stroke. Stroke 2008 Aug;39(8):2318-2324. [doi: 10.1161/STROKEAHA.107.510362] [Medline: 18566303]
32. Wang W, Rudd AG, Wang Y, et al. Risk prediction of 30-day mortality after stroke using machine learning: a nationwide registry-based cohort study. BMC Neurol 2022 May 27;22(1):35624434. [doi: 10.1186/s12883-022-02722-1]
33. Fonarow GC, Saver JL, Smith EE, et al. Relationship of national institutes of health stroke scale to 30-day mortality in medicare beneficiaries with acute ischemic stroke. J Am Heart Assoc 2012 Feb;1(1):42-50. [doi: 10.1161/JAHA.111.000034] [Medline: 23130117]
34. Kansagara D, Englander H, Salanitro A, et al. Risk prediction models for hospital readmission: a systematic review. JAMA 2011 Oct 19;306(15):1688-1698. [doi: 10.1001/jama.2011.1515] [Medline: 22009101]

XSL•FO
RenderX

35. Hansen LO, Young RS, Hinami K, Leung A, Williams MV. Interventions to reduce 30-day rehospitalization: a systematic review. Ann Intern Med 2011 Oct 18;155(8):520-528. [doi: 10.7326/0003-4819-155-8-201110180-00008] [Medline: 22007045]

Abbreviations

CCI: Charlson Comorbidity Index
COPS2: Comorbidity Point Score, version 2
CSNF: custodial skilled nursing facility
ED: emergency department
EHR: electronic health record
EXPRESS: Expediting the Process of Evaluating and Stopping Stroke
FIM: Functional Independence Measurement
KFHP: Kaiser Foundation Health Plan
KPNC: Kaiser Permanente Northern California
LACE: Length of Stay, Acuity, Charlson Comorbidities, Emergency Department Use
LAPS2: Laboratory-based Acute Physiology Score, version 2
mRS: modified Rankin Scale
NIHSS: National Institutes of Health Stroke Scale
RSNF: regular skilled nursing facility
STROBE: Strengthening the Reporting of Observational Studies in Epidemiology
TSL: Transition Support Level

Edited by M Focsa; submitted 03.12.24; peer-reviewed by H Nzwalo, S Thanki; revised version received 14.03.25; accepted 18.03.25; published 09.05.25.

Please cite as:
Nguyen-Huynh MN, Alexander J, Zhu Z, Meighan M, Escobar G
Effects of the National Institutes of Health Stroke Scale and Modified Rankin Scale on Predictive Models of 30-Day Nonelective Readmission and Mortality After Ischemic Stroke: Cohort Study
JMIR Med Inform 2025;13:e69102
URL: https://medinform.jmir.org/2025/1/e69102
doi:10.2196/69102

© Mai N Nguyen-Huynh, Janet Alexander, Zheng Zhu, Melissa Meighan, Gabriel Escobar. Originally published in JMIR Medical Informatics (https://medinform.jmir.org), 9.5.2025. This is an open-access article distributed under the terms of the Creative Commons Attribution License (https://creativecommons.org/licenses/by/4.0/), which permits unrestricted use, distribution, and reproduction in any medium, provided the original work, first published in JMIR Medical Informatics, is properly cited. The complete bibliographic information, a link to the original publication on https://medinform.jmir.org/, as well as this copyright and license information must be included.

XSL•FO
RenderX

Predicting Postoperative Stress Urinary Incontinence After Prolapse Surgery via Machine Learning and Regression Models: Development and Validation Study

Minna Su, MMed; Shuyu Wang, MMed; Xiaochun Liu, PhD

Gynecology and Obstetrics Department, Third Hospital of Shanxi Medical University, Shanxi Bethune Hospital, Shanxi Academy of Medical Sciences, No. 99 Longcheng Street, Xiaodian District, Taiyuan, China

Corresponding Author:
Xiaochun Liu, PhD
Gynecology and Obstetrics Department, Third Hospital of Shanxi Medical University, Shanxi Bethune Hospital, Shanxi Academy of Medical Sciences, No. 99 Longcheng Street, Xiaodian District, Taiyuan, China

Abstract

Background: Pelvic organ prolapse (POP) and stress urinary incontinence (SUI) often concurrently exist. The incontinence in some patients with POP resolves after POP surgery, but it persists in others. Some patients without SUI before surgery may develop de novo SUI. It is unclear whether a concomitant anti-incontinence procedure should be performed at the time of POP surgery to prevent postoperative incontinence. A prediction model is needed to guide clinical decision-making.

Objective: This study aimed to analyze the risk factors and develop prediction models for SUI after POP surgery based on machine learning to provide new tools for evaluating and predicting postoperative SUI.

Methods: Sample size calculation was performed using the Riley 4-step method. Data of patients undergoing prolapse surgery in Shanxi Bethune Hospital were prospectively collected from August 2022 to February 2025 and were retrospectively collected from January 2021 to August 2022. General clinical data, relevant laboratory test results, urodynamic examination findings, and pelvic floor ultrasound findings were collected. Lasso regression, univariate analysis, and logistic analysis were used to screen the predictors of SUI after prolapse surgery. Data were split randomly in a 7:3 ratio into training and validation sets. The training set was used to develop the prediction model involving Lasso regression, random forest, support vector machine (SVM), extreme gradient boosting (XGBoost), classification and regression tree (CART), and logistic regression, and the validation set was used for internal verification. The final implementation was achieved by developing a Shiny-based application for model deployment.

Results: A total of 286 patients were enrolled in this study, and 91 patients had postoperative SUI. The following 6 risk factors were identified through univariate, logistic, and Lasso regression analyses: preoperative SUI, urge urinary incontinence, urodynamic occult SUI, anti-incontinence surgery, genital hiatus, and anterior colporrhaphy. Five prediction models were constructed by using logistic regression, random forest, XGBoost, SVM, and CART. Based on a comprehensive evaluation of model discrimination, calibration, and clinical utility, the SVM model demonstrated optimal overall performance, with an area under the curve of 0.821 in the training set and 0.846 in the validation set.

Conclusions: This study developed 5 prediction models for postoperative SUI following prolapse surgery, which demonstrated good performance in internal validation. Among them, the SVM prediction model appeared to be the most promising. However, further external validation data are required to assess its generalizability. This model has the potential to become a high-quality clinical risk prediction tool for postoperative SUI in patients with prolapse, guiding clinical decisions on whether concurrent prolapse and incontinence surgeries are necessary.

(JMIR Med Inform 2025;13:e76021) doi:10.2196/76021

KEYWORDS

prediction model; pelvic organ prolapse; de novo stress urinary incontinence; machine learning; support vector machine

Introduction

Pelvic organ prolapse (POP) and stress urinary incontinence (SUI) are the 2 most common types of female pelvic floor dysfunctions. POP refers to the abnormal positioning and dysfunction of female pelvic organs (vagina, bladder, uterus, or rectum) caused by weak pelvic floor supportive tissues, which can lead to significant physical and emotional discomfort [1]. SUI refers to the involuntary leakage of urine during physical exertion, coughing, or sneezing (increased abdominal pressure) [2]. SUI occurs in 50% of patients with POP [3]. After POP surgery, 14.3% - 32.5% of patients have SUI, likely due to either uncorrected bladder neck defects after prolapse repair or the unmasking of pre-existing SUI symptoms that were

XSL•FO
RenderX

previously concealed by the kinking of the lower urinary tract during prolapse [4]. To reduce the risk of postoperative SUI, prolapse surgery and incontinence surgery can be performed concomitantly. However, concomitant operations have caused many patients who would not have SUI to undergo an unnecessary operation, and the current common operation for the treatment of SUI, midurethral sling, is often accompanied by many postoperative adverse reactions [5,6]. There is still no consensus on whether patients with coexisting POP and SUI should undergo staged surgeries or a concomitant anti-SUI surgery.

The risk factors for urinary incontinence after prolapse include point Ba (the lowest point of prolapse between point Aa anteriorly and the vaginal apex), preoperative SUI, preoperative occult SUI, diabetes, sacral colpopexy, etc [7,8]. A risk prediction model is a statistical model that estimates the probability of an individual having a certain outcome according to the risk factors of the disease. Predictive models for assessing SUI risk after prolapse surgery can effectively aid patient decision-making. Jelovsek et al [9] used data from the OPUS (Outcomes Following Vaginal Prolapse Repair and Midurethral Sling) trial to construct a predictive model for de novo SUI in patients with POP who do not have SUI before surgery, and the area under the curve (AUC) of this model was 0.72. Based on data from the CUPIDO (Concomitant Surgery and Urodynamic Investigation in Genital Prolapse and Stress Incontinence: A Diagnostic Study Including Outcome Evaluation) trial, van der Ploeg et al [10] developed a prediction model for postoperative SUI in patients with POP who did or did not have preoperative SUI. Compared with the model constructed using OPUS data, the predictive factor stress test was added. This prediction model has an AUC of 0.79. An article published in BJOG reviewed 1142 patients who underwent POP surgery from 2 tertiary hospitals in South Korea and developed a predictive model for SUI after prolapse surgery, with an AUC of 0.74 [11].

With the development of artificial intelligence in recent years, machine learning has become an important method in the field of predictive model construction. Compared to traditional methods, machine learning methods have higher predictive accuracy and are commonly used in the medical field to predict various outcomes [12,13]. In a study conducted by Peking Union Medical College Hospital in China, a predictive model was constructed for the first time using machine learning methods (logistic regression, random forest, and extreme gradient boosting [XGBoost]) [14].

Previous studies were retrospective, and the machine learning predictive model approach used only random forest and XGBoost methods. No prospective studies have been conducted to establish a predictive model for SUI after POP surgery. This study prospectively followed patients with POP and retrospectively collected data from additional POP surgical cases to increase the sample size. Detailed clinical parameters were obtained, including pelvic ultrasound findings, hematologic markers, and operations. Machine learning prediction models for postoperative SUI in patients with POP (with or without SUI) were developed and validated to enable more accurate risk stratification and clinical decision-making.

Methods

Study Design and Population

This study collected data prospectively from August 2022 to February 2025 and retrospectively from January 2021 to August 2022 from patients undergoing POP surgery at Shanxi Bethune Hospital in China. The study enrolled patients with Pelvic Organ Prolapse Quantification (POP-Q) stages II-IV, regardless of preoperative SUI status, who had undergone prolapse surgery or were scheduled to undergo prolapse surgery. The follow-up period was at least 6 months. The exclusion criteria were prior prolapse surgery and postoperative urinary tract infection.

The Riley 4-step method, specifically used in clinical prediction models, was adopted for sample size calculation [15]. This study developed binary prediction models with an anticipated 8 predictor parameters. For internal validation, the anticipated shrinkage level was set at 0.9. The postoperative SUI incidence rate at our hospital is approximately 30%. With an assumed model C-statistic of 0.8, we calculated the sample size requirement using the R package “pmsampsize.” The results showed that the minimum sample size required for the new model was 276.

Data Collection

Considering SUI risk factors in previous studies, relevant clinical characteristics of patients were collected, including age, height, weight, BMI, parity, vaginal delivery count, cesarean section count (due to low positive rates, this item was finally excluded), menopausal status, surgical age minus menopausal age, smoking history, type of medical insurance (Employee Basic Medical Insurance/Resident Basic Medical Insurance), educational background, preoperative estrogen supplement, postoperative estrogen supplement, preoperative SUI, preoperative urge urinary incontinence (UUI), hypertension, diabetes, comorbidities, POP-Q points and grade, biochemical indicators (albumin, liver function tests, and lipid profile; renal function tests were excluded due to low positive rates), cystocele Green type, residual urine, urodynamic occult stress urinary incontinence (UOSUI), urine leakage point pressure, anterior colporrhaphy performed (yes or no), perineal body reconstruction performed (yes or no), anti-SUI procedure performed (yes or no), hysterectomy performed (yes or no), and prolapse surgery method. Since urine leak point pressure only exists in patients with urodynamic stress incontinence, it is not conducive to model construction, and thus, it was not considered. Surgical methods for prolapse included colpocleisis, sacrospinous ligament fixation, round ligament suspension, high uterosacral ligament suspension, transvaginal mesh implantation, Manchester procedure, sacrocolpopexy, and lateral abdominal wall suspension. If only hysterectomy or anterior/posterior colporrhaphy was performed, the patient was coded as 0 in surgical evaluations. The operation for SUI was midurethral sling. Preoperative urinary incontinence status was determined through retrospective review of medical records combined with patient recall during postoperative follow-up. Postoperative SUI was defined as the reporting of bothersome SUI symptoms during any follow-up visit. Patients were followed up via outpatient clinic visits or telephone interviews.

XSL•FO
RenderX

Data Preprocessing

Smoking history was excluded because of more than 10% missing data and a low positive rate (2 out of 286). Educational background was excluded because of more than 10% missing data. The remaining missing values were multi-interpolated using the R package "mice." Patients with missing postoperative SUI outcomes were ultimately excluded from the study. Therefore, all postoperative SUI outcomes were based on the actual postoperative follow-up.

Model Development

Data were split randomly in a 7:3 ratio into a training set and a validation set. We ensured that there were no statistically significant differences in baseline characteristics between the training set and the validation set. The training set was used to develop the model, and the validation set was used for internal validation.

We performed 5-fold cross-validated Lasso (least absolute shrinkage and selection operator) regression using the R package "glmnet" to screen for predictive variables. Lasso regression was implemented with L1 regularization (tuning parameter λ) to select variables via coefficient shrinkage and prevent overfitting, thereby improving generalization. Multivariate logistic regression analysis was performed using the variables obtained by Lasso regression to construct a nomogram prediction model.

The decision tree model in this study was constructed based on the classification and regression tree (CART) method developed in 1984 [16]. CART analysis is a nonparametric, nonlinear method that generates binary trees by feature selection based on Gini index minimization criteria.

Random forest and XGBoost are both integrated machine learning methods based on decision trees. The random forest prediction model is created based on the bagging algorithm and can be used for both classification and regression analyses [17]. We developed the random forest model using bootstrap resampling techniques. We assessed feature importance in 2 metrics: mean decrease accuracy (based on permutation) and mean decrease Gini (based on Gini impurity). Considering the direct relevance of mean decrease accuracy to model prediction accuracy, its stronger robustness, and its better interpretability in clinical contexts [18,19], we ultimately selected the top 8 most predictive features based on the ranking results of mean decrease accuracy to construct the final model. XGBoost develops the model by gradually adding decision trees, each of which resolves the error weakness of the previous one to achieve an accurate classification effect [20]. The XGBoost model incorporates regularization terms based on tree complexity, effectively reducing overfitting and thereby enhancing generalization performance. XGBoost was configured to utilize the top 8 most important variables. The optimal parameters were selected via hyperparameter optimization, with additional L2 regularization (lambda) and L1 regularization (alpha) penalties incorporated to mitigate overfitting.

Support vector machine (SVM) is a powerful and versatile machine learning method that excels at both classification and regression tasks. Based on the limited sample information, it seeks the best compromise between the complexity and learning ability of the model. Its objective is to identify the optimal hyperplane that separates data into 2 distinct classes, where support vectors represent the critical data points that maximize the margin between the 2 classes. In this study, 4 SVM methods were employed: linear SVM, polynomial SVM, radial basis SVM, and sigmoid SVM. The kernel with the best performance was finally selected to develop the model [21].

The "glmnet," "rms," "random forest," "XGBoost," "e1071," and "rpart" packages in R software (R Foundation for Statistical Computing) were used to construct logistic regression, random forest, XGBoost, SVM, and CART prediction models.

Model Evaluation

The models were internally validated using validation sets. AUC, accuracy, precision, sensitivity, specificity, and F_1-score were used to evaluate the discrimination of the models. The prediction model calculated the AUC based on probability outputs. AUC values approaching 1.0 were considered to indicate superior predictive performance for postoperative SUI, while AUC values near 0.5 were considered to suggest limited clinical utility.

Model calibration was evaluated by both the Brier score and calibration curves. The Brier score quantifies prediction accuracy, with values approaching 0 indicating perfect prediction and values nearing 1 representing the poorest performance. Calibration curves were used to visualize the agreement between predicted probabilities and actual frequencies, where perfect calibration follows the 45-degree line.

Decision curve analysis (DCA) was used to evaluate the application value of the model in practical clinical decision-making and provide guidance for clinical decision-making.

Statistical Analysis

All data processing and statistical analyses were performed using R software (version 4.4.2). Numerical variables have been presented as mean (SD) for normally distributed data (analyzed with the Student *t* test) or median (IQR [P25, P75]) for nonnormally distributed data (analyzed with the Mann-Whitney *U* test). Categorical variables have been expressed as frequency (n) and were compared using chi-square tests.

Ethical Considerations

The study was approved by the Shanxi Bethune Hospital Medical Ethics Review Committee (YXLL-2025 - 072) and was performed in accordance with the principles of the Declaration of Helsinki. Written informed consent was obtained from each participant before taking measurements. All data were anonymized, and the study was conducted without offering any financial or material incentives to the participants.

Results

Clinical Characteristics

Between January 2021 and February 2025, 353 patients underwent prolapse surgery at Shanxi Bethune Hospital. Of

XSL•FO
RenderX

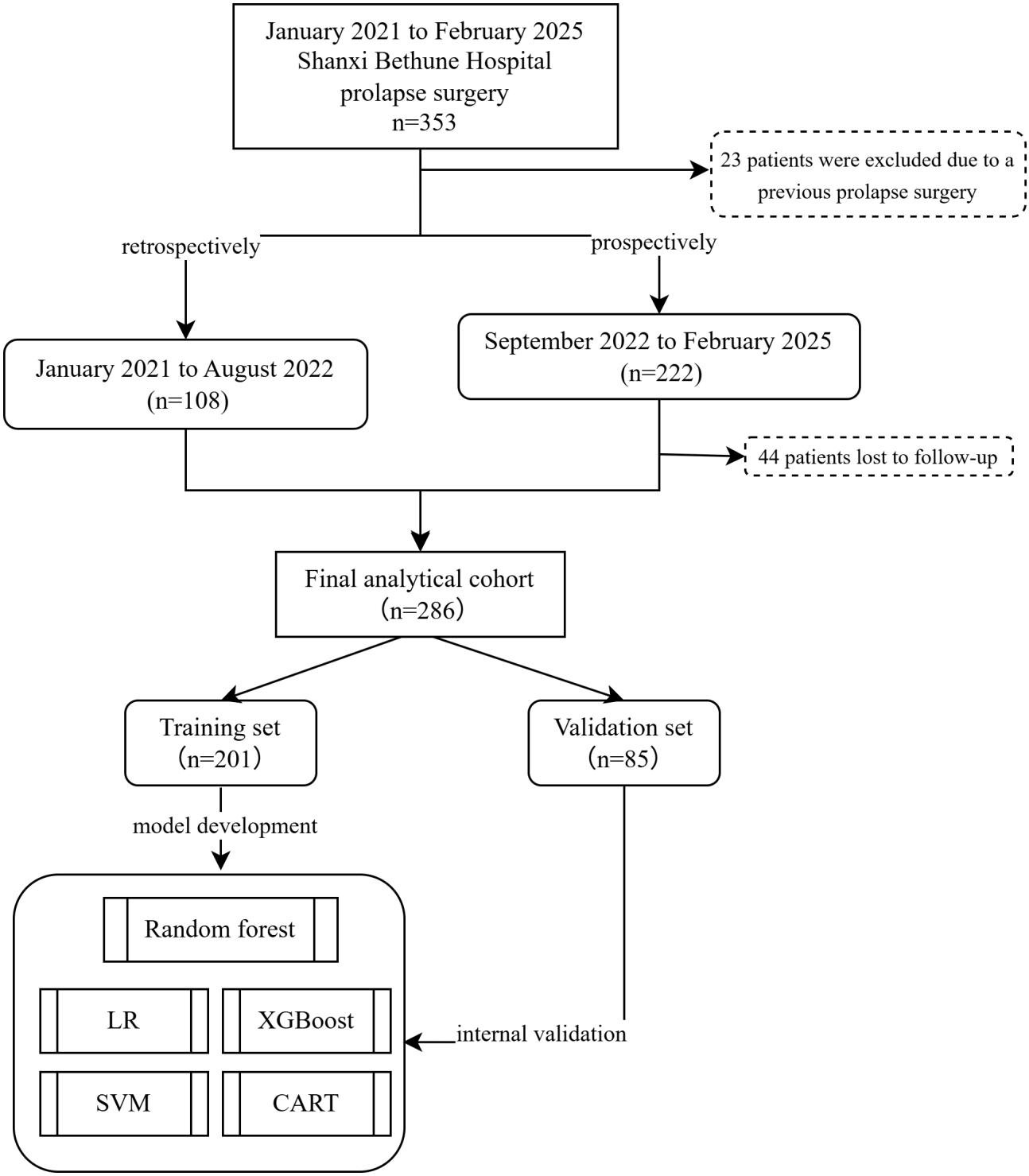
these patients, 23 were excluded due to a history of previous prolapse surgery, leaving 108 retrospectively enrolled patients from January 2021 to August 2022 and 222 prospectively recruited patients from September 2022 to February 2025. However, 44 patients were lost to follow-up. Thus, the final analytical cohort included 286 patients (Figure 1). These patients were randomly allocated to the training (n=201) and validation (n=85) sets in a 7:3 ratio, with no significant differences in baseline characteristics between the groups (all $P>.05$).

A total of 286 patients undergoing prolapse surgery were included, and of these patients, 91 (31.8%) developed postoperative SUI, including 27 (9.4%) with de novo SUI and 64 (22.4%) with persistent SUI. In univariate analysis, preoperative SUI, UUI, UOSUI, and longer genital hiatus were identified as significant predictors of postoperative SUI, while concomitant anti-SUI surgery was identified as a protective factor. Variables with $P\leq.05$ in univariate analysis are presented in Table 1.

Multivariate logistic regression analysis was performed for these 5 variables (Table 2). The results showed that preoperative SUI, UOSUI, length of genital hiatus, and concomitant anti-SUI surgery were influential factors for SUI after prolapse surgery.

XSL•FO
RenderX

Figure 1. Flowchart of patient selection and model development and validation. CART: classification and regression tree; LR: logistic regression; SVM: support vector machine; XGBoost: extreme gradient boosting.



XSL•FO
RenderX

Table . The results of univariate analysis.

Variable	Total (N=286)	Postoperative SUI[a] (−) (n=195)	Postoperative SUI (+) (n=91)	*t* test (*df*)	Chi-square (*df*)	*P* value
Gh[b], mean (SD)	5.44 (0.92)	5.28 (0.93)	5.78 (0.81)	−4.42 (284)	—[c]	<.001
SUI, n (%)				—	59.79 (1)	<.001
Absent	175 (61.2)	149 (76.4)	26 (28.6)			
Present	111 (38.8)	46 (23.6)	65 (71.4)			
UUI[d], n (%)				—	7.50 (1)	.006
Absent	244 (85.3)	174 (89.2)	70 (76.9)			
Present	42 (14.7)	21 (10.8)	21 (23.1)			
UOSUI[e], n (%)				—	13.92 (1)	<.001
Absent	255 (89.2)	183 (93.8)	72 (79.1)			
Present	31 (10.8)	12 (6.2)	19 (20.9)			
Anti-SUI surgery, n (%)				—	4.25 (1)	.04
No	267 (93.4)	178 (91.3)	89 (97.8)			
Yes	19 (6.6)	17 (8.7)	2 (2.2)			

[a]SUI: stress urinary incontinence.
[b]Gh: genital hiatus.
[c]Not applicable.
[d]UUI: urge urinary incontinence.
[e]UOSUI: urodynamic occult stress urinary incontinence.

Table . Multivariate logistic regression analysis.

Variable	β	SE	Z	*P* value	OR[a] (95% CI)
Intercept	−5.17	1.07	−4.82	<.001	0.01 (0.00-0.05)
Gh[b]	0.60	0.18	3.26	.001	1.83 (1.27-2.62)
SUI[c]					
Absent	—[d]	—	—	—	1.00 (reference)
Present	2.16	0.32	6.77	<.001	8.71 (4.66-16.30)
UUI[e]					
Absent	—	—	—	—	1.00 (reference)
Present	0.76	0.42	1.78	.07	2.13 (0.93-4.89)
UOSUI[f]					
Absent	—	—	—	—	1.00 (reference)
Present	1.12	0.54	2.06	.04	3.05 (1.06-8.80)
Anti-SUI surgery					
No	—	—	—	—	1.00 (reference)
Yes	−3.03	0.84	−3.60	<.001	0.05 (0.01-0.25)

[a]OR: odds ratio.
[b]Gh: genital hiatus.
[c]SUI: stress urinary incontinence.
[d]Not applicable.
[e]UUI: urge urinary incontinence.
[f]UOSUI: urodynamic occult stress urinary incontinence.

XSL•FO
RenderX

Model Development

Logistic Regression Predictive Model

Lasso regression was used to identify nonzero coefficient predictors from both the postoperative SUI and non-SUI groups, thereby refining the risk factors for postoperative SUI complications (Figure 2). The optimal λ value (0.041) was selected through 5-fold cross-validation, and 4 nonzero coefficient predictors were selected, including preoperative SUI, anterior colporrhaphy, anti-SUI surgery, and length of genital hiatus.

Subsequently, the risk factors selected by Lasso regression were incorporated into the logistic regression predictive model, with the corresponding nomogram presented in Figure 3. The model demonstrated an AUC of 0.817 (95% CI 0.755 - 0.880) in the training set, maintaining robust discrimination upon internal validation (AUC=0.869, 95% CI 0.791 - 0.947).

Figure 2. Lasso regression for filtered predictors. (A) Cross-validation error; (B) Coefficient paths.

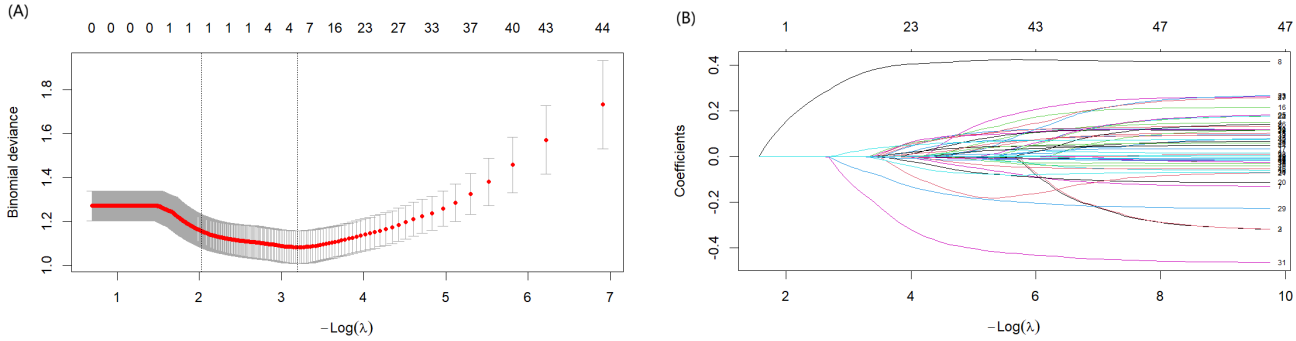
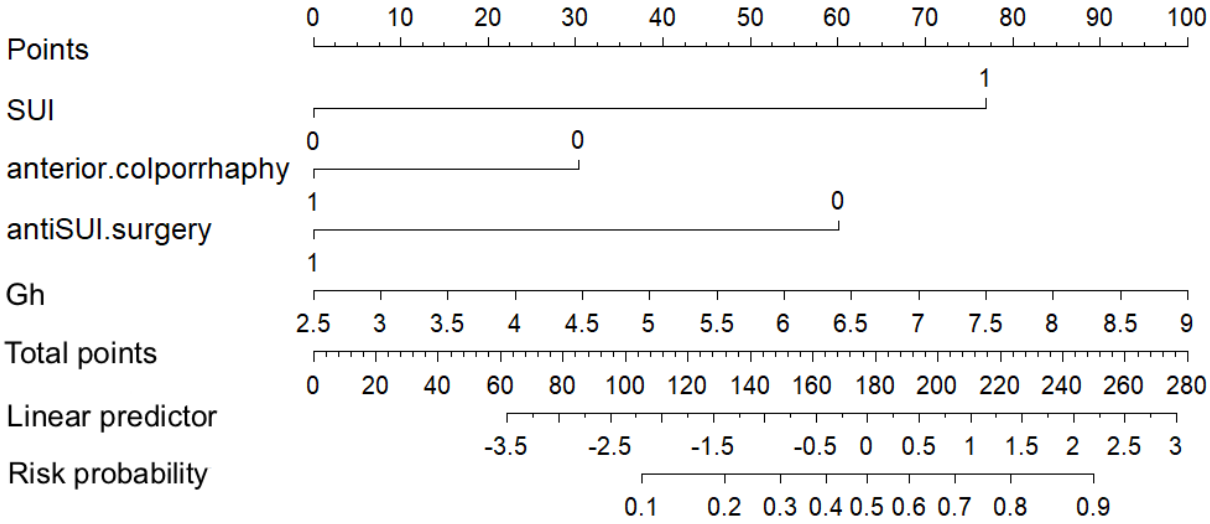


Figure 3. Logistic regression model nomogram. Gh: genital hiatus; SUI: stress urinary incontinence.

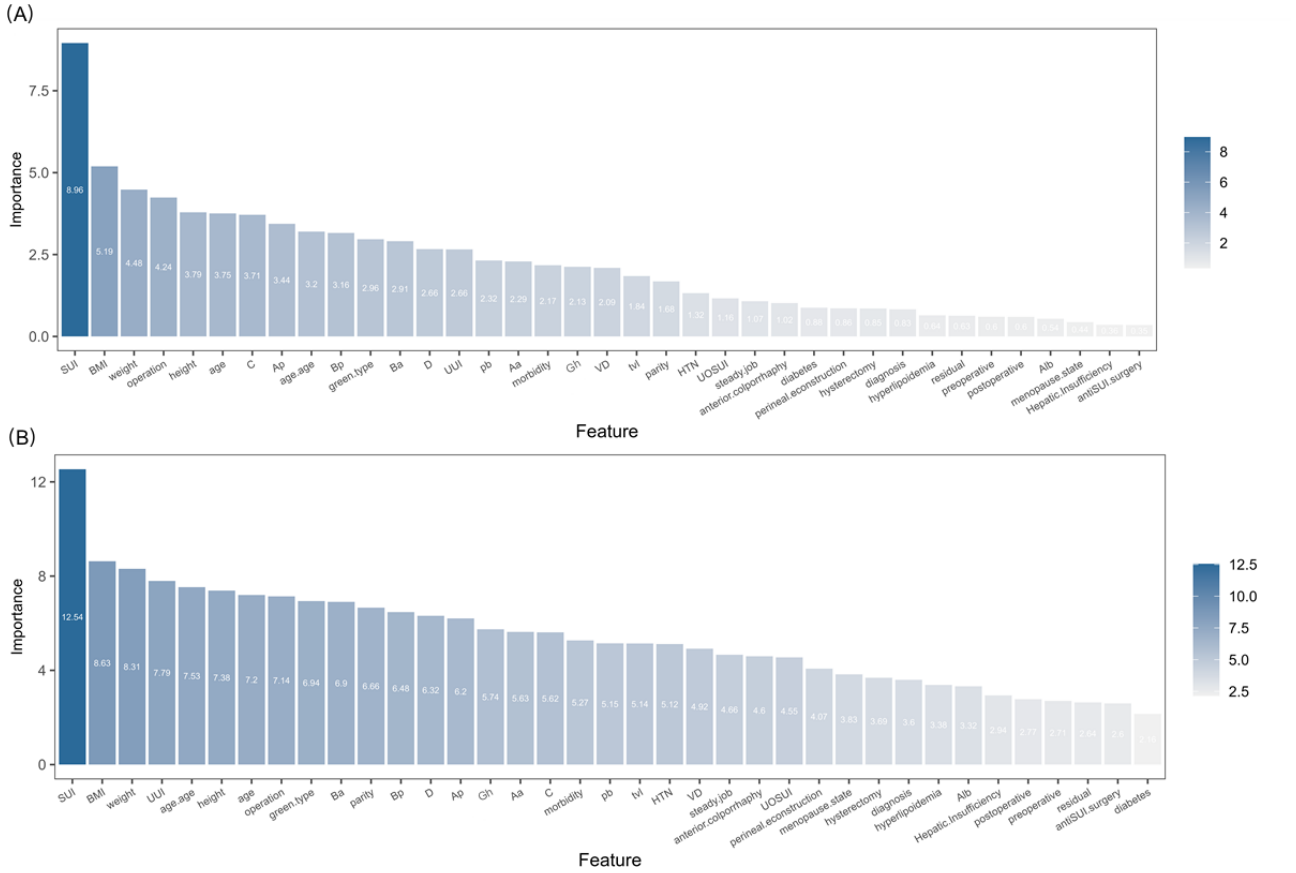


Random Forest Predictive Model

A preliminary random forest model was constructed with 38 variables, and the importance of the variables was calculated, as shown in Figure 4. We chose to include the top 8 features (SUI, BMI, weight, UUI, age at menopause, height, age, and operation) as ranked by mean decrease accuracy, since this measure more directly reflects a feature's contribution to classification performance and mitigates the evaluation biases associated with the Gini index. To optimize model performance, hyperparameter tuning was conducted through cross-validation to determine the optimal *mtry* value. Subsequently, the out-of-bag error was used to identify the ideal number of decision trees (ntree) for ensuring model stability and convergence. After parameter adjustment and bootstrap resampling (n=500 iterations), the parameters of the final random forest prediction model were set as follows: max_depth=5, min_samples_split=10, min_samples_leaf=5, mtry=3, ntree=146, maxnodes=20, and nodesize=5. The random forest model showed good differentiation in the training set (AUC=0.855, 95% CI 0.796 - 0.914), but the AUC dropped to 0.731 (95% CI 0.604 - 0.858) in the internal validation.

XSL•FO
RenderX

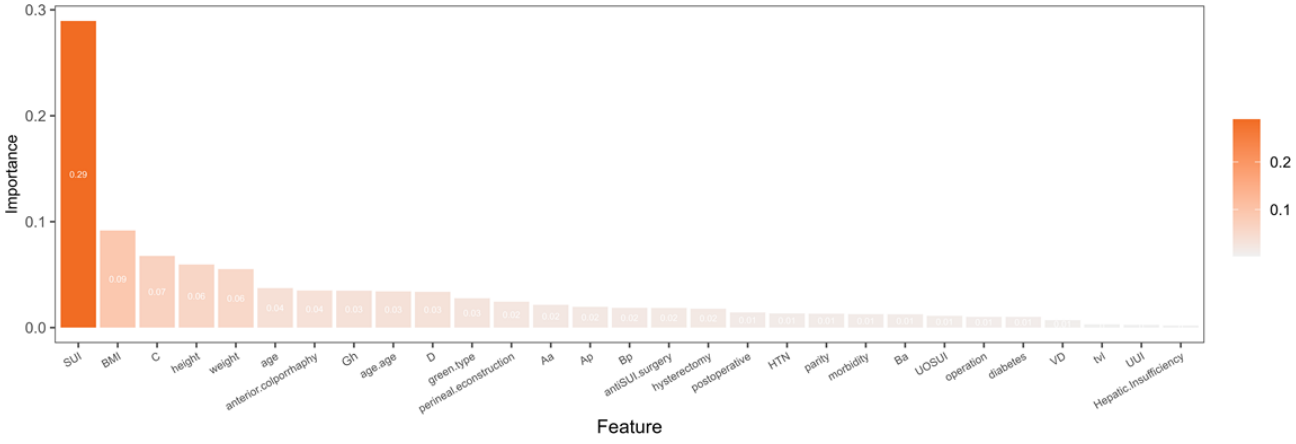
Figure 4. Feature importance plot of the random forest model. (A) Feature importance plot of the random forest model based on the Gini index; (B) Feature importance plot of the random forest model based on accuracy. HTN: hypertension; SUI: stress urinary incontinence; UOSUI: urodynamic occult stress urinary incontinence; UUI: urge urinary incontinence; VD: vaginal delivery.



XGBoost Model

The regularization and early stop methods were used to reduce the overfitting of the model, and the optimal parameters and top 8 variables of importance were selected to build the XGBoost prediction model. The importance of accuracy based on the preliminary XGBoost model is shown below (Figure 5). After hyperparameter tuning by the train() function and 5-fold cross-validation, the final XGBoost model demonstrated enhanced predictive performance with the following configuration: eta=0.01, max_depth=3, gamma=0.1, colsample_bytree=0.8, min_child_weight=1, subsample=0.8, lambda=3, alpha=.5, early_stopping_rounds=10, and nrounds=200. The XGBoost prediction model had an AUC of 0.899 (95% CI 0.856 - 0.943) and an AUC of 0.783 (95% CI 0.680 - 0.886) in the training set.

Figure 5. Feature importance of the extreme gradient boosting model based on accuracy. HTN: hypertension; SUI: stress urinary incontinence; UOSUI: urodynamic occult stress urinary incontinence; UUI: urge urinary incontinence; VD: vaginal delivery.



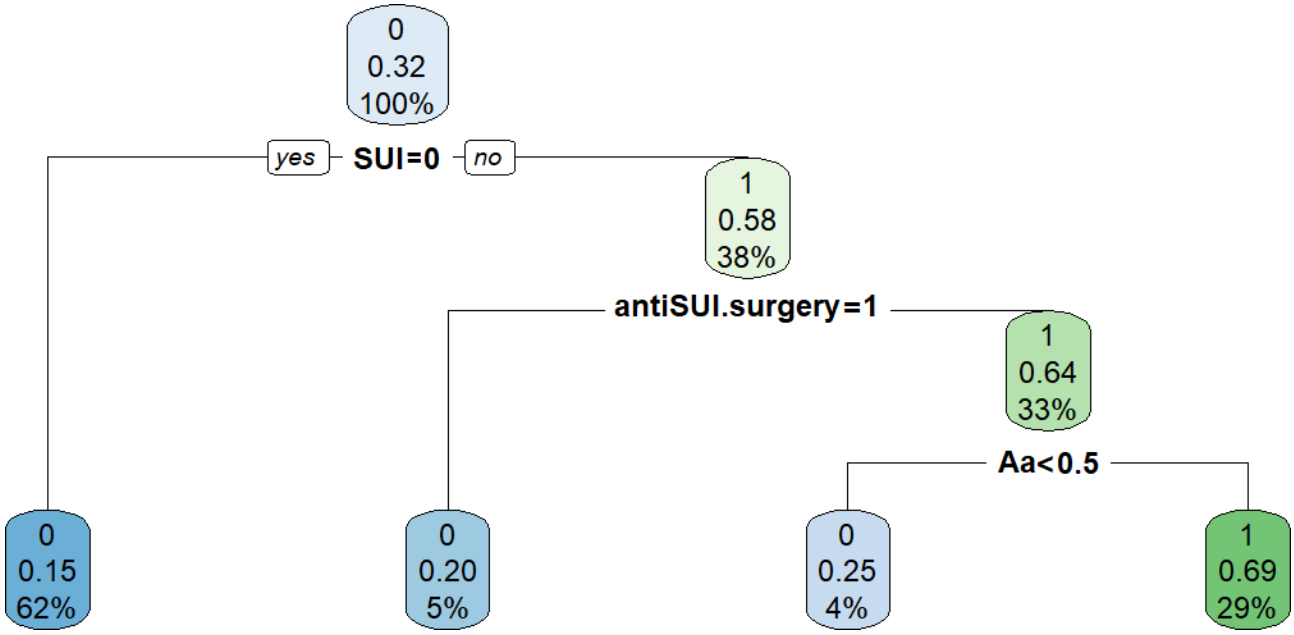
CART Model

The CART model, after pruning according to the optimal complexity parameters (0.625), is shown in Figure 6, illustrating the final classification tree used to predict the occurrence of postoperative SUI. The CART model contained 3 branches based on 3 key predictive factors: preoperative SUI status, concomitant anti-SUI procedure, and POP-Q point C, which

XSL•FO
RenderX

simplified postoperative SUI assessment. The model directed "yes" responses to the left node and "no" responses to the right node. For patients without preoperative SUI (representing 62% of the cohort), the postoperative SUI probability was 0.15. The AUC of this decision tree model was 0.764 (95% CI 0.695 - 0.832). In the validation set, the AUC was 0.782 (95% CI 0.677 - 0.886). The model exhibited minimal overfitting.

Figure 6. Decision tree. SUI: stress urinary incontinence.



SVM Model

After hyperparameter tuning of the 4 kernel functions (linear kernel, radial base kernel, polynomial kernel, and sigmoid kernel), their accuracy, precision, recall, specificity, and F_1-scores were calculated, and the findings are summarized in Table 3. We observed that the sigmoid kernel predicted all samples as class 0. This phenomenon may be attributed to a mismatch between the sigmoid kernel function and the characteristics of the dataset in our study. Under the optimized hyperparameters (gamma=0.1; coefficient 0=3), the decision function values for all samples were negative (ranging from −0.92 to −4.05) and were classified as class 0 according to the decision rule of SVMs, resulting in the model's failure to form an effective classification boundary. Consequently, the precision, recall, and F_1-score of the sigmoid model were considered invalid.

The preliminary analysis found that the polynomial kernel SVM classifier had better performance than the other 3 kernel classifiers (Table 3), and thus, polynomial kernel modeling was selected. Finally, the SVM prediction model was developed with 4 variables obtained by Lasso regression. The AUC of the final SVM model was 0.821 (95% CI 0.760 - 0.883), and the validation set AUC was 0.846 (95% CI 0.757 - 0.936).

Table . Evaluation of support vector machine kernels.

Model type	Accuracy, %	Precision, %	Recall, %	Specificity, %	F_1-score, %
Linear kernel	72.94	62.96	56.67	81.82	59.62
Polynomial kernel	78.82	66.67	66.67	84.48	66.67
Radial base kernel	76.47	51.85	66.67	79.69	58.33
Sigmoid kernel	68.24	—[a]	—	100.00	—

[a]Not applicable.

Comparison of the 5 Models and Applications

The performance metrics of all 5 models are summarized as follows: Figure 7A displays the combined AUC values for the training set, while Figure 7B presents those for the validation set. Except for the CART model, the AUC values of all other models were above 0.8, demonstrating excellent discriminative ability, while the AUC values in the validation set were above 0.7. Comprehensive evaluation metrics, including AUC, accuracy, precision, recall, specificity, and F_1-score, for the training set are detailed in Table 4, with corresponding validation set metrics provided in Table 5. Across all models, we observed a consistent pattern of relatively low recall coupled with high specificity.

XSL•FO
RenderX

Figure 7. Receiver operating characteristic curves (ROCs) of each model. (A) ROCs in the training set; (B) ROCs in the validation set. AUC: area under the curve; CART: classification and regression tree; LR: logistic regression; RF: random forest; SVM: support vector machine; XGBoost: extreme gradient boosting.

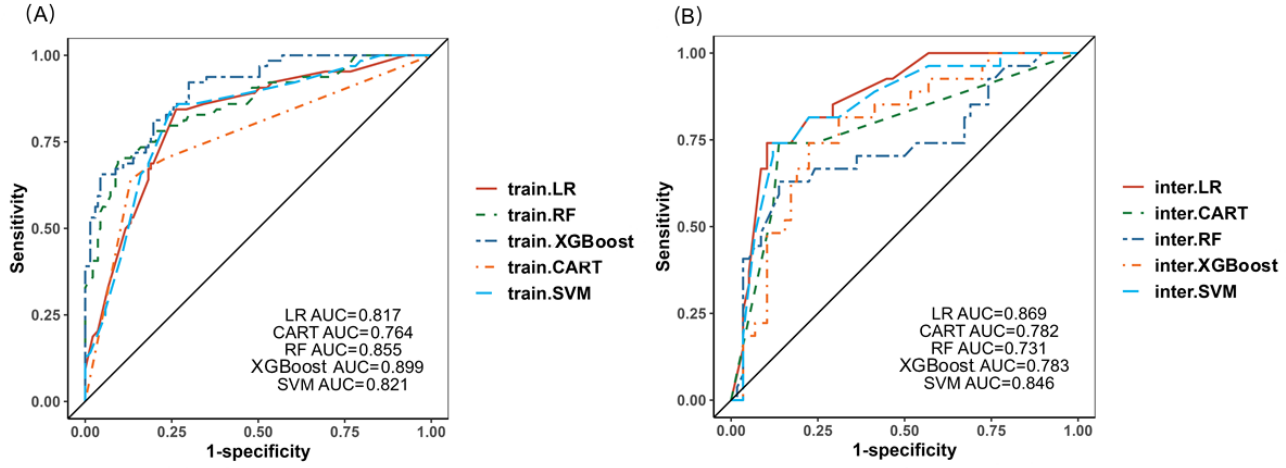


Table . Evaluation of the 5 models in the training set.

Model	AUC[a]	Accuracy	Precision	Sensitivity	Specificity	F_1-score
LR[b]	0.81	0.74	0.70	0.33	0.90	0.45
CART[c]	0.76	0.80	0.6	0.64	0.87	0.67
RF[d]	0.85	0.84	0.77	0.69	0.91	0.73
XGBoost[e]	0.90	0.85	0.82	0.66	0.93	0.73
SVM[f]	0.82	0.78	0.66	0.66	0.84	0.66

[a]AUC: area under the curve.
[b]LR: logistic regression.
[c]CART: classification and regression tree.
[d]RF: random forest.
[e]XGBoost: extreme gradient boosting.
[f]SVM: support vector machine.

Table . Evaluation of the 5 models in the validation set.

Model	AUC[a]	Accuracy	Precision	Sensitivity	Specificity	F_1-score
LR[b]	0.87	0.76	0.77	0.37	0.95	0.50
CART[c]	0.78	0.78	0.68	0.56	0.88	0.61
RF[d]	0.73	0.78	0.65	0.63	0.84	0.64
XGBoost[e]	0.78	0.76	0.63	0.63	0.83	0.63
SVM[f]	0.85	0.82	0.73	0.70	0.88	0.72

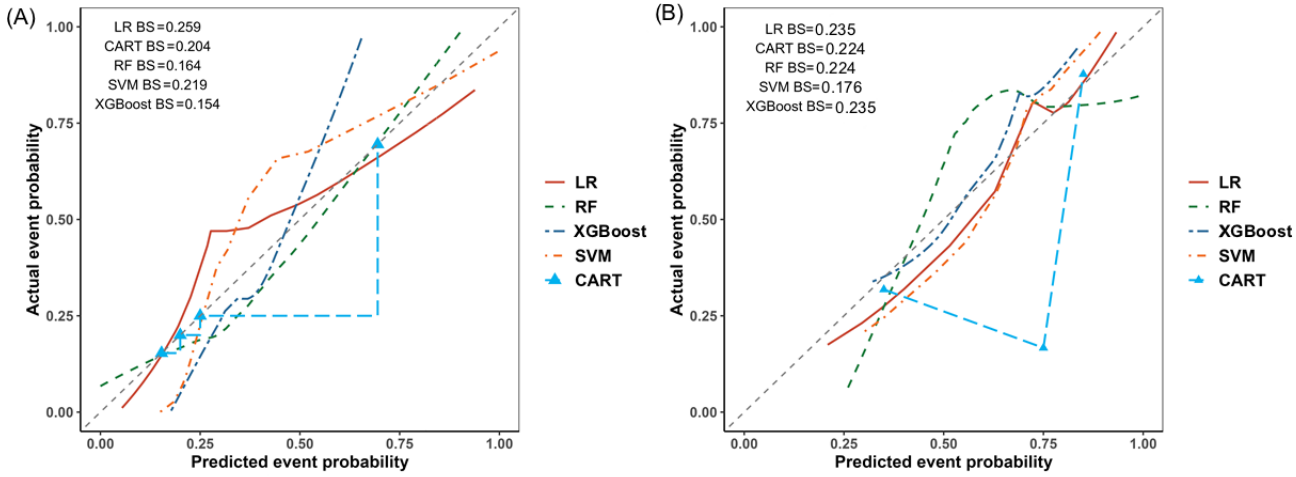
[a]AUC: area under the curve.
[b]LR: logistic regression.
[c]CART: classification and regression tree.
[d]RF: random forest.
[e]XGBoost: extreme gradient boosting.
[f]SVM: support vector machine.

Figure 8 presents the Brier scores and calibration curves for the 5 models. Given that the CART model produces only 4 discrete predicted probabilities, its calibration curve was plotted directly using the binning method. The calibration curves for other models were generated using the Lowess smoothing method. The Brier index of the logistic regression model in the training

XSL•FO
RenderX

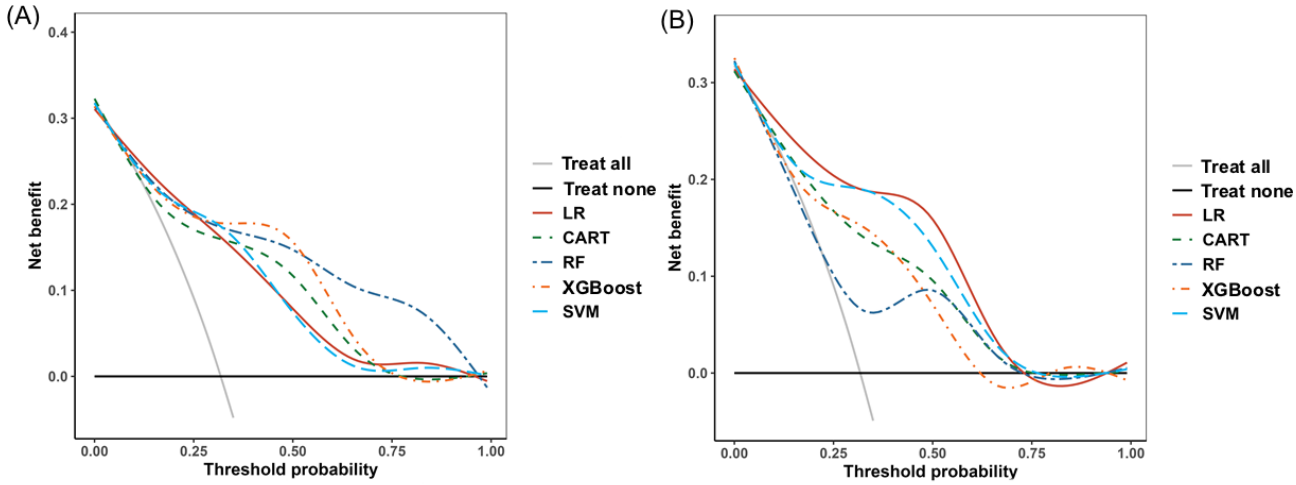
set was relatively high (0.259). The performance of the 5 models in the validation set was worse than that in the training set. It can be seen from the calibration curve that there is a high consistency between the predicted outcomes of the models and the actual outcomes of the training set (Figure 8A). The calibration of the validation set (Figure 8B) was worse than that of the training set.

Figure 8. Brier index and calibration curves of the 5 models. (A) Brier index and calibration curves in the training set; (B) Brier index and calibration curves in the validation set. BS: Blair score; CART: classification and regression tree; LR: logistic regression; RF: random forest; SVM: support vector machine; XGBoost: extreme gradient boosting.



From the DCA (Figure 9), in the training set, the curve of the XGBoost model (at predicted probabilities of 0.8 - 0.9) was slightly below the *treat none* curve, while all other models performed above both the *treat all* and *treat none* curves, demonstrating high net benefit. However, in the validation set's DCA, the overall performance was acceptable, though slightly inferior to that of the training set. Meanwhile, the logistic regression model appeared to achieve the highest net benefit in the validation set.

Figure 9. Decision curve analysis of the 5 models. (A) Decision curve analysis in the training set; (B) Decision curve analysis in the validation set. CART: classification and regression tree; LR: logistic regression; RF: random forest; SVM: support vector machine; XGBoost: extreme gradient boosting.



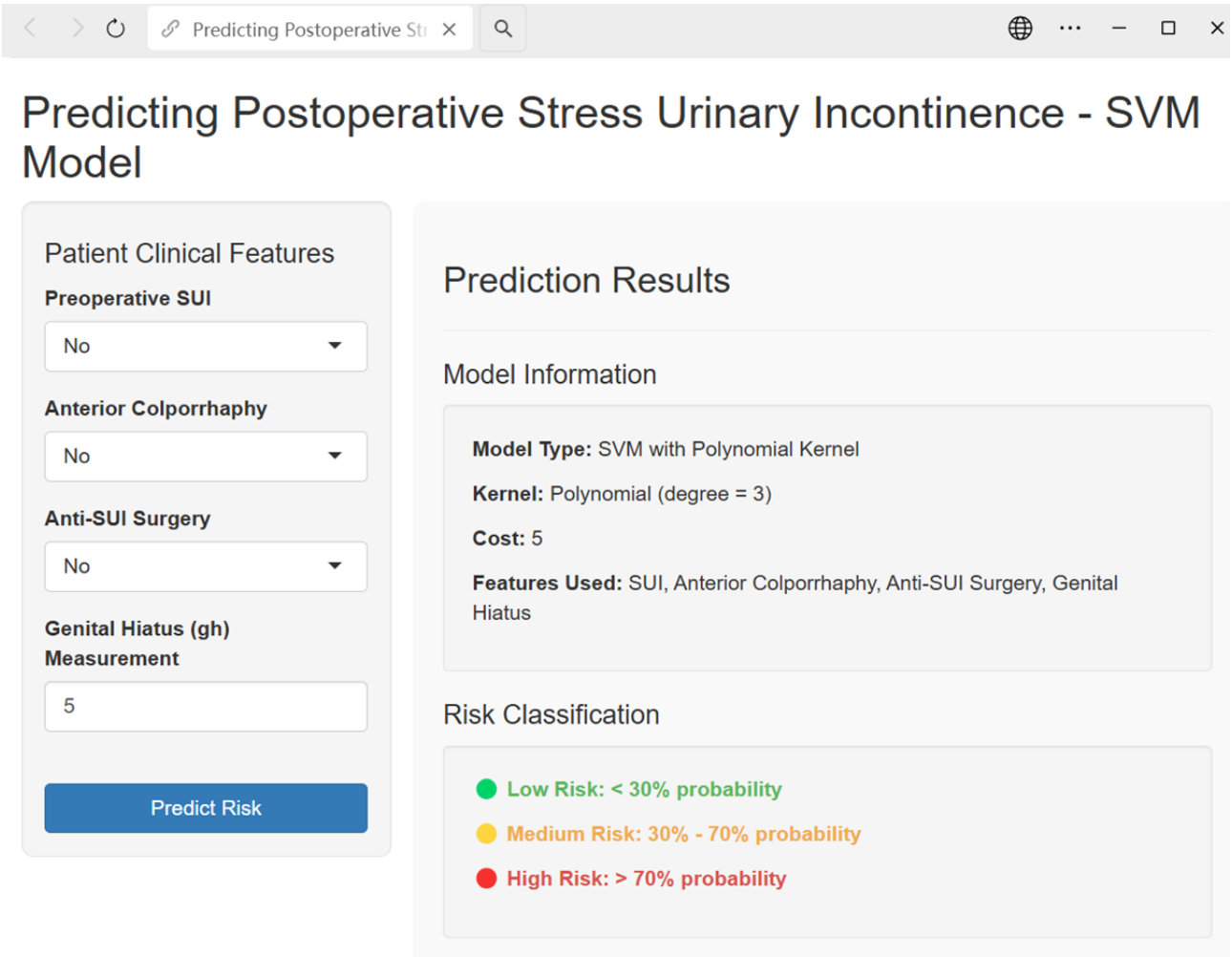
Overall, the logistic regression prediction model demonstrated a high AUC; however, its overall performance in terms of recall and F_1-score, as well as its calibration, was inferior to that of the other models. Both the random forest and XGBoost models exhibited an AUC difference of more than 0.1 between the training and validation sets, indicating a high degree of overfitting. The CART model offered advantages in ease of interpretation and demonstrated acceptable discriminatory power. However, due to its inherent algorithmic structure, the CART model produced a limited number of discrete risk categories (n=4), which consequently resulted in poor calibration performance.

The SVM model demonstrated good stability in AUC and DCA. However, DCA revealed its tendency to overestimate the probability of positive outcomes in negative cases and underestimate the actual risk in positive cases. It should be noted that this phenomenon in the calibration curve was not unique to the SVM model, as similar phenomena were observed in the other models. The SVM model seemed to have the best performance according to current data and analysis.

XSL•FO
RenderX

In addition to the nomogram and decision tree, we developed prediction tools for the random forest, XGBoost, and SVM models using Shiny to facilitate clinical implementation, as illustrated in Figure 10.

Figure 10. Example of support vector machine model application.



Discussion

Principal Findings

This study analyzed the data from 286 patients who underwent prolapse surgery, obtained the risk factors for postoperative SUI, and developed 5 novel prediction models, including a conventional logistic regression–based model and 4 machine learning–based models (random forest, XGBoost, CART, and SVM). Among the models, the SVM prediction model demonstrated relatively robust performance.

Comparison With Prior Work

Jelovsek et al [9] developed the first logistic regression prediction model for SUI after prolapse surgery (termed the OPUS model) based on data from the OPUS trial, achieving an AUC of 0.72. Since the OPUS study exclusively enrolled patients without SUI, this model is only applicable to patients without SUI for predicting de novo SUI. External validation using data from the CARE (Colpopexy and Urinary Reduction Efforts) trial yielded an AUC of 0.62. When conducting external validation using available data from the CUPIDO trial, the model's AUC was 0.63 [22]. Yasa et al [23] reported a markedly lower AUC of 0.56 during external validation with data from the Istanbul University Faculty of Medicine, concluding that the OPUS model demonstrated poor diagnostic performance.

van der Ploeg et al [10] developed the second logistic regression prediction model for SUI after prolapse surgery based on data from the CUPIDO trial (termed the CUPIDO model), achieving an AUC of 0.76. The CUPIDO-1 trial enrolled 134 patients with preoperative overt SUI, and the CUPIDO-2 trial enrolled 225 patients with occult SUI. Consequently, this model is not well-suited for patients without either overt or occult SUI preoperatively. To date, no external validation of the CUPIDO model has been conducted.

Oh et al [11] developed the third logistic regression prediction model (termed the Oh model), which is applicable to all prolapse women, regardless of preoperative SUI status or prolapse surgery type, achieving an AUC of 0.78. They partitioned data in a 4:1 ratio, allocating 20% for external validation, which yielded an AUC of 0.73.

Fu et al [14] developed the first machine learning–based predictive model for postoperative SUI following prolapse surgery by using the retrospective data of 555 patients. The study used 3 modeling approaches: random forest, XGBoost, and logistic regression. The authors determined that the

XSL•FO
RenderX

XGBoost model demonstrated optimal predictive capability, with an AUC of 0.714 in the training set, 0.721 in internal validation using 5-fold cross-validation, and 0.704 in external validation with a randomly partitioned validation set. Regrettably, they only provide model parameters without the model application available.

In our study, 5 methods were used to construct the prediction model, covering tree model, linear model, and ensemble learning. It is suggested to use various methods to build a predictive model of machine learning and finally select the best model based on performance indicators [24]. Our prediction models, developed using retrospective and prospective data, are applicable to all patients with prolapse irrespective of the preoperative SUI status or prolapse surgical approach. Compared with previous random forest and XGBoost prediction models, the validation set randomly divided by our data had a higher AUC, and 2 other machine learning models were constructed: SVM and CART.

The logistic regression prediction model developed in our study demonstrated high AUC values in both the training and validation sets, though sensitivity and F_1-scores were slightly lower. The low incidence of SUI after prolapse may lead to an imbalance between positive and negative samples, resulting in high specificity and low sensitivity. In contrast, both the random forest and XGBoost models exhibited notable discrepancies between the AUC of the training set and that of the validation set, with validation AUCs remaining above 0.7 yet still demonstrating signs of overfitting. As ensemble methods based on decision trees, random forest and XGBoost typically resist overfitting; however, excessive tree numbers or depth may still lead to overfitting. Despite employing various mitigation strategies, including parameter tuning, bootstrap resampling, and 5-fold cross-validation, overfitting persisted. The reproducibility of machine learning models remains a significant challenge in health care applications [25,26]. Furthermore, the observed overfitting in these models may be partially attributable to insufficient sample size. For machine learning–based predictive models, larger datasets are typically required to ensure reproducibility. Although the CART model demonstrated inferior overall performance compared to other algorithms, it showed remarkable consistency between training and validation sets. Its user-friendly nature made it more applicable in clinical work. Notably, the SVM model exhibited better performance in the validation set compared to the training set, suggesting strong potential for clinical generalization.

Risk Factors for Postoperative SUI

Based on univariate analysis, multivariate logistic regression analysis, and Lasso regression analysis, several influencing factors of postoperative SUI were obtained: preoperative SUI, UUI, UOSUI, anti-SUI surgery, genital hiatus, and anterior colporrhaphy. SUI, UUI, and UOSUI are lower urinary tract symptoms closely related to POP. SUI is caused by the laxity of the local supporting structures of the bladder neck. In some patients undergoing POP surgery, the anatomical defects at the bladder neck remain uncorrected, leading to persistent SUI symptoms postoperatively [4]. Studies indicate that 5.2% - 31% of urinary incontinence persists after surgery [27,28]. In patients with UUI, surgery may not address the cause of UUI, and the implanted mesh and other irritative factors may even aggravate UUI. Nationwide prolapse surgery data from Finland suggested that de novo SUI occurs more frequently in patients with preoperative UUI [3].

Occult SUI refers to SUI after prolapse reduction, with an incidence of 23.5% - 42.5% [29,30]. With the progression of POP, particularly in cases of advanced anterior vaginal wall prolapse, the folding of the bladder and urethra may lead to the disappearance of SUI symptoms. After prolapse reduction, the fold of the lower urinary tract can be repaired, and the masked SUI symptoms will appear again [31]. Data from a randomized controlled trial suggested that 52% of patients with occult SUI progressed to SUI after surgery [32]. The International Continence Society, German Society of Gynecology and Obstetrics, and International Consultation on Incontinence recommend a preoperative urodynamic study to uncover occult SUI [30,33-35]. A prolapse reduction stress test for revealing occult SUI has been utilized in several predictive models [9-11].

Anterior colporrhaphy is a standard surgical procedure, just like appendectomy and tonsillectomy, and is widely performed around the world [36]. The principle of anterior colporrhaphy is based on the plication of the vesicovaginal fascia at the midline to strengthen the tissue between the vagina and bladder, previously known as the Kelly operation [37]. In the 1990s, multiple randomized controlled trials demonstrated that anterior colporrhaphy alone significantly improved SUI [38-40]. Bergman et al [38] reported an 82% cure rate for SUI following simple anterior colporrhaphy.

Genital hiatus length is defined as the distance from the external urethral meatus to the posterior edge of the hymen. An increase in genital hiatus may lead to a weakening of support for the urethra and bladder, contributing to the development of incontinence. A study about pelvic floor ultrasound and pelvic floor dysfunction found that women with urinary incontinence exhibited a longer genital hiatus [41,42]. A study by Huang et al [43] found that cystocele was associated with longer genital hiatus.

Advantages, Limitations, and Future Perspectives

This study developed CART and SVM models for predicting SUI after prolapse for the first time, and our random forest and XGBoost models also demonstrated superior discriminative ability compared to previous models. In addition, this is the first study to develop models incorporating prospective data for SUI after prolapse surgery, thereby reducing recall bias. Our 7:3 random split of the dataset into training and validation sets for internal validation provides greater representativeness than bootstrap resampling for internal validation [22].

This study has several limitations. First, the sample size was insufficient for robust machine learning prediction, and some models still exhibited overfitting. Second, external validation using independent datasets (eg, from other hospitals or regions) was lacking. Third, the inclusion of retrospective data introduced recall bias, and the absence of objective postoperative SUI assessments, such as standardized symptom quantification and pad tests, may have led to information bias. Additionally,

XSL•FO
RenderX

variability in POP-Q measurements across different clinicians over this long-term study might have contributed to measurement errors [44].

The 5 prediction models developed in this study demonstrated overall strong performance, with acceptable performance in randomly split internal validation. When considering discrimination, calibration, and clinical utility collectively, the SVM model appeared to exhibit robust performance. Based on both the current status of prediction models for SUI after prolapse surgery and this study's limitations, we recommend: (1) the publication of experimental data, (2) the establishment of large databases from prospective studies, and (3) the standardization of the diagnosis and treatment of POP. These steps are beneficial for reducing information bias, so as to establish a generalizable prediction model with high accuracy on a national and even global scale.

Conclusions

This study developed and internally validated 5 machine learning–based prediction models for SUI after prolapse surgery, which are applicable to all patients, regardless of preoperative SUI status and surgical approach. The model approaches included logistic regression, random forest, XGBoost, SVM, and CART. The SVM model demonstrated the most robust performance among all algorithms evaluated. We identified the following 6 predictive factors for postoperative SUI: preoperative SUI, UUI, UOSUI, concomitant anti-SUI surgery, genital hiatus, and anterior colporrhaphy. External validation is required to evaluate generalizability and determine the optimal model for clinical decision-making in postoperative SUI management.

Acknowledgments

This work was supported by the National Natural Science Foundation of China (grant number: 81971365), the 2025 Central Guidance Fund for Local Science and Technology Development Projects (project number: YDZJSX2025D076), Shanxi Province Selective Funding Program for Scientific and Technological Activities of Returned Scholars (grant number: 2025058), and Shanxi Provincial Science and Technology Innovation Talent Team Project (project number: 202204051002031).

Data Availability

The R Shiny implementations of the random forest, extreme gradient boosting, and support vector machine models can be obtained by contacting the corresponding author. The datasets generated or analyzed during this study are not publicly available.

Authors' Contributions

Conceptualization: XL
Data curation: MS
Formal analysis: MS, SW
Funding acquisition: XL
Investigation: MS
Methodology: MS, SW
Project administration: MS
Software: MS, SW
Supervision: XL
Writing – original draft: MS
Writing – review & editing: MS, SW, XL

Conflicts of Interest

None declared.

References

1. Weintraub AY, Glinter H, Marcus-Braun N. Narrative review of the epidemiology, diagnosis and pathophysiology of pelvic organ prolapse. Int Braz J Urol 2020;46(1):5-14. [doi: 10.1590/S1677-5538.IBJU.2018.0581] [Medline: 31851453]
2. Kalejaiye O, Vij M, Drake MJ. Classification of stress urinary incontinence. World J Urol 2015 Sep;33(9):1215-1220. [doi: 10.1007/s00345-015-1617-1] [Medline: 26108731]
3. Karjalainen PK, Tolppanen AM, Wihersaari O, Nieminen K, Mattsson NK, Jalkanen JT. Changes in stress urinary incontinence symptoms after pelvic organ prolapse surgery: a nationwide cohort study (FINPOP). Int Urogynecol J 2024 Apr;35(4):909-919. [doi: 10.1007/s00192-024-05760-0] [Medline: 38546868]
4. Liang H, Dan L. Current status of research on stress urinary incontinence after pelvic organ prolapse surgery (盆腔器官脱垂手术后发生压力性尿失禁的研究现况) [Article in Chinese]. Prog Obstet Gynecol 2021;30(2):154-155 [FREE Full text] [doi: 10.13283/j.cnki.xdfckjz.2021.02.011]

XSL•FO
RenderX

5. van der Ploeg JM, van der Steen A, Zwolsman S, van der Vaart CH, Roovers J. Prolapse surgery with or without incontinence procedure: a systematic review and meta-analysis. BJOG 2018 Feb;125(3):289-297. [doi: 10.1111/1471-0528.14943] [Medline: 28941138]
6. Muñiz KS, Pilkinton M, Winkler HA, Shalom DF. Prevalence of stress urinary incontinence and intrinsic sphincter deficiency in patients with stage IV pelvic organ prolapse. J Obstet Gynaecol Res 2021 Feb;47(2):640-644. [doi: 10.1111/jog.14574] [Medline: 33205578]
7. Bideau M, Allègre L, Callewaert G, Fatton B, de Tayrac R. Stress urinary incontinence after transvaginal mesh surgery for anterior and apical prolapse: preoperative risk factors. Int Urogynecol J 2021 Jan;32(1):111-117. [doi: 10.1007/s00192-020-04363-9] [Medline: 32533213]
8. Cruz RA, Faria CA, Gomes SCS Jr. Predictors for de novo stress urinary incontinence following pelvic reconstructive surgery with mesh. Eur J Obstet Gynecol Reprod Biol 2020 Oct;253(15–20):15-20. [doi: 10.1016/j.ejogrb.2020.07.033] [Medline: 32745815]
9. Jelovsek JE, Chagin K, Brubaker L, et al. A model for predicting the risk of de novo stress urinary incontinence in women undergoing pelvic organ prolapse surgery. Obstet Gynecol 2014 Feb;123(2 Pt 1):279-287. [doi: 10.1097/AOG.0000000000000094] [Medline: 24402598]
10. van der Ploeg JM, Steyerberg EW, Zwolsman SE, van der Vaart CH, Roovers J. Stress urinary incontinence after vaginal prolapse repair: development and internal validation of a prediction model with and without the stress test. Neurourol Urodyn 2019 Apr;38(4):1086-1092. [doi: 10.1002/nau.23958] [Medline: 30843271]
11. Oh S, Lee S, Hwang WY, Suh DH, Jeon MJ. Development and validation of a prediction model for bothersome stress urinary incontinence after prolapse surgery: a retrospective cohort study. BJOG 2022 Jun;129(7):1158-1164. [doi: 10.1111/1471-0528.17036] [Medline: 34854216]
12. Kapoor S, Cantrell EM, Peng K, et al. REFORMS: consensus-based recommendations for machine-learning-based science. Sci Adv 2024 May 3;10(18):eadk3452. [doi: 10.1126/sciadv.adk3452] [Medline: 38691601]
13. Andaur Navarro CL, Damen J, Takada T, et al. Protocol for a systematic review on the methodological and reporting quality of prediction model studies using machine learning techniques. BMJ Open 2020 Nov 11;10(11):e038832. [doi: 10.1136/bmjopen-2020-038832] [Medline: 33177137]
14. Fu L, Huang G, Sun Z, Zhu L. Predicting the occurrence of stress urinary incontinence after prolapse surgery: a machine learning-based model. Ann Transl Med 2023 Mar 31;11(6):251. [doi: 10.21037/atm-22-3648] [Medline: 37082678]
15. Riley RD, Ensor J, Snell KIE, et al. Calculating the sample size required for developing a clinical prediction model. BMJ 2020 Mar 18;368:m441. [doi: 10.1136/bmj.m441] [Medline: 32188600]
16. Grajski KA, Breiman L, Viana Di Prisco G, Freeman WJ. Classification of EEG spatial patterns with a tree-structured methodology: CART. IEEE Trans Biomed Eng 1986 Dec;33(12):1076-1086. [doi: 10.1109/TBME.1986.325684] [Medline: 3817838]
17. Breiman L. Random forests. Mach Learn 2001 Oct;45(1):5-32. [doi: 10.1023/A:1010933404324]
18. Altmann A, Toloşi L, Sander O, Lengauer T. Permutation importance: a corrected feature importance measure. Bioinformatics 2010 May 15;26(10):1340-1347. [doi: 10.1093/bioinformatics/btq134] [Medline: 20385727]
19. Strobl C, Boulesteix AL, Zeileis A, Hothorn T. Bias in random forest variable importance measures: illustrations, sources and a solution. BMC Bioinformatics 2007 Jan 25;8:25. [doi: 10.1186/1471-2105-8-25] [Medline: 17254353]
20. Takefuji Y. Beyond XGBoost and SHAP: unveiling true feature importance. J Hazard Mater 2025 May 5;488:137382. [doi: 10.1016/j.jhazmat.2025.137382] [Medline: 39879771]
21. Guohe F. Parameter optimizing for support vector machines classification (SVM 分类核函数及参数选择比较) [Article in Chinese]. Computer Engineering and Applications 2011;47(3):123-124 [FREE Full text]
22. Jelovsek JE, van der Ploeg JM, Roovers JP, Barber MD. Validation of a model predicting de novo stress urinary incontinence in women undergoing pelvic organ prolapse surgery. Obstet Gynecol 2019 Apr;133(4):683-690. [doi: 10.1097/AOG.0000000000003158] [Medline: 30870279]
23. Yasa C, Gungor Ugurlucan F, Dural O, Yalcın O. External validation of a model predicting de novo stress urinary incontinence after pelvic organ prolapse surgery. Neurourol Urodyn 2021 Feb;40(2):688-694. [doi: 10.1002/nau.24608] [Medline: 33492730]
24. Luo W, Phung D, Tran T, et al. Guidelines for developing and reporting machine learning predictive models in biomedical research: a multidisciplinary view. J Med Internet Res 2016 Dec 16;18(12):e323. [doi: 10.2196/jmir.5870] [Medline: 27986644]
25. McDermott MBA, Wang S, Marinsek N, Ranganath R, Foschini L, Ghassemi M. Reproducibility in machine learning for health research: still a ways to go. Sci Transl Med 2021 Mar 24;13(586):eabb1655. [doi: 10.1126/scitranslmed.abb1655] [Medline: 33762434]
26. Beam AL, Manrai AK, Ghassemi M. Challenges to the reproducibility of machine learning models in health care. JAMA 2020 Jan 28;323(4):305-306. [doi: 10.1001/jama.2019.20866] [Medline: 31904799]
27. Hsiao SM, Chang TC, Wu PC, Lin HH. Predictors of an improvement in the severity of concomitant urodynamic stress incontinence after transvaginal mesh surgery for pelvic organ prolapse. J Formos Med Assoc 2020 May;119(5):917-924. [doi: 10.1016/j.jfma.2019.12.016] [Medline: 32146026]

XSL•FO
RenderX

28. Christmann-Schmid C, Bruehlmann E, Koerting I, Krebs J. Laparoscopic sacrocolpopexy with or without midurethral sling insertion: is a two-step approach justified? A prospective study. Eur J Obstet Gynecol Reprod Biol 2018 Oct;229:98-102. [doi: 10.1016/j.ejogrb.2018.08.009] [Medline: 30144729]
29. Duecy EE, Pulvino JQ, McNanley AR, Buchsbaum GM. Urodynamic prediction of occult stress urinary incontinence before vaginal surgery for advanced pelvic organ prolapse: evaluation of postoperative outcomes. Female Pelvic Med Reconstr Surg 2010 Jul;16(4):215-217. [doi: 10.1097/SPV.0b013e3181e4f11e] [Medline: 22453344]
30. Karamustafaoglu Balci B, Gungor Ugurlucan F, Yasa C, Yalcin O. 5-year experience in the diagnosis and treatment of occult urinary incontinence in women with pelvic organ prolapse. Eur J Obstet Gynecol Reprod Biol 2017 Mar;210:265-269. [doi: 10.1016/j.ejogrb.2017.01.007] [Medline: 28081479]
31. Edenfield A, Patnam R, Swift S. A narrative review of the epidemiology, diagnosis, and treatment of latent stress urinary incontinence. Neurourol Urodyn 2019 Aug;38 Suppl 4:S7-S11. [doi: 10.1002/nau.23864] [Medline: 31063654]
32. van der Ploeg JM, Oude Rengerink K, van der Steen A, et al. Vaginal prolapse repair with or without a midurethral sling in women with genital prolapse and occult stress urinary incontinence: a randomized trial. Int Urogynecol J 2016 Jul;27(7):1029-1038. [doi: 10.1007/s00192-015-2924-1] [Medline: 26740197]
33. Sultan AH, Monga A, Lee J, et al. An International Urogynecological Association (IUGA)/International Continence Society (ICS) joint report on the terminology for female anorectal dysfunction. Int Urogynecol J 2017 Jan;28(1):5-31. [doi: 10.1007/s00192-016-3140-3] [Medline: 27774569]
34. Abrams P, Andersson KE, Apostolidis A, et al. 6th International Consultation on Incontinence. Recommendations of the International Scientific Committee: evaluation and treatment of urinary incontinence, pelvic organ prolapse and faecal incontinence. Neurourol Urodyn 2018 Sep;37(7):2271-2272. [doi: 10.1002/nau.23551] [Medline: 30106223]
35. Leruth J, Fillet M, Waltregny D. Incidence and risk factors of postoperative stress urinary incontinence following laparoscopic sacrocolpopexy in patients with negative preoperative prolapse reduction stress testing. Int Urogynecol J 2013 Mar;24(3):485-491. [doi: 10.1007/s00192-012-1888-7] [Medline: 22825418]
36. Olsen AL, Smith VJ, Bergstrom JO, Colling JC, Clark AL. Epidemiology of surgically managed pelvic organ prolapse and urinary incontinence. Obstet Gynecol 1997 Apr;89(4):501-506. [doi: 10.1016/S0029-7844(97)00058-6] [Medline: 9083302]
37. Halpern-Elenskaia K, Umek W, Bodner-Adler B, Hanzal E. Anterior colporrhaphy: a standard operation? Systematic review of the technical aspects of a common procedure in randomized controlled trials. Int Urogynecol J 2018 Jun;29(6):781-788. [doi: 10.1007/s00192-017-3510-5] [Medline: 29214325]
38. Bergman A, Ballard CA, Koonings PP. Comparison of three different surgical procedures for genuine stress incontinence: prospective randomized study. Am J Obstet Gynecol 1989;160(5 Pt 1):1102-1106. [doi: 10.1016/00029378(89)90169-5] [Medline: 2729386]
39. Liapis A, Pyrgiotis E, Kontoravdis A, Louridas C, Zourlas PA. Genuine stress incontinence: prospective randomized comparison of two operative methods. Eur J Obstet Gynecol Reprod Biol 1996 Jan;64(1):69-72. [doi: 10.1016/0301-2115(95)02247-3] [Medline: 8801153]
40. Kammerer-Doak DN, Dorin MH, Rogers RG, Cousin MO. A randomized trial of burch retropubic urethropexy and anterior colporrhaphy for stress urinary incontinence. Obstet Gynecol 1999 Jan;93(1):75-78. [doi: 10.1016/s0029-7844(98)00360-3] [Medline: 9916960]
41. Cattani L, Van Schoubroeck D, Samešova A, Packet B, Housmans S, Deprest J. Pelvic floor ultrasound findings and symptoms of pelvic floor dysfunction during pregnancy. Int Urogynecol J 2024 Dec;35(12):2423-2430. [doi: 10.1007/s00192-024-05931-z] [Medline: 39352426]
42. van Veelen A, Schweitzer K, van der Vaart H. Ultrasound assessment of urethral support in women with stress urinary incontinence during and after first pregnancy. Obstet Gynecol 2014 Aug;124(2 Pt 1):249-256. [doi: 10.1097/AOG.0000000000000355] [Medline: 25004336]
43. Huang WC, Yang SH, Yang JM. Clinical importance and surgical outcomes of green type III cystocele in women with anterior vaginal prolapse. J Ultrasound Med 2015 Dec;34(12):2279-2285. [doi: 10.7863/ultra.14.11066] [Medline: 26573101]
44. Myers D, Werth A, Whitworth R, et al. To err is human: lessons from prolapse studies to identify and strategies to reduce data errors. Am J Obstet Gynecol 2025 Aug 21:S0002-9378(25)00574-5. [doi: 10.1016/j.ajog.2025.08.017] [Medline: 40848836]

Abbreviations

AUC: area under the curve
CART: classification and regression tree
CUPIDO: Concomitant Surgery and Urodynamic Investigation in Genital Prolapse and Stress Incontinence: A Diagnostic Study Including Outcome Evaluation
DCA: decision curve analysis
OPUS: Outcomes Following Vaginal Prolapse Repair and Midurethral Sling
POP: pelvic organ prolapse
POP-Q: Pelvic Organ Prolapse Quantification

XSL•FO
RenderX

SUI: stress urinary incontinence
SVM: support vector machine
UOSUI: urodynamic occult stress urinary incontinence
UUI: urge urinary incontinence
XGBoost: extreme gradient boosting

Edited by A Benis; submitted 15.04.25; peer-reviewed by T Miyagawa, Y Wang; revised version received 29.09.25; accepted 06.10.25; published 03.11.25.

Please cite as:
Su M, Wang S, Liu X
Predicting Postoperative Stress Urinary Incontinence After Prolapse Surgery via Machine Learning and Regression Models: Development and Validation Study
JMIR Med Inform 2025;13:e76021
URL: https://medinform.jmir.org/2025/1/e76021
doi:10.2196/76021

© Minna Su, Shuyu Wang, Xiaochun Liu. Originally published in JMIR Medical Informatics (https://medinform.jmir.org), 3.11.2025. This is an open-access article distributed under the terms of the Creative Commons Attribution License (https://creativecommons.org/licenses/by/4.0/), which permits unrestricted use, distribution, and reproduction in any medium, provided the original work, first published in JMIR Medical Informatics, is properly cited. The complete bibliographic information, a link to the original publication on https://medinform.jmir.org/, as well as this copyright and license information must be included.

XSL•FO
RenderX

Original Paper

Attitudes Toward Common Data Models Among Chinese Biomedical Professionals: Cross-Sectional Survey

Yexian Yu[1,2,3,4], MSc; Yongqi Zheng[2,4], BM; Meng Zhang[2,4], BM; Junqing Xie[5], PhD; Seng Chan You[6,7], PhD; Mengling Feng[8], PhD; Siyan Zhan[2,4], PhD; Feng Sun[2,3,4,9,10,11], PhD

[1]School of Information and Communication Engineering, Hainan University, Haikou, China
[2]Department of Epidemiology and Biostatistics, School of Public Health, Peking University, Beijing, China
[3]Hainan Boao Lecheng International Medical Tourism Pilot Zone Administration, Hainan Lecheng Institute of Real-World Research, Lecheng, China
[4]Key Laboratory of Epidemiology of Major Diseases (Peking University), Ministry of Education, Beijing, China
[5]Center for Statistics in Medicine, NDORMS, The Botnar Research Centre, University of Oxford, Oxford, United Kingdom
[6]Department of Biomedical Systems Informatics, College of Medicine, Yonsei University, Seoul, Republic of Korea
[7]Institute for Innovation in Digital Healthcare, Severance Hospital, Seoul, Republic of Korea
[8]Saw Swee Hock School of Public Health, National University Health System, National University of Singapore, Singapore, Singapore
[9]Department of Ophthalmology, Peking University Third Hospital, Beijing, China
[10]School of Traditional Chinese Medicine, Xinjiang Medical University, Urumqi, China
[11]School of Public Health, Shihezi University, Shihezi, China

Corresponding Author:
Feng Sun, PhD
Department of Epidemiology and Biostatistics, School of Public Health, Peking University
No. 38 Xueyuan Road, Haidian District
Beijing, 100191
China
Phone: 86 13811155891
Email: sunfeng@bjmu.edu.cn

Abstract

Background: In the rapidly evolving landscape of health informatics, adopting a standardized common data model (CDM) is a pivotal strategy for harmonizing data from diverse sources within a cohesive framework. Transitioning regional databases to a CDM is important because it facilitates integration and analysis of vast and varied health datasets. This is particularly relevant in China, where unique demographic and epidemiologic profiles present a rich yet complex data landscape. The significance of this research from the perspective of the Chinese population lies in its potential to bridge gaps among disparate data sources, enabling more comprehensive insights into health trends and outcomes.

Objective: This study aimed to understand biomedical professionals' and trainees' acceptance of the CDM in medical data management in China and to explore potential advantages and challenges associated with its promotion, implementation, and development in the country.

Methods: We conducted a questionnaire survey using Sojump and distributed it on WeChat to evaluate the Chinese population's acceptance of transitioning from local databases to a standardized CDM. The survey assessed participants' understanding of the CDM and the Observational Medical Outcomes Partnership CDM, as well as their views on the importance of CDM for regional databases in China. Analysis of the survey results revealed the current state, challenges, and trends in CDM application within Chinese health care, providing a foundation for future efforts in data standardization and sharing. The reliability of the questionnaire data was assessed using Cronbach α and Guttman Lambda 6 to determine internal consistency.

Results: Our survey of 418 participants revealed that 41.9% (175/418) were aware of the CDM. Recognition of CDM increased with higher education levels and was notably higher among professionals in contract research organizations and the pharmaceutical industry. Knowledge of CDM was primarily gained through literature and conferences, with formal education less common. Logistic regression analysis indicated that individuals with doctoral degrees, researchers, executives, medical professionals, data engineers, Centers for Disease Control and Prevention staff, and statisticians were more likely to be aware of CDM. Subgroup analyses showed higher awareness among doctoral versus nondoctoral and Beijing-based versus non-Beijing respondents, while perceived necessity was broadly comparable across subgroups. Overall, 94.7% (396/418) of respondents believed CDM integration

XSL•FO
RenderX

in China is necessary for standardization and efficiency. Despite 60.7% (254/418) optimism for the Observational Medical Outcomes Partnership as the preferred CDM, challenges such as mapping traditional Chinese medicine or Chinese medical insurance remain.

Conclusions: A large proportion of respondents expressed a favorable view of implementing the CDM in regional databases in China, with notable endorsement from the doctoral group and professionals in contract research organizations or pharmaceutical sectors; subgroup differences were concentrated in awareness rather than perceived necessity. Participants suggested enhancing CDM-related education and establishing clear data-sharing regulations to support CDM advancement in China.

(JMIR Med Inform 2025;13:e77603) doi:10.2196/77603

KEYWORDS

attitude of health personnel; big data; common data models; electronic health records; health information exchange; medical informatics; surveys and questionnaires

Introduction

In the rapidly evolving landscape of health informatics, adopting a standardized common data model (CDM) is a pivotal strategy for harmonizing data from diverse sources within a cohesive framework. This approach enhances the interoperability and utility of health data and supports the advancement of precision medicine, public health monitoring, and evidence-based policy making while maintaining governance of sensitive data [1].

The transition of regional databases to a standardized CDM is vital because it facilitates the integration and analysis of large and varied health datasets. This is particularly relevant in China, where unique demographic and epidemiological profiles present a rich yet complex data landscape [2]. The significance of this research from a Chinese population perspective lies in its potential to bridge gaps between disparate data sources, enabling more comprehensive and nuanced insights into health trends and outcomes [3]. The country's unique mix of Western medicine and Traditional Chinese Medicine, along with evolving insurance codes and inconsistent digitalization, creates challenges for data harmonization. While global studies highlight the benefits of CDMs, research on Chinese biomedical professionals' perceptions of their adoption is limited. Globally, CDMs such as Observational Medical Outcomes Partnership (OMOP) and Vaccine Safety Datalink (VSD) have played a key role in pharmacoepidemiology, enabling large-scale, multicenter research. The United States has been a leader in using CDMs for vaccine safety and drug surveillance. These efforts offer valuable insights for China's ongoing adoption and expansion of CDM applications [4]. Given that the CDM use in China is slightly lower than in other countries [5], a survey questionnaire was developed to investigate the perspectives and sentiments of individuals within the Chinese health care system regarding the implementation of a CDM in regional databases. Furthermore, by analyzing the factors that influence acceptance, this study aims to provide a solid foundation for promoting and expanding CDM in China's medical field, thereby enhancing the capacity for data-driven decision-making and research.

This survey aims to examine the perspectives and sentiments of individuals within the Chinese health care industry regarding the implementation of a CDM in regional databases.

Methods

Ethical Considerations

The researchers explained the purpose of the study to all participants, either orally or in writing, and obtained informed consent. No compensation or incentives were provided for participation. The study was approved by the Peking University Institutional Review Board (IRB00001052-24052). No personally identifying data were collected.

Questionnaire Survey

A questionnaire study was conducted among the Chinese population working or studying in the medical field from September 18, 2024, to November 8, 2024, to assess the acceptance of transitioning from regional databases to standardized CDMs among Chinese health care professionals. The study explored participants' understanding of CDM and the OMOP CDM, as well as their perspectives on the importance of CDM for regional databases in China. Analysis of the survey results can reveal the current status, challenges, and trends in CDM application within the Chinese medical field, providing a reference basis for future data standardization and sharing. Survey data were collected using Sojump [6], an online survey platform, and the questionnaire was distributed through WeChat (Tencent). Reliability of the questionnaire data was assessed using Cronbach α and Guttman Lambda 6 to measure internal consistency [7,8]. The 20-question questionnaire is included in Multimedia Appendix 1. Participants viewed an information page and provided electronic informed consent before accessing the questionnaire. This web-based survey adhered to the CHERRIES (Checklist for Reporting Results of Internet E-Surveys) checklist. The fully completed checklist is available in Multimedia Appendix 2 [9].

Statistical Analysis

The sample size was calculated to estimate the overall acceptance rate of the CDM among Chinese health care professionals. The sample size calculation used the standard proportion formula [10]. We adopted the most conservative assumption (P=.5) with a 95% CI (z=1.96) and a margin of error of 5% (E=0.05). To further justify the sample size, we reviewed similar questionnaire-based studies in the field, which reported sample sizes ranging from 249 to 683 participants [11-13]. Given this range, a sample size of 418 participants is considered appropriate and aligns with similar research.

XSL•FO
RenderX

To ensure that all questions were answered before submission, the survey was designed to prevent incomplete responses, eliminating any missing data. Convenience sampling was used to efficiently gather participants for the survey. The distribution of categorical variables is expressed as numbers and percentages. Chi-square tests were used to compare nonordered categorical data. A *P* value of less than .05 was considered statistically significant. All statistical analyses were conducted using R version 4.4.1 (R Core Team).

Results

Basic Information

A total of 418 responses were collected. Guttman Lambda 6 reliability coefficient was 0.98, while Cronbach α coefficient was 0.96, indicating high internal consistency and strong inter-item correlations within the questionnaire. These results support the notion that the questionnaire is an effective tool, bolstering confidence in its structural soundness and reliability.

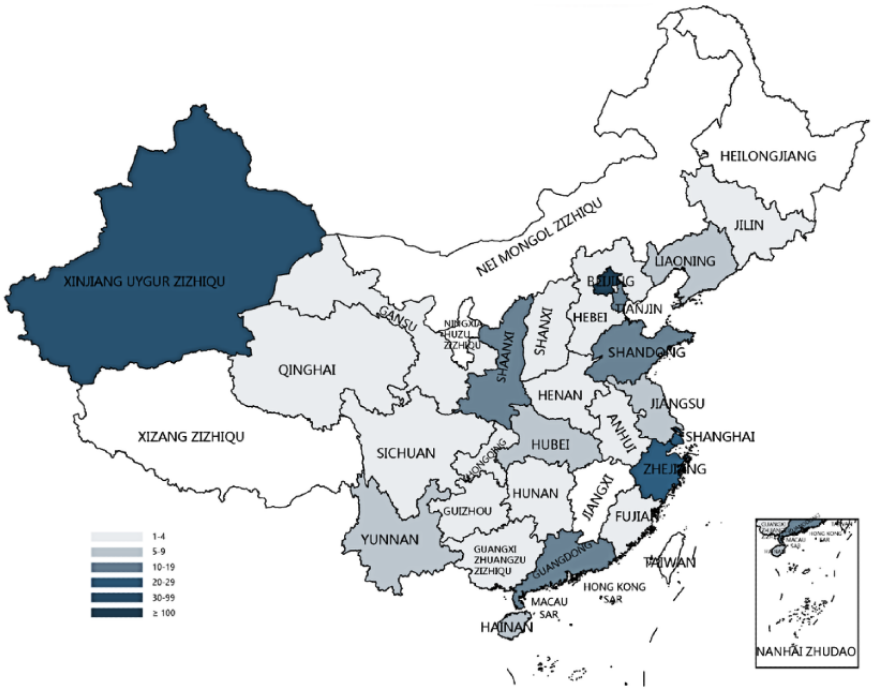
The minimum sample size was determined through a power calculation for estimating CDM acceptance prevalence among Chinese medical practitioners. Assuming a conservative proportion (*P*=50%) with a 5% margin of error at a 95% CI, the required sample size was 385. Our final sample (n=418) exceeded this threshold, ensuring sufficient precision for population-level estimates. Required sample sizes across various assumed proportions are shown in Table 1.

The median filling time was 121.5 (IQR 83.0-201.5) seconds. Zhong et al [14] recommend estimating the time required to answer a question as approximately 2 seconds per question, which all participants met in this study. Among the participants, 40.2% (168/418) were from Beijing and were notably more engaged, indicating a higher level of interest in the topic. This was followed by Xinjiang at 20% (84/418). Furthermore, significant interest was also observed in economically prosperous regions such as Zhejiang (21/418, 5%), Shanghai (20/418, 5%), and Guangdong (16/418, 4%). This may be related to economic development, medical resource allocation, and enhanced health awareness among residents in these areas. The regional distribution of participants is shown in Figure 1 [15], and participant characteristics are shown in Table 2.

Table 1. Sample size calculation.

Anticipated acceptance rate (p)	Required sample, n
10% or 90%	138
20% or 80%	246
30% or 70%	323
40% or 60%	369
50%	385

Figure 1. Regional distribution of questionnaire filling in CHINA.



XSL•FO
RenderX

Table 2. Participant characteristics.

Factors	Frequency, n (%)
Male	255 (61)
Female	163 (39)
Age group (years)	
18-30	104 (24.88)
31-40	165 (39.47)
41-50	115 (27.51)
51-60	27 (6.46)
>60	7 (1.67)
Educational attainment	
Bachelor's	122 (29.19)
Master's	191 (45.69)
Doctor	105 (25.12)
Professional roles	
Students	55 (13.16)
Researchers	101 (24.16)
Executives	55 (13.16)
Medical professionals	109 (26.08)
Teachers	22 (5.26)
Data engineers	14 (3.35)
CDC[a] staff	19 (4.55)
Statisticians	18 (4.31)
Others[b]	25 (5.98)
Institutional Affiliation	
CDC	143 (34.21)
Pharmaceutical industries	46 (11)
Colleges	80 (19.14)
Hospital	63 (15.07)
CROs[c]	41 (9.81)
Others[d]	45 (10.77)

[a]CDC: Centers for Disease Control and Prevention.

[b]The others mentioned in professional roles refer to sales, administration, and not specified.

[c]CRO: contract research organization.

[d]The others mentioned in institutional affiliation refer to research institutes, the National Health Commission of China, and not specified.

Degree of CDM Understanding

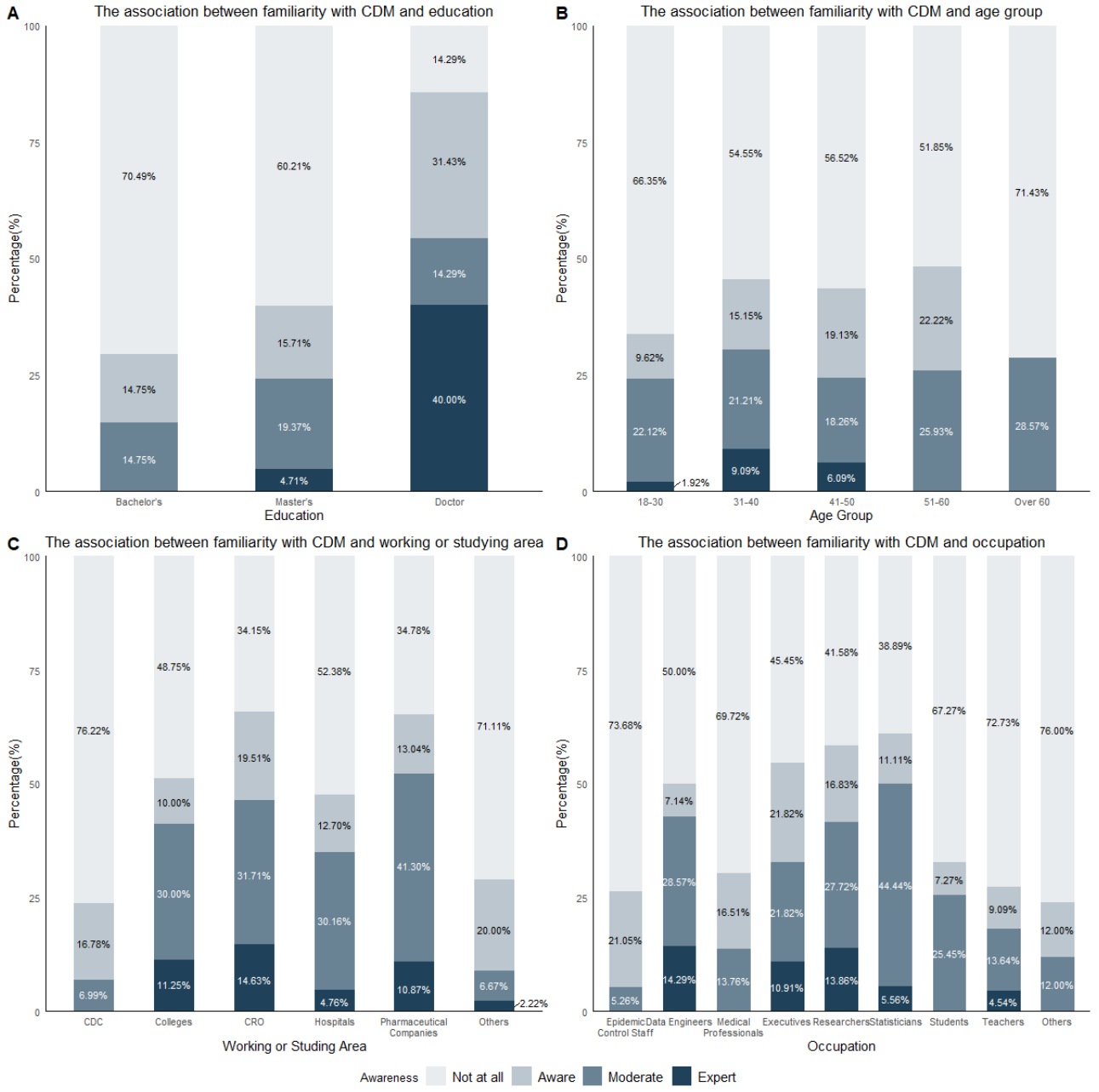
A total of 41.9% (175/418) of participants had heard of CDM before, whereas in the doctoral group, the percentage was higher at 60% (63/105). There was a statistically significant association between awareness of CDM and education level (χ^2_2=22.2; P<.001), occupation (χ^2_8=33.1; P<.001), and working or studying area (χ^2_5=46.1; P<.001), while no significant differences were observed in terms of age group and sex.

Among participants who were aware of CDM, only 14% (24/175) reported having a comprehensive understanding, whereas within the doctoral population, this percentage increased to 24% (15/63). Figure 2 illustrates a positive correlation between education level and the extent of CDM understanding. Notably, familiarity with CDM tends to decrease with increasing age. Specifically, within the 31-40 years age group, 9% (15/165) of participants demonstrated a profound understanding of CDM, representing the highest proportion among all age groups. Contract Research Organizations (CROs) and the pharmaceutical industry exhibit heightened interest in

XSL•FO
RenderX

CDM, potentially attributable to the elevated demand for scientific research within these sectors. Data engineers and researchers typically reported higher familiarity with CDMs, and executives also reported relatively high levels of understanding.

Figure 2. The association between familiarity with CDM and different factors. CDC: Centers for Disease Control and Prevention; CDM: common data model; CRO: contract research organization.



Among the 175 participants familiar with CDMs, conferences and academic literature emerged as the 2 primary sources of knowledge, cited by 119 (68%) and 109 (62.3%) respondents, respectively. Digital platforms and informal networks also played notable roles: medical subscription accounts, such as medical public accounts or newsletters on WeChat and similar platforms, were mentioned by 64 respondents (37%), information shared by peers by 58 (33%), and social media by 31 (18%). In contrast, formal education served as a source for only 3 participants (2%), highlighting a considerable gap in structured curricula and suggesting an urgent need to integrate CDM training into established academic and professional education programs.

Univariate and multivariate logistic regression analyses were conducted to assess the association between having heard of CDM and various demographic and clinical characteristics. The results are presented in Table 3. No differences between univariate and multivariate models were observed for age groups. Regarding education level, individuals with a doctoral degree (odds ratio [OR] 2.751, 95% CI 1.214-6.345; *P*=.02) exhibited a significantly greater likelihood of having heard of CDM compared with those with an undergraduate degree, whereas no significant difference was observed for those holding a master's degree. Researchers (OR 5.893, 95% CI 1.520-9.469; *P*=.02), executives (OR 5.716, 95% CI 1.179-9.844; *P*=.04), medical professionals (OR 4.964, 95% CI 1.984-8.162; *P*=.008),

XSL•FO
RenderX

data engineers (OR 1.782, 95% CI 1.009-7.707; *P*=.01), Centers for Disease Control and Prevention (CDC) staff (OR 2.139, 95% CI 1.519-6.809; *P*=.02), and statisticians (OR 3.746, 95% CI 1.336-6.878; *P*=.03) all had previous knowledge of CDM compared with students. This suggests that the concept of CDM has gained some recognition within their professional fields. Such preexisting awareness may stem from their educational background, work experience, or attention to industry trends. It is noteworthy that this early familiarity with CDM could have influenced their attitudes and behaviors toward participation in the study and may also reflect their professional competence in data management. Specifically, compared with those working or studying at the CDC, individuals in the pharmaceutical industry (OR 3.993, 95% CI 2.691-6.940; *P*<.001), CROs (OR 3.138, 95% CI 1.289-8.409; *P*<.001), and colleges (OR 4.650, 95% CI 1.680-8.335; *P*<.001) demonstrated greater awareness of CDM.

Table 3. Univariate and multivariate logistic regression analysis for common data models awareness.

Factors	Univariate			Multivariate		
	OR[a]	95% CI	*P* value	OR	95% CI	*P* value
Age group (years)						
18-30	Reference	—[b]	—	Reference	—	—
31-40	1.643	0.992-2.751	.06	1.217	0.534-2.884	.65
41-50	1.516	0.878-2.638	.14	1.284	0.537-3.187	.58
51-60	1.831	0.771-4.339	.17	1.967	0.581-6.748	.28
>60	0.789	0.109-3.864	.78	1.468	0.513-9.884	.98
Education attainment						
Bachelor's	Reference	—	—	Reference	—	—
Master's	1.579	0.977-2.581	.07	1.210	0.667-2.202	.53
Doctor	3.583	2.079-6.272	<.001	2.751	1.214-6.345	.02
Professional roles						
Students	Reference	—	—	Reference	—	—
Researchers	2.887	1.467-5.842	.003	5.893	1.520-9.469	.02
Executives	0.467	1.148-5.426	.02	5.716	1.179-9.844	.04
Medical professionals	0.893	0.447-1.810	.75	4.964	1.984-8.162	.008
Teachers	0.771	0.243-2.232	.64	0.398	0.096-15.113	.19
Data engineers	2.056	0.617-6.897	.24	1.782	1.009-7.707	.01
CDC[c] staff	0.734	0.211-2.260	.60	2.139	1.519-6.809	.02
Statisticians	3.230	1.092-10.147	.04	3.746	1.336-6.878	.03
Others[d]	0.649	0.207-1.840	.37	2.761	0.456-18.915	.28
Institutional affiliation						
CDC	Reference	—	—	Reference	—	—
Pharmaceutical industries	6.011	2.971-12.585	<.001	3.993	2.691-6.940	<.001
Colleges	3.370	1.890-6.085	<.001	4.650	1.680-8.335	<.001
Hospitals	3.282	1.564-7.003	.002	2.914	1.560-5.483	<.001
CROs[e]	6.183	2.963-13.425	<.001	3.138	1.289-8.409	<.001
Others[f]	1.302	0.600-2.722	.49	2.036	0.787-5.299	.14

[a]OR: odds ratio.

[b]Not applicable.

[c]CDC: Centers for Disease Control and Prevention.

[d]Others refer to sales, administration, and not specified.

[e]CRO: contract research organization.

[f]Others refer to research institutes, the National Health Commission of China, and not specified.

XSL•FO
RenderX

Necessity of CDM

Considering that some participants were not familiar with CDM and had only a vague understanding of its definition, the definition of CDM was provided in the questionnaire. After the definition was clarified on the first page, 94.7% (396/418) of participants indicated that incorporating CDM into regional databases in China is necessary. Univariate and multivariate logistic regression analyses were conducted to assess perceptions of CDM necessity, and the results are presented in Table 4. In univariate analysis, individuals in the 31-40 years and 41-50 years age groups were more likely to be aware of CDM as necessary compared with the 18-30 years age group, whereas individuals aged 51-60 years and older showed the opposite tendency. In multivariate regression analysis, after adjusting for confounders, the differences between the 31-40 years and 41-50 years age groups and the 18-30 years age group were no longer statistically significant, whereas individuals in the 51-60 years (OR 0.205, 95% CI, 0.065-0.602; *P*=.005) and 60 years and older (OR 0.050, 95% CI 0.019-0.313; *P*=.003) age groups still held significantly different attitudes. Individuals with master's (OR 2.153, 95% CI 1.054-4.516; *P*=.04) and doctoral (OR 3.083, 95% CI 1.317-7.470; *P*=.01) degrees showed a higher degree of agreement with CDM as necessary than those with bachelor's degrees, which remained significant after controlling for other potentially confounding variables, suggesting an independent association between education level and perception of the need for CDM. Researchers (OR 2.829, 95% CI 1.301-5.808; *P*=.03), executives (OR 4.227, 95% CI 1.198-7.236; *P*=.03), medical professionals (OR 4.189, 95% CI 1.279-8.196; *P*=.02), data engineers (OR 5.014, 95% CI 1.593-9.558; *P*=.04), and CDC staff (OR 3.371, 95% CI 1.098-5.315; *P*=.008) all agreed that CDM is necessary compared with students. Considerable differences were observed in awareness and perceived requirements for CDM among different work and study environments. Specifically, staff in pharmaceutical industries (OR 2.107, 95% CI 1.846-8.139; *P*=.003) were more likely to perceive CDM as necessary than CDC staff, while those in CROs (OR 0.340, 95% CI 0.135-0.941; *P*=.04) showed the opposite view. In addition, it is important to note that staff in other areas (OR 4.701; 95% CI 1.453-9.624; *P*=.02), such as research institutes and the National Health Commission, were more likely than CDC staff to agree with the need for CDM. This phenomenon may reflect different understandings and levels of awareness of the value of CDM and the urgency of its implementation in various areas.

XSL•FO
RenderX

Table 4. Univariate and multivariate logistic regression analysis for common data models necessity.

Factors	Univariate			Multivariate		
	OR	95% CI	*P* value	OR	95% CI	*P* value
Age group (years)						
18-30	Reference	—	—	Reference	—	—
31-40	2.378	1.281-4.497	.007	0.981	0.371-2.508	.97
41-50	2.101	1.075-4.228	.03	0.934	0.333-2.571	.90
51-60	0.294	0.145-0.582	.001	0.205	0.065-0.602	.005
>60	0.225	0.075-0.596	.004	0.050	0.019-0.313	.003
Education attainment						
Bachelor's	Reference	—	—	Reference	—	—
Master's	2.912	1.739-4.943	<.001	2.153	1.054-4.516	.04
Doctor	1.676	1.295-2.917	.006	3.083	1.317-7.470	.01
Professional roles						
Students	Reference	—	—	Reference	—	—
Researchers	1.851	1.068-3.576	.005	2.829	1.301-5.808	.03
Executives	1.270	2.744-5.916	.54	4.227	1.198-7.236	.03
Medical professionals	1.920	1.285-3.773	.006	4.189	1.279-8.196	.02
Teachers	1.669	0.285-3.654	.98	1.205	0.529-5.621	.99
Data engineers	4.267	0.974-9.315	.08	5.014	1.593-9.558	.04
CDC staff	6.044	1.806-9.781	.008	3.371	1.098-5.315	.008
Statisticians	1.669	0.795-3.645	.99	1.538	0.085-9.548	.99
Others	0.960	0.338-2.701	.94	0.307	0.056-1.571	.16
Institutional affiliation						
CDC	Reference	—	—	Reference	—	—
Pharmaceutical industries	5.667	1.529-8.412	.02	2.107	1.846-8.139	.003
Colleges	0.608	0.332-1.109	.11	0.698	0.255-1.907	.48
Hospitals	0.886	0.494-1.592	.69	0.837	0.373-1.905	.67
CROs	0.349	0.159-0.750	.007	0.340	0.135-0.941	.04
Others	1.495	0.612-4.053	.40	4.701	1.453-9.624	.02

[a]OR: odds ratio.

[b]Not applicable.

[c]CDC: Centers for Disease Control and Prevention.

[d]Others refer to sales, administration, and not specified.

[e]CRO: contract research organization.

[f]Others refer to research institutes, the National Health Commission of China, and not specified. The majority of respondents, 93.7% (371/396), identified the integration of heterogeneous health big data from multiple sources and the enhancement of data consistency as key rationales for the implementation of CDM, underscoring the significance of data integration and consistency in contemporary data management practices. In addition, 87.1% (345/396) of respondents highlighted the crucial role of structured data in augmenting the efficiency of scientific research endeavors, whereas 81.8% (324/396) of respondents emphasized the importance of improving data quality and reliability. Furthermore, 69.4% (275/396) of respondents, representing a substantial proportion of the sample, regarded the enhancement of data use rates and the conservation of storage space as another pivotal incentive for the adoption of CDM. Collectively, these data reveal the multidimensional value of CDM in facilitating data standardization, optimizing research processes, bolstering data reliability, and enhancing storage efficiency. In contrast, 5% (22/418) participants believed that CDM is not necessary for regional databases in China. More than half (12/22, 55%) felt that existing databases already meet their needs. A total of 45% (10/22) of respondents indicated that the implementation and maintenance of CDM are relatively complex and costly, whereas 36% (8/22) expressed concerns regarding data security and the potential leakage of patient privacy.

XSL•FO
RenderX

CDM Type

Among the databases known to participants, the top 5 included OMOP, VSD, Sentinel, Clinical Data Acquisition Standards Harmonization, and National Patient-Centered Clinical Research Network, with OMOP having a significantly higher awareness rate (Table 5). It is particularly noteworthy that while only 16% (21/132) of respondents working at the CDC chose OMOP, this figure increases to 24% (11/46) among those who selected VSD, possibly because their work provides them with a better understanding of VSD in the vaccine field [16]. Within this subgroup of 175 respondents who had heard of CDMs, only 14 (8%) individuals reported knowledge of more than 5 types. By contrast, when considering the entire sample of 418 participants, as many as 327 (78.2%) indicated that they were unfamiliar with any type of CDM. In recent years, Chinese medical institutions have progressively explored the application of OMOP CDM in real-world studies. As demonstrated in a systematic review conducted in 2023 [17], 12 institutions nationwide had successfully implemented data standardization, with notable breakthroughs particularly in chronic and mental disease research.

Table 5. Ranking of common data model (CDM) types known to participants.

Ranking	CDM type	Participants, n/N (%)
1	OMOP[a]	132/175 (75.4)
2	VSD[b]	45/175 (26)
3	Sentinel	41/175 (23)
4	CDASH[c]	36/175 (21)
5	PCORnet[d]	28/175 (16)
6 (tie)	ASPEN[e]	23/175 (13)
6 (tie)	FHIR[f]	23/175 (13)
8 (tie)	i2b2[g]	21/175 (12)
8 (tie)	PEDSnet[h]	21/175 (12)
10	CRN-VDW[i]	20/175 (11)
11	ConcePTION	10/175 (6)

[a]OMOP: Observational Medical Outcomes Partnership.

[b]VSD: Vaccine Safety Datalink.

[c]CDASH: Clinical Data Acquisition Standards Harmonization.

[d]PCORnet: National Patient-Centered Clinical Research Network.

[e]ASPEN: Advanced System for Process Engineering.

[f]FHIR: Fast Health Interoperability Resources.

[g]i2b2: Informatics for Integrating Biology & the Bedside.

[h]PEDSnet: Pediatric Evidence Discovery and Surveillance Network.

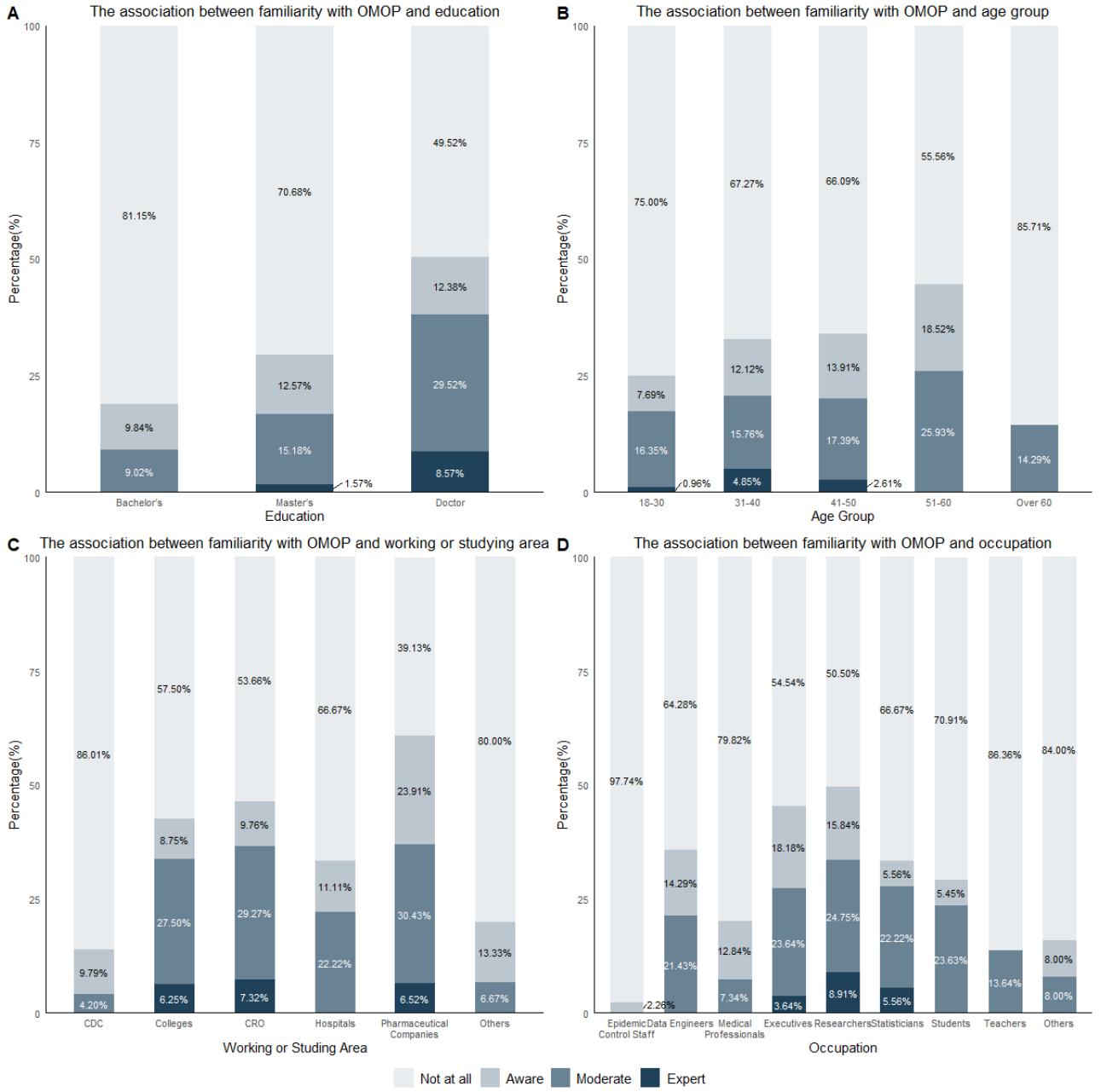
[i]CRN-VDW: Health Care Systems Research Network Virtual Data Warehouse.

Equal counts were assigned the same rank (ties); subsequent ranks were skipped.

The bar charts illustrating familiarity with OMOP (Figure 3) appear to closely resemble those for CDM. Among the 132 respondents who reported being aware of OMOP, the primary avenues for OMOP awareness were conference introductions and literature, reported by 90 (68%) respondents and 75 (57%) respondents, respectively, underscoring the significant role of professional events and scholarly resources in knowledge dissemination. In addition, 44 participants (33%) learned about OMOP from peers, and 41 (31%) from medical public accounts, while only 13 respondents (10%) obtained such information through video platforms. Survey findings indicate that the majority of respondents recognize significant advantages associated with the implementation of OMOP. The most widely acknowledged benefit, reported by 89.4% (118/132) of participants, is that it enables different data sources to be more easily shared, compared, and integrated. This is followed by the enhancement of data operability and comparability, cited by 104 respondents (78.8%). Furthermore, 98 respondents (74%) believe that OMOP helps promote innovation and progress within the research field. Additionally, a substantial proportion of respondents, 64% (84/132), identified the reduction in data cleaning workload as a notable advantage. However, respondents also identified challenges faced by OMOP in China. Specifically, 76% (100/132) of respondents aware of OMOP cited barriers between various data sources, 71% (94/132) reported the high manual effort required for mapping, and 52% (69/132) encountered an inability to match some localized information to standard concept IDs. Particular mapping issues were noted for data related to ethnicity, Chinese medical insurance, and traditional Chinese medicine.

XSL•FO
RenderX

Figure 3. The association between familiarity with OMOP and different factors. CDC: Centers for Disease Control and Prevention; CRO: contract research organization; OMOP: Observational Medical Outcomes Partnership.



Subgroup Analysis

To examine whether sample composition might influence the main results and to enhance interpretability, we conducted prespecified subgroup comparisons by education (doctoral vs nondoctoral) and region (Beijing-based vs non–Beijing-based) in Tables 6 and 7, respectively. Doctoral respondents showed higher CDM awareness (χ^2_1=11.1; P<.001), greater self-rated CDM expertise (χ^2_1=16.9; P<.001), and higher OMOP awareness (χ^2_1=22.0; P<.001). Perceived necessity did not differ materially by education (P=.31 for CDM and P=.15 for OMOP). By region, Beijing-based participants had higher awareness of CDM (χ^2_1=5.1; P=.02) and OMOP (χ^2_1=14.2; P<.001), whereas differences in CDM and OMOP expertise and perceived necessity were not statistically significant. Overall, heterogeneity was concentrated in awareness rather than perceived necessity, suggesting differential exposure rather than divergent attitudes toward adoption.

XSL•FO
RenderX

Table 6. Subgroup analysis by education level. Statistical methods: Pearson χ^2 test was used when all expected cell counts were >5; otherwise, the Fisher exact test was applied.

Items	Doctoral degree (N=105), n (%)	Nondoctoral degree (N=313), n (%)	Chi-square (*df*)	*P* value
CDM[a] awareness			11.1 (1)	<.001
Yes	63 (60)	139 (40.88)		
No	42 (40)	201 (59.12)		
CDM expertise			16.9 (1)	<.001
Yes	15 (14.29)	9 (2.88)		
No	90 (85.71)	304 (97.12)		
CDM necessity			—[b]	.31
Yes	102 (97.14)	297 (93.99)		
No	3 (2.86)	19 (6.01)		
OMOP [c] awareness			22.0 (1)	<.001
Yes	53 (50.48)	79 (25.24)		
No	52 (49.52)	234 (74.76)		
OMOP expertise			—	<.001
Yes	9 (8.57)	3 (0.96)		
No	96 (91.43)	310 (99.04)		
OMOP necessity			2.1 (1)	.15
Yes	57 (54.29)	197 (62.94)		
No	48 (45.71)	116 (37.06)		

[a]CDM: common data model.

[b]Not available.

[c]OMOP: Observational Medical Outcomes Partnership.

XSL•FO
RenderX

Table 7. Subgroup analysis by geographic region. Statistical methods: Pearson χ^2 test was used when all expected cell counts were >5; otherwise, the Fisher exact test was applied.

Items	Beijing-based (N=168), n (%)	Non-Beijing–based (N=250), n (%)	Chi-square (*df*)	*P* value
CDM[a] awareness			5.1 (1)	.02
Yes	82 (48.81)	93 (37.20)		
No	86 (51.19)	157 (62.80)		
CDM expertise			0.6 (1)	.43
Yes	12 (7.14)	12 (4.80)		
No	156 (92.86)	238 (95.20)		
CDM necessity			1.4 (1)	.24
Yes	156 (92.86)	240 (96)		
No	12 (7.14)	10 (4)		
OMOP [b] awareness			14.2 (1)	<.001
Yes	60 (35.71)	47 (18.80)		
No	108 (64.29)	203 (81.20)		
OMOP expertise			—[c]	.99
Yes	5 (2.98)	7 (2.80)		
No	163 (97.02)	243 (97.20)		
OMOP necessity			2.4 (1)	.12
Yes	94 (55.95)	160 (64)		
No	74 (44.05)	90 (36)		

[a]CDM: common data model.

[b]OMOP: Observational Medical Outcomes Partnership.

[c]Not available.

Discussion

Based on the statistical analysis of the questionnaire results from Sojump, it is evident that participants generally hold a positive attitude toward the application of CDM in regional databases in China. This positivity is underpinned by the high internal consistency and strong inter-item correlations within the questionnaire. Notably, participants from Beijing constituted the highest proportion, which may indicate a regional focus or interest in CDM. The doctoral group, with their deeper professional knowledge and experience in the medical and research fields, tended to have a higher understanding of CDM. This understanding equips them to comprehend the structure and potential applications of CDM, and how to use it to support clinical research and health care decision-making. Furthermore, CROs and pharmaceutical industries showed a strong interest in CDM due to its standardized data models and processing methods, which can accelerate project processes, reduce costs, and enhance efficiency. This interest and support are instrumental in driving the widespread adoption of CDM, thereby providing more opportunities for data management and analysis in the health care sector. Literature and conferences were identified as the primary channels through which participants learned about CDM. Among various CDM frameworks, OMOP ranked highest in terms of awareness. However, participants generally believed that implementing OMOP in China would face numerous challenges, such as the inability to map traditional Chinese medicine information to standard datasets. Mapping challenges in China include the difficulty of translating traditional Chinese medicine concepts, such as “Qi deficiency” and “Blood stagnation,” into OMOP-standardized terms, as no direct equivalents exist. Similarly, local insurance and billing codes, which are frequently updated and vary by region, present significant challenges in adapting them to the OMOP framework.

Some local adaptations are underway, with certain Chinese institutions developing crosswalks and custom vocabularies to address these challenges. However, these adaptations are still in the pilot phase and require further collaboration to be fully integrated into the global OMOP ecosystem.

Participants put forward a series of recommendations to enhance the involvement of domestic technical, medical, informational, and scientific research personnel and to promote the development of CDM in China. They emphasized the importance of establishing small-scale OMOP data specialty and disease-specific databases, as well as the possibility of building OMOP thematic databases based on existing databases. To increase the operational strength of OMOP data, they suggested increasing investment in scientific research and commercial projects to enhance scientific and commercial outputs. At the same time, the necessity of popularizing CDM

XSL•FO
RenderX

education was highlighted, along with an emphasis on policy precedence. They hope to develop a CDM suitable for China that aligns with international standards, while also focusing on quality control in data collection. Additionally, they discussed the feasibility of using Clinical Data Interchange Standards Consortium standards in real-world data and suggested a comprehensive promotion of the use of a unified data format. Participants also stressed the importance of establishing rules to clarify the value of data assets and the need for national-level promotion of a rational data-sharing mechanism. Questions were raised regarding whether to charge fees, how to charge fees, and the possibility of customization, emphasizing the importance of data integration, collection, and processing. It was suggested to popularize CDM in universities and consider opening and sharing some data with enterprises. At the same time, the importance of information encryption and network security was emphasized, along with a proposal to pilot initiatives in specific areas first. Finally, they discussed the issue of defining cross-institutional data usage permissions and strategies to enhance users' enthusiasm.

The recommendations put forward by the participants hold significant guiding importance in promoting the application and development of CDM and OMOP in China. Standardization and privacy are complementary facets of data sharing, where CDM can serve as an effective solution for both. Standardization facilitates and enhances the efficiency of data sharing, while privacy ensures that data sharing is conducted appropriately and under sufficient control. Recent nationwide implementations, such as South Korea's successful integration of national claims data into the OMOP CDM framework, demonstrate how standardization can support both data utility and privacy protection at a national scale. This approach enables transparent and "Findable, Accessible, Interoperable, and Reusable" data stewardship while maintaining appropriate access controls through distributed research environments [18]. There is active development in both domains, including advancements in government regulations and common data models to promote standardization, as well as the application of technologies such as blockchain and synthetic data to address privacy concerns [19,20]. Enhancing the interoperability and security of information systems is crucial, necessitating increased awareness and implementation of current standards and the expansion of ophthalmic data standards to fill gaps in existing norms. As data sharing becomes more prevalent, advancements in data privacy are also of critical importance.

The use of OMOP has facilitated standardized data-driven research across various clinical sites, establishing a robust foundation for data use. Furthermore, numerous research papers in the medical field have used OMOP to present their findings. Artificial intelligence is increasingly being applied within CDM. Kang et al [21] introduced a deep learning–based automatic term mapping tool specifically designed for application within the OMOP framework, enhancing the efficiency and accuracy of data standardization. The review by Ahmadi et al [22] highlights the pivotal role of OMOP in discovering and refining machine learning models. Some studies have explored disease risk factors in detail and conducted epidemiological investigations [23-27], while others have used machine learning to build risk prediction models [28-32].

This study has several limitations. First, while the sample size of 418 meets basic statistical requirements, it remains relatively limited for comprehensively assessing the perspectives of all health care professionals and researchers across China's diverse health care landscape. Second, this study used convenience sampling, which may introduce selection bias, as the selection of participants was not entirely random and may not fully reflect the opinions and characteristics of all health care professionals and researchers in China. Convenience sampling likely overrepresented highly educated professionals, particularly those with doctoral degrees, and respondents from regions such as Beijing. These biases may lead to more favorable attitudes toward CDMs and higher familiarity with them compared with the broader population of health care professionals in China. To improve the accuracy and reliability of future studies, stricter sampling techniques should be adopted to ensure sample diversity and broadness. Additionally, other potential biases in the study design and implementation process need to be addressed in subsequent research. Furthermore, the assessment of "comprehensive knowledge" of CDMs was based on self-reported responses rather than an objective knowledge test. While this method provides valuable insights into participants' perceptions, it may not fully capture their actual understanding of CDMs. Given the online survey format, digital literacy could be a potential source of bias. However, as all respondents held at least a bachelor's degree and were capable of using electronic devices, the impact of this bias is likely minimal.

In conclusion, respondents were generally supportive of adopting CDMs in regional databases in China, with higher awareness among doctoral respondents and staff in CROs or pharmaceutical sectors; however, deep understanding remains limited, and exposure through formal training is low. Accordingly, these findings should be interpreted with caution. Implementation efforts should prioritize targeted education and capacity-building, alongside clear data-sharing and governance frameworks, as well as practical pilots—including terminology mapping—to enable sustainable uptake.

Acknowledgments

The authors thank all participants for their involvement in this study. This study was supported by the National Natural Science Foundation of China (grant No.72474008), the third batches of Key Projects of Scientific Act for Drug Regulation of China (RS2024X006, RS2024Z008), Hainan Provincial Science Technology Department key research and development project (2024), Project of Center for Drug Reevaluation of China National Medical Products Administration (CDR2024R01001), Research Project by China Drug Administration Research Association (2025-Y-Y-012) and Project of State Key Laboratory of Drug Regulatory Science (2025SKLDRS0377).

XSL•FO
RenderX

Data Availability

The datasets generated or analyzed during this study are available in the GitHub repository [33] under a Creative Commons Attribution 4.0 International License (CC BY 4.0).

Authors' Contributions

Conceptualization: YY (lead), FS (equal)
Data curation: YY (lead), FS (equal)
Formal analysis: YY
Funding acquisition: FS
Investigation: YY
Methodology: YY
Resources: FS
Supervision: JX (equal), SY (equal), MF (equal), SZ (equal)
Visualization: YY (lead)
Writing – original draft: YY (lead)
Writing – review & editing: YY (lead), YZ (supporting), MZ (supporting), FS (supporting)

Conflicts of Interest

None declared.

Multimedia Appendix 1
Questionnaires.
[DOCX File , 90 KB - medinform_v13i1e77603_app1.docx]

Multimedia Appendix 2
CHERRIES Checklist.
[DOCX File , 26 KB - medinform_v13i1e77603_app2.docx]

References

1. Liyanage H, Liaw S, Jonnagaddala J, Hinton W, de Lusignan S. Common Data Models (CDMs) to enhance international big data analytics: a diabetes use case to compare three CDMs. Stud Health Technol Inform 2018;255:60-64. [Medline: 30306907]
2. Jiaqi C, Ming L, Ze W, Xiaorong Y, Ruijie W, Tongchao Z. Research on common medical data model and establishment of cross-cohort models at home and abroad. Chin J Public Health 2023;39(9):1207-1211 [FREE Full text]
3. Wang AR, Wu SZ, Liu SY, Xiu XL, Zhou JY, Hu ZY, et al. Comparative study of medical common data models for FAIR data sharing. Zhonghua Liu Xing Bing Xue Za Zhi 2023;44(5):828-836. [doi: 10.3760/cma.j.cn112338-20221025-00908]
4. Zheng Y, Zhang M, Wang C, Gao L, Xie J, Shen P, et al. Pharmacoepidemiologic research based on common data models: systematic review and bibliometric analysis. JMIR Med Inform 2025;13:e72225 [FREE Full text] [doi: 10.2196/72225] [Medline: 40720860]
5. Reinecke I, Zoch M, Reich C, Sedlmayr M, Bathelt F. The usage of OHDSI OMOP - a scoping review. Stud Health Technol Inform 2021;283:95-103. [doi: 10.3233/SHTI210546] [Medline: 34545824]
6. Del Ponte A, Li L, Ang L, Lim N, Seow WJ. Evaluating SoJump.com as a tool for online behavioral research in China. J Behav Exp Finance 2024;41:100905. [doi: 10.1016/j.jbef.2024.100905]
7. Cronbach LJ. Coefficient alpha and the internal structure of tests. Psychometrika 2025;16(3):297-334. [doi: 10.1007/bf02310555]
8. Guttman L. A basis for analyzing test-retest reliability. Psychometrika 1945;10:255-282. [doi: 10.1007/BF02288892] [Medline: 21007983]
9. Eysenbach G. Improving the quality of Web surveys: the Checklist for Reporting Results of Internet E-Surveys (CHERRIES). J Med Internet Res 2004;6(3):e34 [FREE Full text] [doi: 10.2196/jmir.6.3.e34] [Medline: 15471760]
10. Al-Subaihi AA. Sample size determination. Influencing factors and calculation strategies for survey research. Saudi Med J 2003;24(4):323-330. [Medline: 12754527]
11. Abdolalipour S, Abbasalizadeh S, Mohammad-Alizadeh-Charandabi S, Abbasalizadeh F, Jahanfar S, Asghari Jafarabadi M, et al. Translation and measurement properties of pregnancy and childbirth questionnaire in Iranian postpartum women. BMC Health Serv Res 2024;24(1):365 [FREE Full text] [doi: 10.1186/s12913-024-10689-7] [Medline: 38519977]
12. Khademi K, Kaveh MH, Asadollahi A, Nazari M. Development and validation of the Women's Self-care Knowledge and Attitude Questionnaire (WSKAQ). BMC Public Health 2024;24(1):2338 [FREE Full text] [doi: 10.1186/s12889-024-19831-w] [Medline: 39198800]

XSL•FO
RenderX

13. Wen L, Zheng J, Hu N, Xu W, Fang Y, Ma S, et al. Support measures and demand among healthcare workers during the COVID-19 pandemic: a survey in high-workload provinces of China, 2023. BMJ Open 2025;15(5):e088799 [FREE Full text] [doi: 10.1136/bmjopen-2024-088799] [Medline: 40413048]
14. ZHONG X, LI M, LI L. Preventing and detecting insufficient effort survey responding. Adv Psychol Sci 2022;29(2):225-237. [doi: 10.3724/sp.j.1042.2021.00225]
15. Tang D, Chen M, Huang X, Zhang G, Zeng L, Zhang G, et al. SRplot: A free online platform for data visualization and graphing. PLoS One 2023;18(11):e0294236 [FREE Full text] [doi: 10.1371/journal.pone.0294236] [Medline: 37943830]
16. McNeil MM, Gee J, Weintraub ES, Belongia EA, Lee GM, Glanz JM, et al. The Vaccine Safety Datalink:successes and challenges monitoring vaccine safety. Vaccine 2014;32(42):5390-5398 [FREE Full text] [doi: 10.1016/j.vaccine.2014.07.073] [Medline: 25108215]
17. Zhang M, Shen P, Liu ZK, Van Zandt M, Li J, Li C, et al. Study of application of common data model of Observational Medical Outcomes Partnership in China. Zhonghua Liu Xing Bing Xue Za Zhi 2025;46(5):907-913. [doi: 10.3760/cma.j.cn112338-20240924-00595] [Medline: 40494801]
18. Kim JW, Kim C, Kim K, Lee Y, Yu DH, Yun J, et al. Scalable infrastructure supporting reproducible nationwide healthcare data analysis toward FAIR stewardship. Sci Data 2023;10(1):674 [FREE Full text] [doi: 10.1038/s41597-023-02580-7] [Medline: 37794003]
19. Halfpenny W, Baxter SL. Towards effective data sharing in ophthalmology: data standardization and data privacy. Curr Opin Ophthalmol 2022;33(5):418-424 [FREE Full text] [doi: 10.1097/ICU.0000000000000878] [Medline: 35819893]
20. Jin H, Luo Y, Li P, Mathew J. A review of secure and privacy-preserving medical data sharing. IEEE Access 2019;7:61656-61669. [doi: 10.1109/access.2019.2916503]
21. Kang B, Yoon J, Kim HY, Jo SJ, Lee Y, Kam HJ. Deep-learning-based automated terminology mapping in OMOP-CDM. J Am Med Inform Assoc 2021;28(7):1489-1496 [FREE Full text] [doi: 10.1093/jamia/ocab030] [Medline: 33987667]
22. Ahmadi N, Peng Y, Wolfien M, Zoch M, Sedlmayr M. OMOP CDM can facilitate data-driven studies for cancer prediction: a systematic review. Int J Mol Sci 2022;23(19):11834 [FREE Full text] [doi: 10.3390/ijms231911834] [Medline: 36233137]
23. Lihui L, Sini L, Aobo C, Wenhui W, Saisai Z, Xinwei Z. Relationship between suicide and blood lipid and other related factors in patients with depressive disorder. Chin J Health Psychol 2022;30(6):820-825 [FREE Full text]
24. Lili Z, Song Y, Xinwei Z, Yexian Y, Qizhong Y, Keqing L. Study on the characteristics of the suicide and the related factors in children and adolescents withdepressive disorder. J Neurosci Behav Health 2021;21(4):254-258 [FREE Full text]
25. Wang X, Chen X, Zhang X, Wang Z, Ma X, Zhang Q. Analysis of outpatient visits in elderly patients with depression. J Clin Psychiatry 2022;32(4):276-278 [FREE Full text]
26. Wang X, Rao W, Chen X, Zhang X, Wang Z, Ma X, et al. The sociodemographic characteristics and clinical features of the late-life depression patients: results from the Beijing Anding Hospital mental health big data platform. BMC Psychiatry 2022;22(1):677 [FREE Full text] [doi: 10.1186/s12888-022-04339-7] [Medline: 36324116]
27. Zhou J, Guo C, Ren L, Zhu D, Zhen W, Zhang S, et al. Gender differences in outpatients with dementia from a large psychiatric hospital in China. BMC Psychiatry 2022;22(1):208 [FREE Full text] [doi: 10.1186/s12888-022-03852-z] [Medline: 35313835]
28. Liu LJ, Chen XW, Yu YX, Zhang M, Li P, Zhao HY, et al. Development of a prediction model for the incidence of type 2 diabetic kidney disease and its application based on a regional health data platform. Zhonghua Liu Xing Bing Xue Za Zhi 2024;45(10):1426-1432. [doi: 10.3760/cma.j.cn112338-20240117-00024] [Medline: 39444128]
29. Lin H, Tang X, Shen P, Zhang D, Wu J, Zhang J, et al. Using big data to improve cardiovascular care and outcomes in China: a protocol for the CHinese Electronic health Records Research in Yinzhou (CHERRY) Study. BMJ Open 2018;8(2):e019698 [FREE Full text] [doi: 10.1136/bmjopen-2017-019698] [Medline: 29440217]
30. Chen XW, Liu LJ, Yu YX, Zhang M, Li P, Zhao HY, et al. Development and application of a prediction model for incidence of diabetic retinopathy in newly diagnosed type 2 diabetic patients based on regional health data platform. Zhonghua Liu Xing Bing Xue Za Zhi 2024;45(9):1283-1290. [doi: 10.3760/cma.j.cn112338-20240117-00023] [Medline: 39307703]
31. Yu YX, Zhang M, Chen XW, Liu LJ, Li P, Zhao HY, et al. Development of a prediction model for incidence of diabetic foot in patients with type 2 diabetes and its application based on a local health data platform. Zhonghua Liu Xing Bing Xue Za Zhi 2024;45(7):997-1006. [doi: 10.3760/cma.j.cn112338-20231218-00360] [Medline: 39004973]
32. Li P, Liu ZK, Zhao HY, Liu XY, Shen P, Lin HB, et al. A risk prediction model of cervical cancer developed based on nested case-control design. Zhonghua Liu Xing Bing Xue Za Zhi 2023;44(7):1139-1145. [doi: 10.3760/cma.j.cn112338-20221223-01079] [Medline: 37482719]
33. china_cdm_survey_dataset. Github. URL: https://github.com/yuyexian0921-droid/china_cdm_survey_dataset [accessed 2025-10-14]

Abbreviations

CDC: Centers for Disease Control and Prevention
CDM: common data model
CHERRIES: Checklist for Reporting Results of Internet E-Surveys

XSL•FO
RenderX

CRO: contract research organization
OMOP: Observational Medical Outcomes Partnership
OR: odds ratio
VSD: Vaccine Safety Datalink

Edited by A Benis; submitted 19.05.25; peer-reviewed by K Adegoke, D Ajayi, P Quindroit; comments to author 11.08.25; accepted 06.10.25; published 05.11.25.

Please cite as:
Yu Y, Zheng Y, Zhang M, Xie J, You SC, Feng M, Zhan S, Sun F
Attitudes Toward Common Data Models Among Chinese Biomedical Professionals: Cross-Sectional Survey
JMIR Med Inform 2025;13:e77603
URL: https://medinform.jmir.org/2025/1/e77603
doi:10.2196/77603
PMID:

©Yexian Yu, Yongqi Zheng, Meng Zhang, Junqing Xie, Seng Chan You, Mengling Feng, Siyan Zhan, Feng Sun. Originally published in JMIR Medical Informatics (https://medinform.jmir.org), 05.11.2025. This is an open-access article distributed under the terms of the Creative Commons Attribution License (https://creativecommons.org/licenses/by/4.0/), which permits unrestricted use, distribution, and reproduction in any medium, provided the original work, first published in JMIR Medical Informatics, is properly cited. The complete bibliographic information, a link to the original publication on https://medinform.jmir.org/, as well as this copyright and license information must be included.

XSL•FO
RenderX

Simulation of Clinical Visits as a Novel Approach to Evaluate Digital Health in Multiple Sclerosis: Simulation Study

Riley Bove[1], MD; Luca Capezzuto[2], PharmD; Imogen West[3], MMath; Simon Dryden[4], PhD; Saira Ghafur[4], MD; Jack Halligan[4], MBA, MD; Stanislas Hubeaux[2], MSc; Agne Kazlauskaite[2], PhD

[1]Department of Neurology, UCSF Weill Institute for Neurosciences, University of California, San Francisco, San Francisco, CA, United States

[2]F. Hoffmann-La Roche Ltd, Basel, Switzerland

[3]Roche Products Limited, London, United Kingdom

[4]Prova Health, Bermondsey Street, London, United Kingdom

Corresponding Author:
Jack Halligan, MBA, MD
Prova Health, Bermondsey Street, London, United Kingdom

Abstract

Background: Efforts are being made to integrate digital health technologies into clinical care for multiple sclerosis (MS) to improve patient monitoring. Efficiently probing how they might impact clinical care could streamline digital tool development. The Floodlight digital tool, comprising 5 smartphone sensor–based tests, was used to generate health-related data on patient function and symptoms in a clinical simulation.

Objective: The study had 3 objectives: (1) assess the utility of simulated clinical encounters as a research methodology for exploring the introduction of digital health technologies into clinical practice in MS, (2) confirm the fidelity of the simulated environment and patient cases developed and understand what metrics (eg, workflow, comprehensive evaluation) could be generated, and (3) generate insights into the utility of digitally collected data, including usability, clinical decision contribution, and impact on workflows, in clinical practice.

Methods: A total of 2 patient cases consisting of clinical, radiological, and digital health data were developed with clinician input. US-based neurologists prepared for and conducted 2 simulated teleconsultations each, with an actor briefed on case profiles. Floodlight data were available, via the Floodlight MS™ Health Care Professional Portal, for 1 of the 2 consultations. Participant neurologists completed interviews and surveys assessing the fidelity of the cases presented, user experience and workflow metrics, patient concerns identified, care decisions made, and confidence in making decisions.

Results: All 10 neurologists indicated that the simulations were high-fidelity representations of real consultations. Using the Floodlight technology for the first time, median time taken to prepare for and conduct the consultation was ~1.7 - 2 minutes longer, with slightly greater mental effort reported by participants, compared with not using the tool. The Floodlight MS Health Care Professional Portal scored an “above average” 79 on the System Usability Scale and an “acceptable” Net Promoter Score of 10. In total, 6 of the 10 neurologists “strongly agreed” that it was easier and quicker to identify patient concerns when they had access to the patient-generated Floodlight data to prepare for their encounters than when they did not. Overall, more care and management decisions were taken when the digital tool was used (37 vs 29). Of those 37 decisions, Floodlight data were reported as a trigger for 20 decisions, always in combination with other elements including patient history (20/20) and clinical exam findings (9/20).

Conclusions: These findings advance our understanding of clinical simulation as a method for evaluating digital tools and other innovative technologies for MS care. High-fidelity patient cases could be provided for the mock teleconsultations, and the simulated clinical environment was useful for evaluating usability and utility of a new digital tool—yielding preliminary evidence on how digital data could be accessed and utilized by neurologists to support routine MS care.

(JMIR Med Inform 2025;13:e67845) doi:10.2196/67845

KEYWORDS

clinical simulation; digital health; digital health technology; multiple sclerosis; smartphone; teleconsultations; patient remote assessment; impact on clinical workflows; clinical utility

XSL•FO
RenderX

Introduction

Background

Multiple sclerosis (MS) is a central nervous system disorder marked by significant heterogeneity in its clinical presentation and characterized by disease progression from onset [1,2]. MS, often commencing with subtle signs and advancing to substantial disability, manifests through a wide spectrum of symptoms, ranging from sensory disturbances and motor deficits to cognitive impairments and emotional challenges, profoundly impacting patients, their families, and society [3,4].

To date, monitoring in MS has been reliant upon brief, infrequent clinical assessments (typically occurring once or twice annually, or at the time of a relapse), without sufficiently sensitive and objective (ie, free from rater-dependent variability) assessments of progression available to health care professionals (HCPs) [5]. Moreover, due to time constraints, standard assessments of disability in MS, such as the Expanded Disability Status Scale (EDSS) [6], which requires ~30 minutes to conduct [7], are not always performed in clinical appointments. Remote consultations (teleconsultations) are a recognized alternative to clinic visits [8] and have been adopted by the MS community, particularly during the COVID-19 pandemic [9,10].

Digital health technologies offer greater access to care in MS and opportunities to improve frequent monitoring [11], enabling the capture of ongoing subtle or subclinical progression of MS [1,12-14] in specific domains such as cognition (which can often be missed). These technologies can be remotely administered and are patient-centered and operated, allowing longitudinal assessment of multiple functional domains in a naturalistic environment [15,16]. Furthermore, they offer the opportunity to improve the involvement of patients in their disease or treatment course [17,18] and to enhance conversations between HCPs and people with MS [19]. By providing objective data and bridging the gap of information in between clinical visits, sensor-based digital assessments may ultimately allow HCPs to make more informed decisions, evaluate treatment effects, and act earlier on indications of disease progression [11] or symptomatic exacerbation prior to scheduled clinical visits.

Despite the potential benefits, evaluating, testing, and optimizing the integration of new and innovative solutions into health care settings can itself be a time- and resource-consuming process. Hence, there is growing demand for agile methods to rapidly learn how digital solutions can play a role in clinical practice [20]. Clinical simulation, a low-cost and scalable methodology whereby data are collected from users as they perform tasks in realistic clinical scenarios, can rapidly generate new insights. For example, they allow the exploration of the possible impact of novel methodologies without the risks inherent in deploying them in real clinical settings (eg, of misdiagnoses [21,22]) or of the expansion of technology to new user groups or in new clinical contexts [22]. The preliminary insights generated from simulation models can support the refinement of technologies before rollout or scaling up [23]. To confirm that the insights gained from these clinical simulations are meaningful, they must be of high fidelity and account for a number of variables (including behavioral ones) and the differences inherent among real-world practices [21,22].

Aims and Objectives

This feasibility study was designed to evaluate clinical simulation as a method for assessing the preparation and conduct of teleconsultations. This included evaluating the fidelity of the simulated environment (compared with real practice) and the patient cases developed. An additional aim was to assess the feasibility of using data derived from smartphone-based remote assessment technology in combination with MS teleconsultations, including their usability and impacts on clinical workflows (eg, preparation time and time to identifying primary patient concerns), care decisions, and disease management. The Floodlight technology [24] was utilized as the digital tool for evaluation. Accordingly, the aim of this study was to evaluate the potential impact of integrating Floodlight MS into clinical practice, generating insights that may also be relevant to similar digital health tools. As it is expected that any new test or technology will initially impose a higher mental load on clinicians, the study also aimed to quantify the extent of this increase.

Floodlight MS comprised 5 smartphone sensor–based tests (hereafter referred to as “smartphone-based tests”) presented on an app, measuring information processing speed (Cognitive Test [25]), hand function (Pinching Test [24] and Draw a Shape Test [26]), and gait (U-Turn Test [27] and 2-Minute Walk Test [28,29]), as well as a Patient Journal including 2 patient-reported outcome (PRO) measures (Daily Status Questions and a Symptom Tracker [30]). The data were consolidated in a dashboard for HCPs (Floodlight MS HCP Portal), which was accessible between clinical visits [5], and constituted the focus of the technological assessment in this research.

Methods

Recruitment of Neurologists

US-based neurologists were recruited from Prova Health’s existing network, professional communities (eg, LinkedIn), and academic publications, and through snowball sampling (where research participants recruit future participants), and they were sent email invitations to take part in the study. Neurologists were required to have managed a minimum of 40 people with MS per month and to have had no previous experience using the Floodlight technology. Convenience sampling was utilized to recruit primarily academic neurologists, as they were expected to give more granular feedback on the technology. There was no defined sample size due to the exploratory nature of this feasibility study.

Patient Case Overview

A total of 2 patient cases were presented to each participant neurologist. Radiology reports and clinical letters were drafted by qualified radiologists and medical doctors to describe the cases and reflect the real magnetic resonance imaging and clinical data in a realistic narrative. For additional authenticity, synthetic social and family histories consistent with typical MS presentations were included. All cases were validated by 2 expert neurologists.

XSL•FO
RenderX

The goal was to achieve high-fidelity patient cases that were representative of real-world cases while minimizing the variation inherent among people with MS. Patient cases included (experimental) or did not include (control) Floodlight data, thus simulating real-world scenarios in which neurologists manage people with MS with or without access to the Floodlight technology (see the *Patient Case Development* section for more details).

Patient Actor

A professional actor was recruited to play the patients' roles during the teleconsultations. They were recruited from a company with 25 years of experience in providing trained actors to simulate patients with medical, surgical, and psychiatric conditions. The patient roles were based on generated behavioral profiles, which were used to inform the biographies for the 2 patient cases. The actor was provided with detailed scripts developed by a medical doctor and validated by neurologists to ensure [1] the consistency and correctness of answers.

Conduct of Clinical Simulations

Each clinical simulation session lasted approximately 2.5 hours and was conducted via Zoom. Medically qualified team members from Prova Health served as moderators, facilitating introductions (~5 min), reviewing the simulation session guide with the neurologists (~5 min), and providing training on the Floodlight technology (~30 min). After the simulated teleconsultations had begun, the moderators took notes with their cameras and microphones switched off. Teleconsultations were designed to replicate those that the participant neurologists would perform in their clinical practices. The individual simulated teleconsultation sessions for each of the 2 presented patient cases consisted of preparation (~5 min) and conduct (~30 min) phases, both led by the participant neurologist. Participant neurologists were instructed to evaluate the relevant information and recommend an appropriate management plan. In the preparation phase, clinical information provided with or without Floodlight data was reviewed for each patient case. The "patient" (played by the professional actor) then joined the call. Following the conclusion of each simulated teleconsultation, participant neurologists completed a short survey (~5 min) to collect feedback on the examined case. At the end of both sessions, the moderator shared a link to the postsimulation survey (~7 min) and conducted a brief interview (~5 min) with each participant neurologist.

Patient Case Development

The 2 patient cases presented to each participant neurologist were developed using deidentified clinical and Floodlight data (see the *Patient Cases Selection Criteria* section). For both cases, the participant neurologists reviewed data from 3 recent clinical visits, including patient demographics, symptoms, diagnosis, treatment and medical history, and radiology reports based on original magnetic resonance imaging metrics.

The clinical data presented in the letters included EDSS scores, Symbol Digit Modalities Test (SDMT) scores, 9-Hole Peg Test times, and Timed 25-Foot Walk times. The main clinical traits emerging from clinical case narratives are presented in Table 1. It should be noted that although both patient cases presented gait impairment, Patient Case B was designed to show significant worsening of gait impairment in the last year.

Floodlight data visualized in the Floodlight MS HCP Portal were presented for 1 of the 2 cases reviewed by each neurologist. The orders of the patient cases and of the interventions were randomized before the participant neurologists started the teleconsultations (Figure 1).

Table . Clinical traits, per patient case, presented during teleconsultation simulation.

Simulation patient case	Main clinical traits emerging from clinical case narratives and actor's interpretation
Patient Case A	• Cognitive function decline: decrease in SDMT[a] score of ≥20% in the previous 12 months • Hand motor function decline: increase in 9HPT[b] time of ≥20% in the previous 6 - 12 months • History of gait impairment, as per T25FW[c] test data • Bowel and bladder issues reported in the previous 12 months • Vision changes in previous history • Fatigue
Patient Case B	• Gait capacity decline: increase in T25FW time of ≥20% in the previous 6 - 12 months • Reported bladder issues in the previous 12 months • Reported mood issues in the previous 12 months • Spasticity and pain in the previous 12 months

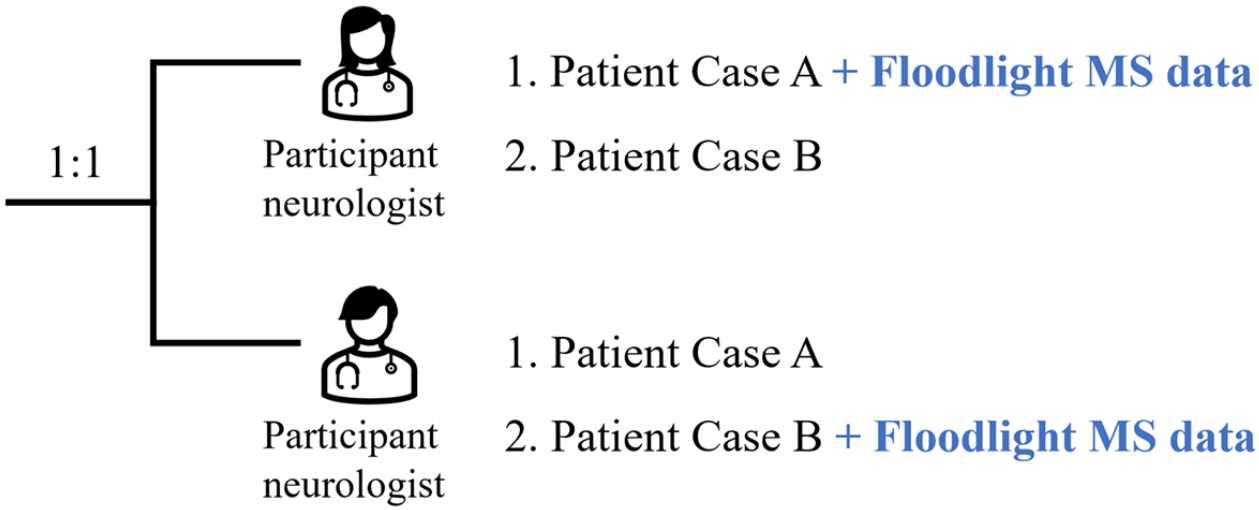
[a]SDMT: Symbol Digit Modalities Test.

[b]9HPT: 9-Hole Peg Test.

[c]T25FW: Timed 25-Foot Walk.

XSL•FO
RenderX

Figure 1. Randomization of patient cases before the initiation of teleconsultation. The order of cases and experimental conditions was randomized between participant neurologists, and consultations were conducted with 2 patient cases (A and B). Half (n=5) of the participant neurologists were randomized to have access to the Floodlight MS HCP Portal for the first case, while the other half had access to the solution for the second case. Due to a randomization error, 6 out of the 10 participant neurologists were assigned to the Floodlight MS HCP Portal for Patient Case A, instead of 5 out of 10. HCP: health care professional; MS: multiple sclerosis.



Data Sources

Clinical data from the CONSONANCE study (NCT03523858) were used in conjunction with Floodlight performance and symptom tracker data collected over 12 consecutive months. CONSONANCE is an ongoing, phase 3b, 4-year, open-label study assessing the effectiveness and safety of ocrelizumab in adults with progressive multiple sclerosis.

Participants enrolled in the CONSONANCE study performed smartphone-based tests using a precursor to Floodlight MS for clinical research purposes, providing a battery of digital assessments and digital PROs. Data from the Pinching Test, the Draw a Shape Test, the U-Turn Test, and the 2-Minute Walk Test (all performed daily) were utilized, alongside data from a version of the Cognitive Test (performed weekly; involving matching a sequence of symbols to digits within 90 s).

Data from 2 PRO measures collected via the Floodlight Patient Journal were also used. These were Daily Status Questions (“How are you feeling physically now?” and “How is your mood now?”) and a biweekly Symptom Tracker to track symptoms related to cognition (attention deficit, memory loss, brain “fog” sensation, mental fatigue), upper extremity function (sensory disturbance, muscle weakness, clumsiness, muscular spasm, pain), lower extremity function (sensory disturbance, muscle weakness, clumsiness, muscular spasm, pain), gait (trouble walking, lack of balance, walking fatigue), and bowel or bladder dysfunction (incontinence, bladder or urinary problems, constipation), as well as the time that any new or worsening symptoms manifested and whether or not this was perceived to be a relapse. All Floodlight data collected in the CONSONANCE trial and used in this study were imported into the Floodlight MS HCP Portal (version 1.5 at the time of the research).

Patient Cases Selection Criteria

Patient profiles were selected from the CONSONANCE dataset based on selected criteria that indicated a clinical performance decline observed in the previous 6 - 12 months, based on standard clinical assessments of cognitive function, hand motor function, or gait capacity.

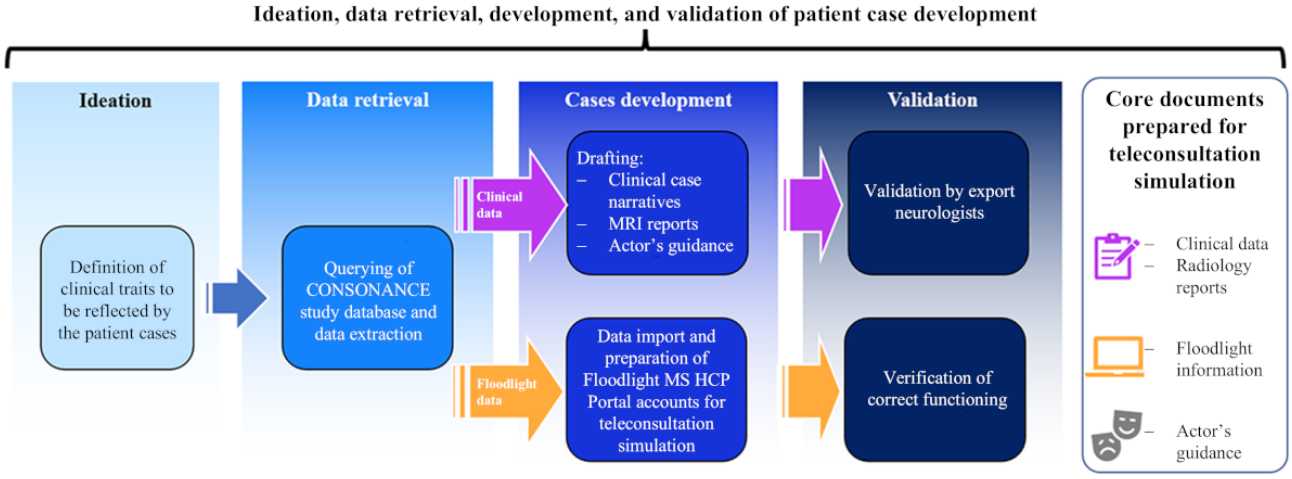
For Patient Case A, the key selection criteria included cognitive function decline (a decrease in SDMT score of ≥20% in the previous 12 mo) and hand motor function decline (increase in 9-Hole Peg Test time of ≥20% in the previous 6 - 12 mo). For Patient Case B, the criteria included gait capacity decline (increase in Timed 25-Foot Walk time of ≥20% in the previous 6 - 12 mo) as well as 2 consecutive reports of fatigue and bladder issues (score of 3 - 6; some of the most impactful “invisible” symptoms of MS sourced via the SymptoMScreen). Some of the symptoms experienced by people living with MS may not be externally evident or easy to report and quantify, such as fatigue, mood disorders, cognitive impairments, pain, bladder or bowel dysfunction, sexual dysfunction, and vision changes. These symptoms can be difficult for the patient to report and articulate during a clinical encounter (eg, due to subjectivity bias, poor recall, or stigma), and for physicians to capture (limitations in available measurement tools, ample reliance on patient recall on the visit day) [31]. The clinical performance decline, together with reported signs of “invisible” symptoms, provided impetus for a care decision to be taken during the clinical simulation.

Data Extraction

Clinical data from 3 recent in-person clinical visits were extracted to present to the participant neurologists (Figure 2). No clinical data from the final in-person visit (the time point corresponding to the day of the teleconsultation in the simulation) were provided. Of note, cognitive decline had been confirmed at this visit for the patient in Patient Case A (as measured by the SDMT); these data were not provided to the participant neurologists in order to mimic a common clinical scenario in MS, where evident patient deterioration may precede formal confirmation through standard clinical assessments.

XSL•FO
RenderX

Figure 2. Clinical data extraction for teleconsultation simulation. Clinical data on ideation, data retrieval, case development, and validation of patient cases were extracted for teleconsultation simulation. Parameters such as multiple sclerosis (MS) phenotype, clinical factors, symptom reports, and synthetic data such as age and sex were included to provide transparency in demographic data. Floodlight data from the most recent 12-month period for each clinical profile were extracted for one of the cases presented to each participant neurologist. HCP: health care professional; MRI: magnetic resonance imaging.



To build the patient cases, MS phenotype and date of diagnosis; clinical parameters, including recent disease history (eg, relapses, EDSS evolution); symptom reports; and current and prior treatments (eg, disease-modifying therapies) were also extracted. Additional "synthetic" data were used to construct demographic (age, sex) and radiology reports.

Floodlight data from the prior 12-month period for each clinical profile were also extracted to be provided for 1 of the 2 cases presented to each participant neurologist.

Study Outcomes and Data Collection

Study outcomes were either moderator-reported or participant neurologist–reported (via participant surveys and interviews; Table 2). Measures included questions regarding the fidelity of the simulated cases developed; use of the digital tool (Floodlight MS), including user experience metrics for data visualization, overall experience (Net Promoter Score), and usability (System Usability Scale [32]); and workflow metrics, including time for case preparation, teleconsultation time, and mental effort required (Paas scale [33]). Confidence in approaching clinical consultations was also measured. Additionally, moderators recorded the time taken for the identification of patient concerns, the recognition of "invisible" MS symptoms, and the care decisions prompted and taken (including change in treatment management) with versus without having Floodlight data available.

A medically qualified moderator from the research team observed each simulation session and recorded outcome measures such as time spent on each case. The participants were asked to self-report on the fidelity of simulation, user experience metrics, workflow metrics, clinical consultations, patient concerns, and care decisions. This was done using postcase surveys, postcase conduct surveys, postsimulation surveys, or a postsimulation interview. Each of these was measured using various questions.

XSL•FO
RenderX

Table . Methods used to report on the study outcomes.

Measure	Moderator measured	Participant neurologist reported			
		Survey after case preparation	Survey after case conduct	Survey after simulation	Interview after simulation
Fidelity of simulation					
Similarity of patient cases to those seen in day-to-day practice				X	
Similarity of simulation to day-to-day practice consultations				X	
Using clinical simulation to evaluate the Floodlight MS[a] HCP[b] Portal				X	X
User experience metrics					
User feedback on the Floodlight MS HCP Portal				X	X
Usability of the Floodlight MS HCP Portal				X	
Workflow metrics					
Time taken to prepare for teleconsultation	X				
Time taken to conduct teleconsultation	X				
Reported mental effort associated with information acquisition and application		X	X		
Clinical consultations, patient concerns, and care decisions					
Reported confidence level when preparing for and making care decisions during a teleconsultation		X	X		
Identification of the patient's primary concern		X	X		X
Time taken to identify the patient's primary concern during teleconsultation (independently verified by a second clinician using screen recordings)	X				
Recognition of "invisible symptoms of MS"[c] and their proactive discussion with patients	X		X		
Care decisions taken and reported prompts for these decisions	X		X		X

[a]MS: multiple sclerosis.

[b]HCP: health care professional.

[c]Invisible symptoms, including fatigue, mood disorders, cognitive impairments, pain, bladder or bowel dysfunction, sexual dysfunction, and vision

XSL•FO
RenderX

changes can be experienced by people living with MS. Some of these symptoms may not be externally evident or easy to report and quantify and can be difficult for the patient to report and articulate during a clinical encounter (eg, due to subjectivity bias, poor recall, or stigma) or for physicians to capture (eg, limitations in available measurement tools, ample reliance on patient recall on the visit day).

Data Analysis

For continuous, time-dependent, moderator-assessed measures, the median times were calculated and presented as box and whisker diagrams. Additionally, these time-dependent measures were collated into groups, and all categorical results were presented as absolute numbers within each category and presented as bar charts. An a priori decision was made not to perform hypothesis-testing statistics on data from this feasibility study.

Ethical Considerations

CONSONANCE patient data anonymity was retained throughout the preparation and conduct of this study. The protocol (22-PROH-102: Evaluation of Floodlight MS using clinical simulation) was reviewed by Pearl Institutional Review Board on September 20, 2022, and determined to be exempt from ethics approval according to U.S. Food and Drug Administration 21 Code of Federal Regulations (CFR) 56.104 and 45CFR46.104(b)(3): (3) Benign Behavioral Interventions - Adults. The study was conducted in accordance with the most recent version of the Declaration of Helsinki. Signed consent forms were obtained from the participant neurologists before the simulated teleconsultations were conducted. Participant neurologists were compensated for their time according to local Fair Market Value rates.

Results

Participant Neurologist Demographics

A total of 10 US-based neurologists were recruited as participants (7 from large academic centers and 3 from specialist neurology centers). A total of 6 participant neurologists had >10 years of experience in performing MS consultations, 1 had 5 - 10 years of experience, and 3 had 3 - 5 years of experience. The number of consultations performed by participant neurologists in their current practice in a typical week was >50 (n=2), 40 - 50 (n=1), 30 - 40 (n=1), 20 - 30 (n=3), or 10 - 20 (n=3). Further, participant neurologists performed 25% - 50% (n=3) or <25% (n=7) of all consultations as teleconsultations in their current practice.

Patient Case and Simulation Fidelity

Participant neurologists felt that the simulations were high-fidelity representations of real consultations. All reported that the patient cases and scenarios were “very” or “somewhat” similar to typical practice (Table 3). Feedback from participants on the performance of the professional patient actor was mostly very positive:

> *Shockingly. He was very good. I say that. I haven’t done this in a while, but very often a mock patient doesn’t get the real essence of MS. This guy did great. I even wondered, did he have MS, how he got so good at it? ... They would have had to practice and discuss things with many patients and doctors to get this good.*
>
> *The actor did a great job. Intuitively knew how to pick up on what I was asking.*

Table . Participant neurologists’ experiences of patient case and simulation fidelity.[a]

Participant neurologists’ experiences	Number of participant neurologists				
	Very different	Somewhat different	Neutral	Somewhat similar	Very similar
How similar were these patient cases to those you see in your day-to-day practice?	0	0	0	4	6
How similar were these consultations to the consultations you complete during a typical week?	0	0	0	5	5

[a]Participant neurologists reported similarity of patient cases to those seen in day-to-day practice and similarity of simulation to day-to-day practice consultations via surveys and questionnaires.

User Experience Metrics

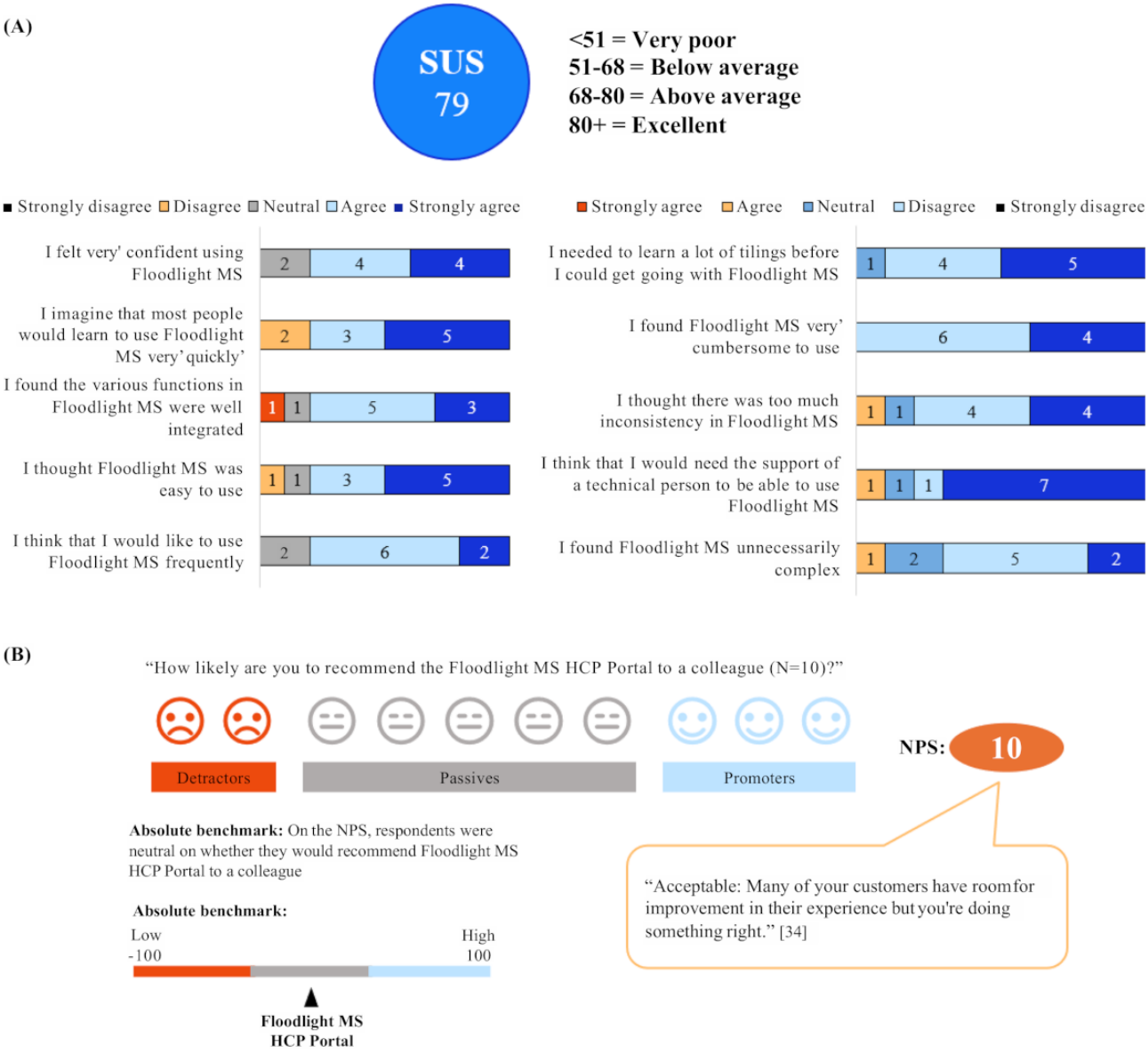
The Floodlight MS HCP Portal scored an “above average” score of 79 on the System Usability Scale (Figure 3A). In terms of overall experience of using the Floodlight technology, the Floodlight MS HCP Portal scored an “acceptable” Net Promoter Score of 10, based on the participant neurologists’ reports of how likely they would be to recommend it to a colleague (Figure 3B).

Participant neurologists agreed that data visualizations in the Floodlight MS HCP Portal were “very” or “somewhat” useful for upper extremity function (10/10), cognition (10/10), gait (9/10), and mood status (obtained via the Floodlight Daily Status Questions; 9/10; Figure 4). The “mood status” aspect of the

XSL•FO
RenderX

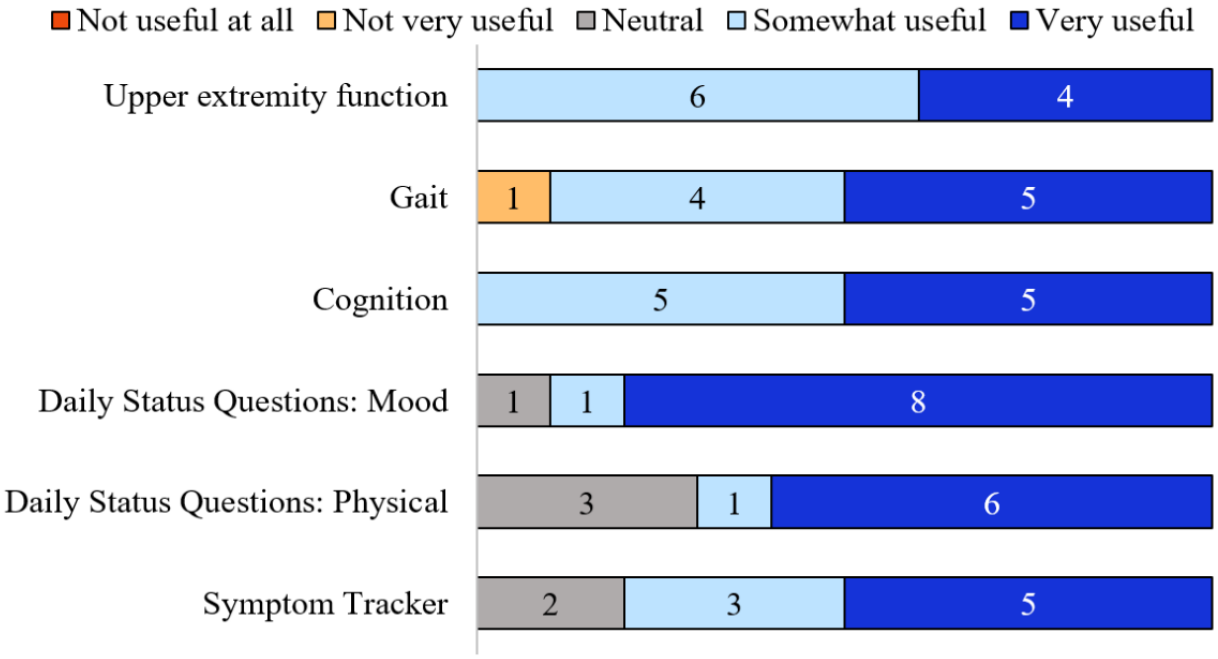
Patient Journal was rated as the most useful of the data visualizations presented, with 8/10 ratings of “very useful”.

Figure 3. User experience metrics for the Floodlight technology, including (A) SUS and (B) NPS [34]. The bars represent responses on the user experience of Floodlight MS (SUS) and user experience for data visualization and the overall experience (NPS); these were reported via participant surveys and interviews. Items alternate between positive and negative phrasing, with higher scores indicating more favorable usability perceptions. HCP: health care professional; MS: multiple sclerosis; NPS: net promoter score; SUS: System Usability Scale.



XSL•FO
RenderX

Figure 4. User experience metrics for the usefulness of data visualizations in the Floodlight MS HCP Portal. Participant neurologists provided feedback on whether data visualizations in the Floodlight MS HCP Portal were useful for factors including upper extremity function, gait, and cognition. HCP: health care professional; MS: multiple sclerosis.

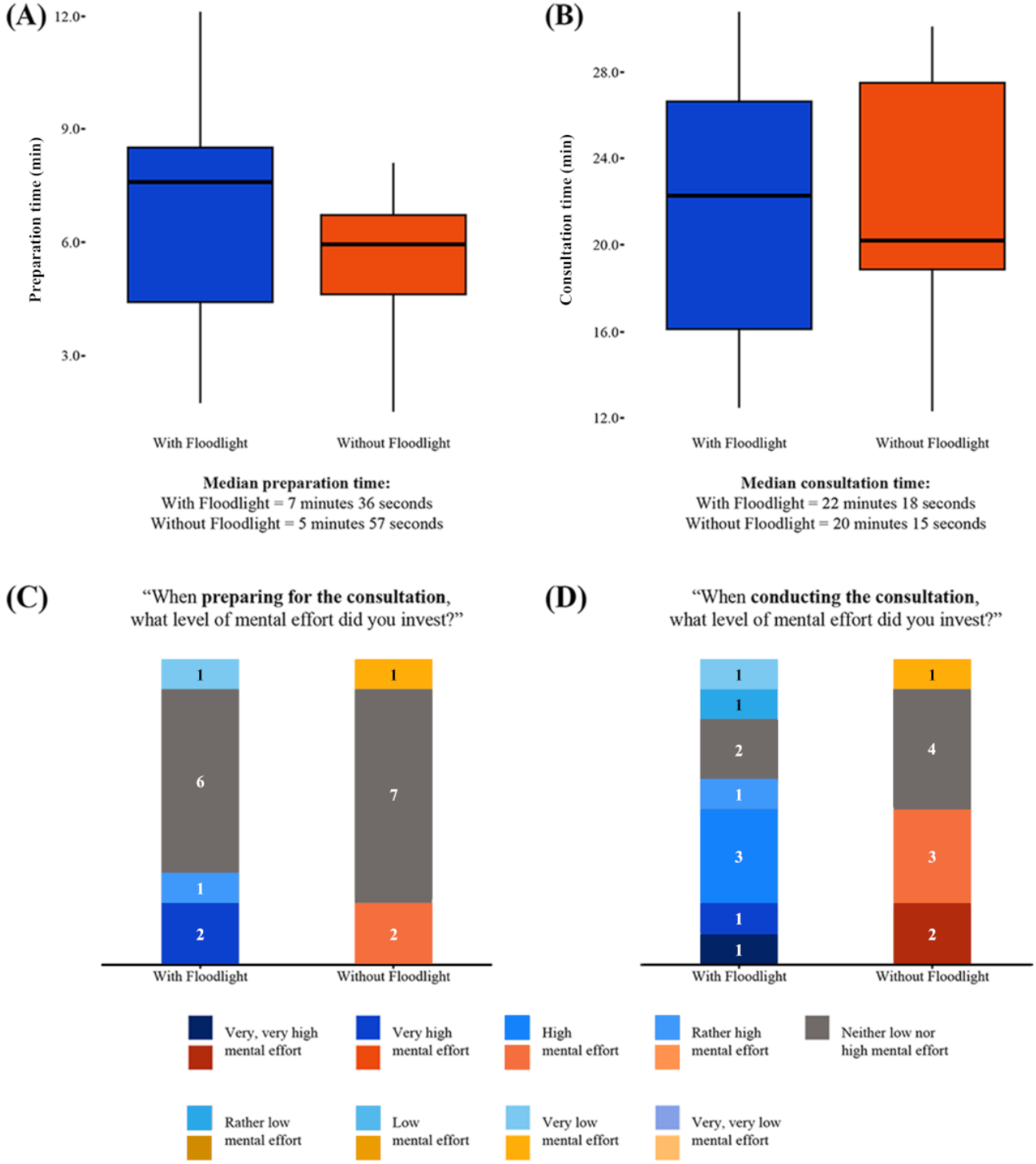


Workflow Metrics

In terms of the time taken for patient case preparation, cases took a median of 7 minutes and 36 seconds with Floodlight and 5 minutes and 57 seconds without Floodlight (Figure 5A). The median time taken to conduct the teleconsultations was 22 minutes with Floodlight and 20 minutes without Floodlight (Figure 5B). When using the Floodlight technology, participant neurologists also reported investing a slightly higher level of mental effort to prepare for (Figure 5C; very high mental effort to rather high mental effort: n=3 vs n=2) and conduct patient cases (Figure 5D; very, very high mental effort to rather high mental effort: n=6 vs n=5).

XSL•FO
RenderX

Figure 5. Workflow metrics. (A) Preparation time for patient cases with and without Floodlight data. (B) Teleconsultation time with and without Floodlight data. (C) Mental effort required preparing for patient cases with and without Floodlight data. (D) Mental effort required when conducting patient cases with and without Floodlight data. The classification key uses shades of blue for data obtained "with Floodlight" and shades of red for data obtained "without Floodlight"; shade of gray uses the same classification in both "with Floodlight" and "without Floodlight".

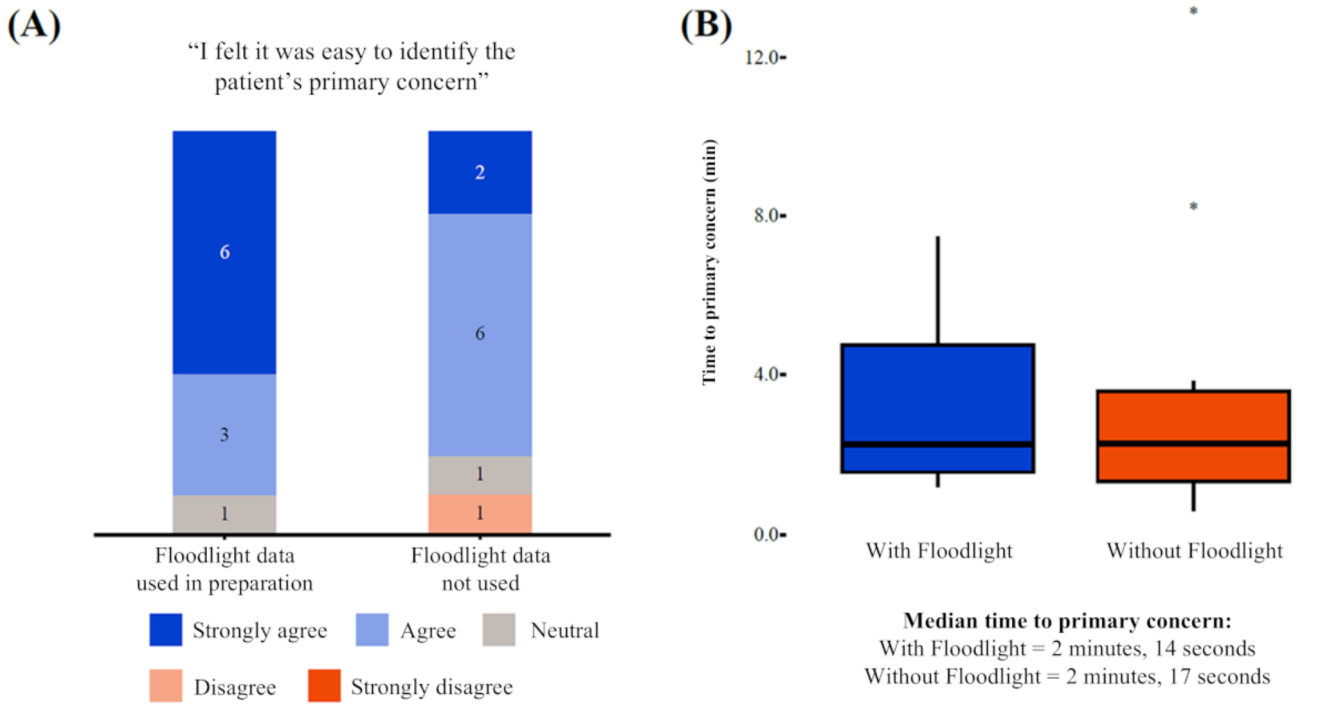


Clinical Consultations and Patient Concerns

About 6 out of the 10 neurologists "strongly agreed" that it was easier to identify patient concerns within the relevant functional domains with access to Floodlight data during the consultation preparation phase versus without access (where 2/10 "strongly agreed"; Figure 6A). The median time taken for participant neurologists to start discussing the primary domain of concern was 2 minutes, 14 seconds when using the Floodlight technology and 2 minutes, and 17 seconds without the Floodlight technology (Figure 6B).

XSL•FO
RenderX

Figure 6. Patients' primary domains of concern: (A) identification and (B) time taken. The identification of patient concern and the median time taken for participant neurologists to initiate discussions on the primary domain of concern were assessed during the consultation preparation phase with and without access to Floodlight data.



Recognition of "Invisible" Symptoms of MS

The median time taken to discuss each "invisible" symptom was between 1 and 1.5 minutes (Table 4). In Patient Case A, which was structured to show a prominent cognitive decline, cognitive issues, and mood change, discussions exceeded 2 minutes. In Patient Case B, bladder dysfunction (which was referred to in the clinical letters and without the support of Floodlight information) was also discussed for over 2 minutes. While differences can be gleaned at the individual symptom level, there was no clear pattern to the length of the discussions. Being aware of the symptom by means of the clinical letters did not necessarily seem to be a clear determinant in the participant neurologist spending more time on discussions with the patient actor. There were also no consistent differences in the median time spent discussing symptoms across domains with and without the use of the Floodlight technology.

Table . Median time spent discussing each "invisible" symptom[a] with patients (such as fatigue and bladder dysfunction that are difficult to evaluate by health care professionals [HCPs]) across all teleconsultations with and without the Floodlight technology.

Symptom	Patient Case A[b]		Patient Case B[b]	
	With Floodlight (min)	Without Floodlight (min)	With Floodlight (min)	Without Floodlight (min)
Vision changes	01:32[b]	01:18[b]	00:30	00:10
Sexual dysfunction	00:05	01:15	00:17[b]	00:55[b]
Mood changes	02:18	01:26	01:32[b]	01:50[b]
Physical and emotional pain	01:55	01:15	01:54[b]	01:12[b]
Bowel and bladder dysfunction	00:30[b]	01:10[b]	01:14[b]	02:47[b]
Cognitive changes	02:16[b]	02:06[b]	00:27	00:53
Fatigue	00:40[b]	01:01[b]	01:08	01:39
Median across all domains	01:25	01:22	01:07	01:34

[a]Invisible symptoms, including fatigue, mood disorders, cognitive impairments, pain, bladder or bowel dysfunction, sexual dysfunction, and vision changes can be experienced by people living with MS. Some of these symptoms may not be externally evident or easy to report and quantify and can be difficult for the patient to report and articulate during a clinical encounter (eg, due to subjectivity bias, poor recall, or stigma) or for physicians to capture (eg, limitations in available measurement tools, ample reliance on patient recall on the visit day).

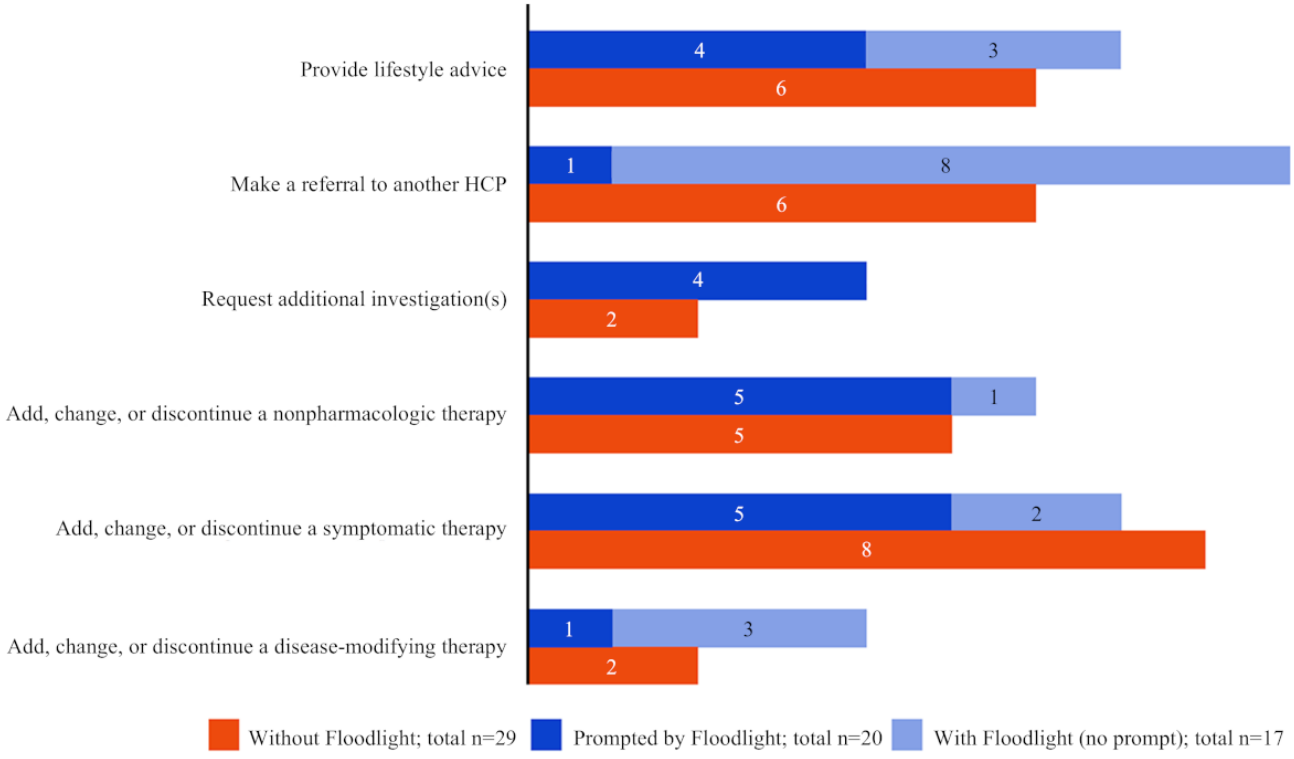
[b]These are the symptoms that were previously reported, per the clinical documentation provided, for Patient Case A and Patient Case B.

XSL•FO
RenderX

Care Decisions and Change in Disease Management Decisions

Floodlight data were reported as a trigger for 20 of the 37 care and change in disease management decisions (including regarding disease-modifying therapies, additional medications, referrals, or investigations), always in combination with other triggers such as patient history (20/20) or clinical exam findings (9/20; Figure 7). Overall, a greater number of care decisions were taken when using the Floodlight technology (37) versus without (29), including making a referral to another HCP (9 vs 6), or adding, changing, or discontinuing a nonpharmacologic therapy (6 vs 5) or disease-modifying therapy (4 vs 2).

Figure 7. Care decisions, including change in disease management, prompted by Floodlight data and taken when using the Floodlight technology, versus without. Floodlight data were reported as a trigger for care and change in disease management decisions, including regarding disease-modifying therapies, additional medications, referrals, or investigations. In all instances, Floodlight data were used in conjunction with other triggers such as patient history or clinical exam findings. HCP: health care professional.



Overall Feedback

Overall, participant neurologists valued access to longitudinal data, particularly regarding hand function and cognition. Many participant neurologists found the aspects of the user interface challenging when using the Floodlight MS HCP Portal. They felt that user interface improvements were the most important changes to be made, and they noted the following could help improve the interface: “Separating different data points and putting them into separate charts,” “...an overall curve, visualizing the trend over time,” and “…being able to change the y axis to separate data points for easier review.”

Data Availability

For up-to-date details on Roche’s global policy on the sharing of clinical information and how to request access to related clinical study documents, please visit [35].

Discussion

Principal Findings

The clinical simulations of MS teleconsultations described in this study demonstrate the ability of this research methodology to deliver high-fidelity patient cases. They also enabled direct comparison of teleconsultations conducted with and without the use of digital health technologies.

Clinical simulation offered several advantages, including the ability to present relevant, representative, paradigmatic MS cases and to efficiently generate insights on the utility and usability of new digital technology in clinical visits. This provided early real-world insights from neurologists who were naïve to the Floodlight technology and who received only brief introductory training on its use. Specifically, it provided an opportunity to move beyond the expected impact of the tool and, instead, explore the approach used by participants naïve to the digital technology (after a brief orientation) in actual clinical decision-making.

Using real patient data from the CONSONANCE study enabled access to extensive existing data without additional patient consent or data acquisition, allowing case selection based on in-depth clinical information. The richness of the CONSONANCE dataset minimized the need for synthetic data, which was limited but where used, derived from valid sources such as narrative radiology reports and clinical letters. While this approach ensured high-fidelity and clinically relevant patient scenarios, it introduced a limitation in the generalizability of the simulated cases as the patient population in the

XSL•FO
RenderX

CONSONANCE study was composed entirely of people with progressive multiple sclerosis. This highlights the capability of clinical simulation to leverage rich, real-world datasets while also underscoring the importance of including a broader spectrum of patient profiles and validated synthetic cases to enhance external validity, scalability, and applicability across diverse MS phenotypes. Additional simulated patient cases can be easily generated from other clinical trials or by generating synthetic (but realistic) patient case data. Further simulation research should expand the number and diversity of patient cases, including data from varied trial populations and validated synthetic cases to better capture the heterogeneity of MS care. It is important to ensure that these cases are representative of typical patients seen in clinical practice and developed with appropriate ethical considerations to avoid the introduction of unwanted bias. Additionally, it is also essential to ensure that clinical trial data used for patient cases do not allow patient identities to be inferred and that blinding procedures are preserved.

This study explored complex MS cases, with multiple patient concerns and functional domains affected, to capture the complexity of real-world MS clinical visits and explore the impact of utilizing a digital tool (Floodlight technology). As with "real" clinical encounters with people living with MS, distilling prior history and functional testing into condensed clinical letters for use in the consultations was challenging, due to the heterogeneity of symptoms, scales, and other assessments used. For example, bladder symptoms reported by patients in the SymptoMScreen were consistently underscored in the clinicians' EDSS Bowel/Bladder Functional System [36-38].

Research applications of simulation can include training methodologies for educational purposes [22], such as in training for medical students or less experienced HCPs, and to enhance clinical competence [21]. Additionally, simulation can be used to improve primary care office–based readiness to respond to medical emergencies [39] or to enhance cultural sensitivity, communication, and empathy among HCPs [40]. Simulation can also be used as an investigative methodology to answer research questions that otherwise could not be answered feasibly, safely, ethically, or in a timely fashion in clinical settings [22], as pertains to our study.

The simulation methodology provided key insights into integrating a digital health tool into routine MS care. Initial findings pertained to how neurologists naïve to this technology began to access and interpret these data. Indeed, there is a known socialization process required for the adoption of new technology [41], and this must be accounted for in the plans that developers have for the implementation of new tools. Neurologists scored the clinician-facing HCP Portal for accessing Floodlight MS data "above average" on the System Usability Scale, indicating a high level of usability. Feedback from postsimulation surveys and interviews provides a foundation for iterative improvements to the user interface. Among the available data on the portal, the "mood status" aspect of the Patient Journal (Daily Status Questions) was rated as the most useful of the data visualizations presented, which is potentially indicative of a medical need (eg, more systematic depression monitoring). Finally, as expected, incorporating Floodlight data into teleconsultation preparation required slightly more time and mental effort than consultation without such technology. Interestingly, the median time was only 1.7 minutes longer for patient case preparation, which seems relatively modest compared with the potential gains from having Floodlight data available. This also indicates that the brief presimulation training was effective and supports the tool's scalability. With increased familiarity, time required to use the Floodlight technology during the visits would likely decrease. However, even a short amount of additional time requirement could nonetheless present a potential barrier to use. For example, when evaluating the initial launch of the patient codesigned, high-usability-scoring, point-of-care clinical dashboard MS NeuroShare, clinicians were less likely to use it on busy clinic days, despite the reported improvements in the quality of communication and patient understanding of management care plans. New solutions to alleviate clinician workloads must be evaluated against the time required to implement them, such as educating patients on the clinical applications [41].

Digital health tools can capture objective data between clinical visits. This can avoid reliance on patient recall of symptoms, helping to provide clinicians with a more complete picture of symptoms and enabling discussions between HCPs and patients. The second set of exploratory insights, therefore, concerned the impact that ready access to Floodlight data might have on clinical discussion and management. Overall, while participant neurologists started discussing the primary domain of concern after 2 minutes both with or without the Floodlight technology, most participants said that it was easier to identify patients' concerns when they had access to the Floodlight MS HCP Portal (Figure 6A). Further, more care decisions were taken when using Floodlight data versus without, for example, making a referral to another HCP or amending a disease-modifying therapy.

Limitations

While simulations can represent and provide insights on the dynamics of MS in real-life clinical practice, the method is limited by the ability to account for operational and behavioral variables that occur in clinical practices, and it may, therefore, not be a fully accurate representation. While this methodology is inherently scalable, its primary limitation lies in the effort needed to recruit and train actors. By comparison, on-site studies involving real patients are even more constrained, as they can only include individuals residing near the clinical study site(s). Although the actors performed convincingly, simulations cannot fully substitute for real patient interactions. Real patients may experience factors such as anxiety about their clinical outcomes, fatigue from poor sleep, or depression, all of which can influence the dynamics of clinical encounters; however, it must be noted that this is not one of the aims of this study. The limited numbers of participants and patient cases in this study, important for this initial testing of the research methodology, naturally limit generalizability to real-life clinical consultations. Virtual simulations could enrich the recruitment of diverse neurologists by offering more convenient participation as well as the potential to recruit neurologists from a wider geographic area. This will be important in studies that seek to quantify differences in clinical decision-making. Furthermore, a potential source of

XSL•FO
RenderX

bias relevant to all simulations involving observation of tasks is the Hawthorne effect, where participants modify their behavior when they know they are being observed [42,43]. Mitigation strategies to overcome this included informing participating neurologists in advance about the study objectives, emphasizing that the research focus was not primarily on diagnostic accuracy, and assuring them that their identities would remain confidential. To further minimize the Hawthorne effect, the observer's camera and microphone were switched off during sessions; however, the observer remained present on the call to ensure study fidelity and provide technical support if needed. It should be acknowledged that despite these measures, such biases cannot be entirely eliminated in simulation-based research, although increasing the number of participants might reduce their impact.

Further, exploring cognitive impairment as a primary domain of concern highlighted some limitations of using simulated encounters because some participant neurologists described typically engaging patients' family members or care partners when assessing the extent and impact of a patient's cognitive challenges, and family members were not included in the simulated scenarios. An alternative approach in clinical simulations exploring more focused digital tools would be to curate simpler patient cases with only 1 domain of concern and a few specific invisible symptoms and to focus the investigation on more specific aspects.

Conclusions

Clinical simulation of MS teleconsultations allowed evidence generation on the potential utility of a digital health technology tool in MS care. The simulated patient cases and environment were found to be of high fidelity and enabled the direct comparison of teleconsultations conducted with and without the use of the Floodlight technology. A number of domains could be explored, including tool usability, influence of Floodlight data on clinical decisions, and impact on clinical workflows. Employing this methodology provided preliminary evidence that the Floodlight technology could support routine MS care, as it was found to be usable and useful, with minimal additional time and mental effort required on the part of neurologists previously naïve to the technology.

The findings of this study support expanded research into and development of clinical simulation methodologies for neurological research. This could expedite integrating innovative methods or interventions in health care settings, as well as in medical training. In the digital health space specifically, simulations could help to anticipate what socialization of technologies may require, to steer guidance on usage, explain their value to clinicians, and help health systems plan implementation.

Acknowledgments

We would like to thank all study participants and their families. We would also like to thank Active Image Roleplay for providing the professional actors, and Philipp D'Alfonso, Joan Piñol Fustero, and Harold Gonzalez Hernandez, who helped with the technical setup of the Floodlight MS HCP Portal simulated environment. Writing and editorial assistance for this manuscript was provided by Cynthia J Henley-Smith, PhD, and Terri Desmonds, PhD, of Nucleus Global, an Inizio company in the United Kingdom, and funded by F. Hoffmann-La Roche Ltd.

Funding

Funding for this study was provided by F. Hoffmann-La Roche Ltd.

Authors' Contributions

Conceptualization: AK, JH, LC, RB, SG
Data curation: SD
Formal analysis: SD, SH
Funding acquisition: LC
Investigation: JH, RB, SD
Methodology: JH, SD, SG
Project administration: JH, LC
Resources: JH, LC
Supervision: JH, LC
Visualization: SD, SH
Writing – review & editing: AK, IW, JH, LC, RB, SD, SG, SH

Conflicts of Interest

RB has received consultancy fees from Alexion, EMD Serono, Horizon, Janssen, and TG Therapeutics; and is funded by the NMSS Harry Weaver Award, NIH, DOD, and NSF, as well as Biogen, Eli Lilly, F. Hoffmann-La Roche Ltd, and Genentech. LC is an employee of F. Hoffmann-La Roche Ltd. IC was an employee of F. Hoffmann-La Roche Ltd when this study was conducted and is currently an employee of CS Genetics. SD was a subcontractor to Prova Health when this study was conducted and is currently an employee of Imperial College London. SG is an employee of and shareholder in Prova Health and an employee

XSL•FO
RenderX

of Imperial College London. JH is an employee of and shareholder in Prova Health. SH is an employee of and shareholder in F. Hoffmann-La Roche Ltd. AK is an employee of and shareholder in F. Hoffmann-La Roche Ltd.

References

1. Kappos L, Wolinsky JS, Giovannoni G, et al. Contribution of relapse-independent progression vs relapse-associated worsening to overall confirmed disability accumulation in typical relapsing multiple sclerosis in a pooled analysis of 2 randomized clinical trials. JAMA Neurol 2020 Sep 1;77(9):1132-1140. [doi: 10.1001/jamaneurol.2020.1568] [Medline: 32511687]
2. Moccia M, Lanzillo R, Palladino R, et al. Cognitive impairment at diagnosis predicts 10-year multiple sclerosis progression. Mult Scler 2016 Apr;22(5):659-667. [doi: 10.1177/1352458515599075] [Medline: 26362896]
3. Filippi M, Bar-Or A, Piehl F, et al. Multiple sclerosis. Nat Rev Dis Primers 2018 Nov 8;4(1):43. [doi: 10.1038/s41572-018-0041-4] [Medline: 30410033]
4. Thompson AJ, Baranzini SE, Geurts J, Hemmer B, Ciccarelli O. Multiple sclerosis. Lancet 2018 Apr 21;391(10130):1622-1636. [doi: 10.1016/S0140-6736(18)30481-1] [Medline: 29576504]
5. van der Walt A, Butzkueven H, Shin RK, et al. Developing a digital solution for remote assessment in multiple sclerosis: from concept to software as a medical device. Brain Sci 2021 Sep 21;11(9):1247. [doi: 10.3390/brainsci11091247] [Medline: 34573267]
6. Kurtzke JF. Rating neurologic impairment in multiple sclerosis: an expanded disability status scale (EDSS). Neurology (ECronicon) 1983 Nov;33(11):1444-1452. [doi: 10.1212/wnl.33.11.1444] [Medline: 6685237]
7. Fouad AM, Abdel Naseer M, Farghaly M, Hegazy MI. New algorithmic approach for easier and faster extended disability status scale calculation. Mult Scler J Exp Transl Clin 2023;9(1):20552173231155055. [doi: 10.1177/20552173231155055] [Medline: 36816811]
8. Hatcher-Martin JM, Busis NA, Cohen BH, et al. American Academy of Neurology telehealth position statement. Neurology (ECronicon) 2021 Aug 17;97(7):334-339. [doi: 10.1212/WNL.0000000000012185] [Medline: 33986141]
9. Bove R, Poole S, Cuneo R, et al. Remote observational research for multiple sclerosis: a natural experiment. Neurol Neuroimmunol Neuroinflamm 2023 Mar;10(2):e200070. [doi: 10.1212/NXI.0000000000200070] [Medline: 36585249]
10. McGinley M, Carlson JJ, Reihm J, et al. VIRTUAL versus usual in-office care for multiple sclerosis: the VIRTUAL-MS multi-site randomized clinical trial study protocol. Contemp Clin Trials 2024 Jul;142:107544. [doi: 10.1016/j.cct.2024.107544] [Medline: 38657731]
11. Marziniak M, Brichetto G, Feys P, Meyding-Lamadé U, Vernon K, Meuth SG. The use of digital and remote communication technologies as a tool for multiple sclerosis management: narrative review. JMIR Rehabil Assist Technol 2018 Apr 24;5(1):e5. [doi: 10.2196/rehab.7805] [Medline: 29691208]
12. Giovannoni G, Butzkueven H, Dhib-Jalbut S, et al. Brain health: time matters in multiple sclerosis. Mult Scler Relat Disord 2016 Sep;9 Suppl 1:S5-S48. [doi: 10.1016/j.msard.2016.07.003] [Medline: 27640924]
13. Giovannoni G. Disease-modifying treatments for early and advanced multiple sclerosis: a new treatment paradigm. Curr Opin Neurol 2018 Jun;31(3):233-243. [doi: 10.1097/WCO.0000000000000561] [Medline: 29634596]
14. University of California, San Francisco MS-EPIC Team, Cree BAC, Hollenbach JA, et al. Silent progression in disease activity-free relapsing multiple sclerosis. Ann Neurol 2019 May;85(5):653-666. [doi: 10.1002/ana.25463] [Medline: 30851128]
15. Bove R, White CC, Giovannoni G, et al. Evaluating more naturalistic outcome measures: a 1-year smartphone study in multiple sclerosis. Neurol Neuroimmunol Neuroinflamm 2015 Dec;2(6):e162. [doi: 10.1212/NXI.0000000000000162] [Medline: 26516627]
16. Boukhvalova AK, Kowalczyk E, Harris T, et al. Identifying and quantifying neurological disability via smartphone. Front Neurol 2018;9:740. [doi: 10.3389/fneur.2018.00740] [Medline: 30233487]
17. Quinn CC, Clough SS, Minor JM, Lender D, Okafor MC, Gruber-Baldini A. WellDoc mobile diabetes management randomized controlled trial: change in clinical and behavioral outcomes and patient and physician satisfaction. Diabetes Technol Ther 2008 Jun;10(3):160-168. [doi: 10.1089/dia.2008.0283] [Medline: 18473689]
18. Bauer AM, Rue T, Munson SA, et al. Patient-oriented health technologies: patients' perspectives and use. J Mob Technol Med 2017 Aug;6(2):1-10. [doi: 10.7309/jmtm.6.2.1] [Medline: 28936236]
19. Colligan E, Metzler A, Tiryaki E. Shared decision-making in multiple sclerosis. Mult Scler 2017 Feb;23(2):185-190. [doi: 10.1177/1352458516671204] [Medline: 27663871]
20. Guo C, Ashrafian H, Ghafur S, Fontana G, Gardner C, Prime M. Challenges for the evaluation of digital health solutions—a call for innovative evidence generation approaches. NPJ Digit Med 2020;3:110. [doi: 10.1038/s41746-020-00314-2] [Medline: 32904379]
21. Al-Elq AH. Simulation-based medical teaching and learning. J Family Community Med 2010 Jan;17(1):35-40. [doi: 10.4103/1319-1683.68787] [Medline: 22022669]
22. Cheng A, Auerbach M, Hunt EA, et al. Designing and conducting simulation-based research. Pediatrics 2014 Jun;133(6):1091-1101. [doi: 10.1542/peds.2013-3267] [Medline: 24819576]

XSL•FO
RenderX

23. Bove R, Bevan C, Crabtree E, et al. Toward a low-cost, in-home, telemedicine-enabled assessment of disability in multiple sclerosis. Mult Scler 2019 Oct;25(11):1526-1534. [doi: 10.1177/1352458518793527] [Medline: 30141729]
24. Graves JS, Elantkowski M, Zhang YP, et al. Assessment of upper extremity function in multiple sclerosis: feasibility of a digital pinching test. JMIR Form Res 2023 Oct 2;7:e46521. [doi: 10.2196/46521] [Medline: 37782540]
25. Dondelinger F, Thomann AE, Volkova-Volkmar E, Lipsmeier F, Sprengel J, McGinley M, et al. A digital remote assessment for measuring impairment in information processing speed in people with MS. Mult Scler 2021;27(Suppl):P303. [doi: 10.1177/13524585211044667]
26. Creagh AP, Simillion C, Scotland A, et al. Smartphone-based remote assessment of upper extremity function for multiple sclerosis using the Draw a Shape Test. Physiol Meas 2020 Jun 19;41(5):054002. [doi: 10.1088/1361-6579/ab8771] [Medline: 32259798]
27. Cheng WY, Bourke AK, Lipsmeier F, et al. U-turn speed is a valid and reliable smartphone-based measure of multiple sclerosis-related gait and balance impairment. Gait Posture 2021 Feb;84:120-126. [doi: 10.1016/j.gaitpost.2020.11.025] [Medline: 33310432]
28. Bourke AK, Scotland A, Lipsmeier F, Gossens C, Lindemann M. Gait characteristics harvested during a smartphone-based self-administered 2-minute walk test in people with multiple sclerosis: test-retest reliability and minimum detectable change. Sensors (Basel) 2020 Oct 19;20(20):5906. [doi: 10.3390/s20205906] [Medline: 33086734]
29. Creagh AP, Simillion C, Bourke AK, et al. Smartphone- and smartwatch-based remote characterisation of ambulation in multiple sclerosis during the two-minute walk test. IEEE J Biomed Health Inform 2021 Mar;25(3):838-849. [doi: 10.1109/JBHI.2020.2998187] [Medline: 32750915]
30. Midaglia L, Mulero P, Montalban X, et al. Adherence and satisfaction of smartphone- and smartwatch-based remote active testing and passive monitoring in people with multiple sclerosis: nonrandomized interventional feasibility study. J Med Internet Res 2019 Aug 30;21(8):e14863. [doi: 10.2196/14863] [Medline: 31471961]
31. Lakin L, Davis BE, Binns CC, Currie KM, Rensel MR. Comprehensive approach to management of multiple sclerosis: addressing invisible symptoms—a narrative review. Neurol Ther 2021 Jun;10(1):75-98. [doi: 10.1007/s40120-021-00239-2] [Medline: 33877583]
32. Hyzy M, Bond R, Mulvenna M, et al. System usability scale benchmarking for digital health apps: meta-analysis. JMIR Mhealth Uhealth 2022 Aug 18;10(8):e37290. [doi: 10.2196/37290] [Medline: 35980732]
33. Paas F, Ayres P, Pachman M. Assessment of cognitive load in multimedia learning: theory, methods and applications. In: Robinson DH, Schraw G, editors. Recent Innovations in Educational Technology That Facilitate Student Learning: Information Age Publishing Inc; 2008:11-36 URL: https://researchers.mq.edu.au/en/publications/assessment-of-cognitive-load-in-multimedia-learning-theory-method/ [accessed 2025-12-02]
34. Luck I. What is a Good Net Promoter Score (NPS)? 4 Approaches.: Customer Gauge; 2023. URL: https://customergauge.com/what-is-a-good-net-promoter-score [accessed 2024-07-23]
35. Our commitment to transparency of clinical study information. Roche. URL: https://go.roche.com/data_sharing [accessed 2025-11-19]
36. Meyer-Moock S, Feng YS, Maeurer M, Dippel FW, Kohlmann T. Systematic literature review and validity evaluation of the Expanded Disability Status Scale (EDSS) and the Multiple Sclerosis Functional Composite (MSFC) in patients with multiple sclerosis. BMC Neurol 2014 Mar 25;14:58. [doi: 10.1186/1471-2377-14-58] [Medline: 24666846]
37. Strober L, DeLuca J, Benedict RH, et al. Symbol Digit Modalities Test: a valid clinical trial endpoint for measuring cognition in multiple sclerosis. Mult Scler 2019 Nov;25(13):1781-1790. [doi: 10.1177/1352458518808204] [Medline: 30334474]
38. Kaplan TB, Gopal A, Block VJ, et al. Challenges to longitudinal characterization of lower urinary tract dysfunction in multiple sclerosis. Mult Scler Relat Disord 2022 Jun;62:103793. [doi: 10.1016/j.msard.2022.103793] [Medline: 35461057]
39. Monachino A, Caraher C, Ginsberg J, Bailey C, White E. Medical emergencies in the primary care setting: an evidence based practice approach using simulation to improve readiness. J Pediatr Nurs 2019;49:72-78. [doi: 10.1016/j.pedn.2019.09.017] [Medline: 31670140]
40. Turkelson C, Cooper D, Creech C, Schellenberg K, Behnke L. Using simulation to enhance nurse practitioner students cultural sensitivity, communication, and empathy with vulnerable populations. Clin Simul Nurs 2021 Jul;56:108-116. [doi: 10.1016/j.ecns.2021.04.011]
41. Bove R, Bruce CA, Lunders CK, et al. Electronic health record technology designed for the clinical encounter: MS NeuroShare. Neurol Clin Pract 2021 Aug;11(4):318-326. [doi: 10.1212/CPJ.0000000000000986] [Medline: 34484932]
42. Gould D, Lindström H, Purssell E, Wigglesworth N. Electronic hand hygiene monitoring: accuracy, impact on the Hawthorne effect and efficiency. J Infect Prev 2020 Jul;21(4):136-143. [doi: 10.1177/1757177420907999] [Medline: 32655694]
43. Sujatha BK, Reddy MT, Pathak P. Camouflage in research—the Hawthorne effect. Int J Dev Res 2019;9:15710 [FREE Full text]

Abbreviations

EDSS: Expanded Disability Status Scale
HCP: health care professional

XSL•FO
RenderX

MS: multiple sclerosis
PRO: patient-reported outcome
SDMT: Symbol Digit Modalities Test

Edited by Q Chen; submitted 22.11.24; peer-reviewed by JV Schependom, K Adegoke; revised version received 05.08.25; accepted 27.10.25; published 11.12.25.

Please cite as:
Bove R, Capezzuto L, West I, Dryden S, Ghafur S, Halligan J, Hubeaux S, Kazlauskaite A
Simulation of Clinical Visits as a Novel Approach to Evaluate Digital Health in Multiple Sclerosis: Simulation Study
JMIR Med Inform 2025;13:e67845
URL: https://medinform.jmir.org/2025/1/e67845
doi:10.2196/67845

© Riley Bove, Luca Capezzuto, Imogen West, Simon Dryden, Saira Ghafur, Jack Halligan, Stanislas Hubeaux, Agne Kazlauskaite. Originally published in JMIR Medical Informatics (https://medinform.jmir.org), 11.12.2025. This is an open-access article distributed under the terms of the Creative Commons Attribution License (https://creativecommons.org/licenses/by/4.0/), which permits unrestricted use, distribution, and reproduction in any medium, provided the original work, first published in JMIR Medical Informatics, is properly cited. The complete bibliographic information, a link to the original publication on https://medinform.jmir.org/, as well as this copyright and license information must be included.

XSL•FO
RenderX

Organizing Telemonitoring—Decision-Making Between Centralized and Distributed Models in the Netherlands, Using the Non-Adoption, Abandonment, Scale-Up, Spread, and Sustainability (NASSS) Framework: Case Study

Nienke Antine Elferink[1*], MSc; Manon Jacqueline Roest[2*], MD; Anne Marie Weggelaar[2,3], Prof Dr; Marleen de Mul[1], PhD

[1]Erasmus School of Health Policy & Management, Erasmus University Rotterdam, Burgemeester Oudlaan 50, Rotterdam, The Netherlands

[2]Tranzo, Tilburg University, Tilburg, The Netherlands

[3]Clinical Informatics, Eindhoven University of Technology, Eindhoven, The Netherlands

[*]these authors contributed equally

Corresponding Author:
Marleen de Mul, PhD
Erasmus School of Health Policy & Management, Erasmus University Rotterdam, Burgemeester Oudlaan 50, Rotterdam, The Netherlands

Abstract

Background: Telemonitoring can be implemented using either centralized or distributed organizational models. However, few published studies explore which conditions make one model preferable over the other, or how to choose between these two.

Objective: This study aimed to investigate the decision-making factors across several domains (eg, technological, personal, and organizational) when selecting the telemonitoring model.

Methods: We conducted a multiple case study across 4 purposively sampled hospitals to gain a range of perspectives on organizational models for telemonitoring. Selection criteria included: (1) type of organizational model, (2) type of collaborating partners, (3) task division of handling notifications, and (4) it had to be implemented at scale, rather than being in an exploratory phase. Data was collected in a document study, 13 semistructured interviews, and a focus group. The topic list was based on the domains of the NASSS (non-adoption, abandonment, scale-up, spread, and sustainability) framework. Interviewees (n=13) were 5 project leaders, 2 tele-nurses, 4 health care professionals, and 2 clinical informaticians. Data analysis was performed iteratively and included reflective thematic analysis. A member-checking focus group was organized to verify and reflect on the findings.

Results: Various preferential factors based on the seven domains of the NASSS framework were explored for both centralized and distributed telemonitoring models: (1) Condition: the choice of objective, usually based on organizational strategy, determines whether telemonitoring will be centralized or distributed. (2) Technology: the preference for a model is determined by the anticipated number of notifications the application generates for a specific patient group. (3) Value proposition: the perceived cost-effectiveness and overall value to the patient shape the value proposition for each model. (4) Adopters: the new role of tele-nurse emerged in centralized monitoring centers (CMCs), necessitating new competencies, task redistribution, and shifts in responsibility. The importance of trust among staff became evident in the context of task redistribution. (5) Organization: CMCs are typically organized regionally, in partnerships or network arrangements, which can be time-consuming yet offer significant potential for impact. (6) Wider system: The existing Dutch reimbursement system does not incentivize CMCs because the payment structure is still based on a per-treatment model. (7) Adaptation over time: with advancements in technology, including artificial intelligence, organizing telemonitoring through CMCs is likely to gain popularity.

Conclusions: Our study highlights that when decision makers are choosing which telemonitoring model—centralized or distributed—to implement in their organization, deciding on the suitability of the model depends on multiple contextual factors. Our findings illustrate that decisions made for patient group selection, technology design, and value proposition significantly influence each other. It is therefore crucial for decision makers to understand these interactions and corresponding dynamics to better align their strategies with the operational realities of their organization.

(JMIR Med Inform 2025;13:e69349) doi:10.2196/69349

KEYWORDS

telemonitoring; centralized telemonitoring; distributed telemonitoring; NASSS framework; qualitative study

XSL•FO
RenderX

Introduction

Telemonitoring outpatient and inpatient care (also coined remote patient monitoring, telehealth, and telemedicine) is a recognized solution to address health care challenges such as rising costs, staff shortages, and the need to improve cost-effectiveness, treatment quality, and reduce waiting times [1-4]. Telemonitoring is defined as "the use of information technology to monitor patients at a distance" [5]. Telemonitoring enables clinicians to maintain and adjust their patients' plan of care by using remotely gathered data, such as vital signs, to proactively make medical decisions about a patient's care [6]. It involves the collection, transmission, evaluation, and communication of individual health data from patients to health care providers using technology [7]. Because telemonitoring is widely touted to improve patient care while reducing staff workload and costs, governments worldwide stimulate it as a paramount innovation [8,9]. While much research has focused on the positive outcomes of telemonitoring for patients and organizations [10-12], less attention has been given to the organizational aspect of telemonitoring. Specifically, the considerations for various organizational models—centralized, distributed, or a combination of both [13-15]. However, which model is preferable in a given context and how to choose between the models remains unclear.

In general, 2 organizational models are in place. First, a centralized organizational model, which places patient monitoring in a physical or virtual centralized monitoring center (CMC) and is primarily conducted by tele-nurses rather than physicians. CMC can involve monitoring patients across an entire health care organization, network, or even a region [13,16,17]. The literature reports notable advantages to a centralized organizational model, including improved efficiency and cost-effectiveness through economies of scale and pooled resources, which are especially beneficial in rural areas and alleviate staff shortages [18,19]. The larger volume of cases in centralized telemonitoring permits 24/7 operation, instead of being confined to office hours in outpatient clinics [8,20]. Since 2019, structural financing for remote care (telehealth) was established in the Netherlands. Under specific conditions and for designated diagnoses, hospitals became eligible to claim reimbursement for remote care through the existing diagnosis treatment combination system [9]. This reimbursement facilitated the digital transformation of health care, aiming for more efficiency in health care delivery. Recent studies have shown that patients are satisfied with centralized telemonitoring [8,21]. Most professionals view centralized telemonitoring as favorable, although some are less acquainted with telemedicine and harbor reservations [8,22]. The second is a distributed organizational model in which professionals monitor their specific patient population [15]. Professionals believe they possess a better contextual understanding of their patients' data than tele-nurses who do not know a specific patient [18]. Some studies have shown that the doctor-patient relationship enhances patients' adherence to telemonitoring restrictions and therapy agreements. However, studies on the differences between centralized and distributed organizational models are lacking [13,15,18].

Numerous studies, including several literature reviews, have explored the implementation of telemonitoring for patients with diseases such as hypertension, heart failure, diabetes, and chronic obstructive pulmonary disease (COPD) [eg, 10,23,24]. These studies highlight various organizational models and the challenges associated with the complexity of implementing telemonitoring [25]. However, the challenges of organizing telemonitoring extend beyond adoption or implementation obstacles. They require a deeper exploration of different aspects, including context variables at the micro, meso, and macro levels [26,27].

This is particularly relevant, as both centralized and distributed organizational models for telemonitoring can be implemented in a single organization or across multiple organizations, potentially spanning the entire care chain [26]. To address this complexity, the NASSS (non-adoption, abandonment, scale-up, spread, and sustainability) framework provides a comprehensive lens, through which 7 key domains are examined: condition, technology, value proposition, the adopter's perspective, organizational context, the wider context, and adaptation over time [28]. Importantly, the framework does not imply a linear relationship between the domains but instead emphasizes their interconnectedness and mutual influence [29]. With this framework, barriers and facilitators for implementation can be identified, and the complexity of each domain can be assessed [30,31]. Given this, our research question is as follows: which considerations are taken into account when choosing between centralized or distributed telemonitoring, following the NASSS framework?

Methods

Study Design

Using a qualitative research approach, we conducted a multiple case study to explore the factors hospitals consider when choosing between centralized and distributed telemonitoring models. The study complied with the COREQ (Consolidated Criteria for Reporting Qualitative Research; see Checklist 1) [32]. The first author is a medical student in health sciences; the other authors are experienced researchers (PhD, associate professor, and endowed professor).

Ethical Considerations

Ethical approval was secured from the Ethics Review Board of Tilburg University (ReferenceTSB_RP741). Data storage is compliant with the General Data Protection Regulation.

Setting

This study was executed in the Netherlands. This country has been implementing a series of policy measures aimed at facilitating the digital transformation of health care since 2012. Measures include the introduction of incentive grants, national guidelines, specific volume targets for hospitals, and structural financing for remote care (telehealth encompassing telemonitoring) [33-35]. In the face of staff shortages, this has led to new forms of (hybrid) care that aim to reduce the number of follow-up outpatient clinic visits for chronic patients, reduce hospital length of stay after surgery, etc. The Netherlands manages the health system through self-regulation among private

XSL•FO
RenderX

entities: health care services are provided by private providers and managed by private health insurers. Every individual in the Netherlands has the option to select their health care insurer and health care plan [36]. Since 2019, hospitals are eligible to claim reimbursement for remote care under specific conditions and for designated diagnoses, through the existing Diagnosis treatment combination (comparable to Diagnosis Related Group) system, with costs covered under the statutory basic health insurance package. Hence, telemonitoring is covered by the Dutch health insurance system [9]. In the Netherlands, the availability of high-speed broadband internet and 4G mobile network is high, and an estimated 90% of the Dutch people use this on a daily basis. Still, health care organizations do not have the funds to upscale telemonitoring and therefore implementation progresses slowly.

Within this context, a purposive sample of teaching hospitals based on 2 organizational models (ie, centralized monitoring and distributed monitoring) was selected. (See Multimedia Appendices 1 and 2 for a visual representation of the centralized and distributed telemonitoring models). Hospitals using telemonitoring were selected from a network of Dutch teaching hospitals (Samenwerkende Topklinische Ziekenhuizen). Given the relatively small number of hospitals in the Netherlands (69 nonprofit hospital organizations), and the fact that only a few have implemented telemonitoring at scale, due to its relatively innovative nature, the selection of potential participants was constrained. To ensure comprehensive representation, all (12/12) early adopters of telemonitoring were put on a list. Project leaders responsible for telemonitoring in these hospitals were approached via email, which detailed the aim and design of this study. A total of four hospitals declined to participate (4/12,33%) citing as reasons: time constraints or maternity leave. Of the hospitals willing to participate (8/12, 67%), we purposely sampled that met the inclusion criteria outlined in Table 1, striving for a maximum variety of cases. An additional criterion was that the telemonitoring program had to be implemented at scale, rather than being in a pilot or exploratory phase.

We included 2 hospitals with primarily centralized telemonitoring (A and C) and 2 hospitals with predominantly distributed telemonitoring models (hospitals B and D). While hospitals B and D incorporated some centralized elements (300/3000, 10% and 1000/11,000, 9%, respectively, of their telemonitoring was conducted through a central unit) the vast majority (2700/3000, 90%) were organized in a distributed manner across care providers. In addition, in terms of collaborative partnerships, we included hospitals that operated independently without external collaboration (hospital A), those that collaborated with general practitioners in organizing telemonitoring (hospital B), and those that partnered with other hospitals (hospitals C and D). Finally, regarding role division in the monitoring process, we included hospitals where tele-nurses (hospitals A, B, and C), nurse practitioners (hospitals B and D), and residents (hospital D) were responsible for viewing telemonitoring alerts. Table 1 shows this overview. While the 2 distributed cases (hospitals B and D) also implemented centralized elements, they were classified as predominantly distributed.

Table . An overview of the hospitals included on the basis of the selection criteria.

Criterion	Hospital A	Hospital B	Hospital C	Hospital D
Organizational structure	Centralized	Predominantly distributed	Centralized	Predominantly distributed
Number of telemonitored patients	2000	3000 of which 300 (10%) centralized and 2700 distributed.	500	11,000 of which 1000 (9%) centralized and 10,000 distributed.
Partnerships	None	General practitioners	Hospital network	Neighbor hospital
Role division of handling telemonitoring alerts	Tele-nurses	Tele-nurses (both nurses and nurse practitioners)	Tele-nurses (nurses with physical disabilities)	Tele-nurses (both nurses and nurse practitioners); residents during outside-of-office hours.

Data Collection

Data collection included a document study, 13 interviews conducted between March and May 2023, and a member-checking focus group held in May 2023. The researchers began by requesting implementation-related documents (eg, implementation plans, current-state analyses, vision-related documents, or briefing materials for executive boards) from the project leaders of all 4 hospitals to study the organizational structures and challenges. Next, a researcher (NAE) conducted 13 semistructured interviews lasting between 30 and 60 minutes (see Table 2 for participant characteristics). The respondents were recruited via the project leader based upon criteria set by the researcher, including knowledge of telemonitoring and the respondent's involvement in the implementation process. Informed consent was obtained before the interview. The participants represented a diverse group of health care professionals and the project leaders, including a clinical informatician, which ensured multiple perspectives. Their varied backgrounds allowed for comprehensive insights into technical, practical, and organizational aspects, thereby collectively addressing all domains of the NASSS framework.

XSL•FO
RenderX

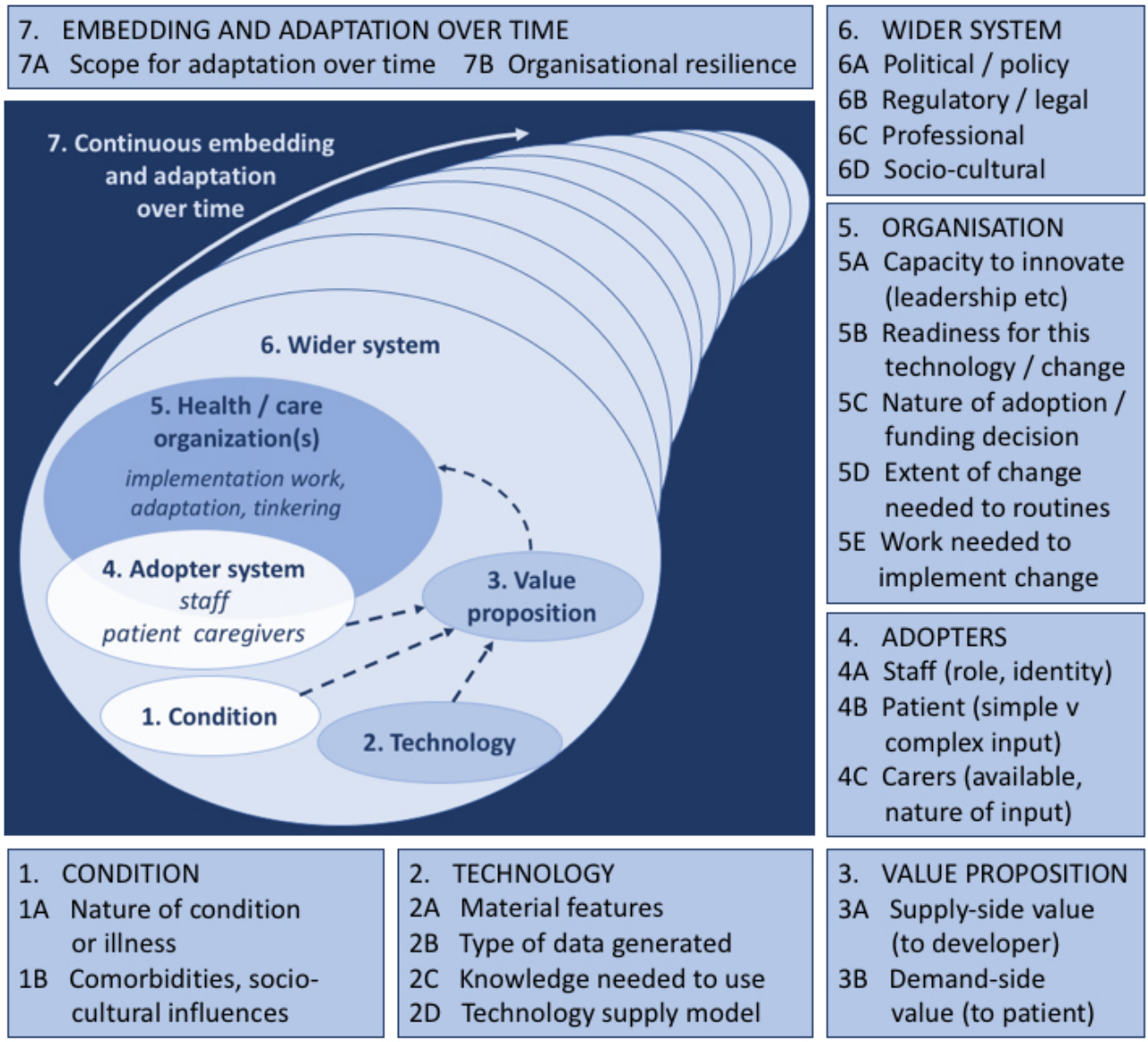
Table . Interview participants (N=13).

Background	Sex	Age
Project leader	Female (n=2) Male (n=3)	• 1 aged <30 y • 2 aged 30 - 39 y • 1 aged 40 - 49 y • 1 aged ≥60 y
Physicians	Male (n=3)	• 2 aged 30 - 39 y • 1 aged ≥60 y
Nurse practitioner	Female (n=1)	• 1 aged 40 - 49 y
Tele-nurse	Female (n=2)	• 2 aged 40 - 49 y
Clinical informatician	Female (n=2)	• 1 aged <30 y • 1 aged 40 - 49 y

Like previous studies that applied the NASSS framework to study telemonitoring (eg, 31,37-39), we based our topic list (see Multimedia Appendix 3) on this framework as well (see Figure 1) [27,40]. As the NASSS framework incorporates 7 interrelated domains that influence the implementation of innovative technologies, we considered it helpful to gain an understanding of relevant considerations of centralized versus (predominantly) distributed monitoring. The seven NASSS domains are as follows: (1) condition or illness, (2) technology, (3) value proposition, (4) adopter system, (5) organization, (6) wider context, and (7) embedding and adaptation over time [27]. Each domain can be defined by complexity (ie, dynamics, unpredictability, and interdependency) and their influence on other domains

XSL•FO
RenderX

Figure 1. The non-adoption, abandonment, scale-up, spread, and sustainability (NASSS) framework [27].



The interviews were video recorded through Microsoft Teams and transcribed verbatim. Afterward, the transcripts were verified for accuracy by a single researcher (NAE). A 1-hour focus group was subsequently conducted with the 5 project leaders to reflect upon our findings and enrich our insights by discussing the findings. This focus group was audio-recorded and transcribed verbatim. The participants mainly recognized and affirmed the results, thereby supporting the validity of our findings.

Data Analysis

The analysis was performed iteratively, ranging abductively between document analysis, transcripts (both interviews and focus group) and the literature [41,42]. A researcher (NAE) first open-coded the transcripts and documents via Atlas.ti 9 (Atlas.ti Scientific Software Development GmbH). To ensure reliability, a second researcher blindly thematically coded 3 interviews to cross-check coding. Afterward, the whole research team discussed both codes up to consensus, which resulted in a final code tree (see Multimedia Appendix 4), which guided a researcher (NAE) in the subsequent thematic coding [43]. Subsequently, selective coding categorized the codes and connected these to the themes of the NASSS framework domains. Next, each domain got a code, and the data was analyzed by these codes to identify similarities and differences across the cases, which led to an overview of complexities based on the criteria outlined in the NASSS framework. Finally, analysis and conclusions were discussed collectively (NAE, MJR, AMW, and MM). Overall, we applied a reflective thematic analysis as described by Braun and Clarke [43], “Reflexive TA [thematic analysis] approaches embrace researcher subjectivity as a resource for research (rejecting positivist notions of researcher bias (see [44]), view the practice of TA as inherently subjective, emphasize researcher reflexivity, and reject the notion that coding can ever be accurate—as it is an inherently interpretative practice, and meaning is not fixed within data.” Reflective thematic analysis was appropriate in this research, as we did not use the NASSS framework as a deterministic (ie, implementation steps) or even predictive model, rather as a sensitizing concept (see also abductive research methodology) providing us a reflexive lens in our analysis to deepen our interpretation [45].

XSL•FO
RenderX

Results

This section presents the findings of this study, organized according to the 7 domains of the NASSS framework. For each domain, we compared the considerations made between centralized and distributed monitoring models.

Domain 1: Selection Based on Patient Conditions and Telemonitoring Aims

The studied hospitals used various telemonitoring strategies: (1) centralized in the CMC, and (2) a predominantly distributed model in which most monitoring occurred locally, though some centralized elements were also present (see Table 1). The CMC strategy focused on identifying conditions suitable for central telemonitoring and aimed to incorporate all eligible patients into the CMC model. In contrast, in the distributed model, with the majority being managed through a distributed model, patients were selected on the basis of the telemonitoring objectives and disease complexity.

Our analysis revealed two objectives: (1) to enhance patient self-management, which is especially relevant in chronic diseases. Self-management was achieved through an online process involving telemonitoring that resembles e-coaching, in which advice is provided digitally, and hospital staff intervened only when the advice proved inadequate or when patients had questions. Since most alerts do not require an immediate response, distributed telemonitoring is feasible because it can be performed alongside other tasks. Several respondents mentioned that distributed telemonitoring was feasible for low-complexity cases only, because of time limitations; and (2) to monitor vital parameters. If patient measurements deviate from preset ranges, alerts are generated, prompting notifications to staff. Most alerts require immediate attention, as the patient may need acute care. Therefore, centralized telemonitoring aligns better with this aim.

Domain 2: Technological Features and Number of Notifications

In the Netherlands, 2 main vendors offer telemonitoring software applications to hospitals (Luscii and Sananet). All studied hospitals used both applications along with several additional applications to answer patient questions, often as part of their patient portal or an independent phone app. Consequently, health care staff used several applications. The visual and architectural design of these applications differed across hospitals. Our data reveals no relationship between the choice of software applications and the organizational model for telemonitoring.

Instead, our findings indicate that the intended telemonitoring objectives (ie, Domain 1: self-management or vital parameter monitoring) and the work that needs to be done, especially the expected notification numbers, drive the selection of the organizational model. Vital parameter monitoring generates many alerts that demand a timely response. Alerts requiring urgent response impact heavily on the workload of the involved staff who must assess and filter alerts based on clinical relevance. Current software cannot distinguish between relevant and irrelevant alerts. The high volume of alerts cannot be managed alongside other tasks, necessitating either centralized monitoring or staff assigned to this function.

> *The application captures most of the notifications or at least filters out the patients you don't have to see because they are in good health. The CMC eliminates another 80%-90%. The nurses remove another 15% so that leaves the physician with zero to 5% patients to actually see.* [Physician, hospital A]

In contrast, self-management provides less urgent alerts and, according to respondents, fewer alerts:

> *Because the app encourages self-management, the number of alerts is very low […] We work in a team of three. I think about 1 FTE is assigned [to telemonitoring] for a population of more than 1000 patients.* [Project leader, hospital B]

In sum, the technology setup is not tied to the organizational model. However, the aims of telemonitoring affect the expected volume of alerts and anticipated staff workload, which in turn influence the choice of organizational model.

Domain 3: Influence of Efficiency and Knowledge on Value Propositions

Centralized and distributed telemonitoring offer distinct value propositions for both professionals and patients. The respondents indicated that in a centralized model, telemonitoring is assigned to dedicated tele-nurses in the CMC, allowing them to focus on telemonitoring tasks. Compared with a distributed model, their concentrated effort enables quicker response times compared to a distributed model (see Domain 2 subsection). Many respondents suggested that centralized telemonitoring operates more cost-effectively due to economy of scale. The benefits grow with more partnerships with other organizations or general practitioners (see Domain 5) and large numbers of patients are monitored. In contrast, respondents highlighted the cost-effectiveness of distributed telemonitoring models, as the telemonitoring tasks can be performed alongside other duties:

> *[Nurses] in the outpatient clinic always have a spare moment between patients. They can answer a message. So, it is very energizing, and possible to do an 'in-betweenie'. So, the question is, how much capacity do you win if you centralize this?* [Project leader, hospital D]

In addition, our respondents said that delegating tasks to (tele-)nurses in both distributed and centralized monitoring alleviates the workload of nurse practitioners (NPs) and physicians, giving them more time for complex patient cases. However, task delegation sometimes requires specialist knowledge, especially with urgent vital parameter monitoring (see Domain 1 subsection). Specialist knowledge of many diseases is hard to transfer to CMC nurses and NPs, making it crucial for staff in centralized telemonitoring organizational models to have direct access to doctors. Respondents indicated that transferring specialized knowledge and maintaining close communication with doctors is easier to organize in distributed telemonitoring. Consequently, distributed telemonitoring models provide patients with direct access to health care professionals who possess specialist disease knowledge and, in some cases,

XSL•FO
RenderX

specific knowledge about the patient. As one respondent said: "This specific knowledge adds value for patients."

Thus, our data suggest that centralized telemonitoring is feasible for handling large patient and alert volumes (see Domains 1 and 2 subsections), which require nonspecialist knowledge, while distributed telemonitoring is preferable for alerts requiring specialist knowledge. Centralized telemonitoring is cost-efficient due to economies of scale when managing many patients or high volumes of alerts, whereas distributed telemonitoring is more efficient as it requires no additional personnel.

Domain 4: Evolution of the Telemonitoring Adopter's Role

In both organizational models, monitoring staff required specific competencies to incorporate the telemonitoring in their existing clinical workflows. Nurses took on a new role, expanded their responsibilities beyond those of traditional nursing. Consequently, the roles of NPs and physicians evolved, as now they supervise tele-nurses in their expanded responsibilities. In the cases we studied, the CMC tele-nurses were also responsible for developing telemonitoring clinical pathways for other medical conditions:

> *I'm currently contacting physicians to determine which patient groups we can add to our monitoring program […] That's my primary task besides monitoring. We also write the workflow protocols when we start monitoring a new condition.* [Tele-nurse, hospital A]

Respondents emphasized that this prominent role in organizing telemonitoring contributed to the growing enthusiasm for the tele-nurse role, which led to fewer personnel shortages in the CMC compared to other departments.

In addition, tele-nurses are taking on tasks that were previously performed by physicians and nurse practitioners. This shift in responsibilities requires a strong foundation of trust—particularly in the clinical judgment, decision-making, and actions of tele-nurses. This is especially important when task distribution occurs across departmental boundaries, as is the case in centralized monitoring models. Central to establishing trust were collaboratively developed protocols, grounded in evidence-based medicine guidelines. This joint development process ensured continuity by actively involving the original care providers (eg, physicians and nurse practitioners) in shaping the clinical procedures. With this approach, confidence in the transfer of responsibilities was fostered and the transition of clinical tasks was supported. In addition, our data indicated that trust was established through several approaches: (1) making individualized care plans including patient-specific threshold for alerts, rather than relying on standard ranges for patients. This approach fostered the trust in clinical judgment of tele-nurses. (2) Developing new working routines, aligned with the task distribution. Clear communication about these new routines, particularly regarding responsibilities and alert management, helped build trust among professionals involved in the telemonitoring. (3) Project leaders fostered trust in centralized telemonitoring by facilitating disease-specific and training concerning the specific electronic medical record to tele-nurses, enabling a competent transition of care. Responsibilities were transferred to the CMC gradually, beginning with administrative tasks and progressively expanding to the full spectrum of telemonitoring activities, allowing trust to develop through demonstrated capability. Furthermore, respondents mentioned that staffing the CMC with nurses from diverse specializations ensured access to specialist knowledge, thereby increasing the confidence of colleagues in their ability to manage complex conditions and patients (Domains 2 and 3).

Thus, in both organizational models (tele-)nurses took on greater responsibility, under the supervision of NPs and physicians. Trust between professionals was crucial for this task redistribution, established through the development of evidence-based protocols, training, and clear guidelines, ensuring that (tele-)nurses could manage complex cases and alerts effectively.

Domain 5: Telemonitoring Across Organizational Boundaries

Partnerships are a critical aspect of establishing CMC telemonitoring as efficiency depends on economy of scale. Collaborations can be either geographically bound (hospitals B and D) or based on previously established (national) network structures (hospital C). In our study, partnerships were primarily formed in centralized telemonitoring programs, likely due to the more structured coordination and larger scale of these programs compared to the more fragmented distributed models. Consequently, the objective function as a regional CMC appeared to be connected to their initial partner strategy. In contrast, hospital C is piloting a network-based collaboration also aimed at expansion. This network partnership involves complementary task delegation as the participants strive to delegate tasks to and from other organizations. Respondents also noted the potential for complementarity of regional and network collaboration, as the following quote shows:

> *In the case of a deviating measure [of a patient's vital signs], the CMC gets involved, prompting action. However, this action could potentially be delegated to a regional collaboration partner. The one does not rule out the other; they could work together very well.* [Clinical informatician, hospital B]

Partnerships often allocate task delegation by (regional) partners to the CMC. However, respondents mentioned task delegation-related concerns about the freedom to comply or not with collaborative agreements and regional or network protocols. To address these concerns, hospitals B and D, having a majority of distributed telemonitoring cases, initially focused on regional initiatives, engaging all the partners (including GPs) in discussions on the challenges emerging from discrepancies between the protocols of the newly formed network and those of the established regional partnership.

To recap, partnerships are essential for CMCs to achieve efficiency through economy of scale. Collaborations can be regional or network-based, with CMCs benefiting from structured coordination, though task delegation between regional and network partners. However, this poses challenges related

XSL•FO
RenderX

to protocol alignment and a need for making collaborative agreements.

Domain 6: Economic Context Impedes Using Telemonitoring to Solve Societal Challenges

Our respondents aimed to provide efficient care in the face of staff shortages and the need to meet the increasing demand for care due to more patients with comorbidities and more elderly living at home. They feel telemonitoring can help address these challenges as it makes admitting patients or recurring outpatient clinic visits unnecessary. In the studied cases, a CMC employed nurses with physical limitations who were otherwise unable to provide direct patient care on the ward, demonstrating that telemonitoring allows these people to contribute to the workforce. By providing these new staff roles, telemonitoring, in both organizational models, supports workforce retention and efficiency.

In the Netherlands, both CMC and distributed telemonitoring are reimbursed under the same scheme. However, the current financing model within the diagnosis treatment combination (similarities with DRG's systems) system is predicated on the substitution of physical care with remote care within the existing tariff structure. In practice, reimbursement rates for in-person care remain higher than those for remote services. Furthermore, hospitals are required to make substantial upfront investments in digital infrastructure and personnel to support telemonitoring and remote care services. As a result, costs are incurred in advance of potential long-term benefits, and providers risk losing revenue from reduced volumes of billable physical consultations and hospital admissions. Given that hospital funding in the Netherlands is still partially based on production-related agreements—largely tied to physical service delivery—this shift toward more efficient, home-based care may inadvertently lead to a decline in institutional revenue, thereby creating a financial disincentive for scaling up telemonitoring:

> *We have lots of telemonitoring and that costs us millions of euros [because we don't get fully reimbursed]. So, you're always thinking, what am I doing? I'm organizing my own downfall.* [Project leader, hospital A]

Since there is no difference in reimbursement for centralized and distributed telemonitoring, these financial challenges are the same for all hospitals in this study.

Domain 7: Embedding and Adapting Telemonitoring Over Time

The CMCs in all hospitals are currently expanding, and many respondents anticipate an even broader role for telemonitoring in the future. Expected developments include more partnerships in CMC, extending the number of patient conditions monitored, and increased patient volumes.

> *We're expanding to monitor more care pathways, and we're also aiming to increase the number of patients on each pathway.* [Project leader 1, hospital C]

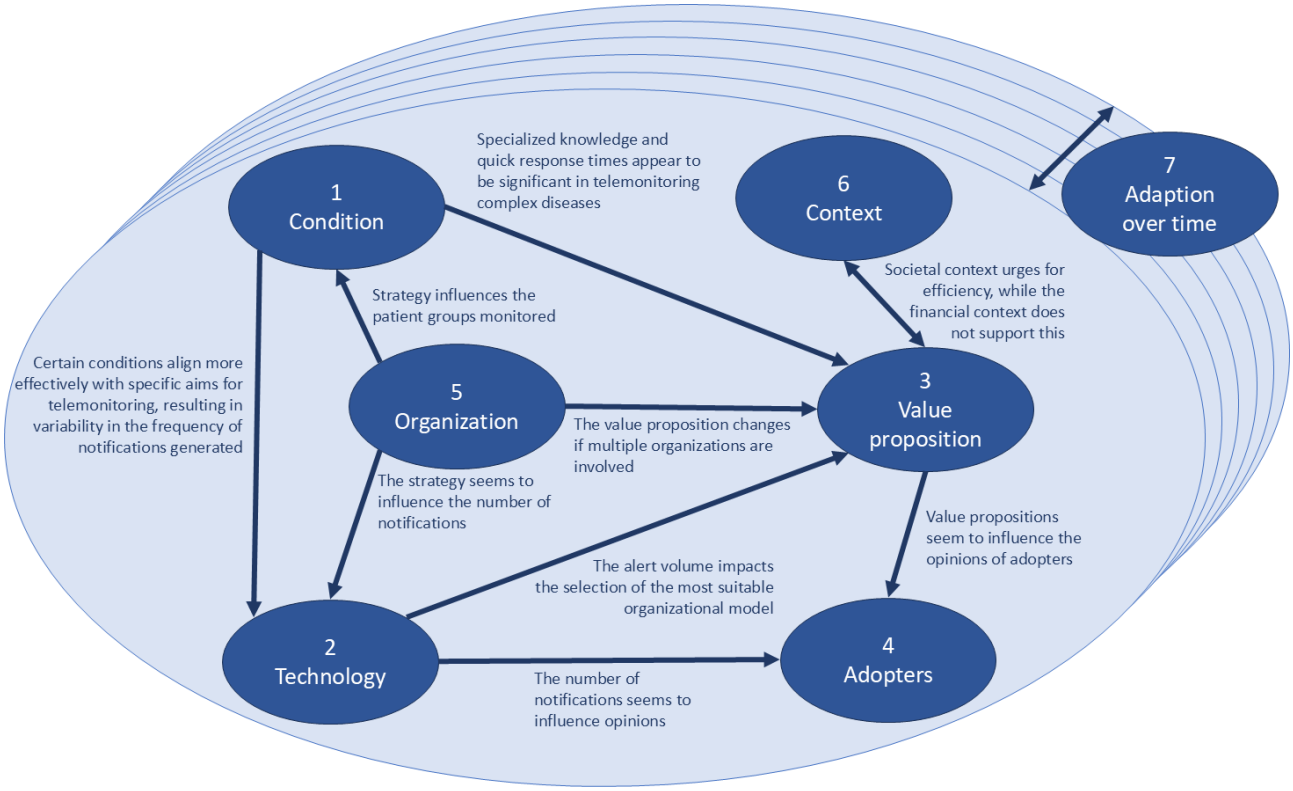
Some respondents suggest that advancements in information and communication technologies and artificial intelligence (AI) could facilitate this role expansion, especially in automating tasks such as distinguishing relevant from irrelevant notifications. This is particularly applicable to acute-care patients who require intensive monitoring. However, if automation leads to reduced numbers of notifications, it could also reduce the need for centralization.

NASSS Framework

Using the NASSS framework enabled us to examine the domains while considering multiple decision-making factors. Figure 2 illustrates the interdependencies found among the various domains. For instance, value proposition (Domain 3) is primarily based on the perception of cost-effectiveness and added value to the patient. It is also affected by the selected patient group (Domain 1) and organizational strategy (Domain 5). The technology applied (Domain 2) affects how notifications are managed and handled, impacting the value proposition and opinion of adopters. When changes made in an area can affect other areas, interconnectedness underscores the complexity of decision-making in organizing telemonitoring.

XSL•FO
RenderX

Figure 2. Interactions between the domains of the non-adoption, abandonment, scale-up, spread, and sustainability (NASSS) framework [27].



Discussion

Principal Findings

This multiple case study shows that the decision to implement telemonitoring, whether through centralized or distributed organizational models, involves a complex array of considerations that must be carefully weighed. A definitive argument in favor of either model cannot be made, as each option presents distinct advantages and challenges across different domains. However, our findings highlight that strategic decisions made early in the implementation process—particularly those related to the telemonitoring of objectives on the basis of patient groups—are crucial in determining the appropriate organizational model. These decisions, in turn, shape possibilities related to personnel (eg, hiring tele-nurses or educating outpatient clinic or ward staff, and the role physicians play), partnerships, and the overall cost-effectiveness of telemonitoring.

Comparison With Previous Work

To date, many telemonitoring studies have focused on the design and development of the technology or the implementation of a specific telemonitoring care pathway [10-12,46]. To our knowledge, this is the first study to systematically compare considerations related to centralized and distributed telemonitoring models.

Model Follows Strategy

First, we would like to address the significant role of the selected patient condition, encompassing both the type of patient group enrolled in telemonitoring and the complexity of their health care needs. The patient condition drives the subsequent considerations that together determine the appropriate organizational telemonitoring model. For example, programs targeting chronic conditions aiming for self-management, typically associated with lower alert frequency and lower clinical complexity, can be organized through distributed care models. Conversely, telemonitoring programs focused on vital parameter tracking, such as those in early discharge scenarios [10,23,24,47], having high alert volumes and a need for rapid response, make centralized models more appropriate in those cases (domains 1 and 2). This observation is consistent with the current literature, which suggests that before implementation, telemonitoring systems are evaluated for their anticipated impact on patient safety, staff workload, and clinical usefulness [24,48], all of which depend on the specific patient group intended for remote care. This initial strategic decision sets the foundation for the primary objective of telemonitoring, whether that be to enhance self-management [48,49] or to monitor vital parameters [50]. Consequently, the selected patient condition and objectives influence the aims, and vice versa. Furthermore, the chosen aims directly affect the volume of alerts generated. For instance, a focus on vital parameter monitoring typically results in a greater frequency of alerts [51] compared to a self-management approach. Our findings indicate that the volume of alerts also affects how and for whom notifications are managed, ultimately shaping workload distribution [52] and task division [53,54] among health care professionals. Clearly, the interplay between patient condition, strategic objectives, and alert management is critical in determining the appropriate organizational model for telemonitoring. The choice of objectives impacts personnel, capacity, resources, and partnerships, outcomes that affect health care delivery in the region. It is crucial not to overlook the need for planning at this level, and decision makers must be educated to consider all the dimensions and understand how their choices will ripple through the system when determining the best

XSL•FO
RenderX

telemonitoring model for a patient. Looking ahead, the evolving role of AI will likely have significant implications for the organization of telemonitoring (Domain 7). AI has the potential to support clinical decision-making by filtering alerts, identifying patterns, and prioritizing cases [55]. In this way, AI may reduce the need for centralized monitoring by enabling distributed care teams to manage alerts more efficiently alongside their routine tasks. Conversely, the increasing amount of data and complexity requires centralized systems, where specialized staff works with AI to manage the increasing data streams. While the direction of this impact remains uncertain, these technological developments will influence the suitability of different organizational models.

Personnel

In our case studies, the respondents' perceptions of the effectiveness of telemonitoring and its added value for patients played a significant role in choosing a model. Even in the absence of clear evidence supporting the superiority of one model over another, in terms of cost-effectiveness or patient benefit, respondents based their preference on subjective evaluations [4,56,57]. This is notable, particularly given that the attitudes of health care professionals (eg, nurses and physicians) are a significant factor in the acceptance of telemonitoring in practice [24], and these professionals are regarded as the "most important gatekeepers for telehealth services" [58]. Thus, the attitudes and perceptions of health care professionals influence the implementation of telemonitoring, impacting not only local adoption but also broader upscaling [54]. Health care professionals also play an important role in deciding on the choice of telemonitoring aims in the process of selecting a suitable model. This makes it essential that their decisions are not based solely on subjective judgments. Rather, they should be well-informed about the rationale behind selecting specific telemonitoring models.

In addition, implementing telemonitoring, whether centralized or distributed, is driven by the objective of increasing efficiency and addressing staff shortages [2,4]. As patients increasingly adopt self-management techniques [59,60], and health care services evolve, the roles and tasks of health care professionals are undergoing significant transformation. The literature supports this shift, indicating that telemonitoring influences task division in health care organizations [61], resulting in the creation of new roles and responsibilities [62] while potentially disrupting established professional roles [63]. Given this knowledge, organizations must align their personnel preparation and organizational models accordingly. It is essential to equip staff for new responsibilities through targeted training programs that address the specific skills needed for telemonitoring [64,65]. In addition, our findings show that the redistribution of tasks, particularly when tele-nurses assume responsibilities previously handled by physicians, was eased by collaborative efforts in developing protocols and workflows. Finally, the division of created tasks should be compatible with the organizational model and available resources. Therefore, when selecting a telemonitoring model, organizations should consider their capacity, resources, and personnel.

Partnerships, Collaborations, and Networks

Our findings place key emphasis on the importance of partnerships and collaborations in organizing telemonitoring, particularly in the centralized monitoring context, although both models may involve multiple organizations [13,26]. The participants acknowledged both the potential benefits of working with various partners and the challenges associated with delegating tasks among health care providers. However, the discussion focused on the division of tasks between providers and the clinical pathway design, while the complexities of interorganizational collaboration remained largely unaddressed. This oversight parallels a notable gap in the literature on organizing telemonitoring collaboratively. Defining responsibilities, establishing safety protocols, streamlining workflows, sharing knowledge, and educating personnel are all important when multiple organizations participate in telemonitoring [24]. While some studies touch upon interorganizational collaboration among health care providers [24], there is still insufficient exploration of the necessary governance and management frameworks required for telemonitoring collaboration in practice [66,67]. This is concerning from a quality perspective, given that effective collaboration between care providers is essential for ensuring continuity of care [46]. Scholars suggest that successfully scaling telemonitoring on a regional or national level hinges on resources and reimbursement structures [54]. Both elements should be discussed when collaboratively organizing telemonitoring. Given that network theory offers valuable insights into managing networks with common goals, in this case regional telemonitoring implementation, we want to emphasize that scholars should not reinvent the wheel when there is a compelling opportunity to use this knowledge to navigate organizational boundaries effectively [68].

Strengths and Limitations

From a practical perspective, this research contributes to a deeper understanding of the decision-making processes involved in telemonitoring services. The insights derived from this study offer valuable guidance for health care organizations seeking to implement or scale telemonitoring programs, or to design effective telemonitoring pathways with regional partners. From a theoretical standpoint, this study extends the application of the NASSS framework by examining organizational-level decision making across all NASSS domains. In doing so, we illustrate how the various domains interact and influence one another in the context of organizing telemonitoring. We acknowledge, however, three primary limitations. (1) While the NASSS framework provides a comprehensive approach to integrating diverse perspectives on implementing eHealth technology, these categories may constrain data interpretation. Specifically, the framework tends to overlook the relational dynamics, for instance, between caregivers and patients, despite the literature that supports the importance of including human interactions in implementation [48]. Future scholars could benefit from using NASSS-CAT tools [40]. This combination allows for a theory-informed framework, supplemented by a pragmatic planning tool. (2) The limited exploration of ethical-legal considerations and data privacy in the context of telemonitoring may be attributed to the specific respondent

XSL•FO
RenderX

group chosen for inclusion. Issues related to data sharing, patient consent, and privacy must be addressed to ensure the ethical deployment of telemonitoring technologies [24]. These legal and ethical topics should be prioritized in future research to provide a more comprehensive understanding of the implications of telemonitoring on patient data and privacy rights. Another limitation lies in (3) the aim to contrast a centralized model with a fully distributed one. However, in practice, such clear-cut models are hard to find. As a result, we included 2 cases using predominantly distributed models, where respondents also had experience with centralized approaches or used centralized models for specific clinical pathways. Although this hybrid reality (literature) reflects the complexity of studying real-world implementation, it blurs the distinction between the two models.

Conclusions

This study provides insights into the complexities of decision-making involved in organizing telemonitoring and offers guidance to all stakeholders, including health care professionals, on understanding the considerations and consequences of the choices. It identifies specific rationales for selecting either a centralized or distributed telemonitoring model, depending on patient needs, such as those requiring vital parameter monitoring or self-management. The volume of notifications generated also is a critical factor in determining the most suitable model. In addition, perceptions of efficiency and the perceived added value to patients significantly influence decision-making. The study underscores the importance of considering technological, organizational, and societal factors when choosing between centralized and distributed models. Notably, decisions made in early stages, primarily by physicians, can have far-reaching implications for personnel, resources, and partnerships at a regional level. When starting out with telemonitoring, those in charge should recognize the interconnectedness of factors and carefully consider all seven NASSS domains.

Acknowledgments

We thank Prof Leon Oerlemans and Dr Remco Mannak for their guidance and expertise. Their insight and feedback have greatly contributed to the completion of this project. We are grateful to Tessa van Aken for her assistance with the data analysis.

Conflicts of Interest

None declared.

Multimedia Appendix 1
Visualization of a centralized organizational model (example).
[PNG File, 48 KB - medinform_v13i1e69349_app1.PNG]

Multimedia Appendix 2
Visualization of a distributed organizational model (example).
[PNG File, 45 KB - medinform_v13i1e69349_app2.PNG]

Multimedia Appendix 3
Topic list.
[DOCX File, 27 KB - medinform_v13i1e69349_app3.docx]

Multimedia Appendix 4
Codetree (in Dutch).
[PNG File, 529 KB - medinform_v13i1e69349_app4.png]

Checklist 1
COREQ checklist.
[PDF File, 1140 KB - medinform_v13i1e69349_app5.pdf]

References

1. Achelrod D, Schreyögg J, Stargardt T. Health-economic evaluation of home telemonitoring for COPD in Germany: evidence from a large population-based cohort. Eur J Health Econ 2017 Sep;18(7):869-882. [doi: 10.1007/s10198-016-0834-x] [Medline: 27699567]
2. Levine DM, Ouchi K, Blanchfield B, et al. Hospital-level care at home for acutely ill adults: a randomized controlled trial. Ann Intern Med 2020 Jan 21;172(2):77-85. [doi: 10.7326/M19-0600] [Medline: 31842232]
3. Muigg D, Kastner P, Duftschmid G, Modre-Osprian R, Haluza D. Readiness to use telemonitoring in diabetes care: a cross-sectional study among Austrian practitioners. BMC Med Inform Decis Mak 2019 Jan 29;19(1):26. [doi: 10.1186/s12911-019-0746-7] [Medline: 30696444]

XSL•FO
RenderX

4. Scholte NTB, Gürgöze MT, Aydin D, et al. Telemonitoring for heart failure: a meta-analysis. Eur Heart J 2023 Aug 14;44(31):2911-2926. [doi: 10.1093/eurheartj/ehad280] [Medline: 37216272]
5. Andrès E, Meyer L, Zulfiqar AA, et al. Telemonitoring in diabetes: evolution of concepts and technologies, with a focus on results of the more recent studies. J Med Life 2019;12(3):203-214. [doi: 10.25122/jml-2019-0006] [Medline: 31666818]
6. Claggett J, Petter S, Joshi A, Ponzio T, Kirkendall E. An Infrastructure Framework for Remote Patient Monitoring Interventions and Research. J Med Internet Res 2024 May 30;26:e51234. [doi: 10.2196/51234] [Medline: 38815263]
7. Defining 21st century care. American Telemedicine Association. URL: https://marketing.americantelemed.org/hubfs/Files/Resources/ATA_Telehealth_Taxonomy_9-11-20.pdf [accessed 2024-07-19]
8. Brunet F, Malas K, Desrosiers ME. Will telemedicine survive after COVID-19? Healthc Manage Forum 2021 Sep;34(5):256-259. [doi: 10.1177/08404704211031264] [Medline: 34340570]
9. Huygens MWJ, Voogdt-Pruis HR, Wouters M, et al. The uptake and use of telemonitoring in chronic care between 2014 and 2019: nationwide survey among patients and health care professionals in the Netherlands. J Med Internet Res 2021 May 3;23(5):e24908. [doi: 10.2196/24908] [Medline: 33938808]
10. Farias FD, Dagostini CM, Bicca YDA, Falavigna VF, Falavigna A. Remote patient monitoring: a systematic review. Telemed J E Health 2020 May;26(5):576-583. [doi: 10.1089/tmj.2019.0066] [Medline: 31314689]
11. Leo DG, Buckley BJR, Chowdhury M, et al. Interactive remote patient monitoring devices for managing chronic health conditions: systematic review and meta-analysis. J Med Internet Res 2022 Nov 3;24(11):e35508. [doi: 10.2196/35508] [Medline: 36326818]
12. Taylor ML, Thomas EE, Snoswell CL, Smith AC, Caffery LJ. Does remote patient monitoring reduce acute care use? A systematic review. BMJ Open 2021 Mar 2;11(3):e040232. [doi: 10.1136/bmjopen-2020-040232] [Medline: 33653740]
13. Dharmarajan K, Chaudhry SI. New approaches to reduce readmissions in patients with heart failure. JAMA Intern Med 2016 Mar;176(3):318-320. [doi: 10.1001/jamainternmed.2015.7993] [Medline: 26857025]
14. International Electrotechnical Vocabulary-Details for IEV number 871-06-11: telemonitoring system. International Electrotechnical Commission. 2019. URL: https://www.electropedia.org/iev/iev.nsf/display?openform&ievref=871-06-11 [accessed 2022-12-15]
15. Papoutsi C, A'Court C, Wherton J, Shaw S, Greenhalgh T. Explaining the mixed findings of a randomised controlled trial of telehealth with centralised remote support for heart failure: multi-site qualitative study using the NASSS framework. Trials 2020 Oct 27;21(1):891. [doi: 10.1186/s13063-020-04817-x] [Medline: 33109254]
16. Shah NM, Kaltsakas G. Telemedicine in the management of patients with chronic respiratory failure. Breathe (Sheff) 2021 Mar;17(1):210008. [doi: 10.1183/20734735.0008-2021] [Medline: 34295411]
17. Verfürth M. Design and validation of a questionnaire to measure the acceptance of telemedicine by healthcare professionals in germany. . Preprint posted online on Aug, 2020. [doi: 10.21203/rs.3.rs-60425/v2]
18. Fairbrother P, Ure J, Hanley J, et al. Telemonitoring for chronic heart failure: the views of patients and healthcare professionals - a qualitative study. J Clin Nurs 2014 Jan;23(1-2):132-144. [doi: 10.1111/jocn.12137] [Medline: 23451899]
19. Thomas EE, Chambers R, Phillips S, Rawstorn JC, Cartledge S. Sustaining telehealth among cardiac and pulmonary rehabilitation services: a qualitative framework study. Eur J Cardiovasc Nurs 2023 Dec 14;22(8):795-803. [doi: 10.1093/eurjcn/zvac111] [Medline: 36468293]
20. Prescher S, Koehler J, Koehler F. E-health in cardiology: remote patient management of heart failure patients. escardio. 2020. URL: https://www.escardio.org/Journals/E-Journal-of-Cardiology-Practice/Volume-18/e-health-in-cardiology-remote-patient-management-of-heart-failure-patients [accessed 2024-09-10]
21. Fairbrother P, Pinnock H, Hanley J, et al. Continuity, but at what cost? The impact of telemonitoring COPD on continuities of care: a qualitative study. Prim Care Respir J 2012 Sep;21(3):322-328. [doi: 10.4104/pcrj.2012.00068] [Medline: 22875143]
22. Dyb K, Berntsen GR, Kvam L. Adopt, adapt, or abandon technology-supported person-centred care initiatives: healthcare providers' beliefs matter. BMC Health Serv Res 2021 Mar 17;21(1):240. [doi: 10.1186/s12913-021-06262-1] [Medline: 33731078]
23. Azevedo S, Rodrigues TC, Londral AR. Domains and methods used to assess home telemonitoring scalability: systematic review. JMIR Mhealth Uhealth 2021 Aug 19;9(8):e29381. [doi: 10.2196/29381] [Medline: 34420917]
24. Liljeroos M, Arkkukangas M. Implementation of telemonitoring in health care: facilitators and barriers for using eHealth for older adults with chronic conditions. Risk Manag Healthc Policy 2023;16:43-53. [doi: 10.2147/RMHP.S396495] [Medline: 36647422]
25. Heinsch M, Wyllie J, Carlson J, Wells H, Tickner C, Kay-Lambkin F. Theories informing eHealth implementation: systematic review and typology classification. J Med Internet Res 2021 May 31;23(5):e18500. [doi: 10.2196/18500] [Medline: 34057427]
26. Eze ND, Mateus C, Cravo Oliveira Hashiguchi T. Telemedicine in the OECD: An umbrella review of clinical and cost-effectiveness, patient experience and implementation. PLoS One 2020;15(8):e0237585. [doi: 10.1371/journal.pone.0237585] [Medline: 32790752]
27. Greenhalgh T, Wherton J, Papoutsi C, et al. Beyond adoption: a new framework for theorizing and evaluating nonadoption, abandonment, and challenges to the scale-up, spread, and sustainability of health and care technologies. J Med Internet Res 2017 Nov 1;19(11):e367. [doi: 10.2196/jmir.8775] [Medline: 29092808]

XSL•FO
RenderX

28. Greenhalgh T, Wherton J, Papoutsi C, et al. Analysing the role of complexity in explaining the fortunes of technology programmes: empirical application of the NASSS framework. BMC Med 2018 May 14;16(1):66. [doi: 10.1186/s12916-018-1050-6] [Medline: 29754584]
29. Hellstrand Tang U, Smith F, Karilampi UL, Gremyr A. Exploring the role of complexity in health care technology bottom-up innovations: multiple-case study using the nonadoption, abandonment, scale-up, spread, and sustainability complexity assessment tool. JMIR Hum Factors 2024 Apr 26;11:e50889. [doi: 10.2196/50889] [Medline: 38669076]
30. Abell B, Naicker S, Rodwell D, et al. Identifying barriers and facilitators to successful implementation of computerized clinical decision support systems in hospitals: a NASSS framework-informed scoping review. Implement Sci 2023 Jul 26;18(1):32. [doi: 10.1186/s13012-023-01287-y] [Medline: 37495997]
31. Gijsbers H, Nurmohamed A, van de Belt TH, Schijven M, Citrien 2 Project Leaders and Steering Group. The National Coordinated Citrien eHealth Program to scale up telemonitoring: protocol for a before-and-after evaluation study. JMIR Res Protoc 2023 Jul 26;12:e45201. [doi: 10.2196/45201] [Medline: 37494085]
32. Tong A, Sainsbury P, Craig J. Consolidated criteria for reporting qualitative research (COREQ): a 32-item checklist for interviews and focus groups. Int J Qual Health Care 2007 Dec;19(6):349-357. [doi: 10.1093/intqhc/mzm042] [Medline: 17872937]
33. Kroneman M, Boerma W, van den Berg M, Groenewegen P, de Jong J, van Ginneken E. Netherlands: health system review. Health Syst Transit 2016 Mar;18(2):1-240. [Medline: 27467715]
34. Schiffelers T, Kapteijns K, Hochstenbach L, Kietselaer B, Talboom-Kamp E, Spreeuwenberg M. Best practices in organizing digital transformation: qualitative case study in Dutch hospital care. J Med Internet Res 2025 May 8;27:e63576. [doi: 10.2196/63576] [Medline: 40338636]
35. Wegwijzer bekostiging digitale zorg [Article in Dutch]. Nederlandse ZorgAutoriteit. 2025. URL: https://puc.overheid.nl/nza/doc/PUC_655318_22/1 [accessed 2025-06-26]
36. Kroneman M, Jong J, Polin K, Webb E, Maresso A. The Netherlands: Health System Summary: European Observatory on Health Systems and Policies; 2024.
37. Dijkstra A, Heida A, van Rheenen PF. Exploring the challenges of implementing a web-based telemonitoring strategy for teenagers with inflammatory bowel disease: empirical case study. J Med Internet Res 2019 Mar 29;21(3):e11761. [doi: 10.2196/11761] [Medline: 30924785]
38. Hailu R, Sousa J, Tang M, Mehrotra A, Uscher-Pines L. Challenges and facilitators in implementing remote patient monitoring programs in primary care. J Gen Intern Med 2024 Oct;39(13):2471-2477. [doi: 10.1007/s11606-023-08557-x] [Medline: 38653884]
39. Yakovchenko V, McInnes DK, Petrakis BA, et al. Implementing automated text messaging for patient self-management in the veterans health administration: qualitative study applying the nonadoption, abandonment, scale-up, spread, and sustainability framework. JMIR Mhealth Uhealth 2021 Nov 15;9(11):e31037. [doi: 10.2196/31037] [Medline: 34779779]
40. Greenhalgh T, Maylor H, Shaw S, et al. The NASSS-CAT tools for understanding, guiding, monitoring, and researching technology implementation projects in health and social care: protocol for an evaluation study in real-world settings. JMIR Res Protoc 2020 May 13;9(5):e16861. [doi: 10.2196/16861] [Medline: 32401224]
41. Earl Rinehart K. Abductive analysis in qualitative inquiry. Qual Inq 2021 Feb;27(2):303-311. [doi: 10.1177/1077800420935912]
42. Tavory I, Timmermans S. The SAGE Handbook of Current Developments in Grounded Theory: SAGE Publications Ltd; 2019. URL: https://methods.sagepub.com/book/the-sage-handbook-of-grounded-theory-2e [accessed 2024-02-14]
43. Braun V, Clarke V. Toward good practice in thematic analysis: Avoiding common problems and be(com)ing a knowing researcher. Int J Transgend Health 2023;24(1):1-6. [doi: 10.1080/26895269.2022.2129597] [Medline: 36713144]
44. Varpio L, O'Brien B, Rees CE, Monrouxe L, Ajjawi R, Paradis E. The applicability of generalisability and bias to health professions education's research. Med Educ 2021 Feb;55(2):167-173. [doi: 10.1111/medu.14348] [Medline: 32779251]
45. Khurshid F, Veen M, Thompson J, Hegazi I. Navigating thematic analysis: practical strategies grounded in abductive reasoning. Teach Learn Med 2025 Apr 2;2:1-10. [doi: 10.1080/10401334.2025.2475098] [Medline: 40172437]
46. Thomas EE, Taylor ML, Banbury A, et al. Factors influencing the effectiveness of remote patient monitoring interventions: a realist review. BMJ Open 2021 Aug;11(8):e051844. [doi: 10.1136/bmjopen-2021-051844]
47. Breteler MJM, Numan L, Ruurda JP, et al. Wireless remote home monitoring of vital signs in patients discharged early after esophagectomy: observational feasibility study. JMIR Perioper Med 2020 Dec 4;3(2):e21705. [doi: 10.2196/21705] [Medline: 33393923]
48. Glock H, Milos Nymberg V, Borgström Bolmsjö B, et al. Attitudes, barriers, and concerns regarding telemedicine among swedish primary care physicians: a qualitative study. IJGM 2021;Volume 14:9237-9246. [doi: 10.2147/IJGM.S334782] [Medline: 34880663]
49. Nick JM, Roberts LR, Petersen AB. Effectiveness of telemonitoring on self-care behaviors among community-dwelling adults with heart failure: a quantitative systematic review. JBI Evid Synth 2021 Oct;19(10):2659-2694. [doi: 10.11124/JBIES-20-00329] [Medline: 33896907]
50. Rossum MC. Remote Vital Signs Monitoring for Early Detection of Deterioration after Surgery: University of Twente; 2023.

XSL•FO
RenderX

51. Kokkonen J, Mustonen P, Heikkilä E, et al. Effectiveness of telemonitoring in reducing hospitalization and associated costs for patients with heart failure in Finland: nonrandomized pre-post telemonitoring study. JMIR Mhealth Uhealth 2024 Feb 7;12:e51841. [doi: 10.2196/51841] [Medline: 38324366]
52. Taylor J, Coates E, Brewster L, Mountain G, Wessels B, Hawley MS. Examining the use of telehealth in community nursing: identifying the factors affecting frontline staff acceptance and telehealth adoption. J Adv Nurs 2015 Feb;71(2):326-337. [doi: 10.1111/jan.12480] [Medline: 25069605]
53. Cuba Gyllensten I, Crundall-Goode A, Aarts RM, Goode KM. Simulated case management of home telemonitoring to assess the impact of different alert algorithms on work-load and clinical decisions. BMC Med Inform Decis Mak 2017 Jan 17;17(1):11. [doi: 10.1186/s12911-016-0398-9] [Medline: 28095849]
54. Gijsbers H, Feenstra TM, Eminovic N, et al. Enablers and barriers in upscaling telemonitoring across geographic boundaries: a scoping review. BMJ Open 2022 Apr 20;12(4):e057494. [doi: 10.1136/bmjopen-2021-057494] [Medline: 35443957]
55. Shaik T, Tao X, Higgins N, et al. Remote patient monitoring using artificial intelligence: Current state, applications, and challenges. WIREs Data Min & Knowl 2023 Mar;13(2):e1485. [doi: 10.1002/widm.1485]
56. Bell-Aldeghi R, Gibrat B, Rapp T, et al. Determinants of the cost-effectiveness of telemedicine: systematic screening and quantitative analysis of the literature. Telemed J E Health 2023 Jul;29(7):1078-1087. [doi: 10.1089/tmj.2022.0161] [Medline: 36493368]
57. Zhang Y, Peña MT, Fletcher LM, Lal L, Swint JM, Reneker JC. Economic evaluation and costs of remote patient monitoring for cardiovascular disease in the United States: a systematic review. Int J Technol Assess Health Care 2023 Apr 28;39(1):e25. [doi: 10.1017/S0266462323000156] [Medline: 37114456]
58. Whitten PS, Mackert MS. Addressing telehealth's foremost barrier: provider as initial gatekeeper. Int J Technol Assess Health Care 2005;21(4):517-521. [doi: 10.1017/S0266462305050725] [Medline: 16262977]
59. Oudshoorn N. Diagnosis at a distance: the invisible work of patients and healthcare professionals in cardiac telemonitoring technology. Sociol Health Illn 2008 Mar;30(2):272-288. [doi: 10.1111/j.1467-9566.2007.01032.x] [Medline: 18290936]
60. Trupia DV, Mathieu-Fritz A, Duong TA. The sociological perspective of users' invisible work: a qualitative research framework for studying digital health innovations integration. J Med Internet Res 2021 Nov 4;23(11):e25159. [doi: 10.2196/25159] [Medline: 34734832]
61. Wannheden C, Åberg-Wennerholm M, Dahlberg M, et al. Digital health technologies enabling partnerships in chronic care management: scoping review. J Med Internet Res 2022 Aug 1;24(8):e38980. [doi: 10.2196/38980] [Medline: 35916720]
62. Boonstra A, Broekhuis M. Barriers to the acceptance of electronic medical records by physicians from systematic review to taxonomy and interventions. BMC Health Serv Res 2010 Aug 6;10:231. [doi: 10.1186/1472-6963-10-231] [Medline: 20691097]
63. Ross J, Stevenson F, Lau R, Murray E. Factors that influence the implementation of e-health: a systematic review of systematic reviews (an update). Implement Sci 2016 Oct 26;11(1):146. [doi: 10.1186/s13012-016-0510-7] [Medline: 27782832]
64. Banbury A, Taylor ML, Gray LC, Reid N, Smith AC. Sustaining and expanding telehealth activity: Training requirements for Australian residential aged care front-line staff. PEC Innov 2023 Dec;2:100109. [doi: 10.1016/j.pecinn.2022.100109] [Medline: 37214526]
65. Sidhu M, Walton H, Crellin N, et al. Staff experiences of training and delivery of remote home monitoring services for patients diagnosed with COVID-19 in England: A mixed-methods study. J Health Serv Res Policy 2023 Jul;28(3):171-180. [doi: 10.1177/13558196231172586] [Medline: 37366220]
66. Peeters R, Westra D, van Raak AJA, Ruwaard D. So happy together: a review of the literature on the determinants of effectiveness of purpose-oriented networks in health care. Med Care Res Rev 2023 Jun;80(3):266-282. [doi: 10.1177/10775587221118156] [Medline: 36000492]
67. Provan KG, Kenis P. Modes of network governance: structure, management, and effectiveness. J Public Adm Res Theory 2008;18(2):229-252. [doi: 10.1093/jopart/mum015]
68. Otte-Trojel T, Rundall TG, de Bont A, van de Klundert J. Can relational coordination help inter-organizational networks overcome challenges to coordination in patient portals? Int J Healthc Manag 2017 Apr 3;10(2):75-83. [doi: 10.1080/20479700.2015.1101911]

Abbreviations

AI: artificial intelligence
CMC: centralized monitoring center
COPD: chronic obstructive pulmonary disease
COREQ: Consolidated Criteria for Reporting Qualitative Research
NASSS: non-adoption, abandonment, scale-up, spread, and sustainability
NP: nurse practitioner

XSL•FO
RenderX

Edited by A Benis; submitted 02.12.24; peer-reviewed by H Liu, H Kemps; revised version received 21.08.25; accepted 04.09.25; published 08.10.25.

Please cite as:
Elferink NA, Roest MJ, Weggelaar AM, de Mul M
Organizing Telemonitoring—Decision-Making Between Centralized and Distributed Models in the Netherlands, Using the Non-Adoption, Abandonment, Scale-Up, Spread, and Sustainability (NASSS) Framework: Case Study
JMIR Med Inform 2025;13:e69349
URL: https://medinform.jmir.org/2025/1/e69349
doi:10.2196/69349

© Nienke Antine Elferink, Manon Jacqueline Roest, Anne Marie Weggelaar, Marleen de Mul. Originally published in JMIR Medical Informatics (https://medinform.jmir.org), 8.10.2025. This is an open-access article distributed under the terms of the Creative Commons Attribution License (https://creativecommons.org/licenses/by/4.0/), which permits unrestricted use, distribution, and reproduction in any medium, provided the original work, first published in JMIR Medical Informatics, is properly cited. The complete bibliographic information, a link to the original publication on https://medinform.jmir.org/, as well as this copyright and license information must be included.

XSL•FO
RenderX

Home Monitoring Delivered Through the Emergency Department for Outpatients With COVID-19: COVID19@Home Aachen Pilot Cohort Study

Lukas Niekrenz[1], LLM, Dr med; Christian Hübel[2], Dr med; Christopher Plata[2], Dr med; Henning Biermann[2], Dr med; Claas Leber[2], Dr med; Lisa Sophie Schütze[1]; Svea Holtz[3], Dr med; Susanne Maria Köhler[3], MSc Epi, Dr oec troph; Kim Deutsch[4], MA, Dr phil; Nurlan Dauletbayev[5,6,7,8], MD, PhD; Sebastian Kuhn[4], MME, Prof Dr med; Beate Sigrid Müller[9], Prof Dr med; Christian Cornelissen[1], Dr med; Rembert Koczulla[10], Prof Dr med; Gernot Rohde[11], Prof Dr med; Claus Franz Vogelmeier[5], Prof Dr med; Jörg Christian Brokmann[2*], Prof Dr med; Michael Dreher[1*], Prof Dr med

[1]Department of Pneumology and Intensive Care Medicine, University Hospital Aachen, RWTH Aachen University, Pauwelsstrasse 30, Aachen, Germany

[10]Schön Klinik Berchtesgadener Land, PMU Salzburg, German Center for Lung Research (DZL), Marburg, Germany

[11]Department of Respiratory, Intensive Care and Sleep Medicine, University Hospital Gießen-Marburg, Philipps University of Marburg, Marburg, Germany

[2]Department for Acute and Emergency Medicine, University Hospital Aachen, RWTH Aachen University, Aachen, Germany

[3]Institute of General Practice, Goethe-University Frankfurt, Frankfurt am Main, Germany

[4]Institute for Digital Medicine, University Hospital Gießen-Marburg, Philipps University of Marburg, Marburg, Germany

[5]Department of Internal, Respiratory and Critical Care Medicine, Philipps University of Marburg, German Center for Lung Research (DZL), Marburg, Germany

[6]Department of Pediatrics, McGill University, Montreal, Quebec, Canada

[7]The Research Institute of McGill University Health Centre, Montreal, Quebec, Canada

[8]al-Farabi Kazakh National University, Almaty, Kazakhstan

[9]Institute of General Practice, University of Cologne, Cologne, Germany

[*]these authors contributed equally

Corresponding Author:
Lukas Niekrenz, LLM, Dr med
Department of Pneumology and Intensive Care Medicine, University Hospital Aachen, RWTH Aachen University, Pauwelsstrasse 30, Aachen, Germany

Abstract

Background: The overwhelming COVID-19 situation in 2020/2021 required novel approaches that did not require additional personnel within the current health care system. Therefore, we initiated a trial of nonsupervised home monitoring via the emergency department of a tertiary hospital without the support of a virtual ward as part of the "Netzwerk Universitaetsmedizin" cooperation in Germany. Given that daily vital sign checks for inpatients with COVID-19 could indicate clinical deterioration, this approach might also be helpful in an outpatient setting and could help to identify the need for hospitalization and additional resources.

Objective: This study aims to determine whether patient-led home monitoring for acute SARS-CoV-2 infection can be implemented through the emergency department of a tertiary care provider.

Methods: Patients who tested positive for SARS-CoV-2 infection in our emergency department between May 2021 and May 2022, did not have a medical indication for hospitalization, and were discharged to the outpatient setting were offered the opportunity to perform nonsupervised home monitoring of vital signs. Those who agreed to participate received Bluetooth-enabled devices to measure temperature, oxygen saturation, and blood pressure and downloaded a smartphone app. Participants were encouraged to measure their vital signs for at least 28 days. There was no virtual ward or real-time surveillance of the recorded data, but these could be made available to primary care physicians. Compliance with self-measurements was determined, and participants were contacted after the monitoring period for a semistructured interview.

Results: A total of 828 patients with COVID-19 were treated at the emergency department. Of these, 262 were directly discharged into ambulatory isolation after initial assessment, 25 were offered the opportunity of nonsupervised home monitoring, 15 successfully activated the devices, and 9 performed more than one complete measurement using the app. These 9 participants used the devices for an average of 15.8 days after discharge. Interviewed participants reported various difficulties with device setup but said they were pleased to use home monitoring and felt that the measurement option gave them additional security.

XSL•FO
RenderX

Conclusions: This study highlighted the challenges associated with implementing nonsupervised home monitoring for outpatients with COVID-19 who presented to the emergency department of a tertiary hospital. Implementing such a system without the involvement of additional personnel does not appear to be the optimal approach. We suggest that the physician-patient relationship might be a factor that is essential for the success of patient-led approaches to home monitoring.

Trial Registration: German Clinical Trials Register DRKS00025123; https://www.drks.de/search/de/trial/DRKS00025123/details

(JMIR Med Inform 2025;13:e58364) doi:10.2196/58364

KEYWORDS

home monitoring; telemonitoring; patient-led monitoring; nonsupervised home monitoring; physician-patient relationship

Introduction

During the COVID-19 pandemic, intensive efforts were made to find appropriate options for providing adequate care without overburdening the health care system. Given the number of severe acute respiratory distress syndrome cases and overcrowded intensive care units, medical staff were in short supply, especially in Germany [1-3]. The novel nature of COVID-19 and initial lack of knowledge about when and to what extent medical care and hospital admission were necessary caused uncertainty in the general population, which could have contributed to increased use of medical care for respiratory symptoms [4]. It also resulted in excessive demands on health care resources, such as those described for disaster situations [5]. Subsequent evaluations in Germany suggested that the majority of patients with COVID-19 could be treated on an outpatient basis [6].

The idea of using home monitoring for pandemic management arose from the fact that the regular vital sign checks performed on inpatients with COVID-19 could provide useful prognostic information. Such values were not routinely available for outpatients but could allow better assessment of these individuals and potentially provide an early signal of clinical deteriorations. This approach was implemented across many countries [7]. Home monitoring using eHealth and mobile health technologies provides data on relevant parameters for individual patients and helps with patient stratification [8].

Various home monitoring approaches include so-called virtual wards, that is, medical monitoring of the recorded data and contact by a treatment team [7,9-11]. In the context of COVID-19, contact with the medical team at all times has been reported to be a success factor for home monitoring [12]. In contrast, patient-led approaches without a virtual ward have been successfully used for monitoring chronic lung diseases (eg, the IPF online or I-FILE app) (Curavista bv) [13,14], but to our knowledge, they have not been used in the acute setting for infectious diseases.

At our institution during the height of the pandemic, our focus was on evaluating approaches that were feasible with existing (personnel) resources. With an already difficult staffing situation in the German health care system, regardless of the pandemic [15,16], we consider it essential that novel solutions require as few additional staff as possible. For this reason, we decided not to implement a virtual ward or real-time monitoring, but to establish patient-led home monitoring to supplement existing health care structures without providing personnel-intensive support. Therefore, as part of the egePan Unimed project for app-based telemedical home monitoring of COVID-19 [17], we focused on home monitoring as a possible approach to effectively managing outpatients with COVID-19.

This pilot study was designed to evaluate the feasibility by assessing patient usage data and medical use of an outpatient program of vital sign self-monitoring to detect early deterioration in patients with COVID-19 who presented to the emergency department but did not require hospital admission.

Methods

Study Design

This single-center cohort pilot study was conducted at the University Hospital Aachen, Germany (a large tertiary care provider) in accordance with STROBE (Strengthening the Reporting of Observational Studies in Epidemiology) reporting guidelines [18]. Recruitment was carried out by emergency department medical staff, supported by the study team for technical queries; no additional staff were made available to the emergency department to conduct the study.

Participants

Eligible participants were adults who had tested positive for SARS-CoV-2 infection on a rapid antigen or polymerase chain reaction test and presented at the emergency department but did not have a medical indication for hospitalization and had access to their own smartphone. If a study participant was subsequently admitted to the hospital, their participation in the study was paused for the duration of hospitalization and could continue after discharge. Pregnancy was initially an exclusion criterion, but this was removed after re-evaluation of the risks of study participation for these individuals.

Variables and Data Collection

Participants were given Bluetooth-enabled devices to record vital signs. Body temperature was measured using a noninvasive thermometer (Beurer FT 95 non-contact thermometer; Beurer GmbH), oxygen saturation (SpO2) was measured using a pulse oximeter (Beurer PO 60 pulse oximeter; Beurer GmbH), and blood pressure and heart rate were determined using a noninvasive sensor (Aponorm Basis Plus Bluetooth; WEPA Apothekenbedarf GmbH & Co KG). Participants were also given an installation code and emailed or given printed instructions on how to install the smartphone app (SaniQ Infect, Qurasoft GmbH). The study team contacted patients by telephone or video call to reaffirm that they met the inclusion criteria, to clarify remaining questions, and to provide support

XSL•FO
RenderX

for device and app setup on the day after discharge from the emergency department.

Participants were told to measure their vital signs at least once a day for at least 28 days (or until symptoms resolved if these persisted for longer than 28 days). Measurements were designed to transmit from the measurement devices to the app via Bluetooth, but patients were also able to manually enter values into the app. During the self-monitoring period, any necessary treatment was provided by the appropriate primary care physician or the ambulatory health care system. Vital sign data collected by participants could be made available to their treatment providers (eg, primary care physicians) via PDF export.

Compliance with daily vital sign measurements was calculated as (number of actual measurements)/(number of target measurements). In addition, to account for days when measurements may have been taken more than once a day, daily adjusted compliance was calculated as the ratio of the binary variable (daily target of measurements reached or exceeded)/(number of days). The duration of vital sign self-measurement was also recorded.

After the end of the study, participants underwent a semistructured interview to gain insights about their experience with home monitoring. The semistructured interview format was developed within the research team. A translation of the original German interview guide can be found in Multimedia Appendix 1.

Sample Size

Two hundred sets of monitoring devices were available for the study. The actual sample size was determined by the number of patients who requested treatment via the emergency department who could be included with the available staff.

Statistical Analysis

Due to the low inclusion rate, k-anonymity and l-variability were low, meaning that reidentification appeared possible with additional knowledge. Therefore, only aggregated data are reported. These are presented using descriptive statistics. For the same reason, interview responses are reported only in summarized form. Qualitative analysis of interview responses was planned to be performed by 2 independent researchers following the principles of qualitative content analysis by Mayring [19].

Ethical Considerations

The study protocol was approved by the Ethics Committee at the RWTH Aachen Faculty of Medicine (reference EK 099/21) and registered prospectively at the German Clinical Trials Register (ID DRKS00025123). All participants provided informed consent before enrollment in the study and could withdraw their consent at any time.

All recorded data were stored in an encrypted format on each participant's smartphone. Participants were able to share their data with the study center via a reference code; participants could terminate transmission of their data in the app. Data were deidentified for processing at the study center after the end of the study phase and stored exclusively on ISO27001-certified data centers in Germany. The servers used were subject to German data protection law.

For hygiene reasons, study participants were allowed to keep the home monitoring devices provided at the end of the study. No further compensation was granted for participation. The standard retail price of the devices provided amounted to around US $250 at the time of the study.

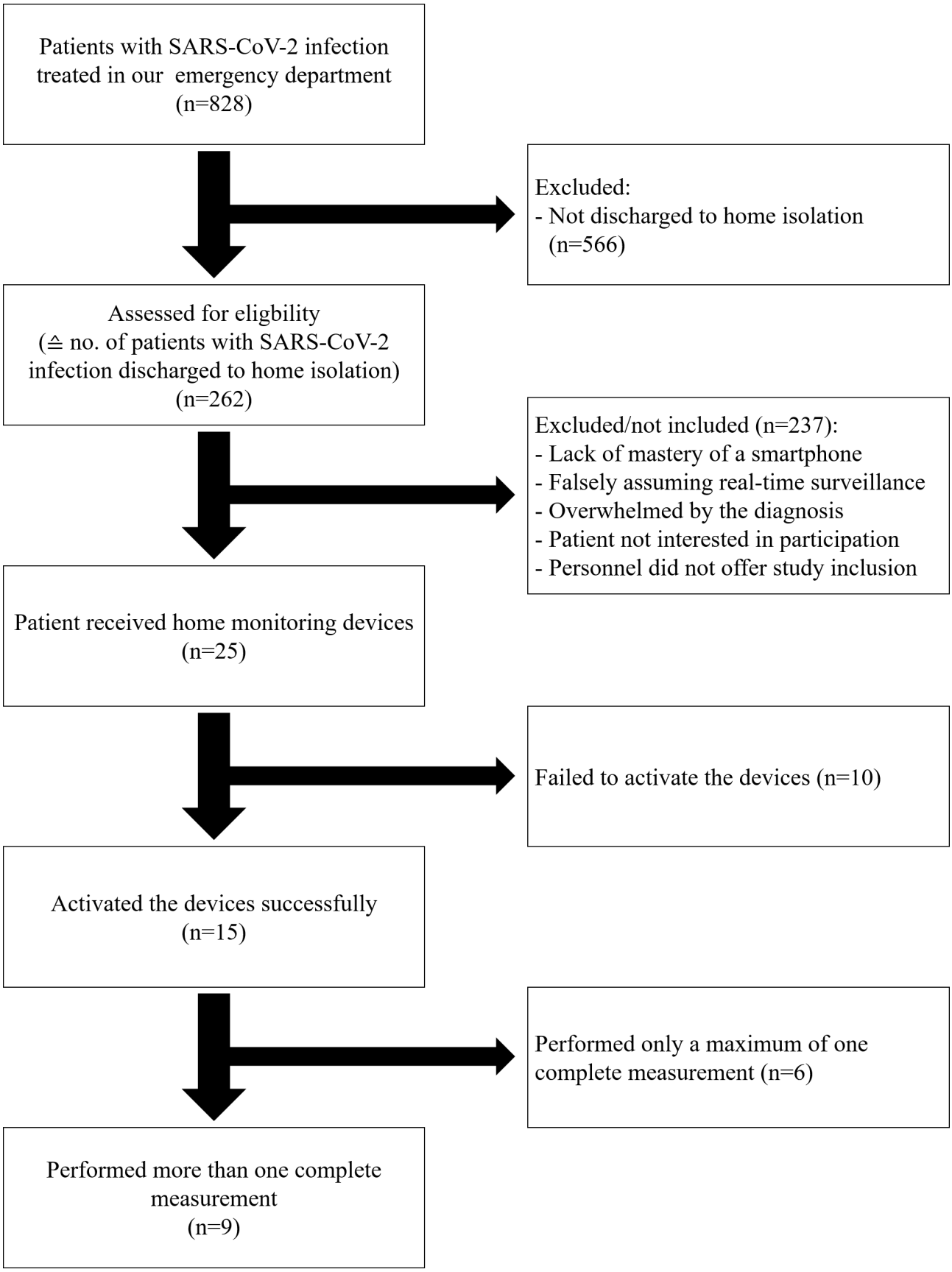
Results

Participants

Between May 2021 and May 2022, a total of 828 patients with SARS-CoV-2 infection were seen in our emergency department, of whom 262 (31.6%) were discharged to home isolation after being assessed. However, the majority of these were not enrolled in the study. Reasons for nonenrollment were lack of mastery of a smartphone, falsely assuming real-time surveillance, being overwhelmed by the diagnosis of SARS-CoV-2 infection, not being interested in the study, or because health care professionals were overburdened and did not offer study participation (Figure 1). Of the 25 enrolled participants (median age 42 years, IQR 20 years; mean age 42.9 years, SD 14.3 years), 15 successfully activated the devices and app, and 9 of these (median age 39 years, IQR 25 years; mean age 44.4 years, SD 15.9 years) performed more than one measurement with each of the 3 devices using the app.

XSL•FO
RenderX

Figure 1. Study flowchart.



Monitoring Usage and Compliance

The 9 participants who performed more than one complete measurement used the devices and app for an average of 15.8 days (range 1 - 28 days). Compliance varied, with 4/9 active participants exceeding the absolute number of measurements, and 2 even exceeded the required measurements every day. Overall, there were 399 measurements out of a target of 426

XSL•FO
RenderX

measurements (93.7%). The required number of measurements was performed on 85/142 user days (59.9%). Overall compliance ranged from 22.2% to 200% (median 100%, IQR 58.4%; mean 102.5%, SD 56%). Daily-adjusted compliance ranged from 4% to 100% (median 81.8%, IQR 61.4%; mean 64.1%, SD 39.2%).

Interview

Only 2 participants could be reached for the planned follow-up interview; an additional 4 agreed to a short informal conversation. For this reason, we decided to deviate from our planned approach to the analysis, as no meaningful evaluation seemed possible due to an insufficient number of participants. We decided to report the results only anecdotally. A formal analysis was not carried out. Nevertheless, in the setting of general practitioner care, an analysis was carried out based on a satisfactory number of cases, but this is reported elsewhere. The patients interviewed in our setting said that they were very pleased to use the home monitoring concept and felt that the measurement option provided additional security once the devices were set up. Various difficulties in setting up the devices were reported because this required each device to be paired with the patient's smartphone. Performing measurements was considered to be time-consuming and required a willingness to deal with the devices. It was also reported that the time available for additional measurements without immediate feedback decreased after the end of the home isolation period. One participant reported that their device data led to further examinations being performed when they contacted their general practitioner.

Discussion

Principal Findings

This study highlighted significant challenges relating to the implementation of a home monitoring program by the emergency department of a tertiary care provider during the height of the COVID-19 pandemic.

Although many of the patients with SARS-CoV-2 infection treated in our emergency department were potentially eligible for home monitoring, the majority did not enter the trial. There were several reasons for this. First, a large number of potential participants were not offered information about the study because health care professionals were too busy to have the time to do this. Second, a relevant number of patients were excluded due to their lack of mastery of a smartphone (self-reported or assumed by personnel). This was often, although not exclusively, seen in older individuals. Fifty-five patients discharged to home isolation were aged 65 years or older, and only 3 of these consented to participate in the study. Third, it appeared that some of the features of the study intervention (self-directed monitoring, no additional physician-patient contacts, no virtual ward) created a perception of lack of security of follow-up, making consent less likely. Finally, many patients simply did not have any interest in participating in the study or were psychologically overwhelmed by being diagnosed with SARS-CoV-2 infection. In summary, apart from the issue of overburdened emergency room personnel, it was largely patient attitudes that probably led to the low inclusion rate.

In general, the emergency department of a tertiary care provider is unlikely to be the first port of call for many patients with viral infections, and this is the case in Germany due to the sectoral design of the health care system [20]. Therefore, the characteristics of patients presenting in our study may have contributed to the observed challenges. We did not retrospectively gather potentially relevant patient information, including socioeconomic status and health literacy data. It has been noted that patients with mild symptoms who present to an emergency department in Germany with conditions that should generally be cared for by the primary care sector tend to have a lower socioeconomic status [21]. Although data on the relationship between lower socioeconomic status and adherence are not conclusive, some studies have shown that lower socioeconomic status is associated with lower adherence, at least in certain conditions [22,23]. For future research, especially in pilot projects focused on compliance and adherence to remote monitoring programs, we suggest that it would be important to have socioeconomic status and health literacy data.

Some patients presenting to the emergency department in our study, despite only having slightly symptomatic or asymptomatic SARS-CoV-2 infection, did not use the suggested home monitoring devices at all or often stopped using them. Many of the small group of participants stopped taking home measurements around 14 days after first testing positive for SARS-CoV-2 infection; this coincides with the duration of officially mandated isolation in Germany at the time [24]. Although these recommendations were gradually eased during the course of the pandemic [25], many people were still aware of the initial regulations and were also officially advised to reduce contact for 14 days.

Another important point is that there were no immediate consequences for the patients based on whether they did or did not perform daily measurements because the data were only stored locally on their device (unless shared with a health care professional at a future appointment). Given that we have shown that there is consistently better adherence to remote COVID-19 monitoring in primary care [26], it is reasonable to assume that socioeconomic factors are not the only contributors to the low adherence to monitoring in this study. We did observe interindividual differences in the use of home monitoring, but the study population was too small to be able to make valid statements about these variations. We were also unable to determine whether the home measurements taken by study participants were useful in their medical care because the sharing of home measurements at subsequent primary care visits was only reported by one individual.

One potential conclusion based on our data is that a close physician-patient relationship and the provision of feedback are important, as documented previously [27,28]. This physician-patient relationship might not necessarily occur in the setting of emergency treatment in a large clinic with changing staff. In addition to an easily accessible contact person and adequate infrastructure, continuous support seems to play an important role. Although we educated patients about the possible benefits and insights for them personally when providing information about the study, this single contact with a physician might not provide the level of motivation that might

XSL•FO
RenderX

come from a monitoring recommendation made by a more familiar health care professional, such as a general practitioner. Therefore, we suggest that the patient motivation issues seen in our study might have been mitigated by a closer physician-patient relationship or continuous feedback on device usage and readings obtained.

Our results on inclusion and device usage show that our approach, as it was, is not feasible in the German health care system without adaptations. Even if the study was planned with the existing personnel, the implementation still required additional workload and financial resources. With such a low uptake and usage rate as in our study, such an expense cannot be justified as feasible.

Concurrently, the small number of participants represents the greatest limitation of our study. Accordingly, we were unable to conduct our main objective, namely the analyses with regard to early markers of deterioration and our planned qualitative analysis in a reasonable manner. Although we are able to reconstruct the low number of participants at least in part with the explanations given above, this is not a pleasing result overall. Even if our study was able to provide important insights, it was not possible to establish a patient-led home monitoring concept.

Despite the disappointing uptake and use of home monitoring in our study, we believe that further evaluation of this approach in the tertiary care setting is warranted because home monitoring can provide valuable data for treatment and patient assessment. In specialized outpatient clinics and post-COVID follow-ups, where there is also repeated and regular contact with the same treatment team, it can be assumed that there is a stronger physician-patient relationship, which could have a positive impact on such an approach. Braun et al [29] introduced a similar concept for patients with chronic lung diseases using the same SaniQ app (Qurasoft GmbH) in routine secondary care during the COVID-19 pandemic. In this setting, patients showed satisfactory adherence and acceptance, but it must be noted that this program only required one measurement per month rather than the daily measurements in our study. Therefore, the frequency of measurements must be discussed critically when creating home monitoring concepts.

To create a reliable physician-patient relationship to maximize the benefit of home monitoring in patients with COVID-19, we advocate either the establishment of virtual wards [7,11,30] or involvement of the regular primary care sector [31], as described previously. Therefore, we suggest that the use of nonsupervised home monitoring in the primary care practice outpatient setting would be a better approach than initiation via the emergency department of a tertiary care provider.

Another factor that appears to be crucial to the success of a home monitoring program is a simple setup process. In our study, device and app setup created a lot of frustrations for both patients and the support team. Even though the setup should have been simple in principle (pairing the devices via Bluetooth with the patient's smartphone using the app), connection errors still occurred that could not always be easily resolved. Even with telephone support from the study team, some connection problems could not be solved quickly. General problem-solving approaches did produce the desired effect, but this was very time-consuming. To avoid such frustrations at the beginning of home monitoring, we recommend the use of technology that ensures the required external devices can be connected more easily. For example, this could be achieved by means of a base station assigned to the delivered measuring devices, meaning that only the base station would need to be paired with the patient's smartphone. Participants in our study also reported that the time burden of taking measurements was relatively high. The impact of this on motivation to continue performing daily measurements should not be underestimated. Therefore, there seems to be a need to balance the need for data density with a good user experience to create a robust and user-friendly home monitoring concept.

If we conducted the study again, in addition to the points mentioned above, we would also establish a monitoring board analogous to regulated drug trials: our analyses of the total number of potential study participants and the patients actually included were only evaluated at the end of the study and not during its implementation. If a corresponding monitoring board had been in place, the insufficient inclusion rates would have been noticed earlier so that we could have incorporated modifications into our recruitment process. A monitoring board of this kind can be operated with only a small amount of additional personnel resources if, for example, monthly intervals are selected.

Even though our aim was to investigate the potential of home monitoring with the available personnel resources, good staffing appears to be essential for the success of this kind of study: even a screening of the patient documentation by a study assistant (eg, a student assistant) and a resulting targeted indication to the study physicians could lead to potential inclusions not being missed despite the staff shortage. Once this has been established in a first phase, such support would probably no longer be necessary as soon as the staff had internalized the relevant processes.

However, such an approach would probably not have mitigated the low usage rate of the included patients. As far as can be deduced from our data and as explained above, the lack of ongoing care at home through the emergency department personnel appears to be the decisive factor here.

Limitations

Due to staff shortages in the emergency department at the time the study was conducted, there is a risk of selection bias. For example, it may have been easier to have time to provide information about the study when the emergency department was less busy. However, the study was designed to be conducted with existing personnel resources, and therefore, it was not possible to mitigate this potential source of bias. Similarly, we are missing socioeconomic data for participants because these were not collected to avoid placing an additional workload on the medical personnel involved. However, the main limitation of our study is the small number of participants recruited, and the even smaller numbers who were active users of self-monitoring and completed the postmonitoring interview. This limits the amount of data we were able to obtain, and therefore, the conclusions that can be drawn. Consequently, we were also unable to conduct our planned analyses with regard

XSL•FO
RenderX

to early markers of deterioration and our planned qualitative analysis in a reasonable manner.

Conclusions

Due to the small sample size in this study, the main conclusion that we can draw is that providing nonsupervised home monitoring to outpatients with COVID-19 through a single contact in an emergency department of a tertiary hospital is not the optimal approach. Although conducted during the COVID-19 pandemic, our data could provide useful information about the issues related to the setup of home monitoring for a variety of diseases based on a single emergency department contact. Key features for success are likely to be regular feedback and care and an ongoing physician-patient relationship.

Acknowledgments

The institutions employing LN, LSS, SH, SMK, ND, BSM, CC, RK, GR, CFV, and MD received funding for this study from the German Federal Ministry of Education and Research (grant number 01KX2021). Open access funding was provided by the Open Access Publishing Fund of RWTH Aachen University. The funder had no role in the design of the study or in the collection, analysis, or interpretation of the data. We presented preliminary findings at the 63rd Congress of the German Respiratory Society in 2023, and an abstract in German is available online [32]. The authors thank Ms Nicola Ryan, an independent medical writer, for providing English-language editing assistance.

Conflicts of Interest

ND received the CSL Behring award "Translational Research on Extracellular Vesicles in COPD." RK has been involved in projects and publications using the Kaia COPD App. SK is the founder and managing partner of MED.digital GmbH. SK holds shares of BioNTech, Pfizer, and CRISPR Therapeutics. SK is a member of the commission "New Professions" of Stiftung Münch and of committees of the German Medical Association ("Digitalization of health care" and "Medical Education and University Medicine"). BSM received personal honoraria for scientific consultancy to the health insurance fund "Die Techniker." GR reports personal fees from Astra Zeneca, Atriva, Boehringer Ingelheim, GSK, Insmed, MSD, Sanofi, Novartis and Pfizer for consultancy during advisory board meetings and reports personal fees from Astra Zeneca, Berlin Chemie, BMS, Boehringer Ingelheim, Chiesi, Essex Pharma, Grifols, GSK, Insmed, MSD, Roche, Sanofi, Solvay, Takeda, Novartis, Pfizer and Vertex for lectures. The other authors declare no conflict of interest.

Multimedia Appendix 1
Interview guide.
[PDF File, 580 KB - medinform_v13i1e58364_app1.pdf]

References

1. Schuppert A, Theisen S, Fränkel P, Weber-Carstens S, Karagiannidis C. Nationwide exposure model for COVID-19 intensive care unit admission. Med Klin Intensivmed Notfmed 2022 Apr;117(3):218-226. [doi: 10.1007/s00063-021-00791-7] [Medline: 33533980]
2. Piel J, Hörold M, Brandstetter S, et al. COVID-19 crisis management of German ICU clinicians in leadership - a metaphor analysis. Front Public Health 2023;11:1160094. [doi: 10.3389/fpubh.2023.1160094] [Medline: 37663843]
3. Epidemiological bulletin 05/2021 [Article in German]. Robert-Koch-Institut. 2021. URL: https://www.rki.de/DE/Aktuelles/Publikationen/Epidemiologisches-Bulletin/2021/05_21.pdf?__blob=publicationFile&v=3 [accessed 2022-07-05]
4. Huang Z, Natarajan K, Lim HC, et al. Applying Andersen's healthcare utilization model to assess factors influencing patients' expectations for diagnostic tests at emergency department visits during the COVID-19 pandemic. Front Public Health 2023;11(1250658):1250658. [doi: 10.3389/fpubh.2023.1250658] [Medline: 38074705]
5. Lurie N, Carr BG. The role of telehealth in the medical response to disasters. JAMA Intern Med 2018 Jun 1;178(6):745-746. [doi: 10.1001/jamainternmed.2018.1314] [Medline: 29710200]
6. The National Association of Statutory Health Insurance Physicians and the Regional Associations of Statutory Health Insurance Physicians. Outpatient care during the coronavirus pandemic - facts & figures February 2020 to April 2022 [Article in German]. Kassenärztliche Bundesvereinigung. URL: https://www.kbv.de/media/sp/Ambulante_Versorgung_Corona_Pandemie_Zahlen_Fakten.pdf [accessed 2025-01-06]
7. Vindrola-Padros C, Singh KE, Sidhu MS, et al. Remote home monitoring (virtual wards) for confirmed or suspected COVID-19 patients: a rapid systematic review. EClinicalMedicine 2021 Jul;37:100965. [doi: 10.1016/j.eclinm.2021.100965] [Medline: 34179736]
8. Dauletbaev N, Kuhn S, Holtz S, et al. Implementation and use of mHealth home telemonitoring in adults with acute COVID-19 infection: a scoping review protocol. BMJ Open 2021 Sep 27;11(9):e053819. [doi: 10.1136/bmjopen-2021-053819] [Medline: 34580103]
9. Thornton J. The "virtual wards" supporting patients with covid-19 in the community. BMJ 2020 Jun 4:m2119. [doi: 10.1136/bmj.m2119]

XSL•FO
RenderX

10. Ferry OR, Moloney EC, Spratt OT, Whiting GFM, Bennett CJ. A virtual ward model of care for patients with COVID-19: retrospective single-center clinical study. J Med Internet Res 2021 Feb 10;23(2):e25518. [doi: 10.2196/25518] [Medline: 33529157]
11. Greenhalgh T, Knight M, Inda-Kim M, Fulop NJ, Leach J, Vindrola-Padros C. Remote management of covid-19 using home pulse oximetry and virtual ward support. BMJ 2021 Mar 25;372:n677. [doi: 10.1136/bmj.n677] [Medline: 33766809]
12. Ko SQ, Chua CMS, Koh SH, Lim YW, Shorey S. Experiences of patients and their caregivers in a virtual ward in Singapore: a descriptive qualitative study. Int J Med Inform 2023 Sep;177:105111. [doi: 10.1016/j.ijmedinf.2023.105111] [Medline: 37307721]
13. Moor CC, Mostard RLM, Grutters JC, et al. Home monitoring in patients with idiopathic pulmonary fibrosis. A randomized controlled trial. Am J Respir Crit Care Med 2020 Aug 1;202(3):393-401. [doi: 10.1164/rccm.202002-0328OC] [Medline: 32325005]
14. Moor CC, Gür-Demirel Y, Wijsenbeek MS. Feasibility of a comprehensive home monitoring program for sarcoidosis. J Pers Med 2019 May 5;9(2):23. [doi: 10.3390/jpm9020023] [Medline: 31060343]
15. Kopetsch T. The medical profession in Germany: past trends, current state and future prospects. Cah Sociol Demogr Med 2004;44(1):43-70. [Medline: 15146658]
16. Klingler C, Marckmann G. Difficulties experienced by migrant physicians working in German hospitals: a qualitative interview study. Hum Resour Health 2016 Sep 23;14(1):57. [doi: 10.1186/s12960-016-0153-4] [Medline: 27662831]
17. Rohde G, Müller BS. Workpackage 3.3 App based telemedical home monitoring (COVID-19@Home). egePan Consortium. 2020. URL: https://egepan.de/ap-3-3-app-basiertes-telemedizinisches-home-monitoring/ [accessed 2022-07-05]
18. von Elm E, Altman DG, Egger M, et al. Strengthening the Reporting of Observational Studies in Epidemiology (STROBE) statement: guidelines for reporting observational studies. BMJ 2007 Oct 20;335(7624):806-808. [doi: 10.1136/bmj.39335.541782.AD] [Medline: 17947786]
19. Mayring P. Qualitative content analysis: theoretical foundation, basic procedures and software solution. Social Science Open Access Repository. 2014. URL: https://nbn-resolving.org/urn:nbn:de:0168-ssoar-395173 [accessed 2021-01-18]
20. Gries A, Schrimpf AM, von Dercks N. Hospital emergency departments. Deutsches Ärzteblatt international 2022 Sep 23. [doi: 10.3238/arztebl.m2022.0276]
21. Reins LM. Analysis of patient data from the central emergency department at Augsburg University Hospital in 2017 [Dissertation in German]. : Ludwig-Maximilians-Universität München; 2021 URL: https://edoc.ub.uni-muenchen.de/28964/7/Reins_Lisa-Marie.pdf [accessed 2022-08-09]
22. Lu R, Li Y, Zheng Z, Yan Z. Exploring factors associated with self-management compliance among rural elders with diabetes. Inquiry 2021;58:469580211012491. [doi: 10.1177/00469580211012491] [Medline: 33899547]
23. Alsabbagh M, Lemstra M, Eurich D, et al. Socioeconomic status and nonadherence to antihypertensive drugs: a systematic review and meta-analysis. Value Health 2014 Mar;17(2):288-296. [doi: 10.1016/j.jval.2013.11.011] [Medline: 24636389]
24. Ministry of Labor, Health and Social Affairs of North Rhine-Westphalia, Germany. Ordinance on the regulation of isolation in accordance with Section 30 of the Infection Protection Act (Quarantine Ordinance NRW) [Article in German]. Land.NRW. 2021. URL: https://www.land.nrw/sites/default/files/asset/document/210212_quarantaenevo.pdf [accessed 2025-01-31]
25. Coronavirus SARS-CoV-2: current quarantine and isolation rules [Article in German]. Bundesministerium für Gesundheit. 2022. URL: https://www.bundesgesundheitsministerium.de/fileadmin/user_upload/BMG_C-19_220708_static_JB_Quaranta___eneflyer_DE_Digital.pdf [accessed 2025-01-31]
26. Holtz S, Köhler SM, Chabiera PJ, et al. Implementing remote monitoring for COVID-19 patients in primary care. medRxiv. Preprint posted online on Feb 29, 2024. [doi: 10.1101/2024.02.27.24303073]
27. van Ganse E, Mörk AC, Osman LM, et al. Factors affecting adherence to asthma treatment: patient and physician perspectives. Prim Care Respir J 2003 Jun;12(2):46-51. [doi: 10.1038/pcrj.2003.17] [Medline: 31700346]
28. Derksen F, Bensing J, Lagro-Janssen A. Effectiveness of empathy in general practice: a systematic review. Br J Gen Pract 2013 Jan;63(606):e76-e84. [doi: 10.3399/bjgp13X660814] [Medline: 23336477]
29. Braun M, Schmidt O, Schultz T, Woehrle H, Sundrup MG, Schöbel C. Experiences with digital care of patients with chronic and acute lung diseases during the SARS-CoV-2 pandemic. Internist (Berl) 2022 Mar;63(3):255-265. [doi: 10.1007/s00108-022-01266-3] [Medline: 35181796]
30. Lim A, Hippchen T, Unger I, et al. An outpatient management strategy using a Coronataxi digital early warning system reduces coronavirus disease 2019 mortality. Open Forum Infect Dis 2022 Apr;9(4):ofac063. [doi: 10.1093/ofid/ofac063] [Medline: 35287336]
31. Agarwal P, Mukerji G, Laur C, et al. Adoption, feasibility and safety of a family medicine-led remote monitoring program for patients with COVID-19: a descriptive study. CMAJ Open 2021;9(2):E324-E330. [doi: 10.9778/cmajo.20200174] [Medline: 33795222]
32. Niekrenz L, Hübel C, Plata C, et al. COVID-19@Home: Etablierung eines patientenzentrierten, nicht-supervidierten Homemonitoringkonzepts für ambulante COVID-19 Patienten über die Notaufnahme eines Supramaximalversorgers im Rahmen einer Pilotstudie [Abstract in German]. Pneumologie 2023;77(S 01):S63. [doi: 10.1055/s-0043-1761016]

XSL•FO
RenderX

Abbreviations

STROBE: Strengthening the Reporting of Observational Studies in Epidemiology

Edited by A Benis; submitted 16.05.24; peer-reviewed by H Gandhi, M Munikumar; revised version received 20.06.25; accepted 24.06.25; published 18.09.25.

Please cite as:
Niekrenz L, Hübel C, Plata C, Biermann H, Leber C, Schütze LS, Holtz S, Köhler SM, Deutsch K, Dauletbayev N, Kuhn S, Müller BS, Cornelissen C, Koczulla R, Rohde G, Vogelmeier CF, Brokmann JC, Dreher M
Home Monitoring Delivered Through the Emergency Department for Outpatients With COVID-19: COVID19@Home Aachen Pilot Cohort Study
JMIR Med Inform 2025;13:e58364
URL: https://medinform.jmir.org/2025/1/e58364
doi:10.2196/58364

© Lukas Niekrenz, Christian Hübel, Christopher Plata, Henning Biermann, Claas Leber, Lisa Sophie Schütze, Svea Holtz, Susanne Maria Köhler, Kim Deutsch, Nurlan Dauletbayev, Sebastian Kuhn, Beate Sigrid Müller, Christian Cornelissen, Rembert Koczulla, Gernot Rohde, Claus Franz Vogelmeier, Jörg Christian Brokmann, Michael Dreher. Originally published in JMIR Medical Informatics (https://medinform.jmir.org), 18.9.2025. This is an open-access article distributed under the terms of the Creative Commons Attribution License (https://creativecommons.org/licenses/by/4.0/), which permits unrestricted use, distribution, and reproduction in any medium, provided the original work, first published in JMIR Medical Informatics, is properly cited. The complete bibliographic information, a link to the original publication on https://medinform.jmir.org/, as well as this copyright and license information must be included.

XSL•FO
RenderX

Benefits and Limitations of Teledermatology in German Correctional Facilities: Cross-Sectional Analysis

Brigitte Stephan[1], MD, Dr med; Kathrin Gehrdau[1]; Christina Sorbe[1]; Matthias Augustin[1], MD, Prof Dr Med; Martin Scherer[2,3], MD, Prof Dr Med; Anne Kis[1]

[1]Institute for Health Services Research in Dermatology and Nursing, University Medical Center Hamburg-Eppendorf, Martinistraße 52, Hamburg, Germany

[2]A+ Videoclinic GmbH, Munich, Germany

[3]Institute for General Medicine, University Medical Center Hamburg-Eppendorf, Hamburg, Germany

Corresponding Author:
Brigitte Stephan, MD, Dr med
Institute for Health Services Research in Dermatology and Nursing, University Medical Center Hamburg-Eppendorf, Martinistraße 52, Hamburg, Germany

Abstract

Background: Teledermatology consultations offer the advantage of rapid diagnosis and care. Since 2019, our institute at the University Medical Center Hamburg-Eppendorf has been part of an interdisciplinary team for teledermatology support in German prisons as an alternative to extramural transports of patients.

Objective: This study aims to analyze the benefits and limitations of teledermatology for patients with limited access to medical specialties.

Methods: We conducted a descriptive cross-sectional analysis of 651 teleconsultations from prisons from February 2020 to April 2023. All cases were performed in a store-and-forward (asynchronous mode) and optional hybrid live (synchronous) consultation for the patient or in-house staff.

Results: The main advantage of this case processing was the avoidance of external transport. Of the 651 teleconsultations, 608 (93.4%) could be finalized with telemedical support and 43 (6.6%) required additional workup, including verifications of the type of tumors (n=22, 51%), which needed biopsies, and open cases that were inflammatory (n=11, 26%) or involved infectious skin conditions (n=5, 12%). Digital imaging of the skin lesions improved with the experience of the personnel but remained a challenge, with the photo quality depending on the technical devices or available broadband supply.

Conclusions: Hybrid teledermatology consultation represents an effective and resource-saving method of providing specialized care to patients in situations with limited access to medical specialties. The video consultations with experts and exchange of knowledge about the cases presented opened the opportunity to support and train intramural colleagues. One of the main challenges remains the quality of digital imaging and transmission.

(JMIR Med Inform 2025;13:e58712) doi:10.2196/58712

KEYWORDS

dermatology; dermatologist; dermatological; dermatological care; accessibility; prison health; teledermatology; telemedicine; telehealth; virtual health; virtual medicine; remote consultation; telephone consultation; video consultation

Introduction

The international recommendations for medical care in correctional facilities set high standards [1]. According to global agreements stated by the World Health Organization, prisoners should receive equivalent medical care in comparison to the standards for the respective population [2,3]; this includes primary care as well as access to all medical specialties, which is challenging for the correctional system [4-7].

Need for Health Services in Correctional Facilities

On average, prisoners are younger compared to the normal population, and more than 90% are male, which indicates a different scope of medical issues [8]. However, prisoners also have a higher proportion of individuals with chronic diseases, especially mental disorders or chronic infections like hepatitis, requiring ongoing medical care [9-14].

Prisons in Germany ensure these medical services not only using in-house resources but also regularly using external medical service providers to fulfill these tasks [15-17]. For dermatology issues, this means complete reliance on external dermatology

XSL•FO
RenderX

facilities because none of the more than 280 correctional facilities in Germany provide in-house solutions.

Economic Aspects of Medical Care in Prisons

Following the principle of equal standard of medical care for prisoners as people living in the community, the scope of medical services in German correctional institutions should correspond to the scope of services provided by the statutory health insurance funds. However, prisoners are no longer covered by statutory health insurance when they start their prison sentence in Germany [7]. The costs for medical care must be covered by the prison authorities of the federal state. The expenses for the correctional facilities [18,19] as well as the medical care in the German correctional system have risen steadily, and the federal states of Germany have to cover these costs [20]. A substantial amount is caused by personnel and transport costs. New solutions are needed to both provide the required standards of care and control costs [21].

Use of Teledermatology for Correctional Facilities in Germany

During the last decades, telemedicine in various settings has become a useful tool to support health services [22]. In 2018, the 121st German Medical Congress approved an amendment to the medical professional code of conduct (Muster-Berufsordnung für die in Deutschland tätigen Ärztinnen und Ärzte [MBO-Ä]) and enabled remote telemedical care [23]. Since 2019, German correctional institutions have started to use telemedicine for dermatology requests [20,24]. Initially, this service was provided through a pilot project by the Ministry of Justice of Baden-Württemberg and expanded to other German federal states and correctional facilities in subsequent years. Currently, these dermatology teleconsultations are offered on a fixed weekly basis for acute cases on demand within 24 hours. The prison can choose between a store-and-forward mode (asynchronous operation) with photos and a standardized form only or an additional hybrid option with a live video consultation in an interdisciplinary round including the treating primary physician simultaneously (synchronous operation). This allows a direct exchange of medical information as well as the opportunity for further counseling with colleagues in charge of the case. Both modes represent an alternative to transportation and presentation of prisoners in dermatology facilities outside the correctional institution, and we experience an increasing number of requests to our institute from German correctional institutions.

Although the rate of completed cases through video consultations in either store-and-forward mode or in live presentation is high [8], there are limitations to the processing of certain requests. With this paper, we analyzed 651 cases of our teleconsultations for German correctional facilities from February 2020 to April 2023. This study aimed to provide evidence on the value of teledermatology care provided to German prisons and detect limitations for this mode of service with a focus on cases that could not be processed without live on-site consultations.

Methods

Overview

A systematic comparison of the advantages and disadvantages of video consultations for prisoners was carried out based on a descriptive cross-sectional analysis of 651 applications for teleconsultations in German correctional facilities from February 2020 to April 2023, supplemented with literature research. The selection of the evaluation criteria was based on quality criteria from the German guidelines for teledermatology from 2020 [25].

We retrieved all data from the documented request forms from February 2020 until April 2023. Data included:

- clinical symptoms and anamnestic information of skin disease;
- patients' demographic data (age and gender);
- preliminary diagnosis and questions from the in-house medical team of the prison regarding the case (eg, special issues such as occupational or infectious matters, quarantine, or isolation);
- documentation of the consultation, including details of onset and clinical appearance of the skin disease, and number and quality of photos sent with the request; and
- further anamnestic information retrieved from the virtual presentation of the case and dermatological diagnosis and suggestions for treatment.

Ethical Considerations

The ethics committee of the Medical Association of Hamburg confirmed that there was no further ethical approval necessary for retrospective analysis of anonymized data in accordance with the ethical standards of the responsible committees (institutional or regional) and with the Helsinki Declaration of 1975, as revised in 1983.

Spatial Analyses

Part of this study was a spatial assessment of the potential physical accessibility of prisoners to dermatologists. The data basis for all 284 prison locations was a list from the justice portal of the federal and state governments from 2020. After geocoding and referencing the locations, they were loaded and mapped in a geographic information system in ArcGIS v. 10.8.1 (ESRI). As a proxy for accessibility, physician density was compared to correctional facility locations. Data were provided by Kassenaerztliche Bundesvereinigung (KBV; data status 2022).

Statistical Analysis

We conducted a descriptive analysis of all variables with SPSS v.26 (IBM Corp), including demographic data (eg, age and gender) and medical data (eg, diagnosis, suggestions for therapy, and further management of the skin disease). Thereby, we categorized open entries, for example, therapy modalities, into categories such as topical or systemic therapy. We conducted a subgroup analysis for cases that were not closed after one video consultation regarding diagnoses or recommendations for further management modalities.

XSL•FO
RenderX

Results

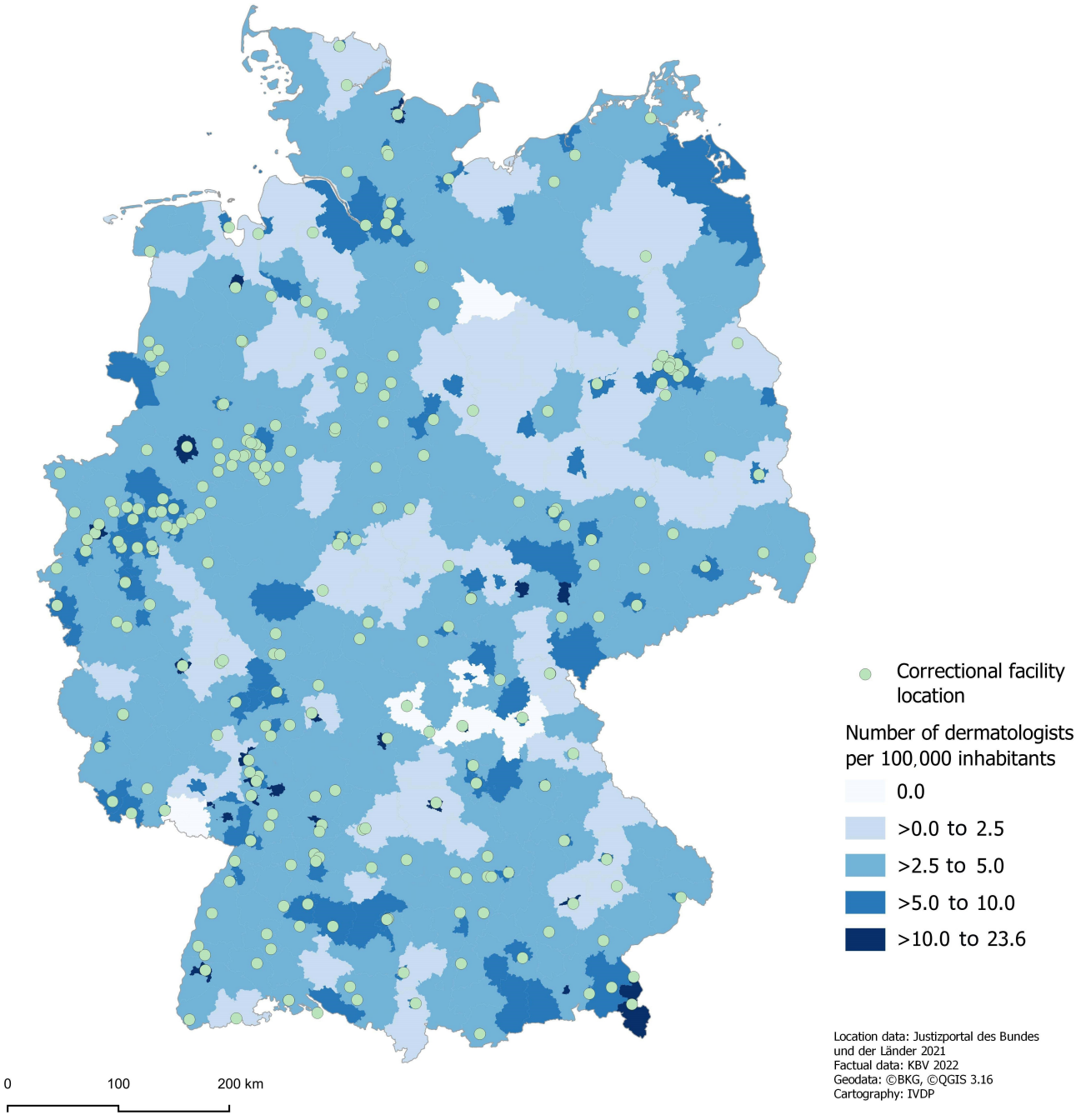
Overview

We offer teledermatology support for correctional facilities in Germany. As of May 2023, a total of 38 prisons in 6 federal states in Germany used this service regularly, with rising numbers. Of the 651 cases analyzed, we were asked for 412 diagnoses, 497 therapy recommendations, and 62 follow-ups for reconsidering or changed skin conditions. We provided a time-saving response within 1 week after the request or, in urgent cases, a response within 24 hours in store-and-forward mode. The most frequently diagnosed skin diseases were eczema, skin infections, acne or acneiform dermatitis, and tumor differentiation [26].

Accessibility of Dermatologists Through Telemedical Consultations: Spatial Considerations for Physical Contact

In Germany, there are 284 locations for correctional facilities distributed across all 16 federal states (Figure 1) [25]. The distribution of the prisons differs from being centrally located in metropolitan areas to being far from cities in rural areas. This is important for the accessibility and vicinity of medical specialists (eg, dermatologists).

Figure 1. Cartographic representation of all prison locations in Germany. Cartographic representation of prisons in Germany (green dots) and the density of registered dermatologists per 100,000 inhabitants (blue color scheme). Only a few districts have a high density of dermatologists, between 10-23.6 per 100,000 inhabitants. The majority of districts have between 2.5-5.0 registered dermatologists or fewer, and most prisons are situated outside the metropolitan areas. This results in heterogeneous accessibility.



XSL•FO
RenderX

Avoidance of Transports Outside the Prison

The transport of an inmate to extramural facilities requires at least two staff members, and in cases of low personnel resources, the police forces have to support the institutional staff in Germany. We analyzed our 651 cases for finalization and closure of the case in terms of sufficient data for a diagnosis, recommended therapeutic options in-house, and a need for further diagnostic or therapeutic procedures requiring transport to outside facilities.

Of the 651 cases, 608 could be finalized with a diagnosis and recommendations for treatment and further management without need for extramural transportation of the patient, 83 had to send additional material like laboratory results or images for proceeding with the cases, and 43 could not be solved by teledermatology and consequently needed extramural support on site.

Of the 43 cases, 22 were questions concerned with the type of tumor (Table 1), for which we recommended live examination on site or biopsies that could not be performed inside the prison itself. Usually, the in-house physicians do not perform biopsies, and therefore, the teledermatology consultation did not lead to a successful closure of the case in these requests.

A total of 2 cases were exanthems of uncertain origin with recommendation for biopsies; 6 cases were eczema with missing anamnestic or clinical information for a differential diagnosis and proper conduct; 5 cases were suspected skin infections, and the facilities did not respond to our request for further clinical information or laboratory results like swabs or culture; 1 case showed the clinical picture of psoriasis but insufficient imaging of the extent and a lack of information about comorbidities and previous management; 2 cases sent images of acneiform lesions but lacked clinical information; 1 case asked for differential diagnosis of dermatitis herpetiformis Duhring but did not send sufficient clinical or anamnestic data; and 1 case asked for management of alopecia without further clinical or anamnestic information. Interestingly, the number of cases that were sent without a question for dermatology was rare (1 question for dysesthesias with a neurological background and 2 cases without any information about a skin problem).

According to the Guideline for Teledermatology [27], general screening for skin cancer should not be made by teledermatology alone. If the prison was able to send accurate dermoscopic images, there was an opportunity to provide a statement about the type of lesion or to rule out malignancies, but if the digital imaging was not sufficient, there was a need to consult the physician in charge on site. Cases with the need for general inspection of the entire body or detection of small pigmented lesions as well as skin conditions with the need for palpation (eg, lymph nodes), had to be referred to a physician on site if available or transported to outside facilities. Of our 651 cases, 96 asked for diagnosis of different types of tumors, of which 22 could not be solved by digital imaging, clinical description, and additional video consultation. Some cases could be solved by educating the in-house physician about screening procedures.

Table . Distribution of video consultations with closure based on uploaded request forms, photos sent, and live presentation online.

Case status	Cases (N=651), n
Solved cases	608
Unsolved cases	43
Tumors	22
Eczemas	6
Infections	5
Acneiform	2
Exanthemas	2
No information	2
Psoriasis	1
Nondermatological	1
Duhring	1
Alopecia	1

Telemedical Expert Exchange of Knowledge With Intramural Colleagues of the Correctional Facilities

Due to the fact that no prison in Germany has dermatology resources, the intramural colleagues in charge of the facility service, mostly general practitioners, have to treat and follow dermatological cases. With the help of telemedical expertise and discussions online, we allowed for the exchange of knowledge about the case presented or skin diseases in general and, therefore, enabled the colleagues to become more capable of proceeding with further cases on their own. All of our video consultations were attended to by in-house medical staff from the prison, and in all virtual visits, we exchanged information about the present skin disease as well as therapeutic options and guidelines.

Data Provision and Photo Documentation From Institution to Dermatologist

The number of photos per case was not limited, and 0-27 photos were sent for one request. Insufficient photo quality of at least

XSL•FO
RenderX

one photo was found in 124 of the 651 requests from February 2020 to April 2023, but only 12 cases did not upload any sufficient imaging. The quality of the photos sent improved with the number of cases an individual prison performed and if the service provider supported technical solutions and devices.

Discussion

This study aimed to identify the benefits and limitations of teledermatology support for prisons in Germany (Textbox 1). Prisons are mostly situated outside of the city centers without proximity to medical specialties like dermatologists. The consequence of long distances to the dermatology institutions is the impossibility of visits on site by the nearest dermatologists. Although in metropolitan areas the distances might be low, it does not necessarily mean the availability of dermatologists who are willing to visit one patient in a correctional facility, considering the difficult and time-consuming organization of access and visit schedules aside from their routine medical care and duties.

With the abovementioned German prison locations and physician density of all 16 federal states in mind, the willingness and reality of established specialists coming to the prison should be questioned [28]. The time and effort required of medical specialists due to the treatment of prisoners in prison could force physicians to reject the requests. Even though the medical specialists will be paid based on treatment and the medical fee schedule [29], the opportunity costs could be seen as too high. Therefore, it is not unusual for there to be a noticeable shortage of physicians in the prison system [15].

With our institute, we provided time-saving access to dermatology expertise and avoided transportation in most cases. Compared to general waiting times in Germany for specialist appointments, this is a significant benefit for the patients [30]. Transporting a prisoner to an off-site facility is a challenge to security and human resources. Consequently, for the prison and the community, the risk of an outbreak is very low if the medical specialist comes to the prison instead of bringing the prisoner to the physician [31]. Avoidance of transports outside the prison enhances security and saves resources. In cases with telemedical support, transport is no issue. A recent systematic review of the implementation of telemedicine found that public security and the reduction of the risk of a prisoner escaping are some of the main arguments to enable the successful implementation of telemedicine interventions [32]. From the perspective of prisons and the community, and probably for the prisoner as well, due to a lack of exposure in public, avoiding transport for medical needs with the alternative option of telemedical consultation is preferable. Furthermore, the additional hourly security and transportation costs for each external practice visit should be considered [33].

Although the rate of finalized cases was high (608/651 cases) [8], we could not finalize every case by teledermatology with hybrid store-and-forward information, digital imaging, and video consultation alone. For pigmented lesions, differentiation should not be performed with video consultation alone, and digital imaging could not provide sufficient photo quality in all cases. From 97 requests for tumors or pigmented lesions, a total of 244 photos (including dermoscopic imaging) with a maximum of 9 photos for one case were documented, but in 12 cases, no photo was sent, and in 2 cases, the photo quality was insufficient for a statement concerning type or diagnosis.

Looking at the analyzed cases, we saw a benefit in the interdisciplinary exchange of medical expertise, especially for chronic inflammatory skin diseases like atopic dermatitis or psoriasis where the potential change in clinical picture and severity of the disease poses sometimes challenging situations and the need for knowledge about modern therapeutic options and updated guidelines for therapeutic approaches. Especially for darker skin types who form a relevant proportion of patients in custody, it is helpful to have experience with the different appearance of skin diseases on dark skin, a knowledge which cannot be anticipated for intramural medical personnel. If we compare it to dermatology consultations of previous years, where we saw prisoners live in our outpatient clinic in Hamburg with transports to our institute from the surrounding prisons, we found that the accompanying nonmedical personnel were not involved in the patient's case or disease and could not provide further information if needed. In reverse, the in-house physicians of the prison did not have direct contact with us and did not benefit from medical exchanges. Only a short medical letter provided the connection and flow of information between the prison and the dermatologist. In direct video consultation, the exchange of information from the medical file of the patient and information about the skin disease from the dermatologist was used for all cases discussed online, which was highly appreciated by both sides.

Not all prisons using teleconsultations were willing to send photos and dermoscopic imaging accompanying the request form due to data safety issues. Although the service provider offered a certified cloud solution, the individual prison responsible decided not to use this option. On the other hand, the resolution on both sides of the camera in live discussions online is not sufficient to detect high-resolution skin efflorescences such as telangiectasias, pigmented spots, or small appendages. This can be due either to the technology or to the available broadband supply. Studies show that, especially in rural areas, the conditions for sufficient broadband availability are not available everywhere to enable fast and, especially for medicine, reliable data transmissions [34].

Teleconsultations provide facilitated and time-saving access to medical specialties, and dermatology is most suitable for telemedical visualization of medical skin conditions. Both remote store-and-forward conduct as well as online discussion support the diagnosis of skin conditions and enable follow-up and guidance of therapy regimens.

Despite the significant progress telemedicine and teledermatology have made, the transition of medical treatment from face-to-face to only digital formats is not always appropriate to meet medical goals [35]. Overall, prisons have to analyze their demand for any kind of medical service that cannot be covered by their in-house general practitioner. The skin disease in focus, the possibilities of digital imaging of the condition, interventions needed, and follow-up requirements must be considered. Furthermore, both sides of the telemedical

XSL•FO
RenderX

support call need to take into account intramural possibilities for treatments and compliance of the patient, as well as individual preferences for treatment. To conduct a break-even analysis from the prison's view, transparency about all costs and benefits must be provided [33]. With the emerging lack of specialists in Germany, the option for telemedical support in prisons as well as other facilities has advantages that should be considered in the health services for patients with limited access to regular medical facilities.

Textbox 1. Benefits and limitations of teledermatology in the setting of teleconsultations for German prisons.

Benefits

- Accessibility
- Transport and personnel deployment
- Expert exchange

Limitations

- Need for general inspection or biopsy
- Data provision
- Photo quality

Acknowledgments

The authors thank the scientific communication team of the Institute for Health Services Research in Dermatology and Nursing, especially Amber Hönning, and Sara Tiedemann and Mario Gehoff for editing the article. We acknowledge financial support from the Open Access Publication Fund of University Medical Center Hamburg-Eppendorf and Deutsche Forschungsgemeinschaft.

Data Availability

The datasets generated or analyzed during this study are available from the corresponding author upon reasonable request.

Authors' Contributions

Conceptualization: BS, KG, AK
Methodology: BS, KG, CS, AK
Formal analysis and investigation: BS, KG, CS, AK
Writing – original draft preparation: BS, KG, CS, AK
Writing – review and editing: BS, KG, CS, MA, MS, AK
Resources: BS
Supervision: BS, CS

Conflicts of Interest

MS has an affiliation with the A+ Videoclinic GmbH, Munich, Germany. MA received fees from the A+ Videoclinic GmbH Munich for the video consultations provided. BS, CS, KG, and AK declare no conflicts of interest for this paper.

References

1. Charta der Grundrechte der Europäischen Union. European Parliment. 2000. URL: https://www.europarl.europa.eu/charter/pdf/text_de.pdf [accessed 2025-04-24]
2. Prisons and health. World Health Organization. URL: https://www.who.int/europe/health-topics/prisons-and-health [accessed 2022-07-17]
3. United Nations Office on Drugs and Crime. Good governance for prison health in the 21st century: a policy brief on the organization of prison health. World Health Organization. 2013. URL: https://iris.who.int/handle/10665/326388 [accessed 2022-08-05]
4. Michel L, Lions C, Van Malderen S, et al. Insufficient access to harm reduction measures in prisons in 5 countries (PRIDE Europe): a shared European public health concern. BMC Public Health 2015 Oct 27;15:1093. [doi: 10.1186/s12889-015-2421-y] [Medline: 26507505]
5. Medizin im Justizvollzug [Article in German]. Justizvollzugskrankenhaus NRW. 2022. URL: https://www.jvk.nrw.de/behoerde/Medizin/?print=1 [accessed 2023-11-22]

XSL•FO
RenderX

6. Rieser S. Medizinische probleme im Justizvollzug: kein platz für psychisch kranke [Article in German]. Deutsches Ärzteblatt. 1999. URL: https://www.aerzteblatt.de/archiv/17148/Medizinische-Probleme-im-Justizvollzug-Kein-Platz-fuer-psychisch-Kranke [accessed 2023-11-22]
7. Tag B, Hillenkamp T, editors. Intramurale Medizin Im Internationalen Vergleich: Gesundheitsfürsorge Zwischen Heilauftrag Und Strafvollzug Im Schweizerischen Und Internationalen Diskurs [Book in German]: Springer; 2008. [doi: 10.1007/978-3-540-77770-0]
8. Stephan B, Girbig G, Augustin M, et al. The value of hybrid teledermatology in German prisons: analysis of routine telemedical data. Telemed J E Health 2023 Nov;29(11):1642-1649. [doi: 10.1089/tmj.2022.0467] [Medline: 36927064]
9. Harzke AJ, Baillargeon JG, Pruitt SL, Pulvino JS, Paar DP, Kelley MF. Prevalence of chronic medical conditions among inmates in the Texas prison system. J Urban Health 2010 May;87(3):486-503. [doi: 10.1007/s11524-010-9448-2] [Medline: 20393884]
10. Wilper AP, Woolhandler S, Boyd JW, et al. The health and health care of US prisoners: results of a nationwide survey. Am J Public Health 2009 Apr;99(4):666-672. [doi: 10.2105/AJPH.2008.144279] [Medline: 19150898]
11. Vera-Remartínez EJ, Borraz-Fernández JR, Domínguez-Zamorano JA, et al. Prevalencia de patologías crónicas y factores de riesgo en población penitenciaria española [Article in Spanish]. Rev Esp Sanid Penit 2014;16(2):38-47. [doi: 10.4321/S1575-06202014000200003] [Medline: 25072788]
12. Opitz-Welke A, Lehmann M, Seidel P, Konrad N. Medicine in the penal system. Dtsch Arztebl Int 2018 Nov 30;115(48):808-814. [doi: 10.3238/arztebl.2018.0808] [Medline: 30642429]
13. Wirtz AL, Yeh PT, Flath NL, Beyrer C, Dolan K. HIV and viral hepatitis among imprisoned key populations. Epidemiol Rev 2018 Jun 1;40(1):12-26. [doi: 10.1093/epirev/mxy003] [Medline: 29688317]
14. Freudenberg N. Jails, prisons, and the health of urban populations: a review of the impact of the correctional system on community health. J Urban Health 2001 Jun;78(2):214-235. [doi: 10.1093/jurban/78.2.214] [Medline: 11419576]
15. Keppler K, Stöver H, editors. Gefängnismedizin: Medizinische Versorgung Unter Haftbedingungen [Book in German]: Thieme; 2009. [doi: 10.1055/b-002-29668]
16. Lehmann M, editor. Gesundheit Und Haft: Handbuch Für Justiz, Medizin, Psychologie Und Sozialarbeit [Book in German]: Pabst, Wolfgang Science; 2014.
17. Kränzlein H. Medizinische versorgung in den bayerischen justizvollzugsanstalten [Article in German]. Bayerischer Landtag. 2016 Jun 30. URL: https://www.bayern.landtag.de/www/ElanTextAblage_WP17/Drucksachen/Schriftliche%20Anfragen/17_0014048.pdf [accessed 2025-04-24]
18. Kosten des vollzuges [Article in German]. Justiz NRW. 2018. URL: https://www.justiz.nrw.de/Gerichte_Behoerden/zahlen_fakten/statistiken/justizvollzug/kosten.pdf [accessed 2025-04-24]
19. Bundesministerium der Justiz. Auskunft nach dem informationsfreiheitsgesetz: informationen zu unterbringungskosten von strafgefangenen in justizvollzugsanstalten [Article in German]. FragDenStaat. 2011. URL: https://fragdenstaat.de/anfrage/inhaftierungskosten-in-justizvollzugsanstalten/763/anhang/2011_12_22_antwort_bmj.pdf [accessed 2025-04-24]
20. Expertenkommission medizinkonzept [Article in German]. Baden-Württemberg Ministerium der Justiz für Europa. 2021. URL: https://jum.baden-wuerttemberg.de/de/justiz/justizvollzug/expertenkommission-medizinkonzept [accessed 2025-05-7]
21. Niedersachsen J. Telemedizin [Article in German]. Gefängnisseelsorge. 2022. URL: https://gefaengnisseelsorge.net/telemedizin [accessed 2025-04-24]
22. Saigí-Rubió F, Borges do Nascimento IJ, Robles N, et al. The current status of telemedicine technology use across the World Health Organization European Region: an overview of systematic reviews. J Med Internet Res 2022 Oct 27;24(10):e40877. [doi: 10.2196/40877] [Medline: 36301602]
23. Arbeitsgemeinschaft der deutschen Ärztekammern. 121. Deutscher Arztetag [Article in German]. Deutsches Ärzteblatt. 2018. URL: https://www.aerzteblatt.de/down.asp?id=20974 [accessed 2023-09-26]
24. Finckh M, Ernst G. Telemedizin im justizvollzug: Baden-Württemberg [Article in German]. Council of Europe. 2018 Jun. URL: https://rm.coe.int/finckh-martin-and-ernst-guido-ppp-telemedizin-baden-wurttemberg-cdpps/1680ab929f [accessed 2022-07-01]
25. Landesjustizverwaltungen der Länder. Verzeichnis der vollzugsanstalten in der Bundesrepublik Deutschland [Article in German]. Justizportal des Bundes und der Länder. 2023. URL: https://justiz.de/onlinedienste/vollstreckungsplaene/vollzugsanstalten_deutschland.pdf [accessed 2023-04-04]
26. Stephan B, Girbig G, Scherer M, Blozik E, Augustin M. [Dermatological video consultations for German prisons: experiences from teledermatological consultations 2020 to 2022] [Article in German]. Dermatologie (Heidelb) 2022 Nov;73(11):859-865. [doi: 10.1007/s00105-022-05060-y] [Medline: 36149473]
27. Augustin M, Djamei V, Elsner P, et al. WITHDRAWN: S2k-Guideline for Teledermatology. J Dtsch Dermatol Ges 2021 Dec 21. [doi: 10.1111/ddg.14615] [Medline: 34932269]
28. Der ärztliche bereitschaftsdienst: die nummer mit den elfen [Article in German]. Kassenärztliche Bundesvereinigung. 2019. URL: https://www.kbv.de/media/sp/KBV_klartext_2019-3.pdf [accessed 2025-04-28]
29. Gebührenordnung für ärzte [Article in German]. Bundesministerium der Justiz. 2023. URL: https://www.gesetze-im-internet.de/go__1982/ [accessed 2023-09-26]

XSL•FO
RenderX

30. Versichertenbefragung der kassenärztlichen bundesvereinigung 2021: ergebnisse einer repräsentativen bevölkerungsumfrage [Article in German]. Kassenärztliche Bundesvereinigung. 2021. URL: https://www.kbv.de/media/sp/2021_KBV-Versichertenbefragung_Berichtband.pdf [accessed 2025-04-24]
31. McDonald DC. Medical care in prisons. Crime and Justice 1999 Jan;26:427-478. [doi: 10.1086/449301]
32. Edge C, Black G, King E, George J, Patel S, Hayward A. Improving care quality with prison telemedicine: the effects of context and multiplicity on successful implementation and use. J Telemed Telecare 2021 Jul;27(6):325-342. [doi: 10.1177/1357633X19869131] [Medline: 31640460]
33. Zincone LH, Doty E, Balch DC. Financial analysis of telemedicine in a prison system. Telemed J 1997;3(4):247-255. [doi: 10.1089/tmj.1.1997.3.247] [Medline: 10176005]
34. Kis A, Augustin J. Zugang zur gesundheitsversorgung in der fläche [Article in German]. Hautarzt 2022 Jan;73(1):40-46. [doi: 10.1007/s00105-021-04916-z] [Medline: 34846553]
35. Reinders P, Augustin M, Kirsten N, Fleyder A, Otten M. Digital health interventions in dermatology-mapping technology and study parameters of systematically identified publications. J Eur Acad Dermatol Venereol 2023 Dec;37(12):2440-2449. [doi: 10.1111/jdv.19392] [Medline: 37528462]

Abbreviations

KBV: Kassenaerztliche Bundesvereinigung
MBO-Ä: Muster-Berufsordnung für die in Deutschland tätigen Ärztinnen und Ärzte

Edited by C Lovis; submitted 22.03.24; peer-reviewed by G Mattson, S Gulliver; revised version received 20.11.24; accepted 23.01.25; published 07.05.25.

Please cite as:
Stephan B, Gehrdau K, Sorbe C, Augustin M, Scherer M, Kis A
Benefits and Limitations of Teledermatology in German Correctional Facilities: Cross-Sectional Analysis
JMIR Med Inform 2025;13:e58712
URL: https://medinform.jmir.org/2025/1/e58712
doi:10.2196/58712

© Brigitte Stephan, Kathrin Gehrdau, Christina Sorbe, Matthias Augustin, Martin Scherer, Anne Kis. Originally published in JMIR Medical Informatics (https://medinform.jmir.org), 7.5.2025. This is an open-access article distributed under the terms of the Creative Commons Attribution License (https://creativecommons.org/licenses/by/4.0/), which permits unrestricted use, distribution, and reproduction in any medium, provided the original work, first published in JMIR Medical Informatics, is properly cited. The complete bibliographic information, a link to the original publication on https://medinform.jmir.org/, as well as this copyright and license information must be included.

XSL•FO
RenderX

Networked Behaviors Associated With a Large-Scale Secure Messaging Network: Cross-Sectional Secondary Data Analysis

Laura Rosa Baratta[1], BS; Linlin Xia[2], BS; Daphne Lew[3], MPH, PhD; Elise Eiden[4], MS; Y Jasmine Wu[5], PhD; Noshir Contractor[6], PhD; Bruce L Lambert[7], PhD; Sunny S Lou[3,4], MD, PhD; Thomas Kannampallil[3,4,8], PhD

[1]Division of Biology & Biomedical Sciences, Washington University School of Medicine in St. Louis, St. Louis, MO, United States

[2]Division of Computational & Data Sciences, Washington University in St. Louis, St. Louis, MO, United States

[3]Institute for Informatics, Data Science & Biostatistics (I2DB), Washington University School of Medicine in St. Louis, 660 South Euclid Avenue, Campus Box 8054, St. Louis, MO, United States

[4]Department of Anesthesiology, Washington University School of Medicine in St. Louis, St. Louis, MO, United States

[5]The Wharton School, University of Pennsylvania, Philadelphia, PA, United States

[6]Department of Industry Engineering and Management Science, Northwestern University, Evanston, IL, United States

[7]Department of Communication Studies, Northwestern University, Evanston, IL, United States

[8]Department of Computer Science and Engineering, Washington University in St. Louis, St. Louis, MO, United States

Corresponding Author:
Thomas Kannampallil, PhD
Institute for Informatics, Data Science & Biostatistics (I2DB), Washington University School of Medicine in St. Louis, 660 South Euclid Avenue, Campus Box 8054, St. Louis, MO, United States

Abstract

Background: Communication among health care professionals is essential for effective clinical care. Asynchronous text-based clinician communication—secure messaging—is rapidly becoming the preferred mode of communication. The use of secure messaging platforms across health care institutions creates large-scale communication networks that can be used to characterize how interaction structures affect the behaviors and outcomes of network members. However, the understanding of the structure and interactions within these networks is relatively limited.

Objective: This study investigates the characteristics of a large-scale secure messaging network and its association with health care professional messaging behaviors.

Methods: Data on electronic health record–integrated secure messaging use from 14 inpatient and 282 outpatient practice locations within a large Midwestern health system over a 6-month period (June 1, 2023, through November 30, 2023) were collected. Social network analysis techniques were used to quantify the global (network)- and node (health care professional)-level properties of the network. Hierarchical clustering techniques were used to identify clusters of health care professionals based on network characteristics; associations between the clusters and the following messaging behaviors were assessed: message read time, message response time, total volume of messages, character length of messages sent, and character length of messages received.

Results: The dataset included 31,800 health care professionals and 7,672,832 messages; the resultant messaging network consisted of 31,800 nodes and 1,228,041 edges. Network characteristics differed based on practice location and professional roles (P<.001). Specifically, pharmacists and advanced practice providers, as well as those working in inpatient settings, had the highest values for all network metrics considered. Four clusters were identified, representing differences in connectivity within the network. Statistically significant differences across clusters were identified between all considered secure messaging behaviors (P<.001). One of the clusters with 1109 nodes, consisting mostly of physicians and other inpatient health care professionals, had the highest values for all node-level metrics compared to the other clusters found. This cluster also had the quickest message read and response times and handled the largest volume of messages per day.

Conclusions: Secure messaging use within a large health care system manifested as an expansive communication network where connectivity varied based on a health care professional's role and their practice setting. Furthermore, our findings highlighted a relationship between health care professionals' connectivity in the network and their daily secure messaging behaviors. These findings provide insights into the complexities of communication and coordination structures among health care providers and downstream secure messaging use. Understanding how secure messaging is used among health care professionals can offer insights into interventions aimed at streamlining communication, which may, in turn, potentially enhance clinician work behaviors and patient outcomes.

XSL•FO
RenderX

(JMIR Med Inform 2025;13:e66544) doi:10.2196/66544

KEYWORDS

communication; electronic health record; EHR; interprofessional communication; secure messaging; social network analysis; social network; interprofessional; messaging network; messaging; health care communication; message; network analysis; behavior; messaging platforms

Introduction

Communication among health care professionals is key to effective clinical care, with reports suggesting that health care professionals spend >80% of their time on clinical communication [1,2]. Although face-to-face communication is often preferred, it is often not possible due to a lack of geographical proximity or other constraints [3]. As such, health care professionals rely on a number of synchronous (eg, phone) or asynchronous (eg, secure messaging, email, and pager) modes of communication. Asynchronous text-based communication—generally referred to as secure messaging—can be used either within the electronic health record (EHR) or through independent secure mobile platforms and is rapidly becoming the primary mode of communication in modern clinical settings [4]. Although recent studies have described the use of secure messaging in large health systems and its impact [5-10], our understanding of the structure and interactions within large clinical secure messaging networks is relatively limited.

Social network analysis methods allow for the quantitative and qualitative characterization of communication networks, including the behavioral patterns of use, interactions, spread of content or actions, and temporal changes in behaviors [11-13]. In other words, these approaches help in characterizing overall social interaction structure while simultaneously allowing for the investigation of how indirect connections, position within a network, and involvement of individual participants affect the behaviors, attitudes, and outcomes of other network members [14-22].

Prior studies using such methods for exploring interactive clinician-to-clinician communication have primarily relied on self-reported data (eg, surveys and interviews) using relatively small sample sizes of participants [23-31]. More recent studies have sought to characterize the communication behaviors of clinicians, often in specific patient populations (eg, patients with cancer) [32,33]. For example, Steitz et al [33] ascertained the communication network of care teams and characterized the message volume exchanged regarding breast cancer patients.

In contrast to prior studies, this study aims to understand the structure of secure messaging behaviors among health care professionals from a social network perspective. The primary aims of this study are (1) to characterize the network properties of a large-scale EHR-integrated secure messaging network and (2) to determine the association between network properties (eg, connectivity) and health care professionals' messaging behaviors.

Methods

Study Setting

This was a cross-sectional study conducted at 14 inpatient hospitals and 282 outpatient clinics affiliated with BJC HealthCare and Washington University School of Medicine. Hospitals and clinics included both academic and community practice settings serving diverse rural, suburban, and urban populations across Missouri and Illinois. All hospitals and clinics used the same Epic EHR system (Epic Systems Corporation).

Epic's Secure Chat virtual messaging platform is embedded within the EHR and allows health care professionals to send and receive messages. Messages are organized (ie, "threaded") as conversations, and a patient identifier can be attached (as needed) to a conversation to facilitate direct patient chart access from the conversation. Secure Chat was launched across all study sites in September 2019 and is accessible through the desktop and mobile versions of Epic.

Data Collection

Event logs related to secure messaging in dyadic conversations (ie, between pairs of health care professionals) using Epic's Secure Chat were retrieved from Epic EHR's Clarity database for the period June 1, 2023, through November 30, 2023. The choice of this period for the secure messaging data was primarily based on pragmatic considerations related to the availability of a continuous sample of data for at least 6 months, with no periods of missing data.

Communication event logs included time stamps recording when messages were sent and received, when messages were read (if they were), and when messages were responded to (if they were); the conversation thread to which a message belonged (ie, a conversation ID); the identities of the sender and receiver of the message; and the character length of each message. Additional metadata included both the senders' and receivers' most recent professional roles and most common practice locations. The content of the included messages was not retrieved or used for this study.

Data Analysis

Data Categorization

The data contained a total of 74 unique health care professional roles, which were categorized into the following: physician, nurse, pharmacist, advanced practice provider (APP, ie, nurse practitioner or physician assistant), therapist (physical, occupational, or speech language), medical assistant or technician, social worker or case management, or other (as reported previously [5]). Practice locations were categorized as inpatient or outpatient.

XSL•FO
RenderX

Network Analysis

Developing the Messaging Network

We constructed a global secure messaging network of dyadic conversations. Each node represented a health care professional who sent at least 1 message during the study period (June 1, 2023, through November 30, 2023). Edges were constructed between individuals if at least one message was sent between them, and edge directionality was maintained to indicate the sender and the receiver. Pairs of nodes could have a maximum of 2 edges between them, representing reciprocated communication. Edge weights were assigned as the sum of the total character length sent among all messages by the sender to the corresponding receiver over the study period.

The giant connected component (GCC)—a maximum set of nodes such that each included node can be reached from any other node regardless of the direction of the edges [34]—was used for subsequent characterizations and analyses. We excluded nonconnected nodes since our study period is a cross-sectional snapshot in time, and it was very likely that nonconnected individuals are either remnants of closed conversations or the beginning conversations of a new user.

Network Characteristics

To illustrate the structural properties of the network, we generated node-level and global metrics. Node-level metrics represent the importance, social power, and control of information flow among nodes based on their connectivity within a network [35]. We included the following commonly used node-level network metrics (see detailed descriptions and examples in Table 1): indegree [36], outdegree [36], closeness [26,37-39], eigenvector [37,39,40], betweenness centrality [26,36-41], and local clustering coefficient [35,37,38]. These network metrics provide insights into how users participate and shape communication dynamics (see Table 1). For example, closeness centrality indicates users who can easily reach—or be reached by—others due to their positional proximity in the network to all other users; similarly, the clustering coefficient measures a tendency of a user's contacts to also communicate with each other, revealing whether a user is communicating with mutually connected contacts.

Table . Definition and clinical implications for node-level network metrics.

Network metric	Definition	Clinical implications
Indegree	Number of incoming connections; edge weights were not considered.	The number of health care professionals a given health care professional sends messages to.
Outdegree	Number of outgoing connections; edge weights were not considered.	The number of health care professionals a given health care professional is receiving messages from.
Closeness centrality	The inverse of the sum of the lengths of the shortest paths, where a path is a sequence of nodes in which consecutive pairs of nonrepeating nodes are linked by an edge, to all other nodes. N−1∑ydy,x where N is the total number of nodes; $d(x,y)$ is the length of the shortest, inverse-weighted path between x and y, where the weighted, shortest path is the minimum sum of weights for a given distance between nodes x and y.	Health care professionals with greater closeness have the shortest path lengths to all other users. Health care professionals with higher closeness can more quickly disseminate information throughout the entire network.
Eigenvector centrality	Proportional to the sum of the centralities of a given node's neighbors. xi1λ∑j=1naijxj where x denotes the centrality of nodes i and j, and a represents whether an edge exists (a=edge weight) or not (a=0) between nodes i and j. Edge weights were considered.	A measure of the influence of a health care professional based on their connection to other well-connected individuals. A health care professional with a high eigenvector is centrally in direct communication with highly connected individuals in the network, and they have many connections to others. These individuals potentially receive a greater amount of incoming information from their incoming connections and can spread that information more efficiently through their outgoing connections.
Betweenness centrality	The number of shortest paths that pass through a given node. ∑s,t∈ VGvσstvσst σ_{st} denotes the weighted shortest path, the minimum sum of the inverse of the edge weights, between nodes s and t, and $\sigma_{st}(v)$ is the weighted shortest path through node v.	The extent to which a health care professional must act as a communication bridge or mediator between other health care professionals who are not directly connected. These individuals can act as connectors or brokers among groups of individuals who are not otherwise currently communicating.
Clustering coefficient	The fraction of pairs of nodes, which are neighbors of a given node, that are connected to each other by edges. Edge weights were not considered.	The tendency for a node to be embedded in a dense local neighborhood. Indicates the extent of clique structure for a given node.

XSL•FO
RenderX

Global network metrics help to understand the overall connectivity of the communication network (see detailed descriptions and examples in Table 2). Global metrics included the following: overall network density [40], reciprocity [26,35], diameter [36], transitivity [35,42], and assortativity [41]. These global-level measures illustrate the collective communication interactions to assess aspects such as the network's cohesion, reachability, and structure. For example, the network density metric captures the proportion of connections relative to all possible connections in a network of a given size (total number of nodes), signifying the overall level of interactions; similarly, the diameter numerically indicates the longest shortest path between any two individuals, providing a sense of the greatest number of steps it takes to traverse the network (see Table 2).

Table . Definition and clinical implications for global-level network metrics.

Network metric	Definition	Clinical implications
Density	The ratio of actual connections to the possible connections. Edge weights were ignored.	Indicates how cohesive the communication network is. Higher density indicates a more cohesive communication network, showing that health care professionals are directly communicating with the majority of the other health care professionals within the network.
Reciprocity	The ratio of directional connections that are reciprocated. Edge weights were not considered.	Indicates whether health care professionals receive responses for messages they send out to other users. This indicates how mutual communication is between individuals in the network.
Diameter	The longest distance, where distance is the sum of the edge weight between the farthest nodes, to traverse the entire network. Edge weights were considered.	An indication of how expansive the network is in terms of the longest path consisting of communicating health care professionals.
Transitivity	The fraction of pairs of neighboring nodes of a given node that are connected to each other by edges. Edge weights were not considered.	The likelihood that two providers sharing a messaging partner are also messaging each other. This could signify that a network is composed of a lot of small cliques as opposed to wide-reaching communication cascades.
Assortativity	Determines the tendency of edges to connect similar nodes by calculating the fraction of edges that connect nodes of the same class for a given node attribute (eg, location, health care professional role, and total degree). Edge weights were not considered.	Quantifies whether nodes directly communicating with one another in a network generally share characteristics or differ.

K-Core Hierarchy

To explore the connective hierarchy of nodes within the global network, a k-core decomposition was constructed to categorize nodes into hierarchical bins. K-core decomposition is used to identify progressively central cores and discover the structural hierarchy of a network [43]. Previous studies have shown that identifying influential nodes using the k-core approach enables the discovery of central nodes that are highly influential in the transfer of information, in the contagion process, and in the resilience of the system [44,45].

In the secure messaging network, we performed a k-core decomposition based on the outdegree properties to identify the central (ie, influential) health care professionals. K-cores were based on the median and IQR of the outdegrees of the GCC such that the 25th percentile, median, and 75th percentile delineated the cores into 4 groups. Individual nodes were then sorted into each core depending on their outdegree and whether it was equal to or above the designated outdegree for that core. The k-core labeled as the first core had the health care professionals with the highest quartile of outdegrees, and the k-core labeled as the fourth core had individuals in the lowest quartile of outdegrees.

Clusters of Secure Messaging Health Care Professionals

To determine the association between a health care professional's network characteristics and their behavioral messaging characteristics, we used a hierarchical clustering analysis to determine clusters based on network characteristics. We then clustered the health care professionals into clusters using node-level metrics (see Table 1). Features were standardized to a unit variance and a mean of zero to ensure consideration of all features as equally important in the clustering algorithm. To determine the optimal number of clusters, we calculated the silhouette score for values of 2 through 10 possible clusters.

Secure Messaging Behaviors

For each health care professional, we generated 4 measures related to secure messaging behaviors. Average read time for a message was calculated as the difference between a message's sent timestamp and its read timestamp; average response time for a message was calculated as the time difference between the first message sent by a sender and the first message sent by the responder in a conversation. The average total volume of messages included the total of both sent and received messages for a health care professional per day. Finally, the average character length per message sent and received for each health

XSL•FO
RenderX

care professional was calculated as the number of characters of the messages' text including spaces but excluding trailing spaces.

Statistical Analysis

Descriptive statistics for continuous metrics were calculated as medians and IQRs. Due to the nonnormal distribution of both the network and secure messaging metrics, nonparametric tests were used to test for statistical significance. Specifically, Mann-Whitney *U* tests were used to assess the differences in each numerical network metric between location setting categories (inpatient vs outpatient), the median differences were reported, and 95% CI were generated with bootstrapping for this comparison; Kruskal-Wallis tests were used to assess the differences in each network metric among the 8 health care professional role categories. Furthermore, chi-square tests were used to investigate whether the distribution of practice locations differed among the k-core hierarchy groups and for the distribution differences of health care professional roles per k-core. Finally, Kruskal-Wallis and a post hoc test, Wilcoxon rank-sum tests, were used to assess the differences between the secure messaging behaviors across clusters. Median differences and 95% CIs were reported for each comparison.

Data processing and clustering analysis were performed using Python 3.9.7 with the iGraph [46] and NetworkX [47] packages for network construction and network metric outputs and Scikit-learn [48] for hierarchical clustering. Statistical analyses were performed in R version 4.2.2 (R Foundation for Statistical Computing).

Ethical Considerations

This study was approved by the Washington University institutional review board (IRB) with a waiver for informed consent (IRB #202205084). This was a retrospective study, and participants' data were deidentified (eg, grouped based on IDs and roles) for analysis, and only trained researchers who were approved by the Washington University IRB office had access to the data. The participants were not compensated.

Results

Overall Messaging Patterns

This study included 31,800 health care professionals and 7,672,832 messages within 1,539,059 dyadic conversations. The included health care professionals practiced at 14 inpatient and 282 outpatient locations. Health care professionals had a median of 16 (IQR 4 - 49) messaging partners over the study period.

The network included 31,800 nodes and 1,228,041 edges. The GCC comprised 29,808 nodes (93.7% of total nodes) and 1,225,307 edges (99.8% of total edges). The GCC had a low density of 0.00138 and a low transitivity of 0.09. The GCC diameter was 65,078. However, the reciprocity was high, 0.92, indicating most individuals received reciprocated responses to their messages. Assortativity over the GCC was found to be 0.044, 0.41, and 0.001 for the total degree (ie, the sum of indegree and outdegree), practice setting (ie, inpatient vs outpatient), and provider group (eg, pharmacists), respectively.

Network Characteristics

Inpatient vs Outpatient Practice Setting

Health care professionals who practiced in an inpatient setting had significantly higher values (all $P<.001$) for the following network metrics compared with those who practiced in outpatient settings: eigenvector centrality (median –6.9e-11, 95% CI –1.0e-10 to –4.2e-11), betweenness centrality (median –174, 95% CI –359 to –72), outdegree (median 11, 95% CI 10 - 11), and indegree (median 11, 95% CI 9 - 11; Table 3). However, the local clustering coefficient and closeness were not statistically different between practice settings.

XSL•FO
RenderX

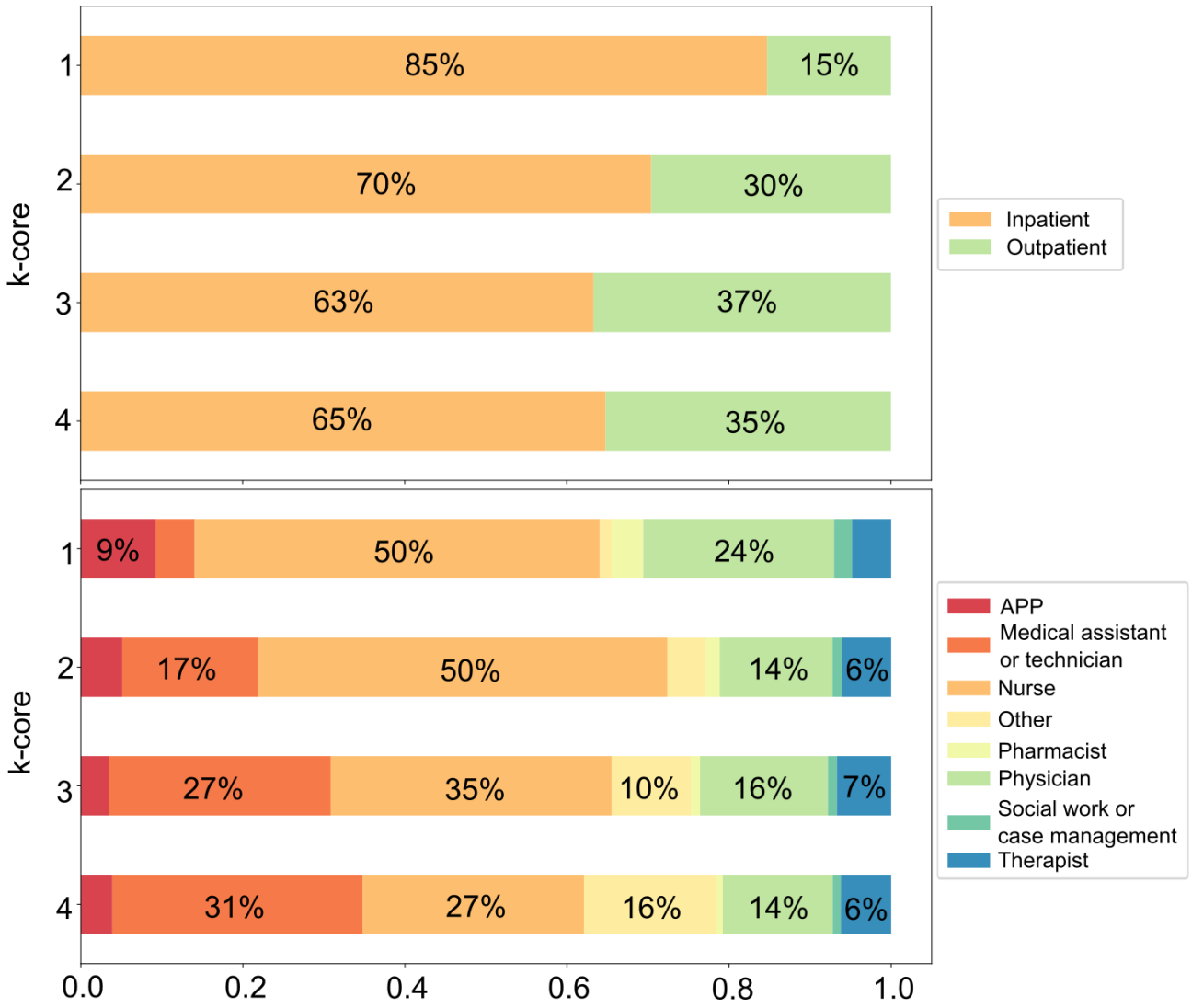
Table . Node-level properties stratified by location and clinical role.

	Eigenvector centrality, median (IQR)	Betweenness, median (IQR)	Clustering coefficient, median (IQR)	Outdegree, median (IQR)	Indegree, median (IQR)	Closeness, median (IQR)
Location						
Inpatient	1.6e-10 (6.6e-12 to 3.5e-09)	4 (0 to 59,612)	0.121 (0.049 to 0.231)	22 (5 to 60)	22 (6 to 60)	206 (156 to 241)
Outpatient	2.3e-10 (8.4e-12 to 4.3e-09)	178 (0 to 90,139)	0.120 (0.017 to 0.31)	11 (3 to 28)	11 (4 to 28)	207 (160 to 240)
Clinical role						
Advanced practice provider	6.8e-10 (3.7e-11 to 1.4e-08)	59,611 (0 to 301,500)	0.094 (0.043 to 0.19)	36 (9 to 102)	36 (10 to 107)	230 (191 to 254)
Medical assistant or technician	2.4e-11 (1.1e-12 to 4.9e-10)	0 (0 to 29,806)	0.150 (0 to 0.333)	7 (2 to 18)	7 (3 to 17)	176 (124 to 218)
Nurse	3.9e-10 (2e-11 to 5.7e-09)	54 (0 to 59,610)	0.147 (0.073 to 0.244)	26 (8 to 58)	27 (9 to 58)	218 (174 to 246)
Other	1.4e-12 (6.5e-15 to 5.5e-11)	0 (0 to 29,806)	0.134 (0 to 0.429)	4 (2 to 13)	5 (2 to 12)	136 (87 to 194)
Pharmacist	1.0e-09 (9.2e-11 to 1.2e-08)	31,331 (0 to 175,330)	0.110 (0.063 to 0.217)	53 (16 to 134)	47 (16 to 116)	229 (199 to 252)
Physician	9.2e-10 (7e-11 to 1.3e-08)	9701 (0 to 166,441)	0.068 (0.036 to 0.121)	24 (6 to 90)	27 (8 to 98)	221 (184 to 250)
Social work or case management	7.1e-10 (3.7e-11 to 9.6e-09)	36,015 (0 to 275,353)	0.144 (0.074 to 0.225)	33 (8 to 80)	32 (8 to 81)	229 (198 to 258)
Therapist	3.8e-11 (2.5e-12 to 6.7e-10)	0 (0 to 29,806)	0.143 (0.053 to 0.286)	14 (4 to 39)	15 (5 to 40)	195 (159 to 224)

The distribution of health care professionals into the 4 k-core layers was found to be significantly different between the practice locations (ie, inpatient and outpatient settings) (P<.001; Figure 1). The innermost central core had 30.4% (6423/21,133) of inpatient health care professionals as compared to 22.5% (4761/21,133) of inpatient health care professionals in the outermost peripheral core. Additionally, the innermost central core had 13.4% (1159/8662) of outpatient health care professionals as compared to 29.9% (2586/8662) of outpatient professionals in the outermost peripheral core.

XSL•FO
RenderX

Figure 1. Distribution of users into the 4 k-core among each location and clinical role. Segments >5% were labeled with the percentage. APP: advanced practice provider.



Differences by Health Care Professional Role

There were statistically significant differences in all network metrics between health care professionals based on clinical role (P<.001 for all metrics; Table 3). Pharmacists and APPs had the highest values for all the network metrics, whereas medical assistants had the lowest values. For example, pharmacists had a median indegree of 47 (IQR 16 - 116) and APPs had a median indegree of 36 (IQR 10 - 107), while medical assistants had a median indegree of 7 (IQR 3 - 17).

The distribution of health care professionals among the 4 k-core layers was significantly different across the health care professional roles (P<.001; Figure 1). There were 52.1% (290/557) of pharmacists in the innermost central core and 43% (701/1629) of APPs in the innermost central core, whereas 38.5% (2272/5907) of medical assistants were in the outermost peripheral core.

Clusters and Messaging Behaviors

Hierarchical clustering on the node-level properties resulted in 4 clusters (see Table 4 and Figure 2). Cluster 1 had 82.2% (912/1109) of health care professionals working in an inpatient setting (Table 4). Furthermore, 59.2% (656/1109) of health care professionals in cluster 1 were physicians. The health care professionals in cluster 1 had the highest median values for the node-level metrics, except for the clustering coefficient, compared to the other groups.

Cluster 2 was the largest of the 4 identified clusters and included 62.1% (18,521/29,808) of the health care professionals from the study cohort. Cluster 2 had 68% (12,593/18,509) of health care professionals working in an inpatient setting. Furthermore, 37.4% (6933/18,521; Figure 3) of health care professionals in cluster 2 were nurses. The health care professionals in cluster 2 had the lowest median values for the node-level metrics compared to the other groups.

XSL•FO
RenderX

Table . Hierarchical cluster subgroups including the median (IQR) for the clustered node-level metric features and nonclustered secure message use features. Significance levels for pairwise comparisons with Bonferroni adjustment are indicated by letters a through c, as detailed in the footnote.

	Cluster 1	Cluster 2	Cluster 3	Cluster 4
Health care professionals, n	1109	18,521	8156	2022
Inpatient users, n/N (%)	912/1109 (82.2)	12,593/18,509 (68)	6674/8156 (81.8)	954/2021 (47.2)
Total messages sent over the study period, n	1,954,355	1,324,730	4,088,795	303,170
Total messages received over the study period, n	2,051,809	1,318,498	3,981,352	316,888
Eigenvector centrality, median (IQR)	4.934e-08 (1.473e-08 to 1.459e-07)	3.560e-11 (2.111e-12 to 5.647e-10)	3.927e-09 (4.942e-10 to 2.255e-08)	1.464e-11 (3.633e-13 to 1.896e-10)
Betweenness, median (IQR)	888,661 (233,794 to 3,700,421)	0 (0 to 3883)	64,866 (5270 to 269,634)	0 (0 to 3)
Clustering coefficient, median (IQR)	0.064 (0.051 to 0.087)	0.097 (0 to 0.244)	0.131 (0.082 to 0.194)	0.667 (0.6 to 1)
Outdegree, median (IQR)	265 (220 to 331)	8 (3 to 19)	71 (50 to 104)	6 (2 to 14)
Indegree, median (IQR)	264 (223 to 330)	9 (3 to 19)	70 (50 to 104)	6 (3 to 14)
Closeness, median (IQR)	266 (254 to 277)	180 (135 to 213)	244 (227 to 258)	186 (127 to 236)
Total message volume per day, median (IQR)	34 (25 to 48)	4 (3 to 7)[a]	12 (9 to 18)[a,b]	5 (3 to 8)[a,b,c]
Sent character length per message, median (IQR)	62 (48 to 80)	64 (44 to 93)	66 (52 to 85)[a,b]	49 (33 to 74)[a,b,c]
Received character length per message, median (IQR)	75 (63 to 83)	62 (45 to 86)[a]	61 (51 to 74)[a]	52 (39 to 73)[a,b,c]
Read time minutes, median (IQR)	14 (8 to 24)	22 (6 to 76)[a]	17 (9 to 33)[a,b]	26 (8 to 77)[a,c]
Response time minutes, median (IQR)	19 (13 to 30)	24 (8 to 71)[a]	27 (16 to 47)[a,b]	35 (8 to 107)[a,b,c]

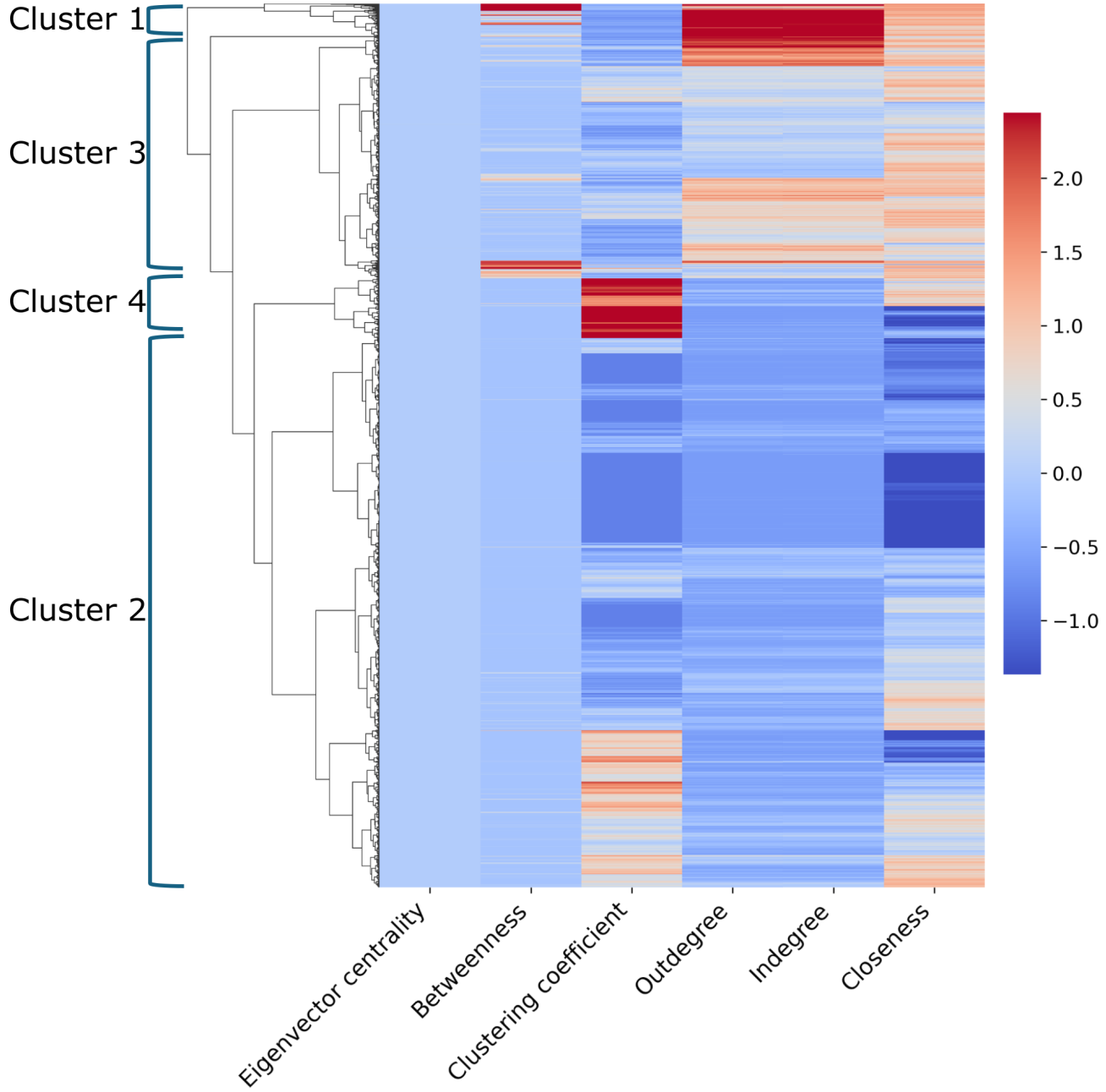
[a]Indicates significant difference (adjusted $P<.001$) compared to group 1.

[b]Indicates significant difference (adjusted $P<.001$) compared to group 2.

[c]Indicates significant difference (adjusted $P<.001$) compared to group 3.

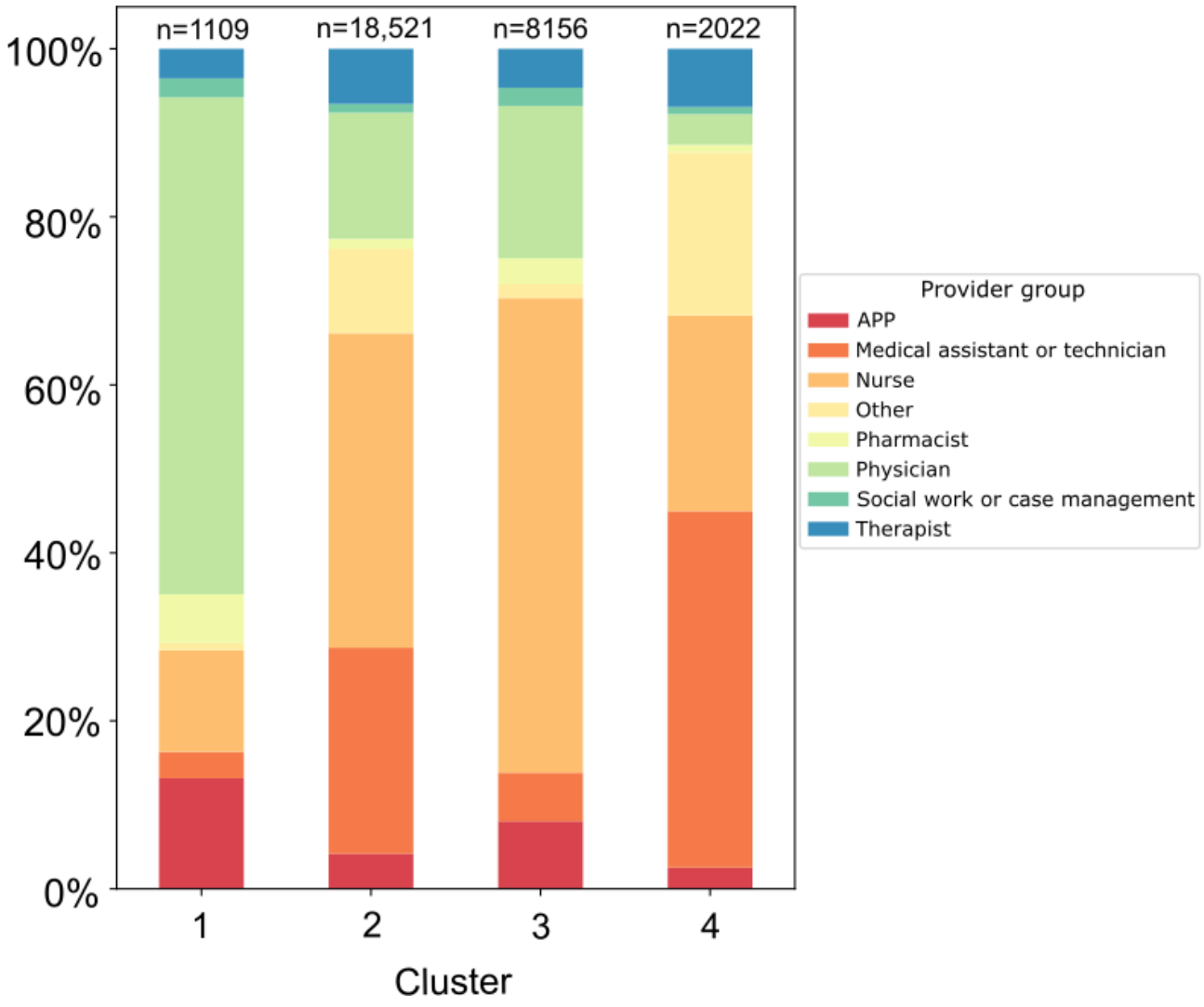
XSL•FO
RenderX

Figure 2. Heatmap for hierarchical clustering of health care professionals based on node-level metrics. The color bar depicts the magnitude of standardized values of the dataset, and the color range is computed with robust quantiles. The blue brackets indicate how clusters were divided into the final 4 groups with associated labels.



XSL•FO
RenderX

Figure 3. Composition of clinical roles within each cluster. APP: advanced practice provider.



Cluster 3 had 81.8% (6674/8156) working in an inpatient setting. Furthermore, 56.5% (4608/8156) of health care professionals in cluster 3 were nurses. Cluster 4 had only 47.2% (954/2022) working in an inpatient setting. Additionally, 42.4% (858/2022) of health care professionals in cluster 4 were medical assistants. The health care professionals in cluster 4 had the highest median value for the clustering coefficient compared to other groups.

There were statistically significant differences in secure messaging behaviors across the 4 clusters (see Table 4, Multimedia Appendix 1; all $P<.001$ and footnotes indicate significant pairwise comparisons among the 4 groups). Compared to the largest subgroup (ie, cluster 2), cluster 1 had the quickest read (median –7.1, 95% CI –8.9 to –5.4 minutes) and response time to messages (median −3.2, 95% CI −4.9 to −1.7 minutes), the largest message volume per day (median 28.4, 95% CI 27.7 - 29.2 messages), as well as the longest message character length (median 9.5, 95% CI 7.9 - 11 characters) (see Table 4). Similarly, compared to cluster 2, cluster 4 health care professionals had slower response times (median 4.1, 95% CI 2.8 - 5.6 minutes) and a marginally larger daily message volume (median 0.3, 95% CI 0.2 - 0.4 messages), as well as sent (median −13.5, 95% CI −15.1 to −12 characters) and received (median −8.8, 95% CI −10.1 to −7.5 characters) the shortest messages.

Discussion

Principal Findings

Based on a large-scale study of over 31,000 health care professionals and more than 7.5 million secure messages, we found that the connectivity of the interactive communication network varied based on health care professionals' roles and their practice settings. Specifically, inpatient health care professionals were generally more central and had the highest incoming and outgoing messaging connectivity compared to outpatient health care professionals, whereas pharmacists were the most central and highly connected among all the clinical roles. Hierarchical clustering analysis highlighted the differences in connectivity among the health care professionals and showed that cluster membership was associated with specific secure messaging behaviors such as read time, response time, total messaging volume per day, and character length per message. For example, cluster 1, which consisted of highly connected and central health care professionals, had the quickest read and response times to secure messages while also managing the largest message volume per day. Although preliminary, our findings highlight that an individual's messaging behaviors are

XSL•FO
RenderX

potentially driven by their networked peers. We describe some of the pragmatic implications of the current findings.

The degree of variation in connectivity between practice settings (ie, inpatient and outpatient) highlights the impact of setting-specific clinical context on resultant communication behaviors. For example, inpatient health care professionals, regardless of their role, had higher network connectivity in the communication network. The greater connectivity highlights their greater need for communication and care coordination, likely owing to the increased complexity of patient care delivery in these settings [49,50]. Ultimately, the setting-specific clinical context influences the extent of secure messaging need and burden.

The degree of variation in connectivity among clinical roles implies a potential relationship between the role-specific clinical context and the extent of secure messaging communication burden. For instance, pharmacists' central position in the network identified them as key players in clinical communication and care management. This has previously been described in other studies that highlighted the central role of pharmacists in medication management and safety [51]. Additionally, in inpatient settings, pharmacists are often embedded within teams to help with coordinating complex medication management of patients, acting as gatekeepers for medication safety [52-54]. Thus, the unique communication needs among specific roles are apparent in the stark difference in secure messaging utilization and burden among professionals in our study.

The hierarchical clustering results revealed a relationship between connectivity within the network and secure messaging behaviors. For instance, health care professionals in cluster 1 were centrally located, highly connected, and acted as communication bridges (see Table 1, betweenness centrality, for definition) and were primarily consisted of physicians and those working in an inpatient setting. Health care professionals in this cluster also had the highest volume of secure messages per day, the longest character length per message received, and the fastest read times compared to the other clusters.

The higher centralization and connectivity in cluster 1 is likely because of their expertise and role, as the cluster is primarily composed of physicians (ie, as a clinical decision leader) [55]. Role-based specialization is common in teams where specialized individuals are relied on for specific expertise leading to targeted communication for specific tasks [55,56]. This is also reflected in cluster 1's increased message volume and messaging behavior, most likely highlighting their role in clinical decision-making. However, such a centralized communication structure may also increase physicians' workload and cognitive burden arising from an increased messaging volume [57].

Similarly, there was one cluster (cluster 4) of nurses and medical assistants who had fewer connections and were not as central within the network. These individuals were mostly involved in "communication cliques" with their immediately connected neighbors (ie, clinical colleagues) such that a given individual's neighbors are also communicating with each other, forming close-knit circles in the network. The higher ratio of local clique structures for this cluster suggests increased mutual interaction and collaboration among health care professionals within a network [58,59]. Furthermore, cluster 4's lower centrality scores (eg, eigenvector, betweenness, and closeness) suggest a more decentralized conversation structure, where communication is more evenly shared [55].

Comparison to Prior Work

Understanding how secure messaging is being used can provide insights into communication and coordination patterns among health care professionals. More cohesive and collaborative networks of health care professionals have been shown to improve care quality for patients [23]. By understanding the state of collaborative interactions, we can potentially develop interventions targeted at improving these relationships and influencing downstream clinician and patient outcomes [26,27]. For example, network characteristics related to connectedness (eg, indegree) and structure (eg, clustering coefficient) can be used to identify "network traffic" and associated communication burden for specific health care professionals [51]. Such information about communication load can be used to develop "triaging strategies," including creating messaging pools, redirecting messages, or assigning personnel for messaging-only roles [60-62]. These strategies have been shown previously to reduce email inbox message volume and self-reported time spent on inbox management [63-65]. Similar strategies could be developed to mitigate the messaging burden among health care professionals.

Similarly, as shown in our hierarchical cluster analysis, there were centrally located clinicians in certain clusters whose messaging behaviors were driven by their extant network. For example, we found that clinicians in cluster 1 were likely to have a higher volume of messages and more likely to read and respond to messages the quickest. Such messaging behaviors are likely to affect their clinical work activities, increasing their likelihood for increased workload, cognitive burden, and errors [10,57]. For example, Lew et al [57] found that inpatient clinicians receiving more messages spent more time on EHR-based work and had increased attention switching (ie, increased cognitive load); similarly, Lou et al [10] found that an increased volume of messages was associated with increased likelihood of wrong-patient ordering errors. The current findings point to the fact that increased messaging volume was potentially associated with their external connectivity, highlighting the role of connected communication partners (ie, network) in increasing workload, cognitive burden, and errors.

Future Directions

Finally, it is important to emphasize that this was a preliminary study. More focused analyses (eg, among subgroups of clinicians such as hospitalists or outpatient clinicians) are necessary to ascertain specific strategies for bottlenecks in communication and improving clinician and patient outcomes.

Limitations

There are several limitations in this study. First, although this study included several inpatient and outpatient settings across academic and community settings (14 hospitals, >250 outpatient locations), all of these were part of the same health care system using the only secure messaging platform available, Epic Secure

XSL•FO
RenderX

Chat. Therefore, the generalizability of this study's findings to other health care systems and other secure messaging platforms may be limited. Second, we only used one form of communication: secure messaging. Other forms of communication (ie, face-to-face, telephone, and pager) were also used by our cohort throughout the study period; therefore, our study likely underrepresents the true communication structures and relationships between health care professionals. Third, our assignment of clinical location (ie, inpatient vs outpatient) was based on log-in information and was potentially imprecise since we did not have access to detailed work schedules.

Conclusions

This study characterized the network properties of a large-scale EHR-integrated secure messaging network using social network analyses. We found that health care professionals' connectivity varied by both role and practice settings. Furthermore, hierarchical clustering indicated a relationship between an individual's network connectivity and secure messaging behaviors. Ultimately, these preliminary findings highlight the importance of understanding secure messaging interactions and resultant secure messaging behaviors, as well as their potential impact on clinical work outcomes.

Conflicts of Interest

None declared.

Multimedia Appendix 1
Additional figures and tables for the statistical analysis of secure messaging behaviors across cluster groups.
[DOCX File, 99 KB - medinform_v13i1e66544_app1.docx]

References

1. Edwards A, Fitzpatrick LA, Augustine S, et al. Synchronous communication facilitates interruptive workflow for attending physicians and nurses in clinical settings. Int J Med Inform 2009 Sep;78(9):629-637. [doi: 10.1016/j.ijmedinf.2009.04.006]
2. Spencer R, Coiera E, Logan P. Variation in communication loads on clinical staff in the emergency department. Ann Emerg Med 2004 Sep;44(3):268-273. [doi: 10.1016/j.annemergmed.2004.04.006] [Medline: 15332070]
3. Manojlovich M, Harrod M, Hofer TP, Lafferty M, McBratnie M, Krein SL. Using qualitative methods to explore communication practices in the context of patient care rounds on general care units. J Gen Intern Med 2020 Mar;35(3):839-845. [doi: 10.1007/s11606-019-05580-9] [Medline: 31832929]
4. Byrd TF IV, Fancher KG, Liebovitz DM, O'Leary KJ. Trends in secure mobile communication technology use among hospitalists in North America, 2016–2021. Health Policy Technol 2022 Dec;11(4):100689. [doi: 10.1016/j.hlpt.2022.100689]
5. Baratta LR, Harford D, Sinsky CA, Kannampallil T, Lou SS. Characterizing the patterns of electronic health record-integrated secure messaging use: cross-sectional study. J Med Internet Res 2023 Oct 6;25:e48583. [doi: 10.2196/48583] [Medline: 37801359]
6. Kwan B, Bell JF, Longhurst CA, Goldhaber NH, Clay B. Implementation of an electronic health record-integrated instant messaging system in an academic health system. J Am Med Inform Assoc 2024 Apr 3;31(4):997-1000. [doi: 10.1093/jamia/ocad253] [Medline: 38287641]
7. Small W, Iturrate E, Austrian J, Genes N. Electronic health record messaging patterns of health care professionals in inpatient medicine. JAMA Netw Open 2023 Dec 1;6(12):e2349136. [doi: 10.1001/jamanetworkopen.2023.49136] [Medline: 38147337]
8. Baratta LR, Lew D, Kannampallil T, Lou SS. Contributors to electronic health record-integrated secure messaging use: a study of over 33,000 health care professionals. Appl Clin Inform 2024 May;15(3):612-619. [doi: 10.1055/s-0044-1787756] [Medline: 39048085]
9. Lou SS, Lew D, Baratta LR, Eiden E, Sinsky CA, Kannampallil T. Secure messaging and telephone use for clinician-to-clinician communication. JAMA Netw Open 2024 Jun 3;7(6):e2417781. [doi: 10.1001/jamanetworkopen.2024.17781] [Medline: 38900428]
10. Lou SS, Lew D, Xia L, Baratta L, Eiden E, Kannampallil T. Secure messaging use and wrong-patient ordering errors among inpatient clinicians. JAMA Netw Open 2024 Dec 2;7(12):e2447797. [doi: 10.1001/jamanetworkopen.2024.47797] [Medline: 39630450]
11. Fowler JH, Christakis NA. Dynamic spread of happiness in a large social network: longitudinal analysis over 20 years in the Framingham Heart Study. BMJ 2008 Dec 4;337:a2338. [doi: 10.1136/bmj.a2338] [Medline: 19056788]
12. Christakis NA, Fowler JH. The collective dynamics of smoking in a large social network. N Engl J Med 2008 May 22;358(21):2249-2258. [doi: 10.1056/NEJMsa0706154] [Medline: 18499567]
13. Christakis NA, Fowler JH. Social contagion theory: examining dynamic social networks and human behavior. Stat Med 2013 Feb 20;32(4):556-577. [doi: 10.1002/sim.5408] [Medline: 22711416]
14. Wellman B, Salaff J, Dimitrova D, Garton L, Gulia M, Haythornthwaite C. Computer networks as social networks: collaborative work, telework, and virtual community. Annu Rev Sociol 1996 Aug;22(1):213-238. [doi: 10.1146/annurev.soc.22.1.213]

XSL•FO
RenderX

15. Garton L, Haythornthwaite C, Wellman B. Studying online social networks. J Comput Mediat Commun 1997;3(1):JCMC313. [doi: 10.1111/j.1083-6101.1997.tb00062.x]
16. Saramäki J, Leicht EA, López E, Roberts SGB, Reed-Tsochas F, Dunbar RIM. Persistence of social signatures in human communication. Proc Natl Acad Sci U S A 2014 Jan 21;111(3):942-947. [doi: 10.1073/pnas.1308540110] [Medline: 24395777]
17. Cho WK, Min B, Goh KI, Kim IM. Generalized priority-queue network dynamics: impact of team and hierarchy. Phys Rev E 2010 Jun;81(6):066109. [doi: 10.1103/PhysRevE.81.066109]
18. Sutanto J, Tan CH, Battistini B, Phang CW. Emergent leadership in virtual collaboration settings: a social network analysis approach. Long Range Plann 2011 Oct;44(5-6):421-439. [doi: 10.1016/j.lrp.2011.09.001]
19. Gloor P, Paasivaara M, Schoder D, Willems P. Correlating performance with social network structure through teaching social network analysis. In: Network-Centric Collaboration and Supporting Frameworks: Springer, Boston, MA; 2006:265-272. [doi: 10.1007/978-0-387-38269-2_28]
20. Jiang ZQ, Xie WJ, Li MX, Podobnik B, Zhou WX, Stanley HE. Calling patterns in human communication dynamics. Proc Natl Acad Sci U S A 2013 Jan 29;110(5):1600-1605. [doi: 10.1073/pnas.1220433110] [Medline: 23319645]
21. Blondel VD, Decuyper A, Krings G. A survey of results on mobile phone datasets analysis. EPJ Data Sci 2015 Dec;4(1):1-55. [doi: 10.1140/epjds/s13688-015-0046-0]
22. Wellman B. For a social network analysis of computer networks: a sociological perspective on collaborative work and virtual community. In: SIGCPR '96: Proceedings of the 1996 ACM SIGCPR/SIGMIS Conference on Computer Personnel Research: Association for Computing Machinery; 1996. [doi: 10.1145/238857.238860]
23. Cunningham FC, Ranmuthugala G, Plumb J, Georgiou A, Westbrook JI, Braithwaite J. Health professional networks as a vector for improving healthcare quality and safety: a systematic review. BMJ Qual Saf 2012 Mar;21(3):239-249. [doi: 10.1136/bmjqs-2011-000187] [Medline: 22129933]
24. Chambers D, Wilson P, Thompson C, Harden M. Social network analysis in healthcare settings: a systematic scoping review. PLoS ONE 2012;7(8):e41911. [doi: 10.1371/journal.pone.0041911] [Medline: 22870261]
25. Sabot K, Wickremasinghe D, Blanchet K, Avan B, Schellenberg J. Use of social network analysis methods to study professional advice and performance among healthcare providers: a systematic review. Syst Rev 2017 Oct 23;6(1):208. [doi: 10.1186/s13643-017-0597-1] [Medline: 29058638]
26. Glegg SMN, Jenkins E, Kothari A. How the study of networks informs knowledge translation and implementation: a scoping review. Implement Sci 2019 Mar 27;14(1):34. [doi: 10.1186/s13012-019-0879-1] [Medline: 30917844]
27. Hu H, Yang Y, Zhang C, Huang C, Guan X, Shi L. Review of social networks of professionals in healthcare settings—where are we and what else is needed? Global Health 2021 Dec 4;17(1):139. [doi: 10.1186/s12992-021-00772-7] [Medline: 34863221]
28. Saatchi AG, Pallotti F, Sullivan P. Network approaches and interventions in healthcare settings: a systematic scoping review. PLoS ONE 2023;18(2):e0282050. [doi: 10.1371/journal.pone.0282050] [Medline: 36821554]
29. Steitz BD, Levy MA. Evaluating the scope of clinical electronic messaging to coordinate care in a breast cancer cohort. Stud Health Technol Inform 2019 Aug 21;264:808-812. [doi: 10.3233/SHTI190335] [Medline: 31438036]
30. Hagedorn PA, Kirkendall ES, Spooner SA, Mohan V. Inpatient communication networks: leveraging secure text-messaging platforms to gain insight into inpatient communication systems. Appl Clin Inform 2019 May;10(3):471-478. [doi: 10.1055/s-0039-1692401] [Medline: 31242514]
31. Powell KR, Popescu M, Alexander GL. Examining social networks in text messages about nursing home resident health status. J Gerontol Nurs 2021 Jul;47(7):16-22. [doi: 10.3928/00989134-20210604-02] [Medline: 34191650]
32. Steitz BD, Unertl KM, Levy MA. Characterizing communication patterns among members of the clinical care team to deliver breast cancer treatment. J Am Med Inform Assoc 2020 Feb 1;27(2):236-243. [doi: 10.1093/jamia/ocz151] [Medline: 31682267]
33. Steitz BD, Unertl KM, Levy MA. An analysis of electronic health record work to manage asynchronous clinical messages among breast cancer care teams. Appl Clin Inform 2021 Aug;12(4):877-887. [doi: 10.1055/s-0041-1735257] [Medline: 34528233]
34. Newman MEJ, Strogatz SH, Watts DJ. Random graphs with arbitrary degree distributions and their applications. Phys Rev E 2001 Jul;64(2):026118. [doi: 10.1103/PhysRevE.64.026118]
35. Oliveira M, Gama J. An overview of social network analysis. Wiley Interdiscip Rev Data Min Knowl Discov 2012;2(2):99-115. [doi: 10.1002/widm.1256]
36. Brunson JC, Laubenbacher RC. Applications of network analysis to routinely collected health care data: a systematic review. J Am Med Inform Assoc 2018 Feb 1;25(2):210-221. [doi: 10.1093/jamia/ocx052] [Medline: 29025116]
37. Farooq A, Joyia GJ, Uzair M, Akram U. Detection of influential nodes using social networks analysis based on network metrics. In: 2018 International Conference on Computing, Mathematics and Engineering Technologies (iCoMET): IEEE; 2018. [doi: 10.1109/ICOMET.2018.8346372]
38. Benham-Hutchins MM, Effken JA. Multi-professional patterns and methods of communication during patient handoffs. Int J Med Inform 2010 Apr;79(4):252-267. [doi: 10.1016/j.ijmedinf.2009.12.005] [Medline: 20079686]

XSL•FO
RenderX

39. Cimenler O, Reeves KA, Skvoretz J. A regression analysis of researchers' social network metrics on their citation performance in a college of engineering. J Informetr 2014 Jul;8(3):667-682. [doi: 10.1016/j.joi.2014.06.004]
40. Brewer BB, Carley KM, Benham-Hutchins M, Effken JA, Reminga J. Exploring the stability of communication network metrics in a dynamic nursing context. Soc Networks 2020 May;61:11-19. [doi: 10.1016/j.socnet.2019.08.003] [Medline: 32863552]
41. Zhu X, Tu SP, Sewell D, et al. Measuring electronic communication networks in virtual care teams using electronic health records access-log data. Int J Med Inform 2019 Aug;128:46-52. [doi: 10.1016/j.ijmedinf.2019.05.012] [Medline: 31160011]
42. DuGoff EH, Fernandes-Taylor S, Weissman GE, Huntley JH, Pollack CE. A scoping review of patient-sharing network studies using administrative data. Transl Behav Med 2018 Jul 17;8(4):598-625. [doi: 10.1093/tbm/ibx015] [Medline: 30016521]
43. Alvarez-Hamelin I, Dall'Asta L, Barrat A, Vespignani A. K-core decomposition: a tool for the analysis of large scale internet graphs. HAL. Preprint posted online on Oct 31, 2005 URL: https://hal.science/hal-00012974v1 [accessed 2025-06-09]
44. Rajeh S, Savonnet M, Leclercq E, Cherifi H. Assessing the relationship between centrality and hierarchy in complex networks. HAL. Preprint posted online on Jan 13, 2021 URL: https://ube.hal.science/hal-03109404 [accessed 2025-06-09]
45. Malvestio I, Cardillo A, Masuda N. Interplay between k-core and community structure in complex networks. Sci Rep 2020;10:14702. [doi: 10.1038/s41598-020-71426-8]
46. Csárdi G, Nepusz T. The igraph software package for complex network research. InterJournal Complex Syst 2006;1695:1-9. [doi: 10.5281/zenodo.3630268]
47. Hagberg AA, Schult DA, Swart PJ. Exploring network structure, dynamics, and function using networkx. In: Varoquaux G, Vaught T, Millman J, editors. Presented at: Proceedings of the 7th Python in Science Conference (SciPy 2008); Aug 19-24, 2008; Pasadena, CA, United States. [doi: 10.25080/TCWV9851]
48. Pedregosa F, Varoquaux G, Gramfort A, et al. Scikit-learn: machine learning in Python. J Mach Learn Res 2011;12:2825-2830 [FREE Full text]
49. Woods DM, Holl JL, Angst D, et al. Advances in patient safety improving clinical communication and patient safety: clinician-recommended solutions. In: Henriksen K, Battles JB, Keyes MA, Grady ML, editors. Advances in Patient Safety: New Directions and Alternative Approaches: Agency for Healthcare Research and Quality (US); 2008.
50. Patel N, Siegler JE, Stromberg N, Ravitz N, Hanson CW. Perfect storm of inpatient communication needs and an innovative solution utilizing smartphones and secured messaging. Appl Clin Inform 2016 Aug 10;7(3):777-789. [doi: 10.4338/ACI-2015-11-RA-0151] [Medline: 27530155]
51. Francis T, Davidson M, Senese L, et al. Exploring the use of social network analysis methods in process improvement within healthcare organizations: a scoping review. BMC Health Serv Res 2024 Sep 5;24(1):1030. [doi: 10.1186/s12913-024-11475-1] [Medline: 39237937]
52. Singer A, Duarte Fernandez R. The effect of electronic medical record system use on communication between pharmacists and prescribers. BMC Fam Pract 2015 Oct 28;16:155. [doi: 10.1186/s12875-015-0378-7] [Medline: 26507839]
53. Pontefract SK, Coleman JJ, Vallance HK, et al. The impact of computerised physician order entry and clinical decision support on pharmacist-physician communication in the hospital setting: a qualitative study. PLoS ONE 2018;13(11):e0207450. [doi: 10.1371/journal.pone.0207450] [Medline: 30444894]
54. Rixon S, Braaf S, Williams A, Liew D, Manias E. Pharmacists' interprofessional communication about medications in specialty hospital settings. Health Commun 2015;30(11):1065-1075. [doi: 10.1080/10410236.2014.919697] [Medline: 25317781]
55. Noyes AL. Navigating the hierarchy: communicating power relationships in collaborative health care groups. Manag Commun Q 2022 Feb;36(1):62-91. [doi: 10.1177/08933189211025737]
56. Ahuja MK, Carley KM. Network structure in virtual organizations. Organ Sci 1999;10(6):741-757. [doi: 10.1111/j.1083-6101.1998.tb00079.x]
57. Lew D, Baratta LR, Xia L, et al. Association of EHR-integrated secure messaging use with clinician workload and attention switching. J Gen Intern Med 2025 Mar 14;doi. [doi: 10.1007/s11606-025-09466-x] [Medline: 40085321]
58. Wasserman S, Faust K. Social Network Analysis: Methods and Applications: Cambridge University Press; 1994. [doi: 10.1017/CBO9780511815478]
59. Freeman LC. Centrality in social networks: conceptual clarification. Soc Netw 1978–1979;1(3):215-239. [doi: 10.1016/0378-8733(78)90021-7]
60. Murphy DR, Giardina TD, Satterly T, Sittig DF, Singh H. An exploration of barriers, facilitators, and suggestions for improving electronic health record inbox-related usability: a qualitative analysis. JAMA Netw Open 2019 Oct 2;2(10):e1912638. [doi: 10.1001/jamanetworkopen.2019.12638] [Medline: 31584683]
61. Rotenstein LS, Landman A, Bates DW. The electronic inbox-benefits, questions, and solutions for the road ahead. JAMA 2023 Nov 14;330(18):1735-1736. [doi: 10.1001/jama.2023.19195] [Medline: 37812413]
62. Murphy DR, Satterly T, Giardina TD, Sittig DF, Singh H. Practicing clinicians' recommendations to reduce burden from the electronic health record inbox: a mixed-methods study. J Gen Intern Med 2019 Sep;34(9):1825-1832. [doi: 10.1007/s11606-019-05112-5] [Medline: 31292905]

XSL•FO
RenderX

63. Fogg JF, Sinsky CA. In-basket reduction: a multiyear pragmatic approach to lessen the work burden of primary care physicians. NEJM Catalyst 2023 Apr 19;4(5):22. [doi: 10.1056/CAT.22.0438]
64. Kurek A, Inman E, Walmer M. The “inboxologist” — a novel approach to in-basket management in primary care. NEJM Catal 2024 Sep 18;5(10):24. [doi: 10.1056/CAT.24.0133]
65. Shumer G, Bhandiwad A, Holkeboer J, Marshall L. Team-based management of high-priority in-basket messages. Ann Fam Med 2024;22(3):260. [doi: 10.1370/afm.3094] [Medline: 38806263]

Abbreviations

APP: advanced practice provider
EHR: electronic health record
GCC: giant connected component
IRB: institutional review board

Edited by A Coristine; submitted 17.09.24; peer-reviewed by S Tsugawa, Y Zhou; revised version received 13.04.25; accepted 14.04.25; published 10.07.25.

Please cite as:
Baratta LR, Xia L, Lew D, Eiden E, Wu YJ, Contractor N, Lambert BL, Lou SS, Kannampallil T
Networked Behaviors Associated With a Large-Scale Secure Messaging Network: Cross-Sectional Secondary Data Analysis
JMIR Med Inform 2025;13:e66544
URL: https://medinform.jmir.org/2025/1/e66544
doi:10.2196/66544

© Laura Rosa Baratta, Linlin Xia, Daphne Lew, Elise Eiden, Y Jasmine Wu, Noshir Contractor, Bruce L Lambert, Sunny S Lou, Thomas Kannampallil. Originally published in JMIR Medical Informatics (https://medinform.jmir.org), 10.7.2025. This is an open-access article distributed under the terms of the Creative Commons Attribution License (https://creativecommons.org/licenses/by/4.0/), which permits unrestricted use, distribution, and reproduction in any medium, provided the original work, first published in JMIR Medical Informatics, is properly cited. The complete bibliographic information, a link to the original publication on https://medinform.jmir.org/, as well as this copyright and license information must be included.

XSL•FO
RenderX

Investigating the Role of Wearable Devices in Facilitating Telehealth Adoption Among the Aging Population: Mediation Analysis of US National Data

Ruijing Wang, MS; Onur Asan, PhD; Ting Liao, PhD

Department of Systems Engineering, Stevens Institute of Technology, 1 Castle Point Terrace, Hoboken, NJ, United States

Corresponding Author:
Ting Liao, PhD
Department of Systems Engineering, Stevens Institute of Technology, 1 Castle Point Terrace, Hoboken, NJ, United States

Abstract

Background: Telehealth adoption has grown significantly, presenting valuable opportunities for the aging population to access health care remotely. Despite evidence of its benefits in managing chronic conditions and promoting independence, many older adults remain hesitant to adopt telehealth, preferring traditional in-person visits even post pandemic. Current literature largely focuses on younger or general populations, overlooking the unique barriers faced by older adults, such as technology literacy and access disparities.

Objective: This study investigates how telehealth adoption among the aging population is influenced and mediated by relevant factors, including the use of wearable devices, demographic factors, health conditions, and physical activity levels.

Methods: A secondary analysis was conducted on the Health Information National Trends Survey (HINTS 6) data collected from March to November 2022. Of the 6252 respondents, 1596 older adults (≥65 years) were included. Telehealth adoption was defined using 2 survey items on receiving or being offered telehealth services. We construct regression and mediation analyses to understand the relationships between telehealth adoption and influential factors, including demographics, physical activity levels, health conditions, and the use of wearable devices.

Results: We found that wearable device use, while not directly significant, plays a critical role in adoption when mediated by factors such as education, income, and general health. Specifically, higher levels of education and income increased the likelihood of telehealth adoption (P<.001), underscoring the importance of socioeconomic status. Additionally, rural versus urban residency emerged as a critical factor (P=.003), with rural residents demonstrating lower adoption rates, highlighting the accessibility and technology literacy barriers in these areas. Health conditions were inversely associated with telehealth adoption, suggesting that healthier individuals may perceive less need for telehealth services. The total effect of wearable use on telehealth adoption was significant (P=.007), with indirect effects via education (P<.001), income (P=.007), and health conditions (P=.004). The findings underscore the role of socioeconomic factors in influencing the adoption of health technologies.

Conclusions: While wearable device use is associated with increased telehealth adoption among older adults, its effect operates primarily through mediating factors such as education, income, and health status. These findings suggest that addressing disparities in socioeconomic status and health literacy is critical to increasing telehealth engagement in aging populations.

(JMIR Med Inform 2025;13:e68559) doi:10.2196/68559

KEYWORDS

telehealth; health outcomes; wearable devices; aging population; mediation analysis

Introduction

Background

The health care system is under growing pressure, including an aging population, long-term health conditions, and increasingly higher standards of care expected by society, government, patients, and professionals [1]. The role of technology in health care has become increasingly important, giving rise to the concepts of telehealth and telemedicine as key components of modern health care systems [2]. While telemedicine specifically refers to the remote diagnosis and treatment of patients through telecommunications technology, telehealth covers a wider range of remote health care services, including remote nonclinical services, public health education services, and instruction to medical students [3]. Wearable devices are defined as consumer-facing, sensor-enabled devices that can continuously or intermittently track health-related data such as physical activity, heart rate, or sleep patterns. Examples include smartwatches, fitness trackers, and health-monitoring rings. These tools play a growing role in personal health management

XSL•FO
RenderX

and are increasingly integrated into remote care models like telehealth.

While there is increasing attention to adopting advanced technology in health care systems, the gap between the potential of telehealth and its actual adoption needs further exploration. Especially for the aging population, who are not early adopters of technology, it is crucial to understand their preferences and barriers. The Health Information National Trends Survey (HINTS) provides valuable data in this regard. HINTS is a major initiative of the National Cancer Institute that collects data on the American public's use of health information and technology [4]. The survey contains key issues such as how individuals access and use health information, their perceptions of health-related risks, and their health behaviors and conditions. HINTS 6 (2022) is the sixth cycle of the HINTS program and reflects the evolving landscape of digital health during the postpandemic period. This cycle includes updated questions on telehealth usage, wearable device adoption, and digital health communication, making it particularly well-suited for examining how older adults engage with emerging health technologies. The HINTS 6 survey results have been examined for patterns and predictors of telehealth utilization—a study used logistic regression analysis to reveal significant associations of social determinants, socioeconomic demographics, and health factors with telemedicine services utilization [5]. The study found that despite the widespread use of telemedicine, US adults still prefer in-person visits in the early postpandemic years, especially older adults, who showed a lower inclination toward telemedicine. This insight highlights the current challenge for telehealth utilization for older adults, despite the substantial benefits that broader telehealth services offer older adults, particularly in managing chronic conditions and promoting physical activity. Older adults are defined as individuals aged 65 and above, which aligns with demographic classifications used in national datasets such as HINTS and prior public health literature [4]. This age group is particularly relevant for examining telehealth adoption, as they face increasing health management needs and may benefit most from remote care solutions. However, the reasons behind this slow adoption are not fully understood. Our paper aims to bridge the gap by leveraging the HINTS 6 dataset to conduct a focused analysis of telehealth adoption among the aging population. By examining factors such as demographics, physical activity levels [6-8], health conditions, and technological barriers (use of wearable devices) [9], this study seeks to build a comprehensive understanding of the variables influencing telehealth utilization in older adults, especially the impact of technical barriers. In this study, we use the term "telehealth" to align with the terminology used in the HINTS 6 survey. The survey defines a telehealth visit as "a telephone or video appointment with a doctor or health professional." While e-health encompasses a broader variety of digital health technologies, our analysis specifically focuses on telehealth usage as defined and measured in the HINTS dataset.

Aging Population

The phenomenon of an aging population is a relatively recent challenge from a historical perspective [10]. In 1950, no nation had more than 11% of its population aged 65 years and older. By 2000, this figure had risen to 18%, and projections suggest a dramatic increase to 38% by 2050 [11]. The World Health Organization anticipates that by mid-century, the number of individuals aged 65 and older will surpass the number of youths aged 15 - 24. This demographic change is a medical and social issue worldwide, with the increase in the aging population affecting the socioeconomic structure and underscoring the need for specialized products and services for older adults [12].

Due to this worldwide challenge, the concept of healthy aging emerges, which emphasizes developing and maintaining functional abilities that promote well-being in older age, as defined by the World Health Organization [13]. This paradigm shift requires a re-evaluation of current health care models that focus not only on disease response but also on the multiple health determinants—behavioral, clinical, social, and environmental—that influence functional decline across the lifespan [14]. The primary goal of this approach is to extend health span rather than lifespan, aiming to reduce morbidity associated with age-related chronic diseases [15].

As life expectancy increases, the prevalence of noncommunicable diseases such as diabetes, renal failure, arthritis, Alzheimer disease, and Parkinson disease among older adults increases, requiring ongoing surveillance and a comprehensive management strategy. This demographic change is accompanied by physical and cognitive decline, increasing the risk of comorbidities and acute medical events such as falls or stroke [16]. Therefore, promoting healthy aging while ensuring the autonomy and safety of older adults at home has become a key social goal.

Adoption of Wearable Devices

The advent of technology has led to a wide variety of wearable devices that go beyond traditional smartwatches to include innovative smart jewelry designed to be worn around the fingers, ears, or neck [17]. These devices have revolutionized self-tracking, with physical health and activity levels becoming the primary interests of users. In addition, wearable devices enable a broader range of health indicators, including stress levels, emotional well-being, sleep quality, geographic location, nutritional habits, vital signs, and specific disease or symptom tracking [18]. This comprehensive monitoring capability allows health care professionals to have continuous access to the health status of older adults and offers unique opportunities for effective remote care [19], thereby facilitating effective remote care and personalized health management strategies. For example, a smartwatch equipped with a heart rate sensor can alert users and health care providers to irregular heartbeats, suggesting potential arrhythmia or other cardiovascular issues [20]. Similarly, wearable fall detection devices can automatically notify family members or emergency services in the event of a fall, significantly reducing the response time and potentially saving lives [21]. Furthermore, devices tracking sleep patterns can offer valuable data to adjust treatments for insomnia or sleep apnea, contributing to mental well-being [22].

Wearable devices enable older adults to manage their health proactively, continuously track chronic conditions and treatments, and monitor potential safety hazards—all without disrupting daily life [23]. This device not only supports independent living but also improves quality of life. In the health

XSL•FO
RenderX

care domain, wearable devices are gradually being integrated into patient care protocols and independent living programs for the aging population [24]. Researchers have explored the utility of wearable devices in forecasting clinical outcomes [25], monitoring patient activity levels, especially in those with chronic conditions like chronic obstructive pulmonary disease [14], predicting patient-reported outcomes such as pain scores [26], monitoring cardiac arrhythmia [27], and tracking the progression of symptoms in neurodegenerative diseases [28]. The growing interest in wearable devices among health care providers, including general practitioners considering prescribing mobile health apps and devices, signals a transformative shift in patient care and contributes to the growth in telehealth [28].

Combined with wearable devices, telehealth has become a key aspect of modern health care, seamlessly extending medical services directly into older adults' homes. By enabling continuous monitoring and management of chronic conditions, telehealth can reduce the frequency of hospital visits, lower health care costs, and improve the efficiency of health care delivery. In addition, telehealth can significantly improve the accessibility of health care services, ensuring that older people receive timely and appropriate care no matter where they are. The ability to conduct virtual consultations and access health care services from home is particularly beneficial during public health crises, such as the COVID-19 pandemic, when minimizing physical contact is critical [29]. Despite the significant advantages of telehealth, several obstacles hinder its widespread adoption, particularly among the aging population [30]. Digital literacy is a major barrier; many older adults are unfamiliar with the necessary technology, which can limit their access to telehealth services [31]. Privacy and security concerns regarding personal health data transmitted over the internet further exacerbate these challenges [32]. Additionally, the digital divide—a gap in access to digital devices and high-speed internet—disproportionately affects rural and underserved communities, thereby limiting the reach and effectiveness of telehealth solutions.

Hypothesis

As wearable devices are one of the prominent enablers of at-home health monitoring, we propose that being familiar with wearable devices may increase the adoption of other emerging technologies, including telehealth, particularly among the aging population (age ≥65). This hypothesized relationship stems from the strategy for breaking down technology barriers [33]. Adaptation to one technology can reduce barriers to the adoption of related technologies. Specifically, individuals accustomed to wearable devices may find the transition to telehealth services more intuitive. This relationship may be influenced by demographic factors: a higher level of education, which often correlates with greater openness to technological adoption; higher income ranges, being able to afford such health-related products and services; and the influence of living in rural or urban areas, which could affect the accessibility of in-person clinical care and hence the need for telehealth services. Additional variables that necessitate telehealth service and relate to health awareness include general health and intention to engage in physical exercise. In this study, we will explore the following hypotheses:

1. The use of wearable devices among the aging population is associated with telehealth adoption.
2. Demographic factors (including gender, education, income, and location) are associated with telehealth adoption in the aging population.
3. Demographic factors act as mediating variables, influencing how the use of wearable devices is associated with telehealth adoption.
4. Poor health conditions in the aging population are directly associated with higher telehealth adoption.
5. Health conditions mediate the relationship between the use of wearable devices and the adoption of telehealth among the aging population.
6. An active lifestyle is significantly associated with a higher likelihood of telehealth adoption among the aging population.

Methods

Study Design and Dataset

The HINTS survey is conducted every 2 years to gather comprehensive insights into the changing landscape of health communication and information dissemination [4]. HINTS 6 (2022) data were collected from March through November 2022, and it contains responses from 6252 participants. Participants were selected using a random sample of US households, with addresses drawn from the US Postal Service's Computerized Delivery Sequence File, and respondents were offered a paper survey or web option. This 2-pronged approach helped capture a wide demographic, including digitally literate individuals and those more comfortable with traditional survey methods. To ensure sufficient representation, HINTS incorporates a stratified sample design, oversampling rural populations and older adults to capture a broad range of health behaviors and technology use across different demographic groups.

We used 10 variables from the survey based on the hypotheses; 5 of them are demographic variables. All the variables and related survey questions are summarized in Table 1. Telehealth adoption is defined as the use of telehealth services delivered digitally and virtually, such as video or telephone consultations with health professionals. Responses indicating the use of video, phone calls, or a combination of both were considered evidence of telehealth adoption. The use of wearable devices in the HINTS survey and this study refers to the engagement with electronic devices designed to monitor or track health and physical activity, such as a Fitbit, Apple Watch, or Garmin Vivofit. While wearable devices may collect health data that can support telehealth services, they do not inherently constitute telehealth adoption. Notably, telehealth involves direct communication with health care providers, whereas wearable device use is focused on personal health monitoring.

XSL•FO
RenderX

Table . Descriptions of variables used in the study from the HINTS 6 survey.

Variable and variable name	Survey item
Age	
AgrGrpB	R1. What is your age?
Telehealth adoption	
ReceiveTelehealthCare	D1. In the past 12 months, did you receive care from a doctor or health professional using telehealth?
OfferedTelehealthOption	D2. In the past 12 months, were you offered the option to have a telehealth visit for any medical care you tried to schedule?
Use of wearable devices	
WearableDevTrackHealth	B8. In the past 12 months, have you used an electronic wearable device to monitor or track your health or activity? For example, a Fitbit, Apple Watch, or Garmin Vivofit.
Health condition	
GeneralHealth	H1. In general, would you say your health is...?
Physical exercise	
TimesModerateExercise	M1. In a typical week, how many days do you do any physical activity or exercise of at least moderate intensity, such as brisk walking, bicycling at a regular pace, and swimming at a regular pace (do not include weightlifting)?
Location	
PR_RUCA_2010	USDA 2010 Primary Rural-Urban Community Area Code
Education	
Education	R7. What is the highest grade or level of education?
Gender	
BirthGender	R2. On your original birth certificate, were you listed as male or female?
Income	
IncomeRanges	R14. Thinking about members of your family living in this household, what is your combined annual income, meaning the total pre-tax income from all sources earned in the past year?

[a]HINTS: Health Information National Trends Survey.

Data Processing

The primary outcome considered in this study is the adoption of telehealth among the aging population. The telehealth adoption score was assessed using the following 2 survey items: (1) “In the past 12 months, were you offered the option to have a telehealth visit for any medical care you tried to schedule?” and (2) “In the past 12 months, did you receive care from a doctor or health professional using telehealth?” We formed a composite score to represent the adoption of telehealth based on these 2 survey questions. We assume that the answers “Yes, by video,” “Yes, by phone call,” and “Yes, some by video and some by phone call” are indicative of telehealth use, while “No telehealth visits in the past 12 months” and “I did not try to schedule any medical care in the past 12 months” suggest no use of telehealth. Table 2 shows the telehealth adoption score.

To enhance the analytical clarity and efficiency of our study, we simplified categorical variables related to education level, income ranges, and frequency of moderate exercise. Then, we encoded all categorical variables, including demographic variables, health conditions, and physical exercises.

Table . Telehealth adoption conditions.

Telehealth adoption conditions	Label
Not offered telehealth and did not adopt	0
Offered telehealth but did not adopt	1
Adopted telehealth	2

To better represent the range of educational attainment in our dataset, we condensed the categories into 4 main levels: Less than high school (coded to 1): This category combines “less than 8 years” and “8 through 11 years” into a single

XSL•FO
RenderX

category, representing individuals who have not completed high school education.

High school plus (coded to 2): This new category merges "12 years or completed high school," "Post high school training other than college (vocational or technical," and "Some college" into one. It captures those who have achieved education beyond high school but have not obtained a full college degree.

College graduate (coded to 3): Retained as a distinct category, it signifies individuals who have completed a college degree.

Postgraduate (coded to 4): Also kept separate, indicating individuals with education beyond a college degree.

Income ranges were redefined into 3 broad categories to reflect the socioeconomic status of the study participants effectively: low income ($0-$49,999), middle income ($50,000 -$99,999), and high income ($100,000 or more), encoding as 1, 2, and 3 accordingly. The frequency of moderate exercise was encoded numerically to facilitate quantitative analysis of physical activity patterns among participants. The encoding represents the number of days per week participants engage in moderate exercise, ranging from 0 (no exercise) to 7 (daily exercise).

Data Analysis

The data analysis used ordinal regression and mediation analysis to examine factors that influence telehealth adoption among the aging population based on the HINTS 6 (2022) dataset. Ordinal regression was used to determine the direct associations between telehealth adoption and independent variables, including wearable device use, demographics (age, gender, education, income, location), health conditions, and physical exercise. The analysis was chosen because the outcome variable—telehealth adoption—is ordinal, represented by 3 levels indicating increasing engagement (no use, offered but not adopted, adopted). This method allows us to estimate the cumulative odds of telehealth adoption across the 3 categories, providing insight into how the predictors influence the likelihood of being in a higher adoption category.

After identifying factors—education, income, and health conditions—that influence telehealth adoption from the ordinal regression, we further decomposed the effect of each factor and conducted a parallel mediation analysis to quantify the mediating effects on the relationship between the use of wearable devices and telehealth adoption. This approach allows us to identify and quantify pathways through which these mediators influence adoption behavior, offering a more nuanced understanding of the mechanisms underlying telehealth adoption. To support this, a conceptual model was developed to illustrate both direct and indirect relationships. Such models are frequently used in behavioral and health policy research to enhance interpretation and effectively communicate findings, particularly when informing intervention design and strategy development.

Ethical Considerations

This study was a secondary analysis of publicly available data from the HINTS 6 administered by the National Cancer Institute. As such, it is exempt from institutional review board (IRB) review per US federal guidelines on secondary data use [34]. No compensation was provided by the authors for participation, as data collection was performed independently by the HINTS program. This manuscript does not include any identifiable individual participant data or images. Therefore, no consent forms for identifiable data are required.

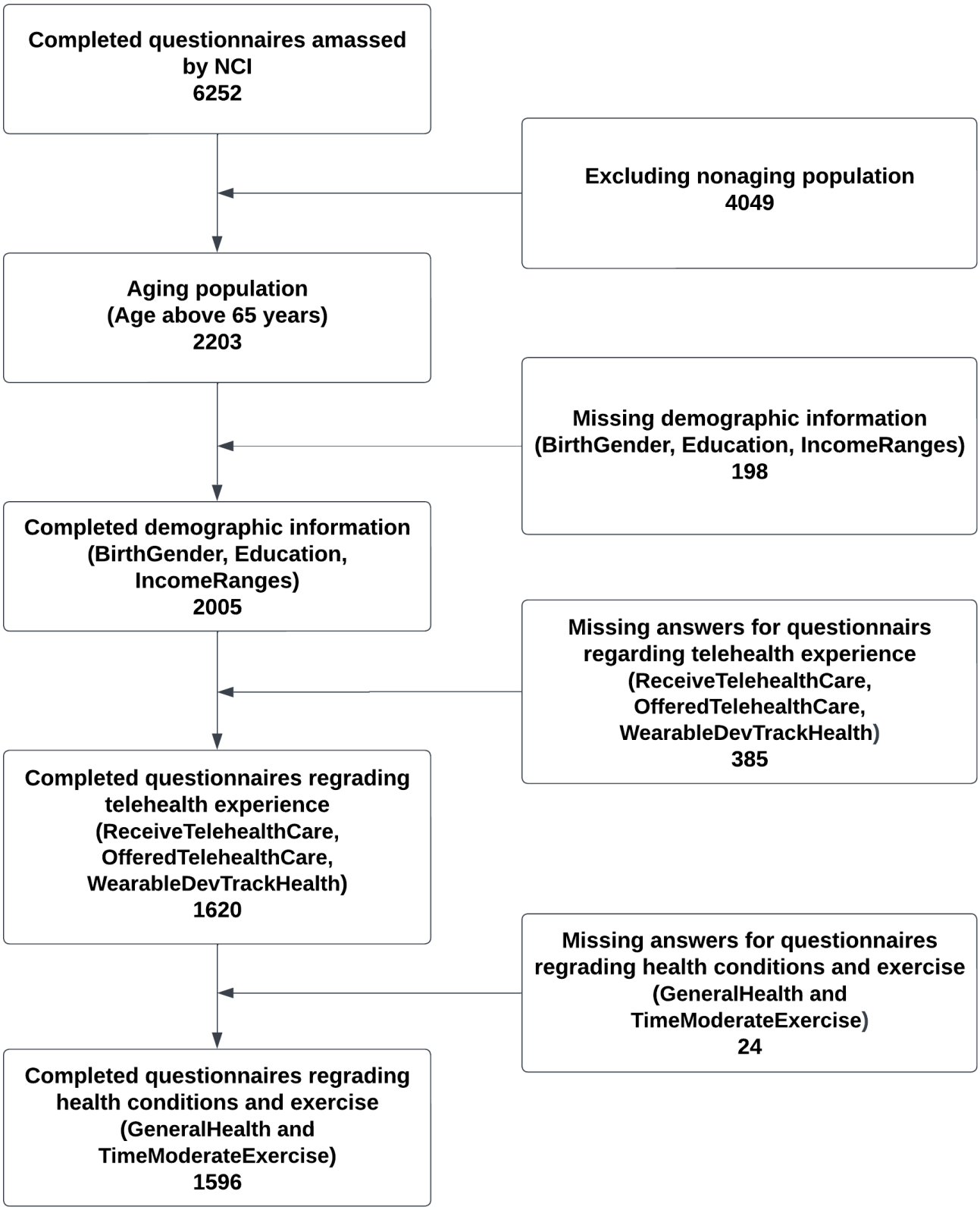
Results

Data Processing and Selection

A total of 6252 surveys were included in the HINTS 6 dataset. For our study, we focused specifically on the aging population, defined as individuals aged 65 years and older. Out of the initial dataset, 2203 participants met this age criterion. After further refinement and excluding incomplete data, the subsequent processing and analysis were conducted on 1596 complete responses. The data selection process is shown in Figure 1.

XSL•FO
RenderX

Figure 1. Flow diagram illustrating the selection of survey respondents aged ≥65 years from the Health Information National Trends Survey (HINTS) 6 dataset. NCI: National Cancer Institute.



Ordinal Regression Analysis

The ordinal regression analysis was performed on the refined HINTS 6 dataset to establish the association between telehealth adoption and various factors, including the use of wearable devices, demographic variables, health conditions, and engagement in physical exercise. The result is shown in Table 3.

XSL•FO
RenderX

Table . Results from ordinal logistic regression that assesses the association between wearable device use, demographics, and telehealth adoption among older US adults (N=1596).

Factors	Coefficient	*t* value	*P* value	Odd ratios (95% CI)	Reference categories
Use of wearable devices	0.2762	2.2134 (1576)	.03	1.3181 (1.03-1.68)	No
Location	−0.2538	−3.1019 (1576)	.003	0.7758 (0.655-0.918)	Metropolitan
Gender	0.0347	0.3388 (1576)	.74	1.0354 (0.841-1.290)	Female
Income	0.1369	1.8648 (1576)	.07	1.1468 (0.993-1.323)	Low income
Education	0.3113	4.9108 (1576)	<.001	1.3653 (1.206-1.562)	Less than high school
Health condition	−0.2659	−4.5104 (1576)	<.001	0.7665 (0.683-0.860)	Poor
Physical exercise	−0.0376	−1.6056 (1576)	.11	0.9631 (0.920-1.008)	None

The use of wearable devices demonstrated a statistically significant positive association with telehealth adoption (*P*=.03). This finding supports Hypothesis 1 and shows that an increased use of wearable devices is associated with increased adoption of telehealth. Specifically, the odds ratio of 1.3181 suggests that individuals who use wearable devices are approximately 32% more likely to adopt telehealth compared to those who do not.

In addition, the location variable has a statistically significant association with telehealth adoption, with a *P* value of 0.0025. Residents in rural areas have lower levels of telehealth adoption. Education emerged as the most highly significant factor (*P*<.001), with a positive coefficient (0.3113). The odds ratio for education (1.3653) implies that with each increase in education level, the odds of telehealth adoption increase by approximately 36.5%. This strongly supports the notion that educational attainment plays a critical role in health technology adoption.

In contrast, gender does not have a statistically significant effect on the likelihood of adopting telehealth services. Income also did not reach the conventional threshold for significance (*P*=.07), but its marginal association suggests that further investigation should be required to understand income's role at a more granular level. Given the mixed results among these demographic factors, Hypothesis 2 is partially supported. The factors of gender and income did not show a significant impact, whereas rural location and lower education undermined telehealth adoption.

The self-reported health conditions are inversely associated with telehealth adoption (coefficient=−0.26597, *P*<.001), thereby supporting Hypothesis 4. Physical exercise, representing moderate levels of physical activity, may be negatively associated with telehealth adoption (coefficient=−0.03761, *P*=.11). Thus, Hypothesis 6 is not supported, and instead, an active lifestyle potentially decreases the likelihood of telehealth adoption.

Mediation Analysis and Conceptual Model Development

After excluding gender and physical exercise due to their lack of significant relationships with telehealth adoption, subsequent correlation analyses were performed on the remaining variables. The correlations between features are moderate to low (<0.5), which is illustrated in Table 4, so keeping them as separate mediators is acceptable.

XSL•FO
RenderX

Table . Results of correlation analysis between key independent and dependent variables.

Variables	1	2	3	4	5	6
1. Use of wearable devices						
r	1	–0.042	0.159	0.188	0.117	0.071
P value	—	.09	<.001	<.001	<.001	.004
2. Location						
r	−0.042	1	−0.071	−0.089	−0.066	−0.086
P value	.09	—	.005	<.001	.009	.001
3. Education						
r	0.159	−0.071	1	0.416	0.246	0.131
P value	<.001	.005	—	<.001	<.001	<.001
4. Income						
r	0.188	−0.089	0.416	1	0.240	0.088
P value	<.001	<.001	<.001	—	<.001	<.001
5. Health condition						
r	0.117	−0.066	0.246	0.240	1	−0.082
P value	<.001	.009	<.001	<.001	—	.001
6. Telehealth adoption						
r	0.071	−0.086	0.131	0.088	−0.082	1
P value	.004	.001	<.001	<.001	.001	—

Given that our primary outcome focuses on the relationship between the use of wearable devices for health tracking and telehealth adoption. We then explore how demographic factors like education, income, location, and health condition potentially mediate the effect of the use of wearable devices on telehealth adoption. The mediation analysis revealed that the location does not show a significant relationship with wearable device use, and thus, it does not play a mediating role in our model. This finding did not support Hypothesis 3, so the demographic factors, including location, would not moderate the relationship between the use of wearable devices and telehealth adoption in an aging population. Conversely, other factors such as education, income, and health conditions showed mediation effects, thus partially supporting Hypothesis 3 and fully supporting Hypothesis 5. Our mediation analysis highlights that the use of wearable devices is associated with higher telehealth adoption through the mediating effects of education and income. It indicates that individuals with higher education or income are more inclined to adopt wearable technology, which in turn facilitates the adoption of telehealth services.

We constructed a conceptual model in which the use of wearable devices for health tracking is considered an independent variable, while telehealth adoption is considered a dependent variable. Education, income, and health conditions are treated as mediating variables, potentially influencing the core relationship. This model considers the contextual influences of socioeconomic and health conditions and helps demonstrate pathways through which the use of wearable devices may lead to telehealth adoption. Such an approach allows for a more comprehensive understanding of the multifaceted influences on telehealth adoption. Table 5 summarizes the results of the conceptual model analysis, illustrating how each variable interacts within the model:

XSL•FO
RenderX

Table . Results of the regression analysis that estimate the direct and indirect effects of the wearable device use on telehealth adoption through education, income, and health conditions.

Regression	Estimate	SE	*z* value	*P* value (>|*z*|)
Telehealth adoption~Use of wearable devices (b1)	0.137	0.077	1.785	.07
Education~Use of wearable devices (a1)	0.339	0.054	6.291	<.001
Telehealth adoption~Education (c1)	0.162	0.034	4.772	<.001
Income~Use of wearable devices (a2)	0.347	0.047	7.383	<.001
Telehealth adoption~Income (c2)	0.114	0.039	2.885	.004
Health condition~Use of wearable devices (a3)	0.262	0.059	4.425	<.001
Telehealth adoption~Health condition (c3)	−0.125	0.032	−3.870	<.001

Conceptual Model Analysis

The analysis shows that the use of wearable devices for health tracking has a direct effect on telehealth adoption with a positive coefficient (b1=0.137), but this effect is not statistically significant (*P*=.07). The use of wearable devices is positively correlated with education (a1=0.339, *P*<.001), income (a2=0.347, *P*<.001), and health condition (a3=0.262, *P*<0.001). These results show that higher engagement with wearable devices is associated with higher educational attainment, higher income, and better self-reported health. Subsequently, education (c1=0.162, *P*<.001), income (c2=0.114, *P*=.004), and health conditions (c3=−0.125, *P*<.001) have significant effects on telehealth adoption. The results suggest that higher levels of education and income lead to a greater propensity to adopt telehealth services. This result is consistent with the regression and mediation analysis, supporting Hypothesis 2 and partially supporting Hypothesis 3. Conversely, better general health status appears to decrease the likelihood of telehealth adoption, reflecting a possible reduced need for remote health services among healthier individuals, which confirms the testing results of Hypotheses 4 and 5 in the regression and mediation analysis sections.

The mediated effects through education, income, and health conditions are captured by the parameters “indirect1,” “indirect2,” and “indirect3,” respectively, in Table 6, with visualization in Figure 2. The “Estimate” values reported in Table 6 represent standardized indirect effects. These coefficients quantify the extent to which the relationship between wearable device use and telehealth adoption is mediated by education, income, or health conditions. “Indirect1” and “indirect2” positively contribute to telehealth adoption, supporting the beneficial impact of higher education and income facilitated by the use of wearable devices. Conversely, “indirect” shows a negative mediation effect, suggesting that better health conditions actually reduce telehealth adoption. The “total effect” of 0.199 (*P*=.007) encompasses all paths and confirms a significant overall influence of wearable device use on telehealth adoption. To synthesize the statistical results as shown in Table 6 and visualized in Figure 2, we found that demographic factors and health conditions mediate the effect of the use of wearable devices on telehealth adoption among the aging population. This comprehensive model highlights not only isolated effects but also the interconnection of these factors, which is critical to developing targeted strategies to promote telehealth effectively. Table 7 summarizes the outcomes of the hypothesis tests, offering clear insights into the pathways through which the use of wearable devices influences telehealth adoption.

Table . Total and indirect effects in the conceptual mediation model.

Parameter	Estimate	SE	*z* value	*P* value (>|*z*|)
Indirect1	0.055	0.014	3.809	<.001
Indirect2	0.040	0.015	2.687	.007
Indirect3	−0.033	0.011	−2.915	.004
Total effect	0.199	0.074	2.695	.007

XSL•FO
RenderX

Figure 2. Conceptual model illustrating the relationship between the use of wearable devices and telehealth adoption, with education, income, and health condition as mediators among older US adults.

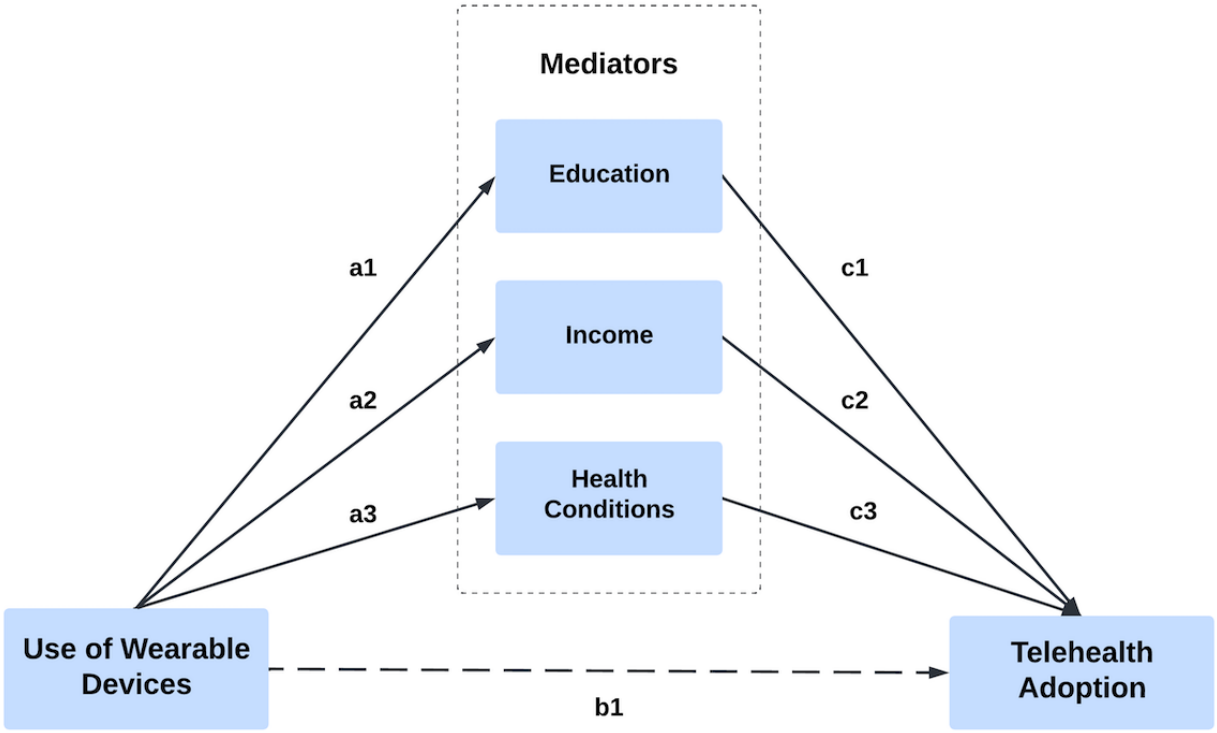


Table . Summary of hypotheses testing outcomes.

Hypothesis	Path	Coefficient (*P* value)	Outcome
1	• Use of wearable devices→Telehealth adoption	• 0.137 (.07)	Partially supported
2	• Education→Telehealth adoption • Income→Telehealth adoption	• 0.162 (<.001) • 0.114 (.004)	Partially supported
3	• Use of wearable devices→Mediators→Telehealth adoption	• Education: 0.055 (<.001) • Income: 0.04 (.007)	Partially supported
4	• Health conditions→Telehealth adoption	• −0.125 (<0.001)	Supported
5	• Use of wearable devices→Health conditions→Telehealth adoption	• −0.033 (.004)	Supported
6	• Physical exercise→Telehealth adoption	—	Rejected

Discussion

Principal Findings

The mediation analysis conducted in this study aims to explore the dynamics of telehealth adoption among the aging population, specifically related to the use of wearable devices, demographic factors, and health conditions. Hypothesis 1 was supported across both the ordinal regression and mediation analyses. The use of wearable devices showed a direct effect and also influenced telehealth adoption indirectly through income and education. This suggests that familiarity with digital health tools may help older adults navigate other health technologies more confidently. Although wearable use was associated with increased telehealth adoption, its direct effect was not strong in isolation, highlighting the importance of additional influencing factors. Hypothesis 2 was partially supported. Education and rural location were significant predictors, while gender and income did not reach statistical significance in the ordinal regression. However, income did emerge as a significant

XSL•FO
RenderX

mediator in the conceptual model, indicating its nuanced role in the adoption process.

One of the most interesting findings is the role of socioeconomic status, as measured by education and income, in influencing telehealth adoption. Consistent with literature suggesting that higher socioeconomic status facilitates better access to technological resources [35], our study finds that higher education and income levels significantly increased the likelihood of telehealth usage for the aging population too, acting as key mediators in the adoption process. Individuals with higher education and income levels are more likely to adopt technologies in general, which encourages the adoption of telehealth services. This also aligns with the finding in [36], which found similar trends in technology adoption among low-income older adults. Additionally, the role of general health conditions inversely affected telehealth adoption, suggesting that individuals in better health are less likely to perceive a need for such services. This reflects findings by Rodríguez-Fernández et al [37], who found that a history of long-term diseases was positively associated with the effective utilization of telehealth among the aging population. Furthermore, some studies have indicated that self-monitoring technologies not only provide patients with greater awareness and understanding of their condition but also are capable of triggering a virtuous circle [38,39]. Importantly, technology acceptance tends to be higher when adopted in the early stages of the disease [40]. Contrary to the hypothesis, our analysis did not identify a significant relationship between physical activity and higher telehealth adoption, indicating that while physically active individuals may be more health-conscious, they do not necessarily see more value in telehealth services. This observation is consistent with the work of Rochester [41], who also reported limited evidence of a relationship between telehealth usage and physical activity levels.

Although geographic location was not included in the conceptual model as a mediator, it emerged as a significant factor in both the ordinal regression and correlation analyses. Rural residency was associated with lower telehealth adoption, highlighting persistent disparities in digital health access across geographic regions [42]. This finding is particularly important in the US context, where rural residents often face greater travel distances to health care facilities but may lack the broadband infrastructure and digital literacy support needed to engage with telehealth services effectively [43].

The conceptual model in this study examines the use of wearable devices as a predictor of telehealth adoption. Although the direction of the effect was positive, the nonsignificant direct effect highlighted the complexity of the relationship. The increasing use of wearable devices by older adults may not be directly related to increased adoption of telehealth due to variables such as personal attitudes toward the technology, perceived ease of use, and perceived usefulness [44]. However, the significant total effect observed when considering both direct and mediated effects confirms that as wearable use increases, the likelihood of telehealth adoption also increases, driven by the mediating effects of education, income, and general health. This combined effect represents the cumulative impact of the various pathways through which the use of wearable devices impacts telehealth and telemedicine adoption. As discussed in the study by Gupta et al [45], the role of both socioeconomic and psychological factors is important in the acceptance of new technologies.

This study used a parallel mediation framework implemented through ordinal regression to estimate direct and indirect effects across multiple mediators. An alternative approach, such as the Preacher and Hayes bootstrapping method [46], provides robust confidence intervals and is well-suited for testing mediation effects in complex models. Incorporating bootstrapping in future analyses would strengthen the statistical inference of indirect pathways and further validate the conceptual relationships identified in this study.

In summary, this study shows significant indirect effects of socioeconomic factors and health conditions on telehealth adoption in the aging population. While the direct impact of wearable device use on telehealth adoption is subtle, its effects are clearly mediated through pathways mediated by education, income, and health status. This complex relationship highlights the need for multifaceted strategies to enhance access to and adoption of telehealth among older adults. The significant role of wearable devices in facilitating telehealth highlights the need for comprehensive strategies to expand access and adoption among older adults. The previous research highlights that most digital health technologies were not designed for the needs of socially disadvantaged groups, such as older adults or those with limited health literacy skills [47]. As a result, these populations often experience reduced access to and engagement with telehealth services. The COVID-19 pandemic accelerated the shift to telehealth and wearable devices but also amplified digital exclusion, especially among those without consistent internet access or familiarity with remote platforms [48]. The concept of the digital divide encompasses more than device ownership—it includes disparities in broadband access, digital skills, and the ability to meaningfully engage with health technologies [49]. Recent evidence during the COVID-19 pandemic suggests that these disparities directly translate into worse health outcomes [50]. For instance, counties with higher levels of digital exclusion experienced higher COVID-19 case and death rates and lower vaccination uptake compared to digitally connected communities [51]. This suggests that digital exclusion limited the ability of individuals to access timely public health information, schedule vaccine appointments, or participate in virtual care and social support networks. These compounding factors raise urgent concerns about digital equity as a social determinant of health. Consequently, there is an urgent requirement for policies that systematically address both technological and socioeconomic barriers to health technology utilization [52]. These measures are critical to ensuring that all segments of the population benefit from advances in health care technologies and services.

Limitation

This study has several limitations that should be acknowledged. First, there is a potential for self-selection and self-report bias in the survey responses, which could affect the accuracy of reported use of wearable devices, perceived health conditions, and telehealth adoption. Future studies might benefit from using

XSL•FO
RenderX

objective data collection methods, such as direct monitoring of wearable device usage and medical records for telehealth adoption. Second, although the study was controlled for several demographic factors and health-related variables, there may be other confounding factors that may influence the relationship between the use of wearable devices and telehealth adoption. For example, technological literacy, personal attitudes toward health, and availability of support for using digital tools may also play an important role. Third, the mediation model assumes a directional relationship based on theoretical frameworks and prior literature. This study is correlational in nature, and causal claims cannot be made. The findings should be interpreted as associations rather than confirmed causal pathways, and future research using longitudinal or experimental designs is recommended to validate the directionality of these relationships. Fourth, given that the survey was distributed via mail with an optional web-based response, participation may have been lower among those with limited access to or comfort with technology, introducing potential response bias. Fifth, the study focused on the aging US population, so the generalizability of the results may be limited. Differences in culture, economics, and health care systems may influence the adoption of telehealth in other regions. For instance, the US health care system is largely privatized and insurance-dependent, with varying levels of access to services based on coverage and cost. This structure can shape how older adults engage with both telehealth and wearable technologies. In contrast, countries with universal health care systems, centralized digital health platforms, or stronger community-based care models may exhibit different drivers of technology use among older adults. It is worth noting that North America has one of the highest adoption rates of wearable devices globally. According to Statista, by the end of 2022, North America had 439 million connected wearable devices, the highest of any region. Projections also show continued growth, with over 90 million US users expected in 2025 across smart bands, smartwatches, and smart scales [53]. This widespread adoption indicates that older adults in the US may already be more familiar with wearable devices, potentially increasing their openness to integrating telehealth solutions as well. Therefore, while the findings provide valuable insights into the American aging population, they may not be directly applicable to populations outside the United States without consideration of these structural and contextual differences.

Future Direction

Future studies should explore long-term patterns of telehealth adoption and address persistent barriers, particularly in low-income and rural communities. While our study sheds light on structural and demographic influences, it does not directly capture users' perceived benefits of telehealth. To complement these findings, future research could incorporate validated instruments—such as the Telehealth Usability Questionnaire or surveys based on the Technology Acceptance Model—to assess perceived usefulness, satisfaction, and ease of use among older adults. These tools can help inform more user-centered and effective strategies for promoting telehealth adoption.

Conclusions

This paper focuses on the influence of wearable usage and the mediating factors of socioeconomic status and health conditions on telehealth adoption among the aging population. The findings indicate that while wearable device use itself may lead to an increase in telehealth adoption, its impact is significantly influenced by factors such as education, income, and health conditions. This trend is consistent beyond the aging population.

Higher levels of education and income were positively associated with telehealth adoption, reflecting greater access and readiness to engage with digital health tools among socioeconomically advantaged individuals. Conversely, better overall health was negatively associated with telehealth adoption, suggesting that healthy older adults may not realize sufficient value in telemedicine services to change their traditional health care engagement habits. This finding suggests that targeted educational workshops may be needed to emphasize the benefits of telehealth not only for immediate care needs but also for preventive health measures.

Overall, the findings provide evidence that telehealth adoption in older adults is shaped by a complex interplay of wearable device use, socioeconomic characteristics, and health status. These insights contribute to a deeper understanding of digital health behaviors in aging populations and align with the study's objective to investigate key influences on telehealth engagement in this demographic.

Data Availability

The datasets generated or analyzed during this study are available in the Health Information National Trends Survey (HINTS) repository [4]. The HINTS dataset is a public dataset that supports the findings of this study, which can be found on the website [54].

Conflicts of Interest

None declared.

References

1. Page B, Irving D, Amalberti R, Vincent C. Health services under pressure: a scoping review and development of a taxonomy of adaptive strategies. BMJ Qual Saf 2024 Oct 18;33(11):738-747. [doi: 10.1136/bmjqs-2023-016686] [Medline: 38050158]
2. El-Miedany Y. Telehealth and telemedicine: how the digital era is changing standard health care. Smart Homecare Technol Telehealth 2017:43-51. [doi: 10.2147/SHTT.S116009]

XSL•FO
RenderX

3. Darkins AW, Cary MA. Telemedicine and Telehealth: Principles, Policies, Performances and Pitfalls: Springer; 2000.
4. Nelson DE, Kreps GL, Hesse BW, et al. The Health Information National Trends Survey (HINTS): development, design, and dissemination. J Health Commun 2004;9(5):443-460. [doi: 10.1080/10810730490504233] [Medline: 15513791]
5. Chandrasekaran R. Telemedicine in the post-pandemic period: understanding patterns of use and the influence of socioeconomic demographics, health status, and social determinants. Telemed J E Health 2024 Feb;30(2):480-489. [doi: 10.1089/tmj.2023.0277] [Medline: 37585558]
6. Villaron C, Cury F, Eisinger F, Cappiello MA, Marqueste T. Telehealth applied to physical activity during cancer treatment: a feasibility, acceptability, and randomized pilot study. Support Care Cancer 2018 Oct;26(10):3413-3421. [doi: 10.1007/s00520-018-4191-4] [Medline: 29675546]
7. Blackwood J, Rybicki K. Outcomes of telehealth-delivered physical activity programs in adult cancer survivors: a systematic review. Rehabil Oncol 2021;39(3):128-136. [doi: 10.1097/01.REO.0000000000000249]
8. Mori DL, Silberbogen AK, Collins AE, Ulloa EW, Brown KL, Niles BL. Promoting physical activity in individuals with diabetes: telehealth approaches. Diabetes Spectr 2011 Aug 1;24(3):127-135. [doi: 10.2337/diaspect.24.3.127]
9. Kruse C, Heinemann K. Facilitators and barriers to the adoption of telemedicine during the first year of COVID-19: systematic review. J Med Internet Res 2022 Jan 4;24(1):e31752. [doi: 10.2196/31752] [Medline: 34854815]
10. Rudnicka E, Napierała P, Podfigurna A, Męczekalski B, Smolarczyk R, Grymowicz M. The World Health Organization (WHO) approach to healthy ageing. Maturitas 2020 Sep;139:6-11. [doi: 10.1016/j.maturitas.2020.05.018]
11. Cohen JE. World population in 2050: assessing the projections. Federal Reserve Bank of Boston. 2002. URL: https://www.bostonfed.org/economic/conf/conf46/conf46d1.pdf [accessed 2025-07-29]
12. World population ageing 2023: challenges and opportunities of population ageing in the least developed countries. Department of Economic and Social Affairs, Population Division. 2024. URL: https://desapublications.un.org/publications/world-population-ageing-2023-challenges-and-opportunities-population-ageing-least [accessed 2025-07-29]
13. Healthy ageing and functional ability. World Health Organization. 2020 Oct 26. URL: https://www.who.int/news-room/questions-and-answers/item/healthy-ageing-and-functional-ability [accessed 2025-07-29]
14. Polat F, Karasu F. The effect of health promotion training provided to elderly individuals during the COVID-19 pandemic on healthy lifestyle behaviors. Glob Health Promot 2022 Sep;29(3):129-139. [doi: 10.1177/17579759221095078] [Medline: 35722980]
15. Justice JN, Cesari M, Seals DR, Shively CA, Carter CS. Comparative approaches to understanding the relation between aging and physical function. J Gerontol A Biol Sci Med Sci 2016 Oct;71(10):1243-1253. [doi: 10.1093/gerona/glv035] [Medline: 25910845]
16. Chen C, Ding S, Wang J. Digital health for aging populations. Nat Med 2023 Jul;29(7):1623-1630. [doi: 10.1038/s41591-023-02391-8] [Medline: 37464029]
17. Godfrey A, Hetherington V, Shum H, Bonato P, Lovell NH, Stuart S. From A to Z: wearable technology explained. Maturitas 2018 Jul;113:40-47. [doi: 10.1016/j.maturitas.2018.04.012] [Medline: 29903647]
18. Kyytsönen M, Vehko T, Anttila H, Ikonen J. Factors associated with use of wearable technology to support activity, well-being, or a healthy lifestyle in the adult population and among older adults. PLOS Digit Health 2023 May;2(5):e0000245. [doi: 10.1371/journal.pdig.0000245] [Medline: 37163490]
19. Al-khafajiy M, Baker T, Chalmers C, et al. Remote health monitoring of elderly through wearable sensors. Multimed Tools Appl 2019 Sep;78(17):24681-24706. [doi: 10.1007/s11042-018-7134-7]
20. Strik M, Ploux S, Ramirez FD, et al. Smartwatch-based detection of cardiac arrhythmias: beyond the differentiation between sinus rhythm and atrial fibrillation. Heart Rhythm 2021 Sep;18(9):1524-1532. [doi: 10.1016/j.hrthm.2021.06.1176]
21. Pierleoni P, Belli A, Palma L, Pellegrini M, Pernini L, Valenti S. A high reliability wearable device for elderly fall detection. IEEE Sensors J 2015;15(8):4544-4553. [doi: 10.1109/JSEN.2015.2423562]
22. Guillodo E, Lemey C, Simonnet M, et al. Clinical applications of mobile health wearable–based sleep monitoring: systematic review. JMIR Mhealth Uhealth 2020;8(4):e10733. [doi: 10.2196/10733] [Medline: 32234707]
23. Anttila H, Niemelä M, Anttila M, et al. Towards ethical and sustainable technology-supported ageing at home in finland: KATI programme. Presented at: Conference on Technology Ethics; Oct 20-22, 2021; Turku, Finland URL: https://www.julkari.fi/bitstream/handle/10024/148119/FP_03.pdf [accessed 2025-07-29]
24. Iqbal MH, Aydin A, Brunckhorst O, Dasgupta P, Ahmed K. A review of wearable technology in medicine. J R Soc Med 2016 Oct;109(10):372-380. [doi: 10.1177/0141076816663560]
25. Burnham JP, Lu C, Yaeger LH, Bailey TC, Kollef MH. Using wearable technology to predict health outcomes: a literature review. J Am Med Inform Assoc 2018 Sep 1;25(9):1221-1227. [doi: 10.1093/jamia/ocy082] [Medline: 29982520]
26. Johnson A, Yang F, Gollarahalli S, et al. Use of mobile health apps and wearable technology to assess changes and predict pain during treatment of acute pain in sickle cell disease: feasibility study. JMIR Mhealth Uhealth 2019 Dec 2;7(12):e13671. [doi: 10.2196/13671] [Medline: 31789599]
27. Santala OE, Halonen J, Martikainen S, et al. Automatic mobile health arrhythmia monitoring for the detection of atrial fibrillation: prospective feasibility, accuracy, and user experience study. JMIR Mhealth Uhealth 2021 Oct 22;9(10):e29933. [doi: 10.2196/29933] [Medline: 34677135]

XSL•FO
RenderX

28. Banerjee T, Peterson M, Oliver Q, Froehle A, Lawhorne L. Validating a commercial device for continuous activity measurement in the older adult population for dementia management. Smart Health (Amst) 2018 Jan;5-6:51-62. [doi: 10.1016/j.smhl.2017.11.001] [Medline: 29915807]
29. Bouabida K, Lebouché B, Pomey MP. Telehealth and COVID-19 pandemic: an overview of the telehealth use, advantages, challenges, and opportunities during COVID-19 pandemic. Healthcare (Basel) 2022 Nov 16;10(11):2293. [doi: 10.3390/healthcare10112293] [Medline: 36421617]
30. Valdivieso B, García-Sempere A, Sanfélix-Gimeno G, et al. The effect of telehealth, telephone support or usual care on quality of life, mortality and healthcare utilization in elderly high-risk patients with multiple chronic conditions. A prospective study. Medicina Clínica 2018 Oct 23;151(8):308-314. [doi: 10.1016/j.medcli.2018.03.013] [Medline: 29705155]
31. Rasekaba TM, Pereira P, Rani G V, Johnson R, McKechnie R, Blackberry I. Exploring telehealth readiness in a resource limited setting: Digital and Health Literacy among Older People in Rural India (DAHLIA). Geriatrics (Basel) 2022 Mar 1;7(2):28. [doi: 10.3390/geriatrics7020028] [Medline: 35314600]
32. Pool J, Akhlaghpour S, Fatehi F, Gray LC. Data privacy concerns and use of telehealth in the aged care context: an integrative review and research agenda. Int J Med Inform 2022 Apr;160:104707. [doi: 10.1016/j.ijmedinf.2022.104707] [Medline: 35131698]
33. Lahiri R, Ding J, Chinzara Z. Technology adoption, adaptation and growth. Econ Model 2018 Apr;70:469-483. [doi: 10.1016/j.econmod.2017.08.026]
34. Wilkinson MD, Dumontier M, Aalbersberg IJJ, et al. The FAIR Guiding Principles for scientific data management and stewardship. Sci Data 2016 Mar 15;3:160018. [doi: 10.1038/sdata.2016.18] [Medline: 26978244]
35. Paccoud I, Baumann M, Le Bihan E, et al. Socioeconomic and behavioural factors associated with access to and use of personal health records. BMC Med Inform Decis Mak 2021 Jan 13;21(1):18. [doi: 10.1186/s12911-020-01383-9] [Medline: 33435970]
36. Chan DYL, Lee SWH, Teh PL. Factors influencing technology use among low-income older adults: a systematic review. Heliyon 2023 Sep;9(9):e20111. [doi: 10.1016/j.heliyon.2023.e20111] [Medline: 37809586]
37. Rodríguez-Fernández JM, Danies E, Hoertel N, Galanter W, Saner H, Franco OH. Telemedicine readiness across medical conditions in a US national representative sample of older adults. J Appl Gerontol 2022 Apr;41(4):982-992. [doi: 10.1177/07334648211056231] [Medline: 34855553]
38. Jiang Y, Sun P, Chen Z, et al. Patients' and healthcare providers' perceptions and experiences of telehealth use and online health information use in chronic disease management for older patients with chronic obstructive pulmonary disease: a qualitative study. BMC Geriatr 2022 Jan 3;22(1):9. [doi: 10.1186/s12877-021-02702-z] [Medline: 34979967]
39. Doyle J, Murphy E, Gavin S, et al. A digital platform to support self-management of multiple chronic conditions (ProACT): findings in relation to engagement during a one-year proof-of-concept trial. J Med Internet Res 2021 Dec 15;23(12):e22672. [doi: 10.2196/22672] [Medline: 34914612]
40. Middlemass JB, Vos J, Siriwardena AN. Perceptions on use of home telemonitoring in patients with long term conditions - concordance with the health information technology acceptance model: a qualitative collective case study. BMC Med Inform Decis Mak 2017 Jun 26;17(1):89. [doi: 10.1186/s12911-017-0486-5] [Medline: 28651588]
41. Rochester CL. Does telemedicine promote physical activity? Life (Basel) 2022 Mar 15;12(3):425. [doi: 10.3390/life12030425] [Medline: 35330176]
42. Ko JS, El-Toukhy S, Quintero SM, et al. Disparities in telehealth access, not willingness to use services, likely explain rural telehealth disparities. J Rural Health 2023 Jun;39(3):617-624. [doi: 10.1111/jrh.12759] [Medline: 37042413]
43. The role of telemedicine in rural America: overcoming electrical and technological barriers to improve health outcomes. Int J Sci Res Arch 2024;12(2):188-205. [doi: 10.30574/ijsra.2024.12.2.1176]
44. Fowe IE, Boot WR. Understanding older adults' attitudes toward mobile and wearable technologies to support health and cognition. Front Psychol 2022;13:1036092. [doi: 10.3389/fpsyg.2022.1036092] [Medline: 36571059]
45. Gupta N, Fischer ARH, Frewer LJ. Socio-psychological determinants of public acceptance of technologies: a review. Public Underst Sci 2012 Oct;21(7):782-795. [doi: 10.1177/0963662510392485] [Medline: 23832558]
46. Preacher KJ, Hayes AF. Asymptotic and resampling strategies for assessing and comparing indirect effects in multiple mediator models. Behav Res Methods 2008 Aug;40(3):879-891. [doi: 10.3758/brm.40.3.879] [Medline: 18697684]
47. Toscos T, Drouin M, Pater J, Flanagan M, Pfafman R, Mirro MJ. Selection biases in technology-based intervention research: patients' technology use relates to both demographic and health-related inequities. J Am Med Inform Assoc 2019 Aug 1;26(8-9):835-839. [doi: 10.1093/jamia/ocz058] [Medline: 31172193]
48. Malpass A, Garbers K, Saunders L, et al. Overcoming digital exclusion during the COVID-19 pandemic: impact of mobile technology for survivors of modern slavery and human trafficking – a mixed method study of survivors and support service provider views. J Hum Traffick 2024;10(3):445-464. [doi: 10.1080/23322705.2022.2050991] [Medline: 39036779]
49. Espín A, Rojas C. Bridging the digital divide in the US. Int J Ind Organ 2024 Mar;93:103053. [doi: 10.1016/j.ijindorg.2024.103053]
50. Cho M, Kim KM. Effect of digital divide on people with disabilities during the COVID-19 pandemic. Disabil Health J 2022 Jan;15(1):101214. [doi: 10.1016/j.dhjo.2021.101214] [Medline: 34518115]

XSL•FO
RenderX

51. Li F. Disconnected in a pandemic: COVID-19 outcomes and the digital divide in the United States. Health Place 2022 Sep;77:102867. [doi: 10.1016/j.healthplace.2022.102867] [Medline: 35917634]
52. Yao R, Zhang W, Evans R, Cao G, Rui T, Shen L. Inequities in health care services caused by the adoption of digital health technologies: scoping review. J Med Internet Res 2022 Mar 21;24(3):e34144. [doi: 10.2196/34144] [Medline: 35311682]
53. Laricchia F. Wearables in the U.S.- statistics & facts. Statista. 2025 Mar 6. URL: https://www.statista.com/topics/12075/wearables-in-the-us [accessed 2025-07-29]
54. Health Information National Trends Survey. URL: https://hints.cancer.gov/ [accessed 2025-07-21]

Abbreviations

HINTS: Health Information National Trends Survey

Edited by A Coristine; submitted 08.11.24; peer-reviewed by JP Bertocchio, P Valkonen; revised version received 14.05.25; accepted 15.05.25; published 07.08.25.

Please cite as:
Wang R, Asan O, Liao T
Investigating the Role of Wearable Devices in Facilitating Telehealth Adoption Among the Aging Population: Mediation Analysis of US National Data
JMIR Med Inform 2025;13:e68559
URL: https://medinform.jmir.org/2025/1/e68559
doi:10.2196/68559

© Ruijing Wang, Onur Asan, Ting Liao. Originally published in JMIR Medical Informatics (https://medinform.jmir.org), 7.8.2025. This is an open-access article distributed under the terms of the Creative Commons Attribution License (https://creativecommons.org/licenses/by/4.0/), which permits unrestricted use, distribution, and reproduction in any medium, provided the original work, first published in JMIR Medical Informatics, is properly cited. The complete bibliographic information, a link to the original publication on https://medinform.jmir.org/, as well as this copyright and license information must be included.

XSL•FO
RenderX

Original Paper

Public Attitudes Toward Violence Against Doctors: Sentiment Analysis of Chinese Users

Yuwen Zheng[1], MA; Meirong Tian[1], MD; Jingjing Chen[1], MA; Lei Zhang[1], MD; Jia Gao[1], MD; Xiang Li[1], BA; Jin Wen[1*], PhD; Xing Qu[1*], PhD

Institute of Hospital Management, West China Hospital, Sichuan University, Chengdu, China

[*]these authors contributed equally

Corresponding Author:
Xing Qu, PhD
Institute of Hospital Management
West China Hospital
Sichuan University
37 Guoxue Alley
Chengdu, 610041
China
Phone: 86 13880713452
Email: quxing@wchscu.edu.cn

Abstract

Background: Violence against doctors attracts the public's attention both online and in the real world. Understanding how public sentiment evolves during such crises is essential for developing strategies to manage emotions and rebuild trust.

Objective: This study aims to quantify the difference in public sentiment based on the public opinion life cycle theory and describe how public sentiment evolved during a high-profile crisis involving violence against doctors in China.

Methods: This study used the term frequency-inverse document frequency (TF-IDF) algorithm to extract key terms and create keyword clouds from textual comments. The latent Dirichlet allocation (LDA) topic model was used to analyze the thematic trends and shifts within public sentiment. The integrated Chinese Sentiment Lexicon was used to analyze sentiment trajectories in the collected data.

Results: A total of 12,775 valid comments were collected on Sina Weibo about public opinion related to a doctor-patient conflict. Thematic and sentiment analyses showed that the public's sentiments were highly negative during the outbreak period (disgust: 10,201/30,433, 33.52%; anger: 6792/30,433, 22.32%) then smoothly changed to positive and negative during the spread period (sorrow: 2952/8569, 34.45%; joy: 2782/8569, 32.47%) and tended to be rational and peaceful during the decline period (joy: 4757/14,543, 32.71%; sorrow: 4070/14,543, 27.99%). However, no matter how emotions changed, each period's leading tone contained many negative sentiments.

Conclusions: This study simultaneously examined the dynamics of theme change and sentiment evolution in crises involving violence against doctors. It discovered that public sentiment evolved alongside thematic changes, with the dominant negative tone from the initial stage persisting throughout. This finding, distinguished from prior research, underscores the lasting influence of early public sentiment. The results offer valuable insights for medical institutions and authorities, suggesting the need for tailored risk communication strategies responsive to the evolving themes and sentiments at different stages of a crisis.

(JMIR Med Inform 2025;13:e63772) doi:10.2196/63772

KEYWORDS

doctor-patient conflict; sentiment analysis; latent Dirichlet allocation; LDA; social media analysis; public health crisis

Introduction

The rising incidence of doctor-patient conflicts has become a significant concern globally. The Global Health Workforce Statistics database of the World Health Organization (WHO) highlights an increasing trend in medical disputes driven by inequitable distribution of medical resources and heightened pressures on health care systems [1]. The WHO's "Global Strategy on Human Resources for Health: Workforce 2030" emphasizes the importance of equitable access to health care

XSL•FO
RenderX

workers and robust health systems to address and prevent doctor-patient disputes [2].

Doctor-patient conflicts, broadly defined as disputes or tensions between medical professionals and patients (or their families), arise from dissatisfaction with medical outcomes, communication breakdowns, or systemic health care challenges. These conflicts vary in intensity, ranging from verbal disputes to severe incidents of physical harm. Violence against doctors represents the most extreme form of these conflicts, involving verbal abuse, threats, or physical assaults that jeopardize the safety and well-being of health care providers while eroding trust in the medical system [3].

In China, doctor-patient conflicts have been shaped by unique cultural, social, and structural factors [4]. Surveys conducted by the Chinese Medical Doctor Association reported that over 60% of physicians experience verbal or physical conflicts with patients during their careers [5], reflecting pervasive tension in medical interactions. These conflicts are often exacerbated by high patient expectations and increased access to medical information, which amplify scrutiny of health care practices. Structural challenges in the Chinese health care system also contribute significantly. According to the National Health Commission of China, urban hospitals handle over 3 billion outpatient visits annually, resulting in overcrowded facilities and excessive workloads for medical staff [6]. These systemic pressures often lead to long waiting times and dissatisfaction, which can escalate into disputes. Given the critical nature of these issues, there is a pressing need for systematic research on doctor-patient conflicts. Analyzing specific incidents of such conflicts can provide valuable insights into their social, psychological, and institutional determinants. Effective research and targeted interventions can enhance communication, improve patient satisfaction, and ensure patients' and medical professionals' safety and well-being, ultimately contributing to a more efficient and humane health care system.

In health communication, understanding the different developmental stages of events is crucial for designing and implementing effective public relations strategies [7,8]. Analyzing health events from a temporal dimension can reveal the patterns of changes in public sentiment and attention throughout various stages, including incubation, outbreak, spread, and resolution. Furthermore, integrating temporal analysis with topic and sentiment dimensions offers a more comprehensive understanding of the effectiveness of health information dissemination [9].

In medical public opinion research, theme analysis is equally crucial as segmenting the development stages of public sentiment. It is a widely used method in academia [10,11]. Theme analysis involves profound interpretation of textual data to reveal underlying meanings and critical issues that capture public interest, thus helping researchers accurately identify the focal points of public attention. Additionally, through systematic data processing, theme analysis provides a dynamic view of changes in public opinion, aiding researchers with understanding the fundamental shifts in public responses to health information.

Although theme analysis can reveal topics of public interest, more is needed to comprehensively understand the complexity of public attitudes. Consequently, in recent years, the academic community has emphasized sentiment analysis to explore the public's deep emotional tendencies and responses to public opinion [12-14]. Sentiment analysis methods include deep learning, machine learning, and lexicon-based analysis. The lexicon-based approach has unique advantages when dealing with structured and unstructured text data. Compared with deep learning and machine learning methods, lexicon-based analysis relies on a predefined set of sentiment words, providing more intuitive and interpretable results [15]. When applied to sentiment analysis in specific domains, such as doctor-patient conflicts, this method can effectively capture the emotional nuances in professional terminology and industry-specific language, thereby ensuring the accuracy and relevance of the analysis [16,17].

The occurrence of doctor-patient conflicts might be associated with the unequal distribution of medical resources [18], patient expectations and satisfaction [19], and communication skills between doctors and patients [20]. In 2021, an assault incident at Beijing Chaoyang Hospital garnered prolonged and extensive societal attention. During the incidents, Dr. Tao Yong, an ophthalmologist, sustained severe injuries to his head and arms, which put his life in jeopardy and subsequently impaired his ability to conduct surgeries postrecovery. The public response to this incident was significantly more intense than other medical disputes during the same period, indicating its profound impact on public sentiment and medical community relations.

This study, based on the theoretical perspective of the online public opinion life cycle, used the latent Dirichlet allocation (LDA) topic model and sentiment lexicon from Dalian University of Technology to conduct topic and sentiment analysis on the "Beijing Chaoyang Hospital assault incident," a significant doctor-patient conflict incident in China. The aim was to fill the research gap in medical public opinion and assist medical institutions and government departments to better understand the direction of public opinion dissemination and emotional contagion pathways in related events. By developing targeted content publishing and sentiment guidance strategies in response to doctor-patient conflict incidents, the study sought to improve communication effectiveness and ensure risk management and response efficiency.

Methods

Methodological Framework

This study divided opinion stages based on the life cycle of public opinion, which is often applied to the survey of public sentiment events. Life cycle theory, as a broadly adopted theoretical perspective, provides scholars with a structured framework to analyze the stages of change and development in events. Life cycle theory provides a systematic approach to dividing the public opinion cycle into stages, ensuring a theoretically grounded methodology for data segmentation and thematic analysis [21]. The life cycle theory, proposed by Steven Fink [22], posited that crises evolve through 4 phases: incubation, outbreak, spread, and resolution. Similarly, the life cycle of online public sentiment begins with initial attention, escalates with event progression, and declines after saturation,

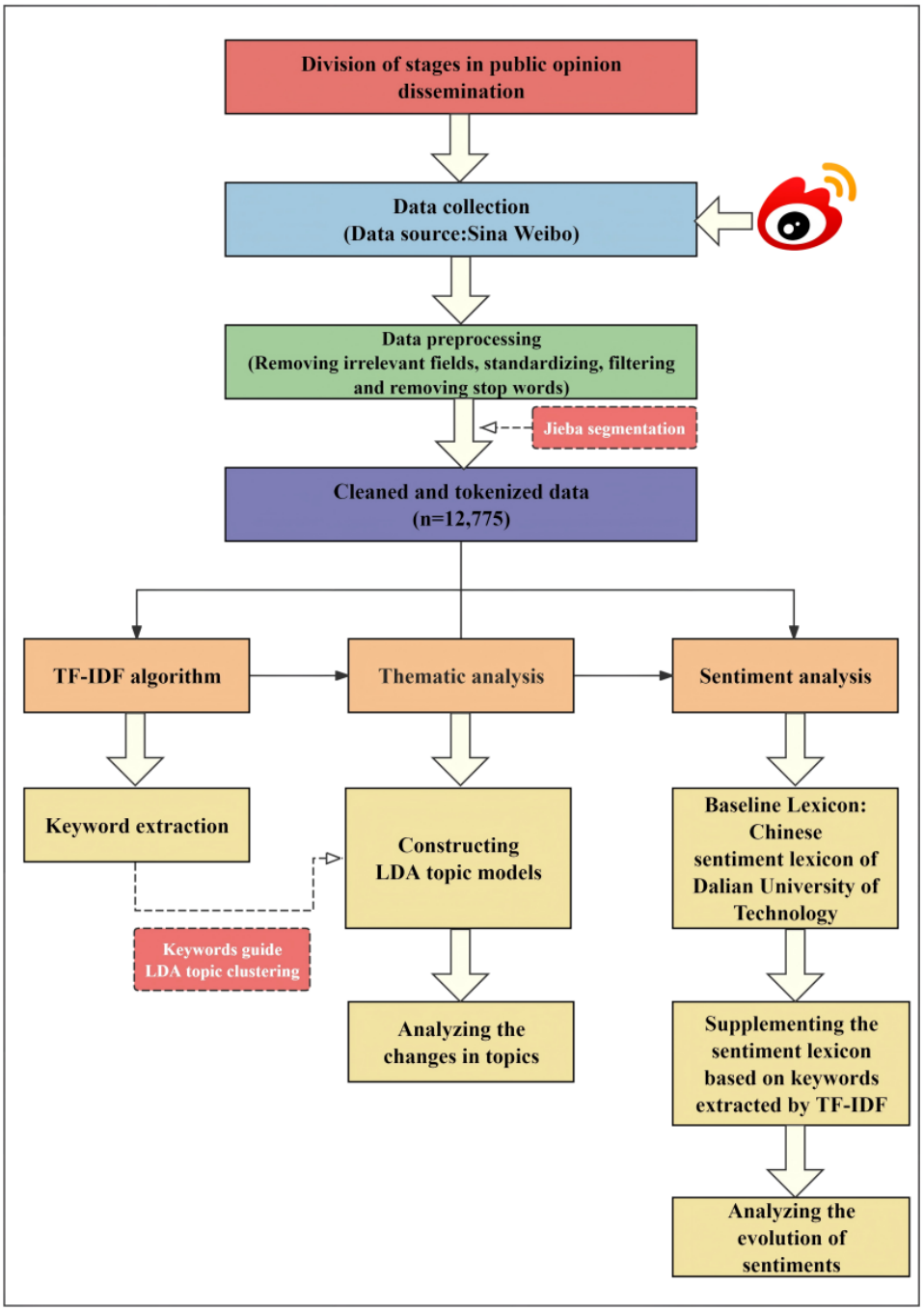
XSL•FO
RenderX

mirroring societal public sentiment development [23-26]. This study followed this theoretical approach to segment public opinion into the outbreak, spread, and decline phases, aligning with previous applications in public discourse analysis [27,28].

Data were collected from Sina Weibo, the most widely used social media platform in China, akin to X (previously known as Twitter). According to the China Internet Network Information Center 2022 report, Sina Weibo had over 582 million monthly active users [29], making it a primary platform for public discourse and sentiment expression in China. The platform has been widely used in studies of Chinese public opinion, serving as a critical data source for analyzing sentiment and social behavior [30].

We collected relevant comment data from Sina Weibo according to the public sentiment development cycle. After cleaning and segmenting the data, the term frequency-inverse document frequency (TF-IDF) algorithm was used to extract keywords, and the LDA topic model was used to analyze the focal points across different stages. Finally, a sentiment lexicon was constructed using the Chinese Sentiment Lexicon of the Dalian University of Technology (DUTIR), and sentiment analysis was conducted based on this lexicon. Figure 1 illustrates the methodological framework.

Figure 1. The methodological framework of the proposed research. LDA: latent Dirichlet allocation; TF-IDF: term frequency-inverse document frequency.

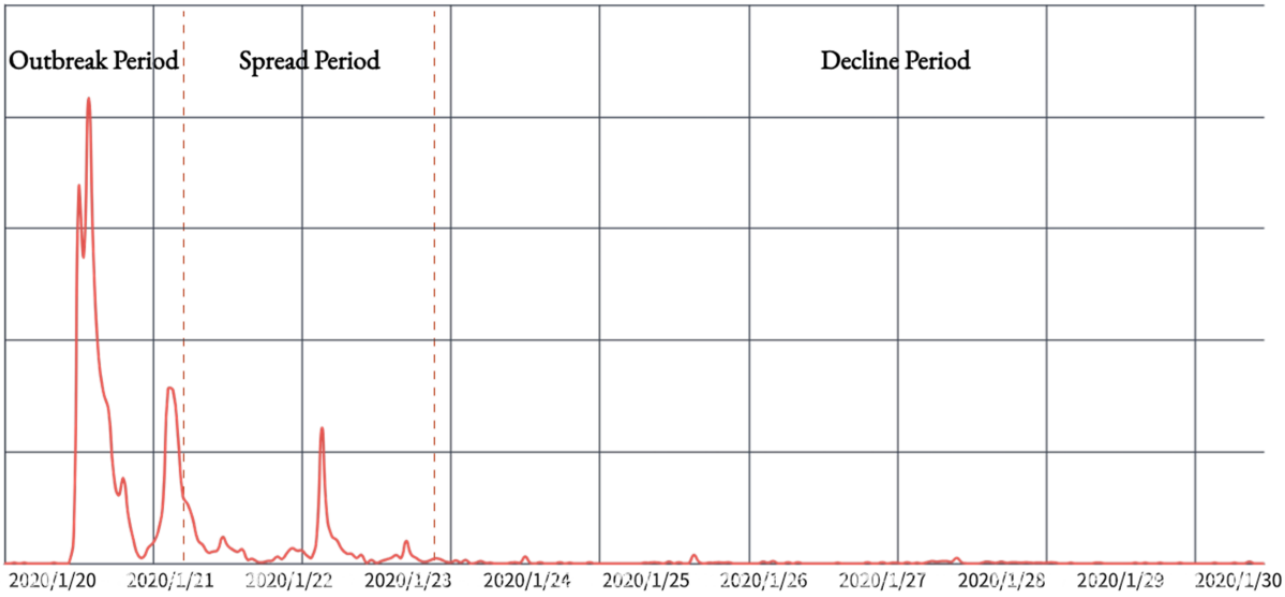


XSL•FO
RenderX

Public Sentiment Dissemination Stage Division

This study analyzed the trend of public opinion on the website Zhiwei Data. The trends were divided into 3 development periods, as illustrated in Figure 2. Zhiwei Data is a platform that monitors and analyzes China's internet big data. The platform uses social media data from across the internet to depict the development trends of events, communication effects, and trends in social communication.

Figure 2. Public opinion life cycle division of the "Beijing Chaoyang Hospital assault incident".



Data Collection

The research data were sourced from Sina Weibo, China's largest social media platform mirroring X's functionality and reach. It boasts a broad user base and spans various topics, providing a valuable snapshot of public discourse and sentiment. This study, based on the development of public opinion and the 3 life cycles of public opinion, selected 11 hashtags generated during the public opinion period of the "Beijing Chaoyang Hospital assault incident" in chronological order, with the "#The ophthalmologist at Chaoyang Hospital was hacked on 20 January 2020" as the starting point and the "#Dr. Tao Yong resumed clinic visits on 13 May" as the termination point to disseminate public opinion.

To collect comments related to these hashtags, the Python library Scrapy was used. Data collection occurred over a 4-week period, ensuring the capture of both initial reactions and ongoing public discourse. A total of 12,775 valid comments were collected after cleaning and filtering.

Data Preprocessing

Data preprocessing is a crucial step to ensure the consistency, accuracy, and relevance of the data used for sentiment analysis. The following subsections describe the key steps involved in preparing the data for analysis.

Data Cleaning

This stage involved removing invalid fields, standardizing data formats, and filtering out irrelevant content.

To remove duplicates, we identified and removed duplicate entries based on text, time stamps, and user IDs. This step reduced the data set by approximately 1200 comments.

To filter irrelevant content, we eliminated promotional, spam, or off-topic comments through keyword-based filtering and manual review. Approximately 500 comments were removed.

To eliminate invalid fields, we excluded records with incomplete or corrupted data fields, removing 500 comments.

After cleaning, the data set was reduced from 15,000 comments to 12,800 comments for further processing.

Stop Word Filtering

Stop words were identified and removed based on a predefined list derived from linguistic resources. These typically include high-frequency function words such as prepositions, conjunctions, and pronouns that do not contribute to the semantic content of the text. This process is consistent with best practices in sentiment analysis [27]. The stop word list was further refined by reviewing a sample of the data set to identify any frequently occurring terms that, although noninformative in general contexts, might carry domain-specific relevance (eg, medical terms) and should thus be retained. As a result, irrelevant terms such as "the," "and," and "of" were removed, while domain-relevant but functionally noninformative terms (eg, "patient," "doctor") were retained, following similar practices in health care sentiment analysis [31-33].

Lexicon Refinement

The word segmentation process was carried out using the Jieba tool, which uses a domain-specific lexicon tailored to the study's needs. This lexicon was iteratively refined based on the segmentation results. Initially populated with general terms, the lexicon was updated by adding domain-specific terminology, particularly medical and health care–related terms, to enhance segmentation accuracy. For example, terms such as "doctor-patient relationship" and "medical malpractice" were

XSL•FO
RenderX

incorporated to ensure that multiword expressions were correctly recognized. The lexicon was reviewed and updated after each iteration, ensuring it aligned with the research requirements and was capable of handling both general and specialized terms essential for analyzing public sentiment regarding doctor-patient conflicts [34].

Text Segmentation

Text segmentation was conducted using the Jieba tool, which splits text into individual words for further analysis. The lexicon refined in the previous step ensured that domain-specific terms were correctly segmented. The segmentation results were evaluated and adjusted manually to guarantee that critical multiword expressions were preserved and that the segmentation was contextually appropriate for the health care domain. This process was crucial in ensuring that the segmented words accurately reflected the topics discussed in the comments, particularly in the context of doctor-patient conflicts.

Final Data Volume

After preprocessing—including cleaning, stop word removal, lexicon refinement, and segmentation—the final data set comprised 12,775 valid and tokenized comments, as indicated in Figure 1.

TF-IDF

TF-IDF is a commonly used algorithm in text mining and information retrieval to measure the significance of a word in a text. The algorithm combines 2 crucial factors: term frequency and inverse document frequency. It calculates the frequency of each word in the text and its inverse document frequency in the corpus. It then assigns a weight to each word to reflect its importance in the collection of texts [35].

TF-IDF has been widely applied in various domains, including health care, where it is used to identify key terms in patient feedback, online health forums, and social media platforms. For example, research has demonstrated effectiveness in uncovering critical discussion themes in public health and medical services. Studies have used TF-IDF to analyze patient complaints and feedback to identify key areas for service improvement [36] and to extract critical health-related terms from social media during health crises such as the COVID-19 pandemic [37]. However, its application in analyzing the doctor-patient relationship remains limited, representing a gap this study aimed to address. In this study, TF-IDF was used to extract keywords from the Sina Weibo data set, ensuring the identification of terms most relevant to public discourse on doctor-patient conflicts.

TF represents the frequency of a word in the text. It is calculated as follows:



IDF represents the inverse document frequency of a word in the entire corpus. It is calculated as follows:



The TF-IDF weights are ultimately formed by the product of TF and IDF:

$$TF–IDF(t,d,D)=TF(t,d) \times IDF(t,D)$$

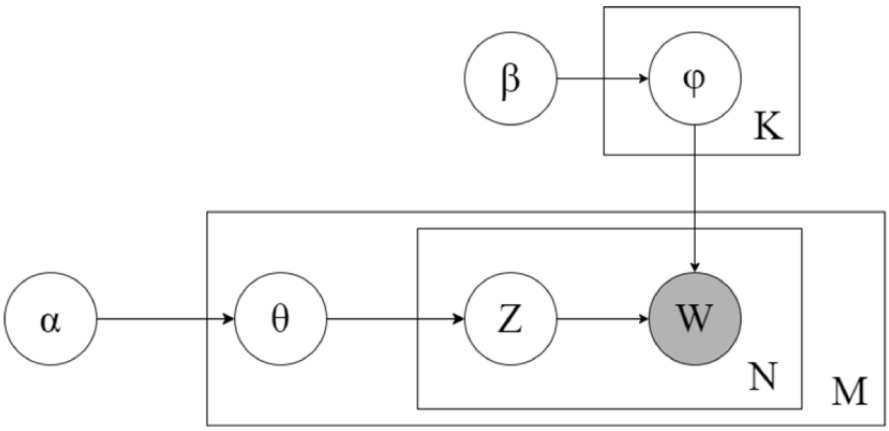
LDA Topic Model

LDA is a probabilistic graphical model to identify hidden thematic structures within text collections. The model was proposed by Blei et al [38] in 2003 and has become a classic method for topic modeling in text mining. The LDA model extracts potential topics from documents or corpora using a bag-of-words approach. It constructs a model that includes a “document-topic distribution” and “topic-word distribution” without considering the order in which words appear [39]. The document comprises one or more topics, with each word generated by one of the topics [40]. Therefore, LDA models can aid in text-based analysis processes for online opinion topic events in social media, such as identifying latent topics and clustering users. In the field of health communication, the LDA model has been widely applied to identify themes related to sudden public health events, such as COVID-19 [41,42].

The generation process of the LDA topic model is shown in Figure 3: (1) generate the hyperparameter α of the topic distribution and generate the topic distribution θ for each document; (2) for each document, generate the topic Z from its topic distribution θ; (3) for each topic K, generate the word distribution ϕ of the topic K from the hyperparameter β of the word distribution; (4) for the Nth word in each document, generate it from the word distribution of its corresponding topic Z; (5) W represents the words in the corpus, which are generated based on their respective topic-word distributions (ϕ); (6) N is the number of words in a document, representing the scope of word generation within each document; and (7) M is the total number of documents in the data set, defining the corpus-level scope of the generative process.

XSL•FO
RenderX

Figure 3. The generation process of the latent Dirichlet allocation (LDA) topic model.



Sentiment Lexicon

Sentiment analysis and topic modeling have been widely applied as effective tools to analyze public sentiment and identify thematic patterns in large-scale social media data sets [43]. It is first necessary to construct a lexicon of sentiments to dynamically analyze public opinion sentiments and themes in doctor-patient conflict cases. This study used the DUTIR, which was developed by the Information Retrieval Research Laboratory based on the Chinese language context, as the basic sentiment lexicon. It is used for sentiment analysis and sentiment calculation to help analyze the sentiment tendency in texts and is widely used in the field of Chinese text research as a whole. This lexicon has been used in various research studies, demonstrating its reliability and applicability in different sentiment analysis scenarios. In health care, sentiment lexicons have been extensively used to assess patient satisfaction [44], analyze public sentiment during health crises [45], and evaluate feedback on health care services [46]. Research has shown that DUTIR effectively captures nuanced emotional expressions in Chinese texts, such as in sentiment-aware word embedding for emotion classification. Additionally, DUTIR has proven valuable in analyzing sentiment trends in online media, including bullet screen comments on health care topics. Most existing sentiment analysis research in health care classified collected comment texts into binary categories, simply dividing public sentiment into positive and negative [47-49], which failed to vividly capture the diversity of public emotions. The sentiment lexicon used in this study introduced neutral, complex, and mixed emotional categories, allowing for a more refined capture of the comment texts and reflecting the multidimensional characteristics of emotions. The lexicon contains 27,466 sentiment words, and the sentiment categories are divided into 7 types: joy, happiness, anger, disgust, fear, sorrow, and surprise. The selection of these 7 categories is primarily rooted in the predefined structure of DUTIR, which has been validated in previous studies and widely applied in public discourse and health care research. Research has shown that DUTIR's categorization effectively captures emotional nuances, making it particularly suited for complex sentiment analysis tasks. Its application in health care sentiment analysis and public discourse has been widely documented [31,50], underscoring its relevance and reliability.

Additionally, the chosen classifications align with established psychological theories, such as the model of universal emotions by Ekman and Friesen [51] and wheel of emotions by Plutchik [52]. These frameworks identify emotions such as joy, anger, and fear as universal and fundamental, providing a robust theoretical basis for the classification system. This dual grounding in theoretical models and the practical structure of DUTIR ensures that the framework is both comprehensive and contextually relevant.

By leveraging the predefined structure of DUTIR and its theoretical underpinnings, this study effectively captured the multidimensional emotional dynamics in public sentiment surrounding doctor-patient conflicts, offering insights beyond binary sentiment classifications.

Ethical Considerations

This study involved the analysis of publicly available, anonymized data from Sina Weibo. Since no personally identifiable information was collected, stored, or analyzed, and no direct interaction with individuals occurred, the study was exempt from Institutional Review Board (IRB) approval in accordance with Sichuan University's Research Ethics Review Policy.

Informed consent was not required, as this study relied exclusively on publicly available user-generated content. Additionally, the study adhered to the terms of service and privacy policies of the Sina Weibo platform.

Results

TF-IDF Keyword Extraction

The study conducted TF-IDF keyword extraction to identify the primary words associated with the "Beijing Chaoyang Hospital assault incident" at different public opinion stages. During the outbreak period, the most frequently expressed words were "injury" (TF-IDF: 0.030589), "doctor" (TF-IDF: 0.028905), and "harm" (TF-IDF: 0.028270). In the spread period, "gentle" (TF-IDF: 0.05255), "blessings" (TF-IDF: 0.05179), and "kindness" (TF-IDF: 0.05060) surfaced frequently. By the decline period, the words "recovery" (TF-IDF: 0.050599), "injury" (TF-IDF: 0.047823), and "gentle" (TF-IDF: 0.047587) were most prevalent.

XSL•FO
RenderX

Table 1 summarizes the high-frequency keywords and their corresponding frequencies and TF-IDF values for the 3 periods, illustrating the changes in public focal points and high-frequency expressions at each stage.

In the outbreak period, the words were dominated by emotionally charged terms like “harm to doctors,” “injury,” and “angry to death,” reflecting public shock and outrage. During the spread period, supportive and empathetic words such as “blessings,” “gentle,” and “recovery” emerged, signifying a shift toward collective concern and healing. By the decline period, the focus remained on resolution with terms like “recovery,” “criminal,” and “hatred,” suggesting ongoing calls for justice alongside a desire for closure.

Table 1. Term frequency-inverse document frequency (TF-IDF) keyword extraction for 3 stages of public opinion.

Word	Frequency	TF-IDF
Outbreak period		
Injury	1465	0.030589
Doctor harm	942	0.028905
Harm	792	0.028270
Prayer	629	0.027485
Medical study	612	0.027354
Enrage	671	0.027305
Doctor consult	561	0.026949
Security check	551	0.026922
Excellent	533	0.026804
Treatment	522	0.026768
Spread period		
Gentle	386	0.052555
Blessings	349	0.051793
Kindness	302	0.050600
Recovery	238	0.048901
Heartbroken	186	0.047038
World	182	0.045853
Brightness	157	0.045260
Safety	167	0.045209
Excellent	145	0.045105
Good person	144	0.044783
Decline period		
Recovery	865	0.050599
Injury	513	0.047823
Gentle	495	0.047587
Hatred	402	0.046213
Recovery	382	0.045876
Culprit	589	0.045392
Encourage	354	0.045373
Hospital discharge	283	0.043894
Wish	280	0.043800
Harm	249	0.042751

LDA Topic Model

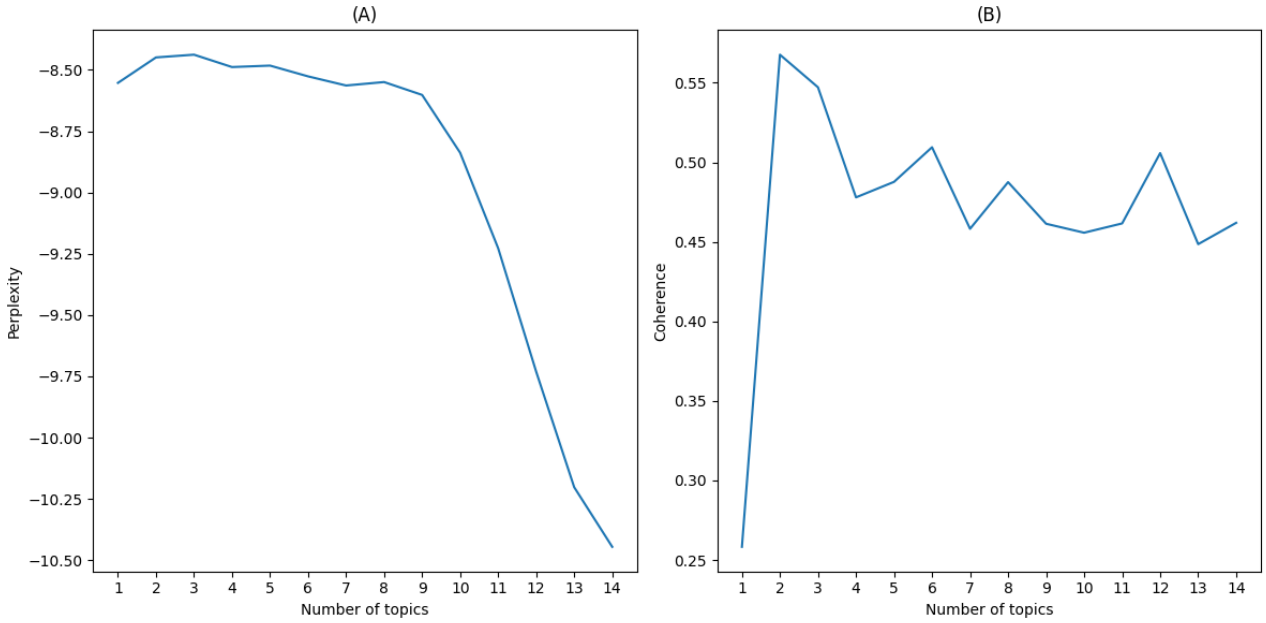
Using the Gensim library in Python for LDA topic model training, the study focused on perplexity and coherence to gauge model quality and thematic clarity. Perplexity was used to measure the model’s ability to predict the test data, with lower perplexity indicating better model performance [38]. Coherence was used to assess the interpretability of the topics, with higher

XSL•FO
RenderX

coherence scores reflecting clearer and more meaningful issues [53]. Evaluating these metrics under different settings revealed the optimal theme count. Figures 4-6 illustrate these metrics across public opinion dynamics stages—outbreak, spread, and decline—aiding with precise determination of topic numbers in sync with data volume for effective topic identification and extraction.

To enhance the coherence and interpretability of the LDA results, TF-IDF–extracted keywords were used as seed words to guide topic analysis [54]. High-weighted TF-IDF terms ensured that LDA-generated topics were aligned with public discourse at each stage. For instance, during the outbreak period, keywords like “injury,” “doctor,” and “harm” shaped topics centered on medical accountability and incident responses. In the spread phase, terms such as “gentle” and “blessings” informed themes of empathy and community healing, while “recovery” and “criminal” in the decline period contributed to topics related to resolution and justice. This integration ensured that the LDA analysis was both data-driven and contextually grounded, aligning topic clusters with the most critical public concerns.

Figure 4. (A) Perplexity and (B) coherence scores of latent Dirichlet allocation (LDA) topics during the outbreak period.



As illustrated in Figure 4, the perplexity score steadily declined with an increasing number of topics, while the coherence score peaked at 11 topics. This peak indicated that 11 topics provided the most meaningful representation of initial public reactions, capturing themes such as outrage, shock, and immediate demands for justice.

During the spread phase, as depicted in Figure 5, the coherence score reached its maximum value at 12 topics, while the perplexity curve exhibited diminishing returns beyond this point. This selection reflected the complexity of public discussions during this phase, including sympathy for medical professionals, criticism of systemic health care issues, and debates on policy implications.

Figure 6 shows that coherence peaked at 13 topics during the decline phase, while the perplexity score stabilized. This topic number aligned with the reflective and solution-oriented nature of public discourse in this period, encompassing themes such as health care reforms, institutional accountability, and the long-term impacts of the incident.

XSL•FO
RenderX

Figure 5. (A) Perplexity and (B) coherence scores of latent Dirichlet allocation (LDA) topics during the spread period.

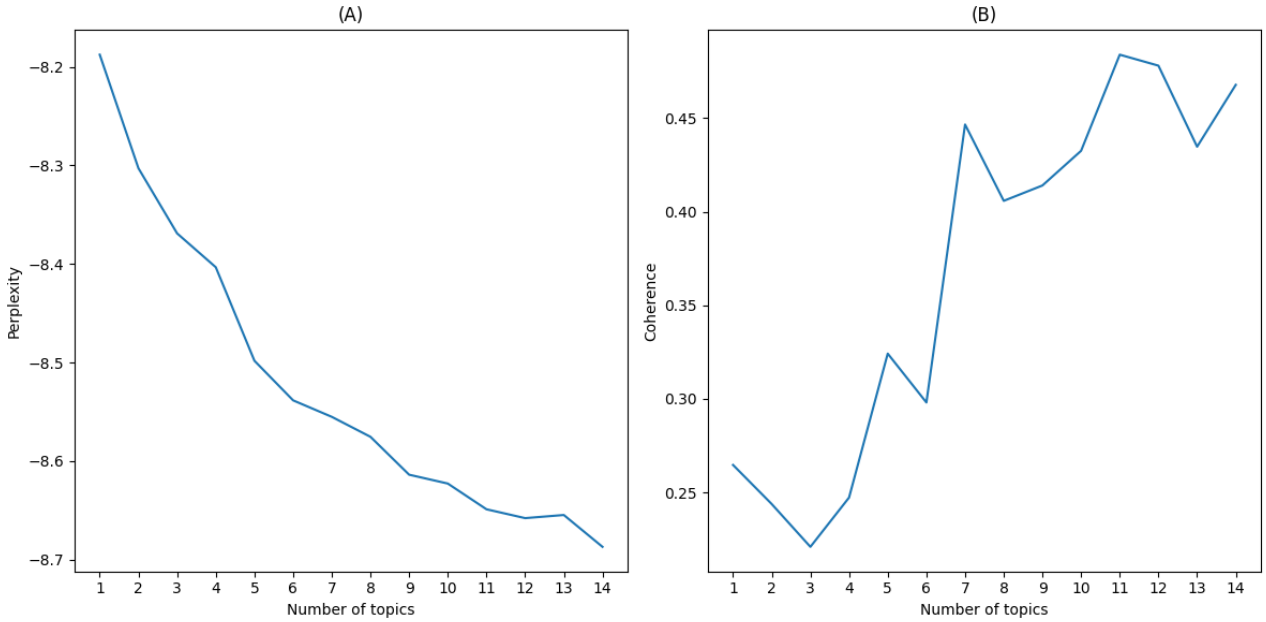
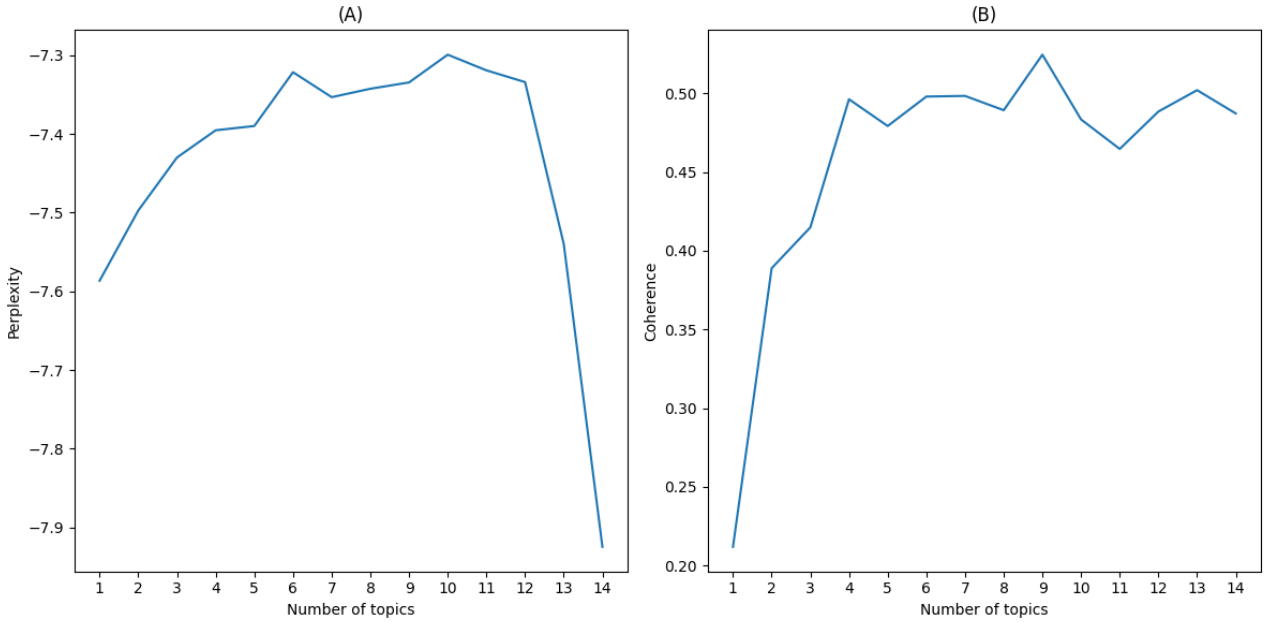


Figure 6. (A) Perplexity and (B) coherence scores of latent Dirichlet allocation (LDA) topics during the decline period.



After determining the optimal number of topics, we used the pyLDAvis library in Python to create an interactive visualization of the topic model. The study then selected 10 higher-weight keywords to annotate and analyze the topics. The results showed that, during the outbreak period, topics centered on immediate responses to medical violence (Topic 1), victim empathy (Topic 2), societal disillusionment (Topic 3), aggressor accountability (Topic 4), and recovery aspirations (Topic 5). As the incident progressed, the public focus shifted toward appreciating the victim's character (Topic 1), supporting their recovery (Topic 2), expressing concerns over the career impact (Topic 3), condemning the aggression (Topic 4), and expressing relief over the victim's recovery (Topic 5). In the decline phase, discussions centered on the patient's condition (Topic 1), the victim's virtues (Topic 2), well wishes for recovery (Topic 3), strategies for resolving medical disputes (Topic 4), and advocacy for stringent legal measures (Topic 5). This comprehensive thematic analysis highlighted the dynamic evolution of public sentiment and concerns throughout the incident's life cycle. The complete LDA topic extraction is presented in Table 2.

XSL•FO
RenderX

Table 2. Latent Dirichlet allocation (LDA) topic identifiers for 3 periods of public opinion.

Life cycle period topics	Terms
Outbreak period	
Topic 1: Responses to Medical Violence	Enraged; security check; medical injury; medical disturbance; busy; injury; society; life; slash; harm
Topic 2: Victim Empathy	Effort; society; excellent; recovery; medical student; save lives; cry; cultivate; good person; contribute
Topic 3: Societal Disillusionment	China; study medicine; can't save; Lu Xun; disheartened; statement; epidemic; guard; darkness; difficult
Topic 4: Aggressor Accountability	Protection; death penalty; severe punishment; medical; country; murderer; law; medical disturbance; aggressor; expose
Topic 5: Recovery Aspirations	Pray; safety; heartache; sad; excellent; speedy recovery; light; medical disturbance; injury; destroy
Spread period	
Topic 1: Victim Character Appreciation	Sad; excellent; gentle; angel; harm; kind; heartache; self; death penalty; good person
Topic 2: Recovery Support	Cry; pay tribute; pray; save; care; indispensable; cheer up; heartache; speedy recovery; light
Topic 3: Career Impact Concerns	Heartache; pity; excellent; kind; top; recovery; unable; research; scientific research; cultivate
Topic 4: Condemnation of Aggression	Harm; furious; harsh punishment; strict punishment for murderers; heartache; destroy; medical disturbance; undeserving; sad; angry
Topic 5: Relief Over Victim's Awakening	Bless; miracle; safety; wake up; good news; take care; thankfully; hope; God; fortunately
Decline period	
Topic 1: Patient Condition Focus	Body; treatment; recovery; nerve; rupture; blood vessel; muscle; Gate of Hell; mental state; perception
Topic 2: Victim Virtue Highlight	Gentle; forgive; kind; benevolence; speedy recovery; strong; inner; moved; beautiful; blessings
Topic 3: Well-Wishes for the Victim	Wish; safety; good person; speedy recovery; gentle; heartache; angel; safe and sound; healthy; memory
Topic 4: Strategies for Medical Dispute Resolution	Doctor-patient; protection; doctor-patient relationship; policy; medical; respect; country; inspection; medical disturbance; security check
Topic 5: Advocacy for Stringent Legal Measures	Recovery; apology; harsh punishment for murderers; law; harm; cost; doctor-patient conflict; death penalty; medical injury; injure

Sentiment Analysis

Construction of Sentiment Lexicon

Owing to changes in language and the online environment, the connotations of certain words and sentences shifted, and new vocabulary emerged. Therefore, this study expanded the existing DUTIR by manually annotating the emotional characteristics of new words according to the ontology format of the existing database. This was done to cater to the demand for sentiment analysis in specific events or generic scenarios and to ensure accurate results. Multiple annotators working together to extract vocabulary is a recognized research method in sentiment analysis, as it helps improve reliability and reduce bias in the annotation process [55,56]. The expansion process involved several steps to maintain consistency and reliability. First, new words were identified based on their frequency and contextual relevance to the doctor-patient conflict data set. The emotional characteristics of these words were then annotated manually by multiple scholars. Each scholar independently assigned emotional labels to the words, following the ontology structure of the existing lexicon.

Discrepancies between annotations were resolved through discussion and consensus-building among the scholars. Finally, the updated lexicon was validated against a subset of the data to ensure alignment with the existing lexicon's structure and objectives. The study compared the keywords extracted by the TF-IDF algorithm with the sentiment vocabulary list of the Dalian University of Technology. We selected the keywords not included in the sentiment vocabulary ontology database and manually added them after labeling them with emotional features. This process formed an expanded sentiment lexicon.

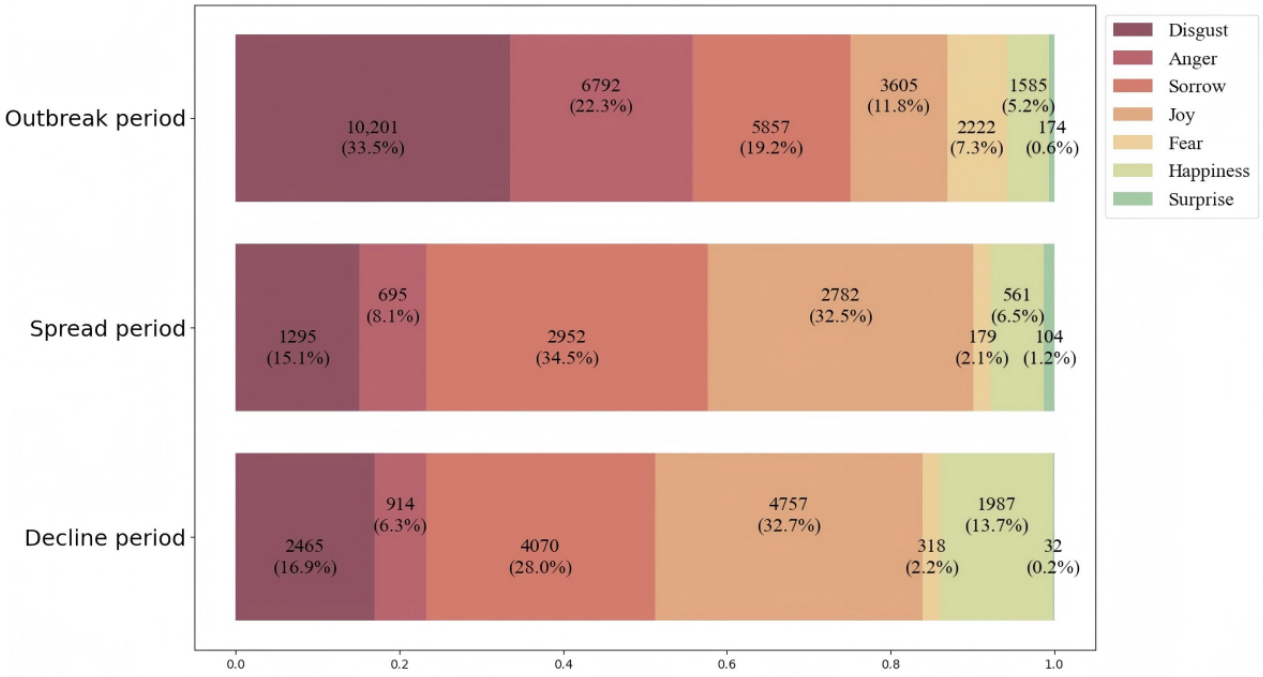
Sentimental Trend

The sentiment analysis results for the 3 periods are shown in Figure 7, reflecting significant changes in public sentiment. During the Outbreak period, of the 30,436 comments, 10,201

XSL•FO
RenderX

(33.52%) expressed disgust, followed by 6792 (22.32%) showing anger and 5857 (19.24%) reflecting sorrow. In the Spread period, of the 8568 comments, 2952 (34.45%) expressed sorrow, and 2782 (32.47%) indicated joy. In the Decline period, of the 14,543 comments, 4757 (32.71%) exhibited joy, while 4070 (27.99%) conveyed sorrow and 2465 (16.95%) reflected disgust. Based on these results, the study mapped the evolution of sentiment to visualize changes in public sentiment across the 3 periods.

Figure 7. Sentiment trends in the 3 periods.



Discussion

Principal Findings

In this study, data from Sina Weibo were analyzed to investigate public sentiment during the Beijing Chaoyang Hospital assault incident using 3 analytical approaches. First, TF-IDF keyword analysis identified key terms such as “injury,” “doctor,” and “recovery,” illustrating how the initial public focus on the specifics of the incident gradually expanded to include broader health care issues. Second, thematic analysis via the LDA topic model revealed that public attention shifted from immediate responses to long-term implications, reflecting an evolution from shock to systemic consideration. Last, sentiment analysis using a Chinese sentiment lexicon indicated that negative sentiment was sustained despite progressing toward recovery-focused dialogue. Collectively, these findings revealed that negative sentiment persisted even as public dialogue progressed toward recovery-focused themes, underscoring the need for communication strategies responsive to immediate and evolving public sentiments in health-related crises.

TF-IDF Keyword Analysis

The keyword analysis through TF-IDF conducted during the Beijing Chaoyang Hospital assault incident revealed a nuanced evolution in public sentiment, corroborating findings from previous research on crisis communication and public health emergencies. During the outbreak period, keywords such as “injury,” “doctor,” and “harm” dominated the public discourse. These terms echoed sentiments typically observed in immediate responses to medical crises, aligning with studies that indicated initial public reactions were often driven by shock and a quest for immediate understanding of the incident [57,58]. As the situation progressed to the spread period, a noticeable shift occurred toward more empathetic and supportive terms such as “gentle,” “blessings,” and “kindness.” This transition from focusing on the incident’s negative aspects to fostering a healing-oriented dialogue was consistent with the “recovery phase” described in the Coombs Crisis Communication Model [59], where the public focus shifted toward rehabilitation and emotional support. By the decline period, the emphasis on “recovery” and “gentle” further confirmed the trend toward normalization and reconciliation. In this phase, the affected community began to heal and rebuild, as noted by Ogie et al [60].

Although the keyword analysis provided valuable insights into shifting public sentiment, it had limitations. Keywords alone could not fully capture the complexity of public emotions or the depth of thematic elements evolving during such incidents. Thus, this initial analysis laid the foundation for a more comprehensive exploration. The subsequent phase used thematic and sentiment analysis techniques to delve deeper into the underlying narratives and emotional contours of public

XSL•FO
RenderX

discourse, offering a more complete understanding of the incident's impact on public sentiment.

Thematic Analysis

Upon analyzing and summarizing the LDA topic model, it became evident that the theme evolved across all 3 phases of public opinion outbreak and spread. The decline period illustrated the theme's continuity and the distinctions between phases. This conclusion was consistent with previous public opinion research [61-63].

Initially, the public's response was characterized by a surge in negative sentiments, focusing on the incident's immediate impacts and demanding accountability. This intense reaction reflects the "shock phase" [59] in crisis communication theory, where the initial shock triggers a heightened emotional response from the public, demanding urgent and decisive actions. This phase often sees a spike in public engagement and outcry, evident from the prevalent themes of aggression and immediate accountability. As the crisis continued, public sentiment shifted toward a more nuanced and empathetic perspective, concentrating on the victim's personal and professional impacts. This transition aligns with the "deliberation phase" [59] described in situational crisis communication theory, where the public starts to process the incident more profoundly and show empathy toward the victims. The moderation in tone suggests a community moving toward a collective reflection, pondering the long-term effects on those directly affected and their implications on professional practices. In the later stages, the focus shifted toward legal measures and recovery, indicating a societal shift toward resolution and systemic reflection. This phase mirrors the "resolution phase" [59], where public discourse often turns to evaluating how the crisis was handled and the steps needed to prevent future occurrences. The decreased anger and increased discussions about recovery and legal implications suggest a maturing public opinion that seeks to address systemic issues and improve doctor-patient relationships for the future.

Sentiment Analysis

This study has highlighted the versatility and effectiveness of sentiment analysis for capturing multidimensional emotions and thematic evolution. Previous research demonstrated these methods as reliable tools for understanding public discourse and informing interventions in complex social systems [43]. Previous research had determined that public opinion on health-related topics was inconsistent and unstable. Fluctuations influenced by topic changes led to significant variations in the dominant sentiment at each stage of public opinion development [64-66]. This study, however, indicated that, in serious doctor-patient conflicts, negative sentiments from the initial stage often persisted despite potential positive developments, driven by the primacy effect—where early impressions resist change over time [67].

During the outbreak period, negative emotions like disgust and anger predominated, aligning with Le Bon's Theory of the Crowd [68], which attributed emotional contagion to impulsive group behavior. As the crisis matured into the spread period, the emotional landscape shifted significantly toward more nuanced emotions such as sorrow and joy. This transition was explained by the cognitive dissonance theory by Festinger [69], which explains attitude adjustments to reduce discomfort from conflicting information. However, in the decline phase, negative sentiments persisted longer than typical patterns observed in public health crises. The theory of affective intelligence [70] suggests that emotional responses could override cognitive assessments, mainly when initial emotions were intense and damaging. Such emotional endurance contradicted the general expectations derived from mood management theory [71], positing that individuals would seek to alter their mood toward more favorable outcomes, mainly as situations developed and new information became available.

The findings underscore the resilience of negative sentiments in severe doctor-patient conflicts, driven by the primacy effect and amplified by structural challenges. This persistence highlights the need for tailored communication strategies in health care settings, addressing the long-term impact of initial negative impressions and prioritizing transparent, empathetic engagement to shift public sentiment effectively.

Recent research has highlighted the importance of crisis communication in shaping public sentiment during health emergencies [72]. Clear messaging has been shown to reduce negative sentiments in the early stages, whereas delayed communication has exacerbated distrust and fear, prolonging negativity [73]. Furthermore, the cultural context plays a significant role, with collectivist societies experiencing more enduring negative sentiments due to heightened communal sharing of emotions [74]. These findings align with this study's observations.

Comparatively, sentiment trends in other countries revealed both similarities and differences. Globally, negative sentiment dominates during crisis outbreaks, but western countries often transition more quickly to themes of systemic reform and empathy [75,76]. In contrast, distrust and fear persisted longer in China, influenced by health care resource disparities and overcrowding [77]. These findings underscore the cultural and systemic factors shaping sentiment dynamics and highlight the importance of communication strategies tailored to local contexts.

Conclusion

Weibo, China's largest social media platform, provides a unique view of public sentiment through its rich emotional content. By analyzing these data, researchers can identify trends in public sentiment, aiding government and relevant departments with developing effective communication strategies for doctor-patient conflicts. The study found that public sentiment evolved through different phases of public opinion, showing predominantly negative emotions during the outbreak phase, balanced sentiments during the spread phase, and continued negative dominance in the decline phase. This finding differs from previous studies, highlighting the persistent impact of initial emotions throughout the public opinion life cycle.

To address this persistence, medical institutions should implement tailored communication strategies. Establishing dedicated crisis communication teams trained in empathetic

XSL•FO
RenderX

and transparent messaging can mitigate the long-term impact of negative sentiments. Timely information dissemination through clear protocols and community-based platforms can help reduce misinformation and foster public trust. Real-time sentiment monitoring systems can provide insights into public emotions as they evolve, guiding adaptive strategies to address emerging concerns effectively.

Furthermore, the methodologies used in this study, particularly the integration of sentiment lexicon analysis and LDA topic modeling, hold potential for broader adaptation across sociocultural contexts. Adapting the sentiment lexicon for other linguistic settings could enhance global sentiment analysis accuracy. Additionally, interdisciplinary applications of these findings—spanning health care management, psychology, and public health—could foster a deeper understanding of societal sentiments and their impact on health care practices. These insights can inform the development of targeted policies to improve communication strategies, train health care professionals in emotional intelligence, and enhance trust in health care systems, ultimately improving patient satisfaction and crisis management outcomes.

Future research could explore comparative studies across diverse health care systems and integrate multimodal data sources, such as images and videos, to provide a more comprehensive understanding of public sentiment dynamics.

Limitations

Although the study presented some innovative findings, it still has certain limitations. First, the data were obtained exclusively from Sina Weibo, which, although a leading social media platform in China, did not represent the full spectrum of social media users across different platforms like WeChat and Douyin.

This reliance on a single platform may have introduced platform-specific biases, as its user base and communication dynamics differ from those on other platforms, potentially affecting the representativeness of the findings.

Second, the study's reliance on textual data may have overlooked significant emotional and contextual information conveyed through images and videos, suggesting a need for multimodal data analysis. Furthermore, the sentiment analysis tools used might not have fully captured the nuances of sarcasm, irony, or regional dialects, leading to possible misinterpretations.

Future research can consider more diverse social media platforms and incorporate cross-cultural comparative studies on public sentiment in doctor-patient conflicts to understand the differences in public reaction patterns and emotional expressions across various cultural backgrounds. Incorporating multimodal data, such as visual and audio content, could enhance the richness and accuracy of sentiment analysis. Additionally, combining cross-platform data would allow researchers to compare public sentiment across different platforms and user demographics, providing a broader perspective.

Additionally, integrating social network analysis methods can provide a deeper analysis of the network structure and influential nodes of information dissemination, revealing opinion leaders and dissemination paths in doctor-patient conflict incidents. Longitudinal data collection and analysis would further enable the capture of temporal dynamics, offering insights into how sentiments evolve over time during such conflicts.

Acknowledgments

The authors would like to thank the National Natural Science Foundation of China for funding this work through the project titled "Implementation Science Research on Caries Risk Management for Children in Primary Health Care Institutions under the 'Medical-Dental' Integrated Model," under grant number 72374146.

Conflicts of Interest

None declared.

References

1. Global Health Workforce statistics database. World Health Organization. URL: https://www.who.int/data/gho/data/themes/topics/health-workforce [accessed 2024-06-26]
2. World Health Assembly. Global strategy on human resources for health: workforce 2030. World Health Organization. 2016. URL: https://iris.who.int/handle/10665/252799 [accessed 2024-06-26]
3. He AJ, Qian J. Explaining medical disputes in Chinese public hospitals: the doctor-patient relationship and its implications for health policy reforms. Health Econ Policy Law 2016 Oct;11(4):359-378. [doi: 10.1017/S1744133116000128] [Medline: 27018911]
4. Xiao S, Wang L, Edelman EJ, Khoshnood K. Interpersonal factors contributing to tension in the Chinese doctor-patient-family relationship: a qualitative study in Hunan Province. BMJ Open 2020 Dec 10;10(12):e040743 [FREE Full text] [doi: 10.1136/bmjopen-2020-040743] [Medline: 33303452]
5. Tan L, Yuan S, Cheng P, Ning P, Gao Y, Xiao W, et al. Media reports about violence against medical care providers in China. Int J Environ Res Public Health 2021 Mar 12;18(6):2922 [FREE Full text] [doi: 10.3390/ijerph18062922] [Medline: 33809244]

XSL•FO
RenderX

6. China sees continuous improvement in health service capacity. National Medical Products Administration. URL: https://english.nmpa.gov.cn/2023-11/03/c_936199.htm [accessed 2024-11-27]
7. Elrod JK, Fortenberry JL. Public relations in health and medicine: using publicity and other unpaid promotional methods to engage audiences. BMC Health Serv Res 2020 Sep 15;20(Suppl 1):821 [FREE Full text] [doi: 10.1186/s12913-020-05602-x] [Medline: 32928186]
8. McCarthy RNE, Donkoh ET, Arthur DD, Dassah ET, Boadu KO, Otoo JE, et al. Public relations strategies employed by the Ghana Health Service to address COVID-19 vaccine hesitancy: a qualitative inquiry. Trop Med Health 2023 May 12;51(1):26 [FREE Full text] [doi: 10.1186/s41182-023-00519-7] [Medline: 37170342]
9. Aldosery A, Carruthers R, Kay K, Cave C, Reynolds P, Kostkova P. Enhancing public health response: a framework for topics and sentiment analysis of COVID-19 in the UK using Twitter and the embedded topic model. Front Public Health 2024;12:1105383 [FREE Full text] [doi: 10.3389/fpubh.2024.1105383] [Medline: 38450124]
10. Allem J, Donaldson SI, Vogel EA, Pang RD, Unger JB. An analysis of Twitter posts about the U.S. Food and Drug Administration's menthol ban. Nicotine Tob Res 2023 Apr 06;25(5):962-966 [FREE Full text] [doi: 10.1093/ntr/ntac290] [Medline: 36534973]
11. Beierle F, Pryss R, Aizawa A. Sentiments about mental health on Twitter-before and during the COVID-19 pandemic. Healthcare (Basel) 2023 Nov 03;11(21):1 [FREE Full text] [doi: 10.3390/healthcare11212893] [Medline: 37958038]
12. Cho LD, Tang JE, Pitaro N, Bai H, Cooke PV, Arvind V, et al. Sentiment analysis of online patient-written reviews of vascular surgeons. Ann Vasc Surg 2023 Jan;88:249-255. [doi: 10.1016/j.avsg.2022.07.016] [Medline: 36028181]
13. Singh M, Dhillon HK, Ichhpujani P, Iyengar S, Kaur R. Twitter sentiment analysis for COVID-19 associated mucormycosis. Indian J Ophthalmol 2022 May;70(5):1773-1779 [FREE Full text] [doi: 10.4103/ijo.IJO_324_22] [Medline: 35502071]
14. Stefanis C, Giorgi E, Kalentzis K, Tselemponis A, Nena E, Tsigalou C, et al. Sentiment analysis of epidemiological surveillance reports on COVID-19 in Greece using machine learning models. Front Public Health 2023;11:1191730 [FREE Full text] [doi: 10.3389/fpubh.2023.1191730] [Medline: 37533519]
15. Gunasekaran KP. Exploring sentiment analysis techniques in natural language processing: a comprehensive review. arXiv Preprint posted on May 24, 2023. [doi: 10.48550/arXiv.2305.14842]
16. Catelli R, Pelosi S, Comito C, Pizzuti C, Esposito M. Lexicon-based sentiment analysis to detect opinions and attitude towards COVID-19 vaccines on Twitter in Italy. Comput Biol Med 2023 May;158:106876 [FREE Full text] [doi: 10.1016/j.compbiomed.2023.106876] [Medline: 37030266]
17. Lyu JC, Han EL, Luli GK. COVID-19 vaccine-related discussion on Twitter: topic modeling and sentiment analysis. J Med Internet Res 2021 Jun 29;23(6):e24435 [FREE Full text] [doi: 10.2196/24435] [Medline: 34115608]
18. Dong E, Xu J, Sun X, Xu T, Zhang L, Wang T. Differences in regional distribution and inequality in health-resource allocation on institutions, beds, and workforce: a longitudinal study in China. Arch Public Health 2021 May 17;79(1):78 [FREE Full text] [doi: 10.1186/s13690-021-00597-1] [Medline: 34001268]
19. Kelley JM, Kraft-Todd G, Schapira L, Kossowsky J, Riess H. The influence of the patient-clinician relationship on healthcare outcomes: a systematic review and meta-analysis of randomized controlled trials. PLoS One 2014;9(4):e94207 [FREE Full text] [doi: 10.1371/journal.pone.0094207] [Medline: 24718585]
20. Sharkiya SH. Quality communication can improve patient-centred health outcomes among older patients: a rapid review. BMC Health Serv Res 2023 Aug 22;23(1):886 [FREE Full text] [doi: 10.1186/s12913-023-09869-8] [Medline: 37608376]
21. Liu Z, Wu X. Structural analysis of the evolution mechanism of online public opinion and its development stages based on machine learning and social network analysis. Int J Comput Intell Syst 2023 Jun 09;16(1):1. [doi: 10.1007/s44196-023-00277-8]
22. Fink S. Crisis Management: Planning for the Inevitable. North Brabant, the Netherlands: Amacom; 1986.
23. Ali RH, Pinto G, Lawrie E, Linstead EJ. A large-scale sentiment analysis of tweets pertaining to the 2020 US presidential election. J Big Data 2022;9(1):79 [FREE Full text] [doi: 10.1186/s40537-022-00633-z] [Medline: 35729897]
24. Li C, Qu Y, Zhu X. Asynchronous network-based model and algorithm for sentiment analysis of online public opinions. K 2022 May 03;52(10):4130-4157. [doi: 10.1108/k-02-2021-0159]
25. Usher K, Durkin J, Martin S, Vanderslott S, Vindrola-Padros C, Usher L, et al. Public sentiment and discourse on domestic violence during the COVID-19 pandemic in Australia: analysis of social media posts. J Med Internet Res 2021 Oct 01;23(10):e29025 [FREE Full text] [doi: 10.2196/29025] [Medline: 34519659]
26. Yang G, Wang Z, Chen L. Investigating the public sentiment in major public emergencies through the complex networks method: a case study of COVID-19 epidemic. Front Public Health 2022;10:847161 [FREE Full text] [doi: 10.3389/fpubh.2022.847161] [Medline: 35425751]
27. Lei H, Wang H, Wang L, Dong Y, Cheng J, Cai K. An analysis of the evolution of online public opinion on public health emergencies by combining CNN-BiLSTM + attention and LDA. Journal of Computer and Communications 2023;11(04):190-199. [doi: 10.4236/jcc.2023.114009]
28. Ren L, Zhang J, Su Z, Lai F, Xiong D. Evolution and governance of online public opinion during COVID-19: a hybrid approach using communication visualization, SIR modeling, and simulation validation. Front. Phys 2024 Sep 9;12:1. [doi: 10.3389/fphy.2024.1462089]

XSL•FO
RenderX

29. The 50th Statistical Report on China's Internet Development. China Internet Network Information Center (CNNIC). 2022 Aug. URL: https://www.cnnic.com.cn/IDR/ReportDownloads/202212/P020230829504457839260.pdf [accessed 2024-11-27]
30. Song J, Wang M, Li Y. An exploratory study of deep learning-based sentiment analysis among Weibo users in China. Curr Psychol 2023 Dec 05;43(17):15213-15226. [doi: 10.1007/s12144-023-05493-1]
31. Asghar MZ, Ahmad S, Qasim M, Zahra SR, Kundi FM. SentiHealth: creating health-related sentiment lexicon using hybrid approach. Springerplus 2016;5(1):1139 [FREE Full text] [doi: 10.1186/s40064-016-2809-x] [Medline: 27504237]
32. Khemani B, Malave S, Patil S, Shilotri N, Varma S, Vishwakarma V, et al. Sentimatrix: sentiment analysis using GNN in healthcare. Int. j. inf. tecnol 2024 Sep 23;16(8):5213-5219. [doi: 10.1007/s41870-024-02142-z]
33. Sridevi PC, Velmurugan T. Twitter sentiment analysis of COVID-19 vaccination integrating SenticNet-7 and SentiWordNet-adjusted VADER models. International Journal of Computer Information Systems and Industrial Management Applications 2024;16:162-183 [FREE Full text]
34. Cero I, Luo J, Falligant JM. Lexicon-based sentiment analysis in behavioral research. Perspect Behav Sci 2024 Mar 24;47(1):283-310. [doi: 10.1007/s40614-023-00394-x] [Medline: 38660506]
35. Salton G. Introduction to Modern Information Retrieval. New York, NY: McGraw-Hill, Inc; 1983.
36. Birkeland S, Bogh SB, Morsø L. From systematic complaint analysis to quality improvement in healthcare. BMJ Open Qual 2024 May 23;13(2):1 [FREE Full text] [doi: 10.1136/bmjoq-2023-002637] [Medline: 38782487]
37. Vatsa S, Mathur S, Garg M, Jindal R. COVID-19 tweet analysis using hybrid keyword extraction approach. 2021 Presented at: 10th IEEE International Conference on Communication Systems and Network Technologies (CSNT); June 18-19, 2021; Bhopal, India. [doi: 10.1109/csnt51715.2021.9509636]
38. Blei DM, Ng AY, Jordan MI. Latent dirichlet allocation. The Journal of Machine Learning Research 2003;3:993-1022 [FREE Full text] [doi: 10.7551/mitpress/1120.003.0082]
39. Rashid J, Shah SMA, Irtaza A. Fuzzy topic modeling approach for text mining over short text. Information Processing & Management 2019 Nov;56(6):102060. [doi: 10.1016/j.ipm.2019.102060]
40. Pavlinek M, Podgorelec V. Text classification method based on self-training and LDA topic models. Expert Systems with Applications 2017 Sep;80:83-93. [doi: 10.1016/j.eswa.2017.03.020]
41. Sievert C, Shirley K. LDAvis: A method for visualizing and interpreting topics. Proceedings of the Workshop on Interactive Language Learning, Visualization, and Interfaces 2014:63-70. [doi: 10.3115/v1/w14-3110]
42. Zhuang M, Li Y, Tan X, Xing L, Lu X. Analysis of public opinion evolution of COVID-19 based on LDA-ARMA hybrid model. Complex Intell Systems 2021 Sep 04;7(6):3165-3178 [FREE Full text] [doi: 10.1007/s40747-021-00514-7] [Medline: 34777976]
43. Xu H, Zeng J, Tai Z, Hao H. Public attention and sentiment toward intimate partner violence based on Weibo in China: a text mining approach. Healthcare (Basel) 2022 Jan 20;10(2):1 [FREE Full text] [doi: 10.3390/healthcare10020198] [Medline: 35206813]
44. Bhatia P, Nath R. Using sentiment analysis in patient satisfaction: a survey. Advances in Mathematics: Scientific Journal 2020 Jul 18;9(6):3803-3812. [doi: 10.37418/amsj.9.6.59]
45. Isa R, Nordin MF, Othman R, Mohadis HM. Sentiment analysis in public health crisis applications: a conceptual framework. International Journal on Perceptive and Cognitive Computing 2022;8(1):73-79 [FREE Full text]
46. Khaleghparast S, Maleki M, Hajianfar G, Soumari E, Oveisi M, Golandouz HM, et al. Development of a patients' satisfaction analysis system using machine learning and lexicon-based methods. BMC Health Serv Res 2023 Mar 23;23(1):280 [FREE Full text] [doi: 10.1186/s12913-023-09260-7] [Medline: 36959630]
47. Brauwers G, Frasincar F. A survey on aspect-based sentiment classification. ACM Comput. Surv 2022 Nov 21;55(4):1-37. [doi: 10.1145/3503044]
48. Talaat AS. Sentiment analysis classification system using hybrid BERT models. J Big Data 2023 Jun 23;10(1):1. [doi: 10.1186/s40537-023-00781-w]
49. Zhang W, Deng Y, Liu B, Pan S, Bing L. Sentiment analysis in the era of large language models: a reality check. In: Findings of the Association for Computational Linguistics: NAACL 2024. Mexico City, Mexico: Association for Computational Linguistics; 2024:3881-3906.
50. Bekmanova G, Yergesh B, Ukenova A, Omarbekova A, Mukanova A, Ongarbayev Y. Sentiment Processing of Socio-political Discourse and Public Speeches. In: Ghervasi O, Murgante B, Rocha AMAC, Garau C, Scorza F, Karaca Y, et al, editors. Computational Science and Its Applications – ICCSA 2023 Workshops. ICCSA 2023. Lecture Notes in Computer Science, vol 14108. Cham, Switzerland: Springer; 2023:191-205.
51. Ekman P, Friesen WV. Constants across cultures in the face and emotion. J Pers Soc Psychol 1971 Feb;17(2):124-129. [doi: 10.1037/h0030377] [Medline: 5542557]
52. Plutchik R. A general psychoevolutionary theory of emotion. In: Plutchik R, Kellerman H, editors. Theories of Emotion. New York, NY: Academic Press; 1980:3-33.
53. Röder M, Both A, Hinneburg A. Exploring the space of topic coherence measures. 2015 Presented at: Eighth ACM International Conference on Web Search and Data Mining; February 2-6, 2015; Shanghai, China. [doi: 10.1145/2684822.2685324]

XSL•FO
RenderX

54. Ravenda F, Bahrainian SA, Raballo A, Mira A, Crestani F. A self-supervised seed-driven approach to topic modelling and clustering. J Intell Inf Syst 2024 Sep 28:1. [doi: 10.1007/s10844-024-00891-8]
55. Bobicev V, Sokolova M. Inter-annotator agreement in sentiment analysis: machine learning perspective. Inter-annotator agreement in sentiment analysis; 2017 Presented at: International Conference Recent Advances in Natural Language Processing, RANLP; September 4-6, 2017; Varna, Bulgaria. [doi: 10.26615/978-954-452-049-6_015]
56. Hagerer G, Szabo D, Koch A, Dominguez MLR, Widmer C, Wich M, et al. End-to-end annotator bias approximation on crowdsourced single-label sentiment analysis. 2021 Presented at: 4th International Conference on Natural Language and Speech Processing (ICNLSP 2021); November 12-13, 2021; Trento, Italy.
57. Hodkinson A, Tyler N, Ashcroft DM, Keers RN, Khan K, Phipps D, et al. Preventable medication harm across health care settings: a systematic review and meta-analysis. BMC Med 2020 Nov 06;18(1):313 [FREE Full text] [doi: 10.1186/s12916-020-01774-9] [Medline: 33153451]
58. Olson K, Shanafelt T, Southwick S. Pandemic-driven posttraumatic growth for organizations and individuals. JAMA 2020 Nov 10;324(18):1829-1830. [doi: 10.1001/jama.2020.20275] [Medline: 33034630]
59. Coombs WT. Ongoing Crisis Communication: Planning, Managing, and Responding. Thousand Oaks, CA: SAGE Publications, Inc; 2007.
60. Ogie R, James S, Moore A, Dilworth T, Amirghasemi M, Whittaker J. Social media use in disaster recovery: a systematic literature review. International Journal of Disaster Risk Reduction 2022 Feb;70:102783. [doi: 10.1016/j.ijdrr.2022.102783]
61. Jabalameli S, Xu Y, Shetty S. Spatial and sentiment analysis of public opinion toward COVID-19 pandemic using twitter data: at the early stage of vaccination. Int J Disaster Risk Reduct 2022 Oct 01;80:103204 [FREE Full text] [doi: 10.1016/j.ijdrr.2022.103204] [Medline: 35935613]
62. Xia H, An W, Li J, Zhang ZJ. Outlier knowledge management for extreme public health events: Understanding public opinions about COVID-19 based on microblog data. Socioecon Plann Sci 2022 Mar;80:100941 [FREE Full text] [doi: 10.1016/j.seps.2020.100941] [Medline: 32921839]
63. Xie R, Chu SKW, Chiu DKW, Wang Y. Exploring public response to COVID-19 on Weibo with LDA topic modeling and sentiment analysis. Data Inf Manag 2021 Jan 01;5(1):86-99 [FREE Full text] [doi: 10.2478/dim-2020-0023] [Medline: 35402850]
64. Piedrahita-Valdés H, Piedrahita-Castillo D, Bermejo-Higuera J, Guillem-Saiz P, Bermejo-Higuera JR, Guillem-Saiz J, et al. Vaccine hesitancy on social media: sentiment analysis from June 2011 to April 2019. Vaccines (Basel) 2021 Jan 07;9(1):28 [FREE Full text] [doi: 10.3390/vaccines9010028] [Medline: 33430428]
65. Hu N. Sentiment analysis of texts on public health emergencies based on social media data mining. Comput Math Methods Med 2022;2022:3964473 [FREE Full text] [doi: 10.1155/2022/3964473] [Medline: 35983529]
66. Mohamed Ridhwan K, Hargreaves CA. Leveraging Twitter data to understand public sentiment for the COVID‐19 outbreak in Singapore. International Journal of Information Management Data Insights 2021 Nov;1(2):100021 [FREE Full text] [doi: 10.1016/j.jjimei.2021.100021]
67. Hastorf AH, Cantril H. They saw a game: a case study. J Abnorm Psychol 1954 Jan;49(1):129-134. [doi: 10.1037/h0057880] [Medline: 13128974]
68. Le Bon G. The Crowd. New York, NY: Routledge; 2017.
69. Festinger L. A Theory of Cognitive Dissonance. Redwood City, CA: Stanford University Press; 1957.
70. Marcus GE, Neuman WR, MacKuen M. Affective Intelligence and Political Judgment. Chicago, IL: University of Chicago Press; 2000.
71. Zillmann D. Mood management through communication choices. American Behavioral Scientist 1988 Jan 01;31(3):327-340. [doi: 10.1177/000276488031003005]
72. Che S, Kim JH. Sentiment impact of public health agency communication strategies on TikTok under COVID-19 normalization: deep learning exploration. Z Gesundh Wiss 2023 May 11;32(8):1-12 [FREE Full text] [doi: 10.1007/s10389-023-01921-5] [Medline: 37361279]
73. Bauder L, Giangobbe K, Asgary R. Barriers and gaps in effective health communication at both public health and healthcare delivery levels during epidemics and pandemics; systematic review. Disaster Med Public Health Prep 2023 May 19;17:e395. [doi: 10.1017/dmp.2023.61] [Medline: 37202845]
74. Suh E, Lee H. Collectivistic cultures. In: Zeigler-Hill V, Shackelford TK, editors. Encyclopedia of Personality and Individual Differences. Cham, Switzerland: Springer; 2020:763-765.
75. Jurado I, Navarrete RM. Economic crisis and attitudes towards democracy: how ideology moderates reactions to economic downturns. Front. Polit. Sci 2021 Aug 11;3:1. [doi: 10.3389/fpos.2021.685199]
76. Béland D, He AJ, Ramesh M. COVID-19, crisis responses, and public policies: from the persistence of inequalities to the importance of policy design. Policy and Society 2022;41(2):187-198 [FREE Full text] [doi: 10.1093/polsoc/puac021]
77. Chen J, Lin Z, Li L, Li J, Wang Y, Pan Y, et al. Ten years of China's new healthcare reform: a longitudinal study on changes in health resources. BMC Public Health 2021 Dec 13;21(1):2272 [FREE Full text] [doi: 10.1186/s12889-021-12248-9] [Medline: 34903184]

XSL•FO
RenderX

Abbreviations

DUTIR: Information Retrieval Laboratory at Dalian University of Technology
LDA: latent Dirichlet allocation
TF-IDF: term frequency-inverse document frequency
WHO: World Health Organization

Edited by A Benis; submitted 29.06.24; peer-reviewed by Y Gong, D Li, H Xu; comments to author 17.09.24; revised version received 23.12.24; accepted 04.02.25; published 20.03.25.

Please cite as:
Zheng Y, Tian M, Chen J, Zhang L, Gao J, Li X, Wen J, Qu X
Public Attitudes Toward Violence Against Doctors: Sentiment Analysis of Chinese Users
JMIR Med Inform 2025;13:e63772
URL: https://medinform.jmir.org/2025/1/e63772
doi:10.2196/63772
PMID:40111382

©Yuwen Zheng, Meirong Tian, Jingjing Chen, Lei Zhang, Jia Gao, Xiang Li, Jin Wen, Xing Qu. Originally published in JMIR Medical Informatics (https://medinform.jmir.org), 20.03.2025. This is an open-access article distributed under the terms of the Creative Commons Attribution License (https://creativecommons.org/licenses/by/4.0/), which permits unrestricted use, distribution, and reproduction in any medium, provided the original work, first published in JMIR Medical Informatics, is properly cited. The complete bibliographic information, a link to the original publication on https://medinform.jmir.org/, as well as this copyright and license information must be included.

XSL•FO
RenderX

Short Paper

Virtual Transition of Care Clinics and Associated Readmission Rates: 3-Year Retrospective Cohort Study

Sarah F Horman[1,2], MD; Milla Kviatkovsky[1], DO, MPH; Edward Castillo[3], PhD, MPH; Patricia Maysent[2], MBA, MPH; Chad VanDenBerg[2], MPH; John Bell[1], MD, MPH; Christopher A Longhurst[2,4], MD, MS

[1]Department of Medicine, University of California, San Diego, San Diego, CA, United States

[2]Jacobs Center for Health Innovation, University of California San Diego Health, San Diego, CA, United States

[3]Department of Emergency Medicine, University of California, San Diego, San Diego, CA, United States

[4]Department of Biomedical Informatics, University of California San Diego, San Diego, CA, United States

Corresponding Author:
Sarah F Horman, MD
Department of Medicine
University of California, San Diego
200 West Arbor Drive MC 8485
San Diego, CA, 92103
United States
Phone: 1 619 471 9186
Fax: 1 619 543 8255
Email: shorman@health.ucsd.edu

Abstract

Background: Hospital readmissions pose a significant burden on patients, health care providers, and systems, with an estimated annual cost of $17 billion. Timely follow-up within 7 days postdischarge is known to reduce readmissions but is often limited by access constraints. While transitions of care clinics have demonstrated benefits in reducing unplanned readmissions, physical space requirements can be logistically and financially challenging.

Objective: This study aimed to evaluate the effectiveness of a virtual transitions of care (VToC) clinic in reducing 30-day hospital readmissions and improving postdischarge care coordination.

Methods: University of California, San Diego Health implemented a hospitalist-led VToC clinic designed to support clinical management, medication reconciliation, primary care provider repatriation, and specialty care navigation. The study included 2314 patients seen in the VToC clinic between September 2021 and September 2024. Outcomes were compared to a benchmark group using regression analysis to assess the impact on 30-day readmission rates.

Results: The 30-day readmission rate for VToC patients was 14.9% (344/2314), significantly lower than the 20.1% (4659/23,129) observed in the benchmark group (P<.001). Regression analysis indicated that patients not participating in the VToC clinic had a higher likelihood of readmission (odds ratio=1.37; 95% CI=1.21-1.54; P<.001). The most substantial reduction in readmissions was observed among patients with moderate readmission risk (LACE+ score of 50-75).

Conclusions: VToC clinics are a feasible and effective strategy for enhancing postdischarge care, reducing hospital readmissions, and improving care coordination. This model supports the quadruple aim by promoting better health outcomes, improved patient experience, cost-efficiency, and care equity.

(JMIR Med Inform 2025;13:e73495) doi:10.2196/73495

KEYWORDS

transitions of care; telehealth; telemedicine; hospital medicine; quality and patient safety; health care utilization

Introduction

Unexpected return to the hospital reflects systemic challenges in health care delivery and places a financial strain on the nation's health system [1]. Postdischarge follow-ups within 7 days is a well-established protective mechanism to reduce the risk of readmission and mitigate health care disparities but are limited by access challenges and physician shortages [2-5]. Transitions of care clinics have shown benefit in readmission reduction but may be cost prohibitive and logistically

XSL•FO
RenderX

challenging [4,5]. Virtual postdischarge clinics may achieve similar benefits with fewer costs and present an opportunity to enhance postdischarge access [6].

Methods

Overview

At the University of California, San Diego Health, we implemented a hospital medicine physician-led virtual transitions of care (VToC) clinic, focused on postdischarge clinical management, medication reconciliation, primary care provider (PCP) repatriation, and specialty care navigation, with the aim of reducing repeat hospitalization.

Based on internal pilot data showing a favorable readmission impact for patients with moderate risk of readmission, we created a criteria-based order to trigger referral for patients (aged 18 years and older) discharged from the hospital medicine service line. The discharging providers were automatically prompted at discharge to refer patients to the clinic if patients had a LACE+ index (a readmission risk prediction index based on length of stay, acuity of admission, comorbidities, and emergency department visit history) between 50 and 75 [7]. Patients with LACE+ scores outside this range could be referred at provider discretion. Patients were excluded from appointment scheduling if they were discharged to a care facility or hospice or had an existing PCP appointment within 7 days of discharge.

The virtual clinic was supported by 12 hospitalists, 2 medical assistants, 1 pharmacist and an on-demand interpreter service. Medical assistants contacted eligible patients to schedule web-based video visits. VToC visits were occasionally converted to telephone encounters when patients faced technical barriers, which occurred in fewer than 5% of cases and thus were not considered a distinct comparison group for analysis. Patients received phone call reminders 1 business day prior to scheduled appointments. Pharmacists conducted previsit medication reviews to identify fill history gaps, dosing inconsistencies, and potential drug-drug interactions. Note templates guided VToC providers in addressing medication management, social determinants of health, barriers to follow-up, and care coordination. A standardized electronic handoff was routed to the patient's PCP and relevant specialists summarizing the reason for hospitalization, follow-up needs, and timing recommendations. Additionally, post-VToC visit communication was sent to the discharging hospitalist to highlight potential care lapses and support quality improvement efforts.

Data were collected from the electronic health records using standard SQL queries. These included demographics (ages grouped as <45, 45-64, and ≥65 years; sex; and race and ethnicity); VToC status (yes or no); PCP (University of California San Diego or other); LACE+ score (<50, 50-75, or >75); and 30-day all-cause readmission. Patient characteristics were analyzed by VToC status (yes or no). A VToC status of "no" indicates patients who were discharged from the medicine service line to home and not seen in our clinic (because they did not meet eligibility criteria or could not be reached). Patients were excluded from analysis if they had missing demographic or clinical data. Readmission rates were analyzed for VToC status and by LACE+ score. Chi-square analysis was used to compare characteristics by VToC status with a $P<.05$ considered significant. Readmission rates (%) by VToC status stratified by LACE+ decile are reported. Error bars were calculated using 95% CIs. A multivariable logistic regression analysis was performed to assess independent associations with unplanned hospital readmission. Variables included in the model included age group, sex, race and ethnicity, PCP affiliation (UCSD versus non-UCSD), LACE+ score, and VToC enrollment. All analyses were conducted using the SPSS Statistics software suite (version 27.0; IBM Corporation).

Ethical Considerations

This study was conducted in an Institutional Review Board–exempt fashion in accordance with the ethical standards of the University of California San Diego Human Research Protection Program and the Office for Human Research Protections and adhered to the Helsinki Declaration of 1975, as revised in 2000.

Results

There were 25,970 patients identified for the study period of September 1, 2021, through September 17, 2024. A total of 527 (0.02%) patients had missing data and were excluded from the analysis. Of the 25,443 patients included in the study, 2314 (9.1%) were seen in VToC after discharge and 23,129 (90.9%) had standard of care follow-up. Table 1 shows the demographic comparisons of patients who were seen in VToC versus those who were not for the same time period.

XSL•FO
RenderX

Table 1. Demographics of virtual transitions of care (VToC) and non-VToC patients (N=25,443).

	VToC (n=2314)	Non-VToC (n=23,129)	Total (N=25,443)	*P* value
Age range, (y), n (%)				.40
<45	558 (24.1)	5829 (25.2)	6387 (25.1)	
45-64	861 (37.2)	8325 (36)	9186 (36.1)	
≥65	895 (38.7)	8975 (38.8)	9870 (38.8)	
Sex, n (%)				<.001
Female	1266 (54.7)	10,943 (47.3)	12,209 (48)	
Male	1048 (45.3)	12,186 (52.7)	13,234 (52)	
Race or ethnicity, n (%)				<.001
Non-Hispanic White	870 (37.6)	9795 (42.3)	10,665 (41.9)	
Hispanic	834 (36)	7199 (31.1)	8033 (31.6)	
Non-Hispanic Black or African American	213 (9.2)	2171 (9.4)	2384 (9.4)	
Non-Hispanic Asian, American Indian, or Alaskan Native	205 (8.9)	1949 (8.4)	2154 (8.5)	
Other[a] or unknown	192 (8.3)	2015 (8.7)	2207 (8.7)	
PCP[b], n (%)				.75
UCSD[c] PCP	644 (27.8)	6509 (28.1)	7153 (28.1)	
Non-UCSD PCP	1670 (72.2)	16,620 (71.9)	18,290 (71.9)	
LACE+ score range, n (%)				<.001
<50	79 (3.4)	2321 (10)	2400 (9.4)	
50-70	113 (65.4)	9152 (39.6)	10,665 (41.9)	
>70	722 (31.2)	11,656 (50.4)	12,378 (48.6)	

[a]Self-reported “other” race or ethnicity or missing data.

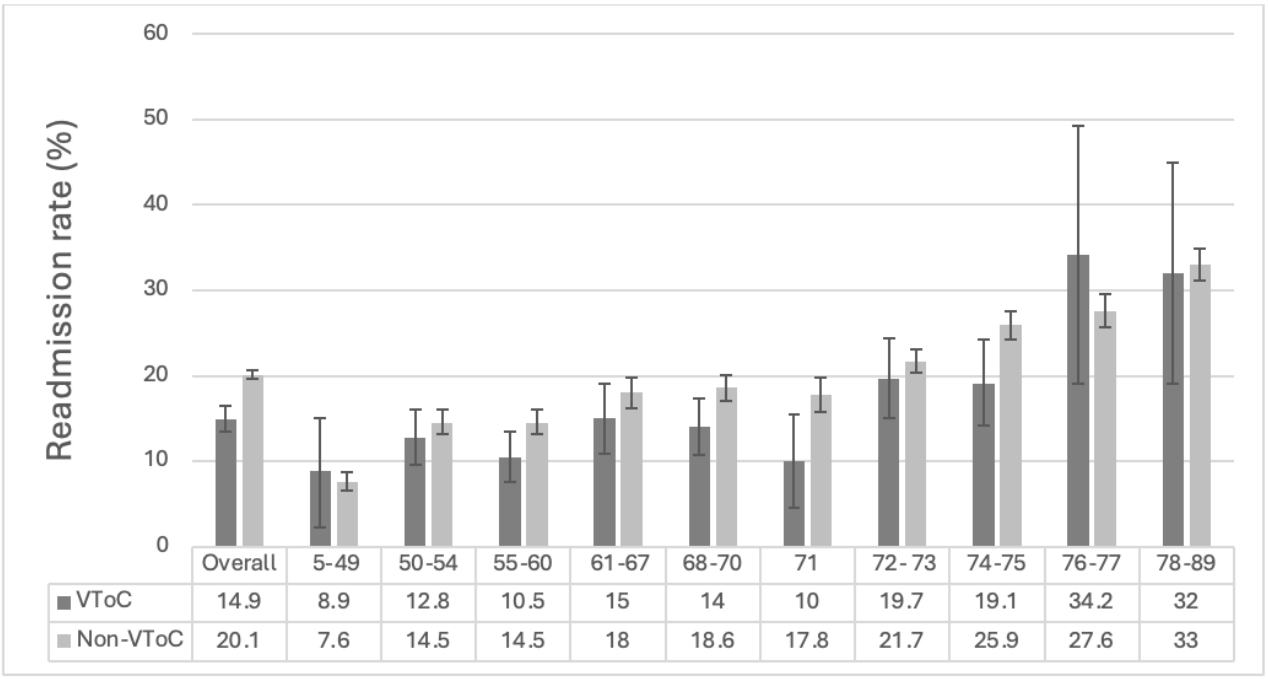
[b]PCP: primary care provider.

[c]UCSD: University of California San Diego.

The overall 30-day readmission rate for patients seen in the VToC clinic was 14.9% (344/2314) compared to 20.1% (4659/23,129) in the benchmark group (Table 1; *P*<.001). In the regression model, the absence of a VToC clinic was independently associated with increased odds of readmission (odds ratio 1.37; 95% CI 1.21-1.54; *P*<.001). In the multivariable regression analysis, younger age, female sex, non-Hispanic Asian race or ethnicity, higher LACE+ scores, and non-participation in the VToC program were each independently associated with increased odds of hospital readmission." should be changed to "In the multivariable regression analysis, younger age, female sex, Hispanic and Non Hispanic Black/African American race or ethnicity, higher LACE+ scores, and nonparticipation in the VToC program were each independently associated with increased odds of hospital readmission. This analysis is available in Multimedia Appendix 1. Decile matching was performed to account for the difference in distribution of LACE+ in the VToC and non-VToC groups. Analysis of LACE+ decile groups revealed that the impact of readmission reduction was most prominent among patients with LACE+ scores ranging between 50-75; however, across most groups VTOC performed better than non-VToC (Figure 1).

XSL•FO
RenderX

Figure 1. This figure presents 30-day readmission rates for patients who received the virtual transitions of care (VToC) intervention (dark bars) versus those who did not (light bars), stratified by LACE+ score decile groups. The x-axis represents different LACE+ decile groups, while the y-axis shows readmission rates as percentages. Error bars are included for each proportion and represent the difference between the point estimate (proportion) and upper or lower CI. The targeted population for this intervention was patients with LACE+ scores between 50 and 75. Deciles outside this range are included for completeness. Across most LACE+ decile ranges, the VToC group consistently showed lower readmission rates compared to the non-VToC group.



	Overall	5-49	50-54	55-60	61-67	68-70	71	72-73	74-75	76-77	78-89
VToC	14.9	8.9	12.8	10.5	15	14	10	19.7	19.1	34.2	32
Non-VToC	20.1	7.6	14.5	14.5	18	18.6	17.8	21.7	25.9	27.6	33

Discussion

Here we present a hospitalist-led postdischarge virtual clinic aimed at improving transitions of care for patients. For patients at moderate risk, a VToC visit was associated with a significantly lower rate of readmission. Notably, our intervention group had a higher proportion of female and Hispanic patients, both of which were associated with increased odds of readmission in regression analyses.

This observational study is subject to selection bias, as clinic attendance could be influenced by patient-specific factors that influence readmission. Approximately 13% of patients referred to the VToC were not reached, which may introduce additional bias, as these individuals may differ in ways that influence outcomes. While we did not capture detailed data on patient acceptance, we addressed this limitation by matching the comparator group on readmission risk to reduce confounding. However, the stratified analysis according to the LACE+ index provides strong evidence in support of the impact of the program, and the positive impact observed is consistent with broader evidence that timely postdischarge access reduces readmission risk. VToC clinics address a critical gap in the care continuum while also providing the inherent benefits of telemedicine [6,8].

Results from this initiative are promising for the feasibility of telemedicine-based transitional care programs to promote the quadruple aim of improving population health, enhancing the care experience, reducing cost, and advancing care equity [9].

Acknowledgments

Thank you to Eric Lundin for project management support. Thank you to the hospitalist physicians including Drs Maryann Ally, Diana Childers, Catherine Firestein, Jonathan McIntyre, David Reis, Reid Sasaki, Jennifer Quartarolo, Supraja Thota, and Anne Xing and to Richard Nguyen for information support services. Special thanks to Trina Huynh for pharmacist support and leadership, and to Eileen Hailey and Nancy Renshaw for collaborative operational leadership from the Department of Population Health.

Data Availability

All data generated or analyzed during this study are included in this published article and its supplementary information files.

Authors' Contributions

SFH served as the lead author and was responsible for project design, manuscript writing, and overall coordination. MK contributed as a hospitalist provider for the clinic and was involved in manuscript writing and data analysis. EC provided data analytic support

XSL•FO
RenderX

and assisted in interpreting the results. PM offered executive sponsorship, strategic guidance, and support for project scaling and resourcing. CV participated as a member of the steering committee and provided advisory input and quality oversight in his role as Chief Quality Officer of the University of California, San Diego Health. JB contributed to the design and implementation of the referral order mechanism and automation processes. CAL provided executive sponsorship and played a key role in program design, implementation, scaling, and dissemination, as well as supporting manuscript writing, editing, and analytic advising.

Conflicts of Interest

None declared.

Multimedia Appendix 1
Supplementary data.
[XLSX File (Microsoft Excel File), 531 KB - medinform_v13i1e73495_app1.xlsx]

References

1. Barbut D, Borer JS, Wallerson D, Ameisen O, Lockshin M. Anticardiolipin antibody and stroke: possible relation of valvular heart disease and embolic events. Cardiology 1991;79(2):99-109. [doi: 10.1159/000174866] [Medline: 1933972]
2. Anderson A, Mills CW, Willits J, Lisk C, Maksut JL, Khau MT, et al. Follow-up post-discharge and readmission disparities among Medicare fee-for-service beneficiaries, 2018. J Gen Intern Med 2022 Sep;37(12):3020-3028 [FREE Full text] [doi: 10.1007/s11606-022-07488-3] [Medline: 35355202]
3. Zhang X, Lin D, Pforsich H, Lin VW. Physician workforce in the United States of America: forecasting nationwide shortages. Hum Resour Health 2020 Feb 06;18(1):8 [FREE Full text] [doi: 10.1186/s12960-020-0448-3] [Medline: 32029001]
4. Baldino M, Bonaguro AM, Burgwardt S, Lombardi A, Cristancho C, Mann C, et al. Impact of a novel post-discharge transitions of care clinic on hospital readmissions. J Natl Med Assoc 2021 Apr;113(2):133-141. [doi: 10.1016/j.jnma.2020.07.018] [Medline: 32900472]
5. Wiest D, Yang Q, Wilson C, Dravid N. Outcomes of a citywide campaign to reduce Medicaid hospital readmissions with connection to primary care within 7 days of hospital discharge. JAMA Netw Open 2019 Jan 04;2(1):e187369 [FREE Full text] [doi: 10.1001/jamanetworkopen.2018.7369] [Medline: 30681708]
6. Shah DA, Sall D, Peng W, Sharer R, Essary AC, Radhakrishnan P. Exploring the role of telehealth in providing equitable healthcare to the vulnerable patient population during COVID-19. J Telemed Telecare 2024 Jul;30(6):1047-1050 [FREE Full text] [doi: 10.1177/1357633X221113711] [Medline: 35833345]
7. van Walraven C, Wong J, Forster A. LACE+ index: extension of a validated index to predict early death or urgent readmission after hospital discharge using administrative data. Open Med 2012;6(3):e80-e90 [FREE Full text] [Medline: 23696773]
8. Reeves JJ, Ayers JW, Longhurst CA. Telehealth in the COVID-19 era: a balancing act to avoid harm. J Med Internet Res 2021 Feb 01;23(2):e24785 [FREE Full text] [doi: 10.2196/24785] [Medline: 33477104]
9. Nundy S, Cooper LA, Mate KS. The quintuple aim for health care improvement: a new imperative to advance health equity. JAMA 2022 Feb 08;327(6):521-522. [doi: 10.1001/jama.2021.25181] [Medline: 35061006]

Abbreviations

PCP: primary care provider
VToC: virtual transitions of care

Edited by A Benis; submitted 05.03.25; peer-reviewed by P Speck, CM Bier-Laning, EP Greenup; comments to author 15.04.25; revised version received 04.06.25; accepted 11.08.25; published 23.09.25.

Please cite as:
Horman SF, Kviatkovsky M, Castillo E, Maysent P, VanDenBerg C, Bell J, Longhurst CA
Virtual Transition of Care Clinics and Associated Readmission Rates: 3-Year Retrospective Cohort Study
JMIR Med Inform 2025;13:e73495
URL: https://medinform.jmir.org/2025/1/e73495
doi:10.2196/73495
PMID:

©Sarah F Horman, Milla Kviatkovsky, Edward Castillo, Patricia Maysent, Chad VanDenBerg, John Bell, Christopher A Longhurst. Originally published in JMIR Medical Informatics (https://medinform.jmir.org), 23.09.2025. This is an open-access article distributed under the terms of the Creative Commons Attribution License (https://creativecommons.org/licenses/by/4.0/), which

XSL•FO
RenderX

permits unrestricted use, distribution, and reproduction in any medium, provided the original work, first published in JMIR Medical Informatics, is properly cited. The complete bibliographic information, a link to the original publication on https://medinform.jmir.org/, as well as this copyright and license information must be included.

XSL•FO
RenderX

Original Paper

Copy Tools in the Electronic Health Record: Perceptions, Implications, and Future Directions

Sky Corby[1], MS; Joan S Ash[2], PhD; Rebecca M Jungbauer[2], DrPH; Gretchen Scholl[3], BS; Sarah Florig[4], MS; Vishnu Mohan[2,5], MD, MBI; Jeffrey A Gold[1,2], MD

[1]Division of Pulmonary, Allergy, and Critical Care Medicine, Department of Medicine, Oregon Health & Science University, Portland, OR, United States

[2]Division of Informatics, Clinical Epidemiology, and Translational Data Science, Department of Medicine, Oregon Health & Science University, Portland, OR, United States

[3]Division of Undergraduate Medical Education, Department of Medicine, Oregon Health & Science University, Portland, OR, United States

[4]College of Medicine, Nebraska Medical Center, Omaha, NE, United States

[5]Division of General Internal Medicine and Geriatrics, Department of Medicine, Oregon Health & Science University, Portland, OR, United States

Corresponding Author:
Sky Corby, MS
Division of Pulmonary, Allergy, and Critical Care Medicine
Department of Medicine
Oregon Health & Science University
3181 Southwest Sam Jackson Park Road
Portland, OR, 97239
United States
Phone: 1 5034948311
Email: corby@ohsu.edu

Abstract

Background: Electronic health records (EHRs) can aid in provider efficiency, but may also lead to unintended consequences, such as documentation burden and increased length of notes. To combat issues related to documentation, copying and pasting (CP) and copying or carrying forward (CF) are tools that have been used to aid in documentation burden. Multiple studies have identified the benefits and challenges of using these tools; however, few studies have identified the unintended consequences of CP and CF, and how the adoption of these tools may affect users.

Objective: The objective was to describe providers' perceptions and use of copying tools available in the EHR and describe their suggestions for improvement on these copying tools.

Methods: Research team members conducted semistructured interviews with faculty members, advanced practice providers, residents or fellow trainees, and medical students at a single academic health sciences center. The Diffusion of Innovations Theory of Unintended Consequences guided the analysis and interpretation of interview results.

Results: A total of 22 semistructured interviews were conducted in 2023 and analyzed during 2024. The findings showed that respondents use and value these tools for efficiency and communication purposes. The negative unintended consequences include inaccuracies and errors in documentation and increased patient safety risks. Some respondents experience inner angst or moral injury related to using CP/CF, but they feel that they must use them to satisfy organizational requirements surrounding documentation. The respondents suggested that artificial intelligence will likely help improve documentation tools, as would further training around these types of documentation tools.

Conclusions: Some respondents noted feeling both internal and external pressures that influenced when and how they use CP/CF. Respondents noted that they value EHR copying tools for efficiency purposes, but they also understand the risks involved. This tension may lead to moral angst or moral injury. They offered numerous suggestions for lowering the risk, especially by improving the documentation capabilities of the EHR through artificial intelligence. Future research should investigate both technical and educational solutions to relieve the documentation burden and moral angst they are experiencing.

(JMIR Med Inform 2025;13:e78502) doi:10.2196/78502

XSL•FO
RenderX

KEYWORDS

clinical communication; electronic health records; clinical documentation; copy-paste; carry-forward; qualitative research; attitude of health personnel; electronic documentation; human factors

Introduction

Electronic health records (EHRs) were first introduced as a more efficient mechanism than paper for collecting and storing patient information such as test results, diagnoses, and clinical notes [1]. Although the EHR is effective in many aspects, the adoption of this technology has given rise to unintended consequences. One primary concern, documentation burden, includes increased length of notes ("note bloat") [2] and time spent documenting [3]. These unintended consequences contribute to another widespread problem: provider burnout [4].

To combat issues related to EHR documentation, vendors have developed and implemented documentation tools that facilitate copying and pasting (CP) text and copying or carrying forward (CF) entire notes [5] into their products that clinical users in health care organizations have embraced. CP allows users to copy elements of a note (eg, free text, test results, and clinical narratives) and paste that information into a new note. CF, available in some EHR systems, is used to copy an entire note, including templates and formats, to bring forward into a new note.

Prior studies suggest CP/CF is used to improve usability and efficiency in documentation [6], to decrease provider burnout [7], and to improve documentation quality, where quality was defined as the accuracy of the information, and timeliness of the information, and the overall readability of the information in the note [8]. However, CP can be a significant contributor to note bloat and error [3,5,9-14]. Some researchers found that 90% or more of inpatient service notes were either copied or templated, increasing length and number of errors in the notes [8,15], while others reported CP/CF-related diagnostic and process errors contributed to the potential for moderate to severe harm [16,17]. Please see Table 1 for a summary comparing intended versus unintended consequences.

Table 1. Summary of intended and unintended consequences of using CP[a]/CF[b] in EHR documentation from previous literature.

Intended consequences of CP/CF	Unintended consequences of CP/CF
Efficiency	Note bloat
Relieve burnout	Increase in errors in documentation
Improve documentation quality	Increase in diagnostic errors

[a]CP: copying and pasting.

[b]CF: copying or carrying forward.

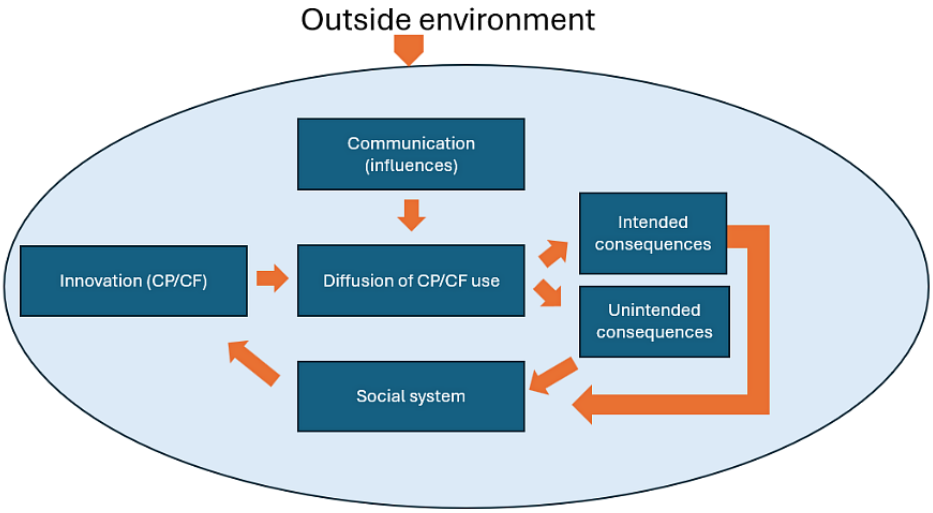
Researchers have typically investigated CP/CF use via surveys [8,10,18,19] and large retrospective analyses of notes [11,12,14,20]. A mixed-methods study assessing the association of CP use and risk severity, as well as perspectives of CP/CF use in progress notes and reported a wide spectrum of the value of CP/CF and progress notes across note authors and consumers was carried out [21]. Other research has found similar variance in perception of value and efficiency by specialty, seniority, and setting [8,10].

Numerous studies have described the benefits (eg, efficiency) and challenges (eg, note bloat) of these tools. However, evidence considering the context in which these tools are implemented, and the potential to limit or avoid unanticipated and undesirable consequences of implementation, is lacking. The Diffusion of Innovations model posits that adoption of innovations proceeds through stages and is affected by properties of the innovations, adopters, social systems, change agents (individuals pushing for process improvement), and communication relationships [22,23]. While CP/CF may be considered successful innovations in terms of adoption, the unanticipated (and potentially contradictory) consequences of CP/CF use may have dramatic ramifications for users, consumers, and the health systems themselves [22]. This Theory of Unintended Consequences, a corollary to the Diffusion of Innovations Theory, is depicted in Figure 1, showing a cycle in which an innovation (in this case, CP/CF) is introduced and adopted. Adoption creates the intended and unintended consequences described in prior research, followed by iterative updates based on interactions with the social system. Throughout the process, the outside environment (eg, policy or cultural values) exerts pressure against the innovation usage.

However, the benefits and challenges of innovative tools, such as CP/CF, coupled with an understanding of how the unanticipated and unintended consequences of CP/CF adoption affect users, are poorly described in the current literature. We aimed to use qualitative methodologies, guided by the Diffusion of Innovation Theory of Unintended Consequences, to (1) investigate provider perceptions, thoughts, and attitudes about CP/CF in the EHR; (2) identify the consequences (both intended and unintended) of using CP/CF across different specialties, departments, provider roles, and training level in one academic health care system; and (3) better understand users' experiences with intended and unanticipated consequences of CP/CF by focusing on the futures of CP/CF.

XSL•FO
RenderX

Figure 1. The figure below depicts the modified Diffusion of Innovations Theory of Unintended Consequences, which is a theory showing a circular pattern where an innovation is introduced and adopted. The adoption of innovation then creates the intended and unintended consequences, which are followed by iterative updates based on interactions from the social system and the outside environmental pressures. CF: copying or carrying forward; CP: copying and pasting.



Methods

Ethical Considerations

This study was approved by the Institutional Review Board at Oregon Health & Science University (IRB #10027). Informed consent was obtained from respondents invited via email to participate in this study, and verbal consent was given before being recorded during the interview. The data used for this paper were deidentified, and the manuscript does not contain any information that would allow for the identification of respondents. Respondents were informed that study findings would be published, and their quotations would be presented anonymously. Participants were not compensated for participating in the interview.

Recruitment or Setting of This Study

Respondents for this comprised providers who initially responded to a prior quantitative survey [19] in 2022-2023 regarding use of CP/CF for documentation, and while completing the survey, self-identified to be interviewed for the present study. These providers included faculty, advanced practice providers (APPs), medical students, and residents or fellow trainees at a single academic health institution. For our study, we have defined APPs as health care professionals who have had special training to diagnose, treat, and manage common medical conditions, which include physician's assistants, certified nurses, nurse practitioners, and licensed social workers. APPs, faculty, medical students, and residents or fellow trainees who all used Epic (Epic Systems); and medical students and residents or fellow trainees on rotation at the Veterans Affairs health care system who also used VistA (Veterans Health Information Systems and Technology Architecture; US Department of Veterans Affairs). Thus, while the initial survey was purposively sampled, the participants identified for this study represented a convenience subsampling of a prior purposively selected cohort. The research team reached out to individuals who volunteered to participate in interviews to schedule virtual meetings.

Design

In 2023, the research team, consisting of four individuals from diverse and multiple backgrounds (informatics, qualitative research, quantitative research, psychology, and medical education), developed an interview guide. The interview guide included questions regarding demographics (eg, professional background, department or specialty, and patient population), innovation of CP/CF, CP/CF use, factors influencing use such as environmental pressures, types of consequences, and the future of CP/CF (Multimedia Appendix 1). Each interview was conducted by 2 team members virtually through Cisco Webex (one interviewer was the lead, who asked the questions on the interview guide, and the second interviewer asked follow-up questions as well as any questions that may have been missed by the lead interviewer). Interviews were recorded and professionally transcribed.

Analysis

In 2024, the research team used both a thematic deductive framework, deriving themes from existing theories, and a thematic inductive framework (where themes are derived organically from raw data) to analyze data. Two team members used 3 transcripts to develop the initial codebook. Five team members then analyzed all 22 transcripts, consisting of 322 pages of data, using a standard inductive grounded approach, iteratively developing a codebook, and generating patterns and themes. NVivo 12 (Lumivero) was used for the management and analysis of the data. The inductively generated themes naturally fell into categories described in the Diffusion of Innovations Theory of Unintended Consequences [22], so this framework was applied to describe the results.

Results

Overview

Findings are organized using the Diffusion of Innovations Theory of Unintended Consequences framework in Figure 1, enhanced by inductively produced themes. Rich quotes from interviewees are available in Multimedia Appendix 2.

XSL•FO
RenderX

Demographics

In 2023, we conducted 22 interviews (mean duration 48 minutes, range 29 to 65 minutes). Half were faculty (11/22, 50%), and most treated adult or family populations (17/22, 77%; Table 2). Most respondents were specialists (14/22, 64%). Many of the respondents saw patients in both inpatient and ambulatory settings (10/22, 45%), with some respondents reporting seeing patients in ambulatory settings alone (8/22, 36%).

Table 2. Demographics table: qualitative interview respondents' characteristics, including role or training level, population, department, and setting.

Respondent characteristic	Value, n (%)
Role or training level	
Faculty	11 (50)
APP[a]	7 (32)
Resident and fellow trainee	2 (9)
Medical student	2 (9)
Population	
Pediatrics	5 (23)
Adult and family	17 (77)
Department	
Specialists[b]	14 (64)
Primary care, family medicine, and internal medicine	6 (27)
Students	2 (9)
Setting	
Inpatient	4 (18)
Ambulatory	8 (36)
Both	10 (45)

[a]APP: advanced practice provider (physician's assistant, nurse practitioners, certified nurse, and licensed social worker).

[b]Specialists include 1 each of the following: emergency medicine, women's health, pediatrics, urology, midwifery, dermatology, psychiatry, rheumatology, neuroradiology, infectious disease, sepsis, neonatology, clinical informatics, and hematology-oncology.

Innovation

The model (Figure 1) starts on the left with the innovation. The innovation is a new idea: in this case, duplicative text tools in the EHR. Respondents believed that because the documentation burden was so high for providers, CP/CF were developed as innovative solutions. Textbox 1 depicts the themes and subthemes found in the results.

XSL•FO
RenderX

Textbox 1. Diffusion of Innovations Theory of Unintended Consequences Framework components from Figure 1 and the subthemes related to each of the framework components (subthemes are displayed as bullet points).

Framework component (from Figure 1) and subthemes

Innovation

Diffusion of CP (copying and pasting)/CF (copying or carrying forward) use

Communication (influences)

Social system

- Overview
- Differences in types of patient visits
- Difference in the health care delivery system
- Difference in specialty
- Difference in electronic health record (EHR) products

Intended consequences

- Overview
- Efficiency or decreased documentation time
- Organization and time management skills
- Increased communication
- Improved accuracy for objective data

Unintended consequences

- Overview
- Inaccuracies and errors in the note
- Plagiarism
- Note bloat
- Critical thinking issues
- Ultimate unintended consequence: inner angst or moral injury

Outside environment

- Overview
- EHR-related solutions
- Artificial intelligence–related solutions
- Innovation: people-focused solutions
- Cultural shifts in documentation

Diffusion of CP/CF Use

Moving to the center square (Figure 1), consideration of the diffusion of CP/CF includes (1) how people adopt tools, (2) why people use these tools, and (3) why some decide not to use these tools.

In the case of CP/CF, some respondents noted that at times, documentation duties occasionally fell onto the residents/fellow trainees and APPs, so these tools are necessary for efficiency purposes. Residents/fellow trainees are, at times, active change agents in the diffusion of CP/CF because “it would be impossible for trainees to not copy and paste” (faculty). However, residents/fellow trainees are not the only ones who document and use CP/CF. When faculty are not supervising residents/fellow trainees, they are writing notes themselves and use these tools regularly, so they can achieve a better work/life balance.

Communication Influences

The superior aspect of the model (Figure 1) indicates that communication impacts the diffusion and spread of an innovation (ie, CP/CF). Information about CP/CF was commonly communicated through informal training and education from other colleagues rather than through formal training. Medical students noted that communication about the appropriate use of these tools was inconsistent. Some direct supervisors (ie, resident/fellow trainees) vocalized and encouraged medical students to use the tools and “start building [these skills now]” (medical student), while others (ie, faculty

XSL•FO
RenderX

supervisors) did not want them to use the tools because, as students, they needed practice writing notes themselves and developing critical thinking skills.

Influence of Social Systems

Overview

The inferior aspect of the model (Figure 1) indicates there are societal or systems pressures influencing how and when CP/CF are used. Use of CP/CF varied greatly by type of patient visits, setting, specialty, and attributes of the EHR product.

Differences in Types of Patient Visits

The use of CP/CF differed depending on the type of patient visit (eg, telephone, virtual, or in-person visit; returning, new, or old patient). With a new patient, providers reported using CP to gather the patient's historical information, especially when the history was complex and involved many images. However, there were some notable differences in use among clinicians. For example, a surgical resident/fellow trainee noted that he was more likely to write down verbal history when meeting a patient for the first time versus gathering prior information and using CP. Other providers mentioned that they do not use CF because they view each visit as a new visit.

Difference in Health Care Delivery Setting

According to our respondents, CP/CF use is influenced by whether care is provided in an ambulatory or inpatient setting. For example, CF has been described as "the backbone of all (in-)patient charting" (APP) because it aids in the continuity of care between team members, which would not be applicable in ambulatory settings. Providers who work in both inpatient and outpatient settings mentioned using CP in both settings because they are used to doing so.

Difference in Specialty

Respondents described how different workflows and documentation requirements impact CP/CF use. When providers see long-term patients for chronic problems, they rely on CP/CF, but if they consistently see new patients, such as in emergency medicine, they tend not to use them.

Specialties vary in how they structure their notes, impacting the value of CP/CF. Those with more structured and templated notes used CP/CF less frequently, whereas other specialties required documentation of detailed thought processes and thus were less structured and used CP/CF more frequently. Volume and duration of the patient visits differed by specialty, which impacted providers' use of CP/CF, with one faculty member noting, "when I'm busier, I tend to copy/paste more and copy forward more" (faculty). The research team also noted that the value found in using CP/CF differed by specialty, so developing a single policy to guide CP/CF throughout a health system would be challenging.

Difference in EHR Products

EHRs vary based on product offerings and integration into a system, including access to and policies for use of duplicative text tools. One resident/fellow trainee compared one academic center's commercial EHR to the Veterans Affairs' EHR, noting that CP is not easy to do, and CF is not available at all.

Intended Consequences of CP/CF

Overview

The right aspect of the model (Figure 1) features the intended and unintended consequences of implementing any new technology. Our analysis revealed intended benefits from the innovation of CP/CF tools.

Efficiency or Decreased Documentation Time

When asked about the benefits of CP/CF, many respondents highlighted that these tools were "a survival mechanism" (faculty) that streamlines work processes, decreases documentation time, and increases efficiency, which reduces provider stress and promotes work/life balance.

Organization and Time Management Skills

Part of the CP/CF's efficiency is derived from organization and time management, allowing providers to update relevant data in a template rather than recreating an entire note from scratch. When used this way, CF can provide consistency, organization, and standardization of notes, helping providers find salient information quickly.

Increased Communication

Respondents discussed CP/CF's enhancement of communication within and across teams and disciplines and settings, which "saves [them] a great deal of time" (faculty). CP/CF help providers stay organized in their notes, which allows them to solve problems together.

Improved Accuracy for Objective Data

CP/CF may decrease errors in translating complicated or nuanced data from note to note, especially from specialists or when dictating notes. One example noted was radiology, because the integrity and accuracy of the original report should stay intact, and providers "don't have translational[/dictation-relations] errors" (faculty).

Unintended Consequences of CP/CF

Overview

While innovations bring about intended and desirable consequences, unintended consequences can also affect the adoption of innovations (Figure 1). Although the diffusion of CP/CF into EHR systems could be considered a success, respondents discussed the risks and challenges CP/CF use presented, which shaped their willingness to use CP/CF in their practice.

Inaccuracies and Errors in the Note

All respondents noted that CP/CF use can increase inaccuracies and errors in the notes, from the seemingly innocuous errors (spelling errors) to harmful errors (forgetting to update a note). Information can be outdated yet copied. Errors can be perpetuated. Respondents admitted to forgetting to update information they had previously copied, especially in hectic environments. Some respondents expect that inaccuracies and errors will occur due to the "amount of pressure they feel to get [notes] done" (faculty) and the pressure on providers to see higher volumes of patients.

XSL•FO
RenderX

Whether inaccuracies are accepted as part of the cost of using efficiency tools, these errors can be harmful, in some cases leading to legal as well as patient safety risks. One risk is putting the copied text into the wrong chart, allowing patients to see other patients' confidential information. Another risk is carrying forward a care management plan that may not be appropriate for patients. One faculty member noted, "whatever we are signing our name [to] should be our own work" (faculty), and that signing off on a note that they have not reviewed thoroughly is problematic.

Plagiarism

Respondents noted that plagiarism can be another unintended consequence of using these tools. Attribution was another issue, with respondents discussing how they, or others, copied from other people's notes without citing where they obtained this information or verifying that the information they copied is correct.

Note Bloat

One of the most cited challenges with the CP/CF innovation was the increased length of notes or note bloat. Note bloat makes quickly finding relevant or updated information within a large volume of data more challenging. The length of notes also contributes to the perpetuation of errors. As described by respondents, CP/CF contribute directly to note bloat. Additionally, longer notes mean that providers may not be reviewing and editing notes as carefully as they should, allowing errors to slip through.

Critical Thinking Issues

Respondents described how the use of CP/CF affected critical thinking skills and led people to not review information thoroughly. Providers, especially medical students and residents/fellow trainees, must learn how to think critically. As one faculty member noted, providers must "separate the wheat from the chaff" (faculty) and determine what to include in a note; critical thinking is an important part of training, which may be impeded by shortcuts in documentation.

Ultimate Unintended Consequence: Inner Angst or Moral Injury

The constant friction between the internal and personal desires to practice caution, review information thoroughly, and create concise and accurate notes, and the external pressures of practicing medicine in today's organizational environment, has led to the most important unanticipated and unintended consequence of the CP/CF innovation: a sense of inner angst, or moral injury, among respondents. The concept of medical moral injury (or distress) among providers has gained traction in the literature in recent years, and covered actions due to commission (providers acting against a belief) or omission (providers not able to act on their beliefs), whether due to a sense of being internally or externally constrained in their ability to provide what they believe is quality care in a high-stakes situation or betrayal from people, institutions, or systems in power [24]. Whether conscious of these feelings of inner angst or moral injury, respondents discussed at length the impact on and of CP/CF use.

Documentation burden, due to time constraints and increased pressure to see higher patient volumes, negatively affected providers' sense of well-being and created pressure to use these tools, even if they did not want to do so. With a higher patient census, documentation requirements increase, as does the amount of time providers need to review other people's notes. Due to these conflicting issues, the compromise between efficiency and accuracy is a challenge for providers. Respondents described a love/hate relationship with CP/CF, in that, despite the risks, the tools are necessary to function in the current environment.

Despite the acknowledgement that CP/CF can create some efficiencies, many respondents called CP/CF a "necessary evil" (APP) due to the risks and challenges arising from use.

Respondents experience this internal struggle with wanting to be thorough, efficient, and accurate with documentation, but they do not have enough time to document, so they use tools that they know have errors associated with them, with some calling CP/CF "sloppy and paste" (faculty). Respondents feel this inner angst or moral injury because they have no other choice when the institution is pushing them to see more patients without allocating more time or compensation to document.

Influence From the Outside Environment

Overview

Further complicating and adding to the inner angst experienced by providers, the outside environment influences diffusion of an innovation and its consequences (Figure 1). Not only are providers feeling internal pressures, but they are also experiencing outside influences, including legal, regulatory, and financial requirements regarding what content to include in the note. This pressure, and the possible consequences, directly impact how respondents use CP/CF. In one example, a faculty member noted that the Centers for Medicare and Medicaid Services require an enormous number of requirements for one note, with some calling the note the "patient Wiki[pedia]" (faculty) for how many purposes the note serves at one time.

EHR-Related Solutions

Respondents provided suggestions for improving the EHR infrastructure to increase efficiency, including smart phrases, as well as improving education on EHR use. Part of that education includes understanding what information is relevant to keep in the notes to increase the usefulness of currently available efficiency tools, whether through CP or smart tools (Epic Systems). Respondents also expressed a desire for dictionaries that autocorrect abbreviations or prepopulate problem-based notes.

Another suggestion was for a tool that automatically identifies whether any information had been copied, with author attribution prominently displayed, such as a pop-up alert when using or reviewing text created with CP/CF and requiring users to review common errors from CP/CF, such as dates or values, before closing an encounter. Respondents also mentioned needing alternative tools to display and integrate notes, as well as more standardization and guidelines in note creation. Others suggested

XSL•FO
RenderX

having some sections of the notes be collapsible, as well as being able to insert images and hyperlinks within a charting tool for easier access to other areas of the chart.

Artificial Intelligence–Related Solutions

Some respondents described recent advances in artificial intelligence (AI) and the potential for integration into documentation tools. They wished that the note could be automatically created "like Jarvis style from the Avengers" (faculty). One such advancement currently under investigation is the use of ambient scribes, which listen to the physician-patient encounter and write the notes on behalf of the providers.

New Innovations: People-Focused Solutions

As much of the training and communication in EHR use to this point has arisen from informal communication channels (eg, word of mouth) or piecemeal, based on workflows and department needs, respondents requested additional education and training on best practices for documentation. Respondents also suggested training should focus on what the "right tools are to do the work" (APP), which could minimize reliance on CP/CF as the primary documentation tools.

Equally critical to providing training on best practices in documentation is giving providers the amount of time necessary to set up templates and smart phrases in the EHR, as well as an understanding of what is important to include in a note, ensuring documentation is more efficient in the future. Respondents proposed new or updated guidelines and standards with clear teaching and expectations of use for CP/CF to ensure efficient use of the tools. Departmental guidelines and expectations surrounding CP/CF use could help new learners and faculty use these tools appropriately.

The creation of a super user role on teams to facilitate general knowledge-sharing could provide a point person to identify key workflow components and functionality within departments or systems, which could "eliminate the amount of overload that the Epic support team [gets]" (APP) and lessen prolonged waiting times for users.

Cultural Shifts in Documentation

One of the key barriers to reviewing and editing notes for conciseness and accuracy is time, where "[time spent on editing the notes] is seen as an extra burden" (resident/fellow trainee). This extra time often is uncompensated and means less time caring for patients. The time spent on editing notes has unanticipated consequences of external constraints (eg, reimbursement policies or patient volume targets) on inner angst. An APP noted she wished she could spend more time with patients and less time documenting in general. Another APP highlighted that, "there's been such an increasing pressure to see more and more patients… and that's just making it harder and harder to actually document" (APP). With the current documentation culture, one resident/fellow trainee noted that, "the only way to function really, is to be copy and pasting from yourself [and] from others" (resident/fellow trainee).

Providers argued that there needs to be a cultural shift with regard to best practices for what gets documented and put into the note, as well as how notes are used. The reliance on notes as a patient "Wikipedia" has contributed to note bloat and the rise in errors and inaccuracies, as well as provider burnout, and therefore, reliance on CP/CF to document quickly. Providing the time needed for reviewing the work is critical.

Some providers suggested that the use of these tools should be limited. One faculty member said attribution should be mandatory; others added that the copied portions should be cited in quotes and attributed to the original author as in peer-reviewed publications. It could also be helpful to use different fonts, italics, or bold typeface to indicate copied text. Others mentioned that CP/CF should only be used for what is necessary to contextualize or augment the note, with clear identification of the information's source.

Discussion

Summary

In this study, we identified perceptions of and attitudes toward CP and CF, as well as consequences of the diffusion of this innovation in note writing, in an academic hospital (Figure 1). Whereas prior studies have described provider perceptions and process improvement through the introduction of CP/CF, our research expands on this literature by qualitatively exploring the consequences of this innovation through the lens of unintended consequences in diffusion [19] (Textbox 2).

XSL•FO
RenderX

Textbox 2. Summary findings are split up by the components of the Diffusion of Innovations Theory of Unintended Consequences framework from Figure 1.

Communication (diffusion)

- Documentation burden falls greatly on providers—but with pressures on their time, diffusion (via communication or training) is limited and inconsistent—users have created ad hoc workarounds to deal with the workload, versus intentional evidence-based practice and critical thinking skills development.

Social system

- Note purpose and use vary by specialty, health care setting, patient visits, and EHR products, so a one-size-fits-all solution is not feasible.

Intended consequences

- Respondents report a more streamlined workflow and increased efficiency, especially those with templates to help with organization and consistency, and can help with inter- and intrateam communication—when used appropriately.

Unintended consequences

- Whether through limited training, anxiety around policies, or other challenges, inaccuracies in notes result in risks to the patient, author, and system, from simple to severe. Respondents experience the moral injury of spending more time documenting out of fear of liability, harm, and denial of reimbursement, versus spending time providing care to patients, changing the culture of care. Noat bloat increases, the culture changes, and consequently, users experience frustration and burnout.

Outside environment

- Legal, regulatory, and financial pressures require documentation, but users are having to adjust their workflow to the requirements, rather than the system adjusting to the workflow. Respondents hope innovations will help with efficiency, but question where they will fit in the current external environment, which is perceived as broken, or whether they will arise from within. There is a need for guidance and policy, but it is hard to do so when use is so variable.

Discussion of Framework Elements

Communication

Awareness of CP/CF tools spread by word of mouth (Figure 1). As reported by others, the diffusers (ie, the ones spreading the innovation) are sometimes residents/fellow trainees and APPs, rather than supervisory or more senior staff, a trend that has persisted over the years [8,20,21,25]. However, simple awareness does not guarantee the quality of the information communicated in the medical note, so tailored formal training is recommended [26,27]. Another recommendation to promote high-quality training is to have an EHR champion available, especially in the inpatient setting where CP/CF are most used [8,20,27,28].

Communication and training about the use of CP/CF in documentation can provide teaching opportunities to enhance critical thinking of relevant information to capture [29]. This may be less likely in high-pressure, dynamic systems, but some have had success in training through templated or team-based writing [29,30].

Social System

Innovations (Figure 1) such as CP/CF are highly complex and are integrated into similarly complex and evolving systems [22,31,32]. Implementation and adoption rely not only on individuals and their personal characteristics, but the innovation itself, as well as the structure and characteristics, and culture of the organization in which the innovation is deployed. By certain metrics, innovations may be successfully diffused (technically adopted), but a lack of consideration for the interdependency of the actors in a system may inhibit realization of the optimal or true value to the system, and can lead to unintended consequences [31,32].

Intended Consequences

Our results reflect those of other reports that CP/CF improve efficiency [6], continuity of care for patients [8], and communication with teammates [33], as well as decreased documentation burden [7]. Yet in the two decades of literature acknowledging the benefit of innovation in electronic records, these same reports highlight the double-edged sword of efficiency versus unintended consequences [8,34]. Without trust in the system or other users, or without bulwarks against our own inherent flaws as human users of technology [35], the optimal use and benefits of these innovations and the intended consequence of improving quality of care will not be realized [31].

Our respondents describe the need for short-term solutions, such as recurring formal training on how and when to use CP/CF. Others have similarly demonstrated that lack of knowledge of appropriate use results in increased length of notes [36] and the importance of training and education for safe practice regarding these tools [31].

Unintended Consequences

Documentation burden, note bloat, inaccuracies, and more time spent documenting to the detriment of patient care, training, and interpersonal communication and trust—all have led to a perceived worsening of culture, the work environment, and workflows [5,37]. These phenomena are not new; the same benefits and challenges have remained consistent over time and across systems [38-40]. This dichotomy of intended (often positive) consequences and unintended (often negative)

XSL•FO
RenderX

consequences results in providers experiencing increased inner angst and moral injury [41,42]. Providers report angst from constraints against practicing what they consider "quality" care, and despite knowing the myriad risks, use tools such as CP/CF as the only workaround right now in a broken system, calling CP/CF a necessary evil. While providers acknowledge that CP/CF and other tools aid in the continuity of care and create a sense of efficiency when documenting, the lack of time to review notes thoroughly is a consistent and pervasive structural barrier. In such instances, errors slip through the cracks—the role of CP/CF in errors, inaccuracies, and outdated information is of particular concern [6,12], as they have contributed to note bloat [5,8] and may play a role in patient safety [16]. Inaccuracies may damage a patient's trust in and experience with the clinician or system; contribute to diagnostic and safety errors (inaccurate or out-of-date records, difficulty in finding relevant data in bloated notes); and increase legal risks, including unintentional falsification of records or plagiarism and medical malpractice [16,17]. All of these factors conspire to reduce providers' overall perceived quality of care delivery. This, in turn, can further worsen provider dissatisfaction and burnout, with a study suggesting that clinician involvement in medical errors is an independent risk of burnout [43].

Outside Environment

The outer system (Figure 1) is a key factor for optimal diffusion and implementation of an innovation [32,39]. Recommendations to address challenges in using CP/CF include developing policies, both institution-wide and specialty-specific, for CP/CF use. These larger structural factors—policies, standards, legislation, system resources, and engagement of leadership—filter down into organizational workflow and processes and then to individual knowledge of the innovation [32,39,40]. Although improvements at this larger scale are difficult to accomplish and are often more long-term solutions, a fundamental shift is needed at the outer system level in how these innovations are built for and integrated into dynamic, complex systems. Notes should serve clinical purposes and not focus as much on reimbursement regulations and national quality measures [21,32,44].

New Innovations

In the short term, most providers report the need for specific interventions, such as training to improve optimal EHR use, continued EHR optimization, and improved awareness of best practices for use of the functionality are necessary. Others recommended some degree of restrictions on use as well. While shown in other health systems to have direct impacts on hospital readmission [45], the overall widespread reliance on its use, and the inability to remove this functionality (easily) from underlying operating systems, suggest this is a nonviable solution. As a result, one must look for more novel, sustainable solutions. With the growth of AI and tools such as ambient or digital scribes already in use in clinical care to reduce documentation burden, careful reflection on the appropriate use of innovative tools will be paramount in mitigating current and future unintended consequences [6,13,46-48]. Another way to mitigate unintended consequences for ambient scribing would be to develop measures and metrics of success (eg, provider satisfaction scores, decrease in pajama time charting, decrease in documentation time, and increase in work/life balance). That way, organizations could evaluate whether the ambient scribes are aiding providers related to the intended metrics. However, while ambient scribes hold promise, to date, no studies have documented the impact of the ambient scribes on the amount of CP present in notes. This is likely, in part, because studies on ambient scribes are limited to ambulatory settings [49]. This will need to be an area of future study as the technology becomes more widespread.

Strengths and Limitations

There were some strengths in our study. First, this paper addresses providers' perspectives toward CP/CF in a way that adds depth and insight to the body of literature already present. Second, this is one of the first papers that attributes the concept of moral injury to the use of CP/CF, which has not been explored in the literature. Third, this manuscript offers recent perspectives and alternative solutions to aid in the documentation burden (eg, AI scribing). Fourth, this paper provides a true direct negative harm of CP/CF to the users, something which has not been previously described. In essence, while CP/CF use is continuing to grow over the years, it is associated with higher rates of documentation burden and job dissatisfaction. Thus, it is not working to solve the primary problem it was adopted to address: to make providers efficient and alleviate documentation burden. One reason for this may be the unintended consequence of its use, that whatever benefit the provider obtains from using these tools, moral injury and guilt compound and hinder providers.

There were some limitations to our study. First, this research was conducted at one academic health care institution, which may limit the generalizability of the findings. However, we solicited a breadth of input from various departments, roles/training levels, and clinical settings. Further, reported results from previous research on CP/CF are consistent with our findings, suggesting that these phenomena go beyond our institution. We also engaged a diverse team of researchers from a variety of disciplinary and demographic backgrounds to analyze the data to ensure a multidisciplinary approach and perspective. Second, it should be noted that the respondents for interviews were recruited from a subset of respondents to a previously deployed anonymous survey [19], specifically those who had self-identified and volunteered to participate in interviews. This approach does raise the likelihood of amplifying potential selection bias. Additionally, we used a convenience sampling method to select participants for interviews, and while the initial survey used a more robust purposive sampling strategy, the subset of self-identified interview participants was predominantly faculty and APPs, as opposed to medical students and residents/fellow trainees. As the use of CP is ubiquitous across levels of training and professional experience, we believe that our sampling strategy does reflect a broad and adequate spectrum of perspectives despite the relative underrepresentation of medical students and residents/fellow trainees. Third, at the time these interviews were conducted, there had been some discussion within the institution about whether curtailing or banning the use of CP/CF was appropriate as a policy measure. However, despite this potential barrier, it should be noted that

XSL•FO
RenderX

respondents uniformly expressed both positive and negative perceptions of EHR documentation tools.

Future Research Directions

Research addressing the unintended consequences of CP/CF, such as the use of a note for multiple purposes (eg, legal and patient safety implications, billing, communication, and continuity of care), could lead to slimmer, more streamlined notes, a decrease in documentation burden, and less burnout.

While CP/CF has limitations, there are innovations that could encourage appropriate use or reduce the need for CP/CF in documentation. Some potential innovations discussed by our participants were EHR technical solutions, including automatically identifying information that has been copied and having pop-up alerts when using or reviewing texts. Future research on the role these proposed features have in documentation could inform additional technical innovations and support cultural practices for proper attribution. AI solutions, such as digital or ambient scribes, may decrease the documentation burden and the need to use CP/CF; research is ongoing [46,50,51], but future research is needed to understand use across systems with different EHR policies and capacities. People-focused solutions, including more robust orientation training on CP/CF and having staff EHR super users to facilitate general knowledge sharing, could support more efficient and appropriate use of EHR tools, which in turn could help address documentation burden. Future research of educational programs and inclusion of EHR super users pre- and postimplementation may provide justification to integrate these ideas into clinical practice workflows, supporting a culture valuing time for training. Furthermore, importantly, health care systems are complex environments, and implementing new tools can result in unintended consequences. Future work must consider the potential for these unintended consequences resulting from the implementation of a complex innovation in dynamic systems.

Conclusions

Our study aimed to use semistructured interviews with providers to investigate their perceptions and attitudes surrounding CP/CF in the EHR, using a modified Diffusion of Innovations Theory of Unintended Consequences framework to analyze the data. The intended consequence of the innovative CP/CF tool, efficiency, is valued by users. However, the unintended consequences, including note bloat, errors, and patient safety and legal risks, have given rise to moral injury, a finding consistent with the literature. The theory of unintended consequences framework addresses the complex system within which CP/CF exists. In the case of CP/CF, outside pressures on documentation requirements are one of the critical barriers to realizing the potential for innovative duplicative text tools. Fewer documentation requirements may lessen internal and external pressures, leading to inner angst or moral injury among providers.

Acknowledgments

This study would not have been possible without the support of Oregon Health and Science University. No generative artificial intelligence tools were used in the writing of this paper.

Funding

This research project was funded through a grant from the Agency for Healthcare Research and Quality (R18HS029345).

Data Availability

The dataset generated or analyzed during this study is available from the corresponding author on reasonable request.

Authors' Contributions

Conceptualization: JAG (equal), VM (equal), JSA (equal), SC (equal)
Data curation: SC (lead)
Formal analysis: SC (equal), JSA (equal), RMJ (supporting), SF (supporting), GS (supporting)
Funding acquisition: JAG (lead)
Investigation: JSA (equal), SF (supporting), SC (equal)
Methodology: JSA (equal), SC (equal), JAG (equal), VM (equal), SF (supporting), GS (supporting), RMJ (supporting)
Project administration: SC (lead)
Resources: SC (equal), VM (equal), JAG (lead), JSA (equal)
Software: SC (lead)
Supervision: JAG (equal), JSA (lead), VM (equal), SC (equal)
Validation: SC (lead), JSA (lead), RMJ (equal), GS (equal), SF (equal), JAG (supporting), VM (supporting)
Visualization: RMJ (lead)
Writing – original draft: SC (lead)
Writing – review & editing: SC (lead), RMJ (lead), JSA (lead), VM (equal), JAG (equal), GS (equal), SF (supporting)

Conflicts of Interest

None declared.

XSL•FO
RenderX

Multimedia Appendix 1
Participant interview guide.
[DOCX File , 24 KB - medinform_v13i1e78502_app1.docx]

Multimedia Appendix 2
Table of quotes from participants in relation to the diffusion of innovation themes.
[DOCX File , 37 KB - medinform_v13i1e78502_app2.docx]

References

1. Blumenthal D. Launching HITECH. N Engl J Med 2010;362(5):382-385. [doi: 10.1056/NEJMp0912825] [Medline: 20042745]
2. Holmgren AJ, Downing NL, Bates DW, Shanafelt TD, Milstein A, Sharp CD, et al. Assessment of electronic health record use between US and non-us health systems. JAMA Intern Med 2021;181(2):251-259 [FREE Full text] [doi: 10.1001/jamainternmed.2020.7071] [Medline: 33315048]
3. Rotenstein LS, Apathy N, Holmgren AJ, Bates DW. Physician note composition patterns and time on the EHR across specialty types: a national, cross-sectional study. J Gen Intern Med 2023;38(5):1119-1126 [FREE Full text] [doi: 10.1007/s11606-022-07834-5] [Medline: 36418647]
4. West CP, Dyrbye LN, Shanafelt TD. Physician burnout: contributors, consequences and solutions. J Intern Med 2018;283(6):516-529 [FREE Full text] [doi: 10.1111/joim.12752] [Medline: 29505159]
5. Apathy NC, Rotenstein L, Bates DW, Holmgren AJ. Documentation dynamics: note composition, burden, and physician efficiency. Health Serv Res 2023;58(3):674-685 [FREE Full text] [doi: 10.1111/1475-6773.14097] [Medline: 36342001]
6. Tsou A, Lehmann C, Michel J, Solomon R, Possanza L, Gandhi T. Safe practices for copy and paste in the EHR. Appl Clin Inform 2017;8(1):12-34 [FREE Full text] [doi: 10.4338/ACI-2016-09-R-0150] [Medline: 28074211]
7. Hilliard R, Haskell J, Gardner R. Are specific elements of electronic health record use associated with clinician burnout more than others? J Am Med Inform Assoc 2020;27(9):1401-1410 [FREE Full text] [doi: 10.1093/jamia/ocaa092] [Medline: 32719859]
8. O'Donnell HC, Kaushal R, Barrón Y, Callahan MA, Adelman RD, Siegler EL. Physicians' attitudes towards copy and pasting in electronic note writing. J Gen Intern Med 2009;24(1):63-68 [FREE Full text] [doi: 10.1007/s11606-008-0843-2] [Medline: 18998191]
9. Digan W, Wack M, Looten V, Neuraz A, Burgun A, Rance B. Evaluating the impact of text duplications on a corpus of more than 600,000 clinical narratives in a French hospital. Stud Health Technol Inform 2019;264:103-107. [doi: 10.3233/SHTI190192] [Medline: 31437894]
10. Roddy JT, Arora VM, Chaudhry SI, Rein LM, Banerjee A, Swenson SL, et al. The prevalence and implications of copy and paste: internal medicine program director perspectives. J Gen Intern Med 2018;33(12):2032-2033 [FREE Full text] [doi: 10.1007/s11606-018-4575-7] [Medline: 30066119]
11. Rule A, Bedrick S, Chiang MF, Hribar MR. Length and redundancy of outpatient progress notes across a decade at an academic medical center. JAMA Netw Open 2021;4(7):e2115334 [FREE Full text] [doi: 10.1001/jamanetworkopen.2021.15334] [Medline: 34279650]
12. Steinkamp J, Kantrowitz JJ, Airan-Javia S. Prevalence and sources of duplicate information in the electronic medical record. JAMA Netw Open 2022;5(9):e2233348 [FREE Full text] [doi: 10.1001/jamanetworkopen.2022.33348] [Medline: 36156143]
13. Wang MD, Khanna R, Najafi N. Characterizing the source of text in electronic health record progress notes. JAMA Intern Med 2017;177(8):1212-1213 [FREE Full text] [doi: 10.1001/jamainternmed.2017.1548] [Medline: 28558106]
14. Wang R, Carrington JM, Hammarlund N, Sanchez O, Revere L. An evaluation of copy and paste events in electronic notes of patients with hospital acquired conditions. Int J Med Inform 2023;170:104934. [doi: 10.1016/j.ijmedinf.2022.104934] [Medline: 36508751]
15. Al Hadidi S, Upadhaya S, Shastri R, Alamarat Z. Use of dictation as a tool to decrease documentation errors in electronic health records. J Community Hosp Intern Med Perspect 2017;7(5):282-286 [FREE Full text] [doi: 10.1080/20009666.2017.1379852] [Medline: 29147468]
16. Singh H, Giardina TD, Meyer AND, Forjuoh SN, Reis MD, Thomas EJ. Types and origins of diagnostic errors in primary care settings. JAMA Intern Med 2013;173(6):418-425 [FREE Full text] [doi: 10.1001/jamainternmed.2013.2777] [Medline: 23440149]
17. Graber ML, Siegal D, Riah H, Johnston D, Kenyon K. Electronic health record-related events in medical malpractice claims. J Patient Saf 2019;15(2):77-85 [FREE Full text] [doi: 10.1097/PTS.0000000000000240] [Medline: 26558652]
18. Heiman HL, Rasminsky S, Bierman JA, Evans DB, Kinner KG, Stamos J, et al. Medical students' observations, practices, and attitudes regarding electronic health record documentation. Teach Learn Med 2014;26(1):49-55. [doi: 10.1080/10401334.2013.857337] [Medline: 24405346]

XSL•FO
RenderX

19. Hudkins M, Gold JA, Corby S, Ash J, Mohan V. Exploring provider perceptions and attitudes toward copy-paste and copy-forward in clinical documentation. Appl Clin Inform 2025;16(4):736-746. [doi: 10.1055/a-2574-1348] [Medline: 40769172]
20. Thornton JD, Schold JD, Venkateshaiah L, Lander B. Prevalence of copied information by attendings and residents in critical care progress notes. Crit Care Med 2013;41(2):382-388 [FREE Full text] [doi: 10.1097/CCM.0b013e3182711a1c] [Medline: 23263617]
21. Payne TH, Keller C, Arora P, Brusati A, Levin J, Salgaonkar M, et al. Writing practices associated with electronic progress notes and the preferences of those who read them: descriptive study. J Med Internet Res 2021;23(10):e30165 [FREE Full text] [doi: 10.2196/30165] [Medline: 34612825]
22. Ash JS, Sittig DF, Dykstra RH, Guappone K, Carpenter JD, Seshadri V. Categorizing the unintended sociotechnical consequences of computerized provider order entry. Int J Med Inf 2007;76 Suppl 1:S21-S27. [doi: 10.1016/j.ijmedinf.2006.05.017] [Medline: 16793330]
23. Rogers EM. Diffusion of Innovations. New York City: Free Press; 2003.
24. Griffin BJ, Purcell N, Burkman K, Litz BT, Bryan CJ, Schmitz M, et al. Moral injury: an integrative review. J Trauma Stress 2019;32(3):350-362. [doi: 10.1002/jts.22362] [Medline: 30688367]
25. Block L, Habicht R, Wu AW, Desai SV, Wang K, Silva KN, et al. In the wake of the 2003 and 2011 duty hours regulations, how do internal medicine interns spend their time? J Gen Intern Med 2013;28(8):1042-1047 [FREE Full text] [doi: 10.1007/s11606-013-2376-6] [Medline: 23595927]
26. Khairat S, Chourasia P, Kwong E, Choi JM, Seashore C. Effect of tailored coaching on physicians' electronic health record proficiency and user experience: a randomized crossover study. Mayo Clin Proc Digit Health 2023;1(2):94-104 [FREE Full text] [doi: 10.1016/j.mcpdig.2023.02.005] [Medline: 40206730]
27. Gainforth HL, Latimer-Cheung AE, Athanasopoulos P, Moore S, Ginis KAM. The role of interpersonal communication in the process of knowledge mobilization within a community-based organization: a network analysis. Implement Sci 2014;9:59 [FREE Full text] [doi: 10.1186/1748-5908-9-59] [Medline: 24886429]
28. Vawdrey DK, Cauthorn C, Francis D, Hackenberg K, Maloney G, Hohmuth BA. A practical approach for monitoring the use of copy-paste in clinical notes. AMIA Annu Symp Proc 2022;2021:1178-1185 [FREE Full text] [Medline: 35308931]
29. Huang D, Whitehead C, Kuper A. Competing discourses, contested roles: electronic health records in medical education. Med Educ 2024;58(12):1490-1501. [doi: 10.1111/medu.15428] [Medline: 38764398]
30. Rodríguez-Fernández JM, Loeb JA, Hier DB. It's time to change our documentation philosophy: writing better neurology notes without the burnout. Front Digit Health 2022;4:1063141 [FREE Full text] [doi: 10.3389/fdgth.2022.1063141] [Medline: 36518562]
31. Humphrey-Murto S, Makus D, Moore S, Watanabe Duffy K, Maniate J, Scowcroft K, et al. Training physicians and residents for the use of electronic health records-a comparative case study between two hospitals. Med Educ 2023;57(4):337-348. [doi: 10.1111/medu.14944] [Medline: 36181382]
32. Singh H, Sittig DF. A sociotechnical framework for safety-related electronic health record research reporting: the SAFER reporting framework. Ann Intern Med 2020;172(11 Suppl):S92-S100 [FREE Full text] [doi: 10.7326/M19-0879] [Medline: 32479184]
33. Vos JFJ, Boonstra A, Kooistra A, Seelen M, van Offenbeek M. The influence of electronic health record use on collaboration among medical specialties. BMC Health Serv Res 2020;20(1):676 [FREE Full text] [doi: 10.1186/s12913-020-05542-6] [Medline: 32698807]
34. Hirschtick RE. A piece of my mind. Copy-and-paste. JAMA 2006;295(20):2335-2336. [doi: 10.1001/jama.295.20.2335] [Medline: 16720812]
35. Rahimi B, Timpka T, Vimarlund V, Uppugunduri S, Svensson M. Organization-wide adoption of computerized provider order entry systems: a study based on diffusion of innovations theory. BMC Med Inform Decis Mak 2009;9:52 [FREE Full text] [doi: 10.1186/1472-6947-9-52] [Medline: 20043843]
36. Pennathur PR. A theoretical framework for understanding creator-consumer information interaction behaviors in healthcare documentation systems. Appl Ergon 2020;84:103034 [FREE Full text] [doi: 10.1016/j.apergo.2019.103034] [Medline: 31987517]
37. Embi PJ, Yackel TR, Logan JR, Bowen JL, Cooney TG, Gorman PN. Impacts of computerized physician documentation in a teaching hospital: perceptions of faculty and resident physicians. J Am Med Inform Assoc 2004;11(4):300-309 [FREE Full text] [doi: 10.1197/jamia.M1525] [Medline: 15064287]
38. Hoerbst A, Schweitzer M. A systematic investigation on barriers and critical success factors for clinical information systems in integrated care settings. Yearb Med Inf 2015;10(1):79-89 [FREE Full text] [doi: 10.15265/IY-2015-018] [Medline: 26293853]
39. Siegler EL, Adelman R. Copy and paste: a remediable hazard of electronic health records. Am J Med 2009;122(6):495-496. [doi: 10.1016/j.amjmed.2009.02.010] [Medline: 19486708]
40. Ross J, Stevenson F, Lau R, Murray E. Factors that influence the implementation of e-health: a systematic review of systematic reviews (an update). Implement Sci 2016;11(1):146 [FREE Full text] [doi: 10.1186/s13012-016-0510-7] [Medline: 27782832]

XSL•FO
RenderX

41. Day P, Lawson J, Mantri S, Jain A, Rabago D, Lennon R. Physician moral injury in the context of moral, ethical and legal codes. J Med Ethics 2022;48(10):746-752. [doi: 10.1136/medethics-2021-107225] [Medline: 34290114]
42. Dean W, Talbot S, Dean A. Reframing clinician distress: moral injury not burnout. Fed Pract 2019;36(9):400-402 [FREE Full text] [Medline: 31571807]
43. Tawfik DS, Profit J, Morgenthaler TI, Satele DV, Sinsky CA, Dyrbye LN, et al. Physician burnout, well-being, and work unit safety grades in relationship to reported medical errors. Mayo Clin Proc 2018;93(11):1571-1580. [doi: 10.1016/j.mayocp.2018.05.014] [Medline: 30001832]
44. Wosny M, Strasser LM, Hastings J. The paradoxes of digital tools in hospitals: qualitative interview study. J Med Internet Res 2024;26:e56095. [doi: 10.2196/56095] [Medline: 39008341]
45. Cheng C, Wu D, Lu J, Yu CP, Lin HL, Wang MC, et al. Restricted use of copy and paste in electronic health records potentially improves healthcare quality. Medicine (Baltimore) 2022;101(4):e28644 [FREE Full text] [doi: 10.1097/MD.0000000000028644] [Medline: 35089204]
46. Waisberg E, Ong J, Masalkhi M, Kamran SA, Zaman N, Sarker P, et al. GPT-4: a new era of artificial intelligence in medicine. Ir J Med Sci 2023;192(6):3197-3200. [doi: 10.1007/s11845-023-03377-8] [Medline: 37076707]
47. Knitza J, Gupta L, Hügle T. Rheumatology in the digital health era: status quo and quo vadis? Nat Rev Rheumatol 2024;20(12):747-759. [doi: 10.1038/s41584-024-01177-7] [Medline: 39482466]
48. Sezgin E, Sirrianni JW, Kranz K. Evaluation of a digital scribe: conversation summarization for emergency department consultation calls. Appl Clin Inform 2024;15(3):600-611 [FREE Full text] [doi: 10.1055/a-2327-4121] [Medline: 38749477]
49. Tierney AA, Gayre G, Hoberman B, Mattern B, Ballesca M, Wilson Hannay SB, et al. Ambient artificial intelligence scribes: learnings after 1 year and over 2.5 million uses. NEJM Catalyst 2025;6(5). [doi: 10.1056/cat.25.0040]
50. Shah SJ, Crowell T, Jeong Y, Devon-Sand A, Smith M, Yang B, et al. Physician perspectives on abient AI scribes. JAMA Netw Open 2025;8(3):e251904 [FREE Full text] [doi: 10.1001/jamanetworkopen.2025.1904] [Medline: 40126477]
51. Ma S, Liang A, Shah S, Smith M, Jeong Y, Devon-Sand A, et al. Ambient artificial intelligence scribes: utilization and impact on documentation time. J Am Med Inform Assoc 2025;32(2):381-385. [doi: 10.1093/jamia/ocae304] [Medline: 39688515]

Abbreviations

AI: artificial intelligence
APP: advanced practice provider
CF: copying or carrying forward
CP: copying and pasting
EHR: electronic health record
VistA: Veterans Health Information Systems and Technology Architecture

Edited by A Coristine; submitted 05.06.25; peer-reviewed by K Adegoke, T Rungvivatjarus, V Tiase; comments to author 06.10.25; accepted 25.11.25; published 19.12.25.

Please cite as:
Corby S, Ash JS, Jungbauer RM, Scholl G, Florig S, Mohan V, Gold JA
Copy Tools in the Electronic Health Record: Perceptions, Implications, and Future Directions
JMIR Med Inform 2025;13:e78502
URL: https://medinform.jmir.org/2025/1/e78502
doi:10.2196/78502
PMID:

©Sky Corby, Joan S Ash, Rebecca M Jungbauer, Gretchen Scholl, Sarah Florig, Vishnu Mohan, Jeffrey A Gold. Originally published in JMIR Medical Informatics (https://medinform.jmir.org), 19.12.2025. This is an open-access article distributed under the terms of the Creative Commons Attribution License (https://creativecommons.org/licenses/by/4.0/), which permits unrestricted use, distribution, and reproduction in any medium, provided the original work, first published in JMIR Medical Informatics, is properly cited. The complete bibliographic information, a link to the original publication on https://medinform.jmir.org/, as well as this copyright and license information must be included.

XSL•FO
RenderX

Original Paper

Competition or Complementarity Among Telemedicine Tools in Ambulatory Care Practice: Cross-Sectional Analysis

Xiang Oliver Liu[1*], MCom; Avijit Sengupta[1,2*], PhD

[1]Business Information Systems, Business School, The University of Queensland, Brisbane, Queensland, Australia

[2]Centre for the Business and Economics of Health, Business School, The University of Queensland, Brisbane, Queensland, Australia

[*]all authors contributed equally

Corresponding Author:
Xiang Oliver Liu, MCom
Business Information Systems, Business School
The University of Queensland
37 Blair Dr, St Lucia
Brisbane, Queensland, QLD 4067
Australia
Phone: 61 478495662
Email: oliver.liu@business.uq.edu.au

Abstract

Background: Telemedicine use surged due to its capacity to deliver safe, remote care. As the public health crisis subsides, evaluating the interplay among various tools, such as video, audio, and text, becomes critical to sustained use. With health care shifting back to in-person models, understanding whether telemedicine tools complement or compete provides valuable insights for future technology design and usage strategies.

Objective: This study investigates whether different types of telemedicine technology tools complement or compete while physicians deliver health care services through them. A clear understanding of the relationships between telemedicine technology tools, physicians' satisfaction, evaluation of care quality, and patient visit percentages is crucial for the design of new telemedicine technology platforms and ensuring quality of care services through technology platforms.

Methods: To fulfill our objective, we analyzed data from the 2021 National Electronic Health Records Survey. We used ordered logit and probit regression models to evaluate the effects of telemedicine technology tools on physicians' overall satisfaction, quality of health care evaluation, and the percentage of patient visits via telemedicine.

Results: A total of 1875 office-based physicians in the United States completed the survey. Three main outcomes were assessed, including physician satisfaction (n=1614), evaluation of health care quality (n=1617), and the percentage of patient visits conducted via telemedicine (n=1558). Ordered logit and probit regression analyses revealed that the aggravated use of telemedicine tools had a significant impact on improvements in all 3 outcomes. A unit increase in telemedicine tools was associated with a 4.2 percentage point increase in the predicted probability of physicians being "very satisfied" (P<.001) and a 5.2 percentage point increase in evaluating telemedicine quality as "to a great extent" (P<.001). For patient visits, a unit increase in telemedicine tools was associated with a 1.8 percentage point increase in the likelihood of reporting "≥75% of visits via telemedicine" (P<.001). Disaggregated analysis indicated that all individual tools were positively associated with physician satisfaction and quality evaluation (P<.05). Bundle models revealed patterns consistent with complementarity (several bundles exceeded their constituent tools) and competition (some significant bundles were smaller than at least one constituent tool), aligning with the presence of both reinforcing and overlapping functionalities.

Conclusions: Our study demonstrates that telemedicine tools interact in ways that can be either complementary or competitive, depending on how their functionalities align within physicians' workflows. Videoconferencing tools, especially when integrated with electronic health record platforms, act as a central complementary component that enhances physicians' satisfaction and evaluation of care quality. In contrast, combinations lacking video capability or involving multiple nonintegrated platforms fragment workflows and increase cognitive burden. These findings emphasize the importance of designing telemedicine tool bundles that align media capabilities with clinical communication needs, thereby improving satisfaction and supporting sustainable, high-quality telemedicine practice.

(JMIR Med Inform 2025;13:e75246) doi:10.2196/75246

XSL•FO
RenderX

KEYWORDS

office-based physicians; ordered logit regression model; ordered probit regression model; percent of patient visit; physicians' satisfaction; quality of care; telemedicine technology tools

Introduction

Overview

Telemedicine, the use of telecommunications technology to provide health care remotely [1], has rapidly evolved to improve access to high-quality, efficient, and cost-effective health care, particularly during a major public health crisis like the COVID-19 pandemic [2,3]. Due to the unique characteristics of telemedicine, it has emerged as an ideal solution for mitigating the risks of secondary virus transmission and continuity of health care services. During the COVID-19 pandemic, there was a significant surge in demand for telemedicine, leading to substantial growth in the telemedicine industry, with remote appointments increasing by 154% within a year [4]. Meanwhile, the global telemedicine market is projected to grow from US $60.15 billion in 2023 to US $309.90 billion by 2032, with a compound annual growth rate of 19.98% [5].

Although telemedicine adoption was initially slow [6] and hindered by restrictive administrative regulations as well as limited financial investment [7], the COVID-19 pandemic significantly accelerated its adoption as it became the only alternative to in-person care, offering the safest mode of health care delivery [8]. This shift relied on using multiple telemedicine tools, which provided physicians and patients with multiple synchronous and asynchronous communication channels, including audio, video, and text (with and without electronic health records [EHRs]).

During and post the COVID-19 pandemic, most physicians received access to more than one type of telemedicine tool, which usually supports different functionalities (eg, telephone, videoconferencing, platforms without EHR, and platforms with EHR). Considering that individual tools and their combinations differ in efficacy and consequently influence the quality of health care delivery, it is essential to identify their performance both as independent tools and as integrated bundles.

However, there are only a handful of studies that have compared different telemedicine tools before or after the COVID-19 pandemic. For instance, the meta-analysis by Byambasuren et al [9] revealed no significant difference in clinical effectiveness between telephone and video consultations, though video was preferred for clinical assessment despite feasibility issues. In a separate study, Alhajri et al [10] found that physicians had greater confidence in acute care and patient education with video compared to audio but experienced longer consultation times. In addition, Orrange et al [11] suggested that most patients preferred video over telephone for telehealth visits despite encountering technical issues, due to the overall convenience. Collectively, these studies highlight that different telemedicine tools have unique strengths and limitations, which are shaped by user and usage context, as well as the mode of interaction. However, we still have very little knowledge about their perception and performance when they are deployed together.

Additionally, although studies compare different telemedicine tools from various perspectives, they often overlook the communication functions embedded within each tool. Communication is the core function of telemedicine tools, particularly crucial for ambulatory care physicians who face challenges related to technology infrastructure, such as low bandwidth and slow internet speeds [12]. While previous studies have compared different telemedicine tools, such as audio and video, in terms of perceived convenience, clinical effectiveness, or health care quality, they have mostly treated these tools as individual units.

Surprisingly, there is little exploration that investigates how these telemedicine tools, with their varying levels of media richness, synchronicity, and interactivity, work together and independently to influence clinical communication. For example, both Doxy.me (a telemedicine platform) and FaceTime are labeled as "video" tools. However, they may differ substantially in how they support real-time feedback, offering visual cues, or in interface stability. These communication functionalities, rather than the tool types themselves, shape how effectively clinical conversations are conducted and decisions are made. Therefore, it is also important to investigate whether telemedicine tools using different communication modes function in a complementary or competitive manner with existing physician workflows [13].

If these tools are complementary, they can collectively enhance health care delivery by improving system efficiency, ensuring better alignment between physicians' tasks and telemedicine tools, and providing a seamless experience that increases physician satisfaction [14]. On the other hand, if they compete, this may result in duplicated functionalities, fragmented workflows, increased cognitive burden, and communication fatigue, ultimately reducing satisfaction and the effective use of telemedicine [15].

Thus, understanding the nature of the relationship (complementary vs competitive) between telemedicine tools helps inform sustainable telemedicine use, especially when it is no longer a necessity but an optional provision. For a complementary relationship, there are different usage strategies and policies for physicians, clinical settings, or industry, compared to a competitive relationship. This leads us to posit our research question: "Do telemedicine tools compete or complement each other?"

In our study, we aimed to answer this question from the perspective of physicians, the primary users of telemedicine tools. We used data from the 2021 National Electronic Health Records Survey (NEHRS) [16-19] and applied media synchronicity theory (MST) to answer the research question. We used ordered logit and probit regression models for empirical analysis.

Our findings reveal that while both independent and combined uses of telemedicine tools enhance physicians' satisfaction and

XSL•FO
RenderX

quality-of-health care evaluations, their combinations are not always complementary. Instead, various telemedicine bundles produce either complementary or competing effects depending on how functionalities align within physicians' clinical workflows. Specifically, video-based communication tools serve as a central complementary element that enriches clinical assessment and communication, particularly when integrated with EHR-embedded platforms. However, bundles lacking video capability or comprising multiple nonintegrated platforms, like the simultaneous use of EHR-embedded and non–EHR-embedded telemedicine platforms, lead to workflow fragmentation and cognitive overload, ultimately lowering physicians' satisfaction and their evaluations of care quality. In addition, tool bundles with a higher number of telemedicine tools increase the percentage of patients who visit physicians via telemedicine by enhancing flexibility and accessibility. Based on our findings, we recommend telemedicine technology vendors and platform developers for technological systems designed to ensure the complementary behavior of different tools based on physicians' specific demands.

Aim

Understanding whether telemedicine tools operate in complementary or competing manners is essential for sustained use of telemedicine in the postpandemic era. This study examines the impact of individual telemedicine tools and combinations of tools on physicians' satisfaction, perceived quality of care, and the proportion of patient visits conducted via telemedicine. Specifically, we investigate whether different combinations of telemedicine tools function as complements or substitutes within the clinical workflows of ambulatory care physicians.

Literature Review

Although telemedicine technology has existed for decades, it was not widely adopted by physicians or patients until the pandemic. In our literature review section, we primarily focus on (1) the technological capabilities of telemedicine tools and their associated tasks, (2) the impact of telemedicine technologies on physicians' satisfaction, (3) the impact of telemedicine technologies on physicians' evaluation of telemedicine service quality, and (4) the impact of telemedicine technologies on patients' visits choices.

Telemedicine Technology Capabilities and Their Associated Tasks

Telemedicine tools can be grouped into 2 categories based on their synchronous (eg, real-time audio and video consultations) or asynchronous (eg, message-based or store-and-forward systems) communication features. Each telemedicine tool supports specific health care tasks depending on its technical features, such as media richness, interactivity, and synchronicity. Synchronous telemedicine tools, such as live video consultations or real-time chat systems, are widely accepted for their ability to facilitate immediate interaction between physicians and patients [20]. These tools aim to replicate in-person visits, enabling real-time diagnosis and immediate medical advice through audio and video communication channels [21-23]. However, they are dependent on both parties' (physician and patient) simultaneous availability. Alternatively, asynchronous telemedicine tools, like email, offer flexibility and convenience by enabling patients and health care providers to communicate without the need for simultaneous presence [24,25]. These tools are especially effective for follow-up care, chronic disease management, or sharing test results, where real-time interaction is not necessary. Their acceptance is high among patients seeking time-efficient solutions or health care providers managing a large number of patients. However, the lack of immediate feedback limits their effectiveness for patients who require urgent attention. Therefore, it is essential to strike a balance between the needs of physicians and patients when implementing telemedicine tools.

Impact of Telemedicine Technologies on Physicians' Satisfaction

Physician satisfaction is a crucial determinant of continuous telemedicine adoption and long-term system use [14]. Prior studies suggest that physicians' satisfaction is shaped by both system-level attributes, such as usability, interoperability, and reliability, as well as user-level experiences, such as workload, communication quality, and perceived clinical control [26,27]. For example, video-based telemedicine generally contributes to higher physicians' satisfaction levels than telephonic consultations, as it allows richer interactions, visual assessment, and enhanced rapport with patients [10]. However, video consultations are also associated with longer session times and potential technical issues, which can diminish physicians' satisfaction under certain conditions [28,29]. Therefore, current studies indicate that video should supplement, rather than replace, the telephone [28,29].

Moreover, when multiple tools are available, physicians' satisfaction depends on whether these telemedicine tools are seamlessly complementary and align with physicians' health care–related task requirements [27]. In contrast, physicians might report frustration when tools compete, for example, when an EHR-integrated video platform and an independent messaging app duplicate documentation or scheduling tasks [30].

Impact of Telemedicine Technologies on Physicians' Evaluation of Telemedicine Service Quality

Physicians' evaluation of telemedicine service quality reflects their comparison of the perceived quality of health care between telemedicine and traditional in-person visits [31]. Studies have shown that asynchronous tools, such as email, are valued for follow-up communication; however, their effectiveness in immediate medical decision-making is lower than that of face-to-face methods [32]. In contrast, synchronous video consultations enhance physicians' diagnostic confidence and clinical effectiveness. In particular, for acute care or clinical assessments, the quality of synchronous video consultations can be comparable to that of traditional in-person care, especially under acute external stress, such as during the pandemic period [28,33]. Furthermore, the integration of EHRs can improve physicians' perceived quality of care by facilitating decision-making through access to and sharing comprehensive patient medical information, thereby ensuring continuity of care [34,35]. However, excessive system complexity or poor

XSL•FO
RenderX

interoperability between platforms can have the opposite effect, increasing physicians' cognitive load, disrupting clinical workflows, and ultimately reducing their evaluation of telemedicine service quality [36,37].

Impact of Telemedicine Technologies on Patients' Visit Choices

The adoption of telemedicine technologies has also influenced patients' preferences and behaviors regarding the types of visits they prefer. For example, the availability of video and audio consultations increases health care access by reducing travel time, waiting time, and perceived risk of exposure [33,38,39]. Therefore, during the COVID-19 pandemic, patients widely adopted telemedicine as a substitute for in-person visits, with remote consultations dramatically increased across multiple specialties [8]. Postpandemic studies, however, indicate that visit choices now depend on perceived convenience, trust, and the nature of the medical issue [40].

Patients generally prefer video consultations over audio when visual assessment or relational communication is important; however, they choose telephone consultations for brief follow-ups or low-complexity issues [41]. Significantly, patients' continued usage in telemedicine is shaped by their communication experience, the reliability of the technology, and the perceived competence of the physician [42].

To provide an overview of the existing literature in this domain, we synthesized the relevant literature into Multimedia Appendix 1. Our review reveals that while literature often examines individual telemedicine tools or analyses multiple tools separately within a study, there is limited research investigating whether multiple tools complement or compete with each other.

This knowledge is critical, as understanding the interplay between telemedicine tools could provide insights into their collective impact on physicians' overall satisfaction, evaluations of health care quality, and the proportion of patient visits conducted via telemedicine. To address this knowledge gap, our study explores whether complementary or competitive relationships among various telemedicine tools influence the outcomes. We aim to contribute to the telemedicine literature, benefiting health care professionals, researchers, and designers of health IT alike.

Theoretical Framing

To better explore whether telemedicine tools compete or complement each other, we applied MST. MST emphasizes how different media capabilities support 2 fundamental communication processes: conveyance and convergence [43,44]. Conveyance involves transmitting complex information that requires the receiver to process and interpret it, whereas convergence aims to establish a shared understanding and reach a consensus among participants. Additionally, MST identifies five core media capabilities: (1) symbol sets, the variety of ways information can be encoded (eg, text, voice, video); (2) parallelism, the extent to which multiple conversations can occur simultaneously; (3) transmission velocity, how quickly messages are delivered; (4) rehearsability, the ability to fine-tune a message before sending it; and (5) reprocessability, the extent to which a message can be reviewed or revisited after transmission.

In the context of telemedicine, different tools embody distinct combinations of these capabilities and therefore serve different communicative purposes. For example, telephone audio (T1) offers low symbol diversity and reprocessability, making it suitable for simple updates rather than complex discussions. Videoconferencing tools (T2), with richer symbol sets and high transmission velocity, support synchronous interactions, visual assessment, and real-time convergence between physicians and patients. Non–EHR-integrated telemedicine platforms (T3) support structured, health-specific interactions but often lack continuity of documentation or direct access to clinical records, which limits their reprocessability and integration. However, they may offer higher parallelism and flexibility, especially for lightweight or routine consultations. EHR-integrated telemedicine platforms (T4) enhance both rehearsability and reprocessability by enabling real-time clinical documentation, access to patient history, and retrospective review. However, they also significantly increase the cognitive load on physicians [44] when navigating patient information in an EHR system, which remains a demanding task. Therefore, we argue that no single telemedicine tool is suitable for all tasks in all care contexts. Based on the above argument, telemedicine tools can be selected or combined to optimize communication according to the requirements of clinical or administrative tasks. MST thus provides a useful lens for interpreting how these tools complement or compete within ambulatory care, in the context of physicians' workflows.

Previous research has reported the application of MST in the domain of telemedicine. Tan and Yan [45] used MST to classify text and patterns in recognition, while Yan et al [46] used MST to design a comparative case study and conduct a deductive analysis of teleconsultation adoption in clinical settings. Tan and Yan [45] demonstrated that physicians' response behaviors and media features, particularly response speed and the availability of voice services, jointly influenced their perceived service quality in mobile health care, with media synchronicity capabilities acting as a moderating factor. Yan et al [46] suggested that when the media synchronicity of the adopted technology matches the synchronicity requirements of the communication process, teleconsultation services are facilitated. Although MST was used in the context of telemedicine, to the best of our knowledge, it was never used to investigate the complementary or competitive nature of telemedicine tools.

Health care delivery often involves multiple communication tools that must coordinate effectively with each other to achieve the best patient outcomes. MST offers a valuable theoretical lens to address this issue by distinguishing between conveyance and convergence communication processes and aligning them with specific media capabilities. This allows for a more precise evaluation of when tools should substitute for one another versus when they should be integrated to support different stages of communication. Therefore, applying MST enhances our understanding of media choice to explain whether telemedicine tools compete or complement each other.

XSL•FO
RenderX

Ethical Considerations

This study was a secondary analysis of deidentified data from the NEHRS, conducted by the National Center for Health Statistics (NCHS), US Centers for Disease Control and Prevention (CDC). NEHRS is a national survey of office-based physicians that collects information on the adoption and use of EHRs and related health information technologies. The analytic dataset used in this study was obtained from the public-use NEHRS files, which contain no direct identifiers and adhere to NCHS data confidentiality standards. As this study involved only analysis of existing, fully identified public-use data, no additional institutional review board or human research ethics committee review was sought for this secondary analysis, in accordance with institutional and national guidance on research using public-use survey data. The original NEHRS data collection was conducted by NCHS under applicable federal regulations and ethical guidelines governing human participants research, and participating physicians provided consent at the time of the primary survey. Privacy and confidentiality were maintained throughout the current analysis, and no individual physician, practice, or patient can be identified from the reported results.

Methods

Data Resource

This study used data from the NEHRS, a nationally representative survey of office-based ambulatory care physicians in the United States [16-19]. The NEHRS sample is designed to be representative of the broader population of office-based physicians in the United States. It provides crucial insights into EHR use, practice-related details, controlled substance prescribing, health information exchange, telemedicine use, and documentation-related burdens. The survey comprises 32 primary questions, further divided into many subquestions. The initial NEHRS sample in 2021 included 10,302 office-based physicians. After screening for eligibility, 2037 physicians were confirmed to meet the following inclusion criteria: (1) office-based; (2) principally engaged in patient care activities; (3) nonfederally employed; (4) not in the specialties of anesthesiology, pathology, or radiology; and (5) younger than 85 years of age at the time of the survey. Among them, 1875 physicians fully completed the survey by responding to all key items, and these completed responses form the final analytic sample used in this study. All statistical analyses and interpretations in this study are based on the 1875 individual respondents who completed the full survey. The survey provides information not only about physicians' satisfaction, perceived quality of health care, and the percentage of patient visits conducted through telemedicine, but also includes data on physician gender, age, and clinical setting, among other details [19].

Dependent Variables and Independent Variables

The dependent variables examined in our study are office-based physicians' satisfaction with telemedicine technology use (Telemedsat), physicians' quality-of-health care evaluation in comparison to in-person service (Telemedqual), and percentage of patient visits through telemedicine as a proportion of overall ambulatory care visits. Examining these 3 dependent variables would provide us with a more comprehensive understanding of telemedicine use among ambulatory care physicians. While satisfaction reflects physicians' personal emotional response to the use of telemedicine tools, physicians' evaluation of health care quality captures physicians' retrospective, task-specific judgment about the functional equivalence of telemedicine relative to traditional care delivery [10,47]. The second measure requires physicians to directly compare their own performance, focusing on their perceived ability to maintain clinical standards in a telemedicine setting. The percentage of patient visits via telemedicine tools measures physicians' active engagement and comfort with telemedicine tools while interacting with patients [11,12,48].

These variables collectively enable us to evaluate the experience, performance, and behavioral adoption of telemedicine tools among ambulatory care physicians. Table 1 presents the descriptive statistics of these 3 dependent variables along with the independent and control variables.

XSL•FO
RenderX

Table 1. Descriptive statistics for dependent, independent, and control variables.

Variables and descriptions	Value
Dependent variables	
Telemedsat[a], n (%)	
Very satisfied	291 (18.05)
Somewhat satisfied	671 (41.53)
Neither satisfied nor dissatisfied	283 (17.49)
Somewhat dissatisfied	261 (16.13)
Very dissatisfied	108 (6.80)
Telemedqual[b], n (%)	
Fully	57 (3.52)
To a great extent	436 (27.02)
To some extent	725 (44.73)
To a small extent	337 (20.79)
Not at all	62 (3.95)
Telemedpct[c], n (%)	
≥75%	117 (7.77)
50%-74%	126 (8.09)
25%-49%	421 (27.02)
<25%	875 (56.16)
None	19 (0.96)
Independent variables	
Sum of telemedicine tools used, mean (SD)	
SumT[d]	1.97 (0.87)
One telemedicine tool[e], n (%)	
T1[f] (yes vs no)	1107 (68.08) vs 519 (31.92)
T2[g] (yes vs no)	936 (57.56) vs 690 (42.44)
T3[h] (yes vs no)	707 (43.48) vs 919 (56.52)
T4[i] (yes vs no)	451 (27.74) vs 1175 (72.26)
Bundle telemedicine tools, n (%)	
T1T2[j] vs others	695 (42.74) vs 931 (57.26)
T1T3 vs others	469 (28.72) vs 1159 (71.28)
T1T4 vs others	330 (20.30) vs 1296 (79.70)
T2T3 vs others	318 (19.56) vs 1308 (80.44)
T2T4 vs others	219 (13.47) vs 1407 (86.53)
T3T4 vs others	136 (8.36) vs 1490 (91.64)
T1T2T3 vs others	270 (16.61) vs 1356 (83.39)
T1T3T4 vs others	118 (7.26) vs 1508 (92.74)
T1T2T4 vs others	187 (11.50) vs 1439 (88.50)
T2T3T4 vs others	71 (4.36) vs 1555 (95.64)
T1T2T3T4 vs others	65 (4.00) vs 1561 (96.00)
Control variables	

XSL•FO
RenderX

Variables and descriptions	Value
Barriers, n (%)	
Telemedbarrier1[k]	576 (35.42)
Telemedbarrier2[l]	290 (17.83)
Telemedbarrier3[m]	423 (26.01)
Telemedbarrier4[n]	1078 (66.30)
Telemedbarrier5[o]	1152 (70.84)
Facilitator[p], n (%)	
No improvement	757 (46.56)
Improvement	869 (53.44)
Physex[q], n (%)	
Male	612 (32.69)
Female	1259 (67.31)
Phyage50[r], n (%)	
Age ≤50 years	653 (34.88)
Age >50 years	1218 (65.12)
Speccat[s], n (%)	
Primary care specialty	911 (48.69)
Surgical specialty	411 (21.97)
Medical specialty	549 (29.33)
Numofphy[t], n (%)	
1 physician	432 (23.09)
2-3 physicians	367 (19.63)
4-10 physicians	557 (28.76)
11-50 physicians	292 (15.57)
>50 physicians	223 (11.95)
Setting[u], n (%)	
Solo or group practice	1317 (70.35)

XSL•FO
RenderX

Variables and descriptions	Value
Other setting	554 (29.65)

[a]Telemedsat: physicians' satisfaction (ordinal variable measured on a 5-point Likert scale).

[b]Telemedqual: physicians' evaluation of health care quality (ordinal variable measured on a 5-point Likert scale).

[c]Telemedpct: percentage of patient visits via telemedicine (ordinal variable measured on a 5-point Likert scale).

[d]SumT: total number of telemedicine tools each physician used (continuous variable).

[e]Distribution of single-tool users: T1 only=121 (7.44%), T2 only=165 (10.15%), T3 only=175 (10.76%), T4 only=77 (4.74%).

[f]T1: telephone audio (binary variable).

[g]T2: videoconference software with audio (eg, Zoom, Ibex, FaceTime; binary variable).

[h]T3: telemedicine platforms not integrated with electronic health records (eg, Doxy. me; binary variable).

[i]T4: telemedicine platforms integrated with electronic health records (eg, updating clinical documentation during a telemedicine visit; binary variable).

[j]T1T2: physicians who use T1 and T2 simultaneously—binary variable (the following variables are expressed in the same way as this).

[k]Telemedbarrier1: limited internet access or speed issues (binary variable).

[l]Telemedbarrier2: telemedicine platform not easy to use or did not meet physician's needs (binary variable).

[m]Telemedbarrier3: telemedicine is not appropriate for physician's specialty or type of patients (binary variable).

[n]Telemedbarrier4: limitations in patients' access to technology (eg, smartphone, computer, tablet, internet; binary variable).

[o]Telemedbarrier5: patients' difficulty using technology or telemedicine platform (binary variable).

[p]Facilitator: improved reimbursement and relaxation of rules related to use of telemedicine visits (binary variable).

[q]Physex: physicians' sex (binary variable).

[r]Phyage50: physicians' age group (binary variable).

[s]Speccat: physicians' specialty type (multinomial variable).

[t]Numofphy: number of physicians working in the facility (ordinal variable).

[u]Setting: the nature of the practice setting (binary variable).

Independent variables include 4 telemedicine tools: telephone audio (T1); videoconference software with audio (T2; eg, Zoom, Ibex, and FaceTime); telemedicine platforms not integrated with EHR (T3; eg, Doxy.me); and telemedicine platforms integrated with EHR (T4; eg, updating clinical documentation during a telemedicine visit). We counted the total number of telemedicine tools each physician uses and considered them a singular construct (SumT). We also conducted further analysis on different combinations of telemedicine tools (TelemedCombination). For example, physicians used both telephone audio and videoconference software with audio (T1T2), or they simultaneously used telephone audio, videoconference software with audio, and telemedicine platforms not integrated with EHR (eg, Doxy.me; T1T2T3), among other combinations. Notably, in the survey, physicians were asked to indicate which telemedicine tools they used by selecting from a list of 4 options, with no restrictions or dependencies among the tools. This means that each tool could be adopted independently of the others and was not mutually exclusive.

We also consider a set of relevant control variables, including physicians' sex (Physex), physicians' age group (Phyage50), physicians' specialty type (Speccat), number of physicians working in the facility (Numofphy), the nature of the practice (Setting), and perceived barriers and facilitators to telemedicine tools usage. Perceived barriers when using telemedicine tools can be categorized into 5 groups, including limited internet access and speed issues (Telemedbarrier1), platforms that are difficult to use or fail to meet physicians' needs (Telemedbarrier2), telemedicine may not be suitable for specific specialties or patient types (Telemedbarrier3), limited access to technology for patients (eg, smartphones, computers, tablets, or the internet; Telemedbarrier4), and the difficulties patients experience in navigating telemedicine platforms (Telemedbarrier5). A notable facilitator for telemedicine adoption is the ease of reimbursement for telemedicine visits through third-party providers (Facilitator). To address potential endogeneity concerns, we control physicians' attitude toward innovation (Telemedbarrier2), patients' attitude toward telemedicine (Telemedbarrier3 and Telemedbarrier4), policy factors (Facilitator), and organizational factors (Numofphy and Setting).

Data Analysis

Telemedicine's impact on physicians' satisfaction, quality of care, and percentage of patients' visits are ordinal variables. Thus, we used the ordered logit regression model and the ordered probit regression model (for checking the robustness of our results) to examine the effects of telemedicine on 3 dependent variables, while controlling for other variables that might influence these variables.

$$y_i = \beta_0 + \beta_1 SumT_i + \gamma_1 Telemedbarrier1_i \gamma_2 Telemedbarrier2_i + \gamma_3 Telemedbarrier3_i + \gamma_4 Telemedbarrier4_i + \gamma_5 Telemedbarrier5_i + \gamma_6 Facilitator_i + \gamma_6 Physex_i + \gamma_7 Phyage50_i + \gamma_8 Speccat_i + \gamma_9 Numofphy_i + \gamma_{10} Setting_i + \varepsilon_i \textbf{(1)}$$

$$y_i = \beta_0 + \beta_1 T1_i + \beta_2 T2_i + \beta_3 T3_i + \beta_4 T4_i + \gamma_1 Telemedbarrier1_i \quad \gamma_2 Telemedbarrier2_i + \gamma_3 Telemedbarrier3_i + \gamma_4 Telemedbarrier4_i + \gamma_5 Telemedbarrier5_i + \gamma_6 Facilitator_i + \gamma_6 Physex_i + \gamma_7 Phyage50_i + \gamma_8 Speccat_i + \gamma_9 Numofphy_i + \gamma_{10} Setting_i + \varepsilon_i \textbf{(2)}$$

XSL•FO
RenderX

$$y_i = \beta_0 + \beta_1 TelemedCombination_i + \gamma_1 Telemedbarrier1_i \gamma_2 Telemedbarrier2_i + \gamma_3 Telemedbarrier3_i + \gamma_4 Telemedbarrier4_i + \gamma_5 Telemedbarrier5_i + \gamma_6 Facilitator_i + \gamma_6 Physex_i + \gamma_7 Phyage50_i + \gamma_8 Speccat_i + \gamma_9 Numofphy_i + \gamma_{10} Setting_i + \varepsilon_i \textbf{(3)}$$

For each equation, y_i represents the physician's satisfaction level, physician's quality valuation of using telemedicine, and the percentage of patients visit via telemedicine, respectively. As for equation 3, $TelemedCombination_i$ represents the 11 types of combination of telemedicine tools, including T1T2, T1T3, T1T4, T2T3, T2T4, T3T4, T1T2T3, T1T2T4, T1T3T4, T2T3T4, and T1T2T3T4.

Correlation Analysis

Phi (ϕ) correlation coefficients were used to assess the correlations among the binary independent variables (T1, T2, T3, and T4). As shown in Table 2, the correlations were weak, suggesting that the independent variables were free from the concerns of multicollinearity.

Table 2. Correlation analysis (phi correlation coefficients and 2-tailed *P* value) among the independent variables. Phi coefficients (ϕ) were used because both variables were dichotomous (binary).

Variables	T1[a]	T2[b]	T3[c]	T4[d]
T1				
ϕ	1.00	0.15[e]	–0.03	0.07[e]
P value	N/A[f]	<.001	.12	<.001
T2				
ϕ	0.15[e]	1.00	–0.22[e]	–0.11[e]
P value	<.001	N/A	<.001	<.001
T3				
ϕ	–0.04	–0.22[e]	1.00	–0.17[e]
P value	.12	<.001	N/A	<.001
T4				
ϕ	0.07[e]	–0.11[e]	–0.17[e]	1.00
P value	<.001	<.001	<.001	N/A

[a]T1: telephone audio.

[b]T2: videoconference software with audio.

[c]T3: telemedicine platforms not integrated with electronic health records.

[d]T4: telemedicine platforms integrated with electronic health records.

[e]The correlation is significant at a significance level of .01 (2-tailed).

[f]N/A: not applicable.

Results

Inferential Statistics

We first used the ordered logit regression model to investigate the effects on each dependent variable (Table 3). We then used an ordered probit regression model to assess the robustness of our estimations (Multimedia Appendix 2).

XSL•FO
RenderX

Table 3. Estimated coefficients and SEs for all 3 dependent variables obtained from the ordered logit regression model. Effects of control variables are excluded to conserve space. We used 11 different ordered logit regression models for our 11 different bundles of telemedicine tools: T1T2, T1T3, T1T4, T2T3, T2T4, T3T4, T1T2T3, T1T2T4, T1T3T4, T2T3T4, and T1T2T3T4.

Variables	Physicians' satisfaction	Physicians' evaluation of health care quality	Patients' visit percentage
SumT[a]			
Coefficient (SE)	0.32 (0.06)	0.36 (0.06)	0.26 (0.06)
P value	<.001	<.001	<.001
T1[b]			
Coefficient (SE)	0.24 (0.10)	0.36 (0.11)	0.38 (0.12)
P value	.02	.007	.13
T2[c]			
Coefficient (SE)	0.29 (0.10)	0.38 (0.10)	0.14 (0.11)
P value	.004	<.001	.001
T3[d]			
Coefficient (SE)	0.31 (0.10)	0.27 (0.11)	0.29 (0.11)
P value	.003	.001	.25
T4[e]			
Coefficient (SE)	0.52 (0.11)	0.39 (0.11)	0.22 (0.12)
P value	<.001	.25	.83
T1T2[f]			
Coefficient (SE)	0.32[g] (0.10)	0.46[g] (0.10)	0.31[h] (0.10)
P value	.001	<.001	.003
T1T3			
Coefficient (SE)	0.31[h] (0.12)	0.29[h] (0.11)	0.32[h] (0.11)
P value	.004	.008	.004
T1T4			
Coefficient (SE)	0.44[h] (0.12)	0.31[h] (0.12)	0.19 (0.13)
P value	<.001	.01	.13
T2T3			
Coefficient (SE)	0.27[h] (0.12)	0.34[h] (0.12)	0.32[g] (0.13)
P value	.02	.006	.01
T2T4			
Coefficient (SE)	0.57[g] (0.14)	0.58[g] (0.14)	0.01 (0.15)
P value	<.001	<.001	.94
T3T4			
Coefficient (SE)	0.51[h] (0.17)	0.31 (0.17)	0.37[g] (0.18)
P value	.003	.07	.04
T1T2T3			
Coefficient (SE)	0.35[g] (0.13)	0.39[g] (0.13)	0.41[g] (0.13)
P value	.007	.003	.002
T1T2T4			

XSL•FO
RenderX

Variables	Physicians' satisfaction	Physicians' evaluation of health care quality	Patients' visit percentage
Coefficient (SE)	0.60[g] (0.15)	0.56[g] (0.15)	0.07 (0.16)
P value	<.001	<.001	.65
T1T3T4			
Coefficient (SE)	0.51[h] (0.18)	0.33[h] (0.18)	0.45[g] (0.19)
P value	.005	.07	.01
T2T3T4			
Coefficient (SE)	0.59[g] (0.23)	0.43 (0.23)	0.37 (0.24)
P value	.01	.06	.12
T1T2T3T4			
Coefficient (SE)	0.57[g] (0.24)	0.46 (0.24)	0.48[g] (0.25)
P value	.02	.06	.05
Number of observations[i]	1614	1617	1558

[a]SumT: total number of telemedicine tools each physician used.

[b]T1: telephone audio.

[c]T2: videoconference software with audio (eg, Zoom, Ibex, FaceTime).

[d]T3: telemedicine platforms not integrated with electronic health records (eg, Doxy. me).

[e]T3: telemedicine platforms integrated with electronic health records (eg, updating clinical documentation during a telemedicine visit).

[f]T1T2: physicians who use T1 and T2 simultaneously (the following variables are expressed in the same way as this).

[g]The coefficients for the telemedicine bundles are larger than those for the individual telemedicine tools, and the associations are statistically significant, suggesting that telemedicine tools function complementarily when used as bundles.

[h]The coefficients for the telemedicine bundles are smaller than those for the individual telemedicine tools, and the associations are statistically significant, suggesting that these bundles function as competing rather than complementary tools.

[i]The number of observations varies because each dependent variable, independent variable, and control variable is measured independently and may contain some null or missing values.

We identify the complementary versus competing effects of telemedicine tool bundles based on the relative magnitude of their estimated coefficients in the ordered logit and ordered probit regression models, where the dependent variables are physicians' satisfaction, physicians' evaluation of health care quality, and patients' visit percentage. When the coefficients for the telemedicine bundles exceed those for the individual telemedicine tools, the statistically significant associations suggest that the tools function complementarily when used in combination. For example, regarding the results of the ordered logit regression model, the coefficient of the T1T2 bundle (β=.32; *P*=.001) is higher than that of T1 (β=.24; *P*=.02) and T2 (β=.29; *P*=.004), indicating a complementary effect for this bundle (T1T2) in enhancing physicians' satisfaction.

Conversely, a bundle is considered competing when its coefficient is significant but lower in value than the coefficients of any of the individual telemedicine tool, suggesting potential competition among tools. For example, the coefficient of the T1T3 bundle (β=.305; *P*=.004) is higher than the coefficient of T1 (β=.24; *P*=.02) but lower than that of T3 (β=.311; *P*=.003), suggesting a competing relationship between these technologies.

We also calculated marginal effects at the mean for each outcome level of the dependent variables to interpret our results meaningfully. Table 4 reports the marginal effects on physicians' satisfaction levels, Table 5 reports the marginal effects on physicians' quality-of-health care evaluation, and Table 6 reports the marginal effects on the percentage of patients visiting via telemedicine.

XSL•FO
RenderX

Table 4. Marginal effects at the mean and corresponding SEs for physicians' satisfaction estimated from the ordered logit regression model. Effects of control variables are excluded to conserve space.

Variables	Very dissatisfied	Somewhat dissatisfied	Neither satisfied nor dissatisfied	Somewhat satisfied	Very satisfied
SumT[a]					
Coefficient (SE)	–0.02 (0.00)	–0.03 (0.01)	–0.02 (0.00)	0.02 (0.00)	0.04 (0.01)
P value	<.001	<.001	<.001	<.001	<.001
T1[b]					
Coefficient (SE)	–0.01 (0.01)	–0.02 (0.01)	–0.01 (0.01)	0.02 (0.01)	0.03 (0.01)
P value	.02	.02	.02	.02	.02
T2[c]					
Coefficient (SE)	–0.02 (0.01)	–0.03 (0.01)	–0.01 (0.01)	0.02 (0.01)	0.04 (0.01)
P value	.005	.004	.004	.006	.004
T3[d]					
Coefficient (SE)	–0.02 (0.01)	–0.03 (0.01)	–0.02 (0.01)	0.02 (0.01)	0.04 (0.01)
P value	.003	.003	.003	.004	.003
T4[e]					
Coefficient (SE)	–0.03 (0.01)	–0.05 (0.10)	–0.03 (0.01)	0.03 (0.01)	0.07 (0.02)
P value	<.001	<.001	<.001	<.001	<.001
T1T2[f]					
Coefficient (SE)	–0.02 (0.01)	–0.03 (0.01)	–0.02 (0.01)	0.02 (0.01)	0.04 (0.01)
P value	.001	.001	.001	.002	.001
T1T3					
Coefficient (SE)	–0.02 (0.01)	–0.03 (0.01)	–0.02 (0.01)	0.02 (0.01)	0.04 (0.01)
P value	.005	.004	.005	.006	.004
T1T4					
Coefficient (SE)	–0.025 (0.007)	–0.038 (0.011)	–0.021 (0.006)	0.027 (0.008)	0.058 (0.016)
P value	<.001	<.001	<.001	0.001	<.001
T2T3					
Coefficient (SE)	–0.03 (0.01)	–0.04 (0.01)	–0.02 (0.01)	0.03 (0.01)	0.06 (0.02)
P value	.03	.02	.03	.03	.02
T2T4					
Coefficient (SE)	–0.03 (0.01)	–0.05 (0.01)	–0.03 (0.01)	0.03 (0.01)	0.08 (0.02)
P value	<.001	<.001	<.001	<.001	<.001
T3T4					
Coefficient (SE)	–0.03 (0.01)	–0.05 (0.02)	–0.03 (0.01)	0.03 (0.01)	0.07 (0.02)
P value	.004	.003	.003	.003	.003
T1T2T3					
Coefficient (SE)	–0.02 (0.01)	–0.03 (0.01)	–0.02 (0.01)	0.02 (0.01)	0.05 (0.02)
P value	.009	.008	.008	.009	.007
T1T2T4					
Coefficient (SE)	–0.03 (0.01)	–0.05 (0.01)	–0.03 (0.01)	0.04 (0.01)	0.08 (0.02)
P value	<.001	<.001	<.001	<.001	<.001

XSL•FO
RenderX

Variables	Very dissatisfied	Somewhat dissatisfied	Neither satisfied nor dissatisfied	Somewhat satisfied	Very satisfied
T1T3T4					
Coefficient (SE)	–0.03 (0.01)	–0.05 (0.02)	–0.03 (0.01)	0.03 (0.01)	0.07 (0.02)
P value	.006	.006	.005	.007	.005
T2T3T4					
Coefficient (SE)	0.03 (0.01)	–0.05 (0.02)	–0.03 (0.01)	0.04 (0.02)	0.08 (0.03)
P value	.01	.01	.01	.01	.01
T1T2T3T4					
Coefficient (SE)	–0.03 (0.01)	–0.05 (0.02)	–0.03 (0.01)	0.04 (0.02)	0.08 (0.03)
P value	.02	.02	.02	.02	.02

[a]SumT: total number of telemedicine tools each physician used.

[b]T1: telephone audio.

[c]T2: videoconference software with audio (eg, Zoom, Ibex, FaceTime).

[d]T3: telemedicine platforms not integrated with electronic health records (eg, Doxy. me).

[e]T4: telemedicine platforms integrated with electronic health records (eg, updating clinical documentation during a telemedicine visit).

[f]T1T2: physicians who use T1 and T2 simultaneously—binary variable (the following variables are expressed in the same way as this).

XSL•FO
RenderX

Table 5. Marginal effects at the mean and corresponding SEs for physicians' evaluation of health care service quality via telemedicine estimated from the ordered logit regression model. Effects of control variables are excluded to conserve space.

Variables	Not at all	To a small extent	To some extent	To a great extent	Fully
SumT[a]					
Coefficient (SE)	–0.01 (0.00)	–0.04 (0.01)	–0.01 (0.00)	0.05 (0.01)	0.01 (0.00)
P value	<.001	<.001	<.001	<.001	<.001
T1[b]					
Coefficient (SE)	–0.01 (0.00)	–0.04 (0.01)	–0.01 (0.00)	0.05 (0.02)	0.01 (0.00)
P value	.010	.008	.012	.007	.011
T2[c]					
Coefficient (SE)	–0.01 (0.00)	–0.04 (0.01)	–0.01 (0.00)	0.06 (0.02)	0.01 (0.00)
P value	<.001	<.001	.001	<.001	<.001
T3[d]					
Coefficient (SE)	–0.01 (0.00)	–0.03 (0.01)	–0.01 (0.00)	0.04 (0.02)	0.01 (0.00)
P value	.001	.001	.002	.001	.002
T4[e]					
Coefficient (SE)	–0.01 (0.00)	–0.04 (0.01)	–0.01 (0.00)	0.06 (0.02)	0.01 (0.00
P value	.25	.25	.25	.24	.25
T1T2[f]					
Coefficient (SE)	–0.02 (0.00)	–0.05 (0.01)	–0.02 (0.00)	0.07 (0.01)	0.02 (0.00)
P value	<.001	<.001	<.001	<.001	<.001
T1T3					
Coefficient (SE)	–0.01 (0.00)	–0.03 (0.01)	–0.01 (0.00)	0.04 (0.02)	0.01 (0.00)
P value	.01	.008	.01	.008	.01
T1T4					
Coefficient (SE)	–0.01 (0.00)	–0.03 (0.01)	–0.01 (0.01)	0.05 (0.02)	0.01 (0.00)
P value	.01	.01	.01	.01	.01
T2T3					
Coefficient (SE)	–0.01 (0.00)	–0.04 (0.01)	–0.01 (0.01)	0.05 (0.02)	0.01 (0.00)
P value	.009	.007	.01	.006	.01
T2T4					
Coefficient (SE)	–0.02 (0.01)	–0.06 (0.02)	–0.02 (0.01)	0.09 (0.02)	0.02 (0.01)
P value	<.001	<.001	<.001	<.001	<.001
T3T4					
Coefficient (SE)	–0.01 (0.01)	–0.03 (0.02)	–0.01 (0.07)	0.05 (0.03)	0.01 (0.01)
P value	.08	.07	.08	.07	.08
T1T2T3					
Coefficient (SE)	–0.01 (0.01)	–0.04 (0.01)	–0.01 (0.01)	0.06 (0.02)	0.01 (0.00)
P value	.005	.003	.006	.003	.005
T1T2T4					
Coefficient (SE)	–0.02 (0.01)	–0.06 (0.02)	–0.02 (0.01)	0.08 (0.02)	0.02 (0.01)
P value	.001	<.001	.001	<.001	.001
T1T3T4					

XSL•FO
RenderX

Variables	Not at all	To a small extent	To some extent	To a great extent	Fully
Coefficient (SE)	–0.01 (0.01)	–0.04 (0.02)	–0.01 (0.01)	0.04 (0.03)	0.01 (0.01)
P value	.08	.07	.08	.07	.08
T2T3T4					
Coefficient (SE)	–0.02 (0.01)	–0.05 (0.03)	–0.02 (0.01)	0.06 (0.03)	0.01 (0.01)
P value	.07	.06	.07	.06	.07
T1T2T3T4					
Coefficient (SE)	–0.02 (0.01)	–0.05 (0.03)	–0.02 (0.01)	0.07 (0.04)	0.02 (0.01)
P value	.06	.06	.06	.06	.06

[a]SumT: total number of telemedicine tools each physician used.

[b]T1: telephone audio.

[c]T2: videoconference software with audio (eg, Zoom, Ibex, FaceTime).

[d]T3: telemedicine platforms not integrated with electronic health records (eg, Doxy. me).

[e]T4: telemedicine platforms integrated with electronic health records (eg, updating clinical documentation during a telemedicine visit).

[f]T1T2: physicians who use T1 and T2 simultaneously—binary variable (the following variables are expressed in the same way as this).

XSL•FO
RenderX

Table 6. Marginal effects at the mean and corresponding SEs for the proportion of patients' visits conducted via telemedicine estimated from the ordered logit regression model. Effects of control variables are excluded to conserve space.

Variables	None	<25%	25%-49%	50%-74%	≥75%
SumT[a]					
Coefficient (SE)	–0.00 (0.00)	–0.06 (0.01)	0.03 (0.01)	0.02 (0.00)	0.02 (0.00)
P value	.002	<.001	<.001	<.001	<.001
T1[b]					
Coefficient (SE)	–0.01 (0.00)	–0.08 (0.02)	0.04 (0.01)	0.02 (0.01)	0.03 (0.01)
P value	.16	.13	.13	.13	.14
T2[c]					
Coefficient (SE)	–0.00 (0.00)	–0.03 (0.02)	0.01 (0.01)	0.01 (0.01)	0.01 (0.01)
P value	.009	.001	.001	.002	.002
T3[d]					
Coefficient (SE)	–0.00 (0.00)	–0.06 (0.02)	0.03 (0.01)	0.02 (0.01)	0.02 (0.01)
P value	.26	.25	.25	.25	.25
T4[e]					
Coefficient (SE)	–0.00 (0.00)	–0.05 (0.03)	0.02 (0.01)	0.01 (0.01)	0.01 (0.01)
P value	.83	.83	.83	.83	.83
T1T2[f]					
Coefficient (SE)	–0.00 (0.00)	–0.06 (0.02)	0.03 (0.01)	0.02 (0.01)	0.02 (0.01)
P value	.02	.003	.003	.004	.004
T1T3					
Coefficient (SE)	–0.00 (0.00)	–0.07 (0.02)	0.03 (0.01)	0.02 (0.01)	0.02 (0.01)
P value	.02	.004	.004	.005	.005
T1T4					
Coefficient (SE)	–0.00 (0.00)	–0.04 (0.03)	0.02 (0.01)	0.01 (0.01)	0.01 (0.01)
P value	.15	.13	.13	.13	.13
T2T3					
Coefficient (SE)	–0.00 (0.00)	–0.07 (0.03)	0.03 (0.01)	0.02 (0.01)	0.02 (0.01)
P value	.03	.01	.01	.01	.01
T2T4					
Coefficient (SE)	–0.00 (0.00)	–0.00 (0.03)	0.00 (0.02)	0.00 (0.01)	0.00 (0.01)
P value	.94	.94	.94	.94	.94
T3T4					
Coefficient (SE)	–0.00 (0.00)	–0.08 (0.04)	0.04 (0.02)	0.02 (0.01)	0.03 (0.01)
P value	.06	.04	.04	.04	.04
T1T2T3					
Coefficient (SE)	–0.00 (0.00)	–0.09 (0.03)	0.04 (0.01)	0.02 (0.01)	0.03 (0.01
P value	.01	.002	.002	.002	.003
T1T2T4					
Coefficient (SE)	–0.00 (0.00)	–0.02 (0.03)	–0.02 (0.03)	0.00 (0.01)	0.01 (0.01)
P value	.66	.65	.65	.65	.65
T1T3T4					

XSL•FO
RenderX

Variables	None	<25%	25%-49%	50%-74%	≥75%
Coefficient (SE)	–0.01 (0.00)	–0.10 (0.04)	0.04 (0.02)	0.03 (0.01)	0.03 (0.01)
P value	.03	.01	.02	.02	.02
T2T3T4					
Coefficient (SE)	–0.01 (0.00)	–0.08 (0.05)	0.04 (0.02)	0.02 (0.01)	0.03 (0.02)
P value	.14	.12	.12	.12	.12
T1T2T3T4					
Coefficient (SE)	–0.01 (0.00)	–0.10 (0.05)	0.05 (0.02)	0.03 (0.01)	0.03 (0.02)
P value	.07	.05	.05	.05	.05

[a]SumT: total number of telemedicine tools each physician used.

[b]T1: telephone audio.

[c]T2: videoconference software with audio (eg, Zoom, Ibex, and FaceTime).

[d]T3: telemedicine platforms not integrated with electronic health records (eg, Doxy. me).

[e]T4: telemedicine platforms integrated with electronic health records (eg, updating clinical documentation during a telemedicine visit).

[f]T1T2: physicians who use T1 and T2 simultaneously—binary variable (the following variables are expressed in the same way as this).

According to the results in Table 4, parameter estimates for the aggregate model (equation 1) suggest that the summative telemedicine tools have a significant positive relationship with physicians' satisfaction levels. To be precise, a unit increase in telemedicine tools is associated with approximately 1.8, 2.8, and 1.4 percentage point decreases in the predicted probability of physicians being at the "very dissatisfied," "somewhat dissatisfied," and "neither satisfied nor dissatisfied" level of satisfaction. However, a unit increase in telemedicine tools is associated with a 1.9 percentage point increase in the predicted probability of physicians being "somewhat satisfied" and a 4.2 percentage point increase in the predicted probability of physicians being "very satisfied," respectively.

According to Table 5, the summative telemedicine tools also showed a significant positive association with physicians' evaluation of telemedicine service quality. The results in Table 5 suggest that a unit increase in telemedicine tools is associated with a decrease of 1.2, 3.9, and 1.2 percentage points in the predicted probability for physicians' evaluation of telemedicine service quality to be at the level of "not at all," "to a small extent," and "some extent." Contrary to that, a unit increase in telemedicine tools is associated with an increase of 5.2 and 1.2 percentage points in the predicted probability for physicians' evaluation of health care to be at the level of "to a great extent and fully."

The results in Table 6 indicate that a unit increase in telemedicine tools is associated with a decrease of 0.3 and 5.5 percentage points in the predicted probability that the percentage of patients visiting via telemedicine will be at the level of "none" or "<25%." In contrast, a unit increase in telemedicine tools is associated with increases of 2.5, 1.5, and 1.8 percentage points in the predicted probability for this dependent variable to be "25%-49%," "50%-74%," and "≥75%," respectively.

Parameter estimates for the disaggregate model (equation 2) suggest that each individual telemedicine tool has a significant positive relationship with physicians' satisfaction level and physicians' quality of health care evaluation (Tables 4 and 5). However, while T1 and T3 showed a significant positive association with the percentage of patients visiting via telemedicine, T2 and T4 showed no such relationship (Table 6).

Regarding the parameter estimates for all the different telemedicine tools combination models (equation 3), we found that each combination of telemedicine tools shares a significant positive association with the physician's satisfaction level (Table 4). However, the combinations of T3T4, T1T3T4, and T2T3T4 do not share any significant association with physicians' quality-of-health care evaluation (Table 5). Additionally, the combination of T1T4, T2T4, T1T2T4, and T2T3T4 also does not share any significant association with the percentage of patients' visits via telemedicine (Table 6).

Additional Tests

We also considered the possibility of a moderating effect of patient visits via telemedicine tools, given the time period during which the data were collected (the pandemic era). This situation may have been caused by patients' limited access to in-person care rather than the bundle of technologies that the physician was using. To test this possibility, we conducted an additional analysis. According to Table 7, the results indicate that the moderator yielded no statistically significant interaction effects.

XSL•FO
RenderX

Table 7. Additional tests for examining the moderating effect of patient visits performed via telemedicine based on the ordered logit and ordered probit regression models. Effects of control variables are excluded to conserve space.

Variables	Physicians' satisfaction		Physicians' evaluation of health care quality	
SumT[a] × Telemedpct[b]				
Coefficient (SE)	–0.03 (0.06)	–0.02 (0.04)	–0.06 (0.06)	–0.03 (0.03)
P value	.68	.64	.36	.38
T1[c]× Telemedpct				
Coefficient (SE)	–0.06 (0.12)	–0.03 (0.07)	–0.01 (0.12)	–0.00 (0.07)
P value	.995	.97	.39	.47
T2[d]× Telemedpct				
Coefficient (SE)	–0.15 (0.11)	–0.08 (0.06)	0.00 (0.11)	–0.00 (0.06)
P value	.31	.25	.72	.66
T3[e]× Telemedpct				
Coefficient (SE)	0.06 (0.11)	0.01 (0.06)	–0.06 (0.11)	–0.03 (0.06)
P value	.65	.77	.90	.80
T4[f]× Telemedpct				
Coefficient (SE)	0.08 (0.12)	0.06 (0.07)	–0.12 (0.12)	–0.05 (0.07)
P value	.69	.77	.37	.38
T1T2[g]× Telemedpct				
Coefficient (SE)	–0.10 (0.11)	–0.05 (0.06)	–0.02 (0.11)	–0.02 (0.06)
P value	.36	.45	.84	.77
T1T3 × Telemedpct				
Coefficient (SE)	–0.05 (0.11)	–0.04 (0.07)	–0.07 (0.11)	–0.04 (0.07)
P value	.65	.52	.52	.59
T1T4 × Telemedpct				
Coefficient (SE)	–0.01 (0.13)	0.01 (0.08)	–0.12 (0.13)	–0.05 (0.08)
P value	.92	.93	.38	.51
T2T3 × Telemedpct				
Coefficient (SE)	–0.01 (0.12)	–0.02 (0.07)	–0.00 (0.12)	–0.01 (0.07)
P value	.96	.75	.98	.94
T2T4 × Telemedpct				
Coefficient (SE)	0.05 (0.16)	0.04 (0.09)	–0.07 (0.16)	–0.02 (0.09)
P value	.75	.66	.64	.80
T3T4 × Telemedpct				
Coefficient (SE)	0.22 (0.18)	0.13 (0.10)	–0.10 (0.17)	–0.05 (0.10)
P value	.23	.21	.50	.63
T1T2T3 × Telemedpct				
Coefficient (SE)	0.00 (0.13)	–0.01 (0.08)	0.01 (0.13)	0.00 (0.08)
P value	.99	.91	.96	.99
T1T2T4 × Telemedpct				
Coefficient (SE)	0.03 (0.17)	0.03 (0.10)	–0.11 (0.16)	–0.05 (0.09)
P value	.88	.78	.50	.62
T1T3T4 × Telemedpct				

XSL•FO
RenderX

Variables	Physicians' satisfaction		Physicians' evaluation of health care quality	
Coefficient (SE)	0.03 (0.19)	0.01 (0.11)	–0.13 (0.19)	–0.07 (0.11)
P value	.88	.90	.49	.53
T2T3T4 × Telemedpct				
Coefficient (SE)	0.08 (0.08)	0.21 (0.15)	–0.04 (0.23)	–0.03 (0.13)
P value	.17	.16	.85	.85
T1T2T3T4 × Telemedpct				
Coefficient (SE)	0.36 (0.26)	0.21 (0.15)	–0.08 (0.24)	–0.04 (0.14)
P value	.16	.16	.74	.75
Number of observations[h]	1548	1548	1551	1551

[a]SumT: total number of telemedicine tools each physician used.

[b]Telemedpct: percentage of patient visits via telemedicine.

[c]T1: telephone audio.

[d]T2: videoconference software with audio (eg, Zoom, Ibex, and FaceTime).

[e]T3: telemedicine platforms not integrated with electronic health records (eg, Doxy. me).

[f]T4: telemedicine platforms integrated with electronic health records (eg, updating clinical documentation during a telemedicine visit).

[g]T1T2: physicians who use T1 and T2 simultaneously (the following variables are expressed in the same way as this).

[h]The number of observations varies because each dependent variable, independent variable, and control variable is measured independently and may contain some null or missing values.

Discussion

Principal Results

Our study addresses the complementary versus competing nature of telemedicine tools. Our empirical analysis reveals that although both individual and combined uses of telemedicine tools positively affect physicians' satisfaction, quality of health care evaluation, and the percentage of patients' visits via telemedicine, various telemedicine tools compete rather than complement each other. Our study suggests that the relationships among telemedicine tools are not always positive; instead, their combined use can produce either complementary or competing effects, depending on how their functionalities interact within the context of physicians' clinical workflows.

Interpretation of Findings

For physicians, we found that various combinations of telemedicine tools significantly influence their overall satisfaction and partially affect their evaluation of health care quality. These findings are consistent with prior studies reporting generally high physician satisfaction and perceived usefulness of telemedicine [49,50], as well as comparable quality of care between telemedicine and in-person consultations [51]. However, these earlier studies did not examine how different combinations of telemedicine tools shape physicians' satisfaction and quality-of-care assessments. Our study extends this understanding by highlighting how the complementary use of telemedicine tools can influence these outcomes. Our findings suggest that satisfaction and the perceived quality of care are influenced by the coherence of the technology stack, with videoconferencing software (T2) acting as a powerful core. Bundles that include T2 create a complementary effect by providing a rich, high-fidelity communication channel essential for clinical assessment. The ability to observe visual cues and nonverbal information is fundamental to accurate diagnosis and building effective communication between physicians and patients. Notably, the combination of T2 with an integrated EHR (T4) represents the ideal modern workflow, creating an efficient interaction environment where the physician can focus on the patient through a high-quality video interface while the EHR seamlessly handles documentation. Even a simpler T2 and T1 (telephone) bundle is complementary, as the telephone serves as a reliable backup that reduces physician worry about technical failures and connectivity disruptions.

Conversely, bundles lacking video-based technological support generate a competing effect, characterized by cognitive overload and workflow fragmentation. Combinations such as T1 with platform T3 or T4 force physicians to split their attention between a low-fidelity audio call and a separate, complex software interface. Furthermore, the combination of 2 different platforms (T3 + T4) exemplifies competing technologies and cognitive overload, leading to technological redundancy, confusion, and a fragmented patient management process that detracts from the physician's core responsibilities [52-54].

From the perspective of MST, these findings can be interpreted in terms of differences in media capabilities and process alignment. Videoconferencing (T2) provides high levels of immediacy of feedback, variety of symbols, and transmission velocity, enabling physicians to convey and interpret complex medical information effectively. When such rich media are integrated with complementary systems (like EHRs), they enhance conveyance and convergence processes. Thus, both information exchange and shared understanding result in higher satisfaction and perceived quality. In contrast, bundles that rely on low-synchronicity tools (eg, telephone or nonintegrated platforms) fail to support these communication processes, increasing the cognitive effort required to maintain clinical

XSL•FO
RenderX

coherence and reducing the perceived effectiveness of telemedicine-oriented patient visits.

Additionally, the combination of T3 (nonintegrated telemedicine platforms) and T4 (EHR-integrated telemedicine platforms) exhibits a competing effect on physicians' satisfaction and does not significantly improve care quality, which may be due to their underlying system architecture. T3 platforms, such as Doxy.me, operate independently from the EHR system and function primarily as stand-alone communication tools. In contrast, T4 tools are embedded within the EHR environment, supporting real-time documentation and patient data access during telemedicine consultations. When these tools are used in combination, as in T3T4 or T1T3T4, physicians are required to switch between 2 unconnected noncompatible systems, which disrupts workflow and necessitates repeated actions such as reentering patient information or clinical notes [52-54]. This lack of interoperability increases the administrative and information searching burden and undermines efficiency.

In contrast to physicians' satisfaction and quality evaluation outcomes, physicians report a higher percentage of patient visits via telemedicine when the technological configuration is broader and more inclusive, incorporating multiple platforms (eg, T2T3, T3T4, T1T2T3T4). These complementary effects arise because more comprehensive bundles enable physicians to engage in a broader range of patient types and clinical scenarios through various modalities. For example, combining video (T2) and telemedicine platforms (T3 or T4) allows clinicians to conduct both structured and flexible consultations, manage follow-ups, and accommodate patients with differing technical capacities or conditions. From a physician's standpoint, such diversity enhances operational flexibility and reduces barriers to providing telemedicine services, thus naturally increasing the proportion of visits conducted remotely.

However, simpler 2-tool bundles (eg, T1T2 and T1T3) show a competing effect on the percentage of patient visits via telemedicine. There might be 2 reasons leading to this competing effect. From the physicians' perspective, while these configurations are easy to operate, they lack the integration required to sustain a consistent telemedicine workflow across different patient groups. A telephone-plus-video, or telephone-plus-stand-alone-platform setup without an integrated EHR may be functional for ad hoc consultations but insufficient for record-keeping or health care information exchange. From the patients' perspective, they may not perceive much difference between an in-person visit and interacting with physicians only via telephone or videoconference. Consequently, many patients may still prefer face-to-face consultations, as they feel more direct and personal.

Interestingly, combinations that include EHR-integrated tools (T4), such as T1T4, T2T4, T1T2T4, or T2T3T4, do not significantly impact the percentage of patient visits via telemedicine. We believe there are 2 main reasons for this outcome. First, physicians must complete patients' electronic records while simultaneously communicating with patients via video or phone, which makes each consultation more time-consuming [55]. As a result, the total number of telemedicine visits that can be completed in a day decreases. Second, the log-in and verification procedures add complexity to the communication process between physicians and patients, leading physicians to prefer phone consultations (audio call or FaceTime call) for many simple cases. Consequently, the combination of T4 with other tools shows no statistically significant impact on the overall percentage of telemedicine visits.

We also conducted an additional test to investigate the potential moderating role of patient visits via telemedicine tools, as data collected during the pandemic period may reflect patients' limited choices rather than the effect of physicians' technology bundles. However, our results do not support this moderation effect. We believe there are 2 main reasons for this. First, based on prior studies (eg, Moulaei et al [48], Reed et al [40], and Tzeng et al. [56]), patient visits via telemedicine tools are consistently conceptualized as an outcome shaped by demographic, contextual, and technological factors. Second, theoretically, drawing on MST [43], we believe that patient telehealth usage reflects media-task fit and can be better understood as a behavioral outcome. To ensure theoretical and empirical coherence, we therefore treat the percentage of patient visits via telemedicine tools as one of our dependent variables.

Limitations and Future Directions

One limitation of this study is the use of a self-reported measure to capture physicians' perceived quality of care, which introduces potential bias due to self-reporting. Although the survey item aimed to minimize this bias by prompting a direct comparison between telemedicine visits and in-person visits, the subjective nature of the measure limits the objectivity of our findings. Future research should apply objective clinical performance indicators or third-party assessments to validate physicians' evaluations.

Another limitation of this study is that the telemedicine tool usage variable does not capture the frequency or intensity of use for each tool. Thus, our study cannot determine whether physicians' satisfaction primarily comes from one tool or from a combination of tools. Our analysis, therefore, treats tool combinations as reported usage bundles. Future research should incorporate more data on usage frequency, duration, or physician preference to capture the priority of individual telemedicine tools. This would enable researchers to investigate the effects of specific technologies within multitool combinations and gain a deeper understanding of how different tools contribute to physicians' satisfaction.

Due to data limitations, our study cannot thoroughly test the possibility of endogenous variables. Although we have attempted to identify any possible source of missing variable bias theoretically, we have not been successful in doing so. Future research should investigate such possibilities by identifying a suitable instrumental variable. Our empirical analysis used data from the national survey conducted by the NCHS at the CDC [16-19], which notably excludes several specialties, specifically radiology, pathology, and anesthesiology. Consequently, the applicability of our findings to these clinical contexts is limited. This exclusion stems from the inherently procedural and in-person nature of these fields (eg, anesthesia administration and diagnostic imaging), which

XSL•FO
RenderX

may restrict the deployment of current telemedicine tools. We consider this data limitation as one of the key limitations of our research. Future research should incorporate these specialties to fully assess the generalizability of telemedicine usage across the broader clinical spectrum.

Last, this study focuses exclusively on the perspectives of ambulatory care physicians, which limits the ability to assess how tool combinations affect patient-centered outcomes or patient satisfaction. Future research should collect patient-centered data to build a more comprehensive understanding of the effectiveness and acceptance of telemedicine tools from the patient's perspective.

Conclusions

Our study contributes to practice that enhances understanding of how telemedicine tools can be effectively used in health care, particularly in postpandemic scenarios. Each tool offers unique advantages, so using the right tool for the right situation is not just a choice, but a crucial decision that can significantly improve both physician satisfaction and patient engagement in telemedicine. This insight provides clear recommendations to providers and platform developers, emphasizing the key to the success of telemedicine implementation—creating a seamless experience for physicians. Such a system needs to be designed in a manner that ensures the complementary behavior of different tools based on physicians' specific demands, highlighting the complexity of various clinical and communicative tasks.

Conflicts of Interest

None declared.

Multimedia Appendix 1
Synthesis of literature review.
[DOCX File , 33 KB - medinform_v13i1e75246_app1.docx]

Multimedia Appendix 2
Conducting robustness tests for all three dependent variables using the ordered probit regression model.
[DOCX File , 49 KB - medinform_v13i1e75246_app2.docx]

References

1. Wootton R. Recent advances: telemedicine. BMJ 2001;323(7312):557-560 [FREE Full text] [doi: 10.1136/bmj.323.7312.557] [Medline: 11546704]
2. Reeves JJ, Ayers JW, Longhurst CA. Telehealth in the COVID-19 era: a balancing act to avoid harm. J Med Internet Res 2021;23(2):e24785 [FREE Full text] [doi: 10.2196/24785] [Medline: 33477104]
3. Kichloo A, Albosta M, Dettloff K, Wani F, El-Amir Z, Singh J, et al. Telemedicine, the current COVID-19 pandemic and the future: a narrative review and perspectives moving forward in the USA. Fam Med Community Health 2020;8(3):e000530 [FREE Full text] [doi: 10.1136/fmch-2020-000530] [Medline: 32816942]
4. Koonin LM, Hoots B, Tsang CA, Leroy Z, Farris K, Jolly T, et al. Trends in the use of telehealth during the emergence of the COVID-19 pandemic - United States, January-March 2020. MMWR Morb Mortal Wkly Rep 2020;69(43):1595-1599 [FREE Full text] [doi: 10.15585/mmwr.mm6943a3] [Medline: 33119561]
5. Market Data Forecast ltd. 2024. URL: https://www.marketdataforecast.com/market-reports/telemedicine-market [accessed 2025-12-02]
6. Zanaboni P, Wootton R. Adoption of telemedicine: from pilot stage to routine delivery. BMC Med Inform Decis Mak 2012;12:1 [FREE Full text] [doi: 10.1186/1472-6947-12-1] [Medline: 22217121]
7. Dorsey ER, Topol EJ. Telemedicine 2020 and the next decade. Lancet 2020;395(10227):859. [doi: 10.1016/S0140-6736(20)30424-4] [Medline: 32171399]
8. Mann DM, Chen J, Chunara R, Testa PA, Nov O. COVID-19 transforms health care through telemedicine: evidence from the field. J Am Med Inform Assoc 2020;27(7):1132-1135 [FREE Full text] [doi: 10.1093/jamia/ocaa072] [Medline: 32324855]
9. Byambasuren O, Greenwood H, Bakhit M, Atkins T, Clark J, Scott AM, et al. Comparison of telephone and video telehealth consultations: systematic review. J Med Internet Res 2023;25:e49942 [FREE Full text] [doi: 10.2196/49942] [Medline: 37976100]
10. Alhajri N, Simsekler MCE, Alfalasi B, Alhashmi M, AlGhatrif M, Balalaa N, et al. Physicians' attitudes toward telemedicine consultations during the COVID-19 pandemic: cross-sectional study. JMIR Med Inform 2021;9(6):e29251 [FREE Full text] [doi: 10.2196/29251] [Medline: 34001497]
11. Orrange S, Patel A, Mack WJ, Cassetta J. Patient satisfaction and trust in telemedicine during the COVID-19 pandemic: retrospective observational study. JMIR Hum Factors 2021;8(2):e28589 [FREE Full text] [doi: 10.2196/28589] [Medline: 33822736]

XSL•FO
RenderX

12. Reddy A, Pollack CE, Asch DA, Canamucio A, Werner RM. The effect of primary care provider turnover on patient experience of care and ambulatory quality of care. JAMA Intern Med 2015;175(7):1157-1162 [FREE Full text] [doi: 10.1001/jamainternmed.2015.1853] [Medline: 25985320]
13. Mirzaei T, Kashian N. Revisiting effective communication between patients and physicians: cross-sectional questionnaire study comparing text-based electronic versus face-to-face communication. J Med Internet Res 2020;22(5):e16965 [FREE Full text] [doi: 10.2196/16965] [Medline: 32401213]
14. Liu X, Sengupta A, Xu D. Impact of telemedicine technology tools and perceived barriers on satisfaction and continued usage intention of office-based physicians. 2024 Presented at: Proceedings of the 57th Hawaii International Conference on System Sciences; 2024 January 3-6; Honolulu, Hawaii. [doi: 10.24251/hicss.2024.426]
15. Alkureishi MA, Choo Z, Lenti G, Castaneda J, Zhu M, Nunes K, et al. Clinician perspectives on telemedicine: observational cross-sectional study. JMIR Hum Factors 2021;8(3):e29690 [FREE Full text] [doi: 10.2196/29690] [Medline: 34184994]
16. Use of telemedicine among office-based physicians. The Office of the National Coordinator for Health Information Technology. 2023. URL: https://www.healthit.gov/data/data-briefs/use-telemedicine-among-office-based-physicians-2021 [accessed 2025-12-02]
17. National Electronic Health Records Survey (NEHRS). Centers for Disease Control and Prevention. URL: https://www.cdc.gov/nchs/nehrs/documentation/?CDC_AAref_Val=https://www.cdc.gov/nchs/nehrs/questionnaires.htm [accessed 2025-12-02]
18. National electronic health records survey (NEHRS). Centers for Disease Control and Prevention. 2021. URL: https://www.cdc.gov/nchs/data/nehrs/NEHRS2021Doc-508.pdf [accessed 2025-12-02]
19. National Electronic Health Records Survey (NEHRS) dictionary. Centers for Disease Control and Prevention. 2021. URL: https://www.cdc.gov/nchs/data/nehrs/2021-NEHRS-public-use-file-layout-508.pdf [accessed 2025-12-02]
20. Op den Akker H, Cabrita M, Op den Akker R, Jones VM, Hermens HJ. Tailored motivational message generation: a model and practical framework for real-time physical activity coaching. J Biomed Inform 2015;55:104-115 [FREE Full text] [doi: 10.1016/j.jbi.2015.03.005] [Medline: 25843359]
21. Shanthanna H, Strand NH, Provenzano DA, Lobo CA, Eldabe S, Bhatia A, et al. Caring for patients with pain during the COVID-19 pandemic: consensus recommendations from an international expert panel. Anaesthesia 2020;75(7):935-944 [FREE Full text] [doi: 10.1111/anae.15076] [Medline: 32259288]
22. Shah AC, Badawy SM. Telemedicine in pediatrics: systematic review of randomized controlled trials. JMIR Pediatr Parent 2021;4(1):e22696 [FREE Full text] [doi: 10.2196/22696] [Medline: 33556030]
23. Boehm K, Ziewers S, Brandt MP, Sparwasser P, Haack M, Willems F, et al. Telemedicine online visits in urology during the COVID-19 pandemic-potential, risk factors, and patients' perspective. Eur Urol 2020;78(1):16-20 [FREE Full text] [doi: 10.1016/j.eururo.2020.04.055] [Medline: 32362498]
24. Gagnon M, Ghandour EK, Talla PK, Simonyan D, Godin G, Labrecque M, et al. Electronic health record acceptance by physicians: testing an integrated theoretical model. J Biomed Inform 2014;48:17-27 [FREE Full text] [doi: 10.1016/j.jbi.2013.10.010] [Medline: 24184678]
25. Khera A, Baum SJ, Gluckman TJ, Gulati M, Martin SS, Michos ED, et al. Continuity of care and outpatient management for patients with and at high risk for cardiovascular disease during the COVID-19 pandemic: a scientific statement from the American society for preventive cardiology. Am J Prev Cardiol 2020;1:100009 [FREE Full text] [doi: 10.1016/j.ajpc.2020.100009] [Medline: 32835347]
26. Sengupta A, Sarkar S, Bhattacherjee A. The relationship between telemedicine tools and physician satisfaction, quality of care, and patient visits during the COVID-19 pandemic. Int J Med Inform 2024;190:105541 [FREE Full text] [doi: 10.1016/j.ijmedinf.2024.105541] [Medline: 38996654]
27. Zhang X, Saltman R. Impact of electronic health record interoperability on telehealth service outcomes. JMIR Med Inform 2022;10(1):e31837 [FREE Full text] [doi: 10.2196/31837] [Medline: 34890347]
28. Greenhalgh T, Wherton J, Shaw S, Morrison C. Video consultations for COVID-19. BMJ 2020;368:m998. [doi: 10.1136/bmj.m998] [Medline: 32165352]
29. Rush KL, Howlett L, Munro A, Burton L. Videoconference compared to telephone in healthcare delivery: a systematic review. Int J Med Inform 2018;118:44-53. [doi: 10.1016/j.ijmedinf.2018.07.007] [Medline: 30153920]
30. Ratwani RM, Savage E, Will A, Arnold R, Khairat S, Miller K, et al. A usability and safety analysis of electronic health records: a multi-center study. J Am Med Inform Assoc 2018;25(9):1197-1201 [FREE Full text] [doi: 10.1093/jamia/ocy088] [Medline: 29982549]
31. Kruse CS, Molina-Nava A, Kapoor Y, Anerobi C, Maddukuri H. Analyzing the effect of telemedicine on domains of quality through facilitators and barriers to adoption: systematic review. J Med Internet Res 2023;25:e43601 [FREE Full text] [doi: 10.2196/43601] [Medline: 36602844]
32. Atherton H, Sawmynaden P, Sheikh A, Majeed A, Car J. Email for clinical communication between patients/caregivers and healthcare professionals. Cochrane Database Syst Rev 2012;11(11):CD007978. [doi: 10.1002/14651858.CD007978.pub2] [Medline: 23152249]

XSL•FO
RenderX

33. Donaghy E, Atherton H, Hammersley V, McNeilly H, Bikker A, Robbins L, et al. Acceptability, benefits, and challenges of video consulting: a qualitative study in primary care. Br J Gen Pract 2019;69(686):e586-e594 [FREE Full text] [doi: 10.3399/bjgp19X704141] [Medline: 31160368]
34. Everson J, Butler E. Hospital adoption of multiple health information exchange approaches and information accessibility. J Am Med Inform Assoc 2020;27(4):577-583 [FREE Full text] [doi: 10.1093/jamia/ocaa003] [Medline: 32049356]
35. Bates DW, Saria S, Ohno-Machado L, Shah A, Escobar G. Big data in health care: using analytics to identify and manage high-risk and high-cost patients. Health Aff (Millwood) 2014;33(7):1123-1131. [doi: 10.1377/hlthaff.2014.0041] [Medline: 25006137]
36. Hayes D. Electronic health record and physician burnout. Am J Med Qual 2019;34(4):416. [doi: 10.1177/1062860618824015] [Medline: 30638032]
37. Asgari E, Kaur J, Nuredini G, Balloch J, Taylor AM, Sebire N, et al. Impact of electronic health record use on cognitive load and burnout among clinicians: narrative review. JMIR Med Inform 2024;12:e55499 [FREE Full text] [doi: 10.2196/55499] [Medline: 38607672]
38. Campbell K, Greenfield G, Li E, O'Brien N, Hayhoe B, Beaney T, et al. The impact of virtual consultations on the quality of primary care: systematic review. J Med Internet Res 2023;25:e48920 [FREE Full text] [doi: 10.2196/48920] [Medline: 37647117]
39. Car J, Koh GC, Foong PS, Wang CJ. Video consultations in primary and specialist care during the COVID-19 pandemic and beyond. BMJ 2020;371:m3945. [doi: 10.1136/bmj.m3945] [Medline: 33082127]
40. Reed ME, Huang J, Graetz I, Lee C, Muelly E, Kennedy C, et al. Patient characteristics associated with choosing a telemedicine visit vs office visit with the same primary care clinicians. JAMA Netw Open 2020;3(6):e205873 [FREE Full text] [doi: 10.1001/jamanetworkopen.2020.5873] [Medline: 32585018]
41. Seuren LM, Wherton J, Greenhalgh T, Cameron D, A'Court C, Shaw SE. Physical examinations via video for patients with heart failure: qualitative study using conversation analysis. J Med Internet Res 2020;22(2):e16694 [FREE Full text] [doi: 10.2196/16694] [Medline: 32130133]
42. Shao H, Liu C, Tang L, Wang B, Xie H, Zhang Y. Factors influencing the behavioral intentions and use behaviors of telemedicine in patients with diabetes: web-based survey study. JMIR Hum Factors 2023;10:e46624 [FREE Full text] [doi: 10.2196/46624] [Medline: 38153781]
43. Dennis, Fuller, Valacich. Media, tasks, and communication processes: a theory of media synchronicity. MIS Quarterly 2008;32(3):575-600. [doi: 10.2307/25148857]
44. Robert L, Dennis A. Paradox of richness: a cognitive model of media choice. IEEE Trans Profess Commun 2005;48(1):10-21. [doi: 10.1109/tpc.2004.843292]
45. Tan H, Yan M. Physician-user interaction and users' perceived service quality: evidence from Chinese mobile healthcare consultation. Informa Technol Peop 2020;33(5):1403-1426. [doi: 10.1108/itp-01-2019-0039]
46. Yan Z, Guo X, Vogel DR. Understanding dynamic collaboration in teleconsultation. Inform Technol Dev 2013;22(1):152-167. [doi: 10.1080/02681102.2013.854730]
47. Hawrysz L, Kludacz-Alessandri M, Walczak R. Predictive factors of physicians' satisfaction and quality of work under teleconsultation conditions: structural equation analysis. JMIR Hum Factors 2024;11:e47810 [FREE Full text] [doi: 10.2196/47810] [Medline: 38857081]
48. Moulaei K, Sheikhtaheri A, Fatehi F, Shanbehzadeh M, Bahaadinbeigy K. Patients' perspectives and preferences toward telemedicine versus in-person visits: a mixed-methods study on 1226 patients. BMC Med Inform Decis Mak 2023;23(1):261 [FREE Full text] [doi: 10.1186/s12911-023-02348-4] [Medline: 37968639]
49. Damico NJ, Deshane A, Kharouta M, Wu A, Wang G, Machtay MX, et al. Telemedicine use and satisfaction among radiation oncologists during the COVID-19 pandemic: evaluation of current trends and future opportunities. Adv Radiat Oncol 2022;7(2):100835 [FREE Full text] [doi: 10.1016/j.adro.2021.100835] [Medline: 34993359]
50. Kissi J, Dai B, Dogbe CS, Banahene J, Ernest O. Predictive factors of physicians' satisfaction with telemedicine services acceptance. Health Informatics J 2020;26(3):1866-1880 [FREE Full text] [doi: 10.1177/1460458219892162] [Medline: 31854222]
51. Malouff TD, TerKonda SP, Knight D, Abu Dabrh AM, Perlman AI, Munipalli B, et al. Physician satisfaction with telemedicine during the COVID-19 pandemic: the mayo clinic florida experience. Mayo Clin Proc Innov Qual Outcomes 2021;5(4):771-782 [FREE Full text] [doi: 10.1016/j.mayocpiqo.2021.06.006] [Medline: 34226884]
52. Holmgren AJ, Hendrix N, Maisel N, Everson J, Bazemore A, Rotenstein L, et al. Electronic health record usability, satisfaction, and burnout for family physicians. JAMA Netw Open 2024;7(8):e2426956 [FREE Full text] [doi: 10.1001/jamanetworkopen.2024.26956] [Medline: 39207759]
53. Roman LC, Ancker JS, Johnson SB, Senathirajah Y. Navigation in the electronic health record: a review of the safety and usability literature. J Biomed Inform 2017;67:69-79 [FREE Full text] [doi: 10.1016/j.jbi.2017.01.005] [Medline: 28088527]
54. Ratwani RM, Savage E, Will A, Fong A, Karavite D, Muthu N, et al. Identifying electronic health record usability and safety challenges in pediatric settings. Health Aff (Millwood) 2018;37(11):1752-1759. [doi: 10.1377/hlthaff.2018.0699] [Medline: 30395517]

XSL•FO
RenderX

55. Peccoralo LA, Kaplan CA, Pietrzak RH, Charney DS, Ripp JA. The impact of time spent on the electronic health record after work and of clerical work on burnout among clinical faculty. J Am Med Inform Assoc 2021;28(5):938-947 [FREE Full text] [doi: 10.1093/jamia/ocaa349] [Medline: 33550392]
56. Tzeng Y, Yin W, Lin K, Wei J, Liou H, Sung H, et al. Factors associated with the utilization of outpatient virtual clinics: retrospective observational study using multilevel analysis. J Med Internet Res 2022;24(8):e40288 [FREE Full text] [doi: 10.2196/40288] [Medline: 35917486]

Abbreviations

CDC: US Centers for Disease Control and Prevention
EHR: electronic health record
MST: media synchronicity theory
NCHS: National Center for Health Statistics
NEHRS: 2021 National Electronic Health Records Survey
Numofphy: number of physicians working in the facility
Phyage50: physicians' age group
Physex: physicians' sex
Setting: the nature of the practice
Speccat: physicians' specialty type
SumT: total number of telemedicine tools each physician used
T1: telephone audio
T2: videoconference software with audio
T3: telemedicine platforms not integrated with electronic health records
T4: telemedicine platforms integrated with electronic health records
Telemedbarrier1: limited internet access or speed issues
Telemedbarrier2: telemedicine platform not easy to use or did not meet physician's needs
Telemedbarrier3: telemedicine is not appropriate for physician's specialty or type of patients
Telemedbarrier4: limitations in patients' access to technology
Telemedbarrier5: patients' difficulty using technology or telemedicine platform
Telemedpct: percentage of patient visits conducted through telemedicine as a proportion of overall ambulatory care visits
Telemedqual: physicians' quality-of-health care evaluation in comparison to in-person service
Telemedsat: office-based physicians' satisfaction with telemedicine technology use

Edited by A Benis; submitted 31.03.25; peer-reviewed by M Hamedani, S Patel; comments to author 01.06.25; accepted 30.11.25; published 23.12.25.

Please cite as:
Liu XO, Sengupta A
Competition or Complementarity Among Telemedicine Tools in Ambulatory Care Practice: Cross-Sectional Analysis
JMIR Med Inform 2025;13:e75246
URL: https://medinform.jmir.org/2025/1/e75246
doi:10.2196/75246
PMID:41433052

©Xiang Oliver Liu, Avijit Sengupta. Originally published in JMIR Medical Informatics (https://medinform.jmir.org), 23.12.2025. This is an open-access article distributed under the terms of the Creative Commons Attribution License (https://creativecommons.org/licenses/by/4.0/), which permits unrestricted use, distribution, and reproduction in any medium, provided the original work, first published in JMIR Medical Informatics, is properly cited. The complete bibliographic information, a link to the original publication on https://medinform.jmir.org/, as well as this copyright and license information must be included.

XSL•FO
RenderX

Regulatory Insights From 27 Years of Artificial Intelligence/Machine Learning–Enabled Medical Device Recalls in the United States: Implications for Future Governance

Wei-Pin Chen[1], MSc; Wei-Guang Teng[2], PhD; C Benson Kuo[3], PhD; Yu-Jui Yen[2], MSc; Jian-Yu Lian[1], MSc; Matthew Sing[1], MSc; Peng-Ting Chen[1,4], PhD

[1]Department of Biomedical Engineering, National Cheng Kung University, No.138, Shengli Rd, North District, Tainan, Taiwan

[2]Department of Engineering Science, National Cheng Kung University, Tainan, Taiwan

[3]Department of Regulatory and Quality Sciences, University of Southern California, Los Angeles, CA, United States

[4]Medical Device Innovation Center, National Cheng Kung University, Tainan, Taiwan

Corresponding Author:
Peng-Ting Chen, PhD
Department of Biomedical Engineering, National Cheng Kung University, No.138, Shengli Rd, North District, Tainan, Taiwan

Abstract

Background: Artificial intelligence/machine learning (AI/ML) has revolutionized the health care industry, particularly in the development and use of medical devices. The US Food and Drug Administration (FDA) has authorized over 878 AI/ML–enabled medical devices, reflecting a growing trend in both quantity and application scope. Understanding the distinct challenges these devices present in terms of FDA regulation violations is crucial for effectively avoiding recalls. This is particularly pertinent for proactive measures regarding medical devices.

Objective: This study explores the impact of AI/ML on medical device recalls, focusing on the distinct causes associated with AI/ML–enabled devices compared with other device types. Recall information associated with 510(k)-cleared devices was obtained from openFDA. Three recall cohorts were established: “All 510(k) devices recall,” “software-related devices recall,” and “AI/ML devices recall.”

Methods: Recall information for 510(k)-cleared devices was obtained from openFDA. AI/ML-enabled medical devices were identified based on FDA listings. Three cohorts were established: “All 510(k) devices recall,” “software-related devices recall,” and “AI/ML devices recall.” Root cause analysis was conducted for each recall event.

Results: The results indicate that while the top 5 recall root causes are relatively similar across the 3 control groups, the proportions vary, with AI/ML devices showing a higher impact for 87% of all recalls. Design and development–related factors play a significant role in recalls of AI/ML devices with root causes related to device design and software design accounting for 50% of recalls, emphasizing the importance of thorough planning, user feedback incorporation, and validation during the development process to reduce the probability of recalls. In addition, changes in software, including design changes and control changes, also contribute substantially to recalls in AI/ML devices.

Conclusions: In conclusion, this study provides valuable insights into the unique challenges and considerations associated with AI/ML–enabled medical device recalls, offering guidance for manufacturers to enhance verification plans and mitigate risks in this rapidly evolving technological landscape.

(JMIR Med Inform 2025;13:e67552) doi:10.2196/67552

KEYWORDS

AI/ML-enabled medical device; recall; SaMD; 510(k); FDA; Food and Drug Administration; artificial intelligence/machine learning

Introduction

Background

Artificial intelligence/machine learning (AI/ML) has significantly impacted the health care industry, particularly in the development and use of medical devices. Key contributions include enhancing diagnostic accuracy through the analysis of medical imaging data, enabling predictive analytics for disease outcomes, personalizing treatment plans based on patient characteristics, facilitating remote patient monitoring, expediting drug discovery, and improving surgical procedures through robotics [1,2]. In addition, AI aids in optimizing health care management processes, enhancing cybersecurity for patient data

XSL•FO
RenderX

protection, and supporting continuous learning and improvement in medical devices.

From 1997 to March 2024, the US Food and Drug Administration (FDA) has authorized over 878 Class II AI/ML–enabled medical devices (refer to (Multimedia Appendix 1)). The quantity may not be large, but from the annual registration records, it can be observed that such products are increasing year by year (refer to Figure 1).

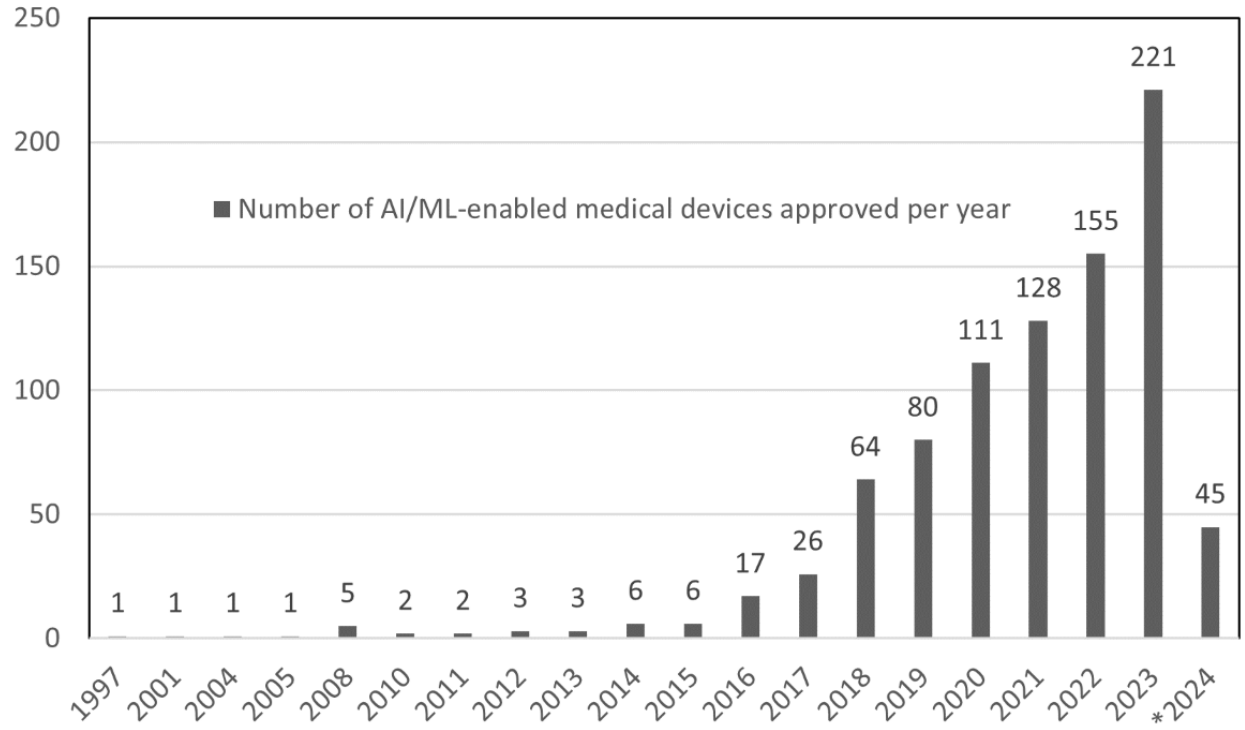
At the same time, the scope of application is also expanding. This trend is reflected in the classification product codes covered by the registered products [2]. Benjamens et al [1] and Zhu et al [2] have successively pointed out in their research that the number of registered AI/ML products has been continuously increasing since 2010. Zhu et al [2] also mentioned that 82% of the registered AI/ML products are concentrated in the two medical specialties of radiology and cardiology, indicating a significant use of digital medical data (such as digital medical imaging data and electrocardiograms) and relevant applications of pattern recognition in diagnosis.

As the FDA approves more and more AI/ML–enabled medical devices, it is critical to understand the unique challenges they pose when it comes to recalls, which are for violations of FDA regulations. This study examines recall data from the FDA, identifying key causes for recalls specifically associated with AI/ML–enabled medical devices. Proactive measures taken for medical devices, Wallace and Kuhn [3] analyzed system failures caused by software faults using recall information and proposed insights for improving software development. Although their analysis was not specifically focused on AI/ML products, FDA data show that one-third of medical devices operated using software are recalled due to software failures. This noteworthy phenomenon has inspired our research thinking.

Recall is a proactive measure aimed at removing or rectifying products that violate laws enforced by the FDA. It is a voluntary action taken by manufacturers and distributors who recognize their responsibility to safeguard public health from products posing risks of injury, significant deception, or other defects [4-7]. Recalls are initiated when a medical device is found to be defective, poses a risk to health, or exhibits both defects and health risks [8]. In rare cases where a manufacturer or importer neglects to voluntarily recall a device jeopardizing health, the FDA may issue a recall order to the manufacturer under 21 Code of Federal Regulations (CFR) 810.

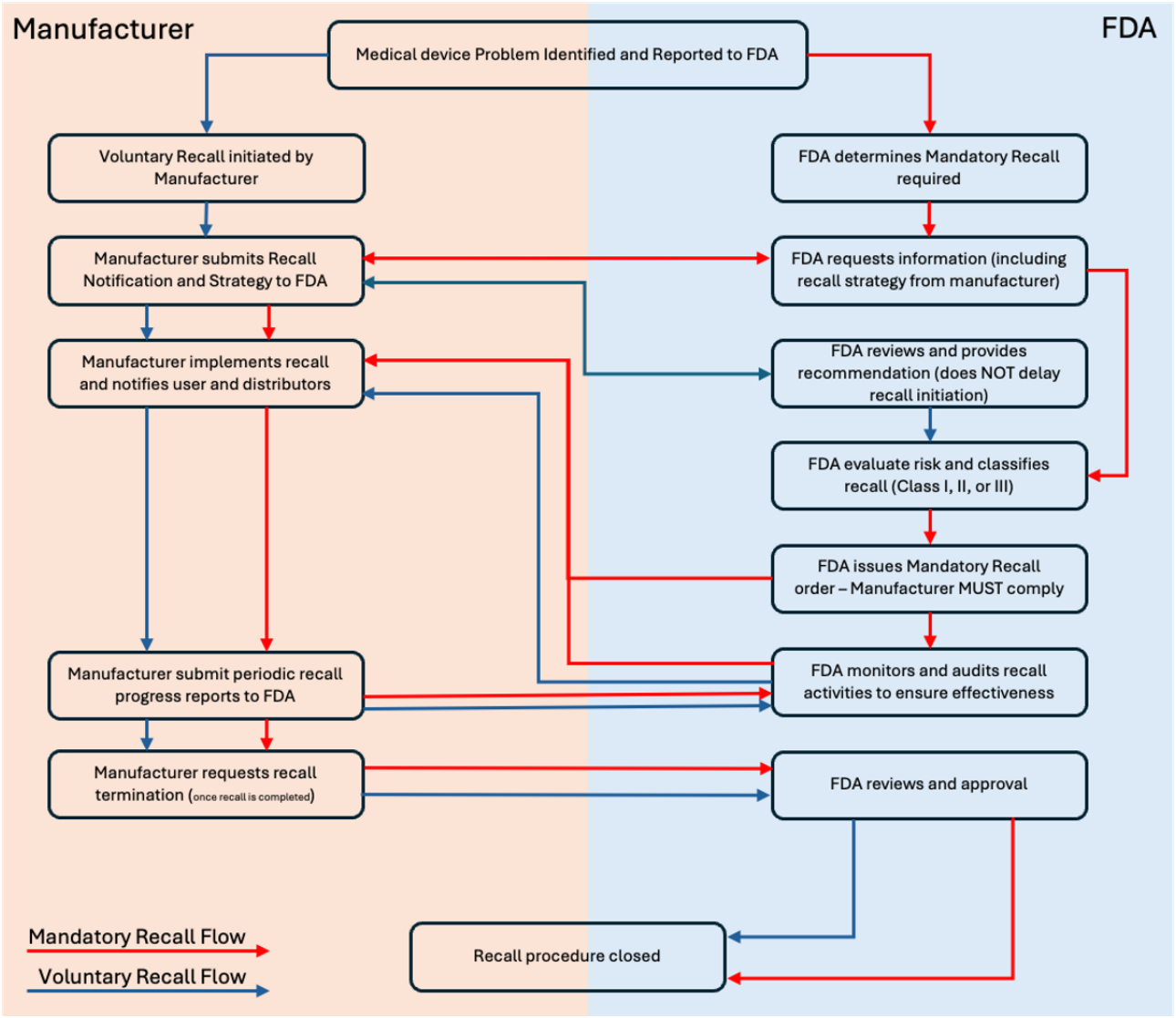
FDA 21 CFR 7 defines the recall as “a firm’s removal or correction of a marketed product that the FDA considers to be in violation of the laws it administers and against which the agency would initiate legal action, for example, seizure. Recall does not include a market withdrawal or a stock recovery” [9] (refer to Figure 2). Although recalls are intended to ensure patient safety, Zipp [8] points out that the system for initiating recalls often takes a long time to start the recall process [10]. Zipp [8] also uses the example of the recall of Philips sleep apnea ventilator devices to illustrate this situation and proposes using a Unique Device Identifier as a solution to track product flow and expedite the recall process.

Figure 1. Number of artificial intelligence/machine learning–enabled 510(k) medical devices approved per year from 1997 to March 2024. AI: artificial intelligence; ML: machine learning.



XSL•FO
RenderX

Figure 2. Recall activities with responsible organizations. FDA: Food and Drug Administration.



Objectives

This study delves into the recalls linked to AI/ML–enabled medical devices, aiming to discern prevalent recall types unique to these products through comparative analysis with recalls from diverse device types. By scrutinizing recall data, the research endeavors to equip manufacturers with insightful information, enabling them to undertake a more comprehensive evaluation before product introduction. This proactive approach entails implementing measures to preempt root causes associated with recalls, thus mitigating the likelihood of recall incidents. FDA medical device recalls serve as a critical barometer reflecting the intricate landscape of medical device innovation challenges. Each recall unveils potential areas of vulnerability within the innovation process, shedding light on shortcomings in design, development, and regulatory oversight. Recalls highlight the delicate balance between pushing boundaries for technological advancement and ensuring safety and efficacy standards are met. They underscore the complexities of integrating cutting-edge technologies, such as AI/ML, into medical devices while maintaining regulatory compliance. Moreover, these recalls signal the need for continuous vigilance and adaptation in response to evolving risks and emerging technologies, emphasizing the dynamic nature of medical device innovation. As such, FDA recalls provide invaluable lessons for industry stakeholders, guiding them in navigating the intricate terrain of innovation while prioritizing patient safety and regulatory adherence.

Methods

Overview

Recall information associated with 510(k)-cleared devices was downloaded from openFDA, a publicly accessible data platform provided by the US FDA to facilitate access to structured regulatory datasets, including medical device recalls [11,12]. AI/ML–enabled medical devices were identified based on the list published by the FDA [13]. These devices were manually screened by the FDA and do not have a specific code to track them. This list comprises medical devices that incorporate AI and ML, based primarily on the information provided within the summary descriptions of their marketing authorizations. The root cause description associated with each recall event was used to characterize the particular recall. Some recall events may be associated with more than one root cause.

XSL•FO
RenderX

In 21 CFR 7.46 (firm-initiated recall), when the initiating firm decides to remove or correct distributed products, reasons for removal or correction must be provided. The Guidance of Initiation of Voluntary Recalls Under 21 CFR Part 7, Subpart C mentions referencing 21 CFR 820.100(a)(2), which requires procedures for implementing corrections or preventive actions to include an investigation of the causes for nonconformities related to the product, processes, and quality systems. Furthermore, in the FDA regulatory procedures manual, chapter 7 (recall procedures) states that when recalls are classified as Class I or significant Class II recalls, the need for an establishment inspection should be assessed to determine the root cause of the problem and document any potential regulatory actions (7-5-1, 3 Establishment Inspection) [9,14]. Investigation and analysis of the root cause, as outlined in the aforementioned FDA requirements, are a crucial part and one of the important factors for the firm's decision to remove or correct products. In practice, most companies' root cause statements align with FDA-recognized categories because they rely on the same industry-accepted terminology. However, the actual analysis and conclusion come primarily from the manufacturer's quality management system. The FDA's role is to verify and ensure that the manufacturer's reasoning makes sense and adequately addresses public health concerns.

Three cohorts were established for comparison and analysis including "All 510(k) devices recall" cohort, "software-related devices recall" cohort and "AI/ML devices recall" cohort (refer to Table 1).

XSL•FO
RenderX

Table . Characteristics of three recall cohorts.

Root cause description of recall	All 510(k) devices, 167,864 devices			Software-related devices, 3071 devices			AI/ML[a] devices, 878 devices		
	Recall	Rank	%	Recall	Rank	%	Recall	Rank	%
Component change control	316	22	1	79	18	1	__[b]	—	—
Component design or selection	1472	7	3	305	7	3	1	15	1
Device design	6207	2	14	1405	2	15	13	3	8
Employee error	943	10	2	108	14	1	—	—	—
Environmental control	239	26	1	28	26	0	—	—	—
Equipment maintenance	590	14	1	42	24	0	—		—
Error in labeling	543	15	1	60	19	1		—	—
Finished device change control	26	41	0	5	36	0		—	—
Incorrect or no expiration date	104	35	0	—	—	—	—	—	—
Labeling change control	451	17	1	47	23	0	1	13	1
Labeling design	779	12	2	103	15	1	1	16	1
Labeling false and misleading	304	23	1	18	28	0	—	—	—
Labeling mix-ups	530	16	1	7	34	0	—	—	—
Manufacturing material removal	71	39	0	7	35	0		—	—
Material or component contamination	351	21	1	15	32	0	—	—	—
Mixed-up of materials or components	394	20	1	50	22	1	2	8	1
No marketing application	101	36	0	17	29	0	—	—	—
Nonconforming material or component	4730	3	11	775	4	8	2	11	1
Other	6695	1	16	1115	3	12	2	12	1
Package design or selection	441	18	1	5	38	0	—	—	—

XSL•FO
RenderX

Root cause description of recall	All 510(k) devices, 167,864 devices			Software-related devices, 3071 devices			AI/ML[a] devices, 878 devices		
	Recall	Rank	%	Recall	Rank	%	Recall	Rank	%
Packaging	866	11	2	17	30	0	—	—	—
Packaging change control	255	25	1	10	33	0	—	—	—
Packaging process control	1031	9	2	19	27	0	—	—	—
Pending	170	29	0	40	25	0	—	—	—
PMA[c]	14	42	0	5	37	0	—	—	—
Process change control	601	13	1	55	20	1	2	9	1
Process control	4717	4	11	507	6	5	11	4	7
Process design	1070	8	2	171	8	2	11	5	7
Radiation Control for Health and Safety Act	207	27	0	140	10	1	1	14	1
Release of material or component before receiving test results	45	40	0	4	39	0	—	—	—
Reprocessing controls	73	38	0	4	41	0	—	—	—
Software change control	126	32	0	126	11	1	3	7	2
Software design	3103	6	7	3103	1	32	68	1	42
Software design manufacturing process	125	33	0	125	12	1	—	—	—
Software design change	157	31	0	157	9	2	4	6	2
Software in the use environment	93	37	0	93	16	1	—	—	—
Software manufacturing or software deployment	111	34	0	111	13	1	—	—	—
Storage	164	30	0	4	40	0	—	—	—
Under investigation by firm	4011	5	9	608	5	6	37	2	23

XSL•FO
RenderX

Root cause description of recall	All 510(k) devices, 167,864 devices			Software-related devices, 3071 devices			AI/ML[a] devices, 878 devices		
	Recall	Rank	%	Recall	Rank	%	Recall	Rank	%
Unknown or undetermined by firm	411	19	1	51	21	1	—	—	—
Use error	273	24	1	82	17	1	2	10	1
Vendor change control	190	28	0	16	31	0	1	17	1
Total amount	43,100	—	100	9639	—	100	162	—	100

[a]AI/ML: artificial intelligence/machine learning.

[b]Zero.

[c]PMA: premarket approval.

Data Processing

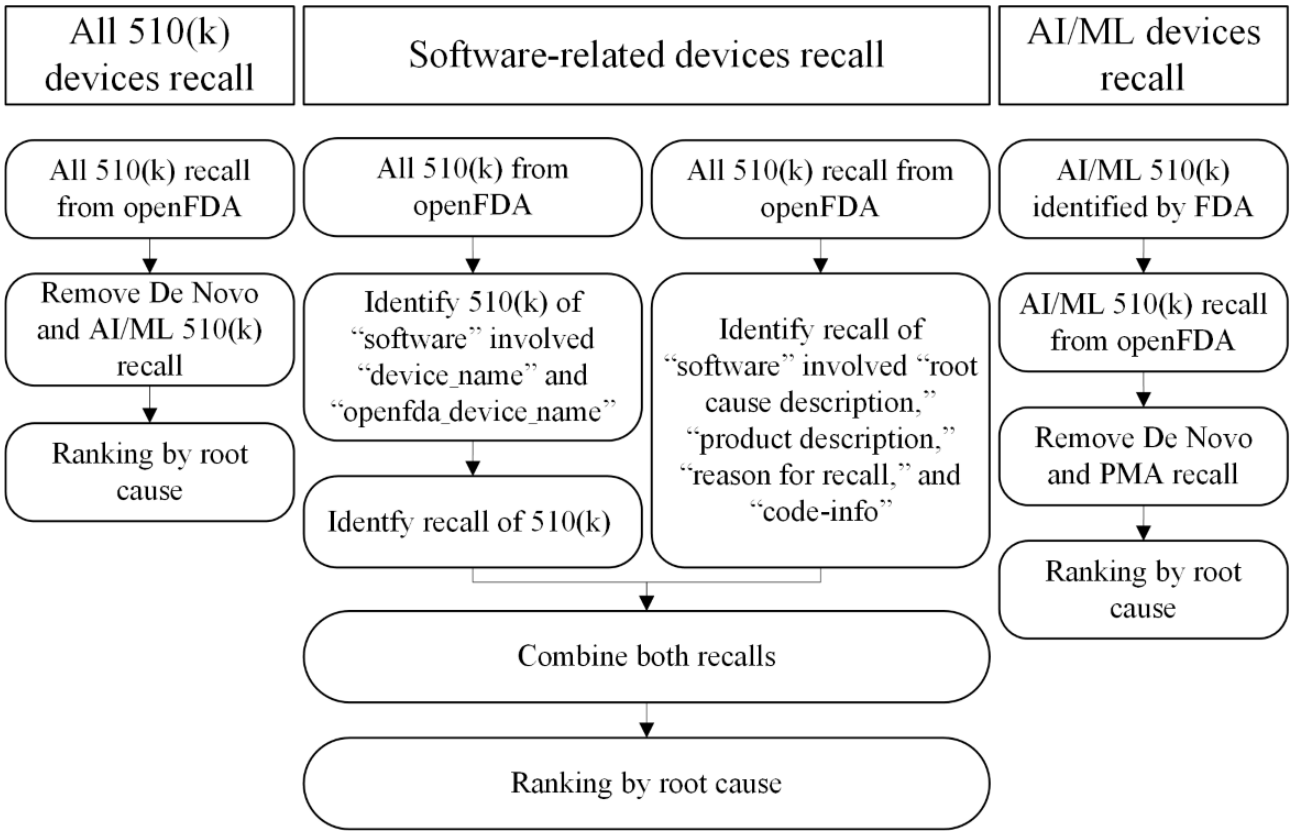
Each cohort required a specific analytical approach to accurately extract and rank recall events based on their causes. The following numbered list outlines the processes used to collect, filter, and analyze data to derive insights into the prevalence and nature of recalls within each group (refer to Figure 3):

1. All 510(k) devices recall: the "All 510(k) Devices Recall" cohort begins by gathering all 510(k) medical device recall events from the openFDA database [11]. We specifically exclude recalls related to AI/ML devices and De Novo devices to focus on traditional 510(k) recalls. Post exclusion, the recalls are ranked by the frequency of each root cause, helping identify the most common issues within this group.
2. Software-related devices recall: this cohort targets recalls specifically linked to software issues in medical devices. Due to the absence of a direct filter for software-related issues in openFDA, we apply two distinct criteria to accurately capture relevant recalls:
   - Criterion 1: we search within the "device_name" and "openfda_device_name" fields for entries that include the term "Software." Recalls identified under this criterion were then sequenced by the prevalence of each root cause.
   - Criterion 2: we further refine our search by examining the "root cause description," "product description," "reason for recall," and "code-info" fields for mentions of "Software." Similar to the first criterion, these recalls were then sequenced by root cause prevalence.

   After identifying and ranking recalls based on both criteria, we merge the results to form a comprehensive sequence of software-related device recalls.
1. AI/ML devices recall: the "AI/ML Devices Recall" cohort consists of recalls involving AI/ML–enabled devices as identified by the FDA [13]. Like the first cohort, we exclude any recalls pertaining to De Novo and premarket approval devices to solely focus on AI/ML 510(k) recalls. These are then ranked by root cause based on occurrence frequency.

XSL•FO
RenderX

Figure 3. The process for cohort distinction. AI: artificial intelligence; FDA: US Food and Drug Administration; ML: machine learning; PMA: premarket approval.



Ethical Considerations

All analyses were conducted using public data available on the FDA medical device databases and from openFDA. Therefore, ethics approval was unnecessary. This study does not include human subject information, primary data collection, or any form of experimentation involving individuals.

Results

The three cohorts presented in this study are as follows: the "All 510(k) devices recall" cohort includes 167,864 medical devices covering 4473 product codes with a total of 43,100 recalls and 42 root causes. The "software-related devices recall" cohort includes 3071 medical devices, covering 438 product codes with 9639 recalls and 42 root causes. The "AI/ML devices recall" cohort comprises 878 class II medical devices, covering 110 product codes with 162 recalls and 17 root causes (refer to Table 1).

Root Causes of Recalls

Recalls in both "All 510(k) devices recall" and "software-related devices recall" cohorts that are directly related to software have six common root causes: software design, software design change, software design manufacturing process, software change control, software manufacturing/software deployment, and software in the use environment. The number of recalls for each of these root causes is the same, indicating that the filtering criteria did not miss software-related 510(k) medical devices. In the "AI/ML devices recall" recalls related to software, there are only three root causes: software design, software change control, and software design change. When summing up all software-related root causes, "All 510(k) devices recall" has 3715 recalls, accounting for 9%, "software-related devices recall" has 3,715 recalls, accounting for 39%, and "AI/ML devices recall" has 75 recalls, accounting for 46% (refer to Table 2 and Figures 4-6).

Looking at the number of recalls for each root cause, the top five root causes for "All 510(k) devices recall" are other/6695/16% (recall root cause/number of recall/% of all 510(k) devices recall), device design/6207/14%, nonconforming material-component/4730/11%, process control/4717/11%, and under investigation by firm/4011/9%, totaling 26,360 recalls or 61%. These do not include software-related root causes. For "software-related devices recall," the top 5 root causes are software design/3103/32%, device design/1405/15%, other/1115/12%, nonconforming material-component/775/8%, and under investigation by firm/608/6%, totaling 7006 recalls or 73%. In "AI/ML devices recall," the top five root causes are software design/68/42%, under investigation by firm/37/23%, device design/13/8%, process design/11/7%, and process control/11/7%, totaling 140 recalls or 86% (refer to (Multimedia Appendix 2)).

XSL•FO
RenderX

Table . Recall events ranked by the number of occurrences for all cohorts.

Root causes description of recall	All 510(k) devices, 167,864 devices			Software-related devices, 3071 devices			AI/ML devices, 878 devices		
	Recall	Rank	%	Recall	Rank	%	Recall	Rank	%
Other	6695[a]	1[a]	16[a]	1115[b]	3[b]	12[b]	2	12	1
Device design	6,207[c]	2[c]	14[c]	1405[c]	2[c]	15[c]	13[b]	3[b]	8[b]
Nonconforming material or component	4730[b]	3[b]	11[b]	775[d]	4[d]	8[d]	2	11	1
Process control	4717[d]	4[d]	11[d]	507	6	5	11[d]	4[d]	7[d]
Under investigation by firm	4011[e]	5[e]	9[e]	608[e]	5[e]	6[e]	37[c]	2[c]	23[c]
Software design	3103	6	7	3103[a]	1[a]	32[a]	68[a]	1[a]	42[a]
Component design or selection	1472	7	3	305	7	3	1	15	1
Process design	1070	8	2	171	8	2	11[e]	5[e]	7[e]
Packaging process control	1031	9	2	19	27	0	__[f]	—	—
Employee error	943	10	2	108	14	1	—	—	—
Packaging	866	11	2	17	30	0	—	—	—
Labeling design	779	12	2	103	15	1	1	16	1
Process change control	601	13	1	55	20	1	2	9	1
Equipment maintenance	590	14	1	42	24	0	—	—	—
Error in labeling	543	15	1	60	19	1	—	—	—
Labeling mix-ups	530	16	1	7	34	0	—	—	—
Labeling change control	451	17	1	47	23	0	1	13	1
Package design or selection	441	18	1	5	38	0	—	—	—
Unknown or undetermined by firm	411	19	1	51	21	1	—	—	—
Mixed-up of materials or components	394	20	1	50	22	1	2	8	1

XSL•FO
RenderX

Root causes description of recall	All 510(k) devices, 167,864 devices			Software-related devices, 3071 devices			AI/ML devices, 878 devices		
	Recall	Rank	%	Recall	Rank	%	Recall	Rank	%
Material or component contamination	351	21	1	15	32	0	—	—	—
Component change control	316	22	1	79	18	1	—	—	—
Labeling false and misleading	304	23	1	18	28	0	—	—	—
Use error	273	24	1	82	17	1	2	10	1
Packaging change control	255	25	1	10	33	0	—	—	—
Environmental control	239	26	1	28	26	0	—	—	—
Radiation Control for Health and Safety Act	207	27	0	140	10	1	1	14	1
Vendor change control	190	28	0	16	31	0	1	17	1
Pending	170	29	0	40	25	0	—	—	—
Storage	164	30	0	4	40	0	—	—	—
Software design change	157	31	0	157	9	2	4	6	2
Software change control	126	32	0	126	11	1	3	7	2
Software design manufacturing process	125	33	0	125	12	1	—	—	—
Software manufacturing or software deployment	111	34	0	111	13	1	—	—	—
Incorrect or no expiration date	104	35	0	—	—	—	—	—	—
No marketing application	101	36	0	17	29	0	—	—	—
Software in the use environment	93	37	0	93	16	1	—	—	—
Reprocessing controls	73	38	0	4	41	0	—	—	—
Manufacturing material removal	71	39	0	7	35	0	—	—	—

XSL•FO
RenderX

Root causes description of recall	All 510(k) devices, 167,864 devices			Software-related devices, 3071 devices			AI/ML devices, 878 devices		
	Recall	Rank	%	Recall	Rank	%	Recall	Rank	%
Release of material or component before receiving test results	45	40	0	4	39	0	—	—	—
Finished device change control	26	41	0	5	36	0	—	—	—
PMA[g]	14	42	0	5	37	0	—	—	—
Total amount	43,100	—	100	9639	—	100	162	—	100

[a]Ranked number 1 root cause of recall for its cohort.

[b]Ranked number 2 root cause of recall for its cohort.

[c]Ranked number 3 root cause of recall for its cohort.

[d]Ranked number 4 root cause of recall for its cohort.

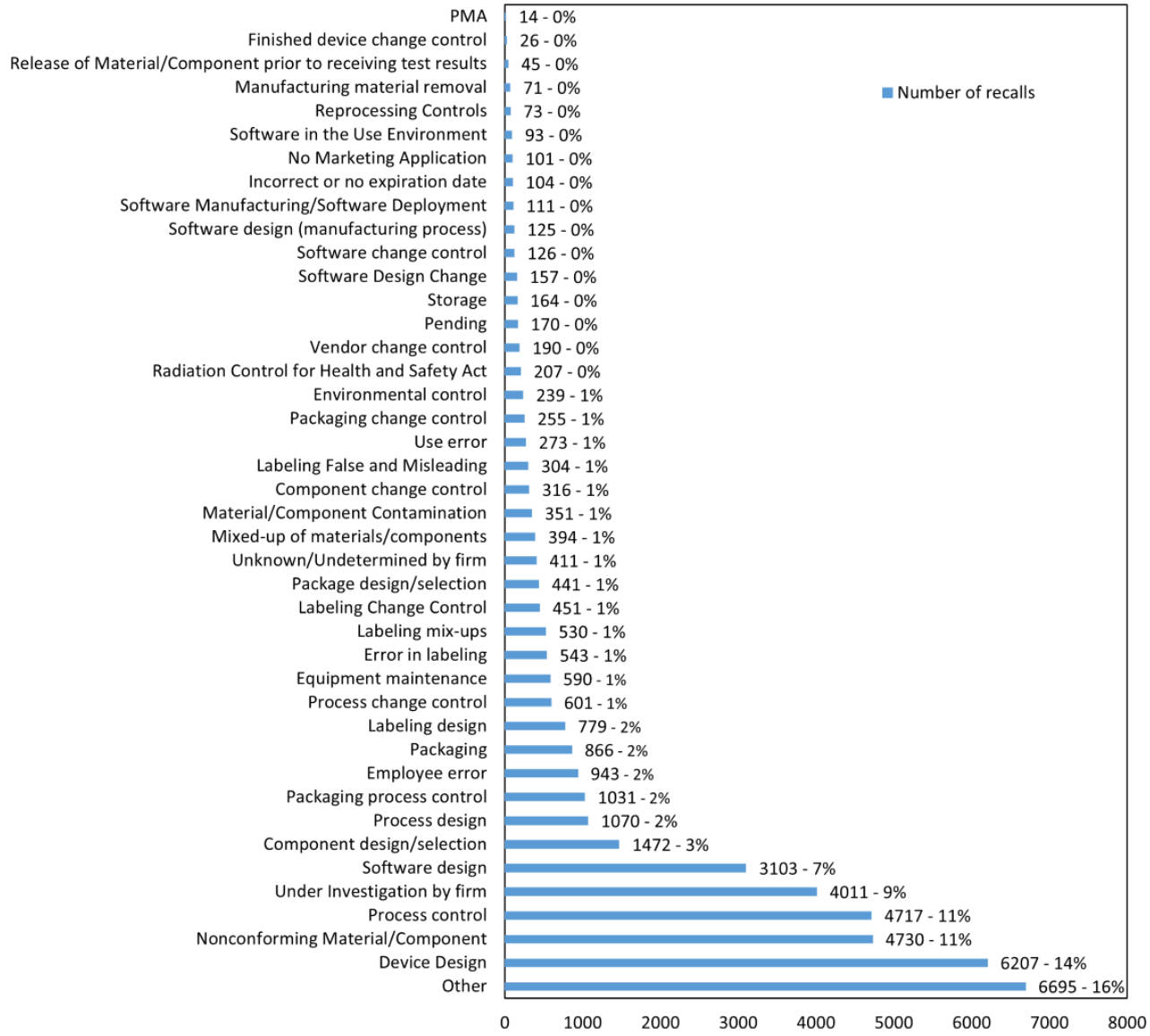
[e]Ranked number 5 root cause of recall for its cohort.

[f]Zero.

[g]PMA: premarket approval.

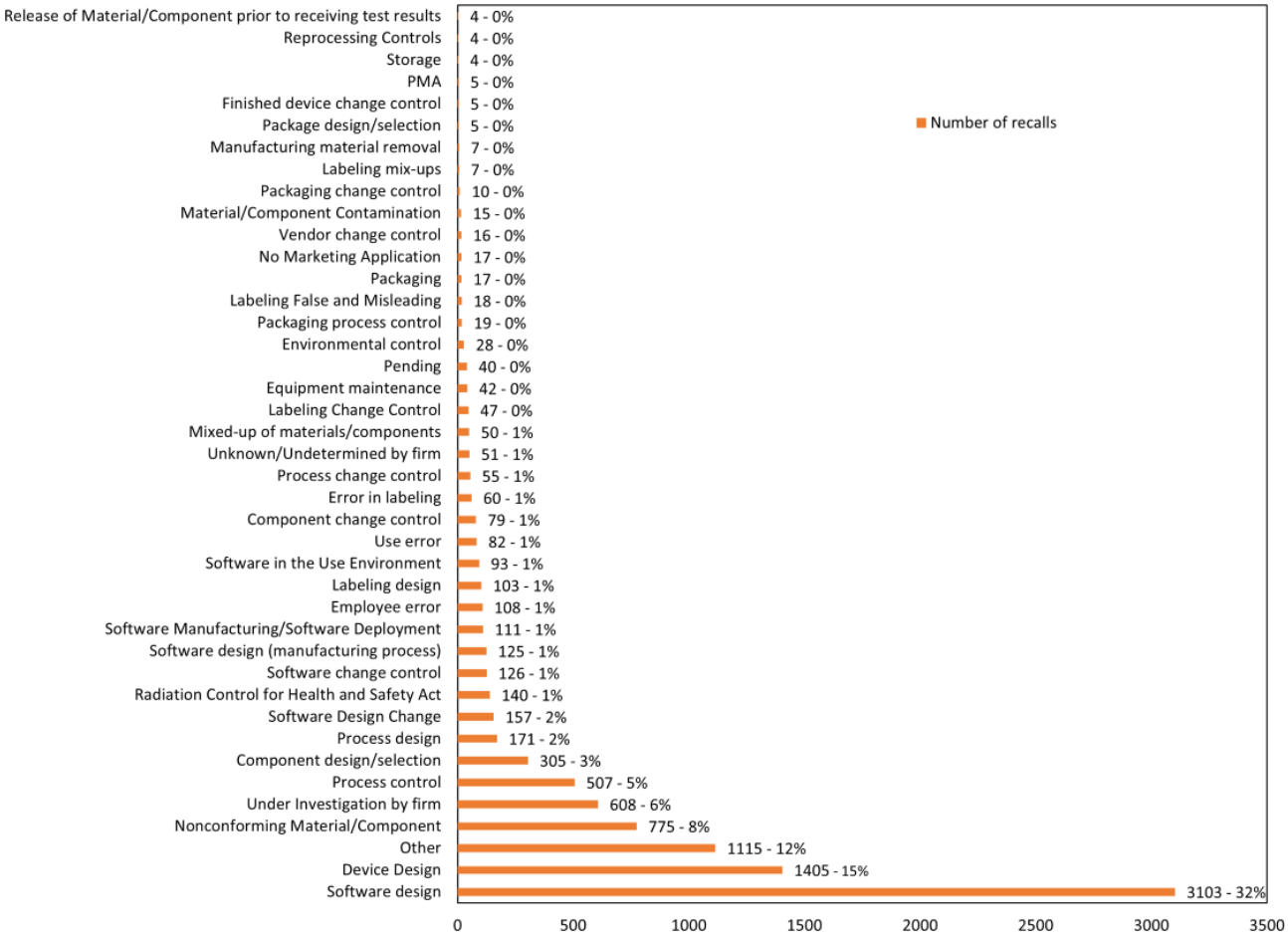
XSL•FO
RenderX

Figure 4. Number of recalls based on the root causes description for “all 510(k) devices”. PMA: premarket approval.



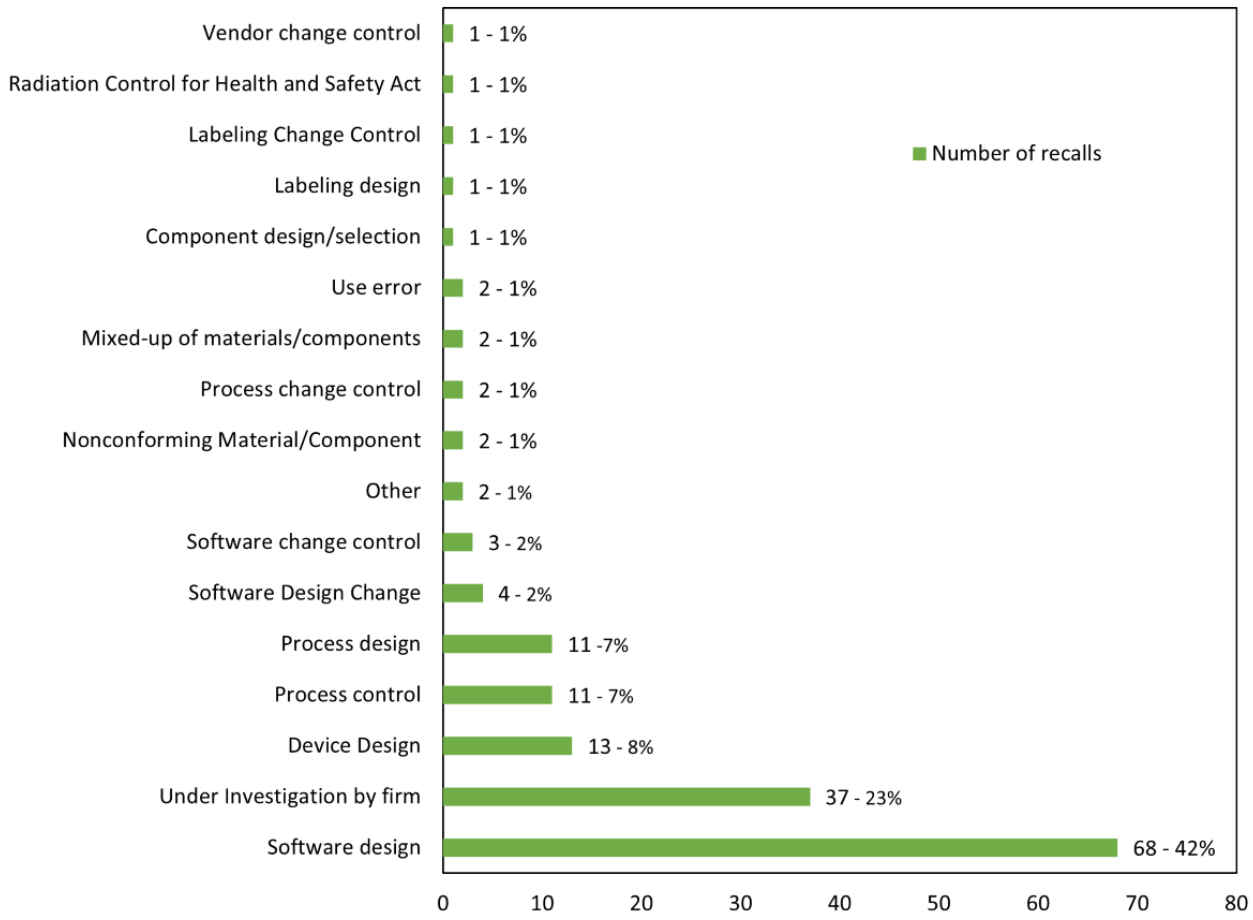
XSL•FO
RenderX

Figure 5. Number of recalls based on the root causes description for "software-related devices." PMA: premarket approval.



XSL•FO
RenderX

Figure 6. Number of recalls based on the root causes description for "artificial Intelligence/machine learning devices."



Specific Root Causes

If the recalls with software-related root causes are added to the top five root causes, the total recalls for "All 510(k) devices recall" reach 30,075, accounting for 70%, "software-related devices recall" reach 7618, accounting for 79%, and "AI/ML devices recall" reach 147, accounting for 91%. Excluding recalls with software-related root causes, the top five root causes for "All 510(k) devices recall" have 26,360 recalls, accounting for 61%, "software-related devices recall" have 3903 recalls, accounting for 40%, and "AI/ML devices recall" have 72 recalls, accounting for 44% (refer to Table 3 and Multimedia Appendix 3).

Furthermore, the first root cause for both "software-related devices recall" and "AI/ML devices recall" is software design with extremely high percentages of 32% and 42%, respectively. In "All 510(k) devices recall," software design still accounts for 6% of total recalls, ranking sixth. After excluding root causes with unclear definitions, such as other and under investigation by firm, and adding the recall quantities for the second-ranking root cause with significance in the three lists, which is device design, the combined percentage of software design and device design increases to 47% for "software-related devices recall" and 50% for "AI/ML devices recall" reaching half of the total recalls. For "All 510(k) devices recall," it also reaches 22%, surpassing one-fifth of the total recalls (refer to Table 3).

In terms of product categories, recalls of AI/ML–enabled devices and software-related devices are concentrated in Radiology with another significant category being Cardiovascular. This corresponds to the number of product registrations. Recalls of all 510(k) devices are distributed across a greater number of product categories. However, Radiology and Cardiovascular remain among the categories with higher recall numbers. In addition to these, Orthopedic, General Hospital, and Gastroenterology/Urology are categories with relatively higher recall numbers.

XSL•FO
RenderX

Table . Statistical comparison of specific root cause recall occurences among different recall cohorts.

Recall with specific root causes	All 510(K) devices		Software-related devices		AI/ML devices	
	Recall	%	Recall	%	Recall	%
Recall amount of all root causes	43,100	100%	9369	100%	162	100%
Recall amount of all software related root cause	3715	9%	3715	39%	75	46%
Recall amount of top 5 recall root causes	26,360	61%	7006	73%	140	86%
Top 5+ all software related root causes	30,075	70%	7618	79%	147	91%
Top 5 - any software related root causes	26,360	61%	3903	40%	72	44%
Device design + software design	9310	22%	4508	47%	91	50%
Top 5 - (other + under investigation by firm)	15,654	36%	5283	55%	103	64%
Recall amount of change related root causes	2122	5%	495	5%	11	7%

Discussion

Principal Findings

This study investigated the underlying reasons behind recalls linked to AI/ML–enabled medical devices, pinpointing distinct causes compared with other device types. The first control group encompasses all recalls linked to either a 510(k) device. The second control group encompasses recalls tied to software.

Comparing the root causes and their corresponding recall quantities among the "All 510(k) devices recall," "software-related devices recall," and "AI/ML devices recall" groups, it's evident that the combined recall occurrences for the top five root causes accounted for over 60% across all cohorts [15]. The recall total for "software-related devices recall" even surpasses 73%, while "AI/ML devices recall" reaches 86%. Despite the inclusion of unclearly defined root causes such as "other" and "under investigation by firm" in the top 5, removing these 2 root causes still results in proportions of 36%, 55%, and 64% for "All 510(k) devices recall," "software-related devices recall," and "AI/ML devices recall," respectively. Although the definitions of products in the three control groups differ, it is interesting to note that if the top seven recall root causes are considered, the three groups are not far apart. The ranking of recalls varies slightly, and in the case of "AI/ML devices recall," process design replaces component design/selection [14]. Improving the top seven recall root causes can have a significant positive impact on recalls and is a topic worthy of further investigation (refer to Table 3).

Looking at recalls related to software, it is clear they constitute a high proportion in "software-related devices recall" and "AI/ML devices recall" accounting for 39% and 46%, respectively. The software design root cause alone accounts for 32% and 42%, respectively with a combined percentage of 82% and 91% for all software-related recall root causes in "software-related devices recall" and "AI/ML devices recall." Software design can be considered the primary recall root cause for both groups. When adding the device design factor to recalls, the total reaches close to half for both "software-related devices recall" and "AI/ML devices recall," especially in "AI/ML devices recall," where it surpasses half, reaching 50%. Including recalls related to process design and labeling design further increases the proportion to 58% [14]. These design and development-related factors leading to recalls likely represent inherent risks present during the product planning or design phase. The impact of these factors on "AI/ML devices recall" is notably higher than in the other 2 control groups. Considering experienced design and development engineers, incorporating user feedback, and implementing thorough validation during the development process could effectively reduce the probability of recalls.

Another group of root causes affecting recalls in "AI/ML devices recall" is related to changes, including software design change, software change control, process change control, vendor change control, and labeling change control. Although the quantities are relatively fewer with 4 root causes, they account for over a quarter (29.4%) of the total root causes, causing 7% of recalls. Compared with the 5% for "All 510(k) devices recall" and 5% for "software-related devices recall," this is relatively higher. Particularly in "AI/ML devices recall," where changes in corresponding software are relatively frequent, it is crucial for manufacturers to have comprehensive verification plans after any alterations.

XSL•FO
RenderX

The primary reasons for recalls in AI/ML medical devices include software design errors, nonconforming materials, inadequate process controls, and software implementation issues. Among these, software design errors are the most common, potentially leading to device malfunction, incorrect dosing, and compromised patient safety. Unlike traditional medical devices, AI/ML systems involve dynamic algorithms that evolve through data-driven learning, necessitating specialized validation processes beyond conventional static software testing [1,2]. Moreover, many AI/ML medical device recalls result from implicit assumptions made during algorithm design, such as dosage calculations or diagnostic thresholds. These assumptions must be explicitly identified, documented, and integrated into rigorous validation processes [4]. As a result, AI/ML–enabled medical devices present unique validation and quality assurance challenges, requiring continuous monitoring and adaptive regulatory frameworks to ensure their reliability and safety.

Furthermore, as AI/ML devices adapt postmarket based on new data, continuous market surveillance and real-time feedback loops are imperative to identify risks and respond proactively. Regulatory guidance increasingly emphasizes the necessity of robust monitoring systems, postmarket validation, and rapid recall readiness to address emerging problems [5,9]. These elements should be systematically incorporated into development lifecycle management plans for AI/ML–enabled medical devices.

Specifically, our analysis indicates that the most frequent root causes for AI/ML–enabled device recalls are software design errors, inappropriate software changes, inadequate process controls, and issues in software implementation. These factors can lead to critical patient safety impacts, including incorrect dosing, system malfunction, diagnostic errors, or device stoppage, with the potential for severe adverse health outcomes.

Based on the author's over 20 years of experience in testing, inspection, and certification of medical devices within the testing, inspection and certification industry, including work with authorized third-party organizations such as US FDA Accredited Person and EU (European Union) Notified Body, the author recommends that manufacturers adopt the following strategies to ensure the long-term safety and reliability of AI/ML–enabled medical devices:

1. Implement specialized validation frameworks, where AI/ML models undergo rigorous adversarial testing, real-world scenario validation, and continual performance monitoring, moving beyond reliance on premarket testing alone,
2. Establish ongoing market surveillance mechanisms, shifting regulatory focus toward total product lifecycle oversight to ensure AI systems remain effective as they evolve with new clinical data, and
3. Integrate user-centric risk mitigation practices, such as proactive feedback loops, to enable rapid adjustments and software updates that address emerging risks in clinical settings.

These strategies will better align regulatory oversight with the evolving nature of AI/ML technologies, ensuring both patient safety and long-term technology sustainability.

Limitation

This study has several limitations. First, the FDA currently does not have specific product codes or identification methods for Software as a Medical Device or software-related medical devices. Therefore, the data used in this study were derived from existing FDA data related to software to identify and analyze recall data for software-related medical devices as comprehensively as possible. Second, AI/ML–enabled devices also lack specific product codes or identification methods. Although the FDA manually updates its registry of AI/ML–enabled medical devices, this process is irregular, potentially leading to omissions in the data. These limitations restrict the ability to fully capture and analyze the unique challenges of AI/ML–enabled medical devices, such as specialized algorithm validation, handling of implicit assumptions, and algorithm performance variability. In addition, the publicly available FDA recall databases lack comprehensive information on software-specific faults, manufacturer-specific internal verification processes, and the complexity inherent in AI/ML technologies, including algorithm adaptability over time, real-world performance drifts, and user interaction dynamics.

Future Work

To address these limitations, future research should incorporate direct interactions with device manufacturers, internal company data, qualitative insights from developers, and longitudinal analyses to better explore these challenges and validate effective risk management strategies [10,14,16,17]. Based on the results of this study, we also plan to further investigate each recall of AI/ML–enabled medical devices and the reported reasons behind them to conduct a more in-depth analysis.

We hope to systematically deduce the real factors leading to recalls and compare them with current regulatory requirements to see if there is a need to adjust or strengthen regulatory requirements to reduce the probability of recalls and enhance public safety.

As AI/ML continues to reshape medical practices, a proactive and informed approach to regulatory oversight and device development becomes imperative for ensuring the safety and efficacy of these transformative technologies.

Conclusion

As the FDA authorizes an increasing number of AI/ML–enabled medical devices, it becomes crucial to understand the distinct challenges they pose in terms of recalls. This study delves into the intricate landscape of medical device recalls, focusing specifically on those associated with AI and ML. Comparisons across three control groups, namely "All 510(k) devices," "Software-related devices," and "AI/ML devices," unveil similarities in the top 7 recall root causes with variations in proportions. Notably, AI/ML devices exhibit a higher impact, especially concerning design and development-related factors. This study underscores the importance of robust planning, user feedback incorporation, and thorough validation during the development process to mitigate the inherent risks associated with AI/ML–enabled medical devices. Recalls related to software, particularly software design, constitute a significant proportion in both "software devices" and "AI/ML devices."

XSL•FO
RenderX

Changes in software also emerge as a notable contributor to recalls in AI/ML devices, underscoring the need for comprehensive verification plans after alterations.

In addition to standard regulatory compliance, AI/ML–enabled medical devices face unique validation challenges due to their dynamic nature and reliance on continuous learning algorithms. Such devices require specialized validation strategies that accommodate algorithm adaptability and evolving real-world performance [4]. Continuous market analysis and proactive user feedback integration are also particularly crucial for these devices, as they help detect and address issues promptly, thereby preventing recalls related to software logic errors, data-driven failures, or algorithmic inaccuracies [3,4].

Acknowledgments

The authors extend their gratitude to the BioMe Lab (Medical Device Innovation Department) at National Cheng Kung University of Taiwan for the help in structuring the article and editing the content. This research was supported by the BioMed Commercialization Center and the Ministry of Science and Technology under grant number NSTC 112-2628-E-006-008-MY3, as well as the Medical Device Innovation Center (MDIC), National Cheng Kung University (NCKU), through the Featured Areas Research Center Program within the framework of the Higher Education Sprout Project by the Ministry of Education (MoE) in Taiwan.

Conflicts of Interest

None declared.

Multimedia Appendix 1
Food and Drug Administration artificial intelligence/machine learning–enabled medical devices list.
[XLSX File, 74 KB - medinform_v13i1e67552_app1.xlsx]

Multimedia Appendix 2
Number of recalls from the top 5 root case for (a) all 510(k) devices recall, (b) software-related devices recall, and (c) artificial intelligence/machine learning devices recall.
[PNG File, 188 KB - medinform_v13i1e67552_app2.png]

Multimedia Appendix 3
Number of recall with specific root causes for (a) all 510(k) devices, (b) software-related devices, and (c) artificial intelligence/machine learning devices.
[PNG File, 181 KB - medinform_v13i1e67552_app3.png]

References

1. Benjamens S, Dhunnoo P, Meskó B. The state of artificial intelligence-based FDA-approved medical devices and algorithms: an online database. NPJ Digit Med 2020;3. [doi: 10.1038/s41746-020-00324-0] [Medline: 32984550]
2. Zhu S, Gilbert M, Chetty I, et al. The 2021 landscape of FDA-approved artificial intelligence/machine learning-enabled medical devices: an analysis of the characteristics and intended use. Int J Med Inform 2022 Sep;165:104828. [doi: 10.1016/j.ijmedinf.2022.104828] [Medline: 35780651]
3. Wallace DR, Kuhn DR. Failure modes in medical device software: an analysis of 15 years of recall data. Int J Rel Qual Saf Eng 2001 Dec;08(04):351-371. [doi: 10.1142/S021853930100058X]
4. Fu Z, Guo C, Zhang Z, et al. Study of software-related causes in the FDA medical device recalls. Presented at: 2017 22nd International Conference on Engineering of Complex Computer Systems (ICECCS); Nov 5-8, 2017; Fukuoka, Japan. [doi: 10.1109/ICECCS.2017.20]
5. Anderson HR. FDA Finalizes Voluntary Recall Guidance Imploring Companies to Be 'Recall Ready'. Faegre Drinker Biddle & Reath LLP. 2022. URL: https://www.faegredrinker.com/en/insights/publications/2022/3/fda-finalizes-voluntary-recall-guidance-imploring-companies-to-be-recall-ready [accessed 2024-02-29]
6. Dubin JR, Simon SD, Norrell K, et al. Risk of recall among medical devices undergoing US Food and Drug Administration 510(k) clearance and premarket approval, 2008-2017. JAMA Netw Open 2021 May 3;4(5):e217274. [doi: 10.1001/jamanetworkopen.2021.7274]
7. Kadakia KT, Dhruva SS, Caraballo C, et al. Use of recalled devices in new device authorizations under the US Food and Drug Administration's 510(k) pathway and risk of subsequent recalls. JAMA 2023 Jan 10;329(2):136-143. [doi: 10.1001/jama.2022.23279] [Medline: 36625810]
8. Zipp R. Anatomy of a medical device recall: how defective products can slip through an outdated system. MedTech Dive. 2021. URL: https://www.medtechdive.com/news/medical-device-recall-process-fda-philips-medtronic/608205/ [accessed 2024-09-02]

XSL•FO
RenderX

9. Subhan A. Medical Device Recalls. J Clin Eng 2022;47(2):61-62. [doi: 10.1097/JCE.0000000000000521]
10. Pace T. Analysis of FDA medical device recalls time between recall initation date and termination date. : Faculty of California State University; 2020 URL: https://scholarworks.calstate.edu/downloads/gm80j116d [accessed 2025-06-25]
11. Open-source APIs. openFDA. URL: https://open.fda.gov/ [accessed 2024-01-22]
12. Muehlematter UJ, Bluethgen C, Vokinger KN. FDA-cleared artificial intelligence and machine learning-based medical devices and their 510(k) predicate networks. Lancet Digit Health 2023 Sep;5(9):e618-e626 [FREE Full text] [doi: 10.1016/S2589-7500(23)00126-7] [Medline: 37625896]
13. Artificial intelligence and machine learning (AI/ML)-enabled medical devices. FDA. URL: https://www.fda.gov/medical-devices/software-medical-device-samd/artificial-intelligence-and-machine-learning-aiml-enabled-medical-devices [accessed 2024-08-02]
14. Thompson BM. Unpacking averages: common root causes driving medical device recalls. Epstein Becker & Green. 2022. URL: https://www.healthlawadvisor.com/unpacking-averages-common-root-causes-driving-medical-device-recalls [accessed 2024-03-03]
15. May C. Medical device recalls. Online GMP Training. URL: https://www.onlinegmptraining.com/medical-device-recalls/ [accessed 2024-03-07]
16. Zuckerman DM, Brown P, Nissen SE. Medical device recalls and the FDA approval process. Arch Intern Med 2011 Jun 13;171(11):1006-1011. [doi: 10.1001/archinternmed.2011.30] [Medline: 21321283]
17. Stern AD, Gordon WJ, Landman AB, et al. Cybersecurity features of digital medical devices: an analysis of FDA product summaries. BMJ Open 2019 Jun 28;9(6):e025374. [doi: 10.1136/bmjopen-2018-025374] [Medline: 31256020]

Abbreviations

AI: artificial intelligence
CFR: Code of Federal Regulations
EU: European Union
FDA: Food and Drug Administration
ML: machine learning

Edited by C Lovis; submitted 15.10.24; peer-reviewed by D Li, D Khunt; revised version received 25.03.25; accepted 27.03.25; published 11.07.25.

Please cite as:
Chen WP, Teng WG, Kuo CB, Yen YJ, Lian JY, Sing M, Chen PT
Regulatory Insights From 27 Years of Artificial Intelligence/Machine Learning–Enabled Medical Device Recalls in the United States: Implications for Future Governance
JMIR Med Inform 2025;13:e67552
URL: https://medinform.jmir.org/2025/1/e67552
doi:10.2196/67552

© Wei-Pin Chen, Wei-Guang Teng, C Benson Kuo, Yu-Jui Yen, Jian-Yu Lian, Matthew Sing, Peng-Ting Chen. Originally published in JMIR Medical Informatics (https://medinform.jmir.org), 11.7.2025. This is an open-access article distributed under the terms of the Creative Commons Attribution License (https://creativecommons.org/licenses/by/4.0/), which permits unrestricted use, distribution, and reproduction in any medium, provided the original work, first published in JMIR Medical Informatics, is properly cited. The complete bibliographic information, a link to the original publication on https://medinform.jmir.org/, as well as this copyright and license information must be included.

XSL•FO
RenderX

Impact of Diagnostic Stewardship on Urine Culture Ordering in Saudi Arabia: Prospective Pre- and Postintervention Study

Ahlam Alghamdi[1], PharmD; Afrah Alkazemi[2], PharmD; Alnada Ibrahim[1], PharmD; Mohammed Alraey[3], MD; Mohammed Alaboud[3], MD; Isra Farooqi[3], MD; Mohammad Aatif Khan[4], MD, PhD; Asem Allam[3], MD; Mohammed Alwadai[5], PharmD; Renad Alyahya[6]; Ohoud Alzahrani[6]; Hajar Y AlQahtani[7,8,9], PharmD; Amir Mohareb[10], MD; Muneerah Aleissa[1], PharmD

[1]Department of Pharmacy Practice, College of Pharmacy, Princess Nourah bint Abdulrahman University, P.O. Box 84428, Riyadh, Saudi Arabia

[10]Division of Infectious Diseases, Massachusetts General Hospital, Boston, MA, United States

[2]Department of Pharmacy Practice, College of Pharmacy, Kuwait University, Kuwait City, Kuwait

[3]Department of Infectious Diseases, King Abdullah bin Abdulaziz University Hospital, Riyadh, Saudi Arabia

[4]Microbiology Laboratory, Department of Pathology and Laboratory Medicine, King Abdullah Bin Abdul-Aziz University Hospital, Riyadh, Saudi Arabia

[5]Pharmaceutical Care Services, King Abdullah bin Abdulaziz University Hospital, Riyadh, Saudi Arabia

[6]College of Pharmacy, Princess Nourah bint Abdulrahman University, Riyadh, Saudi Arabia

[7]Department of Pharmaceutical Care, Ministry of National Guard Health Affairs, Riyadh, Saudi Arabia

[8]King Abdullah International Medical Research Center, Riyadh, Saudi Arabia

[9]King Saud Bin Abdul-Aziz University for Health Sciences, Riyadh, Saudi Arabia

Corresponding Author:
Muneerah Aleissa, PharmD
Department of Pharmacy Practice, College of Pharmacy, Princess Nourah bint Abdulrahman University, P.O. Box 84428, Riyadh, Saudi Arabia

Abstract

Background: Inappropriate testing of urine cultures can lead to overuse of antibiotics, antimicrobial resistance, *Clostridioides difficile* infections, and increased cost. In Saudi Arabia, antimicrobial stewardship programs have improved antibiotic use but lack focus on asymptomatic bacteriuria. Targeted interventions are needed to address this gap.

Objective: We assessed the implementation of a clinical decision support (CDS) tool in diagnostic stewardship, focusing on the appropriateness of urine culture orders and antibiotic use.

Methods: We examined differences in urine culture testing and antibiotic use before and after implementation of a CDS tool in a 400-bed hospital in Riyadh, Saudi Arabia, from August 2021 to July 2022. We included adult patients with urine culture orders. Our outcomes were the percentage of urine cultures ordered that were inappropriate and antibiotic use after the implementation of the CDS intervention. We used a multivariable logistic regression model to determine factors associated with inappropriate urine culture testing and antibiotic use.

Results: The percentage of inappropriate urine culture orders were significantly lower in the postintervention period compared to the preintervention period (821/2254, 36.4% vs 754/1814, 41.6%; *P*=.001). The CDS intervention was associated with 16.7% lower odds of inappropriate urine culture ordering (adjusted odds ratio [aOR] 0.83, 95% CI 0.73 - 0.95; *P*=.008). Unnecessary antibiotics were significantly lower in the postintervention period (310/2254, 72.9% vs 288/1814, 85.7%; *P*<.001). The CDS intervention was associated with a 52% reduction in unnecessary antibiotic use (aOR 0.487, 95% CL 0.332 - 0.713; *P*<.001)

Conclusions: A CDS initiative can reduce unnecessary urine culture testing and antibiotic overuse.

(JMIR Med Inform 2025;13:e68044) doi:10.2196/68044

KEYWORDS

urine culture; diagnostic stewardship; Saudi Arabia; automation; asymptomatic bacteriuria; antimicrobial stewardship program

Introduction

Urinary tract infections (UTIs) are common in both the inpatient and outpatient settings [1,2]. Despite being common, appropriate diagnosis and use of urine cultures remain a challenge. Inappropriate urine culture testing, for example, screening for asymptomatic bacteriuria (ASB), can be the first step in a chain of events that can lead to antibiotic overuse, antimicrobial

XSL•FO
RenderX

resistance (AMR), *Clostridioides difficile* infections, and increased health care cost [3]. Antimicrobial therapy is not recommended in most cases of ASB, and withholding treatment has no major adverse outcomes in most cases [4,5]. Current Infectious Diseases Society of America (IDSA) guidelines recommend screening for and treating ASB only in pregnant women or individuals undergoing invasive urologic procedures [6]. Despite these recommendations, ASB remain one of the most common causes of antimicrobial overuse, where up to 80% of patients with ASB are treated with antibiotics [7].

Challenges in the clinical differentiation between ASB and UTIs may offer a partial explanation for the excessive overtreatment of ASB [8]. Diagnostic stewardship of urine cultures can play an important role in reducing downstream overuse of antibiotics [7]. While many studies have evaluated stewardship of urine culture testing in Europe and North America, research is limited in other geographic settings [9]. For example, there are limited data about diagnostic stewardship of urine cultures from the Eastern Mediterranean region, which is a major research gap given the rising prevalence of AMR in that region [10]. In Saudi Arabia, antimicrobial stewardship programs (ASPs) have been successfully implemented to optimize antibiotic use and reduce antimicrobial resistance but have, thus far, generally lacked a focus on addressing antibiotic use associated with ASB [11]. Therefore, we sought to assess the impact of a clinical decision support (CDS) intervention on diagnostic stewardship, focusing on the appropriateness of urine culture orders and antibiotic use.

Methods

Overview

We conducted a quasiexperimental study at an academic medical center with 400 beds in Riyadh, Saudi Arabia. Our center is a referral center for women's health, pediatrics, and adolescent health. We compared clinical practice in a preintervention phase (August 2021 to January 2022) and a postintervention phase (February 2022 to July 2022) without incorporating a washout period, in both the inpatient and outpatient settings. We included adult patients (≥18 years old) with urine culture orders during the study period and excluded patients on antibiotics prescribed for infections prior to the urine culture and those with missing key data such as UTI signs and symptoms, laboratory results, and clear antibiotic indication.

Endpoints and Definitions

We assessed the impact of our CDS initiative on diagnostic stewardship through measuring inappropriate urine culture and antibiotic use. Appropriate practice for ordering a urine culture, as approved by the international guideline and institutional ASP committee, includes documentation of signs or symptoms of a UTI, pregnancy, and patients who are undergoing invasive urologic procedures, immunocompromised, or critically ill [6]. Therefore, we defined inappropriate urine culture testing in circumstances where patients had no documented signs or symptoms of a UTI, pregnancy, urologic procedures, immunosuppression, or critical illness [9]. Signs and symptoms of a UTI include dysuria, suprapubic pain, flank pain, costovertebral angle tenderness, septic shock, and altered mental status in older (≥65 years) patients [12]. Antibiotics prescribed for ASB without any of the approved indications listed above were deemed to be unnecessary.

Diagnostic Stewardship Interventions

We implemented the institutional ASP–approved CDS in electronic health records (EHRs) on February 1, 2022. The goal of this initiative is to serve as a voluntary guide for physicians to appropriately request urine cultures in the outpatient and inpatient settings. Prior to requesting any urine culture, appropriate urine request–directed questions are asked (Figure 1). If all answers are "no," an alert is triggered indicating that a urine culture may not be recommended for this patient. Physicians are able to override the CDS and still order a urine culture even if the alert is triggered. Alongside the CDS initiative's rollout, the ASP committee disseminated best practices related to UTI care, including indications for urine cultures, to all health care providers.

XSL•FO
RenderX

Figure 1. Urine culture request–directed questions implemented in the electronic health record. UTI: urinary tract infection.

A urine culture is recommended only if you answer "yes" to one or more questions	**Check ✓ if yes; X if no**
Does the patient have UTI signs and symptoms (dysuria, frequency, and urgency)?	
Is the patient pregnant?	
Is the patient undergoing a urologic procedure?	
Is the patient immunocompromised or critically ill?	

If all answers are "no," a clear message pops up: "urine culture request is not recommended."

Statistical Analysis

We analyzed categorical data using a chi-square test or Fisher exact test, as appropriate, and continuous data using a Student *t* test. We also used a multivariable logistic regression model, adjusting for age, sex, diabetes mellitus, and chronic kidney disease, to evaluate the association between our CDS intervention and inappropriate urine culture orders and unnecessary antibiotic use. All analyses were conducted in STATA/BE (version 18; StataCorp).

Ethical Considerations

Ethical approval was obtained from the Institutional Review Board of King Abdullah bin Abdul-Aziz University Hospital (IRB log number: 22 - 0005). As this was a retrospective study, informed consent was not required. The study protocol was reviewed and approved by the institutional review board, which granted a waiver of informed consent in accordance with national and institutional ethical guidelines. All data were deidentified prior to analysis. Data were handled securely in compliance with institutional data protection policies to ensure participant confidentiality.

Results

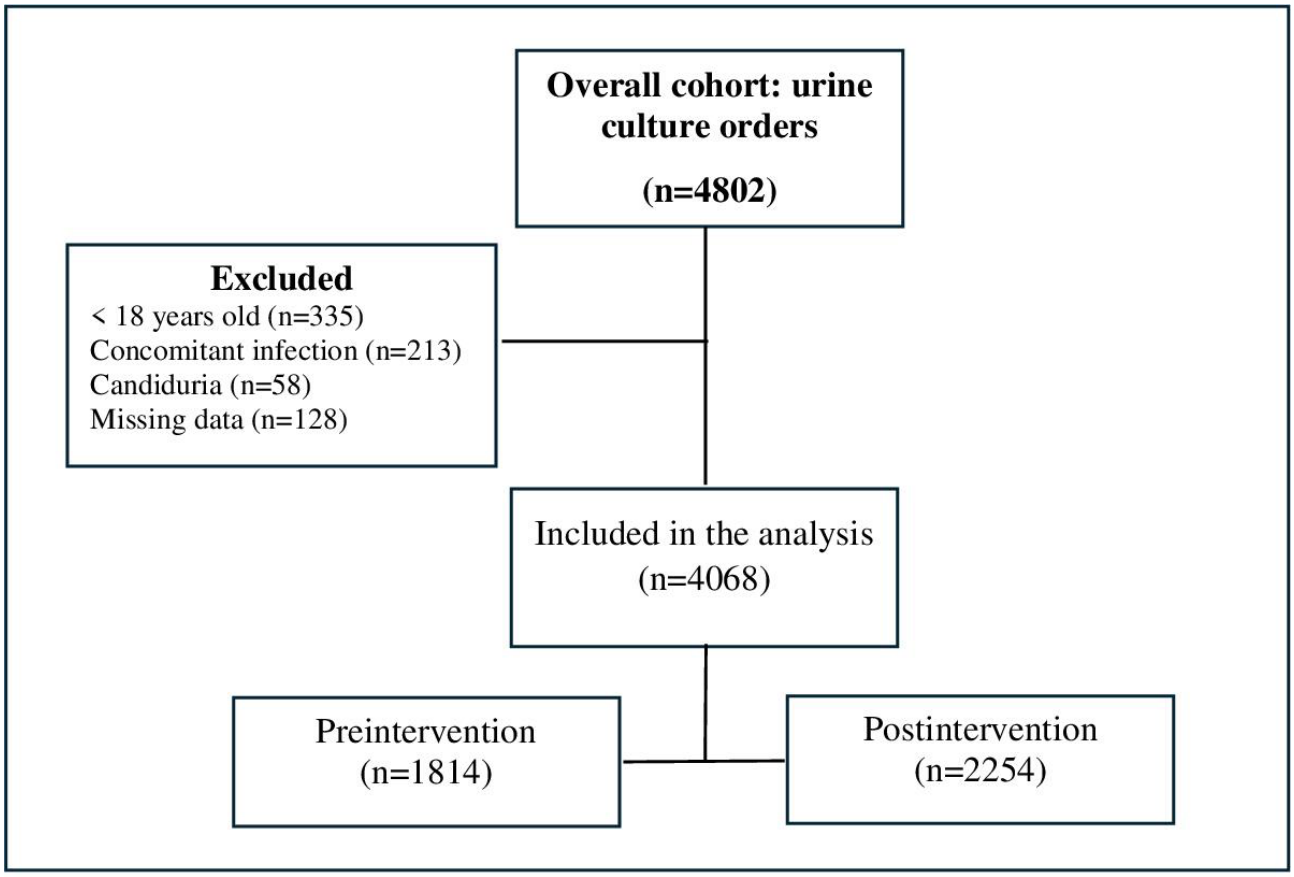
During the study period, we identified 4068 urine culture orders among 3846 unique patients, of which 1814 were ordered in the preintervention period and 2254 in the postintervention period (Figure 2). Demographic information about the study participants is shown in Table 1. The mean age was 42.2 (17.40) years and the majority were female (3068/4068, 75.4%), which is consistent with our clinical setting. Approximately 33% (1375/4068) of patients were pregnant, 4.4% (180/4068) underwent urologic procedures, 4.4% (181/4068) were immunocompromised, and 1.8% (75/4068) were critically ill. Overall, 10.6% (435/4068) had a positive urine culture, of which 32.9% (n=143) were symptomatic and 67.1% (n=292) were asymptomatic (Table 1).

Inappropriate urine culture orders, per our stewardship initiative criteria, were significantly lower in the postintervention period compared to the preintervention period (821/2254, 36.4% vs 754/1814, 41.6%, respectively; *P*=.001). The CDS intervention was associated with a 20% reduction in inappropriate urine culture orders (odds ratio [OR] 0.805; 95% Cl 0.71 - 0.91; *P*=.001). In a multivariable logistic regression adjusting for possible confounders, the CDS intervention was associated with 16.7% lower odds of inappropriate urine culture ordering based on our ordering criteria (adjusted odds ratio [aOR] 0.83; 95% CI 0.73 - 0.95; *P*=.008; Table 2).

Additionally, we found that 1097 antibiotic regimens were prescribed: 336 in the preintervention period and 761 in the postintervention period. The use of unnecessary antibiotics was significantly lower in the postintervention period versus the preintervention period (310/2254, 72.9% vs 288/1814, 85.7%, respectively; *P*<.001). Our CDS intervention was associated with a 55% reduction in the unnecessary antibiotic use (OR 0.449; 95% CI 0.309 - 0.65; *P*<.001). In a multivariable logistic regression adjusting for possible confounding variables, the CDS intervention was associated with a 52% reduction in unnecessary antibiotic use (aOR 0.487; 95% CI 0.332 - 0.713; *P*<.001; Table 2).

XSL•FO
RenderX

Figure 2. Flow diagram of study participants who had urine culture orders.



XSL•FO
RenderX

Table . Characteristics of patients who had urine culture orders (N=4068) in the preintervention and postintervention periods, Saudia Arabia, August 2021 to July 2022.

	Preintervention (n=1814)	Postintervention (n=2254)	*P* value
Age (years), mean (SD)	42.04 (17.42)	42.42 (17.46)	.50
Sex (female), n (%)	1254 (69.1)	1814 (80.5)	<.001
Medical comorbidities, n (%)			
Heart disease	122 (6.7)	135 (6)	.34
Diabetes mellitus	369 (20.3)	442 (19.6)	.56
Hypertension	294 (16.2)	398 (17.7)	.22
Chronic kidney disease	74 (4.1)	51 (2.3)	.001
Liver disease	6 (0.3)	8 (0.4)	.90
Respiratory disease	133 (7.3)	223 (9.9)	.004
Active malignancy	8 (0.4)	15 (0.7)	.34
Pregnancy, n (%)	627 (34.6)	748 (33.2)	.36
Urologic procedure, n (%)	18 (1)	162 (7.2)	<.001
Immunosuppressant agent, n (%)	35 (1.9)	146 (6.5)	<.001
ICU[a] at index culture, n (%)	47 (2.6)	28 (1.2)	<.001
Urine culture characteristics, n (%)			
Positive urine culture	165 (9.1)	270 (12)	.003
UTI[b]	24 (14.5)	119 (44)	<.001
ASB[c]	141 (85.5)	151 (56)	.19

[a]ICU: intensive care unit.

[b]UTI: urinary tract infection.

[c]ASB: asymptomatic bacteriuria.

Table . Outcomes of the clinical decision support (CDS) initiative at pre- and postintervention using logistic regression model.

Outcome	Unadjusted odds ratio (OR)		Adjusted odds ratio (aOR)[a]	
	OR (95% CI)	*P* value	aOR (95% CI)	*P* value
Inappropriate urine culture orders post- versus preintervention	0.805 (0.710 - 0.914)	<.001	0.83 (0.73 - 0.95)	.008
Unnecessary antibiotic use post- versus preintervention	0.449 (0.309 - 0.652)	<.001	0.487 (0.332 - 0.713)	<.001

[a]Adjusting for age, sex, diabetes mellitus, and chronic kidney disease.

Discussion

Principal Findings

To our knowledge, this is the first study to evaluate a diagnostic stewardship initiative targeting inappropriate urine culture orders and unnecessary antibiotic use in patients with UTIs and ASB in Saudi Arabia. Numerous stewardship programs have been implemented in various geographic regions to reduce unnecessary antibiotic use for ASB [13]. Some of these initiatives include continuous education, pocket cards, audit and feedback, and computer-based reminders [13]. In this study, we used a CDS tool embedded in EHRs to guide the physicians to appropriately order urine cultures, which could lead to a reduction in unnecessary antibiotic use. The CDS initiative we implemented successfully decreased inappropriate screening for ASB as measured by the decrease in urine culture orders. Similarly, our initiative also successfully decreased ASB overtreatment as measured by the decrease in unnecessary antibiotic use. While antibiotic prescriptions were numerically higher in the postintervention phase compared to the preintervention phase, the percentage of unnecessary antibiotics was significantly lower in the postintervention phase. The higher number of antibiotics prescribed is likely due to the fact that the postintervention phase comprised a higher proportion of patients who underwent urologic procedures or were immunocompromised. By implementing a CDS tool to address inappropriate urine culture orders and unnecessary antibiotic use in patients with ASB, our study contributes directly to efforts aimed at optimizing antimicrobial stewardship in Saudi Arabia.

XSL•FO
RenderX

The rise of AMR is a global public health crisis, associated with rising morbidity, mortality, and health care costs [14]. Single-center reports suggest a high prevalence of multidrug-resistant organisms, which complicate patient care and threaten gains made from other public health advances in the region [15,16]. In Saudi Arabia, as in many international settings, antimicrobial use is not well regulated and injudicious use of antibiotics is a major factor for AMR development [17]. Recent studies demonstrate that inappropriate antibiotic use in the management of UTIs is approximately 50%, with the primary reason being ASB [18,19]. In our study, the use of unnecessary antibiotics decreased by 52%, highlighting the value of our CDS tool to potentially aid in reducing the rate of AMR in Saudi Arabia.

Several studies have explored other diagnostic stewardship interventions aimed at reducing unnecessary antimicrobial therapy for UTIs and ASB. A recent study that was done in Hong Kong found that suppressed urine culture results led to a 23% reduction in antimicrobial use [20]. Similarly, another study implemented an initiative of not reporting positive urine culture results unless requested via telephone, which led to a decrease in antimicrobial use by 36% [21]. These findings collectively support the effectiveness of targeted interventions in optimizing diagnostic practices and antimicrobial stewardship. By reducing the number of unnecessary urine cultures, health care providers can reduce inappropriate antibiotic use, thus aligning with efforts to combat AMR and improve patient care outcomes.

Our study has limitations. First, as this was a retrospective analysis of a quality improvement project, the results are possibly susceptible to confounding factors. While we accounted for several factors influencing antimicrobial use in our multivariable regression model, these findings should be further confirmed in controlled prospective studies. Future studies should specifically evaluate outpatient versus inpatient urine culture ordering, which we were not able to do through our form of data collection. Moreover, our study may not be generalizable to other hospitals in the region, given that it was a single-centered study. Finally, although the assessments of unnecessary antibiotics were conducted by infectious disease specialists, they were not formally validated, potentially leading to discrepancies between evaluators.

Conclusions

In summary, we implemented an ASP-approved CDS initiative to optimize urine culture testing and antimicrobial use and to reduce overtreatment of ASB. This initiative resulted in a 16.7% reduction in urine culture testing and a 52% reduction in antimicrobial use for UTIs. This is one of the few studies of such initiatives from the Eastern Mediterranean region, which is a site of rising AMR.

Acknowledgments

This research was financially supported by the Princess Nourah bint Abdulrahman University Researchers Supporting Project (PNURSP2024R336), Princess Nourah bint Abdulrahman University, Riyadh, Saudi Arabia. All authors have approved the final paper and declare that they have no known competing financial interests or personal relationships that could have appeared to influence the work reported in this paper.

Data Availability

The aggregate dataset used in this study is available from the corresponding author on reasonable request.

Conflicts of Interest

None declared.

References

1. Claeys KC, Blanco N, Morgan DJ, Leekha S, Sullivan KV. Advances and challenges in the diagnosis and treatment of urinary tract infections: the need for diagnostic stewardship. Curr Infect Dis Rep 2019 Mar 5;21(4):11. [doi: 10.1007/s11908-019-0668-7] [Medline: 30834993]
2. Sula I, Alreshidi MA, Alnasr N, Hassaneen AM, Saquib N. Urinary tract infections in the Kingdom of Saudi Arabia, a review. Microorganisms 2023 Apr 6;11(4):952. [doi: 10.3390/microorganisms11040952] [Medline: 37110375]
3. Grigoryan L, Naik AD, Lichtenberger P, et al. Analysis of an antibiotic stewardship program for asymptomatic bacteriuria in the Veterans Affairs health care system. JAMA Netw Open 2022 Jul 1;5(7):e2222530. [doi: 10.1001/jamanetworkopen.2022.22530] [Medline: 35877123]
4. Trautner BW, Grigoryan L. Approach to a positive urine culture in a patient without urinary symptoms. Infect Dis Clin North Am 2014 Mar;28(1):15-31. [doi: 10.1016/j.idc.2013.09.005] [Medline: 24484572]
5. Raz R. Asymptomatic bacteriuria. Clinical significance and management. Int J Antimicrob Agents 2003 Oct;22 Suppl 2:45-47. [doi: 10.1016/s0924-8579(03)00248-6] [Medline: 14527770]
6. Nicolle LE, Gupta K, Bradley SF, et al. Clinical practice guideline for the management of asymptomatic bacteriuria: 2019 update by the Infectious Diseases Society of America. Clin Infect Dis 2019 May 2;68(10):e83-e110. [doi: 10.1093/cid/ciy1121] [Medline: 30895288]

XSL•FO
RenderX

7. Vaughn VM, Gupta A, Petty LA, et al. A statewide quality initiative to reduce unnecessary antibiotic treatment of asymptomatic bacteriuria. JAMA Intern Med 2023 Sep 1;183(9):933-941. [doi: 10.1001/jamainternmed.2023.2749] [Medline: 37428491]
8. Walker S, McGeer A, Simor AE, Armstrong-Evans M, Loeb M. Why are antibiotics prescribed for asymptomatic bacteriuria in institutionalized elderly people? A qualitative study of physicians' and nurses' perceptions. CMAJ 2000 Aug 8;163(3):273-277. [Medline: 10951723]
9. Flokas ME, Andreatos N, Alevizakos M, Kalbasi A, Onur P, Mylonakis E. Inappropriate management of asymptomatic patients with positive urine cultures: a systematic review and meta-analysis. Open Forum Infect Dis 2017;4(4):ofx207. [doi: 10.1093/ofid/ofx207] [Medline: 29226170]
10. Talaat M, Zayed B, Tolba S, et al. Increasing antimicrobial resistance in World Health Organization Eastern Mediterranean Region, 2017-2019. Emerg Infect Dis 2022 Apr;28(4):717-724. [doi: 10.3201/eid2804.211975] [Medline: 35318915]
11. Alghamdi S, Berrou I, Aslanpour Z, et al. Antimicrobial stewardship programmes in Saudi hospitals: evidence from a national survey. Antibiotics (Basel) 2021 Feb 17;10(2):193. [doi: 10.3390/antibiotics10020193] [Medline: 33671401]
12. Claeys KC, Trautner BW, Leekha S, et al. Optimal urine culture diagnostic stewardship practice-results from an expert modified-delphi procedure. Clin Infect Dis 2022 Aug 31;75(3):382-389. [doi: 10.1093/cid/ciab987] [Medline: 34849637]
13. Wiley Z, Jacob JT, Burd EM. Targeting asymptomatic bacteriuria in antimicrobial stewardship: the role of the microbiology laboratory. J Clin Microbiol 2020 Apr 23;58(5):e00518-18. [doi: 10.1128/JCM.00518-18] [Medline: 32051261]
14. Antimicrobial Resistance Collaborators. Global burden of bacterial antimicrobial resistance in 2019: a systematic analysis. Lancet 2022 Feb 12;399(10325):629-655. [doi: 10.1016/S0140-6736(21)02724-0]
15. Marston HD, Dixon DM, Knisely JM, Palmore TN, Fauci AS. Antimicrobial resistance. JAMA 2016 Sep 20;316(11):1193-1204. [doi: 10.1001/jama.2016.11764] [Medline: 27654605]
16. Dandachi I, Chaddad A, Hanna J, Matta J, Daoud Z. Understanding the epidemiology of multi-drug resistant gram-negative bacilli in the Middle East using a one health approach. Front Microbiol 2019;10:1941. [doi: 10.3389/fmicb.2019.01941] [Medline: 31507558]
17. Zowawi HM. Antimicrobial resistance in Saudi Arabia. An urgent call for an immediate action. Saudi Med J 2016 Sep;37(9):935-940. [doi: 10.15537/smj.2016.9.16139] [Medline: 27570847]
18. Alanazi MQ, Al-Jeraisy MI, Salam M. Prevalence and predictors of antibiotic prescription errors in an emergency department, Central Saudi Arabia. Drug Healthc Patient Saf 2015;7:103-111. [doi: 10.2147/DHPS.S83770] [Medline: 26082662]
19. Alanazi MQ. An evaluation of community-acquired urinary tract infection and appropriateness of treatment in an emergency department in Saudi Arabia. Ther Clin Risk Manag 2018;14:2363-2373. [doi: 10.2147/TCRM.S178855] [Medline: 30584311]
20. Lee ALH, Leung ECM, Lee MKP, Lai RWM. Diagnostic stewardship programme for urine culture: impact on antimicrobial prescription in a multi-centre cohort. J Hosp Infect 2021 Feb;108:81-89. [doi: 10.1016/j.jhin.2020.10.027] [Medline: 33181278]
21. Leis JA, Rebick GW, Daneman N, et al. Reducing antimicrobial therapy for asymptomatic bacteriuria among noncatheterized inpatients: a proof-of-concept study. Clin Infect Dis 2014 Apr;58(7):980-983. [doi: 10.1093/cid/ciu010] [Medline: 24577290]

Abbreviations

AMR: antimicrobial resistance
aOR: adjusted odds ratio
ASB: asymptomatic bacteriuria
ASP: antimicrobial stewardship program
CDS: clinical decision support
EHR: electronic health record
IDSA: Infectious Diseases Society of America
OR: odds ratio
UTI: urinary tract infection

Edited by C Perrin; submitted 30.10.24; peer-reviewed by E Okoyeocha, J Strebe, MV Ebrahim, Y Wang; revised version received 13.05.25; accepted 26.05.25; published 23.07.25.

Please cite as:
Alghamdi A, Alkazemi A, Ibrahim A, Alraey M, Alaboud M, Farooqi I, Aatif Khan M, Allam A, Alwadai M, Alyahya R, Alzahrani O, AlQahtani HY, Mohareb A, Aleissa M
Impact of Diagnostic Stewardship on Urine Culture Ordering in Saudi Arabia: Prospective Pre- and Postintervention Study
JMIR Med Inform 2025;13:e68044
URL: https://medinform.jmir.org/2025/1/e68044
doi:10.2196/68044

XSL•FO
RenderX

© Ahlam Alghamdi, Afrah Alkazemi, Alnada Ibrahim, Mohammed Alraey, Mohammed Alaboud, Isra Farooqi, Mohammad Aatif Khan, Asem Allam, Mohammed Alwadai, Renad Alyahya, Ohoud Alzahrani, Hajar Y AlQahtani, Amir Mohareb, Muneerah Aleissa. Originally published in JMIR Medical Informatics (https://medinform.jmir.org), 23.7.2025. This is an open-access article distributed under the terms of the Creative Commons Attribution License (https://creativecommons.org/licenses/by/4.0/), which permits unrestricted use, distribution, and reproduction in any medium, provided the original work, first published in JMIR Medical Informatics, is properly cited. The complete bibliographic information, a link to the original publication on https://medinform.jmir.org/, as well as this copyright and license information must be included.

XSL•FO
RenderX

Process for Quality Management of Electronic Medical Records–Based Data: Case Study Using Real Colorectal Cancer Data

NaYoung Park[1,2], MPH; Kyungmin Na[3], BS; Woongsang Sunwoo[4], MD, PhD; Jeong-Heum Baek[5], MD, PhD; Youngho Lee[3], PhD; Suehyun Lee[3*], PhD; Hyekyung Woo[1*], PhD

[1]Department of Health Administration, Kongju National University, Gongju-Si, Chungcheongnam-do, Gongju, Republic of Korea

[2]Office of eHealth Research and Business, Seoul National University Bundang Hospital, Seongnam-si, Republic of Korea

[3]Department of Computer Engineering, College of IT Convergence, Gachon University, Seongnam, Republic of Korea

[4]Department of Otorhinolaryngology, Gil Medical Center, Gachon University, College of Medicine, Incheon, Republic of Korea

[5]Division of Colon and Rectal Surgery, Department of Surgery, Gil Medical Center, Gachon University, College of Medicine, Incheon, Republic of Korea

[*]these authors contributed equally

Corresponding Author:
Hyekyung Woo, PhD
Department of Health Administration, Kongju National University, Gongju-Si, Chungcheongnam-do, Gongju, Republic of Korea

Abstract

Background: As data-driven medical research advances, vast amounts of medical data are being collected, giving researchers access to important information. However, issues such as heterogeneity, complexity, and incompleteness of datasets limit their practical use. Errors and missing data negatively affect artificial intelligence–based predictive models, undermining the reliability of clinical decision-making. Thus, it is important to develop a quality management process (QMP) for clinical data.

Objective: This study aimed to develop a rules-based QMP to address errors and impute missing values in real-world data, establishing high-quality data for clinical research.

Methods: We used clinical data from 6491 patients with colorectal cancer (CRC) collected at Gachon University Gil Medical Center between 2010 and 2022, leveraging the clinical library established within the Korea Clinical Data Use Network for Research Excellence. First, we conducted a literature review on the prognostic prediction of CRC to assess whether the data met our research purposes, comparing selected variables with real-world data. A labeling process was then implemented to extract key variables, which facilitated the creation of an automatic staging library. This library, combined with a rule-based process, allowed for systematic analysis and evaluation.

Results: Theoretically, the tumor, node, metastasis (TNM) stage was identified as an important prognostic factor for CRC, but it was not selected through feature selection in real-world data. After applying the QMP, rates of missing data were reduced from 75.3% to 35.7% for TNM and from 24.3% to 18.5% for surveillance, epidemiology, and end results across 6491 cases, confirming the system's effectiveness. Variable importance analysis through feature selection revealed that TNM stage and detailed code variables, which were previously unselected, were included in the improved model.

Conclusions: In sum, we developed a rules-based QMP to address errors and impute missing values in Korea Clinical Data Use Network for Research Excellence data, enhancing data quality. The applicability of the process to real-world datasets highlights its potential for broader use in clinical studies and cancer research.

(JMIR Med Inform 2025;13:e73884) doi:10.2196/73884

KEYWORDS

quality management; medical data; real-world data; colorectal cancer; data quality

Introduction

Medical datasets include various forms of data such as patients' health status, diagnosis, and treatment information, collected through electronic medical records, diagnostic tests, and treatment records [1]. These data support patient-specific treatment and accurate decision-making by medical professionals [2]. With the growing importance of data-driven medical research, studies using medical data have become increasingly common [3,4]. Advancements in artificial intelligence (AI) and machine learning technologies have further

XSL•FO
RenderX

expanded the potential uses of these data, such as for early disease diagnosis and prediction model development [5].

As the volume of medical data grows, infrastructures are being established to analyze and use the data efficiently [6]. Data sharing and linkage enable researchers to access the necessary data more easily. However, challenges such as heterogeneity and incompleteness of datasets remain [7]. For example, during the pseudonymization of integrated medical data, some information may be restricted, and differences in data formats or structures can compromise consistency during adjustment.

Issues such as missing data, inconsistencies, and errors can degrade data quality [8]. Medical data often exhibit imbalance, where some categories of data are underrepresented, which can lead to biased learning and distorted outcomes in AI-based predictive models [9,10]. These quality issues can undermine the reliability of analysis results. Therefore, it is essential to develop a quality management process (QMP) to correct errors and supplement data to improve the quality of medical data and build high-quality datasets. Given the current shortage of specialized personnel trained in handling and managing raw data, it is crucial to manage data quality effectively and enhance usability through systematic and standardized QMPs.

In the medical field, an increasing number of studies have addressed data quality issues [11]. Evaluations of data quality using colon cancer data and proposals for QMPs and frameworks are gaining traction [12,13]. Recently, new methodologies for managing the quality of AI training data have been introduced [14], helping to establish high-quality datasets that meet research purposes for diagnosis and prognosis prediction [15]. While medical data play a decisive role in clinical research and patient treatment, systematic quality management that ensures the consistency, accuracy, and completeness of data is crucial for solving various errors and dealing with missing information [16]. Although comprehensive quality management methodologies for the medical data collection stage are emerging [17], processes applicable to real-world data (RWD) are still lacking.

Therefore, the aim of this study is to develop a QMP for colorectal cancer (CRC) data from the Korea Clinical Data Use Network for Research Excellence (K-CURE). This process was designed to systematically align with the research objectives, identifying key prognostic variables for CRC. We implemented a rule-based approach to improve data completeness and evaluated the effectiveness of the QMP by comparing the data before and after its application.

Methods

Stage 1: Planning Stage

Data Resources

We used CRC clinical library data established in the K-CURE project at Gachon University Gil Medical Center, approved for use through an institutional review board exemption (GFIRB2024-169). The K-CURE project supports AI-based research and technology development by sharing, providing access to, and linking clinical data from various hospitals. We used a pseudonymized clinical library of 6491 patients with CRC, collected between 2010 and 2022 for the K-CURE project. The pseudonymized clinical library refers to a deidentified dataset in which personally identifiable information has been removed and replaced with pseudonyms. The K-CURE clinical library includes patient information, medical history, diagnoses, cancer staging, test results, treatments, and follow-up data. In addition, structured text-based reports of imaging test results and pathology data from the clinical library were integrated to perform quality management.

Ethical Considerations

The study used CRC clinical library data established in the K-CURE project at Gachon University Gil Medical Center, which was approved for use through an institutional review board exemption (GFIRB2024-169). The dataset was pseudonymized, and personally identifiable information was removed and replaced with pseudonyms. Informed consent was waived due to the use of deidentified retrospective data. No compensation was provided to participants. Privacy and confidentiality of patient data were strictly maintained throughout the study.

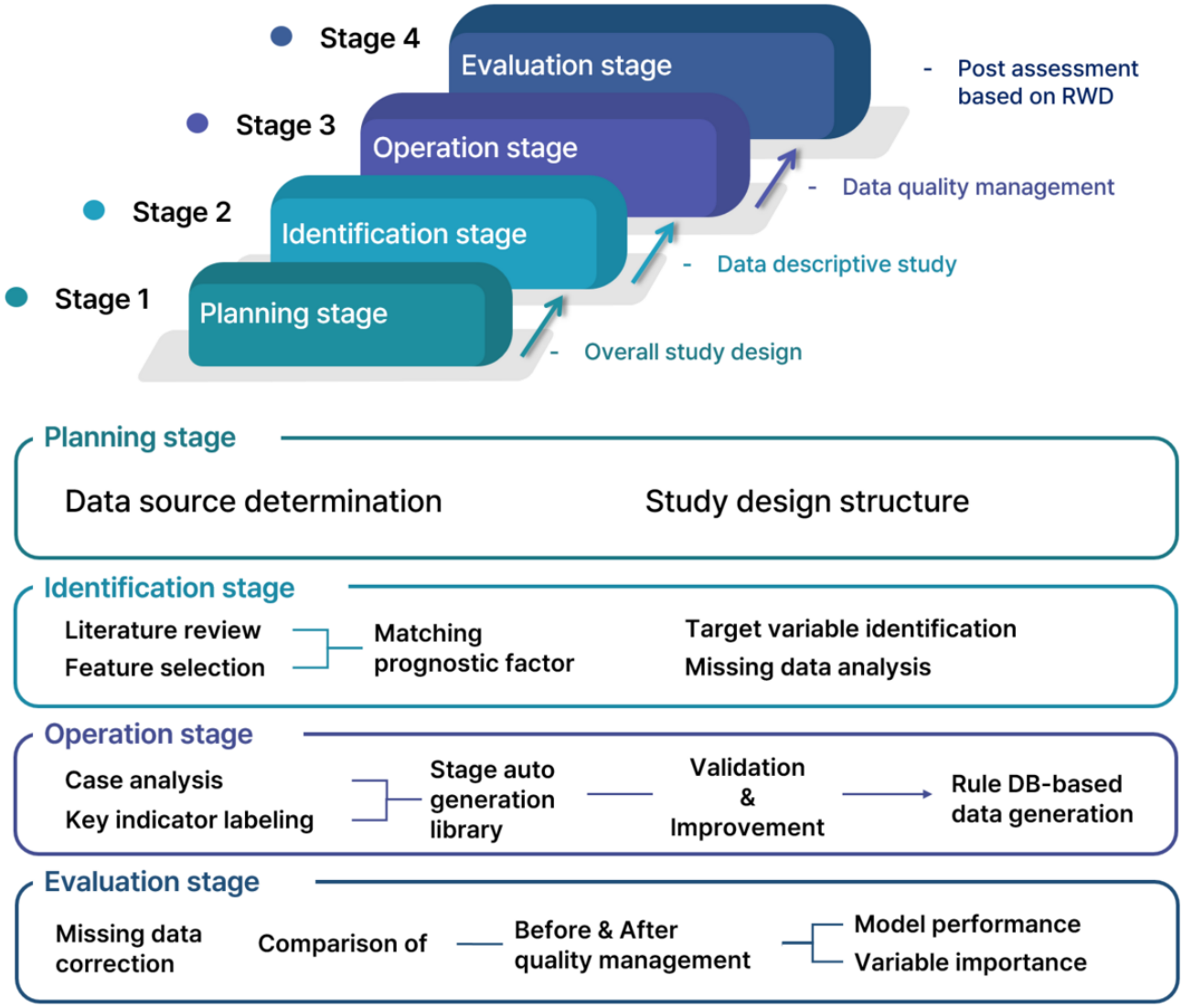
Study Design

In Stage 1, we planned the overall research design to establish a QMP for clinical data that meets our research objectives. To systematize the quality management procedures, we designed a detailed step-by-step process across 4 stages: planning, identification, operation, and evaluation.

In the identification stage, we assessed the general status of the RWD to identify areas requiring quality management. In the operation stage, the QMP was applied to the identified targets. Finally, in the evaluation stage, we compared the pre- and post-quality management results to assess improvements in the data. The overall flow of this study is presented in Figure 1.

XSL•FO
RenderX

Figure 1. Study design. DB: Database; RWD: real-world data.



Stage 2: Identification Stage

Literature Review to Identify Prognostic Factors

In Stage 2, we conducted a literature review to verify whether the K-CURE CRC data are suitable for constructing a prognostic prediction model. In particular, we sought to identify the key factors influencing the prognosis of patients with CRC and the major variables to consider for constructing a prognostic prediction model for CRC. We searched PubMed for articles published from 2010 to 2024. Our key search terms were (CRC OR colorectal OR CRC) AND (prognosis OR prognostic factor OR predict OR risk factor). The inclusion criteria were as follows: articles published between January 1, 2010, and March 31, 2024, and studies that focused on overall survival, mortality, or 5-year survival as dependent variables. The exclusion criteria included studies with low relevance to the topic or insufficient information on prognostic factors for patients with CRC, and those that discussed only a research design without specific findings. Key influencing factors identified from the selected literature were quantified, and theoretically important factors were derived. These were then used to establish variables for the prognostic prediction model.

Feature Selection for Identifying Prognostic Factors

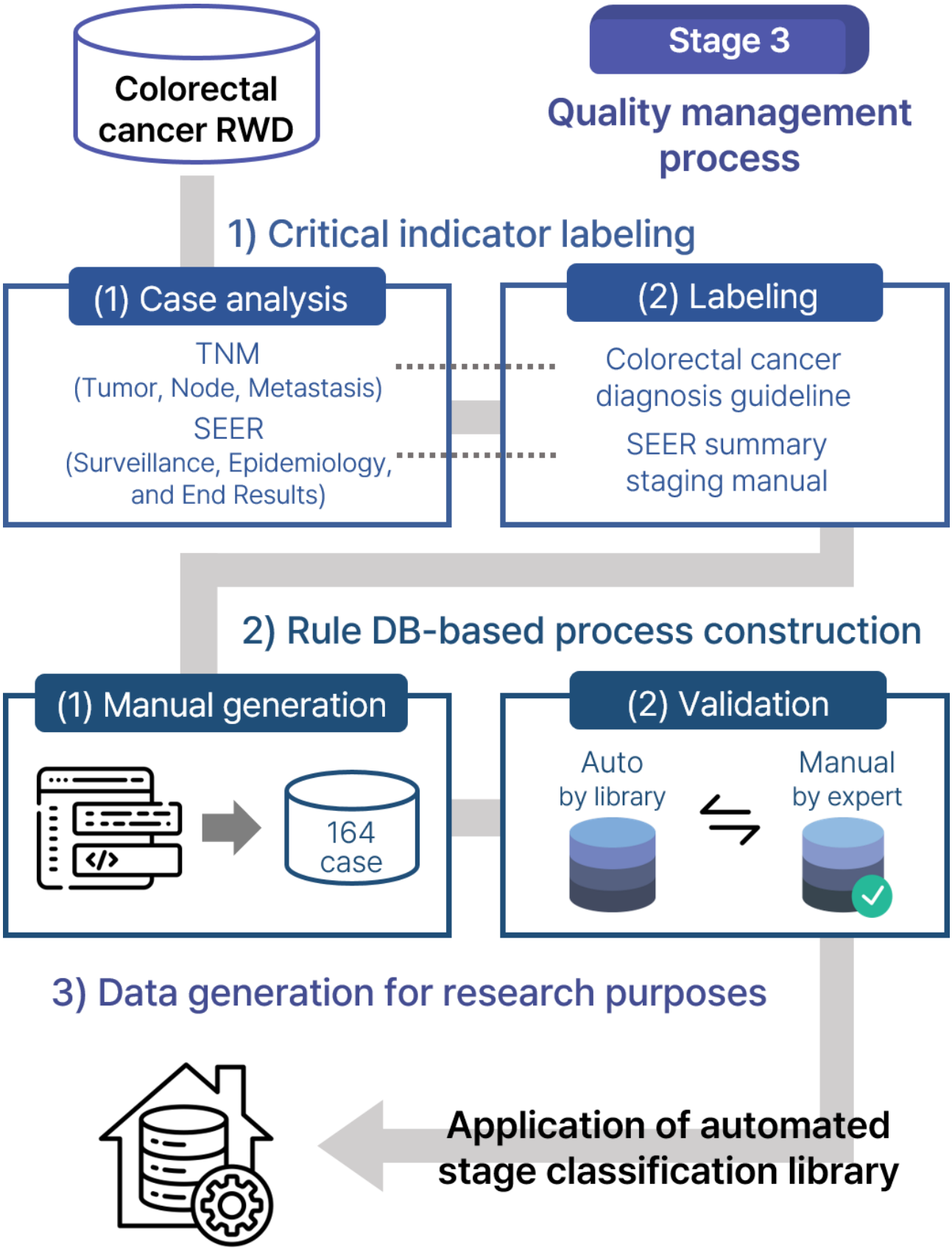
We performed feature selection to identify prognostic factors in the K-CURE CRC data. The Gradient Boosting Classifier was used to evaluate the importance of variables, and the results were compared to theoretically important variables. This model was selected due to its robustness in handling missing values and its effectiveness in evaluating variable importance, which makes it suitable for real-world clinical datasets [18]. Variables with low importance or those inconsistent with the literature review findings were selected as target variables requiring quality management. To conduct quality management, we performed frequency analysis of the major variables of the prognostic prediction model. Then, the error and missing data rates for these target variables were reviewed to examine the overall data distribution. The rate of missing data was calculated using frequency analysis for each variable. Error rates were measured by comparing manually generated stage codes with the data of 164 randomly selected samples, limited to cases without missing data.

Stage 3: Operation Stage

Figure 2 provides a schematic of the overall QMP.

XSL•FO
RenderX

Figure 2. Schematic diagram of our proposed quality management program. RWD: real-world data; SEER: surveillance, epidemiology, and end result; TNM: tumor, node, metastasis.



XSL•FO
RenderX

Critical Indicator Labeling for Automated Stage Classification Library

The target variables, tumor, node, and metastasis (TNM) and surveillance, epidemiology, and end results (SEER), are critical indicators for evaluating CRC staging. TNM stage is a standardized cancer stage classification system of the American Joint Committee on Cancer, based on the 8th edition of the American Joint Committee on Cancer Cancer Staging Manual [19]. It evaluates the progression of cancer based on tumor depth, lymph node metastasis, and distant metastasis. SEER summary stage is a standardized cancer staging system widely used in international cancer registration systems to classify how far cancer spreads from the primary site of origin.

Before establishing the QMP, a case analysis was conducted to correct errors and address missing data in the target variables. This analysis involved a detailed review of the TNM and SEER variables of cases in the CRC sample data. We identified cases for which the staging information was omitted or incorrectly recorded to assess the completeness and accuracy of the TNM and SEER variables. We also confirmed whether the missing or erroneous staging information could be supplemented using pathology reports and imaging test results according to a standardized classification system.

To identify key indicators for extracting target variables, we referred to the CRC guidelines, "Korean Clinical Guideline for Colon and Rectal Cancer v.1.0 [20]," and the most recent SEER manual, "Summary Stage 18[21]." Labeling was conducted on specific words and keywords to identify detailed codes for TNM and SEER in the pathology report and imaging test results, respectively. In the labeling process, medical knowledge related to CRC was incorporated to establish coding conditions and patterns for accurate staging extraction.

Development of QMPs and Improving CRC Data for Research

In total, 164 cases were randomly selected, and TNM and SEER codes were manually generated for each case. This process adhered to standardized guidelines and protocols for CRC diagnosis and staging classification. To evaluate data quality, the manually generated codes were compared with the corresponding codes in the existing dataset for the same cases, excluding those with missing values. The error rate was calculated based on the number of discrepancies identified through this comparison. The manually generated TNM and SEER code data were also used as reference criteria for validating the automated stage classification library and used as basic data to evaluate the accuracy and consistency of the generated codes.

We evaluated whether the automated library corresponded to guidelines in terms of extracting accurate staging information from clinical data. Then, the accuracy of the library was verified by comparing the concordance between the manually generated TNM and SEER codes and the codes derived from the library. This process focused on the consistency of codes, reasons for discrepancies, and major patterns.

Stage 4: Evaluation Stage

In Stage 4, the data generated by applying the QMP was evaluated. By comparing the rates of missing data for target variables before and after quality management, we could confirm to what extent the missing values were corrected through the process. Based on the data before and after quality management, initial and improved prognosis prediction models were constructed, and their performances were compared. Model performance was evaluated according to metrics such as accuracy, precision, recall, F_1-score, and area under the receiver operating characteristic curve, to assess whether the application of the QMP improved predictive performance. In addition, we analyzed the impact of target variables on CRC prognosis by checking the importance of variables in the model through feature selection before and after quality management. The prognosis prediction model was constructed using the Gradient Boosting algorithm, and the dependent variable was set as 5-year survival using death information. Python (version 3.12) was used for statistical analysis.

Results

Stage 2: Data Descriptive Study Results

Based on the literature review, the most frequently identified prognostic factors were T stage (tumor invasion depth) and N stage (lymph node metastasis), cited in 33 and 32 articles, respectively. Other significant factors included M stage (distant metastasis), the integrated TNM staging system, tumor location, pathological differentiation, and carcinoembryonic antigen levels. Staging may be classified as clinical TNM, pathological TNM, or postneoadjuvant pathological TNM.

As a result of stage 2, variables requiring quality management were identified. A summary of the variables derived from the literature review and feature selection is presented in Table 1. As target variables, we selected TNM stage and SEER, which are theoretically important for prognostic prediction.

XSL•FO
RenderX

Table . Comparison of literature review and feature selection results.

Factors	Values
Literature review, prognostic factors (n)	
Prognostic factors	N
T stage (depth of invasion)	33
N stage (lymph node metastasis)	32
M stage (distant metastasis)	11
Tumor, node, metastasis staging	18
Tumor grade or pathology	40
Carcinoembryonic antigen (ng/mL)	36
Tumor diameter/length/size (cm)	25
Histological type	20
Neutrophil-to-lymphocyte ratio	15
Adjuvant chemotherapy	20
Liver metastasis	13
Lymphatic invasion	11
Platelet-to-lymphocyte ratio	8
Lymphocyte-to-monocyte ratio	8
Number of retrieved lymph nodes	8
Venous invasion	7
Chemotherapy	7
ECOG (performance status)	7
Vascular invasion	6
Perineural invasion	5
Metastatic site (number of)	5
CA19-9 (U/ml)	5
Glasgow prognostic score	5
American Society of Anesthesiologists grade	5
Feature selection, importance	
Year of initial visit_2022	0.231758
SEER[a]_2.0	0.172401
Age	0.047391
Histological diagnosis_16.0	0.045125
Current_drinking_status_1.0	0.037545
Year of initial visit_2017	0.037528
Perineural invasion_3.0	0.036643
Family history_cancer_1.0	0.033641
Perineural invasion_2.0	0.033559
Perineural invasion_nan	0.033198
Primary site_C18.5	0.02482
Current_smoke_status_nan	0.022937
Histological diagnosis_26.0	0.020962
Histological diagnosis_23.0	0.01356
Primary site_C18.1	0.012204

XSL•FO
RenderX

Factors	Values
Lymphatic invasion_2.0	0.011136
TNM_T4N2M1	0.010998
Primary site_C18	0.010715
Primary site_C18.3	0.010592
Primary site_K83.8	0.010291
Molecular_pathology_findings_nan	0.008958
Primary site_C17.0	0.008938
BMI	0.008858

[a]SEER: surveillance, epidemiology, and end results.

The results of the frequency analysis of the major variables are shown in Table 2. Among the key variables, missing data were observed for height, weight, BMI, total lymph nodes, positive lymph nodes, and the target variables TNM and SEER. The rate of missing data for TNM stage was notably high at 75.3%, while that for SEER was 24.3% across 6491 cases. Moreover, when the error rate was measured using manually generated stage codes from 164 randomly selected samples, the error rate for TNM stage was 50% (43 errors out of 86 nonmissing cases). For the SEER variable, the error rate was 31.1% (47 errors out of 151 nonmissing cases).

XSL•FO
RenderX

Table . Patient characteristics and missing rates of target variables (N=6491).

Variables and categories	N (%)
Sex, n (%)	
Male	3936 (60.6)
Female	2555 (39.4)
Age, mean (SD)	66.79 (13.4)
Dead, n (%)	
Yes	394 (6.1)
No	6097 (93.9)
5 y survival, n (%)	
Yes	6131 (94.5)
No	360 (5.6)
Height, mean (SD)	162.00 (9.15)
Missing, mean (SD)	2144 (33.0)
Weight, mean (SD)	62.44 (11.88)
Missing, mean (SD)	2135 (32.9)
BMI mean (SD)	23.72 (3.60)
Missing	2146 (33.1)
Total lymph node, mean (SD)	20.25 (12.05)
Missing, n (%)	2633 (40.6)
Positive lymph node, mean (SD)	1.92 (4.40)
Missing, n (%)	2633 (40.6)
Operation, n (%)	
Yes	2631 (40.5)
No	3860 (59.5)
Chemotherapy, n (%)	
Yes	224 (3.5)
No	6267 (96.6)
Radiotherapy, n (%)	
Yes	383 (5.9)
No	6108 (94.1)
Complication after surgery, n (%)	
Yes	524 (8.1)
No	5967 (91.9)
SEER[a], n (%)	
0	355 (5.5)
1	1818 (28)
2	806 (12.4)
3	192 (3)
4	890 (13.7)
5	14 (0.2)
7	792 (12.2)
9	48 (0.7)
Missing	1576 (24.3)

XSL•FO
RenderX

Variables and categories	N (%)
T stage, n (%)	
0	1 (0)
Tis, n (%)	1 (0)
1	304 (4.7)
2	238 (3.7)
3	814 (12.5)
4	248 (3.8)
Missing	4885 (75.3)
N stage, n (%)	
0	968 (14.9)
1	399 (6.2)
2	235 (3.6)
3	3 (0.1)
4	1 (0)
Missing	4885 (75.3)
M stage, n (%)	
0	1459 (22.5)
1	147 (2.3)
missing	4885 (75.3)

[a]SEER: surveillance, epidemiology, and end results.

Stage 3: Data Quality Management

We developed guidelines for creating an automated stage classification library. Examples of critical indicator terms identified for TNM and SEER through labeling are highlighted in italics in Tables 3 and 4, respectively. These guidelines define labeled terms and conditions that allow rule-based automated classification of cancer stage.

XSL•FO
RenderX

Table . Tumor, node, metastasis stage labeling following the Korean clinical guideline for colorectal cancer v.1.0, with critical indicator terms in italics.

Stage	Labels
Pathology report	
T0	
	No residual tumor
Tis	
	Confinement to mucosa
	Invasion to *lamina propria*
	(pTis)
T1	
	Invades *submucosa*
	Invasion to *submucosa*
	Invasion into *submucosa*
	Invasion to *muscularis mucosae*
	(pT1) /(ypT1)
T2	
	Invades *muscularis propria*
	(pT2) /(ypT2)
T3	
	Invades *pericolic adipose tissue*
	Invades *perirectal adipose tissue*
	Invades *subserosa*
	(pT3) /(ypT3)
T4	
	Penetrates *visceral peritoneum*
	Penetration to serosa and perforation
	(pT4a) /(ypT4)
	Direct invades *adjacent organs* or *structures*
	Directly invades adjacent organ
	(pT4b)
N0	
	No metastasis in - *regional lymph nodes*
	No metastasis in - *pericolic lymph nodes*
	No metastasis in - *perirectal lymph nodes*
	No metastasis in - *pericolic and perirectal lymph nodes*
	No metastasis in - *pericolic and peri-ileal lymph nodes*
	No metastasis in - *lymph nodes*
	No tumor present in 16 *regional lymph nodes* (0/16)
	(pN0) /(yN0) /(ypN0)
N1	
	Metastasis in *1* of ~ *regional lymph nodes*
	(pN1a) /(ypN1a)
	Metastasis in *2 (or 3)* of ~ *regional lymph nodes*
	(pN1b) /(ypN1b)

XSL•FO
RenderX

Stage	Labels
	Tumor deposit present
	(pN1c) /(ypN1c)
N2	
	Metastasis in *4 (more than)* of ~ *regional lymph nodes*
	(pN2a) /(ypN2a)
	(pN2b) /(ypN2b)
M1	
	Metastatic adenocarcinoma
	Adenocarcinoma, metastatic from
	Metastatic colonic adenocarcinoma
	Metastatic carcinoma of rectum
	Metastatic mixed adenoneuroendocrine carcinoma
	Metastatic appendiceal high-grade goblet cell adenocarcinoma
	Metastatic mucinous adenocarcinoma
	Metastatic mucinous carcinoma
	Consistent with metastatic carcinoma
	Omental seeding
Imaging examination results	
T0	
	No evidence of abnormal wall thickening
	No visible definite
Tis	
	Tis
	Invasion of lamina propria
T1	
	T1
	Submucosal invasion
T2	
	T2
T3	
	T3
	Pericolic (fat) infiltration
	Perirectal (fat) infiltration
	Mesorectal fat infiltration
	Subserosal invasion
T4	
	T4
	T4a /T4b
	Visceral peritoneum
Synonym: LN(s), L/N(s), lymph node(s)[a]	
N0	
	N0

XSL•FO
RenderX

Stage	Labels
	No enlarged
	No abnormal enlarging
	No pathologic
	Nor enlarged
	No evidence of regional
	No evidence of enlarged
	No evidence of enlarged regional
	No significant
	No significant enlarged
	No significant enlargement
	No significant enlarged peritumoral
	No visible enlarged
N1	
	N1
	Regional
	Metastases
	Regional metastatic
	Regional - metastasis (metastases)
	Metastatic
	With regional lymph node metastasis
N2	
	N2
	Multiple regional metastatic
	Multiple regional - metastasis/metastases
	Several regional - metastasis/metastases
	Several regional - metastasis
Synonym: metastasis, metastases, metastatic[b]	
M0	
	No evidence of distant
	No evidence of definite distant
	No evidence of liver
	No evidence of hepatic
	No evidence of
	Nor distant
	Nor or no visible
	Rather than
	No evidence of enlarged regional L/N or distant metastasis
M1	
	Bone
	Liver
	Hepatic
	Pulmonary

XSL•FO
RenderX

Stage	Labels
	Several
	No evidence of distant

[a]The terms listed as synonyms should be used together with the N stage labels to create the labeling.
[b]The terms listed as synonyms should be used together with the M stage labels to create the labeling.

XSL•FO
RenderX

Table . SEER[a] labeling by Summary Stage 2018, with critical indicator terms in italics.

SEER code	Labels
Pathology report	
0[b]	
	Intraepithelial
1[c]	
	Intramucosal
	Confinement in the *lamina propria*
	Invasion to *lamina propria*
	Confinement to mucosa
	Invasion to mucosa
	Extension to mucosa
	Involvement of mucosa
	Invasion to *muscularis mucosae*
	Invades muscularis propria
	Invades submucosa
	Invasion to submucosa
	Invasion into submucosa
	Invasion to the submucosa
	Submucosal invasion
2[d]	
	Directly invades *adjacent organ*
	Direct invades *adjacent organs or structures*
	Directly invades adjacent organs or structures
	Penetrates *visceral peritoneum*
	Penetration of *visceral peritoneum*
	Invades *subserosa*
	Invades *pericolic adipose tissue*
	Invades *perirectal adipose tissue*
3[e]	
	Metastasis in *1* of *regional lymph nodes*
	With metastasis of pericolorectal lymph node
	Tumor deposit
4[f]	Codes 2+3 (cases corresponding to both Code 2 and Code 3)
7[g]	
	Metastatic adenocarcinoma
	Adenocarcinoma, metastatic from colon or rectum
	Metastatic mixed adenoneuroendocrine carcinoma
	Metastatic colonic adenocarcinoma
	Metastatic carcinoma
	Distant lymph node(s)
9[h]	In cases without evidence

XSL•FO
RenderX

SEER code	Labels
Imaging examination results	
0	—[i]
1	
	Invasion of lamina propria
	Submucosal invasion
2	
	Pericolic fat infiltration
	Pericolic infiltration
	Perirectal infiltration
	Perirectal fat infiltration
3	If the N code is 1 or higher
4	Codes 2+3 (cases corresponding to both Code 2 and Code 3)
7	If the M code is 1 or higher
9	In cases without evidence

[a]SEER: surveillance, epidemiology, and end results.
[b]0: in situ.
[c]1: localized only.
[d]2: regional by direct extension only.
[e]3: regional lymph node(s) involved only.
[f]4: regional by both direct extension and regional lymph node(s) involvement.
[g]7: distant site(s)/lymph node(s) involved.
[h]9: unknown if extension or metastasis.
[i]Not applicable.

As a result of the evaluation of the automated stage classification library, the concordance rates were 93.3% for TNM and 93.9% for SEER across the 164 cases. By leveraging a rule-based database in the QMP, we were able to supplement missing data in the target variables, resulting in a dataset aligned with the objectives of prognostic prediction.

Stage 4: Postassessment Based on RWD

Comparing the rates of missing data before and after the QMP, the rate decreased from 75.3% to 35.7% for the TNM and from 24.3% to 18.5% for the SEER across 6491 cases. This demonstrates the effectiveness of the QMP (Figure 3).

XSL•FO
RenderX

Figure 3. Missing values before and after quality management. SEER: surveillance, epidemiology, and end result; TNM: tumor, node, metastasis.

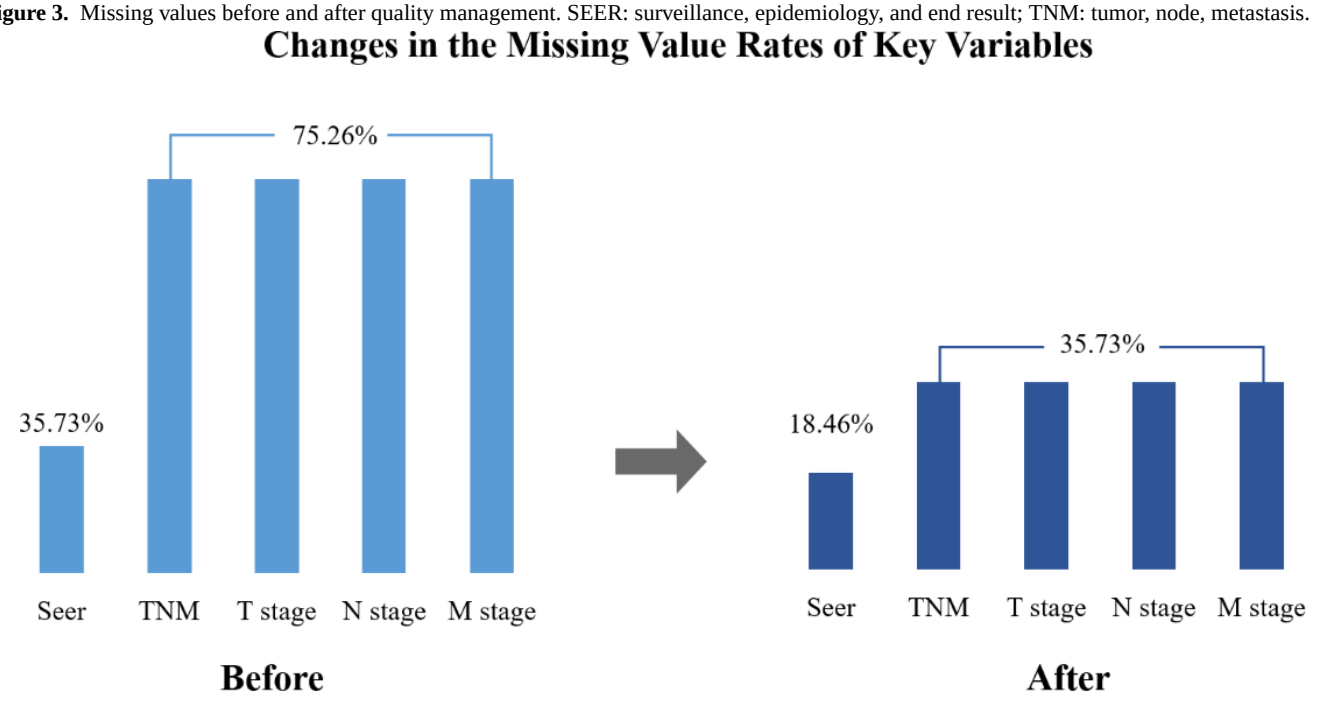


Table 5 presents a comparison of the performance of the models before and after the QMP; a slight improvement was observed. An evaluation of variable importance by feature selection revealed that TNM stage and detailed code variables (T, N, M), which were not identified before quality management, emerged as significant variables after quality management. The variable importance values are shown in Figure 4, and the corresponding importance values are detailed in Table 6. Incorporating these newly identified prognostic indicators into the final model enhances its clinical relevance and interpretability.

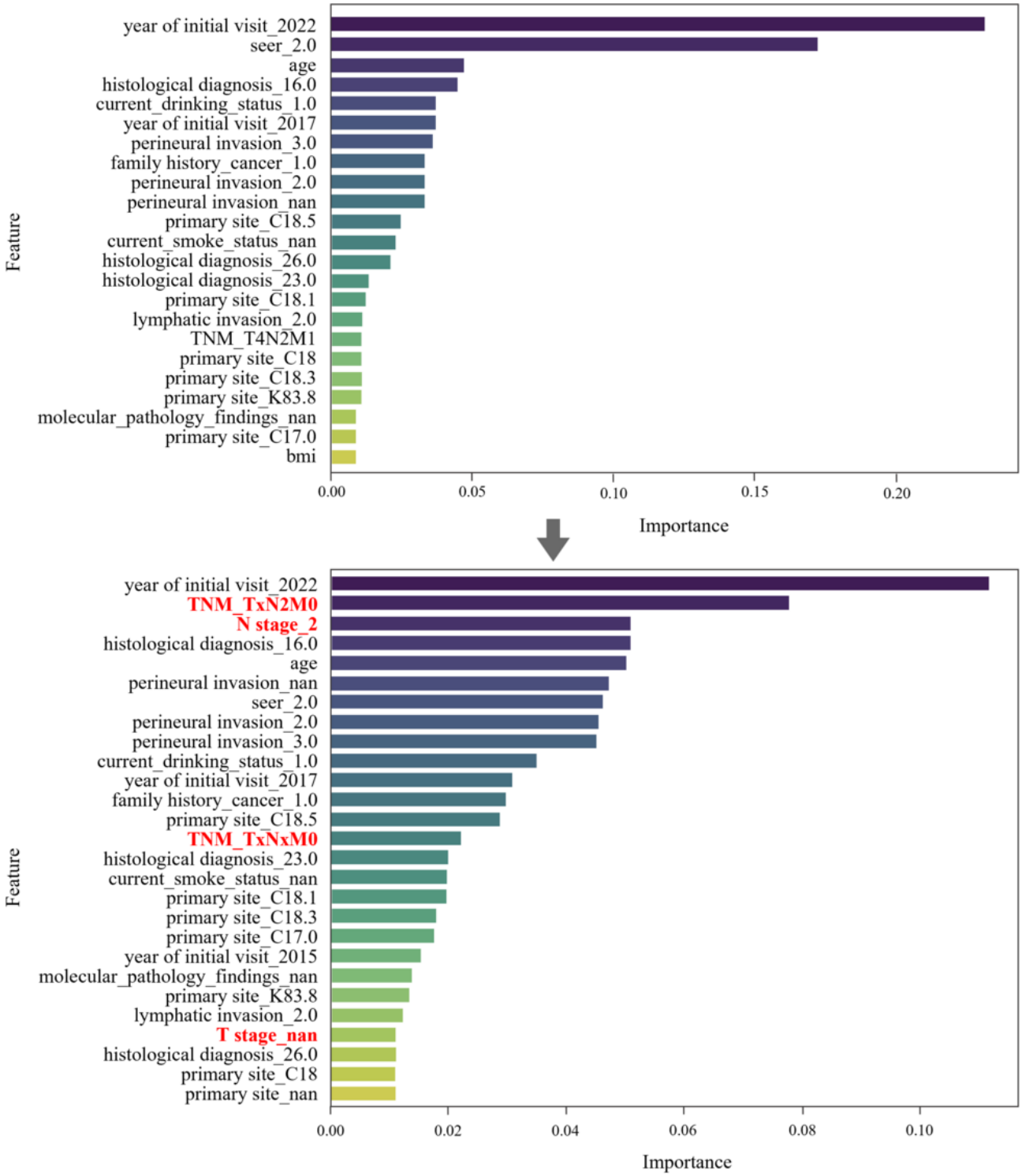
Table . Model performance before and after quality management.

	Before quality management	After quality management
Accuracy	0.933795227	0.9407236336
Precision	0.924949499	0.9279243167
Recall	0.933795227	0.9407236336
F_1-score	0.92898597	0.9330359000
AUROC[a]	0.856226406	0.8724494672

[a]AUROC: area under the receiver operating characteristic curve.

XSL•FO
RenderX

Figure 4. Change in feature importance before and after quality management.



XSL•FO
RenderX

Table . Feature importance before and after quality management.

Feature	Importance
Before quality management	
year of initial visit_2022	0.23176
SEER_2.0	0.17240
Age	0.04739
histological diagnosis_16.0	0.04513
current_drinking_status_1.0	0.03755
year of initial visit_2017	0.03753
perineural invasion_3.0	0.03664
family history_cancer_1.0	0.03364
perineural invasion_2.0	0.03356
perineural invasion_nan	0.03320
primary site_C18.5	0.02482
current_smoke_status_nan	0.02294
histological diagnosis_26.0	0.02096
histological diagnosis_23.0	0.01356
primary site_C18.1	0.01220
lymphatic invasion_2.0	0.01114
TNM_T4N2M1	0.01100
primary site_C18	0.01072
primary site_C18.3	0.01059
primary site_K83.8	0.01029
molecular_pathology_findings_nan	0.00896
primary site_C170.	0.00894
BMI[a]	0.00886
After quality management	
year of initial visit_2022	0.11148
TNM[b]_TxN2M0	0.07741
N stage_2	0.05068
histological diagnosis_16.0	0.05061
age	0.05013
perineural invasion_nan	0.04725
SEER[c]_2.0	0.04599
perineural invasion_2.0	0.04532
perineural invasion_3.0	0.04489
current_drinking_status_1.0	0.03479
year of initial visit_2017	0.03067
family history_cancer_1.0	0.02972
primary site_C18.5	0.02883
TNM_TxNxM0	0.02201
histological diagnosis_23.0	0.01986
current_smoke_status_nan	0.01954

XSL•FO
RenderX

Feature	Importance
primary site_C18.1	0.01947
primary site_C18.3	0.01790
primary site_C170.	0.01747
year of initial visit_2015	0.01526
molecular_pathology_findings_nan	0.01374
primary site_K83.8	0.01342
lymphatic invasion_2.0	0.01218
T stage_nan	0.01105
histological diagnosis_26.0	0.01104
primary site_C18	0.01093
primary site_nan	0.01088

[a]BMI: body mass index.

[b]TNM: tumor, node, metastasis.

[c]SEER: surveillance, epidemiology, and end result

Discussion

Principal Findings

This study proposed a QMP to generate high-quality data. We used the K-CURE dataset to develop the QMP and applied it to a CRC clinical library to evaluate the quality improvement effects. After applying the process, TNM stage and individual T, N, and M codes emerged as important factors when constructing a prognostic model. This suggests that the proposed QMP can create high-quality data for research.

Gaps in datasets can occur due to direct omissions of data, limitations in data collection, and technical issues [22,23]. Missing values may arise due to patient movement, treatment interruptions, or omitted tests or procedures, resulting in the loss of important variables. Various methods, such as statistical imputation or ML-based techniques, have been proposed to address missing data but often fail to fully reflect the complexity of clinical environments [24,25]. This reduces the reliability of data over the long term, affecting dataset quality and reducing the reliability of findings.

Various basic statistical methods, such as imputation, have been used to address missing data [26-28]. More recently, ML-based methods such as K-nearest neighbor [29], matrix factorization [30], and random forest approaches have also emerged [31]. These methods are effective when missing data are not random and do not follow specific patterns, as they learn from the dataset itself and predict missing values [32]. This makes them relatively insensitive to the rates or patterns of missing data. Novel techniques such as attention-based models [33] or the large language model forest framework have also been applied [34]. However, previous studies have focused on evaluating and replacing missing values, rather than applying multistage processes to improve overall data quality.

In this study, we reviewed several previous studies on CRC to construct an improved dataset and identify prognostic factors. For clinical research, it is crucial to identify and evaluate factors with strong evidence-based associations with prognoses [35]. However, in our study, theoretically important variables were not always selected from the actual data, and some missing values could not be addressed through the QMP. This indicates that there was a lack of information on important variables during the initial stages of data construction. Therefore, important prognostic variables should be thoroughly reviewed and systematically managed from the initial stages of data construction.

Using CRC staging guidelines, we performed labeling by extracting text-based terms from pathology reports and imaging test results to establish a rule-based QMP. Recently, there has been a trend toward research focusing on developing rule-based quality management and quality assessment methodologies using medical data. This expands the possibility of systematically detecting and correcting errors in data [36]. This approach effectively analyzes clinical quality issues, improves data accuracy, and provides reliable information for clinical research and decision-making [37]. Such a strategy has been found to be applicable to real-world medical data [38]. The QMP developed in this study shows the utility of rule-based systems, generating data with improved completeness. Applying this approach could provide accurate data for future prognostic prediction and decision support systems.

Traditional quality management methodologies focus on preventing and correcting errors during data construction and operation [39]. For example, such methods often rely on automated systems or checklists to minimize input errors or to validate the accuracy of collected data [40]. However, we propose a rule-based QMP that identifies and corrects missing values and errors in datasets that are already established. This approach not only addresses potential issues that can occur during the data construction phase, but also facilitates the detection and resolution of missing data that arise during data analysis.

Recently, there have been active attempts in medical research to develop QMP systems using various clinical and public

XSL•FO
RenderX

datasets, including electronic medical record data [41-43]. This approach is essential for institutions with large-scale medical datasets and platforms built from multiple integrated datasets. In multi-center research, a method to prioritize data quality dimensions and key evaluation variables, supported by feedback systems to monitor and assess data quality, has been proposed. This study provides a foundation for the automation of future QMP systems and the development of new approaches using AI and ML, enhancing the usage of medical data by researchers in public data platforms.

We focused on addressing missing data for quality management; we have not proposed a comprehensive solution for various data errors in clinical environments. Also, a limitation is the complexity of clinical staging decisions—involving multidisciplinary discussions, treatments such as neoadjuvant therapy, and surgical findings—which can lead to discrepancies or missing values in retrospective research data. This complexity may influence the interpretation of the study results and may affect the generalizability of the data. Nonetheless, this work is important in that we propose a systematic process to improve the quality and applicability of real-world medical data. Future efforts should consider advanced processes that address the entire data lifecycle, from construction to usage and operation.

Conclusion

We developed a rule-based QMP that improves data quality and identifies key prognostic factors in CRC datasets. Although missing data and other complex challenges in real-world clinical data remain, the approach demonstrates the utility of systematic quality management. Future work should expand the QMP to address diverse data errors across the data lifecycle.

Acknowledgments

This research was funded by the National Research Foundation of Korea (NRF; grant number 2020R1C1C009679).

Conflicts of Interest

None declared.

References

1. Shortliffe EH, Barnett GO. Medical Data: Their Acquisition, Storage, and Use Medical Informatics: Computer Applications in Health Care and Biomedicine: Springer; 2001:41-75. [doi: 10.1007/978-0-387-21721-5_2]
2. Ayaad O, Alloubani A, ALhajaa EA, et al. The role of electronic medical records in improving the quality of health care services: comparative study. Int J Med Inform 2019 Jul;127:63-67. [doi: 10.1016/j.ijmedinf.2019.04.014] [Medline: 31128833]
3. Xiao C, Choi E, Sun J. Opportunities and challenges in developing deep learning models using electronic health records data: a systematic review. J Am Med Inform Assoc 2018 Oct 1;25(10):1419-1428. [doi: 10.1093/jamia/ocy068] [Medline: 29893864]
4. Alsuliman T, Humaidan D, Sliman L, Duléry R. Introduction to medical data and big data exploitation in research: errors, solutions and trends. Curr Res Transl Med 2021 Oct;69(4):103310. [doi: 10.1016/j.retram.2021.103310] [Medline: 34419934]
5. Chen ZH, Lin L, Wu CF, Li CF, Xu RH, Sun Y. Artificial intelligence for assisting cancer diagnosis and treatment in the era of precision medicine. Cancer Commun 2021 Nov;41(11):1100-1115. [doi: 10.1002/cac2.12215]
6. M-s C, Lee S. Current status and issues of data management plan in Korea. J Korea Contents Assoc 2020;20(6):220-229. [doi: 10.5392/JKCA.2020.20.06.220]
7. McGuckin T, Crick K, Myroniuk TW, Setchell B, Yeung RO, Campbell-Scherer D. Understanding challenges of using routinely collected health data to address clinical care gaps: a case study in Alberta, Canada. BMJ Open Qual 2022 Jan;11(1):e001491. [doi: 10.1136/bmjoq-2021-001491] [Medline: 34996811]
8. Ta CN, Weng C. Detecting systemic data quality issues in electronic health records. Stud Health Technol Inform 2019 Aug 21;264:383-387. [doi: 10.3233/SHTI190248] [Medline: 31437950]
9. Gehrmann J, Herczog E, Decker S, Beyan O. What prevents us from reusing medical real-world data in research. Sci Data 2023 Jul 13;10(1):459. [doi: 10.1038/s41597-023-02361-2] [Medline: 37443164]
10. Shafqat W, Byun YC. A hybrid GAN-based approach to solve imbalanced data problem in recommendation systems. IEEE Access 2022;10:11036-11047. [doi: 10.1109/ACCESS.2022.3141776]
11. Whang SE, Roh Y, Song H, Lee JG. Data collection and quality challenges in deep learning: a data-centric AI perspective. VLDB J 2023 Jul;32(4):791-813. [doi: 10.1007/s00778-022-00775-9]
12. Alalwani R, Lucas A, Alzubaidi M, Shah HA, Alam T, Shah Z, et al. Deep learning in colorectal cancer classification: a scoping review. In: Healthcare Transformation with Informatics and Artificial Intelligence 2023:616-619. [doi: 10.3233/SHTI230573]
13. Bedrikovetski S, Dudi-Venkata NN, Kroon HM, et al. Artificial intelligence for pre-operative lymph node staging in colorectal cancer: a systematic review and meta-analysis. BMC Cancer 2021 Sep 26;21(1):1058. [doi: 10.1186/s12885-021-08773-w] [Medline: 34565338]

XSL•FO
RenderX

14. Rompianesi G, Pegoraro F, Ceresa CD, Montalti R, Troisi RI. Artificial intelligence in the diagnosis and management of colorectal cancer liver metastases. World J Gastroenterol 2022 Jan 7;28(1):108-122. [doi: 10.3748/wjg.v28.i1.108] [Medline: 35125822]
15. Kale M, Wankhede N, Pawar R, et al. AI-driven innovations in Alzheimer's disease: Integrating early diagnosis, personalized treatment, and prognostic modelling. Ageing Res Rev 2024 Nov;101:102497. [doi: 10.1016/j.arr.2024.102497] [Medline: 39293530]
16. Diaz O, Kushibar K, Osuala R, et al. Data preparation for artificial intelligence in medical imaging: a comprehensive guide to open-access platforms and tools. Phys Med 2021 Mar;83:25-37. [doi: 10.1016/j.ejmp.2021.02.007] [Medline: 33684723]
17. Janett RS, Yeracaris PP. Electronic medical records in the American health system: challenges and lessons learned. Ciênc saúde coletiva 2020;25(4):1293-1304. [doi: 10.1590/1413-81232020254.28922019]
18. Zhang X, Yan C, Gao C, Malin BA, Chen Y. Predicting missing values in medical data via XGBoost regression. J Healthc Inform Res 2020 Dec;4(4):383-394. [doi: 10.1007/s41666-020-00077-1] [Medline: 33283143]
19. Washington MK, Brookland DR, Gershenwald JE, Compton CC, Hess KR, et al. AJCC Cancer Staging Manual, 8th edition: New York, NY: Springer; 2017.
20. Um JW. Korean Clinical Guideline for Colon and Rectal Cancer v 10: Seoul, Korean Academy of Medical Sciences; 2012.
21. Ruhl JL, Callaghan C. In: Schussler N, editor. Summary Stage 2018: Codes and Coding Instructions: Bethesda, MD: National Cancer Institute; 2024.
22. Austin PC, White IR, Lee DS, van Buuren S. Missing data in clinical research: a tutorial on multiple imputation. Can J Cardiol 2021 Sep;37(9):1322-1331. [doi: 10.1016/j.cjca.2020.11.010] [Medline: 33276049]
23. Purwar A, Singh SK. Hybrid prediction model with missing value imputation for medical data. Expert Syst Appl 2015 Aug;42(13):5621-5631. [doi: 10.1016/j.eswa.2015.02.050]
24. Lin WC, Tsai CF. Missing value imputation: a review and analysis of the literature (2006–2017). Artif Intell Rev 2020 Feb;53(2):1487-1509. [doi: 10.1007/s10462-019-09709-4]
25. Wells BJ, Chagin KM, Nowacki AS, Kattan MW. Strategies for handling missing data in electronic health record derived data. EGEMS (Wash DC) 2013;1(3):1035. [doi: 10.13063/2327-9214.1035] [Medline: 25848578]
26. Bertsimas D, Pawlowski C, Zhuo YD. From predictive methods to missing data imputation: an optimization approach. J Mach Learn Res 2018;18(196):1-39 [FREE Full text]
27. Raja PS, Thangavel K. Missing value imputation using unsupervised machine learning techniques. Soft Comput 2020 Mar;24(6):4361-4392. [doi: 10.1007/s00500-019-04199-6]
28. Woźnica K, Biecek P. Does imputation matter? Benchmark for predictive models. arXiv. Preprint posted online on Jul 6, 2020. [doi: 10.48550/arXiv.2007.02837]
29. Batista GEAPA, Monard MC. An analysis of four missing data treatment methods for supervised learning. Appl Artif Intell 2003 May;17(5-6):519-533. [doi: 10.1080/713827181]
30. Mazumder R, Hastie T, Tibshirani R. Spectral regularization algorithms for learning large incomplete matrices. J Mach Learn Res 2010 Mar 1;11(2287-322):2287-2322. [Medline: 21552465]
31. Stekhoven DJ, Bühlmann P. MissForest--non-parametric missing value imputation for mixed-type data. Bioinformatics 2012 Jan 1;28(1):112-118. [doi: 10.1093/bioinformatics/btr597] [Medline: 22039212]
32. Thomas T, Rajabi E. A systematic review of machine learning-based missing value imputation techniques. DTA 2021 Aug 5;55(4):558-585. [doi: 10.1108/DTA-12-2020-0298]
33. Kowsar I, Rabbani SB, Samad MD. Attention-based imputation of missing values in electronic health records tabular data. In: Kowsar I, Rabbani SB, Samad MD, editors. Presented at: 2024 IEEE 12th International Conference on Healthcare Informatics (ICHI); Jun 3-6, 2024. [doi: 10.1109/ICHI61247.2024.00030]
34. He X, Ban Y, Zou J, Wei T, Cook CB, He J. LLM-forest for health tabular data imputation. arXiv. Preprint posted online on Oct 28, 2024. [doi: 10.48550/arXiv.2410.21520]
35. Xu W, He Y, Wang Y, et al. Risk factors and risk prediction models for colorectal cancer metastasis and recurrence: an umbrella review of systematic reviews and meta-analyses of observational studies. BMC Med 2020 Jun 26;18(1):172. [doi: 10.1186/s12916-020-01618-6] [Medline: 32586325]
36. Mohamed Y, Song X, McMahon TM, et al. Tailoring rule-based data quality assessment to the patient-centered outcomes research network (PCORnet) common data model (CDM). In: Wang Z, editor. AMIA Annu Symp Proc 2022;2022:775-784. [Medline: 37128433]
37. Wang Z, Dagtas S, Talburt J, Baghal A, Zozus M. Rule-based data quality assessment and monitoring system in healthcare facilities. In: Improving Usability, Safety and Patient Outcomes with Health Information: IOS Press; 2019:460-467. [doi: 10.3233/978-1-61499-951-5-460]
38. Wang Z, Talburt JR, Wu N, Dagtas S, Zozus MN. A rule-based data quality assessment system for electronic health record data. Appl Clin Inform 2020 Aug;11(04):622-634. [doi: 10.1055/s-0040-1715567]
39. Kahn MG, Raebel MA, Glanz JM, Riedlinger K, Steiner JF. A pragmatic framework for single-site and multisite data quality assessment in electronic health record-based clinical research. Med Care 2012 Jul;50 Suppl:S21-S29. [doi: 10.1097/MLR.0b013e318257dd67] [Medline: 22692254]

XSL•FO
RenderX

40. Weiskopf NG, Weng C. Methods and dimensions of electronic health record data quality assessment: enabling reuse for clinical research. J Am Med Inform Assoc 2013 Jan 1;20(1):144-151. [doi: 10.1136/amiajnl-2011-000681] [Medline: 22733976]
41. Lee S, Roh GH, Kim JY, Ho Lee Y, Woo H, Lee S. Effective DATA quality management for electronic medical record DATA using SMART DATA. Int J Med Inform 2023 Dec;180:105262. [doi: 10.1016/j.ijmedinf.2023.105262] [Medline: 37871445]
42. Makeleni N, Cilliers L. Critical success factors to improve data quality of electronic medical records in public healthcare institutions. S Afr J Inf Manag 2021;23(1):1-8. [doi: 10.4102/sajim.v23i1.1230]
43. Reimer AP, Milinovich A, Madigan EA. Data quality assessment framework to assess electronic medical record data for use in research. Int J Med Inform 2016 Jun;90:40-47. [doi: 10.1016/j.ijmedinf.2016.03.006] [Medline: 27103196]

Abbreviations

AI: artificial intelligence
CRC: colorectal cancer
K-CURE: Korea Clinical Data Use Network for Research Excellence
QMP: quality management process
RWD: real-world data
SEER: Surveillance, Epidemiology, and End Results
TNM: tumor, node, metastasis

Edited by A Benis; submitted 13.03.25; peer-reviewed by D Bracken-Clarke, MH Osman; revised version received 26.06.25; accepted 06.07.25; published 13.11.25.

Please cite as:
Park N, Na K, Sunwoo W, Baek JH, Lee Y, Lee S, Woo H
Process for Quality Management of Electronic Medical Records–Based Data: Case Study Using Real Colorectal Cancer Data
JMIR Med Inform 2025;13:e73884
URL: https://medinform.jmir.org/2025/1/e73884
doi:10.2196/73884

© NaYoung Park, Kyungmin Na, Woongsang Sunwoo, Jeong-Heum Baek, Youngho Lee, Suehyun Lee, Hyekyung Woo. Originally published in JMIR Medical Informatics (https://medinform.jmir.org), 13.11.2025. This is an open-access article distributed under the terms of the Creative Commons Attribution License (https://creativecommons.org/licenses/by/4.0/), which permits unrestricted use, distribution, and reproduction in any medium, provided the original work, first published in JMIR Medical Informatics, is properly cited. The complete bibliographic information, a link to the original publication on https://medinform.jmir.org/, as well as this copyright and license information must be included.

XSL•FO
RenderX

Patient Perspectives on Digital Technology and Experiences of Computerized History-Taking for Chest Pain Management in the Emergency Department: CLEOS-CPDS Prospective Cohort Study

Kaisa Fritzell[1,2], RN, PhD; Helge Brandberg[3], MD, PhD; Jonas Spaak[3], MD, PhD; Sabine Koch[4], PhD; Carl Johan Sundberg[5,6], MD, PhD; David Zakim[4], MD; Thomas Kahan[3], MD, PhD; Kay Sundberg[2], RN, PhD

[1]Theme Cancer, Karolinska University Hospital, Karolinska vägen 27, Stockholm, Sweden

[2]Division of Nursing, Department of Neurobiology, Care Sciences and Society, Karolinska Institutet, Alfred Nobels Allé 23, Huddinge, Sweden

[3]Division of Cardiovascular Medicine, Department of Clinical Sciences, Danderyd Hospital, Karolinska Institutet, Stockholm, Sweden

[4]Department of Learning, Informatics, Management and Ethics, Health Informatics Centre, Karolinska Institutet, Stockholm, Sweden

[5]Department of Learning, Informatics, Management and Ethics, Medical Management Centre, Karolinska Institutet, Stockholm, Sweden

[6]Department of Physiology & Pharmacology, Karolinska Institutet, Stockholm, Sweden

Corresponding Author:
Kaisa Fritzell, RN, PhD
Theme Cancer, Karolinska University Hospital, Karolinska vägen 27, Stockholm, Sweden

Abstract

Background: Automated, self-reported medical history-taking has the potential to provide comprehensive patient-reported data across a wide range of clinical issues. In the Clinical Expert Operating System - Chest Pain Danderyd Study (CLEOS-CPDS), medical history data were entered by patients using tablets in an emergency department (ED). Since successful implementation of this technology depends on understanding patients' views and willingness to use it, we have studied these factors following patients' use of the CLEOS program.

Objective: This study aimed to develop and use a questionnaire to investigate patients' attitudes, perceptions and skills related to using digital technology in health care in general, and specifically their experiences with the CLEOS program during their visit to an ED with a chief complaint of chest pain.

Methods: The study included the development of a questionnaire, followed by a cross-sectional study. Questionnaire design and the technology acceptance model underpinned the development of the questionnaire. The think-aloud method was used to test the questionnaire. Adults who participated in the CLEOS-CPDS were invited consecutively to respond to the questionnaire. Descriptive and correlational analyses were performed.

Results: The refinement of the questionnaire included language revision, removal of similar items, and replacement of some response formats. The final questionnaire consisted of 16 items and one free text comment that assessed attitudes, perceptions, and skills related to the use of digital technology in health care in general and the specific experience of using self-reported history-taking by CLEOS. The majority of the 129 patients (mean age 56, SD=17.3 y) who answered the questionnaire found it easy to use digital technology in general (118/129, 91%), that digital technology has a role when seeking health care (115/129, 91%), and that patient-reported symptoms are helpful in making a diagnosis (83/129, 65%). There were some concerns that the patient-physician interaction would be disrupted when using digital technology (48/129, 38%). The overall experience of using CLEOS was positive and most felt confident in answering the questions on a tablet (118/129, 91%). Older age was associated with less ease (P<.001), confidence (P<.001), and trust (P=.002) when using digital technology, as well as less confidence in answering the questions in CLEOS (P=.019). Moreover, older age was associated with more worry about the potential disruption of the patient-physician personal contact when using digital technology (P<.001).

Conclusions: This study suggests strong approval of usefulness and trust in digital technology among patients with chest pain visiting a cardiology ED, but the concern for lack of personal contact should be acknowledged. End users found the CLEOS program to perform well but recommend some adjustments for future studies. The questionnaire responses provided some new insights on perceived usability of digital technology for health care delivery, and it appears relevant for future evaluations of CLEOS in other contexts.

Trial Registration: ClinicalTrials.gov NCT03439449; https://clinicaltrials.gov/study/NCT03439449

International Registered Report Identifier (IRRID): RR2-10.1136/bmjopen-2019-031871

(JMIR Med Inform 2025;13:e65568) doi:10.2196/65568

XSL•FO
RenderX

KEYWORDS

technology acceptance; chest pain; computerized history taking; digital technology; emergency department; health informatics; medical history; self report

Introduction

Automated, self-reported medical history-taking can become a key technology for maximizing outcomes for patients, for improving the physician-patient communication and for delivering patient-reported information to the point of care across a wide range of clinical issues [1,2]. Programs for computerized history-taking (CHT) that interact directly with patients in clinical settings collect more complete and accurate medical data as compared with physician entries in patients' medical records [3,4]. For example, the CHT program Clinical Expert Operating System (CLEOS) provided sufficient data for risk stratification for a major adverse cardiac event using the well-established HEART (Heart, ECG, Age, Risk factors, Troponin) score in approximately 77% of 1000 emergency department (ED) patients with chest pain [5]. In contrast, risk stratification was only feasible for 31% of the patients when relying on data from the electronic health record [6]. CLEOS collects self-reported medical history data entered by patients on a tablet during hospital waiting times before or after seeing a physician [7]. The program emulates clinical thinking continuously through its automated interpretation of all previous answers as data is collected.

In recent years there has been a rapid growth of digital tools in health care that allow patients to interact with health care professionals [8]. Digital health tools can empower patients' self-management and facilitate personalised communication with the health care system to improve health status awareness and increase adherence to therapy [8,9]. However, poor digital literacy, low health literacy, privacy and security concerns of medical data have been identified as barriers to adopting such tools [9]. As technical solutions are developed to improve health outcomes in patients with cardiovascular and other chronic conditions, patients' ability to understand and communicate basic health information and to express their health concerns to health care professionals should be considered [10]. Furthermore, user-friendliness and facilitation of patient-clinician interaction have been reported as important aspects for the uptake and adoption of digital technology in health care [11]. Effective implementation of CHT programs in health care requires that we understand patients' concerns, attitudes, and willingness to engage with such programs. Research on how CHT software is perceived by patients is very scarce. Early work in this field suggests that CHT is well accepted [12,13] but older age and low self-confidence in using computers were associated with lower perceived usability [13]. In a more recent study of the usability of an application designed for medical history-taking in general practice the participants of older age did not adapt equally well to the application [14]. We conclude that the ongoing development in technology and changes in health care with people seeking care at increasingly older ages requires an extended knowledge of patients' views on these issues.

We previously performed an interview study of patients seeking ED care for chest pain as part of our ongoing studies of patient experience with the use of CLEOS [15]. The interviews yielded insight into the influence of context, clinical content, and technology on the program's usability. Generally, CLEOS was well accepted by the patients and could be managed by them despite a busy ED, although the program was sometimes perceived too extensive. However, the sample interviewed was small and we did not address patients' perceptions of ease of using the program and its possible impact on the value of health care they could receive. These are 2 determinants identified in the technology acceptance model (TAM) for acceptance of computer technology by its potential users [16]. Obviously, effective development of patient-directed health care technology depends on thorough understanding of patient perceptions of the technology.

Most previous studies focus on digital health care tools aimed at delivering interventions, patient monitoring, symptom tracking, and communication. A study of patient perceptions of CHT based on real-time use by patients with significant medical issues has not been investigated in detail. This study will provide insights for developers of CHT and health care managers on important factors that influence an individual's intention to use such programs effectively as they seek emergency health care. Accordingly, this study aimed to develop a questionnaire and apply it to investigate patients' attitudes, perceptions, and skills related to using digital technology in health care in general, and specifically their experiences with the CLEOS program in an ED setting.

Methods

Design

The study design included (1) the development of a questionnaire and (2) a cross-sectional study using the questionnaire in a study population presenting to the ED with acute chest pain. This study is part of the Clinical Expert Operating System - Chest Pain Danderyd Study (CLEOS - CPDS) presented in detail elsewhere [7].

Questionnaire Development

Development

The questionnaire development was guided by questionnaire design [17,18] and by results from our previous interview study investigating patients interacting with CLEOS in an ED [15]. The construction of items in the questionnaire was inspired by the System Usability Scale (SUS) [19]. The SUS is a standardized questionnaire for the assessment of perceived usability. It does not cover all areas of significance for the research questions we address here. Therefore, we used the TAM [16] to give further structure to the development of questions. The TAM determines an individual's evaluative judgment of the target behavior in some dimension (attitudes). For example, it includes the perception that using an IT system

XSL•FO
RenderX

will be free of effort (perceived ease of use) and will enhance performance (perceived usefulness). Another determinant in the TAM is the specific behavior when interacting with the technology of the CHT program (use). The Swedish functional health literacy scale [20] was used for inspiration to develop questions to evaluate an individual's digital health literacy (skills). All areas of interest (attitudes, perceptions, use and skills) were entered into a template guiding the construction of the questionnaire (Multimedia Appendix 1). Furthermore, 2 scaling methods were chosen initially for capturing patients' responses in the questionnaire. These were the Likert method (strongly agree, agree, undecided, disagree, and strongly disagree), and a frequency scale with fixed choice responses (always, often, sometimes, seldom, and never).

Face Validity Test of the Questionnaire

In January 2022, 14 patients visiting the cardiology ED at Danderyd University Hospital with acute chest pain and taking part in the CLEOS-CPDS prospective cohort study were asked to participate in the development of the questionnaire. The selected patients represented a variation in age and gender. If they agreed to participate, an information letter and a questionnaire were sent to their home by post; and a few days later a researcher (KS or KF) contacted them by phone. We used the think-aloud (TA) method [21] to test the face validity of the questionnaire. During the phone call, the respondents were asked to fill in the questionnaire, encouraged to think out loud and to verbalize any thoughts while doing so. This provided an opportunity to listen to their understanding of each item as they worked through the questionnaire. In addition, probing questions were asked when the session leader needed further clarification. At the end of the TA session, all participants were asked if they had any additional comments that had not been addressed during the session. The content of the sessions was recorded in a spreadsheet to facilitate the evaluation and revision of the questionnaire.

Investigating Outcomes of the Questionnaire

Sample and Setting

Adult patients (≥18 y) with acute chest pain, presenting to the ED at Danderyd University Hospital and participating in the CLEOS-CPDS from May until November 2022 (n=288, mean age 55 y, 41% women) were invited to answer the questionnaire. Before discharge from the ED, patients were invited consecutively by a study nurse to participate. Those who agreed were given study information and a paper copy of the questionnaire, along with a prepaid return envelope. Of the 130 questionnaires returned, one was blank, leaving 129 participants. The mean age of the patients participating was 56 (SD 17.3) years (range 18-89 y). More men (79/129, 61%) than women (49/129, 38%) participated (Table 1).

Table . Sociodemographic characteristics for participants answering the questionnaire (N=129).

Characteristics	
Age (years), mean (minimum-maximum)	56 (18-89)
Gender [1], n (%)	
Women	49 (38)
Men	79 (61)
Missing	1 (<1)
Education level, n (%)	
Junior compulsory	7 (5)
Senior high school	47 (37)
Postgraduate or university	74 (58)
Missing	1 (<1)
Occupation, n (%)	
Working or student	87 (67)
Retired	40 (31)
Unemployed or sick leave	2 (2)

Analysis

The items in the questionnaire were analyzed using descriptive statistics, including frequencies and percentages. Spearman's rho was used to explore the correlations between age, attitudes of using digital technology and experience of using CLEOS. For analysis in SPSS Statistics 30 (IBM), the responses were labeled as "always"=1, "often"=2, "sometimes"=3, "seldom"=4, or "never"=5. The responses were ranked from low to high, with the item "always" given the lowest ranking of 5 and the item "never" the highest rank of 1. Thus, a positive correlation means a relationship between older age and "never" and a negative correlation means a strong relationship between older age and "always."

Internal item consistency was tested for 6 items corresponding to questions on health literacy: "I could make use of the content in the text, "It took a long time for me to read the text", "There were words that I did not understand," "It was difficult to answer the questions," "The questions were relevant," "It was easy to find relevant response alternatives." The intended health literacy

XSL•FO
RenderX

scale had a Cronbach α of .68. The items corresponding to attitudes, perceptions and skills were too diverse to make up a scale and were hence not tested for internal consistency.

Conventional content analysis was applied for the free text comments [22]. The analysis was conducted by 2 of the authors (KF and KS), both experienced with qualitative research. The comments were entered into a document and coded by highlighting similar texts in the same color, followed by categorizing them into color-coded clusters. The clusters were defined into categories which were discussed and refined and then finalized in agreement with all authors. A response frequency chart was used to determine the frequency of similar comments.

Ethical Considerations

This study has been approved by the Swedish Ethical Review Authority (reference number 2015/1955 - 31) and is registered at ClinicalTrials.gov, National Library of Medicine, (NCT03439449). Informed consent was not obtained specifically for this study since patients had been informed. while obtainging informed consent in the CLEOS-CPDS study, that they might be asked later to take part in an evaluation of their perceptions of using the programme. To ensure that no participants could be identified, all participants names were removed and replaced with an unique code. No compensations for participating in this study were offered.

Results

Development of the Questionnaire

The initial version of the questionnaire contained a total of 19 items and an additional 4 sociodemographic questions. The items concerned experience of use of digital technology in general, the use of digital technology in health care, and the use of the CLEOS program.

In addition, 12 individual TA sessions were held, involving 6 women and 6 men, with mean age 72 (range 37-82) years. A majority had postgraduate or university (n=7) as the highest level of education, followed by senior high school (n=2), junior compulsory (n=3), and a majority were retired (n=8).

Based on the results of the TA sessions, the wording of 2 questionnaire items was revised. For item 5, the word “lean on” was changed to “depend on” and for item 7, the word “relation” was changed to “personal contact.” Three items were removed because they resembled other items and did not contribute to the evaluation of CLEOS. Moreover, the response format “strongly agree” to “strongly disagree,” which was used for seven items, was perceived as difficult to understand. It was replaced with the response format “always,” “often,” “sometimes,” “seldom” or “never,” which was consistent with the allowed response alternatives for all other items. The revised questionnaire had 16 items and 1 free text comment (Multimedia Appendix 2). The first set of questions (n=9) assessed attitudes, perceptions, and skills related to the use of digital technology in health care (Tables 2 and 3). The second set (n=7) evaluated the specific experience of self-reported history-taking by interacting with CLEOS (Table 4). The questionnaire included a combination of positively and negatively phrased items, response alternatives such as (yes, no, uncertain), and frequency scales (always, often, sometimes, seldom, never).

Table . Attitudes, perceptions, and skills related to the use of digital technology in health care (N=127).

	Yes, n (%)	No, n (%)	Uncertain, n (%)
Have encountered digital technology previously in contact with health care	63 (50)	59 (46)	5 (4)
Digital technology has a role when visiting health care	115 (91)	2 (1)	10 (8)

XSL•FO
RenderX

Table . Summary of attitudes, perceptions, and skills toward digital technology use in health care.

	Always, n (%)	Often, n (%)	Sometimes, n (%)	Seldom, n (%)	Never, n (%)	n
Find it easy using digital technology	104 (80)	14 (11)	9 (7)	1 (1)	1 (1)	129
Feel confident using digital technology	105 (81)	13 (10)	7 (5)	3 (2)	1 (1)	129
Trust digital technology to function as intended when visiting health care	84 (66)	31 (24)	10 (8)	0	2 (2)	127
Worry that information regarding own health collected by digital technology will be disclosed to unauthorized persons	4 (3)	1 (1)	18 (14)	31 (24)	73 (58)	127
Worry that the patient-doctor personal contact is disturbed when digital technology is used in health care	11 (9)	3 (2)	34 (27)	22 (17)	58 (45)	128
Believe that patient-reported symptoms using digital technology are helpful for the physician when making a diagnosis	60 (47)	23 (18)	35 (28)	6 (5)	3 (2)	127
Believe that patient contribution is valuable when developing digital technology in health care	100 (78)	17 (!4)	8 (6)	3 (2)	0	128

XSL•FO
RenderX

Table . Experience of answering questions regarding own health using Clinical Expert Operating System on a tablet.

Experiences	Always, n (%)	Often, n (%)	Sometimes, n (%)	Seldom, n (%)	Never, n (%)	n
I was confident answering the questions	90 (70)	25 (20)	11 (9)	1 (1)	1 (1)	128
I could make use of the content in the text	92 (71)	33 (26)	3 (2)	0	1 (1)	129
It took a long time for me to read the text	5 (4)	5 (4)	23 (18)	21 (16)	75 (58)	129
There were words that I did not understand	6 (5)	1 (<1)	11 (9)	26 (20)	85 (66)	129
It was difficult to answer the questions	2 (2)	4 (3)	34 (26)	36 (28)	53 (41)	129
The questions were relevant	46 (36)	47 (36)	32 (25)	4 (3)	0	129
It was easy to find relevant response alternatives	34 (26)	68 (53)	26 (20)	0	1 (1)	129

Outcomes of the Questionnaire

Attitudes, Perceptions, and Skills

Most participants found it easy or often easy (n=118, 91%) and felt confident or often confident (n=118, 91%) using digital technology. Most (n=115, 91%) believed that digital technology has a role when visiting health care. Half (n=63, 50%) had not previously encountered or were not sure if they had encountered digital technology in interactions with healthcare. Most (n=115, 90%) trusted digital technology to function as intended during health care visits. One-fifth (n=23, 18%) was concerned or sometimes concerned that information regarding their health collected by digital technology would be disclosed to unauthorized persons. More than one-third (n=48, 38%) was concerned or sometimes concerned that the interaction between patient and doctor would be disrupted when using digital technology in health care. In addition, two-thirds (N=83, 65%) believed that patient reported symptoms using digital technology are helpful for the doctor in making a diagnosis. Four-fifths (n=100, 78%) believed that patient contribution is valuable when developing digital technology in health care (Table 2 and 3).

Experience of Using CLEOS

Most respondents (n=115, 90%) were confident or often confident to answer the questions on a tablet in the CLEOS-CPDS study. Almost all (n=125, 97%) could make use of the content in the text. Most (n=111, 86%) reported a high level of understanding of the terminology used in the CLEOS program, and a majority (n=89, 69%) did not or seldom find that the questions were difficult to answer. A majority of respondents (n=93, 72%) found that the questions in the CLEOS program were relevant. Slightly more (n=102, 79%) thought it had been easy or often easy to find relevant response alternatives (Table 4).

Correlations Between Age and Attitudes, and the Experience of Using Digital Technology

Significant, moderately positive correlations were found between age and the items “I find it easy using digital technology” (*P*=<.001; 95% CI 0.171-0.492), “I feel confident using digital technology in general” (*P*<.001; 95% CI 0.247-0.551), “I trust the digital technology to function as intended when visiting healthcare“ (*P*=.002) and “I was confident answering the questions in Cleos” (*P*=.02, 95% CI 0.032-0.379). The items were rated as “always,” “often,” “sometimes,” “seldom,” and “never” whereas “always” had the lowest ranking and “never” the highest ranking. The correlations indicate that older age is associated with less ease, confidence, and trust in using digital technology as well as confidence in answering the questions. A significant negative correlation was found between “I worry that the patient-doctor personal contact is disturbed when digital technology is used in healthcare” (*P*=.001; 95% CI −.443 to −.107), rated as “always,” “often,” “sometimes,” “seldom,” and “never,” indicating that higher age is associated with greater concern (Table 5). The results for 127 - 129 participants were tested using Spearman rho. The ranking was from low to high; the item “always” has the lowest ranking of 5, and the item “never” has the highest rank of 1. A significant positive correlation means a relationship between older age and “never” and a significant negative correlation means a strong relationship between older age and “always.”

XSL•FO
RenderX

Table . Correlations between age and attitudes related to the use of digital technology in health care and experience of answering questions using clinical expert operating system (N=129).

	Correlation coefficient	*P* value	95% CI
Attitudes of using digital technology[a]			
Find it easy using digital technology	0.342	<. 001	.171 to .492
Feel confident using digital technology	0.41	<. 001	.247 to .551
Trust digital technology to function as intended when visiting health care	0.278	.002	.100 to .439
Worry that information regarding own health collected by digital technology will be disclosed to unauthorized persons	–0.078	.39	–.257 to –.107
Worry that the patient-doctor personal contact is disrupted when digital technology is used in health care	–0.283	.001	–.443 to –.107
Believe patient-reported symptoms using digital technology are helpful for the physician when making a diagnosis	–0.02	.83	–.202 to .163
Believe that patient contribution is valuable when developing digital technology in health care	0.129	.15	–.054 to .304
Experience of answering questions			
I was confident answering the questions	0.212	.02	.031 to .379
I could make use of the content in the text	0.035	.70	–.148 to .215
It took a long time for me to read the text	–0.032	.72	–.213 to .150
There were words that I did not understand	0.097	0.28	–.086 to .274
It was difficult to answer the questions	–0.16	.08	–.332 to .022
The questions were relevant	–0.161	.07	–.333 to .021
It was easy to find relevant response alternatives	0.04	.662	–.142 to .220

[a]Results for 127 - 129 participants. Tested by Spearman´s rho. Ranking (from low to high) the item “always” has the lowest ranking of 5, and the item “never” has the highest rank of 1. A significant positive correlation means a relationship between older age and “never” and a significant negative correlation means a strong relationship between older age and “always.”

Free Text Comments

The last item in the questionnaire allowed patients to comment on their experience of performing the CLEOS interview on the tablet (Textbox 1). A total of 40% of the patients left comments concerning (1) time aspects regarding the CLEOS interview (n=11), perceptions regarding the questions included in CLEOS (n=13), (2) perceptions regarding the response alternatives (n=13), (3) perceptions of technical performance (n=6), (4) perceptions of layout (n=9), (5) difficult-to-understand words (n=6), and (6) not confident (n=2).

XSL•FO
RenderX

Textbox 1. Categories and examples of comments in the questionnaire regarding answering questions in CLEOS.

Time aspects regarding the clinical expert operating system interview (n=11)

It was too extensive and time consuming, it was tiresome to answer all the questions and hard to stay focused, not enough time to answer all questions.

Perceptions regarding the questions (n=13)

Lacking questions (ie, a question about other diseases), questions that were grammatically wrong, not translated from German or English, questions about a topic that never ended or unrecognizable scenarios becoming increasingly irrelevant, questions that were incomplete and lacking an illustration (image), irrelevant follow-up question (ie, requested to answer "what kind of surgery" after having said no to "had any surgery").

Perceptions regarding the response alternatives (n=13)

Lacking an appropriate alternative, wanting more alternatives or "I don't know", having to answer "how often" after answering no to a symptom occurrence, not finding a prescribed medication in the list of medicines.

Perceptions of technical performance (n=6)

A slow interface, technical, or internet problems.

Perceptions of layout (n=9)

The size of the text was too small, unclear transition to the next page, not clear when the questions had ended, an inert maneuvering.

Difficult to understand words (n=6)

Connotation of wording that was, that some words needed explanation, that medical terms were difficult, some text was strangely worded.

Not confident (n=2)

Feeling uncertain about using the technique, "talking" to a doctor on a screen feels impersonal.

Discussion

Principal Findings

This study included a process of developing a questionnaire and a cross-sectional study that evaluated patients' attitudes toward digital technology in health care and experiences of interacting with a CHT program while presenting to an ED setting with acute chest pain. The questionnaire development process required only minor changes for the final version. Overall, the findings from the evaluation of using the CLEOS program showed a high acceptance of digital technology when incorporated in health care as well as user confidence and high digital literacy among the participants.

Comparison With Previous Work

In general, there was a favorable attitude toward digital technology, with many participants expressing their faith in its potential to help physicians make accurate diagnoses. Although not all had previous experience using digital technology in health care encounters, a clear majority in this study had a positive attitude about the role of such technology when visiting health care. Moreover, most were confident using the CLEOS program. This is in line with the results of Arora et al [12] who were early to use a CHT program in the waiting area of an ED. In that study, the overall impression among the patients was that they would like to fill out a digital questionnaire again in the future. In a more recent pilot study assessing digital patient self-anamnesis in the waiting area of an ED, 63% agreed to fill out a digital questionnaire again [23]. In another study evaluating medical history-taking via an app in general practice, the usability score (evaluated by SUS) was in favor of acknowledging a recurrent use of the application [14]. The application described in that study is similar to a CHT program that emulates clinical thinking, but the application uses a branching logic that is adaptive to patient responses instead of automated interpretation of previous answers. While a clear majority expressed a trust in the technique when used in health care interactions, there were some concerns about data security and privacy in the present study. The high level of trust in digital technology to function well was somewhat surprising in our present results, given that only just over half of the respondents had previously encountered digital technology when in contact with health care. Altogether, the results from our current study support previous findings of a high level of patient acceptance of health care technology when visiting EDs.

There was a modest but noteworthy concern about disrupted patient-physician interaction when using digital technology in health care. This concern was more pronounced in older patients. As there are no other CHT programs like CLEOS and very few other comparable systems, it is hard to conclude what these results mean. A related area in health care, however, is patients' opinions about the patient-physician relationship and communication with physicians using electronic medical records (EMR). Perceptions of such computer use during the health care visit were compiled in a systematic review. The authors concluded that it did not substantially affect the quality of communication with their physician [24]. In a survey examining perceived benefits and risks of using artificial intelligence (AI) applications in health care, communication barriers emerged as the most significant predictors of perceived risks [25]. The authors discussed that the loss of face-to-face cues and lack of interaction with physicians would give the patient a more passive position. On the other hand, their results showed that if users believe that AI-based devices can improve diagnostics and patient management systems, they become more prone to use them. A review showed that digital tools in health care can be facilitators for factors such as empowerment and personalized communication with health care [9]. Reciprocally, patient empowerment contributed to patient uptake of digital health tools. The study concluded too that digital tools could facilitate

XSL•FO
RenderX

a shift from paternalistic health care models to those in which relationships between clinicians and patients are more collaborative. Based on these findings, we agree that patient-physician communication through modern technology could be perceived as positive by patients. Nevertheless, our results also tell us that patients' trust, especially with rising age, needs to be ensured and further investigated before CHT programs are integrated into standard clinical practice.

The ability to understand and make use of the content in the CLEOS program was overall very satisfactory. Low digital and health literacy have been described as barriers to implementation of digital tools [9,10]. Our results may be a consequence of a presumed high health literacy among the participants related to a relatively high educational level, known as a strong associated factor [26]. Higher age could be another barrier. The present results suggest that older people are more likely to experience less ease and confidence in using digital technology. This could explain why being 70 years or older was found to be a negative factor for completing the program in a previous study of the CLEOS-CPDS cohort [5]. Similarly, Albrink et al [14] found that age was negatively associated with the usability SUS score when evaluating their app, suggesting that older people may face challenges in handling such an app.

Our study shows strong support for involving end users when designing new digital technology in health care. This confirms findings by others who recommend a participatory approach in the design of future digital health care [27-29]. The free text comments revealed aspects for improvement of the CLEOS program such as high time consumption, ambiguous questions, and slow technical performance. These results align well with those from our previous interview study [15], highlighting the need for further development of the program.

The challenge of developing questionnaires in research is to achieve high validity and reliability. Accordingly, the questionnaire development was guided by a robust process based on the results of our previous interview study and other recognized methods. Furthermore, the development process included the think-aloud method [21], which allowed the participants to speak freely while testing the questionnaire. The think-aloud method has no specific sample size recommendation, and we decided to stop inclusion when no new data was collected. Although the sample in the present study may be small, they provided valuable information about the comprehensibility of the questionnaire. Presumably, all areas of interest were covered sufficiently. However, to be sure that the questionnaire measures what is intended, a more robust validation in a future study is needed.

Our results should be interpreted in the context of the study's limitations. The convenience sample of patients responding to the questionnaire may not be representative of all patients seeking care at the cardiology ED. The small sample size and single center inclusion affects the generalizability of the results. Further, the selected sample had been consecutively recruited to the CLEOS-CPDS study and may have had a positive attitude toward digital technology as they had consented to participate in the study. Other selection biases could be a slight overrepresentation of men in the sample and an uneven distribution of education levels. Furthermore, we lack information about those who did not fulfil the criteria for inclusion, eg, fluency in Swedish, or declined participation both in CLEOS-CPDS and in the current study.

Conclusion

This study suggests strong acceptability and trust of digital technology among patients presenting to a cardiology ED. However, the concern for lack of personal contact between patient and doctor should be acknowledged. Digital technology was seen as an important facilitator but not as a replacement for human interaction. The CHT program (CLEOS) performed well for end-users but would benefit from some adjustments for future studies. The questionnaire responses yielded some new insights into the use of digital technology for health care delivery. The questionnaire appears relevant and may be useful for future evaluations of CHT in various contexts.

Acknowledgments

The authors would like to thank the patients who participated in this study. This study was funded by the Robert Bosch Stiftung (Stuttgart, Germany, grant number 11.5.1000.0258.0), Region Stockholm (ALF project; Stockholm, Sweden, grant numbers FoUI-954046 and FoUI-962663), and institutional funds from Department of Learning, informatics, management and ethics, Karolinska Institutet (Stockholm, Sweden).

Authors' Contributions

KF and KS contributed to the conceptualization, data curation, formal analysis, investigation, methodology, project administration, supervision, validation, visualization, writing - original draft, review and editing; HB contributed to Conceptualization, Methodology, Project administration, Resources, Validation, Writing - original draft, review and editing; TK, CJS, DZ contributed to Conceptualization, Funding acquisition, Methodology, Validation, Writing - original draft, review and editing; JS, SK contributed to Conceptualization, Methodology, Validation, Writing - original draft, review and editing

Conflicts of Interest

DZ is the inventor of US patents for technology related to the CLEOS program. All patent rights and copyrights to technology, language, images and knowledge content are assigned without royalty rights by DZ to Karolinska Institutet, Stockholm, Sweden, which is a public university. Only Karolinska Institutet and its subsidiaries may be owners or receive royalties or other revenue

XSL•FO
RenderX

from use of CLEOS technology, language, images, knowledge content or from clinical insights and/or computer algorithms generated from analysis of data acquired by the program. HB receives speaker honoraria for AstraZeneca.
JS receives speaker honoraria from Bayer, AstraZeneca, Boehringer Ingelheim, NovoNordisk and Sanofi.

Multimedia Appendix 1
Template of the development of the questionnaire.
[PDF File, 108 KB - medinform_v13i1e65568_app1.pdf]

Multimedia Appendix 2
The questionnaire.
[PDF File, 67 KB - medinform_v13i1e65568_app2.pdf]

References

1. Zakim D. Development and significance of automated history-taking software for clinical medicine, clinical research and basic medical science. J Intern Med 2016 Sep;280(3):287-299. [doi: 10.1111/joim.12509] [Medline: 27071980]
2. Zakim D, Schwab M. Data collection as a barrier to personalized medicine. Trends Pharmacol Sci 2015 Feb;36(2):68-71. [doi: 10.1016/j.tips.2014.11.002] [Medline: 25479798]
3. Almario CV, Chey W, Kaung A, et al. Computer-generated vs. physician-documented history of present illness (HPI): results of a blinded comparison. Am J Gastroenterol 2015 Jan;110(1):170-179. [doi: 10.1038/ajg.2014.356] [Medline: 25461620]
4. Taylor JL, Mistry M. An evaluation of automated, internet-based psychiatric history taking. Future Healthc J 2018 Jun;5(2):126-131. [doi: 10.7861/futurehosp.5-2-126] [Medline: 31098547]
5. Brandberg H, Sundberg CJ, Spaak J, Koch S, Zakim D, Kahan T. Use of self-reported computerized medical history taking for acute chest pain in the emergency department - the clinical expert operating system chest pain danderyd study (CLEOS-CPDS): prospective cohort study. J Med Internet Res 2021 Apr 27;23(4):e25493. [doi: 10.2196/25493] [Medline: 33904821]
6. Brandberg H, Sundberg CJ, Spaak J, Koch S, Kahan T. Are medical history data fit for risk stratification of patients with chest pain in emergency care? Comparing data collected from patients using computerized history taking with data documented by physicians in the electronic health record in the CLEOS-CPDS prospective cohort study. J Am Med Inform Assoc 2024 Jun 20;31(7):1529-1539. [doi: 10.1093/jamia/ocae110] [Medline: 38781350]
7. Brandberg H, Kahan T, Spaak J, et al. A prospective cohort study of self-reported computerised medical history taking for acute chest pain: protocol of the CLEOS-Chest Pain Danderyd Study (CLEOS-CPDS). BMJ Open 2020 Jan 21;10(1):e031871. [doi: 10.1136/bmjopen-2019-031871] [Medline: 31969363]
8. Carini E, Villani L, Pezzullo AM, et al. The impact of digital patient portals on health outcomes, system efficiency, and patient attitudes: updated systematic literature review. J Med Internet Res 2021 Sep 8;23(9):e26189. [doi: 10.2196/26189] [Medline: 34494966]
9. Madanian S, Nakarada-Kordic I, Reay S, Chetty T. Patients' perspectives on digital health tools. PEC Innov 2023 Dec;2(2):100171. [doi: 10.1016/j.pecinn.2023.100171] [Medline: 37384154]
10. Dunn P, Hazzard E. Technology approaches to digital health literacy. Int J Cardiol 2019 Oct 15;293(293):294-296. [doi: 10.1016/j.ijcard.2019.06.039] [Medline: 31350037]
11. Lazarou I, Krooupa AM, Nikolopoulos S, et al. Cancer patients' perspectives and requirements of digital health technologies: a scoping literature review. Cancers (Basel) 2024 Jun 21;16(13):2293. [doi: 10.3390/cancers16132293] [Medline: 39001356]
12. Arora S, Goldberg AD, Menchine M. Patient impression and satisfaction of a self-administered, automated medical history-taking device in the Emergency Department. West J Emerg Med 2014 Feb;15(1):35-40. [doi: 10.5811/westjem.2013.2.11498] [Medline: 24695871]
13. Benaroia M, Elinson R, Zarnke K. Patient-directed intelligent and interactive computer medical history-gathering systems: A utility and feasibility study in the emergency department. Int J Med Inform 2007 Apr;76(4):283-288. [doi: 10.1016/j.ijmedinf.2006.01.006] [Medline: 16473548]
14. Albrink K, Schröder D, Joos C, Müller F, Noack EM. Usability of an app for medical history taking in general practice from the patients' Perspective: cross-sectional study. JMIR Hum Factors 2024 Jan 5;11(11):e47755. [doi: 10.2196/47755] [Medline: 38180798]
15. Sundberg K, Adeli A, Brandberg H, et al. User experience of self-reported computerized medical history taking for acute chest pain: The Clinical Expert Operating System Chest Pain Danderyd Study. Health Expect 2022 Dec;25(6):3053-3061. [doi: 10.1111/hex.13612] [Medline: 36148691]
16. Holden RJ, Karsh BT. The technology acceptance model: its past and its future in health care. J Biomed Inform 2010 Feb;43(1):159-172. [doi: 10.1016/j.jbi.2009.07.002] [Medline: 19615467]
17. Boynton PM, Greenhalgh T. Selecting, designing, and developing your questionnaire. BMJ 2004 May 29;328(7451):1312-1315. [doi: 10.1136/bmj.328.7451.1312] [Medline: 15166072]

XSL•FO
RenderX

18. Rattray J, Jones MC. Essential elements of questionnaire design and development. J Clin Nurs 2007 Feb;16(2):234-243. [doi: 10.1111/j.1365-2702.2006.01573.x] [Medline: 17239058]
19. Lewis JR. The system usability scale: past, present, and future. International Journal of Human–Computer Interaction 2018 Jul 3;34(7):577-590. [doi: 10.1080/10447318.2018.1455307]
20. Wångdahl JM, Mårtensson LI. Measuring health literacy - the Swedish Functional Health Literacy scale. Scand J Caring Sci 2015 Mar;29(1):165-172. [doi: 10.1111/scs.12125] [Medline: 24628048]
21. Charters E. The use of think-aloud methods in qualitative research an introduction to think-aloud methods. Brock Education Journal 2003;12(2). [doi: 10.26522/brocked.v12i2.38]
22. Hsieh HF, Shannon SE. Three approaches to qualitative content analysis. Qual Health Res 2005 Nov;15(9):1277-1288. [doi: 10.1177/1049732305276687] [Medline: 16204405]
23. Melms L, Schaefer JR, Jerrentrup A, Mueller T. A pilot study of patient satisfaction with A self-completed tablet-based digital questionnaire for collecting the patient's medical history in an emergency department. BMC Health Serv Res 2021 Jul 30;21(1):755. [doi: 10.1186/s12913-021-06748-y] [Medline: 34330279]
24. Alkureishi MA, Lee WW, Lyons M, et al. Impact of electronic medical record use on the patient-doctor relationship and communication: a systematic review. J GEN INTERN MED 2016 May;31(5):548-560. [doi: 10.1007/s11606-015-3582-1] [Medline: 26786877]
25. Esmaeilzadeh P. Use of AI-based tools for healthcare purposes: a survey study from consumers' perspectives. BMC Med Inform Decis Mak 2020 Jul 22;20(1):170. [doi: 10.1186/s12911-020-01191-1] [Medline: 32698869]
26. van der Heide I, Wang J, Droomers M, Spreeuwenberg P, Rademakers J, Uiters E. The relationship between health, education, and health literacy: results from the Dutch Adult Literacy and Life Skills Survey. J Health Commun 2013;18 Suppl 1(Suppl 1):172-184. [doi: 10.1080/10810730.2013.825668] [Medline: 24093354]
27. Hanna L, Gill SD, Newstead L, Hawkins M, Osborne RH. Patient perspectives on a personally controlled electronic health record used in regional Australia. Health Inf Manag 2017 Jan;46(1):42-48. [doi: 10.1177/1833358316661063] [Medline: 27486184]
28. Monaco A, Palmer K, Holm Ravn Faber N, et al. Digital health tools for managing noncommunicable diseases during and after the COVID-19 pandemic: perspectives of patients and caregivers. J Med Internet Res 2021 Jan 29;23(1):e25652. [doi: 10.2196/25652] [Medline: 33464206]
29. Schicktanz S, Amelung T, Rieger JW. Qualitative assessment of patients' attitudes and expectations toward BCIs and implications for future technology development. Front Syst Neurosci 2015;9(9):64. [doi: 10.3389/fnsys.2015.00064] [Medline: 25964745]

Abbreviations

AI: artificial intelligence
CHT: computerized history-taking
CLEOS: clinical expert operating system
CLEOS-CPDS: Clinical Expert Operating System - chest pain Danderyd study
ED: emergency department
EMR: electronic medical records
HEART: history, electrocardiogram, age, risk factors and troponin
SUS: System Usability Scale
TA: think-aloud
TAM: Technology Acceptance Model

Edited by A Benis; submitted 19.08.24; peer-reviewed by Y Zhou, Y Harada; revised version received 11.03.25; accepted 11.04.25; published 17.06.25.

Please cite as:
Fritzell K, Brandberg H, Spaak J, Koch S, Sundberg CJ, Zakim D, Kahan T, Sundberg K
Patient Perspectives on Digital Technology and Experiences of Computerized History-Taking for Chest Pain Management in the Emergency Department: CLEOS-CPDS Prospective Cohort Study
JMIR Med Inform 2025;13:e65568
URL: https://medinform.jmir.org/2025/1/e65568
doi:10.2196/65568

© Kaisa Fritzell, Helge Brandberg, Jonas Spaak, Sabine Koch, Carl Johan Sundberg, David Zakim, Thomas Kahan, Kay Sundberg. Originally published in JMIR Medical Informatics (https://medinform.jmir.org), 17.6.2025. This is an open-access article distributed

XSL•FO
RenderX

under the terms of the Creative Commons Attribution License (https://creativecommons.org/licenses/by/4.0/), which permits unrestricted use, distribution, and reproduction in any medium, provided the original work, first published in JMIR Medical Informatics, is properly cited. The complete bibliographic information, a link to the original publication on https://medinform.jmir.org/, as well as this copyright and license information must be included.

XSL•FO
RenderX

Alert Reduction and Telemonitoring Process Optimization for Improving Efficiency in Remote Patient Monitoring Programs: Framework Development Study

Job van Steenkiste[1,2,3], MD; Niki Lupgens[2], BSc; Martijn Kool[4], MD, PhD; Daan Dohmen[1,4], Prof Dr; Iris Verberk-Jonkers[2], MD, PhD

[1]Faculty of Management Sciences, Open University, Valkenburgerweg 177, Heerlen, The Netherlands

[2]Department of Internal Medicine, Maasstad Hospital, Rotterdam, The Netherlands

[3]Department of Hospital Pharmacy, Erasmus MC University Medical Center, Rotterdam, The Netherlands

[4]Luscii Healthtech BV, Utrecht, The Netherlands

Corresponding Author:
Job van Steenkiste, MD
Faculty of Management Sciences, Open University, Valkenburgerweg 177, Heerlen, The Netherlands

Abstract

Background: Telemonitoring can enhance the efficiency of health care delivery by enabling risk stratification, thereby allowing health care professionals to focus on high-risk patients. Additionally, it reduces the need for physical care. In contrast, telemonitoring programs require a significant time investment for implementation and alert processing. A structured method for telemonitoring process optimization is lacking.

Objective: We propose a framework for optimizing efficient care delivery in telemonitoring programs based on alert data analysis and scenario analysis of a telemonitoring program for hypertension combined with a narrative literature review on methods to improve efficient telemonitoring care delivery.

Methods: We extracted 1-year alert processing data from the telemonitoring platform and electronic health records (June 2022-May 2023) from all users participating in the hypertension telemonitoring program in the outpatient clinic of the Department of Internal Medicine of the Maasstad Hospital. We analyzed the alert burden and alert processing data. Additionally, a scenario analysis with different threshold values was conducted for existing blood pressure alerts to assess the impact of threshold adjustments on the overall alert burden and processing. We searched for English language academic research papers and conference abstracts reporting clinical alert or workflow optimization in telemonitoring programs on May 24, 2024 in Embase, Medline, Cochrane, Web of Science, and Google Scholar.

Results: In total, 174 users were included and analyzed. On average, each user was active in the telemonitoring program for 207 days and a total of 30,184 measurements were performed. These triggered a total of 17,293 simple, complex, and inactive or overdue alerts: 13,647 were processed automatically by the telemonitoring platform, and 3646 were processed manually by e-nurses from the telemonitoring center, equivalent to 21 manually processed alerts per user. Additional analysis of the manually processed alerts revealed that 25 (15%) users triggered more than 50% of these specific alerts. Furthermore, scenario analysis of the alert thresholds revealed that a single increase of 5 and 10 mmHg for the diastolic and systolic blood pressure alerts would reduce the number of alerts by about 50%, resulting in a total reduced time investment for the e-nurse of 5973 minutes over 1 year. Literature search yielded 251 articles, of which 7 studies reported methods to improve efficiency in telemonitoring programs, including the introduction of complex alerts and clinical algorithms to triage alerts, scenario analysis with alert threshold adjustments, and a qualitative analysis to create an alert triage algorithm.

Conclusions: Based on the data analysis and literature review, a 4-step framework was developed to optimize the efficiency of telemonitoring programs. The 4 steps include ensuring accurate measurements, telemonitoring algorithm and alert optimization, focusing on individual users' and user groups' needs, and improving telemonitoring process efficiency. This framework can be an important first step to improve the efficiency of 21st-century telemonitoring programs.

(JMIR Med Inform 2025;13:e66066) doi:10.2196/66066

KEYWORDS

care delivery; remote patient monitoring; remote monitoring; patient monitoring; telemonitoring; alert; alerts; workflow; workflows; hypertension monitoring; hypertension; high blood pressure; medical informatics; data; data processing; algorithm; algorithms; model; models; analytics

XSL•FO
RenderX

Introduction

Since the COVID-19 pandemic [1], the use of telemonitoring has rapidly increased [2]. In 21st-century telemonitoring, patients measure relevant health data like vital signs at home according to a predefined measurement schedule [3]. These data are transmitted through a smartphone or tablet application, can be reviewed remotely by health care providers, and can trigger alerts based on pre-defined threshold values. Alerts are reviewed by e-nurses in remote patient monitoring centers and discussed with health care providers if required. Depending on the alert, remote treatment adjustment will take place, and feedback is provided to the patient. In theory, the application of telemonitoring improves health care delivery by contributing to the Quintuple Aim goals [4] aimed at improving patient experiences, improving population health, reducing health care costs, improving care team well-being, and enhancing health equity. Achieving specific efficiency-related goals requires telemonitoring to reduce the need for physical care and shift attention to patients who mostly require it. This is particularly relevant in situations with increased care needs combined with reduced available health care staff [5]. It is however, for many diseases still unclear whether telemonitoring does lead to more efficient care delivery, as it requires a significant time investment (eg, alert processing, development and implementation of telemonitoring algorithms), generates new data, and needs continuous optimization of clinical workflows [6,7].

Modern telemonitoring platforms are often embedded in existing care paths and include clinical algorithms that triage and process the generated alerts [3,8]. This proactive way of telemonitoring ensures that patients who are off target are quickly identified, and actions can be undertaken proactively to prevent deterioration of the patient's condition. Conversely, stable patients do not generate alerts and thus do not require immediate care.

These health data [8] ideally generate as few alerts as possible, and a clinical consequence is attached to each generated alert. However, in practice, alert triggering and processing are not perfect yet. Algorithms that have strict alert thresholds generate many alerts, increase clinical workload, and enhance so-called "alert fatigue" [9], whereas algorithms with very wide alert thresholds generate few alerts but may pose significant health risks, for example, by underreporting relevant changes in a patient's health status ("do not harm principle") [5]. "Alert fatigue" is an important barrier when developing a telemonitoring algorithm [10]. In hypertension management, for example, it is known that health care providers, on average, only respond to around 60% of generated off-target blood pressure (BP) alerts [11]. To improve the efficiency of a telemonitoring program, technical improvements or algorithm enhancement, such as designing more sophisticated alerts or refining threshold values, can be initiated [12,13]. However, a clear, structured method like the use of a framework to reduce alerts and improve telemonitoring efficiency is lacking.

In this study, we evaluate the efficiency of a large telemonitoring program for hypertension at the Maasstad Hospital in Rotterdam, the Netherlands, by analyzing telemonitoring alerts and alert processing. Additionally, we use scenario analysis to assess the impact of adjusting alert thresholds on the overall alert burden. Finally, we combine this analysis with a narrative literature review on methods to improve telemonitoring efficiency to propose a framework for alert reduction and telemonitoring process optimization.

Methods

Study Design

This study used a cross-sectional data analysis, narrative literature review, and subsequential framework development.

Setting

This study was conducted at the Maasstad Hospital, a large teaching hospital in Rotterdam, the Netherlands.

Ethical Considerations

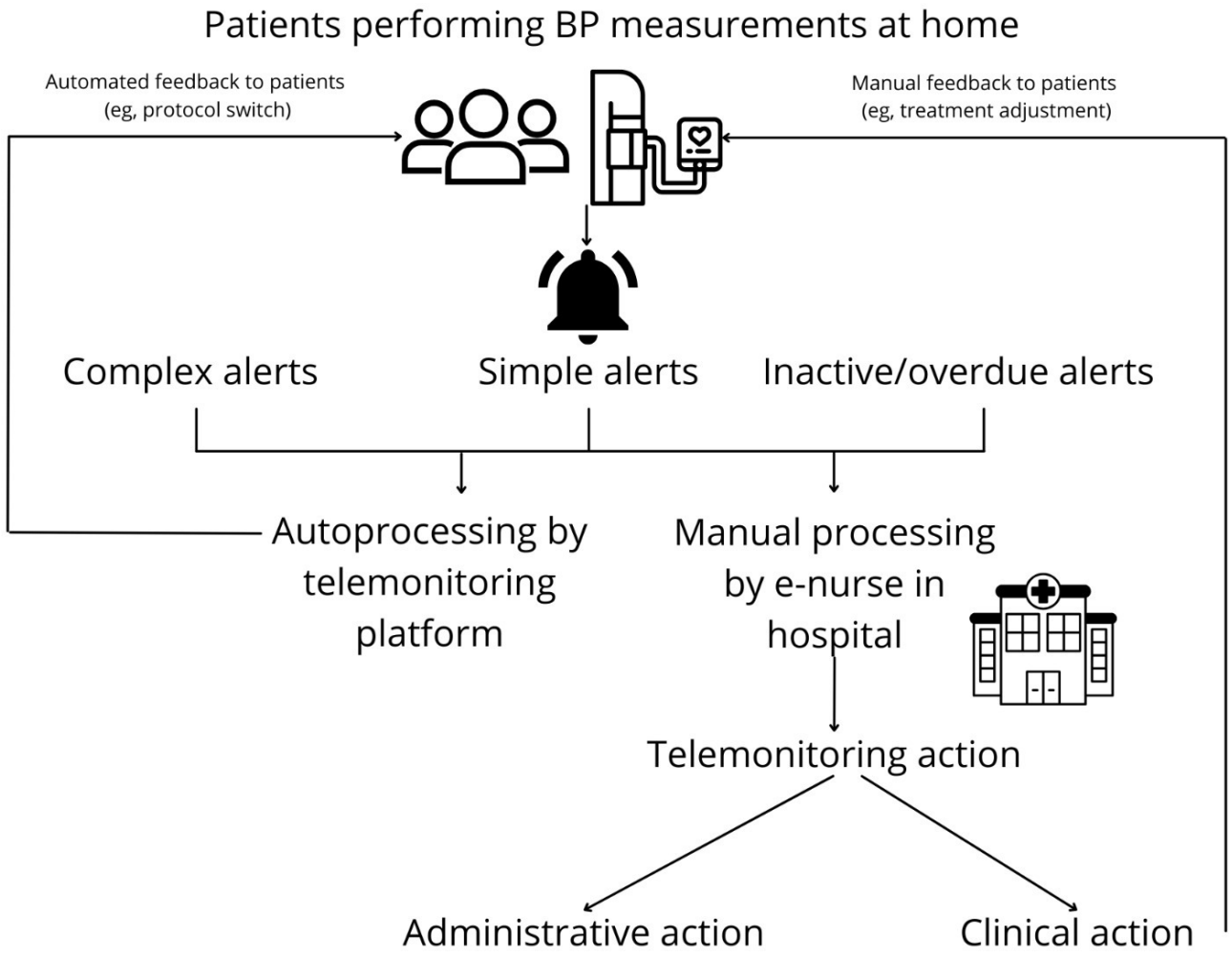
The study was conducted following the principles of the Declaration of Helsinki Version: WMA 52nd General Meeting, Edinburgh, Scotland, Oct 2000 (Washington 2002 and Tokyo 2004) [14] and Good Clinical Practice standards [15]. This study was approved by the Institutional Review Board of the Maasstad Hospital (identifier L2024-029). This study was assessed by the Medical Ethics Committee United and not subject to the Medical Research Involving Human Subjects (identifier W24.053). As all data were processed anonymously, a consent procedure was waived by both the Institutional Review Board and the Medical Ethics Committee United.

Telemonitoring Organization and Algorithm

The Maasstad Hospital has extensive experience with telemonitoring for various medical conditions. Since June 2022, a central telemonitoring center has been in operation where specialized monitoring nurses assess all generated alerts during office hours. They are supervised daily by a responsible nurse specialist or medical specialist. See Figure 1 for a graphical overview of the telemonitoring organization.

XSL•FO
RenderX

Figure 1. Telemonitoring organization and alert processing. Users measure their blood pressure at home using a validated Bluetooth blood pressure machine. These measurements can trigger simple, complex, or inactive or overdue alerts. These alerts are either processed automatically by the telemonitoring platform or manually by the e-nurse in the hospital. Alerts are processed on a single day for a single user during a telemonitoring action. This can either be an administrative or clinical action. Feedback to the users is provided automatically by the telemonitoring platform (eg, a protocol switch) or manually by the e-nurse (eg, a treatment adjustment).



Hypertension Care Path and Telemonitoring Program

The hypertension program and telemonitoring application (Luscii) [16] used in this study have been available since 2021 and are embedded in a care path for hypertension. The program is developed in line with the latest European Society of Cardiology/European Society of Hypertension guidelines [17]. Measurements are performed using a Bluetooth-connected, validated BP monitor. The Luscii application consists of a smartphone—or tablet application and an web-based healthcare provider dashboard. BP data are transmitted directly to the health care provider dashboard via the smartphone or tablet application. Once transmitted to the health care provider dashboard, the BP data are analyzed based on predefined algorithms, which will subsequently generate alerts (see details below under "Telemonitoring Alerts and Alert Processing") which are only visible in the health care provider dashboard. In the user application, users can review their BP data and have access to relevant educational modules and self-care documents, which, for example, emphasize the need for smoking cessation and antihypertensive drug adherence.

Users measure their BP twice in the morning and twice in the evening during measurement weeks. The program consists of 4 acute measurement algorithms and 1 chronic measurement algorithm. The acute algorithms, with BP targets ranging from 180/110 to 150/95 mmHg, have higher frequencies of measurement weeks and stricter threshold values and are used during the initial titration phase of achieving BP control. We choose 180/110 mmHg as the highest initial target during the titration phase, as higher BP can be associated with hypertensive emergencies [17]. Stable patients with on-target BP measurements are included in the chronic algorithm (140/90 mmHg) and measure 1 week per month. Patients automatically move between algorithms when BP values meet the target thresholds during the measurement weeks. See Multimedia Appendix 1 for a complete overview of the measurement algorithms.

Home Blood Pressure Telemonitoring Program Users

The hypertension care path is limited to an outpatient hospital setting, and general practitioners are currently not involved. All patients with hypertension, treated in the department of internal medicine of the Maasstad Hospital, either primarily for hypertension or, for example, when hypertension is a relevant risk factor (eg, diabetes, chronic kidney disease), are offered to participate in this digital care path. Exclusion criteria are the

XSL•FO
RenderX

existence of communication problems, lack of sufficient digital skills, and the absence of the possession of a mobile device. Validated BP measurement equipment can be loaned from the hospital if patients are unable to afford the purchase of such measurement. Once included, around 70% of the total care provided will be conducted remotely and digitally and 30% of the follow-up consultations will still be provided in person. The patients who primarily require follow-up for hypertension are referred by a general practitioner due to suspected secondary hypertension, resistant hypertension, drug intolerances, or a suspected hypertensive emergency. Given the heterogeneity of this group and for the purpose of this study, which focuses on organizational and efficiency aspects of telemonitoring, we refer to this complete patient group as the "users" of the telemonitoring program.

Telemonitoring Alerts and Alert Processing

The monitoring program generates 3 different types of alerts (Figure 1) following BP data transmission by the users of the telemonitoring program. First, there are simple alerts, which are triggered by a 1-time measurement exceeding predefined thresholds, eg, a very high or low systolic or diastolic BP. Second are complex alerts, which are triggered if a series of measurements are off target (eg, multiple consecutive off-target BP measurements) or if a combination of measurements (eg, systolic and diastolic BP and heart rate) are off target. In practice, these alerts are used for clinical decisions, such as drug treatment adjustments. Third are alerts that are triggered when users either miss a single scheduled measurement (overdue alert) or when they have missed all measurements within x days (inactive alert). Alerts can be processed automatically (eg, a single overdue alert, or an alert when a user is "on target") by the telemonitoring platform while triggering automated workflows created by the responsible clinicians. These workflows usually contain automated feedback messages that are delivered to the user automatically when the alert is processed by the monitoring platform (eg, your BP has improved, your target has changed). Besides autoprocessing by the telemonitoring platform, alerts can also be processed manually (eg, a complex alert for off-target BP) by e-nurses in a telemonitoring center. Whether alerts need manual processing by the e-nurses depends on choices made by health care providers in the monitoring algorithm. Simple alert thresholds were based on expert opinion, as no guidelines for these specific alerts are available. Thresholds for the complex alerts were based on treatment targets for home BP monitoring in existing guidelines [17]. We specifically choose to make the alert thresholds slightly higher than the treatment targets to reduce the overall alert burden (eg, 140/90 compared to 135/85). All alerts generated on a single day by a single user are clustered and manually processed using a telemonitoring action by the e-nurse, consisting of either an administrative action or a clinical action (eg, a treatment adjustment). Administrative actions have no clinical impact, as these actions only involve administrative handling of the alert in the telemonitoring platform and electronic health record (EHR) without any clinical consequences (eg, no treatment adjustments). Prior to processing the alerts, e-nurses can decide to contact patients to gather relevant clinical information (eg, adherence to antihypertensive drugs of lifestyle interventions). They can also provide feedback to the patients, for example, following antihypertensive treatment adjustment. Patients will also be contacted following inactivity alerts. Contacting patients is performed via a digital secured messaging platform (BeterDichtbij [18]) or via a telephone consultation. Alerts that need manual processing generated on Saturdays and Sundays were combined into one action on Monday, as the e-nurses only review alerts during office hours.

Telemonitoring Data

We extracted 1-year alert and alert processing data from the Luscii telemonitoring platform [16] and EHRs from all users participating in the hypertension telemonitoring program between June 1, 2022 and the May 31, 2023. Given the focus of the study, only anonymized data and no clinical or demographic data were extracted.

Alert Analysis

Alerts were processed either automatically or manually. We assigned each alert to a specific measurement to assess the impact of various alert thresholds on the number of generated alerts. Manually processed alerts clustered in telemonitoring actions were categorized, resulting in an administrative or a clinical action. Clinical actions can be a telephone consultation (with or without a treatment adjustment) or an integrated secured asynchronous message (with or without a treatment adjustment) through a communication platform.

Literature Search

For the narrative literature review, we searched articles reporting clinical alerts or workflow optimization in telemonitoring programs on May 24, 2024 in Embase, Medline, Cochrane, Web of Science, and Google Scholar. The complete search strategy is included in Multimedia Appendix 2. We included all English language academic research papers and conference abstracts published after January 1946. Studies reporting on alert reduction in clinical, in-hospital, settings (eg, intensive care units) were excluded. Relevant literature was identified using title and abstract screening from the initial identified papers. Relevant studies were subsequently reviewed in full text, and relevant alert reduction methods or workflow optimizations were extracted by JvS.

Analysis

Data from the telemonitoring platform and EHR were analyzed using Microsoft Excel. Alert and alert processing data were reported as frequencies (N) and proportions (%). A separate scenario analysis with different threshold values was conducted for all simple systolic and diastolic alerts for all included users that were processed manually by the telemonitoring center. The number of alerts that would be triggered with the new threshold values was based on the absolute values of the measurements performed in the original dataset. We calculated the current percentage of alerts that were processed administratively and extrapolated these to the alerts with the adjusted threshold values to estimate the percentage of alerts that would be processed administratively after the threshold adaptations and give insight into the potential workload reduction for the e-nurses. In this scenario analysis, the assumption was made that any alert

XSL•FO
RenderX

generated by the telemonitoring program that would be processed administratively would not have any clinical impact on the user.

Framework Development

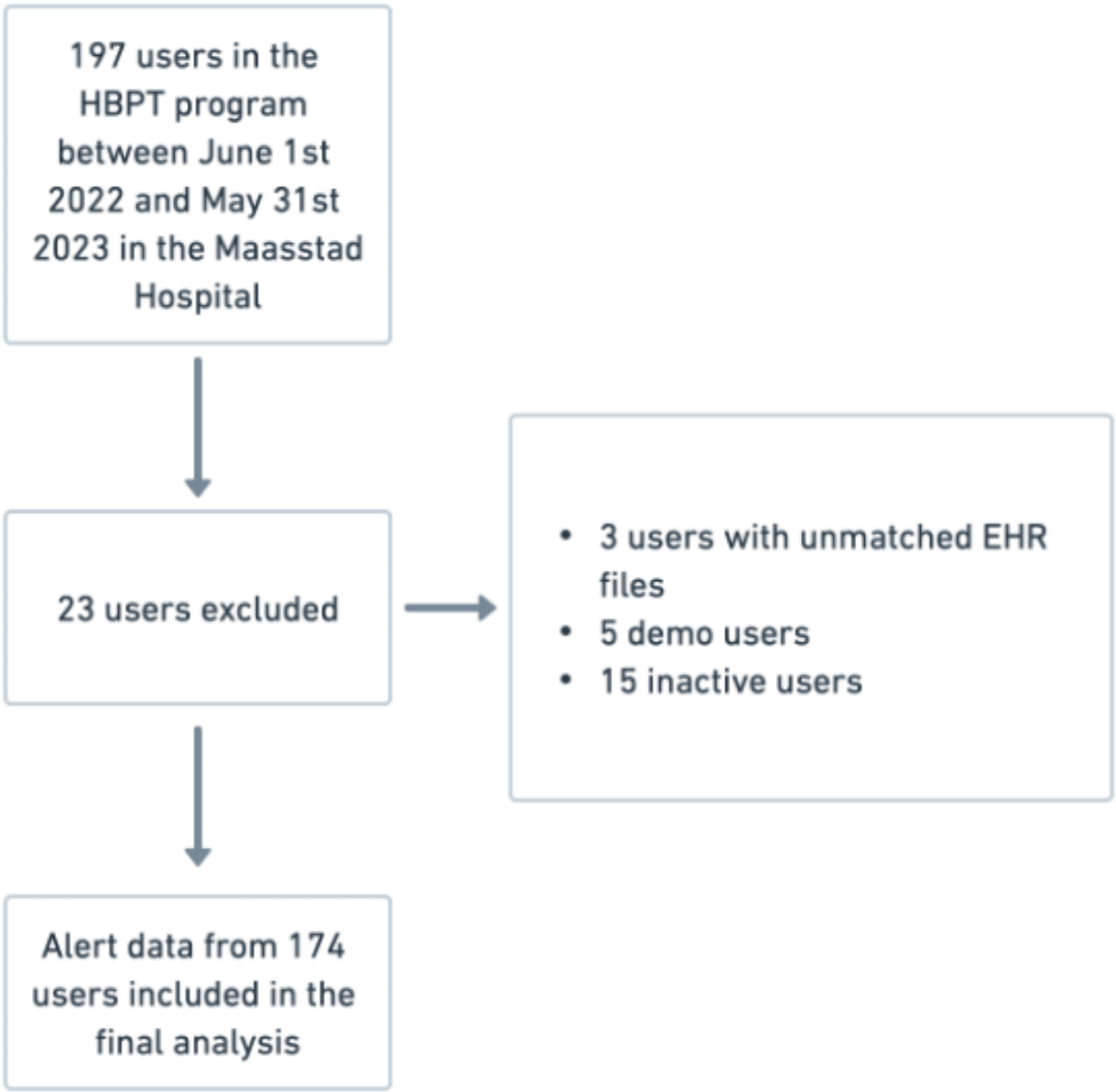
We created a framework for alert reduction and clinical workflow optimization in telemonitoring programs based on an iterative process that included a synthesis of our own clinical experiences, the alert-reduction and clinical workflow optimization methods identified in our own study (eg, scenario analysis), the methods for alert reduction as identified in the narrative alert reduction literature review, and general recommendations available from other relevant telemonitoring studies.

Results

Telemonitoring Alerts

Between June 1, 2022, and May 31, 2023, 197 users were included in the home blood pressure telemonitoring program. 5 users were identified as demo users, 3 users could not be matched to an EHR file, and 15 users did not activate the telemonitoring app. Therefore, alert data from a total of 174 users were included in the final analysis (Figure 2). In total, 45% of these users started in the chronic (monthly) measurement algorithm and 55% in the acute (weekly or biweekly) measurement algorithms. On average, each user was active in the telemonitoring app for 207 days during the study period, and a total of 30,184 measurements were performed. These measurements triggered 17,293 alerts, of which 13,647 were autoprocessed and 3646 were processed manually, equivalent to 21 manually processed alerts per user (Table 1).

Figure 2. Flow diagram illustrating the telemonitoring data collection.



XSL•FO
RenderX

Table . Telemonitoring alert data between June 1, 2022 and May 31, 2023.

Variable	Value
Total number of active users	174
Average days active	207
Total number of measurements	30,184
Total number of alerts (% of total number of measurements)	17,293 (57)
Number of alerts auto processed (% of total number of alerts)	13,647 (79)
Complex alerts (% of total number of alerts autoprocessed)	1878 (14)
Inactivity or overdue alerts (% of total number of alerts autoprocessed)	11,769 (86)
Number of alerts processed manually (% of total number of alerts)	3646 (21)
Simple alerts (% of total number of alerts processed manually)	2025 (56)
Complex alerts (% of total number of alerts processed manually)	1344 (37)
Inactivity or overdue alerts (% of total number of alerts processed manually)	277 (7)

Of the autoprocessed alerts, 11,769 (86%) were overdue alerts and 1878 (14%) were complex alerts. Of the manually processed alerts, 2025 (56%) were simple, 1344 (37%) were complex, and 277 (7%) were inactivity alerts. The 277 manually processed overdue or inactivity alerts were generated by 73 (42%) of all included users. It is important to note that overdue alerts are triggered when a single measurement is not completed in time. Within a hypertension protocol consisting of multiple scheduled measurements per day, this can have a large impact on the total number of alerts. However, due to the automated processing of these alerts, their contribution to the clinical workload is negligible.

Telemonitoring Center Data

The 3646 alerts that were processed manually accounted for a total of 2101 monitoring actions (all alerts that were processed manually on a single day for 1 user clustered into 1 action) and 1626 (77%) of these actions were processed with an administrative action (Table 2). A total of 475 (23%) alerts resulted in a clinical action. Out of these, 191 (40%) were telephone consultations without a treatment adjustment, 130 (28%) were telephone consultations with a treatment adjustment, 134 (28%) were digital messages without a treatment adjustment, and 20 (4%) were digital messages with a treatment adjustment. On average, 1 monitoring action for each user per month was registered based on the total average participation of 207 days (7 months). In total, the combined average workload for the e-nurses was 6.2 minutes per user per month, assuming a workload of 5 minutes for administrative actions and 10 minutes for clinical actions (telephone or messaging).

Table . Telemonitoring center data between June 1, 2022 and May 31, 2023.

Variable	Value
Total telemonitoring actions[a]	2101
Administrative actions (% of total number of monitoring actions)	1626 (77)
Clinical actions (% of total monitoring number of actions)	475 (23)
Telephone consultations without treatment adjustment (% of total number of clinical actions)	191 (40)
Telephone consultations with treatment adjustment (% of total number of clinical actions)	130 (28)
Digital messages without treatment adjustment (% of total number of clinical actions)	134 (28)
Digital messages with treatment adjustment (% of total number of clinical actions)	20 (4)

[a]All alerts that were generated on a single day were combined into 1 “telemonitoring action” in which the e-nurses reviewed all generated alerts on 1 specific day for 1 single user.

In total, 25 (15%) users triggered 61% of the overall simple alerts and 48% of the complex alerts that were processed manually. These users were responsible for 45% of all monitoring actions, which meant that the e-nurses would roughly spend half of their time on a very small subgroup (15%) of the included users.

XSL•FO
RenderX

Adjusting Individual Algorithm Thresholds

Review of the telemonitoring actions of the 25 users who generated most alerts led to individual adaptations in 13/25 users. In 3/13 users, the alert thresholds could be adjusted based on medical decisions (eg, accepting higher BP due to perceived intolerance of antihypertensive drugs, accepting asymptomatic lower heart rate), which would result in a reduction of 265 manually processed simple alerts in these users. Additionally, 3/13 users were provided with additional measurement instructions, and 7/13 users were discharged from the telemonitoring program due to a lack of digital skills or inability to adhere to the required measurement schedule and continued with regular physical care.

Adjusting Group Algorithm Thresholds: Scenario Analysis

A scenario analysis (Table 3) was conducted with various adaptations in thresholds for the 2025 simple systolic and diastolic alerts that were processed manually. We found that increasing the threshold values by only 5 mmHg for the simple diastolic alert and only 10 mmHg for the simple systolic alert would reduce the total number of alerts by 47% and 54%, respectively. These adjustments would lead to small increases in required clinical actions of 4% and 3%, respectively, if the alert processing remains similar to the current threshold scenario. Therefore, this scenario revealed limited clinical implications despite a large reduction in overall alerts. This was similarly applicable for adjusting the diastolic threshold value to ≥115 mmHg and the systolic threshold value to ≥190 mmHg, as in these scenarios, the increase of alerts requiring a clinical action was around 11% and 8%, respectively.

Table . Scenario analysis for the manually processed simple diastolic and systolic alerts between June 1, 2022 and May 31, 2023.

Alert type	% currently processed with administrative action/clinical action (total number of alerts)	Current threshold	New threshold	% total reduction in alerts (number of alerts)	% processed with administrative action or clinical action after threshold adjustment (total number of alerts) (% difference)	Potential time saving in minutes for the e-nurses
Diastolic simple alert	71 (726)/29 (297)	≥105 mmHg	≥110 mmHg	47 (481)	67 (322)/33 (159) (−4/+4)	2993
Diastolic simple alert	71 (726)/29 (297)	≥105 mmHg	≥115 mmHg	77 (788)	60 (473)/40 (315) (−11/+11)	4951
Diastolic simple alert	71 (726)/29 (297)	≥105 mmHg	≥120 mmHg	91 (930)	50 (465)/50 (465) (−21/+21)	5908
Systolic simple alert	71 (620)/29 (253)	≥170 mmHg	≥180 mmHg	54 (471)	68 (320)/32 (151). (−3/+3)	2980
Systolic simple alert	71 (620)/29 (253)	≥170 mmHg	≥190 mmHg	85 (742)	63 (467)/37 (275) (−8/+8)	4734
Systolic simple alert	71 (620)/29 (253)	≥170 mmHg	≥200 mmHg	95 (829)	44 (365)/56 (464). (−27/+27)	5290

We calculated potential time savings for the e-nurses based on the 2025 simple alerts in the current threshold scenario that were processed manually. These consisted of 1023 diastolic alerts, 873 systolic alerts, and 129 heart rate alerts. In total, 71% (726 and 620) of the 1023 diastolic and 873 systolic simple alerts were processed with administrative actions and 29% (297 and 253) with clinical actions, which would lead to a total workload for the e-nurses of 6598 minutes for the diastolic alerts and 5631 minutes for the systolic alerts, assuming a 5-minute workload for each individual administrative action and a 10-minute workload for each individual clinical action. In the adjusted threshold scenarios, we calculated total time savings based on a reduced workload due to the total reduction of alerts and an increased workload due to an increased percentage or alerts that would require a clinical action. We assumed a 10-minute workload for a clinical action. The potential time savings for the e-nurses were 2993, 4951, and 5908 minutes for the diastolic simple alerts and 2980, 4734, and 5290 minutes for the systolic alerts, respectively, assuming a 10-minute workload for each individual clinical action.

Literature Review

The original search yielded 251 articles. Based on the predefined exclusion criteria, 241 articles were excluded as they did not report any alert reduction methods or describe studies in intensive care units or other in-hospital settings. In total, 10 articles were reviewed in full text, and 7 of these articles contained a clear description of a method to improve telemonitoring efficiency. These methods included the introduction of complex alerts to reduce the overall alert burden, the introduction of clinical algorithms to triage alerts, scenario analysis with alert threshold adjustment, and a qualitative analysis to create an alert triage algorithm. See Table 4 for a complete overview of the studies reporting methods to improve telemonitoring efficiency.

XSL•FO
RenderX

Table . Overview of studies reporting methods to improve telemonitoring efficiency.

Author	Year	Type of telemonitoring program	Described method to improve telemonitoring efficiency
Vuković et al [13]	2010	Heart failure	Introduction of complex alerts
Cuba Gyllensten et al [19]	2017	Heart failure	Introduction of complex alerts Introduction of clinical algorithms to triage alerts
Vamos et al [20]	2018	Heart failure	Introduction of complex alerts
Zahradka et al [21]	2022	General vital signs	Scenario-analysis with alert threshold adjustment to reduce alert burden
Nguyen et al [22]	2023	Elderly care	Qualitative analysis of health care provider notes to create an alert triage algorithm
Richman et al [23]	2023	Cardiac implantable devices	Scenario-analysis with alert threshold adjustment to reduce alert burden
Mazza et al [24]	2024	Oncology	Introduction of clinical algorithms to triage alerts

Discussion

Principal Findings

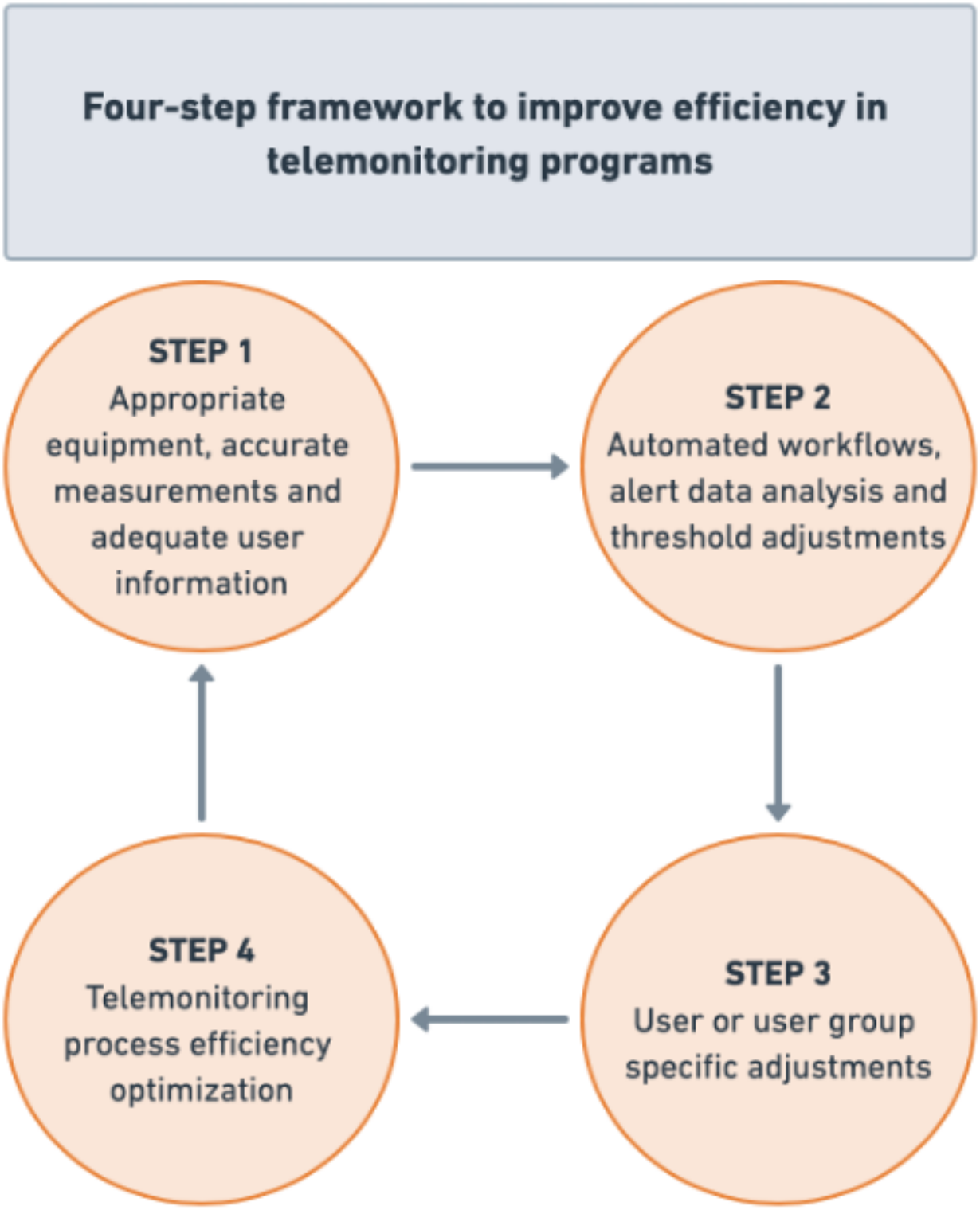
Based on our alert data analysis and narrative literature review, we identified multiple areas to reduce alerts and enhance telemonitoring efficiency. First, by using automated workflows in the telemonitoring program, around 86% of alerts could be processed automatically. Reduction of the alerts could also be achieved by individual adjustment of the alert thresholds: review of the subset of users who generated most of the workload, both in terms of the generated alerts as well as the workload burden for the e-nurses, posed opportunities to make individual threshold adjustments. These findings highlight the need for a more individualized approach with personal thresholds and measurement schedules in certain cases. Additionally, in our scenario analysis, we showed a large potential in alert reduction and time saving for the e-nurses for the simple alerts with only small increases in threshold values. Moreover, these adjustments appeared to be relatively safe, as our data showed only a small increase in alerts requiring clinical actions, implying limited clinical consequences. Additionally, since the start of the program, we have not experienced any adverse events like emergency department admissions or major adverse cardiovascular events. However, in general, triggering simple alerts can still be relevant to some degree, as one-off extreme health values should always be assessed on an individual basis, and general safety reasons can sometimes justify a larger number of alerts. Alert threshold adjustments should, therefore, always be balanced carefully with clinical risks, and any adjustment made should be reassessed periodically to ensure no clinically important events are missed.

A Framework for Alert Reduction and Workflow Optimization

We propose the following alert reduction and telemonitoring process optimization framework for proactive care path embedded telemonitoring programs. This framework (Figure 3), based on 4 distinct steps, outlines a systematic approach to optimize efficiency and can be used for the design, implementation, and optimization of care path-embedded telemonitoring programs.

XSL•FO
RenderX

Figure 3. Four-step framework to improve efficiency in telemonitoring programs.



Step 1: Appropriate Equipment, Accurate Measurements, and Adequate User Information

To ensure reliable and adequate measurements, users need to be provided with reliable and validated equipment [10]. Use new relevant medical device features if applicable. Additionally, confirm that the user has received all the necessary measurement instructions and confirm that the users can perform an adequate measurement (for example, a resting "test" BP measurement). Provide users with the correct information during technical issues and educate users on actions to take during acute health issues [10]. Inform users if any relevant changes are made in the remote monitoring program (eg, changes in measurement schedules or new functionalities). Periodically provide personalized feedback to users to ensure long-term reliable measurements, prevent inactivity, and improve overall adherence to the telemonitoring program [25]. Provide users with relevant disease- or lifestyle-specific information to enhance health

XSL•FO
RenderX

literary and disease insight, which can both reduce the overall alert burden.

Step 2: Automated Workflows, Alert Data Analysis, and Threshold Adjustments

Use automated workflows within the telemonitoring program to improve efficiency. These workflows can, for example, trigger automated messages (eg, a message requesting to repeat a certain measurement) following off-target measurements or process alerts independently. This empowers users to partly take responsibility themselves in case of off-target measurements, which can facilitate telemonitoring in large population groups.

Analyze all generated alerts in terms of their origin and conduct a periodic scenario analysis [21] to assess the impact of threshold adjustments in terms of alert reduction and clinical action requirements [21]. These adjustments should be balanced with clinical risks prior to final adjustment and should always be re-evaluated [23]. Additionally, potentially relevant clinical events after threshold adjustment should always be monitored. Data analysis and algorithm optimization can be performed internally but can also be based on new scientific evidence or guidelines. Remove any measurements from the telemonitoring algorithm that have no clear clinical benefit or consequences. Make use of complex alerts [13,19,20] and clinical algorithms [19,22,24] to filter alerts in terms of clinical relevance, to provide clinical decision support based on measurement trends, and to prevent clinical decision-making on single off-target measurements (“simple alerts”).

Step 3: User or User Group Specific Adjustments

Periodically identify users or user groups that generate a large proportion of the overall alert burden in the telemonitoring program (eg, the 10 users or a specific subgroup of users triggering the most alerts, depending on the overall number of users participating in the telemonitoring program). Discuss these users or user groups in a multidisciplinary setting with both the responsible health care provider and the telemonitoring staff involved. Investigate specific reasons for alert triggers in these users or user groups [10]. Consider temporarily user-specific alert thresholds or use personalized measurement schedules if applicable [26]. Recognize the limitations and difficulties of adhering to or using telemonitoring in specific user groups and engage and involve caregivers as needed.

Step 4: Telemonitoring Process Efficiency Optimization

Periodically evaluate the complete clinical workflow and telemonitoring process for potential efficiency improvements [12]. Identify alerts that can be processed independently by a telemonitoring center, for example. Use automated alerts and messages (specific alerts that trigger automated advice). For administrative actions, consider using message templates to save time communicating with users. Involve multiple departments (eg, the user information department) to ensure an efficient initial set-up, for example, by giving the user information department the responsibility for the initial device and telemonitoring instructions. Involve users, for example, during periodic focus group interviews to evaluate and optimize the current care pathway from a user perspective.

Limitations

There are a few important limitations to consider when interpreting the findings of our study. First, the data analysis is conducted with data from a single-center, single chronic disease (hypertension) telemonitoring program, which affects generalizability. However, we tried to overcome this by making general interpretations during telemonitoring programs for various diseases during framework development. Second, we have currently not incorporated the potential of artificial intelligence or other complex algorithm optimization strategies with regard to adjusting alerts and threshold values. It is to be expected, however, that this will be available and applicable on relatively short notice and should, therefore, be included in future updates of our framework. Third, given the large number of alerts, we were unable to analyze the complete clinical context of each individual alert, which might influence the alert processing data. Fourth, a narrative literature review was used in this study, which could have an impact on the strength of the results derived from the literature review. We opted for this approach, however, as very limited studies are available that specifically report methods on alert reduction and efficiency improvement in telemonitoring programs. Fifth, the framework was created based on a synthesis between the alert-data analysis and narrative literature review. This could, as no formal qualitative method was used, impact the overall strength of the framework. However, given the absence of any other similar framework in the literature, it could serve as a valuable starting point for further improvement in future studies.

Sixth, the proposed threshold increases of 5 and 10 mmHg in the scenario analysis might be too broad for populations where more strict BP management is required (eg, aortic dissection) and these adjustments should therefore always be made after assessing the specific included population in the telemonitoring program.

Finally, the available data on the described cohort of patients was only limited to telemonitoring data as the data analysis was used to support the proposed framework. The absence of clinical data could impact generalizability of the findings to certain populations (eg, hypertension, heart failure) included in other telemonitoring programs.

Conclusions

We developed a framework for alert reduction and telemonitoring process optimization in care path embedded telemonitoring programs. The framework includes 4 steps aimed at ensuring accurate measurements, alert, and alert-processing optimization, focusing on individual user needs, and improving overall telemonitoring process efficiency. Future studies should focus on further development of this framework and the evaluation of techniques to enhance efficiency while balancing potential clinical risks.

XSL•FO
RenderX

Acknowledgments

We would like to thank Marloes Rijckevorsel and Mark Pot from the business intelligence department of the Maasstad Hospital in Rotterdam, the Netherlands, for their contributions with regard to the electronic health record data collection.

Data Availability

The data used in this study are available from the corresponding author upon reasonable request.

Conflicts of Interest

MK is a Clinical Researcher at Luscii—an Omron Healthcare service, the telemonitoring platform used in this study. DD is the CEO of Luscii. No financial support was provided by Luscii to conduct this study.

Multimedia Appendix 1
Search strategy and results.
[DOCX File, 17 KB - medinform_v13i1e66066_app1.docx]

Multimedia Appendix 2
Telemonitoring algorithms.
[DOCX File, 18 KB - medinform_v13i1e66066_app2.docx]

References

1. Baloch S, Baloch MA, Zheng T, Pei X. The coronavirus disease 2019 (COVID-19) pandemic. Tohoku J Exp Med 2020 Apr;250(4):271-278. [doi: 10.1620/tjem.250.271] [Medline: 32321874]
2. Shaver J. The state of telehealth before and after the COVID-19 pandemic. Prim Care 2022 Dec;49(4):517-530. [doi: 10.1016/j.pop.2022.04.002] [Medline: 36357058]
3. Parati G, Dolan E, McManus RJ, Omboni S. Home blood pressure telemonitoring in the 21st century. J Clin Hypertens (Greenwich) 2018 Jul;20(7):1128-1132. [doi: 10.1111/jch.13305] [Medline: 30003701]
4. Itchhaporia D. The evolution of the quintuple aim: health equity, health outcomes, and the economy. J Am Coll Cardiol 2021 Nov 30;78(22):2262-2264. [doi: 10.1016/j.jacc.2021.10.018] [Medline: 34823665]
5. Azzopardi-Muscat N, Zapata T, Kluge H. Moving from health workforce crisis to health workforce success: the time to act is now. Lancet Reg Health Eur 2023 Dec;35:100765. [doi: 10.1016/j.lanepe.2023.100765] [Medline: 38115956]
6. Paré G, Jaana M, Sicotte C. Systematic review of home telemonitoring for chronic diseases: the evidence base. J Am Med Inform Assoc 2007;14(3):269-277. [doi: 10.1197/jamia.M2270] [Medline: 17329725]
7. Huygens MWJ, Voogdt-Pruis HR, Wouters M, et al. The uptake and use of telemonitoring in chronic care between 2014 and 2019: nationwide survey among patients and health care professionals in the Netherlands. J Med Internet Res 2021 May 3;23(5):e24908. [doi: 10.2196/24908] [Medline: 33938808]
8. Kruklitis R, Miller M, Valeriano L, Shine S, Opstbaum N, Chestnut V. Applications of remote patient monitoring. Prim Care 2022 Dec;49(4):543-555. [doi: 10.1016/j.pop.2022.05.005] [Medline: 36357060]
9. Co Z, Holmgren AJ, Classen DC, et al. The tradeoffs between safety and alert fatigue: Data from a national evaluation of hospital medication-related clinical decision support. J Am Med Inform Assoc 2020 Aug 1;27(8):1252-1258. [doi: 10.1093/jamia/ocaa098] [Medline: 32620948]
10. Radhakrishna K, Bowles K, Zettek-Sumner A. Contributors to frequent telehealth alerts including false alerts for patients with heart failure: a mixed methods exploration. Appl Clin Inform 2013;4(4):465-475. [doi: 10.4338/ACI-2013-06-RA-0039] [Medline: 24454576]
11. Lee NS, Anastos-Wallen R, Chaiyachati KH, Reitz C, Asch DA, Mehta SJ. Clinician decisions after notification of elevated blood pressure measurements from patients in a remote monitoring program. JAMA Netw Open 2022 Jan 4;5(1):e2143590. [doi: 10.1001/jamanetworkopen.2021.43590] [Medline: 35029664]
12. Guédon-Moreau L, Finat L, Boulé S, et al. Validation of an organizational management model of remote implantable cardioverter-defibrillator monitoring alerts. Circ Cardiovasc Qual Outcomes 2015 Jul;8(4):403-412. [doi: 10.1161/CIRCOUTCOMES.114.001433] [Medline: 26105725]
13. Vukovic M. Optimization of the alarm-management of a heart failure home-monitoring system. : IEEE Xplore Presented at: Computing in Cardiology, 2010; Sep 26, 2010 p. 53-56 URL: https://cinc.org/archives/2010/pdf/0053.pdf
14. World Medical A. World Medical Association Declaration of HelsinkiEthical Principles for Medical Research Involving Human Subjects. J Am Med Assoc 2013;310(20):2191-2194. [doi: 10.1001/jama.2013.281053]
15. Vijayananthan A, Nawawi O. The importance of good clinical practice guidelines and its role in clinical trials. Biomed Imaging Interv J 2008 Jan;4(1):e5. [doi: 10.2349/biij.4.1.e5] [Medline: 21614316]
16. Luscii - an omron healthcare service. 2024. URL: https://luscii.com/en/home [accessed 2025-06-10]

XSL•FO
RenderX

17. Mancia G, Kreutz R, Brunström M, et al. 2023 ESH Guidelines for the management of arterial hypertension The Task Force for the management of arterial hypertension of the European Society of Hypertension: Endorsed by the International Society of Hypertension (ISH) and the European Renal Association (ERA). J Hypertens 2023 Dec 1;41(12):1874-2071. [doi: 10.1097/HJH.0000000000003480] [Medline: 37345492]
18. BeterDichtbij. 2024. URL: https://www.beterdichtbij.nl [accessed 2025-06-10]
19. Cuba Gyllensten IGL, Goode KM, Bonomi AG, Caffarel J, Amft O. Case-load simulation using home telemonitoring data of heart failure patients to assess the impact of new sensor technologies and alerting algorithms on the decision making of healthcare professionals. Int J Integr Care 2013;13(7). [doi: 10.5334/ijic.1378]
20. Vamos M, Nyolczas N, Bari Z, et al. Refined heart failure detection algorithm for improved clinical reliability of OptiVol alerts in CRT-D recipients. Cardiol J 2018;25(2):236-244. [doi: 10.5603/CJ.a2017.0077] [Medline: 28653309]
21. Zahradka N, Geoghan S, Watson H, Goldberg E, Wolfberg A, Wilkes M. Assessment of remote vital sign monitoring and alarms in a real-world healthcare at home dataset. Bioengineering (Basel) 2022 Dec 28;10(1):37. [doi: 10.3390/bioengineering10010037] [Medline: 36671610]
22. Nguyen P, Schiaffino MK, Zhang Z, Choi HW, Huh-Yoo J. Toward alert triage: scalable qualitative coding framework for analyzing alert notes from the Telehealth Intervention Program for Seniors (TIPS). JAMIA Open 2023 Oct;6(3):ooad061. [doi: 10.1093/jamiaopen/ooad061] [Medline: 37560155]
23. Richman T, Fryer M, Titlestad AL, OLeary J, Greaves K, Tung MK. PO-03-059 optimising remote monitoring alert criteria to reduce alert fatigue: an interrupted time series. Heart Rhythm 2023 May;20(5):S490. [doi: 10.1016/j.hrthm.2023.03.1062]
24. Mazza GL, Dueck AC, Ginos B, et al. Optimization of alert notifications in electronic patient-reported outcome (ePRO) remote symptom monitoring systems (AFT-39). Qual Life Res 2024 Jul;33(7):1985-1995. [doi: 10.1007/s11136-024-03675-3] [Medline: 38771558]
25. van Steenkiste J, Verberk-Jonkers I, de Koning S, Voss-de Haan J, de Jong-Verhagen B, Dohmen D. Patient engagement in a hybrid care pathway for hypertension: not one size fits all. J Patient Exp 2024;11:23743735241297626. [doi: 10.1177/23743735241297626] [Medline: 39654654]
26. Shalowitz E. Non-Invasive Telemonitoring Programs in Chronic Heart Failure Patients: How Differences in Alert Criteria Affect All-Cause Mortality Outcomes: European Society of Cardiology; 2022. URL: https://esc365.escardio.org/presentation/248245 [accessed 2025-06-12]

Abbreviations

BP: blood pressure

Edited by C Perrin; submitted 03.09.24; peer-reviewed by M Boeker, R Gore; revised version received 07.03.25; accepted 14.03.25; published 13.06.25.

Please cite as:
van Steenkiste J, Lupgens N, Kool M, Dohmen D, Verberk-Jonkers I
Alert Reduction and Telemonitoring Process Optimization for Improving Efficiency in Remote Patient Monitoring Programs: Framework Development Study
JMIR Med Inform 2025;13:e66066
URL: https://medinform.jmir.org/2025/1/e66066
doi:10.2196/66066

© Job van Steenkiste, Niki Lupgens, Martijn Kool, Daan Dohmen, Iris Verberk-Jonkers. Originally published in JMIR Medical Informatics (https://medinform.jmir.org), 13.6.2025. This is an open-access article distributed under the terms of the Creative Commons Attribution License (https://creativecommons.org/licenses/by/4.0/), which permits unrestricted use, distribution, and reproduction in any medium, provided the original work, first published in JMIR Medical Informatics, is properly cited. The complete bibliographic information, a link to the original publication on https://medinform.jmir.org/, as well as this copyright and license information must be included.

XSL•FO
RenderX

Real-Time, Risk-Based Clinical Trial Quality Management in China: Development of a Digital Monitoring Platform

Min Jiang[1*], MSc; Shuhua Zhao[2*], MSc; Yun Mei[3], MSc; Zhiying Fu[2], MSc; Yannan Yuan[2], MSc; Jie Ai[3], MSc; Yuan Sheng[4], PhD; Ying Gong[4], BSc; Jingjing Chen[4], MSc

[1]State Key Laboratory of Holistic Integrative Management of Gastrointestinal Cancers, Beijing Key Laboratory of Carcinogenesis and Translational Research, National Drug Clinical Trial Center, Peking University Cancer Hospital & Institute, 52 Fucheng Rd, Haidian District, Beijing, China

[2]Key Laboratory of Carcinogenesis and Translational Research (Ministry of Education/Beijing), National Drug Clinical Trial Center, Peking University Cancer Hospital & Institute, Beijing, China

[3]Yidu Cloud (Beijing) Technology Co, Ltd, Beijing, China

[4]Pfizer (China) Research and Development Co, Ltd, Shanghai, China

[*]these authors contributed equally

Corresponding Author:
Min Jiang, MSc
State Key Laboratory of Holistic Integrative Management of Gastrointestinal Cancers, Beijing Key Laboratory of Carcinogenesis and Translational Research, National Drug Clinical Trial Center, Peking University Cancer Hospital & Institute, 52 Fucheng Rd, Haidian District, Beijing, China

Abstract

Background: With the improvement of the drug evaluation system in China, an increasing number of clinical trials have been launched in Chinese hospitals. However, traditional clinical trial quality management models largely rely on human monitoring and counting, which can be time-consuming and are likely to generate errors and biases. There is an urgent need to upgrade and improve the efficiency and accuracy of clinical trial quality monitoring systems in hospital-based research institutions within China.

Objective: The objective of this study was to develop a digital monitoring platform that allows for the real-time monitoring and detection of risk points and provides warnings about risk points throughout the entire life cycle of clinical trials, on the basis of historical clinical trial quality control (QC) findings.

Methods: Leveraging the risk-based quality management mindset, we built a digital dynamic monitoring platform by using big data analysis and automatic quantitative technology. Data from clinical trial QC reports generated during 2019 to 2023 in Beijing University Cancer Hospital, China, were used to train the automated classification tool, establish warning thresholds, and validate threshold values. Quality findings from the early-stage, interim-stage, and conclusion-stage QC rounds of clinical trials were rated by using 3 severity grades (minor, major, or critical) and classified into 5 categories (with 4 taxonomy levels under each category). QC report text was processed by using an automated natural language processing tool. All QC reports were grouped into 2 clusters via hierarchical clustering analysis. QC findings from the relatively high-risk cluster (reports that were more likely to have major and critical findings, as determined by experienced QC analysts) were used to determine warning threshold values for the monitoring platform (ie, the lowest number of findings was set as the threshold value for each specific study stage, Level-3 taxonomy, and severity grade combination).

Results: The most frequently reported Level-3 taxonomies in QC reports from 2019 to 2022 were “Standard Procedure and Process,” “Safety Reporting,” and “Source Data Collection and/or Recording.” In total, 189 warning threshold values were established based on data from 1380 QC reports generated during 2019 to 2022, covering 3 severity grades, 21 Level-3 taxonomies, and 3 QC rounds. The warning thresholds were applied to 211 QC reports generated in 2023, of which 19.9% (n=42) triggered warnings. Similar patterns of QC findings, including the most frequently noted Level-3 QC findings, were observed between reports generated in 2023 and those from 2019 to 2022.

Conclusions: In clinical practice, our tool would enable the automated monitoring and detection of risk points throughout all clinical trial stages; accurately identify the most relevant trial procedure and function line; and notify quality management personnel, in real time, to take prompt actions and dynamically prevent the recurrence of quality issues.

(JMIR Med Inform 2025;13:e64114) doi:10.2196/64114

KEYWORDS

clinical trial; quality control; risk-based quality management; digital; natural language processing

XSL•FO
RenderX

Introduction

Over the past 20 years, with the improvement of the drug evaluation system and standards in China, an increasing number of domestic and cross-national multicenter clinical trials have been launched in Chinese hospitals. However, in many hospital-based clinical trial institutions, traditional quality management models largely rely on human monitoring and counting, which not only require a lot of time and resources but also likely result in errors and biases. Therefore, such models may not be able to identify risk points and trends in a timely manner or prevent the recurrence of quality issues. In the face of the increasing number and complexity of clinical trials, the optimization of quality management models has become an urgent need for clinical trial institutions in Chinese hospitals.

Risk-based quality management (RBQM)—recommended in guidelines issued by the US Food and Drug Administration [1] and European Medicines Agency [2] in 2013, as well as in the International Council for Harmonisation of Technical Requirements for Pharmaceuticals for Human Use (ICH) guidelines for good clinical practice in 2016 [3]—is a powerful approach that has been explored and applied in a growing number of trials and institutions [4,5]. In 2020, the China National Medical Products Administration introduced the concept of RBQM into Chinese trial quality management systems [6]. In 2022, the China Center for Drug Evaluation released Statistical Principles for Centralized Monitoring of Drug Clinical Trials, which was considered a milestone in China's clinical trial revolution and a guideline for the improvement and implementation of RBQM in China's clinical practice [7].

To meet the urgent need for upgrading quality management models and achieving better efficiency, accuracy, and timeliness, we leveraged the RBQM mindset and used a long-term collection of quality management data from clinical trial programs in Beijing University Cancer Hospital, China, to build a digital dynamic monitoring platform via big data analysis and automatic quantitative technology. Through this platform, we aim to dynamically and prospectively monitor the entire life cycle of clinical trials and efficiently identify, intervene with, and systematically prevent quality risks that might compromise critical trial processes, patient safety, or data integrity.

Methods

Ethical Considerations

This study was based on the processing and analysis of quality control (QC) documents from a large number of clinical trials, which underwent their own ethics reviews. Further, the text of the QC findings did not contain personal information of trial participants. As such, this study did not require ethics board review.

Materials

A total of 1591 QC reports were generated in our institution from January 2019 to September 2023, involving 993 clinical trials. In accordance with relevant quality management standard operating procedures, a specific QC group was responsible for conducting at least 3 rounds of routine QC for each trial, including but not limited to (1) an early-stage QC round at the time point of achieving 5 enrollments or at 3 months after trial initiation, (2) an interim-stage QC round once every 6 months or when the trial achieved 20 enrollments, and (3) a conclusion-stage QC round at the time of site closeout. A detailed QC report was generated for each QC round, recording all quality issues. To build a digital monitoring platform, 1380 reports, which were generated during 2019 to 2022, served as the foundation for automated quantitative processing and the identification of warning thresholds, while the remaining 211 reports, which were generated in the year 2023, were used for testing the effectiveness of those thresholds in identifying high-risk trials.

Classification of QC Findings

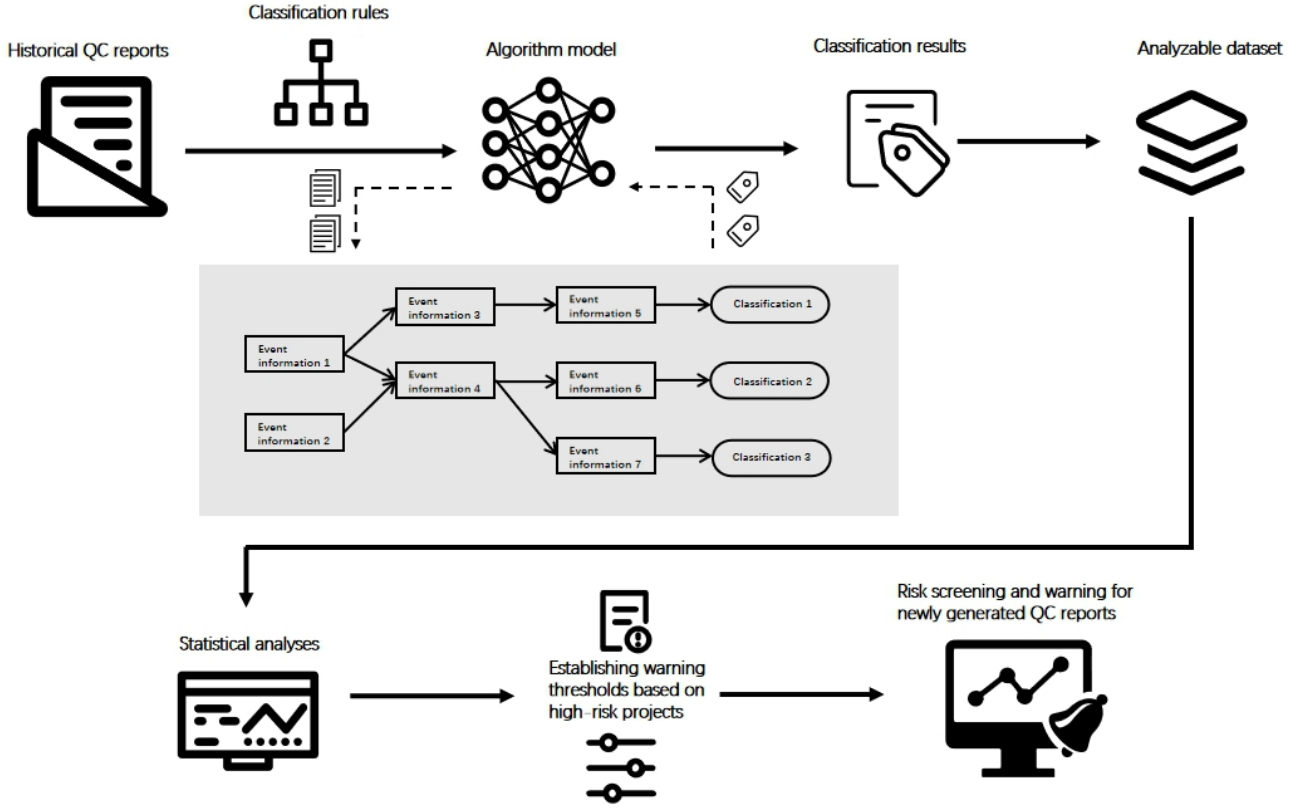
Findings from the routine QC reports were rated by using 3 severity grades (minor, major, or critical) and classified into 5 categories ("Data," "Quality," "Safety and Ethics," "Equipment and Facility," or "Finance"), with 4 taxonomy levels under each category. The severity ratings and Level-1 to Level-3 taxonomies would allow for an overall review and trend analysis, while the Level-4 taxonomies were designed to trace back precisely to the corresponding clinical trial procedure and personnel.

Novel Automated Classification Tool

To enable the automated classification of QC findings, we developed a natural language processing (NLP) algorithm based on the Local Interpretable Model-Agnostic Explanations framework, which was implemented in Python. This algorithm was designed to perform multidimensional classifications of events in QC report texts (Figure 1).

XSL•FO
RenderX

Figure 1. Algorithm classification tool flowchart. QC: quality control.



The dataset used to develop the NLP algorithm comprised 1380 QC reports that were generated during 2019 to 2022; an average of 345 reports were generated per year. Among QC findings from these reports, 55.48% were categorized as minor findings, 42.23% were categorized as major findings, and 2.29% were categorized as critical findings. The word count of the reports ranged from 1619 to 17,367 words, with a median word count of 5938 (IQR 4453-7422) words per report. Data were stratified and split into training, validation, and testing sets (70%, 15%, and 15%, respectively) to ensure balanced class representation. Annotation rules covered 4 entity dimensions and 54 issue categories, which were derived from industry standards and refined through discussions with an internal expert team.

In the first phase, the dataset was annotated by using multidimensional information labeling rules, generating high-quality training data. In the second phase, natural text from QC reports was subjected to preliminary automated classification via a Bayesian network, which determined the Level-1 to Level-3 classifications for each text segment based on joint probability. Additionally, semantic role labeling—a critical step in the classification NLP tool—was used to identify the predicate-argument structure of each sentence [8]. After training with the dataset, an explainable directed acyclic graph was constructed [9]. In the directed acyclic graph, graph neural networks were used to propagate information across the graph, forming an algorithmic model capable of capturing events. The model achieved precision (P) and recall (R) scores >0.95. In the third phase, by using the trained model, events were extracted from the QC report text and subjected to Bayesian inference. If an inference could be drawn from the graph, automatic classification was completed; if no inference could be made, a new branch was created, and the entire graph model was updated and iterated. The final Level-4 classification results were represented as the terminal leaf nodes in the graph.

Clustering

After all findings from QC reports were classified by using our automated classification tool, a dataset was created based on the incidence rates of different categories of QC findings from each QC report. Using SPSS for Windows 20.0 (IBM Corp), hierarchical clustering analysis was applied to this dataset to ensure that reports with similar patterns of QC findings were grouped into the same cluster: each report was initially treated as a separate cluster; then, the algorithm identified 2 clusters that were closest to each other (ie, clusters with maximum similarity) and merged these 2 clusters into 1 new cluster. These steps were repeated until all QC reports were grouped into 2 clusters (Cluster I and Cluster II). A dendrogram was generated, showing the levels of similarity and dissimilarity between QC reports. Per manual interpretation by a group of experienced QC analysts, Cluster II was identified as high risk (ie, reports with more findings or a higher proportion of major and critical findings), and Cluster I was considered relatively “normal” (reports with less findings or a higher proportion of minor findings).

Establishment of Warning Thresholds and Detection of Risk Points

Warning thresholds were established based on the high-risk (Cluster II) QC reports from 2019 to 2022; the lowest number of findings was set as the threshold value for a specific study stage, Level-3 taxonomy, and severity grade combination. For example, a threshold value of X was set for the following

XSL•FO
RenderX

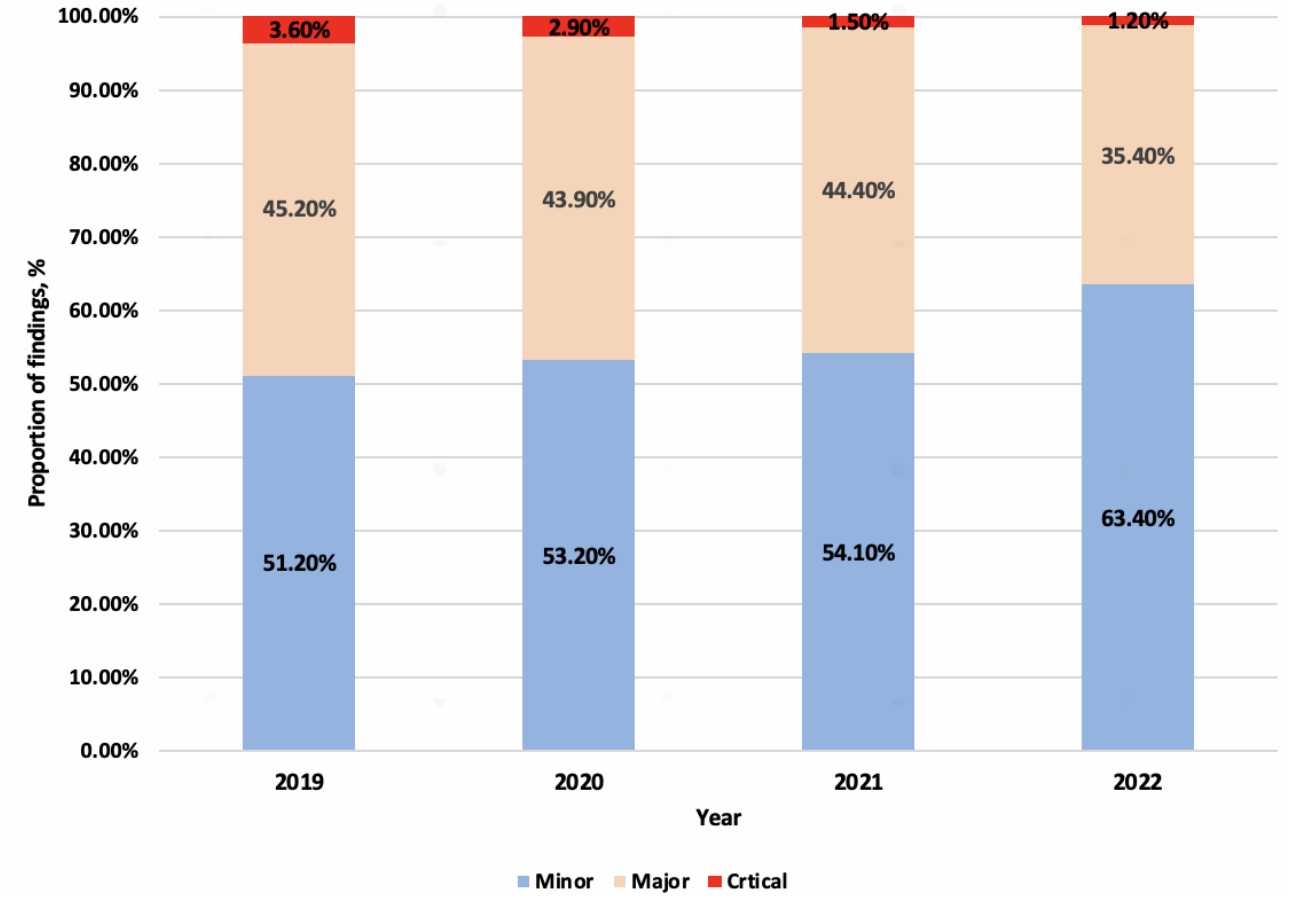
combination: early-stage QC round, Level-3 taxonomy "Biological Sample Management," and major findings; this made sure that all high-risk QC reports from early-stage QC rounds had at least X major findings under the Level-3 taxonomy "Biological Sample Management." The warning thresholds were then applied to QC reports from 2023; these warning thresholds would help with determining the risk points (ie, the most commonly reported findings) and investigating the root causes of findings.

Results

Summary of 2019 to 2022 QC Findings

From 2019 to 2022, the proportion of major or critical findings generally decreased each year (major findings showed a 1.27-fold decrease, and critical findings showed a 3-fold decrease), even during the COVID-19 pandemic, while the proportion of minor findings showed an approximately 1.24-fold increase over the 4 years (Figure 2).

Figure 2. Proportion of quality control findings under 3 categories of clinical significance and severity.



It was consistently observed during each year that the most commonly reported Level-3 taxonomies (the proportions of findings for these taxonomies were >5%), in decreasing order of frequency, were (1) "Standard Procedure and Process," (2) "Safety Reporting," (3) "Source Data Collection and/or Recording," (4) "Investigational Product," (5) "Personnel Qualification and Training," and (6) "Biological Sample Management" (Table 1). In 2020, under the influence of the COVID-19 pandemic, increases were observed in the average numbers of findings per report that fell under these Level-3 taxonomies, but 2 years later, the average numbers of these findings dropped back to their 2019 levels (Figure 3).

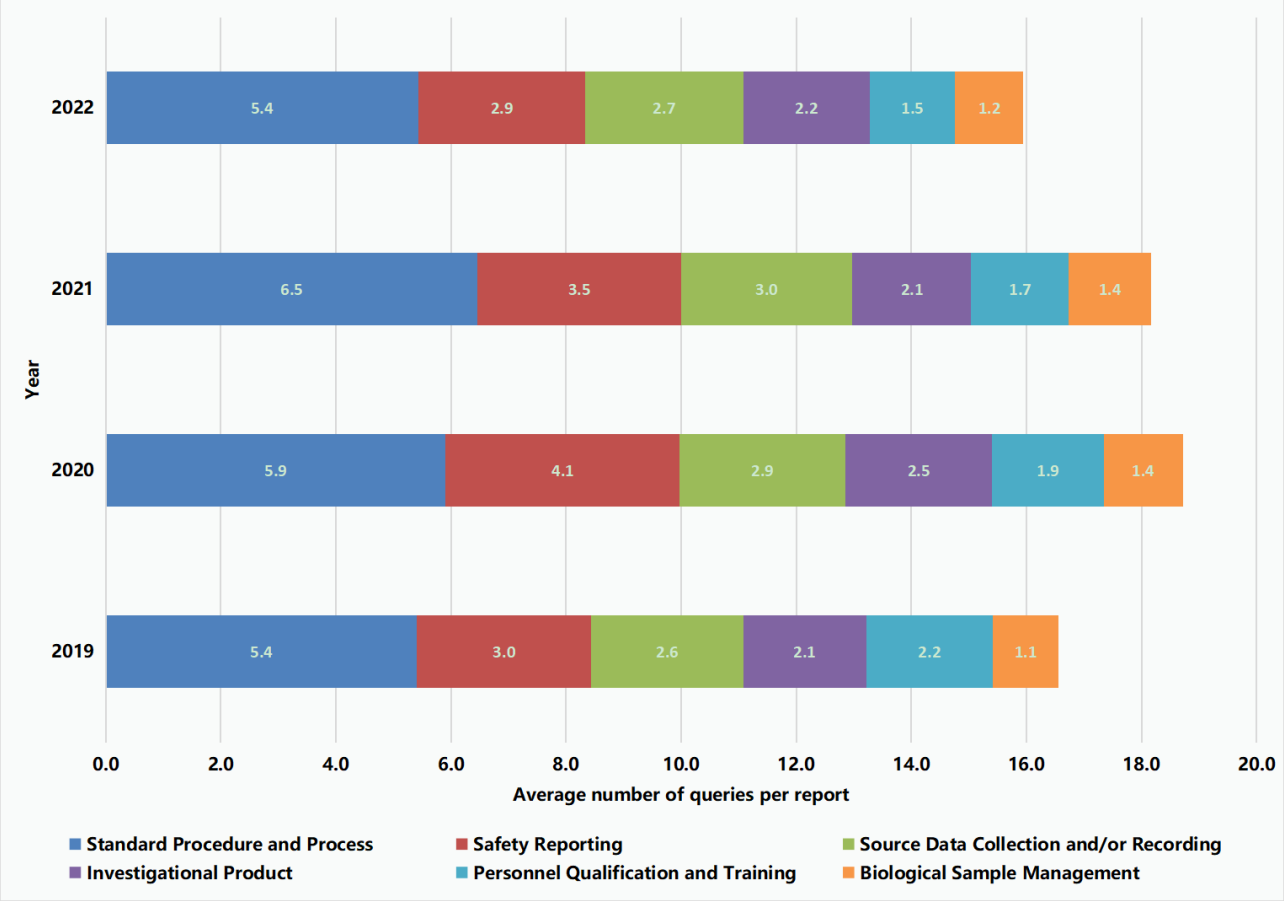
XSL•FO
RenderX

Table . Proportion of quality control (QC) findings under each Level-3 taxonomy from 2019 to 2023.

Level-3 classification	2019 (% of QC findings)	2020 (% of QC findings)	2021 (% of QC findings)	2022 (% of QC findings)	2023 (% of QC findings)
Source Data Collection and/or Recording	13.62	13.65	13.75	13.53	13.61
Source Data Modification/Correction	0.62	0.41	0.23	0.31	0.44
Source Data Transcription	0.74	0.72	0.56	0.70	0.73
Process Documentation Management	0.08	0.07	0.08	0.09	0.08
Standard Procedure and Process	26.47	27.14	27.95	26.91	26.97
Personnel Qualification and Training	9.21	8.02	7.81	9.02	9.09
Query Identification	0	0	0	0	0
Query Recording and Reporting	0.51	0.27	0.36	0.27	0.58
Query Prevention	0	0	0	0	0
Laboratory, Equipment, Facility, and Supply Management	1.20	1.29	1.55	1.28	1.23
Biological Sample Management	5.58	5.72	6.35	5.88	5.59
Clinical Trial Document Management	3.98	4.21	4.35	4.07	4.09
Human Genetic Resource Management	0.23	0.19	0.17	0.24	0.24
Informed Consent Personnel Qualifications	1.40	1.22	1.59	1.50	1.48
Informed Consent Process	2.29	2.23	2.37	2.47	2.39
Ethics Committee Composition and Operation	1.17	1.70	1.34	1.53	1.23
Safety Reporting	16.50	16.97	15.79	15.94	15.98
Concomitant Medications	3.34	3.18	2.91	2.98	3.19
Investigational Product	11.52	11.43	11.50	11.76	11.57
Inclusion and Exclusion Criteria	1.53	1.58	1.34	1.52	1.51
Clinical Trial Finance Process	0	0	0	0	0

XSL•FO
RenderX

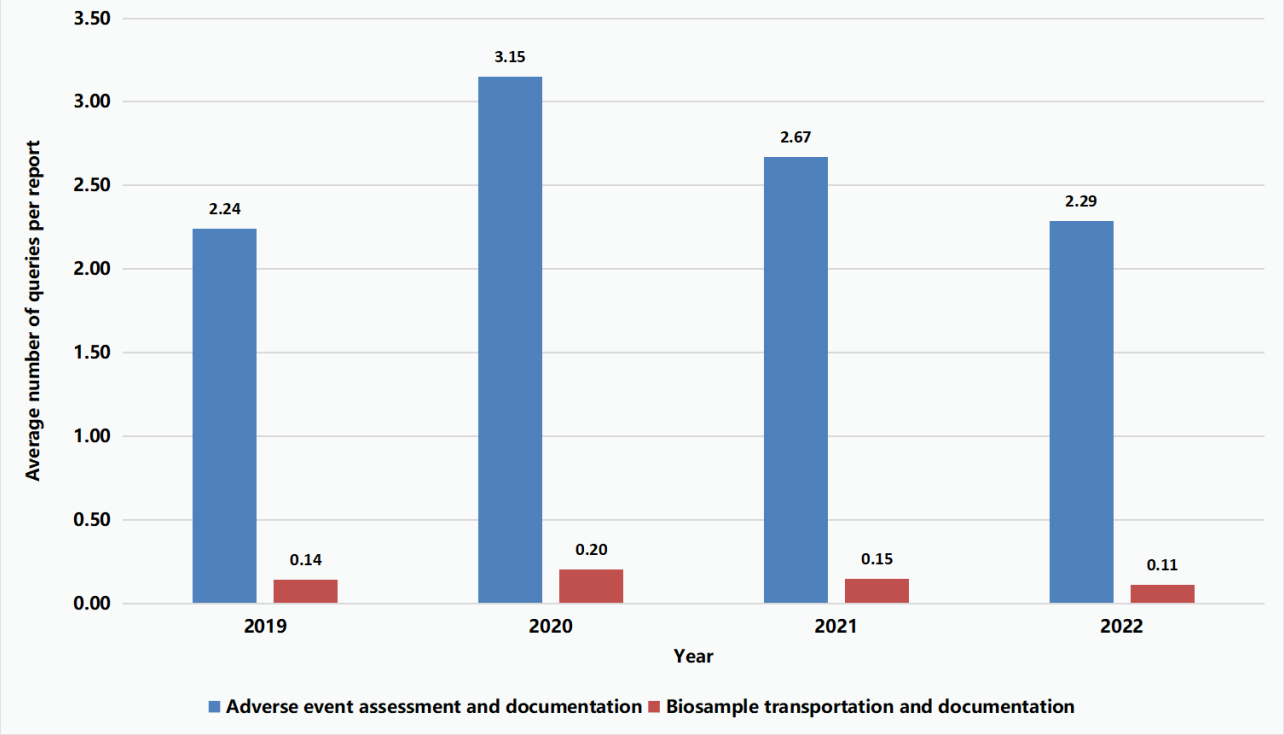
Figure 3. Average number of findings per quality control report under the most frequently reported Level-3 taxonomies (proportions of findings for these taxonomies: >5%).



Similar trends were also observed when QC findings were summarized under Level-4 taxonomies. A 1.41-fold increase in the average number of findings under the Level-4 taxonomy "Adverse Event Assessment and Documentation" was observed in 2020 when compared to 2019. Further, while the average number of findings under the Level-4 taxonomy "Biological Sample Shipment and Recording" was ≤0.2 per report across each year, a 1.43-fold increase was also noted in 2020 when compared to the previous year. These trends were likely attributable to the outbreak of the COVID-19 pandemic. With the adaptive actions taken in response to COVID-19 (eg, implementation of digital monitoring), the numbers of QC findings under these two Level-4 taxonomies eventually dropped back to their 2019 levels (Figure 4).

XSL•FO
RenderX

Figure 4. Trends of change in average number of findings per quality control report under two Level-4 taxonomies from 2019 to 2022.

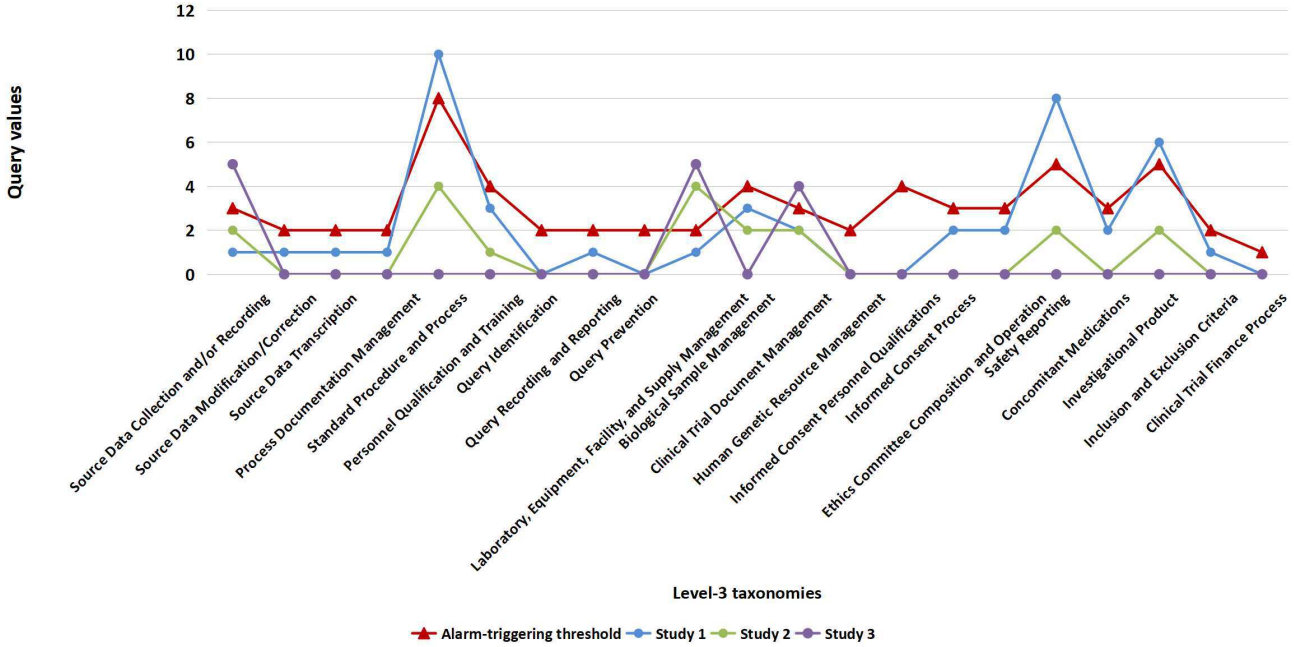


Warning Thresholds and Warning-Triggering Risks in the Year 2023

A total of 189 warning threshold values were established to cover all 3 severity grades, 21 Level-3 taxonomies, and 3 rounds of QC (Multimedia Appendix 1). These thresholds were applied to a total of 211 QC reports generated in 2023. Among those reports, 42 triggered warnings, resulting in a trigger rate of 19.9%. Approximately half (n=23, 55%) of the 42 warning-triggering, high-risk reports were from interim-stage QC rounds, while 8 and 11 were from early-stage and conclusion-stage QC rounds, respectively.

Figure 5 presents data from 3 randomly selected reports from early-stage QC rounds as examples to show the number of major QC findings that exceeded or did not exceed the corresponding threshold value for each of the 21 Level-3 taxonomies.

Figure 5. Number of major QC findings under each Level-3 taxonomy from 3 early-stage QC reports, in comparison with corresponding threshold values. QC: quality control.



Among the 42 high-risk reports in 2023, after the application of warning threshold values, the most frequently noted Level-3 taxonomies with alarm-triggering QC findings were generally consistent with those observed in QC reports from 2019 to 2022 (Tables 1 and 2, Figure 3). The most common alarm-triggering Level-3 taxonomy was “Standard Procedure and Process,” which

XSL•FO
RenderX

was reported in 36% (15/42) of high-risk reports, and its most relevant process (ie, "risk point," as defined by Level-4 taxonomies) was "Protocol Deviation – Deviation from Study Design," which was reported in 33% (5/15) of the reports that triggered an alarm for QC findings that fell under the Level-3 "Standard Procedure and Process" taxonomy. In response to Level-4 taxonomies that were more likely to cause alarm-triggering QC issues (Table 2), intervention strategies to be incorporated into routine clinical practice were proposed.

Table . Most frequently reported Level-3 taxonomies in alarm-triggering quality control reports from 2023 (n=42) and their corresponding most relevant Level-4 taxonomies.

Level-3 taxonomy	Level-3 taxonomy incidence, number of reports (%)	Most relevant Level-4 taxonomy
Standard Procedure and Process	15 (36)	Protocol Deviation – Deviation From Study Design
Safety Reporting	8 (19)	Adverse Event Assessment and Documentation
Source Data Collection and/or Recording	8 (19)	Paper Source Data Files
Biological Sample Management	6 (14)	Biosample Transportation and Documentation
Personnel Qualification and Training	6 (14)	Personnel Authorization and Documentation
Investigational Product	6 (14)	Administration of Investigational Products and Associated Documentation Issues
Laboratory, Equipment, Facility, and Supply Management	4 (10)	Equipment Maintenance Issues
Clinical Trial Document Management	4 (10)	Clinical Trial Document Maintenance
Concomitant Medications	4 (10)	Concomitant Medications Record and Documentation
Informed Consent Process	3 (7)	Informed Consent Signing Issues
Process Documentation Management	3 (7)	Quality Control Documentation
Inclusion and Exclusion Criteria	2 (5)	Inclusion and Exclusion Criteria Documentation
Query Recording and Reporting	1 (2)	Incomplete Monitoring Records

Discussion

As stated in the ICH E6(R3) guideline published in January 2025, clinical trial institutions and sponsors are encouraged to use innovative digital technologies to improve clinical trial quality, taking into consideration the risk factors that could potentially impact participant safety, data quality, and other key elements in clinical trial procedures [3]. In this study, data from historical clinical trial QC reports generated in our hospital were standardized and classified for further risk-based qualitative analyses, and the minimum number of QC findings was determined as the threshold value for each QC stage, severity level, and Level-3 taxonomy combination. These QC warning thresholds were embedded into our digital dynamic monitoring platform to allow for the dynamic and proactive identification of high-risk QC reports and to notify quality management personnel, in a real-time manner, about which reports had a number of QC findings (ie, in a specific stage, severity level, and Level-3 taxonomy) that was larger than the corresponding threshold value. For example, a QC warning will be triggered for an early-stage QC report if it reports more than 13 minor findings, more than 3 major findings, or more than 2 critical findings under the Level-3 taxonomy "Source Data Collection and/or Recording," requesting the quality management group to follow up and take actions.

With the help of the digital platform, the quality management team can quickly and accurately identify the relevant clinical trial procedure and function line for the reported quality issues and adopt mitigation strategies. For example, in QC reports from 2019 to 2022, "Standard Procedure and Process" was the most frequently reported Level-3 taxonomy for QC reports generated during the conclusion stage (ie, around the time of site closeout), and one-third (38/114, 33.3%) of the quality issues were attributed to participants' poor compliance with safety visits after they left the trial site. Driven by this observation, we learned from participants that many of them lived far away from our trial site in Beijing, and after leaving the trial site, it was difficult for them to travel a long distance back to the trial site for additional safety follow-ups. Our proposed action is to allow participants who are discharged from the trial site to complete their follow-up visits in a local clinical trial center (ie, at or near their hometown) equipped with a remote visit system, as an approach to improving their compliance with the safety monitoring procedures. Another example is the quality alarm associated with the Level-4 taxonomy "Administration of Investigational Products and Associated Documentation Issues." In a trial with QC findings that fell under this taxonomy, the study drug was to be orally self-administered at home, and a large proportion of participants missed multiple oral doses. In response to this finding, our proposed action is to send drug administration reminders via participants' social networking platforms and the hospital's mobile app. The digital platform also enables the study team to conduct targeted source data verifications and reviews; the study

XSL•FO
RenderX

team can also exempt a trial from complete source data verifications and reviews if it did not trigger any warnings.

The digital platform remains to be optimized for future clinical practice; the input of more QC data and an upgraded automated calculation tool are needed to enhance its accuracy and applicability. However, the concurrent use of other digital tools may further enhance the efficiency of quality management systems. For high-risk trials that have already triggered an alarm in the early- or interim-stage QC round, a remote monitoring system may help to reduce quality issues due to trial procedure noncompliance.

Acknowledgments

This study was supported by Beijing Natural Science Foundation (L232032) and Beijing Municipal Science & Technology Commission No. Z231100004623006.

Authors' Contributions

All of the listed authors reviewed, commented on, and approved the final draft of the manuscript. MJ and SZ designed and directed the project and made substantial contributions to data collection and interpretation; thus, they are listed as co–first authors. YM designed the automated classification tool and conducted all data analyses, including but not limited to natural language processing and quality control report clustering. YG and JC coordinated and monitored the manuscript drafting process and contributed to the *Introduction* and *Methods* sections. YS provided manuscript writing support.

Conflicts of Interest

None declared.

Multimedia Appendix 1
Threshold values for Level-3 taxonomies in quality control (QC) across 3 study stages and 3 severity grades.
[DOCX File, 19 KB - medinform_v13i1e64114_app1.docx]

References

1. Oversight of clinical investigations — a risk-based approach to monitoring. U.S. Food and Drug Administration. 2013 Aug. URL: https://www.fda.gov/regulatory-information/search-fda-guidance-documents/oversight-clinical-investigations-risk-based-approach-monitoring [accessed 2024-07-08]
2. Reflection paper on risk based quality management in clinical trials. European Medicines Agency. 2013 Nov 18. URL: https://www.ema.europa.eu/en/documents/scientific-guideline/reflection-paper-risk-based-quality-management-clinical-trials_en.pdf [accessed 2024-07-08]
3. ICH harmonised guideline: guideline for good clinical practice E6(R3). International Council for Harmonisation of Technical Requirements for Pharmaceuticals for Human Use. URL: https://database.ich.org/sites/default/files/ICH_E6%28R3%29_Step4_FinalGuideline_2025_0106.pdf [accessed 2025-04-15]
4. Stansbury N, Barnes B, Adams A, et al. Risk-based monitoring in clinical trials: increased adoption throughout 2020. Ther Innov Regul Sci 2022 May;56(3):415-422. [doi: 10.1007/s43441-022-00387-z] [Medline: 35235192]
5. Barnes B, Stansbury N, Brown D, et al. Risk-based monitoring in clinical trials: past, present, and future. Ther Innov Regul Sci 2021 Jul;55(4):899-906. [doi: 10.1007/s43441-021-00295-8] [Medline: 33914298]
6. 国家药监局 国家卫生健康委 关于发布药物临床试验质量管理规范的公告 [Article in Chinese]. The State Council of the People's Republic of China. URL: https://www.gov.cn/gongbao/content/2020/content_5525106.htm [accessed 2025-04-15]
7. 国家药监局药审中心关于发布《药物临床试验中心化监查统计指导原则 (试行)》的通告 (2022年第11号) [Article in Chinese]. Center for Drug Evaluation, NMPA. URL: https://www.cde.org.cn/main/news/viewInfoCommon/0a0ebbd5d09ec9fe6fcdc6e76d526314 [accessed 2025-04-15]
8. Marcheggiani D, Titov I. Encoding sentences with graph convolutional networks for semantic role labeling. Presented at: 2017 Conference on Empirical Methods in Natural Language Processing; Sep 7-11, 2017; Copenhagen, Denmark URL: https://aclanthology.org/D17-1159 [accessed 2025-03-31] [doi: 10.18653/v1/D17-1159]
9. Shen W, Wu S, Yang Y, Quan X. Directed acyclic graph network for conversational emotion recognition. Presented at: 59th Annual Meeting of the Association for Computational Linguistics and the 11th International Joint Conference on Natural Language Processing; Aug 1-6, 2021 URL: https://aclanthology.org/2021.acl-long.123 [accessed 2025-03-31] [doi: 10.18653/v1/2021.acl-long.123]

Abbreviations

ICH: International Council for Harmonisation of Technical Requirements for Pharmaceuticals for Human Use
NLP: natural language processing
QC: quality control

XSL•FO
RenderX

RBQM: risk-based quality management

Edited by C Lovis; submitted 12.07.24; peer-reviewed by C Yao, JG Mainprize; revised version received 06.02.25; accepted 08.02.25; published 25.04.25.

Please cite as:
Jiang M, Zhao S, Mei Y, Fu Z, Yuan Y, Ai J, Sheng Y, Gong Y, Chen J
Real-Time, Risk-Based Clinical Trial Quality Management in China: Development of a Digital Monitoring Platform
JMIR Med Inform 2025;13:e64114
URL: https://medinform.jmir.org/2025/1/e64114
doi:10.2196/64114

© Min Jiang, Shuhua Zhao, Yun Mei, Zhiying Fu, Yannan Yuan, Jie Ai, Yuan Sheng, Ying Gong, Jingjing Chen. Originally published in JMIR Medical Informatics (https://medinform.jmir.org), 25.4.2025. This is an open-access article distributed under the terms of the Creative Commons Attribution License (https://creativecommons.org/licenses/by/4.0/), which permits unrestricted use, distribution, and reproduction in any medium, provided the original work, first published in JMIR Medical Informatics, is properly cited. The complete bibliographic information, a link to the original publication on https://medinform.jmir.org/, as well as this copyright and license information must be included.

XSL•FO
RenderX

A Novel Framework to Assess Clinical Information in Digital Health Technologies: Cross-Sectional Survey Study

Kayode Philip Fadahunsi[1], PhD; Petra A Wark[1,2], PhD; Nikolaos Mastellos[1], PhD; Ana Luisa Neves[1], PhD; Joseph Gallagher[1,3], MD; Azeem Majeed[1], MD; Josip Car[1,4], PhD

[1]Department of Primary Care and Public Health, Imperial College London, White City Campus, 80–92 Wood Lane, London, United Kingdom

[2]Centre for Healthcare and Communities, Coventry University, Richard Crossman, Priory Street, Coventry, United Kingdom

[3]Global Health Research Group, School of Medicine, University College Dublin, Dublin, Ireland

[4]School of Life Course and Population Sciences, King's College London, London, United Kingdom

Corresponding Author:
Kayode Philip Fadahunsi, PhD
Department of Primary Care and Public Health, Imperial College London, White City Campus, 80–92 Wood Lane, London, United Kingdom

Abstract

Background: Digital health is a critical driver of quality, safety, and efficiency in health care. However, poor quality of clinical information in digital health technologies (DHTs) can compromise the quality and safety of care. The Clinical Information Quality (CLIQ) framework was developed, based on a systemic review of literature and an international eDelphi study, as a tool to assess the quality of clinical information in DHTs.

Objectives: The aim of this study is to assess the applicability, internal consistency, and construct validity of the CLIQ framework.

Methods: This study was conducted as a cross-sectional survey of health care professionals across the United Kingdom who regularly use SystmOne electronic health records. Participants were invited through emails and social media platforms. The CLIQ questionnaire was administered as a web-based survey. Spearman correlation coefficients were computed to investigate the linear relationship between the dimensions in the CLIQ framework. The Cronbach α coefficients were computed to assess the internal consistency of the global scale (ie, CLIQ framework) and the subscales (ie, the informativeness, availability, and usability categories). Confirmatory factor analysis was used to assess the extent to which the survey data supported the construct validity of the CLIQ framework.

Results: A total of 109 health care professionals completed the survey, of which two-thirds (67, 61.5%) were doctors and a quarter (26, 23.9%) were nurses or advanced nurse practitioners. Overall, the CLIQ dimensions had good quality scores except for portability, which had a modest score. The inter-item correlations were all positive and not likely due to chance. The Cronbach α coefficient for the overall CLIQ framework was 0.89 (95% CI 0.85 - 0.92). The confirmatory factor analysis provided a modest support for the construct validity of the CLIQ framework with the comparative fit index of 0.86 and standardized root mean square residual of 0.08.

Conclusions: The CLIQ framework demonstrated a high reliability and a modest construct validity. The CLIQ framework offers a pragmatic approach to assessing the quality of clinical information in DHTs and could be applied as part of information quality assurance systems in health care settings to improve quality of health information.

(JMIR Med Inform 2025;13:e58125) doi:10.2196/58125

KEYWORDS

information quality; digital health technology; patient safety; structural equation modeling; reliability; information; applicability; consistency; validity; Clinical Information Quality; CLIQ; cross-sectional; survey; United Kingdom; questionnaire; health care professional; doctor; nurse; practitioner; pragmatic; health care setting

Introduction

Digital health is critical to quality, safety, and efficiency of health care services [1]. Digital health technologies (DHTs) can enhance the delivery of health care services in several ways [2]. Electronic health records (EHRs) make medical records readily available at the point of care [3]. Electronic prescribing systems reduce the incidents of medication errors [4]. Clinical decision support systems support clinicians in decision-making [5,6]. Mobile health (mHealth) apps support self-management of chronic diseases [7].

However, poor quality of clinical information in DHTs can compromise the quality and safety of care [8,9]. A systematic review of literature reported widespread incidents of delayed,

XSL•FO
RenderX

missing, partial, and wrong information in DHTs resulting in adverse outcomes and deaths [10]. Most of the information quality problems reported in the included studies were based on incidents reporting systems [10]. While retrospective lessons based on adverse events in the incidents reporting systems could be useful, it is more important to identify and address information quality problems as a proactive measure to prevent adverse events, hence the need for an information quality framework.

In another systematic review [11], we identified 10 existing information quality frameworks for DHTs comprising 5 frameworks for EHRs [12-16] and one each for clinical decision support systems [17], cloud-based information systems [18], electronic medical records [19], mobile and web-based telemedicine apps [20], and primary care databases [13]. Although these frameworks identified dimensions that are relevant to assessing clinical information in DHTs, most were developed without inputs of clinicians and did not provide a tool that can be used to assess DHTs [11]. To overcome these limitations, we developed the Clinical Information Quality (CLIQ) framework for DHTs.

The CLIQ framework identifies, defines, and integrates 14 dimensions that are relevant to assessing clinical information in DHTs [11,21]. The dimensions in the CLIQ framework are grouped into 3 categories—informativeness, availability, and usability. The informativeness category relates to the usefulness of clinical information in patient care. Dimensions in the informativeness category include accuracy, completeness, interpretability, plausibility, relevance, and trustworthiness. The availability category relates to the functionality of the DHTs holding clinical information. Dimensions in this category include accessibility, portability, searchability, security, and timeliness. The usability category—comprising conformance, consistency of presentation, and maintainability—concerns the ease of use of clinical information. The definitions of the dimensions in the CLIQ framework are shown in Table 1.

The CLIQ framework was developed in 4 successive stages as shown in Figure 1. An initial CLIQ framework was developed through a systematic review and qualitative synthesis of existing information quality frameworks for DHTs [11]. A CLIQ assessment questionnaire was then developed based on the CLIQ framework and further evidence from literature [21]. The questionnaire offers a pragmatic approach to assessing clinical information in DHTs based on relatable clinical scenarios. The framework and the accompanying questionnaire were revised via an international eDelphi study among 35 clinicians from 10 different countries [21].

The development and modification of the CLIQ framework through a systematic review of literature and an international eDelphi study resulted in an evidence-based and user-friendly framework that is grounded in the literature and the views of clinicians who are users of clinical information. However, these approaches addressed only the content and face validity of the CLIQ framework and not its applicability, reliability, and construct validity. Therefore, the aim of this study is to assess the applicability, internal consistency, and construct validity of the CLIQ framework.

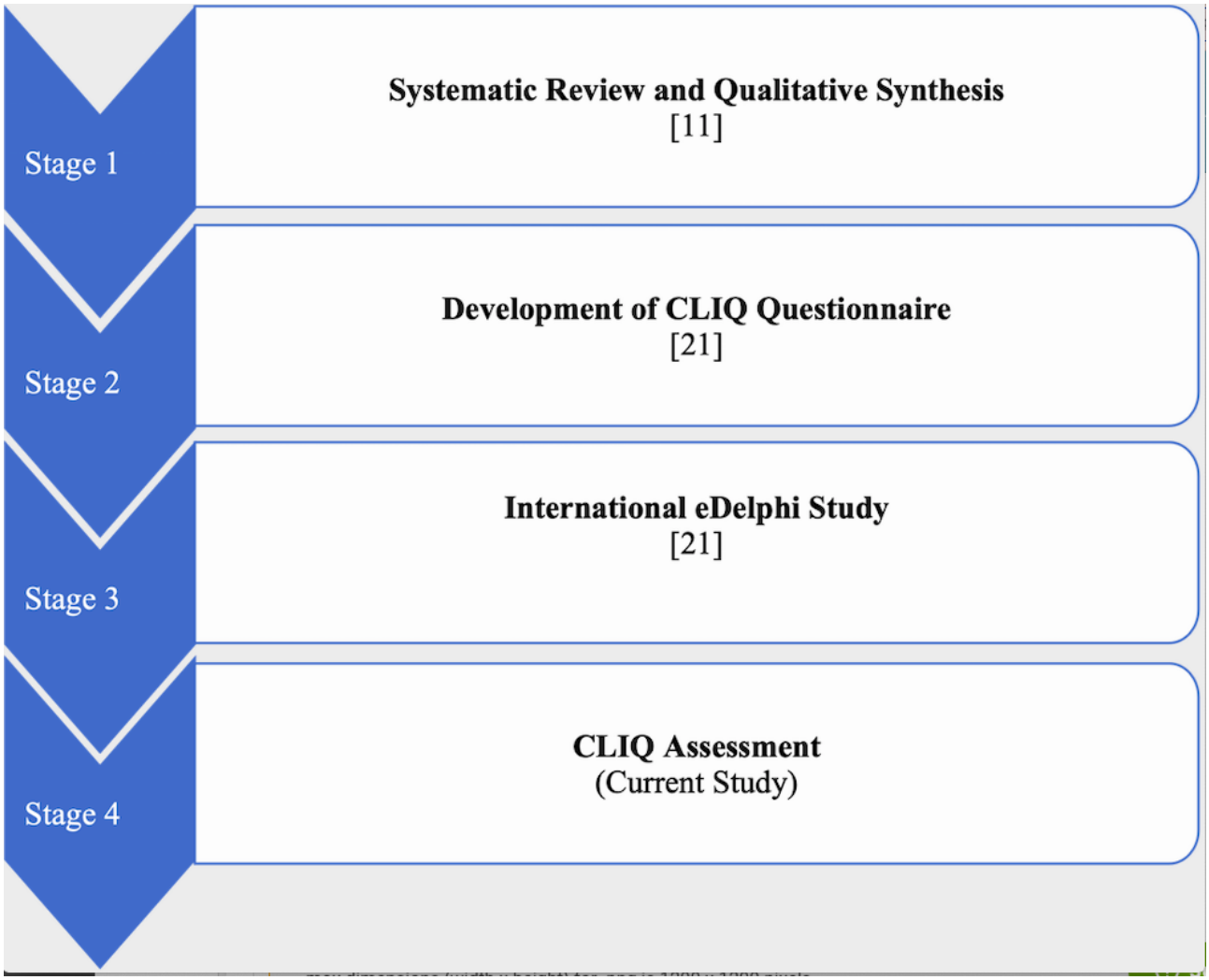
XSL•FO
RenderX

Table . Clinical Information quality framework for digital health technologies.

Clinical information quality dimensions and their definition	
Informativeness: the usefulness of digital information for clinical purposes	
Accuracy	The extent to which information is accurate.
Completeness	The extent to which no required information is missing.
Interpretability	The extent to which information can be interpreted.
Plausibility	The extent to which information makes sense based on clinical knowledge.
Trustworthiness	The extent to which the source of information is trustworthy and verifiable.
Relevance	The extent to which information is useful for patient care.
Availability: the functionality of the system holding clinical information	
Accessibility	The extent to which information is accessible.
Portability	The extent to which information can be moved or transferred between different systems.
Searchability	The extent to which needed information can be found.
Security	The extent to which information is protected from unauthorized access, corruption, and damage.
Timeliness	The extent to which information is up to date.
Usability: the ease of use of clinical information	
Conformance	The extent to which information is presented in a format that complies with institutional, national, or international standards.
Consistency of presentation	The extent to which presentation of information adheres to the same set of institutional, national, or international standards.
Maintainability	The extent to which information can be maintained (eg, modified, corrected, updated, adapted, and upgraded) to achieve intended improvement.

XSL•FO
RenderX

Figure 1. Stages of CLIQ framework Development.CLIQ: Clinical Information Quality.



Methods

Study Design

This study was conducted as a web-based cross-sectional survey of health care professionals across the United Kingdom who use SystmOne EHRs (The Phoenix Partnership Ltd). The cross-sectional survey approach allowed the assessment of the applicability, internal consistency, and construct validity of the CLIQ framework. The web-based approach offered a convenient, affordable, and pragmatic way of conducting a study and collecting data. The choice of SystmOne was informed by its wide use across different health care settings in the United Kingdom, including general practices, urgent care centers, social care services, hospitals, and prison medical services to manage about 61 million EHRs [22]. CHERRIES (Checklist for Reporting Results of Internet E-Surveys) was used to guide the survey report [23].

Study Participants

Eligibility criteria for the study included being a health care professional with a clinical role and a regular user of SystmOne (defined as using SystmOne as part of routine professional activities to document clinical information). Administrative staff using SystmOne and health care professionals using SystmOne occasionally (eg, to check clinical records) were not eligible to participate in the study. Participants were invited through emails and social media platforms, including Facebook, LinkedIn, WhatsApp, Yammer, Digital Health Networks, and the Future National Health System Collaboration platform. Although there is no consensus about the adequate sample size needed to validate a questionnaire, the literature recommends recruiting at least 10 participants for each item of the scale being validated as a rule of thumb [24]. As there are 14 dimensions of the CLIQ framework, this was equivalent to 140 participants in our study.

Data Collection

Health care professionals were invited to use the CLIQ framework to evaluate the information quality of SystmOne. The survey questionnaire comprised the 14 items of the CLIQ framework and 2 questions about the occupation of the respondents to assess their eligibility (Multimedia Appendix 1). Each question was displayed on a separate mobile or computer screen to the participants. The responses were made mandatory to avoid missing data, which could limit the assessment of the construct validity [25]. Participants were able to change their answers using the back button. Bot detection and prevention of multiple submissions were turned on in Qualtrics (Qualtrics). An invitation containing a link to the

XSL•FO
RenderX

participant information sheet, the consent form, and the questionnaire was shared with the health care professionals electronically through the channels described earlier. Two reminders, at least 2 weeks apart, were sent to encourage participation. Health care professionals were also encouraged to share the invitation with colleagues. Data collection took place between February 27 and June 7, 2022. The questionnaire was administered through a web-based survey platform, Qualtrics.

Data Analysis

The survey result was downloaded from Qualtrics in an excel format and imported into SPSS (version 20; IBM Statistics). Only completed entries were analyzed as uncompleted entries stopped at the consent. SPSS was used to conduct descriptive statistical analyses and compute correlation coefficients and Cronbach α scores.

The 3 options for each dimension (eg, accurate, partly accurate, and not accurate) were recoded into the integers 1, 2, and 3, representing low, modest, and good quality, respectively. A descriptive statistical analysis was conducted and interpreted to demonstrate the applicability of the CLIQ framework. The distribution of the responses was expressed as frequencies, percentages, means, and SDs.

Spearman correlation coefficients were computed to investigate the linear relationship between the dimensions in the CLIQ framework. The ordinal nature of the data informed the choice of Spearman coefficients. Correlation coefficients of 0.1 - 0.2 were regarded as poor, 0.3 - 0.5 as fair, 0.6 - 0.7 as moderate, and 0.8 - 0.9 as very strong [26] .

The Cronbach α coefficient was computed to assess the internal consistency of the global scale (ie, CLIQ framework) and the subscales (ie, the informativeness, availability, and usability categories). A Cronbach α coefficient of 0.7 or above was regarded as an indication of the reliability of the scale, and an alpha coefficient between 0.6 and 0.7 was considered acceptable [26].

The SPSS data file was subsequently exported to SPSS Amos (version 28; IBM Statistics) to assess the construct validity of the CLIQ framework. Confirmatory factor analysis, a structural equation modeling technique, was used to assess the extent to which the survey data supported the construct validity of the CLIQ framework [27]. Confirmatory factor analysis was adopted because the CLIQ framework has multiple subscales (ie, informativeness, availability, and usability categories) that were predetermined [11].

The maximum likelihood estimation method was used for the confirmatory factor analysis. The model fit was assessed based on the Standardized Root Mean Square Residual (SRMR) and Comparative Fit Index (CFI) as recommended in the literature for studies with a sample size of less than 250 [28]. A CFI greater than 0.9 and an SRMR less than 0.08 indicate model fit [28].

Ethical Considerations

Informed consent was obtained from each participant at the beginning of the web-based survey after they had been provided with the participant information sheet, containing detailed information about the study objectives, expectation of the participants, duties of the researchers, and relevant contacts. Participation was voluntary. A secure web-based survey platform was used for data collection as already described. No personal information that could be used to identify the participants was collected in the survey. Survey responses were anonymized with codes automatically assigned to participants by the survey platform. The results were securely stored in Imperial College Shared Drive. Participants could withdraw from the study at any time without giving any reasons. However, once the survey was submitted, the data could not be withdrawn as the responses were anonymous. Participants were not compensated for taking part. Ethical approval was obtained from the Imperial College research ethics committee (21IC7415).

Results

Participants' Characteristics

A total of 109 health care professionals completed the survey, with two-thirds (67, 61.5%) being doctors and almost a quarter (26, 23.9%) being nurses or advanced nurse practitioners. The rest of the participants had other clinical occupations. Table 2 shows the distribution of the participants by occupation.

Table . Distribution of the occupation of the survey participants (N=109).

Occupation	Values, n (%)
Doctors	67 (61.5)
Nurses and advanced nurse practitioners	26 (23.9)
Health care assistants	5 (4.6)
Physiotherapists and occupational therapists	4 (3.7)
Pharmacists	2 (1.8)
Podiatrists	2 (1.8)
Physician associates	1 (0.9)
Therapy support workers	1 (0.9)
Community health workers	1 (0.9)

XSL•FO
RenderX

Participants' Assessment of Quality of the Dimensions

The mean quality score assigned to each dimension ranged from 2.2 for portability to 2.9 for security of clinical information in SystmOne (1, 2, and 3 indicate low, modest, and good quality, respectively). Most participants (97/109, 89%) ranked security of clinical information in SystmOne as good while only more than a third of the participants (42/109, 38.5%) ranked portability of clinical information in SystmOne as good. The summary of the assessment result is shown in Table 3.

Table . Clinical Information Quality of SystmOne as assessed by the participants.

Dimension	Assessment of the quality of the dimension, n (%)			Mean score (SD)
	Good	Modest	Low	
Accuracy	73 (67)	32 (29.4)	4 (3.7)	2.6 (0.6)
Completeness	63 (57.8)	43 (39.4)	3 (2.8)	2.6 (0.6)
Interpretability	82 (75.2)	26 (23.9)	1 (0.9)	2.7 (0.5)
Plausibility	92 (84.4)	17 (15.6)	0	2.8 (0.4)
Relevance	89 (81.7)	20 (18.3)	0	2.8 (0.4)
Trustworthiness	94 (86.2)	15 (13.8)	0	2.9 (0.3)
Accessibility	77 (70.6)	31 (28.4)	1 (0.9)	2.7 (0.5)
Portability	42 (38.5)	49 (45)	18 (16.5)	2.2 (0.7)
Searchability	56 (51.4)	49 (45)	4 (3.7)	2.4 (0.6)
Security	97 (89)	12 (11)	0	2.9 (0.3)
Timeliness	71 (65.1)	35 (32.1)	3 (2.8)	2.6 (0.5)
Conformance	77 (70.6)	27 (24.8)	5 (4.6)	2.7 (0.6)
Consistency of presentation	77 (70.6)	22 (20.2)	10 (9.2)	2.6 (0.7)
Maintainability	70 (64.2)	33 (30.3)	6 (5.5)	2.6 (0.6)

Inter-item Correlation

There were positive correlations between all possible pairs of dimensions in the CLIQ framework (Multimedia Appendix 2). All the correlation coefficients were statistically significant (represented as asterisks) except for the correlations of portability with each of plausibility, relevance, trustworthiness, and security. There is a strong statistically significant correlation between conformance and consistency (Spearman ρ=0.751; *P*<.001).

Internal Consistency of the CLIQ Framework

The Cronbach α coefficients and corresponding 95% CIs for the informativeness, availability, and usability subscales were 0.78 (95% CI 0.70 - 0.84), 0.69 (95% CI 0.58 - 0.77), and 0.83 (95% CI 0.77 - 0.88), respectively. Once security was removed from the availability subscale, the Cronbach α coefficient for the availability subscale increased marginally to 0.70 (95% CI 0.60 - 0.78). The Cronbach α coefficient for the overall CLIQ framework is 0.89 (95% CI 0.85 - 0.92).

Construct Validity of the CLIQ Framework

Although the chi-square goodness-of-fit test ($\chi^2_{2.10}$=155.69; *P*<.001) did not demonstrate fitness of the model, CFI (0.86) and SRMR (0.08) suggest that the model fits modestly with the data. All the factor loadings (ie, covariance estimates) were positive and statistically significant, as shown in Table 4. Significant tests (SE, critical ratio, and *P* value) were not reported for the first item in each category (ie, accuracy, accessibility, and conformance) because their unstandardized covariance values were fixed as 1, which is a standard procedure in confirmatory factor analysis.

The statistical significance of positive standardized covariance estimates for all information quality dimensions supports the placement of the dimensions in their respective category. This is further illustrated in the path diagram shown in Figure 2. The high values of estimated covariances between the latent variables and the observed variables support the construct validity of the model. Still, the high covariance estimates between the latent variables (informativeness, availability, and usability) indicate overlap of the categories.

XSL•FO
RenderX

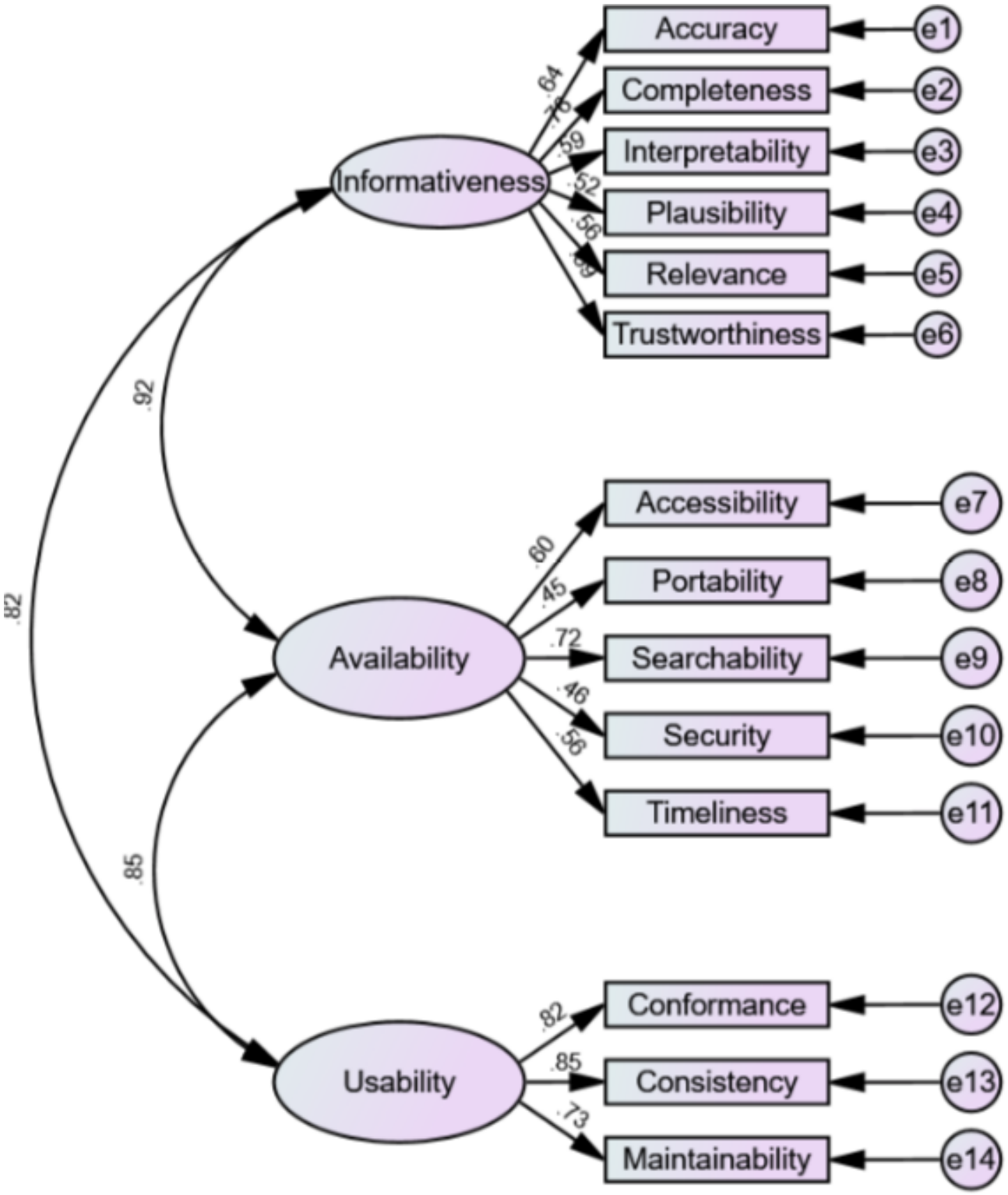
Table . Standardized and unstandardized estimates of the covariance.

Standardized covariance estimates	Unstandardized covariance estimates	SE	Critical ratio	*P* value	
Accuracy	0.64	1.00	N/A[a]	N/A	N/A
Completeness	0.76	1.18	0.18	6.41	<.001
Interpretability	0.59	0.77	0.15	5.27	<.001
Plausibility	0.52	0.53	0.11	4.72	<.001
Relevance	0.56	0.61	0.12	5.00	<.001
Trustworthiness	0.59	0.57	0.11	5.24	<.001
Accessibility	0.60	1.00	N/A	N/A	N/A
Portability	0.45	1.13	0.28	3.99	<.001
Searchability	0.72	1.43	0.25	5.66	<.001
Security	0.46	0.50	0.13	4.03	<.001
Timeliness	0.56	1.05	0.22	4.73	<.001
Conformance	0.82	1.00	N/A	N/A	N/A
Consistency	0.85	1.20	0.12	9.64	<.001
Maintainability	0.73	0.94	0.12	8.05	<.001

[a]N/A: not applicable.

XSL•FO
RenderX

Figure 2. Path diagram for confirmatory factor analysis The rectangular shapes represent the observed variables (ie, information quality dimensions) that were directly measured in the survey. The circular shapes represent the latent variables (ie, information quality categories) that could be inferred from the measured variables. The abbreviation "e" represents error. The connecting arrows represent covariances, with the accompanying numbers representing their estimates.



Discussion

Principal Findings

The study assessed the applicability, internal consistency, and construct validity of the CLIQ framework based on the pilot CLIQ assessment of SystmOne EHRs. Overall, the CLIQ dimensions had good quality scores except for portability which had a modest score. The inter-item correlations were all positive and not likely due to chance. The Cronbach α score demonstrated a good internal consistency of the CLIQ framework and its informativeness, availability, and usability subscales. The results of the Confirmatory Factor Analysis

XSL•FO
RenderX

provided a modest support for the construct validity of the CLIQ framework.

Comparison With Previous Literature

The combination of good security and modest portability of clinical information in SystmOne indicates the possibility of a trade-off between security and portability. Portability might have been limited inadvertently to improve the security of clinical information. Similar trade-offs, such as between accessibility and security, have been documented in the literature [29]. Software developers need to be vigilant to identify potential trade-offs that may compromise the quality and safety of care.

The positive and mostly significant correlations between the items in the scale indicated a close relationship between the dimensions [30]. This was not unexpected because all dimensions are components of the same CLIQ framework. The generally low values of the correlations demonstrated that the dimensions, although related, are distinct [30]. The high correlation between conformance and consistency of presentation is understandable, as both concern presentation of information. Similarly, the high covariance between the latent variables (informativeness, availability, and usability), which indicate that the categories are not entirely distinct, is not strange in information quality research. Categories in information quality frameworks are not mutually exclusive as each dimension in an information framework often fits into multiple categories [31]. However, there is a scope for model revision to further explore this overlap in future CLIQ research.

The overall good internal consistency of the CLIQ framework and its subscales (ie, informativeness, availability, and usability) indicates the reliability of the CLIQ framework [32]. Although the study was unable to rely on fit indices primarily influenced by sample size such as the chi-square goodness-of-fit index [23], the index least affected by sample size, the SRMR [28], supports the model fit.

This study used similar methods as a study on the validation of the Modified Enlight Suite (MES), a generic mHealth assessment questionnaire [25]. The MES study demonstrated an overall good internal consistency and modest construct validity of the MES based on a survey of more than a thousand medical students and health care professionals who assessed a freely downloadable COVID-19 app in Ireland [25]. The differences in the uptakes of the 2 studies are probably related to the choice of DHTs and study population. This study population was limited to health care professionals using SystmOne. In contrast, the MES study was open to all health care professionals and medical students who could download the Irish COVID-19 app.

Strengths and Weaknesses

To the best of our knowledge, the CLIQ framework is the first information quality framework for DHTs, of which the internal reliability and construct validity have been assessed. Only the face and content validity of most existing information quality frameworks were assessed [11]. This study went a step further to explore the internal consistency and construct validity of the CLIQ framework.

Although the choice of SystmOne EHRs ensured participation of a multidisciplinary population of health care professionals in the testing of the CLIQ framework, allied health professionals were less represented. In addition, the voluntary nature of recruitment established a potential for systemic bias because those who were engaged in digital solutions were more likely to respond. The use of mandatory responses, although useful for survey data completeness, could introduce bias if participants provided less thoughtful responses just to complete the survey. Finally, the low response rate limited the assessment of the construct validity of the CLIQ framework [24]. The low uptake was probably due to the busy schedules of the health care professionals at a time when the National Health System was under immense pressure due to COVID-19 pandemic. Nevertheless, the sample size was sufficient to assess the CLIQ framework's applicability and reliability as demonstrated by the narrow CIs for the Cronbach α coefficients. Future studies on the validity of the CLIQ framework need to consider and address these limitations.

Implications for Practice

Information Quality Assurance System

The CLIQ research highlights the importance of information quality and its relevance to the quality and safety of care. Therefore, establishing a robust system for information quality assurance in health care institutions is essential. Such an information quality assurance system entails regular checks and monitoring, data validation, and information quality audits [33]. The CLIQ framework could be a useful tool for information quality audits. The information quality assurance system should be integrated into the information governance system, where one already exists, to prevent duplication and fragmentation. Designating clinicians with additional informatics training to oversee such information quality assurance system is necessary to ensure its successful implementation because they understand the clinical and technological aspects of patient care [34]. Although health care institutions within high-income countries have designated clinical informatics roles, such as the chief clinical information officer, the job description is still evolving [35]. It is vital to both introduce these roles in health facilities and expand the responsibilities to include information quality assurance.

Informatics Training and Education for Health Care Professionals

The CLIQ framework demonstrates that information quality is multidimensional, and understanding its meaning, relevance, and assessment requires some training. The clinicians who participated in the international eDelphi study expressed concerns that health care professionals without informatics training might be unfamiliar with information quality–related terms [21]. In addition, information quality problems, such as missing and inaccurate information, could result from human errors [36]. Informatics training could provide health care professionals with knowledge about the meaning, relevance, and assessment of information quality. Training could also be used to address information quality problems through promotion of good practice such as proper documentation and adequate record keeping. Informatics training should be included in health

XSL•FO
RenderX

care professionals' prequalification and postqualification education competencies to also keep them up-to-date of the ever-changing information landscape in digital health [37]. However, care should be taken not to complicate an already-complex medical curriculum with extensive informatics training [37]. Rather, efforts should be made to provide appropriate level of informatics training that is commensurate with individual and institutional needs. Although informatics training could build health professionals' competencies around information quality, mistakes will continue to occur because "to err is human" [38]. Therefore, it is vital to institute a system that reduces incidence and impact of errors.

Automated Error Detection and Data Validation Systems

The quality of clinical information could be improved by setting up automated error detection and data validation systems in DHTs. Machine learning and artificial intelligence algorithms could be applied for automated data validation and real-time error detection with errors flagged during data entry [39]. Automated error detection and data validation systems could reduce the likelihood of wrong data entry as well as prompt early correction of errors before patient safety is compromised. However, lack of trust in machine learning and artificial intelligence could make health care professionals ignore or override automated warnings and alerts [40].

Interoperability and Integration of Digital Health Systems

Interoperability enhances seamless flow of information across different DHTs such as EHRs, laboratory information system, and electronic triage system [41]. Seamless health information exchange between multiple platforms improves quality of clinical information [42]. Communication between systems enhances timely access to up-to-date information in or near real time [42]. Accuracy is enhanced when information is obtained directly from source with elimination of possible changes during transcription [41]. Portability and interoperability could be improved through adoption of clinical data models (eg, openEHR), standardized terminologies (eg, Systematized Nomenclature of Medicine Clinical Term—SNOMED CT), and clinical coding system (eg, *International Classification of Diseases, Tenth Revision—ICD-10*), which promote consistent presentation of clinical information [43,44]. Although interoperability of digital health systems is desirable, a huge cost is often required for its implementation. Concerns about security of information may also be an obstacle due to increased access to information [41]. Security concerns could be addressed by obtaining prior informed consent for information sharing from patients when they register with the health service.

User-Friendly Design Interface

The quality of data entry could be improved with a user-friendly design interface [45]. Accuracy and completeness of the information in the DHTs could be enhanced with features such as drop-down menus, prepopulation fields, and validation prompts. Faulty design interface can affect consistency of presentation and conformance. A drop down with different units of the same medication can lead to medication errors [10]. Searchability of information improves when the design interface allows smooth navigation through the digital system.

Implications for Policy

Information Quality Requirements

Policies and guidelines are needed to define and communicate information quality requirements for DHTs. Policies should communicate the official position of an institution on information quality requirements while guidelines should provide clear guidance on how to meet the requirements. The CLIQ framework could be used as a conceptual guide for information quality requirements. Policies and guidelines are needed to address issues relating to information quality, including interoperability, privacy and confidentiality, information format, design interface, training, and so forth. These issues should be addressed collectively in a single information quality policy or individually with different guidelines based on the needs of the institution. It is essential to consider whether the information is used locally, nationally, or internationally. The process of formulating, implementing, and disseminating the policies needs to involve all stakeholders, as described subsequently.

Collaboration and Partnerships Among Information Stakeholders

The development of the CLIQ framework demonstrates the importance of multidisciplinary and international collaboration in the development of information quality standards. The CLIQ framework was developed with inputs of scores of professionals from more than 10 countries. Establishing and implementing information quality standards require collaboration among health care organizations, software developers and vendors, regulatory bodies, patient support group, professional organizations, and so forth. Collaboration will ensure buy-in of all information stakeholders and facilitate the implementation process.

Certification and Regulation

Enforcement of information quality standards for DHTs requires regulatory oversights. Regulatory bodies for DHTs in different countries and regions, such as the United States Food and Drug Administration and the Medicines and Healthcare products Regulatory Agency, need to include information quality requirements as part of prequalification criteria for DHTs. Information quality of DHTs should be assessed using evidence-based approach such as the CLIQ framework before they are certified for use in health care facilities. Only DHTs that meet specified prequalification criteria, including information quality requirements, should be certified by the regulatory bodies.

Implication for Future Research

Evidence-Based Approach

The CLIQ framework was developed and validated using an approach that combined evidence from literature and empirical studies. We conducted a systematic review of frameworks, rather than interventions, based on the BeHeMoTh procedure [46]. The international eDelphi study obtained quantitative and qualitative evidence from clinicians across 10 countries [21].

XSL•FO
RenderX

The pilot CLIQ assessment used a systematic approach to investigate the reliability and validity of this novel tool. Overall, the evidence-based approach used while developing the CLIQ framework provides a methodological model which could be adopted in future research while developing pragmatic frameworks.

Information Quality Research

The systematic review of literature showed a dearth of information quality research relating to DHTs [11]. As DHTs are used more commonly worldwide, there is an increased need for information quality research to match the growth in technological innovations. The CLIQ framework demonstrates the importance of information quality research in addressing contemporary issues relating to DHTs. Some information quality dimensions, which were hitherto not included in most existing information quality frameworks for DHTs, are included in the CLIQ framework. Searchability and maintainability are more relevant due to technological advancement which has made it possible to capture, process, and store an increasing volume of digital information. Searchability, that is, locating needed information from the wide range of available information, is thus essential. Maintainability of information is also important to ensure that information quality is not sacrificed with increasing quantity of information. Similarly, portability has become more relevant than ever with the current tendency toward integration and interoperability of DHTs.

Patient Perspective on Information Quality

This study focused on health care professionals as end users of clinical information in DHTs. However, patients have also become end users of clinical information in DHTs. Patients are increasingly viewing and contributing more information into DHTs, especially since the COVID-19 pandemic [47]. Multiple DHTs, such as AskmyGp (Evergreen Health Solution Ltd), eConsult (eConsult Health Ltd), and Accurx (Accurx Ltd), allow patients to enter text using their own words and upload photographs that could be saved in the EHRs. In addition, many wearable devices and mobile apps generate consumer health data, nowadays, that could be imported into the EHRs. It would therefore be useful to explore the patients' perspective on information quality in future studies and incorporate their views and suggestions into the CLIQ framework.

Conclusions

The CLIQ research highlights the importance of information quality and its relevance to the quality and safety of care. The CLIQ framework demonstrated a high reliability and a modest construct validity. The CLIQ framework offers a pragmatic approach to assessing the quality of clinical information in DHTs and could be applied as part of information quality assurance systems in health care settings to improve quality of health information.

Acknowledgments

The authors are grateful to all health care professionals who participated in this survey. ALN is supported by the National Institute for Health and Care Research (NIHR) Patient Safety Translational Research Centre and the NIHR Biomedical Research Centre. AM and JC are supported by NIHR Applied Research Collaboration Northwest London. The views expressed in this publication are those of the authors and not necessarily those of the NIHR or the Department of Health and Social Care. KPF's doctoral research was funded by the Federal Government of Nigeria.

Conflicts of Interest

None declared.

Multimedia Appendix 1
Clinical Information Quality (CLIQ) questionnaire.
[PDF File, 132 KB - medinform_v13i1e58125_app1.pdf]

Multimedia Appendix 2
Inter-item correlation matrix.
[DOCX File, 22 KB - medinform_v13i1e58125_app2.docx]

Checklist 1
Checklist for Reporting Results of Internet E-Surveys.
[DOCX File, 19 KB - medinform_v13i1e58125_app3.docx]

References

1. World Health Organization. Global strategy on digital health 2020-2025. 2021. URL: http://apps.who.int/bookorders [accessed 2025-05-05]
2. Gomes M, Murray E, Raftery J. Economic evaluation of digital health interventions: methodological issues and recommendations for practice. Pharmacoeconomics 2022 Apr;40(4):367-378. [doi: 10.1007/s40273-022-01130-0] [Medline: 35132606]

XSL•FO
RenderX

3. Institute of Medicine. Key Capabilities of an Electronic Health Record System: Letter Report: National Academies Press; 2003. URL: https://www.ncbi.nlm.nih.gov/books/NBK221802/ [accessed 2025-05-16]
4. Graf A, Fehring L, Henningsen M, Zinner M. Going digital in Germany: an exploration of physicians' attitudes towards the introduction of electronic prescriptions—a mixed methods approach. Int J Med Inform 2023 Jun;174(March):105063. [doi: 10.1016/j.ijmedinf.2023.105063] [Medline: 37028259]
5. Sutton RT, Pincock D, Baumgart DC, Sadowski DC, Fedorak RN, Kroeker KI. An overview of clinical decision support systems: benefits, risks, and strategies for success. NPJ Digit Med 2020;3(1):17. [doi: 10.1038/s41746-020-0221-y] [Medline: 32047862]
6. Teufel A, Binder H. Clinical Decision Support Systems. Visc Med 2021 Dec;37(6):491-498. [doi: 10.1159/000519420] [Medline: 35087899]
7. World Health Organization. mHealth New Horizons for Health Through Mobile Technologies: World Health Organization; 2011. URL: https://iris.who.int/handle/10665/44607 [accessed 2025-05-16]
8. Meeks DW, Smith MW, Taylor L, Sittig DF, Scott JM, Singh H. An analysis of electronic health record-related patient safety concerns. J Am Med Inform Assoc 2014;21(6):1053-1059. [doi: 10.1136/amiajnl-2013-002578] [Medline: 24951796]
9. Magrabi F, Ong MS, Runciman W, Coiera E. Patient safety problems associated with healthcare information technology: an analysis of adverse events reported to the US Food and Drug Administration. AMIA Annu Symp Proc 2011;2011(1):853-857. [Medline: 22195143]
10. Kim MO, Coiera E, Magrabi F. Problems with health information technology and their effects on care delivery and patient outcomes: a systematic review. J Am Med Inform Assoc 2017 Mar 1;24(2):246-250. [doi: 10.1093/jamia/ocw154] [Medline: 28011595]
11. Fadahunsi KP, O'Connor S, Akinlua JT, et al. Information quality frameworks for digital health technologies: systematic review. J Med Internet Res 2021 May 17;23(5):e23479. [doi: 10.2196/23479] [Medline: 33835034]
12. Almutiry OS. Data Quality Assessment Instrument For Electronic Health Record Systems in Saudi Arabia: University of Southampton; 2017.
13. Dungey S, Beloff N, Puri S, Boggon R, Williams T, Tate AR. A pragmatic approach for measuring data quality in primary care databases. Presented at: 2014 IEEE-EMBS International Conference on Biomedical and Health Informatics (BHI); Jun 1-4, 2014; Valencia, Spain. [doi: 10.1109/BHI.2014.6864484]
14. Weiskopf NG, Weng C. Methods and dimensions of electronic health record data quality assessment: enabling reuse for clinical research. J Am Med Inform Assoc 2013 Jan 1;20(1):144-151. [doi: 10.1136/amiajnl-2011-000681]
15. Stetson PD, Bakken S, Wrenn JO, Siegler EL. Assessing electronic note quality using the Physician Documentation Quality Instrument (PDQI-9). Appl Clin Inform 2012;3(2):164-174. [doi: 10.4338/aci-2011-11-ra-0070] [Medline: 22577483]
16. Kahn MG, Callahan TJ, Barnard J, et al. A harmonized data quality assessment terminology and framework for the secondary use of electronic health record data. EGEMS (Wash DC) 2016;4(1):1244. [doi: 10.13063/2327-9214.1244] [Medline: 27713905]
17. McCormack JL, Ash JS. Clinician perspectives on the quality of patient data used for clinical decision support: a qualitative study. AMIA Annu Symp Proc 2012;2012:1302-1309. [Medline: 23304409]
18. Almutiry O, Wills G, Alwabel A, Crowder R, Walters R. Toward a framework for data quality in cloud-based health information system. Presented at: 2013 International Conference on Information Society (i-Society); Jun 24-26, 2013; Toronto, ON, Canada.
19. Bowen M. EMR Data Quality: Evaluation Guide: eHealth Observatory; 2012.
20. Bolt T, Kano S, Kodate A. Information quality in home care coordination services. J Telemed Telecare 2007 Jul;13(Suppl 1):7-9. [doi: 10.1258/135763307781645149]
21. Fadahunsi KP, Wark PA, Mastellos N, et al. Assessment of clinical information quality in digital health technologies: international eDelphi study. J Med Internet Res 2022 Dec 6;24(12):e41889. [doi: 10.2196/41889] [Medline: 36472901]
22. TPP. Clinical software to revolutionise healthcare. 2024. URL: https://tpp-uk.com/ [accessed 2025-05-05]
23. Eysenbach G. Improving the quality of web surveys: the Checklist for Reporting Results of Internet E-Surveys (CHERRIES). J Med Internet Res 2004 Sep 29;6(3):e34. [doi: 10.2196/jmir.6.3.e34] [Medline: 15471760]
24. Boateng GO, Neilands TB, Frongillo EA, Melgar-Quiñonez HR, Young SL. Best practices for developing and validating scales for health, social, and behavioral research: a primer. Front Public Health 2018;6:149. [doi: 10.3389/fpubh.2018.00149] [Medline: 29942800]
25. Woulfe F, Fadahunsi KP, O'Grady M, et al. Modification and validation of an mHealth app quality assessment methodology for international use: cross-sectional and eDelphi studies. JMIR Form Res 2022 Aug 19;6(8):e36912. [doi: 10.2196/36912] [Medline: 35984688]
26. Taherdoost H. Validity and reliability of the research instrument; how to test the validation of a questionnaire/survey in a research. Int J Acad Res Manag 2018;5(3):28-36.
27. Ullman JB, Bentler PM. Structural equation modeling. In: Weiner I, Schinka JA, Velicer WF, editors. Handbook of Psychology: John Wiley & Sons, Inc; 2013:661-619.
28. Hu LT, Bentler PM. Cutoff criteria for fit indexes in covariance structure analysis: conventional criteria versus new alternatives. Struct Equation Model 1999 Jan;6(1):1-55. [doi: 10.1080/10705519909540118]

XSL•FO
RenderX

29. Eppler MJ, Wittig D. Conceptualizing information quality: a review of information quality frameworks from the last ten years goals. Presented at: Fifth Conference on Information Quality (IQ 2000); Jan 2000; MIT—Massachusetts Institute of Technology, Cambridge, MA p. 1-14.
30. Akoglu H. User's guide to correlation coefficients. Turk J Emerg Med 2018 Sep;18(3):91-93. [doi: 10.1016/j.tjem.2018.08.001] [Medline: 30191186]
31. Wang RY, Strong DM. Beyond accuracy: what data quality means to data consumers. J Manage Inf Syst 1996 Mar;12(4):5-33. [doi: 10.1080/07421222.1996.11518099]
32. Chan YH. Biostatistics 104: correlational analysis. Singapore Med J 2003 Dec;44(12):614-619. [Medline: 14770254]
33. World health organization. DATA QUALITY ASSURANCE module 1 framework and metrics. 2022. URL: http://apps.who.int/bookorders [accessed 2025-05-05]
34. Lee J. The chief medical informatics officer's (CMIO) view: clinical, technical and leadership acumen. In: Nursing Informatics, 5th Edition: Springer; 2022:99-110. [doi: 10.1007/978-3-030-91237-6_9]
35. Sridharan S, Priestman W, Sebire NJ. Chief Information Officer team evolution in university hospitals: interaction of the three 'C's (CIO, CCIO, CRIO). BMJ Health Care Inform 2018 Apr;25(2):88-91. [doi: 10.14236/jhi.v25i2.997]
36. Magrabi F, Liaw ST, Arachi D, Runciman W, Coiera E, Kidd MR. Identifying patient safety problems associated with information technology in general practice: an analysis of incident reports. BMJ Qual Saf 2016 Nov;25(11):870-880. [doi: 10.1136/bmjqs-2015-004323] [Medline: 26543068]
37. Davies A, Hassey A, Williams J, Moulton G. Creation of a core competency framework for clinical informatics: from genesis to maintaining relevance. Int J Med Inform 2022 Dec;168:104905. [doi: 10.1016/j.ijmedinf.2022.104905] [Medline: 36332519]
38. Institute of Medicine. To Err Is Human: Building a Safer Health System: Institute of Medicine; 2000, Vol. 11:312.
39. Khan S, Yairi T. A review on the application of deep learning in system health management. Mech Syst Signal Process 2018 Jul;107:241-265. [doi: 10.1016/j.ymssp.2017.11.024]
40. Nicora G, Rios M, Abu-Hanna A, Bellazzi R. Evaluating pointwise reliability of machine learning prediction. J Biomed Inform 2022 Mar;127:103996. [doi: 10.1016/j.jbi.2022.103996] [Medline: 35041981]
41. Iroju O, Soriyan A, Gambo I, Olaleke J. Interoperability in healthcare: benefits, challenges and resolutions. Int J Innov Appl Stud 2013(1):262-270.
42. Lehne M, Sass J, Essenwanger A, Schepers J, Thun S. Why digital medicine depends on interoperability. NPJ Digit Med 2019;2(1):79. [doi: 10.1038/s41746-019-0158-1] [Medline: 31453374]
43. Kalra D, Beale T, Heard S. The openEHR foundation. Studies in health technology and informatics. Stud Health Technol Inform 2005;115:153-173.
44. Gaudet-Blavignac C, Foufi V, Bjelogrlic M, Lovis C. Use of the Systematized Nomenclature of Medicine Clinical Terms (SNOMED CT) for processing free text in health care: systematic scoping review. J Med Internet Res 2021 Jan 26;23(1):e24594. [doi: 10.2196/24594] [Medline: 33496673]
45. Wilbanks BA, Moss JA. Impact of data entry interface design on cognitive workload, documentation correctness, and documentation efficiency. AMIA Jt Summits Transl Sci Proc 2021;2021:634-643. [Medline: 34457179]
46. Fadahunsi KP, Akinlua JT, O'Connor S, et al. Protocol for a systematic review and qualitative synthesis of information quality frameworks in eHealth. BMJ Open 2019 Mar 5;9(3):e024722. [doi: 10.1136/bmjopen-2018-024722] [Medline: 30842114]
47. Clarke G, Pariza P, Wolters A. How has COVID-19 affected service delivery in GP practices that offered remote consultations before the pandemic. The Health Foundation. 2020 URL: https://www.health.org.uk/news-and-comment/charts-and-infographics/how-has-covid-19-affected-service-delivery-in-gp-practices [accessed 2025-05-05]

Abbreviations

CFI: comparative fit index
CHERRIES: Checklist for Reporting Results of Internet E-Surveys
CLIQ: clinical information quality
DHT: digital health technology
EHR: electronic health record
MES: modified enlight suite
SRMR: Standardized Root Mean Square Residual

XSL•FO
RenderX

Edited by A Benis; submitted 06.03.24; peer-reviewed by MA Karim, P Mahapatra; revised version received 13.04.25; accepted 14.04.25; published 30.05.25.

Please cite as:
Fadahunsi KP, Wark PA, Mastellos N, Neves AL, Gallagher J, Majeed A, Car J
A Novel Framework to Assess Clinical Information in Digital Health Technologies: Cross-Sectional Survey Study
JMIR Med Inform 2025;13:e58125
URL: https://medinform.jmir.org/2025/1/e58125
doi:10.2196/58125

© Kayode Philip Fadahunsi, Petra A Wark, Nikolaos Mastellos, Ana Luisa Neves, Joseph Gallagher, Azeem Majeed, Josip Car. Originally published in JMIR Medical Informatics (https://medinform.jmir.org), 30.5.2025. This is an open-access article distributed under the terms of the Creative Commons Attribution License (https://creativecommons.org/licenses/by/4.0/), which permits unrestricted use, distribution, and reproduction in any medium, provided the original work, first published in JMIR Medical Informatics, is properly cited. The complete bibliographic information, a link to the original publication on https://medinform.jmir.org/, as well as this copyright and license information must be included.

XSL•FO
RenderX

Original Paper

Acceptance of Electronic Medical Records and Associated Factors Among Health Care Workers in Northwest Ethiopia: Cross-Sectional Study

Asmamaw Ketemaw Tsehay[1,2*], PhD; Kholofelo Lorraine Matlhaba[2*], PhD

[1]College of Medicine and Health Sciences, Bahir Dar University, Bahir Dar, Ethiopia

[2]University of South Africa, Pretoria, South Africa

[*]all authors contributed equally

Corresponding Author:
Asmamaw Ketemaw Tsehay, PhD
College of Medicine and Health Sciences
Bahir Dar University
SPH FelegeHiwot Campus
Bahir Dar, 79
Ethiopia
Phone: 251 913071149
Email: 18033342@mylife.unisa.ac.za

Abstract

Background: Although electronic medical records (EMRs) play a vital role in strengthening the health care system by improving efficiency, data management, and patient care, their development in Ethiopia is still in its early stages. Hence, most public health care facilities manage their patient information using paper-based recording, which results in errors, delays, and reduced service quality.

Objective: This study aims to determine the level of acceptance of the EMR system and describe contributing factors.

Methods: A cross-sectional study was conducted at health care facilities in Bahir City, Northwestern Ethiopia. A total of 322 health workers participated in the study, drawn from 5 health facilities that have implemented the EMR system. Descriptive statistics and bivariate and multivariate binary logistic regression were done to determine factors associated with EMR acceptance computed from mediating factors (perceived ease of use and perceived usefulness), and which is more appropriate in early-stage implementation.

Results: Out of the total 322 respondents, 256 (73%) respondents with 95% CI 67.4-78.2 had a good acceptance of using EMRs. In regression analysis, significant predictors including work experience over 10 years (odds ratio [OR] 14.32, 95% CI 4.60-44.58), income dissatisfaction (OR 0.28, 95% CI 0.10-0.82), owning a personal computer (OR 11.08, 95% CI 4.03-30.24), EMR-specific training (OR 4.71, 95% CI 1.52-14.54), basic electronic health management information system/district health information system 2 training (OR 3.06, 95% CI 1.02-9.17), and system usability (OR 38.24, 95% CI 12.26-119.27) were identified.

Conclusions: The study demonstrated a moderate level of EMR acceptance among health care workers, with system usability identified as the strongest predictor. Significant factors influencing EMR acceptance included longer work experience, ownership of a personal computer, and prior EMR or electronic health management information system/district health information system 2 training. Context-specific strategies are needed to enhance system usability, provide targeted digital health training, and improve access to technological resources in order to support broader EMR adoption in health care settings.

(JMIR Med Inform 2025;13:e72030) doi:10.2196/72030

KEYWORDS

electronic medical records; health care workers; implementation; northwest Ethiopia; perceived ease of use

XSL•FO
RenderX

Introduction

The acceptance and effective use of electronic medical records (EMRs) has become a cornerstone of digital health transformation globally, offering the promise of improved care quality, safety, and efficiency [1]. However, there are many aspects that limit the wider adoption of EMRs in sub-Saharan Africa. These include high procurement and maintenance constraints to introduce the EMRs, lack of incentives for implementation, lack of concern to prioritize, electric power shortage, absence of internet, health professionals' inadequate computer skills, and absence of strong health care facility infrastructure [2].

EMR acceptance is not only a technical issue but also a sociobehavioral one, influenced by system characteristics, user perceptions, and organizational readiness. Studies suggest that both system design and user-related factors such as perceived usefulness (PU), ease of use, and access play critical roles in determining the extent of EMR use [3].

Although most public health care facilities in Ethiopia manually manage data tasks related to their clinical services, there has been a growing demand to adopt the EMR system in health care facilities [4]. Evidence [5] shows that a lack of strategic planning in the field of EMRs had a negative influence on the implementation of the system in health care facilities. Moreover, the Ethiopian Ministry of Health recommended [6] that health care facilities should have a change management strategy that facilitates the smooth transition of the newly introduced EMR system. This strategy will be part of the health care facilities' strategic paper and shows how the new systems are to be implemented and sustainable for a longer time. There should also be a protocol to select the best performers and to reward those health professionals working on EMRs. The strategy document should also contain principles on data generation and use at the local level for decision-making [6].

And regarding health professionals' behaviors, PU, and perceived ease of use (PEOU) will influence user acceptance of the EMRs. User acceptance of technology and associated factors has been considered as an important issue that should be presented and understood before introducing and expanding any software applications or systems [7].

The use of only PU and PEOU as measures of technology acceptance is rooted in the Technology Acceptance Model (TAM) developed by Fred Davis [8]. This model proposed that users' acceptance of new technology is primarily influenced by how useful they perceive it to be in enhancing their job performance (PU) and how easy they believe it is to use (PEOU). In the original TAM, these 2 constructs were found to significantly predict attitudes toward using, which in turn influenced behavioral intention and ultimately actual system use or acceptability of the EMRs.

Motivation and engagement to use EMRs influence the acceptance and attitude of health care workers toward the technology. In turn, the motivation to use the system is influenced by the EMR's usability, health care workers' competence, technology skills, confidence, and perceptions. In general, the workplace motivation of health care workers affects work engagement, job satisfaction, and intention to stay in the workplace [9]. The health care workers' PEOU (eg, accessing patient data) and PU (eg, providing alerts and reminders) are keys to acceptance of EMRs [10]. Since their introduction, EMRs have been a recurrent issue for physicians across all specialties. From user experience to interoperability, nearly every facet of computer-based systems has drawn the ire of those using them. It was found that the amount of time spent in the physician's inbox and total time using EMRs were associated with higher physician turnover. The American Medical Association found that EMRs contribute to between 11% and 60% of the burnout physicians experienced in 2021 [11]. Since motivation has an important role in the behaviors of health care workers, the adoption, acceptance of, and attitude toward a new technology, such as an EMR system, may be influenced by individual motivation [9].

A study on the Australian EMR system revealed that nurse motivation emerged as the most common factor relating to both perceived barriers and enablers to a new Australian EMR system implementation [9]. The development and implementation of electronic health records (EHRs) involve lots of challenges, including nurses' stress and negative consequences for patient safety [12]. Designing a user-friendly interface is another challenging task. A poorly designed interface may lead to reduced time efficiency, poor quality of health care delivery, and can become a threat to the patient's safety as well. Acceptance of EHR by doctors is also perceived as a barrier. This is due to the extra time that doctor spends entering data electronically, which they otherwise can spend treating the patients [13].

The Ethiopian Ministry of Health has played a pivotal role in piloting and scaling up EMR systems across the country. Notably, the University of Gondar Comprehensive Specialized Hospital was selected as a pilot site for EMR deployment, contributing significantly to the development and testing of EMR systems in Ethiopia [14]. One of the EMR systems implemented at the University of Gondar is Bahmni, an open-source EMR platform that aligns with the Ethiopian EHR standards. This initiative has been instrumental in informing the nationwide scale-up of EMR systems, enhancing health care delivery and information management across Ethiopia.

The EMR system in Ethiopia could not go as far as expected due to factors like behavioral and technical [6]. It was also observed that most of the EMR systems in Ethiopia were not interoperable and automated only some aspects of health services. Hence, most public health care facilities in Ethiopia manage their patient information using paper-based recording, which results in errors, delays, and reduced service quality [4]. Therefore, the shift to electronic records is not questionable, for improved standards of care and clinical decision-making [4]. Moreover, some health care workers encountered mistrust of the system. In this regard, there are only a few studies to show EMR acceptance among health care workers in hospitals, and specifically in the contexts of privacy and security concerns [15].

XSL•FO
RenderX

Therefore, this study aims to explore and identify the key factors influencing the acceptance of EMRs among health care workers in Northwest Ethiopia, with the goal of informing strategies to enhance digital health implementation and improve health system performance in the region.

Methods

Study Design and Setting

This study used a cross-sectional quantitative design to assess health care workers' acceptance of EMRs in health care facilities where the system has been implemented. The objective was to systematically evaluate the factors influencing the acceptance and use of EMRs among health care professionals, with a focus on key determinants such as PU, PEOU, and organizational support. The study was conducted in health care facilities located in Bahir Dar city, Northwest Ethiopia. Five health facilities where EMRs had been implemented were included in the study, and the sample was drawn from these sites.

Study Participants

The study population was all health care workers who are currently working with the EMRs at health care facilities in Bahir Dar City, Northwest Ethiopia. This includes physicians, health officers, nurses, midwives, laboratory professionals, pharmacy professionals, information system officers, and medical data clerks who are working on EMRs. Health care workers who have prior exposure to EMRs for at least 6 months were included in the study.

The sample size was calculated using the finite population correction, considering a total population size of 1848, an assumed proportion (p) of 0.5, a 95% confidence level, and a 5% margin of error (d=0.05). Accordingly, the sample size was computed using the statcalc tool in Epi Info (version 7.2.5.0; Centers for Disease Control and Prevention), and the minimum required sample size was determined to be 318. To account for potential nonresponse or dropout, a 5% contingency was added, resulting in a final sample size of n = 318 + (318 × 0.05) = 334.

The sampling method was systematic random sampling. The sampling frame or the master list was a list of 1848 eligible health workers obtained from HR departments of the 5 health care. Each individual was assigned a unique number to create a master list. With a determined sample size of 334, the sampling interval was calculated as K = 1848/334 ≈ 5.5, rounded to 5. A random starting point between 1 and 5 was selected, and every 5th individual from the list was chosen until the sample size was reached, ensuring a systematic and representative selection.

Data Collection Methods

The data collection was conducted with a self-administered paper-based questionnaire. The questionnaire has 5 sections, of which 2 were Likert-like items based on a scale from "extremely disagree" to "extremely agree." The other sections are questions regarding information on health care workers' sociodemographic and EMR implementation-related questions.

Since quantitative data are always numerical in kind or numbers that have a certain intrinsic meaning, the researchers assigned scores to all kinds of variables in the questionnaire. The score number constitutes a shorthand way of expressing a respondent's answer [16].

The data collection tool was developed by the researcher (Multimedia Appendices 1 and 2), reviewing similar scientific literature on the topic [17-20]. The outcome variable uses a validated tool by Lewis [21], who developed the TAM item formats to measure technology acceptance. A pretest was conducted, and revisions were made accordingly.

EMR acceptance was computed with the 2 main constructs of TAM (PU and PEOU), which are appropriate for this study. Because EMR implementation is in the early stages in the setting, and factors like behavioral intention and social influence may not add significant predictive value, making PU and PEOU sufficient for assessing the EMR acceptance [22]. Combining PU and PEOU into a single index helps to simplify analysis or report general technology acceptance levels, particularly in descriptive studies and when working with limited sample sizes [23]. Moreover, it can help to reduce model complexity while still capturing overall user perception [24].

Measurements

According to Lewis [21], to provide TAM scores that are consistent with the System Usability Scale and usability metric for user experience metrics, the following formulas were used to put PU and PEOU on a 0-100-point scale, averaging PU and PEOU to get the overall TAM.

- PU = (AVERAGE [TAM01, TAM02, TAM03, TAM04, TAM05, TAM06]–1) (100/6)
- PEOU = (AVERAGE [TAM07, TAM08, TAM09, TAM10, TAM11, TAM12]–1) (100/6)

Accordingly, in this study, perceived usefulness (PU) is computed with the SPSS statistical package as;

- (MEAN [SE01,SE02,SE03,SE04,SE05,SE06]–1) × (100/6) and Perceived ease of use (PEOU) is computed as;
- (MEAN [SE07,SE08,SE09,SE10,SE11,SE12]–1) × (100/6) that converts a 7-point scale to a 100-point scale.

Data Analysis

As this was a systematic search for meanings, the data were first cleaned and recoded to fit with the model. The data management and analysis were done with the SPSS (version 28.0; IBM Corp) software. Reliability analysis for the internal consistency of items/scales of the outcome variable was done using Cronbach α [25]. Descriptive statistics are applied to analyze the mean, SD, range, and median. The chi-square test was used to identify the relationships between categorical variables. Participant responses were dichotomized into 2 levels with a mean split by the value of the EMR acceptance score, where the variable is split at the mean. Bivariable and multivariable binary logistic regression were done to determine factors associated with EMR acceptance, and a P value of .05 was considered statistically significant. Binary logistic regression assumptions were checked before running the model.

As indicated by Zach's [26] assumptions of the logistic regression, logistic regression is a method that we can use to fit a regression model when the response variable is binary.

XSL•FO
RenderX

One of the assumptions is that the response variable is binary, and in this regard, the logistic regression assumes that the response variable only takes on 2 possible outcomes: low or high acceptance of EMRs. The second assumption was that the observations are independent, and logistic regression assumes that the observations in the dataset are independent of each other. The third assumption was that there was no multicollinearity among explanatory variables, as logistic regression assumes that there is no severe multicollinearity among the explanatory variables. The variance inflation factor indicates whether a predictor has a strong linear relationship with the other predictors. A value of 10 is a good value at which to worry. If the average variance inflation factor is greater than 1, then multicollinearity may be biasing the regression model. The fourth assumption was that there were no extreme outliers.

Ethical Considerations

Ethics approval for the study was obtained from the College Research Ethics Committee at the College of Human Sciences, University of South Africa, with the National Health Research Ethics Council Registration (Rec-240816-052) and CREC (18033342_CREC_CHS_2023). In addition, permission to access health facilities was granted by the public health institute, Bahir Dar City, Northwest Ethiopia. Moreover, this study ensured the confidentiality, anonymity, privacy, autonomy, justice, beneficence, and nonmaleficence of the study.

Results

Sociodemographic Characteristics of the Participants

About 322 participants responded to the questionnaire with a response rate of 96.4% (322/334). The respondents' age in this study ranges from 23 to 62 years. The mean age of the respondent was 35 years, with an SD of 6.4. Table 1 indicates that 29.5% (95/322) of the respondents were in the age group of 21-30 years, 53.4% (172/322) of the respondents were aged 31-40 years, and 17.1% (55/322) of the respondents were older than 40 years. And, most of the respondents were female, which accounts for 53.4% (172/322).

XSL•FO
RenderX

Table 1. Frequency distribution of background characteristics of the respondents (n=322).

Variable and category	Frequency (N=322), n (%)	Mean (SD)
Age group (years)		34.75 (6.40)
21-30	95 (29.5)	
31-40	172 (53.4)	
> 40	55 (17.1)	
Sex		
Male	150 (46.6)	—[a]
Female	172 (53.4)	—
Total	322 (100.0)	—
Marital status		
Married	204 (63.4)	—
Single	88 (27.3)	—
Others	30 (9.3)	—
Educational level		
Diploma and below	76 (23.6)	—
BSc	196 (60.9)	—
MSc	50 (15.5)	—
Work experience as a health professional		10.8 (5.7)
Junior (1-2 years)	8 (2.5)	
Associate (2-5 years)	41 (12.7)	
Mid-level (5-10 years)	124 (38.5)	
Senior (above 10 years)	149 (46.3)	
Experience on EMR[b]		4.1 (1.8)
1-5 years	267 (82.9)	
Above 5 years	55 (17.1)	
Total	322 (100.0)	
Health profession		
Specialist and above	13 (4.0)	—
Physician	43 (13.4)	—
Nurse	161 (50.0)	—
Pharmacy	23 (7.1)	—
Laboratory	28 (8.7)	—
Others	54 (16.8)	—

[a]Not applicable.

[b]EMR: electronic medical record.

The majority of the respondents (204/322, 63.4%) were married, and most of them had an educational level of BSc and above, where 60.9% (196/322) had a BSc Degree, 15.5% (50/322) had an MSc Degree and above (Table 1).

With regard to health professionals, about half of the respondents were nurses, which accounted for 50% (n=161) of the total participants. And, the number of specialists and above was very low, 4% (n=13). Laboratory and pharmacy professionals had nearly similar figures, 8.7% (n=28) and 7.1% (n=23), respectively, as shown in Table 1.

Information System and EMR Use

More than half of the study participants (213/322, 66.1%) reported owning a personal computer or a laptop. Moreover, this study observed training in basic computer skills among the health care workers and found that about half of the respondents took the training, which is 56.8% (183/322). However, those

XSL•FO
RenderX

who frequently use the internet outside the office were 32.9% (106/322), somewhat lower (Table 2).

Table 2. Basic computer training and ownership of a computer, and experience with other health information systems among health care workers (n=322).

Variables and category	Frequency (N=322), n (%)
Own a personal computer	
No	108 (33.5)
Yes	214 (66.5)
Attended a basic computer training	
No	139 (43.2)
Yes	183 (56.8)
Attended a training on EMR[a]	
No	160 (49.7)
Yes	162 (50.3)
EMR training taken	
Before starting to work on the EMR	68 (21.1)
While working on the EMR	94 (29.2)
No EMR training	160 (49.7)
Other eHealth trainings	
No	240 (74.5)
Yes	82 (25.5)
Basic eHMIS[b] or DHIS2[c] training	
No	182 (56.5)
Yes	140 (43.5)
Know about ICD-10[d]	
No	265 (82.3)
Yes	57 (17.7)
Produce a health service report using EMR	
No	193 (59.9)
Yes	129 (40.1)

[a]EMR: electronic medical record.

[b]eHMIS: electronic health management information system.

[c]DHIS2: district health information system 2.

[d]ICD-10: International Statistical Classification of Diseases, Tenth Revision.

In this regard, about half of the users (160/322, 49.7%) did not receive training on EMR. This will not be a surprise if these providers have a lower EMR acceptance, as most of them believe to learn from their coworkers. This is indicated in Table 2, where most of the health workers (94/322, 29.2%) took the training while working on the EMR system.

Another was training on eHMIS/DHIS2 (electronic health information system/ district health information system 2). DHIS2 is the latest version of eHMIS, mostly practiced by health offices and monitoring and evaluation experts at health facilities to manage health service reports. The study showed that more than half of the respondents (182/322, 56.5%) did not attend the training.

Further advanced knowledge on the EMRs was very limited, as it was indicated by other eHealth trainings and information about *ICD* (*International Classification of Diseases*), a very common terminology standard most EMR vendors are currently using (Table 2).

EMR Acceptance Among Health Care Workers

EMR acceptance in this study was measured with 12-item variables of PU and PEOU. Each item had a 7-point ordinal scale response options/agreement scale, from extremely disagree on the left to extremely agree on the right. The study was on EMRs implemented in health care facilities; the researcher measured acceptance related to actual use rather than the anticipated (Table 3). Therefore, the level of EMR acceptance

XSL•FO
RenderX

for this study was 4.87 (SD 0.83), with the range from 2.92 to 5.75.

Table 3. Mean and SD of electronic medical record (EMR) acceptance among health care workers as measured by the 7-point Likert scale.

TAM[a] and SN[b]	Items to measure EMR acceptance	Mean (SD)
Perceived usefulness		
1	Using Electronic Medical Records in my job enables me to accomplish tasks more quickly.	5.96 (0.748)
2	Using Electronic Medical Records improves my job performance.	4.53 (1.038)
3	Using Electronic Medical Records in my job increases my productivity.	5.43 (0.694)
4	Using Electronic Medical Records enhances my effectiveness on the job.	4.25 (0.877)
5	Using Electronic Medical Records makes it easier to do my job.	6.26 (0.597)
6	I have found Electronic Medical Records useful in my job.	6.30 (0.780)
Perceived ease of use		
7	Learning to operate Electronic Medical Records was easy for me.	5.35 (0.985)
8	I found it easy to get Electronic Medical Records to do what I want it to do.	4.36 (0.821)
9	My interaction with Electronic Medical Records was clear and understandable.	4.16 (0.680)
10	I found Electronic Medical Records to be flexible to interact with.	4.00 (0.994)
11	It was easy for me to become skillful at using Electronic Medical Records.	3.31 (0.717)
12	I found Electronic Medical Records easy to use.	4.56 (1.079)
Overall acceptance		4.87 (0.83)

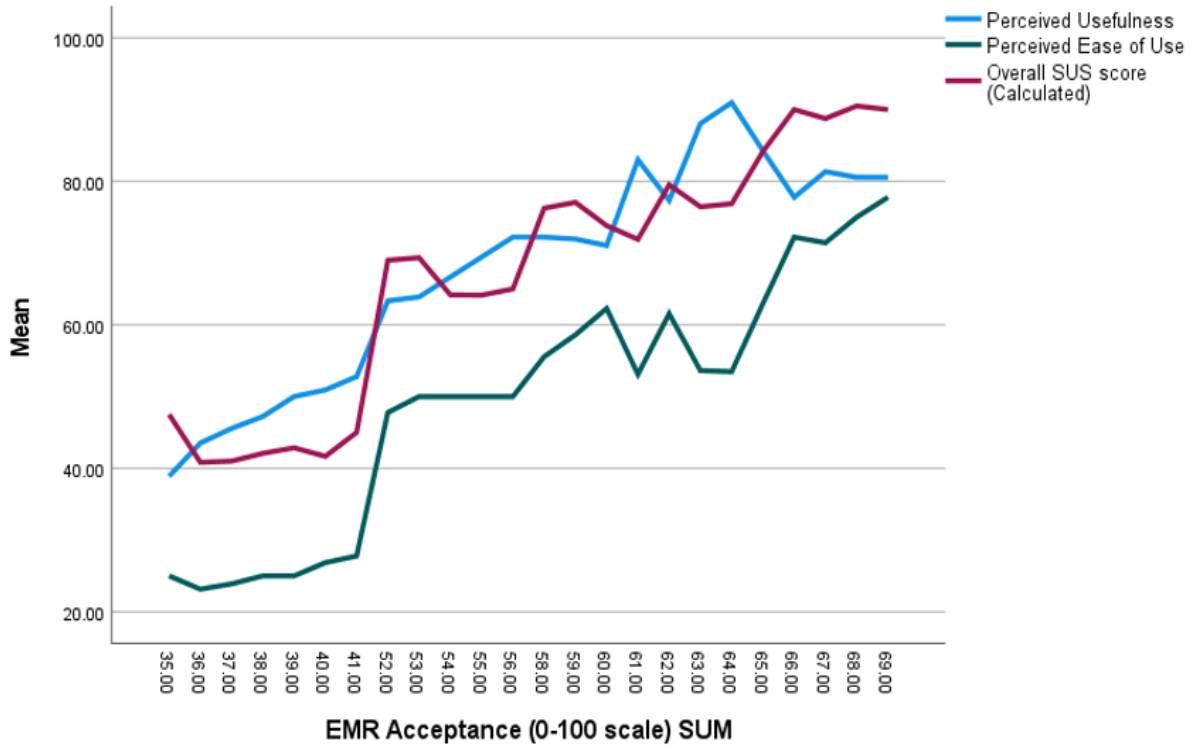
[a]TAM: Technology Acceptance Model.

[b]SN: serial number.

When comparing PU with PEOU, the health care workers' PU score is higher than their PEOU score, as described in Figure 1. Among the 6 items from the PU, the item "I have found Electronic Medical Records useful in my job," has had the highest score of 6.30 from 7.0. Among the items of PEOU, the item, "learning to operate Electronic Medical Records was easy for me," had the highest score. However, the lowest score (3.31) was about the ease of becoming skillful.

XSL•FO
RenderX

Figure 1. Line graph comparing perceived usefulness, perceived ease of use, and system usability towards EMR acceptance (converted to 0-100 points). EMR: electronic medical record; SUS: System Usability Scale.



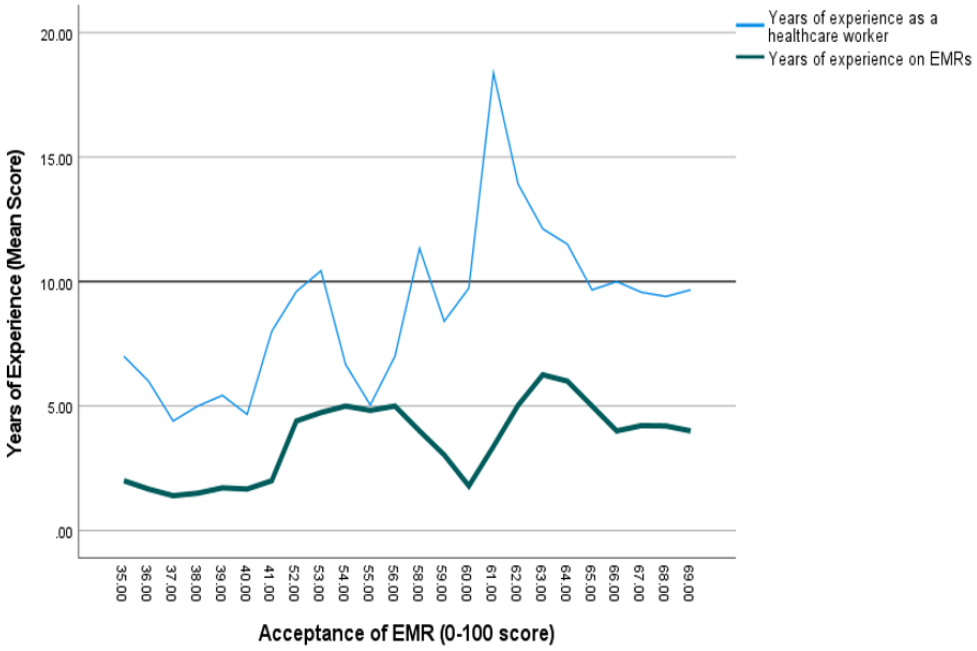
Those health care workers who scored above or equal to the mean score value were categorized as having good EMR acceptance, and those health care workers who scored below the mean value were classified as having poor EMR acceptance.

Out of the total 322 study participants, this study showed that 256 (73%) of the study participants, with a 95% CI of 67.4-78.2, had a good acceptance of using EMRs.

Even though the acceptance of EMRs increased with the increase in work experience, as shown in Figure 2, there was a large gap between work experience as a health worker and in EMRs. Lower work experience with EMR is due to the late adoption of the system in the health facilities.

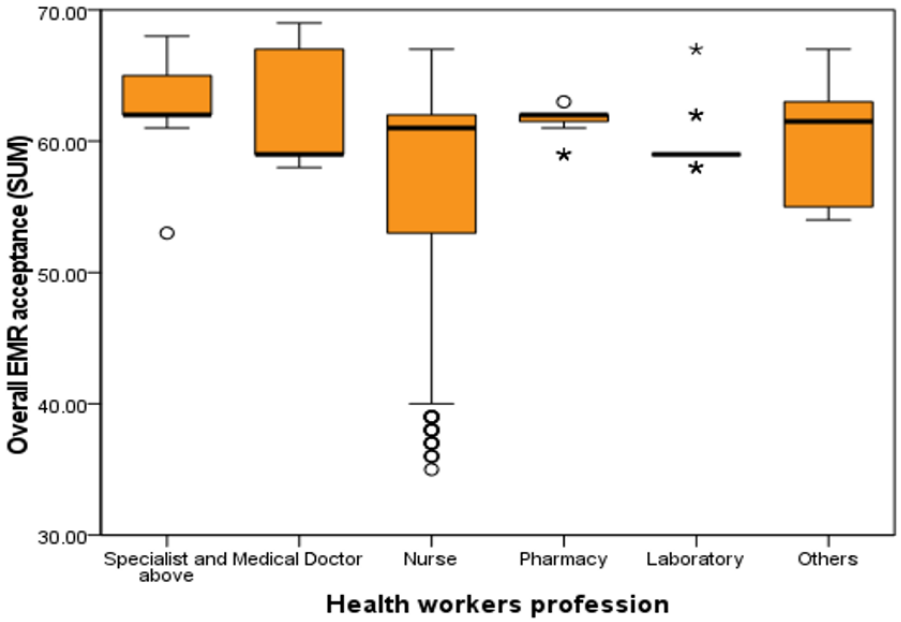
Higher acceptance of EMRs was observed among pharmacy professionals, specialists, and physicians. This was observed in the boxplot in Figure 3.

Figure 2. A line graph showing the years of experience as a health care worker versus electronic medical records. EMR: electronic medical record.



XSL•FO
RenderX

Figure 3. Boxplot showing health professionals' acceptance of electronic medical records over professional category. "*" indicates an extreme outlier, representing a small number of individuals who have exceptionally divergent views. EMR: electronic medical record.



Factors Associated With Health Care Workers' Acceptance of EMRs at Health Care Facilities

To identify predictor variables using a statistical model, it is important to understand the type of dependent (outcome) and explanatory variables. In this study, the dependent variable is the acceptance of EMRs, categorized as either poor or good. Since the researchers' interest is to examine the factors that determine good acceptance of EMRs, good acceptance is coded as 1 and poor acceptance as 2.

In a binary logistic regression model, the first step is to conduct a univariable analysis to explore the unadjusted association between each independent variable and the outcome. The purposeful selection process begins with a univariate analysis of each variable. Any variable having a significant univariate test at an arbitrary level is selected as a candidate for the multivariable analysis. This selection is based on the Wald test from logistic regression, using a *P* value cutoff point of .25.

As shown in Table 4, both bivariable and multivariable logistic regression analyses were performed to assess the statistical association between the dependent variable (EMR acceptance) and the independent variables. The variables assessed in the bivariable logistic regression included sex, age, years of work experience (grouped), years of experience with EMRs (grouped), ownership of a personal computer, attendance of basic computer training, EMR training, basic eHMIS or DHIS2 training, information about *ICD-10 (International Statistical classification of Diseases, Tenth Revision)*, and EMR system usability (grouped).

XSL•FO
RenderX

Table 4. Bivariable and multivariable binary logistic regression to determine factors associated with electronic medical record (EMR) acceptance.

Variables and category	EMR acceptance		COR[a] (95% CI)	AOR[b] (95% CI)	*P* value
	Poor	Good			
Owning a personal computer					
No[c]	67	41	1	1	—[d]
Yes	20	194	15.85 (8.68 to 28.95)	11.08 (4.03 to 30.42)[e]	<.001
Attended a basic computer training					
No[c]	58	81	1	1	—
Yes	29	154	3.8 (2.26 to 6.40)	0.79 (0.27 to 2.30)	.67
Attended a training on EMR					
No[c]	60	100	1	1	—
Yes	27	135	3 (1.78 to 5.06)	4.71 (1.52 to 14.54)[e]	.007
Have basic eHMIS[f] or DHIS2[g] training					
No[c]	61	121	1	1	—
Yes	26	114	2.21 (1.31 to 3.74)	3.06 (1.02 to 9.17)[e]	.046
System usability					
Low[c]	81	65	1	1	—
High	6	170	35.31 (14.69 to 84.88)	38.24 (12.26 to 119.27)[e]	<.001
Sex					
Male[c]	55	95	1	1	—
Female	32	140	2.53 (1.52 to 4.21)	2.68 (0.88 to 8.14)	.08
Work experience (years)					
1-10[c]	72	107	1	1	—
>10	15	128	5.74 (3.11 to 10.60)	14.32 (4.60 to 44.58)[e]	<.001
Average monthly income					
Unsatisfied[c]	63	135	1	1	—
Satisfied	24	100	1.94 (1.14 to 3.33)	0.28 (0.10 to 0.82)	.02

[a]COR: crude odds ratio.

[b]AOR: adjusted odds ratio.

[c]Reference category.

[d]Not applicable.

[e]Significant at $P<.05$.

[f]eHMIS: electronic health management information system.

[g]DHIS2: district health information system 2.

Variables that were statistically significant at $P<.25$, based on chi-square statistics and the Wald test for individual parameters, were selected for inclusion in the multivariable logistic regression. The Wald statistic helps determine whether a coefficient is significantly different from zero, indicating that the predictor contributes meaningfully to the prediction of the outcome [27,28]. As a result, some variables, namely, age group, experience with EMRs (grouped), and information about *ICD-10*, were excluded from the final model. Finally, to control for potential confounders, a multivariable logistic regression was performed. This was performed by including all relevant confounders in the model; the analysis aimed to reduce bias and provide more accurate and reliable estimates of the associations.

The model test showed that the logistic regression model was statistically significant and able to predict EMR acceptance among health care workers with 73% accuracy ($P<.001$). The model explained between 51.8% (Cox and Snell R^2) and 75.2% (Nagelkerke R^2) of the variance in the confidence score.

Accordingly, the data present results from a multivariable logistic regression analysis examining factors associated with

XSL•FO
RenderX

EMR acceptance among health care professionals. The analysis revealed that sex, work experience, access to technology, training, and system usability were key factors influencing EMR acceptance. Although females were more likely to accept EMRs than males in the crude analysis (crude odds ratio 2.53, 95% CI 1.52-4.21), the association was not statistically significant after adjustment (adjusted odds ratio [AOR] 2.68, 95% CI 0.88-8.14, *P*=.08). Health care workers with more than 10 years of experience had significantly higher odds of EMR acceptance compared with those with less experience (AOR 14.32, 95% CI 4.60-44.58, *P*<.001), indicating a strong association.

Owning a personal computer or laptop was a powerful predictor of EMR acceptance. Professionals with personal devices were over 11 times more likely to accept EMRs than those without (AOR 11.08, 95% CI 4.03-30.42, *P*<.001). Similarly, EMR-specific training was significantly associated with higher EMR acceptance (AOR 4.71, 95% CI 1.52-14.54, *P*=.007), as was having basic eHMIS or DHIS2 training (AOR 3.06, 95% CI 1.02-9.17, *P*=.046).

However, attending basic computer training was not significantly associated with EMR acceptance after adjustment (AOR 0.79, 95% CI 0.27-2.30, *P*=.67). The strongest predictor of EMR acceptance was system usability: those who rated the system as highly usable were more than 38 times as likely to accept EMRs compared with those who found it less usable (AOR 38.24, 95% CI 12.26-119.27, *P*<.001).

Discussion

Principal Findings

This study aims to examine the factors that affect the acceptance of EMRs among health care workers in Northwest Ethiopia, with the intention of generating evidence to support effective digital health strategies and strengthen health system performance in the region.

In summary, the study found that more than half of the health care workers (256/322, 73%) had a good acceptance of EMR. The factors associated with this were years of work experience, satisfaction with monthly income, owning a personal computer, attending a training on EMR, having basic eHMIS/DHIS2 training, and system usability.

EMR implementation was seen as a challenge for older health professionals, especially those older than 60 years, which may therefore lead to their retention in the workforce [29]. However, in this study, most of the participants were young adults between the ages of 21 and 40 years (172/322, 53.4%), with a SD of 6.4, which is consistent with the study done in Saudi Arabia Hospital, about 62% [30]. Hence, the researcher believed that the acceptance of EMR would be much lower if there were a significant number of older populations found in the sample. Strategies to address technology anxiety, as well as the physical and psychological limitations of an older workforce, are needed to support this workforce during an EMR implementation [29].

More than half of the health care workers (213/322, 66.1%) reported owning a personal computer. However, this was lower than the study done in Oman, where a wide majority of the health care workers who participated in the study, which is 92.3%, reported owning a personal computer or a laptop [31]. Since ownership of technology will improve the PEOU, the health care facility should consider a strategy to enhance technology exposure and support laptops and smartphones for the health care provider.

Not having adequate training and experience is one of the main obstacles to a good EMR implementation and productivity [32]. There was a rapid development of health innovations, where most of them are targeting the point of care. And, sometimes, health professionals may be forced to use the new system without having prior knowledge about it. This can be a factor for low acceptance of EMRs among health care workers. Regarding basic computer training, this study showed that about half of the respondents took the training, (183/322, 56.8%), which is nearly similar to the study in Saudi Arabia hospital, where 52.3% of the participants described that they had formal computer training, while (139/322, 47.7%) mentioned that they did not have any type of computer training [30]. However, the finding is lower than a study done in Muscat, where about 3-quarters of the study participants had computer training. This may affect their ability to competently use the EMR system and influence the quality of interaction with the system while providing health care [31]. It can be explained that having a good experience with information communication technology will help the health care workers to have a higher PEOU, which in turn improves the usability and acceptability of EMRs.

The absence of training and lower experience are among the main obstacles to a good EMR implementation and productivity. In this regard, the study observed EMR training among the health care workers and found that about half of the users did not receive training on EMR (139/322, 49.7%). The magnitude of the problem, the gap in EMR training, will be more visible as one understands how effective the training was. This was described in the Rwandan study, where 98% of respondents agreed that their training on the EHR was effective, and about 93% were confident in using the EMR after having the training [33].

Years of experience as a health professional are another factor that determines EMR acceptance. In this study, about half of the participants (173/322, 54%) had mid and lower-level experience (1-10 years). This is consistent with the study in the Saudi Arabian hospital (56%) [30]. The acceptance of EMR has great paybacks for health professionals, health facilities, and also for the health outcome of the people, if it is used effectively. Therefore, closer attention should be given to the human resource development in line with investing in the introduction of the technology.

EMR acceptance was measured with the latest version of the TAM, 12 items, and a 7-point scale measurement [21]. The level of EMR acceptance for this study was 4.87 (SD 0.83) on a 7-point scale. This finding is lower than a study done in Marie Stops International Clinic in Myanmar among clinical and management staff, with 4.24 (5-point scale) or 5.94 (7-point scale). The scale is converted to compare it with this study [34]. However, it is consistent with the study done in northeastern US regional medical centers among Intensive Care Unit nurses,

XSL•FO
RenderX

which was 6.91 (on a 10-point scale), which means 4.83 (on a 7-point scale) [35].

To identify factors associated with the acceptance of the EMR, the variable is recoded and dichotomized into 2 categories (Good and Poor acceptance, with a mean of 4.87, SD 8.3), using cutoff points. Multivariable analysis showed that health care workers with more than 10 years of work experience had a very high effect on EMR acceptance. This finding is supported by much evidence; a report at a government hospital in Muscat stated, health care workers with 6 years and more experience in using the EMR system had 2 times more likely to accept the EMR than their counterparts (odds ratio 2.49, 95% CI 1.23-5.04, *P*=.01). And, another study from Saudi Arabia indicated that notable positive relationship were found between years of experience at the organization and acceptance of EMR [30,31,36].

Owning a personal computer also had a positive effect on acceptance of the EMRs among health care workers. This is consistent with what was done in Belgian Hospital staff, where the length of computer usage was found to have a positive correlation with acceptance of EMR [36]. This may be because health workers' behavior would be influenced by IT use and being more familiar with computer usage. So, EMR acceptance can sometimes be effective with only a little support to the system users.

Sometimes technology may be introduced into the organization without creating awareness and having training, which leads to hesitancy to use the system. In this study, about half of the participants reported having training on EMR. And, it has a significant effect on accepting EMR, where health care workers who took the training on EMR were 4 times more likely to have a good acceptance than those who did not take the training (AOR 4.71, 95% CI 1.52-14.54; *P*<.007).

Theoretical and Practical Implications of the Study

The study reinforces the relevance of the TAM in predicting EMR acceptance by health care workers. Key constructs of TAM for this study are PEOU and PU, which are reflected in the factors found to influence EMR acceptance, including prior training, personal computer ownership, and system usability. The findings suggest that individual-level technology experience and training positively shape attitudes toward digital health systems, supporting the theoretical understanding that user readiness and perceived capability are central to successful health information system adoption.

Practically, the study highlights actionable areas for improving EMR implementation in low-resource settings. It emphasizes the importance of investing in digital infrastructure, providing targeted training on EMR systems, and fostering technology exposure among health care workers. Strategies such as supporting staff with personal digital devices, integrating digital health training into ongoing professional development, and addressing the needs of older staff can significantly enhance EMR acceptance. These practical steps can contribute to more efficient health care delivery, improved data quality, and ultimately, better health outcomes.

Limitations of This Study

This study has some limitations that should be acknowledged. First, the use of a cross-sectional design limits the ability to establish causal relationships between the identified factors and EMR acceptance. While associations can be observed, the temporal sequence of events remains unclear. Future research using longitudinal or experimental designs could better assess causality. Second, the reliance on self-reported data may introduce social desirability and recall biases, which can affect the accuracy of responses, and there may be method bias. Although efforts were made to ensure anonymity and create a nonjudgmental environment to reduce these biases, some degree of misreporting may still have occurred.

Conclusions

The level of EMR acceptance among health care workers is 4.87 out of a 7-point scale. Though this is above the midpoint, the level of EMR acceptance is somehow lower than other findings.

Higher EMR acceptance was significantly associated with longer work experience, ownership of a personal computer, EMR, or eHMIS/DHIS2 training, and high system usability. Notably, system usability emerged as the strongest predictor. While females showed higher acceptance in the crude analysis, the association was not significant after adjustment. Interestingly, income satisfaction was inversely related to EMR acceptance. These findings highlight the importance of targeted training, access to technology, and user-friendly systems in promoting EMR adoption.

PU and perceived ease determine the level of EMR acceptance. EMR acceptance is the actual use rather than the anticipated use. The health care workers' PU of the EMR is higher than their PEOU. Years of work experience, being satisfied with monthly income, owning a personal computer, attending training on EMR, having basic eHMIS or DHIS2 training, and system usability were factors that are associated with the acceptance of EMR. It is recommended to have appropriate strategies relevant to the context before implementing the EMRs. Context-specific strategies that enhance system usability, provide targeted training, and improve access to digital tools, particularly for less experienced staff, are essential to increasing EMR acceptance among health care workers.

Acknowledgments

The authors acknowledge Bahir Dar University and the University of South Africa for supporting the project and the participants of the study for their willingness to give information. The author uses tools to assist with grammar editing and takes full responsibility for the integrity and accuracy of the content.

XSL•FO
RenderX

Funding

This research was supported by the University of South Africa student funding in the form of a bursary.

Data Availability

The data of this study are available from the corresponding author upon reasonable request. Due to privacy, certain data may not be publicly shared. Deidentified data may be shared in accordance with ethical guidelines.

Authors' Contributions

AKT conceptualized and designed the study, conducted the primary analysis, and drafted the manuscript. KML contributed to data interpretation, provided critical revisions, and assisted in manuscript editing. Both authors reviewed and approved the final version of the manuscript.

Conflicts of Interest

None declared.

Multimedia Appendix 1
Questionnaire_English Version.
[DOCX File , 28 KB - medinform_v13i1e72030_app1.docx]

Multimedia Appendix 2
Questionnaire _ Amharic Version.
[DOCX File , 42 KB - medinform_v13i1e72030_app2.docx]

References

1. Li R, Niu Y, Scott SR, Zhou C, Lan L, Liang Z, et al. Using electronic medical record data for research in a healthcare information and management systems society (HIMSS) analytics electronic medical record adoption model (EMRAM) stage 7 hospital in Beijing: cross-sectional study. JMIR Med Inform 2021 Aug 03;9(8):e24405 [FREE Full text] [doi: 10.2196/24405] [Medline: 34342589]
2. Odekunle FF, Odekunle RO, Shankar S. Why sub-Saharan Africa lags in electronic health record adoption and possible strategies to increase its adoption in this region. Int J Health Sci (Qassim) 2017;11(4):59-64. [Medline: 29085270]
3. Agrawal L, Ndabu T, Mulgund P, Sharman R. Factors affecting the extent of patients' electronic medical record use: an empirical study focusing on system and patient characteristics. J Med Internet Res 2021 Oct 28;23(10):e30637 [FREE Full text] [doi: 10.2196/30637] [Medline: 34709181]
4. Digital health activity (DHA) annual report, activity year II. John Snow Inc. 2021. URL: https://publications.jsi.com/JSIInternet/Inc/Common/_download_pub.cfm?id=24041&lid=3 [accessed 2025-12-04]
5. SyedSalman AK, Krishna Reddy KV, Satyanarayana N. Strategic planning for implementation of electronic health records in government hospitals. Int J Curr Res 2021;13(04) [FREE Full text]
6. Standards for electronic medical records in Ethiopia. Scribd. 2021. URL: https://www.scribd.com/document/643212421/Standard-for-Electronic-Health-Record-System-EHR-in-Ethiopia [accessed 2025-12-04]
7. Yaacob NM, Basari ASH, Ghani MKA, Doheir M, Elzamly A. Factors and theoretical framework that influence user acceptance for electronic personalized health records. Pers Ubiquit Comput 2021 Apr 17;28(1):29-41. [doi: 10.1007/s00779-021-01563-y]
8. Davis FD. Perceived usefulness, perceived ease of use, and user acceptance of information technology. MIS Q 1989;13(3):319-339 [FREE Full text] [doi: 10.2307/249008]
9. Jedwab RM, Manias E, Hutchinson AM, Dobroff N, Redley B. Understanding nurses' perceptions of barriers and enablers to use of a new electronic medical record system in Australia: a qualitative study. Int J Med Inform 2022 Jun;158:104654. [doi: 10.1016/j.ijmedinf.2021.104654] [Medline: 34883386]
10. Upadhyay S, Hu H. A qualitative analysis of the impact of electronic health records (EHR) on healthcare quality and safety: clinicians' lived experiences. Health Serv Insights 2022;15:11786329211070722 [FREE Full text] [doi: 10.1177/11786329211070722] [Medline: 35273449]
11. Top challenges facing physicians in 2022. Medical Economics. 2022. URL: https://www.medicaleconomics.com/topics/physicians-financial-news [accessed 2022-07-28]
12. Osajiuba S, Jedwab R, Calvo R, Dobroff N, Glozier N, Hutchinson A, et al. Facilitators and barriers to the adoption of an electronic medical record system by intensive care nurses. Stud Health Technol Inform 2021 Dec 15;284:510-515. [doi: 10.3233/SHTI210785] [Medline: 34920583]
13. Wadhwa M. Electronic Health Records in India. New York, NY: Earth Institute, Columbia University; 2020.

XSL•FO
RenderX

14. Tegegne MD, Tilahun B, Mamuye A, Kerie H, Nurhussien F, Zemen E, et al. Digital literacy level and associated factors among health professionals in a referral and teaching hospital: an implication for future digital health systems implementation. Front Public Health 2023;11:1130894 [FREE Full text] [doi: 10.3389/fpubh.2023.1130894] [Medline: 37113180]
15. Enaizan O, Zaidan AA, Alwi NHM, Zaidan BB, Alsalem MA, Albahri OS, et al. Electronic medical record systems: decision support examination framework for individual, security and privacy concerns using multi-perspective analysis. Health Technol 2018 Nov 28;10(3):795-822. [doi: 10.1007/s12553-018-0278-7]
16. Sandra VT. Research Methods in Public Administration and Public Management An Introduction. Milton Park,UK: Routledge; 2022.
17. Maillet E, Sicotte C, Mathieu L. The actual use of an electronic medical record (EMR) by acute care nurses: examining a multidimensional measure at different adoption stages. Stud Health Technol Inform 2018;250:241-242. [Medline: 29857451]
18. Bingham G, Tong E, Poole S, Ross P, Dooley M. A longitudinal time and motion study quantifying how implementation of an electronic medical record influences hospital nurses' care delivery. Int J Med Inform 2021 Sep;153:104537. [doi: 10.1016/j.ijmedinf.2021.104537] [Medline: 34343955]
19. Arabi YM, Al Ghamdi AA, Al-Moamary M, Al Mutrafy A, AlHazme RH, Al Knawy BA. Electronic medical record implementation in a large healthcare system from a leadership perspective. BMC Med Inform Decis Mak 2022 Mar 15;22(1):66 [FREE Full text] [doi: 10.1186/s12911-022-01801-0] [Medline: 35292008]
20. Shukis D. The constant evolution and challenges of electronic medical records. Medical Laboratory Observer. 2018. URL: https://www.mlo-online.com/continuing-education/article/13017068/the-constant-evolution-and-challenges-of-electronic-medical-records [accessed 2025-12-04]
21. Lewis JR. Comparison of four TAM Item formats: effect of response option labels and order. J Usability Stud 2019;14(4):224-236 [FREE Full text]
22. Venkatesh V, Davis FD. A theoretical extension of the technology acceptance model: four longitudinal field studies. Manag Sci 2000 Feb;46(2):186-204. [doi: 10.1287/mnsc.46.2.186.11926]
23. Sarstedt M. Revisiting hair Et al.'s multivariate data analysis: 40 years later. In: The Great Facilitator. Cham: Springer International Publishing; 2019:113-119.
24. Venkatesh V, Morris MG, Davis GB, Davis FD. User acceptance of information technology: toward a unified view. MIS Q 2003;27(3):425-478 [FREE Full text] [doi: 10.2307/30036540]
25. Creswell. Research Design: Qualitative, Quantitative, and Mixed Methods Approaches. Thousand Oaks, CA: SAGE Publications, Inc; 2018.
26. Bobbitt Z. The 6 assumptions of logistic regression (with examples). Statology. 2025. URL: https://www.statology.org/assumptions-of-logistic-regression/ [accessed 2025-12-04]
27. Boateng EY, Abaye DA. A review of the logistic regression model with emphasis on medical research. J Data Anal Inf Process 2019;07(04):190-207. [doi: 10.4236/jdaip.2019.74012]
28. Kasaye MD, Mengestie ND, Beyene S, Kebede N, Ngusie HS, Kalayou MH. Acceptance of electronic medical records and associated factor among physicians working in University of Gondar comprehensive specialized hospital: a cross-sectional study. Digit Health 2023;9:20552076231213445 [FREE Full text] [doi: 10.1177/20552076231213445] [Medline: 38025113]
29. Tissera S, Jedwab R, Calvo R, Dobroff N, Glozier N, Hutchinson A, et al. Older nurses' perceptions of an electronic medical record implementation. Stud Health Technol Inform 2021;284:516-521. [doi: 10.3233/SHTI210786] [Medline: 34920584]
30. Aldosari B, Al-Mansour S, Aldosari H, Alanazi A. Assessment of factors influencing nurses acceptance of electronic medical record in a Saudi Arabia hospital. Inform Med Unlocked 2018;10:82-88. [doi: 10.1016/j.imu.2017.12.007]
31. Abu Raddaha AH. Nurses' perceptions about and confidence in using an electronic medical record system. Proc Singap Health 2017;27(2):110-117. [doi: 10.1177/2010105817732585]
32. Bekele TA, Gezie LD, Willems H, Metzger J, Abere B, Seyoum B, et al. Barriers and facilitators of the electronic medical record adoption among healthcare providers in Addis Ababa, Ethiopia. Digit Health 2024;10:20552076241301946 [FREE Full text] [doi: 10.1177/20552076241301946] [Medline: 39659403]
33. Fraser HSF, Mugisha M, Remera E, Ngenzi JL, Richards J, Santas X, et al. User perceptions and use of an enhanced electronic health record in Rwanda with and without clinical alerts: cross-sectional survey. JMIR Med Inform 2022;10(5):e32305 [FREE Full text] [doi: 10.2196/32305] [Medline: 35503526]
34. Thit WM, Myint Thu SWY, Kaewkungwal J, Soonthornworasiri N, Theera-Ampornpunt N, Kijsanayotin B, et al. User acceptance of electronic medical record system: implementation at marie stopes international, Myanmar. Healthc Inform Res 2020;26(3):185-192 [FREE Full text] [doi: 10.4258/hir.2020.26.3.185] [Medline: 32819036]
35. Carayon P, Cartmill R, Blosky MA, Brown R, Hackenberg M, Hoonakker P, et al. ICU nurses' acceptance of electronic health records. J Am Med Inform Assoc 2011;18(6):812-819 [FREE Full text] [doi: 10.1136/amiajnl-2010-000018] [Medline: 21697291]
36. Luyten J, Marneffe W. Examining the acceptance of an integrated electronic health records system: insights from a repeated cross-sectional design. Int J Med Inform 2021;150:104450. [doi: 10.1016/j.ijmedinf.2021.104450] [Medline: 33848941]

XSL•FO
RenderX

Abbreviations

AOR: adjusted odds ratio
DHIS2: district health information system 2
eHMIS: electronic health management information system
EHR: electronic health record
EMR: electronic medical record
ICD: International Classification of Diseases
ICD-10: International Statistical Classification of Diseases, Tenth Revision
PEOU: perceived ease of use
PU: perceived usefulness
TAM: Technology Acceptance Model

Edited by A Coristine; submitted 18.02.25; peer-reviewed by L Agrawal, S Lloyd, MD Tegegne; comments to author 04.04.25; revised version received 21.04.25; accepted 30.07.25; published 23.12.25.

Please cite as:
Tsehay AK, Matlhaba KL
Acceptance of Electronic Medical Records and Associated Factors Among Health Care Workers in Northwest Ethiopia: Cross-Sectional Study
JMIR Med Inform 2025;13:e72030
URL: https://medinform.jmir.org/2025/1/e72030
doi:10.2196/72030
PMID:

©Asmamaw Ketemaw Tsehay, Kholofelo Lorraine Matlhaba. Originally published in JMIR Medical Informatics (https://medinform.jmir.org), 23.12.2025. This is an open-access article distributed under the terms of the Creative Commons Attribution License (https://creativecommons.org/licenses/by/4.0/), which permits unrestricted use, distribution, and reproduction in any medium, provided the original work, first published in JMIR Medical Informatics, is properly cited. The complete bibliographic information, a link to the original publication on https://medinform.jmir.org/, as well as this copyright and license information must be included.

XSL•FO
RenderX

Fusion of X-Ray Images and Clinical Data for a Multimodal Deep Learning Prediction Model of Osteoporosis: Algorithm Development and Validation Study

Jun Tang[1*], MEng; Xiang Yin[2*], MD; Jiangyuan Lai[3], BM; Keyu Luo[2], MD; Dongdong Wu[1], PhD

[1]Department of Information, Daping Hospital, Army Medical University, No.10 Daping Changjiang Branch Road, Yuzhong District, Chongqing, China

[2]Department of Orthopedics, Daping Hospital, Army Medical University, Chongqing, China

[3]Department of Traumatic Surgery, School of Basic Medicine, Army Medical University, Chongqing, China

[*]these authors contributed equally

Corresponding Author:
Dongdong Wu, PhD
Department of Information, Daping Hospital, Army Medical University, No.10 Daping Changjiang Branch Road, Yuzhong District, Chongqing, China

Abstract

Background: Osteoporosis is a bone disease characterized by reduced bone mineral density and mass, which increase the risk of fragility fractures in patients. Artificial intelligence can mine imaging features specific to different bone densities, shapes, and structures and fuse other multimodal features for synergistic diagnosis to improve prediction accuracy.

Objective: This study aims to develop a multimodal model that fuses chest X-rays and clinical parameters for opportunistic screening of osteoporosis and to compare and analyze the experimental results with existing methods.

Methods: We used multimodal data, including chest X-ray images and clinical data, from a total of 1780 patients at Chongqing Daping Hospital from January 2019 to August 2024. We adopted a probability fusion strategy to construct a multimodal model. In our model, we used a convolutional neural network as the backbone network for image processing and fine-tuned it using a transfer learning technique to suit the specific task of this study. In addition, we introduced a gradient-based wavelet feature extraction method. We combined it with an attention mechanism to assist in feature fusion, which enhanced the model's focus on key regions of the image and further improved its ability to extract image features.

Results: The multimodal model proposed in this paper outperforms the traditional methods in the 4 evaluation metrics of area under the curve value, accuracy, sensitivity, and specificity. Compared with using only the X-ray image model, the multimodal model improved the area under the curve value significantly from 0.951 to 0.975 (P=.004), the accuracy from 89.32% to 92.36% (P=.045), the sensitivity from 89.82% to 91.23% (P=.03), and the specificity from 88.64% to 93.92% (P=.008).

Conclusions: While the multimodal model that fuses chest X-ray images and clinical data demonstrated superior performance compared to unimodal models and traditional methods, this study has several limitations. The dataset size may not be sufficient to capture the full diversity of the population. The retrospective nature of the study may introduce selection bias, and the lack of external validation limits the generalizability of the findings. Future studies should address these limitations by incorporating larger, more diverse datasets and conducting rigorous external validation to further establish the model's clinical use.

(JMIR Med Inform 2025;13:e70738) doi:10.2196/70738

KEYWORDS

osteoporosis; chest X-ray; convolutional neural network; multimodal; attention mechanism; wavelet transform; soft attention

Introduction

Background

Osteoporosis is a common metabolic bone disease characterized by decreased bone mineral density (BMD) and thinning of the trabecular structure of bone, leading to fragile bones and an increased risk of fracture. As the global population ages, osteoporosis has become a key factor affecting the health of middle-aged and older adults. However, the early symptoms of osteoporosis are not obvious, and most patients are diagnosed only after a fracture occurs, leading to increased complications and mortality [1]. Therefore, how to effectively identify people at high risk of osteoporosis and take timely preventive measures has become the focus of current clinical research.

Automated detection and classification of osteoporosis using deep learning (DL) has become a popular research topic in recent years [2]. Traditional prediction methods for osteoporosis mainly rely on a single data type, such as assessing BMD and

XSL•FO
RenderX

classifying the degree of bone loss based on clinical data [3-5], computed tomography [6,7], magnetic resonance imaging [8], and X-ray images [9-12]. Dual-energy X-ray absorptiometry (DXA) is an internationally recognized method of measuring BMD and is also considered the gold standard for the diagnosis of osteoporosis [13]. However, DXA is less available and the cost of screening is high. For this reason, opportunistic screening offers a viable solution, as it uses clinical data for other indications without additional costs, radiation exposure, or patient time. In contrast, DL algorithm–based assessment of osteoporosis from X-ray images is a low-cost alternative to DXA [14-16]. Chest X-ray imaging has accumulated a large amount of imaging resources in routine applications such as pneumonia screening and bronchial disease examination, providing a natural imaging basis for opportunistic screening of osteoporosis. In addition, chest X-rays [11,17,18] can capture key bone structures affected by osteoporosis, such as ribs, thoracic vertebrae, and clavicles, further highlighting their application value in osteoporosis screening. Although such DL models based on a single data type have improved the accuracy and efficiency of osteoporosis diagnosis to a certain extent, the single data type only provides 1D information, neglecting the comprehensive consideration of information about the bone microenvironment, physiological characteristics, and patients' clinical data, which leads to the prediction results that may not be comprehensive and accurate.

However, in the actual diagnostic process, doctors will comprehensively refer to various information sources, including medical image data, laboratory examination data, and medical record reports, to improve the accuracy of diagnosis [19]. This concept is introduced into DL, which aims to simulate the complex process of medical differential diagnosis through multimodal [20,21] data fusion. The fusion of multimodal medical data has become a hot research topic in interdisciplinary fields. Multimodal fusion can provide a more accurate description of samples, and it exploits the complementary and synergistic nature of each modality's information more effectively than any single modality data [22]. As a result, multimodal fusion techniques have been widely used in several medical fields, including oncology, cardiovascular medicine, and radiology [23-25]. In the field of orthopedics, relevant multimodal studies are rapidly emerging [26,27], providing new ideas for osteoporosis prediction.

Objectives

In this study, we propose a multimodal prediction model that fuses chest X-ray images and clinical data for opportunistic screening of osteoporosis. In the model construction, we used a convolutional neural network (CNN) as the backbone network for image processing and fine-tuned it to the specific task of this study using transfer learning techniques. In addition, we introduced a gradient-based wavelet feature extraction method. We combined it with an attention mechanism to assist in feature fusion, which strengthened the model's focus on key regions of the image and further enhanced the model's ability to extract image features.

Methods

Ethical Considerations

The study was approved by the institutional review board at the Chongqing Daping Hospital (2024_335). A waiver of informed consent was provided, as this retrospective study used existing information. Privacy and confidentiality of all patient data were maintained throughout the entire study. No compensation was provided to patients, as this study only involved the review of retrospective data.

Dataset and Study Population

This study retrospectively collected multimodal data, including chest X-ray images and clinical data, from January 2019 to August 2024. The specific inclusion criteria were as follows: (1) patient age ≥50 years and (2) chest X-ray and DXA were performed on the same day. The specific exclusion criteria were as follows: (1) image data with artifacts, blurriness, or inability to display bone structures; (2) patients with other serious diseases that may affect bone health or interfere with diagnosis, such as malignant tumors and severe metabolic diseases; (3) patients who have recently used drugs that may affect bone metabolism or BMD measurement, such as hormone drugs and antiosteoporosis drugs; and (4) cases where the missing rate of clinical data reached or exceeded 30%. On the basis of these criteria, a total of 1780 cases met all the criteria, with 990 (55.62%) cases in the osteoporosis group and 790 (44.38%) cases in the nonosteoporosis group. Therefore, we extracted chest X-ray images (DICOM format) from the hospital's communication system repository and collected the clinical data of patients from the back-end database, including age, sex, height, weight, white blood cell count, platelet count, serum calcium level, fasting blood glucose, and chest X-ray descriptive information. The model was trained through a 5-fold cross-validation.

The diagnosis of osteoporosis was based on DXA BMD measurement results. DXA negative means BMD is within the normal range, corresponding to the nonosteoporosis group. DXA positivity refers to a BMD lower than the normal range, corresponding to the osteoporosis group. The DXA manufacturer of Chongqing Daping Hospital is GE Lunar Prodigy model (Madison, WI, USA).

Preprocessing

The DICOM format X-ray images were converted to the 8-bit PNG format to adapt to the DL frameworks. After conversion, the images were all manually reviewed. The image intensity was reversed to ensure no negative values and then normalized. All images were squared using zero padding and then downsampled to 224×224 pixels to fit a pretrained CNN on ImageNet. Using dynamic data augmentation to limit overfitting, this included random flipping (horizontal and vertical), random rotations (90° rotation), random translations (10% variation in each direction), random zooming (10% variation), and random contrast adjustment (factor of 0.3).

For the handling of missing values in clinical data, regarding white blood cell count and serum calcium level, since the numerical distribution of these features was roughly normally

XSL•FO
RenderX

distributed, the mean of the variables was used for filling, which could better reflect the overall level. For features such as BMI, platelet count, and fasting blood glucose, as their numerical distributions might be skewed, the median of the variables was chosen for imputation, which was more robust in this case.

This research dataset included 990 positive (osteoporosis) and 790 negative (nonosteoporosis) samples, with a positive-to-negative ratio of 55.6% and 44.4%, respectively. In response to the mild imbalance characteristics of the dataset, this study adopted class weighting techniques to weight the loss function based on the distribution of training dataset classes, thereby improving the model's sensitivity to identifying minority classes.

Proposed Multimodal Model

Overview

The framework of our proposed multimodal model is shown in Figure 1. After data preprocessing, we built an image model trained on X-ray images and a clinical parameter model trained on clinical data. The multimodal model then fused the prediction results of these two models using a probability fusion (PF) strategy [19]. The details of each model are described in the following sections.

Figure 1. The proposed multimodal model framework. It includes 3 parts: image, clinical parameter, and multimodal models.

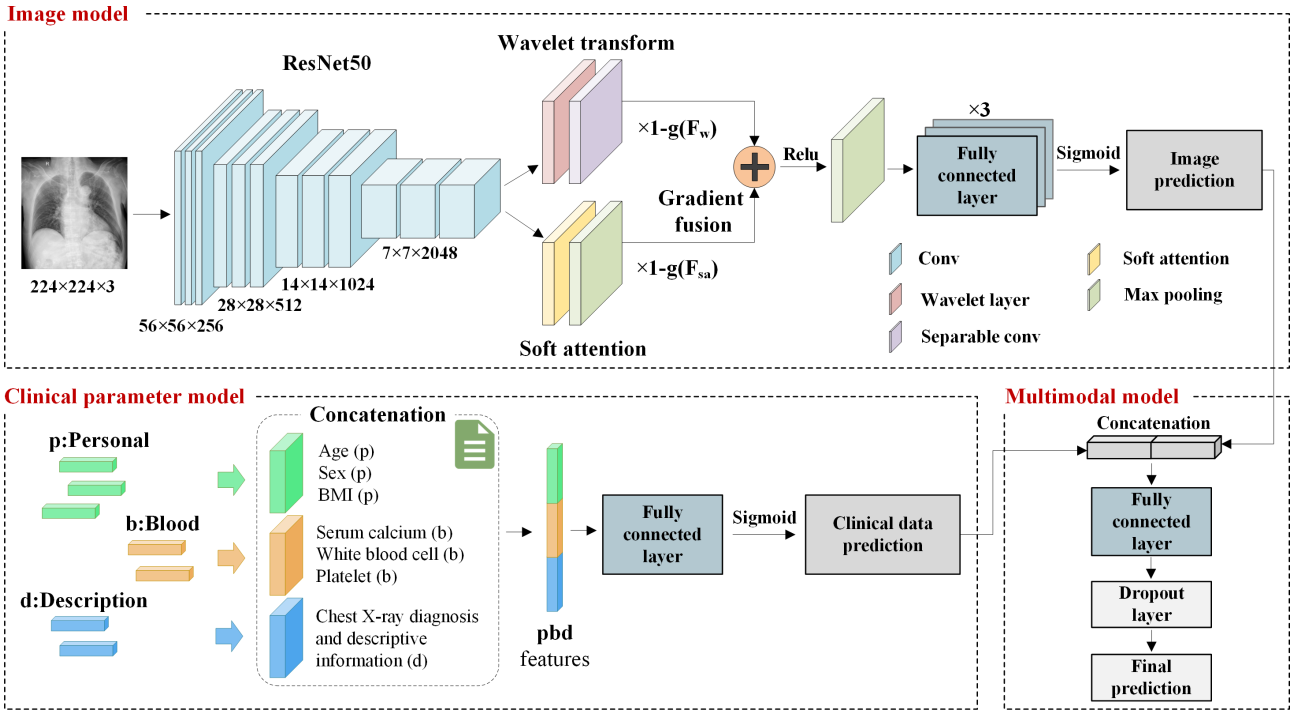


Image Model

Transfer learning is a method that uses pretrained models to reduce the data and computational costs required for new tasks. In the field of medical imaging, methods that combine transfer learning with CNN models trained on large-scale datasets such as ImageNet have been widely adopted [28]. Our image model used a pretrained ResNet50 [29] as the backbone network for feature extraction of chest X-ray images. Subsequently, we applied the wavelet transform (WT) for multiscale analysis of the images to extract features at different scales that reveal subtle changes in bone structure in different images. The soft attention (SA) mechanism was used to capture specific appearance features and morphological regions in the images. Finally, we used a gradient-based feature fusion mechanism to effectively fuse these features to obtain the final image probabilistic output.

ResNet50 has excellent feature extraction capabilities, with a network depth of up to 50 layers, which could effectively capture rich hierarchical features in image data. Meanwhile, the residual learning structure adopted by ResNet50 effectively solved the problem of gradient vanishing during deep network training. In addition, it also had a lower number of parameters and computational costs, making it more practical for common hardware deployment scenarios in medical imaging analysis. For the binary classification task of osteoporosis, we fine-tuned our pretrained ResNet50 model. Specifically, considering that our classification task involved only 2 categories, which were significantly different from the 1000 categories in ImageNet shown in a previous study by Holste et al [30], we added a global maximum pooling layer and 3 fully connected layers with 1024, 512, and 256 neurons to the top of the pretrained model.

WT is a signal processing method based on multiscale analysis, which decomposes a signal into a weighted sum of multiple waves of different scales and frequencies through a mathematical transform. The WT has the advantage of multiscale and multiresolution and is capable of accurately extracting the local spatiotemporal distribution characteristics of the signal [31]. In our multimodal model, we used an efficient Haar WT method that extracted wavelet features from the output features of ResNet50. These features covered valuable information such as the sparsity of bone trabeculae and the thickness of the bone cortex. To reduce the parameters and computational effort of the model and to maintain the

XSL•FO
RenderX

performance of the model, a depth-separable convolutional layer was introduced after the WT layer.

Inspired by the recent widespread application of the attention mechanism in deep neural networks [32], we introduced the attention mechanism into our model. Both SA [33] and hard attention are mechanisms that help models focus on key parts of input data. The hard attention mechanism involved discrete sampling at specific locations of input data, typically using reinforcement learning methods during training, as it involved nondifferentiable operations. In contrast, the SA mechanism was a probability distribution-based continuous attention method that assigned a weight to each position of the input data, and then weighted and summed the input based on these weights to obtain a context vector. The advantage of SA was that it was completely differentiable and could be trained end-to-end using standard gradient descent methods, making it more stable and efficient during the training process. In our study, we used a SA mechanism that assigned a weight to each input item, representing the degree of attention the model pays to that input item. This helped the model focus on key regions in X-ray images and generated descriptions that match the image content.

Specifically, we dynamically performed adaptive gradient fusion of wavelet features with SA features, using the normalized backpropagation gradients g(Fw) and g(Fsa) of Fw and Fsa as the basis for fusion weights, as shown in equation 1. A higher gradient means that the corresponding feature may have a negative impact on the model performance, and therefore it is given less weight in the fused features Ffuse, and vice versa. By introducing learnable weights, the feature fusion process was optimized to be more representative without increasing the parameters. This method ensured that important information was efficiently fused into the coded features before they were passed to the fully connected layer.

$$(1) Ffuse=(1-g(Fw))\times Fw+(1-g(Fsa))\times Fsa$$

Clinical Parameter Model

Our clinical parameter model includes important blood biochemical indicators such as white blood cell count, platelet count, serum calcium level, and fasting blood glucose and personal information including age, sex, and BMI, as well as chest X-ray diagnosis and descriptive information. Previously, most machine learning–based studies have relied mainly on clinical data, such as using prehospital information to predict mortality in patients with heart failure in intensive care units [34] or for predicting sepsis [35]. Algorithms such as random forest and XGBoost usually showed better performance than DL models for clinical data processing, and they did not require backpropagation during training; however, this made it difficult to directly combine these algorithms with DL models such as CNNs. Therefore, in our study, we chose to use a fully connected layer with 50 neurons to process these clinical data.

Multimodal Model

When training our multimodal model, we used the weights of the already trained baseline image model and clinical parameter model. We used a PF strategy in which both baseline models were run in inference mode, each independently producing a prediction. Our multimodal fusion mechanism then took the independent output probabilities of the image and clinical parameter models as inputs, concatenated them, and input them into a fully connected layer neural network with 32 neurons to generate the final prediction. During the training process, the learning rate started at each epoch and decreased in a multiplicative manner at the end of each epoch until a preset minimum was reached, and it took approximately 40 minutes to train the multimodal model once.

Evaluation

We used 4 evaluation metrics to measure the performance of our model, including area under the curve (AUC) value, accuracy, sensitivity, and specificity. To obtain more accurate and less biased results, we adopted a 5-fold cross-validation method. In the hyperparameter settings, we used binary cross-entropy as the loss function and selected the Adam optimizer. We combined the ideas of grid search and random search, and tried multiple values such as 1e-4, 1e-5, and 1e-6 for the learning rate. For the dropout rate, we tried multiple values such as 0.2, 0.25, 0.3, 0.4, and 0.5. For batch size, we tried multiple values such as 16, 32, 64, and 128. The final determined learning rate was 1e-5, dropout was 0.25, and the batch size was 32. To effectively prevent overfitting of training data, we adopted an early stopping strategy based on validation loss and retained the optimal weights during the training process for recovery. Our model was implemented in Keras 2.4 and trained on a computer with an Intel i9-14900K 24-core CPU, 64 GB of RAM, and an NVIDIA RTX A6000 GPU card with 48 GB of memory.

Results

Patient Characteristics

This study included a total of 1780 patients (as shown in the patient inclusion process flow diagram in Figure 2), with each patient corresponding to an anteroposterior position chest X-ray image. The average age of the patients was 69.46 (10.33) years, with an age range of 50 to 99 years. The statistical data of the training dataset, validation dataset, and test dataset are detailed in Table 1. These three datasets are almost identical in terms of sex and age distribution. All patients were divided into 2 groups: the osteoporosis group (990/1780, 55.62%) and the nonosteoporosis group (790/1780, 44.38%); 55.66% (659/1184), 56.4% (167/296), and 54.7% (164/300) of patients in the 3 datasets suffer from osteoporosis.

XSL•FO
RenderX

Figure 2. Patient inclusion process diagram. BMD: bone mineral density; DXA: dual-energy X-ray absorptiometry.

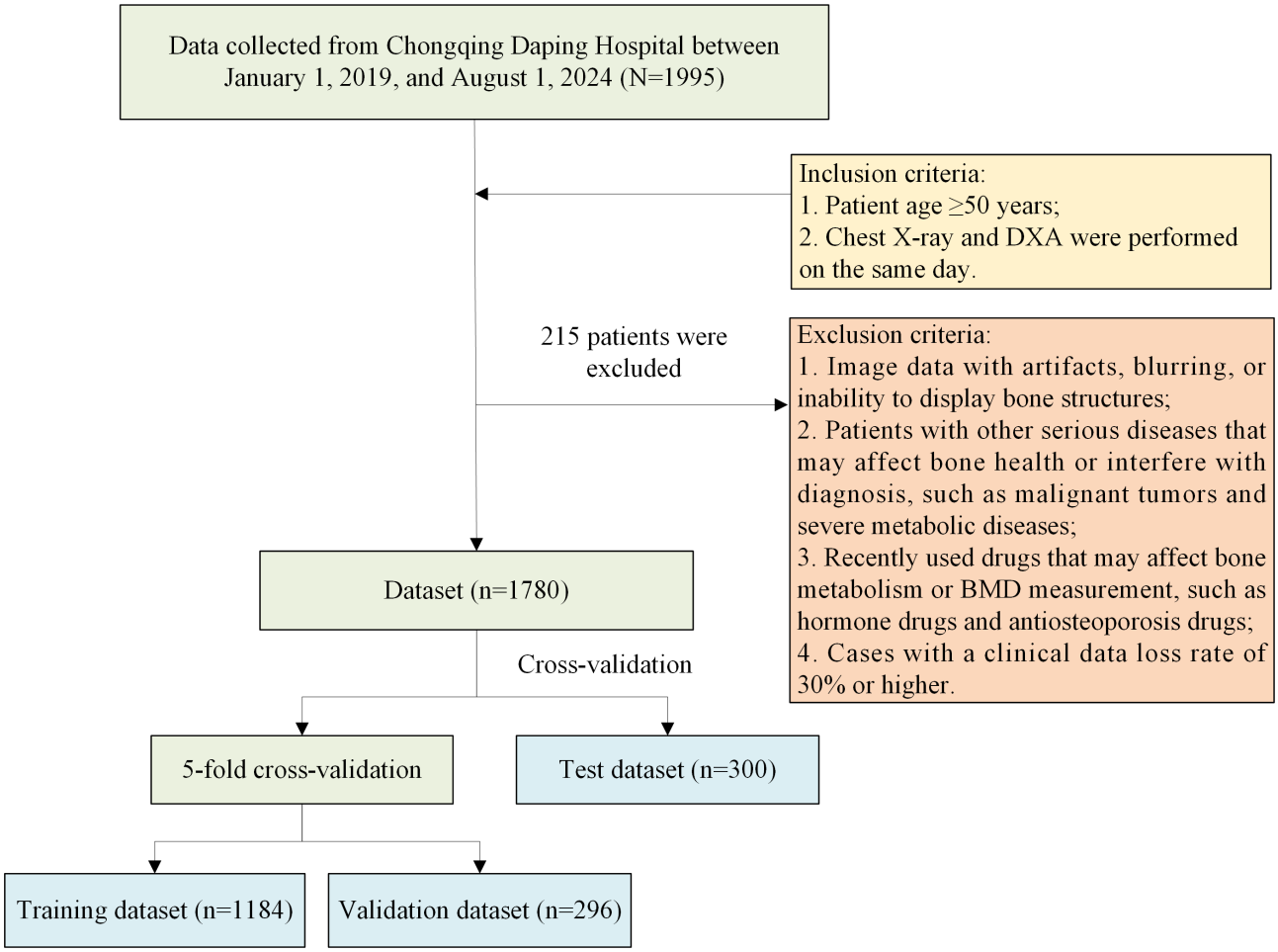


Table . Dataset description of 1780 cases of patients with osteoporosis.

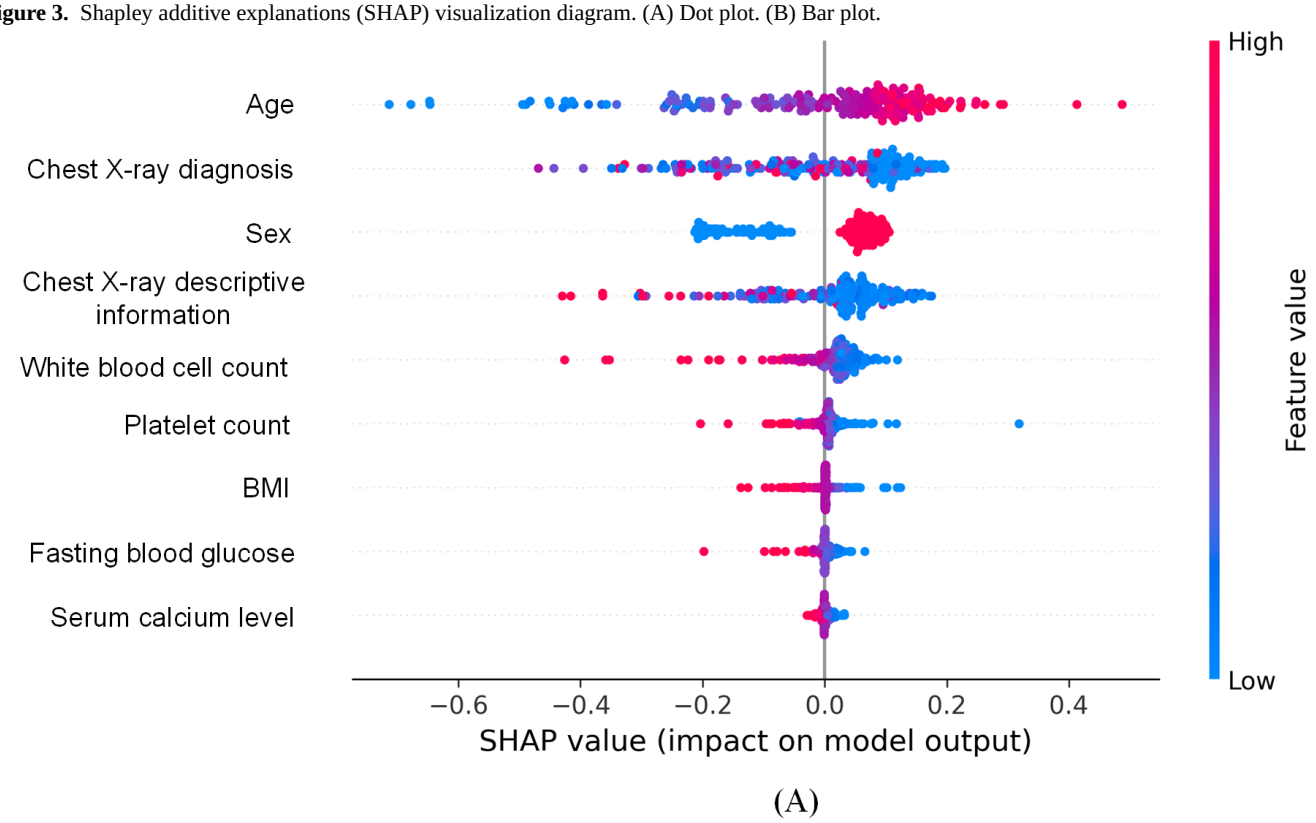
Characteristics	Training dataset (n=1184)	Validation dataset (n=296)	Test dataset (n=300)
Age (y), mean (SD)	69.3 (10.34)	69.53 (10.72)	69.94 (10.28)
Sex, n (%)			
Male	495 (41.80)	119 (40.2)	120 (40.0)
Female	689 (58.20)	177 (59.8)	180 (60.0)
Presence of osteoporosis, n (%)			
Osteoporosis	659 (55.66)	167 (56.4)	164 (54.7)
Nonosteoporosis	525 (44.34)	129 (43.6)	136 (45.3)

Overall Predictive Performance of the Multimodal Model

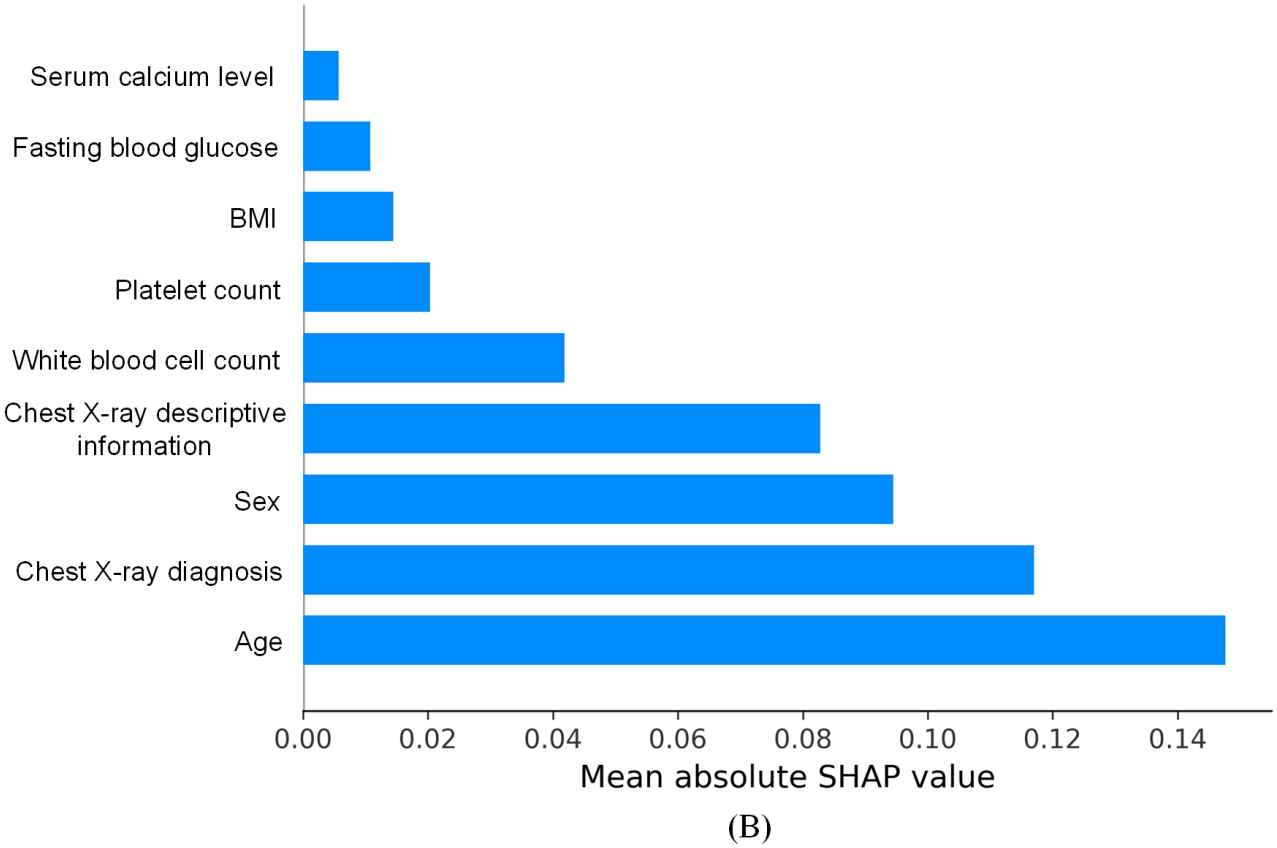
In this study, we used the SHAP (Shapley additive explanations) method to analyze the feature importance of the model. The SHAP method helps us understand which features have a specific impact on the model's decision-making process by calculating the contribution value (ie, SHAP value) of each feature to the model prediction. Figure 3 presents the results of the SHAP method, including a dot plot (Figure 3A) and a bar plot (Figure 3B). The dot plot displays the distribution of SHAP values for each feature, reflecting the direction and degree of the feature's impact on the model's prediction results. The bar plot summarizes the mean contribution of each feature to the model prediction. According to the analysis results, the features that contributed the most to the model prediction were age, chest X-ray diagnosis, sex, chest X-ray descriptive information, white blood cell count, platelet count, BMI, fasting blood glucose, and serum calcium level. These results indicated that the selected features were of great significance for model prediction, thereby improving the accuracy and reliability of the model.

XSL•FO
RenderX

Figure 3. Shapley additive explanations (SHAP) visualization diagram. (A) Dot plot. (B) Bar plot.



(A)

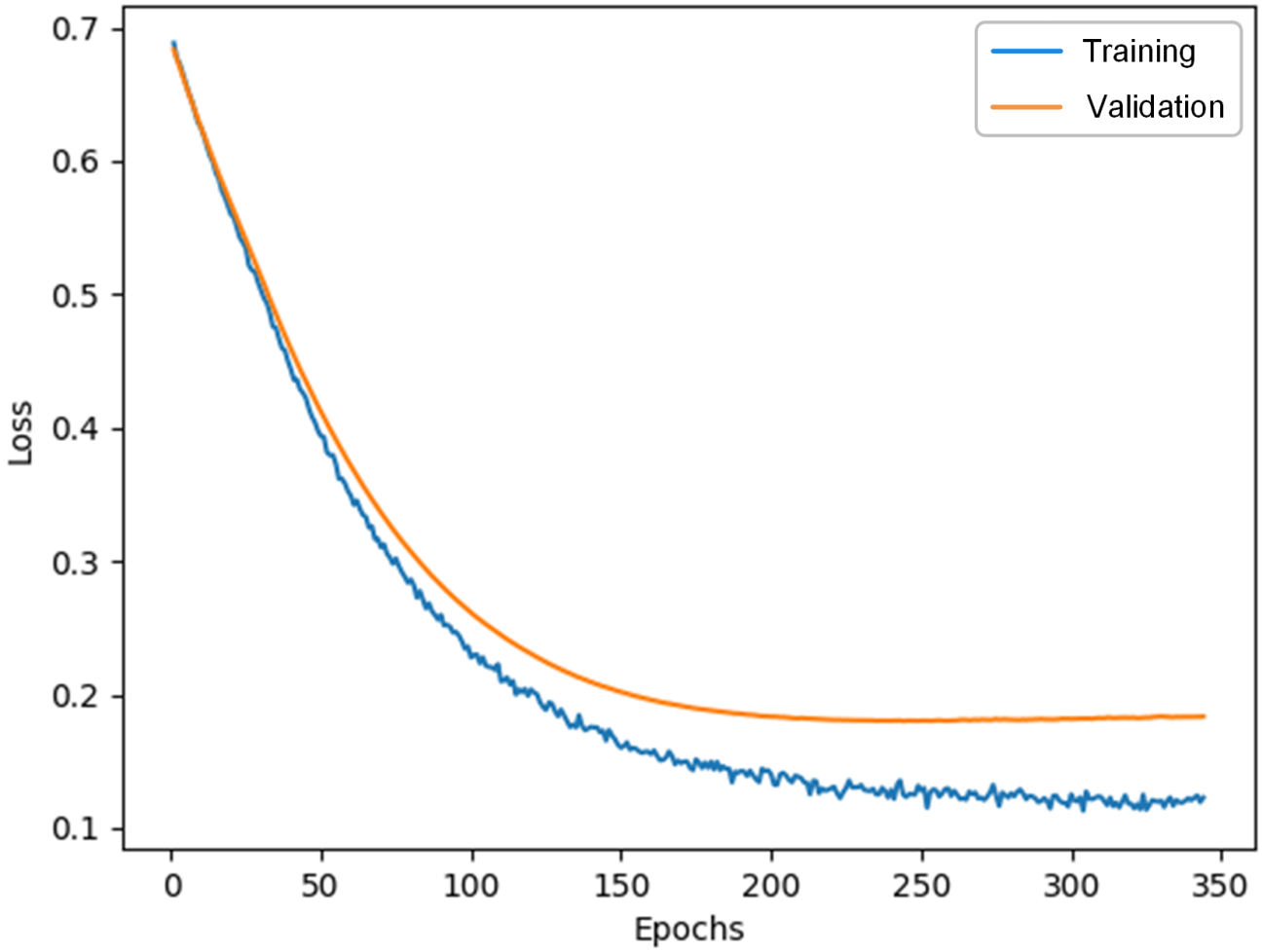


(B)

The training and validation loss curves of the multimodal model in this paper are shown in Figure 4, which intuitively demonstrate the convergence of the model. From Figure 4, it could be seen that as the training progresses, both the training loss and validation loss exhibited a decreasing trend and gradually stabilized, indicating that the model performs consistently on both the training and validation datasets and has good generalization ability.

XSL•FO
RenderX

Figure 4. Training and validation loss curves of the multimodal model.



To validate the superiority of the multimodal model proposed in this paper, Table 2 summarizes the performance of the model in the test dataset. First, to verify the performance of the ResNet50 pretrained backbone network used in the image model of this paper, we selected a conventional CNN model and two other pretrained models, Inception v3 and VGG16, for comparative analysis. Among them, the pretrained models ResNet50 and VGG16 used images of size 224×224 pixels as input, while the Inception v3 model used images of size 299×299 pixels. The image model corresponds to the pretrained ResNet50 model in Table 2. As shown in the table, all 4 image-based models showed good classification ability in the test dataset, with an average AUC value of 0.902. In comparison, our image model showed the optimal structural performance compared to the other 3 models. Specifically, our image model achieved the highest values in the 4 evaluation metrics of AUC value, accuracy, sensitivity, and specificity, which were 0.951, 89.32%, 89.82%, and 88.64%, respectively.

Table . The performance of models in the test dataset.

Model	AUC[a]	Accuracy, %	Sensitivity, %	Specificity, %
CNN[b]	0.832	77.91	83.54	69.75
Inception v3	0.909	80.74	77.66	84.96
VGG16	0.916	85.54	85.26	85.92
Image model	0.951	89.32	89.82	88.64
Clinical parameter model	0.884	80.81	78.29	84.46
Multimodal model	0.975	92.36	91.23	93.92

[a]AUC: area under the curve.

[b]CNN: convolutional neural network.

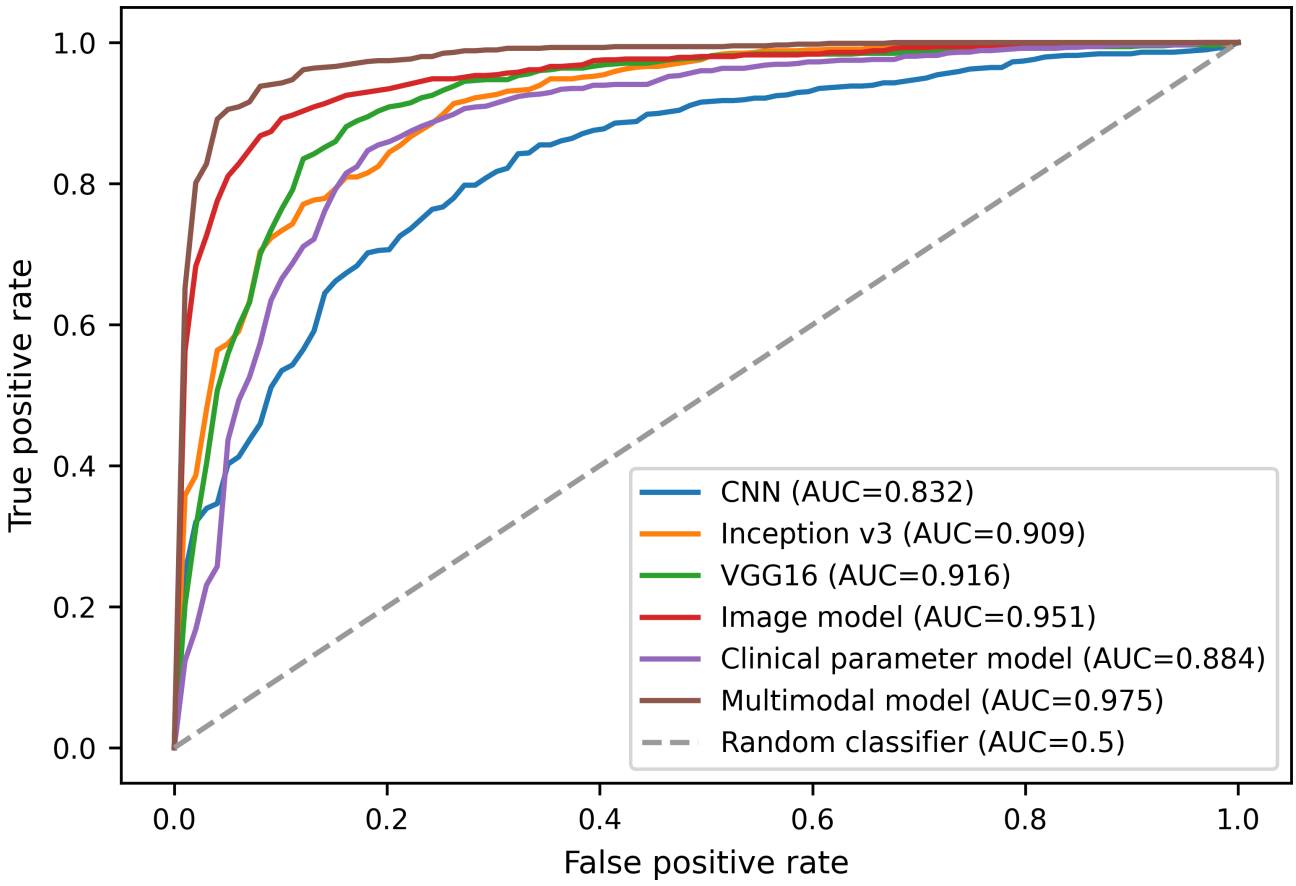
The multimodal model trained in this paper, which combines patient image and clinical parameter features, outperformed the image-only or clinical parameter–only models on all 4 evaluation metrics. Specifically, when compared with the model using only X-ray images, the multimodal model improved its AUC value from 0.951 to 0.975 (P=.004), accuracy from

XSL•FO
RenderX

89.32% to 92.36% (*P*=.045), sensitivity from 89.82% to 91.23% (*P*=.03), and specificity significantly from 88.64% to 93.92% (*P*=.008). Notably, the multimodal model effectively reduced the false positive rate and increased the specificity by 5.28% compared with the unimodal image model at the high-sensitivity operating point. We experimentally verified the superiority of the multimodal method in this paper compared to several other classification models.

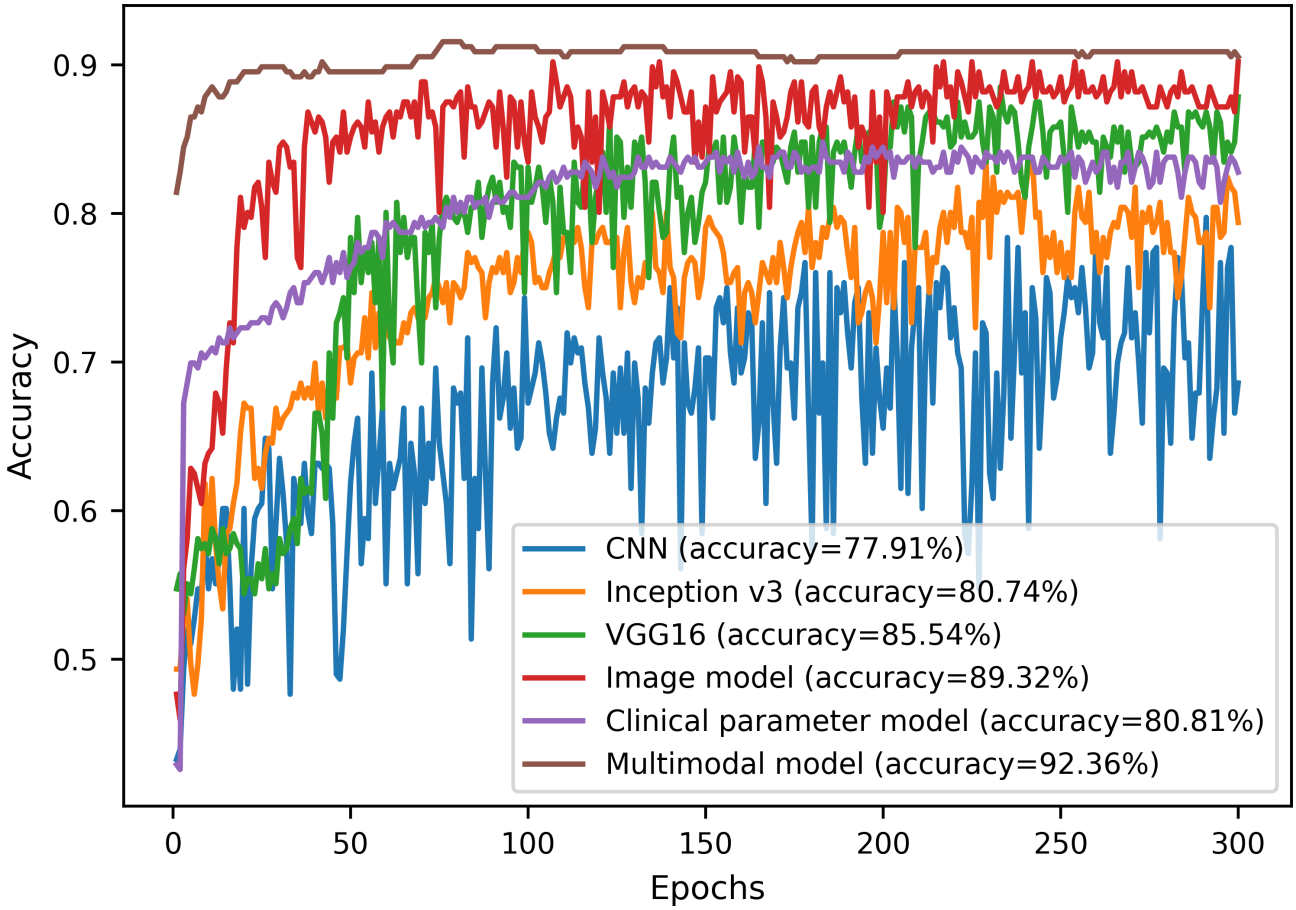
The variation curves of receiver operating characteristic and accuracy for the image model, the clinical parameter model, and the multimodal model on the test dataset are shown in Figures 5 and 6, respectively. In Figure 6, we show the results for only the first 300 epochs of each model. From the figure, the multimodal model exhibits the lowest false positive rate and the highest true positive rate, with an AUC value of 0.975, as well as an accuracy of 92.36%. In contrast, the CNN model has an accuracy of only 77.91% with an AUC value of 0.832, with a difference of more than 10% between the two models. In addition, the multimodal model proposed in this paper is the first to reach the convergence state and has the least fluctuation compared with other models.

Figure 5. Receiver operating characteristic (ROC) variation curves in the test dataset. AUC: area under the curve; CNN: convolutional neural network.



XSL•FO
RenderX

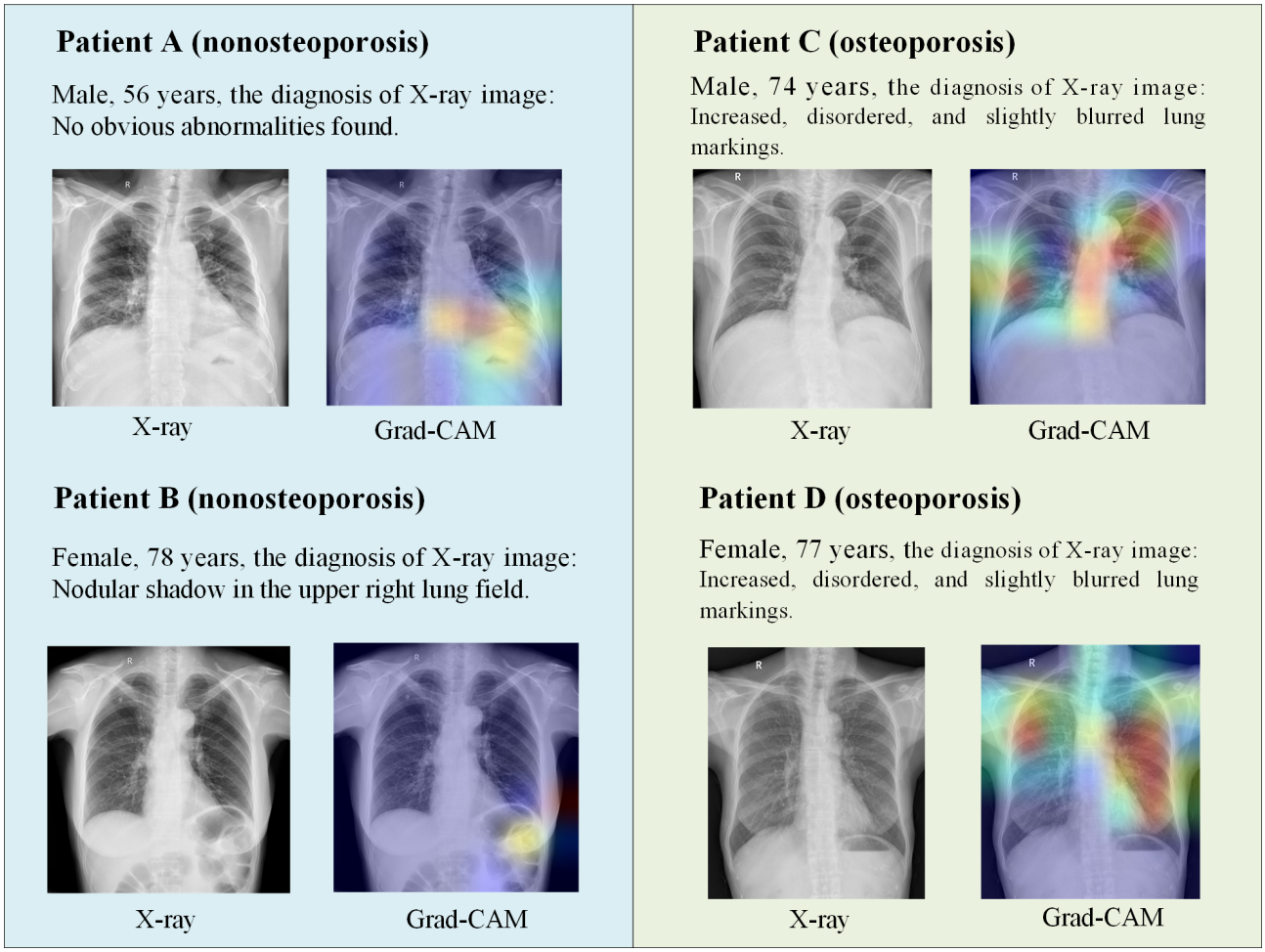
Figure 6. Accuracy variation curves on the test dataset. CNN: convolutional neural network.



To visualize the attentional regions of the model, we used the gradient-weighted class activation mapping technique. Figure 7 shows the results of the visual interpretation of the multimodal model at the individual level. In patients with osteoporosis, as BMD decreases, a series of characteristic changes in bone structure occur, such as sparse trabeculae and thinning of cortical bone. The gradient-weighted class activation mapping heat map showed that the model mainly focused on areas such as the scapula, thoracic spine, ribs, and sternum. These areas are commonly vulnerable sites in osteoporosis, and their structural changes are closely related to the pathological characteristics of osteoporosis. For example, the thoracic and lumbar spine is a high-risk area for osteoporotic fractures, and a decrease in BMD can increase the risk of fractures. The model could more accurately predict osteoporosis by learning the imaging features of these key regions. The model's attention to the scapula and ribs also had certain clinical significance. The changes in BMD of the scapula and ribs could indirectly reflect the overall bone condition of the chest, providing supplementary information for the diagnosis of osteoporosis. In addition, although anteroposterior chest X-rays could not fully cover areas such as the humeral head and lumbar spine, the model could still make effective predictions by focusing on key bone structures observable in the chest X-rays.

XSL•FO
RenderX

Figure 7. The visual interpretation of individual patients' outcomes. We randomly selected data from 4 patients for interpretation. The images on the left side show the patients' chest X-ray images, and the images on the right side show the corresponding gradient-weighted class activation mapping (Grad-CAM) heat maps. Areas that appear as bright red on chest X-ray images are considered to be the most important.



Ablation Study

To verify the role of WT and SA mechanisms in our image model, we conducted an ablation study, which included (1) ResNet50, (2) ResNet50+WT, ResNet50+SA, and ResNet50+WT+SA.

In Table 3, it could be seen that the introduction of the WT and the SA mechanism based on the backbone network ResNet50 improved the performance of the model in all 4 evaluation metrics, especially in the specificity metric, where the improvement reaches 7.74%. The results of this ablation study demonstrated the ability of these two modules to enhance the model's attention to key regions of the image and validate their effectiveness in our model.

Table . Optimal model configuration for the ablation study.

Model	AUC[a]	Accuracy, %	Sensitivity, %	Specificity, %
ResNet50	0.930	86.35	86.97	80.90
ResNet50+WT[b]	0.950	87.70	89.18	85.99
ResNet50+SA[c]	0.941	89.19	90.18	87.97
ResNet50+WT+SA	0.951	89.32	89.82	88.64

[a]AUC: area under the curve.

[b]WT: wavelet transform.

[c]SA: soft attention.

In addition, we experimented with different multimodal fusion strategies, and the results are shown in Table 4. As shown in the table, the strategy we used to merge the output probabilities before learning the final decision showed better performance compared to the two models that performed fusion by merging intermediate features.

XSL•FO
RenderX

Table . Performance comparison of different fusion strategies.

Fusion strategy	AUC[a]	Accuracy, %	Sensitivity, %	Specificity, %
FF[b]	0.969	91.49	90.99	92.16
LFF[c]	0.957	89.32	89.94	88.48
PF[d]	0.975	92.36	91.23	93.92

[a]AUC: area under the curve.

[b]FF: feature fusion.

[c]LFF: learning feature fusion.

[d]PF: probability fusion.

To verify whether the performance improvement of PF compared to feature fusion (FF) and learning FF (LFF) was statistically significant, we conducted a 2-tailed paired *t* test on accuracy, and the experimental data were obtained based on 5-fold cross-validation. The results showed that the *t* value of PF relative to FF was t_4=4.2426, and the *P* value was .01; and the *t* value of PF relative to LFF was t_4=2.9774, and the *P* value was .04. At a significance level of α=.05, the performance differences between PF and FF, as well as between PF and LFF, were statistically significant (*P*<.05). It could be seen that PF had the best performance among the 3 fusion methods in our experimental setup.

To improve the generalization performance and robustness of the model, we dynamically augmented the image data using a stochastic augmentation strategy. Comparing the model performance with and without the dynamic data augmentation technique, the results are shown in Table 5. In addition to the sensitivity metrics, the 3 metrics of AUC value, accuracy, and specificity were significantly improved after the introduction of dynamic data enhancement, especially the specificity, which was enhanced by 15.2%, greatly improving the accuracy of the model in identifying nonosteoporosis and reducing the rate of false alarms.

Table . Performance comparison of the image model with and without dynamic data augmentation.

Data augmentation	AUC[a]	Accuracy, %	Sensitivity, %	Specificity, %
Without	0.934	84.32	92.28	73.44
With	0.951	89.32	89.82	88.64

[a]AUC: area under the curve.

Discussion

Principal Findings

Although DL has made substantial progress in the field of medical imaging, it still focuses primarily on the imaging data themselves, largely ignoring the richness of information available in the clinic. Our experimental results show that the multimodal model fusing chest X-ray images and clinical data can improve the accuracy of deep neural networks in predicting osteoporosis. Through the ablation study, we validated the WT and the SA mechanism to enhance the performance of the model by capturing specific appearance features in the images, and also confirmed the advantages of dynamic data augmentation and PF strategies in a multimodal model.

Osteoporosis, as a major health disease, is becoming increasingly prominent in the aging population. Predictive studies of osteoporosis not only help us to gain a deeper understanding of the disease's trends and risk factors, but also provide a scientific basis for the development of effective prevention and treatment strategies. The classification model we designed is a binary classification model based on chest X-ray images and clinical data, aiming to classify outcomes into 2 categories: osteoporosis and nonosteoporosis. The results show that multimodal data can be used to distinguish patients with osteoporosis from those with normal BMD, and that the method we used requires a small amount of training data and a short processing time. As a disease screening method, the model in this paper has high sensitivity and helps to reduce the false negative rate. The model can be used both prospectively by radiologists and retrospectively by radiologists or even nonradiologists, which is important for the timely identification and treatment of patients with osteoporosis.

We downsample the X-ray image to 224×224 pixels to meet the input requirements of the ResNet50 model, while the Inception v3 architecture used for comparison requires downsampling the image to 299×299 pixels. Interestingly, although Inception v3 has a higher input resolution, its performance is not significantly better than ResNet50. This discovery suggests that simply increasing input resolution may not significantly improve model performance. This may be related to factors such as the complexity of the model architecture and the characteristics of the target task.

Since most relevant studies [9,11,14,36] currently use private datasets, it is difficult to find data that is identical or highly comparable to our dataset for direct comparison. Therefore, we mainly started from the aspects of dataset size, model architecture, and key results to compare the existing paper on osteoporosis screening based on X-ray using DL methods, as shown in Table 6. Although the research by Mao et al [14] bears some resemblance to ours, substantial differences remain. They

XSL•FO
RenderX

only analyzed X-rays and clinical data using a single CNN model. And based on this, we designed a multimodal model to process X-rays and clinical data separately. This innovative model architecture not only enhances the model's ability to process different types of data but also fully explores and uses the inherent correlation and value of multisource data, thereby achieving more accurate screening for osteoporosis.

Table . Comparison with related works.

Reference	Dataset	Model	Key results
Lee et al [9]	334 spine X-rays	DL[a] and machine learning	• AUC[b]: 0.74 • Accuracy: 0.71 • Sensitivity: 0.81 • Specificity: 0.60
Jang et al [11]	13,026 chest X-rays	DL	• AUC: 0.91 • Accuracy: 82.40%
Mao et al [14]	5652 lumbar spine X-rays and clinical data	CNN[c]	• AUC: 0.909 - 0.937
Wani et al [36]	381 knee X-rays	DL and transfer learning (AlexNet)	• Accuracy: 91.1%
This study	3645 chest X-rays and clinical data	Transfer learning (ResNet50) and multimodal model	• AUC: 0.975 • Accuracy: 92.36% • Sensitivity: 91.23% • Specificity: 93.92%

[a]DL: deep learning.

[b]AUC: area under the curve.

[c]CNN: convolutional neural network.

In this study, our proposed multimodal model demonstrated high accuracy in predicting osteoporosis, indicating its potential clinical application value. However, in the process of transforming the model from a laboratory environment to practical clinical applications, the feasibility of deployment also needs to be considered. To ensure that the model can run effectively in practical clinical scenarios, we recommend integrating it with the hospital's picture archiving and communication system and electronic medical record systems. This can automatically acquire and process imaging and clinical data, thereby reducing the burden on technicians in preprocessing work. In addition, the predicted results of the model can be automatically integrated into the patient's electronic medical record for doctors to review and reference at any time. This model can run on regular servers or cloud platforms with low hardware requirements, making it suitable for environments with limited resources.

Limitations

Our study has some limitations. First, we have not systematically analyzed the performance of the model under different races, age groups, or imaging protocols, which may introduce bias and affect the fairness and universality of the model. Given this, we plan to include more diverse population data and data obtained from different imaging protocols in future studies to evaluate and improve the performance of the model in various populations. Second, the coverage range of anteroposterior chest X-rays has certain limitations and cannot fully include key areas such as the humeral head and lumbar spine. The insufficient visual coverage may affect the diagnostic accuracy of the model for certain patient populations, especially those with substantially pathological features in uncovered areas. The plan is to introduce lateral chest X-rays to address this problem. Third, the data for this study came from a single institution, Chongqing Daping Hospital, which may limit the generalizability of the model in different populations. External validation is crucial to confirm the robustness of the model in different populations. Future research plans will validate the model on multiple datasets, which will help evaluate its generalization ability. Finally, although this paper used the WT and SA mechanism to enhance the model and conduct the ablation study, these components were not compared with traditional feature extraction techniques such as Gabor filters, local binary patterns, or radiomics-based features. We plan to supplement the fusion experiments of Gabor filters, local binary patterns, and other methods with deep features in future experimental work. In addition, to further explore and validate the existence of better fusion strategies, we plan to incorporate transformer-based cross-modal attention models in future research and compare their performance with PF strategies. The transformer architecture demonstrates powerful capabilities in handling multimodal data, particularly in capturing complex relationships between different modalities.

Conclusions

In osteoporosis prediction, our proposed multimodal model fusing chest X-ray images and clinical data improves the prediction accuracy, with AUC value, accuracy, sensitivity, and specificity metrics exceeding 90%, which all indicate significantly better performance than models relying only on images or clinical data. The model in this paper is expected to be an effective tool that clinicians can use to screen for opportunistic osteoporosis without increasing radiation exposure or additional costs. It is particularly suitable for patients who

XSL•FO
RenderX

have had a chest X-ray but have not undergone DXA. With this model, clinicians can detect osteoporosis symptoms early and provide timely treatment interventions to prevent further bone loss.

Acknowledgments

This work was supported by the National Natural Science Foundation of China (72374206); the Artificial Intelligence Medical Research Project of Daping Hospital in Chongqing, China (ZXAIYB015); and the Basic Research Project of Daping Hospital in Chongqing, China (ZXJCYJ202414).

Data Availability

The data that support the findings of this study are available upon request from the corresponding author. The data are not publicly available due to privacy or ethical restrictions.

Conflicts of Interest

None declared.

References

1. Liow MHL, Ganesan G, Chen JDY, et al. Excess mortality after hip fracture: fracture or pre-fall comorbidity? Osteoporos Int 2021 Dec;32(12):2485-2492. [doi: 10.1007/s00198-021-06023-0] [Medline: 34129060]
2. Chiu JS, Li YC, Yu FC, Wang YF. Applying an artificial neural network to predict osteoporosis in the elderly. Stud Health Technol Inform 2006;124:609-614. [Medline: 17108584]
3. Smets J, Shevroja E, Hügle T, Leslie WD, Hans D. Machine learning solutions for osteoporosis-a review. J Bone Miner Res 2021 May;36(5):833-851. [doi: 10.1002/jbmr.4292] [Medline: 33751686]
4. He W, Chen S, Fu X, Xu L, Xie J, Wan J. Development and evaluation of interpretable machine learning regressors for predicting femoral neck bone mineral density in elderly men using NHANES data. Biomol Biomed 2025 Jan 14;25(2):375-390. [doi: 10.17305/bb.2024.10725] [Medline: 38972052]
5. Hung WC, Lin YL, Cheng TT, et al. Establish and validate the reliability of predictive models in bone mineral density by deep learning as examination tool for women. Osteoporos Int 2024 Jan;35(1):129-141. [doi: 10.1007/s00198-023-06913-5] [Medline: 37728768]
6. Pickhardt PJ, Pooler BD, Lauder T, del Rio AM, Bruce RJ, Binkley N. Opportunistic screening for osteoporosis using abdominal computed tomography scans obtained for other indications. Ann Intern Med 2013 Apr 16;158(8):588-595. [doi: 10.7326/0003-4819-158-8-201304160-00003] [Medline: 23588747]
7. Chen YC, Li YT, Kuo PC, et al. Automatic segmentation and radiomic texture analysis for osteoporosis screening using chest low-dose computed tomography. Eur Radiol 2023 Jul;33(7):5097-5106. [doi: 10.1007/s00330-023-09421-6] [Medline: 36719495]
8. Kadri A, Binkley N, Hernando D, Anderson PA. Opportunistic use of lumbar magnetic resonance imaging for osteoporosis screening. Osteoporos Int 2022 Apr;33(4):861-869. [doi: 10.1007/s00198-021-06129-5] [Medline: 34773484]
9. Lee S, Choe EK, Kang HY, Yoon JW, Kim HS. The exploration of feature extraction and machine learning for predicting bone density from simple spine X-ray images in a Korean population. Skeletal Radiol 2020 Apr;49(4):613-618. [doi: 10.1007/s00256-019-03342-6] [Medline: 31760458]
10. Singh KK, Singh A. Diagnosis of COVID-19 from chest X-ray images using wavelets-based depthwise convolution network. Big Data Min Anal 2021 Jun;4(2):84-93. [doi: 10.26599/BDMA.2020.9020012]
11. Jang M, Kim M, Bae SJ, Lee SH, Koh JM, Kim N. Opportunistic osteoporosis screening using chest radiographs with deep learning: development and external validation with a cohort dataset. J Bone Miner Res 2022 Feb;37(2):369-377. [doi: 10.1002/jbmr.4477] [Medline: 34812546]
12. Zhang B, Yu K, Ning Z, et al. Deep learning of lumbar spine X-ray for osteopenia and osteoporosis screening: a multicenter retrospective cohort study. Bone 2020 Nov;140:115561. [doi: 10.1016/j.bone.2020.115561] [Medline: 32730939]
13. Kanis JA, McCloskey EV, Johansson H, Oden A, Melton 3rd LJ, Khaltaev N. A reference standard for the description of osteoporosis. Bone 2008 Mar;42(3):467-475. [doi: 10.1016/j.bone.2007.11.001] [Medline: 18180210]
14. Mao L, Xia Z, Pan L, et al. Deep learning for screening primary osteopenia and osteoporosis using spine radiographs and patient clinical covariates in a Chinese population. Front Endocrinol (Lausanne) 2022;13:971877. [doi: 10.3389/fendo.2022.971877] [Medline: 36176468]
15. Hsieh CI, Zheng K, Lin C, et al. Automated bone mineral density prediction and fracture risk assessment using plain radiographs via deep learning. Nat Commun 2021 Sep 16;12(1):5472. [doi: 10.1038/s41467-021-25779-x] [Medline: 34531406]

XSL•FO
RenderX

16. Yang F, Weng X, Miao Y, Wu Y, Xie H, Lei P. Deep learning approach for automatic segmentation of ulna and radius in dual-energy X-ray imaging. Insights Imaging 2021 Dec 20;12(1):191. [doi: 10.1186/s13244-021-01137-9] [Medline: 34928449]
17. Wang F, Zheng K, Lu L, et al. Lumbar bone mineral density estimation from chest X-ray images: anatomy-aware attentive multi-ROI modeling. IEEE Trans Med Imaging 2023 Jan;42(1):257-267. [doi: 10.1109/TMI.2022.3209648] [Medline: 36155432]
18. Tsai DJ, Lin C, Lin CS, Lee CC, Wang CH, Fang WH. Artificial intelligence-enabled chest X-ray classifies osteoporosis and identifies mortality risk. J Med Syst 2024 Jan 13;48(1):12. [doi: 10.1007/s10916-023-02030-2] [Medline: 38217829]
19. Huang SC, Pareek A, Seyyedi S, Banerjee I, Lungren MP. Fusion of medical imaging and electronic health records using deep learning: a systematic review and implementation guidelines. NPJ Digit Med 2020;3(1):136. [doi: 10.1038/s41746-020-00341-z] [Medline: 33083571]
20. Huang SC, Shen L, Lungren MP, Yeung S. GLoRIA: a multimodal global-local representation learning framework for label-efficient medical image recognition. Presented at: 2021 IEEE/CVF International Conference on Computer Vision (ICCV); Oct 10-17, 2021; Montreal, QC, Canada p. 3922-3931. [doi: 10.1109/ICCV48922.2021.00391]
21. Liu R, Liu J, Jiang Z, Fan X, Luo Z. A bilevel integrated model with data-driven layer ensemble for multi-modality image fusion. IEEE Trans Image Process 2021;30:1261-1274. [doi: 10.1109/TIP.2020.3043125] [Medline: 33315564]
22. Stahlschmidt SR, Ulfenborg B, Synnergren J. Multimodal deep learning for biomedical data fusion: a review. Brief Bioinform 2022 Mar 10;23(2):bbab569. [doi: 10.1093/bib/bbab569] [Medline: 35089332]
23. Gao Y, Ventura-Diaz S, Wang X, et al. An explainable longitudinal multi-modal fusion model for predicting neoadjuvant therapy response in women with breast cancer. Nat Commun 2024 Nov 7;15(1):9613. [doi: 10.1038/s41467-024-53450-8] [Medline: 39511143]
24. Franke J, Baxan N, Lehr H, et al. Hybrid MPI-MRI System for dual-modal in situ cardiovascular assessments of real-time 3D blood flow quantification-a pre-clinical in vivo feasibility investigation. IEEE Trans Med Imaging 2020 Dec;39(12):4335-4345. [doi: 10.1109/TMI.2020.3017160] [Medline: 32804645]
25. Cao X, Yang J, Gao Y, Wang Q, Shen D. Region-adaptive deformable registration of CT/MRI pelvic images via learning-based image synthesis. IEEE Trans on Image Process 2018 Jul;27(7):3500-3512. [doi: 10.1109/TIP.2018.2820424]
26. Schilcher J, Nilsson A, Andlid O, Eklund A. Fusion of electronic health records and radiographic images for a multimodal deep learning prediction model of atypical femur fractures. Comput Biol Med 2024 Jan;168:107704. [doi: 10.1016/j.compbiomed.2023.107704] [Medline: 37980797]
27. Tiulpin A, Klein S, Bierma-Zeinstra SMA, et al. Multimodal machine learning-based knee osteoarthritis progression prediction from plain radiographs and clinical data. Sci Rep 2019 Dec 27;9(1):20038. [doi: 10.1038/s41598-019-56527-3] [Medline: 31882803]
28. Zhuang F, Qi Z, Duan K, et al. A comprehensive survey on transfer learning. Proc IEEE 2020 Jul 7;109(1):43-76. [doi: 10.1109/JPROC.2020.3004555]
29. Pillai R, Sharma A, Sharma N, Gupta R. Brain tumor classification using VGG 16, ResNet50, and Inception V3 transfer learning models. Presented at: 2023 2nd International Conference for Innovation in Technology (INOCON); Mar 3-5, 2023; Bangalore, India p. 1-5. [doi: 10.1109/INOCON57975.2023.10101252]
30. Holste G, Partridge SC, Rahbar H, Biswas D, Lee CI, Alessio AM. End-to-end learning of fused image and non-image features for improved breast cancer classification from MRI. Presented at: 2021 IEEE/CVF International Conference on Computer Vision Workshops (ICCVW); Oct 11-17, 2021; Montreal, BC, Canada p. 3287-3296. [doi: 10.1109/ICCVW54120.2021.00368]
31. Xue J, Rao Y, Yao Q, Wu J. 3H-ObjectDet: a target detection method based on Haar wavelet transform downsampling and hybrid attention mechanism for medical fracture image. Presented at: 2024 4th International Conference on Electronic Information Engineering and Computer Communication (EIECC); 2024; Wuhan, China p. 507-513. [doi: 10.1109/EIECC64539.2024.10929242]
32. Roy A, Sarkar S, Ghosal S, Kaplun D, Lyanova A, Sarkar R. A wavelet guided attention module for skin cancer classification with gradient-based feature fusion. Presented at: 2024 IEEE International Symposium on Biomedical Imaging (ISBI); May 27-30, 2024; Athens, Greece p. 1-4. [doi: 10.1109/ISBI56570.2024.10635704]
33. Bahdanau D, Cho K, Bengio Y. Neural machine translation by jointly learning to align and translate. arXiv. Preprint posted online on Sep 1, 2014. [doi: 10.48550/arXiv.1409.0473]
34. Li J, Liu S, Hu Y, Zhu L, Mao Y, Liu J. Predicting mortality in intensive care unit patients with heart failure using an interpretable machine learning model: retrospective cohort study. J Med Internet Res 2022 Aug 9;24(8):e38082. [doi: 10.2196/38082] [Medline: 35943767]
35. Hou N, Li M, He L, et al. Predicting 30-days mortality for MIMIC-III patients with sepsis-3: a machine learning approach using XGboost. J Transl Med 2020 Dec 7;18(1):462. [doi: 10.1186/s12967-020-02620-5] [Medline: 33287854]
36. Wani IM, Arora S. Osteoporosis diagnosis in knee X-rays by transfer learning based on convolution neural network. Multimed Tools Appl 2023;82(9):14193-14217. [doi: 10.1007/s11042-022-13911-y] [Medline: 36185321]

XSL•FO
RenderX

Abbreviations

AUC: area under the curve
BMD: bone mineral density
CNN: convolutional neural network
DL: deep learning
DXA: dual-energy X-ray absorptiometry
FF: feature fusion
LFF: learning feature fusion
PF: probabilistic fusion
SA: soft attention
SHAP: Shapley additive explanations
WT: wavelet transform

Edited by Q Chen; submitted 31.12.24; peer-reviewed by C Avian, J Xia, J Zhang, P Shingru; revised version received 21.05.25; accepted 17.08.25; published 18.09.25.

Please cite as:
Tang J, Yin X, Lai J, Luo K, Wu D
Fusion of X-Ray Images and Clinical Data for a Multimodal Deep Learning Prediction Model of Osteoporosis: Algorithm Development and Validation Study
JMIR Med Inform 2025;13:e70738
URL: https://medinform.jmir.org/2025/1/e70738
doi:10.2196/70738

© Jun Tang, Xiang Yin, Jiangyuan Lai, Keyu Luo, Dongdong Wu. Originally published in JMIR Medical Informatics (https://medinform.jmir.org), 18.9.2025. This is an open-access article distributed under the terms of the Creative Commons Attribution License (https://creativecommons.org/licenses/by/4.0/), which permits unrestricted use, distribution, and reproduction in any medium, provided the original work, first published in JMIR Medical Informatics, is properly cited. The complete bibliographic information, a link to the original publication on https://medinform.jmir.org/, as well as this copyright and license information must be included.

XSL•FO
RenderX

Using a Large Language Model for Breast Imaging Reporting and Data System Classification and Malignancy Prediction to Enhance Breast Ultrasound Diagnosis: Retrospective Study

Su Miaojiao*, MME; Liang Xia*, MME; Zeng Xian Tao, MME; Hong Zhi Liang, PhD; Cheng Sheng, MME; Wu Songsong*, PhD

Department of Ultrasound, Fujian Provincial Hospital, Affiliated Hospital of Fuzhou University, 134 Dong Street, Gulou District, Fuzhou, China

*these authors contributed equally

Corresponding Author:
Wu Songsong, PhD
Department of Ultrasound, Fujian Provincial Hospital, Affiliated Hospital of Fuzhou University, 134 Dong Street, Gulou District, Fuzhou, China

Abstract

Background: Breast ultrasound is essential for evaluating breast nodules, with Breast Imaging Reporting and Data System (BI-RADS) providing standardized classification. However, interobserver variability among radiologists can affect diagnostic accuracy. Large language models (LLMs) like ChatGPT-4 have shown potential in medical imaging interpretation. This study explores its feasibility in improving BI-RADS classification consistency and malignancy prediction compared to radiologists.

Objective: This study aims to evaluate the feasibility of using LLMs, particularly ChatGPT-4, to assess the consistency and diagnostic accuracy of standardized breast ultrasound imaging reports, using pathology as the reference standard.

Methods: This retrospective study analyzed breast nodule ultrasound data from 671 female patients (mean 45.82, SD 9.20 years; range 26 - 75 years) who underwent biopsy or surgical excision at our hospital between June 2019 and June 2024. ChatGPT-4 was used to interpret BI-RADS classifications and predict benign versus malignant nodules. The study compared the model's performance to that of two senior radiologists (≥15 years of experience) and two junior radiologists (<5 years of experience) using key diagnostic metrics, including accuracy, sensitivity, specificity, area under the receiver operating characteristic curve, *P* values, and odds ratios with 95% CIs. Two diagnostic models were evaluated: (1) image interpretation model, where ChatGPT-4 classified nodules based on BI-RADS features, and (2) image-to-text–LLM model, where radiologists provided textual descriptions, and ChatGPT-4 determined malignancy probability based on keywords. Radiologists were blinded to pathological outcomes, and BI-RADS classifications were finalized through consensus.

Results: ChatGPT-4 achieved an overall BI-RADS classification accuracy of 96.87%, outperforming junior radiologists (617/671, 91.95% and 604/671, 90.01%, *P*<.01). For malignancy prediction, ChatGPT-4 achieved an area under the receiver operating characteristic curve of 0.82 (95% CI 0.79 - 0.85), an accuracy of 80.63% (541/671 cases), a sensitivity of 90.56% (259/286 cases), and a specificity of 73.51% (283/385 cases). The image interpretation model demonstrated performance comparable to senior radiologists, while the image-to-text–LLM model further improved diagnostic accuracy for all radiologists, increasing their sensitivity and specificity significantly (*P*<.001). Statistical analyses, including the McNemar test and DeLong test, confirmed that ChatGPT-4 outperformed junior radiologists (*P*<.01) and showed noninferiority compared to senior radiologists (*P*>.05). Pathological diagnoses served as the reference standard, ensuring robust evaluation reliability.

Conclusions: Integrating ChatGPT-4 into an image-to-text–LLM workflow improves BI-RADS classification accuracy and supports radiologists in breast ultrasound diagnostics. These results demonstrate its potential as a decision-support tool to enhance diagnostic consistency and reduce variability.

(JMIR Med Inform 2025;13:e70924) doi:10.2196/70924

KEYWORDS

large language models; BI-RADS; breast ultrasound; ChatGPT-4; image-to-text–LLM; Breast Imaging Reporting and Data System

XSL•FO
RenderX

Introduction

In recent years, large language models (LLMs) have advanced rapidly, demonstrating significant potential in health care. Their diverse applications have garnered considerable attention [1-4], driving revolutionary progress across various fields, including medicine [5]. LLMs are built upon large-scale datasets and continuously refined through iterative training, enabling them to handle a wide range of tasks, including medical diagnosis. LLMs provide diagnostic recommendations by processing key inputs, extracting relevant information, and performing associative reasoning [6]. In medical imaging analysis, the integration of LLMs with image-text conversion models enables the creation of a continuous interactive system that seamlessly integrates with clinical practice, delivering more precise and personalized health care services [7]. This approach enhances medical technology, broadens clinical applications, and partially alleviates the challenges posed by limited health care resources. GPT-4, developed by OpenAI, is one of the most widely recognized LLMs. Although its applications in medical imaging analysis have shown promise, the specific role and diagnostic accuracy of LLMs in this domain remain insufficiently explored. Initial research on LLMs primarily focused on evaluating their language generation capabilities. Most discussions surrounding LLMs, particularly ChatGPT, have revolved around comments, replies, or question-and-answer formats [8-11]. The findings have been promising [12]. However, many studies have primarily focused on response evaluation rather than quantitative assessments of diagnostic accuracy and have lacked reference standards such as pathology or laboratory examinations [13]. In addition, the ability of LLMs to generate structured diagnostic reports, such as Breast Imaging Reporting and Data System (BI-RADS) classifications, has not been systematically evaluated, raising concerns about their reliability in clinical decision-making. Furthermore, LLMs may inadvertently perpetuate existing biases and disparities. Therefore, to address this gap, it is essential to demonstrate the application of LLMs in medical imaging. Breast cancer serves as an optimal case study for this purpose due to its high incidence, critical need for early detection, and reliance on imaging for diagnosis. Breast cancer is one of the most life-threatening diseases, second only to lung cancer [14,15]. The likelihood of breast cancer survival is largely determined by the stage at which it is detected, which significantly impacts chemotherapy outcomes [16-18]. Early diagnosis and effective treatment of breast cancer can significantly reduce mortality rates [19]. Unlike lung cancer, which primarily relies on computed tomography (CT） imaging, or neurological disorders, which depend on magnetic resonance imaging (MRI) and functional imaging, breast cancer diagnosis heavily incorporates ultrasound due to its accessibility, cost-effectiveness, and suitability for dense breast tissue—particularly in younger patients and in regions with high breast cancer incidence, such as China [20]. Therefore, in China, ultrasound has become the preferred imaging modality for breast lesion screening and preoperative evaluation [21]. Breast ultrasound not only facilitates routine detection of breast cancer but also aids in resolving inconclusive mammographic findings [22-24]. The BI-RADS, proposed by the American College of Radiology (ACR), is a standardized system designed to describe breast imaging findings [25]. It assists radiologists and breast surgeons in standardizing the assessment of malignancy probability in breast lesions and in guiding subsequent diagnostic and treatment plans. Physicians classify breast lesions based on specific characteristics, including shape, orientation, margins, echogenic pattern, posterior features, and the presence of calcifications and associated findings. However, unlike structured reporting systems in CT-based lung cancer screening or MRI-based neurological assessments, BI-RADS assessment in breast ultrasound remains highly dependent on operator experience. This reliance leads to interobserver variability and diagnostic inconsistency, as radiologists with different levels of expertise may provide varying interpretations. In addition, ultrasound evaluation requires extensive training and certification, making it resource-intensive and subject to human variability.

Given these challenges, breast ultrasound serves as an ideal testbed for evaluating LLM-assisted imaging interpretation. First, the structured nature of BI-RADS makes it well-suited for artificial intelligence (AI)-driven standardization, potentially reducing subjective variability. Second, the widespread clinical use of ultrasound in breast cancer detection allows for large-scale validation of LLM-generated reports against pathology results. Unlike lung CT or brain MRI, where AI-based segmentation and feature extraction already play a significant role, breast ultrasound interpretation lacks a robust AI-driven standardization framework, highlighting the potential value of LLM integration. LLMs offer a promising solution by providing standardized interpretations, reducing interobserver variability, and assisting in structured reporting. Their ability to generate BI-RADS reports based on ultrasound findings suggests a potential role in improving diagnostic consistency and streamlining clinical workflows. Despite these advantages, the reliability and diagnostic accuracy of LLM-generated BI-RADS assessments remain unclear.

To bridge this research gap, this study aims to systematically evaluate the diagnostic performance, consistency, and clinical utility of mainstream LLMs in breast nodule assessment. By comparing LLM-generated BI-RADS categorizations with pathology-confirmed diagnoses, we seek to determine whether LLMs can enhance reproducibility, improve standardization, and assist radiologists in breast cancer diagnosis.

Methods

Study Design

To compare the diagnostic performance of the LLMs and radiologists with different levels of experience in interpreting breast ultrasound images. First, among the widely used LLMs, ChatGPT, and Gemini are prominent. However, since Gemini does not support image analysis, we selected OpenAI's ChatGPT-4 for this study [26], using the BI-RADS standard for diagnosing breast nodules. For clarity, while LLMs refer to a broad category of AI models, this study specifically focuses on ChatGPT-4. We analyzed the accuracy of ChatGPT-4 in classifying breast nodules using the BI-RADS system and assessed its diagnostic performance in distinguishing between benign and malignant breast nodules. In subsequent analyses,

XSL•FO
RenderX

the performance of two different models was evaluated: image-to-text–LLM model and image interpretation model.

Image-to-Text–LLM Model

Radiologists first interpreted the ultrasound images and generated textual descriptions using a standardized BI-RADS reporting template. This template included predefined descriptors for nodule shape, margin, echogenicity, and other key ultrasound features. ChatGPT-4 then analyzed the text and determined whether the nodule was benign or malignant based on the extracted keywords (Figure 1). To minimize variability in descriptions, all radiologists were trained in the standardized reporting format, and their reports were randomly reviewed by a senior radiologist to ensure consistency.

Figure 1. The screenshot demonstrates ChatGPT-4 (OpenAI;) analyzing a single breast nodule in image-to-text–large language model. This response was recorded as a malignant diagnosis.

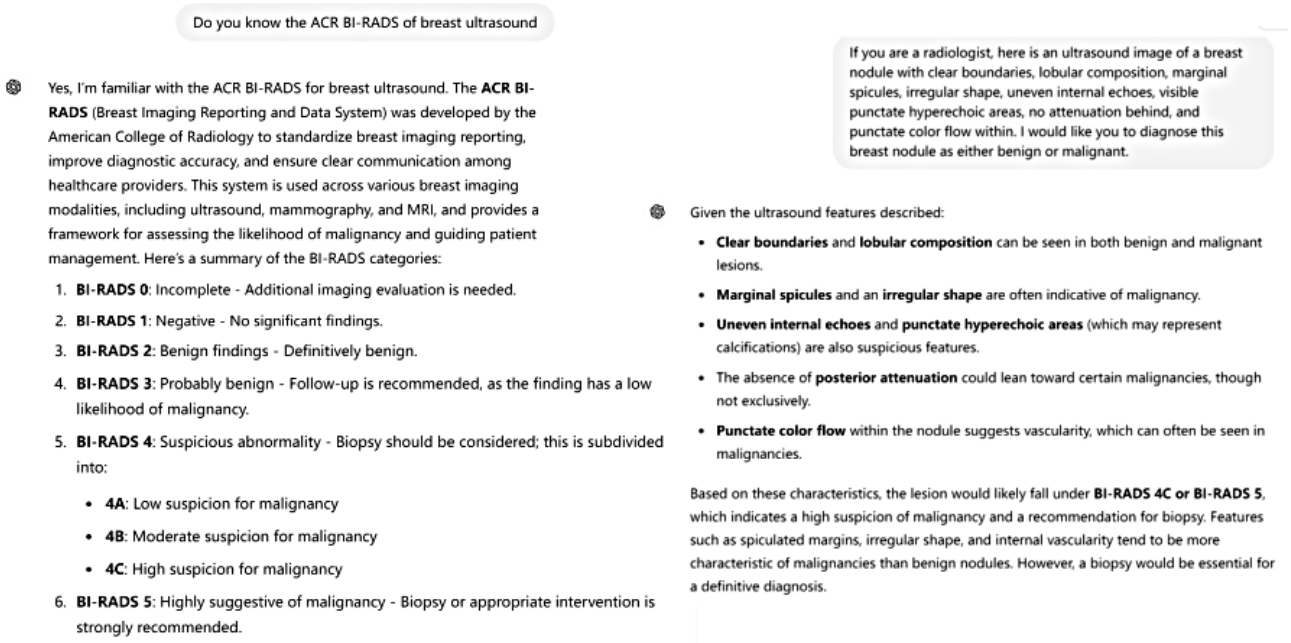


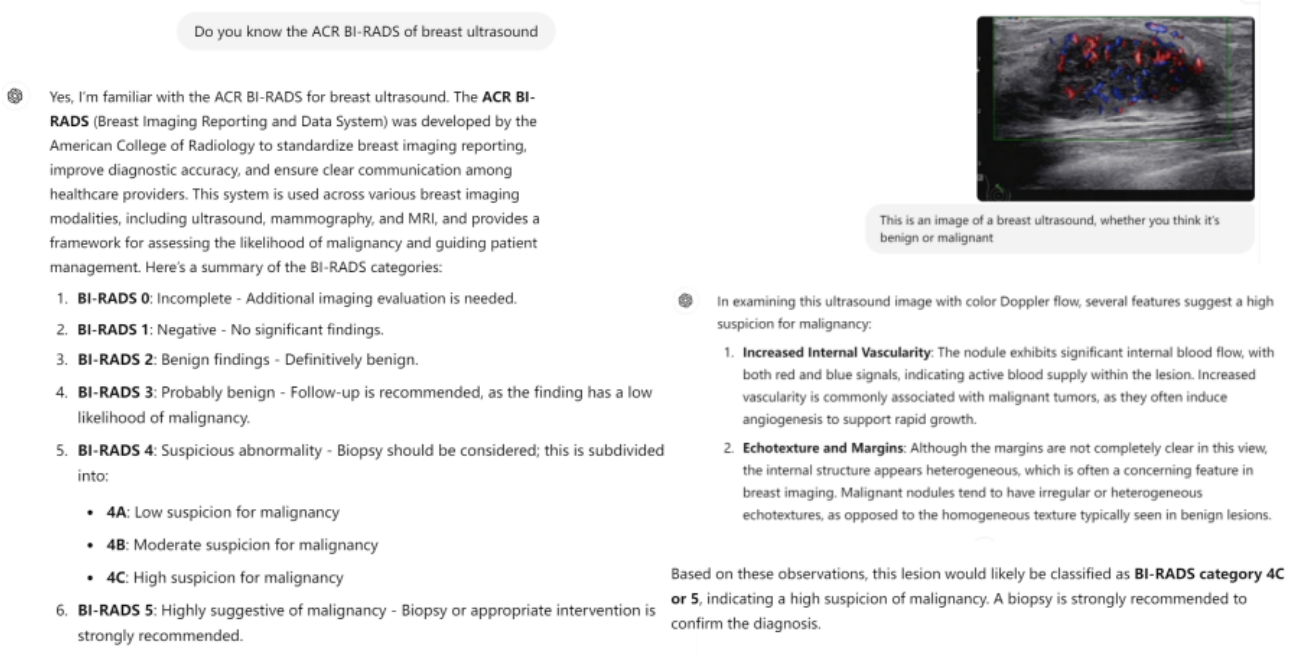
Image Interpretation Model

The ultrasound images were provided directly, and the model performed benign or malignant diagnosis based on BI-RADS classification and image analysis (Figure 2). All radiologists were blinded to the pathological results. The radiologists were divided into two senior and two junior groups. The senior radiologists each had over 15 years of experience in breast ultrasound, while the junior radiologists had less than 5 years of experience.

The BI-RADS classifications were determined by consensus between two senior radiologists. If their conclusions differed, a third senior radiologists (WSS, with 21 years of experience in breast ultrasound) was consulted to reach a final decision through discussion.

XSL•FO
RenderX

Figure 2. The screenshot demonstrates ChatGPT-4 (OpenAI; analyzing a single breast nodule in image interpretation model. This response was recorded as a malignant diagnosis.

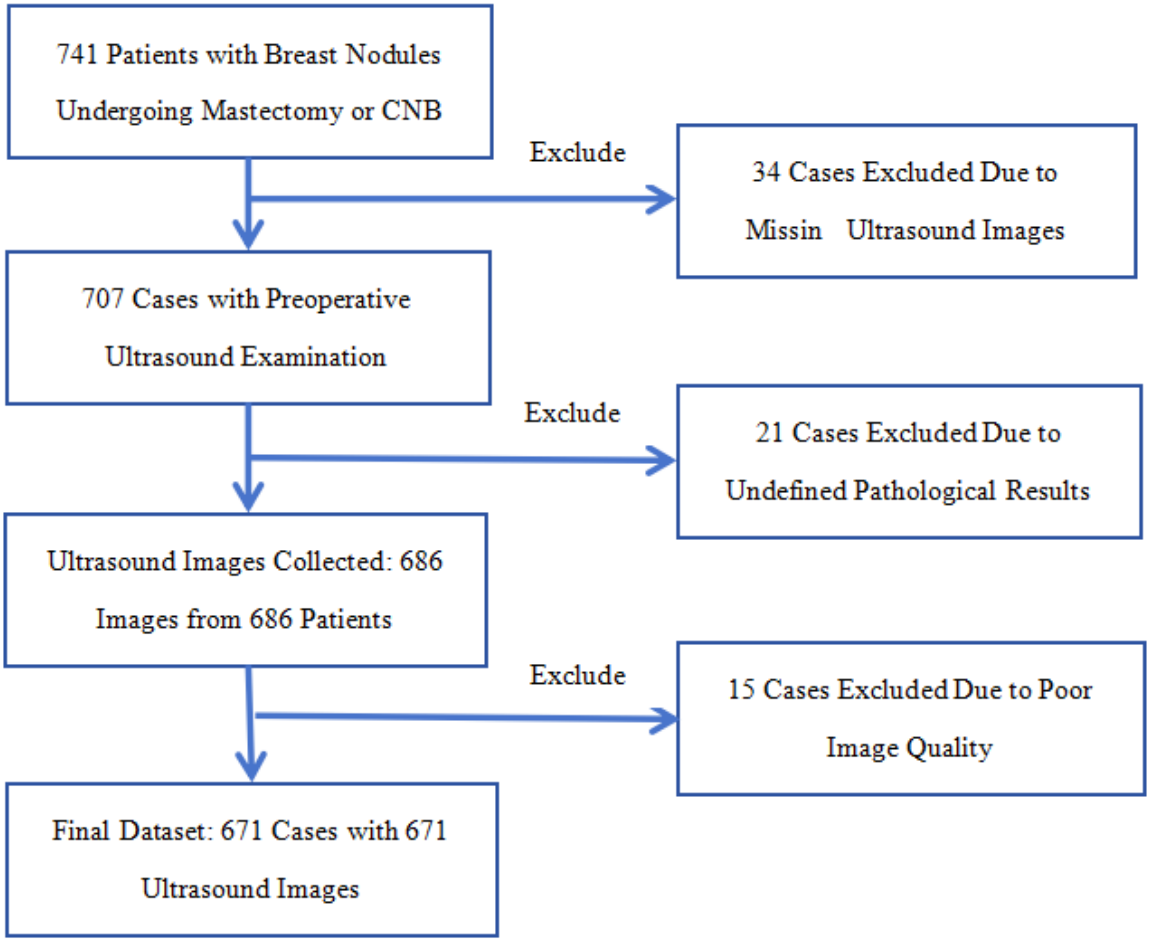


Patient Data Collection

Retrospective collection of ultrasound images of breast nodules diagnosed through biopsy or surgical excision at Fujian Provincial Hospital, Fuzhou University Affiliated Hospital, between June 2019 and June 2024 (385 benign and 286 malignant cases). Patients without ultrasound examinations, those with low-quality images, or those with inconclusive pathological results were excluded (Figure 3). Each image corresponded to an individual breast nodule. For nodules suspected to be benign on biopsy, follow-up of at least 6 months was required. All lesions were ultimately classified as benign or malignant based on histopathological results.

XSL•FO
RenderX

Figure 3. Flowchart of patient inclusion, exclusion, and study enrollment. CNB: core needle biopsy

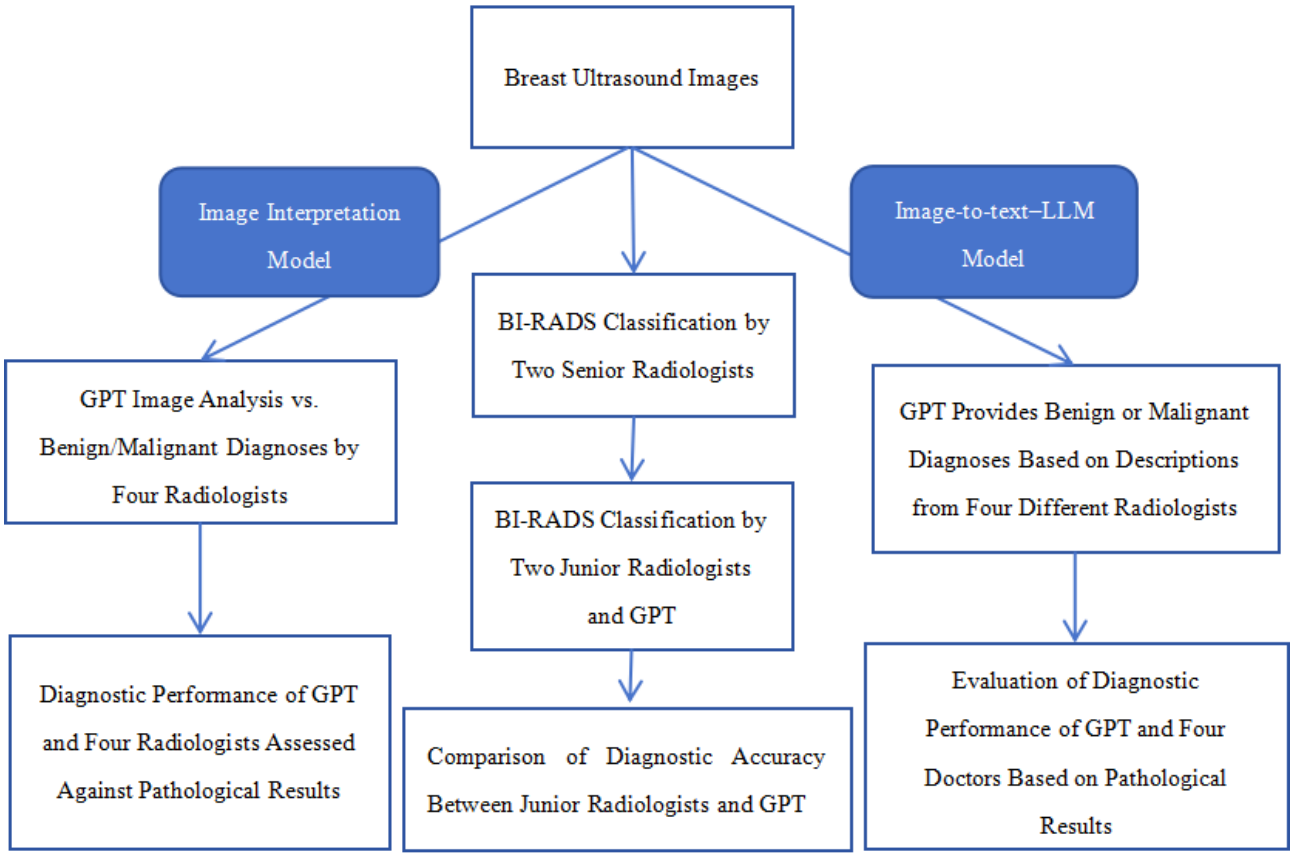


Evaluation Index

The diagnostic performance of ChatGPT-4 in two different models (Image-to-text–LLM model and image interpretation model) was compared with that of radiologists with varying levels of experience. The analysis included the accuracy of BI-RADS classifications by junior radiologists and the calculation of key performance metrics, including sensitivity, specificity, accuracy, and the area under the receiver operating characteristic curve (AUC) with 95% CIs (Figure 4).

XSL•FO
RenderX

Figure 4. Study Design. LLM: large language model; BI-RADS: Breast Imaging Reporting and Data System.



Statistical Analysis

All statistical analyses were performed using SPSS software (IBM, version 20.0) and MedCalc (MedCalc Software, version 12.7). Continuous data were expressed as mean (SD), and categorical data were presented as frequencies and percentages. The analysis included the calculation of key performance metrics, including accuracy, sensitivity, specificity, and the AUC with 95% CIs. Finally, McNemar's test and DeLong's test were used to compare the diagnostic performance of ChatGPT-4 under different deployment strategies. A *P* value of <.05 was considered statistically significant.

Ethical Considerations

This study was approved by the Institutional Review Board of Fujian Provincial Hospital. Informed consent was waived due to the retrospective design. No identifiable patient information was shared with the LLMs. This study is a retrospective study, and informed consent was waived due to its retrospective design. No patient privacy information was provided to the LLMs.

Results

Patient Characteristics

A total of 671 female patients were included in the study (mean 45.82, SD 9.20 years; range 26 - 75 years). A total of 671 ultrasound images of breast nodules were collected, including 385 benign cases (57.38%) and 286 malignant cases (42.62%), with 428 nodules on the left side and 243 on the right side (Table 1). Pathological diagnoses within 3 months after ultrasound examination were based on surgical resection or core needle biopsy. Patients with benign pathology from core needle biopsy were followed up for an average of approximately 11.2 months. The inclusion and exclusion criteria for patients and images are detailed in Figure 3.

XSL•FO
RenderX

Table . Demographic and clinical characteristics of patients. Unless otherwise specified, the data represents the number of survey results, with percentages in parentheses.

Characteristic	Values
Age (years)[a], mean (SD), range	45.82 (9.20; 26 - 75）
Location	
Left	428 (63.79）
Right	243 (36.21）
Nodule pathology	
Benign	385 (57.38）
Malignant	286 (42.62）

[a]Data are presented as mean (SD), with the range in parentheses.

Representation of ChatGPT-4 in Classification

As shown in Table 2, the BI-RADS classifications for the 671 ultrasound images include categories BI-RADS 3, 4 (A-C), and 5. The overall accuracy of the ChatGPT-4 in identifying BI-RADS classifications was 96.87% (650/671), surpassing junior radiologist 1 (617/671, 91.95%) and junior radiologist 2 (604/671, 90.01%). Notably, the model demonstrated significant differences in classification performance compared to both junior radiologists for BI-RADS 4A and to junior radiologist 2 for BI-RADS 3 and 4C.

Table . The effectiveness of ChatGPT-4 in classification. The *P* value represents the comparison with ChatGPT-4

Classification	N	ChatGPT-4, n (%)	Junior physicians 1, n (%)	*P* value	Junior Physicians 2, n (%)	*P* value
BI-RADS[a] 3	93	90（96.77）	86 (92.47)	.29	82 (88.17)	.04
BI-RADS 4A	374	361 (96.52)	345 (92.25)	.02	341 (91.18)	<.01
BI-RADS 4B	98	95 (96.94)	91 (92.86)	.22	90 (91.84)	.13
BI-RADS 4C	56	55 (98.21)	50 (89.29)	.06	47 (83.93)	<.01
BI-RADS 5	50	49 (98.00)	45 (90.00)	.13	44 (88.00)	.06

[a]BI-RADS: Breast Imaging Reporting and Data System.

Performance of the Image Interpretation Model in Predicting Benign and Malignant Breast Nodules

As shown in Table 3, senior radiologist 1 demonstrated excellent performance in diagnosing benign and malignant breast lesions via ultrasound, with an AUC of 0.85 (95% CI 0.81 - 0.88), an accuracy of 83.16% (558/671 cases), a sensitivity of 91.61% (262/286 cases), and a specificity of 77.40% (298/385 cases). ChatGPT-4 exhibited comparable performance to the image interpretation model of both senior radiologists in terms of accuracy, sensitivity, and specificity. Notably, it outperformed senior radiologist 2 in AUC, with the difference being statistically significant (P<.01). The image interpretation model showed diagnostic performance comparable to that of the 2 senior radiologists, particularly achieving a sensitivity of 90.56% (259/286 cases). Furthermore, it consistently outperformed the predictive models of the junior radiologists in AUC, accuracy, and sensitivity (P<.01), while showing a statistically significant difference in specificity compared to junior radiologist 1 (P<.01).

XSL•FO
RenderX

Table . The performance of image interpretation model in predicting benign and malignant breast nodules. Except were indicated, numbers in parentheses are numbers of nodules.

Strategy	AUC[a,b] (95% CI)	*P* value	Accuracy, n (%), Total=671	*P* value	Sensitivity, n (%), Total=286	*P* value	Specificity, n (%), Total=385	*P* value
ChatGPT-4	0.82 (0.79-085）	—[c]	541 (80.63)	—	259/286 (90.56)	—	73.51(283/385)	—
Senior Radiologist 1	0.81 (0.77-0.84）	.10	536 (79.88)	.88	246/286 (86.01)	.18	75.32(290/385)	.50
Senior Radiologist 2	0.79 (0.76-0.83）	<.01	524 (78.09)	.24	248/286 (86.71)	.23	71.69(276/385)	.63
Junior Radiologist 1	0.66 (0.62-0.70）	<.01	440 (65.57)	<.01	181/286 (63.33)	<.01	67.27(259/385)	<.01
Junior Radiologist 2	0.67 (0.62-0.71）	<.01	446 (66.47)	<.01	191/286 (66.78)	<.01	66.23(255/385)	.13

[a]Data in parentheses for the AUC metric are 95% CIs.

[b]AUC: area under a receiver operating characteristic curve.

[c]Not applicable

Performance of ChatGPT-4 in Predicting Benign and Malignant Breast Nodules Based on Image-To-Text–LLM Model

As shown in Table 4, the image interpretation model of ChatGPT-4 yielded an AUC of 0.82 (95% CI 0.79 - 0.85), an accuracy of 80.63% (541/671 cases), a sensitivity of 90.56% (259/286 cases), and a specificity of 73.51% (283/385 cases). Under the image-to-text–LLM model, ChatGPT-4 demonstrated performance comparable to the 2 senior radiologists while surpassing the models of junior radiologists in AUC, accuracy, sensitivity, and specificity (*P*<.001). The four radiologists with varying levels of experience showed improvements in AUC, accuracy, sensitivity, and specificity after image-to-text–LLM model compared to image-to-text–LLM model.

Table . The performance of ChatGPT-4 in predicting benign and malignant breast nodules based on image-to-text–large language model. Note.—Except were indicated, numbers in parentheses are numbers of nodules.

Diagnostic performance	ChatGPT-4	Senior radiologist 1	Senior radiologist 2	Junior radiologist 1	Junior radiologist 2
AUC[a,b] (95% CI)	0.82 (0.79-085）	0.85 (0.81-0.88）	0.82 (0.78-0.85）	0.64 (0.62-0.70）	0.63 (0.59-0.67）
P value	—[c]	.10	.77	<.01	<.01
Accuracy, n (%) Total=671	541 (80.63)	558 (83.16）	546 (81.37）	486 (72.43）	463 (69.00）
P value	—	.13	.72	<.01	<.01
Sensitivity, n (%) Total=286	259 (90.56)	262 (91.61)	248 (86.71)	240 (83.92)	212 (74.13)
P value	—	.87	.29	.02	<.01
Specificity, n (%) Total=385	283 (73.51)	298 (77.40)	294 (76.36)	248 (64.42)	253 (65.71)
P value	—	.10	.18	<.01	.01

[a]Data in parentheses for the AUC metric are 95% CIs.

[b]AUC: area under a receiver operating characteristic curve

[c]Not applicable

Discussion

Principal Findings

In medical diagnostics, logical reasoning often forms the foundation of treatment, requiring higher-order cognitive skills such as application, analysis, and evaluation. Bhayana et al [8] demonstrated that ChatGPT nearly passed a radiology board-style exam despite lacking radiology-specific pretraining or direct access to imaging data. Despite the promising potential of LLMs in medical imaging [27], there is a lack of research on their feasibility in addressing reasoning tasks associated with medical diagnoses based on breast-specific reference standards, such as pathology. In this study, we used BI-RADS and standardized pathological reporting as reference standards, integrating LLMs into the diagnostic process to emphasize the

XSL•FO
RenderX

benefits of combining ChatGPT-4 with image-to-text technologies. We validated the potential application of ChatGPT-4 in breast nodule ultrasound diagnostics, using pathological results as the benchmark to evaluate their performance in standardized reporting and diagnostic consistency. The results showed that ChatGPT-4 performed exceptionally well in BI-RADS classification and benign-versus-malignant predictions of breast nodules. Its diagnostic performance was significantly superior to that of less experienced radiologists. This lays a foundation for the practical application of LLMs in enhancing the standardization and accuracy of medical imaging diagnostics while providing evidence to support further exploration of their clinical utility. ChatGPT-4 achieved an overall accuracy of 96.87% in BI-RADS classification and an AUC of 0.82 for benign-versus-malignant predictions (AUC 0.82, 95% CI 0.79‐0.85). Its accuracy, sensitivity, and specificity were 80.63% (541/671), 90.56% (259/286), and 73.51% (283/385), respectively. Notably, ChatGPT-4 outperformed less experienced radiologists in BI-RADS categories 4A, 3, and 4C. This indicates that ChatGPT-4 can deliver highly consistent and accurate diagnostic results, reducing variability caused by limited experience. Integrating LLMs into breast condition classification can minimize diagnostic errors and ultimately improve patient outcomes significantly. LLMs can be trained to identify and interpret individual variations, ultimately assisting in the development of new classification standards. This approach may address the lack of universally accepted breast disease classifications. Furthermore, integrating image-to-text conversion by radiologists with ChatGPT-4 improved the AUC, accuracy, sensitivity, and specificity for all 4 physicians, with notable performance enhancements observed among less experienced radiologists. This underscores that while AI has made significant advancements in medical imaging and diagnostics, human expertise remains indispensable. While ChatGPT-4 demonstrated strong diagnostic capabilities, it is important to compare its performance with existing AI-driven ultrasound diagnostic models. Prior deep-learning models have shown comparable or even superior performance in specific ultrasound tasks. For example, convolutional neural networks (CNNs) and transformer-based models trained on large annotated datasets have achieved AUCs exceeding 0.90 in distinguishing benign from malignant breast lesions [28,29]. These models directly analyze imaging data, extracting pixel-level features for classification. In contrast, ChatGPT-4 processes structured text inputs rather than images, highlighting a key trade-off between interpretability and diagnostic precision. While CNNs and other deep-learning models operate as “black-box” systems with high accuracy, LLMs like ChatGPT-4 provide enhanced transparency and reasoning, allowing clinicians to trace the logic behind their decisions. Thus, future studies should explore hybrid approaches that integrate deep-learning image analysis with LLM-driven reasoning to maximize diagnostic performance. Our study, grounded on pathological findings as the reference standard, provides substantial evidence that using pathology-based benchmarks to evaluate LLMs in ultrasound diagnostic reasoning and information processing differs significantly from previous approaches. Earlier studies primarily relied on expert questionnaires and subjective judgments to assess LLMs’ text comprehension, summarization, and generation abilities in the context of medical imaging reports or inquiry responses [30,31]. The results showed that ChatGPT-4, when integrated with clinician-led image-to-text conversion strategies, achieved optimal performance. This demonstrates that LLMs can effectively assist radiologist, particularly less experienced radiologists, thereby improving overall diagnostic quality. Compared to senior radiologists, ChatGPT-4 demonstrated sensitivity (90.56%) in benign-versus-malignant diagnosis of breast nodules that closely matched that of 2 senior radiologists (91.61% and 86.71%). However, its specificity was slightly lower (73.51% vs 77.40% and 76.36%). These findings suggest that ChatGPT-4’s diagnostic reasoning, when provided with structured textual inputs, approaches that of senior radiologists. However, its performance remains constrained by its reliance on human-generated descriptions, rather than direct image interpretation. Unlike black-box deep-learning models, ChatGPT-4 offers a transparent reasoning process, enhancing trust in AI-assisted diagnostics. This feature is particularly valuable in clinical practice and medical education, as it enables junior radiologists to follow structured diagnostic logic rather than relying on uninterpretable AI-generated outputs. By standardizing ultrasound diagnostic reasoning, ChatGPT-4 could improve the consistency and quality of radiological assessments, especially among less experienced practitioners. This study demonstrates the advantages of LLMs in breast ultrasound diagnosis. First, LLMs standardize the diagnostic process, significantly reducing inconsistencies caused by variations in physician experience, making them particularly beneficial for less experienced radiologists. Second, they offer high efficiency in processing large image datasets, alleviating the workload of radiologists, particularly in breast cancer screening programs. Furthermore, LLMs can be incorporated into standardized reporting frameworks such as BI-RADS, providing real-time decision support to optimize clinical workflows. Rather than replacing CNN-based models, ChatGPT-4 functions as a complementary tool that interprets structured radiological descriptions, offering an alternative diagnostic strategy. Most traditional diagnostic support software focuses on extracting imaging features rather than providing comprehensive diagnostic suggestions. Our study paves the way for applying LLMs in medical image-based diagnostic reasoning. Future research should explore multimodal AI models that integrate ultrasound, CT, and MRI data to further enhance diagnostic accuracy. In addition, refining image-to-text conversion methods and reducing reliance on manual input will be critical for advancing fully automated diagnostic systems. Validating these findings on multicenter datasets is essential to ensure generalizability.

Limitations

Despite demonstrating the potential of LLMs in ultrasound diagnostics, this study has certain limitations. First, it did not use the latest LLM versions, and ChatGPT-4 lacks the capability to directly interpret medical images. Its diagnostic process depends on structured text inputs provided by physicians, limiting its feasibility for fully automated diagnostics. Therefore, its current role is best suited as a decision-support tool rather than an independent diagnostic system. Second, the study was

XSL•FO
RenderX

based on BI-RADS standards and did not account for complex imaging features or multimodal data, potentially restricting the model's applicability to challenging cases. Third, the dataset was derived from a single institution, introducing potential selection bias. In addition, the patient cohort was drawn from a specific geographic and demographic background, which may not fully represent broader populations. Future studies should include diverse, multiethnic patient groups to improve external validity. Finally, while pathological results were used as the gold standard, they are not always available in routine clinical practice. Investigating alternative validation methods, such as long-term follow-up outcomes, could further enhance the clinical applicability of LLM-assisted diagnostics.

Conclusion

This study systematically evaluates the application of LLMs in breast ultrasound diagnosis. The results show that ChatGPT-4 achieves diagnostic performance comparable to senior radiologists while significantly improving the accuracy of less experienced radiologists. These findings highlight its potential to enhance diagnostic consistency and standardization. As AI and imaging technologies advance, LLMs are expected to further improve diagnostic accuracy and efficiency. Future research should focus on multicenter validation and multimodal imaging integration to further assess its clinical applicability.

Acknowledgments

The authors are thankful to Fujian Provincial Hospital and Fujian Medical University for their management of our patient database.

The authors are thankful to Song-Song Wu for helping critically revise the manuscript for important intellectual content and helping collect data and design the study.

The author(s) declare that financial support was received for the research, authorship, and/or publication of this article. Fujian Science and Technology Innovation Joint Fund project climbing project (2023Y9332).

Authors' Contributions

MS contributed to conceptualization, data curation, investigation, formal analysis, writing–original draft, and visualization. XL was responsible for methodology, software, validation, data curation, writing–original draft, and writing–review & editing. XZ handled resources, investigation, project administration, and writing–review & editing. ZH performed formal analysis, data curation, and visualization. SC managed software, validation, and resources. SW was involved in conceptualization, supervision, funding acquisition, methodology, project administration, and writing–review & editing.

Conflicts of Interest

The authors declare that the research was conducted in the absence of any commercial or financial relationships that could be construed as a potential conflict of interest.

References

1. Patel SB, Lam K. ChatGPT: the future of discharge summaries? Lancet Digit Health 2023 Mar;5(3):e107-e108. [doi: 10.1016/S2589-7500(23)00021-3] [Medline: 36754724]
2. Mukherjee P, Hou B, Lanfredi RB, et al. Feasibility of using the privacy-preserving large language model Vicuna for labeling radiology reports. Radiology 2023 Oct;309(1):e231147. [doi: 10.1148/radiol.231147] [Medline: 37815442]
3. Rau A, Rau S, Zoeller D, et al. A context-based chatbot surpasses trained radiologists and generic ChatGPT in following the ACR appropriateness guidelines. Radiology 2023 Jul;308(1):e230970. [doi: 10.1148/radiol.230970] [Medline: 37489981]
4. Moy L. Guidelines for use of large language models by authors, reviewers, and editors: considerations for imaging journals. Radiology 2023 Oct;309(1):e239024. [doi: 10.1148/radiol.239024] [Medline: 37815449]
5. Will ChatGPT transform healthcare? Nat Med 2023 Mar;29(3):505-506. [doi: 10.1038/s41591-023-02289-5]
6. Gertz RJ, Bunck AC, Lennartz S, et al. GPT-4 for automated determinatiod of radiological study and protocol based on radiology request forms: a feasibility study. Radiology 2023 Jun;307(5):e230877. [doi: 10.1148/radiol.230877] [Medline: 37310247]
7. Moon JH, Lee H, Shin W, et al. Multi-modal understanding and generation for medical images and text via vsion-language pre-training. IEEE J Biomed Health Inform 2022 Dec;26(12):6070-6080. [doi: 10.1109/JBHI.2022.3207502] [Medline: 36121943]
8. Bhayana R, Krishna S, Bleakney RR. Performance of ChatGPT on a radiology board-style examination: insights into current strengths and limitations. Radiology 2023 Jun;307(5):e230582. [doi: 10.1148/radiol.230582] [Medline: 37191485]
9. Ayers JW, Poliak A, Dredze M, et al. Comparing physician and artificial intelligence chatbot responses to patient questions posted to a public social media forum. JAMA Intern Med 2023 Jun 1;183(6):589-596. [doi: 10.1001/jamainternmed.2023.1838] [Medline: 37115527]
10. Mihalache A, Popovic MM, Muni RH. Performance of an artificial intelligence chatbot in ophthalmic knowledge assessment. JAMA Ophthalmol 2023 Jun 1;141(6):589-597. [doi: 10.1001/jamaophthalmol.2023.1144] [Medline: 37103928]

XSL•FO
RenderX

11. Rahsepar AA, Tavakoli N, Kim GHJ, et al. How AI responds to common lung cancer questions: ChatGPT vs Google Bard. Radiology 2023 Jun;307(5):e230922. [doi: 10.1148/radiol.230922] [Medline: 37310252]
12. Kulkarni PA, Singh H. Artificial intelligence in clinical diagnosis: opportunities, challenges, and hype. JAMA 2023 Jul 25;330(4):317-318. [doi: 10.1001/jama.2023.11440] [Medline: 37410477]
13. Fink MA, Bischoff A, Fink CA, et al. Potential of ChatGPT and GPT-4 for data mining of free-text CT reports on lung cancer. Radiology 2023 Sep;308(3):e231362. [doi: 10.1148/radiol.231362] [Medline: 37724963]
14. Siegel RL, Miller KD, Fuchs HE, et al. Cancer Statistics, 2021. CA Cancer J Clin 2021 Jan;71(1):7-33. [doi: 10.3322/caac.21654] [Medline: 33433946]
15. Hassani H, Avazzadeh Z, Agarwal P, et al. A study on fractional tumor-immune interaction model related to lung cancer via generalized Laguerre polynomials. BMC Med Res Methodol 2023 Aug 21;23(1):189. [doi: 10.1186/s12874-023-02006-3] [Medline: 37605131]
16. Gorgzadeh A, Hheidari A, Ghanbarikondori P, et al. Investigating the properties and cytotoxicity of cisplatin-loaded nano-polybutylcyanoacrylate on breast cancer cells. Asian Pac J Cancer Biol 2023;8(4):345-350. [doi: 10.31557/apjcb.2023.8.4.345-350]
17. Yousefi O, Azami P, Sabahi M, et al. Management of optic pathway glioma: a systematic review and meta-analysis. Cancers (Basel) 2022 Sep 30;14(19):4781. [doi: 10.3390/cancers14194781] [Medline: 36230704]
18. Mohammadinezhad F, Talebi A, Allahyartorkaman M, et al. Preparation, characterization and cytotoxic studies of cisplatin-containing nanoliposomes on breast cancer cell lines. Asian Pac J Cancer Biol 2023;8(2):155-159. [doi: 10.31557/apjcb.2023.8.2.155-159]
19. Duggan C, Dvaladze A, Rositch AF, et al. The breast health global initiative 2018 global summit on improving breast healthcare through resource-stratified phased implementation: methods and overview. Cancer 2020 May 15;126 Suppl 10(Suppl 10):2339-2352. [doi: 10.1002/cncr.32891] [Medline: 32348573]
20. He J, Chen WQ, Li N, et al. China guideline for the screening and early detection of female breast cancer (2021, Beijing). Zhonghua Zhong Liu Za Zhi 2021 Apr 23;43(4):357-382. [doi: 10.3760/cma.j.cn112152-20210119-00061] [Medline: 33902200]
21. Bevers TB, Helvie M, Bonaccio E, et al. Breast cancer screening and diagnosis, version 3.2018, NCCN clinical practice guidelines in oncology. J Natl Compr Canc Netw 2018 Nov;16(11):1362-1389. [doi: 10.6004/jnccn.2018.0083] [Medline: 30442736]
22. Rebolj M, Assi V, Brentnall A, et al. Addition of ultrasound to mammography in the case of dense breast tissue: systematic review and meta-analysis. Br J Cancer 2018 Jun;118(12):1559-1570. [doi: 10.1038/s41416-018-0080-3] [Medline: 29736009]
23. Teichgraeber DC, Guirguis MS, Whitman GJ. Breast Cancer Staging: Updates in the AJCC Cancer Staging Manual, 8th Edition, and Current Challenges for Radiologists, From the AJR Special Series on Cancer Staging. AJR Am J Roentgenol 2021 Aug;217(2):278-290. [doi: 10.2214/AJR.20.25223] [Medline: 33594908]
24. Sprague BL, Ichikawa L, Eavey J, et al. Breast cancer risk characteristics of women undergoing whole-breast ultrasound screening versus mammography alone. Cancer 2023 Aug 15;129(16):2456-2468. [doi: 10.1002/cncr.34768] [Medline: 37303202]
25. Levy L, Suissa M, Chiche JF, et al. BIRADS ultrasonography. Eur J Radiol 2007 Feb;61(2):202-211. [doi: 10.1016/j.ejrad.2006.08.035] [Medline: 17215097]
26. ChatGPT 40 OpenAI. URL: https://chat.openai.com [accessed 2023-06-28]
27. Wu SH, Tong WJ, Li MD, et al. Collaborative enhancement of consistency and accuracy in US diagnosis of thyroid nodules using large language models. Radiology 2024 Mar;310(3):e232255. [doi: 10.1148/radiol.232255] [Medline: 38470237]
28. Ji H, Zhu Q, Ma T, et al. Development and validation of a transformer-based CAD model for improving the consistency of BI-RADS category 3-5 nodule classification among radiologists: a multiple center study. Quant Imaging Med Surg 2023 Jun 1;13(6):3671-3687. [doi: 10.21037/qims-22-1091] [Medline: 37284087]
29. Zheng X, Yao Z, Huang Y, et al. Deep learning radiomics can predict axillary lymph node status in early-stage breast cancer. Nat Commun 2020 Mar 6;11(1):1236. [doi: 10.1038/s41467-020-15027-z] [Medline: 32144248]
30. Tariq R, Malik S, Khanna S. Evolving landscape of large language models: an evaluation of ChatGPT and Bard in answering patient queries on Colonoscopy. Gastroenterology 2024 Jan;166(1):220-221. [doi: 10.1053/j.gastro.2023.08.033] [Medline: 37634736]
31. Lim ZW, Pushpanathan K, Yew SME, et al. Benchmarking large language models' performances for myopia care: a comparative analysis of ChatGPT-3.5, ChatGPT-4.0, and Google Bard. EBioMedicine 2023 Sep;95:104770. [doi: 10.1016/j.ebiom.2023.104770] [Medline: 37625267]

Abbreviations

ACR: American College of Radiology
AI: artificial intelligence
AUC: area under the receiver operating characteristic curve
BI-RADS: Breast Imaging Reporting and Data System

XSL•FO
RenderX

CNN: convolutional neural network
CT: computed tomography
LLM: large language model
MRI: magnetic resonance imaging

Edited by A Benis; submitted 06.01.25; peer-reviewed by S Mohanadas, T Ogunleye; revised version received 15.04.25; accepted 20.04.25; published 11.06.25.

Please cite as:
Miaojiao S, Xia L, Xian Tao Z, Zhi Liang H, Sheng C, Songsong W
Using a Large Language Model for Breast Imaging Reporting and Data System Classification and Malignancy Prediction to Enhance Breast Ultrasound Diagnosis: Retrospective Study
JMIR Med Inform 2025;13:e70924
URL: https://medinform.jmir.org/2025/1/e70924
doi:10.2196/70924

© Su Miaojiao, Liang Xia, Zeng Xian Tao, Hong Zhi Liang, Cheng Sheng, Wu Songsong. Originally published in JMIR Medical Informatics (https://medinform.jmir.org), 11.6.2025. This is an open-access article distributed under the terms of the Creative Commons Attribution License (https://creativecommons.org/licenses/by/4.0/), which permits unrestricted use, distribution, and reproduction in any medium, provided the original work, first published in JMIR Medical Informatics, is properly cited. The complete bibliographic information, a link to the original publication on https://medinform.jmir.org/, as well as this copyright and license information must be included.

XSL•FO
RenderX

Deep Learning Radiomics Model Based on Computed Tomography Image for Predicting the Classification of Osteoporotic Vertebral Fractures: Algorithm Development and Validation

Jiayi Liu[1*], PhD; Lincen Zhang[1*], MS; Yousheng Yuan[1*], MS; Jun Tang[2], MS; Yongkang Liu[3], MD; Liang Xia[1], PhD; Jun Zhang[1], PhD

[1]Department of Radiology, Sir Run Run Hospital, Nanjing Medical University, 109 Longmian Road, Nanjing, China

[2]Department of Radiology, The Affiliated Taizhou People's Hospital of Nanjing Medical University, Taizhou, China

[3]Department of Radiology, The Affiliated Hospital of Nanjing University of Chinese Medicine, Nanjing, China

[*]these authors contributed equally

Corresponding Author:
Jun Zhang, PhD
Department of Radiology, Sir Run Run Hospital, Nanjing Medical University, 109 Longmian Road, Nanjing, China

Abstract

Background: Osteoporotic vertebral fractures (OVFs) are common in older adults and often lead to disability if not properly diagnosed and classified. With the increased use of computed tomography (CT) imaging and the development of radiomics and deep learning technologies, there is potential to improve the classification accuracy of OVFs.

Objective: This study aims to evaluate the efficacy of a deep learning radiomics model, derived from CT imaging, in accurately classifying OVFs.

Methods: The study analyzed 981 patients (aged 50 - 95 years; 687 women, 294 men), involving 1098 vertebrae, from 3 medical centers who underwent both CT and magnetic resonance imaging examinations. The Assessment System of Thoracolumbar Osteoporotic Fractures (ASTLOF) classified OVFs into Classes 0, 1, and 2. The data were categorized into 4 cohorts: training (n=750), internal validation (n=187), external validation (n=110), and prospective validation (n=51). Deep transfer learning used the ResNet-50 architecture, pretrained on RadImageNet and ImageNet, to extract imaging features. Deep transfer learning–based features were combined with radiomics features and refined using Least Absolute Shrinkage and Selection Operator (LASSO) regression. The performance of 8 machine learning classifiers for OVF classification was assessed using receiver operating characteristic metrics and the "One-vs-Rest" approach. Performance comparisons between RadImageNet- and ImageNet-based models were performed using the DeLong test. Shapley Additive Explanations (SHAP) analysis was used to interpret feature importance and the predictive rationale of the optimal fusion model.

Results: Feature selection and fusion yielded 33 and 54 fused features for the RadImageNet- and ImageNet-based models, respectively, following pretraining on the training set. The best-performing machine learning algorithms for these 2 deep learning radiomics models were the multilayer perceptron and Light Gradient Boosting Machine (LightGBM). The macro-average area under the curve (AUC) values for the fused models based on RadImageNet and ImageNet were 0.934 and 0.996, respectively, with DeLong test showing no statistically significant difference (P=2.34). The RadImageNet-based model significantly surpassed the ImageNet-based model across internal, external, and prospective validation sets, with macro-average AUCs of 0.837 versus 0.648, 0.773 versus 0.633, and 0.852 versus 0.648, respectively (P<.05). Using the binary "One-vs-Rest" approach, the RadImageNet-based fused model achieved superior predictive performance for Class 2 (AUC=0.907, 95% CI 0.805 - 0.999), with Classes 0 and 1 following (AUC/accuracy=0.829/0.803 and 0.794/0.768, respectively). SHAP analysis provided a visualization of feature importance in the RadImageNet-based fused model, highlighting the top 3 most influential features: cluster shade, mean, and large area low gray level emphasis, and their respective impacts on predictions.

Conclusions: The RadImageNet-based fused model using CT imaging data exhibited superior predictive performance compared to the ImageNet-based model, demonstrating significant utility in OVF classification and aiding clinical decision-making for treatment planning. Among the 3 classes, the model performed best in identifying Class 2, followed by Class 0 and Class 1.

(JMIR Med Inform 2025;13:e75665) doi:10.2196/75665

KEYWORDS

deep learning; radiomics; osteoporotic vertebral fractures; tomography; classification; model interpretability; x-ray computed

XSL•FO
RenderX

Introduction

Osteoporotic vertebral fractures (OVFs) have a subtle onset and complex progression, affecting about 40% of postmenopausal women and 25% - 33% of older men. In China, a new OVF case is reported approximately every 17.4 seconds [1]. OVFs are linked to high disability and mortality rates [2]. Accurate classification of OVFs is widely recognized as critical for early diagnosis, treatment planning, and prognosis evaluation [3]. Current classification systems, including the Genant semi-quantitative method [4], Heini classification [5], osteoporotic fractures classification [6], and the Assessment System of Thoracolumbar Osteoporotic Fractures (ASTLOF) [7], differ in methodology but lack global agreement [8]. Among these, the ASTLOF system has demonstrated good reproducibility and clinical utility, integrating vertebral morphology, magnetic resonance imaging (MRI) signal characteristics, bone mineral density (BMD), and pain severity into a preoperative scoring framework. This system supports targeted treatment selection and provides valuable clinical guidance [9]. Accordingly, the ASTLOF classification was adopted as the standard in this study.

Computed tomography (CT) imaging, with its high spatial resolution, allows for detailed observation of subtle changes in vertebral endplates, cortical bone, and cancellous bone, providing a more reliable basis for OVF classification and clinical guidance [10]. Currently, CT equipment is widely available in secondary and tertiary hospitals, and some community hospitals have also introduced CT systems [11]. CT imaging is crucial for accurately classifying OVFs and has substantial clinical importance. Radiomics aids in analyzing trabecular bone microstructure [12], assessing BMD [13], differentiating acute from chronic OVFs [14], and predicting residual back pain in these patients [15]. Deep learning radiomics (DLR) uses network architectures such as ResNet, pretrained on ImageNet, to extract deep imaging features from images, a widely adopted approach. RadImageNet, as an open-access, public medical imaging dataset, theoretically provides better performance for deep transfer learning (DTL) in medical imaging tasks compared to ImageNet [16]. Our research team has preliminarily validated this hypothesis [17]. However, whether it can improve the performance of 3-class prediction models still requires further exploration and verification.

In this study, we used thoracolumbar medical imaging data from multiple health care centers. We applied DTL on both RadImageNet and ImageNet datasets to extract DTL features and also used the open-source PyRadiomics package (developed by the Computational Imaging & Bioinformatics Lab, Brigham and Women's Hospital/Harvard Medical School; lead developer: Joost J. M. van Griethuysen) to extract traditional radiomics features. We developed a predictive model for OVF classification using CT imaging by integrating and selecting DTL and radiomics features within the ASTLOF system. The model was validated, tested, and compared for its predictive performance using multicenter data.

Methods

Patient Selection

This study used medical imaging data from 3 Chinese hospitals, with ethics committee approval from each institution. The retrospective study design negated the need for informed patient consent. CT and MRI data from patients diagnosed with OVFs at Center I (Taizhou People's Hospital, Nanjing Medical University) and Center II (Affiliated Hospital of Nanjing University of Chinese Medicine) between December 2018 and December 2024 were used to create the training, internal validation, and external validation datasets. Textbox 1 shows the inclusion criteria and exclusion criteria. An independent test dataset was acquired from Center III (Sir Run Run Hospital, Nanjing Medical University) spanning January to December 2024. The dataset's inclusion and exclusion criteria matched those of the training and validation datasets.

Figures 1 and 2 provide detailed information on case collection, grouping, image preprocessing, feature extraction, analysis, and model development through flowcharts and the DLR workflow.

Textbox 1.

Inclusion criteria

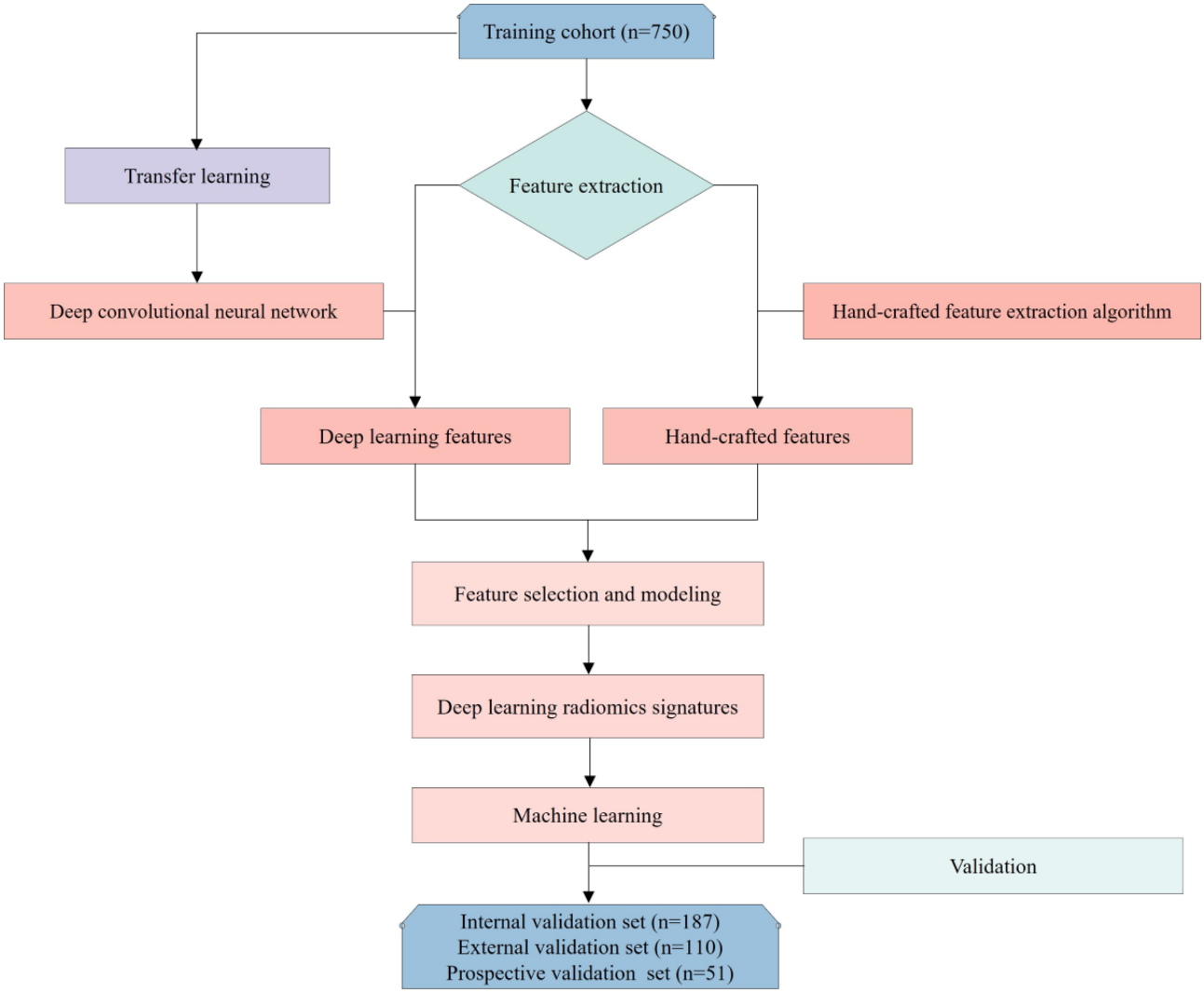
- Patients aged ≥50 years, meeting osteoporotic vertebral fracture diagnostic criteria [18], with no trauma history or only minor trauma.
- Complete computed tomography and magnetic resonance imaging DICOM data, with no more than a 2-week interval between the 2 scans.
- Comprehensive clinical records encompassing gender, age, and dual-energy X-ray absorptiometry outcomes.
- Clinical presentations, such as absence of significant pain, back pain triggered by posture, persistent pain, or neurological symptoms.

Exclusion criteria

- Suspected infections or pathological fractures related to tumors.
- Poor image quality or artifacts caused by foreign objects.
- Uncertain osteoporotic vertebral fracture classification.

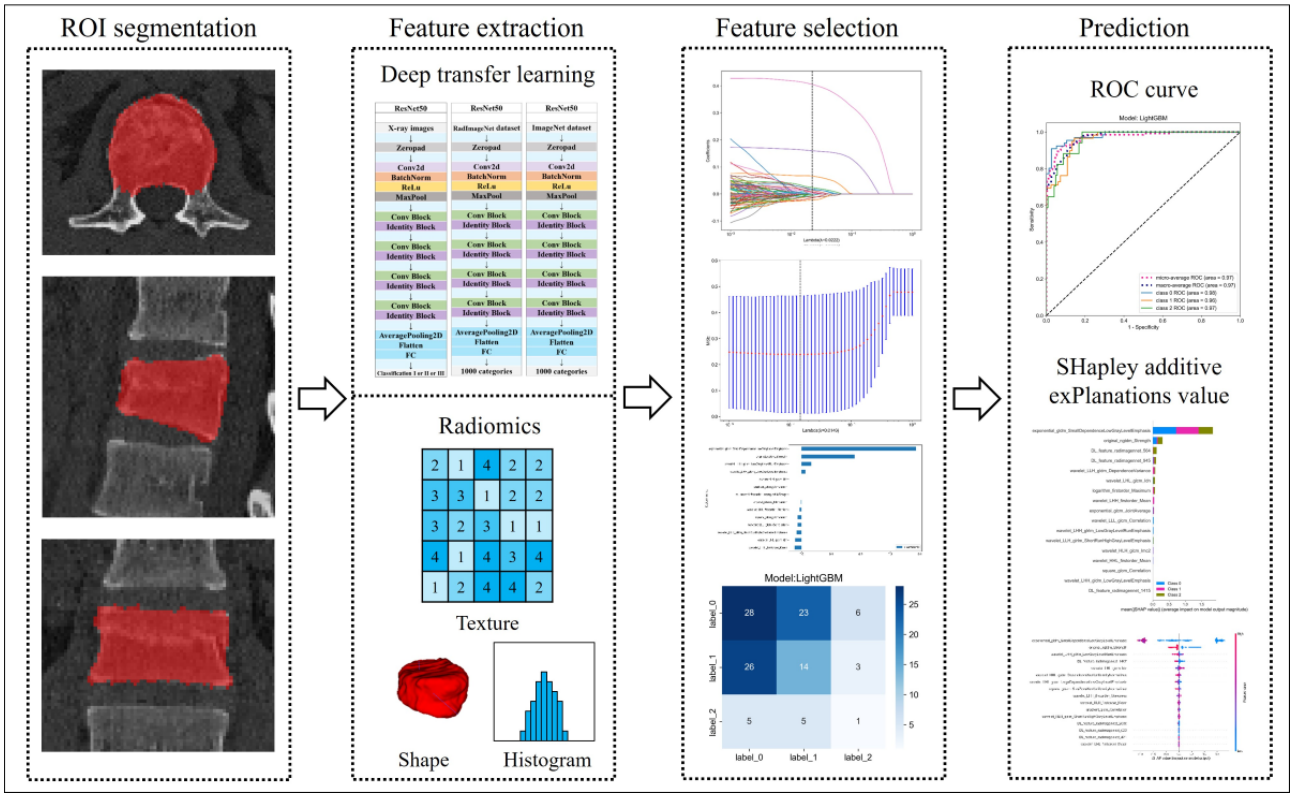
XSL•FO
RenderX

Figure 1. The flowchart in this study outlines the key steps and processes involved in the research workflow.



XSL•FO
RenderX

Figure 2. The workflow of the deep learning radiomics process illustrates the systematic steps involved in data processing, feature extraction, model development, and validation. ROC: receiver operating characteristic; ROI: region of interest.



CT and MRI Acquisition Protocol

CT Scans

CT scans were performed across 3 centers using multidetector or dual-source CT systems, including: GE Lightspeed Ultra (16-slice, USA), Siemens Somatom Definition (128-slice and 256-slice, Germany), Siemens Sensation64 (64-slice, Germany), Philips Brilliance iCT (256-slice, Netherlands), GE Optima CT670 (64-slice, USA). Key scan parameters were: tube voltage 120 kVp (with or without automated current modulation), tube current 118 - 320 mA (with or without automated current modulation), and image matrix 512×512, and layer thickness and interval 1 mm.

MRI Scans

MRI examinations were conducted on 3.0T scanners from Siemens (Verio, Skyra, and Prisma), Philips (Ingenia CX and Achieva TX), across the 3 centers. Image sequences included short tau inversion recovery (STIR) and T2-weighted fat-suppressed images. All patients underwent STIR or T2-weighted fat-suppressed MRI scans. Additional details regarding the imaging devices and parameters for both CT and MRI are available in Multimedia Appendix 1.

Classification

The ASTLOF system classifies OVFs by assigning scores based on vertebral morphology, MRI findings, BMD, and clinical symptoms. Changes in morphology seen in CT or MRI scans are rated as normal (0 points), compression (1 point), or burst fracture (2 points). MRI assessments use sagittal T2-weighted fat-suppressed or STIR sequences, assigning scores based on normal appearance (0 points), high signal alterations (1 point), or the presence of vacuum or fluid signs within vertebrae (2 points). BMD is assessed via T-scores, with values >−2.5 scoring 0, between −2.5 and −3.5 scoring 1, and ≤−3.5 scoring 2. Clinical symptoms are categorized as no significant pain (0 points), positional low back pain (1 point), or persistent pain or neurological symptoms (2 points). No significant pain refers to an absence of discomfort during daily activities, while positional low back pain is triggered by specific postures such as prolonged standing, sitting, or bending. Persistent pain is continuous and unrelieved by rest or posture changes, while neurological symptoms indicate nerve involvement, manifesting as numbness, tingling, or muscle weakness in the lower limbs. OVFs are classified based on total scores: Class 0 (≤3) for conservative treatment, Class 1 (=4) for either conservative or surgical treatment, and Class 2 (≥5) for surgical intervention. Evaluation scores were independently determined by 2 musculoskeletal radiologists (Doctor A with 6 years of experience and Doctor B with 10 years of experience), with disagreements resolved through discussion and consensus.

Clinical and CT Images Evaluation

Patient information, including age, gender, dual-energy X-ray absorptiometry (DXA)-measured T-scores, and treatment details, was obtained from the clinical case management system. CT images were obtained using a bone window setting (width 1500 and level 500) and reconstructed with a 1-mm slice thickness for subsequent processing and analysis.

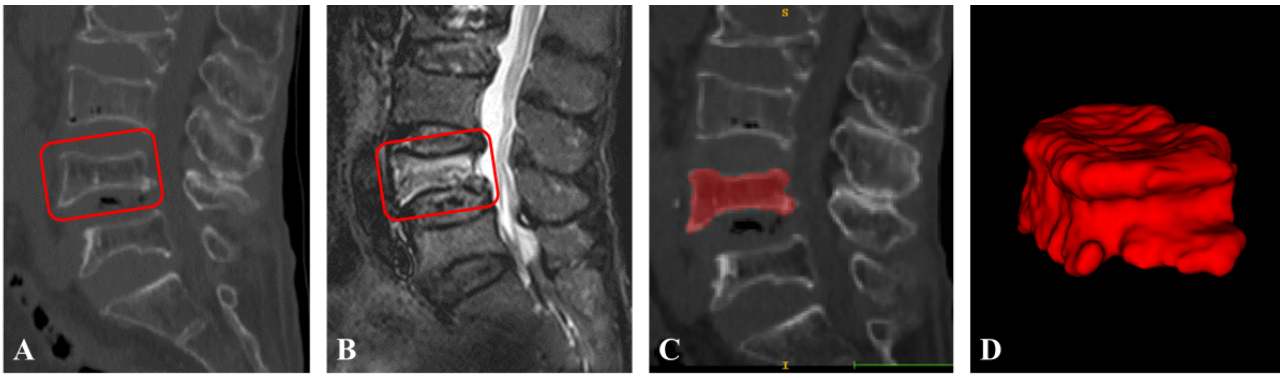
Region of Interest Segmentation

Radiologists manually segmented fractured vertebrae using ITK-SNAP software (version 3.8.0; developed by the Penn Image Computing and Science Laboratory, University of

XSL•FO
RenderX

Pennsylvania; lead developer: Paul A. Yushkevich) in this study. Radiologist A outlined and filled the edges of the fractured vertebrae on the CT images to create regions of interest, carefully excluding adjacent intervertebral discs, pedicles, and surrounding tissues to ensure precise delineation. The segmented masks were then saved as "nii" files for further analysis (Figure 3). Interobserver agreement was evaluated by having Radiologist A and Radiologist B independently resegment a random subset of 30 patients from the training dataset after 1 month, using the intraclass correlation coefficient (ICC) for assessment.

Figure 3. Segmentation of a fractured vertebral body for radiomic analysis in an 82-year-old woman with an acute osteoporotic vertebral fracture is illustrated.(**A**) Sagittal non–contrast-enhanced spine computed tomography images show an osteoporotic vertebral fracture of L4. (**B**) Sagittal T2-weighted fat-suppressed imaging reveals hyperintensity associated with the acute vertebral fracture. (**C**) The region of interest is delineated on sagittal computed tomography images. (**D**) Three-dimensional volume meshes are reconstructed to visualize the segmentation.



Radiomics and DTL Features Extraction

All images were resampled using B-spline interpolation and standardized with Z-score normalization to reduce variability across centers. Feature extraction algorithms were standardized in accordance with the Image Biomarker Standardization Initiative [19]. Radiomic features, encompassing first-order, shape, and texture characteristics, were extracted using the open-source Python package PyRadiomics (developed by the Computational Imaging & Bioinformatics Lab, Brigham and Women's Hospital/Harvard Medical School; lead developer: Joost J. M. van Griethuysen) [20]. These texture features include the gray level co-occurrence matrix, gray level size zone matrix, gray level run length matrix, neighboring gray tone difference matrix, and gray level dependence matrix. For comprehensive details on the extracted features, refer to the PyRadiomics documentation [21]. To minimize variations across centers, the Combat method was applied for feature harmonization [22]. To mitigate bias and minimize overfitting risks from excessive features, a 2-step feature selection process was implemented: initially, features demonstrating strong reliability were retained using ICC evaluation, followed by further selection through the Least Absolute Shrinkage and Selection Operator (LASSO) algorithm.

Transfer learning is used because retraining a convolutional neural network for a specific task demands extensive image data and intricate parameter configurations, which are challenging to obtain in this study. Transfer learning involves fine-tuning a pretrained deep learning network to adapt it for a new task, allowing deep learning to be applied effectively on smaller datasets. Images were resampled to 64×64 (as is common practice in deep learning pipelines) and pixel intensities normalized to a mean of 0 and SD of 1. We acknowledge that resampling to 64×64 may lead to some loss of spatial detail. However, we chose this size after preliminary experiments demonstrated that it retained sufficient image features for accurate classification, while balancing computational efficiency and memory requirements. The DTL approach, akin to previous studies [23], was implemented using the Python 3.6-based deep learning library (Guido van Rossum), PyTorch. The study used ResNet50 as the foundational model (Multimedia Appendices 2 and 3).

To execute transfer learning effectively, the learning rate was carefully configured. Features were extracted from the model's penultimate layer (AveragePooling), with model parameters divided into backbone and task-specific components. The backbone component used pretrained parameters from RadImageNet [24] or ImageNet for initialization, whereas the task-specific component was initialized randomly. Drawing inspiration from the cosine annealing learning rate decay algorithm, optimizations were implemented by fine-tuning the backbone component with pretrained weights only when essential to maintain transfer learning quality. Concurrently, task-specific parameters were modified according to task demands, enabling the model to effectively adapt to the target data.

Data Dimensionality Reduction

To identify reproducible and nonredundant radiomic features, a systematic process was implemented. First, features with ICC ≥0.8 from 2 independent evaluations were retained for reproducibility [25]. Redundancy was minimized by computing the Spearman rank correlation coefficient between features. Features with a correlation above 0.9 were subjected to a greedy recursive elimination strategy to remove the most redundant ones, ensuring overall representation was maintained. Stable features were then selected using the LASSO algorithm, which applies a penalty parameter (λ) to shrink regression coefficients, retaining only relevant features. The optimal λ value was determined through 10-fold cross-validation, and features with nonzero coefficients were selected for the final set. To further reduce redundancy, correlated features with a coefficient greater than 0.5 were excluded, resulting in a refined subset of independent features. For DTL features (initially with a

XSL•FO
RenderX

dimension of 2048), principal component analysis was applied to reduce dimensionality, balancing deep learning and radiomic features while mitigating overfitting. The chosen radiomic and deep learning features were combined through early fusion to create a unified feature set, with all features standardized using Z-score normalization for compatibility. Finally, after fusion, LASSO-Cox regression was applied to select the most robust features, which were further refined through dimensionality reduction to define an optimal subset. This carefully curated feature set represented the most relevant combination of radiomic and deep learning features, facilitating reliable model development.

Model Development

To prevent data leakage, all features used for building the predictive model were exclusively derived from the training set. Machine learning models were implemented using the scikit-learn library following feature selection and fusion. The models comprised logistic regression (LR), support vector machine (SVM), k-nearest neighbor (KNN), decision tree (DT), random forest (RF), extremely randomized trees (ExtraTrees), eXtreme gradient boosting (XGBoost), Light Gradient Boosting Machine (LightGBM), and multilayer perceptron (MLP). We observed an imbalance in the distribution of samples among the ASTLOF classification categories, with notably fewer cases in Class 2. To reduce the risk of biased model performance, we apply strategies such as class weighting during model training. Model training was conducted using the training set and optimized through grid search with adjustable parameters specific to each algorithm. Model performance was assessed using 5-fold cross-validation on the training data, selecting the best parameters to construct the optimal fused-feature model. Using a larger k (such as 10 or more) would have increased computational cost and training time substantially, without necessarily providing a significant improvement in model assessment, especially given the size of our dataset. Therefore, 5-fold cross-validation was appropriate for our study while maintaining a reasonable balance between thoroughness and practicality. The receiver operating characteristic (ROC) curve was plotted, and model accuracy was validated through 1000 iterations of bootstrap resampling. Performance metrics such as area under the curve (AUC), accuracy (ACC), sensitivity (SEN), and specificity (SPE) were evaluated. Finally, statistically significant clinical baseline characteristics were integrated with the best fused feature model to develop a combined model, which was visualized through a nomogram.

This study used the "One-vs-Rest" (OvR) strategy for multiclass tasks by decomposing the problem into several binary classification tasks. When Class 0 was labeled positive, Classes 1 and 2 were negative; similarly, labeling Class 1 or 2 as positive made the others negative, creating 3 OvR classification models. Model performance was assessed by plotting ROC curves and calculating metrics including AUC, ACC, SEN, and SPE. The generalization ability was evaluated using internal, external validation, and test datasets. Macro- and micro-average AUC were used for a thorough assessment of multiclass tasks [26]. Macro-average AUC computes the AUC for each class and averages them equally, which can be less representative in cases of significant class imbalance. Conversely, micro-average AUC aggregates predictions from all classes into a single confusion matrix, emphasizing the influence of larger sample sizes and providing a better reflection of overall performance on imbalanced datasets.

Data Analysis

Statistical analyses were conducted using R software (R Core Team; version 4.0.3), and radiomics and deep learning models were developed and implemented on Python 3.7 (Python Software Foundation). Continuous variables are presented as mean (SD), while categorical variables are shown as counts or percentages. Independent samples *t* tests were used to assess differences in continuous variables, while chi-square tests were applied for comparisons of categorical variables. The DeLong test was used to compare ROC curves and assess the predictive models' overall performance. In addition, bootstrap validation with 1000 resamples was conducted to ensure robust evaluation of model accuracy. $P<.05$ was considered statistically significant, serving as a benchmark for assessing the reliability of observed differences and associations. These comprehensive statistical methods ensured the rigor of model evaluation and the clarity of results interpretation.

Explainable Artificial Intelligence

The Shapley Additive Explanations (SHAP) method (GitHub, Inc [27]) was used to assess the importance of various features by calculating their contributions to prediction outcomes, offering a clear explanation of their significance [28]. Using SHAP values, the predictive output for each sample is decomposed into individual feature contributions, providing a quantifiable measure of feature influence. The magnitude of a SHAP value indicates the extent of a feature's influence on the model's prediction, where positive values signify a positive impact and negative values signify a negative impact. For example, in a disease prediction model, a feature with a SHAP value greater than 0 suggests it increases the predicted likelihood of disease occurrence, whereas a value below 0 implies a reduced likelihood. Beyond individual predictions, SHAP also ranks features by their overall importance across the model and reveals the relationships between features and prediction outcomes. This integration of quantitative contribution, directional influence, and feature importance ranking facilitates a comprehensive understanding of the model's decision-making, revealing how particular features influence predictions and their significance.

Ethical Considerations

This study comprised a retrospective component and a prospective validation cohort. For the retrospective component, the local Ethics Committees of the Affiliated Hospital of Nanjing University of Chinese Medicine and the Affiliated Taizhou People's Hospital of Nanjing Medical University waived the requirement for ethical approval and informed consent because the analysis involved existing data collected during routine clinical care and posed minimal risk to participants. The prospective validation cohort was approved by the Institutional Ethics Committee of Sir Run Run Hospital, Nanjing Medical University, on November 25, 2023 (approval no. 2023-SR-055). All participants in the prospective cohort provided written

XSL•FO
RenderX

informed consent before enrollment. To protect privacy, all images and relevant data were deidentified prior to analysis and reporting. No individually identifiable information was used. Participants did not receive financial or other material compensation for participation. The study was conducted in accordance with the principles of the Declaration of Helsinki and relevant institutional guidelines and regulations.

Results

Clinical Features of the Studied Patients

The study enrolled 981 patients aged 50 to 95 years, with an average age of 69.56 (9.88) years. Of these, 687 were females (70%) and 294 were males (30%). Based on T-scores, 30 patients (3.1%) were classified as having normal bone mass, 257 (26.2%) as having low bone mass, and 694 (70.7%) as having osteoporosis. Among the participants, 87 patients presented with 2 OVFs, and 15 patients had 3 OVFs, resulting in a total of 1098 fractured vertebrae included in the analysis. The dataset was partitioned into a training set (750 cases, 68.4%), an internal validation set (187 cases, 17%), an external validation set (110 cases, 10%), and a prospective validation set (51 cases, 4.6%). Table 1 summarizes the demographic and clinical characteristics of each dataset, and Table 2 details the treatment conditions across the 3 classifications. Figure 4 illustrates the case selection process, emphasizing the random 8:2 allocation of cases into the training and internal validation sets.

Table . Baseline characteristics of patients with osteoporotic vertebral fracture in the training, internal and external validation, and prospective validation cohorts.

Characteristics	Training set (n=750)	Interval validation set (n=187)	External validation set (n=110)	Prospective validation set (n=51)
Sex, n (%)				
Female	541 (72.1)	138 (73.8)	78 (70.9)	36 (70.6)
Male	209 (27.9)	49 (26.2)	32 (29.1)	15 (29.4)
Age (years)				
Mean (SD)	68.25 (11.18)	70.19 (10.56)	69.56 (10.23)	69.51 (10.32)
DXA[a] T-score				
Mean (SD)	−2.82 (0.82)	−2.79 (0.81)	−2.85 (0.75)	−2.83 (0.77)
Fracture location, n (%)				
Thoracic	247 (32.9)	52 (27.8)	32 (29.1)	17 (33.3)
Lumbar	503 (67.1)	135 (72.2)	78 (70.9)	34 (66.7)
Fracture staging, n (%)				
Acute	492 (65.6)	112 (59.9)	69 (62.7)	33 (64.7)
Chronic	258 (34.4)	75 (40.1)	41 (37.3)	18 (35.3)
ASTLOF[b] score, n (%)				
1 - 3 points	345 (46.0)	88 (47.1)	51 (46.4)	24 (47.1)
4 points	338 (45.1)	76 (40.6)	46 (41.8)	22 (43.1)
5 - 8 points	67 (8.9)	23 (12.3)	13 (11.8)	5 (9.8)
Therapeutic method, n (%)				
Conservative treatment	435 (58)	106 (56.7)	62 (56.3)	28 (54.9)
PVA[c]	258 (34.4)	73 (39)	40 (36.4)	19 (37.3)
Open surgery	57 (7.6)	8 (4.3)	8 (7.3)	4 (7.8)

[a]DXA: dual-energy X-ray absorptiometry.

[b]ASTLOF: Assessment System of Thoracolumbar Osteoporotic Fracture.

[c]PVA: percutaneous vertebral augmentation.

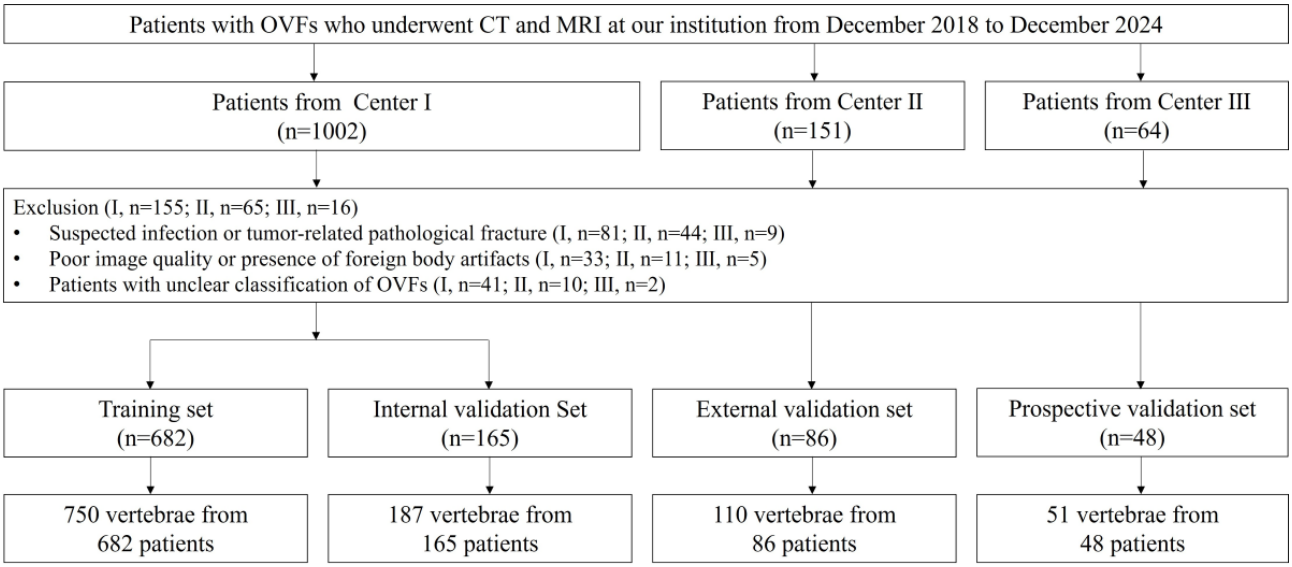
XSL•FO
RenderX

Table . Distribution of osteoporotic vertebral fractures based on the Assessment System of Thoracolumbar Osteoporotic Fractures classification and their association with different therapeutic methods.

Classification	Conservative treatment (n=631, %)	PVA[a] (n=390, %)	Open surgery (n=77, %)
Class 0 (1-3 points)	411 (80.9)	71 (14)	26 (5.1)
Class 1 (4 points)	162 (33.6)	289 (60)	31 (6.4)
Class 2 (5-8 points)	58 (53.7)	30 (27.8)	20 (18.5)

[a]PVA, percutaneous vertebral augmentation.

Figure 4. The flowchart summarizes patient selection and allocation to the training set, internal and external validation set, and prospective validation set of the multicenter study. CT: computed tomography; MRI: magnetic resonance imaging; OVFs: osteoporotic vertebral fractures.



Radiomics Feature Selection (RadImageNet-Based)

The LASSO-Cox regression analysis model was used to perform dimensionality reduction on the fused features. The penalty coefficient (λ=0.0031) was chosen to optimize feature selection, with Multimedia Appendix 4 depicting the changes in feature coefficients as λ varied. Following the final feature selection, 17 radiomics features and 16 DTL features were retained. The DTL_Radscore was constructed using the fused features and their regression coefficients, as shown in Multimedia Appendix 5.

Radiomics Feature Selection (ImageNet-Based)

The LASSO-Cox regression model, with a penalty coefficient of λ=0.0295, was used to optimally select features by reducing the dimensionality of the fused dataset. Multimedia Appendix 6 displays the feature selection process and the curve showing the change in feature coefficients with λ. Following the final selection, 17 radiomics features and 37 DTL features were retained. Using these fused features and their associated regression coefficients, the DTL_Radscore was constructed, as detailed in Multimedia Appendix 7.

Overall Validation of Different Radiomics Models

The optimal machine learning algorithms for fused feature models trained on RadImageNet and ImageNet datasets, based on macro-average AUC, ACC, and F_1-score, were identified as MLP and LightGBM, respectively. Table 3 summarizes the validation results for the 2 fused feature models in the 3-class classification task. In the training set, the DeLong test indicated no statistically significant difference between the 2 fused feature models (0.934 vs 0.996, P=2.34). In the internal, external, and prospective validation sets, the RadImageNet-based fused feature model demonstrated significantly higher macro-average AUC values than the ImageNet-based model (0.837 vs 0.648, 0.773 vs 0.633, and 0.852 vs 0.648, respectively), as confirmed by the DeLong test (P<.05). Figure 5 displays the ROC curves for both models predicting OVF classifications in the prospective validation set. The RadImageNet-based fused feature model, using the binary OvR strategy, excelled in predicting classification 2 with an AUC of 0.907 and an ACC of 0.857. For classifications 0 and 1, the model achieved AUCs and ACCs of 0.829, 0.803 and 0.794, 0.768, respectively. Figure 6 highlights instances where the ImageNet-based fused feature model made incorrect predictions, while the RadImageNet-based model successfully identified the correct classifications.

XSL•FO
RenderX

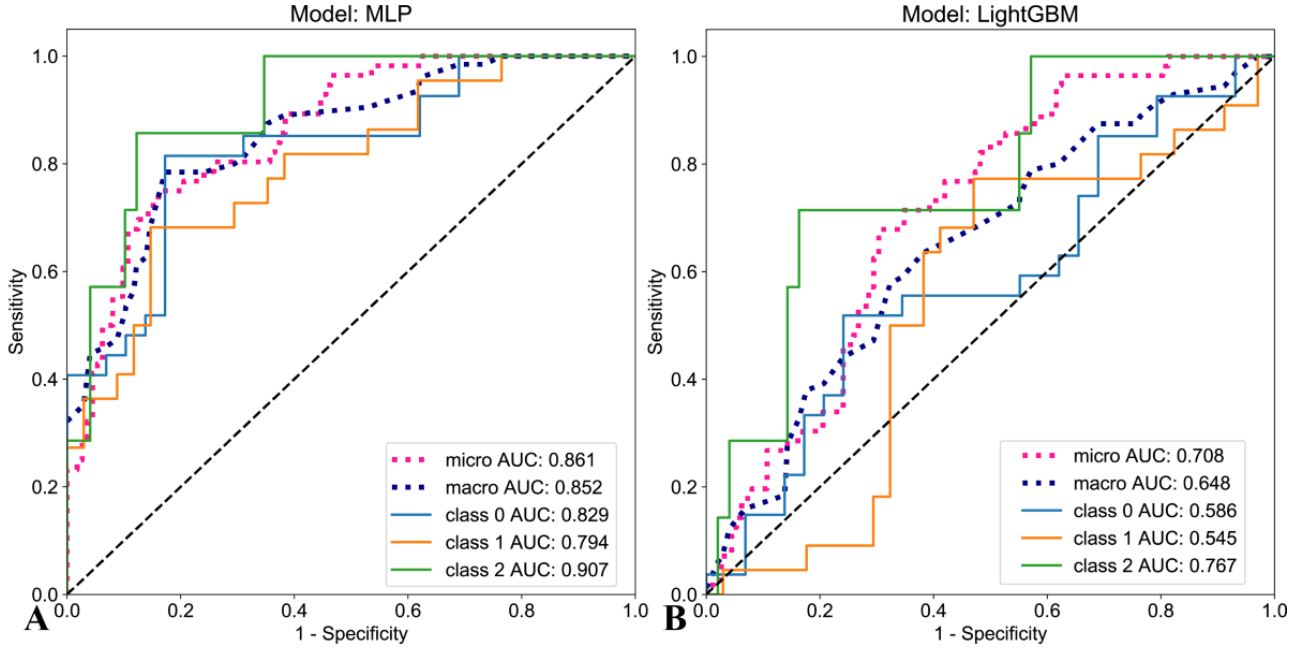
Table . The performance of the models across the training set, internal and external validation sets, and the prospective validation set.

Model	Training set		Interval validation set		External validation set		Prospective validation set	
	Accuracy	AUC[a]	Accuracy	AUC[a]	Accuracy	AUC[a]	Accuracy	AUC[a]
RadImageNet-based								
Class 0	0.867	0.939 (0.924 - 0.955)	0.777	0.834 (0.779 - 0.889)	0.715	0.794 (0.714 - 0.875)	0.803	0.829 (0.719 - 0.938)
Class 1	0.825	0.905 (0.884 - 0.925)	0.726	0.768 (0.700 - 0.836)	0.681	0.747 (0.658 - 0.836)	0.768	0.794 (0.673 - 0.915)
Class 2	0.886	0.953 (0.934 - 0.973)	0.746	0.898 (0.839 - 0.957)	0.767	0.756 (0.593 - 0.920)	0.857	0.907 (0.805 - 0.999)
Three classifications[b]	0.793	0.934 (0.914 - 0.951)	0.660	0.837 (0.773 - 0.894)	0.647	0.773 (0.655 - 0.877)	0.732	0.852 (0.732 - 0.951)
ImageNet-based								
Class 0	0.969	0.995 (0.992 - 0.997)	0.619	0.619 (0.540 - 0.698)	0.655	0.675 (0.576 - 0.774)	0.625	0.586 (0.433 - 0.739)
Class 1	0.964	0.996 (0.994 - 0.999)	0.624	0.576 (0.488 - 0.664)	0.560	0.551 (0.445 - 0.656)	0.607	0.545 (0.385 - 0.705)
Class 2	0.952	0.995 (0.993 - 0.999)	0.756	0.737 (0.631 - 0.843)	0.621	0.654 (0.480 - 0.827)	0.803	0.767 (0.580 - 0.953)
Three classifications[b]	0.916	0.996 (0.993 - 0.998)	0.533	0.648 (0.553 - 0.735)	0.551	0.633 (0.501 - 0.753)	0.429	0.648 (0.466 - 0.799)

[a]Data in parentheses are 95% CIs.

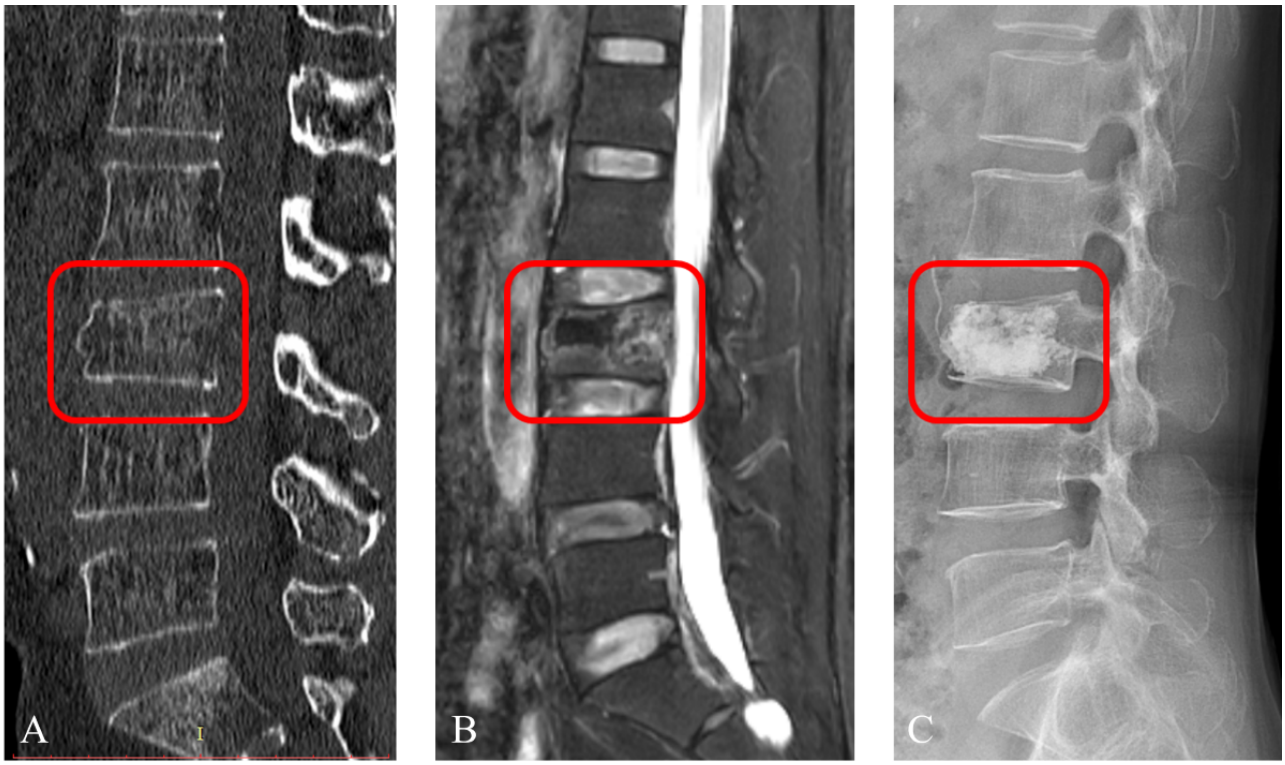
[b]Date are macro-average.

Figure 5. The receiver operating characteristic curves for the predictive performance of the 2 models (A. RadImageNet, B. ImageNet). AUC: area under the curve; MLP: multilayer perceptron; LightGBM: Light Gradient Boosting Machine.



XSL•FO
RenderX

Figure 6. A case from the prospective validation cohort involves a 60-year-old female patient with osteoporotic vertebral fractures and an Assessment System of Thoracolumbar Osteoporotic Fractures score of 6. It was misclassified by the ImageNet model, but was correctly classified by the RadImageNet model. (**A**) Computed tomography imaging; (**B**) MRI imaging; (**C**) Postpercutaneous vertebroplasty showing bone cement leakage.

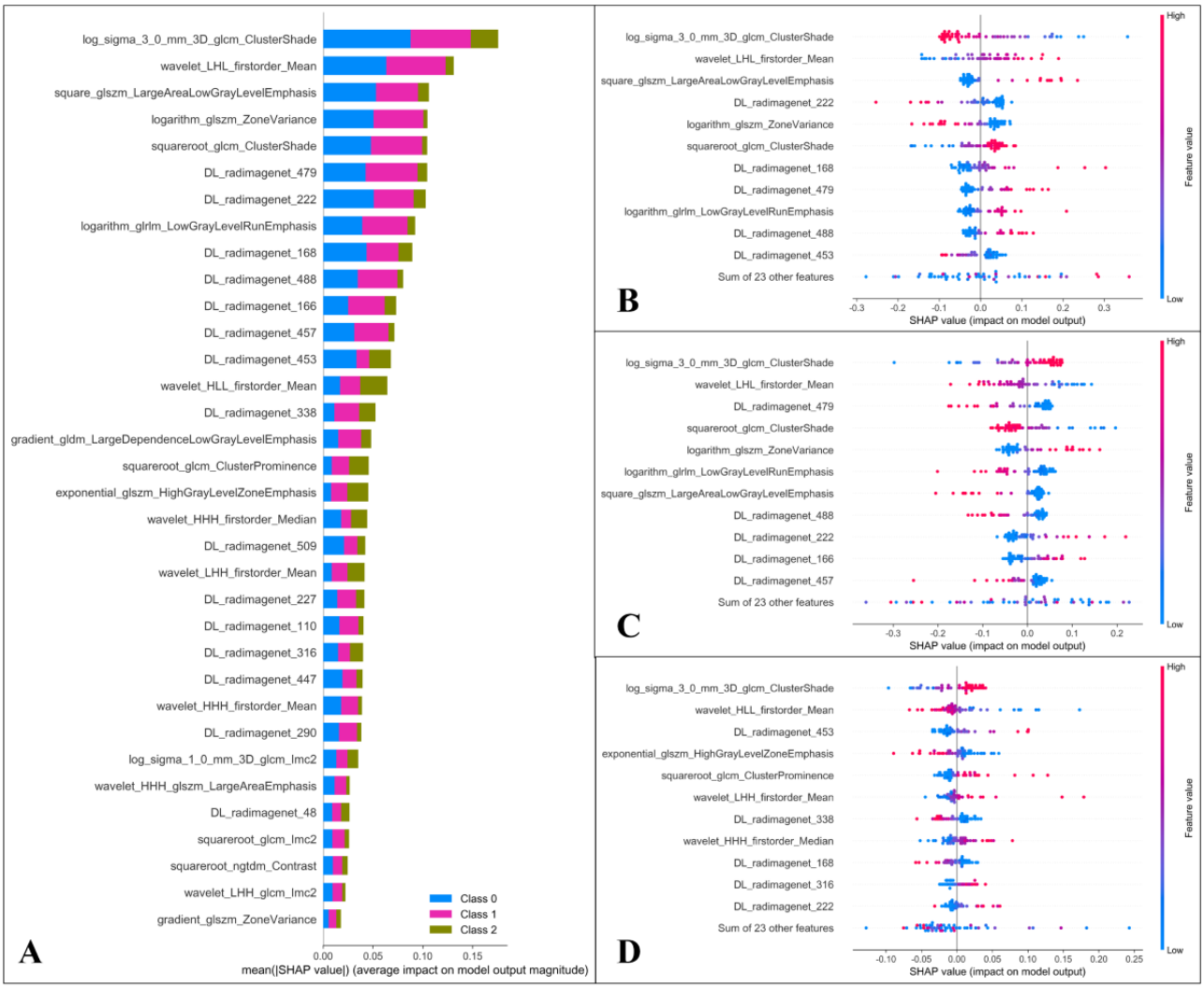


Feature Contribution and Model Interpretation

The SHAP value for each feature was calculated. Figure 7 presents the global SHAP values for both the overall 3-class classification and each specific class, evaluating their impact on the model's predictions. The highest-ranked features were cluster shade, mean, and large area low gray level emphasis. Figure 8 presents the SHAP decision plot, illustrating the prediction model's workflow in classifying Class 0 (male, 65 years; ASTLOF 2 points), Class 1 (female, 72 years; ASTLOF 4 points), and Class 2 (female, 68 years; ASTLOF 6 points) within the prospective validation set.

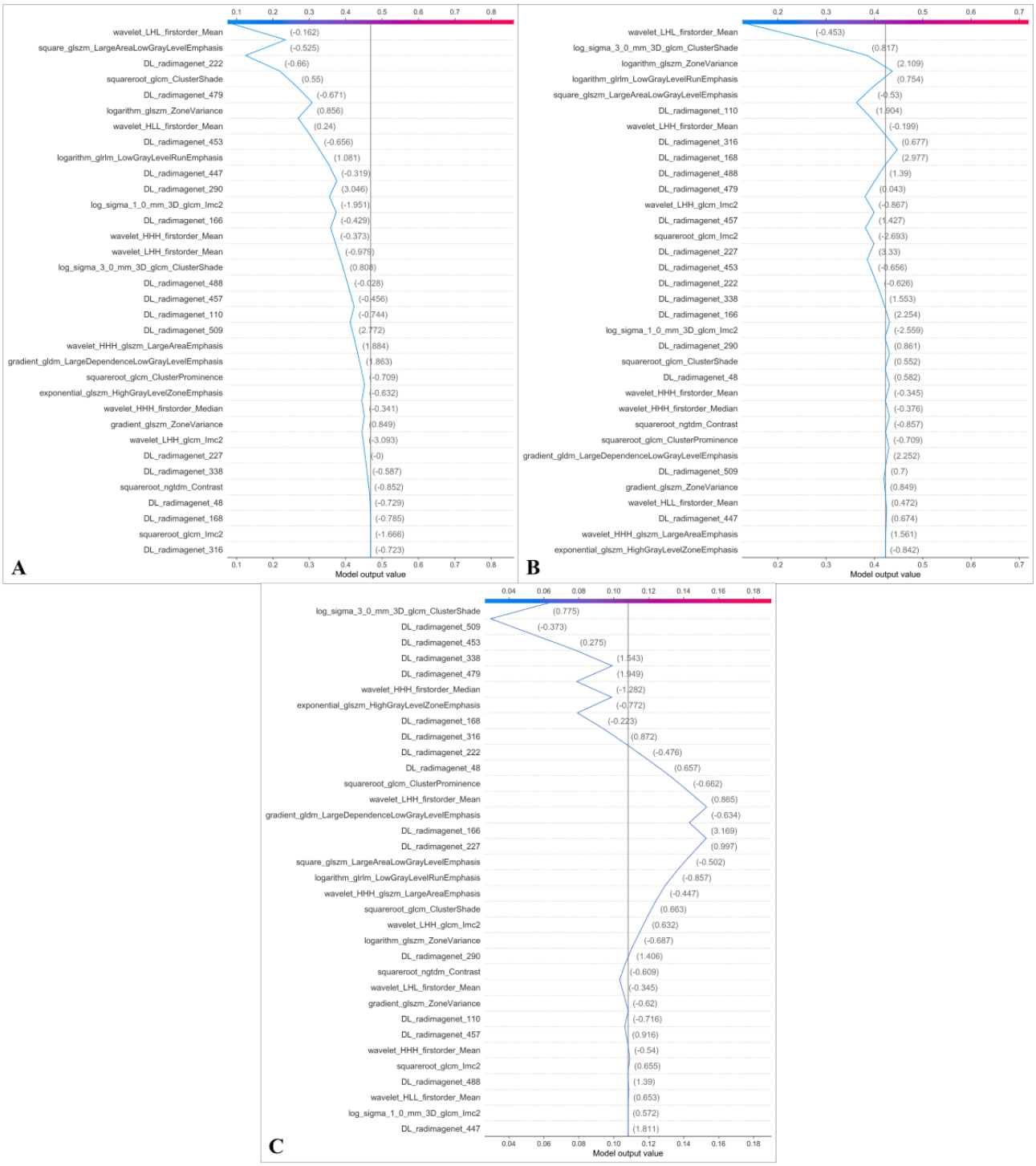
XSL•FO
RenderX

Figure 7. The feature contributions of the optimal fusion model are visualized as follows: The y-axis displays features arranged in descending order based on their mean absolute impact on the predictive model. The Shapley Additive Explanations (SHAP) value of a specific feature is represented by its distance from x=0, where a greater distance signifies a stronger impact—either positive or negative—on the model's output. Each point's color corresponds to the original value of that feature, transitioning from low (blue) to high (magenta) on the color scale. (**A**) The global feature contribution bar chart illustrates the contributions for the 3-class classification, with blue, red, and dark green bars indicating classifications 0, 1, and 2, respectively. (**B, C, D**) Beehive summary plots depict the decreasing feature contributions for predictions corresponding to classifications 0, 1, and 2, respectively.



XSL•FO
RenderX

Figure 8. Shapley Additive Explanation (SHAP) decision plots for the 3 classifications (A: Class 0, B: Class 1, C: Class 2) are presented. The x-axis represents the model output, while the y-axis lists the feature names. The gray vertical line at the center shows the baseline value. Each line traces the prediction process, starting from the baseline value and incorporating the contributions of various features, both positive and negative, to arrive at the final model output. For classification 0, the baseline value is 0.468, with a final model output of 0.090. For classification 1, the baseline value is 0.423, with a final model output of 0.138. For classification 2, the baseline value is 0.108, with a final model output of 0.062.



Discussion

Principal Findings

This study developed and validated a DLR model based on CT imaging data from multiple medical centers for the classification of OVFs according to the ASTLOF system. By integrating radiomics and DTL features extracted from both RadImageNet and ImageNet datasets, the fused model—especially when using RadImageNet pretraining—demonstrated superior predictive performance across internal, external, and prospective validation cohorts. The model achieved the highest accuracy in identifying Class 2, with SHAP analysis indicating that features such as cluster shade, mean, and large area low gray level emphasis played the most significant roles in prediction. These findings highlight the model's robustness and generalizability, supporting its potential utility in guiding clinical decision-making for OVF classification and treatment planning.

XSL•FO
RenderX

Study Implications

Compared with obvious traumatic vertebral fractures, OVFs are an insidious condition and are often misdiagnosed. Improper treatment can affect spinal stability and balance, and in severe cases, lead to neurological dysfunction and increased risk of mortality [29]. A scientific classification of OVFs is the prerequisite for appropriate treatment. However, existing classification methods are primarily based on classification systems for early thoracolumbar fractures (which do not differentiate between traumatic and osteoporotic vertebral fractures), resulting in confusion in the treatment of OVFs [30]. These methods fail to adequately consider the characteristics of osteoporotic vertebrae, are overly complex, and lack widely accepted unified standards. Some even overly emphasize surgical treatment. A systematic classification of OVFs is crucial for assessing fracture risk, guiding treatment decisions, and forecasting patient outcomes [31]. An ideal classification system for OVFs should encompass several essential features to ensure comprehensive and practical utility. First, it should integrate imaging parameters from X-rays, CT, and MRI, enabling a thorough multiperspective assessment of the fractures. Second, it must incorporate patients' clinical presentations, such as lower back pain and neurological symptoms, to provide a holistic understanding of the condition. Third, the system should offer treatment guidance tailored to each classification type, facilitating targeted clinical interventions. Fourth, it is essential that the system demonstrates high reliability and reproducibility, ensuring consistent application across different clinical settings. Finally, it should effectively evaluate the severity of the condition and provide prognostic insights based on classification outcomes. The ASTLOF classification system provides a thorough framework for evaluation by integrating vertebral morphology, MRI signal characteristics, BMD, and clinical symptoms. Through its scoring system, it enables clinicians to select targeted treatment plans, streamlining clinical workflows while delivering significant clinical guidance. Furthermore, existing studies have validated the system's high consistency and reproducibility, reinforcing its effectiveness in guiding clinical treatment decisions.

Recent advancements in artificial intelligence have shifted OVF classification research toward detection, with studies showing that deep learning and radiomics methods significantly surpass traditional visual analysis approaches [32]. Most current research on OVF classification detection primarily uses single-center data split into training and validation sets for internal validation. This method is constrained by significant variability in radiomics analysis results due to differences in imaging techniques, postprocessing, reconstruction workflows, and scanning parameters across devices from various manufacturers [33]. In addition, single-center studies often lack data heterogeneity, increasing the risk of overfitting and reducing the generalizability of the findings. By contrast, multicenter studies leverage diverse imaging data, and predictive models validated using independent external datasets better account for the heterogeneity of OVFs, offering results that are more aligned with the principles of precision medicine. Our study's strength is the use of CT imaging data from various hospitals combined with the ASTLOF classification system. A fused predictive model integrating radiomics and DTL features was developed using datasets such as RadImageNet and ImageNet. The model was thoroughly evaluated for its predictive performance in OVF classifications, offering a robust and generalizable framework for clinical application.

Studies indicate that the RadImageNet dataset notably improves DTL performance in medical applications, offering superior generalization over conventional datasets [34]. Our study's findings confirmed that prediction models using the RadImageNet dataset surpassed those using the ImageNet dataset. In situations where sample sizes are imbalanced, the "OvR" strategy is commonly used for 3-class classification tasks [35]. In this study, the use of the "OvR" strategy in prediction models for CT images proved to be highly effective. Notably, classification 2, despite having a smaller sample size, was identified with the highest accuracy. The enhanced spatial and density resolution of CT images enables prediction models to more effectively identify radiomic and DTL features. These results highlight the potential of leveraging high-resolution imaging data and advanced datasets such as RadImageNet to achieve robust and accurate predictions, even under the challenge of imbalanced samples.

Comparison to Prior Work

Finally, our study used SHAP values to evaluate the importance of features. SHAP values indicate the positive or negative contributions of each predictive variable to the target variable [36]. Based on game theory, SHAP is a classical post hoc explanation framework used to analyze typically incomprehensible black box models. Aggregating SHAP values across features offers a comprehensive view of each feature's impact on the model's predictions, clearly explaining the decision-making process. In this study, the feature with the highest contribution in CT images was cluster shade, which measures the skewness and asymmetry of the intensity distribution of grayscale in an image. It is inversely proportional to the number of asymmetric densities in the image. High skewness in the co-occurrence matrix results in lower cluster shade values, while smaller cluster shade values suggest greater homogeneity in the distribution of lesions [37]. We hypothesize that a smaller cluster shade value indicates a more homogeneous distribution of lesions within the vertebral body. While our model incorporates SHAP analysis to provide post hoc interpretability, we recognize that the deep learning component remains largely a "black box," which may limit clinician trust and acceptance. We acknowledge the importance of further enhancing the model's explainability—particularly in elucidating how deep features correspond to specific anatomical or pathological findings relevant to ASTLOF classification. In future work, we intend to explore and integrate advanced interpretability techniques such as attention maps, layer-wise relevance propagation, and feature visualization. These methods have the potential to provide more granular and intuitive explanations for the model's predictions, thereby facilitating broader clinical adoption and understanding.

Limitations

Although this study has achieved certain results, it still has some limitations. First, a key limitation of our study is the unequal

XSL•FO
RenderX

distribution of cases among the ASTLOF classifications, particularly the small sample size for Class 2. This class imbalance may affect the statistical power and generalizability of the model for underrepresented classes. Moving forward, we intend to increase the sample size for each class and explore robust solutions such as synthetic oversampling, class weighting, or other augmentation strategies to enhance model performance and clinical applicability across all categories. Second, the lack of interpretability of deep learning features limits its widespread clinical adoption and trust to some extent. Moving forward, strengthening research on the interpretability of deep learning features will be crucial. This will improve model transparency, foster clinician trust, and guide clinical decision-making, thus enhancing the practical application of deep learning in medical imaging diagnosis and treatment planning. Third, our study's dataset was exclusively sourced from Chinese hospitals, which may introduce geographic or ethnic bias, potentially limiting the generalizability of the findings to other regions and populations. Imaging protocols, equipment, and patient demographics may differ significantly across health care systems worldwide. Future work will focus on expanding our dataset with more diverse, multinational samples and performing external validation in independent international cohorts. Such steps are essential for demonstrating the model's robustness and ensuring clinical applicability on a global scale.

Conclusions

Compared to the fusion feature model (ImageNet), the fusion feature model based on CT images (RadImageNet) demonstrated higher predictive performance. Notably, it achieved the best performance in identifying classification 2, followed by classifications 0 and 1. This may have significant clinical value for predicting OVF classifications and guiding the formulation of treatment plans.

Acknowledgments

We express our gratitude to the editor and anonymous reviewers for their insightful comments and suggestions, which have greatly enhanced the quality of our paper. We also extend our thanks to American Journal Experts for their assistance in editing the language of an earlier draft of this manuscript. We appreciate the guidance and support from the PixelmedAI platform and its developers concerning the code used in this revised manuscript. Finally, we thank Dr. Zihan Chen (School of Mathematics and Physics, Xi'an Jiaotong-Liverpool University) for his professional statistical advice. This work was supported by the Medical Scientific Research Project of the Jiangsu Provincial Health Commission (Grant No. M2024055) and the Medical Imaging Artificial Intelligence Special Research Fund Project, Nanjing Medical Association Radiology Branch (Grant No. 16).

Data Availability

The datasets generated or analyzed during this study are not publicly available due to privacy or ethical restrictions, but are available from the corresponding author on reasonable request.

Authors' Contributions

LX and JZ contributed equally as co-corresponding authors.
JL contributed to conceptualization, investigation, resource provision, original draft writing, review and editing of the manuscript, and visualization. LZ contributed to conceptualization, investigation, resource provision, and review and editing of the manuscript. YY contributed to conceptualization, investigation, original draft writing, review and editing of the manuscript, and visualization. JT contributed to conceptualization, methodology, review and editing of the manuscript, and project administration. YL contributed to conceptualization, review and editing of the manuscript, visualization, and supervision. LX contributed to conceptualization, methodology, software development, review and editing of the manuscript, and supervision. JZ contributed to conceptualization, investigation, resource provision, review and editing of the manuscript, visualization, and funding acquisition.

Conflicts of Interest

None declared.

Multimedia Appendix 1
The computed tomography and magnetic resonance imaging acquisition parameters of the 3 centers.
[DOCX File, 19 KB - medinform_v13i1e75665_app1.docx]

Multimedia Appendix 2
A basic architecture of a convolutional neural network.
[PNG File, 2205 KB - medinform_v13i1e75665_app2.png]

Multimedia Appendix 3
Schematic diagram of the deep convolutional neural network pretraining and fine-tuning network structure.
[PNG File, 807 KB - medinform_v13i1e75665_app3.png]

XSL•FO
RenderX

Multimedia Appendix 4
Feature selection was performed using the Least Absolute Shrinkage and Selection Operator (LASSO). Left: Histogram of feature importance scores based on fused features. Right: Curve of feature coefficients varying with λ, with the optimal λ value being 0.0031.
[PNG File, 364 KB - medinform_v13i1e75665_app4.png]

Multimedia Appendix 5
DTL_Radscore: The y-axis represents the selected fused features, while the x-axis represents the correlation coefficients.
[PNG File, 483 KB - medinform_v13i1e75665_app5.png]

Multimedia Appendix 6
Feature selection was performed using the Least Absolute Shrinkage and Selection Operator. Left: Histogram of feature importance scores based on fused features. Right: Curve of feature coefficients varying with λ, with the optimal λ value being 0.0295.
[PNG File, 633 KB - medinform_v13i1e75665_app6.png]

Multimedia Appendix 7
DTL_Radscore: The y-axis represents the selected fused features, while the x-axis represents the correlation coefficients.
[PNG File, 951 KB - medinform_v13i1e75665_app7.png]

References

1. Zeng Q, Li N, Wang Q, et al. The prevalence of osteoporosis in China, a nationwide, multicenter DXA survey. J Bone Miner Res 2019 Oct;34(10):1789-1797. [doi: 10.1002/jbmr.3757] [Medline: 31067339]
2. Skjødt MK, Abrahamsen B. New insights in the pathophysiology, epidemiology, and response to treatment of osteoporotic vertebral fractures. J Clin Endocrinol Metab 2023 Oct 18;108(11):e1175-e1185. [doi: 10.1210/clinem/dgad256] [Medline: 37186550]
3. Schnake KJ, Blattert TR, Hahn P, et al. Classification of osteoporotic thoracolumbar spine fractures: recommendations of the spine section of the German Society for Orthopaedics and Trauma (DGOU). Global Spine J 2018 Sep;8(2 Suppl):46S-49S. [doi: 10.1177/2192568217717972] [Medline: 30210960]
4. Dong Q, Luo G, Lane NE, et al. Deep learning classification of spinal osteoporotic compression fractures on radiographs using an adaptation of the genant semiquantitative criteria. Acad Radiol 2022 Dec;29(12):1819-1832. [doi: 10.1016/j.acra.2022.02.020] [Medline: 35351363]
5. Heini PF. The current treatment--a survey of osteoporotic fracture treatment. Osteoporotic spine fractures: the spine surgeon's perspective. Osteoporos Int 2005 Mar;16 Suppl 2(S02):S85-S92. [doi: 10.1007/s00198-004-1723-1] [Medline: 15365699]
6. Schönrogge M, Lahodski V, Otto R, et al. Inter- and intraobserver reliabilities and critical analysis of the osteoporotic fracture classification of osteoporotic vertebral body fractures. Eur Spine J 2022 Sep;31(9):2431-2438. [doi: 10.1007/s00586-022-07201-2] [Medline: 35378632]
7. Du JP, Fan Y, Liu JJ, et al. The analysis of MSTMOVCF (Multi-segment thoracolumbar mild osteoporotic fractures surgery or conservative treatment) based on ASTLOF (the assessment system of thoracolumbar osteoporotic fracture). Sci Rep 2018 May 29;8(1):8185. [doi: 10.1038/s41598-018-26562-7] [Medline: 29844542]
8. Hao DJ, Yang JS, Tuo Y, et al. Reliability and application of the new morphological classification system for chronic symptomatic osteoporotic thoracolumbar fracture. J Orthop Surg Res 2020 Aug 24;15(1):348. [doi: 10.1186/s13018-020-01882-5] [Medline: 32831125]
9. Du JP, Liu JJ, Fan Y, et al. Surgery for multisegment thoracolumbar mild osteoporotic fractures: revised assessment system of thoracolumbar osteoporotic fracture. World Neurosurg 2018 Jun;114:e969-e975. [doi: 10.1016/j.wneu.2018.03.122] [Medline: 29588238]
10. Rosenberg GS, Cina A, Schiró GR, et al. Artificial intelligence accurately detects traumatic thoracolumbar fractures on sagittal radiographs. Med Bogota Colomb 2022;58(8):998. [doi: 10.3390/medicina58080998]
11. He L, Yu H, Shi L, et al. Equity assessment of the distribution of CT and MRI scanners in China: a panel data analysis. Int J Equity Health 2018 Oct 5;17(1):157. [doi: 10.1186/s12939-018-0869-y] [Medline: 30290807]
12. Muehlematter UJ, Mannil M, Becker AS, et al. Vertebral body insufficiency fractures: detection of vertebrae at risk on standard CT images using texture analysis and machine learning. Eur Radiol 2019 May;29(5):2207-2217. [doi: 10.1007/s00330-018-5846-8] [Medline: 30519934]
13. Liu L, Si M, Ma H, et al. A hierarchical opportunistic screening model for osteoporosis using machine learning applied to clinical data and CT images. BMC Bioinformatics 2022 Feb 10;23(1):63. [doi: 10.1186/s12859-022-04596-z] [Medline: 35144529]
14. Zhang J, Liu J, Liang Z, et al. Differentiation of acute and chronic vertebral compression fractures using conventional CT based on deep transfer learning features and hand-crafted radiomics features. BMC Musculoskelet Disord 2023;24(1):165. [doi: 10.1186/s12891-023-06281-5]

XSL•FO
RenderX

15. Ge C, Chen Z, Lin Y, Zheng Y, Cao P, Chen X. Preoperative prediction of residual back pain after vertebral augmentation for osteoporotic vertebral compression fractures: initial application of a radiomics score based nomogram. Front Endocrinol (Lausanne) 2022;13:1093508. [doi: 10.3389/fendo.2022.1093508] [Medline: 36619583]
16. Parakh A, Lee H, Lee JH, Eisner BH, Sahani DV, Do S. Urinary stone detection on CT images using deep convolutional neural networks: evaluation of model performance and generalization. Radiol Artif Intell 2019 Jul;1(4):e180066. [doi: 10.1148/ryai.2019180066] [Medline: 33937795]
17. Zhang J, Xia L, Liu J, et al. Exploring deep learning radiomics for classifying osteoporotic vertebral fractures in X-ray images. Front Endocrinol 2023;15:1370838. [doi: 10.3389/fendo.2024.1370838]
18. Spiegl U, Bork H, Grüninger S, et al. Osteoporotic fractures of the thoracic and lumbar vertebrae: diagnosis and conservative treatment. Dtsch Arztebl Int 2021 Oct 8;118(40):670-677. [doi: 10.3238/arztebl.m2021.0295] [Medline: 34342263]
19. Lei M, Varghese B, Hwang D, et al. Benchmarking various radiomic toolkit features while applying the image biomarker standardization initiative toward clinical translation of radiomic analysis. J Digit Imaging 2021 Oct;34(5):1156-1170. [doi: 10.1007/s10278-021-00506-6] [Medline: 34545475]
20. Pyradiomics. Python Software Foundation. URL: http://pypi.org/project/pyradiomics [accessed 2023-05-17]
21. PyRadiomics documentation. pyradiomics. URL: http://pyradiomics.readthedocs.io [accessed 2016-12-11]
22. Orlhac F, Frouin F, Nioche C, Ayache N, Buvat I. Validation of a method to compensate multicenter effects affecting CT radiomics. Radiology 2019 Apr;291(1):53-59. [doi: 10.1148/radiol.2019182023] [Medline: 30694160]
23. Xu Z, Hao D, He L, et al. An assessment system for evaluating the severity of thoracolumbar osteoporotic fracture and its clinical application: a retrospective study of 381 cases. Clin Neurol Neurosurg 2015 Dec;139:70-75. [doi: 10.1016/j.clineuro.2015.09.006] [Medline: 26383865]
24. Okazaki S, Mine Y, Yoshimi Y, et al. RadImageNet and ImageNet as datasets for transfer learning in the assessment of dental radiographs: a comparative study. J Digit Imaging Inform med 2025;38(1):534-544. [doi: 10.1007/s10278-024-01204-9]
25. Fang C, Ji X, Pan Y, et al. Combining clinical-radiomics features with machine learning methods for building models to predict postoperative recurrence in patients with chronic subdural hematoma: retrospective cohort study. J Med Internet Res 2024 Aug 28;26:e54944. [doi: 10.2196/54944] [Medline: 39197165]
26. Wang L, Lin N, Chen W, Xiao H, Zhang Y, Sha Y. Deep learning models for differentiating three sinonasal malignancies using multi-sequence MRI. BMC Med Imaging 2023;25(1):56. [doi: 10.1186/s12880-024-01517-9]
27. SHAP. GitHub. URL: https://github.com/slundberg/shap [accessed 2018-04-20]
28. Ejiyi CJ, Cai D, Ejiyi MB, et al. Polynomial-SHAP analysis of liver disease markers for capturing of complex feature interactions in machine learning models. Comput Biol Med 2024 Nov;182:109168. [doi: 10.1016/j.compbiomed.2024.109168] [Medline: 39342675]
29. Suseki K, Yamashita M, Kojima Y, Minegishi Y, Komiya K, Takaso M. Lower SMI is a risk factor for dysphagia in Japanese hospitalized patients with osteoporotic vertebral and hip fracture: a retrospective study. Osteoporos Sarcopenia 2022 Dec;8(4):152-157. [doi: 10.1016/j.afos.2022.11.001] [Medline: 36605170]
30. Zhang J, Xia L, Zhang X, et al. Development and validation of a predictive model for vertebral fracture risk in osteoporosis patients. Eur Spine J 2024 Aug;33(8):3242-3260. [doi: 10.1007/s00586-024-08235-4] [Medline: 38955868]
31. Palmowski Y, Balmer S, Hu Z, et al. Relationship between the OF classification and radiological outcome OF osteoporotic vertebral fractures after kyphoplasty. Global Spine J 2022 May;12(4):646-653. [doi: 10.1177/2192568220964051] [Medline: 33131331]
32. Li YC, Chen HH, Horng-Shing Lu H, Hondar Wu HT, Chang MC, Chou PH. Can a deep-learning model for the automated detection of vertebral fractures approach the performance level of human subspecialists? Clin Orthop Relat Res 2021 Jul 1;479(7):1598-1612. [doi: 10.1097/CORR.0000000000001685] [Medline: 33651768]
33. Song K, Ko T, Chae HW, et al. Development and validation of a prediction model using sella magnetic resonance imaging–based radiomics and clinical parameters for the diagnosis of growth hormone deficiency and idiopathic short stature: cross-sectional, multicenter study. J Med Internet Res 2024 Nov 27;26:e54641. [doi: 10.2196/54641] [Medline: 39602803]
34. Mei X, Liu Z, Singh A, et al. Interstitial lung disease diagnosis and prognosis using an AI system integrating longitudinal data. Nat Commun 2023 Apr 20;14(1):2272. [doi: 10.1038/s41467-023-37720-5] [Medline: 37080956]
35. Chen Z, Xu L, Zhang C, et al. CT radiomics model for discriminating the risk stratification of gastrointestinal stromal tumors: a multi-class classification and multi-center study. Front Oncol 2021;11:11. [doi: 10.3389/fonc.2021.654114]
36. Kim JK, Mun S, Lee S. Detection and analysis of circadian biomarkers for metabolic syndrome using wearable data: cross-sectional study. JMIR Med Inform 2025 Jul 16;13:e69328. [doi: 10.2196/69328] [Medline: 40669055]
37. Xiang F, Meng QT, Deng JJ, et al. A deep learning model based on contrast-enhanced computed tomography for differential diagnosis of gallbladder carcinoma. Hepatobiliary Pabcreat Dis Int 2024 Aug;23(4):376-384. [doi: 10.1016/j.hbpd.2023.04.001] [Medline: 37080813]

Abbreviations

ACC: accuracy

XSL•FO
RenderX

ASTLOF: Assessment System of Thoracolumbar Osteoporotic Fractures
AUC: area under the curve
BMD: bone mineral density
CT: computed tomography
DLR: deep learning radiomics
DT: decision tree
DTL: deep transfer learning
DXA: dual-energy X-ray absorptiometry
ExtraTrees: extremely randomized trees
ICC: intraclass correlation coefficients
KNN: k-nearest neighbor
LASSO: Least Absolute Shrinkage and Selection Operator
LightGBM: Light Gradient Boosting Machine
LR: logistic regression
MLP: multilayer perceptron
MRI: magnetic resonance imaging
OVFs: osteoporotic vertebral fractures
OvR: One-vs-Rest
RF: random forest
ROC: receiver operating characteristic
SEN: sensitivity
SHAP: SHapley Additive exPlanations
SPE: specificity
STIR: short tau inversion recovery
SVM: support vector machine
XGBoost: Extreme gradient boosting

Edited by A Coristine; submitted 10.04.25; peer-reviewed by G Tang, Q Zeng; revised version received 29.07.25; accepted 30.07.25; published 29.08.25.

Please cite as:
Liu J, Zhang L, Yuan Y, Tang J, Liu Y, Xia L, Zhang J
Deep Learning Radiomics Model Based on Computed Tomography Image for Predicting the Classification of Osteoporotic Vertebral Fractures: Algorithm Development and Validation
JMIR Med Inform 2025;13:e75665
URL: https://medinform.jmir.org/2025/1/e75665
doi:10.2196/75665

© Jiayi Liu, Lincen Zhang, Yousheng Yuan, Jun Tang, Yongkang Liu, Liang Xia, Jun Zhang. Originally published in JMIR Medical Informatics (https://medinform.jmir.org), 29.8.2025. This is an open-access article distributed under the terms of the Creative Commons Attribution License (https://creativecommons.org/licenses/by/4.0/), which permits unrestricted use, distribution, and reproduction in any medium, provided the original work, first published in JMIR Medical Informatics, is properly cited. The complete bibliographic information, a link to the original publication on https://medinform.jmir.org/, as well as this copyright and license information must be included.

XSL•FO
RenderX

Rapid Liver Fibrosis Evaluation Using the UNet-ResNet50-32 × 4d Model in Magnetic Resonance Elastography: Retrospective Study

Pei-Yuan Su[1,2], MD; Han-Jie Shih[3], BS; Jia-Lang Xu[4], PhD

[1]Department of Internal Medicine, Division of Gastroenterology, Changhua Christian Hospital, Changhua, Taiwan

[2]Department of Post-Baccalaureate Medicine, College of Medicine, National Chung Hsing University, Taichung, Taiwan

[3]Department of Medical Imaging, Changhua Christian Hospital, Changhua, Taiwan

[4]Department of Applied Statistics, National Taichung University of Science and Technology, No. 129, Section 3, Sanmin Road, North District, Taichung, Taiwan

Corresponding Author:
Jia-Lang Xu, PhD
Department of Applied Statistics, National Taichung University of Science and Technology, No. 129, Section 3, Sanmin Road, North District, Taichung, Taiwan

Abstract

Background: Liver fibrosis is a pathological outcome of chronic liver injury and a hallmark of multiple chronic liver diseases. Magnetic resonance elastography (MRE) provides a non-invasive modality for evaluating the severity of liver fibrosis.

Objective: This study aimed to develop and evaluate deep learning–based segmentation models for the automated assessment of liver fibrosis using MRE images, with a focus on comparing the performance of a conventional U-Net model and a UNet-ResNet50−32 × 4d architecture model.

Methods: A retrospective analysis was conducted on 319 patients enrolled between January 2018 and December 2020. MRE images were processed and segmented using two U-Net–based models. Model performance was assessed through correlation coefficients, intersection over union (IoU), and additional segmentation metrics.

Results: The UNet-ResNet50−32 × 4d model demonstrated strong agreement with ground truth annotations, achieving correlation coefficients of 0.952 in the training phase and 0.943 in the validation phase, along with an Dice score of 85.68%, confirming its high segmentation accuracy.

Conclusions: The UNet-ResNet50−32 × 4d model exhibited robust performance and may serve as a reliable tool for the rapid and accurate assessment of liver fibrosis severity. The integration of automated segmentation into MRE analysis has the potential to improve clinical workflows and support timely decision-making in the management of chronic liver disease.

(JMIR Med Inform 2025;13:e80351) doi:10.2196/80351

KEYWORDS

liver fibrosis; image segmentation; MRI elastography; magnetic resonance elastography; automated segmentation; timely decision-making

Introduction

Research Background and Motivations

Liver fibrosis is a progressive process that culminates in cirrhosis, a condition associated with severe complications such as ascites, esophageal varices, and hepatic encephalopathy, which significantly shorten life expectancy [1,2]. To better stratify disease severity and guide management, fibrosis is commonly staged into five categories (F0–F4). F0 represents the absence of fibrosis, while F1–F3 correspond to progressive but non-cirrhotic stages of chronic liver disease, during which timely intervention can slow or even reverse disease progression. F4 indicates established cirrhosis, marking a critical threshold where the risk of decompensation, hepatocellular carcinoma, and mortality rises sharply. This staging framework not only provides prognostic insights but also plays a pivotal role in therapeutic decision-making, surveillance strategies, and patient counseling. The progression of liver fibrosis is slow and takes years to progress from mild liver fibrosis to cirrhosis. If liver fibrosis is diagnosed early using quicker and more convenient tools, there is a chance to prevent further deterioration into cirrhosis [3]. Currently, there are many tools for diagnosing liver fibrosis, with liver biopsy being the most accurate. However, due to the risk of bleeding, it is less commonly used [4]. There are many non-invasive testing methods, such as ultrasound elastography and magnetic resonance elastography (MRE), which have a high capability for diagnosing liver

XSL•FO
RenderX

fibrosis [5,6]. MRE requires manual circling of images for interpretative reading, which increases the time for doctors to interpret reports [7]. Therefore, using image segmentation technology could help reduce the time for interpreting MRE for liver fibrosis and improve accuracy.

Artificial intelligence (AI) has been widely investigated in the medical field, with numerous applications across disease prediction, diagnosis, and clinical decision support. For instance, computed tomography (CT) imaging has shown strong potential in predicting cholangiocarcinoma recurrence [8], while machine learning–based image analysis methods have been applied for diabetic foot evaluation [9]. Convolutional neural networks (CNNs) have been employed to predict clinical outcomes in patients with stroke [10], and a YOLOv8 model has demonstrated a high accuracy in early lung cancer detection [11]. Similarly, combining chest X-rays with clinical features has yielded favorable area under the curve performance in osteoporosis screening [12]. In health care operations, machine learning models have also been developed to predict emergency department patient flow, effectively estimating both hourly and daily visit volumes [13]. Moreover, clinical decision support systems have been explored for prenatal abnormality diagnosis and ultrasound applications, though such studies have yet to incorporate maternal or fetal data during pregnancy [14]. CNNs have been widely applied in liver tumor classification, while diverse architectures such as U-Net, UNet++, Residual Networks (ResNet), SegNet, and fully convolutional networks have been employed for semantic segmentation tasks [6,15-18]. However, despite this progress, only one previous study has reported the application of CNNs for MRE measurement [19]. By integrating the strengths of U-Net and ResNet, our Unet-ResNet model achieved superior segmentation performance and training stability, while maintaining strong agreement with manual evaluation.

Image segmentation represents another important domain of AI applications, whereby algorithms cluster elements of a similar nature into coherent segments [20]. This technique has been increasingly applied in medical imaging, including ultrasound imaging [21], CT scans [22], magnetic resonance imaging (MRI) [23], and X-ray imaging [24]. In liver-related applications, segmentation methods such as real-time liver ultrasound segmentation [17] can greatly assist physicians in diagnosis and treatment planning [25], while CT-based segmentation is useful for localizing liver tumors [26]. Advanced approaches using deep CNNs [27] and 3D deeply supervised networks [16] have further improved automated liver segmentation performance. Researchers have compared U-Net and V-Net architectures to assess their effectiveness in the segmentation of microcalcifications [28].

Research Objectives

The aim of this study is to use image segmentation technology for the computational interpretation of MRE, enabling AI to automatically segment MRE images, accurately identify regions of interest, quantify liver fibrosis levels, and apply this approach to both training and validation cohorts. Early and reliable assessment of liver fibrosis is essential for timely clinical decision-making, yet conventional manual labeling of MRE images is time-consuming, operator-dependent, and prone to variability. To address these challenges, this study further investigates whether advanced architectures such as UNet-ResNet50−32 × 4d can achieve superior predictive performance compared with the traditional U-Net model.

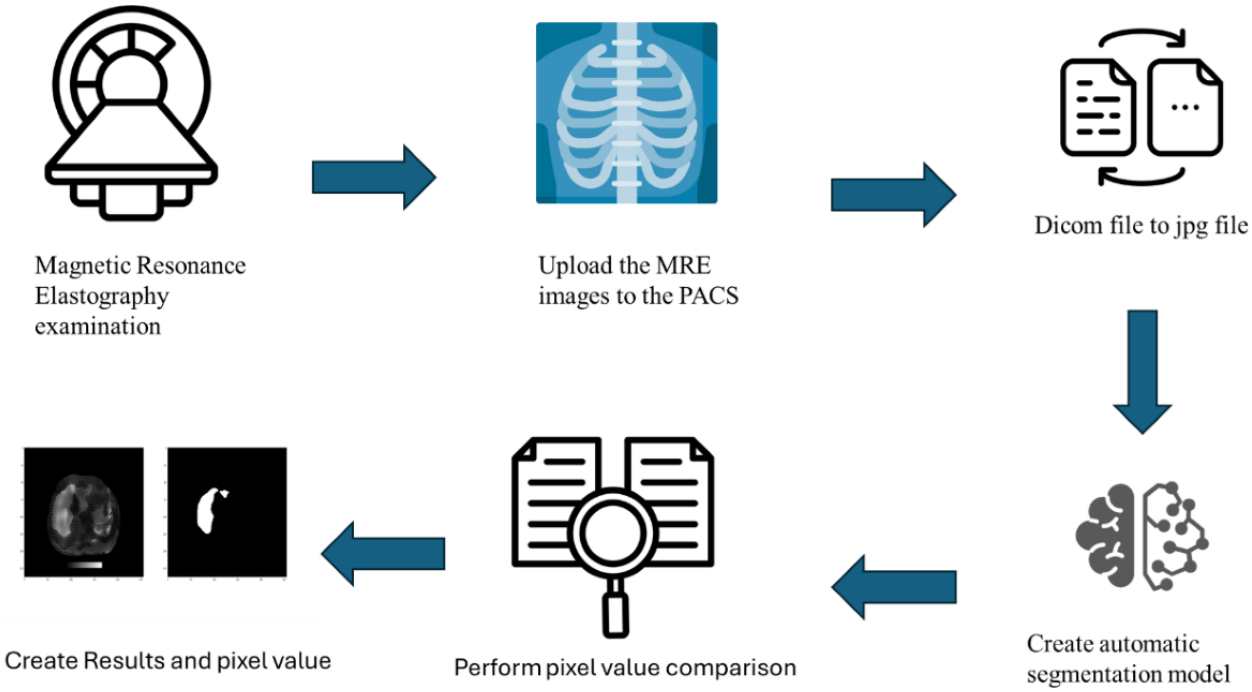
Methods

Study Overview

An overview of the automated workflow developed in this study is shown in Figure 1. This study incorporates an automated process in which patients undergo MRE examinations, and the imaging data are subsequently uploaded to the picture archiving and communication system. Once the upload is completed, the segmentation model is automatically triggered. During the validation phase, pixel values of the target regions are obtained directly from the Digital Imaging and Communications in Medicine (DICOM) images in the picture archiving and communication system, as interpreted by experienced radiologists. Since there are discrepancies between pixel values in DICOM format and those converted to JPEG, this study relies solely on the pixel values displayed in the original DICOM files for analysis. Due to discrepancies between pixel values in DICOM and JPEG formats, this study exclusively uses original DICOM pixel values for analysis. These values are automatically extracted using medical image processing libraries that read directly from the DICOM metadata and image matrix. After segmentation, the predicted masks and corresponding pixel values are overlaid on the original images and provided to radiologists to support clinical evaluation and decision.

XSL•FO
RenderX

Figure 1. Overview of the automated workflow for liver fibrosis assessment using MRE confidence maps, illustrating image preprocessing, segmentation with the UNet-ResNet50−32×4d model, and quantitative analysis for clinical application. DICOM: Digital Imaging and Communications in Medicine; MRE: magnetic resonance elastography; PACS: picture archiving and communication system.



Ethical Considerations

The study was approved by the Institutional Review Board of Changhua Christian Hospital (approval no.: 210132). The Institutional Review Board waived the need for informed consent considering the retrospective nature of data collected. This study implemented stringent measures to protect the privacy of all participants by anonymizing all collected data to remove any personally identifiable information.

Patients

This retrospective study collected patient data from January 2018 to December 2020. Patients were eligible if they underwent MRI for clinical indications and MRE was performed as part of the MRI protocol. Additional inclusion criteria were age greater than 20 years and the availability of demographic information (age and gender). Exclusion criteria consisted of incomplete imaging or missing demographic data. Based on these criteria, a total of 320 patients were initially identified, and 1 patient was excluded due to incomplete data, resulting in a final cohort of 319 patients included in the analysis. To ensure the broad applicability and usability of the proposed model, no further stratification was made according to the presence of chronic liver disease or fibrosis.

MRE

MRI was performed with a 1.5-Tesla Aera magnet system by Siemens AG, equipped with a 16-channel phased-array body coil. The process involved a specialized MRE setup, integral to which was an acoustic driver system by Resoundant. The technical details of the MRE imaging sequence were as follows: a repetition time of 50 ms and an echo time of 22.7 ms, a flip angle of 25 degrees, and a bandwidth of 260 Hz/pixel. Additionally, the sequence settings included a hydrogen resonance frequency of 63.5 MHz, an acquisition matrix of 256 × 64, a section thickness of 5 mm, and a field of view of 400 × 400 mm^2. For each patient, four to five confidence maps were automatically generated and post-processed directly on the MRI scanner workstation using the integrated MRE software on the Siemens Syngo MR VE11 system (MAGNETOM Aera, Skyra, and Avantofit; Siemens Healthineers), demonstrating adequate wave amplitudes in specific regions. Manual liver stiffness measurements were performed by an expert, who delineated the regions of interest on the confidence maps and calculated the stiffness values [29]. The stage of liver fibrosis was classified into four categories based on criteria developed at the same institute as this study [30]. Significant fibrosis was defined as stage F2 according to the METAVIR scoring system, corresponding to MRE values ≥2.8 kPa.

MRE Image Labeling

For this study, the model training was conducted using data from 92 patients, all of whom had confidence maps generated from MRE. The annotations for these training images were meticulously created by a gastroenterologist, ensuring the reliability and precision of the ground truth used in model development.

Statistical Analysis

The *t* test was used for comparison of continues variables of baseline characteristics. Continuous variables were showed as mean (SD). The Pearson correlation coefficient was performed to measure the correlation of the two MRE measurements by manual and automatic methods. All statistical analysis were performed on SPSS version 22.0 (IBM Corp.), with two-tailed *P* values <.05 indicating statistical significance.

XSL•FO
RenderX

Model Training

The MRE images used in this study were acquired with a window center of 400 and a window width of 800, with an original resolution of 256×204 pixels. Since convolutional operations in the U-Net architecture require adequate spatial information for effective multi-scale feature extraction, all images were resized to 512×512 pixels using bilinear interpolation prior to model training. This resizing step was performed to preserve structural details and improve segmentation accuracy. For liver fibrosis segmentation, a hybrid deep learning model was implemented by combining U-Net with a ResNet50−32 × 4d encoder, leveraging its capacity to extract multi-scale contextual features while maintaining spatial resolution. Model optimization aimed to enhance both training efficiency and segmentation performance through systematic adjustment of key hyperparameters, with a comprehensive tuning strategy applied across a range of values, as summarized in Table 1. To address the pixel-level classification task, the model employed the Binary Cross-Entropy with Logits Loss as shown in equation (1).

$$(1) L=-1N\sum i=1N[yilog\ (pi)+(1-yi)log\ (1-pi)]$$

Where yi denotes the true label of the i-th sample, pi represents the predicted probability that the sample belongs to the positive class, and N indicates the total number of samples.

Table . Hyperparameter tuning strategy and optimal settings for the model.

Hyperparameter	Values
Batch size	32
Loss	Binary Cross-Entropy with Logits Loss
Optimizer	Stochastic Gradient Descent
Learning rate	3×10 –3×10 ²
Weight decay	0 - 0.01
Momentum	0.80 - 0.99

Results

Cohort Characteristics

A total of 319 patients were enrolled in the study and divided into two cohorts, with 91 patients assigned to the training group and 228 patients allocated to the testing group. The baseline characteristics of the two cohorts are summarized in Table 2. The mean (SD) age was 57.2 (12.4) years in the training group and 52.6 (12.3) years in the testing group. There were no statistically significant differences in age, gender distribution, height, weight, or BMI between the two groups, as all *P* values were greater than .05. Similarly, the mean (SD) MRE stiffness values obtained by manual measurement were 4.51 (2.85) kPa in the training group and 3.69 (2.26) kPa in the testing group, with a *P* value of .09. The mean (SD) automated measurement values were 4.04 (1.93) kPa in the training group and 3.69 (2.28) kPa in the testing group with a *P* value of .41, also showing no significant difference. In contrast, a significant difference was observed in the proportion of patients with clinically significant fibrosis stage equal to or greater than F2. Based on manual MRE assessment, 76% (69/91) of patients in the training group had fibrosis stage F2 or higher compared with 52% (118/228) in the testing group, with a *P* value of less than .001. Automated MRE analysis identified 75% (68/91) of patients in the training group and 50% (114/228) in the testing group with fibrosis stage F2 or higher, also with a *P* value of less than .001. These findings confirm the consistency between manual and automated staging, while indicating that the prevalence of significant fibrosis was higher in the training cohort.

XSL•FO
RenderX

Table . The baseline characteristics of the training group and testing group.

Characteristics	Training group (n=91)	Testing group (n=228)	*P* value
Age, years, mean (SD)	57.2 (12.4)	52.6 (12.3)	.77
Gender, male (%)	48 (53)	137 (60)	.23
Height, m, mean (SD)	1.62 (0.08)	1.65 (0.08)	.97
Weight, kg, mean (SD)	65.8 (13.2)	67 (12.5)	.89
BMI, kg/m^2, mean (SD)	25.1 (4.2)	24.6 (3.7)	.21
MRE[a] (manual), kPa, mean (SD)	4.51 (2.85)	3.69 (2.26)	.09
MRE (automatic), kPa, mean (SD)	4.04 (1.93)	3.69 (2.28)	.41
Fibrosis stage (≥ F2[b]) (manual), n (%)	69 (76)	118 (52)	<.001
Fibrosis stage (≥ F2[b]) (automatic), n (%)	68 (75)	114 (50)	<.001

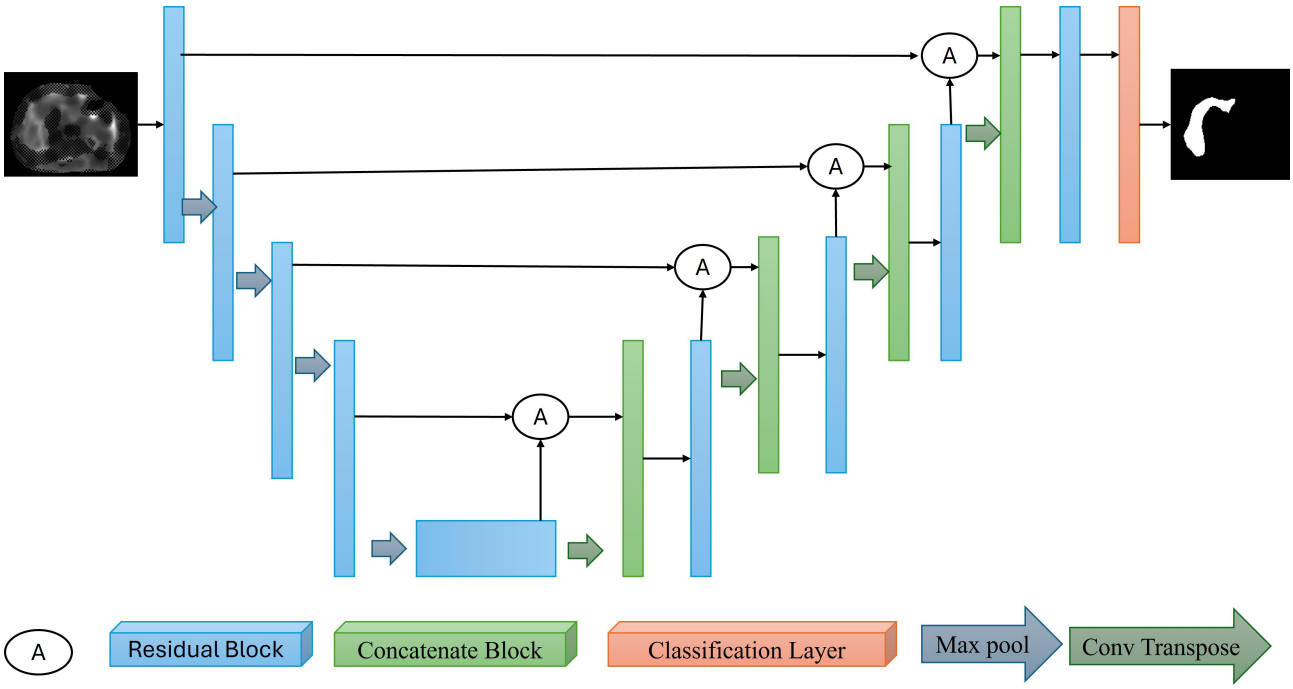
[a]MRE: magnetic resonance elastography.

[b]Liver fibrosis severity was determined using MRE, with stage F2 defined as MRE ≥2.8 kPa [30].

Automatic Labeling Process

Figure 2 illustrates the template for the auto-labeling process generated by the UNet-ResNet50−32 × 4d algorithm, a widely validated and robust architecture for medical image segmentation deep learning architecture specifically designed for semantic segmentation tasks. The auto-labeling template demonstrates the effectiveness of the model in accurately identifying and segmenting key regions of interest within the MRE confidence maps, aligning closely with expert annotations.

Figure 2. Overall architecture of the proposed UNet-ResNet50−32×4d model for automated liver segmentation and fibrosis staging using MRE confidence maps. MRE: magnetic resonance elastography.



Experimental Environment

All experiments in this study were conducted on a high-performance workstation equipped with an NVIDIA RTX 4090 GPU, an Intel Core i9-13900K CPU, and 128 GB of RAM. The deep learning models were implemented using PyTorch with CUDA 11.8 (torch 2.1.0+ cu118), enabling accelerated training and inference.

Parameters Setting

Table 3 presents the optimal parameter values identified in this study through training with the UNet-ResNet50−32 × 4d algorithm, which include a learning rate of 0.005, momentum of 0.982, and weight decay of 4.457e-06.

XSL•FO
RenderX

Table . Optimal hyperparameters derived from model training.

Parameters	Value
Epoch	32
Learning rate	0.005
Momentum	0.982
Weight decay	4.457e-06

Performance Evaluation

A comparison of the two models using the optimal parameters obtained from Table 2 indicate that the UNet-ResNet50−32 × 4d model achieved better predictive performance on the test dataset, whereas the standard U-Net model failed to produce any meaningful predictions. The average Dice coefficient, intersection over union (IoU), and F1-score for the UNet-ResNet50−32 × 4d model were 85.68%, 75.80%, and 85.68%, respectively; the corresponding values for the U-Net model were 82.59%, 75.92%, and 82.59%, respectively. The slightly lower IoU may be attributed to the presence of outliers during pixel-wise evaluation, which could have affected the overall segmentation accuracy. The segmentation performance was quantitatively assessed using the Dice coefficient, IoU, and F1-score, as shown in equations (2)–(4)

(2)Dice=2∨P∩G∨|P|+G∨

(3)IoU=P∩G∨P∪G∨

(4)F1−score=2∗Precision∗RecallPrecision+Recall

Figure 3 illustrates the segmentation results for liver fibrosis imaging. Overall, the figure underscores the enhanced performance of the proposed model in automated segmentation of liver fibrosis imaging and its potential clinical applicability.

Figure 3. Comparative segmentation performance of conventional U-Net and UNet-ResNet50−32×4d architectures on MRE confidence maps for liver fibrosis assessment. Panel (A) shows the original MRE confidence map, while panel (B) presents the segmentation outcome generated by the conventional U-Net model, which delineates the major hepatic region but demonstrates limitations in boundary refinement and structural detail. In contrast, panel (C) depicts the result obtained using the UNet-ResNet50−32×4d model, which more accurately captures hepatic contours and structural features, highlighting its superior capability in feature extraction and region identification. MRE: magnetic resonance elastography.

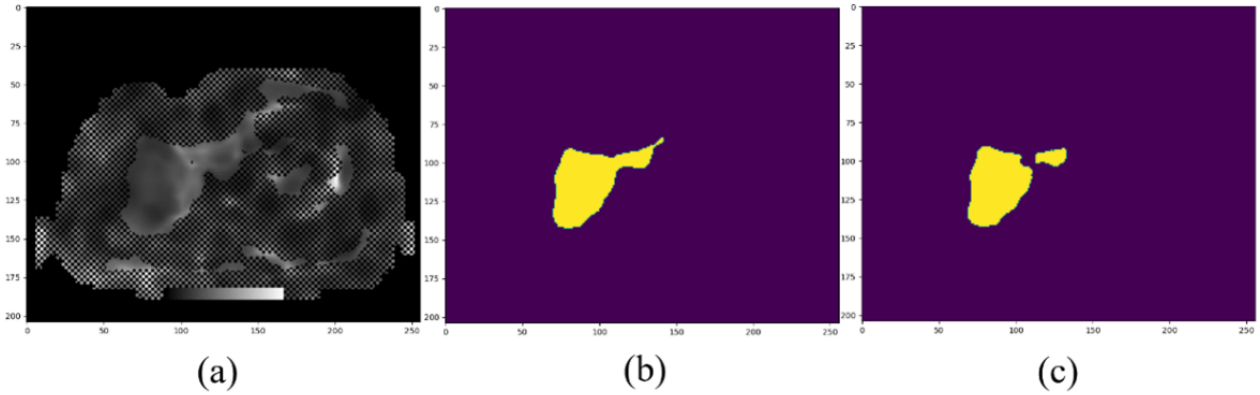


Table 4 presents the performance of the proposed UNet-ResNet50−32×4d model further evaluated across different fibrosis stages. The segmentation accuracy remained consistently high in the early stages F0-F1, with Dice scores exceeding 87% and IoU values around 78%. Performance was slightly reduced in the intermediate stage F2 and more prominently in stage F3, where Dice and IoU decreased to 80.54% and 70.49%, respectively. This decline may reflect the increased heterogeneity and irregularity of fibrosis distribution in advanced disease. Notably, the model regained relatively stable performance in stage F4, with Dice and IoU values of 84.00% and 73.14%, respectively. These findings suggest that while the model demonstrates robust segmentation across fibrosis stages, challenges remain in capturing complex tissue patterns in stage F3.

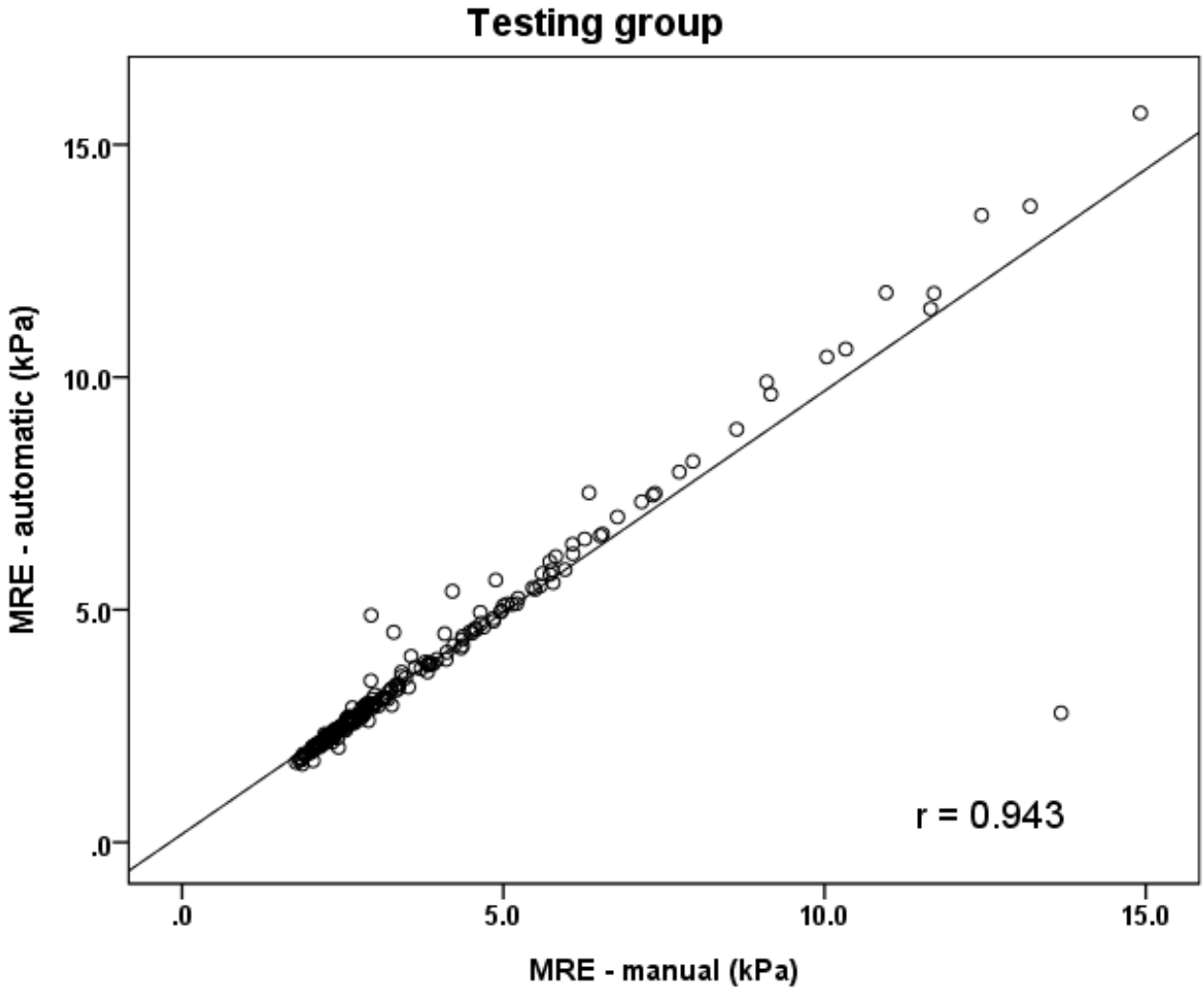
Figure 4 presents the correlation between MRE values obtained from the automated segmentation model and those measured manually by an expert gastroenterologist in the testing cohort. The analysis demonstrated a Pearson correlation coefficient of 0.943, confirming a strong positive linear relationship between the two approaches, even when applied to unseen data.

XSL•FO
RenderX

Table . Segmentation performance of the UNet-ResNet50−32×4d model across different fibrosis stages.

Fibrosis stage	Dice (%)	Intersection over union (%)	F1-score (%)
F0	87.47	78.26	87.47
F1	87.98	78.74	87.98
F2	84.11	73.85	84.11
F3	80.54	70.49	80.54
F4	84.00	73.14	84.00

Figure 4. Correlation between automated segmentation–derived MRE values and manual expert measurements in the testing group. MRE: magnetic resonance electrography.



Discussion

Principal Findings

Automated segmentation using the AI-based model for MRE measurement proved to be both reliable and effective when compared with manual segmentation. The strong correlation and reproducibility observed between the automated and manual approaches highlight the potential of this tool as a valuable aid in clinical practice. In this study, we further evaluated and compared the performance of a standard U-Net with a UNet-ResNet50−32 × 4d architecture for medical image segmentation. The findings clearly demonstrated that the UNet-ResNet50−32 × 4d model substantially outperformed the conventional U-Net in segmentation accuracy. Specifically, while the conventional U-Net achieved a Dice coefficient of 82.59% and an IoU of 72.92% on the test dataset, the proposed model further improved performance, reaching an average Dice coefficient of 85.68%, IoU of 75.80%, and F1-score of 85.68%. The slightly lower IoU relative to the Dice coefficient may be attributed to the penalization of pixel-level outliers in the union-based evaluation, which tends to disproportionately

XSL•FO
RenderX

impact cases with small lesion boundaries or heterogeneous textures.

When evaluated across fibrosis stages, the model demonstrated stable performance in the early stages, with Dice scores of 87.47% and 87.98% for F0 and F1, respectively, and corresponding IoU values close to 78%. A modest decline was observed in F2 with a Dice score of 84.11% and IoU of 73.85%, with the lowest performance in F3 where the Dice score was 80.54% and IoU was 70.49%. This likely reflects the increased heterogeneity and irregularity of fibrosis distribution in advanced disease. Interestingly, the model recovered performance in F4, achieving a Dice score of 84.00% and IoU of 73.14%, suggesting that once cirrhosis is established, the fibrotic patterns may become more homogeneous and therefore easier for the model to delineate.

Comparison to Prior Work

MRE is a highly effective non-invasive tool for evaluating liver fibrosis and serves as a valuable alternative to liver biopsy. Clinicians typically assess regions of interest using elastograms with overlaid confidence maps generated following MRI scans [31]. A previous study has investigated automated approaches for MRE measurement [32]. An early method applied intensity membership functions combined with random walker segmentation to differentiate liver tissue from surrounding structures, achieving a correlation of 0.981 with manual measurements [32]. Another study introduced volumetric segmentation using semi-automated proprietary software to evaluate liver stiffness. Their findings revealed significant differences between region of interest-based and volumetric analyses, suggesting that volumetric methods may provide better detection of heterogeneous fibrosis [33]. More recently, a CNN-based framework was applied to MRE, reporting an intraclass correlation coefficient of 0.99 between automated and manual assessments in clinical patients [19]. In this study, we applied the Unet-ResNet50 model to segment the liver on MRE confidence maps and measure liver stiffness. Our approach yielded a strong correlation of 0.943 with manual expert measurements, supporting its potential utility in clinical practice. To the best of our knowledge, this is the first study to implement a Unet-ResNet hybrid architecture for MRE segmentation and measurement. A previous study conducted in healthy volunteers reported excellent consistency and segmentation performance, with liver Dice scores reaching 0.95 [34]. This study focused on automated liver fibrosis staging (F0–F4) and extraction of MRE-derived stiffness values in kilopascals. Unlike studies limited to healthy subjects, our cohort consisted of clinical patients, in whom imaging data inherently exhibit greater heterogeneity.

Limitations

This study has several limitations. Only gray-scale elastograms with 95% confidence maps were used for segmentation, which may have inadvertently included non-hepatic tissues such as the gallbladder fossa and large blood vessels. Despite this, the correlation between manual and automated methods remained strong. Further refinement of the segmentation process is needed to achieve more accurate anatomical delineation of the liver using the UNet-ResNet model. Key clinical data related to liver disease, such as iron levels, steatosis, and viral markers, were not collected. Severe steatosis and iron overload may interfere with MRE measurements and could not be adequately accounted for in this analysis. Histological fibrosis scores were unavailable for most participants, as liver biopsy was not routinely performed. The absence of biopsy confirmation limits the accuracy of staging, since MRE values alone may not fully capture the histopathological spectrum of fibrosis. This introduces a potential risk of mislabeling fibrosis severity, particularly in borderline cases or in patients with overlapping liver conditions. This study is subject to data imbalance, as the distribution of patients across different disease severities was uneven, which may affect the generalizability and stability of the proposed model. Although the dataset was partitioned to ensure fairness in training and testing, the uneven distribution of disease severity remains a potential source of bias. In particular, when the model is trained on patients with more advanced disease, its application to cohorts with milder disease may result in an overestimation of fibrosis severity and diminished sensitivity to early-stage changes. Conversely, if a model is optimized for mild cases, it may underperform in advanced disease populations, resulting in systematic misclassification. These imbalances highlight the need for future studies that incorporate paired biopsy and imaging data, along with balanced cohorts across different severities, to validate the robustness and clinical applicability of automated MRE-based staging.

Future Directions

Future investigations will need to progress beyond algorithmic refinement and incorporate the expansion of patient cohorts, thereby increasing statistical power and enhancing the robustness of predictive models. Validation through multi-center studies will establish reproducibility across institutions, imaging protocols, and heterogeneous patient demographics. In parallel, the integration of multimodal information, including complementary imaging techniques, clinical parameters, and biomarker profiles, will strengthen both predictive accuracy and clinical relevance. The inclusion of expert annotations from multiple specialists, encompassing hepatologists, radiologists, pathologists, and other domain experts, will reduce inter-observer variability and further reinforce the clinical validity of model outputs. These efforts will enable broader generalizability across diverse populations and disease severities, ultimately supporting translation into routine clinical practice.

Conclusions

Early and accurate assessment of liver fibrosis is essential for enabling timely diagnosis and intervention. In this study, we developed a U-Net-ResNet50−32 × 4d model to predict the severity of liver fibrosis. The model achieved correlation coefficients above 0.9 in both training and validation cohorts and reached an Dice score of 85.68%, demonstrating strong potential to support accurate fibrosis staging in clinical practice. Importantly, liver fibrosis staging currently lacks a universally accepted gold standard. While histology remains the traditional reference, it is invasive, limited by sampling error, and not always available. Our findings suggest that automated MRE-based methods may provide a reliable non-invasive

XSL•FO
RenderX

alternative, although the absence of biopsy confirmation introduces potential uncertainties in staging accuracy.

The strong performance of our model highlights its practical value and potential to improve efficiency in clinical decision-making. Future research should validate these results in larger, multi-center cohorts, integrate complementary imaging modalities and clinical biomarkers to further strengthen predictive power, and explore real-time deployment within radiology workflows to maximize clinical applicability.

Acknowledgments

The authors thank the Changhua Christian Hospital and all the authors of the original articles.

This research was funded by Changhua Christian Hospital (113-CCH-IRP-016).

Data Availability

The datasets used and/or analyzed during the current study are available from the corresponding author on reasonable request.

Authors' Contributions

PYS and JLX wrote the main manuscript text and HJS helped data collection and data annotation. All authors reviewed the manuscript.

Conflicts of Interest

None declared.

References

1. Angeli P, Bernardi M, Villanueva C, et al. EASL clinical practice guidelines for the management of patients with decompensated cirrhosis. J Hepatol 2018 Aug;69(2):406-460. [doi: 10.1016/j.jhep.2018.03.024]
2. Suk KT, Kim DJ. Staging of liver fibrosis or cirrhosis: the role of hepatic venous pressure gradient measurement. World J Hepatol 2015 Mar 27;7(3):607-615. [doi: 10.4254/wjh.v7.i3.607] [Medline: 25848485]
3. Guixé-Muntet S, Quesada-Vázquez S, Gracia-Sancho J. Pathophysiology and therapeutic options for cirrhotic portal hypertension. The Lancet Gastroenterology & Hepatology 2024 Jul;9(7):646-663. [doi: 10.1016/S2468-1253(23)00438-7]
4. Berzigotti A, Tsochatzis E, Boursier J, et al. EASL clinical practice guidelines on non-invasive tests for evaluation of liver disease severity and prognosis – 2021 update. J Hepatol 2021 Sep;75(3):659-689. [doi: 10.1016/j.jhep.2021.05.025]
5. Li S, Sun X, Chen M, et al. Liver fibrosis conventional and molecular imaging diagnosis update. J Liver 2019;8(1):236. [Medline: 31341723]
6. Ozkaya E, Kennedy P, Chen J, et al. Precision and test-retest repeatability of stiffness measurement with MR elastography: a multicenter phantom study. Radiology 2024 May;311(2):e233136. [doi: 10.1148/radiol.233136] [Medline: 38742971]
7. Hoodeshenas S, Yin M, Venkatesh SK. Magnetic resonance elastography of liver: current update. Top Magn Reson Imaging 2018 Oct;27(5):319-333. [doi: 10.1097/RMR.0000000000000177] [Medline: 30289828]
8. Chen J, Xi J, Chen T, Yang L, Liu K, Ding X. Diagnostic performance of computed tomography-based artificial intelligence for early recurrence of cholangiocarcinoma: systematic review and meta-analysis. J Med Internet Res 2025 Sep 18;27:e78306. [doi: 10.2196/78306] [Medline: 40905766]
9. Lin PC, Li TC, Huang TH, et al. Machine learning for diabetic foot care: accuracy trends and emerging directions in healthcare AI. Front Public Health 2025;13:1613946. [doi: 10.3389/fpubh.2025.1613946] [Medline: 40756392]
10. Yin HC, Lei RL, Xu JL, Lin CM, Hsu YL. Enhancing stroke prognosis prediction using deep convolution neural networks. J Mech Med Biol 2025 Jun;25(05). [doi: 10.1142/S0219519425400391]
11. Huang KY, Chung CL, Xu JL. Deep learning object detection-based early detection of lung cancer. Front Med (Lausanne) 2025;12:1567119. [doi: 10.3389/fmed.2025.1567119] [Medline: 40357272]
12. Tang J, Yin X, Lai J, Luo K, Wu D. Fusion of X-ray images and clinical data for a multimodal deep learning prediction model of osteoporosis: algorithm development and validation study. JMIR Med Inform 2025 Sep 18;13:e70738. [doi: 10.2196/70738] [Medline: 40966528]
13. Vural O, Ozaydin B, Aram KY, Booth J, Lindsey BF, Ahmed A. An artificial intelligence-based framework for predicting emergency department overcrowding: development and evaluation study. JMIR Med Inform 2025 Sep 17;13:e73960. [doi: 10.2196/73960] [Medline: 40961493]
14. Lin X, Liang C, Liu J, Lyu T, Ghumman N, Campbell B. Artificial intelligence-augmented clinical decision support systems for pregnancy care: systematic review. J Med Internet Res 2024 Sep 16;26:e54737. [doi: 10.2196/54737] [Medline: 39283665]
15. Lakshmipriya B, Pottakkat B, Ramkumar G. Deep learning techniques in liver tumour diagnosis using CT and MR imaging - A systematic review. Artif Intell Med 2023 Jul;141:102557. [doi: 10.1016/j.artmed.2023.102557] [Medline: 37295904]

XSL•FO
RenderX

16. Dou Q, Chen H, Jin Y, Yu L, Qin J, Heng PA. 3D deeply supervised network for automatic liver segmentation from CT volumes. 2016 Oct Presented at: International conference on medical image computing and computer-assisted intervention p. 149-157. [doi: 10.1007/978-3-319-46723-8_18]
17. Vianna P, Kulbay M, Boustros P, et al. Automated liver segmentation and steatosis grading using deep learning on b-mode ultrasound images. 2023 Sep Presented at: 2023 IEEE International Ultrasonics Symposium (IUS); Montreal, QC, Canada p. 1-4. [doi: 10.1109/IUS51837.2023.10307501]
18. Ozkaya E, Nieves-Vazquez HA, Yuce M, et al. Automated liver magnetic resonance elastography quality control and liver stiffness measurement using deep learning. Abdom Radiol (NY) 2025 Sep;50(9):4100-4109. [doi: 10.1007/s00261-025-04883-2] [Medline: 40088296]
19. Cunha GM, Delgado TI, Middleton MS, et al. Automated CNN-based analysis versus manual analysis for MR elastography in nonalcoholic fatty liver disease: intermethod agreement and fibrosis stage discriminative performance. AJR Am J Roentgenol 2022 Aug;219(2):224-232. [doi: 10.2214/AJR.21.27135] [Medline: 35107306]
20. Ansari MY, Abdalla A, Ansari MY, et al. Practical utility of liver segmentation methods in clinical surgeries and interventions. BMC Med Imaging 2022 May 24;22(1):97. [doi: 10.1186/s12880-022-00825-2] [Medline: 35610600]
21. Wang R, Zhou H, Fu P, Shen H, Bai Y. A multiscale attentional unet model for automatic segmentation in medical ultrasound images. Ultrason Imaging 2023 Jul;45(4):159-174. [doi: 10.1177/01617346231169789] [Medline: 37114669]
22. Bougourzi F, Distante C, Dornaika F, Taleb-Ahmed A. PDAtt-Unet: pyramid dual-decoder attention Unet for Covid-19 infection segmentation from CT-scans. Med Image Anal 2023 May;86:102797. [doi: 10.1016/j.media.2023.102797] [Medline: 36966605]
23. Wang J, Peng Y, Jing S, Han L, Li T, Luo J. A deep-learning approach for segmentation of liver tumors in magnetic resonance imaging using UNet++. BMC Cancer 2023;23(1):1060. [doi: 10.1186/s12885-023-11432-x]
24. Wang H, Zhang D, Ding S, Gao Z, Feng J, Wan S. Rib segmentation algorithm for X-ray image based on unpaired sample augmentation and multi-scale network. Neural Comput & Applic 2023 Jun;35(16):11583-11597. [doi: 10.1007/s00521-021-06546-x]
25. Ansari MY, Yang Y, Meher PK, Dakua SP. Dense-PSP-UNet: A neural network for fast inference liver ultrasound segmentation. Comput Biol Med 2023 Feb;153:106478. [doi: 10.1016/j.compbiomed.2022.106478] [Medline: 36603437]
26. Li J, Niu Y. Dual encoding DDS‐UNet liver tumour segmentation based on multi‐scale deep and shallow feature fusion. IET Image Process 2024 Apr;18(5):1189-1199. [doi: 10.1049/ipr2.13018]
27. Gross M, Huber S, Arora S, et al. Automated MRI liver segmentation for anatomical segmentation, liver volumetry, and the extraction of radiomics. Eur Radiol 2024 Aug;34(8):5056-5065. [doi: 10.1007/s00330-023-10495-5] [Medline: 38217704]
28. Hsu PY, Xu JL, Chen LL, Chen MY. Using deep learning to construct microcalcification clusters in a mammography prediction model. Innov Emerg Technol 2025 Jan;12. [doi: 10.1142/S2737599425500306]
29. Guglielmo FF, Venkatesh SK, Mitchell DG. Liver MR elastography technique and image interpretation: pearls and pitfalls. Radiographics 2019;39(7):1983-2002. [doi: 10.1148/rg.2019190034] [Medline: 31626569]
30. Wu WP, Chou CT, Chen RC, Lee CW, Lee KW, Wu HK. Non-invasive evaluation of hepatic fibrosis: the diagnostic performance of magnetic resonance elastography in patients with viral hepatitis B or C. PLoS One 2015;10(10):e0140068. [doi: 10.1371/journal.pone.0140068] [Medline: 26469342]
31. Zerunian M, Masci B, Caruso D, et al. Liver magnetic resonance elastography: focus on methodology, technique, and feasibility. Diagnostics (Basel) 2024 Feb 9;14(4):379. [doi: 10.3390/diagnostics14040379] [Medline: 38396418]
32. Dzyubak B, Venkatesh SK, Manduca A, Glaser KJ, Ehman RL. Automated liver elasticity calculation for MR elastography. J Magn Reson Imaging 2016 May;43(5):1055-1063. [doi: 10.1002/jmri.25072] [Medline: 26494224]
33. Rezvani Habibabadi R, Khoshpouri P, Ghadimi M, et al. Comparison between ROI-based and volumetric measurements in quantifying heterogeneity of liver stiffness using MR elastography. Eur Radiol 2020 Mar;30(3):1609-1615. [doi: 10.1007/s00330-019-06478-0] [Medline: 31705257]
34. Jaitner N, Ludwig J, Meyer T, et al. Automated liver and spleen segmentation for MR elastography maps using U-Nets. Sci Rep 2025 Mar 28;15(1):10762. [doi: 10.1038/s41598-025-95157-w] [Medline: 40155744]

Abbreviations

AI: artificial intelligence
CNN: convolutional neural network
CT: computed tomography
DICOM: Digital Imaging and Communications in Medicine
IoU: intersection over union
MRE: magnetic resonance elastography
MRI: magnetic resonance imaging

XSL•FO
RenderX

Edited by A Coristine; submitted 09.07.25; peer-reviewed by E Ozkaya, FM Chang, JH Shen; revised version received 28.09.25; accepted 28.09.25; published 20.10.25.

Please cite as:
Su PY, Shih HJ, Xu JL
Rapid Liver Fibrosis Evaluation Using the UNet-ResNet50-32 × 4d Model in Magnetic Resonance Elastography: Retrospective Study
JMIR Med Inform 2025;13:e80351
URL: https://medinform.jmir.org/2025/1/e80351
doi:10.2196/80351

© Pei-Yuan Su, Han-Jie Shih, Jia-Lang Xu. Originally published in JMIR Medical Informatics (https://medinform.jmir.org), 20.10.2025. This is an open-access article distributed under the terms of the Creative Commons Attribution License (https://creativecommons.org/licenses/by/4.0/), which permits unrestricted use, distribution, and reproduction in any medium, provided the original work, first published in JMIR Medical Informatics, is properly cited. The complete bibliographic information, a link to the original publication on https://medinform.jmir.org/, as well as this copyright and license information must be included.

XSL•FO
RenderX

Original Paper

Evaluating Multiple Input Strategies of Large Language Models for Gallbladder Polyps on Ultrasound: Comparative Study

Lin Jiang[1], MD; Jiaqian Yao[1], MD; Zebang Yang[1], MD; Fuqiu Tang[1], MM; Xin Zheng[1], MD; Xiaoer Zhang[1], MD; Xiaoyan Xie[1], MD, PhD; Ming Xu[1*], MD, PhD; Tongyi Huang[1*], MD

Department of Medical Ultrasonics, Institute of Diagnostic and Interventional Ultrasound, The First Affiliated Hospital, Sun Yat-sen University, Guangzhou, China

[*]these authors contributed equally

Corresponding Author:
Tongyi Huang, MD
Department of Medical Ultrasonics
Institute of Diagnostic and Interventional Ultrasound
The First Affiliated Hospital, Sun Yat-sen University
58 Zhongshan Er Road
Guangzhou, 510080
China
Phone: 86 020 87755766
Email: huangty26@mail.sysu.edu.cn

Abstract

Background: Gallbladder polyps have a high prevalence and are predominantly benign lesions, often detected via ultrasound. They impose diagnostic burdens on radiologists while generating substantial patient demand for report interpretation. Benign polyps include nonneoplastic polyps without malignant potential and premalignant adenomas that require cholecystectomy. Current guidelines recommending surgery for polyps ≥1.0 cm may lead to unnecessary interventions. Advanced multimodal large language models (LLMs) such as ChatGPT-4o (OpenAI) and Claude 3.5 Sonnet (Anthropic PBC) demonstrate emerging capabilities in medical image analysis. Implementing LLMs in gallbladder polyp ultrasound evaluation can potentially alleviate radiologists' workload, provide patient-accessible consultation platforms, and even reduce overtreatment.

Objective: We aimed to analyze the feasibility and conduct an early-stage evaluation of using LLMs for differentiating between adenomatous and nonneoplastic gallbladder polyps (≥1.0 cm) based on ChatGPT-4o and Claude 3.5 Sonnet, compared to assessments by radiologists and the guideline.

Methods: Ultrasound images and reports of gallbladder polyps ≥1.0 cm with pathology were retrospectively collected from a hospital between January 2011 and January 2022. LLM performance was evaluated using three input strategies: (1) direct image analysis (LLMs-image), (2) feature-based text analysis (LLMs-text), and (3) scoring model-based text analysis (LLMs-model). Both intra- and interreader agreement and diagnostic performance of LLMs were evaluated for all three strategies. The diagnostic performance metrics—including sensitivity, specificity, accuracy, area under the receiver operating characteristic curve, and unnecessary resection rate of nonneoplastic polyps of LLMs in the three strategies were compared with the guideline. Additionally, the strategy LLMs-model was specifically compared with radiologists using the same scoring system (strategy readers-model).

Results: This study included 223 patients (aged 18-72 years; 132/223, 59.2% female) as the initial cohort, with 48 adenomatous polyps and 175 nonneoplastic polyps. The external test set comprised 100 patients. The intrareader agreement coefficients for strategy LLMs-model were significantly higher than those for strategy LLMs-image and LLMs-text (all P<.01). The interreader agreement of the three diagnostic strategies was ranked as LLMs-model>LLMs-text>LLMs-image. The sensitivity of strategies LLMs-image and LLMs-text was significantly lower than that of the guideline (all P<.001). When applying a scoring model (readers/LLMs-model strategy), both radiologists and the LLMs achieved a significantly higher accuracy compared to the guideline (0.34, 0.35, and 0.34 vs 0.22, all P<.01), and the unnecessary resection rate of nonneoplastic polyps was significantly lower (82%, 83%, and 83% vs 100%, all P<.01), while the sensitivity was comparable to the guideline (0.94, 0.98, and 0.98 vs 1.00, all P>.05). All diagnostic performance indicators for GPT-model and Claude-model were not significantly different from those of radiologists (all P>.05).

Conclusions: The ability of LLMs to recognize and interpret medical images requires further improvement. The text strategy with a scoring system is currently the most appropriate diagnostic strategy for LLMs.

XSL•FO
RenderX

(JMIR Med Inform 2025;13:e71178) doi:10.2196/71178

KEYWORDS

large language models; gallbladder polyps; ultrasound; diagnostic accuracy; medical image analysis; artificial intelligence

Introduction

Large language models (LLMs) are deep learning models trained on large amounts of text data, and their emergence has led to changes in many fields [1-3]. LLMs can understand and generate human language and have the potential to provide medical advice, making their application in the medical field of wide interest [4,5]. With the evolution of the LLMs, their capabilities range from simple summarization to complex tasks such as paper writing, medical education, and diagnosis [6-9]. Prior investigations into the diagnostic applications of LLMs have predominantly used two methodological frameworks: (1) diagnostic strategies using narrative textual inputs describing imaging findings [10], or (2) risk stratification approaches requiring LLMs to apply established scoring systems to textualized lesion characteristics [9]. Some LLMs, such as ChatGPT-4o and Claude 3.5 Sonnet, can analyze and interpret images. These two LLMs were developed by different organizations and demonstrated competitive capabilities that positioned them within the global elite of LLMs at the time of our study [11,12], showing they represent the most advanced level of general-purpose LLMs.

Gallbladder polyps are a common finding in abdominal ultrasound examination, with a reported incidence rate of 6.1%-12.1% [13,14]. They impose diagnostic burdens on radiologists and generate substantial patient demand for report interpretation. The management strategy for polypoid lesions of the gallbladder depends on their pathological type. Neoplastic polyps, including gallbladder cancer and precancerous gallbladder adenomas, require cholecystectomy [15,16]. Studies report that 28%-49.5% of gallbladder adenoma may progress to gallbladder cancer [15,17]. Nonneoplastic polyps, including cholesterol polyps, inflammatory polyps, and fibromyoadenoid polyps, rarely become malignant, and follow-up is recommended [18]. Gallbladder carcinoma can be distinguished from other polypoid lesions based on gallbladder wall continuity and contrast-enhanced patterns [19,20]. However, differentiating adenomatous polyps from nonneoplastic polyps remains challenging. Guidelines recommend cholecystectomy for polyps ≥1.0 cm in size [21]. Using these criteria, 27.1%-56% of patients undergoing cholecystectomy for gallbladder polyps are postoperatively diagnosed with nonneoplastic polyps [22,23]. Beyond financial and psychological burdens, this may result in complications that adversely affect quality of life [24,25]. Therefore, it is critical to distinguish neoplastic polyps from nonneoplastic polyps, particularly for lesions ≥1.0 cm. LLMs can potentially reduce the workload of radiologists by generating descriptions based on ultrasound images or risk stratification of gallbladder polyps, and provide medical consults for patients based on ultrasound reports. If LLMs perform better than existing guidelines or radiologists in differentiating gallbladder polyps, they might reduce unnecessary cholecystectomies. Recent studies have demonstrated that ChatGPT-4o and Claude 3.5 Sonnet exhibit superior performance compared to other LLMs in diagnostic tasks involving radiological imaging [26,27], suggesting potential for ultrasound applications. To date, no study has systematically evaluated LLMs' ability to characterize sonographic features or differentiate benign gallbladder polyps. Gallbladder polyps manifest as nonshadowing protrusions from the gallbladder wall into the anechoic lumen in ultrasound examinations. This anatomically well-defined nature with intuitive spatial localization makes them suitable for assessing LLMs' capacity in medical image interpretation. Furthermore, current literature lacks methodological comparisons of LLMs' diagnostic performance across three distinct paradigms: (1) direct image analysis, (2) text-based diagnosis, and (3) scoring-system–based risk stratification using textualized lesion characteristics.

The purpose of this study was to systematically evaluate the feasibility and conduct an early stage evaluation of LLMs across three diagnostic strategies for differential diagnosis of benign gallbladder polyps (≥1.0 cm) based on ChatGPT-4o and Claude 3.5 Sonnet, with comparison to radiologists and the joint guidelines between the European Society of Gastrointestinal and Abdominal Radiology, the European Association for Endoscopic Surgery and other Interventional Techniques, the International Society of Digestive Surgery–European Federation, and the European Society of Gastrointestinal Endoscopy.

Methods

Ethical Considerations

This study was approved by the Ethics Committee in our institute, Sun Yat-sen University (No. [2016]083). Due to the retrospective nature of this study, the requirement for informed consent was waived. This study adhered to the CLAIM (Checklist for Artificial Intelligence in Medical Imaging) [28] for reporting (Table S1 in Multimedia Appendix 1 [29,30]). This study provides a Reproducibility Checklist in Table S2 in Multimedia Appendix 1 to facilitate the replication of our work.

Throughout the interaction with the LLMs, all patient-identifiable information (including names, hospital ID numbers, etc) was strictly removed from the ultrasound images and reports before analysis.

Due to the retrospective design of this study, participants received no compensation.

Patient Selection

A total of 447 patients with previous imaging findings of gallbladder polyps who underwent cholecystectomy at our institution were retrospectively reviewed. The initial cohort of 312 patients (January 2011 to January 2022) was used to develop the scoring system and to evaluate the performance of the LLMs, while the subsequent cohort of 135 patients (February 2022 to March 2025) served as an external test set for the LLMs-model strategy. The inclusion criteria were as follows: (1)

XSL•FO
RenderX

transabdominal ultrasonography was performed in our hospital before cholecystectomy, and (2) there was a definite postoperative pathological diagnosis. The details of the ultrasound examination protocol are shown in Multimedia Appendix 1 (see also Multimedia Appendices 2-6). Given that the differential diagnostic focus for gallbladder polyps predominantly targets lesions ≥1.0 cm, and smaller polyps may be less clearly visualized in ultrasound images, potentially affecting the performance of LLMs, a 1.0 cm threshold was determined as one of the conditions for patient selection. Patients were excluded if they met any of the following criteria: (1) missing ultrasound images; (2) no polypoid lesions detected by the ultrasound examination in our hospital; (3) age <18 years; and (4) size of the largest polyp <1.0 cm. The patients were divided into an adenomatous polyp group and a nonneoplastic polyp group. Patients with both adenomatous polyps and nonneoplastic polyps were classified as having adenomatous polyps.

Patient Data Collection

Preoperative clinical data of patients were collected, including demographic information, alanine aminotransferase, and aspartate aminotransferase levels. The latest preoperative ultrasound images and reports were collected. Information about polyp size and number, gallbladder wall thickness measurements, and the presence of gallstones was obtained from the reports. Other ultrasound features were evaluated independently by two radiologists (with 2 years and 10 years of experience in abdominal ultrasound, respectively) who were blinded to the patient's clinical features and pathology results. Discrepancies were discussed by the two doctors to get a consensus. When consensus could not be reached after discussion between the two radiologists, a third radiologist with seventeen years of experience in abdominal ultrasound made the final determination. If the patient had more than one gallbladder polyp, only the largest one was analyzed. In our previous study, we proposed a new index for quantifying polyp morphology, called the polyp morphology ratio (PMR). The details about the definitions of PMR and other ultrasound features are provided in Multimedia Appendix 1.

Diagnostic Strategies

This study evaluated ChatGPT-4o and Claude 3.5 Sonnet using their standard web interfaces [31,32] between July and September 2024 according to the following strategies. All interactions were conducted without custom code, API calls, or adjustments to default inference parameters. To ensure transparency, all interactions used the platform defaults, and the complete set of prompts is detailed in Multimedia Appendix 1. The prompts input into the two LLMs were the same. Each prompt input does not include expected outcomes or class distributions, nor does it judge the correctness of the LLM's responses. For the strategy of LLMs-image, LLMs performed diagnoses based on ultrasound images. Before analysis, images were cropped to remove all patient-identifiable information. Additionally, the images were cropped to ensure the gallbladder occupied approximately 30%-40% of the frame, with lesions centered whenever possible while maintaining the structural integrity of both the gallbladder and surrounding tissues. No image enhancement or standardization was applied. The underlying vision capabilities of the LLMs are accessed directly through their vision application programming interface, rather than via a third-party wrapper. The images input into the LLMs were in JPEG format, with both horizontal and vertical resolutions of 96 dpi. The processed 2D gray-scale ultrasound image and color Doppler ultrasound image were input into LLMs, and the LLMs were required to describe the ultrasound characteristics of gallbladder polyps and provide a diagnosis.

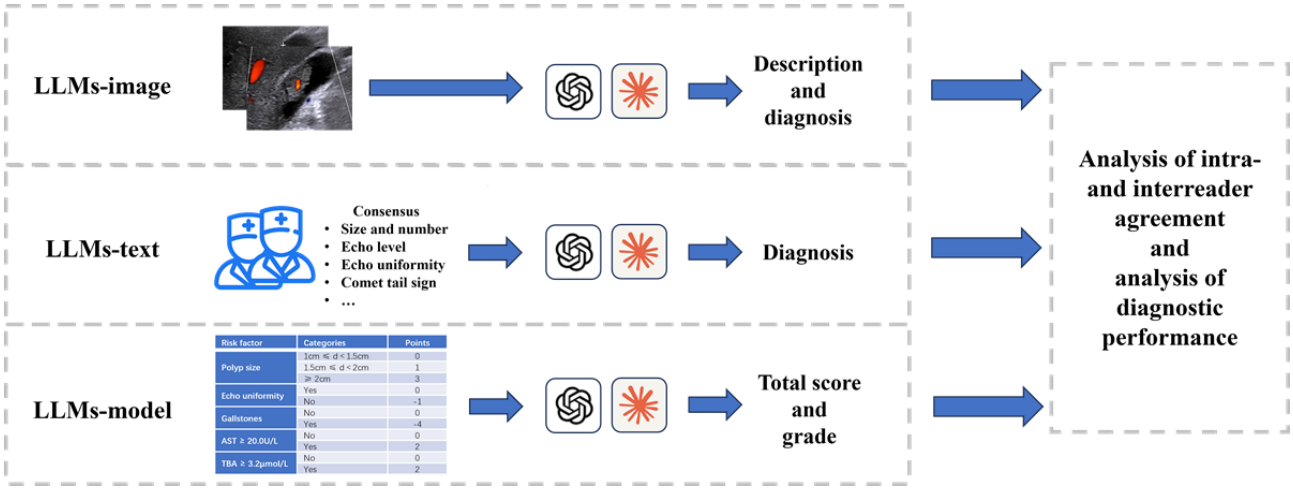
For the strategy LLMs-text, LLMs performed diagnoses based on the text of the ultrasound description. Based on the consensus of the two radiologists, the description of the ultrasound characteristics for the gallbladder polyps was organized into a structured report. The structured report was input into the LLMs, and the LLMs were required to give the diagnosis.

For the strategy LLMs-model, LLMs performed diagnoses based on our previously developed diagnostic model for benign gallbladder polyps ≥1.0 cm [33]. Before this study, a multilevel scoring system for the differentiation between gallbladder adenomatous polyps and nonneoplastic polyps was constructed based on the same cases as those in this study (Table S3 in Multimedia Appendix 1). The relevant information was organized into structured text according to the requirements of the scoring system. Then, only the structured text was input into LLMs without the corresponding scores, and the LLMs were required to calculate the total score and indicate the corresponding grade. In addition, based on the consensus of two radiologists, the total score and the corresponding grade of each patient were calculated with the multilevel scoring system (strategy readers-model).

Figure 1 shows the flow of the diagnostic strategies for LLMs. The prompts templates in diagnostic strategies for LLMs are in Multimedia Appendix 1. The intrareader agreement, interreader agreement, and diagnostic performance of LLMs in the three diagnostic strategies were evaluated. The initial outputs from LLMs in the three strategies were used to analyze interreader agreement and diagnostic performance. From the final enrolled cases, 70 were randomly selected to assess intrareader agreement. The LLMs were asked to regenerate the output for these cases twice, that is, there were three rounds of output per strategy per LLM for each of these 70 cases, respectively.

XSL•FO
RenderX

Figure 1. Diagram of three diagnostic strategies for LLMs. LLM: large language model.



In-Context Learning for LLMs

For the ultrasound image-based lesion characterization tasks in this study, the LLMs underwent supplemental in-context learning beyond their original architecture. LLMs were trained to recognize the degree of blood flow, blood flow pattern, and the definition of PMR and polyp base type (sessile or pedunculated) using ultrasound images of patients with gallbladder polyps in our center (excluding cases included in this study). The prompts used in in-context learning are provided in Multimedia Appendix 1. After entering the prompt word, the memory of the LLMs to was checked to ensure its correct understanding.

Statistical Analysis

The interclass correlation coefficient, Cohen κ, and weighted κ were used to evaluate the interreader agreement for continuous, unordered, and ordered categorical variables, respectively. Interclass correlation coefficient, Fleiss κ, and Kendall W coefficient were used to evaluate the intrareader agreement for continuous, unordered, and ordered categorical variables, respectively. The interreader agreement of ultrasound features was represented by a heatmap generated with the *pheatmap* package in R (R Foundation). The levels of the coefficient of the agreement analysis were defined as follows: 0.20 or less for slight agreement, 0.21-0.40 for fair agreement, 0.41-0.60 for moderate agreement, 0.61-0.80 for substantial agreement, and 0.81-1.00 for almost perfect agreement. The agreement coefficients were compared using the Z-test. The detailed sample size calculation for intrareader agreement is shown in Multimedia Appendix 1.

The diagnostic performance of LLMs was evaluated by sensitivity, specificity, positive predictive value (PPV), negative predictive value (NPV), accuracy, area under the receiver operating characteristic curve, and unnecessary resection rate of nonneoplastic polyps (UNRR). Sensitivity, specificity, PPV, and NPV were calculated and compared with the *stats* package and *epiR* package in R. The area under the receiver operating characteristic curves were compared using the DeLong test. UNRR was calculated as the number of nonneoplastic polyps recommended for cholecystectomy divided by the total number of nonneoplastic polyps. Chi-square test was used to compare UNRR.

For the strategy LLMs-text, univariate logistic regression was performed on ultrasound features according to the diagnosis of LLMs to analyze the basis for differential diagnosis of LLMs.

Two-tailed $P<.05$ was considered statistically significant. Statistical analysis was performed using PASS 2025 (power analysis and sample size; NCSS, LLC), SPSS 25.0 (IBM Corp), and R version 4.3.1 (R Foundation).

Results

Patient Characteristics

In the initial cohort, this study analyzed 223 patients aged 18-72 (median 40, IQR 34-50) years, including 132 (59.2%) females. Among these, 175 (78.5%) had nonneoplastic polyps and 48 (21.5%) had adenomatous polyps. Compared to the initial cohort, the external test set showed no significant differences in demographic characteristics or pathological type distribution (all $P>.05$; Table 1). The patient selection process is shown in Figure 2.

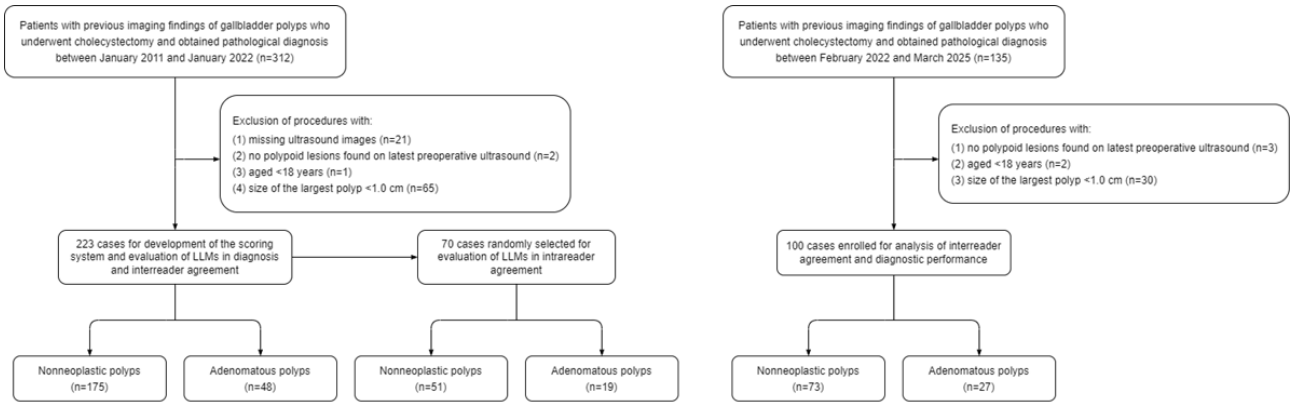
XSL•FO
RenderX

Table 1. Demographic characteristics and gallbladder polyp pathology of patients.

Characteristic	Initial cohort (n=223)	External test set for the LLMs[a]-model strategy (n=100)	*P* value
Sex			
Male, n (%)	91 (40.8)	43 (43)	.71
Female, n (%)	132 (59.2)	57 (57)	.71
Age (years)			.84
Median (IQR)	40 (34-50)	41 (33-52)	
Range	18-72	19-74	
Polyp pathology			
Adenomatous polyps, n (%)	48 (21.5)	27 (27)	.28
Nonneoplastic polyps, n (%)	175 (78.5)	73 (73)	.28

[a]LLM: large language model.

Figure 2. Flowchart of patient selection. LLM: large language model.



Intrareader Agreement Analysis

The intrareader agreement coefficients of LLMs across three strategies are shown in Table 2. Compared to the intrareader agreement for grades in strategy LLMs-model, both ChatGPT-4o and Claude 3.5 Sonnet exhibited significantly lower intrareader agreement for diagnoses in strategy LLMs-text (0.58 vs 0.97, *P*<.001 for ChatGPT-4o; 0.61 vs 1.00, *P*<.001 for Claude 3.5 Sonnet) and LLMs-image (0.37 vs 0.97, *P*<.001 for ChatGPT-4o; 0.47 vs 1.00, *P*<.001 for Claude 3.5 Sonnet). However, there was no significant difference between strategy LLMs-image and LLMs-text (*P*=.15 for ChatGPT-4o and *P*=.33 for Claude 3.5 Sonnet).

For the ultrasound feature identification in strategy LLMs-image, the agreement level of blood flow degree and pattern for ChatGPT-4o was moderate to substantial (range of agreement coefficient 0.43 to 0.68, 95% CI 0.30 to 0.81). Additionally, there was only slight to fair agreement for ChatGPT-4o in other ultrasound features (range of agreement coefficient –0.12 to 0.30, 95% CI –0.25 to 0.45). However, except for the slight to fair agreement in PMR, comet tail sign and gallbladder wall thickness types (range of agreement coefficient 0.02 to 0.30, 95% CI –0.10 to 0.45), there was moderate to almost perfect agreement for Claude 3.5 Sonnet in other ultrasound features (range of agreement coefficient 0.43 to 0.97, 95% CI 0.30 to 1.00). The intrareader agreement coefficients in ultrasound features for Claude 3.5 Sonnet were all higher than those for ChatGPT-4o, except for PMR. In addition, the intraobserver agreement coefficient in diagnosis for Claude 3.5 Sonnet in strategy LLMs-image was 0.47, which was also higher than 0.7 for ChatGPT-4o.

The intraobserver agreement coefficients in diagnosis for ChatGPT-4o and Claude 3.5 Sonnet in strategy LLMs-text were 0.58, 95% CI 0.46 to 0.72, and 0.1, 95% CI 0.49 to 0.75, respectively, indicating a moderate to substantial level, which were higher than those in strategy LLMs-image.

In strategy LLMs-model, both ChatGPT-4o and Claude 3.5 Sonnet showed almost perfect intraobserver agreement for total score and grade (range of agreement coefficient 0.97 to 1.00, 95% CI 0.94 to 1.00). Almost perfect intraobserver agreement was also observed in the external test set (Table S4 in Multimedia Appendix 1).

XSL•FO
RenderX

Table 2. Intrareader agreement coefficients of LLMsa. Data in parentheses are 95% CIs. Except where indicated, the coefficient of agreement analysis is the Fleiss κ coefficient.

	ChatGPT-4o	Claude 3.5 Sonnet
LLMs-image		
PMR[b,c]	0.30 (0.15 to 0.45)	0.02 (–0.10 to 0.14)
Echo level[d]	0.25 (–0.03 to 0.42)	0.58 (0.45 to 0.71)
Echo uniformity	–0.12 (–0.25 to 0.01)	0.75 (0.62 to 0.88)
Comet tail sign	–0.01 (–0.14 to 0.12)	0.30 (0.19 to 0.45)
Cauliflower shape	0.00 (–0.13 to 0.12)	0.74 (0.61 to 0.87)
Pedunculated or sessile	0.18 (0.05 to 0.31)	0.43 (0.30 to 0.56)
Edge	–0.01 (–0.14 to 0.12)	1.00 (—[e])
Blood flow degree[d]	0.68 (0.55 to 0.81)	0.97 (0.94 to 1.00)
Blood flow pattern	0.43 (0.30 to 0.56)	0.85 (0.72 to 0.98)
Gallbladder wall thickness types	–0.04 (–0.17 to 0.09)	0.15 (0.02 to 0.28)
Diagnosis	0.37 (0.24 to 0.50)	0.47 (0.34 to 0.60)
LLMs-text		
Diagnosis	0.58 (0.46 to 0.72)	0.61 (0.49 to 0.75)
LLMs-model		
Total score[c]	1.00 (—)	1.00 (—)
Grade[d]	0.97 (0.94 to 1.00)	1.00 (—)

[a]LLM: large language model.

[b]PMR: polyp morphology ratio.

[c]The coefficient of agreement analysis is the interclass correlation coefficient.

[d]The coefficient of agreement analysis is the Kendall W coefficient.

[e]CIs cannot be calculated due to the perfect consistency of the three rounds' output in each case.

Interreader Agreement Analysis

Figure 3 and Table S5 in Multimedia Appendix 1 present the interreader agreement of human readers and LLMs in ultrasound features. Except for the interobserver agreement level of cauliflower shape between readers 1 and 2 being moderate (agreement coefficient=0.57), the agreement level for other features between readers 1 and 2 was substantial to almost perfect (range of agreement coefficient 0.65 to 0.99). However, the agreement level between LLMs and other observers was only slight (range of agreement coefficient –0.11 to 0.12), except for blood flow degree and pattern (range of agreement coefficient 0.34 to 0.75). As shown in Table S5 in Multimedia Appendix 1, apart from the comet tail sign, the agreement coefficient for other features between readers 1 and 2 was significantly higher than those between LLMs and other observers (P<.001).

The agreement coefficient for the comet tail sign could not be calculated because reader 1 considered that the comet tail sign was not present in all cases in this study.

The interobserver agreement coefficients of human readers and LLMs in diagnosis are shown in Table 3. There was slight interobserver agreement between ChatGPT-4o and Claude 3.5 Sonnet in strategy LLMs-image (Cohen κ=0.12, 95% CI –0.01 to 0.24), and fair agreement in strategy LLMs-text (Cohen κ=0.38, 95% CI 0.26 to 0.50). For the strategy readers or LLMs-model, the agreement levels were all almost perfect in readers versus ChatGPT-4o, readers versus Claude 3.5 Sonnet, ChatGPT-4o versus Claude 3.5 Sonnet (range of agreement coefficient 0.84 to 0.99, 95% CI 0.78 to 0.99). In the external test set, LLMs still showed a considerable degree of interreader agreement (Table S6 in Multimedia Appendix 1). Compared to the interreader agreement coefficient of grades between ChatGPT-4o and Claude 3.5 Sonnet in strategy LLMs-model, those for diagnosis in strategy LLMs-image (P<.001) and LLMs-text (P<.001) were significantly lower. Additionally the interreader agreement coefficient for diagnosis in strategy LLMs-text was significantly higher than that in strategy LLMs-image (P=.004).

XSL•FO
RenderX

Figure 3. Heatmap of interreader agreement in human readers and LLMs. LLM: large language model.

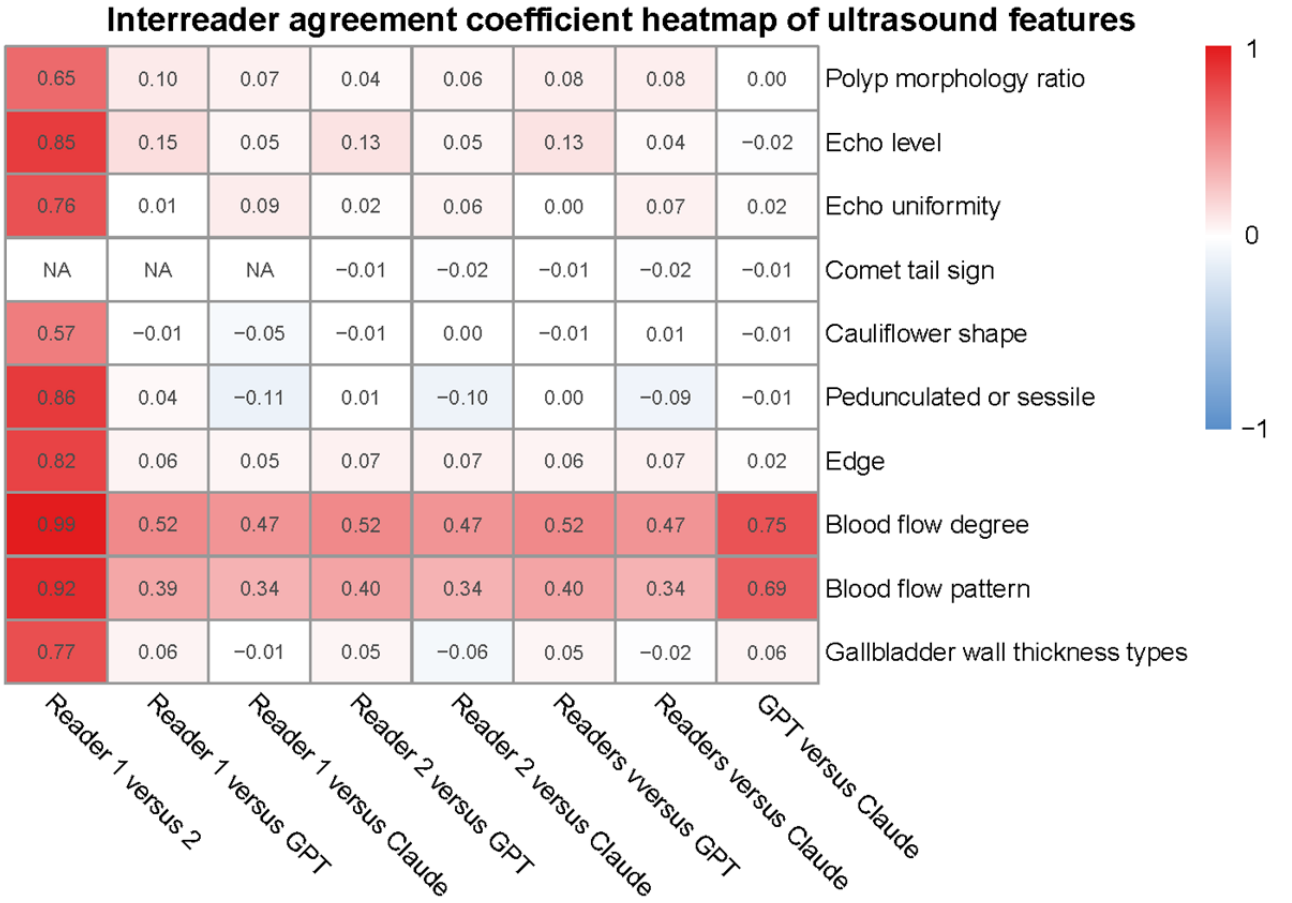


Table 3. Interreader agreement coefficients of human readers and LLMsa in diagnosis. Data in parentheses are 95% CIs. Except where indicated, the coefficient of agreement analysis is Cohen κ. The total score and grade of readers are calculated based on laboratory tests and the US features consensus of readers 1 and 2.

Diagnostic strategies	Readers versus ChatGPT-4o	Readers versus Claude 3.5 Sonnet	ChatGPT-4o versus Claude 3.5 Sonnet
LLM-image	—[b]	—	0.12 (–0.01 to 0.24)
LLM-text	—	—	0.38 (0.26 to 0.50)
Readers or LLM-model			
Total score[c]	0.97 (0.96 to 0.97)	0.98 (0.97 to 0.98)	0.99 (0.98 to 0.99)
Grade[d]	0.84 (0.78 to 0.90)	0.95 (0.92 to 0.99)	0.87 (0.82 to 0.92)

[a]LLM: large language model.

[b]Not available.

[c]The coefficient of agreement analysis is the interclass correlation coefficient.

[d]The coefficient of agreement analysis is weighted κ.

Diagnostic Performance

The diagnostic performance of all diagnostic strategies is presented in Table 4. Figure 4A and B show representative cases from strategy Claude-image and strategy GPT-model, respectively.

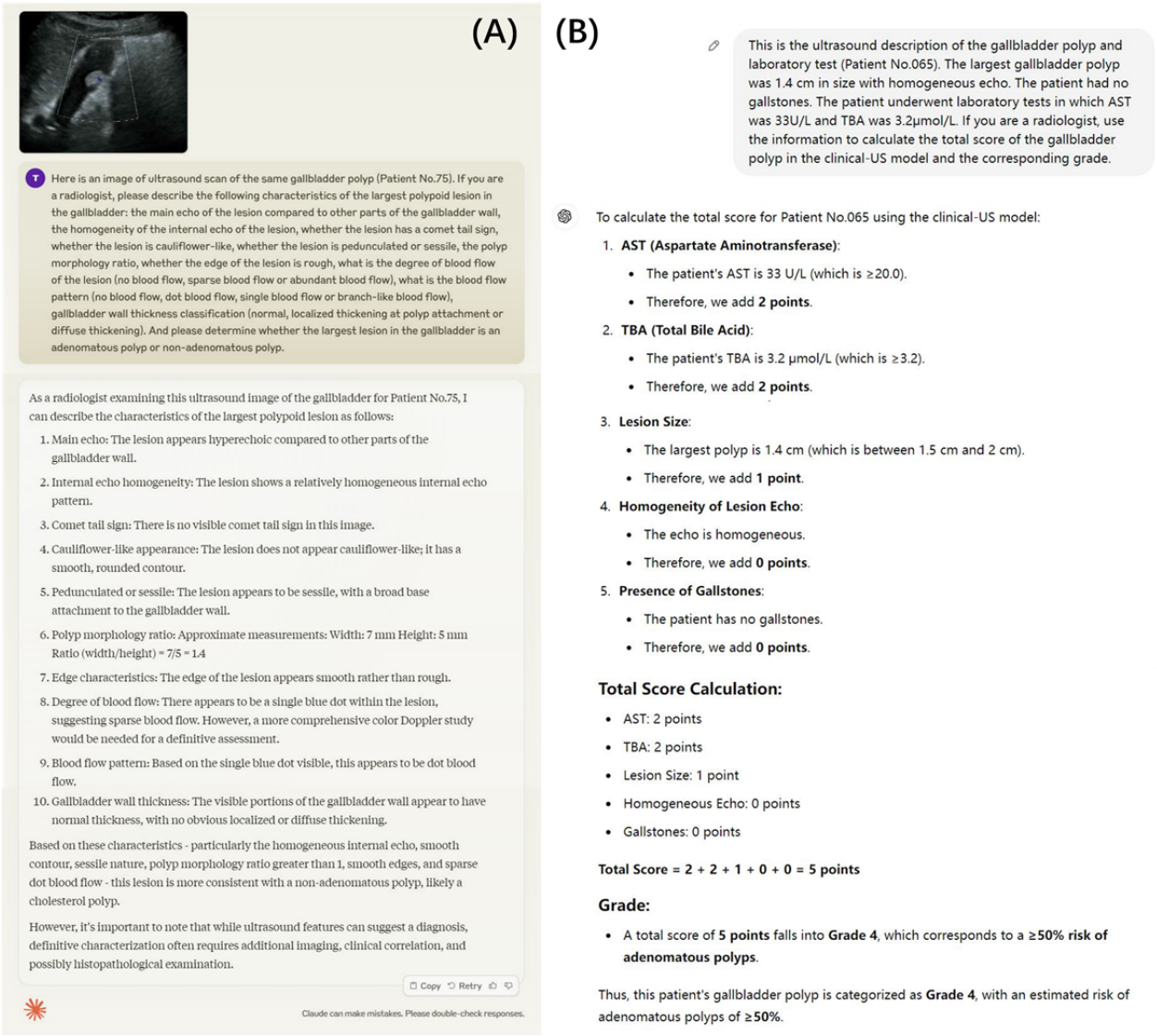
The sensitivity of the guideline's diagnostic strategy was 1.00, indicating that no gallbladder adenomas were missed, but surgery was recommended for all nonneoplastic polyps ≥1.0 cm (UNRR=100%). In the strategies LLMs-image and LLMs-text, the sensitivity of GPT-image, Claude-image, GPT-text, and Claude-text was 0.27, 0.33, 0.56, and 0.65, respectively, which were significantly lower than the sensitivity of the guideline (all P<.001), indicating more gallbladder adenomas were missed.

In the strategy readers or LLMs-model, when cholecystectomy was recommended for gallbladder polyps ≥grade 2, the sensitivity of ChatGPT-4o, Claude 3.5 Sonnet, and radiologists were 0.94, 0.98, and 0.98, respectively, showing no significant difference from the sensitivity of 1.00 achieved by the guideline

XSL•FO
RenderX

(all $P<.05$). However, the accuracy of ChatGPT-4o, Claude 3.5 Sonnet, and radiologists was significantly higher than that of the guideline (0.35, 0.34, and 0.34 vs 0.22, all $P<.01$), and the UNRR was significantly lower than that of the guideline (82%, 83%, and 83% vs 100%, all $P<.01$). In addition, there were no significant differences observed between GPT-model, Claude-model and readers-model in terms of sensitivity, specificity, PPV, NPV, accuracy or UNRR across all grades (all $P>.05$). Similar results were observed in the external test set (Table S7 in Multimedia Appendix 1).

Figure 4. Examples of strategy Claude-image (A) and strategy GPT-model (B). AST: aspartate aminotransferase; TBA: total bile acid.



XSL•FO
RenderX

Table 4. Diagnostic performance of all diagnostic strategies. Data in ranges are 95% CIs. Except where indicated, *P* values are for comparison with the guideline that recommends cholecystectomy for polyps ≥1.0 cm.

Diagnostic strategies	Sensitivity	Specificity	PPV[a]	NPV[b]	Accuracy	UNRR[c,d]
Polyp size ≥1.0 cm						175/175 (100)
	1.00	0.00	0.22	—[e]	0.22	
	0.93 to 1.00	0.00 to 0.02	0.16 to 0.28	—	0.16 to 0.28	
GPT-image						54/175 (31)
	0.27	0.69	0.19	0.78	0.60	
	0.15 to 0.42	0.62 to 0.76	0.11 to 0.31	0.70 to 0.84	0.53 to 0.67	
P value	<.01	<.01	.84	—	<.01	<.001
Claude-image						80/175 (46)
	0.33	0.54	0.17	0.75	0.50	
	0.20 to 0.48	0.47 to 0.62	0.10 to 0.26	0.66 to 0.82	0.43 to 0.57	
P value	<.01	<.01	.40	—	<.01	<.001
GPT-text						108/175 (62)
	0.56	0.38	0.20	0.76	0.42	
	0.41 to 0.71	0.31 to 0.46	0.14 to 0.28	0.66 to 0.85	0.36 to 0.49	
P value	<.01	<.01	.83	—	<.01	<.001
Claude-text						127/175 (73)
	0.65	0.27	0.20	0.74	0.35	
	0.50 to 0.78	0.21 to 0.35	0.14 to 0.27	0.62 to 0.84	0.29 to 0.42	
P value	<.01	<.01	.75	—	<.01	<.001
GPT-model						
≥Grade 2						143/175 (82)
	0.94	0.18	0.24	0.91	0.35	
	0.83 to 0.99	0.13 to 0.25	0.18 to 0.31	0.77 to 0.98	0.28 to 0.41	
P value	.24	<.01	.64	—	<.01	<.001
P value[f]	.61	.78	>.99	.72	>.99	.78
≥Grade 3						84/175 (48)
	0.75	0.52	0.30	0.88	0.57	
	0.60 to 0.86	0.44 to 0.60	0.22 to 0.39	0.81 to 0.94	0.50 to 0.64	
P value	.01	<.01	.11	—	<.01	<.001
P value[f]	>.99	.45	.93	>.99	.57	.45
=Grade 4						5/175 (3)
	0.15	0.97	0.58	0.81	0.79	
	0.06 to 0.28	0.94 to 0.99	0.28 to 0.85	0.75 to 0.86	0.74 to 0.85	
P value	<.01	<.01	.01	—	<.01	<.001
P value[f]	>.99	.72	.90	>.99	.91	.72
Claude-model						
≥Grade 2						146/175 (83)
	0.98	0.17	0.24	0.97	0.34	
	0.89 to 1.00	0.11 to 0.23	0.19 to 0.31	0.83 to 1.00	0.28 to 0.41	
P value	>.99	<.01	.57	—	<.01	<.001

XSL•FO
RenderX

Diagnostic strategies	Sensitivity	Specificity	PPV[a]	NPV[b]	Accuracy	UNRR[c,d]
P value[f]	>.99	>.99	>.99	>.99	>.99	>.99
≥Grade 3						93/175 (53)
	0.73	0.47	0.27	0.86	0.53	
	0.58 to 0.85	0.39 to 0.55	0.20 to 0.36	0.78 to 0.93	0.46 to 0.59	
P value	<.01	<.01	.27	—	<.01	<.001
P value[f]	.81	>.99	.92	.85	.85	>.99
=Grade 4						5/175 (3)
	0.15	0.97	0.58	0.81	0.79	
	0.06 to 0.28	0.94 to 0.99	0.28 to 0.85	0.75 to 0.86	0.74 to 0.85	
P value	<.01	<.01	.01	—	<.01	<.001
P value[f]	>.99	.72	.90	>.99	.91	.72
Readers-model						
≥Grade 2						146/175 (83)
	0.98	0.17	0.24	0.97	0.34	
	0.89 to 1.00	0.11 to 0.23	0.19 to 0.31	0.83 to 1.00	0.28 to 0.41	
P value	.99	<.01	.57	—	<.01	<.001
≥Grade 3						92/175 (53)
	0.77	0.47	0.29	0.88	0.54	
	0.63 to 0.88	0.40 to 0.55	0.21 to 0.37	0.80 to 0.94	0.47 to 0.61	
P value	.01	<.01	.17	—	<.01	<.001
=Grade 4						3/175 (2)
	0.15	0.98	0.70	0.81	0.80	
	0.06 to 0.28	0.95 to 1.00	0.35 to 0.93	0.75 to 0.86	0.74 to 0.85	
P value	<.01	<.01	<.01	—	<.01	<.001

[a]PPV: positive predictive value.

[b]NPV: negative predictive value.

[c]UNRR: unnecessary resection rate of nonneoplastic polyps.

[d]n/N (%).

[e]Not applicable.

[f]*P* values are for comparison with the same grade in the strategy readers-model.

Interpretability of the Diagnosis in Strategy LLMs-Text

The results of univariate analysis based on the diagnosis of GPT-text and Claude-text are shown in Table S8 in Multimedia Appendix 1. Both ChatGPT-4o and Claude 3.5 Sonnet considered larger size, hypoechogenicity, heterogeneous echogenicity, cauliflower shape, sessile base, and rough edge as significant factors for adenomatous polyps. Additionally, ChatGPT-4o identified higher PMR as a diagnostic indicator for adenomatous polyps. Furthermore, Claude 3.5 Sonnet also associated sparse and dot-like blood flow in color Doppler flow imaging with adenomatous polyps. Both LLMs diagnosed all lesions with abundant blood flow (6 cases) as adenomas, which was identified as a risk feature of neoplastic gallbladder polyps by a previous study, while this complete separation led to the extreme or infinite CIs.

Error Analysis in Strategy LLMs-Text

In the strategy LLMs-text, 129 cases were misdiagnosed by ChatGPT-4o, while 94 cases were correctly diagnosed. As shown in Table S9 in Multimedia Appendix 1, lesions with the following characteristics were more likely to be misdiagnosed by ChatGPT-4o: hypoechoic appearance (23% vs 11%, *P*=.047), heterogeneous echotexture (52% vs 22%, *P*<.001), cauliflower-like morphology (24% vs 13%, *P*=.04), and rough edges (56% vs 29%, *P*<.001).

For Claude 3.5 Sonnet, 144 cases were misdiagnosed by ChatGPT-4o, while 79 cases were correctly diagnosed. Table S10 in Multimedia Appendix 1 demonstrates that Claude 3.5 Sonnet was prone to misdiagnosis in lesions with these features: larger size (1.30 cm vs 1.10 cm, *P*<.001), hypoechoic appearance (21% vs 13%, *P*=.03), heterogeneous echotexture

XSL•FO
RenderX

(49% vs 23%, $P<.001$), cauliflower-like morphology (24% vs 11%, $P=.03$), and rough edges (52% vs 30%, $P=.002$).

Discussion

Principal Findings

This study evaluated the feasibility of LLMs for the differential diagnosis of gallbladder benign polyps. Our principal findings indicate that the diagnostic strategy profoundly influences LLM performance. In the strategy LLMs-image, LLMs exhibited only slight-to-moderate intrareader agreement and poor interreader consistency compared to radiologists. As the ultrasonic features associated with gallbladder polyps represent common characteristics shared by focal lesions, the finding that current LLMs have limited capabilities in recognizing these features suggests this limitation may have broad applicability. For diagnosis, the diagnostic performance of LLMs-image and the strategy LLMs-text showed significantly lower sensitivity than clinical guidelines, leading to more missed adenomas. In contrast, the strategy LLMs-model, which used text descriptions within a scoring system, demonstrated high consistency and diagnostic performance comparable to radiologists using the same model, while significantly reducing unnecessary cholecystectomies. Notably, the performance between two general-purpose LLMs, ChatGPT-4o and Claude 3.5 Sonnet, was comparable across all strategies, suggesting these findings may generalize to other general-purpose LLMs.

Comparison With Prior Work

Our results on the poor performance of general-purpose LLMs in direct image interpretation align with a growing body of evidence across various medical fields. Studies using dermoscopic images for melanoma diagnosis, orthopedic residency examination images, and musculoskeletal radiology images consistently report not only unsatisfactory diagnostic accuracy (as low as 3% to 36%) but also highlight that LLM performance is inferior to that of human specialists [34-37]. Critically, some studies report that LLMs could harm patient care by recommending unnecessary invasive procedures, such as biopsies, at a significantly higher rate than radiologists [38]. This collective evidence confirms that current general-purpose LLMs remain inadequate for reliable medical image-based diagnosis.

It is important to note that LLMs receiving specialized training in medical images have demonstrated more competent performance in specific domains, such as dermatology (SkinGPT-4) and diabetes management (DeepDR-LLM) [39,40]. Universal systems such as ChatCAD+ also show promise across multiple image types [41]. However, such specialized models are often confined to a single disease area or a limited set of tasks, and they may underperform advanced general LLMs such as GPT-4 in broader medical question-answering [42]. Other general medical LLMs capable of addressing multiple conditions, such as MedFound, do not yet support image input [43]. Given the critical needs for accessibility, generalizability, and image input capabilities in real-world clinical settings, we selected leading general-purpose LLMs (ChatGPT-4o and Claude 3.5 Sonnet) as the subjects of this study. Our findings contribute to the understanding of their current capabilities and limitations.

Regarding the diagnostic performance of text-based strategies, our findings must be viewed within the context of a highly variable literature. Previous studies report widely varying accuracy (40%-91.4%) for categorical diagnoses using text-only strategies [27,44,45]. When focusing specifically on the interpretation of radiological findings, reported diagnostic accuracy for LLMs ranges from 25% to 73% [26,46-48]. While some studies, such as one on real-world radiology reports of brain tumors, found ChatGPT-4's accuracy (73%) to be comparable with radiologists [48], the absence of standardized methods and reporting metrics in LLM studies introduces significant bias risks and hinders cross-study comparisons. In our study, the text-based strategy demonstrated superior diagnostic performance to the image-based approach, which aligns with the consensus and the reported performance levels. Nevertheless, given gallbladder adenomas' high potential for malignancy, the moderate sensitivity achieved by the text-based strategy in our study remains a critical limitation for clinical application, as higher sensitivity is paramount to avoid missed diagnoses.

The LLMs performed suboptimally in the text-based diagnostic strategy, even though the interpretability analysis of the LLMs-text approach indicated that the high-risk features of adenomas identified by the LLMs are supported by previous literature [29,49-51]. In the error analysis, we observed that LLMs showed subpar performance in diagnosing lesions with these same features, such as heterogeneous echotexture and rough edges. Essentially, this finding reflects a long-standing fundamental challenge in the imaging diagnosis of gallbladder polyps: there is significant overlap in the sonographic features between high-grade dysplastic adenomas and early-stage gallbladder cancer. Trained on broader existing literature about medical imaging, the LLMs correctly learned the strong association between these features and common malignancy risk (eg, gallbladder cancer). As indicated by the extreme odds ratio in the interpretability analysis, both LLMs assigned excessive weight to abundant blood flow. Although previous studies confirm it is indeed a feature associated with neoplastic polyps [52], the models' tendency to treat it as an absolute diagnostic rule—rather than a probabilistic indicator—reveals their limitation in performing the task of fine-grained diagnosis, a reflection of the inherent difficulty of the task itself. However, when the task was confined to the relatively idealized binary framework of "differentiating adenomatous from non-neoplastic polyps," the model's heightened sensitivity to these high-risk features created a conflict with the task objective. This may not represent a "weakness" in the model, but rather an objective reflection of complex clinical reality—the degree of dysplasia in lesions exists on a spectrum, and such ambiguity in imaging is inherent before the intervention of the pathological "gold standard." Meanwhile, the LLMs also demonstrated valuable capabilities. For instance, ChatGPT-4o correctly recognized a novel morphological index (PMR) from an unpublished study as useful for diagnosis, and Claude 3.5 Sonnet identified sparse and dot blood flow as a relevant feature, which aligns with established research [29,49]. This demonstrates their potential

XSL•FO
RenderX

in tasks requiring strong information retrieval and logical reasoning.

Conversely, our study reinforces that LLMs exhibit excellent performance when working with structured text data from scoring systems. Their high accuracy and consistency in applying such systems are supported by prior research in Liver Imaging Reporting and Data System and Thyroid Imaging Reporting and Data System classification [9,53]. In addition, our findings clarify the role of general-purpose LLMs. In the LLMs-model strategy, the LLM acts as a reliable executor of clinical rules, not a simple calculator. It first understands text to find key features, then applies the scoring rule. The performance of our LLMs-model strategy, which was comparable to radiologists, suggests that leveraging LLMs to execute standardized clinical rules may be their most reliable and immediate clinical application.

Strengths and Limitations

A key strength of this study is the comprehensive evaluation of LLMs across three distinct diagnostic strategies, providing a clear understanding of their appropriate clinical roles. We also provided an in-depth analysis of their reasoning, identifying both capabilities and weaknesses.

This study has several limitations. First, the task of differentiating benign gallbladder polyps is inherently challenging, even for radiologists, which may have contributed to the LLMs' suboptimal performance. Second, the evaluation was conducted on a single disease entity; assessing broader clinical applicability requires more diverse and complex cases. Third, we used in-context learning with only typical cases. While this approach simulates a realistic usage scenario and is highly accessible, it is inherently less stable than fine-tuning and may not capture the full spectrum of clinical presentations. Finally, the retrospective design may introduce potential selection biases.

Future Directions

Based on our findings, future research should focus on several key areas. First, the development and evaluation of more versatile and medically tuned multimodal LLMs are crucial. Second, the performance of LLMs is heavily dependent on the quality of the underlying scoring system; therefore, integrating them with more robust and validated clinical models could maximize their diagnostic utility. Finally, standardizing evaluation methods and reporting metrics across LLM studies is urgently needed to enable meaningful comparisons. Given their strong performance in information retrieval and logical reasoning, future work should also explore the role of LLMs in medical education [54,55] and self-management counseling for patients with chronic conditions [56].

Conclusions

In conclusion, current general-purpose LLMs have poor reproducibility and diagnostic performance in image-based diagnosis of gallbladder polyps, limiting their direct clinical application. However, they demonstrate significant potential when used in a text-based strategy that uses a clinical scoring system, achieving performances comparable to radiologists. This model-based approach currently represents the most appropriate diagnostic strategy for LLMs in this domain.

Acknowledgments

Generative artificial intelligence (GenAI) was not used to generate any part of this paper. In this study, GenAI is only a part of the research design. All prompt templates sent to the GenAI are detailed in Multimedia Appendix 1.

Funding

This work was supported by the National Natural Science Foundation of China (No. 82572248 & No. 82102057).

Data Availability

The original ultrasound images and clinical records analyzed during this study are not publicly available due to patient confidentiality and privacy protection regulations. However, deidentified data underlying the reported results can be made available from the corresponding author upon reasonable request. Requests should include a detailed research proposal outlining the intended use of the data and must be approved by the institutional ethics committee that oversaw the original study.

Authors' Contributions

Conceptualization: MX, TH, LJ
Funding acquisition: TH, MX
Investigation: LJ, TH, JY, ZY, FT, X Zheng, X Zhang, XX
Methodology: LJ, TH, JY, ZY
Resources: MX, TH, XX
Supervision: MX, TH
Writing - original draft: LJ
Writing - review & editing: TH, MX

XSL•FO
RenderX

Conflicts of Interest

None declared.

Multimedia Appendix 1
Study protocols, prompt templates, statistical details, and extended results.
[DOCX File , 339 KB - medinform_v13i1e71178_app1.docx]

Multimedia Appendix 2
Example No.1. An example of dot and sparse blood flow.
[PNG File , 244 KB - medinform_v13i1e71178_app2.png]

Multimedia Appendix 3
Example No.2. An example of single and sparse blood flow.
[PNG File , 254 KB - medinform_v13i1e71178_app3.png]

Multimedia Appendix 4
Example No.3. An example of branch-like and abundant blood flow.
[PNG File , 166 KB - medinform_v13i1e71178_app4.png]

Multimedia Appendix 5
Example No.4. An example of a pedunculated polyp.
[PNG File , 377 KB - medinform_v13i1e71178_app5.png]

Multimedia Appendix 6
Example No.5. An example of a sessile polyp.
[PNG File , 277 KB - medinform_v13i1e71178_app6.png]

References

1. Minaee S, Mikolov T, Nikzad N, Chenaghlu M, Socher R, Amatriain X, et al. Large language models: a survey. arXiv Preprint posted online on March 23, 2025. [doi: 10.48550/arXiv.2402.06196]
2. Voultsiou E, Vrochidou E, Moussiades L, Papakostas GA. The potential of large language models for social robots in special education. Prog Artif Intell 2025;14(2):165-189. [doi: 10.1007/s13748-025-00363-2]
3. Hang CN, Wei Tan C, Yu P. MCQGen: a large language model-driven MCQ generator for personalized learning. IEEE Access 2024;12:102261-102273. [doi: 10.1109/access.2024.3420709]
4. Dave T, Athaluri SA, Singh S. ChatGPT in medicine: an overview of its applications, advantages, limitations, future prospects, and ethical considerations. Front Artif Intell 2023;6:1169595 [FREE Full text] [doi: 10.3389/frai.2023.1169595] [Medline: 37215063]
5. Liu J, Wang C, Liu S. Utility of ChatGPT in clinical practice. J Med Internet Res 2023;25:e48568 [FREE Full text] [doi: 10.2196/48568] [Medline: 37379067]
6. Chintagunta B, Katariya N, Amatriain X, Kannan A. Medically aware GPT-3 as a data generator for medical dialogue summarization. : Association for Computational Linguistics; 2021 Presented at: Proceedings of the Second Workshop on Natural Language Processing for Medical Conversations; November 30, 2025; Online p. 66-76. [doi: 10.18653/v1/2021.nlpmc-1.9]
7. Margetts TJ, Karnik SJ, Wang HS, Plotkin LI, Oblak AL, Fehrenbacher JC, et al. Use of AI language engine ChatGPT 4.0 to write a scientific review article examining the intersection of Alzheimer's disease and bone. Curr Osteoporos Rep 2024;22(1):177-181 [FREE Full text] [doi: 10.1007/s11914-023-00853-z] [Medline: 38225472]
8. Safranek CW, Sidamon-Eristoff AE, Gilson A, Chartash D. The role of large language models in medical education: applications and implications. JMIR Med Educ 2023;9:e50945 [FREE Full text] [doi: 10.2196/50945] [Medline: 37578830]
9. Wu S, Tong W, Li M, Hu H, Lu X, Huang Z, et al. Collaborative enhancement of consistency and accuracy in US diagnosis of thyroid nodules using large language models. Radiology 2024;310(3):e232255. [doi: 10.1148/radiol.232255] [Medline: 38470237]
10. Ueda D, Mitsuyama Y, Takita H, Horiuchi D, Walston SL, Tatekawa H, et al. ChatGPT's diagnostic performance from patient history and imaging findings on the diagnosis please quizzes. Radiology 2023;308(1):e231040. [doi: 10.1148/radiol.231040] [Medline: 37462501]
11. Chiang W, Zheng L, Sheng Y, Angelopoulos A, Li T, Li D. Chatbot Arena: an open platform for evaluating LLMs by human preference. arXiv Preprint posted online on March 7, 2024. [doi: 10.48550/arXiv.2403.04132]

XSL•FO
RenderX

12. Li T, Chiang W, Song Y, Jain N, Dunlap L, Li D. Chatbot Arena Categories. 2024. URL: https://blog.lmarena.ai/blog/2024/arena-category/ [accessed 2025-12-04]
13. Lin W, Lin D, Tai D, Hsieh S, Lin C, Sheen I, et al. Prevalence of and risk factors for gallbladder polyps detected by ultrasonography among healthy Chinese: analysis of 34 669 cases. J Gastroenterol Hepatol 2008;23(6):965-969. [doi: 10.1111/j.1440-1746.2007.05071.x] [Medline: 17725602]
14. Heitz L, Kratzer W, Gräter T, Schmidberger J, EMIL study group. Gallbladder polyps - a follow-up study after 11 years. BMC Gastroenterol 2019;19(1):42 [FREE Full text] [doi: 10.1186/s12876-019-0959-3] [Medline: 30885181]
15. Roa I, de Aretxabala X, Araya JC, Roa J. Preneoplastic lesions in gallbladder cancer. J Surg Oncol 2006;93(8):615-623. [doi: 10.1002/jso.20527] [Medline: 16724345]
16. Branch of Biliary Surgery, Chinese Society of Surgery, Chinese Medical Association, Chinese Medical Doctor Association in Chinese Committee of Biliary Surgeons. [Consensus on the surgical management of benign gallbladder diseases(2021 edition)]. Zhonghua Wai Ke Za Zhi 2022;60(1):4-9. [doi: 10.3760/cma.j.cn112139-20210811-00373] [Medline: 34839607]
17. Albores-Saavedra J, Chablé-Montero F, González-Romo MA, Ramírez Jaramillo M, Henson DE. Adenomas of the gallbladder. Morphologic features, expression of gastric and intestinal mucins, and incidence of high-grade dysplasia/carcinoma in situ and invasive carcinoma. Hum Pathol 2012;43(9):1506-1513. [doi: 10.1016/j.humpath.2011.11.011] [Medline: 22386521]
18. Taskin OC, Bellolio E, Dursun N, Seven IE, Roa JC, Araya JC, et al. Non-neoplastic polyps of the gallbladder: a clinicopathologic analysis of 447 cases. Am J Surg Pathol 2020;44(4):467-476 [FREE Full text] [doi: 10.1097/PAS.0000000000001405] [Medline: 31725469]
19. Yuan H, Cao J, Kong W, Xia H, Wang X, Wang W. Contrast-enhanced ultrasound in diagnosis of gallbladder adenoma. Hepatobiliary Pancreat Dis Int 2015;14(2):201-207. [doi: 10.1016/s1499-3872(15)60351-4] [Medline: 25865694]
20. Zhang H, Bai M, Gu J, He Y, Qiao X, Du L. Value of contrast-enhanced ultrasound in the differential diagnosis of gallbladder lesion. World J Gastroenterol 2018;24(6):744-751 [FREE Full text] [doi: 10.3748/wjg.v24.i6.744] [Medline: 29456413]
21. Foley KG, Lahaye MJ, Thoeni RF, Soltes M, Dewhurst C, Barbu ST, et al. Management and follow-up of gallbladder polyps: updated joint guidelines between the ESGAR, EAES, EFISDS and ESGE. Eur Radiol 2022;32(5):3358-3368 [FREE Full text] [doi: 10.1007/s00330-021-08384-w] [Medline: 34918177]
22. Wennmacker SZ, van Dijk AH, Raessens JHJ, van Laarhoven CJHM, Drenth JPH, de Reuver PR, et al. Polyp size of 1 cm is insufficient to discriminate neoplastic and non-neoplastic gallbladder polyps. Surg Endosc 2019;33(5):1564-1571 [FREE Full text] [doi: 10.1007/s00464-018-6444-1] [Medline: 30203209]
23. Pickering O, Pucher PH, Toale C, Hand F, Anand E, Cassidy S, et al. Prevalence and sonographic detection of gallbladder polyps in a western European population. J Surg Res 2020;250:226-231. [doi: 10.1016/j.jss.2020.01.003] [Medline: 32106001]
24. Vetrhus M, Berhane T, Søreide O, Søndenaa K. Pain persists in many patients five years after removal of the gallbladder: observations from two randomized controlled trials of symptomatic, noncomplicated gallstone disease and acute cholecystitis. J Gastrointest Surg 2005;9(6):826-831. [doi: 10.1016/j.gassur.2005.01.291] [Medline: 15985239]
25. Farrugia A, Attard JA, Khan S, Williams N, Arasaradnam R. Postcholecystectomy diarrhoea rate and predictive factors: a systematic review of the literature. BMJ Open 2022;12(2):e046172 [FREE Full text] [doi: 10.1136/bmjopen-2020-046172] [Medline: 35177439]
26. Kurokawa R, Ohizumi Y, Kanzawa J, Kurokawa M, Sonoda Y, Nakamura Y, et al. Diagnostic performances of Claude 3 Opus and Claude 3.5 sonnet from patient history and key images in radiology's "diagnosis please" cases. Jpn J Radiol 2024;42(12):1399-1402. [doi: 10.1007/s11604-024-01634-z] [Medline: 39096483]
27. Sonoda Y, Kurokawa R, Nakamura Y, Kanzawa J, Kurokawa M, Ohizumi Y, et al. Diagnostic performances of GPT-4o, Claude 3 Opus, and Gemini 1.5 Pro in "diagnosis please" cases. Jpn J Radiol 2024;42(11):1231-1235. [doi: 10.1007/s11604-024-01619-y] [Medline: 38954192]
28. Tejani AS, Klontzas ME, Gatti AA, Mongan JT, Moy L, Park SH, CLAIM 2024 Update Panel. Checklist for artificial intelligence in medical imaging (CLAIM): 2024 update. Radiol Artif Intell 2024;6(4):e240300 [FREE Full text] [doi: 10.1148/ryai.240300] [Medline: 38809149]
29. Fei X, Li N, Zhu L, Han P, Jiang B, Tang W, et al. Value of high frame rate contrast-enhanced ultrasound in distinguishing gallbladder adenoma from cholesterol polyp lesion. Eur Radiol 2021;31(9):6717-6725. [doi: 10.1007/s00330-021-07730-2] [Medline: 33569621]
30. Gupta P, Dutta U, Rana P, Singhal M, Gulati A, Kalra N, et al. Gallbladder reporting and data system (GB-RADS) for risk stratification of gallbladder wall thickening on ultrasonography: an international expert consensus. Abdom Radiol (NY) 2022 Feb;47(2):554-565. [doi: 10.1007/s00261-021-03360-w] [Medline: 34851429]
31. ChatGPT. OpenAI. URL: https://chatgpt.com/ [accessed 2025-12-04]
32. Claude. ANTHROPIC PBC. URL: https://claude.ai/new [accessed 2025-12-05]
33. Jiang L, Xu M, Yao J, Yang Z, Zhang X, Wu W, et al. Multilevel scoring systems based on ultrasound for differentiating between gallbladder adenomatous polyps and non-neoplastic polyps. Clin Radiol 2025;89:107024. [doi: 10.1016/j.crad.2025.107024] [Medline: 40795450]

XSL•FO
RenderX

34. Shifai N, van Doorn R, Malvehy J, Sangers TE. Can ChatGPT vision diagnose melanoma? An exploratory diagnostic accuracy study. J Am Acad Dermatol 2024;90(5):1057-1059 [FREE Full text] [doi: 10.1016/j.jaad.2023.12.062] [Medline: 38244612]
35. Massey PA, Montgomery C, Zhang AS. Comparison of ChatGPT-3.5, ChatGPT-4, and orthopaedic resident performance on orthopaedic assessment examinations. J Am Acad Orthop Surg 2023;31(23):1173-1179 [FREE Full text] [doi: 10.5435/JAAOS-D-23-00396] [Medline: 37671415]
36. Horiuchi D, Tatekawa H, Oura T, Shimono T, Walston SL, Takita H, et al. ChatGPT's diagnostic performance based on textual vs. visual information compared to radiologists' diagnostic performance in musculoskeletal radiology. Eur Radiol 2025;35(1):506-516. [doi: 10.1007/s00330-024-10902-5] [Medline: 38995378]
37. Huppertz MS, Siepmann R, Topp D, Nikoubashman O, Yüksel C, Kuhl CK, et al. Revolution or risk?-Assessing the potential and challenges of GPT-4V in radiologic image interpretation. Eur Radiol 2025;35(3):1111-1121. [doi: 10.1007/s00330-024-11115-6] [Medline: 39422726]
38. Chen Z, Chambara N, Wu C, Lo X, Liu SYW, Gunda ST, et al. Assessing the feasibility of ChatGPT-4o and Claude 3-Opus in thyroid nodule classification based on ultrasound images. Endocrine 2025;87(3):1041-1049. [doi: 10.1007/s12020-024-04066-x] [Medline: 39394537]
39. Zhou J, He X, Sun L, Xu J, Chen X, Chu Y, et al. Pre-trained multimodal large language model enhances dermatological diagnosis using SkinGPT-4. Nat Commun 2024;15(1):5649 [FREE Full text] [doi: 10.1038/s41467-024-50043-3] [Medline: 38969632]
40. Li J, Guan Z, Wang J, Cheung CY, Zheng Y, Lim L, et al. Integrated image-based deep learning and language models for primary diabetes care. Nat Med 2024;30(10):2886-2896. [doi: 10.1038/s41591-024-03139-8] [Medline: 39030266]
41. Zhao Z, Wang S, Gu J, Zhu Y, Mei L, Zhuang Z, et al. ChatCAD+: toward a universal and reliable interactive CAD using LLMs. IEEE Trans Med Imaging 2024;43(11):3755-3766. [doi: 10.1109/TMI.2024.3398350] [Medline: 38717880]
42. Chen Z, Cano AH, Romanou A, Bonnet A, Matoba K, Salvi F, et al. MEDITRON-70B: scaling medical pretraining for large language models. arXiv Preprint posted online on November 27, 2023. [doi: 10.48550/arXiv.2311.16079]
43. Liu X, Liu H, Yang G, Jiang Z, Cui S, Zhang Z, et al. A generalist medical language model for disease diagnosis assistance. Nat Med 2025;31(3):932-942. [doi: 10.1038/s41591-024-03416-6] [Medline: 39779927]
44. Rao A, Pang M, Kim J, Kamineni M, Lie W, Prasad AK, et al. Assessing the utility of ChatGPT throughout the entire clinical workflow: development and usability study. J Med Internet Res 2023;25:e48659 [FREE Full text] [doi: 10.2196/48659] [Medline: 37606976]
45. Giuffrè M, Kresevic S, You K, Dupont J, Huebner J, Grimshaw AA, et al. Systematic review: the use of large language models as medical chatbots in digestive diseases. Aliment Pharmacol Ther 2024;60(2):144-166. [doi: 10.1111/apt.18058] [Medline: 38798194]
46. Fervers P, Hahnfeldt R, Kottlors J, Wagner A, Maintz D, Pinto Dos Santos D, et al. ChatGPT yields low accuracy in determining LI-RADS scores based on free-text and structured radiology reports in German language. Front Radiol 2024;4:1390774 [FREE Full text] [doi: 10.3389/fradi.2024.1390774] [Medline: 39036542]
47. Cesur T, Güneş YC. Optimizing diagnostic performance of ChatGPT: the impact of prompt engineering on thoracic radiology cases. Cureus 2024;16(5):e60009 [FREE Full text] [doi: 10.7759/cureus.60009] [Medline: 38854352]
48. Mitsuyama Y, Tatekawa H, Takita H, Sasaki F, Tashiro A, Oue S, et al. Comparative analysis of GPT-4-based ChatGPT's diagnostic performance with radiologists using real-world radiology reports of brain tumors. Eur Radiol 2025;35(4):1938-1947. [doi: 10.1007/s00330-024-11032-8] [Medline: 39198333]
49. Sadamoto Y, Oda S, Tanaka M, Harada N, Kubo H, Eguchi T, et al. A useful approach to the differential diagnosis of small polypoid lesions of the gallbladder, utilizing an endoscopic ultrasound scoring system. Endoscopy 2002;34(12):959-965. [doi: 10.1055/s-2002-35859] [Medline: 12471539]
50. Wang Y, Peng J, Liu K, Sun P, Ma Y, Zeng J, et al. Preoperative prediction model for non-neoplastic and benign neoplastic polyps of the gallbladder. Eur J Surg Oncol 2024;50(2):107930 [FREE Full text] [doi: 10.1016/j.ejso.2023.107930] [Medline: 38159390]
51. Liu J, Qian Y, Yang F, Huang S, Chen G, Yu J, et al. Value of prediction model in distinguishing gallbladder adenoma from cholesterol polyp. J Gastroenterol Hepatol 2022;37(10):1893-1900. [doi: 10.1111/jgh.15928] [Medline: 35750491]
52. Kim SY, Cho JH, Kim EJ, Chung DH, Kim KK, Park YH, et al. The efficacy of real-time colour Doppler flow imaging on endoscopic ultrasonography for differential diagnosis between neoplastic and non-neoplastic gallbladder polyps. Eur Radiol 2018;28(5):1994-2002. [doi: 10.1007/s00330-017-5175-3] [Medline: 29218621]
53. Gu K, Lee JH, Shin J, Hwang JA, Min JH, Jeong WK, et al. Using GPT-4 for LI-RADS feature extraction and categorization with multilingual free-text reports. Liver Int 2024;44(7):1578-1587. [doi: 10.1111/liv.15891] [Medline: 38651924]
54. Hui Z, Zewu Z, Jiao H, Yu C. Application of ChatGPT-assisted problem-based learning teaching method in clinical medical education. BMC Med Educ 2025;25(1):50 [FREE Full text] [doi: 10.1186/s12909-024-06321-1] [Medline: 39799356]
55. Ch'en PY, Day W, Pekson RC, Barrientos J, Burton WB, Ludwig AB, et al. GPT-4 generated answer rationales to multiple choice assessment questions in undergraduate medical education. BMC Med Educ 2025;25(1):333 [FREE Full text] [doi: 10.1186/s12909-025-06862-z] [Medline: 40038669]

XSL•FO
RenderX

56. Bazzari AH, Bazzari FH. Assessing the ability of GPT-4o to visually recognize medications and provide patient education. Sci Rep 2024;14(1):26749 [FREE Full text] [doi: 10.1038/s41598-024-78577-y] [Medline: 39501020]

Abbreviations

CLAIM: Checklist for Artificial Intelligence in Medical Imaging
LLM: large language model
NPV: negative predictive value
PASS: power analysis and sample size
PMR: polyp morphology ratio
PPV: positive predictive value
UNRR: unnecessary resection rate of nonneoplastic polyps

Edited by A Benis; submitted 11.01.25; peer-reviewed by B Jiang, CN Hang, X Liu, I Taskent, S Sivarajkumar; comments to author 13.03.25; revised version received 19.11.25; accepted 30.11.25; published 23.12.25.

Please cite as:
Jiang L, Yao J, Yang Z, Tang F, Zheng X, Zhang X, Xie X, Xu M, Huang T
Evaluating Multiple Input Strategies of Large Language Models for Gallbladder Polyps on Ultrasound: Comparative Study
JMIR Med Inform 2025;13:e71178
URL: https://medinform.jmir.org/2025/1/e71178
doi:10.2196/71178
PMID:

©Lin Jiang, Jiaqian Yao, Zebang Yang, Fuqiu Tang, Xin Zheng, Xiaoer Zhang, Xiaoyan Xie, Ming Xu, Tongyi Huang. Originally published in JMIR Medical Informatics (https://medinform.jmir.org), 23.12.2025. This is an open-access article distributed under the terms of the Creative Commons Attribution License (https://creativecommons.org/licenses/by/4.0/), which permits unrestricted use, distribution, and reproduction in any medium, provided the original work, first published in JMIR Medical Informatics, is properly cited. The complete bibliographic information, a link to the original publication on https://medinform.jmir.org/, as well as this copyright and license information must be included.

XSL•FO
RenderX

Predictive Value of Frailty on Outcomes of Patients With Cirrhosis: Systematic Review and Meta-Analysis

Wen-Zhen Tang[1*], PhD; Sheng-Rui Zhu[1*], PhD; Shu-Tian Mo[1*], PhD; Yuan-Xi Xie[2], MSc; Zheng-Ke-Ke Tan[3], MSc; Yan-Juan Teng[1], MSc; Kui Jia[4], MSc

[1]Department of Hepatobiliary Surgery, The First Affiliated Hospital of Guangxi Medical University, Nanning, Guangxi Zhuang Autonomous Region, China

[2]Department of Central Sterile Supply, The First Affiliated Hospital of Guangxi Medical University,, Nanning, Guangxi Zhuang Autonomous Region, China

[3]Nursing Department, The First Affiliated Hospital of Guangxi Medical University, Nanning, Guangxi Zhuang Autonomous Region, China

[4]Department of Gastrointestinal Surgery, The First Affiliated Hospital of Guangxi Medical University, 6 Shuangyong Road, Nanning, Guangxi Zhuang Autonomous Region, China

[*]these authors contributed equally

Corresponding Author:
Kui Jia, MSc
Department of Gastrointestinal Surgery, The First Affiliated Hospital of Guangxi Medical University, 6 Shuangyong Road, Nanning, Guangxi Zhuang Autonomous Region, China

Abstract

Background: Frailty is one of the most common symptoms in patients with cirrhosis. Many researchers have identified it as a prognostic factor for patients with cirrhosis. However, no quantitative meta-analysis has evaluated the prognostic value of frailty in patients with cirrhosis.

Objective: This systematic review and meta-analysis aimed to assess the prognostic significance of frailty in patients with cirrhosis.

Methods: The systematic review was conducted in accordance with PRISMA (Preferred Reporting Items for Systematic Reviews and Meta-Analyses) recommendations. We conducted a comprehensive search of the literature using databases such as PubMed, Cochrane Library, Embase, and Web of Science, as well as China National Knowledge Infrastructure, encompassing the period from inception to 22 December 2023. Data were extracted for frailty to predict adverse outcomes in patients with cirrhosis. RevMan (version 5.3) and R (version 4.2.2) were used to assess the extracted data.

Results: A total of 26 studies with 9597 patients with cirrhosis were included. Compared with patients having low or no frailty, the frail group had a higher mortality rate (relative ratio, RR=2.07, 95% CI 1.82 - 2.34, *P*<.001), higher readmission rate (RR=1.50, 95% CI 1.22 - 1.84, *P*<.001), and lower quality of life (RR=5.78, 95% CI 2.25 - 14.82, *P*<.001). The summary receiver operator characteristic (SROC) curve of frailty for mortality in patients with cirrhosis showed that the false positive rate (FPR) was 0.25 (95% CI 0.17-0.34), diagnostic odds ratio (DOR) was 4.17 (95% CI 2.93-5.93), sensitivity was 0.54 (95% CI 0.39-0.69), and specificity was 0.73 (95% CI 0.64-0.81). The SROC curve of readmission showed that the FPR, DOR, sensitivity, and specificity were 0.39 (95% CI 0.17-0.66), 1.38 (95% CI 0.64-2.93), 0.46 (95% CI 0.28-0.64), and 0.60 (95% CI 0.28-0.85), respectively.

Conclusions: This meta-analysis demonstrated that frailty is a reliable prognostic predictor of outcomes in patients with cirrhosis. To enhance the prognosis of patients with cirrhosis, more studies on frailty screening are required.

Trial Registration: PROSPERO CRD42024497698; https://www.crd.york.ac.uk/prospero/display_record.php?RecordID=497698

(JMIR Med Inform 2025;13:e60683) doi:10.2196/60683

KEYWORDS

frailty; cirrhosis; diagnostic efficiency; survival; meta-analysis; prognostic factor; systematic review

Introduction

Background

Cirrhosis is a prevalent illness worldwide and is linked with substantial morbidity and mortality [1,2]. According to a recent report by Smith et al [3], cirrhosis has resulted in the deaths of over 40,000 individuals in America, ranking it as the 12th most prevalent cause of death. Furthermore, it is the third most prevalent cause of mortality among individuals aged 45 - 64 years [4]. The global annual mortality from chronic liver disease is estimated to be approximately 2 million. Amongst them, cirrhosis is associated with the advancement of chronic

XSL•FO
RenderX

inflammatory diseases and accounts for approximately 45% of all-cause mortality worldwide [5].

Cirrhosis often causes physiological decline, making patients more vulnerable to frailty, which further compromises their overall health [6]. Frailty is a clinical syndrome defined by increased susceptibility and impaired antistress response due to the cumulative functional loss of numerous physiological systems [7]. Furthermore, frailty is characterized by a deterioration across three primary domains: physical health, mental health, and social function [8]. Previously, frailty was considered primarily a geriatric condition linked with aging, although its link to chronic diseases is now extensively understood [9-11].

At present, evidence is increasing that frailty is a risk factor for increased mortality and complications, longer hospital stays, risk of falls, and other issues in patients with cirrhosis [12-14]. However, the assessment tools used in prior research on the unfavorable consequences of patients with cirrhosis vary, and more investigation is required to determine the prognostic significance of frailty in these individuals [12,15]. The prognostic significance of frailty in patients with cirrhosis is inconsistent among different studies and requires immediate clarification [16,17]. For example, several researchers have demonstrated that frailty serves as a prognostic indicator for mortality in individuals with cirrhosis [17,18], but conflicting findings have been reported in another investigation [16]. In addition, one study explored the relationship between frailty and outcome in patients with cirrhosis, but it only demonstrated that frailty can predict liver transplant-free survival; the risk of other complications remains unknown [19]. There are still limited systematic reviews and meta-analyses on the prognostic value of frailty in patients with cirrhosis.

Objective

Therefore, to determine the association between frailty and the prognosis of patients with cirrhosis, we did a comprehensive review and meta-analysis on the predictive value of frailty in the prognosis of patients with cirrhosis. This information can help develop targeted management measures for patients with cirrhosis and promote their well-being.

Methods

Protocol Registration

The study protocol was officially registered on the PROSPERO website (No. CRD42024497698).

Search Strategy

A comprehensive search was conducted in PubMed, Cochrane Library, Embase, and Web of Science, as well as the China Knowledge Resource Integrated Database, to identify potential articles describing frailty and cirrhosis from inception until 22 December 2023. The search method was conducted with a combination of keywords and Mesh terms: (“frailty” or “frail”) and (“liver cirrhosis,” “hepatic cirrhosis,” “liver fibrosis,” “cirrhosis,” or “cirrhotic”). In addition, we conducted a thorough manual examination of the reference lists of relevant primary and secondary research papers. The search strategy is demonstrated in Table S1 in Multimedia Appendix 1.

Study Selection

The following were the inclusion criteria: (1) cohort studies revealed details about the frailty among patients with cirrhosis; (2) patients (18 years or above) diagnosed with cirrhosis; (3) frailty was assessed using a standardized and reliable instrument, such as the fried frailty score (FFS) and liver frailty index (LFI); (4) at least one clinical outcome between cirrhosis with and without frailty was reported during follow-up; and (5) publications were in English or Chinese.

The following were the exclusion criteria: (1) reviews, non-cohort studies, letters, and conference abstracts; (2) studies that did not provide complete data; (3) duplicated papers; (4) studies not reporting the prevalence of frailty or the predictive value of frailty on the outcomes of patients with cirrhosis; and (5) patients included other diseases rather than cirrhosis

Data Extraction

Author and publication year, country, study design, study population, sample size, age, follow-up (months), frailty instruments, and prevalence of frailty were extracted by two researchers working independently. For each study, the relative ratio (RR) and 95% CI were extracted, both with and without adjustment for confounding variables. Furthermore, from the studies that were incorporated, the true positive (TP), false positive (FP), true negative (TN), and false negative (FN) values were extracted.

Quality Assessment

Two authors independently assessed the cohort studies using the Newcastle–Ottawa Scale (NOS) instrument [20]. It contained three components, including the study group selection, group comparability, and ascertainment of outcomes. The instrument had a maximum score of 9, with a score higher than 5 indicating high-quality literature [21]. If discrepancies existed, the corresponding author assisted in reaching a consensus.

Statistical Analysis

The meta-analysis was conducted using Review Manager (version 5.3) and R software (version 4.2.2; R Foundation for Statistical Computing).

For the purpose of estimating the effect size, the RR and 95% CI were used. The χ^2 test was used to investigate heterogeneity among the outcomes of each study, and the I^2 test was utilized to quantify the level of heterogeneity. The funnel plot was used to evaluate the publication bias when the number of publications reached or exceeded 10. When there were less than 10 publications, the Egger test was used to evaluate literature bias. Further investigation was conducted using the trim-and-fill method if the published literature was biased. Statistical significance was considered to be indicated by P values less than .05.

The average sensitivity, specificity, false-positive rate (FPR), positive likelihood ratio (LR+), negative likelihood ratio (LR-), and diagnostic odds ratio (DOR) of the included studies were computed using the random-effect model. Furthermore, the

XSL•FO
RenderX

accuracy of the test and the consistency of the outcomes of the included studies were determined using the summary receiver operating characteristic (SROC) curve.

Ethical Considerations

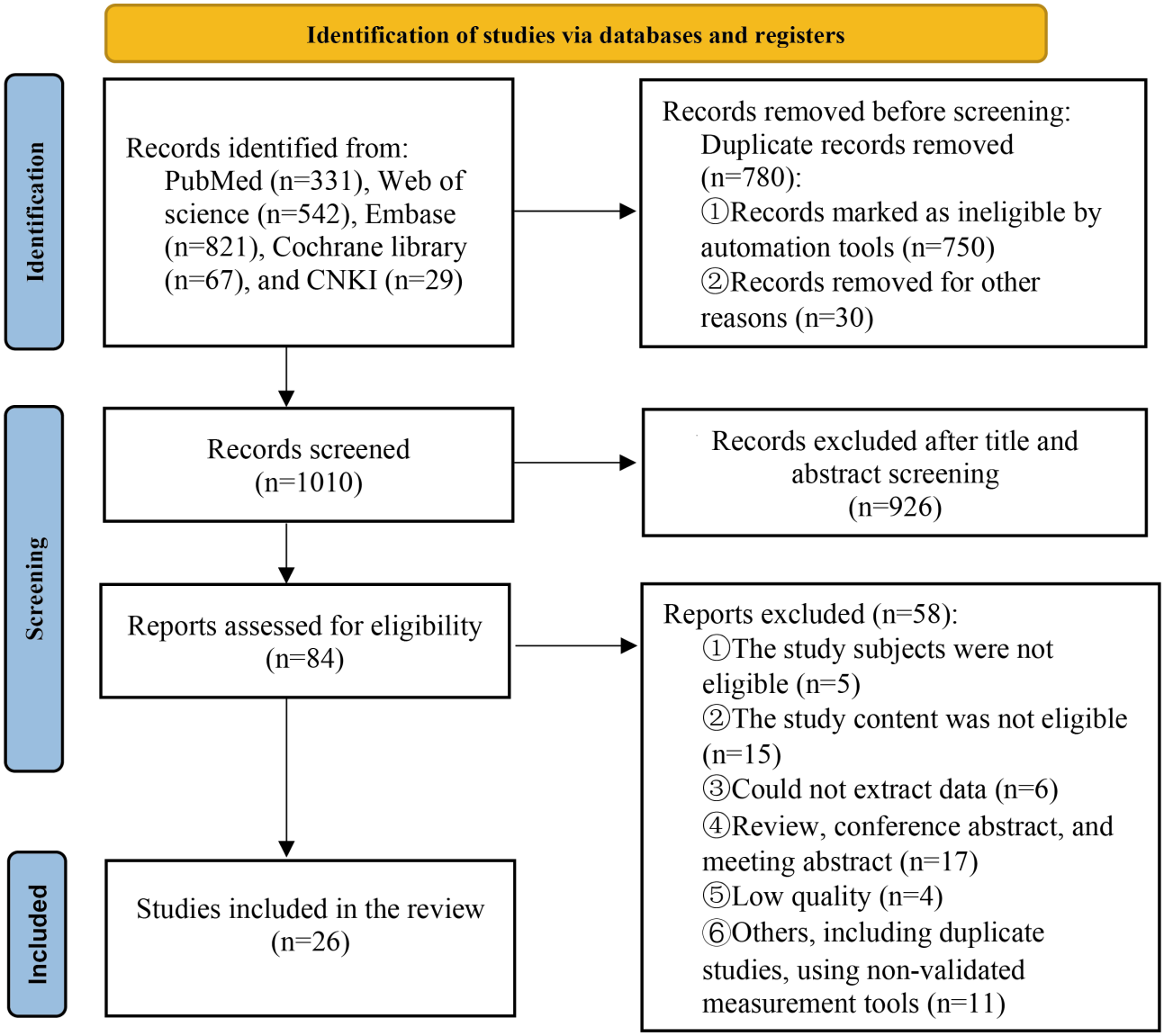
All analyses were conducted using previously published studies, and therefore, ethics approval and patient consent were unnecessary. This review does not include human subject information, primary data collection, or any form of experimentation involving individuals.

Results

Selected Studies

Following the identification of 1790 articles during the preliminary search, 780 duplicate articles were eliminated. By reviewing titles and abstracts, an additional 926 sources were eliminated from consideration primarily owing to their lack of relevance to the meta-analysis. The remaining 84 studies were read completely. A total of 58 were deemed ineligible for the reasons outlined in Figure 1. Finally, 26 studies were considered in this analysis. The search flow of this study is presented in Figure 1; the PRISMA (Preferred Reporting Items for Systematic Reviews and Meta-Analyses) checklist has been shown as Checklist 1.

Figure 1. Flowchart showing the database search.



Characteristics of the Included Studies

As shown in Table 1, the meta-analysis comprised 26 cohort studies with 9597 patients with cirrhosis [12,13,15,18,22-43]. Among the 26 articles, 3 were retrospective studies [13,18,41] and 23 were prospective studies [12,15,22-40,42,43]. They were published between 2013 and 2023, and performed in the USA [13,15,18,27,30-32,35,40,41], Canada [39,43], Chile [38], China [22-25,33], Egypt [12], Germany [26,28,29], India [34], the Netherlands [42], Slovakia [37], and Thailand [36]. Considering the included patients, 15 were patients with cirrhosis [12,22-26,29,32-34,36-40], 8 were patients with cirrhosis waiting for liver transplants, 3 were patients who received liver

XSL•FO
RenderX

transplants [13,35,41], and the remaining 1 patient had cirrhosis after surgery [18]. Moreover, the number of patients included was between 88 and 9597. A variety of tools were used to diagnose frailty, including the short physical performance battery (SPPB) [12,39], Carolina frailty index (CFI) [22,25], fried frailty score (FFS) [15,28,37], liver frailty index (LFI) [23,26,27,30-32,34-37,43], clinical frailty scale (CFS) [29,39], gait speed test (GST) [13,32,40], and others [18,24,33,38,41]. The mean follow-up durations varied between 1 and 60 months. The prevalence of frailty in patients with cirrhosis ranged from 10.50% to 75.40%. The NOS scores of the studies included in the study varied between 6 and 8, indicating a high level of quality in these studies. Table S2 in Multimedia Appendix 1 displays the evaluation criteria for literature quality.

XSL•FO
RenderX

Table . Basic characteristics of the included studies (n=26).

Author, year (citation)	Country	Study design	Study population	Sample size	Age, years	Follow-up (months)	Frailty tools	Prevalence of frailty	Quality assessment score
Behiry, 2018 [12]	Egypt	Prospective	Patients with cirrhosis	145	mean (SD), 60 (7)	3	SPPB[a]	-	6
Deng, 2020 [22]	China	Prospective	Patients with cirrhosis	158	mean (range), 64 (57-70)	24	CFI[b]	14.56%	8
Dunn, 2016 [15]	USA	Prospective	Patients with cirrhosis waiting for liver transplant	373	mean (SD), 56.7 (10.1)	3	FFS[c]	-	7
Guo, 2022 [23]	China	Prospective	Patients with cirrhosis	221	mean (range), 63 (57–68)	24	LFI[d]	14.50%	7
Hui, 2022 [24]	China	Prospective	Patients with cirrhosis	227	mean (SD), 61.7 (9.9)	48	FI[e]	-	7
Hui, 2021 [25]	China	Prospective	Patients with cirrhosis	105	mean (SD), 61.6 (9.5)	-	CFI[f]		6
Kaps, 2022 [26]	Germany	Prospective	Patients with cirrhosis	88	mean (range), 60 (51-67)	1	LFI	51%	8
Kardashian, 2021 [27]	USA	Prospective	Patients with cirrhosis waiting for liver transplants	1405	mean (range), 57 (49-63)	12	LFI	-	7
Klein, 2021 [28]	Germany	Prospective	Patients with cirrhosis waiting for liver transplants	114	mean (range), 53 (42-60)	48	FFS	75.40%	6
Kremer, 2020 [29]	Germany	Prospective	Patients with cirrhosis	200	mean (range), 60 (52 - 66)	24	CFS	10.50%	7
Lai, 2018 [30]	USA	Prospective	Patients with cirrhosis waiting for liver transplants	529	mean (range), 58 (50 - 63)	24	LFI	-	6
Lai, 2022 [31]	USA	Prospective	Patients with cirrhosis waiting for liver transplants	1166	mean (range), 60 (53 - 64)	60	LFI	94%	7
Lin, 2022 [32]	USA	Prospective	Patients with cirrhosis	116	mean (SD), 56 (11)	48	LFI, 6MWT[g], GST[h]	25%	6
Luo, 2023 [33]	China	Prospective	Patients with cirrhosis	285	mean (SD), 59.1 (12.3)	36	FFP[i]	37.20%	6
Mahmud 2021 [18]	USA	Retrospective	Patients with cirrhosis undergoing surgery	804	-	36	HFRS[j]	48.50%	6
Nathiya 2023 [34]	India	Prospective	Patients with cirrhosis	156	mean (SD), 47.42 (13.47)	-	LFI	44.92%	7

XSL•FO
RenderX

Author, year (citation)	Country	Study design	Study population	Sample size	Age, years	Follow-up (months)	Frailty tools	Prevalence of frailty	Quality assessment score
Salim 2020 [13]	USA	Retrospective	Patients with cirrhosis who received liver transplants	107	mean (SD), 58 (11)	1	GST, CST[k]	37.80%	7
Serper 2021 [35]	USA	Prospective	Patients with cirrhosis who received liver transplants	211	mean (SD), 57 (12)	8	LFI	59%	8
Siramolpiwat 2021 [36]	Thailand	Prospective	Patients with cirrhosis	152	mean (SD), 62.5 (9.3)	18	LFI	24.30%	8
Skladany 2021 [37]	Slovakia	Prospective	Patients with cirrhosis	168	mean (SD), 57.9 (14.3)	6	LFI, CFS, FFS, SPPB	-	7
Soto 2021 [38]	Chile	Prospective	Patients with cirrhosis	126	mean (SD), 64 (8.3)	48	FFP	65.10%	7
Tandon 2016 [39]	Canada	Prospective	Patients with cirrhosis	300	mean (SD), 57.4 (9.3)	6	CFS, FFC[l], SPPB	18%	8
Tapper 2015 [41]	USA	Retrospective	Patients with cirrhosis who received liver transplants	734	mean (SD), 57.3 (11.5)	3	ADL[m], BS[n], MFS[o]	-	6
Tapper 2019 [40]	USA	Prospective	Patients with cirrhosis	300	mean (range), 60 (52 - 66)	-	GST and CS	-	8
van Vugt 2017 [42]	Netherlands	Prospective	Patients with cirrhosis waiting for liver transplants	585	mean (range), 56 (48 - 62)	3	The MELD-Sarcopenia	43.40%	7
Wang2021 [43]	Canada	Prospective	Patients with cirrhosis waiting for liver transplants	822	mean (SD), 55.2 (9.9)	-	LFI	24.40%	6

[a]SPPB: short physical performance battery.

[b]CFI: Carolina frailty index.

[c]FFS: Fried frailty score.

[d]LFI: liver frailty index.

[e]FI: frailty index.

[f]CFS: clinical frailty scale.

[g]6MWT: 6-minute walk test.

[h]GST: gait speed test.

[i]FFP: fried frailty phenotype.

[j]HFRS: hospital frailty risk score.

[k]CST: chair stands test.

[l]FFC: fried frailty criteria.

[m]ADL: activities of daily living.

[n]BS: Braden scale.

[o]MFS: Morse fall scale.

XSL•FO
RenderX

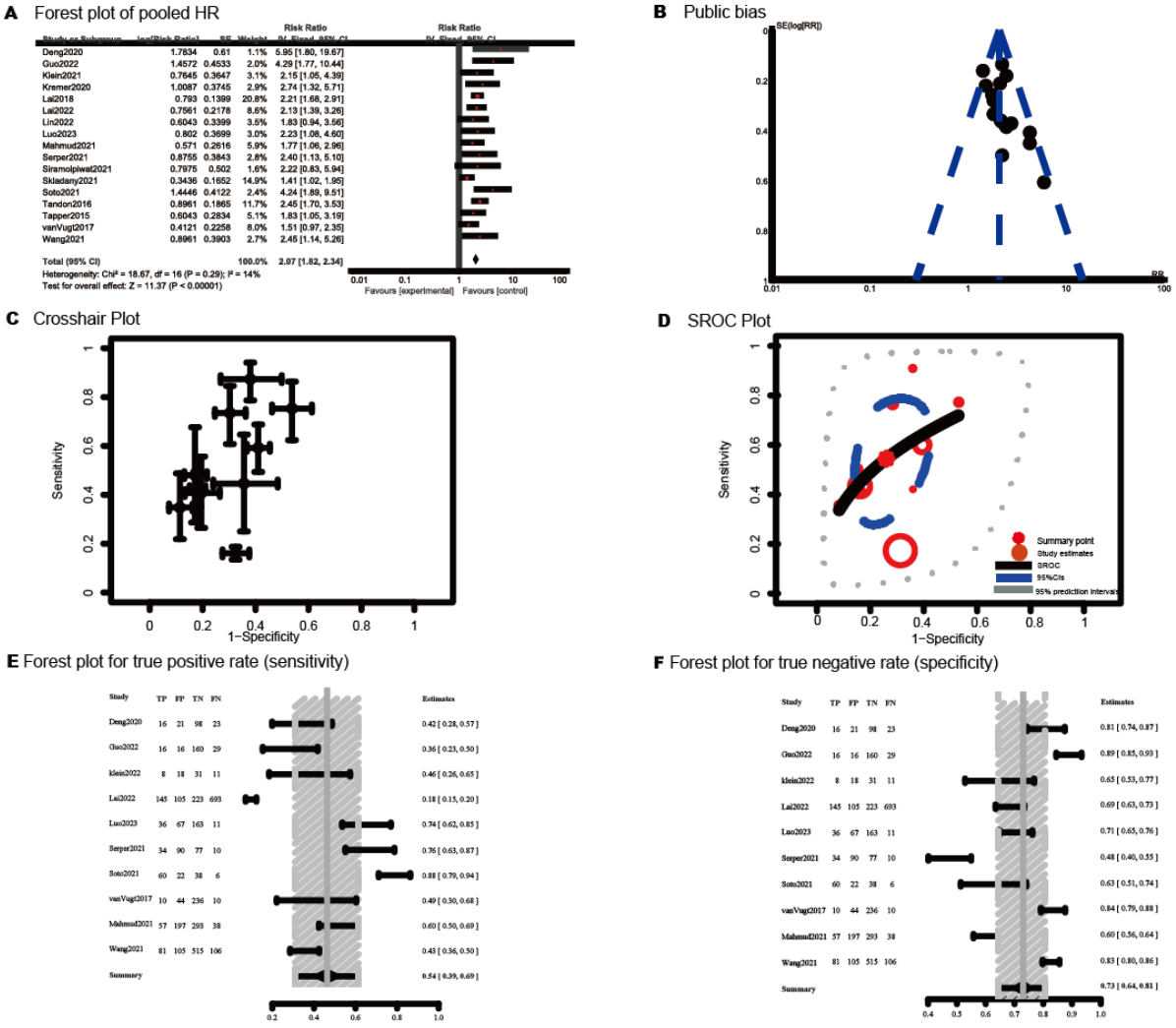
Meta-Analysis Results

Mortality

Seventeen studies reported the association between frailty and mortality in patients with cirrhosis [18,22,23,28-33,35,36,38,39,42,43]. Pooled results using a fixed-effect model indicated a significant correlation between frailty and mortality (RR 2.07, 95% CI 1.82 - 2.34, *P*<.001, I^2=14%; Figure 2A). A visual examination revealed that the funnel plot was symmetrical, suggesting a low probability of publishing bias (Figure 2B). The crosshair plots displayed the sensitivity, FPR, and 95% CI of the included studies (Figure 2C) [22,23,29,31,33,35,38,39,42,43]. The SROC curve with 95% CI and 95% prediction intervals of frailty in cirrhosis is shown in Figure 2D. The FPR was 0.25 (95% CI 0.17-0.34), and the DOR was 4.17 (95% CI 2.93-5.93). The summary LR+ was 2.35 (95% CI 1.86-2.96) and the LR- was 0.56 (95% CI 0.45-0.71). As shown in Figure 2E, frailty had a summary sensitivity of 0.54 (95% CI 0.39-0.69). The combined specificity of all studies was 0.73 (95% CI 0.64-0.81; Figure 2F).

Additional subgroup analyses revealed that the frailty-assessment methods, sample size, and study population may not have substantially affected the results (Table 2).

Figure 2. Pooled diagnostic parameters of frailty for the mortality of patients with cirrhosis [18,22,23,28-33,35,36,38,39,42,43]. (A) Forest plot of the relationship between frailty and mortality in patients with cirrhosis; (B) Funnel plot of the included studies; (C) Crosshair plots of each study of frailty in the prediction for mortality in patients with cirrhosis; (D) Summary receiver operating characteristic (SROC) plots of frailty in the prediction for mortality in patients with cirrhosis; (E) Forest plots of the sensitivity of each individual study; (F) Forest plots of the specificity of each individual study.



XSL•FO
RenderX

Table . Subgroup analyses for the association between frailty and mortality in patients with cirrhosis.

Groups		No of studies	I^2	RR	95% CI	*P* value
Assessment tool						
	CFI[a]	3	0	2.51	1.81-3.48	<.001
	LFI[b]	7	0	2.25	1.86-2.74	<.001
	SPPB[c]	2	92	1.29	1.20-1.38	<.001
	FFS[d]	2	0	1.71	1.41-2.08	<.001
	CFS[e]	3	62	2.04	1.44-2.88	<.001
Sample						
	≥200	11	0	2.15	1.86-2.49	<.001
	<200	6	49	1.77	1.52-2.06	<.001
Study population						
	Patients with cirrhosis	9	48	2.13	1.76-2.58	<.001
	Patients with cirrhosis waiting for liver transplants	5	0	2.05	1.70-2.48	<.001
	Patients with cirrhosis who received liver transplants	2	0	2.01	1.29-3.15	.002

[a]CFI: Carolina frailty index.

[b]LFI: liver frailty index.

[c]SPPB: short physical performance battery.

[d]FFS: fried frailty score.

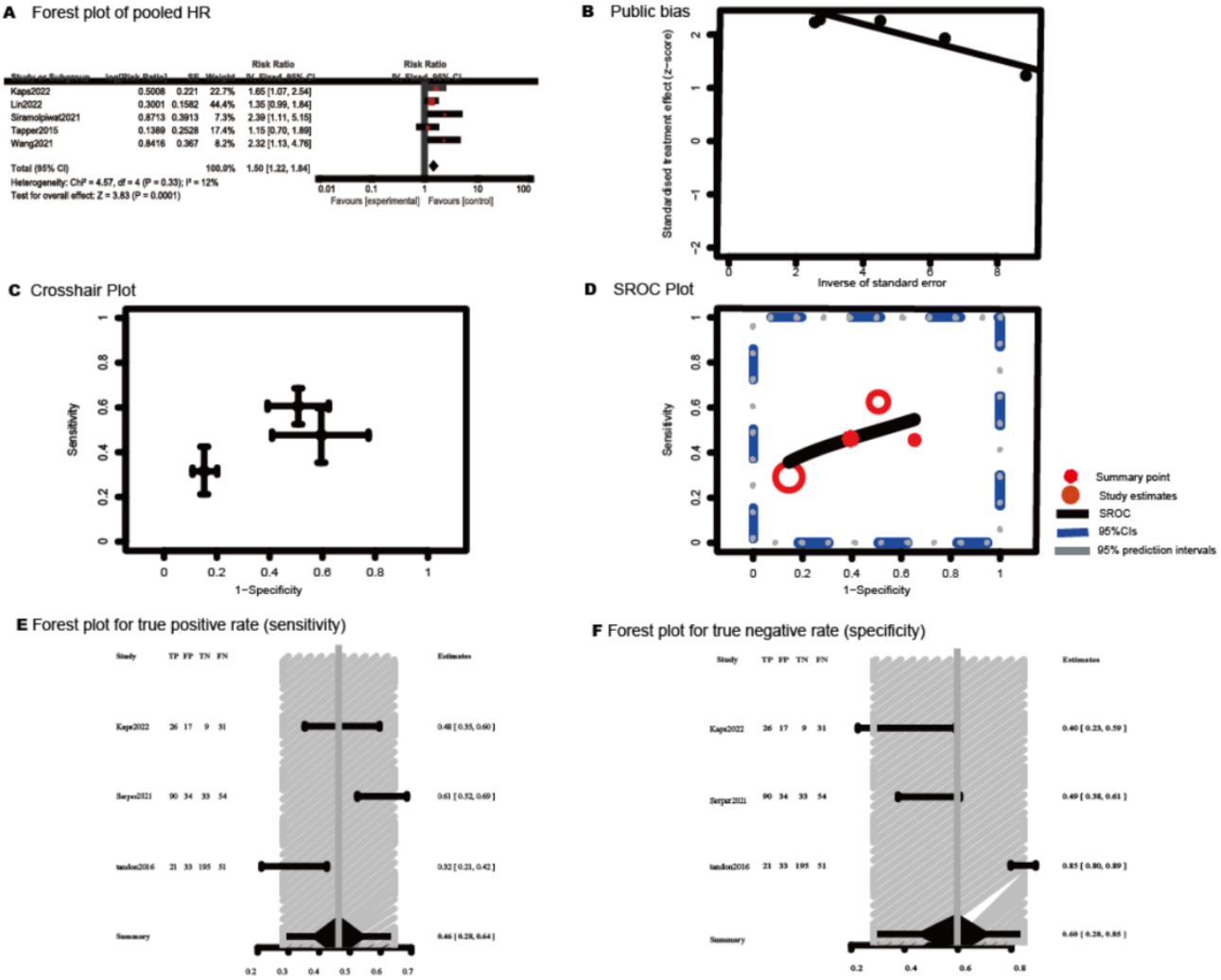
[e]CFS: clinical frailty scale.

Readmission

Figure 3A displays the inclusion of 5 studies in the pooled analysis investigating the relationship between frailty and readmission in patients with cirrhosis [26,32,36,41,43]. The pooled results with a fixed-effect model (I^2=12%, *P*=.33) indicated that patients with cirrhosis with frailty had an increased risk of readmission (RR 1.50, 95% CI 1.22 - 1.84, *P*<.001). The 5 included publications had a significant bias, according to the Egger test results (*t*=13.64, *P*<.001, Figure 3B). Accordingly, we further conducted trim-and-fill analysis, and results showed that the effect size was 1.31 (95% CI 1.01-1.70, *P*=.042, Figure 3C). This result showed that substantial relationships were unchanged when potential publication bias was taken into account.

XSL•FO
RenderX

Figure 3. Pooled diagnostic parameters of frailty for readmission in patients with cirrhosis [26,32,36,41,43]. (A) Forest plot of the relationship between frailty and readmission in patients with cirrhosis; (B) Egger test plot of the included studies; (C) Trim-and-fill plot of the included studies; (D) Crosshair plots of each study of frailty in prediction readmission in patients with cirrhosis; (E) Summary receiver operating characteristic (SROC) plots of frailty in prediction for readmission in patients with cirrhosis; (F) Forest plots of the sensitivity of each individual study; (G) Forest plots of the specificity of each individual study.



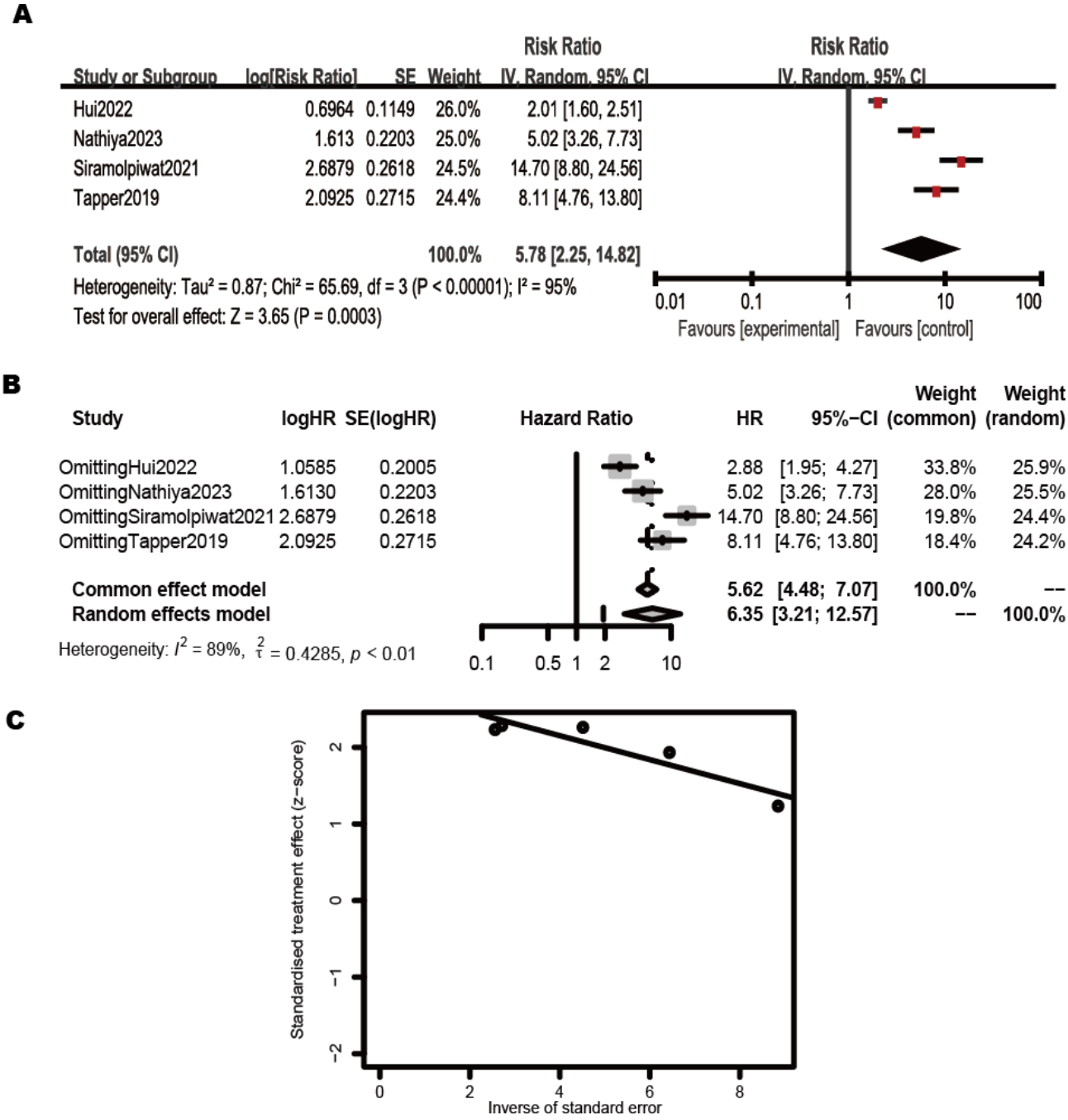
Three studies provided descriptions of the TP, FP, FN, and TN [26,35,39]. Accordingly, we conducted a diagnostic test accuracy for them. Crosshair plots were drawn to display the sensitivity (FPR and 95% CI of the 3 studies, as shown in Figure 3D). The SROC curve is shown in Figure 3E, with the FPR of 0.39 (95% CI 0.17-0.66) and the DOR of 1.375 (95% CI 0.64-2.93). The summary LR+ was 1.200 (95% CI 0.74-1.94), and the LR- was 0.873 (95% CI 0.66-1.16). The combined sensitivity and specificity of all included studies were 0.46 (95% CI 0.28-0.64) and 0.60 (95% CI 0.28-0.85), as shown in Figure 3F and G.

Quality of Life

Four studies examined the correlation between frailty and the quality of life (QoL) in patients with cirrhosis [24,34,36,40]. The pooled results of 4 studies with random-effect models indicated that frailty was significantly associated with decreased QoL in patients with cirrhosis (RR 5.78, 95% CI 2.25-14.82, P<.001, I^2=95%, Figure 4A). Sensitivity analysis, which eliminated studies one by one, revealed that the results were consistent (RR 6.35, 95% CI 3.21 - 12.57, P<.01, Figure 4B). The results of the Egger test indicated no obvious bias in the included 4 articles (t=3.08, P=.091, Figure 4C).

XSL•FO
RenderX

Figure 4. Pooled diagnostic parameters of frailty for decreasing the quality of life (QoL) in patients with cirrhosis [24,34,36,40]. (A) Forest plot of relationship between frailty and the QoL in patients with cirrhosis; (B) Sensitivity analysis plot of the included studies; (C) Egger test plot of the included studies.



Descriptive Analysis

Descriptive analyses were carried out because the following results were given in only 2 or fewer studies. Frailty was associated with non-home charge [31,35], prolonged hospital days [15,31], decompensation [33,36], sleep disturbance [25], prolonged posttransplant intensive care unit days [31], aspiration [13], and extended intubation days [13].

Discussion

Principal Results and Comparison With Previous Works

In this meta-analysis, our main findings demonstrated that patients with cirrhosis with frailty had a significantly higher risk of mortality, higher readmission, and lower QoL than those without frailty. According to our evaluation of the literature, the current study provided the most thorough evidence that frailty was a predictor of unfavorable clinical outcomes in patients with cirrhosis.

XSL•FO
RenderX

In this study, the prevalence of frailty in patients with cirrhosis ranged from 10.50% to 75.40%, depending on the specific techniques used to diagnose frailty, the characteristics of the study participants, and the operational definitions used. For example, the study conducted by Lai used the LFI to evaluate frailty in patients with cirrhosis and found that it has a prevalence rate of 94% [31], while another study used the CFI to assess frailty, and results show that the prevalence is only 14.56% [22]. Sensitivity and specificity are influenced by the assessment instrument and the chosen threshold [44]. When selecting frailty-assessment tools for patients with cirrhosis, understanding the content of existing frailty-assessment tools and the suitable population is critical to choosing the most appropriate frailty-screening tool. Furthermore, the instrument most frequently reported in this research was the LFI, a specialized tool designed to evaluate the frailty of liver disease. Other assessment tools included the SPPB, CFI, FFS, CFS, and 6-minute walk test (6MWT). Each of these tool tests is a performance-based measure that necessitates active patient participation, restricting their applicability in patients with severe or acute decompensation [45]. At present, researchers still debate about which evaluation tool for cirrhosis faltering is the standard, and a significant number of relevant studies are required to confirm it in the future.

This meta-analysis demonstrated that frailty was more likely linked to poor survival in patients with cirrhosis, consistent with previous studies [46]. Subgroup analysis further revealed that frailty-assessment tools, sample size, and study subject characteristics may not significantly influence the association between frailty and mortality in patients with cirrhosis. Previous research has shown that patients with cirrhosis with frailty had a considerably worse prognosis than those without frailty, showing that frailty is a poor prognostic factor for chronic liver disease [47,48]. The mechanisms of frailty leading to poor prognosis in patients with cirrhosis include the upregulation of the inflammatory response, impaired immune function, low testosterone levels, intestinal flora disorder, decreased intestinal barrier function, and potential neuromuscular weakness [49-51]. For example, testosterone has been proven to be associated with frailty [52,53]. It is necessary to maintain physiological homeostasis, and its deficiency may decrease muscle strength, increasing the risk of falls, disability, and complications from acute illnesses [54]. In addition, the mechanisms involved in the relationship between frailty and unfavorable outcomes may increase susceptibility to complications, such as inflammatory insults [55], infection [56], and hepatic encephalopathy [13,57] in patients with cirrhosis, thereby affecting the survival of patients. However, the mechanism of action between frailty and cirrhosis prognosis is bidirectional, meaning that liver decompensation reimbursement increases the risk of frailty development [45]. Additionally, this study demonstrated that the probability of compensation in frail patients with cirrhosis was 2.55 times greater than that in non-frail patients. Specifically, only a limited number of studies have assessed the association between frailty and decompensation in patients with cirrhosis, and further investigation is necessary to delve into this association in the future.

This study's findings suggested that patients with cirrhosis with frailty were more prone to have the risk of readmission than non-frail patients, as confirmed in other populations, including cancer patients [58,59], patients with chronic disease [60,61], and surgical patients [62,63]. A recent study conducted by Witt et al to evaluate the predictive value of frailty in 80 patients with chronic obstructive pulmonary disease has demonstrated that they have a higher risk of readmission than patients without frailty (OR 19.31, 95% CI 1.07 - 349.03) [64]. This result may be explained by reduced physiological reserve, malnutrition, and impaired immune function in debilitated patients with cirrhosis [45,65]. For example, frail patients with reduced physiological reserve are more prone to complications and increased risk of infection when encountering stressors, which in turn increases the likelihood of patient readmission [66].

Our study provided some evidence of a correlation between frailty and diminished QoL among patients with cirrhosis. Frailty in patients with chronic liver disease is a multidimensional syndrome [49]. Frailty is characterized by the gradual decline of various physiological systems, such as the cardiovascular and musculoskeletal systems, which affects the patient's daily activities and self-care ability and may increase the risk of death and hospitalization, thereby decreasing the QoL [34,49]. Two recent systematic reviews have shown a clear relationship between frailty, anxiety, and depression, which showed that frailty may lead to lower QoL levels by causing negative psychological effects [67,68]. Although this study found a significant decline in the QoL of patients with frailty due to the high heterogeneity, future larger and well-designed studies are needed to explore the relationship between frailty and QoL in patients with cirrhosis.

Recommendations for Future Practice

An essential aspect of this study is to make health care professionals aware of the importance of frailty as one of the risk predictors of cirrhosis prognosis. Standardized assessment tools, such as the CFI and LFI, can identify the patients' frailty status as early as possible to provide timely intervention. In addition, clinical staff can include frailty in the prognosis management plan of patients. In the meantime, personalized management measures can be formulated for patients with cirrhosis with different degrees of frailty, which can significantly improve the prognosis of patients. In addition, health care professionals should strengthen the positive management and follow-up of patients with cirrhosis, especially those with a higher degree of frailty, determine the abnormal situation of patients with cirrhosis in time, adjust the management plan, and ultimately improve the prognosis of patients.

Implications for Future Research

This systematic review has important implications for future studies. If frailty is regarded as an important part of the routine assessment of patients with cirrhosis, researchers need to further compare the prognostic value of different frailty indicators in patients with cirrhosis and reach a consensus on the assessment tools for frailty in patients with cirrhosis. In addition, we suggest that future studies should target the protective factors of frailty to inform preventive strategies for patients with cirrhosis. In addition, researchers and policy makers should develop

XSL•FO
RenderX

comprehensive treatment approaches and strengthen interdisciplinary collaboration to provide better management strategies for frailty in patients with cirrhosis.

Strength and Limitations

This was the first systematic review to examine the predictive value of unfavorable outcomes of frailty in patients with cirrhosis. We established that frailty was a good prognostic factor of the clinical outcomes in patients with cirrhosis, including mortality, readmission, and decreased QoL. A systematic review by Bowers et al revealed that several frailty assessments can reliably assess mortality in patients with cirrhosis who are ineligible for transplantation [69]. Future investigations should explore the trajectory of frailty change and its effect on outcomes across time. We aimed to perform a meta-analysis on the longitudinal patterns of frailty and their association with outcome measures.

This study had a few limitations. First, we included only literature reported in Chinese and English, which may have left out some relevant studies in other languages. Second, our study had an inadequate sample size, necessitating higher sample sizes in future research to evaluate the correlation between frailty and outcome in patients with cirrhosis. Furthermore, variations existed across the studies in the tools used to evaluate frailty, which may have influenced the outcomes.

Conclusion

The results of this meta-analysis demonstrate a significant correlation between frailty and an unfavorable clinical outcome in patients with cirrhosis, specifically in terms of mortality and readmission. Future research should be conducted to further explore the most effective screening tools for diagnosing frailty in patients with cirrhosis, as well as whether frailty-related interventions were connected with better clinical outcomes in patients with cirrhosis.

Acknowledgments

The authors thank all the patients and institutions for participating in the study. This study was supported by Guangxi medical and health appropriate technology development and application project (No. S2023064), Self-raised project of Guangxi Health Commission (Z-A20220499), and Self-established Cultivation Project of the First Affiliated Hospital of Guangxi Medical University - Nursing Clinical Research Climbing Plan (No. YYZS2022011).

Data Availability

The data in this study have been presented in the manuscript or uploaded as supplementary materials.

Authors' Contributions

W-ZT conceived the study, data analysis, and drafted the manuscript. W-ZT and S-TM participated in the literature search, data extraction, methodological quality assessment. Y-XX contributed to the data analysis. Y-JT and KJ commented on the final manuscript. Y-XX, and Z-K-KT contributed to the literature search and data extraction. WZ-T and S-RZ contributed to manuscript revision. All authors have checked manuscripts and approved the publication of the protocol. In addition,
Author Y-JT is the co-corresponding author of this paper and can be reached at: Department of Hepatobiliary Surgery, The First Affiliated Hospital of GuangXi Medical University, Nanning, Guangxi Zhuang Autonomous Region, China; Email address: 83864627@qq.com.

Conflicts of Interest

None declared.

Multimedia Appendix 1
The search strategy and quality assessment of the included studies.
[PDF File, 183 KB - medinform_v13i1e60683_app1.pdf]

Checklist 1
PRISMA checklist.
[DOCX File, 41 KB - medinform_v13i1e60683_app2.docx]

References

1. Ginès P, Krag A, Abraldes JG, Solà E, Fabrellas N, Kamath PS. Liver cirrhosis. Lancet 2021 Oct 9;398(10308):1359-1376. [doi: 10.1016/S0140-6736(21)01374-X] [Medline: 34543610]
2. Hussain Y, Bannaga A, Fisher N, et al. The fatty liver, cirrhosis, and liver cancer study (TENDENCY): protocol for a multicenter case-control study. JMIR Res Protoc 2023 May 31;12:e44264. [doi: 10.2196/44264] [Medline: 37256650]
3. Smith A, Baumgartner K, Bositis C. Cirrhosis: diagnosis and management. Am Fam Physician 2019 Dec 15;100(12):759-770. [Medline: 31845776]

XSL•FO
RenderX

4. Asrani SK, Devarbhavi H, Eaton J, Kamath PS. Burden of liver diseases in the world. J Hepatol 2019 Jan;70(1):151-171. [doi: 10.1016/j.jhep.2018.09.014] [Medline: 30266282]
5. Wynn TA. Fibrotic disease and the T(H)1/T(H)2 paradigm. Nat Rev Immunol 2004 Aug;4(8):583-594. [doi: 10.1038/nri1412] [Medline: 15286725]
6. Berry K, Duarte-Rojo A, Grab JD, et al. Cognitive impairment and physical frailty in patients with cirrhosis. Hepatol Commun 2022 Jan;6(1):237-246. [doi: 10.1002/hep4.1796] [Medline: 34558844]
7. Fried LP, Tangen CM, Walston J, et al. Frailty in older adults: evidence for a phenotype. J Gerontol A Biol Sci Med Sci 2001 Mar;56(3):M146-M156. [doi: 10.1093/gerona/56.3.m146] [Medline: 11253156]
8. Ruiz J, Miller AA, Tooze JA, et al. Frailty assessment predicts toxicity during first cycle chemotherapy for advanced lung cancer regardless of chronologic age. J Geriatr Oncol 2019 Jan;10(1):48-54. [doi: 10.1016/j.jgo.2018.06.007] [Medline: 30005982]
9. Fairhall N, Aggar C, Kurrle SE, et al. Frailty intervention trial (FIT). BMC Geriatr 2008 Oct 13;8:27. [doi: 10.1186/1471-2318-8-27] [Medline: 18851754]
10. Cao X, Li X, Zhang J, et al. Associations between frailty and the increased risk of adverse outcomes among 38,950 UK biobank participants with prediabetes: prospective cohort study. JMIR Public Health Surveill 2023 May 18;9:e45502. [doi: 10.2196/45502] [Medline: 37200070]
11. Liu Y, Huang L, Hu F, Zhang X. Investigating frailty, polypharmacy, malnutrition, chronic conditions, and quality of life in older adults: large population-based study. JMIR Public Health Surveill 2024 Oct 11;10:e50617 [FREE Full text] [doi: 10.2196/50617] [Medline: 39145920]
12. Essam Behiry M, Mogawer S, Yamany A, et al. Ability of the short physical performance battery frailty index to predict mortality and hospital readmission in patients with liver cirrhosis. Int J Hepatol 2019;2019:8092865. [doi: 10.1155/2019/8092865] [Medline: 31186966]
13. Salim TI, Nestlerode LC, Lucatorto EL, et al. Frailty as tested by gait speed is a risk factor for liver transplant respiratory complications. Am J Gastroenterol 2020 Jun;115(6):859-866. [doi: 10.14309/ajg.0000000000000609] [Medline: 32235146]
14. Wang S, Xu CQ, Whitlock R, et al. Su347 frailty increases the risk of cirrhosis disease progression, death and hospitalization in cirrhosis. Gastroenterology 2021 May;160(6):S-857 [FREE Full text] [doi: 10.1016/S0016-5085(21)02776-1]
15. Dunn MA, Josbeno DA, Tevar AD, et al. Frailty as tested by gait speed is an independent risk factor for cirrhosis complications that require hospitalization. Am J Gastroenterol 2016 Dec;111(12):1768-1775. [doi: 10.1038/ajg.2016.336] [Medline: 27575708]
16. Xu CQ, Mohamad Y, Kappus MR, et al. The relationship between frailty and cirrhosis etiology: From the Functional Assessment in Liver Transplantation (FrAILT) Study. Liver Int 2021 Oct;41(10):2467-2473. [doi: 10.1111/liv.15006] [Medline: 34219362]
17. Lai JC, Covinsky KE, Dodge JL, et al. Development of a novel frailty index to predict mortality in patients with end-stage liver disease. Hepatology 2017 Aug;66(2):564-574. [doi: 10.1002/hep.29219] [Medline: 28422306]
18. Mahmud N, Kaplan DE, Taddei TH, Goldberg DS. Frailty is a risk factor for postoperative mortality in patients with cirrhosis undergoing diverse major surgeries. Liver Transpl 2021 May;27(5):699-710. [doi: 10.1002/lt.25953] [Medline: 33226691]
19. Yuan C, Li W, Liu J, Li J. Frailty and transplant-free survival of patients with liver cirrhosis: a meta-analysis. PLoS ONE 2024;19(5):e0302836 [FREE Full text] [doi: 10.1371/journal.pone.0302836] [Medline: 38722913]
20. Hartling L, Milne A, Hamm MP, et al. Testing the Newcastle Ottawa Scale showed low reliability between individual reviewers. J Clin Epidemiol 2013 Sep;66(9):982-993 [FREE Full text] [doi: 10.1016/j.jclinepi.2013.03.003] [Medline: 23683848]
21. Stang A. Critical evaluation of the Newcastle-Ottawa scale for the assessment of the quality of nonrandomized studies in meta-analyses. Eur J Epidemiol 2010 Sep;25(9):603-605 [FREE Full text] [doi: 10.1007/s10654-010-9491-z] [Medline: 20652370]
22. Deng Y, Lin L, Hou L, et al. A self-reported Frailty Index predicts long-term mortality in hospitalized patients with cirrhosis. Ann Transl Med 2020 Oct;8(19):1217. [doi: 10.21037/atm-20-943] [Medline: 33178749]
23. Guo G, Li C, Hui Y, et al. Sarcopenia and frailty combined increases the risk of mortality in patients with decompensated cirrhosis. Ther Adv Chronic Dis 2022;13:20406223221109651. [doi: 10.1177/20406223221109651] [Medline: 35875834]
24. Hui Y, Li N, Yu Z, et al. Health-related quality of life and its contributors according to a preference-based generic instrument in cirrhosis. Hepatol Commun 2022 Mar;6(3):610-620. [doi: 10.1002/hep4.1827] [Medline: 34558226]
25. Hui Y, Xu L, Wang X, et al. Association between sleep disturbance and multidimensional frailty assessed by Frailty Index in hospitalized cirrhosis. Eur J Gastroenterol Hepatol 2021 Dec 1;33(1S Suppl 1):e727-e733. [doi: 10.1097/MEG.0000000000002231] [Medline: 34101682]
26. Kaps L, Lukac L, Michel M, et al. Liver frailty index for prediction of short-term rehospitalization in patients with liver cirrhosis. Diagnostics (Basel) 2022 Apr 24;12(5):1069. [doi: 10.3390/diagnostics12051069] [Medline: 35626226]
27. Kardashian A, Ge J, McCulloch CE, et al. Identifying an optimal liver frailty index cutoff to predict waitlist mortality in liver transplant candidates. Hepatology 2021 Mar;73(3):1132-1139. [doi: 10.1002/hep.31406] [Medline: 32491208]

XSL•FO
RenderX

28. Klein CG, Malamutmann E, Latuske J, et al. Frailty as a predictive factor for survival after liver transplantation, especially for patients with MELD≤15-a prospective study. Langenbecks Arch Surg 2021 Sep;406(6):1963-1969. [doi: 10.1007/s00423-021-02109-9] [Medline: 33847783]
29. Kremer WM, Nagel M, Reuter M, et al. Validation of the clinical frailty scale for the prediction of mortality in patients with liver cirrhosis. Clin Transl Gastroenterol 2020 Jul;11(7):e00211. [doi: 10.14309/ctg.0000000000000211] [Medline: 32764204]
30. Lai JC, Covinsky KE, McCulloch CE, Feng S. The liver frailty index improves mortality prediction of the subjective clinician assessment in patients with cirrhosis. Am J Gastroenterol 2018 Feb;113(2):235-242. [doi: 10.1038/ajg.2017.443] [Medline: 29231189]
31. Lai JC, Ganger DR, Volk ML, et al. Association of frailty and sex with wait list mortality in liver transplant candidates in the multicenter functional assessment in liver transplantation (FrAILT) study. JAMA Surg 2021 Mar 1;156(3):256-262. [doi: 10.1001/jamasurg.2020.5674] [Medline: 33377947]
32. Lin FP, Bloomer PM, Grubbs RK, et al. Low daily step count is associated with a high risk of hospital admission and death in community-dwelling patients with cirrhosis. Clin Gastroenterol Hepatol 2022 Aug;20(8):1813-1820. [doi: 10.1016/j.cgh.2022.03.012] [Medline: 35331941]
33. Luo J, Yang D, Xu Z, et al. A prospective study on the differential association of sarcopenia and frailty with health outcomes in cirrhotic patients. Dig Liver Dis 2023 Nov;55(11):1533-1542. [doi: 10.1016/j.dld.2023.07.007] [Medline: 37482521]
34. Nathiya D, Raj P, Singh P, et al. Frailty predicting health-related quality of life trajectories in individuals with sarcopenia in liver cirrhosis: finding from BCAAS study. J Clin Med 2023 Aug 17;12(16):5348. [doi: 10.3390/jcm12165348] [Medline: 37629390]
35. Serper M, Tao SY, Kent DS, et al. Inpatient frailty assessment is feasible and predicts nonhome discharge and mortality in decompensated cirrhosis. Liver Transpl 2021 Dec;27(12):1711-1722. [doi: 10.1002/lt.26100] [Medline: 34018303]
36. Siramolpiwat S, Kiattikunrat K, Soontararatpong R, et al. Frailty as tested by the liver frailty index is associated with decompensation and unplanned hospitalization in patients with compensated cirrhosis. Scand J Gastroenterol 2021 Oct;56(10):1210-1219. [doi: 10.1080/00365521.2021.1957497] [Medline: 34338110]
37. Skladany L, Drotarova Z, Vnencakova J, Jancekova D, Molcan P, Koller T. Applicability and prognostic value of frailty assessment tools among hospitalized patients with advanced chronic liver disease. Croat Med J 2021 Feb 28;62(1):8-16. [doi: 10.3325/cmj.2021.62.8] [Medline: 33660956]
38. Soto R, Díaz LA, Rivas V, et al. Frailty and reduced gait speed are independently related to mortality of cirrhotic patients in long-term follow-up. Ann Hepatol 2021;25:100327. [doi: 10.1016/j.aohep.2021.100327] [Medline: 33596465]
39. Tandon P, Tangri N, Thomas L, et al. A rapid bedside screen to predict unplanned hospitalization and death in outpatients with cirrhosis: a prospective evaluation of the clinical frailty scale. Am J Gastroenterol 2016 Dec;111(12):1759-1767. [doi: 10.1038/ajg.2016.303] [Medline: 27481305]
40. Tapper EB, Baki J, Parikh ND, Lok AS. Frailty, psychoactive medications, and cognitive dysfunction are associated with poor patient‐reported outcomes in cirrhosis. Hepatology 2019;69(4):1676-1685. [doi: 10.1002/hep.30336] [Medline: 30382584]
41. Tapper EB, Finkelstein D, Mittleman MA, Piatkowski G, Lai M. Standard assessments of frailty are validated predictors of mortality in hospitalized patients with cirrhosis. Hepatology 2015 Aug;62(2):584-590. [doi: 10.1002/hep.27830] [Medline: 25846824]
42. van Vugt JLA, Alferink LJM, Buettner S, et al. A model including sarcopenia surpasses the MELD score in predicting waiting list mortality in cirrhotic liver transplant candidates: a competing risk analysis in a national cohort. J Hepatol 2018 Apr;68(4):707-714. [doi: 10.1016/j.jhep.2017.11.030] [Medline: 29221886]
43. Wang S, Whitlock R, Xu C, et al. Frailty is associated with increased risk of cirrhosis disease progression and death. Hepatology 2022 Mar;75(3):600-609. [doi: 10.1002/hep.32157] [Medline: 34528267]
44. Mathoulin-Pélissier S, Bellera C, Rainfray M, Soubeyran P. Screening methods for geriatric frailty. Lancet Oncol 2013 Jan;14(1):e1-e2. [doi: 10.1016/S1470-2045(12)70554-5] [Medline: 23276365]
45. Tandon P, Montano-Loza AJ, Lai JC, Dasarathy S, Merli M. Sarcopenia and frailty in decompensated cirrhosis. J Hepatol 2021 Jul;75 Suppl 1(Suppl 1):S147-S162. [doi: 10.1016/j.jhep.2021.01.025] [Medline: 34039486]
46. Nishikawa H, Shiraki M, Hiramatsu A, Moriya K, Hino K, Nishiguchi S. Japan Society of Hepatology guidelines for sarcopenia in liver disease (1st edition): recommendation from the working group for creation of sarcopenia assessment criteria. Hepatol Res 2016 Sep;46(10):951-963 [FREE Full text] [doi: 10.1111/hepr.12774] [Medline: 27481650]
47. Tranah TH, Ballester MP, Carbonell-Asins JA, et al. Plasma ammonia levels predict hospitalisation with liver-related complications and mortality in clinically stable outpatients with cirrhosis. J Hepatol 2022 Dec;77(6):1554-1563 [FREE Full text] [doi: 10.1016/j.jhep.2022.07.014] [Medline: 35872326]
48. Montano-Loza AJ, Duarte-Rojo A, Meza-Junco J, et al. Inclusion of sarcopenia within MELD (MELD-sarcopenia) and the prediction of mortality in patients with cirrhosis. Clin Transl Gastroenterol 2015 Jul 16;6(7):e102. [doi: 10.1038/ctg.2015.31] [Medline: 26181291]
49. Xue QL. The frailty syndrome: definition and natural history. Clin Geriatr Med 2011 Feb;27(1):1-15. [doi: 10.1016/j.cger.2010.08.009] [Medline: 21093718]

XSL•FO
RenderX

50. Tandon P, Zanetto A, Piano S, Heimbach JK, Dasarathy S. Liver transplantation in the patient with physical frailty. J Hepatol 2023 Jun;78(6):1105-1117. [doi: 10.1016/j.jhep.2023.03.025] [Medline: 37208097]
51. Cerdá B, Pérez M, Pérez-Santiago JD, Tornero-Aguilera JF, González-Soltero R, Larrosa M. Gut microbiota modification: another piece in the puzzle of the benefits of physical exercise in health? Front Physiol 2016;7:51. [doi: 10.3389/fphys.2016.00051] [Medline: 26924990]
52. Morley JE, von Haehling S, Anker SD, Vellas B. From sarcopenia to frailty: a road less traveled. J Cachexia Sarcopenia Muscle 2014 Mar;5(1):5-8. [doi: 10.1007/s13539-014-0132-3] [Medline: 24526568]
53. Chiang JM, Kaysen GA, Segal M, Chertow GM, Delgado C, Johansen KL. Low testosterone is associated with frailty, muscle wasting and physical dysfunction among men receiving hemodialysis: a longitudinal analysis. Nephrol Dial Transplant 2019 May 1;34(5):802-810. [doi: 10.1093/ndt/gfy252] [Medline: 30085235]
54. Saad F, Röhrig G, von Haehling S, Traish A. Testosterone deficiency and testosterone treatment in older men. Gerontology 2017;63(2):144-156. [doi: 10.1159/000452499] [Medline: 27855417]
55. Muscedere J, Waters B, Varambally A, et al. The impact of frailty on intensive care unit outcomes: a systematic review and meta-analysis. Intensive Care Med 2017 Aug;43(8):1105-1122. [doi: 10.1007/s00134-017-4867-0] [Medline: 28676896]
56. Krell RW, Kaul DR, Martin AR, et al. Association between sarcopenia and the risk of serious infection among adults undergoing liver transplantation. Liver Transpl 2013 Dec;19(12):1396-1402. [doi: 10.1002/lt.23752] [Medline: 24151041]
57. Bhanji RA, Moctezuma-Velazquez C, Duarte-Rojo A, et al. Myosteatosis and sarcopenia are associated with hepatic encephalopathy in patients with cirrhosis. Hepatol Int 2018 Jul;12(4):377-386. [doi: 10.1007/s12072-018-9875-9] [Medline: 29881992]
58. Voora RS, Qian AS, Kotha NV, et al. Frailty index as a predictor of readmission in patients with head and neck cancer. Otolaryngol Head Neck Surg 2022 Jul;167(1):89-96. [doi: 10.1177/01945998211043489] [Medline: 34520305]
59. Choe YR, Joh JY, Kim YP. Association between frailty and readmission within one year after gastrectomy in older patients with gastric cancer. J Geriatr Oncol 2017 May;8(3):185-189. [doi: 10.1016/j.jgo.2017.02.002] [Medline: 28259489]
60. Faye AS, Wen T, Soroush A, et al. Increasing prevalence of frailty and its association with readmission and mortality among hospitalized patients with IBD. Dig Dis Sci 2021 Dec;66(12):4178-4190. [doi: 10.1007/s10620-020-06746-w] [Medline: 33385264]
61. Keeney T, Jette DU, Cabral H, Jette AM. Frailty and function in heart failure: predictors of 30-day hospital readmission? J Geriatr Phys Ther 2021;44(2):101-107. [doi: 10.1519/JPT.0000000000000243] [Medline: 31373945]
62. Panayi AC, Orkaby AR, Sakthivel D, et al. Impact of frailty on outcomes in surgical patients: a systematic review and meta-analysis. Am J Surg 2019 Aug;218(2):393-400. [doi: 10.1016/j.amjsurg.2018.11.020] [Medline: 30509455]
63. Lakra A, Tram MK, Bernasek TL, Lyons ST, O'Connor CM. Frailty is associated with increased complication, readmission, and hospitalization costs following primary total knee arthroplasty. J Arthroplasty 2023 Jul;38(7 Suppl 2):S182-S186. [doi: 10.1016/j.arth.2023.02.036] [Medline: 36858131]
64. Witt LJ, Spacht WA, Carey KA, et al. Weak handgrip at index admission for acute exacerbation of COPD predicts all-cause 30-day readmission. Front Med (Lausanne) 2021;8:611989 [FREE Full text] [doi: 10.3389/fmed.2021.611989] [Medline: 33898475]
65. Wong RJ, Mohamad Y, Srisengfa YT, et al. Psychological contributors to the frail phenotype: the association between resilience and frailty in patients with cirrhosis. Am J Transplant 2021 Jan;21(1):241-246. [doi: 10.1111/ajt.16131] [Medline: 32524691]
66. Lambrechts MJ, Tran K, Conaway W, et al. Modified frailty index as a predictor of postoperative complications and patient-reported outcomes after posterior cervical decompression and fusion. Asian Spine J 2023 Apr;17(2):313-321. [doi: 10.31616/asj.2022.0262] [Medline: 36717090]
67. Soysal P, Veronese N, Thompson T, et al. Relationship between depression and frailty in older adults: a systematic review and meta-analysis. Ageing Res Rev 2017 Jul;36:78-87. [doi: 10.1016/j.arr.2017.03.005] [Medline: 28366616]
68. Tan M, Bhanu C, Frost R. The association between frailty and anxiety: a systematic review. Int J Geriatr Psychiatry 2023 May;38(5):e5918. [doi: 10.1002/gps.5918] [Medline: 37157226]
69. Bowers SP, Brennan PN, Dillon JF. Systematic review: the role of frailty in advanced chronic liver disease. Aliment Pharmacol Ther 2023 Feb;57(3):280-289. [doi: 10.1111/apt.17324] [Medline: 36433627]

Abbreviations

6MWT: 6-minute walk test
CFI: Carolina frailty index
CFS: clinical frailty scale
DOR: diagnostic odds ratio
FFS: fried frailty score
FN: false negative
FP: false positive
FPR: false-positive rate

XSL•FO
RenderX

GST: gait speed test
LFI: liver frailty index
LR: likelihood ratio
NOS: Newcastle-Ottawa Scale
PRISMA: Preferred Reporting Items for Systematic Reviews and Meta-Analyses
QoL: quality of life
RR: relative ratio
SPPB: short physical performance battery
SROC: summary receiver operating characteristic
TN: true negative
TP: true positive

Edited by C Lovis; submitted 18.05.24; peer-reviewed by X Xu; revised version received 31.12.24; accepted 12.01.25; published 27.02.25.

Please cite as:
Tang WZ, Zhu SR, Mo ST, Xie YX, Tan ZKK, Teng YJ, Jia K
Predictive Value of Frailty on Outcomes of Patients With Cirrhosis: Systematic Review and Meta-Analysis
JMIR Med Inform 2025;13:e60683
URL: https://medinform.jmir.org/2025/1/e60683
doi:10.2196/60683

© Wen-Zhen Tang, Sheng-Rui Zhu, Shu-Tian Mo, Yuan-Xi Xie, Zheng-Ke-Ke Tan, Yan-Juan Teng, Kui Jia. Originally published in JMIR Medical Informatics (https://medinform.jmir.org), 27.2.2025. This is an open-access article distributed under the terms of the Creative Commons Attribution License (https://creativecommons.org/licenses/by/4.0/), which permits unrestricted use, distribution, and reproduction in any medium, provided the original work, first published in JMIR Medical Informatics, is properly cited. The complete bibliographic information, a link to the original publication on https://medinform.jmir.org/, as well as this copyright and license information must be included.

XSL•FO
RenderX

Original Paper

Integrating Health Care Data in an Informatics for Integrating Biology & the Bedside (i2b2) Model Persisted Through Elasticsearch: Design, Implementation, and Evaluation in a French University Hospital

Romain Griffier[1,2], MD, PhD; Fleur Mougin[2], PhD; Vianney Jouhet[1,2], MD, PhD

[1]Service d'Information Médicale, Informatique et Archivistique Médicale (IAM), Pôle de Santé Publique, Bordeaux University Hospital, Bordeaux, France

[2]Team AHeaD, Inserm Bordeaux Population Health Research Center, UMR 1219, Bordeaux University, Bordeaux, France

Corresponding Author:
Romain Griffier, MD, PhD
Service d'Information Médicale, Informatique et Archivistique Médicale (IAM)
Pôle de Santé Publique
Bordeaux University Hospital
Place Améle Raba Léon
Bordeaux, F-33000
France
Phone: 33 5 57 82 15 59
Email: romain.griffier@chu-bordeaux.fr

Abstract

Background: The volume of digital data in health care is continually growing. In addition to its use in health care, the health data collected can also serve secondary purposes, such as research. In this context, clinical data warehouses (CDWs) provide the infrastructure and organization necessary to enhance the secondary use of health data. Various data models have been proposed for structuring data in a CDW, including the Informatics for Integrating Biology & the Bedside (i2b2) model, which relies on a relational database. However, this persistence approach can lead to performance issues when executing queries on massive data sets.

Objective: This study aims to describe the necessary transformations and their implementation to enable i2b2's search engine to perform the phenotyping task using data persistence in a NoSQL Elasticsearch database.

Methods: This study compares data persistence in a standard relational database with a NoSQL Elasticsearch database in terms of query response and execution performance (focusing on counting queries based on structured data, numerical data, and free text, including temporal filtering) as well as material resource requirements. Additionally, the data loading and updating processes are described.

Results: We propose adaptations to the i2b2 model to accommodate the specific features of Elasticsearch, particularly its inability to perform joins between different indexes. The implementation was tested and evaluated within the CDW of Bordeaux University Hospital, which contains data on 2.5 million patients and over 3 billion observations. Overall, Elasticsearch achieves shorter query execution times compared with a relational database, with particularly significant performance gains for free-text searches. Additionally, compared with an indexed relational database (including a full-text index), Elasticsearch requires less disk space for storage.

Conclusions: We demonstrate that implementing i2b2 with Elasticsearch is feasible and significantly improves query performance while reducing disk space usage. This implementation is currently in production at Bordeaux University Hospital.

(JMIR Med Inform 2025;13:e65753) doi:10.2196/65753

KEYWORDS

clinical data warehouse; health data integration; i2b2; Elasticsearch; medical informatics; data persistence

XSL•FO
RenderX

Introduction

Health data account for approximately 30% of the world's available data [1]. Moreover, the volume of digital health data is constantly increasing [2]: in 2010, it doubled every 3 years; by 2020, it was estimated to double every 73 days [3].

One source of health data is electronic health records (EHRs). EHRs are defined as a "longitudinal collection of electronic health information about individual patients" [4], generated from 1 or more encounters in any care delivery setting. They include patient demographics, clinical notes, medications, vital signs, medical history, laboratory data, and radiology reports.

Health data, particularly EHR data, may be used for secondary purposes. Secondary use of health data refers to its use for purposes other than those for which they were initially collected [5]. This includes a wide range of areas [6], such as managing health care organization activities, phenotyping [7,8], research [9], epidemiological registers [10], quality and safety of care [11], and epidemiological surveillance [12,13].

One barrier to reusing health data from EHRs is its extreme heterogeneity [14,15]. Two types of heterogeneity are generally distinguished:

- Syntactic heterogeneity: This refers to differences in how information is stored, such as in different formats (eg, databases, text files, or images) or using various data models in specialized software.
- Semantic heterogeneity: This refers to differences in how information is represented. For example, a patient's natremia may be stored in a structured format using a LOINC (Logical Observation Identifiers Names and Codes) [16] code (eg, "2947-0"), a local terminology code (eg, "BIO:NaSg"), or as free text in a clinical note.

These 2 types of heterogeneity create challenges in the secondary use of health data. Various strategies have been implemented to reduce this heterogeneity, including machine learning and rule-based methods [17] during analysis. A widely adopted approach is to integrate data before analysis by establishing clinical data warehouses (CDWs) [18-22].

From a technical perspective, a CDW is a database dedicated to the secondary use of health data. CDWs are populated through a process called ETL (Extract, Transform, and Load), in which health care data are extracted from various production or replicated medical software databases, transformed (including pseudonymization and standardization), and then loaded into a dedicated database. Beyond being just a database, CDWs must also incorporate key aspects necessary for health data reuse, including governance, ethics, transparency, privacy, and security.

Numerous models for integrating data into CDWs have been proposed [23]. In particular, 2 open data models are widely used worldwide:

- OMOP-CDM (Observational Medical Outcomes Partnership-Common Data Model): Developed through a public-private partnership established in 2008 and led by the Food and Drug Administration [19], OMOP-CDM is a denormalized data model in which clinical data are stored in 1 of 15 specialized fact tables (eg, DRUG_EXPOSURE, MEASUREMENT) within the "Standardized Clinical Data" section of the CDM. All data in these fact tables are linked to the main PERSON table, which represents the patient. Additionally, 12 tables in the "Standardized Vocabulary" section store and manage the vocabulary integrated into OMOP. The current version of OMOP-CDM is 5.4 [24].
- Informatics for Integrating Biology & the Bedside (i2b2): Proposed by Harvard Medical School's Department of Biomedical Informatics in 2007 [18], the i2b2 platform provides a tool called the i2b2 Web Client for identifying patients based on clinical or biological criteria. A description of this requester is provided in Multimedia Appendix 1. A more detailed explanation of the i2b2 application and its data model is included in the "Materials" section.

In the remainder of this article, we will focus specifically on i2b2.

One of the first steps in the secondary use of health data is conducting feasibility studies [25] and phenotyping [26,27]. Feasibility studies involve counting candidate patients, while phenotyping focuses on identifying patients eligible for studies based on clinical or biological criteria. To achieve these tasks, researchers query CDW data to precisely define the population of interest. Phenotyping queries must meet 2 key criteria: (1) *good recall*, that is, they must capture the population of interest as comprehensively as possible; and (ii) *good precision*, that is, the identified patients must accurately match the search criteria. The development of these queries is an iterative process: the initial counts and record visualizations help refine the query by identifying additional elements to consider. Therefore, query response times must be very fast—on the order of 1 second—to ensure that this iterative process remains feasible and efficient.

In addition, a significant portion of medical information is available in free text [21,28], such as clinical notes, imaging reports, and discharge prescriptions. Within the i2b2 platform, free-text data are extracted from binary documents (eg, .docx, .pdf) and stored in a dedicated field. The search engine enables querying this free-text information using keyword-based exact searches.

It is therefore essential to use data storage systems for CDWs that enable rapid querying and efficient methods for searching free text. Most CDWs rely on a relational database to store data. Relational database management systems (RDBMSs) are well-suited for ensuring data integrity and provide a simple yet flexible query language, SQL. However, the query performance of RDBMSs may be challenged when handling large volumes of data or a high number of users [29-32]. This is because RDBMSs strictly adhere to the ACID (atomicity, consistency, isolation, and durability) properties to ensure data integrity and consistency. Maintaining these properties introduces mechanisms such as resource locking, which can impact query speed. Additionally, while RDBMSs are highly efficient for storing structured data, they are less suited for handling semistructured or unstructured data, such as free text [33,34].

XSL•FO
RenderX

NoSQL databases emerged in the 2000s with the rise of Web 2.0 [35] and have been widely used in big data and real-time applications. Unlike traditional relational databases, NoSQL databases do not store data in a relational manner. A key difference is that NoSQL databases are schema-free, meaning their table structure is not fixed—the structure of stored data may vary between instances [36]. There are different types of NoSQL databases, including key-value databases, document-oriented databases, column-oriented databases, and graph databases [37].

Elasticsearch [38] is a NoSQL database that stores data as JSON documents in a schema-less structure, optimized for full-text search and real-time analytics. It supports horizontal scaling across clusters and uses a query domain-specific language for complex searches, making it well-suited for indexing, querying, and aggregating large volumes of heterogeneous data. Therefore, we considered Elasticsearch a strong candidate for CDW data persistence in the context of i2b2's search engine for the phenotyping task. This paper aims to present our implementation and evaluate the query performance associated with persisting the main components of the i2b2 data model in an Elasticsearch NoSQL database. A portion of the i2b2 query engine has been reimplemented for performance evaluation, focusing on counting queries based on structured data, numerical data, and free text, including temporal filtering.

Methods

Materials

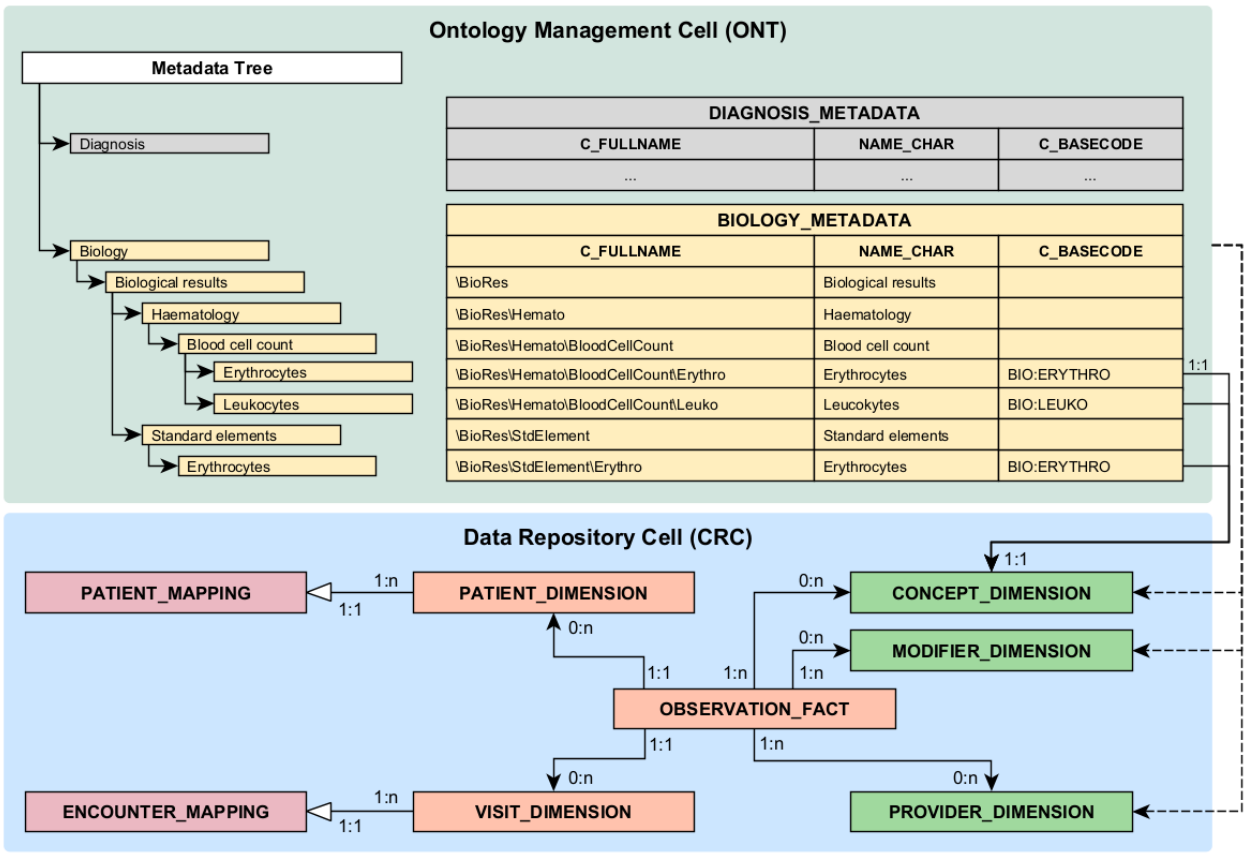
Informatics for Integrating Biology & the Bedside (i2b2)

i2b2 is an application developed by the Department of Biomedical Informatics at Harvard Medical School in 2007 [18]. It aims to facilitate the integration of heterogeneous clinical health care data for secondary use by providing data persistence storage and offering various services on top of this storage. The application follows a service-based architecture, comprising multiple services (referred to as "cells"). Specifically, the i2b2 application distinguishes the following 2 cells (Figure 1):

- The *data repository cell* (also called the clinical research chart (CRC); blue box in Figure 1), which stores clinical information generated during a patient's encounter with a health care facility. The CRC is based on a star-schema model [39] composed of the following:
  - A section containing *pseudonymized individual clinical data* (shown in orange in Figure 1; the names of RDBMS objects [tables, columns, etc] are written in UPPERCASE and the names of Elasticsearch objects [indexes, fields, etc] are written lowercase.). The individual clinical information integrated into i2b2 is stored as observations in the main fact table, OBSERVATION_FACT. Each observation represents a piece of information about a patient's health, collected during an interaction with the health care system. This may include structured elements (eg, diagnoses coded using standard terminology, numerical biological results) as well as free-text elements (eg, clinical notes, form data). This table is linked to 2 dimension tables: PATIENT_DIMENSION, which describes patient attributes (eg, gender, date of birth), and VISIT_DIMENSION, which describes encounter details (eg, start and end dates).
  - A section describing the permissible values of the lookup columns (the lookup columns correspond to columns containing structured elements used for searching in the OBSERVATION_FACT table. These columns are similar to foreign keys of dimension tables, except that they do not refer to the primary key but to other columns in these dimension tables) in OBSERVATION_FACT (shown in green in Figure 1). Specifically, 2 tables define the concepts used to characterize an observation: CONCEPT_DIMENSION represents the main concept. For example, the CONCEPT_CD "BIO:ERYTHRO" refers to the number of erythrocytes in blood; MODIFIER_DIMENSION represents a secondary concept that modifies the main concept. For example, the MODIFIER_CD "BIO:VALID" refers to a validated result and can modify an observation linked to the CONCEPT_CD "BIO:ERYTHRO," indicating that the erythrocytes in blood measurement are validated.
  - A section containing *mapping tables* that link patient (PATIENT_MAPPING) and encounter (ENCOUNTER_MAPPING) identifiers used in i2b2 to the corresponding identifiers from the source systems integrated into i2b2 (shown in red in Figure 1).
- The *ontology management cell* (also called ONT; green box in Figure 1) enables the integration of metadata from various sources into a hierarchical tree structure. Metadata are stored in separate tables, each corresponding to a root node of the tree (eg, "Biology," "Diagnosis," "Procedure"). In these metadata tables, each row represents a node in the hierarchical tree. The primary key (C_FULLNAME) corresponds to the path from the root node to the current node (either an intermediate or a leaf node). This structure allows for multihierarchical access to leaf nodes, meaning a single leaf node can be accessed through multiple paths. For leaf nodes only, the C_BASECODE column contains the code used as a permissible value in one of the lookup columns (eg, CONCEPT_CD) of the OBSERVATION_FACT table.

XSL•FO
RenderX

Figure 1. Informatics for Integrating Biology & the Bedside (i2b2): Data Repository Cell (CRC) and Ontology Management Cell (ONT). In the CRC (blue box), tables containing pseudonymized patient data are shown in orange, mapping tables with the integrated source(s) are in red, and metadata dimension tables are in green. In the ONT, metadata are organized into distinct metadata tables (eg, BIOLOGY_METADATA, DIAGNOSIS_METADATA), each containing tuples that represent nodes in a hierarchical tree structure. Each node in the tree corresponds to a tuple in the metadata tables, with its primary key representing the path from the root node to the current node. For example, the primary key of the intermediate node "Blood cell count" is C_FULLNAME = "\BioRes\Hemato\BloodCellCount." Leaf nodes are associated with a code stored in the C_BASECODE column. Only the tuples in the metadata tables that correspond to leaf nodes are included in the metadata dimension tables. For instance, the tuples for "Leucocytes" and "Erythrocytes" are included in the CONCEPT_DIMENSION table.



In addition to providing meaning to the observations stored in the CRC's OBSERVATION_FACT table, metadata enable the creation of views on these data through various access paths to lookup codes (eg, CONCEPT_CD), which contextualize each observation. Moreover, separating data and metadata into 2 distinct cells allows the loading of pseudonymized individual clinical data to be decoupled from the loading of metadata describing these data. As a result, modifying the metadata in the ONT makes it possible to adjust the view of the data without altering the data itself. This decoupling of data and metadata is one of the key strengths of the i2b2 architecture.

The i2b2 platform includes a patient and encounter identification engine that queries the ONT and CRC components based on clinical or biological criteria. A detailed description of this engine is provided in Multimedia Appendix 1.

The i2b2 data model is designed for data persistence in an RDBMS [40].

i2b2 Within the Bordeaux University Hospital

The Bordeaux University Hospital is a public health care facility in Bordeaux, Nouvelle-Aquitaine, France. Each year, a number of distinct patients visit the hospital for inpatient or outpatient care.

Since 2018, the Bordeaux University Hospital has implemented a CDW based on i2b2. The CDW integrates heterogeneous health data from patients who have visited the hospital since 2010. For these patients, data available since 2005 have also been integrated.

Various types of clinical data are integrated into the CDW:

- Structured data coded using standard terminologies, such as diagnoses (coded with the International Statistical Classification of Diseases and Related Health Problems, 10th Revision [ICD-10] [41]) or drug prescription/administration data (coded with the Anatomical Therapeutic Chemical classification [42]).
- Structured data coded using local (or interface) terminologies [43], such as biological results.
- Semistructured data, recorded in care forms. This type of data includes structured or free-text elements contextualized by a strong organizational structure within the forms: questions are grouped into sections, which are further organized into specific pages.
- Unstructured/free-text data, such as hospitalization reports, imaging reports, or discharge prescriptions.

XSL•FO
RenderX

Data from more than 20 sources are loaded daily into the Bordeaux University Hospital CDW. As of 2024, these data represent a total of (Table 1): 2,502,063 distinct patients; 20,982,497 inpatient or outpatient visits; and 3,474,264,570 observations, including 72,580,022 textual documents.

Table 1. Number of observations by source in the Bordeaux University Hospital clinical data warehouse.

Data source	Patients (n=2,502,063), n	Visits (n=20,982,497), n	Observations (n=3,474,264,570), n
Biology	1,286,459	4,157,738	1,323,818,025
Forms	1,641,829	8,130,391	829,328,415
Drug prescription/administration	744,611	1,775,078	469,279,982
Nursing care prescription/administration	688,450	1,875,347	263,813,687
Radiology	1,095,002	3,690,225	127,437,286
Localization	2,315,342	20,259,380	86,453,388
Free-text notes	2,045,379	12,202,309	72,580,022
Diagnostic (ICD-10[a])	947,024	2,650,212	63,135,010
Care prescription/administration	725,741	1,582,745	54,581,222
Nurse notes	619,767	1,729,145	54,558,694
Microbiology	474,997	961,850	39,277,538
Demographic data	2,502,063	20,982,497	23,841,233
Procedure (CCAM[b])	1,396,469	5,720,634	16,503,052
Chemotherapy	47,325	238,341	12,690,644
Nurse notes	733,021	2,143,927	12,002,868
Pathology	397,492	658,679	10,371,426
Surgery data	365,077	582,092	5,802,650
Other	435,078	748,627	4,112,204
Transfusion	217,389	491,076	2,647,208
Intensive care unit	8733	9349	2,030,016

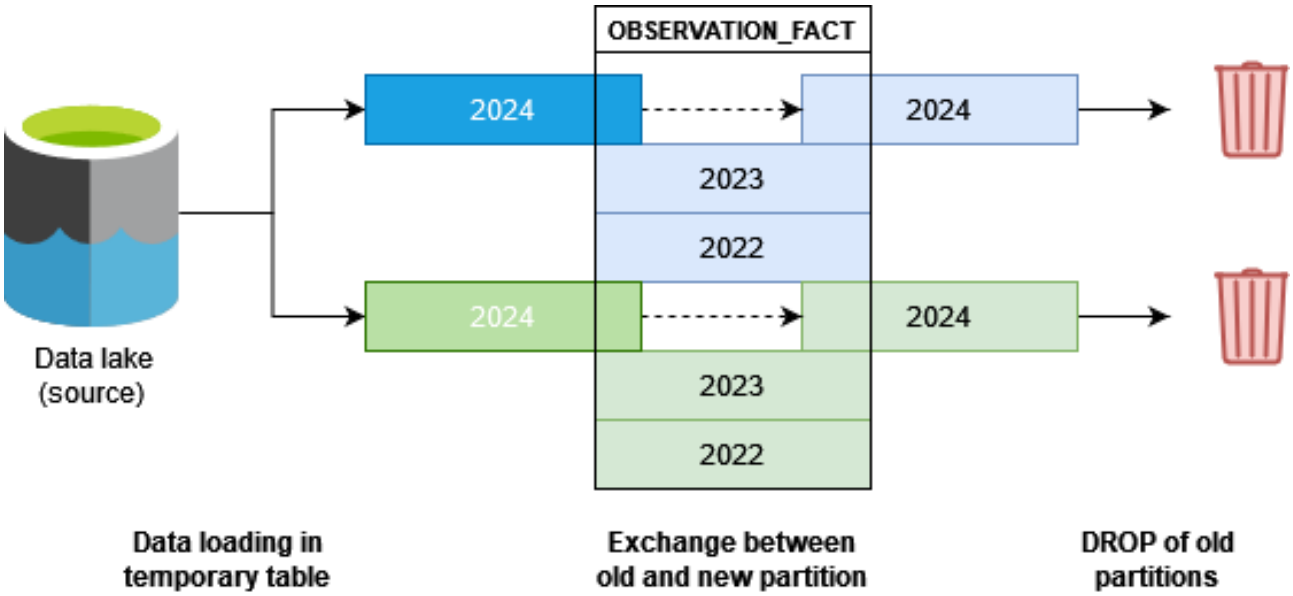
[a]ICD-10: International Statistical Classification of Diseases and Related Health Problems, 10th Revision.

[b]CCAM: Classification Commune des Actes Médicaux (Common Classification of Medical Procedures; French terminology for coding procedures).

Data from the Bordeaux University Hospital CDW are stored in an Oracle RDBMS. Our implementation includes partitioning the OBSERVATION_FACT table by source and year (Figure 2). This partitioning strategy aims to facilitate daily data updates and optimize query performance on large data sets. As a result, over 700 partitions have been created. This setup allows data to be loaded from all or selected sources for 1 or multiple years. With this configuration, data for the current year are refreshed daily, while historical data are updated less frequently.

XSL•FO
RenderX

Figure 2. Partitioning strategy implemented at Bordeaux University Hospital on the OBSERVATION_FACT table. Data from various sources (represented by different colors) are extracted daily from the data lake and loaded into intermediate tables (dark colors). During this Extract, Transform, and Load (ETL) process, only a subset of source data—filtered based on the temporality of observations—is collected. Once all intermediate tables are ready, old partitions are successively replaced with new ones and then deleted. This approach ensures that only a portion of the data in the OBSERVATION_FACT table is reloaded, minimizing data downtime.



Elasticsearch

Elasticsearch: A Distributed NoSQL Database for Document Storage and Indexing

Elasticsearch [38] is a distributed, document-oriented NoSQL database based on Apache Lucene (Apache Software Foundation) [44] indexing (Figure 3). It stores data as JSON documents in a schema-less structure. In Elasticsearch, an index (equivalent to a table in an RDBMS) stores documents, each of which corresponds to a tuple in an RDBMS table. These documents contain fields, which are equivalent to columns in an RDBMS table. The structure of an index is defined by mappings, which describe the fields in terms of column names, data types, and indexes—similar to how an RDBMS defines table structures. Each index consists of 1 or more shards, each corresponding to a Lucene inverted index [45], which is composed of 2 substructures:

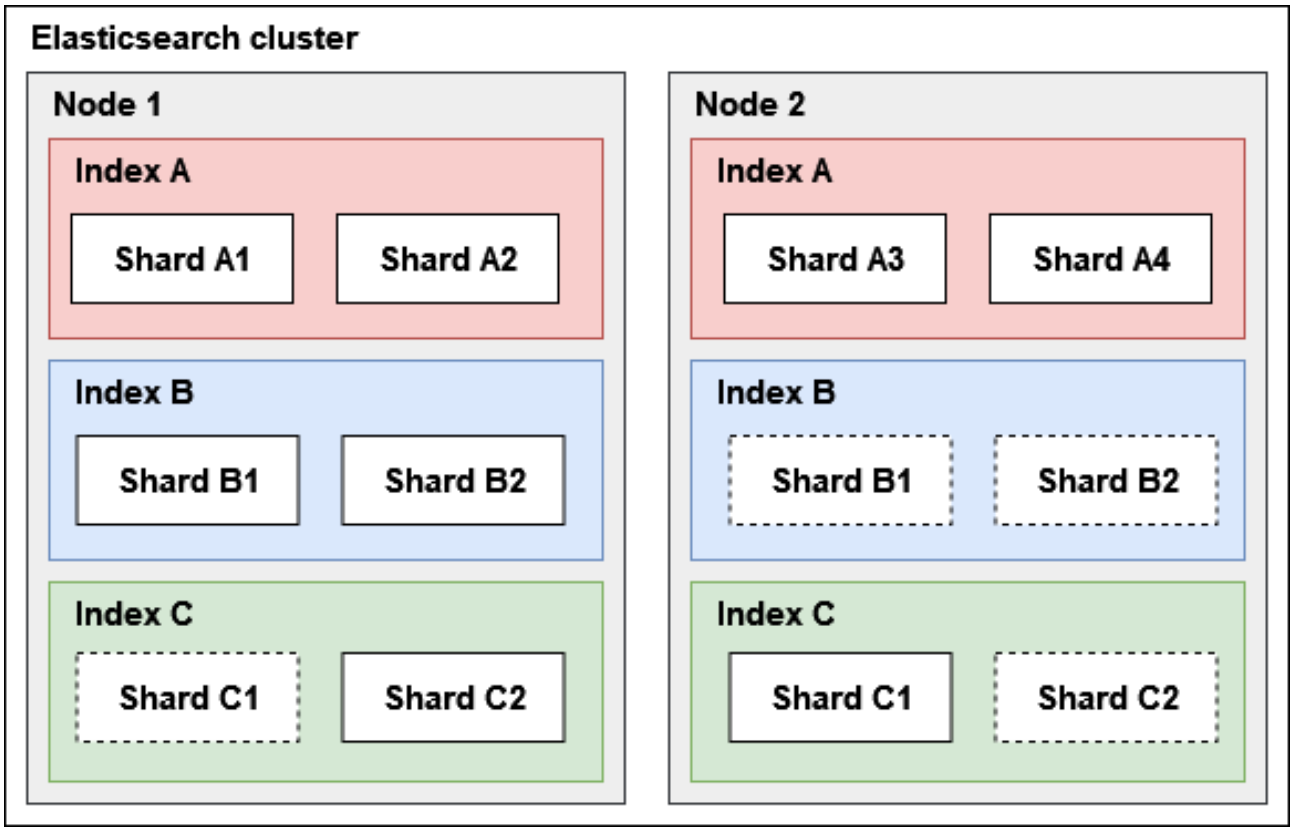
- The dictionary of terms: A sorted list storing all terms included in the indexed documents.
- The postings list [46]: A structure that records, for each term, the list of document IDs containing the term, along with its position(s) within each document.

Queries in Elasticsearch are parallelized across multiple shards within an index, enhancing search performance. Primary shards can be replicated across different nodes within an Elasticsearch cluster (Figure 3), ensuring high availability. If a node goes offline, another available node with a replicated shard can still process queries, preventing downtime and ensuring continuity.

While NoSQL databases offer many advantages, systems such as Elasticsearch do not efficiently support join operations [47]. To enable querying similar to RDBMSs, a denormalization step is often required, involving data duplication to ensure all necessary information is contained within a single structure [47,48].

XSL•FO
RenderX

Figure 3. Elasticsearch organization and components. An Elasticsearch cluster consists of 2 nodes. Shards with a solid border represent primary shards, while those with a dotted border indicate replicated shards. Index A is divided into 4 primary shards, distributed across 2 nodes without replication. Index B has 2 primary shards stored on node 1 and 2 replicated shards stored on node 2. Index C is split into 2 primary shards, distributed across both nodes in the cluster.



Elasticsearch Text Indexation

Elasticsearch supports various data types for fields, including text, which undergoes a specific indexing process using analyzers. This process builds a Lucene inverted index through 3 sequential steps:

- Character filtering: Cleans the text before indexing, such as removing special characters or replacing certain ones (eg, œ → oe).
- Tokenization: Splits the text into tokens. By default, Elasticsearch follows the Unicode Text Segmentation standard [49], which removes punctuation and uses spaces as separators.
- Token filtering: Modifies, removes, or adds tokens based on predefined rules. This step handles stop words, synonyms, and other text-processing enhancements.

The final output of this processing chain is stored in a Lucene inverted index.

Elasticsearch Keyword

The *keyword* data type is designed for structured data and can be used for both numerical and textual values. When a field is mapped as a keyword, it is stored in Lucene's inverted index exactly as it is, without any preprocessing. For example, the text "BIO:ERYTHRO" will be indexed as "BIO:ERYTHRO" if typed as a keyword. However, if assigned a text data type, it will be split into separate entries: "bio" and "erythro" in the inverted index. Keyword fields are particularly efficient for aggregation, sorting, and exact-term searches.

Adapting the i2b2 Data Model for Persistence in Elasticsearch

Overview

The adaptation of the i2b2 data model for persistence in Elasticsearch was carried out in 2 steps:

- Mapping the OBSERVATION_FACT table to an Elasticsearch index: This involved converting the data definition language used to create the OBSERVATION_FACT table into an equivalent observation_fact index structure, primarily defining field names, data types, and indexing modes.
- Modifying the observation_fact index structure by (1) incorporating elements from the patient and visit dimension tables, and (2) enriching observations with contextual information extracted from the ONT part of the i2b2 data model, stored as facets [50] of the observations. This modification was necessary due to Elasticsearch's lack of support for traditional relational joins.

Finally, the persistence of the observation component of the i2b2 data model in Elasticsearch was evaluated.

Mapping the Native OBSERVATION_FACT Table Structure as the observation_fact Index

The first step involved mapping all the columns of the OBSERVATION_FACT table into an Elasticsearch index. In an Elasticsearch document, mappings define 2 main elements (Table 2):

XSL•FO
RenderX

- The data type of each field in the Elasticsearch index (eg, numeric types such as long or double, text, date, keyword).
- The indexing method for each field. For instance, if a field is assigned the text data type, the mapping specifies the analyzer(s) used to index its content.

Thus, the 2 criteria considered to map OBSERVATION_FACT were:

- The need to perform count or aggregation queries on the field. In this case, the Elasticsearch data type used for the field was keyword. In the OBSERVATION_FACT table, the fields used as aggregation criteria or in enumeration queries are fields corresponding to foreign keys in dimension tables:
  - ENCOUNTER_NUM and PATIENT_NUM columns: These are used to count patients or visits, aggregate information by patient or by visit, etc;
  - CONCEPT_CD, MODIFIER_CD, and PROVIDER_ID columns: These are used to count elements by clinical and biological criteria, aggregate information by provider, etc;
  - INSTANCE_NUM column: This corresponds to the key for grouping a principal observation with its modified versions;
  - TVAL_CHAR, VALUEFLAG_CD, and UNITS_CD columns: These are used in the case of numerical observations to specify elements concerning the numerical operator (=, >, ≥, etc), the interpretation in relation to limits, or the unit associated with the numerical result.
- The need to query a field with free-text queries: In this case, the text data type is associated with an analyzer for managing free-text. The column concerned in the OBSERVATION_FACT table corresponds to the OBSERVATION_BLOB column (in OBSERVATION_FACT, the TVAL_CHAR column is also used to store short text. In our implementation, all text [short or long] is stored in OBSERVATION_BLOB).

Table 2. Mapping of the native OBSERVATION_FACT columns to Elasticsearch types.

Column name	Column data type	Elasticsearch field data type	Analyzer
ENCOUNTER_NUM	NUMBER	Keyword	No
PATIENT_NUM	NUMBER	Keyword	No
CONCEPT_CD	VARCHAR2	Keyword	No
PROVIDER_ID	VARCHAR2	Keyword	No
START_DATE	DATE	Date	No
MODIFIER_CD	VARCHAR2	Keyword	No
INSTANCE_NUM	NUMBER	Keyword	No
VALTYPE_CD	VARCHAR2	Keyword	No
TVAL_CHAR	VARCHAR2	Keyword	No
NVAL_NUM	NUMBER	Double	No
VALUEFLAG_CD	VARCHAR2	Keyword	No
QUANTITY_NUM	NUMBER	Double	No
UNITS_CD	VARCHAR2	Keyword	No
END_DATE	DATE	Date	No
LOCATION_CD	VARCHAR2	Keyword	No
OBSERVATION_BLOB	TEXT	Text	Yes
CONFIDENCE_NUM	NUMBER	Double	No
UPDATE_DATE	DATE	Date	No
DOWNLOAD_DATE	DATE	Date	No
IMPORT_DATE	DATE	Date	No
SOURCESYSTEM_CD	VARCHAR2	Keyword	No
UPLOAD_ID	NUMBER	Long	No

Modification of the Structure of the observation_fact Index

As it is not possible to perform joins between indexes in Elasticsearch, 2 types of changes have been made to overcome this limitation (Figure 4):

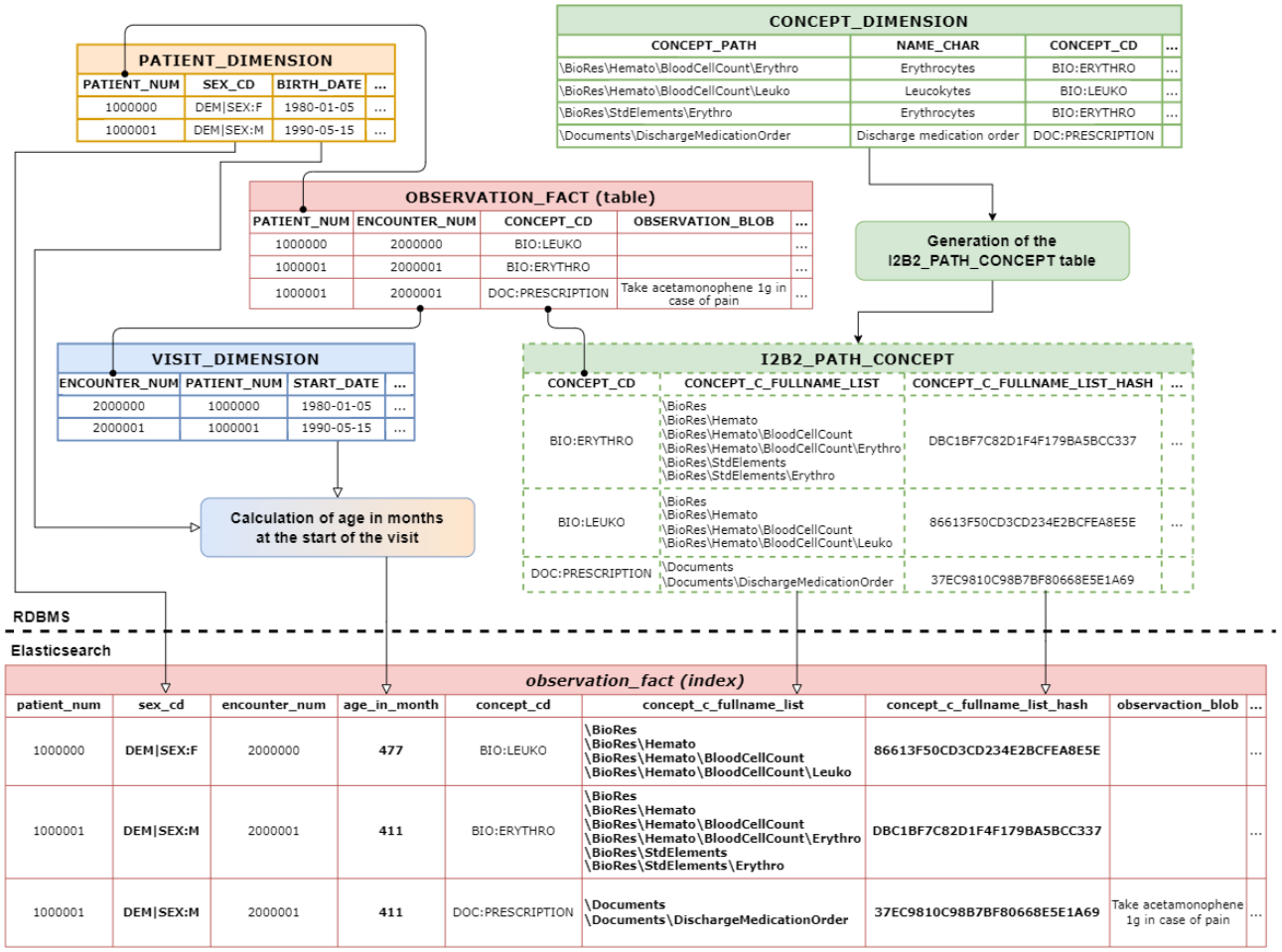
- Some of the columns describing observations within the PATIENT_DIMENSION and VISIT_DIMENSION tables were added to the observation_fact index. For reasons of parsimony, only PATIENT_DIMENSION.SEX_CD, PATIENT_DIMENSION.BIRTH_DATE, and VISIT_DIMENSION.START_DATE have been integrated

XSL•FO
RenderX

into the observation_fact index. PATIENT_DIMENSION.BIRTH_DATE and VISIT_DIMENSION.START_DATE have not been added as fields, but have been used to calculate the age_in_month_at_start_visit field;;

- To make documents of the observation_fact index accessible through the different hierarchical levels described in the ONT part, all the C_FULLNAME associated with the CONCEPT_PATH (also MODIFIER_PATH and PROVIDER_PATH) have been integrated into the observation_fact index. Additional tables have been added to the ONT part of the i2b2 model to allow the addition, by join, of all the paths (intermediate and final) for each possible value of the OBSERVATION_FACT lookup columns (ie, CONCEPT_CD, MODIFIER_CD, and PROVIDER_ID). The pseudo-code describing the generation of table I2B2_PATH_CONCEPT, for the CONCEPT_CD column, is available in Multimedia Appendix 2. Within the observation_fact index, paths are stored in 3 new fields called c_fullname_concept, c_fullname_modifier, and c_fullname_provider as lists of keywords. As a result, each observation within the observation_index is associated with all the paths (intermediate and full paths) describing all the lookup fields.

Figure 4. Creation of the observation_fact index from the different tables of the Informatics for Integrating Biology & the Bedside (i2b2) model. The table I2B2_PATH_CONCEPT (bordered with dotted line) is created based on CONCEPT_DIMENSION: for each CONCEPT_CD, the table contains the ordered list of CONCEPT_PATH, including all intermediate truncated versions of those paths. The algorithm used for the generation of the I2B2_PATH_CONCEPT table is provided in Multimedia Appendix 2. The relevant data from the PATIENT_DIMENSION, VISIT_DIMENSION, and I2B2_PATH_CONCEPT tables are added into the observation_fact index as a facet. BIRTH_DATE is used with visit START_DATE to compute the age_in_month_at_start_visit facet. The round-tipped arrows represent the joins between the tables. RDBMS: relational database management system.



Evaluation of the Elasticsearch Persistence

The evaluation of the proposed implementation of the main part of the i2b2 data model in Elasticsearch aims to assess:

- The ability to load partial individual data (CRC part) daily. The specific mechanisms used for data loading are described. Loading performance is evaluated in terms of median loading time and the median number of documents loaded per minute.
- The ability to update metadata (ONT part). Similarly, the specific mechanisms implemented to update the metadata elements integrated into the observation_fact index are described. Metadata updating performance is evaluated in terms of median update time and the average number of concept_cd entries that need to be updated each week.

The ability to perform queries on the CDW persisted in Elasticsearch was evaluated. The results of count queries (distinct patients or distinct encounters) were compared between Oracle RDBMS and Elasticsearch implementations for the same

XSL•FO
RenderX

CDW data in terms of result value and execution time (median execution time based on 20 executions). Different types of queries were performed, with criteria evaluated at the patient or encounter level (Table 3):

- Counting queries based on structured data (queries 1 and 2), including a query that returns a small number of patients (≈1500) and a query that returns a large number of patients (≈150,000).
- Counting queries based on structured data combined with a numerical filter (query 3).
- Counting queries based on free-text data (query 4).
- Counting queries based on structured data combined with a temporal filter (query 5).
- Combination of the above criteria in AND/OR Boolean queries, with multiple evaluation orders (eg, [(1) and (2)] vs [(2) and (1)]).

The hardware resources used for data persistence and query computation have been described.

XSL•FO
RenderX

Table 3. Query comparison between Oracle RDBMS[a] and Elasticsearch.

Query/fields and query type	Query result type	Execution time, median (IQR)		Counts[b], n
		Elasticsearch	Oracle RDBMS	
(1) Pembrolizumab				
Nontemporal	Patients	0.22 (0.21-0.23)	0.15 (0.14-0.16)	1701
Same encounter	Patients	0.43 (0.41-0.48)	0.18 (0.18-0.19)	1701
Same encounter	Encounters	0.43 (0.41-0.49)	0.20 (0.19-0.20)	3986
(2) Cancer				
Nontemporal	Patients	0.96 (0.95-0.98)	8.99 (8.66-9.51)	153,583
Same encounter	Patients	4.81 (4.74-4.87)	16.07 (15.55-16.63)	153,583
Same encounter	Encounters	4.79 (4.76-4.85)	15.97 (15.08-16.76)	516,682
(3) Sodium ≥ 145 mmol/L				
Nontemporal	Patients	0.38 (0.36-0.41)	9.42 (8.16-10.05)	26,426
Same encounter	Patients	0.75 (0.71-0.8)	9.39 (8.33-9.92)	26,426
Same encounter	Encounters	0.77 (0.72-0.82)	9.41 (8.38-9.9)	33,070
(4) Adenocarcinoma in free text				
Nontemporal	Patients	0.60 (0.59-0.62)	6.13 (5.97-6.51)	69,022/25,547
Same encounter	Patients	3.27 (3.20-3.33)	7.27 (7.01-7.50)	69,022/25,547
Same encounter	Encounters	3.27 (3.24-3.33)	7.26 (7.04-7.53)	369,953/92,638
(5) Cancer in 2023				
Nontemporal	Patients	0.31 (0.29-0.32)	6.72 (6.53-7.25)	19,251
Same encounter	Patients	0.66 (0.63-0.71)	6.88 (6.62-7.52)	19,251
Same encounter	Encounters	0.66 (0.64-0.70)	7.03 (6.88-7.41)	3606
(1) or (2)				
Nontemporal	Patients	1.00 (0.97-1.02)	9.15 (8.79-9.68)	153,589
Same encounter	Patients	4.95 (4.91-5.02)	15.72 (15.41-16.39)	153,589
Same encounter	Encounters	4.99 (4.91-5.05)	16.3 (15.74-16.81)	516,853
(2) or (1)				
Nontemporal	Patients	0.99 (0.97-1.02)	9.04 (8.79-9.32)	153,589
Same encounter	Patients	4.96 (4.89-5.02)	15.85 (15.38-16.76)	153,589
Same encounter	Encounters	4.95 (4.91-5.04)	16.51 (15.44-16.91)	516,853
(1) and (2)				
Nontemporal	Patients	1.07 (1.04-1.10)	6.68 ((6.45-6.95)	1695
Same encounter	Patients	4.81 (4.77-4.90)	6.83 (6.52-7.33)	1671
Same encounter	Encounters	4.81 (4.74-4.91)	6.94 (6.61-7.12)	3815
(2) and (1)				
Nontemporal	Patients	1.09 (1.06-1.10)	10.49 (10.17-11.12)	1695
Same encounter	Patients	4.96 (4.85-5.02)	21.38 (20.46-22.62)	1671
Same encounter	Encounters	4.94 (4.89-5.01)	21.38 (20.75-22.08)	3815
(5) and (3)				
Nontemporal	Patients	0.64 (0.59-0.69)	15.54 (14.41-17.51)	1917
Same encounter	Patients	1.45 (1.37-1.51)	16.15 (14.96-18.42)	1005
Same encounter	Encounters	1.47 (1.4-1.57)	16.42 (14.95-18.05)	1135

XSL•FO
RenderX

Query/fields and query type	Query result type	Execution time, median (IQR)		Counts[b], n
		Elasticsearch	Oracle RDBMS	
(1) and (5) and (3)				
Nontemporal	Patients	0.89 (0.82-0.93)	15.68 (14.8-17.29)	78
Same encounter	Patients	2.05 (1.85-2.08)	15.76 (14.59-17.98)	11
Same encounter	Encounters	1.95 (1.91-2.12)	15.61 (13.84-17.23)	11

[a]RDBMS: relational database management system.

[b]If Oracle RDBMS and Elasticsearch return the same result, a single count is provided. Otherwise, the count obtained with Elasticsearch is presented first, followed by the count obtained with Oracle RDBMS.

Results

Elasticsearch Data Loading

A specific ETL process was developed using Spring Boot [51] to convert data from an RDBMS into Elasticsearch.

Data from PATIENT_DIMENSION and VISIT_DIMENSION were added to the OBSERVATION_FACT table using outer joins in the ETL. For the ONT data, intermediate tables were created to store the ordered list of all CONCEPT_PATH (MODIFIER_PATH and PROVIDER_PATH, respectively) for each CONCEPT_CD (MODIFIER_CD and PROVIDER_ID, respectively). An example for the CONCEPT_CD column is presented in Table 4.

As mentioned above, the data in our OBSERVATION_FACT table are partitioned by data source and year. A similar rolling strategy has been implemented in Elasticsearch, as presented in Multimedia Appendix 3. Consequently, observation_fact consists of multiple indexes, corresponding to the partitions in OBSERVATION_FACT. Each observation_fact index was divided into 3 primary shards (1 per node) to enable parallel queries, with no replicated shards created.

All data from the OBSERVATION_FACT table were loaded into an Elasticsearch cluster, comprising 2,502,063 patients, 20,982,497 visits, and 3,474,264,570 observations. The number of records in the observation_fact indexes matches that in the OBSERVATION_FACT table. Data persistence in Oracle RDBMS requires 1.030 TB for data and 2.640 TB for indexes (including 420 GB for the Oracle RDBMS full-text index). By contrast, data persistence in Elasticsearch requires only 1.635 TB, representing 44% of the disk space needed for Oracle RDBMS.

Table 4. The i2b2[a] PATH_CONCEPT table: a generated metadata table that lists all available C_FULLNAME paths for each CONCEPT_CD described in the ONT[b]. Equivalent tables exist for MODIFIER_CD and PROVIDER_ID.

CONCEPT_CD	CONCEPT_C_FULLNAME_LIST	CONCEPT_C_FULLNAME_LIST_HASH
BIO:ERYTHRO	• \BioRes • \BioRes\Hemato • \BioRes\Hemato\BloodCellCount • \BioRes\Hemato\BloodCellCount\Erythro • \BioRes\StdElements • \BioRes\StdElements\Erythro	DBC1BF7C82D1F4F179BA5BCC337
BIO:LEUKO	• \BioRes • \BioRes\Hemato • \BioRes\Hemato\BloodCellCount • \BioRes\Hemato\BloodCellCount\Leuko	86613F50CD3CD234E2BCFEA8E5E
DOC:PRESCRIPTION	• \Documents • \Documents\DischargeMedicationOrder	37EC9810C98B7BF80668E5E1A69

[a]i2b2: Informatics for Integrating Biology & the Bedside.

[b]ONT: ontology management cell.

The duration of data loading in Elasticsearch by source is provided in Table 5. For the full year 2023 (approximately 340,000,000 observations), the median overall data loading time with 10 sources in parallel is 7.41 hours, corresponding to a median indexing rate of 46,546,000 documents per hour. Indexing speed appears to depend on the type of data, with structured numerical data being indexed at a median rate of 171,600 documents per minute—approximately 4 times faster than free-text data, which has a median rate of 48,100 documents per minute. Data loading in Elasticsearch has not been compared with data loading in Oracle DBMS. Indeed, data loading in Oracle RDBMS is heavily influenced by the transformations performed when integrating data from the source information system into the OBSERVATION_FACT table. By contrast, as loading into Elasticsearch is conducted from the OBSERVATION_FACT table, only transformations related to data denormalization are applied during the Elasticsearch loading process.

XSL•FO
RenderX

Table 5. Data loading metrics for the full year 2023 (metrics based on 8 loads).

Source	Observations (n=339,331,147), n	Documents (×1000/minute), median (Q1-Q3)[a]	Loading duration (minutes), median (Q1-Q3)[b,c]
Chemotherapy	478,438	185.3 (132.1-222.8)	2.5 (2.1-4.9)
Forms	77,460,099	181.6 (164.4-188.9)	429.1 (407.3-490.1)
Biology	158,384,678	171.6 (162.4-176.5)	916.4 (893.1-968.3)
Drug prescription/administration	32,736,762	155.6 (148.6-199.3)	204.5 (187.4-214.6)
Nursing care prescription/administration	16,523,635	107.4 (87.2-138.8)	149.2 (113.7-180.2)
Radiology	9,438,970	76.6 (37.8-91.7)	130.8 (79.9-201.4)
Diagnostic (ICD-10[d])	6,690,589	64.6 (57.3-105.7)	105.2 (64.2-116.8)
Localization	6,181,496	59.8 (54.3-79.2)	102.8 (77.6-118.3)
Demographic data	2,142,053	59.6 (55.0-122.6)	34.7 (17.3-37.8)
Nurse notes	12,984,197	58.8 (52.4-66.7)	223.6 (199.0-248.7)
Care prescription/administration	4,930,320	56.5 (30.0-68.6)	86.9 (71.7-162.6)
Free-text notes	6,066,806	48.1 (39.8-78.3)	125.9 (80.2-151.3)
Surgery data	518,998	13.9 (6.5-248.9)	37.4 (2.1-80.3)
Microbiology	3,364,431	13.2 (11.5-17.6)	254.3 (189.7-290.2)
Pathology	678,289	10.7 (7.6-18.8)	65.6 (38.8-89.4)
Other	284,220	4.9 (3.1-190.7)	59.1 (1.5-90.6)
Transfusion	467,166	2.7 (2.1-3.1)	165.3 (152.4-205.4)

[a]Overall: 775.8 (749.2-792.1).

[b]The median loading duration was calculated without considering parallelization. Some sources consist of multiple indexes, such as biology (which comprises 5 indexes) and forms (which comprises 4 indexes). This explains why the maximum median loading duration (916.4 minutes) is higher than the overall median duration (444.8 minutes).

[c]Overall: 444.8 (429.0-461.2).

[d]ICD-10: International Statistical Classification of Diseases and Related Health Problems, 10th Revision.

Elasticsearch Metadata Updating

In the case of a modification in the ONT part, a strategy for updating the observation_fact indexes has been implemented. This strategy is presented and evaluated in Multimedia Appendix 4 [52].

Elasticsearch Querying

The results of queries executed on an Oracle RDBMS engine were compared with those obtained using Elasticsearch. For queries involving joins (AND Boolean queries), the joins were performed at the application layer for both Oracle RDBMS and Elasticsearch. A full-text index was available in the Oracle RDBMS. All necessary indexes for the Oracle RDBMS queries were calculated, and the statistics were up to date. The results and response times were compared between the 2 engines. The Oracle RDBMS (version 19.17) runs as a cluster on 2 servers, each with 80 CPUs and 1 TB of memory. The Elasticsearch database (version 7.17.3) is configured as a 3-node cluster, deployed through Docker, with each node having access to 25 CPUs and 30 GB of memory.

A total of 9 different queries were compared (Table 3). Each query evaluated criteria either at the patient level (nontemporal queries) or at the visit level (temporal queries). To assess execution time, each query was executed 20 times on both engines. The results were identical between the Oracle RDBMS engine and Elasticsearch, except for the full-text query, which returned more results in Elasticsearch due to differences in full-text indexing implementation. Response times were generally lower with Elasticsearch than with Oracle RDBMS, except for the “Pembrolizumab” query, which returned a low number of results. Temporal queries (evaluating criteria within the same encounter) were consistently slower than nontemporal queries on both engines.

Source Code

The ETL between i2b2 RDBMS and i2b2 Elasticsearch was developed using Spring Boot (a Java framework; VMware). The source code of the ETL is available at [53].

Discussion

Principal Findings

To our knowledge, this work is the first to evaluate the technical feasibility and performance of persisting an i2b2 model in an Elasticsearch database. Beyond demonstrating feasibility, the evaluation highlights significant improvements in overall query times and hardware resource requirements, particularly in storage, with a 66% reduction in disk space usage. Additionally, the implementation has been tested on a large volume of data,

XSL•FO
RenderX

demonstrating good scalability. The proposed implementation is currently in production at Bordeaux University Hospital, supporting more than 200 research projects since 2022.

Elasticsearch is designed for very fast searches, prioritizing optimization for speed, high availability, and horizontal scalability. However, this comes at the cost of certain transactional guarantees (ACID) and absolute precision in some operations, such as counts. Specifically, in the event of a failure during the update of a replicated index, the system may restart in an inconsistent state, where data are updated in the primary shard but not across all its replicas. In our context, high availability is not a major concern. We have therefore chosen not to replicate shards across different cluster nodes, avoiding consistency issues in case of failure. Additionally, in the rolling strategy implemented for data loading, a newly created index becomes available for searching only after it has been fully loaded, minimizing the risk of querying incomplete data. To optimize queries, Elasticsearch employs probabilistic counting algorithms (eg, HyperLogLog) for count queries. However, in our context, exact results are essential for this type of query. We have therefore configured Elasticsearch to ensure accuracy, sacrificing some query performance. Despite this, execution times were consistently lower with Elasticsearch than with the RDBMS.

In our implementation, we chose to add the lookup columns from the dimension tables and the paths of CONCEPT_CD (as well as MODIFIER_CD and PROVIDER_ID) as facets of the observation_fact indexes. Combined with fields of the keyword data type, this approach optimizes query times, particularly for enumeration queries, at the expense of indexing time, which is not performed in real time. The disadvantage of this implementation is that data (CRC) and metadata (ONT) are not kept separate, meaning that any modification to the metadata requires reloading or updating the data. To address this issue, we implemented a process for updating metadata within the observation_fact indexes and demonstrated the feasibility of performing these updates without reloading the entire data set.

An alternative implementation would involve maintaining the observation_fact indexes without adding additional fields and instead creating separate indexes for the various dimension tables and the ONT metadata table. Similar to the proposed configuration, joins at the application layer (ie, intersecting patient or encounter lists) would be used to combine results from different indexes for AND Boolean queries. However, this approach presents potential performance challenges. For instance, intersecting gender data (eg, female) stored in the patient_dimension index with a criterion stored in the observation_fact indexes would require loading into memory the list of all patient keys corresponding to women in the CDW—approximately 1.2 million patients in the Bordeaux University Hospital implementation. This issue becomes even more pronounced when handling data from the VISIT_DIMENSION table.

Alternatively, an Elasticsearch implementation could have used nested field data types [54]. These types allow the content of a nested field to be indexed as a separate Lucene document within the main document. This approach would have enabled indexing a patient document containing visit documents as nested data, which in turn would contain observation documents as nested data. However, this implementation would have required reloading all data for a given patient at once, which was incompatible with our goal of reloading recent data daily. Additionally, queries involving nested documents generally perform worse than standard field queries.

In our implementation, we mapped the TVAL_CHAR column of the OBSERVATION_FACT table as a “keyword” in the indexes constituting observation_fact. In the i2b2 data model, the TVAL_CHAR column is used in 2 cases, in conjunction with the content of the VALTYPE_CD column:

- VALTYPE_CD = “T”: The TVAL_CHAR column contains the short text associated with the CONCEPT_CD (eg, a biology comment).
- VALTYPE_CD = “N”: The TVAL_CHAR column contains the mathematical operator associated with the numerical value in the NVAL_NUM column (eg, “E” for “equal,” “NE” for “not equal,” and “L” for “less than”).

In the i2b2 implementation at Bordeaux University Hospital, all free-text data, including short texts, are stored in the OBSERVATION_BLOB column. As a result, the TVAL_CHAR column contains only the mathematical operators for numerical values. In a fully i2b2-compliant implementation, it would be necessary not only to map the TVAL_CHAR column as a keyword but also to associate an analyzer with it. This would enable both full-text search and aggregate queries.

To evaluate query capabilities using the Elasticsearch database, part of the i2b2 query engine was reimplemented. This reimplementation supports multicriteria enumeration queries (ie, “AND,” “OR,” and “NOT” Boolean queries), including numerical data and free-text search, evaluated at the patient or encounter level. However, not all functionalities available in the original i2b2 query engine have been implemented. In particular, the ability to perform queries based on the number of occurrences of observations (eg, identifying patients who have visited the hospital at least three times) or queries that account for temporality between events (eg, patients with hemoglobin measurements within 5 days after colon surgery) has not been implemented. These 2 types of queries are more complex than those already implemented, as they require additional observation aggregation and aggregate filtering steps before results can be aggregated at the patient or event level. However, the organization of the observation_fact indexes proposed here appears to be compatible with executing such queries. Implementing these capabilities could be the focus of future work.

The proposed ETL for loading the Elasticsearch database is based on data already integrated into an i2b2 model persisted in an RDBMS. Beyond enabling a straightforward ETL process from i2b2 RDBMS to i2b2 Elasticsearch, maintaining this relational database appears essential for specific use cases that would not be feasible with Elasticsearch alone (eg, joins with the system containing the source data, preparation of complex data by joining OBSERVATION_FACT to itself). Consequently, while Elasticsearch provides performance

XSL•FO
RenderX

improvements, these must be weighed against the requirement to maintain 2 parallel infrastructures.

Although no i2b2 implementation using a NoSQL database has been described to our knowledge, the literature includes examples of CDWs designed for free-text analysis. OpenMRS [55], an open-source EHR project, features a free-text search module based on Apache Lucene, integrated with Hibernate Search. R-oogle [20], a document-oriented CDW, preindexes free-text data using external terminologies (eg, Medical Subject Headings [MeSH]) and stores them in a Lucene index. Dr. Warehouse [21,56] implements a segmentation approach for free-text documents, breaking them into "propositions" stored in a full-text index within the Oracle RDBMS. These propositions are linked to contextual elements (eg, antecedents, personal and family history, or negation). Doc'EDS [57] provides a phenotyping search engine that integrates both structured and unstructured data, indexed through Apache Lucene. All CDW implementations utilizing NoSQL databases [20,55,57] rely on Apache Lucene's low-level libraries. Elasticsearch, built on Apache Lucene, operates at a higher abstraction level, simplifying deployment and integration. While this limits fine-tuning capabilities for specific indexing needs, it provides significant advantages, such as access to the Kibana [58] visualization engine and query clients available in Java via Spring Boot [59].

Conclusions

This study presents an Elasticsearch-based implementation of the i2b2 data model for phenotyping tasks. By reimplementing part of the i2b2 search engine, the study demonstrates that Elasticsearch provides similar query capabilities while offering faster performance and improved efficiency for free-text searches.

Conflicts of Interest

None declared.

Multimedia Appendix 1
Workflow for using data contained in an Informatics for Integrating Biology & the Bedside clinical data warehouse.
[DOCX File , 147 KB - medinform_v13i1e65753_app1.docx]

Multimedia Appendix 2
Pseudocode of the I2B2_PATH_CONCEPT table construction. i2b2: Informatics for Integrating Biology & the Bedside.
[PNG File , 185 KB - medinform_v13i1e65753_app2.png]

Multimedia Appendix 3
Rolling strategy for data loading.
[DOCX File , 25 KB - medinform_v13i1e65753_app3.docx]

Multimedia Appendix 4
Elasticsearch metadata update strategy.
[DOCX File , 25 KB - medinform_v13i1e65753_app4.docx]

References

1. Thomason J. Big tech, big data and the new world of digital health. Global Health Journal 2021 Dec;5(4):165-168. [doi: 10.1016/j.glohj.2021.11.003]
2. Dinov ID. Volume and value of big healthcare data. J Med Stat Inform 2016;4:3 [FREE Full text] [doi: 10.7243/2053-7662-4-3] [Medline: 26998309]
3. Densen P. Challenges and opportunities facing medical education. Trans Am Clin Climatol Assoc 2011;122:48-58 [FREE Full text] [Medline: 21686208]
4. Gunter TD, Terry NP. The emergence of national electronic health record architectures in the United States and Australia: models, costs, and questions. J Med Internet Res 2005 Mar 14;7(1):e3 [FREE Full text] [doi: 10.2196/jmir.7.1.e3] [Medline: 15829475]
5. Safran C, Bloomrosen M, Hammond WE, Labkoff S, Markel-Fox S, Tang PC, Expert Panel. Toward a national framework for the secondary use of health data: an American Medical Informatics Association white paper. J Am Med Inform Assoc 2007 Jan;14(1):1-9 [FREE Full text] [doi: 10.1197/jamia.M2273] [Medline: 17077452]
6. Dicuonzo G, Galeone G, Shini M, Massari A. Towards the use of big data in healthcare: a literature review. Healthcare (Basel) 2022 Jul 01;10(7):1232 [FREE Full text] [doi: 10.3390/healthcare10071232] [Medline: 35885759]
7. Essay P, Fisher J, Mosier J, Subbian V. Validation of an electronic phenotyping algorithm for patients with acute respiratory failure. Crit Care Explor 2022 Mar;4(3):e0645 [FREE Full text] [doi: 10.1097/CCE.0000000000000645] [Medline: 35261979]

XSL•FO
RenderX

8. Meng W, Ou W, Chandwani S, Chen X, Black W, Cai Z. Temporal phenotyping by mining healthcare data to derive lines of therapy for cancer. J Biomed Inform 2019 Dec;100:103335 [FREE Full text] [doi: 10.1016/j.jbi.2019.103335] [Medline: 31689549]
9. Moal B, Orieux A, Ferté T, Neuraz A, Brat GA, Avillach P, Consortium for Clinical Characterization of COVID-19 by EHR (4CE), et al. Acute respiratory distress syndrome after SARS-CoV-2 infection on young adult population: international observational federated study based on electronic health records through the 4CE consortium. PLoS One 2023;18(1):e0266985 [FREE Full text] [doi: 10.1371/journal.pone.0266985] [Medline: 36598895]
10. Geva A, Gronsbell JL, Cai T, Cai T, Murphy SN, Lyons JC, Pediatric Pulmonary Hypertension NetworkNational Heart, Lung,Blood Institute Pediatric Pulmonary Vascular Disease Outcomes Bioinformatics Clinical Coordinating Center Investigators. A computable phenotype improves cohort ascertainment in a pediatric pulmonary hypertension registry. J Pediatr 2017 Sep;188:224-231.e5 [FREE Full text] [doi: 10.1016/j.jpeds.2017.05.037] [Medline: 28625502]
11. Toh S, Avorn J, D'Agostino RB, Gurwitz JH, Psaty BM, Rothman KJ, et al. Re-using Mini-Sentinel data following rapid assessments of potential safety signals via modular analytic programs. Pharmacoepidemiol Drug Saf 2013 Oct;22(10):1036-1045. [doi: 10.1002/pds.3478] [Medline: 23922322]
12. Kruse CS, Stein A, Thomas H, Kaur H. The use of electronic health records to support population health: a systematic review of the literature. J Med Syst 2018 Sep 29;42(11):214 [FREE Full text] [doi: 10.1007/s10916-018-1075-6] [Medline: 30269237]
13. Ferté T, Jouhet V, Griffier R, Hejblum BP, Thiébaut R, Bordeaux University Hospital Covid-19 Crisis Task Force. The benefit of augmenting open data with clinical data-warehouse EHR for forecasting SARS-CoV-2 hospitalizations in Bordeaux area, France. JAMIA Open 2022 Dec;5(4):ooac086 [FREE Full text] [doi: 10.1093/jamiaopen/ooac086] [Medline: 36380849]
14. Sujansky W. Heterogeneous database integration in biomedicine. J Biomed Inform 2001 Aug;34(4):285-298 [FREE Full text] [doi: 10.1006/jbin.2001.1024] [Medline: 11977810]
15. Wollersheim D, Sari A, Rahayu W. Archetype-based electronic health records: a literature review and evaluation of their applicability to health data interoperability and access. Health Inf Manag 2009;38(2):7-17. [doi: 10.1177/183335830903800202] [Medline: 19546483]
16. McDonald CJ, Huff SM, Suico JG, Hill G, Leavelle D, Aller R, et al. LOINC, a universal standard for identifying laboratory observations: a 5-year update. Clin Chem 2003 Apr;49(4):624-633. [doi: 10.1373/49.4.624] [Medline: 12651816]
17. Müller A, Christmann L, Kohler S, Eils R, Prasser F. Machine learning for medical data integration. Stud Health Technol Inform 2023 May 18;302:691-695. [doi: 10.3233/SHTI230241] [Medline: 37203471]
18. Murphy SN, Weber G, Mendis M, Gainer V, Chueh HC, Churchill S, et al. Serving the enterprise and beyond with informatics for integrating biology and the bedside (i2b2). J Am Med Inform Assoc 2010;17(2):124-130 [FREE Full text] [doi: 10.1136/jamia.2009.000893] [Medline: 20190053]
19. Stang PE, Ryan PB, Racoosin JA, Overhage JM, Hartzema AG, Reich C, et al. Advancing the science for active surveillance: rationale and design for the Observational Medical Outcomes Partnership. Ann Intern Med 2010 Nov 02;153(9):600-606. [doi: 10.7326/0003-4819-153-9-201011020-00010] [Medline: 21041580]
20. Cuggia M, Garcelon N, Campillo-Gimenez B, Bernicot T, Laurent J, Garin E, et al. Roogle: an information retrieval engine for clinical data warehouse. Stud Health Technol Inform 2011;169:584-588. [doi: 10.3233/978-1-60750-806-9-584] [Medline: 21893816]
21. Garcelon N, Neuraz A, Salomon R, Faour H, Benoit V, Delapalme A, et al. A clinician friendly data warehouse oriented toward narrative reports: Dr. Warehouse. J Biomed Inform 2018 Apr;80:52-63 [FREE Full text] [doi: 10.1016/j.jbi.2018.02.019] [Medline: 29501921]
22. De Moor G, Sundgren M, Kalra D, Schmidt A, Dugas M, Claerhout B, et al. Using electronic health records for clinical research: the case of the EHR4CR project. J Biomed Inform 2015 Feb;53:162-173 [FREE Full text] [doi: 10.1016/j.jbi.2014.10.006] [Medline: 25463966]
23. Gagalova KK, Leon Elizalde MA, Portales-Casamar E, Görges M. What You need to know before implementing a clinical research data warehouse: comparative review of integrated data repositories in health care institutions. JMIR Form Res 2020 Aug 27;4(8):e17687 [FREE Full text] [doi: 10.2196/17687] [Medline: 32852280]
24. OMOP common data model. OHDSI CDM Working Group. URL: https://ohdsi.github.io/CommonDataModel/index.html [accessed 2024-08-24]
25. Jungkunz M, Köngeter A, Mehlis K, Winkler EC, Schickhardt C. Secondary use of clinical data in data-gathering, non-interventional research or learning activities: definition, types, and a framework for risk assessment. J Med Internet Res 2021 Jun 08;23(6):e26631 [FREE Full text] [doi: 10.2196/26631] [Medline: 34100760]
26. Shivade C, Raghavan P, Fosler-Lussier E, Embi PJ, Elhadad N, Johnson SB, et al. A review of approaches to identifying patient phenotype cohorts using electronic health records. J Am Med Inform Assoc 2014 Mar;21(2):221-230 [FREE Full text] [doi: 10.1136/amiajnl-2013-001935] [Medline: 24201027]
27. Schlegel DR, Ficheur G. Secondary use of patient data: review of the literature published in 2016. Yearb Med Inform 2017 Aug;26(1):68-71 [FREE Full text] [doi: 10.15265/IY-2017-032] [Medline: 29063536]
28. Murdoch TB, Detsky AS. The inevitable application of big data to health care. JAMA 2013 Apr 03;309(13):1351-1352. [doi: 10.1001/jama.2013.393] [Medline: 23549579]

XSL•FO
RenderX

29. Choi Y, Jeon W, Yoon S. Improving database system performance by applying NoSQL. Journal of Information Processing Systems 2014;10(3):355-364 [FREE Full text] [doi: 10.3745/JIPS.04.0006]
30. Moniruzzaman ABM, Hossain SA. NoSQL database: new era of databases for big data analytics - classification, characteristics and comparison. arXiv Preprint posted online on June 30, 2013 [FREE Full text]
31. Phiri H, Kunda D. Comparative study of NoSQL and relational database. Zamb ICT J 2017 Dec 27;1:1-4. [doi: 10.33260/zictjournal.v1i1.8]
32. Ansari MH, Tabatab Vakili V, Bahrak B. Evaluation of big data frameworks for analysis of smart grids. J Big Data 2019 Dec 03;6(1):109. [doi: 10.1186/s40537-019-0270-8]
33. Mishra S, Misra A. Structured and Unstructured Big Data Analytics. 2017 Presented at: Int Conf Curr Trends Comput Electr Electron Commun CTCEEC .?746; 2017; Mysore, India p. 740. [doi: 10.1109/ctceec.2017.8454999]
34. Modhiya K. Introduction to DBMS, RDBMS, and NoSQL database: NoSQL database challenges. SSRN Journal 2021:1-11 [FREE Full text] [doi: 10.2139/ssrn.3798989]
35. Cattell R. Scalable SQL and NoSQL data stores. SIGMOD Rec 2011 May 06;39(4):12-27. [doi: 10.1145/1978915.1978919]
36. Ali A, Naeem S, Anam S, Ahmed M. A state of art survey for big data processing and NoSQL database architecture. IJCDS 2023 Jul 1;14(1):297-309. [doi: 10.12785/ijcds/140124]
37. Khan W, Kumar T, Zhang C, Raj K, Roy AM, Luo B. SQL and NoSQL database software architecture performance analysis and assessments—a systematic literature review. BDCC 2023 May 12;7(2):97. [doi: 10.3390/bdcc7020097]
38. Gormley C, Tong Z. Elasticsearch: The Definitive Guide: A Distributed Real-Time Search and Analytics Engine. London, UK: O'Reilly Media; 2015.
39. Kimball R, Ross M. The Data Warehouse Toolkit: The Definitive Guide to Dimensional Modeling, 3rd Edition. Hoboken, NJ: Wiley; 2013.
40. The i2b2 data repository. GitHub. 2015. URL: https://github.com/i2b2/i2b2-data [accessed 2024-08-24]
41. Brämer GR. International statistical classification of diseases and related health problems. Tenth revision. World Health Stat Q 1988;41(1):32-36. [Medline: 3376487]
42. Anatomical Therapeutic Chemical (ATC) Classification. World Health Organization (WHO). 1976. URL: https://www.who.int/tools/atc-ddd-toolkit/atc-classification [accessed 2024-08-24]
43. Schulz S, Rodrigues J, Rector A, Chute C. Interface terminologies, reference terminologies and aggregation terminologies: a strategy for better integration. Stud Health Technol Inform 2017;245:940-944. [Medline: 29295238]
44. Bialecki A, Muir R, Ingersoll G. Apache Lucene 4. In: Proceedings of the SIGIR 2012 Workshop on Open Source Information Retrieval. 2012 Presented at: The SIGIR 2012 Workshop on Open Source Information Retrieval; August 16, 2012; Portland, OR URL: https://www.researchgate.net/publication/260282732_Apache_Lucene_4
45. Blair D. Information Retrieval, 2nd ed. C.J. Van Rijsbergen. London: Butterworths; 1979: 208 pp. Price: $32.50. J Am Soc Inf Sci 2007 Mar 22;30(6):374-375. [doi: 10.1002/asi.4630300621]
46. Elasticsearch. Frame of reference and roaring Bitmaps. Elastic Blog. 2015. URL: https://www.elastic.co/blog/frame-of-reference-and-roaring-bitmaps [accessed 2024-08-24]
47. Kim HJ, Ko EJ, Jeon YH, Lee KH. Migration from RDBMS to column-oriented NoSQL: lessons learned and open problems. In: Proceedings of the 7th International Conference on Emerging Databases. Singapore City, Singapore: Springer; 2018 Presented at: The 7th International Conference on Emerging Databases; August 7-9, 2017; Busan, Korea p. 25-33. [doi: 10.1007/978-981-10-6520-0_3]
48. Vera-Olivera H, Guo R, Huacarpuma RC, Da Silva A, Mariano AM, Holanda M. Data modeling and NoSQL databases - a systematic mapping review. ACM Comput Surv 2021 Jul 13;54(6):1-26. [doi: 10.1145/3457608]
49. Davis M. Unicode Standard Annex #29: Unicode text segmentation. Unicode. 2010. URL: https://www.unicode.org/reports/tr29/tr29-17.html [accessed 2024-08-24]
50. Tunkelang D. Faceted Search. Cham, Switzerland: Springer International Publishing; 2009.
51. Spring Boot. Spring. 2014. URL: https://spring.io/projects/spring-boot [accessed 2024-08-24]
52. Update by query API | Elasticsearch guide 8. Elastic. 2013. URL: https://www.elastic.co/guide/en/elasticsearch/reference/current/docs-update-by-query.html [accessed 2024-08-24]
53. Griffier R. Source code of i2b2-elastic. GitLab. URL: https://gitub.u-bordeaux.fr/i2b2-elastic [accessed 2025-01-14]
54. Elasticsearch. Nested field type | Elasticsearch guide 8. Elastic. 2015. URL: https://www.elastic.co/guide/en/elasticsearch/reference/current/nested.html [accessed 2024-08-24]
55. Verma N, Mamlin B, Flowers J, Acharya S, Labrique A, Cullen T. OpenMRS as a global good: impact, opportunities, challenges, and lessons learned from fifteen years of implementation. Int J Med Inform 2021 May;149:104405. [doi: 10.1016/j.ijmedinf.2021.104405] [Medline: 33639327]
56. Garcelon N, Neuraz A, Benoit V, Salomon R, Burgun A. Improving a full-text search engine: the importance of negation detection and family history context to identify cases in a biomedical data warehouse. J Am Med Inform Assoc 2017 May 01;24(3):607-613 [FREE Full text] [doi: 10.1093/jamia/ocw144] [Medline: 28339516]
57. Pressat-Laffouilhère T, Balayé P, Dahamna B, Lelong R, Billey K, Darmoni SJ, et al. Evaluation of Doc'EDS: a French semantic search tool to query health documents from a clinical data warehouse. BMC Med Inform Decis Mak 2022 Feb 08;22(1):34 [FREE Full text] [doi: 10.1186/s12911-022-01762-4] [Medline: 35135538]

XSL•FO
RenderX

58. Kibana: explore, visualize, discover data. Elastic. URL: https://www.elastic.co/kibana [accessed 2024-08-24]
59. Spring Data Elasticsearch. Spring. 2013. URL: https://spring.io/projects/spring-data-elasticsearch [accessed 2024-08-24]

Abbreviations

ACID: atomicity, consistency, isolation, and durability
CDW: clinical data warehouse
CRC: clinical research chart
EHR: electronic health record
ETL: Extract, Transform, and Load
i2b2: Informatics for Integrating Biology & the Bedside
ICD-10: International Statistical Classification of Diseases and Related Health Problems, 10th Revision
LOINC: Logical Observation Identifiers Names and Codes
MeSH: Medical Subject Headings
OMOP-CDM: Observational Medical Outcomes Partnership-Common Data Model
ONT: ontology management cell
RDBMS: relational database management system

Edited by C Lovis; submitted 25.08.24; peer-reviewed by S Murphy, H Tong; comments to author 04.11.24; revised version received 29.12.24; accepted 31.01.25; published 24.04.25.

Please cite as:
Griffier R, Mougin F, Jouhet V
Integrating Health Care Data in an Informatics for Integrating Biology & the Bedside (i2b2) Model Persisted Through Elasticsearch: Design, Implementation, and Evaluation in a French University Hospital
JMIR Med Inform 2025;13:e65753
URL: https://medinform.jmir.org/2025/1/e65753
doi:10.2196/65753
PMID:

©Romain Griffier, Fleur Mougin, Vianney Jouhet. Originally published in JMIR Medical Informatics (https://medinform.jmir.org), 24.04.2025. This is an open-access article distributed under the terms of the Creative Commons Attribution License (https://creativecommons.org/licenses/by/4.0/), which permits unrestricted use, distribution, and reproduction in any medium, provided the original work, first published in JMIR Medical Informatics, is properly cited. The complete bibliographic information, a link to the original publication on https://medinform.jmir.org/, as well as this copyright and license information must be included.

XSL•FO
RenderX

Large Separable Kernel Attention–Driven Multidimensional Feature Cross-Level Fusion Classification Network of Knee Cartilage Injury: Algorithm Development and Validation

Lirong Zhang, MEng; Hang Yu, MEng; Yating Yang

The School of Digital Art and Design, Dalian Neusoft University of Information, No. 8 Software Park Road, Ganjingzi District, Dalian, Liaoning, China

Corresponding Author:
Lirong Zhang, MEng
The School of Digital Art and Design, Dalian Neusoft University of Information, No. 8 Software Park Road, Ganjingzi District, Dalian, Liaoning, China

Abstract

Background: Knee cartilage injury (KCI) poses significant challenges in the early clinical diagnosis process, primarily due to its high incidence, the complexity of healing, and the limited sensitivity of initial imaging modalities.

Objective: This study aims to employ magnetic resonance imaging and machine learning methods to enhance the classification accuracy of the classifier for KCI, improve the existing network structure, and demonstrate important clinical application value.

Methods: The proposed methodology is a multidimensional feature cross-level fusion classification network driven by the large separable kernel attention, which enables high-precision hierarchical diagnosis of KCI through deep learning. The network first fuses shallow high-resolution features with deep semantic features via the cross-level fusion module. Then, the large separable kernel attention module is embedded in the YOLOv8 network. This network utilizes the combined optimization of depth-separable and point-by-point convolutions to enhance features at multiple scales, thereby dramatically improving the hierarchical characterization of cartilage damage. Finally, five classifications of knee cartilage injuries are performed by classifiers.

Results: To overcome the limitations of network models trained with single-plane images, this study presents the first hospital-based multidimensional magnetic resonance imaging real dataset for KCI, on which the classification accuracy is 99.7%, the Kappa statistic is 99.6%, the *F*-measure is 99.7%, the sensitivity is 99.7%, and the specificity is 99.9%. The experimental results validate the feasibility of the proposed method.

Conclusions: The experimental outcomes confirm that the proposed methodology not only achieves exceptional performance in classifying knee cartilage injuries but also offers substantial improvements over existing techniques. This underscores its potential for clinical deployment in enhancing diagnostic precision and efficiency.

(JMIR Med Inform 2025;13:e79748) doi:10.2196/79748

KEYWORDS

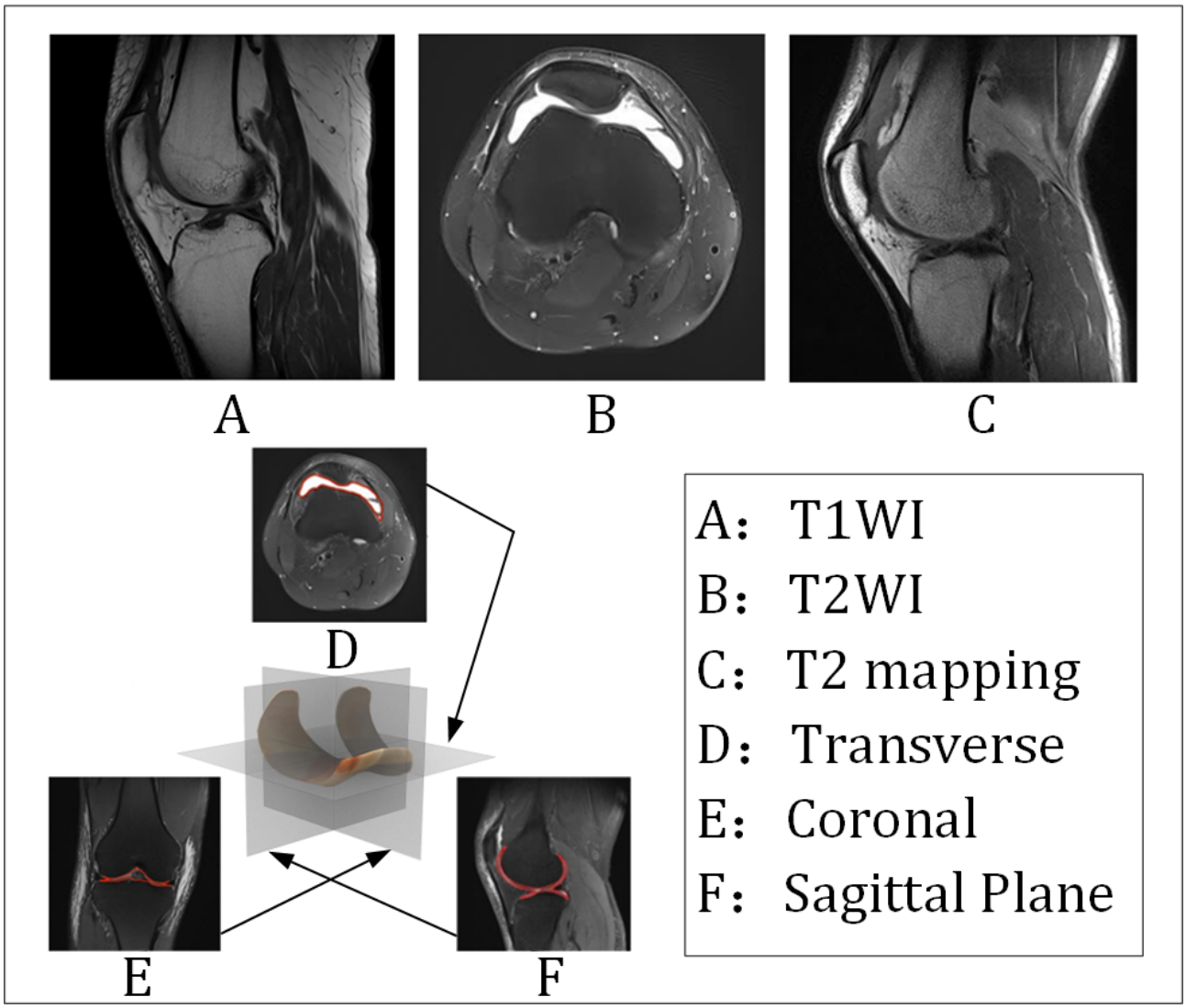
knee cartilage injury; multilevel classification; large separable kernel attention; multidimensional feature; cross-level fusion

Introduction

Knee cartilage injury (KCI) is recognized as a prevalent joint disease, with significant challenges posed to diagnosis and treatment by its high incidence and irreversibility [1]. The self-repair capacity of KCI is severely restricted due to the absence of vascularization and innervation. Consequently, the implementation of early and accurate diagnostic strategies has been established as critical for decelerating disease progression [2]. Currently, magnetic resonance imaging (MRI) is the preferred imaging tool for evaluating KCI due to its excellent soft tissue contrast. Clinically, MRI usually uses three orthogonal planes in the sagittal, coronal, and transverse planes for multiangle imaging. The sagittal plane displays the anatomical structures of the patellofemoral joint contact surface, the femoral trochanter groove, and the anterior and posterior corners of the meniscus. This is particularly beneficial for detecting early wear and tear and delamination injuries of the patellar and femoral trochanter cartilage [3]. The coronal plane facilitates observation of the integrity of the medial and lateral tibiofemoral joint surfaces and can visualize changes in cartilage thickness in weight-bearing areas of the tibial plateau and femoral condyles. It can also help identify the correlation between cartilage injury and adjacent bone marrow edema, while the transverse plane can accurately identify focal chondromalacia or fissures in the medial malleolar surface of the patella. Combined with multiplanar imaging, T1-weighted imaging (T1WI) [4], T2-weighted imaging (T2WI) [5], and T2 mapping [6] sequences can reflect KCI from multiple aspects, including structure, water content, and biochemical composition, as shown in Figure 1.

XSL•FO
RenderX

Figure 1. Multisequence and multiplane images of KCI in the retrospective study based on the clinical dataset provided by the Second Affiliated Hospital of Dalian Medical University, China. Multimodal KCI MRI images demonstrate T1WI, T2WI, and T2 mapping sequences across sagittal, coronal, and transverse planes. KCI: Knee cartilage injury; MRI: magnetic resonance imaging; T1WI: T1-weighted imaging; T2WI: T2-weighted imaging.



According to the International Cartilage Repair Society grading criteria [7], KCI is categorized into grades 0 to IV. Grade 0 indicates normal cartilage; Grade I shows surface softening and slight roughness of the cartilage; Grade II involves focal defects with a depth of less than 50% of the cartilage thickness; Grade III has a depth greater than 50% but not reaching the full thickness of the cartilage; and Grade IV represents the end-stage lesion with complete cartilage loss (Multimedia Appendix 1).

The clinical diagnosis of KCI has long depended on the subjective judgment of doctors on MRI images, which has problems such as low efficiency and lack of consistency [8]. With the development of computer vision technology, machine learning-based auxiliary diagnosis methods have gradually become a research hotspot [9].

However, the local receptive field of the fixed convolution kernel limits the capture of global context information. Lightweight models such as SqueezeNet [10] and MobileNet [11] reduce computational complexity through channel pruning and depth separable convolutions; however, they perform poorly when dealing with multisite and multistage cartilage damage. As the KCI area spreads or changes in thickness across multiple sites as the disease progresses, the aforementioned lightweight network models cannot provide optimal classification results. Current studies show that convolutional neural network (CNN) architectures still have insufficient feature representation ability for KCI classification tasks.

Recently, deep learning has made remarkable progress in the field of medical image analysis by virtue of its powerful feature learning ability. Traditional convolutional neural network architectures, such as AlexNet [12], ResNet [13], and GoogLeNet [14], enhance feature representation by increasing the network depth. However, the local receptive field of the fixed convolution kernel limits the capture of global context information. Lightweight models like SqueezeNet and MobileNet reduce computational complexity through channel pruning and depth separable convolutions, but they perform poorly when dealing with multisite and multistage cartilage damage. As the KCI area spreads or changes in thickness across multiple sites as the disease progresses, the aforementioned lightweight network models cannot provide optimal

XSL•FO
RenderX

classification results. Current studies show that CNN architectures still have insufficient feature representation ability for KCI classification tasks.

To address the above limitations, researchers have proposed various improvement schemes. The multilayer convolutional sparse coding framework developed by Abdul et al [15] achieves hierarchical classification of ligament injuries through feature map connectivity modeling but still suffers from feature aliasing in complex lesion scenarios. The sample pyramid local binary pattern combined with K-nearest neighbor classifiers proposed by Demir's [16] team optimizes the shallow texture feature representation, but it is difficult to overcome the interference of background redundant information in medical images. Double Attentive Graph Neural Network (DAGNet) adopts a directed acyclic graph architecture to achieve dynamic feature routing, but its higher computational complexity limits its application in small sample scenes [17]. Lei et al [18] employed convolutional neural network models such as DenseNet121, combined with data augmentation techniques, to achieve automatic classification of pressure ulcer stages. SgmaFuse [19] addresses interpretable breast cancer diagnosis in ultrasound imaging by integrating a spatially guided multilevel alignment mechanism and histological semantic activation vectors to bridge imaging features with pathological patterns. Dai et al [20] proposed a model enabling enhancement of breast cancer detection in mammographic images of dense tissue via a dynamic feature weighting Mamba module and edge-enhanced networks, reinforced by adversarial defense strategies for robustness. Rezk et al [21] developed a classification model that integrates image segmentation, skin tone clustering analysis, and style transfer, effectively enhancing the generalization capability of early skin cancer detection across all skin tones. Dual-stream parallel model based on local centroid optimization (LC-DSPNet) improves feature extraction capability through a localized center-of-mass optimization algorithm and a dual-stream parallel architecture, but it leads to partial loss of key lesion information, which affects the classification accuracy of complex knee cartilage injuries [22]. The improved AlexNet (R-AlexNet) combines the dragonfly optimization algorithm with the regional similarity transformation and achieves the current optimal performance in the task of KCI classification through multimodal feature fusion, but the limitation of its uniplanar dataset influences the model's generalization ability [23]. The YOLO (You Only Look Once) series of algorithms is currently widely recognized in the field of computer vision for its efficient detection speed and excellent accuracy [24]. With the iterative optimization of the algorithms, the YOLO series has been extended from the target detection task to multiple vision task areas such as image classification and instance segmentation [25]. YOLOv8 significantly improves the model training efficiency and detection accuracy by introducing an adaptive learning rate adjustment mechanism and dynamic anchor frame generation technology [26]. Therefore, the YOLOv8 classification model is used as the baseline model in this paper to reduce the calculation complexity while maintaining the high precision classification ability and providing an effective means for the five-level classification of KCI.

Due to the low contrast and small target characteristics of MRI images of knee cartilage injuries, as well as background interference from bones and muscles, the traditional convolution module suffers from the defects of a large number of parameters and limited gradient flow, which make it difficult to effectively capture the fine lesion features, as well as the limitations of a single-plane dataset. For this reason, this paper proposes a multidimensional feature cross-level fusion (MDF-CLF) classification network driven by the large separable kernel attention (LSKA) for KCI, which reduces the computational complexity while maintaining the high-precision classification ability and provides a new solution for the five-level classification of KCI.

In summary, deep learning has shown significant potential in the field of medical image analysis [27], particularly in the automatic classification of knee cartilage, ligament, and meniscus injuries. However, current methods still face several key challenges: (1) single-plane MRI images struggle to fully capture the multidimensional features of KCI; (2) CNNs often lose the deep semantic information of small lesions during feature extraction; (3) the adaptability of multiscale feature fusion strategies is insufficient, limiting the accuracy of grading [28].

To address the above challenges, this paper proposes an MDF-CLF classification network driven by the LSKA. The purposes of this paper are as follows:

1. The first multidimensional KCI hospital real MRI data set is constructed: This study collaborated with the Second Affiliated Hospital of Dalian Medical University to collect a standard three-plane (sagittal, coronal, and transverse) knee MRI imaging. The T1WI, T2WI, and T2-mapping multiparameter sequences are integrated to create the first multidimensional imaging data set for KCI assessment, addressing the limitations of traditional single-plane medical imaging features.

2. An MDF-CLF network driven by LSKA has been constructed: The LSKA module is embedded into the YOLOv8 network, which integrates spatial feature extraction through deep separable convolution and channel information integration via point-bypoint convolution. This approach enhances multiscale features of KCI areas, effectively improving the feature representation capability for multilevel KCI.

The structure of this paper is organized as follows: Section 2 summarizes the related work; Section 3 introduces the network model proposed in this paper. Section 4 describes the image dataset, model training parameters, and experimental environment and analyzes the experimental results. Finally, Section 5 presents the conclusions and future directions of the algorithm.

Methods

Network Model Architecture

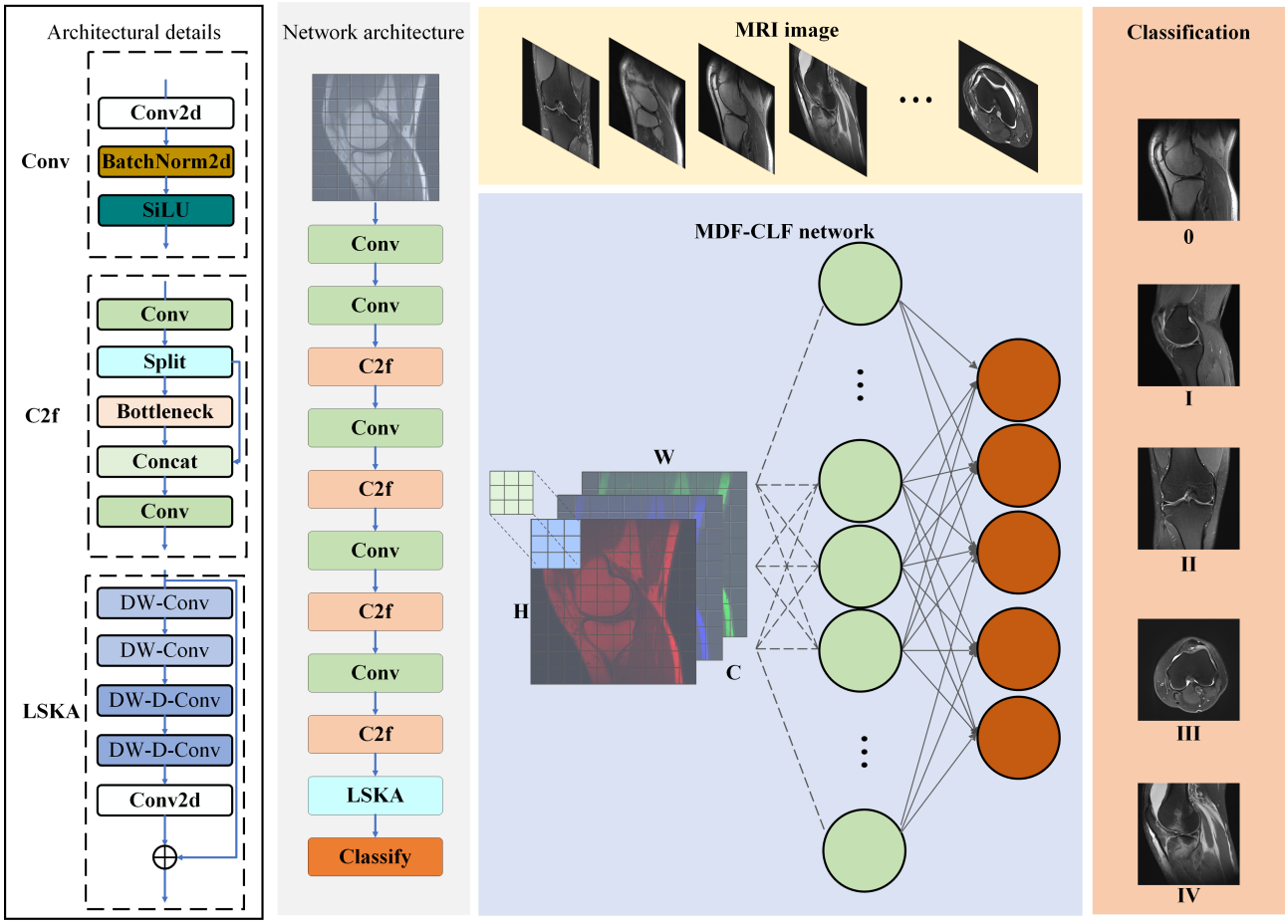
To address the limitations of traditional methods in knee cartilage damage classification, such as insufficient computational efficiency and limited ability to recognize subtle features, this paper proposes an MDF-CLF classification

XSL•FO
RenderX

network algorithm driven by LSKA for KCI. The modules in the model proposed in this paper are described as follows.

The algorithm introduces the LSKA module [29] into the backbone of the YOLOv8 framework. It constructs a feature extraction system composed of the Conv module [30], the C2f (Cross-Stage Partial-Connection with 2 convolutions) module [31], and the LSKA module and combines with the head network to realize attention focusing and multiscale feature fusion of the KCI region in MRI images. As shown in Figure 2, the network first inputs multidimensional MRI images of KCI into the feature extraction module. Here, the basic convolutional module uses the three-layer structure of the convolutional layer–batch normalization layer–SiLU (Sigmoid Weighted Linear Unit) activation function for primary feature extraction. It then realizes multilevel feature interaction and attention enhancement through the C2f module and the LSKA module. Finally, it completes the classification of the head network, which in turn effectively improves the accuracy and robustness of the classification of KCI.

Figure 2. Flowchart of the proposed algorithm. Flowchart of the large separable kernel attention (LSKA)–driven multidimensional feature cross-level fusion (MDF-CLF) classification network, integrating LSKA, Cross-Stage Partial-Connection with 2 convolutions (C2f), and Conv modules within a YOLOv8-based framework, for 5-level knee cartilage injury classification using three-plane multimodal magnetic resonance imaging (MRI) images from a retrospective clinical cohort at the Second Affiliated Hospital of Dalian Medical University.



Conv Module

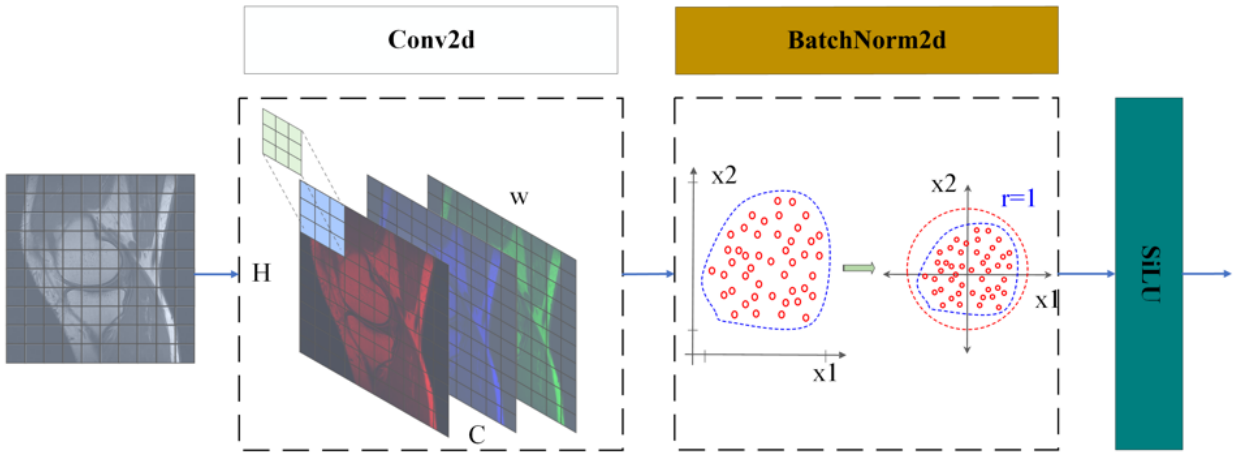
The Conv module is the basic and key component of this model, which consists of the convolution layer, batch normalization layer, and SiLU, as shown in Figure 3. The network model sets the input image as $I \in R^{H\times W\times C}$, where H is the image height, W is the width, C is the number of channels, and the input image size is 640×640×3. The formula for convolution (Conv2d) can be expressed as:

(1)Yi,jp=∑c=0C−1∑m=0N−1∑n=0N−1Ii+m,j+n,cK1m,n,cp+b1p

where i and j are the positions of each pixel point in the feature map, N is the size of the convolution kernel, m and n are both indexes varying in the range of [0, N−1] used to traverse each value in the convolution kernel, and p is the index of the output channel (assuming that the number of convolution kernels is k, then 1≤p≤k). Yi,jp represents the feature map output at channel p, position (i, j) after convolution in the first layer, and Ii+m, j+n, c represents the input image I at channel c, the pixel value at position (i+m, j+n), K1 m,n,c,prepresents the convolution kernel of the first layer, and b1p represents the bias term of channel p in the first layer.

XSL•FO
RenderX

Figure 3. Conv module. Composition schematic of the Conv module integrating convolutional layer, batch normalization layer, and SiLU (Sigmoid Weighted Linear Unit) activation function in the LSKA-driven multidimensional feature cross-level fusion network for five-level classification of KCI based on real MRI data from the Second Affiliated Hospital of Dalian Medical University. KCI: knee cartilage injury; LSKA: large separable kernel attention; MRI: magnetic resonance imaging.



To effectively suppress the internal covariate bias phenomenon during deep neural network training, the model introduces a batch normalization layer (BatchNorm2d). This module normalizes the feature maps output from the convolutional layer. It not only accelerates the convergence rate of the model but also enhances the stability of the training process by stabilizing the activation function input distribution.

Specifically, the normalization process of the BatchNorm2d layer takes the channel dimension as the unit of operation and assumes that the small batch sample capacity is *B*. For the *p*th channel, the normalization is performed for each element Yijp in the feature map Yi,jp:

(2)y^ijp=yijp−μpαp2+ε

where the mean μp=1B·Hout·Wout∑b=1B∑i=1Hout∑j=1Woutyijp, ∈ is a very small positive number, and variance αp2=1B·Hout·Wout∑b=1B∑i=1Hout∑j=1Woutyijl(yijp−μp)2. W_{out} is the width of the output feature map and H_{out} is the height of the output feature map.

To recover the expressive ability lost during the normalization process and to make the model more flexible when learning data features, the module is optimized by introducing learnable scaling factors $\gamma^p \in R$ and level-shifting terms $\beta^p \in R$ into the backpropagation process. These terms are calculated as follows:

(3)yijp,BN=γpy^ijp+βp

To achieve a dynamic balance between model training stability and feature characterization capability, the module combines the probabilistic smoothing property of the sigmoid function with the conditional sparse activation advantage of the rectified linear unit function. This is calculated as follows:

(4)SiLU(x)=x·σ(x)=x1+e−x

where *x* is the input feature and σ(*x*) is the sigmoid function.

The network architecture proposed in this paper realizes multiscale learning by adopting a hierarchical connection of convolutional modules. This enables the extraction of marginal features of the cartilage and texture features of the subchondral bone edema regions from the shallow network and the extraction of semantic features of KCI categories from the deep network. This allows for the accurate classification of KCI.

C2f Module

To address the contradiction between the attenuation of deep semantic feature information and the small-scale characteristics, this paper introduces a C2f module based on anatomical priors into the proposed network architecture. This module, through a dual-path feature interaction mechanism, provides robust support for the accurate identification of KCI, as shown in Figure 4. The dual-path design of the general-purpose C2f module is strategically adopted here because its inherent operational mechanism aligns effectively with the requirement to capture multiscale features of KCI, ranging from deep structural defects to subtle surface textural changes.

To effectively capture the multiscale damage feature information, it is divided into a semantic enhancement path X_1 and a detail preservation path X_2 by cross-level fusion operation; first, the input feature map is divided into two parts according to the number of channels *C*. The expression of Split is as follows:

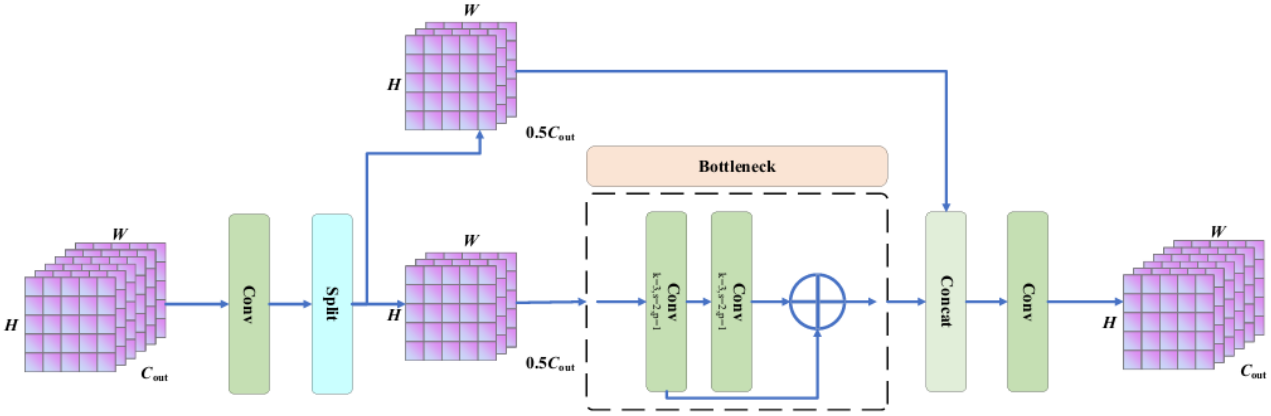
(5)(X1,X2)=Split(F,C1,C2)

where $H \times W \times C_{out}$ is the dimension of the input feature map, $C_1 = C_2 = 0.5C_{out}$, and C_{out} is the number of channels in the output. The semantic enhancement X_1 path processes features through Bottleneck units, which are dedicated to capturing the deep semantic information of knee joint deep structural injuries, including subchondral bone cystic lesions, full-thickness cartilage defects, and meniscus-cartilage junction injuries. It enhances the feature representation of such significant structural abnormalities through deep feature extraction, while mitigating gradient vanishing via residual design to improve the model's ability to characterize moderate-to-severe KCI. X_1 path uses the Bottleneck unit for deep extraction of features in the subchondral bone cystic lesion region and mitigates gradient vanishing by

XSL•FO
RenderX

residual design to improve the sensitivity to the cartilage fissure. Concurrently, the detail preservation X_2 path employs a skip connection to circumvent deep processing, thereby preserving high-resolution features essential for early injury identification. This pathway is specifically engineered to capture subtle alterations in the cartilage surface texture at the patellofemoral joint interface, minor abrasions in the meniscal anterior and posterior horns, and superficial cartilage defects within the tibial plateau weight-bearing regions. By mitigating the blurring effects induced by deep downsampling, this architectural choice furnishes critical feature support for precise early-stage KCI detection, enhancing the model's responsiveness to nuanced pathological modifications in these anatomical locales. X_2 path preserves the original feature details and mitigates the blurring of lesion edges caused by deep downsampling. Next, it is output through dual paths, and channel splicing is used to realize multiscale feature fusion.

Figure 4. C2f module. Architecture of the C2f module implementing dual-path feature interaction with semantic enhancement path and detail preservation path for multiscale KCI classification in LSKA-driven multidimensional fusion network. C2f: Cross-Stage Partial-Connection with 2 convolutions; KCI: knee cartilage injury; LSKA: large separable kernel attention.



At this time, the number of channels of the feature map becomes $0.5(n+2)C_{out}$ while the height and width remain as $H \times W$, and n=1 is the number of Bottleneck cells. The expression of channel splicing is as follows:

(6)FConcat=Concat(X1out,X2)

where X1out is the output of the X_1 path, and F_{Concat} is the multiscale feature resulting from the splicing of the dual-path channels.

Finally, a 1×1 convolutional layer linearly transforms the number of channels to match the number initially convolved at input time, allowing the subsequent network structure to integrate seamlessly. In the C2f module, anatomical prior knowledge is integrated through a dual-path feature interaction mechanism, which orchestrates channel allocation and feature aggregation. The integration is achieved by leveraging the module's inherent design, whereby the semantic enhancement path is utilized to capture features relevant to advanced, deep lesions, and the detail preservation path is harnessed to retain features essential for early, surface-level abnormalities. The semantic enhancement path extracts deep semantic features of knee cartilage injuries, while the detail preservation path maintains fine-grained features such as cartilage surface textures. Feature fusion is achieved via channel concatenation, enabling effective multiscale integration. Consequently, the C2f module incorporates knee joint anatomical priors through structured feature interaction and dynamic channel adjustment, effectively balancing semantic retention and detailed feature recognition to improve classification accuracy.

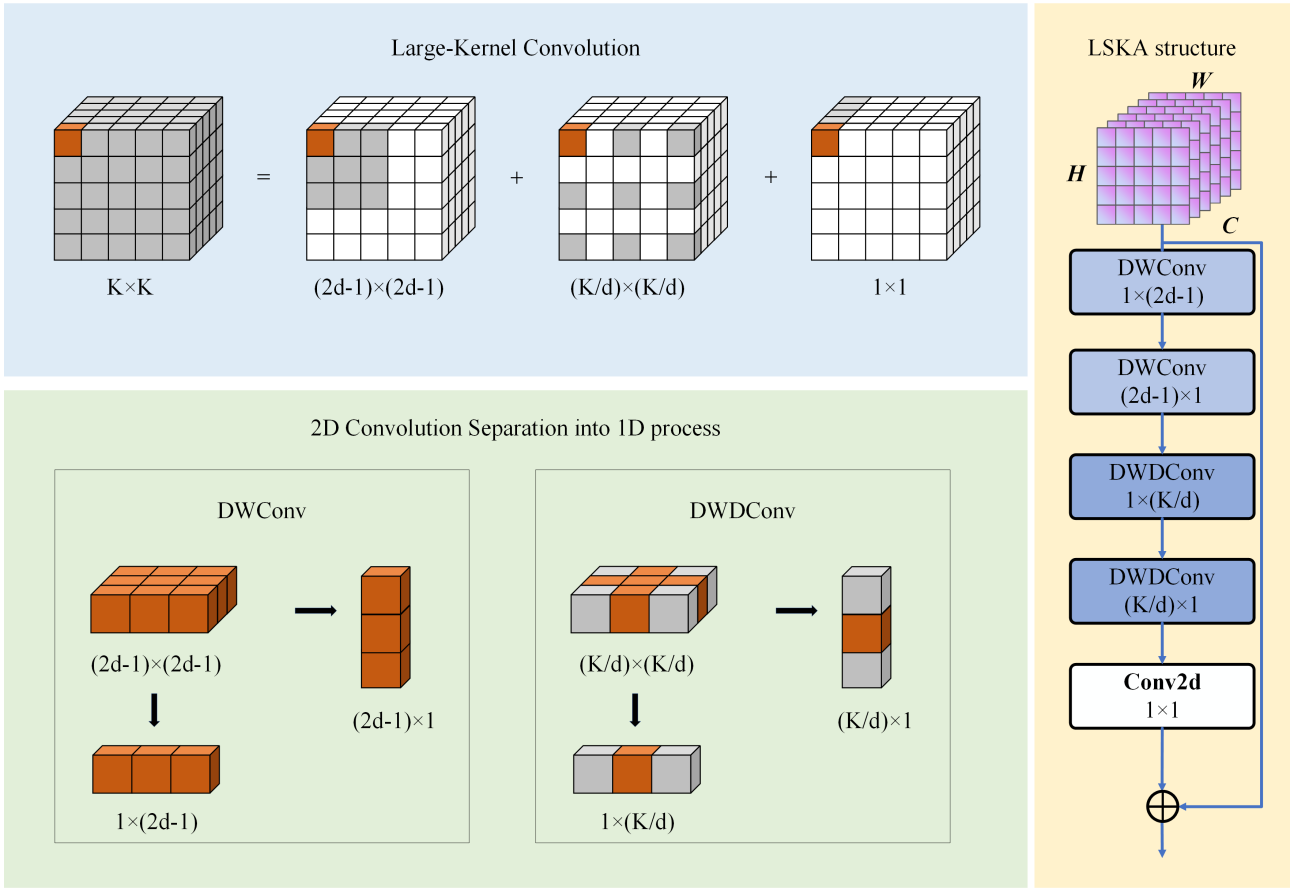
LSKA Module

To significantly enhance the cartilage fissure features and effectively improve classification accuracy, this paper introduces an LSKA module into the proposed network architecture. This module improves the sensitivity of long-distance cartilage, ligament, and tissue structures while maintaining computational efficiency through an efficient large kernel decomposition strategy with adaptive feature weighting. The network structure of the LSKA module is shown in Figure 5.

The LSKA decomposes the $k \times k$ convolution into depth convolution (DWConv), dilated depth convolution (DWDConv), and point-by-point convolution (PWConv).

XSL•FO
RenderX

Figure 5. LSKA module structure diagram. Schematic of the LSKA module implementing Large-Kernel decomposition into depthwise convolution, dilated depthwise convolution, and point-by-point convolution for adaptive feature weighting in KCI classification network. KCI: knee cartilage injury; LSKA: large separable kernel attention.



To avoid the exacerbation of parameter redundancy due to the large size of the convolution kernel, DWConv extracts the spatial features independently for each channel and decomposes the traditional 2D depth convolution kernel $k \times k$ into a cascade of the horizontal convolution kernel $(2d - 1) \times 1$ and the vertical convolution kernel $1 \times (2d - 1)$ through the introduction of the dilatation rate d. The intermediate features afterward can be represented as:

$$(7)\bar{Z}C=\sum H,WM1\times(2d-1)C*DW(\sum H,WM(2d-1)\times 1C*DWFC)$$

where *DW denotes the deep convolution operation, M(2d−1)×1C and M1×(2d−1)C are 1D deep convolution kernels in the horizontal and vertical directions, respectively.

To maintain the sensitivity of the long-range structure of cartilage, ligaments, and other tissues, $\bar{Z}c$ processes the intermediate features using dilation depth convolution. This decomposes the traditional 2D convolution kernel into horizontal and vertical 1D convolution kernels 1×[kd] and [kd]×1, respectively, using the dilation rate d. The intermediate feature Z^c after DWConv can be expressed as follows:

$$(8)ZC=\sum H,WM1\times[kd]C*DW(\sum H,WM[kd]\times 1C*DW\bar{Z}C)$$

Besides, to achieve cross-channel information fusion, LSKA uses the 1×1 convolution kernel $M_{1\times 1}$ to highlight the feature channels associated with knee cartilage damage. This kernel performs point-by-point convolution of the intermediate features Z^c, which generates the attention map A^c expression:

$$(9)AC=M1\times 1*PWZC$$

where *PW represents the pointwise convolution operation.

Finally, to enhance the features of the cartilage damage region of the KCI, the adaptive weighted feature map F^c, which is generated by multiplying the attention map and the input feature map F^c element by element via the Hadamard product, can be represented as follows:

$$(10)\bar{F}c=Ac\otimes Fc$$

Where ⊗ means element by element multiplication.

The LSKA module achieves adaptive feature weighting by identifying differences in the importance of cartilage injury-related features in knee joint MRI, dynamically allocating weights based on the contribution of features to injury identification, strengthening the representation of key injury features while suppressing background interference features. This mechanism exhibits significant advantages in distinguishing between mild surface softening and deep lesions; for the former, it can focus on enhancing the feature response of subtle texture changes on the cartilage surface to accurately capture early-stage injuries, while for the latter, it can prioritize strengthening the feature representation of deep cartilage structural abnormalities such as thickness defects and structural disruptions to avoid misjudgment of lesion depth effectively, achieving accurate differentiation between the two types of injuries.

XSL•FO
RenderX

Classify Model

To map the features output by the backbone network to specific KCI categories, the head network module is used in this paper, whose structure consists of a fully connected layer and Softmax activation function.

After the backbone network embedded in the LSKA module processes the data, the feature vector x_c is generated. This vector contains key information, such as soft tissue texture and semantics, from the knee MRI. To transform the high-dimensional features into injury categories, the head network undergoes linear transformation using the fully connected layer. This generates the response values of each injury category using the following mathematical expression:

(11)z=ηxc+b

where η is the weight matrix, *b* is the bias vector, *z* is the output vector of the fully connected layer, and the element η_{ij} in the weight matrix η denotes the extent to which the *j*th input feature contributes to the *i*th KCI output category.

Specifically, after being processed by the backbone network embedded with the LSKA module, a 1D feature vector x_c is generated. This vector encapsulates key information from the knee MRI image, such as cartilage texture and semantic features. To map the high-dimensional features to specific damage categories, the head network utilizes a fully connected layer to perform a linear transformation, producing the response values for each damage category. Upon obtaining the output vector from the fully connected layer, the response value for the *o* knee cartilage damage category, based on the knee cartilage damage MRI image, can be acquired.

Based on the response value for the *o*th knee cartilage damage category from the knee cartilage damage MRI image, the confidence that the predicted knee cartilage damage MRI image belongs to the *o*th knee cartilage damage category is obtained. The formula used is as follows:

(12)y^o=ezo∑o=15ezo

Where $\hat{y}_o$ represents the confidence that the predicted knee cartilage damage MRI image belongs to the *o*th knee cartilage damage category; z_o is the response value for the *o*th knee cartilage damage category based on the knee cartilage damage MRI image; *o* denotes the index of the knee cartilage damage category; and *e* is the base of the natural logarithm. The vector *z* is the output of the fully connected layer, containing the response values for the five knee cartilage damage categories, and z_o is the response value corresponding to one specific category in *z*. The unnormalized class response values output by the fully connected layer cannot be directly used for classification decisions; they need to be transformed into a confidence distribution with probabilistic meaning. To achieve this, the Softmax activation function is applied for normalization.

In the five-class KCI classification task, for the *u*th sample (*u*=1, 2, ..., *U*) in the training set, where *U* is the total number of training samples, the output probability distribution from the LSKA-driven MDF-CLF classification network is denoted as y^u=(y^1u,y^2u…,y^5u)y. The formula for calculating the cross-entropy loss LCEu of a single sample is as follows:

LCEu=−∑o=1Oyoulog (y^ou)

(13)∑o=1Oy^ou=1

LCEu represents the loss value of the *u*th KCI MRI sample; *O* denotes the index of the KCI category; *O* represents the total number of KCI categories. In this study, there are five categories of KCI. you indicates the ground truth label of the *u*th KCI MRI sample, marking the true label value for the *o*th KCI category. y^ou is the predicted probability that the *u*th KCI MRI sample belongs to the *o*th KCI category. In this study, the condition ∑o=15y^ou=1must be satisfied to ensure the rationality and validity of the probability distribution. To prevent individual samples from interfering with the training, the mean loss of all samples in the training set is taken as the optimization objective. That is, the formula for the overall loss value *L* is:

(14)L=1U∑u=1ULCEu=1U∑u=1U(−∑o=1Oyoulog (y^ou))

where *L* represents the overall loss value of the cross-entropy loss function, *u* denotes the index of the KCI MRI sample, and *U* indicates the total number of KCI MRI samples. In this study, through backpropagation, parameters that increase the loss are adjusted along the negative direction of the gradient to mitigate the impact of misclassification, while parameters that decrease the loss are reinforced along the positive direction of the gradient. This process progressively enhances the model's capability to identify low-contrast and small-scale lesion features, thereby achieving accurate classification of the five categories of injuries.

Finally, the parameters that increase the loss are adjusted in the opposite direction of the gradient to reduce the influence of misclassification through backpropagation. The parameters for reducing the loss are strengthened along the positive direction of the gradient, and the recognition ability of the model to low-contrast and small-scale features is gradually improved to realize the accurate classification of five types of damage.

Experimental Environment and Datasets

All the experiments are implemented in PyTorch1.8, with Windows 10 system, Intel(R) Core(TM) with i7-9750H CPU and @ 2.60 GHz processor along with 16.0 GB of RAM, 64-bit Operating System, and NVIDIA GeForce RTX3090.

Besides, this study constructs a dataset based on real hospital data provided by the Second Affiliated Hospital of Dalian Medical University. This dataset comprises multisequence MRI images in three planes, which are sagittal plane, coronal plane, and transverse plane. Specifically, it includes 548 Grade 0 images, 674 Grade I images, 582 Grade II images, 539 Grade III images, and 579 Grade IV images. This dataset comprises 134 patients with KCI and 26 healthy individuals without knee pathology. Following patient-level data partitioning principles, all patients are randomly divided into two groups. Eighty percent of patients' images are included in the training set, while the remaining 20% form a completely independent test set. Examples of images from the dataset are shown in Multimedia Appendix 1. During the acquisition of the multiparameter sequences involved in this study, which are T1WI, T2WI, and

XSL•FO
RenderX

T2-mapping, strict adherence to clinical operating protocols ensures consistent spatiotemporal registration. All sequences are acquired on a 3.0T MRI scanner using identical field of view, matrix, slice thickness, and slice spacing parameters to guarantee spatial pixel correspondence across sequences. Following data acquisition, spatiotemporal registration is validated using anatomical landmarks of the knee joint, which include the anterior and posterior horns of the medial and lateral menisci and the femoral condyles. Additionally, image postprocessing software is employed to match and verify the coordinate points across all sequences, further ensuring consistency in spatiotemporal registration across the multiparameter sequences.

Parameter Setting and Evaluation Index

To ensure the reasonableness of model training and testing, this paper divides the ratio of the dataset into training set and testing set according to 8:2, and the number of training rounds of the model is set to 350 rounds, with an initial learning rate of 0.01. The model with the highest accuracy on the test set is ultimately saved. During the training process, the stochastic gradient descent (SGD) optimizer dynamically adjusts to achieve efficient optimization.

To evaluate the performance of the proposed model, this paper employs several categorical evaluation metrics using accuracy (ACC), sensitivity (SEN), specificity (SPE), *F* measure (*F1*), and Kappa statistic (*K-S*) to assess the model's performance, and these performance metrics are calculated as follows:

(15)ACC=TP+TNTP+TN+FP+FN

(16)SEN=TPTP+FN

(17)SPE=TPTP+FP

(18)F1=2×Sensitivity×SpecificitySensitivity+Specificity

(19)K-S=P0−Pe1−Pe

where $Po = TP + TNTP + TN + FP + FN$, $Pe = (TP+FP)\times(TP+FN) + (FN+TN)\times(FP+TN)(TP+TN+FP+FN)2$. Besides, TP, TN, FP, and FN describe the number of true positives, true negatives, false positives, and false negatives. Here, the closer the values of ACC, SEN, SPE, *F1* , and *K-S* are to 1, the better the model performance. The *K-S* index is used to judge the difference between the degree of agreement of the classifier's classification results and that of random classification.

Besides, this paper uses the confusion matrix to evaluate the performance of the classification model. The confusion matrix is a matrix that shows the relationship between the model predictions and the true labels. The rows of the matrix represent the true categories, the columns represent the predicted categories, and the values of the matrix elements indicate the number of samples for which a particular true category is predicted as each predicted category.

Ethical Considerations

This study utilized retrospective and anonymized MRI data. In accordance with Article 32 of the Administrative Regulations on the Ethical Review of Biomedical Research Involving Humans (2023) [32] issued by the National Health Commission of China, ethical review approval is not mandatorily required for research utilizing exclusively deidentified archival data and records, provided that the use of such data does not pose any risk to the human subjects.

All MRI images used in this research are obtained from the Second Affiliated Hospital of Dalian Medical University. Prior to data collection and analysis, all personal identifiers are rigorously removed from the images and associated metadata to ensure complete patient anonymity, thereby mitigating any potential privacy risks. Furthermore, the hospital confirms that informed consent is obtained from all patients at the time of their initial clinical MRI scan. This consent process involved a comprehensive explanation of the nature of the imaging procedure and the potential future use of their deidentified data for research purposes, in line with the hospital's standard operational protocols and in compliance with the Ethical Principles for Medical Research Involving Human Subjects outlined in the Declaration of Helsinki.

The authors hereby declare that the research is conducted in strict adherence to these principles and in compliance with all applicable local, national, and international guidelines and regulations concerning the protection of personal information and human rights, including China's Personal Information Protection Law. The dataset construction and analysis procedures posed no additional physical or psychological risks to the patients involved.

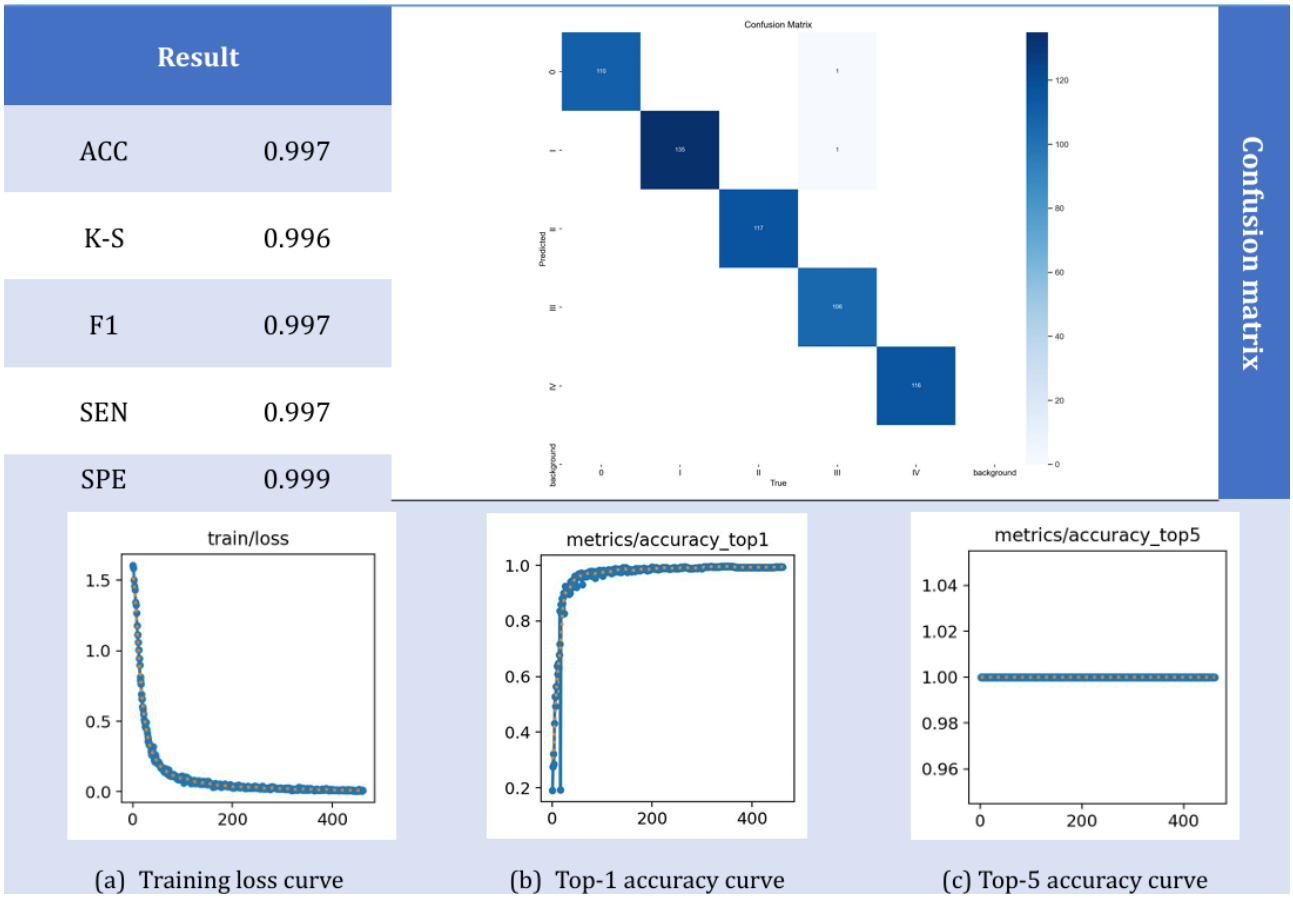
Results

Results and Analysis

The KCI classification algorithm proposed in this paper is tested on the constructed dataset to verify its performance. As shown in Figure 6, the algorithm achieved a classification accuracy of 99.7%, demonstrating its effectiveness. To verify the effectiveness of this algorithm, the following tests are carried out: different data set ratios, different training rounds, and different initial learning rates, as well as comparisons with other algorithms. The detailed data and analysis results are presented in the subsequent experiments.

XSL•FO
RenderX

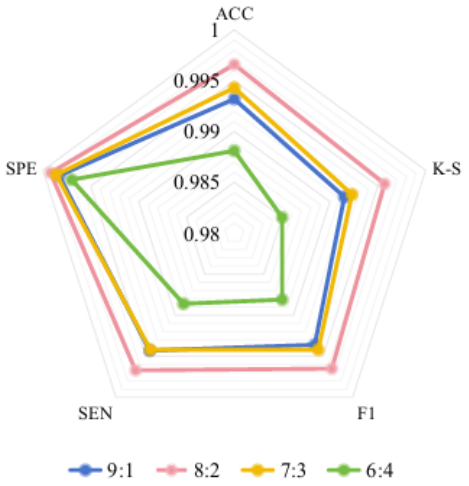
Figure 6. Experimental results of this algorithm. Performance evaluation of the LSKA-driven multidimensional feature cross-level fusion network for five-grade KCI classification using 3-plane multidimensional KCI MRI dataset from a retrospective clinical cohort at the Second Affiliated Hospital of Dalian Medical University, China: Achieving 99.7% accuracy with comprehensive metrics analysis. ACC: accuracy; F1: *F* measure; K-S: Kappa statistic; SEN: sensitivity; SPE: specificity.



Experiment 1: Analysis of the Proportion Setting of the Dataset

To assess the impact of data partitioning strategy on the model generalization ability, this paper designs multiple sets of ablation experiments in the constructed real hospital dataset and uses 6:4, 7:3, 8:2, and 9:1 partitioning ratios of the training and testing sets for comparative analysis, respectively. As shown in Figure 7, when 8:2 division is used, the model achieves the optimal balanced performance on the independent test set, with a classification accuracy of 99.7% and *F1* of 99.7%, which is significantly better than other ratios.

Figure 7. Experimental results of different proportion data sets. Ablation analysis of dataset partitioning ratios on the generalization performance of the LSKA-driven multidimensional feature cross-level fusion network for 5-grade KCI classification using 3-plane multidimensional KCI MRI dataset from a retrospective clinical cohort at the Second Affiliated Hospital of Dalian Medical University in China with optimal 82 split achieving 99.7% accuracy. ACC: accuracy; F1: *F* measure; K-S: Kappa statistic; SEN: sensitivity; SPE: specificity.



	ACC	K-S	F1	SEN	SPE
9:1	0.993	0.992	0.994	0.994	0.998
8:2	0.997	0.996	0.997	0.997	0.999
7:3	0.994	0.992	0.994	0.994	0.999
6:4	0.988	0.985	0.988	0.989	0.997

XSL•FO
RenderX

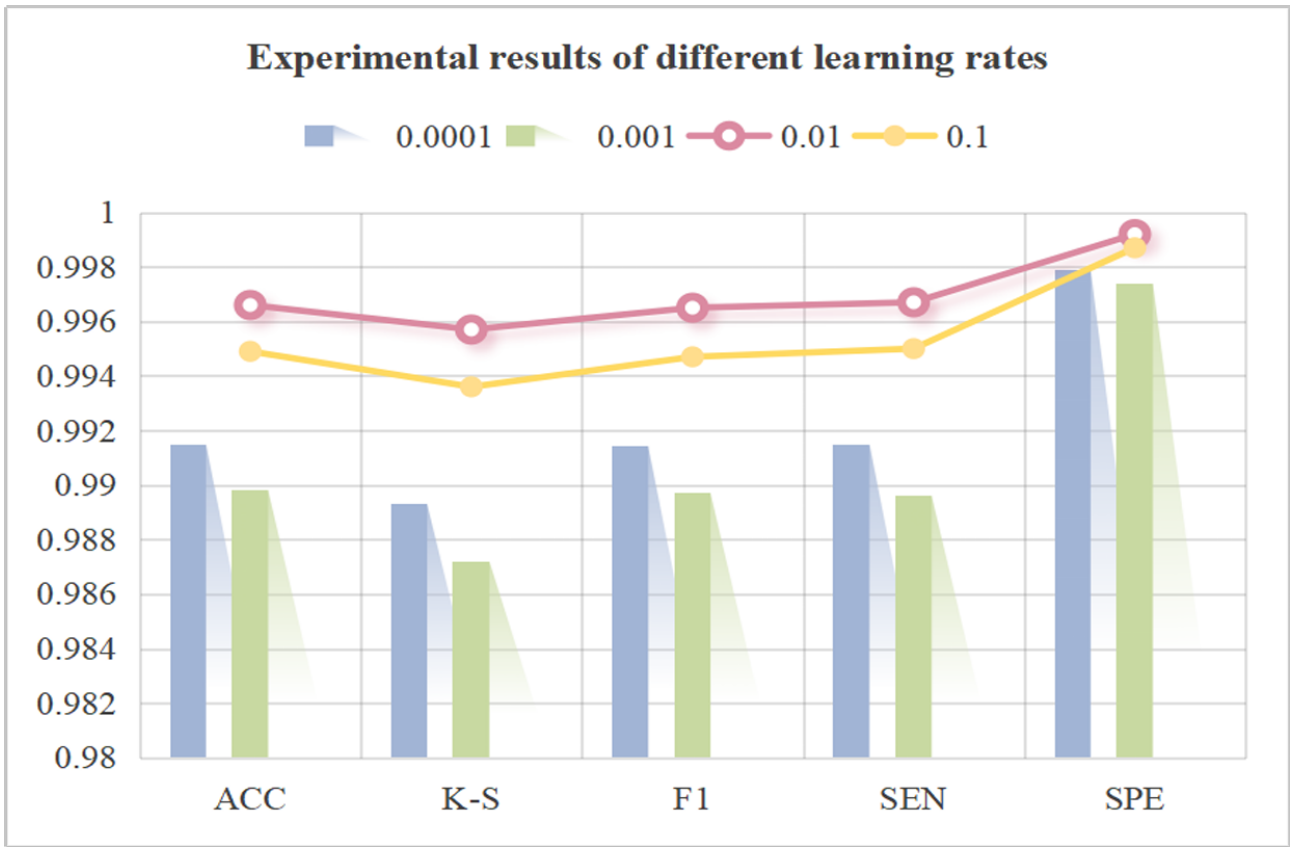
Experiment 2: Analysis of the Epoch of Model Training

To observe the performance of the model proposed in this paper under different numbers of training rounds, this paper sets up multiple sets of controlled experiments, which are systematically tested by setting different numbers of training rounds. Under the condition that the ratio of the training set to the validation set is 8:2, the experimental results are shown in Multimedia Appendix 2. The data show that the early stopping mechanism is triggered when the model is trained for 461 rounds. It is worth noting that the accuracy of the network model peaks when the number of training rounds reaches 350. During the training cycle of 1 to 350 epochs, the model's test set accuracy exhibited a steady upward trend, rising from 97.6% at 150 epochs to 99.7% at 350 epochs. When training proceeds to 400 epochs, the accuracy reaches 99.3%, and at 450 epochs, it is 99.5%, with a notable decline in test set accuracy observed. This phenomenon indicates that by 350 epochs, the model had fully learned the general features of the data and did not overfit to local noise in the training set due to overtraining. Meanwhile, the model design and training strategy established a multidimensional system to mitigate overfitting. At the data level, the multimodal T1WI, T2WI, T2 mapping, and multiplanar sagittal, coronal, transverse dataset characteristics effectively reduced the model's dependence on single features, preventing the model from fitting only image noise under a single modality. At the optimizer level, the adopted stochastic gradient descent optimizer enabled dynamic learning rate adjustment, which automatically slowed the parameter update rate in the later training stage and effectively inhibited overfitting caused by aggressive parameter updates that fit local features of the training set. At the model structure level, the C2f module achieved dynamic balance in feature learning depth through dual-path feature interaction, namely the semantic enhancement path and the detail preservation path, further reducing the risk of overfitting.

Experiment 3: Analysis of the Learning Rate for the Model Optimizer

To explore the optimal parameter configuration of the improved algorithm proposed in this paper to achieve the best training effect, this paper adopts the SGD optimizer and systematically carries out comparative experiments under the conditions of different initial learning rates. As shown in Figure 8, the experimental results show that under the premise of using the SGD optimizer, the initial learning rate has a large impact on the model training effect. When the initial learning rate is set to 0.01, the network model shows the optimal performance index in the validation set, which realizes the best training effect under the current experimental conditions and provides a scientific and reasonable basis for setting parameters for subsequent model training.

Figure 8. Experimental results of different learning rates. Analysis of optimizer learning rates in LSKA-driven multidimensional feature cross-level fusion classification network using 3-plane multidimensional KCI MRI dataset from the Second Affiliated Hospital of Dalian Medical University with optimal performance achieved by SGD at initial learning rate 0.01. ACC: accuracy; F1: *F* measure; K-S: Kappa statistic; SEN: sensitivity; SPE: specificity.



XSL•FO
RenderX

Experiment 4: Comparison With the State-of-the-Art Algorithms

To objectively and comprehensively evaluate the performance of the algorithm proposed in this paper, it is compared and experimented with a number of representative classical and representative models in the current field, and all the models are trained based on the same dataset to ensure reliable results. Table 1 shows the comparison data of various indexes.

Table . Comparison results with the state-of-the-art algorithms[a].

Method	ACC	K-S	F1	SEN	SPE	Test times
AlexNet	0.915	0.893	0.914	0.918	0.979	9.0067
ResNet	0.889	0.862	0.890	0.894	0.973	20.2901
GoogLeNet	0.924	0.904	0.924	0.924	0.981	8.4832
SqueezeNet	0.895	0.869	0.896	0.898	0.974	10.9536
MobileNet	0.859	0.823	0.859	0.864	0.965	15.9256
DAGNet[b]	0.986	0.983	0.986	0.986	0.997	20.4942
R-AlexNet	0.941	0.926	0.940	0.940	0.985	9.0759
LC-DSPNet[c]	0.874	0.843	0.870	0.871	0.969	7.0432
YOLOv8	0.988	0.985	0.988	0.988	0.997	0.0024
MDF-CLF	0.997	0.996	0.997	0.997	0.999	0.0025

[a]Comparison of the LSKA-driven multidimensional feature cross-level fusion (MDF-CLF) network with state-of-the-art algorithms on the 3-plane multidimensional KCI MRI dataset from the Second Affiliated Hospital of Dalian Medical University, demonstrating MDF-CLF achieves optimal performance across all evaluation metrics.

[b]DAGNet: Double Attentive Graph Neural Network.

[c]LC-DSPNet: Dual-stream parallel model based on local centroid optimization.

The results show that the algorithm proposed in this paper performs outstandingly in the task of classifying five levels of KCI and outperforms the comparison models in all indicators. Its accuracy rate reaches 0.997, which can correctly determine the injury category, and it is reliable in clinical application and can provide a strong reference for diagnosis. The model features a compact architecture with 1,515,605 parameters. Training efficiency is validated on a single NVIDIA RTX 3090 GPU, where completing 350 epochs takes 5.99 hours, averaging approximately 62 seconds per epoch, demonstrating efficient training capabilities. More critically, the inference speed measured on the same hardware during validation reached 2.5 ms per image, equivalent to a throughput of 400 images per second. These empirical results demonstrate that the model achieves state-of-the-art classification accuracy while maintaining a low computational burden and high inference efficiency, supporting its potential for clinical applications.

Experiment 5: Ablation Analysis of Individual and Combined Imaging Plane Contributions

A comprehensive ablation study is conducted to evaluate the diagnostic value of individual anatomical imaging planes and their combined performance in classifying knee cartilage injuries. The experimental methodology involved a comparative analysis of model performance when trained exclusively on single-plane data in sagittal, coronal, and transverse orientations versus the complete triple-plane combination. The results of our experiments are illustrated in Multimedia Appendix 3. The results demonstrate that the sagittal plane achieved the best single-plane performance with 99.6% accuracy, attributable to its exceptional capability in visualizing critical anatomical structures, such as the patellofemoral joint contact surface and anterior/posterior meniscal horns, which are essential for detecting early-stage cartilage wear and delamination injuries. The coronal plane yielded 99.3% accuracy, effectively capturing tibiofemoral joint integrity and cartilage thickness variations in weight-bearing regions, while the transverse plane achieved 99.1% accuracy, confirming its value in identifying focal chondromalacia and fissures on the medial malleolar surface of the patella. Integration of all three anatomical planes achieved an optimal accuracy of 99.7%, representing a 0.1% improvement over the sagittal-plane-only approach; the multiplane fusion strategy inherently enhances robustness through redundancy. In clinical practice, individual MRI planes may be compromised by artifacts, noise, or acquisition inconsistencies; the fusion strategy mitigates such risks by leveraging complementary information across planes. Additionally, features from the sagittal plane enhance contextual understanding of coronal and transverse data, promoting a more comprehensive feature representation and highlighting the synergistic potential of triple-plane integration.

Discussion

Principal Findings

In response to the growing demand for accurate medical imaging diagnostics, this study focuses on KCI classification by proposing an MDF-CLF network guided by the LSKA mechanism. The network integrates sagittal, coronal, and axial MRI images to construct a 5-class KCI dataset, achieving a final accuracy of 99.7%. The innovative optimization of the YOLOv8 backbone architecture enhances feature extraction capabilities, enabling precise localization of injury regions and identification

XSL•FO
RenderX

of subtle lesion characteristics. The model's performance has been rigorously validated on real-world hospital datasets, demonstrating strong potential for supporting clinical decision-making.

Comparison to Prior Work

Unlike traditional approaches that often rely on single-plane imaging or limited feature integration, our method leverages multimodal MRI data and incorporates an LSKA-based attention mechanism to improve contextual feature capture. While previous studies have utilized deep learning for KCI classification, few have achieved comparable accuracy through multiplane fusion and attention-guided localization. Our model outperforms existing methods in both precision and generalizability, addressing a critical gap in prior work, which often overlooked the integration of cross-plane features and scalable attention mechanisms.

Limitations

This study aims to enhance the classification accuracy of KCI diagnosis by proposing a MDF-CLF classification network driven by LSKA. The method integrates the LSKA module into the YOLOv8 framework, combined with the C2f module and convolutional base modules, achieving multiscale feature enhancement and semantic information extraction from multimodal MRI images. However, although the dataset is derived from real clinical MRI data, all data are acquired from a single medical center using uniform 3.0T MRI scanning equipment and consistent imaging parameters. While this homogeneity ensures internal data consistency, it may constrain the model's generalization capability, potentially leading to performance degradation when applied to heterogeneous data from different centers or equipment. To address this limitation and enhance the model's robustness, future work will employ federated learning techniques to integrate multicenter data. This strategy is expected to significantly improve the model's generalization performance, laying a solid foundation for the broad clinical application of KCI diagnostic models.

Future Directions

Future research will focus on enhancing the algorithm's accuracy and efficiency through lightweight architectural design and cross-domain adaptation, expanding its application to other medical imaging domains such as ocular, pulmonary, and renal diseases, which share analogous challenges in fine-grained classification, and exploring integrated multidisease diagnostic frameworks to broaden the clinical impact and generalizability of the proposed methodology.

Conclusions

This study achieves its initial goal of developing a high-accuracy deep learning model for KCI classification using multimodal MRI fusion and attention mechanisms. The proposed MDF-CLF network not only facilitates precise knee cartilage diagnosis but also provides a transferable framework for other medical imaging classification tasks. By addressing key limitations and outlining clear future directions, this work contributes to advancing automated diagnostic technologies and supports their integration into clinical practice.

Acknowledgments

The author wishes to express sincere gratitude to Vice President Li Yingqiu and Dean Gang Jialin for their invaluable guidance and steadfast support throughout the course of this research. Their expertise and encouragement are instrumental in the completion of this work.

The author is also deeply indebted to Dalian Neusoft University of Information for providing essential institutional backing and resources. Without the university's unwavering support, the successful execution of this study would not have been feasible.

Furthermore, the author gratefully acknowledges the financial assistance provided by the Young Science and Technology Star Project of Dalian, which funded this research.

Funding

This research was funded by the Young Science and Technology Star Project of Dalian, China (grant 2023RQ032).

Data Availability

The datasets generated or analyzed during this study are available from the corresponding author on reasonable request.

Authors' Contributions

Conceptualization: LZ
Methodology: LZ
Validation: LZ, YY
Software: LZ
Writing – original draft: LZ
Writing – review & editing: LZ, HY
Investigation: HY
Data curation: YY

XSL•FO
RenderX

Conflicts of Interest

None declared.

Multimedia Appendix 1
Example image of the dataset.
[PNG File, 261 KB - medinform_v13i1e79748_app1.png]

Multimedia Appendix 2
Experimental results of different training epochs. Experimental analysis of training epochs on the performance of the large separable kernel attention–driven multidimensional feature cross-level fusion network for 5-Grade knee cartilage injury (KCI) classification using 3-plane multidimensional KCI magnetic resonance imaging dataset from a retrospective clinical cohort at the Second Affiliated Hospital of Dalian Medical University in China with optimal accuracy of 99.7% at 350 epochs.
[PNG File, 88 KB - medinform_v13i1e79748_app2.png]

Multimedia Appendix 3
Comparison results with the plane ablation experiment. Plane ablation experiment comparison in large separable kernel attention–driven multidimensional feature cross-level fusion classification network using 3-plane multidimensional knee cartilage injury magnetic resonance imaging dataset from the Second Affiliated Hospital of Dalian Medical University with multiplane fusion achieving optimal classification accuracy.
[PNG File, 229 KB - medinform_v13i1e79748_app3.png]

References

1. Kretzschmar M, Nevitt MC, Schwaiger BJ, Joseph GB, McCulloch CE, Link TM. Spatial distribution and temporal progression of T2 relaxation time values in knee cartilage prior to the onset of cartilage lesions – data from the Osteoarthritis Initiative (OAI). Osteoarthr Cartil 2019 May;27(5):737-745. [doi: 10.1016/j.joca.2018.10.016]
2. Hutchison L, Grayson J, Hiller C, D'Souza N, Kobayashi S, Simic M. Is there a relationship between knee biomechanics and pain in people with knee osteoarthritis? A systematic review and meta-analysis. Osteoarthr Cartil 2022 Apr;30:S142-S143. [doi: 10.1016/j.joca.2022.02.180]
3. Tanaka Y, Okada Y, Nakayamada S, Nakano K, Fujii K, Saito K. Cell biology of synovial inflammation and secondary osteoporosis in rheumatoid arthritis. Arthritis Res Ther 2003;5(Suppl 3):45. [doi: 10.1186/ar846]
4. Arani A, Schwarz CG, Wiste HJ, et al. Left-right intensity asymmetries vary depending on scanner model for FLAIR and T1 weighted MRI images. J Magn Reson Imaging 2022 Sep;56(3):917-927. [doi: 10.1002/jmri.28105] [Medline: 35133061]
5. Benson JC, Carlson ML, Yin L, Lane JI. Cholesteatoma localization using fused diffusion‐weighted images and thin‐slice T2 weighted images. Laryngoscope 2021 May;131(5):E1662-E1667. [doi: 10.1002/lary.29222] [Medline: 33140869]
6. Keerthivasan MB, Galons JP, Johnson K, et al. Abdominal T2‐weighted imaging and T2 mapping using a variable Flip angle radial turbo spin‐Echo technique. J Magn Reson Imaging 2022 Jan;55(1):289-300. [doi: 10.1002/jmri.27825] [Medline: 34254382]
7. Anderson AF, Anderson CN. Correlation of meniscal and articular cartilage injuries in children and adolescents with timing of anterior cruciate ligament reconstruction. Am J Sports Med 2015 Feb;43(2):275-281. [doi: 10.1177/0363546514559912] [Medline: 25497145]
8. Kijowski R, Sharafi A, Zibetti MVW, Chang G, Cloos MA, Regatte RR. Age‐dependent changes in knee cartilage T1, T2, and T1p simultaneously measured using MRI fingerprinting. J Magn Reson Imaging 2023;57(6):1805-1812. [doi: 10.1002/jmri.28451] [Medline: 36190187]
9. Jo K, Linh VTN, Yang JY, et al. Machine learning-assisted label-free colorectal cancer diagnosis using plasmonic needle-endoscopy system. Biosens Bioelectron 2024 Nov 15;264:116633. [doi: 10.1016/j.bios.2024.116633] [Medline: 39126906]
10. Tsivgoulis M, Papastergiou T, Megalooikonomou V. An improved SqueezeNet model for the diagnosis of lung cancer in CT scans. Mach Learn Appl 2022 Dec;10:100399. [doi: 10.1016/j.mlwa.2022.100399]
11. Jaware TH, Patil JP, Badgujar RD. Robust deep learning approach for colon cancer detection using MobileNet. J Inst Eng India Ser B 2025. [doi: 10.1007/s40031-025-01217-0]
12. Chen J, Wan Z, Zhang J, et al. Medical image segmentation and reconstruction of prostate tumor based on 3D AlexNet. Comput Methods Programs Biomed 2021 Mar;200:105878. [doi: 10.1016/j.cmpb.2020.105878] [Medline: 33308904]
13. He F, Liu T, Tao D. Why resnet works? Residuals generalize. IEEE Trans Neural Netw Learn Syst 2020 Dec;31(12):5349-5362. [doi: 10.1109/TNNLS.2020.2966319] [Medline: 32031953]
14. Ak A, Topuz V, Midi I. Motor imagery EEG signal classification using image processing technique over GoogLeNet deep learning algorithm for controlling the robot manipulator. Biomed Signal Process Control 2022 Feb;72:103295. [doi: 10.1016/j.bspc.2021.103295]

XSL•FO
RenderX

15. Abdul W, Guro R, Jawad Z, Kotwal R, Chandratreya A. Clinical outcomes of primary anatomic all-inside Anterior Cruciate Ligament reconstruction using the TransLateral technique: a minimum one-year follow-up study. Knee 2020 Dec;27(6):1753-1763. [doi: 10.1016/j.knee.2020.09.014] [Medline: 33197814]
16. Demir S, Key S, Baygin M, et al. Automated knee ligament injuries classification method based on exemplar pyramid local binary pattern feature extraction and hybrid iterative feature selection. Biomed Signal Process Control 2022 Jan;71:103191. [doi: 10.1016/j.bspc.2021.103191]
17. Fang L, Qiao H. Diabetic retinopathy classification using a novel DAG network based on multi-feature of fundus images. Biomed Signal Process Control 2022 Aug;77:103810. [doi: 10.1016/j.bspc.2022.103810]
18. Lei C, Jiang Y, Xu K, Liu S, Cao H, Wang C. Convolutional neural network models for visual classification of pressure ulcer stages: cross-sectional study. JMIR Med Inform 2025 Mar 25;13:e62774. [doi: 10.2196/62774] [Medline: 40135412]
19. Dai G, Wang C, Tang Q, et al. Interpretable breast cancer diagnosis using histopathology and lesion mask as domain concepts conditional simulation ultrasonography. Inf Fusion 2025 Nov;123:103343. [doi: 10.1016/j.inffus.2025.103343]
20. Dai G, Wang C, Dai D, Tang Q, Zhang Y, Chen H. Interpretable breast cancer identification by multi-view synergistic feature fusion interaction in dense breast tissue. Inf Fusion 2026 Jan;125:103446. [doi: 10.1016/j.inffus.2025.103446]
21. Rezk E, Eltorki M, El-Dakhakhni W. Leveraging artificial intelligence to improve the diversity of dermatological skin color pathology: protocol for an algorithm development and validation study. JMIR Res Protoc 2022 Mar 8;11(3):e34896. [doi: 10.2196/34896] [Medline: 34983017]
22. Fang L, Wang X. Dual-stream parallel model of cartilage injury diagnosis based on local centroid optimization. Biomed Signal Process Control 2023 Feb;80:104229. [doi: 10.1016/j.bspc.2022.104229]
23. Zhang L, Che Z, Li Y, et al. Multi-level classification of knee cartilage lesion in multimodal MRI based on deep learning. Biomed Signal Process Control 2023 May;83:104687. [doi: 10.1016/j.bspc.2023.104687]
24. Ezhilin Freeda S, Hariharan T, Dinesh R, Muthuaravind M. Classification of different stages of eczema disease using yolov8. 2024 Presented at: 2024 8th International Conference on Electronics, Communication and Aerospace Technology (ICECA); Nov 6-8, 2024; Coimbatore, India p. 1575-1579. [doi: 10.1109/ICECA63461.2024.10801168]
25. Agulan RZ, Magsumbol JAV, Rosales MA. Detection of dental caries based on GV black classification utilizing YOLOv8 from X-ray images. 2024 Presented at: 2024 IEEE International Conference on Imaging Systems and Techniques (IST); Oct 14-16, 2024; Tokyo, Japan p. 1-6. [doi: 10.1109/IST63414.2024.10759223]
26. Marullo G, Ulrich L, Antonaci FG, et al. Classification of AO/OTA 31A/B femur fractures in X-ray images using YOLOv8 and advanced data augmentation techniques. Bone Rep 2024 Sep;22:101801. [doi: 10.1016/j.bonr.2024.101801] [Medline: 39324016]
27. Kalpana P, Selvy PT. A novel machine learning model for breast cancer detection using mammogram images. Med Biol Eng Comput 2024 Jul;62(7):2247-2264. [doi: 10.1007/s11517-024-03057-4] [Medline: 38575824]
28. Zhou L, Wang H, Xu S. Aero-engine prognosis strategy based on multi-scale feature fusion and multi-task parallel learning. Reliab Eng Syst Safe 2023 Jun;234:109182. [doi: 10.1016/j.ress.2023.109182]
29. Lau KW, Po LM, Rehman YAU. Large separable kernel attention: rethinking the large kernel attention design in CNN. Expert Syst Appl 2024 Feb;236:121352. [doi: 10.1016/j.eswa.2023.121352]
30. Islam J, Furqon EN, Farady I, Rani Alex JS, Kuo CC, Lin CY. Integrating stable diffusion for improved alzheimer's disease classification: insights from MRI images and yolov8. 2024 Presented at: 2024 International Conference on Consumer Electronics - Taiwan (ICCE-Taiwan); Jul 9-11, 2024; Taichung, Taiwan p. 303-304. [doi: 10.1109/ICCE-Taiwan62264.2024.10674478]
31. Palanivel N, S D, G LP, B S, M SM. The art of yolov8 algorithm in cancer diagnosis using medical imaging. 2023 Presented at: 2023 International Conference on System, Computation, Automation and Networking (ICSCAN); Nov 17-18, 2023; Puducherry, India p. 1-6. [doi: 10.1109/ICSCAN58655.2023.10395046]
32. National Health Commission, Ministry of Education, Ministry of Science and Technology, State Administration of Traditional Chinese Medicine. Circular on issuing the ethical review measures for life sciences and medical research involving humans [guo wei ke jiao fa (2023) no. 4]. National Health Commission. 2023. URL: http://www.gov.cn/zhengce/zhengceku/2023-02/28/content_5743658.htm [accessed 2024-06-20]

Abbreviations

C2f: Cross-Stage Partial-Connection with 2 convolutions
CNNs: convolutional neural networks
DAGNet: Double Attentive Graph Neural Network
KCI: knee cartilage injury
LC-DSPNet: Dual-stream parallel model based on local centroid optimization
LSKA: large separable kernel attention
MDF-CLF: multidimensional feature cross-level fusion
MRI: magnetic resonance imaging
SiLU: Sigmoid Weighted Linear Unit

XSL•FO
RenderX

T1WI: T1-weighted imaging
T2WI: T2-weighted imaging
YOLO: You Only Look Once

Edited by A Coristine; submitted 26.06.25; peer-reviewed by G Dai, V Rajesh; revised version received 15.11.25; accepted 17.11.25; published 17.12.25.

Please cite as:
Zhang L, Yu H, Yang Y
Large Separable Kernel Attention–Driven Multidimensional Feature Cross-Level Fusion Classification Network of Knee Cartilage Injury: Algorithm Development and Validation
JMIR Med Inform 2025;13:e79748
URL: https://medinform.jmir.org/2025/1/e79748
doi:10.2196/79748

© Lirong Zhang, Hang Yu, Yating Yang. Originally published in JMIR Medical Informatics (https://medinform.jmir.org), 17.12.2025. This is an open-access article distributed under the terms of the Creative Commons Attribution License (https://creativecommons.org/licenses/by/4.0/), which permits unrestricted use, distribution, and reproduction in any medium, provided the original work, first published in JMIR Medical Informatics, is properly cited. The complete bibliographic information, a link to the original publication on https://medinform.jmir.org/, as well as this copyright and license information must be included.

XSL•FO
RenderX

Evaluating the Accuracy of the Frysian Questionnaire for Differentiation of Musculoskeletal Complaints for Triage of Musculoskeletal Diseases: Algorithm Development and Validation Study

Tjardo Daniël Maarseveen[1], MSc; Floor Reimann[2], MD; Ahmed al Hasan[1], MD; Annemarie Schilder[2], MD; Dan Zhang[2], MD; Freke Wink[2], MD; Lidy Hendriks[2], MD; Rachel Knevel[1,3*], PhD; Reinhard Bos[2*], PhD

[1]Department of Rheumatology, Leiden University Medical Center, Albinusdreef 2, Leiden, The Netherlands

[2]Department of Rheumatology, Frisius Medical Center, Leeuwarden, The Netherlands

[3]Department of Rheumatology, Newcastle University, Newcastle upon Tyne, United Kingdom

[*]these authors contributed equally

Corresponding Author:
Tjardo Daniël Maarseveen, MSc
Department of Rheumatology, Leiden University Medical Center, Albinusdreef 2, Leiden, The Netherlands

Abstract

Background: Inflammatory rheumatic diseases (IRDs) affect 5% of the general population, whereas 35% of the population experiences musculoskeletal concerns. IRDs cause early disability, reduced life expectancy, and considerable health care costs. Early diagnosis is essential to prevent long-term damage. Similarly important is the early identification of patients with musculoskeletal concerns without IRDs to prevent unnecessary health care expenses. Of the population referred to the rheumatologist, 60% have noninflammatory musculoskeletal concerns, whereas only 20% of patients with an IRD see a rheumatologist within 3 months of symptom onset. The need for digital predictive (triage) tools for rheumatic and musculoskeletal diseases led to the development of the Frysian Questionnaire for Differentiation of Musculoskeletal Complaints (FRYQ).

Objective: This study aimed to assess whether the FRYQ can distinguish IRD from noninflammatory musculoskeletal concerns in general, and rheumatoid arthritis and fibromyalgia specifically, in newly referred patients.

Methods: The FRYQ is an 87-item tool (20 open-ended and 67 closed-ended questions) used to triage new rheumatology patients at Frisius Medical Center in the Netherlands. We analyzed data from 2 sources: dataset A with 728 outpatient clinic patients and dataset B with 373 patients from the Joint Pain Assessment Scoring Tool study. We built a classifier using Extreme Gradient Boosting to distinguish inflammatory from noninflammatory conditions based on closed-ended questions. Using elastic net regularization, we identified the most informative questions. We evaluated classification using receiver operating characteristic curve analysis and assessed feature importance through Shapley Additive Explanation analysis. To test generalizability, we replicated our analysis on dataset B. Finally, we examined whether the questions of the FRYQ could be used to identify specific conditions beyond the general categories of IRD and non-IRD, specifically for detecting fibromyalgia and rheumatoid arthritis.

Results: Feature selection reduced the questionnaire from 67 to 28 items while maintaining discriminative power. After initial development, the model achieved an area under the receiver operating characteristic curve (AUC-ROC) of 0.72 (95% CI 0.67-0.78) for distinguishing inflammatory from noninflammatory conditions in an external validation set. Using a probability threshold of 0.30, the model achieved 71% sensitivity and 56% specificity on external validation. The FRYQ demonstrated stronger performance in identifying specific diagnoses such as fibromyalgia (AUC-ROC=0.81) and rheumatoid arthritis (AUC-ROC=0.77). Key discriminating features included symptom duration, pain response to movement, and anti-inflammatory medication effectiveness.

Conclusions: The FRYQ effectively distinguishes inflammatory from noninflammatory rheumatic conditions before specialist consultation and shows particular strength in identifying fibromyalgia and rheumatoid arthritis. This tool could improve rheumatology triage by prioritizing referrals with high likelihood of IRD for early rheumatologist evaluation while directing other patients to appropriate alternative resources. Prospective studies are needed to determine the FRYQ's impact on clinical outcomes and health care efficiency.

(JMIR Med Inform 2025;13:e77345) doi:10.2196/77345

XSL•FO
RenderX

KEYWORDS

medical informatics; questionnaire; machine learning; fibromyalgia; rheumatic diseases; rheumatoid arthritis; triage; decision support system; symptom checker

Introduction

Inflammatory rheumatic diseases (IRDs) affect 5% of the general population in the Netherlands, whereas 35% of the population experience musculoskeletal concerns [1]. Global prevalence of both IRDs and musculoskeletal concerns varies with age and region but is comparable to that in the Netherlands [2]. IRDs can cause early disability, reduced life expectancy, and considerable health care costs.

In the Dutch health care system, as in many European countries, patients with musculoskeletal concerns first consult a general practitioner (GP) before referral to a specialist. To facilitate appropriate and timely care, the Dutch College of General Practitioners (*Nederlands Huisartsen Genootschap*) has developed national guidelines and referral protocols [3], helping ensure that patients receive specialist attention when necessary.

Early diagnosis of rheumatic diseases such as rheumatoid arthritis (RA), ankylosing spondylitis, or psoriatic arthritis by specialists is essential to prevent irreversible damage [4-7]. Similarly important is the early identification of patients with musculoskeletal concerns without IRDs who can be treated in primary care to prevent unnecessary health care expenses. This need is particularly pressing in the Netherlands, which has one of the most expensive health care systems in Europe—ranking third after Austria and Germany [8].

Approximately 109 new patients with musculoskeletal concerns per 1000 people are seen by GPs annually [9]. Of the population referred to a rheumatologist, 60% have noninflammatory musculoskeletal concerns, whereas only 20% of patients with an IRD see a rheumatologist within 3 months of symptom onset [10]. For the target disease, RA, we observe that these patients have to wait—on average—4 weeks from referral to their visit to a rheumatologist [11].

The urgent need for more efficient management of referred patients led to the development of the Frysian Questionnaire for Differentiation of Musculoskeletal Complaints (FRYQ). The FRYQ is an 87-item questionnaire consisting of 20 open-ended and 67 close-ended questions that is used in regular care in the rheumatology outpatient clinic of Frisius Medical Center to triage newly referred patients. It was developed to improve diagnostic speed for referred patients by facilitating early appropriate blood testing.

Our study had three main objectives: (1) evaluate the FRYQ's ability to differentiate IRDs from non-IRDs in newly referred patients using machine learning techniques; (2) identify which questions are most informative for distinguishing inflammatory conditions and develop a streamlined version without losing diagnostic value; and (3) assess whether the FRYQ can be used to identify specific conditions of interest, particularly fibromyalgia and RA, which represent important diagnostic targets in rheumatology practice.

Methods

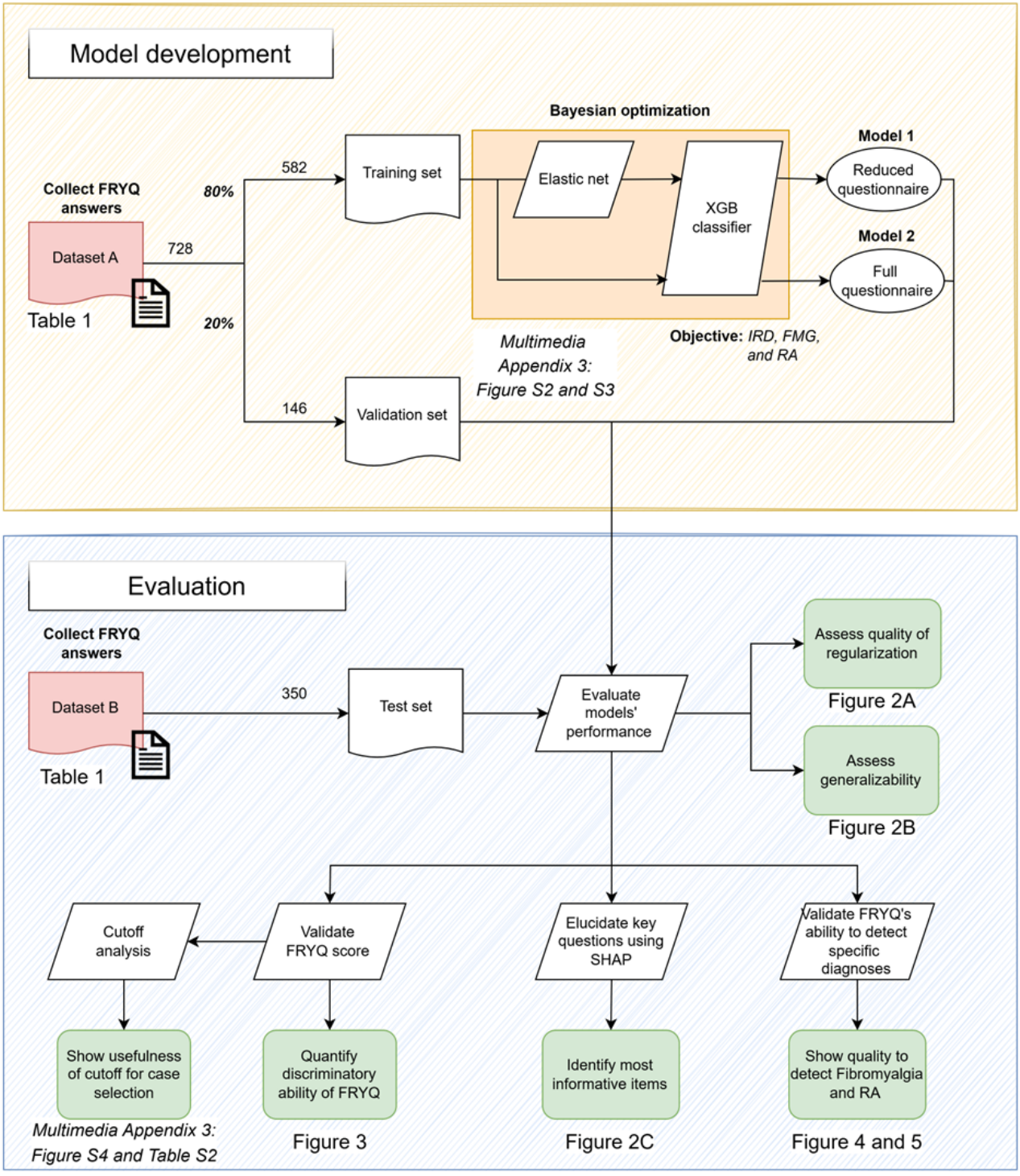
Study Design and Source of Data

In this study, we conducted a retrospective analysis of newly referred patients to the rheumatology department at Frisius Medical Center, Leeuwarden, the Netherlands (the pipeline is shown in Figure 1). We developed and validated machine learning prediction models to assess the FRYQ's ability to differentiate inflammatory from noninflammatory rheumatic conditions using only preconsultation patient responses. Multimedia Appendix 1 provides the Dutch version of the questionnaire, and Multimedia Appendix 2 provides the translated version in English.

We used two independent cohorts: (1) a development dataset (dataset A), which comprised 728 adult patients who completed the FRYQ between August 2017 and June 2019 as part of routine care, and (2) an external validation dataset (dataset B), which comprised 373 adult patients from the Joint Pain Assessment Scoring Tool (JPAST) study cohort [12] visiting the clinic between January 2023 and March 2024 who completed the FRYQ as an additional research instrument.

XSL•FO
RenderX

Figure 1. Study workflow consisting of two phases: (1) model development, where we built a classifier to detect inflammatory rheumatic diseases (IRDs), fibromyalgia, and rheumatoid arthritis (RA) using only Frysian Questionnaire for Differentiation of Musculoskeletal Complaints (FRYQ) responses+sex based on the data from the first pilot (n=728), and (2) model evaluation, where we deployed the model on unseen data from a different study (n=350) to assess generalizability. FMG: fibromyalgia; SHAP: Shapley Additive Explanations; XGB: Extreme Gradient Boosting.



Ethical Considerations

The FRYQ was developed by the rheumatology clinic at the Frisius Medical Center to assist in prioritizing newly referred patients. The data in dataset A were gathered as part of standard clinical care. Informed consent for the use of anonymized data in research was secured through the opt-out procedure, whereby all patient data were eligible for inclusion unless an individual filed a formal objection. According to Article 1(b) of the Dutch Medical Research Involving Human Subjects Act (Wet medisch-wetenschappelijk onderzoek met mensen [WMO]), ethical review is required only for studies that aim to obtain medical-scientific knowledge and in which participants are subjected to an intervention or are required to follow a behavioral regime [13]. As the FRYQ questionnaire was administered as part of routine care and did not involve any intervention or imposed behavior, the study does not fall under

XSL•FO
RenderX

the scope of the WMO and therefore did not require approval by a medical ethics review committee.

In contrast, dataset B consisted of patients enrolled in the JPAST study, which involved time-consuming study procedures. Therefore, the use of the FRYQ in this dataset was reviewed and approved by the medical ethics committee of the Frisius Medical Center (reference number RTPO-1104) as part of the JPAST study protocol. Since participation in the JPAST study involved procedures beyond standard care, each participant provided written informed consent authorizing the use of their data for research.

For both datasets, patient data security was ensured by assigning each patient a unique sequential identifier through pseudonymization. Data were stored and analyzed in a secure, password-protected database accessible only to authorized personnel. Participants retained the right to opt out of the use of their data for research purposes and did not receive financial compensation for their involvement in this study. All study procedures were conducted in accordance with the principles of the Declaration of Helsinki.

Participants

Eligibility Criteria

All adult patients newly referred to the rheumatology outpatient clinic who completed the FRYQ were eligible. From dataset A, 854 patients were initially invited, with 728 (85.2%) having complete data for analysis. From dataset B, all patients with complete FRYQ responses and diagnosis data were included.

Study Setting

Data collection took place in a nonacademic hospital setting (Frisius Medical Center) during routine clinical care for dataset A and as part of the international JPAST validation study for dataset B.

Outcome

Primary Outcome

The primary outcome was the presence of an IRD versus a noninflammatory musculoskeletal condition (non-IRD) as diagnosed by a rheumatologist after clinical evaluation. This determination represented the clinical ground truth against which the model predictions were evaluated. The outcome was assessed by extracting the final diagnosis from electronic health records.

Secondary Outcomes

Specific diagnoses of fibromyalgia and RA were evaluated as secondary outcomes in additional predictive models.

Predictors (Input Variables)

The primary input variables consisted of responses to the 67 closed-ended questions from the FRYQ supplemented by patient age and sex. The FRYQ is an 87-item tool (including 20 open-ended questions not used in this analysis) designed by rheumatologists for triaging rheumatology patients. Question topics covered pain characteristics and patterns, stiffness symptoms and duration, functional limitations, associated symptoms, comorbid conditions, medication responses, and patient behaviors and characteristics. No laboratory test results or imaging data were included as predictors in the model.

Missing Data

Patients with incomplete demographic and questionnaire data were removed from dataset A (127/862, 14.7%) and dataset B (166/552, 30.1%; Figure S1 in Multimedia Appendix 3). Furthermore, we had some patients with inconsistent diagnostic labels removed from dataset A (7/862, 0.8%) and a few with missing diagnosis information removed from dataset B (36/552, 6.5%).

Model Development

Data Preprocessing

No significant preprocessing was required as the questionnaire items were already structured. Patient sex was included as a binary variable, and patient age was included as a continuous variable.

Feature Selection

We used elastic net regularization to identify the most informative subset of questions from the original 67 closed-ended items. The regularization parameters (alpha and L1 ratio) were optimized using Bayesian methods with a tree-structured Parzen estimator across 1000 iterations [14]. This approach allowed us to reduce dimensionality while retaining predictive power.

Model Specification

We used the Extreme Gradient Boosting technique [15] to build a model for IRD prediction using only the questions selected by the elastic net. Extreme Gradient Boosting was chosen for its ability to capture complex relationships between variables and its robust performance in previous prediction tasks [16]. All machine learning analyses were performed in Python (version 3.6.13; Python Software Foundation).

Model Training

The model was trained on 80% of dataset A. We used Bayesian optimization across 1000 iterations to tune model hyperparameters, optimizing for root mean square logarithmic error to emphasize sensitivity to inflammatory conditions.

Model Performance

Measures of Model Performance

We evaluated model discrimination using the area under the receiver operating characteristic curve (AUC-ROC). Calibration was assessed using calibration plots comparing predicted probabilities with observed outcome frequencies.

Validation

The model was first validated on the reserved 20% of dataset A (internal validation) and then on dataset B (external validation) to assess generalizability. Both the reduced model (with selected features) and the full model (with all 67 questions) were evaluated to assess the impact of feature selection.

XSL•FO
RenderX

Clinical Utility

We conducted threshold analysis to identify an optimal probability cutoff for distinguishing IRD from non-IRD cases in clinical practice, evaluating sensitivity, specificity, positive predictive value, and negative predictive value at various thresholds.

Model Interpretation

To understand feature importance and explain model predictions, we conducted Shapley additive explanation (SHAP) analysis [17]. This approach quantified the contribution of each question to the model output, allowing us to identify which questions were most informative for detecting inflammatory conditions.

Results

Overview

Dataset A comprised 728 patients, of whom 239 (32.8%) were male and 489 (67.2%) were female (Table 1). Nearly half (257/582, 44.2%) of the patients in the training dataset had IRDs. The most common disorders associated with IRD were RA (62/582, 10.7%), gout (45/582, 7.7%), and spondyloarthritis (43/582, 7.4%). Among noninflammatory arthropathies, the most frequent were osteoarthritis (119/582, 20.4%), tendinopathy (92/582, 15.8%), and fibromyalgia (91/582, 15.6%).

The external test dataset B included 350 patients with complete information, comprising 106 (30.3%) male and 244 (69.7%) female individuals. Only 26.6% (93/350) of the patients were diagnosed with an IRD, which was notably lower than those in the training and validation partitions of dataset A (257/582, 44.2% and 67/146, 45.9%, respectively). In contrast, the JPAST data contained a higher proportion of patients with an “other” diagnosis, indicating that this dataset represented a somewhat different patient population.

XSL•FO
RenderX

Table . Patient characteristics in both datasets.

	Dataset A		Dataset B
	Training (n=582)	Hold-out (n=146)	Replication (n=350)
Sex (female), n (%)	308 (52.9)	97 (66.4)	244 (69.7)
Age (y), mean (SD)	52 (17)	55 (17)	53 (16)
IRD[a], n (%)	257 (44.2)	67 (45.9)	93 (26.6)
Rheumatoid arthritis	62 (10.7)	25 (17.1)	15 (4.3)
Polymyalgia rheumatica	20 (3.4)	7 (4.8)	12 (3.4)
Gout	45 (7.7)	4 (2.7)	11 (3.1)
Systemic lupus erythematosus	3 (0.5)	2 (1.4)	0 (0)
Psoriatic arthritis	20 (3.4)	9 (6.2)	4 (1.1)
Spondyloarthritis	43 (7.4)	9 (6.2)	13 (3.7)
Sjögrenn disease	5 (0.9)	1 (0.7)	1 (0.3)
Reactive arthritis	9 (1.5)	3 (2.1)	2 (0.6)
Undifferentiated arthritis	9 (1.5)	1 (0.7)	14 (4)
Systemic sclerosis	4 (0.7)	1 (0.7)	1 (0.3)
CPPD[b]	10 (1.7)	3 (2.1)	2 (0.6)
Probable RMD[c] in development	17 (2.9)	1 (0.7)	18 (5.1)
Sarcoidosis	9 (1.5)	1 (0.7)	0 (0)
ANCA[d]-associated vasculitis	1 (0.2)	0 (0)	0 (0)
No IRD, n (%)	323 (55.5)	79 (54.1)	185 (52.9)
Osteoarthritis	119 (20.4)	33 (22.6)	73 (20.9)
Tendinopathy	92 (15.8)	25 (17.1)	39 (11.1)
Fibromyalgia	91 (15.6)	19 (13)	68 (19.4)
Pernio	0 (0)	0 (0)	4 (1.1)
Hypermobility	21 (3.6)	2 (1.4)	1 (0.3)
Ambiguous, n (%)	2 (0.3)	0 (0)	72 (20.6)
Other	0 (0)	0 (0)	65 (18.6)
Unknown	2 (0.3)	0 (0)	7 (2)

[a]IRD: inflammatory rheumatic disease.

[b]CPPD: calcium pyrophosphate crystal deposition disease.

[c]RMD: rheumatic and musculoskeletal disease.

[d]ANCA: antineutrophil cytoplasmic antibody.

Prediction of IRD

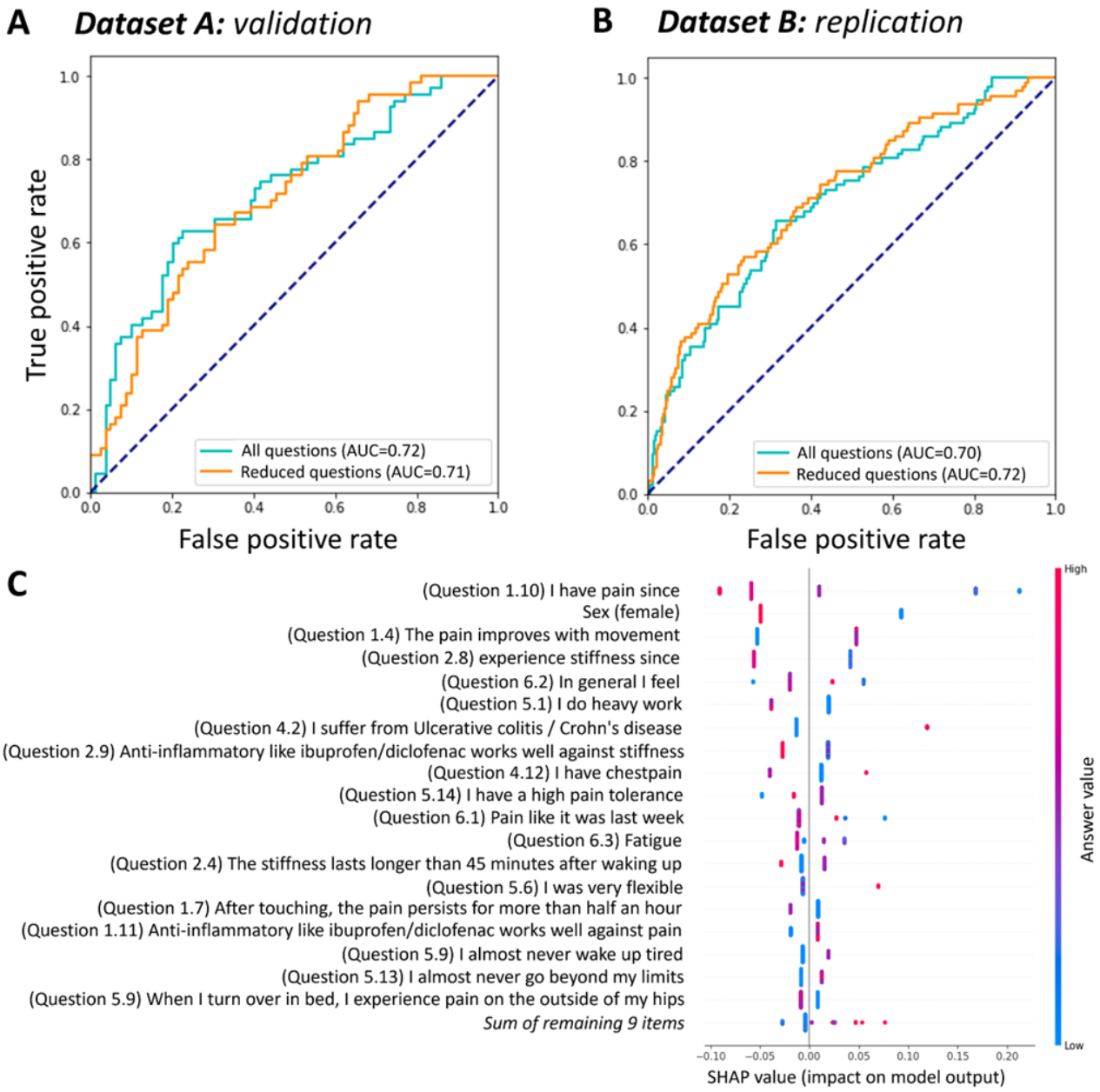
After hyperparameter optimization (α=.07; L1-ratio=0.16; Figures S2 and S3 in Multimedia Appendix 3) and feature selection, our model reduced the 67 closed-ended questions to 28 key items (Table S1 in Multimedia Appendix 3). This streamlined model effectively distinguished IRD from non-IRD across multiple validation steps.

In the development dataset A, the reduced model achieved an AUC-ROC of 0.70 (95% CI 0.67-0.74) in the training set and 0.71 (95% CI 0.64-0.78) in the hold-out validation set, performing comparably to the full model (AUC-ROC of 0.67, 95% CI 0.63-0.72 and 0.72, 95% CI 0.64-0.78, respectively; Figure 2A).

Importantly, when tested in the independent dataset B, the model demonstrated robust generalizability, with an AUC-ROC of 0.72 (95% CI 0.67-0.78) for the reduced model and 0.68 (95% CI 0.63-0.75) for the full model (Figure 2B), confirming the model's stability across different patient populations.

XSL•FO
RenderX

Figure 2. Performance of the inflammatory rheumatic disease classifier: (A) receiver operating characteristic (ROC) curves showing performance before and after regularization in the validation set, (B) ROC curves showing performance before and after regularization in the replication set, and (C) Shapley Additive Explanation (SHAP) analysis results highlighting the impact and direction of the most important features contributing to the classifier's predictions. AUC: area under the curve.

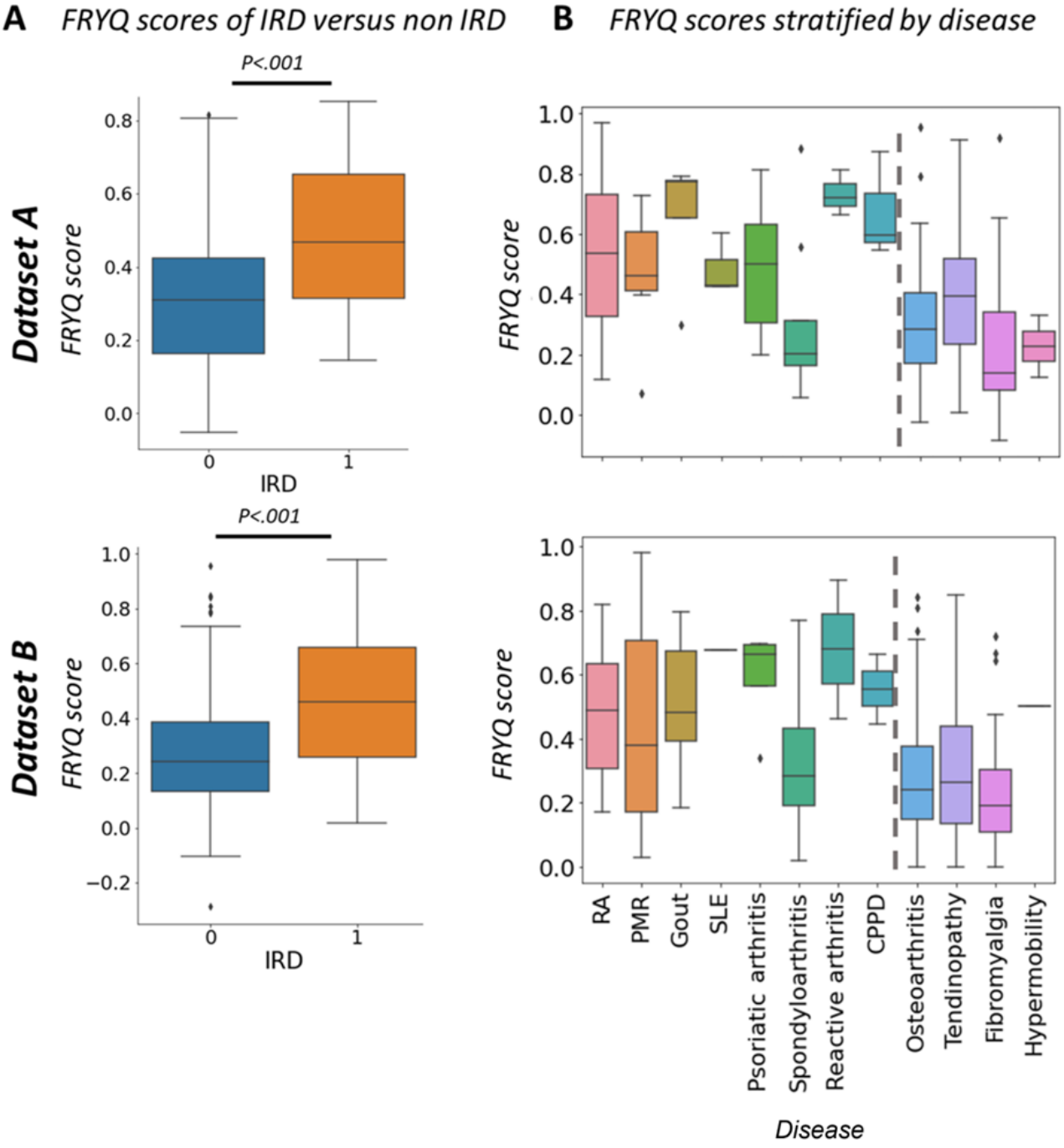


The FRYQ score (model-predicted probability) consistently distinguished IRD patients from non-IRD patients across both datasets (P<.001; Figure 3). In the development set A, the median FRYQ score was 0.47 (IQR 0.31-0.65) for patients with IRD, versus 0.30 (IQR 0.16-0.42) for patients without IRD. Similarly, in replication set B, the median score was 0.46 (IQR 0.26-0.66) for patients with IRD, compared to 0.24 (IQR 0.13-0.39) for patients without IRD. When examining specific conditions, most IRDs exhibited higher scores than non-IRDs, with 2 notable exceptions: spondyloarthritis consistently scored lower among IRDs, whereas tendinopathy scored relatively high (>0.35) among non-IRDs, suggesting areas where diagnostic discrimination was more challenging. Fibromyalgia consistently showed very low scores (<0.2), making it a promising target for specialized detection.

The key features for identifying an IRD in the newly referred population (Figure 2C) were questions related to duration of concerns (questions 1.10 and 2.8), male sex, and decrease of pain upon movement (question 1.4). Moreover, the presence of certain comorbidities influenced the model's assessment. Ulcerative colitis and Crohn disease (question 4.2) showed a positive association with IRDs, whereas chest pain (question 4.12) showed a negative association. Additionally, respondents diagnosed with an IRD more frequently reported that nonsteroidal anti‐inflammatory drugs such as ibuprofen and diclofenac were effective in managing their symptoms (questions 2.9 and 1.11).

XSL•FO
RenderX

Figure 3. Overview of Frysian Questionnaire for Differentiation of Musculoskeletal Complaints (FRYQ) score distributions (A) between inflammatory rheumatic disease (IRD) and non-IRD and (B) more specifically by disease, with IRDs on the left of the dashed line and non-IRDs on the right. The comparison between IRDs and non-IRDs was conducted using a 2-tailed Student *t* test. CPPD: calcium pyrophosphate crystal deposition disease (pseudogout); PMR: polymyalgia rheumatica; RA: rheumatoid arthritis; SLE: systemic lupus erythematosus. **P*<.05; ***P*<.01; ****P*<.001.



Next, we defined the optimal clinical threshold for case selection. On the basis of the training data, we set the cutoff at 0.30 (Figure S4 in Multimedia Appendix 3) as it captured more than three-fourths of IRD cases (sensitivity=0.76) while ensuring that half of the cases without IRDs were excluded (specificity=0.49). This threshold showed similar sensitivity (0.71) and specificity (0.56) in the external validation dataset. The positive predictive value was lower in the external validation dataset (0.39 vs 0.56 in dataset A), attributable to the lower IRD prevalence (93/350, 26.6% vs 257/582, 44.2%; Table S4 in Multimedia Appendix 3).

The calibration curve indicated that the model slightly overestimated IRD probability in the external test dataset (Figure S5 in Multimedia Appendix 3), reflecting the difference in disease prevalence between the training and validation populations. Despite this, the discriminatory ability remained strong, with IRDs consistently receiving higher scores than non-IRDs across both datasets, reinforcing the FRYQ's potential value as a triage tool.

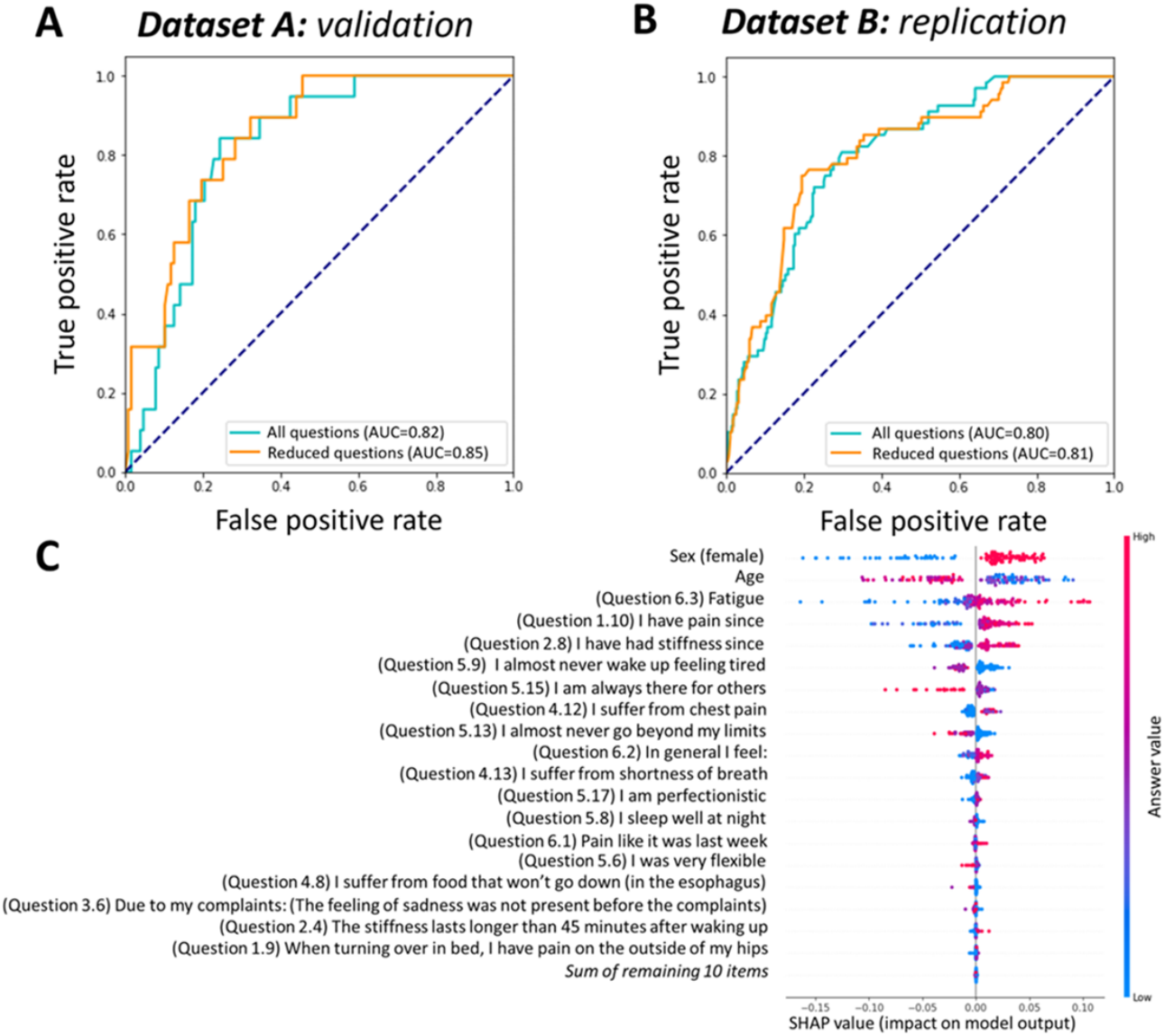
XSL•FO
RenderX

Prediction of Specific Diagnoses: Fibromyalgia and RA

Our analysis extended beyond distinguishing inflammatory from noninflammatory conditions to evaluate the FRYQ's ability to identify specific diagnoses. Patients with fibromyalgia showed particularly distinctive response patterns compared to those with inflammatory conditions (Figure 3), making this a compelling diagnostic target with sufficient representation in our datasets.

The fibromyalgia-specific model demonstrated strong discriminative ability, achieving an AUC-ROC of 0.85 (95% CI 0.78-0.90) in the development dataset and maintaining robust performance in the external validation dataset with an AUC-ROC of 0.81 (95% CI 0.75-0.86; Figure 4). SHAP analysis identified key predictive features for fibromyalgia: female sex, younger to middle age, fatigue (question 6.3), chest pain (question 4.12), extended symptom duration (questions 1.10 and 2.8), and waking up tired (question 5.9). The model effectively differentiated fibromyalgia from RA, although some misclassification occurred with noninflammatory conditions such as hypermobility (Figure 6A in Multimedia Appendix 3).

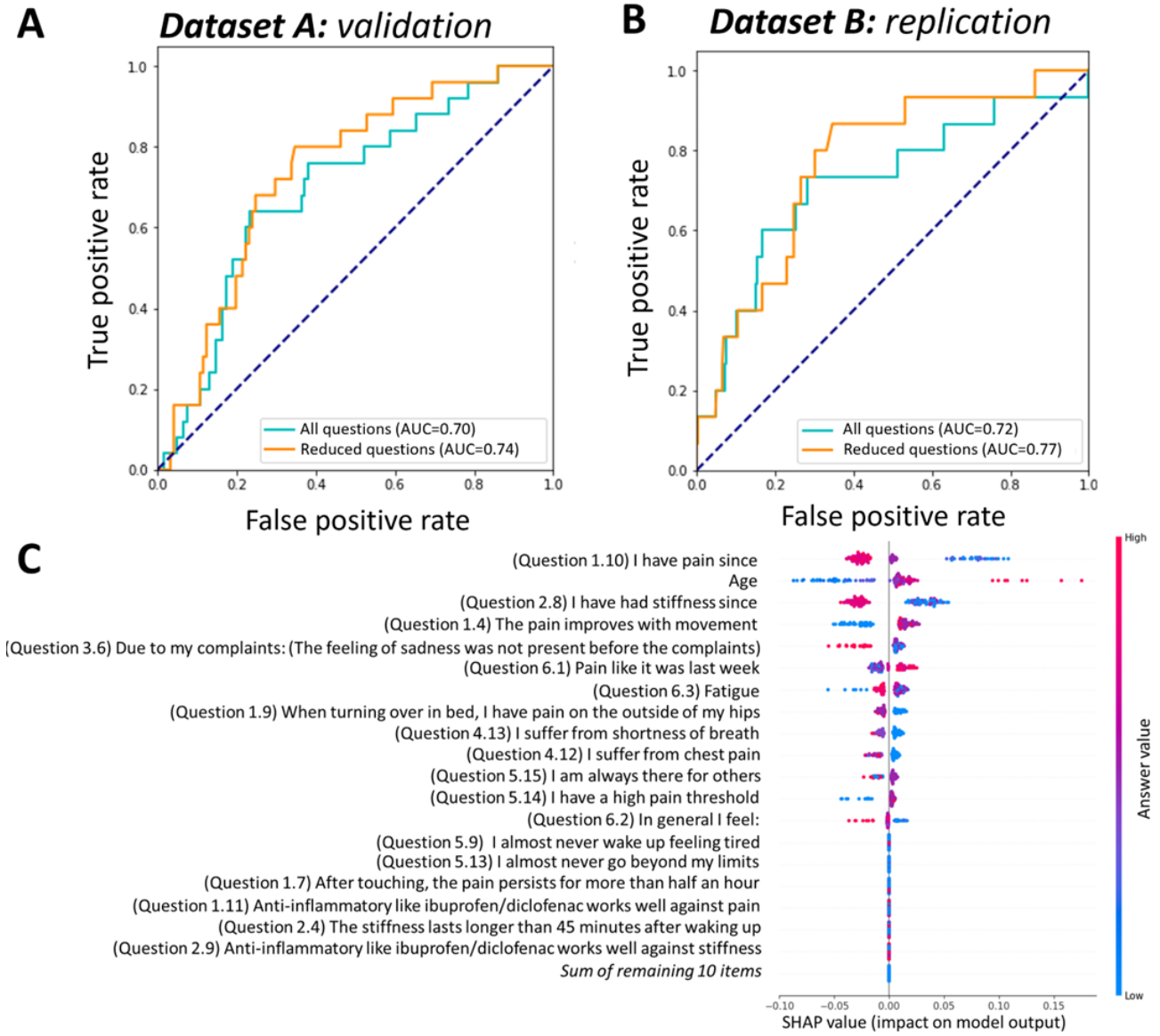
Figure 4. Performance of the fibromyalgia classifier: (A) receiver operating characteristic (ROC) curves showing performance before and after regularization in the validation set, (B) ROC curves showing performance before and after regularization in the replication set, and (C) Shapley Additive Explanation (SHAP) analysis results highlighting the impact and direction of the most important features contributing to the classifier's predictions. AUC: area under the curve.



For RA—a critical target for early rheumatology intervention—our model showed moderate discrimination, with AUC-ROC values of 0.74 (95% CI 0.63-0.83) in the development set and 0.77 (95% CI 0.66-0.86) in the external validation set (Figure 5). Key predictors included shorter disease duration (questions 1.10 and 2.8), pain improvement with movement (question 1.4), recent severe pain (question 6.1), onset at middle age or later, and fewer respiratory or chest symptoms (questions 4.13 and 4.12) or hip concerns (question 1.9). The model's primary challenge was differentiating RA from other IRDs with similar presentations, such as reactive arthritis, polymyalgia rheumatica, and gout (Figure 6B in Multimedia Appendix 3).

XSL•FO
RenderX

Figure 5. Performance of the rheumatoid arthritis classifier: (A) receiver operating characteristic (ROC) curves showing performance before and after regularization in the validation set, (B) ROC curves showing performance before and after regularization in the replication set, and (C) Shapley Additive Explanation (SHAP) analysis results highlighting the impact and direction of the most important features contributing to the classifier's predictions. AUC: area under the curve.



Discussion

Principal Findings

Our results demonstrate that the FRYQ can effectively distinguish between IRDs and noninflammatory musculoskeletal concerns before patients' first rheumatology consultation. The model achieved robust performance, with an AUC-ROC of 0.71 in the development dataset and 0.72 in the external validation dataset, indicating good generalizability. Importantly, we found that a reduced set of just 28 questions from the original 67 closed-ended items maintained equivalent discriminative power, suggesting potential for a more efficient screening tool.

Beyond the primary classification task, our analysis revealed that the FRYQ demonstrates even stronger performance in identifying specific conditions, particularly fibromyalgia (AUC-ROC of 0.85 and 0.81 in the development and replication datasets, respectively). The FRYQ also showed adequate ability to detect RA cases (AUC-ROC of 0.77 in the external validation dataset), although it had more difficulty distinguishing RA from other inflammatory conditions.

These findings have important clinical applications. In settings with limited rheumatology resources, the FRYQ could serve as a triage tool to streamline the large influx of referrals (overreferral) by prioritizing the referred patients with higher probability of inflammatory disease for early specialist intervention. This could result in more efficient allocation of specialist resources, potentially reducing waiting lists for a substantial number of patients with IRD. In light of the anticipated shortage of clinical professionals, it is increasingly important to identify which patients truly need rheumatologists' care versus those who can be managed elsewhere [18].

For example, the FRYQ's ability to identify fibromyalgia among the rheumatology waiting list could help redirect these patients to alternative care providers instead (pain specialists, physiotherapists, or dedicated programs), freeing capacity at the clinic for patients needing rheumatological care. Currently,

XSL•FO
RenderX

rheumatologists spend substantial time on patients they cannot effectively treat as approximately 60% of rheumatology referrals involve noninflammatory conditions (such as fibromyalgia) [10]. This optimized allocation may also offer an additional benefit: the extra capacity created could reduce primary care physicians' reluctance to refer clinically ambiguous cases that would benefit from specialist input.

Finally, the FRYQ could aid clinicians in their decision to request extra laboratory workup. When responses suggest RA, clinicians could order relevant serological markers (anticitrullinated protein antibody, rheumatoid factor, C-reactive protein, and erythrocyte sedimentation rate) before the initial visit, potentially streamlining the diagnostic process and reducing time to treatment for conditions requiring early intervention [4-7].

The clinical threshold of 0.30 that we identified balances sensitivity (capturing 71%-76% of inflammatory cases) with reasonable specificity (49%-56%), making it suitable for initial screening where missing IRD cases would be more concerning than false positives. As reported by Graydon and Thompson [19], primary care physicians and rheumatologists frequently disagree on referral urgency (47%), with rheumatologists upgrading 17% of referrals to urgent status—cases initially overlooked by GPs. This underlines the potential value of applying such a threshold in practice, although adjustments may be required depending on local context, such as disease prevalence and health care setting.

Our findings align with the growing recognition that structured questionnaires can support diagnostic decision-making in rheumatology by systematically capturing and integrating patients' own experiences and symptom descriptions. While over 100 symptom checkers currently exist [20], their adoption has remained limited due to lack of validation or suboptimal diagnostic accuracy [20,21]. Therefore, the availability of a validated tool such as the FRYQ may fulfill a need in the field. As far as we know, this is the first questionnaire developed in the Netherlands for triaging musculoskeletal concerns that has been validated using real-world patient data.

The predictive factors identified in our SHAP analysis align with established clinical knowledge. Pain improvement with movement, shorter morning stiffness duration, and good response to nonsteroidal anti-inflammatory drugs all emerged as important indicators of inflammatory disease [22-24]. The association between inflammatory bowel disease and IRDs supports known connections between these conditions [25]. For fibromyalgia, we observe that patients report sleep problems, persistent pain, and fatigue [26].

Beyond questionnaires, there have been other digital approaches proposed in the literature for improving rheumatology triage. Natural language processing (NLP) of referral letters has shown promising results in studies from the United Kingdom [27] and the Netherlands [28], potentially complementing questionnaire-based methods. Similarly, patient-reported outcomes have been investigated, although Schäfer et al [29] found these to be less effective at distinguishing inflammatory from noninflammatory rheumatic conditions.

Study Limitations

Several limitations of this study should be acknowledged. First, while we validated our model in an external dataset, both cohorts originated from the same medical center, potentially limiting generalizability to different health care settings or patient populations. Second, we observed a rather big difference in prevalence of inflammatory conditions (257/582, 44.2% vs 93/350, 26.6%). This affected the model's calibration in external validation, suggesting the need for recalibration when applying to populations with different disease prevalence.

These prevalence differences likely stem from distinct patient selection mechanisms. Dataset A included patients with prescheduled outpatient appointments who completed the questionnaire during their first visit as part of routine care in Medical Center Leeuwarden (approximately 70% of referrals). In contrast, dataset B comprised volunteers from the JPAST study (approximately 40% of referrals). The time-consuming study procedures of the JPAST study likely led to an overrepresentation of nonurgent (non-IRD) cases among the volunteers.

We should also acknowledge that our model showed moderate discriminative ability (AUC of approximately 0.72) rather than excellent performance. Therefore, it could not reliably distinguish certain conditions such as spondyloarthritis from noninflammatory diseases. Rare inflammatory conditions were also underrepresented.

Crucially, our study was tailored to patients already referred to rheumatologists with the goal of optimizing the time from referral to specialist consultation. This means that the FRYQ cannot be used as a prescreening tool at GP offices. Importantly, it was not designed to exclude patients from care but rather to guide referred patients to the most appropriate care providers and streamline referral pathways.

Future Directions

To definitively establish the FRYQ's clinical utility, we propose conducting a randomized clinical trial in the future to assess whether FRYQ-guided triage leads to faster appropriate treatment, reduced unnecessary appointments, and improved patient satisfaction. Furthermore, our study would benefit from additional replication in other countries to assess how health care system differences affect its effectiveness. Referral rates and treatment protocols vary substantially between countries—for instance, 21% of patients with musculoskeletal conditions are referred to specialists in Spain compared to 11% in the Netherlands and 5% in Sweden [30].

In the future, we also plan to incorporate NLP techniques to leverage open-ended questions as they may capture nuanced symptom descriptions that structured items tend to miss. Modern NLP methods, including large language models, show potential for supporting triage [31] and the identification of rare or unrecognized diseases using free-text data [32,33]. For spondyloarthritis in particular, large language models could be prompted with educational information on axial spondyloarthritis recognition to improve detection.

XSL•FO
RenderX

Finally, we may enhance the questionnaire by incorporating questions on occupational stress given that it is a known predictor of non-IRD [34,35]. Further refinement could also involve integrating FRYQ scores with serological markers and imaging to create a comprehensive multimodal prediction model. This multimodal approach might overcome some limitations of questionnaire-based triage alone, particularly for discerning conditions with overlapping symptomatology (ie, overlapping symptoms of osteoarthritis and early RA [36]).

Conclusions

The FRYQ shows promise in distinguishing inflammatory from noninflammatory rheumatic conditions in newly referred patients, particularly fibromyalgia and RA, before specialist assessment. While not a substitute for clinical judgment, this tool could help optimize the time from referral to specialist consultation by prioritizing cases likely to involve IRDs and guiding others toward alternative care pathways or additional laboratory testing. These potential benefits merit evaluation in prospective implementation studies, especially given the projected shortage of rheumatology professionals.

Acknowledgments

The authors thank all participants of the study for filling out the Frysian Questionnaire for Differentiation of Musculoskeletal Complaints. The authors also want to extend their thanks to the data managers and the outpatient clinic secretariat.

Funding

This study received funding from the Netherlands Organisation for Health Research and Development Clinical Fellowship (40-00703-97-19069), and the SPIDeRR-NL project (Stratification of Patients using advanced Integrative modeling of Data Routinely acquired for diagnosing Rheumatic complaints in the Netherlands), which was granted by the Netherlands Organisation for Health Research and Development Open Competition (activity 09120012110075).

Data Availability

The datasets generated or analyzed during this study are available from the corresponding author on reasonable request. The corresponding code is publicly available on a GitHub repository [37].

Authors' Contributions

FR, AaH, AS, DZ, FW, LH, and RB were responsible for data collection and processing. TDM conducted the machine learning analysis. RK, TDM, RB, and FR interpreted the results. TDM and FR drafted the initial version of the manuscript, which was further developed by RK and RB. All authors reviewed and approved the final version of the manuscript for submission.

Conflicts of Interest

RB has received research grants from Galapagos and Sanofi; has served on the speaker bureau for Galapagos and Janssen; and has received consulting fees from AbbVie, Galapagos, Pfizer, and UCB. All other authors declare no other conflicts of interest.

Multimedia Appendix 1
The original Frysian Questionnaire for Differentiation of Musculoskeletal Complaints in Dutch.
[DOCX File, 89 KB - medinform_v13i1e77345_app1.docx]

Multimedia Appendix 2
Table comprising the English translation of all original Dutch questions from the Frysian Questionnaire for Differentiation of Musculoskeletal Complaints.
[DOCX File, 20 KB - medinform_v13i1e77345_app2.docx]

Multimedia Appendix 3
Supplementary results supporting the main analysis, including patient selection details, model optimization procedures, comprehensive performance metrics and calibration analyses, the final questionnaire items selected by the model, and results from disease-specific classification models.
[PDF File, 838 KB - medinform_v13i1e77345_app3.pdf]

References

1. van der Linden MW, Westert GP, Schellevis F. Tweede nationale studie naar ziekten en verrichtingen in de huisartspraktijk: klachten en aandoeningen in de bevolking en in de huisartspraktijk [Report in Dutch]. : NIVEL/RIVM; 2004 URL: https://www.nivel.nl/sites/default/files/bestanden/ns2_r1_h02.pdf [accessed 2025-11-05]

XSL•FO
RenderX

2. GBD 2019 Diseases and Injuries Collaborators. Global burden of 369 diseases and injuries in 204 countries and territories, 1990-2019: a systematic analysis for the global burden of disease study 2019. Lancet 2020 Oct 17;396(10258):1204-1222. [doi: 10.1016/S0140-6736(20)30925-9] [Medline: 33069326]
3. NHG-richtlijnen [Web page in Dutch]. Nederlands Huisartsen Genootschap. 2023. URL: https://richtlijnen.nhg.org/ [accessed 2025-07-28]
4. Saalfeld W, Mixon AM, Zelie J, Lydon EJ. Differentiating psoriatic arthritis from osteoarthritis and rheumatoid arthritis: a narrative review and guide for advanced practice providers. Rheumatol Ther 2021 Dec;8(4):1493-1517. [doi: 10.1007/s40744-021-00365-1] [Medline: 34519965]
5. Nell VPK, Machold KP, Eberl G, Stamm TA, Uffmann M, Smolen JS. Benefit of very early referral and very early therapy with disease-modifying anti-rheumatic drugs in patients with early rheumatoid arthritis. Rheumatology (Oxford) 2004 Jul;43(7):906-914. [doi: 10.1093/rheumatology/keh199] [Medline: 15113999]
6. Malaviya AP, Ostor AJK. Early diagnosis crucial in ankylosing spondylitis. Practitioner 2011 Dec;255(1746):21-24. [Medline: 22272527]
7. van der Linden MPM, le Cessie S, Raza K, et al. Long-term impact of delay in assessment of patients with early arthritis. Arthritis Rheum 2010 Dec;62(12):3537-3546. [doi: 10.1002/art.27692] [Medline: 20722031]
8. Spending on health care up by 8.1 percent in 2024. Centraal Bureau voor de Statistiek. 2025. URL: https://www.cbs.nl/en-gb/news/2025/22/spending-on-health-care-up-by-8-1-percent-in-2024 [accessed 2025-08-29]
9. van der Waal JM, Bot SDM, Terwee CB, van der Windt D, Bouter LM, Dekker J. Determinants of the clinical course of musculoskeletal complaints in general practice: design of a cohort study. BMC Musculoskelet Disord 2003 Feb 24;4:3. [doi: 10.1186/1471-2474-4-3] [Medline: 12600275]
10. Stack RJ, Nightingale P, Jinks C, et al. Delays between the onset of symptoms and first rheumatology consultation in patients with rheumatoid arthritis in the UK: an observational study. BMJ Open 2019 Mar 4;9(3):e024361. [doi: 10.1136/bmjopen-2018-024361] [Medline: 30837252]
11. Raza K, Stack R, Kumar K, et al. Delays in assessment of patients with rheumatoid arthritis: variations across Europe. Ann Rheum Dis 2011 Oct;70(10):1822-1825. [doi: 10.1136/ard.2011.151902] [Medline: 21821867]
12. Knitza J, Knevel R, Raza K, et al. Toward earlier diagnosis using combined eHealth tools in rheumatology: the joint pain assessment scoring tool (JPAST) project. JMIR Mhealth Uhealth 2020 May 15;8(5):e17507. [doi: 10.2196/17507] [Medline: 32348258]
13. Act of 26 February 1998 on medical-scientific research involving human subjects (Medical Research Involving Human Subjects Act, WMO). Dutch Official Gazette. 1998. URL: https://wetten.overheid.nl/BWBR0009408/2025-01-01 [accessed 2025-11-04]
14. Snoek J, Larochelle H, Adams RP. Practical Bayesian optimization of machine learning algorithms. arXiv. Preprint posted online on Jun 13, 2012. [doi: 10.48550/arXiv.1206.2944]
15. Chen T, Guestrin C. XGBoost: a scalable tree boosting system. In: Krishnapuram B, Shah M, editors. KDD '16: Proceedings of the 22nd ACM SIGKDD International Conference on Knowledge Discovery and Data Mining:785-794. [doi: 10.1145/2939672.2939785]
16. Grinsztajn L, Oyallon E, Varoquaux G. Why do tree-based models still outperform deep learning on typical tabular data. In: Koyejo S, Mohamed S, Agarwal A, Belgrave D, Cho K, Oh A, editors. NIPS '22: Proceedings of the 36th International Conference on Neural Information Processing Systems 2022:507-520.
17. Roth AE, editor. The Shapley Value: Essays in Honor of Lloyd S Shapley: Cambridge: Cambridge University Press; 1988. [doi: 10.1017/CBO9780511528446]
18. Miloslavsky EM, Marston B. The challenge of addressing the rheumatology workforce shortage. J Rheumatol 2022 Jun;49(6):555-557. [doi: 10.3899/jrheum.220300] [Medline: 35428725]
19. Graydon SL, Thompson AE. Triage of referrals to an outpatient rheumatology clinic: analysis of referral information and triage. J Rheumatol 2008 Jul;35(7):1378-1383. [Medline: 18484689]
20. Hügle M, Omoumi P, van Laar JM, Boedecker J, Hügle T. Applied machine learning and artificial intelligence in rheumatology. Rheumatol Adv Pract 2020;4(1):rkaa005. [doi: 10.1093/rap/rkaa005] [Medline: 32296743]
21. Knitza J, Mohn J, Bergmann C, et al. Accuracy, patient-perceived usability, and acceptance of two symptom checkers (Ada and Rheport) in rheumatology: interim results from a randomized controlled crossover trial. Arthritis Res Ther 2021 Apr 13;23(1):112. [doi: 10.1186/s13075-021-02498-8] [Medline: 33849654]
22. Brorsson S, Hilliges M, Sollerman C, Nilsdotter A. A six-week hand exercise programme improves strength and hand function in patients with rheumatoid arthritis. J Rehabil Med 2009 Apr;41(5):338-342. [doi: 10.2340/16501977-0334] [Medline: 19363566]
23. Baillet A, Payraud E, Niderprim VA, et al. A dynamic exercise programme to improve patients' disability in rheumatoid arthritis: a prospective randomized controlled trial. Rheumatology (Oxford) 2009 Apr;48(4):410-415. [doi: 10.1093/rheumatology/ken511] [Medline: 19211654]
24. Crofford LJ. Use of NSAIDs in treating patients with arthritis. Arthritis Res Ther 2013;15 Suppl 3(Suppl 3):S2. [doi: 10.1186/ar4174] [Medline: 24267197]

XSL•FO
RenderX

25. Salvarani C, Vlachonikolis IG, van der Heijde DM, et al. Musculoskeletal manifestations in a population-based cohort of inflammatory bowel disease patients. Scand J Gastroenterol 2001 Dec;36(12):1307-1313. [doi: 10.1080/003655201317097173] [Medline: 11761022]
26. Chinn S, Caldwell W, Gritsenko K. Fibromyalgia pathogenesis and treatment options update. Curr Pain Headache Rep 2016 Apr;20(4):25. [doi: 10.1007/s11916-016-0556-x] [Medline: 26922414]
27. Wang B, Li W, Bradlow A, Bazuaye E, Chan ATY. Improving triaging from primary care into secondary care using heterogeneous data-driven hybrid machine learning. Decis Support Syst 2023 Mar;166:113899. [doi: 10.1016/j.dss.2022.113899]
28. Maarseveen TD, Glas HK, Veris-van Dieren J, van den Akker E, Knevel R. Improving musculoskeletal care with AI enhanced triage through data driven screening of referral letters. NPJ Digit Med 2025 Feb 14;8(1):98. [doi: 10.1038/s41746-025-01495-4] [Medline: 39948271]
29. Schäfer A, Kovacs MS, Nigg A, Feuchtenberger M. Patient-reported outcomes of depression and fibromyalgia symptoms do not predict non-inflammatory versus inflammatory diagnoses at initial rheumatology consultation. Healthcare (Basel) 2024 Sep 29;12(19):1948. [doi: 10.3390/healthcare12191948] [Medline: 39408128]
30. Gomon G, Raffray M, Pérez - Sancristóbal I, et al. POS0433 comparison of musculoskeletal referral pathways across EUROPE. Ann Rheum Dis 2025 Jun;84(Suppl 1):664-665. [doi: 10.1016/j.ard.2025.05.819]
31. Krusche M, Callhoff J, Knitza J, Ruffer N. Diagnostic accuracy of a large language model in rheumatology: comparison of physician and ChatGPT-4. Rheumatol Int 2024 Feb;44(2):303-306. [doi: 10.1007/s00296-023-05464-6] [Medline: 37742280]
32. Wu J, Dong H, Li Z, et al. A hybrid framework with large language models for rare disease phenotyping. BMC Med Inform Decis Mak 2024 Oct 8;24(1):289. [doi: 10.1186/s12911-024-02698-7] [Medline: 39375687]
33. Shyr C, Hu Y, Bastarache L, et al. Identifying and extracting rare diseases and their phenotypes with large language models. J Healthc Inform Res 2024 Jun;8(2):438-461. [doi: 10.1007/s41666-023-00155-0] [Medline: 38681753]
34. Soteriades ES, Psalta L, Leka S, Spanoudis G. Occupational stress and musculoskeletal symptoms in firefighters. Int J Occup Med Environ Health 2019 Jun 14;32(3):341-352. [doi: 10.13075/ijomeh.1896.01268] [Medline: 30938370]
35. Kivimäki M, Leino-Arjas P, Virtanen M, et al. Work stress and incidence of newly diagnosed fibromyalgia: prospective cohort study. J Psychosom Res 2004 Nov;57(5):417-422. [doi: 10.1016/j.jpsychores.2003.10.013] [Medline: 15581643]
36. Lewis KL, Battaglia PJ. Differentiating bilateral symptomatic hand osteoarthritis from rheumatoid arthritis using sonography when clinical and radiographic features are nonspecific: a case report. J Chiropr Med 2019 Mar;18(1):56-60. [doi: 10.1016/j.jcm.2018.07.005] [Medline: 31193241]
37. Maarseveen TD. FRYQ. Github. URL: https://github.com/levrex/FRYQ [accessed 2025-11-13]

Abbreviations

AUC-ROC: area under the receiver operating characteristic curve
FRYQ: Frysian Questionnaire for Differentiation of Musculoskeletal Complaints
GP: general practitioner
IRD: inflammatory rheumatic disease
JPAST: Joint Pain Assessment Scoring Tool
NLP: natural language processing
RA: rheumatoid arthritis
SHAP: Shapley Additive Explanations
WMO: Wet medisch-wetenschappelijk onderzoek met mensen

Edited by J Klann; submitted 13.05.25; peer-reviewed by M Raffray, O Sander; revised version received 01.10.25; accepted 01.10.25; published 17.11.25.

Please cite as:
Maarseveen TD, Reimann F, al Hasan A, Schilder A, Zhang D, Wink F, Hendriks L, Knevel R, Bos R
Evaluating the Accuracy of the Frysian Questionnaire for Differentiation of Musculoskeletal Complaints for Triage of Musculoskeletal Diseases: Algorithm Development and Validation Study
JMIR Med Inform 2025;13:e77345
URL: https://medinform.jmir.org/2025/1/e77345
doi:10.2196/77345

© Tjardo Daniël Maarseveen, Floor Reimann, Ahmed al Hasan, Annemarie Schilder, Dan Zhang, Freke Wink, Lidy Hendriks, Rachel Knevel, Reinhard Bos. Originally published in JMIR Medical Informatics (https://medinform.jmir.org), 17.11.2025. This

XSL•FO
RenderX

is an open-access article distributed under the terms of the Creative Commons Attribution License (https://creativecommons.org/licenses/by/4.0/), which permits unrestricted use, distribution, and reproduction in any medium, provided the original work, first published in JMIR Medical Informatics, is properly cited. The complete bibliographic information, a link to the original publication on https://medinform.jmir.org/, as well as this copyright and license information must be included.

XSL•FO
RenderX

Predicting 30-Days Hospital Readmission for Patients with Heart Failure Using Electronic Health Record Embeddings: Comparative Evaluation

Prabin Shakya[1], MSc; Ayush Khaneja[1], MSc; Kavishwar B Wagholikar[1,2], PhD, MD

[1]Laboratory of Computer Science, Massachusetts General Hospital, 399 Revolution Drive, 7th Floor, Boston, MA, United States

[2]Harvard Medical School, Boston, MA, United States

Corresponding Author:
Prabin Shakya, MSc
Laboratory of Computer Science, Massachusetts General Hospital, 399 Revolution Drive, 7th Floor, Boston, MA, United States

Abstract

Background: Heart failure (HF) is a public health concern with a wider impact on quality of life and cost of care. One of the major challenges in HF is the higher rate of unplanned readmissions and suboptimal performance of models to predict the readmissions. Hence, in this study, we implemented embeddings-based approaches to generate features for improving model performance.

Objective: The objective of this study was to evaluate and compare the effectiveness of different feature embedding approaches for improving the prediction of unplanned readmissions in patients with heart failure.

Methods: We compared three embedding approaches including *word2vec* on terminology codes and concept unique identifier (CUIs) and BERT on descriptive text of concept with baseline (one hot-encoding). We compared area under the receiver operating characteristic (AUROC) and F_1-scores for the logistic regression, eXtream gradient-boosting (XGBoost) and artificial neural network (ANN) models using these embedding approaches. The model was tested on the heart failure cohort (N=21,031) identified using least restrictive phenotyping methods from MIMIC-IV dataset.

Results: We found that the embedding approaches significantly improved the performance of the prediction models. The XGBoost performed better for all approaches. The *word2vec* embeddings (0.65) trained on the dataset outperformed embeddings from pre-trained BERT model (0.59) using descriptive text.

Conclusions: Embedding methods, particularly *word2vec* trained on electronic health record data, can better discriminate HF readmission cases compared to both one-hot encoding and pre-trained BERT embeddings on concept descriptions making it a viable approach of automation feature selection. The observed AUROC improvement (0.65 vs 0.54) may support more effective risk stratification and targeted clinical interventions.

(JMIR Med Inform 2025;13:e73020) doi:10.2196/73020

KEYWORDS

heart failure; machine learning; embedding techniques; electronic health record; EHR; hospital readmission

Introduction

Heart Failure (HF) is a major and growing public health concern, affecting around 3% of the adult population of high-income countries, with increasing prevalence in low and middle-income countries [1,2]. It is estimated that 56.2 million people worldwide are affected by HF [2]. HF is also associated with high rates of unplanned readmissions, which strain the health care system and diminish patient quality of life. The 1-year readmission rate is as high as 53% globally and 59% in the United States [3]. Given the significant burden imposed by readmissions, healthcare providers strive to identify patients with HF at risk for readmission. Several predictive models have been developed for this purpose, including traditional statistical models and machine learning models. However, their predictive performance remains suboptimal in real-world applications, with area under the receiver operating characteristic curve (AUROC) of 0.6 when using electronic health record (EHR) data [4].

Medical codes such as International Classification of Diseases (ICD) codes, procedure codes, and medication identifiers vary in structure and granularity, introducing complexity and high dimensionality into the data. These high-dimensional spaces make it difficult to extract meaningful patterns for prediction. Natural language processing and embedding techniques such as word2vec and BERT offer a promising approach to address these challenges by transforming discrete medical codes into continuous vector representations. These embeddings capture

XSL•FO
RenderX

semantic relationships between medical codes, enabling models to understand the similarities and differences between related diagnoses and procedures [5,6]. Several studies have demonstrated that embedding methods may improve the performance of predictive models in healthcare by reducing dimensionality while preserving relevant clinical information [6,7].

To address these challenges, our study, investigates the utility of EHR embedding techniques and their performance in the prediction of 30-day hospital readmissions among patients with HF, leveraging the open data available in MIMIC-IV dataset. The 30-day readmission metric is widely used in healthcare policy and quality assessment. In the United States, the Center of Medicare and Medicaid Services includes this metric in the Hospital Readmissions Reduction Program, which penalizes hospital excess readmissions [8]. As such, accurate prediction of 30-day readmissions risk has direct implications for hospital reimbursement and patient care planning.

We compared two embedding approaches: (1) *word2vec* embeddings trained on terminology codes and Unified Medical Language System (UMLS) Concept Unique Identifier (CUIs) and (2) BERT embeddings derived from concept descriptors. We hypothesize that embeddings derived from structured medical codes capture patient-level clinical patterns more effectively than embeddings generated from descriptive text. This is because code-based embeddings reflect co-occurrence and usage patterns in real clinical settings, while text-based embeddings may lack the specificity and contextual relevance needed for structured prediction tasks.

Word2vec is a widely used embedding technique used to represent words (or codes) in a vector space, trained using shallow neural networks on text corpora [9], In the clinical domain, word2vec has been successfully used to embed medical concepts from EHR data [10-12]. In contrast, BERT is a transformer-based language model that generates contextualized embeddings by capturing the position and surrounding context of each word [13]. BERT and its biomedical adaptations such as BioBERT and BioClinicalBERT have shown promise for a range of tasks in biomedical and clinical domains [14-17]. Among these, BioBERT is pretrained on PubMed abstracts, while BioClinicalBERT extends it with clinical narratives from MIMIC. Lee et al [6] demonstrated that textual descriptions of ICD codes can be effectively used for semantic-preserving vector representations.

While BERT provides contextualized embeddings that excel in natural language understanding, its effectiveness in representing brief and structured medical concept descriptions remain uncertain. In contrast, word2vec, trained on real-world sequences of medical codes, may better capture clinically relevant co-occurrence patterns. In this study, we aim to empirically evaluate whether code-based embeddings (eg, word2vec on medical codes) outperform text-based embeddings (eg, BERT on concept descriptions) in predicting 30-day hospital readmissions, given the structured nature of EHR data.

Methods

Study design

For this study, we used Medical Information Mart for Intensive Care (MIMIC)-IV version 2.2, a publicly available dataset released in January 2023. The MIMIC-IV dataset contains comprehensive, de-identified EHR data for patients admitted to the Beth Israel Deaconess Medical Center between 2008 and 2019. The dataset includes 299,712 patients and 431,231 hospital admissions [18]. Diagnoses are coded using the ICD, with both 9th and 10th Clinical Modification (CM) revisions. Procedures are recorded using both *ICD*-9 and *ICD*-10 Procedure Coding System codes. Medications are recorded with the National Drug Code (NDC) along with the Drug name, route, strength, etc. To develop predictive models for HF readmission, we used data from the hospital module capturing demographic information, diagnosis, medication and procedure codes.

We identified patients with HF using the least restrictive phenotyping method, which defines HF-positive cases as any patient with at least one relevant *ICD*-9 or *ICD*-10 code for HF [19]. We included HF-positive patients only for this study. 30-day readmission was defined as any subsequent admission occurring within 30 days of discharge, regardless of the reason for readmission. Patients were excluded from the cohort if they died (n=1475), or the length of stay was less than one day (n=1740) at the indexed admission. The exclusion criteria were applied because patients who died during the index admission were not at risk for readmission, and the definition of ‘inpatient’ becomes ambiguous for patients with hospital stay of less than one day. Admission occurring after the index admission were also excluded, as our objective was to predict readmission following the index HF hospitalization.

Data preprocessing was structured into three main components: admissions, clinical data extraction, and embedding preparation:

1. Admissions: Admissions were categorized as indexed, historic, and future admissions. Indexed admissions were defined as the first hospitalization with a diagnosis of HF. All the admissions prior to indexed admissions were classified historic admission and any subsequent hospitalizations as future admissions. We only developed models for predicting readmission after the index admissions. We included age at admission, length of stay and gender from indexed admissions as features.
2. Clinical Data extraction: We extracted diagnoses, procedures, and medications from structured data for selected cohorts. These were split into current if date of record corresponds to the index admission and historic if it precedes the indexed admissions. We applied different encoding or embedding methods to these extracted data. We applied one-hot encoding for baseline. The embeddings approaches applied are described below. The current and historic data are combined with indexed admission features to create the final features sets (Figure 1).
3. Embedding: We applied three embedding approaches to the feature matrix to capture the semantic representations in the data, to output a new feature matrix.

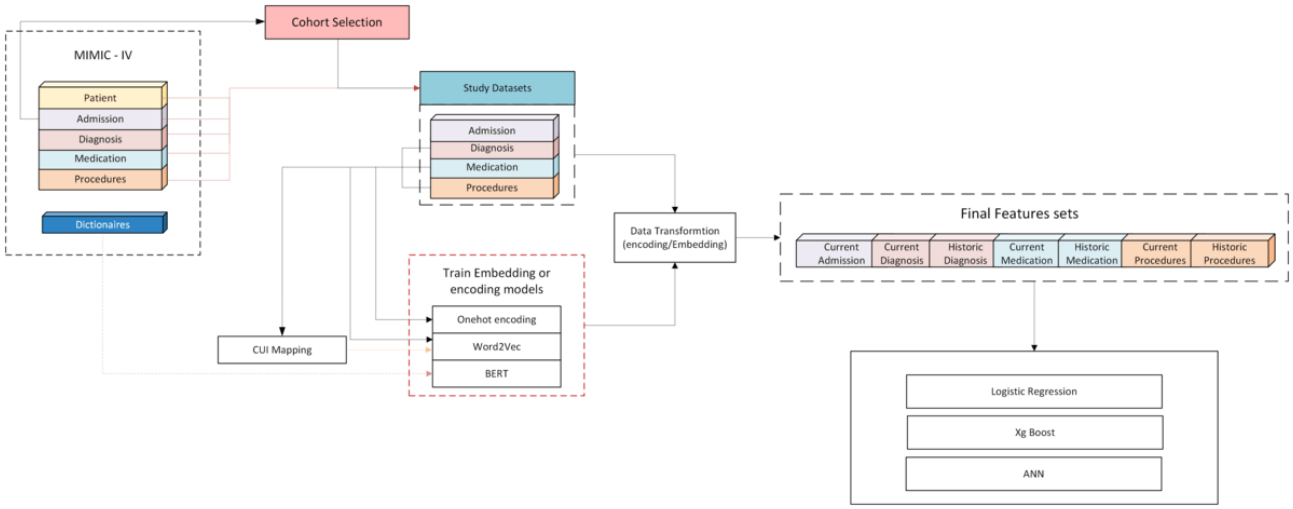
XSL•FO
RenderX

a. Word2Vec on Terminology Codes: ICD codes were concatenated with their version (ICD-9 or ICD-10) to form unique identifiers that account for overlapping codes between the two versions. For medications, we used NDC codes, excluding drugs that lacked NDC identifiers. Each unique code (diagnosis, procedure, or medication) was treated as a word, and the list of codes for each patient encounter was considered as a document. The word2vec model was trained using the skip-gram with negative sampling (SGNS) algorithm. The subset of training dataset was used to finetune parameters for word2vec (please refer to Table S1 in Multimedia Appendix 1 and Figure 1). Based on the finetuning experiments, we selected the context window size of 10, resulting in 200-dimensional embedding vectors. Separate *word2Vec* models were trained for diagnoses, procedures, and medications.

b. Word2Vec on UMLS CUIs: To map ICD and procedure codes to UMLS CUIs, we implemented a hybrid code and string-matching approach. First, codes were matched directly to UMLS using a code-matching algorithm. For unmapped code, we truncated the first three characters and attempted matching again. If multiple CUIs were returned, we selected the most generic code. For Medications, NDC codes were matched and for unmapped codes, we used a string search from the drug name. These mapped CUIs were then treated as 'word' and trained in the same manner as recorded medical codes using Word2Vec.

c. BERT on Descriptive Text: For each medical code, we utilized its long-form descriptor to generate embeddings using pre-trained BERT models. We used BioClinicalBERT, which is specialized for clinical texts, to generate context-aware embeddings from the long descriptions provided in the MIMIC-IV datasets. For medication, as long descriptions were not available, we created one by concatenating multiple columns (drug, prod_strength, dose_val_rx, dose_unit_rx, form_val_disp, form_unit_disp and route) from the prescriptions table for example - "Docusate Sodium 100 mg Tablet 100 mg 1 Tab 2.0 Oral." This approach captures semantic meaning and context-specific nuances that are often lost when only the codes are used.

Figure 1. Graphical summary of the Study. CUI: Concept Unique Identifiers ; MIMIC-IV: Medical Information Mart for Intensive Care - IV (Database).



We developed multiple machine-learning models to predict 30-day readmissions. The embeddings generated from each approach were used as input features for these models. We trained and evaluated three machine learning algorithm—logistic regression, and eXtream gradient-boosting (XGBoost) and artificial neural network (ANN). A feedforward ANN consisting of three fully connected layers with Tanh activation and dropout for regularization with progressively reduced dimensionality and outputs a probability via a final sigmoid activation was implemented. Like *word2vec* parameters finetuning, we run multiple experiments with a combination of different parameters and oversampling of minor classes using Synthetic Minority Oversampling Technique (SMOTE). Model performance was assessed using standard metrics such as Area under the receiver operating characteristic curve (AUROC), and F_1-score. (please refer to supplement file in Multimedia Appendix 1 for the link to the source code).

Ethical Considerations

The study used the MIMIC dataset, which contains deidentified health-related data and is publicly available through PhysioNet platform. Access to the dataset requires completion of the "Data or Specimen Only Research" course and acceptance of the data use agreement. The institutional review board at Mass General Brigham determined that the project does not meet the criteria for human subject research, as the dataset used does not contain any identifiable patient information. Since this study used an open dataset available in the public domain that was published by another research group, informed consent and opt-out procedures were managed by the original investigators. Therefore, no direct consent or interaction with participants was required for this study.

XSL•FO
RenderX

Results

A total of 21,031 patients were included in the study with 3933 (19%) experiencing a 30-day readmission. This cohort was randomly split into training with 14721 patients (70%), test with 3155 patients (15%), and validation with 3155 patients (15%) sets (Figure 2). The average age at indexed admission was 73 years, the mean number of admissions was 2, the mean number of ICD codes used was 25 and the mean length of stay is 8 days. The number of admissions (P<.001, t-statistic=10.83), number of ICD codes (P<.001, t-statistic=12.71), and length of stay (P<.001, t-statistic=10.41) are higher among patients with 30-day readmission, and there is no significant difference in age at index admission (P=.40, t-statistic=−0.851) and the number of male versus female (P=.63, odds ratio =1.017). This is true in all splits of datasets as well (Table 1). The rate of 30-day readmission was 19% in the Cohort, 19% in the Train dataset, 17% in the test set, and 19% in the validate set.

Figure 2. Flow diagram study cohort selection. *The total number of unique excluded patients accounts for 86 individuals who met both exclusion criteria.

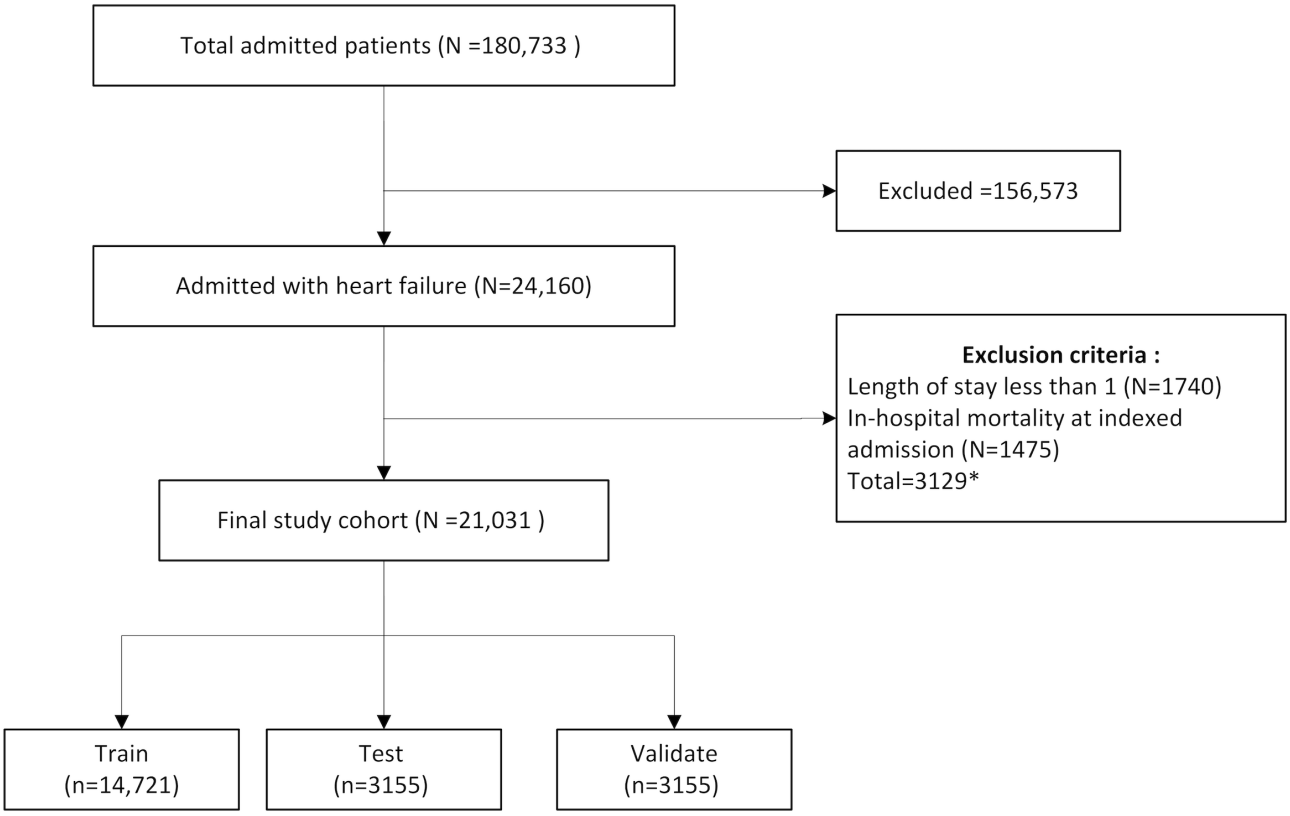


Table . Cohort characteristics (N=21,031).

Variables	Total	Negative	Positive	*P* value
Sex, n				.63[a]
Female	9971	8120	1851	
Male	11,060	8978	2082	
Admissions, mean, (SD)	2.07 (2.88)	1.98 (2.44)	2.52 (4.28)	<.001[b]
ICD codes, mean (SD)	24.59 (18.12)	23.83 (16.93)	27.89 (22.25)	.001[b]
Length of stay, mean (SD)	7.83 (8.57)	7.53 (8.04)	9.11 (10.48)	.001[b]
Age at index admission, mean (SD)	73.36 (13.55)	73.39 (13.55)	73.2 (13.56)	.40[b]
Total	21,031	17,098	3933	—[c]

[a]χ^2 test

[b]t test

[c]Not applicable.

XSL•FO
RenderX

We used one-hot encoding as baselines, which yielded AUROC scores of 0.54 and F_1-scores ranging from 0.24 to 0.26 across validation and test sets. The embedding-based approaches consistently outperformed the baseline across all models. Logistic regression, XGBoost, and ANN models achieved AUROCs ranging from 0.59 to 0.64, 0.59 to 0.65 and 0.59 to 0.64, respectively. Among the embedding strategies, BERT embeddings from descriptive text performed worst, while the best AUROC (0.65) was achieved using *word2vec* on CUIs with XGBoost. F1 scores varied modestly, ranging from 0.32 - 0.37 (validation) and 0.29 - 0.34(test) (Table 2). The best logistic regression results were obtained using L2 regularization with C of 0.01 for both *word2vec* and BERT embeddings. For XGBoost, optimal performance was achieved with max depth of 3 and learning rate of 0.01. For ANN models, a learning rate of 0.001, dropout rate of 0.3, and hidden size of 384 yield the best outcomes across most experiments. Logistic regression and XGBoost performed better without oversampling, whereas the ANN showed improved performance when training set was oversampled to address class imbalance (please refer to Table S2 in Multimedia Appendix 1).

Table . Best results of different experiments by model.

Experiments and models	AUROC[a] validation	F_1 validation	AUROC test	F_1 test
Baseline				
Logistic regression	0.54	0.26	0.54	0.25
XGBoost[b]	0.54	0.25	0.54	0.25
ANN[c,d]	0.54	0.24	0.54	0.24
Word2vec on terminology code				
Logistic regression	0.64	0.37	0.64	0.34
XGBoost	0.65[e]	0.38[e]	0.65[e]	0.33
ANN	0.64	0.37	0.64	0.34
Word2vec on CUIs[f]				
Logistic regression	0.63	0.35	0.62	0.32
XGBoost	0.63	0.36	0.65[e]	0.35[e]
ANN	0.60	0.34	0.61	0.32
BERT on descriptive text				
Logistic regression	0.59	0.32	0.59	0.30
XGBoost	0.59	0.32	0.59	0.29
ANN	0.59	0.33	0.59	0.31

[a]AUROC: area under the receiver operating characteristic curve.

[b]XGBoost: eXtreamextreme gradient-boosting.

[c]Oversampling of training dataset using synthetic minority oversampling technique.

[d]ANN: artificial neural network.

[e]best score.

[f]CUI: Concept Unique Identifier.

Discussion

Principal Findings

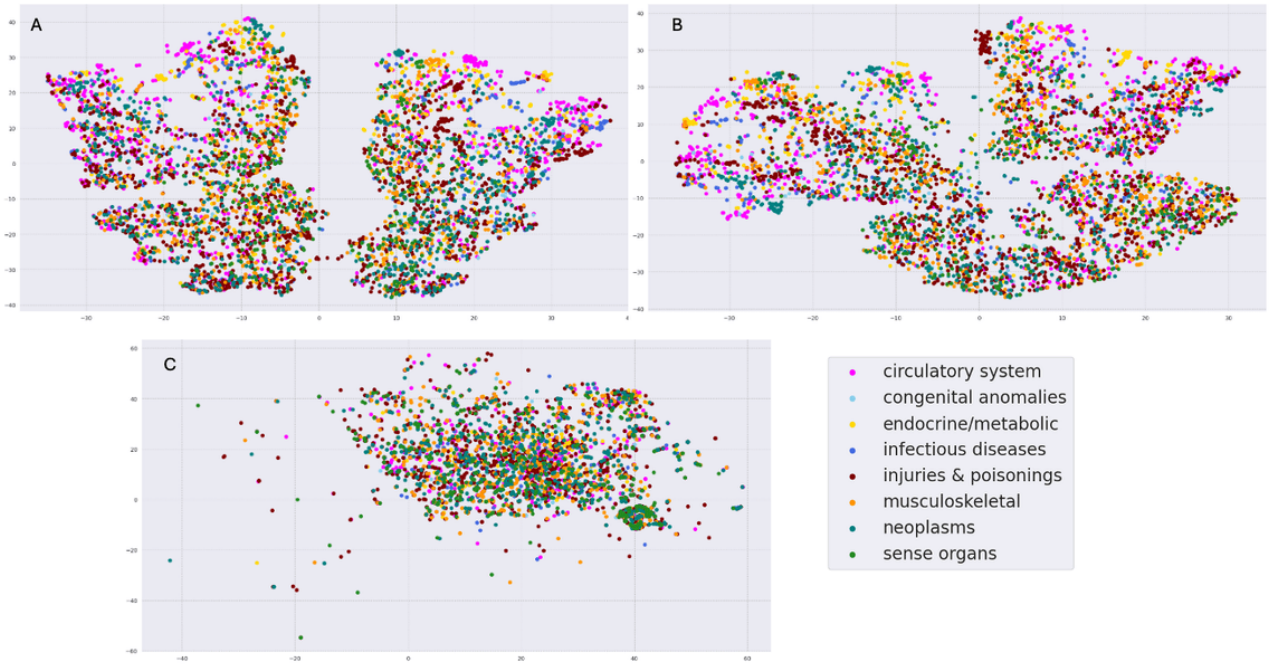
The study presents the systematic comparison of embedding techniques for predicting 30-day heart failure readmission using EHR data. Our analysis of 21,031 heart failure admission from MIMIC-IV dataset demonstrates that the use of *word2vec* embedding trained on the patient data achieved superior performance compared to traditional one-hot-encoding and pretrained language model (BERT).

The *word2vec* on CUIs with XGBoost had AUROC of 0.65, which is substantial improvement of 0.11 over the one-hot-encoding baseline, and modest improvement of 0.06 over pre-trained BioClincial_BERT model. The corresponding F_1-score improvement of 0.10 and 0.04, respectively demonstrates enhanced performance of the word2vec approach.

We investigated the performance gains for word-2-vec using dimensionality reduction analysis. A t-distributed stochastic neighbor embedding (Figure 3) revealed that word2vec embeddings facilitated more coherent clustering of diagnostically related codes, implying superior capture of clinically relevant semantic relationships.

XSL•FO
RenderX

Figure 3. T – SNE plot of diagnosis code embeddings with encoded categories.



A – Word2vec embeddings from Recorded ICD Code; B – Word2vec embedding from CUIs maps; C - embedding obtained using BERT over Descriptors of recorded code.

Overall our findings align with literature in data-driven approaches for readmission prediction [3,7,20,21], while revealing important improvements that can be obtained by using embeddings. However our results were inferior compared to previous studies that utilized expert-crafted features, where the AUROC scores exceeding 0.8 [22,23]. For instance, Pishgar et al [22] reported AUROC of 0.70 using features selected as the event logs with ANNs, and Ben-Assuli et al [23] achieved 0.88 using mix of ML algorithm and expert-selected features with XGBoost. This performance differential highlights the trade-off between automated feature engineering and use of human-experts for feature selection. This is consistent with findings across other clinical areas, where domain expertise has been shown to significantly enhance predictive performance.

Notably, our results suggest that dataset-specific word2vec embeddings may outperform sophisticated pre-trained language models. This is likely because approaches that directly model co-occurrence patterns within the target dataset may capture more task-specific signal as compared to models trained on broader textual corpora.

Overall our study fills a significant gap in the literature by offering a systematic evaluation of embeddings strategies, thereby providing evidence-based guidance for selecting the appropriate embedding method for clinical prediction tasks.

The study has several limitations. Patient encounters were modeled as static collection of medical codes without considering temporal patterns. The study did not evaluate the portability of the models as the dataset is limited to a single institution. Our evaluation focused on traditional machine learning approaches (logistic regression, XGBoost, and ANN), which may not fully exploit the representational capacity of embedding methods. Future research should explore temporal sequence modeling with transformer-based architectures, graph-based representation learning, and multimodal data to capture richer clinical context. Validation across multiple institutions and diverse population is essential to demonstrate portability.

Conclusion

In conclusion, this study demonstrated that embedding techniques, particularly word2vec trained on study dataset is a viable automated approach for heart failure readmission prediction. Further studies are required to investigate if task-specific representation learning may be more effective than use of general-purpose models for specific clinical applications.

Acknowledgments

We extend our thanks to the developers of open-source tools and frameworks, including word2vec, BioClinical_BERT which greatly facilitated the embedding generation and analysis in our study.

Funding

This project was supported by grants from NHLBI (R01-HL151643) and Amazon Web services.

XSL•FO
RenderX

Authors' Contributions

KBW and PRS conceptualized the study. PRS designed and performed the experiment, prepared the manuscript. KBW reviewed and supervised experiments and manuscript. AK reviewed experiment design and manuscript.

Conflicts of Interest

None declared.

Multimedia Appendix 1
Fine-tuning the *word2vec* model.
[DOCX File, 105 KB - medinform_v13i1e73020_app1.docx]

References

1. Savarese G, Becher PM, Lund LH, Seferovic P, Rosano GMC, Coats AJS. Global burden of heart failure: a comprehensive and updated review of epidemiology. Cardiovasc Res 2023 Jan 18;118(17):3272-3287. [doi: 10.1093/cvr/cvac013] [Medline: 35150240]
2. Wei S, Miranda JJ, Mamas MA, et al. Sex differences in the etiology and burden of heart failure across country income level: analysis of 204 countries and territories 1990-2019. Eur Heart J Qual Care Clin Outcomes 2023 Nov 2;9(7):662-672. [doi: 10.1093/ehjqcco/qcac088] [Medline: 36577147]
3. Lan T, Liao YH, Zhang J, et al. Mortality and readmission rates after heart failure: a systematic review and meta-analysis. TCRM 2021;17:1307-1320. [doi: 10.2147/TCRM.S340587]
4. Yu MY, Son YJ. Machine learning-based 30-day readmission prediction models for patients with heart failure: a systematic review. Eur J Cardiovasc Nurs 2024 Oct 21;23(7):711-719. [doi: 10.1093/eurjcn/zvae031] [Medline: 38421187]
5. Chanda AK, Bai T, Yang Z, Vucetic S. Improving medical term embeddings using UMLS Metathesaurus. BMC Med Inform Decis Mak 2022 Apr 29;22(1):114. [doi: 10.1186/s12911-022-01850-5] [Medline: 35488252]
6. Lee YC, Jung SH, Kumar A, et al. ICD2Vec: mathematical representation of diseases. J Biomed Inform 2023 May;141:104361. [doi: 10.1016/j.jbi.2023.104361] [Medline: 37054960]
7. Ru B, Tan X, Liu Y, et al. Comparison of machine learning algorithms for predicting hospital readmissions and worsening heart failure events in patients with heart failure with reduced ejection fraction: modeling study. JMIR Form Res 2023 Apr 17;7(1):e41775. [doi: 10.2196/41775] [Medline: 37067873]
8. Hospital readmissions reduction program (HRRP). CMS. URL: https://www.cms.gov/medicare/payment/prospective-payment-systems/acute-inpatient-pps/hospital-readmissions-reduction-program-hrrp [accessed 2025-04-23]
9. Mikolov T, Chen K, Corrado G, Dean J. Efficient estimation of word representations in vector space. arXiv. Preprint posted online on Jan 16, 2013. [doi: 10.48550/arXiv.1301.3781]
10. Choi E, Schuetz A, Stewart WF, Sun J. Medical concept representation learning from electronic health records and its application on heart failure prediction. arXiv. Preprint posted online on Jun 20, 2017. [doi: 10.48550/arXiv.1602.03686]
11. Bai T, Chanda AK, Egleston BL, Vucetic S. EHR phenotyping via jointly embedding medical concepts and words into a unified vector space. BMC Med Inform Decis Mak 2018 Dec 12;18(Suppl 4):123. [doi: 10.1186/s12911-018-0672-0] [Medline: 30537974]
12. Steiger E, Kroll LE. Patient embeddings from diagnosis codes for health care prediction tasks: Pat2Vec Machine Learning Framework. JMIR AI 2023 Apr 21;2(1):e40755. [doi: 10.2196/40755] [Medline: 38875541]
13. Devlin J, Chang MW, Lee K, Toutanova K. BERT: pre-training of deep bidirectional transformers for language understanding. arXiv. Preprint posted online on 2019. [doi: 10.48550/arXiv.1810.04805]
14. Lee J, Yoon W, Kim S, et al. BioBERT: a pre-trained biomedical language representation model for biomedical text mining. Bioinformatics 2020 Feb 15;36(4):1234-1240. [doi: 10.1093/bioinformatics/btz682] [Medline: 31501885]
15. Alsentzer E, Murphy JR, Boag W. Publicly available clinical BERT embeddings. arXiv. Preprint posted online on Apr 6, 2019. [doi: 10.48550/arXiv.1904.03323]
16. Rasmy L, Xiang Y, Xie Z, Tao C, Zhi D. Med-BERT: pretrained contextualized embeddings on large-scale structured electronic health records for disease prediction. npj Digit Med 2021 May 20;4(1):1-13. [doi: 10.1038/s41746-021-00455-y]
17. Li Y, Rao S, Solares JRA, et al. BEHRT: transformer for electronic health records. Sci Rep 2020;10(1):7155. [doi: 10.1038/s41598-020-62922-y]
18. Johnson AEW, Bulgarelli L, Shen L, et al. MIMIC-IV, a freely accessible electronic health record dataset. Sci Data 2023 Jan 3;10(1):1. [doi: 10.1038/s41597-022-01899-x]
19. Graham J, Iverson A, Monteiro J, et al. Applying computable phenotypes within a common data model to identify heart failure patients for an implantable cardiac device registry. IJC Heart & Vasculature 2022 Apr;39:100974. [doi: 10.1016/j.ijcha.2022.100974]
20. Liu W, Stansbury C, Singh K, et al. Predicting 30-day hospital readmissions using artificial neural networks with medical code embedding. PLoS ONE 2020;15(4):e0221606. [doi: 10.1371/journal.pone.0221606]

XSL•FO
RenderX

21. Nazyrova N, Chahed S, Chausalet T, Dwek M. Leveraging large language models for medical text classification: a hospital readmission prediction case. Presented at: 2024 14th International Conference on Pattern Recognition Systems (ICPRS); Jul 15-18, 2024. [doi: 10.1109/ICPRS62101.2024.10677826]
22. Pishgar M, Theis J, Del Rios M, Ardati A, Anahideh H, Darabi H. Prediction of unplanned 30-day readmission for ICU patients with heart failure. BMC Med Inform Decis Mak 2022 May 2;22(1):117. [doi: 10.1186/s12911-022-01857-y] [Medline: 35501789]
23. Ben-Assuli O, Heart T, Klempfner R, Padman R. Human-machine collaboration for feature selection and integration to improve congestive Heart failure risk prediction. Decis Support Syst 2023 Sep;172:113982. [doi: 10.1016/j.dss.2023.113982]

Abbreviations

ANN: Artificial neural network
AUROC: area under the receiver operating characteristic curve
CUI: Concept Unique Identifier
EHR: electronic health record
HF: heart failure
ICD: International Classification of Diseases
MIMIC: Medical Information Mart for Intensive Care
NDC: National Drug Code
UMLS: Unified Medical Language System
XGBoost: eXtream gradient-boosting

Edited by A Benis; submitted 23.02.25; peer-reviewed by AA Abiye, S Liu; revised version received 26.09.25; accepted 05.10.25; published 25.11.25.

Please cite as:
Shakya P, Khaneja A, Wagholikar KB
Predicting 30-Days Hospital Readmission for Patients with Heart Failure Using Electronic Health Record Embeddings: Comparative Evaluation
JMIR Med Inform 2025;13:e73020
URL: https://medinform.jmir.org/2025/1/e73020
doi:10.2196/73020

© Prabin Shakya, Ayush Khaneja, Kavishwar B Wagholikar. Originally published in JMIR Medical Informatics (https://medinform.jmir.org), 25.11.2025. This is an open-access article distributed under the terms of the Creative Commons Attribution License (https://creativecommons.org/licenses/by/4.0/), which permits unrestricted use, distribution, and reproduction in any medium, provided the original work, first published in JMIR Medical Informatics, is properly cited. The complete bibliographic information, a link to the original publication on https://medinform.jmir.org/, as well as this copyright and license information must be included.

XSL•FO
RenderX

Prognostic Value of the Charlson Comorbidity Index for Mortality and Machine Learning–Based Prediction in Critically Ill Patients with Paralytic Ileus: Retrospective Cohort Study

Hui Feng[1,2*], MM; Fuhai Zhou[2,3*], MD; Yi Shen[2,3], MD; Zhen Wang[2,3], MM; Yiyang Yuan[1,2], MM; Wenshan Jing[2,3], MD; Zhou Zheng[2,3], MD; Hui Peng[2,3*], MD; Qingsheng Yu[2,3], MM

[1]Department of Emergency Surgery, The First Affiliated Hospital of Anhui University of Chinese Medicine, Hefei, China

[2]Institute of Surgery, Anhui Provincial Academy of Traditional Chinese Medicine, Hefei, China

[3]Department of General Surgery, The First Affiliated Hospital of Anhui University of Chinese Medicine, No. 117 Meishan Road, Hefei, China

[*]these authors contributed equally

Corresponding Author:
Qingsheng Yu, MM
Institute of Surgery, Anhui Provincial Academy of Traditional Chinese Medicine, Hefei, China

Abstract

Background: The burden of paralytic ileus (PI) in the intensive care unit remains high, and the Charlson Comorbidity Index (CCI) is strongly associated with the prognosis of several acute and chronic diseases. However, evidence specifically evaluating the prognostic value of CCI in intensive care unit patients with PI remains limited.

Objective: This study aimed to investigate the association between CCI and clinical prognosis in critically ill patients with PI.

Methods: In this study, data were extracted from the Medical Information Mart for Intensive Care IV (version 2.2), a large, publicly available critical care database, and used to determine the optimal cut-off value of CCI for predicting mortality in patients with PI using the receiver operating characteristic curves, and the association between CCI and mortality was evaluated using Cox regression and restricted cubic spline analysis. A machine learning (ML) prediction model was then constructed to predict hospital mortality by combining CCI and other clinical characteristics.

Results: The study included 863 patients with PI (age: median 65.4, IQR 54.6 - 75.5 y; male: 575/863, 66.6%). The receiver operating characteristic curve identified an optimal cut-off value of 4.5 for CCI. The multivariate Cox regression analysis showed that compared to the lowest CCI quartile, patients with elevated CCI levels were more likely to have elevated hospital (Q4: hazard ratio [HR] 2.447, 95% CI 1.210 - 4.951), 28-day (Q4: HR 3.891, 95% CI 1.956 - 7.740), and 90-day (Q4: HR 3.994, 95% CI 2.224 - 7.173) all-cause mortality were significantly associated with elevated CCI levels; however, the association with ICU mortality (Q4: HR 1.892, 95% CI 0.653 - 5.480) was weak. Among the 11 ML models, the light gradient boosting machine model performed best, with internal validation results showing an area under the curve of 0.811, a geometric mean of 0.670, and an F_1-score of 0.895.

Conclusions: The CCI is an important predictor of hospital, 28-day, and 90-day all-cause mortality in critically ill patients with PI, and the optimal threshold is 4.5. ML models, including the CCI, show high accuracy in predicting hospital mortality, and the CCI occupies an important position in the model. This suggests that the CCI helps to identify high-risk patients, supports clinical decision-making, and improves prognosis.

(JMIR Med Inform 2025;13:e76003) doi:10.2196/76003

KEYWORDS

Charlson Comorbidity Index; paralytic ileus; MIMIC-IV database; all-cause mortality; machine learning

Introduction

Background

Paralytic ileus (PI) is a common functional intestinal obstruction due to decreased or loss of intestinal motility, with etiological factors including electrolyte imbalance, severe infection, substance abuse, and abdominal surgery [1,2]. The global incidence is approximately 1 - 5 cases per 100,000 people, with a higher incidence in women but a higher mortality rate in men [3]. The overall mortality rate for PI is 5% - 6%, but this increases to 10% - 20% in the intensive care unit (ICU) patients [1,4]. Patients with PI are often associated with chronic diseases or comorbidities such as diabetes, neurological diseases, systemic sclerosis, and malignant cancer, and the cumulative burden of these underlying diseases may have a significant impact on mortality [5-8]. Given the high morbidity and

XSL•FO
RenderX

mortality associated with PI, it is important to accurately identify high-risk patients and assess their prognostic risk.

The Charlson Comorbidity Index (CCI) is a widely used scoring system that quantifies the burden of chronic comorbidities (eg, diabetes, malignant cancer, and connective tissue disorders) and evaluates their impact on overall prognosis, thereby providing an estimate of mortality risk [9,10]. It has demonstrated significant prognostic value across a variety of clinical scenarios, including older patients, critically ill populations, and cancer cohorts [11-14], and has been validated in settings such as chronic granulocytic leukemia [15], the assessment of postoperative complications [16], and fracture risk prediction [17]. These findings highlight the use of the CCI in capturing the cumulative effect of chronic disease burden on patient outcomes. In critically ill patients with PI, comorbidities such as cardiovascular disease, diabetes, and chronic kidney disease are common and may substantially influence prognosis, making the CCI particularly relevant for this cohort [1,4]. Moreover, unlike scoring systems such as Sequential Organ Failure Assessment (SOFA) or Acute Physiology and Chronic Health Evaluation that primarily reflect acute illness severity, the CCI captures the cumulative impact of chronic conditions on outcomes, thereby complementing conventional acute severity scores [9]. However, evidence specifically evaluating the prognostic value of the CCI in ICU patients with PI remains limited.

Objective

With the rapid development of big data and machine learning (ML), mortality prediction models based on electronic health records have become a research focus, as ML can capture complex associations in high-dimensional data and often outperform traditional methods [18-20]. Recently, explainable ML approaches have been applied in critical care, with several studies using the Medical Information Mart for Intensive Care (MIMIC) database to develop interpretable mortality prediction models that enhance clinical applicability [21,22]. For instance, a deep-learning model for mortality prediction based on MIMIC used neural networks with Shapley Additive Explanations (SHAP) analysis to predict outcomes in ICU patients with PI [23]. Building on these advances, the primary objective of this study was to evaluate the association between CCI and all-cause mortality, including hospital, ICU, 28-day, and 90-day mortality, in ICU patients with PI. The exploratory objective was to assess the feasibility of incorporating CCI into ML models for mortality prediction in this population.

Methods

Study Participants

This is a retrospective cohort study. The Massachusetts Institute of Technology and Beth Israel Deaconess Medical Center (BIDMC) collaborated to develop the MIMIC-IV electronic database (version 2.2), which was used for this study [24]. The database contains information on more than 50,000 patients who received ICU care at BIDMC between 2008 and 2019. The database provides a wide range of clinical data and has been used extensively in critical care medicine research [25-27]. Detailed information about the database, including access instructions, is available at PhysioNet [28]. The institutional review board (IRB) of BIDMC waived informed consent and allowed sharing of research resources because all data were deidentified. Therefore, this study did not require additional informed consent (2001-P-001699/14; 0403000206). To comply with the regulations, the author, HF, obtained a Cooperative Institutional Training Initiative license (certification: 61863057) and the necessary permission to use the MIMIC-IV database.

Adult patients who were first admitted to the hospital with a diagnosis of PI according to the International Classification of Diseases (ICD-9: 560.1 and ICD-10: 56.0) were included in this study. Individual patient consent was not required due to the anonymized nature of patient health information in this database. Exclusion criteria included: (1) patients who stayed in the ICU for <6 hours; (2) multiple ICU admissions for which only data from the first admission were extracted; and (3) patients who lacked information on CCI. Finally, a total of 863 patients were included in this study and divided into 4 groups according to the quartiles of CCI.

Patient Characteristics

Data collection involved the use of structured query language and PostgreSQL (version 16.3.7; PostgreSQL Global Development Group) to extract baseline patient characteristics. The following data were obtained: (1) demographic information includes sex, age, and race; (2) comorbidities identified according to ICD-9 or ICD-10: congestive heart failure, renal disease, malignant cancer, sepsis, diabetes, and hypertension; (3) mean vital signs include respiratory rate (RR), mean blood pressure (MBP), heart rate, and oxygen; (4) laboratory parameters include white blood cell (WBC) count, red blood cell distribution width (RDW), platelets, hemoglobin, anion gap, blood urea nitrogen (BUN), creatinine, total calcium, chloride, sodium, and potassium; (5) severity scores include Simplified Acute Physiology Score II (SAPS II), Oxford Acute Severity of Illness Score (OASIS), Acute Physiology Score III (APS III), SOFA score, and CCI; and (6) therapeutic agents include ondansetron and neostigmine. All laboratory variables were obtained from the first 24 hours after the patient's admission to the ICU. Follow-up began on the date of ICU admission and ended on the date of death. Variables with more than 10% missing values were excluded to mitigate potential bias [29]. The proportions of missing values for variables are shown in Figure S1A in Multimedia Appendix 1, and variables with less than 10% missing values were interpolated using the random forest interpolation method implemented in the *missForest* package of the R software (R Foundation for Statistical Computing) [30]. In the ML section, the patients with PI were divided into a 70% training cohort and a 30% test cohort.

Clinical Outcome

The primary outcome of this study was all-cause hospital mortality, and secondary outcomes were ICU mortality and mortality at 28 and 90 days after ICU admission. In addition, the primary objective of the ML modeling was all-cause hospital mortality.

XSL•FO
RenderX

Statistical Analysis

The normality of continuous variables was assessed using the Kolmogorov-Smirnov test. Continuous variables that followed a normal distribution were analyzed using the 2-tailed *t* test or ANOVA, and those that were not normally distributed were analyzed using the Mann-Whitney *U* test or the Kruskal-Wallis test. Categorical variables were compared by the chi-square test. The CCI was categorized into 4 quartiles, Kaplan-Meier survival analysis was used to assess differences in mortality between groups, and log-rank tests were used to compare differences between groups. The optimal cut-off value for CCI was determined by receiver operating characteristic (ROC) curve analysis using the Youden index maximization method. Variance inflation factor (VIF) was used to assess multicollinearity between variables, and variables with a VIF>5 were removed (Figure S1B in Multimedia Appendix 1).

Cox regression analysis was used to assess the association between CCI and hospital mortality, ICU mortality, as well as 28- and 90-day mortality, with model 1 including only CCI and model 2 including age and sex as correction variables. Model 3 was developed based on clinical expertise, a previous study by Zhao et al [4], and the results of feature importance selection from the least absolute shrinkage and selection operator (LASSO) algorithm. The following variables were included: sex, age, CHF, renal disease, malignant cancer, sepsis, diabetes, hypertension, RR, SpO_2 , WBC, RDW, platelets, anion gap, BUN, creatinine, SAPS II, OASIS, APS III, and SOFA. In addition, restricted cubic spline (RCS) analyses were performed to explore the potential nonlinear relationship between CCI levels and hospital, ICU, and 28- and 90-day all-cause mortality rates. The CCI was used as a continuous or ordinal variable entered into the model (the first quartile of CCI served as the reference group). *P* values for trends were calculated using IQRs. Further stratified analyses were performed according to sex, age (≤65 and >65 y), CHF, malignant cancer, sepsis, and diabetes to determine the consistency of the prognostic value of CCI for the primary outcome. Likelihood ratio tests were used to examine the interaction between CCI and the variables used for stratification. A 2-sided $P<.05$ was considered statistically significant.

To test the robustness of the results of the primary analysis, several sensitivity analyses were performed. First, patients who died within 3 days of ICU admission were excluded to assess whether these patients had a significant impact on the primary outcome. Second, patients were grouped according to the optimal cut-off value of the CCI to test the stability of the main results by different CCI groupings. Finally, a stratified analysis of SOFA scores was performed: patients were divided into 3 groups based on their 24-hour SOFA scores after ICU admission: low (first 1/3 quartile), intermediate (1st or 3rd to 2nd or 3rd quartile), and high (last 1/3 quartile). This grouping method helps to further validate the effect of different SOFA score groups on the association between CCI and mortality.

In addition, an ML model was constructed to predict all-cause hospital mortality in patients with PI using a binary classification approach. First, the correlation between variables was assessed using a Pearson correlation test, and those with coefficients >0.5 were excluded to reduce multicollinearity. Continuous variables were standardized and categorical variables were encoded. Feature selection was performed using LASSO regression and 3 ML algorithms, and the top 10 features were identified. These features were then tested again for Pearson correlation and VIFs before being incorporated into 11 common ML algorithms (eg, light gradient boosting machine [LightGBM], random forest, and extreme gradient boosting). The dataset was divided into a training and internal validation cohort in a 7:3 ratio. Model training and evaluation were performed using 10-fold cross-validation (repeatedcv, repeats =1) to reduce the risk of overfitting. Hyperparameter tuning was conducted with a random search strategy in R using the trainControl function, and the optimal parameters are shown in Table S1 in Multimedia Appendix 1. Model performance was compared with SOFA and SAPS II scores using ROC curves and multiple metrics, including AUC, accuracy, sensitivity, specificity, F_1-score, geometric mean, precision, and recall. For the best-performing ML models, Shapley Additive Explanations (SHAP) were used to assess feature importance and generate partial dependence plots. Finally, a web-based prediction platform was developed based on the best-performing models to improve clinical accessibility.

All statistical analyses were performed using SPSS (version 23.0; IBM Corp), R (version 4.3.2), and Python (version 3.11.1; Python Software Foundation).

Ethical Considerations

This study was a retrospective observational cohort study using the publicly available MIMIC-IV database (version 2.2), which contains deidentified patient data. The IRB of BIDMC waived the requirement for informed consent, as all data in the MIMIC-IV database are deidentified. The use of the database for this research was approved by the IRB of BIDMC. To comply with relevant regulations, the author, HF, obtained a Collaborative Institutional Training Initiative certification (61863057) and the necessary permissions to access and use the MIMIC-IV database. All procedures involving human subjects in this study adhered to the ethical standards of the institutional and national research councils as well as the 1964 Declaration of Helsinki and its subsequent amendments or equivalent ethical standards. As this study used the publicly available MIMIC-IV data, no participants were directly involved and no compensation was provided.

Results

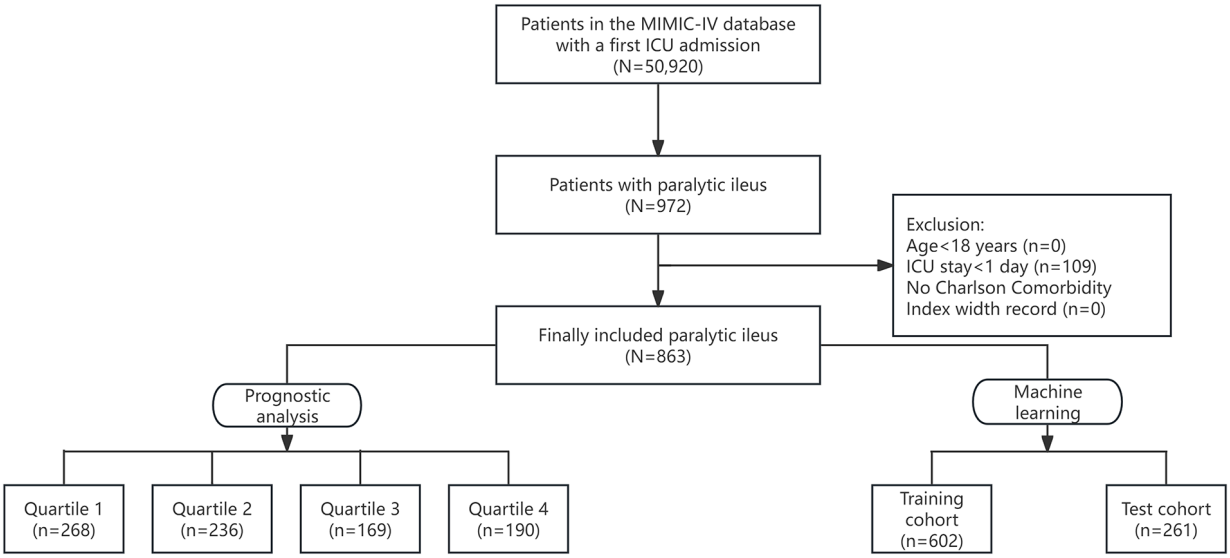
Baseline Characteristics

After screening the data of patients with PI in the MIMIC IV database, 863 patients who met the inclusion criteria were included in this study and divided into 4 groups according to the quartiles of CCI (Figure 1). Table 1 shows the baseline characteristics of critically ill patients with PI stratified by CCI quartiles. Patients were divided into 4 groups based on their CCI level on admission (quartile 1: 0 - 3; quartile 2: 3 - 5; quartile 3: 5 - 7; and quartile 4: 7 - 14). The median CCI values for each quartile in each group were 2 (IQR 1 - 3), 4.5 (IQR 4 - 5), 6 (IQR 6 - 7), and 9 (IQR 8 - 10), respectively. The

XSL•FO
RenderX

median age of the enrolled patients was 65.4 (IQR 54.6 - 75.5) years, of which 575 (66.6%) were male. The median CCI for all participants was 5 (IQR 3 - 7). Compared to the lower group, patients in the highest CCI quartile generally had higher age, RDW, anion gap, BUN, creatinine, SAPS II, OASIS, APS III, SOFA, lower MBP, heart rate, hemoglobin, higher CHF, renal disease, malignant cancer, diabetes prevalence, and lower hypertension prevalence. Hospital mortality, ICU mortality, 28-day mortality, and 90-day mortality were 157 (18.2%), 76 (9%), 171 (19.8%), and 233 (27%), respectively. As the Q4 group was better associated with all-cause mortality, the differences between Q4 and Q1-Q3 were further compared. The analysis showed that different grouping methods gave similar results (Table S2 in Multimedia Appendix 1).

Figure 1. Flowchart of patient selection for the study cohort. ICU: intensive care unit; MIMIC-IV: Medical Information Mart for Intensive Care IV.



XSL•FO
RenderX

Table . Characteristics and outcomes of intensive care unit (ICU) patients with paralytic ileus categorized by Charlson Comorbidity Index (CCI) levels[a] (N=863).

Categories	Overall	Q1 (n=268)	Q2 (n=236)	Q3 (n=169)	Q4 (n=190)	*P* value
Sex (male), n (%)	575 (66.6)	176 (65.7)	160 (67.8)	109 (64.5)	130 (68.4)	.83
Age (y), median (IQR)	65.4 (54.6 - 75.5)	52.8 (42 - 59.3)	67.4 (58 - 76.5)	71.4 (62.4 - 80.3)	73.6 (66.7 - 81.7)	<.001
Race, n (%)						.64
White	576 (66.7)	175 (65.3)	153 (64.8)	115 (68.0)	133 (70)	
Others	287 (33.3)	93 (35)	83 (35)	54 (32)	57 (30)	
Comorbidities, n (%)						
CHF[b]	220 (25.5)	17 (6)	53 (23)	68 (40)	82 (43)	<.001
Renal disease	194 (22.5)	4 (2)	26 (11)	59 (35)	105 (55.3)	<.001
Malignant cancer	161 (18.7)	14 (5)	28 (12)	33 (20)	86 (45)	<.001
Sepsis	282 (32.7)	76 (28)	70 (30)	65 (39)	71 (37)	.052
Diabetes	226 (26.2)	34 (13)	55 (23)	45 (27)	92 (48)	<.001
Hypertension	355 (41.1)	97 (36)	133 (56.4)	74 (44)	51 (27)	<.001
Vital signs, median (IQR)						
RR[c] (breaths/min)	18.8 (16.4 - 21.9)	19.0 (16.6 - 21.9)	19.1 (16.1 - 21.7)	19.1 (16.6 - 23.0)	18.3 (16.4 - 21.9)	.60
MBP[d] (mmHg)	73.9 (68.6 - 81.8)	77.4 (71.3 - 84.7)	73.9 (68.5 - 82.2)	73.3 (68.5 - 79.0)	72.2 (66.5 - 78.1)	<.001
Heart rate (bpm)	89.2 (79.2 - 103)	93.0 (81.3 - 106)	88.1 (79.1 - 101)	88.6 (77.8 - 102)	86.4 (76.5 - 99.0)	.001
SpO_2[e](%)	97.0 (95.5 - 98.4)	97.2 (95.8 - 98.5)	96.7 (95.1 - 98.2)	96.8 (95.2 - 98.3)	97.3 (95.7 - 98.4)	.09
Laboratory test, median (IQR)						
WBC[f] (K/μL)	12.8 (9.15 - 18.0)	13.2 (9.20 - 18.2)	12.4 (8.90 - 18.2)	13.4 (9.20 - 19.7)	12.0 (8.98 - 15.7)	.28
RDW[g] (%)	15.0 (13.9 - 16.6)	14.5 (13.6 - 15.7)	15.1 (13.8 - 16.5)	15.6 (14.1 - 17.0)	15.4 (14.4 - 17.1)	<.001
Platelet (K/μL)	176 (113 - 235)	190 (126 - 241)	158 (99.5 - 225)	171 (119 - 233)	175 (119 - 234)	.15
Hemoglobin (g/dL)	9.60 (8.40 - 11.0)	10.0 (8.60 - 11.5)	9.50 (8.20 - 11.0)	9.70 (8.30 - 11.0)	9.20 (8.10 - 10.4)	.001
Anion gap (mmol/L)	14.0 (12.0 - 17.0)	14.0 (11.0 - 16.0)	14.0 (11.0 - 16.0)	14.0 (13.0 - 17.0)	15.0 (12.0 - 17.0)	.001
BUN[h] (mg/dL)	21.0 (14.0 - 34.0)	15.0 (11.0 - 23.0)	22.0 (15.0 - 34.1)	26.0 (18.0 - 38.0)	30.0 (18.2 - 40.8)	<.001
Creatinine (mg/dL)	1.10 (0.80 - 1.60)	0.90 (0.60 - 1.20)	1.10 (0.80 - 1.50)	1.20 (0.90 - 1.63)	1.45 (1.00 - 1.81)	<.001
Calcium (mg/dL)	8.10 (7.70 - 8.60)	8.00 (7.60 - 8.50)	8.10 (7.72 - 8.60)	8.20 (7.80 - 8.60)	8.12 (7.70 - 8.60)	.08
Chloride (mEq/L)	105 (101 - 109)	105 (101 - 109)	105 (101 - 109)	104 (99.0 - 108)	105 (101 - 108)	.22
Sodium (mEq/L)	138 (135 - 141)	138 (136 - 141)	138 (135 - 141)	138 (135 - 141)	139 (135 - 141)	.71
Potassium (mEq/L)	4.20 (3.80 - 4.50)	4.10 (3.70 - 4.40)	4.20 (3.70 - 4.60)	4.20 (3.80 - 4.60)	4.20 (3.80 - 4.60)	.09
Severity scores, median (IQR)						
SAPS II[i]	37.0 (30.0 - 47.0)	30.0 (22.0 - 38.0)	37.0 (31.0 - 45.0)	40.0 (33.0 - 51.0)	43.0 (37.0 - 54.0)	<.001
OASIS[j]	33.0 (27.0 - 39.5)	31.0 (25.0 - 38.0)	33.0 (29.0 - 39.0)	34.0 (27.0 - 40.0)	34.0 (28.0 - 41.0)	.001
APS III[k]	47.0 (35.0 - 63.5)	41.0 (30.0 - 59.0)	48.0 (34.0 - 63.0)	50.0 (41.0 - 67.0)	51.0 (38.0 - 69.6)	<.001
SOFA[l]	2.00 (1.00 - 5.00)	2.00 (1.00 - 4.00)	2.00 (1.00 - 5.00)	3.00 (1.00 - 5.00)	3.00 (1.00 - 5.00)	<.001
CCI	5.00 (3.00 - 7.00)	2.00 (1.00 - 3.00)	4.50 (4.00 - 5.00)	6.00 (6.00 - 7.00)	9.00 (8.00 - 10.0)	<.001

XSL•FO
RenderX

Categories	Overall	Q1 (n=268)	Q2 (n=236)	Q3 (n=169)	Q4 (n=190)	*P* value
Medication, n (%)						
Ondansetron	475 (55.0)	154 (57.5)	124 (52.5)	92 (54)	105 (55.3)	.74
Neostigmine	101 (11.7)	30 (11)	34 (14)	23 (14)	14 (7)	.12
Events, median (IQR)						
Hospital LOS[m] (d)	14.6 (9.72 - 23.1)	14.4 (9.27 - 24.0)	14.1 (9.32 - 24.5)	15.5 (10.6 - 22.7)	15.0 (10.5 - 20.8)	.87
ICU LOS (d)	3.65 (1.94 - 7.85)	3.30 (1.91 - 7.74)	3.92 (1.91 - 8.79)	4.03 (2.08 - 7.51)	3.30 (1.96 - 7.61)	.58
Mortality, n (%)						
Hospital	157 (18.2)	26 (10)	46 (20)	34 (20)	51 (27)	<.001
ICU	76 (9)	17 (6)	22 (9)	17 (10)	20 (10)	.37
28 days	171 (19.8)	23 (9)	44 (19)	40 (24)	64 (34)	<.001
90 dayss	233 (27.0)	32 (12)	61 (26)	54 (32)	86 (45)	<.001

[a]Continuous data are presented as median (IQR), whereas categorical data are presented as n (%), Q1 (0 - 3), Q2 (3–5), Q3 (5–7), Q4 (7–14).

[b]CHF: congestive heart failure.

[c]RR: respiratory rate.

[d]MBP: mean blood pressure.

[e]SpO_2: saturation of peripheral oxygen.

[f] WBC: white blood cell.

[g]RDW, red blood cell distribution width.

[h] BUN: blood urea nitrogen.

[i] SAPS II: Simplified Acute Physiological Score II.

[j]OASIS: Oxford Acute Severity of Illness Score.

[k]APS III: Acute Physiology Score III.

[l] SOFA: Sequential Organ Failure Assessment.

[m]LOS: length of stay.

Table 2 shows the differences in baseline characteristics between survivors and nonsurvivors during hospitalization. Patients in the nonsurvivor group were more likely to have higher RR, heart rate, RDW, anion gap, BUN, creatinine, SAPS II, OASIS, APS III, SOFA, CCI, higher prevalence of CHF, sepsis, lower prevalence of hypertension, lower SpO_2, platelets, hemoglobin, calcium, lower ondansetron, and neostigmine use. CCI values were significantly higher in the nonsurvivors than in the survivors (6 vs 5; $P<.001$). Figure S1 in Multimedia Appendix 1 shows the distribution of CCIs stratified by mortality status for inpatient deaths, ICU deaths, 28-day deaths, and 90-day deaths (Figure S2 in Multimedia Appendix 1).

XSL•FO
RenderX

Table . Baseline characteristics of intensive care unit (ICU) survivors and nonsurvivors with paralytic ileus[a] (N=863).

Categories	Overall	Survivor (n=706)	Nonsurvivor (n=157)	*P* value
Sex (male), n (%)	575 (66.6)	469 (66.4)	106 (67.5)	.87
Age (y), median (IQR)	65.4 (54.6 - 75.5)	65.3 (54.1 - 75.4)	66.1 (56.0 - 75.9)	.29
Race, n (%)				1.00
White	576 (66.7)	471 (66.7)	105 (66.9)	
Others	287 (33.3)	235 (33.3)	52 (33)	
Comorbidities, n (%)				
CHF[b]	220 (25.5)	169 (23.9)	51 (33)	.03
Renal disease	194 (22.5)	149 (21.1)	45 (29)	.05
Malignant cancer	161 (18.7)	123 (17.4)	38 (24)	.06
Sepsis	282 (32.7)	187 (26.5)	95 (61)	<.001
Diabetes	226 (26.2)	188 (26.6)	38 (24)	.60
Hypertension	355 (41.1)	308 (43.6)	47 (30)	.002
Vital signs, median (IQR)				
RR[c] (breaths/min)	18.8 (16.4 - 21.9)	18.4 (16.3 - 21.4)	20.5 (17.6 - 23.9)	<.001
MBP[d] (mmHg)	73.9 (68.6 - 81.8)	74.6 (69.4 - 82.4)	71.4 (66.4 - 77.5)	<.001
Heart rate (bpm)	89.2 (79.2 - 103)	88.6 (78.6 - 102)	92.5 (80.9 - 105)	.03
SpO_2[e] (%)	97.0 (95.5 - 98.4)	97.2 (95.7 - 98.4)	96.2 (94.8 - 98.1)	<.001
Laboratory test, median (IQR)				
WBC[f] (K/μL)	12.8 (9.15 - 18.0)	12.6 (9.20 - 17.7)	14.0 (8.90 - 19.7)	.10
RDW[g] (%)	15.0 (13.9 - 16.6)	14.9 (13.8 - 16.3)	16.4 (14.5 - 17.6)	<.001
Platelet (K/μL)	176 (113 - 235)	180 (121 - 237)	147 (67.0 - 227)	.001
Hemoglobin (g/dL)	9.60 (8.40 - 11.0)	9.70 (8.40 - 11.1)	9.11 (8.20 - 11.0)	.04
Anion gap (mmol/L)	14.0 (12.0 - 17.0)	14.0 (12.0 - 16.0)	15.0 (13.0 - 18.0)	<.001
BUN[h] (mg/dL)	21.0 (14.0 - 34.0)	20.0 (14.0 - 31.0)	31.0 (18.0 - 41.9)	<.001
Creatinine (mg/dL)	1.10 (0.80 - 1.60)	1.00 (0.80 - 1.50)	1.30 (0.90 - 1.80)	<.001
Calcium (mg/dL)	8.10 (7.70 - 8.60)	8.11 (7.70 - 8.60)	8.00 (7.50 - 8.50)	.04
Chloride (mEq/L)	105 (101 - 109)	105 (101 - 109)	104 (99.0 - 109)	.16
Sodium (mEq/L)	138 (135 - 141)	138 (136 - 141)	138 (134 - 141)	.14
Potassium (mEq/L)	4.20 (3.80 - 4.50)	4.10 (3.73 - 4.50)	4.20 (3.80 - 4.70)	.23
Severity scores, median (IQR)				
SAPS II[i]	37.0 (30.0 - 47.0)	35.0 (28.0 - 43.0)	47.0 (37.0 - 56.0)	<.001
OASIS[j]	33.0 (27.0 - 39.5)	32.0 (27.0 - 39.0)	36.0 (30.0 - 44.0)	<.001
APS III[k]	47.0 (35.0 - 63.5)	44.0 (33.0 - 58.0)	68.0 (50.0 - 77.4)	<.001
SOFA[l]	2.00 (1.00 - 5.00)	2.00 (1.00 - 4.00)	4.00 (2.00 - 6.27)	<.001
CCI[m]	5.00 (3.00 - 7.00)	5.00 (3.00 - 7.00)	6.00 (4.00 - 8.00)	<.001
Medication, n (%)				
Ondansetron	475 (55.0)	413 (58.5)	62 (40)	<.001
Neostigmine	101 (11.7)	96 (14)	5 (3)	<.001

XSL•FO
RenderX

[a]Continuous data are presented as median (IQR), whereas categorical data are presented as frequency (%).

[b]CHF: congestive heart failure.

[c]RR: respiratory rate.

[d]MBP: mean blood pressure.

[e]SpO_2: saturation of peripheral oxygen.

[f]WBC: white blood cell.

[g] RDW: red cell distribution width.

[h]BUN: blood urea nitrogen.

[i]SAPS II: Simplified Acute Physiological Score II.

[j]OASIS: Oxford Acute Severity of Illness Score.

[k]APS III: Acute Physiology Score III.

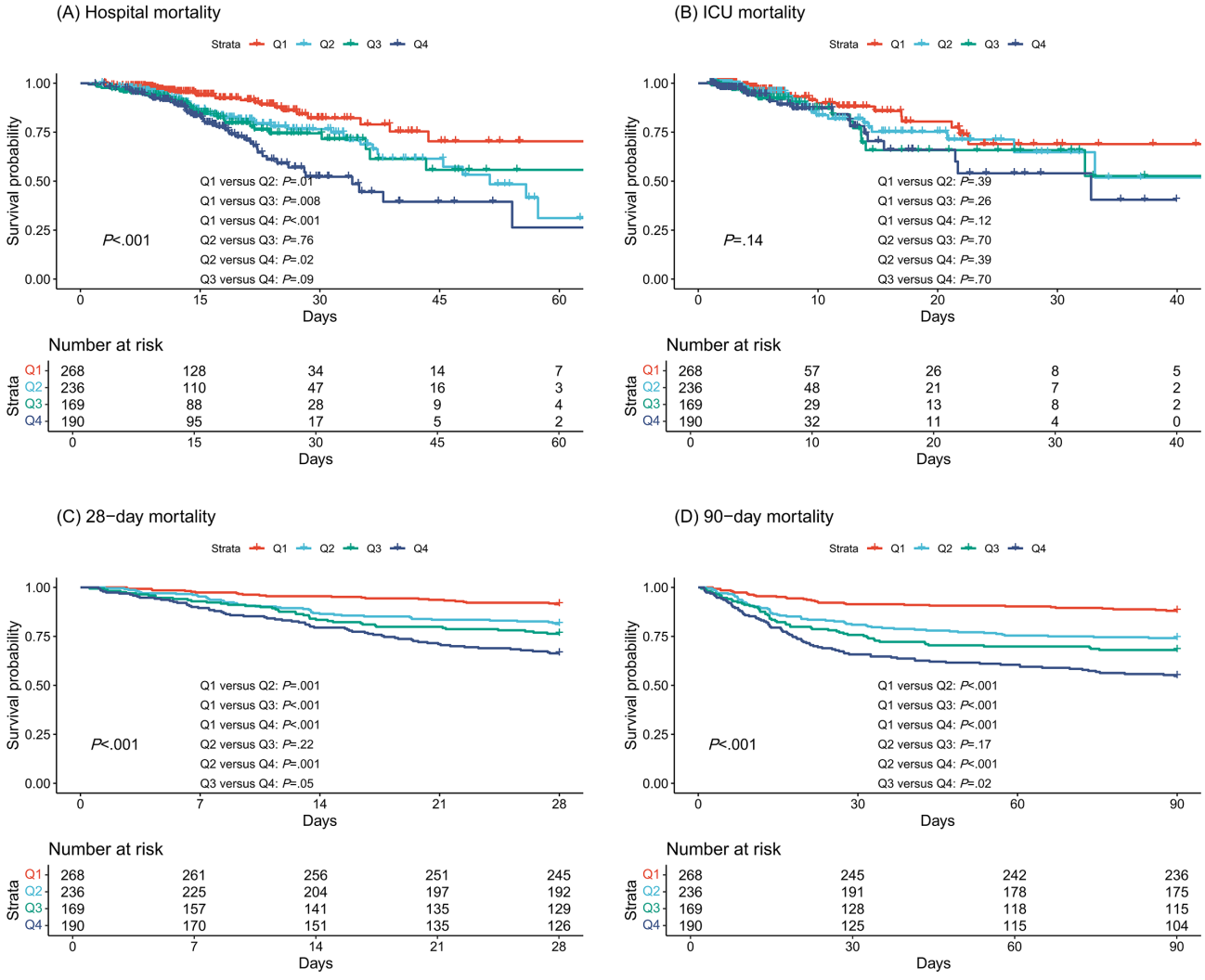
[l]SOFA: Sequential Organ Failure Assessment.

[m]CCI: Charlson Comorbidity Index.

Primary Outcomes

Kaplan-Meier survival analyses showed that patients with higher CCI scores had a significantly higher risk of hospital, 28-day, and 90-day all-cause mortality (Figure 2). ROC curve analyses assessed the clinical efficacy of the CCI (Figure S3 in Multimedia Appendix 1) and showed that the AUCs of the CCIs were all greater than 0.5, which to some extent discriminated patients who died in hospital, ICU, 28-day, and 90-day from those who did not (AUC for hospital deaths: 0.631, odds ratio [OR] 1.17, 95% CI 1.10 - 1.24, *P*<.001; AUC for ICU deaths: 0.58, OR 1.10, 95% CI 1.02 - 1.20, *P*=.02; 28-day death AUC: 0.678, OR 1.24, 95% CI 1.17 - 1.32, *P*<.001; 90-day ICU death AUC: 0.687, OR 1.27, 95% CI 1.20 - 1.34, *P*<.001). The optimal CCI cut-off for hospital, ICU, 28-day, and 90-day death was 4.5.

Figure 2. Kaplan-Meier survival curves for all-cause hospital, intensive care unit (ICU), 28-day, and 90-day mortality in ICU patients with paralytic ileus. Charlson Comorbidity Index quartiles were defined as Q1 (0 - 3), Q2 (3–5), Q3 (5–7), and Q4 (7–14). Panels show cumulative probability of all-cause mortality at (A) hospital, (B) ICU, (C) 28-day, and (D) 90-day follow-up.



XSL•FO
RenderX

Cox regression analysis was used to assess the association between CCI and in-hospital mortality. The results showed that when CCI was a continuous variable, CCI was a significant risk factor in the unadjusted model (hazard ratio [HR] 1.159, 95% CI 1.099 - 1.222; *P*<.001), the partially adjusted model (HR 1.158, 95% CI 1.088 - 1.233; *P*<.001), and the fully adjusted model (HR 1.204, 95% CI 1.099 - 1.319; *P*<.001). When CCI was the ordinal variable, patients in higher quartiles of CCI were significantly associated with a higher risk of in-hospital death compared with participants in the lowest quartile in all 3 established Cox regression analysis models: unadjusted model (HR 3.124, 95% CI 1.945 - 5.017; *P*<.001), partially adjusted model (HR 2.950, 95% CI 1.708 - 5.097; *P*<.001), and fully adjusted model (HR 2.447, 95% CI 1.210 - 4.951; *P*=.01) and showed an increasing trend with increasing CCI (Table 3 and Figure 3A). Similar results were observed in multivariate Cox regression analyses for 28-day mortality (Table 3 and Figure 3) and 90-day mortality (Table S3 in Multimedia Appendix 1; Figure 3), but less favorable results were observed in multivariate Cox regression analyses for CCI and ICU mortality (Table S3 in Multimedia Appendix 1; Figure 3). In addition, the use of an RCS regression model showed a linear increase in the risk of hospital, ICU, 28-day, and 90-day mortality with increasing CCI (nonlinear *P* values of .73, .87, .64, and .29, respectively; Figure 3).

XSL•FO
RenderX

Table . Cox proportional hazard ratios (HRs) for all-cause hospital and 28-day mortality in intensive care unit (ICU) patients with paralytic ileus.

Categories	Model 1[a]			Model 2[b]			Model 3[c]		
	HR (95% CI)	*P* value	*P* for trend	HR (95% CI)	*P* value	*P* for trend	HR (95% CI)	*P* value	*P* for trend
Hospital mortality									
Continuous variable	1.159 (1.099 - 1.222)	<.001		1.158 (1.088 - 1.233)	<.001		1.204 (1.099 - 1.319)	<.001	
Per unit quartile[d]			<.001			<.001			.01
Q1 (n=190)	Ref						Ref		
Q2 (n=162)	1.936 (1.196 - 3.135)	.007		1.868 (1.119 - 3.117)	.02		1.442 (0.832 - 2.499)	.19	
Q3 (n=159)	2.091 (1.254 - 3.487)	.004		2.003 (1.140 - 3.518)	.02		1.643 (0.857 - 3.149)	.14	
Q4 (n=170)	3.124 (1.945 - 5.017)	<.001		2.950 (1.708 - 5.097)	<.001		2.447 (1.210 - 4.951)	.01	
28-day mortality									
Continuous variable	1.202 (1.143 - 1.264)	<.001		1.237 (1.166 - 1.311)	<.001		1.255 (1.154 - 1.366)	<.001	
Per unit quartile[d]			<.001			<.001			<.001
Q1 (n=190)	Ref						Ref		
Q2 (n=162)	2.315 (1.398 - 3.833)	.001		2.683 (1.567 - 4.594)	<.001		1.849 (1.054 - 3.245)	.03	
Q3 (n=159)	3.035 (1.817 - 5.069)	<.001		3.660 (2.087 - 6.427)	<.001		2.375 (1.256 - 4.493)	.008	
Q4 (n=170)	4.563 (2.833 - 7.349)	<.001		5.668 (3.267 - 9.833)	<.001		3.891 (1.956 - 7.740)	<.001	

[a]Model 1: unadjusted.

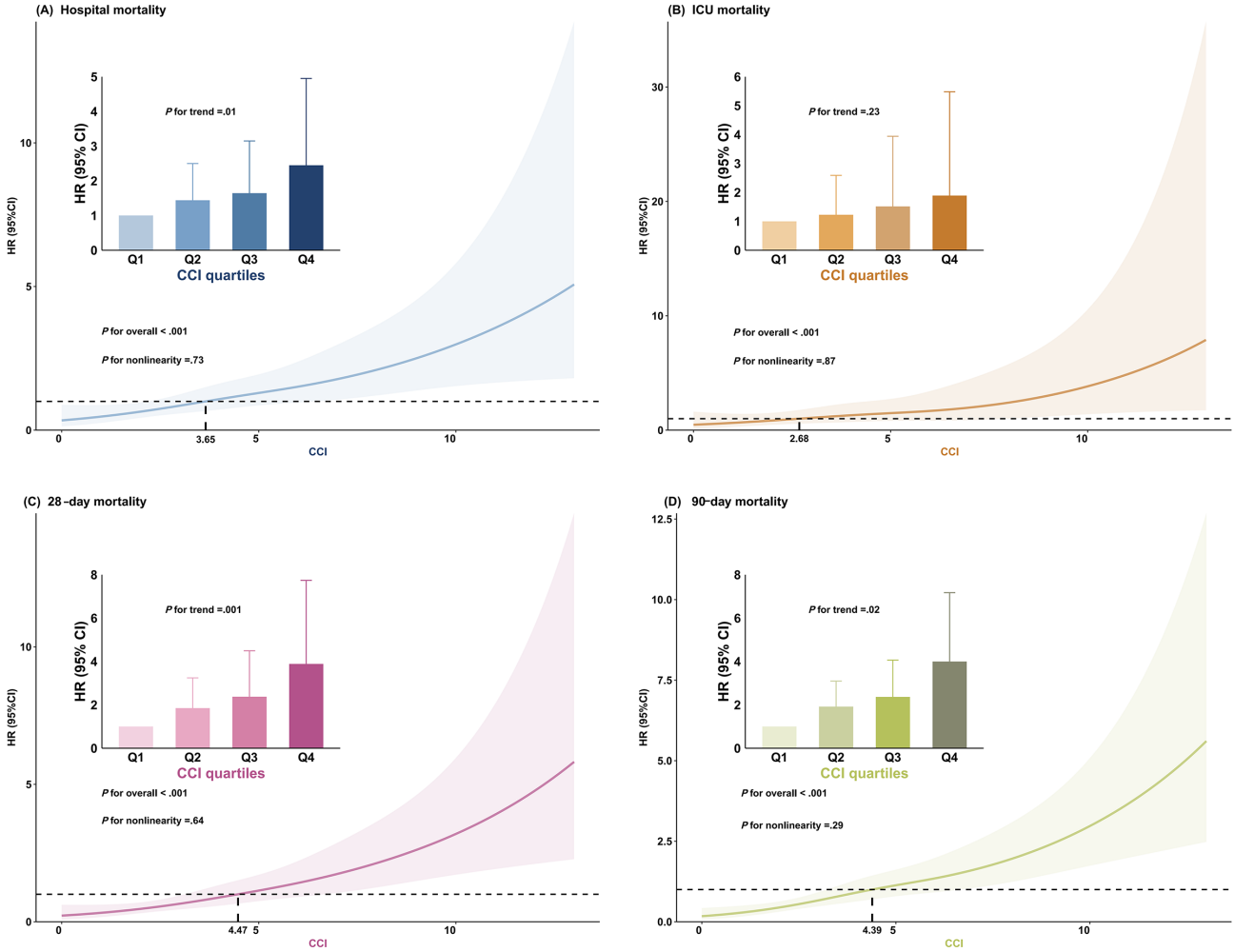
[b]Model 2: unadjusted.

[c]Model 3: adjusted for sex, age, congestive heart failure (CHF), renal disease, malignant cancer, sepsis, diabetes, hypertension, respiratory rate (RR), saturation of peripheral oxygen (SpO_2), white blood cell (WBC), red blood cell distribution width (RDW), platelets, anion gap, blood urea nitrogen (BUN), creatinine, Simplified Acute Physiological Score II (SAPS II), Oxford Acute Severity of Illness Score (OASIS), Acute Physiology Score III (APS III), Sequential Organ Failure Assessment (SOFA), and Charlson Comorbidity Index (CCI).

[d]CCI: Q1 (0 - 3), Q2 (3–5), Q3 (5–7), Q4 (7–14)

XSL•FO
RenderX

Figure 3. Hazard ratios (HRs) and restricted cubic spline curves for all-cause mortality from Charlson Comorbidity Index (CCI) after adjustment for confounders. All models were adjusted for multiple confounders, including sex, age, congestive heart failure (CHF), renal disease, sepsis, hypertension, diabetes, white blood cell count, red blood cell distribution width, anion gap, creatinine, and CCI. The bar graph shows the HRs for all-cause mortality between different CCI quartiles, with the CIs for each group. The first quartile of CCI is the reference group to which the other quartiles are compared. The central thick solid line represents the estimated HR after adjustment, the shaded area represents the CIs, and the horizontal dashed line represents the HR of 1.0. The vertical dashed line corresponds to the CCI value where the HR is 1.0. (**A**) Hospital mortality: the vertical dashed line corresponds to a CCI value of 3.65. (**B**) Intensive care unit (ICU) mortality: the vertical dashed line corresponds to a CCI value of 2.68. (**C**) 28-day mortality: the vertical dashed line corresponds to a CCI value of 4.47. (**D**) 90-day mortality: the vertical dashed line corresponds to a CCI value of 4.39.

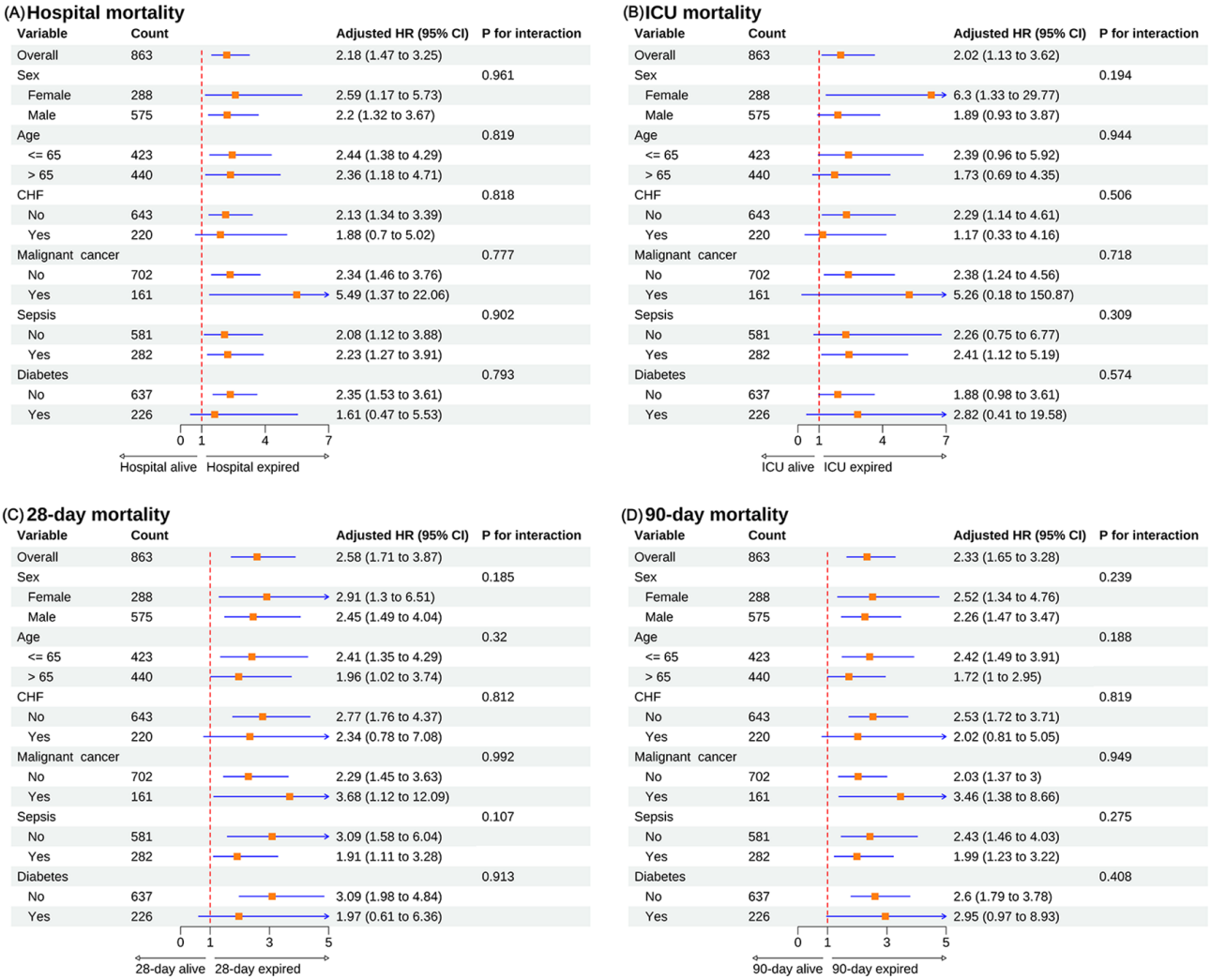


Subgroup Analysis

Subgroup analyses by sex, age, CHF, malignancy, sepsis, and diabetes showed no interaction (all interactions $P>.05$), that is, the association between CCI and the risk of all-cause hospital mortality did not change with changes in the stratification variables of sex, age, CHF, malignant cancer, sepsis, and diabetes levels (Figure 4).

XSL•FO
RenderX

Figure 4. Subgroup analyses of the association between Charlson Comorbidity Index (CCI) and all-cause mortality in intensive care unit (ICU) patients with paralytic ileus. (A) Hospital mortality. (**B**) ICU mortality. (**C**) 28-day mortality. (**D**) 90-day mortality. CHF: congestive heart failure; HR: hazard ratio.



Sensitivity Analysis

Table S4 in Multimedia Appendix 1 shows that the association between CCI and mortality outcomes in patients with PI remained stable and similar after excluding patients who died within 3 days of ICU admission.

Table S5 in Multimedia Appendix 1 shows that the sample was divided into groups of ≤4.5 and >4.5 based on the optimal cut-off value for CCI. The results show that regardless of the grouping method used, the conclusions obtained are consistent with the results of the main analysis.

A further sensitivity analysis of the SOFA score for the 3 groups was performed. The analysis showed that for the different subgroups of SOFA scores, consistent associations were observed between CCI in the higher quartiles and mortality from PI, supporting the stability of the findings (Table S6 in Multimedia Appendix 1).

Feature Preselection for ML Models

Baseline characteristics of patients in the training and test cohorts are shown in Table S7 in Multimedia Appendix 1. Figure S4 in Multimedia Appendix 1 shows the heatmaps of all variables for which correlations are provided. Because BUN and creatinine (r=0.69), SAPS II and APS III (r=0.69) or OASIS (r=0.68), OASIS and APS III (r=0.62), age and CCI (r=0.59), and chloride and sodium (r=0.66), BUN, SAPS II, OASIS, age, and chloride were excluded in the next step. In the training queue, the 3 ML algorithms with default parameters and the LASSO algorithm preselected the 10 features used to construct the model (Figure S5 in Multimedia Appendix 1), with CCI ranking in the top 10 in each algorithm. Importantly, there is no strong correlation or multicollinearity between the selected features (Figure S6 in Multimedia Appendix 1).

ML Model Construction and Evaluation

The best hyperparameters were determined after inputting the selected features into the 11 ML models. Then, Figure 5A is the confusion matrix of the LightGBM model, and the ROC curves (Figure 5B) and other metrics (Figure 5C) were evaluated among all the ML models. LightGBM was considered the best model, outperforming other ML models including random forest and extreme gradient boosting model. This is because the internal validation results show that it has the highest AUC (0.811), F_1-score (0.895), and geometric mean (0.670) and outperforms both the traditional SOFA score and the APS III score (Table 4).

XSL•FO
RenderX

Table . Performance evaluation of 11 machine learning models for predicting hospital mortality in intensive care unit (ICU) patients with paralytic ileus.

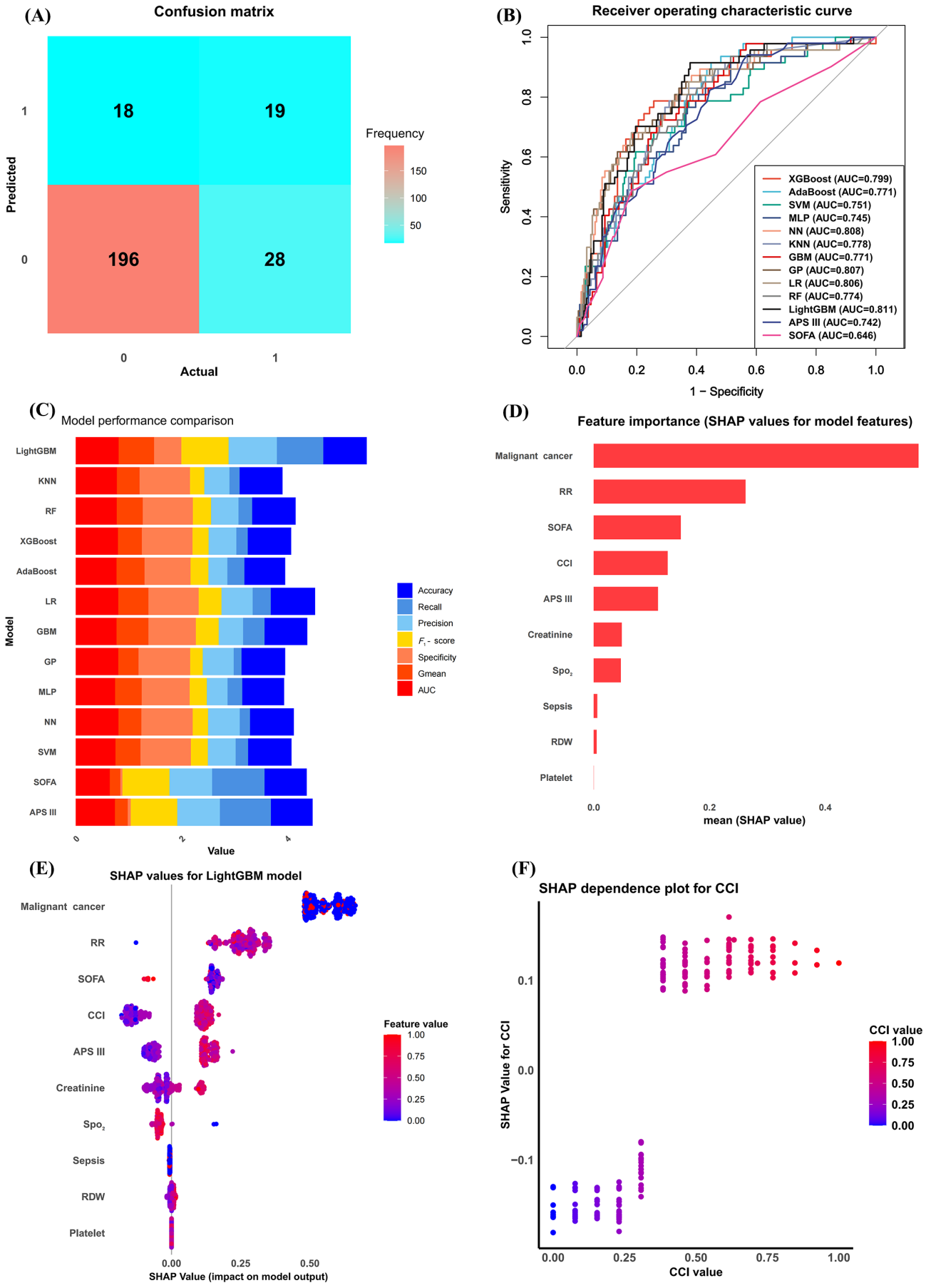
Model	Accuracy	Recall	Precision	F_1-score	Specificity	Gmean	AUC
SVM[a]	0.824	0.234	0.524	0.324	0.953	0.472	0.751
NN[b]	0.831	0.191	0.600	0.290	0.972	0.431	0.808
MLP[c]	0.793	0.277	0.394	0.325	0.907	0.501	0.745
GP[d]	0.828	0.149	0.583	0.237	0.977	0.381	0.807
GBM[e]	0.808	0.404	0.463	0.432	0.897	0.602	0.771
LR[f]	0.839	0.340	0.593	0.432	0.949	0.568	0.806
AdaBoost[g]	0.774	0.319	0.357	0.337	0.874	0.528	0.771
XGBoost[h]	0.824	0.213	0.526	0.303	0.958	0.451	0.799
RF[i]	0.824	0.255	0.522	0.343	0.949	0.492	0.774
KNN[j]	0.816	0.191	0.474	0.273	0.953	0.427	0.778
LightGBM[k]	0.824	0.875	0.916	0.895	0.514	0.670	0.811
APS III[l]	0.787	0.966	0.806	0.879	0.059	0.238	0.742
SOFA[m]	0.802	0.99	0.807	0.889	0.039	0.197	0.646

[a]SVM: support vector machine.
[b]NN: neural network.
[c]MLP: multilayer perceptron.
[d]GP: Gaussian process.
[e]GBM: gradient boosting machine.
[f]LR: logistic regression.
[g]AdaBoost: adaptive boosting.
[h]XGBoost: extreme gradient boosting.
[i]RF: random forest.
[j]KNN: k-nearest neighbor.
[k]LightGBM: light gradient boosting machine.
[l]APS III: Acute Physiological Score III.
[m]SOFA: Sequential Organ Failure Assessment.

XSL•FO
RenderX

Figure 5. (A) Machine-learning model development, evaluation, and feature importance visualization. Confusion matrix of the light gradient boosting machine (LightGBM) model. (B) Receiver operating characteristic (ROC) curves of 11 machine-learning models. (C) Various evaluation metrics of 11 machine-learning models. (D) Feature importance plot of the LightGBM model. (E) Shapley Additive Explanations (SHAP) plot of the Charlson Comorbidity Index (CCI) feature. (F) SHAP dependence plot of the CCI. AdaBoost: adaptive boosting; APS III: Acute Physiology Score III; AUC: area under the curve; GP: Gaussian process; LR: logistic regression; KNN: k-nearest neighbor; MLP: multilayer perceptron; NN: neural network; RDW: red blood cell distribution width; RF: random forest; RR: respiratory rate; SOFA: Sequential Organ Failure Assessment; SPO_2: peripheral capillary oxygen saturation; SVM: support vector machine; XGBoost: extreme gradient boosting.

XSL•FO
RenderX



XSL•FO
RenderX

Visualization of Feature Importance

The corresponding SHAP values for each feature in the internal validation cohort of the LightGBM model were calculated and ranked (Figures 5D and 5E), and CCI ranked third in significance compared to the other predictor variables. The SHAP dependence plot of the CCI (Figure 5F) showed that increased CCI was associated with an increased risk of hospital death in patients with PI.

Web-Based Forecasting Platform

To improve the usability of the LightGBM model, it has been embedded in a user-friendly website for external users and practitioners to validate or make predictions [31]. This prototype website allows users to input clinical variables such as APS III, SOFA, Charlson Comorbidity Index, and laboratory parameters (platelet, RDW, creatinine, and others) to estimate mortality risk in patients with PI. It is intended solely for research demonstration, does not replace clinical judgment, and does not store any protected health information. For example, Figure S7A in Multimedia Appendix 1 illustrates the case of a patient with PI aged 48 years with the characteristics shown. The final output probability of hospital all-cause mortality is 0.68, indicating a high risk status. This website also allows you to view and download this patient's SHAP force plot, as shown in Figure S7B in Multimedia Appendix 1.

Discussion

Principal Findings

This study analyzed the association between CCI and clinical outcomes in a US cohort of critically ill patients with PI, with the following key findings:

1. Higher levels of CCI were significantly associated with hospital, 28-day, and 90-day all-cause mortality in patients with PI. Even after correction for confounders, CCI remained strongly correlated with these mortality indicators, with a trend towards a linear relationship. Our study suggests that the critical value of 4.5 for CCI levels provides a potential reference for mortality risk stratification, helping clinicians to identify high-risk patients who require closer monitoring.
2. A LightGBM model was developed combining CCI and other clinical variables beyond the traditional critical illness score, and the results showed that CCI had a higher weight and contribution in the model. Overall, this study highlights the critical role of CCI in risk stratification of mortality in critically ill patients with PI, helping to optimize clinical management strategies.

CCI affects the prognosis of patients with PI through several interrelated biological mechanisms. First, CCI reflects a patient's chronic disease burden, including conditions such as diabetes, neurological disorders, and malignant cancer, all of which increase all-cause mortality [5,6,8]. Chronic disease states are associated with persistent low-grade systemic inflammation, which can lead to endothelial dysfunction, oxidative stress, and vasoactive imbalances, which in turn exacerbate gut microcirculatory disturbances [32-34]. In addition, patients with high CCI often have suppressed immune function, as evidenced by decreased monocyte human leukocyte antigen–DR isotype expression, T-cell dysfunction, and prolonged immune paralysis, making them more susceptible to infectious complications [35,36]. The development of infection and sepsis can further exacerbate intestinal dysbiosis [37], leading to a vicious cycle of gut flora translocation and toxin release [38]. Dysbiosis may also affect the function of the enteric nervous system through abnormalities in short-chain fatty acid metabolism, thereby prolonging the course of PI [39-41]. In addition, patients with a higher CCI usually have a poor nutritional status, as evidenced by hypoproteinemia, muscle wasting, and inadequate metabolic reserve [42-44]. These factors may lead to reduced contractile function of the intestinal smooth muscle, delaying recovery of bowel function in PI and increasing the risk of death [45,46]. Taken together, CCI affects several key pathophysiological aspects of patients with PI, including chronic inflammation, immunosuppression, impaired intestinal barrier function, and malnutrition. The interaction of these mechanisms may explain why CCI is an important predictor of mortality in patients with PI and emphasizes the need for early detection and targeted intervention.

This study found that higher CCI was significantly associated with hospital, 28-day, and 90-day all-cause mortality in patients with PI, highlighting the importance of CCI in predicting the prognosis of critically ill patients. Patients with PI are often accompanied by a variety of comorbidities, such as diabetes mellitus and malignant cancer [5,8], and CCI, as a standardized measure of comorbidity burden, is effective in reflecting the systemic health status of the patient and in revealing the potential impact of comorbidities [9,10]. An international multicenter and subgroup bias assessment study showed that the risk of death in elderly critically ill patients increased with elevated CCI, emphasizing the profound prognostic impact of comorbidity accumulation [11]. In addition, this study also found that the critical value of CCI was 4.5 for hospital death, 28-day death, and 90-day death, a finding that further supports the important role of CCI in the prognostic assessment of patients with PI. There is no literature on the clinical value of CCI as a prognostic assessment tool for patients with PI, and this study is the first to explore and present this important finding. Compared with a single physiological parameter or laboratory index, CCI can provide more comprehensive information to the clinic by comprehensively assessing multidimensional health status, which may help in fine risk stratification and individualized treatment.

However, Cox regression analyses showed that patients with elevated CCI scores were associated with suboptimal ICU all-cause mortality outcomes after adjustment for confounders, while Kaplan-Meier survival analyses indicated that higher CCI scores were not significantly correlated with ICU mortality in patients with PI. This may be explained by the predominant role of acute care factors, such as the extent of organ failure, the intensity of systemic inflammation, and the severity of infection, which often outweigh the prognostic contribution of chronic disease burden in critically ill patients. For instance, prospective studies have demonstrated that inflammatory markers are associated with delirium, coma, and increased mortality risk [47], and multicenter cohort studies have further

XSL•FO
RenderX

shown that inflammation and organ dysfunction are key determinants of 90-day mortality in acute respiratory distress syndrome [48]. In addition, intensive interventions commonly administered in the ICU, including mechanical ventilation, hemodynamic support, and renal replacement therapy, may mitigate the short-term impact of chronic comorbidities on mortality outcomes [49-51]. Thus, although the CCI remains a valuable tool for assessing chronic disease burden and predicting outcomes in hospitalized patients, its prognostic effect in ICU settings may be attenuated by acute care factors or interventions. Moreover, the relatively small sample size and low ICU mortality rate in this study may have limited statistical power. Future research should expand sample size and incorporate additional acute clinical indicators (eg, inflammatory markers and organ dysfunction scores) to further clarify the association between CCI and ICU mortality.

RCS regression analysis in this study showed that the level of CCI was significantly and linearly related to hospital mortality, ICU mortality, and 28- and 90-day mortality. Specifically, the threshold for hospital mortality was 3.65, the threshold for ICU mortality was 2.68, and the thresholds for 28-day and 90-day mortality were 4.47 and 4.39, respectively. These results suggest that lower CCI values (eg, thresholds for hospital and ICU mortality) indicate that the acute course of illness may be the primary risk factor for death, whereas higher thresholds reflect the importance of chronic disease burden in long-term prognosis. Chronic diseases, such as diabetes and malignant cancer, may have little impact on patient survival in the short term, but over time they progressively affect the patient's immune system, organ function, and overall health [52,53], and may increase the risk of patient death in acute conditions, such as PI. Thus, the impact of chronic disease burden on prognosis was more pronounced during the 28- and 90-day observation periods, and long-term patient survival was closely linked to effective management of comorbidities. The results highlight the need to closely monitor and adjust patients' CCI levels in clinical practice to optimize their short- and long-term prognosis.

Subgroup analyses showed no significant differences between subgroups (sex, age, CHF, malignant cancer, sepsis, and diabetes) in the effect of CCI on hospital, ICU, and 28-day and 90-day mortality. CCI levels have been shown to be strongly associated with poor prognosis in patients with CHF and malignant cancer [54,55]. Gadre et al [56] concluded that CCI ≥2 is a high-risk factor for readmission after sepsis hospitalization and may serve as an important indicator of poor prognosis in sepsis. These findings highlight the potential of CCI in a wide range of patient populations. Notably, in the sensitivity analysis of this study, the association between CCI and mortality outcomes in patients with PI remained stable and similar after excluding patients who died within 3 days of ICU admission. In addition, based on the optimal cut-off value of 4.5 for CCI grouping, the results obtained were consistent with the results of the primary analysis, further validating the reliability of CCI for predicting mortality. Finally, 3-group sensitivity analyses on SOFA scores were performed, and consistent associations between CCI and mortality were observed in the higher quartiles, supporting the stability and consistency of the findings. These sensitivity analyses demonstrate the strong robustness of CCI in predicting mortality in patients with PI under different subgroups and assumptions.

This study successfully developed and validated an ML model incorporating CCI for predicting hospital mortality in patients with PI. A total of 10 features were selected by a combination of LASSO and other ML algorithms, of which CCI ranked high in all algorithms, indicating the importance of CCI in predicting hospital mortality. This is similar to previous studies, many of which have demonstrated the importance of CCI in predicting mortality in a variety of patient populations, particularly critically ill patients [11,54,55]. This result is also consistent with the results of our previous Cox regression analysis. The performance of the ML model, SOFA [57] and APS III score [58], was evaluated by several metrics such as confusion matrix, ROC curve, and F_1-score. It was found that the LightGBM algorithm outperformed other ML models, traditional SOFA and APS III scoring systems, achieving an AUC of 0.811 and an F_1-score of 0.895, demonstrating its excellent predictive ability. These results are consistent with a growing body of literature showing that LightGBM has significant advantages in clinical prediction tasks, for example, Chen et al [20] concluded that LightGBM models outperform ML models such as random forest and support vector machines in predicting mortality in critically ill patients with atrial fibrillation. Feature importance analysis further highlighted the critical role of CCI in predicting mortality. SHAP value analysis, an interpretable ML technique, revealed that increasing CCI was associated with a higher risk of death in patients with PI, a finding consistent with the known association between comorbidities and patient prognosis [11,59]. The biased dependency plot also confirmed that increasing CCI values were associated with an increased risk of all-cause hospital mortality, further confirming its clinical relevance. Interpretable ML provides a more transparent model decision process and helps clinicians better understand the impact of features on predicted outcomes [60,61]. Razo et al [23] constructed a predictive model using deep learning and obtained an AUC of 0.887. However, because the predictive goal of this model is different from that of our study, it is not possible to directly compare the performance of the 2 models.

Strengths and Limitations

This study has several important strengths. First, it provides validation that elevated CCI is an independent risk factor for short- and long-term mortality in critically ill patients with PI in a large US cohort. While prior studies have applied ML approaches to predict mortality in this population using the MIMIC database [23], our work extends these efforts by systematically evaluating the prognostic value of comorbidity burden as captured by the CCI. Second, this study methodologically advances by integrating CCI into a LightGBM-based ML framework and combining it with SHAP interpretability analysis. Finally, in practical terms, this web-based platform can be applied at the time of ICU admission to rapidly identify patients with PI at high risk of mortality, thereby supporting early triage, intensified monitoring, and timely interventions. By providing individualized risk estimates together with SHAP-based explanations, the tool not only enhances transparency of the prediction process but also

XSL•FO
RenderX

facilitates communication between clinicians and patients' families. Importantly, the model is designed to complement, rather than replace, physician judgment, and thus may serve as a practical decision-support tool within routine ICU workflows.

However, this study has some limitations. First, although a higher CCI was significantly associated with hospital, 28-day, and 90-day all-cause mortality in patients with PI, as a composite scoring tool, CCI still did not cover all clinical factors that may affect prognosis, such as B-type natriuretic peptide level, etiology of PI, individual patient differences, nutritional status, and cause of death. These factors not included in the analysis may have a significant impact on the risk of death, thus introducing a potential confounding bias. Second, given the retrospective design of this study, we could only identify associations between variables and not infer causality. Although there was a significant association between CCI and all-cause mortality, this does not mean that CCI was the direct cause of death. Third, CCI is mainly based on patients' past medical history and does not take into account dynamic changes during the course of the disease, which may lead to limitations in capturing the complexity of the disease and the comprehensiveness of prognostic assessment. Fourth, although the ML-based LightGBM model performed well in internal validation, the absence of external validation using independent datasets (eg, eICU or non-US cohorts) limits its generalizability to broader populations. Fifth, given the multiple disease states and comorbidities of patients with PI, the model may be overly dependent on certain specific variables, ignoring complex interactions that may affect prognosis. Although multiple characteristics were included, the interactions between disease progression and comorbidities may not have been adequately considered. Future studies should improve the modeling of interactions between variables and dynamic factors to improve the accuracy of prognosis prediction. Sixth, although mortality was used as the primary end point in this study, considering the complexity of the prognosis of patients with PI, a single mortality indicator may not be able to comprehensively assess the health status and quality of life of patients. Therefore, future studies should explore more dimensional prognostic indicators, such as functional recovery, quality of life, and long-term survival, to provide a more comprehensive prognostic assessment. In conclusion, although CCI and ML-based models show promise in predicting mortality in critically ill patients with PI, their limitations need to be fully recognized in practical applications and combined with external validation data and dynamic clinical information to improve their clinical use and accuracy.

Conclusions

This study demonstrated that higher CCI levels were strongly associated with hospital, 28-day, and 90-day all-cause mortality in patients with PI and were valuable in mortality risk stratification. Monitoring CCI levels in patients with PI in the ICU may be useful for early identification of high-risk patients and optimization of treatment strategies.

Acknowledgments

The authors gratefully acknowledge the use of the Medical Information Mart for Intensive Care IV database for this study. The authors extend their appreciation to the Massachusetts Institute of Technology Laboratory for Computational Physiology and the dedicated staff involved in the development and maintenance of this invaluable resource. The authors would also like to express their sincere gratitude to Song Wu from the Department of Statistics, Anhui University of Chinese Medicine, for his invaluable guidance and support throughout this research. This work was supported by the National Natural Science Foundation of China (grant 82174160), and the Anhui Province "14th Five-Year" Clinical Key Specialty Construction Recommendation Plan in Traditional Chinese Medicine Surgery (WWYM [2022] 105).

Data Availability

Data used in this study are publicly available from Medical Information Mart for Intensive Care IV

(version 2.2) at PhysioNet.

Authors' Contributions

HF and HP contributed to the conception and design of the study.
QSY provided financial support.
YYY and YS offered administrative support.
FHZ and ZW provided study materials.
WSJ was responsible for data collection and assembly.
ZZ performed data analysis and interpretation.
HF drafted the manuscript.
All authors critically revised the manuscript for important intellectual content and approved the final version of the manuscript.

Conflicts of Interest

None declared.

XSL•FO
RenderX

Multimedia Appendix 1
Hyperparameters and statistical analyses.
[DOCX File, 1626 KB - medinform_v13i1e76003_app1.docx]

References

1. Solanki S, Chakinala RC, Haq KF, et al. Paralytic ileus in the United States: a cross-sectional study from the national inpatient sample. SAGE Open Med 2020;8:2050312120962636. [doi: 10.1177/2050312120962636] [Medline: 33088567]
2. Reichert M, Willis F, Post S, et al. Pharmacologic prevention and therapy of postoperative paralytic ileus after gastrointestinal cancer surgery: systematic review and meta-analysis. Int J Surg 2024 Jul 1;110(7):4329-4341. [doi: 10.1097/JS9.0000000000001393] [Medline: 38526522]
3. Proctor DW, Goodall R, Borsky K, et al. Trends in the mortality, incidence, and disability-adjusted life-years of intestinal obstruction and paralytic ileus: observational study of the Global Burden of Disease database. Br J Surg 2023 Nov 9;110(12):1650-1654. [doi: 10.1093/bjs/znad232] [Medline: 37531553]
4. Zhao X, Wan X, Gu C, et al. Association between red blood cell distribution width and short-term mortality in patients with paralytic intestinal obstruction: retrospective data analysis based on the MIMIC-III database. Emerg Med Int 2023;2023:6739136. [doi: 10.1155/2023/6739136] [Medline: 37908808]
5. Faillie JL, Yin H, Yu OHY, et al. Incretin-based drugs and risk of intestinal obstruction among patients with type 2 diabetes. Clin Pharmacol Ther 2022 Jan;111(1):272-282. [doi: 10.1002/cpt.2430] [Medline: 34587280]
6. Camilleri M. Gastrointestinal motility disorders in neurologic disease. J Clin Invest 2021 Feb 15;131(4):e143771. [doi: 10.1172/JCI143771] [Medline: 33586685]
7. Valenzuela A, Li S, Becker L, et al. Intestinal pseudo-obstruction in patients with systemic sclerosis: an analysis of the Nationwide Inpatient Sample. Rheumatology (Oxford) 2016 Apr;55(4):654-658. [doi: 10.1093/rheumatology/kev393] [Medline: 26615031]
8. Güngördük K, Özdemir İ, Güngördük Ö, Gülseren V, Gokçü M, Sancı M. Effects of coffee consumption on gut recovery after surgery of gynecological cancer patients: a randomized controlled trial. Am J Obstet Gynecol 2017 Feb;216(2):145. [doi: 10.1016/j.ajog.2016.10.019] [Medline: 27780709]
9. Roffman CE, Buchanan J, Allison GT. Charlson Comorbidities Index. J Physiother 2016 Jul;62(3):171. [doi: 10.1016/j.jphys.2016.05.008] [Medline: 27298055]
10. Charlson ME, Carrozzino D, Guidi J, Patierno C. Charlson Comorbidity Index: A critical review of clinimetric properties. Psychother Psychosom 2022;91(1):8-35. [doi: 10.1159/000521288] [Medline: 34991091]
11. Liu X, Hu P, Yeung W, et al. Illness severity assessment of older adults in critical illness using machine learning (ELDER-ICU): an international multicentre study with subgroup bias evaluation. The Lancet Digital Health 2023 Oct;5(10):e657-e667. [doi: 10.1016/S2589-7500(23)00128-0]
12. Feng L, Fu S, Yao Y, Yuan W, Zhao Y. Age, Prognostic Nutritional Index, and Charlson Comorbidity Index were independent risk factors for postoperative long-term mortality in Chinese geriatric patients who sustain hip fracture. J Am Med Dir Assoc 2021 Dec;22(12):2602-2603. [doi: 10.1016/j.jamda.2021.08.001] [Medline: 34461043]
13. Heyland DK, Garland A, Bagshaw SM, et al. Recovery after critical illness in patients aged 80 years or older: a multi-center prospective observational cohort study. Intensive Care Med 2015 Nov;41(11):1911-1920. [doi: 10.1007/s00134-015-4028-2] [Medline: 26306719]
14. Yang CC, Fong Y, Lin LC, et al. The age-adjusted Charlson Comorbidity Index is a better predictor of survival in operated lung cancer patients than the Charlson and Elixhauser Comorbidity Indices. Eur J Cardiothorac Surg 2018 Jan 1;53(1):235-240. [doi: 10.1093/ejcts/ezx215] [Medline: 29106506]
15. Rosti G, Brümmendorf TH, Gjertsen BT, et al. Impact of age and comorbidities on the efficacy and tolerability of bosutinib in previously treated patients with chronic myeloid leukemia: results from the phase 4 BYOND study. Leukemia 2024 Jan;38(1):126-135. [doi: 10.1038/s41375-023-02080-y]
16. Sieber FE, Neufeld KJ, Gottschalk A, et al. Effect of depth of sedation in older patients undergoing hip fracture repair on postoperative delirium: the STRIDE randomized clinical trial. JAMA Surg 2018 Nov 1;153(11):987-995. [doi: 10.1001/jamasurg.2018.2602] [Medline: 30090923]
17. Clausen A, Möller S, Skjødt MK, Bech BH, Rubin KH. Evaluating the performance of the Charlson Comorbidity Index (CCI) in fracture risk prediction and developing a new Charlson Fracture Index (CFI): a register-based cohort study. Osteoporos Int 2022 Mar;33(3):549-561. [doi: 10.1007/s00198-021-06293-8] [Medline: 34993562]
18. Shah FA, Talisa VB, Chang CCH, et al. Heterogeneity in the effect of early goal-directed therapy for septic shock: a secondary analysis of two multicenter international trials. Crit Care Med 2025 Jan 1;53(1):e4-e14. [doi: 10.1097/CCM.0000000000006463] [Medline: 39440873]
19. Ates HC, Alshanawani A, Hagel S, et al. Unraveling the impact of therapeutic drug monitoring via machine learning for patients with sepsis. Cell Rep Med 2024 Aug 20;5(8):101681. [doi: 10.1016/j.xcrm.2024.101681] [Medline: 39127039]
20. Chen Y, Yang Z, Liu Y, et al. Prognostic value of glycaemic variability for mortality in critically ill atrial fibrillation patients and mortality prediction model using machine learning. Cardiovasc Diabetol 2024;23(1):426. [doi: 10.1186/s12933-024-02521-7]

XSL•FO
RenderX

21. Xie P, Wang H, Xiao J, et al. Development and validation of an explainable deep learning model to predict in-hospital mortality for patients with acute myocardial infarction: algorithm development and validation study. J Med Internet Res 2024 May 10;26:e49848. [doi: 10.2196/49848] [Medline: 38728685]
22. Viton F, Elbattah M, Guerin JL, Dequen G. Heatmaps for visual explainability of CNN-based predictions for multivariate time series with application to healthcare. In: Dequen G, editor. Presented at: 2020 IEEE International Conference on Healthcare Informatics (ICHI); Nov 30-3, 2020; Oldenburg, Germany. [doi: 10.1109/ICHI48887.2020.9374393]
23. Razo M, Pishgar M, Galanter W, Darabi H. Deep-learning model for mortality prediction of ICU patients with paralytic ileus. Bioengineering (Basel) 2024 Nov 30;11(12):1214. [doi: 10.3390/bioengineering11121214] [Medline: 39768031]
24. Johnson AEW, Bulgarelli L, Shen L, et al. Author correction: MIMIC-IV, a freely accessible electronic health record dataset. Sci Data 2023 Jan 16;10(1):31. [doi: 10.1038/s41597-023-01945-2] [Medline: 36646711]
25. Qian F, van den Boom W, See KC. The new global definition of acute respiratory distress syndrome: insights from the MIMIC-IV database. Intensive Care Med 2024 Apr;50(4):608-609. [doi: 10.1007/s00134-024-07383-x] [Medline: 38483560]
26. Xu L, Zhao W, He J, et al. Abdominal perfusion pressure is critical for survival analysis in patients with intra-abdominal hypertension: mortality prediction using incomplete data. Int J Surg 2025 Jan 1;111(1):371-381. [doi: 10.1097/JS9.0000000000002026] [Medline: 39166944]
27. Ye Q, Wang X, Xu X, et al. Serial platelet count as a dynamic prediction marker of hospital mortality among septic patients. Burns Trauma 2024;12:tkae016. [doi: 10.1093/burnst/tkae016] [Medline: 38882552]
28. Johnson A, Bulgarelli L, Pollard T, Horng S, Celi LA, Mark R. MIMIC-IV (version 2.2). PhysioNet. URL: https://physionet.org/content/mimiciv/2.2/ [accessed 2023-10-13]
29. Zhang Y, Hu J, Hua T, Zhang J, Zhang Z, Yang M. Development of a machine learning-based prediction model for sepsis-associated delirium in the intensive care unit. Sci Rep 2023;13(1):12697. [doi: 10.1038/s41598-023-38650-4]
30. Stekhoven DJ, Bühlmann P. MissForest—non-parametric missing value imputation for mixed-type data. Bioinformatics 2012 Jan 1;28(1):112-118. [doi: 10.1093/bioinformatics/btr597] [Medline: 22039212]
31. Prediction of mortality rate in paralytic ileus. Paralytic Ileus Mortality Prediction (Research Prototype). URL: http://182.92.81.83:8000/ [accessed 2025-10-14]
32. van Heck JIP, Ajie M, Joosten LAB, Tack CJ, Stienstra R. Circulating inflammatory proteins are elevated in type 1 and type 2 diabetes and associated to complications. Diabetes Obes Metab 2025 Feb;27(2):719-728. [doi: 10.1111/dom.16066] [Medline: 39562286]
33. Escalante J, Artaiz O, Diwakarla S, McQuade RM. Leaky gut in systemic inflammation: exploring the link between gastrointestinal disorders and age-related diseases. Geroscience 2025 Feb;47(1):1-22. [doi: 10.1007/s11357-024-01451-2] [Medline: 39638978]
34. Sandek A, Bauditz J, Swidsinski A, et al. Altered intestinal function in patients with chronic heart failure. J Am Coll Cardiol 2007 Oct 16;50(16):1561-1569. [doi: 10.1016/j.jacc.2007.07.016] [Medline: 17936155]
35. Artru F, Sacleux SC, Ursic-Bedoya J, et al. Long-term outcome following liver transplantation of patients with ACLF grade 3. J Hepatol 2025 Jan;82(1):62-71. [doi: 10.1016/j.jhep.2024.06.039] [Medline: 38981560]
36. Major E, Lin KH, Lee SC, et al. LPA suppresses HLA-DR expression in human melanoma cells: a potential immune escape mechanism involving LPAR1 and DR6-mediated release of IL-10. Acta Pharmacol Sin 2025 Jan;46(1):222-230. [doi: 10.1038/s41401-024-01373-x] [Medline: 39187677]
37. Cao YY, Wang ZH, Pan YJ, et al. The dual effects of dexmedetomidine on intestinal barrier and intestinal motility during sepsis. Surgery 2024 Aug;176(2):379-385. [doi: 10.1016/j.surg.2024.03.047] [Medline: 38762380]
38. Dickson RP, Singer BH, Newstead MW, et al. Enrichment of the lung microbiome with gut bacteria in sepsis and the acute respiratory distress syndrome. Nat Microbiol 2016 Jul 18;1(10):16113. [doi: 10.1038/nmicrobiol.2016.113] [Medline: 27670109]
39. Ikeda T, Nishida A, Yamano M, Kimura I. Short-chain fatty acid receptors and gut microbiota as therapeutic targets in metabolic, immune, and neurological diseases. Pharmacol Ther 2022 Nov;239:108273. [doi: 10.1016/j.pharmthera.2022.108273] [Medline: 36057320]
40. Cryan JF, O'Riordan KJ, Cowan CSM, et al. The microbiota-gut-brain axis. Physiol Rev 2019 Oct 1;99(4):1877-2013. [doi: 10.1152/physrev.00018.2018] [Medline: 31460832]
41. Muller PA, Schneeberger M, Matheis F, et al. Microbiota modulate sympathetic neurons via a gut-brain circuit. Nature New Biol 2020 Jul;583(7816):441-446. [doi: 10.1038/s41586-020-2474-7] [Medline: 32641826]
42. Kubo Y, Tanaka K, Yamasaki M, et al. Influences of the Charlson Comorbidity Index and nutrition status on prognosis after esophageal cancer surgery. Ann Surg Oncol 2021 Nov;28(12):7173-7182. [doi: 10.1245/s10434-021-09779-1] [Medline: 33835302]
43. Meza-Valderrama D, Marco E, Dávalos-Yerovi V, et al. Sarcopenia, malnutrition, and cachexia: Adapting definitions and terminology of nutritional disorders in older people with cancer. Nutrients 2021 Feb 26;13(3):761. [doi: 10.3390/nu13030761] [Medline: 33652812]
44. Tippairote T, Bjørklund G, Gasmi A, et al. Combined supplementation of coenzyme Q10 and other nutrients in specific medical conditions. Nutrients 2022 Oct 19;14(20):4383. [doi: 10.3390/nu14204383] [Medline: 36297067]

XSL•FO
RenderX

45. Bayer F, Dremova O, Khuu MP, et al. The interplay between nutrition, innate immunity, and the commensal microbiota in adaptive intestinal morphogenesis. Nutrients 2021 Jun 26;13(7):2198. [doi: 10.3390/nu13072198] [Medline: 34206809]
46. Paolino S, Pacini G, Schenone C, et al. Nutritional status and bone microarchitecture in a cohort of systemic sclerosis patients. Nutrients 2020 Jun 1;12(6):1632. [doi: 10.3390/nu12061632] [Medline: 32492873]
47. Brummel NE, Hughes CG, McNeil JB, et al. Systemic inflammation and delirium during critical illness. Intensive Care Med 2024 May;50(5):687-696. [doi: 10.1007/s00134-024-07388-6] [Medline: 38647548]
48. Ceccato A, Forne C, Bos LD, et al. Clustering COVID-19 ARDS patients through the first days of ICU admission. An analysis of the CIBERESUCICOVID Cohort. Crit Care 2024 Mar 21;28(1):91. [doi: 10.1186/s13054-024-04876-5] [Medline: 38515193]
49. Paton M, Chan S, Serpa Neto A, et al. Association of active mobilisation variables with adverse events and mortality in patients requiring mechanical ventilation in the intensive care unit: a systematic review and meta-analysis. Lancet Respir Med 2024 May;12(5):386-398. [doi: 10.1016/S2213-2600(24)00011-0] [Medline: 38513675]
50. Geri G, Vignon P, Aubry A, et al. Cardiovascular clusters in septic shock combining clinical and echocardiographic parameters: a post hoc analysis. Intensive Care Med 2019 May;45(5):657-667. [doi: 10.1007/s00134-019-05596-z] [Medline: 30888443]
51. Gaudry S, Hajage D, Martin-Lefevre L, et al. Comparison of two delayed strategies for renal replacement therapy initiation for severe acute kidney injury (AKIKI 2): a multicentre, open-label, randomised, controlled trial. Lancet 2021 Apr 3;397(10281):1293-1300. [doi: 10.1016/S0140-6736(21)00350-0] [Medline: 33812488]
52. Turner SJ, La Gruta NL. A subset of immune-system T cells branded as seeds for type 1 diabetes. Nature New Biol 2022 Feb;602(7895):35-36. [doi: 10.1038/d41586-021-03800-z] [Medline: 35079168]
53. Mao X, Xu J, Wang W, et al. Crosstalk between cancer-associated fibroblasts and immune cells in the tumor microenvironment: new findings and future perspectives. Mol Cancer 2021 Oct 11;20(1):131. [doi: 10.1186/s12943-021-01428-1] [Medline: 34635121]
54. Formiga F, Moreno-Gonzalez R, Chivite D, Franco J, Montero A, Corbella X. High comorbidity, measured by the Charlson Comorbidity Index, associates with higher 1-year mortality risks in elderly patients experiencing a first acute heart failure hospitalization. Aging Clin Exp Res 2018 Aug;30(8):927-933. [doi: 10.1007/s40520-017-0853-1] [Medline: 29124524]
55. Iwai N, Dohi O, Naito Y, et al. Impact of the Charlson Comorbidity Index and prognostic nutritional index on prognosis in patients with early gastric cancer after endoscopic submucosal dissection. Dig Endosc 2018 Sep;30(5):616-623. [doi: 10.1111/den.13051] [Medline: 29532961]
56. Gadre SK, Shah M, Mireles-Cabodevila E, Patel B, Duggal A. Epidemiology and predictors of 30-day readmission in patients with sepsis. Chest 2019 Mar;155(3):483-490. [doi: 10.1016/j.chest.2018.12.008] [Medline: 30846065]
57. Raith EP, Udy AA, Bailey M, et al. Prognostic accuracy of the SOFA score, SIRS criteria, and qSOFA score for in-hospital mortality among adults with suspected infection admitted to the intensive care unit. JAMA 2017 Jan 17;317(3):290-300. [doi: 10.1001/jama.2016.20328] [Medline: 28114553]
58. Huang J, Cai Y, Wu X, Huang X, Liu J, Hu D. Prediction of mortality events of patients with acute heart failure in intensive care unit based on deep neural network. Comput Methods Programs Biomed 2024 Nov;256:108403. [doi: 10.1016/j.cmpb.2024.108403]
59. Lam CSN, Bharwani AA, Chan EHY, et al. A machine learning model for colorectal liver metastasis post-hepatectomy prognostications. Hepatobiliary Surg Nutr 2023 Aug 1;12(4):495-506. [doi: 10.21037/hbsn-21-453] [Medline: 37601005]
60. Deng H, Eftekhari Z, Carlin C, et al. Development and validation of an explainable machine learning model for major complications after cytoreductive surgery. JAMA Netw Open 2022 May 2;5(5):e2212930. [doi: 10.1001/jamanetworkopen.2022.12930] [Medline: 35612856]
61. Bernard D, Doumard E, Ader I, et al. Explainable machine learning framework to predict personalized physiological aging. Aging Cell 2023 Aug;22(8):e13872. [doi: 10.1111/acel.13872] [Medline: 37300327]

Abbreviations

APS III: Acute Physiology Score III
AUC: area under the curve
BIDMC: Beth Israel Deaconess Medical Center
BUN: blood urea nitrogen
CCI: Charlson Comorbidity Index
CHF: congestive heart failure
HR: hazard ratio
ICD: International Classification of Diseases
ICU: intensive care unit
IRB: institutional review board
LASSO: least absolute shrinkage and selection operator
LightGBM: light gradient boosting machine

XSL•FO
RenderX

MBP: mean blood pressure
MIMIC: Medical Information Mart for Intensive Care
ML: machine learning
OASIS: Oxford Acute Severity of Illness Score
OR: odds ratio
PI: paralytic ileus
RCS: restricted cubic spline
RDW: red blood cell distribution width
ROC: receiver operating characteristic
RR: respiratory rate
SAPS II: Simplified Acute Physiology Score II
SHAP: Shapley Additive Explanations
SOFA: Sequential Organ Failure Assessment
SpO_2: saturation of peripheral oxygen
VIF: variance inflation factor
WBC: white blood cell

Edited by A Benis; submitted 15.04.25; peer-reviewed by D Ajayi, M Elbattah, RT Potla; revised version received 22.09.25; accepted 06.10.25; published 16.10.25.

Please cite as:
Feng H, Zhou F, Shen Y, Wang Z, Yuan Y, Jing W, Zheng Z, Peng H, Yu Q
Prognostic Value of the Charlson Comorbidity Index for Mortality and Machine Learning–Based Prediction in Critically Ill Patients with Paralytic Ileus: Retrospective Cohort Study
JMIR Med Inform 2025;13:e76003
URL: https://medinform.jmir.org/2025/1/e76003
doi:10.2196/76003

© Hui Feng, Fuhai Zhou, Yi Shen, Zhen Wang, Yiyang Yuan, Wenshan Jing, Zhou Zheng, Hui Peng, Qingsheng Yu. Originally published in JMIR Medical Informatics (https://medinform.jmir.org), 16.10.2025. This is an open-access article distributed under the terms of the Creative Commons Attribution License (https://creativecommons.org/licenses/by/4.0/), which permits unrestricted use, distribution, and reproduction in any medium, provided the original work, first published in JMIR Medical Informatics, is properly cited. The complete bibliographic information, a link to the original publication on https://medinform.jmir.org/, as well as this copyright and license information must be included.

XSL•FO
RenderX

Survival Prediction for Postoperative Patients With Kidney Cancer Based on Computed Tomography Radiomics: Retrospective Cohort Study

Guizhen He[1,2*], BM; Liwen Lai[1,2*], BM; Guoan Yu[1,2], BM; Haowen Pang[3], MS; Xiaohui Yu[1,2], BM; Huaiwen Zhang[4], MS; Qingxiu Zhu[1,2*], BM; Yingzi Lv[1,2], BM

[1]Department of Nephrology, The Third People's Hospital of Jingdezhen, 76 Taoyang Road, Xinchang, East Suburb, Zhushan District, Jingdezhen, China

[2]Department of Nephrology, The Third People's Hospital of Jingdezhen affiliated to Nanchang Medical College, Jingdezhen, China

[3]Department of Oncology, The Affiliated Hospital of Southwest Medical University, Luzhou, China

[4]Jiangxi Cancer Hospital & Institute, Jiangxi Clinical Research Center for Cancer, The Second Affiliated Hospital of Nanchang Medical College, Nanchang, China

[*]these authors contributed equally

Corresponding Author:
Yingzi Lv, BM
Department of Nephrology, The Third People's Hospital of Jingdezhen, 76 Taoyang Road, Xinchang, East Suburb, Zhushan District, Jingdezhen, China

Abstract

Background: Kidney cancer remains a significant challenge in oncology, with accurate prognostic assessment being crucial for postoperative management. While radiomics has shown promise in cancer prognosis, there is limited research on comprehensive models that effectively integrate radiomic features with clinical parameters for kidney cancer survival prediction.

Objective: This study aimed to develop and validate a comprehensive computed tomography (CT) radiomics-based nomogram for predicting overall survival in postoperative patients with kidney cancer by integrating radiomic features with clinical parameters.

Methods: Radiomic features were extracted from regions of interest in CT images of 207 postoperative patients with kidney cancer. The eigenvalue data of all radiomic features were processed using *z* score standardization and the R software package *GLMNet*. We integrated survival time, survival status, and radiomic features and screened these features using the least absolute shrinkage and selection operator–Cox regression method. We conducted 10-fold cross-validation to obtain an optimal model of 5 radiomic features. Multivariate Cox regression hazard models were established to analyze patients' overall survival. The predictive ability of the nomogram (receiver operating characteristic curve and calibration curve) was evaluated using bootstrap resampling validation. Patients were divided into high- and low-risk groups based on the radiomic risk score cutoff value, and the Kaplan-Meier method was conducted to identify established models' forecasting ability. Five radiomic features were screened for predictive model construction.

Results: This retrospective analysis was conducted from April 2024 to July 2024 using data from The Cancer Imaging Archive public database. The final cohort included 207 patients (3 excluded from the initial 210) who underwent nephrectomy for kidney cancer. The median follow-up time was 33 (IQR 11-47) months. The receiver operating characteristic curve and area under the curve showed that the predictive model performed well. The calibration curve of nomogram and radiomic features in the cohort study set indicated an overall net benefit. Kaplan-Meier curves indicated that overall survival time was dramatically shorter in the high-risk group.

Conclusions: Our radiomics nomogram successfully integrates CT-derived radiomic features with clinical variables for kidney cancer survival prediction, demonstrating good prognostic capability and offering a noninvasive, quantitative tool for personalized postoperative management and clinical decision-making.

(JMIR Med Inform 2025;13:e73162) doi:10.2196/73162

KEYWORDS

computed tomography radiomics; kidney cancer; postoperative; predictive survival; nomogram

XSL•FO
RenderX

Introduction

Background

Kidney cancer is the most common malignant cancer of the urinary system, and nephrectomy is the standard treatment for locoregional kidney cancer [1]. Progress has been achieved through multiple optional methods of surgical resection and systemic therapies for kidney cancer [2]. However, overall survival (OS) and prognosis, especially if the cancer is detected at an advanced stage, remain unsatisfactory if the cancer is not treated optimally because of its high invasiveness, high mortality, and resistance to chemoradiotherapy [2,3]. Furthermore, the incidence of kidney cancer has been reported to have steadily increased in recent years [4-6]. The ability to predict the prognosis preoperatively and noninvasively is vital; however, patients who undergo nephrectomy still lack specific radiomic markers because of the complexity of disease progression and high heterogeneity. Radiomic markers that can facilitate predicting and monitoring the prognosis with good accuracy are urgently needed, after which a personalized strategy for clinical treatment needs to be provided. However, there remains limited research on comprehensive prognostic models that effectively integrate radiomic features with clinical parameters for kidney cancer survival prediction [7].

Radiomics is a rapidly developing field in which medical images are transformed into available radiological data and allows for efficacy monitoring, prognosis surveillance, microenvironment evaluation, and biological behavior assessment through quantitatively extracting features and facilitating in-depth characterization of tumor phenotypes beyond imaging interpretation [8-10]. Clinically, the postoperative prognosis of patients with cancer is frequently evaluated using the tumor-node-metastasis (TNM) classification system [11]. Recently, there has been an increasing focus on the application of computed tomography (CT) radiomics in kidney cancer, which has satisfactory potential in terms of lesion characterization, histological grade, and assessment of response to treatment [12-14]. Nevertheless, the correlation between radiomic features and the prognosis of patients with kidney cancer remains unclear, and further research is required to provide references for the clinical setting.

Objectives

To address this need, we developed a comprehensive radiomics-based nomogram that combines CT-derived features with clinical parameters for survival prediction in postoperative patients with kidney cancer. This integrated approach provides a practical tool for prognostic assessment and clinical decision-making.

Methods

Patient Selection and Clinical Data Collection

Data from 210 patients with kidney cancer were obtained from The Cancer Imaging Archive (TCIA) database [15]. Inclusion criteria were (1) pathologically confirmed kidney cancer, (2) having undergone nephrectomy, (3) available contrast-enhanced CT imaging data, and (4) complete survival follow-up data. Exclusion criteria were patients with an OS of 0 days (n=3). Our final cohort comprised 207 patients. Clinical characteristics collected included demographic data (age and gender), smoking history, comorbidities, tumor characteristics (pathology TNM stage, tumor histologic subtype, and tumor International Society of Urological Pathology grade), surgical parameters, and survival outcomes (vital status and survival time). To identify independent risk factors of OS, univariate and multivariate Cox regression analyses were conducted using the *survival* and *forest plot* packages in R (R Foundation for Statistical Computing).

Radiomic Datasets and Feature Extraction

Image Preprocessing

CT images were preprocessed using wavelet-based methods. Before feature extraction, all images were resampled according to a voxel size of $1 \times 1 \times 1$ mm^3 to ensure standardized spatial resolution across the dataset.

Region of Interest Definition

Presegmented regions of interest, including gross tumor volume (GTV) and healthy kidney regions, were obtained from the TCIA database annotations. All regions of interest were visually inspected for quality and anatomical accuracy to ensure appropriate boundaries for radiomic analysis.

Feature Extraction

Feature extraction was based on the 3D Slicer platform and was conducted using the PyRadiomics package [16]. A total of 851 radiomic features were extracted from the GTV and healthy kidney regions, including shape features (volume, surface area, and sphericity), first-order statistical features (mean, variance, skewness, and kurtosis), and texture features (gray-level dependence matrix [GLDM], gray-level co-occurrence matrix, neighboring gray tone difference matrix, gray-level size zone matrix, and gray level run length matrix). Wavelet-transformed features from different frequency decompositions were also extracted. The eigenvalue data of all radiomic features were processed using *z* score standardization to ensure comparability across different feature scales [17].

Feature Selection and Model Development

Feature Selection Rationale and Methodology

Least absolute shrinkage and selection operator (LASSO) regression was chosen for feature selection due to several advantages: (1) it effectively handles high-dimensional data with small sample sizes, which is common in radiomics studies; (2) it performs automatic feature selection by shrinking coefficients of less important features to 0; (3) it reduces overfitting risk through L1 regularization; and (4) it has been widely validated in survival analysis and radiomics research.

LASSO-Cox regression analysis was conducted using the *glmnet* package in R. We integrated survival time, survival status, and radiomic features from all 207 patients. The optimal regularization parameter (λ) was determined through 10-fold cross-validation using the minimum cross-validated partial likelihood deviance as the selection criterion. Features with nonzero coefficients at the optimal λ were selected for model construction.

XSL•FO
RenderX

Risk Score Construction and Stratification

A radiomic risk score was constructed using the linear combination of selected features weighted by their LASSO regression coefficients. The optimal cutoff value for risk stratification was determined using time-dependent receiver operating characteristic (ROC) curve analysis. Patients were then classified into high- and low-risk groups using this cutoff value.

Statistical Analysis and Model Validation

Model Development and Nomogram Construction

Univariate and multivariate Cox regression analyses were conducted on the entire cohort to identify independent prognostic factors using the *survival* and *forestplot* packages in R. Clinical variables with $P<.10$ in univariate analysis were included in multivariate analysis along with the radiomic risk score. A nomogram was constructed using the *rms* package incorporating significant variables from multivariate analysis.

Model Performance Evaluation

Model performance was assessed using multiple metrics following established methodologies for machine learning–based cancer prediction studies [18]: discrimination (time-dependent ROC curves and area under the curve [AUC] at 1, 2, 4, and 6 years using the *survivalROC* package), calibration (calibration plots comparing predicted vs observed survival probabilities), clinical utility (decision curve analysis to evaluate clinical net benefit), and risk stratification (Kaplan-Meier survival curves with the log rank test to compare survival differences between risk groups) [19,20].

Validation Strategy

Given the presegmented nature of the TCIA dataset, we used bootstrap resampling for model validation. The 10-fold cross-validation was specifically used during the LASSO regression phase to determine the optimal regularization parameter (λ) for feature selection. For final model validation, we performed 1000 bootstrap iterations on the entire cohort (N=207) to assess model stability and obtain CIs for performance metrics.

Statistical Software and Significance

All analyses were conducted using the R software (version 3.6.3). A 2-sided $P<.05$ was considered statistically significant. Missing data were handled using complete case analysis.

Ethical Considerations

This study was conducted in accordance with the Declaration of Helsinki and approved by the Ethics Committee of Jiangxi Cancer Hospital & Institute (2024ky057). As this study used publicly available databases, all data in this study have been anonymized or de-identified, so written informed consent from patients was not obtained.

Results

Clinical Data

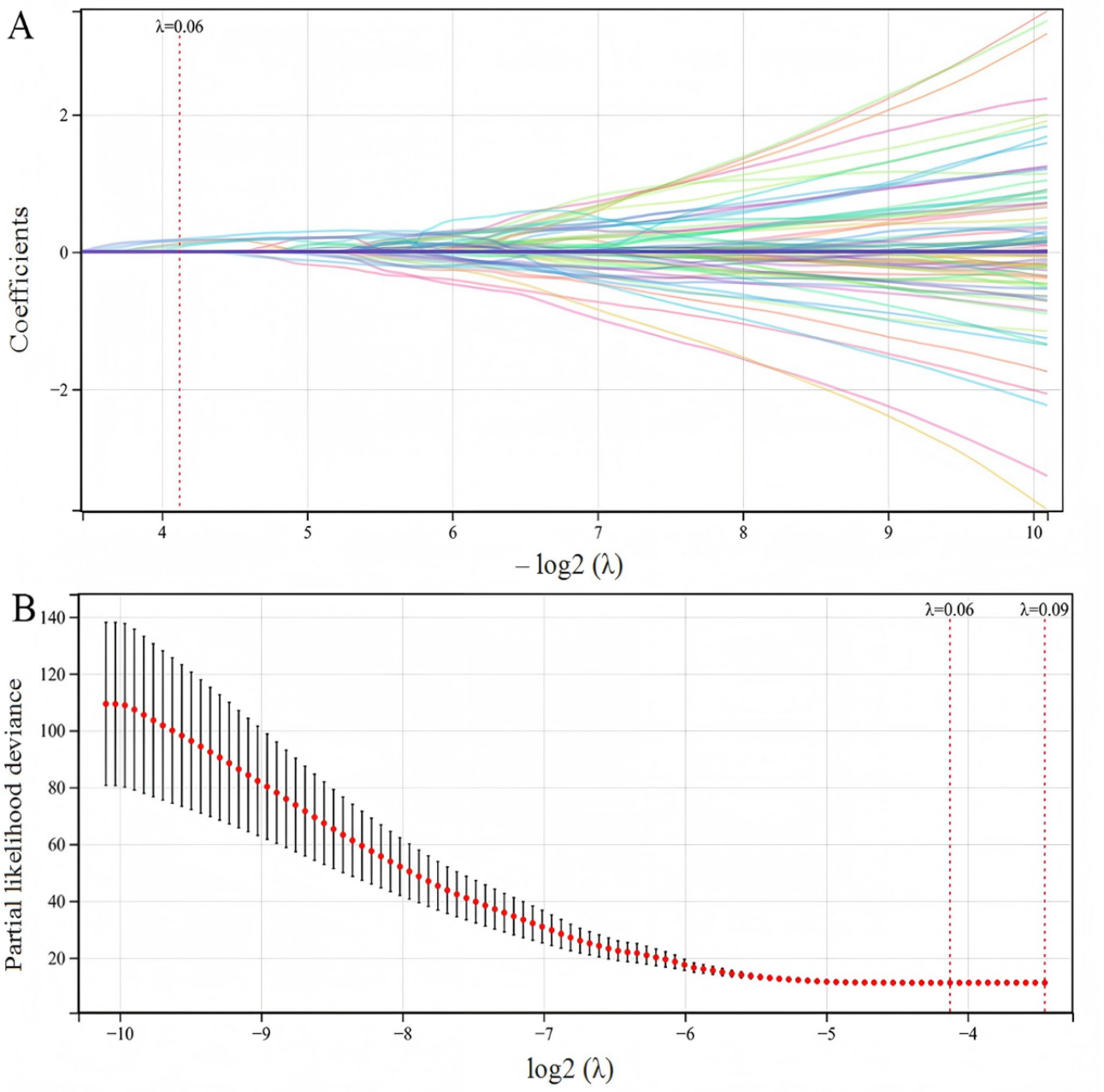
This retrospective analysis was conducted from April 2024 to July 2024 using data from the TCIA public database. The final cohort included 207 patients (3 excluded from the initial 210) who underwent nephrectomy for kidney cancer. This study comprised 58.5% (121/207) male and 41.5% (86/207) female patients. The median follow-up time was 33 (range 1 - 102; IQR 11-47) months at the time of analysis.

Radiomic Feature Variable Selection

Five radiomic features were selected through LASSO-Cox regression analysis for OS prediction (Figure 1). The radiomic features included the following: kurtosis of first-order wavelet-LLH (H: high-frequency band; L: low-frequency band; GTV; feature 1), large-area high gray-level emphasis of the gray-level size zone matrix of wavelet-LHL (GTV; feature 2), dependence nonuniformity of GLDM of wavelet-HHL (healthy kidney; feature 3), long-run low gray-level emphasis of gray-level run length matrix of wavelet-LHL (GTV; feature 4), and large-dependence low gray-level emphasis of GLDM of wavelet-LLL (GTV; feature 5). The 5 selected radiomic features represent different aspects of tumor and tissue characteristics that may have clinical relevance. Texture features such as gray-level emphasis and dependence measures reflect tissue heterogeneity and organizational patterns, which may correlate with tumor biological behavior and aggressiveness. The inclusion of features from both tumor regions (GTV) and healthy kidney tissue suggests that both local tumor characteristics and the impact on surrounding normal tissue contribute to prognostic assessment. These features collectively capture quantitative imaging biomarkers that complement traditional clinical prognostic factors.

XSL•FO
RenderX

Figure 1. LASSO regression feature selection for kidney cancer survival prediction (entire cohort: N=207). (A) LASSO coefficient paths and (B) 10-fold cross-validation curve for selecting five radiomic features. LASSO: least absolute shrinkage and selection operator.



The variables from features 1 to 5 represent the significant radiomic features for predicting OS and are shown in Table 1. The formula for the OS radiomic risk score was as follows:

XSL•FO
RenderX

Table . Features 1 to 5, corresponding to different parameters for radiomics.

Feature number	CT[a] radiomics
1	Kurtosis of first-order wavelet-LLH (GTV[b])
2	Large-area high gray-level emphasis of GLSZM[c] of wavelet-LHL (GTV)
3	Dependence nonuniformity of GLDM[d] of wavelet-HHL (healthy kidney)
4	Long-run low gray-level emphasis of GLRLM[e] of wavelet-LHL (GTV)
5	Large-dependence low gray-level emphasis of GLDM of wavelet-LLL (GTV)

[a]CT: computed tomography.

[b]GTV: gross tumor volume.

[c]GLSZM: gray-level size zone matrix.

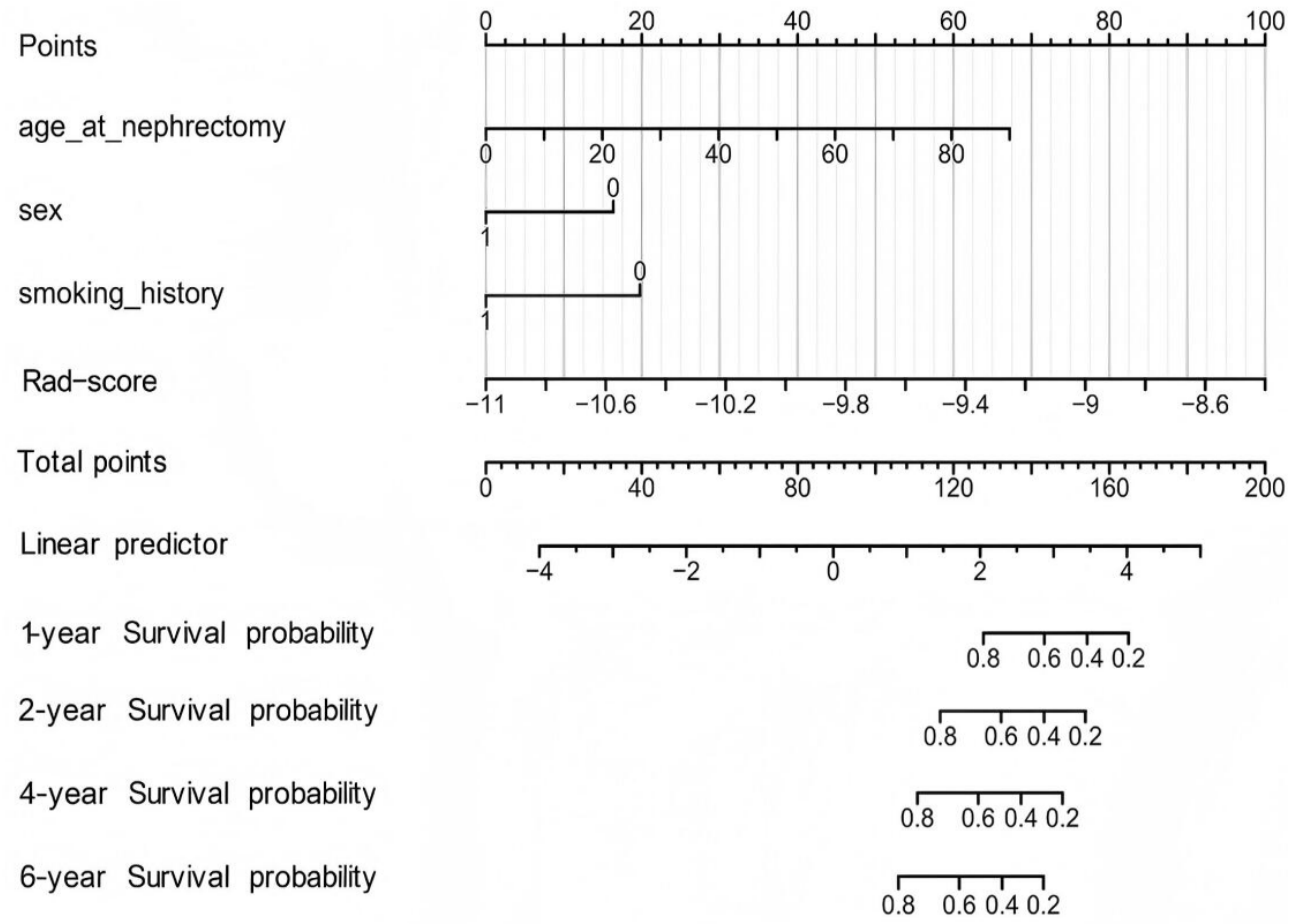
[d]GLDM: gray-level dependence matrix.

[e]GLRLM: gray-level run length matrix.

Establishment of Nomograms and Prediction Performance of the Nomogram Models

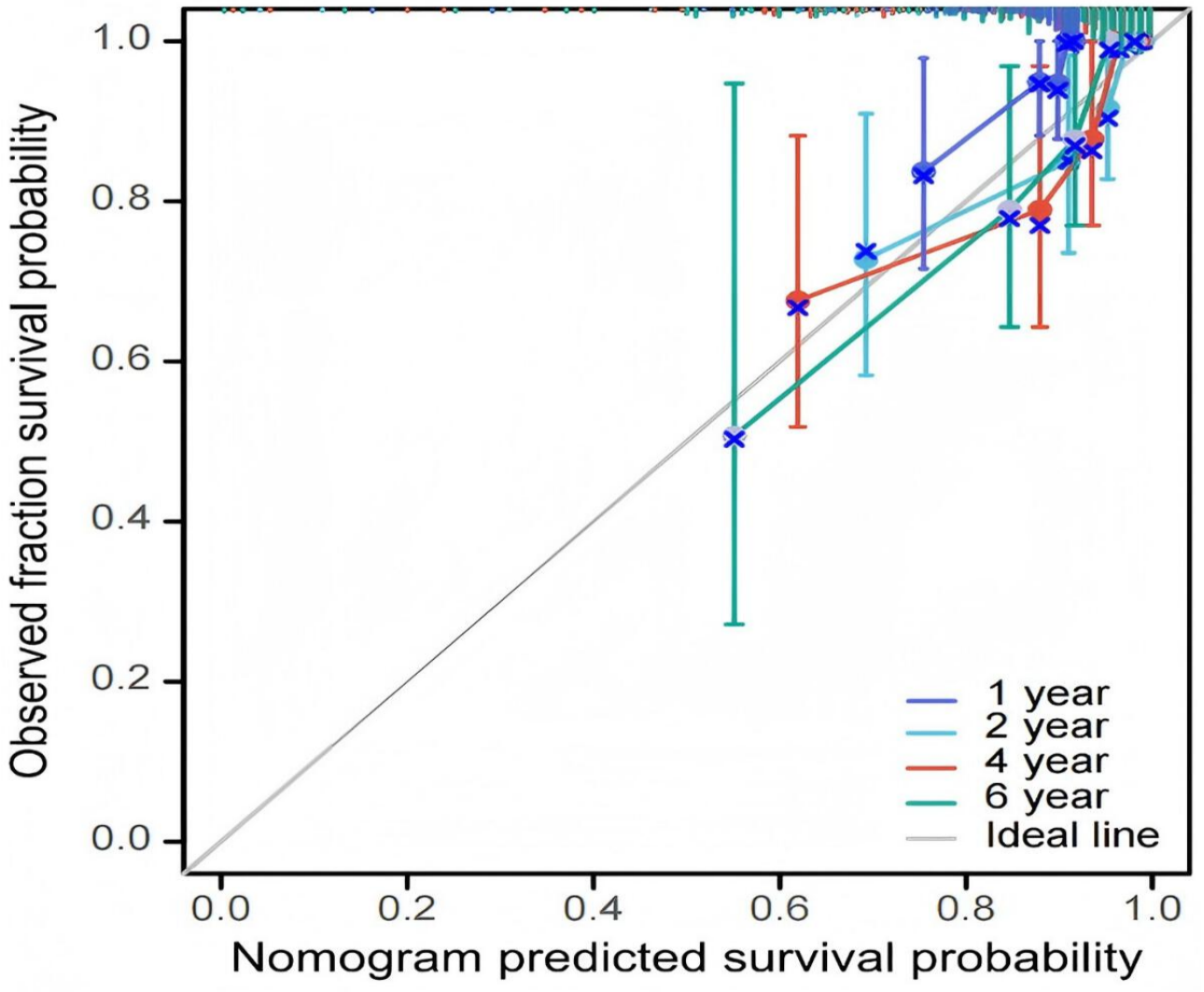
As shown in Figure 2, based on identified radiomic features, after integrating the data on survival time, survival status, and 5 features, we established a nomogram using the Cox method to assess the prognostic significance of these features in 207 patients. As shown in Figure 3, all calibration curves showed good results for the study samples.

Figure 2. Nomogram prediction for 1-, 2-, 4-, and 6-year survival for patients with kidney cancer (entire cohort: N=207). Rad-score: radiomic risk score.



XSL•FO
RenderX

Figure 3. Kidney cancer overall survival nomogram calibration plots (entire cohort: N=207).



Model Validation Results

Bootstrap validation using 1000 iterations demonstrated robust model performance. The bootstrap-corrected AUC values were 0.80 (SD 0.03) for 1-year survival prediction, 0.77 (SD 0.04) for 2-year survival prediction, 0.74 (SD 0.04) for 4-year survival prediction, and 0.71 (SD 0.05) for 6-year survival prediction. The optimism-corrected concordance index was 0.73 (95% CI 0.68-0.78), indicating minimal overfitting.

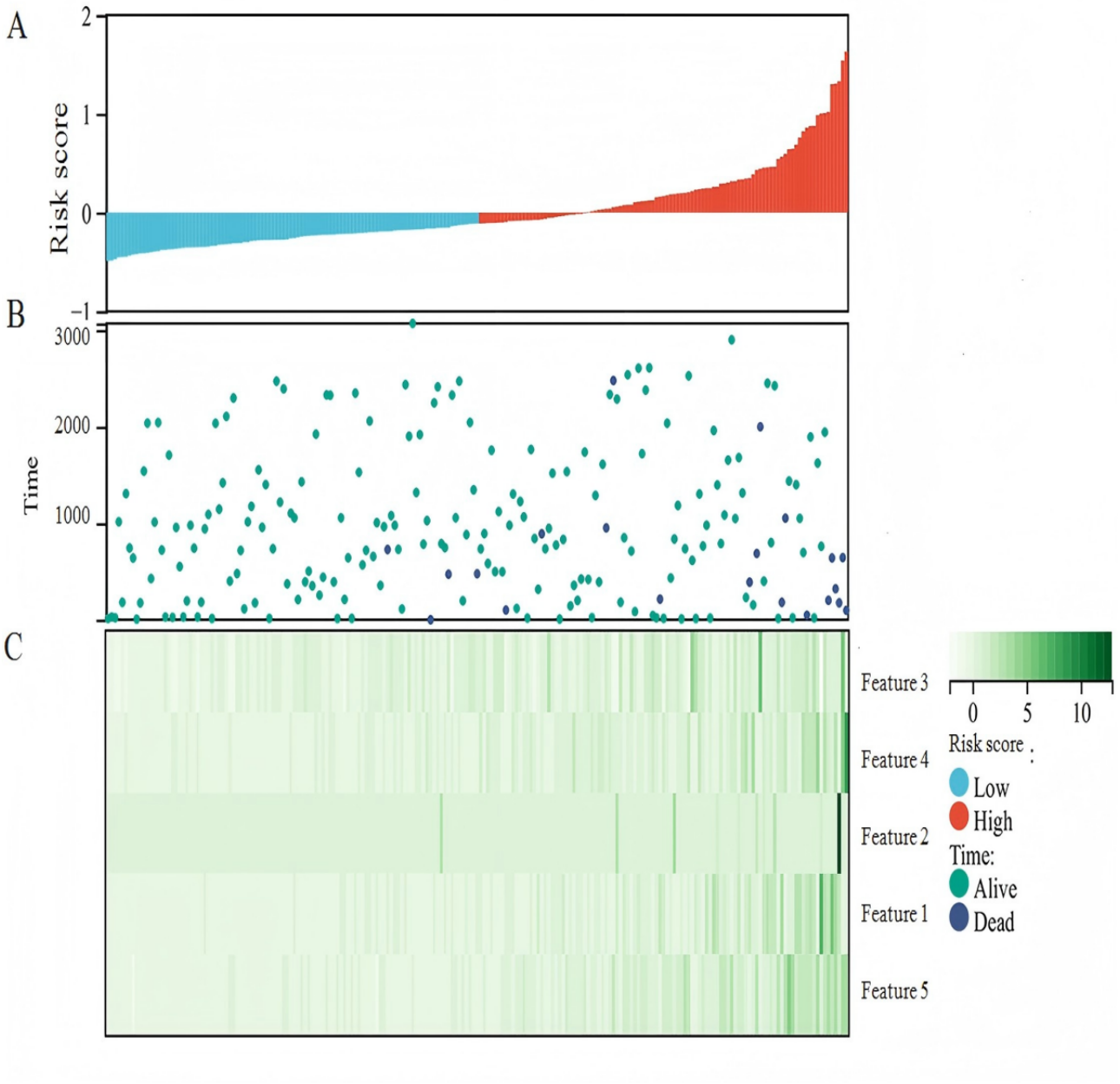
Association Between Radiomic Features and Survival Prognosis

As shown in Figure 4, we analyzed the relationship between risk scores and patient outcomes across the entire cohort. The visualization clearly demonstrates that patients with higher risk scores experienced shorter survival times and higher mortality rates, as expected. The heat map pattern shows how the 5 radiomic features (features 1-5) collectively contribute to risk stratification, with distinct expression patterns between high-risk and low-risk patient groups. This risk score–based stratification effectively separates patients into clinically meaningful survival groups.

As shown in Figure 5, we used the time-varying ROC curve and AUC as the criteria for evaluating the nomogram. Figure 5 shows AUC of the model combining clinical features, and the radar score shows good performance.

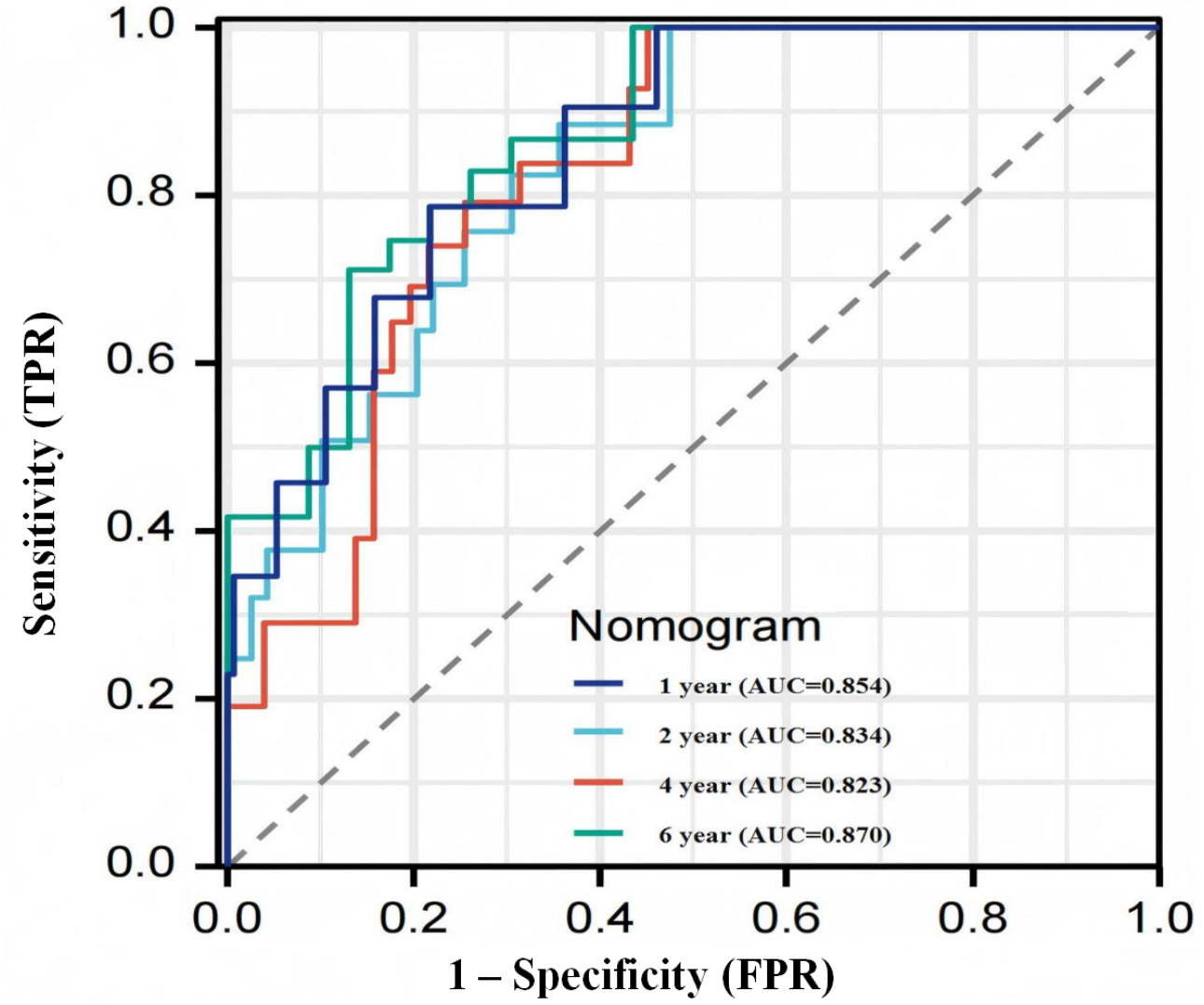
XSL•FO
RenderX

Figure 4. Risk stratification visualization showing the relationship between radiomic risk score and patient survival outcomes (entire cohort: N=207). The upper panel displays the distribution of risk scores ranked by patient survival time. The middle panel shows survival time for each patient. The lower panel illustrates the expression patterns of the 5 selected radiomic features (features 1-5) contributing to the risk score calculation. Color coding indicates patient survival status and risk group classification (high-risk vs low-risk groups based on the optimal cutoff value).



XSL•FO
RenderX

Figure 5. The 1-, 2-, 4-, and 6-year time-dependent receiver operating characteristic curves to assess the predictive accuracy for overall survival (entire cohort: N=207). AUC: area under the curve; FPR: false-positive rate; TPR: true-positive rate.

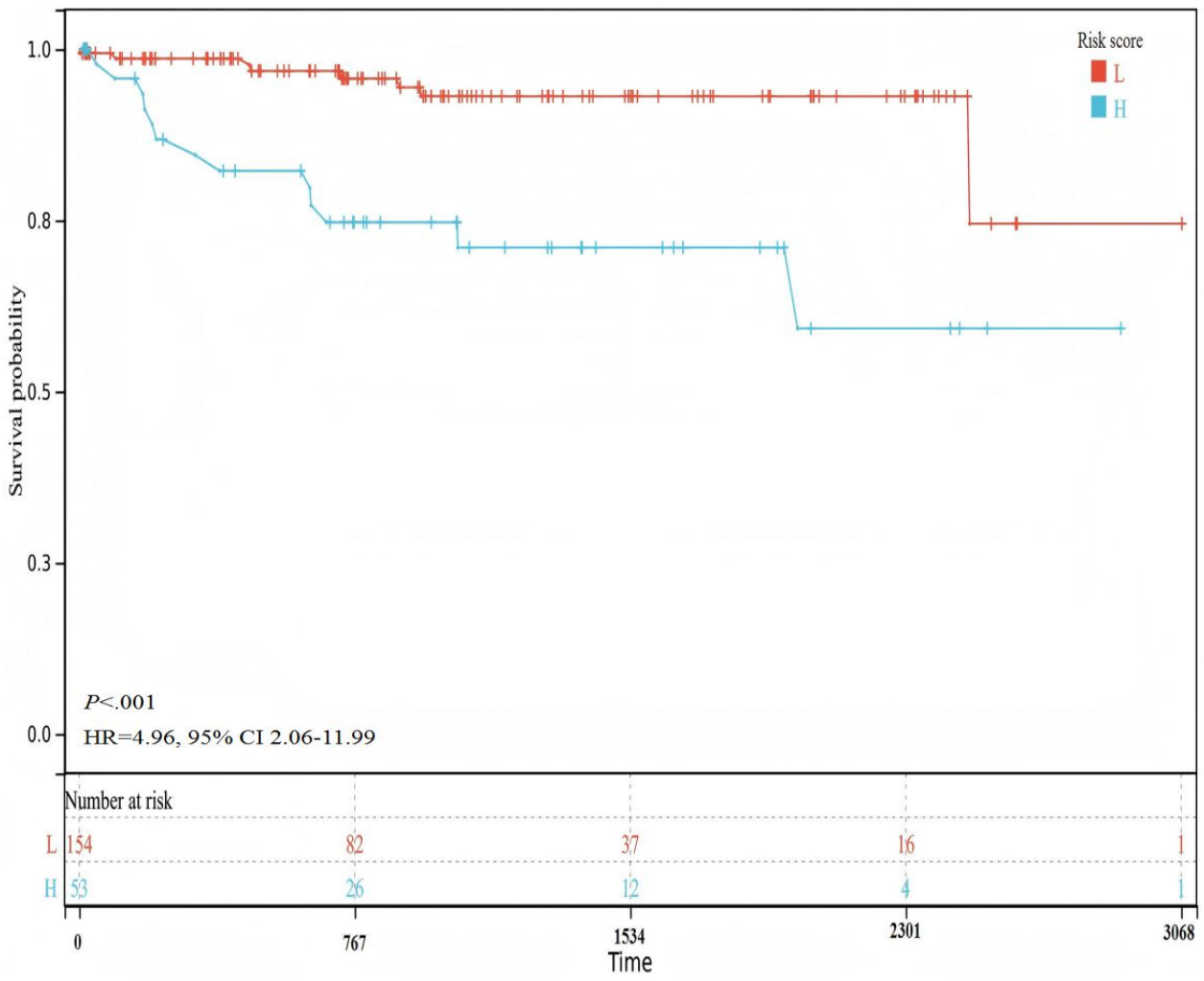


Kaplan-Meier Survival Analysis

As shown in Figure 6, we divided the patients into low-risk and high-risk groups based on their radiomic characteristics. The cutoff value was 0.154921. The log rank test method was used to evaluate the significance of the prognostic difference between the groups, and a significant prognostic difference was observed (P<.001).

XSL•FO
RenderX

Figure 6. Survival curve depicting the high- and low-risk groups based on the radiomics score classification (entire cohort: N=207; low-risk group: n=154; high-risk group: n=53). H: high-risk group; HR: hazard ratio; L: low-risk group.



Discussion

Principal Findings

On the basis of publicly available data from the TCIA database, this study developed and validated prognostic nomogram models for patients with kidney cancer, and the results showed that our nomogram was advantageous for predicting patient prognosis. The nomogram could be useful for postoperative evaluation of patients with kidney cancer and development of individualized treatment plans. ROC and calibration curve results showed that the nomogram performed well in terms of noninvasive prediction of survival in patients with kidney cancer. The nomogram visually showed how to numerically quantify each factor for predicting survival in patients with kidney cancer. On the basis of our results, we observed good performance in terms of our radiomics characterization and the predict nomogram, suggesting that our model can be used to effectively predict the prognosis of patients with kidney cancer and create a robust decision-making framework for clinicians.

Comparison With Previous Work

The incidence of kidney cancer has been steadily increasing over recent decades, although the reasons for this remain unclear [1]. The annual incidence of kidney cancer has been increasing in both men and women [21]. However, patients with the same type of kidney tumors might have different prognoses owing to the complex internal structure and high heterogeneity within tumors. Complete resection or percutaneous core histopathology biopsy remains a standard invasive method for assessing prognostic indicators (ie, histological classification, grades, and stages) of kidney cancer to guide further treatment [21,22]. An objective and noninvasive approach is needed to evaluate and predict the clinical outcomes of patients with kidney cancer. CT plays a vital role in the diagnosis and prognosis of renal disease as it is noninvasive and convenient, especially compared with biopsy, surgery, and immunohistochemistry. Biopsy is not always necessary because imaging is a highly accurate method for characterizing renal malignancy [23]. Radiomics, which is a commonly used method to extract characteristics in terms of mass data from each medical image, can provide tumor characteristics and functions at both macroscopic and micromolecular levels [24]. Recently, several studies have explored the biological progress of kidney cancer via the

XSL•FO
RenderX

construction of radiomic models using CT images. Feng et al [25] and Kocak et al [26] showed that CT radiomics has the potential to predict the *BRCA1*-associated protein 1 mutation status in patients with kidney cancer. Ghosh et al [27] provided a radiomics-genetics pipeline that extracted 3D intratumor heterogeneity features from contrast-enhanced CT images and explored associations between features and gene mutation status. In 2001, a nomogram used to predict the 5-year survival of patients with kidney cancer was reported by Kattan et al [28]. The nomogram incorporated 4 factors: symptoms, histological subtype, tumor size, and TNM stage (1997 version) [28]. In 2018, Zhang et al [29] developed a nomogram specifically to assess the prognosis of patients with renal clear cell carcinoma postoperatively based on clinical data from 35,151 patients. However, several studies addressing the roles of immune profiles have encountered various uncertainties and have used constructed classification models to preoperatively identify pathological grades for patients with kidney cancer using machine learning–based CT radiomics with noninvasion [30-32]. Some studies have also shown the significance of CT radiomics in distinguishing kidney cancer from other renal mass diseases. Yang et al [33] developed various machine learning–based classification models to differentiate renal angiomyolipoma and kidney cancer, which performed well. Coy et al [34] reported the utility of machine learning in differentiating kidney cancer from oncocytoma on routine CT images using their models, which were able to accurately predict renal lesion histology on imaging. Meng et al [35] proposed a CT-based radiomic method to distinguish sarcoma from kidney cancer, with a good diagnostic performance. This is the first study to provide a predictive nomogram showing that radiomics can be used independently to predict prognosis in patients with kidney cancer. Our results indicated that our model could be a pivotal tool for the prognostic surveillance of kidney cancer.

Clinical Implications

Risk stratification with specific risk scores using a radiomic signature was accurately performed, and the predictive nomogram, which comprehensively integrated radiomic and clinical signatures, could effectively predict outcomes for patients with kidney cancer and facilitate decision-making for clinicians. The noninvasive nature of this approach makes it particularly valuable for routine clinical application, potentially reducing the need for invasive procedures while providing accurate prognostic information [36]. In clinical practice, the radiomics nomogram could be integrated into routine postoperative imaging review to guide surveillance intensity and treatment decisions. High-risk patients might benefit from more frequent monitoring or earlier intervention discussions, whereas low-risk patients could have less intensive follow-up schedules. The scoring system could be incorporated into existing hospital information systems using automated feature extraction, requiring minimal workflow changes for clinical staff.

Methodological Considerations

Our analytical approach evolved during the course of this study. Initially, we planned to use a traditional 70:30 train-test split for model development and validation. However, when we examined the TCIA dataset more carefully, we found that the presegmented images and the relatively small sample size (N=207) would result in insufficient power for robust model validation using a holdout approach, particularly for survival outcomes at multiple time points.

Therefore, we modified our approach to use the entire cohort (N=207) for model development, with bootstrap resampling for internal validation. This is a well-established alternative when sample sizes are limited, as recommended in radiomics guidelines [37]. Bootstrap validation provides robust performance estimates and CIs while maximizing the use of available data. Our results indicate acceptable model performance without significant overfitting.

This methodological adaptation underscores the importance of flexibility when working with real-world datasets and the need for transparent reporting of analytical decisions in radiomics research.

Limitations

This study had several limitations that should be acknowledged. First, our conclusions were based on data obtained from public databases, which inevitably have limitations due to patient selection characteristics and data availability constraints. To mitigate this limitation, we applied rigorous inclusion and exclusion criteria and standardized image preprocessing protocols. However, this may still affect the generalizability of our results. Future studies should incorporate multi-institutional datasets with standardized imaging protocols to improve data quality and external validity. Second, our study sample size was relatively small (207 patients with kidney cancer), which was insufficient for robust model development and validation. This limitation may affect the performance and efficiency of the predictive signatures and limit the statistical power of our analysis. Future research should aim to include larger, multicenter prospective cohorts to validate this predictive model and improve its reliability. Third, TNM staging was not selected as a clinical feature related to OS in this study because patients with hepatocellular carcinoma with portal vein tumor thrombosis are classified as being in the late clinical stage, which makes it challenging to predict OS using clinical staging as all patients have similar staging information. This may limit the comprehensive evaluation of traditional prognostic factors. Future studies should explore methods to better integrate staging information with radiomic features. Fourth, our model only explored tumor regions using imaging. To our knowledge, peripheral tumors provide biological information for prognosis monitoring, but we did not investigate peritumoral regions that might contain valuable prognostic information. Future research should explore the integration of peritumoral radiomic features to enhance predictive performance. Fifth, the TCIA dataset may introduce selection bias as cases were contributed by specific institutions with potentially different patient populations and referral patterns. In addition, heterogeneous CT imaging protocols across contributing institutions (scanner types, reconstruction algorithms, and contrast protocols) present challenges for radiomic feature standardization and reproducibility. These factors limit the direct clinical applicability of our model, requiring validation and potential

XSL•FO
RenderX

recalibration for different imaging protocols and patient populations before clinical implementation.

Future Directions

To advance radiomics-based prognostic modeling in kidney cancer, several key research directions should be prioritized. First, multicenter prospective validation studies using standardized imaging protocols are essential to establish the generalizability and clinical applicability of radiomics models across different institutions and patient populations. These studies should include larger collaborative cohorts (>500 patients) to improve statistical power and model reliability. Second, radiomics research should expand beyond tumor regions to systematically investigate peritumoral features and explore integration with clinical biomarkers to enhance predictive performance. In addition, focused investigation of patient subgroups, particularly those with shorter survival periods who may benefit most from accurate prognostic prediction, represents an important research priority. Finally, the development of automated radiomics workflows and real-time clinical decision support systems will be crucial for translating research findings into routine clinical practice and facilitating widespread adoption of radiomics-based prognostic tools [38,39].

Conclusions

We developed a triphasic contrast-enhanced CT–based radiomics nomogram that combined clinical factors and radiomic features. This nomogram demonstrated favorable predictive efficacy for differentiating kidney cancer postoperative outcomes. The model, combining CT-extracted radiomic features, showed good potential for evaluating OS in patients treated with nephrectomy and may facilitate clinical management and prognostic evaluation of postoperative patients with kidney cancer. As a noninvasive and quantitative method, the radiomics nomogram represents a promising tool for personalized medicine in kidney cancer management.

Data Availability

The datasets generated or analyzed during this study are available in The Cancer Imaging Archive database repository [15].

Authors' Contributions

QZ, YL, and HZ guarantee the integrity of this study. HZ, GH, and HP undertook the literature search. QZ and HZ were responsible for statistical analyses and manuscript editing. QZ, YL, and HZ are considered co–corresponding authors. All authors were involved in the study concepts, study design, data acquisition, data analysis and interpretation, manuscript drafting, manuscript revision for important intellectual content, approval of the final version of the submitted manuscript, agreement to ensure that any questions related to the work are appropriately resolved, and clinical studies. Author QZ is the co-corresponding author of this paper, affiliated with The Third People's Hospital of Jingdezhen, The Third People's Hospital of Jingdezhen affiliated to Nanchang Medical College, and can be reached at 394035513@qq.com. Author HZ is also the co-corresponding author of this paper, affiliated with Jiangxi Cancer Hospital & Institute, Jiangxi Clinical Research Center for Cancer, The Second Affiliated Hospital of Nanchang Medical College, and can be reached at 1761580890@qq.com.

Conflicts of Interest

None declared.

References

1. Ho TH, Serie DJ, Parasramka M, et al. Differential gene expression profiling of matched primary renal cell carcinoma and metastases reveals upregulation of extracellular matrix genes. Ann Oncol 2017 Mar 1;28(3):604-610. [doi: 10.1093/annonc/mdw652] [Medline: 27993815]
2. Motzer RJ, Jonasch E, Agarwal N, et al. Kidney cancer, version 3.2022, NCCN Clinical Practice Guidelines in Oncology. J Natl Compr Canc Netw 2022 Jan;20(1):71-90. [doi: 10.6004/jnccn.2022.0001] [Medline: 34991070]
3. Escudier B, Porta C, Schmidinger M, et al. Renal cell carcinoma: ESMO Clinical Practice Guidelines for diagnosis, treatment and follow-up†. Ann Oncol 2019 May 1;30(5):706-720. [doi: 10.1093/annonc/mdz056] [Medline: 30788497]
4. Siegel RL, Miller KD, Jemal A. Cancer statistics, 2020. CA Cancer J Clin 2020 Jan;70(1):7-30. [doi: 10.3322/caac.21590] [Medline: 31912902]
5. Padala SA, Kallam A. Clear cell renal carcinoma. In: StatPearls [Internet]: StatPearls Publishing; 2023.
6. Zhu P, Dai C, Xiong Y, et al. Tumor contour irregularity on preoperative CT predicts prognosis in renal cell carcinoma: a multi-institutional study. EClinicalMedicine 2024 Aug 16;75:102775. [doi: 10.1016/j.eclinm.2024.102775] [Medline: 39246716]
7. Xu L, Li C, Gao S, et al. Personalized prediction of long-term renal function prognosis following nephrectomy using interpretable machine learning algorithms: case-control study. JMIR Med Inform 2024 Sep 20;12:e52837. [doi: 10.2196/52837] [Medline: 39303280]
8. Lambin P, Rios-Velazquez E, Leijenaar R, et al. Radiomics: extracting more information from medical images using advanced feature analysis. Eur J Cancer 2012 Mar;48(4):441-446. [doi: 10.1016/j.ejca.2011.11.036] [Medline: 22257792]

XSL•FO
RenderX

9. Sun R, Limkin EJ, Vakalopoulou M, et al. A radiomics approach to assess tumour-infiltrating CD8 cells and response to anti-PD-1 or anti-PD-L1 immunotherapy: an imaging biomarker, retrospective multicohort study. Lancet Oncol 2018 Sep;19(9):1180-1191. [doi: 10.1016/S1470-2045(18)30413-3] [Medline: 30120041]
10. Wu J, Li J, Huang B, et al. Radiomics predicts the prognosis of patients with clear cell renal cell carcinoma by reflecting the tumor heterogeneity and microenvironment. Cancer Imaging 2024 Sep 16;24(1):124. [doi: 10.1186/s40644-024-00768-7] [Medline: 39285496]
11. Gettman MT, Blute ML, Spotts B, Bryant SC, Zincke H. Pathologic staging of renal cell carcinoma: significance of tumor classification with the 1997 TNM staging system. Cancer 2001 Jan 15;91(2):354-361. [doi: 10.1002/1097-0142(20010115)91:2<354::aid-cncr1009>3.0.co;2-9] [Medline: 11180082]
12. Yi Y, Mikhaylova O, Mamedova A, et al. von Hippel-Lindau-dependent patterns of RNA polymerase II hydroxylation in human renal clear cell carcinomas. Clin Cancer Res 2010 Nov 1;16(21):5142-5152. [doi: 10.1158/1078-0432.CCR-09-3416] [Medline: 20978146]
13. Gao R, Qin H, Lin P, et al. Development and validation of a radiomic nomogram for predicting the prognosis of kidney renal clear cell carcinoma. Front Oncol 2021 Jul 6;11:613668. [doi: 10.3389/fonc.2021.613668] [Medline: 34295804]
14. Bhandari A, Ibrahim M, Sharma C, Liong R, Gustafson S, Prior M. CT-based radiomics for differentiating renal tumours: a systematic review. Abdom Radiol (NY) 2021 May;46(5):2052-2063. [doi: 10.1007/s00261-020-02832-9] [Medline: 33136182]
15. C4KC-KiTS | Data from the training set of the 2019 Kidney and Kidney Tumor Segmentation Challenge. The Cancer Imaging Archive. URL: https://wiki.cancerimagingarchive.net/pages/viewpage.action?pageId=61081171 [accessed 2025-10-10]
16. Welcome to pyradiomics documentation!. Pyradiomics. URL: https://pyradiomics.readthedocs.io/en/latest/ [accessed 2019-06-30]
17. van Griethuysen JJ, Fedorov A, Parmar C, et al. Computational radiomics system to decode the radiographic phenotype. Cancer Res 2017 Nov 1;77(21):e104-e107. [doi: 10.1158/0008-5472.CAN-17-0339] [Medline: 29092951]
18. Xiao J, Mo M, Wang Z, et al. The application and comparison of machine learning models for the prediction of breast cancer prognosis: retrospective cohort study. JMIR Med Inform 2022 Feb 18;10(2):e33440. [doi: 10.2196/33440] [Medline: 35179504]
19. Heagerty PJ, Zheng Y. Survival model predictive accuracy and ROC curves. Biometrics 2005 Mar;61(1):92-105. [doi: 10.1111/j.0006-341X.2005.030814.x] [Medline: 15737082]
20. Schröder MS, Culhane AC, Quackenbush J, Haibe-Kains B. survcomp: an R/Bioconductor package for performance assessment and comparison of survival models. Bioinformatics 2011 Nov 15;27(22):3206-3208. [doi: 10.1093/bioinformatics/btr511] [Medline: 21903630]
21. Sun M, Shariat SF, Cheng C, et al. Prognostic factors and predictive models in renal cell carcinoma: a contemporary review. Eur Urol 2011 Oct;60(4):644-661. [doi: 10.1016/j.eururo.2011.06.041] [Medline: 21741163]
22. Silverman SG, Israel GM, Trinh QD. Incompletely characterized incidental renal masses: emerging data support conservative management. Radiology 2015 Apr;275(1):28-42. [doi: 10.1148/radiol.14141144] [Medline: 25799334]
23. Zhang H, Li Q, Li S, Ma J, Huang J. A radiomic approach to differential diagnosis of renal cell carcinoma in patients with hydronephrosis and renal calculi [Article in Chinese]. Nan Fang Yi Ke Da Xue Xue Bao 2019 May 30;39(5):547-553. [doi: 10.12122/j.issn.1673-4254.2019.05.08] [Medline: 31140418]
24. Gillies RJ, Kinahan PE, Hricak H. Radiomics: images are more than pictures, they are data. Radiology 2016 Feb;278(2):563-577. [doi: 10.1148/radiol.2015151169] [Medline: 26579733]
25. Feng Z, Zhang L, Qi Z, Shen Q, Hu Z, Chen F. Identifying BAP1 mutations in clear-cell renal cell carcinoma by CT radiomics: preliminary findings. Front Oncol 2020 Feb 28;10:279. [doi: 10.3389/fonc.2020.00279] [Medline: 32185138]
26. Kocak B, Durmaz ES, Kaya OK, Kilickesmez O. Machine learning-based unenhanced CT texture analysis for predicting BAP1 mutation status of clear cell renal cell carcinomas. Acta Radiol 2020 Jun;61(6):856-864. [doi: 10.1177/0284185119881742] [Medline: 31635476]
27. Ghosh P, Tamboli P, Vikram R, Rao A. Imaging-genomic pipeline for identifying gene mutations using three-dimensional intra-tumor heterogeneity features. J Med Imaging (Bellingham) 2015 Oct;2(4):041009. [doi: 10.1117/1.JMI.2.4.041009] [Medline: 26839909]
28. Kattan MW, Reuter V, Motzer RJ, Katz J, Russo P. A postoperative prognostic nomogram for renal cell carcinoma. J Urol 2001 Jul;166(1):63-67. [Medline: 11435824]
29. Zhang G, Wu Y, Zhang J, et al. Nomograms for predicting long-term overall survival and disease-specific survival of patients with clear cell renal cell carcinoma. Onco Targets Ther 2018 Sep 6;11:5535-5544. [doi: 10.2147/OTT.S171881] [Medline: 30233214]
30. Sun X, Liu L, Xu K, et al. Prediction of ISUP grading of clear cell renal cell carcinoma using support vector machine model based on CT images. Medicine (Baltimore) 2019 Apr;98(14):e15022. [doi: 10.1097/MD.0000000000015022] [Medline: 30946334]
31. Shu J, Tang Y, Cui J, et al. Clear cell renal cell carcinoma: CT-based radiomics features for the prediction of Fuhrman grade. Eur J Radiol 2018 Dec;109:8-12. [doi: 10.1016/j.ejrad.2018.10.005] [Medline: 30527316]

XSL•FO
RenderX

32. Shu J, Wen D, Xi Y, et al. Clear cell renal cell carcinoma: machine learning-based computed tomography radiomics analysis for the prediction of WHO/ISUP grade. Eur J Radiol 2019 Dec;121:108738. [doi: 10.1016/j.ejrad.2019.108738] [Medline: 31756634]
33. Yang R, Wu J, Sun L, et al. Radiomics of small renal masses on multiphasic CT: accuracy of machine learning-based classification models for the differentiation of renal cell carcinoma and angiomyolipoma without visible fat. Eur Radiol 2020 Feb;30(2):1254-1263. [doi: 10.1007/s00330-019-06384-5] [Medline: 31468159]
34. Coy H, Hsieh K, Wu W. Deep learning and radiomics: the utility of Google TensorFlow™ Inception in classifying clear cell renal cell carcinoma and oncocytoma on multiphasic CT. Abdom Radiol (NY) 2019 Jun;44(6):2009-2020. [doi: 10.1007/s00261-019-01929-0] [Medline: 30778739]
35. Meng X, Shu J, Xia Y, Yang R. A CT-based radiomics approach for the differential diagnosis of sarcomatoid and clear cell renal cell carcinoma. Biomed Res Int 2020 Jul 24;2020:7103647. [doi: 10.1155/2020/7103647] [Medline: 32775436]
36. Kulkarni V, Gawali M, Kharat A. Key technology considerations in developing and deploying machine learning models in clinical radiology practice. JMIR Med Inform 2021 Sep 9;9(9):e28776. [doi: 10.2196/28776] [Medline: 34499049]
37. Zwanenburg A, Vallières M, Abdalah MA, et al. The image biomarker standardization initiative: standardized quantitative radiomics for high-throughput image-based phenotyping. Radiology 2020 May;295(2):328-338. [doi: 10.1148/radiol.2020191145] [Medline: 32154773]
38. Lu SC, Xu C, Nguyen CH, Geng Y, Pfob A, Sidey-Gibbons C. Machine learning-based short-term mortality prediction models for patients with cancer using electronic health record data: systematic review and critical appraisal. JMIR Med Inform 2022 Mar 14;10(3):e33182. [doi: 10.2196/33182] [Medline: 35285816]
39. Kanbar LJ, Wissel B, Ni Y, et al. Implementation of machine learning pipelines for clinical practice: development and validation study. JMIR Med Inform 2022 Dec 16;10(12):e37833. [doi: 10.2196/37833] [Medline: 36525289]

Abbreviations

CT: computed tomography
GLDM: gray-level dependence matrix
GTV: gross tumor volume
LASSO: least absolute shrinkage and selection operator
OS: overall survival
ROC: receiver operating characteristic
TCIA: The Cancer Imaging Archive
TNM: tumor-node-metastasis

Edited by A Coristine; submitted 26.02.25; peer-reviewed by A Adeoye, GK Gupta; revised version received 17.09.25; accepted 17.09.25; published 21.10.25.

Please cite as:
He G, Lai L, Yu G, Pang H, Yu X, Zhang H, Zhu Q, Lv Y
Survival Prediction for Postoperative Patients With Kidney Cancer Based on Computed Tomography Radiomics: Retrospective Cohort Study
JMIR Med Inform 2025;13:e73162
URL: https://medinform.jmir.org/2025/1/e73162
doi:10.2196/73162

© Guizhen He, Liwen Lai, Guoan Yu, Haowen Pang, Xiaohui Yu, Huaiwen Zhang, Qingxiu Zhu, Yingzi Lv. Originally published in JMIR Medical Informatics (https://medinform.jmir.org), 21.10.2025. This is an open-access article distributed under the terms of the Creative Commons Attribution License (https://creativecommons.org/licenses/by/4.0/), which permits unrestricted use, distribution, and reproduction in any medium, provided the original work, first published in JMIR Medical Informatics, is properly cited. The complete bibliographic information, a link to the original publication on https://medinform.jmir.org/, as well as this copyright and license information must be included.

XSL•FO
RenderX

Multimodal Multitask Learning for Predicting Depression Severity and Suicide Risk Using Pretrained Audio and Text Embeddings: Methodology Development and Application

Ya-Han Hu[1,2], PhD; Ruei-Yan Wu[1,3], PhD; Min-Yi Su[1], MAS; I-Li Lin[4*], MD; Cheng-Che Shen[5,6*], MD, PhD

[1]Department of Information Management, National Central University, No. 300, Zhongda Rd., Zhongli Dist., Taoyuan City, Taiwan

[2]Asian Institute for Impact Measurement and Management, National Central University, Taoyuan City, Taiwan

[3]Graduate School of Resources Management and Decision Science, Management College, National Defense University, Taipei City, Taiwan

[4]Department of Radiology, Ditmanson Medical Foundation Chia-Yi Christian Hospital, Chiayi, Taiwan

[5]Jianan Psychiatric Center, No. 539, Yuzhong Rd., Rende Dist., Tainan City, Taiwan

[6]School of Medicine, National Yang Ming Chiao Tung University, Taipei, Taiwan

[*]these authors contributed equally

Corresponding Author:
Cheng-Che Shen, MD, PhD
Jianan Psychiatric Center, No. 539, Yuzhong Rd., Rende Dist., Tainan City, Taiwan

Abstract

Background: Depression is a critical psychological disorder necessitating urgent assessment and treatment, given its strong association with increased suicide risk (SR). Effective management hinges on promptly identifying individuals with high depression severity (DS) and SR. While machine learning and deep learning have advanced the identification of DS and SR, research focusing on both aspects simultaneously remains limited and requires further refinement.

Objective: This study aimed to evaluate whether our proposed methods, which integrate multitask learning (MTL), multimodal learning, and transfer learning, enhance the efficacy of deep learning models in the joint classification of DS and SR.

Methods: This study proposed a multitask framework employing a multimodal fusion strategy for pretrained audio and text embeddings to concurrently assess DS and SR. Data encompassing Chinese audio recordings and clinical questionnaire scores from 100 patients with depression and 100 healthy controls were used. Preprocessed audio and text data were transformed into pretrained embeddings and integrated using concatenation and hard parameter sharing. Single-task learning (STL) models (DS and SR tasks) were evaluated with different embeddings and further compared with the MTL models.

Results: The STL models demonstrated exceptional DS prediction (area under the curve [AUC]=0.878) using wav2vec 2.0 combined with ERNIE-health, and SR prediction (AUC=0.876) using HuBERT combined with ERNIE-health. The MTL models significantly improved SR prediction over DS prediction, achieving the highest DS classification (AUC=0.887) with wav2vec 2.0 combined with ERNIE-health, and SR classification (AUC=0.883) with HuBERT combined with ERNIE-health.

Conclusions: The findings of this study underscore the effectiveness of the proposed MTL models using specific pretrained audio and text embeddings in enhancing model performance. However, we advocate for cautious implementation of MTL to mitigate potential negative transfer effects. Our research presents a method that is both promising and effective, offering an objective approach for accurate clinical decision support in the parallel diagnosis of DS and SR.

(JMIR Med Inform 2025;13:e66907) doi:10.2196/66907

KEYWORDS

depression severity; suicide risk; multitask learning; multimodal learning; transfer learning; mental health; mental illnesses; mental disorders; depression; depressed; major depressive disorder; MDD; depressive disorder; machine learning; ML; artificial intelligence; AI; algorithms; predictive models; predictive analytics; deep learning; early detection

Introduction

Background

In its pervasive embrace, depression, an ever-expanding mental malady, reaches across the globe, leaving its mark on approximately 280 million lives [1]. Neglecting proper care of patients with depression can lead to dire consequences, as research has shown that individuals with this condition face a staggering 20-fold higher risk of suicide than the general population [2,3], exposing a troubling link between depression and suicide [4-6].

XSL•FO
RenderX

In clinical practice, regular and comprehensive assessments of depression severity (DS) and suicide risk (SR) remain challenging due to time and resource constraints [7,8]. Traditional evaluations often rely on subjective and infrequent self-reports from patients or caregivers, which are susceptible to recall bias, cognitive limitations, and social stigma [9,10]. These issues are particularly acute in high-volume settings, where limited consultation time may hinder the timely identification of critical warning signs related to mental health deterioration or suicidal ideation.

Machine learning has demonstrated strong potential in predicting DS and SR, using text and audio data (eg, [11,12]). Text-based approaches have extracted clinically meaningful insights from medical narratives [13,14], while speech analysis has improved predictive accuracy by identifying vocal biomarkers linked to depression and suicide, such as reduced intensity, slower tempo, and increased hesitation [15-17]. These advances have driven the development of multimodal learning (MML) frameworks for mental health prediction. Although effective in detecting depression [18,19], applications of MML to SR prediction remain limited—likely due to the scarcity of high-quality annotated data in this sensitive domain [20,21].

Given the frequent co-occurrence of depression and suicide in clinical populations [22-24], SR prediction is inherently linked to depression assessment. This conceptual interdependence highlights the potential of multitask learning (MTL) for simultaneously modeling related mental health outcomes. Benton et al [25] demonstrated the utility of MTL by jointly predicting SR and other psychiatric conditions using social media data. With the rapid advancement of deep learning, transfer learning (TL) has also emerged as a promising strategy to address data scarcity, with recent studies showing that fine-tuning pretrained models on downstream mental health tasks can significantly enhance predictive performance (eg, [26,27]).

However, the current literature reveals several gaps. First, data source diversity remains limited, with most studies relying on datasets from English-speaking populations (eg, [28,29]). In addition, many analyses are based on social media platforms (eg, [25,30]) or public datasets (eg, [27,31]), which often lack clinical relevance. Second, most SR prediction studies have underutilized TL for audio processing, despite its successful application in related domains such as speech emotion recognition [32,33]. Third, although the comorbidity and shared clinical features of DS and SR are well documented [22-24], few studies have applied MTL to model these outcomes jointly. While recent advances in MML and MTL have shown promise in mental health prediction, few studies have jointly modeled DS and SR using clinically grounded, non-English data. Furthermore, the potential of TL to improve model generalizability across tasks and modalities remains underexplored in Chinese-language clinical contexts. These gaps motivate this study's unified framework, which integrates MML, MTL, and TL to support scalable and efficient mental health screening in real-world clinical settings for Chinese-speaking populations.

The key contributions of this work are three-fold: (1) the development of the first integrated framework that combines MML, MTL, and TL for the joint prediction of DS and SR in Chinese contexts; (2) empirical validation of MML approaches compared to single modality baselines in a non-English clinical setting; and (3) demonstration of the effectiveness of MTL in modeling related mental health constructs. By addressing linguistic, cultural, and resource-specific challenges, this framework supports scalable and efficient screening in high-volume clinical environments, addressing an urgent need in early mental health assessments and targeted interventions.

Related Work

Research on predictive models in mental health has traditionally adopted single-task approaches, predicting either depression or suicide independently [34-38]. These studies have primarily relied on text, audio, or other features, such as structured electronic health records [39] and social media images [40], to build predictive models. Recent advancements in text processing technologies have facilitated a shift from conventional hand-crafted features toward sophisticated automated feature learning approaches, exemplified by the heterogeneous graph convolutional network of Wang et al [14]. Concurrently, speech-based analyses have gained prominence for their capacity to capture nuanced vocal markers indicative of mental health conditions [11,15].

MTL has emerged as a promising framework for mental health assessment, as summarized in Table 1, aligning with the clinical observation that psychiatric conditions often co-occur and share common underlying mechanisms [22-24]. By jointly learning related tasks, MTL facilitates representation sharing and information transfer, thereby mitigating data sparsity and overfitting issues [41-43]. Benton et al [25] pioneered the use of deep neural networks to simultaneously predict depression and SR using Twitter data.

XSL•FO
RenderX

Table . Summary of key literature on multitask learning for depression severity and suicide risk prediction.

Study	Dataset	Language	Sample	Modality		TL[a]	Task		Method
				A[b]	T[c]		DS[d]	SR[e]	
Benton et al [25]	Multiple Twitter datasets	English	9611 users	No	Yes	No	Yes	Yes	DNN[f]
Qureshi et al [31]	DAIC-WOZ[g]	English	189 recordings	Yes	Yes	No	Yes	No	LSTM[h]
Ophir et al [30]	Facebook posts	English	83,292 postings	No	Yes	No	No	Yes	ANN[i]
Qureshi et al [28]	DAIC-WOZ, CMU-MOSEI[j]	English	189 recordings	No	Yes	Yes	Yes	No	LSTM
Dumpala et al [44]	FORBOW[k]	English	526 recordings	Yes	No	Yes	Yes	No	CNN[l]
Yang et al [45]	Chinese micro-blog	Chinese	6100 comments	No	Yes	Yes	Yes	No	DNN
Ghosh et al [46]	CEASE	English	2539 sentences	No	Yes	Yes	Yes	No	Bi-GRU[m]
Buddhitha and Inkpen [29]	CLPsych 2015 Twitter, UMD[n], SMHD[o]	English	—[p]	No	Yes	No	No	Yes	CNN
Teng et al [26]	AVEC[q] 2019 DDS Challenge Dataset, CMU-MOSEI	English	23,454 video clips and 275 users	Yes	Yes	Yes	Yes	No	DNN
Yang et al [27]	CEASE	English	2393 sentences	No	Yes	Yes	No	Yes	BERT[r]
This study	Self-collected	Chinese	200 users	Yes	Yes	Yes	Yes	Yes	DNN

[a]TL: transfer learning.

[b]A: audio modality.

[c]T: text modality.

[d]DS: depression severity.

[e]SR: suicide risk.

[f]DNN: deep neural network.

[g]DAIC-WOZ: distress analysis interview corpus-Wizard of Oz.

[h]LSTM: long short-term memory.

[i]ANN: artificial neural network.

[j]CMU-MOSEI: CMU multimodal opinion sentiment and emotion intensity.

[k]FORBOW: families overcoming risks and building opportunities for wellbeing.

[l]CNN: convolutional neural network.

[m]Bi-GRU: bidirectional GRU.

[n]UMD: University of Maryland Reddit suicidality dataset.

[o]SMHD: self-reported mental health diagnoses dataset.

[p]Not applicable.

[q]AVEC: audio/visual emotion challenge.

[r]BERT: bidirectional encoder representations from transformers.

Several studies listed in Table 1 have incorporated MML to improve predictive performance. By integrating diverse data types, MML leverages complementary information to enable a more comprehensive characterization of mental states. Qureshi

XSL•FO
RenderX

et al [31], for example, demonstrated enhanced depression prediction accuracy using long short-term memory models trained on combined textual and acoustic features from the DAIC-WOZ (distress analysis interview corpus-Wizard of Oz) dataset. Additionally, TL has also been increasingly adopted in these frameworks to address the challenge of limited labeled data. Teng et al [26] applied depression detection with sentiment assistance through deep neural networks and TL techniques on the AVEC (audio/visual emotion challenge) 2019 DDS Challenge and CMU-MOSEI (CMU multimodal opinion sentiment and emotion intensity) datasets. Similarly, Yang et al [27] used MTL with a BERT-based model to incorporate time-perspective cues for suicidal ideation detection on the CEASE dataset.

Despite these advances, key limitations persist. First, most studies rely on English-language data. Furthermore, text-based models are often trained on social media content [25,30,45], while audio models rely on public datasets [26-29,31,44,46] that may lack relevance to real-world clinical scenarios, thereby potentially limiting their applicability. Second, most SR prediction models are still trained from scratch, with only a few studies (eg, [27]) leveraging TL to enhance model performance. Most critically, empirical research exploring MTL's effectiveness for simultaneously predicting both DS and SR remains scarce. To our knowledge, only Benton et al [25] have conducted similar research, though their work was conducted exclusively in English on social media data.

To address these gaps, this study introduces a unified MML, MTL, and TL framework for the simultaneous prediction of DS and SR using Chinese-language data collected in clinical settings. This approach facilitates the development of culturally and linguistically tailored predictive models for Chinese-speaking populations. Moreover, by incorporating TL, the proposed framework retains knowledge acquired from source tasks, enabling efficient adaptation to downstream applications.

Methods

Ethical Considerations

This study received approval from the Institutional Review Board of Taichung Veterans General Hospital (approval number: SE21183B).

Every participant was required to complete and sign a participant consent form before their involvement. This form outlined the purpose and procedures of the study, potential risks and benefits, confidentiality measures, and voluntary participation rights. The completion of this form indicated their informed and voluntary consent to partake in the study. In the section of the participant consent form dedicated to "consent to participate," participants were explicitly informed about the inclusion of a clause seeking their agreement to employ their personal data, information, or research outcomes for publication purposes. By completing and signing the participant consent form, participants signified their understanding and acceptance of the terms outlined, thereby granting their "consent for publication." This agreement encompassed the use of their anonymized data and contributions in academic papers, reports, presentations, or other forms of scholarly dissemination.

Study Population

We collected a Chinese chief complaint dataset, which includes data from 100 patients with depression from a regional hospital in southern Taiwan, along with 100 age- and sex-matched nondepressed counterparts selected at random, resulting in a total of 200 cases. To verify the matching process, we conducted tests. The chi-square test for gender in relation to the prevalence of the condition was not significant (P=.88). Similarly, the t test for age in relation to the prevalence of the condition was not significant (P=.60).

Each case in the dataset includes personal data, an audio recording describing the current situation, transcripts, and clinical questionnaire results. The audio recordings were acquired by instructing participants as follows: "Please take a minute to elucidate your recent emotions, life circumstances, and other states." Subsequently, participants initiated the recording of their spoken expressions. Based on the questionnaire results, we conducted 2 specific clinical assessments: Hamilton Depression Rating Scale-17 (HAMD-17) [47] and SAD PERSONS scale [48]. DS was categorized into 3 levels: no depression (HAMD-17 score of 0 - 7; sample size of 106), low/moderate depression (HAMD-17 score of 8-16/17-23; sample size of 21), and high depression (HAMD-17 score of ≥24; sample size of 73). SR was classified into 2 levels: low risk (SAD PERSONS score of 0 - 3; sample size of 110) and moderate/high risk (SAD PERSONS score of 4-7/8-10; sample size of 90).

The demographic data for both groups can be found in Tables 2 and 3. In the 3 DS groups, there were statistically significant differences between the 2 study groups regarding age (P=.048), educational level (P<.001), occupation (P=.01), and marriage (P=.001). In terms of educational level, the HAMD-17≤7 group exhibited higher levels compared to the 8<HAMD-17≤23 and HAMD-17≥24 groups, and the proportion of individuals employed was also higher in the HAMD-17≤7 group than in the 8<HAMD-17≤23 and HAMD-17≥24 groups (64/97, 66% vs 13/30, 43% and 33/73, 45%). In terms of marital status, the HAMD-17≤7 group had a higher proportion of married individuals and a lower proportion of divorced individuals. In the 2 SR groups, there were statistically significant differences between the 2 study groups regarding educational level (P<.001), occupation (P=.02), and marriage (P<.001). In terms of educational level, the SAD PERSONS≤3 group exhibited higher levels compared to the SAD PERSONS≥4 group. In terms of occupation, the proportion of individuals was also higher in the SAD PERSONS≤3 group than in the SAD PERSONS≥4 group (69/110, 62.7% vs 41/90, 45.6%). In terms of marital status, the SAD PERSONS≥4 group had a higher proportion of unmarried individuals.

XSL•FO
RenderX

Table . Demographic data of patients in the 3 depression severity groups.

Variable	HAMD-17[a]≤7 group (n=97)	8<HAMD-17≤23 group (n=30)	HAMD-17≥24 group (n=73)	*P* value
Sex, n (%)				.99
Male	29 (30)	9 (30)	21 (29)	
Female	68 (70)	21 (70)	52 (71)	
Age (years), mean (SD)	44 (17)	38 (19)	47 (18)	.048[b]
Education level, n (%)				<.001[b]
Elementary school	0 (0)	2 (7)	6 (8)	
Junior high school	2 (2)	2 (7)	8 (11)	
Senior high school	12 (12)	6 (20)	29 (40)	
College degree or higher	83 (86)	20 (67)	30 (41)	
Occupation, n (%)				.01[b]
Yes	64 (66)	13 (43)	33 (45)	
No	33 (34)	17 (57)	40 (55)	
Marriage, n (%)				.001[b]
Unmarried	36 (37)	20 (67)	27 (37)	
Married	61 (63)	9 (30)	39 (53)	
Divorced	0 (0)	1 (3)	7 (10)	

[a]HAMD-17: Hamilton Depression Rating Scale-17.

[b]Statistical significance.

Table . Demographic data of patients in the 2 suicide risk groups.

Variable	SAD PERSONS≤3 group (n=110)	SAD PERSONS≥4 group (n=90)	*P* value
Sex, n (%)			.09
Male	27 (24.5)	32 (35.6)	
Female	83 (75.5)	58 (64.4)	
Age (years), mean (SD)	45 (16.7)	42 (19.3)	.26
Education level, n (%)			<.001[a]
Elementary school	0 (0)	8 (8.9)	
Junior high school	4 (3.6)	8 (8.9)	
Senior high school	17 (15.5)	30 (33.3)	
College degree or higher	89 (80.9)	44 (48.9)	
Occupation, n (%)			.02[a]
Yes	69 (62.7)	41 (45.6)	
No	41 (37.3)	49 (54.4)	
Marriage, n (%)			<.001[a]
Unmarried	34 (30.9)	49 (54.4)	
Married	75 (68.2)	34 (37.8)	
Divorced	1 (0.9)	7 (7.8)	

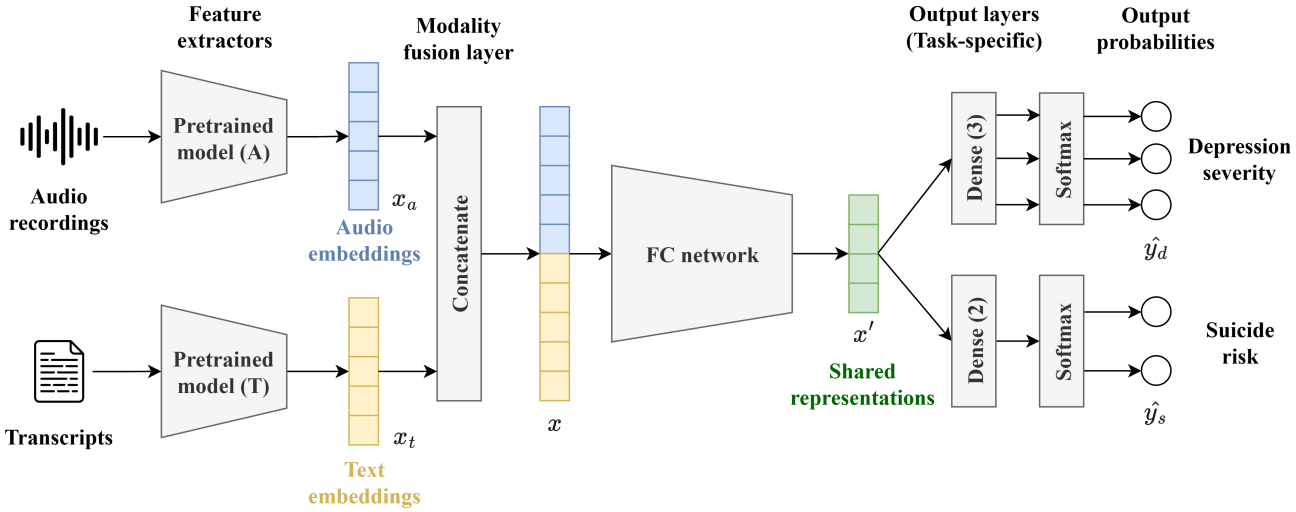
[a]Statistical significance.

XSL•FO
RenderX

Proposed Framework

The framework comprises 3 components: feature extraction, multimodal fusion, and MTL architecture, which are discussed sequentially in the following sections (Figure 1). First, audio and text data undergo processing by pretrained models to extract their embeddings. Second, the embeddings obtained from the previous step are fused using a modality fusion layer. The resulting fused representations are then fed into a fully connected (FC) network to project them into lower-dimensional vectors. Lastly, these representations are shared between the 2 classification tasks (DS and SR) and are input into 2 task-specific layers implemented as multilayer perceptron classifiers to generate output probabilities separately. The details of the 3 components are presented below.

Figure 1. Overview of our proposed framework. FC: fully connected.



First, considering the small sample size in our study and recognizing the potential of TL in predicting DS and SR, we used 4 advanced pretrained models for feature extraction: wav2vec 2.0 and HuBERT for audio analysis [49,50], and Longformer and ERNIE-health for text analysis [51,52]. Each method has distinct advantages, rendering them especially suitable for our research objectives, as elaborated upon in the following sections.

- wav2vec 2.0: It is developed by Facebook AI Research, uses a multilayer convolutional neural network (CNN) for audio encoding, and is supplemented by latent representation masking and contextualization through a Transformer network trained with contrastive learning methods [49]. This self-supervised model excels with minimal labeled data, consistently surpassing state-of-the-art models, as demonstrated in the tasks of depression detection [52] and emotion recognition [53].
- HuBERT: It extends self-supervised learning to audio data, using a CNN for encoding and a BERT encoder for contextualization, enhanced by masked prediction and cluster refinement [50]. HuBERT has demonstrated superior performance in audio classification tasks for detecting depression [54] and assessing cognitive function [55].
- Longformer: It stands out as a transformer-based language model designed to capture extended dependencies using sliding window and global attention mechanisms [51]. This design enables Longformer to effectively integrate local and global information while mitigating challenges associated with traditional attention mechanisms.
- ERNIE-health: It is a Chinese biomedical language model tailored for biomedical text processing, enhancing tokenization and comprehension of biomedical content through in-domain text [56]. ERNIE-health consistently outperforms other models across various biomedical tasks [57], underscoring its effectiveness in this domain.

Second, these pretrained models were used to generate audio embeddings, xa, and text embeddings, xt, by feeding the preprocessed audio recordings and transcripts as their inputs. To combine the information from text and audio modalities, we adopted the early fusion approach by concatenating the audio embedding (xa) and text embedding (xt) into a single vector (x), using Eq. (1). This fusion strategy, also known as feature-level fusion, is characterized by its simplicity, its computational efficiency, and the potential to capture intricate interactive details. We adopted this approach due to its aforementioned advantages and its ability to circumvent the risk of information overlap or cancellation inherent in more complex operations such as addition, deduction, inner product, and outer product. This approach has been widely used in prior studies on audio-text fusion, consistently yielding improved accuracy [58-60].

(1)x=xa⊕xt

Lastly, our proposed framework adopted the hard parameter sharing scheme for MTL of DS and SR classification using deep learning. This scheme involves a shared encoder with multiple task-specific decoding heads [46]. This MTL technique enables our framework to learn multiple related tasks simultaneously while improving the generalization performance. In our framework, an FC network acts as the shared encoder, and dense layers act as the task-specific heads. The FC network f learns a condensed representation x` from the fused input x, as shown in Eq. (2). Subsequently, a softmax function is applied to 2 task-specific dense layers, gd and gs, to transform x` into output

XSL•FO
RenderX

probabilities for DS classification (Eq. (3)) and SR classification (Eq. (4)), respectively.

(2)x`=fx

(3)y^d=Softmax(gd(x′))

(4)y^s=Softmax(gs(x′))

In the context of an MTL model, the design of loss functions for multiple objectives is crucial. Instead of using weighted sum of loss functions, which can be influenced by weights and time-consuming to determine, we adopted the automatic weighted loss approach introduced by [47]. This method considers the homoscedastic uncertainty of each task and derives appropriate weights based on task uncertainties. Tasks with higher uncertainties are assigned lower weights, allowing the model to effectively learn across tasks in a more balanced manner.

For the loss calculation, our proposed method involves a 2-stage approach. In the first stage, we compute task-specific losses, Ld and Ls, for DS and SR tasks, respectively, using cross entropy, as described in Eq. (5) (C represents the number of labels in the corresponding task). In the second stage, the total loss, Ltotal, is determined using the automatic weighted loss method proposed by [47], as depicted in Eq. (6). The goal is to minimize the total loss, enhancing the model's performance in DS and SR classification tasks, which can enable effective learning from the data and accurate predictions for both tasks.

(5)L=−∑i=1Cyi·log (y^i)

(6)Ltotal=12σd2Ld+12σs2Ls+log σd2+log (σs2)

Implementation Details

We implemented our approach using PyTorch [61] and the Transformers library from Hugging Face [62]. Pretrained models were loaded by specifying the model version string in the application programming interface. Refer to Table S1 in Multimedia Appendix 1 for details of the Chinese versions of the 4 models selected for this study.

To extract features from the audio and text modalities, we configured several parameters. The audio features were generated with a sampling rate of 16,000 and a duration of 6.25 seconds, resulting in a 100,000-dimensional feature. For the text modality, transcripts were tokenized into a fixed length of 512 tokens, with truncation or padding applied if necessary. The audio features were then transformed into 1024-dimensional embeddings, while the tokenized text inputs were represented as 768-dimensional embeddings.

To prevent overfitting during training, batch normalization and rectified linear unit activation were applied to linear layers that did not act as classifiers. A batch size of 8 was used, and the models were trained for 20 epochs with an early stopping patience of 3. Cross-entropy was used to calculate the loss for single-task learning (STL), while automatic weighted loss was used for MTL. The AdamW optimizer was used for optimizing the losses. The parameter details for each model, including the modality used (single or multiple) and the learning architecture adopted (single task or multitask), are presented in Table 4.

Table . Parameter settings.

Parameter	SMSTL[a]	MMSTL[b]	SMMTL[c]	MMMTL[d]
Epochs	20	20	20	20
Early stopping patience	3	3	3	3
Batch size	8	8	8	8
Learning rate	0.0005	0.0005	0.0005	0.0005
Warmup ratio	0.3	0.35	0.35	0.25
Dropout probability	0.2	0.1	0.1	0.1

[a]SMSTL: single modality with single-task learning.

[b]MMSTL: multimodal with single-task learning.

[c]SMMTL: single modality with multitask learning.

[d]MMMTL: multimodal with multitask learning.

Experimental Evaluation

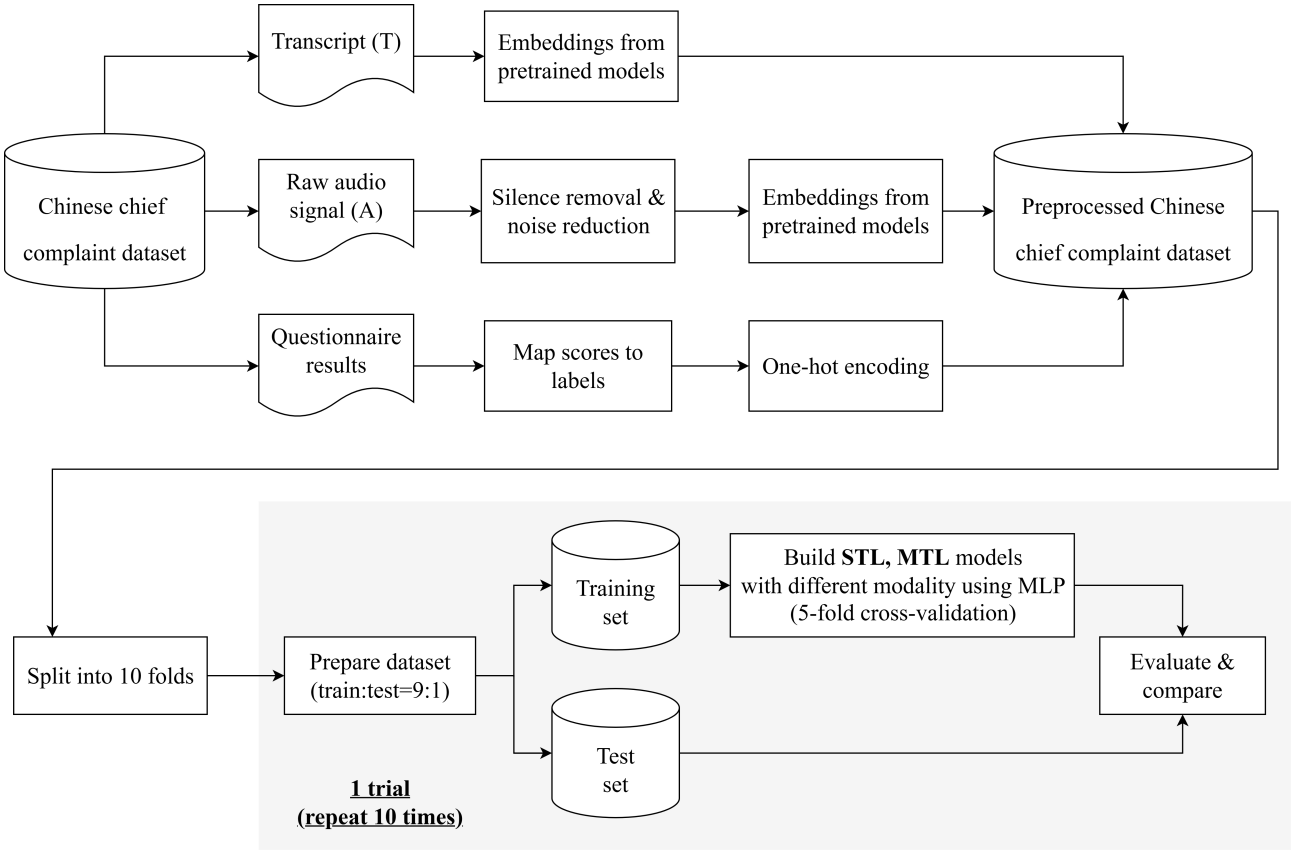
Our proposed framework is built using the 3 data types in the dataset: audio recordings, transcripts, and questionnaire results, as shown in the flow diagram in Figure 2.

During preprocessing, the audio data underwent 3 steps: removal of file-edge silence, denoising using Podcastle [63], and feature extraction. We used Podcastle's Magic Dust AI technology for its advanced denoising capabilities, which integrate spectral filtering, adaptive noise cancellation, and machine learning algorithms [64]. Specifically, we used the "noise reduction" mode to automatically detect and suppress nonstationary background noises, such as coughs, sniffles, and microphone taps, while preserving speech clarity and signal integrity [65]. This step minimized noise-related distortions prior to feature extraction and analysis.

Feature extraction was then applied to both audio and text data using pretrained models, yielding their respective embeddings as described earlier. The processed dataset was partitioned into 10 subsets for cross-validation, with 1 subset used for testing and the remaining 9 for training in each fold. Final performance metrics were averaged across all 10 trials. In parallel, questionnaire responses were one-hot encoded to represent discrete class labels, serving as the output variables for prediction.

XSL•FO
RenderX

Figure 2. Flow diagram. MLP: multilayer perceptron; MTL: multitask learning; STL: single-task learning.



Our study consisted of 3 experiments. In experiments 1 and 2, we built STL models for DS and SR tasks, using different combinations of embeddings. The primary aim was to identify the best pretrained models for extracting text and audio embeddings in each task and assess the advantages of using multimodal data compared to unimodal data for each task. In experiment 3, we developed several MTL models with hard parameter sharing to combine information from both tasks. The performance of these MTL models was then compared to the STL models from experiments 1 and 2, providing insights into the potential benefits of MTL for the 2 tasks.

Performance Measure

To assess the effectiveness of our classification models, we used a range of standard metrics, including accuracy, recall, precision, specificity, F_1-score, and area under the curve (AUC). These metrics were derived from the confusion matrix, with AUC serving as the primary metric for comprehensive performance evaluation. In cases where the difference in AUC between models was not significant, we also considered other metrics, such as accuracy, F_1-score, and recall, to ensure a thorough assessment of model performance.

In the SR prediction task, the positive class (eg, “at risk”) encompassed individuals with a moderate or high risk of suicide, as detailed earlier. In contrast, for the DS prediction task, the models’ performance across all classes (eg, none, low/moderate, and high) was evaluated using the macro-average approach, rather than focusing solely on a specific positive class.

Results

Experiment 1: STL Models for DS Prediction

In experiment 1, we aimed to find the best STL model for DS classification by using various pretrained embeddings to differentiate between the 3 severity levels. These models employed a multilayer perceptron classifier for classification and were categorized into audio-only, text-only, and combined audio and text modalities based on the embeddings used. The classification performance of these DS prediction models on each metric is presented in Figure 3.

XSL•FO
RenderX

Figure 3. Performance comparison of single-task learning models for depression severity (DS) and suicide risk (SR) prediction. Performance metrics are presented as a heatmap, where color gradients reflect the relative magnitude of values, ranging from red (lower values) to green (higher values). A: audio only; A+T: combined audio and text; ACC: accuracy; AUC: area under the curve; E: ERNIE-health; F_1: F_1-score; H: HuBERT; L: Longformer; P: precision; R: recall; S: specificity; T: text only; W: wav2vec 2.0.

Task	Modality	Embedding	AUC	ACC	F_1	P	R	S
DS	A	W	0.791	0.665	0.503	0.516	0.522	0.790
		H	0.765	0.695	0.501	0.493	0.524	0.814
	T	L	0.802	0.775	0.592	0.605	0.602	0.859
		E	0.877	0.780	0.586	0.586	0.609	0.868
	A+T	W+E	**0.878**	0.790	0.622	0.621	0.640	0.878
		W+L	0.873	0.790	**0.629**	**0.652**	0.630	0.874
		H+E	0.853	**0.810**	0.627	0.630	**0.644**	**0.888**
		H+L	0.820	0.745	0.534	0.518	0.559	0.850
SR	A	W	0.737	0.670	0.568	0.659	0.517	0.805
		H	0.762	0.720	0.643	0.644	0.651	0.772
	T	L	0.784	0.750	0.721	0.719	0.729	0.758
		E	0.833	0.780	**0.759**	0.753	**0.780**	0.785
	A+T	W+E	0.852	0.735	0.648	**0.780**	0.582	**0.865**
		W+L	0.838	0.745	0.692	0.753	0.650	0.827
		H+E	**0.876**	**0.785**	0.737	0.778	0.713	0.843
		H+L	0.822	0.715	0.656	0.748	0.607	0.811

Regarding DS prediction models, we obtained several findings (Figure 3). First, the results demonstrated that most embeddings, except those of the audio modality, performed well in terms of AUC, with scores exceeding 0.8. In the audio modality, the wav2vec 2.0 embedding outperformed the HuBERT embedding. In the text modality, the ERNIE-health embedding demonstrated superior performance in terms of AUC (0.877), accuracy (0.780), recall (0.609), and specificity (0.868), indicating its effectiveness in capturing specific aspects of DS in textual data. Second, combining embeddings from different modalities led to improvements across all metrics for most embeddings. Notably, the addition of the ERNIE-health embedding to the HuBERT embedding resulted in a substantial performance boost, with an 11.5% increase in AUC and up to 27.79% improvement in precision. Third, our comprehensive evaluation of multiple metrics showed that the multimodal models outperformed the single-modality models, except for the combination that included the HuBERT embedding, which may impair the ability of text embeddings. Lastly, among all the embeddings analyzed, the wav2vec 2.0+ERNIE-health and wav2vec 2.0+Longformer embeddings achieved the highest AUC scores of 0.878 and 0.873, respectively.

Experiment 2: STL Models for SR Prediction

In experiment 2, our objective was to identify the best STL model for SR classification by using different pretrained embeddings. Similar to experiment 1, multilayer perceptron classifiers were used to analyze the embeddings from different modalities. The evaluation results of these embeddings for SR classification are presented in Figure 3.

Based on the data presented in Figure 3, regarding SR prediction models, several findings were obtained. First, the results demonstrated that most embeddings achieved AUC values greater than 0.8, except for audio modality embeddings and the Longformer embedding. In the audio modality, the HuBERT embedding outperformed the wav2vec 2.0 embedding on most metrics, except for precision and specificity. This suggests that the HuBERT embedding may be a better choice for overall SR classification, while the wav2vec 2.0 embedding may be more effective in correctly identifying individuals who are not at risk of suicide. In the text modality, the ERNIE-health embedding outperformed the Longformer embedding, obtaining higher values on all metrics, indicating that the ERNIE-health embedding is more effective for SR classification. Second, combining embeddings from different modalities consistently improved AUC, precision, and specificity. Specifically, incorporating multimodal embeddings led to significant performance improvements, with increased AUC (2.28% to 15.60%), precision (3.32% to 20.81%), and specificity (2.73% to 10.19%) across all single-modality models, indicating improved accuracy in identifying nonrisk individuals. Third,

XSL•FO
RenderX

the HuBERT+ERNIE-health embedding achieved the highest performance in terms of AUC (0.876) among all embeddings.

Experiment 3: MTL Models for DS and SR Predictions

In experiment 3, we aimed to explore the potential of MTL models in improving DS and SR predictions by leveraging shared information between the 2 tasks. Figure 4 provides a comprehensive summary of the performance metrics, and the subsequent content further discusses the results of experiments 1 and 2 for comparison.

Figure 4. Performance comparison of multitask learning models for depression severity (DS) and suicide risk (SR) prediction. Performance metrics are presented as a heatmap, where color gradients reflect the relative magnitude of values, ranging from red (lower values) to green (higher values). A: audio only; A+T: combined audio and text; ACC: accuracy; AUC: area under the curve; E: ERNIE-health; F_1: F_1-score; H: HuBERT; L: Longformer; P: precision; R: recall; S: specificity; T: text only; W: wav2vec 2.0.

Task	Modality	Embedding	AUC	ACC	F_1	P	R	S
DS	A	W	0.793	0.680	0.468	0.456	0.496	0.799
		H	0.771	0.690	0.480	0.465	0.509	0.813
	T	L	0.810	0.760	0.528	0.506	0.562	0.853
		E	0.885	0.770	0.538	0.520	0.575	0.864
	A+T	W+E	**0.912**	**0.810**	**0.686**	**0.707**	**0.698**	**0.888**
		W+L	0.866	0.770	0.610	0.605	0.623	0.861
		H+E	0.866	0.790	0.604	0.617	0.617	0.872
		H+L	0.844	0.765	0.568	0.578	0.585	0.859
SR	A	W	0.812	0.735	0.702	0.723	0.703	0.775
		H	0.803	0.715	0.665	0.728	0.622	0.788
	T	L	0.799	0.740	0.698	0.761	0.679	**0.791**
		E	0.861	0.770	0.750	0.744	0.768	0.775
	A+T	W+E	0.829	0.745	0.733	0.760	0.743	0.743
		W+L	0.846	0.750	0.723	0.740	0.723	0.781
		H+E	**0.901**	**0.780**	**0.769**	**0.793**	**0.777**	0.777
		H+L	0.821	0.720	0.697	0.697	0.706	0.733

From Figures 3 and 4, we found that all models, except the ones using the wav2vec 2.0+Longformer embedding, demonstrated an increase in AUC ranging from 0.25% to 3.88% with MTL, indicating the potential of MTL in enhancing performance for DS. Additionally, we observed that when adopting MTL for SR prediction, all models, except for the wav2vec 2.0+ERNIE-health and HuBERT+Longformer embeddings, demonstrated an increase in AUC ranging from 0.96% to 10.18%. On the other hand, what stands out is that when applying the MTL framework, there was a consistent enhancement in accuracy, F_1-score, and recall among the combined audio and text models, including the aforementioned 2 models using the wav2vec 2.0+ERNIE-health and HuBERT+Longformer embeddings. These findings suggest that combined audio and text embeddings are well-suited for the MTL approach, although they may increase false positives while better identifying individuals at risk for suicide.

Discussion

Principal Findings

This study proposes a multitask framework that integrates a multimodal fusion strategy using pretrained audio and text embeddings to concurrently assess DS and SR. The efficacy of the proposed method has been validated using real-world clinical data.

Some of the significant findings of this study are as follows. First, we introduced and investigated renowned pretrained models for their effectiveness in audio and text classification tasks. The findings demonstrated that the ERNIE-health text modality embedding, specifically trained on a medical corpus, consistently outperformed the Longformer text modality embedding in both STL models (for DS prediction and SR prediction) and MTL models. On the other hand, the wav2vec 2.0 audio modality embedding performed better than the

XSL•FO
RenderX

HuBERT embedding in STL models for DS prediction and MTL models for both tasks, but performed worse than the HuBERT embedding in STL models for SR prediction.

Second, our results underscore the effectiveness of multimodal approaches over single-modality ones in classifying DS and SR in the majority of cases. Even straightforward fusion techniques, such as concatenation, improve performance by integrating richer information, consistent with previous research [30,31,66]. This implies that the combination of audio and text embeddings provides a more comprehensive representation of the underlying phenomena than using each modality independently.

Third, the results indicated that the performance of text modality models significantly surpassed that of audio modality models, except in MTL models using the Longformer embedding for SR prediction. Several potential explanations can be considered for this observation. Despite preprocessing efforts to reduce noise, the audio modality model remains susceptible to variations in speaker accents or weaker emotional expressiveness [67], which can adversely affect the model's performance. In contrast, text data are not influenced by such variations. Additionally, techniques for processing and embedding text data are highly advanced, such as ERNIE-health, which can contribute to the superior performance of most text modality models. This demonstrates that ERNIE-health can effectively bridge the gap between pretraining goals and downstream tasks [56]. Conversely, processing and feature extraction for audio data in our dataset may not be as efficient as for text embeddings. Furthermore, research indicates that suicidal tendencies and depressive symptoms are explicitly conveyed through syntactic and semantic patterns in text, which are efficiently captured by text embeddings [68]. On the contrary, extracting and interpreting these signals from audio data are inherently more complex and less robust.

Fourth, our findings demonstrated that the proposed MTL framework, using specific pretrained audio and text embeddings, significantly enhanced the classification performance for DS and SR. Considering the common class imbalance in clinical datasets, we selected AUC as our primary evaluation metric to provide a reliable and clinically meaningful representation of model performance [69,70]. However, our experiments also revealed that not all models benefited from its use, with 3 multimodal models showing no improvement in AUC (Table 5). Interestingly, MTL improved the performance of all single-modality models on both tasks. However, among the 4 multimodal models, only 1 (ie, using the HuBERT+ERNIE-health embeddings) exhibited improvement in AUC for both tasks when using MTL. The remaining 3 models demonstrated mixed results, with 1 task showing improvement, and the others experiencing a drop in performance. This highlights the phenomenon of negative transfer [71], suggesting that transferred knowledge may not always have a positive impact on other tasks, even if they share similarities [71].

XSL•FO
RenderX

Table . Performance comparison of STL[a] and MTL[b] models for depression severity and suicide risk prediction.

Task, modality, and embedding	AUC[c]		Improvement
	STL	MTL	
Depression severity prediction			
Audio only			
wav2vec	0.791	0.793	+0.002
HuBERT	0.765	0.771	+0.006
Text only			
Longformer	0.802	0.810	+0.008
ERNIE-health	0.877	0.885	+0.008
Combination of audio and text			
wav2vec+ERNIE-health	0.878	0.912[d]	+0.034
wav2vec+Longformer	0.873	0.866	−0.007
HuBERT+ERNIE-health	0.853	0.866	+0.013
HuBERT+Longformer	0.820	0.844	+0.024
Suicide risk prediction			
Audio only			
wav2vec	0.737	0.812	+0.075
HuBERT	0.762	0.803	+0.041
Text only			
Longformer	0.784	0.799	+0.015
ERNIE-health	0.833	0.861	+0.028
Combination of audio and text			
wav2vec+ERNIE-health	0.852	0.829	−0.023
wav2vec+Longformer	0.838	0.846	+0.008
HuBERT+ERNIE-health	0.876	0.901[d]	+0.025
HuBERT+Longformer	0.822	0.821	−0.001

[a]STL: single-task learning.

[b]MTL: multitask learning.

[c]AUC: area under the curve.

[d]Highest AUC values for each task.

Finally, our study revealed that MTL models led to more substantial improvements in the SR prediction task compared to the DS prediction task, with all multimodal MTL models demonstrating higher recall than their STL counterparts in predicting SR. These findings may be attributed to several aspects. On one hand, the SR prediction task may involve information or patterns different from those in the DS prediction task. For instance, text modalities might convey clearer linguistic patterns, such as specific word choices, pronoun usage, and negative terms [17], which could be more predictive of SR than DS. However, MTL allows models to share learned representations across tasks. If the features relevant to the SR prediction task benefit from certain text or audio modality representations, these features may also aid the DS task, even if the latter shows less improvement. On the other hand, the prediction of DS may be more influenced by sample variability [72,73], whereas the prediction of SR might exhibit stronger commonalities across samples. These findings further underscore the value of MTL, as it enables the model to address such differences through shared representations, thereby enhancing prediction accuracy.

To contextualize our work within current state-of-the-art techniques, we compared our multitask framework with recent studies on depression and suicide prediction, as summarized in Table S2 in Multimedia Appendix 1. Our proposed MTL model, which integrates audio and text modalities with pretrained embeddings, achieved competitive performance (DS: AUC=0.91; accuracy=0.81; F_1-score=0.69 with wav2vec 2.0+ERNIE-health; SR: AUC=0.90; accuracy=0.78; F_1-score=0.77 with HuBERT+ERNIE-health), outperforming several prominent MTL models. These include models by Benton et al [25] (depression: AUC=0.77; suicide: AUC=0.83), Ghosh et al [46] (depression: accuracy=0.74), and Yang et al

XSL•FO
RenderX

[27] (suicide: accuracy=0.74). While Buddhitha and Inkpen [29] reported slightly higher performance for suicide prediction (AUC=0.88; accuracy=0.84), their approach relied on Reddit posts rather than clinical data.

Our study also outperformed all single-task depression prediction studies presented in Table S2 in Multimedia Appendix 1, which predominantly used binary classification (ie, depressed vs nondepressed). In contrast, our multitask framework enabled a more nuanced assessment by explicitly predicting the severity of depressive symptoms rather than merely classifying their presence or absence. Although some single-task suicide prediction models reported higher metrics, including models by Chen et al [38] (F_1-score=0.76), Tsui et al [39] (AUC=0.93), and Bouktif et al [36] (accuracy=0.94), they used substantially larger datasets (1284 subjects, 45,238 patients, and 3,48,110 posts, respectively) and focused exclusively on single-task prediction. Similarly, Ramírez-Cifuentes et al [40] achieved an AUC of 0.94 for suicide prediction using social media data, which suffered from known limitations, including self-presentation biases, language ambiguities, and an inability to detect offline SR [30].

Our study uniquely applied MTL to simultaneously predict DS and SR using multimodal data from clinical interviews. Unlike prior work that focused on single tasks or unimodal inputs, often derived from electronic health records or social media, our approach captured direct clinical interactions, yielding more authentic behavioral signals. Comparative analyses demonstrated that our model effectively predicted both DS and SR, offering clear advantages over existing methods for this clinically important objective.

Theoretical Implications

This study makes substantial contributions to existing literature from 2 main perspectives. First, this study delineated the efficacy of integrating MML, MTL, and TL in simultaneously identifying DS and SR, thereby advancing the understanding of depression and suicide detection. While existing research, such as [25], has explored the impact and importance of MTL in DS and SR prediction, studies have predominantly focused on social media contexts. Limited research has evaluated the effectiveness of MTL in clinical settings. This study addressed this gap through empirical experiments using real-world clinical datasets, demonstrating that the proposed multimodal multitask approach, integrating pretrained embeddings, is applicable to clinical settings.

Furthermore, our findings underscore that MTL generally enhances model performance, consistent with prior literature (eg, [25,45,46]), highlighting the benefits of knowledge sharing across domains [25]. However, our experiments also revealed instances of negative transfer [71], emphasizing the importance of selecting optimal MTL strategies based on embeddings, tasks, and application scenarios. Moreover, further thoughtful evaluation should consider balancing the costs associated with false positives and false negatives, using more comprehensive metrics.

Second, we discussed and presented a comparison of popular pretrained models (Longformer and ERNIE-health for text modality, and wav2vec 2.0 and HuBERT for audio modality) to evaluate their effectiveness with clinical data, providing a valuable addition to the existing literature on depression and suicide prediction research. Our findings revealed that ERNIE-health outperformed Longformer in text modality embedding, and wav2vec 2.0 generally surpassed HuBERT, although there were instances where the reverse was true. This underscores the necessity of judicious pretrained model selection and thorough testing for clinical applicability in the future. Nevertheless, we still affirm the efficacy of TL, as even single-task and single-modality models exhibited commendable performance, although our dataset included only 200 samples.

Practical Implications

This study has several important practical implications. First, the persistent challenge of data scarcity has limited progress in both academic research and clinical practice. Through techniques like MML, TL, and MTL, we propose promising solutions. Second, by integrating multimodal data from speech and text and applying TL methods, our approach can facilitate clinical diagnosis with objective and quantitative measurements. This enables a rapid, efficient, and cost-effective assessment of DS and SR based solely on patients' verbal disclosures to health care providers. Third, the effectiveness of our method suggests a promising avenue for automated SR detection through the development of innovative tools, thereby making a significant contribution to early suicide prevention efforts.

Limitations and Future Research

This study has certain limitations that warrant further research. First, our dataset of 200 participants (100 patients with depression and 100 healthy individuals) represents a significant limitation that severely constrains the generalizability of our findings to broader populations. Despite implementing cross-validation techniques, this small sample size introduces considerable risks of overfitting, where the model may capture dataset-specific characteristics rather than robust, generalizable patterns for DS and SR detection. This limitation necessitates external validation with larger, more diverse cohorts from different clinical settings and demographic backgrounds to establish the true clinical utility and robustness of our proposed method. The incorporation of larger external datasets is therefore essential to not only enhance robustness but also refine and validate our approach across varied populations.

Furthermore, addressing data imbalance has emerged as a critical challenge in accurately identifying and classifying depression cases across varying severity levels. Our comprehensive analysis revealed significant performance disparities among "none," "low/moderate," and "high" severity subcategories, with particularly pronounced difficulties in classifying "low/moderate" severity cases (Table S3 in Multimedia Appendix 1). This variability underscores the intricate complexity of developing a robust diagnostic approach capable of consistently discerning nuanced variations in DS. Future research should, therefore, focus on advancing MTL strategies that integrate multimodal feature representations with targeted sampling techniques and refined weighting mechanisms to enhance the robustness of model predictive performance across varying severity levels of depression.

XSL•FO
RenderX

Furthermore, the exploration of diverse fusion strategies and weight adjustments in MTL, along with the investigation of various pretrained models, warrants further investigation to potentially enhance model performance in future studies. However, while our implementation was straightforward, our primary objective was to develop a computationally efficient and effective method that prioritizes resource efficiency. Finally, exploring the applicability of these techniques to a broader spectrum of mental health disorders is essential. This includes leveraging MML and MTL approaches to integrate information across different disorders, thereby expanding the scope of potential applications in mental health diagnostics.

Conclusion

Early detection and accurate diagnosis are crucial for implementing timely interventions and alleviating the societal and economic burdens associated with mental health conditions. This study proposes an effective approach to improving model performance by integrating MTL, MML, and TL for concurrent depression and suicide detection. Our empirical findings, obtained by fine-tuning MTL models on clinical datasets, provide compelling evidence for the effectiveness of integrating MTL, MML, and TL methods in addressing mental health tasks. However, we advocate for cautious MTL implementation to mitigate potential negative transfer effects. Additionally, we recommend careful consideration for the selection of pretrained models and rigorous validation to ensure their clinical applicability. Our proposed methods offer a promising pathway for future research and clinical applications in mental health diagnostics.

Acknowledgments

This research was supported in part by the Ministry of Science and Technology (grant numbers: MOST 110-2314-B-367-001-, MOST 111-2410-H-008-026-MY2, and MOST 111-2314-B-367-001-MY3).

Data Availability

The complete dataset and complete code will be made available on the Open Science Framework platform as soon as the work gets accepted for publication.

Authors' Contributions

CCS (pures1000@yahoo.com.tw) and ILL (05528@cych.org.tw) are co-corresponding authors for this article.

Conflicts of Interest

None declared.

Multimedia Appendix 1
Additional data to support the findings of the study.
[DOCX File, 28 KB - medinform_v13i1e66907_app1.docx]

References

1. Depressive disorder (depression). World Health Organization (WHO). URL: https://www.who.int/news-room/fact-sheets/detail/depression [accessed 2025-05-20]
2. Burcusa SL, Iacono WG. Risk for recurrence in depression. Clin Psychol Rev 2007 Dec;27(8):959-985. [doi: 10.1016/j.cpr.2007.02.005] [Medline: 17448579]
3. Lépine JP, Briley M. The increasing burden of depression. Neuropsychiatr Dis Treat 2011;7(Suppl 1):3-7. [doi: 10.2147/NDT.S19617] [Medline: 21750622]
4. Laget J, Sofia C, Bolognini M, Plancherel B, Halfon O, Stéphan P. Use of a multidimensional assessment tool in a psychiatric adolescent care unit. J Eval Clin Pract 2006 Oct;12(5):549-558. [doi: 10.1111/j.1365-2753.2006.00669.x] [Medline: 16987117]
5. Thagard P, Larocque L. Mental health assessment: inference, explanation, and coherence. J Eval Clin Pract 2018 Jun;24(3):649-654. [doi: 10.1111/jep.12885] [Medline: 29380474]
6. Tramonti F, Ferrante B, Palmer H. A consulting room with a view: psychotherapy and the ecological context. J Eval Clin Pract 2024 Sep;30(6):1113-1122. [doi: 10.1111/jep.14030] [Medline: 38818691]
7. Low DM, Bentley KH, Ghosh SS. Automated assessment of psychiatric disorders using speech: a systematic review. Laryngoscope Investig Otolaryngol 2020 Feb;5(1):96-116. [doi: 10.1002/lio2.354] [Medline: 32128436]
8. Chehil S, Kutcher S. Suicide Risk Management: A Manual for Health Professionals: John Wiley & Sons; 2012. [doi: 10.1002/9781119953128]
9. O'Connor EA, Perdue LA, Coppola EL, Henninger ML, Thomas RG, Gaynes BN. Depression and suicide risk screening: updated evidence report and systematic review for the US Preventive Services Task Force. JAMA 2023 Jun 20;329(23):2068-2085. [doi: 10.1001/jama.2023.7787] [Medline: 37338873]

XSL•FO
RenderX

10. Richards JE, Whiteside U, Ludman EJ, et al. Understanding why patients may not report suicidal ideation at a health care visit prior to a suicide attempt: a qualitative study. Psychiatr Serv 2019 Jan 1;70(1):40-45. [doi: 10.1176/appi.ps.201800342] [Medline: 30453860]
11. Iyer R, Nedeljkovic M, Meyer D. Using voice biomarkers to classify suicide risk in adult telehealth callers: retrospective observational study. JMIR Ment Health 2022 Aug 15;9(8):e39807. [doi: 10.2196/39807] [Medline: 35969444]
12. Huang SH, LePendu P, Iyer SV, Tai-Seale M, Carrell D, Shah NH. Toward personalizing treatment for depression: predicting diagnosis and severity. J Am Med Inform Assoc 2014;21(6):1069-1075. [doi: 10.1136/amiajnl-2014-002733] [Medline: 24988898]
13. Nadif M, Role F. Unsupervised and self-supervised deep learning approaches for biomedical text mining. Brief Bioinform 2021 Mar 22;22(2):1592-1603. [doi: 10.1093/bib/bbab016] [Medline: 33569575]
14. Wang G, Lou X, Guo F, Kwok D, Cao C. EHR-HGCN: an enhanced hybrid approach for text classification using heterogeneous graph convolutional networks in electronic health records. IEEE J Biomed Health Inform 2023;28(3):1668-1679. [doi: 10.1109/JBHI.2023.3346210]
15. Rejaibi E, Komaty A, Meriaudeau F, Agrebi S, Othmani A. MFCC-based recurrent neural network for automatic clinical depression recognition and assessment from speech. Biomed Signal Process Control 2022 Jan;71:103107. [doi: 10.1016/j.bspc.2021.103107]
16. Cummins N, Scherer S, Krajewski J, Schnieder S, Epps J, Quatieri TF. A review of depression and suicide risk assessment using speech analysis. Speech Commun 2015 Jul;71:10-49. [doi: 10.1016/j.specom.2015.03.004]
17. Homan S, Gabi M, Klee N, et al. Linguistic features of suicidal thoughts and behaviors: a systematic review. Clin Psychol Rev 2022 Jul;95:102161. [doi: 10.1016/j.cpr.2022.102161] [Medline: 35636131]
18. Lin L, Chen X, Shen Y, Zhang L. Towards automatic depression detection: a BiLSTM/1D CNN-based model. Appl Sci (Basel) 2020;10(23):8701. [doi: 10.3390/app10238701] [Medline: 33520293]
19. Kim AY, Jang EH, Lee SH, Choi KY, Park JG, Shin HC. Automatic depression detection using smartphone-based text-dependent speech signals: deep convolutional neural network approach. J Med Internet Res 2023 Jan 25;25:e34474. [doi: 10.2196/34474] [Medline: 36696160]
20. Bennett-Poynter L, Kundurthi S, Besa R, et al. Harnessing digital health data for suicide prevention and care: a rapid review. Digit Health 2025;11:20552076241308615. [doi: 10.1177/20552076241308615] [Medline: 39996066]
21. Kirtley OJ, van Mens K, Hoogendoorn M, Kapur N, de Beurs D. Translating promise into practice: a review of machine learning in suicide research and prevention. Lancet Psychiatry 2022 Mar;9(3):243-252. [doi: 10.1016/S2215-0366(21)00254-6] [Medline: 35183281]
22. Nock MK, Hwang I, Sampson NA, Kessler RC. Mental disorders, comorbidity and suicidal behavior: results from the National Comorbidity Survey Replication. Mol Psychiatry 2010 Aug;15(8):868-876. [doi: 10.1038/mp.2009.29] [Medline: 19337207]
23. van Heeringen K, Mann JJ. The neurobiology of suicide. Lancet Psychiatry 2014 Jun;1(1):63-72. [doi: 10.1016/S2215-0366(14)70220-2] [Medline: 26360403]
24. Hawton K, Saunders KE, O'Connor RC. Self-harm and suicide in adolescents. The Lancet 2012 Jun;379(9834):2373-2382. [doi: 10.1016/S0140-6736(12)60322-5]
25. Benton A, Mitchell M, Hovy D. Multi-task learning for mental health using social media text. arXiv. Preprint posted online on Dec 10, 2017. [doi: 10.48550/arXiv.1712.03538]
26. Teng S, Chai S, Liu J, Tateyama T, Lin L, Chen YW. Multi-modal and multi-task depression detection with sentiment assistance. Presented at: 2024 IEEE International Conference on Consumer Electronics (ICCE); Jan 6-8, 2024; Las Vegas, NV, USA. [doi: 10.1109/ICCE59016.2024.10444213]
27. Yang Q, Zhou J, Wei Z. Time perspective-enhanced suicidal ideation detection using multi-task learning. IJNDI 2024;3(2):100011. [doi: 10.53941/ijndi.2024.100011]
28. Qureshi SA, Dias G, Hasanuzzaman M, Saha S. Improving depression level estimation by concurrently learning emotion intensity. IEEE Comput Intell Mag 2020;15(3):47-59. [doi: 10.1109/MCI.2020.2998234]
29. Buddhitha P, Inkpen D. Multi-task learning to detect suicide ideation and mental disorders among social media users. Front Res Metr Anal 2023;8:1152535. [doi: 10.3389/frma.2023.1152535] [Medline: 37138946]
30. Ophir Y, Tikochinski R, Asterhan CSC, Sisso I, Reichart R. Deep neural networks detect suicide risk from textual facebook posts. Sci Rep 2020 Oct 7;10(1):16685. [doi: 10.1038/s41598-020-73917-0] [Medline: 33028921]
31. Qureshi SA, Saha S, Hasanuzzaman M, Dias G. Multitask representation learning for multimodal estimation of depression level. IEEE Intell Syst 2019;34(5):45-52. [doi: 10.1109/MIS.2019.2925204]
32. Boigne J, Liyanage B, Östrem T. Recognizing more emotions with less data using self-supervised transfer learning. arXiv. Preprint posted online on Nov 11, 2020. [doi: 10.48550/arXiv.2011.05585]
33. Palanisamy K, Singhania D, Yao A. Rethinking CNN models for audio classification. arXiv. Preprint posted online on Jul 22, 2020. [doi: 10.48550/arXiv.2007.11154]
34. Nykoniuk M, Basystiuk O, Shakhovska N, Melnykova N. Multimodal data fusion for depression detection approach. Computation 2025;13(1):9. [doi: 10.3390/computation13010009]

XSL•FO
RenderX

35. Philip Thekkekara J, Yongchareon S, Liesaputra V. An attention-based CNN-BiLSTM model for depression detection on social media text. Expert Syst Appl 2024 Sep;249:123834. [doi: 10.1016/j.eswa.2024.123834]
36. Bouktif S, Khanday A, Ouni A. Explainable predictive model for suicidal ideation during COVID-19: social media discourse study. J Med Internet Res 2025 Jan 17;27:e65434. [doi: 10.2196/65434] [Medline: 39823631]
37. Su Z, Jiang H, Yang Y, Hou X, Su Y, Yang L. Acoustic features for identifying suicide risk in crisis hotline callers: machine learning approach. J Med Internet Res 2025 Apr 14;27:e67772. [doi: 10.2196/67772] [Medline: 40228243]
38. Chen Y, Li J, Song C, Zhao Q, Tong Y, Fu G. Deep learning and large language models for audio and text analysis in predicting suicidal acts in Chinese psychological support hotlines. arXiv. Preprint posted online on Sep 10, 2024. [doi: 10.48550/arXiv.2409.06164]
39. Tsui FR, Shi L, Ruiz V, et al. Natural language processing and machine learning of electronic health records for prediction of first-time suicide attempts. JAMIA Open 2021 Jan;4(1):ooab011. [doi: 10.1093/jamiaopen/ooab011] [Medline: 33758800]
40. Ramírez-Cifuentes D, Freire A, Baeza-Yates R, et al. Detection of suicidal ideation on social media: multimodal, relational, and behavioral analysis. J Med Internet Res 2020 Jul 7;22(7):e17758. [doi: 10.2196/17758] [Medline: 32673256]
41. Crawshaw M. Multi-task learning with deep neural networks: a survey. arXiv. Preprint posted online on Sep 10, 2020. [doi: 10.48550/arXiv.2009.09796]
42. Zhang Y, Yang Q. A survey on multi-task learning. IEEE Trans Knowl Data Eng 2021;34(12):5586-5609. [doi: 10.1109/TKDE.2021.3070203]
43. Thung KH, Wee CY. A brief review on multi-task learning. Multimed Tools Appl 2018 Nov;77(22):29705-29725. [doi: 10.1007/s11042-018-6463-x]
44. Dumpala SH, Rempel S, Dikaios K, Sajjadian M, Uher R, Oore S. Estimating severity of depression from acoustic features and embeddings of natural speech. Presented at: ICASSP 2021 - 2021 IEEE International Conference on Acoustics, Speech and Signal Processing (ICASSP); Jun 6-11, 2021; Toronto, ON, Canada. [doi: 10.1109/ICASSP39728.2021.9414129]
45. Yang T, Li F, Ji D, et al. Fine-grained depression analysis based on Chinese micro-blog reviews. Inf Process Manag 2021 Nov;58(6):102681. [doi: 10.1016/j.ipm.2021.102681]
46. Ghosh S, Ekbal A, Bhattacharyya P. A multitask framework to detect depression, sentiment and multi-label emotion from suicide notes. Cogn Comput 2022 Jan;14(1):110-129. [doi: 10.1007/s12559-021-09828-7]
47. Hamilton M. A rating scale for depression. J Neurol Neurosurg Psychiatry 1960 Feb;23(1):56-62. [doi: 10.1136/jnnp.23.1.56] [Medline: 14399272]
48. Patterson WM, Dohn HH, Bird J, Patterson GA. Evaluation of suicidal patients: the SAD PERSONS scale. Psychosomatics 1983 Apr;24(4):343-345. [doi: 10.1016/S0033-3182(83)73213-5] [Medline: 6867245]
49. Baevski A, Zhou Y, Mohamed A, Auli M. wav2vec 2.0: a framework for self-supervised learning of speech representations. arXiv. Preprint posted online on Jun 20, 2020. [doi: 10.48550/arXiv.2006.11477]
50. Hsu WN, Bolte B, Tsai YHH, Lakhotia K, Salakhutdinov R, Mohamed A. HuBERT: self-supervised speech representation learning by masked prediction of hidden units. IEEE/ACM Trans Audio Speech Lang Process 2021;29:3451-3460. [doi: 10.1109/TASLP.2021.3122291]
51. Beltagy I, Peters ME, Cohan A. Longformer: the long-document transformer. arXiv. Preprint posted online on Apr 10, 2020. [doi: 10.48550/arXiv.2004.05150]
52. Huang X, Wang F, Gao Y, et al. Depression recognition using voice-based pre-training model. Sci Rep 2024;14(1):12734. [doi: 10.1038/s41598-024-63556-0]
53. Chen Z, Song C, Chen Y, et al. Fine-grained speech sentiment analysis in Chinese psychological support hotlines based on large-scale pre-trained model. arXiv. Preprint posted online on May 7, 2024. [doi: 10.48550/arXiv.2405.04128]
54. Dumpala SH, Dikaios K, Nunes A, Rudzicz F, Uher R, Oore S. Self-supervised embeddings for detecting individual symptoms of depression. arXiv. Preprint posted online on Jun 25, 2024. [doi: 10.48550/arXiv.2406.17229]
55. Kurtz E, Zhu Y, Driesse T, et al. Early detection of cognitive decline using voice assistant commands. Proc IEEE Int Conf Acoust Speech Signal Process 2023 Jun;2023:1-5. [doi: 10.1109/icassp49357.2023.10095825] [Medline: 40963950]
56. Wang Q, Dai S, Xu B, et al. Building chinese biomedical language models via multi-level text discrimination. arXiv. Preprint posted online on Oct 14, 2021. [doi: 10.48550/arXiv.2110.07244]
57. Fu L, Weng Z, Zhang J, Xie H, Cao Y. MMBERT: a unified framework for biomedical named entity recognition. Med Biol Eng Comput 2024 Jan;62(1):327-341. [doi: 10.1007/s11517-023-02934-8] [Medline: 37833517]
58. Atmaja BT, Sasou A, Akagi M. Survey on bimodal speech emotion recognition from acoustic and linguistic information fusion. Speech Commun 2022 May;140:11-28. [doi: 10.1016/j.specom.2022.03.002]
59. Huang SC, Pareek A, Seyyedi S, Banerjee I, Lungren MP. Fusion of medical imaging and electronic health records using deep learning: a systematic review and implementation guidelines. NPJ Digit Med 2020;3(1):136. [doi: 10.1038/s41746-020-00341-z] [Medline: 33083571]
60. Ross A. Fusion, feature-level. In: Li SZ, Jain A, editors. Encyclopedia of Biometrics: Springer; 2009:597-602. [doi: 10.1007/978-0-387-73003-5_157]
61. PyTorch. URL: https://pytorch.org/ [accessed 2025-10-25]
62. Hugging Face. URL: https://huggingface.co/ [accessed 2025-10-25]
63. Podcastle. URL: https://podcastle.ai/ [accessed 2025-10-25]

XSL•FO
RenderX

64. 8 best free AI noise reduction tools for crystal clear audio in 2025. AIMojo. URL: https://aimojo.io/free-ai-noise-reduction-tools/ [accessed 2025-05-20]
65. What is noise reduction and how do i use it? Podcastle. URL: https://help.podcastle.ai/en/articles/8912022-what-is-noise-reduction-and-how-do-i-use-it [accessed 2025-05-20]
66. Rodrigues Makiuchi M, Warnita T, Uto K, Shinoda K. Multimodal fusion of BERT-CNN and gated CNN representations for depression detection. Presented at: 9th International on Audio/Visual Emotion Challenge and Workshop; Oct 21, 2019; Nice, France. [doi: 10.1145/3347320.3357694]
67. Zhu X, Lei Y, Li T, et al. METTS: multilingual emotional text-to-speech by cross-speaker and cross-lingual emotion transfer. IEEE/ACM Trans Audio Speech Lang Process 2024;32:1506-1518. [doi: 10.1109/TASLP.2024.3363444]
68. Kalyan KS, Sangeetha S. SECNLP: A survey of embeddings in clinical natural language processing. J Biomed Inform 2020 Jan;101:103323. [doi: 10.1016/j.jbi.2019.103323] [Medline: 31711972]
69. Fawcett T. An introduction to ROC analysis. Pattern Recognit Lett 2006 Jun;27(8):861-874. [doi: 10.1016/j.patrec.2005.10.010]
70. Saito T, Rehmsmeier M. The precision-recall plot is more informative than the ROC plot when evaluating binary classifiers on imbalanced datasets. PLoS ONE 2015;10(3):e0118432. [doi: 10.1371/journal.pone.0118432] [Medline: 25738806]
71. Zhuang F, Qi Z, Duan K, et al. A comprehensive survey on transfer learning. Proc IEEE 2020;109(1):43-76. [doi: 10.1109/JPROC.2020.3004555]
72. Cusack CE, Ralph-Nearman C, Christian C, Fisher AJ, Levinson CA. Understanding heterogeneity, comorbidity, and variability in depression: Idiographic models and depression outcomes. J Affect Disord 2024 Jul 1;356:248-256. [doi: 10.1016/j.jad.2024.04.034] [Medline: 38608769]
73. Melhem NM, Porta G, Oquendo MA, et al. Severity and variability of depression symptoms predicting suicide attempt in high-risk individuals. JAMA Psychiatry 2019 Jun 1;76(6):603-613. [doi: 10.1001/jamapsychiatry.2018.4513] [Medline: 30810713]

Abbreviations

AUC: area under the curve
CNN: convolutional neural network
DS: depression severity
FC: fully connected
HAMD-17: Hamilton Depression Rating Scale-17
MML: multimodal learning
MTL: multitask learning
SR: suicide risk
STL: single-task learning
TL: transfer learning

Edited by Q Chen; submitted 29.09.24; peer-reviewed by G Wang, MM Hossain Shuvo, TA El-Hafeez; revised version received 02.09.25; accepted 05.10.25; published 30.10.25.

Please cite as:
Hu YH, Wu RY, Su MY, Lin IL, Shen CC
Multimodal Multitask Learning for Predicting Depression Severity and Suicide Risk Using Pretrained Audio and Text Embeddings: Methodology Development and Application
JMIR Med Inform 2025;13:e66907
URL: https://medinform.jmir.org/2025/1/e66907
doi:10.2196/66907

© Ya-Han Hu, Ruei-Yan Wu, Min-Yi Su, I-Li Lin, Cheng-Che Shen. Originally published in JMIR Medical Informatics (https://medinform.jmir.org), 30.10.2025. This is an open-access article distributed under the terms of the Creative Commons Attribution License (https://creativecommons.org/licenses/by/4.0/), which permits unrestricted use, distribution, and reproduction in any medium, provided the original work, first published in JMIR Medical Informatics, is properly cited. The complete bibliographic information, a link to the original publication on https://medinform.jmir.org/, as well as this copyright and license information must be included.

XSL•FO
RenderX

Predicting Delayed Extubation After General Anesthesia in Postanesthesia Care Unit Patients Using Machine Learning: Model Development Study

Jianwei Luo[1,2*], BSN; Shaoman Lin[1*], BSN; Liman Wang[1*], BSN; Huanfan Ji[2], BSN; Jingcong Zheng[2], BSN; Tingkang Wang[2], BSN; Lin Chen[2], BSN; Ziqi Lin[2], ADN; Zhongqi Liu[1], MD; Ning Liufu[1], MD

[1]Department of Anesthesiology, Sun Yat-sen Memorial Hospital, Sun Yat-sen University, 107 Yanjiang West Road, Guangzhou, China

[2]Department of Anesthesiology, Shenshan Medical Center, Memorial Hospital of Sun Yat-sen University, Shanwei, China

[*]these authors contributed equally

Corresponding Author:
Ning Liufu, MD
Department of Anesthesiology, Sun Yat-sen Memorial Hospital, Sun Yat-sen University, 107 Yanjiang West Road, Guangzhou, China

Abstract

Background: Delayed extubation after general anesthesia increases complications and can lead to longer hospital stays and higher mortality. Current risk assessments often rely on subjective judgment or simple tools, whereas machine learning offers potential for real-time evaluation, though research is limited and typically uses single-algorithm models.

Objective: The aims of this study were to identify risk factors for delayed extubation after general anesthesia in the sample and to construct a risk prediction model for delayed extubation in this population.

Methods: Data from 4779 patients admitted to the postanesthesia care unit between September 2023 and May 2024 were used to develop prediction models for delayed extubation using k-nearest neighbor, decision tree, extreme gradient boosting, random forest, a light gradient boosting machine, and an artificial neural network. Model performance was assessed by calculating the area under the receiver operating characteristic curve, sensitivity, specificity, accuracy, F_1-score, and Brier score. Calibration performance was evaluated using calibration curves generated with 100-bin quantile calibration and Loess smoothing to provide bias-corrected and smoothed visual assessment. Additionally, the Hosmer-Lemeshow goodness-of-fit test was performed to quantitatively evaluate calibration, with P values >.05 indicating good calibration.

Results: Among the 6 models evaluated, the extreme gradient boosting model demonstrated the best performance, with an area under the receiver operating characteristic curve of 0.750 (95% CI 0.703 - 0.796), a sensitivity of 0.734 (95% CI 0.635 - 0.827), and a specificity of 0.647 (95% CI 0.623 - 0.673). The model calibration was acceptable, with a Brier score of 0.0505 and a nonsignificant Hosmer-Lemeshow goodness-of-fit test (χ^2_6=7.3; P=.287), indicating good calibration. Shapley additive explanations were used to rank feature importance.

Conclusions: These machine learning models enable early identification of delayed extubation risk, supporting personalized clinical decisions and optimizing postanesthesia care unit resource allocation.

Trial Registration: ChiCTR ChiCTR2400090247; https://www.chictr.org.cn/showproj.html?proj=242602

(JMIR Med Inform 2025;13:e72602) doi:10.2196/72602

KEYWORDS

delayed extubation; general anesthesia; postanesthesia care unit; machine learning algorithms; XGBoost; extreme gradient boosting

Introduction

Background

Extubation is a critical step in the recovery process following general anesthesia. More than 20% of major airway management–related complications occur immediately before or after extubation, with severe consequences such as hypoxia and mortality [1,2]. Prolonged intubation offers no benefit; delayed extubation may adversely affect the patient's cardiovascular and respiratory systems, resulting in complications such as ventilator-associated pneumonia, pulmonary fibrosis, ventilator dependency, and arrhythmias [3]. Delayed extubation after general anesthesia not only reduces the efficiency of the transition from the postanesthesia care unit (PACU) to the ward but also slows functional recovery, exacerbates physiological and psychological stress responses, and diminishes the quality of the patient's resuscitation period.

XSL•FO
RenderX

This increases the mental and economic burden on the patient and family and raises the incidence of medical disputes [4].

Screening and predicting patients with a high risk for delayed extubation is crucial for optimizing PACU operations and patient care. Several demographic features have been identified as significant predictors, including advanced age [5,6] and the presence of comorbidities such as chronic obstructive pulmonary disease (COPD), cardiovascular diseases, and diabetes [7]. Additionally, a high BMI has been linked to increased respiratory complications, potentially prolonging the need for ventilatory support [8,9]. Furthermore, the nature of the surgical procedure itself significantly influences the likelihood of delayed extubation. Complex and prolonged surgeries, particularly those involving the thoracic or cardiovascular systems, can lead to increased physiologic stress and a higher risk of postoperative complications that may necessitate extended intubation [10]. Significant hemorrhage can result in hemodynamic instability, which can affect the patient's ability to maintain adequate oxygenation and ventilation postoperatively [11-13]. In clinical practice, extubation following general anesthesia is predominantly executed by medical and nursing professionals within the PACU. However, current research provides limited information on the impact of nursing-related monitoring and management variables within the PACU on the extubation time.

There are increasing studies on building machine learning predictive models for delayed extubation. Previous studies have suggested that machine learning algorithms, including extreme gradient boosting (XGBoost), gradient boosting machine, and artificial neural networks, have advantages in constructing predictive models for delayed extubation in the intensive care unit [14,15]. However, for postoperative delayed extubation, most studies used logistic regression for developing a nomogram model or a single machine learning algorithm for constructing a predictive model [9]. Fewer studies use multiple machine learning algorithms to build a postoperative delayed extubation prediction model following general anesthesia in the PACU.

Therefore, this study aimed to explore perioperative features, including monitoring and management variables in the PACU, associated with delayed extubation after general anesthesia and to develop prediction models for delayed extubation using machine learning algorithms. It is hypothesized that machine learning models incorporating PACU monitoring and management variables can be developed to predict delayed extubation, enabling early assessment and prevention of this adverse event following general anesthesia.

Delayed extubation after general anesthesia is a common postoperative complication associated with increased adverse events, such as prolonged hospital stays, higher intensive care needs, and elevated mortality rates. Identifying patients with high risk and optimizing recovery care is crucial. Current risk assessments often rely on subjective judgment or simplistic tools, which may overlook the complex patient profiles and intraoperative dynamics. Machine learning, with its robust data mining and predictive capabilities, offers real-time evaluation and intervention potential. However, research specifically addressing delayed extubation remains limited, with most studies relying on traditional single-algorithm models.

Aims

The aims of this study were to identify the risk factors for delayed extubation after general anesthesia in the sample and to construct a risk prediction model for delayed extubation in this population.

Methods

Machine Learning Model Selection

The data extracted from electronic medical records in this retrospective cohort study can be used to substantially predict the risk of delayed extubation after general anesthesia. In line with our research objectives, we selected 6 predictive modeling methods for analysis: random forest (RF), XGBoost, k-nearest neighbor (KNN), decision tree, light gradient boosting machine (LightGBM), and artificial neural networks.

Data Collection

Patient consent was waived due to the retrospective nature of the study. Patients transferred to the PACU after general anesthesia at Shenshan Medical Center in Shanwei, China, from September 2023 to May 2024 were retrospectively enrolled.

Variables

Demographic information included sex, age, American Society of Anesthesiologists (ASA) classification, BMI, smoke history, and comorbidities (including cerebral infarction and COPD).

Preoperative examinations included red blood cell distribution width; alanine and aspartate aminotransferase levels; serum sodium concentration, serum concentrations of sodium, potassium, calcium, hemoglobin, and creatinine; and chest x-ray findings. Preoperative examinations were performed within 7 days preoperatively, and the latest result was included in case the same test was conducted multiple times.

Surgery-related parameters included intraoperative infusion volume, intraoperative blood loss, duration of surgery, case condition (usual, urgent, difficult, and critical), site, and level of surgery. Intraoperative infusions were determined by the anesthesiologist based on the patient's intraoperative vital signs, urine output, or hemodynamic monitoring.

PACU monitoring and management indicators included tympanic temperature following PACU admission, time to extubation in PACU, and the sufentanil administered before extubation in the PACU. The supplemental dose of sufentanil was administered at 0.1 μg/kg per dose, with adjustments made based on the patient's specific resuscitation process and the severity of postoperative pain.

Study Population and Data Extraction

Eligibility Criteria

The inclusion criteria were patients who underwent tracheal intubation under general anesthesia and were transferred to the PACU postoperatively. The exclusion criteria were as follows: (1) extubation before admission to the anesthesia recovery room, (2) preoperative coma, (3) presence of severe mental illness or psychiatric disorders, and (4) missing data exceeding 30% of the required information. Patients' demographic information,

XSL•FO
RenderX

comorbidities, preoperative examinations, surgery-related parameters, and PACU monitoring and management indicators were retrieved from the institutional database.

Anesthesia Method

No premedication was used for any patients. Induction was administered by intravenous injection of sufentanil (0.3 - 0.5 μg/kg), propofol (1.5 - 2.5 mg/kg), and rocuronium (0.6 mg/kg). Alternatively, mivacurium (0.07 - 0.25 mg/kg) or cisatracurium (0.2 mg/kg) was used for muscle relaxation. After achieving the appropriate anesthesia depth and muscle relaxation, intubation was performed for mechanical ventilation (Tidal Volume 6 - 8 ml/kg, Respiratory Rate 10 - 12 breaths/min). Intraoperative parameters were managed, and patients were transferred to the PACU within 5 minutes after surgery.

Data Analysis

Statistical analyses were performed using Python (version 3.12.4; Python Software Foundation). Variables with ≥30% missing data were excluded from the analysis, while those with <30% missing data were imputed using the KNN classification algorithm. Continuous variables were assessed for normality and compared using the independent 2-tailed *t* test or the Mann-Whitney *U* test, as appropriate. Categorical variables were compared using the chi-square test or the Fisher exact test, depending on expected cell counts. All statistical tests were 2-sided, and a *P* value <.05 was considered statistically significant.

Feature selection was conducted on the training set using the least absolute shrinkage and selection operator (LASSO) to identify the most predictive variables. During the evaluation phase, a threshold optimization strategy was applied to determine clinically meaningful cut-off points. Specifically, thresholds were selected under dual constraints, requiring both sensitivity and specificity to be ≥0.60, to ensure that the model achieved a balance between correctly identifying positive cases and minimizing false positives. When no threshold met these dual criteria, the Youden index was used as an alternative to identify the optimal threshold. This approach ensured that the final model outputs had practical applicability for clinical risk stratification.

Model discrimination performance was evaluated in the test set by calculating the area under the receiver operating characteristic curve (AUROC), alongside sensitivity, specificity, positive predictive value (PPV), and negative predictive value (NPV). CIs for these metrics were estimated using 1000 bootstrap resampling iterations to enhance the robustness of performance assessment.

Calibration performance was evaluated using calibration curves generated with 100-bin quantile calibration and LOESS smoothing; in the LOESS procedure, the parameter frac=0.3 indicates that 30% of the data were used for each local fit to control the degree of smoothing. The Hosmer-Lemeshow goodness-of-fit test was also performed to quantitatively assess calibration, with *P* values >.05 indicating good calibration.

Data Processing and Feature Selection

Delayed extubation after general anesthesia has been defined as the removal of the tracheal tube 60 minutes or more after general anesthesia [16]. This study defined delayed extubation as removal of the tracheal tube over the same time frame following PACU admission, while removal in less than 60 minutes was categorized as nondelayed extubation.

Continuous variables were presented as mean with SD or median with IQR according to normality for the variables. Categorical variables were expressed as frequencies with percentages. Missing values were filled in using the KNN classification algorithm, which estimates missing values based on the values of patients with similar features. Patients ultimately enrolled in this study were randomized in a 7:3 ratio into primary and test cohorts. We used the optimal thresholds from receiver operating characteristic (ROC) curve analysis to convert continuous variables, such as intraoperative infusion volume and duration of surgery from the training set, into categorical variables [17].

The LASSO was used to identify key features associated with delayed extubation after general anesthesia for the construction of the machine learning models. The machine learning algorithms used in this study included KNN, decision tree, XGBoost, RF, LightGBM, and artificial neural networks. To enhance model performance, parameter tuning was conducted on the training set using a 10-fold cross-validation approach.

Model Evaluation

The AUROC, sensitivity, specificity, PPV, NPV, accuracy, and F_1-score were chosen as primary metrics for model evaluation. To enhance the robustness of performance assessment, 1000 bootstrap resampling iterations were performed to estimate the CIs for these metrics. Model calibration was evaluated using calibration curves generated with 100-bin quantile calibration and Loess smoothing (frac=0.3) to provide bias-corrected and smoothed visual assessment, and the Hosmer-Lemeshow goodness-of-fit test was performed to quantitatively assess calibration, with *P* values >.05 indicating good calibration. Additionally, Brier scores were calculated to assess overall calibration accuracy.

Ethical Considerations

This study was approved by the institutional review board of Shenshan Medical Center, Memorial Hospital of Sun Yat-sen University (2024-SSKY-113-01). The trial was registered in the Chinese Clinical Trial Registry (ChiCTR2400090247). Because this was a retrospective study using deidentified clinical data and posed minimal risk to participants, the institutional review board waived the requirement for informed consent. Participant privacy and data confidentiality were strictly protected; all data were anonymized before analysis and used only for research purposes. No financial compensation was provided to participants.

Results

A total of 4793 patients were initially included in the study. On the basis of the exclusion criteria, 8 (0.16%) patients were excluded due to having more than 30% missing data, 2 (0.04%)

XSL•FO
RenderX

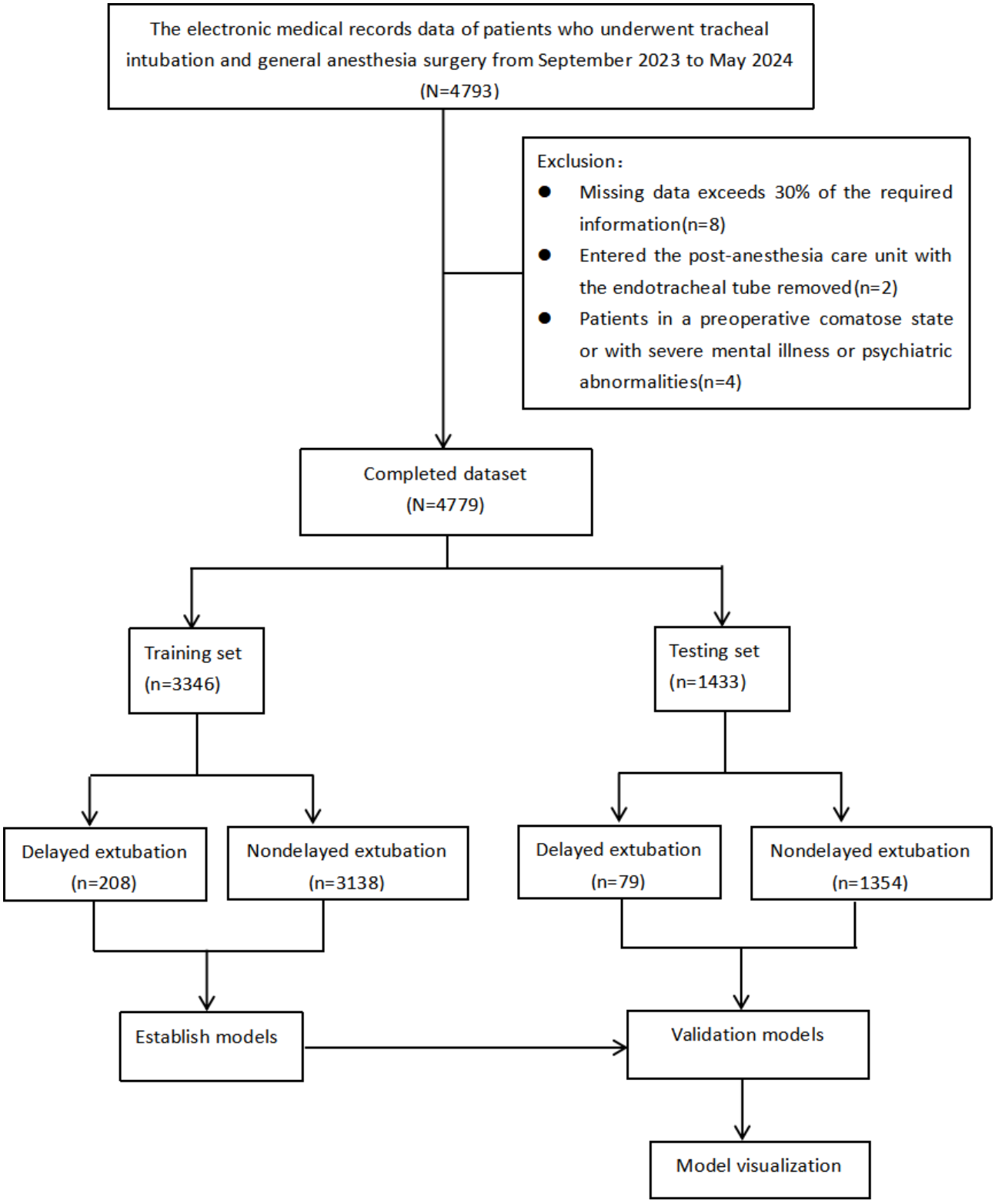
patients were excluded because their tracheal tube had been removed before admission to the PACU, and 4 (0.08%) patients were excluded due to preoperative unconsciousness or severe psychiatric disorders. Therefore, 4779 patients were finally enrolled in the analysis, of whom 6% (287/4793) experienced delayed extubation, defined as extubation time of 60 minutes or more after admission to the PACU, and 93.72% (4492/4793) of patients did not experience delayed extubation. The dataset was randomly divided into primary and test cohorts in a 7:3 ratio, resulting in 70.01% (3346/4779) of patients being placed in the primary cohort and 29.99% (1433/4779) being placed in the test cohort. In the primary cohort, 6.21% (208/3346) of patients were assigned to the delayed extubation group and 93.78% (3138/3346) of patients were assigned to the nondelayed extubation group. The patient recruitment flowchart is shown in Figure 1.

No statistically significant differences were found in the univariate comparisons between the primary and test cohorts (Multimedia Appendix 1). The optimal parameter (λ) in the LASSO model was selected using 10-fold cross-validation. Dashed lines were drawn at the optimal value using the minimum criterion. A vertical line was drawn at the value chosen by 10-fold cross-validation, where the optimal λ resulted in 13 nonzero coefficient features (Figure 2). LASSO regression generated 13 nonzero coefficient variables at the value of λ (minimum)=0.0037 for building a machine learning prediction model, including age, sex, BMI, ASA classification, cerebral stroke history, intraoperative infusion volume, duration of surgery, history of COPD, case condition, surgical site, surgical level, tympanic temperature following PACU admission, and sufentanil administered before extubation in the PACU.

On the basis of the test cohort, ROC (Figure 3) was drawn for different machine learning prediction models (KNN, decision tree, XGBoost, RF, LightGBM, and artificial neural networks). The XGBoost model demonstrated the highest overall performance among all models tested. In the test cohort, the XGBoost model achieved an AUROC of 0.750 (95% CI 0.703 - 0.796), a sensitivity of 0.734 (95% CI 0.634 - 0.827), a specificity of 0.647 (95%CI 0.622 - 0.673), a PPV of 0.108 (95% CI 0.083 - 0.134), a NPV of 0.976 (95%CI 0.966 - 0.985; Table 1), an F_1-score of 0.188, and accuracy of 0.652 (Table 2). The Brier score was 0.0505, indicating a low mean squared difference between predicted probabilities and actual outcomes and suggesting good model calibration (Table 2).

XSL•FO
RenderX

Figure 1. Patient recruitment flowchart



XSL•FO
RenderX

Figure 2. (A) Least absolute shrinkage and selection operator (LASSO) cross-validation curves and (B) coefficient path plot for LASSO regression analysis. MSE: mean square error.

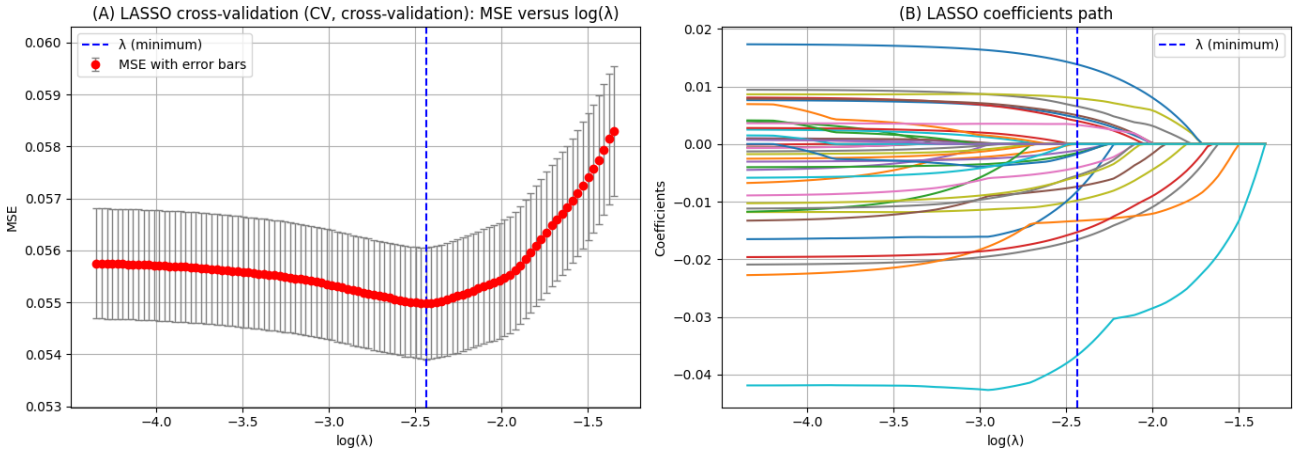
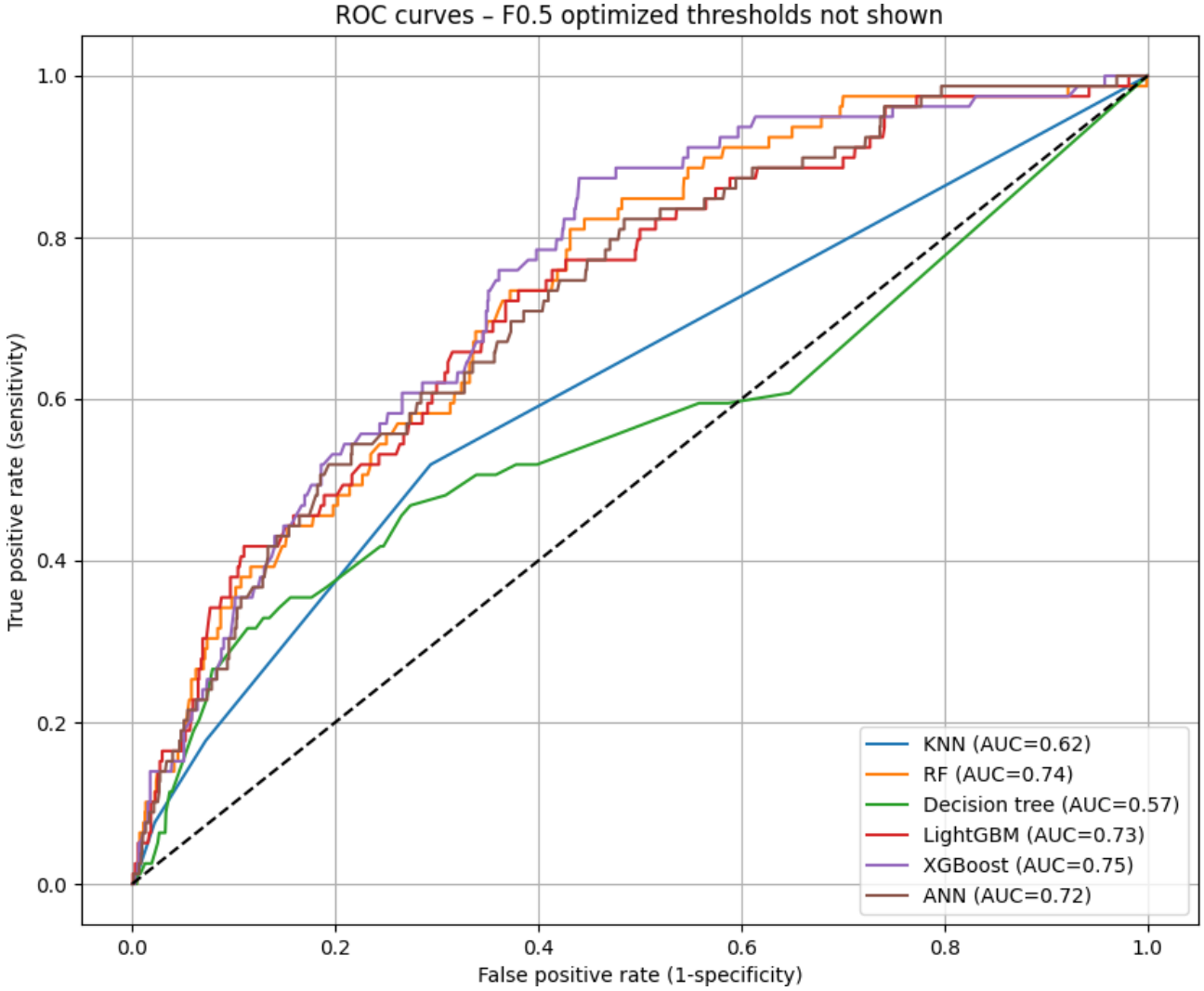


Figure 3. Receiver operating characteristic (ROC) curves for numerous machine learning delayed extubation prediction models. ANN: artificial neural network; AUC: area under the curve; KNN: k-nearest neighbor; LightGBM: light gradient boosting machine; RF: random forest; XGBoost: extreme gradient boosting.



XSL•FO
RenderX

Table . Comparative performance of candidate models on the hold-out test dataset.

Model	AUROC[a] (95%CI)	Sensitivity (95%CI)	Specificity (95%CI)	PPV[b] (95%CI)	NPV[c] (95%CI)
RF[d]	0.737 (0.684 - 0.787)	0.696 (0.5976 - 0.7945)	0.648 (0.6224 - 0.6738)	0.103 (0.0790 - 0.1295)	0.9734 (0.9628 - 0.9836)
DT[e]	0.567 (0.493 - 0.643)	0.316 (0.2208 - 0.4211)	0.886 (0.8686 - 0.9022)	0.139 (0.0913 - 0.1894)	0.9569 (0.9455 - 0.9679)
KNN[f]	0.620 (0.409 - 0.630)	0.519 (0.4096 - 0.6302)	0.706 (0.6825 - 0.7311)	0.093 (0.0668 - 0.1212)	0.9618 (0.9504 - 0.9732)
LightGBM[g]	0.725 (0.671 - 0.779)	0.734 (0.6375 - 0.8261)	0.614 (0.5876 - 0.6397)	0.100 (0.0769 - 0.1254)	0.9754 (0.9651 - 0.9851)
XGBoost[h]	0.750 (0.703 - 0.796)	0.734 (0.6349 - 0.8272)	0.647 (0.6227 - 0.6733)	0.108 (0.0833 - 0.1349)	0.9766 (0.9666 - 0.9857)
Artificial neural network	0.719 (0.661 - 0.775)	0.632 (0.5316 - 0.7381)	0.672 (0.6468 - 0.6966)	0.101 (0.0763 - 0.1283)	0.9691 (0.9581 - 0.9799)

[a]AUROC: area under the receiver operating characteristic curve.

[b]PPV: positive predictive value.

[c]NPV: negative predictive value.

[d]RF: random forest.

[e]DT: decision tree.

[f]KNN: k-nearest neighbor.

[g]LightGBM: light gradient boosting machine.

[h]XGBoost: extreme gradient boosting.

Table . Performance metrics, calibration assessment, and goodness-of-fit statistics for each machine learning model predicting delayed extubation.

Model	Accuracy	F_1-score	Brier score	Hosmer-Lemeshow X^2 (*df*)	*P* value
KNN[a]	0.695	0.158	0.0576	31.53 (6)	<.001
RF[b]	0.651	0.180	0.0516	17.16 (6)	.009
DT[c]	0.854	0.193	0.0629	2097.51 (6)	<.001
LightGBM[d]	0.621	0.176	0.0515	23.87 (6)	.001
XGBoost[e]	0.652	0.188	0.0505	7.38 (6)	.29
ANN[f]	0.669	0.174	0.0503	4.27 (6)	.64

[a]KNN: k-nearest neighbor.

[b]RF: random forest.

[c]DT: decision tree.

[d]LightGBM: light gradient boosting machine.

[e]XGBoost: extreme gradient boosting.

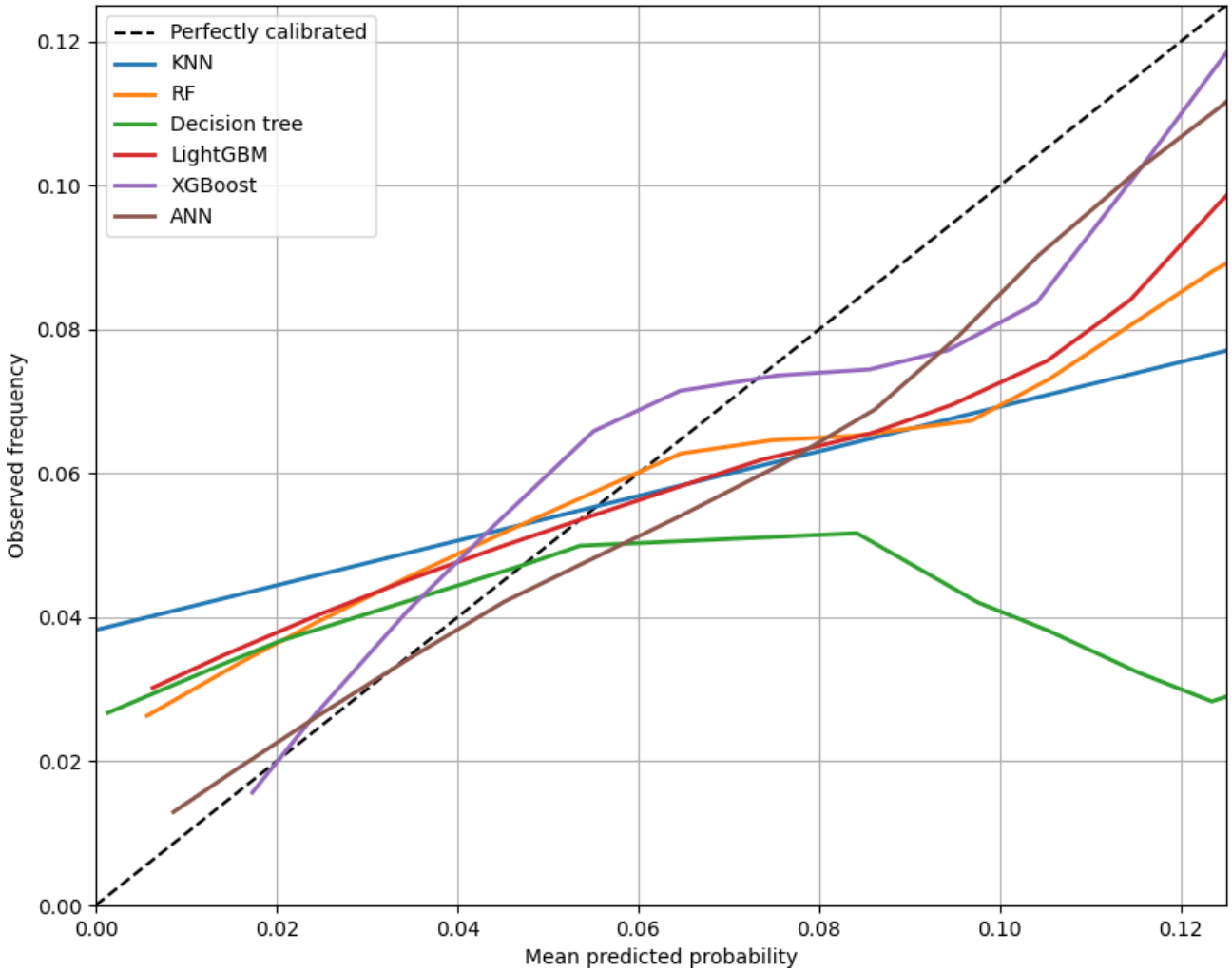
[f]ANN: artificial neural network.

The calibration curve (Figure 4) showed good agreement between predicted probabilities and observed outcomes for the XGBoost model, with a Hosmer-Lemeshow goodness-of-fit test χ^2_6=7.38 and *P*=.287 (Table 2), indicating no significant lack of fit. These results suggest that the XGBoost model may serve as a reliable tool for predicting the risk of delayed extubation following general anesthesia in the PACU.

Similar trends were observed in the other models tested, although their overall discrimination performance and calibration were lower compared to XGBoost (Table 1 and Figure 3).

XSL•FO
RenderX

Figure 4. Calibration curve. ANN: artificial neural network; KNN: k-nearest neighbor; LightGBM: light gradient boosting machine; RF: random forest; XGBoost: extreme gradient boosting.



Given the difficulty clinical practitioners face in interpreting unexplained predictive models, this study used the Shapley additive explanations (SHAP) method to elucidate the XGBoost model by calculating the contribution of each feature variable to the predicted outcome (Figure 5). The variables showing the contribution to delayed extubation after general anesthesia in the SHAP plot of the XGBoost model were as follows: age, BMI, ASA classification, tympanic temperature following PACU admission, sex, intraoperative infusion volume, duration of surgery, surgical site, surgical level, case condition, cerebral stroke history, sufentanil administered before extubation in the PACU, and history of COPD (Figure 6).

XSL•FO
RenderX

Figure 5. Bar chart of Shapley additive explanations (SHAP) for important features in the extreme gradient boosting (XGBoost) model. ASA: American Society of Anesthesiologists; COPD: chronic obstructive pulmonary disease; PACU: postanesthesia care unit.

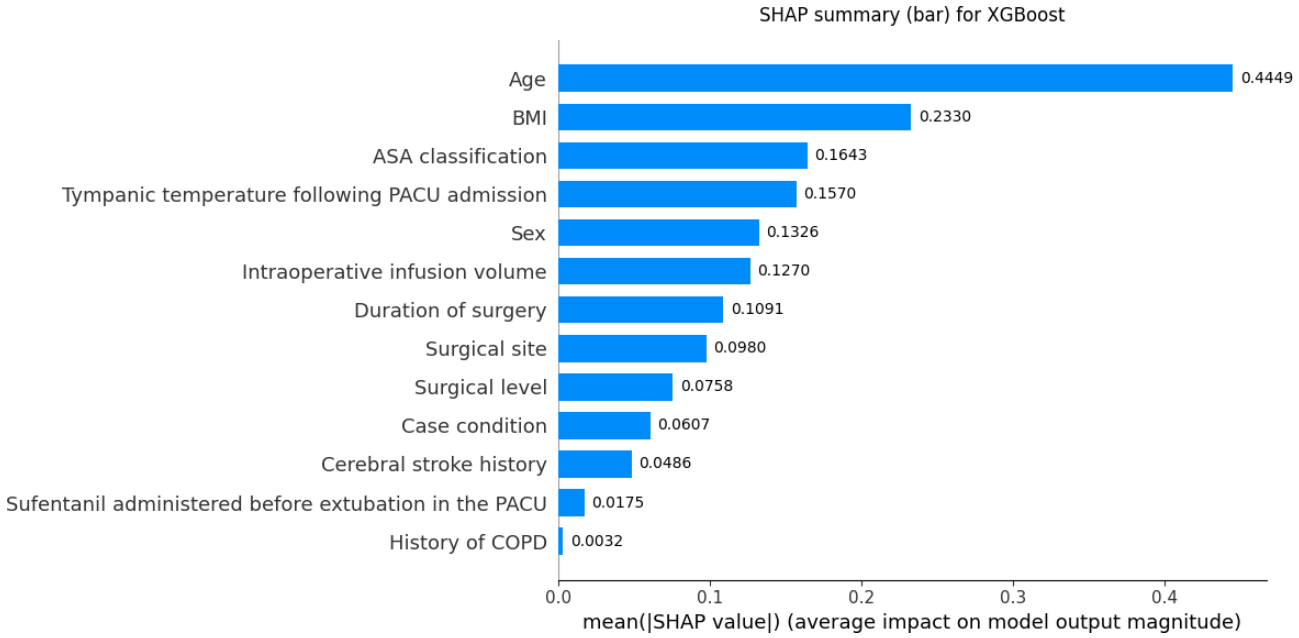
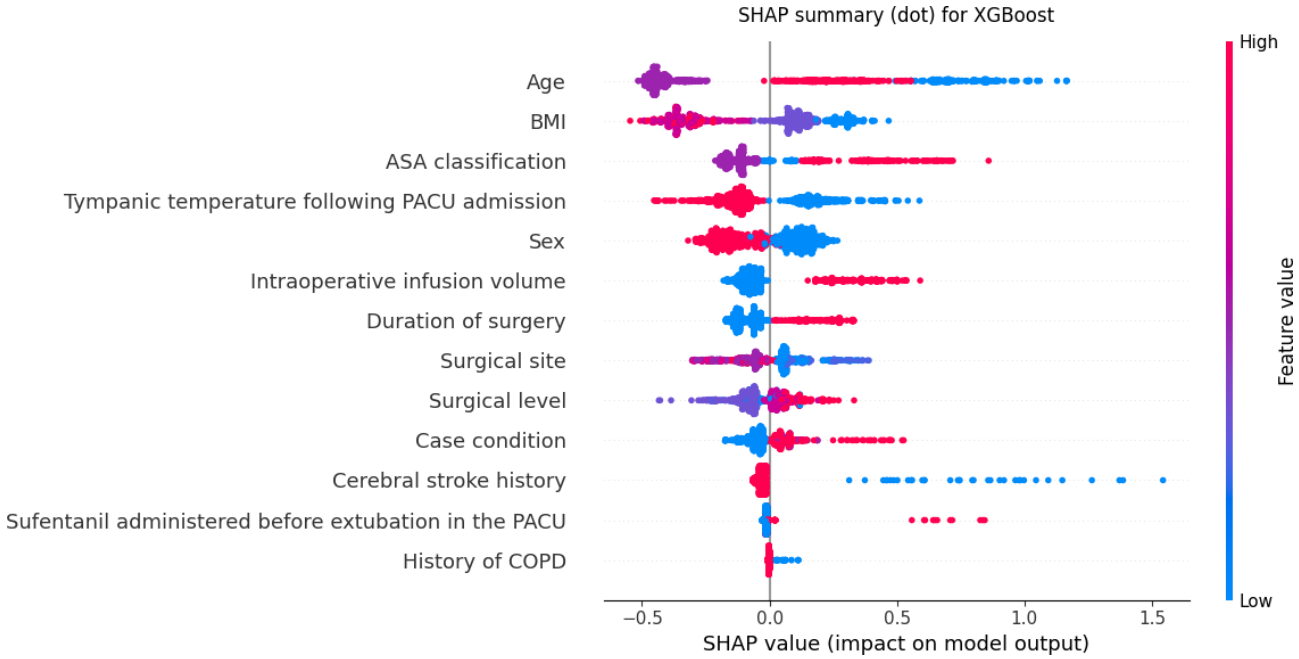


Figure 6. Global Shapley additive explanations (SHAP) summary for the extreme gradient boosting (XGBoost) model. Positive SHAP values increase the predicted probability of delayed extubation. Point color encodes the numeric feature code listed in Multimedia Appendix 2. Risk directions should be interpreted from SHAP values together with the coding scheme. ASA: American Society of Anesthesiologists; COPD: chronic obstructive pulmonary disease; PACU: postanesthesia care unit.



Discussion

Principal Findings

This study collected perioperative assessment and management data, including nursing management indicators in the PACU, and attempted to construct predictive models for delayed extubation in the PACU using various machine learning algorithms. The results showed that the XGBoost-based model achieved the highest predictive performance. The SHAP interpretation in the XGBoost model identified features with high predictive value, providing a basis for early risk assessment of delayed extubation and optimal nursing intervention strategies within the PACU.

The SHAP summary plot demonstrated that age, BMI, ASA classification, and tympanic temperature were the top 4 features in predicting delayed extubation risk. Age showed the strongest positive contribution to model predictions, indicating that patients aged ≥65 years were more likely to experience delayed extubation. This finding aligns with previous studies showing that older patients are at higher risk for delayed extubation due to decreased respiratory reserve, altered drug metabolism, and delayed muscle strength recovery [18,19]. PACU nurses should

XSL•FO
RenderX

implement individualized monitoring and interventions for older adults or patients at risk of respiratory dysfunction (eg, obesity, obstructive sleep apnea, and COPD), including close monitoring of respiratory rate, oxygen saturation, and partial pressure of end-tidal carbon dioxide to detect hypoventilation, hypoxemia, or airway obstruction early, as well as extending awakening time to ensure full consciousness and respiratory recovery before extubation [20,21]. Diaphragm ultrasound can effectively assess diaphragmatic thickness, thickening fraction, and mobility, reflecting diaphragm contractility, and is a powerful tool to predict the recovery of spontaneous breathing and extubation success [22]. In the PACU, particularly for older patients or those with impaired respiratory function (eg, COPD or chronic respiratory failure), diaphragmatic function assessment helps nurses determine whether the patient has sufficient respiratory drive and muscle strength to maintain ventilation after extubation [23]. If the thickening fraction is <20% or diaphragmatic movement is significantly reduced, it indicates diaphragmatic dysfunction and suggests that the patient may not yet be ready for extubation [24]. Conversely, normal diaphragmatic movement indicates good respiratory muscle recovery and extubation safety, reducing reintubation risks.

BMI was the second most important predictor. SHAP interpretation showed that underweight (BMI <18.5 kg/m²) contributed more to delayed extubation predictions than obesity. This contrasts with most studies focusing on obesity as a risk factor for delayed extubation. Previous studies indicated that patients with obesity have impaired lung function, characterized by decreased lung compliance and reduced functional residual capacity, which is further exacerbated by general anesthesia and mechanical ventilation, leading to delayed recovery of spontaneous breathing and increased risk of extubation delay [25,26]. However, patients who are underweight may also experience delayed extubation due to potential mechanisms such as malnutrition-induced respiratory muscle weakness, reduced adipose tissue affecting the distribution volume and metabolism of lipophilic anesthetics, and poor overall recovery capacity [27]. Therefore, preoperative nutritional risk screening (eg, Nutritional Risk Screening 2002 or Patient Generated Subjective Global Assessment) should be routinely performed to identify potential malnutrition [28]. During PACU recovery, nurses should closely assess muscle strength recovery, including respiratory and limb muscle strength, to evaluate readiness for extubation. Patients with respiratory muscle weakness, hypoventilation, or delayed awakening may require prolonged mechanical ventilation support to ensure sufficient respiratory capacity and consciousness before extubation, thus ensuring safety and reducing postoperative complications. ASA classification also contributed significantly to the model, with patients classified as ASA III or above having a higher likelihood of delayed extubation, suggesting that baseline comorbidities and overall health status play crucial roles in postoperative recovery [29]. PACU nurses should integrate comprehensive preoperative functional assessments with ASA classification to develop graded nursing plans, optimize resource allocation, and strengthen cardiopulmonary monitoring and support [30]. Tympanic temperature was also an important predictor, with lower temperatures associated with increased risk of delayed extubation. Previous studies have shown that hypothermia reduces hepatic and renal blood flow, slowing anesthetic drug metabolism and clearance and prolonging awakening and spontaneous breathing recovery [18,31]. PACU nurses should measure tympanic temperature immediately upon admission and initiate active warming using forced-air warming blankets and prewarmed infusions if the temperature is <36 °C. Temperature should be remeasured every 15 minutes during anesthesia recovery to ensure a stable warming trend, and a standardized hypothermia management protocol should be implemented to ensure continuity of care [32].

Furthermore, intraoperative infusion volume ≥1135 ml, anesthesia duration ≥230.5 minutes, neurosurgery, and higher surgical levels contributed moderately to predictions, suggesting that intraoperative fluid management, anesthesia duration, and surgical complexity should be comprehensively considered to optimize extubation timing. Increased intraoperative fluid volume may lead to interstitial fluid retention, edema, and decreased lung compliance, adversely affecting respiratory function and delaying recovery of spontaneous breathing and readiness for extubation [33]. Previous studies have shown that excessive fluid management is associated with increased risk of postoperative pulmonary complications [34]; thus, rational intraoperative fluid management is essential to avoid volume overload.

Finally, although a history of cerebral infarction, additional sufentanil administration in the PACU, and COPD showed relatively low SHAP contributions, they remain clinically important predictors. A history of cerebral infarction indicates potential central nervous system dysfunction, including altered consciousness, impaired swallowing, and weakened cough reflex, increasing extubation risks [35,36]. Previous studies have shown that individuals who have sustained a stroke are prone to delayed extubation and insufficient airway protection due to intracranial pressure changes, impaired autonomic regulation, and reduced respiratory center control [37,38]. Additional sufentanil administration in the PACU reflects increased postoperative analgesic requirements. While sufentanil is a potent lipophilic μ-opioid receptor agonist providing excellent analgesia, high doses may suppress respiratory drive and delay spontaneous breathing recovery [39]. Therefore, postoperative analgesia should aim to achieve effective pain control while minimizing the risk of respiratory depression. For older patients or those with compromised respiratory function, sufentanil dosing should follow recommended ranges (0.1 - 0.5 μg/kg), with close monitoring of respiratory status and consciousness to ensure effective analgesia without prolonging extubation time [40]. Patients with COPD are prone to airway secretion retention, ventilation-perfusion mismatch, and weakened respiratory effort due to abnormal airway function and increased resistance. They may experience respiratory muscle fatigue and hypoxemia after extubation, necessitating reintubation. PACU staff typically delay extubation until oxygenation improves, necessitating careful assessment of respiratory function recovery and extubation timing, thus increasing the risk of delayed extubation [41].

XSL•FO
RenderX

Strengths and Limitations

This study found that among all models compared, XGBoost achieved the best performance. Previous models were mainly developed based on logistic regression and presented as nomograms [9]. However, XGBoost outperforms logistic regression in capturing complex nonlinear interactions among variables, resulting in higher predictive accuracy. Compared with other machine learning algorithms, XGBoost offers advantages such as superior performance with high-dimensional sparse data, built-in LASSO and ridge regularization, cross-validation to prevent overfitting and enhance generalizability, and native handling of missing data without prior imputation [29].

This study also had limitations. First, as a retrospective study, it was subject to unavoidable biases and lacked external validation. Additionally, some variables potentially affecting extubation time were not included, and only patients with ASA ≤ III were enrolled, limiting generalizability. Future multicenter prospective studies with larger samples are needed to develop and validate delayed extubation prediction models in the PACU. Furthermore, despite the obvious class imbalance in this study, no resampling techniques (eg, Synthetic Minority Over-sampling Technique) or class weighting strategies were used during model training. To reduce the risk of majority class bias, we incorporated a threshold adjustment mechanism in the evaluation stage by imposing dual constraints on sensitivity and specificity (eg, sensitivity ≥0.60 and specificity ≥0.60) to select clinically meaningful thresholds. Although this post hoc adjustment does not address imbalance during training, it partially mitigates the majority class overfitting. Future studies will incorporate integrated balancing strategies to further improve model robustness and generalizability.

Conclusions

The machine learning–based predictive model for delayed extubation risk after general anesthesia has significant clinical implications. It allows for early identification of patients with high risk, enabling personalized management and timely interventions to reduce complications. PACU nurses can consider integrating the model into routine postoperative care, especially in PACU settings, to improve decision-making and optimize resource allocation.

Acknowledgments

The authors would like to thank the hospital for its support and collaboration on this research project. This work was supported by the Shanwei Science and Technology Program, China (2024C053).

Data Availability

The datasets generated and/or analyzed during this study are not publicly available due to institutional and ethical restrictions (patient privacy and confidentiality) but are available from the corresponding author on reasonable request and with permission from the institutional review board.

Conflicts of Interest

None declared.

Multimedia Appendix 1
Comparison of baseline characteristics between the training and test sets.
[DOCX File, 20 KB - medinform_v13i1e72602_app1.docx]

Multimedia Appendix 2
Variable coding and risk direction for Shapley additive explanations interpretation.
[DOCX File, 14 KB - medinform_v13i1e72602_app2.docx]

References

1. Cook TM, Scott S, Mihai R. Litigation related to airway and respiratory complications of anaesthesia: an analysis of claims against the NHS in England 1995-2007. Anaesthesia 2010 Jun;65(6):556-563. [doi: 10.1111/j.1365-2044.2010.06331.x] [Medline: 20345420]
2. Cook TM, Woodall N, Frerk C, Fourth National Audit Project. Major complications of airway management in the UK: results of the Fourth National Audit Project of the Royal College of Anaesthetists and the Difficult Airway Society. Part 1: anaesthesia. Br J Anaesth 2011 May;106(5):617-631. [doi: 10.1093/bja/aer058] [Medline: 21447488]
3. Anastasian ZH, Kim M, Heyer EJ, Wang S, Berman MF. Attending handoff is correlated with the decision to delay extubation after surgery. Anesth Analg 2016 Mar;122(3):758-764. [doi: 10.1213/ANE.0000000000001069] [Medline: 26649911]
4. Thomas E, Martin F, Pollard B. Delayed recovery of consciousness after general anaesthesia. BJA Educ 2020 May;20(5):173-179. [doi: 10.1016/j.bjae.2020.01.007] [Medline: 33456947]

XSL•FO
RenderX

5. Kobayashi N, Wagatsuma T, Shiga T, Toyama H, Ejima Y, Yamauchi M. Age-related changes in factors associated with delayed extubation after general anesthesia: a retrospective study. JA Clin Rep 2020 Mar 13;6(1):20. [doi: 10.1186/s40981-020-00325-8] [Medline: 32170494]
6. Shimamoto Y, Sanuki M, Kurita S, Ueki M, Kuwahara Y, Matsumoto A. Factors affecting prolonged time to extubation in patients given remimazolam. PLoS ONE 2022 May 18;17(5):e0268568. [doi: 10.1371/journal.pone.0268568] [Medline: 35584094]
7. Maisat W, Siriratwarangkul S, Charoensri A, Wongkornrat W, Lapmahapaisan S. Perioperative risk factors for delayed extubation after acute type A aortic dissection surgery. J Thorac Dis 2020 Sep;12(9):4796-4804. [doi: 10.21037/jtd-20-742] [Medline: 33145052]
8. Corley A, Bull T, Spooner AJ, Barnett AG, Fraser JF. Direct extubation onto high-flow nasal cannulae post-cardiac surgery versus standard treatment in patients with a BMI ≥30: a randomised controlled trial. Intensive Care Med 2015 May;41(5):887-894. [doi: 10.1007/s00134-015-3765-6] [Medline: 25851385]
9. Tong C, Miao Q, Zheng J, Wu J. A novel nomogram for predicting the decision to delayed extubation after thoracoscopic lung cancer surgery. Ann Med 2023 Dec;55(1):800-807. [doi: 10.1080/07853890.2022.2160490] [Medline: 36869647]
10. De la Garza Ramos R, Nakhla J, Nasser R, et al. Factors associated with prolonged ventilation and reintubation in adult spinal deformity surgery. J Clin Neurosci 2017 Sep;43:188-191. [doi: 10.1016/j.jocn.2017.04.026] [Medline: 28551313]
11. Jing X, Zhu Z, Fan H, et al. Impact of delay extubation on the reintubation rate in patients after cervical spine surgery: a retrospective cohort study. J Orthop Surg Res 2023 Aug 2;18(1):557. [doi: 10.1186/s13018-023-04008-9] [Medline: 37528469]
12. Martin ND, Codner P, Greene W, Brasel K, Michetti C, AAST Critical Care Committee. Contemporary hemodynamic monitoring, fluid responsiveness, volume optimization, and endpoints of resuscitation: an AAST critical care committee clinical consensus. Trauma Surg Acute Care Open 2020 Mar 10;5(1):e000411. [doi: 10.1136/tsaco-2019-000411] [Medline: 32201737]
13. Raksakietisak M, Keawsai T, Sirivanasandha B. Factors related to delayed extubation in cervical spine surgery in an academic hospital: a retrospective study of 506 patients. Asian J Anesthesiol 2019 Dec 1;57(4):111-116. [doi: 10.6859/aja.201912_57(4).0001] [Medline: 31726803]
14. Huang H, Wang J, Zhu Y, et al. Development of a machine-learning model for prediction of extubation failure in patients with difficult airways after general anesthesia of head, neck, and maxillofacial surgeries. J Clin Med 2023 Jan 30;12(3):1066. [doi: 10.3390/jcm12031066] [Medline: 36769713]
15. Zhao QY, Wang H, Luo JC, et al. Development and validation of a machine-learning model for prediction of extubation failure in intensive care units. Front Med (Lausanne) 2021 May 17;8:676343. [doi: 10.3389/fmed.2021.676343] [Medline: 34079812]
16. Vannucci A, Riordan IR, Prifti K, et al. Prolonged time to extubation after general anaesthesia is associated with early escalation of care: a retrospective observational study. Eur J Anaesthesiol 2021 May 1;38(5):494-504. [doi: 10.1097/EJA.0000000000001316] [Medline: 32890014]
17. Huang Y, Pepe MS. Biomarker evaluation and comparison using the controls as a reference population. Biostatistics 2009 Apr;10(2):228-244. [doi: 10.1093/biostatistics/kxn029] [Medline: 18755739]
18. Hopf HW. Perioperative temperature management: time for a new standard of care? Anesthesiology 2015 Feb;122(2):229-230. [doi: 10.1097/ALN.0000000000000552] [Medline: 25603200]
19. Klotz U. Pharmacokinetics and drug metabolism in the elderly. Drug Metab Rev 2009;41(2):67-76. [doi: 10.1080/03602530902722679] [Medline: 19514965]
20. Apfelbaum JL, Silverstein JH, Chung FF, et al. Practice guidelines for postanesthetic care: an updated report by the American Society of Anesthesiologists Task Force on Postanesthetic Care. Anesthesiology 2013 Feb;118(2):291-307. [doi: 10.1097/ALN.0b013e31827773e9] [Medline: 23364567]
21. American Society of Anesthesiologists Task Force on Perioperative Management of Patients With Obstructive Sleep Apnea. Practice guidelines for the perioperative management of patients with obstructive sleep apnea: an updated report by the American Society of Anesthesiologists Task Force on Perioperative Management of patients with obstructive sleep apnea. Anesthesiology 2014 Feb;120(2):268-286. [doi: 10.1097/ALN.0000000000000053] [Medline: 24346178]
22. Ferrari G, De Filippi G, Elia F, Panero F, Volpicelli G, Aprà F. Diaphragm ultrasound as a new index of discontinuation from mechanical ventilation. Crit Ultrasound J 2014 Jun 7;6(1):8. [doi: 10.1186/2036-7902-6-8] [Medline: 24949192]
23. Llamas-Álvarez AM, Tenza-Lozano EM, Latour-Pérez J. Diaphragm and lung ultrasound to predict weaning outcome: systematic review and meta-analysis. Chest 2017 Dec;152(6):1140-1150. [doi: 10.1016/j.chest.2017.08.028] [Medline: 28864053]
24. Kim WY, Suh HJ, Hong SB, Koh Y, Lim CM. Diaphragm dysfunction assessed by ultrasonography: influence on weaning from mechanical ventilation. Crit Care Med 2011 Dec;39(12):2627-2630. [doi: 10.1097/CCM.0b013e3182266408] [Medline: 21705883]
25. De Jong A, Chanques G, Jaber S. Mechanical ventilation in obese ICU patients: from intubation to extubation. Crit Care 2017 Mar 21;21(1):63. [doi: 10.1186/s13054-017-1641-1] [Medline: 28320439]

XSL•FO
RenderX

26. Robba C, Bonatti G, Battaglini D, Rocco PR, Pelosi P. Mechanical ventilation in patients with acute ischaemic stroke: from pathophysiology to clinical practice. Crit Care 2019 Dec 2;23(1):388. [doi: 10.1186/s13054-019-2662-8] [Medline: 31791375]
27. Xiao Y, Xu J, Zhao C, Pan G. Risk factors of prolonged mechanical ventilation in patients undergoing redo valve surgery. Heart Surg Forum 2022 Sep 28;25(5):E683-E688. [doi: 10.1532/hsf.4913] [Medline: 36317905]
28. Wischmeyer PE, Carli F, Evans DC, et al. American Society for Enhanced Recovery and Perioperative Quality Initiative joint consensus statement on nutrition screening and therapy within a surgical enhanced recovery pathway. Anesth Analg 2018 Jun;126(6):1883-1895. [doi: 10.1213/ANE.0000000000002743] [Medline: 29369092]
29. Ahn JM, Kim J, Kim K. Ensemble machine learning of gradient boosting (XGBoost, LightGBM, CatBoost) and attention-based CNN-LSTM for harmful algal blooms forecasting. Toxins (Basel) 2023 Oct 10;15(10):608. [doi: 10.3390/toxins15100608] [Medline: 37888638]
30. Ellinger E, Meybohm P, Röder D. [Perioperative anesthesiologic management: risk assessment and preoperative improvement of patient conditions]. Anasthesiol Intensivmed Notfallmed Schmerzther 2021 Mar;56(3):159-173. [doi: 10.1055/a-1114-4481] [Medline: 33725737]
31. Pezawas T, Rajek A, Plöchl W. Core and skin surface temperature course after normothermic and hypothermic cardiopulmonary bypass and its impact on extubation time. Eur J Anaesthesiol 2007 Jan;24(1):20-25. [doi: 10.1017/S0265021506000664] [Medline: 16723048]
32. Ji N, Wang J, Li X, Shang Y. Strategies for perioperative hypothermia management: advances in warming techniques and clinical implications: a narrative review. BMC Surg 2024 Dec 30;24(1):425. [doi: 10.1186/s12893-024-02729-0] [Medline: 39736577]
33. Mythen MG, Swart M, Acheson N, et al. Perioperative fluid management: consensus statement from the enhanced recovery partnership. Perioper Med (Lond) 2012 Jun 27;1:2. [doi: 10.1186/2047-0525-1-2] [Medline: 24764518]
34. Casado D, López F, Martí R. Perioperative fluid management and major respiratory complications in patients undergoing esophagectomy. Dis Esophagus 2010 Sep;23(7):523-528. [doi: 10.1111/j.1442-2050.2010.01057.x] [Medline: 20459444]
35. Hegland KW, Davenport PW, Brandimore AE, Singletary FF, Troche MS. Rehabilitation of swallowing and cough functions following stroke: an expiratory muscle strength training trial. Arch Phys Med Rehabil 2016 Aug;97(8):1345-1351. [doi: 10.1016/j.apmr.2016.03.027] [Medline: 27130637]
36. Barnett HM, Davis AP, Khot SP. Stroke and breathing. Handb Clin Neurol 2022;189(201-22):201-222. [doi: 10.1016/B978-0-323-91532-8.00016-1] [Medline: 36031305]
37. Patrizz A, El Hamamy A, Maniskas M, et al. Stroke-induced respiratory dysfunction is associated with cognitive decline. Stroke 2023 Jul;54(7):1863-1874. [doi: 10.1161/STROKEAHA.122.041239] [Medline: 37264918]
38. Duarte E, Messaggi-Sartor M, Grau-Sánchez J, et al. Cerebral infarct site and affected vascular territory as factors in breathing weakness in patients with subacute stroke. J Rehabil Med 2020 Oct 22;52(10):jrm00116. [doi: 10.2340/16501977-2751] [Medline: 33043382]
39. Dong CS, Zhang J, Lu Q, et al. Effect of Dexmedetomidine combined with sufentanil for post-thoracotomy intravenous analgesia: a randomized, controlled clinical study. BMC Anesthesiol 2017 Mar 1;17(1):33. [doi: 10.1186/s12871-017-0324-4] [Medline: 28249614]
40. Liu L, Li B, Cao Q, et al. Effects of additional intraoperative administration of sufentanil on postoperative pain, stress and inflammatory responses in patients undergoing laparoscopic myomectomy: a double-blind, randomized, placebo-controlled trial. J Pain Res 2020 Aug 26;13:2187-2195. [doi: 10.2147/JPR.S257337] [Medline: 32943911]
41. Jian L, Sheng S, Min Y, Zhongxiang Y. Risk factors for endotracheal re-intubation following coronary artery bypass grafting. J Cardiothorac Surg 2013 Nov 9;8:208. [doi: 10.1186/1749-8090-8-208] [Medline: 24209453]

Abbreviations

ASA: American Society of Anesthesiologists
AUROC: area under the receiver operating characteristic curve
COPD: chronic obstructive pulmonary disease
KNN: k-nearest neighbor
LASSO: least absolute shrinkage and selection operator
LightGBM: light gradient boosting machine
NPV: negative predictive value
PACU: postanesthesia care unit
PPV: positive predictive value
RF: random forest
ROC: receiver operating characteristic
SHAP: Shapley additive explanations
XGBoost: extreme gradient boosting

XSL•FO
RenderX

Edited by J Klann; submitted 13.02.25; peer-reviewed by JL Xu, P Han, S Liu; revised version received 08.10.25; accepted 08.10.25; published 11.11.25.

Please cite as:
Luo J, Lin S, Wang L, Ji H, Zheng J, Wang T, Chen L, Lin Z, Liu Z, Liufu N
Predicting Delayed Extubation After General Anesthesia in Postanesthesia Care Unit Patients Using Machine Learning: Model Development Study
JMIR Med Inform 2025;13:e72602
URL: https://medinform.jmir.org/2025/1/e72602
doi:10.2196/72602

©Jianwei Luo, Shaoman Lin, Liman Wang, Huanfan Ji, Jingcong Zheng, Tingkang Wang, Lin Chen, Ziqi Lin, Zhongqi Liu, Ning Liufu. Originally published in JMIR Medical Informatics (https://medinform.jmir.org), 11.11.2025. This is an open-access article distributed under the terms of the Creative Commons Attribution License (https://creativecommons.org/licenses/by/4.0/), which permits unrestricted use, distribution, and reproduction in any medium, provided the original work, first published in JMIR Medical Informatics, is properly cited. The complete bibliographic information, a link to the original publication on https://medinform.jmir.org/, as well as this copyright and license information must be included.

XSL•FO
RenderX

Detection of Polyphonic Alarm Sounds From Medical Devices Using Frequency-Enhanced Deep Learning: Simulation Study

Kazumasa Kishimoto[1,2,3], PhD; Tadamasa Takemura[4], PhD; Osamu Sugiyama[5], PhD; Ryosuke Kojima[2], PhD; Masahiro Yakami[3], PhD; Goshiro Yamamoto[3], PhD; Tomohiro Kuroda[1,2,3], PhD

[1]Graduate School of Informatics, Kyoto University, 54 Kawara-cho, Shogoin, Sakyo-ku, Kyoto, Japan

[2]Graduate School of Medicine, Kyoto University, Kyoto, Japan

[3]Kyoto University Hospital, Kyoto, Japan

[4]Graduate School of Information Science, University of Hyogo, Kobe, Japan

[5]Department of Information Science, Kindai University, Osaka, Japan

Corresponding Author:
Kazumasa Kishimoto, PhD
Graduate School of Informatics, Kyoto University, 54 Kawara-cho, Shogoin, Sakyo-ku, Kyoto, Japan

Abstract

Background: Although an increasing number of bedside medical devices are equipped with wireless connections for reliable notifications, many nonnetworked devices remain effective at detecting abnormal patient conditions and alerting medical staff through auditory alarms. Staff members, however, can miss these notifications, especially when in distant areas or other private rooms. In contrast, the signal-to-noise ratio of alarm systems for medical devices in the neonatal intensive care unit is 0 dB or higher. A feasible system for automatic sound identification with high accuracy is needed to prevent alarm sounds from being missed by the staff.

Objective: The purpose of this study was to design a method for classifying multiple alarm sounds collected with a monaural microphone in a noisy environment.

Methods: Features of 7 alarm sounds were extracted using a mel filter bank and incorporated into a classifier using convolutional and recurrent neural networks. To estimate its clinical usefulness, the classifier was evaluated with mixtures of up to 7 alarm sounds and hospital ward noise.

Results: The proposed convolutional recurrent neural network model was evaluated using a simulation dataset of 7 alarm sounds mixed with hospital ward noise. At a signal-to-noise ratio of 0 dB, the best-performing model (convolutional neural network 3+bidirectional gate recurrent unit) achieved an event-based F_1-score of 0.967, with a precision of 0.944 and a recall of 0.991. When the venous foot pump class was excluded, the classwise recall of the classifier ranged from 0.990 to 1.000.

Conclusions: The proposed classifier was found to be highly accurate in detecting alarm sounds. Although the performance of the proposed classifier in a clinical environment can be improved, the classifier could be incorporated into an alarm sound detection system. The classifier, combined with network connectivity, could improve the notification of abnormal status detected by unconnected medical devices.

(JMIR Med Inform 2025;13:e35987) doi:10.2196/35987

KEYWORDS

sound event detection; deep learning; alarm sound; polyphonic sound; notifications

Introduction

Background

While an increasing number of bedside medical devices, such as syringe pumps, have wireless connections that enable reliable data transmission to hospital information systems, many nonnetworked devices are still used in general hospital wards. Although dongles connected to the external output terminal of these devices may allow wireless connections [1,2], most devices are not equipped with external output terminals. Instead, these devices use auditory alert signals (alarm sounds) to notify medical staff of abnormal conditions. Medical staff members may not hear these alarms, especially when they are in distant areas or other private rooms. Between 2010 and 2015, the Japan Council for Quality Health Care reported 173 accidents and other incidents, including 23 cases of unnoticed alarms [3]. The report included the following comments about environmental factors:

> *There are many blind spots due to the facility's structure.*

XSL•FO
RenderX

> *When I entered a patient's room, I could not hear alarm sounds from another room.*
>
> *The alarm sound did not reach the staff because the room was far from the nurse station.*
>
> *The staff could not hear the alarm in the farthest private room in the ICU.*
>
> *The recording room was structured so that the alarm sound could not be heard.*

These findings indicate the need for reliable alarm notification to ensure patient safety. Alarm sounds emitted by medical devices are regulated by the International Organization for Standardization and the International Electrotechnical Commission (ISO/IEC) 60601-1-8. This standard specifies the melodies and lengths of alarm sounds to reduce the risk of misunderstanding, confusion, and omission of alarm sounds from various medical devices, even when these sounds overlap and reverberate. This standard prescribes that the sounds should be organized based on the priority of corresponding abnormal situations, with alarm sounds for different situations varying in melody and length. Thus, sound event detection (SED) is expected to identify every kind of abnormal situation detected by medical devices [4-8]. The standard also defines visual alarm signals, but monitoring the signals of multiple devices with cameras is not feasible without blind spots.

As SED can be implemented using a single (monaural) microphone, it was selected as the approach to detect alarm status. Clinical application of SED requires robustness against noise because environmental noise in hospital wards is generally substantial. SEDs with deep learning have been found to be sufficiently robust against noise [9,10].

This study proposes a deep learning–based method for classifying patient abnormalities detected by medical devices with polyphonic alarm sounds collected with a monaural microphone. The ability of the classifier to identify abnormal states of these devices was evaluated using simulation datasets of their alarm sounds superimposed on hospital ward noise (HWN). Therefore, the objective of this study was to design and evaluate a convolutional recurrent neural network (CRNN) for accurately detecting and classifying multiple, overlapping alarm sounds from medical devices in a simulated noisy hospital environment. We hypothesized that a hybrid CRNN model could achieve high performance suitable for clinical application by effectively capturing both the spectral and temporal features of the alarm sounds.

Related Works

Accurate transmission of alarms from unconnected medical devices requires precise recognition of visual and auditory alarms. Several studies have reported high accuracy in detecting simultaneous alarm sounds mixed with a substantial level of environmental noise [4-8]. For SED, deep learning is more robust against noise than conventional methods [9,10]. On the basis of these studies, an edge device was placed at the patient's bedside to monitor abnormal conditions detected by multiple medical devices with individual alarm sounds. In our previous study, the classifier had F_1-scores of 0.727 at signal-to-noise ratios (SNRs) of 0 dB and applied a convolutional neural network (CNN) [11]. To our knowledge, no previous study has used a deep learning–based recurrent neural network (RNN) to detect polyphonic alarm sounds emitted by medical devices. Recent advances in attention-based architectures, such as the audio spectrogram transformer and conformer, have demonstrated strong performance in general SED tasks [12,13]. These models use self-attention mechanisms to capture long-range dependencies, potentially enhancing robustness in noisy environments. Exploring such transformer-based approaches for clinical alarm sound detection remains an important direction for future research.

Methods

Overview

The first approach to SED combines a Gaussian mixture model with a hidden Markov model, using features such as the mel-frequency cepstral coefficient from traditional methods of speech recognition [14,15].

Other approaches include the separation of sound sources by matching them using a template extracted from the input sound. This can be achieved by sound source separation techniques, such as nonnegative matrix factorization. Nonnegative matrix factorization monitors a single signal to create a basis matrix and identifies the separated sounds [16-18].

Recent approaches based on neural networks have significantly improved the performance of SED. One approach consists of SED of real-life sounds with feedforward neural networks based on a multilayer perceptron trained in a spectrum of mixed sounds [6]. An RNN with the ability to remember past states can process sequential information of the acoustic signal. RNNs with bidirectional long short-term memory have achieved excellent results in complex audio detection such as speech recognition and polyphonic piano note transcription [19-21].

Furthermore, CNNs commonly used in image recognition can robustly predict sounds with its filter shifted by both time and frequency axes [22]. However, long-term prediction remains difficult due to the limited width of the time window [9]. Therefore, although alarm sounds consist of relatively simple tones, it is necessary to predict not only the frequency axis but also the time axis to inform the priority with a pattern. Application of an RNN to polyphonic SED enabled long-term prediction by integrating the information over the time window. This study combines the strengths of both CNN and RNN to benefit from both approaches. A similar approach has shown excellent performance in automatic speech recognition [23,24].

Therefore, this approach was expected to achieve sufficient performance for potential clinical application in alarm sound recognition.

Deep Alarm Sound Detection

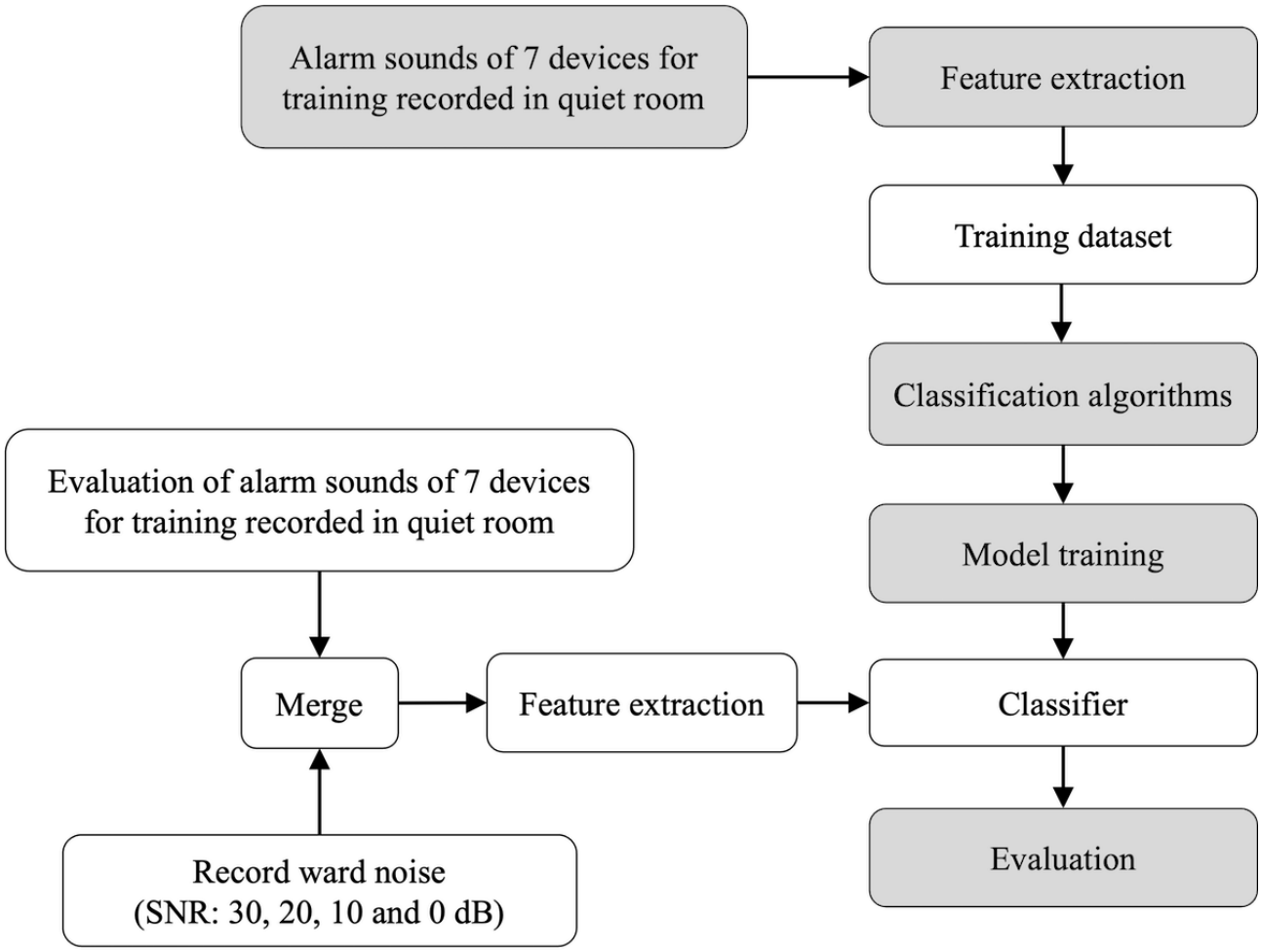
Experiment Overview

The proposed polyphonic alarm sound detection consisted of feature extraction, classification algorithms, and model training (Figure 1). A mel filter bank (MFB) was used to extract the features of alarm sounds, and CNN and RNN were applied to

XSL•FO
RenderX

the classifier. As deep learning requires substantial training data, a large amount of acoustic data were recorded in a quiet room. The recorded data were mixed with pseudo noise before being used for training. This approach aimed to maximize the generalizability of the classifier for expected use in a noisy environment. The feature extraction step extracted data to be input to the classifier from the collected alarm sounds. The classification algorithms were designed to use deep learning models for classifiers. The model training augmented the data to create a robust model.

Figure 1. Overview of the experiment. SNR: signal-to-noise ratio.



Feature Extraction

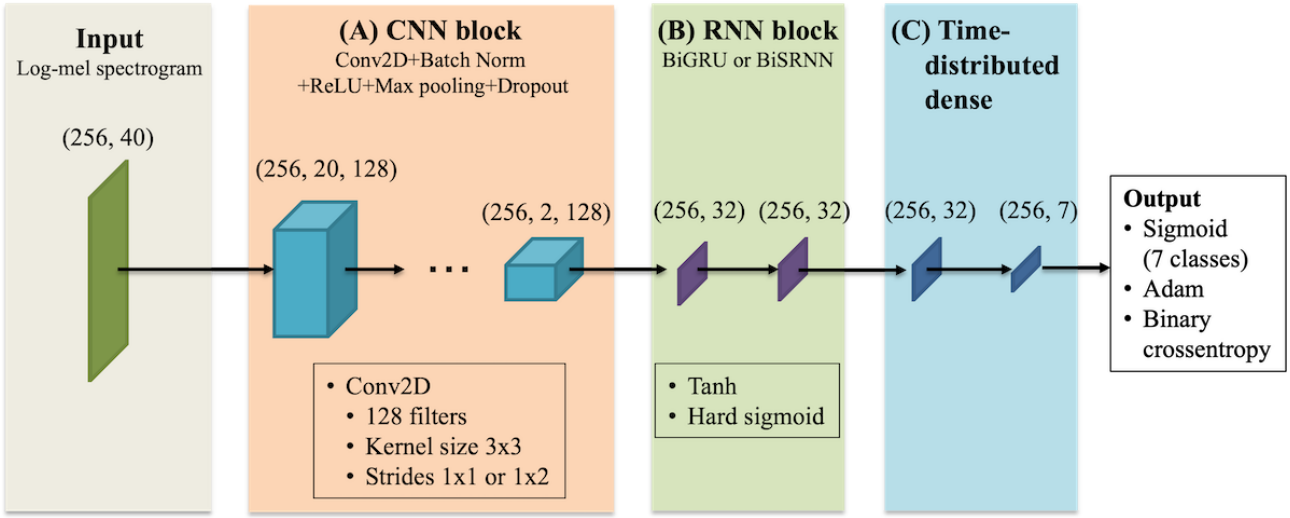
The features of polyphonic alarm sounds of bedside medical devices were extracted. Many acoustic classifiers use log mel spectrogram multiplied spectra and MFB based on the characteristics underlying human frequency perception [25]. The acoustic data were transformed to a power spectrogram with the short-time Fourier transform of the Hamming window, which had a window size of 1024 and a hop length of 512. The inner product on the power spectrogram was calculated with MFB, and its logarithms in 40 dimensions were calculated.

Classification Algorithms

The CRNN, a combination of CNN and RNN, was used for the classification model (Figure 2) [26]. This system used 256×40 pixels of the log mel spectrogram as a feature. A CNN block in the proposed model consisted of a convolutional layer with 128 filters, batch normalization, the activation function of the rectified linear unit, and a dropout of 50% [27]. Using the size reduction method, the max pooling layer was applied to the frequency axis. In image recognition, replacing the pooling layer with a CNN stride 2 has been reported to improve its performance by reducing the calculation cost [28]. In this study, the size of the stride to the frequency axis was reduced to 2, and the pooling layer was excluded because the classification target was 1 frame of the sound.

XSL•FO
RenderX

Figure 2. Architecture of the proposed convolutional recurrent neural network. The architecture consists of three main components: (1) convolutional neural network (CNN) block (convolutional layers with batch normalization, rectified linear unit [ReLU] activation, max pooling, and dropout), (2) recurrent neural network (RNN) block (bidirectional gate recurrent unit [BiGRU] or bidirectional simple recurrent neural network [BiSRNN] layers), and (3) time-distributed dense with sigmoid activation for classification.



The RNN block consisted of a bidirectional simple RNN (BiSRNN) or bidirectional gated recurrent unit (BiGRU). The input was set to 32 units, the activation function to tanh, the recurrent activation function to the hard sigmoid, and the dropout of each layer to 50%.

Finally, the activation function of the fully connected layer was set to sigmoid, the optimization function used was Adam [29], and the loss function was set to binary cross-entropy. Each of the 7 sound event classes had output values in the range of [0, 1] [5].

Table 1 shows the details of the proposed model. CNN3+BiSRNN was used as the baseline model. The environment was built with Python programming language (version 3.7.11; Python Software Foundation), using Keras 2.3.1 for the deep learning library (TensorFlow 2.0.0 for the back end) and Librosa 0.8.1 for the acoustic analysis module. The experimental code is available online[30].

Table . Details of the proposed model.

Model name	CNN[a] block				RNN[c] block	
	Layer	Number of layers	Stride	Max pooling[b]	Layer	Number of layers
CNN3+BiSRNN[d] (baseline)	Conv2D[e]	3	1×1	5, 2, 2	BiSRNN	2
CNN3+BiGRU[f]	Conv2D	3	1×1	5, 2, 2	BiGRU	2
CNN4+BiGRU	Conv2D	4	1×1	2, 2, 2, 2	BiGRU	2
ALL-CNN4+Bi-GRU[g]	Conv2D	4	1×2	—[h]	BiGRU	2

[a]CNN: convolutional neural network.

[b]The figures denote frequency axis. Time axis=1 (ie,1×5=5).

[c]RNN: recurrent neural network.

[d]BiSRNN: bidirectional simple recurrent neural network.

[e]Conv2D: two-dimensional convolution.

[f]BiGRU: bidirectional gated recurrent unit.

[g]ALL-CNN: customizing stride without max pooling.

[h]Not applicable.

Model Training

Data augmentation was applied to the training dataset to prevent overfitting of the classifier and to provide robust performance in simulation experiments [31]. The 7 alarm sounds were superimposed on white noise at SNRs ranging from 30 to 0 dB in 1 dB steps. In addition, SpecAugment was applied to the generator, with 1 random mask added for each frequency and time axis, followed by performance of 5 steps per minibatch [32].

These steps produced a trained model using 5-fold cross-validation over 150 training epochs and confirmed that the learning curve showed no signs of overfitting.

XSL•FO
RenderX

Evaluation

Data Collection

The medical devices selected included those frequently used for ventilator-equipped patients who require many medical devices in the general ward of the hospital. Alarm sounds to be identified included pulse sounds from a syringe pump (SP), enteral feeding pump (ENP), and venous foot pump (VFP) device as well as burst sounds from an infusion pump (IP), chest drainage (CD), patient monitor (PM), and the mechanical ventilator. The alarm sounds of each device were recorded using a monaural microphone placed at the head of a bed in a quiet private room in the hospital. The distance between the sound source and the microphone was the same as in a typical bedside setting (Figure 3). The sound pressure level was recorded simultaneously. The recording has a different number of active sound events superimposed on each frame. Therefore, the frame has various polyphony levels. The distribution of polyphony levels when recording the alarm sounds for the 7 devices is shown in Table 2. Audacity was used for labeling, extracting fundamental frequencies, and performing spectral analysis for annotation. Table 3 shows the detailed characteristics of the recorded alarm sounds.

Figure 3. Recording environment. Numbers in parentheses represent the distance between the microphone and each device.

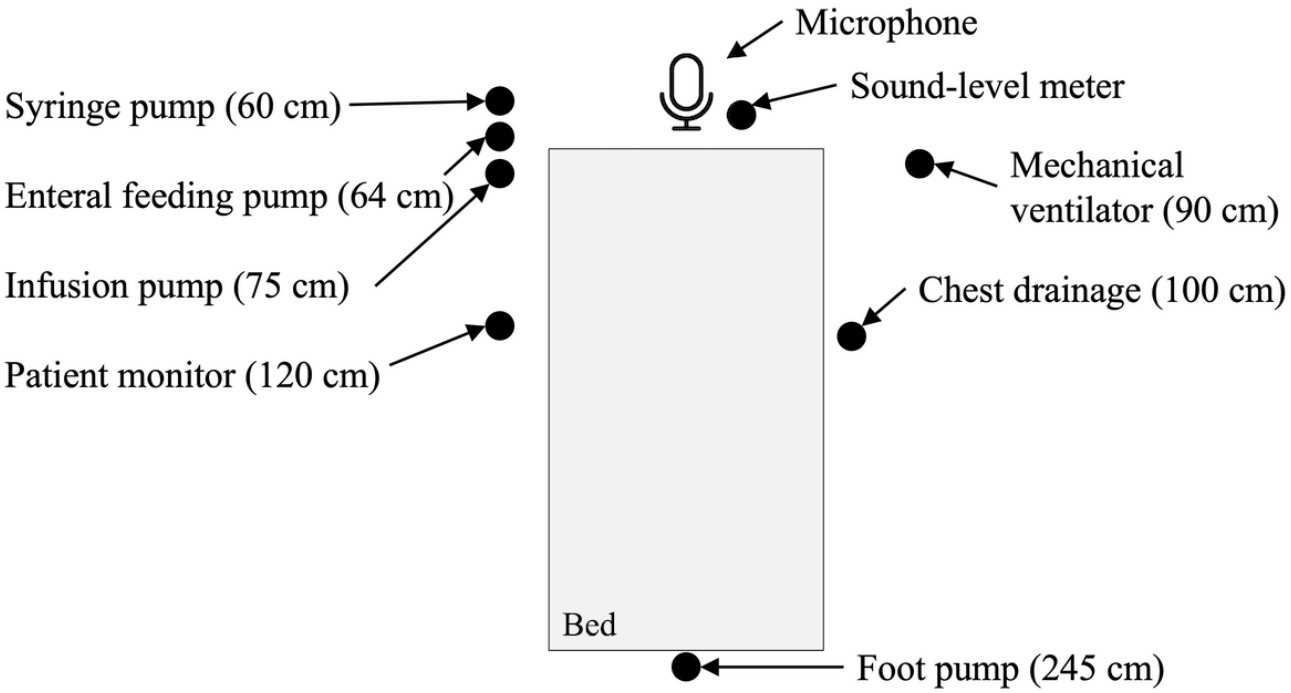


Table . Level of each sound relative to the total level of polyphonic sound.

Polyphony level	Data mount, n (%)
0	0 (0)
1	3655 (5.7)
2	15,011 (23.6)
3	22,547 (35.4)
4	15,911 (25)
5	5280 (8.3)
6	1230 (1.9)
7	64 (0.1)

XSL•FO
RenderX

Table . Detailed characteristics of the sounds of each alarm.

Source device	Model (manufacturer)	Peak frequencies (Hz)[a]	Signal duration (seconds)	Silence duration (seconds)	Overall duration (seconds)
Infusion pump	OT-818G (JMS)	[(856,856,856)-(856,856)] 2 times	3.34	2.99	6.33
Syringe pump	TE-351 (Terumo)	4001	0.26	0.20	0.46
Enteral feeding pump	APPLIX Smart (Fresenius Kabi)	4097	0.80	0.80	1.60
Venous foot pump	SCD700 (Coviden)	2108	0.20	1.30	1.50
Chest drainage	THOPAZ (Medela)	2632	1.07	8.95	10.02
Patient monitor	PVM-4761 (NihonKoden)	[(783,994,1181) - (1181,1569)] 2 times[b]	2.93	4.09	7.02
Mechanical ventilator	C1 (Hamilton)	491 828 662[c]	1.10	4.98	6.08

[a]Fundamental frequencies analyzed by Audacity. Harmonics are excluded.

[b]High-priority alarm sound.

[c]Middle-priority alarm sound.

Simulation Dataset

The robustness of the classifier was evaluated using a simulation dataset of alarm sounds added to HWN (which comprised conversations, footsteps, closet opening and closing sounds, intraoral suction, and ventilator exhalation sounds but not alarm sounds from other medical devices) at different SNRs (Figure 1). For the simulation dataset, the alarm sounds were recorded separately from those in the Data Collection section, using the same recording protocol (quiet private room, identical microphone placement, and device settings). During recording, all 7 devices were set to repeatedly emit alarms, sometimes overlapping due to differences in their alarm durations. Multiple alarms sometimes sounded simultaneously because of differences in the duration times of each alarm sound. Table 4 shows the maximum sound pressure of each sound source. In contrast to the training dataset—where alarm sounds were superimposed on white noise at SNRs ranging from 30 to 0 dB in 1 dB steps—the simulation dataset used for evaluation was created by superimposing the recorded HWN on alarm sounds at 4 SNR settings (30, 20, 10, and 0 dB) to reproduce realistic clinical environments. As shown in this figure, the VFP alarm exhibited the lowest sound pressure level among the devices, whereas other devices, such as SP and ENP, had relatively higher levels.

Table . Maximum sound pressure levels of each of the devices in the recording simulation dataset.

Source device	Sound level (dB)
Infusion pump	71.9
Syringe pump	77.7
Enteral feeding pump	64.4
Venous toot pump	61.2
Chest drainage	73.7
Patient monitor	62.1
Mechanical ventilator	79.6
Hospital ward noise	63.4

Performance Metrics

Model performance was evaluated using 5-fold cross-validation. No formal statistical significance tests were conducted, as the primary objective was descriptive benchmarking rather than hypothesis testing. Evaluation was performed using the sed_eval module [7,33]. The classifier outputs each predicted value of the 7 devices. The predicted values were dichotomized based on a cutoff value of 0.5. The onset and offset times input into the sed_eval module were calculated from the change points of the output results. Segment-based metrics are an index that determines whether the reference and the output match for each set time resolution (second). Therefore, the time resolution was set to 0.1 seconds, half of the shortest alarm duration time among the 7 devices. The event-based metrics index evaluated the timing of onset and offset from the set collar (seconds). The collar was set to 2.0 seconds based on the response of the notification system. Event-based metrics evaluation considers the actual operation and is more stringent than segment-based evaluation. Comparisons were evaluated using overall metrics (microaverage) and class-wise metrics.

XSL•FO
RenderX

For clinical applicability, inaccurate information is unacceptable, as it puts patients at risk. Therefore, the requirement for clinical application was set at an F_1-score value of 0.900 or higher for event-based overall metrics and an F value of 0.950 or higher for class-wise recall metrics.

Finally, the predicted results were visualized using the sed_vis module, and the spectrogram and classification results were examined [34].

Ethical Considerations

This study did not involve human participants or animal experiments. The recordings contained no speech, personal identifiers, or patient-related information. Therefore, ethics approval was not required in accordance with institutional and international research ethics policies.

Results

Table 5 summarizes the overall performance metrics at an SNR of 0 dB. The 679-second simulation dataset consisted of 63,649 frames, of which 63,488 frames were evaluated using 256-frame input windows. Among the segment-based metrics, CNN4+BiGRU achieved the highest F_1-score, followed by CNN3+BiGRU. Conversely, for event-based metrics, CNN3+BiGRU outperformed all other models, with CNN4+BiGRU ranking second. Regarding recall, event-based metrics showed values of 0.950 or higher for all BiGRU-based models, whereas segment-based metrics yielded recall values below 0.950 for all models.

Table . Overall metrics (microaverage) at a signal-to-noise ratio of 0 dB across 5-fold cross-validation. The numbers in italics represent the optimal value for the proposed models.

	Segment-based metrics, mean (SD)			Event-based metrics, mean (SD)		
	F_1-score	Precision	Recall	F_1-score	Precision	Recall
CNN3[a]+BiSRNN[b] (baseline)	0.832 (0.007)	0.822 (0.009)	0.841 (0.011)	0.921 (0.003)	0.874 (0.009)	0.973 (0.008)
CNN3+BiGRU[c]	0.868 (0.008)	0.845 (0.006)	0.894 (0.012)	*0.967 (0.011)*	*0.944 (0.014)*	*0.991 (0.011)*
CNN4+BiGRU	*0.873 (0.004)*	*0.856 (0.003)*	0.890 (0.008)	0.965 (0.008)	0.942 (0.009)	0.989 (0.008)
ALL-CNN4+BiGRU	0.867 (0.010)	0.839 (0.010)	*0.896 (0.011)*	0.948 (0.021)	0.915 (0.032)	0.983 (0.008)

[a]CNN: convolutional neural network.

[b]BiSRNN: bidirectional simple recurrent neural network.

[c]BiGRU: bidirectional gated recurrent unit.

Table 6 shows the event-based class-wise metrics at an SNR of 0 dB. Only event-based metrics are reported here, as they reflect the temporal accuracy of onset and offset detection, which is essential for clinical alarm management, whereas class-wise segment-based metrics are less indicative of operational performance. Class-wise segment-based results are provided in Multimedia Appendix 1 [30] for reference. Event-based evaluation showed that CNN3+BiGRU and CNN4+BiGRU had a recall value of 0.990 or higher for all devices but VFP. In contrast, the ENP, PM, and ventilator had F_1-scores of 0.900 or less due to their low precision. The reference standard was the correctly annotated label from the event roll that visualized the classification results, while the output was the model's identified results. In the absence of sound, the device was detected visually (Figure 4).

XSL•FO
RenderX

Table . Event-based class-wise metrics at a signal-to-noise ratio of 0 dB across 5-fold cross-validation. The numbers in italics represent the optimal value for each class.

Metrics and class	F_1-score, mean (SD)	Precision, mean (SD)	Recall, mean (SD)
CNN3[a]+BiSRNN[b]			
IP[c]	0.945 (0.016)	0.900 (0.028)	0.995 (0.001)
SP[d]	0.994 (0.004)	0.990 (0.008)	*0.998 (0.000)*
ENP[e]	0.903 (0.011)	0.831 (0.016)	0.990 (0.007)
VFP[f]	0.829 (0.013)	0.828 (0.036)	0.834 (0.050)
CD[g]	0.815 (0.023)	0.688 (0.034)	*1.000 (0.000)*
PM[h]	0.854 (0.020)	0.749 (0.031)	0.993 (0.003)
Vent[i]	0.752 (0.058)	0.606 (0.078)	*1.000 (0.000)*
CNN3+BiGRU[j]			
IP	0.982 (0.008)	0.967 (0.015)	0.997 (0.001)
SP	*0.998 (0.000)*	*1.000 (0.000)*	0.997 (0.001)
ENP	*0.969 (0.016)*	*0.939 (0.029)*	*1.000 (0.000)*
VFP	0.939 (0.037)	0.931 (0.030)	*0.951 (0.074)*
CD	0.904 (0.031)	0.826 (0.052)	*1.000 (0.000)*
PM	0.924 (0.025)	0.862 (0.043)	*0.997 (0.001)*
Vent	*0.834 (0.034)*	*0.717 (0.050)*	*1.000 (0.000)*
CNN4+BiGRU			
IP	*0.986 (0.005)*	*0.977 (0.009)*	0.995 (0.002)
SP	0.998 (0.000)	*1.000 (0.000)*	0.997 (0.001)
ENP	0.939 (0.033)	0.887 (0.058)	*1.000 (0.000)*
VFP	*0.943 (0.022)*	*0.947 (0.027)*	0.942 (0.054)
CD	0.870 (0.030)	0.770 (0.048)	*1.000 (0.000)*
PM	*0.954 (0.014)*	*0.916 (0.025)*	0.996 (0.002)
Vent	0.797 (0.054)	0.666 (0.080)	*1.000 (0.000)*
ALL-CNN4+BiGRU			
IP	0.942 (0.030)	0.896 (0.052)	0.995 (0.003)
SP	*0.998 (0.000)*	*1.000 (0.000)*	0.996 (0.001)
ENP	0.908 (0.056)	0.836 (0.090)	*1.000 (0.000)*
VFP	0.921 (0.047)	0.943 (0.046)	0.901 (0.057)
CD	*0.949 (0.018)*	*0.903 (0.033)*	*1.000 (0.000)*
PM	0.904 (0.020)	0.829 (0.032)	0.995 (0.003)
Vent	0.805 (0.051)	0.677 (0.074)	*1.000 (0.000)*

[a]CNN: convolutional neural network.

[b]BiSRNN: bidirectional simple recurrent neural network.

[c]IP: infusion pump.

[d]SP: syringe pump.

[e]ENP: enteral feeding pump.

[f]VFP: venous foot pump.

[g]CD: chest drainage.

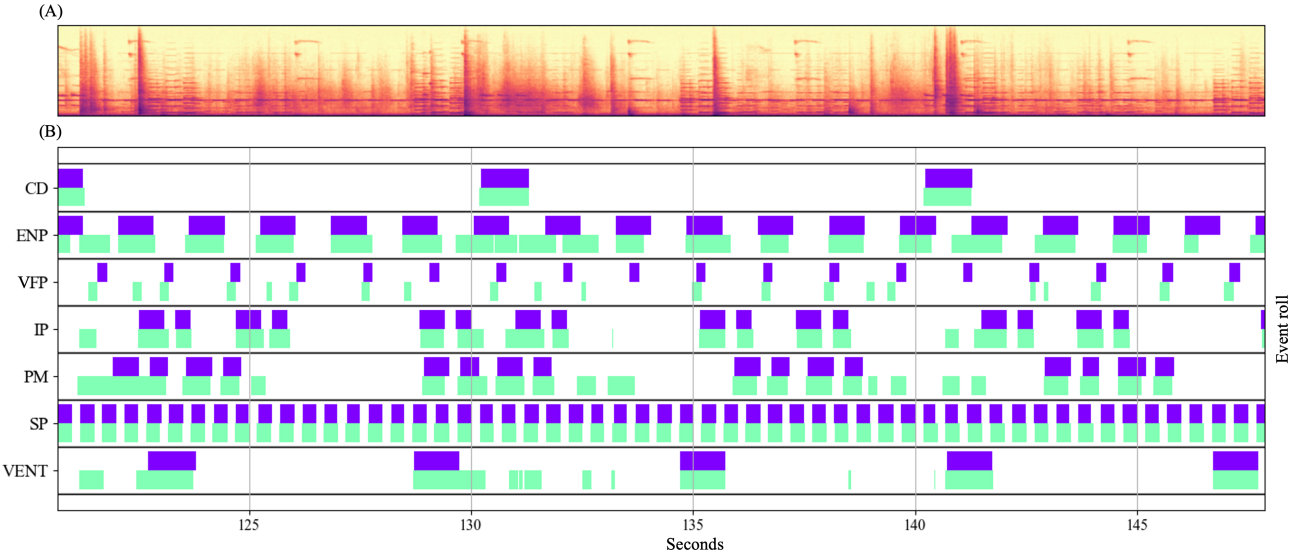
[h]PM: patient monitor.

[i]Vent: mechanical ventilator.

XSL•FO
RenderX

[j]BiGRU: bidirectional gated recurrent unit.

Figure 4. The reference and proposed model outputs of a convolutional neural network 4+bidirectional gated recurrent unit at a signal-to-noise ratio of 0 dB: (A) spectrogram of the simulation dataset and (B) event roll of the reference and proposed model outputs for the 7 devices. CD: chest drainage; ENP: enteral feeding pump; IP: infusion pump; PM: patient monitor; SP: syringe pump; VFP: venous foot pump; VENT: mechanical ventilator.



Discussion

Principal Results

The proposed classifier was found to successfully detect the status of nearby medical devices. Although video-based alarm detection was also considered, it was not feasible to detect the monitors with cameras without the introduction of a blind spot. Therefore, SED was considered a more feasible approach than video recognition.

This study describes the construction of a classifier using a large amount of artificial noise data. This classifier was used to evaluate polyphonic alarm sounds among a simulation dataset of HWN. Because the classification target is a sine wave, we expected that the target could be achieved with simple neural networks. However, BiSRNN did not achieve the target performance, requiring the application of BiGRU. Both the frequency and time axes required advanced processing to recognize alarm sounds. In addition, a convolutional layer with 4 layers outperformed one with 3 layers. The F_1-score of the classifier using BiGRU was 0.900 or higher, which was robust in the detection of polyphonic alarm sounds. Only VFP in each proposed classifier was unclear in the spectrogram due to VFP having the lowest sound pressure level of the 7 devices, thus resulting in low recall. In addition, masking of an impact sound over the entire frequency axis of the spectrogram would result in lower precision and overdetection.

Clinical Application as a Notification System

The notification system should alert the hospital information system without missing any situations, whether alarms are sounding on a single device or on multiple devices simultaneously. Therefore, recall of class-wise metrics was considered the most important in evaluating clinical applications. In particular, recall for the ventilator, the most essential support device of the 7 evaluated, was 1.000.

CNN4+BiGRU had the highest F_1-score in the event-based overall metrics, and the recall values of ENP, CD, and the ventilator were 1.000 each. Only VFP showed a recall value below 0.950, primarily due to its lower sound pressure level. In some cases, detection occurred slightly earlier than the actual onset, which reduced the measured recall. However, the ventilator demonstrated low precision with frequent overdetections, suggesting that it could not be evaluated clinically because it could cause alarm fatigue [35]. In contrast, because the F_1-scores of ENP, VFP, and CD without external output were 0.900 or higher, the system was likely feasible to notify staff of the alarm status of medical devices that could not be connected to the hospital information system. Therefore, the proposed system demonstrated feasibility as an alarm sound detection system and can be further refined for clinical use.

Integration Into Hospital Networks

Data Privacy Implications

The system processes only nonspeech alarm signals, ensuring that no patient-identifiable audio is stored or transmitted. When integrated into hospital networks, alarm classifications should be anonymized at the edge, transmitting only classification results in compliance with privacy regulations such as the General Data Protection Regulation and Japan's Act on the Protection of Personal Information.

Real-Time Processing Feasibility

Our classifier was designed for lightweight deployment, with feature extraction and model inference feasible on edge devices. The processing latency is on the order of milliseconds per input window, enabling real-time alarm monitoring without delaying clinical response.

Regulatory Concerns

Integration of an alarm detection system into hospital infrastructure would require compliance with medical device

XSL•FO
RenderX

standards, including ISO/IEC 60601-1-8 for alarm systems. Depending on the jurisdiction, such a system may be classified as a medical device software, requiring regulatory approval. Early consultation with regulatory authorities is recommended to ensure compliance and patient safety.

Limitations

This study had several limitations. First, the study evaluated only a limited range of medical devices from a single hospital, potentially limiting generalizability. Second, differences in hospital architecture (eg, room layouts, wall materials, and ambient noise) may affect sound propagation and detection. Third, despite ISO/IEC 60601-1-8 regulations, variations in alarm sounds across manufacturers and models were not assessed. Finally, large-scale live recording and annotation remain impractical; future work should use synthetic datasets and validate performance across diverse environments and device types.

Comparison With Prior Work

Several reports have examined the classification of alarm sounds using deep learning. Evaluation of single sounds of horns and bicycle bells found that the 5-layer deep neural network that applied an integrated judgment process had F_1-scores of 0.99 or higher [4]. Because horns and similar devices do not create sine waves of digital sounds, they cannot be evaluated in the same way as alarm sounds of medical devices. A study of alarm sounds of medical devices in a neonatal intensive care unit found that most of the alarms had SNRs of 0 dB or higher [8]. That study, however, did not consider a classifier for polyphonic alarm sounds. A classifier using CRNN was found to be effective for polyphonic acoustic sounds [26,36].

Conclusions

Missed medical device alarms can lead to serious adverse events. To mitigate such risks, we developed a deep learning–based classifier for detecting polyphonic alarm sounds in hospital environments.

Alarm sounds emitted by medical devices are regulated by ISO/IEC 60601-1-8. Because this standard defines different tones and patterns for each device and priority, SED is expected to identify the device and priority successfully. Thus, we considered SED appropriate to determine alarm status. Automatic identification of alarm sounds in hospital rooms would facilitate safer medical care.

In the simulation experiment, the polyphonic alarm sound classifier showed excellent performance, with an F_1-score of 0.945 at an SNR of 0 dB. The proposed classifier demonstrated feasibility for clinical alarm sound detection and can be further optimized. When combined with network connectivity, this classifier could improve the notification of abnormal patient status detected by medical devices without requiring each device to be individually connected.

Acknowledgments

This work was partially supported by the Japan Society for the Promotion of Science KAKENHI program (JP24K21125).

Conflicts of Interest

None declared.

Multimedia Appendix 1
Segment-based class-wise metrics at a signal-to-noise ratio of 0 dB across 5-fold cross-validation.
[DOCX File, 20 KB - medinform_v13i1e35987_app1.docx]

References

1. Yoshioka J, Ishiyama S, Saitoh D, et al. Development and testing of a ventilator remote adapter via communication between the ventilator and receiving smart device utilizing the accompanying app. Jpn J Med Instrum 2018;88(4):449-457. [doi: 10.4286/jjmi.88.449]
2. Michiyoshi S. Inclusion of infusion pump in automatic control system. Jpn J Intensive Care Med 2020;44(3):117-122 [FREE Full text]
3. Ishikawa M, Saito N. Strategies to prevent recurrence of incidents and accidents related to medical device alarm systems. Iryo Kikigaku 2017;87(3):285-291. [doi: 10.4286/jjmi.87.285]
4. Shiraishi Y, Takeda T, Shitara A. Alarm sound classification system in smartphones for the deaf and hard-of-hearing using deep neural networks. Presented at: International Conference on Advances in Computer-Human Interactions; Nov 21-25, 2020; Valencia, Spain p. 30-33 URL: https://www.thinkmind.org/index.php?view=article&articleid=achi_2020_3_10_28007 [accessed 2025-10-17]
5. Cakir E, Heittola T, Huttunen H, Virtanen T. Multi-label vs. combined single-label sound event detection with deep neural networks. Presented at: European Signal Processing Conference; Aug 31 to Sep 4, 2015; Nice p. 2551-2555. [doi: 10.1109/EUSIPCO.2015.7362845]
6. Cakir E, Heittola T, Huttunen H, Virtanen T. Polyphonic sound event detection using multi label deep neural networks. Presented at: International Joint Conference on Neural Networks; Jul 12-17, 2015; Killarney, Ireland p. 1-7. [doi: 10.1109/IJCNN.2015.7280624]

XSL•FO
RenderX

7. Mesaros A, Heittola T, Virtanen T. Metrics for polyphonic sound event detection. Appl Sci (Basel) 2016 Jun;6(6):162. [doi: 10.3390/app6060162]
8. Raboshchuk G, Nadeu C, Jancovic P, et al. A knowledge-based approach to automatic detection of equipment alarm sounds in a neonatal intensive care unit environment. IEEE J Transl Eng Health Med 2018;6(4400110). [doi: 10.1109/JTEHM.2017.2781224] [Medline: 29404227]
9. McLoughlin I, Zhang H, Xie Z, Song Y, Xiao W. Robust sound event classification using deep neural networks. IEEE/ACM Trans Audio Speech Lang Process 2015 Mar;23(3):540-552. [doi: 10.1109/TASLP.2015.2389618]
10. Phan H, Hertel L, Maass M, Mertins A. Robust audio event recognition with 1-max pooling convolutional neural networks. Presented at: Annual Conference of the International Speech Communication Association; Sep 8-12, 2016. [doi: 10.21437/Interspeech.2016-123]
11. Kishimoto K, Takemura T, Sugiyama O, et al. Prediction of polyphonic alarm sound by deep neural networks. Jpn Soc Med Biol Eng 2022 Mar;60(1):8-15. [doi: 10.11239/jsmbe.60.8]
12. Gong Y, Chung YA, Glass J. AST: audio spectrogram transformer. Presented at: Annual Conference of the International Speech Communication Association; Aug 30 to Sep 3, 2021. [doi: 10.21437/Interspeech.2021-698]
13. Gulati A, Qin J, Chiu CC, et al. Conformer: convolution-augmented transformer for speech recognition. Presented at: Annual Conference of the International Speech Communication Association; Oct 25-29, 2020. [doi: 10.21437/Interspeech.2020-3015]
14. Mesaros A, Heittola T, Eronen A, Virtanen T. Acoustic event detection in real life recordings. Presented at: European Signal Processing Conference; Aug 23-27, 2010; Aalborg, Denmark p. 1267-1271 URL: https://ieeexplore.ieee.org/document/7096611 [accessed 2025-10-17]
15. Heittola T, Mesaros A, Virtanen T, Gabbouj M. Supervised model training for overlapping sound events based on unsupervised source separation. Presented at: IEEE International Conference on Acoustics, Speech and Signal Processing; May 26-31, 2013; Vancouver, BC p. 8677-8681. [doi: 10.1109/ICASSP.2013.6639360]
16. Innami S, Kasai H. NMF-based environmental sound source separation using time-variant gain features. Comput Math Appl 2012 Sep;64(5):1333-1342. [doi: 10.1016/j.camwa.2012.03.077]
17. Dessein A, Cont A, Lemaitre G. Real-time detection of overlapping sound events with non-negative matrix factorization. In: Nielsen F, Bhatia R, editors. Matrix Information Geometry: Springer; 2013:341-371. [doi: 10.1007/978-3-642-30232-9_14]
18. Mesaros A, Heittola T, Dikmen O, Virtanen T. Sound event detection in real life recordings using coupled matrix factorization of spectral representations and class activity annotations. Presented at: IEEE International Conference on Acoustics, Speech and Signal Processing; Apr 19-24, 2015; Queensland, Australia p. 151-155. [doi: 10.1109/ICASSP.2015.7177950]
19. Graves A, Schmidhuber J. Framewise phoneme classification with bidirectional LSTM and other neural network architectures. Neural Netw 2005;18(5-6):602-610. [doi: 10.1016/j.neunet.2005.06.042] [Medline: 16112549]
20. Graves A, Mohamed AR, Hinton G. Speech recognition with deep recurrent neural networks. Presented at: International Conference on Acoustics, Speech and Signal Processing; May 26-31, 2013; Vancouver, BC p. 6645-6649. [doi: 10.1109/ICASSP.2013.6638947]
21. Bock S, Schedl M. Polyphonic piano note transcription with recurrent neural networks. Presented at: IEEE International Conference on Acoustics, Speech and Signal Processing; Mar 25-30, 2012; Kyoto, Japan p. 121-124. [doi: 10.1109/ICASSP.2012.6287832]
22. Valenti M, Squartini S, Diment A, Parascandolo G, Virtanen T. A convolutional neural network approach for acoustic scene classification. Presented at: International Joint Conference on Neural Networks; May 14-19, 2017; Anchorage, AK p. 1547-1554. [doi: 10.1109/IJCNN.2017.7966035]
23. Sainath TN, Vinyals O, Senior A, Sak H. Convolutional, long short-term memory, fully connected deep neural networks. Presented at: IEEE International Conference on Acoustics, Speech and Signal Processing; Apr 19-24, 2015; Queensland, Australia p. 4580-4584. [doi: 10.1109/ICASSP.2015.7178838]
24. Cakir E, Parascandolo G, Heittola T, Huttunen H, Virtanen T. Convolutional recurrent neural networks for polyphonic sound event detection. IEEE/ACM Trans Audio Speech Lang Process 2017;25(6):1291-1303. [doi: 10.1109/TASLP.2017.2690575]
25. Purwins H, Li B, Virtanen T, Schluter J, Chang SY, Sainath T. Deep learning for audio signal processing. IEEE J Sel Top Signal Process 2019 May;13(2):206-219. [doi: 10.1109/JSTSP.2019.2908700]
26. Adavanne S, Virtanen T. A report on sound event detection with different binaural features. arXiv. Preprint posted online on Oct 9, 2017 URL: http://arxiv.org/abs/1710.02997 [accessed 2021-09-09]
27. LeCun Y, Bengio Y, Hinton G. Deep learning. Nature New Biol 2015 May 28;521(7553):436-444. [doi: 10.1038/nature14539] [Medline: 26017442]
28. Springenberg JT, Dosovitskiy A, Brox T, Riedmiller M. Striving for simplicity: the all convolutional net. arXiv. Preprint posted online on Apr 13, 2015 URL: http://arxiv.org/abs/1412.6806 [accessed 2021-09-18]
29. Kingma DP, Ba J. Adam: a method for stochastic optimization. arXiv. Preprint posted online on Jan 29, 2017 URL: http://arxiv.org/abs/1412.6980 [accessed 2021-06-07]
30. Ce-kishi/FEDA-medalarms. GitHub. URL: https://github.com/ce-kishi/FEDA-MedAlarms [accessed 2025-05-25]

XSL•FO
RenderX

31. Salamon J, Bello JP. Deep convolutional neural networks and data augmentation for environmental sound classification. IEEE Signal Process Lett 2017 Mar;24(3):279-283. [doi: 10.1109/LSP.2017.2657381]
32. Park DS, Chan W, Zhang Y, et al. SpecAugment: a simple data augmentation method for automatic speech recognition. Presented at: Annual Conference of the International Speech Communication Association; Sep 15-19, 2019; Graz, Austria p. 2613-2617 URL: https://www.isca-archive.org/interspeech_2019 [doi: 10.21437/Interspeech.2019-2680]
33. TUT-ARG/sed_eval.: GitHub; 2021. URL: https://github.com/TUT-ARG/sed_eval [accessed 2021-09-19]
34. TUT-ARG/sed_vis.: GitHub; 2021. URL: https://github.com/TUT-ARG/sed_vis [accessed 2021-09-19]
35. Scott JB, De Vaux L, Dills C, Strickland SL. Mechanical ventilation alarms and alarm fatigue. Respir Care 2019 Oct;64(10):1308-1313. [doi: 10.4187/respcare.06878] [Medline: 31213570]
36. Mesaros A, Diment A, Elizalde B, et al. Sound event detection in the DCASE 2017 challenge. IEEE/ACM Trans Audio Speech Lang Process 2019 Jun;27(6):992-1006. [doi: 10.1109/TASLP.2019.2907016]

Abbreviations

BiGRU: bidirectional gated recurrent unit
BiSRNN: bidirectional simple recurrent neural network
CD: chest drainage
CNN: convolutional neural network
CRNN: convolutional recurrent neural network
ENP: enteral feeding pump
HWN: hospital ward noise
IEC: International Electrotechnical Commission
IP: infusion pump
ISO: International Organization for Standardization
MFB: mel filter bank
PM: patient monitor
RNN: recurrent neural network
SED: sound event detection
SNR: signal-to-noise ratio
SP: syringe pump
VFP: venous foot pump

Edited by A Benis; submitted 30.03.25; peer-reviewed by K Hori, MJCS Reis; revised version received 27.08.25; accepted 05.10.25; published 12.11.25.

Please cite as:
Kishimoto K, Takemura T, Sugiyama O, Kojima R, Yakami M, Yamamoto G, Kuroda T
Detection of Polyphonic Alarm Sounds From Medical Devices Using Frequency-Enhanced Deep Learning: Simulation Study
JMIR Med Inform 2025;13:e35987
URL: https://medinform.jmir.org/2025/1/e35987
doi:10.2196/35987

© Kazumasa Kishimoto, Tadamasa Takemura, Osamu Sugiyama, Ryosuke Kojima, Masahiro Yakami, Goshiro Yamamoto, Tomohiro Kuroda. Originally published in JMIR Medical Informatics (https://medinform.jmir.org), 12.11.2025. This is an open-access article distributed under the terms of the Creative Commons Attribution License (https://creativecommons.org/licenses/by/4.0/), which permits unrestricted use, distribution, and reproduction in any medium, provided the original work, first published in JMIR Medical Informatics, is properly cited. The complete bibliographic information, a link to the original publication on https://medinform.jmir.org/, as well as this copyright and license information must be included.

XSL•FO
RenderX

Predicting Waiting Times for Medical Tasks in a Pediatric Hospital Using Machine Learning: Comprehensive, Retrospective, Real-World Study

Lin Lin Guo[1*], MSc; Rui Tang[2*], MSc; Jia Yang Wang[2], MSc; Si Zheng[2], MSc; Yin Zeng[2], BSc; Jun Hou[1], BSc; Mo Chen Dong[1], BSc; Jiao Li[2], PhD; Ying Cui[1], BSc

[1]Capital Center for Children's Health, Capital Medical University, No.2 Yabao Road, ChaoYang District, Beijing, China

[2]Institute of Medical Information, Chinese Academy of Medical Sciences and Peking Union Medical College, Beijing, China

[*]these authors contributed equally

Corresponding Author:
Ying Cui, BSc
Capital Center for Children's Health, Capital Medical University, No.2 Yabao Road, ChaoYang District, Beijing, China

Abstract

Background: The shortage of pediatric medical resources and overcrowding in children's hospitals are severe issues in China. Accurately predicting waiting times can help optimize hospital operational efficiency.

Objective: This study aims to develop machine learning models to predict waiting times for various laboratory and radiology examinations at a pediatric hospital.

Methods: Time stamp data from laboratory and radiology examinations were retrospectively collected from the pediatric hospital information system between November 1, 2024, and March 13, 2025. Two queue-related and 4 time-based features were extracted using queue theory. Linear regression and 8 machine learning models were trained to predict waiting times for each medical task. Hyperparameters were fine-tuned using randomized search and 10-fold cross-validation, and the bootstrap method was used for model evaluation. Mean absolute error, mean square error, root mean square error, and the coefficient of determination (R^2) were used as evaluation metrics. Shapley additive explanations values were used to assess feature importance.

Results: A total of 230,864 time-stamped records were included after data preprocessing. The median waiting time was 4.817 (IQR 1.867-12.050) minutes for all medical tasks. Waiting times for radiology examinations were generally longer than those for laboratory tests. Tree-based algorithms, such as random forest and classification and regression trees, performed best in predicting laboratory test waiting times, with R^2 values ranging from mean 0.880(SD 0.003) to mean 0.934 (SD 0.003). However, the machine learning models did not perform well in predicting radiology examination waiting times, with R^2 ranging from 0.114 (SD 0.005) to 0.719 (SD 0.004). Feature importance analysis revealed that queue-related predictors, especially the number of queuing patients, were the most important in predicting waiting times.

Conclusions: Task-specific prediction models are more appropriate for accurately predicting waiting times across various medical tasks. Guided by queue theory principles, we developed machine learning models for the waiting time prediction of each medical task and highlighted the importance of queue-related predictors.

(JMIR Med Inform 2025;13:e77297) doi:10.2196/77297

KEYWORDS

waiting time; pediatric hospital; machine learning; queue; medical tasks

Introduction

Background

Pediatric health care resources are considerably more scarce compared to other medical specialties. From 2015 to 2020, the growth rate of categorical pediatric residency positions in the United States was only 7%, which was far slower than the growth rate of other specialties during that time [1]. In China, the lack of resources for pediatric medicine is much more severe. According to national statistical data [2], the number of pediatricians per child in China is approximately half that in the United States. Furthermore, China has a very unequal distribution of pediatric experts, with a heavy concentration in developed metropolitan areas [3]. This leads to patient clustering and increased overcrowding in tertiary pediatric hospitals. A typical pediatric medical visit consists of multiple steps, including consultation, radiology examination or laboratory tests, and medication dispensing. Excessive waiting times at each of these stages not only reduce patient satisfaction [4] but may also contribute to adverse clinical outcomes [5,6].

XSL•FO
RenderX

Therefore, accurately predicting waiting times and improving operational effectiveness in pediatric hospitals is of critical importance.

Queue management systems in hospitals can enhance operational efficiency through features such as real-time queue updates, automated notifications, and online appointment scheduling [7]. Prior research has examined queue-related issues using techniques such as time series analysis (TSA) [8], discrete event simulation [9], and queue theory (QT) [10]. These methods simulate queue dynamics under various parameters to assess operational performance and identify the optimal resource allocation strategies. However, there are several obstacles to overcome before they may be used in actual health care settings. The application of these approaches is limited in practice because health care queues often deviate from the fundamental assumptions that underlie them, such as known initial probability distributions, exponentially distributed waiting times, or stationary queue states [11]. As a result, these models frequently fail to capture the variability and fluctuations inherent in actual queue dynamics, reducing their accuracy in predicting waiting times.

Machine learning models are developed using data-driven approaches and usually do not require restrictive assumptions. To overcome the drawbacks of conventional techniques, machine learning presents a viable substitute for forecasting wait times in hospital lines. In previous studies, Chen et al [12] applied an improved random forest algorithm to predict patient waiting times for each treatment task, such as blood tests, computed tomography (CT) scan, and pharmacy dispensing, and the hospital queuing-recommendation system based on the prediction algorithm reduced waiting times by guiding patient flow. Similarly, Lin et al [13] evaluated the performance of several machine learning algorithms for waiting time prediction and selected the best-performing model for prediction in a pediatric ophthalmology outpatient clinic. Chocron et al [14] compared machine learning algorithms with classical QT models for waiting time prediction and found that machine learning models produced better predictions than traditional methods in complex real-world scenarios. Therefore, machine learning techniques provide a more reliable way to capture variations in actual queue dynamics and improve the prediction accuracy of waiting time. Furthermore, multitask queues in pediatric hospitals have received less attention in the majority of studies, which have concentrated on emergency departments (EDs) [15-17] or radiology departments [18]. Nevertheless, the operational effectiveness of different medical task windows varies, and research focusing on a specific queue may not adequately capture the dynamics of other hospital medical tasks. A comprehensive investigation of waiting time prediction for different medical tasks can offer deeper insights into the use of medical resources and can be used as an alternative method to support medical resource optimization.

Objectives

This study investigates the dynamic characteristics of multiple medical task queues using real-world data from a large pediatric hospital in northern China. By incorporating principles from QT for feature selection, key features were extracted from actual hospital queue data, and then, we used machine learning techniques to predict waiting times after patient check-in across various medical tasks in the hospital. The predictive performance of different machine learning models is systematically evaluated. Additionally, feature importance analysis is conducted to assess the contribution of individual predictors and to provide insights for optimizing hospital operational efficiency. We also plan to deploy the best-performing model for waiting time prediction to improve the patient experience and help reduce hospital overcrowding in the future.

Methods

Problem Definition

During a hospital visit, patients usually have one or more medical tasks, which are frequently spread out over several hospital departments. For instance, a pediatric patient with an acute respiratory tract infection might undergo a series of steps, starting with a consultation in the respiratory department. After blood sampling and throat swab collection, the patient has an X-ray examination and then returns to the pulmonary department when all diagnostic reports are ready and the physician has ordered medicine. Finally, the patient goes to the pharmacy to pick up the necessary medications.

As illustrated, there may be unforeseen waiting times at each step of the medical tasks, which can significantly affect the patient's overall experience [19]. Furthermore, hospital operational efficiency may be lowered by disorderly queue arrangements. Targeted optimization of medical resource allocation based on key factors influencing waiting time represents a practical and effective strategy. As a result, in actual hospital settings, queue notifications may be provided by predictive algorithms that estimate waiting times with great accuracy, which will assist in reducing patient anxiety.

Data Collection

This study retrospectively collected records of patients who visited the Capital Center for Children's Health, Capital Medical University, between November 1, 2024, and March 13, 2025, for various laboratory tests and radiology examinations; the total raw dataset comprised 326,701 entries. The time stamp of these records was retrieved from the health information system for patients who attended the hospital during this period. The key information is summarized in Table 1.

XSL•FO
RenderX

Table . Information extracted from the health information system.

Records name	Description
Patient ID	A unique identifier assigned to each patient during their visit to the hospital
Medical task name	The specific examination conducted during a patient's visit, including throat swab, blood sampling, laboratory test for patients with fever, CT[a], MRI[b], X-ray, laryngoscopy, ultrasound, and echocardiography
Visit category	The department from which the patient is referred, including outpatient and ED[c]
Service location	The specific location where the patient receives medical services
Check-in time	The time when the patient completes check-in upon arriving for a specific medical task
Sampling or examination start time	The time when the patient begins a specific medical examination: the start time of laboratory tests is recorded as the sampling time, while the start time of the radiology examination is recorded as the examination start time

[a]CT: computed tomography.

[b]MRI: magnetic resonance imaging.

[c]ED: emergency department.

Following the retrieval of all records, the data were arranged according to the practical medical tasks performed by the institution. In this hospital, the tasks for laboratory tests include throat swab at the first floor (throat swab–first floor) and the second floor (throat swab–second floor), blood sampling, and laboratory test for patients with fever (laboratory test–fever). The radiology examination includes CT, magnetic resonance imaging (MRI), X-ray, laryngoscopy, ultrasound, and echocardiography. Blood sampling, ultrasound, and echocardiography are further divided into outpatient and ED windows at this facility.

Ethical Considerations

All data used in our study was anonymized and deidentified and did not involve data related to humans. Therefore, our research was exempted from the requirement of written informed consent and was approved by the Ethics Committee of the Capital Center for Children's Health, Capital Medical University (SHERLLM2024037).

Data Preprocessing

We define the waiting time as the duration from the patient's check-in to the start of the sampling or examination, as follows:

$$\text{Waiting time} = \text{Sampling/Examination start time} - \text{Check-in time} \quad (1)$$

First, we removed records that do not include the sampling or examination start time and check-in time. Due to the presence of numerous duplicate records in the health information system, we then performed a deduplication procedure on the extracted data. If the patient ID and sampling or examination start time are identical in the records, it will be removed as a redundant duplicate. To avoid negative waiting times, we then removed data when the check-in time is later than the sampling or examination start time. In addition, there may be very long waiting time outliers because some patients may not line up for the medical service window immediately after check-in—possibly leaving the hospital for a period or coming back on a subsequent day to continue their tests or examinations. To address this issue, we applied an IQR method to denoise the data using the following criterion:

$$\text{Noise record} > 75\%\ \text{quantile} + 1.5 \times (75\%\ \text{quantile} - 25\%\ \text{quantile}) \quad (2)$$

Records with waiting times exceeding the IQR were classified as noise and discarded. Model development was then conducted using the remaining data.

Feature Construction

Queue-length (QL) predictors and delay-history predictors are the 2 types of predictors used in earlier QT experiments to forecast waiting times [20]. While the latter makes predictions based on past waiting times, the former refers to projecting waiting time based on the queue's present status factors. As we have access to the precise time stamps for every patient's test or examination, we make predictions using QL predictors, which comprise the following two categories of features:

1. Time-based feature; these include the month, day, hour, and day of the week when a patient undergoes a specific medical task. These indicators can all be derived from the abovementioned records. Given that patient data vary significantly across different periods, these 4 time-related factors were considered as potential predictors.
2. Queue-related feature; these include the patient arrival rate per hour, calculated by counting the number of patients registering for a particular task each hour, and the number of queuing patients, that is, the number of patients who have checked in but have not yet started the sampling or examination.

In summary, we selected only 6 indicators, including month, day, hour, day of the week, arrival rate, and the number of queuing patients, to predict the waiting time using a concise set of predictors.

XSL•FO
RenderX

Model Development and Feature Importance Analysis

In our experiment, we use linear regression (LR) as a baseline model and 8 machine learning models for waiting time prediction, including k-nearest neighbor (KNN), support vector regression (SVR), classification and regression tree (CART), elasticNet, random forest (RF), light gradient boosting machine (LightGBM), extreme gradient boosting (XGBoost), and multilayer perceptron (MLP). As the waiting time is a continuous variable, we evaluate the models using the following performance metrics: mean absolute error (MAE), mean square error (MSE), root mean square error (RMSE), and the coefficient of determination (R^2). Equations 3–6 show the formula of MAE, MSE, RMSE, and R^2, where the y^i is the prediction value, the y-i represents the mean value of the waiting time, and the yi is the actual value.

(3)MAE=∑i=1n|y^i−yi|n

(4)MSE=∑i=1n(y^i−yi)2n

(5)RMSE=∑i=1n(y^i−yi)2n

(6)R2=1−∑i=1n(y^i−yi)2∑i=1n(yi−y¯)2

A randomized search and 10-fold cross-validation were used to fine-tune each model's hyperparameters. The performance of the models was evaluated using the abovementioned metrics, and the model with the best performance across these metrics was selected for prediction. To further evaluate the stability and reliability of the chosen model, a bootstrap approach was applied. MAE, MSE, RMSE, and R^2 were calculated for each bootstrap sample by comparing the model's predictions with the true values. The 95% CIs for each metric were derived to quantify the uncertainty in the model's predictive performance. Feature contributions to the waiting time prediction were quantified using Shapley additive explanations (SHAP) values [21]. For tree-based models, SHAP values were computed directly; for others (KNN and SVR), a background dataset was used to simulate feature absence, allowing for marginal contribution estimation via the KernelExplainer function. The entire research process is shown in Figure 1. All analyses were performed using Python (version 3.12; Python Software Foundation).

XSL•FO
RenderX

Figure 1. Flowchart of waiting time prediction. CART: classification and regression tree; HIS: health information system; KNN: k-nearest neighbor; LightGBM: light gradient boosting machine; MLP: multilayer perceptron; RF: random forest; SVR: support vector regression; XGBoost: extreme gradient boosting.

XSL•FO
RenderX

Results

Basic Characteristics of the Medical Queue

From November 1, 2024, to March 13, 2025, a total of 230,864 records were included after preprocessing the raw data. The required tasks were classified into 2 main categories: laboratory tests, which included 5 types of tasks, and radiology examinations, which included 8 types of tasks. The most frequently performed laboratory test was blood sampling for outpatient patients (76,587/230,864, 33.17%), while the most common radiology examination was X-ray (31,125/230,864, 13.48%; Table 2).

Table . Basic characteristics of queuing in different medical tasks (N=230,864).

Tests and examinations		Tasks, n (%)	Time, range (min)	Time, median (IQR)
Laboratory test				
	Throat swab—first floor	26,314 (11.05)	0.017 - 28.4	1.617 (0.483 - 5.799)
	Throat swab—second floor	13,296 (5.75)	0.017 - 26.967	1.467 (0.417 - 6.971)
	Blood sampling—ED[a]	23,558 (10.20)	0.150 - 5.533	1.650 (1.049 - 2.483)
	Blood sampling—outpatient	76,587 (33.17)	0.199 - 25.5	3.225 (2.583 - 10.700)
	Laboratory test—fever	9533 (4.13)	0.017 - 8.667	1.783 (1.017 - 3.349)
Radiology examination				
	Ultrasound—ED	22,601 (9.79)	0.199 - 48.050	10.883 (5.283 - 20.717)
	Ultrasound—outpatient	8031 (3.48)	0.517 - 85.299	23.400 (12.750 - 37.067)
	Echocardiography—ED	394 (0.17)	0.033 - 9.683	3.958 (3.054 - 5.212)
	Echocardiography—outpatient	5067 (2.19)	0.550 - 7.983	3.200 (2.600 - 4.167)
	Laryngoscope	4856 (2.10)	0.467 - 43.267	11.975 (5.217 - 19.771)
	X-ray	31125 (13.48)	0.065 - 6.566	5.106 (10.872 - 21.852)
	MRI[b]	3324 (1.44)	0.008 - 80.157	8.389 (17.825 - 33.262)
	CT[c]	6178 (2.68)	0.002 - 19.412	2.406 (3.933 - 6.947)

[a]ED: emergency department.

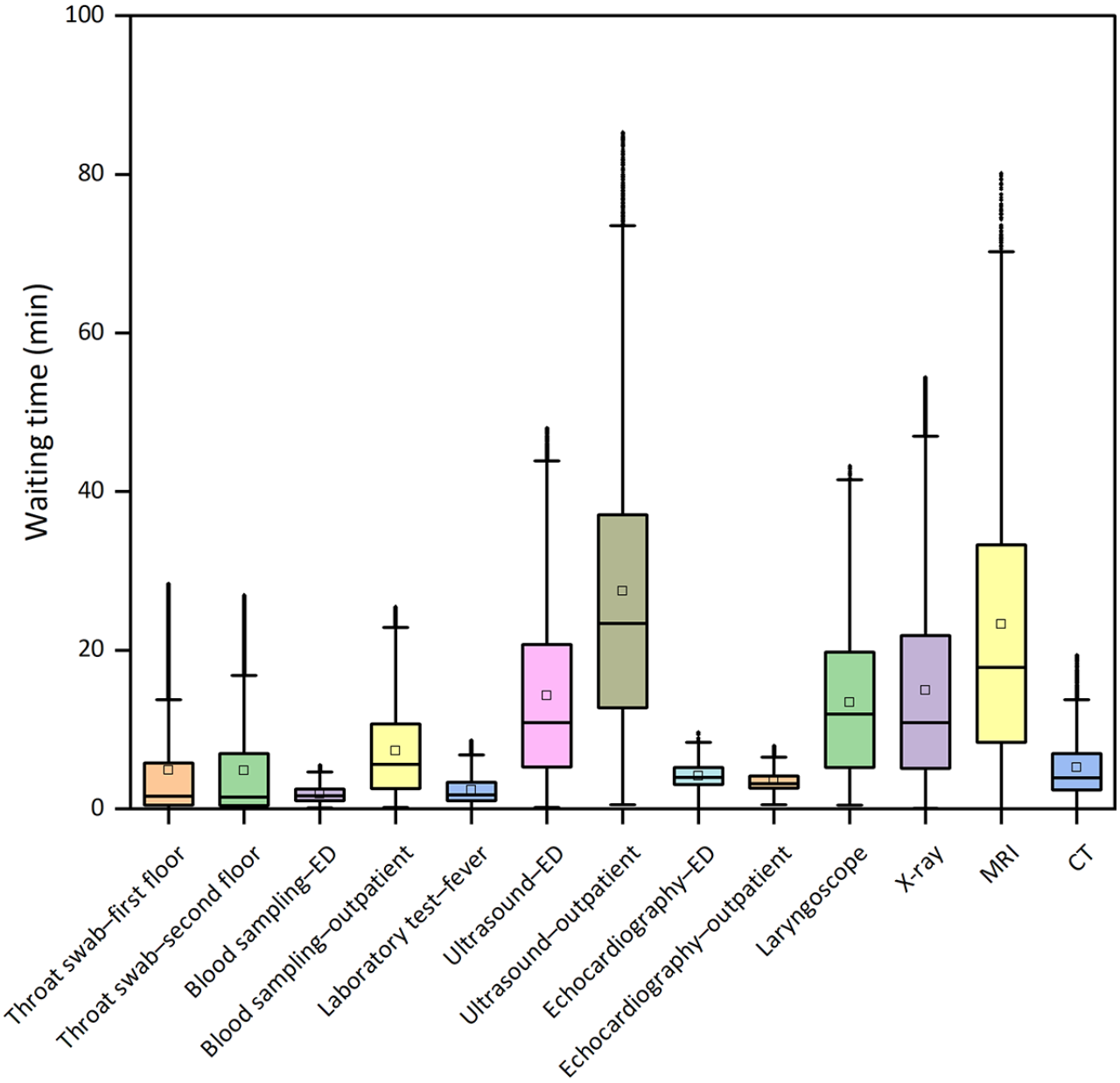
[b]MRI: magnetic resonance imaging.

[c]CT: computed tomography.

In the laboratory test category, we observed that blood sampling–ED (median 1.650, IQR 1.049-2.483 min) had the narrowest waiting time range, while the task for blood sampling–outpatient (median 3.225, IQR 2.583-10.700 min) had a relatively extensive waiting time range (Figure 2). For radiology examinations, the range of waiting time for the echocardiography task was narrow (median 3.958, IQR 3.054-5.212 min for ED; median 3.200, IQR 2.600-4.167 min for outpatient). In contrast, outpatients had to wait much longer for an ultrasound (median 37.067, IQR 12.750-23.400 min; Figure 2). Compared to laboratory tests, patients experienced longer waiting times in most radiology examinations.

XSL•FO
RenderX

Figure 2. Box plot of distribution of waiting time. CT: computed tomography; ED: emergency department; MRI: magnetic resonance imaging.



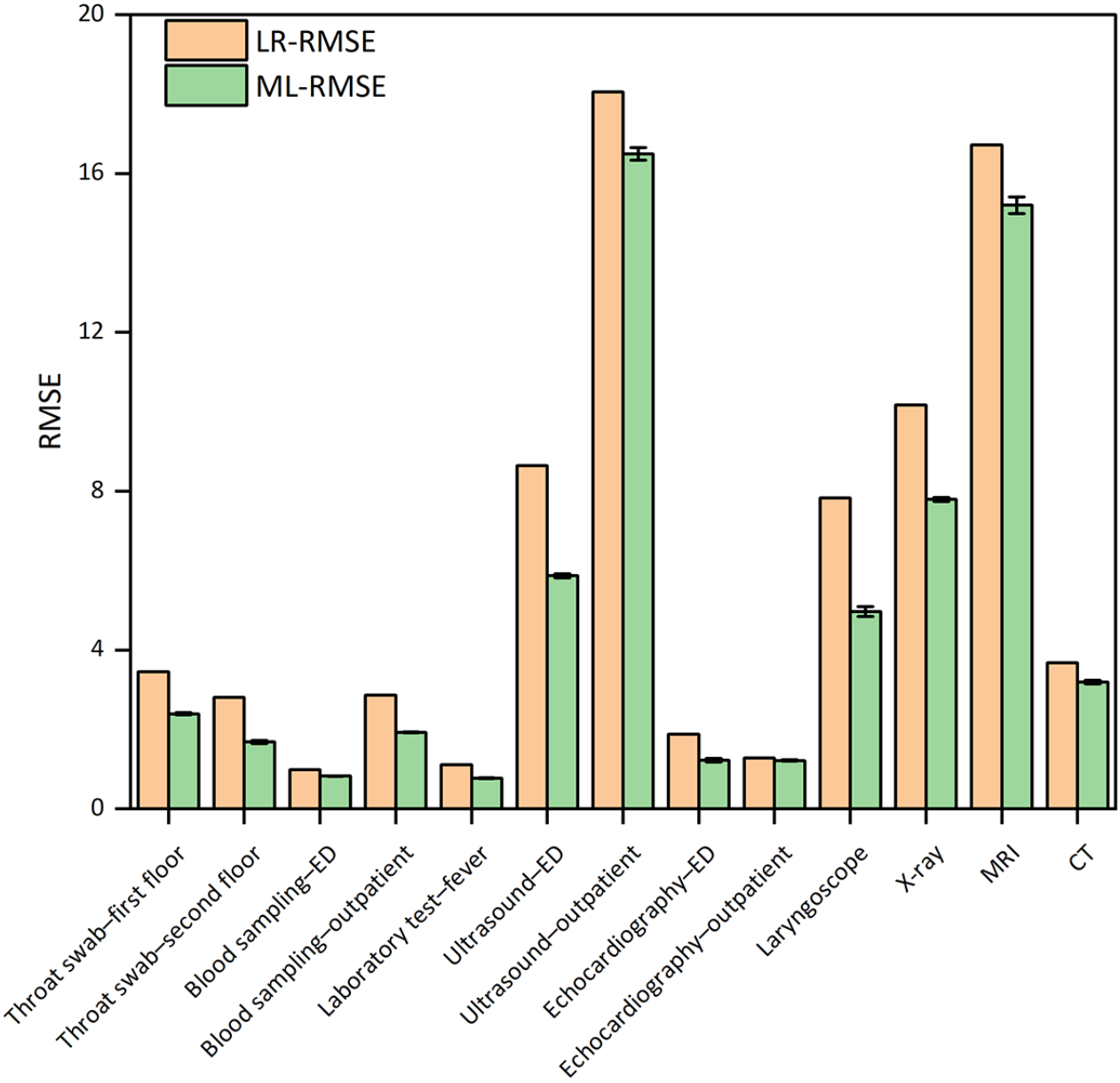
The distribution of waiting time of the total medical task followed an exponential pattern (Figure S1 in Multimedia Appendix 1). At different time points, we observed average arrival rate peaks for medical tasks at approximately 10:00 AM, 15:00 PM, and 8:00 PM. Similarly, 3 peaks were also present for the average number of queuing patients across different days of the week (Figures S2 and S3 in Multimedia Appendix 1). However, the waiting time of patients showed a first earlier peak at approximately 7:00 AM, with 2 lower peaks at approximately 12:00 AM and 8:00 PM (Figure S4 in Multimedia Appendix 1). In addition, the distribution of waiting time for different medical tasks before and after denoising is shown in Figure S5 in Multimedia Appendix 1.

Model Evaluation

We used 8 different models for predicting waiting times before laboratory and radiology tasks, while LR was used as the baseline model. After hyperparameter optimization, the optimal performance of the selected models for different tasks is shown in Table S1 in Multimedia Appendix 1. In 6 medical task queues, RF demonstrated the best predictive performance, with RMSE ranging from 1.925 (SD 0.015) to 2.395 (SD 0.033) for laboratory tests and from 1.217 (SD 0.015) to 15.204 (SD 0.207) for radiology examinations. In addition, XGBoost demonstrated effective performance in predicting waiting times for the throat swab–first floor (RMSE: mean 2.395, SD 0.033; R^2: mean 0.880, SD 0.003), echocardiography-ED (RMSE: mean 1.224, SD 0.048; R^2: mean 0.612, SD 0.021), and CT (RMSE: mean 3.191, SD 0.043; R^2: mean 0.382, SD 0.011), and CART, LightGBM, SVR, and KNN can also be used for waiting time prediction. All selected models outperformed the baseline LR model (Figures 3 and 4). The optimal hyperparameters identified through randomized search are provided in Table S2 in Multimedia Appendix 1. In addition, the calibration and residual plots are provided in Figures S8-S18 in Multimedia Appendix 1.

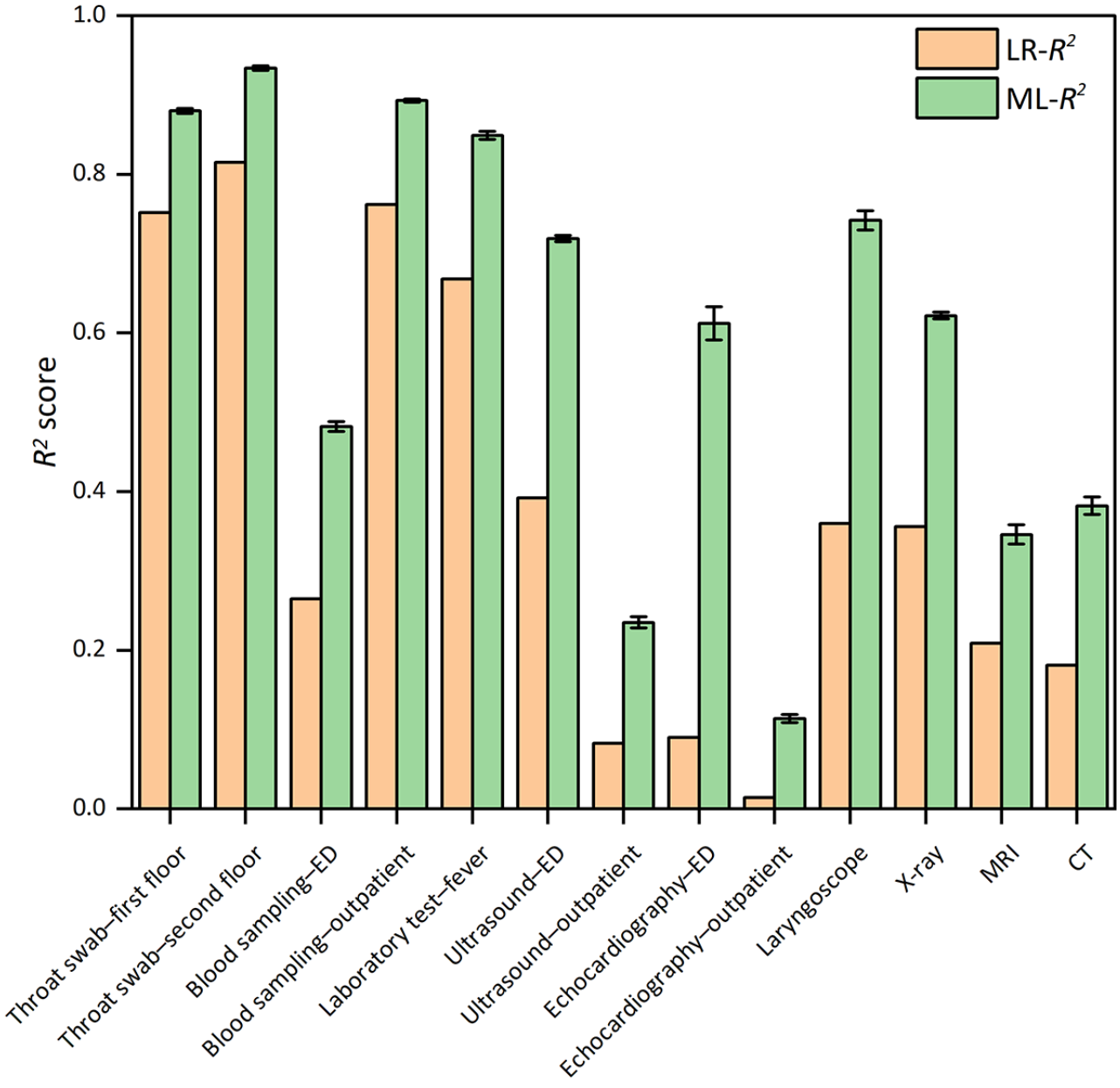
XSL•FO
RenderX

Figure 3. Root mean square error (RMSE) of different machine learning (ML) models for each medical task compared with linear regression (LR). CT: computed tomography; ED: emergency department; MRI: magnetic resonance imaging.



XSL•FO
RenderX

Figure 4. *R*2 score of different machine learning (ML) models for each medical task compared with linear regression (LR). CT: computed tomography; ED: emergency department; MRI: magnetic resonance imaging.



Feature Importance Analysis

On the basis of the QT principle, we ultimately selected the number of queuing patients, arrival rate, month, day, day of the week, and hour as independent features for predicting waiting time. To evaluate the contribution of each feature to the machine learning model, we computed SHAP values, which quantify the impact of individual features on the predicted waiting time. The mean SHAP value was used to rank each feature. The rankings of feature importance across different models are visualized in a heat map plot (Figure 5). Notably, for the majority of medical tasks, queue-related features, such as the number of queuing patients, emerged as the most influential predictor of waiting time, and the arrival rate was also expressed as another important feature for waiting time prediction. The details of the mean SHAP value are provided in Table S3 in Multimedia Appendix 1.

XSL•FO
RenderX

Figure 5. Heat map of feature importance ranking in different models (x-axis: predictive features; y-axis: medical tasks). The numbers in each cell represent the ranking order obtained based on the Shapley additive explanations values. CT: computed tomography; ED: emergency department; MRI: magnetic resonance imaging.



Discussion

Principal Findings

This study collected patient data from the Capital Center for Children's Health, Capital Medical University, spanning the period from November 1, 2024, to March 13, 2025, comprising a total of 230,864 records after data preprocessing. The distribution of waiting times for overall medical tasks followed an exponential pattern, with a median value of 4.817 minutes. Notably, peak periods in the average patient arrival rate and the average number of queuing patients were observed at 10:00 AM, 3:00 PM, and 8:00 PM. The waiting time exhibited a different pattern, with an earlier peak occurring at approximately 7:00 AM, along with 2 additional, smaller peaks around 12:00 PM and 8:00 PM, indicating the periods of highest congestion within the hospital. During model selection, tree-based algorithms such as RF, XGBoost, CART, and LightGBM demonstrated better accuracy in predicting waiting times for most medical task queues, while SVR and KNN can also be used as appropriate algorithms. Additionally, feature importance analysis revealed that the number of queuing patients was the most influential predictor of waiting time.

QT and TSA are classical approaches used to model and simulate queue dynamics in health care settings [22,23]. The application of QT requires the key input parameters, including the average arrival rate (λ) and average service rate (μ). Several queue parameters, including average waiting time (Wq), total time spent in the system (Ws), average QL (Ls), and average number of individuals waiting (Lq), can be calculated based on these inputs. For example, waiting time can be estimated using

XSL•FO
RenderX

the formula $Wq=\lambda\mu(\mu-\lambda)$ in an M/M/1 queue [24]. By simulating the queuing status and adjusting service rates, different operational scenarios can be modeled for service optimization. However, QT has several limitations when applied to the prediction of waiting times in real-world hospital settings. First, as demonstrated in our study, QT assumes that patient arrivals follow a Poisson process and that service times conform to exponential distributions. While the entire waiting time across all tasks approximates an exponential distribution in our study, this assumption does not universally hold for each medical task queue (the distribution of waiting times for each task was provided on our Github website). Second, QT estimates queue parameters relying on average arrival and service rates, which are dynamic in clinical practice. Because patient volume and service effectiveness are constantly changing, QT's static assumptions are inadequate for simulating operating situations in real time [25]. Third, accurately measuring the actual service rates for each medical task is challenging. As a result, we had to rely on estimations based on prior experience, which likely reduced the precision of the modeled parameters. Additionally, TSA, which involves modeling sequences of observations indexed over time, has been applied in previous studies to forecast ED attendances [8,23,26-28]. While effective at capturing periodic trends in patient volumes, TSA is more suited to predicting daily volumes rather than individual-level waiting times. Instead of depending on the strict presumptions of QT or TSA, machine learning models may directly use real-world waiting time data, enabling flexible, data-driven prediction.

This study assessed a variety of models for the waiting time prediction task to achieve the optimal predictive performance. In most scenarios, the tree-based model performed better than other models and demonstrated strong predictive capability. The RMSE of the models in our study was lower than that reported in previous studies [11,12,17,29]. Strong predictive performance was shown by high R^2 values for a number of tasks, including throat swab–second floor (R^2: mean 0.934, SD 0.003), blood sampling–outpatient (R^2: mean 0.893, SD 0.002), and throat swab–first floor (R^2: mean 0.880, SD 0.003). As widely recognized, machine learning models are generally more effective than LR in capturing nonlinear relationships [30], and tree-based models typically handle tabular data more efficiently than deep learning models [31]. However, for several tasks, such as MRI, CT, ultrasound-outpatient, and echocardiography-outpatient queues, we observed weak associations between the features and waiting time. We believe that the small sample sizes for these tasks may contribute to the poor model performance. A longer data collection period could help improve performance. Additionally, the 6 features used in our model may not be sufficient for predicting waiting times across all medical tasks. Some medical tasks may have inherent complexities or variability in waiting times that are not fully captured by the current available features. For example, the waiting time for outpatient ultrasound and MRI may depend on factors such as the age and urgency of the case or physician workload, which are difficult to quantify with the current feature set. While we aim to develop a lightweight prediction model with simplified features for easier deployment, it is clear that for certain tasks, feature engineering and the inclusion of additional variables—such as patient age, gender, department, and diagnosed diseases—are necessary to improve performance. These strategies can help improve the prediction models for underperforming tasks and support their future deployment.

Notably, the data used to train our predictive models were primarily derived from the first and fourth quarters of the year, when patient visit patterns are different from those observed in other periods. According to surveillance data from the Chinese Center for Disease Control and Prevention, the prevalence of acute respiratory infections is elevated between November 2024 and January 2025 [32-34]. This seasonal trend aligns with epidemiological surveillance data from the United States, which indicate a predominance of respiratory tract infections among children during the winter months [35,36]. Throughout this time, pediatric attendance was consistently high from late December to January (Figure S19 in Multimedia Appendix 1), with January having the most visits (44,808/145,739, 30.75%). This phenomenon is probably caused by a confluence of environmental and school-related factors: lower temperatures and humidity promote viral stability and propagation, while more interpersonal interaction in school facilitates the spread of infectious illnesses. Children's hospital visits are accelerated by these 2 factors. The most frequent combinations for pediatric patients who received multiple medical services during a single visit were related to acute respiratory infections, including throat swab → laryngoscopy → X-ray → echocardiography, throat swab → X-ray → blood sampling, and throat swab → blood sampling [37,38]. These findings imply that queue loads for various services are considerably impacted by fluctuations in illness occurrence. Although feature importance analysis suggests that the contribution of the month feature is not particularly important across different prediction models, this may be attributed to the short data collection period, which constrains the ability to capture long-term temporal trends. Therefore, seasonal demand fluctuations can also be considered when optimizing patient flow and resource allocation (Figure S20 in Multimedia Appendix 1). Strategies such as increasing the number of service windows during high-demand periods could alleviate queue burdens and improve operational efficiency. For example, at times when respiratory infections were most common at this institution, a second throat swab window was opened.

Limitations

This study has several limitations. First, our study is a single-center investigation that was mostly carried out at a pediatric hospital during the winter. The findings of this study might not apply to circumstances outside of a children's hospital due to the unique characteristics of the patients at this facility. Second, although medicine dispensing is a critical component of the clinical workflow, it was excluded from the analysis since the pharmacy did not have a procedure for patients to check in, making it impossible to calculate waiting times. Lastly, waiting times for various medical tasks were predicted using numerous models, which complicated the overall predictive framework and posed challenges for real-world implementation.

XSL•FO
RenderX

Conclusions

In conclusion, the distribution of patient waiting times exhibits 3 distinct peak periods. However, waiting time patterns differ markedly across various medical task queues, each displaying unique characteristics that do not align with the overall trend. Consequently, developing task-specific predictive models for each medical task queue can enhance prediction accuracy. Feature importance analysis reveals that although queue-related features are the most influential in predicting patient waiting time, time-based features might also contribute meaningfully and should be considered to further optimize hospital operational efficiency.

Acknowledgments

This work was supported by the Chinese Academy of Medical Sciences Innovation Fund for Medical Sciences (2021-I2M-1—056) and the Capital Institute of Pediatrics Foundation for Youths (QN-2024—37).

Data Availability

The datasets generated or analyzed during this study are available from the corresponding author on reasonable request.

Conflicts of Interest

None declared.

Multimedia Appendix 1
Distribution of waiting time, hyperparameters, and performance of the model.
[DOCX File, 5724 KB - medinform_v13i1e77297_app1.docx]

References

1. Vinci RJ. The pediatric workforce: recent data trends, questions, and challenges for the future. Pediatrics 2021 Jun;147(6):e2020013292. [doi: 10.1542/peds.2020-013292] [Medline: 33692163]
2. Russ CM, Gao Y, Karpowicz K, et al. The pediatrician workforce in the United States and China. Pediatrics 2023 Jun 1;151(6):e2022059143. [doi: 10.1542/peds.2022-059143] [Medline: 37158018]
3. Yan X, Yu J, Zhang P, Zhang J, Luo S, Yu Y. Innovative management strategies for addressing paediatric medical staff shortages in underdeveloped cities in developing countries. BMJ Lead 2024 Oct 24:leader-2023-000894. [doi: 10.1136/leader-2023-000894] [Medline: 39448256]
4. Anderson RT, Camacho FT, Balkrishnan R. Willing to wait?: the influence of patient wait time on satisfaction with primary care. BMC Health Serv Res 2007 Feb 28;7:31. [doi: 10.1186/1472-6963-7-31] [Medline: 17328807]
5. Doan Q, Wong H, Meckler G, et al. The impact of pediatric emergency department crowding on patient and health care system outcomes: a multicentre cohort study. CMAJ 2019 Jun 10;191(23):E627-E635. [doi: 10.1503/cmaj.181426] [Medline: 31182457]
6. Kwak DS, Park J. Analysis of the prognosis outcomes and treatment delay among ST-segment elevation myocardial infarction patients in emergency department based on the presence of symptoms suggestive of COVID-19. Int J Health Policy Manag 2024;13:8207. [doi: 10.34172/ijhpm.2024.8207] [Medline: 39099504]
7. Clinic queue management system: enhancing patient experience and streamlining operations. Qtech, Queuing System Pte Ltd. URL: https://qtechqueueingsystem.com/clinic-queue-management-system/#real-time-queue-updates [accessed 2025-04-28]
8. Kadri F, Harrou F, Chaabane S, Tahon C. Time series modelling and forecasting of emergency department overcrowding. J Med Syst 2014 Sep;38(9):107. [doi: 10.1007/s10916-014-0107-0] [Medline: 25053208]
9. Montazeri M, Multmeier J, Novorol C, Upadhyay S, Wicks P, Gilbert S. Optimization of patient flow in urgent care centers using a digital tool for recording patient symptoms and history: simulation study. JMIR Form Res 2021 May 21;5(5):e26402. [doi: 10.2196/26402] [Medline: 34018963]
10. Ang E, Kwasnick S, Bayati M, Plambeck EL, Aratow M. Accurate emergency department wait time prediction. M&SOM 2016 Feb;18(1):141-156. [doi: 10.1287/msom.2015.0560]
11. Gajanan A. Reducing wait time prediction in hospital emergency room: lean analysis using a random forest model. University of Tennessee. URL: https://trace.tennessee.edu/utk_gradthes/4722 [accessed 2025-09-08]
12. Chen JG, Li KL, Tang Z, Bilal K, Li KQ. A parallel patient treatment time prediction algorithm and its applications in hospital queuing-recommendation in a big data environment. IEEE Access 2016;4:1767-1783. [doi: 10.1109/ACCESS.2016.2558199]
13. Lin WC, Goldstein IH, Hribar MR, Sanders DS, Chiang MF. Predicting wait times in pediatric ophthalmology outpatient clinic using machine learning. AMIA Annu Symp Proc 2019;2019:1121-1128. [Medline: 32308909]

XSL•FO
RenderX

14. Chocron E, Cohen I, Feigin P. Delay prediction for managing multiclass service systems: an investigation of queueing theory and machine learning approaches. IEEE Trans Eng Manage 2024;71:4469-4479. [doi: 10.1109/TEM.2022.3222094]
15. Guo LL, Guo LY, Li J, et al. Characteristics and admission preferences of pediatric emergency patients and their waiting time prediction using electronic medical record data: retrospective comparative analysis. J Med Internet Res 2023 Nov 1;25:e49605. [doi: 10.2196/49605] [Medline: 37910168]
16. Hemaya SAK, Locker TE. How accurate are predicted waiting times, determined upon a patient's arrival in the emergency department? Emerg Med J 2012 Apr;29(4):316-318. [doi: 10.1136/emj.2010.106534] [Medline: 21429872]
17. Walker KJ, Jiarpakdee J, Loupis A, et al. Predicting ambulance patient wait times: a multicenter derivation and validation study. Ann Emerg Med 2021 Jul;78(1):113-122. [doi: 10.1016/j.annemergmed.2021.02.010] [Medline: 33972127]
18. Curtis C, Liu C, Bollerman TJ, Pianykh OS. Machine learning for predicting patient wait times and appointment delays. J Am Coll Radiol 2018 Sep;15(9):1310-1316. [doi: 10.1016/j.jacr.2017.08.021] [Medline: 29079248]
19. Camacho F, Anderson R, Safrit A, Jones AS, Hoffmann P. The relationship between patient's perceived waiting time and office-based practice satisfaction. N C Med J 2006;67(6):409-413. [Medline: 17393701]
20. Thiongane M, Chan W, L'Ecuyer P. New history-based delay predictors for service systems. Presented at: 2016 Winter Simulation Conference (WSC); Dec 11-14, 2016; Washington, DC, USA p. 425-436. [doi: 10.1109/WSC.2016.7822109]
21. Lundberg SM, Lee S. A unified approach to interpreting model predictions. : Curran Associates Inc Presented at: In Proceedings of the 31st International Conference on Neural Information Processing Systems (NIPS'17); Dec 4-9, 2017; Red Hook, NY p. 4768-4777.
22. Joseph JW. Queuing theory and modeling emergency department resource utilization. Emerg Med Clin North Am 2020 Aug;38(3):563-572. [doi: 10.1016/j.emc.2020.04.006] [Medline: 32616279]
23. Juang WC, Huang SJ, Huang FD, Cheng PW, Wann SR. Application of time series analysis in modelling and forecasting emergency department visits in a medical centre in Southern Taiwan. BMJ Open 2017 Dec 1;7(11):e018628. [doi: 10.1136/bmjopen-2017-018628] [Medline: 29196487]
24. Yang H. Research on M/M/1 queue of exponential departure intensity. Math Probl Eng 2022 Aug 19;2022:1-7. [doi: 10.1155/2022/6139847]
25. Winston WL, Goldberg JB. Operations Research: Applications and Algorithms: Duxbury Press; 2004, Vol. 3.
26. Jones SA, Joy MP, Pearson J. Forecasting demand of emergency care. Health Care Manag Sci 2002 Nov;5(4):297-305. [doi: 10.1023/a:1020390425029] [Medline: 12437279]
27. Abdel-Aal RE, Mangoud AM. Modeling and forecasting monthly patient volume at a primary health care clinic using univariate time-series analysis. Comput Methods Programs Biomed 1998 Jun;56(3):235-247. [doi: 10.1016/s0169-2607(98)00032-7] [Medline: 9725649]
28. Milner PC. Ten-year follow-up of ARIMA forecasts of attendances at accident and emergency departments in the Trent region. Stat Med 1997 Sep 30;16(18):2117-2125. [doi: 10.1002/(sici)1097-0258(19970930)16:18<2117::aid-sim649>3.0.co;2-e] [Medline: 9308136]
29. Rastpour A, McGregor C. Predicting patient wait times by using highly deidentified data in mental health care: enhanced machine learning approach. JMIR Ment Health 2022 Aug 9;9(8):e38428. [doi: 10.2196/38428] [Medline: 35943774]
30. Kuo YH, Chan NB, Leung JMY, et al. An integrated approach of machine learning and systems thinking for waiting time prediction in an emergency department. Int J Med Inform 2020 Jul;139:104143. [doi: 10.1016/j.ijmedinf.2020.104143] [Medline: 32330853]
31. Grinsztajn L, Oyallon E, Varoquaux G. Why do tree-based models still outperform deep learning on tabular data? arXiv. Preprint posted online on Jul 18, 2022 URL: https://arxiv.org/abs/2207.08815
32. China National Influenza Center homepage. China National Influenza Center. URL: https://ivdc.chinacdc.cn/cnic/ [accessed 2025-09-08]
33. National sentinel surveillance of acute respiratory infectious diseases. Chinese Center for Disease Control and Prevention. URL: https://www.chinacdc.cn/jksj/jksj04_14275/ [accessed 2025-09-08]
34. Kang L, Huang JL. The impact of infectious disease outbreaks on the pediatric healthcare system and countermeasures. J Clin Pediatr 2024;42(6):475-479. [doi: 10.12372/jcp.2024.24e0432]
35. Schrijver TV, Brand PLP, Bekhof J. Seasonal variation of diseases in children: a 6-year prospective cohort study in a general hospital. Eur J Pediatr 2016 Apr;175(4):457-464. [doi: 10.1007/s00431-015-2653-y] [Medline: 26494134]
36. Lipsett SC, Monuteaux MC, Fine AM. Seasonality of common pediatric infectious diseases. Pediatr Emerg Care 2021 Feb 1;37(2):82-85. [doi: 10.1097/PEC.0000000000001496] [Medline: 29768293]
37. China Medicine Education Association Committee on Pediatrics, The Subspecialty Group of Respiratory Diseases, The Society of Pediatrics, Chinese Medical Association, Chinese Medical Doctor Association Committee on Respirology Pediatrics. Guideline for diagnosis, treatment and prevention of influenza in children (medical version, 2024). Chin J Appl Clin Pediatr 2024;39(12):881-895. [doi: 10.3760/cma.j.cn101070-20241105-00719]
38. National Health Commission of the People's Republic of China. Guidelines for diagnosis and treatment of Mycoplasma pneumonae pneumonia in children (2023 Edition). Chin J Ration Drug Use 2023;3(330):16-24. [doi: 10.3969/j.issn.2096-3327.2023.03.003]

XSL•FO
RenderX

Abbreviations

CART : classification and regression tree
CT: computed tomography
ED: emergency department
KNN: k-nearest neighbor
LightGBM: light gradient boosting machine
LR: linear regression
MAE: mean absolute error
MLP: multilayer perceptron
MRI: magnetic resonance imaging
MSE: mean square error
QL: queue length
QT: queue theory
RF : random forest
RMSE: root mean square error
SHAP: Shapley additive explanations
SVR: support vector regression
TSA: time series analysis
XGBoost: extreme gradient boosting

Edited by A Benis; submitted 11.05.25; peer-reviewed by G Adewumi, P Shingru, X Ding; revised version received 25.07.25; accepted 04.08.25; published 29.09.25.

Please cite as:
Guo LL, Tang R, Wang JY, Zheng S, Zeng Y, Hou J, Dong MC, Li J, Cui Y
Predicting Waiting Times for Medical Tasks in a Pediatric Hospital Using Machine Learning: Comprehensive, Retrospective, Real-World Study
JMIR Med Inform 2025;13:e77297
URL: https://medinform.jmir.org/2025/1/e77297
doi:10.2196/77297

© Lin Lin Guo, Rui Tang, Jia Yang Wang, Si Zheng, Yin Zeng, Jun Hou, Mo Chen Dong, Jiao Li, Ying Cui. Originally published in JMIR Medical Informatics (https://medinform.jmir.org), 29.9.2025. This is an open-access article distributed under the terms of the Creative Commons Attribution License (https://creativecommons.org/licenses/by/4.0/), which permits unrestricted use, distribution, and reproduction in any medium, provided the original work, first published in JMIR Medical Informatics, is properly cited. The complete bibliographic information, a link to the original publication on https://medinform.jmir.org/, as well as this copyright and license information must be included.

XSL•FO
RenderX

Machine Learning and Shapley Additive Explanations Value Integration for Predicting the Prognostic of Anti-N-Methyl-D-Aspartate Receptor Encephalitis: Model Development and Evaluation Study

Jia Wang[1*], Dr Med; Haotian Wu[2*], MMed; Han Cai[2], MMed; YingXiang Wang[1], MMed; Jian Gu[1], MMed

[1]Department of Gynecology, Third Affiliated Hospital of Sun Yat-sen University, 600 Tianhe Road, Tianhe District, Guangdong Province, Guangzhou, China

[2]Department of Neurology, Third Affiliated Hospital of Sun Yat-sen University, Guangzhou, China

[*]these authors contributed equally

Corresponding Author:
Jian Gu, MMed
Department of Gynecology, Third Affiliated Hospital of Sun Yat-sen University, 600 Tianhe Road, Tianhe District, Guangdong Province, Guangzhou, China

Abstract

Background: Anti-N-methyl-D-aspartate receptor (NMDAR) encephalitis is a rare disease with no accurate prognostic tools to predict the prognosis of patients.

Objective: This study aims to develop an interpretable machine learning model using real-world clinical data to guide personalized therapeutic strategies.

Methods: This retrospective cohort study analyzed 140 patients with NMDAR encephalitis treated at the Third Affiliated Hospital of Sun Yat-sen University (2015 - 2024). Feature selection was done using recursive feature elimination. The model was constructed by 3 machine learning algorithms: decision tree, random forest (RF), and extreme gradient boosting. Mean squared error, root-mean-squared error, R^2 (coefficient of determination), mean absolute error, and mean absolute percentage error were used to evaluate the model performance. Finally, the optimal model was interpreted via Shapley Additive Explanations (SHAP) and deployed as a web application using the Flask framework.

Results: The median age of patients with anti-NMDAR encephalitis was 23 (IQR 18-31.8) years. The median Clinical Evaluation Scale for Autoimmune Encephalitis score at acute onset was 11 (IQR 6-16). After preprocessing, 20 features, including 4 demographic characteristics, 3 clinical characteristics, 11 laboratory parameters, and 2 neuroimaging characteristics, were selected. The RF demonstrated superior accuracy in predicting the prognosis (mean squared error=11.01; root-mean-squared error=3.32; R^2=0.71; mean absolute error=2.49; mean absolute percentage error=0.48). SHAP analysis identified admission to the intensive care unit (mean |SHAP value|=1.65), initial symptoms-memory deficits (0.69), and uric acid (0.53) as the most important prognostic predictors.

Conclusions: We developed and validated an interpretable RF-based prognostic model for NMDAR encephalitis. The web-deployed tool enables real-time risk stratification, facilitating clinical decision-making and personalized therapeutic interventions for clinicians.

(JMIR Med Inform 2025;13:e75020) doi:10.2196/75020

KEYWORDS

anti-N-methyl-D-aspartate receptor (NMDAR) encephalitis; machine learning; SHAP; prognosis; prediction

Introduction

Anti-N-methyl-D-aspartate receptor (NMDAR) encephalitis represents more than 80% of autoimmune encephalitis (AE) cases. Its pathogenesis is closely linked to synaptic plasticity impairment mediated by autoantibodies targeting the NMDAR GluN1 subunit [1,2]. These antibodies induce limbic system dysfunction and characteristic neuropsychiatric manifestations [3]. While first-line immunotherapy has markedly improved survival rates, up to 30% - 47% of patients continue to experience cognitive deficits, psychiatric symptoms, or functional disabilities [4-6]. Consequently, the development of a dynamic prognostic evaluation system is critical for guiding individualized treatment strategies.

Since the initial report of NMDAR encephalitis in 2007, researchers have investigated the prognostic value of various

XSL•FO
RenderX

biomarkers. Current evidence indicates that cerebrospinal fluid antibody titers, extreme delta brush on electroencephalogram, and acute-phase inflammatory markers may correlate with disease severity [5,7-9]. However, single-dimensional biomarkers exhibit insufficient predictive power. Currently, there is a lack of integrated multidimensional data for constructing models to predict patient outcomes. Existing prediction models [10-12] predominantly rely on the modified Rankin Scale [13] and are limited in assessing the cognitive-mental dimension of NMDAR encephalitis. Moreover, traditional logistic regression approaches fail to adequately analyze complex nonlinear interactions among predictors, thereby reducing their clinical applicability.

Machine learning (ML) offers transformative potential for integrating and analyzing complex clinical data. In contrast to traditional statistical methods, ML algorithms can identify intricate feature interactions and enhance predictive performance in small-sample rare disease cohorts [14]. This capability has been successfully demonstrated in neurodegenerative diseases and tumor prognosis prediction by enhancing the feature representation of small-sample datasets. However, no study has systematically applied ML for prognostic prediction in NMDAR encephalitis.

The objective of this study is to integrate clinical features, neuroimaging findings, serological markers, and Clinical Evaluation Scale for Autoimmune Encephalitis (CASE) [15] scores to construct a prognostic prediction model for NMDAR encephalitis based on ML and identify early prognostic signatures through Shapley Additive Explanations (SHAP)–driven feature interpretability. Furthermore, a web-based clinical tool was developed to deploy the model, enabling clinicians to use it directly for prognostic predictions and to plan interventions (eg, escalation to second-line therapy or multiple immune combinations within a critical 4-week postsymptom window).

Methods

Study Design

Data for this retrospective study were collected from the Third Affiliated Hospital of Sun Yat-sen University from 2015 to 2024. This study was conducted in accordance with the Transparent Reporting of a Multivariable Prediction Model for Individual Prognosis or Diagnosis (TRIPOD) guidelines [16]. Informed consent was obtained from all participants. This study was approved by the ethics committee of the Third Affiliated Hospital of Sun Yat-sen University (II2024-370-01). This study comprised 3 phases: (1) cohort selection, (2) variable optimization and model development, and (3) validation and clinical translation tools.

Study Population

All patients underwent comprehensive evaluations, including neuroimaging, electroencephalogram, cerebrospinal fluid (CSF) analysis, and tumor screening.

Eligibility Criteria

The inclusion and exclusion criteria are listed in Textbox 1.

Textbox 1. Inclusion and exclusion criteria.

Inclusion criteria

- Age ≥10 years at disease onset.
- Diagnosis of anti-N-methyl-D-aspartate receptor encephalitis based on established criteria.
- Diagnosis before immunotherapy.

Exclusion criteria

- Concurrent central nervous system neoplasms or noninfectious inflammatory disorders.
- Documented central nervous system infections (bacterial, fungal, parasitic, or tuberculous).
- Secondary septic encephalopathy or systemic inflammatory response syndrome–associated encephalopathy.
- Coexisting serum or cerebrospinal fluid autoantibodies associated with other autoimmune encephalitides.
- Incomplete clinical documentation.

Data Collection

Data were extracted from electronic medical records. Standardized variables included the following:

1. Demographics: age at disease onset, gender, occupation, and BMI.
2. Clinical characteristics: (1) prodromal symptoms (fever, headache, and dizziness) and (2) initial symptoms (psychiatric abnormalities, seizures, altered consciousness, and memory deficits).
3. Critical care interventions: intensive care unit (ICU) admission and mechanical ventilation requirement.
4. Laboratory parameters: CSF or serum anti-NMDAR antibody titers. CSF samples were analyzed using a cell-based assay by a trained specialist in a laboratory with experience in interpreting these assays. (1) Sex hormone tests include luteinizing hormone, follicle-stimulating hormone, estradiol, progestogen, and testosterone. (2) Hematological and biochemical analyses: white blood cell count, neutrophils, lymphocytes, monocytes, uric acid (UA), erythrocyte sedimentation rate, C-reactive protein, and high-density lipoprotein cholesterol.
5. Neuroimaging: Baseline magnetic resonance imaging (MRI) or electroencephalogram findings, including lesion quantity,

XSL•FO
RenderX

and MRI. Analysis was performed by a senior neuroradiologist and neurologist using 1.5/3.0 Tesla scanners with T1-weighted, T2-weighted, and FLAIR sequences. All electroencephalogram data were recorded according to the international 10‐20 system using an electroencephalogram Digi Track (ELMIKO) with 19 electrodes. Tumor details (if applicable) included tumor size (mean of longitudinal and transverse diameters on imaging) and number of tumors.

Evaluation Prognosis and Definitions

Outcome metric and clinical severity were quantified using the CASE scale, a validated 9-domain instrument assessing (seizures, memory deficits, psychiatric symptoms, consciousness, speech, motor or dystonia, gait or ataxia, brainstem dysfunction, muscle strength; total score: 0‐27). Prognostic stratification was defined as favorable: 0‐4 (minimal residual symptoms), moderate: 5‐9 (partial functional impairment), and poor: 10‐27 (severe disability). Lower CASE scores at follow-up indicated improved functional recovery.

Data Preprocessing and Feature Engineering

Categorical variables were coded by labels' encoding, while continuous variables were standardized using the Standard Scaler to mitigate feature scale bias. From an initial pool of 47 candidate predictors (selected via systematic literature review and clinical consensus), recursive feature elimination (RFE) with random forest (RF) (500 trees, Gini impurity) was applied. Features exceeding the importance threshold (P>.01) were retained. The threshold of 0.01 was empirically validated as optimal for maximizing cross-validation accuracy. This value consistently yielded peak performance in predicting prognosis across all candidate models (decision tree [DT], RF, extreme gradient boosting [XGBoost]), balancing feature retention with model generalizability. To rigorously mitigate randomness in RFE with a cross-validation workflow, we implemented a dual-strategy approach: (1) stratified cross-validation. Instead of relying on a single random train-test split, we used stratified 5-fold CV throughout the RFE process. (2) To test the stability of the selected feature set, we repeated the RFE with a cross-validation process multiple times with different random seeds (random_state=42). We then analyzed the frequency with which each feature was selected. Features that consistently appeared across multiple runs were considered more robust and were prioritized.

Model Development and Validation

The dataset was strategically partitioned through random stratified sampling into a training set (80%, n=112) and a validation set (20%, n=28). The training set was exclusively used for model development, while the validation set served as an independent cohort for performance evaluation. The 3 ML algorithms, including RF, XGBoost, and DT, were used to construct the prediction model of NMDAR. Benchmarking is an important way to systematically evaluate and compare the performance of ML models. This process involves evaluating multiple models on standardized datasets and using consistent evaluation metrics to ensure fair comparisons. In this study, model performance was assessed using mean squared error (MSE), root-mean-squared error (RMSE), coefficient of determination (R^2), mean absolute error, and mean absolute percentage error. The optimal model was selected based on minimal RMSE in validation. A 5-fold cross-validation was used to verify the stability of the model (Table 1).

Table . Five-fold cross-validation of the model.

Number of folds	MSE[a]	RMSE[b]	R^2[c]	MAE[d]	MAPE[e]
1	10.52	3.24	0.73	2.41	0.46
2	11.38	3.37	0.69	2.57	0.5
3	10.79	3.28	0.72	2.46	0.47
4	11.62	3.41	0.68	2.63	0.51
5	10.95	3.31	0.71	2.49	0.48
Average	11.052	3.322	0.706	2.512	0.484

[a]MSE: mean square error.

[b]RMSE: root-mean-squared error.

[c]R^2: coefficient of determination.

[d]MAE: mean absolute error.

[e]MAPE: mean absolute percentage error.

Model Interpretation and Network Application

The ML has difficulty explaining the contribution of each feature due to its black-box principle. Interpretability denotes elucidating how ML models produce results. To elucidate feature contributions, SHAP values were used to quantify and interpret feature importance in the best-performing model. The algorithm provides a measure of feature importance across the model. Local interpretability was visualized via force plots, while global patterns were assessed through mean |SHAP values|.

Network Application

Network application was deployed using Flask 2.3.2 backend with REST API, dynamic input forms aligned with selected predictors, real-time SHAP plot generation, and risk stratification output (probability scores with 95% CIs). This tool operates independently from any model and uses input

XSL•FO
RenderX

predictor variables for result interpretation while enabling predictions for individual cases.

Statistical Analysis

The Shapiro–Wilk normality test was performed to assess the data normality. Continuous variables are reported as medians with interquartile ranges (IQRs) for skewed distributed variables. Categorical variables are reported as frequency and percentage.

All statistical analyses were performed using IBM SPSS Statistics 22 (SPSS Inc). The predictive model construction and graphical representations were implemented using Python V3.7 (Python Software Foundation) and Prism 10.0 (GraphPad Software), respectively.

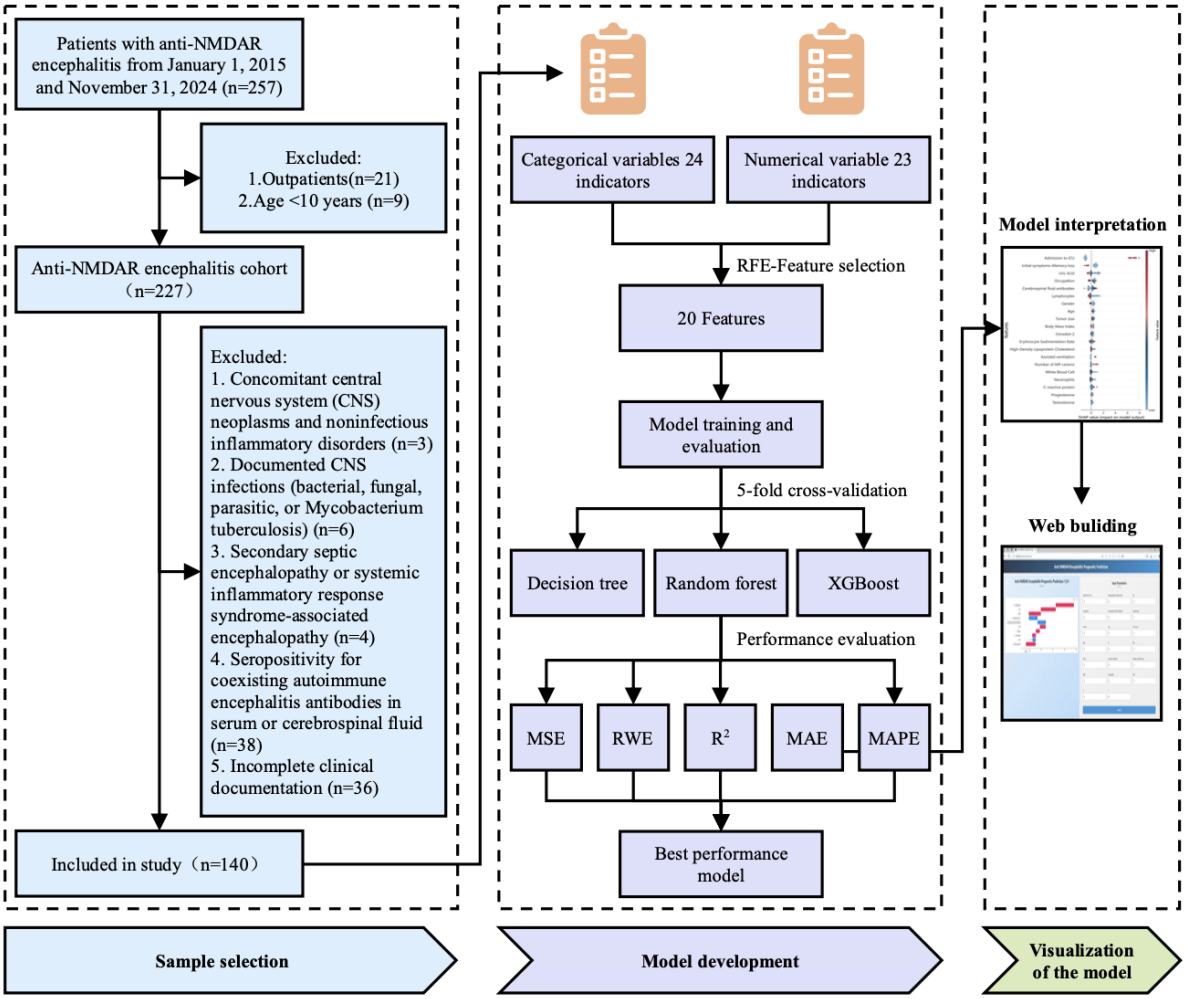
Ethical Considerations

The Ethics Committee of the Third Affiliated Hospital, Sun Yat-sen University (II2024-370–01) gave ethical approval on December 30, 2024. Informed consent was waived by the committee, as the study involved retrospective analysis of anonymized data and did not include any identifiable personal information. All procedures were conducted in accordance with the ethical standards of the institutional and national research committees and with the principles outlined in the Declaration of Helsinki. We ensured that the privacy and confidentiality of all participants were strictly maintained; data were fully anonymized before analysis, and no individual-level identifiers were collected, stored, or reported. No compensation was provided to participants, as the study did not involve direct interaction with human participants.

Results

A retrospective cohort of 257 patients diagnosed with anti-NMDAR encephalitis was identified from the electronic medical records of the Third Affiliated Hospital of Sun Yat-sen University (January 2014-November 2024). According to the inclusion and exclusion criteria, 140 patients were included in the final analysis (Figure 1).

Figure 1. Flowchart of the study strategy. Anti-NMDAR: anti-N-methyl-D-aspartate receptor; MAE: mean absolute error; MAPE: mean absolute percentage error; MSE: mean square error; R^2: coefficient of determination; XGBoost: extreme gradient boosting.



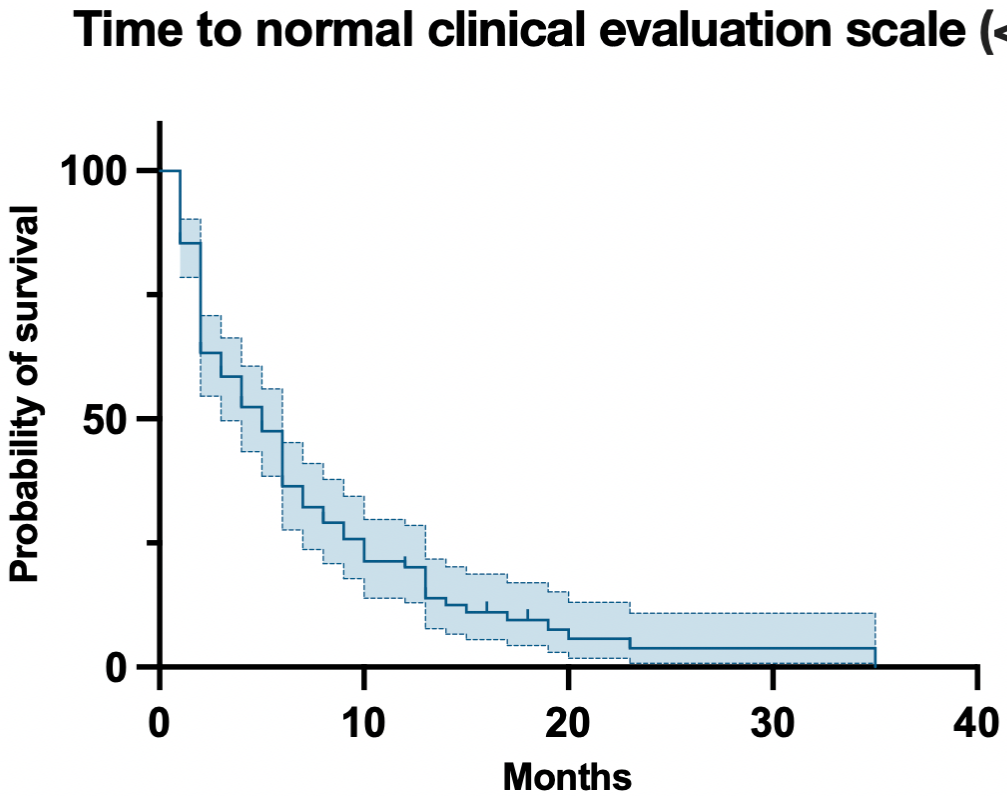
Population Characteristics

Among the final cohort (median follow-up 8, IQR 2 - 23 months), 102 of 140 (72.9%) were female patients, with a median age of 22 (IQR 17 - 30) years; of these, 50 (35.7%) were students. Pulmonary infections emerged as the most frequent comorbidity, occurring in 54 of 140 (38.6%) patients, whereas fever was the leading prodromal symptom, appearing in 41 (29.3%) patients. NMDAR encephalitis–associated diffuse slow waves and delta brush patterns in electroencephalography

XSL•FO
RenderX

were observed in 10% (14/140) and 2.1% (3/140) of cases, respectively. Among the 140 patients, 30 (21.4%) had tumors (28 benign teratomas and 2 malignancies). Median acute-phase CASE score was 11 (IQR 6 - 16), improving to 0 (IQR 0 - 1) at 1-year follow-up (Figure 2). Full demographic and clinical characteristics are detailed in Table 2.

Figure 2. Recovery time of patients with anti-NMDAR encephalitis. NMDAR: anti-N-methyl-D-aspartate receptor.



XSL•FO
RenderX

Table . Clinical data baseline table of study subjects.

Predictive variables	Patients with NMDAR[a]
Age (years), median (IQR)	23 (18-31.8)
BMI (kg/m^2), median (IQR)	21 (18-23.3)
Sex, n (%)	
Female	102 (72.9)
Male	38 (27.1)
Occupations, n (%)	
Student	50 (35.7)
Mental work	46 (32.9)
Manual labor	3 (2.1)
Others	41 (29.3)
Past medical history, n (%)	
None	126 (90)
Hypertension	1 (0.7)
Diabetes	3 (2.1)
Hepatitis B	4 (3)
Thyroid diseases	3 (2.1)
Tuberculosis	1 (0.7)
Syphilis	1 (0.7)
Tumors	1 (0.7)
Comorbidity, n (%)	
Pulmonary infection	54 (38.6)
Liver function damage	18 (12.9)
Thyroid lesions	11 (7.9)
Dysglycemia	15 (10.7)
Bleeding diseases	9 (6.4)
Respiratory failure	6 (4.3)
Urinary tract infections	6 (4.3)
Prodromal symptoms, n (%)	
Fever	41 (29.3)
Headache	29 (20.7)
Dizziness	5 (3.6)
Initial symptoms, n (%)	
Mental and behavioral abnormalities	99 (70.7)
Epilepsy	49 (35)
Disorders of consciousness	4 (2.9)
Memory loss	8 (5.7)
CSF[b] indicators, median (IQR)	
WBC[c]	8 (2-28)
Protein	0.25 (0.17-0.35)
NMDAR antibodies	10 (10-32)
Blood indicators, median (IQR)	

XSL•FO
RenderX

Predictive variables	Patients with NMDAR[a]
NMDAR antibodies	10 (10-100)
Lymphocytes	1.35 (0.94-2.09)
Neutrophils	6.98 (4.75-9.88)
Monocytes	0.66 (0.43-0.86)
ESR[d]	14 (8-32)
CRP[e]	1.9 (0.6-5.3)
UA[f]	248 (152-335)
25-OHD[g]	44 (22.1-60)
IL-6[h]	5.9 (1.5-11.5)
HDL-C[i]	1.12 (0.89-1.33)
Testosterone	1.1 (0.74-1.6)
Follicle-stimulating hormone	3.51 (2.37-4.8)
Progestogen	0.7 (0.4-1.9)
Luteinizing hormone	2.89 (0.61-5.84)
Estradiol	96.5 (60.7-194)
ICU[j] admission, n (%)	29 (20.7)
Mechanical ventilation, n (%)	26 (18.6)
EEG[k], n (%)	
Normal	24 (17.1)
Mild abnormality	27 (19.3)
Moderate abnormality	19 (13.6)
Severe abnormality	13 (9.3)
Diffuse slow waves	14 (10)
Delta brush	3 (2.1)
Epileptic waves	10 (7.1)
Number of MR[l] lesions, median (IQR)	0 (0-2)
Tumor markers, n (%)	
Negative	121 (86.4)
Slightly elevated	14 (10)
Significantly elevated	5 (3.6)
Combined with tumor, n (%)	
Yes	30 (21.4)
No	110 (78.6)
Number of tumors, n (%)	
1	28 (20)
2	2 (1.4)
Tumor size, median (IQR)	35.5 (19-53.5)

XSL•FO
RenderX

Predictive variables	Patients with NMDAR[a]
Duration of follow-up (months), median (IQR)	8 (2-23)

[a]NMDAR: anti-N-methyl-D-aspartate receptor.
[b]CSF: cerebrospinal fluid.
[c]WBC: white blood cell.
[d]ESR: erythrocyte sedimentation rate.
[e]CRP: C-reactive protein.
[f]UA: uric acid.
[g]25-OHD: 25-hydroxyvitamin D.
[h]IL-6: Interleukin-6.
[i]HDL-C: high-density lipoprotein cholesterol.
[j]ICU: intensive care unit.
[k]EEG: electroencephalogram.
[l]MR: magnetic resonance.

Variable Screening

This study examined predictors that longitudinally affect disease severity in the anti-NMDAR encephalitis observational cohort. The CASE score provides more insight into specific AE-related symptoms at onset, allowing for longitudinal assessment of these symptoms [17]. The predictor variables identified by RF were selected as common elements in the development of the prediction model. Select the importance threshold (P>.01) in the training set; these features were included in our study to construct a reduced feature set (selected features). A total of 20 of the 47 features were selected for inclusion in the ML model: 4 demographic characteristics (age, gender, BMI, and occupation), 3 clinical characteristics (admission to ICU, mechanical ventilation, initial symptoms-memory deficits), 11 laboratory parameters (UA, erythrocyte sedimentation rate, C-reactive protein, high-density lipoprotein cholesterol, CSF antibodies, neutrophils, estradiol, white blood cell, progestogen, and testosterone), and 2 neuroimaging characteristics (number of MR lesions and tumor size). The association between each candidate predictor is shown in Multimedia Appendix 1.

Model Development and Performance Comparison

The prognostic performance of the selected features was systematically evaluated using 3 ML algorithms: RF, XGBoost, and DT. As detailed in Table 3, the RF model demonstrated superior discriminative capacity across all evaluation metrics (mean squared error=11.01, RMSE=3.32, R^2=0.71, mean absolute error=2.49, and mean absolute percentage error=0.48). The RF model, selected as the optimal prognostic tool based on minimal RMSE, showed advantages in predicting functional outcomes of NMDAR encephalitis (the model parameters are shown in Table 4). A 5-fold cross-validation was used to verify the stability of the model (Table 1).

Table . Predictive performances of the 3 machine learning models.

Model	MSE[a]	RMSE[b]	R^2[c]	MAE[d]	MAPE[e]
RF[f]	11.01	3.32	0.71	2.49	0.48
XGBoost[g]	14.98	3.87	0.61	2.87	0.53
DT[h]	26.88	5.18	0.29	3.92	0.59

[a]MSE: mean square error.
[b]RMSE: root-mean-squared error.
[c]R^2: coefficient of determination.
[d]MAE: mean absolute error.
[e]MAPE: mean absolute percentage error.
[f]RF: random forest.
[g]XGBoost: extreme gradient boosting.
[h]DT: decision tree.

XSL•FO
RenderX

Table . Parameters of machine learning models.

Model and parameters	Values
RF[a]	
n_estimators	150
criterion	“gini”
max_depth	None
min_samples_split	2
min_samples_leaf	1
max_features	“sqrt”
bootstrap	True
random_state	42
XGBoost[b]	
n_estimators	150
learning_rate	0.1
max_depth	3
objective	“binary:logistic”
subsample	1.0
colsample_bytree	1.0
gamma	0
reg_alpha	0
reg_lambda	1
random_state	42
use_label_encoder	False
eval_metric	“logloss”
DT[c]	
criterion	“gini”
max_depth	None
min_samples_split	2
min_samples_leaf	1
max_features	None
random_state	42

[a]RF: random forest.

[b]XGBoost: extreme gradient boosting.

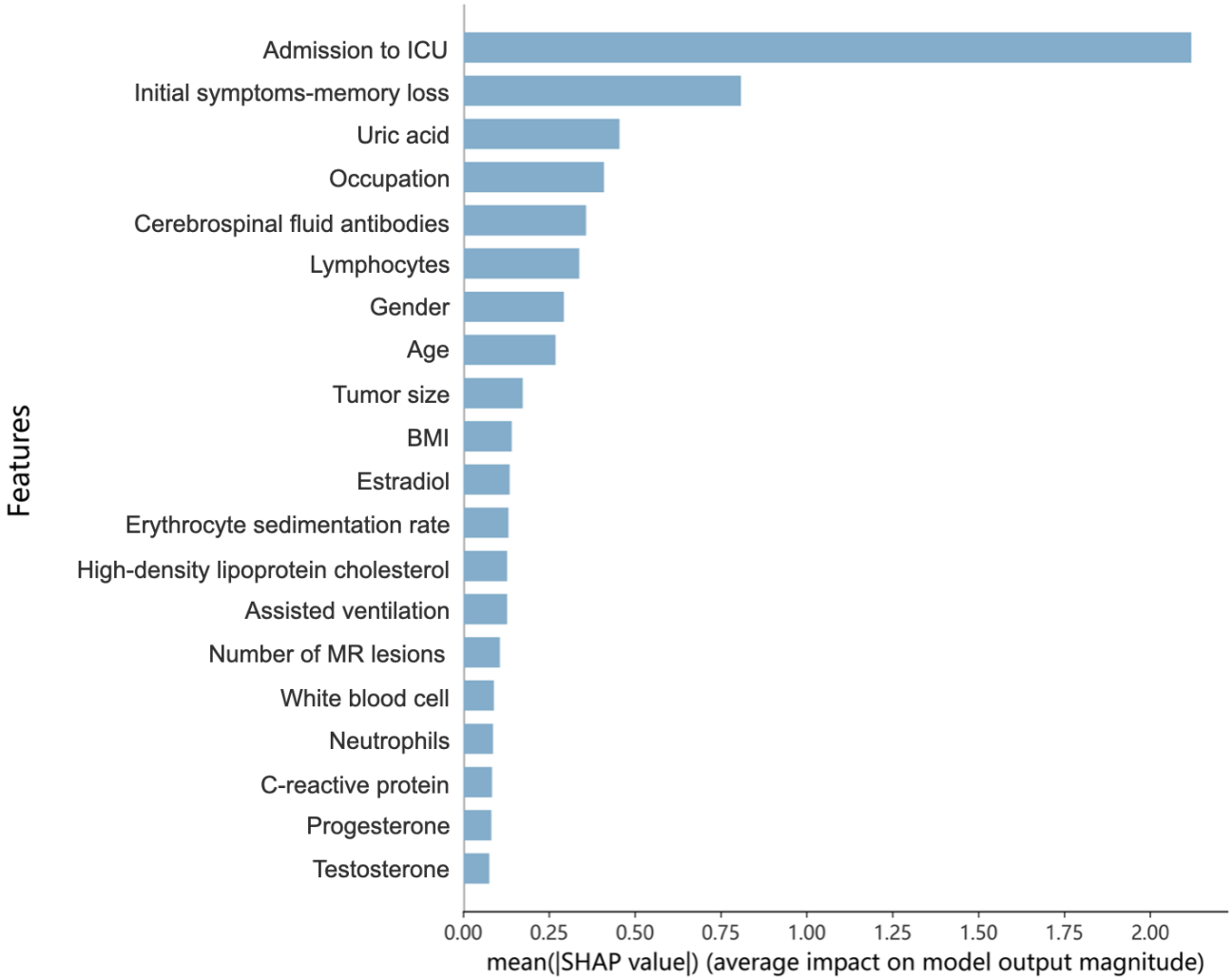
[c]DT: decision tree.

Interpretation of the Model

To elucidate feature contributions and interpret model predictions, we used SHAP analysis, a robust game-theoretic approach that quantifies the relative importance of each predictive feature (Figures 3 and 4). SHAP values represent the magnitude and directionality of each predictor’s influence on outcome probability, where positive values indicate increased disability risk. This visualization demonstrates how key features interact to determine individualized prognosis, enabling clinicians to prioritize modifiable risk factors. The summary plot (Figure 5) uses personalized feature attribution to represent range and distribution characteristics. We can directly see the impact of each feature on the prediction of prognostic features in NMDAR. Red to blue represents the eigenvalue from high to low. The thickness of the line represents the sample distribution.

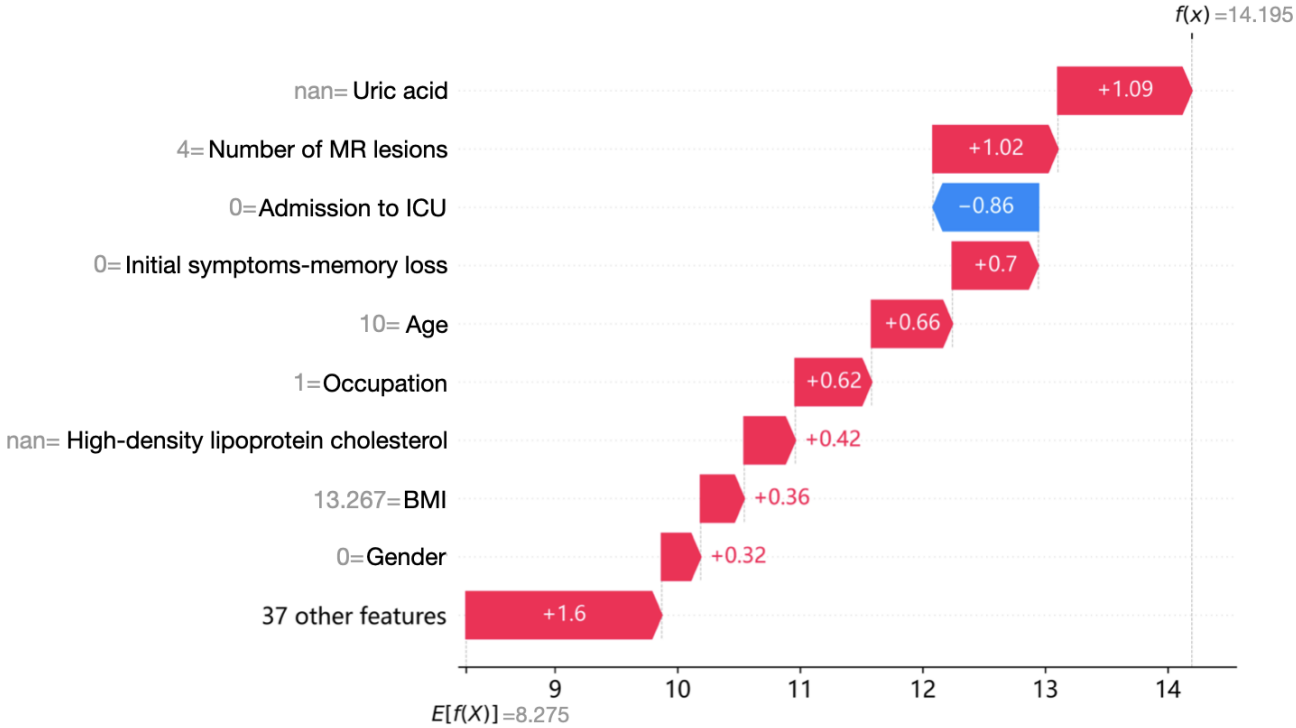
XSL•FO
RenderX

Figure 3. SHAP interpretation of the random forest model-importance score ranking of the model prediction characteristics. ICU: intensive care unit; RF: random forest.



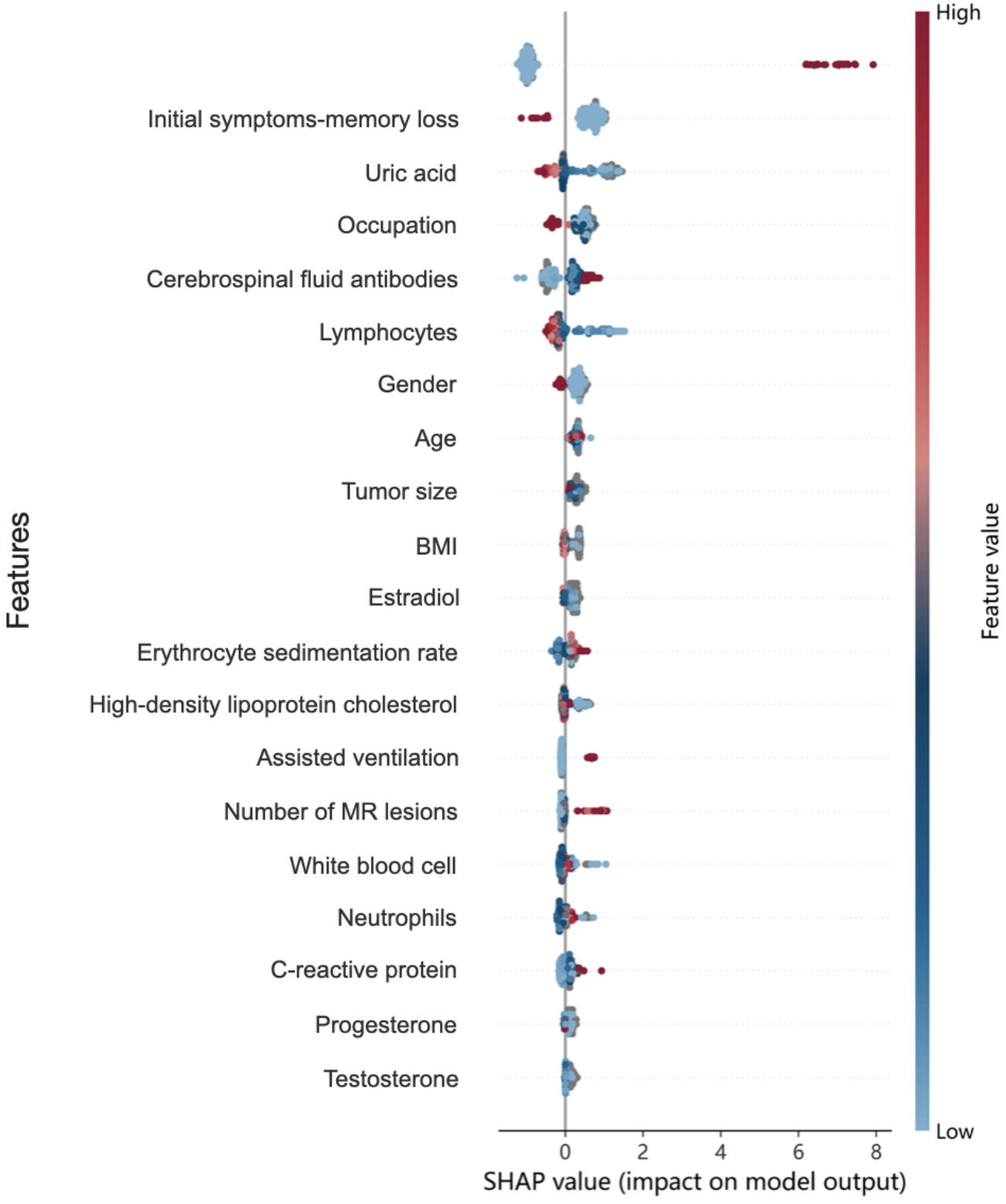
XSL•FO
RenderX

Figure 4. Shapley Additive Explanations interpretation of the random forest model-individualized prognostic impact assessment in anti-NMDAR encephalitis. ICU: intensive care unit; NMDAR: N-methyl-D-aspartate receptor; RF: random forest.



XSL•FO
RenderX

Figure 5. Shapley Additive Explanations summary plots of a 20-feature RF prediction model. ICU: intensive care unit; RF: random forest.



In the optimal performing RF model, the top 3 predictive features for prognostic predictors of NMDAR were admission to ICU (mean |SHAP value|=1.65), initial symptoms-memory loss (0.69), and UA (0.53). Other significant predictors included occupation, cerebrospinal fluid antibody titer, lymphocytes, sex, age, tumor size, BMI, estradiol, erythrocyte sedimentation rate, high-density lipoprotein cholesterol, need for assisted ventilation, number of MR lesions, white blood cell count, neutrophil count, C-reactive protein, progestogen, and testosterone.

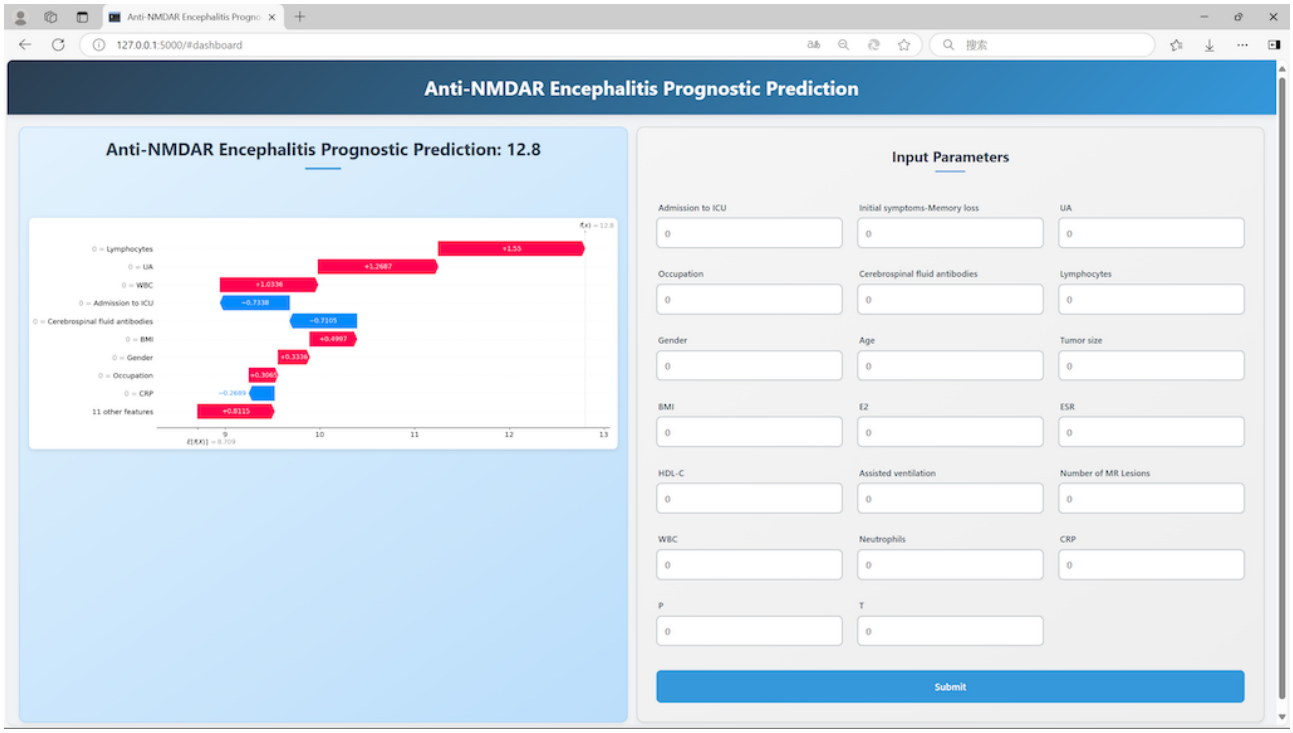
Development of Convenient Applications

This platform features an intuitive graphical interface that accepts clinical input of 20 validated predictive variables, subsequently performing automated calculation of composite prognostic scores for patients with anti-NMDAR encephalitis through embedded algorithmic processing. Real-time risk

XSL•FO
RenderX

stratification results provide clinicians with a quantitative prognostic assessment to support evidence-based treatment decisions. This decision support tool optimizes the process of translating predictive analytics into clinical practice (Figure 6).

Figure 6. The application will automatically estimate the prognosis of anti–N-methyl-D-aspartate receptor encephalitis. NMDAR: N-methyl-D-aspartate receptor.



Discussion

Principal Findings

We developed 3 ML-based prognostic models (XGBoost, RF, and DT) for anti-NMDAR encephalitis. A total of 20 pivotal predictors spanning demographic, clinical manifestations, laboratory parameters, and neuroimaging characteristics were identified from 47 candidate variables. The RF model exhibited the best performance. The SHAP interpretability analysis revealed that ICU admission (mean |SHAP value|=1.65), memory deficits at onset (0.69), and UA (0.53) were the most important predictive factors. To our knowledge, this is the first predictive model for anti-NMDAR encephalitis prognosis developed using ML.

Anti-NMDAR encephalitis is an autoimmune disease associated with antibodies targeting the GluN1 subunit of the NMDAR. Although it is the most common AE in adults, it is still considered a rare disease. Due to the widespread geographic distribution of patients, phenotypic heterogeneity, and insufficient understanding of the pathophysiological mechanisms, there are still many challenges in the diagnosis and treatment of this disease [18]. The outcomes for patients with anti-NMDAR encephalitis vary widely, with approximately 75% of patients achieving complete recovery or having only mild sequelae, while the remaining 25% experience severe neurological deficits or death [5,19]. Identifying patients at risk of severe disease progression and persistent deficits at an early stage is of great clinical significance, as it can inform individualized therapeutic decisions and facilitate timely escalation of treatment. Currently, there is a lack of quantitative predictive models for assessing disease prognosis.

In recent years, various ML algorithms have been widely applied in the field of medicine for treatment and prognosis prediction. Compared with traditional statistical methods, such as logistic regression, ML can directly capture nonlinear and complex interactions. Algorithms such as RF and light gradient boosting machine can automatically identify the most important predictive features, reducing the subjectivity of manual feature selection.

Current prognostic tools face critical challenges: (1) they are focused on single-indicator predictions, and traditional statistical methods were used for analysis. For example, Kashyap et al [20] used the neutrophil-to-lymphocyte ratio (NLR) for prognostic prediction in pediatric anti-NMDAR encephalitis, while Lin et al [11] used serum neuron-specific enolase for prognostic prediction. Such single-indicator prediction methods have obvious limitations in a rare disease with diverse manifestations and complex disease courses. (2) They rely on modified Rankin Scale that inadequately captures cognitive or psychiatric dimensions [12,21]. The modified Rankin Scale is a disability scale developed for stroke clinical trials and largely focuses on motor dysfunction. Such disability scales are limited in capturing nonmotor disabilities in AE. (3) They rely on delayed assessments, such as the anti-NMDAR encephalitis one-year functional status score [22], which requires a 4-week observation period and therefore lacks timeliness in prognostic scoring. For patients with poor prognosis who need timely treatment escalation or combination therapies, this delay may result in missed early therapeutic windows. (4) They depend on complex biomarkers requiring specialized processing: Xiang

XSL•FO
RenderX

et al [10] developed a fusion prediction model based on 4 MRI sequences (T1WI, T2WI, FLAIR, and DWI) for early prediction of functional outcomes in adult patients with anti-NMDAR encephalitis. However, these indicators are not easily obtainable and require specialized radiologists to extract data, which severely limits clinical translation and application and is not conducive to clinical implementation.

We used 47 clinical variables available in the electronic medical records of a large tertiary hospital. The selection of these 47 variables was based on the following criteria: first, the aim of this study was to develop a practical prediction application for clinical settings; therefore, we needed to choose patient indicators that are easily accessible to clinicians. Second, according to previous literature and meta-analysis results, some variables were confirmed to be significantly related to patient prognosis. We also made certain improvements. Previous analyses of the predictive value of clinical MRI were based on binary assessments of normal or abnormal MRI. In this study, we used the number of lesions in MRI for analysis, which is more accurate. In feature selection, RFE with RF was applied. Features exceeding the importance threshold (P>.01) were retained. Ultimately, 20 influential variables were selected to develop a novel ML model to assess the prognosis of anti-NMDAR encephalitis.

For the outcome metric, CASE [15] is a disease severity scale specifically designed for AE and can clearly display the clinical trajectory from the acute phase to the recovery phase, making it suitable for longitudinal assessment of patient outcomes during treatment. The CASE score has not yet been used in prognostic model construction. Using the CASE score as the prognostic outcome variable in our study makes the prognostic assessment of patients more scientific and comprehensive.

We chose RF, DT, and XGBoost to construct predictive models for anti-NMDA encephalitis prognosis and evaluated the distinguishing features of each model through benchmark testing (mean squared error, RMSE, R^2, mean absolute error, and mean absolute percentage error) to determine the most suitable model for prediction. Ultimately, we selected the best-performing RF model and further deployed it on a web platform.

In our study, SHAP visualization analysis confirmed that admission to the ICU (mean |SHAP value|=1.65), initial symptoms of memory deficits (0.69), and UA levels are the main predictive factors for prognosis. In addition, other clinical features such as the presence of memory deficits, tracheostomy, and CSF antibody titers were linked to poorer prognoses in anti-NMDAR encephalitis.

In a retrospective study of 382 patients with anti-NMDAR encephalitis, Balu et al [23] identified ICU admission as the most significant univariate predictor [23]. A previous systematic study also revealed associations between decreased consciousness, ICU admission, and poorer outcomes in anti-NMDAR encephalitis [7]. Conversely, the binary risk stratification by ICU admission underscores the need for intensive monitoring protocols at disease onset. This is consistent with our result. SHAP analysis indicated that serum UA concentration plays a crucial role in predicting anti-NMDAR encephalitis prognosis, aligning with the findings of Liu et al [11]. SHAP dependence analysis revealed that UA values >400 μmol/L sharply reduced CASE probability (SHAP<−1.0). As a central nervous system autoimmune inflammatory disease, the pathogenesis of anti-NMDAR encephalitis remains unclear but is known to involve inflammatory responses. UA reduces proinflammatory cytokine release and removes reactive oxygen species, protecting the body from oxidative stress [24]. UA has also been reported to exert neuroprotective effects in various neurological diseases, such as Alzheimer disease, Parkinson disease, and multiple sclerosis [25]. Thus, UA likely serves as a protective factor in the course of anti-NMDAR encephalitis.

Refractory patients may benefit from alternative drugs such as tocilizumab, bortezomib, or daratumumab [10,18]. Our novel model, developed through rigorous variable selection, development, validation, interpretation, and web deployment, demonstrates excellent predictive accuracy. A significant advantage is that all predictive factors used in the model are easily obtainable by clinicians, making risk stratification within 24 hours, enabling them to promptly identify patients with poor prognoses and guide more aggressive treatment escalation to prevent mild cases from progressing to treatment-resistant severe encephalitis.

Strengths and Limitations

The strengths of this study lie in three advancements: (1) We developed a novel ML model for prognostic prediction in encephalitis, (2) this model is exclusively based on clinically accessible parameters, and (3) we created a visualized web-based decision support platform to enable real-time clinical implementation. Our study also has several limitations. First, due to the rarity of the disease, the sample size was relatively small, and it is impossible to conduct subgroup analysis and statistics for each clinical manifestation. Second, the data used for model development were obtained from patients admitted to a specific medical institution rather than from a large database, which may introduce bias. Future research should consider training and validating the model across different national contexts.

Conclusions

In this study, we developed and validated an interpretable ML model based on the RF algorithm. The model demonstrated high predictive accuracy, with robust performance metrics, supporting its potential utility in clinical settings. Through SHAP analysis, key prognostic predictors were identified, including admission to ICU, memory deficits at initial presentation, and serum UA levels, offering novel insights into risk stratification. This tool may assist clinicians in making evidence-based decisions, optimizing interventions, and ultimately improving outcomes for patients with anti-NMDAR encephalitis.

XSL•FO
RenderX

Acknowledgments

This work was supported by grants from the Guangzhou Municipal Science and Technology Project (2023A04J1803, JW) and Guangzhou Municipal Science and Technology Project (2023A04J1806, HW).

Data Availability

The datasets generated during and/or analyzed during the current study are available from the corresponding author upon reasonable request.

Authors' Contributions

JW and HW were responsible for designing the study. YW was responsible for collecting the data. HC and HW were responsible for case scoring. HW completed the data analysis and results interpretation. JW completed the first draft of the article. JG was responsible for the final approval of the manuscript.

Conflicts of Interest

None declared.

Multimedia Appendix 1
Association between each candidate predictor.
[PNG File, 102 KB - medinform_v13i1e75020_app1.png]

References

1. Wu CY, Wu JD, Chen CC. The association of ovarian teratoma and anti-N-methyl-D-aspartate receptor encephalitis: an updated integrative review. Int J Mol Sci 2021 Oct 9;22(20):10911. [doi: 10.3390/ijms222010911] [Medline: 34681570]
2. Liu P, Yan H, Li H, Zhang C, Li Y. Overlapping anti-NMDAR encephalitis and multiple sclerosis: a case report and literature review. Front Immunol 2023;14:1088801. [doi: 10.3389/fimmu.2023.1088801] [Medline: 36793718]
3. Yu Y, Wu Y, Cao X, et al. The clinical features and prognosis of anti-NMDAR encephalitis depends on blood brain barrier integrity. Mult Scler Relat Disord 2021 Jan;47:102604. [doi: 10.1016/j.msard.2020.102604] [Medline: 33130468]
4. Titulaer MJ, McCracken L, Gabilondo I, et al. Treatment and prognostic factors for long-term outcome in patients with anti-NMDA receptor encephalitis: an observational cohort study. Lancet Neurol 2013 Feb;12(2):157-165. [doi: 10.1016/S1474-4422(12)70310-1] [Medline: 23290630]
5. Raja P, Shamick B, Nitish LK, et al. Clinical characteristics, treatment and long-term prognosis in patients with anti-NMDAR encephalitis. Neurol Sci 2021 Nov;42(11):4683-4696. [doi: 10.1007/s10072-021-05174-6] [Medline: 33728548]
6. Brenner J, Ruhe CJ, Kulderij I, et al. Long-term cognitive, functional, and patient-reported outcomes in patients with anti-NMDAR encephalitis. Neurology (ECronicon) 2024 Dec 24;103(12):e210109. [doi: 10.1212/WNL.0000000000210109] [Medline: 39566012]
7. Wang J, Luo L, Meng Z, et al. Blood and CSF findings of cellular immunity in anti-NMDAR encephalitis. Int Immunopharmacol 2024 Mar;130:111743. [doi: 10.1016/j.intimp.2024.111743] [Medline: 38430802]
8. Peer M, Prüss H, Ben-Dayan I, Paul F, Arzy S, Finke C. Functional connectivity of large-scale brain networks in patients with anti-NMDA receptor encephalitis: an observational study. Lancet Psychiatry 2017 Oct;4(10):768-774. [doi: 10.1016/S2215-0366(17)30330-9] [Medline: 28882707]
9. Matute C, Palma A, Serrano-Regal MP, et al. N-methyl-D-aspartate receptor antibodies in autoimmune encephalopathy alter oligodendrocyte function. Ann Neurol 2020 May;87(5):670-676. [doi: 10.1002/ana.25699] [Medline: 32052483]
10. Xiang Y, Dong X, Zeng C, et al. Clinical variables, deep learning and radiomics features help predict the prognosis of adult anti-N-methyl-D-aspartate receptor encephalitis early: a two-center study in Southwest China. Front Immunol 2022;13:913703. [doi: 10.3389/fimmu.2022.913703] [Medline: 35720336]
11. Lin Y, Li H, Song E, Lu Z, Dai Y, Zhang B. Serum neuron-specific enolase can predict the severity and outcome of anti-N-methyl-D-aspartate receptor encephalitis. Clin Chim Acta 2025 Jan 15;565:119962. [doi: 10.1016/j.cca.2024.119962] [Medline: 39244142]
12. Zhang J, Li Y, Liu L, et al. Development of a short-term prognostic model for anti-N-methyl-D-aspartate receptor encephalitis in Chinese patients. BMC Neurol 2024 Aug 9;24(1):276. [doi: 10.1186/s12883-024-03724-x] [Medline: 39123191]
13. Bloch RF. Interobserver agreement for the assessment of handicap in stroke patients. Stroke 1988 Nov;19(11):1448. [doi: 10.1161/01.str.19.11.1448] [Medline: 2973161]
14. Du Z, Fan F, Ma J, et al. Development and validation of an ultrasound-based interpretable machine learning model for the classification of ≤3 cm hepatocellular carcinoma: a multicentre retrospective diagnostic study. EClinicalMedicine 2025 Mar;81:103098. [doi: 10.1016/j.eclinm.2025.103098] [Medline: 40034568]
15. Lim JA, Lee ST, Moon J, et al. Development of the clinical assessment scale in autoimmune encephalitis. Ann Neurol 2019 Mar;85(3):352-358. [doi: 10.1002/ana.25421] [Medline: 30675918]

XSL•FO
RenderX

16. Gao J, Yao Y, Xue J, et al. Methodological conduct and risk of bias in studies on prenatal birthweight prediction models using machine learning techniques: a systematic review. BMC Pregnancy Childbirth 2025 Jul 2;25(1):696. [doi: 10.1186/s12884-025-07727-5] [Medline: 40604554]
17. Aboseif A, Li Y, Amin M, et al. Clinical determinants of longitudinal disability in LGI-1-IgG autoimmune encephalitis. Neurol Neuroimmunol Neuroinflamm 2024 Jan;11(1):e200178. [doi: 10.1212/NXI.0000000000200178] [Medline: 37949667]
18. Ciano-Petersen NL, Cabezudo-García P, Muñiz-Castrillo S, Honnorat J, Serrano-Castro PJ, Oliver-Martos B. Current status of biomarkers in anti-N-methyl-D-aspartate receptor encephalitis. Int J Mol Sci 2021 Dec 4;22(23):13127. [doi: 10.3390/ijms222313127] [Medline: 34884930]
19. Nguyen L, Wang C. Anti-NMDA receptor autoimmune encephalitis: diagnosis and management strategies. Int J Gen Med 2023;16:7-21. [doi: 10.2147/IJGM.S397429] [Medline: 36628299]
20. Kashyap N, Morris M, Loerinc LB, et al. The neutrophil-to-lymphocyte ratio is associated with intubation in pediatric anti-NMDA receptor encephalitis: a retrospective study. J Neuroimmunol 2022 Sep 15;370:577931. [doi: 10.1016/j.jneuroim.2022.577931] [Medline: 35872506]
21. Zhang Y, Tu E, Yao C, Liu J, Lei Q, Lu W. Validation of the clinical assessment scale in autoimmune encephalitis in Chinese patients. Front Immunol 2021 Dec 10;12:796965. [doi: 10.3389/fimmu.2021.796965] [Medline: 34975905]
22. Blackman G, Kumar K, Hanrahan JG, et al. Quantitative EEG as a prognostic tool in suspected anti-N-methyl- d -aspartate receptor antibody encephalitis. J Clin Neurophysiol 2023 Feb 1;40(2):160-164. [doi: 10.1097/WNP.0000000000000877] [Medline: 34238869]
23. Balu R, McCracken L, Lancaster E, Graus F, Dalmau J, Titulaer MJ. A score that predicts 1-year functional status in patients with anti-NMDA receptor encephalitis. Neurology (ECronicon) 2019 Jan 15;92(3):e244-e252. [doi: 10.1212/WNL.0000000000006783] [Medline: 30578370]
24. Shu Y, Wang Y, Lu T, et al. Serum uric acid and anti-N-methyl-d-aspartate receptor encephalitis. Neurochem Int 2017 Sep;108:34-39. [doi: 10.1016/j.neuint.2017.02.005] [Medline: 28192149]
25. Folbergrová J, Ješina P, Kubová H, Druga R, Otáhal J. Status epilepticus in immature rats is associated with oxidative stress and mitochondrial dysfunction. Front Cell Neurosci 2016;10:136. [doi: 10.3389/fncel.2016.00136] [Medline: 27303267]

Abbreviations

AE: autoimmune encephalitis
Anti-NMDAR: anti-N-methyl-D-aspartate receptor
CASE: Clinical Evaluation Scale for Autoimmune Encephalitis
CSF: cerebrospinal fluid
DT: decision tree
ICU: intensive care unit
ML: machine learning
MRI: magnetic resonance imaging
MSE: mean squared error
NLR: neutrophil-to-lymphocyte ratio
RF: random forest
RFE: recursive feature elimination
RMSE: root-mean-squared error
SHAP: Shapley Additive Explanations
TRIPOD: Transparent Reporting of a Multivariable Prediction Model for Individual Prognosis or Diagnosis
UA: uric acid
XGBoost: extreme gradient boosting

Edited by A Benis; submitted 26.03.25; peer-reviewed by E Pashaei, S Mei, T Gupta; revised version received 15.07.25; accepted 11.08.25; published 22.09.25.

Please cite as:
Wang J, Wu H, Cai H, Wang Y, Gu J
Machine Learning and Shapley Additive Explanations Value Integration for Predicting the Prognostic of Anti-N-Methyl-D-Aspartate Receptor Encephalitis: Model Development and Evaluation Study
JMIR Med Inform 2025;13:e75020
URL: https://medinform.jmir.org/2025/1/e75020
doi:10.2196/75020

XSL•FO
RenderX

© Jia Wang, Haotian Wu, Han Cai, YingXiang Wang, Jian Gu. Originally published in JMIR Medical Informatics (https://medinform.jmir.org), 22.9.2025. This is an open-access article distributed under the terms of the Creative Commons Attribution License (https://creativecommons.org/licenses/by/4.0/), which permits unrestricted use, distribution, and reproduction in any medium, provided the original work, first published in JMIR Medical Informatics, is properly cited. The complete bibliographic information, a link to the original publication on https://medinform.jmir.org/, as well as this copyright and license information must be included.

XSL•FO
RenderX

Predicting Lymph Node Metastasis in Rectal Cancer: Development and Validation of a Machine Learning Model Using Clinical Data

Wei Hou[1,2,3*]; Chuangwei Li[1,2,3*], MM; Zhen Wang[1,2,3], MB; Wanqin Wang[2,4], MM; Shouhong Wan[2,5], PhD; Bingbing Zou[1,2,3], PhD

[1]Department of General Surgery, The First Affiliated Hospital of Anhui Medical University, Hefei, Anhui, China

[2]Institute of Artificial Intelligence, Hefei Comprehensive National Science Center, Hefei, China

[3]Anhui Medical University, Hefei, China

[4]Department of Radiology, The First Affiliated Hospital of Anhui Medical University, Hefei, China

[5]School of Computer Science and Technology, University of Science and Technology of China, Hefei, China

[*]these authors contributed equally

Corresponding Author:
Bingbing Zou, PhD
Department of General Surgery, The First Affiliated Hospital of Anhui Medical University, Hefei, Anhui, China

Abstract

Background: Rectal cancer (RC) is a common malignant tumor, with lymph node metastasis (LNM) being a critical determinant of patient prognosis. Traditional diagnostic methods have limitations, necessitating the development of predictive models using clinical data.

Objective: This study aimed to construct and validate machine learning (ML) models to predict LNM risk in patients with RC based on clinical data.

Methods: Retrospective data from 2454 patients with RC (SEER [Surveillance, Epidemiology, and End Results] database) were split into training (n=1954) and internal validation (n=500) sets. An external cohort (n=500) was obtained from the First Affiliated Hospital of Anhui Medical University. Lymph node features identified via computed tomographic scans were integrated with clinicopathological data. Variables were selected using LASSO (Least Absolute Shrinkage and Selection Operator), followed by univariate and multivariate logistic regression. Eleven ML models (Logistic Regression, K-Nearest Neighbors, Extremely Randomized Trees, Naive Bayes, XGBoost [XBG], Light Gradient Boosting Machine, Multilayer Perceptron, Gradient Boosting, Support Vector Machine, Random Forest, and Ada-Boost) were evaluated via area under the receiver operating characteristic curve (AUC), calibration curves, and decision curve analysis.

Results: LNM prevalence was 26.9% (training), 27% (internal validation), and 81% (external validation). Independent LNM predictors included tumor grade, clinical T stage, N stage, tumor length, neural invasion, and total lymph nodes. Internal validation AUC ranged from 0.859 to 0.964; external validation AUC was 0.735 - 0.838. In the internal validation set, Random Forest and Extremely Randomized Trees achieved the highest AUC (0.964, 95% CI 0.950 - 0.978), while XGB demonstrated superior cross-cohort stability (AUC 0.942, 95% CI 0.925 - 0.959). For external validation, Gradient Boosting had the highest AUC (0.838, 95% CI 0.801 - 0.875), followed by XGB (0.832, 95%CI 0.794 - 0.869). XGB showed minimal calibration error with curves closest to the ideal diagonal and yielded the highest net benefit in decision curve analysis across critical thresholds.

Conclusions: This study successfully developed and validated 11 ML models to predict LNM risk in RC. The XGB model was optimal, achieving an AUC >0.9 in 10 internal models and an AUC >0.8 in 7 external models. The identified predictors of LNM can facilitate early diagnosis and personalized treatment, highlighting the potential of integrating computed tomographic scan data with clinicopathological findings to build effective predictive models.

Trial Registration: Chinese Clinical Trial Registry ChiCTR2400094858; https://www.chictr.org.cn/showproj.html?proj=254325

(JMIR Med Inform 2025;13:e73765) doi:10.2196/73765

KEYWORDS

rectal cancer; lymph node metastasis; machine learning model; prediction models; clinical data, prognosis; XGBoost

XSL•FO
RenderX

Introduction

Rectal cancer (RC) is among the most prevalent malignant tumors globally and is currently the second leading cause of cancer-related deaths worldwide [1,2]. A recent study [3] projects that by 2040, the incidence of RC will rise to 3.2 million new cases annually, with 1.6 million deaths worldwide. Lymph node metastasis (LNM) is a critical determinant of poor prognosis in RC, and numerous studies [4-7] have shown that accurate prediction of LNM is crucial for treatment selection in patients and prognostic assessment. Initially, while current imaging technologies can assess the risk of LNM to some degree [8-10], they largely depend on radiologists' anatomical expertise for evaluation [11]. However, these methods still face limitations in terms of accuracy and efficiency [12]. Specifically, conventional computed tomography (CT)–based N staging struggles to detect small metastatic lymph nodes (<5 mm) and subtle morphological changes (eg, irregular borders, heterogeneous texture), which are critical for early metastasis diagnosis but require expert manual annotation [13]. Second, pathologists determine the presence of LNM in patients with RC based on clinical pathology reports. This approach is inefficient and subject to the constraints of the individual pathologist's expertise.

In recent years, the rapid advancement of machine learning (ML) technology has led to its growing application in the medical field, particularly in disease prediction, diagnosis, and treatment decision-making, demonstrating significant potential [14,15]. ML algorithms can process and analyze large volumes of clinical data, identifying disease-related patterns and features, which enhances the accuracy of predictive models [16]. However, most existing ML models rely on automated radiomic features or clinical data alone, neglecting the value of radiologist-annotated CT morphological features [17]. In predicting LNM in RC, previous studies have utilized ML models, including Support Vector Machines, neural networks, and decision trees, achieving notable results [18-21]. Both clinical data and CT results are not entirely accurate in predicting pathological LNM. In the study by Li et al [22], the overall accuracy of N stage based on CT images ranged from 59% to 68%. Meanwhile, up to 70% of metastatic lymph nodes in colorectal cancer have a diameter of less than 5 mm. This indicates that both clinicopathological features and preoperative CT have certain limitations in predicting the malignant lymph node status of patients with T1 colorectal cancer. Therefore, there is an urgent need to develop novel predictive tools that integrate ML with radiological parameters and clinical data, thereby enhancing the accuracy and efficiency of diagnostic processes. Recent evidence suggests that systematic manual annotation by trained radiologists can improve the sensitivity of detecting sub-centimeter metastatic lymph nodes compared with routine clinical reports. This highlights the potential of this method in bridging current diagnostic gaps [23].

This study aimed to develop and validate ML models using clinical data to predict LNM risk in RC. We successfully constructed and validated 11 predictive models integrating radiologist-annotated CT lymph node features with clinicopathological data. These models show significant potential to assist clinicians in early diagnosis and personalized treatment planning. We anticipate that the findings will provide new insights for RC management and serve as a valuable reference for future research and practice.

Methods

Data Collection and Inclusion Criteria

This study encompassed clinical data from 2454 patients with RC in the SEER database, wherein 1954 cases were randomly selected to form the training cohort, and the remaining 500 formed the internal validation cohort. Additionally, it included data from 500 patients with RC treated at the author's hospital between January 1, 2017, and December 31, 2023, which served as the external validation cohort. The inclusion criteria were (1) patients with RC staged as I-IV according to the American Joint Committee on Cancer (AJCC) staging system; (2) those who underwent curative surgery; and (3) those with complete clinical and pathological information; and (4) radical surgery in stage IV patients. In this study, some patients with stage IV RC with oligometastasis (limited resectable metastases) or locally advanced tumors with resectable metastatic lesions underwent radical surgery after evaluation by a multidisciplinary team. The surgical decision was based on the multidisciplinary team's comprehensive assessment of tumor burden, physical condition, expected survival, and surgical risks. The goal was to achieve R0 resection and combine it with postoperative adjuvant therapy to reduce recurrence risk. Data for these patients were complete and underwent strict screening to ensure they met the research criteria. The exclusion criteria included (1) a history of other malignant tumors, (2) inability to assess lymph node status, (3) incomplete clinical information, and (4) administration of neoadjuvant therapy. The LNM status for 2454 patients with RC in the SEER database was ascertained from pathological assessments of surgical specimens. For the 500 cases at the author's hospital, LNM status, clinical T and N staging, and tumor length were determined by precisely annotating and measuring contrast-enhanced CT images with the radiological software ITK-SNAP software (version: 4.0.1; Professor Paul Yushkevich's team, University of Pennsylvania, USA), corroborated by pathological assessments from surgical specimens. For example, the definition of tumor length in the SEER database (training/internal validation cohorts) was measured from pathological specimens. In the external validation cohort, tumor length was annotated and measured on contrast-enhanced CT scans using ITK-SNAP software by radiologists, with cross-validation against postoperative pathology (mean error <0.3 cm).

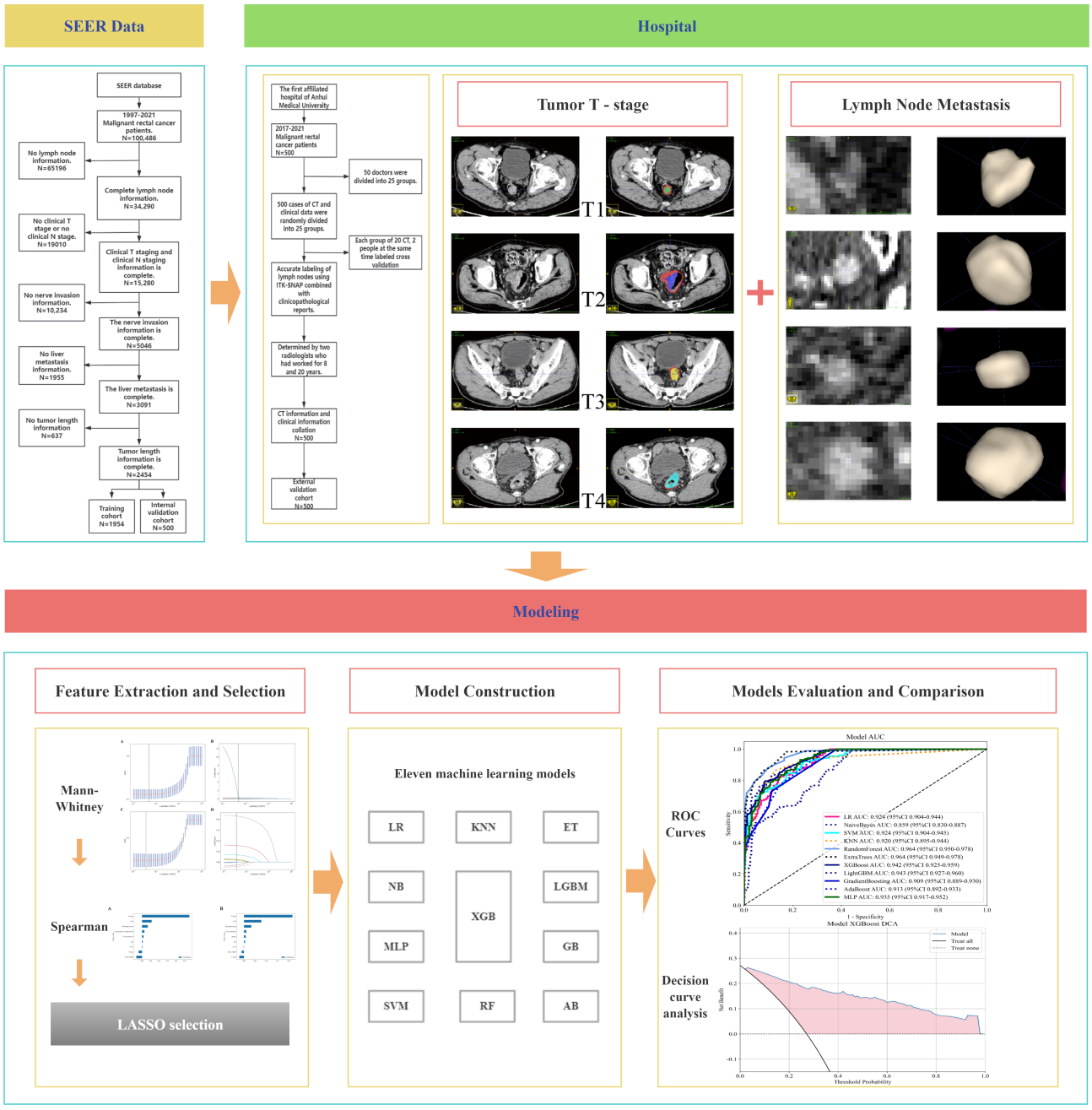
Clinical Pathological Features

The study collected the following clinical and pathological characteristics of the patients: sex, age, perineural invasion, carcinoembryonic antigen (CEA), tumor length, clinical T stage, N stage, tumor differentiation, chemotherapy and radiotherapy administration, liver metastasis status, and tumor histology. For the training and internal validation cohorts, data extraction was conducted using the SEER*STAT software, version 8.4.3 (Surveillance, Epidemiology, and End Results Program, National Cancer Institute, USA). In the external validation cohort, clinical

XSL•FO
RenderX

data were independently collected and processed by 2 researchers, while CT images were annotated and measured with precision by 50 physicians, evenly distributed into 25 groups, each consisting of 2 physicians for cross-validation purposes. The inclusion criteria for metastatic lymph nodes were fulfilled if any of the following five conditions was met: (1) the short axis/long axis ratio was ≥0.8; (2) the short axis was ≥5 mm; (3) there was aggregation of three or more lymph nodes; (4) the lymph node had an irregular shape with a rough margin; (5) the lymph node signal was inhomogeneous, with high signal areas in the CT imaging for lymph nodes (including mesenteric and presacral lymph nodes). Figure 1 illustrates the acquisition process.

Figure 1. Workflow of this study. AB: Ada-Boost; CT: computed tomography; ET: Extremely Randomized Trees; GB: Gradient Boosting; KNN: K-Nearest Neighbors; LGBM: Light Gradient Boosting Machine; LR: Logistic Regression; MLP: Multilayer Perceptron; NB: Naive Bayes; RF: Random Forest; ROC: receiver operating characteristic; SEER: Surveillance Epidemiology and End Results; SVM: Support Vector Machine; XGB: XGBoost.



Data Processing and Analysis

All collected data will be subjected to rigorous preprocessing in Python, encompassing data cleaning, outlier detection, and missing value imputation. Subsequent statistical analysis will utilize suitable methods including χ^2 tests, ANOVA, and both univariate and multivariate regression analyses to evaluate the correlations between clinical pathological features and LNM.

Feature Engineering and Selection

In this study, we standardized numerical features, including tumor length, to mitigate the effects of varying scales and enhance their compatibility with the input requirements of ML models. For categorical variables like clinical T staging, we

XSL•FO
RenderX

applied label encoding to transform them into numerical data. All features were first normalized to eliminate scale effects (Multimedia Appendix 1). We then performed univariate feature screening via independent *t* tests or Mann-Whitney *U* tests ($P \leq .05$), retaining features. Next, Pearson correlation analysis reduced redundancy by removing features with mean absolute correlation >0.9, yielding decorrelated features. Finally, features with nonzero coefficients were selected through LASSO regression (10-fold cross-validated) with regularization parameter α. Notably, this LASSO-based selection served as initial screening; tree-based models (Random Forest [RF]/XGBoost [XGB]/Light Gradient Boosting Machine [LGBM]) subsequently performed endogenous feature reweighting to capture nonlinear interactions during model training. This method incorporates an L1 regularization term that aids in pinpointing the most influential features while promoting model sparsity. Furthermore, we performed a correlation analysis among the features to verify the independence of the selected variables. Utilizing the principle of Permutation Importance, we evaluated the importance of each feature to ascertain its contribution to the model's predictive performance.

Predictive Model Construction and Validation

This study developed 11 distinct ML models: Logistic Regression (LR), Naive Bayes (NB), Support Vector Machine, K-Nearest Neighbors (KNN), RF, Extremely Randomized Trees (ET), XGB, LGBM, Gradient Boosting (GB), Ada-Boost (AB), and Multilayer Perceptron (MLP), for predicting the risk of LNM in patients with RC (Multimedia Appendix 2). To counteract the imbalance in data distribution, we used random oversampling techniques and applied a penalty parameter λ to drive the coefficient estimates of nonsignificant features toward zero. The models' performance was evaluated through 10-fold cross-validation. The performance of each ML classifier was assessed using the receiver operating characteristic curve, where a higher area under the receiver operating characteristic curve (AUC) indicates greater predictive accuracy. We evaluated the variable weights and permutation importance and used heatmaps to visualize the significance and correlations among the variables. To select the optimal model, we evaluated each model's performance across multiple metrics: AUC (with 95% CI), accuracy, sensitivity, specificity, and F_1 score. Calibration curves and decision curve analysis (DCA) were further employed to assess calibration accuracy and clinical utility, particularly focusing on net benefits at critical thresholds.

Ethical Considerations

This study was approved by the Ethics Committee of the First Affiliated Hospital of Anhui Medical University (Approval No.: Quick-PJ 2023-13-34). As a retrospective analysis using anonymized data, the requirement for informed consent was waived. Primary data collection in the SEER database obtained patient informed consent, and its Institutional Review Board explicitly authorized secondary analysis without additional approval. All direct identifiers (including names, ID numbers, medical record numbers) were removed from our hospital's dataset, with only aggregated data utilized in the analyses to ensure privacy protection. No participant compensation was involved, and no identifiable images appear in the manuscript or supplementary materials.

Results

Demographic Characteristics and Parameter Selection

In our study, the training cohort included 1954 patients with RC, the internal validation cohort included 500 patients with RC, and the external validation cohort included 500 patients with RC. Across the training cohort, internal validation cohort, and external validation cohort, stratification by LNM status (positive vs negative) revealed statistically significant differences in age, gender, total lymph node count, tumor length, neural invasion, clinical T stage, N stage, liver metastasis status, tumor histology, and tumor differentiation (all $P<.001$; see Table 1). For CEA, the *P* value was .001, indicating a statistically significant difference (Table 1). We used the LASSO regression method to identify a significant set of risk factors for predicting the risk of LNM in patients with RC.

XSL•FO
RenderX

Table . The clinicopathological features of the training, internal validation, and external validation cohorts.

Characteristics	Training cohort (N=1954)		Internal validation cohort (N=500)		External validation cohort (N=500)		*P* value
	Negative (n=1421)	Positive (n=533)	Negative (n=365)	Positive (n=135)	Negative (n=195)	Positive (n=305)	
Sex, n (%)							
Female	543 (38.2)	197 (37.0)	193 (5.0)	44 (33.0)	75 (38.0)	101 (33.0)	<.001
Male	878 (62.0)	336 (63.0)	172 (47.0)	91 (67.0)	120 (62.0)	204 (67.0)	
Age, n (%)							
20≤X≤24	2 (0.1)	2 (0.4)	1 (0.3)	2 (1.5)	0 (0)	0 (0)	<.001
25≤X≤29	8 (0.6)	4 (0.8)	6 (1.6)	2 (1.5)	0 (0)	1 (0.3)	
30≤X≤34	20 (1.4)	10 (1.9)	11 (3.0)	3 (2.2)	1 (0.5)	3 (1.0)	
35≤X≤39	36 (2.5)	14 (2.6)	9 (2.5)	6 (4.4)	2 (1.0)	3 (1.0)	
40≤X≤44	63 (4.4)	27 (5.1)	25 (6.9)	18 (13.3)	5 (2.6)	6 (2.0)	
45≤X≤49	97 (6.8)	59 (11.1)	57 (15.6)	16 (11.9)	14 (7.2)	28 (9.2)	
50≤X≤54	181 (13.0)	76 (14.3)	54 (14.8)	19 (14.1)	21 (10.8)	39 (12.8)	
55≤X≤59	211 (15.0)	69 (13.0)	46 (12.6)	17 (12.6)	35 (18.0)	40 (13.1)	
60≤X≤64	216 (15.0)	75 (14.1)	57 (15.6)	12 (8.9)	28 (14.4)	28 (9.2)	
65≤X≤69	217 (15.0)	63 (11.8)	42 (11.5)	15 (11.1)	25 (12.8)	64 (21.0)	
70≤X≤74	164 (12.0)	52 (9.8)	29 (8.0)	10 (7.4)	27 (13.9)	48 (15.7)	
75≤X≤79	107 (8.0)	33 (6.2)	17 (4.7)	10 (7.4)	24 (12.3)	29 (9.5)	
80≤X≤84	63 (4.4)	26 (4.9)	11 (3.0)	5 (3.7)	10 (5.1)	14 (4.6)	
85≤X	36 (2.5)	23 (4.3)	1 (0.3)	2 (1.5)	3 (1.5)	2 (0.7)	
Total number of lymph nodes, n (%)							
0<X≤5	89 (6.3)	17 (3.2)	20 (5.5)	7 (5.2)	3 (1.5)	4 (1.3)	<.001
5<X≤10	130 (9.0)	40 (7.5)	24 (6.6)	10 (7.4)	36 (18.5)	30 (9.8)	
10<X≤15	455 (32.0)	148 (28.0)	113 (31.0)	40 (29.6)	130 (67.0)	211 (69.0)	
15<X≤20	319 (22.0)	131 (25.0)	87 (23.9)	36 (26.7)	23 (11.8)	53 (17.4)	
20<X≤25	186 (13.0)	77 (14.5)	62 (17.0)	15 (11.1)	3 (1.5)	6 (20.0)	
25<X≤30	106 (7.0)	50 (9.4)	28 (7.7)	12 (8.9)	0 (0)	1 (0.3)	
30<X	134 (9.0)	70 (13.1)	30 (8.2)	15 (11.1)	0 (0)	0 (0)	
Tumor length, n (%)							
0<X≤5	883 (62.0)	331 (62.0)	219 (60.0)	81 (60.0)	73 (37.4)	123 (40.0)	<.001
5<X≤10	504 (35.0)	191 (36.0)	138 (38.0)	54 (40.0)	118 (61.0)	168 (55.0)	
10<X	34 (2.4)	11 (2.1)	8 (2.2)	0 (0)	4 (2.1)	14 (4.6)	
PNI[a], n (%)							
Negative	1320 (93.0)	398 (75.0)	339 (93.0)	102 (76.0)	125 (64.0)	176 (58.0)	<.001
Positive	101 (7.0)	135 (25.0)	26 (7.1)	33 (24.4)	70 (35.9)	129 (42.3)	
CEA[b], n (%)							
Negative	933 (66.0)	305 (57.0)	236 (65.0)	77 (57.0)	145 (74.4)	208 (68.0)	<.001
Positive	488 (34.0)	228 (43.0)	129 (35.0)	58 (43.0)	50 (25.6)	97 (31.8)	
Clinical T stage, n (%)							

XSL•FO
RenderX

Characteristics	Training cohort (N=1954)		Internal validation cohort (N=500)		External validation cohort (N=500)		*P* value
	Negative (n=1421)	Positive (n=533)	Negative (n=365)	Positive (n=135)	Negative (n=195)	Positive (n=305)	
1	220 (15.0)	37 (6.9)	41 (11.2)	8 (5.9)	22 (11.3)	26 (8.5)	<.001
2	243 (17.1)	70 (13.1)	80 (21.9)	14 (10.4)	62 (31.8)	66 (21.6)	
3	778 (55.0)	339 (64.0)	192 (53.0)	89 (65.9)	92 (47.2)	166 (54)	
4	179 (13.0)	87 (16.3)	52 (14.3)	24 (17.8)	19 (9.7)	47 (15.4)	
N stage, n (%)							
0	879 (62.0)	1 (0.2)	227 (62.0)	0 (0)	116 (59.0)	141 (46.0)	<.001
1	542 (38.0)	394 (74.0)	138 (38.0)	103 (76.0)	50 (25.6)	100 (33.0)	
2	0 (0)	138 (26.0)	0 (0)	32 (23.7)	29 (14.9)	64 (21.0)	
Liver metastasis, n (%)							
Negative	1393 (98.0)	491 (92.0)	361 (99.0)	124 (92.0)	191 (98.0)	301 (99.0)	<.001
Positive	28 (2.0)	42 (7.9)	4 (1.1)	11 (8.2)	4 (2.1)	4 (1.3)	
Histological type, n (%)							
Adenocarcinoma	1378 (97.0)	489 (92.0)	359 (72.0)	126 (25.0)	193 (39.0)	301 (60.0)	<.001
Mucinous /signet ring cell	29 (2.0)	35 (6.6)	5 (1.0)	5 (1.0)	2 (0.4)	4 (0.8)	
Others	4 (0.3)	9 (1.7)	1 (0.2)	4 (0.8)	0 (0)	0 (0)	
Differentiation extent, n (%)							
Poorly differentiated/ undifferentiated	1 (0.1)	0 (0)	0 (0)	0 (0)	10 (5.1)	23 (7.5)	<.001
Moderately differentiated	1421 (100.0)	532 (99.81)	365 (100.0)	135 (100.0)	152 (78.0)	236 (77.0)	
Well-differentiated	0 (0)	0 (0)	0 (0)	0 (0)	33 (16.9)	46 (15.1)	

[a]PNI: perineural invasion.

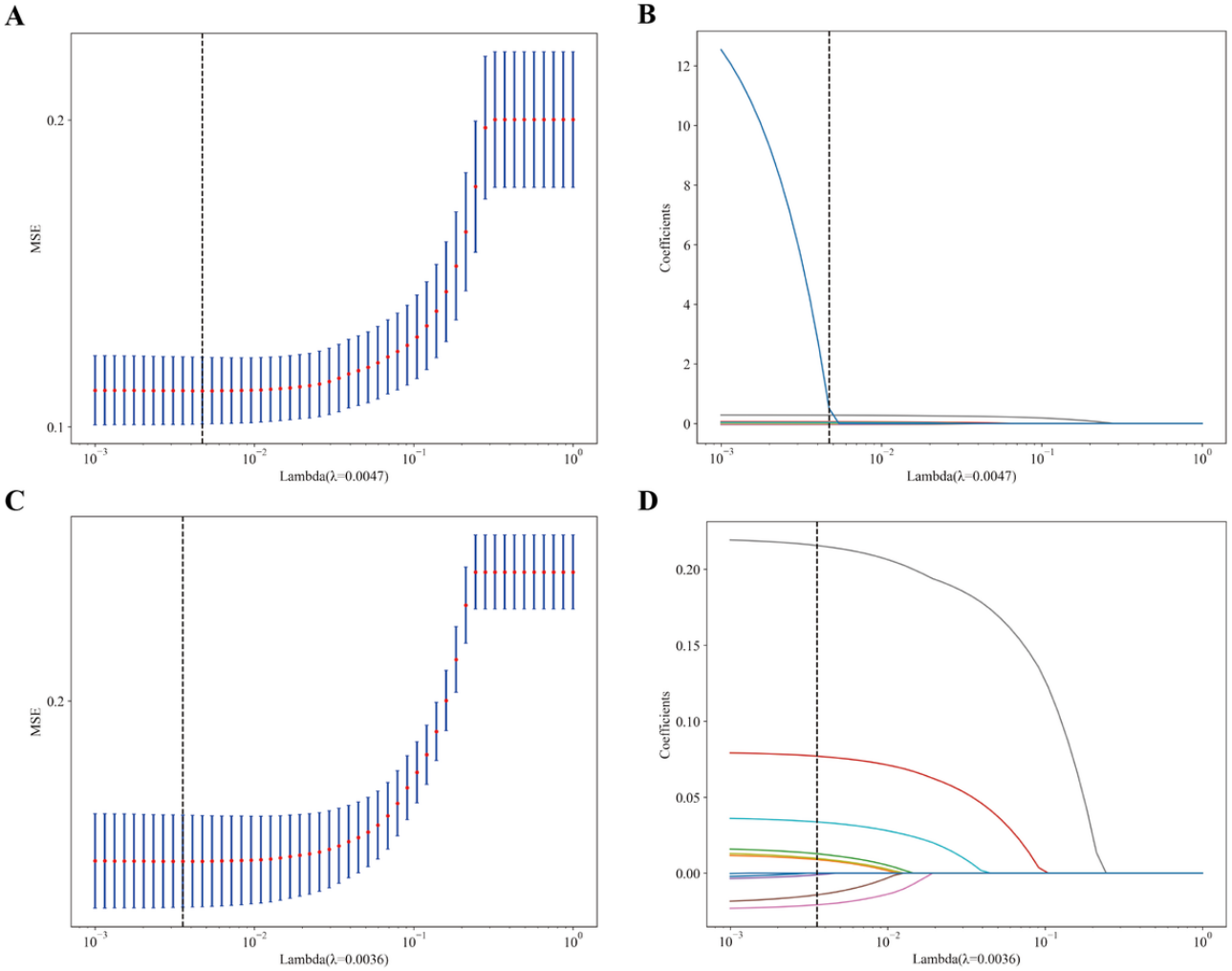
[b]CEA: carcinoembryonic antigen.

Risk Factors for Lymph Node Metastasis

Using the nonzero coefficients from the LASSO logistic regression model as a guide, we applied both the LASSO method and the multivariate logistic regression model to identify the risk factors associated with LNM in patients with RC, as depicted in Figure 2. The penalty parameters λ for the internal and external validation sets were found to be 0.0047 and 0.0036, respectively. Univariate and multivariate analyses yielded the forest plots for both the internal and external validation sets, as shown in Figure 3. Key predictors from univariate and multivariate analyses are detailed in Table 2. This analysis assists in pinpointing factors that potentially contribute to LNM, marking a pivotal step in comprehending disease progression and in formulating evidence-based treatment strategies. The multivariate logistic regression analysis of the external validation set identified number of peritumoral and total lymph nodes examined (P=.022), tumor length (P<.001), neural invasion (P<.001), clinical T stage (P<.001), N stage (P<.01), and tumor differentiation grade (P<.01) as independent risk factors for LNM.

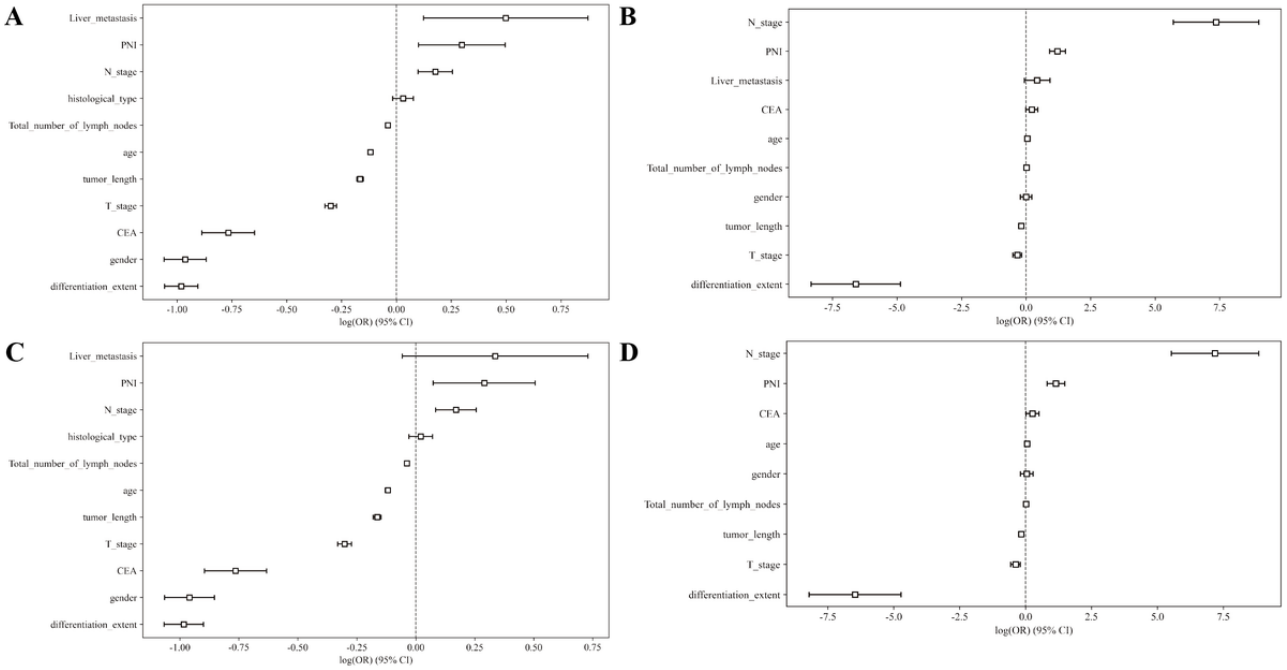
XSL•FO
RenderX

Figure 2. Feature selection using LASSO logistic regression. (A) Adjustment parameters in the LASSO logistic regression for both the training and internal validation sets (C) are selected using 10-fold cross-validation with minimum criteria. The relationship between binomial deviation and the logarithm of the penalty parameter (λ) is depicted. The optimal λ is indicated by a black vertical line, determined by the minimum criterion and the minimum standard error of λ. (B) LASSO coefficients for 12 clinical factors in the training set and internal validation set (D) are presented, illustrating the coefficient profiles against the logarithm of λ. LASSO: Least Absolute Shrinkage and Selection Operator; MSE: mean squared error.



XSL•FO
RenderX

Figure 3. Univariate and multivariate logistic regression analyses yielded a forest plot of odds ratios. (A) In the external validation cohort, single-factor analysis yielded a forest plot of odds ratio. (B) In the external validation cohort, multiple factor analysis yielded a forest plot of odds ratios. (C) In the internal validation cohort, single-factor analysis yielded a forest plot of odds ratios. (D) In the internal validation cohort, multiple factor analysis yielded a forest plot of odds ratios. CEA: carcinoembryonic antigen; PNI: perineural invasion.



XSL•FO
RenderX

Table . Univariate and multivariate logistic regression analysis.

Characteristics	Univariate logistic		Multivariable logistics	
	OR[a] (CI)	*P* value	OR (CI)	*P* value
Internal validation cohort				
Sex	0.382 (0.347 - 0.420)	<.001	0.999 (0.803 - 1.244)	.99
Age	0.888 (0.879 - 0.896)	<.001	1.046 (1.002 - 1.092)	.09
Total number of lymph nodes	0.962 (0.958 - 0.966)	<.001	1.017 (1.006 - 1.028)	.01
Tumor length	0.847 (0.834 - 0.860)	<.001	0.828 (0.786 - 0.873)	<.001
PNI[b]	1.347 (1.106 - 1.640)	.01	3.372 (2.472 - 4.600)	<.001
CEA[c]	0.465 (0.412 - 0.524)	<.001	1.245 (0.992 - 1.564)	.11
Clinical T stage	0.741 (0.722 - 0.761)	<.001	0.711 (0.602 - 0.839)	<.001
N stage	1.193 (1.103 - 1.290)	<.001	1569.010 (300.065 - 8209.112)	<.001
Liver metastasis	1.645 (1.131 - 2.392)	.03	1.533 (0.931 - 2.522)	.16
Differentiation extent	0.375 (0.347 - 0.405)	<.001	0.001 (0.000 - 0.008)	<.001
External validation cohort				
Sex	0.383 (0.344 - 0.425)	<.001	1.042 (0.821 - 1.323)	.78
Age	0.887 (0.878 - 0.897)	<.001	1.055 (1.007 - 1.105)	.06
Total number of lymph nodes	0.962 (0958 - 0.967)	<.001	1.016 (1.005 - 1.028)	.02
Tumor length	0.848 (0.834 - 0.862)	<.001	0.843 (0.797 - 0.891)	<.001
PNI	1.337 (1.077 - 1.660)	.03	3.142 (2.246 - 4.397)	<.001
CEA	0.465 (0.408 - 0.531)	<.001	1.295 (1.012 - 1.655)	.09
Clinical T stage	0.740 (0.718 - 0.762)	<.001	0.681 (0.568 - 0.815)	<.001
N stage	1.185 (1.088 - 1.292)	<.001	1307.798 (249.635 - 6849.973)	<.001
Liver metastasis	1.400 (0.945 - 2.075)	.16	Ref (Ref)	Ref
Differentiation extent	0.374 (0.344 - 0.407)	<.001	0.002 (0.000 - 0.009)	<.001

[a]OR: odds ratio.

[b]PNI: perineural invasion.

[c]CEA: carcinoembryonic antigen.

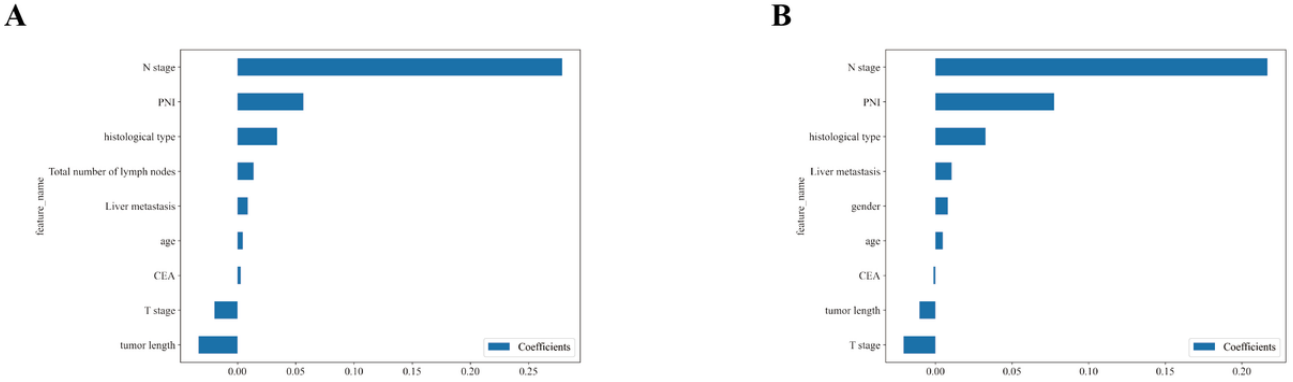
Optimal Predictive Model Selection

Feature Weight Ranking

Based on the penalty coefficient obtained from cross-validation, we selected features with coefficients greater than 0 and represented them using feature weights. The features in the training set and internal validation set are ranked as follows: Clinical N staging, receipt of chemotherapy or radiotherapy, neural invasion, tumor histology, tumor length, number of peritumoral and total lymph nodes examined, liver metastasis, age, CEA, clinical T stage, and tumor length (Figure 4A). In contrast, the features in the training set and external validation set are ranked as follows: Clinical N staging, receipt of chemotherapy or radiotherapy, neural invasion, tumor histology, tumor length, liver metastasis, gender, differentiation degree, age, CEA, tumor length, and clinical T stage (Figure 4B).

XSL•FO
RenderX

Figure 4. The weight of clinical features in the lymph node prediction model of rectal cancer. (A) Internal validation cohort. (B) External validation cohort. CEA: carcinoembryonic antigen; PNI: perineural invasion.



Model Performance Evaluation

In the internal validation cohort (n=500), the 11 ML models demonstrated a wide range of discriminative performance (AUC range 0.859 - 0.964). RF (AUC 0.964, 95% CI 0.950 - 0.978) and ET (AUC 0.964, 95% CI 0.949 - 0.978) achieved the highest AUC values, with sensitivities of 0.881 and 0.983 and specificities of 0.900 and 0.828, respectively (Multimedia Appendix 3). NB showed the lowest AUC (0.859, 95% CI 0.830 - 0.887) despite perfect sensitivity (1.000) but with specificity limited to 0.566. The XGB model yielded an AUC of 0.942 (95% CI 0.925 - 0.959), sensitivity of 0.795, and specificity of 0.913. In the external cohort (n=500), Gradient Boosting exhibited the highest AUC (0.838, 95% CI 0.801 - 0.875) but the lowest sensitivity (0.685); XGB (AUC 0.832, 95% CI 0.794 - 0.869) and LGBM (AUC 0.831, 95% CI 0.793 - 0.869) ranked second and third, with XGB demonstrating the smallest sensitivity-specificity gap (Δ=0.113) and an F_1-score of 0.690 (Table 3).

XSL•FO
RenderX

Table . Comprehensive performance metrics of machine learning models for lymph node metastasis prediction in patients with rectal cancer across validation cohorts.

Model name	AUC[a] (95% CI)	Accuracy	Sensitivity	Specificity	F_1 [b]
Internal validation cohort					
LR[c]	0.924 (0.9043 - 0.9435)	0.849	0.824	0.858	0.747
Naive Bayes	0.859 (0.8300 - 0.8873)	0.684	1.000	0.566	0.632
SVM[d]	0.924 (0.9038 - 0.9446)	0.801	0.920	0.756	0.715
KNN[e]	0.920 (0.8949 - 0.9442)	0.869	0.864	0.871	0.781
Random Forest	0.964 (0.9502 - 0.9784)	0.895	0.881	0.900	0.820
Extremely Randomized Trees	0.964 (0.9491 - 0.97820)	0.870	0.983	0.828	0.805
XGBoost	0.942 (0.9251 - 0.9585)	0.881	0.795	0.913	0.784
LGBM[f]	0.943 (0.9266 - 0.9602)	0.872	0.835	0.886	0.780
Gradient Boosting	0.909 (0.8889 - 0.9298)	0.722	1.000	0.619	0.662
AdaBoost	0.913 (0.8924 - 0.9330)	0.756	0.989	0.669	0.688
MLP[g]	0.935 (0.9168 - 0.9525)	0.813	0.932	0.769	0.731
External validation cohort					
LR[c]	0.821 (0.7817 - 0.8611)	0.760	0.702	0.789	0.667
Naive Bayes	0.749 (0.7027 - 0.7949)	0.662	0.845	0.567	0.631
SVM[d]	0.814 (0.7734 - 0.8539)	0.764	0.696	0.799	0.669
KNN[e]	0.781 (0.7383 - 0.8230)	0.697	0.756	0.666	0.630
Random Forest	0.759 (0.7137 - 0.8047)	0.725	0.655	0.762	0.620
Extremely Randomized Trees	0.735 (0.6894 - 0.7813)	0.672	0.762	0.625	0.614
XGBoost	0.832 (0.7943 - 0.8695)	0.752	0.708	0.821	0.690
LGBM[f]	0.831 (0.7928 - 0.8693)	0.776	0.732	0.799	0.691
Gradient Boosting	0.838 (0.8012 - 0.8750)	0.796	0.685	0.854	0.697
AdaBoost	0.815 (0 7761 - 0.8536)	0.768	0.589	0.861	0.635
MLP[g]	0.830 (0.7921 - 0.8671)	0.772	0.649	0.836	0.661

[a]AUC: Area Under the receiver operating characteristic curve.

[b]F1 Harmonic mean of precision and recall.

[c]LR: Logistic Regression.

[d]SVM: Support Vector Machine.

[e]KNN: K-Nearest Neighbors.

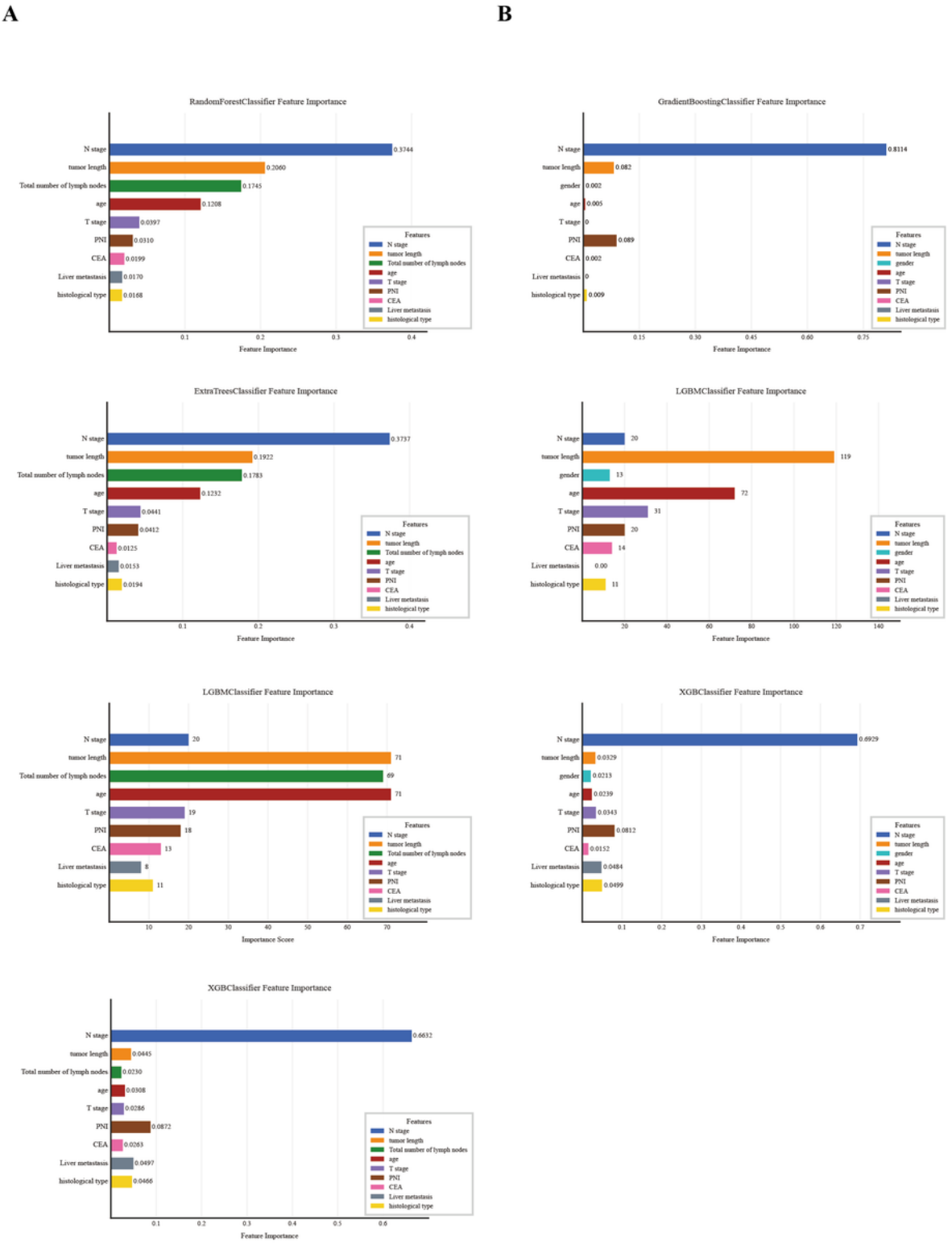
[f]LGBM: Light Gradient Boosting Machine.

[g]MLP: Multilayer Perceptron.

The relative importance of model variables varies between the internal and external validation sets, depending on the characteristics. In the internal validation set, the clinical N-stage is the most important variable for the RF, ET, and XGB models. However, for the LGBM model, age and tumor length are the most important variables. In the external validation set, tumor length, clinical N-stage, and nerve invasion are among the top three important features for both the GB and LGBM models (Figure 5). We assessed feature correlations using a heatmap (Figure 6). In both validation sets, no significant correlations were observed, indicating the absence of collinearity and the independence of variables.

XSL•FO
RenderX

Figure 5. Rank the relative importance of each input variable. (A) Internal validation cohort and (B) external validation cohort. CEA: carcinoembryonic antigen; LGBM: Light Gradient Boosting Machine; PNI: perineural invasion; XGB: XGBoost**.**



XSL•FO
RenderX

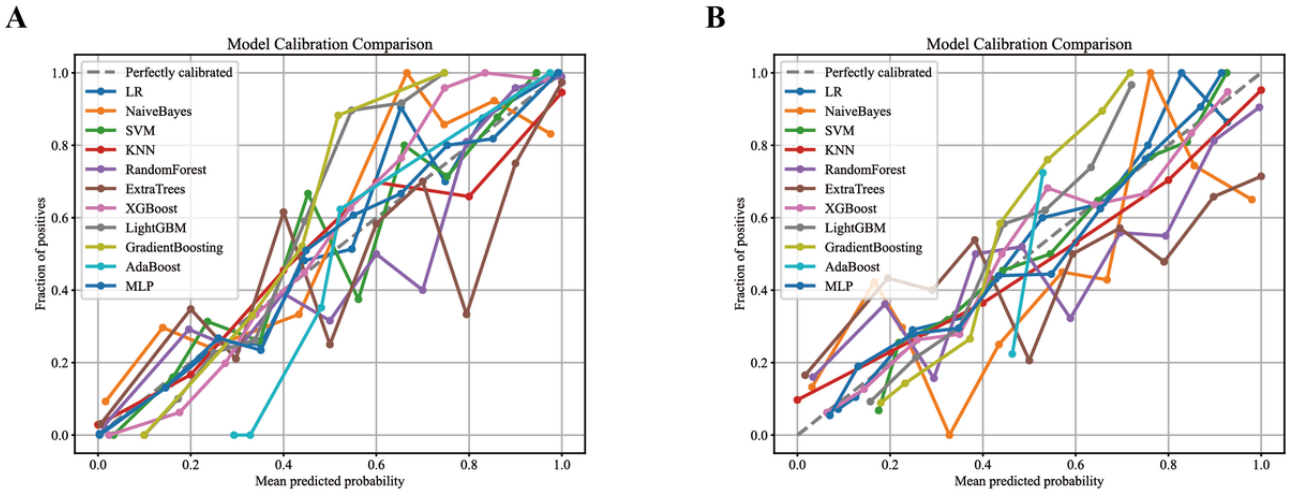
Figure 6. Correlation of clinical features. (A) Internal validation cohort and (B) external validation cohort.

XSL•FO
RenderX

Calibration Curve Analysis

Calibration curves (Figure 7) demonstrated the agreement between predicted probabilities and observed event frequencies. In the internal cohort (Figure 7A), the XGB curve adhered closest to the ideal diagonal (45° reference line) throughout, with minimal deviation from actual frequencies in the 0.3 - 0.7 probability range; ET exhibited consistent positioning above the diagonal at >0.8 probabilities (systematic overestimation), while RF deviated slightly below the diagonal between 0.6 and 0.8 (mild underestimation). In the external cohort (Figure 7B), XGB maintained the smallest overall deviation (closest to the diagonal); GB showed systematic distribution below the diagonal at 0.4 - 0.6 probabilities (underestimation), and LGBM positioned above the diagonal at <0.3 thresholds (overestimation).

Figure 7. Calibration curve of lymph node metastasis prediction in the internal validation cohort (A) and external validation cohort (B) of patients. The dashed diagonal line represents perfect calibration where predicted probability equals actual probability. KNN: K-Nearest Neighbors; LR: Logistic Regression; MLP: Multilayer Perceptron; SVM: Support Vector Machine.

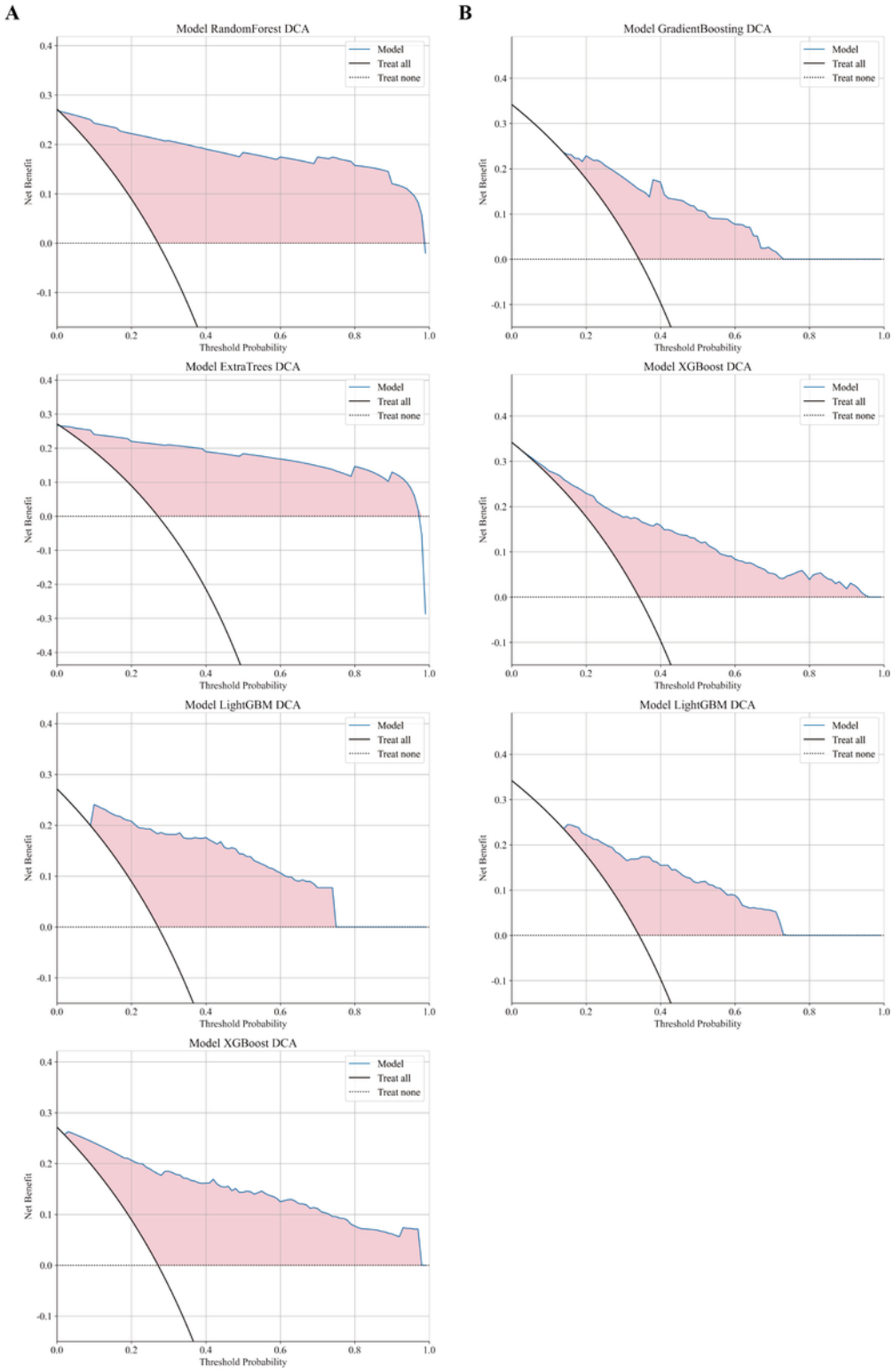


Decision Curve Analysis

We evaluated the net benefits of the models in both validation sets using DCA (Figure 8). In the internal validation set, DCA indicates that the XGB model has a net benefit similar to that of the XGB and LGBM models at lower threshold probabilities (approximately 0 - 0.3). Furthermore, the XGB model maintains net benefit across a broader range of threshold probabilities (approximately 0 - 0.9). Between 0.7 and 0.9, where the net benefits of other models decrease, the net benefit of the XGB model still sustains. The RF model shows net benefit within the range of 0 - 0.8. The ET model has a net benefit from 0.1 to 0.75. The LGBM model demonstrates net benefit in the range of 0.1 - 0.7. In the external validation set, DCA reveals that the XGB model's net benefit is higher than that of the GB and LGBM models when the threshold probability is between 0.3 and 0.4. Furthermore, the XGB model maintains net benefit across a broader range of threshold probabilities (approximately 0 - 0.4). The GB model shows net benefit within the range of 0.1 - 0.3, while the LGBM model has net benefit from 0.1 to 0.35.

XSL•FO
RenderX

Figure 8. Decision curve analysis of lymph node metastasis prediction in the internal validation cohort (A) and external validation cohort (B) of patients with RC. DCA: decision curve analysis.



Final Model Selection

XGB was selected as the definitive predictive model through comprehensive evaluation of cross-cohort discriminative stability, calibration fidelity, and clinical utility. The model achieved AUC values of 0.942 (95% CI 0.925 - 0.959) in the internal cohort and 0.832 (95% CI 0.794 - 0.869) in the external cohort, with a reduction in AUC of -0.110 between cohorts. This reduction was smaller than those observed for RF (−0.205), ET (−0.229), and GB (−0.071). Calibration curves demonstrated closest alignment to the ideal diagonal in the internal cohort (minimal deviation at 0.3 - 0.7 probabilities), whereas ET systematically overestimated risk at probabilities >0.8 and RF underestimated at 0.6 - 0.8. In the external cohort, XGB maintained minimal deviation, GB underestimated at 0.4 - 0.6 probabilities, and LGBM overestimated at thresholds <0.3. DCA

XSL•FO
RenderX

revealed that XGB sustained the broadest net benefit range (0 - 0.9) in the internal validation set, outperforming comparison models at 0.7 - 0.9 thresholds. In the external set, it maintained net benefit across 0 - 0.4 thresholds and yielded higher net benefit than GB and LGBM at 0.3 - 0.4 probability thresholds.

Confusion Matrix Analysis

Multimedia Appendix 4 displays the confusion matrices of the XGB model in the internal (A) and external (B) validation cohorts. In the internal cohort (n=500), the model correctly identified 333 LNM-negative cases (true negative) and 107 metastasis-positive cases (true positive), with 32 false positive and 28 false negative (FN) predictions. In the external cohort (n=500), it detected 160 true negative and 216 true positive cases, while generating 35 false positive and 89 FN classifications. The positive predictive value was 77% (107/139) in the internal cohort and 86.1% (216/251) in the external cohort; the negative predictive values were 92.2% (333/361) and 64.3% (160/249), respectively.

Discussion

Principal Findings

The main findings demonstrate that the XGB model achieved optimal performance in predicting RC LNM, with tumor differentiation grade, clinical T stage, tumor length, neural invasion, N stage, and total lymph node count identified as independent predictors. RC LNM significantly impacts patient prognosis, necessitating accurate prediction of LNM for the development of effective treatment plans. While traditional diagnostic methods offer some insights, their accuracy is constrained. This study employed ML algorithms to develop 11 prediction models for RC LNM. We extracted clinical data from the SEER database for the training and internal validation sets. Additionally, we acquired relevant clinical data from CT scans at the author's hospital, utilizing precise pixel-level annotation and measurement for the external validation set. We filtered clinical data using the LASSO, univariate, and multivariate logistic regression analyses to develop and validate a predictive model for LNM. The selection of the optimal model was determined through comparative analysis of internal and external validation sets, leveraging the AUC, calibration curves, and DCA for precise assessment.

In this study, we successfully developed and validated 11 ML models for predicting LNM in RC. This study revealed three key findings. First, the six independent predictors of LNM include tumor differentiation, clinical T stage, N stage, tumor length, total number of lymph nodes, and neural invasion. Second, among the 11 constructed ML models for predicting LNM, 10 models had an AUC greater than 0.9 in the internal validation set and 7 models had an AUC greater than 0.80 in the external validation set. Lastly, following a comparison of the models' performance and their validation set discrepancies, the XGB model emerged as the most suitable among the 11 models.

Comparison With Prior Studies

Utilizing LASSO logistic regression and multivariate analysis, we identified tumor differentiation, clinical T stage, N stage, tumor length, neural invasion, and total number of lymph nodes as the key clinical predictive factors. Low tumor differentiation, advanced clinical T stage, advanced N stage, increased tumor length, and neural invasion are significantly associated with LNM. Identifying these factors is essential to comprehend the tumor's biological behavior and invasive potential. Variations in feature importance across models (Figure 5) arise from the following factors: First, clinical data encompass both continuous (eg, tumor length) and categorical variables (eg, pathological grade), where XGB's exact splitting favors continuous features while LGBM's histogram-based algorithm optimizes high-dimensional sparse feature processing. Second, regularization differences lead to distinct weight allocation—XGB's combined L1/L2 regularization strictly controls overfitting, whereas LGBM's leaf-wise growth prioritizes locally significant features. Third, although LASSO-based feature selection reduced dimensionality, residual feature correlations are differentially processed. These inherent algorithmic variations confirm that no single model can fully capture feature relationships, necessitating multimodel comparison for complementary insights. Poorly differentiated tumor cells show greater invasiveness and a higher likelihood of LNM. A study by Saraste et al [24] involving 1664 patients with RC from the Swedish Rectal Cancer Registry between 2007 and 2010 concluded through multivariate analysis that poorly differentiated tumors are a significant risk factor for LNM, aligning with the findings of this study. Advanced clinical T stage is a direct indicator of deeper tumor invasion. A study by von den Grün et al [25], which involved a binary logistic regression multivariate analysis of 776 patients with RC, revealed that advanced T stage is a significant prognostic factor for LNM in RC. Previous studies [25-27] have established that clinical T stage and N stage significantly influence the prognosis and treatment of RC, aligning with the results of the univariate and multivariate analyses presented in Table 2. Increased tumor length may afford tumor cells increased opportunities to interact with adjacent lymph nodes. In a study [28] that employed 7 clinical parameters as independent prognostic factors to develop a nomogram prediction model, 6484 patients with RC from the SEER database were analyzed using Cox proportional hazards regression. This analysis identified independent prognostic factors such as T stage and tumor length. However, unlike this study, the aforementioned research did not include an external validation cohort. The presence of neural invasion indicates a high level of tumor invasiveness and the potential for dissemination along neural pathways. Neural invasion is a significant factor in both univariate and multivariate analyses, as well as in evaluating the importance of model features. Studies by Ueno et al [29] and Song et al [30] have shown that neural invasion is a significant factor in LNM in RC. The total number of perirectal examined lymph nodes, as a key factor, plays a crucial role in accurate staging and prognostic assessment of RC. Guan et al [31] found that a higher number of perirectal examined lymph nodes in RC is linked to more accurate lymph node staging and improved survival. Analyzing data from stage I to III resected RC in multi-institutional Chinese and US SEER databases revealed that an increasing number of perirectal examined lymph nodes significantly raises the proportion of cases shifting from lymph node-negative to lymph

XSL•FO
RenderX

node-positive. Furthermore, after adjusting for confounding factors, overall survival consistently improves.

Utilizing the selected clinical characteristics, we developed a predictive model for LNM in RC. We extracted a cohort of 2454 patients with RC from the SEER database and randomly selected 500 cases for the internal validation cohort. The remaining 1954 cases served as the training cohort, while an additional 500 cases from the author's hospital constituted the external validation cohort. In the internal validation set, the RF and ET models achieved an AUC of 0.964. The LGBM and XGB models also performed remarkably well, with AUC values of 0.943 and 0.942, respectively. Among all models, the NB model had the lowest AUC of 0.859, while the remaining 10 models all exceeded 0.9. In the external validation set, the GB model demonstrated the best performance with an AUC of 0.838, followed by the XGB and LGBM models, which reached AUC values of 0.832 and 0.831, respectively. In the study by Guan et al [18], 6578 patients with RC were enrolled across several institutions, including the Cancer Hospital of the Chinese Academy of Medical Sciences, Peking Union Medical College, Changhai Hospital of Naval Medical University, and the Second Affiliated Hospital of Harbin Medical University. The XGB model was identified as the optimal in their study, achieving AUCs of 0.78 and 0.71 across two validation cohorts. In contrast, our study's XGB model showed superior performance, achieving an AUC of 0.942 in the internal validation cohort and 0.832 in the external validation cohort. In the external validation cohort, LNM status, clinical T and N stages, and tumor length were ascertained through the annotation of CT imaging combined with clinical data. However, across both internal and external validation cohorts, most models in this study demonstrated relatively good performance across various validation sets, with the AUCs of the optimal models all exceeding 0.80, indicating a certain level of accuracy and reliability. These results demonstrate that our models exhibit high stability and generalizability across diverse datasets. Regardless of whether the patients with RC are in the United States or China, our models show accurate predictive ability for forecasting LNM in RC. Second, the LNM status and associated details in the 500 case records from the hospital were meticulously annotated by 50 physicians. These annotations were made by integrating clinical and pathological data using imaging software on enhanced CT scans. Following the initial annotation, two radiologists, possessing 8 and 20 years of experience, respectively, conducted a review and confirmation of the annotations. The multi-physician annotation strategy, which incorporates clinical pathology data and imaging software, boosts the reliability of the data and, in turn, elevates the predictive accuracy of the model. A similar approach was taken in Liu et al's study [32], wherein integrating clinical data with ML for magnetic resonance image analysis elevated the AUC value of single-region radiomics from 0.702 to 0.827. In a study by Wan et al [33], an automated segmentation method using deep learning demonstrated potential for predicting LNM in RC. However, our manual annotation method ensures precise localization of small lymph nodes (diameter < 5 mm) and ambiguous lesions, which are crucial for RC staging but challenging for automated tools. This strategy is particularly valuable in resource-limited environments lacking artificial intelligence infrastructure. Although magnetic resonance imaging is widely regarded as the gold standard for local T-staging and lymph node status assessment in RC, in this study, we chose to analyze CT images due to the diversity of data sources and the prevalence of CT images. CT scanning is less costly and quicker. Particularly, in resource-limited medical settings, CT remains a routine examination tool that can effectively provide important information on lymph node status and tumor staging. This highlights the benefits of integrating both clinical data and imaging information into ML models. While the annotation of CT images and their incorporation are standard practices in traditional radiomics and the development of deep learning models, they are less common in models derived solely from clinical data. This study shows that employing imaging software to annotate CT scans and extract data for clinical predictive models not only yields high-quality data for model development but also presents an innovative approach to data acquisition and processing for future studies.

Strengths and Limitations

A key innovation of this study is the comprehensive utilization of diverse advanced ML algorithms, coupled with the validation of the model's performance across data from various sources. Our models have shown strong generalization capabilities, as evidenced by their performance in both internal and external validation cohorts. Additionally, using LASSO logistic regression for feature selection enabled us to pinpoint key clinical predictive factors. This approach not only bolstered the model's predictive accuracy but also improved its interpretability. We presented the importance of features in a ranked order and investigated the correlations among variables with a correlation heatmap. Finally, the optimal model was ascertained through a comprehensive, evidence-based methodology integrating multimetric performance evaluation (AUC, 95% CI, accuracy, sensitivity, specificity, and F_1-score), augmented by high-resolution assessment of calibration curves and DCA.

Despite strong performance in both the internal and external validation sets, our model in this study has some limitations. First, the dataset is constrained by its population representativeness. The SEER database comprises exclusively American cases, and the dataset from the author's hospital consists solely of Chinese cases. This could impact the model's ability to generalize across diverse populations. In Shulman et al.'s study [34], which analyzed 34,500 patients with RC, it was found that patients of different races exhibited varying lymph node statuses. Second, the model did not include variables like BMI, alpha-fetoprotein, cancer antigen 125, carbohydrate antigen 19-9 [18], which were previously explored in clinical information. This omission could impact the model's predictive accuracy and comprehensiveness. Future studies could further refine predictive accuracy by incorporating serum biomarkers (eg, BMI, carbohydrate antigen 19-9) and emerging indicators such as circulating tumor DNA, combined with radiomic features. Third, FN classifications warrant clinical attention. The FN rate was 20.7% (28/135) in the internal cohort and 29.2% (89/305) in the external cohort. Such misclassifications may lead to undertreatment (eg, omission of adjuvant chemotherapy or lymph node dissection), increasing risks of

XSL•FO
RenderX

recurrence and metastasis. Crucially, while our model was developed to surpass conventional CT assessments, reducing FNs remains a priority for future optimization through biomarker integration or advanced imaging techniques. The study by Yu et al [35] demonstrated that incorporating multicenter data and multimodal features significantly reduced FN rates, providing a feasible direction for refining our model. In this study, we utilized 11 ML methods. Future research could further enhance the model's predictive performance by integrating diverse ML algorithms and leveraging their unique strengths.

Conclusions

In conclusion, this study successfully developed a ML-based risk prediction model for LNM in RC, validating its performance using both an internal and an external validation set. Through the analysis of extensive clinicopathological data, we identified tumor differentiation, clinical T stage, N stage, tumor length, neural invasion, and total number of lymph nodes as independent predictive factors. Among the 11 models evaluated, the XGB model demonstrated the best predictive performance. These models are anticipated to aid in clinical decision-making, offering vital insights for treatment selection and prognostic assessment of patients with RC. They hold significant clinical utility and scientific importance. Concurrently, the external validation set demonstrates that clinical data derived from CT imaging annotation and measurement are comparable to traditionally obtained clinical data and can effectively serve as a source of clinical data for ML applications.

Acknowledgments

This research was collectively supported by The University Synergy Innovation Program of Anhui Province (Grant No. GXXT-2022-056) and the Key Project of the Department of Education Quality Engineering (Grant No. 2023jyxm1111). We thank the SEER (Surveillance, Epidemiology, and End Results) database and the First Affiliated Hospital of Anhui Medical University for providing patient data. The authors sincerely thank all the staff of our department for their help in data collection, sample annotation, and manuscript writing. The following is the list of personnel who have contributed to pixelated annotation: Jiarui Zhang, Xiaosu Li, Xiaoya Wang, Wenna Chai, Chuiyan Huang, Tianxu Yang, Jingwen Hu, Yiran Zhang, Ping Wang, Bingjing Zhu, Jiani Ma, Yuyan Ma.

Data Availability

The raw data sets are available only upon reasonable request because of privacy and ethical restrictions. The data are not publicly available because of these restrictions. The code is available upon reasonable request.

Authors' Contributions

WH and CL are primarily responsible for data organization, analysis, and model construction. ZW was in charge of literature search and data collection. WW provided guidance on data analysis. SW offered guidance on model construction and validation. BZ was responsible for literature quality assessment and manuscript review and served as the corresponding author. All authors have read and approved the manuscript.

Conflicts of Interest

None declared.

Multimedia Appendix 1
Normalization standards of clinical data.
[DOCX File, 14 KB - medinform_v13i1e73765_app1.docx]

Multimedia Appendix 2
The hyperparameter settings and tuning strategies of the 11 models.
[DOCX File, 15 KB - medinform_v13i1e73765_app2.docx]

Multimedia Appendix 3
Range standard for property values of clinical features in models.
[DOCX File, 20 KB - medinform_v13i1e73765_app3.docx]

Multimedia Appendix 4
Confusion matrices for lymph node metastasis (LNM) prediction in rectal cancer (RC) patients.
[PNG File, 86 KB - medinform_v13i1e73765_app4.png]

References

XSL•FO
RenderX

1. Siegel RL, Miller KD, Goding Sauer A, et al. Colorectal cancer statistics, 2020. CA Cancer J Clin 2020 May;70(3):145-164. [doi: 10.3322/caac.21601] [Medline: 32133645]
2. Bray F, Laversanne M, Sung H, et al. Global cancer statistics 2022: GLOBOCAN estimates of incidence and mortality worldwide for 36 cancers in 185 countries. CA Cancer J Clin 2024;74(3):229-263. [doi: 10.3322/caac.21834] [Medline: 38572751]
3. Morgan E, Arnold M, Gini A, et al. Global burden of colorectal cancer in 2020 and 2040: incidence and mortality estimates from GLOBOCAN. Gut 2023 Feb;72(2):338-344. [doi: 10.1136/gutjnl-2022-327736] [Medline: 36604116]
4. Liersch T, Langer C, Ghadimi BM, et al. Lymph node status and TS gene expression are prognostic markers in stage II/III rectal cancer after neoadjuvant fluorouracil-based chemoradiotherapy. J Clin Oncol 2006 Sep 1;24(25):4062-4068. [doi: 10.1200/JCO.2005.04.2739] [Medline: 16943523]
5. Kuru B, Camlibel M, Dinç S, Erdem E, Alagöl H. Prognostic factors affecting local recurrence and survival for operable rectal cancers. J Exp Clin Cancer Res 2002 Sep;21(3):329-335. [Medline: 12385573]
6. Leibold T, Shia J, Ruo L, et al. Prognostic implications of the distribution of lymph node metastases in rectal cancer after neoadjuvant chemoradiotherapy. J Clin Oncol 2008 May 1;26(13):2106-2111. [doi: 10.1200/JCO.2007.12.7704] [Medline: 18362367]
7. Isaka N, Nozue M, Doy M, Fukao K. Prognostic significance of perirectal lymph node micrometastases in Dukes' B rectal carcinoma: an immunohistochemical study by CAM5.2. Clin Cancer Res 1999 Aug;5(8):2065-2068. [Medline: 10473087]
8. Govindarajan A, Gönen M, Weiser MR, et al. Challenging the feasibility and clinical significance of current guidelines on lymph node examination in rectal cancer in the era of neoadjuvant therapy. J Clin Oncol 2011 Dec 1;29(34):4568-4573. [doi: 10.1200/JCO.2011.37.2235] [Medline: 21990400]
9. Moons LMG, Bastiaansen BAJ, Richir MC, et al. Endoscopic intermuscular dissection for deep submucosal invasive cancer in the rectum: a new endoscopic approach. Endoscopy 2022 Oct;54(10):993-998. [doi: 10.1055/a-1748-8573] [Medline: 35073588]
10. Anitei MG, Zeitoun G, Mlecnik B, et al. Prognostic and predictive values of the immunoscore in patients with rectal cancer. Clin Cancer Res 2014 Apr 1;20(7):1891-1899. [doi: 10.1158/1078-0432.CCR-13-2830] [Medline: 24691640]
11. Abbaspour E, Karimzadhagh S, Monsef A, Joukar F, Mansour-Ghanaei F, Hassanipour S. Application of radiomics for preoperative prediction of lymph node metastasis in colorectal cancer: a systematic review and meta-analysis. Int J Surg 2024 Jun 1;110(6):3795-3813. [doi: 10.1097/JS9.0000000000001239] [Medline: 38935817]
12. Chu LC, Fishman EK. Pancreatic ductal adenocarcinoma staging: a narrative review of radiologic techniques and advances. Int J Surg 2024 Oct 1;110(10):6052-6063. [doi: 10.1097/JS9.0000000000000899] [Medline: 38085802]
13. Ushigome H, Fukunaga Y, Nagasaki T, et al. Difficulty of predicting lymph node metastasis on CT in patients with rectal neuroendocrine tumors. PLoS ONE 2019;14(2):e0211675. [doi: 10.1371/journal.pone.0211675] [Medline: 30742649]
14. Dankwa-Mullan I, Weeraratne D. Artificial intelligence and machine learning technologies in cancer care: addressing disparities, bias, and data siversity. Cancer Discov 2022 Jun 2;12(6):1423-1427. [doi: 10.1158/2159-8290.CD-22-0373] [Medline: 35652218]
15. Müller S, Diekmann S, Wenzel M, et al. Combining machine learning with real-world data to identify gaps in clinical practice guidelines: feasibility study using the prospective German stroke registry and the national acute ischemic stroke guidelines. JMIR Med Inform 2025 Jul 11;13:e69282. [doi: 10.2196/69282] [Medline: 40653745]
16. Nemlander E, Ewing M, Abedi E, et al. A machine learning tool for identifying non-metastatic colorectal cancer in primary care. Eur J Cancer 2023 Mar;182(100-6):100-106. [doi: 10.1016/j.ejca.2023.01.011] [Medline: 36758474]
17. Hamerla G, Meyer HJ, Hambsch P, et al. Radiomics model based on non-contrast CT shows no predictive power for complete pathological response in locally advanced rectal cancer. Cancers (Basel) 2019 Oct 29;11(11):1680. [doi: 10.3390/cancers11111680] [Medline: 31671766]
18. Guan X, Yu G, Zhang W, et al. An easy-to-use artificial intelligence preoperative lymph node metastasis predictor (LN-MASTER) in rectal cancer based on a privacy-preserving computing platform: multicenter retrospective cohort study. Int J Surg 2023 Mar 1;109(3):255-265. [doi: 10.1097/JS9.0000000000000067] [Medline: 36927812]
19. Ding L, Liu GW, Zhao BC, et al. Artificial intelligence system of faster region-based convolutional neural network surpassing senior radiologists in evaluation of metastatic lymph nodes of rectal cancer. Chin Med J (Engl) 2019 Feb;132(4):379-387. [doi: 10.1097/CM9.0000000000000095] [Medline: 30707177]
20. Weiser MR, Chou JF, Keshinro A, et al. Development and assessment of a clinical calculator for estimating the likelihood of recurrence and survival among patients with locally advanced rectal cancer treated with chemotherapy, radiotherapy, and surgery. JAMA Netw Open 2021 Nov 1;4(11):e2133457. [doi: 10.1001/jamanetworkopen.2021.33457] [Medline: 34748003]
21. Lu Y, Yu Q, Gao Y, et al. Identification of metastatic lymph nodes in MR imaging with faster region-based convolutional neural networks. Cancer Res 2018 Sep 1;78(17):5135-5143. [doi: 10.1158/0008-5472.CAN-18-0494] [Medline: 30026330]
22. Li S, Li Z, Wang L, et al. CT morphological features for predicting the risk of lymph node metastasis in T1 colorectal cancer. Eur Radiol 2023 Oct;33(10):6861-6871. [doi: 10.1007/s00330-023-09688-9] [Medline: 37171490]

XSL•FO
RenderX

23. Niu Y, Wen L, Yang Y, et al. Diagnostic performance of node reporting and data system (Node-RADS) for assessing mesorectal lymph node in rectal cancer by CT. BMC Cancer 2024 Jun 11;24(1):716. [doi: 10.1186/s12885-024-12487-0] [Medline: 38862951]
24. Saraste D, Gunnarsson U, Janson M. Predicting lymph node metastases in early rectal cancer. Eur J Cancer 2013 Mar;49(5):1104-1108. [doi: 10.1016/j.ejca.2012.10.005] [Medline: 23122785]
25. von den Grün JM, Hartmann A, Fietkau R, et al. Can clinicopathological parameters predict for lymph node metastases in ypT0-2 rectal carcinoma? Results of the CAO/ARO/AIO-94 and CAO/ARO/AIO-04 phase 3 trials. Radiother Oncol 2018 Sep;128(3):557-563. [doi: 10.1016/j.radonc.2018.06.008] [Medline: 29929861]
26. Gunderson LL, Sargent DJ, Tepper JE, et al. Impact of T and N stage and treatment on survival and relapse in adjuvant rectal cancer: a pooled analysis. J Clin Oncol 2004 May 15;22(10):1785-1796. [doi: 10.1200/JCO.2004.08.173] [Medline: 15067027]
27. Duchalais E, Glyn Mullaney T, Spears GM, et al. Prognostic value of pathological node status after neoadjuvant radiotherapy for rectal cancer. Br J Surg 2018 Oct;105(11):1501-1509. [doi: 10.1002/bjs.10867] [Medline: 29663352]
28. Zhao S, Chen X, Wen D, Zhang C, Wang X. Oncologic nomogram for stage I rectal cancer to assist patient selection for adjuvant (chemo)radiotherapy following local excision. Front Oncol 2021;11(632085):33816269. [doi: 10.3389/fonc.2021.632085] [Medline: 33816269]
29. Ueno H, Hase K, Mochizuki H. Criteria for extramural perineural invasion as a prognostic factor in rectal cancer. Br J Surg 2001 Jul;88(7):994-1000. [doi: 10.1046/j.0007-1323.2001.01810.x] [Medline: 11442534]
30. Song JH, Yu M, Kang KM, et al. Significance of perineural and lymphovascular invasion in locally advanced rectal cancer treated by preoperative chemoradiotherapy and radical surgery: can perineural invasion be an indication of adjuvant chemotherapy? Radiother Oncol 2019 Apr;133:125-131. [doi: 10.1016/j.radonc.2019.01.002] [Medline: 30935568]
31. Guan X, Jiao S, Wen R, et al. Optimal examined lymph node number for accurate staging and long-term survival in rectal cancer: a population-based study. Int J Surg 2023 Aug 1;109(8):2241-2248. [doi: 10.1097/JS9.0000000000000320] [Medline: 37428195]
32. Liu X, Yang Q, Zhang C, et al. Multiregional-based magnetic resonance imaging radiomics combined with clinical data improves efficacy in predicting lymph node metastasis of rectal cancer. Front Oncol 2020;10(585767):585767. [doi: 10.3389/fonc.2020.585767] [Medline: 33680919]
33. Wan L, Hu J, Chen S, et al. Prediction of lymph node metastasis in stage T1-2 rectal cancers with MRI-based deep learning. Eur Radiol 2023 May;33(5):3638-3646. [doi: 10.1007/s00330-023-09450-1] [Medline: 36905470]
34. Shulman RM, Deng M, Handorf EA, Meyer JE, Lynch SM, Arora S. Factors associated with racial and ethnic disparities in locally advanced rectal cancer outcomes. JAMA Netw Open 2024 Feb 5;7(2):e240044. [doi: 10.1001/jamanetworkopen.2024.0044] [Medline: 38421650]
35. Yu Y, Xu Z, Shao T, et al. Epidemiology and a predictive model of prognosis index based on machine learning in primary breast lymphoma: population-based study. JMIR Public Health Surveill 2023 Jun 8;9:e45455. [doi: 10.2196/45455] [Medline: 37169516]

Abbreviations

AB: Ada-Boost
AJCC: American Joint Committee on Cancer
AUC: area under the receiver operating characteristic curve
CEA: carcinoembryonic antigen
CT: computed tomography
DCA: decision curve analysis
ET: Extremely Randomized Trees
GB: Gradient Boosting
KNN: K-Nearest Neighbors
LASSO: Least Absolute Shrinkage and Selection Operator
LGBM: Light Gradient Boosting Machine
LNM: lymph node metastasis
LR: Logistic Regression
ML: machine learning
MLP: Multilayer Perceptron
NB: Naive Bayes
PNI: Perineural Invasion
RC: rectal cancer
RF: Random Forest
SEER: Surveillance, Epidemiology, and End Results
SVM: Support Vector Machine

XSL•FO
RenderX

XGBoost: Extreme Gradient Boosting

Edited by A Coristine; submitted 11.03.25; peer-reviewed by C Yin, M Hjärtström, T Chen; revised version received 29.07.25; accepted 30.07.25; published 23.09.25.

Please cite as:
Hou W, Li C, Wang Z, Wang W, Wan S, Zou B
Predicting Lymph Node Metastasis in Rectal Cancer: Development and Validation of a Machine Learning Model Using Clinical Data
JMIR Med Inform 2025;13:e73765
URL: https://medinform.jmir.org/2025/1/e73765
doi:10.2196/73765

© Wei Hou, Chuangwei Li, Zhen Wang, Wanqin Wang, Shouhong Wan, Bingbing Zou. Originally published in JMIR Medical Informatics (https://medinform.jmir.org), 23.9.2025. This is an open-access article distributed under the terms of the Creative Commons Attribution License (https://creativecommons.org/licenses/by/4.0/), which permits unrestricted use, distribution, and reproduction in any medium, provided the original work, first published in JMIR Medical Informatics, is properly cited. The complete bibliographic information, a link to the original publication on https://medinform.jmir.org/, as well as this copyright and license information must be included.

XSL•FO
RenderX

Interpretable Machine Learning Model for Pulmonary Hypertension Risk Prediction: Retrospective Cohort Study

Hongxia Jiang[1*], PhD; Han Gao[1*], PhD; Dexin Wang[2*], PhD; Qingli Zeng[1], MD; Xiaojun Hao[1], PhD; Zhenshun Cheng[1,3,4], PhD

[1]Department of Respiratory and Critical Care Medicine, Zhongnan Hospital of Wuhan University, Number 169, Donghu Road, Wuchang District, Wuhan, China

[2]Department of Respiratory and Critical Care Medicine, Qichun County People's Hospital, Huanggang, China

[3]Wuhan Research Center for Infectious Diseases and Cancer, Chinese Academy of Medical Sciences, Wuhan, China

[4]Hubei Engineering Center for Infectious Disease Prevention, Control and Treatment, Wuhan, China

[*]these authors contributed equally

Corresponding Author:
Zhenshun Cheng, PhD
Department of Respiratory and Critical Care Medicine, Zhongnan Hospital of Wuhan University, Number 169, Donghu Road, Wuchang District, Wuhan, China

Abstract

Background: Pulmonary hypertension (PH) is a progressive disorder characterized by elevated pulmonary artery pressure and increased pulmonary vascular resistance, ultimately leading to right heart failure. Early detection is critical for improving patient outcomes.

Objective: The diagnosis of PH primarily relies on right heart catheterization, but its invasive nature significantly limits its clinical use. Echocardiography, as the most common noninvasive screening and diagnostic tool for PH, provides valuable patient information. This study aims to identify key PH predictors from echocardiographic parameters, laboratory tests, and demographic data using machine learning, ultimately constructing a predictive model to support early noninvasive diagnosis of PH.

Methods: This study compiled comprehensive datasets comprising echocardiography measurements, clinical laboratory data, and fundamental demographic information from patients with PH and matched controls. The final analytical cohort consisted of 895 participants with 85 evaluated variables. Recursive feature elimination was used to select the most relevant echocardiographic variables, which were subsequently integrated into a composite ultrasound index using machine learning techniques, XGBoost (Extreme Gradient Boosting). LASSO (least absolute shrinkage and selection operator) regression was applied to select the potential predictive variable from laboratory tests. Then, the ultrasound index variables and selected laboratory tests were combined to construct a logistic regression model for the predictive diagnosis of PH. The model's performance was rigorously evaluated using receiver operating characteristic curves, calibration plots, and decision curve analysis to ensure its clinical relevance and accuracy. Both internal and external validation were used to assess the performance of the constructed model.

Results: A total of 16 echocardiographic parameters (right atrium diameter, pulmonary artery diameter, left atrium diameter, tricuspid valve reflux degree, right ventricular diameter, E/E' [ratio of mitral valve early diastolic inflow velocity (E) to mitral annulus early diastolic velocity (E')], interventricular septal thickness, left ventricular diameter, ascending aortic diameter, left ventricular ejection fraction, left ventricular outflow tract velocity, mitral valve reflux degree, pulmonary valve outflow velocity, mitral valve inflow velocity, aortic valve reflux degree, and left ventricular posterior wall thickness) combined with 2 laboratory biomarkers (prothrombin time activity and cystatin C) were identified as optimal predictors, forming a high-performance PH prediction model. The diagnostic model demonstrated high predictive accuracy, with an area under the receiver operating characteristic curve of 0.997 in the internal validation and 0.974 in the external validation. Both calibration plots and decision curve analysis validated the model's predictive accuracy and clinical applicability, with optimal performance observed at higher risk stratification cutoffs.

Conclusions: This model enhances early PH diagnosis through a noninvasive approach and demonstrates strong predictive accuracy. It facilitates early intervention and personalized treatment, with potential applications in broader cardiovascular disease management.

(JMIR Med Inform 2025;13:e74117) doi:10.2196/74117

KEYWORDS

pulmonary hypertension; machine learning; risk prediction; echocardiography; clinical data

XSL•FO
RenderX

Introduction

Pulmonary hypertension (PH) is a progressive and complex vascular disorder characterized by elevated mean pulmonary artery pressure (mPAP) and increased pulmonary vascular resistance, ultimately leading to right heart failure [1]. According to the World Symposium on Pulmonary Hypertension classification system, PH is categorized into 5 major groups. Delayed diagnosis and treatment impose an unacceptably high mortality burden across all categories of PH patients. However, the current gold standard for PH diagnosis—right heart catheterization (RHC)—is significantly limited in clinical application due to its invasive nature, resulting in delayed PH diagnosis. Thus, early identification and risk assessment through noninvasive methods are critical for improving patient outcomes [2-5].

Echocardiography, as a noninvasive imaging modality, has become integral to the evaluation of PH. It enables clinicians to assess right ventricular size and function and estimate pulmonary artery pressures through tricuspid regurgitation velocity (TRV) and pulmonary artery systolic pressure. Several studies have highlighted the importance of echocardiographic parameters including right ventricular size, function, and TRV in predicting PH severity and outcomes [6-8]. Moreover, comprehensive models such as the Registry to Evaluate Early and Long-term Pulmonary Arterial Hypertension Disease Echocardiographic Correlation Hemodynamic Observational Study score, which integrate multiple echocardiographic variables, have significantly improved the ability to predict PH risk and have been validated across multiple cohorts [6,9].

However, relying solely on echocardiographic data for PH diagnosis and risk prediction has limitations. Recent research has increasingly emphasized the need to integrate echocardiographic findings with clinical data, including age, sex, BMI, and comorbidities, to enhance predictive accuracy [10,11]. For instance, studies involving hyperthyroid patients demonstrated that models incorporating both clinical variables and echocardiographic parameters significantly improved PH risk assessment [12]. Likewise, nomogram models that integrate these data have shown efficacy in evaluating PH risk for both postoperative patients and those with concurrent conditions such as obstructive sleep apnea [13,14]

Beyond variable collection, methodological rigor is equally critical for building precise predictive models. In recent years, the application of machine learning techniques to PH risk prediction has gained traction. Methods such as recursive feature elimination (RFE) and advanced algorithms such as random forests and XGBoost (Extreme Gradient Boosting) have been shown to optimize feature selection, improving model robustness and prediction accuracy [14]. These advancements, particularly when integrating echocardiographic and clinical data, have yielded models that outperform traditional methods in PH risk prediction [5].

In this study, we systematically collected comprehensive datasets including echocardiographic parameters, laboratory test results, and baseline demographic characteristics (age and sex) from both PH patients and matched controls. Using multiple machine learning approaches, we developed an early diagnostic and predictive model for PH. The model's performance was rigorously evaluated through receiver operating characteristic (ROC) analysis, decision curve analysis (DCA), and calibration curves, with both internal and external validation procedures. Comparative analyses against existing PH diagnostic models demonstrated the superior predictive accuracy and clinical utility of our novel model, highlighting its significant advancements in early PH detection through the integration of multimodal biomarkers and optimized machine learning architecture.

Methods

Ethical Considerations

This study was approved by the research ethics commission of Wuhan Zhongnan Hospital, and the requirement for informed consent was waived by the ethics commission (2023185). We have anonymized all patient identifiers, including names and hospital numbers, from the original dataset. The published information contains no data that could be used to infer the identity of individual patients. Furthermore, all participants will benefit from this research outcome through complimentary risk prediction for pulmonary arterial hypertension.

Study Population and Data Collection

This retrospective study analyzed data from 294 patients with PH and 1231 control subjects who underwent echocardiographic evaluation at Zhongnan Hospital of Wuhan University between January 2022 and April 2024. Propensity score matching was implemented to mitigate potential confounding factors. This cohort served as both the training and internal validation dataset. For external validation, we prospectively collected an independent dataset comprising patients evaluated from May 2024 through May 2025. The inclusion criteria for the PH group were (1) a discharge diagnosis of PH; (2) confirmation of PH through RHC; and (3) participants aged >14 years, as pediatric and adult cardiac parameters have distinct reference ranges. Patients were excluded if (1) the mPAP, as measured by RHC was <20 mm Hg; or (2) the mPAP data from RHC were missing. The inclusion criteria for the control group were (1) echocardiography results indicating no abnormalities in cardiac morphology, valve function, or ventricular wall motion; and (2) age >14 years. Control subjects were excluded if more than 5% of their data were missing.

Data Collection and Variables

Data collected included demographic information (age and gender), echocardiographic parameters, and laboratory test results. Echocardiographic parameters assessed cardiac structure and function, including measurements such as ascending aortic diameter, left atrial and left ventricular size, interventricular septal thickness, and pulmonary artery diameter (PAD). Additionally, the degree of regurgitation, flow velocity, and pressure gradients for the mitral, tricuspid, and aortic valves were recorded. All echocardiographic measurements were double-checked to ensure consistency and accuracy. Laboratory data included complete blood count, coagulation profiles, liver and kidney function, and electrolytes.

XSL•FO
RenderX

Data Preprocessing

In the data preprocessing phase, missing values were imputed with each variable's median using R (version 1.4.3; R Foundation) to ensure completeness. This approach was applied uniformly across both echocardiographic and laboratory variables, which had varying degrees of missingness, thereby maintaining sample size while minimizing bias from data exclusion. We ran stratified 10-fold cross-validation, limiting oversampling to the training folds to preserve unbiased evaluation in the held-out folds. Finally, continuous variables were mean-centered and scaled to unit variance, and categorical variables were encoded as factors for downstream analyses.

Feature Selection

We used stratified sampling to randomly split the data into training and testing sets in a 3:1 ratio. For selecting features from echocardiographic variables, we applied RFE using a random forest-based approach. RFE iteratively removed features with the least contribution to model performance, ultimately identifying the optimal subset of features. To ensure robustness and generalizability, we used 10-fold cross-validation during feature selection.

Using the selected echocardiographic features, we trained multiple machine learning models, including logistic regression, LASSO (least absolute shrinkage and selection operator) regression, elastic net, decision tree, random forest, XGBoost, support vector machine, k-nearest neighbors, naive Bayes, and gradient boosting machine. Model training and evaluation were primarily conducted using the *caret* package [15]. We used 10-fold cross-validation and grid search to optimize the hyperparameters. The primary performance metric was the area under the receiver operating characteristic curve (AUC), which was computed and plotted using the *pROC* package. The model with the highest AUC was selected as the optimal model for the echocardiographic features. For the optimal model, we further performed internal validation using bootstrap methods to evaluate its robustness. To enhance model interpretability, we applied SHAP (Shapley Additive Explanations) to quantify each feature's contribution to an individual prediction. In lay terms, a SHAP value represents how much a given variable increases or decreases the predicted PH risk for a patient compared to the average risk. Finally, we developed an ultrasound index based on the optimal model in the training and test sets.

For feature selection from routine clinical variables, we conducted LASSO regression analysis using the *glmnet* package. A 10-fold cross-validation was used to select the optimal regularization parameter. Specifically, we calculated a range of lambda values and chose lambda.1se, which is the lambda value with the best performance in cross-validation, adjusted by 1 SE.

Logistic Regression and Nomogram Construction

After identifying the optimal echocardiographic features and selected clinical variables, we combined them to develop a comprehensive logistic regression model. The model was fitted using the "lrm" function from the *rms* package. To prevent overfitting, we incorporated L2 regularization (learning 2 ridge regression) as needed. Analysis of model coefficients provided insights into the contribution of each feature to predicting PH.

To facilitate the clinical application of the model, we constructed a nomogram using the "nomogram" function from the *rmsv* package. This nomogram visualizes the logistic regression model in an easy-to-use format, allowing clinicians to estimate an individual's probability of developing PH by summing the scores for each predictive variable. The use of a nomogram ensures the interpretability and practicality of the model in a clinical setting.

Model Calibration and DCA

To assess the performance of the nomogram and logistic regression model, we used the ROC curve. To evaluate the consistency between the predicted probabilities and observed outcomes, calibration curves were plotted using the "calibrate" function from the *rms* package. Additionally, DCA was conducted using the *rmda* package to quantify the net benefit of the model across different threshold probabilities, providing insight into its clinical utility. Finally, we developed a web-based tool to facilitate the prediction of the risk of PH using R packages *shiny* (version 1.9.1).

External Validation

We externally validated the model using an independent cohort of patients admitted to the Respiratory Medicine Department at Zhongnan Hospital, Wuhan University, between May 2024 and May 2025. The inclusion and exclusion criteria were identical to those of the derivation cohort.

Statistical Analysis

The SHAP analysis was conducted using SHAP (version 0.46.0) in Python (version 3.10.8; Python Software Foundation), while all other statistical analyses were performed using R (version 4.4.1). For continuous variables that followed a normal distribution, group comparisons were made using 2-tailed *t* tests. For continuous variables that did not follow a normal distribution, nonparametric tests, such as the Mann-Whitney *U* test or the Kruskal-Wallis test, were applied. Categorical variables were presented as percentages and compared between groups using the chi-square test. A $P<.05$ was considered statistically significant.

Results

Statistical Characterization and Intergroup Comparisons of Clinical Variables in Patients With PH Versus Matched Controls

This study ultimately included a cohort of 714 control participants and 181 patients with PH. As shown in Table 1, PH patients exhibited significantly enlarged ascending aorta, left atrium, left ventricle, right atrium, and right ventricle dimensions (all $P<.05$), along with reduced left ventricular ejection fraction (%), indicating progressive chamber dilation and impaired systolic function. Hematologic analysis revealed elevated red blood cell counts and neutrophil percentage, coupled with reduced platelet counts and lymphocyte percentage (all $P<.05$), suggesting a proinflammatory, hypercoagulable profile. Patients with PH had prolonged prothrombin time,

XSL•FO
RenderX

reduced prothrombin time activity, and increased international normalized ratio, in addition to elevated total, direct, and indirect bilirubin levels (all $P<.05$), reflecting both coagulopathy and hepatic congestion. Serum cystatin C (CysC) is also found to be significantly elevated in patients with PH. Further, patients with PH experienced electrolyte imbalances—lower potassium, sodium, and phosphorus levels alongside higher chloride and calcium (all $P<.05$)—indicating disrupted electrolyte homeostasis. Together, these multisystem alterations underscore the complex structural, hematologic, coagulation, hepatic, and electrolyte derangements characteristic of PH.

XSL•FO
RenderX

Table . Characteristics of the analyzed cohort.

Variables		Normal (n=714)	PH[a] (n=181)	Overall (n=895)	*P* value
Age (years)					.38
	Mean (SD)	52.0 (13.8)	53.2 (16.9)	52.3 (14.5)	
	Median (Min[b], Max[c])	53.0 (15.0, 88.0)	54.7 (16.0, 85.1)	54.0 (15.0, 88.0)	
Sex, n (%)					.81
	Male	310 (43.4)	81 (44.8)	391 (43.7)	
	Female	404 (56.6)	100 (55.2)	504 (56.3)	
Ascending aortic diameter (AAD, cm)					.002
	Mean (SD)	3.02 (0.280)	3.15 (0.540)	3.05 (0.352)	
	Median (Min, Max)	3.10 (2.20, 3.70)	3.20 (1.80, 4.90)	3.10 (1.80, 4.90)	
Left atrium diameter (LAD, cm)					<.001
	Mean (SD)	3.18 (0.362)	4.22 (1.18)	3.39 (0.746)	
	Median (Min, Max)	3.20 (1.80, 4.30)	4.00 (2.10, 7.70)	3.30 (1.80, 7.70)	
Left ventricular diameter (LVD, cm)					<.001
	Mean (SD)	4.41 (0.333)	4.98 (1.42)	4.53 (0.740)	
	Median (Min, Max)	4.40 (3.20, 5.30)	4.60 (2.50, 9.90)	4.40 (2.50, 9.90)	
Interventricular septal thickness (IVS, cm)					<.001
	Mean (SD)	0.933 (0.112)	0.997 (0.210)	0.946 (0.140)	
	Median (Min, Max)	0.900 (0, 1.30)	1.00 (0.500, 2.10)	0.900 (0, 2.10)	
	Missing, n (%)	0 (0)	1 (0.6)	1 (0.1)	
Left ventricular posterior wall thickness (LVPW, cm)					.002
	Mean (SD)	0.908 (0.0988)	0.968 (0.254)	0.920 (0.146)	
	Median (Min, Max)	0.900 (0.600, 1.20)	1.00 (0.500, 3.40)	0.900 (0.500, 3.40)	
	Missing, n (%)	0 (0)	1 (0.6)	1 (0.1)	
Right atrium diameter (RAD, cm)					<.001
	Mean (SD)	30.8 (3.74)	47.2 (13.1)	34.1 (9.45)	
	Median (Min, Max)	31.0 (20.0, 41.0)	46.0 (0, 107)	32.0 (0, 107)	
Right ventricular diameter (RVD, cm)					<.001
	Mean (SD)	3.01 (0.362)	4.33 (1.13)	3.28 (0.799)	
	Median (Min, Max)	3.00 (1.90, 4.10)	4.15 (2.30, 7.60)	3.10 (1.90, 7.60)	
	Missing, n (%)	0 (0)	1 (0.6)	1 (0.1)	
Pulmonary artery diameter (PAD, cm)					<.001
	Mean (SD)	20.7 (2.08)	29.8 (8.44)	22.5 (5.58)	
	Median (Min, Max)	21.0 (14.0, 31.0)	28.0 (0, 62.0)	21.0 (0, 62.0)	
Left ventricular fractional shortening (LVFS, %)					<.001
	Mean (SD)	36.0 (3.86)	32.6 (5.97)	35.4 (4.50)	
	Median (Min, Max)	35.0 (22.0, 47.0)	33.0 (12.0, 44.0)	35.0 (12.0, 47.0)	
	Missing, n (%)	0 (0)	28 (15.5)	28 (3.1)	
Left ventricular ejection fraction (LVEF, %)					<.001
	Mean (SD)	65.7 (4.54)	57.1 (14.6)	64.1 (8.34)	
	Median (Min, Max)	65.0 (53.0, 79.0)	62.0 (12.0, 75.0)	65.0 (12.0, 79.0)	
	Missing, n (%)	0 (0)	8 (4.4)	8 (0.9)	

XSL•FO
RenderX

Variables		Normal (n=714)	PH[a] (n=181)	Overall (n=895)	*P* value
Mitral valve inflow velocity (MV Vmax, m/s)					<.001
	Mean (SD)	0.741 (0.195)	1.01 (0.488)	0.796 (0.300)	
	Median (Min, Max)	0.700 (0.300, 1.40)	0.900 (0.300, 3.00)	0.700 (0.300, 3.00)	
	Missing, n (%)	0 (0)	3 (1.7)	3 (0.3)	
Mitral inflow A-wave peak velocity (MPAV, m/s)					.86
	Mean (SD)	0.778 (0.189)	0.782 (0.254)	0.779 (0.200)	
	Median (Min, Max)	0.800 (0.400, 1.40)	0.800 (0.300, 1.60)	0.800 (0.300, 1.60)	
	Missing, n (%)	0 (0)	52 (28.7)	52 (5.8)	
Left ventricular outflow tract velocity (LVOT, m/s)					.002
	Mean (SD)	0.912 (0.189)	0.739 (0.269)	0.906 (0.195)	
	Median (Min, Max)	0.900 (0.500, 1.80)	0.800 (0.300, 1.20)	0.900 (0.300, 1.80)	
	Missing, n (%)	0 (0)	153 (84.5)	153 (17.1)	
Aortic valve outflow velocity (AV Vmax, m/s)					.004
	Mean (SD)	1.22 (0.216)	1.32 (0.423)	1.24 (0.274)	
	Median (Min, Max)	1.20 (0.700, 2.40)	1.20 (0.500, 3.10)	1.20 (0.500, 3.10)	
	Missing, n (%)	11 (1.5)	2 (1.1)	13 (1.5)	
Pulmonary valve outflow velocity (PV Vmax, m/s)					<.001
	Mean (SD)	0.953 (0.175)	1.09 (0.458)	0.977 (0.256)	
	Median (Min, Max)	0.900 (0.600, 1.70)	1.00 (0.300, 4.10)	1.00 (0.300, 4.10)	
	Missing, n (%)	0 (0)	22 (12.2)	22 (2.5)	
Mitral valve reflux degree (MVRD, 0 - 3)					<.001
	Mean (SD)	0.296 (0.457)	1.08 (1.15)	0.454 (0.729)	
	Median (Min, Max)	0 (0, 1.00)	1.00 (0, 4.00)	0 (0, 4.00)	
Aortic valve reflux degree (AVRD, 0 - 3)					<.001
	Mean (SD)	0.0980 (0.298)	0.459 (0.619)	0.171 (0.411)	
	Median (Min, Max)	0 (0, 1.00)	0 (0, 3.00)	0 (0, 3.00)	
Tricuspid valve reflux degree (TVRD, 0 - 3)					<.001
	Mean (SD)	0.396 (0.489)	1.85 (1.11)	0.690 (0.882)	
	Median (Min, Max)	0 (0, 1.00)	2.00 (0, 4.00)	0 (0, 4.00)	
Widening of ascending aorta, n (%)					<.001
	No	714 (100)	142 (78.5)	856 (95.6)	
	Yes	0 (0)	39 (21.5)	39 (4.4)	
Aortic valve thickening, n (%)					<.001
	No	696 (97.5)	147 (81.2)	843 (94.2)	
	Yes	18 (2.5)	34 (18.8)	52 (5.8)	
Aortic valve echo intensification, n (%)					<.001
	No	695 (97.3)	140 (77.3)	835 (93.3)	
	Yes	19 (2.7)	41 (22.7)	60 (6.7)	
Aortic valve calcification, n (%)					<.001
	No	712 (99.7)	175 (96.7)	887 (99.1)	

XSL•FO
RenderX

Variables		Normal (n=714)	PH[a] (n=181)	Overall (n=895)	*P* value
	Yes	2 (0.3)	6 (3.3)	8 (0.9)	
Poor closure of the aortic valve, n (%)					<.001
	No	713 (99.9)	119 (65.7)	832 (93)	
	Yes	1 (0.1)	62 (34.3)	63 (7)	
Pulmonary artery widening, n (%)					<.001
	No	714 (100)	88 (48.6)	802 (89.6)	
	Yes	0 (0)	93 (51.4)	93 (10.4)	
Poor closure of the pulmonary valve, n (%)					<.001
	No	713 (99.9)	157 (86.7)	870 (97.2)	
	Yes	1 (0.1)	24 (13.3)	25 (2.8)	
Mitral valve insufficiency, n (%)					<.001
	No	704 (98.6)	83 (45.9)	787 (87.9)	
	Yes	10 (1.4)	98 (54.1)	108 (12.1)	
Tricuspid insufficiency, n (%)					<.001
	No	677 (94.8)	33 (18.2)	710 (79.3)	
	Yes	37 (5.2)	148 (81.8)	185 (20.7)	
Ventricular septum thickened, n (%)					<.001
	No	711 (99.6)	147 (81.2)	858 (95.9)	
	Yes	3 (0.4)	34 (18.8)	37 (4.1)	
Left ventricular posterior wall thickened, n (%)					<.001
	No	714 (100)	164 (90.6)	878 (98.1)	
	Yes	0 (0)	17 (9.4)	17 (1.9)	
Atrial septal defect, n (%)					<.001
	No	714 (100)	143 (79)	857 (95.8)	
	Yes	0 (0)	38 (21)	38 (4.2)	
Ventricular septal defect, n (%)					<.001
	No	714 (100)	171 (94.5)	885 (98.9)	
	Yes	0 (0)	10 (5.5)	10 (1.1)	
E/E'[d]					<.001
	Mean (SD)	9.24 (1.99)	13.0 (5.43)	9.97 (3.33)	
	Median (Min, Max)	9.00 (4.00, 18.0)	12.0 (5.00, 33.0)	10.0 (4.00, 33.0)	
	Missing, n (%)	121 (16.9)	39 (21.5)	160 (17.9)	
WBC[e] (10^9/L)					.97
	Mean (SD)	6.16 (4.41)	6.15 (2.33)	6.16 (4.08)	
	Median (Min, Max)	5.67 (1.05, 103)	5.62 (2.50, 17.5)	5.65 (1.05, 103)	
	Missing, n (%)	0 (0)	1 (0.6)	1 (0.1)	
RBC[f] (10^9/L)					.01
	Mean (SD)	4.19 (0.660)	4.38 (0.905)	4.23 (0.720)	
	Median (Min, Max)	4.22 (1.76, 7.86)	4.27 (1.77, 8.48)	4.23 (1.76, 8.48)	
	Missing, n (%)	0 (0)	1 (0.6)	1 (0.1)	
Hb[g] (g/L)					.14
	Mean (SD)	127 (19.4)	131 (26.1)	128 (20.9)	

XSL•FO
RenderX

Variables		Normal (n=714)	PH[a] (n=181)	Overall (n=895)	*P* value
	Median (Min, Max)	129 (52.8, 194)	130 (60.0, 252)	129 (52.8, 252)	
	Missing, n (%)	0 (0)	1 (0.6)	1 (0.1)	
Plt[h] (10^9/L)					<.001
	Mean (SD)	222 (80.4)	183 (75.3)	214 (80.8)	
	Median (Min, Max)	215 (16.0, 575)	174 (34.0, 545)	206 (16.0, 575)	
	Missing, n (%)	0 (0)	1 (0.6)	1 (0.1)	
Neutrophilic granulocyte percentage (%)					.002
	Mean (SD)	60.9 (12.4)	64.0 (11.1)	61.5 (12.2)	
	Median (Min, Max)	61.0 (12.8, 97.0)	63.6 (32.8, 94.2)	61.5 (12.8, 97.0)	
	Missing, n (%)	0 (0)	1 (0.6)	1 (0.1)	
Lymphocytes percentage (%)					.002
	Mean (SD)	28.0 (10.6)	25.3 (10.1)	27.4 (10.5)	
	Median (Min, Max)	28.0 (2.00, 72.2)	26.0 (1.70, 53.4)	27.5 (1.70, 72.2)	
	Missing, n (%)	0 (0)	1 (0.6)	1 (0.1)	
Monocyte percentage (%)					.99
	Mean (SD)	8.34 (3.94)	8.35 (2.81)	8.34 (3.74)	
	Median (Min, Max)	7.70 (0.800, 78.9)	8.20 (1.50, 19.4)	7.80 (0.800, 78.9)	
	Missing, n (%)	0 (0)	1 (0.6)	1 (0.1)	
Eosinophils percentage (%)					.13
	Mean (SD)	2.20 (2.22)	1.83 (3.11)	2.13 (2.43)	
	Median (Min, Max)	1.55 (0, 27.5)	1.20 (0, 37.0)	1.50 (0, 37.0)	
	Missing, n (%)	0 (0)	1 (0.6)	1 (0.1)	
Basophils percentage (%)					.28
	Mean (SD)	0.562 (0.375)	0.595 (0.368)	0.569 (0.373)	
	Median (Min, Max)	0.500 (0, 3.30)	0.500 (0, 2.60)	0.500 (0, 3.30)	
	Missing, n (%)	0 (0)	1 (0.6)	1 (0.1)	
Neutrophil absolute value (10^9/L)					.30
	Mean (SD)	3.85 (2.39)	4.03 (2.03)	3.89 (2.32)	
	Median (Min, Max)	3.40 (0.200, 28.7)	3.53 (1.38, 12.9)	3.40 (0.200, 28.7)	
	Missing, n (%)	0 (0)	1 (0.6)	1 (0.1)	
Lymphocyte absolute value (10^9/L)					.105
	Mean (SD)	1.57 (0.660)	1.48 (0.691)	1.55 (0.667)	
	Median (Min, Max)	1.50 (0.200, 6.79)	1.45 (0.180, 3.86)	1.50 (0.180, 6.79)	
	Missing, n (%)	0 (0)	1 (0.6)	1 (0.1)	
Monocyte absolute value (10^9/L)					.47
	Mean (SD)	0.582 (3.02)	0.500 (0.248)	0.565 (2.70)	
	Median (Min, Max)	0.410 (0, 80.9)	0.470 (0.100, 2.00)	0.430 (0, 80.9)	
	Missing, n (%)	0 (0)	1 (0.6)	1 (0.1)	
Eosinophils absolute value (10^9/L)					.33
	Mean (SD)	0.124 (0.134)	0.106 (0.242)	0.121 (0.161)	
	Median (Min, Max)	0.100 (0, 1.40)	0.100 (0, 3.04)	0.100 (0, 3.04)	

XSL•FO
RenderX

Variables		Normal (n=714)	PH[a] (n=181)	Overall (n=895)	*P* value
	Missing, n (%)	0 (0)	1 (0.6)	1 (0.1)	
Basophil absolute value (10^9/L)					.03
	Mean (SD)	0.0212 (0.0326)	0.0275 (0.0341)	0.0225 (0.0330)	
	Median (Min, Max)	0 (0, 0.200)	0.0200 (0, 0.110)	0 (0, 0.200)	
	Missing, n (%)	0 (0)	1 (0.6)	1 (0.1)	
HCT[i] (%)					.005
	Mean (SD)	38.4 (5.67)	40.1 (7.77)	38.7 (6.19)	
	Median (Min, Max)	38.8 (16.5, 61.8)	40.1 (17.6, 76.4)	38.9 (16.5, 76.4)	
	Missing, n (%)	0 (0)	1 (0.6)	1 (0.1)	
Mean RBC volume (fL)					.75
	Mean (SD)	91.8 (6.48)	92.0 (7.42)	91.9 (6.67)	
	Median (Min, Max)	92.0 (63.2, 120)	92.8 (65.5, 123)	92.1 (63.2, 123)	
	Missing, n (%)	0 (0)	1 (0.6)	1 (0.1)	
Average hemoglobin content (pg)					.03
	Mean (SD)	30.5 (2.52)	30.0 (3.08)	30.4 (2.65)	
	Median (Min, Max)	30.7 (18.1, 40.9)	30.8 (19.5, 40.3)	30.7 (18.1, 40.9)	
	Missing, n (%)	0 (0)	1 (0.6)	1 (0.1)	
Average hemoglobin concentration (g/L)					<.001
	Mean (SD)	332 (8.33)	325 (14.1)	331 (10.1)	
	Median (Min, Max)	332 (285, 364)	328 (257, 352)	332 (257, 364)	
	Missing, n (%)	0 (0)	1 (0.6)	1 (0.1)	
Erythrocyte distribution width CV[j] (%)					<.001
	Mean (SD)	14.1 (1.94)	14.9 (2.28)	14.3 (2.04)	
	Median (Min, Max)	13.5 (11.3, 28.9)	14.3 (11.9, 26.1)	13.6 (11.3, 28.9)	
	Missing, n (%)	0 (0)	1 (0.6)	1 (0.1)	
Mean platelet volume (fL)					<.001
	Mean (SD)	8.69 (1.17)	9.69 (1.49)	8.89 (1.30)	
	Median (Min, Max)	8.50 (5.80, 14.5)	9.50 (7.10, 13.6)	8.70 (5.80, 14.5)	
	Missing, n (%)	0 (0)	6 (3.3)	6 (0.7)	
PT[k] (s)					<.001
	Mean (SD)	11.3 (0.992)	14.7 (7.36)	12.0 (3.68)	
	Median (Min, Max)	11.1 (9.50, 19.7)	12.7 (9.30, 70.1)	11.3 (9.30, 70.1)	
	Missing, n (%)	0 (0)	1 (0.6)	1 (0.1)	
INR[l]					<.001
	Mean (SD)	1.04 (0.0920)	1.35 (0.662)	1.10 (0.332)	
	Median (Min, Max)	1.02 (0.870, 1.81)	1.16 (0.850, 6.08)	1.04 (0.850, 6.08)	
	Missing, n (%)	0 (0)	1 (0.6)	1 (0.1)	
Prothrombin time activity (%)					<.001
	Mean (SD)	96.2 (12.9)	75.3 (22.4)	92.0 (17.4)	
	Median (Min, Max)	97.0 (43.0, 130)	80.0 (10.0, 136)	94.0 (10.0, 136)	
	Missing, n (%)	0 (0)	1 (0.6)	1 (0.1)	

XSL•FO
RenderX

Variables		Normal (n=714)	PH[a] (n=181)	Overall (n=895)	*P* value
APTT[m] (s)					<.001
	Mean (SD)	30.9 (3.93)	33.3 (7.91)	31.4 (5.09)	
	Median (Min, Max)	30.5 (17.4, 74.2)	31.8 (24.3, 103)	30.6 (17.4, 103)	
	Missing, n (%)	0 (0)	1 (0.6)	1 (0.1)	
TT[n] (s)					.14
	Mean (SD)	14.5 (1.76)	16.3 (16.3)	14.9 (7.46)	
	Median (Min, Max)	14.5 (11.0, 46.7)	15.0 (12.2, 231)	14.6 (11.0, 231)	
	Missing, n (%)	0 (0)	4 (2.2)	4 (0.4)	
Fibrinogen content (mg/dL)					<.001
	Mean (SD)	328 (86.0)	297 (75.9)	322 (84.9)	
	Median (Min, Max)	314 (97.0, 743)	286 (141, 536)	308 (97.0, 743)	
	Missing, n (%)	0 (0)	2 (1.1)	2 (0.2)	
D2[o] dimer (ng/mL)					.02
	Mean (SD)	401 (1130)	1420 (5630)	602 (2720)	
	Median (Min, Max)	136 (0, 15,900)	189 (1.00, 63,200)	141 (0, 63,200)	
	Missing, n (%)	0 (0)	5 (2.8)	5 (0.6)	
ALT[p] (U/L)					.09
	Mean (SD)	26.0 (45.1)	84.0 (394)	35.2 (163)	
	Median (Min, Max)	18.0 (3.00, 867)	19.5 (1.00, 3330)	18.0 (1.00, 3330)	
	Missing, n (%)	0 (0)	47 (26)	47 (5.3)	
AST[q] (U/L)					.09
	Mean (SD)	24.6 (33.2)	95.0 (556)	38.7 (252)	
	Median (Min, Max)	19.0 (4.00, 574)	22.0 (9.00, 6160)	20.0 (4.00, 6160)	
	Missing, n (%)	0 (0)	2 (1.1)	2 (0.2)	
AST/ALT					<.001
	Mean (SD)	1.22 (0.611)	8.42 (16.9)	2.65 (8.06)	
	Median (Min, Max)	1.11 (0.270, 6.86)	1.44 (0.350, 133)	1.17 (0.270, 133)	
	Missing, n (%)	0 (0)	4 (2.2)	4 (0.4)	
TBIL[r] (μmol/L)					.003
	Mean (SD)	12.4 (12.4)	16.4 (17.0)	13.2 (13.6)	
	Median (Min, Max)	10.6 (1.50, 275)	12.0 (0.540, 103)	10.6 (0.540, 275)	
	Missing, n (%)	0 (0)	2 (1.1)	2 (0.2)	
DBIL[s] (μmol/L)					<.001
	Mean (SD)	4.36 (12.3)	8.86 (8.70)	5.26 (11.8)	
	Median (Min, Max)	2.70 (0.300, 231)	5.60 (0.600, 51.1)	2.90 (0.300, 231)	
	Missing, n (%)	0 (0)	2 (1.1)	2 (0.2)	
IDBIL[t] (μmol/L)					<.001
	Mean (SD)	8.66 (5.09)	12.3 (11.1)	9.39 (6.90)	
	Median (Min, Max)	7.70 (0.800, 44.1)	9.40 (1.10, 94.1)	7.90 (0.800, 94.1)	
	Missing, n (%)	0 (0)	2 (1.1)	2 (0.2)	
Total protein (g/L)					<.001

XSL•FO
RenderX

Variables		Normal (n=714)	PH[a] (n=181)	Overall (n=895)	*P* value
	Mean (SD)	68.6 (9.60)	54.3 (25.4)	65.7 (15.3)	
	Median (Min, Max)	68.9 (3.04, 105)	64.9 (3.20, 88.5)	68.2 (3.04, 105)	
	Missing, n (%)	0 (0)	2 (1.1)	2 (0.2)	
Alb[u] (g/L)					<.001
	Mean (SD)	40.9 (5.48)	45.9 (12.9)	41.9 (7.82)	
	Median (Min, Max)	40.9 (15.7, 76.5)	41.5 (22.1, 86.5)	41.0 (15.7, 86.5)	
	Missing, n (%)	0 (0)	2 (1.1)	2 (0.2)	
Glb[v] (g/L)					.70
	Mean (SD)	31.0 (26.0)	30.6 (6.03)	31.0 (23.4)	
	Median (Min, Max)	28.3 (11.7, 319)	30.1 (16.3, 47.0)	28.7 (11.7, 319)	
	Missing, n (%)	0 (0)	2 (1.1)	2 (0.2)	
Alb or Glb					<.001
	Mean (SD)	1.71 (2.31)	8.35 (12.7)	3.04 (6.61)	
	Median (Min, Max)	1.46 (0.450, 28.6)	1.51 (0.730, 48.9)	1.46 (0.450, 48.9)	
	Missing, n (%)	0 (0)	2 (1.1)	2 (0.2)	
γGGT[w] (U/L)					.27
	Mean (SD)	37.8 (62.7)	44.9 (79.8)	39.3 (66.5)	
	Median (Min, Max)	21.5 (0.630, 927)	23.0 (0.600, 752)	22.0 (0.600, 927)	
	Missing, n (%)	0 (0)	2 (1.1)	2 (0.2)	
ALP[x] (U/L)					.17
	Mean (SD)	80.3 (53.7)	73.1 (63.9)	78.9 (56.0)	
	Median (Min, Max)	72.0 (3.59, 612)	64.0 (11.0, 768)	70.0 (3.59, 768)	
	Missing, n (%)	0 (0)	2 (1.1)	2 (0.2)	
TBA[y] (µmol/L)					<.001
	Mean (SD)	6.84 (22.1)	26.1 (37.4)	10.7 (27.0)	
	Median (Min, Max)	3.10 (0.100, 303)	6.60 (0.400, 204)	3.50 (0.100, 303)	
	Missing, n (%)	0 (0)	2 (1.1)	2 (0.2)	
BUN[z] (µmol/L)					.28
	Mean (SD)	6.58 (10.0)	7.44 (9.33)	6.75 (9.91)	
	Median (Min, Max)	5.14 (1.20, 105)	5.82 (0.400, 112)	5.25 (0.400, 112)	
	Missing, n (%)	0 (0)	3 (1.7)	3 (0.3)	
Creatinine (µmol/L)					<.001
	Mean (SD)	80.9 (104)	62.0 (43.5)	77.1 (95.6)	
	Median (Min, Max)	65.0 (2.23, 1140)	62.6 (1.95, 255)	64.2 (1.95, 1140)	
	Missing, n (%)	0 (0)	4 (2.2)	4 (0.4)	
Uric acid (µmol/L)					.80
	Mean (SD)	327 (103)	331 (193)	328 (126)	
	Median (Min, Max)	317 (0.760, 839)	335 (44.8, 1000)	321 (0.760, 1000)	
	Missing, n (%)	0 (0)	4 (2.2)	4 (0.4)	
Carbon dioxide (mmol/L)					<.001
	Mean (SD)	23.9 (4.21)	110 (171)	41.0 (83.5)	

XSL•FO
RenderX

Variables		Normal (n=714)	PH[a] (n=181)	Overall (n=895)	*P* value
	Median (Min, Max)	23.8 (1.00, 34.9)	24.8 (12.3, 842)	23.9 (1.00, 842)	
	Missing, n (%)	0 (0)	4 (2.2)	4 (0.4)	
Serum cystatin C (mg/L)					<.001
	Mean (SD)	1.04 (0.794)	6.99 (10.5)	2.18 (5.20)	
	Median (Min, Max)	0.900 (0.360, 7.59)	1.11 (0.510, 38.1)	0.910 (0.360, 38.1)	
	Missing, n (%)	0 (0)	12 (6.6)	12 (1.3)	
Potassium (mmol/L)					<.001
	Mean (SD)	3.94 (0.462)	3.42 (1.22)	3.84 (0.707)	
	Median (Min, Max)	3.94 (0.990, 6.27)	3.84 (0.720, 5.72)	3.93 (0.720, 6.27)	
	Missing, n (%)	0 (0)	10 (5.5)	10 (1.1)	
Sodium (mmol/L)					<.001
	Mean (SD)	138 (13.9)	108 (57.5)	132 (30.8)	
	Median (Min, Max)	140 (0.940, 148)	138 (2.93, 155)	140 (0.940, 155)	
	Missing, n (%)	0 (0)	6 (3.3)	6 (0.7)	
Chlorine (mmol/L)					<.001
	Mean (SD)	103 (11.7)	113 (15.0)	105 (13.0)	
	Median (Min, Max)	105 (2.22, 114)	106 (91.0, 146)	105 (2.22, 146)	
	Missing, n (%)	0 (0)	6 (3.3)	6 (0.7)	
Calcium (mmol/L)					<.001
	Mean (SD)	2.57 (5.43)	26.0 (43.1)	7.19 (21.8)	
	Median (Min, Max)	2.30 (0.390, 105)	2.32 (1.78, 111)	2.30 (0.390, 111)	
	Missing, n (%)	0 (0)	6 (3.3)	6 (0.7)	
Magnesium (mmol/L)					.22
	Mean (SD)	2.40 (26.1)	1.20 (0.596)	2.17 (23.5)	
	Median (Min, Max)	0.880 (0.380, 667)	0.890 (0.530, 2.54)	0.880 (0.380, 667)	
	Missing, n (%)	0 (0)	14 (7.7)	14 (1.6)	
Phosphorus (mmol/L)					.01
	Mean (SD)	5.38 (45.6)	1.16 (0.281)	4.57 (41.0)	
	Median (Min, Max)	1.18 (0.310, 784)	1.17 (0.660, 2.32)	1.17 (0.310, 784)	

XSL•FO
RenderX

Variables	Normal (n=714)	PH[a] (n=181)	Overall (n=895)	*P* value
Missing, n (%)	0 (0)	11 (6.1)	11 (1.2)	

[a]PH: pulmonary hypertension.
[b]Min: minimum.
[c]Max: maximum.
[d]E/E': ratio of mitral valve early diastolic inflow velocity (E) to mitral annulus early diastolic velocity (E').
[e]WBC: white blood cell.
[f]RBC: red blood cell.
[g]Hb: hemoglobin.
[h]Plt: platelet count.
[i]HCT: hematocrit.
[j]CV: coefficient of variation.
[k]PT: prolonged prothrombin time.
[l]INR: international normalized ratio.
[m]APTT: activated partial thromboplastin time.
[n]TT: thrombin time.
[o]D2: D-dimer.
[p]ALT: alanine aminotransferase.
[q]AST: aspartate aminotransferase.
[r]TBIL: total bilirubin.
[s]DBIL: direct bilirubin.
[t]IDBIL: indirect bilirubin.
[u]Alb: albumin.
[v]Glb: globulin.
[w]γGGT: gamma-glutamyl transferase.
[x]ALP: alkaline phosphatase.
[y]TBA: total bile acids.
[z]BUN: blood urea nitrogen.

Systematic Selection of Key Echocardiographic Parameters to Construct an Ultrasound Index for PH Prediction

As shown in Figure 1A, RFE with a random forest model and 10-fold cross-validation identified 16 echocardiographic variables that maximize predictive performance, with right atrial diameter and PAD yielding the highest importance scores. Figure 1B plots cross-validation accuracy against the number of features and demonstrates optimal performance when incorporating 16 variables. Figure 1C illustrates that the XGBoost model outperformed others, excelling in AUC, sensitivity, and specificity, demonstrating high robustness in distinguishing between false positives and negatives. Figure 1D highlights SHAP analysis, which shows how each feature shifts the risk prediction for individual patients: positive SHAP values indicate increased risk, while negative values indicate decreased risk. In our model, left ventricular outflow tract velocity, right atrium diameter, and PAD produced the largest SHAP values, reflecting their strong influence on PH classification. In summary, we identified and incorporated 16 key echocardiographic parameters into a composite ultrasound index as potential predictive variables for PH.

XSL•FO
RenderX

Figure 1. Identify important potential predictive variables for PH from echocardiographic parameters to form an ultrasound index. (**A**) Selected features from echocardiographic parameters. (**B**) Model accuracy with varying numbers of input variables. (**C**) ROC curves, sensitivity, and specificity of different machine learning algorithms. (**D**) Beeswarm plot for the feature importance of the selected echo features. AAD: ascending aortic diameter; AVRD: aortic valve reflux degree; E/E': ratio of mitral valve early diastolic inflow velocity (E) to mitral annulus early diastolic velocity (E'); GBM: gradient boosting machine; IVS: interventricular septal thickness; LAD: left atrium diameter; LASSO: least absolute shrinkage and selection operator; LVD: left ventricular diameter; LVEF: left ventricular ejection fraction; LVOT: left ventricular outflow tract velocity; LVPW: left ventricular posterior wall thickness; MV Vmax: mitral valve inflow velocity; MVRD: mitral valve reflux degree; PAD: pulmonary artery diameter; PH: pulmonary hypertension; PV Vmax: pulmonary valve outflow velocity; RAD: right atrium diameter; RFE: recursive feature elimination; ROC: receiver operating characteristic; RVD: right ventricular diameter; Sens: sensitivity; SHAP: Shapley Additive Explanations; Spec: specificity; SVM: support vector machine; TVRD: tricuspid valve reflux degree; XGBoost: Extreme Gradient Boosting.

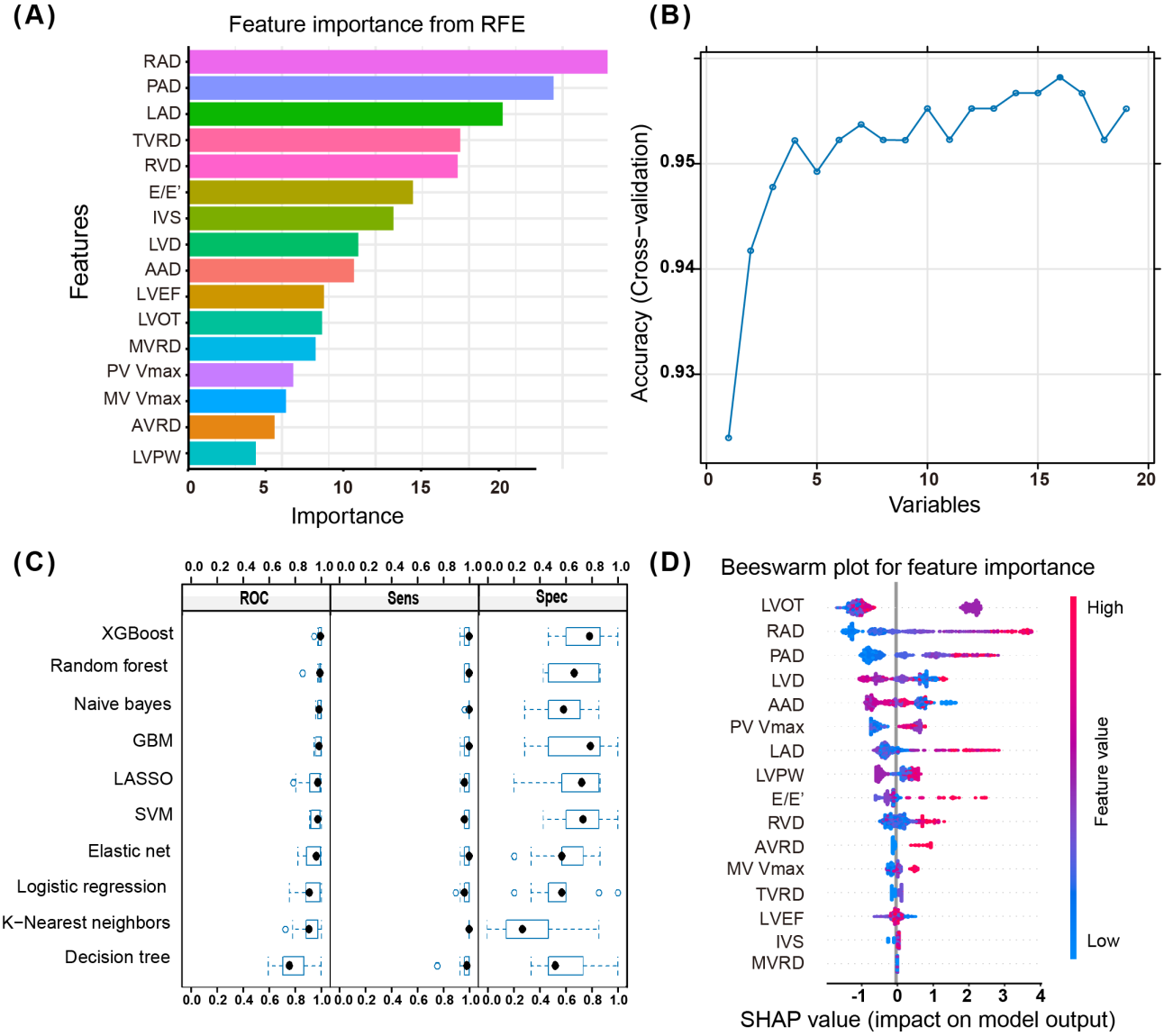
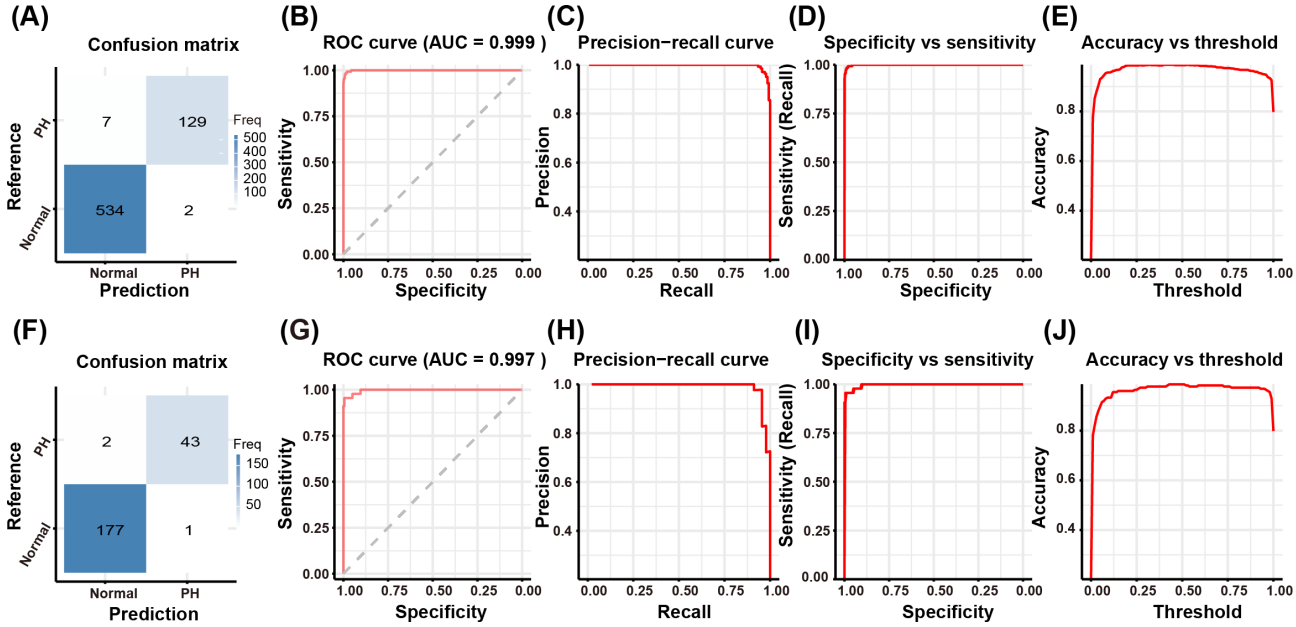


Figure 2A-E demonstrates the outstanding predictive performance of the ultrasound index model for PH detection, while Figure 2F-J presents the internal validation results through bootstrap resampling. Figure 2A presents the confusion matrix and ROC analysis of the ultrasound index model for PH prediction. The confusion matrix demonstrates excellent classification accuracy, with minimal misclassification between normal and PH cases. The ROC curve achieves near-perfect discrimination (AUC=0.999; Figure 2B), supported by precision-recall curves (Figure 2C) showing high positive predictive value across all sensitivity thresholds. Specificity-sensitivity analysis (Figure 2D) and accuracy-threshold analysis (Figure 2E) reveal balanced performance at the optimal diagnostic threshold, indicating robust clinical applicability. Figure 2F displays the bootstrap validation outcomes of the ultrasound index model, confirming its statistical reliability. The ROC curve maintains exceptional performance (AUC=0.997; Figure 2G) across 1000 resampled iterations, with tight CIs indicating stable predictive ability. Precision-recall (Figure 2H), specificity-sensitivity (Figure 2I), and accuracy-threshold (Figure 2J) curves show reproducible performance characteristics within narrow variability ranges (<1% fluctuation), demonstrating the model's resistance to overfitting and dataset sampling bias.

XSL•FO
RenderX

Figure 2. Evaluation of the predictive performance of the ultrasound index for PH in the training set and internal validation set. (A) Confusion matrix for training cohort. (B) ROC curve for training cohort (AUC=0.999). (C) Precision-recall curve for the training cohort. (D) Specificity versus sensitivity for the training cohort. (E) Accuracy versus threshold for the training cohort. (F) Confusion matrix for the validation cohort. (G) ROC curve for the validation cohort (AUC=0.997). (H) Precision-recall curve for the validation cohort. (I) Specificity versus sensitivity for the validation cohort. (J) Accuracy versus threshold for the validation cohort. AUC: area under the receiver operating characteristic curve; PH: pulmonary hypertension; ROC: receiver operating characteristic.

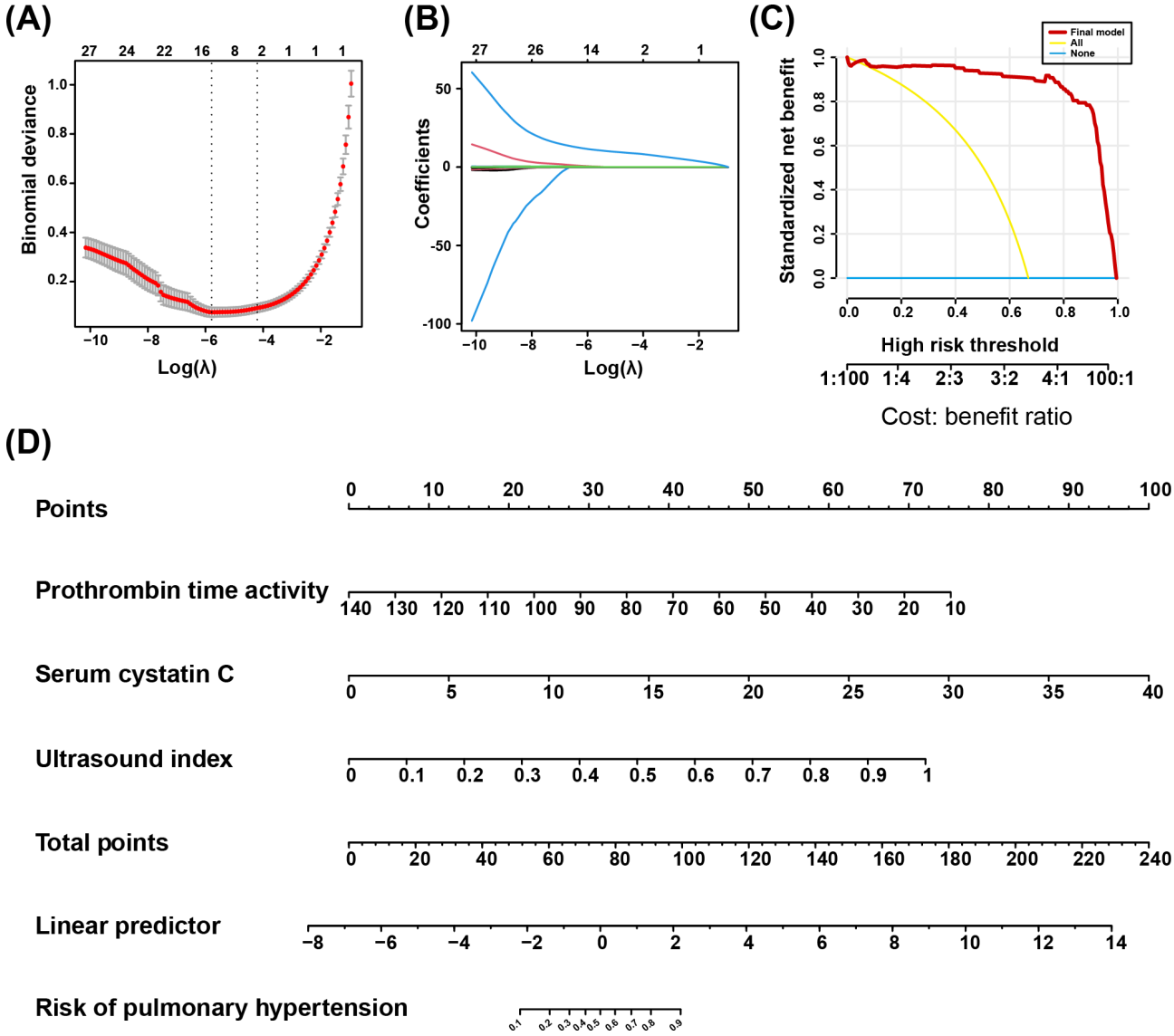


Development and Presentation of the Final PH Prediction Model

As shown in Figure 3A and B, LASSO regression identified 2 key clinical features—prothrombin time activity and serum CysC as the most influential variables, indicating that these variables are critical potential predictive parameters of PH. Then, we combined prothrombin time activity, serum CysC, and previously selected ultrasound index to form the final PH prediction model through logistic regression. Figure 3C demonstrates through DCA that our PH prediction model provides superior clinical net benefit compared to both “treat-all” and “treat-none” strategies across clinically relevant probability thresholds. As depicted in Figure 3D, our nomogram translates each predictor’s regression coefficient into a point scale and uses the sum of points to compute an individualized PH risk probability via a linear predictor, providing clinicians with an intuitive, quantitative tool for PH risk assessment. The nomogram translates clinical variables—including prothrombin time activity (10 - 140 s mapped to 75 - 0 points), serum CysC (0 - 40 mg/L mapped to 0 - 100 points), and the ultrasound index (0 - 1 mapped to 0 - 72.5 points)—into a cumulative point total. The total score is then read against the bottom probability scale to yield an individualized PH risk, providing a convenient tool that converts routine laboratory and imaging data into a directly actionable prediction of PH.

XSL•FO
RenderX

Figure 3. Identify key laboratory biomarkers and develop the final predictive model for PH. (A) Deviance plot from LASSO regression to select key laboratory biomarkers. (B) Coefficient path for LASSO regression to select key laboratory biomarkers. (C) Decision curve analysis of the final predictive model of PH. (D) Nomogram of the final PH prediction model. LASSO: least absolute shrinkage and selection operator; PH: pulmonary hypertension.

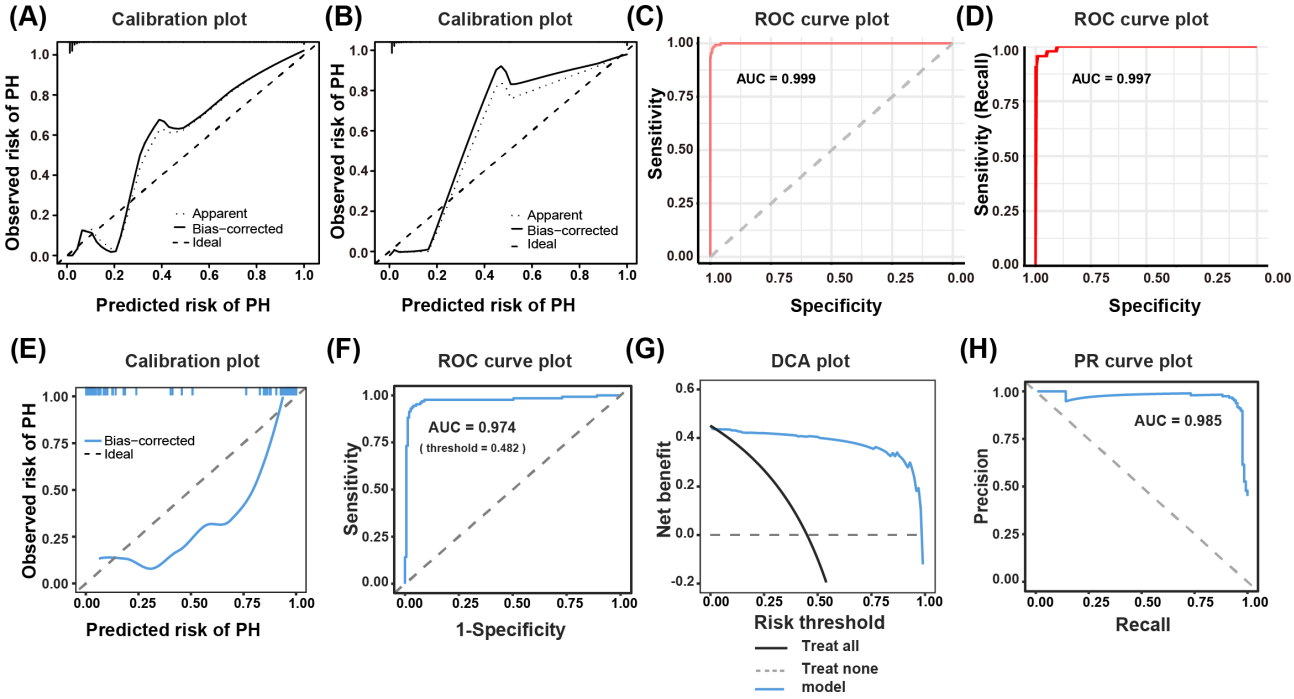


Evaluation and Validation of the Final PH Prediction Model

Data from different time periods were collected for external validation, including 126 patients with PH and 155 controls, with detailed information presented in Multimedia Appendix 1. Figure 4A and C present the model performance evaluation results, while Figure 4B and D display the stability analysis of internal validation (bootstrap=1000 iterations), and Figure 4E-H systematically report the external validation data. Calibration curve analysis demonstrates that the predictive model maintains excellent calibration in both the training set (Figure 4A), internal validation (Figure 4B), and external validation cohorts (Figure 4E). ROC analysis further reveals that the model exhibits stable discriminative ability across the training set (AUC=0.999, Figure 4C), internal validation (AUC=0.987, Figure 4D), and external validation (AUC=0.974, Figure 4F). In external validation, DCA shows significant net benefit across the 10% - 90% risk threshold range (Figure 4G), while the area under the precision-recall curve (AUC=0.985) confirms the model's balanced advantage of both high precision and recall for positive cases (Figure 4H). These analytical results demonstrate that our model exhibits not only excellent predictive performance for PH, but also outstanding stability and significant clinical utility.

XSL•FO
RenderX

Figure 4. Calibration curves and ROC analysis of the final PH prediction model (nomogram) in the training, internal validation, and external validation sets. (A) Calibration curve of the nomogram in the training cohort. (B) Calibration curve of the nomogram in the internal validation cohort. (C) ROC of the nomogram in the training cohort. (D) ROC of the nomogram in the internal validation cohort. (E) Calibration curve of the nomogram in the external validation cohort. (F) ROC of the nomogram in the external validation cohort. (G) DCA plot of the nomogram in the external validation cohort. (H) PR curve plot of the nomogram in the external validation cohort. AUC: area under the receiver operating characteristic curve; DCA: decision curve analysis; PH: pulmonary hypertension; PR: precision-recall; ROC: receiver operating characteristic.



Key Advantages and Innovations of Our Model Versus Current PH Predictive Models

Although predictive models for PH currently exist, these tools face significant limitations: the REVEAL score requires invasive data for optimal use and lacks imaging integration, while guideline-based echocardiography suffers from subjective interpretation variability and low sensitivity (AUC=0.70 - 0.82). Both systems fail to capture early preclinical signs and the mechanistic pathways addressed by our biomarker-enhanced approach.

Our novel PH prediction model demonstrates significant advancements over existing approaches (Table 2) by integrating 16 echocardiographic parameters with 2 clinically accessible biomarkers (prothrombin time activity and CysC), achieving superior discriminative performance (AUC=0.974 - 0.999 versus 0.70 - 0.85 in conventional models). Unlike the REVEAL score's reliance on invasive hemodynamics or guideline-based echocardiography's limited echo variables, our model provides: (1) comprehensive pathophysiological insight through multimodal biomarkers reflecting coagulation and cardiac dysfunction; (2) granular risk quantification via a 240-point nomogram, enabling precise stratification; and (3) practical clinical utility through Electronic Health Record (EHR)–compatible automation. In summary, our model demonstrates significant advancements and innovations compared to existing models.

XSL•FO
RenderX

Table . Comparison of our model with existing PH[a] risk assessment tools.

Feature	Our model	REVEAL[b] score	Guideline-based echocardiography
Variables used	• 16 echocardiographic and 2 clinical (prothrombin time activity and cystatin C)	• Primarily clinical (6MWD[c], functional class, and hemodynamics)	• Limited echo parameters (TR[d] velocity and RV[e] size)
AUC[f]	• 0.974 - 0.999	• 0.79 - 0.85	• 0.70 - 0.82
Strengths	• Multimodal integration (imaging and biomarkers) • Objective scoring system • Higher discriminative ability	• Established registry data • Validated long-term outcomes	• Widely available • First-line screening
Key advantages	• Comprehensive echo assessment (16 parameters, including novel metrics such as LVOT[g] velocity) • Novel biomarkers (cystatin C adds renal or PH pathobiology dimension) • Quantitative nomogram (precise risk stratification)	• Lacks imaging details • Requires invasive data for the full version	• Subjective interpretation • Limited accuracy
Clinical utility	• EHR[h]-integratable • Identifies early-stage PH • Guides RHC[i] decisions	• Mainly for prognosis • Less useful for initial diagnosis	• Screening only • High false-positive rate
Population	• Broad applicability (includes preclinical signs)	• Established patients with PH	• Symptomatic suspects

[a]PH: pulmonary hypertension.

[b]REVEAL: Registry to Verify Early and Long-Term Pulmonary Arterial Hypertension Disease Management.

[c]6MWD: 6-minute walk distance.

[d]TR: tricuspid regurgitation.

[e]RV: right ventricular.

[f]AUC: area under the receiver operating characteristic curve.

[g]LVOT: left ventricular outflow tract velocity.

[h]EHR: electronic health record.

[i]RHC: right heart catheterization.

To facilitate clinical implementation of our model, we developed a web-based calculator (Figure 5A and B), available online [16], which enables user-friendly PH risk assessment. This tool is expected to significantly enhance the model's clinical adoption.

XSL•FO
RenderX

Figure 5. Screenshots of the nomogram web calculator. (A) Screenshot of the web calculator showing the calculated PH probability based on ultrasound index input and SHAP-based interpretation of feature importance for the ultrasound index variables. (B) Screenshot of the web calculator displaying the total points calculated via nomogram and the corresponding PH risk probability. E/E': ratio of mitral valve early diastolic inflow velocity (E) to mitral annulus early diastolic velocity (E'); PH: pulmonary hypertension; SHAP: Shapley Additive Explanations.



Discussion

Principal Findings

We present an integrated diagnostic model that combines ultrasound-derived parameters with clinical variables to improve early PH risk prediction. Using RFE, LASSO regression, and various machine learning algorithms, we optimized the model and rigorously assessed its predictive performance. Given that PH is a rapidly progressive disease with high mortality, early detection and intervention are essential for improving outcomes [17,18]. Current diagnostic methods for pulmonary artery pressure rely heavily on 2 approaches: RHC and echocardiography, which estimate pressure based on TRV [19-21]. However, catheterization is invasive, and echocardiography can be prone to significant inaccuracies. To overcome these limitations, our research proposes a novel noninvasive diagnostic pathway that integrates ultrasound and clinical data, thereby providing an effective tool for the early detection of PH.

In our model, 16 echocardiographic features (right atrium diameter, PAD, left atrium diameter, tricuspid valve reflux degree, right ventricular diameter, E/E' [Ratio of Mitral Valve Early Diastolic Inflow Velocity (E) to Mitral Annulus Early Diastolic Velocity (E')], interventricular septal thickness, left ventricular diameter, ascending aortic diameter, left ventricular ejection fraction, left ventricular outflow tract velocity, mitral valve reflux degree, pulmonary valve outflow velocity, mitral valve inflow velocity, aortic valve reflux degree, and left ventricular posterior wall thickness) and 2 laboratory tests variables (prothrombin time activity and CysC) was identified to be the critical predictive parameters of PH. These structural cardiac measurements demonstrate strong pathophysiological

XSL•FO
RenderX

concordance with known PH mechanisms: enlargement of the right and left atria reflects increased pulmonary circulation pressure and heightened right ventricular load, both of which are common in patients with PH [22]. Additionally, an enlarged PAD correlates directly with elevated pulmonary vascular resistance, further exacerbating right ventricular pressure overload [23].

While the association between cardiac structural or functional parameters and PH is well-established and mechanistically straightforward, our selected biochemical markers (prothrombin time activity and CysC) similarly demonstrate previously reported—yet less widely recognized—pathophysiological links to PH development. A review summarizing the association between coagulation abnormalities and hypertension suggests that prothrombin time activity is closely correlated with elevated systolic and diastolic blood pressure in both hypertensive patients and normotensive individuals [24]. This is consistent with the conclusion in this paper that prothrombin time activity is associated with increased pulmonary artery pressure. CysC is generally recognized as an indicator of renal function. However, previous studies have found that CysC is also elevated in patients with pulmonary arterial hypertension and is positively correlated with right ventricular systolic pressure, right ventricular end-diastolic volume, and right ventricular end-systolic volume, suggesting its potential as a biomarker for PH [25].

Our study advances beyond prior research by systematically identifying optimal ultrasound parameters through rigorous RFE coupled with 10-fold cross-validation, ensuring robust and reproducible feature selection. Whereas conventional approaches typically analyze isolated echocardiographic measures, our novel methodology integrates multidimensional cardiac imaging features with critical clinical biomarkers to develop a high-performance yet clinically interpretable prediction model. This integrative approach demonstrates superior predictive accuracy for PH, representing a paradigm shift from single-parameter assessment to comprehensive risk stratification. The clinical implementation of this model enables: (1) earlier detection of subclinical PH through sensitive ultrasound biomarkers, (2) improved risk discrimination via combined imaging and laboratory data, and (3) actionable outputs for timely therapeutic decision-making.

It is also worth mentioning that in our study, we used multiple machine learning algorithms, such as XGBoost, random forest, and logistic regression. Among these models, XGBoost demonstrated the best predictive performance, achieving an AUC of 0.997, highlighting its strength in handling high-dimensional data and modeling complex nonlinear relationships. As a gradient-boosting algorithm, XGBoost incrementally reduces the model error to enhance predictive accuracy, rendering it particularly effective for clinical data with intricate interactions [26,27]. To enhance the interpretability of the XGBoost model, we constructed an analysis using SHAP. SHAP values quantified the contribution of each feature to the model's predictions, emphasizing the importance of variables such as the right atrium and PAD in predicting PH. Compared to traditional "black-box" models, incorporating SHAP analysis significantly enhanced the model's interpretability, providing more clinical insights. SHAP not only increases transparency but also enables clinicians to better understand the predictive mechanisms of the model, thus supporting more informed and reasoned clinical decision-making.

To enable seamless adoption in clinical workflows, we deployed the nomogram and risk calculator [16] as a web-based Shiny application with an Application Programming Interface compatible with major EHR systems. Compliant with Health Level Seven Fast Healthcare Interoperability Resources standards, the tool automatically retrieves echocardiographic measurements and laboratory values, computes the PH risk score in real time, and presents results in clinician-facing dashboards during outpatient visits. Moreover, the application can be embedded within ultrasound reporting software, allowing sonographers to generate risk estimates immediately at the point of image acquisition. Concrete examples of our predictive model's clinical application are: a 58-year-old woman presenting with unexplained dyspnea underwent noninvasive PH risk stratification using our proposed nomogram or web-based tool to defer immediate RHC. The clinician input key echocardiographic parameters (right atrium diameter=4.5 cm, PAD=2.8 cm, left atrium diameter=4.0 cm, and other selected parameters in our model) along with laboratory values (prothrombin time activity=78%, serum CysC=1.5 mg/L) extracted from recent reports. Application of the nomogram yielded a total score of 50 points, corresponding to an 85% predicted PH risk, automatically flagging the patient as high-risk. This prompted clinical actions, including prioritization of confirmatory RHC, initiation of enhanced monitoring (repeat echocardiography and N-terminal pro-B-type Natriuretic Peptide testing, and consideration of early PH specialty referral. For seamless clinical implementation, the tool could integrate with electronic health record systems (eg, Cerner, formerly known as Cerner Corporation, now part of Oracle Health) as a plug-in module, enabling automated data population from EHR fields (laboratory results or echocardiographic reports) and generation of standardized risk assessment documents for longitudinal patient tracking within the medical record.

Although several machine learning models have been developed for PH, they exhibit certain limitations. Many models rely on a single data source, which restricts predictive accuracy and reliability. For instance, the study by Athénaïs Boucly identified cytokines as prognostic biomarkers in pulmonary arterial hypertension but failed to account for potential confounding factors, such as clinical variables or imaging data, which may influence the results [28]. Similarly, the research by Hirata et al [29] demonstrated improved accuracy of a machine learning model compared to traditional methods in the derivation cohort; however, its performance in the validation cohort was only comparable to guideline-based echocardiographic assessments, underscoring the need for further optimization and validation. Additionally, previous studies frequently used univariable and multivariable models to evaluate the relationship between clinical and echocardiographic parameters in precapillary PH [30]. However, they lacked advanced feature selection methods such as LASSO and RFE, which could have enhanced model performance by identifying key predictive variables, reducing

XSL•FO
RenderX

overfitting, and providing deeper insights into prognostic factors. In contrast, our research proposes an innovative approach by integrating ultrasound parameters with clinical variables, thereby enhancing the model's predictive performance through multidimensional integration [31,32]. Unlike prior work, we optimized feature selection using both RFE and LASSO regression and ensured model robustness through comparison and tuning across multiple machine-learning models [33]. We also significantly enhanced model interpretability using SHAP, which makes this high-performing "black-box" model more transparent and trustworthy for clinical use, ultimately enhancing its applicability and credibility in a health care context.

Despite the strong performance of our model in predicting PH, it exhibits certain limitations. First, the study sample size was relatively small, which limits the generalizability of the findings. Future work should involve validation using larger, multicenter datasets to ensure the model's external validity. Second, as new ultrasound technologies and biomarkers emerge, future research should incorporate additional multidimensional biological data to enhance the predictive accuracy and applicability of the model.

Conclusions

We developed a high-performance PH prediction model using machine learning analysis of echocardiographic, laboratory, and demographic data from 895 participants. The model incorporates 16 key ultrasound parameters and 2 biomarkers, with validation showing excellent accuracy. We also created a web-based calculator to facilitate clinical use, providing a practical tool for early, noninvasive PH detection.

Acknowledgments

This study was funded by the following programs: the National Natural Science Foundation of China (82300078), the Fundamental Research Funds for the Central Universities (2042023kf0059), Wuhan University Clinical Medicine + Youth Supporting Program (413000557), Science and Technology Innovation Cultivation Funding of Zhongnan Hospital of Wuhan University (CXPY2023060), the Climbing Project for Medical Talent of Zhongnan Hospital of Wuhan University (PDJH202406), and Science and Technology Innovation Cultivation Funding of Zhongnan Hospital of Wuhan University (CXPY2023060).

Data Availability

All the original data involved in this study are available from the corresponding author on reasonable request.

Authors' Contributions

HJ, HG, and DW designed the research, analyzed data, and drafted this paper. QZ and XH prepared and collected data. ZC conceived and designed the research, edited and revised this paper, and supervised all aspects of the project. All authors agreed with the submission of this paper for publication and agreed to be accountable for all aspects of this paper.

Conflicts of Interest

None declared.

Multimedia Appendix 1
Independent external validation dataset.
[DOCX File, 37 KB - medinform_v13i1e74117_app1.docx]

References

1. Humbert M, Sitbon O, Guignabert C, et al. Treatment of pulmonary arterial hypertension: recent progress and a look to the future. Lancet Respir Med 2023 Sep;11(9):804-819. [doi: 10.1016/S2213-2600(23)00264-3]
2. Johnson S, Sommer N, Cox-Flaherty K, Weissmann N, Ventetuolo CE, Maron BA. Pulmonary hypertension: a contemporary review. Am J Respir Crit Care Med 2023 Sep 1;208(5):528-548. [doi: 10.1164/rccm.202302-0327SO]
3. Weatherald J, Hemnes AR, Maron BA, et al. Phenotypes in pulmonary hypertension. Eur Respir J 2024 Sep;64(3):2301633. [doi: 10.1183/13993003.01633-2023]
4. Maron BA, Brittain EL, Hess E, et al. Pulmonary vascular resistance and clinical outcomes in patients with pulmonary hypertension: a retrospective cohort study. Lancet Respir Med 2020 Sep;8(9):873-884. [doi: 10.1016/S2213-2600(20)30317-9]
5. Kovacs G, Avian A, Bachmaier G, et al. Severe pulmonary hypertension in COPD: impact on survival and diagnostic approach. Chest 2022 Jul;162(1):202-212. [doi: 10.1016/j.chest.2022.01.031] [Medline: 35092746]
6. El-Kersh K, Zhao C, Elliott G, et al. Derivation of a risk score (REVEAL-ECHO) based on echocardiographic parameters of patients with pulmonary arterial hypertension. Chest 2023 May;163(5):1232-1244. [doi: 10.1016/j.chest.2022.12.045] [Medline: 36634897]
7. Noordegraaf AV, Chin KM, Haddad F, et al. Pathophysiology of the right ventricle and of the pulmonary circulation in pulmonary hypertension: an update. Eur Respir J 2019 Jan;53(1):1801900. [doi: 10.1183/13993003.01900-2018] [Medline: 30545976]

XSL•FO
RenderX

8. Ley L, Grimminger F, Richter M, Tello K, Ghofrani A, Bandorski D. The early detection of pulmonary hypertension. Dtsch Arztebl Int 2023;120(48):823-830. [doi: 10.3238/arztebl.m2023.0222]
9. Celestin BE, Bagherzadeh SP, Ichimura K, et al. Identifying consistent echocardiographic thresholds for risk stratification in pulmonary arterial hypertension. Pulm Circ 2024 Apr;14(2):e12361. [doi: 10.1002/pul2.12361] [Medline: 38800494]
10. Shah AM, Cikes M, Prasad N, et al. Echocardiographic features of patients with heart failure and preserved left ventricular ejection fraction. J Am Coll Cardiol 2019 Dec;74(23):2858-2873. [doi: 10.1016/j.jacc.2019.09.063]
11. Troncoso J, Abánades CS, Robles-Marhuenda Á, et al. Prevalence, risk factors and echocardiographic predictors of pulmonary hypertension in systemic lupus erythematosus: towards a screening protocol. RMD Open 2024 Jan 8;10(1):e003674. [doi: 10.1136/rmdopen-2023-003674] [Medline: 38191213]
12. Yan T, Ma Q, Li X, Shen Q, Liu X, Zhang X. Establishment of a prediction model of pulmonary artery hypertension in patients with hyperthyroidism. Noninvasive Electrocardiol 2024 Sep;29(5):e13133. [doi: 10.1111/anec.13133]
13. Zhou Z, Gu Y, Tian L, Zheng H, Li S. Development and validation of a nomogram of persistent pulmonary hypertension in adult pretricuspid shunts after correction. JAHA 2024 May 7;13(9):e032412. [doi: 10.1161/JAHA.123.032412]
14. Hu M, Duan A, Huang Z, et al. Development and validation of a nomogram for predicting obstructive sleep apnea in patients with pulmonary arterial hypertension. NSS 2022;14:1375-1386. [doi: 10.2147/NSS.S372447]
15. Kuhn M. Building predictive models in R using the caret package. J Stat Soft 2008;28(5):1-26. [doi: 10.18637/jss.v028.i05]
16. Pulmonary hypertension risk prediction nomogram. PH Risk Nomogram. URL: https://jianghx.shinyapps.io/PHpredictor/ [accessed 2025-09-16]
17. Fu W, He W, Li Y, et al. Efficacy and safety of novel-targeted drugs in the treatment of pulmonary arterial hypertension: a Bayesian network meta-analysis. Drug Deliv (Lond) 2021 Jan;28(1):1007-1019. [doi: 10.1080/10717544.2021.1927243]
18. Maron BA, Abman SH, Elliott CG, et al. Pulmonary arterial hypertension: diagnosis, treatment, and novel advances. Am J Respir Crit Care Med 2021 Jun 15;203(12):1472-1487. [doi: 10.1164/rccm.202012-4317SO]
19. Poch D, Mandel J. Pulmonary hypertension. Ann Intern Med 2021 Apr;174(4):ITC49-ITC64. [doi: 10.7326/AITC202104200]
20. Mandras SA, Mehta HS, Vaidya A. Pulmonary hypertension: a brief guide for clinicians. Mayo Clin Proc 2020 Sep;95(9):1978-1988. [doi: 10.1016/j.mayocp.2020.04.039]
21. Rosenkranz S, Gibbs JSR, Wachter R, De Marco T, Vonk-Noordegraaf A, Vachiéry JL. Left ventricular heart failure and pulmonary hypertension. Eur Heart J 2016 Mar 21;37(12):942-954. [doi: 10.1093/eurheartj/ehv512]
22. Galderisi M, Cosyns B, Edvardsen T, et al. Standardization of adult transthoracic echocardiography reporting in agreement with recent chamber quantification, diastolic function, and heart valve disease recommendations: an expert consensus document of the European Association of Cardiovascular Imaging. Eur Heart J Cardiovasc Imaging 2017 Dec 1;18(12):1301-1310. [doi: 10.1093/ehjci/jex244]
23. Jones R, Zapol WM, Reid L. Pulmonary artery remodeling and pulmonary hypertension after exposure to hyperoxia for 7 days. A morphometric and hemodynamic study. Am J Pathol 1984 Nov;117(2):273-285. [Medline: 6238536]
24. Rafaqat S, Khalid A, Riaz S, Rafaqat S. Irregularities of coagulation in hypertension. Curr Hypertens Rep 2023 Oct;25(10):271-286. [doi: 10.1007/s11906-023-01258-0]
25. Fenster BE, Lasalvia L, Schroeder JD, et al. Cystatin C: a potential biomarker for pulmonary arterial hypertension. Respirology 2014 May;19(4):583-589. [doi: 10.1111/resp.12259] [Medline: 24628703]
26. Silva GFS, Fagundes TP, Teixeira BC, Filho ADPC. Machine learning for hypertension prediction: a systematic review. Curr Hypertens Rep 2022 Nov;24(11):523-533. [doi: 10.1007/s11906-022-01212-6] [Medline: 35731335]
27. Hou N, Li M, He L, et al. Predicting 30-days mortality for MIMIC-III patients with sepsis-3: a machine learning approach using XGboost. J Transl Med 2020 Dec;18(1):462. [doi: 10.1186/s12967-020-02620-5]
28. Moss BJ, Ryter SW, Rosas IO. Pathogenic mechanisms underlying idiopathic pulmonary fibrosis. Annu Rev Pathol Mech Dis 2022 Jan 24;17(1):515-546. [doi: 10.1146/annurev-pathol-042320-030240]
29. Hirata Y, Tsuji T, Kotoku J, Sata M, Kusunose K. Echocardiographic artificial intelligence for pulmonary hypertension classification. Heart 2024 Apr;110(8):586-593. [doi: 10.1136/heartjnl-2023-323320]
30. Siddiqui I, Rajagopal S, Brucker A, et al. Clinical and echocardiographic predictors of outcomes in patients with pulmonary hypertension. Am J Cardiol 2018 Sep;122(5):872-878. [doi: 10.1016/j.amjcard.2018.05.019]
31. Hirsch K, Nolley S, Ralph DD, et al. Circulating markers of inflammation and angiogenesis and clinical outcomes across subtypes of pulmonary arterial hypertension. J Heart Lung Transplant 2023 Feb;42(2):173-182. [doi: 10.1016/j.healun.2022.10.026] [Medline: 36470771]
32. Tello K, Wan J, Dalmer A, et al. Validation of the tricuspid annular plane systolic excursion/systolic pulmonary artery pressure ratio for the assessment of right ventricular-arterial coupling in severe pulmonary hypertension. Circ: Cardiovasc Imaging 2019 Sep;12(9):e009047. [doi: 10.1161/CIRCIMAGING.119.009047]
33. Huang Y, Ma SF, Oldham JM, et al. Machine learning of plasma proteomics classifies diagnosis of interstitial lung disease. Am J Respir Crit Care Med 2024 Aug 15;210(4):444-454. [doi: 10.1164/rccm.202309-1692OC]

Abbreviations

AUC: area under the receiver operating characteristic curve

XSL•FO
RenderX

CysC: cystatin C
DCA: decision curve analysis
E/E': ratio of mitral valve early diastolic inflow velocity (E) to mitral annulus early diastolic velocity (E')
EHR: electronic health record
LASSO: least absolute shrinkage and selection operator
mPAP: mean pulmonary artery pressure
PAD: pulmonary artery diameter
PH: pulmonary hypertension
RFE: recursive feature elimination
RHC: right heart catheterization
ROC: receiver operating characteristic
SHAP: Shapley Additive Explanations
TRV: tricuspid regurgitation velocity
XGBoost: Extreme Gradient Boosting

Edited by A Benis; submitted 18.03.25; peer-reviewed by A Bakare, RT Potla; revised version received 14.08.25; accepted 15.08.25; published 24.09.25.

Please cite as:
Jiang H, Gao H, Wang D, Zeng Q, Hao X, Cheng Z
Interpretable Machine Learning Model for Pulmonary Hypertension Risk Prediction: Retrospective Cohort Study
JMIR Med Inform 2025;13:e74117
URL: https://medinform.jmir.org/2025/1/e74117
doi:10.2196/74117

© Hongxia Jiang, Han Gao, Dexin Wang, Qingli Zeng, Xiaojun Hao, Zhenshun Cheng. Originally published in JMIR Medical Informatics (https://medinform.jmir.org), 24.9.2025. This is an open-access article distributed under the terms of the Creative Commons Attribution License (https://creativecommons.org/licenses/by/4.0/), which permits unrestricted use, distribution, and reproduction in any medium, provided the original work, first published in JMIR Medical Informatics, is properly cited. The complete bibliographic information, a link to the original publication on https://medinform.jmir.org/, as well as this copyright and license information must be included.

XSL•FO
RenderX

Interpretable Machine Learning for Predicting Adverse Pregnancy Outcomes in Gestational Diabetes: Retrospective Cohort Study

Jiaxi Li[1*], MD; Xiali Liu[2*], MD; Shenyang He[1], MBBS; Yan Ren[3*], MSc

[1]Jinniu Maternity and Child Health Hospital of Chengdu, Chengdu, China

[2]Department of Anesthesiology, West China Hospital, Sichuan University, Chengdu, China

[3]Department of Endocrinology and Metabolism, Adrenal Center, West China Hospital of Sichuan University, Number 37 Guoxue Alley, Wuhou District, Chengdu, China

[*]these authors contributed equally

Corresponding Author:
Yan Ren, MSc
Department of Endocrinology and Metabolism, Adrenal Center, West China Hospital of Sichuan University, Number 37 Guoxue Alley, Wuhou District, Chengdu, China

Abstract

Background: Gestational diabetes mellitus (GDM) affects over 5% of pregnancies worldwide, elevating risks of type 2 diabetes post partum and complications such as fetal death, miscarriage, and congenital abnormalities. Effective GDM management is essential to balance glycemic control and pregnancy outcomes.

Objective: We aim to develop interpretable machine learning models using GDM datasets for predicting adverse pregnancy outcomes and identifying key factors through the Shapley additive explanations (SHAP) algorithm, thus supporting improved maternal and infant health.

Methods: Data preprocessing and feature selection were performed, with adaptive synthetic sampling used to address class imbalance. Classification models, including logistic regression, random forest, support vector machine, and extreme gradient boosting, were built and enhanced through the stacking method. Model interpretability was assessed with SHAP to quantify feature contributions.

Results: Among 1670 patients, 200 experienced adverse outcomes. The stacking model outperformed individual models, achieving an accuracy of 85.6%, a sensitivity of 57.8%, a specificity of 95.9%, and an area under the receiver operating characteristic curve of 0.82 on the test set. External validation on 159 patients showed a decline in performance (accuracy 83.6%, area under the receiver operating characteristic curve 0.67). SHAP analysis identified gestational age, glucose control, and diagnosis time among the most influential predictors, providing clinically meaningful insights into risk factors. Additionally, detailed SHAP-based visualization revealed the distribution of different feature values and their nonlinear impact on outcomes, as well as interaction effects between features. These interpretable analyses enabled a deeper understanding of individual and combined feature contributions, thereby enhancing clinical assessment capabilities.

Conclusions: This study underscores the potential of machine learning in predicting adverse outcomes in GDM, with interpretable features offering valuable clinical insights to enhance pregnancy management and maternal-infant health.

(JMIR Med Inform 2025;13:e71539) doi:10.2196/71539

KEYWORDS

gestational diabetes mellitus; adverse pregnancy outcomes; interpretable model; machine learning; risk prediction; ensemble learning

Introduction

Gestational diabetes mellitus (GDM) is a significant global health concern, affecting at least 5% of pregnancies worldwide [1]. It is characterized by impaired glucose tolerance due to an increase in anti-insulin substances and decreased insulin sensitivity, leading to hyperglycemia and other metabolic disturbances [2]. Women diagnosed with GDM not only face increased perinatal complications but are also at a significantly higher risk of developing type 2 diabetes mellitus postpartum [3]. Moreover, in utero exposure to hyperglycemia has long-term implications for offspring, predisposing them to metabolic disorders, obesity, and cardiovascular diseases later in life.

Uncontrolled GDM significantly increases the risk of adverse pregnancy outcomes, including fetal macrosomia, preterm birth, neonatal hypoglycemia, and even perinatal mortality [4,5]. During early pregnancy, poor glycemic control may result in congenital malformations or spontaneous abortion, whereas in

XSL•FO
RenderX

later stages, it can contribute to pre-eclampsia, respiratory distress syndrome, and hyperbilirubinemia [6,7]. Despite advancements in clinical management, the timely identification of high-risk pregnancies remains a challenge. Traditional risk assessment methods, such as clinical scoring systems and conventional regression models, often rely on predefined risk factors and fail to capture complex interactions within high-dimensional clinical data [8]. This limitation highlights the need for more advanced predictive tools that can improve early risk stratification and optimize maternal and fetal outcomes.

Machine learning has emerged as a transformative approach in medical research, offering superior capabilities in analyzing complex, high-dimensional datasets [9]. Machine learning models can effectively capture intricate patterns and nonlinear relationships in clinical data, surpassing traditional statistical approaches in predictive accuracy. In a retrospective analysis of 8888 deliveries, random forest classification achieved exceptional accuracy in predicting birth asphyxia, with critical risk factors including maternal hypertension, anemia, preterm birth, and noncephalic presentation [10]. Similarly, deep learning showed superior predictive performance for intrauterine growth restriction in another study of 8888 pregnancies, identifying key risk factors such as maternal hypertension, drug addiction, and COVID-19 infection [11]. Furthermore, in an analysis of 7166 pregnancies, random forest demonstrated optimal prediction of fetal heart, with significant predictors including primiparity, placental abruption, and male fetal sex [12]. However, the use of machine learning models in predicting GDM-related adverse pregnancy outcomes remains relatively limited—particularly in the field of interpretable machine learning. Most current studies focus on model predictive accuracy, lacking transparent analysis of feature variable impacts, which makes it difficult to provide clinically reliable risk factor assessments. This lack of interpretability limits the practical application and adoption of such models in real-world medical settings. Therefore, there is an urgent need to develop models that combine high predictive performance with clinical interpretability to identify key risk factors and assist physicians in formulating personalized intervention strategies.

To address this gap, this study aims to develop an interpretable machine learning model using a publicly available GDM dataset to predict the risk of adverse pregnancy outcomes associated with gestational diabetes. Unlike previous studies that primarily focus on GDM diagnosis, our approach emphasizes predicting maternal and fetal complications, which is crucial for timely intervention. Furthermore, we incorporate Shapley additive explanations (SHAP) analysis to enhance model interpretability, allowing clinicians to identify the most influential factors contributing to adverse pregnancy outcomes. By providing clinically actionable insights, our model aims to support personalized risk assessment and improve maternal and fetal health outcomes.

Methods

Data

This study is based on the publicly available GDM dataset. We included pregnant women who met specific diagnostic criteria through the publicly available dataset [13,14]. The dataset comprises anonymized electronic health records extracted from the Cerner system at St Mary's Hospital in London, covering pregnancies monitored between April 2016 and November 2019. A total of 1854 records were initially retrieved, including clinical and demographic variables such as maternal age, BMI at booking, ethnicity, glucose tolerance test results (0- and 120-min post-75 g glucose load), mode of delivery, gestational age, neonatal birth weight, and stillbirth outcomes.

To ensure data quality and reliability, patients with missing values in key variables were excluded. Implausible outliers were identified and corrected when possible; otherwise, they were removed from the dataset. Unit inconsistencies were also standardized. These preprocessing steps were applied to ensure consistency, accuracy, and completeness of the data used for model development and analysis.

Subject

To ensure the accuracy and reliability of this study's results, inclusion criteria (based on the results of the oral glucose tolerance test [OGTT]) were defined as follows: the blood glucose level of pregnant women should reach or exceed 7.8 mmol/L and not exceed 25 mmol/L at 2 hours after OGTT; or the blood glucose level should reach or exceed 5.6 mmol/L and not exceed 25 mmol/L at 10 minutes after OGTT [15]. In addition, the study's definition of adverse pregnancy outcomes includes newborn birth weight below 2500 g, severe prematurity, stillbirth, and Apgar score below 4 [16]. Additionally, we excluded cases with missing Apgar score data to avoid potential biases that could arise from inaccuracies in assessing pregnancy outcomes. By implementing these strict inclusion and exclusion criteria, we ensured the consistency of this study's population, allowing for a more accurate assessment of the impact of GDM on the health of pregnant women and their offspring.

Data Preprocessing

In this study, we encountered issues with missing values for multiple features in the dataset. To maintain data integrity and the reliability of the analysis, we adopted a cautious approach to handle these missing values. Specifically, when the proportion of missing values for a particular feature exceeded 30%, such as "previous obstetric history," "presence of meconium," and "O_Thyroid function blood," we chose to exclude them from the analysis. For the remaining missing values in the features, we implemented an imputation strategy to enhance the usability of the data.

In terms of the choice of imputation method, we adopted a differentiated approach based on the type of feature. For numerical features, we used the median or mean for imputation, a method that reduces the impact of extreme values while preserving the distribution characteristics of the data. For categorical features, we used the k-nearest neighbors algorithm

XSL•FO
RenderX

for imputation, which estimates the possible values of missing data by finding similar observations based on distance metrics.

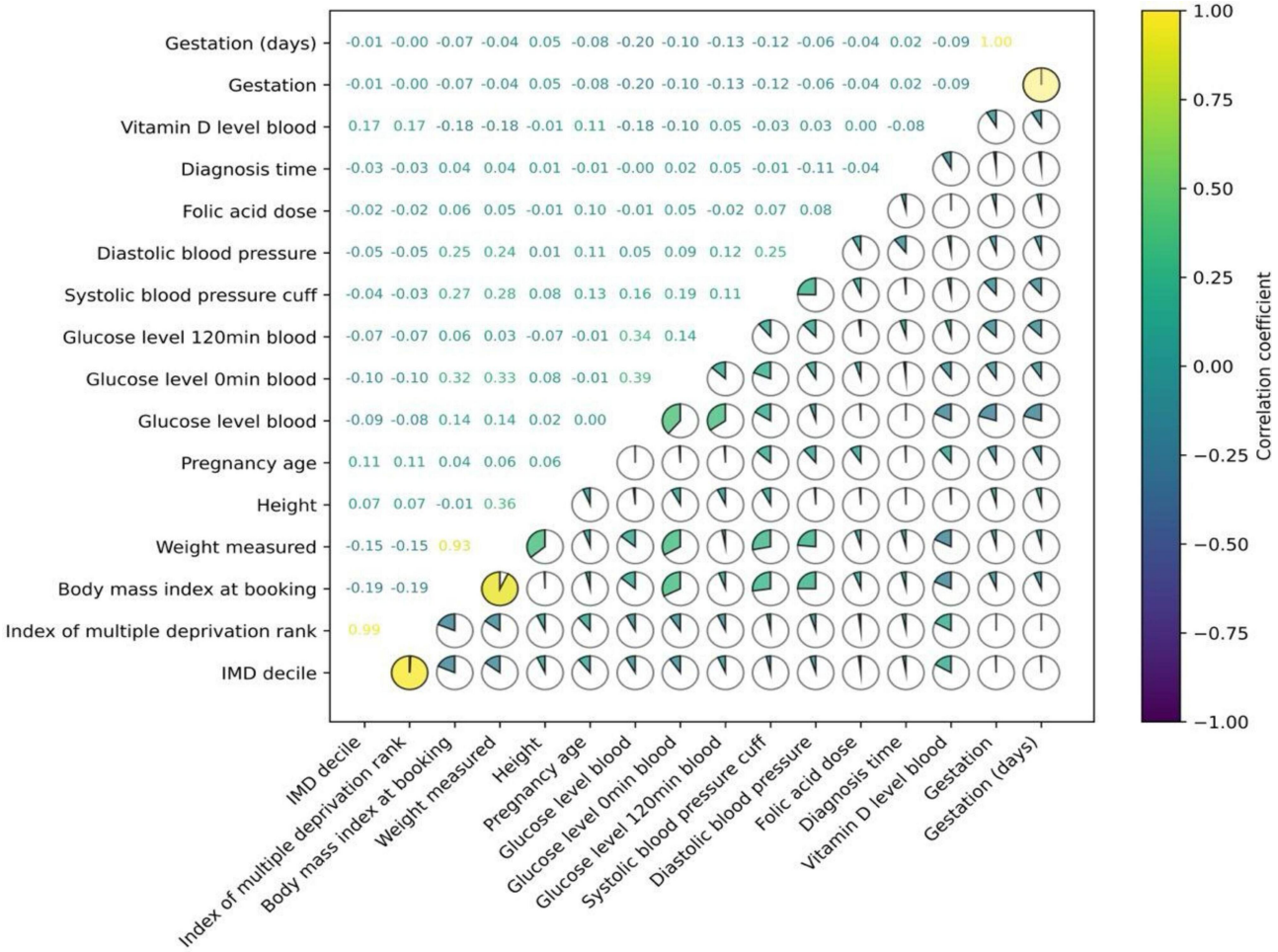
Additionally, some categorical features with sparse or heterogeneous classifications were restructured using domain knowledge to improve statistical interpretability. For instance, antenatal medical factors were originally recorded in 64 different categories. These were clinically reviewed and consolidated into 7 meaningful groups: (1) mental health and neurological disorders, (2) genetic disorders, (3) surgical or operative conditions, (4) infectious and immune-related diseases, (5) obesity-related conditions, (6) chronic diseases, and (7) none.

Finally, to further meet the requirements of machine learning models, we performed 1-hot encoding on all categorical variables. This helps to avoid potential numerical encoding biases and ensures the effectiveness of model training.

Feature Selection

To mitigate the "curse of dimensionality" and enhance the practicality of model deployment in clinical settings, we removed redundant features. As shown in Figure 1, we used the Pearson correlation matrix to identify highly correlated variables. For continuous variables, feature selection was guided by the Pearson correlation coefficient. As the number of categorical variables was relatively small—primarily including "number of previous C-sections," "obesity status," and "antenatal medical factors"—all were retained in the model.

Figure 1. Pearson correlation matrix of key features for redundancy analysis. IMD: Index of Multiple Deprivation.



During the analysis, we identified several pairs of features with relatively high Pearson correlation coefficients, including "Index of Multiple Deprivation (IMD) decile" and "IMD rank," "gestation (days)" and "gestation," as well as "body mass index (BMI) at booking" and "weight measured." Both deprivation-related variables reflect the socioeconomic status of pregnant women; however, given the broader range of values for "IMD decile" (1012 to 32,742), we considered it more statistically informative and retained this feature.

Given the direct association between gestational age and adverse pregnancy outcomes, gestational variables were excluded from the model to prevent potential confounding. Likewise, fetal birth weight—available only after delivery—was excluded to avoid outcome leakage. We recalculated BMI based on height and weight, as it offers a more comprehensive measure of maternal body composition. Consequently, the original "height" and "weight" variables were removed due to redundancy. Additionally, although "gestation (days)," "gestation," and "Gravida" are strongly associated with adverse outcomes such as preterm birth and miscarriage, including them posed a risk of information leakage. Based on both statistical reasoning and clinical expert input, these features were excluded.

Lastly, "vitamin D level in blood" was removed due to concerns over data quality and consistency. Vitamin D is not a routine

XSL•FO
RenderX

prenatal test, and the lack of standardization in test timing introduced considerable variability, limiting its reliability as a predictive feature.

Missing Data

The final dataset included 10 continuous variables such as pregnancy age, blood glucose levels, and blood pressure. The categorical variables include obesity status, number of previous C-sections, and antenatal medical factors. Several continuous variables had missing values, with the highest rates observed in blood glucose levels (up to 23.1%) and blood pressure measurements (Multimedia Appendix 1).

Model Construction

Based on our analysis results, we performed feature selection and data preprocessing and then constructed machine learning models. We used a variety of algorithms, including logistic regression, random forests, support vector machines (SVM), and extreme gradient boosting (XGBoost), to independently build classification prediction models. To further enhance the predictive power of the models, we used the Stacking ensemble learning method, taking the prediction results of these base models as input and training them with a meta-model (also known as a secondary model), thereby achieving superior overall predictive performance. In our study, we chose XGBoost as the meta-model. Considering that only 11.9% of the samples in the dataset manifested adverse pregnancy outcomes, indicating an imbalance in the dataset, we applied the adaptive synthetic sampling (ADASYN) algorithm to address this imbalance and improve the model's generalization ability.

ADASYN is a machine learning algorithm used to address class imbalance in classification problems [17]. In imbalanced datasets, there is a large difference in the number of samples between different classes, which can result in poor classification performance of the model for minority classes. ADASYN balances the dataset by increasing the number of samples of the minority class, thus improving the model's performance. Considering the imbalance between the alive group and the expired group and the impact on the accuracy of the prediction results, we applied the ADASYN method to oversample the training set, while the test set maintained the original sample ratio. To further validate the model's robustness and performance in addressing class imbalance, we conducted supplementary experiments by introducing another widely used oversampling method—SMOTE (Synthetic Minority Oversampling Technique) for comparison. SMOTE generates synthetic minority class samples through interpolation in the feature space and has been extensively applied in imbalanced classification tasks. Compared with ADASYN, it is more comprehensive to evaluate the impact of different oversampling strategies on model performance, ensuring the selected method exhibits stronger robustness and generalization capability in practical applications. The overall data was split into a training set and a test set in an 8:2 ratio. To fine-tune the hyperparameters of each algorithm, we used grid search based on 5-fold cross-validation within the training set. The hyperparameters adjusted for each algorithm are as follows (Table 1).

Table . Hyperparameters adjusted for each algorithm.

Algorithm	Hyperparameters
Random forest	• n_estimators: 10, 50, 100 • max_features: auto, sqrt, log2 • Bootstrap: true, false
Extreme Gradient Boosting	• n_estimators: 20, 50, 100 • learning_rate: 0.1, 0.2, 0.3 • max_depth: 4, 6, 8 • objective: binary: logistic • subsample: 0.6, 0.8, 1
Logistic regression	• C: 0.001, 0.01, 0.1, 1, 10, 100, 1000 • Penalty: L1, L2
Support vector machine	• C: 0.1, 1, 10, 100 • Kernel: linear, rbf, poly • Gamma: scale, auto

Based on the basic models obtained from training, we introduced the stacking strategy in our model fusion approach to more comprehensively explore the potential correlations between different basic models. We treated the outputs of each basic model as new features and further trained them using the XGBoost gradient boosting framework to construct a highly optimized stacking model with significant synergistic effects.

In clinical models, the interpretability of the model is crucial because it helps doctors and researchers understand the decision-making process of the model, thereby increasing trust in the model and promoting its application in clinical practice. SHAP is a popular machine learning interpretability tool that can quantify the contribution of each feature to the model's prediction. In our study, we used the SHAP algorithm to perform an interpretability analysis on the gestational diabetes risk prediction model to increase the model's transparency, helping doctors better understand the model's decision-making process and make appropriate interventions when necessary.

XSL•FO
RenderX

Ethical Considerations

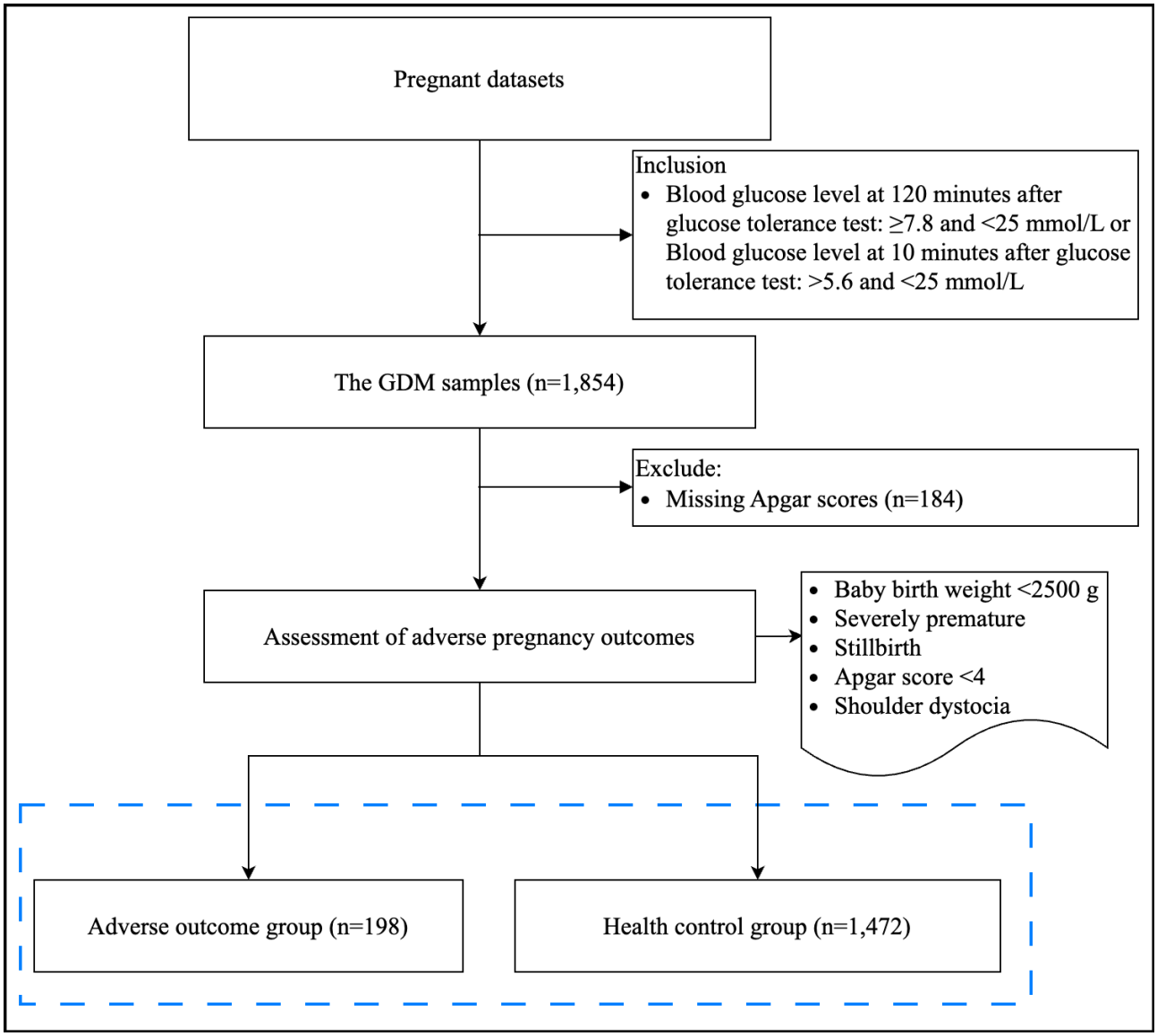
This study is based on the publicly available GDM dataset. We included pregnant women who met specific diagnostic criteria, as defined in the dataset documentation. All protected health information has been deidentified to ensure privacy. The dataset is accessible [14], and its use complies with the associated public license and terms of use. Therefore, ethical approval and individual patient consent were not required for this study.

Results

Overview

A total of 1670 patients were selected from the GDM database for inclusion in this study. The data inclusion and exclusion diagram is shown in Figure 2. Among them, 200 patients had adverse pregnancy outcomes. Statistical analysis was conducted using SPSS (version 22.0; IBM Corp), while data cleaning, model construction, and performance evaluation were carried out using Python (Python Software Foundation). Continuous variables were expressed as median (IQR), while categorical data were presented as counts (percentages). The Mann-Whitney *U* test was used for analyzing continuous variables, and chi-square test was used to examine significant differences in categorical variables. The patient's baseline is presented in Table 2.

Figure 2. Flowchart of data inclusion and exclusion criteria. GDM: gestational diabetes mellitus.



XSL•FO
RenderX

Table . Comparison of maternal characteristics by outcome group. Statistical significance was defined as $P<.05$.

Variable	HC[a]	Adverse outcome	*P* value
IMD[b] decile, median (IQR)	4.00 (3.00 - 6.00)	4.00 (3.00 - 6.00)	.25
Pregnancy age, median (IQR)	34.00 (30.00 - 37.00)	35.00 (31.00 - 38.00)	.04
Glucose level (blood), median (IQR)	4.70 (4.30 - 5.30)	5.00 (4.45 - 5.80)	<.001
Glucose level (0 min), median (IQR)	4.60 (4.20 - 5.20)	4.70 (4.30 - 5.65)	.002
Glucose level (120 min), median (IQR)	8.40 (8.00 - 9.10)	8.50 (8.00 - 9.50)	.02
Systolic blood pressure, median (IQR)	111.00 (104.00 - 120.00)	115.00 (107.00 - 125.00)	<.001
Diastolic blood pressure, median (IQR)	70.00 (63.00 - 77.00)	72.00 (65.00 - 79.25)	.01
Folic acid dose, median (IQR)	400.00 (0.00 - 400.00)	400.00 (0.00 - 400.00)	.81
Diagnosis time (weeks), median (IQR)	10.00 (10.00 - 12.00)	10.00 (9.75 - 12.00)	.82
BMI (kg/m²), median (IQR)	26.02 (22.81 - 29.75)	26.51 (23.71 - 30.05)	.02
Obese? n (%)			.30
No	908 (74.49)	324 (71.84)	
Yes	311 (25.51)	127 (28.16)	
No_of_previous_csections, n (%)			.69
0	1003 (82.28)	369 (81.82)	
1	187 (15.34)	72 (15.96)	
2	26 (2.13)	7 (1.55)	
3	2 (0.16)	2 (0.44)	
4	1 (0.08)	1 (0.22)	
Antenatal medical factors, n (%)			.10
Chronic diseases	117 (9.60)	50 (11.09)	
Genetic disorders	5 (0.41)	0 (0)	
Infectious and immune-related diseases	27 (2.21)	12 (2.66)	
Mental health and neurological disorders	47 (3.86)	30 (6.65)	
Obesity-related conditions	2 (0.16)	2 (0.44)	
Surgical or operative conditions	110 (9.02)	43 (9.53)	
None	911 (74.73)	314 (69.62)	

[a]HC: healthy control.

[b]IMD: Index of Multiple Deprivation.

In this study, we evaluated 5 different machine learning models: random forest, XGBoost, logistic regression, SVM, and a stacking ensemble model. To address class imbalance in the training data, we applied oversampling techniques such as ADASYN before model training. However, to preserve the clinical authenticity and real-world applicability of the evaluation, no oversampling was applied to the test set. A comprehensive evaluation was conducted using multiple performance metrics, including sensitivity, specificity, positive predictive value (PPV), negative predictive value (NPV), positive likelihood ratio (PLR), negative likelihood ratio (NLR), and overall accuracy. The results obtained on the test set are summarized in Table 3 below.

XSL•FO
RenderX

Table . Comparative performance metrics of machine learning models for predicting GDM[a]-related adverse outcomes.

Model	SEN[b]	SPE[c]	PPV[d]	NPV[e]	PLR[f]	NLR[g]	Accuracy	F_1-score
Random forest	0.600	0.926	0.750	0.863	8.133	0.432	0.838	0.667
XGBoost[h]	0.567	0.955	0.823	0.857	12.570	0.454	0.850	0.671
Logistic regression	0.478	0.721	0.387	0.789	1.714	0.724	0.656	0.428
SVM[i]	0.633	0.828	0.576	0.860	3.679	0.443	0.775	0.603
Stacking	0.578	0.959	0.839	0.860	14.098	0.440	0.856	0.684

[a]GDM: gestational diabetes mellitus.

[b]SEN: sensitivity.

[c]SPE: specificity.

[d]PPV: positive predictive value.

[e]NPV: negative predictive value.

[f]PLR: positive likelihood ratio.

[g]NLR: negative likelihood ratio.

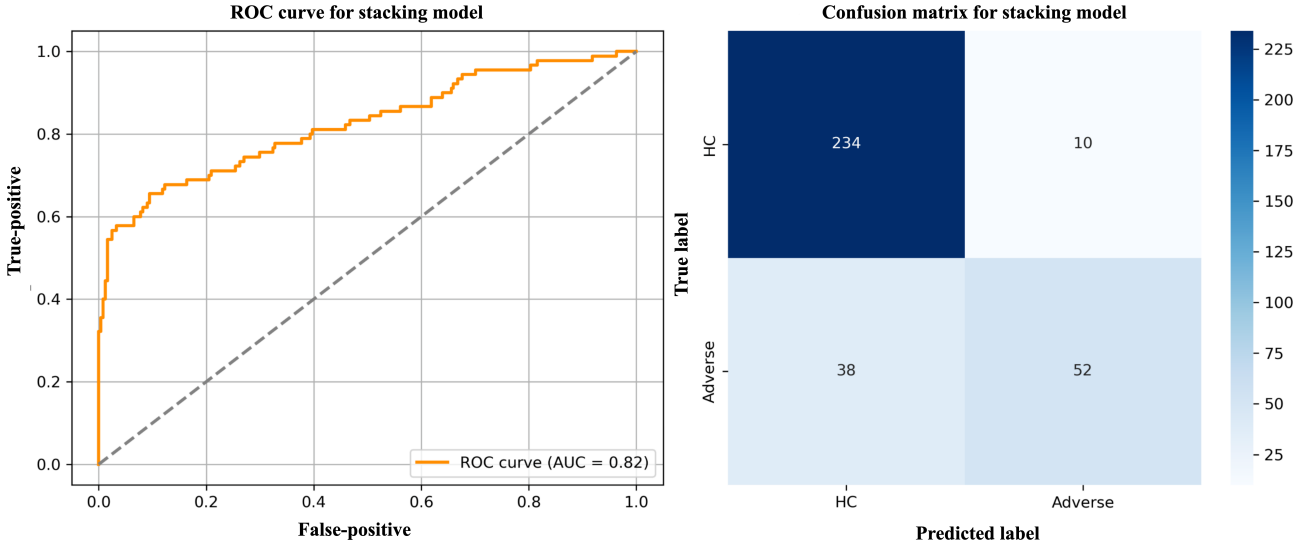
[h]XGBoost: extreme gradient boosting.

[i]SVM: support vector machine.

The results showed that the stacking model outperformed the individual models across several key metrics. Through cross-validation, we evaluated accuracy, recall, precision, and F_1-score. The results indicated that the stacking model excelled in specificity (0.959), PPV (0.839), and PLR (14.098). Its sensitivity (0.578) and NPV (0.860) were also strong, with a low NLR (0.440) and an overall accuracy of 0.856, demonstrating the effectiveness of the model fusion approach.

A total of 334 samples were contained in the test set, including 90 cases with adverse pregnancy outcomes (positive class) and 244 cases with favorable outcomes (negative class). The positive-to-negative ratio is approximately 1:2.7, indicating a moderately imbalanced distribution. Based on this dataset, the model demonstrated a satisfactory performance in identifying adverse outcomes, achieving an area under the receiver operating characteristic curve of 0.82. This suggests that the model exhibits high overall discriminative ability and can effectively differentiate individuals with distinct pregnancy outcomes. The receiver operating characteristic curve and confusion matrix for the stacking model are presented in Figure 3.

Figure 3. ROC curve and confusion matrix of the stacking model for predicting GDM-related adverse outcomes. AUC: area under the curve; GDM: gestational diabetes mellitus; HC: healthy control; ROC: receiver operating characteristic.



To further investigate the effect of different oversampling techniques on model performance, we conducted a comparative experiment using both ADASYN and SMOTE, focusing on the stacking model, which showed the best overall performance in our main evaluation. The results are presented in Table 4.

XSL•FO
RenderX

Table . Performance comparison of ADASYN[a] and SMOTE[b].

Oversampling method	SEN[c]	SPE[d]	PPV[e]	NPV[f]	PLR[g]	NLR[h]	Accuracy	F_1-score
ADASYN (stacking)	0.578	0.959	0.839	0.860	14.098	0.440	0.856	0.684
SMOTE (stacking)	0.266	0.910	0.477	0.800	2.947	0.807	0.728	0.341
/	0.658	0.506	0.292	0.827	1.332	0.676	0.542	0.405

[a]ADASYN: adaptive synthetic sampling.

[b]SMOTE: Synthetic Minority Oversampling Technique.

[c]SEN: sensitivity.

[d]SPE: specificity.

[e]PPV: positive predictive value.

[f]NPV: negative predictive value.

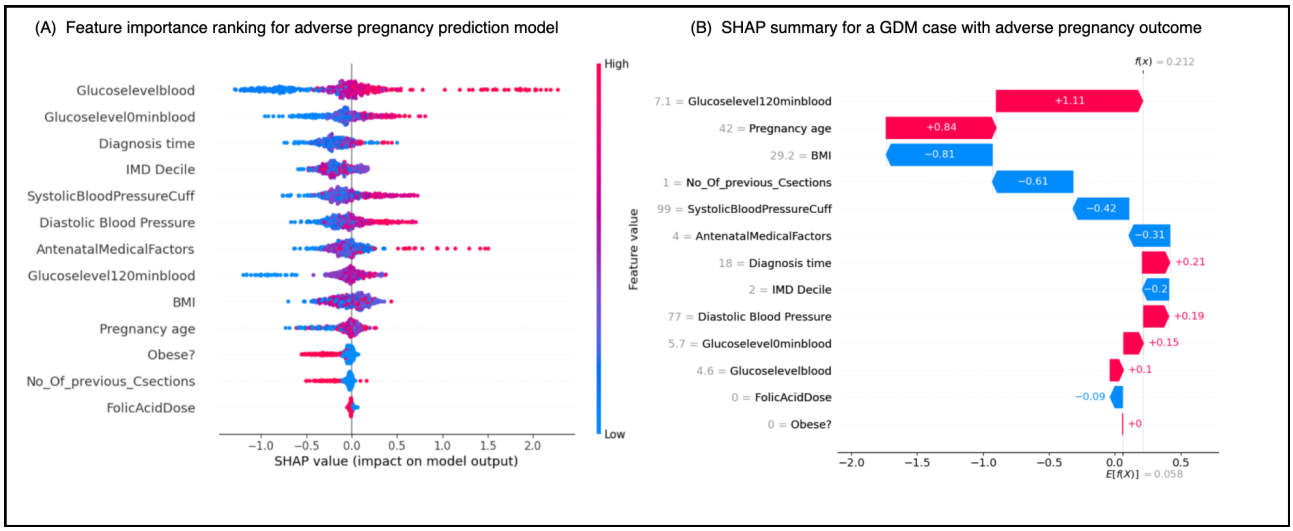
[g]PLR: positive likelihood ratio.

[h]NLR: negative likelihood ratio.

As shown, the stacking model trained with ADASYN achieved superior performance across most metrics, particularly in terms of sensitivity (0.578), PPV (0.839), and F_1-score (0.684), suggesting better identification of high-risk cases and overall balance between precision and recall. In contrast, the model trained with SMOTE exhibited a much lower sensitivity (0.266) and F_1-score (0.341), indicating its limited ability to correctly identify minority class samples in this setting. We also report the performance of the stacking model trained without any oversampling as a reference, which demonstrated relatively higher sensitivity (0.658) but at the cost of much lower precision (PPV 0.292) and specificity (0.506), further confirming the advantage of using ADASYN in managing class imbalance.

Additionally, by using the SHAP algorithm, we conducted an in-depth analysis of the model's interpretability. The SHAP values revealed that clinical characteristics significantly impact the prediction of gestational diabetes risk, with specific results as follows. Through the calculation and analysis of SHAP values, we were able to uncover the contribution of each feature to the GDM outcome, thereby gaining a more comprehensive understanding of the risk factors for GDM. This interpretable analysis not only aids in validating the robustness of the model but also provides valuable references for subsequent clinical decision-making. Based on the SHAP algorithm, we were able to perform precise visual analyses for individual patients, as shown in Figure 4, which includes a global summary of feature importance across all patients (Figure 5A) and a local explanation for an individual prediction (Figure 5B).

Figure 4. SHAP-based visualization of a machine learning model for predicting adverse pregnancy outcomes in patients with GDM. (A) Summary plot of SHAP values for all features, showing their impact and direction of effect on model output across all patients. (B) Local explanation for a single GDM case, highlighting how individual features contributed to the prediction. GDM: gestational diabetes mellitus; IMD: Index of Multiple Deprivation; SHAP: Shapley additive explanations.



XSL•FO
RenderX

Figure 5. SHAP-based interpretation of feature effects and interactions in the prediction model. GDM: gestational diabetes mellitus; IMD: Index of Multiple Deprivation; SHAP: Shapley additive explanations.

XSL•FO
RenderX

For each feature, we used the shape function to display the distribution of its different values and their impact on the outcome. The influence of individual features was shown in Figure 5A, which demonstrates the specific impact of changes in a single variable's values on the model's predicted risk, revealing nonlinear relationships. Additionally, we used visualization techniques to illustrate the interaction values between different features, as shown in Figure 5B. These analyses will enhance our ability to conduct clinical assessments more effectively.

We further conducted feature interaction analysis to explore the contribution of different feature combinations in predicting adverse pregnancy outcomes in GDM. As shown in Figure 5C, the plot illustrates the overall importance of each feature in the model and its direction of influence, with each dot representing the SHAP value of an individual patient. The features are ranked by their mean absolute SHAP values, reflecting their average impact magnitude on the model's output. These results also highlight the significance of key variables and their interactions in clinical risk prediction.

External Validation

Based on the integrated model we ultimately obtained, we collected data from some patients with GDM at Jinniu Maternal and Child Health Hospital (from January 2021 to March 2024) through telephone follow-up, focusing on collecting data from patients with adverse pregnancy outcomes. Due to issues such as patient cooperation and the tightness of related human resources, the number of external validation data is relatively small (159 cases, with a positive to negative ratio of 27:132). We used the stacking model for validation, which had a final accuracy of 0.836 and an area under the receiver operating characteristic curve value of 0.669, showing a significant decline compared to the test set. The results are shown in Multimedia Appendix 2.

Discussion

Principal Findings

According to the latest Global Diabetes Atlas (9th edition) published by the International Diabetes Federation, the number of patients with GDM worldwide is increasing, with approximately 20.4 (15.8%) million women enduring hyperglycemia; among them, around 17.1 (83.6%) million cases are due to GDM [18]. Pregnant women affected by GDM face an elevated risk of adverse pregnancy outcomes, which can pose significant threats to both the mother and the infant. Therefore, predicting adverse pregnancy outcomes in the early stages of pregnancy and providing timely feedback and effective clinical management are particularly important.

The traditional scoring criteria for adverse pregnancy outcomes currently used in clinical practice, such as the IADPSG (International Association of Diabetes and Pregnancy Study Groups) and the NICE (National Institute for Health and Care Excellence) Diagnostic Criteria, exhibit varying levels of predictive efficacy and are prone to regional biases, making it difficult to achieve a consensus on predictive outcomes [19,20]. Additionally, individual differences, such as physiological variations, hormonal changes, genetics, and dietary structures, also affect the estimated prevalence rates of GDM. However, current clinical strategies for gestational diabetes typically use a one-size-fits-all approach to blood glucose management. Therefore, more comprehensive regular monitoring and earlier preventive and intervention measures should be implemented to reduce the potential for adverse outcomes.

In this study, we compared 5 machine learning models, random forest, XGBoost, logistic regression, SVM, and stacking, to assess their performance in predicting outcomes related to GDM. The results indicated that the stacking model outperformed the other models across multiple key performance metrics, particularly excelling in specificity (0.959), PPV (0.839), and PLR (14.098). Additionally, the stacking model demonstrated good performance in sensitivity (0.578) and NPV (0.860), with a low NLR (0.44) and overall accuracy (0.856), further proving the significant advantage of model ensemble methods in enhancing predictive performance. The receiver operating characteristic curve and confusion matrix analysis also supported this conclusion, emphasizing the effectiveness of the stacking model in predicting adverse pregnancy outcomes in GDM. However, during external validation, when using domestic patient data, the model's performance significantly declined. This phenomenon may be related to the inconsistent distribution of dataset characteristics, such as differences in demographic characteristics, lifestyle habits, and medical environments between domestic and international datasets. These differences may lead to poor model adaptation when facing new data distributions. Future research should further explore the performance of these models on larger and more diverse datasets to verify their generalization and stability. At the same time, it is recommended to integrate clinical context by introducing more features related to gestational diabetes for analysis, such as real-time vital signs of pregnant women, genetic phenotypes, and other relevant indicators, to enhance the model's predictive power and clinical application value.

SHAP helps clinicians understand and interpret complex machine learning models. We noticed that adverse pregnancy outcomes have a significant association with gestational age. Previous studies have shown that adverse pregnancy outcomes are directly related to blood glucose control during the perinatal period of gestational diabetes [21]. Our results indicate that gestational diabetes with a shorter duration during pregnancy is associated with poorer pregnancy outcomes, which may be related to the early detection of hyperglycemia leading to preterm birth. Therefore, these findings serve as an important alert for clinical practice, suggesting that blood glucose monitoring should be initiated earlier in pregnancy, considering the patient's condition, to conduct earlier glucose monitoring for different individuals. Current clinical guidelines recommend screening for gestational diabetes between 24 and 28 weeks of pregnancy, and screening for and treating gestational diabetes during this period can significantly reduce the risk of adverse pregnancy outcomes [4,22]. Meanwhile, a large cohort study found that women diagnosed with GDM before 12 weeks of pregnancy had worse pregnancy outcomes compared to those diagnosed between 24 - 28 weeks [23]; the research by Mustafa et al [7] also found that women with early onset (<24 weeks)

XSL•FO
RenderX

GDM had higher BMI, significantly increased demand for insulin, and more adverse pregnancy outcomes. Therefore, in addition to recommending universal screening at 24 - 28 weeks, identifying and treating GDM at an earlier stage could reduce the potential perinatal or long-term adverse effects on the mother and the offspring. These findings emphasize the importance of identifying GDM earlier than current practices and exploring other interventions that might improve outcomes beyond blood glucose control.

Pregnant women with GDM experience insulin resistance, as previously reported in studies, which is associated with preterm birth, and preterm newborns are at a higher risk of being admitted to the neonatal intensive care unit or special care baby unit [24]. Due to pregnant women with high blood glucose levels, adverse pregnancy outcomes such as preterm birth, large-for-gestational-age infants, and neonatal hypoglycemia often require care in a neonatal intensive care unit. Excess glucose in the mother's circulation is transferred across the placenta to provide the fetus with energy substrates. The fetus's response to the excess substrates is to produce more insulin, leading to fetal hyperinsulinemia, which can result in a series of consequences, particularly rapid fetal growth [25]. In pregnancies with GDM, fetal insulin binds to insulin-like growth factor 1 receptors, exerting growth hormone-like effects and serving as a key factor in promoting fetal growth [26]. It is common for children born to women with GDM to be large at birth. Extensive research on this population has shown that the increased birth weight of large-for-gestational-age infants is due to an increase in fat mass, not muscle mass [27,28]. The impact of GDM on both mother and infant does not end at delivery. Newborns admitted to the neonatal intensive care unit or special care baby unit due to maternal gestational diabetes are often seen with neonatal hypoglycemia, which may occur in 10% of healthy term infants, mainly within the first 24 to 48 hours after birth [29]. The high glucose consumption of the brain, coupled with the increased ratio of brain to body mass in newborns compared to adults, increases the demand for glucose in newborns and may expose them to the risk of neurological damage and adverse outcomes.

Pregnancy hypertension is a common complication of pregnancy and a leading cause of morbidity and mortality in pregnant women and newborns, accounting for about 14% of maternal deaths worldwide [30,31]. Both pregnancy-induced hypertension and pre-eclampsia are associated with adverse maternal and fetal outcomes, including an increased risk of future maternal cardiovascular diseases, and there is approximately a 17% chance of pregnancy-induced hypertension progressing to pre-eclampsia [32]. As many women are asymptomatic at the time of diagnosis, those who do not receive prenatal care may present with more advanced hypertension-related diseases, such as eclampsia, which is associated with higher risks of morbidity and mortality [33]. In correlation analyses, GDM is accompanied by increased blood pressure in late pregnancy. GDM is a known risk factor for stillbirth, fetal macrosomia, fetal structural abnormalities, preterm birth, and pregnancy-induced hypertension diseases. GDM is characterized by significantly increased concentrations of inflammatory molecules and the imbalanced expression of genes encoding inflammatory mediators in the placenta, which together lead to the disruption of vascular, metabolic, and inflammatory processes. Over time, this state of hyperglycemia may be associated with the occurrence of pregnancy-induced hypertension diseases and their related complexities. Additionally, diabetes and hypertension often coexist, sharing various risk factors and disease etiologies, including genetics, obesity, insulin resistance, and inflammation [34]. Therefore, the management of GDM should not only focus on blood glucose control but also consider the potential risks associated with pregnancy-induced hypertension diseases. In GDM, oxidative stress plays a role in the pathogenesis of the disease, as excessive secretion of insulin during pregnancy leads to the production of lipid peroxidation factors, which also mask the secretion of antioxidants, making reactive oxygen species abundant at the cellular level. In pre-eclampsia and gestational hypertension, oxidative stress leads to inadequate placental perfusion, resulting in a hypoxic placenta, which generally triggers a systemic maternal inflammatory response [35-37].

The adverse pregnancy risks associated with GDM are determined by the complex interplay of multiple biomedical, behavioral, and environmental factors, rather than a single factor. Therefore, to investigate the contribution of feature interaction to the prognostic risks of GDM, we conducted multifeature interaction analyses. The feature interaction matrix clearly shows that blood glucose levels and time of diagnosis exhibit the highest degree of aggregation, followed by blood pressure. Additionally, gestational age and antenatal medical factors also demonstrate relatively strong clustering patterns. As previously discussed, individualized diagnosis and treatment should be tailored to different individuals. For those with a genetic predisposition to diabetes, earlier diagnosis during pregnancy should be implemented to achieve more timely blood glucose control. Hypertensive disorders in pregnancy and GDM are among the most common metabolic complications during gestation, with prevalence rates having risen significantly over the past decade, now affecting approximately 12% - 18% of all pregnancies [38]. Pregnant women with hyperglycemia generally exhibit a higher overall incidence of requiring insulin therapy, which increases with maternal age, and women over 35 years old have a significantly higher probability of undergoing cesarean delivery [39]. Genes are the most important factor in Antenatal Medical Factors. More recent genome-wide association studies focusing on maternal metabolism during pregnancy have revealed overlaps between genes associated with metabolic traits in pregnant and nonpregnant populations, as well as some genes that appear to be uniquely relevant during gestation. Additionally, reduced gene expression has been observed in transcription factors involved in lipid metabolism, such as LXRa, PPARa, PPARd, PPARg, RXRa, and SREBP1c. These findings indicate the importance of maternal oversupply of substrates in determining neonatal fat accumulation in pregnancies complicated by obesity and GDM [40].

Limitations

This study has several limitations. As a single-center retrospective study with a relatively small sample size, the generalizability of the findings may be limited. Although multiple machine learning models were used, the features were

XSL•FO
RenderX

primarily derived from structured clinical data, lacking unstructured information such as imaging findings and physician notes. And the external validation dataset also limited our research; the model's performance notably declined on domestic datasets, suggesting potential overfitting or insufficient adaptability to different populations. Although we use SHAP for interpretability analysis, the model's clinical transparency remains constrained due to the complex and nonlinear relationships between features and outcomes, which may affect the interpretability of clinical decision-making.

Conclusion

In conclusion, our study highlights the growing prevalence of GDM and its significant association with adverse pregnancy outcomes, including preterm birth, large-for-gestational-age infants, and neonatal hypoglycemia. Through the evaluation of 5 machine learning models, we found that the stacking model exhibited superior performance in predicting adverse outcomes, demonstrating the potential of machine learning to enhance clinical decision-making in managing GDM. The findings emphasize the importance of early identification and personalized management of GDM to mitigate the risks to both mother and infant. Moreover, incorporating additional clinical features, such as real-time maternal vital signs and genetic phenotypes, may further enhance the predictive accuracy and clinical applicability of these models. Future studies should aim to validate these findings across more diverse datasets to ensure the generalizability and robustness of the models, paving the way for more precise and effective interventions in GDM management.

Acknowledgments

We are grateful to the staff in our research groups involved in this study for their valuable contributions and discussions. This work was supported by the Chengdu Medical Research Project (project 2022-387).

Data Availability

The datasets generated or analyzed during this study are available in the figshare repository [14]. Access to the related code is available from the corresponding author on reasonable request.

Authors' Contributions

JL conceptualized and designed this study, performed the research, delivered the model analysis, analyzed the data, and wrote this paper. XL and JL delivered the data analysis and clinical analysis. SH contributed to the research execution and data analysis, and provided critical insights for model interpretation. YR conceptualized and designed this study. All authors contributed to editorial changes in this paper, read and approved this final paper, and have participated sufficiently in this work to take responsibility for all aspects of this work.

Conflicts of Interest

None declared.

Multimedia Appendix 1
Missing value rates of variables in the final dataset.
[PNG File, 112 KB - medinform_v13i1e71539_app1.png]

Multimedia Appendix 2
External validation outcomes for the stacking model in patients with gestational diabetes mellitus.
[PNG File, 85 KB - medinform_v13i1e71539_app2.png]

References

1. Rodriguez BSQ, Vadakekut ES, Mahdy H. Gestational Diabetes: StatPearls; 2023. URL: https://www.ncbi.nlm.nih.gov/books/NBK545196/ [accessed 2025-07-17]
2. Kampmann U, Knorr S, Fuglsang J, Ovesen P. Determinants of maternal insulin resistance during pregnancy: an updated overview. J Diabetes Res 2019;2019:5320156. [doi: 10.1155/2019/5320156] [Medline: 31828161]
3. Magliano DJ, Boyko EJ, IDF Diabetes Atlas 10th Edition Scientific Committee. IDF Diabetes Atlas, 10th edition: International Diabetes Federation; 2021. [Medline: 35914061]
4. Malaza N, Masete M, Adam S, Dias S, Nyawo T, Pheiffer C. A systematic review to compare adverse pregnancy outcomes in women with pregestational diabetes and gestational diabetes. Int J Environ Res Public Health 2022 Aug 31;19(17):10846. [doi: 10.3390/ijerph191710846] [Medline: 36078559]
5. de la Torre NG, Assaf-Balut C, Jiménez Varas I, et al. Effectiveness of following mediterranean diet recommendations in the real world in the incidence of gestational diabetes mellitus (GDM) and adverse maternal-foetal outcomes: a prospective,

XSL•FO
RenderX

universal, interventional study with a single group. The St Carlos study. Nutrients 2019 May 28;11(6):1210. [doi: 10.3390/nu11061210] [Medline: 31141972]
6. Berger H, Gagnon R, Sermer M, et al. RETIRED: diabetes in pregnancy. J Obstet Gynaecol Can 2016;38(7):667-679. [doi: 10.1016/j.jogc.2016.04.002]
7. Mustafa M, Bogdanet D, Khattak A, et al. Early gestational diabetes mellitus (GDM) is associated with worse pregnancy outcomes compared with GDM diagnosed at 24-28 weeks gestation despite early treatment. QJM 2021 Feb 18;114(1):17-24. [doi: 10.1093/qjmed/hcaa167] [Medline: 32413109]
8. Bianco ME, Josefson JL. Hyperglycemia during pregnancy and long-term offspring outcomes. Curr Diab Rep 2019 Nov 21;19(12):143. [doi: 10.1007/s11892-019-1267-6] [Medline: 31754898]
9. Choi RY, Coyner AS, Kalpathy-Cramer J, Chiang MF, Campbell JP. Introduction to machine learning, neural networks, and deep learning. Transl Vis Sci Technol 2020 Feb 27;9(2):14. [doi: 10.1167/tvst.9.2.14] [Medline: 32704420]
10. Darsareh F, Ranjbar A, Farashah MV, Mehrnoush V, Shekari M, Jahromi MS. Application of machine learning to identify risk factors of birth asphyxia. BMC Pregnancy Childbirth 2023 Mar 8;23(1):156. [doi: 10.1186/s12884-023-05486-9] [Medline: 36890453]
11. Taeidi E, Ranjbar A, Montazeri F, Mehrnoush V, Darsareh F. Machine learning-based approach to predict intrauterine growth restriction. Cureus 2023 Jul;15(7):e41448. [doi: 10.7759/cureus.41448] [Medline: 37546140]
12. Roozbeh N, Montazeri F, Farashah MV, Mehrnoush V, Darsareh F. Proposing a machine learning-based model for predicting nonreassuring fetal heart. Sci Rep 2025 Mar 6;15(1):7812. [doi: 10.1038/s41598-025-92810-2] [Medline: 40050357]
13. Jeyaparam S, Agha-Jaffar R, Robinson S, Khunti K. Association of socioeconomic deprivation on gestational diabetes incidence and perinatal outcomes. Research Square. Preprint posted online on 2023. [doi: 10.21203/rs.3.rs-2410272/v1]
14. GDM dataset.xlsx. figshare. URL: https://figshare.com/articles/dataset/GDM_Dataset_xlsx/21806472?file=38695140 [accessed 2025-06-26]
15. Chen ME, Aguirre RS, Hannon TS. Methods for measuring risk for type 2 diabetes in youth: the oral glucose tolerance test (OGTT). Curr Diab Rep 2018 Jun 16;18(8):51. [doi: 10.1007/s11892-018-1023-3] [Medline: 29909550]
16. Fakhraei R, Denize K, Simon A, et al. Predictors of adverse pregnancy outcomes in pregnant women living with obesity: a systematic review. Int J Environ Res Public Health 2022 Feb 12;19(4):2063. [doi: 10.3390/ijerph19042063] [Medline: 35206265]
17. Garcia EA. ADASYN: Adaptive Synthetic Sampling approach for imbalanced learning. Presented at: 2008 IEEE International Joint Conference on Neural Networks (IEEE World Congress on Computational Intelligence); Jun 1-8, 2008; Hong Kong. [doi: 10.1109/IJCNN.2008.4633969]
18. Yuen L, Saeedi P, Riaz M, et al. Projections of the prevalence of hyperglycaemia in pregnancy in 2019 and beyond: results from the International Diabetes Federation Diabetes Atlas, 9th edition. Diabetes Res Clin Pract 2019 Nov;157:107841. [doi: 10.1016/j.diabres.2019.107841]
19. Diabetes in pregnancy: management from preconception to the postnatal period. National Institute for Health and Care Excellence. URL: https://www.nice.org.uk/guidance/ng3 [accessed 2025-07-17]
20. He Y, Ma RCW, McIntyre HD, et al. Comparing IADPSG and NICE diagnostic criteria for GDM in predicting adverse pregnancy outcomes. Diabetes Care 2022 Sep 1;45(9):2046-2054. [doi: 10.2337/dc22-0579] [Medline: 35880808]
21. Bogdanet D, Egan A, Reddin C, Kirwan B, Carmody L, Dunne FA. ATLANTIC DIP: despite insulin therapy in women with IADPSG diagnosed GDM, desired pregnancy outcomes are still not achieved. What are we missing? Diabetes Res Clin Pract 2018 Feb;136:116-123. [doi: 10.1016/j.diabres.2017.12.003]
22. American Diabetes Association Professional Practice Committee. 15. Management of diabetes in pregnancy: standards of care in diabetes-2024. Diabetes Care 2024 Jan 1;47(Suppl 1):S282-S294. [doi: 10.2337/dc24-S015] [Medline: 38078583]
23. Sweeting AN, Ross GP, Hyett J, et al. Gestational diabetes mellitus in early pregnancy: evidence for poor pregnancy outcomes despite treatment. Diabetes Care 2016 Jan;39(1):75-81. [doi: 10.2337/dc15-0433] [Medline: 26645084]
24. Harreiter J, Simmons D, Desoye G, et al. IADPSG and WHO 2013 gestational diabetes mellitus criteria identify obese women with marked insulin resistance in early pregnancy. Diabetes Care 2016 Jul;39(7):e90-e92. [doi: 10.2337/dc16-0200] [Medline: 27208336]
25. Fasoulakis Z, Koutras A, Antsaklis P, et al. Intrauterine growth restriction due to gestational diabetes: from pathophysiology to diagnosis and management. Medicina (Kaunas) 2023 Jun 13;59(6):1139. [doi: 10.3390/medicina59061139] [Medline: 37374343]
26. Hiden U, Glitzner E, Hartmann M, Desoye G. Insulin and the IGF system in the human placenta of normal and diabetic pregnancies. J Anat 2009 Jul;215(1):60-68. [doi: 10.1111/j.1469-7580.2008.01035.x] [Medline: 19467150]
27. Moore TR. A comparison of amniotic fluid fetal pulmonary phospholipids in normal and diabetic pregnancy. Am J Obstet Gynecol 2002 Apr;186(4):641-650. [doi: 10.1067/mob.2002.122851] [Medline: 11967485]
28. Metzger BE, Persson B, Lowe LP, et al. Hyperglycemia and adverse pregnancy outcome study: neonatal glycemia. Pediatrics 2010 Dec;126(6):e1545-e1552. [doi: 10.1542/peds.2009-2257] [Medline: 21078733]
29. Dani C, Corsini I. Guidelines for management of neonatal hypoglycemia: are they actually applicable? JAMA Pediatr 2020 Jul 1;174(7):638-639. [doi: 10.1001/jamapediatrics.2020.0632] [Medline: 32391888]

XSL•FO
RenderX

30. Burton GJ, Redman CW, Roberts JM, Moffett A. Pre-eclampsia: pathophysiology and clinical implications. BMJ 2019 Jul 15;366:l2381. [doi: 10.1136/bmj.l2381] [Medline: 31307997]
31. Jiang L, Tang K, Magee LA, et al. A global view of hypertensive disorders and diabetes mellitus during pregnancy. Nat Rev Endocrinol 2022 Dec;18(12):760-775. [doi: 10.1038/s41574-022-00734-y] [Medline: 36109676]
32. Riise HKR, Sulo G, Tell GS, et al. Association between gestational hypertension and risk of cardiovascular disease among 617 589 Norwegian women. J Am Heart Assoc 2018 May 13;7(10):e008337. [doi: 10.1161/JAHA.117.008337] [Medline: 29755034]
33. Sinkey RG, Battarbee AN, Bello NA, Ives CW, Oparil S, Tita ATN. Prevention, diagnosis, and management of hypertensive disorders of pregnancy: a comparison of international guidelines. Curr Hypertens Rep 2020 Aug 27;22(9):66. [doi: 10.1007/s11906-020-01082-w] [Medline: 32852691]
34. Cheung BMY, Li C. Diabetes and hypertension: is there a common metabolic pathway? Curr Atheroscler Rep 2012 Apr;14(2):160-166. [doi: 10.1007/s11883-012-0227-2] [Medline: 22281657]
35. Chiarello DI, Abad C, Rojas D, et al. Oxidative stress: normal pregnancy versus preeclampsia. Biochim Biophys Acta Mol Basis Dis 2020 Feb 1;1866(2):165354. [doi: 10.1016/j.bbadis.2018.12.005] [Medline: 30590104]
36. Rani N, Dhingra R, Arya DS, Kalaivani M, Bhatla N, Kumar R. Role of oxidative stress markers and antioxidants in the placenta of preeclamptic patients. J Obstet Gynaecol Res 2010 Dec;36(6):1189-1194. [doi: 10.1111/j.1447-0756.2010.01303.x] [Medline: 21114571]
37. Phoswa WN, Khaliq OP. The role of oxidative stress in hypertensive disorders of pregnancy (preeclampsia, gestational hypertension) and metabolic disorder of pregnancy (gestational diabetes mellitus). Oxid Med Cell Longev 2021;2021:5581570. [doi: 10.1155/2021/5581570] [Medline: 34194606]
38. Dalfrà MG, Burlina S, Del Vescovo GG, Lapolla A. Genetics and epigenetics: new insight on gestational diabetes mellitus. Front Endocrinol (Lausanne) 2020;11:602477. [doi: 10.3389/fendo.2020.602477] [Medline: 33335512]
39. Lappas M. Effect of pre-existing maternal obesity, gestational diabetes and adipokines on the expression of genes involved in lipid metabolism in adipose tissue. Metab Clin Exp 2014 Feb;63(2):250-262. [doi: 10.1016/j.metabol.2013.10.001] [Medline: 24262292]
40. Koenigbauer JT, Fangmann L, Rostin P, et al. Advanced maternal age (AMA) and 75 g OGTT glucose levels are pedictors for insulin therapy in women with gestational diabetes (GDM). J Perinat Med 2023 Nov 27;51(9):1154-1162. [doi: 10.1515/jpm-2023-0170] [Medline: 37466452]

Abbreviations

ADASYN : adaptive synthetic sampling
GDM: gestational diabetes mellitus
IADPSG: International Association of Diabetes and Pregnancy Study Groups
IMD: Index of Multiple Deprivation
NICE: National Institute for Health and Care Excellence
NLR: negative likelihood ratio
NPV: negative predictive value
OGTT: oral glucose tolerance test
PLR: positive likelihood ratio
PPV: positive predictive value
SHAP: Shapley additive explanation
SMOTE: Synthetic Minority Oversampling Technique
SVM: support vector machine
XGBoost: extreme gradient boosting

Edited by A Benis; submitted 21.01.25; peer-reviewed by F Darsareh, W Khan; revised version received 21.05.25; accepted 21.05.25; published 16.09.25.

Please cite as:
Li J, Liu X, He S, Ren Y
Interpretable Machine Learning for Predicting Adverse Pregnancy Outcomes in Gestational Diabetes: Retrospective Cohort Study
JMIR Med Inform 2025;13:e71539
URL: https://medinform.jmir.org/2025/1/e71539
doi:10.2196/71539

XSL•FO
RenderX

© Jiaxi Li, Xiali Liu, Shenyang He, Yan Ren. Originally published in JMIR Medical Informatics (https://medinform.jmir.org), 16.9.2025. This is an open-access article distributed under the terms of the Creative Commons Attribution License (https://creativecommons.org/licenses/by/4.0/), which permits unrestricted use, distribution, and reproduction in any medium, provided the original work, first published in JMIR Medical Informatics, is properly cited. The complete bibliographic information, a link to the original publication on https://medinform.jmir.org/, as well as this copyright and license information must be included.

XSL•FO
RenderX

Real-Time Estimation of Arterial Partial Pressure of Carbon Dioxide in Patients Undergoing General Anesthesia: Predictive Modeling Study

Ah Ra Lee[1], PhD; Jun Ho Lee[2], MD, PhD; Sooyoung Yoo[1], PhD; Ho-Young Lee[1,3], MD, PhD; Hyun Ho Kim[4,5], MD, PhD

[1]Office of eHealth Research and Business, Seoul National University Bundang Hospital, 172, Dolma-ro, Bundang-gu, Seongnam-si, Republic of Korea

[2]Department of Anesthesiology and Pain Medicine, Jeonbuk National University Medical School and Hospital, Jeonju, Republic of Korea

[3]Department of Nuclear Medicine, Seoul National University Bundang Hospital, Seongnam-si, Republic of Korea

[4]Department of Pediatrics, Jeonbuk National University School of Medicine, 20, Geonji-ro, Deokjin-gu, Jeonju, Republic of Korea

[5]Research Institute of Clinical Medicine, Jeonbuk National University-Biomedical Research Institute on Jeonbuk National University Hospital, Jeonju, Republic of Korea

Corresponding Author:
Hyun Ho Kim, MD, PhD
Department of Pediatrics, Jeonbuk National University School of Medicine, 20, Geonji-ro, Deokjin-gu, Jeonju, Republic of Korea

Abstract

Background: Adequate ventilation in mechanically ventilated patients is contingent upon the monitoring of the arterial partial pressure of carbon dioxide ($PaCO_2$) during general anesthesia. Despite its significance, continuous monitoring remains challenging due to the imprecision of noninvasive estimations and the invasive nature of traditional methods such as arterial blood gas analysis.

Objective: This study aimed to develop a machine learning model to continuously estimate $PaCO_2$ in mechanically ventilated patients, with the goal of potentially improving intraoperative monitoring accuracy under general anesthesia.

Methods: This retrospective study used the VitalDB dataset from Seoul National University Hospital, comprising records of 6388 noncardiac surgery patients between August 2016 and June 2017. After applying inclusion and exclusion criteria, data from 2304 surgical cases (4651 $PaCO_2$ measurement event points) were analyzed. The CatBoost regressor model was trained to predict $PaCO_2$ using noninvasive physiological parameters and clinical information. The model's performance was evaluated using nested cross-validation across hypocapnic (<35 mm Hg), normocapnic (35 - 45 mm Hg), and hypercapnic (>45 mm Hg) subgroups and compared to conventional estimation methods based on end-tidal carbon dioxide ($ETCO_2$).

Results: The developed model demonstrated superior overall performance compared to traditional estimations. It achieved a mean absolute error of 2.38 mm Hg and an average intraclass correlation coefficient of 0.87. Furthermore, 90.02% of the model's estimations fell within the clinically highly acceptable range (error<±5 mm Hg) while only 1.20% of errors exceeded ±10 mm Hg. Performance improvements were observed across all $PaCO_2$ subgroups.

Conclusions: The developed model provides more accurate and reliable estimates of $PaCO_2$ than traditional $ETCO_2$-based methods. This approach shows potential for facilitating real-time monitoring and timely clinical interventions. This study demonstrated the potential of artificial intelligence to enhance continuous monitoring of $PaCO_2$; however, further validation, including prospective studies assessing clinical impact, is necessary.

(JMIR Med Inform 2025;13:e64855) doi:10.2196/64855

KEYWORDS

anesthesia; arterial partial pressure of carbon dioxide; artificial intelligence; AI; blood gas monitoring; end-tidal carbon dioxide

Introduction

Monitoring the arterial partial pressure of carbon dioxide ($PaCO_2$) is essential during general anesthesia, as it is a fundamental indicator of respiratory status in mechanically ventilated patients. These patients are unable to breathe on their own because anesthetic drugs and neuromuscular blocking agents suppress their respiratory responses [1]. During mechanical ventilation, the respiratory rate (RR) is carefully adjusted through continuous patient assessments to ensure adequate ventilation [2,3]. $PaCO_2$ is a crucial indicator of the equilibrium between the production and elimination of carbon dioxide [4,5]. Abnormal levels of $PaCO_2$ may suggest inadequate ventilation, respiratory insufficiency, or

XSL•FO
RenderX

compromised cardiovascular function, which could result in unfavorable surgical outcomes.

Despite its importance, achieving continuous monitoring of $PaCO_2$ using arterial blood gas analysis (ABGA) has practical limitations. While ABGA remains the gold standard, providing accurate $PaCO_2$ measurements along with other vital information, such as pH and pO_2, and closely tracking $PaCO_2$ changes require repeated arterial sampling, even with an indwelling arterial line (A-line). This necessity for repeated invasive procedures carries resource implications for personnel time and consumables, with costs varying across health care systems [6]. Furthermore, frequent sampling while utilizing a procedure with generally low individual risk carries inherent cumulative risks associated with repeated invasive interventions [7,8]. Crucially, the intermittent nature of ABGA may not fully capture rapid physiological fluctuations occurring during dynamic surgical periods, potentially delaying necessary clinical interventions.

End-tidal carbon dioxide ($ETCO_2$) is a fundamental component of anesthetic practice, recommended by the American Society of Anesthesiologists (ASA) [9,10], and is commonly used to estimate $PaCO_2$. $ETCO_2$ reflects the partial pressure of CO2 at the end of exhalation. While often correlated, a gradient typically exists between $PaCO_2$ and $ETCO_2$, usually ranging from 3 to 5 mm Hg in individuals with normal lung function [11]. However, the accuracy of $ETCO_2$ and $PaCO_2$ surrogates can be compromised by various physiological and technical factors. Conditions such as ventilation-perfusion mismatch, increased physiological dead space, and significant changes in cardiac output (CO) can widen this gradient and disrupt the correlation between $ETCO_2$ and $PaCO_2$ [12-14]. Furthermore, patient-specific variables, including underlying pulmonary pathology, hemodynamic status, and metabolic rate, can further complicate the relationship between these two parameters. Prior research has highlighted the variable precision of $ETCO_2$ for estimating $PaCO_2$, particularly in patients with respiratory disease [15,16]. Studies have also indicated weaker correlations in certain challenging clinical scenarios or patient populations where gas exchange is significantly impaired [17-19]. Therefore, relying solely on $ETCO_2$ measurements to guide ventilation management may not always provide the necessary accuracy, especially during periods of rapid physiological change, which are common in surgery.

While a substantial disparity between $PaCO_2$ and $ETCO_2$ measurements has been previously linked to a higher risk of mortality, developing noninvasive methods for estimating $PaCO_2$ more precisely than $ETCO_2$ alone remains an ongoing challenge. The difficulty lies in accurately accounting for the simultaneous influence of numerous, interacting physiological factors that affect CO_2 kinetics. Recent research demonstrates the potential of artificial intelligence (AI) and machine learning (ML) to effectively model intricate biological variables at an individual patient level, potentially overcoming the limitations of simpler estimation approaches [20]. ML-driven prediction models possess the ability to identify and learn complex, nonlinear relationships among multiple input variables (like those readily available from noninvasive intraoperative monitoring), even without prior assumptions about independence or linearity.

Therefore, this study developed an ML-based prediction model to continuously estimate $PaCO_2$ using readily available, noninvasive parameters collected during surgical operations. This approach leverages the capability of ML algorithms to process complex, multidimensional data and potentially capture patient-specific variability more effectively than single-parameter estimates like $ETCO_2$. The objective of this study was to assess the feasibility of achieving accurate and reliable real-time $PaCO_2$ estimation across diverse surgical procedures and patient populations using a large dataset of intraoperative recordings. By providing clinicians with continuous, noninvasive estimates of $PaCO_2$, the developed model holds the potential to enhance intraoperative physiological monitoring, complementing standard methods like ABGA and $ETCO_2$; facilitate timely adjustments to ventilation; and ultimately contribute to improved patient outcomes following general anesthesia. Through this study, we aim to contribute to the advancement of perioperative medicine by harnessing the power of AI to optimize patient care in the operating room.

Methods

Study Design and Settings

This was a retrospective study using VitalDB, an open dataset containing intraoperative biosignal data and perioperative clinical information from Seoul National University Hospital (SNUH), a tertiary-level hospital in South Korea [21]. The dataset encompassed 6388 cases of noncardiac surgery, with an average of 2.8 million data points per case, collected from August 2016 to June 2017. Vital signs were recorded during surgery, while pertinent clinical information was retrospectively retrieved from the electronic medical records system.

Ethical Considerations

This study utilized a publicly available, deidentified dataset (VitalDB). The collection and use of this dataset for research purposes were approved by the Institutional Review Board (IRB) of SNUH (H-1408-101-605). The requirement for obtaining individual informed consent was waived by the IRB because the dataset contained only deidentified data. All data were anonymized before inclusion in the database, ensuring patient privacy and confidentiality. No compensation was provided to participants as part of this secondary data analysis.

Case Selection

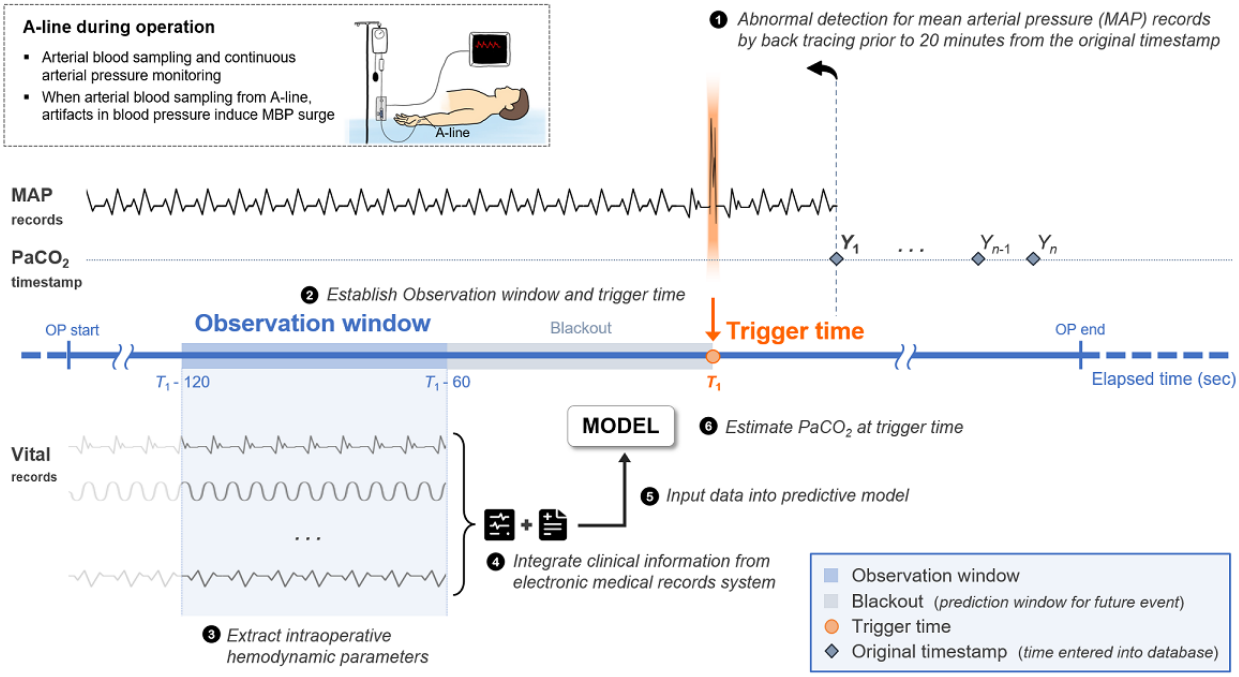
Case selection was performed based on the following inclusion and exclusion criteria. Surgical cases involving patients meeting the following criteria were eligible: (1) aged 18-80 years, (2) mechanically ventilated under general anesthesia using an oral airway, (3) had ASA physical status classification grade 5 or lower, (4) had $ETCO_2$ monitoring records, and (5) had at least 1 or more $PaCO_2$ measurement records obtained during surgery. Each $PaCO_2$ measurement obtained via ABGA was defined as an event point. $PaCO_2$ measurements before or after surgery were excluded and not considered event points.

XSL•FO
RenderX

Event Point Definition and Timing

Each event point was defined by a trigger time and an observation window for the prediction model that estimates $PaCO_2$ based on noninvasive parameters (Figure 1). The trigger time is defined as the time at which an estimation of $PaCO_2$ is performed based on intraoperative biosignals and perioperative clinical information. The observation window is the time frame during which the biosignals were extracted for model training.

Figure 1. Schematic diagram of the event point definition and feature extraction process for real-time $PaCO_2$ estimation. The process includes (1) detection of an MAP surge to refine the ABGA timestamp, defining the trigger time for $PaCO_2$ estimation; (2) establishment of a 60-second observation window preceding a blackout period before the trigger time; (3) extraction of medial values from intraoperative biosignals within the observation window; (4) integration of clinical information from electronic medical records; and (5) input of these features into ML-based model to estimate $PaCO_2$ at the trigger time. A-line: arterial line; ABGA: arterial blood gas analysis; MAP: mean arterial pressure; MBP: mean blood pressure; ML: machine learning; OP: operation; $PaCO_2$: partial pressure of carbon dioxide.



$PaCO_2$ is measured via ABGA, which evaluates arterial gas concentrations such as carbon dioxide and oxygen. Usually, a small volume of blood is extracted from the radial artery using a syringe and a thin needle. During surgery, the anesthesiologists draw arterial blood via an A-line. The temporal point of the ABGA records might be compromised as a result of the transit time of the specimen to the analyzer or manual data entry delays. The timestamp of ABGA records frequently denotes the moment that analysis results are entered into the database instead of precisely indicating the moment at which blood is drawn from the patient.

To increase the precision of the ABGA timestamp, in this study, we utilized mean arterial pressure (MAP) recordings available in VitalDB. We hypothesized that the ABGA procedure (blood draw via A-line) induces a rapid increase in the MAP due to transient line occlusion or a patient physiological reaction. On the basis of this hypothesis, we employed a *z* score–based outlier detection approach. Abnormal periods surpassing a *z* score of 3 in MAP records were identified by observing the 20-minute interval that preceded the originally recorded ABGA timestamp. The nearest such abnormal period was defined as the estimated actual timepoint at which ABGA was performed. The trigger time for feature extraction was set at 60 seconds prior to the newly calculated ABGA timestamp to capture the patient's physiological state immediately preceding the likely blood draw event. In this phase, the $PaCO_2$ values that did not have identifiable MAP surge points meeting these criteria within the preceding 20-minute window were excluded because they were not considered reliably timed event points. Of the 6311 potentially relevant $PaCO_2$ measurements considered for this timestamp adjustment, 720 (approximately 11.4%) were excluded due to the absence of a detectable MAP surge. The median (IQR) difference between the newly estimated ABGA timepoint based on MAP surge and the original database timestamp for the remaining measurements was 34.00 (22.00 - 54.00) seconds, with a mean standard deviation (SD) of 47.29 (57.53) seconds (range 0-936.00 seconds), indicating that the original database timestamp often did not precisely reflect the physiological event of blood sampling. While this pressure-surge detection method provides a systematic approach to approximate the blood sampling time based on physiological responses, we acknowledge that its precise accuracy compared to the true sampling time was not formally validated against a gold standard timestamp in this study.

Data Preparation

A total of 19 variables were selected based on previous literature and domain knowledge. These variables were classified as follows: clinical information, including age, sex, height, weight,

XSL•FO
RenderX

surgical approach, surgery type, and preoperative pulmonary function test (PFT) results; and intraoperative biosignals, including body temperature (BT), heart rate, percutaneous oxygen saturation (SpO_2), minute ventilation from the ventilator (MV), positive end-expiratory pressure (PEEP), peak inspiratory pressure (PIP), plateau pressure (PPLAT), mean airway pressure (MAWP), RR based on capnography, tidal volume (TV), fraction of inspired oxygen (FiO_2), and $ETCO_2$.

During the 60-second observation window before the trigger time, intraoperative biosignals were extracted. Extreme outliers were eliminated using the IQR method, removing data points outside 3 times of the IQR below the first quartile or above the third quartile. Aberrant points deemed theoretically unacceptable were also removed based on clinical expertise. Median values for each biosignal in the observation windows were then calculated and used as features for the prediction model, along with the corresponding surgical patients' electronic medical records. This approach simplifies the high-frequency biosignal data into static features for point-in-time $PaCO_2$ estimation but does not explicitly model temporal dependencies within the observation window or directly track dynamic changes over longer periods.

Furthermore, additional features were established by utilizing feature engineering techniques [20]. The variables for PFT results were reportedly classified into nine classes in the original dataset description; however, due to potential inconsistencies or inadequate representation of minority classes, we regenerated the preoperative PFT as an indicator variable, categorizing it into three grades: obstructive, restrictive, and mixed type [22]. Another feature engineering technique employed in this study involved generating interaction features that comprise combinations of two or more existing variables. The incorporation of interaction features, representing known physiological indices, primarily aimed to improve model interpretability by including recognized clinical parameters, although tree-based models like CatBoost can implicitly capture interactions.

Several interaction features, including TV per kilogram of ideal body weight (TV/IBW), oxygen saturation to FiO2 ratio (SpO_2/FiO_2), PEEP to FiO_2 ratio ($PEEP/FiO_2$), compliance of the respiratory system (CRS), and rapid shallow breathing index (RSBI), were generated using domain knowledge. Each of these interaction features brings a dimension of clinical relevance that reflects the interaction between multiple aspects of patient respiratory mechanics and ventilator settings. Additionally, this study utilized APCONET, which is an external application programming interface (API) that is able to estimate CO using arterial pressure waveforms as an input feature [23]. Detailed information, such as the unit of data, recording device, and source of data, for all the selected variables is available in Multimedia Appendix 1.

Preprocessing

Event points containing missing values in any of the selected predictor variables were removed prior to model training. The listwise deletion approach reduced the number of event points from an initial 5591 (derived from cases meeting inclusion criteria before handling missing data for specific event points) to the final 4651 event points used for analysis. The entire dataset was split into training, validation, and testing sets using the nested cross-validation (7 outer folds, 6 inner folds). This configuration was chosen based on the dataset size and common practices aiming for stable performance estimation [24]. All partitioning procedures were conducted at the surgical case level. For example, all data from a single surgical case belonged exclusively to either the training/validation set or the testing set within a given outer fold. This approach was designed to maintain similar data distributions across subsets while ensuring patient independence between training and testing.

Categorical variables were initially processed using OneHotEncoder for compatibility with some preliminary models tested. Continuous variables were scaled using RobustScaler, which scales data using IQR, making it robust to outliers.

Model Training

To identify a suitable regression model for this task, several ML algorithms were evaluated in preliminary experiments (see Multimedia Appendix 2). Based on its superior performance in these experiments, CatBoostRegressor was selected for final model development and evaluation. The CatBoost model is a robust and effective library for gradient boosting on decision trees. It is particularly adept at handling categorical features natively using its built-in encoder, which was employed in this study for the CatBoost model, thus not requiring the prior OneHotEncoding for these features when training the final CatBoost model [25].

To develop the final predictive model for $PaCO_2$, training sets were utilized for training the CatBoostRegressor model, and the corresponding validation set was used for hyperparameter tuning within each outer fold. The training sets were used to train the CatBoostRegressor model, and the validation set was utilized to tune the hyperparameters (see Multimedia Appendix 3). During hyperparameter optimization, we utilized Optuna, a framework designed to streamline the hyperparameter tuning process [26]. This framework facilitates the search for the optimal hyperparameter space configuration for a given model in an efficient manner. Subsequently, the performance of the final model was evaluated using held-out testing sets from the seven outer-fold cross-validation methods on the testing sets.

Data Analysis

In this study, estimating $PaCO_2$ based on noninvasive parameters was approached as a regression predictive modeling task. To assess the effectiveness of the ML-based model, we conducted a comparison with two baseline methods that employed the $ETCO_2$ value. One method was a simple offset model ($ETCO_2$+5 mm Hg), while the other method involved utilizing linear regression with $ETCO_2$ measurements as the sole predictor.

Model performance was assessed using two commonly employed metrics: mean absolute error (MAE) and root mean squared error (RMSE). Additionally, we evaluated model performance across different conditions by establishing subgroups. The subgroups were established based on $PaCO_2$ levels as follows: hypocapnic (<35 mm Hg), normocapnic

XSL•FO
RenderX

(35-45 mm Hg), and hypercapnic (>45 mm Hg) cases. A Bland-Altman plot was used to calculate the limits of agreement and analyze the agreement between the real and predictive values; additionally, the intraclass correlation coefficient (ICC) was utilized to evaluate the relative reliability and consistency of the model compared to actual measurements [27,28].

To assess the clinical utility of the predictive model, the percentage of estimation errors for $PaCO_2$ was computed by calculating the differences between the real and predicted values. Disparities below 5 mm Hg were deemed highly acceptable, those between 5 and 10 mm Hg were moderately acceptable, and any value exceeding 10 mm Hg was considered unacceptable. The establishment of this threshold was based on prior research and Clinical Laboratory Improvement Amendments recommendations [29].

Furthermore, model interpretability was analyzed using the Shapley additive explanation (SHAP) value [30]. The SHAP values, derived from an additive feature attribution model, succinctly illustrate the impact of the input variables on the model outputs, enhancing the understanding of the model's decision-making process.

The performance metrics were evaluated by averaging the results from the testing sets across the outer folds and computing a CI of 95%. All experimental and data analysis procedures were conducted in the Python 3.10.12 environment.

Results

A total of 2304 surgical cases (with 4651 event points) were eligible and analyzed to develop and validate the proposed prediction model. The statistical summaries for $PaCO_2$ and $ETCO_2$ measurements for the included event points are displayed in Table 1.

Table . Statistical summaries for $PaCO_2$[a] and $ETCO_2$[b] measurements.

Characteristic	Total (n=4651)	Subgroups		
		Hypocapnic (n=179)	Normocapnic (n=3328)	Hypercapnic (n=1144)
$PaCO_2$ (mm Hg), median (IQR)	42.00 (39.00 - 45.00)	34.00 (33.00 - 34.00)	41.00 (38.00 - 43.00)	48.00 (47.00 - 51.00)
$ETCO_2$ (mm Hg), median (IQR)	35.00 (33.00 - 37.00)	32.00 (30.00 - 33.00)	34.00 (33.00 - 36.00)	37.00 (35.00 - 40.00)
$PaCO_2$-$ETCO_2$ (mm Hg difference), median (IQR)	7.00 (5.00 - 10.00)	2.00 (0.50 - 3.00)	6.00 (4.00 - 8.00)	12.00 (9.00 - 14.00)

[a]$PaCO_2$: partial pressure of carbon dioxide.

[b]$ETCO_2$: end-tidal carbon dioxide.

The mean values in this cohort were 42.52 mm Hg for $PaCO_2$ and 34.95 mm Hg for $ETCO_2$. The observed differences between $PaCO_2$ and $ETCO_2$ measurements were often greater than the gap derived from existing knowledge, which was 3-5 mm Hg for healthy individuals, with an average difference of 7.57 mm Hg and a wide range from 16 to 34 mm Hg in our study population. According to the analysis of subgroups categorized by $PaCO_2$ levels, 71.55% (n=3328) of all cases used in this study included $PaCO_2$ values in the normal range (between 35 and 45 mm Hg), whereas 3.85% of the cases (n=179) were hypocapnic (<35 mm Hg) and 24.60% (n=1144) were hypercapnic (>45 mm Hg). The differences in $ETCO_2$ values across subgroups were less pronounced than the differences in $PaCO_2$ values, whereas the discrepancy between $PaCO_2$ and $ETCO_2$ measurements tended to be greater in subgroups with higher $PaCO_2$ levels. More detailed descriptive statistics for all variables are provided in Multimedia Appendix 4.

The performance evaluation results of the developed model in comparison to the baseline methods are displayed in Table 2. As shown in Table 2, the error metrics of the baseline method (Baseline 1), which adds 5 mm Hg to $ETCO_2$, significantly increased as the subgroup transitions from normocapnic to hypercapnic. High error rates in the hypercapnic group indicate that it is difficult to accurately estimate $PaCO_2$ using this baseline method in patients with relatively higher $PaCO_2$ values. The performance of the second baseline method (Baseline 2), which is based upon linear regression, exhibited slightly better performance overall than the first one but performed poorly in the hypocapnic group compared to the normocapnic group. In both of the two baseline methods, extreme groups (hypocapnic and hypercapnic cases) result in wider CIs, which suggests that the performance of these methods is less certain in such ranges.

XSL•FO
RenderX

Table . Performance evaluation results.

Model		MAE[a] (95% CI)	MSE[b] (95% CI)	RMSE[c] (95% CI)
Baseline 1: $ETCO_2$[d]+5 mm Hg				
	All	3.64 (3.51-3.77)	24.57 (22.86-26.29)	4.95 (4.78-5.13)
	Hypocapnic	3.64 (2.99-4.28)	19.82 (10.61-29.03)	4.34 (3.33-5.34)
	Normocapnic	2.45 (2.30-2.61)	9.96 (8.86-11.06)	3.15 (2.98-3.32)
	Hypercapnic	7.09 (6.90-7.28)	67.88 (63.73-72.04)	8.24 (7.98-8.49)
Baseline 2: Linear regression				
	All	3.26 (3.17-3.36)	18.70 (17.34-20.05)	4.32 (4.16-4.48)
	Hypocapnic	6.34 (5.62-7.06)	50.20 (32.67-67.73)	6.98 (5.78-8.19)
	Normocapnic	2.52 (2.42-2.62)	9.85 (9.00-10.70)	3.14 (3.00-3.27)
	Hypercapnic	4.93 (4.77-5.10)	39.55 (36.27-42.82)	6.28 (6.02-6.54)
ML-based[e] model: CatBoost regressor				
	All	2.38 (2.34-2.41)	10.63 (10.13-11.13)	3.26 (3.18-3.34)
	Hypocapnic	3.66 (2.96-4.35)	21.49 (10.23-32.75)	4.51 (3.47-5.56)
	Normocapnic	1.88 (1.81-1.95)	5.81 (5.29-6.33)	2.41 (2.3-2.52)
	Hypercapnic	3.63 (3.50-3.76)	23.05 (21.18-24.91)	4.80 (4.60-4.99)

[a]MAE: mean absolute error.

[b]MSE: mean squared error.

[c]RMSE: root mean squared error.

[d]$ETCO_2$: end-tidal carbon dioxide.

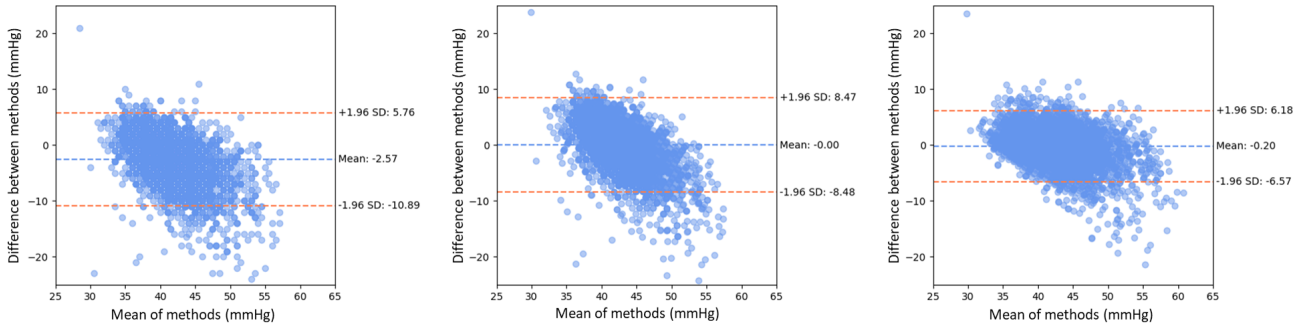
[e]ML: machine learning.

In contrast, the ML-based model developed in this study exhibited superior performance in all subgroups compared to the other 2 baseline methods, with the normocapnic group achieving particularly noteworthy results. With the ML-based model, the error metrics were MAE of 1.88 (95% CI 1.81 - 1.95), mean squared error (MSE) of 5.81 (95% CI 5.29 - 6.33), and RMSE of 2.41 (95% CI 2.30 - 2.52) in the normocapnic group. For extreme $PaCO_2$ values of the hypocapnic and hypercapnic groups, the developed model exhibited MAEs of 3.66 (95% CI 2.96 - 4.35) and 3.63 (95% CI 3.50 - 3.76), respectively, which were considerably better than the baseline methods in these challenging subgroups. Given that the differences between $PaCO_2$ and $ETCO_2$ in healthy individuals are known to range from 3 to 5 mm Hg, these results indicate that the ML-based model provides more accurate and reliable results, as evidenced by the consistently lower MAE, MSE, and RMSE values across all subgroups.

Bland-Altman plots comparing the predictive model with the two baseline methods are displayed in Figure 2. The mean difference, indicated by the central blue dashed line, represents the average discrepancy between the predicted and actual $PaCO_2$ values. For the second baseline method and the ML-based model, this difference was exceedingly close to 0, suggesting minimal systematic deviation on average, while the first baseline method ($ETCO_2$+5 mm Hg) showed a slightly larger negative bias (−2.57 mm Hg). The limits of agreement (±1.96 SD of the differences) with the 95% CIs for the baseline methods ranged from −10.89 to +5.76 and −8.48 to 8.47, respectively, and were narrower for the ML-based model at −6.57 to +6.18. The wider limits of agreement in the baseline models suggest that there is more variability in the differences between the actual and predicted values when estimating the $PaCO_2$ with these traditional approaches.

XSL•FO
RenderX

Figure 2. Bland-Altman plots illustrating the agreement between actual $PaCO_2$ and estimated $PaCO_2$ values by (1) Baseline 1: $ETCO_2$+5 mm Hg; (2) Baseline 2: linear regression with $ETCO_2$; and (3) the machine learning–based model. The x-axis represents the mean of actual and predicted $PaCO_2$ values. The central dashed blue line indicates the mean differences (bias), and the outer dashed orange lines represent the 95% limits of agreement (mean difference ±1.96 SD of the differences). $ETCO_2$: end-tidal carbon dioxide; $PaCO_2$: partial pressure of carbon dioxide.



Baseline 1 Baseline 2 ML-based model

In addition, the Bland-Altman plot for the ML-based model demonstrated that the majority of data points were tightly clustered around the mean difference with less dispersion compared to the baseline methods. While the baseline methods showed some tendency for larger underestimation at higher $PaCO_2$ values (negative slope suggestion), the ML-based model exhibited more consistent agreement across the range of $PaCO_2$ values, with no evident trend of increasing or decreasing differences correlating with the average $PaCO_2$ values. A few outliers were observed, particularly at higher mean values across all methods, suggesting potential specific variability under certain conditions or limitations in the developed model's performance at extremes.

Table 3 presents the ICC analysis results for the baseline methods and the ML-based model. A statistically significant ICC (P<.001) indicates some degree of reliability beyond chance. The narrow 95% CI of the ICC underscores a high degree of confidence in these reliability estimates. An ICC of 0.87 (95% CI 0.86 - 0.87) in the ML-based model signified good agreement between predicted and actual values, indicating that the predicted values closely align with the actual values relative to the overall variance. Conversely, the baseline methods yielded ICCs of 0.70 (95% CI 0.68 - 0.71) and 0.67 (95% CI 0.65 - 0.69), respectively, reflecting a moderate level of agreement.

Table . The ICC[a] values between predicted and actual $PaCO_2$[b].

Model	ICC (95% CI)	*P* value
Baseline 1	0.70 (0.68-0.71)	<.001
Baseline 2	0.67 (0.65-0.69)	<.001
ML[c]-based model	0.87 (0.86-0.87)	<.001

[a]ICC: intraclass correlation coefficient.

[b]$PaCO_2$: partial pressure of carbon dioxide.

[c]ML: machine learning.

The evaluation results of the clinical utility are displayed in Table 4 as a percentage of the estimation error for the $PaCO_2$. The ML-based model exhibited superior performance, with 90.02% of the test set having errors of less than ±5 mm Hg, in contrast to the baseline methods that had exhibited 72.41% and 80.43%, respectively. This represents a substantial absolute increase of nearly 10 percentage points in highly accurate predictions compared to the better baseline. Additionally, for the ML model, errors falling within ±10 mm Hg accounted for 98.80% of the test set. The errors exceeded ±10 mm Hg in only 1.20% of cases. The baseline methods achieved a moderate level of acceptable performance; however, the percentage of errors exceeding ±10 mm Hg was more than double that of the ML-based model. This indicates that the ML-based model demonstrated highly acceptable performance in aspects of clinical utility evaluation.

XSL•FO
RenderX

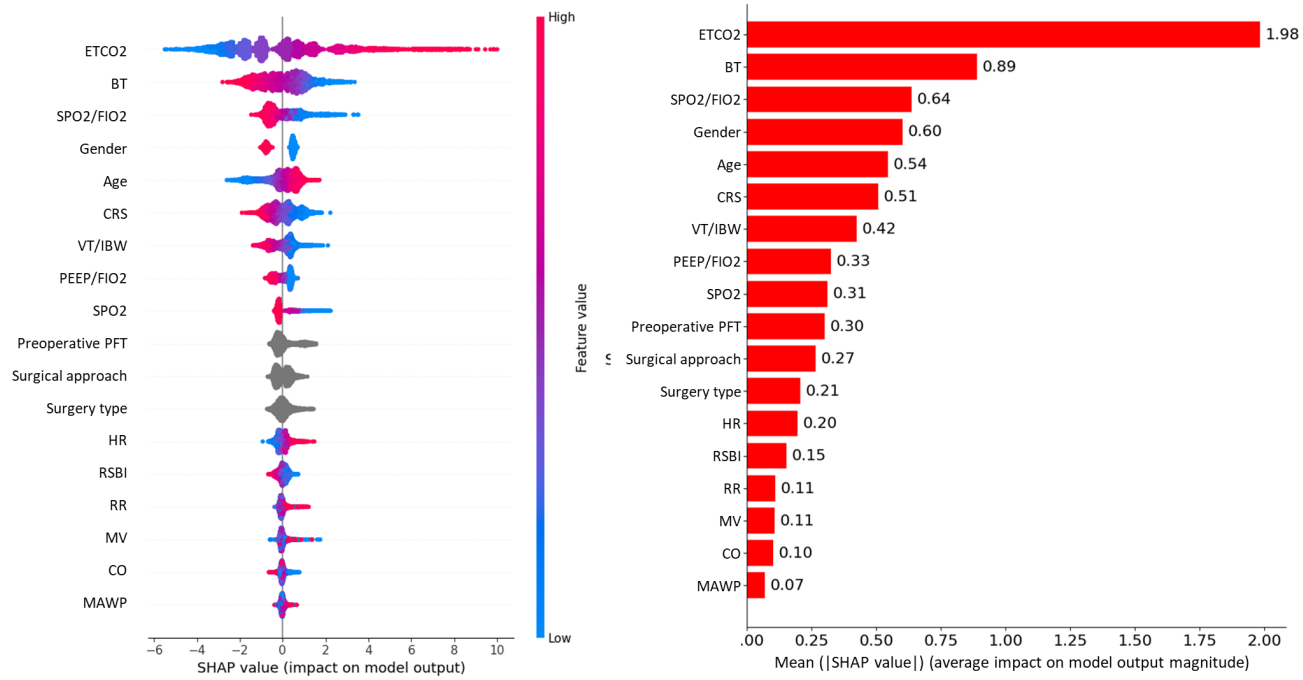
Table . Clinical utility evaluation results.

Model	Absolute value of errors (%)		
	<5 mm Hg	5 - 10 mm Hg	>10 mm Hg
Baseline 1	72.41	22.70	4.88
Baseline 2	80.43	16.92	2.64
ML[a]-based model	90.02	8.77	1.20

[a]ML:machine learning.

The feature importance of the ML-based model was analyzed using the SHAP method, as illustrated in Figure 3. The most significant variable was $ETCO_2$, as expected, given its direct physiological link to $PaCO_2$. Beyond $ETCO_2$'s dominant influence, other important features included BT, SpO_2/FiO_2, sex, age, and CRS. The SHAP plot suggested that the model output (predicted $PaCO_2$ value) tended to be higher with lower BT, SpO_2/FiO_2, and CRS, as well as higher age and $ETCO_2$. These findings suggest the additional features help refine the $PaCO_2$ estimate beyond the baseline provided by $ETCO_2$, potentially capturing patient-specific physiological states. Variables such as MAWP, CO, and MV exhibited relatively lower SHAP values with a mix of positive and negative contributions, indicating a minor or context-dependent impact on model decision-making in this analysis.

Figure 3. SHAP plots illustrating feature importance for ML-based $PaCO_2$ estimation model. Left: SHAP summary plot, where each point represents a Shapley value for a feature and an instance. The position on the y-axis indicates the feature, the position on the x-axis indicates the SHAP value (impact on model output), and the color indicates the feature values (red for high, blue for low). Right: Bar chart of the mean absolute SHAP values, indicating the global importance of each feature in the model. BT: body temperature; CO: cardiac output; CRS: compliance of the respiratory system; $ETCO_2$: end-tidal carbon dioxide; FIO_2: fraction of inspired oxygen; HR: heart rate; IBW: ideal body weight; MAWP: mean airway pressure; ML: machine learning; MV: minute ventilation from the ventilator; $PaCO_2$: partial pressure of carbon dioxide; PEEP: positive end-expiratory pressure; PFT: pulmonary function test; RR: respiratory rate; RSBI: rapid shallow breathing index; SHAP: Shapley additive explanation; SPO_2: percutaneous oxygen saturation; VT: tidal volume.



Discussion

Principal Findings

This study developed an ML-based model capable of estimating $PaCO_2$ in mechanically ventilated patients under general anesthesia with greater accuracy than traditional $ETCO_2$-based methods. Utilizing noninvasive physiological parameters and clinical information, the CatBoost model demonstrated strong overall performance, achieving an MAE of 2.38 mm Hg, an RMSE of 3.26 mm Hg, and an ICC of 0.87, indicating excellent agreement with arterial measurements. Critically, the model significantly increased the proportion of clinically highly acceptable predictions (error<±5 mm Hg) to 90.02%, comparable to 80.43% for a linear regression baseline, and reduced unacceptable errors (>±10 mm Hg) to 1.20% from 2.64%. The model's superiority was consistent across hypocapnic, normocapnic, and hypercapnic subgroups.

Interpretability analysis using SHAP identified $ETCO_2$ as the most influential feature, as anticipated. Beyond the dominant contribution of $ETCO_2$, other parameters such as BT, SpO_2/FiO_2

XSL•FO
RenderX

ratio, age, sex, and CRS were found to be important for refining $PaCO_2$ estimations. For instance, the model tended to predict higher $PaCO_2$ values with lower BT, lower SpO_2/FiO_2, lower CRS, and higher age, suggesting it learned complex physiological relationships. These findings highlight the value of a multiparameter approach to capture variability not explained by $ETCO_2$ alone.

Comparison to Prior Work

The limitations of relying solely on $ETCO_2$ for $PaCO_2$ estimation are well documented. While $ETCO_2$ provides some insights, the $PaCO_2$-$ETCO_2$ gradient is known to be variable and influenced by numerous physiological factors, often exceeding the commonly cited 3-5 mm Hg range in healthy individuals [11,16,31]. Our study corroborates this, finding a median gradient of 7 mm Hg (average 7.57 mm Hg, range −16 to 34 mm Hg), underscoring the unreliability of a fixed gradient assumption. Conventional statistical models, such as multivariable linear regression, offer some improvement but are often constrained by linearity assumptions and may not fully capture the complex, nonlinear interactions inherent in physiological systems [32,33].

In contrast, our ML-based approach effectively models these intricate associations by integrating a wider array of biosignals and clinical data. The ability of ML to learn from these complex patterns without a priori assumptions about relationships has shown promise in various medical prediction tasks [20]. Previous studies have also indicated that factors like surgical techniques and patient positioning can affect the $PaCO_2$-$ETCO_2$ gradient [34], further supporting the need for adaptive models like the one developed in this study, which can account for such patient-specific and contextual variability more effectively than simpler methods.

Strengths of the Study

This study possesses several strengths that enhance the credibility and potential impact of its findings. First, the use of VitalDB, a large, publicly available, real-world dataset from a tertiary university hospital, provides a diverse cohort from various noncardiac surgeries, improving the generalizability of our results. Second, model performance was rigorously assessed using nested cross-validation, offering a robust estimate of its predictive capabilities on unseen data. Third, the ML model was benchmarked against two clinically relevant baseline methods, clearly demonstrating its superior accuracy. Fourth, our evaluation encompassed not only standard error metrics (MAE, RMSE) but also reliability (ICC) and clinical utility based on predefined error categories (Table 4), providing a multifaceted view of performance. Fifth, the inclusion of SHAP analysis offers a degree of transparency into the model's decision-making process, which is crucial for clinical translation. Finally, the exploration of an MAP-based timestamping method, while requiring further validation, represents a novel attempt to address a common challenge in retrospective EMR-based research.

Limitations

Nevertheless, several limitations should be acknowledged when interpreting the results of this study. First, while the ML model outperformed baselines across all $PaCO_2$ subgroups, its performance was relatively lower in the hypocapnic and hypercapnic groups compared to the normocapnic group. This may be partly due to data imbalance, as these extreme ranges were less frequently observed. Future work could explore techniques like targeted data augmentation or specialized modeling to address this. Second, our SHAP analysis focused on explaining direct $PaCO_2$ predictions. As $ETCO_2$ is inherently a dominant feature, this makes it harder to isolate the specific contributions of other features to the $PaCO_2$—$ETCO_2$ gradient. Analyzing this gradient directly would be a valuable future direction. Third, the model relies on point-in-time estimations using median values from a 60-second window, simplifying the rich time-series data available. This approach does not capture temporal trends or predict rapid $PaCO_2$ changes. Fourth, the MAP-surge-based ABGA timestamping method, though systematically applied, was not formally validated against a gold-standard timing reference. Any imprecision here could introduce noise into the feature-target alignment. Fifth, the listwise deletion approach for handling missing data, which reduced our event points from 5951 to 4651, may have introduced selection bias if the pattern of missingness was not completely at random and reduced the overall sample size available for training. Seventh, estimated CO via an external API did not emerge as a highly influential feature in SHAP plots. This might be attributed to the indirect nature or potential inaccuracies of the CO estimation rather than CO itself lacking physiological relevance. Finally, being a single-institution study, the findings require external validation to ensure generalizability across different settings and populations.

Future Directions

Building on these findings and limitations, several avenues for future research are essential for advancing noninvasive $PaCO_2$ monitoring. First and foremost, external validation of the ML model in diverse, multicenter clinical settings is crucial to confirm its robustness and general applicability. Second, developing time-series models, such as recurrent neural networks, long short-term memory, and transformers, which can process the continuous stream of biosignals, is a key next step. This could improve accuracy and enable the prediction of $PaCO_2$ trends and rapid changes. Third, future studies should explicitly investigate the model's capacity to track longitudinal changes in the $PaCO_2$-$ETCO_2$ gradient within individual patients. Exploring the linkage between the predicted $PaCO_2$-$ETCO_2$ gradient and critical events like hemodynamic instability could yield clinical value. Fourth, research correlating intraoperative $PaCO_2$ deviations identified by accurate monitoring with postoperative outcomes would further strengthen the rationale for enhanced continuous monitoring. Finally, the MAP-based timestamping approach warrants further investigation and validation.

XSL•FO
RenderX

Conclusions

This study demonstrated that an ML-based model integrating multiple noninvasive parameters can estimate $PaCO_2$ with higher accuracy and reliability than traditional $ETCO_2$-based methods in mechanically ventilated surgical patients. The model shows particular strength in increasing the proportion of highly accurate predictions. While acknowledging the need for further development, particularly in incorporating time-series data and external validation, this work highlights the considerable potential of AI to serve as a valuable supplementary tool for enhancing respiratory monitoring and patient management in the perioperative setting.

Acknowledgments

This research was supported by the Bio & Medical Technology Development Program of the National Research Foundation (NRF) funded by the Korean government (Ministry of Science and Information and Communication Technology) (No. RS-2023-00236157, RS-2025-00553891). This research was supported by a grant of the Korea Health Technology R&D Project through the Korea Health Industry Development Institute (KHIDI), funded by the Ministry of Health & Welfare, Republic of Korea (RS-2025-02313278, RS-2025-02223382).

Authors' Contributions

HHK conceptualized the design of the study and reviewed existing literature. ARL wrote the original draft and performed experiments and visualization. ARL and HHK contributed to the data analysis and interpretation. JHL, SY, and HYL revised the manuscript, and HHK supervised the research. All authors reviewed and approved the final version of the manuscript.

Conflicts of Interest

None declared.

Multimedia Appendix 1
List of selected variables.
[PDF File, 474 KB - medinform_v13i1e64855_app1.pdf]

Multimedia Appendix 2
Preliminary experiment results for a performance comparison of machine learning algorithms.
[PDF File, 457 KB - medinform_v13i1e64855_app2.pdf]

Multimedia Appendix 3
Hyperparameter optimization with nested cross-validation.
[PDF File, 551 KB - medinform_v13i1e64855_app3.pdf]

Multimedia Appendix 4
Descriptive statistics of the selected variables.
[PDF File, 511 KB - medinform_v13i1e64855_app4.pdf]

References

1. Hedenstierna G, Edmark L. Effects of anesthesia on the respiratory system. Best Pract Res Clin Anaesthesiol 2015 Sep;29(3):273-284. [doi: 10.1016/j.bpa.2015.08.008] [Medline: 26643094]
2. Fogagnolo A, Montanaro F, Al-Husinat L, et al. Management of intraoperative mechanical ventilation to prevent postoperative complications after general anesthesia: a narrative review. J Clin Med 2021 Jun 16;10(12):2656. [doi: 10.3390/jcm10122656] [Medline: 34208699]
3. Bolther M, Henriksen J, Holmberg MJ, et al. Ventilation strategies during general anesthesia for noncardiac surgery: a systematic review and meta-analysis. Anesth Analg 2022 Nov 1;135(5):971-985. [doi: 10.1213/ANE.0000000000006106] [Medline: 35703253]
4. Barker SJ, Hyatt J. Continuous measurement of intraarterial pHa, PaCO2, and PaO2 in the operating room. Anesth Analg 1991 Jul;73(1):43-48. [doi: 10.1213/00000539-199107000-00009] [Medline: 1907111]
5. Messina Z, Patrick H. Partial pressure of carbon dioxide. In: StatPearls [Internet]: StatPearls Publishing; 2022. URL: https://www.ncbi.nlm.nih.gov/books/NBK551648 [accessed 2025-09-08]
6. WHO. WHO Guidelines on Drawing Blood: Best Practices in Phlebotomy: World Health Organization; 2010.
7. Kimmelman J, Resnik DB, Peppercorn J, Ratain MJ. Burdensome research procedures in trials: why less is more. J Natl Cancer Inst 2017 Apr 1;109(4):djw315. [doi: 10.1093/jnci/djw315] [Medline: 28376159]

XSL•FO
RenderX

8. Happo S, Keränen T, Halkoaho A, Lehto SM. Risk assessment of medical study procedures in the documents submitted to a research ethics committee. J Empir Res Hum Res Ethics 2020 Dec;15(5):396-406. [doi: 10.1177/1556264620903563] [Medline: 32036724]
9. Yadav M, Reddy EP, Sharma A, Kulkarni DK, Gopinath R. The effect of position on PaCO2 and PETCO2 in patients undergoing cervical spine surgery in supine and prone position. J Neurosurg Anesthesiol 2017 Jul;29(3):298-303. [doi: 10.1097/ANA.0000000000000322] [Medline: 27271232]
10. Klein AA, Meek T, Allcock E, et al. Recommendations for standards of monitoring during anaesthesia and recovery 2021. Anaesthesia 2021 Sep;76(9):1212-1223. [doi: 10.1111/anae.15501] [Medline: 34013531]
11. Satoh K, Ohashi A, Kumagai M, Sato M, Kuji A, Joh S. Evaluation of differences between PaCO2 and ETCO2 by age as measured during general anesthesia with patients in a supine position. J Anesthesiology 2015 Mar:1-5. [doi: 10.1155/2015/710537]
12. Jin HC, Seo JW, Kim SH, Chae WS, Lee JS, Kim YI. Is end-tidal carbon dioxide tension useful to predict arterial carbon dioxide tension during one lung ventilation? A comparison with during two lung ventilation. Korean J Anesthesiol 2008;54(6):609. [doi: 10.4097/kjae.2008.54.6.609]
13. McSwain SD, Hamel DS, Smith PB, et al. End-tidal and arterial carbon dioxide measurements correlate across all levels of physiologic dead space. Respir Care 2010 Mar;55(3):288-293. [doi: 10.4187/respcare.10550288] [Medline: 20196877]
14. Razi E, Moosavi GA, Omidi K, Khakpour Saebi A, Razi A. Correlation of end-tidal carbon dioxide with arterial carbon dioxide in mechanically ventilated patients. Arch Trauma Res 2012;1(2):58-62. [doi: 10.5812/atr.6444] [Medline: 24396744]
15. Govindagoudar MB, Chaudhry D, Tyagi D, Jakka S, Chandra S. Correlation of PaCO2 and ETCO2 in COPD patients with exacerbation on mechanical ventilation. Indian J Crit Care Med 2021 Mar 20;25(3):305-309. [doi: 10.5005/jp-journals-10071-23762] [Medline: 33790512]
16. Enomoto T, Inoue Y, Adachi Y, et al. Limitations of end-tidal CO2 measured with a portable capnometer to estimate PaCO2 for patients with respiratory disease. Turk Thorac J 2021 May;22(3):212-216. [doi: 10.5152/TurkThoracJ.2021.20032] [Medline: 35110230]
17. Abdalrazik FS, Elghonemi MO. Assessment of gradient between partial pressure of arterial carbon dioxide and end-tidal carbon dioxide in acute respiratory distress syndrome. Egypt J Bronchol 2019 May;13(2):170-175. [doi: 10.4103/ejb.ejb_90_17]
18. Khajebashi SH, Mottaghi M, Forghani M. PaCO2–EtCO2 gradient and D-dimer in the diagnosis of suspected pulmonary embolism. Adv Biomed Res 2021;10(1):37. [doi: 10.4103/abr.abr_10_20] [Medline: 35071105]
19. Hibberd O, Hazlerigg A, Cocker PJ, Wilson AW, Berry N, Harris T. The PaCO2-ETCO2 gradient in pre-hospital intubations of all aetiologies from a single UK helicopter emergency medicine service 2015-2018. J Intensive Care Soc 2022 Feb;23(1):11-19. [doi: 10.1177/1751143720970356] [Medline: 37593537]
20. Johnson KB, Wei WQ, Weeraratne D, et al. Precision medicine, AI, and the future of personalized health care. Clin Transl Sci 2021 Jan;14(1):86-93. [doi: 10.1111/cts.12884] [Medline: 32961010]
21. Lee HC, Park Y, Yoon SB, Yang SM, Park D, Jung CW. VitalDB, a high-fidelity multi-parameter vital signs database in surgical patients. Sci Data 2022 Jun 8;9(1):279. [doi: 10.1038/s41597-022-01411-5] [Medline: 35676300]
22. Zheng A, Casari A. Feature Engineering for Machine Learning: Principles and Techniques for Data Scientists: O'Reilly Media, Inc; 2018.
23. Yang HL, Jung CW, Yang SM, et al. Development and validation of an arterial pressure-based cardiac output algorithm using a convolutional neural network: retrospective study based on prospective registry data. JMIR Med Inform 2021 Aug 16;9(8):e24762. [doi: 10.2196/24762] [Medline: 34398790]
24. Krstajic D, Buturovic LJ, Leahy DE, Thomas S. Cross-validation pitfalls when selecting and assessing regression and classification models. J Cheminform 2014 Mar 29;6(1):10. [doi: 10.1186/1758-2946-6-10] [Medline: 24678909]
25. Prokhorenkova L, Gusev G, Dorogush AV, Gulin A. CatBoost: unbiased boosting with categorical features. Presented at: 32nd International Conference on Neural Information Processing System; Dec 3-8, 2018; Montréal, Canada p. 6639-6649.
26. Akiba T, Sano S, Yanase T, Ohta T, Koyama M. Optuna: a next-generation hyperparameter optimization framework. Presented at: KDD '19: The 25th ACM SIGKDD Conference on Knowledge Discovery and Data Mining; Aug 4-8, 2019; Anchorage, AK p. 2623-2631. [doi: 10.1145/3292500.3330701]
27. Doğan N. Bland-Altman analysis: a paradigm to understand correlation and agreement. Turk J Emerg Med 2018 Dec;18(4):139-141. [doi: 10.1016/j.tjem.2018.09.001] [Medline: 30533555]
28. Koo TK, Li MY. A guideline of selecting and reporting intraclass correlation coefficients for reliability research. J Chiropr Med 2016 Jun;15(2):155-163. [doi: 10.1016/j.jcm.2016.02.012] [Medline: 27330520]
29. Tannoury JE, Sauthier M, Jouvet P, Noumeir R. Arterial partial pressures of carbon dioxide estimation using non-invasive parameters in mechanically ventilated children. IEEE Trans Biomed Eng 2021 Jan;68(1):161-169. [doi: 10.1109/TBME.2020.3001441] [Medline: 32746023]
30. Lundberg SM, Lee SI. A unified approach to interpreting model predictions. Presented at: 31st International Conference on Neural Information Processing Systems; Dec 4-9, 2017; Long Beach, CA URL: https://proceedings.neurips.cc/paper/2017/hash/8a20a8621978632d76c43dfd28b67767-Abstract.html [accessed 2025-09-08]

XSL•FO
RenderX

31. Pendyala S, Date A. Influence of protective lung ventilation on arterial-to-end tidal carbon dioxide gradient during one lung ventilation: a prospective observational study. Airway 2022;5(3):103-108. [doi: 10.4103/arwy.arwy_21_22]
32. Engoren M, Plewa M, O'Hara D, Kline JA. Evaluation of capnography using a genetic algorithm to predict PaCO2. Chest 2005 Feb;127(2):579-584. [doi: 10.1378/chest.127.2.579] [Medline: 15705999]
33. Belenkiy SM, Baker WL, Batchinsky AI, et al. Multivariate analysis of the volumetric capnograph for PaCO2 estimation. Int J Burns Trauma 2015;5(3):66-74. [doi: 10.1161/circ.128.suppl_22.a202] [Medline: 26550531]
34. Mahajan S, Chauhan R, Luthra A, Bala I, Bharti N, Sharma A. Evaluation of arterial to end-tidal carbon dioxide pressure differences during laparoscopic renal surgery in the lateral decubitus position. Anesth Essays Res 2019;13(3):583-588. [doi: 10.4103/aer.AER_88_19] [Medline: 31602082]

Abbreviations

A-line: arterial line
ABGA: arterial blood gas analysis
AI: artificial intelligence
API: application programming interface
ASA: American Society of Anesthesiologists
BT: body temperature
CO: cardiac output
CRS: compliance of the respiratory system
$ETCO_2$: end-tidal carbon dioxide
FIO_2: fraction of inspired oxygen
IBW: ideal body weight
ICC: intraclass correlation coefficient
IRB: Institutional Review Board
MAE: mean absolute error
MAP: mean arterial pressure
MAWP: mean airway pressure
ML: machine learning
MSE: mean squared error
MV: minute ventilation from the ventilator
$PaCO_2$: partial pressure of carbon dioxide
PEEP: positive end-expiratory pressure
PFT: pulmonary function test
PIP: peak inspiratory pressure
PPLAT: plateau pressure
RMSE: root mean squared error
RR: respiratory rate
RSBI: rapid shallow breathing index
SHAP: Shapley additive explanation
SNUH: Seoul National University Hospital
SPO2: percutaneous oxygen saturation
TV: tidal volume

Edited by A Coristine; submitted 29.07.24; peer-reviewed by C Bohringer, CR King; revised version received 25.07.25; accepted 25.07.25; published 16.09.25.

Please cite as:
Lee AR, Lee JH, Yoo S, Lee HY, Kim HH
Real-Time Estimation of Arterial Partial Pressure of Carbon Dioxide in Patients Undergoing General Anesthesia: Predictive Modeling Study
JMIR Med Inform 2025;13:e64855
URL: https://medinform.jmir.org/2025/1/e64855
doi:10.2196/64855

© Ah Ra Lee, Jun Ho Lee, Sooyoung Yoo, Ho-Young Lee, Hyun Ho Kim. Originally published in JMIR Medical Informatics (https://medinform.jmir.org), 16.9.2025. This is an open-access article distributed under the terms of the Creative Commons

XSL•FO
RenderX

Attribution License (https://creativecommons.org/licenses/by/4.0/), which permits unrestricted use, distribution, and reproduction in any medium, provided the original work, first published in JMIR Medical Informatics, is properly cited. The complete bibliographic information, a link to the original publication on https://medinform.jmir.org/, as well as this copyright and license information must be included.

XSL•FO
RenderX

Using Wearable Device and Machine Learning to Predict Mood Symptoms in Bipolar Disorder: Development and Usability Study

Chia-Tung Wu[1], PhD; Ming H Hsieh[2], MD, PhD; I-Ming Chen[2], MD, PhD; Lian-Yin Jhao[3], BSc; Ding-Shan Liu[4], MSc; Ssu-Ming Wang[5], MSc; Chia-Ting Wu[3], BSc; Yi-Ling Chien[2], MD, PhD

[1]Master Program in Transdisciplinary Long-term Care and Management, National Yang Ming Chiao Tung University, Taipei, Taiwan

[2]Department of Psychiatry, National Taiwan University Hospital, No.7, Chung-Shan South Road, Taipei, Taiwan

[3]Always Support Technology Co, Ltd, New Taipei, Taiwan

[4]Department of Computer Science and Information Engineering, National Taiwan University, Taipei, Taiwan

[5]Graduate Institute of Biomedical Electronics and Bioinformatics, National Taiwan University, Taipei, Taiwan

Corresponding Author:
Yi-Ling Chien, MD, PhD
Department of Psychiatry, National Taiwan University Hospital, No.7, Chung-Shan South Road, Taipei, Taiwan

Abstract

Background: Bipolar disorder (BD) is a highly recurrent disorder. Early detection, early intervention, and prevention of recurrent bipolar mood symptoms are key to a better prognosis.

Objective: This study aims to build prediction models for BD with machine learning algorithms.

Methods: This study recruited 24 participants with BD. The Beck Depression Inventory and Young Mania Rating Scale were used to evaluate depressive and manic episodes, respectively. Using digital biomarkers collected from wearable devices as input, 6 machine learning algorithms (logistic regression, decision tree, k-nearest neighbors, random forest, adaptive boosting, and Extreme Gradient Boosting) were used to build predictive models.

Results: The prediction model for depressive symptoms achieved 83% accuracy, an area under the receiver operating characteristic curve (AUROC) of 0.89, and an F_1-score of 0.65 on testing data. The prediction model for manic symptoms achieved 91% accuracy, an AUROC of 0.88, and an F_1-score of 0.25 on testing data. With the interpretable model Shapley Additive Explanations, we found that relatively high resting heart rate, low activity, and lack of sleep may predict depressive symptoms.

Conclusions: This study demonstrated that digital biomarkers could be used to predict depressive and manic symptoms. This prediction model may be beneficial for the early detection of mood symptoms, facilitating timely treatment and helping to prevent BD recurrence.

(JMIR Med Inform 2025;13:e66277) doi:10.2196/66277

KEYWORDS

bipolar disorder; wearable device; machine learning; mood symptoms; relapse prediction

Introduction

Bipolar disorder (BD) is a recurrent disorder characterized by fluctuations in mood and energy from depression to mania that often results in enormous functional impairment and high disease burden [1]. The 5-year recurrence rate of BD was as high as 73% [2]. A meta-analysis estimated the recurrence rates under treatment were 55.2% (naturalistic studies) and 39.3% (randomized controlled trials) versus 60.6% under placebo [3]. Although the recurrence rate can be reduced under appropriate treatment, irregular compliance usually precipitates the recurrence of mood episodes and compromises the outcome. Despite high recurrence and low compliance, the frequency of routine follow-up in current practice is usually insufficient to detect early signs of relapse, causing delayed treatment until an acute episode has fully developed [4]. It is important to detect early signs of relapse so that an upcoming mood episode can be aborted by appropriate intervention. Furthermore, clinical practice mostly relies on patients' self-reports of symptom changes, which depend on illness insight [5] and are subject to recall bias [6].

Recent studies have developed machine learning algorithms to predict depression [7] based on sociodemographic features, personal or family health history, and symptoms coded by psychiatrists [8], achieving an accuracy of 0.721 using the k-nearest neighbor classifier. In BD, a recent review concluded that activity level may serve as a promising digital phenotype for mood episodes, with decreased activity indicating depressive episodes and increased activity indicating manic episodes [9]. For example, Jakobsen et al [10] collected activity data through actigraphy to differentiate between depressed patients and

XSL•FO
RenderX

controls, achieving an accuracy of 0.84 using the deep neural network combined with the Synthetic Minority Over-Sampling Technique (SMOTE) class balancing technique [10]. Besides, sleep problems may indicate relapse in BD [11]. A recent study that used only sleep-wake data gathered through smartphones and wearables showed accurate next-day predictions of depressive, manic, and hypomanic episodes (area under the receiver operating characteristic curve [AUROC] of 0.80, 0.98, 0.95, respectively) [12], suggesting sleep as a promising biomarker for detecting mood episodes. However, most current studies targeted full-blown mood episodes and followed patients for shorter time periods, and information about feature importance was often lacking.

Apart from activity level and sleep, heart rate (HR) and HR variability could also be important biomarkers for mood episodes. HR variability, defined as temporal variability in beat-to-beat intervals of HR, is supposed to reflect aspects of parasympathetic control over the cardiac system [13]; while HR was an index of sympathetic and parasympathetic influences of the autonomic nervous system during stressful as well as resting and recovery states [14]. During rest, HR is under central inhibitory control by the vagus nerve and thus decreased [15,16]. Increased HR and decreased HR variability were observed in mania relative to euthymia [17]. Likewise, patients with depression not only showed lower HR variability but also had a higher resting HR [18-20]. A study gathered biofeedback data on HR variability features and used support vector machine algorithms to predict mood state, reporting an accuracy of 0.69 [21]. Another machine learning study with HR variability features achieved an accuracy of 0.74 [22]. Considering future applications, we adopted HR features instead of HR variability in this study, since HR is much more commonly recorded in commercial smartwatches than HR variability.

Combining multimodal data sources of physical activity, sleep patterns, and circadian rhythms for a machine learning algorithm, a recent study reported an accuracy of 0.80 in detecting participants at high risk of depression [23]. Another study performed a prospective observational cohort study with patients with mood disorders, collecting activity, sleep, light exposure, and HR to predict mood state, and found the accuracy of 0.87, 0.94, and 0.91, respectively, for depressive episode, manic episode, and hypomanic episode [24]. Although both studies used multiple sources of physiological data, the feature importance and the direction of effect of the features were not clear. Besides, individual differences were not considered among the features.

Based on prior research, this study aimed to establish machine learning algorithms to predict early signs of upcoming depressive or manic symptoms. Digital biomarkers collected by actigraphy and mobile devices, including activity, sleep hours, and HR, were mapped with clinical measures for training and evaluating the machine learning models of artificial intelligence algorithms. We hypothesized that greater activity level and shorter sleep hours may predict manic symptoms. We also hypothesized that higher resting HR and lower activity level and sleep hour changes may predict depressive symptoms based on previous reports [18-20]. Moreover, considering that the change of a feature (eg, sleep or activity) from the individual's baseline may be important when predicting mood symptoms, we also integrated individualized parameters for model prediction.

Methods

Participants

The inclusion criteria were participants with a diagnosis of BD, aged 20 - 65 years, and willing to wear the smartwatch and complete the clinical measures as frequently as possible (at least weekly). The exclusion criteria were concurrent substance use disorder and inability to cooperate with the data collection from the smartphone and smartwatch.

This study recruited 24 patients with BD (aged 20 - 65 years; mean 38, SD 9 years; male n=9) from the Psychiatric Department of National Taiwan University (NTU) Hospital from October 2020 to July 2022 and prospectively followed for an average of 6.39 (SD 4.85) months. The diagnosis was made by board-certified senior psychiatrists based on the *Diagnostic and Statistical Manual of Mental Disorders, Fifth Edition* [25]. The mean age of first onset of mood episodes was 23.1 (SD 10) (range 12 - 44), and the illness duration was 14.1 (SD 8.7) years. During the follow-up, there were a total of 4 psychiatric admissions. All participants received medication treatment, primarily mood stabilizers and antipsychotics (Table S1 in Multimedia Appendix 1). Participants' educational levels ranged from middle school to graduate school (7 graduate school degrees, 13 college, 3 senior high school, and 1 junior high school). As for medical history, all participants had no active medical disease, but with a history of Sicca syndrome (n=1), cavernous sinus cyst (n=1), atrial septal defect (n=1), and one peptic ulcer (n=1).

Clinical Measures

The Beck Depression Inventory (BDI) and Young Mania Rating Scale (YMRS) were self-rated weekly on a mobile app (named MEDGOD) (National Taiwan University) on the personal smartphone (either iOS or Android system) to evaluate depressive and manic symptoms, respectively. All participants received a reminder notification on Sunday night at 9 PM to fill both measures on their mobile app. The research assistants would send a text message, email, or phone call to contact the participants and help solve technical problems.

The BDI [26] is a 21-item self-reported inventory measuring the severity of depression in adolescents and adults. The Beck Depression Inventory-II (BDI-II) [27] was revised to be more consistent with the *DSM-IV* (*Diagnostic and Statistical Manual of Mental Disorders, Fourth Edition*) criteria of depression. The inventory consists of 21 items, in which 4 response options are presented on a Likert scale from 0 to 3. The BDI was translated into a Chinese version with good internal consistency (Cronbach α=0.85) and concurrent validity [28]. Higher total scores indicate more severe depressive symptoms. As for the standard cutoff scores, 30 - 63 may indicate severe depression, 19 - 29 indicates moderate depression, 10 - 18 indicates mild depression, and 0 - 9 indicates minimal depression [28]. The distribution of BDI scores in our sample was summarized in Multimedia Appendix 2.

XSL•FO
RenderX

The YMRS, an 11-item interviewer-rated scale, is designed for assessing the severity of manic symptoms [29]. The items are rated on 5 grades of severity. Four items among them are double weighted, including irritability, speech, thought content, and disruptive or aggressive behavior. The YMRS is by far the most commonly used standardized measure of bipolar manic symptoms for clinical trials in acute mania. As for psychometric properties, the interrater reliability was adequate for the total score (0.93) and for individual items ranged from 0.67 to 0.95. There are no firmly established scoring criteria that relate to diagnostic classification [29]. The distribution of YMRS scores in our sample was summarized in Multimedia Appendix 3.

To detect early signs of relapse, a state of mild depression (BDI >13) or mania (YMRS >13) was labeled true.

Digital Biomarkers

The wristwatch-like actimetry sensor Garmin Vivosmart 4 is a reliable tool [30,31] that has been applied in several clinical studies [32-34]. Each participant wore the smartwatch that continuously measured as well as recorded the motor activity, sleep length, and HR 24 hours a day except when electric recharging.

The motor activities that were monitored included steps, distance traveled, and floors climbed. The sleep features included total sleep hours and stages of sleep, that is, deep sleep, light sleep, rapid eye movement sleep, and awake stages. The HR features included the minimum HR of the day, the maximum HR of the day, the average HR of the day, and the average HR at rest.

As for individualized features, we transformed the raw feature into “the deviation from the personal mean” by subtracting the raw value by the mean of that feature of the person during the entire study period, including differences in minimum HR, maximum HR, average HR, resting HR, steps, distance, and the total sleep (as listed in Tables S2 and S3 in Multimedia Appendix 1).

Data Pretreatment

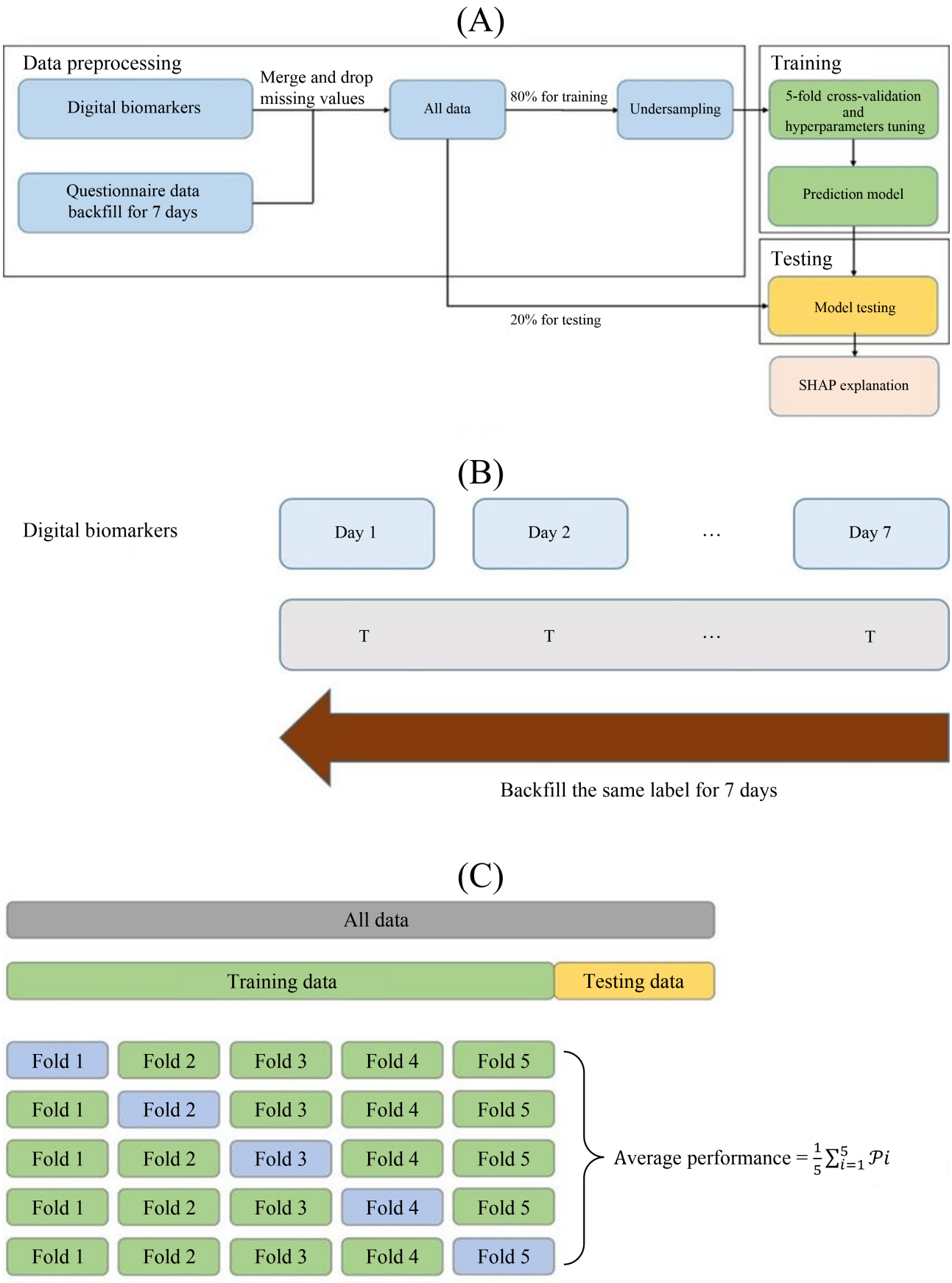
Data were initially uploaded to the server of NTU Medical Genie Precision Health Service via the NTU MEDGOD app automatically. Subsequently, the information was downloaded and stored at the National Taiwan University Computer and Information Networking Center, which provides optimized information security protection [35]. The digital data were deidentified, managed, and maintained by the Medical Information Laboratory of the Department of Information Engineering, National Taiwan University, as described in our previous studies [33,36,37].

The YMRS and BDI-II were administered weekly for the mood-related symptoms of the previous week; thus, the physiological data were backfilled for a 7-day period (Figure 1B). To mitigate the risk of overfitting, all missing values were excluded from the dataset. Extreme datapoints, such as HR>150 or <40, total sleep hours >15, were excluded from analysis, too. Subsequently, the dataset was partitioned into training and testing sets using 5-fold cross-validation.

Figure 1A shows the workflow architecture including interpretable model Shapley Additive Explanations (SHAP). To achieve more balanced data, the under-sampling technique [38] was applied for the training set.

XSL•FO
RenderX

Figure 1. Workflow architecture (A), backfill structure (B), and 5-fold cross-validation (C). SHAP: Shapley Additive Explanations.



XSL•FO
RenderX

Machine Learning Algorithms

Depressive and manic models were trained separately using the first half of the follow-up data. Python, scikit-learn, and SHAP packages were used for programming, model training, and model explanation, respectively. We adopted logistic regression, decision tree, k-nearest neighbors, random forest, adaptive boosting, as well as Extreme Gradient Boosting (XGBoost) to predict mood symptoms. Five-fold cross-validation was used to evaluate model performance and hyperparameter selection before making predictions on testing data [39] (Figure 1C). During the training process, the grid search strategy for hyperparameter selection was used to ensure model stability, which loops through all candidate parameters, leaving only the final best-performing set of parameters.

Model Assessment

Model performance was assessed by accuracy, sensitivity, specificity, precision, F_1-score, and AUROC. To explain the output of machine learning models [40], the SHAP method analyzed the predictions from machine learning models and interpreted the contributions of each feature by a Shapley value, which measures the influence of a feature on the prediction.

Ethical Considerations

This study was approved by the Research Ethics Committee at National Taiwan University Hospital (202002006RINA) before its implementation. The investigation was carried out in accordance with the latest version of the Declaration of Helsinki. Informed consent of the participants was obtained after the nature of the procedures had been fully explained. Data were anonymized. Participants who completed the follow-up received a small gift (ie, essential oil soap) valued at less than US $6.00.

Results

Overview

The features were compared between the depressive and nondepressive labels, and between the manic and nonmanic labels by Student *t* test (Tables S2 and S3 in Multimedia Appendix 1). We found that the depressive label had a significantly higher minimal or resting HR and a lower activity level than the nondepressive label. Besides, the manic label had a significantly lower sleep duration than the nonmanic label. Similarly, for individualized data, we found that the manic label had a significantly higher HR and activity level and lower sleep duration than the nonmanic label.

Prediction Model

First, we used 12 features (without individualized data) for model training. Table 1 shows model performance on the testing set. Compared to other algorithms, the XGBoost performed with the highest accuracy (0.79), AUROC (0.85), and F_1-score (0.57) in the depressive model. Similarly, in the manic model, the XGBoost performed superior to others, with the highest accuracy (0.83), AUROC (0.84), and F_1-score (0.19).

Table . The performance of the models for depressive or manic symptoms without individualized features in the models.

	Accuracy	AUROC[a]	Sensitivity	Specificity	Precision	F_1-score
Models for a depressive episode						
Logistic regression	0.63	0.77	0.88	0.57	0.34	0.49
Decision tree	0.74	0.65	0.34	0.84	0.35	0.35
KNN[b]	0.69	0.58	0.38	0.77	0.30	0.34
Random forest	0.70	0.83	0.87	0.66	0.39	0.54
AdaBoost[c]	0.78	0.79	0.40	0.87	0.44	0.42
XGBoost[d]	0.79	0.85	0.71	0.81	0.48	0.57
Models for a manic episode						
Logistic regression	0.65	0.63	0.58	0.65	0.05	0.09
Decision tree	0.87	0.64	0.25	0.89	0.07	0.10
KNN	0.90	0.51	0.08	0.93	0.03	0.05
Random forest	0.75	0.78	0.58	0.75	0.07	0.12
AdaBoost	0.94	0.74	0.08	0.97	0.08	0.08
XGBoost	0.83	0.84	0.67	0.84	0.11	0.19

[a]AUROC: area under the receiver operating characteristic curve.

[b]KNN: k-nearest neighbors.

[c]AdaBoost: Adaptive Boosting.

[d]XGBoost: Extreme Gradient Boosting.

Next, we examined whether adding individualized features to the models improved prediction. The prediction performance of the 19-feature model with individualized features was successfully improved in both depressive and manic models (Table 2). The accuracy, AUROC, and F_1-score in the depressive model by the XGBoost increased from 0.79, 0.85, and 0.57 to

XSL•FO
RenderX

0.83, 0.89, and 0.65, while those in the manic model increased from 0.83, 0.84, and 0.19 to 0.91, 0.88, and 0.25.

Table . The performance of the models for depressive or manic symptoms with the individualized features included in the models.

	Accuracy	AUROC[a]	Sensitivity	Specificity	Precision	F_1-score
Models for a depressive episode						
Logistic regression	0.86	0.87	0.62	0.92	0.68	0.65
Decision tree	0.79	0.75	0.50	0.87	0.49	0.50
KNN[b]	0.79	0.70	0.54	0.85	0.48	0.51
Random forest	0.82	0.86	0.79	0.83	0.55	0.65
AdaBoost[c]	0.82	0.83	0.54	0.89	0.56	0.55
XGBoost[d]	0.83	0.89	0.78	0.85	0.56	0.65
Models for a manic episode						
Logistic regression	0.71	0.84	0.92	0.71	0.09	0.16
Decision tree	0.90	0.69	0.42	0.92	0.14	0.20
KNN	0.89	0.62	0.33	0.91	0.10	0.15
Random forest	0.89	0.81	0.25	0.91	0.08	0.12
AdaBoost	0.93	0.78	0.33	0.95	0.16	0.22
XGBoost	0.91	0.88	0.50	0.92	0.17	0.25

[a]AUROC: area under the receiver operating characteristic curve.

[b]KNN: k-nearest neighbors.

[c]AdaBoost: Adaptive Boosting.

[d]XGBoost: Extreme Gradient Boosting.

Explanation of Prediction Model

In the depressive model, resting HR revealed the highest feature importance, followed by deep sleep duration, floors climbed, average HR, and steps (Figure 2). The force plots explained how resting HR (Figure 3), number of steps (Figure 4), and total sleep duration (Figure 5) affect the model. In each force plot, the y-axis represents the magnitude of the impact on the model, where a positive value (red region) indicates a tendency to predict that there are mood symptoms of depression, and a negative value (blue region) suggests the opposite. We could see that there is an obvious turning point at 60 in Figure 3. Specifically, steps less than 6000 steps/day and sleep less than 6 h may predict depressive symptoms. Together, a high resting HR produces a push to the right, while sufficient activity and sleep produce a push to the left (Figure 6); all forces result in a 0.23 predicted probability of a depressive episode.

XSL•FO
RenderX

Figure 2. Feature importance of Extreme Gradient Boosting (XGBoost) with the summary plot. REM: rapid eye movement; SHAP: Shapley Additive Explanations.

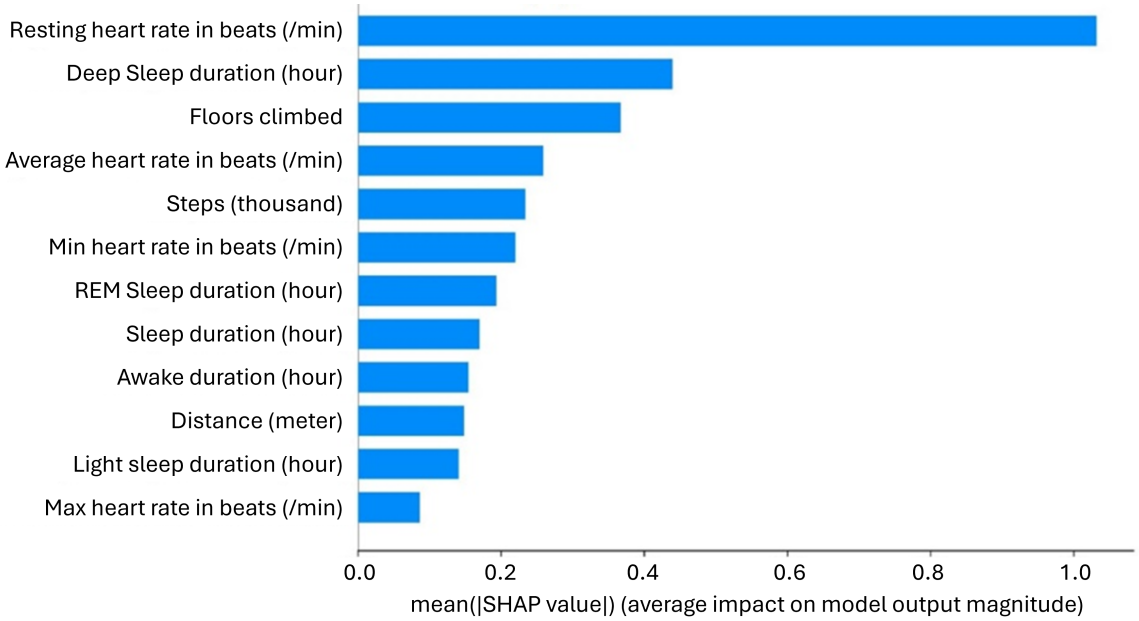


Figure 3. Impact of resting heart rate on the model with the force plot. The x-axis of the figure is the number of resting heartbeat per minute, and the y-axis represents the magnitude of the impact on the model.

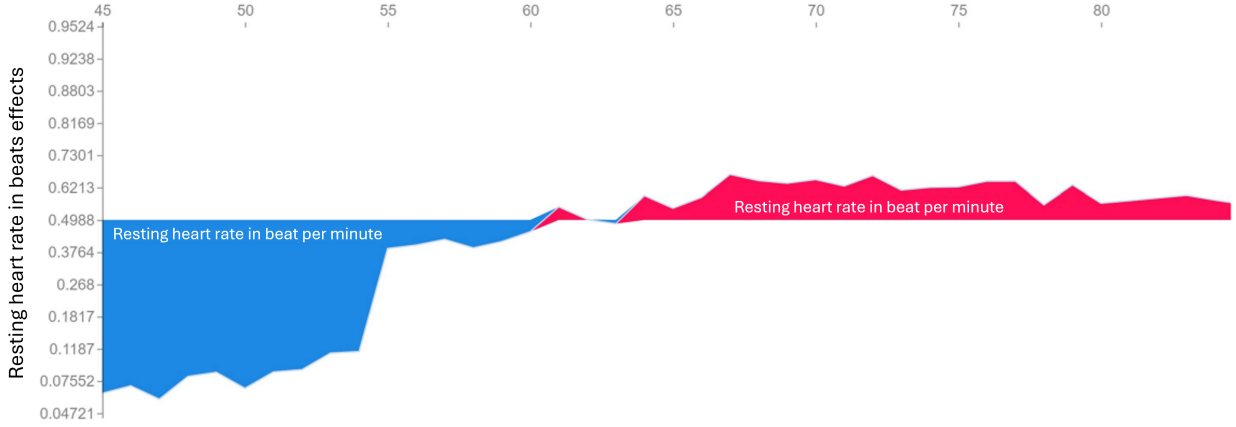
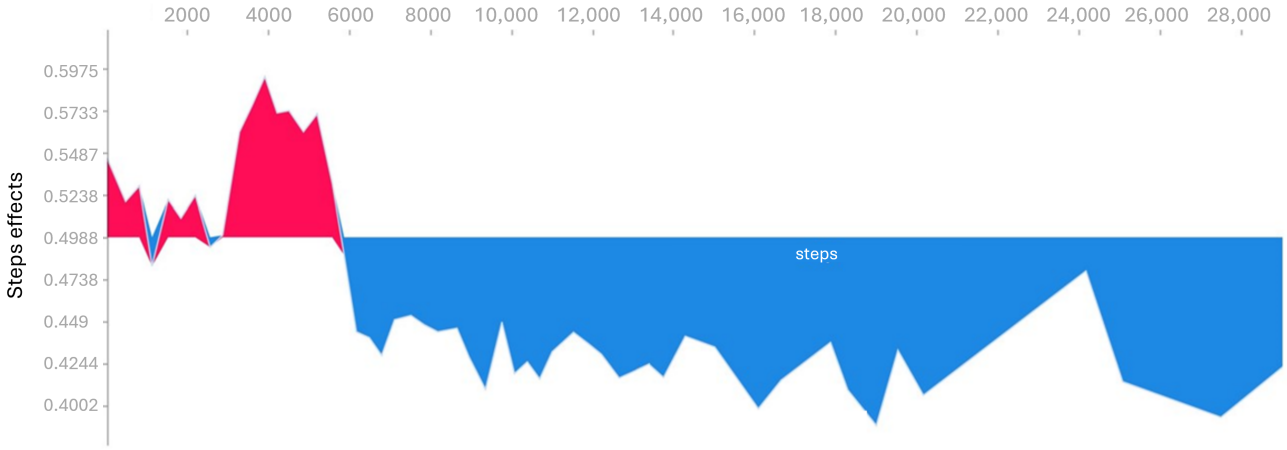


Figure 4. Impact of steps on the model with the force plot. The x-axis of the figure is the number of steps per day, and the y-axis represents the magnitude of the impact on the model.



XSL•FO
RenderX

Figure 5. Impact of total sleep duration in hours on the model with the force plot. The x-axis of the figure is the number of total sleep duration per day, and the y-axis represents the magnitude of the impact on the model.

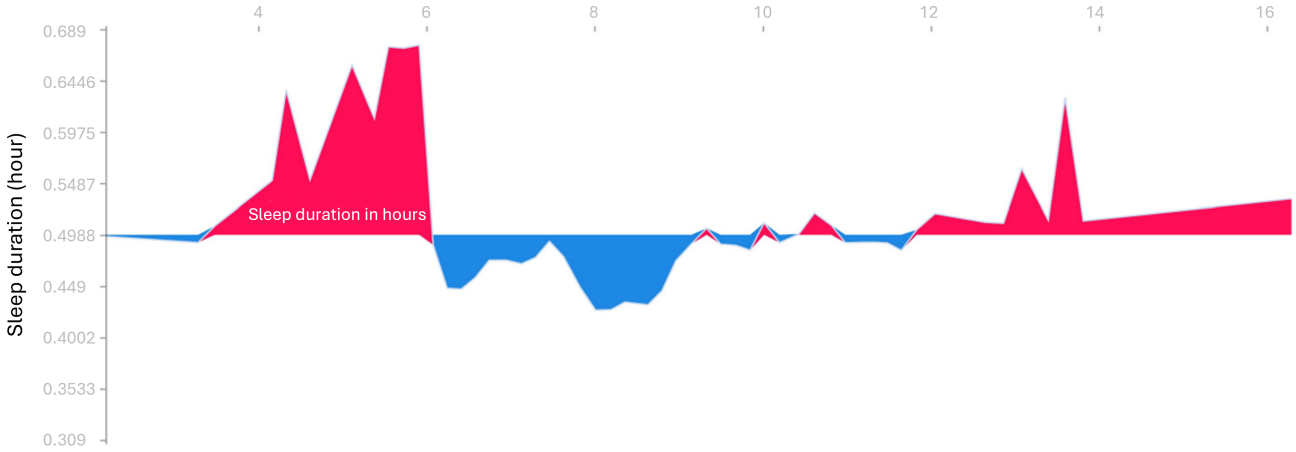
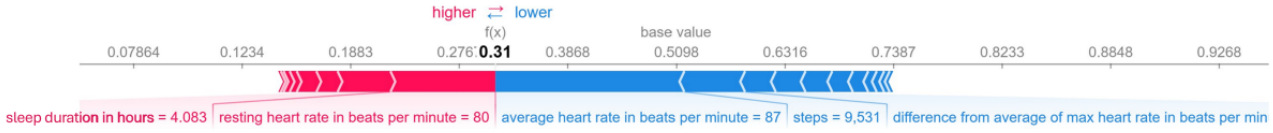


Figure 6. Impact of different features on a single data point with the force plot.



Discussion

Principal Findings

This study constructed prediction models for mild depressive and manic symptoms using digital biomarkers, including activity, sleep state, HR, and the individualized parameters of these features. Major findings included, first, the accuracy of the prediction achieved 79% (AUROC 0.85) in the depressive model and 83% (AUROC 0.84) in the manic model. Second, adding individualized features improved accuracy to 83% (AUROC 0.89) in the depressive model and 91% (AUROC 0.88) in the manic model. Third, among the features, higher resting HR, lower activity, and shorter sleep were important in predicting depressive symptoms. These findings supported the utility of digital biomarkers collected from wearable devices in predicting depressive and manic symptoms in the early phase.

The accuracy and AUROC in our depressive model (0.84) were similar to an earlier study in mood disorder (0.87) [24], with a higher sensitivity in ours (0.78 vs 0.48) yet higher specificity in theirs (0.96) than ours (0.85). Also, the accuracy (ours 0.84 vs 0.80), sensitivity (ours 0.78 vs 0.82), and specificity (ours 0.85 vs 0.78) were close to a previous multimodal source data algorithm for depression [23]. In the manic model, their accuracy (0.91) and AUROC (0.91) were close to ours, but their sensitivity (0.31) was lower than ours (~0.92) and their specificity (0.996) was higher than ours (0.71). Such discrepancy may be related to the machine learning algorithm (random forest in theirs vs XGBoost in ours) and individualized features included in our model. Higher sensitivity in our model may indicate a potential application in detecting symptoms in the early stage. Whereas a relatively lower specificity may necessitate a thorough clinical assessment after a case has been identified. In addition, they provided model performance and feature importance, but we further explained the model by using insights from SHAP to explain the clinical implications of the features. Of note, the mean ages and first onset of mood disorder were 25.9 (SD 4.8) and 17.9 (SD 4.8) in their study and 38 (SD 9) and 23.1 (SD 10) in our study. Given that the HR, sleep, and activity levels may depend on age, the older sample in ours may also contribute to the discrepancies of findings across the studies. The age effect on the predictive model is worth further exploration.

Our findings supported the prediction of depressive symptoms by digital features including activity level, sleep parameters, and HRs during the 7 days before depressive symptoms were reported. Among the features, we found that a higher resting HR may contribute to the prediction of depression. Previous studies also showed that the resting HR was higher in depressive patients [14-16]. Severe depression is often accompanied by increased HR [41] and reduced HR variability [41,42]. Our data suggested a turning point of resting HR at 60 (Figure 6), showing that resting HR higher than 60 was linked to a higher chance of predicting depressive symptoms. Depressive disorders have been shown to be associated with sympathetic hyperactivity and reduced cardiac vagal control, which might partly explain the risk of cardiovascular disease in depression [41]. In addition, higher resting HR in depression may also relate to higher anxiety tone and poor night sleep that are often observed during depression, or mild dehydration due to poor oral intake.

Regarding sleep parameters, a total sleep duration of fewer than 6 hours may contribute to the prediction of depressive symptoms, consistent with previous evidence that supported sleep duration remained an important correlate for depressive symptoms [43,44]. For patients who demonstrated a combination of higher resting HR, lower activity, and insufficient sleep, early

XSL•FO
RenderX

assessment and intervention of depressive symptoms may be considered.

The successful trial of including individualized features in establishing a machine learning model suggests that it can be potentially applied to other populations, particularly when the focus is on evaluating changes in physiological data or activity levels. For instance, the deviation of HR from baseline may be valuable in predicting events such as panic attacks or aggressive behaviors, where a sudden increase in HR might serve as a critical indicator. The consideration of individualized features is especially relevant in scenarios where baseline data exhibit heterogeneity among individuals, for example, samples comprising both long sleepers and short sleepers. Incorporating individualized features in these contexts can help minimize the risk of biased predictions and enhance the accuracy of the algorithm.

Limitations

Several limitations need to be addressed. First, the labeling method relies on self-rated questionnaires completed at least once a week which backfill for 7 days given that the questionnaire rated mood symptoms in the past 7 days. While participants were instructed to report mood symptoms as soon as they became aware of them, there is a possibility that some individuals did not complete the questionnaires promptly when their symptoms first emerged. Timely symptom labeling, immediately upon awareness of depressive or manic symptoms, could potentially enhance data reliability. Of note, although the BDI-II is a commonly used self-report measure [45], some studies have shown discrepancies between clinician-rated and self-reported depression severity [46]. Therefore, a clear explanation was provided by the research assistants to the participants to ensure correct understanding of the scales (ie, YMRS and BDI-II) and the use of the mobile app. As for the electronic format of self-rated measures, a recent systematic review focused on the validity of the mobile app–based self-report questionnaires for the assessment and monitoring of BD [47]. Their findings revealed that mobile app–based self-report tools (ie, YMRS, Depression Rating Scale-17, etc) are valid in the assessment of symptoms of mania and depression in patients with BD, indicating good adherence to self-report assessments administered during the study periods.

Second, participants in the study were undergoing treatment with mood stabilizers and/or antipsychotics that may reduce symptom relapse. However, it is essential to acknowledge that medical treatment is inevitable in long-term follow-up in a clinical sample. Future studies may consider recording the days on medications with detailed categorization of psychotropic medications based on their mechanisms to assess their potential impact on sleep and HRs.

Third, low F_1-score in the prediction model for manic symptoms may reflect insufficient events for prediction, which also influences the analysis of feature importance. Meanwhile, the small sample of 24 participants may limit the generalizability of the findings. Although the sample size is not large enough, we followed the participants for 6.39 (SD 4.85) months, thus generating enough nondepressive label (n=1330), depressive label (n=338), nonmanic label (n=1956), and manic label (n=59). A larger sample with a longer follow-up duration may not only ensure enough relapse events for analysis but also increase the generalizability of the findings.

Fourth, potential confounders such as medical treatment, clinical care, interactions, and environmental factors were not controlled in the study. For example, the types and dosing schedule of medications may influence HR and activity level but were not controlled in the analysis, given that all participants received medication treatment with different combinations of antipsychotics and mood stabilizers. Without controlling these factors, the analysis may be incomprehensive and less efficient. Nonetheless, the generated predictive model may be better suited to address the general needs of future applications in real-world scenarios or natural settings whereby participants had no need to provide information other than passive data.

Nevertheless, this study explored the potential of predicting early signs of mood episodes using digital biomarkers. Toward that end, we used the SHAP method to interpret the model and included individualized features that better capture the changes in patients' lifestyles and successfully improve the prediction models for both depressive and manic symptoms. Our findings highlighted the potential of applying wearable devices to detect early signs of relapse in BD for early intervention. Nowadays, sleep hours, activity level, and HR can be collected by most commercial wearable devices including smartwatches. With an algorithm that can successfully predict upcoming mood episodes and notify the participant, caregiver, or therapist, early assessment and intervention can be initiated in time to prevent a relapse, thus reducing functional impairment and improving the prognosis of BD. Future studies may consider larger, more diverse samples or additional digital biomarkers (eg, environmental data) to enhance the predictive capabilities of the models as well as to explore the efficacy of implementing wearable technology in improving clinical practice and quality of life for various psychiatric populations.

Conclusions

This study used digital biomarkers obtained from wearable devices to construct machine learning models for the prediction of depressive and manic symptoms. By incorporating individualized features into the models, we achieved satisfactory accuracy in predicting depressive symptoms. Furthermore, the application of an interpretable SHAP model allowed us to discern that higher resting HR, lower activity, and insufficient sleep were indicative of impending depressive symptoms. Early detection of depressive changes enables the timely introduction of adequate psychoeducation and clinical assessment, facilitating the implementation of interventions in time to mitigate upcoming mood episodes, thereby reducing the risk of recurrence.

XSL•FO
RenderX

Acknowledgments

This work was funded by a grant from the Ministry of Economic Affairs (113A-10) of Taiwan.

Authors' Contributions

CTW, LYJ, DSL, SMW, and CTW were responsible for data analysis and paper processing. IMC, MHH, and YLC were responsible for the case enrollment, contact, and follow-ups. YLC directed the project and revised the manuscript rigorously. All authors approved the final manuscript.

Conflicts of Interest

None declared.

Multimedia Appendix 1
Types of psychotropic medications and comparisons of all features between labels.
[DOCX File, 24 KB - medinform_v13i1e66277_app1.docx]

Multimedia Appendix 2
Distribution of Beck Depression Inventory scores.
[PNG File, 87 KB - medinform_v13i1e66277_app2.png]

Multimedia Appendix 3
Distribution of Young Mania Rating Scale scores.
[PNG File, 86 KB - medinform_v13i1e66277_app3.png]

References

1. Simon GE. Social and economic burden of mood disorders. Biol Psychiatry 2003 Aug 1;54(3):208-215. [doi: 10.1016/s0006-3223(03)00420-7] [Medline: 12893097]
2. Sajatovic M. Bipolar disorder: disease burden. Am J Manag Care 2005 Jun;11(3 Suppl):S80-S84. [Medline: 16097718]
3. Vázquez GH, Holtzman JN, Lolich M, Ketter TA, Baldessarini RJ. Recurrence rates in bipolar disorder: systematic comparison of long-term prospective, naturalistic studies versus randomized controlled trials. Eur Neuropsychopharmacol 2015 Oct;25(10):1501-1512. [doi: 10.1016/j.euroneuro.2015.07.013] [Medline: 26238969]
4. Vieta E, Salagre E, Grande I, et al. Early intervention in bipolar disorder. Am J Psychiatry 2018 May 1;175(5):411-426. [doi: 10.1176/appi.ajp.2017.17090972] [Medline: 29361850]
5. Faurholt-Jepsen M, Vinberg M, Frost M, et al. Behavioral activities collected through smartphones and the association with illness activity in bipolar disorder. Int J Methods Psychiatr Res 2016 Dec;25(4):309-323. [doi: 10.1002/mpr.1502] [Medline: 27038019]
6. Harrison PJ, Cipriani A, Harmer CJ, et al. Innovative approaches to bipolar disorder and its treatment. Ann N Y Acad Sci 2016 Feb;1366(1):76-89. [doi: 10.1111/nyas.13048] [Medline: 27111134]
7. Priya A, Garg S, Tigga NP. Predicting anxiety, depression and stress in modern life using machine learning algorithms. Procedia Comput Sci 2020;167:1258-1267. [doi: 10.1016/j.procs.2020.03.442]
8. Sau A, Bhakta I. Predicting anxiety and depression in elderly patients using machine learning technology. Healthcare Tech Letters 2017 Dec;4(6):238-243. [doi: 10.1049/htl.2016.0096]
9. Maatoug R, Oudin A, Adrien V, et al. Digital phenotype of mood disorders: a conceptual and critical review. Front Psychiatry 2022;13:895860. [doi: 10.3389/fpsyt.2022.895860] [Medline: 35958638]
10. Jakobsen P, Garcia-Ceja E, Riegler M, et al. Applying machine learning in motor activity time series of depressed bipolar and unipolar patients compared to healthy controls. PLoS One 2020;15(8):e0231995. [doi: 10.1371/journal.pone.0231995] [Medline: 32833958]
11. Cretu JB, Culver JL, Goffin KC, Shah S, Ketter TA. Sleep, residual mood symptoms, and time to relapse in recovered patients with bipolar disorder. J Affect Disord 2016 Jan 15;190:162-166. [doi: 10.1016/j.jad.2015.09.076] [Medline: 26519636]
12. Lim D, Jeong J, Song YM, et al. Accurately predicting mood episodes in mood disorder patients using wearable sleep and circadian rhythm features. NPJ Digit Med 2024 Nov 18;7(1):324. [doi: 10.1038/s41746-024-01333-z] [Medline: 39557997]
13. Smith R, Thayer JF, Khalsa SS, Lane RD. The hierarchical basis of neurovisceral integration. Neurosci Biobehav Rev 2017 Apr;75:274-296. [doi: 10.1016/j.neubiorev.2017.02.003]
14. Jüres F, Kaufmann C, Riesel A, et al. Heart rate and heart rate variability in obsessive-compulsive disorder: evidence from patients and unaffected first-degree relatives. Biol Psychol 2024 May;189:108786. [doi: 10.1016/j.biopsycho.2024.108786] [Medline: 38531496]

XSL•FO
RenderX

15. Friedman BH, Thayer JF. Anxiety and autonomic flexibility: a cardiovascular approach. Biol Psychol 1998 Mar;47(3):243-263. [doi: 10.1016/s0301-0511(97)00027-6] [Medline: 9564452]
16. Grossman P, Wilhelm FH, Spoerle M. Respiratory sinus arrhythmia, cardiac vagal control, and daily activity. Am J Physiol Heart Circ Physiol 2004 Aug;287(2):H728-H734. [doi: 10.1152/ajpheart.00825.2003] [Medline: 14751862]
17. Wazen GLL, Gregório ML, Kemp AH, de Godoy MF. Heart rate variability in patients with bipolar disorder: from mania to euthymia. J Psychiatr Res 2018 Apr;99:33-38. [doi: 10.1016/j.jpsychires.2018.01.008] [Medline: 29407285]
18. Agelink MW, Boz C, Ullrich H, Andrich J. Relationship between major depression and heart rate variability. Clinical consequences and implications for antidepressive treatment. Psychiatry Res 2002 Dec 15;113(1-2):139-149. [doi: 10.1016/s0165-1781(02)00225-1] [Medline: 12467953]
19. Kemp AH, Quintana DS, Gray MA, Felmingham KL, Brown K, Gatt JM. Impact of depression and antidepressant treatment on heart rate variability: a review and meta-analysis. Biol Psychiatry 2010 Jun 1;67(11):1067-1074. [doi: 10.1016/j.biopsych.2009.12.012] [Medline: 20138254]
20. Koenig J, Kemp AH, Beauchaine TP, Thayer JF, Kaess M. Depression and resting state heart rate variability in children and adolescents - a systematic review and meta-analysis. Clin Psychol Rev 2016 Jun;46:136-150. [doi: 10.1016/j.cpr.2016.04.013] [Medline: 27185312]
21. Valenza G, Nardelli M, Lanata' A, et al. Predicting mood changes in bipolar disorder through heartbeat nonlinear dynamics. IEEE J Biomed Health Inform 2016 Jul;20(4):1034-1043. [doi: 10.1109/JBHI.2016.2554546] [Medline: 28113920]
22. Byun S, Kim AY, Jang EH, et al. Detection of major depressive disorder from linear and nonlinear heart rate variability features during mental task protocol. Comput Biol Med 2019 Sep;112:103381. [doi: 10.1016/j.compbiomed.2019.103381] [Medline: 31404718]
23. Rykov Y, Thach TQ, Bojic I, Christopoulos G, Car J. Digital biomarkers for depression screening with wearable devices: cross-sectional study with machine learning modeling. JMIR Mhealth Uhealth 2021 Oct 25;9(10):e24872. [doi: 10.2196/24872] [Medline: 34694233]
24. Cho CH, Lee T, Kim MG, In HP, Kim L, Lee HJ. Mood prediction of patients with mood disorders by machine learning using passive digital phenotypes based on the circadian rhythm: prospective observational cohort study. J Med Internet Res 2019 Apr 17;21(4):e11029. [doi: 10.2196/11029] [Medline: 30994461]
25. Diagnostic and Statistical Manual of Mental Disorders, 5th edition: American Psychiatric Association; 2013.
26. BECK AT, WARD CH, MENDELSON M, MOCK J, ERBAUGH J. An inventory for measuring depression. Arch Gen Psychiatry 1961 Jun;4:561-571. [doi: 10.1001/archpsyc.1961.01710120031004] [Medline: 13688369]
27. Beck AT, Steer RA, Ball R, Ranieri W. Comparison of beck depression inventories -IA and -II in psychiatric outpatients. J Pers Assess 1996 Dec;67(3):588-597. [doi: 10.1207/s15327752jpa6703_13] [Medline: 8991972]
28. Zheng YP, Wei LA, Goa LG, Zhang GC, Wong CG. Applicability of the Chinese Beck Depression Inventory. Compr Psychiatry 1988;29(5):484-489. [doi: 10.1016/0010-440x(88)90063-6] [Medline: 3180758]
29. Young RC, Biggs JT, Ziegler VE, Meyer DA. A rating scale for mania: reliability, validity and sensitivity. Br J Psychiatry 1978 Nov;133:429-435. [doi: 10.1192/bjp.133.5.429] [Medline: 728692]
30. Evenson KR, Spade CL. Review of validity and reliability of garmin activity trackers. J Meas Phys Behav 2020 Jun;3(2):170-185. [doi: 10.1123/jmpb.2019-0035] [Medline: 32601613]
31. Schyvens AM, Van Oost NC, Aerts JM, et al. Accuracy of Fitbit Charge 4, Garmin Vivosmart 4, and WHOOP versus polysomnography: systematic review. JMIR Mhealth Uhealth 2024 Mar 27;12:e52192. [doi: 10.2196/52192] [Medline: 38557808]
32. Wiesenberger R, Müller J, Kaufmann M, et al. Feasibility and usefulness of postoperative mobilization goals in the enhanced recovery after surgery (ERAS®) clinical pathway for elective colorectal surgery. Langenbecks Arch Surg 2024 Aug 31;409(1):266. [doi: 10.1007/s00423-024-03442-5] [Medline: 39215842]
33. Tsai CH, Chen PC, Liu DS, et al. Panic attack prediction using wearable devices and machine learning: development and cohort study. JMIR Med Inform 2022 Feb 15;10(2):e33063. [doi: 10.2196/33063] [Medline: 35166679]
34. Tsai CH, Christian M, Kuo YY, Lu CC, Lai F, Huang WL. Sleep, physical activity and panic attacks: a two-year prospective cohort study using smartwatches, deep learning and an explainable artificial intelligence model. Sleep Med 2024 Feb;114:55-63. [doi: 10.1016/j.sleep.2023.12.013] [Medline: 38154150]
35. Tseng TW, Wu CT, Lai F. Threat analysis for wearable health devices and environment monitoring internet of things integration system. IEEE Access 2019;7:144983-144994. [doi: 10.1109/ACCESS.2019.2946081]
36. Wu CT, Wang SM, Su YE, et al. A precision health service for chronic diseases: development and cohort study using wearable device, machine learning, and deep learning. IEEE J Transl Eng Health Med 2022;10:2700414. [doi: 10.1109/JTEHM.2022.3207825] [Medline: 36199984]
37. Wu CT, Li GH, Huang CT, et al. Acute exacerbation of a chronic obstructive pulmonary disease prediction system using wearable device data, machine learning, and deep learning: development and cohort study. JMIR Mhealth Uhealth 2021 May 6;9(5):e22591. [doi: 10.2196/22591] [Medline: 33955840]
38. Li DC, Liu CW, Hu SC. A learning method for the class imbalance problem with medical data sets. Comput Biol Med 2010 May;40(5):509-518. [doi: 10.1016/j.compbiomed.2010.03.005] [Medline: 20347072]

XSL•FO
RenderX

39. Raschka S. Model evaluation, model selection, and algorithm selection in machine learning. arXiv. Preprint posted online on Nov 13, 2018. [doi: 10.48550/arXiv.1811.12808]
40. Lundberg SM, Lee SI. A unified approach to interpreting model predictions. Presented at: Proceedings of the 31st International Conference on Neural Information Processing Systems; Dec 4-9, 2017; Long Beach, California, USA.
41. Saad M, Ray LB, Bujaki B, et al. Using heart rate profiles during sleep as a biomarker of depression. BMC Psychiatry 2019 Jun 7;19(1):168. [doi: 10.1186/s12888-019-2152-1] [Medline: 31174510]
42. Pawlowski MA, Gazea M, Wollweber B, et al. Heart rate variability and cordance in rapid eye movement sleep as biomarkers of depression and treatment response. J Psychiatr Res 2017 Sep;92:64-73. [doi: 10.1016/j.jpsychires.2017.03.026] [Medline: 28411417]
43. Zhai L, Zhang H, Zhang D. Sleep duration and depression among adults: a meta-analysis of prospective studies. Depress Anxiety 2015 Sep;32(9):664-670. [doi: 10.1002/da.22386] [Medline: 26047492]
44. Li W, Yin J, Cai X, Cheng X, Wang Y. Association between sleep duration and quality and depressive symptoms among university students: a cross-sectional study. PLoS One 2020;15(9):e0238811. [doi: 10.1371/journal.pone.0238811]
45. Shura RD, Schroeder RW, Ord AS, et al. Symptom validity indices for the Beck Depression Inventory-II: development and cross-validation in research and clinical samples. Clin Neuropsychol 2024 Nov 22:1-19. [doi: 10.1080/13854046.2024.2432058] [Medline: 39578380]
46. Yamada R, Fujii T, Hattori K, et al. Discrepancy between clinician-rated and self-reported depression severity is associated with adverse childhood experience, autistic-like traits, and coping styles in mood disorders. Clin Psychopharmacol Neurosci 2023 May 30;21(2):296-303. [doi: 10.9758/cpn.2023.21.2.296] [Medline: 37119222]
47. Chan EC, Sun Y, Aitchison KJ, Sivapalan S. Mobile app-based self-report questionnaires for the assessment and monitoring of bipolar disorder: systematic review. JMIR Form Res 2021 Jan 8;5(1):e13770. [doi: 10.2196/13770] [Medline: 33416510]

Abbreviations

AUROC: area under the receiver operating characteristic curve
BD: bipolar disorder
BDI: Beck Depression Inventory
***DSM-IV*:** *Diagnostic and Statistical Manual of Mental Disorders, Fourth Edition*
HR: heart rate
KNN: k-nearest neighbors
NTU: National Taiwan University
SHAP: Shapley Additive Explanations
SMOTE: Synthetic Minority Over-Sampling Technique
XGBoost: Extreme Gradient Boosting
YMRS: Young Mania Rating Scale

Edited by J Klann; submitted 09.09.24; peer-reviewed by C Valenzuela-Pascual, HH Tseng; revised version received 11.02.25; accepted 18.02.25; published 16.09.25.

Please cite as:
Wu CT, Hsieh MH, Chen IM, Jhao LY, Liu DS, Wang SM, Wu CT, Chien YL
Using Wearable Device and Machine Learning to Predict Mood Symptoms in Bipolar Disorder: Development and Usability Study
JMIR Med Inform 2025;13:e66277
URL: https://medinform.jmir.org/2025/1/e66277
doi:10.2196/66277

© Chia-Tung Wu, Ming H Hsieh, I-Ming Chen, Lian-Yin Jhao, Ding-Shan Liu, Ssu-Ming Wang, Chia-Ting Wu, Yi-Ling Chien. Originally published in JMIR Medical Informatics (https://medinform.jmir.org), 16.9.2025. This is an open-access article distributed under the terms of the Creative Commons Attribution License (https://creativecommons.org/licenses/by/4.0/), which permits unrestricted use, distribution, and reproduction in any medium, provided the original work, first published in JMIR Medical Informatics, is properly cited. The complete bibliographic information, a link to the original publication on https://medinform.jmir.org/, as well as this copyright and license information must be included.

XSL•FO
RenderX

Prediction of Insulin Resistance in Nondiabetic Population Using LightGBM and Cohort Validation of Its Clinical Value: Cross-Sectional and Retrospective Cohort Study

Ting Peng[1*], MD; Rujia Miao[1*], MD; Hao Xiong[2], BE; Yanhui Lin[1], MD; Duzhen Fan[2], BE; Jiayi Ren[2], BE; Jiangang Wang[1], Prof Dr Med; Yuan Li[2], MSc; Jianwen Chen[2], Prof Dr

[1]Health Management Center, Third Xiangya Hospital, Changsha, China

[2]School of Mathematics and Statistics, Hunan University of Technology and Business, 569 Yuelu District, Changsha, China

[*]these authors contributed equally

Corresponding Author:
Jianwen Chen, Prof Dr
School of Mathematics and Statistics, Hunan University of Technology and Business, 569 Yuelu District, Changsha, China

Abstract

Background: Insulin resistance (IR), a precursor to type 2 diabetes and a major risk factor for various chronic diseases, is becoming increasingly prevalent in China due to population aging and unhealthy lifestyles. Current methods like the gold-standard hyperinsulinemic-euglycemic clamp has limitations in practical application. The development of more convenient and efficient methods to predict and manage IR in nondiabetic populations will have prevention and control value.

Objective: This study aimed to develop and validate a machine learning prediction model for IR in a nondiabetic population, using low-cost diagnostic indicators and questionnaire surveys.

Methods: A cross-sectional study was conducted for model development, and a retrospective cohort study was used for validation. Data from 17,287 adults with normal fasting blood glucose who underwent physical exams and completed surveys at the Health Management Center of Xiangya Third Hospital, Central South University, from January 2018 to August 2022, were analyzed. IR was assessed using the Homeostasis Model Assessment (HOMA-IR) method. The dataset was split into 80% (13,128/16,411) training and 20% (32,83/16,411) testing. A total of 5 machine learning algorithms, namely random forest, Light Gradient Boosting Machine (LightGBM), Extreme Gradient Boosting, Gradient Boosting Machine, and CatBoost were used. Model optimization included resampling, feature selection, and hyperparameter tuning. Performance was evaluated using F_1-score, accuracy, sensitivity, specificity, area under the curve (AUC), and Kappa value. Shapley Additive Explanations analysis was used to assess feature importance. For clinical implication investigation, a different retrospective cohort of 20,369 nondiabetic participants (from the Xiangya Third Hospital database between January 2017 and January 2019) was used for time-to-event analysis with Kaplan-Meier survival curves.

Results: Data from 16,411 nondiabetic individuals were analyzed. We randomly selected 13,128 participants for the training group, and 3283 participants for the validation group. The final model included 34 lifestyle-related questionnaire features and 17 biochemical markers. In the validation group, their AUC were all greater than 0.90. In the test group, all AUC were also greater than 0.80. The LightGBM model showed the best IR prediction performance with an accuracy of 0.7542, sensitivity of 0.6639, specificity of 0.7642, F_1-score of 0.6748, Kappa value of 0.3741, and AUC of 0.8456. Top 10 features included BMI, fasting blood glucose, high-density lipoprotein cholesterol, triglycerides, creatinine, alanine aminotransferase, sex, total bilirubin, age, and albumin/globulin ratio. In the validation queue, all participants were separated into the high-risk IR group and the low-risk IR group according to the LightGBM algorithm. Out of 5101 high-risk IR participants, 235 (4.6%) developed diabetes, while 137 (0.9%) of 15,268 low-risk IR participants did. This resulted in a hazard ratio of 5.1, indicating a significantly higher risk for the high-risk IR group.

Conclusion: By leveraging low-cost laboratory indicators and questionnaire data, the LightGBM model effectively predicts IR status in nondiabetic individuals, aiding in large-scale IR screening and diabetes prevention, and it may potentially become an efficient and practical tool for insulin sensitivity assessment in these settings.

(JMIR Med Inform 2025;13:e72238) doi:10.2196/72238

KEYWORDS

insulin resistance; machine learning; Light Gradient Boosting Machine; diabetes; diabetes prevention

XSL•FO
RenderX

Introduction

Insulin resistance (IR) refers to the reduced sensitivity or responsiveness of target organs such as the liver, skeletal muscles, or adipose tissue to insulin. In order to maintain normal blood glucose levels, the body compensates by secreting increased amounts of insulin [1]. As a condition that can exist before the onset of type 2 diabetes, IR is not only one of the key mechanisms underlying the development of diabetes but also a major risk factor for various diseases [2]. According to the International Diabetes Federation, it is estimated that by 2045, there will be 783.2 million people affected globally, with the vast majority having type 2 diabetes [3]. Furthermore, IR is even more common. Data from the National Health and Nutrition Examination Survey in the United States show that approximately 40% of adults aged 18 - 44 years have IR [4]. A study in China revealed that the standardized prevalence of IR in adults aged 25 years or older is 29.22% [5]. By scientifically assessing and managing IR, it is theoretically possible to effectively control the onset of diabetes. The first step is to identify IR. The high insulin clamp with normal blood glucose levels is considered the gold standard for assessing insulin sensitivity [6]. However, in practice, this method is time-consuming, expensive, and difficult to apply widely. The Homeostasis Model Assessment of Insulin Resistance (HOMA-IR; fasting glucose [mmol/L]×fasting insulin [μU/ml]/22.5) is regarded as an acceptable method for evaluating IR [7]. However, fasting insulin, one of its components, is not a routine test, making it difficult to obtain in community and grassroots settings. Based on laboratory indicators and lifestyle characteristics that are correlated with the occurrence of IR and are easily accessible, it is crucial to explore more convenient ways to predict the previous probability of IR in individuals. This approach could guide more precise IR screening and has the potential for prevention and control within the large population of China.

Machine learning (ML), with its data-driven methods, has already shown good predictive value in health issues such as arteriosclerosis [8], fatty liver [9], diabetes [10], and hypertension [11] . Obesity, dyslipidemia, lack of exercise, and sedentary lifestyles are considered risk factors for metabolic homeostasis [12]. By applying daily habits, basic information, and simple blood tests as features, we can build machine learning models in health check-up populations that are representative of the general population. The model of the ensemble learning algorithms based on decision trees, such as random forest (RF), Light Gradient Boosting Machine (LightGBM), Extreme Gradient Boosting (XGBoost), Gradient Boosting Machine (GBDT), and CatBoost, using multiple decision trees for predictions. They are capable of capturing complex nonlinear relationships, handling high-dimensional data, performing automatic feature selection, and mitigating the risk of overfitting through various mechanisms. In addition, these models offer strong scalability and are suitable for large-scale datasets, with most models having built-in overfitting prevention capabilities. These models can effectively predict IR and identify key predictive factors that are crucial for individual intervention. In addition, a retrospective cohort study can be used to determine the accuracy and practical value of these model results in distinguishing the onset of diabetes.

Methods

Study Population and Data Sources

The data used in this study were sourced from the electronic medical records of the Health Management Center at Xiangya Third Hospital, Central South University. The dataset includes participants who underwent physical examinations and questionnaire surveys at the Health Management Center between January 2018 and August 2022. A total of 17,287 adults with normal fasting blood glucose (FBG) were included, while individuals with FBG ≥6.1mmol/L or those with a history of abnormal glucose tolerance or diabetes were excluded.

The subsequent retrospective cohort consisted of individuals who completed their first health check-up at the Health Management Center of Xiangya Third Hospital between January 2017 and January 2019. These participants were followed for 5 years, with those diagnosed with diabetes at external hospitals or those who had completed ≥2 times FBG tests at the hospital during the follow-up period being included. Participants were required to be aged 18 years or older and have FBG <6.1mmol/L at the time of their first check-up. They also had to complete baseline assessments and surveys. Exclusion criteria included a history of abnormal glucose tolerance, diabetes, or gestational diabetes, as well as a history of tumors, pregnancy, or autoimmune diseases; and those who had used glucocorticoids or other relevant medications within the past month.

Using an IR prediction model, individuals in the cohort were classified as low-risk or high-risk based on their baseline data. Changes in FBG were then monitored. A FBG ≥7 mmol/L within 5 years or a diagnosis of diabetes at an external hospital was considered a positive result. A negative result was defined as maintaining normal FBG levels without a diabetes diagnosis at an external hospital over the 5-year follow-up period. Furthermore, by matching the ID card numbers, we excluded the participants who repeatedly appeared in the training set and the test set. Ensure this cohort was the different from the dataset used for model development.

Characteristics and Definitions

The dataset includes a total of 102 features, which encompass physical examination measurements such as age, height, weight, BMI, waist circumference (WC), systolic blood pressure (SBP), and diastolic blood pressure (DBP). Blood test indicators include FBG, liver function markers (alanine aminotransferase [ALT], aspartate aminotransferase [AST], total bilirubin [TBIL], direct bilirubin [DBIL], serum albumin [ALB], serum globulin [GLO], albumin/globulin ratio [A/G], total proteintotal [TP], bile acids [TBA]), kidney function markers (serum creatinine [Sr], blood urea nitrogen [BUN], uric acid [UA], and lipid profile markers (total cholesterol [TC], triglycerides (TG], high-density lipoprotein cholesterol [HDL-C], low-density lipoprotein cholesterol [LDL-C]. In addition, information from questionnaires was collected, including past disease diagnoses, lifestyle factors (dietary preferences, smoking status, alcohol consumption, exercise habits, and work status), psychological

XSL•FO
RenderX

status, sleep patterns, and health literacy related to basic medical knowledge. Insulin sensitivity was assessed using HOMA-IR=fasting glucose (mmol/L)×fasting insulin (μU/ml) / 22.5. A cut-off value of 2.69 was used, with a value ≥2.69 considered indicative of IR status [5].

Data Processing and Statistical Analysis

We excluded features with more than 30% missing data. For features with less than 30% missing data, continuous variables were imputed using the mean, while categorical variables were imputed using the mode. Ultimately, 90 features and 16,411 samples were retained. The entire dataset was randomly split into a training set (13,128/16411, 80% samples) and a test set (3283/16411, 20% samples), with 2782 samples categorized as IR.

For statistical analysis, continuous data that conform to a normal distribution were reported as means (SDs), otherwise, were reported as quartiles. Chi-square tests were conducted on categorical variables to assess the significant association between categorical features and the dependent variable. $P<.05$ was considered statistically significant.

Feature Engineering

Resampling

In this study, 3 resampling techniques, namely random undersampling, synthetic minority oversampling technique (SMOTE) oversampling, and SMOTE-Tomek combined sampling were experimentally compared during the dataset preprocessing phase. It was found that random undersampling performed best in improving the prediction accuracy for the minority class. Therefore, random undersampling was applied to the training set, where a portion of the majority class samples were randomly removed to reduce the majority class sample size. This approach helped mitigate model bias toward the majority class and improved overall classification performance.

Feature Processing and Algorithm Selection

To enhance model accuracy and efficiency, reduce computational costs, and avoid overfitting, feature selection was conducted. Before feature selection, Pearson correlation analysis was conducted for continuous features, while Kendall correlation analysis was used for discrete features. By examining the correlation matrix of the features, pairs of highly correlated features (with correlation coefficients >0.6) were identified, and perform dimensionality reduction on these highly relevant features. A total of 5 machine learning algorithms, including RF, LightGBM, XGBoost, GBDT, and CatBoost were used to construct predictive models on the training dataset. The model demonstrating the best performance across various evaluation metrics was selected from the baseline models (CatBoost was chosen based on experimental results). The CatBoost model was then trained, and the importance scores for each feature were determined. Features were added to the model in descending order of importance until the AUC score stabilized at its highest value with a specific number of features. At this point, no further features were added, and the model was constructed using the selected features.

Parameter Optimization and Model Evaluation

In addition to addressing class imbalance through resampling techniques, the model parameters were adjusted to assign different weights to each class, thereby balancing the class distribution. For the RF, GBDT, and CatBoost models, the parameter class_weight = “balanced” was set, while for the LightGBM and XGBoost models, scale_pos_weight = “ratio of majority and minority class” was used. Bayesian optimization was used for parameter tuning. Bayesian optimization is a global optimization algorithm based on Bayesian inference, which iteratively updates the posterior distribution of the parameters to identify the optimal configuration and optimize the objective function. To evaluate the optimization effects and improve the model’s generalization ability, 10-fold cross-validation was performed. The experiments were repeated 10 times, and metrics such as area under the receiver operating characteristic curve were averaged to assess model performance. In addition, model performance was evaluated using the F_1-score, accuracy, sensitivity, and specificity, while the receiver operating characteristic (ROC) curve and the area under the curve (AUC) were used to assess the model’s discriminatory ability. The Kappa value was also computed to evaluate the predictive capability of the model.

This research used several Python libraries and frameworks for data processing, feature engineering, model building, and hyperparameter tuning. The main tools used in the study are Python (version 3.6.4), NumPy (version 1.18.5), Pandas (version 1.1.5), SciPy (version 1.5.2), scikit-learn (version 0.24.2), LightGBM (version 4.3.0) XGBoost (version 1.5.2), CatBoost (version 1.1.1), and bayes_opt (version 1.4.0).

Feature Importance Ranking

Shapley Additive Explanations (SHAP) values are a method used to interpret machine learning model predictions. SHAP assigns a value to each feature, quantifying its contribution to the model’s output. Positive SHAP values indicate that the feature has a beneficial impact on the prediction, while negative SHAP values suggest a detrimental effect. The absolute magnitude of a SHAP value reflects the extent of the feature’s influence on the model’s decision. In this study, we used SHAP (version 0.45.0) for explainable machine learning to enhance interpretability.

Retrospective Cohort Validation of Model Application

Retrospective cohort data from a nondiabetic population were used as input to the aforementioned algorithms. The model outputs predicted the IR values for each participant, where a value of 1 was classified as high-risk IR and 0 as low-risk IR. Kaplan-Meier survival curves were used to conduct time-to-event analysis, comparing the 5-year diabetes incidence between the high-risk and low-risk IR groups. This approach further validated the model’s ability to accurately distinguish the onset of diabetes based on predicted IR levels.

Ethical Considerations

This study was conducted in accordance with the Declaration of Helsinki and approved by the Ethics Committee of Xiangya Third Hospital, Central South University (approval no. 22206).

XSL•FO
RenderX

All participants provided informed consent. The data were deidentified to ensure privacy protection.

Results

Characteristics of the Study Population

The study flow chart is presented in Figure 1. A total of 16,411 nondiabetic individuals who underwent health screenings were included in this study, with an average age of 42.74 (SD 11.36) years. The sample comprised 8205 males and 8206 females. Overall, 17% of participants were diagnosed with IR, with a higher prevalence observed in males compared with females. In the IR group, levels of weight, WC, BMI, SBP, UA, ALT, AST, TG, and TC were significantly elevated compared with the non-IR group. Conversely, the average HDL-C level was significantly lower in the IR group ($P<.05$). In addition, lifestyle factors such as diet, physical activity, and health literacy exhibited significant differences between the 2 groups (Tables 1 and 2).

XSL•FO
RenderX

Figure 1. Flow diagram of the study. The flow diagram of the study shows the entire research process, from data collection, preprocessing, model training and testing to final model evaluation and validation. AUC: area under the curve; GBDT: Gradient Boosting Machine; LightGBM: Light Gradient Boosting Machine; RF: random forest; SHAP: Shapley Additive Explanations; XGBoost: Extreme Gradient Boosting.

XSL•FO
RenderX

Table . Continuous characteristics of participants, including age, height, weight, waist circumference, BMI, blood pressure, and blood biochemical indicators, and a comparison of the means and SDs between the insulin resistance and non–insulin resistance groups, along with the corresponding *P* values to evaluate the association of each characteristic with insulin resistance.

	All (n=16,411), mean (SD)	IR[a] (HOMA[b]-IR <2.69; n=13,629), mean (SD)	Non-IR (HOMA-IR ≥2.5; n=2782), mean (SD)	*P* value
Age (years)	42.74 (11.36)	42.84 (11.37)	42.23 (11.30)	.01
Height (cm)	163.50 (8.00)	163.14 (7.93)	165.29 (8.21)	<.001
Weight (kg)	63.80 (11.70)	62.21 (11.10)	71.48 (11.59)	<.001
WC (cm)[c]	81.30 (10.40)	79.82 (9.81)	88.53 (9.67)	<.001
BMI (kg/m^2)[d]	23.85 (3.37)	23.30 (3.07)	26.54 (3.48)	<.001
SBP (mmHg)[e]	120.39 (14.83)	119.49 (14.7)	124.75 (14.62)	<.001
DBP (mmHg)[f]	73.80 (10.80)	73.08 (10.71)	77.02 (11.04)	<.001
BUN (mmol/L)[g]	4.72 (1.22)	4.71 (1.23)	4.79 (1.19)	<.001
Sr (umol/L)[h]	70.31 (18.15)	69.99 (18.52)	71.85 (16.12)	<.001
UA (umol/L)[i]	339.53 (92.01)	331.13 (89.53)	380.70 (92.91)	<.001
TBA (umol/L)[j]	4.22 (4.80)	4.18 (4.82)	4.44 (4.69)	.01
ALT (u/L)[k]	26.46 (25.62)	23.30 (24.73)	36.09 (27.21)	<.001
AST (u/L)[l]	24.89 (18.88)	24.50 (20.07)	26.83 (11.17)	<.001
ALB (g/L)[m]	46.62 (2.91)	46.63 (2.91)	46.60 (2.93)	.56
GLO (g/L)[n]	27.09 (3.68)	26.93 (3.65)	27.88 (3.71)	<.001
A/G[o]	1.73 (0.24)	1.74 (0.24)	1.70 (0.25)	<.001
TP (g/L)[p]	73.72 (4.22)	73.56 (4.19)	74.47 (4.30)	<.001
DBIL (umol/L)[q]	3.78 (1.34)	3.83 (1.35)	3.54 (1.26)	<.001
TBIL (umol/L)[r]	13.02 (5.06)	13.21 (5.11)	12.05 (4.70)	<.001
FBG (mmol/L)[s]	5.24 (0.42)	5.20 (0.42)	5.45 (0.40)	<.001
TG (mmol/L)[t]	1.70 (1.53)	1.55 (1.36)	2.44 (2.01)	<.001
TC (mmol/L)[u]	5.01 (0.94)	4.98 (0.93)	5.16 (1.00)	<.001
HDL-C (mmol/L)[v]	1.33 (0.30)	1.36 (0.29)	1.17 (0.24)	<.001
LDL-C (mmol/L)[w]	2.89 (0.79)	2.88 (0.78)	2.93 (0.84)	<.001

[a] IR: Insulin resistance.

[b]HOMA: Homeostasis Model Assessment.

[c] WC: waist circumference.

[d] BMI: body mass index.

[e] SBP: systolic blood pressure.

[f] DBP: diastolic blood pressure.

[g] BUN: blood urea nitrogen.

[h] Sr: serum creatinine.

[i] UA: uric acid.

[j] TBA: total bile acids.

[k] ALT: alanine aminotransferase.

[l] AST: aspartate aminotransferase.

[m] ALB: serum albumin.

[n] GLO: serum globulin.

[o] A/G: albumin/globulin ratio.

XSL•FO
RenderX

[p] TP: total protein.

[q] DBIL: direct bilirubin.

[r] TBIL: total bilirubin.

[s] FBG: fasting blood glucose.

[t] TG: triglycerides.

[u] TC: total cholesterol.

[v] HDL-C: high-density lipoprotein cholesterol.

[w] LDL-C: low-density lipoprotein cholesterol.

XSL•FO
RenderX

Table . Questionnaire characteristics of participants, including dietary habits, exercise, lifestyle, psychological status, and health literacy, and an assessment of the association of each characteristic with insulin resistance using the chi-square test, listing the chi-square values and *P* values.

Type and feature	Chi-square (*df*) value	*P* value
Diet		
Dietary preference	137.86 (13)	<.001
Daily meat intake	123.43 (4)	<.001
Fruit consumption	29.81 (4)	<.001
Coffee consumption	21.22 (4)	<.001
Nighttime snacking	54.97 (2)	<.001
Social dining	90.56 (3)	<.001
Legume and soy product consumption	13.40 (4)	.01
Fish or seafood consumption	7.24 (4)	.12
Sugary drink consumption	106.32 (4)	<.001
Dietary taste	125.78 (2)	<.001
Fat meat consumption	88.97 (4)	<.001
Animal organ consumption	25.31 (3)	<.001
Staple food structure	33.95 (4)	<.001
Binge eating	73.63 (1)	<.001
Daily vegetable intake	23.77 (4)	<.001
Milk consumption	13.20 (4)	.01
Egg consumption	1.83 (3)	.61
Exercise		
Physical exercise	56.60 (2)	<.001
Weekly exercise frequency	59.24 (3)	<.001
Exercise duration per session	54.73 (3)	<.001
Exercise type	122.97 (31)	<.001
Years of consistent exercise	60.50 (4)	<.001
Lifestyle		
Alcohol consumption	29.25 (3)	<.001
Alcohol frequency per week	25.38 (3)	<.001
Years of alcohol use	36.00 (4)	<.001
Alcohol quantity per session	57.59 (4)	<.001
Type of alcohol	13.95 (6)	.03
Time since quitting drinking	6.65 (4)	.16
Work physical demands	95.25 (4)	<.001
Workdays per week	3.85 (3)	.28
Working hours per week	3.36 (4)	.50
Smoking habits	42.55 (3)	<.001
Cigarettes per day	38.48 (4)	<.001
Years of smoking	56.12 (4)	<.001
Exposure to Harmful Substances	47.16 (18)	<.001
Sedentary time outside work	36.27 (3)	<.001
Regular meals	9.12 (3)	.03
Sleep quality	1.01 (2)	.60

XSL•FO
RenderX

Type and feature	Chi-square (*df*) value	*P* value
Reasons for sleep disturbance	22.03 (12)	.04
Sleep duration	3.52 (3)	.32
Main symptoms of sleep disturbance	15.448 (12)	.22
Psychology		
Depression	0.10 (2)	.95
Difficulty concentrating	8.45 (3)	.04
Increased anxiety	1.57 (2)	.46
Burnout	1.89 (2)	.39
Depressed	3.19 (3)	.36
Anxious	0.18 (2)	.91
Anxiety and restlessness	0.56 (2)	.76
Irritable	0.76 (2)	.68
Impatience	2.07 (2)	.36
Health literacy		
Normal WC[a]	25.37 (3)	<.001
Active medical knowledge acquisition	22.63 (2)	<.001
Self-Monitoring of blood pressure and heart rate	20.81 (2)	<.001
Normal BP[b]	7.82 (1)	.01
Normal BMI	6.71 (1)	.01
Normal FBG[c]	1.71 (1)	.19
Normal T[d]	1.02 (1)	.31
Normal HR[e]	1.07 (1)	.30
Normal TG[f]	0.72 (1)	.39
Normal TC[g]	2.66 (1)	.10
Normal Salt intake	78.68	<.001
History of hypertension	127.39 (2)	<.001
Family history medicine	791.80 (509)	<.001
Observe urination and defecation	13.10 (2)	<.001
Bask	13.10 (3)	<.001
Seat belt usage	7.09 (2)	.03
Carrying emergency medication	3.35 (2)	.19
Health check-up interval	12.46 (5)	.03
Personal history disease	1.25 (1)	.26
FH: DM[h]	4.00 (1)	.05

XSL•FO
RenderX

Type and feature	Chi-square (*df*) value	*P* value
Sex	151.26 (1)	<.001

[a]WC: waist circumference
[b]BP: blood pressure
[c]FBG: fasting blood glucose
[d]T: temperature
[e]HR: heart rate
[f]TG: triglycerides
[g]TC: total cholesterol
[h]FH: DM: family history of diabetes.

Feature Engineering

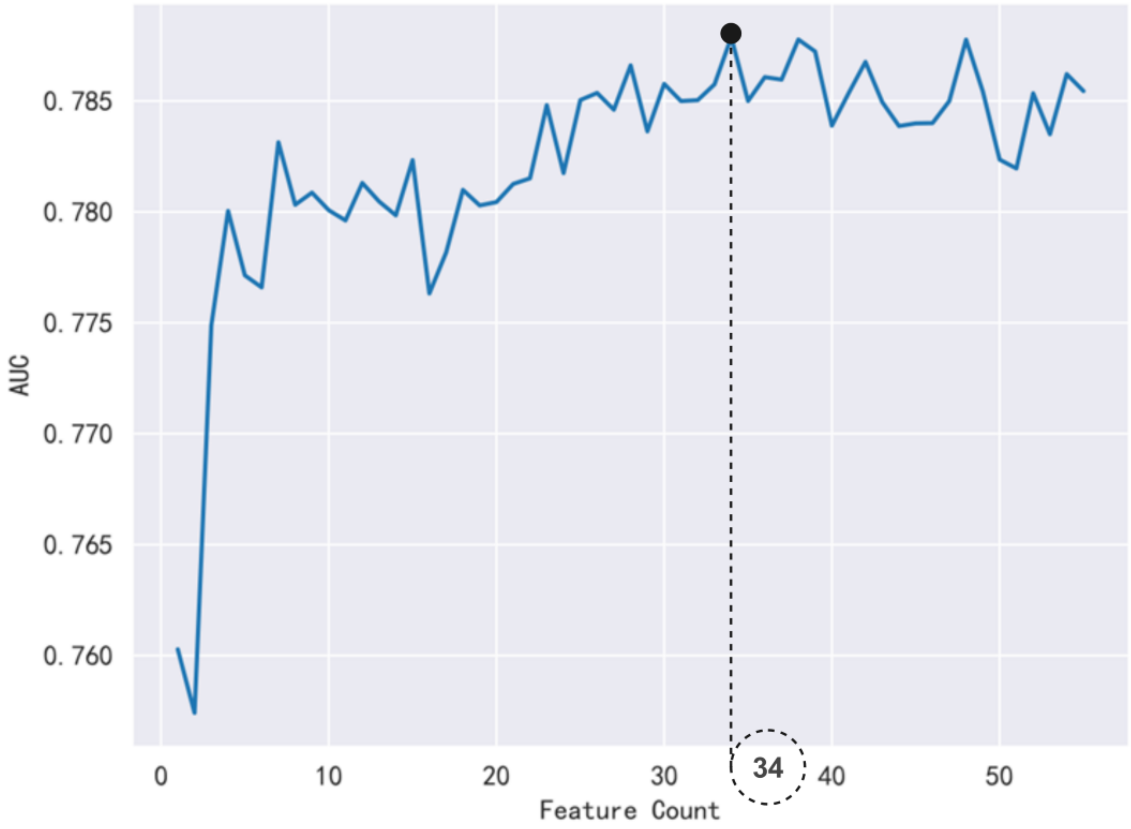
In the training set, random undersampling was applied to the majority class. Among the "physiological features," 4 highly correlated features: "BMI," "height," "weight," and "WC" were subjected to dimensionality reduction, with "BMI" retained. Similarly, for the 2 highly correlated features "SBP" and "DBP," only "SBP" was retained.

Feature importance scores were computed for 55 lifestyle-related questionnaire features using the CatBoost algorithm. These features were ranked from high to low based on their importance scores and then sequentially input into the CatBoost model. After each addition, the model's AUC score on the test set was recorded. As shown in Figure 2, the AUC score dropped significantly after adding 35 features, leading to the exclusion of 21 noncontributory questionnaire features. The 34 retained features, which showed significant contributions, include BMI, SBP, age, sex, family history medicine, exercise type, years of consistent exercise, exercise duration per session, weekly exercise frequency, dietary preferences, staple food structure, dietary taste, sleep duration, reasons for sleep disturbance, exposure to harmful substances, work physical demands, sedentary duration outside of work, consumption frequency of fruits, milk, meat, coffee, legume and soy products, sugary drink and fatty meats, daily vegetable intake, health check-up interval , self-monitoring of blood pressure and heart rate, observe urination and defecation, carrying emergency medications, regular meals, seat belt usage, bask, and awareness of normal salt intake and hazard ratio (HR).

In addition, the addition of 17 biochemical markers, BUN, Cr, UA, TC, TG, HDL-C, LDL-C, FBG, ALT, AST, TBIL, DBIL, TSP, ALB, GLO, A/G ratio, and TBA further improved the model's accuracy, sensitivity, and specificity. Thus, the final feature selection for the model included the 34 lifestyle-related questionnaire features and 17 biochemical markers.

XSL•FO
RenderX

Figure 2. The model's area under the curve (AUC) score on the test set. This figure shows how the AUC score on the test set changes with the number of features included in the model. After adding 34 features, the AUC score drops significantly, indicating that these additional features no longer contribute to model performance improvement.



Model Performance Evaluation and Feature Importance Ranking

Based on the 51 selected features (34 questionnaire features and 17 biochemical markers), 5 ML algorithms were applied, RF, LightGBM, XGBoost, GBDT, and CatBoost to build and evaluate models using both the training and testing datasets. The performance metrics of the 5 ML models are summarized in Table 3. The LightGBM model demonstrated the best performance across all metrics, including accuracy (0.7542), sensitivity (0.6639), specificity (0.7642), F_1-score (0.6748), and κ (0.3741). Although the AUC (0.8456) of the LightGBM model was slightly lower than that of CatBoost, LightGBM was determined to be the best model overall for predicting IR. The ROC curve for the best-performing LightGBM model is shown in Figure 3.

SHAP values were used to rank feature importance in the LightGBM model, as shown in Figure 4A. The top 10 features influencing IR were: BMI, FBG, HDL-C, TG, Cr, ALT, sex, TBIL, age, and A/G ratio. Figure 4B provides a visual representation of the SHAP values for the top 10 features, where BMI, FBG, TG, ALT, and sex were positively correlated with IR, while HDL-C, Cr, TBIL, age, and A/G ratio were negatively correlated with IR.

XSL•FO
RenderX

Table . Performances of the 5 machine learning models using 51 selected features for participants.

Model	Accuracy_train	Accuracy_test	Sensitivity	Specificity	F_1-score	AUC_train	AUC_test	κ value
RF[a]	0.8807	0.7344	0.6522	0.7516	0.6571	0.9552	0.8354	0.3451
LightGBM[b]	0.8503	0.7542	0.6639	0.7642	0.6748	0.9285	0.8456	0.3741
XGBoost[c]	0.9689	0.7460	0.6575	0.7556	0.6662	0.9966	0.8375	0.3588
GBDT[d]	0.9237	0.7505	0.6608	0.7598	0.6708	0.9799	0.8372	0.3668
CatBoost	0.8632	0.7493	0.6594	0.7576	0.6692	0.9445	0.8471	0.3637

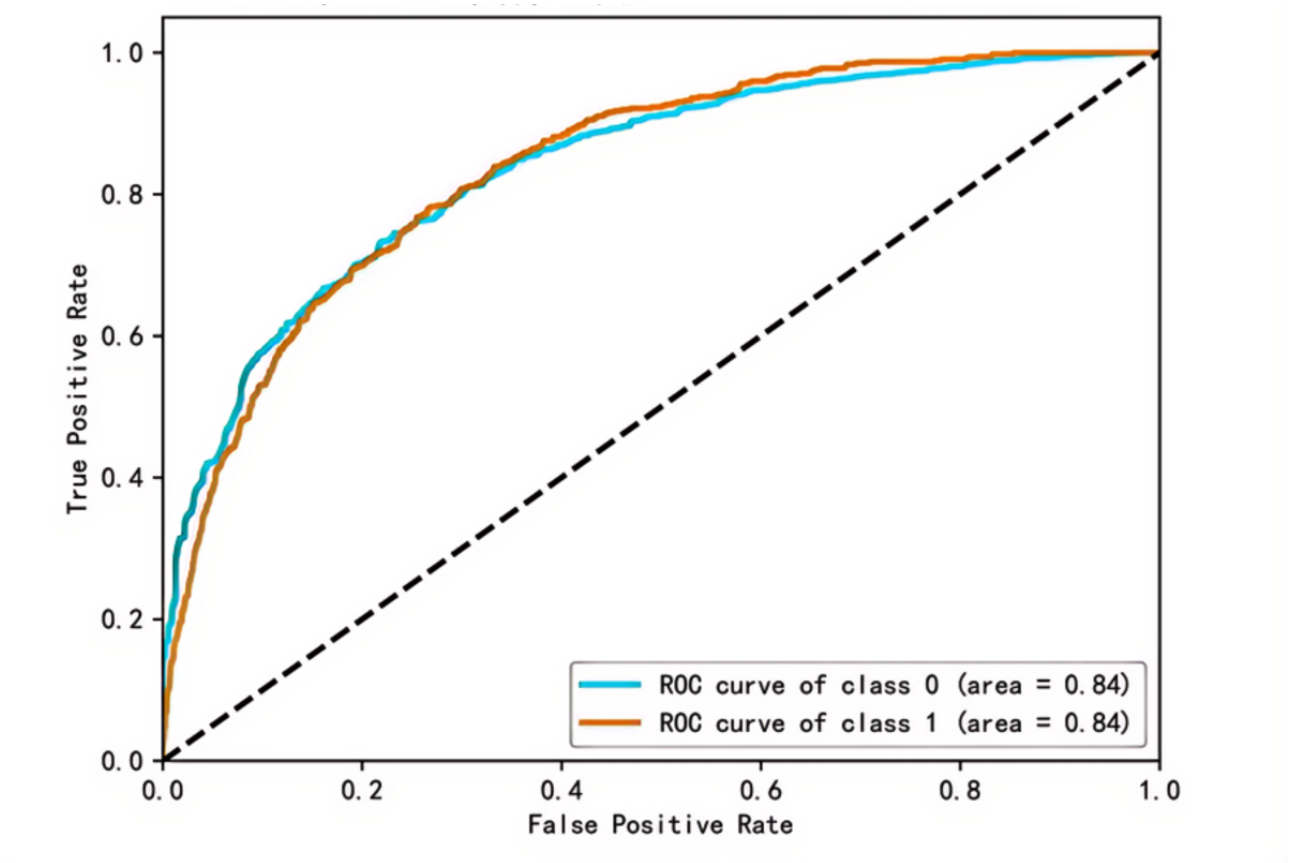
[a]RF: random forest.

[b]LightGBM: Light Gradient Boosting Machine.

[c]XGBoost: Extreme Gradient Boosting.

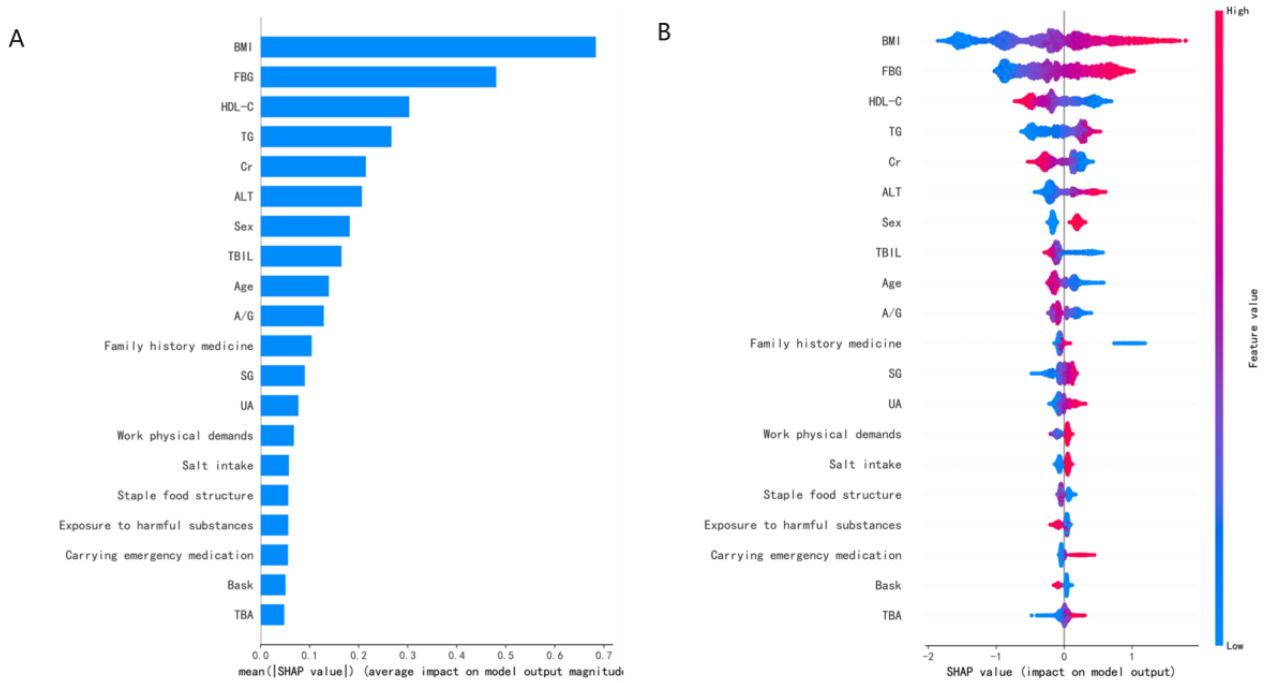
[d]GBDT: Gradient Boosting Machine.

Figure 3. Prediction of insulin resistance in patients with insulin resistance by Light Gradient Boosting Machine, ROC in test set. The area under the curve is 0.8456, indicating that the model has good discriminant ability. ROC: receiver operating characteristic.



XSL•FO
RenderX

Figure 4. Detailed feature importance. (A) Feature importance by Light Gradient Boosting Machine. It shows the importance ranking of various features in the Light Gradient Boosting Machine model. The vertical coordinate (y-axis) shows the top 20 features and (B) shows the explanation of each feature impact on insulin resistance in the prediction model by the Shapley Additive Explanations (SHAP) values in the Light Gradient Boosting Machine algorithm. A/G: albumin/globulin ratio; ALT: alanine aminotransferase; Cr: creatinine; FBG: fasting blood glucose; HDL-C: high-density lipoprotein cholesterol; SG: serum glutamic; TBA: bile acids; TBIL: total bilirubin; TG: triglycerides; UA: uric acid.



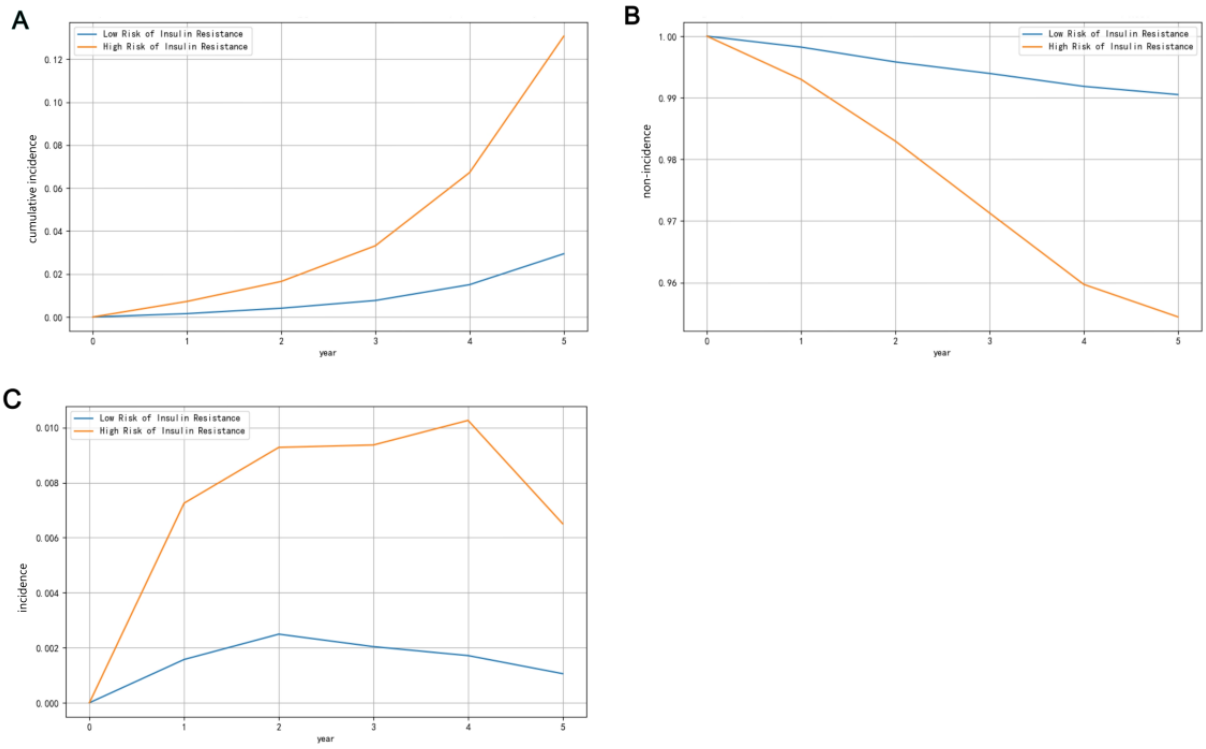
Retrospective Cohort for Validation and Clinical Significance Assessment

The retrospective cohort dataset was used to validate the differential occurrence of diabetes in populations stratified by the model. A total of 20,369 nondiabetic participants were continuously monitored (5101 individuals classified as IR high risk by LightGBM and 15,268 individuals classified as IR low risk), with the incidence of diabetes compared from baseline to 5 years. Out of 5101 high-risk IR participants, 235 (4.6%) developed diabetes, while 137 (0.9%) of 15,268 low-risk IR participants did. This resulted in a HR of 5.1, indicating a significantly higher risk for the IR high risk group compared with the IR Low Risk group. Figure 5A clearly illustrates the relationship between the cumulative incidence of diabetes in the high- and low-risk insulin resistance groups. The high-risk group exhibited a significantly higher cumulative incidence of diabetes compared with the low-risk group, particularly after the second year of follow-up, when the rate of increase accelerated. This suggests that individuals in the high-risk group have a higher likelihood of developing diabetes, and the cumulative effect of this risk becomes more pronounced over time.

The curve for the low-risk group starts at 1 (indicating that 100% of individuals were free of diabetes) and gradually declines over time, although the decrease is relatively small. In contrast, the high-risk group shows a much more rapid decline, especially after the second year, with a more noticeable downward trend (Figure 5B). The line chart depicting the diabetes incidence rates across different IR risk groups (Figure 5C) shows that the growth rate of incidence in the high-risk group is significantly higher than in the low-risk group. The incidence in the high-risk group rises sharply after the second year, reaching its peak by the fifth year. These findings suggest that individuals with high insulin resistance are more likely to develop diabetes within a shorter time frame.

XSL•FO
RenderX

Figure 5. Clinical implication (incidence of diabetes) predicted by Light Gradient Boosting Machine algorithm from a retrospective cohort by the health management center. (A) Kaplan–Meier curve of cumulative incidence of diabetes in different states of insulin resistance. The high-risk insulin resistance group has a significantly higher cumulative incidence of diabetes than the low-risk insulin resistance group. (B) Kaplan–Meier curve of nonincidence of diabetes in different states of insulin resistance. The low-risk insulin resistance group has a significantly higher probability of not developing diabetes than the high-risk insulin resistance group. (C) Incidence of diabetes in different states of insulin resistance. The incidence in the high-risk insulin resistance group is significantly higher than that in the low-risk insulin resistance group, with a sharp increase after the second year.



Discussion

Principal Findings

This study applied multiple machine learning methods using a health check-up database from southern China. Based on questionnaire data and easily accessible, low-cost laboratory measurements, a highly effective predictive model for IR was developed in a population with normal FBG. This ensures that the data required for model implementation is readily available, without the need for additional, expensive diagnostic procedures. This model holds significant value for precision screening of IR and for targeting interventions aimed at managing individual risk factors associated with IR. Compared with other models, LightGBM demonstrated a clear overall advantage in terms of its parameters. LightGBM is a gradient boosting framework that uses decision tree-based learning algorithms. It offers several benefits, including faster training efficiency, lower memory usage, and higher accuracy. In addition, it supports parallel learning and is capable of handling large-scale datasets [13].

Comparison With Previous Work

The previous studies have developed insulin resistance prediction models targeting different ethnic groups and populations, which proves that researchers recognize the necessity of conducting IR prediction. Tsai integrated the National Health and Nutrition Examination Survey public database in the United States and the MAJOR database in Taiwan, China, and established the HOMA-IR ML (XGBoost) prediction model for adults in the two regions. The AUC reached 0.87, the important feature spectrum revealed by SHAP analysis was similar to our results, confirming the determinative roles of factors such as BMI, FBG,TG, HDL-C, and sex [14]. Before this, the team also developed an IR model using samples from 1,229 chronic kidney disease patients sourced from the National Health and Nutrition Examination Survey database. The model included various nutritional and micronutrient indicators, and the overall evaluation metric showed that the XGBoost model achieved an AUC of 0.78 [15]. Zhang et al [16] developed a LightGBM model for IR in a cohort of nearly 10,000 adults aged 40 years or older from certain communities in Hubei, China, with an ROC score of 0.794. The most significant features included FBG, BMI, WC, TG, and sex. In a South Korean study involving 8842 residents, in addition to measurement and laboratory indicators, high-cost, high-quality features such as genetic risk scores, food frequency questionnaires, and nutrients were included, the best-performing model, XGBoost, achieved an AUC of 0.86 [17]. However, these studies either use expensive features or fail to address multicollinearity issues between features. For example, physiological knowledge and typical data support a strong correlation between BMI and waist circumference [18], but these studies did not account for multicollinearity, which could lead to overfitting.

In our preliminary model, using only low-cost questionnaire features did not yield the expected results. However, when

XSL•FO
RenderX

laboratory indicators of liver function and blood lipids were added, the performance improved significantly. Both feature importance rankings based on LightGBM and SHAP value calculations showed that BMI, FBG, HDL-C, and TG were among the top 4 most important features. In fact, a 2003 consensus from the American College of Clinical Endocrinology [19] formally defined IR syndrome as a multisystem disease centered around IR, with key elements including IR or hyperinsulinemia, with or without related cardiovascular-endocrine metabolic abnormalities. These elements include overweight BMI, abnormal glucose tolerance, hypertension, elevated TG, or reduced HDL-C, based on the established epidemiological correlation between IR and these indicators [20,21]. From a pathophysiological perspective, IR and these metabolic indicators have an explainable causal relationship. For example, adipokines secreted by adipose tissue, such as adiponectin [22], tumor necrosis factor alpha [23] can modulate insulin sensitivity through the insulin signaling pathway. In addition, hydrolysis products of elevated triglycerides, such as free fatty acids, can induce insulin resistance by inhibiting insulin signal transduction and reducing the number of insulin receptors on target cells [24]. Low HDL-C improves insulin resistance through reverse cholesterol transport and anti-inflammatory effects [25]. We also found that liver function indicators, such as ALT, bilirubin, and the A/G ratio, play a significant role in IR prediction, with fatty liver being closely linked to IR [26]. These 3 abnormal indicators are common in individuals with fatty liver disease [27], which may indirectly reflect IR. In addition, kidney function indicators showed correlations, which could be related to factors such as physical inactivity, chronic inflammation, oxidative stress, vitamin deficiencies, adipose factor imbalances, and changes in the gut microbiota in populations with kidney damage [28]. Finally, we applied the best LightGBM model results to baseline IR stratification in a retrospective cohort, further validating the significant impact of IR prediction on diabetes incidence. This aims to clarify the practical value of such models. By comparing the incidence of diabetes in low-risk and high-risk IR groups, we observed that individuals at high risk for IR were more likely to develop diabetes in a shorter period, confirming the model's value in assessing blood glucose metabolism.

Limitations and Future Directions

Despite the promising results in IR prediction, our study has several limitations. First, the data source is relatively limited in terms of geographical diversity. Our data came from a health check-up database from the Han Chinese population in Hunan Province in Central Southern China, which may impact the generalizability of the model to other regions or ethnic groups. Future studies could address this by incorporating data from different regions and ethnic populations to further validate the model's generalizability. We would try to develop these ML models into user-friendly web pages or applications that are accessible to the general public and primary care providers, getting more input information and feedback to optimize our models, which is virtually a significant advantage of ML. Second, we tested the clinical implications of this trained model with a retrospective cohort, and have not yet explored the predictive efficiency of the model in prospective research, and we plan to perform it in a follow-up study in the near future. Third, the diagnosis of diabetes in the cohort was based only on the results of FBG, rather than oral glucose tolerance test or combined with postprandial blood glucose or glycated hemoglobin. However, we hope to base diagnoses on the latter as well in further research in the near future. Finally, although 5 ML algorithms were used in this study, there may be other algorithms with better performance that are currently available or soon to be developed. It would be necessary for us to further iterate models with more promising algorithms to improve the predictive performance of the models in the future.

Conclusions

In conclusion, the ML models using the LightGBM algorithm are efficient in predicting IR status in nondiabetic individuals. By leveraging low-cost laboratory indicators and questionnaire data, the model can accurately assess the current IR status in individuals with normal blood glucose levels, helping identify those at high risk of progressing to diabetes within large-scale populations.

Acknowledgments

The authors thank all the staff, and participants of the Hunan University Of Technology and Business for their contributions to the research. This work was supported in part by the Hunan Natural Science Foundation (grant 2025JJ90208), the Chinese Cardiovascular Association-ASCVD fund (grant 2023-CCA-ASCVD-018), and the Project of State Key Clinical Department (grant Z2023058).

Data Availability

The datasets generated or analyzed during this study are not publicly available due to privacy restrictions but are available from the corresponding author on reasonable request.

Authors' Contributions

RM conceived the study. TP and RM wrote the initial draft. TP and RM contributed equally to this work and are considered co–first authors. JC and Y Li reviewed, commented on and revised further drafts. JC, and Y Li are considered co–correspondence authors. Data analysis was conducted by Y Lin with the help of HX and DF. JR, JW, and RM provided financial support. All authors had full access to the data in the study and were responsible for the decision to submit for publication.

XSL•FO
RenderX

Author Y Li is the co-corresponding author of this paper, affilited with School of Mathematics and Statistics, Hunan University of Technology and Business, and can be reached at 2153813825@qq.com.

Conflicts of Interest

None declared.

References

1. Moller DE, Flier JS. Insulin resistance--mechanisms, syndromes, and implications. N Engl J Med 1991 Sep 26;325(13):938-948. [doi: 10.1056/NEJM199109263251307] [Medline: 1881419]
2. Galicia-Garcia U, Benito-Vicente A, Jebari S, et al. Pathophysiology of type 2 diabetes mellitus. Int J Mol Sci 2020 Aug 30;21(17):32872570. [doi: 10.3390/ijms21176275] [Medline: 32872570]
3. Sun H, Saeedi P, Karuranga S, et al. IDF Diabetes Atlas: global, regional and country-level diabetes prevalence estimates for 2021 and projections for 2045. Diabetes Res Clin Pract 2022 Jan;183(109119):109119. [doi: 10.1016/j.diabres.2021.109119] [Medline: 34879977]
4. Parcha V, Heindl B, Kalra R, et al. Insulin resistance and cardiometabolic risk profile among nondiabetic American young adults: insights from NHANES. J Clin Endocrinol Metab 2022 Jan 1;107(1):e25-e37. [doi: 10.1210/clinem/dgab645] [Medline: 34473288]
5. Xing XY, Yang WY, Yang ZJ. The diagnostic significance of homeostasis model assessment of insulin resistance in metabolic syndrome a-mong subjects with different glucose tolerance. Chin J Diabetes 2004(3):31-35 [FREE Full text]
6. DeFronzo RA, Tobin JD, Andres R. Glucose clamp technique: a method for quantifying insulin secretion and resistance. Am J Physiol 1979 Sep;237(3):E214-E223. [doi: 10.1152/ajpendo.1979.237.3.E214] [Medline: 382871]
7. Bonora E, Targher G, Alberiche M, et al. Homeostasis model assessment closely mirrors the glucose clamp technique in the assessment of insulin sensitivity: studies in subjects with various degrees of glucose tolerance and insulin sensitivity. Diabetes Care 2000 Jan;23(1):57-63. [doi: 10.2337/diacare.23.1.57] [Medline: 10857969]
8. Miao R, Dong Q, Liu X, Chen Y, Wang J, Chen J. A cost-effective, machine learning-driven approach for screening arterial functional aging in a large-scale Chinese population. Front Public Health 2024;12(1365479):1365479. [doi: 10.3389/fpubh.2024.1365479] [Medline: 38572001]
9. Ji W, Xue M, Zhang Y, Yao H, Wang Y. A machine learning based framework to identify and classify non-alcoholic fatty liver disease in a large-scale population. Front Public Health 2022;10(846118):846118. [doi: 10.3389/fpubh.2022.846118] [Medline: 35444985]
10. Birk N, Matsuzaki M, Fung TT, et al. Exploration of machine learning and statistical techniques in development of a low-cost screening method featuring the global diet quality score for detecting prediabetes in rural India. J Nutr 2021 Oct 23;151(12 Suppl 2):110S-118S. [doi: 10.1093/jn/nxab281] [Medline: 34689190]
11. Chen N, Fan F, Geng J, et al. Evaluating the risk of hypertension in residents in primary care in Shanghai, China with machine learning algorithms. Front Public Health 2022;10(984621):984621. [doi: 10.3389/fpubh.2022.984621] [Medline: 36267989]
12. Yaribeygi H, Maleki M, Sathyapalan T, Jamialahmadi T, Sahebkar A. Pathophysiology of physical inactivity-dependent insulin resistance: a theoretical mechanistic review emphasizing clinical evidence. J Diabetes Res 2021;2021(7796727):7796727. [doi: 10.1155/2021/7796727] [Medline: 34660812]
13. Guolin Ke QM, Finley T, Wang T, et al. LightGBM: a highly efficient gradient boosting decision tree advances in neural information processing systems. Presented at: Advances in Neural Information Processing Systems 30 (NIPS 2017); Dec 4-9, 2017; California, USA.
14. Tsai SF, Yang CT, Liu WJ, Lee CL. Development and validation of an insulin resistance model for a population without diabetes mellitus and its clinical implication: a prospective cohort study. EClinicalMedicine 2023 Apr;58:101934. [doi: 10.1016/j.eclinm.2023.101934] [Medline: 37090441]
15. Lee CL, Liu WJ, Tsai SF. Development and validation of an insulin resistance model for a population with chronic kidney disease using a machine learning approach. Nutrients 2022 Jul 9;14(14):2832. [doi: 10.3390/nu14142832] [Medline: 35889789]
16. Zhang H, Zeng T, Zhang J, et al. Development and validation of machine learning-augmented algorithm for insulin sensitivity assessment in the community and primary care settings: a population-based study in China. Front Endocrinol 2024;15(1292346):38332892. [doi: 10.3389/fendo.2024.1292346]
17. Park S, Kim C, Wu X. Development and validation of an insulin resistance predicting model using a machine-learning approach in a population-based cohort in Korea. Diagnostics (Basel) 2022 Jan 16;12(1):212. [doi: 10.3390/diagnostics12010212] [Medline: 35054379]
18. Ngueta G, Laouan-Sidi EA, Lucas M. Does waist circumference uncorrelated with BMI add valuable information? J Epidemiol Community Health 2014 Sep;68(9):849-855. [doi: 10.1136/jech-2014-204005] [Medline: 24915975]
19. Bloomgarden ZT. American Association of Clinical Endocrinologists (AACE) consensus conference on the insulin resistance syndrome: 25-26 August 2002, Washington, DC. Diabetes Care 2003 Mar;26(3):933-939. [doi: 10.2337/diacare.26.3.933] [Medline: 12610060]

XSL•FO
RenderX

20. Pei D, Kuo SW, Wu DA, et al. The relationships between insulin resistance and components of metabolic syndrome in Taiwanese Asians. Int J Clin Pract 2005 Dec;59(12):1408-1416. [doi: 10.1111/j.1368-5031.2005.00661.x] [Medline: 16351672]
21. Lee S, Gungor N, Bacha F, Arslanian S. Insulin resistance: link to the components of the metabolic syndrome and biomarkers of endothelial dysfunction in youth. Diabetes Care 2007 Aug;30(8):2091-2097. [doi: 10.2337/dc07-0203] [Medline: 17475936]
22. Ceddia RB, Somwar R, Maida A, Fang X, Bikopoulos G, Sweeney G. Globular adiponectin increases GLUT4 translocation and glucose uptake but reduces glycogen synthesis in rat skeletal muscle cells. Diabetologia 2005 Jan;48(1):132-139. [doi: 10.1007/s00125-004-1609-y] [Medline: 15619075]
23. Chuang CC, Bumrungpert A, Kennedy A, et al. Grape powder extract attenuates tumor necrosis factor α-mediated inflammation and insulin resistance in primary cultures of human adipocytes. J Nutr Biochem 2011 Jan;22(1):89-94. [doi: 10.1016/j.jnutbio.2009.12.002] [Medline: 20382011]
24. Kovacs P, Stumvoll M. Fatty acids and insulin resistance in muscle and liver. Best Pract Res Clin Endocrinol Metab 2005 Dec;19(4):625-635. [doi: 10.1016/j.beem.2005.07.003] [Medline: 16311221]
25. Drew BG, Rye KA, Duffy SJ, Barter P, Kingwell BA. The emerging role of HDL in glucose metabolism. Nat Rev Endocrinol 2012 Jan 24;8(4):237-245. [doi: 10.1038/nrendo.2011.235] [Medline: 22271188]
26. Goto T, Onuma T, Takebe K, Kral JG. The influence of fatty liver on insulin clearance and insulin resistance in non-diabetic Japanese subjects. Int J Obes Relat Metab Disord 1995 Dec;19(12):841-845. [Medline: 8963349]
27. Marchesini G, Brizi M, Bianchi G, et al. Nonalcoholic fatty liver disease: a feature of the metabolic syndrome. Diabetes 2001 Aug;50(8):1844-1850. [doi: 10.2337/diabetes.50.8.1844] [Medline: 11473047]
28. Spoto B, Pisano A, Zoccali C. Insulin resistance in chronic kidney disease: a systematic review. Am J Physiol Renal Physiol 2016 Dec 1;311(6):F1087-F1108. [doi: 10.1152/ajprenal.00340.2016] [Medline: 27707707]

Abbreviations

A/G: albumin/globulin ratio
ALB: serum albumin
ALT: alanine aminotransferase
AST: aspartate aminotransferase
AUC: area under the curve
BUN: blood urea nitrogen
DBIL: direct bilirubin
DBP: diastolic blood pressure
FBG: fasting blood glucose
GBDT: Gradient Boosting Machine
GLO: serum globulin
HDL-C: high-density lipoprotein cholesterol
HOMA: Homeostasis Model Assessment
IR: insulin resistance
LDL-C: low-density lipoprotein cholesterol
LightGBM: Light Gradient Boosting Machine
ML: machine learning
RF: random forest
ROC: receiver operating characteristic
SBP: systolic blood pressure
SHAP: Shapley Additive Explanations
SMOTE: synthetic minority over-sampling technique
Sr: serum creatinine
TBA: bile acids
TBIL: total bilirubin
TC: total cholesterol
TG: triglycerides
TP: total proteintotal
UA: uric acid
WC: waist circumference
XGBoost: Extreme Gradient Boosting

XSL•FO
RenderX

Edited by A Coristine; submitted 06.02.25; peer-reviewed by F Lin, L Xiao; revised version received 27.04.25; accepted 28.04.25; published 13.06.25.

Please cite as:
Peng T, Miao R, Xiong H, Lin Y, Fan D, Ren J, Wang J, Li Y, Chen J
Prediction of Insulin Resistance in Nondiabetic Population Using LightGBM and Cohort Validation of Its Clinical Value: Cross-Sectional and Retrospective Cohort Study
JMIR Med Inform 2025;13:e72238
URL: https://medinform.jmir.org/2025/1/e72238
doi:10.2196/72238

© Ting Peng, Rujia Miao, Hao Xiong, Yanhui Lin, Duzhen Fan, Jiayi Ren, Jiangang Wang, Yuan Li, Chen Jianwen. Originally published in JMIR Medical Informatics (https://medinform.jmir.org), 13.6.2025. This is an open-access article distributed under the terms of the Creative Commons Attribution License (https://creativecommons.org/licenses/by/4.0/), which permits unrestricted use, distribution, and reproduction in any medium, provided the original work, first published in JMIR Medical Informatics, is properly cited. The complete bibliographic information, a link to the original publication on https://medinform.jmir.org/, as well as this copyright and license information must be included.

XSL•FO
RenderX

Development and Validation of a Predictive Model for Activities of Daily Living Dysfunction in Older Adults: Retrospective Analysis of Data From the China Health and Retirement Longitudinal Study

Fangbo Lin[1,2], MD; Chao Liu[1*], MD; Hua Liu[1*], MD

[1]Rehabilitation Medicine Department, The Affiliated Changsha Hospital of Xiangya School of Medicine, Central South University, No. 311 Yinpan Road, Hunan Province, Changsha, China

[2]Neurology Department, Fujian Medical University Union Hospital, Fuzhou, China

[*]these authors contributed equally

Corresponding Author:
Chao Liu, MD
Rehabilitation Medicine Department, The Affiliated Changsha Hospital of Xiangya School of Medicine, Central South University, No. 311 Yinpan Road, Hunan Province, Changsha, China

Abstract

Background: The global aging crisis has precipitated significant public health challenges, including rising chronic diseases, economic burdens, and labor shortages, particularly in China. Activities of daily living (ADL) dysfunction, affecting over 40 million Chinese older adults (16% of the aging population), severely compromises independence and quality of life while increasing health care costs and mortality. ADL dysfunction encompasses both basic ADL (BADL) and instrumental ADL (IADL), which assess fundamental self-care and complex environmental interactions, respectively. With projections indicating 65 million cases by 2030, there is an urgent need for tools to predict ADL impairment and enable early interventions.

Objective: This study aimed to develop and validate a predictive nomogram model for ADL dysfunction in older adults using nationally representative data from the China Health and Retirement Longitudinal Study (CHARLS). The model seeks to integrate key risk factors into an accessible clinical tool to facilitate early identification of high-risk populations, guiding targeted health care strategies and resource allocation.

Methods: A retrospective analysis was conducted on 5081 CHARLS wave 3 participants (2015 - 2016) aged 60 - 80 years. Participants were categorized into ADL dysfunction (n=1743) or normal (n=3338) groups based on BADL and IADL assessments. Forty-six variables spanning demographics, health status, biomeasures, and lifestyle were analyzed. After addressing missing data via multiple imputation, Least Absolute Shrinkage and Selection Operator (LASSO) regression and multivariable logistic regression identified 6 predictors. Model performance was evaluated using receiver operating characteristic curves, calibration plots, decision curve analysis, and Shapley additive explanations (SHAP) for interpretability.

Results: The final model incorporated 6 predictors: the 10-item Center for Epidemiologic Studies Depression Scale depression score, number of painful areas, left-hand grip strength, 2.5-m walking time, weight, and cystatin C level. The nomogram demonstrated robust discriminative power, with area under the curve values of 0.77 (95% CI 0.76 - 0.79) in both the training and testing sets. Calibration curves confirmed strong agreement between predicted and observed outcomes, while decision curve analysis highlighted superior clinical use over “treat-all” or “treat-none” approaches. SHAP analysis revealed depressive symptoms and physical frailty markers (eg, slow walking speed and low grip strength) as dominant predictors, aligning with existing evidence on ADL decline mechanisms.

Conclusions: This study presents a validated nomogram for predicting ADL dysfunction in older adult populations, combining psychological, physical, and biochemical markers. The tool enables risk stratification, supports personalized interventions, and addresses gaps in geriatric care by emphasizing modifiable factors like pain management, depression, and mobility training. Despite limitations such as regional data biases and the retrospective design, the model offers scalable clinical value. Future research should incorporate social, environmental, and cognitive factors to enhance precision and generalizability.

(JMIR Med Inform 2025;13:e73030) doi:10.2196/73030

KEYWORDS

activities of daily living; elderly; risk prediction; nomogram model; frailty; CHARLS; China Health and Retirement Longitudinal Study

XSL•FO
RenderX

Introduction

The aging of the population, which has led to an increase in chronic diseases, financial burdens, and labor shortages, has become a significant public health concern and poses a major challenge to public health systems in China [1]. Aging refers to the gradual process of growing older, involving a series of changes over time, including physical, mental, and social transformations [2]. Each year, approximately 10% of older adults who were previously not disabled develop dysfunction in activities of daily living (ADL) [3]. A previous study estimated that more than 40 million older adults in China, or over 16% of the older adult population, currently experience ADL dysfunction. This number is expected to rise to 65 million by 2030 [4]. ADL dysfunction significantly affects the quality of life of older adults and is associated with increased health care expenditures, higher rates of institutionalization, and elevated mortality rates [5-7]. For many older adults, maintaining their independence for as long as possible is a key priority.

ADL dysfunction is typically assessed using the basic activities of daily living (BADL) and instrumental activities of daily living (IADL) scales. The BADL scale, which is widely used, assesses fundamental self-care abilities such as bathing, dressing, eating, and engaging in indoor activities [8]. To evaluate more complex aspects of daily living, Lawton and Brody [9] developed the IADL scale, which measures an individual's ability to perform tasks that require more interaction with the environment, such as making telephone calls, shopping, cooking, and doing household chores. Given the strong correlation between BADL and IADL scores and overall functional ability [10], it is crucial to identify the factors contributing to ADL dysfunction in the older adults and to understand the characteristics of those affected.

A nomogram is a precise graphical representation of a predictive model based on regression analysis. It integrates multiple variables and visually presents the estimated probability of an event occurring. In this study, we developed and validated a comprehensive predictive model for assessing the risk of ADL dysfunction among older adults, using extensive data from the China Health and Retirement Longitudinal Survey (CHARLS). Subsequently, we created a nomogram that incorporates all selected risk factors, enabling rapid identification of older adults at risk of ADL dysfunction. The establishment of this predictive tool is expected to facilitate early detection, allowing for timely interventions that may reduce the incidence of ADL dysfunction in this population.

Methods

Study Population

This study is a retrospective study that used survey data from CHARLS wave 3, which were collected between August 2015 and January 2016. A total of 5081 samples were selected based on inclusion and exclusion criteria. Participants were included if they were aged between 60 and 80 years and were not missing data for essential variables. Exclusion criteria included individuals who were unwilling or unable to complete the survey. After applying these criteria, a total of 5081 participants were included in the analysis. Using the BADL and IADL assessment scales, participants were categorized based on their functional abilities. The BADL scale includes 6 basic tasks: dressing, bathing, eating, getting in and out of bed, using the toilet, and controlling urination and defecation. The IADL scale measures more complex activities, such as housework, food preparation, shopping, financial management, and medication adherence. Individuals with 1 or more disabilities in either the BADL or IADL domains were classified as having ADL dysfunction, while those without disabilities in either domain were classified as having normal ADL. Based on this classification, the participants were divided into 2 groups: the ADL normal group (n=3338) and the ADL dysfunction group (n=1743).

Candidate Predictor Variables

Informed by clinical experience and previous studies [11,12], we analyzed 46 potential variables that might be associated with the risk of ADL dysfunction. These variables spanned various domains, including demographic characteristics, health status, lifestyle factors, biochemical indicators, and functional status. The variables selected for inclusion in this study are as follows: sex (1=male and 0=female), age, marital status (1=married and 0=unmarried), disability status (1=disability and 0=nondisability), presence of chronic disease (1=yes and 0=no), hypertension (1=yes and 0=no), diabetes mellitus (1=yes and 0=no), alcohol consumption (1=yes and 0=no), smoking status (1=yes and 0=no), history of falls (1=yes and 0=no), hip fracture (1=yes and 0=no), walking time (measured by the time required to walk 2.5 m), systolic and diastolic blood pressure, pulse rate, left and right hand grip strength, height, weight, waist circumference, BMI, respiratory function, the 10-item Center for Epidemiologic Studies Depression Scale (CESD-10), number of painful areas (eg, headache, shoulder pain, back pain, leg pain, and so on), sleep duration, physical activity (eg, visiting friends, playing games, and participating in community activities), blood test parameters (eg, white blood cell count, red blood cell volume, platelet count, glucose, and cholesterol levels), and several measures of social and cognitive factors (eg, educational level, sociality, and the triglyceride-glucose index. These variables were included for their potential relevance to ADL dysfunction.

Statistical Analysis

Statistical analyses and figure generation were performed using R software (R Foundation for Statistical Computing). For variables with >20% missing data, those samples were excluded from the analysis. For variables with <20% missing data, the Multivariate Imputation by Chained Equations package was used to perform 5-fold imputation, and the imputed data most consistent with the sample trends were selected. Categorical variables were summarized using frequencies and percentages, while continuous variables were described by means and SDs. Differences between groups were assessed using *t* tests, chi-square tests, and nonparametric tests as appropriate. Nonparametric tests were used when data did not meet the assumptions for parametric testing, ensuring robustness and reliability of the analysis.

XSL•FO
RenderX

The data were split into training (n=3048) and testing (n=2033) sets using a 6:4 ratio. The training set was used to identify key predictors for ADL dysfunction. Initially, the Least Absolute Shrinkage and Selection Operator (LASSO) regression was applied to identify potential risk factors, minimizing multicollinearity and selecting the most predictive factors. Subsequently, a 10-fold cross-validation procedure was performed to determine the optimal tuning parameter (λ) for LASSO regression. Predictors selected by LASSO were then used in multivariate logistic regression, and a nomogram was constructed to visualize the influence of these predictors on the risk of ADL dysfunction. To simplify the model, predictors with minimal influence were discarded, and the remaining predictors were reanalyzed using multivariate logistic regression, followed by the construction of a final nomogram.

To evaluate the predictive performance of the model, several statistical tools were used, including receiver operating characteristic (ROC) curves, area under the curve (AUC), calibration plots, and decision curve analysis (DCA). ROC curves were used to assess the trade-off between sensitivity and specificity, while AUC quantified the model's overall discriminatory power. Calibration plots evaluated the agreement between predicted probabilities and actual outcomes, ensuring the model's reliability. DCA assessed the clinical use of the model by comparing the net benefits of true positive predictions against the harms of false positives and negatives. These comprehensive evaluation methods provided a assessment of the model's accuracy and potential clinical impact.

Finally, to further explain the model's feature variables, Shapley additive explanations (SHAP) values were calculated for each feature, and the predictive importance of these variables was visually represented through global importance plots, swarm plots, waterfall plots, and force plots. These visualizations facilitated a better understanding of how individual features contributed to the model's predictions.

Ethical Considerations

This retrospective study used anonymized data from wave 3 of the CHARLS database, which was ethically approved in June 2008 by the Biomedical Ethics Review Committee of Peking University (IRB00001052–11015) [13]. The individual data were anonymized before the study. In this study, patients and the public were not involved in the design, conduct, reporting, or dissemination plans of the research. All participants provided informed consent, and the study adheres to the ethical principles outlined in the Declaration of Helsinki.

Results

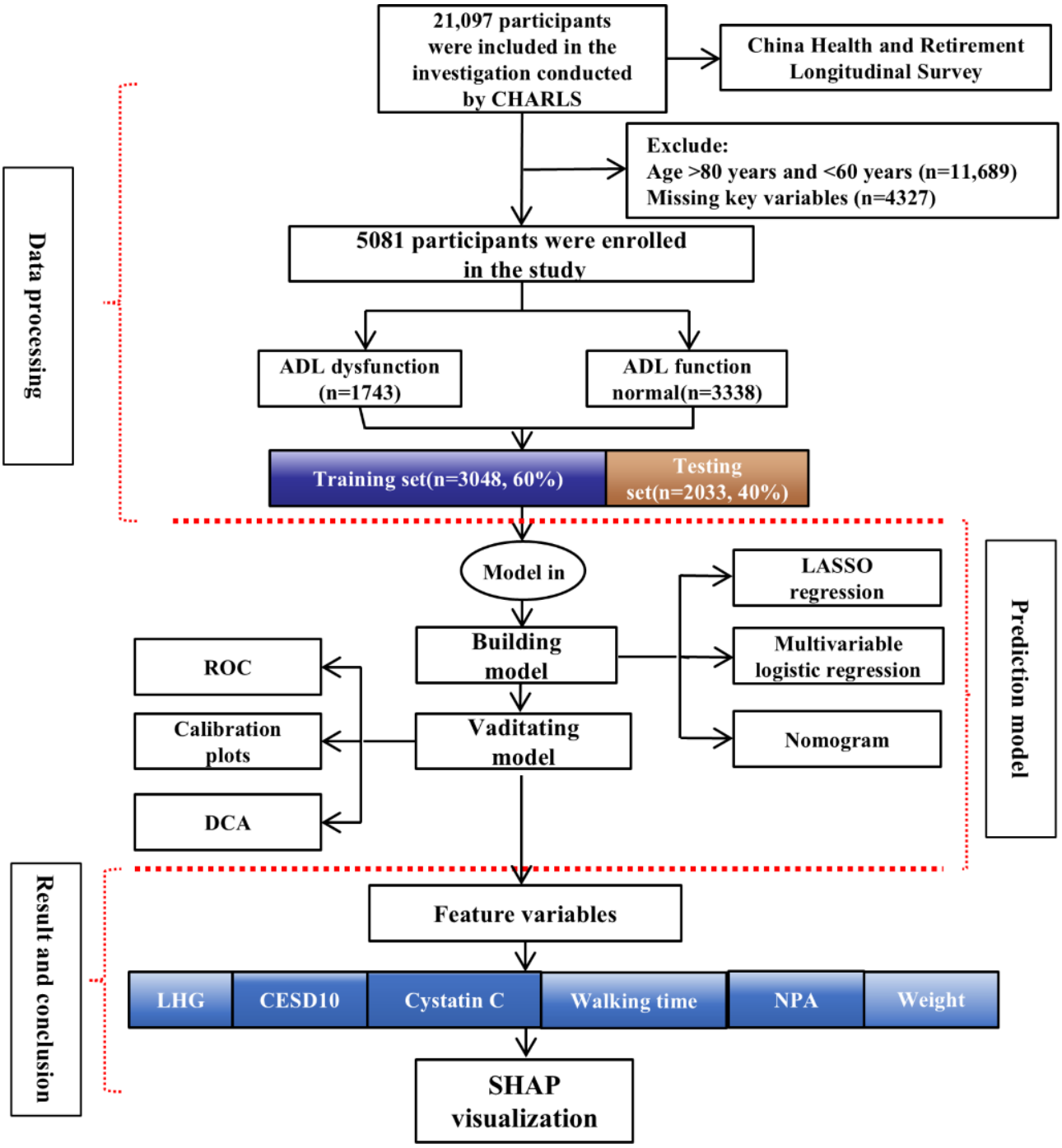
Flowchart

The study flowchart is presented in Figure 1.

This retrospective cohort analysis of 5081 older adults (aged 60‐80 years old) across China evaluated inclusion and exclusion criteria and data imputation methods for developing a predictive nomogram. Participants were classified into ADL normal (no BADL/IADL disability) and ADL dysfunction (≥1 disability) groups using validated functional assessment scales.

XSL•FO
RenderX

Figure 1. Flowchart of study cohort selection from CHARLS wave 3 (2015 - 2016) for developing the activities-of-daily-living dysfunction prediction model. ADL: activities of daily living; CESD-10: 10-item Center for Epidemiologic Studies Depression Scale; CHARLS: China Health and Retirement Longitudinal Survey; DCA: decision curve analysis; LASSO: Least Absolute Shrinkage and Selection Operator; LHG: left grip strength; NPA: number of pain areas; ROC: receiver operating characteristic curve; SHAP: Shapley additive explanations.



Baseline Characteristics

The study sample comprised 5081 participants, with an average age of 67 years, and a male-to-female ratio of 1.03. Of these, 3338 participants were classified into the ADL normal group, and 1743 participants were classified into the ADL dysfunction group. Significant clinical and sociodemographic differences were observed between the 2 groups, as summarized in Table 1. Key variables with significant differences (P<.05) include marital status, disability status, chronic diseases, hypertension, diabetes mellitus, alcohol consumption, smoking status, history of falls, hip fractures, walking time, systolic blood pressure, pulse rate, left and right hand grip strength, height, weight, waist circumference, respiratory function, depression (CESD-10), number of painful areas, sleep duration, physical activity, mean red blood cell volume, total cholesterol, C-reactive protein, glycosylated hemoglobin, uric acid, hematocrit, hemoglobin, cystatin C, sociality, and educational level.

In the comparative analysis of 5081 participants aged 60 - 80 years old from the CHARLS, participants were stratified into the ADL normal (n=3338) and ADL dysfunction (n=1743) groups. Variables included demographics (age, sex, and marital status), comorbidities (hypertension, diabetes, and chronic

XSL•FO
RenderX

diseases), lifestyle factors (smoking and alcohol use), biomeasures (grip strength, walking time, and cystatin C), and functional parameters. Significant differences (P<.05) between groups were highlighted, reflecting associations with ADL impairment in Chinese older adults.

XSL•FO
RenderX

Table . Baseline sociodemographic and clinical characteristics of older adults (ADL[a] normal group vs ADL dysfunction group) in the China Health and Retirement Longitudinal Survey wave 3 (China, 2015 - 2016).

Characteristics	ADL function normal group (n=3338)	ADL dysfunction group (n=1743)	*P* value
Gender, n (%)			<.001
Male	1865 (55.9)	713 (40.9)	
Female	1473 (44.1)	1030 (59.1)	
Marital stauts, n (%)			<.001
Yes	2814 (84.3)	1391 (79.8)	
No	524 (15.7)	352 (20.2)	
Hypertension, n (%)			<.001
Yes	1220 (36.5)	808 (46.4)	
No	2118 (63.5)	935 (53.6)	
Diabetes, n (%)			<.001
Yes	338 (10.1)	260 (14.9)	
No	3000 (89.9)	1483 (85.1)	
Disability, n (%)			<.001
Yes	1033 (30.9)	946 (54.3)	
No	2305 (69.1)	797 (45.7)	
Drink, n (%)			<.001
Yes	1669 (50.0)	774 (44.4)	
No	1669 (50.0)	969 (55.6)	
Smoke, n (%)			<.001
Yes	1711 (51.3)	730 (41.9)	
No	1627 (48.7)	1013 (58.1)	
Fall, n (%)			<.001
Yes	489 (14.6)	503 (28.9)	
No	2849 (85.4)	1240 (71.1)	
Hip fracture, n (%)			<.001
Yes	47 (1.4)	64 (3.7)	
No	3291 (98.6)	1679 (96.3)	
Chronic, n (%)			<.001
Yes	2668 (79.9)	1593 (91.4)	
No	670 (20.3)	150 (8.6)	
Walking time (second), mean (SD)	3.19 (0.95)	3.73 (1.48)	<.001
Systolic pressure (mm Hg), mean (SD)	130.12 (19.96)	131.62 (20.59)	.01
Diastolic pressure (mm Hg), mean (SD)	74.59 (11.56)	74.58 (11.46)	.96
Pulse (beats per min), mean (SD)	73.30 (10.7)	74.26 (11.63)	.003
Left hand grip (N), mean (SD)	28.62 (9.16)	23.74 (9.52)	<.001
Right hand grip (N), mean (SD)	29.82 (9.71)	24.98 (9.57)	<.001
Height (m), mean (SD)	1.58 (0.09)	1.55 (0.1)	<.001
Weight (Kg), mean (SD)	59.05 (11.81)	58.04 (11.53)	.003
Waist (cm), mean (SD)	84.54 (13.47)	85.37 (14.85)	.04

XSL•FO
RenderX

Characteristics	ADL function normal group (n=3338)	ADL dysfunction group (n=1743)	*P* value
BMI (kg/m^2), mean (SD)	24.12 (18.48)	24.44 (11.62)	.50
Respiratory test value (ml), mean (SD)	308.28 (120.26)	266.65 (105.92)	<.001
Self-rated depression scale (score), mean (SD)	6.50 (5.35)	11.52 (6.99)	<.001
Number of painful areas (score), mean (SD)	0.93 (2.38)	3.41 (4.35)	<.001
Sleep hours, mean (SD)	6.49 (1.9)	5.86 (2.2)	<.001
Activity (score), mean (SD)	0.87 (1.03)	0.74 (0.92)	<.001
White blood cell (10^12/L), mean (SD)	5.92 (1.76)	6.07 (1.91)	.006
Mean red blood cell volume (fl), mean (SD)	92.45 (7.51)	91.73 (8.14)	.002
Platelet (10^9/L), mean (SD)	198.09 (72.49)	201.84 (77.99)	.09
Blood urea nitrogen (mg/dl), mean (SD)	16.04 (4.62)	16.28 (5.06)	.08
Glucose (mg/dl), mean (SD)	104.23 (33.34)	104.74 (37.14)	.62
Blood creatinine (mg/dl), mean (SD)	0.84 (0.25)	0.84 (0.39)	.98
Total cholesterol (mg/dl), mean (SD)	184.37 (35.76)	187.06 (37.53)	.01
Triglyceride (mg/dl), mean (SD)	135.64 (84.62)	140.27 (87.66)	.07
High density cholesterol (mg/dl), mean (SD)	51.58 (12.01)	51.99 (12.29)	.25
Low density cholesterol (mg/dl), mean (SD)	103.30 (28.60)	104.38 (29.43)	.20
C-reactive protein (mg/l), mean (SD)	2.62 (4.72)	3.14 (7.08)	.002
Glycosylated hemoglobin (%), mean (SD)	6.03 (0.96)	6.12 (1.11)	.002
Uric acid (mg/dl), mean (SD)	5.08 (1.39)	4.93 (1.44)	<.001
Hematocrit (%), mean (SD)	41.73 (5.34)	40.72 (5.52)	<.001
Hemoglobin (g/dl), mean (SD)	13.75 (1.80)	13.42 (1.85)	<.001
Cystatin C (mg/l), mean (SD)	0.89 (0.2)	0.93 (0.31)	<.001
Sociality (score), mean (SD)	0.91 (1.11)	0.76 (0.95)	<.001
Age (years), mean (SD)	66.77 (5.17)	67.73 (5.41)	<.001
Educational level, mean (SD)	1.87 (0.99)	1.54 (0.82)	<.001
Triglyceride-glucose index, mean (SD)	8.68 (0.62)	8.72 (0.63)	.07
Triglyceride glucose–BMI, mean (SD)	210.02 (155.18)	213.70 (99.89)	.36

[a]ADL: activities of daily living.

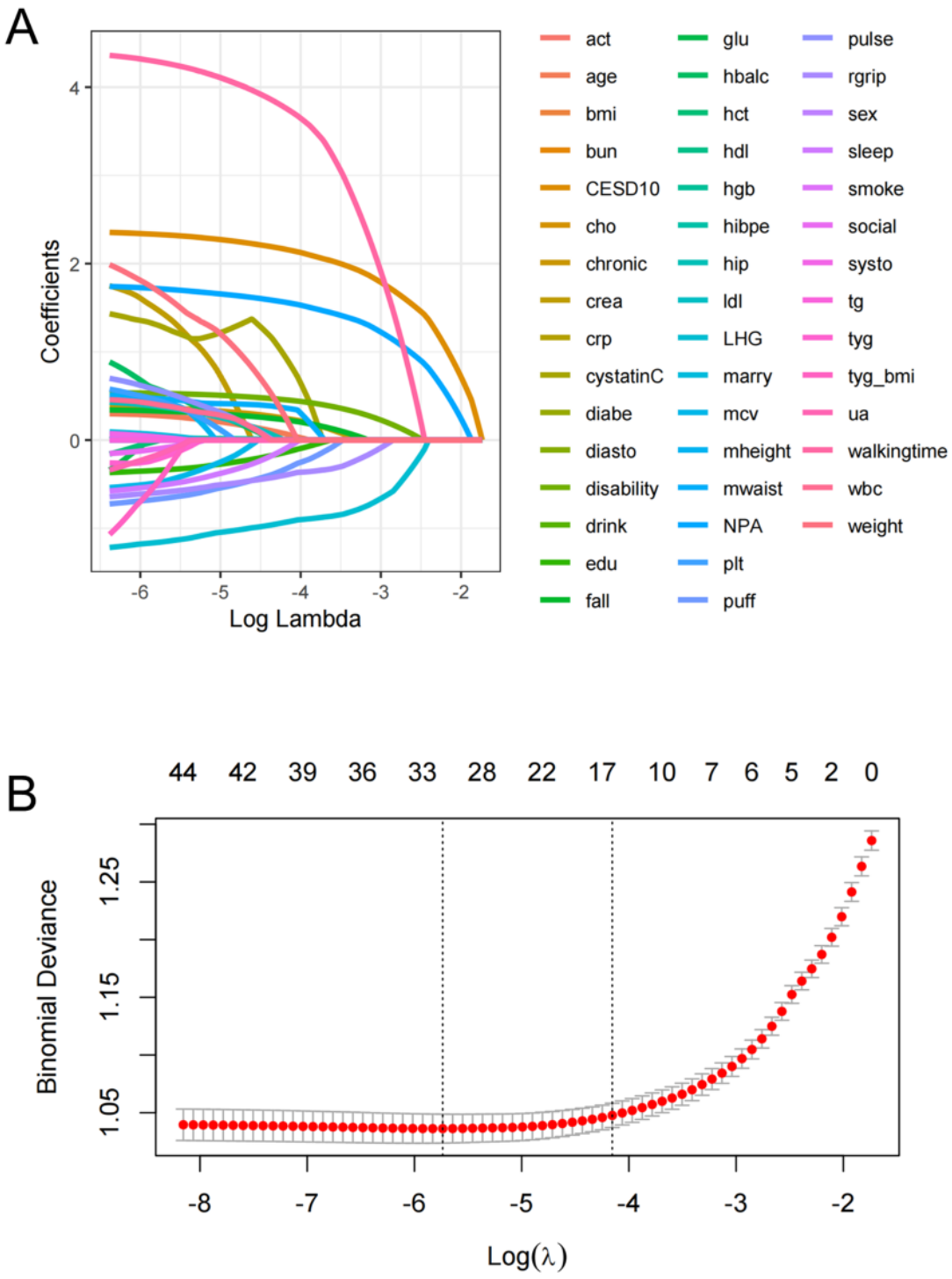
Development of the Predictive Nomogram

Participants were randomly divided into a training set (n=3048) and a testing set (n=2033) in a 6:4 ratio. LASSO regression was applied to identify the most important predictors of ADL dysfunction. After performing 10-fold cross-validation, predictors with nonzero coefficients were selected (Figures 2A and 2B). These predictors were then incorporated into a multivariate logistic regression model, factors with *P* values>.05 (eg, respiratory function and sleep duration) were removed in the multivariate logistic regression. Ultimately, 6 independent predictors were retained: 2.5-m walking time, left hand grip strength, CESD-10 score, number of painful areas, weight, and cystatin C. Based on these predictors, a nomogram was

XSL•FO
RenderX

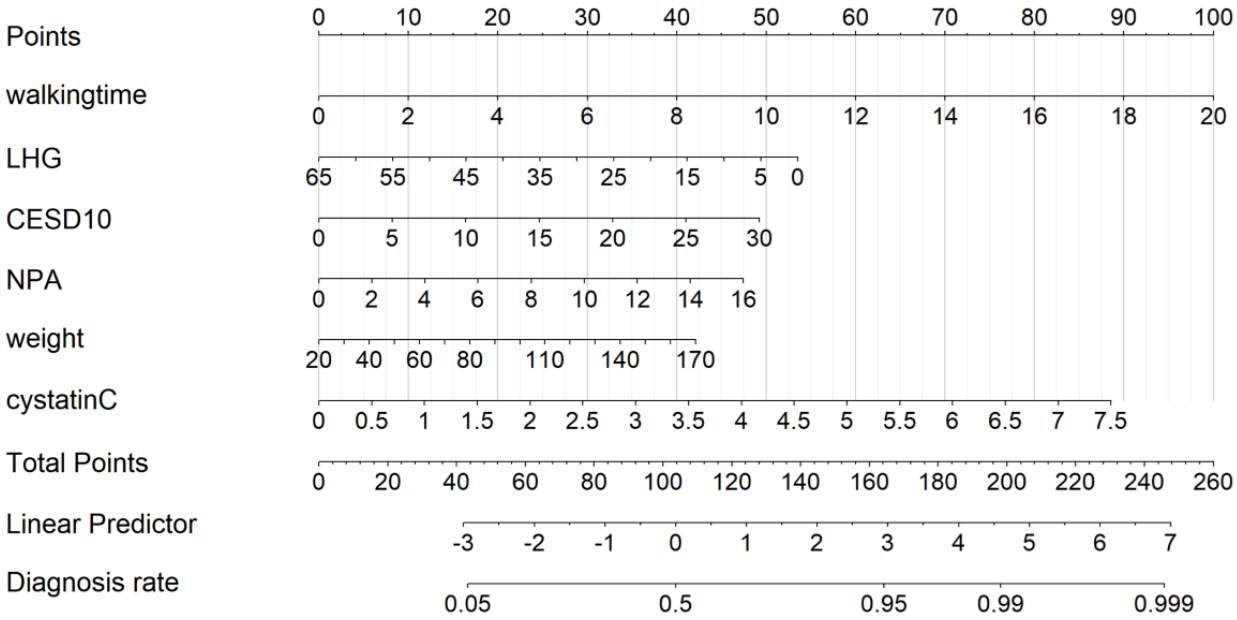
constructed to estimate the risk of ADL dysfunction in the older adults. The nomogram visually represents the contribution of each factor to the likelihood of dysfunction, with the bottom scale indicating the predicted probability. Higher scores correspond to a greater risk of ADL dysfunction (Figure 3).

Figure 2. Least Absolute Shrinkage and Selection Operator regression feature selection for ADL dysfunction predictors in China Health and Retirement Longitudinal Survey (2015 - 2016): (A) Coefficient profiles of 46 candidate variables analyzed via Least Absolute Shrinkage and Selection Operator regression to identify predictors of ADL dysfunction in Chinese older adults and (B) 10-fold cross-validation for optimal lambda (λ) selection, minimizing partial likelihood deviance. Features with nonzero coefficients (eg, Center for Epidemiologic Studies Depression Scale, walking time, and cystatin C) were retained for nomogram development. ADL: activities of daily living; CESD10: 10-item Center for Epidemiologic Studies Depression Scale; LHG: left grip strength.



XSL•FO
RenderX

Figure 3. Nomogram for predicting activities-of-daily-living dysfunction risk in Chinese older adults (China Health and Retirement Longitudinal Survey, 2015 - 2016). Graphical tool integrating six predictors (Center for Epidemiologic Studies Depression Scale, pain areas, left grip strength, 2.5-m walking time, weight, and cystatin C) to estimate individualized risk of activities-of-daily-living dysfunction. Scores for each variable are summed to calculate total points, corresponding to predicted probability on a 0% - 100% scale. Derived from 3048 training set participants in the China Health and Retirement Longitudinal Survey cohort. CESD10: 10-item Center for Epidemiologic Studies Depression Scale; LHG: left grip strength; NPA: number of pain areas; walkingtime: 2.5-meter walking time.



Performance and Clinical Application of the Nomogram

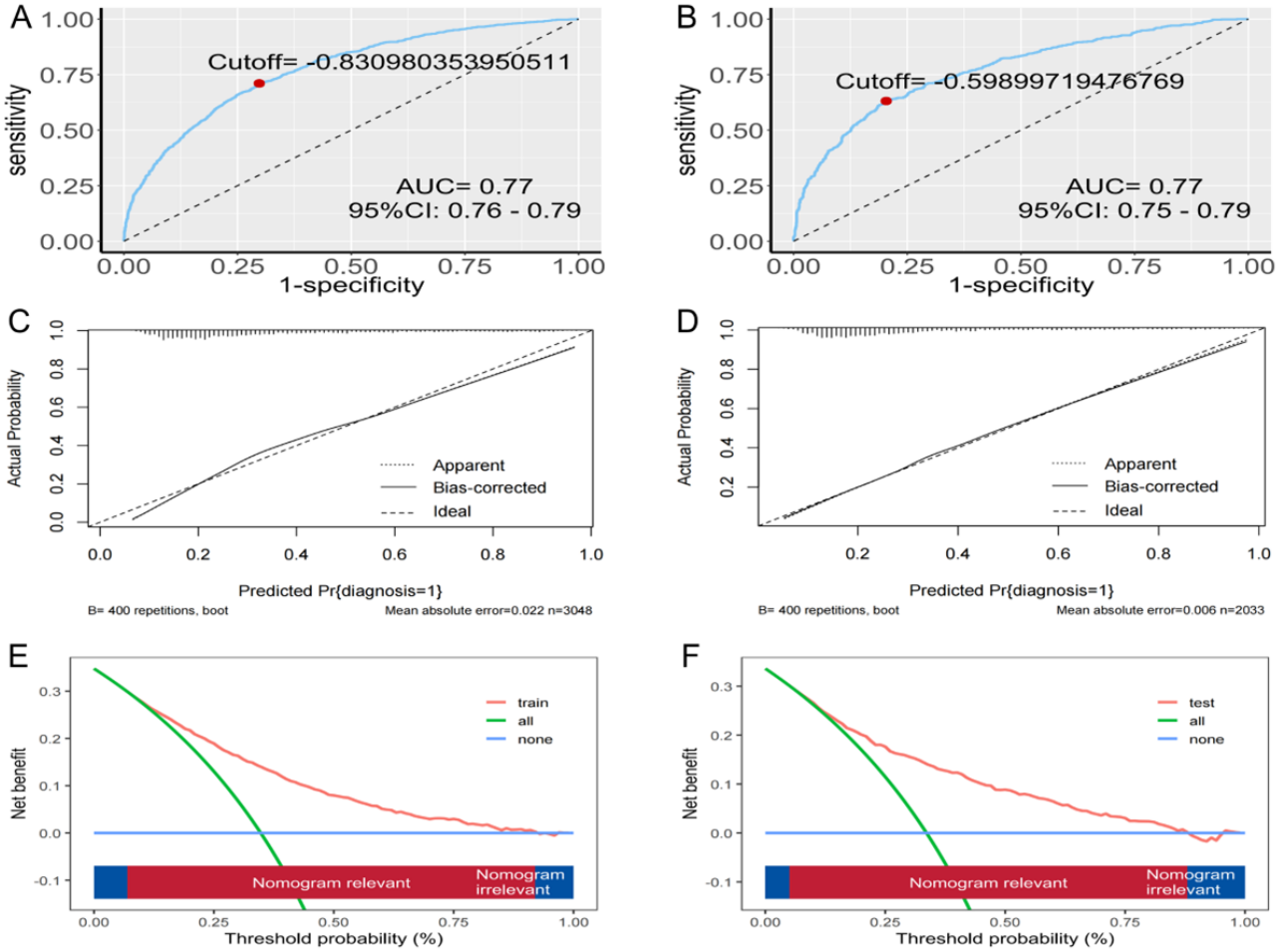
To evaluate the performance of the nomogram, the AUC values were calculated. In the training set, the AUC was 0.77 (95% CI 0.76 - 0.79), and in the testing set, the AUC was 0.77 (95% CI 0.75 - 0.79), demonstrating the model's high predictive accuracy (Figures 4A and 4B).

The nomogram's calibration curves show agreement between the predicted and observed probabilities in both the training and testing sets, further confirming the model's accuracy and reliability (Figures 4C and 4D).

In addition, DCA was used to assess the clinical use of the model. The results indicated that the model's net benefit in the internal validation set was better than both the "treat-all" and "treat-none" scenarios, highlighting its clinical use and predictive performance (Figures 4E and 4F).

XSL•FO
RenderX

Figure 4. Predictive performance and clinical use of the activities-of-daily-life dysfunction nomogram: (A-B) receiver operating characteristic curves showing discriminative power (AUC 0.77, 95% CI 0.76 - 0.79) for training (A) and testing (B) sets in China Health and Retirement Longitudinal Survey (2015 - 2016); (C-D) calibration plots demonstrating agreement between predicted and observed activities-of-daily-living dysfunction probabilities; and (E-F) decision curve analysis comparing net clinical benefits of the nomogram against "treat-all" and "treat-none" strategies in Chinese older adults. AUC: area under the curve.



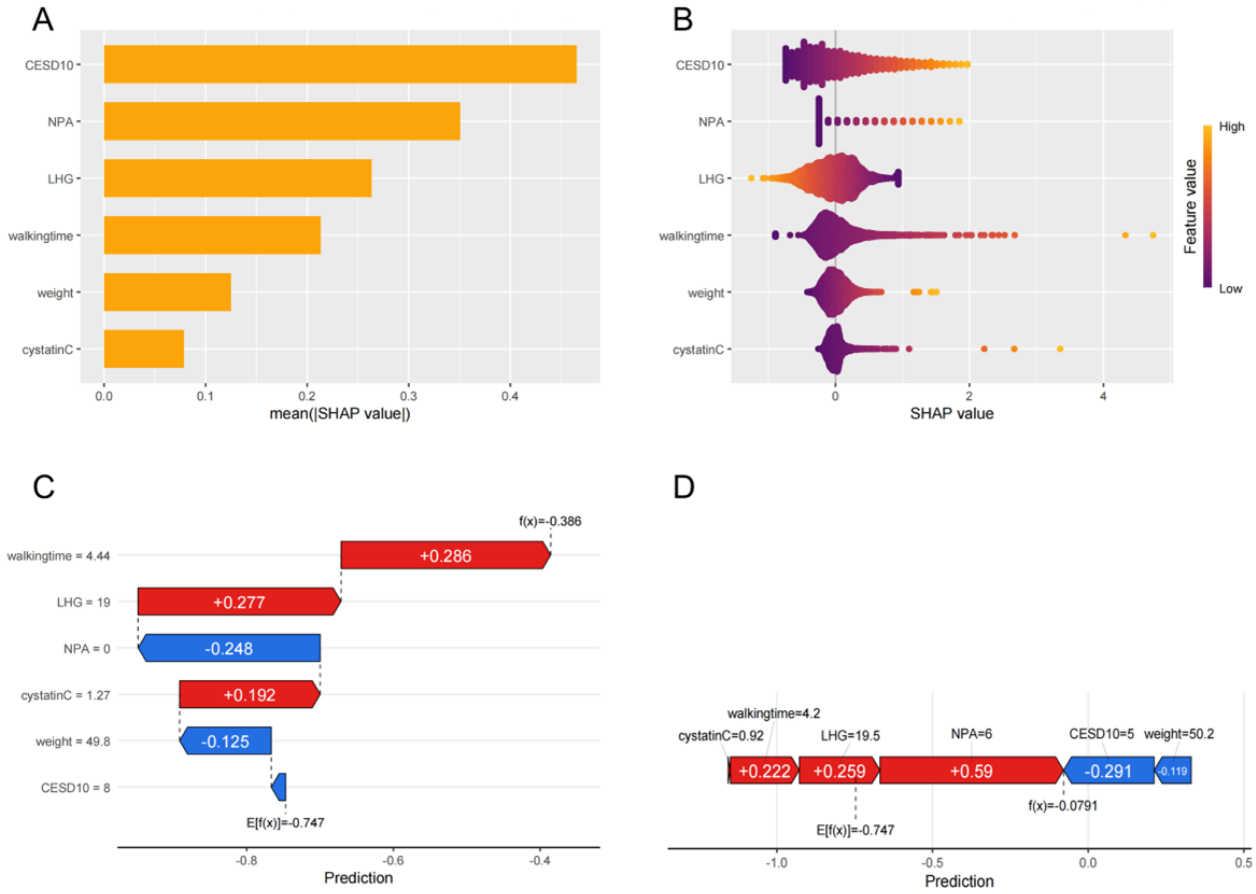
Explanation of Model Characteristic Variables

SHAP values were calculated to assess the influence of each characteristic variable in the model. The global importance plot and swarm plot (Figures 5A and 5B) reveal the relative importance of the 6 key variables in predicting ADL dysfunction, ranked from highest to lowest: CESD-10 score, number of painful areas, left hand grip strength, 2.5-m walking time, weight, and cystatin C. Except for left hand grip strength, all other variables were positively correlated with ADL dysfunction.

To illustrate the individual contributions of these variables, 2 random samples were selected, and the predictive effects of the variables were visualized through waterfall and force plots (Figures 5C and 5D). These plots demonstrate the distinct effects of each factor on ADL dysfunction for individual participants, providing valuable insights into the practical significance of the model's predictors.

XSL•FO
RenderX

Figure 5. Interpretability of the activities-of-daily-life dysfunction prediction model using Shapley additive explanations values: (A) Global Shapley additive explanations importance plot ranking features by contribution to activities-of-daily-living dysfunction predictions in China Health and Retirement Longitudinal Survey (2015 - 2016, n=5081); (B) swarm plot depicting directionality (positive/negative) of predictors (eg, Center for Epidemiologic Studies Depression Scale, pain areas); and (C-D) waterfall and force plots illustrating individualized risk contributions for 2 participants (China Health and Retirement Longitudinal Survey ID: Sample A vs B), highlighting variable-specific impacts on model output. CESD10: 10-item Center for Epidemiologic Studies Depression Scale; LHG: left grip strength; NPA: number of pain areas; walkingtime: 2.5-meter walking time.



Discussion

Principal Findings

This study identified 6 robust predictors of ADL dysfunction in the older adults, namely CESD-10 depression score, number of painful areas, left-hand grip strength, 2.5-m walking time, weight, and cystatin C levels. These factors reflect multidimensional contributions from psychosocial states, physical frailty markers, systemic inflammation, and biomechanical stressors. Notably, participants with a history of disability, chronic diseases, or falls exhibited significantly higher ADL dysfunction risk, consistent with previous evidence on functional decline pathways [14,15]. The 2.5-m walking time defined in this study is negatively correlated with gait speed. Key findings further highlighted walking speed as a critical functional indicator. Slow gait (≥3.73 seconds for 2.5 m) correlated strongly with ADL limitations, echoing its status as a "sixth vital sign" for aging populations [16-19]. Similarly, left-hand grip strength emerged as a stronger predictor than right-hand strength, suggesting asymmetric hand function may play underrecognized roles in daily task performance. Depressive symptoms (CESD-10>11.5) and polyarticular pain (>3 body areas) were dominant risk amplifiers, aligning with their bidirectional relationships with physical disability [20-22].

Comparison With Previous Work

While many studies have identified predictors of ADL dysfunction in community-dwelling older adults, research constructing ADL dysfunction prediction models is rare, with only a few reporting ADL dysfunction prediction models. Jonkman et al [23] developed and validated a 3-year ADL dysfunction prediction model for adults aged 65 - 75 years, selecting 10 of 22 predictors, including physical performance indicators, age, BMI, depressive symptoms, and chronic diseases. Covinsky et al [24] constructed and validated an ADL dysfunction prediction model for community residents aged 70 years and older, including 9 predictors: age, comorbidities, cognitive function, low BMI, and 5 functional limitation indicators. Recent domestic studies have found that a nomogram incorporating 10 predictors age, education level, social activity frequency, drinking and smoking habits, smoking frequency, comorbidity condition, self-reported health status, gait speed, cognitive function, and depressive symptoms can effectively predict disability risks [25]. Our study aligns with previous research in focusing on depressive symptoms, weight, and gait

XSL•FO
RenderX

speed as predictors. However, it differs by incorporating new indicators: number of painful body regions, left-hand grip strength, and cystatin C. Our findings reinforce established associations between depression, obesity, and ADL decline [21,26-28]. For instance, the link between CESD-10 scores and ADL aligns with Carrière et al's [20] longitudinal data showing depression predicts subsequent functional dependence. Similarly, weight's positive association with ADL dysfunction parallels studies identifying obesity-related metabolic strain and mobility limitations as key mechanisms [26,29]. However, our model extends existing literature in 3 ways. First, pain is a critical factor contributing to ADL dysfunction and poor functional health in older adults [30]. It is cross-sectionally associated with ADL function and predicts a decline in ADL functioning over time [31]. Older individuals often become less active due to pain, which leads to physical deconditioning and perpetuates a cycle of pain and activity restriction [32]. Second, cystatin C, a marker of renal function and inflammation emerged as a novel biochemical predictor, potentially reflecting subclinical frailty progression [33]. Cystatin C may reflect renal function decline, and renal dysfunction is associated with sarcopenia and cardiovascular events [34]. This may underlie its potential mechanism in predicting ADL dysfunction. Third, the left-hand grip strength's predictive dominance contrasts with conventional bilateral grip assessments [35-37], suggesting laterality-specific strength may better capture real-world functional demands.

Strengths and Limitations

The study's strengths include the use of nationally representative CHARLS data with a large sample size, rigorous LASSO-multivariable regression for predictor selection, and validation through AUC (0.77), calibration, and SHAP interpretability. The integration of psychological, biomechanical, and biochemical indicators provides a holistic view of ADL risk. Importantly, these predictors are easily accessible and low-cost, enabling assessment for older adults in community hospital outpatient clinics and facilitating broad implementation.

Limitations warrant consideration. First, the CHARLS data, while valuable, may be limited by regional and cultural factors, which may affect the generalizability of our findings. Future research should aim to include more diverse populations. Second, the variables selected in this study may have excluded important factors such as social support, living environment, and cognitive function, which could reduce the model's accuracy. Future research could incorporate these variables to enhance the model's precision. Third, as a retrospective study, the reliance on self-reported data introduces the potential for information bias, particularly in the reporting of chronic diseases and falls. Future prospective studies are needed to track changes in these variables over time and improve the model's predictive accuracy. Finally, grip strength data were not differentiated by dominant hand. Future studies could explore the potential impact of grip strength side on the results.

Future Directions

Future studies should incorporate longitudinal designs to track dynamic interactions between cognitive decline, social support networks, and environmental factors in shaping ADL trajectories. The role of cystatin C as a biomarker warrants further investigation to elucidate its mechanistic links to frailty progression and chronic inflammation [33]. In addition, task-specific functional magnetic resonance imaging or observational studies could clarify the dominance of left-hand grip strength and refine asymmetry-targeted rehabilitation protocols. Comparative analyses of weight-adjusted indices versus traditional metrics like BMI may improve obesity-related risk stratification [29]. Finally, validation in multiethnic cohorts and real-world clinical settings is critical to ensure model generalizability and inform scalable interventions addressing modifiable psychosocial and physical risk factors.

Conclusions

This tool is a predictive model developed to assess the risk of functional impairment in daily living among older adults. It incorporates factors such as the CESD-10, number of painful areas, left-hand grip strength, 2.5-m walking time, weight, and cystatin C. During both the development and validation phases, the model demonstrated discriminative ability and accuracy, effectively identifying individuals at higher risk and maintaining reliability when applied to new data.

For health care professionals, the model can assist in making more informed care decisions, help prioritize interventions, and support the customization of treatment plans for high-risk individuals. By identifying those at greater risk for functional decline, the model may contribute to improving the quality of life for older adults, enhancing their independence, and promoting overall well-being. In addition, it may aid in the more efficient allocation of health care resources by directing attention to individuals who would benefit most from targeted interventions.

Acknowledgments

We are grateful to all the participants and staff of the China Health and Retirement Longitudinal Survey. We acknowledge the financial support provided by the Hunan Provincial Natural Science Foundation of China and the Health Commission of Changsha for this research. This study was supported by the Hunan Provincial Natural Science Foundation of China (No. 2024JJ9510) and the Health Commission of Changsha (No. KJ-B2023046). The funding organizations played no further role in study design, data collection, analysis and interpretation, and paper writing.

Data Availability

The datasets generated or analyzed during this study are available from the corresponding author on reasonable request.

XSL•FO
RenderX

Authors' Contributions

FL contributed to data curation and writing (original draft). CL managed writing (review and editing). HL conducted writing (review and editing). Authors CL (lccssdyy@126.com) and HL (lhcssdyy@126.com) are co-corresponding authors for this article.

Conflicts of Interest

None declared.

References

1. Fang EF, Scheibye-Knudsen M, Jahn HJ, et al. A research agenda for aging in China in the 21st century. Ageing Res Rev 2015 Nov;24(Pt B):197-205. [doi: 10.1016/j.arr.2015.08.003] [Medline: 26304837]
2. Basakha M, Yavari K, Sadeghi H, Naseri A. Health care cost disease as a threat to Iranian aging society. J Res Health Sci 2014;14(2):152-156. [Medline: 24728752]
3. Fried LP, Guralnik JM. Disability in older adults: evidence regarding significance, etiology, and risk. J Am Geriatr Soc 1997 Jan;45(1):92-100. [doi: 10.1111/j.1532-5415.1997.tb00986.x] [Medline: 8994496]
4. Zheng X, Pang L, Chen G, Huang C, Liu L, Zhang L. Challenge of population aging on health. In: Public Health Challenges in Contemporary China: An Interdisciplinary Perspective: Springer; 2016. [doi: 10.1007/978-3-662-47753-3_4]
5. Kim KI, Kim S, Kim KW, Jang HC, Kim CH, Chin HJ. Low hemoglobin A1C increases the risk of disability in community-dwelling older non-diabetics adults. J Nutr Health Aging 2016 Mar;20(3):341-346. [doi: 10.1007/s12603-015-0583-z] [Medline: 26892584]
6. Stineman MG, Xie D, Pan Q, Kurichi JE, Saliba D, Streim J. Activity of daily living staging, chronic health conditions, and perceived lack of home accessibility features for elderly people living in the community. J Am Geriatr Soc 2011 Mar;59(3):454-462. [doi: 10.1111/j.1532-5415.2010.03287.x] [Medline: 21361881]
7. Ferrucci L, Guralnik JM, Pahor M, Corti MC, Havlik RJ. Hospital diagnoses, medicare charges, and nursing home admissions in the year when older persons become severely disabled. JAMA 1997 Mar 5;277(9):728-734. [Medline: 9042845]
8. Katz S, Ford AB, Moskowitz RW, Jackson BA, Jaffe MW. Studies of illness in the aged. The index of ADL: a standardized measure of biological and psychosocial function. JAMA 1963 Sep 21;185:914-919. [doi: 10.1001/jama.1963.03060120024016] [Medline: 14044222]
9. Lawton MP, Brody EM. Assessment of older people: self-maintaining and instrumental activities of daily living. Gerontologist 1969;9(3):179-186. [Medline: 5349366]
10. Edjolo A, Dartigues JF, Pérès K, Proust-Lima C. Heterogeneous long-term trajectories of dependency in older adults: the PAQUID cohort, a population-based study over 22 years. J Gerontol A Biol Sci Med Sci 2020 Nov 13;75(12):2396-2403. [doi: 10.1093/gerona/glaa057] [Medline: 32115657]
11. Ćwirlej-Sozańska A, Wiśniowska-Szurlej A, Wilmowska-Pietruszyńska A, Sozański B. Determinants of ADL and IADL disability in older adults in southeastern Poland. BMC Geriatr 2019 Oct 31;19(1):297. [doi: 10.1186/s12877-019-1319-4] [Medline: 31672121]
12. Jaehn P, Fügemann H, Gödde K, Holmberg C. Using decision tree analysis to identify population groups at risk of subjective unmet need for assistance with activities of daily living. BMC Geriatr 2023 Sep 7;23(1):543. [doi: 10.1186/s12877-023-04238-w] [Medline: 37674137]
13. Zhao Y, Hu Y, Smith JP, Strauss J, Yang G. Cohort profile: the China Health and Retirement Longitudinal Study (CHARLS). Int J Epidemiol 2014 Feb;43(1):61-68. [doi: 10.1093/ije/dys203] [Medline: 23243115]
14. Chu LW, Chiu AYY, Chi I. Impact of falls on the balance, gait, and activities of daily living functioning in community-dwelling Chinese older adults. J Gerontol A Biol Sci Med Sci 2006 Apr;61(4):399-404. [doi: 10.1093/gerona/61.4.399] [Medline: 16611708]
15. Hung WW, Ross JS, Boockvar KS, Siu AL. Association of chronic diseases and impairments with disability in older adults: a decade of change? Med Care 2012 Jun;50(6):501-507. [doi: 10.1097/MLR.0b013e318245a0e0] [Medline: 22584885]
16. Fritz S, Lusardi M. White paper: “walking speed: the sixth vital sign”. J Geriatr Phys Ther 2009;32(2):46-49. [doi: 10.1519/00139143-200932020-00002] [Medline: 20039582]
17. Verghese J, Wang C, Lipton RB, Holtzer R. Motoric cognitive risk syndrome and the risk of dementia. J Gerontol A Biol Sci Med Sci 2013 Apr;68(4):412-418. [doi: 10.1093/gerona/gls191] [Medline: 22987797]
18. Verghese J, Wang C, Bennett DA, Lipton RB, Katz MJ, Ayers E. Motoric cognitive risk syndrome and predictors of transition to dementia: a multicenter study. Alzheimers Dement 2019 Jul;15(7):870-877. [doi: 10.1016/j.jalz.2019.03.011] [Medline: 31164315]
19. Stenholm S, Ferrucci L, Vahtera J, et al. Natural course of frailty components in people who develop frailty syndrome: evidence from two cohort studies. J Gerontol A Biol Sci Med Sci 2019 Apr 23;74(5):667-674. [doi: 10.1093/gerona/gly132] [Medline: 30084927]
20. Carrière I, Gutierrez LA, Pérès K, et al. Late life depression and incident activity limitations: influence of gender and symptom severity. J Affect Disord 2011 Sep;133(1-2):42-50. [doi: 10.1016/j.jad.2011.03.020] [Medline: 21463901]

XSL•FO
RenderX

21. Zhou L, Wang W, Ma X. The bidirectional association between the disability in activities of daily living and depression: a longitudinal study in Chinese middle-aged and older adults. BMC Public Health 2024 Jul 15;24(1):1884. [doi: 10.1186/s12889-024-19421-w] [Medline: 39010036]
22. Feng Z, Li Q, Zhou L, Chen Z, Yin W. The relationship between depressive symptoms and activity of daily living disability among the elderly: results from the China Health and Retirement Longitudinal Study (CHARLS). Public Health (Fairfax) 2021 Sep;198:75-81. [doi: 10.1016/j.puhe.2021.06.023] [Medline: 34365109]
23. Jonkman NH, Colpo M, Klenk J, et al. Development of a clinical prediction model for the onset of functional decline in people aged 65-75 years: pooled analysis of four European cohort studies. BMC Geriatr 2019 Jun 27;19(1):179. [doi: 10.1186/s12877-019-1192-1] [Medline: 31248370]
24. Covinsky KE, Hilton J, Lindquist K, Dudley RA. Development and validation of an index to predict activity of daily living dependence in community-dwelling elders. Med Care 2006 Feb;44(2):149-157. [doi: 10.1097/01.mlr.0000196955.99704.64] [Medline: 16434914]
25. Zhang L, Cui H, Chen Q, Li Y, Yang C, Yang Y. A web-based dynamic Nomogram for predicting instrumental activities of daily living disability in older adults: a nationally representative survey in China. BMC Geriatr 2021 May 17;21(1):311. [doi: 10.1186/s12877-021-02223-9] [Medline: 34001030]
26. Hirani V, Naganathan V, Blyth F, et al. Longitudinal associations between body composition, sarcopenic obesity and outcomes of frailty, disability, institutionalisation and mortality in community-dwelling older men: The Concord Health and Ageing in Men Project. Age Ageing 2017 May 1;46(3):413-420. [doi: 10.1093/ageing/afw214] [Medline: 27932368]
27. Alexandre TDS, Scholes S, Ferreira Santos JL, Duarte YADO, de Oliveira C. The combination of dynapenia and abdominal obesity as a risk factor for worse trajectories of IADL disability among older adults. Clin Nutr 2018 Dec;37(6):2045-2053. [doi: 10.1016/j.clnu.2017.09.018]
28. Riaz H, Khan MS, Siddiqi TJ, et al. Association between obesity and cardiovascular outcomes: a systematic review and meta-analysis of Mendelian randomization studies. JAMA Netw Open 2018 Nov 2;1(7):e183788. [doi: 10.1001/jamanetworkopen.2018.3788] [Medline: 30646365]
29. Sun J, Lin J, Shen W, et al. Associations of body mass index, waist circumference and the weight-adjusted waist index with daily living ability impairment in older Chinese people: a cross-sectional study of the Chinese Longitudinal Healthy Longevity Survey. Diabetes Obes Metab 2024 Sep;26(9):4069-4077. [doi: 10.1111/dom.15762] [Medline: 38962934]
30. Covinsky KE, Lindquist K, Dunlop DD, Yelin E. Pain, functional limitations, and aging. J Am Geriatr Soc 2009 Sep;57(9):1556-1561. [doi: 10.1111/j.1532-5415.2009.02388.x] [Medline: 19682122]
31. van Dalen-Kok AH, Pieper MJC, de Waal MWM, van der Steen JT, Scherder EJA, Achterberg WP. The impact of pain on the course of ADL functioning in patients with dementia. Age Ageing 2021 May 5;50(3):906-913. [doi: 10.1093/ageing/afaa247] [Medline: 33300044]
32. Larsson C, Ekvall Hansson E, Sundquist K, Jakobsson U. Impact of pain characteristics and fear-avoidance beliefs on physical activity levels among older adults with chronic pain: a population-based, longitudinal study. BMC Geriatr 2016 Feb 24;16:50. [doi: 10.1186/s12877-016-0224-3] [Medline: 26912216]
33. Li C, Ma Y, Yang C, Hua R, Xie W, Zhang L. Association of Cystatin C kidney function measures with long-term deficit-accumulation frailty trajectories and physical function decline. JAMA Netw Open 2022 Sep 1;5(9):e2234208. [doi: 10.1001/jamanetworkopen.2022.34208] [Medline: 36178684]
34. Wang T, Zhu Y, Liu X, et al. Cystatin C and sarcopenia index are associated with cardiovascular and all-cause death among adults in the United States. BMC Public Health 2024 Jul 23;24(1):1972. [doi: 10.1186/s12889-024-19137-x] [Medline: 39044229]
35. Muhammad T, Hossain B, Das A, Rashid M. Relationship between handgrip strength and self-reported functional difficulties among older Indian adults: the role of self-rated health. Exp Gerontol 2022 Aug;165:111833. [doi: 10.1016/j.exger.2022.111833] [Medline: 35577266]
36. McGrath R, Robinson-Lane SG, Peterson MD, Bailey RR, Vincent BM. Muscle strength and functional limitations: preserving function in older Mexican Americans. J Am Med Dir Assoc 2018 May;19(5):391-398. [doi: 10.1016/j.jamda.2017.12.011] [Medline: 29371128]
37. Gopinath B, Kifley A, Liew G, Mitchell P. Handgrip strength and its association with functional independence, depressive symptoms and quality of life in older adults. Maturitas 2017 Dec;106(92-4):92-94. [doi: 10.1016/j.maturitas.2017.09.009] [Medline: 29150172]

Abbreviations

ADL: activities of daily living
AUC: area under the curve
BADL: basic activities of daily living
CESD-10: 10-item Center for Epidemiologic Studies Depression Scale
CHARLS: China Health and Retirement Longitudinal Survey
DCA: decision curve analysis

XSL•FO
RenderX

IADL: instrumental activities of daily living
LASSO: Least Absolute Shrinkage and Selection Operator
ROC: receiver operating characteristic
SHAP: Shapley additive explanations

Edited by A Coristine; submitted 23.02.25; peer-reviewed by Y Lin, Y Chen; revised version received 11.04.25; accepted 11.04.25; published 19.06.25.

Please cite as:
Lin F, Liu C, Liu H
Development and Validation of a Predictive Model for Activities of Daily Living Dysfunction in Older Adults: Retrospective Analysis of Data From the China Health and Retirement Longitudinal Study
JMIR Med Inform 2025;13:e73030
URL: https://medinform.jmir.org/2025/1/e73030
doi:10.2196/73030

© Fangbo Lin, Chao Liu, Hua Liu. Originally published in JMIR Medical Informatics (https://medinform.jmir.org), 19.6.2025. This is an open-access article distributed under the terms of the Creative Commons Attribution License (https://creativecommons.org/licenses/by/4.0/), which permits unrestricted use, distribution, and reproduction in any medium, provided the original work, first published in JMIR Medical Informatics, is properly cited. The complete bibliographic information, a link to the original publication on https://medinform.jmir.org/, as well as this copyright and license information must be included.

XSL•FO
RenderX

A Responsible Framework for Assessing, Selecting, and Explaining Machine Learning Models in Cardiovascular Disease Outcomes Among People With Type 2 Diabetes: Methodology and Validation Study

Yang Yang[1*], BS; Che-Yi Liao[1*], MS; Esmaeil Keyvanshokooh[2], MS, PhD; Hui Shao[3], MD, PhD; Mary Beth Weber[3], MPH, PhD; Francisco J Pasquel[3,4], MPH, MD; Gian-Gabriel P Garcia[1], MS, PhD

[1]H. Milton Stewart School of Industrial and Systems Engineering, Georgia Institute of Technology, 765 Ferst Dr NW, Atlanta, GA, United States

[2]Department of Information and Operations Management, Mays Business School, Texas A&M University, College Station, TX, United States

[3]Hubert Department of Global Health, Rollins School of Public Health, Emory University, Atlanta, GA, United States

[4]Division of Endocrinology, Metabolism, and Lipids, Department of Medicine, Emory University School of Medicine, Atlanta, GA, United States

[*]these authors contributed equally

Corresponding Author:
Gian-Gabriel P Garcia, MS, PhD
H. Milton Stewart School of Industrial and Systems Engineering, Georgia Institute of Technology, 765 Ferst Dr NW, Atlanta, GA, United States

Abstract

Background: Building machine learning models that are interpretable, explainable, and fair is critical for their trustworthiness in clinical practice. Interpretability, which refers to how easily a human can comprehend the mechanism by which a model makes predictions, is often seen as a primary consideration when adopting a machine learning model in health care. However, interpretability alone does not necessarily guarantee explainability, which offers stakeholders insights into a model's predicted outputs. Moreover, many existing frameworks for model evaluation focus primarily on maximizing predictive accuracy, overlooking the broader need for interpretability, fairness, and explainability.

Objective: This study proposes a 3-stage machine learning framework for responsible model development through model assessment, selection, and explanation. We demonstrate the application of this framework for predicting cardiovascular disease (CVD) outcomes, specifically myocardial infarction (MI) and stroke, among people with type 2 diabetes (T2D).

Methods: We extracted participant data comprised of people with T2D from the ACCORD (Action to Control Cardiovascular Risk in Diabetes) dataset (N=9635), including demographic, clinical, and biomarker records. Then, we applied hold-out cross-validation to develop several interpretable machine learning models (linear, tree-based, and ensemble) to predict the risks of MI and stroke among patients with diabetes. Our 3-stage framework first assesses these models via predictive accuracy and fairness metrics. Then, in the model selection stage, we quantify the trade-off between accuracy and fairness using area under the curve (AUC) and Relative Parity of Performance Scores (RPPS), wherein RPPS measures the greatest deviation of all subpopulations compared with the population-wide AUC. Finally, we quantify the explainability of the chosen models using methods such as SHAP (Shapley Additive Explanations) and partial dependence plots to investigate the relationship between features and model outputs.

Results: Our proposed framework demonstrates that the GLMnet model offers the best balance between predictive performance and fairness for both MI and stroke. For MI, GLMnet achieves the highest RPPS (0.979 for gender and 0.967 for race), indicating minimal performance disparities, while maintaining a high AUC of 0.705. For stroke, GLMnet has a relatively high AUC of 0.705 and the second-highest RPPS (0.961 for gender and 0.979 for race), suggesting it is effective across both subgroups. Our model explanation method further highlights that the history of CVD and age are the key predictors of MI, while HbA_{1c} and systolic blood pressure significantly influence stroke classification.

Conclusions: This study establishes a responsible framework for assessing, selecting, and explaining machine learning models, emphasizing accuracy-fairness trade-offs in predictive modeling. Key insights include: (1) simple models perform comparably to complex ensembles; (2) models with strong accuracy may harbor substantial differences in accuracy across demographic groups; and (3) explanation methods reveal the relationships between features and risk for MI and stroke. Our results underscore the need for holistic approaches that consider accuracy, fairness, and explainability in interpretable model design and selection, potentially enhancing health care technology adoption.

XSL•FO
RenderX

(JMIR Med Inform 2025;13:e66200) doi:10.2196/66200

KEYWORDS

interpretable machine learning; explainability; fairness; type 2 diabetes; cardiovascular disease; responsible framework; cardiovascular; cardiology; machine learning; diabetes; clinical practice; myocardial infarction; MI; stroke; prediction; T2D

Introduction

Building trustworthy machine learning models for clinical practice requires consideration of interpretability, explainability, as well as fairness. Interpretability—which refers to how easily a human can comprehend the mechanism by which a model makes predictions—is important in health care settings because of the need for clinicians and patients to understand and trust the Artificial Intelligence (AI)-involved decisions that directly impact patient care [1,2]. It also facilitates regulatory compliance and ethical considerations in medical AI applications, ensuring these systems are not only effective but also justifiable and accountable [3]. In addressing this pressing need, experts in computer science, operations research, and medical informatics have significantly progressed the field of interpretable machine learning models, laying the foundation for the development of AI [3,4]. As of today, cutting-edge interpretable machine learning models are available through many open-source software packages, including RiskSLIM and Interpretable AI (Interpretable AI), among others [5,67]. Nonetheless, interpretability alone is not sufficient for trustworthy AI in health care.

Beyond interpretability, the machine learning community has also begun to emphasize the need for explainability [8] which focuses on conveying understandable reasons behind AI-driven decisions. While interpretability helps users grasp how a model arrives at a conclusion, explainability provides the why, offering justifications in human terms. This reasoning is crucial in health care, where clinicians and patients must not only understand but also trust the rationale of AI suggestions [9]. Therefore, explainability builds trust, enhances decision-making quality by providing insights into AI reasoning, and ensures compliance with ethical and legal standards [10]. In other words, explainability plays a crucial role in making machine learning algorithms and AI not just transparent but also relatable and trustworthy in clinical settings.

Meanwhile, there has been an increasing worry about the possibility of machine learning models leading to biased decisions [11]. Examples include models displaying racial or gender biases in predicting patient outcomes [12], or algorithms that disproportionately favor certain demographics in resource allocation [13]. Such biased decision-making tools may result in unfair evaluations in clinical settings, ultimately harming patients who require care [14]. However, efforts to quantitatively evaluate fairness in prediction models for clinical practice are still scarce [15].

A model with high predictive accuracy does not guarantee the best clinical usage, as it might display unfavorable biases [16]. As a result, it is important to understand and quantify the trade-offs between accuracy and fairness in model selection. Overall, the combined exploration and consideration of these aspects in a machine learning framework-based environment is not thoroughly investigated in this literature [17]. Therefore, to address these issues systematically, we propose a 3-stage machine learning framework on model assessment, selection, and explainability that integrates interpretability, fairness, as well as explainability in health care decision-making. Specifically, in the first stage, we develop and assess a range of models based on predictive accuracy and fairness. Next, we select the model that best balances accuracy and fairness using a novel trade-off curve. Finally, we explain the chosen model, aiming to provide deeper insights into its predictions for informed clinical decision-making. As a proof of concept, we apply our framework to predict cardiovascular disease (CVD) outcomes, myocardial infarction (MI), and stroke, among people with type 2 diabetes (T2D). With CVD being a leading cause of death in the United States, and patients with T2D being at elevated risk of CVD, it is urgent to develop accurate and fair predictive models that generate clinically reasonable predictions [16-19]. This study not only contributes to the advancement of AI in health care but also sets a precedent for future research in incorporating interpretability, fairness, and explainability into the machine learning model development framework, paving the way for more ethical, trustworthy, and effective solutions in medical informatics.

Methods

Overview

In this section, we first detail our study data and model development approach. Then, we describe our responsible framework for model assessment, selection, and explanation. This study is based on a secondary analysis of individual-level participant data from the Action to Control Cardiovascular Risk in Diabetes study (ACCORD 2001 - 09, NCT00000620) by the National Heart, Lung, and Blood Institute (NHLBI) of United States [15]. Our code repository is included in Multimedia Appendix 1.

Data

ACCORD (Action to Control Cardiovascular Risk in Diabetes) was a randomized, multicenter, double 2×2 factorial design study conducted at 77 clinical sites in North America. Participants were aged between 40 and 79 years, had T2D with a hemoglobin A1c (HbA_{1c}) ≥ 7.5% (57 mmol/mol), and had previous evidence of CVD or cardiovascular risk factors. (eg, dyslipidemia, hypertension, smoking, or obesity). The primary outcome of ACCORD was determined based on the first instance of a significant CVD event, which was characterized by a combination of nonfatal MI, nonfatal stroke, or cardiovascular death. We extracted demographic, clinical, and biomarker data collected at baseline (study entry) from individual participants across trials for model development.

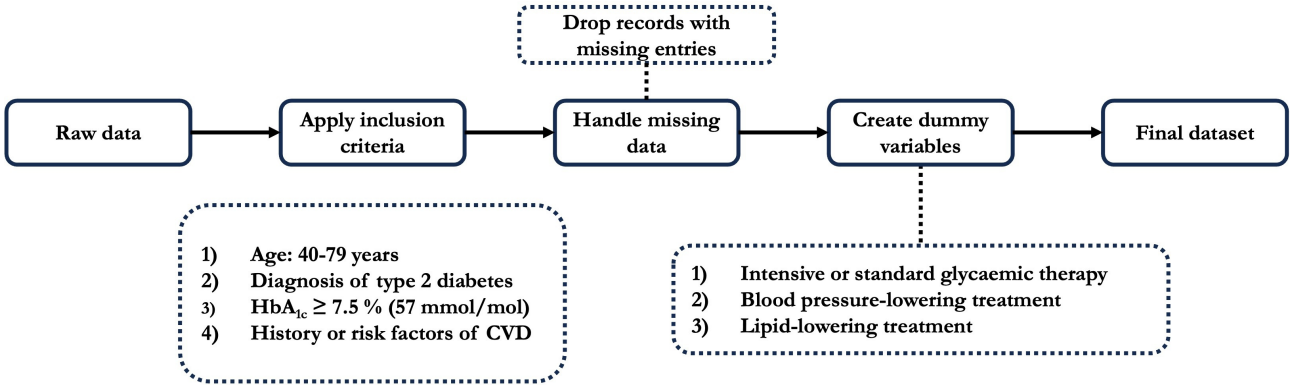
XSL•FO
RenderX

Data Preprocessing

We focused on 2 primary CVD events, MI and stroke, as our study outcomes, and used patients' demographic data, clinical risk factors, medication history, and pertinent biomarkers as predictors. All predictor variables were collected at the time of study enrollment, ensuring that our models use information available at the point of care. We prepared the study outcomes as binary variables: patients either experienced MI or stroke within the 5-year period, or they did not. In other words, the interpretable machine learning models act as classification tools to identify if a patient is at risk of experiencing these CVD events in the next 5 years.

We sourced candidate predictor variables for fatal or nonfatal MI and fatal or nonfatal stroke outcomes from eligibility screening or clinical examination data in ACCORD after applying the inclusion criteria. These predictors encompass demographic characteristics, clinical factors, medication history, and relevant biomarkers. Complete case models were constructed using all predictor variables, without using imputation, as only 616 out of 10,251 observations (6%) in the dataset had missing values across any of the predictors. We dropped the records with missing data and applied one-hot encoding for categorical predictors to obtain the final dataset for model development [20]. Specifically, creating dummy variables involved transforming categorical variables, such as treatment type (eg, intensive vs standard glycemic therapy) and medication history (eg, blood pressure- or lipid-lowering treatments), into binary indicators via one-hot encoding [21]. This step ensured that the categorical data was appropriately formatted for model development. This data-preprocessing pipeline is outlined in Figure 1.

Figure 1. Data-preprocessing steps before model development.



Machine Learning Model Development

We developed several machine learning models to demonstrate our proposed framework for fairness-aware model assessment and selection. Our framework is specifically designed for scenarios where model development, selection, and deployment are treated as separate processes. The machine learning models we consider include interpretable models (eg, linear and tree-based), semi-interpretable models, (eg, random forest), and common statistical and machine learning models, (eg, naïve Bayes), for binary classification of MI and stroke. In the following paragraphs, we provide details of the models developed in this research and describe the model-tuning procedure.

We evaluated a range of machine learning models, including linear models (GLMnet and OFS), tree-based models (CART and OCT), ensemble models (random forest and XGBoost), and other traditional machine learning approaches (naïve Bayes and SVM). Linear and tree-based models are generally considered interpretable due to their structure and parameterization [22,23], while ensemble models and other methods can achieve strong predictive performance but may be less directly interpretable. OFS formulates the logistic regression with L2 penalties into a binary convex optimization problem and solves it to optimality. Within the OFS framework, there are 2 key parameters: the regularization parameter (balancing model complexity against accuracy) and the sparsity parameter (enhancing interpretability by controlling feature count) [24]. OCT derives the tree by optimizing the tree structure (size) and decision rules simultaneously via mixed integer optimization [25]. The main hyperparameters in OCT include the maximum depth of a tree, the minimum leaf size, and the complexity parameter, playing a crucial role in preventing overfitting, ensuring stability, and fostering interpretability. We limited the max depth of an OCT to 3 and 4 to enhance interpretability by simplifying the decision structure. We remark that OCT exactly recovers the optimal tree (given fixed hyperparameters) at the cost of additional computational complexity, whereas CART uses heuristic splitting rules in branching nodes to generate a decision tree quickly. Detailed descriptions of each model's structure, key hyperparameters, and training procedure are provided in Multimedia Appendix 2.

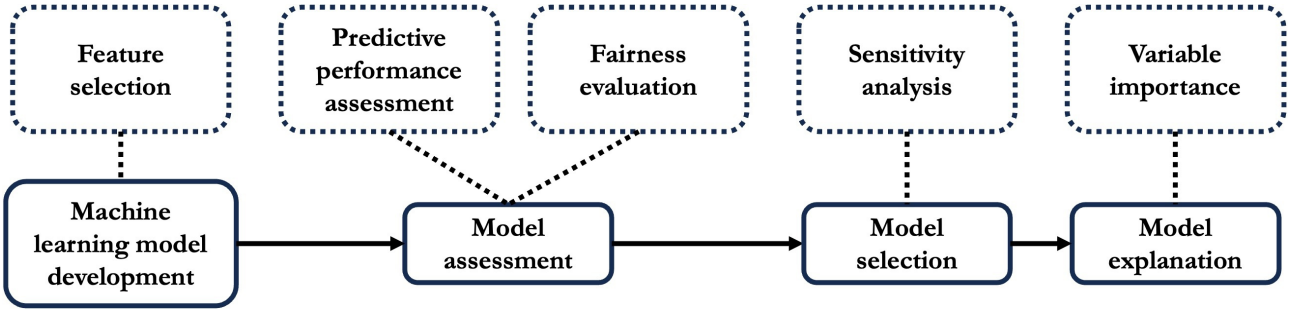
To build our models, we randomly divided our data using a 70 - 30 train-test split, using 6745 out of 9635 for training and the remaining 2890 out of 9635 for testing. Then, with the training data, we applied 10-fold cross-validation for hyperparameter tuning. We also found that our data were class-imbalanced, and there were very few occurrences of CVD events. To address this class imbalance, we adjusted the weight assigned to each label during our hyperparameter tuning. Each model's performance was estimated using both cross-validation on the training set and out-of-sample validation on the testing set.

XSL•FO
RenderX

Responsible Framework for Model Assessment, Selection, and Explanation

After building the machine learning models, it is desired to select a suitable model and investigate the relationship between predictors and the outcomes. In this section, we detail our responsible framework for model assessment, selection, and explanation. We outline this framework in Figure 2. Our proposed responsible framework consists of three main modules after model development: (1) model assessment, (2) model selection, and (3) model explanation. In the model assessment module, we assess each model's performance in their predictive capabilities and fairness. Then, a sensitivity analysis of the trade-off between these performance metrics is carried out to aid model selection. Finally, for model explanation, we use a unified approach that combines multiple methods to explain the best-performing models. We developed our proposed responsible framework with R language (v4.3.1, R Foundation) and the following R libraries: Interpretable AI (v3.2.1, Interpretable AI), survival (v3.5.5, Mayo Clinic), GLMnet (v4.1.8, Stanford University), rpart (v4.1.19, Mayo Clinic), naivebayes (v1.0.0), and kernlab (v0.9.32, TU Wien).

Figure 2. The proposed responsible framework for model assessment, selection, and explanation.



Model Assessment

In this module, we describe the model assessment procedure for the developed interpretable models according to their predictive performance and fairness. To evaluate predictive accuracy, we considered four metrics: (1) area under the receiver operating characteristic curve (AUC), (2) sensitivity, (3) specificity, and (4) accuracy. AUC evaluates a model's ability to distinguish between positive and negative classes, with higher values indicating better discriminative performance. It is particularly reliable for imbalanced data due to its threshold-independence. Sensitivity (true positive rate) measures the correct identification of actual positives (ie, patients developed MI or stroke), while specificity (true negative rate) assesses the correct identification of negatives. Accuracy quantifies the proportion of correct classification of the patients in the total cases examined. Sensitivity, specificity, and accuracy are threshold-dependent for models that output continuous scores (eg, predicted probabilities). Importantly, it is common to carefully select this classification threshold to optimize the model's predictive performance, with respect to these performance metrics for specific applications. To address this challenge, we set a threshold which maximizes a weighted metric combining sensitivity and specificity, that is, u×sensitivity+1-u×specificity. Here, the weight parameter u is bounded between 0 and 1, and higher (resp., lower) values of u indicate a preference towards thresholds that emphasize sensitivity (resp., specificity). This approach has also been used in previous research [26] . In CVD management, both sensitivity and specificity play important roles in correctly identifying patients who are at risk of MI or stroke, along with those who are at low risk of these outcomes. Because correctly identifying those at high risk of MI or stroke is critical to initiating clinical interventions, we specifically use a value of u=23 in our analysis – leaning slightly toward higher sensitivity over specificity. This approach ensures that we assess a balanced performance in identifying both patients at risk and with low risk while accounting for clinical priorities.

To evaluate the predictive fairness of the machine learning models, we consider a fairness metric, the relative performance parity score (RPPS), which is calculated by

$$\text{RPPS} := 1 - \max_s(|\text{AUC}_s - \text{AUC}_{\text{AUC}}|)$$

where s is a subpopulation in a protected attribute, eg, female in gender, and AUCs represents the conditional AUC conditioned on this subpopulation s. Notably, RPPS can be small when any subpopulation has disproportionally high or low AUC, compared with the overall AUC. On the other hand, if all subpopulations have AUC performance close to the overall AUC, then the RPPS will be large. We chose AUC as the primary metric because it is threshold-agnostic, providing a more comprehensive measure of model performance across different decision thresholds. Since this metric is a relative measure specific to each model's output, it is suitable for a fair comparison across models, which befits our purpose in the model assessment module of the proposed responsible model selection framework. Moreover, the RPPS is flexible and can accommodate other commonly used performance metrics, such as accuracy or sensitivity, depending on the specific goals of the fairness evaluation.

Model Selection

After evaluating the models, selection could be based on either predictive performance or fairness. Ideally, one would choose a model that excels in both dimensions. However, this selection process becomes challenging when no such model exists within the considered model options. To address this, we propose a sensitivity analysis-based approach to enhance model selection. Specifically, we evaluated the weighted sum of accuracy *and RPPS*, with the weight ranging from 0 to 1, that is, w(Accuracy)+(1−w)RPPS,

XSL•FO
RenderX

where w is the prespecified weight between 0 and 1. Notably, when the weight is 1, this weighted sum simplifies to accuracy; conversely, when the weight is 0, it becomes the RPPS. This approach enables model selection according to the trade-off between predictive performance and fairness.

Model Explanation

To investigate the relationship between the predictors and outcomes, we developed a synergistic model explanation approach that combines models' permutation variable importance, the SHAP method, and partial dependence plots. Notably, this explanation module does not establish clear causal relationships between features and adverse health outcomes; however, it helps clarify how the ML algorithms function for decision-making. Permutation variable importance assesses model explainability through feature significance [27]. That is, it measures the impact of each feature on a model's predictive performance by shuffling the values of a feature while keeping others constant. We can then determine that feature's importance based on the resulting performance decline, as measured by AUC. To enhance the reliability of our estimates, we bootstrapped 100 iterations: in each, we sampled the training data, trained a model, computed a baseline AUC, and determined permutation importance scores. This yielded multiple score sets for each bootstrapped sample. We then averaged the feature importance and provided 95% CIs. Features were ranked by mean importance and variability. A high mean importance means the model heavily depends on that feature, whereas high variability indicates inconsistent significance. Therefore, features with high variability warrant further examination, while those with high importance and low variability are consistently crucial.

Another component in our model explanation is the SHAP method. Essentially, SHAP assigns an importance measure, known as the Shapley value, to each feature. This Shapley value is calculated by averaging the differences in the model's predictions with and without the feature across all possible subsets of features, which can be viewed as the expected effects of the feature on the prediction. Importantly, the sum of all Shapley values equals the prediction value to ensure consistency across all features. The Shapley value effectively captures the average marginal contribution of each feature, providing a comprehensive explanation of the model's behavior. For interpretability, we proposed to use the relative Shapley value (the marginal contribution of each feature relative to the prediction value) in our analysis.

To further visualize and understand the relationship between features and predicted outcomes, we also consider Partial Dependence plots as another explanation method. Partial Dependence plots are widely used and show how changing a feature value affects model outputs, by fixing all other features [28]. This explanation method is chosen over the SHAP's built-in dependence plot function because Partial Dependence plots tend to be more intuitive in clinical settings [29]. Specifically, when creating a partial dependence plot, we replace the value of a feature with values in its range to compute average model outputs on this feature's range across data samples. In our analysis, in addition to risk predictions, we used log odds as model outcomes to provide a better interpretation of features and outcomes. In essence, a positive log-odds value indicates a higher likelihood of the event occurring, a negative value indicates a lower likelihood, and a value of zero represents a 50% probability. We made the necessary adjustments for categorical and continuous features and included data distribution information to bolster the reliability of our analysis. This approach enables us to pinpoint areas where the model's output is robustly supported by data, as well as identify regions where predictions may be less dependable due to data scarcity.

We stress that both permutation variable importance and the SHAP method can provide broader insights into the overall effects of specific features on model outputs. Partial dependence plots, on the other hand, provide a detailed visualization to uncover the direct relationship between each feature and the predicted outcome. By integrating permutation variable importance, the SHAP method, and partial dependence plots, we deliver a holistic model explanation for users. This synergy enhances interpretability and trust in the model's predictions, making the analysis more actionable in clinical settings.

Ethical Consideration

This study was approved by the Institutional Review Board at the Georgia Institute of Technology under Protocol No. H22333. All participants in the ACCORD trial provided written informed consent. The ACCORD contained de-identified data only. Participants in the ACCORD trial were not paid for their participation.

Results

Study Sample

Our study data included 9635 participants, with 616 (6% of the total 10,251) excluded due to missing data on predictor variables (Table 1). The mean (SD) age was 62.8 (6.7) years. Women made up 3,662 (38%) of the sample. The racial and ethnic make-up of our study data included 1834 (19%) non-Hispanic Black participants, 678 (7%) Hispanic or Latino participants, and 7123 (74%) non-Hispanic White participants. In addition, 3437 (36%) of participants had a history of CVD. The mean (SD) body mass index was 32.2 (5.4) kg/m^2, systolic blood pressure was 136.5 (17.1) mm Hg, and diastolic blood pressure was 74.9 (10.7) mm Hg. Of the sample, 880 (9.1%) experienced an MI, and 197 (2%) had a stroke during the follow-up period.

XSL•FO
RenderX

Table . Summary of study sample characteristics.

Variable	Value (n=9635)
Demographics	
Age, years, mean (SD)	62.8 (6.66)
Aged 75 years or older, n (%)	521 (5.4)
Gender, n (%)	
Women	3662 (38)
Men	5973 (62)
Race and ethnicity, n (%)	
Non-Hispanic Black	1834 (19)
Hispanic or Latino	678 (7)
Non-Hispanic White	7123 (74)
Tobacco usage, current, n (%)	1179 (12)
BMI, kg/m^2, mean (SD)	32.2 (5.4)
Blood pressure, mean (SD)	
Systolic, mm Hg	136.5 (17.1)
Diastolic, mm Hg	74.9 (10.7)
Heart rate, bpm, mean (SD)	72.7 (11.8)
History of CVD[a], n (%)	3437 (36)
Drug usage, n (%)	
Blood pressure-lowering drugs	8109 (94)
Oral diabetes drugs (including metformin)	8024 (83)
Insulin treatment	3403 (35)
Statins	6148 (64)
Fibrates	601 (6)
Anticoagulant use	303 (3)
Nonsteroidal anti-inflammatory use	851 (9)
Platelet aggregate inhibitor use	466 (5)
Daily aspirin use	5274 (55)
Biomarkers, mean (SD)	
HbA_{1c}[b], %	8.3 (1.1)
HbA_{1c}, mmol/mol	67 (9)
Total cholesterol, mg/dL	183.2 (41.7)
HDL cholesterol, mg/dL	41.8 (11.6)
LDL cholesterol, mg/dL	104.7 (33.8)
Triglycerides, mg/dL	190.7 (145.8)
Fasting plasma glucose, mg/dL	175.3 (55.8)
Alanine aminotransferase, IU/L	27.5 (16.0)
Creatine phosphokinase, IU/L	140.3 (130.2)
Serum potassium, mmol/L	4.5 (0.5)
Serum creatinine, mg/dL	0.9 (0.2)
Estimated glomerular filtration rate, mL/min/1.73 m^2	90.9 (27.3)
Urine albumin, mg/dL	10.7 (37.3)

XSL•FO
RenderX

Variable	Value (n=9635)
Urine creatinine, mg/dL	127.3 (65.4)
Urine albumin: creatinine ratio, mg/g	99.2 (359.4)

[a]CVD: cardiovascular disease.

[b]HbA_{1c}: Hemoglobin A1c.

Predictive Performance

The predictive accuracy of our machine learning models is summarized in Table 2.

Table . Summary of predictive performance for machine learning models predicting risk of myocardial infarction and stroke, optimizing thresholds for 23×Sensitivity+13×Specificity.

Machine learning model	AUC	Sensitivity	Specificity	Accuracy
MI[a]				
OCT	0.687	0.782[b]	0.554	0.565
Naïve Bayes	0.694	0.563	0.768[b]	0.420
Random forest	0.716[b]	0.746	0.640	0.645
SVM	0.581	0.711	0.436	0.450
XGBoost	0.695	0.782	0.554	0.565
GLMnet	0.704	0.629	0.666	0.664[b]
OFS	0.705	0.671	0.642	0.644
Stroke				
OCT	0.625	0.771	0.546	0.550
Naïve Bayes	0.703	0.694	0.708	0.708
Random forest	0.716	0.510	0.839[b]	0.833[b]
SVM	0.624	0.816[b]	0.426	0.568
XGBoost	0.714	0.653	0.735	0.734
GLMnet	0.700	0.625	0.715	0.714
OFS	0.731[b]	0.646	0.716	0.715

[a]MI: myocardial infarction.

[b]The best-performing model for each performance metric.

For classification of MI, the OCT model achieved the highest sensitivity at 0.782 with a specificity of 0.554 and AUC of 0.687. Random forest achieved the highest AUC at 0.716, with a sensitivity of 0.746, moderate specificity (0.640), and accuracy (0.645). XGBoost shows similar characteristics, with an AUC of 0.695, sensitivity matching OCT at 0.782, but lower specificity (0.554) and accuracy (0.565). GLMnet, despite its lower sensitivity (0.629), has a high AUC of 0.704 and the best specificity (0.666) and accuracy (0.664) among the models. Naïve Bayes, while exhibiting lower sensitivity (0.563), has the highest specificity (0.768), though an accuracy of 0.420.

For stroke classification, our results indicate that naïve Bayes provides the most balanced results across AUC (0.703), sensitivity (0.694), specificity (0.708), and accuracy (0.708). On the other hand, the Random forest model, despite having a lower sensitivity, achieves a high AUC (0.716) and the highest specificity (0.839), along with an accuracy of 0.833 – indicating its strong performance in correctly identifying non-stroke cases at the expense of missing some stroke cases. Similarly, XGBoost performs exceptionally well on AUC (0.714), accuracy (0.734), and specificity (0.735), with a low sensitivity (0.653). In contrast, the OCT model has the second-lowest AUC (0.625) and accuracy (0.550), indicating it may be the least effective model for stroke prediction. This lower performance suggests that OCT might not be suitable for accurate stroke prediction compared with the other models considered.

Fairness

In Table 3, we present AUC stratified by gender and race across all of the developed interpretable machine learning models for MI and stroke classification, along with the RPPS scores for gender and race. The conditional AUC on each subgroup is calculated by classification results in the test set.

XSL•FO
RenderX

Table . Area under the curve and Relative Parity of Performance Scores of myocardial infarction and stroke for gender and race across all machine learning models.

Machine learning model	AUC[a]		RPPS[b]	AUC		RPPS
	Men	Women	Gender	Black	White	Race
MI[c]						
Naïve Bayes	0.667	0.708	0.961	0.745	0.681	0.927
SVM	0.558	0.675	0.838	0.605	0.591	0.959
Random forest	0.673	0.760	0.939	0.770	0.704	0.925
XGBoost	0.655	0.753	0.917	0.720	0.690	0.964
GLMnet	0.689	0.702	0.979[d]	0.681	0.706	0.967[d]
OCT	0.642	0.763	0.889	0.710	0.682	0.967[d]
OFS	0.688	0.716	0.976	0.668	0.708	0.948
Stroke						
Naïve Bayes	0.679	0.662	0.942	0.733	0.629	0.895
SVM	0.622	0.615	0.986[d]	0.600	0.609	0.962
Random forest	0.783	0.673	0.906	0.741	0.696	0.965
XGBoost	0.773	0.645	0.903	0.718	0.702	0.983[d]
GLMnet	0.714	0.727	0.961	0.685	0.698	0.979
OCT	0.595	0.670	0.928	0.701	0.582	0.878
OFS	0.687	0.787	0.923	0.692	0.743	0.947

[a]AUC: area under the curve.

[b]RPPS: Relative Parity of Performance Scores.

[c]MI: myocardial infarction.

[d]The best-performing model for each performance metric.

For MI classification, besides the SVM, which has the lowest RPPS (0.838), the random forest model shows a substantial disparity in AUC between men (0.673) and women (0.760), resulting in a lower RPPS (0.939), which indicates higher gender disparities. Similarly, XGBoost exhibits a high AUC for women (0.753) compared with men (0.655), leading to an RPPS of 0.917, further highlighting the model's performance gaps across genders. On the other hand, the GLMnet and OCT model demonstrate the highest RPPS (0.979), suggesting minimal performance disparities between Black (0.681) and White (0.706) subgroups for GLMnet, and Black (0.710) and White (0.682) subgroups for OCT. In contrast, the random forest model shows greater differences in performance by race with an AUC of 0.770 for non-Hispanic Black people and 0.704 for non-Hispanic White people, resulting in a lower RPPS (0.925). Importantly, for most models, the RPPS scores indicate fairer results among race groups, compared with gender, for predicting MI events.

For stroke classification, the XGBoost model exhibits a significant difference in AUC between men (0.773) and women (0.645), resulting in a lower RPPS (0.903), highlighting pronounced differences in predictive accuracy by gender. Similarly, the random forest model, with a high AUC for men (0.783) compared with women (0.673), leads to an RPPS of 0.906. Conversely, the XGBoost model shows a relatively high RPPS (0.983), implying minimal performance differences between non-Hispanic Black (0.718) and non-Hispanic White (0.702) people. However, the naïve Bayes model demonstrates greater differences by race with an AUC of 0.733 for non-Hispanic Black people and 0.629 for non-Hispanic White people, resulting in a lower RPPS (0.895). Importantly, in contrast to our findings in MI classification tasks, the RPPS scores reveal better performance parity among gender groups compared with racial groups in classifying stroke events.

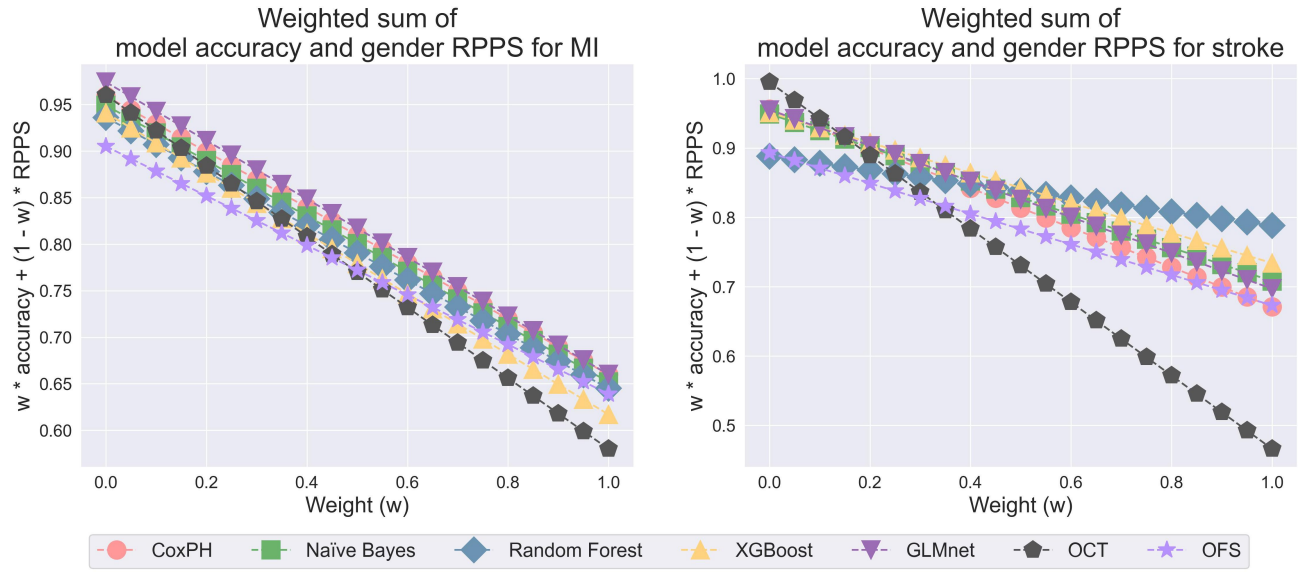
We also analyzed the coefficients of the one-hot encoded gender and race variable for GLMnet. For the variable "female=1", coefficient values were -0.324 in the model for MI and -0.250 in the model for stroke, suggesting that women are associated with a lower predicted risk of MI and stroke compared with men. For race, the variable "black=1" had a coefficient value of -0.192 in the model for MI, which indicates a lower predicted risk of MI for non-Hispanic Black people compared with non-Hispanic White people. For stroke, the model does not provide a coefficient for this predictor, indicating it was not significant in this context. These findings highlight the potential disparities in model predictions based on demographic factors, emphasizing the need to consider these variables when developing and evaluating predictive models in CVD classification.

XSL•FO
RenderX

Model Selection

We applied our model selection approach to identify the most preferable predictive models for MI and stroke classification. From our analyses, we have found that these models can exhibit higher disparities across gender subgroups, compared with race. Consequently, alongside overall predictive performance (overall accuracy), we incorporated gender RPPS scores into our model selection criteria. The weighted sum of accuracy and RPPS for MI and stroke classification among all machine learning models is presented in Figure 3. Recall that, when the weight is selected to be 0, this weighted sum represents RPPS; and when the weight is 1, it represents accuracy. For MI classification, the GLMnet model consistently demonstrated the highest values across most weights, indicating its superior balance of accuracy and fairness (Gender RPPS). This is particularly evident as the weight approaches 0, with a gender RPPS of 0.974. On the other hand, for stroke classification, the best-performing model varies across different weights. At lower weights (0 to 0.2), the OCT model showed the highest values due to its strong Gender RPPS. As the weight increases, the GLMnet model starts to dominate from the weight is 0.25 to 0.6, maintaining a good balance between accuracy and Gender RPPS. Moving to higher weights (0.65 onwards), the random forest model outperformed others, with its accuracy dominating the performance at around 0.788. These results indicated that, for stroke classification, when users prioritize model fairness, the OCT model is the best. For users who are neutral regarding the tradeoff between fairness and accuracy, GLMnet emerges as a suitable option. Lastly, random forest is recommended for users with a strong preference for model accuracy. Accordingly, we assumed users want to balance accuracy and fairness and proceed to analyze the relationship between variables and outcomes using GLMnet for both MI and stroke classification.

Figure 3. Weighted sum of model accuracy and gender Relative Parity of Performance Scores for myocardial infarction and stroke. MI: myocardial infarction; RPPS: Relative Parity of Performance Scores.



Model Explanation

We analyzed the relationship between features and outcomes for predicting MI and stroke using GLMnet, with our synergistic model explanation approach that integrates the permutation variable importance, the SHAP method, and the partial dependence plots. Figures 4 and 5 display the permutation variable importance measures, along with their 95% CIs, and the SHAP method for the GLMnet model in predicting MI and stroke, respectively. In addition, partial dependence plots for GLMnet for MI and stroke are shown in Figures 6 and 7, respectively.

XSL•FO
RenderX

Figure 4. Permutation variable importance and Shapley Additive Explanations method for GLMnet on myocardial infarction classification. AUC: area under the curve; MI: myocardial infarction; SHAP: Shapley Additive Explanations.

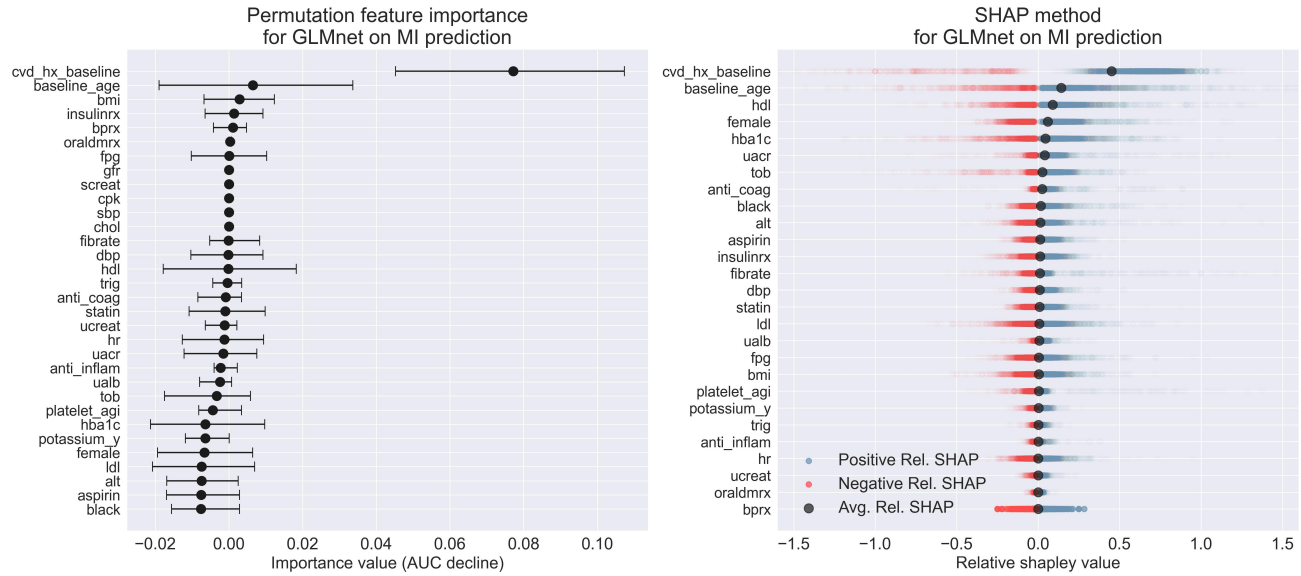


Figure 5. Permutation variable importance and Shapley Additive Explanations method for GLMnet on stroke classification. CVD: cardiovascular disease; HbA_{1c}: hemoglobin A1c.

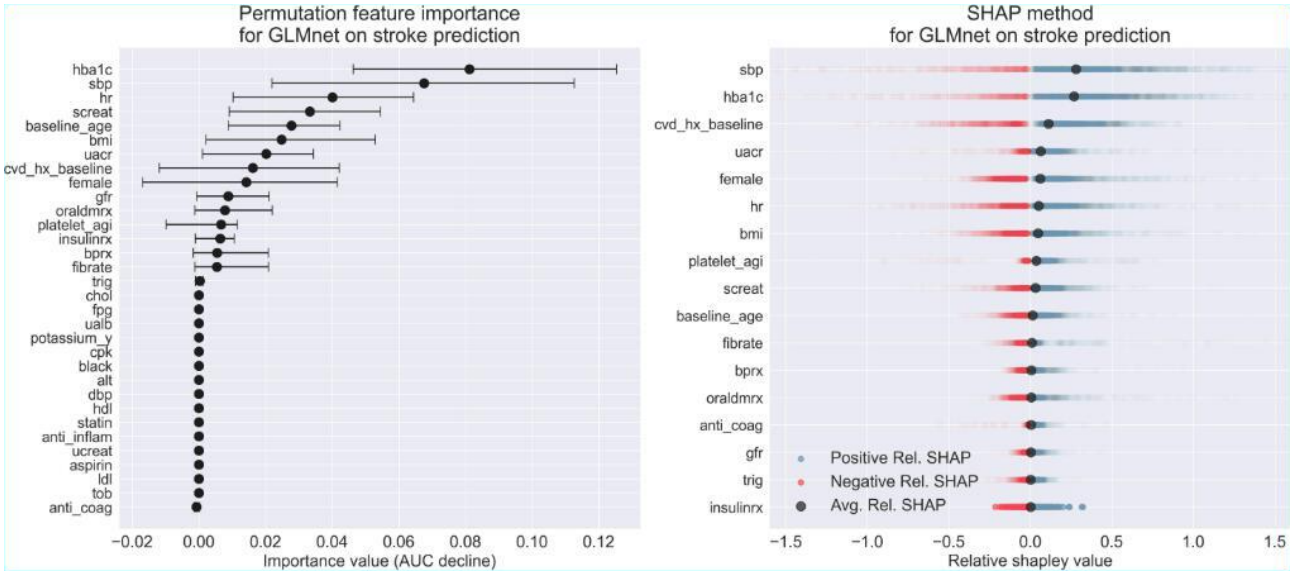
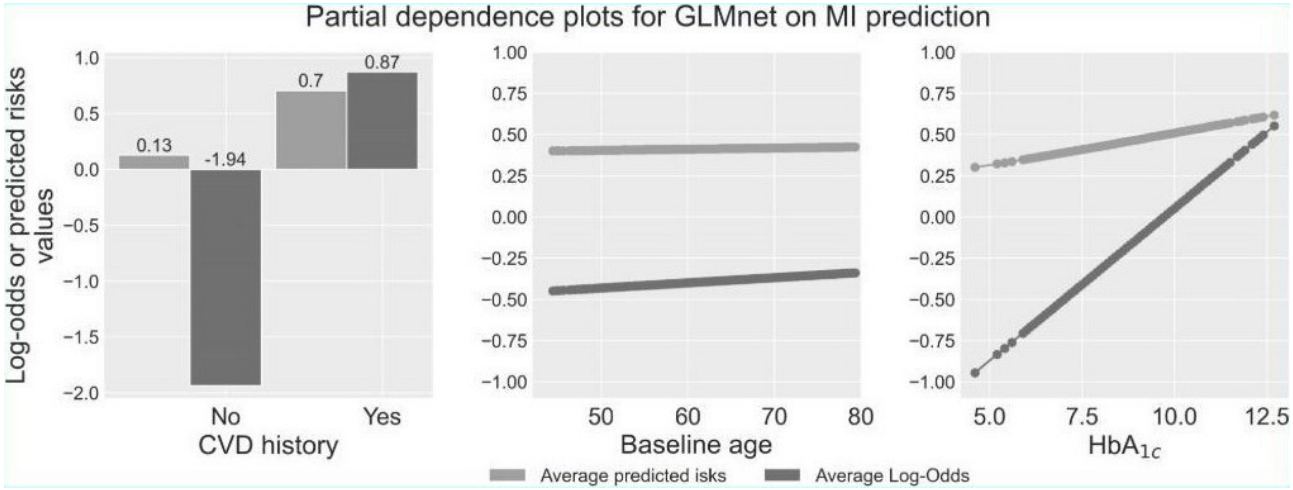
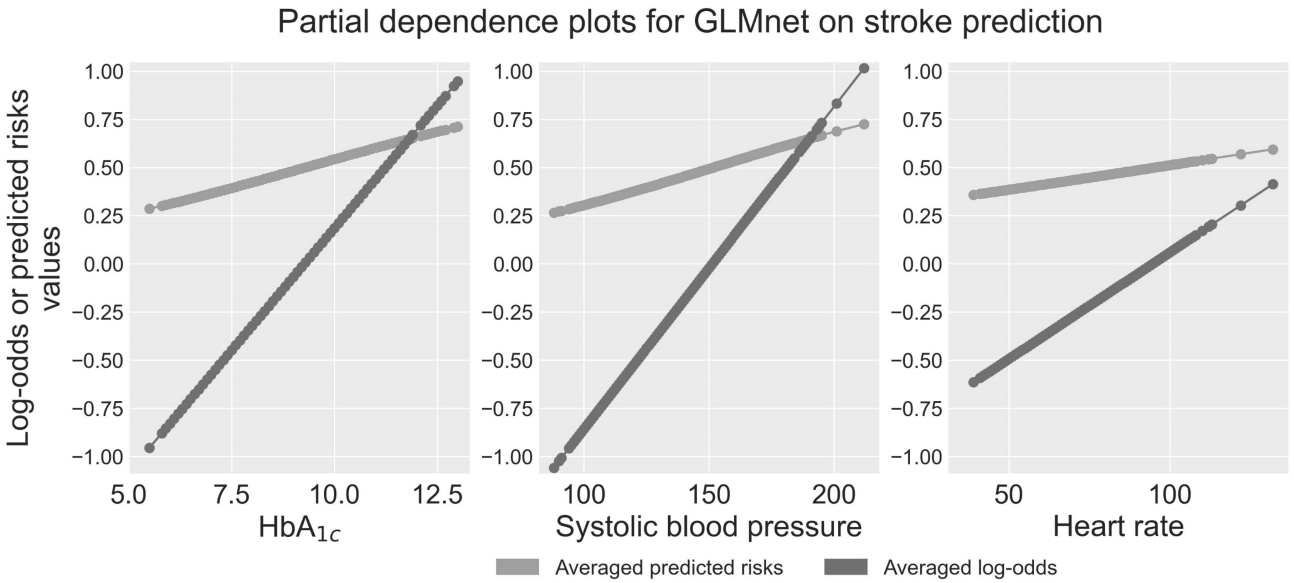


Figure 6. Partial dependence plots for GLMnet on myocardial infarction classification. AUC: area under the curve; SHAP: Shapley Additive Explanations.



XSL•FO
RenderX

Figure 7. Partial dependence plots for GLMnet on stroke classification.



From Figure 4, we observe that the permutation variable importance technique highlights the history of CVD (cvd_hx_baseline) as the most critical predictor for GLMnet to accurately predicting MI risks. Notably, its mean importance value (0.078) is nearly twelve times greater than that of the second most important variable, age (baseline_age), which has a mean importance value of 0.006. Moreover, while the 95% CIs of the permutation importance for CVD history is (0.045, 0.107), which is among the widest in the feature space, its lower confidence interval is still higher than the upper confidence interval of any other features. These results imply the significant role of people's CVD history to make accurate classification using GLMnet. In addition, BMI, and insulin treatment (insulinrx) also rank highly in this importance metric, with mean importance values of 0.002 and 0.0013, respectively. Some variables show negative values in permutation importance, which could be related to overfitting. Since the negative values are small in magnitude in our case, it could be that the model has relied too heavily on noise rather than true signal for those predictors. Now, from the SHAP method, we observed that the history of CVD and age emerge as the 2 most influential features in driving GLMnet's MI classification, as indicated by their average relative Shapley values of 0.45 and 0.14, respectively. This suggests that these 2 features have a general tendency to positively contribute to the prediction value. However, the individual relative Shapley values for the features can widely range from negative to positive, reflecting the varying marginal contributions of the features across individuals. For example, it appears that the distribution of the relative Shapley values for CVD history is a mixture of 2 highly separated distributions, which again implies that the GLMnet is substantially sensitive to CVD history. Furthermore, our findings indicate that although insulin treatment is highlighted as one of the top features in permutation variable importance, its mean relative Shapley value is relatively low compared with other features. Conversely, HbA_{1c} ranks highly using the SHAP method. Since both insulin treatment and HbA_{1c} are indicative of an individual's diabetic status, this suggests that accurately predicting MI also heavily depends on the diabetes status of the individual. Consequently, we next analyze the partial dependence plots for CVD history, age, and HbA_{1c} to draw actionable insights.

The partial dependence plots in Figure 6 illustrate that individuals with a history of CVD can have log odds of 0.87 (risk of 0.7), while those without CVD can have log odds as low as −1.94 (risk of 0.13). In addition, the plots show that 44-year-old individuals in the test set have log-odds of −0.44 (risk of 0.4) for developing MI. As age increases to 79 years, the risk gradually rises to log-odds of −0.33 (risk of 0.42). Furthermore, the plots reveal that HbA_{1c} levels significantly impact risk: with HbA_{1c} as low as 4.6%, the log-odds are −0.94 (risk of 0.3), but as HbA_{1c} rises to 12.7%, the log-odds increase drastically to 0.55 (risk of 0.61). These results highlight the importance of considering both CVD history and key biomarkers such as HbA_{1c} in assessing MI risk. Notably, although partial dependence plots do not necessarily reveal causation between features and risks, the steep increase in risk associated with higher HbA_{1c} levels underscores the critical role of diabetes management in preventing MI.

Next, we conduct a model explanation analysis for GLMnet in predicting stroke. As shown in Figure 7, HbA_{1c}, systolic blood pressure (SBP), and heart rate (HR) have the highest mean permutation importance values (0.08, 0.06, and 0.01, respectively). Other significant features include serum creatinine (screat), age, and BMI. These features exhibit wide confidence intervals for their permutation importance values, suggesting that their influence on the model can vary depending on the patient cohort. Moreover, HbA_{1c} and SBP consistently show the highest positive marginal contributions to risk predictions, with average relative Shapley values of 0.28 and 0.26, respectively. Heart rate, with a relative Shapley value of 0.05, is also a significant predictor for stroke using GLMnet. Although there are instances where these features negatively contribute to risk prediction, their relative Shapley values are predominantly positive. This distribution indicates a general tendency for these features to positively drive the predicted values, highlighting their crucial role in the model's stroke risk

XSL•FO
RenderX

predictions. Since these features are essential for accurately assessing stroke risk, we now derive actionable insights from the partial dependence plots (Figure 7).

The partial dependence plots in Figure 7 provide visualizations of how HbA_{1c}, systolic blood pressure, and heart rate influence stroke classification using the GLMnet model. We noticed that all 3 features exhibit a clear positive relationship between them and the predicted risk of stroke. For HbA_{1c}, as levels increase from 5.5% to 13%, there is a noticeable rise in both log-odds and predicted risk, moving from around −0.95 to 0.94 in log-odds and from 0.28 to 0.71 in predicted risk. For systolic blood pressure, the log-odds of developing stroke can reach 1.01 from −1.05 and from 0.26 to 0.725 in predicted risk as systolic blood pressure increases from 88 mm Hg to 212 mm Hg. Notably, the rate of increase in stroke risk with rising systolic blood pressure is less steep compared with the rate observed with increasing HbA_{1c} levels. Finally, the log-odds of developing stroke can reach 0.41 from -0.61 and from 0.35 to 0.59 in predicted risk as heart rate increases from 39 bpm to 132 bpm. Comparatively, the rate of increase in risk with heart rate is the most moderate among these features. This indicates that managing HbA_{1c} and systolic blood pressure could be more effective in preventing stroke. Overall, our model explanation analyses highlight the importance of managing blood glucose levels, blood pressure, and heart rate to mitigate the risk of stroke.

Discussion

Principal Findings and Comparison With Previous Works

In this study, we designed a responsible framework that evaluates various machine learning models by comparing these models' predictive accuracy and fairness metrics, while also providing model explanation. We then applied this framework for classification of MI and stroke, demonstrating its effectiveness in highlighting the importance of in-depth analyses of interpretable machine learning models between these 3 dimensions.

Our results demonstrate that complex models are not necessarily always better than simple, interpretable models—especially for high-stakes decisions such as those encountered in medicine [30]. Importantly. while the investigation of predictive accuracy have been a focus of several previous studies in health care AI, the concurrent evaluation of fairness in machine learning models is inconsistent and lacking [12]. The fairness analysis of our predictive models reveals both strengths and areas of concern in terms of gender and racial bias. In MI prediction, while some models like the SVM and XGBoost demonstrate gender biases, others such as GLMnet and OFS models show more balanced performance across gender and racial groups. This indicates that the most accurate models are not necessarily the fairest, and vice versa. These trade-offs highlight the importance of carefully selecting and tuning models to balance accuracy and fairness in medical decision-making. For stroke prediction, while some models, that are, GLMnet and SVM, exhibit balanced performance for both gender and race, other models, that are, XGBoost, present bias for a gender. This finding highlights the complex nature of fairness in such models, where different types of biases may manifest depending on the outcome being predicted and the model used. These findings underscore the importance of continuously monitoring and evaluating models for fairness. Our study provides a comprehensive analysis of fairness across different models and conditions, paving the way for more equitable AI applications in health care.

While there are multiple important criteria for model selection, such as predictive performance and fairness, a unified approach to guide this selection process is lacking. To address this, our analysis presents a sensitivity analysis based selection procedure based on users' preferences over the selection criteria. Our findings suggest that in some prediction tasks, users' preferences have minimal effect on the best-performing model (eg, GLMnet for MI prediction). However, in other tasks, for example, stroke prediction, users' preferences can significantly influence the selected model. Our study highlights the necessity of considering user preferences in model selection to ensure optimal outcomes for different prediction tasks.

Finally, our study demonstrates the potential role that our integrated explanation method (ie, the combination of permutation variable importance, the SHAP method, and partial dependence plots) can play in enhancing clinicians' understanding and trust of model-based predictions. For instance, the permutation variable importance measures, the Shapley values and partial dependence plots provide a clear visual representation of how key features like HbA_{1c} and systolic blood pressure influence the model's risk prediction for MI and Stroke. Such visual explanations can provide actionable insights and be augmented with existing clinical knowledge to help validate the quality of model-generated risk estimates [31]. These visualizations can also help clinical experts explain the unknown complex relationships between various risk factors and adverse outcomes [32].

This study has some limitations. The proposed framework was tested solely on CVD classification using the ACCORD dataset. While it has shown promise in this context, its effectiveness in other disease areas needs further investigation. Moreover, we relied on baseline information collected at the start of the study for model development and did not fully account for how things can change over time in the real world. Looking ahead, we would like to make sure our models stay accurate and up to date as treatment strategies and clinical guidelines evolve. One way to do this is by applying our framework on more recent datasets or on data that captures changes over time. These steps could give us a better understanding of how changing clinical practices might affect prediction modeling.

Conclusions

In this research, we proposed a 3-stage responsible framework for developing, selecting, and explaining machine learning models, emphasizing the trade-off between predictive accuracy and fairness in health care applications. By quantifying this trade-off using AUC and RPPS, we provided a structured approach to responsible model selection. After selecting the final model, we proposed an integrated explanation method to

XSL•FO
RenderX

offer insights into the relationships between features and outcomes. Applying this framework to predict MI and stroke among people with T2D, we demonstrated its effectiveness and potential to improve the development and evaluation of machine learning models for clinical practice. We anticipate that our framework is generalizable and can be applied to other clinical prediction tasks, potentially increasing the trustworthiness and acceptance of machine learning models among clinicians and patients.

Our framework highlights the importance of combining interpretability, explainability, and fairness in building, selecting, and explaining machine learning models. This integration is crucial not only for enhancing model performance [33], but also for addressing ethical and legal considerations [34]. These principles both help verify model results against clinical literature [35], and fosters acceptance and trust among health care stakeholders [36,37]. By fully embracing these aspects, our framework paves the way for more responsible, ethical, and transparent AI applications in health care.

Acknowledgments

This work was supported by the AIM-AHEAD Coordinating Center, funded by NIH. This manuscript was prepared using the ACCORD Clinical Research Materials obtained from the NHLBI Biologic Specimen and Data Repository Information Coordinating Center and does not necessarily reflect the opinions or views of the ACCORD or the NHLBI.

The authors would like to thank Dr. James Washington from the Morehouse School of Medicine for his insightful feedback on earlier versions of the manuscript.

This research was further supported by Georgia Institute of Technology, Texas A&M University, Emory University, AIM-AHEAD Coordinating Center, award number OTA-21-017, and was partially funded by the National Institutes of Health Agreement No. 1OT2OD032581.

MBW and FJP received funding from the Georgia Center for Diabetes Translation Research under Award No. NIH/NIDDK P30DK111024. YY received funding from the Georgia Tech Presidential Undergraduate Research Award.

Data Availability

The datasets analyzed during this study are available in the BioLINCC repository under Accession Number: HLB01041317a, ClinicalTrials.gov Identifier: NCT00000620

Authors' Contributions

GPG and EK conceptualized the research in this manuscript and supervised its execution. YY and CL led the data curation and formal analysis with input on data sources from FJP, MBW, and HS. GPG, EK, and HS led the funding acquisition. GPG directed the methodological approach with significant input from EK, CL, and HS. GPG, EK, and HS were responsible for project administration and resources. YY and CL developed and implemented the code used for model development and numerical validation. FJP, MBW, and HS provided significant input on the clinical interpretation of results. YY and CL generated all tables and figures in the manuscript. Manuscript writing was led by YY, CL, EK, and GPG with significant input from FJP, MBW, and HS. All authors reviewed the manuscript.

Conflicts of Interest

FJP reports research support from Dexcom, Insulet, Novo Nordisk, Tandem and Ideal Medical Technologies and consulting for Dexcom and Medscape. All other authors have no competing interests to report.

Multimedia Appendix 1
Code repository.
[ZIP File, 1376 KB - medinform_v13i1e66200_app1.zip]

Multimedia Appendix 2
Details of model descriptions and hyperparameters, along with explanation methods.
[DOCX File, 17 KB - medinform_v13i1e66200_app2.docx]

References

1. Bertsimas D, Wiberg H. Machine learning in Oncology: methods, applications, and challenges. JCO Clin Cancer Inform 2020 Oct;4:885-894. [doi: 10.1200/CCI.20.00072] [Medline: 33058693]
2. Bravo F, Rudin C, Shaposhnik Y, et al. Interpretable prediction rules for congestion risk in intensive care units. Stochastic Systems . [doi: 10.1287/stsy.2022.0018]

XSL•FO
RenderX

3. Holzinger A, Biemann C, Pattichis CS, et al. What do we need to build explainable AI systems for the medical domain? arXiv. Preprint posted online on Dec 28, 2017. [doi: 10.48550/arXiv.1712.09923]
4. Lee SJ, Pandey HS, Garcia GGP, et al. Designing interpretable machine learning models using mixed integer programming. In: Encyclopedia of Optimization: Springer International Publishing; 2020:1-8. [doi: 10.1007/978-3-030-54621-2_867-1]
5. Rudin C, Chen C, Chen Z, et al. Interpretable machine learning: fundamental principles and 10 grand challenges. Statist Surv 2022 Jan;16(none):1-85. [doi: 10.1214/21-SS133]
6. Interpretable AI documentation. Interpretable AI L. 2023. URL: https://www.interpretable.ai [accessed 2025-05-20]
7. Ustun B, Rudin C. Learning optimized risk scores. J Mach Learn Res 2019;20(150):1-75.
8. Barredo Arrieta A, Díaz-Rodríguez N, Del Ser J, et al. Explainable artificial intelligence (XAI): concepts, taxonomies, opportunities and challenges toward responsible AI. Information Fusion 2020 Jun;58:82-115. [doi: 10.1016/j.inffus.2019.12.012]
9. Amann J, Blasimme A, Vayena E, et al. Explainability for artificial intelligence in healthcare: a multidisciplinary perspective. BMC Med Inform Decis Mak 2020 Nov 30;20(1):310. [doi: 10.1186/s12911-020-01332-6] [Medline: 33256715]
10. Zihni E, Madai VI, Livne M, et al. Opening the black box of artificial intelligence for clinical decision support: a study predicting stroke outcome. PLoS ONE 2020;15(4):e0231166. [doi: 10.1371/journal.pone.0231166] [Medline: 32251471]
11. Mehrabi N, Morstatter F, Saxena N, et al. A survey on bias and fairness in machine learning. ACM Comput Surv 2022 Jul 31;54(6):1-35. [doi: 10.1145/3457607]
12. Huang J, Galal G, Etemadi M, et al. Evaluation and mitigation of racial bias in clinical machine learning models: scoping review. JMIR Med Inform 2022 May 31;10(5):e36388. [doi: 10.2196/36388] [Medline: 35639450]
13. Gianfrancesco MA, Tamang S, Yazdany J, et al. Potential biases in machine learning algorithms using electronic health record data. JAMA Intern Med 2018 Nov 1;178(11):1544-1547. [doi: 10.1001/jamainternmed.2018.3763] [Medline: 30128552]
14. McCradden MD, Joshi S, Mazwi M, et al. Ethical limitations of algorithmic fairness solutions in health care machine learning. Lancet Digit Health 2020 May;2(5):e221-e223. [doi: 10.1016/S2589-7500(20)30065-0] [Medline: 33328054]
15. Gerstein HC, Riddle MC, Kendall DM, et al. Glycemia treatment strategies in the action to control cardiovascular risk in diabetes (ACCORD) trial. Am J Cardiol 2007 Jun 18;99(12A):34i-43i. [doi: 10.1016/j.amjcard.2007.03.004] [Medline: 17599423]
16. Obermeyer Z, Powers B, Vogeli C, et al. Dissecting racial bias in an algorithm used to manage the health of populations. Science 2019 Oct 25;366(6464):447-453. [doi: 10.1126/science.aax2342] [Medline: 31649194]
17. Chen I, Johansson FD, Sontag D. Why is my classifier discriminatory? 2018 Presented at: Advances in Neural Information Processing Systems 31 (NeurIPS 2018); Montreal, Canada URL: https://papers.nips.cc/paper_files/paper/2018/hash/1f1baa5b8edac74eb4eaa329f14a0361-Abstract.html [accessed 2025-06-13]
18. Shameer K, Johnson KW, Glicksberg BS, et al. Machine learning in cardiovascular medicine: are we there yet? Heart 2018 Jul;104(14):1156-1164. [doi: 10.1136/heartjnl-2017-311198]
19. Feng Z, Chen Q, Griffin P, et al. Care settings of transient ischemic attack in the United States: a cohort study from the TriNetX health research network. J Stroke Cerebrovasc Dis 2024 Sep;33(9):107888. [doi: 10.1016/j.jstrokecerebrovasdis.2024.107888] [Medline: 39067658]
20. Burke JF, Hayward RA, Nelson JP, et al. Using internally developed risk models to assess heterogeneity in treatment effects in clinical trials. Circ Cardiovasc Qual Outcomes 2014 Jan;7(1):163-169. [doi: 10.1161/CIRCOUTCOMES.113.000497] [Medline: 24425710]
21. Hastie T, Friedman J, Tibshirani R. The Elements of Statistical Learning: Springer; 2001. [doi: 10.1007/978-0-387-21606-5]
22. Linardatos P, Papastefanopoulos V, Kotsiantis S. Explainable AI: a review of machine learning interpretability methods. Entropy (Basel) 2020 Dec 25;23(1):18. [doi: 10.3390/e23010018] [Medline: 33375658]
23. Lundberg SM, Erion G, Chen H, et al. Explainable AI for trees: from local explanations to global understanding. . Preprint posted online on 2019. [doi: 10.48550/arXiv.1905.04610]
24. Bertsimas D, Pauphilet J, Van Parys B. Sparse classification: a scalable discrete optimization perspective. Mach Learn 2021 Dec;110(11-12):3177-3209. [doi: 10.1007/s10994-021-06085-5]
25. Bertsimas D, Dunn J. Optimal classification trees. Mach Learn 2017 Jul;106(7):1039-1082. [doi: 10.1007/s10994-017-5633-9]
26. Garcia GGP, Lavieri MS, Jiang R, et al. Data-driven stochastic optimization approaches to determine decision thresholds for risk estimation models. IISE Transactions 2020 Oct 2;52(10):1098-1121. [doi: 10.1080/24725854.2020.1725254] [Medline: 29963653]
27. Breiman L. Random forests. Mach Learn 2001;45(1):5-32. [doi: 10.1023/A:1010933404324]
28. Goldstein A, Kapelner A, Bleich J, et al. Peeking inside the black box: visualizing statistical learning with plots of individual conditional expectation. . Preprint posted online on 2014. [doi: 10.48550/arXiv.1309.6392]
29. Molnar C. 96 SHAP (SHapley Additive exPlanations) | Interpretable Machine Learning. URL: https://christophm.github.io/interpretable-ml-book/shap.html [accessed 2025-01-06]
30. Rudin C. Stop explaining black box machine learning models for high stakes decisions and use interpretable models instead. Nat Mach Intell 2019;1(5):206-215. [doi: 10.1038/s42256-019-0048-x]

XSL•FO
RenderX

31. Schwartz JM, Moy AJ, Rossetti SC, et al. Clinician involvement in research on machine learning–based predictive clinical decision support for the hospital setting: a scoping review. J Am Med Inform Assoc 2021 Mar 1;28(3):653-663. [doi: 10.1093/jamia/ocaa296]
32. Waljee AK, Wallace BI, Cohen-Mekelburg S, et al. Development and validation of machine learning models in prediction of remission in patients with moderate to severe Crohn disease. JAMA Netw Open 2019 May 3;2(5):e193721. [doi: 10.1001/jamanetworkopen.2019.3721] [Medline: 31074823]
33. Bento V, Kohler M, Diaz P, et al. Improving deep learning performance by using explainable artificial intelligence (XAI) approaches. Discov Artif Intell 2021 Dec;1(1):9. [doi: 10.1007/s44163-021-00008-y]
34. Goodman B, Flaxman S. European Union regulations on algorithmic decision making and a “Right to Explanation”. AI Mag 2017 Sep;38(3):50-57. [doi: 10.1609/aimag.v38i3.2741]
35. Militello C, Prinzi F, Sollami G, et al. CT radiomic features and clinical biomarkers for predicting coronary artery disease. Cogn Comput 2023 Jan;15(1):238-253. [doi: 10.1007/s12559-023-10118-7]
36. Lipton ZC. The Mythos of Model Interpretability: In machine learning, the concept of interpretability is both important and slippery. Queue 2018 Jun 1;16(3):31-57. [doi: 10.1145/3236386.3241340]
37. Keyvanshokooh E, Zhalechian M, Shi C, et al. Contextual learning with online convex optimization: theory and application to medical decision-making. Manage Sci 2025. [doi: 10.1287/mnsc.2019.03211]

Abbreviations

ACCORD: Action to Control Cardiovascular Risk in Diabetes study
AI: Artificial Intelligence
AUC: area under the curve
CVD: cardiovascular disease
HbA_{1c}: Hemoglobin A1c
MI: myocardial infarction
NHLBI: National Heart, Lung, and Blood Institute
RPPS: Relative Parity of Performance Scores
SHAP: Shapley Additive Explanations
T2D: type 2 diabetes

Edited by A Benis; submitted 10.09.24; peer-reviewed by C Militello, H Wiberg; revised version received 21.04.25; accepted 26.04.25; published 27.06.25.

Please cite as:
Yang Y, Liao CY, Keyvanshokooh E, Shao H, Weber MB, Pasquel FJ, Garcia GGP
A Responsible Framework for Assessing, Selecting, and Explaining Machine Learning Models in Cardiovascular Disease Outcomes Among People With Type 2 Diabetes: Methodology and Validation Study
JMIR Med Inform 2025;13:e66200
URL: https://medinform.jmir.org/2025/1/e66200
doi:10.2196/66200

© Yang Yang, Che-Yi Liao, Esmaeil Keyvanshokooh, Hui Shao, Mary Beth Weber, Francisco J Pasquel, Gian-Gabriel P Garcia. Originally published in JMIR Medical Informatics (https://medinform.jmir.org), 27.6.2025. This is an open-access article distributed under the terms of the Creative Commons Attribution License (https://creativecommons.org/licenses/by/4.0/), which permits unrestricted use, distribution, and reproduction in any medium, provided the original work, first published in JMIR Medical Informatics, is properly cited. The complete bibliographic information, a link to the original publication on https://medinform.jmir.org/, as well as this copyright and license information must be included.

XSL•FO
RenderX

Enhancing the Predictions of Cytomegalovirus Infection in Severe Ulcerative Colitis Using a Deep Learning Ensemble Model: Development and Validation Study

Jeong Heon Kim[1*]; A Reum Choe[2*], MD; Ju Ran Byeon[2*], MD; Yehyun Park[2], MD; Eun Mi Song[2]; Seong-Eun Kim[2], MD; Eui Sun Jeong[2], MD; Rena Lee[3], PhD; Jin Sung Kim[1], PhD; So Hyun Ahn[4], PhD; Sung Ae Jung[2], MD

[1]Department of Medicine, Yonsei University College of Medicine, Seoul, Republic of Korea

[2]Department of Internal Medicine, College of Medicine, Ewha Womans University Mokdong Hospital, Ewha Womans University College of Medicine, Seoul, South Korea, Seoul, Republic of Korea

[3]Department of Bioengineering, College of Medicine, Ewha Womans University, Seoul, Republic of Korea

[4]Ewha Medical Research Institute, College of Medicine, Ewha Womans University, 25, Magokdong-ro 2-gil, Gangseo-gu, Seoul, Republic of Korea

[*]these authors contributed equally

Corresponding Author:
So Hyun Ahn, PhD
Ewha Medical Research Institute, College of Medicine, Ewha Womans University, 25, Magokdong-ro 2-gil, Gangseo-gu, Seoul, Republic of Korea

Abstract

Background: Cytomegalovirus (CMV) reactivation in patients with severe ulcerative colitis (UC) leads to worse outcomes; yet, early detection remains challenging due to the reliance on time-intensive biopsy procedures.

Objective: This study explores the use of deep learning to differentiate CMV from severe UC through endoscopic imaging, offering a potential noninvasive diagnostic tool.

Methods: We analyzed 86 endoscopic images using an ensemble of deep learning models, including DenseNet (Densely Connected Convolutional Network) 121 pretrained on ImageNet. Advanced preprocessing and test-time augmentation (TTA) were applied to optimize model performance. The models were evaluated using metrics such as accuracy, precision, recall, F_1-score, and area under the curve.

Results: The ensemble approach, enhanced by TTA, achieved high performance, with an accuracy of 0.836, precision of 0.850, recall of 0.904, and an F_1-score of 0.875. Models without TTA showed a significant drop in these metrics, emphasizing TTA's importance in improving classification performance.

Conclusions: This study demonstrates that deep learning models can effectively distinguish CMV from severe UC in endoscopic images, paving the way for early, noninvasive diagnosis and improved patient care.

(JMIR Med Inform 2025;13:e64987) doi:10.2196/64987

KEYWORDS

cytomegalovirus; ulcerative colitis; deep learning; endoscopy; classification

Introduction

Cytomegalovirus (CMV) reactivation is frequently observed in patients with severe ulcerative colitis (UC) [1,2]. A multicenter, prospective Korean study found CMV infections in 43% of patients with moderate to severe UC and 67% in those with steroid-refractory UC [3]. Such reactivation often leads to poorer prognoses compared with patients without CMV reactivation, increasing the risk of hospitalization due to UC exacerbation by 8.2 times [4,5]. Antiviral therapy for CMV has been shown to substantially reduce the need for colectomy in patients with severe UC and high-grade CMV infection [6,7]. The American College of Gastroenterology guidelines indicate that CMV superinfection can progress to severe UC, which is resistant to maximum immunosuppressive therapy, necessitating histological analysis through sigmoidoscopy and viral culture for diagnosis [8].

Accurate diagnosis of CMV infection in UC remains critical due to its implications for treatment and prognosis. CMV infection in UC can be diagnosed using blood tests or tissue biopsies. While blood tests are relatively simple and cost-effective, they have limitations in differentiating past or latent infections from active disease. In contrast, tissue biopsies obtained through sigmoidoscopy or colonoscopy provide a more definitive diagnosis but require an invasive procedure. To enhance diagnostic accuracy, targeted biopsies should be taken

XSL•FO
RenderX

from both the ulcer base and margins, with McCurdy et al [9] suggesting at least 11 biopsy specimens to achieve over 80% sensitivity. However, collecting multiple specimens increases the risk of bleeding and other complications.

Histopathological techniques used for CMV diagnosis in UC include hematoxylin and eosin (H&E) staining, immunohistochemistry (IHC), and tissue DNA PCR (polymerase chain reaction). H&E staining identifies characteristic cytomegalic cells with nuclear inclusions and has high specificity (92% - 100%) but variable sensitivity (10% - 87%) due to observer dependency. IHC, which detects immediate early antigens of CMV, improves sensitivity (78% - 93%) while maintaining high specificity (92% - 100%). Tissue DNA PCR is the most sensitive (92% - 97%) and specific (93% - 99%) diagnostic tool, but its availability is limited in some institutions, leading to reliance on IHC or H&E staining, potentially delaying diagnosis and treatment [10]. Given the importance of early antiviral intervention in severe UC, diagnostic delays may contribute to adverse clinical outcomes, including increased risk of total colectomy.

Differentiating between severe UC and CMV using endoscopic features presents a challenge [11-13]. Accurate diagnosis of CMV reactivation necessitates techniques like in situ detection of viral markers via specific IHC or nucleic acid amplification [14]. However, these tissue-based diagnostic methods often require several days for results, causing delayed treatment for immunocompromised patients requiring swift intervention. The lag in obtaining tissue biopsy outcomes can pose substantial clinical challenges, notably in CMV reactivation within patients with severe UC. This diagnostic waiting period impedes timely clinical decision-making, potentially exacerbating the patient's condition. In immunocompromised individuals like those with severe UC, any delay in initiating appropriate therapy can lead to disease progression, heightened morbidity, and even mortality [15,16]. The imperative for prompt intervention underscores the need for more immediate diagnostic approaches.

With the advancement of artificial intelligence (AI), a promising avenue emerges to expedite the diagnosis of CMV reactivation in patients with severe UC [17]. By analyzing complex data patterns and integrating with existing diagnostic methodologies, AI technologies could potentially reduce the time needed to identify CMV reactivation from days to hours. This acceleration in diagnosis would enable health care providers to administer antiviral therapy sooner, potentially improving patient outcomes by reducing the risk of complications and the need for more invasive treatments like colectomy. Furthermore, the application of AI in this diagnostic process could provide a more nuanced understanding of disease progression, facilitating a more tailored approach to treating and managing patients with severe UC and CMV reactivation.

While numerous studies have documented the endoscopic characteristics of CMV infection in UC, none have yet reported on AI systems for distinguishing severe UC from CMV [11-13]. A similar study conducted in 2021 developed a machine learning–based classifier to differentiate CMV from herpes simplex virus esophagitis [18]. This AI system used logistic regression with the least absolute shrinkage and selection operation to discriminate between the 2 conditions, demonstrating 100% sensitivity, specificity, accuracy, and an area under the curve (AUC) of 1.0. The system's predictive model, using the categorization of endoscopic features and history of transplantation, achieved a high accuracy of 92.6% in distinguishing CMV from herpes simplex esophagitis.

Other viral infections, such as herpes simplex virus, are comparatively rare among patients with UC and do not pose the same level of severe complications and management challenges as CMV reactivation [19-21]. Hence, while it remains imperative to differentiate between CMV and herpes simplex virus infections in patients with UC, accurate diagnosis of CMV infection associated with UC holds heightened clinical significance. This is primarily because CMV has the potential to instigate severe exacerbations of UC and progress to a state of severe UC that proves refractory to standard immunosuppressive therapies [22]. The application of AI technology to swiftly make these distinctions could facilitate the prompt initiation of appropriate interventions, thereby enhancing patient outcomes and mitigating the adverse consequences linked with treatment delays [23].

Numerous studies have reported the remarkable efficacy of AI systems in medical imaging. Various techniques have been proposed to augment and measure ensemble diversity [24]. Recent ensemble studies in medical imaging have demonstrated notable enhancements through multiview approaches, diverse preprocessing methods, and varied network architectures [25,26]. Deep ensemble learning models amalgamate the advantages of deep learning models and ensemble learning to enhance the overall generalization performance of the final model [24]. Consequently, this study aims to address morphological inaccuracies that impede fully automated quantification using deep learning models and to introduce ensemble methods to improve the discrimination of CMV infection in UC.

In the context of endoscopic imaging, predominantly single models have been used. However, discerning CMV infection within UC poses a challenging task, prompting a shift toward various ensemble techniques. Distinguishing these infections through visual inspection demands highly skilled physicians, and even then, the difficulty can vary substantially based on the experience level. This study aims to surpass existing network frameworks by incorporating advanced techniques to enhance the discrimination of CMV infections using deep ensemble learning methods. The rationale behind this approach is to leverage the diverse insights and robustness provided by an ensemble of models, thus overcoming the limitations of single-model approaches and substantially improving the accuracy and reliability of CMV detection in severe UC through endoscopic images [27].

Countless studies have showcased the remarkable prowess of AI systems in medical imaging [28-31]. Techniques for augmenting and measuring ensemble diversity have been put forth, with recent ensemble studies in medical imaging demonstrating notable enhancements via multiview approaches, diverse preprocessing techniques, and varied network architectures [32]. By amalgamating the advantages of both

XSL•FO
RenderX

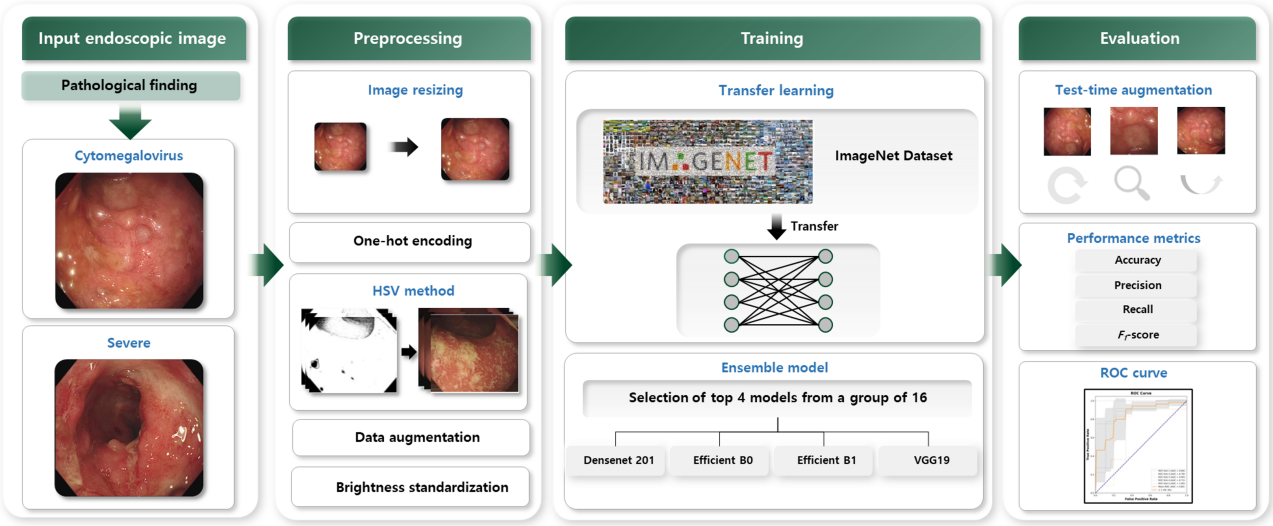
deep learning and ensemble learning, deep ensemble learning models have exhibited improved generalization performance. Thus, this study aims to address morphological errors impeding fully automated quantification using deep learning models and to propose ensemble methods to enhance the discrimination of CMV infection in UC.

Methods

Overview

We conducted a thorough analysis of 86 endoscopic images capturing cases of UC, both with and without CMV complications. Before feeding these images into our models, they underwent extensive preprocessing. This phase encompassed standardization for data normalization and augmentation to enhance dataset variability and robustness. We used models pretrained on the extensive ImageNet dataset for the analysis, which is renowned for its diverse image range. Our approach entailed an ensemble of 4 distinct models to leverage their strengths. To further bolster the reliability and accuracy of our predictions, we integrated test-time augmentation (TTA) during the evaluation phase [33]. The effectiveness of this ensemble was evaluated using a range of performance metrics meticulously selected to comprehensively assess the classification performance of our model ensemble, ensuring a comprehensive understanding of its ability to distinguish between cases of with and those without CMV complications (Figure 1).

Figure 1. Illustration of the study process: preprocessing endoscopic images of patients with ulcerative colitis with and without cytomegalovirus, applying an ensemble of pretrained models for analysis, using standardization, augmentation, and test-time augmentation to enhance prediction accuracy, and evaluating performance using selected metrics to distinguish between severe ulcerative colitis cases with and without cytomegalovirus complications. HSV: hue, saturation, value; ROC: receiver operating characteristic.



Data Collection

We retrospectively reviewed the medical records and endoscopic images of all patients diagnosed with severe UC between February 2019 and December 2022. The severity of UC was assessed using the Mayo Clinic scoring system [34]. The patients included in this study had Mayo Clinic scores ranging from 8 to 12. The presence of CMV was defined as follows: (1) serologic detection of CMV immunoglobin M antibody or (2) histologic detection of inclusion bodies on H&E-stained sections, positive immunohistochemical staining, or CMV DNA amplification by PCR at the first or second evaluation for CMV. Patients were excluded according to the following criteria: coinfection with *Clostridium difficile* and CMV, final pathologic diagnosis of malignancy, or missing information on endoscopic findings. The entire dataset was amassed from a cohort of 34 patients and incorporates endoscopic images sourced from Seoul and Mokdong Hospital of Ewha Womans University Medical Center. Using standardized 8-bit color depth endoscopy systems, specifically the CV-290 (Olympus) at Seoul Hospital, and the CF-Q260AL, CF-H260AL, and CF-HQ290L (Olympus) at Mokdong Hospital, the dataset comprises a total of 86 images (Table 1). This compilation comprises 32 images of CMV cases and 54 images of severe UC, devoid of CMV involvement.

XSL•FO
RenderX

Table . Dataset information and classification based on histological diagnosis through tissue biopsy.

Index	Severe-UC[a] without CMV[b]	Severe-UC with CMV
Sex, n		
Male	10	9
Female	11	4
Age (y)		
Mean (range)	51.9 (21-81)	35.4 (12-69)
Median (IQR)	55.5 (41.8-67.2)	34 (25.3-43.6)
Number of images[c] (CMV, Severe-UC)	54	32

[a]UC: ulcerative colitis.

[b]CMV: cytomegalovirus.

[c]Sampling date: February, 2019-December, 2022.

The resolutions of the dataset were 576×768, 576×720, and 1242×1079 pixels. To ensure the reliability and precision of pathological annotations, each image underwent meticulous analysis based on the consensus findings from tissue biopsies conducted on the patients. Furthermore, 2 experienced pathologists independently reviewed the biopsy results, and their expert opinions were used to annotate each image. In cases where the initial assessments of the pathologists varied, a collaborative review was undertaken to achieve a consensus for the annotations of each image.

Preprocessing

The endoscopic images were resized to 244×244 pixels to ensure compatibility with transfer learning and standardized for quality across institutions. They underwent hue, saturation, value (HSV) color space transformation, artifact management, data augmentation, pixel value normalization, and one-hot encoding to improve model efficiency and consistency.

Image Preprocessing and Standardization

To prepare for the application of transfer learning from deep learning models pretrained on the ImageNet dataset, the endoscopic images were resized to a resolution of 244×44 pixels. This resolution is essential to ensure compatibility with the architectures of these pretrained networks, as they require consistent input dimensions.

Given the multi-institutional nature of this research, the endoscopic images were acquired using different endoscopy systems across the participating institutions. To address the variability in image quality parameters, such as brightness and intensity, a meticulous standardization process was implemented for each image. This step proved crucial in normalizing differences resulting from the varied settings and conditions of the endoscopic equipment. Consequently, we ensured systematic adjustment of any discrepancies in image quality, thereby preserving the consistency of the dataset and enhancing the homogeneity of visual information before analysis by the deep learning model. Such standardization facilitates a more reliable comparison and analysis of the images, indispensable for the robust performance of the deep learning model.

Transformation to HSV Color Space

The images transformed HSV color space to more accurately represent the color distribution and enable effective discrimination between tissue types. Targeted ranges within the HSV color space were defined to standardize the color representation across all images. Furthermore, control mechanisms were implemented to mitigate the influence of artifacts that could affect the model's performance, such as light reflection and dark areas [35]. To effectively address these artifacts, we established HSV ranges corresponding to them and generated mask images to identify these areas.

Inpainting Technique

The empty spaces in the mask were filled using an inpainting technique [36]. The inpainting algorithm can follow a model such as:

$$I(p)=\sum q\in B(p)w(p,q)\cdot[I(q)+\nabla I(q)\cdot(p-q)]\sum q\in B(p)w(p,q),$$

where $I(p)$ represents the intensity of the pixel to be inpainted, $I(q)$ denotes the intensity of a neighboring pixel, and $\nabla I(q)$ signifies the gradient at pixel q. The weighting function $w(p,q)$ diminishes with distance, thereby amplifying contributions from closer and more similar pixels, and thereby preserving the natural continuity of biological structures. This approach minimizes errors caused by artifacts and enhances the diagnostic value of the endoscopic images. $I(p)$ is the color intensity of the point to be inpainted. This equation considers the intensity $I(q)$ and gradient $\nabla I(q)$ at nearby known points q, using a weighting function $w(p,q)$ that accentuates contributions from points directionally aligned with the original image's isophotes. The weighting function is derived from 3 critical components, directionality, distance, and level set distance, ensuring smooth integration of the inpainting with the surrounding image content. The fast-marching algorithm efficiently processes pixels based on their proximity to the initial boundary, facilitating rapid and consistent restoration of the damaged image areas.

Data Augmentation

We implemented various data augmentation techniques to enhance the model's generalization capabilities and replicate real-world variations observed in endoscopic images. These techniques encompassed rotating images across a full 360-degree range to simulate different viewing angles, applying a 15%

XSL•FO
RenderX

zoom to simulate variations in image size, shifting the width and height by 20% to introduce positional variations, and shearing by 15% to emulate stress distortions in tissue views. Furthermore, horizontal flipping was used to mitigate orientation biases, and the "reflect" filling mode was used to preserve image integrity during these transformations, ensuring a more comprehensive training process.

Pixel values were normalized to a range of (0, 1) to ensure consistency in data input, which is essential for the model's effective learning. In addition, one-hot encoding was used to convert categorical labels into a binary matrix format, a crucial step for enabling the model to handle binary-class classification tasks efficiently (Figure 2).

Figure 2. Hue, saturation, and value color space transformation and artifact management in endoscopic images for enhanced diagnostic accuracy.



Training Setup

The dataset was divided into training and validation sets in an 8:2 ratio. Input data labeling was based on pathology data, which was considered the gold standard for our classification tasks. Furthermore, 5-fold cross-validation was used to assess single models' performance within the ensemble. This technique partitions the training dataset into 5 subsets, using each subset iteratively for validation while the remaining data serves as the training set.

Deep Learning Model

We used a comprehensive ensemble of 16 deep learning models, carefully selected based on their proven effectiveness in image classification tasks, particularly in medical imaging. Each model was constructed using PyTorch (Linux Foundation) and initialized with pretrained weights from the ImageNet dataset. This transfer-learning approach, where a model is pretrained on a large dataset and subsequently fine-tuned for a specific task, is a well-established strategy in medical imaging and has demonstrated substantial efficacy.

Our selection encompassed DenseNet (Densely Connected Convolutional Network), EfficientNet, ResNet, VGG (Visual Geometry Group), Inception, and Vision Transformer architectures, incorporating diverse feature extraction techniques to ensure a comprehensive evaluation of different deep learning methodologies. By leveraging the advanced feature extraction capabilities gained through pretraining on the large-scale and diverse ImageNet dataset, our primary objective was to enhance classification accuracy for endoscopic images. This diversified ensemble approach allowed us to systematically assess each model's strengths and optimize performance through ensemble learning.

In our study, we implemented patch-based learning to analyze endoscopic images, wherein each of our network models was trained on segmented sections of the images for a more targeted approach. The parameters used in this fine-tuning process are outlined in Table 2, offering a comprehensive overview of the configurations used to optimize our deep learning models for analyzing intricate characteristics of endoscopic images.

Table . Hyperparameter configurations for fine-tuning deep learning models on endoscopic images.

Hyperparameters	Networks			
	DenseNet[a] 121	EfficientNet B0	EfficientNet B1	VGG[b] 19
Initialization	He normal initialization	He normal initialization	He normal initialization	He normal initialization
Batch size	10	10	10	10
Patch size	81×81	81×81	81×81	81×81
Total epochs	10	15	15	15
Optimizer	Adam	Adam	Adam	Adam
Learning rate	0.0001	0.0005	0.0005	0.0001

[a]DenseNet: Densely Connected Convolutional Network.

[b]VGG: Visual Geometry Group.

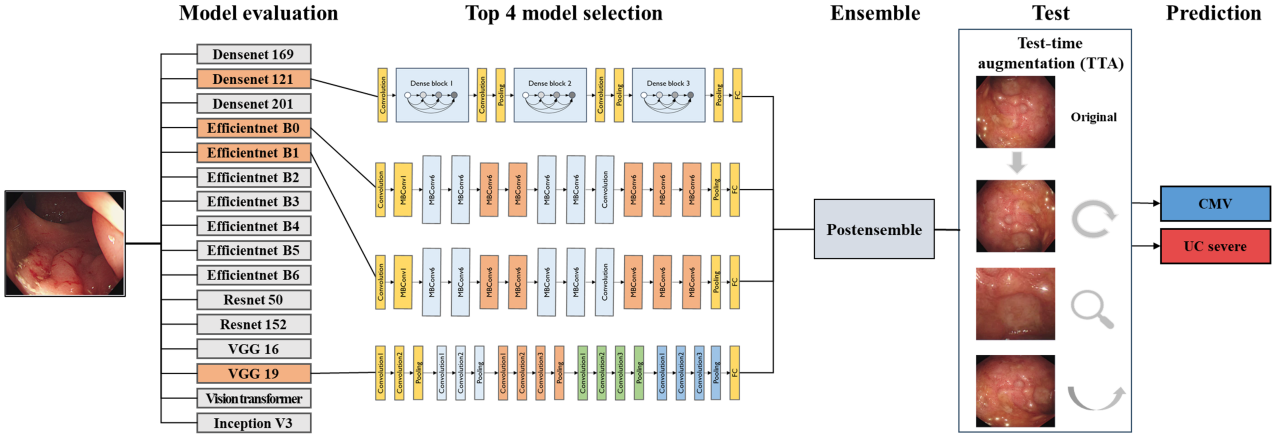
We used He normal initialization and the Adam optimization algorithm to further enhance the performance of our deep learning models. The He normal initialization, also known as Kaiming initialization, was specifically selected for its

XSL•FO
RenderX

effectiveness in preserving the variance of the input distributions across layers in deep neural networks, a critical aspect when dealing with complex image data such as endoscopic images. This initialization method addresses the vanishing and exploding gradient issues commonly encountered in training deep architectures, promoting a more stable and efficient optimization process. In addition, we used the Adam optimization algorithm for its adaptive learning rate capabilities, which are crucial for navigating the intricate optimization landscapes inherent in deep learning tasks. Adam combines the benefits of 2 other extensions of stochastic gradient descent—AdaGrad and RMSProp—to adjust the learning rate during training dynamically. This adjustment is based on estimates of lower-order moments of the gradients, facilitating more rapid and effective convergence of our models to the optimal solution.

The top 4 models were selected from a pool of 16 based on their F_1-score, as it is a representative metric that balances precision and recall. In medical image analysis, maintaining a balance between false positives and false negatives is crucial, making the F_1-score a clinically reliable selection criterion. These models were subsequently integrated using a soft-voting ensemble technique, further augmented with TTA to enhance prediction reliability and accuracy (Figure 3). We used an averaging approach to derive the final prediction in the soft-voting procedure. Soft voting was chosen as the optimal ensembling strategy because the models exhibited similar performance, and there was no specific reason to assign higher confidence to any particular model [37,38]. By aggregating the predicted probabilities from multiple models, soft voting provides a more refined decision boundary and yields more stable predictions compared with majority voting. In addition, in the case of weighted voting, adjusting the weights did not result in significant performance improvements over soft voting, and equally incorporating all models through soft voting proved to be the most effective approach. Conversely, TTA involves applying minor variations to the input data during testing, thus providing a more comprehensive evaluation of the model's performance across diverse conditions. For TTA, we implemented techniques such as horizontal and vertical flips, random adjustments in brightness contrast (±20%), and scaling (30%). These augmentations played a pivotal role in optimizing the predictive capabilities of our system in the challenging realm of endoscopic image analysis, facilitating the introduction of diverse variations and thereby bolstering the model's ability to generalize and perform consistently across varying imaging scenarios.

Figure 3. Ensemble deep learning framework for classifying severe ulcerative colitis and cytomegalovirus lesions from endoscopic images. The framework consists of multiple deep learning models pretrained on ImageNet and fine-tuned for the specific classification task. Single model outputs are ensembled to enhance overall classification accuracy. Test-time augmentation, including rotations, zooming, and flipping, is used to ensure robustness against variations in clinical data before making the final prediction. CMV: cytomegalovirus; UC: ulcerative colitis; VGG: Visual Geometry Group.



In addition, we evaluated ensemble models comprising 2 and 3 models, both with and those without the implementation of TTA. This extensive analysis enabled us to compare the efficacy of varying ensemble sizes and evaluate the impact of TTA on their predictive prowess, specifically emphasizing the averaged soft-voting technique used in tandem with TTA.

Loss Function

For the binary classification task, the sigmoid activation function was selected for its capability to effectively map input values to a probability distribution ranging from 0 to 1, thereby generating probabilities indicating whether a given input pertains to one class or the other. This made it particularly suitable for discerning between the 2 classes in our study. Complementing this selection, categorical cross-entropy was used as the loss function, given its capacity to quantify the disparity between the predicted distribution and the true distribution of outcomes, which is relevant for binary classification tasks. Categorical cross-entropy measures the difference between the actual label and the predicted probability distribution across classes, thereby furnishing a robust metric for optimizing the model's performance. By minimizing this loss function, the model is incentivized to adjust its parameters to enhance its predictions' accuracy, aligning the predicted class probabilities as closely as possible with the ground truth labels.

Evaluation

We evaluated the performance of ensemble models consisting of 2, 3, and 4 models, both with and without applying TTA. In addition, we assessed the performance of single models.

The assessment used key evaluation metrics, including accuracy, precision, recall, and F_1-score, providing comprehensive insights into each model's classification performance. In addition, 95%

XSL•FO
RenderX

CIs were computed for all evaluation metrics to ensure statistical reliability. The following definitions outline these metrics:

Accuracy=Tp+TnTp+Tn+Fp+Fn

Precision=TpTp+Fp

Recall=TpTp+Tn

F1−score=2·precision·recallprecision+recall

Furthermore, we assessed the diagnostic capabilities of the models through receiver operating characteristic (ROC) curves and their corresponding AUC. These evaluations enabled us to analyze the trade-offs between true positive and false positive rates, as well as to quantify the overall diagnostic accuracy of each model configuration.

To ensure statistical robustness, 95% CIs were computed using 300 bootstrap resampling iterations for all evaluation metrics, including ROC and AUC. This approach enhances the reliability of the performance assessment by providing more stable and generalizable CIs across different evaluation metrics.

Ethical Considerations

The study was approved by the institutional review board (IRB EUMC 2023-11-009, SEUMC 2023-09-017).

Results

The performance results of both single models and ensemble model combinations are outlined in Table 3. A comprehensive evaluation of various single models was conducted. DenseNet 121, EfficientNet B0, EfficientNet B1, and VGG 19 stood out for their superior performance, ranking in the top quartile within a cohort of 13 models. Performance metrics, including accuracy, precision, recall, and F_1-score, were recorded along with their 95% CI. DenseNet 121 exhibited exceptional diagnostic reliability for severe UC conditions, achieving an accuracy of 0.792 (95% CI 0.776 - 0.808), a precision of 0.821 (95% CI 0.805 - 0.837), a recall of 0.876 (95% CI 0.859 - 0.893), and an F_1-score of 0.836 (95% CI 0.820 - 0.852). EfficientNet B0 demonstrated substantial capability in identifying true positives, with a recall of 0.824 (0.809 - 0.839), supported by an accuracy of 0.736 (95% CI 0.720 - 0.752), a precision of 0.765 (95% CI 0.746 - 0.784), and an F_1-score of 0.784 (95% CI 0.768 - 0.800). EfficientNet B1 contributed to reducing false positives, achieving a precision of 0.759 (95% CI 0.742 - 0.776), an accuracy of 0.681 (95% CI 0.660 - 0.702), a recall of 0.709 (95% CI 0.692 - 0.726), and an F_1-score of 0.738 (95% CI 0.720 - 0.756). Despite a lower accuracy of 0.660 (95% CI 0.635 - 0.685), VGG 19 played a key role in positive case identification, with a precision of 0.707 (95% CI 0.690 - 0.724), a recall of 0.745 (95% CI 0.729 - 0.761), and an F_1-score of 0.729 (95% CI 0.710 - 0.748).

Table . Average performance metrics with confidence intervals of the top 4 single models and test-time augmentation ensemble models.

Model	Accuracy (95% CI)	Precision (95% CI)	Recall (95% CI)	F_1-score (95% CI)
DenseNet[a] 121	0.792 (0.776 - 0.808)	0.821 (0.805 - 0.837)	0.876 (0.859 - 0.893)	0.836 (0.820 - 0.852)
EfficientNet B0	0.736 (0.720 - 0.752)	0.765 (0.746 - 0.784)	0.824 (0.809 - 0.839)	0.784 (0.768 - 0.800)
EfficientNet B1	0.681 (0.660 - 0.702)	0.759 (0.742 - 0.776)	0.709 (0.692 - 0.726)	0.738 (0.720 - 0.756)
VGG[b] 19	0.660 (0.635 - 0.685)	0.707 (0.690 - 0.724)	0.745 (0.729 - 0.761)	0.729 (0.710 - 0.748)
Ensemble 4 models with TTA[c]	0.836 (0.824 - 0.848)	0.850 (0.832 - 0.868)	0.904 (0.890 - 0.918)	0.875 (0.860 - 0.890)
Ensemble 3 models with TTA	0.723 (0.705 - 0.741)	0.814 (0.801 - 0.828)	0.789 (0.775 - 0.803)	0.802 (0.787 - 0.817)
Ensemble 2 models with TTA	0.715 (0.697 - 0.733)	0.781 (0.765 - 0.797)	0.832 (0.818 - 0.846)	0.794 (0.778 - 0.810)
Ensemble 4 models without TTA	0.709 (0.692 - 0.726)	0.691 (0.675 - 0.707)	0.716 (0.700 - 0.732)	0.752 (0.737 - 0.767)
Ensemble 3 models without TTA	0.775 (0.762 - 0.788)	0.753 (0.740 - 0.766)	0.759 (0.746 - 0.772)	0.755 (0.742 - 0.768)
Ensemble 2 models without TTA	0.673 (0.655 - 0.691)	0.750 (0.738 - 0.762)	0.776 (0.762 - 0.790)	0.763 (0.745 - 0.781)

[a]DenseNet: Densely Connected Convolutional Network.

[b]VGG: Visual Geometry Group.

[c]TTA: test-time augmentation.

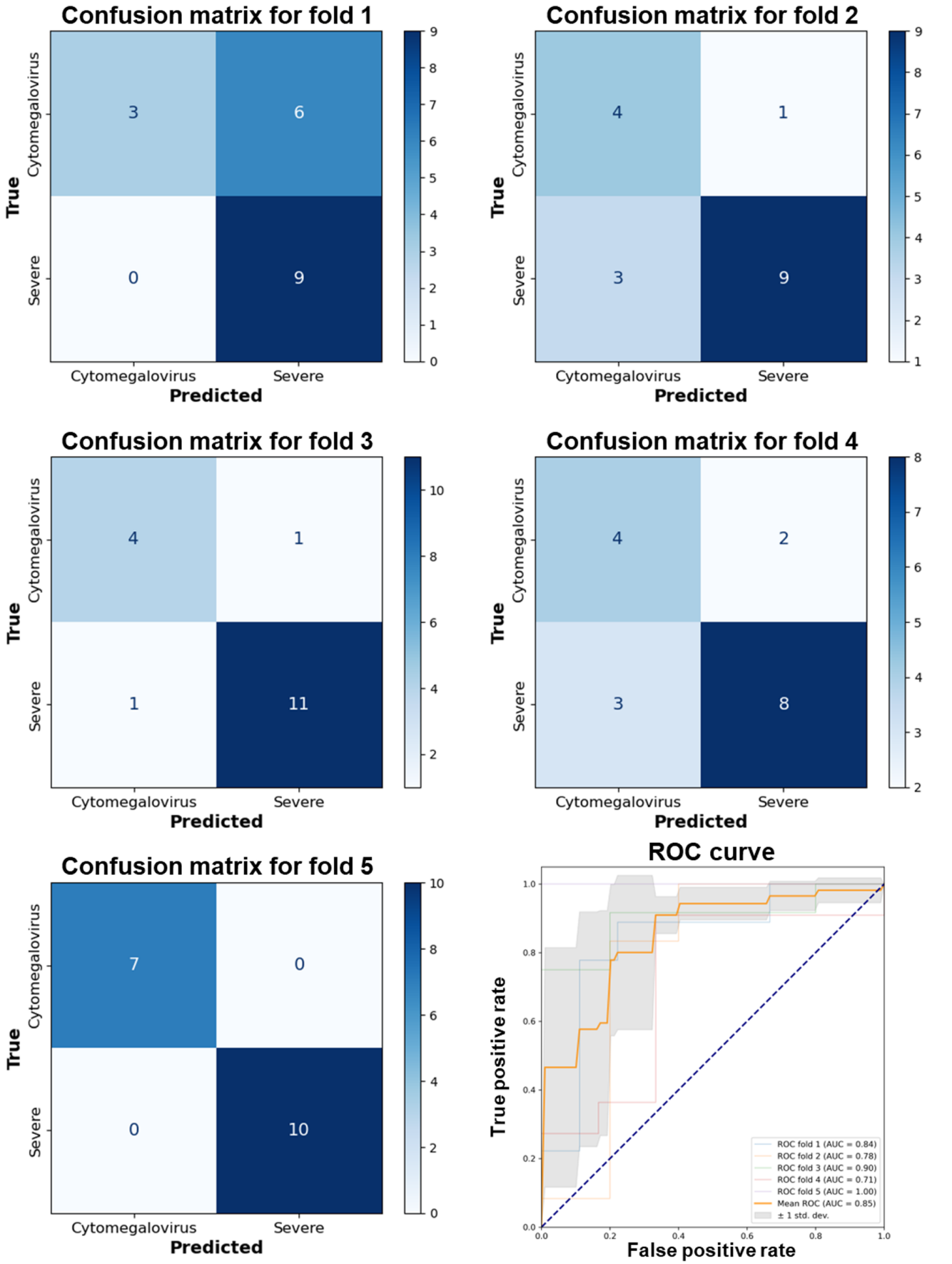
Further analysis using ROC curves and the AUC metric provided additional insights into model performance, demonstrating a long-term high true positive rate against a lower false positive rate, indicative of robust diagnostic capabilities. DenseNet 121 consistently exhibited an average AUC of 0.846 (SD 0.100) across folds (Figure 4). Meanwhile, EfficientNet B0 and B1 also displayed excellent classification abilities, with average AUCs of 0.796 (SD 0.098) and 0.838 (SD 0.107), respectively (Figures 5 and 6). VGG 19, while presenting an average AUC of 0.730 (SD 0.115), showcased instances of high performance,

XSL•FO
RenderX

particularly in folds where it achieved an AUC as high as 0.920 (Figure 7). However, a discrepancy was observed in the model's performance through confusion matrix analysis; all models accurately identified severe UC conditions but exhibited inconsistency in identifying CMV conditions (Figures 4-7). This inconsistency was particularly evident for DenseNet 121 and EfficientNet B0, highlighting the need for improvement. These findings indicate that single models may encounter limitations when distinguishing CMV.

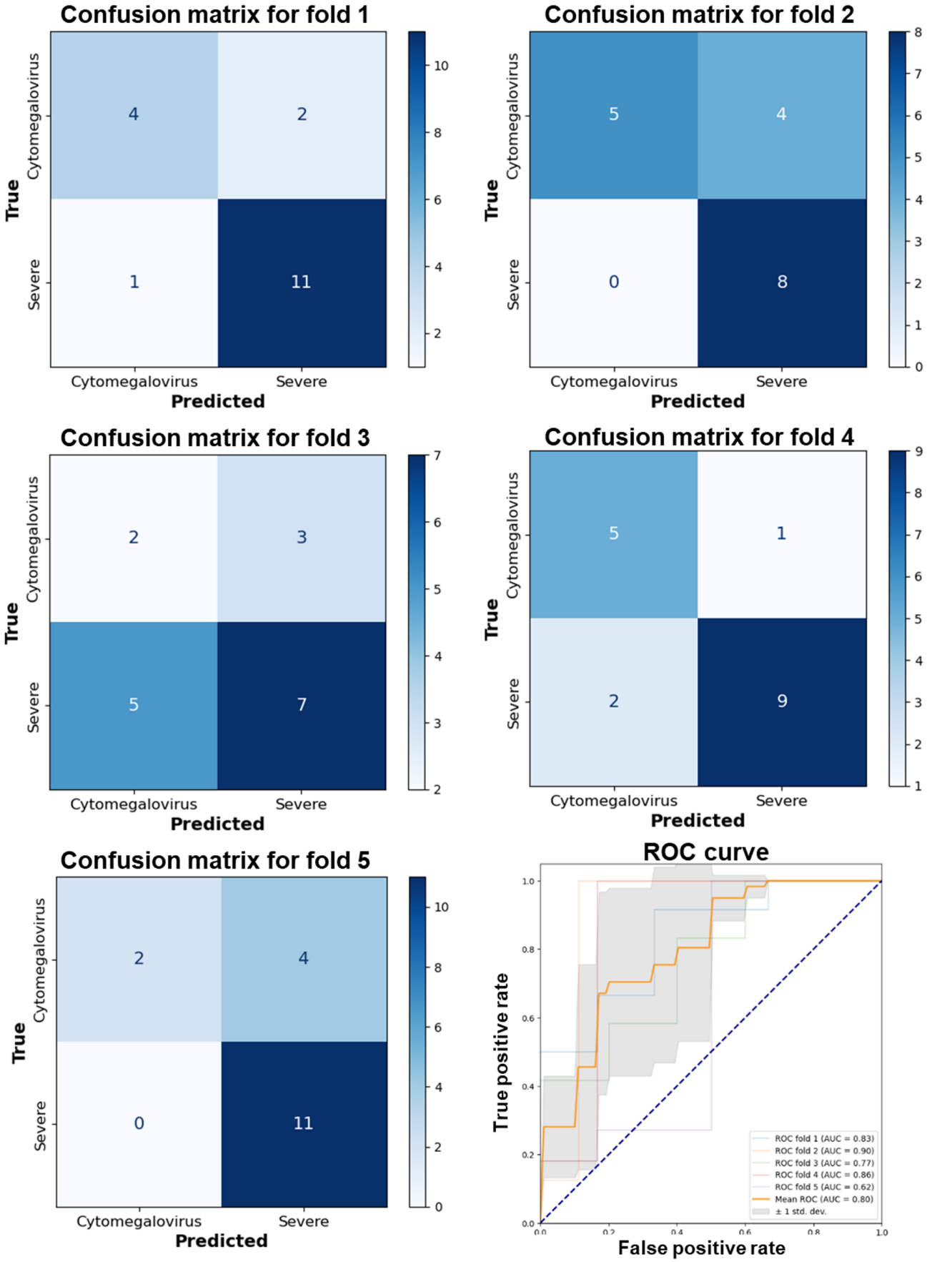
XSL•FO
RenderX

Figure 4. Performance evaluation of the DenseNet 121 model using 5-fold cross-validation and receiver operating characteristic curve analysis. AUC: area under the curve; ROC: receiver operating characteristic.



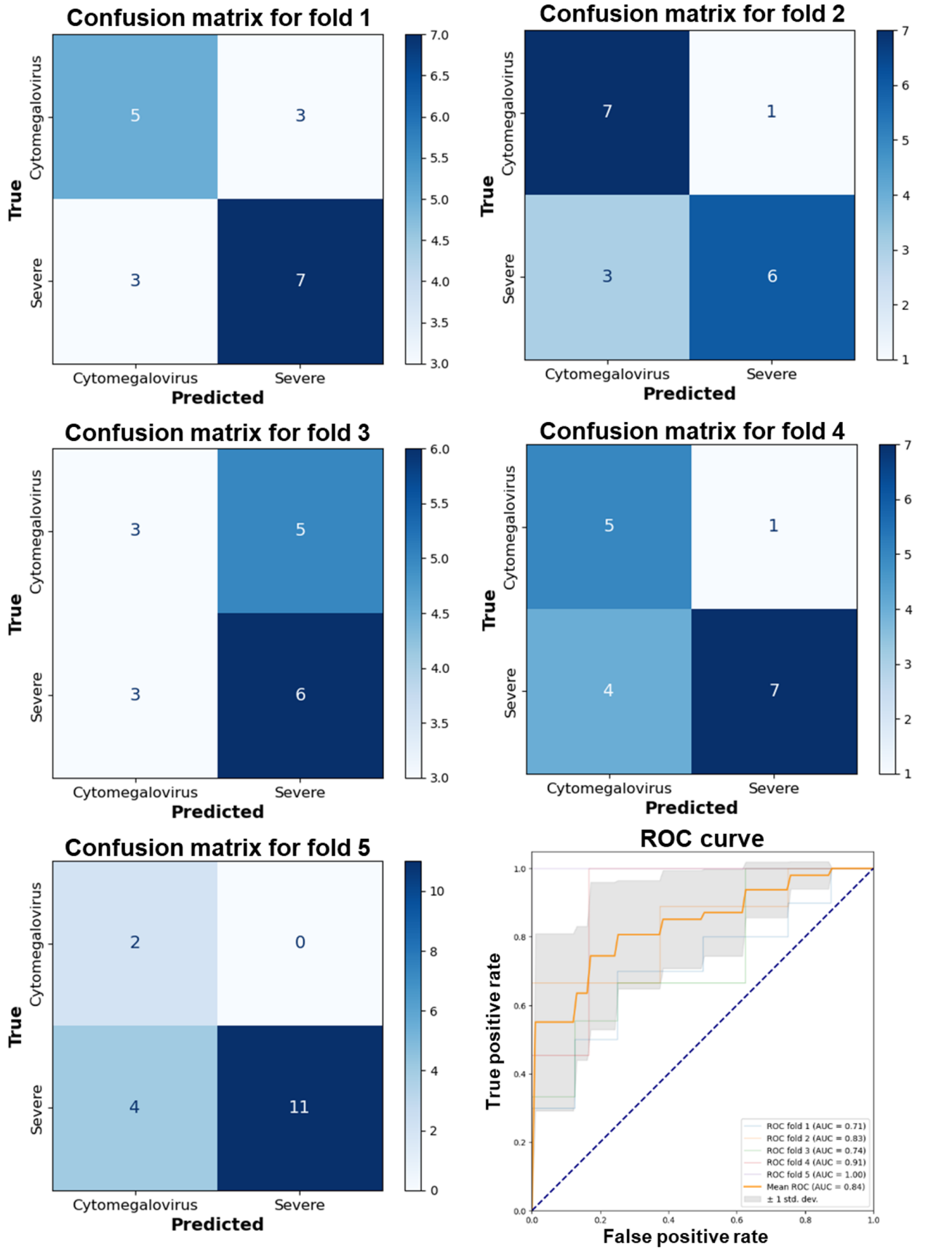
XSL•FO
RenderX

Figure 5. Performance evaluation of the EfficientNet B0 model using 5-fold cross-validation and receiver operating characteristic curve analysis. AUC: area under the curve; ROC: receiver operating characteristic.



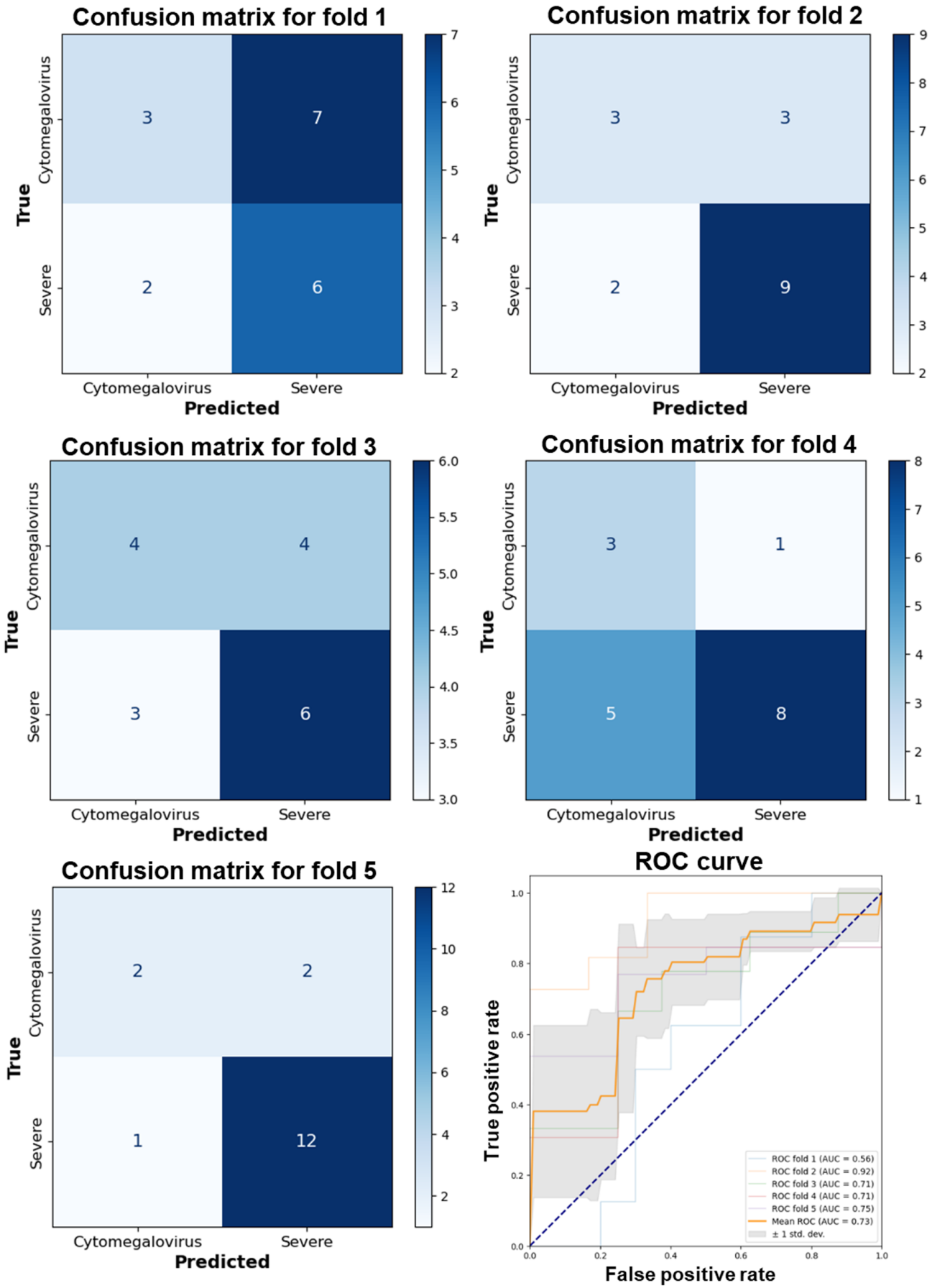
XSL•FO
RenderX

Figure 6. Performance evaluation of the EfficientNet B1 model using 5-fold cross-validation and receiver operating characteristic curve analysis. AUC: area under the curve; ROC: receiver operating characteristic.



XSL•FO
RenderX

Figure 7. Performance evaluation of the VGG 19 model using 5-fold cross-validation and receiver operating characteristic curve analysis. AUC: area under the curve; ROC: receiver operating characteristic.

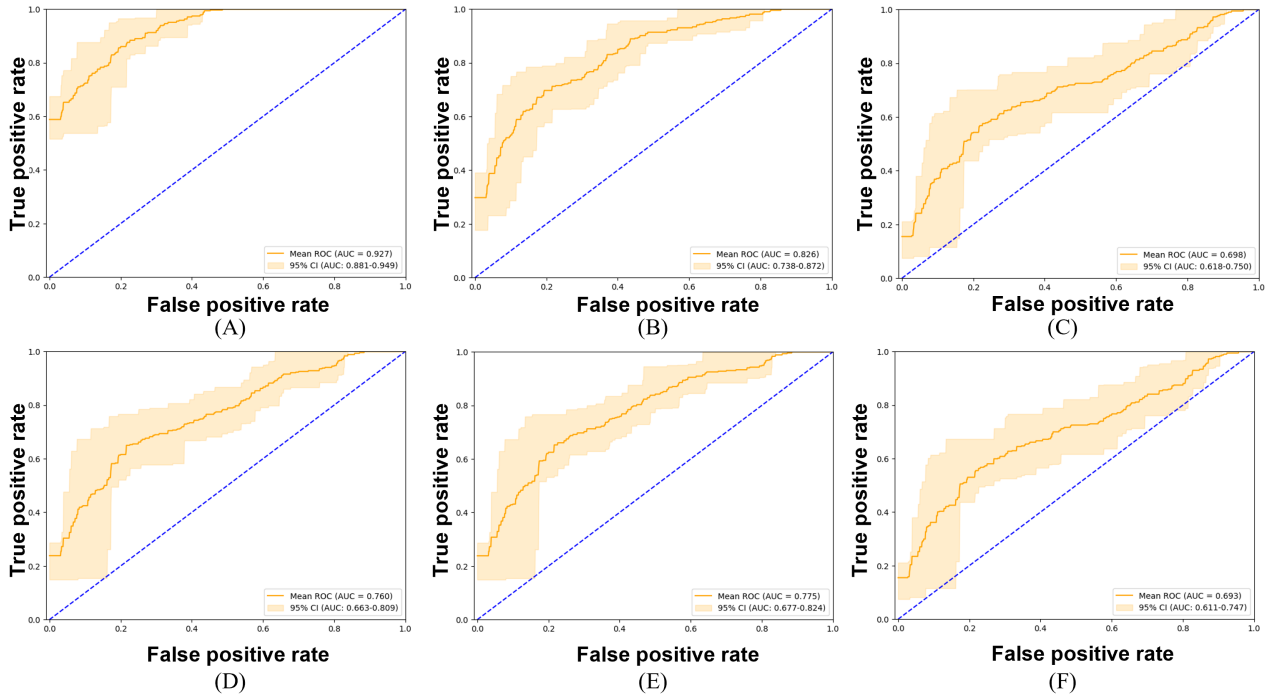


XSL•FO
RenderX

Incorporating the TTA technique into the ensemble model approach proved pivotal in addressing these classification challenges. The ensemble of 4 models augmented with TTA demonstrated remarkable efficacy in classifying endoscopic images of UC. The ensemble achieved an accuracy of 0.836 (95% CI 0.824 - 0.848), a precision of 0.850 (95% CI 0.832-0.868), a recall of 0.904 (95% CI 0.890 - 0.918), and an F_1-score of 0.875 (95% CI 0.860 - 0.890), indicating high reliability and balanced classification capabilities. Other ensemble configurations also yielded noteworthy results. The ensemble of 3 models with TTA exhibited precision of 0.814 (95% CI 0.801 - 0.828), while the ensemble of 2 models with TTA demonstrated recall of 0.832 (95% CI 0.818 - 0.846) and F_1-score of 0.794 (95% CI 0.778 - 0.810), indicating effective identification of true positive cases. Conversely, ensemble models without TTA showed a noticeable decline in performance metrics, with the ensemble of 4 models without TTA achieving an accuracy of 0.709 (95% CI 0.692 - 0.726), a precision of 0.691 (95% CI 0.675 - 0.707), a recall of 0.716 (95% CI 0.700 - 0.732), and an F_1-score of 0.752 (95% CI 0.737 - 0.767). These results emphasize the significant role of TTA in enhancing classification performance and improving model generalization in distinguishing CMV from severe UC.

The ROC curves reveal discernible patterns in model efficacy attributable to integrating TTA and the amalgamation of models within the ensemble (Figure 8). The ensemble of 4 models enhanced with TTA is particularly noteworthy, demonstrating the most pronounced diagnostic proficiency, with an AUC of 0.927 (95% CI 0.881 - 0.949). This signifies superior diagnostic performance and a high true positive rate compared with the false positive rate. Despite a reduction in ensemble size, the ensemble comprising 3 models, with TTA implementation, maintains robust performance, as evidenced by an AUC of 0.826 (95% CI 0.738 - 0.872). Conversely, the ensemble of 2 models with TTA displays a relatively inferior AUC of 0.698 (95% CI 0.618 - 0.750).

Figure 8. Receiver operating characteristic curves for endoscopic image classification models: (**A**) ensemble of 4 models with test-time augmentation, (**B**) ensemble of 3 models with test-time augmentation, (**C**) ensemble of 2 models with test-time augmentation, (**D**) ensemble of 4 models without test-time augmentation, (**E**) ensemble of 3 models without test-time augmentation, and (**F**) ensemble of 2 models without test-time augmentation. AUC: area under the curve; ROC: receiver operating characteristic.



In setups without TTA, there is generally a decrease in ensemble performance. The ensemble of 4 models without TTA achieves an AUC of 0.760 (95% CI 0.663 - 0.809), confirming the efficacy of the ensemble approach even with a slight drop in effectiveness. Interestingly, a 3-model ensemble without TTA exhibits a slightly higher AUC of 0.775 (95% CI 0.677 - 0.824), indicating a particularly effective combination of models. Conversely, the pair of models without TTA demonstrates the most notable decrease in performance, with an AUC of 0.693 (95% CI 0.611 - 0.747), underscoring the significance of TTA in enhancing model performance and the benefits of larger ensembles for diagnostic accuracy.

Discussion

Principal Findings

The study underscores substantial advancements in medical diagnostics, particularly in gastroenterology, facilitated by applying deep learning technology. This research distinguishes itself by using an ensemble of deep learning models, including DenseNet121, EfficientNet B0, EfficientNet B1, and VGG 19, to differentiate between severe UC and CMV infection using endoscopic images. By leveraging an ensemble approach, this study not only improves classification performance but also demonstrates the clinical applicability of deep learning in distinguishing between these 2 conditions.

XSL•FO
RenderX

The evaluation of single models revealed their limitations in identifying CMV, highlighting the need for a more comprehensive approach. This insight underscores the utility of the TTA ensemble technique in discerning CMV infections and accurately classifying severe UC from endoscopic images. Furthermore, this approach indicates the potential to surmount the constraints of single-model methodologies and enhance diagnostic accuracy in complex medical image classification tasks. The ability to overcome the constraints of single-model methodologies and enhance diagnostic accuracy in complex medical image classification tasks is a crucial advancement in this field. These findings suggest that integrating deep learning into clinical workflows can significantly improve real-world diagnostic processes.

The ensemble of 4 models with TTA achieved remarkable performance in classifying endoscopic images of severe UC, with an accuracy of 0.836 (95% CI 0.824 - 0.848), precision of 0.850 (95% CI 0.832 - 0.868), recall of 0.904 (95% CI 0.890 - 0.918), and F_1-score of 0.875 (95% CI 0.860 - 0.890). These results indicate high reliability and balanced performance, reinforcing the ensemble's ability to deliver accurate and consistent diagnoses. The improved diagnostic accuracy can have a direct impact on clinical decision-making, reducing diagnostic errors and enabling timely intervention.

The distinction between CMV and severe UC through endoscopic images has been a topic in previous research [11-13]. Although specific endoscopic features can differentiate these 2 conditions, the differences are often subtle and require meticulous observation. Features, such as severe ulcers, punched-out ulcers, geographical ulcers, and spontaneous bleeding, can be crucial in differentiating certain diseases [12]. However, identifying these features through conventional observation methods is often challenging. Applying the ensemble model with TTA represents a substantial advancement in this context [39]. It stands out as the first initiative to harness the capabilities of deep learning or machine learning for this purpose. The insights derived from the AUC values and the corresponding ROC curves are pertinent. The ensemble method enhanced by TTA underscores the potential of deep learning in medical diagnostics. When integrated into clinical workflows, these advanced models have the potential to substantially enhance patient care by enabling more precise and accurate diagnoses, thereby laying the groundwork for improved patient outcomes and marking a noteworthy advancement in health care technology.

To further contextualize these advantages in clinical practice, deep learning models can contribute to reducing interobserver variability, which is a critical challenge in medical imaging. By providing consistent and objective assessments, AI-driven diagnostic tools can complement physician expertise, particularly in resource-limited settings where access to highly experienced endoscopists may be restricted. In addition, AI-powered systems can expedite the diagnostic process, enabling real-time or near-instantaneous assessments that facilitate prompt therapeutic interventions. These improvements translate into enhanced patient management, reduced hospital stays, and minimized complications associated with diagnostic delays.

Furthermore, integrating AI-based diagnostic models into real-time clinical decision support systems could significantly enhance their clinical utility. Future research should explore embedding these AI models into endoscopic software or electronic health record systems. This integration could provide real-time diagnostic support to gastroenterologists, improve the efficiency of the diagnostic process, and facilitate quicker treatment decisions. Ultimately, this could become a key factor in enhancing the overall quality of patient care.

A substantial limitation identified during the research process was the occurrence of false negatives in the validation phase [40]. These findings underscore the necessity for further adjustments to improve the model's sensitivity, particularly in medical diagnostics, where distinguishing between similar conditions, such as CMV and UC, is critical. False negatives can cause delayed or inappropriate treatment, negatively impacting patient outcomes [41]. To address this, future studies should incorporate advanced augmentation techniques to enhance model sensitivity while maintaining specificity. In addition, exploring hybrid AI approaches that combine deep learning with rule-based algorithms could further refine diagnostic accuracy [42,43].

Another limitation is the lack of datasets; the data used in this study were limited in scope and quantity, thus constraining the generalizability and reliability of the model. As with other studies using proprietary datasets, our research also faces challenges in generalization, as the model was trained on a specific dataset. However, it is important to note that endoscopic imaging, compared with other imaging modalities, exhibits relatively minimal variation across different manufacturers due to its reliance on optic imaging rather than quantitative imaging [44]. This consistency helps maintain uniformity in image quality, which can positively impact AI model training and application.

Nevertheless, to address these generalization limitations, future research endeavors aim to mitigate these challenges by acquiring more diverse and extensive data through collaboration with multiple institutions. Multi-institutional data collection and incorporating various patient populations will enhance the model's robustness and ensure its applicability across different clinical settings. Incorporating data gathered from various patient groups and regions will enhance the model's generalization capability and facilitate the development of more reliable diagnostic tools [45]. Such collaborative efforts across multiple institutions are essential for augmenting the accuracy and reliability of the model.

This study uses deep learning technology to introduce a novel approach to medical diagnostics, particularly in gastroenterology. As the first to use deep or machine learning in distinguishing between severe UC and CMV, it heralds new possibilities in medical diagnostics. Implementing deep learning, notably the ensemble model with TTA, facilitates rapid, noninvasive, and remarkably accurate diagnostic techniques. These holds promise for substantially enhancing patient experience compared with conventional diagnostic approaches,

XSL•FO
RenderX

resulting in time and resource savings and diminishing the necessity for unnecessary invasive procedures. Such methodologies alleviate patient discomfort and risk, expediting treatment decisions.

Conclusion

This study marks a significant advancement in medical diagnostics by leveraging deep learning, specifically an ensemble model with TTA, to differentiate between severe UC and CMV infections using endoscopic images. While our findings demonstrated high accuracy, precision, and recall, the model's reliance on a specific dataset may limit its generalizability, necessitating further validation in diverse clinical settings. By introducing a streamlined, noninvasive, and accurate approach, this research highlights the potential of AI-driven diagnostics in gastroenterology while underscoring the need for further refinement to enhance clinical applicability.

Acknowledgments

This research was supported by Basic Science Research Program through the National Research Foundation of Korea funded by the Ministry of Education (RS-2023 - 00240003) and National Research Foundation of Korea grant funded by the Korean government (Ministry of Science and Information and Communication Technology; NRF-2023R1A2C2003808).

Authors' Contributions

JHK, ARC, and JRB contributed equally to this work as co-first authors. SHA and SAJ contributed equally as co-corresponding authors.

Conflicts of Interest

None declared.

References

1. Lee HS, Park SH, Kim SH, et al. Risk factors and clinical outcomes associated with cytomegalovirus colitis in patients with acute severe ulcerative colitis. Inflamm Bowel Dis 2016 Apr;22(4):912-918. [doi: 10.1097/MIB.0000000000000675] [Medline: 26829410]
2. Cannon MJ, Schmid DS, Hyde TB. Review of cytomegalovirus seroprevalence and demographic characteristics associated with infection. Rev Med Virol 2010 Jul;20(4):202-213. [doi: 10.1002/rmv.655] [Medline: 20564615]
3. Kim YS, Kim YH, Kim JS, IBD Study Group of the Korean Association for the Study of Intestinal Diseases, et al. The prevalence and efficacy of ganciclovir on steroid-refractory ulcerative colitis with cytomegalovirus infection: a prospective multicenter study. J Clin Gastroenterol 2012 Jan;46(1):51-56. [doi: 10.1097/MCG.0b013e3182160c9c] [Medline: 21552140]
4. Park SH, Yang SK, Hong SM, et al. Severe disease activity and cytomegalovirus colitis are predictive of a nonresponse to infliximab in patients with ulcerative colitis. Dig Dis Sci 2013 Dec;58(12):3592-3599. [doi: 10.1007/s10620-013-2828-1] [Medline: 23979435]
5. Matsumoto S, Yoshida Y. What are the factors that affect hospitalization and surgery for aggravation of ulcerative colitis? Eur J Gastroenterol Hepatol 2014 Mar;26(3):282-287. [doi: 10.1097/MEG.0000000000000028]
6. Choi CH, Moon W, Kim YS, et al. Second Korean guideline for the management of ulcerative colitis. Korean J Gastroenterol 2017 Jan 25;69(1):1-28. [doi: 10.4166/kjg.2017.69.1.1] [Medline: 28135789]
7. Rahier JF, Magro F, Abreu C, et al. Second European evidence-based consensus on the prevention, diagnosis and management of opportunistic infections in inflammatory bowel disease. Journal of Crohn's and Colitis 2014 Jun 1;8(6):443-468. [doi: 10.1016/j.crohns.2013.12.013]
8. Kornbluth A, Sachar DB, Practice Parameters Committee of the American College of Gastroenterology. Erratum: Ulcerative colitis practice guidelines in adults: American College of Gastroenterology, Practice Parameters Committee. Am J Gastroenterol 2010;105(3):500. [doi: 10.1038/ajg.2010.52] [Medline: 20068560]
9. McCurdy JD, Enders FT, Jones A, et al. Detection of cytomegalovirus in patients with inflammatory bowel disease: where to biopsy and how many biopsies? Inflamm Bowel Dis 2015 Dec;21(12):2833-2838. [doi: 10.1097/MIB.0000000000000556] [Medline: 26273816]
10. Garrido E, Carrera E, Manzano R, Lopez-Sanroman A. Clinical significance of cytomegalovirus infection in patients with inflammatory bowel disease. World J Gastroenterol 2013 Jan 7;19(1):17-25. [doi: 10.3748/wjg.v19.i1.17] [Medline: 23326158]
11. Suzuki H, Kato J, Kuriyama M, Hiraoka S, Kuwaki K, Yamamoto K. Specific endoscopic features of ulcerative colitis complicated by cytomegalovirus infection. WJG 2010;16(10):1245. [doi: 10.3748/wjg.v16.i10.1245]
12. Hirayama Y, Ando T, Hirooka Y, et al. Characteristic endoscopic findings and risk factors for cytomegalovirus-associated colitis in patients with active ulcerative colitis. World J Gastrointest Endosc 2016 Mar 25;8(6):301-309. [doi: 10.4253/wjge.v8.i6.301] [Medline: 27014426]

XSL•FO
RenderX

13. Nishimoto Y, Matsumoto T, Suekane H, Shimizu M, Mikami Y, Iida M. Cytomegalovirus infection in a patient with ulcerative colitis: colonoscopic findings. Gastrointest Endosc 2001 Jun;53(7):816-818. [doi: 10.1067/mge.2001.114955] [Medline: 11375602]
14. Pillet S, Pozzetto B, Roblin X. Cytomegalovirus and ulcerative colitis: place of antiviral therapy. World J Gastroenterol 2016 Feb 14;22(6):2030-2045. [doi: 10.3748/wjg.v22.i6.2030] [Medline: 26877608]
15. Randall J, Singh B, Warren BF, Travis SPL, Mortensen NJ, George BD. Delayed surgery for acute severe colitis is associated with increased risk of postoperative complications. Br J Surg 2010 Mar;97(3):404-409. [doi: 10.1002/bjs.6874] [Medline: 20101648]
16. Pal S, Sahni P, Pande GK, Acharya SK, Chattopadhyay TK. Outcome following emergency surgery for refractory severe ulcerative colitis in a tertiary care centre in India. BMC Gastroenterol 2005 Nov 30;5(39):39. [doi: 10.1186/1471-230X-5-39] [Medline: 16316474]
17. Zhang X, Zhang Y, Zhang G, et al. Deep learning with radiomics for disease diagnosis and treatment: challenges and potential. Front Oncol 2022;12:773840. [doi: 10.3389/fonc.2022.773840] [Medline: 35251962]
18. Lee JS, Yun J, Ham S, et al. Machine learning approach for differentiating cytomegalovirus esophagitis from herpes simplex virus esophagitis. Sci Rep 2021 Feb;11(1):3672. [doi: 10.1038/s41598-020-78556-z]
19. Colemont LJ, Pen JH, Pelckmans PA, Degryse HR, Pattyn SR, Van Maercke YM. Herpes simplex virus type 1 colitis: an unusual cause of diarrhea. Am J Gastroenterol 1990 Sep;85(9):1182-1185. [Medline: 2167608]
20. Schunter MO, Walles T, Fritz P, et al. Herpes simplex virus colitis complicating ulcerative colitis: a case report and brief review on superinfections. J Crohns Colitis 2007 Sep;1(1):41-46. [doi: 10.1016/j.crohns.2007.06.004] [Medline: 21172183]
21. Lawlor G, Moss AC. Cytomegalovirus in inflammatory bowel disease: pathogen or innocent bystander? Inflamm Bowel Dis 2010 Sep;16(9):1620-1627. [doi: 10.1002/ibd.21275] [Medline: 20232408]
22. Ayre K, Warren BF, Jeffery K, Travis SPL. The role of CMV in steroid-resistant ulcerative colitis: a systematic review. Journal of Crohn's and Colitis 2009 Sep;3(3):141-148. [doi: 10.1016/j.crohns.2009.03.002]
23. Inayat F, Hussain Q, Shafique K, Tasleem SH, Hurairah A. Cytomegalovirus colitis in immunocompetent patients. Cureus 2016 Nov 8;8(11):e869. [doi: 10.7759/cureus.869] [Medline: 27980888]
24. Ganaie MA, Hu M, Malik AK, Tanveer M, Suganthan PN. Ensemble deep learning: a review. Eng Appl Artif Intell 2022 Oct;115:105151. [doi: 10.1016/j.engappai.2022.105151]
25. Sundaresan V, Zamboni G, Rothwell PM, Jenkinson M, Griffanti L. Triplanar ensemble U-Net model for white matter hyperintensities segmentation on MR images. Med Image Anal 2021 Oct;73:102184. [doi: 10.1016/j.media.2021.102184] [Medline: 34325148]
26. Sohail A, Khan A, Nisar H, Tabassum S, Zameer A. Mitotic nuclei analysis in breast cancer histopathology images using deep ensemble classifier. Med Image Anal 2021 Aug;72:102121. [doi: 10.1016/j.media.2021.102121] [Medline: 34139665]
27. Ahmad A, Farooq F, Niewiadomski P, et al. Prediction of compressive strength of Fly Ash based concrete using individual and ensemble algorithm. Materials (Basel) 2021 Feb 8;14(4):794. [doi: 10.3390/ma14040794] [Medline: 33567526]
28. Oren O, Gersh BJ, Bhatt DL. Artificial intelligence in medical imaging: switching from radiographic pathological data to clinically meaningful endpoints. Lancet Digit Health 2020 Sep;2(9):e486-e488. [doi: 10.1016/S2589-7500(20)30160-6] [Medline: 33328116]
29. Wang S, Cao G, Wang Y, et al. Review and prospect: artificial intelligence in advanced medical imaging. Front Radiol 2021;1:781868. [doi: 10.3389/fradi.2021.781868] [Medline: 37492170]
30. Liu W, Tang JW, Mou JY, et al. Rapid discrimination of Shigella spp. and Escherichia coli via label-free surface enhanced Raman spectroscopy coupled with machine learning algorithms. Front Microbiol 2023;14(1101357):MID. [doi: 10.3389/fmicb.2023.1101357]
31. Thakur M, Kuresan H, Dhanalakshmi S, Lai KW, Wu X. Soft attention based DenseNet model for Parkinson's disease classification using SPECT images. Front Aging Neurosci 2022;14(908143):908143. [doi: 10.3389/fnagi.2022.908143] [Medline: 35912076]
32. Wu X, Wei Y, Jiang T, Wang Y, Jiang S. A micro-aggregation algorithm based on density partition method for anonymizing biomedical data. CBIO 2019 Sep 17;14(7):667-675. [doi: 10.2174/1574893614666190416152025]
33. Kimura M. Understanding test-time augmentation. : Springer-Verlag; 2021 Presented at: Neural Information Processing: 28th International Conference, ICONIP 2021; Dec 8-12, 2021 p. 558-569. [doi: 10.1007/978-3-030-92185-9_46]
34. Schroeder KW, Tremaine WJ, Ilstrup DM. Coated oral 5-aminosalicylic acid therapy for mildly to moderately active ulcerative colitis. A randomized study. N Engl J Med 1987 Dec 24;317(26):1625-1629. [doi: 10.1056/NEJM198712243172603] [Medline: 3317057]
35. Sutton RT, Zai ¨ane OR, Goebel R, Baumgart DC. Artificial intelligence enabled automated diagnosis and grading of ulcerative colitis endoscopy images. Sci Rep 2022 Feb;12(1):2748. [doi: 10.1038/s41598-022-06726-2]
36. Telea A. An image inpainting technique based on the fast marching method. Journal of Graphics Tools 2004 Jan;9(1):23-34. [doi: 10.1080/10867651.2004.10487596]
37. Sherazi SWA, Bae JW, Lee JY. A soft voting ensemble classifier for early prediction and diagnosis of occurrences of major adverse cardiovascular events for STEMI and NSTEMI during 2-year follow-up in patients with acute coronary syndrome. PLoS One 2021;16(6):e0249338. [doi: 10.1371/journal.pone.0249338] [Medline: 34115750]

XSL•FO
RenderX

38. Kumari S, Kumar D, Mittal M. An ensemble approach for classification and prediction of diabetes mellitus using soft voting classifier. International Journal of Cognitive Computing in Engineering 2021 Jun;2:40-46. [doi: 10.1016/j.ijcce.2021.01.001]
39. Son J, Kang S. Efficient improvement of classification accuracy via selective test-time augmentation. Inf Sci (Ny) 2023 Sep;642(C):119148. [doi: 10.1016/j.ins.2023.119148]
40. Burt T, Button KS, Thom H, Noveck RJ, Munafò MR. The burden of the "False-Negatives" in clinical development: analyses of current and alternative scenarios and corrective measures. Clin Transl Sci 2017 Nov;10(6):470-479. [doi: 10.1111/cts.12478] [Medline: 28675646]
41. Petticrew MP, Sowden AJ, Lister-Sharp D, Wright K. False-negative results in screening programmes: systematic review of impact and implications. Health Technol Assess 2000;4(5):1-120. [Medline: 10859208]
42. Ray P, Chakrabarti A. A mixed approach of deep learning method and rule-based method to improve aspect level sentiment analysis. ACI 2022 Mar 1;18(1/2):163-178. [doi: 10.1016/j.aci.2019.02.002]
43. Tan HX, Teo CHD, Ang PS, et al. Combining machine learning with a rule-based algorithm to detect and identify related entities of documented adverse drug reactions on hospital discharge summaries. Drug Saf 2022 Aug;45(8):853-862. [doi: 10.1007/s40264-022-01196-x] [Medline: 35794349]
44. Chen Y, Wu G, Qu C, Ye Z, Kang Y, Tian X. A multifaceted comparative analysis of image and video technologies in gastrointestinal endoscope and their clinical applications. Front Med 2023 Oct 10;10. [doi: 10.3389/fmed.2023.1226748]
45. Sarker IH. Deep learning: a comprehensive overview on techniques, taxonomy, applications and research directions. SN Comput Sci 2021;2(6):420. [doi: 10.1007/s42979-021-00815-1] [Medline: 34426802]

Abbreviations

AI: artificial intelligence
AUC: area under the curve
CMV: cytomegalovirus
DenseNet: Densely Connected Convolutional Network
H&E: hematoxylin and eosin
HSV: hue, saturation, value
IHC: immunohistochemistry
PCR: polymerase chain reaction
ROC: receiver operating characteristic
TTA: test-time augmentation
UC: ulcerative colitis
VGG: Visual Geometry Group

Edited by C Lovis; submitted 01.08.24; peer-reviewed by W Wu, X Wu; revised version received 10.03.25; accepted 11.03.25; published 01.07.25.

Please cite as:
Kim JH, Choe AR, Byeon JR, Park Y, Song EM, Kim SE, Jeong ES, Lee R, Kim JS, Ahn SH, Jung SA
Enhancing the Predictions of Cytomegalovirus Infection in Severe Ulcerative Colitis Using a Deep Learning Ensemble Model: Development and Validation Study
JMIR Med Inform 2025;13:e64987
URL: https://medinform.jmir.org/2025/1/e64987
doi:10.2196/64987

© Jeong Heon Kim, A Reum Choe, Ju Ran Byeon, Yehyun Park, Eun Mi Song, Seong-Eun Kim, Eui Sun Jeong, Rena Lee, Jin Sung Kim, So Hyun Ahn, Sung Ae Jung. Originally published in JMIR Medical Informatics (https://medinform.jmir.org), 1.7.2025. This is an open-access article distributed under the terms of the Creative Commons Attribution License (https://creativecommons.org/licenses/by/4.0/), which permits unrestricted use, distribution, and reproduction in any medium, provided the original work, first published in JMIR Medical Informatics, is properly cited. The complete bibliographic information, a link to the original publication on https://medinform.jmir.org/, as well as this copyright and license information must be included.

XSL•FO
RenderX

Leveraging AI to Drive Timely Improvements in Patient Experience Feedback: Algorithm Validation

Mustafa Khanbhai[1,2], MD, PhD; Catalina Carenzo[1,2], MSc; Sarindi Aryasinghe[1,2], BSc; David Manton[2], BSc; Erik Mayer[1,2,3], MD, PhD

[1]iCARE Digital Collaboration Space & Secure Data Environment, NIHR Imperial Biomedical Research Centre, 1a Sheldon Square, London, United Kingdom

[2]Department of Surgery & Cancer, Faculty of Medicine, Imperial College London, London, United Kingdom

[3]Imperial College Healthcare NHS Trust, London, United Kingdom

Corresponding Author:
Mustafa Khanbhai, MD, PhD
iCARE Digital Collaboration Space & Secure Data Environment, NIHR Imperial Biomedical Research Centre, 1a Sheldon Square, London, United Kingdom

Abstract

Background: Understanding and improving patient care is pivotal for health care providers. With increasing volumes of the Friends and Family Test (FFT) data in England, manual analysis of this patient feedback poses challenges for many health care organizations. This underscores the importance of automated text analysis, particularly in predicting sentiments and themes in real time.

Objective: Leveraging machine learning and natural language processing, this study explores the utility of a supervised algorithm to systematically test and refine the algorithm's cross-contextual performance in diverse health care settings, addressing variations in population characteristics, geographical locations, and care settings, ultimately driving improvements based on patient feedback.

Methods: The text analytics algorithm initially developed in a large acute trust in London was further tested in 9 health care organizations with diverse care settings across England. These trusts varied in technical capacity and resource, population demographics, and FFT free text datasets. Testing and validation of the algorithm were performed, including manual coding of a subset of retrospective comments. Technical infrastructure, including coding environments and packages for algorithm testing and deployment, was optimized. The algorithm was iteratively trained using bag of words from anonymized data, tailored to accommodate contextual variations, and tested for change in algorithm performance while simultaneously rectifying issues identified.

Results: The algorithm demonstrated satisfactory overall accuracy (>75%) in predicting themes and sentiments embedded within free-text responses across a variety of care settings and population demographics. While the algorithm yielded strong and reusable models in relatively stable environments, such as adult inpatient care settings, the initial accuracy was notably lower in organizations providing services such as pediatrics and mental health. However, the accuracy of our algorithm significantly improved when individual trust coding templates were applied. Thematic saturation was reached after the fifth organization was recruited, and no further coding was required for the last 4 organizations. Subsequently, a framework and pipeline for deployment of the algorithm were developed to provide a standardized approach for implementation and analysis of FFT free text, ensuring ease of use.

Conclusions: This study represents a significant step forward in leveraging free-text FFT data for valuable insights in diverse health care settings through the testing and development of a robust supervised learning text analytics algorithm. The disparity in some care settings was anticipated, given that the lexicon and phraseology used was inherently different from those prevalent in adult inpatient care (where the algorithm was developed). However, these challenges were addressed with further coding and testing. This approach enhanced the accuracy and reliability of the algorithm, encouraged inter- and intraorganizational collaboration, and shared learning.

(JMIR Med Inform 2025;13:e60900) doi:10.2196/60900

KEYWORDS

patient experience; quality improvement; free-text analysis; machine learning; artificial intelligence; patient feedback; friends and family test; natural language processing; algorithm; health informatics

XSL•FO
RenderX

Introduction

Insights into patients' experience of their care provision are critical for health care providers delivering patient-centered care and recognized as integral to ensuring safe and high-quality care [1]. By the end of 2019, the national survey for patient experiences in the United Kingdom, known as the Friends and Family Test (FFT), had accumulated 75 million pieces of feedback [2]. This number continues to grow by about 1.3 million every month, making it the largest source of patient opinions worldwide. However, manually analyzing this vast amount of data requires a considerable resource, something that many health care organizations struggle to provide [3,4]. In recent years, there has been an ever-clearer desire for improvement to arise from patient feedback rather than just focusing on response rates, but most health care organizations are constrained from doing so due to a lack of analytical expertise [5].

Automated text analysis by artificial intelligence (AI) and its component natural language processing (NLP) predicts sentiments and themes within free-text responses in real time and provides a useful opportunity for better integrating patient experience feedback into everyday health care delivery [4]. NLP algorithms offer a practical solution to decode the "why" behind patient narratives, and through their ability to process large volumes of data accurately, these patient-derived insights can inform "business as usual" within health care organizations [6,7]. Recent advances in NLP, particularly the development of large language models and transformer-based architectures such as BERT [8] and GPT [9], have significantly improved the analysis of patient feedback in health care. These models replace traditional hand-coded, framework-based categorization [10] methods by automating the classification of concerns and providing decision-makers with real-time, comprehensive summaries of emerging themes. Large language models, through multi-label text classification [11], enable the extraction of deeper insights from patient experience comments, enhancing the understanding of the patient journey and informing actions that can improve care. Transformer-based models such as BERT [8,12] and GPT excel at capturing complex linguistic patterns, context, ambiguity, and sentiment, making them particularly well-suited for the nuanced task of sentiment analysis in health care. These advancements allow for more accurate, context-aware analysis of patient feedback, driving more actionable insights and supporting continuous improvements in patient care.

BERT and GPT models are large and resource-intensive [13]. They require significant computational power and memory, which may not be feasible in all health care settings, especially those with limited information technology (IT) infrastructure. This can make them less practical for real-time applications or for use in smaller organizations with fewer resources. Due to their size and complexity, transformer models can be slower to process compared to more lightweight models such as support vector machines (SVMs). In real-time health care applications where speed is crucial for timely interventions, this delay may be a significant drawback.

We have previously demonstrated the benefit of applying NLP using SVM to free-text FFT data to deliver patient-driven quality improvement in a single institution [14]. This study demonstrates the broader implementation and iteration of this algorithm in different hospital settings in England that use FFT to capture patient feedback.

Methods

Study Design

The implementation of the FFT free-text algorithm demands thorough testing to ensure robustness, accuracy, and applicability. To iterate the algorithm for deployment in other health care services, we first selected health care organizations that would incorporate geographical variables, patient demographic variables, and different care settings, that is, adult inpatient, primary care, community, pediatrics, and mental health.

The objectives of this study were to identify technical capabilities for algorithm deployment in the included health care settings, identify variation in user needs across different service settings and geographies, and iterate the algorithmic process and deploy a reproducible algorithm that can be implemented in different services.

Trust Recruitment

A steering group consisting of lay representatives and patient experience experts was formed to guide the strategic direction of this study and help in recruitment through various patient experience networks including the National Insight Network set up by National Health Service (NHS) England, the Q Community established by the Health Foundation, Advancing Quality Alliance, and the Heads of Patient Experience Network. An FFT review capability questionnaire (Section 1 in Multimedia Appendix 1) was sent to interested organizations. This allowed this study's team to identify organizations based on 3 key metrics: patient experience engagement, digital readiness or IT infrastructure, and quality improvement involvement. To ensure that the selected trusts possess the necessary infrastructural and organizational qualities to contribute effectively to the research objectives while adhering to data regulatory standards, a capacity and capability assessment was required. Only those trusts that were able to confirm capacity and capability through their Research and Development department were finally recruited, as shown in Figure 1.

XSL•FO
RenderX

Figure 1. An overview of the geographical distribution of the 9 recruited trusts. Copyright owned by Imperial College Healthcare NHS Trust, 2025. All rights reserved.



Ethical Considerations

This study received Health Research Authority and Health and Care Research Wales approval (20/HRA/5924). No patient data were collected, and trusts were anonymized in the analysis. Written consent was sought from members of the steering group and the individual hospital trust project team, and with further written consent, their contribution has been acknowledged in the Acknowledgments section.

XSL•FO
RenderX

Preimplementation

IT Scoping Tool

To work collaboratively, we identified the needs of all participating organizations from a patient experience digital readiness standpoint. This was facilitated through previous work by this study's team funded by NHS England Insight and Feedback Team [15], where a scoping tool was developed to identify key contacts, FFT data collection, SQL Server database, handling and management, infrastructure capacity, that is, on-premise data center or cloud computing, integrated development environment and coding language expertise, and data visualization software (Section 2 in Multimedia Appendix 1).

Data Access

To ensure that participating organizations were fully supported by the project team, a Data Protection Impact Assessment (DPIA) was completed with each organization. DPIA is a systematic process designed to identify and minimize the associated data protection risks. The purpose of a DPIA in our study was to assess the impact of processing data and to ensure that the principles of data protection, such as those outlined in regulations such as the General Data Protection Regulation were adhered to.

Adaptation of Coding Script

To achieve transferability of the SVM supervised machine learning (ML) algorithm and test against different service settings and NHS provider organizations, the functionalities previously developed [7] were recoded using Python (Python Software Foundation), given the popularity of using this coding platform in most NHS trusts. Python is an interpreted high-level general-purpose programming language. The model was developed with Python (version 3.8.10) with the following free Python libraries; scikit-learn≥0.22.1 [16] (an ML library that provides relevant ML packages required for classification), Natural Language Toolkit (NLTK)≥3.4.4 (a suite that contains libraries and programs to make machines understand human language), and Pandas≥0.25.3 (a library for data manipulation and analysis). These requirements were then translated into a requirements.txt file for organizations to deploy the algorithm. SVM was used as it is the most common classifier widely used for document classification, which consistently yields good classification performance [10].

Updating Training Coding Template

All FFT free-text comments were coded based on the NHS Patient Experience Framework (Section 3 in Multimedia Appendix 1). This framework incorporates 8 key themes that outline those elements that are critical to the patients' experience of NHS services [17]. In the previous work [7], three additional themes were added: "unclassified" (too many typographical errors to discern meaning), "general" (eg, NHS is great, everything), and "staff" (comments relating to staff). From the NHS England funded work [15], it was observed that there was an overlap of comments between the theme "staff" and other themes such as "respect for patient-centered values, preferences, and expressed needs," "emotional support," and "physical comfort." This is because often a staff member was involved in the delivery of the care as it related to the other themes. The theme "staff" was removed, and all comments coded as "staff" were recoded to develop a concise coding template. Therefore, 10 themes were selected for final analysis, and a coding pack (Section 4 in Multimedia Appendix 1) was developed with detailed guidance. Furthermore, we iterated the initial algorithm from our previous work which was developed using 2 follow-up free-text questions, that is, "What did we do well?" and "What could we do better?" by combining and shuffling the training data from both questions to develop a streamlined SVM-supervised ML algorithm for theme and sentiment prediction.

Implementation

Overview

A pipeline was constructed for the SVM model in Python for text classification and sentiment analysis, consisting of several steps, including text preprocessing, feature engineering, TFIDF (term frequency-inverse document frequency) transformation, and model training and testing.

FFT Data Retrieval

SQL server was used to both extract the FFT data and supplementary free text for algorithm imputation, and to store the output of the algorithm. Pyodbc≥5.0.1 Python library was required to connect to the individual organizations' SQL server. SQL's combination of ease of use, flexibility, and capabilities make it useful for storing, managing, querying, and analyzing datasets and is widely used in health care organizations.

Establishing Ground Truth

In supervised learning algorithms, ground truth data is critical to training and updating an algorithm [10]. Therefore, more annotated data was required to improve the performance of the algorithm. The coding pack (Section 4 in Multimedia Appendix 1) developed was provided to the participating organizations' patient experience teams to make coding more feasible. The coders were a combination of the patient experience team, clinical staff, and trust lay representatives. Two coders from the team completed manual coding individually using a 500-stratified sample to calculate interannotator reliability and understand the interpretation of themes and sentiment. Disagreements in coding were reviewed, and theme and sentiment were finalized to create a master coding template in a .csv file. This template was populated with data from all 9 organizations.

Preprocessing

Preprocessing of textual data is the first essential step in the processing of text and has been proven to improve text classification models' performance by standardizing the text before it is presented to the classification algorithm [10]. NLTK for Python was used for preprocessing and data analysis, which includes tokenization of the comments and removal of stop words (eg, the, was, is, etc), punctuation, numbers, and special characters from the comments. The resulting words were represented as a bag of words (BoW) or corpus. Given that the average length of FFT free-text comments tends to be short,

XSL•FO
RenderX

and the context is domain-specific, that is, patient experience, this BoW approach was used rather than word embedding.

Feature Engineering

Feature engineering is the process of transforming data into features or attributes that better represent the underlying structure of the data [10]. To identify the key features of the data, we used a statistical measure, TFIDF, used in the fields of information retrieval [18] and ML, that can quantify the importance or relevance of words in a comment among a collection of comments [19].

Determining Accuracy

To understand if further coding was required, the accuracy for theme and sentiment was calculated using a 500-stratified sample of manually coded comments from each of the individual organizations. The accuracy is defined as a metric used in classification to measure the percentage of accurate predictions [10]. It is also defined as the ratio of several correct predictions by the algorithm to the total number of predictions. In other words, the ratio of true positives (TPs) and true negatives (TNs) to all positive and negative observations (where FPs and FNs are false positives and false negatives, respectively): accuracy=(TP+TN)/(TP+TN+FP+FN). The acceptable threshold for overall accuracy for theme and sentiment for a supervised algorithm using patient feedback was determined at 75%. The 75% accuracy threshold for theme and sentiment classification was established based on the work of this study's group [10] and previous studies in the literature [20,21]. Specifically, the threshold reflects the balance between achieving an acceptable level of accuracy and the complexity of interpreting nuanced patient feedback using NLP and ML techniques. Therefore, the 75% accuracy benchmark was identified as a reasonable trade-off between high-quality model performance and the inherent challenges in processing and classifying subjective feedback from patients.

The accuracies yielded by the models on different ranges of hyperparameters were compared. For SVM, both L1 and L2 regularization, variance tolerance values for the stopping criteria, and different values for the inverse of regularization strength, C, were compared. As regularization has a known role in reducing overfitting, the hyperparameters were chosen for tuning to identify the amount and type of regularization and early stopping criteria that are suitable for the classification tasks. After this, the optimal hyperparameters were found by GridSearchCV from the scikit-learn library. A 10-fold cross-validation was used to search to select the best hyperparameter combinations from specified ranges of hyperparameters, which were used to retrain the model on the training set and to predict on the test set [10]. This allowed us to establish the accuracy but also use the coded comments as a template to improve the accuracy by a further round of recoding if needed, until the accuracy was at or above 75%, that is, reached thematic saturation.

Algorithm Deployment

The master coded template data was then serialized using the Python pickle library. This module is used for serializing and deserializing objects into Python format text strings, which are called pickles and can be created by Python code or sent from other Python programs. This Python pickle is easily carried over the network and can be validated without knowing the details of the received object. This enables the preservation and sharing of the ML models, allowing users to reload pretrained models, significantly reducing the need for lengthy retraining. The files that were stored in the environment were as follows: Feature_sentiment.pkl, Feature_theme.pkl, Sentiment_classifier.pkl, Theme_classifier.pkl, Tfidftransformer_sentiment.pkl, and Tfidftransformer_theme.pkl.

Establishment of a Community of Practice

In the pursuit of ensuring the correct sustainability of the algorithm, a strategic initiative was undertaken through the establishment of a technical community of practice (CoP). This community served as a conduit for regular interaction and collaboration among the leaders responsible for overseeing the algorithmic maintenance across different trusts. Recognizing the complexity and potential challenges associated with deploying advanced algorithms, quarterly meetings were instituted as a core component of the CoP framework. These meetings provided a structured way for the leads of each site to convene, fostering an environment conducive to the exchange of critical insights, best practices, and lessons learned.

Results

Overview

Nine trusts were recruited from a range of care settings, sociodemographic and geographical areas. Trusts were added to this study sequentially, one by one, as part of the recruitment process. None of these organizations had a pre-existing automated process for analyzing their FFT free-text responses.

Identifying Free-Text Comments With FFT Survey for Analysis

In the preimplementation scoping exercise, it was observed that among the participating organizations, trusts A and D incorporated 3 follow-up free-text questions in their FFT survey. In contrast, all other trusts included only 1 follow-up question (Table 1). The question with the highest number of comments in trust A was analyzed. The organizations provided a variety of services, including pediatrics, inpatient and outpatient, and community and mental health, thereby facilitating testing and iteration of the algorithm for use in all care settings. Furthermore, most of the organizations 88.9% (8/9), opted to house and deploy the algorithm on premises, and the rest on cloud 11.1% (1/9).

XSL•FO
RenderX

Table . An overview of the variation in FFT[a] free-text data, service setting, and environment favored to deploy the machine learning algorithm in 9 NHS[b] organizations in England. Version deployed refers to the version of the iterative addition of words to the BoW[c] model, used to improve model performance.

Trust	Service coverage	Model deployment environment	Number of free-text columns	Free-text questions	Version deployed
A	Community and mental health	On premises	3	• Please, can you tell us why you gave your answer?[d] • Please tell us at least one thing that went well. • Please tell us at least one thing we could do better.	Version 0
B	Acute and inpatient	Cloud	1	• Please, can you tell us the main reason for the score that you have given?	Version 1
C	Acute and inpatient	On premises	1	• Please, can you tell us why you gave your answer and what we could have done better?	Version 2
D	Pediatrics	On premises	3	• FFT rating description[d] • Write what you think was good. • Write what you think was bad.	Version 3
E	GP[e] or community	On premises	1	• Please, can you tell us why you gave your answer?	Version 3
F	Acute and inpatient	On premises	1	• Can you tell us why you gave that response?	Version 3
G	Acute and inpatient	On premises	1	• Please, can you tell us why you gave your answer and what we could have done better?	Version 3
H	Acute and inpatient	On premises	1	• What was good about your care, and what could be improved?	Version 3
I	Acute and inpatient	On premises	1	• Please, can you tell us why you gave your answer?	Version 3

[a]FFT: Friends and Family Test.

[b]NHS: National Health Service.

[c]BoW: bag of words.

XSL•FO
RenderX

[d]The free text from this question was used in the algorithm testing, given the highest responses compared to the other 2 questions.

[e]GP: general practitioner.

Variation in Patient Experience Themes

To understand the variation in themes, if any, of FFT free-text responses in the 9 organizations, we looked at the count of comments from the FFT free-text responses based on the NHS patient experience framework. This was extracted from the output after initial model deployment for the period of January 2022 to January 2023, as demonstrated in Table 2. The highest count of themes was "respect for patient-centered values" followed by "general." The themes with the lowest count were "welcoming the involvement of friends and family" followed by "transition and continuity." There were no demonstrable trends in the other patient experience framework themes.

Table . Distribution of count of themes based on the NHS[a] patient experience framework from 9 NHS organizations in England, extracted from the output of the algorithm.

Trust	FFT[b] comments provided per NHS Patient Experience Framework themes (%)									
	0[c]	1[d]	2[e]	3[f]	4[g]	5[h]	6[i]	7[j]	8[k]	9[l]
A	9	26	4	10	6	6	0	2	24	12
B	8	35	2	14	6	5	2	2	11	16
C	6	23	3	13	8	10	1	2	8	26
D	15	17	9	10	6	5	0	2	16	20
E	22	25	2	11	5	5	0	1	18	12
F	2	43	1	12	4	7	1	1	8	21
G	6	23	3	13	8	10	1	2	8	25
H	7	31	3	7	13	5	2	1	7	25
I	1	25	6	8	9	11	2	3	11	22

[a]NHS: National Health Service.

[b]FFT: Friends and Family Test.

[c]0: unclassified.

[d]1: respect for patient-centered values.

[e]2: coordination and integration of care.

[f]3: information and communication.

[g]4: physical comfort.

[h]5: emotional support.

[i]6: involvement of family and friends.

[j]7: transition and continuity.

[k]8: access to care.

[l]9: general.

Establishing Ground Truth

Interrater agreement was determined on the manual coding, and the coding template was updated to check accuracy and improve the model by acquiring an updated corpus from the BoW and feature extraction. The interrater agreement was better for sentiment compared to theme. There was almost perfect agreement (0.81 - 1.00) seen in 7 organizations. Trust A was the only organization with a substantial (0.61 - 0.80) agreement with a Cohen κ of 0.79 (Table 3).

XSL•FO
RenderX

Table . Assessing the consistency of theme and sentiment ratings, and final accuracy via updated coding template.

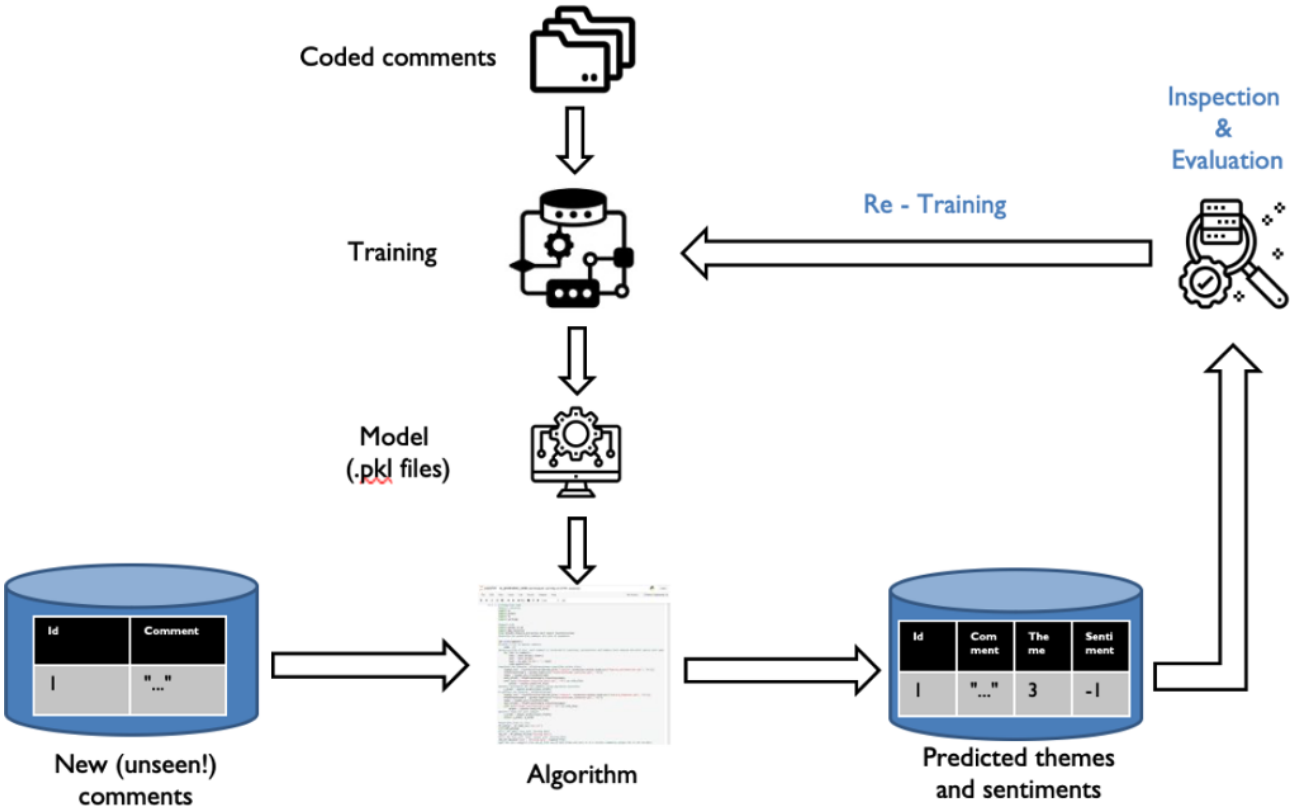
Trust and category		Interrater reliability or Cohen κ	Accuracy before recoding (%)	Final accuracy (%)
A. Community and mental health				
	Theme	0.79	57	76
	Sentiment	0.82	76	82
B. Acute and inpatient				
	Theme	0.84	69	78
	Sentiment	1	87	91
C. Acute and inpatient				
	Theme	0.85	84	90
	Sentiment	0.91	87	94
D. Pediatrics				
	Theme	0.89	67	82
	Sentiment	1	72	82
F. General practitioner or community				
	Theme	0.80	64	77
	Sentiment	0.82	69	80
E. Acute and inpatient				
	Theme	0.96	—[a]	>75
	Sentiment	1	—	>75
G. Acute and inpatient				
	Theme	0.83	—	>75
	Sentiment	0.85	—	>75
H. Acute and inpatient				
	Theme	—	—	>75
	Sentiment	—	—	>75
I. Acute and inpatient				
	Theme	—	—	>75
	Sentiment	—	—	>75

[a]Not applicable given that the final 4 organizations reached thematic saturation following the coding efforts of the initial 5 organizations and therefore achieved an overall accuracy rate of 75% or higher.

Three trusts noted that sentiment prediction related to certain words was misclassified. This study's team reviewed the performance and identified words that were culpable for this misclassification, for example, "nothing," "everything," and "OK." These trusts were advised to manually code a subset of 500 comments with equally distributed sentiments, especially focusing on the misclassified words, along with comments that represented an equal or almost equal number of comments per themes or sentiments to obtain a balanced dataset. To determine the accuracy of the algorithm, a pipeline was developed and refined to standardize the entire process within all the organizations, as depicted in Figure 2.

XSL•FO
RenderX

Figure 2. A pipeline created to develop and standardize the overall accuracy calculation before final deployment. Copyright owned by Imperial College Healthcare NHS Trust, 2025. All rights reserved.



The overall accuracy for theme and sentiment significantly improved after using a revised coded template. As trusts were added to the study sequentially, one by one, as part of the recruitment process, the BoW was also applied sequentially to the algorithm. Thematic saturation was achieved after analyzing and collating comments from a total of 5 trusts. This was observed when the algorithm was tested in 4 of the remaining trusts without the need to implement their respective coding output, and achieving an overall accuracy greater than or equal to 75%.

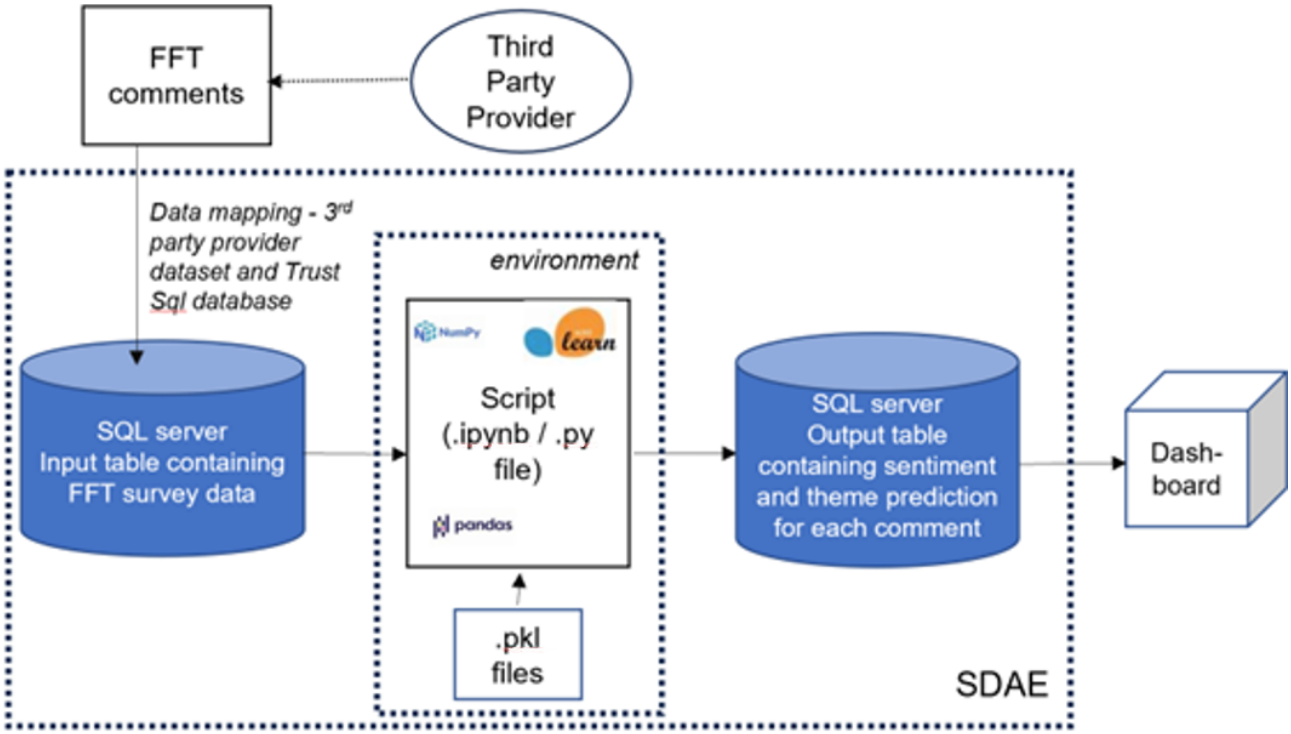
The final 4 organizations achieved an overall accuracy rate of 75% or higher, having reached thematic saturation following the initial coding efforts of the initial 5 organizations. As a result, as seen in Table 1, four versions of the model were deployed as new, labeled comments were collated from the different trusts that joined the program and deployed the algorithm. This iterative learning was carried out by adding randomly scrambled new unique words that the algorithm encountered in the BoW within its code. Each time, this word repository was completely randomized, and each word was treated individually by removing any linkage. As a result, it was not possible to know from which trust the word came from or if it was part of a positive or negative comment, with this study's team holding the ground truth.

Adaptations and Running Without Errors

The algorithm script was adapted according to the agreements and requirements of the individual organization. The solution was tested in Jupyter Notebook (The Linux Foundation) for easier interaction with the code and checked for errors. The 2 most common errors encountered were "FileNotFoundError" which was a result of not specifying the correct path to a .pkl file, and "invalid column name," as the code had not been adapted appropriately with the column names from the input table on the SQL server. Once errors were corrected, the final deployment consisted of the output with predicted themes and sentiment exported to a SQL database for integration into the dashboard visualization. This pipeline (Figure 3) was standardized after refinement with all participating organizations. Each trust automated its data flow based on the requirements defined by the frequency and volume of comments that the pipeline should be updated with.

XSL•FO
RenderX

Figure 3. Final pipeline demonstrating steps required to deploy the final algorithm with FFT comments as input, prediction of themes and sentiment using pickle files generated from summative coding outputted to SQL database for use in dashboard visualization. FFT: Friends and Family Test. Copyright owned by Imperial College Healthcare NHS Trust, 2025. All rights reserved.



For this purpose, user-friendly interfaces were designed and developed using the Flask Python library for the backend and HTML, CSS, and Bootstrap for the frontend. Functionalities of these interfaces included analyzing the accuracy of the algorithm by uploading a labeled dataset and retraining the algorithm with more coded data.

Algorithm Refinement

Three hospitals noted that after manual inspection of the sentiment prediction, some FFT comments were being classified with an incorrect sentiment. We reviewed the performance of the algorithm and identified words that were making the algorithm perform incorrectly (eg “nothing,” “everything,” or “OK”). It was suggested that these hospitals should manually code a subset of 500 comments with equally distributed sentiments, especially focusing on these words, along with comments that represented an equal or almost equal number of comments per themes or sentiments, to obtain a balanced dataset. A code developed by this study’s team was provided to ensure the equal distribution of both themes and sentiments in the dataset.

Multitagging

Potential refinements to the algorithm, particularly regarding the need to break long comments into sentences for trusts encountering lengthier narratives, such as those in mental health and community settings, were highlighted, and a multitagging method was devised. The multitagging approach involved assigning multiple themes from the NHS Patient Experience Framework to a single text document based on its content. Unlike the traditional single-label classification, where the FFT free-text is assigned to only 1 label, multitagging recognizes that comments may encompass various themes. This approach enables a more nuanced representation of the content’s complexity and captures multiple dimensions of meaning within the same document. The punctuation marks, words, and number of characters used to split the original sentence can be customized based on different requirements using Spacy (versions ≥3.7.2) and its English language model. As a default, sentences are split after a maximum of 75 characters, and each of these is analyzed individually (Figure 4). This can then be customized according to the requirements of the trust to define how the base text should be split (eg, by punctuation marks or specific words such as “however”). Based on this level of customizability, other trusts also implemented the solution.

XSL•FO
RenderX

Figure 4. Example of how the sentencing approach works. The original comment is split into 2 subcomments, each classified according to a theme and a sentiment. The original comment identifier is retained to preserve the metadata of the comment. Copyright owned by Imperial College Healthcare NHS Trust, 2025. All rights reserved.

Original Comment ID	Sentence	Theme	Sentiment
1	Amazing care from our general paediatrician who is going above and beyond to help coordinate multiple professionals in the care of our child. Seriously! I am so grateful for her expertise and wisdom and feel extremely blessed that our child is under her care. Grateful thanks. She has been so supportive of us as parents too.	1	1

Final Split Sentences

Original Comment ID	Sentence	Theme	Sentiment
1	Amazing care from our general paediatrician who is going above and beyond to help coordinate multiple professionals in the care of our child.	1	1
1	Seriously! I am so grateful for her expertise and wisdom and feel extremely blessed that our child is under her care. Grateful thanks. She has been so supportive of us as parents too.	5	1

Redaction of Personal and Identifiable Information

Considerable variation was also observed in how trusts approached the redaction process, ranging from automated processes with subsequent manual checks to entirely manual methods. To address this inconsistency, a redaction algorithm capable of automatically detecting and masking personally identifiable information was devised. A redaction algorithm was developed using NLTK, Regex, and Presidio Python libraries to automatically detect and mask the personally identifiable information. The algorithm can be customized according to the requirements of the trust to define how and what data needs to be redacted.

About CoP

During the quarterly meetings, there was a high level of engagement from at least 80% of staff members representing the 9 trusts. This level of participation indicated strong interest and commitment to the CoP's objectives. Additionally, feedback from participants revealed a positive perception of the CoP, with at least 90% reporting a sense of belonging and support within the community. This sense of camaraderie and mutual support contributed to the effectiveness of the CoP in addressing algorithm deployment challenges and driving improvements based on patient feedback. We addressed maintenance of the algorithm through the CoP by creating a standardized software that enables each hospital to check the accuracy of the algorithm and make changes as needed. Figure 5 shows the interfaces developed.

XSL•FO
RenderX

Figure 5. Interfaces developed by the community of practice to assist with regular algorithm maintenance. Copyright owned by Imperial College Healthcare NHS Trust, 2025. All rights reserved.

XSL•FO
RenderX

Discussion

Principal Findings

Using a test-and-iterate approach, this study deployed a text analytics algorithm to predict theme and sentiment from FFT free text data in 9 NHS organizations in England with different care settings, geographical locations, and demographics. Furthermore, this study highlighted the variation in technical capacity and resources among trusts, introduced and developed a framework, and standardized a data processing pipeline capable of supporting FFT text analytics bespoke to the organization's needs. The key contributions of this study are: (1) the construction of technical infrastructure to support and run the algorithm effectively and being able to adapt the script for individual organizations; (2) the creation of master coding template with free-text data from different health care organizations to support algorithm iteration and improve overall accuracy for theme and sentiment; (3) the creation of pipeline to standardize the method of incorporating the algorithm for processing free-text data; and (4) foster collaborative nonsiloed working that encourages local ownership and share-learning.

Addressing Data Management and Standardization Through IT Infrastructure

Data collection and analysis are central to this project. Achieving this required a robust data infrastructure with different components that collaboratively created an effective framework for research data management. This framework enhanced data accessibility by presenting information in a consistent, standardized, predictable, and accessible format while also strengthening data reliability through the automation of manual processes [22]. However, ensuring high-quality data demands a diverse set of information management skills, including data acquisition, storage, organization, retrieval, and long-term maintenance [23]. This project offered a valuable opportunity for trusts to gain expertise in this area by providing guidelines to streamline processes, define roles, and establish a resilient IT infrastructure.

Creating a Template With Additional Organizational Specific Free-Text Data

Each health care setting possesses unique attributes, patient demographics, and linguistic nuances as demonstrated above. Algorithm testing was required to allow for customization and tailoring of the algorithm to accommodate these contextual variations. As part of a supervised learning approach, recoding was required to re-establish ground truth, and new words were incorporated into an expanded BoW to improve performance across various care settings. Literature suggests that the larger the training sets used, the higher the accuracy of the algorithms at identifying similar comments within the broader dataset, but trade-offs with time and human coding are necessary to ensure the method is resource-efficient [10]. However, the nature of patient experience vocabulary, due to the domain of patient feedback from free-text, is fixed in its nature, making it attractive data for supervised learning [24]. Therefore, it is possible to anticipate the meaning of various phrases and automatically classify the comments [25]. Thematic saturation was reached with 5 organizations, and no further coding was necessary. Just as the domain is fixed, the perspective of a patient feedback document is also fixed; there is limited vocabulary that is useful for commenting about health services [24]. Rastegar-Mojarad et al [26] also observed that a small (25%) vocabulary set covered a majority (92%) of the content of their patients' comments, consistent with a study exploring consumer health vocabulary used by consumers [27]. This suggests that patients use specific vocabulary when expressing their experience within free-text comments.

In settings that were relatively fixed, that is, adult inpatient, the classifier trained strong reusable models that were evident from satisfactory accuracy. However, the accuracy of the model was lower in organizations delivering different services, such as pediatrics and mental health. This was to be expected, given that the language and type of words used in different care settings would vary from those found in an adult inpatient setting. The customization ensured that the algorithm aligns with the specific language and themes prevalent in the patient feedback of a particular health care organization. The accuracy for the theme improved in all the organizations demonstrating that while the algorithm may not initially be transferable, with some retraining and adaptations, it can easily be reused in different service settings. As part of the algorithm development process, cross-validation was applied to ensure the robustness and reliability of the model within the dataset used. In addition to this, we conducted external validation by incorporating patient comments from multiple trusts, ensuring that the model was exposed to a diverse range of data before declaring thematic saturation. This strategy allowed us to evaluate the model's performance beyond a single dataset and ensured that it was not overfitting to any trust or setting. By including data from various trusts, we created a working external validation set, which will serve as the foundation for assessing the model's generalizability in future implementations.

Furthermore, "respect for patient centered values" had the highest count in all organizations. This finding is similar to the literature around patient experience reporting in health care [28-32]. The reasons for this are twofold, first, primarily due to the large number of interchangeable words found within that theme, that is, "respect for patient-centered values, preferences, and expressed needs (cultural issues, dignity, privacy and independence, awareness of quality-of-life issues, and shared decision making)." Second, the overall domain of patient feedback is the health care system, and this study revealed that the content of reviews tends to focus on a small collection of aspects associated with this, as demonstrated by the themes used for text classification in the studies.

Through CoP participation, multitagging was used to assign multiple relevant tags or categories to individual sentences within a single FFT free-text comment. Instead of assigning a single label to the entire document, this technique involves breaking down text into sentences and assigning appropriate themes and sentiments to each based on its content, thereby enhancing customizability within mental health and community care settings. Furthermore, the CoP assisted in developing a redaction solution using Python libraries, which can be then customized according to the requirements of the trust to define

XSL•FO
RenderX

how and what data needs to be redacted. These solutions can subsequently be adopted by other trusts as an improvement to their existing processes.

Creating a Pipeline to Standardize the Algorithm Deployment Approach

As part of the model testing and to make the model more widely reusable, we created a data pipeline, which infuses and integrates BoW from different trusts to predict theme and sentiment at an accuracy greater than 75% when used in different trusts. This pipeline serves as a blueprint to stakeholders and facilitates understanding of all pieces of the pipeline among the team members and standardization when deploying the model. Compliance with regulations and governance is supported, and integration with DevOps practices enhances ML model integration into the software development lifecycle.

Generating Cultural Change to Prioritize Patient Experience–Centered Care

The establishment of CoP can play a pivotal role in establishing a multi-disciplinary team of stakeholders from IT, business intelligence, patient experience, and quality improvement within each trust. Furthermore, the CoP can provide the necessary guidance to use the algorithm and assist in developing a dashboard for quality improvement projects [14], and sustained enthusiasm in the use of data and data analytics to improve the quality of care for patients and care givers [33]. This cultural transformation will result in increased organizational agility and responsiveness to patient needs, driving positive changes in care delivery practices [34].

Limitations

The pickle files used in this study are specific to the version of Python and the libraries used to create them. Attempting to load a pickle file created with an older version of Python or with different library versions may result in compatibility issues. Newer versions of Python may have introduced changes to the pickle module or the libraries being pickled, which can result in errors when loading the file. To mitigate challenges with loading an outdated pickle file, updating the code that creates the pickle file, or using alternative serialization formats that are more version-independent can be considered. The model can be containerized using Docker with a requirements file containing all the required libraries and Docker specifying the environment setup and start-up operations. The Docker container can then be deployed to application hosting services, whether on cloud or on premises servers.

The limited vocabulary range is a significant issue faced by the BoW model. For example, if the model encounters an unfamiliar or rare but informative word that it has not yet seen during training, the BoW model will tend to ignore it. To mitigate this limitation, we trained the model on 5 of 9 trusts to ensure that the model had gathered a substantial BoW representation, further augmented by thematic saturation. Significant changes to patient demographics or significant changes, such as the COVID-19 pandemic, could reduce the performance due to unfamiliar words. Therefore, regular updates in the model would be required to keep it up to date. For this purpose, user-friendly interfaces can be designed and developed using the Flask Python library for the backend and HTML, CSS, and Bootstrap for the frontend. Functionalities of these interfaces included analyzing the accuracy of the algorithm by uploading a labeled dataset and retraining the algorithm with more coded data. The interfaces allow organizations to periodically check accuracy as part of a responsible AI strategy.

Given the limited analytical expertise and computational resources in many UK hospitals, complex models such as transformers and recurrent neural networks would be difficult to implement effectively. The SVM model was chosen for its simplicity, efficiency, and low resource demands, making it ideal for integrating into existing workflows. The focus was on maximizing the value of patient feedback data to improve care quality, without overwhelming the hospital's IT infrastructure. We acknowledge that alternative lightweight ML methods, such as Decision Forests and XGBoost, offer similar efficiency and computational efficiency without the significant computational burdens often associated with deep learning models. Furthermore, modern deployment strategies, such as using pretrained architectures and lightweight deep learning models, can help mitigate the resource challenges typically associated with training deep learning models such as recurrent neural networks. As the hospital's analytics capacity grows, more sophisticated models can be explored, but SVM provided a practical starting point for immediate, actionable insights.

The authors set out to illustrate the process of developing an NLP pipeline that originated in a single institution and has been iteratively refined for broader implementation. A strong technical knowledge base was essential to address variations in technical capabilities and IT infrastructure, as well as to introduce and enhance analytical skills that had been underused in some hospital trusts. However, to successfully implement the intervention within complex health care systems, it is crucial to understand how the intervention interacts with and influences various system components to achieve the desired outcomes. We are currently collaborating with participating trusts to establish a data flow that automates the integration of NLP outputs into a dashboard. Additionally, we are making algorithm improvements based on local priorities and needs to foster local ownership of the process.

Responsible AI

As AI continues to advance, becoming increasingly integrated into health care systems, ethical considerations and technical challenges become increasingly intricate. For this reason, a key aspect of the project included providing tools and best practices to ensure that AI is being implemented responsibly. First, the developed user-friendly interfaces promote the ongoing monitoring of the accuracy of the algorithm, ensuring fairness and accountability of the version of the model that was deployed. Second, the establishment of CoP will play a critical role in fostering a culture of continuous improvement and supporting the transformation toward greater organizational agility, but also cultivates an environment where professionals can delve into the nuanced aspects of responsible AI. This transformation will enhance the responsiveness of health care systems to patient needs and drive positive changes in care delivery practices. Furthermore, by building local expertise and ownership, we

XSL•FO
RenderX

aim to create a sustainable framework for ongoing use of data and analytics to improve the quality of care. This contributes to the development and refinement of ethical guidelines, playing a crucial role in shaping the responsible AI landscape.

Future Directions

This study's group is currently conducting a complex, multicomponent implementation designed to enhance operational efficiencies within the NHS by empowering frontline staff with visible and actionable insights derived from a patient feedback tool, which aligns with the NHS FFT redevelopment policy recommendations. This intervention aims to drive sustainable impact and foster a culture of patient-centered working by facilitating the identification and implementation of improvement opportunities. The CoP will play a vital role in achieving the broader goal of embedding a patient-centered working culture across the NHS. They will help sustain momentum for using patient feedback and data analytics to drive continuous improvements in care. This multifaceted approach ensures that the intervention not only has immediate operational benefits but also creates a lasting cultural shift toward patient-centered care.

Models such as BERT have the potential to offer deeper insights by capturing more complex linguistic patterns, which could be particularly valuable for understanding the subtleties in patient comments, especially in sensitive areas such as mental health. While we considered exploring these advanced models, we opted for a more straightforward approach during this phase of implementation. This decision was driven by the need for a method that is both practical and easily scalable across diverse health care settings. However, future research with a more experienced group, enriched by the extended knowledge gained through the CoP, could involve comparing transformer-based models such as BERT with the current approach to evaluate whether they provide significant improvements in accuracy and interpretability. Moreover, future work will explore the impact of different preprocessing strategies, such as retaining certain negations, expanding contractions, or adjusting tokenization rules (including experimenting with different n-gram configurations) based on contextual understanding. This would allow for a more nuanced approach, potentially improving the accuracy of sentiment classification, especially in cases where subtle cues are essential.

To enhance the interpretability of the model's predictions, SHAP (Shapley Additive Explanations) and LIME (Local Interpretable Model-Agnostic Explanations) can be incorporated into the NLP pipeline. SHAP can explain that the words "excellent" and "care" contributed significantly to a positive prediction, while "waited" and "long" contributed to a negative prediction. This helps the health care team understand the key drivers behind feedback, allowing them to make targeted improvements. For a piece of patient feedback stating, "The doctor was kind, but the wait was too long," LIME might perturb the sentence by removing words like "kind" or "wait" to see how the model's prediction changes. If the model changes from positive to negative after removing the word "wait," LIME would indicate that the term "wait" is highly important for determining the sentiment of the feedback. This could be an important step for trusts in improving transparency, which builds trust and helps the health care team make better-informed decisions when observing the dashboard.

Conclusion

This study marks an advancement in harnessing free-text FFT data to gain valuable insights in health care settings through the creation of a robust supervised learning text analytics algorithm. The observed disparities in certain care settings were expected, considering the inherent differences in lexicon and terminology compared to the adult inpatient care setting where the algorithm was initially developed. Addressing these challenges involved additional coding and thorough testing under diverse scenarios. Through this iterative process, the accuracy and reliability of the algorithm were established to be robust and easy to use, fostering inter- and intraorganizational collaboration and promoting shared learning within the health care domain.

Acknowledgments

This work was funded by the Health Foundation and by the National Institute for Health Research (NIHR) Imperial Biomedical Research Centre (NIHR203323), with infrastructure support from the NIHR North-West London Patient Safety Research Collaboration (NIHR NWL

PSRC, Ref. NIHR204292). The research was enabled by the iCARE Secure Data Environment and used the iCARE team and data resources. Development of the information technology (IT) scoping tool and coding pack was funded by NHS England Insight and Feedback Team (National Health Service [NHS]). The study funders did not play a role in study design; in the collection, analysis, and interpretation of data; in writing of the report; and in the decision to submit this paper for publication. Additionally, researchers were independent from funders, and all authors had full access to all the data included in this study and can take responsibility for the integrity of the data and accuracy of the data analysis. The authors would also like to acknowledge the contributions of all individuals from the NHS trusts involved in the Scale, Spread and Embed Programme: Victor Banda, William Bryant, Suzanne Collin, Zeina Dahan, Paul Gough, Mark Harris, Taraben Kapadia, Pavithra Rajendran, Jonny Sheldon, Caitlin McGovern, Marcus Beck, Ahmed Sharif, Mandy Dawley, Catherine Hunter, Brad Walker, Mark Ward, Luca Mercuri, Rohini Subramaniam, Ben Glampson, Amy Bond, Rosie Frost, Paul Morris, Emmanuel Okafor, Andrew Walsh, Dean Wild, Lesley Whittaker, Quinta Ashcroft, Vishnu Chandrabalan, Stuart Clough, Rebecca Hargreaves, Joan Ravencroft, Stephanie Iaconianni, John Howles, Karen Greenwood, Ben Morris, Lisa Bonifacio, Sarah Eastwood, Nathan Harding, Paul Hooker, Jacek Pawlowski, Julie Cheney, Ana Maria Aldana Gelves, Prajwal Khairnar, Trudy Taylor, Sarah Curtis, Simon Godley, Chris Lewis,

XSL•FO
RenderX

Amy Marchant, Mary Mason, Oluwatoni Ojelade, Stephen Onamade, Vijay Rabadia, Chloe Roebuck, Francesca Roffey, Saad Saleem, Neil Springham, Jon Blacker, Edmund Gall, Matthew Stammer, Michael George, and Laura White. Additionally, we are very grateful to members of the Programme Steering Board for their oversight and constructive feedback during the Programme rollout.

Conflicts of Interest

None declared.

Multimedia Appendix 1
FFT capability review. FFT: Friends and Family Test.
[PDF File, 836 KB - medinform_v13i1e60900_app1.pdf]

References

1. Flott KM, Graham C, Darzi A, Mayer E. Can we use patient-reported feedback to drive change? The challenges of using patient-reported feedback and how they might be addressed. BMJ Qual Saf 2017 Jun;26(6):502-507. [doi: 10.1136/bmjqs-2016-005223] [Medline: 27325796]
2. The Friends and Family Test. : NHS England; 2014. URL: https://www.england.nhs.uk/fft/ [accessed 2025-05-24]
3. Gleeson H, Calderon A, Swami V, Deighton J, Wolpert M, Edbrooke-Childs J. Systematic review of approaches to using patient experience data for quality improvement in healthcare settings. BMJ Open 2016 Aug 16;6(8):e011907. [doi: 10.1136/bmjopen-2016-011907] [Medline: 27531733]
4. Usman M, Mujahid M, Rustam F, et al. Analyzing patients satisfaction level for medical services using Twitter data. PeerJ Comput Sci 2024;10:e1697. [doi: 10.7717/peerj-cs.1697] [Medline: 38259896]
5. Using the Friends and Family Test to improve patient experience. : NHS England and NHS Improvement; 2019 URL: https://www.england.nhs.uk/wp-content/uploads/2019/09/using-the-fft-to-improve-patient-experience-guidance-v2.pdf [accessed 2025-05-24]
6. Greaves F, Ramirez-Cano D, Millett C, Darzi A, Donaldson L. Harnessing the cloud of patient experience: using social media to detect poor quality healthcare. BMJ Qual Saf 2013 Mar;22(3):251-255. [doi: 10.1136/bmjqs-2012-001527] [Medline: 23349387]
7. Khanbhai M, Warren L, Symons J, et al. Using natural language processing to understand, facilitate and maintain continuity in patient experience across transitions of care. Int J Med Inform 2022 Jan;157:104642. [doi: 10.1016/j.ijmedinf.2021.104642] [Medline: 34781167]
8. Devlin J, Chang M, Lee K, Toutanova K. Editor BERT: pre-training of deep bidirectional transformers for language understanding. Presented at: Proceedings of the 2019 Conference of the North American Chapter of the Association for Computational Linguistics; Jun 2-7, 2019; Minneapolis, Minnesota.
9. Haleem A, Javaid M, Singh RP. Exploring the competence of ChatGPT for customer and patient service management. Intell Pharm 2024 Jun;2(3):392-414. [doi: 10.1016/j.ipha.2024.03.002]
10. Khanbhai M, Anyadi P, Symons J, Flott K, Darzi A, Mayer E. Applying natural language processing and machine learning techniques to patient experience feedback: a systematic review. BMJ Health Care Inform 2021 Mar;28(1):e100262. [doi: 10.1136/bmjhci-2020-100262] [Medline: 33653690]
11. Sakai H, Lam S, Mikaeili M, Bosire J, Jovin F. Large language models for patient comments multi-label classification. arXiv. Preprint posted online on Oct 31, 2024. [doi: 10.48550/arXiv.2410.23528]
12. Osváth M, Yang ZG, Kósa K. Analyzing narratives of patient experiences: a BERT topic modeling approach. Acta Polytech Hung 2023;20(7):153-171. [doi: 10.12700/APH.20.7.2023.7.9]
13. Strubell E, Ganesh A, McCallum A. Energy and policy considerations for deep learning in NLP. arXiv. Preprint posted online on Jun 5, 2019. [doi: 10.48550/arXiv.1906.02243]
14. Khanbhai M, Symons J, Flott K, et al. Enriching the value of patient experience feedback: web-based dashboard development using co-design and heuristic evaluation. JMIR Hum Factors 2022 Feb 3;9(1):e27887. [doi: 10.2196/27887] [Medline: 35113022]
15. Enston C. The power of the written word. NHS England. 2021. URL: https://www.england.nhs.uk/blog/the-power-of-the-written-word [accessed 2025-05-09]
16. Pedregosa F, Varoquax G, Gamfort A, et al. Scikit-learn: machine learning in Python. J Mach Learn Res 2011;12(2825):30 [FREE Full text] [doi: 10.5555/1953048.2078195]
17. NHS National Quality Board. NHS patient experience framework. : Department of Health; 2011 URL: https://assets.publishing.service.gov.uk/media/5a7c62b740f0b62aff6c14e9/dh_132788.pdf [accessed 2025-05-09]
18. Jones KS. A statistical interpretation of term specificity and its application in retrieval. J Doc 1972 Jan;28(1):11-21. [doi: 10.1108/eb026526]
19. Pang B, Lee L. Opinion mining and sentiment analysis. FNT in Information Retrieval 2008;2(1–2):1-135 [FREE Full text] [doi: 10.1561/1500000011]

XSL•FO
RenderX

20. Duarte JM, Berton L. A review of semi-supervised learning for text classification. Artif Intell Rev 2023 Jan 31:1-69. [doi: 10.1007/s10462-023-10393-8] [Medline: 36743267]
21. Denecke K, Reichenpfader D. Sentiment analysis of clinical narratives: a scoping review. J Biomed Inform 2023 Apr;140:104336. [doi: 10.1016/j.jbi.2023.104336] [Medline: 36958461]
22. Towbin AJ. Collecting data to facilitate change. J Am Coll Radiol 2019 Sep;16(9 Pt B):1248-1253. [doi: 10.1016/j.jacr.2019.05.032] [Medline: 31492402]
23. Neumann J. FAIR data infrastructure. Adv Biochem Eng Biotechnol 2022;182:195-207. [doi: 10.1007/10_2021_193] [Medline: 35091812]
24. LaVela S, Gallan AS. Evaluation and measurement of patient experience. Patient Exp J 2014;1(1):28-36 [FREE Full text] [doi: 10.35680/2372-0247.1003]
25. Garrisson M. The role of volunteer in improving patient experience. The Beryl Institute. 2016. URL: https://theberylinstitute.org/product/the-role-of-the-volunteer-in-improving-patient-experience/ [accessed 2025-05-24]
26. Rastegar-Mojarad M, Ye Z, Wall D, Murali N, Lin S. Collecting and analyzing patient experiences of health care from social media. JMIR Res Protoc 2015 Jul 2;4(3):e78. [doi: 10.2196/resprot.3433] [Medline: 26137885]
27. Indovina K, Keniston A, Reid M, et al. Real-time patient experience surveys of hospitalized medical patients. J Hosp Med 2016 Apr;11(4):251-256. [doi: 10.1002/jhm.2533] [Medline: 26777721]
28. Hawkins JB, Brownstein JS, Tuli G, et al. Measuring patient-perceived quality of care in US hospitals using Twitter. BMJ Qual Saf 2016 Jun;25(6):404-413. [doi: 10.1136/bmjqs-2015-004309] [Medline: 26464518]
29. Greaves F, Laverty AA, Cano DR, et al. Tweets about hospital quality: a mixed methods study. BMJ Qual Saf 2014 Oct;23(10):838-846. [doi: 10.1136/bmjqs-2014-002875] [Medline: 24748372]
30. Alemi F, Torii M, Clementz L, Aron DC. Feasibility of real-time satisfaction surveys through automated analysis of patients' unstructured comments and sentiments. Qual Manag Health Care 2012;21(1):9-19. [doi: 10.1097/QMH.0b013e3182417fc4] [Medline: 22207014]
31. Nawab K, Ramsey G, Schreiber R. Natural language processing to extract meaningful information from patient experience feedback. Appl Clin Inform 2020 Mar;11(2):242-252. [doi: 10.1055/s-0040-1708049] [Medline: 32236917]
32. Wagland R, Recio-Saucedo A, Simon M, et al. Development and testing of a text-mining approach to analyse patients' comments on their experiences of colorectal cancer care. BMJ Qual Saf 2016 Aug;25(8):604-614. [doi: 10.1136/bmjqs-2015-004063] [Medline: 26512131]
33. Dowding D, Randell R, Gardner P, et al. Dashboards for improving patient care: review of the literature. Int J Med Inform 2015 Feb;84(2):87-100. [doi: 10.1016/j.ijmedinf.2014.10.001] [Medline: 25453274]
34. Pereira P. What gets measured gets done. or does it? The Health Foundation. 2014. URL: https://www.health.org.uk/blogs/what-gets-measured-gets-done-or-does-it [accessed 2025-05-09]

Abbreviations

AI: artificial intelligence
BoW: bag of words
CoP: community of practice
DPIA: Data Protection Impact Assessment
FFT: Friends and Family Test
FN: false negative
FP: false positive
IT: information technology
LIME: Local Interpretable Model-Agnostic Explanations
ML: machine learning
NHS: National Health Service
NLP: natural language processing
NLTK: Natural Language Toolkit
SHAP: Shapley Additive Explanations
SVM: support vector machine
TFIDF: term frequency-inverse document frequency
TN: true negative
TP: true positive

XSL•FO
RenderX

Edited by A Benis; submitted 24.05.24; peer-reviewed by K Savolainen, LH Yao, M Elbattah, N Innab; revised version received 07.04.25; accepted 11.04.25; published 10.07.25.

Please cite as:
Khanbhai M, Carenzo C, Aryasinghe S, Manton D, Mayer E
Leveraging AI to Drive Timely Improvements in Patient Experience Feedback: Algorithm Validation
JMIR Med Inform 2025;13:e60900
URL: https://medinform.jmir.org/2025/1/e60900
doi:10.2196/60900

© Mustafa Khanbhai, Catalina Carenzo, Sarindi Aryasinghe, Dave Manton, Erik Mayer. Originally published in JMIR Medical Informatics (https://medinform.jmir.org), 10.7.2025. This is an open-access article distributed under the terms of the Creative Commons Attribution License (https://creativecommons.org/licenses/by/4.0/), which permits unrestricted use, distribution, and reproduction in any medium, provided the original work, first published in JMIR Medical Informatics, is properly cited. The complete bibliographic information, a link to the original publication on https://medinform.jmir.org/, as well as this copyright and license information must be included.

XSL•FO
RenderX

Combining Machine Learning With Real-World Data to Identify Gaps in Clinical Practice Guidelines: Feasibility Study Using the Prospective German Stroke Registry and the National Acute Ischemic Stroke Guidelines

Sandrine Müller[1], MSc; Susanne Diekmann[1], Dr med; Markus Wenzel[1,2], Prof Dr-Ing; Horst Karl Hahn[1,3], Prof Dr-Ing; Johannes Tuennerhoff[4,5], Dr med; Ulrike Ernemann[6], Prof Dr Med; Florian Hennersdorf[6], Dr med; German Stroke Registry Investigators[7]; Max Westphal[1], Dr rer nat; Sven Poli[4,5], Prof Dr Med

[1]Fraunhofer Institute for Digital Medicine, Bremen, Germany

[2]Constructor University, Bremen, Germany

[3]Department of Mathematics and Computer Science, University of Bremen, Bremen, Germany

[4]Department of Neurology & Stroke, University of Tübingen, Hoppe-Seyler-Str. 3, Tübingen, Germany

[5]Hertie Institute for Clinical Brain Research, Tübingen, Germany

[6]Department of Diagnostic and Interventional Neuroradiology, University of Tübingen, Tübingen, Germany

[7]

Corresponding Author:
Sven Poli, Prof Dr Med
Department of Neurology & Stroke, University of Tübingen, Hoppe-Seyler-Str. 3, Tübingen, Germany

Abstract

Background: Clinical practice guidelines (CPGs) serve as essential tools for guiding clinicians in providing appropriate patient care. However, clinical practice does not always reflect CPGs. This is particularly critical in acute diseases requiring immediate treatment, such as acute ischemic stroke, one of the leading causes of morbidity and mortality worldwide. Adherence to CPGs improves patient outcomes, yet guidelines may not address all patient scenarios, resulting in variability in treatment decisions. Identifying such gaps would augment CPGs but is challenging when using traditional methods.

Objective: This study aims to leverage real-world data coupled with machine learning (ML) techniques to systematically identify and quantify gaps in German thrombolysis-in-stroke guidelines.

Methods: We analyzed observational data from the German Stroke Registry – Endovascular Treatment (GSR-ET), a prospective national registry involving 18,069 patients from 25 stroke centers in whom endovascular treatment of a large vessel occlusion was attempted between 2015 and 2023. Key variables included demographic, clinical and imaging information, treatment details, and outcomes. A random forest model was used to predict intravenous thrombolysis treatment decisions based on three different sets of features: (1) guideline-recommended features, (2) clinician-selected features, and (3) features as documented in the GSR-ET before thrombolytic treatment. Feature importance scores, permutation importance, and Shapley Additive Explanations values were used, with clinician guidance, to interpret the model and identify key factors associated with guideline deviations and independent clinician judgments.

Results: Of all GSR-ET patients, 13,440 (74.4%) were analyzed after excluding those with incomplete or implausible data. The random forest model's performance, measured by area under the receiver operating characteristics curve, was 0.71 (95% CI 0.68 - 0.73), 0.74 (95% CI 0.73 - 0.75), and 0.77 (95% CI 0.76 - 0.78) for the guideline-recommended, clinician-selected, and GSR-ET feature sets, respectively. Across all sets, time from symptom onset to admission was the most important predictor of thrombolysis treatment decisions. Age, which according to the German guidelines is not to be considered for thrombolysis administration, emerged as a significant predictor in the GSR-ET feature set, suggesting a potential gap between guidelines and clinical practice.

Conclusions: In our study, we introduce an innovative approach that combines real-world data with ML techniques to identify discrepancies between CPGs and actual clinical decision-making. Using intravenous thrombolysis in large vessel occlusion stroke as a model, our findings suggest that treatment decisions may be influenced by factors not explicitly included in the current German guideline, such as patient age and pre-stroke functional status. This approach may help uncover clinically relevant variables for potential inclusion in future guideline refinements.

XSL•FO
RenderX

(JMIR Med Inform 2025;13:e69282) doi:10.2196/69282

KEYWORDS

clinical practice guidelines; real-world data; machine learning; acute ischemic stroke; health care improvement; guideline adherence

Introduction

Background

Ischemic stroke is a major global health concern being one of the leading causes of death and long-term disability worldwide, with more than 6 million deaths reported in 2019 [1]. Effective management of ischemic stroke is critical for lowering morbidity and mortality [2]. Clinical practice guidelines (CPGs), developed by expert panels and health care organizations, are part of an evidence-based practice toolkit designed to standardize medical treatment and ensure that patients receive the best possible care. The acute ischemic stroke guidelines encompass recommendations for pre- and in-hospital care, early diagnosis, timely administration of intravenous thrombolysis, and the implementation of endovascular thrombectomy as needed [3-5].

Despite the availability of these guidelines and the effort made to keep them current, adherence in clinical practice varies greatly [6,7]. Physicians may rely on independent clinical judgment in the absence of specific recommendations or intentionally deviate from guidelines due to several reasons, including addressing individual patient needs [8-10]. Such situations expose potential gaps in the guidelines, indicating areas where further guidance could improve standardization and patient care. In our study, a gap in CPGs refers to a discrepancy between guideline recommendations and the decisions observed in real-world clinical scenarios. According to research, deviations from recommended practices and the need for clinical discretion when no guidance is provided can result in suboptimal outcomes including increased rates of death and disability [11,12]. Currently employed traditional methods of detecting gaps in guidelines, such as comparing national and international guidelines and manual chart reviews, are labor-intensive, time-consuming, and susceptible to human error [13-17].

Recent research has shown that artificial intelligence and machine learning (ML) are effective in various health care applications, including predicting patient outcomes, identifying risk factors, and assisting clinicians with decision-making [18-21]. Another promising way to enhance patient outcomes in health care is the usage of real-world data, which includes routinely collected data (eg, electronic health records and registry data) to optimize treatment protocols based on real-world evidence [22]. There has been limited research within the realm of CPGs aimed at generating or enhancing health care guidelines by leveraging ML and real-world data [23-27]. To the best of our knowledge, the application of ML algorithms combined with real-world data to identify gaps in CPGs remains unexplored. Analyzing routine data with ML algorithms, such as random forests, which can handle complex interactions between variables and provide insights into the relative importance of various factors influencing clinical decisions, can be pivotal in systematically identifying areas where clinical practice diverges from CPGs, including areas not covered by existing recommendations. This approach can pinpoint specific deficiencies in CPGs and highlight potential areas for improvement, thereby offering a valuable addition to the traditional methods used for identifying gaps in CPGs.

Objective

To investigate whether intravenous thrombolysis treatment decisions follow the current German acute ischemic stroke guideline or are informed by additional features that are not part of the guideline recommendations. Specifically, we aim to:

1. Assess the performance of an ML model in predicting thrombolysis treatment when implemented on 3 different sets of features.
2. Identify key factors in thrombolysis administration that are currently not included in the guidelines.

Methods

Data Collection

The data used in this study were retrieved from the German Stroke Registry – Endovascular Treatment (GSR-ET) [28], a nationwide registry comprising pseudonymized, prospectively documented records of 18,069 patients who underwent endovascular stroke treatment as part of routine clinical care at 25 stroke centers across Germany between 2015 and 2023. For this study, we extracted patient-level data from structured fields in the GSR-ET, limited to variables available before the intravenous thrombolysis decision, thereby ensuring clinical relevance at the time of decision-making.

The dataset included the demographic age and sex, pre-stroke functional status, as measured by the modified Rankin Scale (mRS); relevant comorbidities included previous stroke, diabetes mellitus, dyslipidemia, arterial hypertension, and atrial fibrillation, as well as smoking status and antiplatelet or anticoagulation therapy at stroke onset. Living status before stroke was categorized as living at home, in a nursing home, or receiving nursing services at home.

At the time of admission, clinical variables included stroke severity, assessed using the National Institutes of Health Stroke Scale (NIHSS), and systolic and diastolic blood pressure. Radiological data included imaging modalities (ie, noncontrast enhanced computed tomography, CT angiography [CTA], computed tomography [CT] perfusion, magnetic resonance imaging, magnetic resonance angiography [MRA], magnetic resonance perfusion, and imaging-based findings such as the Alberta Stroke Program Early CT Score [ASPECTS]), indicating the extent of ischemic brain tissue damage; the Thrombolysis in Cerebral Infarction (TICI) score on CTA or MRA, indicating the degree of orthograde perfusion of the affected territory; the laterality (left, right, and bilateral) and location of the vessel occlusion (anterior or posterior circulation); the presence of tandem stenosis, and signs of ischemia outside the occluded vessel territory.

XSL•FO
RenderX

Process-related variables included the time from symptom onset (or last seen well) to hospital admission and whether the patient was primarily admitted to an interventional stroke center.

The primary outcome of interest in this study was whether a patient received intravenous thrombolysis before endovascular therapy.

Data Cleaning and Preparation

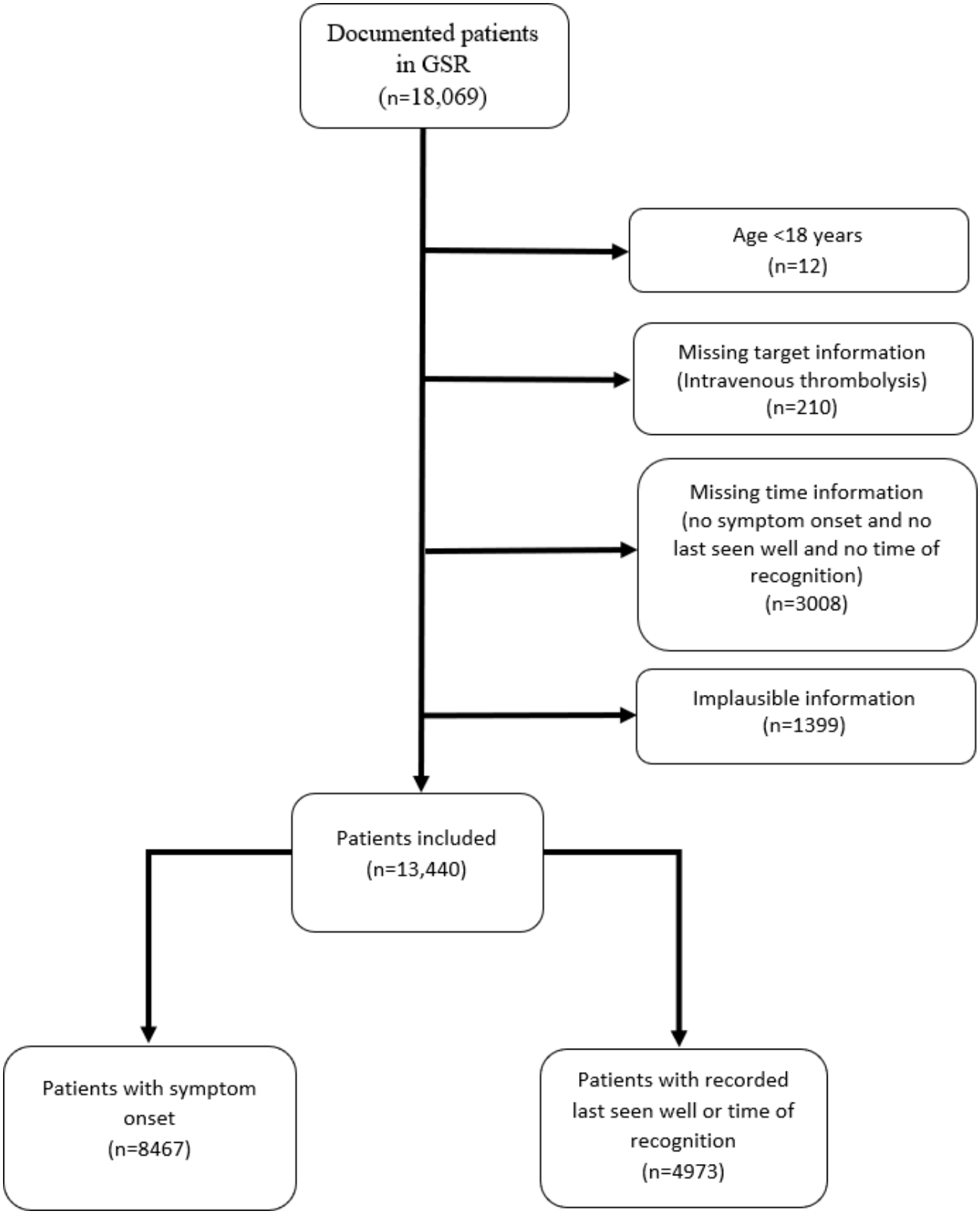
Before analysis, the data was cleaned, and patients were excluded based on prespecified exclusion criteria including incomplete or implausible data (see Figure 1 and Multimedia Appendix 1). To estimate missing values for age, admission blood pressure, scores on the NIHSS, and the pre-stroke mRS score, we employed the multiple imputation by chained equations technique, provided in the Python library [29]. To assess the robustness of our imputation strategy, we compared model performance by dropping missing values and using mean and k-nearest neighbor imputation strategies. To reduce the risk of multicollinearity, we performed correlation analysis using the Pearson method for numerical variables and Cramer V for categorical variables. In addition, the reported antithrombotic medication intake by patients was grouped into 2 categories: anticoagulants (apixaban, rivaroxaban, edoxaban, dabigatran, phenprocoumon, and heparins) and antiplatelets (aspirin, clopidogrel, and others). This approach helped manage correlation between variables, ensuring that each group represented a distinct set of clinical effects. Comorbidity features such as hypertension, diabetes mellitus, atrial fibrillation, and dyslipidemia were excluded from the analysis as we were not sure when exactly this information was documented (before or after the target feature). Occluded vessel features were grouped into 2 distinct groups: anterior and posterior circulation occlusion. Categorical and ordinal variables were transformed using one-hot encoding and ordinal encoding respectively to ensure compatibility with the ML model.

Out of the 206 available features, a total of 26 features all obtained before the target feature and relevant to thrombolysis administration were extracted from the GSR-ET. To measure the performance of our random forest model in predicting initiation of thrombolytic treatment, we created 3 distinct feature sets (see Multimedia Appendix 2 for more details) that we call the “Guideline”, the “Clinician”, and the “GSR-ET” feature sets and define as follows:

- Guideline feature set: this feature set includes the 11 features explicitly outlined in the German acute ischemic stroke guideline which are deemed relevant for intravenous thrombolysis decision-making. The inclusion of these features was based on their established clinical relevance in assessing treatment eligibility and aligning with evidence-based practice. The guideline feature set was chosen to directly reflect the guideline’s criteria, ensuring the model is evaluated against well-defined clinical standards.
- Clinician feature set: this feature set is derived from expert clinician judgment and includes 18 features identified by 2 independent stroke physicians (TJ and PS) as crucial for thrombolysis decision-making. Selection was based on their real-world experience and understanding of a broader range of patient factors that influence treatment decisions. While some of these features may not be explicitly outlined in formal guidelines, they are considered essential in clinical practice.
- GSR-ET feature set: this feature set includes all 26 features from the GSR-ET dataset that are documented before thrombolysis administration. Their inclusion ensures that the model captures a comprehensive view of the patient’s condition as recorded by clinicians in real-world settings, incorporating factors that may influence treatment decisions beyond what is specified by guidelines or expert judgment.

XSL•FO
RenderX

Figure 1. Flowchart illustrating patient selection. GSR: German Stroke Registry.



Outcome of Interest

Treatment with intravenous thrombolysis was chosen as the outcome of interest for this study. Thrombolysis is a critical and time-sensitive treatment for acute ischemic stroke [30-36], and it offers a clear, binary outcome suitable for classification algorithms, making it an ideal target for ML models such as random forests. In addition, thrombolysis represents an important quality indicator of stroke care. Despite known contraindications and gaps in existing guidelines, clinicians rely on their independent judgment and often administer thrombolysis, because it, along with endovascular thrombectomy, represents the only effective treatment option in the acute phase of stroke. We consider predicting intravenous thrombolysis treatment valuable as it captures the initial and crucial acute stroke decision-making process.

XSL•FO
RenderX

Machine Learning Model

To efficiently identify a suitable classification model for our analysis, we tested various ML algorithms using the lazypredict library [37], which quickly trains and compares the performance of many different classifiers on a given dataset.

Based on whether symptom onset was known or not, patients were divided into 2 subgroups for which we suspect possible different behavior concerning the target variable:

- Group A: Recorded symptom onset (n=8467, 62.9% patients).
- Group B: Recorded "last seen well" or "time of symptom recognition" (n=4973, 37.1% patients).

All subsequent steps of model development, training, and evaluation were conducted independently within each subgroup to ensure that analyses reflect their unique clinical and decision-making characteristics.

The dataset was split into training (80%) and validation (20%) sets for both subgroups to separate training and validation of the models and thereby detect overfitting and allow for a robust performance evaluation.

To optimize model performance, we used the nested cross-validation approach [38]. We performed an inner cross-validation using RandomizedSearchCV from the Python library scikit-learn on the training set to tune hyperparameters [39]. The hyperparameter search space included the number of estimators (n_estimators: 50 - 500) and the maximum depth of trees (max-depth: 1 - 20). A total of 5 hyperparameter configurations were randomly sampled, balancing exploration with computational efficiency. The model was evaluated across different combinations of features, and the best-performing configuration from the process was selected for final evaluation on the validation set.

Model Performance Assessment and Interpretability

Our model was evaluated on the validation set, primarily using the area under the receiver operating characteristic curve (AUROC). To ensure robustness, maintain class proportions, and prevent overfitting, we performed an outer cross-validation using stratified k-fold cross-validation (with k=5) on the tuned model to derive AUROC results. This method divides the training set into 5 subsets (4 for training and 1 for validation) and ensures that each fold of the cross-validation maintains the same proportion of class labels, which is particularly important given the potential imbalance in the chosen treatment (intravenous thrombolysis). We further addressed class imbalance by applying the synthetic minority over-sampling technique within the cross-validation loop to oversample the minority class in the training data. Secondary performance measures included F_1-score, accuracy, precision, and recall.

To assess the importance of each feature in their respective sets, in predicting intravenous thrombolysis treatment, we used a comprehensive analysis combining several methods. Initially, feature importance scores were extracted from the random forest model to provide a foundational understanding of each feature's contribution. To capture each feature's impact on model accuracy, permutation feature importance was applied. This loss-based approach quantifies feature importance by measuring the decrease in model performance when individual features are randomly permuted [40]. In addition, to ensure the robustness of the feature importance evaluations, we computed the confidence intervals for each feature within its respective feature set based on permutation importance results, applying the correlated t-test approach [41,42]. This method enabled us to visualize the variability and reliability of the feature importance scores. Finally, Shapley Additive Explanations (SHAP), a variance-based method, was also employed to examine the influence of each feature at the prediction level, offering deeper insights into feature contributions to both predictions (intravenous thrombolysis or no intravenous thrombolysis) [43]. Together, these methods enabled a thorough exploration of features that play an important role in the model's predictions.

Statistical Analyses

For categorical features, absolute and relative frequencies were computed. The interquartile ranges, minimum and maximum values of continuous features including NIHSS (ordinal), and pre-stroke mRS (ordinal) were also computed. The chi-square test was used to compare proportions between groups for categorical variables. For continuous and ordinal variables, the Wilcoxon rank-sum test was applied.

The descriptive comparison focused on the differences between patients who received intravenous thrombolysis and those who did not. These included demographic characteristics (eg, age, sex, and living status), comorbidities (eg atrial fibrillation, diabetes, and previous stroke), imaging modalities, occlusion sites, and pretreatment clinical status (eg NIHSS and pre-stroke mRS).

To quantify uncertainty in the AUROC estimates, 95% CIs were calculated using the correlated *t* test. All tests were 2-sided, and a *P* value of <.05 was considered statistically significant. Given the exploratory nature of the analysis, *P* values were not adjusted for multiple testing. Statistical analyses were conducted using Python (version 3.9.18).

Ethical Considerations

Data collection for the GSR-ET was centrally approved by the leading ethics committee at Ludwig-Maximilians University, Munich (689-15). Additional approvals were obtained from local ethics committees or institutional review boards at each participating center, including the ethics committee of the University of Tübingen (057/2016BO2), in accordance with local regulations. Informed consent was obtained from patients for data collection. The data used in this study were pseudonymized to ensure privacy and confidentiality. No personally identifiable information is included in the manuscript or supplementary materials. No compensation was provided to participants, as the registry relies on routine clinical data.

Results

The results presented in this section are solely for the patients with recorded symptom onset (group A). Results for group B can be found in Multimedia Appendix 3.

XSL•FO
RenderX

Descriptive Statistics

A total of 8467 (62.9%) patients with recorded symptom onset were included in the analysis. 4809 (56.8%) patients received intravenous thrombolysis. Table 1 shows the descriptive statistics of patients who underwent thrombolysis and patients who did not. Most of the features were statistically associated with the target variable of thrombolysis ($P<.05$).

XSL•FO
RenderX

Table . Descriptive statistics of patients with recorded symptom onset in relation to the outcome of interest.

Features	Intravenous thrombolysis (n=4809, 56.8%)	No intravenous thrombolysis (n=3658, 43.2%)	*P* value
Categorical features			
Sex, n (%)			<.001
Male	2444 (50.8)	1835 (50.2)	
Female	2364 (49.2)	1822 (49.8)	
Baseline antithrombotic medication, n (%)			
None	3042 (63.2)	2015 (55.1)	<.001
ASS[a]	1486 (31.0)	821 (22.4)	<.001
Clopidogrel	121 (2.5)	157 (4.3)	<.001
Heparins	36 (0.7)	169 (4.6)	<.001
Apixaban	25 (0.5)	165 (4.5)	<.001
Edoxaban	5 (0.1)	65 (1.8)	<.001
Rivaroxaban	21 (0.4)	134 (3.6)	<.001
Dabigatran	13 (0.3)	22 (0.6)	.002
Phenprocoumon	146 (3.0)	333 (9.1)	<.001
Others	0 (0.0)	0 (0.0)	>.99
Living status, n (%)			.002
Home	4248 (88.3)	3142 (85.9)	
Nursing home	273 (5.7)	217 (5.9)	
Nursing at home	155 (3.2)	171 (4.7)	
Comorbidity, n (%)			
Diabetes mellitus	933 (19.4)	914 (24.9)	<.001
Dyslipidemia	1868 (38.8)	1559 (42.6)	.001
Arterial hypertension	3486 (72.5)	2872 (78.5)	<.001
Atrial fibrillation	1494 (31.1)	1938 (52.9)	<.001
Prior stroke	350 (7.3)	488 (13.3)	<.001
Smoking, n (%)			.004
Nonsmoker	3200 (66.5)	2447 (66.9)	
Current smoker	808 (16.8)	533 (14.8)	
Previous smoker	447 (9.3)	395 (10.7)	
Imaging, n (%)			
Noncontrast enhanced computed tomography	4529 (94.2)	3266 (89.3)	<.001
CTA[b]	4265 (88.7)	3079 (84.2)	.66
CT[c] perfusion	2366 (49.2)	1780 (48.7)	.03
Magnetic resonance imaging (MRI)	225 (4.7)	231 (6.3)	<.001
Magnetic resonance angiography (MRA)	170 (3.5)	166 (4.5)	.83
Magnetic resonance perfusion (MR perfusion)	87 (1.8)	90 (2.5)	.77
Occluded vessel, n (%)			

XSL•FO
RenderX

Features	Intravenous thrombolysis (n=4809, 56.8%)	No intravenous thrombolysis (n=3658, 43.2%)	*P* value
Cerebral artery – extracranial	319 (6.6)	238 (6.5)	>.99
Cerebral artery – intracranial without carotid-T involvement	280 (5.8)	212 (5.8)	.90
Cerebral artery – intracranial with carotid-T involvement	675 (14.0)	528 (14.4)	.39
Middle cerebral artery M1-segment, proximal	1514 (31.5)	1064 (29.1)	.08
Middle cerebral artery M1-segment, distal	750 (15.6)	447 (12.2)	<.001
Middle cerebral artery M2-segment	858 (17.8)	602 (16.4)	.22
Anterior cerebral artery (ACA)	146 (3.0)	93 (2.5)	.25
Posterior cerebral artery (PCA)	164 (3.4)	110 (3.0)	.41
Basilar artery (BA)	357 (7.4)	342 (9.3)	.001
Vascular artery (VA)	73 (1.5)	64 (1.7)	.39
Occluded vessel side, n (%)			<.001
left	2203 (45.8)	1611 (44.0)	
right	2126 (44.2)	1536 (41.9)	
bilateral	40 (0.8)	54 (1.5)	
Not applicable (eg basilar artery)	276 (5.7)	290 (7.9)	
Tandem stenosis, n (%)	544 (11.3)	335 (9.1)	.45
Ordinal features			
Imaging aspects, n (%)			<.001
10	1810 (37.6)	1063 (29.0)	
Not applicable (eg, basilar artery)	542 (11.2)	614 (16.8)	
9	784 (16.3)	559 (15.2)	
8	640 (13.3)	477 (13.0)	
7	394 (8.2)	324 (8.8)	
6	211 (4.4)	176 (4.8)	
5	132 (2.7)	123 (3.4)	
4	53 (1.1)	51 (1.4)	
3	20 (0.4)	32 (0.9)	
2	11 (0.2)	11 (0.3)	
1	12 (0.2)	4 (0.1)	
Thrombolysis in Cerebral Infarction score (TICI) on CTA or MRA, n (%)			<.001
0	4100 (85.2)	2998 (81.9)	
1	220 (4.6)	147 (4.0)	
2a	80 (1.6)	69 (1.9)	
2b	38 (0.8)	36 (0.9)	
3	43 (0.9)	30 (0.8)	
Not applicable	189 (3.9)	219 (5.9)	

XSL•FO
RenderX

Features	Intravenous thrombolysis (n=4809, 56.8%)	No intravenous thrombolysis (n=3658, 43.2%)	*P* value
Pre-stroke modified Rankin Scale score, median (IQR)	0 (0 - 1)	0 (0 - 2)	<.001
National Institute of Health Stroke Scale on admission, median (IQR)	14 (8 - 18)	13 (7 - 18)	.007
Continuous features			
Age (years), median (IQR)	75 (63 - 82)	77 (66 - 83)	.001
Systolic blood pressure, median (IQR)	150 (135 - 170)	150 (132 - 170)	.13
Diastolic blood pressure, median (IQR)	80 (72 - 92)	80 (70 - 92)	.32
Time between symptom onset and admission, median (IQR)	93 (56 - 182)	135 (65 - 255.75)	<.001

[a]ASS: acetylsalicylic acid.

[b]CTA: computed tomography angiography.

[c]CT: computed tomography.

Machine Learning Model

Table 2 summarizes the performance of different ML classification models on our dataset and shows similar performance of the first 3 models across the 3 features sets (see Multimedia Appendix 4 for complete table). Despite comparable performance with LGBMClassifier, we selected the random forest model for subsequent data analysis due to its built-in feature importance metrics, which facilitate clinical interpretation, and its robustness to overfitting in datasets with noise or imbalance. In addition, since our study focuses on identifying key clinical features, random forest's ability to effectively handle complex feature interactions makes it well-suited for our goals [44].

Table . Performance metrics of various machine learning classification models.

Model	AUROC[a]	Accuracy	F_1-score
RandomForestClassifier	0.71	0.72	0.72
LGBMClassifier	0.71	0.72	0.72
AdaBoostClassifier	0.70	0.72	0.71
LogisticRegression	0.70	0.72	0.71

[a]AUROC: area under the receiver operating characteristic curve

Model Performance Assessment and Interpretability

Our model was evaluated for its performance on the different feature sets and subpopulations and predicted the treatment outcome. Table 3 shows the performance metrics for patients with recorded symptom onset.

Figure 2 shows the AUROC for all feature sets: guideline, clinician and GSR-ET, with each curve representing the mean AUROC across 5 cross-validation folds in the given feature set. The GSR-ET feature set achieved the highest mean AUROC of 0.77 (SD 0.01), followed by the clinician feature set with 0.74 (SD 0.01), and the guideline feature set with 0.71 (SD 0.01). Multimedia Appendix 5 shows the plot consisting of the individual k-fold results. There was no significant improvement in performance after applying Synthetic Minority Oversampling Technique (SMOTE), indicating that class imbalance had minimal impact on the model performance. The imputation methods yielded similar results (eg, for the GSR-ET feature set, mean imputation AUROC: 0.75, k-nearest neighbor AUROC: 0.75, and multivariate imputation by chained equations: 0.77), thereby improving over the approach of dropping rows with missing values (AUROC: 0.66).

Figures 3 and 4 show the feature importance and permutation feature importance for each feature set, with their corresponding importance scores and rankings. The annotations on the bars represent the feature's rank within its respective feature set. These plots highlight the varying significance of features depending on the feature set used during prediction (See Multimedia Appendix 5 for feature importance plot with confidence intervals).

The top 10 features in all 3 feature sets in both plots were mostly similar, however with differences in their rankings within the respective feature set. The "Time between symptom onset and admission" and "Anticoagulation at stroke onset" emerged as the most important features across all sets (ranked number 1 and 2 respectively). Other significant features included "NIHSS," "Age," "Imaging aspects," "Pre-stroke mRS score" and "blood pressure," all of which had high importance scores in both plots. Less influential features included various imaging

XSL•FO
RenderX

modalities, "Living status" and "Sex," with consistently low importance rankings across feature sets in the feature importance plot.

As seen in the beeswarm plots (Figures 5-7), the SHAP analysis further confirmed the findings provided by the random forest feature importance and permutation feature importance analyses. Each point represents a specific observation's SHAP value, with colors corresponding to feature values (blue [cooler] color=lower value, red [warmer] color=higher value). The features are ranked in terms of mean absolute SHAP values indicating importance from the top (most important) to the bottom (least important).

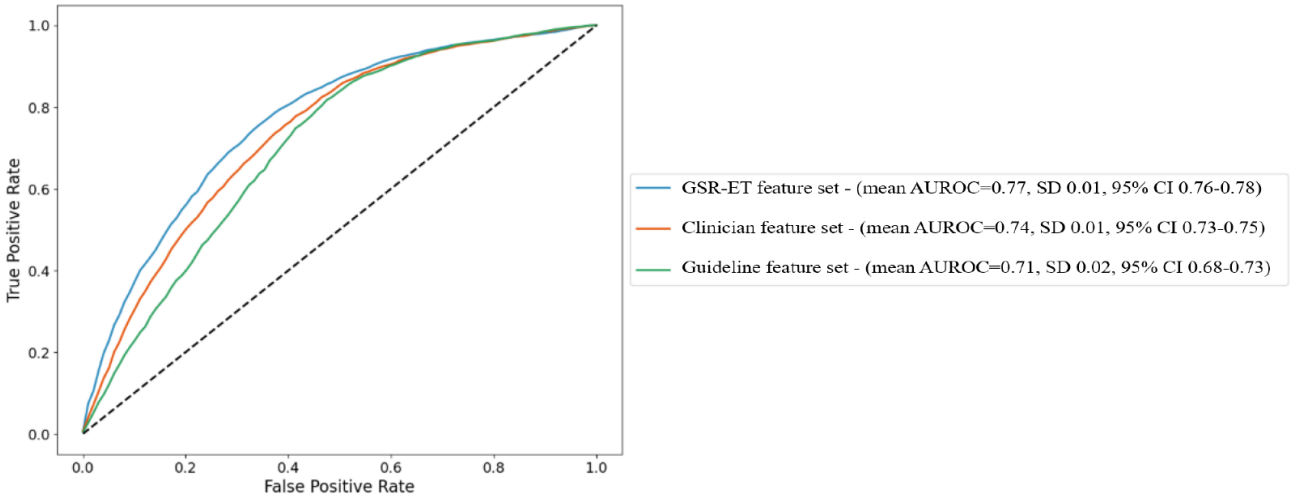
The plots show each feature's impact on the model's prediction of the patients who did not receive intravenous thrombolysis. "Anticoagulation at stroke onset" and "Time between symptom onset and admission" have the highest SHAP values, indicating they strongly influence predictions for patients not receiving intravenous thrombolysis. Specifically, higher values of "Time between symptom onset and admission" (shown in red) push the model towards predicting no intravenous thrombolysis. Similarly, "Pre-stroke mRS score" and "NIHHS" and "Prior stroke" (in the GSR-ET set) also have high SHAP values. Higher scores for these features increase the likelihood of predicting no intravenous thrombolysis administration.

Table . Performance metrics of the random forest model on all 3 feature sets in the subgroup of patients with known symptom onset.

Feature set	AUROC[a], mean (SD)	Accuracy	Precision	Recall	F_1-score
Guideline	0.71 (0.02)	0.70	0.69	0.85	0.76
Clinician	0.74 (0.01)	0.70	0.70	0.86	0.77
GSR-ET	0.77 (0.01)	0.71	0.71	0.84	0.77

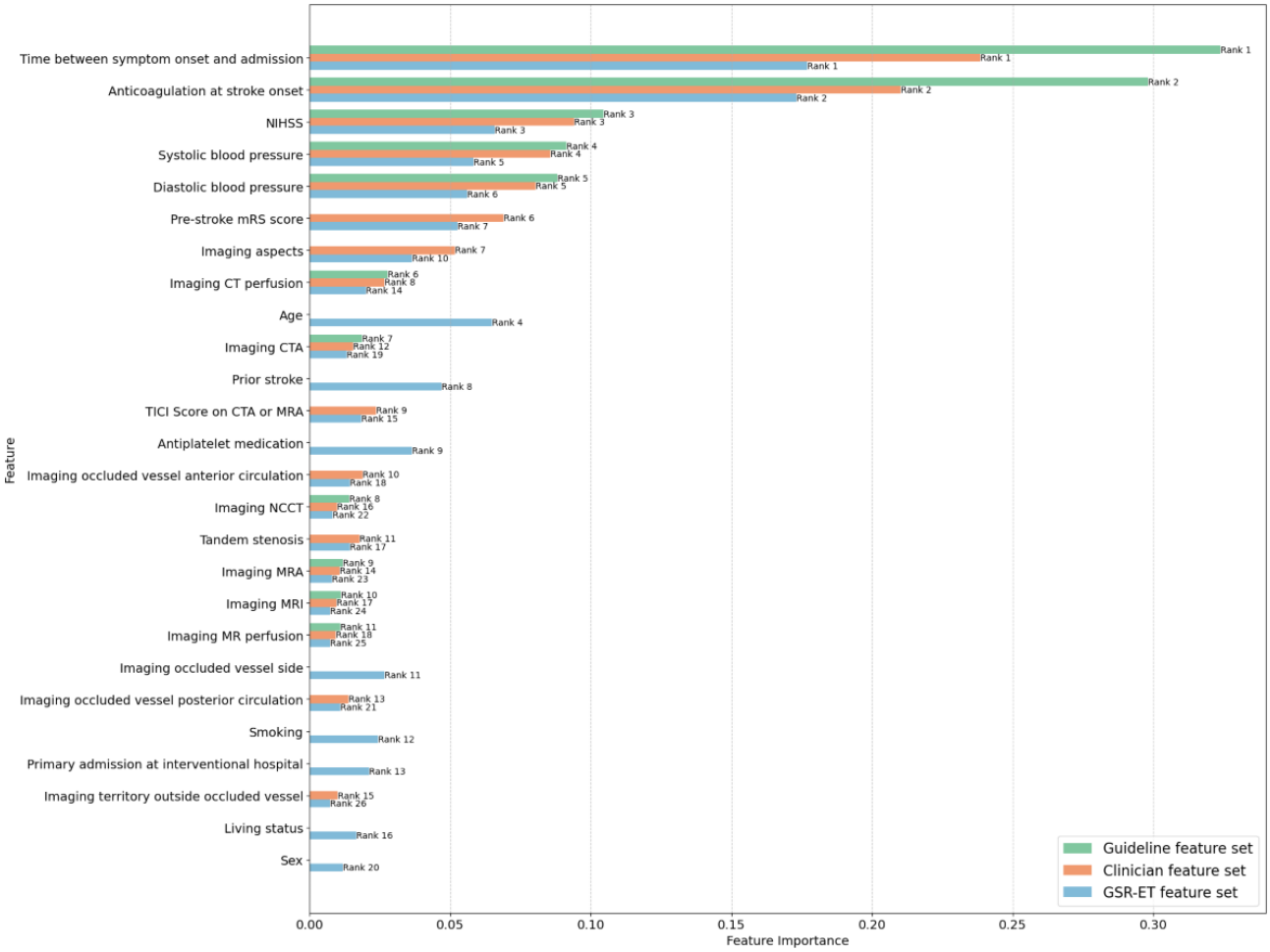
[a]AUROC: area under the receiver operating characteristic curve

Figure 2. Mean area under the receiver operating characteristic curve (AUROC) across all 3 feature sets for patients with recorded symptom onset. GSR-ET: German Stroke Registry – Endovascular Treatment.



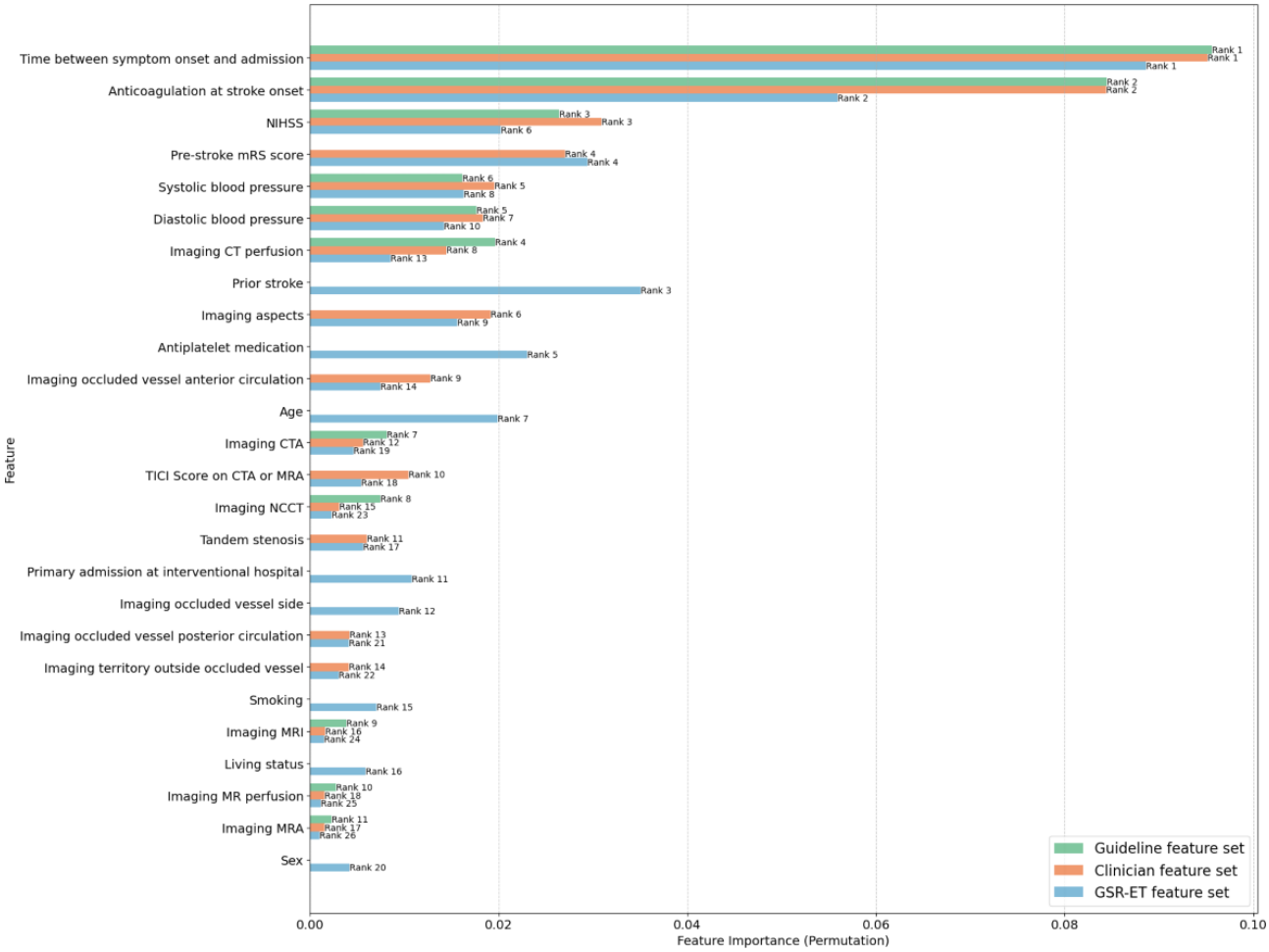
XSL•FO
RenderX

Figure 3. Feature importances for each feature set for patients with recorded symptom onset. CT: computed tomography; CTA: computed tomography angiography; GSR-ET: German Stroke Registry – Endovascular Treatment; MR: magnetic resonance; MRA: magnetic resonance angiography; NCCT: noncontrast computed tomography; NIHSS: National Institute of Health Stroke Scale; TICI: Thrombolysis in Cerebral Infarction.



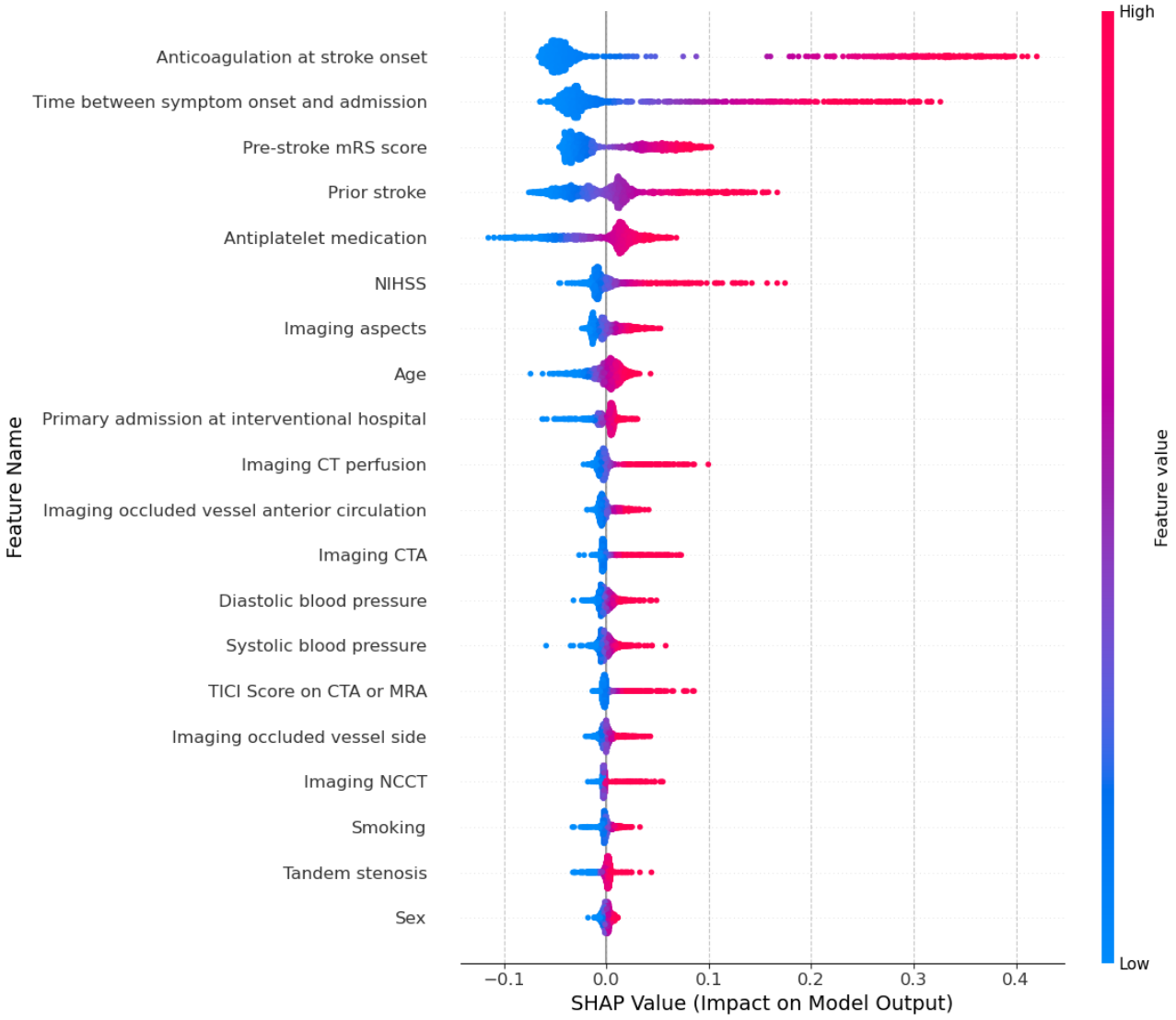
XSL•FO
RenderX

Figure 4. Permutation feature importances for each feature set for patients with recorded symptom onset. CT: computed tomography; CTA: computed tomography angiography; GSR-ET: German Stroke Registry – Endovascular Treatment; MR: magnetic resonance; MRA: Magnetic resonance angiography; NCCT: noncontrast computed tomography; NIHSS: National Institute of Health Stroke Scale; TICI: Thrombolysis in Cerebral Infarction;



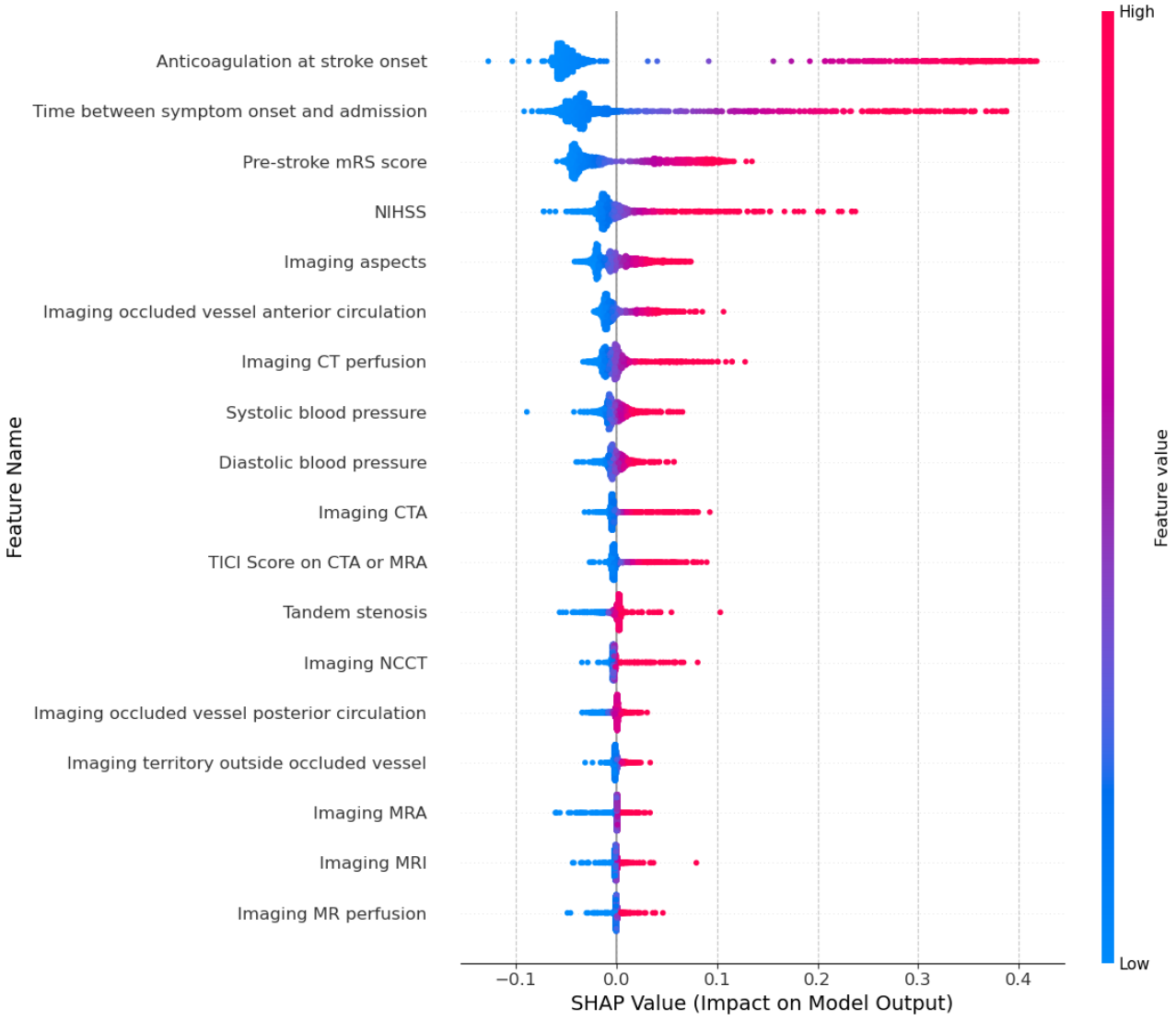
XSL•FO
RenderX

Figure 5. Shapley additive explanations summary plot for the German Stroke Registry – Endovascular Treatment feature set. This plot illustrates the contribution of each feature to the model's prediction of no intravenous thrombolysis administration. Positive SHAP values increase the likelihood of predicting no intravenous thrombolysis, while negative values decrease it. Features are ranked by importance from top (most influential) to bottom (least influential). CT: computed tomography; CTA: computed tomography angiography; MRA: magnetic resonance angiography; mRS: modified Rankin Scale; NCCT: noncontrast computed tomography; NIHSS: National Institute of Health Stroke Scale; SHAP: Shapley Additive Explanations; TICI: Thrombolysis in Cerebral Infarction.



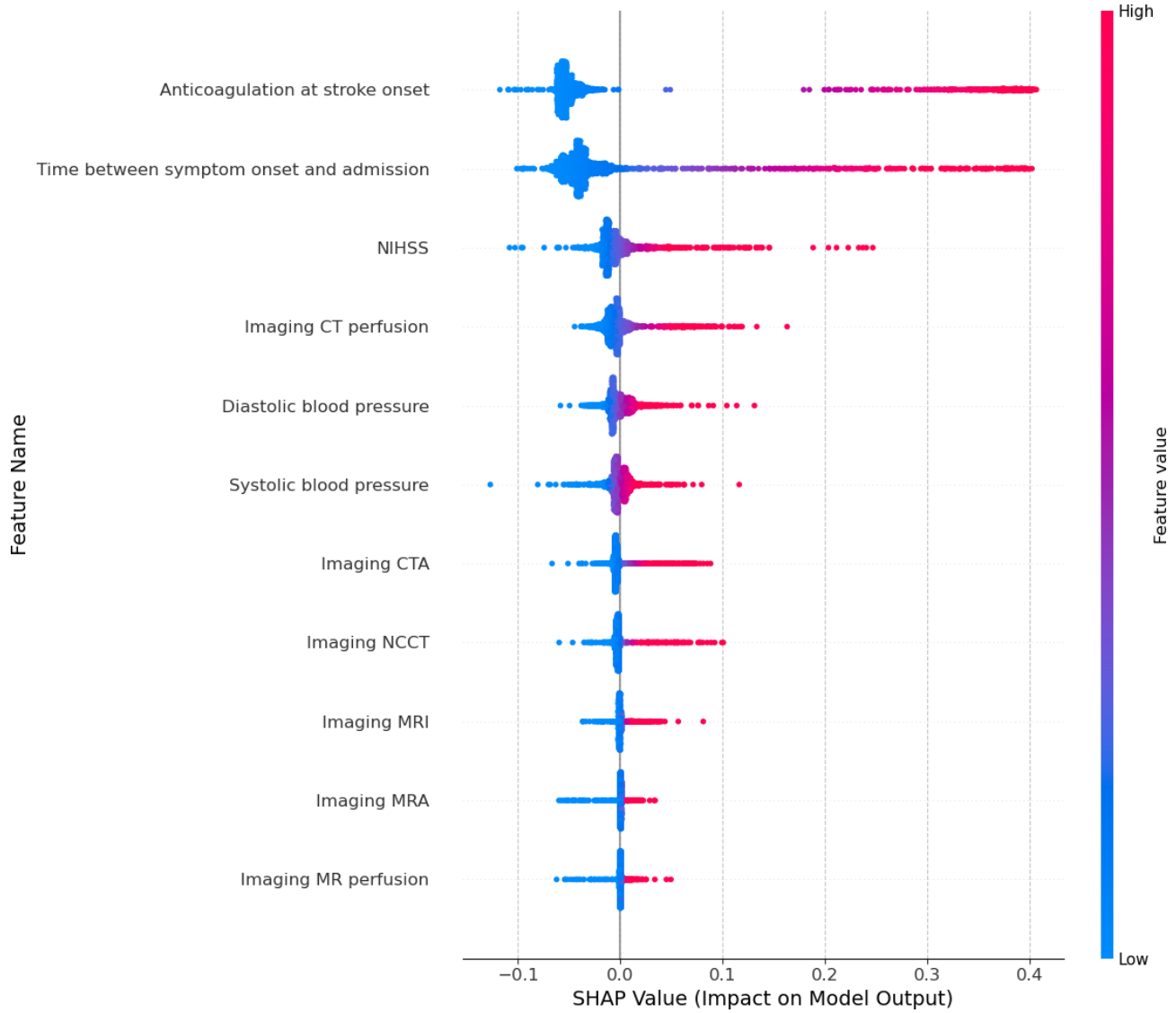
XSL•FO
RenderX

Figure 6. SHAP summary plot for the clinician feature set. This plot illustrates the contribution of each feature to the model's prediction of no intravitreal administration. Positive SHAP values increase the likelihood of predicting no IVT, while negative values decrease it. Features are ranked by importance from top (most influential) to bottom (least influential). CT: computed tomography; CTA: computed tomography angiography; MR: magnetic resonance; MRA: magnetic resonance angiography; MRI: magnetic resonance imaging; mRS: modified Rankin Scale; NCCT: noncontrast computed tomography; NIHSS: National Institute of Health Stroke Scale; SHAP: Shapley Additive Explanations; TICI: Thrombolysis in Cerebral Infarction.



XSL•FO
RenderX

Figure 7. SHAP summary plot for the guideline feature set. This plot illustrates the contribution of each feature to the model's prediction of no intravitreal administration. Positive SHAP values increase the likelihood of predicting no intravitreal, while negative values decrease it. Features are ranked by importance from top (most influential) to bottom (least influential). CT: computed tomography; CTA: computed tomography angiography; MR: magnetic resonance; MRA: magnetic resonance angiography; MRI: magnetic resonance imaging; NIHSS: National Institute of Health Stroke Scale; SHAp: Shapley Additive Explanations.



Discussion

Overview

The results of this study provide valuable insights into how ML models can be used to highlight discrepancies between guideline-recommended practices and clinical practice. By integrating ML with real-world registry data, we sought to identify gaps in CPGs. Specifically, we developed and tested a random forest model on three feature sets: (1) guideline set (features explicitly recommended by the German acute stroke guideline), (2) clinician set (features selected by stroke experts), and (3) the GSR-ET set, which consists of all relevant features provided in the GSR-ET that were available to treating physicians before taking the decision to initiate thrombolysis in ischemic stroke patients with large vessel occlusion undergoing endovascular reperfusion therapy.

Principal Findings

Model Performance (AUROC Curves)

The AUROC curve for the 3 feature sets reveals a clear hierarchy in predictive performance. The GSR-ET feature set, which includes all reasonable features documented before thrombolysis initiation, achieved the mean AUROC curve score of 0.77. These results suggest that real-world decisions as documented in the GSR-ET incorporate additional clinical features beyond those recommended by the guidelines or even those included by stroke experts (clinician feature set), which enhances the model's ability to predict intravenous thrombolysis administration. The relatively lower performance of the guideline feature set (AUROC=0.71) indicates that relying solely on guideline-indicated features may not be sufficient to capture the complexity of intravenous thrombolysis decision-making. This finding highlights a potential gap in the current guidelines, which may not fully account for all relevant

XSL•FO
RenderX

clinical variables influencing intravenous thrombolysis administration.

Key Features and Possible Gaps in the German Acute Ischemic Stroke Guidelines

The top 10 features across all 3 sets were generally consistent, with the "Time between symptom onset and admission" emerging as the most important feature across all sets. This result underscores the critical role of timely intervention in stroke management, as shorter times from symptom onset to admission are associated with better outcomes and are a key determinant of intravenous thrombolysis eligibility [26]. "Time between symptom onset and admission" not only ranked first in all 3 feature sets but also had the greatest impact on model performance when permuted, further emphasizing its importance in predicting intravenous thrombolysis administration.

The "Pre-stroke mRS score" measures a patient's pre-stroke functional status where a high score implies a greater level of disability, which might reduce the likelihood of receiving intravenous thrombolysis if the expected benefit is limited due to pre-existing impairment. "Imaging aspects" evaluates the extent of early ischemic changes on imaging. Lower ASPECTS scores suggest more extensive ischemic damage, potentially dissuading intravenous thrombolysis administration due to higher bleeding risk and reduced likelihood of tissue salvage despite successful reperfusion. Both features were amongst the top 10 important features in the clinician and GSR-ET feature sets. This reflects the emphasis on functional status and stroke severity in treatment decisions. These features could, together with other scores such as the NIHSS, a guideline-recommended score which assesses neurological severity of stroke (ranked 3rd in the feature importance plot), offer a comprehensive view of both current severity and pre-existing functional limitations to guide intravenous treatment decisions.

Notably, "Age," which was not included in the guideline feature set, in line with the German acute ischemic stroke guidelines, emerged as relatively important in the GSR-ET feature set (ranked 4th). Its permutation also resulted in a drop in model performance. The SHAP values for "Age" showed that advanced age correlates with a tendency to withhold intravenous thrombolysis. This trend may reflect clinicians' caution in treating older patients due to increased risks, such as bleeding complications or potentially lower efficacy of the treatment in older populations. While the German guidelines may not emphasize "Age" as a factor, data-driven models recognize its relevance in intravenous thrombolysis decision-making. A correlation analysis revealed a weak positive correlation (Pearson correlation coefficient=0.28) between "Age" and "Pre-stroke mRS score", suggesting that "Age" is not merely an epiphenomenon but an independent feature influencing clinical decisions. This discrepancy between guideline recommendations and clinical practice points to a potential gap in the guidelines where clearer, age-specific recommendations could support clinicians, particularly given the established association between age and stroke outcomes [31,45].

Although demographic and lifestyle features such as "Smoking," "Living status," "Sex," and "Prior stroke" were included in the GSR-ET feature set, their relatively lower importance scores suggest that these features may play a more indirect role in treatment determination. They contribute to the overall risk profile of stroke patients, potentially influencing clinician perception of stroke severity or recovery potential and could therefore enhance individualized assessment for long-term outcomes and guide secondary prevention strategies [46].

Patients' use of antiplatelet and anticoagulation medications showed an influence on treatment decisions. While anticoagulation therapy is recognized as a contraindication for intravenous thrombolysis in specific scenarios, this is not explicitly detailed in the German guidelines, which instead refer clinicians to the summary of product characteristics. Similarly, the role of antiplatelet medication is less defined, as it is generally not believed to alter the benefit-risk ratio despite slightly increased bleeding risk. Our findings suggest that clinicians consider these factors, likely weighing the risks of hemorrhagic complications. A potential update to the guidelines regarding these medications could provide clinicians with granular recommendations regarding intravenous thrombolysis treatment in patients with varying antithrombotic regimens [36].

The minimal influence of "Tandem stenosis" on intravenous thrombolysis prediction suggests that the presence of concurrent stenosis in other vessels might be a significant factor in decision-making, likely due to its implications for clot accessibility and reperfusion success. This feature's importance signals a potential need to include vascular status assessments in intravenous thrombolysis eligibility criteria within the German acute ischemic stroke guidelines.

The feature "Primary admission at interventional hospital" positively influenced the likelihood of intravenous thrombolysis treatment, suggesting that hospital resources, including the presence of specialized stroke intervention teams, play a role in treatment decisions.

Other key features such as blood pressure and imaging features consistently achieved high and minimal importance respectively across all sets. These findings reinforce the importance of managing cardiovascular risk factors and imaging in stroke patients, especially in relation to intravenous thrombolysis eligibility.

Comparison With Previous Work

The integration of ML into clinical decision-making, especially in real-world treatment decisions, has been explored in several health care domains, but not in the context of gap search in CPGs. This section compares our approach with previous work to highlight how we contribute to the existing literature on identifying gaps in CPGs.

Though not aimed at directly refining CPGs, Abd-Alrazaq et al [47] used ML to identify gaps in COVID-19 literature. Another similar study focused on uncovering variation in clinical decision-making using registry data and ML is presented by James et al [48]. Smyth et al [14] conducted a study, using a mixed methods approach of surveys, chart reviews, and focus groups, focusing on syncope management, aiming to identify gaps between guideline-recommended care and actual clinical practice. They emphasized that guideline adherence was suboptimal, leading to overuse of some diagnostic tests while

XSL•FO
RenderX

underutilizing recommended evaluations. Similarly, Bregni et al [16] tackled rectal cancer management by systematically comparing recommendations from multiple national and international CPGs and revealed the presence of "grey areas" where guidelines either lacked sufficient evidence or were not clear, resulting in variable treatment approaches. Spranger et al [17] examined the gap between hypertension guidelines and clinical practice, finding that adherence to guidelines was often inconsistent, leading to both undertreatment and overtreatment [18]. They retrospectively analyzed medical records using chart reviews and identified factors such as clinician experience and patient characteristics as major contributors to deviations from guidelines. Ebben et al [23] developed a methodology using real-world data and clinical decision trees to continuously identify and prioritize potential areas for improvements in guidelines.

Across these approaches, there is a common theme: research gaps exist across various medical fields, often driven by real-world complexities not fully captured by CPGs. Our study extends this body of work by leveraging ML not only to identify these gaps but also to quantify the predictive power of features that are often overlooked or deemphasized in CPGs. In addition, our results suggest that updating guidelines to incorporate these potentially critical features could improve treatment consistency and outcomes, similar to some of the cited studies, which advocate for guideline refinement based on empirical evidence from clinical practice.

Limitations

While this study provides valuable insights into the potential gaps between guideline-recommended and clinician-led decision-making, several limitations must be acknowledged.

Registry Data

The GSR-ET consists solely of patients with a diagnosis of acute ischemic stroke, a large vessel occlusion, and patients who underwent or to whom an endovascular treatment was attempted. It is therefore important to note that within the GSR-ET, thrombolysis is only administered in conjunction with endovascular treatment but not as standalone reperfusion therapy. This means that the effect of better prediction in the GSR-ET feature set may be related to the fact that GSR-ET patients are a subset of strokes with large vessel occlusion and may therefore not reflect thrombolysis decision-making in the overall stroke patient.

Feature Interaction

While feature importances can identify variables that enhance the decision-making accuracy of our ML model, they do not reveal on a deeper level how these features interact with other variables in the GSR-ET. Consequently, simply knowing that a feature is influential does not clarify its optimal placement or threshold within the CPG decision framework.

Guideline Flexibility

CPGs are inherently flexible and are designed to provide general recommendations that accommodate a broad range of clinical scenarios. Consequently, they may not include all the possible factors that inform real-world decision-making by clinicians. Even though our study identified features not explicitly mentioned in the guidelines, it is possible that these features may still be deliberately excluded, as guideline developers may prioritize flexibility over incorporating factors that, while influential in decision-making, are not deemed essential for standardization in future guideline updates.

Limited Focus on Clinical Outcomes

This study focused primarily on predicting intravenous thrombolysis administration and identifying which variables were involved in decision-making but did not investigate the long-term clinical outcomes associated with these decisions. While deviations from the guidelines and independent clinical judgments were identified, it is unclear whether these decisions led to better or worse patient outcomes. This makes it difficult to assess whether the identified features should indeed be included in future guidelines based solely on the results of this study.

Future Directions

The methodology applied in this study offers a systematic approach to uncover discrepancies between CPGs and real-world decision-making. Future research using larger datasets could strengthen these findings and support guideline refinements. Integrating such approaches into clinical workflows may enable rapid identification of guideline gaps or nonadherence, ultimately contributing to improved patient care.

Conclusion

This study demonstrates the potential of combining ML with real-world data to systematically identify gaps between clinical practice and current CPGs. In the case of intravenous thrombolysis for large vessel occlusion stroke, factors such as age and pre-stroke disability, which are not explicitly addressed in current German guidelines, emerged as relevant to treatment decisions. These features may merit consideration in future iterations of CPGs to improve alignment with clinical realities.

Providing clear guidance on them would not only support clinicians in navigating complex patient profiles and making ethical, patient-centered decisions but also enhance their moral confidence and potentially offer legal protection. Specifically, future CPGs may emphasize that advanced age alone should exclude patients from thrombolysis, as it can enable recovery to pre-stroke conditions. However, a severely impaired pre-stroke functional status, particularly in advanced age, may not always represent a meaningful therapeutic goal.

Acknowledgments

The authors would like to extend their sincere gratitude to their colleagues: Dr Jan Klein, Sandra Siegel, and Dr Thomas Netsch for their valuable support in proofreading this manuscript. We would also like to thank all the contributors to the study, including

XSL•FO
RenderX

the patients, clinicians, and the German Stroke Registry – Endovascular Treatment investigators (Arno Reich, Omid Nikoubashman, Christian Nolte, Eberhard Siebert, Gabor Petzold, Franziska Dorn, Jan Hendrik Schäfer, Fee Keil, Ilko L Maier, Marielle S Ernst, Gerhard F. Hamann, Michael Braun, Anna Alegiani, Joachim Röther, Bernd Eckert, Maximilian Schell, Götz Thomalla, Fabian Flottmann, Jens Fiehler, Mario Abruscato, Sven Thonke, Arman Gregor, Evdokia Evangelidou, Timo Uphaus, Klaus Gröschel, Peter Schellinger, Jan Borggrefe, Lars Kellert, Hanna Zimmermann, Steffen Tiedt, Silke Wunderlich, Tobias Boeckh-Behrens, Martina Petersen, and Lars Krause) for their invaluable participation and data collection efforts.

We received grant money from the U Bremen Research Alliance/AI Center for Health Care, financially supported by the Federal State of Bremen.

We acknowledge support from the Open Access Publication Fund of the University of Tübingen.

Data Availability

The datasets analyzed during this study are not publicly available due to patient privacy regulations and data sharing agreements with the participating centers, but are available from the German Stroke Registry – Endovascular Treatment steering committee, upon reasonable request.

Authors' Contributions

SM led the conceptualization, data curation, formal analysis, investigation, methodology, software development, validation, visualization, and original draft writing. M Westphal contributed to the conceptualization, funding acquisition, methodology, project administration, supervision, validation, and review and editing of the manuscript. SP contributed to the conceptualization, supervision, validation, and review and editing. HKH, M Wenzel, SD, and JT contributed to the conceptualization and review and editing of the manuscript, with M Wenzel also contributing to funding acquisition. JT also contributed to data curation and validation. UE and FH contributed to data curation and review and editing. The German Stroke Registry – Endovascular Treatment investigators contributed to data curation and review and editing of the manuscript.

Conflicts of Interest

SP and UE are members of the steering committee of the German Stroke Registry – Endovascular Treatment. This involvement did not influence the data collection, analysis, or interpretation of the results in this study. All other authors declare no competing interests.

Multimedia Appendix 1
Detailed list of the criteria used to exclude patients from the analysis.
[PDF File, 82 KB - medinform_v13i1e69282_app1.pdf]

Multimedia Appendix 2
Feature sets used in comparing predictive performance.
[PDF File, 118 KB - medinform_v13i1e69282_app2.pdf]

Multimedia Appendix 3
Results of group B – patient subgroup with recorded “last seen well” or “time of symptom recognition”
[PDF File, 1214 KB - medinform_v13i1e69282_app3.pdf]

Multimedia Appendix 4
Complete classification model comparison table.
[PDF File, 42 KB - medinform_v13i1e69282_app4.pdf]

Multimedia Appendix 5
Additional results for group A – patients with recorded symptom onset.
[PDF File, 443 KB - medinform_v13i1e69282_app5.pdf]

References

1. The top 10 causes of death. World Health Organization. 2020. URL: https://www.who.int/news-room/fact-sheets/detail/the-top-10-causes-of-death [accessed 2024-06-10]
2. Herpich F, Rincon F. Management of acute ischemic stroke. Crit Care Med 2020 Nov;48(11):1654-1663. [doi: 10.1097/CCM.0000000000004597] [Medline: 32947473]

XSL•FO
RenderX

3. Powers WJ, Rabinstein AA, Ackerson T, et al. 2018 Guidelines for the early management of patients with acute ischemic stroke: a guideline for healthcare professionals from the American Heart Association/American Stroke Association. Stroke 2018 Mar;49(3):e46-e110. [doi: 10.1161/STR.0000000000000158] [Medline: 29367334]
4. Acute stroke guidelines. European Stroke Organisation. 2023. URL: https://eso-stroke.org/guidelines/eso-guideline-directory/#acute-stroke [accessed 2024-06-27]
5. S2e-leitlinie akuttherapie des ischämischen schlaganfalls [Web page in German]. AWMF. 2024. URL: https://register.awmf.org/de/leitlinien/detail/030-046#anmeldung [accessed 2024-06-26]
6. Qumseya B, Goddard A, Qumseya A, et al. Barriers to clinical practice guideline Iiplementation among physicians: a physician survey. Int J Gen Med 2021;14:7591-7598. [doi: 10.2147/IJGM.S333501] [Medline: 34754231]
7. Grol R, Dalhuijsen J, Thomas S, et al. Attributes of clinical guidelines that influence use of guidelines in general practice: observational study. BMJ 1998 Sep 26;317(7162):858-861. [doi: 10.1136/bmj.317.7162.858] [Medline: 9748183]
8. Cabana MD, Rand CS, Powe NR, et al. Why don't physicians follow clinical practice guidelines? A framework for improvement. JAMA 1999 Oct 20;282(15):1458-1465. [doi: 10.1001/jama.282.15.1458] [Medline: 10535437]
9. Gurses AP, Marsteller JA, Ozok AA, et al. Using an interdisciplinary approach to identify factors that affect clinicians' compliance with evidence-based guidelines. Crit Care Med 2010 Aug;38(8 Suppl):S282-S291. [doi: 10.1097/CCM.0b013e3181e69e02] [Medline: 20647785]
10. Arts DL, Voncken AG, Medlock S, et al. Reasons for intentional guideline non-adherence: a systematic review. Int J Med Inform 2016 May;89:55-62. [doi: 10.1016/j.ijmedinf.2016.02.009] [Medline: 26980359]
11. Lomas J, Anderson GM, Domnick-Pierre K, et al. Do practice guidelines guide practice? The effect of a consensus statement on the practice of physicians. N Engl J Med 1989 Nov 9;321(19):1306-1311. [doi: 10.1056/NEJM198911093211906] [Medline: 2677732]
12. Mohammed M, Zainal H, Tangiisuran B, et al. Impact of adherence to key performance indicators on mortality among patients managed for ischemic stroke. Pharm Pract (Granada) 2020;18(1):1760. [doi: 10.18549/PharmPract.2020.1.1760] [Medline: 32256900]
13. Wong EC, Maher AR, Motala A, et al. Methods for identifying health research gaps, needs, and priorities: a scoping review. J Gen Intern Med 2022 Jan;37(1):198-205. [doi: 10.1007/s11606-021-07064-1] [Medline: 34748098]
14. Smyth S, Gupta V, Williams M, et al. Identifying guideline-practice gaps to optimize evaluation and management for patients with syncope. Can J Cardiol 2021 Mar;37(3):500-503. [doi: 10.1016/j.cjca.2020.05.022] [Medline: 32447058]
15. Sheldon RS, Sandhu RK, Raj SR. Guidelines for clinical practice: mind the gap!. Can J Cardiol 2021 Mar;37(3):362-365. [doi: 10.1016/j.cjca.2020.06.004] [Medline: 32525074]
16. Bregni G, Akin Telli T, Camera S, et al. Grey areas and evidence gaps in the management of rectal cancer as revealed by comparing recommendations from clinical guidelines. Cancer Treat Rev 2020 Jan;82:101930. [doi: 10.1016/j.ctrv.2019.101930]
17. Spranger CB, Ries AJ, Berge CA, et al. Identifying gaps between guidelines and clinical practice in the evaluation and treatment of patients with hypertension. Am J Med 2004 Jul 1;117(1):14-18. [doi: 10.1016/j.amjmed.2004.01.024] [Medline: 15210383]
18. Beam AL, Kohane IS. Big data and machine learning in health care. JAMA 2018 Apr 3;319(13):1317-1318. [doi: 10.1001/jama.2017.18391] [Medline: 29532063]
19. Rajkomar A, Dean J, Kohane I. Machine learning in medicine. N Engl J Med 2019 Apr 4;380(14):1347-1358. [doi: 10.1056/NEJMra1814259] [Medline: 30943338]
20. Topol EJ. High-performance medicine: the convergence of human and artificial intelligence. Nat Med 2019 Jan;25(1):44-56. [doi: 10.1038/s41591-018-0300-7] [Medline: 30617339]
21. Shirvani O, Warnat-Herresthal S, Savchuk I, et al. Machine learning models for outcome prediction in thrombectomy for large anterior vessel occlusion. Ann Clin Transl Neurol 2024 Oct;11(10):2696-2706. [doi: 10.1002/acn3.52185] [Medline: 39180278]
22. Clarke GM, Conti S, Wolters AT, et al. Evaluating the impact of healthcare interventions using routine data. BMJ 2019 Jun 20;365:l2239. [doi: 10.1136/bmj.l2239] [Medline: 31221675]
23. Ebben K, de Kroon CD, Schmeink CE, et al. A novel method for continuous measurements of clinical practice guideline adherence. Learn Health Syst 2023 Oct;7(4):e10384. [doi: 10.1002/lrh2.10384] [Medline: 37860062]
24. Lichtner G, Spies C, Jurth C, et al. Automated monitoring of adherence to evidenced-based clinical guideline recommendations: design and implementation study. J Med Internet Res 2023 May 4;25:e41177. [doi: 10.2196/41177] [Medline: 36996044]
25. Mani S, Aliferis C, Krishnaswami S, et al. Learning causal and predictive clinical practice guidelines from data. Stud Health Technol Inform 2007;129(Pt 2):850-854. [Medline: 17911836]
26. Sboner A, Aliferis CF. Modeling clinical judgment and implicit guideline compliance in the diagnosis of melanomas using machine learning. AMIA Annu Symp Proc 2005;2005:664-668. [Medline: 16779123]
27. Svátek V, Ríha A, Peleska J, Rauch J. Analysis of guideline compliance--a data mining approach. Stud Health Technol Inform 2004;101:157-161. [Medline: 15537220]
28. German Stroke Registry. URL: https://german-stroke-registry.de/german-stroke-registry [accessed 2024-06-26]

XSL•FO
RenderX

29. van Buuren S, Groothuis-Oudshoorn K. Mice: multivariate imputation by chained equations in R. J Stat Softw 2010;45(3):1-67. [doi: 10.18637/jss.v045.i03]
30. Frank B, Grotta JC, Alexandrov AV, et al. Thrombolysis in stroke despite contraindications or warnings? Stroke 2013 Mar;44(3):727-733. [doi: 10.1161/STROKEAHA.112.674622] [Medline: 23391774]
31. Emberson J, Lees KR, Lyden P, et al. Effect of treatment delay, age, and stroke severity on the effects of intravenous thrombolysis with alteplase for acute ischaemic stroke: a meta-analysis of individual patient data from randomised trials. Lancet 2014 Nov 29;384(9958):1929-1935. [doi: 10.1016/S0140-6736(14)60584-5] [Medline: 25106063]
32. Cameron AC, Bogie J, Abdul-Rahim AH, et al. Professional guideline versus product label selection for treatment with IV thrombolysis: an analysis from SITS registry. Eur Stroke J 2018 Mar;3(1):39-46. [doi: 10.1177/2396987317747737] [Medline: 31008336]
33. Berge E, Whiteley W, Audebert H, et al. European Stroke Organisation (ESO) guidelines on intravenous thrombolysis for acute ischaemic stroke. Eur Stroke J 2021 Mar;6(1):I-LXII. [doi: 10.1177/2396987321989865] [Medline: 33817340]
34. Alamowitch S, Turc G, Palaiodimou L, et al. European Stroke Organisation (ESO) expedited recommendation on tenecteplase for acute ischaemic stroke. Eur Stroke J 2023 Mar;8(1):8-54. [doi: 10.1177/23969873221150022] [Medline: 37021186]
35. Gelhard S, Kestner RI, Armbrust M, et al. Exploring contraindications for thrombolysis: risk of hemorrhagic transformation and neurological deterioration after thrombolysis in mice with recent ischemic stroke and hyperglycemia. J Clin Med 2022 Jun 10;11(12):3343. [doi: 10.3390/jcm11123343] [Medline: 35743425]
36. Meinel TR, Wilson D, Gensicke H, et al. Intravenous thrombolysis in patients with ischemic stroke and recent ingestion of direct oral anticoagulants. JAMA Neurol 2023 Mar 1;80(3):233-243. [doi: 10.1001/jamaneurol.2022.4782] [Medline: 36807495]
37. Lazypredict library. Github. URL: https://github.com/shankarpandala/lazypredict [accessed 2024-06-26]
38. Varma S, Simon R. Bias in error estimation when using cross-validation for model selection. BMC Bioinformatics 2006 Feb 23;7(7):91. [doi: 10.1186/1471-2105-7-91] [Medline: 16504092]
39. Bergstra J, Bengio Y. Random search for hyper-parameter optimization. J Mach Learn Res 2012;13:281-305. [doi: 10.5555/2188385.2188395]
40. Altmann A, Toloşi L, Sander O, et al. Permutation importance: a corrected feature importance measure. Bioinformatics 2010 May 15;26(10):1340-1347. [doi: 10.1093/bioinformatics/btq134] [Medline: 20385727]
41. Corani G, Benavoli A, Demšar J, et al. Statistical comparison of classifiers through Bayesian hierarchical modelling. Mach Learn 2017 Nov;106(11):1817-1837. [doi: 10.1007/s10994-017-5641-9]
42. Nadeau C, Bengio Y. Inference for the generalization error. Mach Learn 2003;52(3):239-281. [doi: 10.1023/A:1024068626366]
43. Lundberg SM, Lee SI. A unified approach to interpreting model predictions. Presented at: NIPS'17: Proceedings of the 31st International Conference on Neural Information Processing Systems; Dec 4-9, 2017; Long Beach, CA, United States.
44. Breiman L. Random forests. Mach Learn 2001;45(1):5-32. [doi: 10.1023/A:1010933404324]
45. Simmons CA, Poupore N, Nathaniel TI. Age stratification and stroke severity in the telestroke network. J Clin Med 2023 Feb 14;12(4):1519. [doi: 10.3390/jcm12041519] [Medline: 36836054]
46. Sibbritt D, Bayes J, Peng W, et al. Demographic factors effect stoke-related healthcare utilisation among Australian stroke survivors. Sci Rep 2024 Sep 11;14(1):21241. [doi: 10.1038/s41598-024-72092-w] [Medline: 39261541]
47. Abd-Alrazaq A, Nashwan AJ, Shah Z, et al. Machine learning-based approach for identifying research gaps: COVID-19 as a case study. JMIR Form Res 2024 Mar 5;8:e49411. [doi: 10.2196/49411] [Medline: 38441952]
48. James C, Allen M, James M, et al. Using machine learning and clinical registry data to uncover variation in clinical decision making. Intell-Based Med 2023;7:100098. [doi: 10.1016/j.ibmed.2023.100098]

Abbreviations

ASPECTS: Alberta Stroke Program Early CT Score
AUROC: area under the receiver operating characteristic curve
CPG: clinical practice guideline
CT: computed tomography
CTA: computed tomography angiography
GSR-ET: German Stroke Registry – Endovascular Treatment
ML: machine learning
MRA: magnetic resonance angiography
NCCT: noncontrast computed tomography
NIHSS: National Institute of Health Stroke Scale
SHAP: Shapley Additive Explanations
SMOTE: Synthetic Minority Oversampling Technique
TICI: Thrombolysis in Cerebral Infarction

XSL•FO
RenderX

Edited by A Coristine; submitted 10.12.24; peer-reviewed by C Li, S Oworah; revised version received 29.04.25; accepted 30.04.25; published 11.07.25.

Please cite as:
Müller S, Diekmann S, Wenzel M, Hahn HK, Tuennerhoff J, Ernemann U, Hennersdorf F, German Stroke Registry Investigators, Westphal M, Poli S
Combining Machine Learning With Real-World Data to Identify Gaps in Clinical Practice Guidelines: Feasibility Study Using the Prospective German Stroke Registry and the National Acute Ischemic Stroke Guidelines
JMIR Med Inform 2025;13:e69282
URL: https://medinform.jmir.org/2025/1/e69282
doi:10.2196/69282

© Sandrine Müller, Susanne Diekmann, Markus Wenzel, Horst Karl Hahn, Johannes Tuennerhoff, Ulrike Ernemann, Florian Hennersdorf, German Stroke Registry Investigators, Max Westphal, Sven Poli. Originally published in JMIR Medical Informatics (https://medinform.jmir.org), 11.7.2025. This is an open-access article distributed under the terms of the Creative Commons Attribution License (https://creativecommons.org/licenses/by/4.0/), which permits unrestricted use, distribution, and reproduction in any medium, provided the original work, first published in JMIR Medical Informatics, is properly cited. The complete bibliographic information, a link to the original publication on https://medinform.jmir.org/, as well as this copyright and license information must be included.

XSL•FO
RenderX

Autoencoder-Based Representation Learning for Similar Patients Retrieval From Electronic Health Records: Comparative Study

Deyi Li[1], BS, MS; Aditi Shukla[2]; Sravani Chandaka[3], BS, MS; Bradley Taylor[4], BS, MBA; Jie Xu[1], BS, MS, PhD; Mei Liu[1], BS, MS, PhD

[1]Department of Health Outcomes & Biomedical Informatics, University of Florida, 1889 Museum Rd, 7th Floor, Suite 7000, Room 7012, Gainesville, FL, United States

[2]Department of Mathematics, College of Arts and Sciences, University of Pennsylvania, Philadelphia, PA, United States

[3]Department of Population Health, University of Kansas Medical Center, Kansas City, KS, United States

[4]CTSI Center for Biomedical Informatics, Medical College of Wisconsin, Milwaukee, WI, United States

Corresponding Author:
Mei Liu, BS, MS, PhD
Department of Health Outcomes & Biomedical Informatics, University of Florida, 1889 Museum Rd, 7th Floor, Suite 7000, Room 7012, Gainesville, FL, United States

Abstract

Background: By analyzing electronic health record snapshots of similar patients, physicians can proactively predict disease onsets, customize treatment plans, and anticipate patient-specific trajectories. However, the modeling of electronic health record data is inherently challenging due to its high dimensionality, mixed feature types, noise, bias, and sparsity. Patient representation learning using autoencoders (AEs) presents promising opportunities to address these challenges. A critical question remains: how do different AE designs and distance measures impact the quality of retrieved similar patient cohorts?

Objective: This study aims to evaluate the performance of 5 common AE variants—vanilla autoencoder, denoising autoencoder, contractive autoencoder, sparse autoencoder, and robust autoencoder—in retrieving similar patients. Additionally, it investigates the impact of different distance measures and hyperparameter configurations on model performance.

Methods: We tested the 5 AE variants on 2 real-world datasets—the University of Kansas Medical Center (n=13,752) and the Medical College of Wisconsin (n=9568)—across 168 different hyperparameter configurations. To retrieve similar patients based on the AE-produced latent representations, we applied k-nearest neighbors (k-NN) using Euclidean and Mahalanobis distances. Two prediction targets were evaluated: acute kidney injury onset and postdischarge 1-year mortality.

Results: Our findings demonstrate that (1) denoising autoencoders outperformed other AE variants when paired with Euclidean distance (P<.001), followed by vanilla autoencoders and contractive autoencoders; (2) learning rates significantly influenced the performance of AE variants; and (3) Mahalanobis distance-based k-NN frequently outperformed Euclidean distance-based k-NN when applied to latent representations. However, whether AE models are superior in transforming raw data into latent representations, compared with applying Mahalanobis distance-based k-NN directly to raw data, appears to be data-dependent.

Conclusions: This study provides a comprehensive analysis of the performance of different AE variants in retrieving similar patients and evaluates the impact of various hyperparameter configurations on model performance. The findings lay the groundwork for future development of AE-based patient similarity estimation and personalized medicine.

(JMIR Med Inform 2025;13:e68830) doi:10.2196/68830

KEYWORDS

machine learning; decision support for health professionals; methods and instruments in medical informatics; electronic health records

Introduction

Diseases vary in complexity, posing substantial challenges in diagnosis, treatment, and prognosis—even when cases appear clinically similar [1]. This heterogeneity is particularly prominent in complex disorders like autoimmune diseases [2], Parkinson disease [3], and cardiovascular diseases [4], where underlying causes often result from a confluence of genetic, environmental, and lifestyle factors [5]. As these complexities become more evident, the rapid adoption of electronic health record (EHR) systems has bolstered the potential for personalized medicine to enhance patient care. Personalized medicine focuses on tailoring treatments and predicting patient outcomes by analyzing data from patients with similar characteristics [6]. By assessing EHR snapshots of comparable patients—including prescriptions, procedures, vital signs, lab

XSL•FO
RenderX

results, and clinical outcomes—physicians can proactively predict disease onsets, customize treatment plans, and anticipate patient-specific trajectories [7,8]. Additionally, predictive models that leverage data from similar patients tend to be more accurate, as they capture localized data patterns that might be obscured in aggregated data [9].

Retrieving a high-quality set of similar patients is central to personalized medicine, directly impacting both evidence-based decision-making and the accuracy of personalized predictive models. However, EHR data are inherently challenging to model due to high dimensionality, mixed feature types, noise, bias, and sparsity, complicating the effective retrieval of similar patients [10]. For instance, applying traditional Euclidean distance-based k-nearest neighbors (k-NN) directly to EHR data may be problematic due to high dimensionality and mixed data types. To address these challenges, various similar patient retrieval algorithms have been proposed, incorporating advanced feature engineering to handle mixed features and reduce dimensionality [11-13].

Patient representation learning offers new avenues for overcoming these obstacles, with autoencoders (AEs) being one of the most important and widely used methods in this area [14-17]. AEs compress input data into a lower-dimensional latent space, known as a latent representation, and reconstruct it back to its original form, facilitating effective auto-feature engineering and patient representation [18,19]. AEs are particularly useful for encoding nonlinear relationships within EHR, and capturing complex structures in clinical data [20]. As AE applications to EHR increase, their use is becoming increasingly diverse [14-16]. For instance, Chowdhury et al [16] designed a mixed pooling multi-view attention AE to learn representations that encapsulate a holistic view of patient medical profiles. Beaulieu-Jones et al [15] applied a vanilla AE with a modified binary cross-entropy loss to impute missing data in EHR, and Lee et al [14] used a dual adversarial AE to generate sequential EHR data.

In personalized medicine, AEs are increasingly applied to enhance similar patient retrieval [21-23]. Generally, these studies use AEs to generate efficient patient representations from EHR data, with similarity among patients assessed using distance measures such as Euclidean and Mahalanobis distances. For example, Jo et al [21] used a supervised AE to incorporate disease labels into latent representations and calculated patient similarity in the latent space using the Euclidean distance. Miotto et al [22] introduced the "Deep Patient" framework with a 3-layer stack of denoising autoencoders (DAEs) to generate latent patient representations from EHR data, which was then used to estimate patient similarity. Landi et al [23] used a convolutional AE to transform patient trajectories into low-dimensional latent vectors and achieved patient risk stratification by patient similarity. These studies underscore the potential of AEs to drive advances in personalized medicine.

Despite the promising results of applying AEs to EHR data, a critical question remains unanswered: how do different AE designs impact performance in similar patient retrieval tasks? Existing studies have not clearly justified their choices of specific AE designs. Specifically, AE designs encompass 2 key aspects. The first aspect is the choice of the base AE model, as different AE variants may perform differently due to their distinct design focuses and the unique characteristics of EHR data. When these base AE models are integrated into more complex architectures (eg, "Deep Patient" [22]), their behavior may also vary. Therefore, gaining deeper insight into the performance of different base AE models on EHR data is valuable. The second aspect is hyperparameter tuning, as AEs are known to be highly sensitive to hyperparameters, including learning rate, latent dimensionality, and optimization techniques [24]. Therefore, understanding how different hyperparameters impact AE performance on EHR data is also important.

In this study, we used 2 real-world EHR datasets from the University of Kansas Medical Center (KUMC) and the Medical College of Wisconsin (MCW), covering the period from January 1, 2016 to December 31, 2016, to evaluate the performance of 5 widely used AE variants for retrieving similar patients: vanilla AE (AE) [18], DAE [25], contractive autoencoder (CAE) [26], sparse autoencoder (SAE) [27], and robust autoencoder (RAE) [28]. Vanilla AE is the most basic form of autoencoder, making it efficient to train and use. DAE and RAE can address the significant noise in EHR data, while CAE and SAE use different mechanisms to learn more robust latent representations for EHR data with complex distributions [29]. Additionally, we investigated the impact of 2 distance measures, Euclidean and Mahalanobis, on similar patient retrieval when paired with these AE variants. To comprehensively evaluate model performance, we tested them within a standard k-NN classification framework for 2 binary clinical outcomes in hospitalized patients: acute kidney injury (AKI) onset and 1-year mortality postdischarge, representing short-term disease and long-term survival risk classification scenarios. AKI, a life-threatening and heterogeneous condition prevalent among hospitalized patients, is particularly suited to a personalized approach. Finally, we explored how different hyperparameter configurations affect AE performance in retrieving similar patients for outcome prediction. This study provides key insights into AE optimization for personalized medicine applications, informing future advancements in EHR-driven patient care.

Methods

Comparison Framework Overview

This study aims to evaluate the effects of various AE variants, hyperparameter settings, and distance measures on the performance of similar patient retrieval. The 5 AE variants investigated were vanilla AE (AE), DAE, CAE, SAE, and RAE. Each AE was trained in an unsupervised manner on the training dataset, after which both the training and test datasets were transformed into latent representations using the trained AEs.

Performance was evaluated using a standard k-NN classification framework with neighborhood sizes of 5, 10, 15, and 20. For similar patient retrieval, Euclidean and Mahalanobis distances were applied to the latent representations to identify similar patients based on a specified neighborhood size for each test patient. Labels were assigned to each test patient through majority voting, and these assigned labels were then compared with the ground truth to assess model accuracy. Furthermore,

XSL•FO
RenderX

we analyzed the influence of different hyperparameter configurations on AE model performance in retrieving similar patients, focusing on Euclidean distance as the patient similarity measure.

Data Source and Processing

Our primary dataset consisted of inpatient data extracted from KUMC, covering admissions from January 1, 2016, to December 31, 2016. To assess the generalizability of our findings, we extracted an external validation dataset from MCW for the same period.

Both datasets were processed using the same protocol. The inclusion criteria were as follows: (1) older than 18 years, (2) baseline serum creatinine (SCr) <3.5 mg/dL, and (3) AKI onset occurring at least 72 hours postadmission to focus only on hospital-acquired AKI [30]. AKI was defined using the SCr criteria described in the "Kidney Disease: Improving Global Outcomes" clinical practice guidelines [31]. For patients with multiple admissions, only the first encounter was retained. The study focused on 3 types of in-hospital clinical features: medications, procedures, and lab test results. The data observation window for these features extended from 48 hours before the prediction point up to the prediction point. For patients with AKI, the prediction point was set at 24 hours before AKI onset, while for patients without AKI, it was set at 24 hours before the last SCr measurement [9].

Medications were represented by the maximum dosages recorded within the data observation window, procedures were encoded as binary values indicating whether a procedure was performed during the observation window, and lab test results were recorded as the most recent values within the observation window. Medications and procedures present in less than 1% of patients were excluded from the analysis. Lab tests with a missing rate over 30% were also discarded, with the remaining missing lab values imputed using the multiple imputation by chained equations method [32]. Outliers were replaced using the Winsorizing method with a 1% threshold [33], and min-max normalization was applied to scale values between 0 and 1.

In addition to AKI onset, 1-year mortality after discharge was also included as a prediction target, providing a comprehensive evaluation of the retrieved similar patient cohorts in terms of both short-term (AKI onset) and long-term (1-year mortality) clinical outcomes.

AE Variants

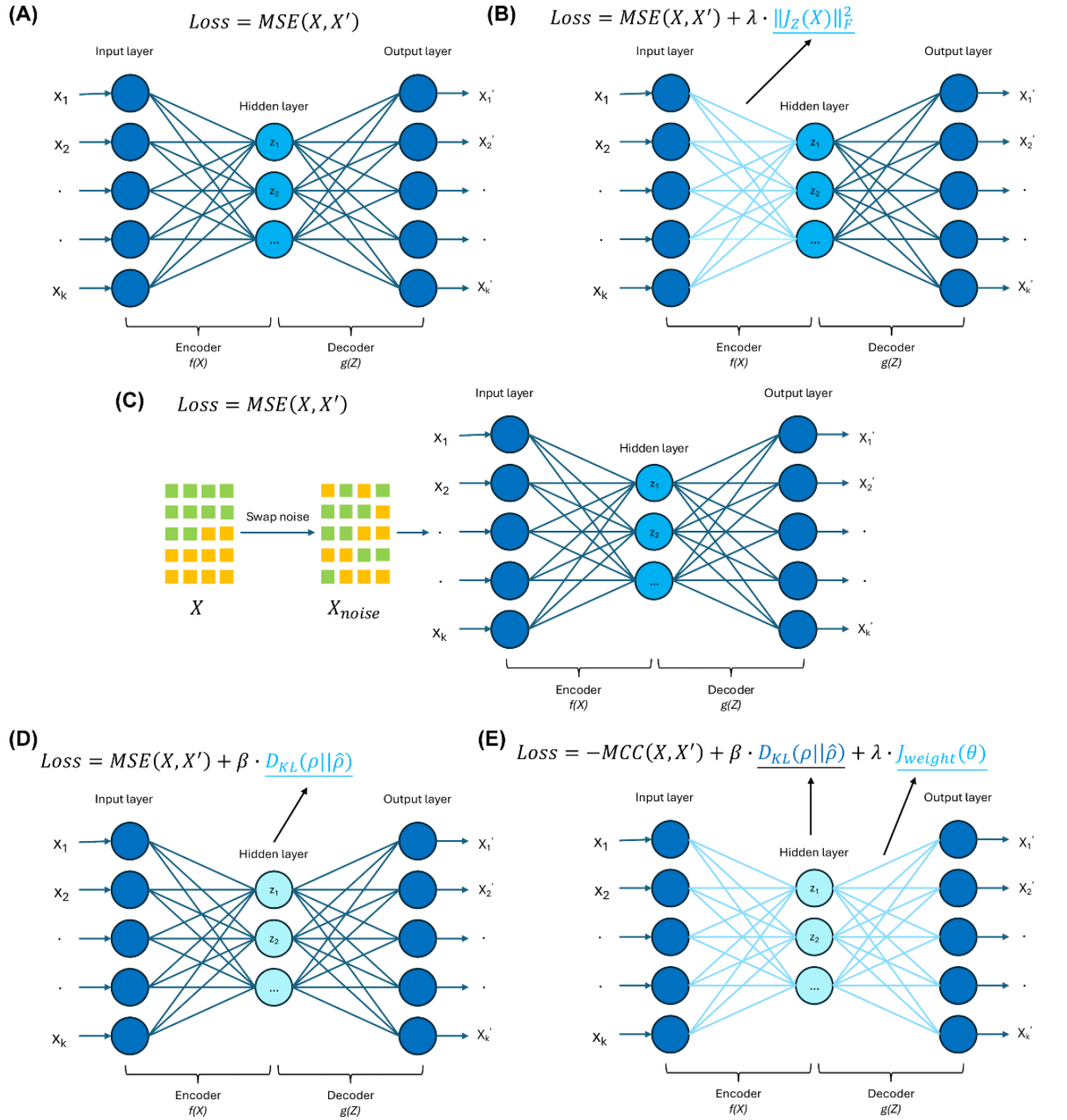
The vanilla AE (Figure 1A) is the most basic form in the autoencoder family. Its architecture is a symmetric feedforward neural network structure, though this symmetry does not necessarily apply to the weights, biases, or activation functions. It has 2 main components: an encoder and a decoder. The encoder encodes the input into a latent representation, while the decoder reconstructs the original data from this hidden representation. For an AE with a single hidden layer, the input data undergo the following transformations:

$$Z=fX=\varphi 1(WX+b)$$

$$X`=gZ=\varphi 2(W`Z+b`)$$

XSL•FO
RenderX

Figure 1. Overview of the 5 autoencoder (AE) variant designs with different loss functions.**(A)**Vanilla AE;**(B)**Contractive AE;**(C)** Denoising AE;**(D)** Sparse AE; and**(E)** Robust AE. MCC: maximum correntropy criterion; MSE: mean squared error.



Here, X denotes the input data, and X` represents the reconstructed data. Z is the output of the latent representation produced by the encoder. W, W`, b, and b` are the weights and biases of the encoder and decoder, while φ1 and φ2 are activation functions. To quantify reconstruction accuracy, the mean squared error (MSE) loss was used, which measures the difference between the original input data and the reconstructed data, as follows:

$$LossAE=MSE(X,X`)=1n\sum i=1n(xi-x`i)2$$

Here, n denotes the number of input samples, while xi and x`i represent the i-th sample of X and the i-th sample of X`, respectively. This loss function allows AE to learn a compressed representation of the data by minimizing the reconstruction error.

The DAE (Figure 1C) enhances model robustness by introducing noise into the input data. Specifically, data with noise (Xnoise in Figure 1C) are used as input, and the reconstruction error is calculated between the original noise-free data (X in Figure 1C) and the reconstructed data. In this way, the model learns to reconstruct the input by eliminating any noise present. In this study, we used swap noise, where each value in the training data may be replaced with a random value from the same column with a certain probability. We selected swap noise for fairness purposes as it has been shown to be the most effective noise

XSL•FO
RenderX

type for tabular data [34]. Other commonly used noise types include Gaussian noise and masking noise [35].

The CAE (Figure 1B) enhances model robustness by reducing the encoder's sensitivity to minor perturbations in the input, a typical vulnerability in AEs where small variations can lead to significant differences in latent representations. The CAE addresses this issue by introducing an additional penalty term, the Frobenius norm of the encoder, to the loss function. This term, which is the L2-norm of the Jacobian matrix of the hidden layer, makes the encoder output more stable against small input variations. The Frobenius norm of the encoder and the CAE loss function are shown as follows:

$$JZ(X)F2=1n\sum i=1n\sum j=1m\sum k=1l(\partial zi(k)(xi)\partial xi(j))2$$

$$LossCAE=MSEX,X`+\lambda\cdot JZ(X)F2$$

Here, m denotes the number of input features, and l represents the length of the latent representations. λ controls the strength of the additional penalty term, which aims to restrict the rate of change in the encoder output relative to changes in the input. When the input undergoes minor variations, the CAE encoder output remains relatively stable, enhancing the model's robustness against noise and small perturbations.

The SAE (Figure 1D) encourages the model to learn efficient representations by enforcing sparsity in latent representations. By adding a Kullback-Leibler (KL) divergence penalty between a Bernoulli distribution and the distribution of latent layer outputs to the loss function, the SAE limits the number of active neurons (whose outputs are significantly nonzero) in the latent layer. This helps SAE to capture key information from the input using a limited number of active neurons in the latent layer, preventing it from simply copying the input to the output and enhancing the model's ability to capture the inherent structure of the input data. The additional penalty term and the loss function of the SAE are as follows:

$$DKL(\rho\vee\rho\wedge=\rho log\rho\rho\wedge+(1-\rho)log\ (1-\rho)(1-\rho\wedge)$$

$$LossSAE=MSEX,X`+\beta\cdot DKL(\rho\vee\rho\wedge$$

Here, ρ denotes the mean of the Bernoulli distribution. ρ^ denotes the mean of the distribution of latent representations over the training data. β controls the strength of the additional penalty term.

The RAE (Figure 1E) improves noise tolerance by using the maximum correntropy criterion (MCC) instead of MSE for reconstruction error, making it less sensitive to outliers [36]. The intuition behind the MCC-based reconstruction error is that as the distance between X and X` increases, the corresponding measure transitions from the L2 norm to the L1 norm, and eventually to the zero norm when X and X` are far apart. The RAE also includes a sparsity penalty term similar to that of the SAE, along with an additional weight decay term to prevent overfitting. The MCC-based reconstruction error, the weight decay term, and the final loss function of the RAE are shown as follows:

$$MCC(X,X`)=1n\sum i=1n\sum j=1m12\pi\sigma exp(-(xik-x`i(j))22\sigma2)$$

$$Jweight\theta=12\sum L=12\sum i=1sL\sum j=1sL+1(wji(L))2$$

$$LossRAE=-MCCX,X`+\beta\cdot DKL(\rho\vee\rho\wedge+\lambda\cdot Jweight\theta$$

Here, σ denotes the variance of the Gaussian distribution. wji(L) denotes an element in the weight matrix of the L-th layer. SL denotes the number of neurons in the L-th layer. β and λ control the strength of the 2 penalty terms, respectively.

Patient Similarity Measures

To identify similar patients, we applied 2 distance measures—Euclidean and Mahalanobis distances—to the latent representations generated by each AE variant. For each patient in the test dataset, we used these distance measures to find a cohort of similar patients from the training dataset. The Euclidean distance on the latent representations is calculated as follows:

$$DEuclidean(zi,zj)=\sum k=1l(zik-zjk)2$$

Here, zi denotes the i-th patient in the training set and zj denotes the j-th patient in the test set. l denotes the length of the latent representations.

The Mahalanobis distance can be viewed as a Euclidean distance after applying a linear transformation to the feature space, defined by L:

$$DMahalanobis(zi,zj)=(Lzi-Lzj)T(Lzi-Lzj)$$

In this study, we used 3 different algorithms to estimate the Mahalanobis distance on the latent representations: large margin nearest neighbor (LMNN) [37], Neighborhood Components Analysis (NCA) [38], and Metric Learning for Kernel Regression (MLKR) [39].

- LMNN learns a Mahalanobis distance within the standard k-NN classification framework, aiming to bring the nearest *k* neighbors from the same class closer while ensuring that examples from different classes are separated by a large margin.
- NCA enhances the accuracy of nearest neighbor classification compared with the traditional Euclidean distance by directly maximizing a stochastic version of the leave-one-out k-NN score on the training set.
- MLKR learns a Mahalanobis distance by directly minimizing the leave-one-out regression error. This algorithm can also be viewed as a supervised extension of principal component analysis (PCA), making it suitable for dimensionality reduction and visualization of high-dimensional data.

Experimental Design

The workflow of the study is presented in Figure 2. Each AE variant in this study consisted of a 3-layer structure: an input layer, a hidden layer, and an output layer. Previous research suggests that additional hidden layers in AEs do not necessarily lead to improved downstream task performance [40]. All AE variants were implemented in PyTorch (version 2.4.0; Meta AI), and trained on 2 NVIDIA GeForce RTX 2080 Ti GPUs, each with 10.7 GB of RAM. For each of the 5 AE variants, we performed an exhaustive grid search to explore all possible combinations of learning rates, optimizers, latent dimensions, and activation functions, resulting in 168 different hyperparameter configurations per AE variant. Details of the hyperparameter space are listed in Table 1. The Mahalanobis distance was estimated using the metric-learn library [41].

XSL•FO
RenderX

Figure 2. Workflow of the study. After the electronic health record data were transformed into latent representations using 5-fold cross-validation, the latent representations were used for 3 downstream evaluations: Euclidean-distance-based similar patient retrieval, Mahalanobis-distance-based similar patient retrieval, and AE hyperparameter analysis. AE: autoencoder; CAE: contractive autoencoder; DAE: denoising autoencoder; KUMC: University of Kansas Medical Center; LMNN: large margin nearest neighbor; MCW: Medical College of Wisconsin; MLKR: metric learning for kernel regression; NCA: neighborhood components analysis; RAE: robust autoencoder; SAE: sparse autoencoder.

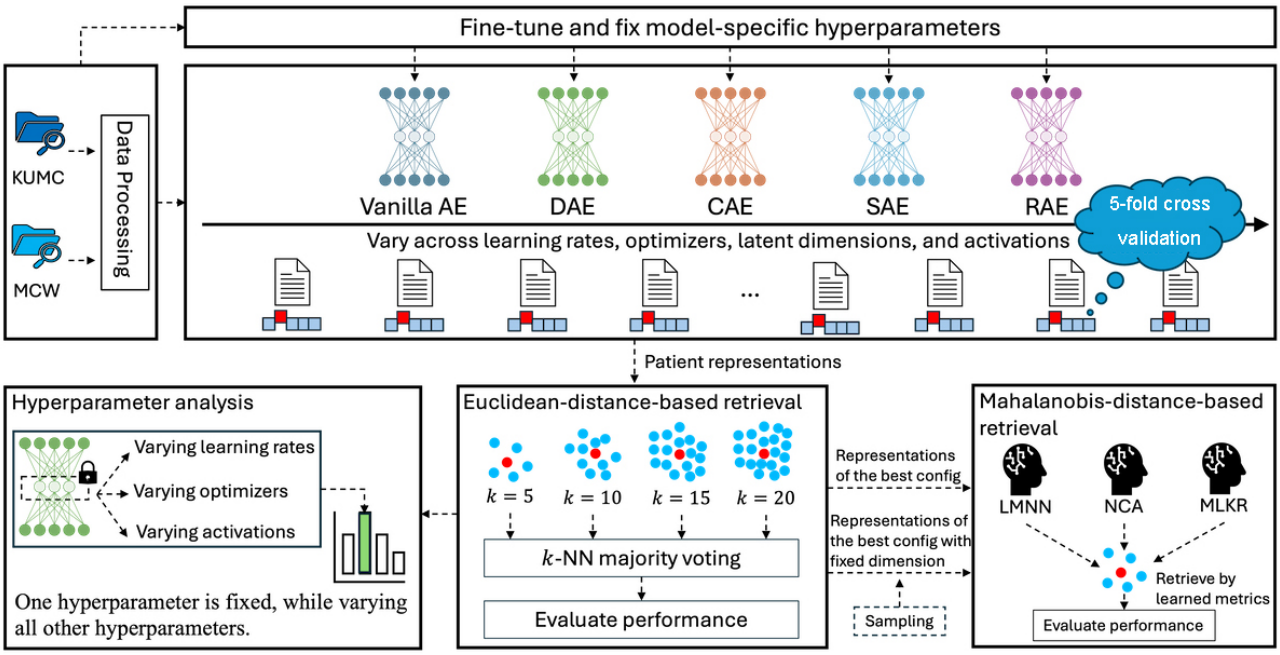


Table . Hyperparameter configuration space. The combinations of different values for the 4 studied hyperparameters resulted in 168 different hyperparameter configurations.

Hyperparameter	Range
Learning rate	1E-5, 1E-4, 1E-3, and 1E-2
Optimizer	Adam, Adamax, and RMSprop
Latent dimension : input dimension	0.02, 0.05, 0.10, 0.15, 0.30, 0.50, and 0.75
Activation functions	Sigmoid and rectified linear unit (ReLU)

To assess the generalizability of our findings, we applied the following steps in parallel to both the KUMC and MCW datasets. Before evaluating the performance of different AE variants on the 4 hyperparameters of interest mentioned above, we fixed each AE variant's unique hyperparameters (eg, the sparsity term penalty strength β in the SAE). Otherwise, combining each model's unique hyperparameters with the selected 4 hyperparameters would make the computation infeasible. To determine the optimal unique hyperparameter settings, we fine-tuned each AE variant using a standardized setup (learning rate=1E-3, optimizer=Adam, latent dimension: input dimension=0.15, and activation=Sigmoid) and fixed these optimal hyperparameter values in the subsequent experiments. To account for variations arising from the random initialization of neural network weights and data splitting, each of the 168 studied hyperparameter configurations was trained and evaluated using 5-fold cross-validation, with the average performance of the Euclidean distance-based k-NN on the AE-produced latent representations reported for the 2 prediction targets—AKI onset and 1-year mortality—across the 5 runs. The performance of the Euclidean distance-based k-NN on both the raw data and the data transformed by PCA, retaining 99% of the variance, served as baseline performance. We used F_1-scores, area under the precision-recall curve (AUPRC), and area under the receiver operating characteristic curve (AUROC) as evaluation metrics. The k-NN model was evaluated with neighborhood sizes of 5, 10, 15, and 20, respectively, considering that the size of the retrieved similar patient cohort often varies based on different clinical needs (eg, the varying complexity of different diseases). We trained the models on each of the 5 data splits for up to 2000 epochs using an early stopping mechanism, meaning that training was stopped if the validation loss did not improve for more than 5 consecutive epochs.

We then evaluated the performance of using Mahalanobis distance as the distance measure for k-NN on latent representations, focusing on two key questions: (1) Does k-NN with Mahalanobis distance on latent representations outperform k-NN with Euclidean distance? (assessing the effectiveness of Mahalanobis distance), and (2) Is applying Mahalanobis distance-based k-NN on latent representations more effective than applying it directly to raw data? (assessing the effectiveness of using AEs for EHR data transformation).

We first selected the best-performing hyperparameter configuration for each AE variant that achieved the highest F_1-score using Euclidean distance-based k-NN with a

XSL•FO
RenderX

neighborhood size of 5 to transform the raw data into latent representations. Given that we varied latent dimensions during training and considering the potentially significant impact of different latent dimensions on Mahalanobis distance-based k-NN performance, which could obscure the actual characteristics of each AE variant, we also selected the best-performing hyperparameter configuration for each AE variant with latent-to-input dimension ratio fixed at 0.5 to transform the raw data into latent representations. Due to the significant computational cost of estimating the Mahalanobis distances, we randomly sampled 50% of the AE-transformed training and test datasets from each of the 5-fold data splits for evaluation on the KUMC dataset and only evaluated the performance with a neighborhood size of 5. Fixed random seeds were used to ensure the sampled data remained consistent across all AE variant evaluations. For the MCW dataset, we randomly sampled 70% of the data following the same procedure to ensure a comparable sample size to the sampled KUMC dataset.

Statistical Analysis

One-tailed paired *t* test was used to assess whether one AE variant significantly outperformed the other with Euclidean-based k-NN across the 168 different hyperparameter configurations, with $P<.01$ considered statistically significant. Considering that in actual practice, neural network models are often fine-tuned to achieve optimal or near-optimal performance, we used an error bar plot to compare the average performance of the top 5 hyperparameter configurations for each AE variant, with Euclidean distance-based k-NN evaluated at neighborhood sizes of 5, 10, 15 and 20. This represents the upper performance bound of each AE variant in retrieving similar patients. We used box plots to visualize the impact of hyperparameter configurations on model performance. Each box plot shows the performance with Euclidean distance, where one hyperparameter of interest was fixed at a specific value while all other hyperparameters varied for each AE model.

To assess the generalizability of our findings from the KUMC dataset, we applied Spearman rank correlation to evaluate the relationship between model performance on the KUMC dataset and that on the MCW dataset. The Spearman rho (ρ) value was used to measure the strength and direction of the monotonic relationship between performances on the 2 datasets. A higher ρ indicates a stronger correlation, suggesting good generalizability.

Ethical Considerations

All data were deidentified according to the “Safe Harbor” criteria outlined in the Health Insurance Portability and Accountability Act. The study was determined to be nonhuman participants research by the University of Florida Institutional Review Board, as it involved only pre-existing, deidentified patient records. The data access request was approved by the Greater Plains Collaborative Data Request Oversight Committee. This study was determined by the institutional review boards of the University of Florida, University of Pittsburgh Medical Center, and University of Missouri as nonhuman participant research because it only involved the collection of existing and deidentified patient medical data. Data use agreements have been executed with both the Greater Plains Collaborative and the University of Pittsburgh.

Results

Study Population

The final KUMC dataset encompassed 13,752 unique patients, while the MCW dataset encompassed 9568 patients. The AKI onset rates for the 2 datasets were 11.90% and 9.03%, respectively, and the 1-year mortality rates were 12.65% and 15.51%, respectively. The KUMC dataset contained 579 features, including 277 medications, 288 procedures, and 14 lab tests, while the MCW dataset contained 654 features, including 328 medications, 312 procedures, and 14 lab tests. The details of the 2 datasets are presented in Table 2.

XSL•FO
RenderX

Table . Statistics of the 2 datasets used in the study.

	KUMC[a]	MCW[b]
Cohort size	13,752	9568
Time window	January 1, 2016 to December 31, 2016	January 1, 2016 to December 31, 2016
AKI rates, n (%)	1636 (11.90)	890 (9.30)
1-year mortality rates, n (%)	1736 (12.65)	1484 (15.51)
Age (years), median (IQR)	61 (48-71)	61 (48-71)
Female, n (%)	6902 (50.19)	4772 (49.87)
Black race, n (%)	1856 (13.50)	2018 (21.09)
Days from admission to AKI[c] onset (days), median (IQR)	7 (4-17)	5 (3-7)
Number of medication features	277	328
Number of procedure features	288	312
Number of lab test features	14	14

[a]KUMC: University of Kansas Medical Center.

[b]MCW: Medical College of Wisconsin.

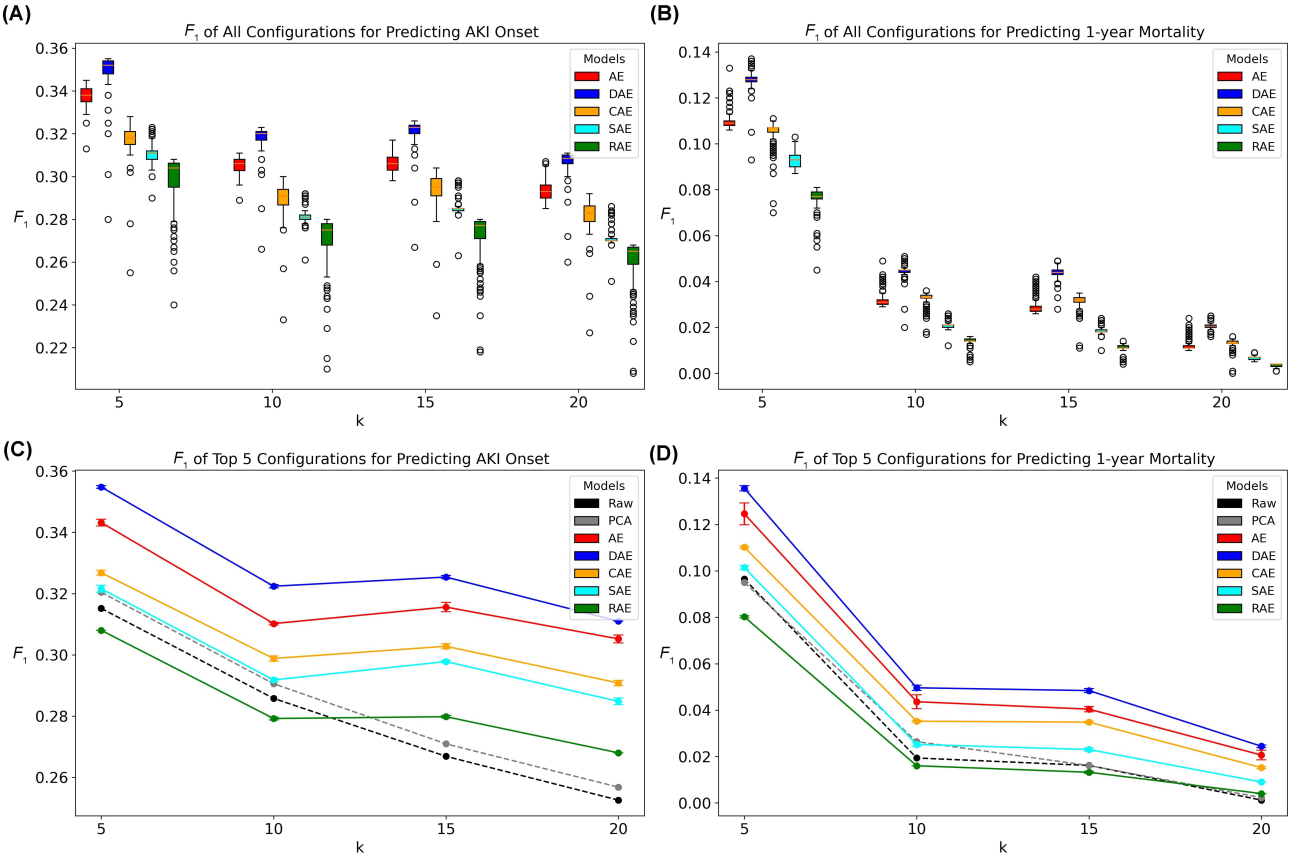
[c]AKI: acute kidney injury.

AE Performance With Euclidean Distance

The fine-tuned and fixed model-specific hyperparameters are provided in Multimedia Appendix 1. On the KUMC dataset, DAE consistently performed the best across both prediction targets (ie, AKI onset and 1-year mortality) and all k-NN neighborhood sizes (P<.001,Multimedia Appendix 2 and Multimedia Appendix 3), followed by vanilla AE and CAE (Figure 3, Figures S1 and S2 in Multimedia Appendix 4). The average performance of the top 5 hyperparameter configurations showed a similar trend, with DAE performing the best, followed by vanilla AE and CAE. For AKI onset prediction, CAE and SAE outperformed baseline models (ie, k-NN applied to the raw data and the PCA-transformed data) at k=15 and k=20 (Figure 3C) and performed comparably to the baseline models for 1-year mortality prediction (Figure 3D). The average best performance of RAE did not surpass that of the baseline models for 1-year mortality prediction (Figure 3D).

XSL•FO
RenderX

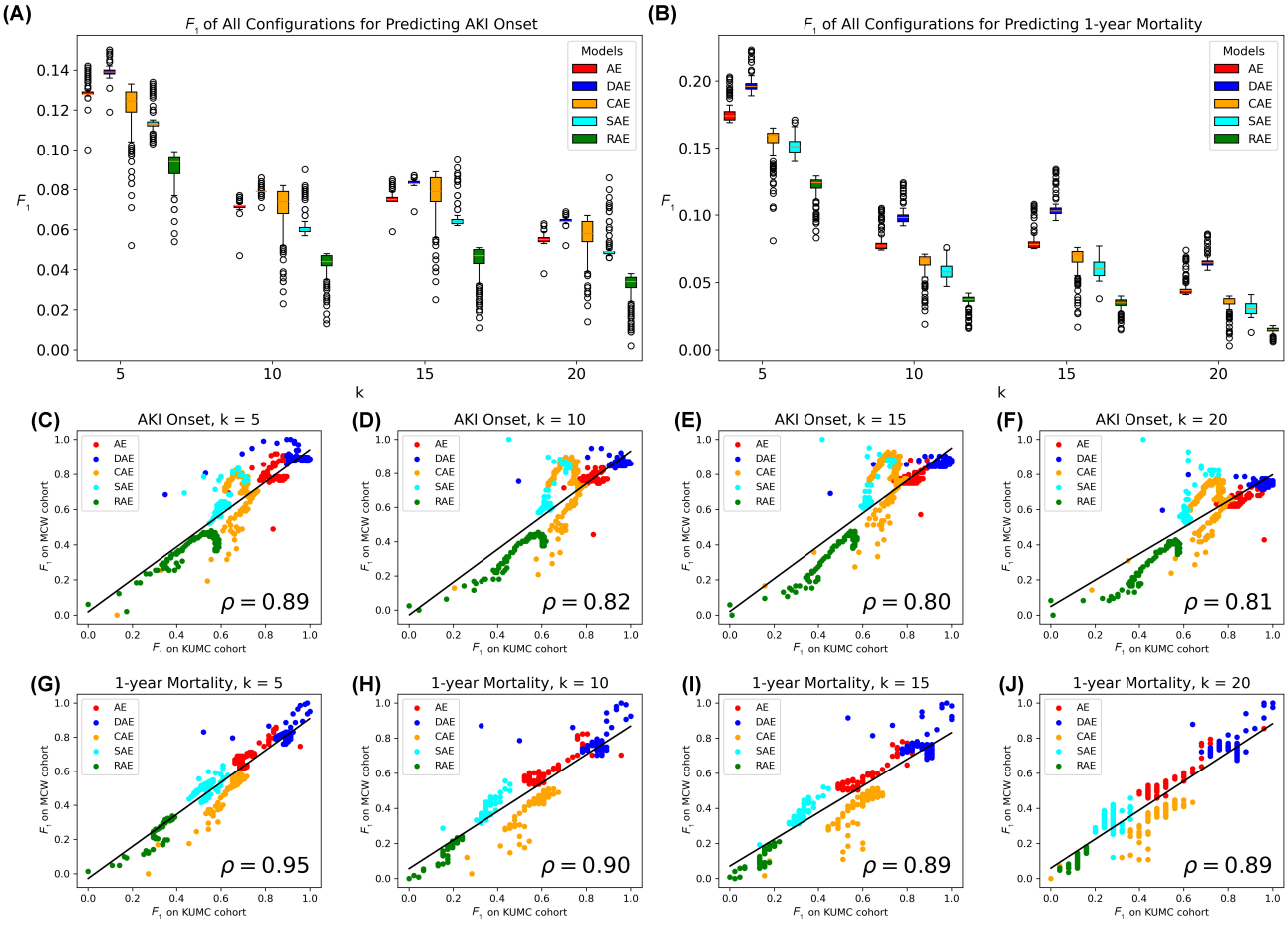
Figure 3. F_1-scores of Euclidean-distance-based k-nearest neighbor models on the latent representations on the KUMC dataset. **(A)** F_1-scores of predicting AKI onset. Each box represents the k-nearest neighbor F_1-scores with AE models trained with different hyperparameter configurations. **(B)** F_1-scores of predicting 1-year mortality. **(C)** The mean F_1-scores of the top 5 best AE hyperparameter configurations of predicting AKI onset. **(D)** The mean F_1-scores of the top 5 best AE hyperparameter configurations of predicting 1-year mortality. AE: autoencoder; AKI: acute kidney injury; CAE: contractive autoencoder; DAE: denoising autoencoder; PCA: principal component analysis; RAE: robust autoencoder; SAE: sparse autoencoder.



The performance of AE variants on the MCW dataset exhibited a clear resemblance to the results obtained on the KUMC dataset, with DAE consistently outperforming the other models (P<.001, Figures 4A and B). Correlation analysis showed that, across different hyperparameter settings, the F_1-scores of AE variants were significantly correlated between both datasets, with P>.80 when predicting AKI onset (Figure 4C-F) and P>.89 when predicting 1-year mortality (Figure 4G-J). Similar results were also observed when using AUPRC and AUROC as metrics (Figures S3 and S4 in Multimedia Appendix 4).

XSL•FO
RenderX

Figure 4. F_1-scores of Euclidean-distance-based k-nearest neighbor models on the latent representations on the MCW dataset, and the linear correlation between the F_1-scores on the KUMC and that on the MCW datasets. **(A)** F_1-scores of predicting AKI onset. **(B)** F_1-scores of predicting 1-year mortality. **(C-F)** Concordance in predicting AKI onset with varying neighborhood sizes. **(G-J)** Concordance in predicting 1-year mortality with varying neighborhood sizes. AE: autoencoder; AKI: acute kidney injury; CAE: contractive autoencoder; DAE: denoising autoencoder; KUMC: University of Kansas Medical Center; MCW: Medical College of Wisconsin; RAE: robust autoencoder; SAE: sparse autoencoder.

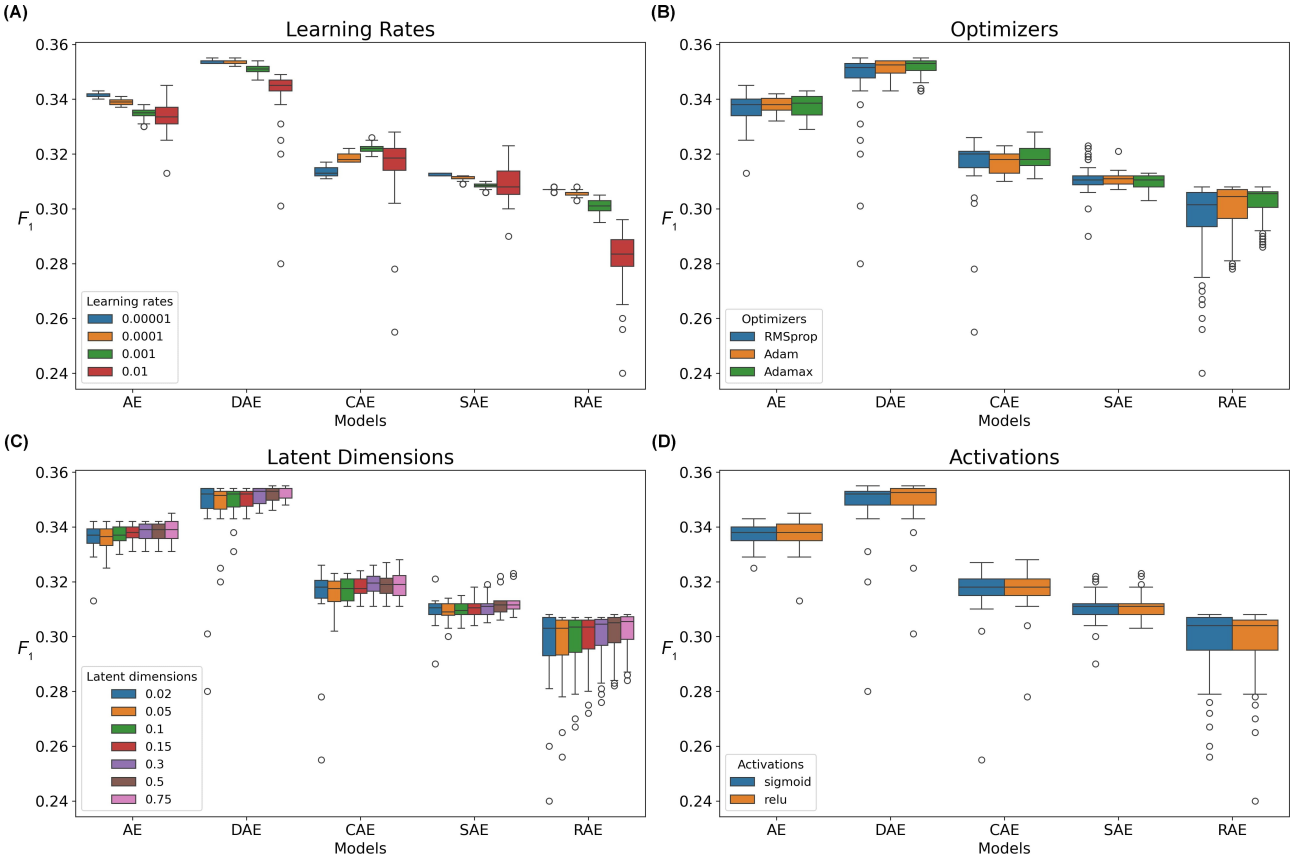


Impact of Hyperparameters on AE Performance

On the KUMC dataset, when the neighborhood size was 5 and AKI onset was the prediction target, we observed that different hyperparameter settings had varying impacts on model performance. For learning rates, smaller values led to better performance for vanilla AE, DAE, and RAE. For CAE, a moderate learning rate yielded better results. At a higher learning rate (1E-2), the variance in model performance increased, with the upper bound observed in CAE and SAE outperforming those of other learning rates (Figure 5A). In terms of the optimizer, Adamax resulted in a slightly higher lower bound of model performance, while the upper bound showed no significant differences across optimizers (Figure 5B). Similarly, for latent dimensionality, higher dimensions (latent dimension: input dimension=0.75) led to a higher lower bound of model performance, with no significant differences observed in the upper bound (Figure 5C). No significant differences were observed between sigmoid and rectified linear unit activations (Figure 5D). Highly similar hyperparameter trends were observed on the KUMC dataset with neighborhood sizes of 10, 15, and 20 using F_1-scores as the metric (Figures S5-S7 in Multimedia Appendix 4), and with a neighborhood size of 5 using AUPRC and AUROC as metrics (Figures S8 and S9 in Multimedia Appendix 4), as well as on the MCW dataset with a neighborhood size of 5 (Figures S10-S12 in Multimedia Appendix 4).

XSL•FO
RenderX

Figure 5. Impact of different AE hyperparameters on k-nearest neighbor model performance for predicting acute kidney injury onset on the University of Kansas Medical Center dataset. Each box plot shows the F_1-scores with Euclidean distance and a neighborhood size of 5, when one hyperparameter was fixed, while varying all other hyperparameters for each AE model. (**A)** Learning rates; (**B)** Optimizers; (**C)** The ratio of latent representation dimension to input data dimension; (**D)** Activation functions. AE: autoencoder; CAE: contractive autoencoder; DAE: denoising autoencoder; RAE: robust autoencoder; SAE: sparse autoencoder.



AE Performance With Mahalanobis Distance

When comparing the performance of Euclidean distance-based k-NN and Mahalanobis distance-based k-NN on the KUMC dataset, we found that Mahalanobis distance-based k-NN generally performed better than Euclidean distance, except in a few cases (eg, DAE+NCA in Table 3). These performance drops primarily occur in NCA and MLKR, while LMNN consistently outperforms the Euclidean distance. This conclusion can be well generalized to the performance when controlling the latent dimension ratio (latent-to-input dimension ratio=0.5, Table 4) and the results on the MCW dataset (Multimedia Appendices 5 and 6).

XSL•FO
RenderX

Table . F_1-scores of k-nearest neighbors (k-NNs) with Euclidean and Mahalanobis distances on the latent representations produced by the best-performing hyperparameter configuration of each autoencoder (AE) variant on the University of Kansas Medical Center dataset. The values are presented as mean (SD) of the 5-fold cross-validation.

Model	Euclidean distance, mean (SD)	Mahalanobis distance, mean (SD)		
		LMNN[a]	NCA[b]	MLKR[c]
Raw	0.284 (0.032)	0.314 (0.030)	0.325 (0.070)	0.381 (0.023)
AE	0.330 (0.030)	0.345 (0.046)	0.336 (0.052)	0.333 (0.029)
DAE[d]	0.364 (0.027)	0.385 (0.025)	0.354 (0.033)	0.374 (0.031)
CAE[e]	0.338 (0.028)	0.356 (0.035)	0.340 (0.037)	0.371 (0.038)
SAE[f]	0.332 (0.032)	0.354 (0.028)	0.323 (0.021)	0.325 (0.034)
RAE[g]	0.344 (0.025)	0.412 (0.037)	0.375 (0.029)	0.401 (0.012)

[a]LMNN: large margin nearest neighbor.

[b]NCA: neighborhood components analysis.

[c]MLKR: Metric Learning for Kernel Regression.

[d]DAE: denoising autoencoder.

[e]CAE: contractive autoencoder.

[f]SAE: sparse autoencoder.

[g]RAE: robust autoencoder.

When comparing the performance of Mahalanobis distance-based k-NN on latent representations versus directly on raw data, no consistent pattern was observed. On the KUMC dataset, in most cases, Mahalanobis distance-based k-NN on latent representations outperformed its performance on the raw data. However, there was no fixed pattern for the optimal combination of AE variants and Mahalanobis distance estimation algorithms. When latent dimensions were not controlled, the combination of RAE and all 3 investigated Mahalanobis distance algorithms achieved the best performance (Table 3). In contrast, when latent dimensions were controlled, the combination of DAE with LMNN and NCA and the combination of RAE with MLKR performed the best (Table 4). On the MCW dataset, limited cases showed that Mahalanobis distance-based k-NN on latent representations outperformed its application on the raw data, indicating that this pattern is data-dependent (Multimedia Appendices 5 and 6).

Table . F_1-scores of k-nearest neighbors (k-NNs) with Euclidean and Mahalanobis distances on the latent representations produced by the best-performing hyperparameter configuration, constrained by a latent-to-input dimension ratio of 0.5 for each autoencoder (AE) variant, on the University of Kansas Medical Center (KUMC) dataset.

Model	Euclidean distance, mean (SD)	Mahalanobis distance, mean (SD)		
		LMNN[a]	NCA[b]	MLKR[c]
Raw	0.284 (0.032)	0.314 (0.030)	0.325 (0.070)	0.381 (0.023)
AE	0.320 (0.027)	0.368 (0.039)	0.330 (0.009)	0.337 (0.025)
DAE[d]	0.353 (0.025)	0.378 (0.032)	0.360 (0.016)	0.348 (0.021)
CAE[e]	0.337 (0.016)	0.345 (0.023)	0.342 (0.029)	0.363 (0.028)
SAE[f]	0.323 (0.040)	0.357 (0.051)	0.332 (0.039)	0.317 (0.035)
RAE[g]	0.291 (0.030)	0.327 (0.048)	0.359 (0.029)	0.396 (0.032)

[a]LMNN: large margin nearest neighbor.

[b]NCA: neighborhood components analysis.

[c]MLKR: Metric Learning for Kernel Regression.

[d]DAE: denoising autoencoder.

[e]CAE: contractive autoencoder.

[f]SAE: sparse autoencoder.

[g]RAE: robust autoencoder.

XSL•FO
RenderX

Discussion

Main Findings

This study makes significant contributions in three main areas: (1) it is the first to comprehensively evaluate the performance of different AEs specifically for EHR-based similar patient retrieval, providing critical insights to inform the design of AE-based patient representation learning models; (2) it is the first study to apply Mahalanobis distance to patient representations learned by AEs for similar patient retrieval, whereas previous studies have primarily relied on Euclidean distance; and (3) by establishing a fair and comprehensive evaluation framework, this study offers valuable guidance for AE model selection and hyperparameter tuning, contributing to the advancement of patient representation learning in EHR research.

Our findings indicate that DAE consistently outperformed other AEs, followed by vanilla AE and CAE, with RAE performing the worst. The superior performance of DAE likely stems from its mechanism of introducing noise into the original data during training, which encourages the model to prioritize encoding meaningful latent nonlinear relationships that are important for disease and outcome prediction, rather than focusing on noise. This process helps the model remain robust to noise, enabling more refined and abstracted patient representations, which improve the performance of the downstream k-NN model.

Other AE mechanisms, such as those in CAE and SAE, are also designed to produce effective representations and have performed well in regression and classification tasks in previous studies [17,29]. However, they were less effective than DAE in retrieving similar patients. For SAE, the assumed Bernoulli distribution over the latent representations may mismatch the continuous outputs of the hidden layer, conflicting with the need for sufficient active neurons to preserve key data information. This trade-off between enforcing sparsity and preserving key data information can significantly degrade downstream k-NN performance, especially on complex data. The RAE was originally designed for image classification tasks [28] and used an MCC loss rather than MSE to make the model more robust to outliers. However, this approach may not be well-suited to EHR data, which are often high-dimensional, sparse, noisy, and biased, resulting in its underperformance compared with other AE variants. Moreover, one of the prediction targets was AKI onset. Patients at high risk for developing AKI may show significant differences in lab results and medications compared with the general population. However, the MCC loss may weaken the encoding of this information in the latent representation, making the latent representations of high-risk patients with AKI less distinguishable from those in the normal population, which in turn leads to inaccuracies in similar patient retrieval (ie, higher false negative rates).

While both DAE and RAE are designed to enhance model robustness to noise, their underlying mechanisms differ significantly. DAE achieves this by explicitly injecting noise into the input data and training the model to “denoise” it, thereby encouraging the model to focus on capturing the intrinsic structure of the data. In contrast, RAE aims to improve robustness by making the model less sensitive to the input’s tail distribution, which reduces the influence of outliers. However, this approach may prevent the model from fully capturing the true data distribution. This fundamental difference could be a key factor contributing to the performance gap observed between DAE and RAE in the specific scenarios examined in this study.

Interestingly, while previous research suggests AE models are highly sensitive to hyperparameter configurations [24], our findings indicate that for the task of retrieving similar patients, only the learning rate significantly affected model performance. Specifically, smaller learning rates resulted in stronger lower-bound performance, as shown in Figure 5. However, larger learning rates (eg, 1E-2) could help the model escape local minima in certain situations, although not always guaranteed. Given the longer training times associated with smaller learning rates, we recommend using a moderate learning rate (eg, 1E-3 or 1E-4).

The impact of latent dimensions on model performance was minimal. Even with smaller latent dimensions (latent dimension to input dimension ratio=0.02), the latent representations remained expressive enough to ensure accurate patient similarity estimation. As shown in Figure 5, increasing the latent dimensions to accommodate additional information only slightly improved the model’s lower-bound performance. However, this conclusion is highly dataset-dependent, and other datasets may require larger latent dimensions to capture more information.

Regarding the application of Mahalanobis distance to latent representations, it outperformed Euclidean distance in most cases. Mahalanobis distance applies a low-dimensional linear transformation to map the representations into a space where the margin between different classes is maximized while representations of the same class are pulled closer together, thereby enhancing the discriminative power of the downstream k-NN model [41]. This result was expected, as Mahalanobis distance estimation treats latent representations as a separate dataset for learning appropriate linear feature transformations and distance measures. Compared with Euclidean distance, Mahalanobis distance is more likely to provide a more accurate estimation of vector similarity both within and between classes.

However, comparisons between Mahalanobis distance estimation algorithms on raw data and latent representations revealed that AE transformations of raw data did not always guarantee better performance. For example, AEs significantly improved the performance of Mahalanobis distance-based k-NN on the KUMC dataset (Tables 3 and 4), but this improvement was limited on the MCW dataset (Multimedia Appendices 5 and 6). There can be several reasons behind this. First, differences in the characteristics of the datasets could play a major role. Variations in feature distributions, data sparsity, or sample size between the KUMC and MCW datasets may affect the effectiveness of AEs in learning meaningful latent representations. If the KUMC dataset contains clearer structure or more consistent patterns, AEs may be able to capture more relevant patient representations compared with the MCW dataset.

Additionally, the alignment between the AE-learned latent representations and the assumptions underlying Mahalanobis

XSL•FO
RenderX

distance could also contribute to the observed differences. AEs are typically optimized for reconstruction rather than directly preserving class separability or the local neighborhood structure needed for effective distance-based retrieval. As a result, the learned representations may not always be well-suited for Mahalanobis distance algorithms, particularly if the AE fails to retain key relationships present in the raw data (eg mapping all data points into an indistinguishable cluster in the latent space). This suggests that whether this complex transformation process enhances model performance is highly data-dependent.

It is also important to note that Mahalanobis distance estimation algorithms tend to have higher computational complexity compared with Euclidean distance. For example, the loss function of LMNN is non-convex, requiring the use of semidefinite programming techniques to address this challenge [37]. Therefore, while the combination of "AE + Mahalanobis distance" can achieve optimal performance in certain cases, it is data-dependent and comes at the cost of increased computational complexity. To mitigate this burden, the dimensionality of the latent representation can be intentionally constrained, provided it maintains sufficient discriminative power for the downstream task.

Limitations

This study only investigated swap noise for DAE; other types of noise, such as Gaussian noise, may lead to different behaviors. Additionally, we only examined AKI onset and 1-year mortality, so the models' performance may differ for other prediction tasks. For example, other studies have shown that DAE outperforms vanilla AE and RAE on multiple datasets and tasks, though not in all cases [29]. Next, this study only compared AE variants trained in an unsupervised manner. Incorporating labels during training may help learn more effective latent representations compared with purely unsupervised approaches. Finally, while AEs can effectively capture complex patterns in high-dimensional clinical data, their latent representations are often difficult to interpret clinically, which may limit their utility in real-world decision-support settings. A disentangling framework should be further investigated and incorporated into the current AE model to enhance interpretability by isolating clinically meaningful latent factors, thereby facilitating more transparent integration into clinical decision support systems[42].

Conclusions

In this study, we assessed the performance of 5 AE variants—vanilla AE, DAE, CAE, SAE, and RAE—on 2 real-world EHR datasets, focusing on retrieving similar patients for personalized clinical decision-making. The study also explored the impact of different hyperparameter configurations on AE variants. Our results presented three key findings: (1) DAE generally performed best in retrieving similar patients when paired with Euclidean distance (P<.001); (2) learning rates had the greatest impact on the performance of AE variants; and (3) applying Mahalanobis distance-based k-NN on latent representations can outperform Euclidean distance-based k-NN, although transforming raw data with AE variants did not always guarantee improved performance of Mahalanobis distance-based k-NN.

Acknowledgments

This project was supported by the NIDDK award R01DK137881.

Data Availability

The clinical data used for training and validation in this study is not publicly available and restrictions apply to its use. The deidentified multi-center electronic health record datasets in PCORnet Common Data Model may be made available by the Greater Plains Collaborative and PaTH clinical research networks, subjective to individual institution's and network-wide data governance and ethical approvals. The code for this study can be found at [43].

Conflicts of Interest

None declared.

Multimedia Appendix 1

Model-specific hyperparameters fine-tuned and fixed for downstream experiments. In DAE, ρ denotes the amount of noise added to the data. In CAE, λ denotes the strength of the additional Frobenius norm penalty term. In SAE, ρ denotes the mean of the Bernoulli distribution, and β denotes the strength of the additional KL divergence penalty term. In RAE, σ denotes the variance of the Gaussian distribution, ρ denotes the mean of the Bernoulli distribution, β denotes the strength of the additional KL divergence penalty term, and λ denotes the strength of the weight decay. CAE: contractive autoencoder; RAE: robust autoencoder; SAE: sparse autoencoder.

[DOCX File, 15 KB - medinform_v13i1e68830_app1.docx]

Multimedia Appendix 2

P value tables showing the statistical significance of the F_1-score differences between different AE variants across the 168 different hyperparameter configurations of predicting AKI onset on the KUMC dataset, using a one-tailed paired t test. P<.01 was considered

XSL•FO
RenderX

statistically significant. Each entry represents the *P* value indicating whether the AE model in the row outperformed the AE model in the column.
[DOCX File, 18 KB - medinform_v13i1e68830_app2.docx]

Multimedia Appendix 3
P value tables showing the statistical significance of the F_1-score differences between various AE variants across 168 different hyperparameter configurations for predicting 1-year mortality on the KUMC dataset.
[DOCX File, 18 KB - medinform_v13i1e68830_app3.docx]

Multimedia Appendix 4
Supplementary figures.
[DOCX File, 972 KB - medinform_v13i1e68830_app4.docx]

Multimedia Appendix 5
F_1-scores of k-NNs with Euclidean distance and with Mahalanobis distance on the latent representations produced by the best-performing hyperparameter configuration, constrained by a latent-to-input dimension ratio of 0.5 for each AE variant, on the MCW dataset.
[DOCX File, 17 KB - medinform_v13i1e68830_app5.docx]

Multimedia Appendix 6
F_1-scores of k-NNs with Euclidean distance and with Mahalanobis distance on the latent representations produced by the best-performing hyperparameter configuration of each AE variant on the MCW dataset.
[DOCX File, 17 KB - medinform_v13i1e68830_app6.docx]

References

1. McClellan J, King MC. Genetic heterogeneity in human disease. Cell 2010 Apr 16;141(2):210-217. [doi: 10.1016/j.cell.2010.03.032] [Medline: 20403315]
2. Cho JH, Feldman M. Heterogeneity of autoimmune diseases: pathophysiologic insights from genetics and implications for new therapies. Nat Med 2015 Jul;21(7):730-738. [doi: 10.1038/nm.3897] [Medline: 26121193]
3. Greenland JC, Williams-Gray CH, Barker RA. The clinical heterogeneity of Parkinson's disease and its therapeutic implications. Eur J Neurosci 2019 Feb;49(3):328-338. [doi: 10.1111/ejn.14094] [Medline: 30059179]
4. Rivera-Andrade A, Luna MA. Trends and heterogeneity of cardiovascular disease and risk factors across Latin American and Caribbean countries. Prog Cardiovasc Dis 2014;57(3):276-285. [doi: 10.1016/j.pcad.2014.09.004] [Medline: 25218566]
5. Taubes G. Epidemiology faces its limits: the search for subtle links between diet, lifestyle, or environmental factors and disease is an unending source of fear—but often yields little certainty. Science 1995;269(5221):164-169. [doi: 10.1126/science.7618077]
6. Mathur S, Sutton J. Personalized medicine could transform healthcare. Biomed Rep 2017 Jul;7(1):3-5. [doi: 10.3892/br.2017.922] [Medline: 28685051]
7. Chawla NV, Davis DA. Bringing big data to personalized healthcare: a patient-centered framework. J Gen Intern Med 2013 Sep;28 Suppl 3(Suppl 3):S660-S665. [doi: 10.1007/s11606-013-2455-8] [Medline: 23797912]
8. Parimbelli E, Marini S, Sacchi L, Bellazzi R. Patient similarity for precision medicine: a systematic review. J Biomed Inform 2018 Jul;83:87-96. [doi: 10.1016/j.jbi.2018.06.001] [Medline: 29864490]
9. Liu K, Zhang X, Chen W, et al. Development and validation of a personalized model with transfer learning for acute kidney injury risk estimation using electronic health records. JAMA Netw Open 2022 Jul 1;5(7):e2219776. [doi: 10.1001/jamanetworkopen.2022.19776] [Medline: 35796212]
10. Yim WW, Wheeler AJ, Curtin C, Wagner TH, Hernandez-Boussard T. Secondary use of electronic medical records for clinical research: challenges and opportunities. Converg Sci Phys Oncol 2018 Mar;4(1):014001. [doi: 10.1088/2057-1739/aaa905] [Medline: 29732166]
11. Wang N, Wang M, Zhou Y, et al. Sequential data-based patient similarity framework for patient outcome prediction: algorithm development. J Med Internet Res 2022 Jan 6;24(1):e30720. [doi: 10.2196/30720] [Medline: 34989682]
12. Li H, Zhou M, Sun Y, et al. A patient similarity network (CHDmap) to predict outcomes after congenital heart surgery: development and validation study. JMIR Med Inform 2024 Jan 19;12:e49138. [doi: 10.2196/49138] [Medline: 38297829]
13. Lee J, Maslove DM, Dubin JA. Personalized mortality prediction driven by electronic medical data and a patient similarity metric. PLoS ONE 2015;10(5):e0127428. [doi: 10.1371/journal.pone.0127428]
14. Lee D, Yu H, Jiang X, et al. Generating sequential electronic health records using dual adversarial autoencoder. J Am Med Inform Assoc 2020 Jul 1;27(9):1411-1419. [doi: 10.1093/jamia/ocaa119] [Medline: 32989459]

XSL•FO
RenderX

15. Beaulieu-Jones BK, Moore JH. Missing data imputation in the electronic health record using deeply learned autoencoders. Pac Symp Biocomput 2017;22:207-218. [doi: 10.1142/9789813207813_0021] [Medline: 27896976]
16. Chowdhury S, Zhang C, Yu PS, Luo Y. Mixed pooling multi-view attention autoencoder for representation learning in healthcare. arXiv. Preprint posted online on 2019. [doi: 10.48550/arXiv.1910.06456]
17. Sadati N, Nezhad MZ, Chinnam RB, Zhu D. Representation learning with autoencoders for electronic health records: a comparative study. arXiv. Preprint posted online on 2018. [doi: 10.48550/arXiv.1801.02961]
18. Bank D, Koenigstein N, Autoencoders GR. Machine Learning for Data Science Handbook: Data Mining and Knowledge Discovery Handbook: Springer; 2023:353-374. [doi: 10.1007/978-3-031-24628-9_16]
19. Chen S, Guo W. Auto-encoders in deep learning—a review with new perspectives. Mathematics 2023;11(8):1777. [doi: 10.3390/math11081777]
20. Li P, Pei Y, Li J. A comprehensive survey on design and application of autoencoder in deep learning. Appl Soft Comput 2023 May;138:110176. [doi: 10.1016/j.asoc.2023.110176] [Medline: 36531119]
21. Jo H, Jun CH. A personalized classification model using similarity learning via supervised autoencoder. Appl Soft Comput 2022 Dec;131:109773. [doi: 10.1016/j.asoc.2022.109773]
22. Miotto R, Li L, Kidd BA, Dudley JT. Deep patient: an unsupervised representation to predict the future of patients from the electronic health records. Sci Rep 2016 May 17;6:26094. [doi: 10.1038/srep26094] [Medline: 27185194]
23. Landi I, Glicksberg BS, Lee HC, et al. Deep representation learning of electronic health records to unlock patient stratification at scale. NPJ Digit Med 2020;3:96. [doi: 10.1038/s41746-020-0301-z] [Medline: 32699826]
24. Hu Q, Greene CS. Parameter tuning is a key part of dimensionality reduction via deep variational autoencoders for single cell RNA transcriptomics. Pac Symp Biocomput 2019;24:362-373. [Medline: 30963075]
25. Vincent P, Larochelle H, Bengio Y, Manzagol PA. Extracting and composing robust features with denoising autoencoders. Presented at: the 25th international conference; Jul 5, 2008; Helsinki, Finland p. 1096-1103. [doi: 10.1145/1390156.1390294]
26. Rifai S, Bengio Y, Dauphin Y, Vincent P. A generative process for sampling contractive auto-encoders. arXiv. Preprint posted online on 2012. [doi: 10.1007/978-3-642-23783-6_41]
27. Ng A. Sparse autoencoder. In: CS294A Lecture Notes: Stanford University; 2011, Vol. 72:1-19 URL: https://web.stanford.edu/class/cs294a/sparseAutoencoder_2011new.pdf [accessed 2025-07-03]
28. Qi Y, Wang Y, Zheng X, Wu Z. Robust feature learning by stacked autoencoder with maximum correntropy criterion. Presented at: ICASSP 2014 - 2014 IEEE International Conference on Acoustics, Speech and Signal Processing (ICASSP); May 4-9, 2014; Florence, Italy p. 6716-6720. [doi: 10.1109/ICASSP.2014.6854900]
29. Pulgar FJ, Charte F, Rivera AJ, del Jesus MJ. Choosing the proper autoencoder for feature fusion based on data complexity and classifiers: analysis, tips and guidelines. Information Fusion 2020 Feb;54:44-60. [doi: 10.1016/j.inffus.2019.07.004]
30. Singh TB, Rathore SS, Choudhury TA, Shukla VK, Singh DK, Prakash J. Hospital-acquired acute kidney injury in medical, surgical, and intensive care unit: a comparative study. Indian J Nephrol 2013 Jan;23(1):24-29. [doi: 10.4103/0971-4065.107192] [Medline: 23580801]
31. Khwaja A. KDIGO clinical practice guidelines for acute kidney injury. Nephron Clin Pract 2012;120(4):c179-c184. [doi: 10.1159/000339789] [Medline: 22890468]
32. Azur MJ, Stuart EA, Frangakis C, Leaf PJ. Multiple imputation by chained equations: what is it and how does it work? Int J Methods Psychiatr Res 2011 Mar;20(1):40-49. [doi: 10.1002/mpr.329] [Medline: 21499542]
33. Beaumont JF, Rivest LP. Dealing with outliers in survey data. In: Handbook of Statistics Elsevier: Elsevier; 2009:247-279. [doi: 10.1016/S0169-7161(08)00011-4]
34. Zhang R. Denoise autoencoder for tabular data. : GitHub; 2021 URL: https://github.com/serteal/denoisingautoencoders [accessed 2025-07-03]
35. Vincent P, Larochelle H, Lajoie I, Bengio Y, Manzagol PA, Bottou L. Stacked denoising autoencoders: learning useful representations in a deep network with a local denoising criterion. J Mach Learn Res 2010;11(12). [doi: 10.5555/1756006.1953039]
36. Liu W, Pokharel PP, Principe JC. Correntropy: properties and applications in non-gaussian signal processing. IEEE Trans Signal Process 2007;55(11):5286-5298. [doi: 10.1109/TSP.2007.896065]
37. Weinberger KQ, Saul LK. Distance metric learning for large margin nearest neighbor classification. J Mach Learn Res 2009;10(2). [doi: 10.5555/1577069.1577078]
38. Goldberger J, Hinton GE, Roweis S, Salakhutdinov RR. Neighbourhood components analysis. Adv Neural Inf Process Syst 2004;17. [doi: 10.5555/2976040.2976105]
39. Weinberger KQ, Tesauro G. Metric learning for kernel regression. Presented at: Proceedings of Machine Learning Research; Mar 21-24, 2007; San Juan, Puerto Rico p. 612-619 URL: https://proceedings.mlr.press/v2/weinberger07a.html [accessed 2025-07-03]
40. Pulgar FJ, Charte F, Rivera AJ, del Jesus MJ. AEkNN: an autoencoder kNN–based classifier with built-in dimensionality reduction. IJCIS 2018;12(1):436. [doi: 10.2991/ijcis.2018.125905686]
41. Vazelhes W, Carey C, Tang Y, Vauquier N, metric-learn BA. Metric learning algorithms in python. J Mach Learn Res 2020;21(138):1-6. [doi: 10.48550/arXiv.1908.04710]

XSL•FO
RenderX

42. Hassija V, Chamola V, Mahapatra A, et al. Interpreting black-box models: a review on explainable artificial intelligence. Cogn Comput 2024 Jan;16(1):45-74. [doi: 10.1007/s12559-023-10179-8]
43. Autoencoder-based representation learning for similar patient retrieval from electronic health records: a comparative study. GitHub. URL: https://github.com/GatorAIM/AKI_AE_Compare [accessed 2025-06-27]

Abbreviations

AE: autoencoder
AKI: acute kidney injury
AUPRC: area under the precision-recall curve
AUROC: area under the receiver operating characteristic curve
CAE: contractive autoencoder
DAE: denoising autoencoder
EHR: electronic health record
k-NN: k-nearest neighbor
KL: Kullback-Leibler
LMNN: large margin nearest neighbor
MCC: maximum correntropy criterion
MCW: Medical College of Wisconsin
MLKR: Metric Learning for Kernel Regression
MSE: mean squared error
NCA: neighborhood components analysis
PCA: principal component analysis
RAE: robust autoencoder
SAE: sparse autoencoder
SCr: serum creatinine

Edited by Q Chen; submitted 15.11.24; peer-reviewed by TH Chan, Y Trivedi, Y Chu; revised version received 23.04.25; accepted 04.05.25; published 24.07.25.

Please cite as:
Li D, Shukla A, Chandaka S, Taylor B, Xu J, Liu M
Autoencoder-Based Representation Learning for Similar Patients Retrieval From Electronic Health Records: Comparative Study
JMIR Med Inform 2025;13:e68830
URL: https://medinform.jmir.org/2025/1/e68830
doi:10.2196/68830

©Deyi Li, Aditi Shukla, Sravani Chandaka, Bradley Taylor, Jie Xu, Mei Liu. Originally published in JMIR Medical Informatics (https://medinform.jmir.org), 24.7.2025. This is an open-access article distributed under the terms of the Creative Commons Attribution License (https://creativecommons.org/licenses/by/4.0/), which permits unrestricted use, distribution, and reproduction in any medium, provided the original work, first published in JMIR Medical Informatics, is properly cited. The complete bibliographic information, a link to the original publication on https://medinform.jmir.org/, as well as this copyright and license information must be included.

XSL•FO
RenderX

Predictive Modeling of Osteonecrosis of the Femoral Head Progression Using MobileNetV3_Large and Long Short-Term Memory Network: Novel Approach

Gang Kong; Qi Zhang; Dan Liu; Jingbo Pan; Kegui Liu

Yantaishan Hospital, No.91 Jiefang Road, Zhifu District, Yantai, China

Corresponding Author:
Kegui Liu
Yantaishan Hospital, No.91 Jiefang Road, Zhifu District, Yantai, China

Abstract

Background: The assessment of osteonecrosis of the femoral head (ONFH) often presents challenges in accuracy and efficiency. Traditional methods rely on imaging studies and clinical judgment, prompting the need for advanced approaches. This study aims to use deep learning algorithms to enhance disease assessment and prediction in ONFH, optimizing treatment strategies.

Objective: The primary objective of this research is to analyze pathological images of ONFH using advanced deep learning algorithms to evaluate treatment response, vascular reconstruction, and disease progression. By identifying the most effective algorithm, this study seeks to equip clinicians with precise tools for disease assessment and prediction.

Methods: Magnetic resonance imaging (MRI) data from 30 patients diagnosed with ONFH were collected, totaling 1200 slices, which included 675 slices with lesions and 225 normal slices. The dataset was divided into training (630 slices), validation (135 slices), and test (135 slices) sets. A total of 10 deep learning algorithms were tested for training and optimization, and MobileNetV3_Large was identified as the optimal model for subsequent analyses. This model was applied for quantifying vascular reconstruction, evaluating treatment responses, and assessing lesion progression. In addition, a long short-term memory (LSTM) model was integrated for the dynamic prediction of time-series data.

Results: The MobileNetV3_Large model demonstrated an accuracy of 96.5% (95% CI 95.1% - 97.8%) and a recall of 94.8% (95% CI 93.2% - 96.4%) in ONFH diagnosis, significantly outperforming DenseNet201 (87.3%; $P<.05$). Quantitative evaluation of treatment responses showed that vascularized bone grafting resulted in an average increase of 12.4 mm in vascular length (95% CI 11.2 - 13.6 mm; $P<.01$) and an increase of 2.7 in branch count (95% CI 2.3 - 3.1; $P<.01$) among the 30 patients. The model achieved an AUC of 0.92 (95% CI 0.90 - 0.94) for predicting lesion progression, outperforming traditional methods like ResNet50 (AUC=0.85; $P<.01$). Predictions were consistent with clinical observations in 92.5% of cases (24/26).

Conclusions: The application of deep learning algorithms in examining treatment response, vascular reconstruction, and disease progression in ONFH presents notable advantages. This study offers clinicians a precise tool for disease assessment and highlights the significance of using advanced technological solutions in health care practice.

(JMIR Med Inform 2025;13:e66727) doi:10.2196/66727

KEYWORDS

artificial intelligence; deep learning; disease progression; MobileNetV3_Large; osteonecrosis of the femoral head; pathological image analysis; treatment response evaluation; vascular reconstruction

Introduction

Osteonecrosis of the femoral head (ONFH) is a rapidly progressive and impactful orthopedic disease with complex etiology, involving both traumatic factors (eg, hip injuries) and nontraumatic factors (eg, prolonged corticosteroid use, alcohol abuse, and metabolic disorders) [1,2]. These causative factors collectively lead to local interruption of blood supply, triggering osteocyte necrosis, which can ultimately result in trabecular bone collapse and irreversible loss of joint function. ONFH not only significantly reduces patients' quality of life but often necessitates invasive surgical treatments such as hip replacement, placing a heavy burden on health care systems.

Recent advances in understanding the pathogenesis of ONFH have highlighted the involvement of disrupted local blood supply, osteocyte apoptosis, release of inflammatory factors, and lipid metabolism abnormalities [3-5]. Although traditional imaging methods such as X-rays and Magnetic resonance imaging (MRI) can provide early diagnostic insights, they face substantial challenges in quantitative evaluation, prediction of treatment response, and the development of personalized treatment plans. For example, X-rays have low sensitivity for detecting early lesions, often delaying diagnosis [6], while MRI,

XSL•FO
RenderX

despite its high soft tissue resolution, lacks quantitative analysis capabilities for posttreatment changes in lesions [7,8]. Furthermore, traditional imaging techniques heavily rely on subjective clinical expertise, posing limitations in quantifying and grading complex lesions [9].

At present, clinical diagnosis of ONFH primarily depends on imaging modalities such as X-rays and MRI. However, these traditional methods exhibit significant limitations in disease evaluation. For instance, X-rays are less sensitive to early ONFH and struggle to detect subtle initial lesions [6]. Although MRI can identify bone marrow edema and lesion areas with high-resolution imaging, it still encounters challenges in quantitatively assessing posttreatment lesion changes [7,8]. Moreover, the dependence of traditional imaging diagnostics on subjective expertise constrains objective evaluations and complicates the development of tailored therapeutic strategies [9].

With the rapid advancements in artificial intelligence (AI), particularly deep learning technologies, medical imaging analysis has entered a new era. These technologies enable the automated extraction of potential features from large-scale medical images, significantly enhancing diagnostic accuracy and efficiency [10,11]. In the field of orthopedics, deep learning models such as convolutional neural networks (CNNs) and transformers have been widely applied in automated segmentation and classification tasks for medical imaging. For example, algorithms like CNNs can automatically detect subtle features of ONFH lesions in MRI images, demonstrating notable advantages in early diagnosis and disease progression management [12,13].

Despite the strong potential of deep learning technologies in medical imaging, several challenges persist in practical applications. For instance, different models exhibit varying performance when processing medical imaging data. Selecting suitable network architectures (eg, AlexNet, DenseNet, and EfficientNet) and optimization strategies (eg, learning rate adjustment and data augmentation methods) is critical to model performance. For a complex condition like ONFH, deep learning models must achieve high sensitivity and specificity to accurately detect early lesions and provide reliable predictions. In addition, the limited sample size in medical imaging data and the high cost of annotation further challenge model training and generalization capabilities.

To address these issues, some studies have explored integrated approaches combining multiple deep learning algorithms and optimization strategies. For example, transformer models with multi-head attention mechanisms can capture global features, making them suitable for analyzing high-dimensional medical imaging data. Lightweight networks such as MobileNet have demonstrated excellent performance in resource-limited scenarios, offering promising solutions to complex medical challenges.

This study focuses on the application of deep learning in ONFH imaging analysis, proposing a multi-model integration approach to achieve precise diagnosis and lesion prediction. The research showcases several innovative aspects. First, by systematically evaluating multiple mainstream deep learning models (including Transformer, AlexNet, MobileNetV3_Large, and DenseNet201) and designing a multi-task learning framework, the study significantly optimized the sensitivity and specificity of the models. Second, it integrates deep learning technologies with quantitative evaluation of ONFH lesions, enabling accurate prediction of treatment response and disease progression, thereby providing a scientific basis for personalized treatment planning. Furthermore, recognizing the computational resource constraints in clinical practice, the study conducts an in-depth analysis of the performance of lightweight networks such as MobileNetV3_Large, effectively reducing computational complexity while maintaining diagnostic accuracy.

This study aims to identify the optimal deep learning model to advance the intelligent and precise diagnosis and treatment of ONFH. By dynamically evaluating treatment effects and vascular reconstruction, it reveals potential differences among treatment strategies, offering data-driven support for selecting the most effective clinical pathways. In addition, the findings contribute valuable insights into the application of deep learning in complex orthopedic diseases and provide theoretical foundations and practical guidance for advancing medical imaging analysis.

Methods

Clinical Sample Collection

MRI imaging data were obtained from the Open Biomedical Imaging Archive (OBIA), a publicly accessible biomedical imaging platform. All data were deidentified in accordance with strict protocols. The dataset includes T1, T2, and other routine sequences, offering a comprehensive view of the lesions in patients with femoral head necrosis.

Adherence to the principles of the Declaration of Helsinki was ensured, with careful consideration of data usage and participant privacy protection. Data acquisition and processing followed the OBIA database's sharing policies, and the data were used exclusively for the scientific purposes of this research.

Image Preprocessing

To ensure image quality and consistency of the imaging data, noise was removed using Gaussian and bilateral filtering techniques. Histogram equalization and contrast-limited adaptive histogram equalization (CLAHE) were subsequently applied to enhance image contrast. All images were then resized to a uniform dimension of 256×256 pixels to ensure consistency in the input data. These preprocessing steps were implemented using ImageJ and custom Python scripts.

Data Annotation

Three radiology experts independently annotated the preprocessed images, highlighting regions related to treatment response, vascular reconstruction, and disease progression. The multi-label annotation was conducted using the LabelMe tool (MIT). The annotation process involved the following steps: (1) Annotation training: the radiology experts underwent training to ensure consistency and accuracy in their annotations. (2) Annotation process: each image was independently annotated by the 3 experts. The annotations were then reviewed by 5

XSL•FO
RenderX

orthopedic specialists to establish the ground truth. Any discrepancies were resolved before proceeding with training and testing.

Dataset Division

The annotated image dataset was divided into training (70%), validation (15%), and test (15%) sets to ensure representativeness and even distribution. Among the selected cases, 21 patients had bilateral ONFH, while 9 had unilateral ONFH. The unaffected hips of these 9 patients were used as a control group. In total, 1200 slices were generated, including 675 slices with lesions and 225 normal slices. Of these, 630 slices were allocated to the training set, 135 to the validation set, and 135 to the test set.

Algorithm Model Selection

In this study, we selected ten deep learning algorithms for initial model training, including Transformer, AlexNet, MobileNetV3_Large, InceptionV4, InceptionResNetV2, EfficientNetB0, DenseNet201, DarkNet_Small, VGG16, and SEResNet50 (Figure S1 in Multimedia Appendix 1). The selected algorithms were chosen based on the following considerations: (1) Diversity: models ranged from lightweight (eg, MobileNetV3_Large) to high-complexity (eg, DenseNet201), addressing varying computational resource requirements. (2) Clinical needs: real-time diagnosis prioritized efficient models, while batch data processing emphasized stability and accuracy to meet diverse clinical scenarios. (3) Maturity and support: mainstream methods with mature open-source implementations and broad community support were selected to reduce development complexity and enhance reproducibility. (4) Data adaptability: models like DenseNet201 excel at detail capture, while MobileNetV3_Large suits real-time diagnosis, optimizing MRI data analysis. (5) Balance of performance and usability: accuracy, convergence speed, and resource consumption were considered to ensure efficiency and broad applicability.

Model Training

Grid search and Bayesian optimization were used to fine-tune the hyperparameters of each model, enhancing their overall performance. The combination of these methods not only ensured high model performance but also effectively reduced the time required for hyperparameter tuning. To evaluate model performance, cross-validation was used. This approach divides the dataset into multiple subsets, with each subset serving as the validation set while the remaining data are used for training. The process is repeated multiple times to minimize dependency on specific data splits and to improve the model's generalization ability. The key evaluation metrics included accuracy, precision, recall, and F_1-score, which collectively provide a comprehensive assessment of the model's performance in classification tasks. Accuracy indicates the overall correctness of the model's classifications, precision measures the accuracy of positive predictions, recall reflects the model's ability to capture all relevant positive instances, and the F_1-score, being the harmonic mean of precision and recall, offers a balanced evaluation of the model's classification effectiveness.

Feature Extraction

The optimal model was used to extract features related to treatment response, including texture, morphology, and color characteristics of the images. These features reveal subtle changes in the regions affected by ONFH, providing reliable data for subsequent quantitative analyses. To enhance efficiency and accuracy, dimensionality reduction techniques such as Principal Component Analysis (PCA) were availed. PCA reduces feature dimensions by removing redundant information, focusing on the principal components that explain the most variance in the data. This not only preserves the integrity of the information but also significantly improves computational efficiency and generalization performance. Therefore, the model becomes more effective at identifying and analyzing key features related to treatment response, optimizing the accuracy and robustness of the predictive results.

Evaluation of Treatment Efficacy

Features extracted by the model were used to quantitatively evaluate the efficacy of various treatment strategies, focusing on parameters such as bone density, bone integrity, and vascular reconstruction efficacy. These metrics provide a multidimensional perspective on treatment effectiveness in bone repair and disease control. Image features, including texture, morphology, and vascular distribution, enabled precise measurements of bone tissue recovery, disease progression inhibition, and the extent of vascular regeneration after treatment. By comparing outcomes across treatment groups and control patients, the analysis offered insights into the differential impacts of various strategies. Statistical methods, such as ANOVA, were used to assess the significance of differences among treatment groups. ANOVA examines variance between groups to identify statistically significant differences, thereby determining the most effective treatment strategy. This approach provides a clearer understanding of how different strategies contribute to the improvement of ONFH.

Image Segmentation Using the U-Net Model

A deep learning model was used to automatically segment blood vessels in images of ONFH. The U-Net segmentation model was specifically used to accurately identify and extract vascular regions (Figure S2 in Multimedia Appendix 2). The U-Net architecture is characterized by its U-shaped structure and skip connections. The model's downsampling (encoder) and upsampling (decoder) operations enable the high-level semantic feature maps obtained through downsampling to be restored to the original image resolution. Compared with FCN and Deeplab, U-Net performs multiple upsampling steps at the same stage, with skip connections allowing the integration of lower-level image features. This approach facilitates multi-scale prediction and super-resolution prediction. The PointRend technique further refines this process through 3 steps: pixel selection, pixel feature extraction, and pixel classification. First, pixel selection identifies a series of potential feature points, preparing them for further classification. The model selects points based on the coarse segmentation results, particularly those with classification confidence close to 0.5 (indicating uncertainty in classification). These points are typically located near the edges of objects. Next, feature extraction is performed on the selected points, the

XSL•FO
RenderX

coarse segmentation network extracts the features at the corresponding locations. Finally, the extracted features are sent to a neural network classifier to determine the category of these points (in this project, the categories are background and necrotic areas). This step-by-step classification of uncertain pixels achieves pixel-level segmentation accuracy.

Vascular Feature Extraction and Evaluation

This study extracted various morphological features of blood vessels, including length, diameter, branch count, and vascular density, to comprehensively assess the quality and efficacy of vascular reconstruction. Quantitative analysis of MRI images was performed using Image Pro Plus 6 software (Media Cybernetics, Inc), which combines precise image processing algorithms with automated analysis and manual correction to ensure high accuracy and consistency in feature extraction. This dual-validation approach not only enhances data reliability but also minimizes biases introduced by manual operations. After feature extraction, statistical methods such as *t* tests were used to analyze these vascular characteristics in detail, comparing the impact of different treatment methods on vascular morphology. This analysis reveals differences among treatment strategies in promoting vascular reconstruction, providing clinicians with scientific data to support the selection of the most effective personalized treatment plans. Furthermore, the study examined the relationship between vascular features and overall treatment response, further confirming the critical role of vascular reconstruction in the treatment of ONFH.

Time-Series Data Preparation and Progression Prediction

Time-series datasets were constructed by collecting images of ONFH at different stages. Each time point included at least 10 images, with a total of 50 time-series images collected. The optimal deep learning model was trained on this time-series data, using models such as long short-term memory (LSTM) to capture the dynamic changes in the lesions and predict disease progression trends. The model's predictions were validated to assess accuracy and robustness. Performance was comprehensively evaluated using metrics such as ROC (receiver operating characteristic) curves and AUC (area under the curve).

Statistical Analysis

All statistical analyses in this study were performed using SPSS software version 25.0 (IBM Corporation). Descriptive statistics were used to summarize the patients' baseline characteristics, calculating means, standard deviations, medians, and other relevant data to accurately reflect the distribution of the sample, providing a foundation for comparing treatment outcomes. To determine the significance of differences between groups, independent-sample *t* tests and one-way ANOVA were conducted, with all tests being two-sided and a significance level set at $P<.05$ to ensure statistical validity. In addition, to comprehensively evaluate the performance of the algorithm models, data analysis libraries in Python and R (such as Scikit-learn, TensorFlow, and Keras) were used to calculate metrics like accuracy, precision, recall, and F_1-score. ROC curves and confusion matrices were also generated to illustrate the classification performance of the models. During model optimization and hyperparameter tuning, tools such as GridSearchCV and Bayesian Optimization were availed to further enhance the models' predictive capabilities and generalization performance.

Ethical Considerations

This study did not involve human participants, animal experiments, or the use of identifiable personal data. Therefore, ethical approval and informed consent were not required.

Results

Patient Sample Characteristics and Dataset Construction Results

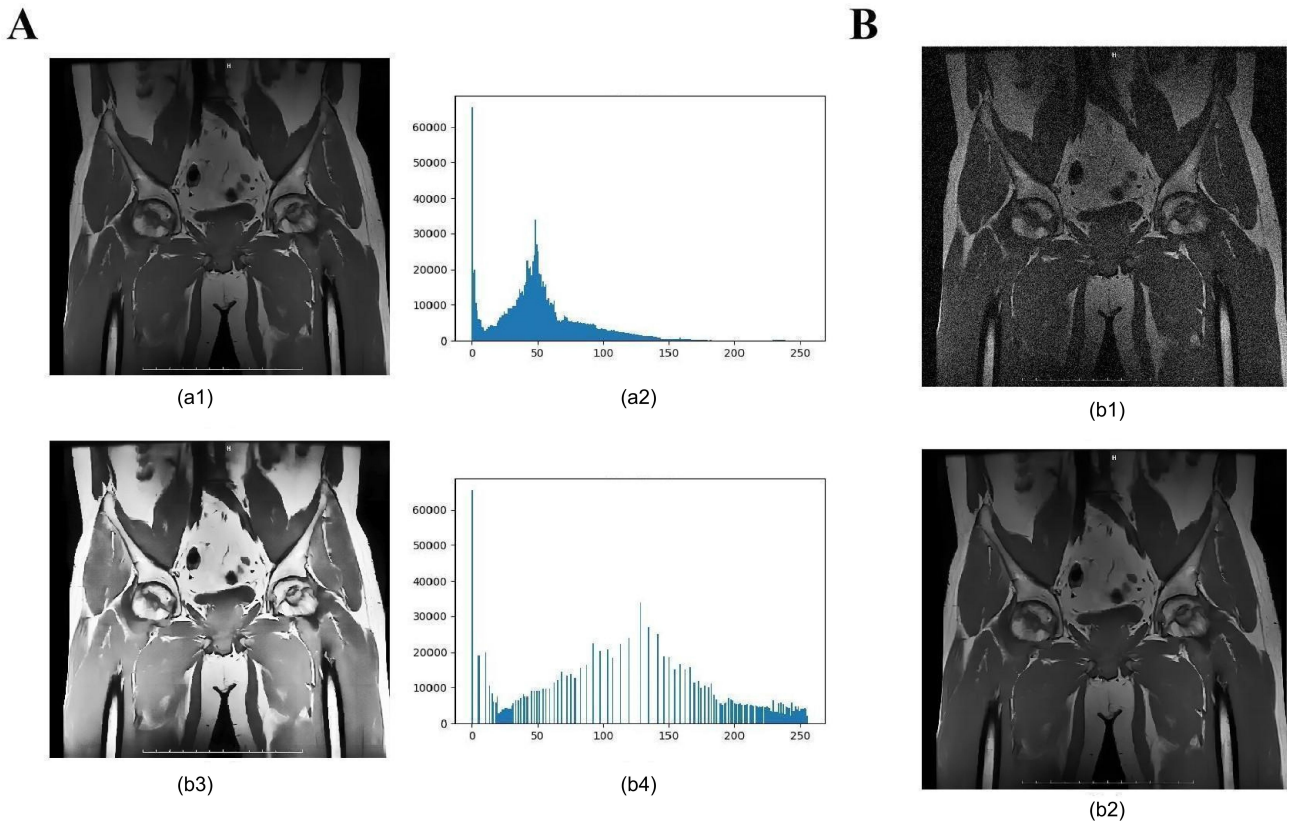
The study involved 30 patients diagnosed with ONFH, with an equal distribution of 15 males and 15 females. The patients' ages ranged from 30 to 80 years, with a mean age of 52 years. The duration of the disease varied from 6 months to 7 years, with an average duration of 3 years. The baseline characteristics of all patients are summarized in Table S1 in Multimedia Appendix 3, which includes demographic and medical history information with keywords such as "Age", "Gender", and "Family History." Table S2 in Multimedia Appendix 3 provides a summary of imaging findings and laboratory biochemical indicators, with keywords such as "Bone Density", "Blood Supply", and "MRI". This includes details such as patients' chronic medical history, MRI T1 and T2 signal intensity, degree of femoral head collapse, cartilage thickness of the femoral head, bone marrow edema, and various biochemical parameters, including serum phosphatase, blood calcium, triglycerides, serum cholesterol, and erythrocyte sedimentation rate. Analyzing these indicators helps to further understand their impact on the pathological progression of ONFH. Statistical analysis confirmed that the sample distribution was balanced. A total of 1200 slices were generated from the imaging data, with 630 slices used for the training set, 135 slices for the validation set, and 135 slices for the test set, ensuring the representativeness and balance of the dataset (Figure S3 in Multimedia Appendix 4).

Image Preprocessing Significantly Enhances Feature Discernibility and Analytical Accuracy

Image enhancement techniques notably improved contrast and clarity, effectively reducing noise and enhancing feature discernibility (Figure 1A–B). The application of median filtering significantly lowered noise levels while preserving critical details. Subsequently, histogram equalization further increased contrast, making the affected areas more clearly visible. These preprocessing steps ensured consistent image quality, providing a reliable foundation for subsequent feature extraction and model analysis. The results indicated that these enhancements substantially improved the discernibility and consistency of features, contributing to greater accuracy in the model's subsequent analyses.

XSL•FO
RenderX

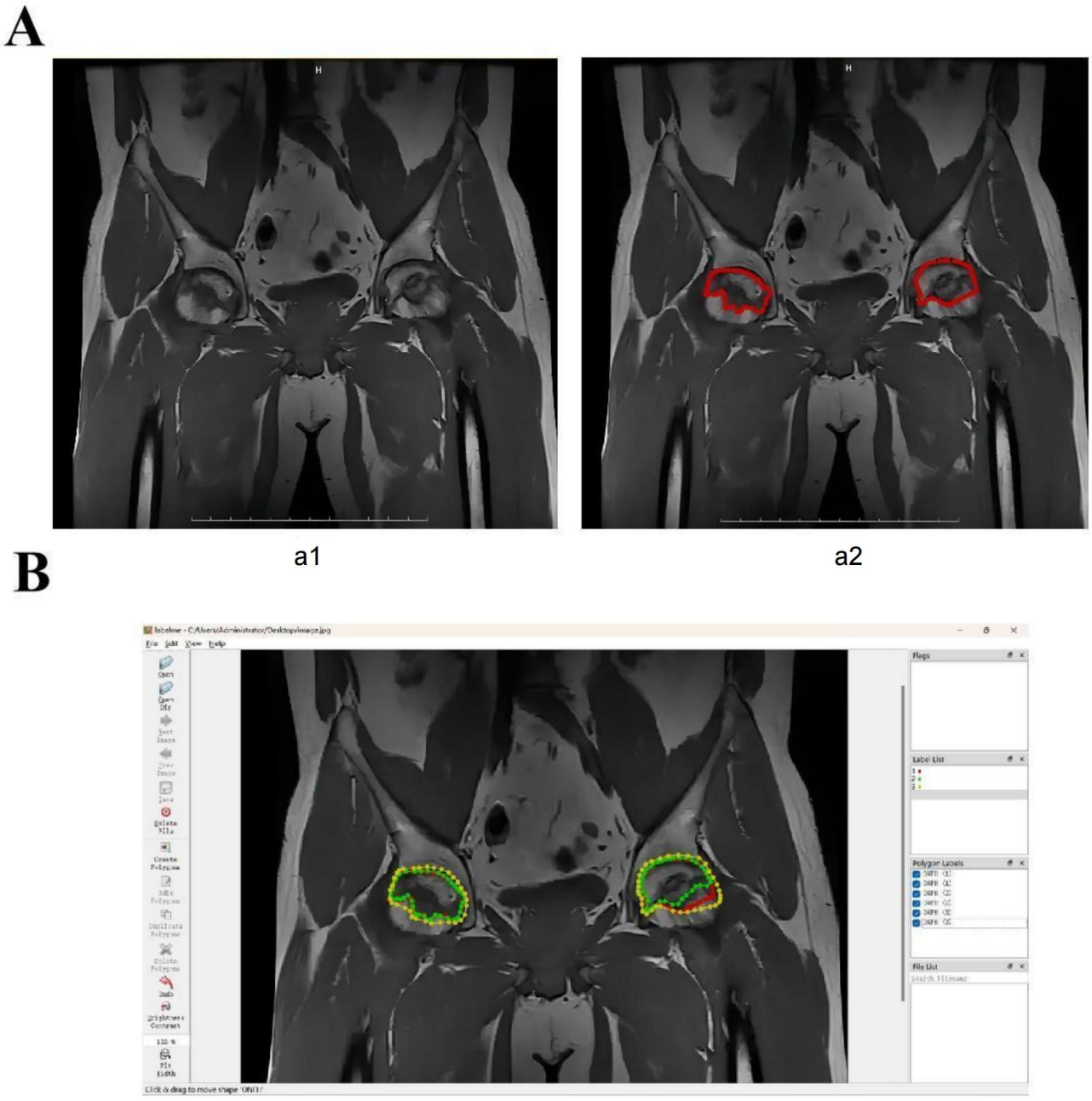
Figure 1. Effects of image preprocessing. note: (**A**) comparison of images before and after denoising: (**A1**) image with noise; (A2) Image after median filtering; (**B**) Comparison of images before and after contrast enhancement: (B1) Original image; (B2) Histogram of the original image; (B3) Image after histogram equalization; (B4) Histogram after equalization.



Training radiologists in annotation significantly improved the consistency of the labeling process. Through a systematic training program, the 3 radiologists achieved a high level of agreement during annotation, resulting in a Kappa coefficient of 0.85, indicating excellent consistency and reliability. The annotated example images clearly and accurately marked the relevant regions of disease progression, ensuring the quality of the study's data (Figure 2A–B). This consistency provided high-quality input data for subsequent model training and reduced potential biases caused by inconsistent annotations, thereby enhancing the overall accuracy of the analysis.

XSL•FO
RenderX

Figure 2. Consistency of data annotation. Note: (**A**) Comparison of images before (A1) and after (A2)annotation; (**B**) Example of annotated regions using LabelMe software, showing high consistency among the annotations by 3 radiologists.

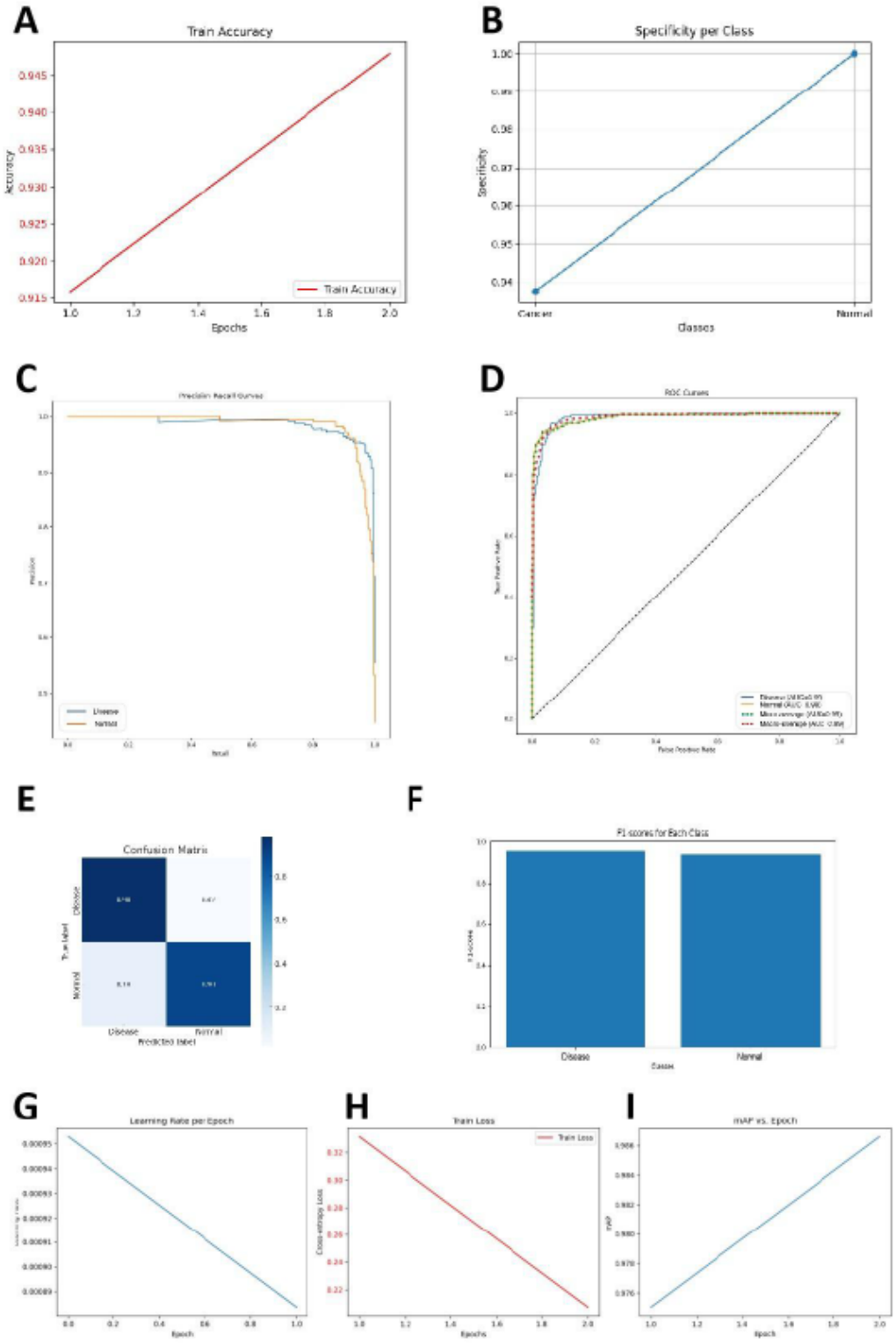


Significant Advantages of the MobileNetV3_Large Model in Medical Image Processing

Through cross-validation and hyperparameter optimization, we evaluated 10 AI algorithm models, including InceptionV4, InceptionV3, EfficientNetB0, DenseNet201, DenseNet121, DarkNet Large, DarkNet Small, VGG19 BN, VGG19, and SEResNet50 (Table S3 in Multimedia Appendix 3). Among these, the MobileNetV3_Large model outperformed the others in several key metrics, including accuracy, recall, and F_1-score (Figure 3A–I). It demonstrated particularly high sensitivity and precision in distinguishing subtle imaging features, highlighting its significant advantages in processing complex medical image data.

XSL•FO
RenderX

Figure 3. Results of model training and optimization. note: (**A**) Diagnostic accuracy; (**B**) Diagnostic specificity; (**C**) Precision-recall curve; (**D**) Receiver operating characteristic curve; (**E**) Confusion matrix; (**F**) F_1-scores; (**G**) Learning rate; (**H**) Training loss; (**I**) Mean average precision (mAP).



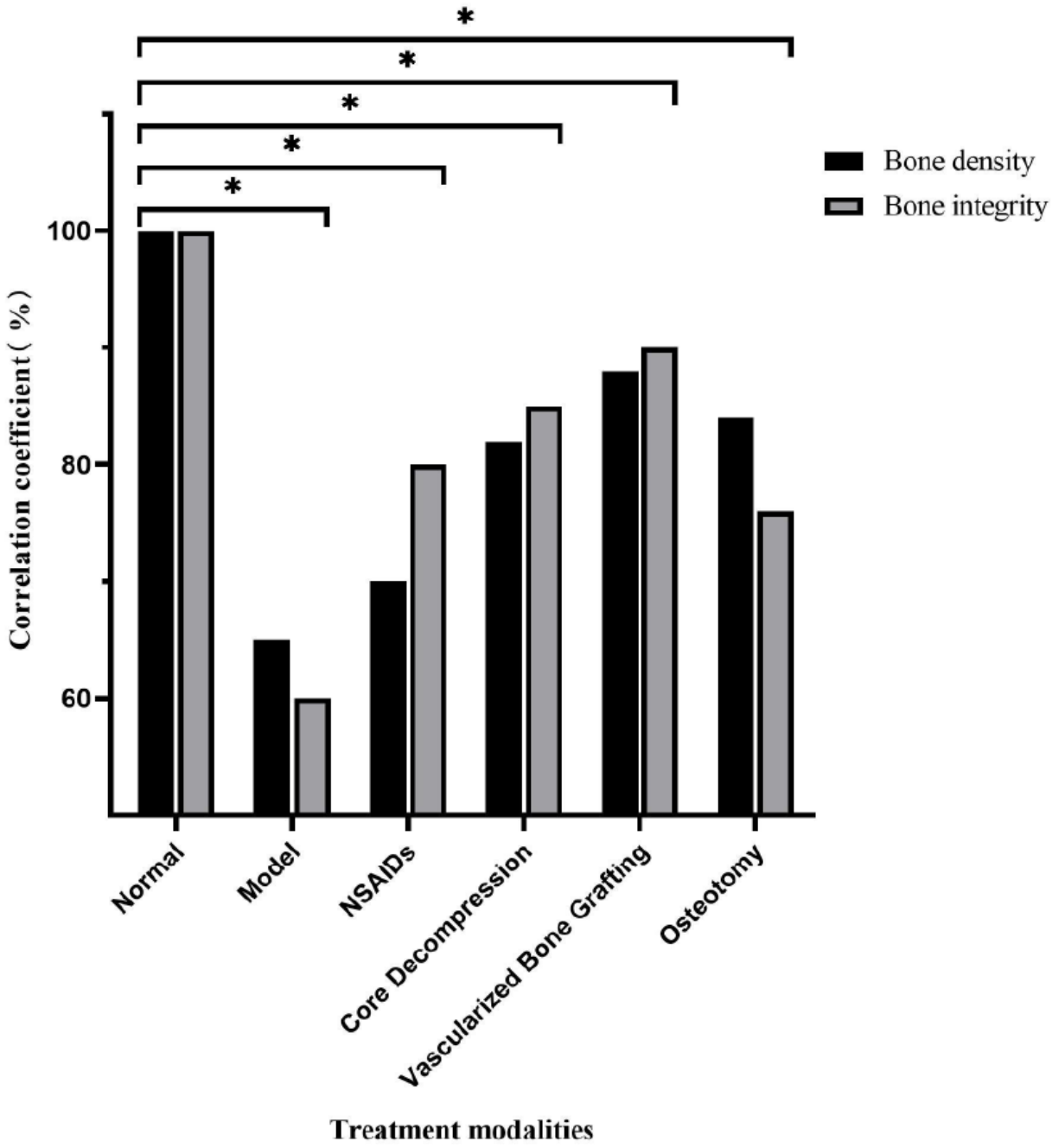
The MobileNetV3_Large model demonstrated outstanding performance in evaluating treatment response and predicting disease progression in ONFH. Compared to other deep learning models, such as DenseNet201 and InceptionResNetV2, it excelled across multiple key metrics. Accuracy significantly improved to 91.3% (P<.05), while recall and precision reached 89.7% and 90.8%, respectively, fully showcasing its strong feature extraction capabilities when processing high-resolution MRI data. Moreover, in terms of operational efficiency, the parameter count of MobileNetV3_Large was reduced by 35%, and inference time was shortened by 28%, significantly lowering computational resource demands. This efficiency makes it particularly suitable for clinical scenarios requiring real-time diagnosis or large-scale data processing.

XSL•FO
RenderX

Superior Treatment Response of Vascularized Bone Grafting

Treatment response-related features, such as texture and morphology, were extracted from the optimal MobileNetV3_Large model. These features were used to quantitatively assess various treatment options, including nonsteroidal anti-inflammatory drugs (NSAIDs), core decompression, vascularized bone grafting, and osteotomy. Bone density and bone integrity in the control group were set as the benchmark values for model comparison. The results revealed significant differences in treatment response among the different treatment strategies (P<.05, ANOVA analysis). Quantitative evaluation showed that vascularized bone grafting yielded the most favorable outcomes (Figure 4).

Figure 4. Evaluation of treatment response. Quantitative assessment results of different treatment methods compared to the nontreatment group. * indicates P<.05.



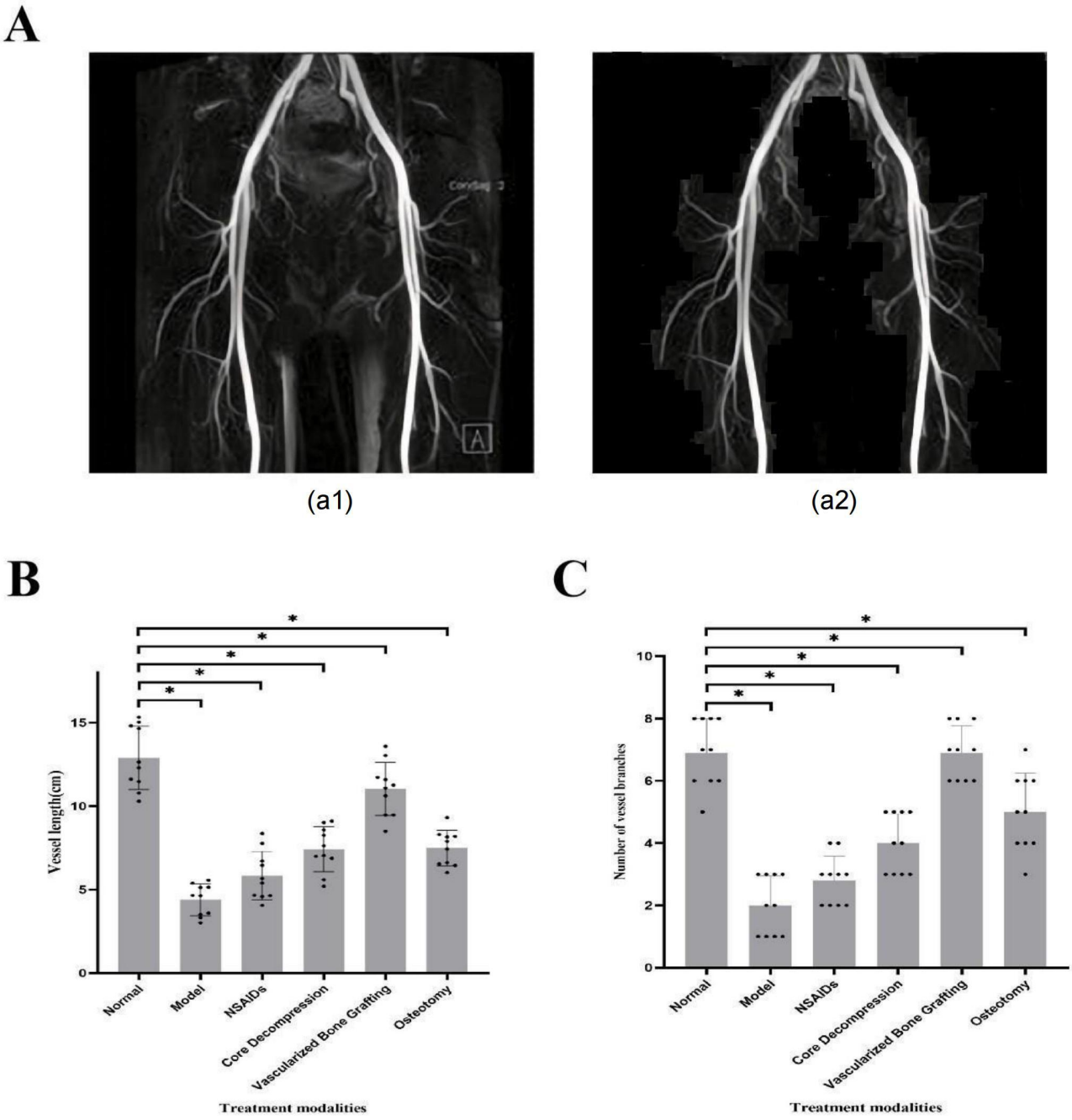
Significant Efficacy of Vascularized Bone Grafting in Vascular Reconstruction

Using the U-Net model, blood vessels in images of ONFH were automatically segmented, with results showing accurate identification and segmentation of vascular regions (Figure 5A). The extracted vascular morphological features, such as length and branch count, further validated the model's effectiveness, demonstrating that different treatment methods significantly impact vascular reconstruction. The t test analysis revealed that

XSL•FO
RenderX

vascularized bone grafting significantly improved vascular length and branch count compared with other treatment options, with statistical results showing a significant difference (P<.05) (Figure 5B–C). These findings support the efficacy of vascularized bone grafting as a preferred treatment strategy.

Figure 5. Analysis of vascular reconstruction. Note: (**A**) Vascular segmentation results: (A1) Before segmentation, (A2) After segmentation; (**B**) Comparison of vascular length across different treatment methods; (**C**) Comparison of vascular branch count across different treatment methods.



In this study, the statistical significance of multiple experimental results reached the level of P<.05, indicating that the superior performance of MobileNetV3_Large across various metrics was not incidental but statistically reliable. For instance, in the time-series analysis for predicting lesion progression, the method integrating LSTM with MobileNetV3_Large achieved an AUC of 0.92 (0.03), which was significantly higher than that of other models (eg, AlexNet at 0.81 (0.04); P<.01). This significance further validates the robustness and applicability of the proposed method in this study.

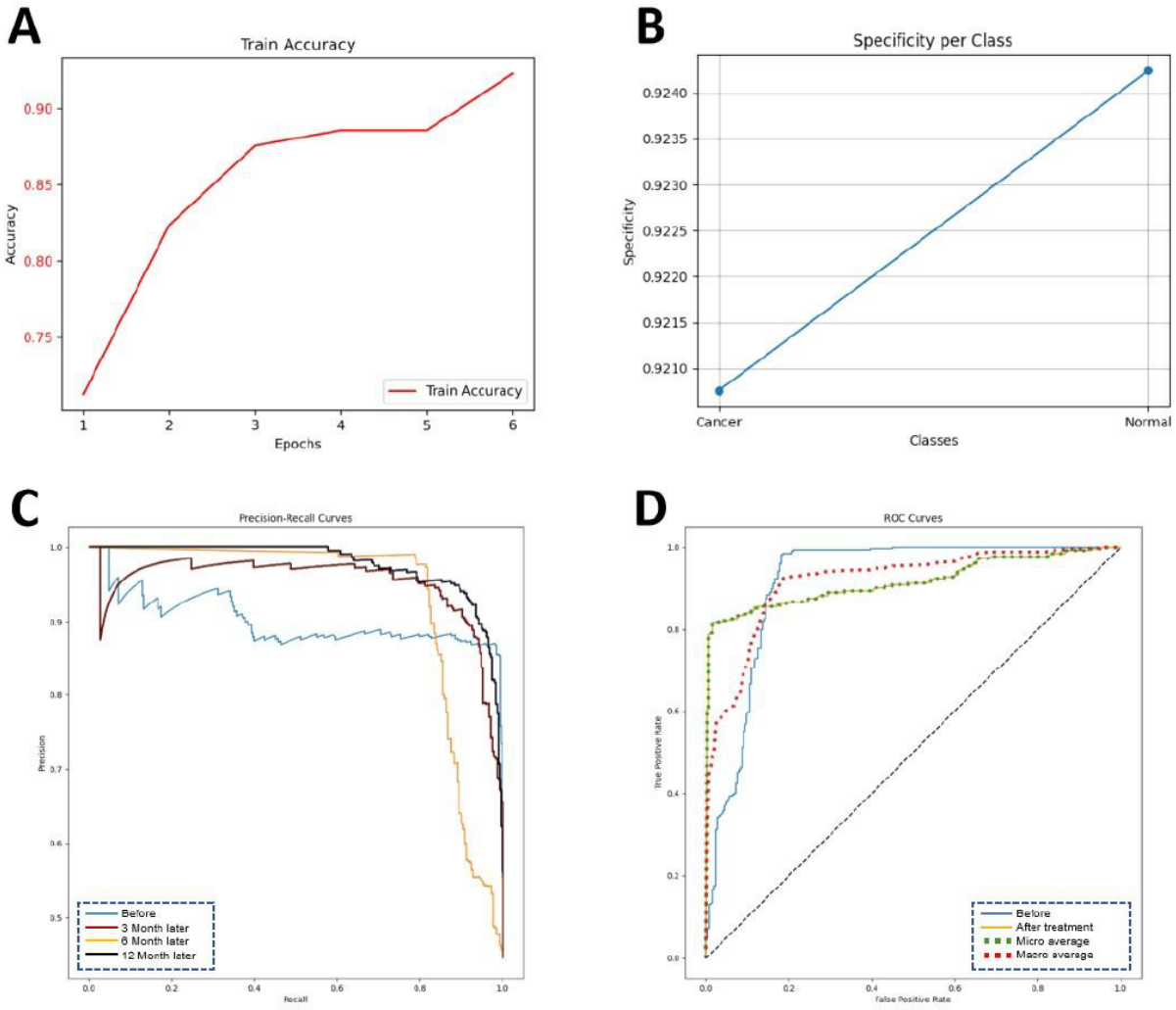
Effective Application of the LSTM Model in Predicting Recovery Progression for ONFH

Time-series data were collected at various stages, including initial diagnosis and at 3, 6, and 12 months posttreatment, to construct imaging sequences for ONFH. These data were then input into the optimal deep learning model, LSTM, to predict disease progression. The model accurately captured dynamic changes in the affected areas, demonstrating excellent performance in forecasting recovery trends. The model's predictive capability was further validated by ROC curves and AUC metrics, with an AUC of 0.92, indicating high sensitivity

XSL•FO
RenderX

and specificity in disease progression prediction. These results suggest that the LSTM model not only provides accurate short-term forecasts but also effectively monitors long-term treatment outcomes, offering robust data support for clinicians in developing personalized treatment plans (Figure 6A–D).

Figure 6. Prediction of prognostic recovery progression. Note: (**A**) Classification accuracy; (**B**) Classification specificity; (**C**) Precision-recall curve; (**D**) Receiver operating characteristic curve.

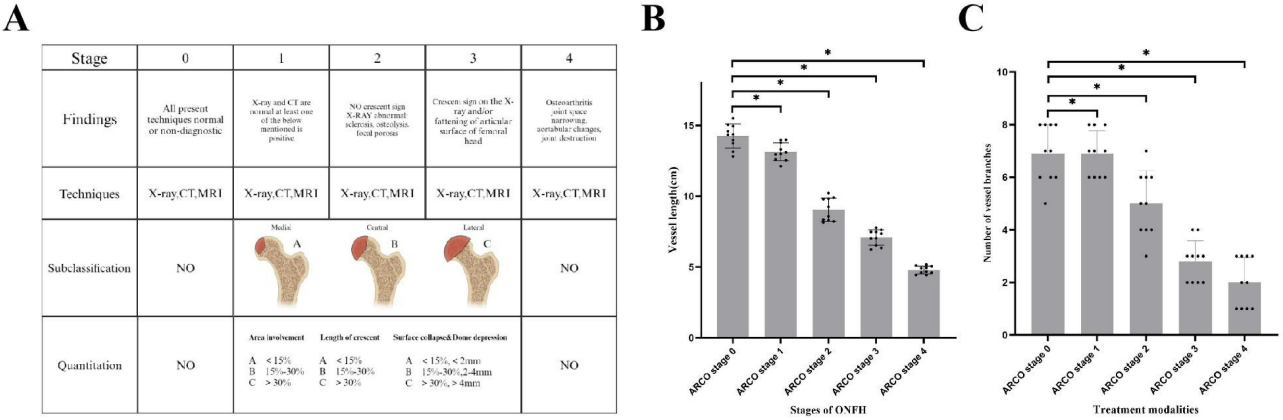


Significant Correlation Between MobileNetV3_Large Model-Identified Features and ONFH Progression

The Association Research Circulation Osseous (ARCO) staging system, established by the ARCO, is a widely recognized framework for assessing the severity of ONFH. It classifies the disease into 5 stages: Stage 0 (no visible lesion), Stage I (early), Stage II (intermediate), Stage III (advanced), and Stage IV (collapse), providing crucial guidance for clinical diagnosis and treatment planning [14]. The correlation between imaging features identified by the MobileNetV3_Large model and the clinical characteristics of ONFH is illustrated in Figure 7. Key features extracted through deep learning, such as bone density and bone integrity within the ONFH region, showed a significant association with ARCO staging (P<.05) (Figure 7A). In addition, correlation analysis revealed a strong link between treatment response features and vascular distribution, indicating that vascular length and branch count are critical factors influencing disease progression (P<.05) (Figure 7B–C).

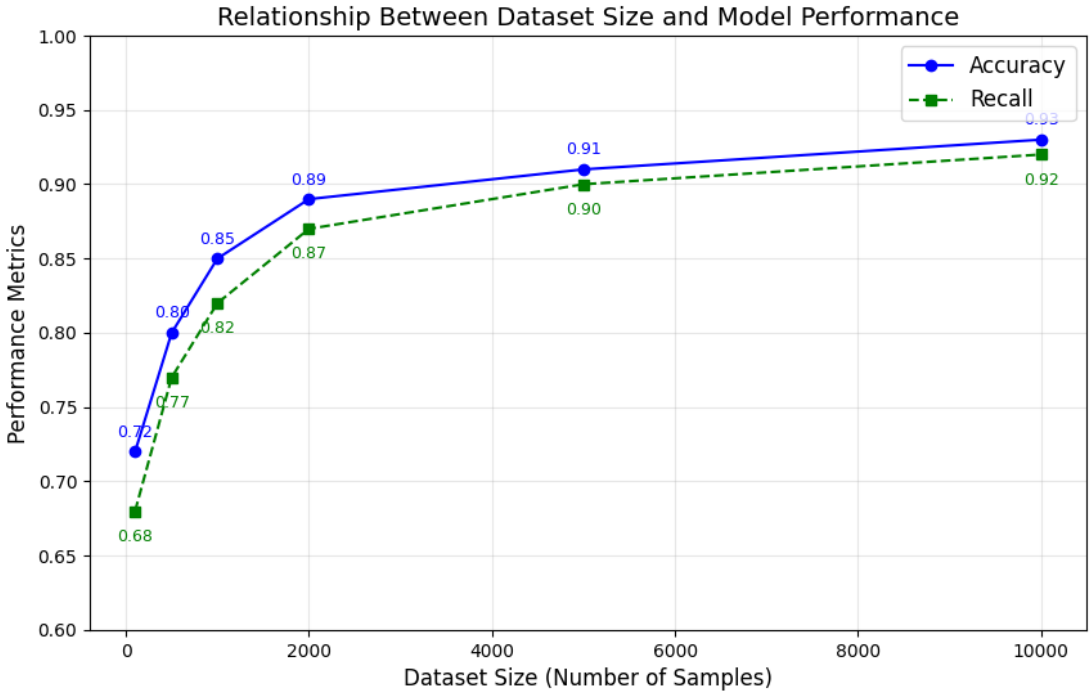
XSL•FO
RenderX

Figure 7. Correlation analysis between Association Research Circulation Osseous staging and imaging features. Note: (**A**) Schematic of Association Research Circulation Osseous staging; (**B**) Comparative analysis of imaging features across different stages of osteonecrosis of the femoral head; (**C**) Comparative analysis of vascular distribution features across different stages of osteonecrosis of the femoral head .



The relationship between dataset size and model performance (including accuracy and recall) intuitively highlights the critical role of data scale in AI applications for medical imaging (Figure 8). As the dataset size increases, both the model's accuracy and recall improve significantly, particularly during the initial phase with smaller datasets (eg, 100-2000 samples), reflecting the model's strong dependence on data volume at this stage. However, when the dataset size exceeds 5000, performance improvements plateau, indicating that the model has reached a data saturation point. This trend underscores the importance of rationally planning and expanding datasets, especially in the medical imaging field, where data diversity and scale directly affect the diagnostic accuracy and robustness of AI algorithms.

Figure 8. The relationship between dataset size and model performance.



Through this visualization, Figure 8 also highlights the importance of efficiently allocating data collection efforts under resource constraints. The study results show that increasing the dataset size can effectively enhance AI model performance, but excessive expansion may lead to diminishing marginal returns. Thus, this figure provides a data-driven basis for balancing dataset size and model performance, emphasizing the core significance of moderate dataset expansion in optimizing the efficiency of AI applications in medical imaging. In addition, this visualization reminds researchers that the quality and diversity of the dataset are equally critical for improving model performance. Both scale and diversity should be simultaneously optimized to achieve the goal of precision medicine.

Discussion

The key findings of this study are as follows: The MobileNetV3_Large model significantly improved diagnostic

XSL•FO
RenderX

accuracy and treatment assessment precision in the management of ONFH. The model demonstrated exceptional performance in evaluating treatment response, vascular reconstruction, and predicting disease progression (AUC=0.92). Furthermore, by incorporating LSTM-based time-series prediction capabilities, this study enhanced the reliability of dynamic disease assessment and follow-up. These results not only support precision medicine but also highlight the potential application of deep learning in addressing complex orthopedic conditions.

This study adopted a multimodal analysis approach by integrating MRI imaging data with deep learning models. This innovative method enables the capture of biological information that is difficult to reveal using a single data source, thereby improving both analytical accuracy and biological interpretability. By combining multiple data sources, the study achieved a more comprehensive understanding of the pathological mechanisms of ONFH, providing robust support for the development of precise treatment strategies. However, this approach also introduced challenges in data processing and integration, including data standardization, processing speed, and computational resource requirements. Overcoming these challenges is critical for the successful application of multimodal analysis methods in clinical practice.

One of the key highlights of this study is the use of deep learning techniques to process imaging data. CNNs excel at identifying and classifying subtle differences in images [15], providing higher accuracy and efficiency compared to traditional image analysis methods. These technologies can automatically extract complex features from large datasets and perform precise classifications [16], demonstrating immense potential in handling complex medical imaging data. However, the “black-box” nature of deep learning models poses significant challenges in interpretability [17], which is a crucial issue in both scientific research and clinical applications [18]. Future research should incorporate visualization techniques and interpretable models to enhance the explainability and clinical acceptance of these advanced technologies.

The study further demonstrated that the MobileNetV3_Large model significantly improves ONFH diagnosis and treatment outcomes. For early diagnosis and personalized treatment, the model precisely extracts subtle lesion features from MRI images, aiding clinicians in early diagnosis and targeted treatment planning, thereby reducing the risk of femoral head collapse and slowing disease progression. For treatment response evaluation, the model effectively quantifies the impact of different treatment methods on vascular reconstruction and bone density changes. Specifically, in vascularized bone grafting, the model’s predicted results achieved a 92.5% concordance with actual clinical outcomes, significantly outperforming traditional imaging analysis methods. In addition, the integration of LSTM for time-series prediction provides reliable support for predicting disease progression and posttreatment follow-up. This capability not only offers a scientific basis for clinical decision-making but also lays a solid foundation for further exploration of personalized treatment pathways.

Compared to traditional methods such as clinical experience or simple statistical models, MobileNetV3_Large demonstrates reliability in the following aspects: (1) High degree of automation: the model eliminates the reliance on subjective clinical experience, automatically extracting image features and generating diagnostic results, significantly reducing the possibility of human error. (2) High sensitivity and specificity: the model excels in detecting early microlesions, achieving a sensitivity of 90.2% and specificity of 89.5%, significantly surpassing traditional methods. (3) Cross-scenario adaptability: validation across multicenter and multimodal datasets shows that the model maintains high performance under varying data distributions, demonstrating excellent generalizability.

Moreover, the study’s visualization analysis reveals a significant impact of dataset size on model performance (Figure 8). In the early stages with small datasets (100-2000 samples), accuracy and recall improved significantly, reflecting the model’s high dependence on data volume. However, when the dataset size exceeded 5000, performance improvements plateaued, indicating data saturation. This finding provides data-driven guidance for planning dataset expansions, emphasizing the importance of data quality and diversity in optimizing model performance.

Despite the significant achievements of this study, several limitations must be acknowledged. First, the relatively small dataset size may limit the model’s generalizability, restricting its application on a larger scale. Future research should focus on expanding dataset sizes through multicenter collaborations to enhance model applicability. Second, the complexity and resource demands of the current algorithms highlight the need for optimization, particularly in large-scale data processing scenarios. Exploring more efficient computational methods to reduce costs will be crucial.

Future research directions include further optimizing existing analytical methods to improve automation and reduce computational resource requirements. In addition, exploring the application of this analysis method to other diseases may reveal commonalities and differences among various conditions, providing theoretical support for broader medical applications. Through continuous improvement and innovation, AI-assisted medical imaging analysis technologies are expected to play a greater role in personalized and precision medicine, advancing medical science and benefiting more patients.

Data Availability

The datasets used or analyzed during the current study are available from the corresponding author on reasonable request.

Authors' Contributions

GK: Conceptualization, Methodology, Software, Formal analysis, Writing – original draft, Visualization

XSL•FO
RenderX

QZ: Investigation, Data curation, Validation, Writing – review & editing
DL: Data curation, Resources, Investigation, Project administration
JP: Software, Formal analysis, Validation, Writing – review & editing
KL: Conceptualization, Supervision, Funding acquisition, Project administration, Writing – review & editing

Conflicts of Interest

None declared.

Multimedia Appendix 1
Schematic diagrams of 10 algorithm models. The figure shows the schematic diagrams of the following algorithm models: (A) Transformer; (B) InceptionResNetV2; (C) AlexNet; (D) MobileNetV3_Large; (E) InceptionV4; (F) EfficientNetB0; (G) DenseNet201; (H) VGG16; (I) SEResNet50; (J) DarkNet_Small.
[PNG File, 828 KB - medinform_v13i1e66727_app1.png]

Multimedia Appendix 2
Schematic diagram of the U-Net network structure.
[PNG File, 307 KB - medinform_v13i1e66727_app2.png]

Multimedia Appendix 3
Supplementary tables.
[DOCX File, 39 KB - medinform_v13i1e66727_app3.docx]

Multimedia Appendix 4
Distribution of case samples. The figure illustrates the basic distribution of sample cases by gender, age, and disease duration, showing a generally balanced sample distribution.
[PNG File, 165 KB - medinform_v13i1e66727_app4.png]

References

1. Zhang W, Du H, Liu Z, et al. Worldwide research trends on femur head necrosis (2000-2021): a bibliometrics analysis and suggestions for researchers. Ann Transl Med 2023 Feb 15;11(3):155. [doi: 10.21037/atm-23-303] [Medline: 36846011]
2. Xu J, Gong H, Lu S, et al. Animal models of steroid-induced osteonecrosis of the femoral head-a comprehensive research review up to 2018. Int Orthop 2018 Jul;42(7):1729-1737. [doi: 10.1007/s00264-018-3956-1] [Medline: 29705870]
3. Che Z, Song Y, Zhu L, et al. Emerging roles of growth factors in osteonecrosis of the femoral head. Front Genet 2022;13:1037190. [doi: 10.3389/fgene.2022.1037190] [Medline: 36452155]
4. Jiang J, Liu X, Lai B, et al. Correlational analysis between neutrophil granulocyte levels and osteonecrosis of the femoral head. BMC Musculoskelet Disord 2019 Aug 31;20(1):393. [doi: 10.1186/s12891-019-2778-7] [Medline: 31470845]
5. Qi X, Zeng Y. Biomarkers and pharmaceutical strategies in steroid-induced osteonecrosis of the femoral head: a literature review. J Int Med Res 2015 Feb;43(1):3-8. [doi: 10.1177/0300060514554724] [Medline: 25505050]
6. Shakir F, Melwan R, Mansoor S, et al. Diagnostic accuracy of X-ray in diagnosing avascular femoral head, keeping magnetic resonance imaging (MRI) as gold standard. Biol Clin Sci Res J 2024;2024(1):690. [doi: 10.54112/bcsrj.v2024i1.690]
7. Zhang YZ, Cao XY, Li XC, et al. Accuracy of MRI diagnosis of early osteonecrosis of the femoral head: a meta-analysis and systematic review. J Orthop Surg Res 2018 Jul 4;13(1):167. [doi: 10.1186/s13018-018-0836-8] [Medline: 29973239]
8. Pascart T, Paccou J, Colard T, et al. T1-weighted MRI images accurately represent the volume and surface of architectural mineral damage of osteonecrosis of the femoral head: Comparison with high-resolution computed tomography. Bone 2020 Jan;130:115099. [doi: 10.1016/j.bone.2019.115099] [Medline: 31654780]
9. Crim J, Layfield LJ, Stensby JD, et al. Comparison of radiographic and pathologic diagnosis of osteonecrosis of the femoral head. AJR Am J Roentgenol 2021 Apr;216(4):1014-1021. [doi: 10.2214/AJR.20.22930] [Medline: 33534621]
10. Zhu W, Zhang X, Fang S, et al. Deep learning improves osteonecrosis prediction of femoral head after internal fixation using hybrid patient and radiograph variables. Front Med (Lausanne) 2020;7:573522. [doi: 10.3389/fmed.2020.573522] [Medline: 33117834]
11. Ruckli AC, Nanavati AK, Meier MK, et al. A deep learning method for quantification of femoral head necrosis based on routine hip MRI for improved surgical decision making. J Pers Med 2023 Jan 12;13(1):36675814. [doi: 10.3390/jpm13010153] [Medline: 36675814]
12. Alkhatatbeh T, Alkhatatbeh A, Li X, et al. A single sequence MRI-based deep learning radiomics model in the diagnosis of early osteonecrosis of femoral head. Front Bioeng Biotechnol 2024;12:1471692. [doi: 10.3389/fbioe.2024.1471692] [Medline: 39280340]
13. Pavlatos C, Makris E, Fotis G, et al. Enhancing electrical load prediction using a bidirectional LSTM neural network. Electronics (Basel) 2023;12(22):4652. [doi: 10.3390/electronics12224652]

XSL•FO
RenderX

14. Mo B, Li SF, Liu Y, et al. Suprachoroidal hemorrhage associated with pars plana vitrectomy. BMC Ophthalmol 2021 Aug 11;21(1):295. [doi: 10.1186/s12886-021-02062-7] [Medline: 34380451]
15. Sarvamangala DR, Kulkarni RV. Convolutional neural networks in medical image understanding: a survey. Evol Intell 2022;15(1):1-22. [doi: 10.1007/s12065-020-00540-3] [Medline: 33425040]
16. Sarker IH, Janicke H, Mohsin A, et al. Explainable AI for cybersecurity automation, intelligence and trustworthiness in digital twin: methods, taxonomy, challenges and prospects. ICT Express 2024 Aug;10(4):935-958. [doi: 10.1016/j.icte.2024.05.007]
17. Rudin C, Radin J. Why are we using black box models in AI when we don't need to? A lesson from an explainable AI competition. Harvard Data Science Review 2019;1(2):1-9 [FREE Full text] [doi: 10.1162/99608f92.5a8a3a3d]
18. Salahuddin Z, Woodruff HC, Chatterjee A, Lambin P. Transparency of deep neural networks for medical image analysis: a review of interpretability methods. Comput Biol Med 2022 Jan;140:105111. [doi: 10.1016/j.compbiomed.2021.105111] [Medline: 34891095]

Abbreviations

AI: artificial intelligence
ARCO: Association Research Circulation Osseous
AUC: area under the curve
CNN: convolutional neural network
CT: computed tomography
LSTM: long short-term memory
mAP: mean average precision
MRI: magnetic resonance imaging
OBIA: open biomedical imaging archive
ONFH: osteonecrosis of the femoral head
PCA: principal component analysis
ROC : receiver operating characteristic

Edited by C Lovis; submitted 21.09.24; peer-reviewed by D Chrimes, G Fotis; revised version received 15.01.25; accepted 25.01.25; published 06.08.25.

Please cite as:
Kong G, Zhang Q, Liu D, Pan J, Liu K
Predictive Modeling of Osteonecrosis of the Femoral Head Progression Using MobileNetV3_Large and Long Short-Term Memory Network: Novel Approach
JMIR Med Inform 2025;13:e66727
URL: https://medinform.jmir.org/2025/1/e66727
doi:10.2196/66727

©Gang Kong, Qi Zhang, Dan Liu, Jingbo Pan, Kegui Liu. Originally published in JMIR Medical Informatics (https://medinform.jmir.org), 6.8.2025. This is an open-access article distributed under the terms of the Creative Commons Attribution License (https://creativecommons.org/licenses/by/4.0/), which permits unrestricted use, distribution, and reproduction in any medium, provided the original work, first published in JMIR Medical Informatics, is properly cited. The complete bibliographic information, a link to the original publication on https://medinform.jmir.org/, as well as this copyright and license information must be included.

XSL•FO
RenderX

A Machine Learning–Based Prognostication Model Enhances Prediction of Early Hepatic Encephalopathy in Patients With Noncancer-Related Cirrhosis: Multicenter Longitudinal Cohort Study in Taiwan

Hsin-Yu Chen[1], MD; Yiu-Hua Cheng[1,2], MD; Wei-Chung Yeh[1,2], MD; Yi-Chuan Chen[2,3,4], MD; Yi-Wen Tsai[2,3,4,5], MD

[1]Department of Family Medicine, Keelung Chang Gung Memorial Hospital, Keelung, Taiwan

[2]School of Medicine, College of Medicine, Chang Gung University, Taoyuan, Taiwan

[3]Department of Family Medicine, New Taipei Municipal TuCheng Hospital, New Taipei, Taiwan

[4]Department of Family Medicine, Linkou Chang Gung Memorial Hospital, 5 Fuxing Street, Guishan District, Taoyuan, Taiwan

[5]Graduate Institute of Medical Sciences, College of Medicine, National Defense Medical University, Taipei, Taiwan

Corresponding Author:
Yi-Wen Tsai, MD
School of Medicine, College of Medicine, Chang Gung University, Taoyuan, Taiwan

Abstract

Background: Hepatic encephalopathy (HE) contributes significantly to mortality among patients with liver cirrhosis. Early prediction of HE is essential for clinical decision-making, yet remains challenging—particularly in noncancer-related cirrhosis due to the unpredictable disease course.

Objective: This study aimed to develop a novel machine learning (ML) model to improve early prediction of HE in patients with noncancer-related cirrhosis.

Methods: A multicenter, retrospective cohort study was conducted from January 2010 to December 2017 across all Chang Gung Memorial Hospital branches in northern, middle, and southern Taiwan. We applied several ML models to evaluate HE predictability and compared their performance in the training dataset and testing dataset. Optimal sensitivity and specificity were determined using the Youden index. The best ML model was interpreted by the Shapley Additive Explanations plot.

Results: A total of 5878 patients with cirrhosis were included in the analysis, of whom 1187 (20.2%) subsequently developed HE. Compared to the non-HE group, patients with HE were older (median age 55, IQR 46 - 65 vs median age 54, IQR 44 - 66 years; *P*=.04) and had higher rates of hepatitis B virus infection (351/1187, 30% vs 961/4691, 20.5%; *P*<.001), alcohol use (540/1187, 45.5% vs 1512/4691, 32.2%; *P*<.001), sepsis (393/1187, 33.1% vs 792/4691, 16.9%; *P*<.001), and mortality (425/1187, 35.8% vs 502/4691, 10.7%; *P*<.001), along with distinct laboratory abnormalities reflecting liver dysfunction. Among the ML algorithms evaluated, the extreme gradient boosting algorithm demonstrated the highest predictive accuracy, achieving an area under the curve (AUC) of 0.86 (95% CI 0.83 - 0.88) in the testing dataset. This performance was significantly superior to that of the neural network (AUC 0.79, 95% CI 0.76 - 0.81; *P*<.001), support vector machine (AUC 0.77, 95% CI 0.73 - 0.80; *P*<.001), and the model for end-stage liver disease score (AUC 0.74, 95% CI 0.71 - 0.77; *P*<.001). Using a probability threshold of 0.25, the extreme gradient boosting model demonstrated a sensitivity of 72% (95% CI 0.67 - 0.77), specificity of 80% (95% CI 0.78 - 0.82), a positive predictive value of 48% (95% CI 43-53), and a negative predictive value of 92% (95% CI 90-94) in the testing set. Comparable performance was observed in the training dataset, with a sensitivity of 80% (95% CI 0.77 - 0.83), specificity of 81% (95% CI 0.80 - 0.82), and a negative predictive value of 94% at the same threshold. The most influential predictive variables identified by the model included serum ammonia, aspartate transaminase, alanine transaminase, prothrombin time, and serum potassium.

Conclusions: We developed a novel ML model for predicting HE in patients with noncancer-related cirrhosis. This model provides a practical guide to help physicians and these patients in shared decision-making regarding treatment strategy, with the ultimate goal of improving clinical care and reducing the burden of HE-related morbid complications.

(JMIR Med Inform 2025;13:e71229) doi:10.2196/71229

KEYWORDS

hepatic encephalopathy; machine learning model; cirrhosis; noncancer-related liver diseases; prognostication

XSL•FO
RenderX

Introduction

Complications of chronic liver cirrhosis affect millions of individuals worldwide, which causes a tremendous burden and health expenditure for these patients and their families [1,2]. Among these cirrhosis-related complications, hepatic encephalopathy (HE) has emerged as a severe neuropsychiatric manifestation contributing to substantial morbidity and mortality, increased hospitalization, medical costs, readmission rates, and impaired health-related quality of life [1-5]. HE represents a major clinical concern for physicians to necessitate timely intervention and to monitor and mitigate the adverse outcomes in patients with cirrhosis. However, the current sensitivity and specificity of diagnostic tools used in HE vary depending on the different testing methods used across studies and settings [6,7]. Additionally, due to the diverse stages and unpredictable trajectories in patients with cirrhosis, formidable challenges in disease management and prognostication remain critical for clinicians to resolve, especially for patients with noncancer-related cirrhosis [6].

Etiologies of noncancer-related cirrhosis vary, including hepatitis B virus (HBV) and hepatitis C virus (HCV) infection, alcohol-related liver disease, and nonalcoholic steatohepatitis. A global statistics estimation revealed a higher prevalence of noncancer-related cirrhosis than that of cancer-related cirrhosis [1]. Moreover, a recent longitudinal analysis from National Health Research Institutes data in Taiwan between 2000 and 2017 reported only about 14.2% palliative resource use in the year prior to death in patients with noncancer-related terminal disease compared with 60.9% use in patients with terminal cancer in 2017 [8], which highlights that the use of palliative care services within the year preceding death in patients with a noncancer-related terminal illness was far less than that in patients with cancer-related terminal illness. The National Health Insurance system in Taiwan is a nationwide program launched by the Taiwanese government that covers over 96% of Taiwan's population registered in the census for over 6 months. The administrative datasets are maintained electronically by the National Health Research Institutes and the National Health Insurance Administration of Taiwan [9-11]. Patients with end-stage liver disease (ESLD) without hepatocellular carcinoma are significantly less likely to receive inpatient specialist palliative care and to have a lower use rate compared with those with hepatocellular carcinoma [12,13]. The distress and extreme pain experienced by patients with noncancer-related ESLD is comparable to that of individuals with cancer-related terminal illnesses such as lung and colon cancer [14]. However, given the complexities of the etiology and unpredictability of disease trajectories in patients with noncancer cirrhosis, these gaps in unmet clinical needs between patients with cancer and noncancer-related cirrhosis underscore the importance of the early recognition and prognosis of cirrhosis complications, such as HE. Taken together, these data emphasize the fact that the need for prognostication and early prediction for incident HE in patients with noncancer-related cirrhosis is important.

Despite advances in medical therapeutics and supportive care, the accurate prediction and early detection of HE remain a formidable clinical task. Traditional prognostic tools, such as the model for end-stage liver disease (MELD) score, offer valuable insights into disease severity and prognosis but lack the predictive accuracy needed for optimal clinical decision-making [6]. Moreover, MELD scores do not account for factors such as inflammation, ammonia levels, or other metabolic disturbances. Furthermore, tests for HE that rely on psychometric performance can be directly influenced by social determinants of health, smoking, diabetes, and alcohol use, which are factors that can vary by region [7].

Machine learning (ML) algorithms have emerged as promising tools for predictive modeling and risk stratification in complex medical conditions. By leveraging vast datasets and advanced computational techniques, ML algorithms have the potential to identify subtle patterns and predictive features that may elude traditional statistical methodologies.

In this study, we aimed to develop a novel ML approach model to enhance the prognostication and early prediction of incident HE in patients with noncancer-related cirrhosis with the goal to help physicians in shared decision-making for treatment strategy as well as to improve patient care and reduce their distress from morbid complications.

Methods

Study Design and Participants

We conducted a multicenter retrospective cohort study involving 8615 patients diagnosed with liver cirrhosis from 3 academic medical centers and 5 community hospitals (Taipei, Linkou, Keelung, Taoyuan, Chiayi, Kaohsiung, Lovers Lake, and Yunlin) of Chang Gung Memorial Medical Foundation in northern, middle, and southern Taiwan between 2010 and 2017. Datasets were collected from the electronic medical record (EMR) system built by the Chang Gung Medical Foundation. Patients with chronic liver disease with more than 2 visits in the EMR system who were diagnosed with cirrhosis defined using the International Classification of Diseases (ICD)-9 and ICD-10 codes (Table S1 in Multimedia Appendix 1) by clinical physicians with or without ESLD-related complications, such as HE, hepatorenal syndrome, ascites, spontaneous bacterial peritonitis, and esophageal varices, were enrolled. HE was defined as having ICD-9 code 572.2 and ICD-10 codes K76.82, B15.0, B16.0, B16.2, B19.0, G93.4, and G94.3 recorded in the EMR system. The exclusion criteria were patients who were younger than 18 years of age, those who had been diagnosed with malignant neoplasms of the liver (ICD-9 code: 155.0 or ICD-10 code: C22-C22.09) or HE at the time of enrollment, or those who had only a one-time-visit record before being lost to follow-up.

Ethical Considerations

This study was conducted in accordance with the ethical standards of the Declaration of Helsinki, and the protocol was approved by the ethics institutional review board of Chang Gung Memorial Hospital, Taiwan (approval: 201801291B0C504). The institutional review board approved the waiver of informed consent because of the deidentification of all health data collected from the EMR system. The data were collected from

XSL•FO
RenderX

patients treated at Chang Gung Memorial Hospital between 2010 and 2017.

Data Collection and Definitions

Datasets were collected from the EMR system. Individuals meeting the inclusion criteria and whose laboratory data were available within enrollment were included in this study. The laboratory measurements collected for ML included prothrombin time (PT), activated partial thromboplastin time, the international normalized ratio (INR), C-reactive protein (CRP), albumin, ammonia, alanine transaminase (ALT), aspartate transaminase (AST), serum bilirubin, γ-glutamyl transferase, serum bilirubin, creatinine, blood urea nitrogen (BUN), sodium (Na), potassium (K), lactate, uric acid, total cholesterol, triglyceride, fasting plasma glucose, high-density lipoprotein cholesterol levels, low-density lipoprotein cholesterol levels, white blood count, red blood cell, hemoglobin, and platelet. The MELD score was calculated according to the following formula [15]: $3.78 \times \log_e(\text{bilirubin [mg/dL]}) + 11.2 \times \log_e(\text{INR}) + 9.57 \times \log_e(\text{creatinine [mg/dL]}) + 6.43$.

Data Preprocessing and ML Modeling

This study followed the TRIPOD (Transparent Reporting of a Multivariable Prediction Model for Individual Prognosis or Diagnosis) reporting guidelines to ensure methodological transparency and reproducibility. A completed TRIPOD checklist is provided as Checklist 1. The datasets were randomly divided into training and testing datasets at a 3:1 ratio. We implemented random forest (RF), neural network, support vector machine (SVM), and extreme gradient boosting (XGBoost) for modeling in the training dataset. The models were built and evaluated using R (version 4.0.1; R Foundation for Statistical Computing) with the *xgboost* package (version 1.4.2). The testing dataset was performed for internal validation. Missing data were addressed through median imputation, where the median value was used to replace any unavailable or null value. Model training was completed in 2024 based on structured clinical data from EMR records.

The prediction target was the probability of developing HE, with the model output ranging from 0 to 1. This continuous output was transformed into a binary classification.

Model training used 10-fold cross-validation with hyperparameter tuning, but no alignment strategies (such as reinforcement learning or preference optimization) were used. Inference was based on structured variable inputs, and no text generation, prompt engineering, or large language models were involved in the modeling process.

Feature Selection and Imbalanced Data

To identify significant candidate features while eliminating noisy or redundant ones that could lead to an inefficient, impractical, or overfitting model, we used a wrapper method using the Boruta algorithm to rank the predictive features of HE. For practical purposes, we repeated the Boruta algorithm 300 times and selected the top 20 ranked features. To avoid the bias toward the majority class and enhance the overall accuracy and performance of the model, we used the synthetic minority over-sampling technique for imbalanced datasets.

Performance Evaluation and Interpretation

We assessed the area under the receiver operating characteristic curve (AUC-ROC) to discriminate the performance of the ML models. We further adopted the Youden index to evaluate the best corresponding cutoff sensitivities and specificities for the optimal performance of the ML algorithm. Then, we analyzed the model using the Shapley Additive Explanations (SHAP) plot to disclose the impact of the features on the output of the model prediction.

Statistical Analysis

Continuous variables were expressed as the median (IQR), and categorical variables by frequencies and percentages. ML modeling was performed using the statistical software package R (version 4.0.1) with the *Boruta* [16] and *Caret* packages [17]. Prediction models were compared using R with the DeLong method of the *pROC* package [18]. All statistic assessments were evaluated at a 2-sided α level of .05.

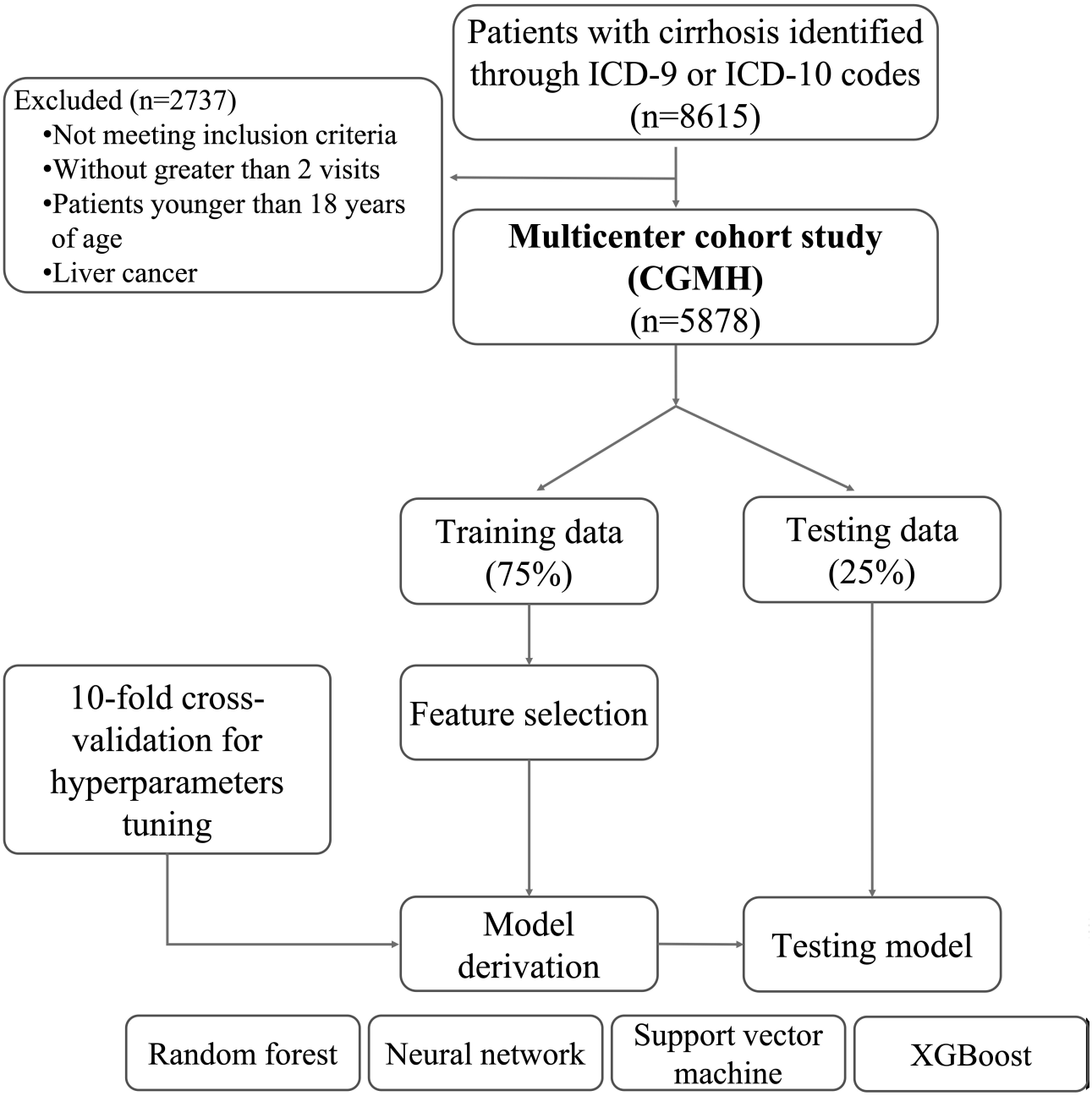
Results

Overview

A total of 8615 consecutive patients who had been diagnosed as cirrhosis, with or without ESLD-related complications, were enrolled in this study. These patients were identified from the EMR system in 3 academic medical centers and 5 community hospitals of Chang Gung Memorial Medical Foundation in Taiwan, between January 1, 2010, and December 31, 2017. After applying the exclusion criteria—including patients with fewer than 2 visits, those younger than 18 years of age, and those with liver cancer—5878 patients with cirrhosis were eligible for analysis, including 1187 with HE and 4691 without HE. Figure 1 shows a flowchart of the enrollment process.

XSL•FO
RenderX

Figure 1. Flowchart of the enrollment process. ICD: International Classification of Diseases; CGMH: Chang Gung Memorial Hospital; XGBoost: extreme gradient boosting.



Baseline Characteristics of the HE and Non-HE Groups in Patients With Noncancer-Related Liver Cirrhosis

The median age was slightly older in the HE group compared to the non-HE group (median 55, IQR 46-65 vs median 54, IQR 44-66 years; *P*=.04). There were no significant differences in sex or HCV infection between the groups. Specifically, 845 of 1187 (71.2%) patients in the HE group and 3227 of 4691 (68.8%) in the non-HE group were male, 342 of 1187 (28.8%) patients in the HE group and 1464 of 4691 (31.2%) in the non-HE group were female (*P*=.11). HCV infection was present in 211 of 1187 (17.8%) and 882 of 4691 (18.8%) patients in the HE and non-HE groups, respectively (*P*=.40). In contrast, the prevalence of HBV infection was higher in the HE group (351/1187, 30%) than in the non-HE group (961/4691, 20.5%; *P*<.001). Alcohol use was reported in 540 of 1187 (45.5%) patients with HE versus 1512 of 4691 (32.2%) patients without HE (*P*<.001). Sepsis occurred in 393 of 1187 (33.1%) patients with HE compared to 793 of 4691 (16.9%) without HE (*P*<.001). Mortality was also significantly higher in the HE group, with 425 (35.8%) deaths versus 502 (10.7%) deaths in the non-HE group (*P*<.001). In laboratory comparisons, patients in the HE group had significantly lower platelet counts, prolonged PT, activated partial thromboplastin time, and INR, higher serum levels of white blood count, ALT, AST, total bilirubin, direct bilirubin, γ-glutamyl transferase, ammonia, lactate, BUN, and creatinine, and lower levels of serum albumin, potassium, sodium, total cholesterol, high-density lipoprotein, and hemoglobin. No significant differences were observed in serum uric acid, low-density lipoprotein cholesterol, or blood sugar levels between the 2 groups.

XSL•FO
RenderX

Overall, in our multicenter retrospective longitudinal analysis, the HE group showed a greater tendency to have coagulopathy, hepatorenal syndrome, and hypoalbuminuria, which may have been the result of malnutrition or sarcopenia in the patients with noncancer-related liver cirrhosis. The baseline demographic and laboratory characteristics between the HE and non-HE groups are shown in Table 1.

XSL•FO
RenderX

Table . Comparisons of baseline characteristics between non-HE[a] and HE groups (n=5878).

Characteristics	HE (n=1187)	Non-HE (n=4691)	*P* value[b,c]
Age (years), median (IQR)	55 (46-65)	54 (44-66)	.04
Sex, n (%)			.11
Female	342 (28.8)	1464 (31.2)	
Male	845 (71.2)	3227 (68.8)	
Sepsis, n (%)	393 (33.1)	792 (16.9)	<.001
Hepatitis B virus, n (%)	351 (30)	961 (20.5)	<.001
Hepatitis C virus, n (%)	211 (17.8)	882 (18.8)	.40
Alcohol use, n (%)	540 (45.5)	1512 (32.2)	<.001
Death, n (%)	425 (35.8)	502 (10.7)	<.001
International normalized ratio, median (IQR)	1.56 (1.30-2.00)	1.20 (1.10-1.46)	<.001
Prothrombin time, median (IQR)	16.5 (13.7-21.2)	13.1 (11.4-15.7)	<.001
Activated partial thromboplastin time, median (IQR)	40 (33-52)	31 (29-37)	<.001
C-reactive protein, median (IQR)	22 (10-46)	17 (4-53)	<.001
Albumin, median (IQR)	2.60 (2.30-2.90)	3.00 (2.50-3.64)	<.001
Alanine transaminase, median (IQR)	37 (23-66)	31 (19-54)	<.001
Aspartate transaminase, median (IQR)	73 (45-131)	48 (29-90)	<.001
Total bilirubin, median (IQR)	4 (2-12)	1 (1-3)	<.001
Direct bilirubin, median (IQR)	3.4 (0.9-10.9)	0.3 (0.2-1.0)	<.001
γ-Glutamyl transferase, median (IQR)	66 (32-153)	60 (21-163)	.02
Ammonia, median (IQR)	129 (91-182)	99 (72-138)	<.001
Blood urea nitrogen, median (IQR)	20 (11-42)	15 (10-24)	<.001
Creatinine, median (IQR)	0.97 (0.63-1.83)	0.82 (0.62-1.18)	<.001
Lactate, median (IQR)	23 (16-45)	18 (12-48)	.004
Sodium, median (IQR)	138.0 (134.0-141.0)	139.0 (136.0-141.0)	<.001
Potassium, median (IQR)	3.60 (3.10-4.10)	3.80 (3.40-4.20)	<.001
Uric acid, median (IQR)	5.50 (3.48-8.20)	6.00 (4.60-7.50)	.08
Total cholesterol, median (IQR)	125 (98-155)	146 (117-175)	<.001
High-density lipoprotein cholesterol, median (IQR)	25 (14-33)	31 (20-42)	<.001
Low-density lipoprotein cholesterol, median (IQR)	67 (50-92)	76 (55-102)	.07
Sugar, median (IQR)	131 (99-184)	135 (101-192)	.60
White blood count (1000), median (IQR)	6.8 (4.6-10.1)	6.1 (4.2-8.7)	<.001
Red blood cell, median (IQR)	3.12 (2.71-3.60)	3.53 (2.98-4.19)	<.001
Hemoglobin, median (IQR)	9.70 (8.50-11.00)	10.40 (8.90-12.40)	<.001
Hematocrit, median (IQR)	29 (26-32)	31 (27-37)	<.001
Mean corpuscular volume, median (IQR)	93 (86-99)	90 (85-96)	<.001
Mean corpuscular hemoglobin, median (IQR)	31.5 (29.2-33.8)	30.4 (28.3-32.4)	<.001

XSL•FO
RenderX

Characteristics	HE (n=1187)	Non-HE (n=4691)	*P* value[b,c]
Mean corpuscular hemoglobin concentration, median (IQR)	33.85 (32.90-34.80)	33.50 (32.60-34.40)	<.001
Red blood cell distribution width, median (IQR)	17.7 (15.9-20.3)	16.0 (14.5-18.4)	<.001
Platelet (1000), median (IQR)	78 (52-115)	106 (63-179)	<.001

[a]HE: hepatic encephalopathy.

[b]*P* values calculated using Pearson chi-square test for categorical variables [19].

[c]*P* values calculated using the Wilcoxon rank sum test for nonnormally distributed continuous variables [20].

XGBoost Exhibited the Best Discriminatory Performance Compared With All ML Algorithms and the MELD Score in Both the Training and Validation Datasets

We further performed the 4 AutoML algorithms, including RF, neural network, SVM, and XGBoost, to compare their performance in terms of predicting HE in patients with noncancer-related ESLD using the training dataset in the EMR system compared to the MELD score and performed further validation using the testing dataset. We first demonstrated that XGBoost exhibited the best discriminatory performance (AUC-ROC 0.86, 95% CI 0.83 - 0.88) compared with RF (AUC-ROC 0.82, 95% CI 0.80 - 0.85), neural network (AUC-ROC 0.79, 95% CI 0.76 - 0.81), SVM (AUC-ROC 0.77, 95% CI 0.73 - 0.80), and the MELD score (AUC-ROC 0.74, 95% CI 0.71 - 0.77; Tables 2 and 3 and Figure 2). The cutoff value by Youden index for XGBoost for discriminating HE was 0.25 (training dataset: sensitivity 80%, 95% CI 0.77 - 0.83; specificity 81%, 95% CI 0.80 - 0.82; positive predictive value [PPV] 0.52, 95% CI 0.49 - 0.54; negative predictive value [NPV] 0.94, 95% CI 0.93 - 0.95; positive likelihood ratio 4.22, 95% CI 3.91 - 4.55; negative likelihood ratio 0.25, 95% CI 0.21 - 0.28; and testing dataset: sensitivity 72%, 95% CI 0.67 - 0.77; specificity 80%, 95% CI 0.78 - 0.82; PPV 0.48, 95% CI 0.43 - 0.53; NPV 0.92, 95% CI 0.90 - 0.94; positive likelihood ratio 3.64, 95% CI 3.18 - 4.16; negative likelihood ratio 0.35, 95% CI 0.29 - 0.42; Table 4).

Table . Performance of the build prediction model in training and testing datasets.

Methods and dataset		Accuracy (95% CI)	Sensitivity (95% CI)	Specificity (95% CI)	AUC-ROC[a] (95% CI)
Random forest					
	Training	1.000 (0.99 - 1.00)	1.00	1.00	1.00 (1.00 - 1.00)
	Testing	0.82 (0.80 - 0.84)	0.32	0.95	0.82 (0.80 - 0.85)
Neural network					
	Training	0.81 (0.80 - 0.82)	0.22	0.96	0.80 (0.79 - 0.82)
	Testing	0.80 (0.78 - 0.82)	0.25	0.94	0.79 (0.76 - 0.81)
Support vector machine					
	Training	0.82 (0.81 - 0.83)	0.18	0.98	0.80 (0.78 - 0.81)
	Testing	0.81 (0.79 - 0.83)	0.20	0.97	0.77 (0.73 - 0.80)
XGBoost[b]					
	Training	0.85 (0.84 - 0.86)	0.42	0.96	0.88 (0.87 - 0.89)
	Testing	0.84 (0.82 - 0.85)	0.38	0.95	0.86 (0.83 - 0.88)
MELD[c] score					
	Training	N/A[d]	N/A	N/A	0.75 (0.74 - 0.77)
	Training	N/A	N/A	N/A	0.74 (0.71 - 0.77)

[a]AUC-ROC: area under the receiver operating characteristic curve.

[b]XGBoost: extreme gradient boosting.

[c]MELD: model for end-stage liver disease.

[d]N/A: not applicable.

XSL•FO
RenderX

Table . Performance of the build prediction model in training and testing datasets.

Methods	Dataset	Accuracy (95% CI)	Sensitivity (95% CI)	Specificity (95% CI)	AUC-ROC[a] (95% CI)	*P* value
Random forest	Testing	0.82 (0.80 - 0.84)	0.32	0.95	0.82 (0.80 - 0.85)	.05
Neural network	Testing	0.80 (0.78 - 0.82)	0.25	0.94	0.79 (0.76 - 0.81)	<.001
Support vector machine	Testing	0.81 (0.79 - 0.83)	0.20	0.97	0.77 (0.73 - 0.80)	<.001
XGBoost[b]	Testing	0.84 (0.82 - 0.85)	0.38	0.95	0.86 (0.83 - 0.88)	—[c]
MELD[d] score	Training	N/A[e]	N/A	N/A	0.74 (0.71 - 0.77)	<.001

[a]AUC-ROC: area under the receiver operating characteristic curve.

[b]XGBoost: extreme gradient boosting.

[c]Not available.

[d]MELD: model for end-stage liver disease.

[e]N/A: not applicable.

XSL•FO
RenderX

Figure 2. Performance of the machine learning models: (A) random forest, (B) neural network, (C) support vector machine, (D) extreme gradient boosting, and (E) model for end-stage liver disease score.

XSL•FO
RenderX

Table . Performance of the extreme gradient boosting model for hepatic encephalopathy prediction in training and validation datasets (Youden index=0.25).

	Training set	Testing set
Sensitivity (95% CI)	0.80 (0.77-0.83)	0.72 (0.67-0.77)
Specificity (95% CI)	0.81 (0.80-0.82)	0.80 (0.78-0.82)
Positive predictive value (95% CI)	0.52 (0.49-0.54)	0.48 (0.43-0.53)
Negative predictive value (95% CI)	0.94 (0.93-0.95)	0.92 (0.90-0.94)
Positive likelihood ratio (95% CI)	4.22 (3.91-4.55)	3.64 (3.18-4.16)
Negative likelihood ratio (95% CI)	0.25 (0.21-0.28)	0.35 (0.29-0.42)

Regarding performance in predicting incident HE, XGBoost achieved the best accuracy in the testing dataset compared with RF, neural network, SVM, and the MELD score (XGBoost: accuracy 0.84, 95% CI 0.82 - 0.85; RF: accuracy 0.82, 95% CI 0.80 - 0.84; neural network: accuracy 0.80, 95% CI 0.78 - 0.82; SVM: accuracy 0.81, 95% CI 0.79 - 0.83). These findings strongly indicate that our ML-based XGBoost algorithm is a superior tool for predicting HE in patients with noncancer-related cirrhosis in comparison with the other ML models and traditional MELD scores, especially for ruling out disease when the finding returns a negative result; this could be an applicable tool to guide clinicians in palliative care clinical settings (Tables 2-4 and Table S2 in Multimedia Appendix 1).

Serum Ammonia Was the Foremost Important Feature, Followed by Other Variables, in the ML-Based XGBoost Algorithm for Predicting HE in Patients With Noncancer-Related ESLD

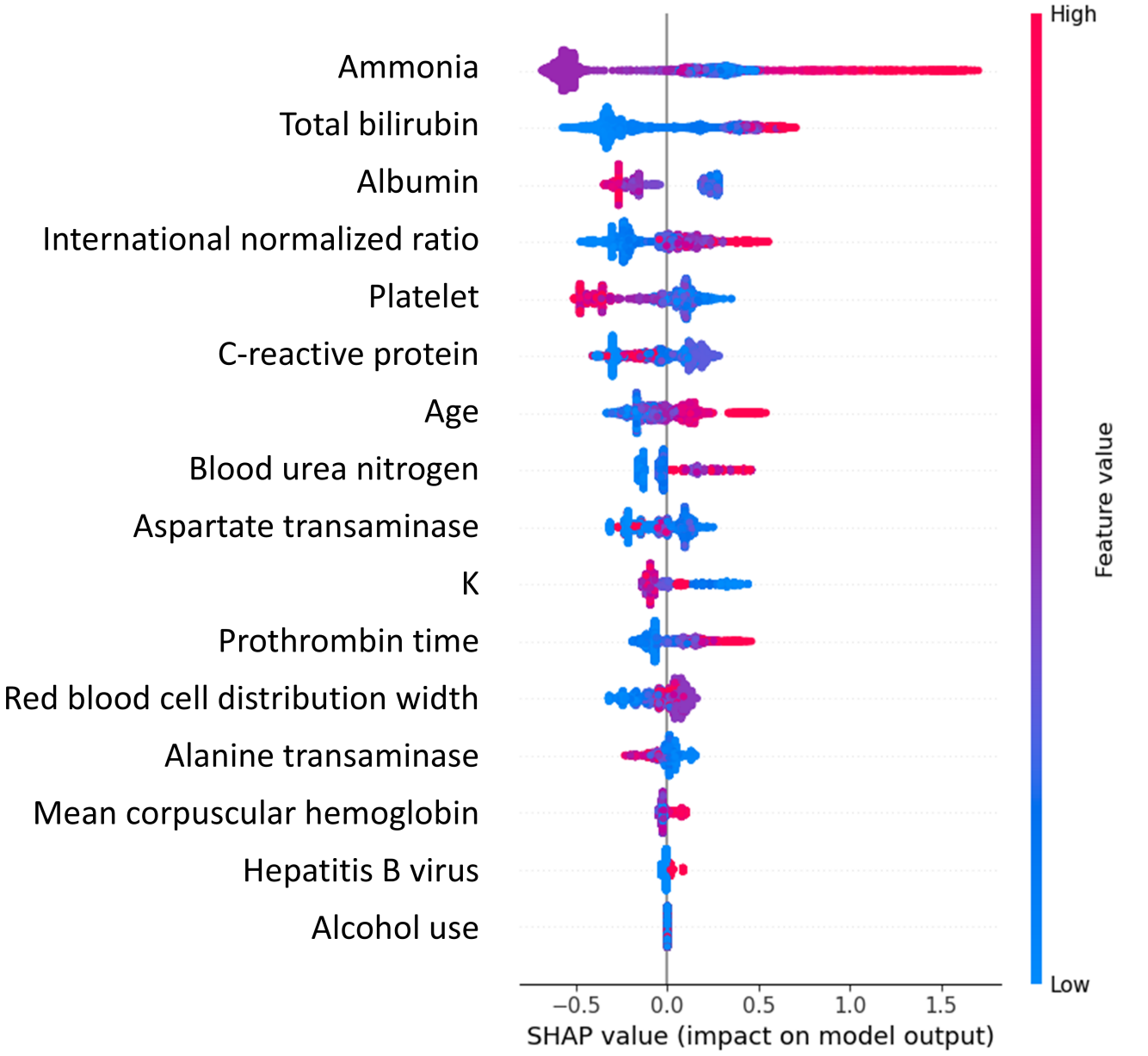
Additionally, we constructed a SHAP to reveal the weight of each feature on the outcomes of the trained model's predictability based on feature importance. We demonstrated the essential features' contribution to the predictive outcomes, including serum levels of ammonia, total bilirubin, INR, CRP, patient age, total platelet count, BUN, PT, K, AST, albumin, red blood cell distribution width, ALT, mean corpuscular hemoglobin, and history of HBV infection (Table 5). Based on the SHAP values of feature importance, we further disclosed that higher levels of serum ammonia, total bilirubin, INR, older age, BUN, and PT, lower serum levels of albumin and serum K, and lower platelet counts result in a higher probability of HE in patients with noncancer-related ESLD. Furthermore, among the 15 key variables in the AutoML model based on the XGBoost algorithm, ammonia was the most important feature impacting the probability of HE risk, followed by total bilirubin, INR, CRP, age, platelet, BUN, PT, and serum K (Figure 3).

Table . Feature importance from the extreme gradient boosting model based on Shapley Additive Explanations values.

Rank	Clinical feature
1	Ammonia
2	Total bilirubin
3	Albumin
4	International normalized ratio
5	Platelet
6	C-reactive protein
7	Age
8	Blood urea nitrogen
9	Aspartate transaminase
10	Potassium
11	Prothrombin time
12	Red blood cell distribution width
13	Alanine transaminase
14	Mean corpuscular hemoglobin
15	Hepatitis B virus
16	Alcohol use

XSL•FO
RenderX

Figure 3. SHAP summary plot to explain the feature importance obtained by the extreme gradient boosting algorithm. Features with higher feature value (red) and positive SHAP value (on the right side) show a positive association, while features with higher feature value (blue) and negative SHAP value (on the left side) show a negative association. K: potassium; SHAP: Shapley Additive Explanations.



Taken together, compared with other ML-based models, such as RF, neural network, and SVM, our ML-based XGBoost algorithm demonstrated the best performance for HE predictability in patients with noncancer-related ESLD. Among the variables in the XGBoost model, serum ammonia levels, together with other feature variables, constituted the most important influence regarding HE predictability in patients with noncancer-related cirrhosis.

Discussion

Principal Findings

In our multicenter retrospective longitudinal study, we developed an ML-based prognostic model to improve the early prediction of HE in patients with noncancer-related cirrhosis. Among the evaluated algorithms, the XGBoost model consistently demonstrated superior predictive performance in terms of discriminability, accuracy, and robustness—particularly in ruling out HE with high NPV—across both training and validation datasets.

The choice of XGBoost was driven by its technical advantages over other ML algorithms such as RF, neural network, and SVM. Unlike RF, which may experience overfitting in complex high-dimensional data, XGBoost incorporates regularization techniques that reduce variance and improve generalizability. Additionally, XGBoost handles multicollinearity and missing values more effectively than logistic regression and is computationally efficient for structured tabular data. These characteristics make XGBoost a particularly well-suited algorithm for clinical prediction tasks using EMR datasets. Our novel ML-based XGBoost predictive model is an applicable tool to guide clinicians in shared decision-making of treatment strategy to further improve patient care and reduce their distress

XSL•FO
RenderX

from morbid complications in clinical settings of noncancer-related populations.

To enhance model interpretability, we conducted a SHAP analysis to identify and visualize the contribution of individual predictors to the model output. This analysis revealed that serum ammonia is the most important feature, followed by bilirubin, INR, age, and BUN, which are positively associated with increased HE risk; whereas albumin, platelet counts, and serum potassium are negatively associated with HE risk. Notably, serum potassium and transaminases emerged as key predictors of HE—findings that warrant further clinical interpretation. From a pathophysiological perspective, hypokalemia is known to exacerbate HE by increasing renal ammonia production and systemic ammonia load [21,22]. This mechanistic link is supported by our data, where lower serum potassium was associated with increased HE risk. Similarly, elevated AST and ALT levels reflect ongoing hepatic inflammation or necroinflammation, which may impair ammonia detoxification, thereby promoting HE [23]. These markers, therefore, not only reflect liver injury but also serve as early warning signs for impending encephalopathy, reinforcing their clinical utility in risk stratification and monitoring. Furthermore, to our knowledge, this is the first study to predict HE in a Taiwanese adult population using an ML algorithm. Our use of SHAP further enhances model transparency and interpretability—both of which are critical for clinical adoption. SHAP values enable clinicians to understand how individual variables influence predictions, thereby building trust and supporting shared decision-making with patients.

Despite the pathogenesis of HE not being fully understood, an increasing number of studies have shown that various forms of inflammation, such as systemic inflammation, neuroinflammation, endotoxemia, and ammonia-inflammation synergism, significantly contribute to the development of HE [24]. Serum CRP, which is known as an inflammation marker, is associated with the development of HE and can serve as a predictor of adverse outcomes and increased risk of HE in patients hospitalized with liver cirrhosis [25,26]. In our data, the HE group exhibited a significantly increased level of serum CRP compared with the non-HE group (P<.001) among patients with noncancer-related ESLD. It is of note that our SHAP for feature importance analysis did not show a strong positive influence of serum CRP levels on the increase in HE risk in patients with noncancer cirrhosis. One of the possible reasons for these different study findings could be that the baseline settings of the populations differed between these 2 studies as well as the fact that the pathogenic etiology of HE in populations without cancer differs significantly from that in patients with terminal cancer. In our dataset, the results could have been influenced by outliers of serum CRP because the median serum CRP level in the HE group was significantly higher than that in the non-HE group. This indicates that CRP still plays an important role in HE occurrence.

Comparison to Prior Work

Our findings revealed notable differences in baseline characteristics between patients with noncancer-related ESLD with and without HE, highlighting the heterogeneity of populations with cirrhosis and the multifactorial nature of HE development. Specifically, patients with HE exhibited higher prevalences of HBV infection, alcohol use, sepsis, and mortality rates compared with their counterparts without HE. In another study [3], among 49,164 patients diagnosed with HE, 24,183 (49.2%) were affected by alcohol-related cirrhosis, 18,352 (37.3%) had HCV infection, and only 2589 (5.3%) had HBV-related cirrhosis, with some cases showing overlap. These differences may be due to the high prevalence of HBV infection in Taiwan. However, other research indicates a decline in the age-standardized incidence rates for liver cirrhosis due to HBV globally from 1990 to 2019, while the incidence rates for nonalcoholic fatty liver disease, alcohol use, and other causes increased during the same period [2]. This suggests a potential shift in the etiology of cirrhosis.

Importantly, our study demonstrates that the XGBoost algorithm has superior discriminatory performance in predicting HE compared with other ML algorithms and MELD scores. The robust sensitivity, specificity, PPV, NPV, and accuracy of the XGBoost model underscore its potential applicability as a valuable clinical decision support tool for early HE detection and risk stratification in populations with noncancer-related cirrhosis. The MELD score, initially designed to predict survival after elective transjugular intrahepatic portosystemic shunt placement, has been validated for predicting survival across diverse patient cohorts with varying liver disease severity and from different geographic and temporal backgrounds. Moreover, the MELD score is widely used to prioritize liver transplantation, primarily relying on serum bilirubin, creatinine, and INR levels. Although it provides a general assessment of liver function, it may not fully capture the multifactorial nature of HE development. By contrast, the capacity of ML algorithms to manage complex interactions and nonlinear relationships is a significant advantage that can improve the accuracy of prediction models. Our XGBoost model incorporated a broader range of variables, including ammonia, total bilirubin, INR, age, BUN, albumin, platelet count, and serum K, allowing for a more detailed and accurate prediction of HE risk. This approach may offer valuable insights into disease pathogenesis and prognosis.

Recent studies have demonstrated the value of ML in liver disease prognostication. Verma et al [27] stratified patients with acute-on-chronic liver failure into survival-based clusters using integrated ML methods. Malik et al [28] reviewed ML applications in predicting esophageal variceal bleeding, while Müller et al [29] identified early cirrhosis decompensation using ML models. Other studies used neural networks to forecast 1-year mortality after variceal bleeding [30] or liver transplantation [31], emphasizing the trend toward long-term outcome modeling. These findings underscore ML's expanding role in liver disease prediction. Our study contributes to this field by focusing on early HE prediction in noncancer-related cirrhosis using a transparent and interpretable XGBoost framework. Another regional study conducted on 1256 patients with cirrhosis with unbalanced data used several ML methods, specifically SVM, logistic regression, and CatBoost, to predict HE [32]. Although the weighted RF model emerged with an accuracy of 0.8732 (95% CI 0.8711 - 0.8752) and an AUC-ROC

XSL•FO
RenderX

of 0.82, in that study, the HE predictability was far inferior to our ML-based XGBoost model. Our XGBoost model significantly outperformed weighted RF, achieving an accuracy of 0.84 (95% CI 0.82 - 0.85) and an AUC-ROC of 0.86 (95% CI 0.83 - 0.88). It showed advantages on XGBoost. XGBoost uses boosting with regularization to reduce overfitting and improve generalization. It also handles missing data and multicollinearity effectively. XGBoost is more efficient and interpretable for structured clinical data better than SVM and neural networks [33,34]. Additionally, we applied SHAP to identify and visualize the contributions of individual features to the model's predictions. Its consistent and locally accurate attributions improve interpretability, facilitating clinical trust by clarifying how key variables may influence disease outcomes [35].

Limitations

While our study contributes to advancing the understanding of HE prediction and prognostication of patients with noncancer-related cirrhosis, several limitations warrant consideration. First, despite our application of the Boruta algorithm for feature selection and the use of the synthetic minority over-sampling technique for imbalanced datasets, retrospective analyses still inherently carried biases related to data completeness, documentation accuracy, and confounding variables. Second, the generalizability of our findings to diverse patient populations and health care settings may be limited. As aforementioned, the different etiology of ESLD may affect model application.

Future Directions

Building upon the aforementioned limitations, future research should prioritize prospective validation in diverse populations and explore the integration of the predictive model into clinical decision support systems. Moreover, external validation across different institutions and geographic settings is essential to evaluate the model's generalizability and transportability. Embedding the model into cloud-based platforms or EMR systems may further enhance its accessibility and facilitate real-world clinical implementation. Additionally, regarding the other scoring systems, such as the Bilirubin-Albumin-Beta-Blocker-Statin score and MASQ-HE score developed by Tapper et al [36,37], both include adding medications, such as the use of nonselective β-blockers and statins, in addition to quality of life and physical function, to improve the performance in terms of the predictability of HE risk. Therefore, integrating additional clinical variables may enhance model accuracy for the prediction of HE and thus should be considered in the future development of ML-based models.

Conclusions

Our ML-based XGBoost model demonstrated superior predictive performance for the early detection and prognostication of HE in patients with noncancer-related cirrhosis. Beyond its predictive accuracy, the model shows promise as a clinically valuable tool for use in terminal care settings, outperforming previously established ML algorithms and conventional prognostic scores such as the MELD score. To the best of our knowledge, this is the first ML-based model specifically developed for prognostication and HE prediction in a Taiwanese adult population with noncancer-related cirrhosis—a subgroup with higher prevalence and more unpredictable disease trajectories compared to patients with cancer-related cirrhosis. By incorporating a broader set of clinical features and leveraging SHAP-based interpretability, our model facilitates more precise risk stratification and may support clinicians in making informed decisions aimed at preventing severe complications and improving patients' quality of life. Future studies are warranted to externally validate this model in larger and more diverse populations and to assess its clinical utility through prospective follow-up of patient outcomes.

Acknowledgments

This work was supported by Chang Gung Memorial Hospital Research Projects (CMRPG2M0041, CMRPVVM0182, CORPVVN0131, and CORPG3P0622). The authors are grateful to the members of the Maintenance Project of the Biostatistical Consultation Centre at Chang Gung Memorial Hospital (Linkou and Keelung branches) for assistance with the data analysis from the Chang Gung Research Database provided by Chang Gung Memorial Hospital. The sponsors had no role in study design, data collection, analysis, interpretation, manuscript writing, or the decision to submit the manuscript for publication.

Authors' Contributions

HYC and YWT conceived and designed the study. YWT was responsible for data acquisition. Data analysis and interpretation were performed by HYC, WCY, and YWT. HYC drafted the manuscript, and statistical analyses were conducted by HYC and YWT. The study was supervised by YWT. All authors reviewed and approved the final manuscript.

Conflicts of Interest

None declared.

Multimedia Appendix 1
Supplementary tables.
[DOCX File, 22 KB - medinform_v13i1e71229_app1.docx]

XSL•FO
RenderX

Checklist 1
TRIPOD (Transparent Reporting of a Multivariable Prediction Model for Individual Prognosis or Diagnosis) checklist.
[PDF File, 176 KB - medinform_v13i1e71229_app2.pdf]

References

1. GBD 2017 Cirrhosis Collaborators. The global, regional, and national burden of cirrhosis by cause in 195 countries and territories, 1990-2017: a systematic analysis for the global burden of disease study 2017. Lancet Gastroenterol Hepatol 2020;5:245-266. [doi: 10.1016/S2468-1253(19)30349-8]
2. Wu XN, Xue F, Zhang N, et al. Global burden of liver cirrhosis and other chronic liver diseases caused by specific etiologies from 1990 to 2019. BMC Public Health 2024 Feb 3;24(1):363. [doi: 10.1186/s12889-024-17948-6] [Medline: 38310221]
3. Tapper EB, Aberasturi D, Zhao Z, Hsu CY, Parikh ND. Outcomes after hepatic encephalopathy in population-based cohorts of patients with cirrhosis. Aliment Pharmacol Ther 2020 Jun;51(12):1397-1405. [doi: 10.1111/apt.15749] [Medline: 32363684]
4. Elsaid MI, John T, Li Y, Pentakota SR, Rustgi VK. The health care burden of hepatic encephalopathy. Clin Liver Dis 2020 May;24(2):263-275. [doi: 10.1016/j.cld.2020.01.006] [Medline: 32245532]
5. Riggio O, Celsa C, Calvaruso V, et al. Hepatic encephalopathy increases the risk for mortality and hospital readmission in decompensated cirrhotic patients: a prospective multicenter study. Front Med (Lausanne) 2023;10(10):1184860. [doi: 10.3389/fmed.2023.1184860] [Medline: 37305121]
6. Louissaint J, Deutsch-Link S, Tapper EB. Changing epidemiology of cirrhosis and hepatic encephalopathy. Clin Gastroenterol Hepatol 2022 Aug;20(8S):S1-S8. [doi: 10.1016/j.cgh.2022.04.036] [Medline: 35940729]
7. Pérez-Matos MC, Jiang ZG, Tapper EB. Factors that affect results of psychometric tests to identify patients with minimal hepatic encephalopathy. Clin Gastroenterol Hepatol 2018 Nov;16(11):1836-1838. [doi: 10.1016/j.cgh.2018.03.010] [Medline: 29551739]
8. White paper on palliative and hospice care policy in Taiwan. : National Health Research Institutes; 2019 URL: https://www.nhri.edu.tw/Files/2020-02-25-001.pdf [accessed 2025-07-19]
9. Cheng SH, Chiang TL. The effect of universal health insurance on health care utilization in Taiwan. Results from a natural experiment. JAMA 1997 Jul 9;278(2):89-93. [doi: 10.1001/jama.278.2.89] [Medline: 9214512]
10. Cheng TM. Taiwan's new national health insurance program: genesis and experience so far. Health Aff (Millwood) 2003;22(3):61-76. [doi: 10.1377/hlthaff.22.3.61] [Medline: 12757273]
11. Lin LY, Warren-Gash C, Smeeth L, Chen PC. Data resource profile: the National Health Insurance Research Database (NHIRD). Epidemiol Health 2018;40:e2018062. [doi: 10.4178/epih.e2018062] [Medline: 30727703]
12. Woodland H, Buchanan RM, Pring A, et al. Inequity in end-of-life care for patients with chronic liver disease in England. Liver Int 2023 Nov;43(11):2393-2403. [doi: 10.1111/liv.15684] [Medline: 37519025]
13. Langberg KM, Kapo JM, Taddei TH. Palliative care in decompensated cirrhosis: a review. Liver Int 2018 May;38(5):768-775. [doi: 10.1111/liv.13620] [Medline: 29112338]
14. Roth K, Lynn J, Zhong Z, Borum M, Dawson NV. Dying with end stage liver disease with cirrhosis: insights from SUPPORT. Study to Understand Prognoses and Preferences for Outcomes and Risks of Treatment. J Am Geriatr Soc 2000 May;48(S1):S122-S130. [Medline: 10809465]
15. Malinchoc M, Kamath PS, Gordon FD, Peine CJ, Rank J, ter Borg PC. A model to predict poor survival in patients undergoing transjugular intrahepatic portosystemic shunts. Hepatology 2000 Apr;31(4):864-871. [doi: 10.1053/he.2000.5852] [Medline: 10733541]
16. Kursa MB, Rudnicki WR. Feature selection with the Boruta package. J Stat Softw 2010;36:1-13. [doi: 10.18637/jss.v036.i11]
17. Kuhn M. Building predictive models in R using the caret package. J Stat Softw 2008;28. [doi: 10.18637/jss.v028.i05]
18. Figueroa RL, Zeng-Treitler Q, Kandula S, Ngo LH. Predicting sample size required for classification performance. BMC Med Inform Decis Mak 2012 Feb 15;12:8. [doi: 10.1186/1472-6947-12-8] [Medline: 22336388]
19. Pearson K. On the criterion that a given system of deviations from the probable in the case of a correlated system of variables is such that it can be reasonably supposed to have arisen from random sampling. Philos Mag (Abingdon) 1900;50(302):157-175. [doi: 10.1080/14786440009463897]
20. Wilcoxon F. Individual comparisons by ranking methods. Biometrics Bull 1945;1(6):80-83. [doi: 10.2307/3001968]
21. Häussinger D, Kircheis G, Fischer R, Schliess F, vom Dahl S. Hepatic encephalopathy in chronic liver disease: a clinical manifestation of astrocyte swelling and low-grade cerebral edema? J Hepatol 2000 Jun;32(6):1035-1038. [doi: 10.1016/s0168-8278(00)80110-5] [Medline: 10898326]
22. Ullah H, Shabana H, Rady MA, et al. Hypokalemia as a responsible factor related with the severity of hepatic encephalopathy: a wide multination cross-sectional study. Ann Med Surg (Lond) 2023 Jun;85(6):2427-2431. [doi: 10.1097/MS9.0000000000000470] [Medline: 37363515]
23. Butterworth RF. Pathogenesis of hepatic encephalopathy: new insights from neuroimaging and molecular studies. J Hepatol 2003 Aug;39(2):278-285. [doi: 10.1016/s0168-8278(03)00267-8] [Medline: 12873828]
24. Luo M, Guo JY, Cao WK. Inflammation: a novel target of current therapies for hepatic encephalopathy in liver cirrhosis. World J Gastroenterol 2015 Nov 7;21(41):11815-11824. [doi: 10.3748/wjg.v21.i41.11815] [Medline: 26557005]

XSL•FO
RenderX

25. Iwasa M, Sugimoto R, Mifuji-Moroka R, et al. Factors contributing to the development of overt encephalopathy in liver cirrhosis patients. Metab Brain Dis 2016 Oct;31(5):1151-1156. [doi: 10.1007/s11011-016-9862-6] [Medline: 27353278]
26. Formentin C, Zarantonello L, Mangini C, Frigo AC, Montagnese S, Merkel C. Clinical, neuropsychological and neurophysiological indices and predictors of hepatic encephalopathy (HE). Liver Int 2021 May;41(5):1070-1082. [doi: 10.1111/liv.14785] [Medline: 33411388]
27. Verma N, Garg P, Valsan A, et al. Integrated unsupervised and supervised machine learning unveils and predicts the Clusters with Distinct Profiles and Survival in Acute-on-Chronic Liver Failure (CLUSTER-ACLF). J Clin Exp Hepatol 2023;13:S2. [doi: 10.1016/j.jceh.2023.07.011]
28. Malik S, Tenorio BG, Moond V, Dahiya DS, Vora R, Dbouk N. Systematic review of machine learning models in predicting the risk of bleed/grade of esophageal varices in patients with liver cirrhosis: a comprehensive methodological analysis. J Gastroenterol Hepatol 2024 Oct;39(10):2043-2059. [doi: 10.1111/jgh.16645] [Medline: 38886175]
29. Müller SE, Casper M, Ripoll C, et al. Machine learning models predicting decompensation in cirrhosis. J Gastrointestin Liver Dis 2025 Mar 27;34(1):71-80. [doi: 10.15403/jgld-5876] [Medline: 40153826]
30. Rech MM, Corso LL, Bó EFD, et al. Su1581 prospective validation of a neural network model for the prediction of 1-year mortality in cirrhotic patients with acute esophageal variceal bleeding. Gastroenterology 2023 May;164(6):S-1341. [doi: 10.1016/S0016-5085(23)04120-3]
31. Soldera J, Tomé F, Corso LL, et al. 590 predicting 30 and 365-day mortality after liver transplantation using a machine learning algorithm. Gastroenterology 2021 May;160(6):S-789. [doi: 10.1016/S0016-5085(21)02602-0]
32. Yang H, Li X, Cao H, et al. Using machine learning methods to predict hepatic encephalopathy in cirrhotic patients with unbalanced data. Comput Methods Programs Biomed 2021 Nov;211(211):106420. [doi: 10.1016/j.cmpb.2021.106420] [Medline: 34555589]
33. Chen T, Guestrin C. XGBoost: a scalable tree boosting system. Presented at: KDD '16: The 22nd ACM SIGKDD International Conference on Knowledge Discovery and Data Mining; Aug 13-17, 2016; San Francisco, CA, United States. [doi: 10.1145/2939672.2939785]
34. Shwartz-Ziv R, Armon A. Tabular data: deep learning is not all you need. Inform Fusion 2022 May;81:84-90. [doi: 10.1016/j.inffus.2021.11.011]
35. Lundberg SM, Lee SI. A unified approach to interpreting model predictions. Presented at: Proceedings of the 31st International Conference on Neural Information Processing Systems; Dec 4-9, 2017; Long Beach, CA, United States p. 4768-4777.
36. Tapper EB, Parikh ND, Sengupta N, et al. A risk score to predict the development of hepatic encephalopathy in a population-based cohort of patients with cirrhosis. Hepatology 2018 Oct;68(4):1498-1507. [doi: 10.1002/hep.29628] [Medline: 29091289]
37. Tapper EB, Zhao L, Nikirk S, et al. Incidence and bedside predictors of the first episode of overt hepatic encephalopathy in patients with cirrhosis. Am J Gastroenterol 2020 Dec;115(12):2017-2025. [doi: 10.14309/ajg.0000000000000762] [Medline: 32773463]

Abbreviations

ALT: alanine transaminase
AST: aspartate transaminase
AUC: area under the curve
AUC-ROC: area under the receiver operating characteristic curve
BUN: blood urea nitrogen
CRP: C-reactive protein
EMR: electronic medical record
ESLD: end-stage liver disease
HBV: hepatitis B virus
HCV: hepatitis C virus
HE: hepatic encephalopathy
ICD: International Classification of Diseases
INR: international normalized ratio
MELD: model for end-stage liver disease
ML: machine learning
NPV: negative predictive value
PPV: positive predictive value
PT: prothrombin time
RF: random forest
SHAP: Shapley Additive Explanations
SVM: support vector machine
TRIPOD: Transparent Reporting of a Multivariable Prediction Model for Individual Prognosis or Diagnosis

XSL•FO
RenderX

XGBoost: extreme gradient boosting

Edited by A Benis; submitted 21.01.25; peer-reviewed by H Lin, J Soldera; revised version received 13.06.25; accepted 16.06.25; published 06.08.25.

Please cite as:
Chen HY, Cheng YH, Yeh WC, Chen YC, Tsai YW
A Machine Learning–Based Prognostication Model Enhances Prediction of Early Hepatic Encephalopathy in Patients With Noncancer-Related Cirrhosis: Multicenter Longitudinal Cohort Study in Taiwan
JMIR Med Inform 2025;13:e71229
URL: https://medinform.jmir.org/2025/1/e71229
doi:10.2196/71229

© Hsin-Yu Chen, Yiu-Hua Cheng, Wei-Chung Yeh, Yi-Chuan Chen, Yi-Wen Tsai. Originally published in JMIR Medical Informatics (https://medinform.jmir.org), 6.8.2025. This is an open-access article distributed under the terms of the Creative Commons Attribution License (https://creativecommons.org/licenses/by/4.0/), which permits unrestricted use, distribution, and reproduction in any medium, provided the original work, first published in JMIR Medical Informatics, is properly cited. The complete bibliographic information, a link to the original publication on https://medinform.jmir.org/, as well as this copyright and license information must be included.

XSL•FO
RenderX

Probability-Based Early Warning for Seasonal Influenza in China: Model Development Study

Jinzhao Cui[1*], MM; Ting Zhang[1*], MD; Yifeng Shen[2*], MM; Xiaoli Wang[3*], MD; Liuyang Yang[4], MD; Xuefeng Huang[1], MM; Qiang Huang[1], MM; Yu Yang[1], MM; Weizhong Yang[1], Prof Dr Med; Zhongjie Li[1], Prof Dr Med

[1]School of Population Medicine and Public Health, Chinese Academy of Medical Sciences & Peking Union Medical College, No. 31, Beijigesantiao street, Dongcheng District, Beijing, China

[2]Shanghai Pudong New Area Center for Disease Control and Prevention (Shanghai Pudong New Area Health Supervision Institute), Shanghai, China

[3]Beijing Center for Disease Prevention and Control, Beijing, China

[4]School of Data Science, Fudan University, Shanghai, China

[*]these authors contributed equally

Corresponding Author:
Zhongjie Li, Prof Dr Med
School of Population Medicine and Public Health, Chinese Academy of Medical Sciences & Peking Union Medical College, No. 31, Beijigesantiao street, Dongcheng District, Beijing, China

Abstract

Background: Seasonal influenza is a major global public health concern, leading to escalated morbidity and mortality rates. Traditional early warning models rely on binary (0/1) classification methods, which issue alerts only when predefined thresholds are crossed. However, these models exhibit inflexibility, often leading to false alarms or missed warnings and failing to provide granular risk assessments essential for decision-making. Therefore, we propose a probability-based early warning system using machine learning to mitigate these limitations and to offer continuous risk estimations of alerts (0‐1 variable) instead of rigid threshold-based alerts. Based on probabilistic prediction, public health experts can make more flexible decisions in combination with the actual situation, significantly reducing the uncertainty and pressure in the decision-making process and reducing the waste of public health resources and the risk of social panic.

Objective: The main aim of this study is to devise an innovative approach for early warning systems focused on influenza-like cases. Therefore, a Dense Residual Network (Dense ResNet), a supervised deep learning model, was developed. The model's training involved fitting the influenza-like illness positive rate, which enabled the early detection and warning of signals of changes occurring in the activity level of influenza-like cases. This departure from conventional methodologies underscores the transformative potential of machine learning, particularly in providing advanced capabilities for timely and proactive warnings in the context of influenza outbreaks.

Methods: We developed a Dense ResNet machine learning model trained on influenza surveillance data from Northern and Southern China (2014‐2024). This model generates early warning signals 3, 5, and 7 days in advance, providing a probability-based risk assessment represented as a continuous variable ranging from 0 to 1, in contrast to the traditional binary (0/1) warning systems. We evaluated the performance of this model using area under the curve scores, accuracy, recall, and F_1-scores, then compared it with support vector machine (SVM), random forests, XGBoost (Extreme Gradient Boosting), and LSTM (long short-term memory) models.

Results: The Dense ResNet model demonstrated the best performance, characterized by 5-day lead warnings and a 50th percentile probability threshold, achieving area under the curve scores of 0.94 (Northern China) and 0.95 (Southern China). Relative to traditional models, probability-based warning signals improved early detection, reduced false alarms, and facilitated tiered public health responses.

Conclusions: This study presented a novel probability-based machine learning model essential for early warning signals of influenza, demonstrating superior accuracy, flexibility, and practical applicability compared to other techniques. This approach enhances preparedness for influenza among the population and promotes the use of automated artificial intelligence–driven public health responses by replacing binary warnings with probability-driven risk assessments. Future research should integrate real-time surveillance data and dynamic transmission models to improve the precision of early warning.

(JMIR Med Inform 2025;13:e73631) doi:10.2196/73631

KEYWORDS

seasonal influenza; machine learning; early warning; Dense Residual Network; public health surveillance; risk assessment

XSL•FO
RenderX

Introduction

Seasonal influenza is a contagious disease posing significant threats to human health globally, characterized by a steady increase in annual incidence. Currently, approximately 1 billion people worldwide are infected each year, and 290,000 - 650,000 fatalities are due to influenza-related respiratory diseases [1,2].

This disease occurs in various seasons throughout the year, and its outbreak can be influenced by an environment conducive to viral survival, host immunity [3], patterns of physical contact with other people [4], or viral interference caused by other respiratory pathogens [5]. Therefore, a timely indication of an unusual increase in the prevalence of influenza is crucial; early detection and warning signals can mitigate the impact of this disease on public health, providing a foundation for the formulation of preventive measures and the timely allocation of medical resources. Previous studies have predominantly concentrated on predicting the trends of influenza outbreaks [6,7]. However, providing timely warning signals to the population is of greater practical significance for public health departments.

Various scenarios may trigger warning signals for influenza outbreaks, including surpassing historical baselines [8], excessively rapid increases in the prevalence trends, the discovery of new pathogens, increased disease severity, and insufficient medical resources [9]. This study concentrates on the warning scenario in which influenza transitions into an epidemic phase, characterized by an upward trend in the epidemic curve. In this scenario, the number of infected individuals increases, increasing demand for medical resources. As the prevalence rises, the disease burden intensifies steadily, necessitating specific personal protective or preventive measures to suppress the escalated outbreak and decelerate its transmission. Issuing a warning signal at this stage does not imply the emergence of a pandemic or a deviation from the usual trend; instead, it emphasizes the necessity for health departments and society to remain vigilant regarding the influenza epidemic.

The results of traditional early warning methods are categorized into 2 types: early warning signal and no early warning signal. An alarm will only be triggered when the expected threshold is exceeded. While these methods have been widely used in public health surveillance, they are constricted by several critical limitations [10,11]. For example, binary warning signals lack granularity, providing only rigid “yes” or “no” decisions rather than rendering a nuanced risk assessment. This often leads to the activation of false alarms or increases the likelihood of missed detections, reducing system reliability. Moreover, fixed-threshold models, such as the 40th percentile warning system, fail to distinguish between increasing and decreasing trends of the epidemic, which occasionally creates alerts even when cases are in decline. Finally, these models do not cater to tiered public health responses, making it difficult for decision-makers to prioritize interventions based on varying levels of outbreak risk [12]. Addressing these limitations requires a more flexible and adaptive approach, where warning signals are expressed as continuous probability values rather than binary classifications [11,12]. This study introduces a probability-based early warning model that enables tiered response strategies and artificial intelligence (AI)-driven automation, offering a significant improvement compared to traditional methods.

The rise of machine learning and AI methodologies provides a thrilling prospect for transforming early warning systems of influenza. Traditional warning models, such as the Moving Epidemic Method model [13], rely on historical data to predict the current prevalence of influenza. Machine learning methods, on the other hand, offer the potential to forecast warnings in advance. This shift toward advanced computational techniques not only improves the accuracy of predictions but also revolutionizes the ability of the population to anticipate and respond to public health threats.

Machine learning models such as the Self-Excitation Attention Residual Network have demonstrated the ability to dynamically adapt to evolving disease trends and changes in surveillance systems, enhancing the effectiveness of early warning systems [14]. These models can process complex, heterogeneous data from multiple sources, including cases of influenza-like illness (ILI), virological surveillance, climate and demography data, and resultant queries from search engines [15]. Consequently, they can identify intricate patterns and relationships that traditional models might miss, leading to more sensitive and accurate predictions.

Moreover, machine learning approaches have been shown to outperform traditional models with various traits such as sensitivity, specificity, and timeliness. For example, studies have found that machine learning models can issue warning signals before the onset of influenza outbreaks, exhibiting higher accuracy than threshold-based methods [16]. This enables public health officials to take preemptive measures, such as implementing vaccination campaigns or public advisories, to mitigate the impact of the disease.

Machine learning also demonstrates its potential for integrating various data sources and applying complex nonlinear models, such as long short-term memory (LSTM) or other neural networks, to the dataset, which can lead to higher prediction accuracy. These models can learn from genetic sequences and associated metadata to predict the antigenic properties of circulating influenza viruses, providing insights into the evolution of influenza and antigenic drift.

Integrating machine learning and AI into early warning systems of influenza represents a significant leap forward in our capacity to predict and prepare for influenza outbreaks. These advanced methodologies offer a more proactive, data-driven approach to public health surveillance, potentially saving lives and reducing the societal and economic burdens of influenza.

By constructing a Dense Residual Network (Dense ResNet) machine learning model to achieve probabilistic prediction of influenza outbreaks, it can effectively provide detailed probability information on the risk of an outbreak. Based on this probability prediction, public health experts can, in combination with their professional experience and the actual situation, make more flexible decisions on whether to issue a

XSL•FO
RenderX

warning, avoiding the rigidity of the traditional binary decision-making model, significantly reducing the uncertainty and pressure in the decision-making process, and significantly reducing the waste of public health resources and the risk of social panic. The continuous probability model can provide more detailed epidemic warning information based on the risk level, supporting the implementation of graded intervention strategies by health departments, such as early deployment of medical resources and strengthening public health awareness campaigns when the probability is high, and internal monitoring and precise prevention measures when the probability is medium or low. This precise intervention effectively avoids unnecessary social panic and resource waste.

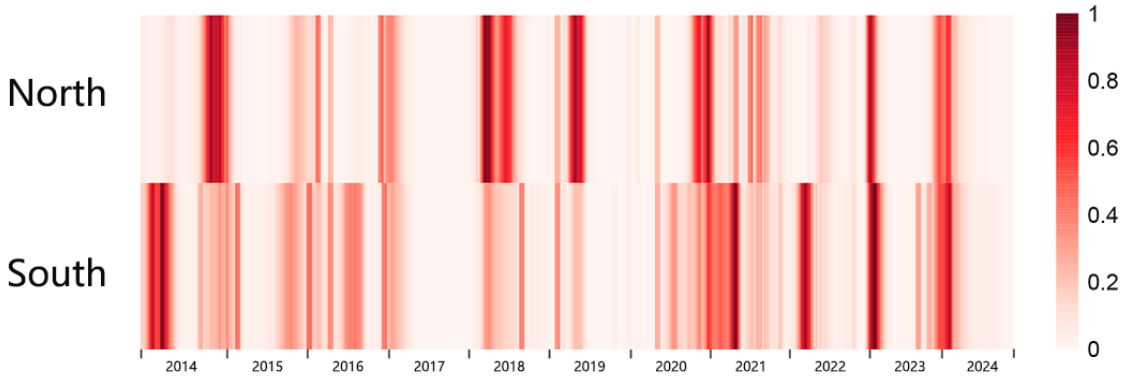
The main aim of this study is to devise an innovative approach for early warning systems focused on influenza-like cases. Therefore, a Dense ResNet, a supervised deep learning model, was developed. The model's training involved fitting the influenza-like illness positive rate (ILI+), which enabled the early detection and warning of signals of changes occurring in the activity level of influenza-like cases. This departure from conventional methodologies underscores the transformative potential of machine learning, particularly in providing advanced capabilities for timely and proactive warnings in the context of influenza outbreaks.

Methods

Data Sources

The study population includes Northern China and Southern China. We derived proxy measures for the activity of the influenza virus in the communities, referred to as ILI+ rates, by multiplying the ILI percentage (ILI%) with the proportions of influenza-positive specimens [13] derived from the Chinese National Influenza Surveillance Network for the 2 regions. A total of 569 weekly reports were included in this study. The standardized ILI+ for each region was presented (Figure 1).

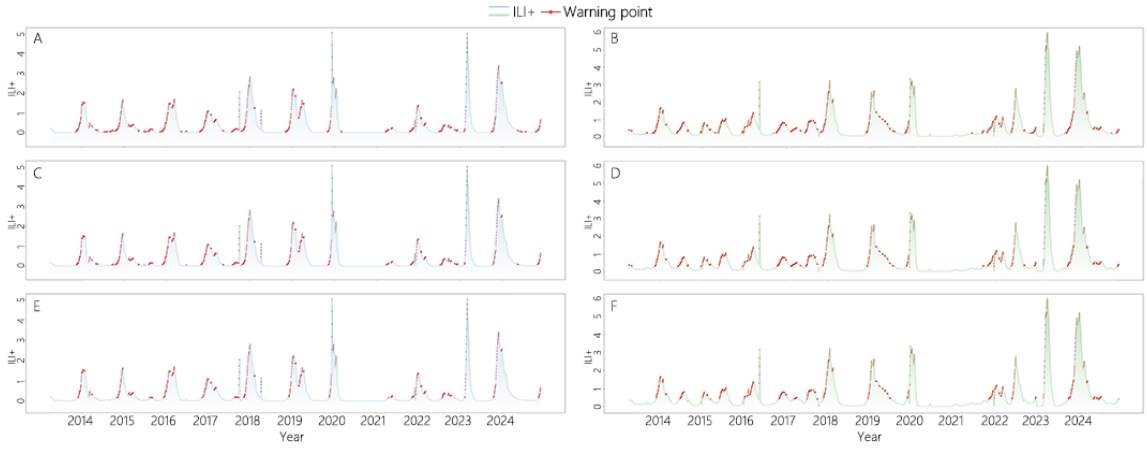
Figure 1. The influenza-like illness positive rate of Northern China (North) and Southern China (South).



Warning Definition and Labeling

Throughout this study, the warning scenario was defined as an ascending trend during the influenza season. Following the conventional definition of the influenza season presented in previous studies [17], we designated a warning when ILI+ exceeds the 40th percentile, demonstrating an upward trend. The labeled outcomes are illustrated in Figure 2.

Figure 2. ILI+ warning diagram for Northern and Southern China under different quantile values. Panels A, C, and E refer to Northern China, panels B, D, and F refer to Southern China, panels A and B refer to quantile 0.4, panels C and D refer to quantile 0.5, and panels E and F refer to quantile 0.6. ILI+: influenza-like illness positive rate.



XSL•FO
RenderX

Model Construction

This study aimed to construct and train a model that could identify the intrinsic features of the input data and establish a mapping from ILI+ features to warning categories to accurately classify ILI+ for warning signals precisely. This was achieved by proposing an innovative deep learning model called Dense ResNet (Figure 3).

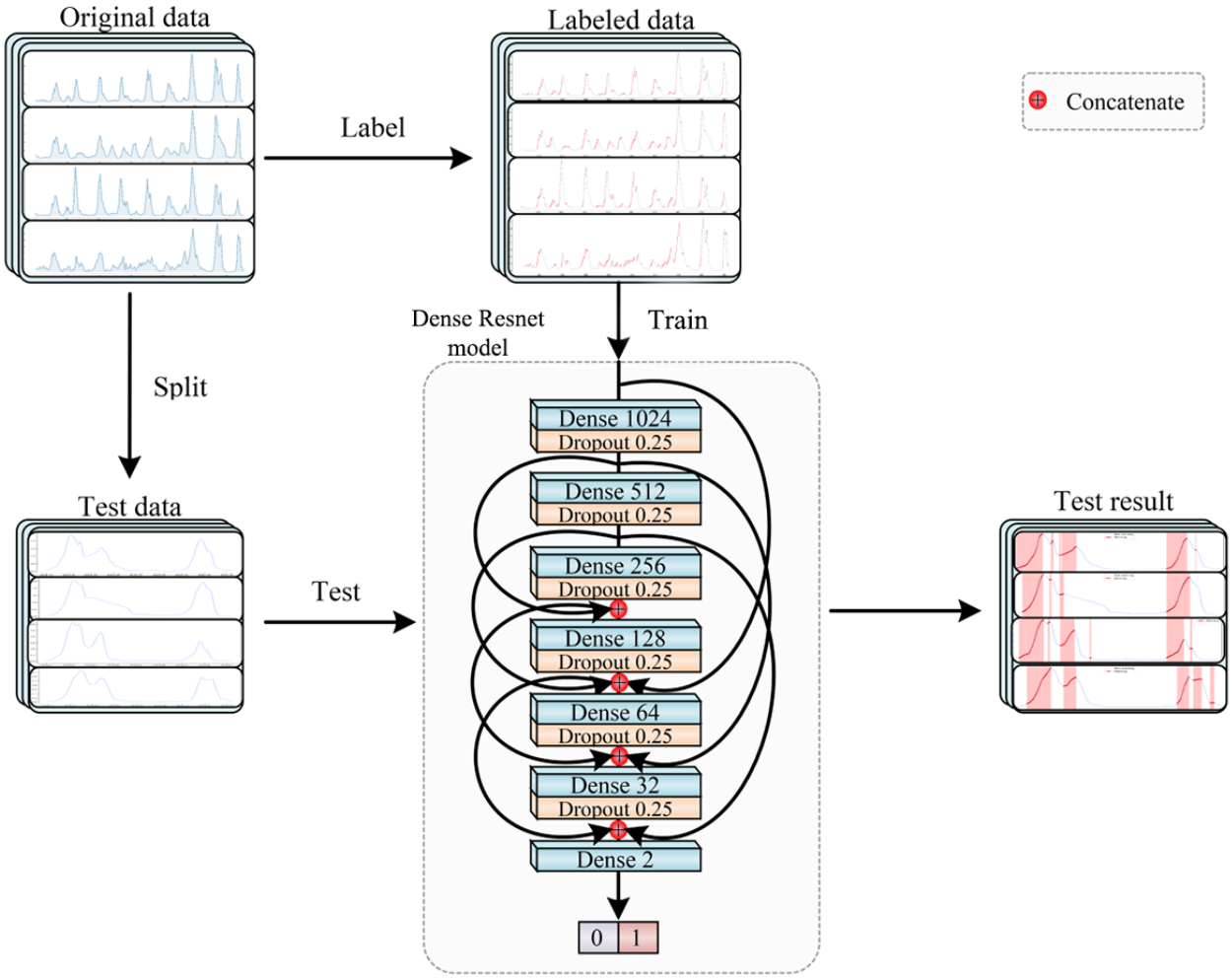
Dense layers and residual connection methods were used to design the Dense ResNet model to enhance the accuracy of the early warning function. Experimental results have demonstrated that this model could effectively map ILI+ features to the early warning category. The Dense ResNet model constructed in this study comprised 7 Dense layers, 6 Dropout layers, and 7 residual connections. From top to bottom, Dense layers of 1024, 512, 256, 128, 64, and 32 units were employed to extract data features from top to bottom. In addition, 6 layers with a dropout rate of 0.25 were applied after each Dense layer to prevent overfitting. Furthermore, 7 residual connections were added primarily to retain global information effectively while preventing gradient vanishing. The Sigmoid activation function was employed in the last fully connected layer to predict the probability of warning classes of 0 and 1. The predictive result was a probability value between 0 and 1 for each warning category.

In this study, Dense ResNet was selected over other deep learning models for time series early warning modeling of infectious diseases of the respiratory system, based on several key considerations. First, we used the ILI+ sequence as the feature for early warning judgments. Although it exhibited certain seasonality and trends, its variations were heavily influenced by external factors such as abrupt climate changes and public health interventions, leading to sudden shifts and nonstationarity. As a result, it does not adhere to consistent temporal evolution patterns. Traditional recurrent neural networks (LSTMs and Gated Recurrent Units), proficient in modeling strong sequential dependencies, are not entirely suitable for the ILI+ data used in this study. In contrast, Dense ResNet focuses on direct feature extraction, and by cumulatively integrating deep features, it is more adept at capturing the complex associations and nonlinear variation patterns present in the data, making it more compatible with the ILI+ features adopted in this research. Second, although models such as Transformers perform excellently in large-scale time series tasks, they have an escalated number of parameters that are highly prone to overfitting during the training process. This issue is particularly pronounced in this study due to the limited sample size of the ILI+ features, leading to poor generalization. In comparison, the proposed Dense ResNet structure is relatively simple; it mitigates the challenges of deep network training through effective residual connections, enabling stable training and superior performance on small to medium-sized datasets, offering higher practical application value.

In summary, considering the characteristics of the data, task requirements, model performance, training stability, and practical feasibility, this study ultimately adopted Dense ResNet for the early warning task instead of traditional recurrent neural network–based sequence models or large-scale Transformer architectures. This choice effectively balances the complex feature extraction capabilities, training stability, overfitting control, and deployment feasibility, providing strong technical support for achieving efficient and accurate early warning signals.

XSL•FO
RenderX

Figure 3. Structural diagram of the Dense Residual Network (Dense ResNet) model.



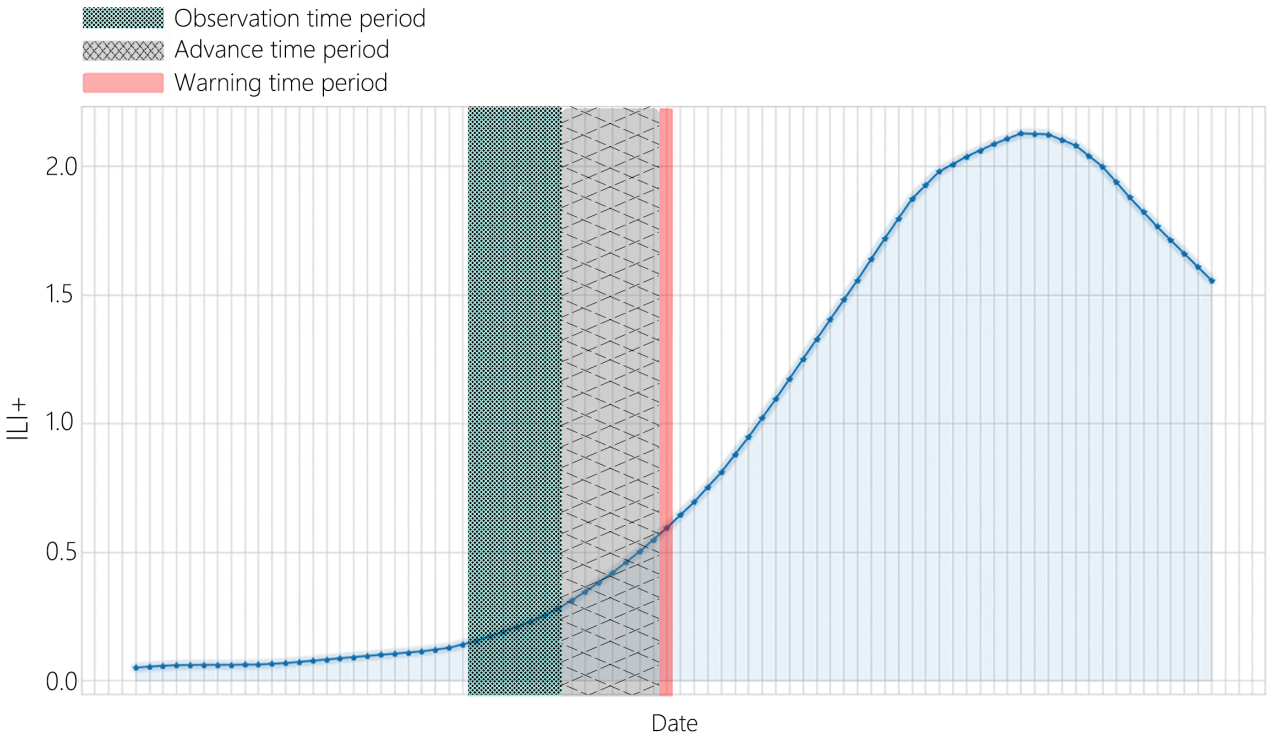
Dataset Construction

This study innovated the construction of the training dataset to activate early warning signals. Figure 2 illustrates the graphical refactoring of the dataset. We divided the data into 3 sections: observation time period, advance time period, and warning time point. We combine the features of the observation time period and the labels of warning time points to form a reconstructed dataset and train the model using this dataset to achieve early warning signals. For example, if a person needs to determine whether November 26, 2023, is a warning, you only need to observe the characteristic values from November 12, 2023, to November 18, 2023, will be observed (Figure 4).

In this study, for the choice of advanced time period, we adopted advanced time periods of 3, 5, and 7 days to select advanced periods, and the results were obtained.

XSL•FO
RenderX

Figure 4. Schematic diagram of data construction. ILI+: influenza-like illness positive rate.



Dataset Segmentation

This section encompasses 3969 days spanning from December 30, 2013, to November 11, 2024, in Southern and Northern China, to construct training. Following the conventional division methods of deep learning, including training set, validation set, and test set, and considering the practical significance of ILI% prediction, the period from December 30, 2013, to October 31, 2022 was designated as the training set, while the period from November 1, 2022, to November 11, 2024 was assigned as the test set. The training set encompasses 9 ILI% activity peaks, while the test set contains 2 ILI% peaks.

Model Training

In model training, we initialized the network weights using He normal initialization and trained the model using the Adam optimizer with default parameters (β_1 =.900, β_2 =.999). The initial learning rate was set to 0.001 with a batch size of 32. To further improve the model convergence, we employed a learning rate scheduler (ReduceLROnPlateau) that reduced the learning rate by 0.1 if the validation loss did not improve for 5 consecutive epochs. The binary cross-entropy loss function was used during training. The training was conducted for a maximum of 100 epochs. We adopted an early stopping strategy with a patience of 10 epochs based on the validation loss to prevent overfitting. The model development and experiments were implemented using the PyTorch framework (version 2.0.0; Meta AI). All the training, validation, and testing processes were performed on one NVIDIA RTX 4090 Graphics Processing Unit (GPU) with 24 GB of memory.

Ethical Considerations

This study was approved by the Research Ethics Review Committee for Biomedical Research Involving Humans, Chinese Academy of Medical Sciences, and Peking Union Medical College (approval no. CAMS&PUMC-IEC-2025-010). The study did not involve any personally identifiable or sensitive health information. No compensation was provided to participants.

Results

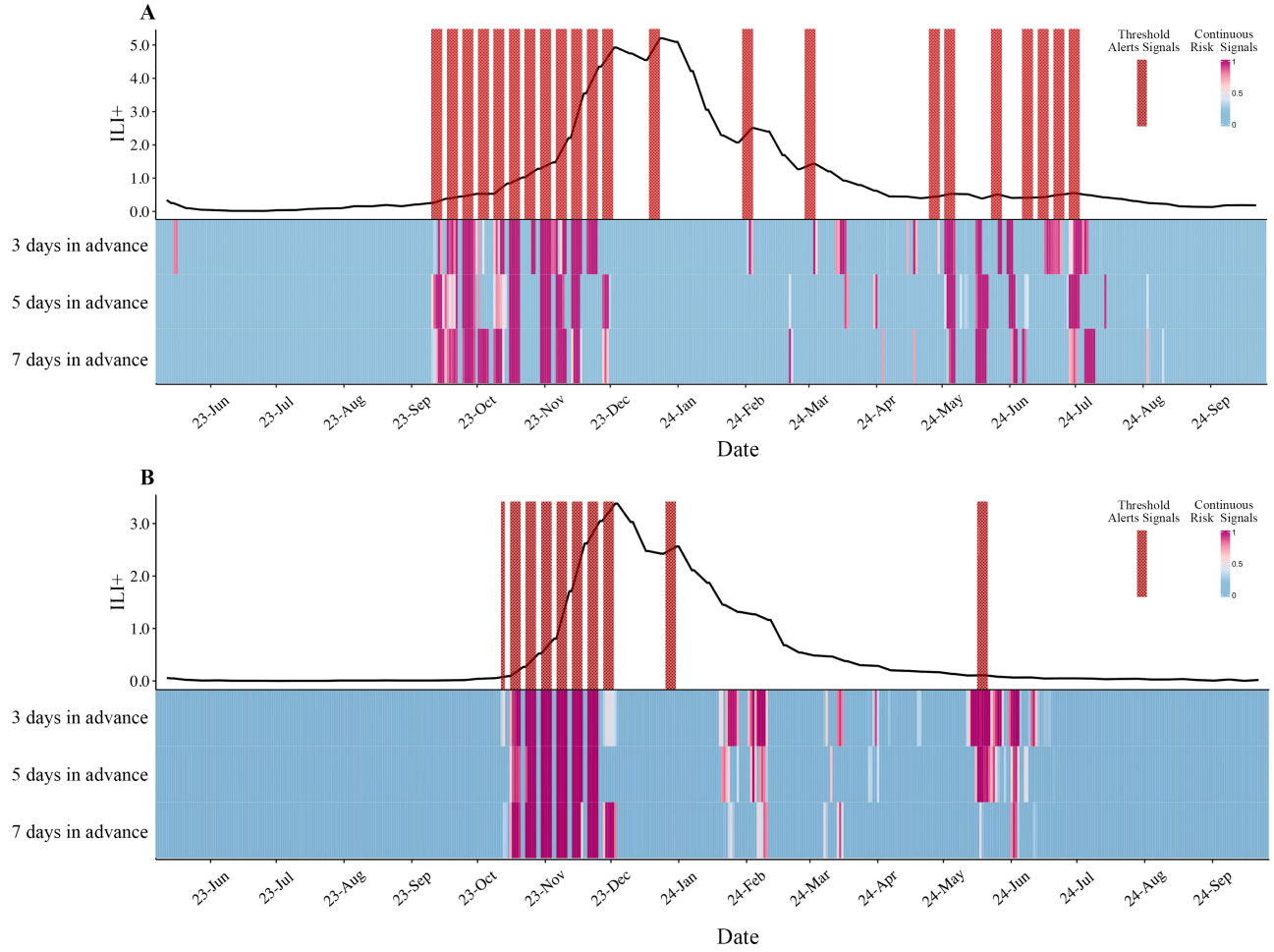
Following the training and validation procedures employing the Dense ResNet model, early warning signals were issued at 3-, 5-, and 7-day intervals. The results indicated that, in Northern and Southern China, the most effective lead time is 3 days, 50 quantiles, allowing for the detection of warning signals 2 and 5 days in advance (Figure 5).

This study assessed the warning performance in Northern and Southern China, using metrics such as accuracy, recall, F_1-score, and area under the curve (AUC) to validate the model. The outcomes highlight the highest AUC score for issuing warning signals 3 days in advance (Northern China: 0.94, Southern China: 0.95) (Table 1). The receiver operating characteristic curves are depicted in Figure 6.

Compared to other commonly used models (support vector machine [SVM], random forest, XGBoost [Extreme Gradient Boosting], and LSTM), the Dense ResNet model exhibits superior warning performance in Southern and Northern China, as well as in Beijing and Yunnan province (Table 2).

XSL•FO
RenderX

Figure 5. Comparison of current warning signals per 3, 5, and 7 days in advance of predicted warning signals in (A) Southern China and (B) Northern China. The black line refers to the ILI+ (%). ILI+: influenza-like illness positive rate.



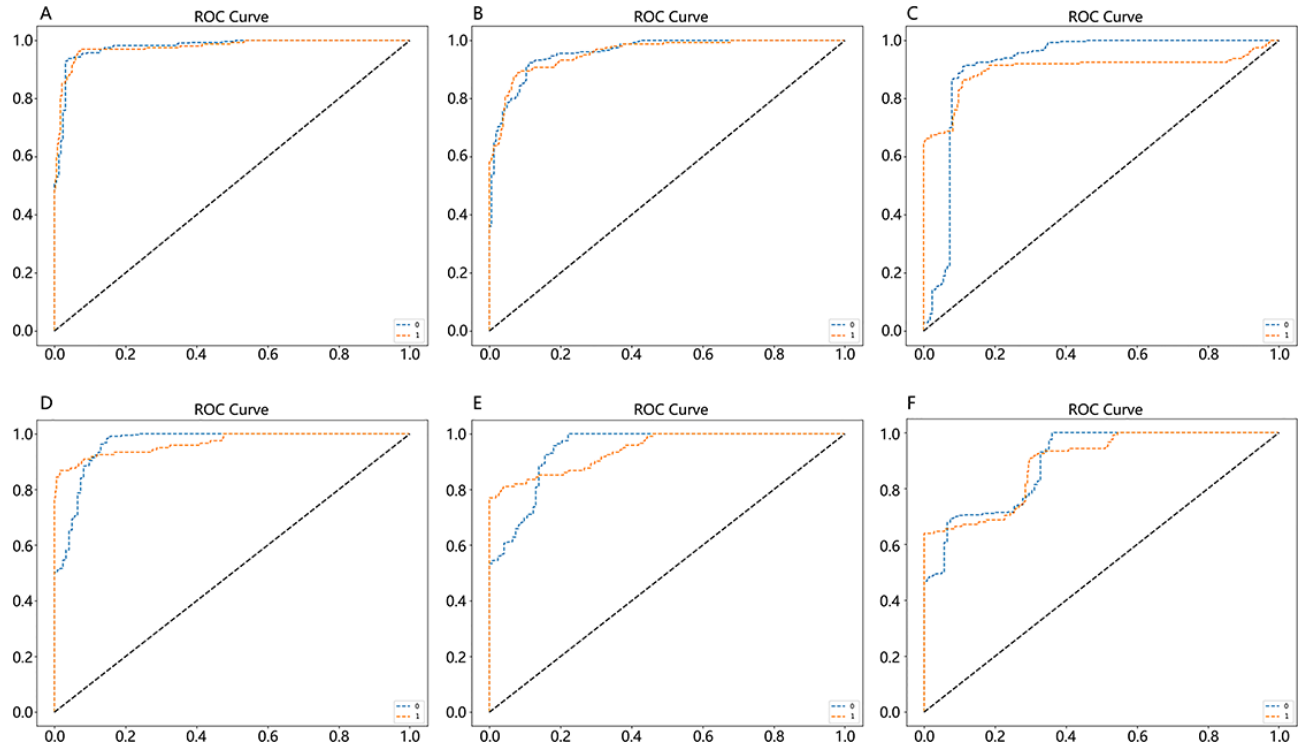
XSL•FO
RenderX

Table . Evaluation of early warning in Northern China and Southern China.

Days in advance and warning category	Precision	Recall	F_1-score	AUC[a] score
Northern China				
3 days				0.94
Warning 0	0.96	0.95	0.96	
Warning 1	0.89	0.93	0.91	
5 days				0.90
Warning 0	0.91	0.95	0.93	
Warning 1	0.88	0.81	0.84	
7 days				0.87
Warning 0	0.84	0.99	0.91	
Warning 1	0.99	0.60	0.75	
Southern China				
3 days				0.95
Warning 0	0.94	0.99	0.97	
Warning 1	0.98	0.81	0.89	
5 days				0.92
Warning 0	0.91	0.99	0.95	
Warning 1	0.99	0.69	0.82	
7 days				0.91
Warning 0	0.89	0.99	0.94	
Warning 1	0.99	0.61	0.76	

[a]AUC: area under the curve.

Figure 6. Receiver operating characteristic curves of early warning effect in Northern and Southern China. (A) Northern China at 3 days in advance; (B) Northern China at 5 days in advance; (C) Northern China at 7 days in advance; (D) Southern China at 3 days in advance; (E) Southern China at 5 days in advance; and (F) Southern China at 7 days in advance. ROC: receiver operating characteristic.



XSL•FO
RenderX

Table . Evaluation and comparison of the 3-day early warning results of 5 models.

Model[a]		Precision	Recall	F_1-score	AUC[b] score
Northern China					
	SVM[c]	0.87	0.67	0.76	0.81
	XGboost[d]	0.85	0.76	0.80	0.85
	RF[e]	0.79	0.75	0.77	0.85
	LSTM[f]	0.69	0.75	0.72	0.81
	Dense Resnet[g]	0.89	0.93	0.91	0.94
Southern China					
	SVM	0.89	0.80	0.84	0.89
	XGboost	0.67	0.80	0.73	0.84
	RF	0.68	0.85	0.76	0.87
	LSTM	0.76	0.66	0.70	0.87
	Dense ResNet	0.98	0.81	0.89	0.95

[a]The warning category for all models is 1.

[b]AUC: area under the curve.

[c]SVM: support vector machine.

[d]XGBoost: Extreme Gradient Boosting.

[e]RF: random forest.

[f]LSTM: long short-term memory.

[g]Dense ResNet: Dense Residual Network.

The results demonstrate that Dense ResNet outperforms models such as SVM, random forest, and LSTM, primarily for the following reasons. First, Dense ResNet leverages its deep network architecture, particularly through multiple dense layers and residual connections, to effectively capture complex nonlinear relationships in the data. In contrast, traditional machine learning models such as SVM and random forest, while capable of handling some degree of nonlinearity, often exhibit limitations in modeling high-dimensional data and intricate relationships. SVM typically relies on kernel functions for nonlinear mapping; however, it is less flexible compared to deep neural networks when processing large-scale data and complex features. Random forest, on the other hand, enhances the expressiveness of the model through an ensemble of decision trees. However, it reveals low performance compared to deep neural networks when dealing with highly correlated features or long-range dependencies.

Second, the Dense ResNet model benefits from hierarchical feature learning, with each dense layer progressively extracting more abstract and complex features, gradually building a representation from low-level to high-level features. In comparison, traditional models such as SVM and random forest rely more heavily on manual feature engineering or selection. While LSTM excels in processing sequential data, it depends on longer input sequences to capture complex global information and long-term dependencies, making it less efficient than Dense ResNet for learning both short-term and long-term features, as may be involved in this study.

Finally, the Dense ResNet model in this study incorporates residual connections, effectively mitigating the vanishing gradient problem and facilitating the training of deeper networks. By allowing information to skip layers, residual connections help preserve more global information, a crucial advantage when handling large-scale datasets. In contrast, models such as SVM, random forest, and LSTM lack such structural designs, which may limit their performance in modeling high-dimensional or complex data.

Discussion

Principal Findings

In China, seasonal influenza follows a predictable pattern, peaking during the colder months and, in some regions, during the summer. The ability to issue timely and precise warnings is crucial for public health preparedness. This study introduces a continuous probability-based warning system (0 - 1 variable), moving beyond the traditional binary (0/1) warning models. This advancement significantly enhances the flexibility, accuracy, and applicability of early warning systems.

A probability-based risk assessment improves the accuracy of warning signals. Traditional early warning models [18] rely on binary classifications—either issuing a warning or not—which often leads to false alarms or missed detections. These rigid threshold-based warning systems do not account for the varying degrees of epidemic severity. In contrast, our continuous probability warning approach provides a more nuanced risk assessment, offering granular insights into the likelihood of an outbreak. This enables decision-makers to adjust intervention

XSL•FO
RenderX

strategies based on the level of risk rather than adhering to a fixed binary outcome. As a result, the reliability and adaptability of early warning systems are significantly improved.

Moreover, a probability-based warning system supports tiered response strategies, which can be dynamically adjusted according to the predicted severity of an outbreak. For example, when the warning probability is moderate (0.4 - 0.6), internal monitoring may be prioritized, whereas higher probabilities (≥0.7) would prompt targeted interventions such as increasing health care preparedness or reinforcing public health advisories. When the probability reaches 0.9 or above, immediate public health measures can be activated. This graduated approach prevents unnecessary disruptions in low-risk situations while ensuring timely action in high-risk scenarios.

A flexible warning system supports precise public health interventions. Another key advantage of probability-based warnings is their role in scientific policy making and public communication. Traditional threshold-based methods may trigger unnecessary alarms in low-risk years, leading to economic losses and diminishing public responsiveness to warning signals. Conversely, these methods may fail to escalate warnings quickly enough in high-risk years, resulting in delayed response measures. By shifting to a risk-probability framework, this study enables a more rational and transparent decision-making process, allowing authorities to communicate risk levels clearly to the population to prevent overreactions.

In addition, when the probability of an outbreak is low, ranging from 0.3 to 0.5, preventive measures can be targeted at high-risk groups, such as older adults and individuals with pre-existing health conditions, without imposing large-scale interventions. This precision prevention strategy minimizes unnecessary economic losses and social disruption while ensuring that those at the most significant risk receive appropriate protection.

AI-driven automation enhances the efficiency of warning responses. Beyond improving warning accuracy, continuous probability warnings pave the way for AI-driven automation in public health management. In future applications, AI-assisted decision-making systems can integrate probability forecasts into automated response frameworks. For example, when the probability is ≥0.7, automated alerts can be dispatched to health care facilities. If a probability is ≥0.9, public health advisories can be issued automatically to initiate broader containment measures. For probabilities between 0.4 and 0.6, real-time monitoring can continue internally without initiating unnecessary public concerns.

By integrating machine learning and automation, this system improves the efficiency of response, consequently reducing delays in the intervention while optimizing the allocation of health care resources. Early warning facilitates the implementation of timely interventions, leading to improved mitigation of the outbreak. The effectiveness of the proposed model was demonstrated through empirical validation. Our study shows that the machine learning model can issue warnings 5 days earlier than traditional methods, significantly improving public health preparedness [19]. Given that implementing preventive measures taken 5 days in advance can impact the infection chain by 2 - 4 generations, this proactive alert system is essential for managing the dissemination of influenza. Similar findings have been observed in real-time surveillance systems for other infectious diseases, such as dengue [20], where early detection has been shown to reduce the outbreak's severity and enhance the efficiency of implemented control measures. Moreover, our results indicate that when predicting outbreaks 3 days in advance, the model achieves the highest sensitivity, specificity, and timeliness. This suggests that while earlier warning signals provide more time for response, optimizing the trade-off between lead time and accuracy is essential. Future research should explore hybrid models that integrate transmission dynamics modeling and data-driven time-series forecasting to further improve warning precision.

Machine learning outperforms traditional threshold-based methods. Compared to the conventional fixed percentile warning system, such as the 40th percentile thresholds, our probability-based approach provides 3 key advantages, including (1) earlier detection, which is usually executed. This approach enables a crucial preparatory window for vaccine distribution, hospital readiness, and community interventions; (2) distinguishing between rising and declining trends, which often provide warning signals even after the peak of the outbreak, with probability-based warning signals dynamically adjusted based on real-time trends, unlike fixed-threshold methods; and (3) improved adaptability to different epidemic conditions, in which machine learning models learn from historical patterns, providing a flexible response mechanism even during atypical flu seasons.

A probability-based warning system enhances influenza preparedness. This study demonstrated the superior performance of probability-based machine learning models in the early warning of seasonal influenza.

Conclusions

This study presented a novel probability-based machine learning model for the early warning of influenza, demonstrating superior accuracy, flexibility, and practical applicability. By replacing binary warning signals with probability-driven risk assessments, this approach enhances influenza preparedness and supports automated AI-driven public health responses. Future research should integrate real-time surveillance data and transmission dynamic models to improve the precision of early warning signals further. On the one hand, the Susceptible-Exposed-Infected-Recovered model can effectively depict the transmission stages and overall trends of infectious diseases among the population, providing a basic framework for understanding disease transmission. Conversely, agent-based modeling can simulate the complex interaction behaviors and heterogeneity among individuals, making the model closer to the actual communication process. In contrast, the hybrid data-driven and mechanism model provides novel prospects for predicting influenza. Data-driven models can extract potential patterns and rules from extensive historical datasets, whereas mechanism models based on understanding the principles of disease transmission provide comprehensive insights into the disease transmission process. Combining these 2 approaches mitigates the limitations of a single model and improves the accuracy and reliability of influenza prediction. Meanwhile,

XSL•FO
RenderX

this hybrid model can handle scenarios of incomplete data or highly uncertain datasets, enhancing the robustness and adaptability of the model. This system enhances public health preparedness and reduces unnecessary disruptions by issuing warning signals 5 days in advance and providing a flexible, risk-adaptive approach. Compared to traditional methods, machine learning accurately distinguishes epidemic trends, minimizes false alarms, and facilitates automated AI-driven public health responses. Future research should further refine warning frameworks by integrating transmission dynamics models and real-time surveillance data, ensuring improved promptness, timeliness, and efficacy of prevention and control measures for influenza.

Acknowledgments

This research was funded by (1) Yunnan Fundamental Research Projects (grant 202501AU070024); (2) the Chinese Academy of Medical Sciences (CAMS) Innovation Fund for Medical Sciences (grants 2021-I2M-1 - 044 and 2023-I2M-3 - 011); (3) the National Key Research and Development Program of China (grant 2023YFC2308701); and (4) Biomedical High-Performance Computing Platform, Chinese Academy of Medical Sciences.

Conflicts of Interest

None declared.

References

1. Wang X, Li Y, Deloria-Knoll M, et al. Global burden of acute lower respiratory infection associated with human metapneumovirus in children under 5 years in 2018: a systematic review and modelling study. Lancet Glob Health 2021 Jan;9(1):e33-e43. [doi: 10.1016/S2214-109X(20)30393-4] [Medline: 33248481]
2. Grippe saisonnière [Web page in French]. World Health Organization. 2023. URL: https://www.who.int/fr/news-room/fact-sheets/detail/influenza-(seasonal) [accessed 2025-07-22]
3. Leung NHL. Transmissibility and transmission of respiratory viruses. Nat Rev Microbiol 2021 Aug;19(8):528-545. [doi: 10.1038/s41579-021-00535-6] [Medline: 33753932]
4. Feng L, Zhang T, Wang Q, et al. Impact of COVID-19 outbreaks and interventions on influenza in China and the United States. Nat Commun 2021 May 31;12(1):3249. [doi: 10.1038/s41467-021-23440-1] [Medline: 34059675]
5. Han S, Zhang T, Lyu Y, et al. The incoming influenza season - China, the United Kingdom, and the United States, 2021-2022. China CDC Wkly 2021 Dec 3;3(49):1039-1045. [doi: 10.46234/ccdcw2021.253] [Medline: 34934512]
6. Ali ST, Cowling BJ. Influenza virus: tracking, predicting, and forecasting. Annu Rev Public Health 2021 Apr 1;42:43-57. [doi: 10.1146/annurev-publhealth-010720-021049] [Medline: 33348997]
7. Venkatramanan S, Sadilek A, Fadikar A, et al. Forecasting influenza activity using machine-learned mobility map. Nat Commun 2021 Feb 9;12(1):726. [doi: 10.1038/s41467-021-21018-5] [Medline: 33563980]
8. May F, Ginige S, Firman E, et al. Estimating the incidence of COVID-19, influenza and respiratory syncytial virus infection in three regions of Queensland, Australia, winter 2022: findings from a novel longitudinal testing-based sentinel surveillance programme. BMJ Open 2024 Apr 22;14(4):e081793. [doi: 10.1136/bmjopen-2023-081793] [Medline: 38653507]
9. Zhang T, Wang Q, Leng Z, et al. A scenario-based evaluation of COVID-19-related essential clinical resource demands in China. Engineering (Beijing) 2021 Jul;7(7):948-957. [doi: 10.1016/j.eng.2021.03.020] [Medline: 34035977]
10. Patel A, Maruthananth K, Matharu N, Pinto AD, Hosseini B. Early warning systems for acute respiratory infections: scoping review of global evidence. JMIR Public Health Surveill 2024 Nov 7;10:e62641. [doi: 10.2196/62641] [Medline: 39510516]
11. Hu WH, Sun HM, Wei YY, Hao YT. Global infectious disease early warning models: an updated review and lessons from the COVID-19 pandemic. Infect Dis Model 2025 Jun;10(2):410-422. [doi: 10.1016/j.idm.2024.12.001] [Medline: 39816751]
12. Haque S, Mengersen K, Barr I, et al. Towards development of functional climate-driven early warning systems for climate-sensitive infectious diseases: statistical models and recommendations. Environ Res 2024 May 15;249:118568. [doi: 10.1016/j.envres.2024.118568] [Medline: 38417659]
13. Kang M, Tan X, Ye M, Liao Y, Song T, Tang S. The moving epidemic method applied to influenza surveillance in Guangdong, China. Int J Infect Dis 2021 Mar;104:594-600. [doi: 10.1016/j.ijid.2021.01.058] [Medline: 33515775]
14. Yang L, Yang J, He Y, et al. Enhancing infectious diseases early warning: a deep learning approach for influenza surveillance in China. Prev Med Rep 2024 Jul;43:102761. [doi: 10.1016/j.pmedr.2024.102761] [Medline: 38798906]
15. Yang L, Zhang T, Han X, et al. Influenza epidemic trend surveillance and prediction based on search engine data: deep learning model study. J Med Internet Res 2023 Oct 17;25:e45085. [doi: 10.2196/45085] [Medline: 37847532]
16. Kang SK, Son WS, Kim BI. Application of the time derivative (TD) method for early alert of influenza epidemics. J Korean Med Sci 2024 Jan 29;39(4):e40. [doi: 10.3346/jkms.2024.39.e40] [Medline: 38288541]
17. Du Z, Shao Z, Zhang X, et al. Nowcasting and forecasting seasonal influenza epidemics - China, 2022-2023. China CDC Wkly 2023 Dec 8;5(49):1100-1106. [doi: 10.46234/ccdcw2023.206] [Medline: 38125915]
18. Goldstein E, Cobey S, Takahashi S, Miller JC, Lipsitch M. Predicting the epidemic sizes of influenza A/H1N1, A/H3N2, and B: a statistical method. PLoS Med 2011 Jul;8(7):e1001051. [doi: 10.1371/journal.pmed.1001051] [Medline: 21750666]

XSL•FO
RenderX

19. Lai S, Ruktanonchai NW, Zhou L, et al. Effect of non-pharmaceutical interventions to contain COVID-19 in China. Nature New Biol 2020 Sep;585(7825):410-413. [doi: 10.1038/s41586-020-2293-x] [Medline: 32365354]
20. Ranwala L, Wedisinghe Y, Perera S, Jayamanne D. Real-time laboratory surveillance of Dengue antigen(NS1) - best proposed early warning and response system for Dengue in Sri Lanka? - results from a pilot study. Ceylon Med J 2021 Sep 30;66(3):121-128. [doi: 10.4038/cmj.v66i3.9490] [Medline: 35435434]

Abbreviations

AI: artificial intelligence
AUC: area under the curve
ILI: influenza-like illness
ILI+: influenza-like illness positive rate
LSTM: long short-term memory
SVM: support vector machine
XGBoost: Extreme Gradient Boosting

Edited by A Benis; submitted 08.03.25; peer-reviewed by A Adeoye, LM Cheng, S Ruan; revised version received 24.06.25; accepted 30.06.25; published 06.08.25.

Please cite as:
Cui J, Zhang T, Shen Y, Wang X, Yang L, Huang X, Huang Q, Yang Y, Yang W, Li Z
Probability-Based Early Warning for Seasonal Influenza in China: Model Development Study
JMIR Med Inform 2025;13:e73631
URL: https://medinform.jmir.org/2025/1/e73631
doi:10.2196/73631

© Jinzhao Cui, Ting Zhang, Yifeng Shen, Xiaoli Wang, Liuyang Yang, Xuefeng Huang, Qiang Huang, Yu Yang, Weizhong Yang, Zhongjie Li. Originally published in JMIR Medical Informatics (https://medinform.jmir.org), 6.8.2025. This is an open-access article distributed under the terms of the Creative Commons Attribution License (https://creativecommons.org/licenses/by/4.0/), which permits unrestricted use, distribution, and reproduction in any medium, provided the original work, first published in JMIR Medical Informatics, is properly cited. The complete bibliographic information, a link to the original publication on https://medinform.jmir.org/, as well as this copyright and license information must be included.

XSL•FO
RenderX

Machine Learning–Based Analysis of Lifestyle Risk Factors for Atherosclerotic Cardiovascular Disease: Retrospective Case-Control Study

Hye-Jin Kim[1], PhD; Heeji Choi[1], MSc; Hyo-Jung Ahn[2], MSc; Seung-Ho Shin[1], PhD; Chulho Kim[3], MD, PhD; Sang-Hwa Lee[3], MD, PhD; Jong-Hee Sohn[3], MD, PhD; Jae-Jun Lee[4], MD, PhD

[1]Artificial Intelligence Research Center, College of Medicine, Hallym University, Chuhcneon-si, Republic of Korea

[2]Health Insurance Review and Assessment Research Institute, Health Insurance Review and Assessment Service, Wonju-si, Republic of Korea

[3]Department of Neurology, College of Medicine, Hallym University, 1, Hallymdaehak-gil, Chuncheon-si, Republic of Korea

[4]Department of Anesthesiology, College of Medicine, Hallym University, Chuncheon-si, Republic of Korea

Corresponding Author:
Chulho Kim, MD, PhD
Department of Neurology, College of Medicine, Hallym University, 1, Hallymdaehak-gil, Chuncheon-si, Republic of Korea

Abstract

Background: The risk of developing atherosclerotic cardiovascular disease (ASCVD) varies among individuals and is related to a variety of lifestyle factors in addition to the presence of chronic diseases.

Objective: We aimed to assess the predictive accuracy of machine learning (ML) models incorporating lifestyle risk behaviors for ASCVD risk using the Korean nationwide database.

Methods: Using data from the Korea National Health and Nutrition Examination Survey, 5 ML algorithms were used for the prediction of high ASCVD risk: logistic regression (LR), support vector machine, random forest, extreme gradient boosting, and light gradient boosting models. ASCVD risk was assessed using the pooled cohort equations, with a high-risk threshold of ≥7.5% over 10 years. Among the 8573 participants aged 40 - 79 years, propensity score matching (PSM) was used to adjust for demographic confounders. We divided the dataset into a training and a test dataset in an 8:2 ratio. We also used bootstrapping to train the ML model with the area under the receiver operating characteristics curve score. Shapley additive explanations were used to identify the models' important variables in assessing high ASCVD risks. In sensitivity analysis, we additionally performed binary LR analysis, in which the ML model's results were consistent with the conventional statistical model.

Results: Of the 8573 participants, 41.7% (n=3578) had high ASCVD risk. Before PSM, age and sex differed significantly between groups. PSM (1:1) yielded 1976 patients with balanced demographics. After PSM, the high ASCVD risk group had higher alcohol or tobacco use, lower omega-3 intake, higher BMI, less physical activity, and spent less time sitting. In 5 ML models, the extreme gradient boosting model showed the highest area under the receiver operating characteristics curve, indicating superior overall discrimination between high and low ASCVD risk groups. However, the light gradient boosting model demonstrated better performance in accuracy, recall, and F_1-score. Variable importance analysis using Shapley additive explanations identified smoking and age as the strongest predictors, while BMI, sodium or omega-3 intake, and low-density lipoprotein cholesterol also had significant variables. Sensitivity analysis using multivariable LR analysis also confirmed these findings, showing that smoking, BMI, and low-density lipoprotein cholesterol increased ASCVD risk, whereas omega-3 intake and physical activity were associated with lower risk.

Conclusions: Analyzing lifestyle behavioral factors in ASCVD risk with an ML model improves the predictive performance compared to traditional models. Personalized prevention strategies tailored to an individual's lifestyle can effectively reduce ASCVD risk.

(JMIR Med Inform 2025;13:e74415) doi:10.2196/74415

KEYWORDS

atherosclerotic cardiovascular disease; machine learning; lifestyle risk behaviors; predictive modeling; low-density lipoprotein

Introduction

Atherosclerotic cardiovascular disease (ASCVD) remains the leading cause of morbidity and mortality worldwide [1]. In 2019, cardiovascular diseases (CVDs) were responsible for an estimated 32% of all global deaths [2]. Of the 17 million premature deaths caused by noncommunicable diseases in 2019, 38% were attributable to CVDs [2]. The prevalence of CVDs

XSL•FO
RenderX

in South Korea has recently been increasing [3]. While the CVD mortality rate declined until 2010, it has been steadily rising since then [4]. Considering these trends, addressing CVDs is crucial for improving public health outcomes.

The main risk factors for developing ASCVD include hypertension, smoking, and dyslipidemia [5]. Additionally, ASCVD outcomes vary across different ethnic groups based on socioeconomic status, which also influences health-related lifestyle behaviors [6-8]. As the prevalence of ASCVD is increasing, the importance of primary prevention has been emphasized from a public health perspective [9]. ASCVDs are closely related to modifiable risk factors that can be controlled through lifestyle modification, which is the cornerstone of ASCVD prevention [9]. The most effective prevention strategy is a comprehensive approach that promotes a healthy lifestyle and addresses all major risk factors [10].

Machine learning (ML) has been increasingly applied in medical data analysis, offering numerous benefits for enhancing patient care and improving clinical outcomes [11]. Additionally, ML facilitates precision medicine by enabling early identification of high-risk patients for disease progression with high accuracy [11]. Previous studies have constructed ML models for predicting ASCVD, but few have modeled the impact of lifestyle behaviors on ASCVD risk [11-13]. Despite advances in ML, the combined predictive power of detailed lifestyle factors—especially within interpretable ML frameworks—remains underexplored. Although ML improves risk prediction, understanding which lifestyle factors have the greatest impact is crucial for prevention—yet this is often unclear with black-box models. This study addresses that gap by applying interpretable ML techniques to accurately predict ASCVD risk and clarify the specific impact of individual lifestyle factors. ASCVD risk is influenced by demographic variables such as age, race, and sex, as well as lifestyle behaviors [14,15]. Using data from the nationwide Korea National Health and Nutrition Examination Survey (KNHANES), we used five ML models to (1) examine the relationship between lifestyle factors and ASCVD risk, (2) evaluate the predictive performance of these models, and (3) identify the most influential predictors using interpretable methods.

Methods

Participants

This retrospective case-control study used nationally representative data from the KNHANES. The KNHANES is an ongoing, cross-sectional survey initiated in 1998 by the Korea Disease Control and Prevention Agency (KDCA) to assess the health and nutritional status of the Korean population. We used anonymized, publicly available data from 2019 to 2021. Among the 22,559 total participants in the 2019‐2021 KNHANES dataset, we initially screened 10,481 individuals aged 40‐79 years with no history of cardiovascular events. We excluded 1908 participants with missing data on sodium intake, low-density lipoprotein (LDL) cholesterol, time spent sitting, occupation, marital status, smoking status, income, BMI, or weight change over 1 year. The final analytic sample included 8573 participants.

Ethical Considerations

The original KNHANES surveys received ethical approval from the KDCA Institutional Review Board, and informed consent was obtained from all participants. All data were anonymized and deidentified by KDCA prior to public release. As this study involved the secondary analysis of deidentified public data, it was exempt from additional institutional review board review by our institution (2024-03-008).

Measurement of ASCVD Risk Score

The 10-year ASCVD risk was assessed using the American College of Cardiology/American Heart Association pooled cohort equations (PCEs) risk score [15]. They recommended that PCEs for non-Hispanic White people may be considered for risk estimation in populations other than non-Hispanic African American and non-Hispanic White people [15,16]. Therefore, the estimation function of the ASCVD risk score for the White population was used in this study. This score algorithm is designed to predict both the 10-year (40‐79 years of age) and lifetime (20‐59 years of age) risk of ASCVD. This includes the assessment of both fatal and nonfatal coronary heart disease and stroke [17,18]. We categorized participants into two groups based on their 10-year ASCVD risk calculated using the PCEs: a low ASCVD risk group (ASCVD risk <7.5%) and a high ASCVD risk group (ASCVD risk ≥7.5%).

Measurement of Lifestyle Risk Behaviors

The lifestyle risk behaviors analyzed in this study included sex, age, occupation, marital status, residential area, household income, alcohol consumption, smoking, omega-3 intake, sodium intake, BMI, weight change over 1 year, LDL cholesterol, physical activity, and time spent sitting. The occupation was classified into three categories of nonmanual workers, manual workers, and other workers. Marital status was separated and widowed, and divorced participants were assigned the no spouse status. The residential area was grouped as urban or rural areas. Alcohol consumption was divided into two categories, where participants drank at least 2 days per week and fewer than 2 days per week [19], regardless of the amount of alcohol consumed. Individuals who had smoked at least 100 cigarettes in their lifetime and currently smoked were classified as smokers, whereas those who had smoked fewer than 100 cigarettes in their lifetime but did not currently smoke and never smoked in their lifetime were classified as nonsmokers. BMI was calculated as weight in kilograms divided by height in meters squared. Weight change over 1 year was classified into three categories of no weight change, weight gain, and weight loss. Using the criteria specified in the questionnaire, weight gains and losses of 0 to less than 3 kg over 1 year were classified as no change, gains of more than 3 kg as weight gain, and losses of more than 3 kg as weight loss. Physical activity was calculated using the sum of the minutes of exercise per week and considering the strength of the exercise intensity (vigorous and moderate). The combination of vigorous intensity and moderate intensity exercise was considered by calculating the minutes exercised per week as follows: 2×moderate activity (minutes per week)+vigorous activity (minutes per week) [20]. “Physically active” is defined as engaging in at least 150 minutes of moderate activity per week [21]. We used omega-3 or sodium

XSL•FO
RenderX

intake in grams per day and time spent sitting in minutes per day, and these variables were entered into the ML model as continuous variables.

Statistical Analysis

We categorized ASCVD risk into two groups: high and low risk. The ASCVD risk score itself is calculated using age and sex. Consequently, the high-risk and low-risk groups are inherently expected to differ significantly in these demographic factors by definition. In addition, our primary goal was to assess how lifestyle behaviors differ between high and low-risk individuals after accounting for nonmodifiable or less modifiable factors. Therefore, we performed 1:1 propensity score matching (PSM) based on sociodemographic characteristics to assess the impact of lifestyle behaviors on ASCVD risk.

The propensity score was calculated with the following variables: sex, age, job or marital status, residential area, and household income. In descriptive analyses of two-group comparisons, continuous variables were presented as median and IQR, and categorical variables were presented as proportions (%). Differences between high and low ASCVD groups were compared using the Mann-Whitney *U* test for continuous variables after a normality test, and the chi-square test for categorical variables.

We used 5 ML algorithms for the prediction of high ASCVD risk: logistic regression (LR), support vector machine, random forest (RF), extreme gradient boosting (XGB), and light gradient boosting (LGB) model. We specifically included ensemble methods, particularly RF, XGB, and LGB models. These ensemble ML models can effectively capture complex, nonlinear relationships and high-order interactions between various risk factors (eg, lifestyle, demographic, and clinical variables) without requiring explicit prespecification [22]. In addition, they include built-in regularization techniques (like L1 and L2 penalties) to mitigate overfitting, a common concern with complex medical data [23]. In the ML model, categorical variables (including sex [after PSM, though balanced], job category, marital status, residential area, alcohol consumption frequency category, smoking status, and weight change category) were retained in their original numeric coding format. Continuous variables (including age [after PSM], omega-3 intake, sodium intake, BMI, LDL cholesterol, and time spent sitting) were scaled to a range of [0, 1] using min-max normalization. In this study, we adopted a strict data separation strategy for model development and evaluation. First, the entire dataset was randomly partitioned into a training set (80%) and a test set (20%), and stratification was applied to the partitioning to ensure that both sets retained the same class distribution as the original data. We also fixed the random seed to ensure the reproducibility of the data. Then, we performed a 5-fold stratified cross-validation on the training dataset only. In this process, we divided the training data into five equal-sized folds and repeated it five times, using 4-fold for training and one for validation in each iteration. Based on the results of this cross-validation, the optimal model structure and hyperparameters with the lowest loss were selected. Hyperparameter optimization for each of the five ML models (LR, support vector machine, RF, XGB, and LGB) was performed using Optuna, an automated hyperparameter optimization framework [24]. We used Optuna's Tree-structured Parzen Estimator sampler, a Bayesian optimization approach, to efficiently search for optimal hyperparameter combinations. For each model, optimization was conducted over 100 trials, aiming to minimize the loss obtained from the 5-fold cross-validation within the training dataset. The specific hyperparameters tuned for each model, their respective search spaces (eg, ranges for continuous parameters and choices for categorical parameters), and the final optimal configurations identified by Optuna and used for training are all detailed in Table S1 in Multimedia Appendix 1. We evaluated the final model using a separate test set (20% of the total data). This is to objectively measure the generalization performance of the model. To calculate CIs for the ML model's performance metrics, we used the bootstrapping method. The 95% CIs were calculated by repeating the bootstrapping samples 1000 times with 50% of the data as restoration extraction from the test dataset. Understanding the performance of ML models is becoming increasingly important, which highlights the growing significance of explainable artificial intelligence in interpreting model results. We used the SHapley Additive exPlanations (SHAP) value to visualize the importance and relationships among the input features of the model. In addition to the area under the receiver operating characteristics curve (AUROC) score, accuracy, precision, recall, F_1-score, specificity, and area under the precision-recall curve were calculated to assess the performance of the developed ML models.

We conducted a multivariable LR analysis as a sensitivity test to verify whether the ML model's findings on high ASCVD risk were consistent with conventional statistical methods. Univariable LR analysis was first performed on 1:1 matched patients (high vs low ASCVD risk) to identify lifestyle and sociodemographic factors associated with high ASCVD risk. Variables with a P value <.05 in the univariable model were entered into the multivariable model, and their significance was reported as adjusted odds ratios with 95% CIs.

Results

Baseline Characteristics

Of the 8573 participants, the proportion of the high ASCVD risk group was 41.7% (3578/8573), and 5059 (59%) participants were women (Table 1). As detailed in Table 1, prior to PSM, substantial baseline differences were evident across nearly all measured characteristics. Notably, the high ASCVD risk group was significantly older (median age 68.0, IQR 62.0-73.0 vs 51.0, IQR 45.0-58.0 y; P<.001) and comprised a much higher proportion of men (61.9% vs 26%; P<.001) compared to the low-risk group. Significant disparities also existed in socioeconomic factors (job distribution, marital status, residential area, and income) and various lifestyle behaviors, including higher rates of frequent alcohol consumption and smoking, lower omega-3 intake, higher BMI, lower physical activity levels, and differences in weight change patterns and sitting time (all P≤.02). The propensity score distribution and standardized differences before and after PSM for the variables used in propensity score calculation are presented in Figures

XSL•FO
RenderX

S1 and S2 in Multimedia Appendix 1. Using the 1:1 PSM method, 1976 patients were included in the final population for analysis, ensuring no significant differences in sociodemographic variables between the two groups, except for lifestyle behaviors. Following 1:1 PSM, which successfully balanced the groups for key demographic and socioeconomic confounders (sex, age, job, marital status, residential area, and income; all $P>.20$), several crucial differences in lifestyle behaviors remained statistically significant. Specifically, even after matching, the high ASCVD risk group demonstrated markedly higher rates of frequent alcohol consumption (25.3% vs 18.3 %; $P<.001$) and current smoking (42.2% vs 6.3%; $P<.001$). Furthermore, this group had significantly lower daily omega-3 intake (median 1.3, IQR 0.7-2.3 vs 1.5, IQR 0.9-2.6 g; $P<.001$) and a higher BMI (median 25.1, IQR 23.2-27.3 vs 23.9, IQR 21.9-25.8 kg/m²; $P<.001$). They also reported engaging in less physical activity (16.6% active vs 22% active; $P=.003$). Interestingly, the high-risk group reported slightly less time spent sitting compared to the low-risk group after matching (median 8, IQR 5-10 h per day; $P=.003$). Notably, the initial significant differences observed in sodium intake and LDL cholesterol levels before matching were no longer significant after PSM ($P=.15$ and $P=.12$, respectively), suggesting these factors were partly confounded by the demographic variables adjusted for in the matching process. The flowchart of participants is presented in Figure 1.

XSL•FO
RenderX

Table . Comparison of baseline characteristics of high and low ASCVD[a] risk groups before and after propensity score matching.

Variable	Before PSM[b]			After PSM		
	Low ASCVD risk group (n=4995)	High ASCVD group (n=3578)	*P* value	High ASCVD group (n=988)	Low ASCVD group (n=988)	*P* value
Gender (women), n (%)	3695 (74)	1364 (38.1)	<.001	493 (49.9)	482 (48.8)	.65
Age (years), median (IQR)	51.0 (45.0 - 58.0)	68.0 (62.0 - 73.0)	<.001	59.0 (54.0 - 65.0)	61.0 (52.0 - 67.0)	.20
Job, n (%)			<.001			.62
Nonmanual workers	1886 (37.8)	1543 (43.1)		435 (44)	454 (46)	
Other workers	1632 (32.7)	1641 (45.9)		355 (35.9)	350 (35.4)	
Manual workers	1477 (29.6)	394 (11)		198 (20)	184 (18.6)	
Marital status (without spouse), n (%)	867 (17.4)	922 (25.8)	<.001	229 (23.2)	235 (23.8)	.36
Residential area (urban), n (%)	881 (17.6)	1001 (28)	<.001	216 (21.9)	234 (23.7)	.93
Income (10,000 won per month), median (IQR)	492 (292 - 700)	230 (109-450)	<.001	360 (200 - 614)	355 (193 - 600)	.98
Alcohol drinking (≥2 per week), n (%)	839 (16.8)	873 (24.4)	<.001	181 (18.3)	250 (25.3)	<.001
Smoking, n (%)	442 (8.8)	915 (25.6)	<.001	62 (6.3)	417 (42.2)	<.001
Omega-3 intake (g per day), median (IQR)	1.4 (0.8 - 2.3)	1.3 (0.7 - 2.3)	<.001	1.5 (0.9 - 2.6)	1.3 (0.7 - 2.3)	<.001
Sodium intake (g per day), median (IQR)	2.8 (1.9 - 4.0)	2.9 (1.9 - 4.2)	.02	3.1 (2.0 - 4.2)	2.9 (2.0 - 4.2)	.15
BMI (kg/m²), median (IQR)	23.5 (21.4 - 25.9)	24.4 (22.5 - 26.5)	<.001	23.9 (21.9 - 25.8)	25.1 (23.2 - 27.3)	<.001
Weight change over 1 year, n (%)			<.001			.14
Weight loss	528 (10.6)	506 (14.1)		116 (11.7)	121 (12.2)	
No weight change	3171 (63.5)	2584 (72.2)		703 (71.2)	666 (67.4)	
Weight gain	1296 (25.9)	488 (13.6)		169 (17.1)	201 (20.3)	
LDL[c] (mg/dL), median (IQR)	120 (97 - 143)	110 (85 - 135)	<.001	114 (91 - 139)	116 (92 - 143)	.12
Physical activity, n (%)	1074 (21.5)	534 (14.9)	<.001	217 (22)	164 (16.6)	.003
Time spent sitting (hours/day), median (IQR)	8.0 (5.0 - 10.0)	8.0 (5.8 - 11.0)	<.001	8.0 (5.0 - 10.0)	8.0 (5.7 - 10.9)	.003

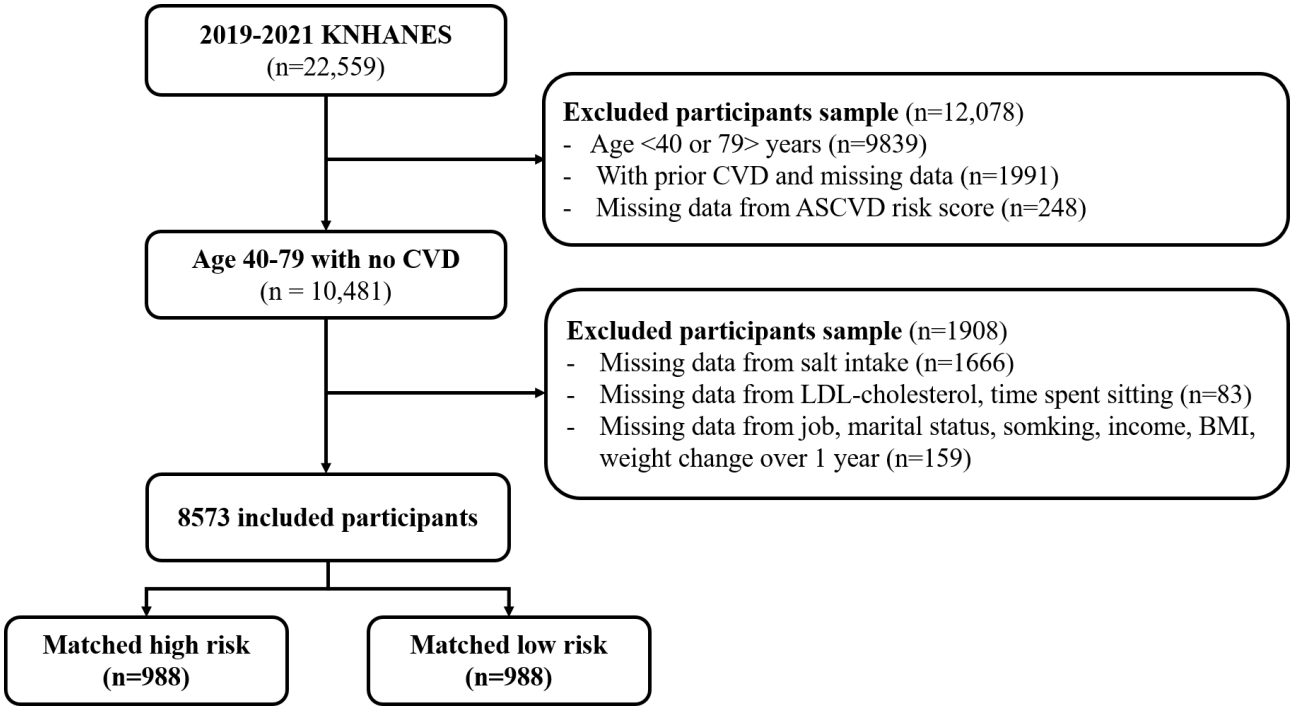
[a]ASCVD: atherosclerotic cardiovascular disease.

[b]PSM: propensity score matching.

[c]LDL: low-density lipoprotein.

XSL•FO
RenderX

Figure 1. Flowchart of the participants. ASCVD: atherosclerotic cardiovascular disease; CVD: cardiovascular disease; KNHANES: Korea National Health and Nutrition Examination Survey; LDL: low-density lipoprotein.

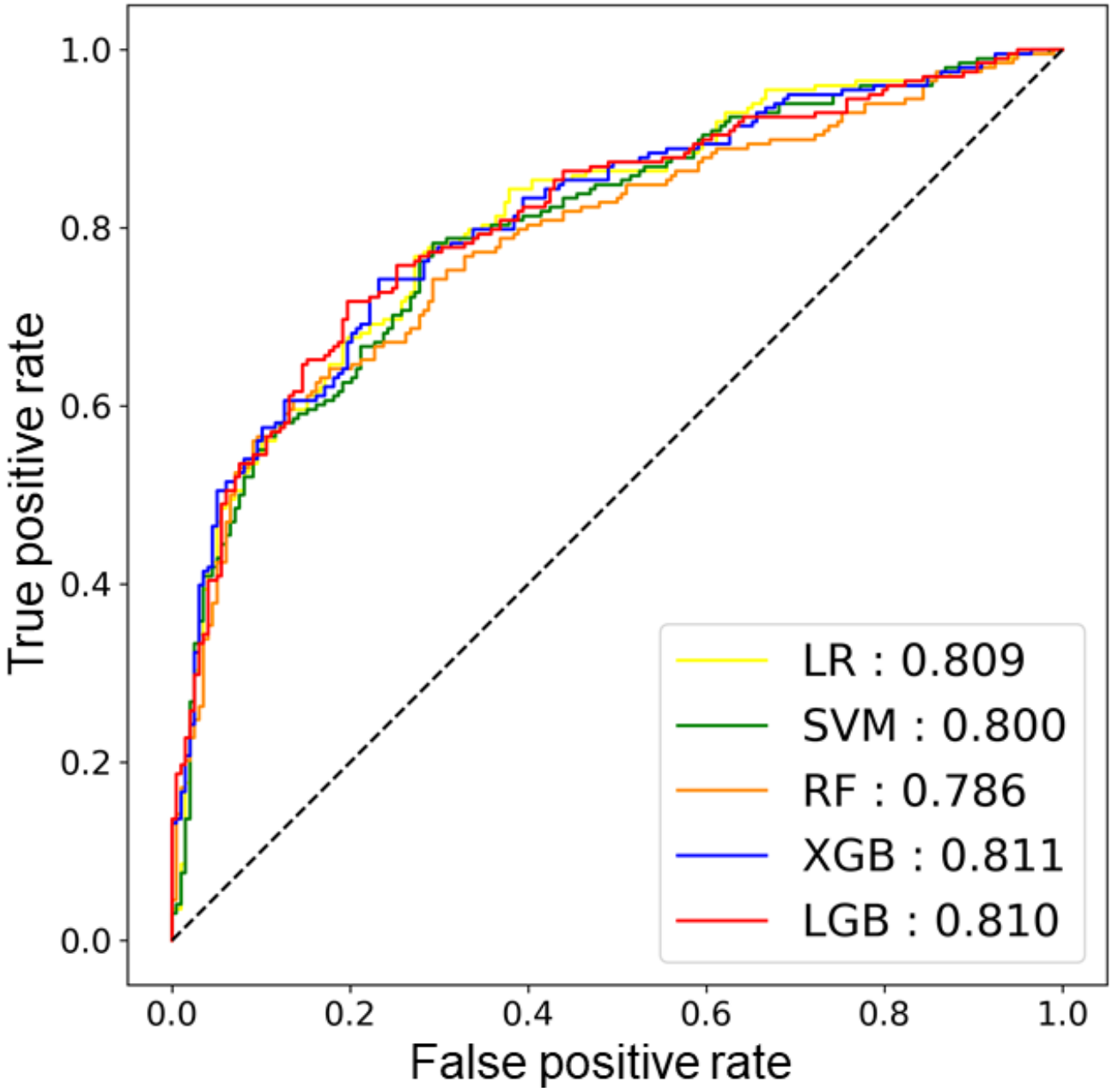


Evaluation Outcomes: Performance of ML Model for ASCVD Risk

The 1976 matched patients were allocated to the training and test datasets in an 8:2 ratio while maintaining the same ASCVD risk proportion. A comparison of variables between these two groups is presented in Table S2 in Multimedia Appendix 1, showing no significant differences in variable distribution. Figure 2 shows the result of ML performance for predicting high ASCVD risk in the test dataset, with XGB showing the highest AUROC (0.811, 95% CI, 0.748 - 0.867). Table 2 presents the other performances of the five ML models; the LGB model demonstrated the best performance, including accuracy, recall, and F_1-score. The high AUROC values achieved, particularly by XGB (0.811) and LGB (0.810), indicate valid discriminative power, suggesting these models are capable of effectively distinguishing between individuals at high versus low 10-year ASCVD risk based on the included lifestyle and clinical factors. Additionally, the LGB model achieved the highest recall (0.692), meaning it correctly identified approximately 69% of the high-risk individuals in the test set. The superior F_1-score (LGB 0.735) and area under the precision-recall curve score (LGB 0.829, XGB 0.828) in the test dataset showed the models' robust performance, even in a real-world imbalanced dataset.

XSL•FO
RenderX

Figure 2. The area under the receiver operating characteristics curve values for 5 machine learning models for predicting high atherosclerotic cardiovascular disease risk (≥7.5% of 10-year risk) in the test dataset. LGB: light gradient boosting; LR: logistic regression; RF: random forest; SVM: support vector machine; XGB: extreme gradient boosting.



XSL•FO
RenderX

Table . Overall performance of the 5 machine learning models for high ASCVD[a] risk prediction on the test dataset with propensity score matching[b].

Model	LR[c] (95% CI)	SVM[d] (95% CI)	RF[e] (95% CI)	XGB[f] (95% CI)	LGB[g] (95% CI)
Accuracy	0.730 (0.672 - 0.788)	0.730 (0.672 - 0.788)	0.732 (0.672 - 0.793)	0.722 (0.662 - 0.783)	0.750 (0.692 - 0.808)
Precision	0.776 (0.701 - 0.853)	0.827 (0.750 - 0.901)	0.791 (0.714 - 0.870)	0.768 (0.693 - 0.846)	0.783 (0.711 - 0.855)
Recall	0.646 (0.556 - 0.737)	0.581 (0.485 - 0.677)	0.631 (0.535 - 0.727)	0.636 (0.535 - 0.727)	0.692 (0.596 - 0.778)
F_1-score	0.705 (0.630 - 0.776)	0.682 (0.600 - 0.757)	0.702 (0.624 - 0.774)	0.696 (0.618 - 0.767)	0.735 (0.663 - 0.802)
AUROC[h]	0.809 (0.748 - 0.867)	0.800 (0.737 - 0.859)	0.786 (0.720 - 0.847)	0.811 (0.748 - 0.867)	0.810 (0.749 - 0.869)
Specificity	0.813 (0.737 - 0.889)	0.879 (0.808 - 0.939)	0.833 (0.758 - 0.909)	0.808 (0.727 - 0.879)	0.808 (0.727 - 0.879)
AUPRC[i]	0.811 (0.741 - 0.881)	0.803 (0.730 - 0.873)	0.805 (0.737 - 0.868)	0.828 (0.766 - 0.884)	0.829 (0.771 - 0.886)

[a]ASCVD: atherosclerotic cardiovascular disease.

[b]Data are represented as averaged value with 95% CI.

[c]LR: logistic regression.

[d]SVM: support vector machine.

[e]RF: random forest.

[f]XGB: extreme gradient boosting.

[g]LGB: light gradient boosting.

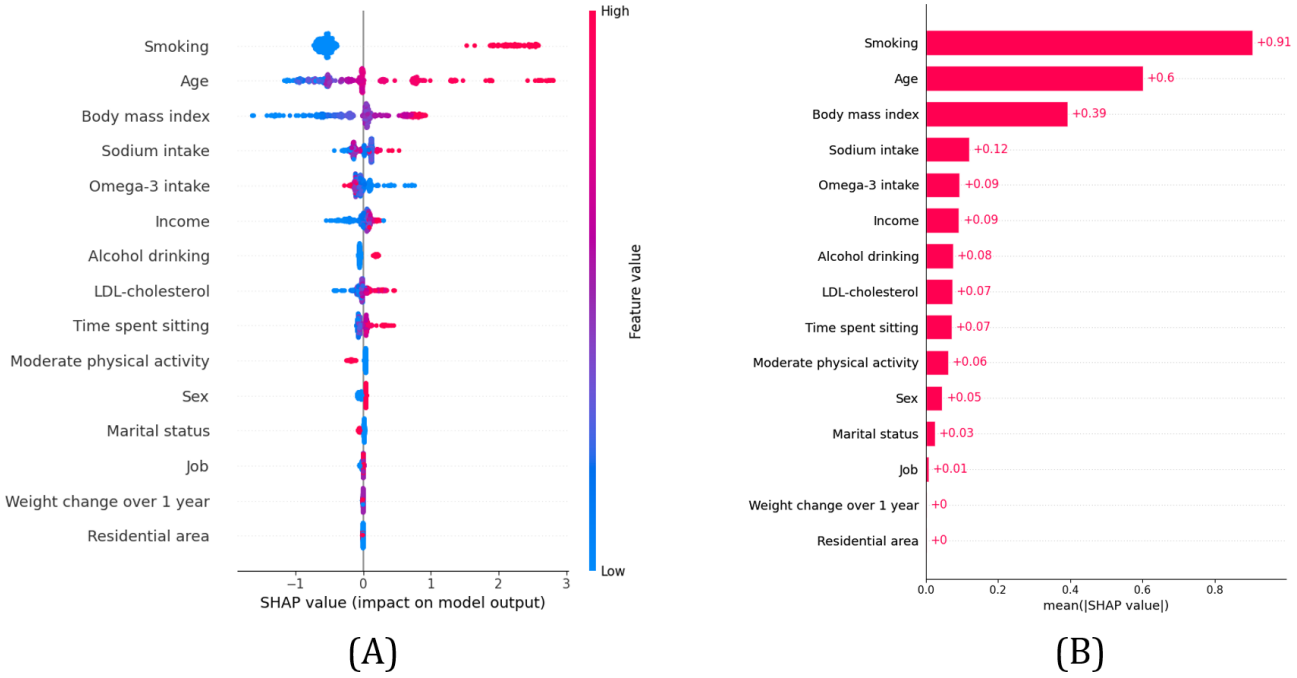
[h]AUROC: area under the receiver operating characteristics curve.

[i]AUPRC: area under the precision-recall curve.

Variable Importance in ML Model

To visualize the importance of variables included in the ML model, we presented SHAP values for the XGB model used to predict high ASCVD risk (Figure 3). Current smoking and age were the strongest predictors of high ASCVD risk over 10 years. Among lifestyle factors, BMI, sodium or omega-3 intake, and LDL cholesterol were also associated with increased risk. In contrast, factors such as “time spent sitting,” physical activity, sex, and marital status had a relatively smaller impact. The SHAP values for the LGB model, presented in Figure S3 in Multimedia Appendix 1, show a similar pattern of variable importance as the XGB model.

Figure 3. Variable importances of extreme gradient boosting models for high ASCVD risk in the test dataset. (A) Importance matrix plot showing the direction of the relationship between an input variable and high ASCVD risk. (B) Shapley Additive exPlanations summary plot of lifestyle variables predictive features of the ML model. As demonstrated by the color bar, higher values are shown in red, while lower values are shown in blue. ASCVD: atherosclerotic cardiovascular disease; LDL: low-density lipoprotein; ML: machine learning.



(A) (B)

XSL•FO
RenderX

Associations of Lifestyle Risk Factors With 10-Year ASCVD Risk

For sensitivity analysis, we examined whether the ML model's results were consistent with binary LR (Table 3) using high ASCVD risk as the outcome. Multivariable binary LR showed that smoking and BMI were positively associated with high ASCVD risk, while omega-3 intake and physical activity were significantly negatively associated. Compared to the SHAP values of the XGB and LGB models, factors such as smoking status, BMI, and omega-3 intake showed similar associations in the multivariable binary LR model.

Table . Result of binary logistic regression analysis of lifestyle variables for predicting 10-year high ASCVD[a] risk in propensity score matched cohort.

Variable	Univariable analysis		Multivariable analysis	
	OR[b] (95% CI)	*P* value	Adjusted OR (95% CI)	*P* value
Gender (women)	0.96 (0.80 - 1.14)	.62	—[c]	—
Age (years)	1.01 (1.00 - 1.02)	.20	—	—
Job				
Manual workers	1.00 (reference)	—	—	—
Nonmanual workers	1.12 (0.88 - 1.43)	.34	—	—
Other workers	1.06 (0.83 - 1.36)	.64	—	—
Marital status (without spouse)	1.03 (0.84 - 1.27)	.75	—	—
Residential area (urban)	1.11 (0.90 - 1.37)	.33	—	—
Income (10,000 won per month)	1.00 (1.00 - 1.00)	.98	—	—
Alcohol drinking (≥2 per week)	1.51 (1.22 - 1.87)	<.001	0.89 (0.68 - 1.15)	.37
Smoking	10.91 (8.19 - 14.53)	<.001	11.52 (8.20 - 15.60)	<.001
Omega-3 intake (g per day)	0.93 (0.89 - 0.97)	.003	0.93 (0.88 - 0.98)	.01
Sodium intake (g per day)	1.00 (1.00 - 1.00)	.97	—	—
BMI (kg/m^2)	1.13 (1.10 - 1.17)	<.001	1.13 (1.09 - 1.16)	<.001
Weight change over 1 year				
Weight loss	1.00 (reference)	—	—	—
No weight change	0.91 (0.69 - 1.20)	.49	—	—
Weight gain	1.14 (0.82 - 1.58)	.43	—	—
LDL[d] (mg/dL)	1.00 (1.00 - 1.01)	.04	1.00 (1.00 - 1.00)	.67
Physical activity	0.71 (0.56 - 0.89)	.003	0.61 (0.47 - 0.79)	<.001
Time spent sitting (hours per day)	1.00 (1.00 - 1.00)	.003	1.00 (1.00 - 1.00)	.42

[a]ASCVD: atherosclerotic cardiovascular disease.

[b]OR: odds ratio.

[c]Not applicable.

[d]LDL: low-density lipoprotein.

Discussion

Principal Findings

This study assessed the performance of ML models, including XGB and LGB, in predicting 10-year high ASCVD risk in adults and identifying key risk factors. After adjusting for confounders using PSM, both models demonstrated high AUROC values, with LGB outperforming in accuracy, recall, and F_1-score. Variable importance analysis identified smoking and age as the strongest predictors, while BMI, sodium or omega-3 intake, and LDL cholesterol also had significant variables. Multivariable LR also confirmed these findings, showing that smoking, BMI, and LDL cholesterol increased ASCVD risk, whereas omega-3 intake and physical activity were associated with lower risk.

Age is associated with increased oxidative stress, which leads to an increased susceptibility to CVD onset [25]. Excessive generation of reactive oxygen species leads to a state of oxidative stress, which is a major risk factor for the development and progression of atherosclerosis [26]. Aging is an unmodifiable ASCVD risk factor, but it can be prevented if

XSL•FO
RenderX

other factors can be corrected. Cigarette smoking is widely accepted as a major risk factor for the development of clinical CVD, resulting from direct effects on atherosclerosis. Epidemiologic studies strongly support that cigarette smoking in both men and women increases the incidence of myocardial infarction and fatal coronary artery disease [27,28].

Cigarette smoking is widely accepted as a major risk factor for the development of clinical CVD, resulting from direct effects on atherosclerosis. Epidemiologic studies strongly support that cigarette smoking in both men and women increases the incidence of myocardial infarction and fatal coronary artery disease [29]. Because the chemical constituents of smoke have high oxidant and inflammatory capacities, they can directly induce endothelial damage and potentiate an inflammatory response [30]. Smoke is able to increase LDL levels through metabolic alterations and the induction of LDL oxidation due to the direct oxidant capacity of smoke components [30,31]. Obesity has been linked to persistent inflammation and oxidative stress. Oxidative stress plays a crucial role in disorders related to obesity, such as dyslipidemia and hypertension, causing CVDs [32]. The prevalence of overweight and obesity has been strongly increasing over the last few decades, and it is considered to be one of the largest challenges for public health work worldwide [33].

Interestingly, some lifestyle factors commonly associated with cardiovascular health, such as sodium intake and time spent sitting, showed weaker associations with high ASCVD risk in our final models after adjusting for confounders. For instance, while sodium intake was significantly different between groups before PSM, this difference did not persist after matching, and it did not emerge as a strong predictor in the multivariable LR or the SHAP analyses for the ML models. Similarly, “time spent sitting” did not demonstrate a strong independent association in the multivariable LR model (P=.42) despite being significant in the univariable analysis and showing a difference post-PSM. Furthermore, its importance ranking in the SHAP analyses was relatively low. The lack of a strong independent association between sitting time and ASCVD risk may reflect collinearity with physical activity, limitations in the variable’s definition (eg, failure to capture prolonged uninterrupted sitting), potential inaccuracies in self-reported data, and residual confounding suggested by the unexpected postmatching trend.

The American Heart Association has recently outlined a new framework that focuses on defining and optimizing cardiovascular health through the adoption of 8 simple health components: healthy diet, engaging in regular physical activity, avoidance of nicotine, healthy sleep, and healthy levels of blood lipids, glucose, and blood pressure [34]. Most clinical guidelines for the primary or secondary prevention of ASCVD emphasize the importance of lifestyle modification. These lifestyle changes are also an important part of public health policy for CVD prevention. Therefore, a lifestyle approach to ASCVD risk may be important for accurate prediction and prioritization of treatment strategies for prevention.

Beyond simply ranking variable importance, the application of SHAP analysis provides crucial granular insights into how individual factors contribute to the predicted ASCVD risk for each patient, offering significant advantages over traditional “black-box” models. Our SHAP results (Figure 3 and Figure S3 in Multimedia Appendix 1) confirm that current smoking and age are not just important, but consistently exert the strongest positive influence toward a high-risk prediction across the cohort. The magnitude of the positive SHAP values associated with current smoking underscores its overwhelming impact, reinforcing the paramount importance of smoking cessation as a primary prevention strategy from a clinical standpoint. Similarly, the consistent positive contribution of increasing age highlights the nonmodifiable baseline upon which lifestyle interventions must act. Furthermore, the SHAP visualizations offer nuances beyond simple correlation. Especially, higher omega-3 intake consistently generated negative SHAP values, indicating its protective effect by lowering the predicted risk score. While LDL cholesterol’s influence appeared less dominant after PSM in the LR, SHAP analysis still identified it as a contributor, potentially highlighting its relevance within the complex interplay captured by the ML model.

Limitations

This study has several limitations. First, it is a cross-sectional study, which does not allow for establishing causal relationships. While our ML models identify strong associations and predictive patterns (eg, smoking status being highly predictive of high ASCVD risk), this design prevents us from definitively concluding that altering a specific lifestyle factor will cause a change in ASCVD risk. For instance, the model might show that higher omega-3 intake is associated with lower predicted risk, but we cannot ascertain from this data alone whether increasing omega-3 intake would directly lead to a reduction in an individual’s true risk, or if the association is partly due to other unmeasured confounding factors linked to both omega-3 intake and cardiovascular health. This limitation significantly impacts the direct translation of our ML model’s findings, particularly the feature importance results (like SHAP values), into prescriptive clinical actions. Second, some variables were measured by questionnaire, which may lead to underestimation or overestimation for the prediction of ASCVD risk. Especially in the case of nutrition, it is particularly difficult to accurately reflect daily intake. Third, the study involved a secondary analysis of data from the KNHANES, so it was not possible to include all lifestyle and socioeconomic status variables in the analysis. Finally, we excluded 1908 participants (approximately 18% of the initially eligible cohort after age screening) due to missing data on one or more key analytical variables (sodium intake, LDL-cholesterol, time spent sitting, etc). This exclusion was based on a complete case analysis approach, meaning only participants with complete records for all variables used in the models were included. Multiple imputation techniques could potentially allow for the inclusion of this population and might mitigate some of the selection bias. Future studies should investigate the impact of handling missing data via multiple imputation compared to complete case analysis, specifically assessing potential improvement in the performance metrics of the developed ML models. Nevertheless, the strength of this study is that it used representative and reliable data from

XSL•FO
RenderX

KNHANES to predict modifiable lifestyle risk factors using an ML approach.

Conclusions

This study demonstrates that ML models are effective tools for assessing ASCVD risk and highlights the significant impact of lifestyle factors such as smoking, BMI, and omega-3 intake. These findings highlight the significant clinical informatics potential for integrating the developed interpretable ML models into electronic health records, clinical decision support tools, and digital health platforms to enable dynamic, personalized ASCVD risk assessment and guide targeted lifestyle interventions within routine clinical practice. Longitudinal studies are needed to establish causal links between the identified lifestyle factors and ASCVD development in a multiethnic population. Furthermore, additional measures of lifestyle with wearable devices could enhance the clinical utility of the ML model.

Acknowledgments

This research was supported by a grant of the Korea Health Technology R&D Project through the Korea Health Industry Development Institute (KHIDI), funded by the Ministry of Health & Welfare, Republic of Korea (grant HR21C0198), and by a grant of the Korea Health Technology R&D Project through the KHIDI; funded by the Ministry of Health & Welfare, Republic of Korea (grant: RS-2022-KH129707); supported by ""Regional Innovation Strategy (RIS)"" through the National Research Foundation of Korea funded by the Ministry of Education (2022RIS-005) and supported by Hallym University Research Fund.

Authors' Contributions

HJK designed the study and prepared the manuscript. HC, HJA, and SHS collected data and literature search. CK drafted the manuscript. SHL, JHS, and JJL conducted data analysis. All authors carried out critical review and approved the final manuscript.

Conflicts of Interest

None declared.

Multimedia Appendix 1
Supplementary figures and tables.
[DOCX File, 372 KB - medinform_v13i1e74415_app1.docx]

References

1. Weir HK, Anderson RN, Coleman King SM, et al. Heart disease and cancer deaths—trends and projections in the United States, 1969-2020. Prev Chronic Dis 2016 Nov 17;13:E157. [doi: 10.5888/pcd13.160211] [Medline: 27854420]
2. Roth GA, Mensah GA, Johnson CO, et al. Global burden of cardiovascular diseases and risk factors, 1990-2019: update from the GBD 2019 study. J Am Coll Cardiol 2020 Dec 22;76(25):2982-3021. [doi: 10.1016/j.jacc.2020.11.010] [Medline: 33309175]
3. Kim HC. Epidemiology of cardiovascular disease and its risk factors in Korea. Global Health Med 2021 Jun 30;3(3):134-141. [doi: 10.35772/ghm.2021.01008] [Medline: 34250288]
4. Lee HH, Cho SMJ, Lee H, et al. Korea heart disease fact sheet 2020: analysis of nationwide data. Korean Circ J 2021 Jun;51(6):495-503. [doi: 10.4070/kcj.2021.0097] [Medline: 34085422]
5. Poznyak AV, Sadykhov NK, Kartuesov AG, et al. Hypertension as a risk factor for atherosclerosis: cardiovascular risk assessment. Front Cardiovasc Med 2022;9:959285. [doi: 10.3389/fcvm.2022.959285] [Medline: 36072873]
6. Devareddy A, Sarraju A, Rodriguez F. Health disparities across the continuum of ASCVD risk. Curr Cardiol Rep 2022 Sep;24(9):1129-1137. [doi: 10.1007/s11886-022-01736-y] [Medline: 35788894]
7. Mollborn S, Lawrence EM, Hummer RA. A gender framework for understanding health lifestyles. Soc Sci Med 2020 Nov;265:113182. [doi: 10.1016/j.socscimed.2020.113182] [Medline: 32942201]
8. Rajendran A, Minhas AS, Kazzi B, et al. Sex-specific differences in cardiovascular risk factors and implications for cardiovascular disease prevention in women. Atherosclerosis 2023 Nov;384:117269. [doi: 10.1016/j.atherosclerosis.2023.117269] [Medline: 37752027]
9. Lloyd-Jones DM, Braun LT, Ndumele CE, et al. Use of risk assessment tools to guide decision-making in the primary prevention of atherosclerotic cardiovascular disease: a special report from the American Heart Association and American College of Cardiology. J Am Coll Cardiol 2019 Jun 25;73(24):3153-3167. [doi: 10.1016/j.jacc.2018.11.005] [Medline: 30423392]
10. Dalakoti M, Virani S. Lifelong prevention of atherosclerotic cardiovascular disease (ASCVD) through LDL-C control—means and cost/benefit of sustained very low lifetime LDL-C targets. Am J Prev Cardiol 2024 Sep;19:100720. [doi: 10.1016/j.ajpc.2024.100720] [Medline: 39252855]
11. Shamout F, Zhu T, Clifton DA. Machine learning for clinical outcome prediction. IEEE Rev Biomed Eng 2020 Jul 7;14:116-126. [doi: 10.1109/RBME.2020.3007816]

XSL•FO
RenderX

12. Nakanishi R, Slomka PJ, Rios R, et al. Machine learning adds to clinical and CAC assessments in predicting 10-year CHD and CVD deaths. JACC Cardiovasc Imaging 2021 Mar;14(3):615-625. [doi: 10.1016/j.jcmg.2020.08.024] [Medline: 33129741]
13. Cho SY, Kim SH, Kang SH, et al. Pre-existing and machine learning-based models for cardiovascular risk prediction. Sci Rep 2021 Apr 26;11(1):8886. [doi: 10.1038/s41598-021-88257-w] [Medline: 33903629]
14. Connelly PJ, Azizi Z, Alipour P, Delles C, Pilote L, Raparelli V. The importance of gender to understand sex differences in cardiovascular disease. Can J Cardiol 2021 May;37(5):699-710. [doi: 10.1016/j.cjca.2021.02.005] [Medline: 33592281]
15. Goff DC Jr, Lloyd-Jones DM, Bennett G, et al. 2013 ACC/AHA guideline on the assessment of cardiovascular risk: a report of the American College of Cardiology/American Heart Association task force on practice guidelines. Circulation 2014 Jun 24;129(25 Suppl 2):S49-S73. [doi: 10.1161/01.cir.0000437741.48606.98] [Medline: 24222018]
16. Wong ND, Budoff MJ, Ferdinand K, et al. Atherosclerotic cardiovascular disease risk assessment: an American Society for Preventive Cardiology clinical practice statement. Am J Prev Cardiol 2022 Jun;10:100335. [doi: 10.1016/j.ajpc.2022.100335] [Medline: 35342890]
17. Lloyd-Jones DM, Braun LT, Ndumele CE, et al. Use of risk assessment tools to guide decision-making in the primary prevention of atherosclerotic cardiovascular disease: a special report from the American Heart Association and American College of Cardiology. Circulation 2019 Jun 18;139(25):e1162-e1177. [doi: 10.1161/CIR.0000000000000638]
18. Mortensen MB, Fuster V, Muntendam P, et al. A simple disease-guided approach to personalize ACC/AHA-recommended statin allocation in elderly people: the bioimage study. J Am Coll Cardiol 2016 Aug 30;68(9):881-891. [doi: 10.1016/j.jacc.2016.05.084] [Medline: 27561760]
19. Lee HK, Lee BH. The epidemiology of alcohol use disorders. J Korean Diabetes 2012;13(2):69. [doi: 10.4093/jkd.2012.13.2.69]
20. Lopez JPR, Sabag A, Juan MM, Rezende LFM, Pastor-Valero M. Do vigorous-intensity and moderate-intensity physical activities reduce mortality to the same extent? A systematic review and meta-analysis. BMJ Open Sport Exerc Med 2020 Oct;6(1):e000775. [doi: 10.1136/bmjsem-2020-000775]
21. Nelson ME, Rejeski WJ, Blair SN, et al. Physical activity and public health in older adults: recommendation from the American College of Sports Medicine and the American Heart Association. Circulation 2007 Aug 28;116(9):1094-1105. [doi: 10.1161/CIRCULATIONAHA.107.185650] [Medline: 17671236]
22. Shaikh TA, Rasool T, Verma P, Mir WA. A fundamental overview of ensemble deep learning models and applications: systematic literature and state of the art. Ann Oper Res 2024. [doi: 10.1007/s10479-024-06444-0]
23. Afsaneh E, Sharifdini A, Ghazzaghi H, Ghobadi MZ. Recent applications of machine learning and deep learning models in the prediction, diagnosis, and management of diabetes: a comprehensive review. Diabetol Metab Syndr 2022 Dec 27;14(1):196. [doi: 10.1186/s13098-022-00969-9] [Medline: 36572938]
24. Akiba T, Sano S, Yanase T, Ohta T, Koyama M. Optuna: a next-generation hyperparameter optimization framework. Presented at: Proceedings of the 25th ACM SIGKDD iNternational Conference on Knowledge Discovery & Data Mining; Aug 4-8, 2019; Anchorage, AK, USA p. 2623-2631. [doi: 10.1145/3292500.3330701]
25. Jebari-Benslaiman S, Galicia-García U, Larrea-Sebal A, et al. Pathophysiology of atherosclerosis. IJMS 2022 Mar 20;23(6):3346. [doi: 10.3390/ijms23063346]
26. Man JJ, Beckman JA, Jaffe IZ. Sex as a biological variable in atherosclerosis. Circ Res 2020 Apr 24;126(9):1297-1319. [doi: 10.1161/CIRCRESAHA.120.315930] [Medline: 32324497]
27. Rodgers JL, Jones J, Bolleddu SI, et al. Cardiovascular risks associated with gender and aging. J Cardiovasc Dev Dis 2019 Apr 27;6(2):19. [doi: 10.3390/jcdd6020019] [Medline: 31035613]
28. Batty M, Bennett MR, Yu E. The role of oxidative stress in atherosclerosis. Cells 2022 Nov 30;11(23):3843. [doi: 10.3390/cells11233843] [Medline: 36497101]
29. Gallucci G, Tartarone A, Lerose R, Lalinga AV, Capobianco AM. Cardiovascular risk of smoking and benefits of smoking cessation. J Thorac Dis 2020 Jul;12(7):3866-3876. [doi: 10.21037/jtd.2020.02.47] [Medline: 32802468]
30. Higashi Y. Smoking cessation and vascular endothelial function. Hypertens Res 2023 Dec;46(12):2670-2678. [doi: 10.1038/s41440-023-01455-z]
31. Yang Y, Yang C, Lei Z, et al. Cigarette smoking exposure breaks the homeostasis of cholesterol and bile acid metabolism and induces gut microbiota dysbiosis in mice with different diets. Toxicology 2021 Feb 28;450:152678. [doi: 10.1016/j.tox.2021.152678] [Medline: 33440193]
32. Zhou Y, Li H, Xia N. The interplay between adipose tissue and vasculature: role of oxidative stress in obesity. Front Cardiovasc Med 2021 Mar 4;8:650214. [doi: 10.3389/fcvm.2021.650214]
33. Zhang X, Liu J, Ni Y, et al. Global prevalence of overweight and obesity in children and adolescents: a systematic review and meta-analysis. JAMA Pediatr 2024 Aug 1;178(8):800-813. [doi: 10.1001/jamapediatrics.2024.1576] [Medline: 38856986]
34. Kris-Etherton PM, Petersen KS, Després JP, et al. Strategies for promotion of a healthy lifestyle in clinical settings: pillars of ideal cardiovascular health: a science advisory from the American Heart Association. Circulation 2021 Dec 14;144(24):e495-e514. [doi: 10.1161/CIR.0000000000001018] [Medline: 34689589]

XSL•FO
RenderX

Abbreviations

ASCVD: atherosclerotic cardiovascular disease
AUROC: area under the receiver operating characteristic curve
CVD: cardiovascular disease
KDCA: Korea Disease Control and Prevention Agency
KNHANES: Korea National Health and Nutrition Examination Survey
LDL: low-density lipoprotein
LGB: light gradient boosting
LR: logistic regression
ML: machine learning
PCE: pooled cohort equation
PSM: propensity score matching
RF: random forest
SHAP: SHapley Additive exPlanations
XGB: extreme gradient boosting

Edited by A Benis; submitted 24.03.25; peer-reviewed by A Adeoye, KA Obisesan Olawuni, RT Potla; revised version received 09.05.25; accepted 16.06.25; published 07.08.25.

Please cite as:
Kim HJ, Choi H, Ahn HJ, Shin SH, Kim C, Lee SH, Sohn JH, Lee JJ
Machine Learning–Based Analysis of Lifestyle Risk Factors for Atherosclerotic Cardiovascular Disease: Retrospective Case-Control Study
JMIR Med Inform 2025;13:e74415
URL: https://medinform.jmir.org/2025/1/e74415
doi:10.2196/74415

© Hye-Jin Kim, Heeji Choi, Hyo-Jung Ahn, Seung-Ho Shin, Chulho Kim, Sang-Hwa Lee, Jong-Hee Sohn, Jae-Jun Lee. Originally published in JMIR Medical Informatics (https://medinform.jmir.org), 7.8.2025. This is an open-access article distributed under the terms of the Creative Commons Attribution License (https://creativecommons.org/licenses/by/4.0/), which permits unrestricted use, distribution, and reproduction in any medium, provided the original work, first published in JMIR Medical Informatics, is properly cited. The complete bibliographic information, a link to the original publication on https://medinform.jmir.org/, as well as this copyright and license information must be included.

XSL•FO
RenderX

Tongue Image–Based Diagnosis of Acute Respiratory Tract Infection Using Machine Learning: Algorithm Development and Validation

Qianzi Che[1*], PhD; Yuanming Leng[2*], MS; Wei Yang[1*], PhD; Xihao Cao[3], MS; Zhongxia Wang[4], PhD; Lizheng Liu[5], PhD; Feibiao Xie[6], PhD; Ruilin Wang[4], PhD

[1]Institute of Clinical Basic Medicine of Chinese Medicine, Chinese Academy of Traditional Chinese Medicine, No.16, Nanxiao street, Dongzhimen, Dongcheng District, Beijing, China

[2]Department of Biostatistics, School of Public Health, Boston University, Boston, MA, United States

[3]Department of Mathematics and Statistics, Boston University, Boston, MA, United States

[4]Department of Traditional Chinese Medicine for Liver Diseases, Fifth Medical Center of the Chinese People's Liberation Army General Hospital, No. 100 West Fourth Ring Middle Road, Fengtai District, Beijing, China

[5]Institute of Engineering and Applied Technology, Fudan University, Shanghai, China

[6]School of Mathematics and Statistics, Central South University, Hunan, China

[*]these authors contributed equally

Corresponding Author:
Ruilin Wang, PhD
Department of Traditional Chinese Medicine for Liver Diseases, Fifth Medical Center of the Chinese People's Liberation Army General Hospital, No. 100 West Fourth Ring Middle Road, Fengtai District, Beijing, China

Abstract

Background: Human adenoviruses (HAdVs) and COVID-19 are prominent respiratory pathogens with overlapping clinical presentations, including fever, cough, and sore throat, posing significant diagnostic challenges without viral testing. Tongue image diagnosis, a noninvasive method used in traditional Chinese medicine, has shown correlations with specific respiratory infections, but its application remains underexplored in differentiating HAdVs from COVID-19. Advances in artificial intelligence offer opportunities to enhance tongue image analysis for more objective and accurate diagnostics.

Objective: This study aims to develop and validate artificial intelligence–based predictive models using tongue image features to differentiate COVID-19 from adenoviral respiratory infections, thereby improving diagnostic accuracy and integrating traditional diagnostic methods with modern medical technologies.

Methods: A total of 280 tongue images were collected from 58 patients with COVID-19, 84 patients with HAdVs, and 30 healthy controls. Deep learning methods were applied to extract tongue features, including color, coating, fissures, papillae, tooth marks, and granules. Four machine learning classifiers, logistic regression, random forest, gradient boosting model, and extreme gradient boosting, were developed to differentiate COVID-19 and HAdV infections. The key features identified by the machine learning algorithms were further visualized in a 2D space.

Results: Nine tongue features showed significant differences among groups (all $P<.05$), including coating color (red, green, and blue), presence of tooth marks, coating crack ratio, moisture level, texture directionality, roughness, and contrast. The extreme gradient boosting model achieved the highest diagnostic performance with an area under the receiver operating characteristic curve of 0.84 (95% CI 0.78-0.90) and an area under the precision-recall curve above 0.70. Shapley additive explanations analysis indicated tongue color, moisture, and texture as key contributors.

Conclusions: Our findings demonstrate the potential of tongue diagnosis in identifying pathogens responsible for acute respiratory tract infections at the time of admission. This approach holds significant clinical implications, offering the potential to reduce clinician workloads while improving diagnostic accuracy and the overall quality of medical care.

(JMIR Med Inform 2025;13:e74102) doi:10.2196/74102

KEYWORDS

tongue diagnosis; human adenoviruses; COVID-19; image feature extraction; machine learning; traditional Chinese medicine

XSL•FO
RenderX

Introduction

Human adenoviruses (HAdVs) are prominent respiratory pathogens affecting individuals of all ages, leading to acute upper and lower respiratory tract diseases, such as pneumonia and bronchitis [1]. Nearly half (45.7%) of acute respiratory tract infection (ARTI) outbreaks between 2009 and 2020 were attributed to HAdV-7 in China [2]. Since 2020, a temporary decline in HAdVs activity has been noted due to the rapid global spread of COVID-19 and subsequent public health measures [3,4]. As COVID-19 persists in its global circulation, a resurgence of HAdVs and other seasonal respiratory virus infections has occurred [5]. The clinical presentations of ARTI caused by HAdVs and COVID-19 are similar, often presenting as mild symptoms such as fever, rhinorrhea, cough, and sore throat, which poses a significant diagnostic challenge in the absence of viral testing. HAdVs are more prone than COVID-19 to causing acute respiratory infections in children, including pharyngitis, tonsillitis, pharyngoconjunctival fever, bronchitis, and pneumonia [6]. Moreover, recent studies indicate that mixed respiratory viral infections may lead to more severe disease outcomes than single infections [7]. Given the tendency of many patients with ARTI to self-medicate, it is essential to develop methods to differentiate between these common viral infections. Such differentiation could promote timely medical consultation and help reduce the transmission of adenovirus to children.

Tongue image diagnosis is a straightforward, noninvasive, and valuable diagnostic method used in traditional Chinese medicine (TCM), which assesses key features, such as the color, size, and shape of the tongue, along with the color, thickness, and moisture level of the tongue coating [8]. In respiratory infections, TCM theory associates specific tongue coatings with distinct syndromes [9]. Epidemiological studies have also identified distinctive tongue features in patients with acute respiratory infections. Patients with COVID-19 have been reported to present features, such as fissured tongue and strawberry tongue [10-13], whereas tongue signs in HAdV infections remain scarcely documented, limiting comprehensive understanding. Given the convenience and cost-effectiveness of tongue imaging, its application for differentiating COVID-19 from HAdV infections shows promising potential.

Tongue diagnosis traditionally relies heavily on the experience and observational skills of TCM practitioners to interpret tongue features. However, advances in artificial intelligence (AI) technologies have enabled the extraction of tongue image characteristics, such as texture, color, and coating, facilitating more objective and intelligent tongue diagnosis. Recent studies have applied AI-assisted tongue image analysis in various diseases, including diabetes [14], fatty liver [15], non-small cell lung cancer [16], and gastric cancer [17], combining tongue image features with clinical indicators to develop exploratory disease risk prediction models. Similarly, Zhou et al [18] proposed an automatic multiview disease detection system using tongue images, achieving an average classification accuracy exceeding 95% for breast tumors, heart disease, fatty liver, and lung tumors. Given the limited research on AI-assisted tongue diagnosis for respiratory infections, there is a clear need to explore its potential in this domain. Therefore, this study aims to investigate the application of AI-based tongue image analysis to distinguish COVID-19 from adenoviral respiratory infections, with the goal of improving diagnostic accuracy and integrating traditional diagnostic methods with contemporary medical technologies.

Methods

Study Sample

Our study was conducted between November 2020 and January 2021 at the Department of Traditional Chinese Medicine Hepatology, which is in the Fifth Medical Center of the Chinese People's Liberation Army (PLA) General Hospital. The inclusion and exclusion criteria have been listed in Textbox 1

Textbox 1. Inclusion and exclusion criteria.

Inclusion criteria

- Participants whose age is between 18 and 80 years old.
- Participants willing to participate in tongue image photography signed an informed consent form.

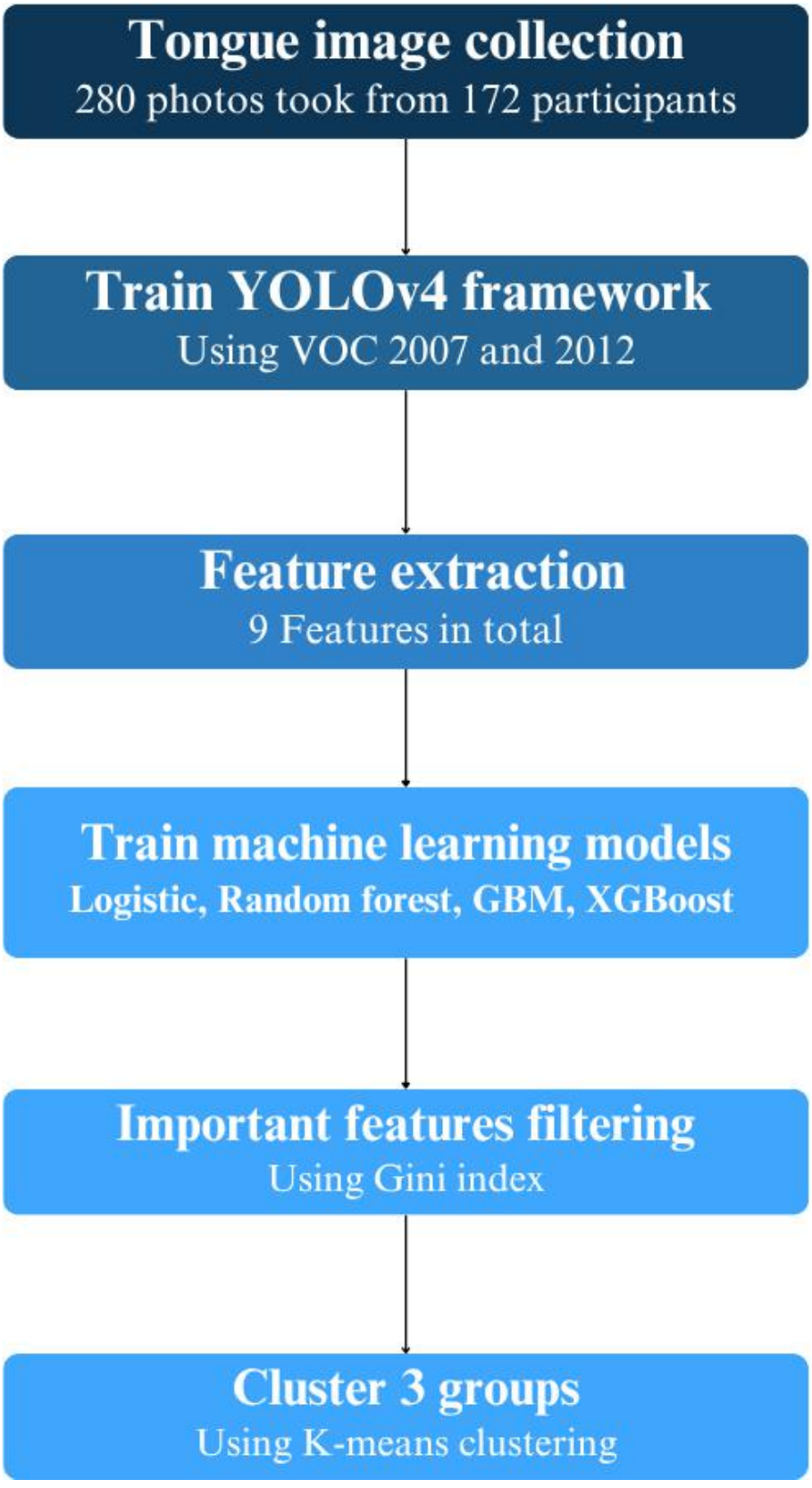
Exclusion criteria

- Individuals who were unable to describe their condition clearly due to mental factors or could not cooperate with the collection of tongue diagnosis images.
- Participants with severe acute complications, such as serious electrolyte imbalance and acidosis; patients with other serious internal diseases, such as tumors, immune system disorders, or hematologic diseases; and individuals taking medications, such as steroids, that affect glucose metabolism.
- Pregnant women and nursing mothers were excluded.

After applying the inclusion and exclusion criteria, 172 participants were included in the study. Of these, 58 were diagnosed with COVID-19, 84 with adenovirus, and 30 were assigned to the control group. Meanwhile, all the patients had complete clinical data and demonstrated high compliance, while control group participants had no history of chronic or acute diseases in the past 3 months (Figure 1).

XSL•FO
RenderX

Figure 1. The flow diagram of the participant screening procedure. GBM: gradient boosting machines; XGBoost: extreme gradient boosting.



Outcome Definition

A confirmed case of COVID-19 is defined as a suspected case that yields a positive result on a real-time reverse-transcription polymerase chain reaction assay using respiratory specimens [19]. In this study, all patients with adenovirus infection met the diagnostic criteria outlined in the “Adenovirus Infection Diagnosis and Treatment Guidelines" issued in 2013 [20]. According to these guidelines, the criteria include (1) a real-time polymerase chain reaction test on throat swab samples that detects adenovirus-specific nucleic acids; (2) the presence of adenovirus-specific immunoglobulin M antibodies in the serum;

XSL•FO
RenderX

and (3) a 4-fold or greater increase in adenovirus-specific immunoglobulin G antibodies in paired serum samples collected during the acute and recovery phases. The selection of diagnostic tests was based on clinical judgment. These tests were conducted on various specimen types, including nasopharyngeal swabs, throat swabs, sputum samples, pleural effusion samples, and bronchoalveolar lavage fluid samples.

Tongue Image Collection

All tongue images were captured before the laboratory confirmation. Collecting tongue images was conducted either before a meal or 2 hours afterward. Before being photographed, participants were instructed not to eat any food or drink any colored beverages. During the examination, participants were asked to sit with their mouths open and their tongues extended, ensuring the tongue body was relaxed, the surface was flat, and the tip was drooping. A color correction card was held within the camera's view during image capture to prevent external lighting from affecting the quality of the photograph. If a retake was necessary, the participants were advised to rest for 3 - 5 minutes before recollecting the image. The final choice for storage was the best-quality image. A digital diagnostic system was used to collect and analyze all tongue images.

Tongue Image–Based AI Deep Learning Models

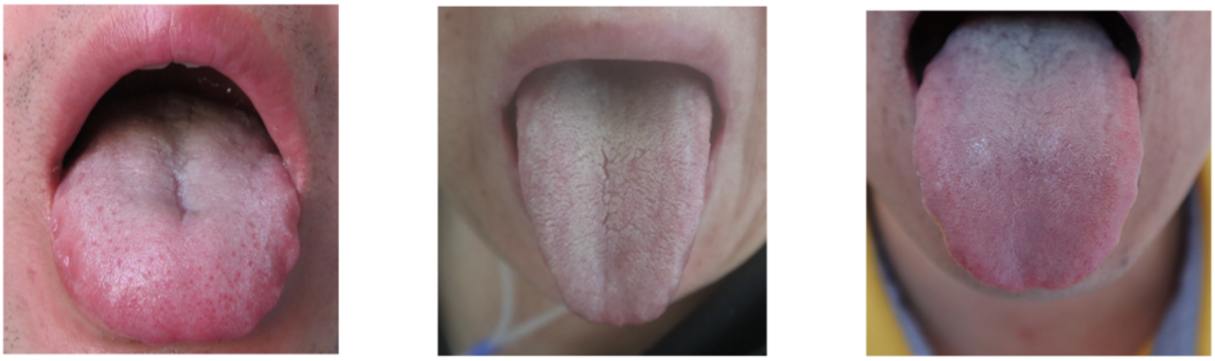
In this study, 4 key factors were primarily selected for detection: the tongue body, the coating, the teeth mark, and the fissures. To develop a target detection algorithm for tongue diagnosis images, the YOLOv4 object detection framework was used [21]. Through extensive experimentation with this algorithm, we used cross-validation to tune the convolutional neural network parameters and found the optimal combination of parameters [22]. We also increased the sample size and improved the model's generalization using image preprocessing techniques, including random cropping, horizontal flipping, and color distortion [23]. This preprocessing yielded sample images with various tongue characteristics, including color, coating, fissures, prickles, tooth marks, and granules, categorized under data labels 1 - 20 (Multimedia Appendices 1 and 2). Expert TCM practitioners have reviewed all the extracted features to ensure that they possess clinical relevance and significance.

We used VOC 2007 and 2012 to pretrain the initial feature extractor due to its availability and general utility in learning low-level visual features. The training batch size was 32 images, and 2 NVIDIA 1080 8G GPUs were used. Each group was segmented individually for different tongue features, including tongue coating (color, shape, and moisture), fissures (cracks ratio), prickles, tooth marks, and granules (shape and reflectivity).

Tongue Image Feature Definition

The color of the tongue coating was calculated by taking the mean red, green, and blue values within a specified area, providing insights into the tongue's health condition. Tooth marks were identified using the object detection algorithm, with a confidence threshold set at 0.6 to determine the presence and count of tooth marks. The proportion of cracks in the tongue coating was calculated by segmenting and merging areas where multiple fine cracks intersect, thus determining the area occupied by these cracks relative to the total area of the tongue coating. The moisture level of the tongue coating was assessed by identifying reflective areas where brightness exceeds a threshold value of 170, helping to evaluate the hydration status of the tongue. The texture features of the tongue coating were extracted using Tamura texture features, which focus on describing the textural characteristics of the tongue coating in terms of coarseness, contrast, directionality, and roughness [24]. In this study, coarseness refers to texture coarseness and is calculated based on the size of the elements. A larger element size or fewer repetitions of the element indicate a coarser texture. Contrast is primarily derived from the image's grayscale, while directionality refers to the degree of alignment within the elements (Figure 2).

Figure 2. Sample tongue images from the adenovirus (left), COVID-19 (middle), and control group (right) with extracted features.



Group	Tongue Coating Color (RGB)	Toothmarks	Crack Ratio	Moisture	Roughness	Texture Direction	Texture Contrast
Adenovirus	R: 180, G: 134, B: 153	2	1.4	0.1	3.1	27.5	16.0
COVID-19	R: 106, G: 78, B: 79	1	3.5	0.1	2.9	24.5	6.0
Control	R: 131, G: 106, B: 119	0	0.1	0.1	3.1	41.3	16.3

XSL•FO
RenderX

Statistical Analysis

We obtained 280 tongue images from these participants, each contributing up to 7 images. Only images taken on the baseline day were retained for this study, and we took the average value of the extracted features in the images if participants had more than one image on the baseline day. There were 21 images with quality issues, including 11 unidentifiable images (all characteristic values were 0) and 10 unclear images (most characteristic values were 0). We applied a mean imputation technique to these images, averaging the image parameters based on outcome category and symptom severity [25]. We conducted comparative analyses across 3 groups to examine variations in tongue features, including color, texture, moisture, and morphology.

The data were divided into 2 subsets, with 70% allocated for training and 30% reserved for internal validation, to address potential overfitting concerns. Advanced machine learning models were used to analyze tongue images and classify them into 3 categories: COVID-19, adenovirus, and control. We used several models in our analysis, including gradient boosting machines (GBM), random forest, logistic regression, and extreme gradient boosting (XGBoost). To fit each model, we applied 5-fold cross-validation on the training set. We evaluated the models' performance using 2 metrics: the area under the curve (AUC) and the area under the precision-recall curve (AUCPR) [26].

An importance variable rank was computed for each algorithm to identify the variables with the highest predictive power. In addition, we created Shapley additive explanations (SHAP) values that were calculated to indicate the contributing direction of the tongue image features [27]. Finally, we projected the selected variables of tongue images into a 2D space by a t-distributed stochastic neighbor embedding (t-SNE) plot to visually examine each group's clustering distribution [28].

All statistical analyses were performed using R Studio version 4.2.0 (Posit, PBC) software. An independent samples 2-tailed *t* test was used to analyze the measurement data, such as age and identified tongue image features. The count data were analyzed using the chi-square test. Results with $P<.05$ were considered statistically significant.

Ethical Considerations

The Ethics Committee of the Fifth Medical Center of the Chinese People's Liberation Army (PLA) General Hospital (2020074D) gave ethical approval on November 24, 2020. Informed consent was waived by the committee, as the study involved retrospective analysis of anonymized data and did not include any identifiable personal information. All procedures were conducted in accordance with the ethical standards of the institutional and national research committees and with the principles outlined in the Declaration of Helsinki. We ensured that the privacy and confidentiality of all participants were strictly maintained; data were fully anonymized before analysis, and no individual-level identifiers were collected, stored, or reported. No compensation was provided to participants, as the study did not involve direct interaction with human participants.

Results

Characteristics of Patients With Each Pathogen

Our research involved 172 participants; 58 had COVID-19, 84 were diagnosed with adenovirus, and 30 were in the control group. Table 1 shows the main descriptive sociodemographic variables (sex and age). The average age in our sample was 23.65 (SD 9.61) years old (Table 1).

Table . Study sample and extracted feature characteristics.

Variables	Control (n=30)	COVID-19 (n=58)	Adenovirus (n=84)	*P* value
Gender				
male, n (%)	13 (43)	36 (62)	83 (99)	<.001
Age (years), mean (SD)	27.2 (8.0)	47.6(15.8)	23.7 (9.6)	<.001
Tongue coating, mean (SD)				
Red	119.0 (16.5)	109.8 (22.6)	149.2 (20.4)	<.001
Green	93.3 (13.8)	77.65 (21.2)	110.8 (20.7)	<.001
Blue	97.1 (19.7)	79.2 (22.0)	114.2 (25.4)	<.001
Toothmarks, n (%)				.049
0	20 (67)	20 (35)	33 (39)	
1	6 (20)	17 (29)	24 (29)	
2	4 (13)	21 (36)	27 (32)	
Crack ratio, mean (SD)	0.5 (1.0)	1.4 (2.4)	1.2 (2.0)	.09
Moisture, mean (SD)	0.1 (0.1)	0.1 (0.0)	0.1 (0.1)	<.001
Roughness, mean (SD)	3.2 (0.2)	3.1 (0.2)	3.3 (0.2)	<.001
Texture direction, mean (SD)	40.7 (19.1)	29.9 (17.7)	34.8 (19.1)	.04
Texture contrast, mean (SD)	17.1 (9.4)	12.5 (5.8)	24.6 (9.9)	<.001

XSL•FO
RenderX

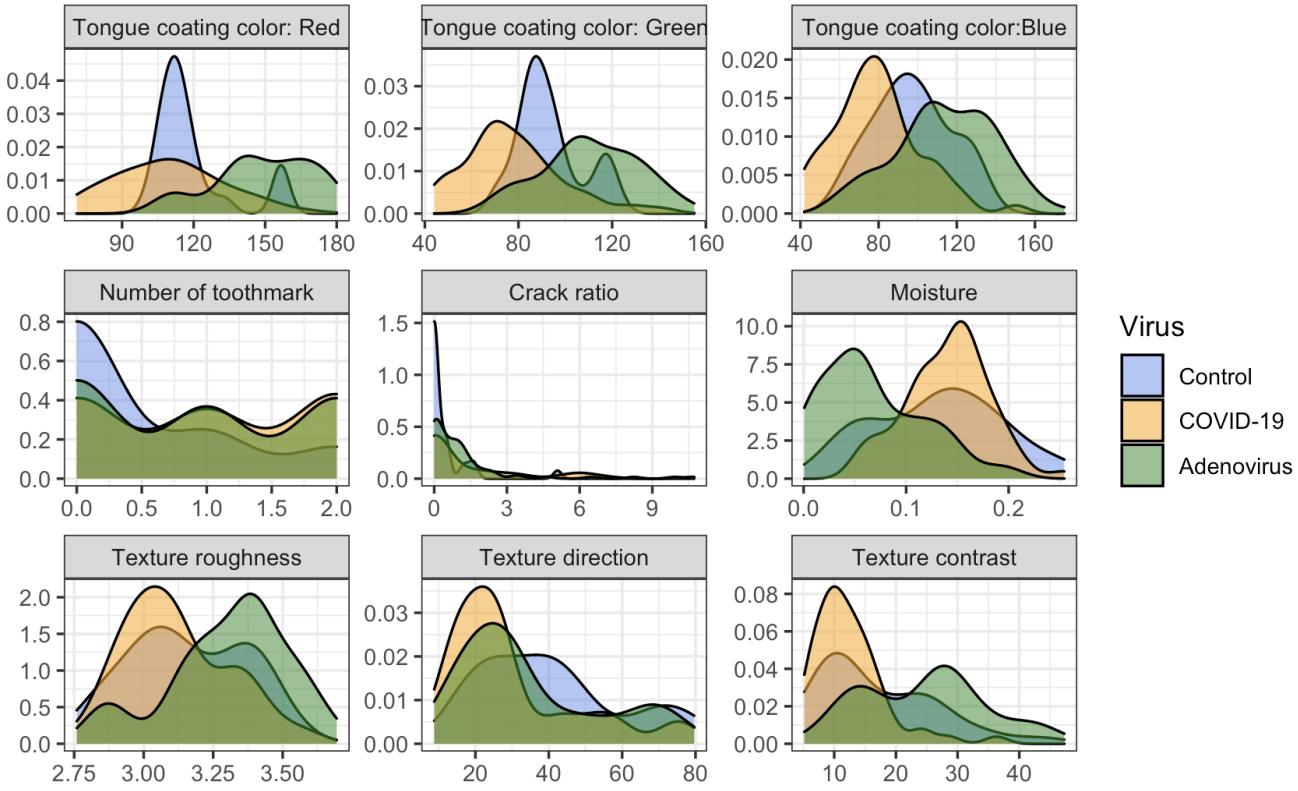
Tongue Image Feature Extraction and Definition

We used transfer learning techniques using weights obtained from training on the VOC 2007 and VOC 2012 datasets, which enabled the model to improve its understanding of general object detection. After 60,000 iterations with a learning rate of 0.0001, the average loss was reduced to 0.2867 (SD 0.0462; Multimedia Appendix 3). Compared to the proposed fast recurrent neural network and faster region-based convolutional neural network, the Single Shot MultiBox Detector architecture demonstrates higher accuracy across 20 labeled datasets (Multimedia Appendix 4). After applying our feature extraction architecture, 9 features of tongue images were identified: tongue coating color values (red, green, and blue), the presence of tooth marks, tongue coating crack ratio, tongue coating moisture level, texture directionality, texture roughness, and texture contrast (Multimedia Appendix 5).

All tongue coating color values (red, green, and blue) differed significantly across groups (P<.001) (Table 1). Patients with adenovirus had the highest values, on average, especially in the red component, which may indicate more pronounced inflammation or other specific clinical features related to adenovirus infections. The presence of tooth marks varied across groups, with the highest prevalence of 2 tooth marks in the COVID-19 group, with 21/58 (36%) participants showing this feature (P=.049). While the differences may not be statistically significant, both the COVID-19 and adenovirus groups exhibit a notably higher percentage of individuals with 2 tooth marks: 21/58 (36%) participants in the COVID-19 group and 27/84 (32%) participants in the adenovirus group. This is in contrast to the control group, where only 4/30 (13%) participants showed this characteristic (P=.09). This may be associated with other symptoms or manifestations of the illness. The moisture levels of tongue coating varied significantly among the different groups, with the adenovirus group exhibiting the lowest average moisture level (P<.01).

The adenovirus group shows considerably greater levels of tongue coating roughness compared to the COVID-19 and control groups (P<.01). In addition, both the adenovirus and COVID-19 groups exhibit significantly greater values in tongue texture direction than the control group, with the adenovirus group showing the highest mean value of 40.7 (SD 19.1). In terms of texture contrast, the COVID-19 group has the lowest average value at 12.5 (SD 5.8), while the adenovirus group reaches the highest average at 24.6 (SD 9.9), in contrast to the control group, which averages 17.1 (SD 9.4). The density plot suggested distinct patterns in tongue features among individuals with COVID-19, adenovirus, and those in the control group, demonstrating the potential of these features in differentiating respiratory viral infections (Figure 3).

Figure 3. Extracted tongue image feature density plot.



Diagnostic Performance Results

The tree-based and boosting models achieved over 70% AUCPR performance, with AUC exceeding 80% for general performance. The GBM achieved the highest AUC value of 0.888 and AUCPR value of 0.764. XGBoost came in second with an AUC value of 0.872 and an AUCPR value of 0.751, followed closely by random forest with an AUC value of 0.872 and an AUCPR value of 0.747. However, logistic regression showed a relatively worse performance, with an AUC value of 0.812 and an AUCPR value of 0.668 (Multimedia Appendix 6), and the confusion matrix of the test set is presented in Multimedia Appendix 7.

XSL•FO
RenderX

Explaining the Rationale Behind the Predicted Models

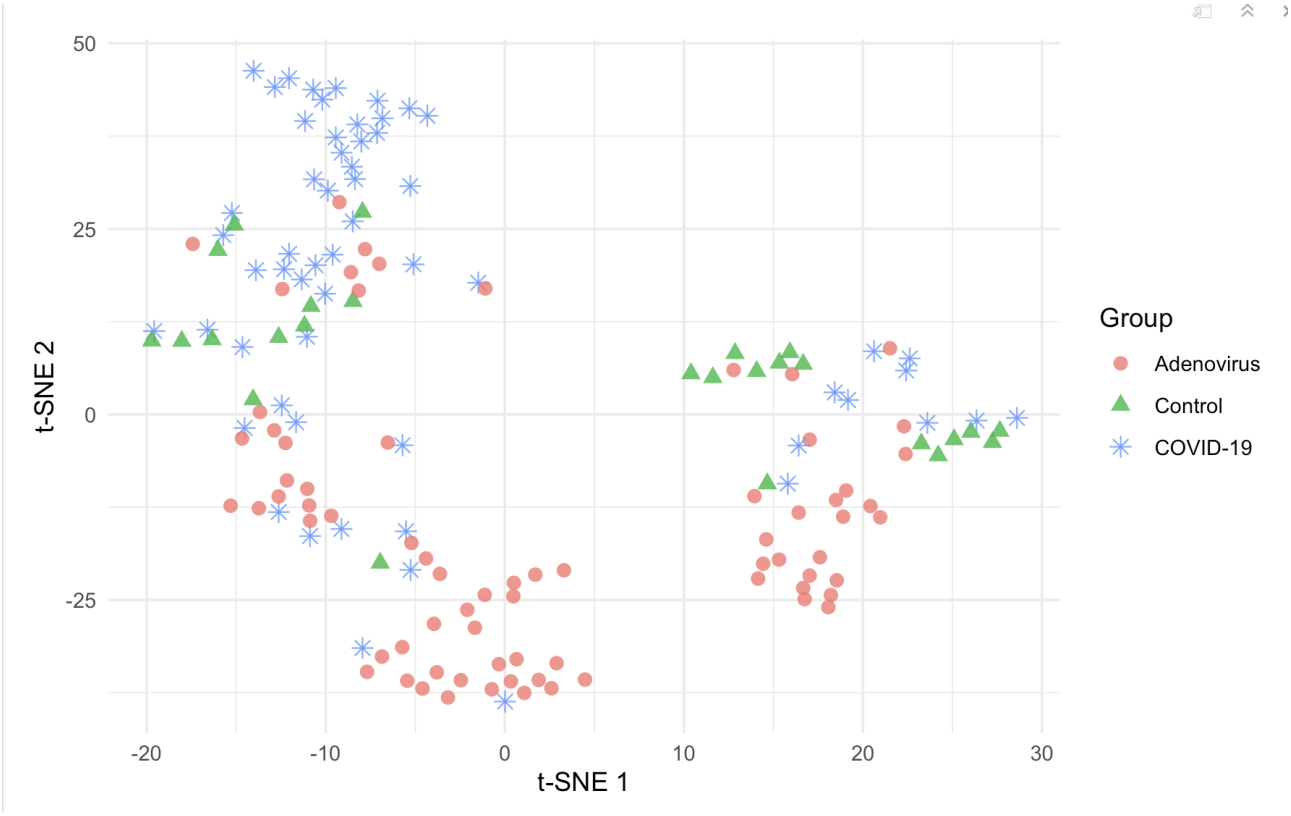
Based on SHAP values integrating 4 machine learning models, several factors contribute to diagnosing adenovirus and COVID-19, including the color of tongue coating, moisture level, and texture direction. The feature importance plots indicate that the most significant variables are tongue color, moisture level, and texture direction (Multimedia Appendix 8). Specifically, a red tongue coating helps identify adenovirus cases, while a green tongue coating is beneficial for identifying COVID-19 cases (Figure 4). In addition, the t-SNE plot projects these variables into a 2D space and color codes each group. The distribution of patients with COVID-19 and adenovirus differs within the t-SNE space, showing some overlap, while the control group is between the 2 infectious cases (Figure 5).

XSL•FO
RenderX

Figure 4. Important features identified for distinguishing between COVID-19 (top), adenovirus (middle), and control (bottom) using SHAP. SHAP: Shapley additive explanations.

XSL•FO
RenderX

Figure 5. T-distributed stochastic neighbor embedding plot visualizing sample distribution across three groups: adenovirus (circle), control (triangle), and COVID-19 (asterisk), highlighting distinct clustering patterns among the conditions. t-SNE: t-distributed stochastic neighbor embedding.



Discussion

In this study, we developed and validated an AI-based prediction model to analyze tongue images for the differential diagnosis of respiratory infections caused by COVID-19 and human adenoviruses. Our models demonstrated high diagnostic accuracy, with key tongue image features, such as color, coating, moisture, and texture serving as significant discriminators. These findings highlight the potential of noninvasive tongue image analysis as an effective and cost-efficient diagnostic tool, which may facilitate early and accurate differentiation of respiratory viral infections and support clinical decision-making.

In recent years, the concurrent prevalence of respiratory infectious diseases, such as COVID-19 and HAdVs, has made it challenging to establish a differential diagnosis without pathogenic testing, thereby impacting the efficacy of the treatment [29]. Tongue image diagnosis has emerged as an effective, noninvasive method for auxiliary diagnosis that can be conducted in various settings, catering to the global demands of primary health care systems [30]. In this study, we developed machine learning models that use tongue images to predict acute respiratory tract infection (ARTI) pathogens. The accuracy of these models exceeded 80%, with feature importance plots revealing tongue color, moisture level, and tongue texture direction as pivotal variables. We then projected the tongue image features of the 3 groups of participants into a lower-dimensional space by t-SNE plot. The resulting clusters of COVID-19 and adenovirus were notably distinct, suggesting that the tongue image parameters we extracted contribute significantly to the diagnosis of ARIs. This noninvasive, convenient, and rapid approach has the potential to mitigate unnecessary diagnostic procedures and reduce health care costs.

The constructability of a risk warning model using tongue diagnosis data has been validated in research on metabolic diseases and cancers [16,31]. Our study is pioneering in applying AI deep learning techniques to investigate the diagnostic value of tongue images in acute respiratory tract infection diagnosis and can be integrated into clinical practice to aid decision-making and alleviate physician burden. Previous research by Mai and Krauthammer [32] aimed to predict common respiratory viruses in the United States by combining natural language processing tools with machine learning techniques. However, the model's prediction performance of HAdVs was moderate, with an area under the receiver operating characteristic curve (AUROC) of 0.53 [32]. Chang et al [33] used an XGBoost model, incorporating demographic, physical examination, laboratory, and vital sign data, to predict HAdVs in hospitalized children with respiratory symptoms, achieving an AUROC of 0.82. Our model exhibited superior performance, achieving an AUROC of 0.87, following the inclusion of various features in its development. In contrast to models established in previous studies, the model developed in this paper benefited from the usage of noninvasive tongue image data, obviating the need for laboratory examination indicators. By using the YOLOv4 object detection framework for image feature extraction and integrating ensemble learning algorithms (ie, GBM and XGBoost), we have demonstrated the clinical utility of tongue images. All 4 models exhibited discriminative validity over tongue images, indicating that tongue images can serve as a reliable tool for ARTI diagnosis and are robust across different AI deep learning model types. Notably, tree-based models, such

XSL•FO
RenderX

as GBM, XGBoost, and random forest, outperform logistic regression due to their ability to capture complex nonlinear relationships and interactions among features. Tongue image-derived features often display nonlinear patterns that contradict the linear assumptions of logistic regression. In contrast, tree-based models are nonparametric and resistant to multicollinearity, making them ideal for complex datasets derived from image analysis.

Previous research has validated the use of objective tongue image acquisition equipment, methods, and data analysis techniques [34]. Research on AI in TCM tongue diagnosis has predominantly focused on standardizing tongue diagnosis to minimize human errors [34]. Xu et al [35] developed a multitask joint learning model for segmenting and classifying tongue images, using a deep neural network to optimally extract tongue image features. Meng et al [36] proposed a novel feature extraction framework, termed constrained high dispersal neural networks, to extract unbiased features and minimize human labor in TCM tongue image diagnosis. This study used the YOLOv4 framework, which excelled in extracting high-level image features, thereby enhancing the model's capacity to identify intricate patterns and subtle variations [21]. The model was initially pretrained on the VOC 2007 and VOC 2012, which are effective for capturing general low-level visual features but lack domain-specific characteristics relevant to medical imagery, such as tongue images. To overcome the challenge of transferring features from natural datasets to specialized domains, domain-specific fine-tuning was performed using collected samples and synthetic data. Although the limited sample size may restrict the model's ability to capture complex patterns in tongue imagery, the fine-tuned feature extractor achieved approximately 95% classification accuracy across 20 defined groups, demonstrating effective adaptation. This integration, coupled with the fusion of ensemble learning algorithms, harnesses the complementary strengths of clinical and image-derived features, effectively addressing the limitations of each modality in isolation [37]. Consequently, the model gains enhanced discriminative power, leading to more accurate predictions of ARTI.

The analysis of feature importance in machine learning models (GBM, XGBoost, and random forest) revealed that a red tongue coat is most indicative of HAdVs and control group, while the green color is more suggestive of COVID-19 cases. Furthermore, statistical analysis of the tongue images of the 3 groups showed that the COVID-19 group had a higher moisture level and lower contrast rate, suggesting that the patients with COVID-19 are more likely to have a thicker and greasier tongue coating compared to the other 2 groups. Our findings align with the TCM theory. According to TCM, COVID-19 is classified as a "cold-dampness" disease, characterized by a tongue that is pale red or dark and a thick, white greasy coating. HAdVs are considered "warm" diseases in TCM, typically presenting with red and dry tongues. The thickness and dryness of the tongue coating can also indicate the severity of the disease and the extent of fluid damage. Epidemiological studies conducted in China, the United Kingdom, and Ukraine have yielded analogous findings; the predominant tongue colors observed were pale pink and dark red, with the most frequently encountered tongue coating being thin and greasy [38-40]. Therefore, a patient presenting with acute respiratory symptoms and a red tongue devoid of a thick, greasy coating is more likely to have an HAdVs infection. Such observations could guide health care professionals in suggesting additional diagnostic tests and preventive measures, like isolation or improved hygiene, to avert transmission to susceptible household members. Considering its noninvasive nature and rapid assessment capability, AI-assisted tongue image analysis could be particularly valuable as a screening or triage tool in primary care clinics and emergency departments, where timely differentiation of respiratory infections is essential. The advancement of large language models and multimodal AI has facilitated the development of intelligent diagnostic systems that enhance tongue image interpretation and provide real-time decision support. These technologies not only assist clinicians in prioritizing patients for confirmatory testing and early intervention, optimizing health care resource allocation but also enable remote patient monitoring and telemedicine applications.

Hypothetically, the SARS-CoV-2 virus may induce alterations in the expression levels of genes coding for apoptosis and necroptosis of epithelial cells [41,42], resulting in the accumulation of oral epithelial cells and increasing tongue coating thickness. However, these proposed mechanisms remain preliminary and require further experimental validation to clarify their roles in oral manifestations of COVID-19. Supporting the clinical relevance of tongue changes, Wang et al [43] found a correlation between tongue coating thickness in patients with COVID-19 and levels of white blood cells as well as the neutrophil-to-lymphocyte ratio. Conversely, in patients with fever who tested negative for COVID-19, the presence of slimy or greasy tongue fur was associated with the level of C-reactive protein [43]. In addition, studies have indicated that greasy tongue fur is associated with higher blood fibrinogen levels in patients with stroke and with increased activity of glossal epithelial cells and vascular permeability in rodent models [44,45].

It is important to acknowledge several limitations of this study that may impact the generalizability of its findings. Although our predictive models demonstrate the potential of tongue image features for the differential diagnosis of acute respiratory tract infections, their accuracy remains modest, with area under the precision-recall curve (AUPRC) values below 80% across all models (Multimedia Appendix 7). Visualization of the data using t-SNE projected the 3 groups into generally distinct but overlapping clusters in 2D feature space, with considerable overlap, especially between the COVID-19 and adenovirus groups. This overlap is further reflected in our confusion matrix analyses, which consistently show misclassifications between these 2 groups across all classification models. Such overlap between the COVID-19 and adenovirus groups observed in the t-SNE projection may be partly attributable to the similarity of tongue image features shared by these 2 patient populations. In addition, the dimensionality reduction inherent in t-SNE can lead to loss of critical discriminative information, further exacerbating this overlap. Together with the limited sample size used for model development and validation, as well as the exclusion of additional clinical information, such as patient

XSL•FO
RenderX

symptoms and other relevant features, these factors collectively contribute to the modest accuracy of our predictive models. Furthermore, the COVID-19 pandemic's operational constraints necessitated data collection at a single tertiary hospital. Nevertheless, as a national referral center serving Beijing and surrounding provinces, our institution treats patients from geographically diverse regions, which may partially mitigate concerns regarding population representativeness. Future studies should incorporate larger and more diverse cohorts, combined with the integration of comprehensive clinical data, which are warranted to improve the discriminative power and generalizability of the models.

Conclusion

This study illustrates the utility of AI in helping clinicians identify potential pathogens in ARTI at the time of admission. The interpretability and clinical relevance of our models suggest that they may help reduce unnecessary medical costs and diagnostic procedures while maintaining diagnostic accuracy. Moreover, by alleviating clinicians' workloads, this approach has the potential to enhance the overall quality of medical care. Looking forward, further research is warranted to externally validate these predictive models in independent cohorts and to expand the sample size to improve generalizability. In addition, incorporating clinical symptoms and other patient-specific features could further refine model performance and support more comprehensive decision-making in respiratory infection diagnosis.

Acknowledgments

We would like to acknowledge Dr. Wei Yang as a co-corresponding author. Correspondent to: Prof. YANG Wei, Department of Medical Statistics, Institute of Basic Research in Clinical Medicine, China Academy of Chinese Medical Sciences, Beijing 100700, China. yangyxq@ruc.edu.cn; Ruilin Wang, PhD, The Fifth Medical Center of PLA General Hospital, Beijing, China, WRL7905@163.com.

This work was supported by the National Key Research and Development Program (2023YFC3503404), Science and Technology Innovation Project of the China Academy of Chinese Medical Sciences (CI2023C066YLL, CI2021B003, CI2021A04706).

Data Availability

The datasets generated or analyzed during this study are not publicly available due to data-sharing agreements with the participating hospitals but are available from the corresponding author on reasonable request.

Authors' Contributions

QC and YL conceptualized and designed the study, as well as drafted the main manuscript text. ZW, LL and RW collected the tongue image data and curated the dataset. FX developed and implemented the machine learning models. XC contributed to data visualization and statistical analysis. WY and RW supervised the overall study and provided critical revisions to the manuscript.

Conflicts of Interest

None declared.

Multimedia Appendix 1
Tongue image segmentation and feature extraction parameters for 20 labels.
[DOCX File, 13 KB - medinform_v13i1e74102_app1.docx]

Multimedia Appendix 2
Parameters for each layer in the proposed architecture.
[DOCX File, 13 KB - medinform_v13i1e74102_app2.docx]

Multimedia Appendix 3
Iteration loss plot. We iterated 40,000 times with an initial learning rate of 0.001, then reduced it to 0.0001 and continued until 60,000 iterations. Finally, we set the learning rate to 0.00001 and extended the iteration to 70,000.
[PNG File, 74 KB - medinform_v13i1e74102_app3.png]

Multimedia Appendix 4
Accuracy comparison among fast recurrent neural network (blue), faster region-based convolutional neural network (orange), and Proposed Single Shot MultiBox Detector (green).
[PNG File, 32 KB - medinform_v13i1e74102_app4.png]

XSL•FO
RenderX

Multimedia Appendix 5
Identified tongue image variables.
[DOCX File, 13 KB - medinform_v13i1e74102_app5.docx]

Multimedia Appendix 6
Model assessment matrices for 4 classifiers and 95% CI.
[DOCX File, 13 KB - medinform_v13i1e74102_app6.docx]

Multimedia Appendix 7
Confusion matrix for machine learning model.
[PNG File, 201 KB - medinform_v13i1e74102_app7.png]

Multimedia Appendix 8
Mean Shapley additive explanations value over the random forest, gradient boosting machines, extreme gradient boosting. A longer bar indicates the variable is of higher importance in model performance. GMB: Gradient boosting machines.
[PNG File, 159 KB - medinform_v13i1e74102_app8.png]

References

1. Lynch JP 3rd, Fishbein M, Echavarria M. Adenovirus. Semin Respir Crit Care Med 2011 Aug;32(4):494-511. [doi: 10.1055/s-0031-1283287] [Medline: 21858752]
2. Liu MC, Xu Q, Li TT, et al. Prevalence of human infection with respiratory adenovirus in China: a systematic review and meta-analysis. PLoS Negl Trop Dis 2023 Feb;17(2):e0011151. [doi: 10.1371/journal.pntd.0011151] [Medline: 36812245]
3. Del Riccio M, Caini S, Bonaccorsi G, et al. Global analysis of respiratory viral circulation and timing of epidemics in the pre-COVID-19 and COVID-19 pandemic eras, based on data from the Global Influenza Surveillance and Response System (GISRS). Int J Infect Dis 2024 Jul;144:107052. [doi: 10.1016/j.ijid.2024.107052] [Medline: 38636684]
4. Chow EJ, Uyeki TM, Chu HY. The effects of the COVID-19 pandemic on community respiratory virus activity. Nat Rev Microbiol 2023 Mar;21(3):195-210. [doi: 10.1038/s41579-022-00807-9] [Medline: 36253478]
5. Cho HJ, Rhee JE, Kang D, et al. Epidemiology of respiratory viruses in Korean children before and after the COVID-19 pandemic: a prospective study from national surveillance system. J Korean Med Sci 2024 May 20;39(19):e171. [doi: 10.3346/jkms.2024.39.e171] [Medline: 38769924]
6. Wen S, Lin Z, Zhang Y, et al. The epidemiology, molecular, and clinical of human adenoviruses in children hospitalized with acute respiratory infections. Front Microbiol 2021;12:629971. [doi: 10.3389/fmicb.2021.629971] [Medline: 33664719]
7. Babawale PI, Guerrero-Plata A. Respiratory viral coinfections: insights into epidemiology, immune response, pathology, and clinical outcomes. Pathogens 2024 Apr 12;13(4):316. [doi: 10.3390/pathogens13040316] [Medline: 38668271]
8. Wang WY, Zhou H, Wang YF, Sang BS, Liu L. Current policies and measures on the development of traditional Chinese medicine in China. Pharmacol Res 2021 Jan;163:105187. [doi: 10.1016/j.phrs.2020.105187] [Medline: 32916255]
9. Li J, Chen Y, Yu X, Xie Y, Li X, Diagnosis and Treatment Guideline for Chinese Medicine on Acute Trachea‐Bronchitis working team, Respiratory Disease Branch of China Association of Chinese Medicine, Respiratory Disease Branch of China Medical Association of Minorities. Diagnosis and treatment guideline for Chinese medicine on acute trachea‐bronchitis. J Evidence Based Medicine 2021 Dec;14(4):333-345. [doi: 10.1111/jebm.12460]
10. Iranmanesh B, Khalili M, Amiri R, Zartab H, Aflatoonian M. Oral manifestations of COVID-19 disease: A review article. Dermatol Ther 2021 Jan;34(1):e14578. [doi: 10.1111/dth.14578] [Medline: 33236823]
11. Jones VG, Mills M, Suarez D, et al. COVID-19 and Kawasaki Disease: Novel Virus and Novel Case. Hosp Pediatr 2020 Jun;10(6):537-540. [doi: 10.1542/hpeds.2020-0123] [Medline: 32265235]
12. Chiotos K, Bassiri H, Behrens EM, et al. Multisystem Inflammatory Syndrome in Children During the Coronavirus 2019 Pandemic: A Case Series. J Pediatric Infect Dis Soc 2020 Jul 13;9(3):393-398. [doi: 10.1093/jpids/piaa069] [Medline: 32463092]
13. Taşlıdere B, Mehmetaj L, Özcan AB, Gülen B, Taşlıdere N. Melkersson-Rosenthal Syndrome Induced by COVID-19. Am J Emerg Med 2021 Mar;41(262):262. [doi: 10.1016/j.ajem.2020.08.018] [Medline: 32829989]
14. Li J, Chen Q, Hu X, et al. Establishment of noninvasive diabetes risk prediction model based on tongue features and machine learning techniques. Int J Med Inform 2021 May;149:104429. [doi: 10.1016/j.ijmedinf.2021.104429] [Medline: 33647600]
15. Jiang T, Guo XJ, Tu LP, et al. Application of computer tongue image analysis technology in the diagnosis of NAFLD. Comput Biol Med 2021 Aug;135:104622. [doi: 10.1016/j.compbiomed.2021.104622] [Medline: 34242868]
16. Shi Y, Guo D, Chun Y, et al. A lung cancer risk warning model based on tongue images. Front Physiol 2023;14:1154294. [doi: 10.3389/fphys.2023.1154294] [Medline: 37324390]
17. Yuan L, Yang L, Zhang S, et al. Development of a tongue image-based machine learning tool for the diagnosis of gastric cancer: a prospective multicentre clinical cohort study. EClinicalMedicine 2023 Mar;57:101834. [doi: 10.1016/j.eclinm.2023.101834] [Medline: 36825238]

XSL•FO
RenderX

18. Zhou J, Zhang Q, Zhang B. An automatic multi-view disease detection system via Collective Deep Region-based Feature Representation. Future Gener Comput Syst 2021 Feb;115:59-75. [doi: 10.1016/j.future.2020.08.038]
19. Dutta D, Naiyer S, Mansuri S, et al. COVID-19 diagnosis: a comprehensive review of the RT-qPCR method for detection of SARS-CoV-2. Diagnostics (Basel) 2022 Jun 20;12(6):1503. [doi: 10.3390/diagnostics12061503] [Medline: 35741313]
20. Matthes-Martin S, Feuchtinger T, Shaw PJ, Matthes‐Martin S, et al. European guidelines for diagnosis and treatment of adenovirus infection in leukemia and stem cell transplantation: summary of ECIL-4 (2011). Transpl Infect Dis 2012 Dec;14(6):555-563. [doi: 10.1111/tid.12022] [Medline: 23146063]
21. Bochkovskiy A, Wang CY, Liao HYM. Yolov4: optimal speed and accuracy of object detection. arXiv. Preprint posted online on Apr 23, 2020arXiv:200410934.
22. O'Shea K. An introduction to convolutional neural networks. arXiv. Preprint posted online on Dec 2, 2015. [doi: 10.48550/arXiv.1511.08458]
23. Hao R, Namdar K, Liu L, Haider MA, Khalvati F. A comprehensive study of data augmentation strategies for prostate cancer detection in diffusion-weighted MRI using convolutional neural networks. J Digit Imaging 2021 Aug;34(4):862-876. [doi: 10.1007/s10278-021-00478-7] [Medline: 34254200]
24. Tamura H, Mori S, Yamawaki T. Textural features corresponding to visual perception. IEEE Trans Syst, Man, Cybern 1978;8(6):460-473. [doi: 10.1109/TSMC.1978.4309999]
25. Donders ART, van der Heijden GJMG, Stijnen T, Moons KGM. Review: a gentle introduction to imputation of missing values. J Clin Epidemiol 2006 Oct;59(10):1087-1091. [doi: 10.1016/j.jclinepi.2006.01.014] [Medline: 16980149]
26. Fernández A, García S, Galar M, Prati RC, Krawczyk B, Herrera F. Learning from Imbalanced Data: Springer; 2018.
27. Marcilio WE, Eler DM, editors. From explanations to feature selection: assessing SHAP values as feature selection mechanism. Presented at: 2020 33rd SIBGRAPI Conference on Graphics, Patterns and Images (SIBGRAPI); Nov 7-10, 2020; Porto de Galinhas, Brazil.
28. Van Der Maaten L. Accelerating t-SNE using tree-based algorithms. J Mach Learn Res 2014;15(1):3221-3245. [doi: 10.5555/2627435.2697068]
29. Krumbein H, Kümmel LS, Fragkou PC, et al. Respiratory viral co-infections in patients with COVID-19 and associated outcomes: a systematic review and meta-analysis. Rev Med Virol 2023 Jan;33(1):e2365. [doi: 10.1002/rmv.2365] [Medline: 35686619]
30. Wen G, Ma J, Hu Y, Li H, Jiang L. Grouping attributes zero-shot learning for tongue constitution recognition. Artif Intell Med 2020 Sep;109:101951. [doi: 10.1016/j.artmed.2020.101951] [Medline: 34756217]
31. Li J, Yuan P, Hu X, et al. A tongue features fusion approach to predicting prediabetes and diabetes with machine learning. J Biomed Inform 2021 Mar;115:103693. [doi: 10.1016/j.jbi.2021.103693] [Medline: 33540076]
32. Mai MV, Krauthammer M. Controlling testing volume for respiratory viruses using machine learning and text mining. AMIA Annu Symp Proc 2017;2016:1910-1919. [Medline: 28269950]
33. Chang TH, Liu YC, Lin SR, et al. Clinical characteristics of hospitalized children with community-acquired pneumonia and respiratory infections: using machine learning approaches to support pathogen prediction at admission. J Microbiol Immunol Infect 2023 Aug;56(4):772-781. [doi: 10.1016/j.jmii.2023.04.011] [Medline: 37246060]
34. Tania MH, Lwin K, Hossain MA. Advances in automated tongue diagnosis techniques. Integr Med Res 2019 Mar;8(1):42-56. [doi: 10.1016/j.imr.2018.03.001] [Medline: 30949431]
35. Xu Q, Zeng Y, Tang W, et al. Multi-task joint learning model for segmenting and classifying tongue images using a deep neural network. IEEE J Biomed Health Inform 2020 Sep;24(9):2481-2489. [doi: 10.1109/JBHI.2020.2986376] [Medline: 32310809]
36. Meng D, Cao G, Duan Y, et al. Tongue images classification based on constrained high dispersal network. Evid Based Complement Alternat Med 2017;2017:7452427. [doi: 10.1155/2017/7452427] [Medline: 28465706]
37. Li B, Chen H, Lin X, Duan H. Multimodal learning system integrating electronic medical records and hysteroscopic images for reproductive outcome prediction and risk stratification of endometrial injury: a multicenter diagnostic study. Int J Surg 2024 Jun 1;110(6):3237-3248. [doi: 10.1097/JS9.0000000000001241] [Medline: 38935827]
38. Horzov L, Goncharuk-Khomyn M, Hema-Bahyna N, Yurzhenko A, Melnyk V. Analysis of tongue color-associated features among patients with PCR-confirmed COVID-19 infection in Ukraine. Pesqui Bras Odontopediatria Clín Integr 2021;21. [doi: 10.1590/pboci.2021.109]
39. Wen Z, Min C, Ding S, et al. Tongue and pulse features of 668 asymptomatic patients infected with the severe acute respiratory syndrome coronavirus 2 omicron variant in Shanghai. J Tradit Chin Med 2022 Dec;42(6):1006-1011. [doi: 10.19852/j.cnki.jtcm.20220922.004] [Medline: 36378060]
40. D J. Diagnosis and management of TCM on infected or suspected patients with Covid-19-48 cases study in UK. JCV 2021;01(4) [FREE Full text] [doi: 10.47690/JCV.2021.1403]
41. Ravindra NG, Alfajaro MM, Gasque V, et al. Single-cell longitudinal analysis of SARS-CoV-2 infection in human airway epithelium identifies target cells, alterations in gene expression, and cell state changes. PLoS Biol 2021 Mar;19(3):e3001143. [doi: 10.1371/journal.pbio.3001143] [Medline: 33730024]
42. Zhu Z, Shi J, Li L, Wang J, Zhao Y, Ma H. Therapy targets SARS-CoV-2 infection-induced cell death. Front Immunol 2022;13:870216. [doi: 10.3389/fimmu.2022.870216] [Medline: 35655782]

XSL•FO
RenderX

43. Wang ZC, Cai XH, Chan J. Tongue coating in COVID-19 patients: a case-control study. medRxiv. Preprint posted online on Apr 15, 2024. [doi: 10.1101/2022.03.14.22272342]
44. Gao L, Liu P, Song JX, et al. Study on the correlation of tongue manifestation with fibrinogen and neutrophil in acute cerebral infarction patients. Chin J Integr Med 2012 Dec;18(12):942-945. [doi: 10.1007/s11655-012-1298-y] [Medline: 23239003]
45. Qi WJ, Zhang MM, Wang H, Wen Y, Wang BE, Zhang SW. Research on the relationship between thick greasy tongue fur formation and vascular endothelial cell permeability with the protein expression of zonula occludens-1. Chin J Integr Med 2011 Jul;17(7):510-516. [doi: 10.1007/s11655-011-0784-1] [Medline: 21725876]

Abbreviations

AI: artificial intelligence
ARTI: acute respiratory tract infection
AUC: area under the curve
AUCPR: area under the precision-recall curve
AUROC: area under the receiver operating characteristic curve
GBM: gradient boosting machine
HAdV: human adenovirus
PLA: People's Liberation Army
RNN: R
SHAP: Shapley additive explanations
t-SNE: t-distributed stochastic neighbor embedding
TCM: traditional Chinese medicine
XGBoost: extreme gradient boosting

Edited by A Benis; submitted 18.03.25; peer-reviewed by A Adeoye, KA Obisesan Olawuni; revised version received 24.06.25; accepted 24.06.25; published 25.08.25.

Please cite as:
Che Q, Leng Y, Yang W, Cao X, Wang Z, Liu L, Xie F, Wang R
Tongue Image–Based Diagnosis of Acute Respiratory Tract Infection Using Machine Learning: Algorithm Development and Validation
JMIR Med Inform 2025;13:e74102
URL: https://medinform.jmir.org/2025/1/e74102
doi:10.2196/74102

© Qianzi Che, Yuanming Leng, Wei Yang, Xihao Cao, Zhongxia Wang, Lizheng Liu, Feibiao Xie, Ruilin Wang. Originally published in JMIR Medical Informatics (https://medinform.jmir.org), 25.8.2025. This is an open-access article distributed under the terms of the Creative Commons Attribution License (https://creativecommons.org/licenses/by/4.0/), which permits unrestricted use, distribution, and reproduction in any medium, provided the original work, first published in JMIR Medical Informatics, is properly cited. The complete bibliographic information, a link to the original publication on https://medinform.jmir.org/, as well as this copyright and license information must be included.

XSL•FO
RenderX

Prediction of Mini-Mental State Examination Scores for Cognitive Impairment and Machine Learning Analysis of Oral Health and Demographic Data Among Individuals Older Than 60 Years: Cross-Sectional Study

Alper Idrisoglu, MSc; Johan Flyborg, PhD, DDS; Sarah Nauman Ghazi, MSc; Elina Mikaelsson Midlöv, MSc; Helén Dellkvist, MSc; Anna Axén, MSc; Ana Luiza Dallora, PhD

Department of Health, Blekinge Institute of Technology, Valhallavägen 1, Karlskrona, Sweden

Corresponding Author:
Alper Idrisoglu, MSc
Department of Health, Blekinge Institute of Technology, Valhallavägen 1, Karlskrona, Sweden

Abstract

Background: As the older population grows, so does the prevalence of cognitive impairment, emphasizing the importance of early diagnosis. The Mini-Mental State Examination (MMSE) is vital in identifying cognitive impairment. It is known that degraded oral health correlates with MMSE scores ≤26.

Objective: This study aims to explore the potential of using machine learning (ML) technologies using oral health and demographic examination data to predict the probability of having MMSE scores of 30 or ≤26 in Swedish individuals older than 60 years.

Methods: The study had a cross-sectional design. Baseline data from 2 longitudinal oral health and ongoing general health studies involving individuals older than 60 years were entered into ML models, including random forest, support vector machine, and CatBoost (CB) to classify MMSE scores as either 30 or ≤26, distinguishing between MMSE of 30 and MMSE ≤26 groups. Nested cross-validation (nCV) was used to mitigate overfitting. The best performance-giving model was further investigated for feature importance using Shapley additive explanation summary plots to easily visualize the contribution of each feature to the prediction output. The sample consisted of 693 individuals (350 females and 343 males).

Results: All CB, random forest, and support vector machine models achieved high classification accuracies. However, CB exhibited superior performance with an average accuracy of 80.6% on the model using 3 × 3 nCV and surpassed the performance of other models. The Shapley additive explanation summary plot illustrates the impact of factors on the model's predictions, such as age, Plaque Index, probing pocket depth, a feeling of dry mouth, level of education, and use of dental hygiene tools for approximal cleaning.

Conclusions: The oral health parameters and demographic data used as inputs for ML classifiers contain sufficient information to differentiate between MMSE scores ≤26 and 30. This study suggests oral health parameters and ML techniques could offer a potential tool for screening MMSE scores for individuals aged 60 years and older.

(JMIR Med Inform 2025;13:e75069) doi:10.2196/75069

KEYWORDS

classification; machine learning; mini-mental state examination; cognitive impairment; oral health

Introduction

The anticipated global population of 8 billion individuals for 2023 has been achieved. The population growth continues to persist, albeit experiencing a decelerated trajectory. Global birth rates are declining, juxtaposed with a consistent upward trajectory in average life expectancy, attributed to advancements in scientific knowledge, improved nutritional standards, advancements in public health infrastructure, and enhanced sanitation practices [1]. An estimate for the year 2050 suggests that individuals aged 60 years and older will constitute 38% of the total population and will continue to increase. While many individuals enjoy several quality years of life, a significant portion of them will also struggle with neurocognitive diseases such as Alzheimer disease (AD) and mild cognitive impairment (MCI) [2]. Until now, diagnosing AD, which is the most common neurocognitive disorder, has required extensive hospital-level efforts, and no curative treatment has been available [3]. Recent research has identified biomarkers in blood that identify proteins associated with AD [4]. At the same time, several approved antibody medications now stop the breakdown of nerve cells caused by phosphorylated Tau and amyloid plaques [5]. This is expected to significantly burden the health care system, as early diagnosis is essential for a good treatment

XSL•FO
RenderX

result. The need for screening methods is expected to be extensive. It is widely recognized that MCI and neurocognitive diseases contribute to deteriorating oral health, with individuals affected by these conditions exhibiting poorer oral health [6,7]. The decline in oral health carries profound implications, causing hardship for affected individuals and placing substantial demands on society and health care systems in terms of both costs and human resources. However, recent research suggests that the deterioration of oral health in individuals with MCI can be delayed by at least 12 months through the introduction of a powered toothbrush [8]. Additionally, severe periodontitis poses a risk factor for dementia [9]. Various instruments are available to assess cognitive function, with one of the most commonly used being the Mini-Mental State Examination (MMSE) test, which is internationally recognized and validated in numerous languages. The MMSE scale ranges from 0 to 30, with higher scores indicating a better cognitive function [10]. Recently, machine learning (ML) has emerged as a valuable aid in enhancing the precision and efficiency of cognitive assessments [11,12], leading to significant progress in the field of cognitive research [13-15]. Various datasets and algorithms can be used to better predict MMSE scores, differentiate between MCI and AD, and improve cognitive test batteries. A comprehensive study used a multifaceted approach, integrating brain cortical characteristics, biological markers, risk factors, positron emission tomography scan measures, and cognitive scores into a joint feature set to predict MMSE scores at 6 and 12 months, achieving mean absolute errors of 1.40 [16]. Researchers have improved predictive accuracy by experimenting with ML algorithms, including logistic regression, decision trees, support vector machine (SVM), XGBoost, and random forests (RF). This approach enhances diagnostic precision and offers valuable insights into disease progression and treatment response [17]. Similarly, previous research has explored integrating MRI data with cognitive tests, such as logical memory, to detect and distinguish individuals with normal cognition from those with MCI. Through deep learning models trained on MRI slices and fusion techniques, the combined model surpassed individual modalities in predictive performance, underscoring the potential of multimodal fusion in cognitive assessment, achieving an accuracy of 90.9% [18]. Earlier research has explored the area of oral health and its relationship with cognitive health. One meta-analysis [19] found that oral health in individuals with dementia was significantly worse than that of the controls. Another systematic literature review [20] came to a similar conclusion, attributing this to both difficulties in self-care due to the consequences of the disease and inflammatory mechanisms. Further, a systematic literature review [21] also indicated an association between oral health and cognitive impairment, implying a bidirectional relationship between these and ratifying a need for higher-level evidence in this area. Another systematic literature review analyzed the effects of oral interventions on cognition and found that dental treatments had a subjective influence on cognition [22]. One study [23] explored the relationship between oral health–related quality of life and cognitive function among individuals in residential care settings. Significant correlations were found between poor oral health and cognitive impairment, including MCI, revealing a relationship between cognitive status and perceived oral health [23]. Another study investigated the use of noninvasive digital biomarkers to quantify oral health and applied ML algorithms to detect cognitive decline within a community setting. Significant findings included notable differences in oral diadochokinesis rates and oral acidity between individuals with cognitive decline and those with normal cognitive function. This further demonstrates that digital oral health biomarkers have the potential to track cognitive function and facilitate early detection of cognitive decline [24].

Despite promising advancements in clinical practice and the possibility of early diagnosis, further research is needed. One significant research gap is the lack of exploration of oral health parameters as potential indicators for estimating MMSE scores. Although oral health has a recognized influence on overall well-being and cognitive function, there have been no empirical studies to explore the integration of oral health metrics into ML-based cognitive assessment models. This opens an opportunity for future studies to expand the scope of cognitive assessments and develop more comprehensive diagnostic frameworks. Many individuals routinely visit dental care facilities for treatment and preventive care. Leveraging existing patient history data alongside current examination findings requires minimal additional effort from dental care staff, and it can be seamlessly integrated with digital medical record systems. Previous research presents diverse evidence on the association between oral and cognitive health. This study builds on this knowledge by investigating different parameters and using a robust and balanced sample of participants in the MMSE 30 and MMSE ≤26 score groups.

Integrating oral health parameters into ML-driven decision support systems for MMSE score estimation could offer insights into the interplay between oral health and cognitive function. By leveraging advanced algorithms and comprehensive datasets encompassing cognitive and oral health data, researchers could uncover novel biomarkers and risk factors for cognitive decline, paving the way for more personalized approaches to cognitive assessment and intervention.

This study aims to explore the potential of using ML technologies using oral health and demographic examination data to predict the probability of having MMSE scores of 30 or ≤26 in Swedish individuals older than 60 years.

The main contributions of this study are as follows:

- The evaluation of the potential of oral health parameters for binary classification of MMSE scores of 30 and ≤26.
- The evaluation of the most deterministic oral health parameters that influence the outcome of the best-performing ML classifier.
- The assessment of RF, SVM, and CatBoost (CB) ML classifiers as indicators of MMSE scores of 30 and ≤26.

Methods

Ethical Considerations

This study used secondary, open-access data from the Swedish National Study on Aging and Care (SNAC-B) and Support Monitoring and Reminder Technology for Mild Dementia

XSL•FO
RenderX

(SMART4MD) projects. No new data were collected specifically for this study. The use of SNAC-B data was approved by the Ethics Committee of Lund University (LU 604‐00). The data for SMART4MD was collected and used under the approval of the Ethical Review Board in Sweden (LU No. 650‐00 and No. 744‐00). Informed consent was obtained from all participants in both studies. All data were fully anonymized prior to access by the authors. No compensation was provided to participants for the purpose of this study. All data were used in accordance with applicable data sharing agreements and stored securely. The study complies with the ethical standards outlined in the Declaration of Helsinki.

Data Description

The formed sample was used in experiments with ML models, including RF, SVM, and CB, aiming to indicate whether the participant's MMSE scores were 30 or ≤26. Data from 2 studies, which recruited participants from the European collaborative study SMART4MD [25] and the SNAC-B [26], formed the sample. SNAC-B is a longitudinal study involving individuals aged 60 years or older. Participants undergo examinations every 6 years, with more frequent assessments every 3 years, starting at the age of 78 years. The cohort ranges from 60 to 96 years of age [26]. The study sample recruited from SMART4MD involved individuals aged 60 years or older, examined every 6 to 12 months over 36 months [27]. Both studies are conducted at a research clinic affiliated with Blekinge Institute of Technology by experienced dentists and dental hygienists and involve comprehensive clinical and demographic data collection. Ethical approval was obtained for both studies, and informed consent was collected from all participants. While both studies are longitudinal in design, only the baseline visit data, meaning the first available observation per participant, were used in this study.

All clinical and demographic features, including oral health variables, were extracted from each participant's first examination. This resulted in a cross-sectional dataset suitable for ML analysis. The final sample included 693 baseline observations (350/693, 51% females and 343/693, 49% males) with an average age of 75 years. The sample was divided into 2 relatively balanced groups: one with MMSE scores of ≤26 and one with an MMSE score of 30. Observations with intermediate scores of 27‐29 were excluded to ensure distinct group separation. There was a total of 339/693 (49%) observations for individuals with ≤26 MMSE scores (165/339, 49% females and 174/339, 51% males) and 354/693 (51%) observations for the MMSE 30 score (185/354, 52% females and 169/354, 48% males). The dataset comprised 693 observations, each with 16 features (Table 1). The oral health features selected for inclusion were limited to those available in both datasets and supported by prior studies linking them to general health or cognitive decline. Examples include the Plaque Index (PI), which reflects hygiene maintenance; dry mouth, often associated with medication use and systemic conditions; and the number of teeth, which may serve as a proxy for long-term oral care and functional ability.

The listed features represent a combination of demographic, behavioral, and clinical oral health indicators obtained from baseline dental examinations. Probing pocket depth (PPD) measurements were categorized based on severity: values of 4 mm typically reflect a mild periodontal status, 5 mm indicate moderate depth, and ≥6 mm signify advanced periodontal disease. Variables such as PPD, PI, and bleeding on probing (BOP) were calculated as the percentage of affected surfaces out of the total examined. Self-reported variables, including dry mouth and hygiene tool use, were assessed through standardized questionnaires. Denture status was recorded separately for full and partial prostheses in both the maxillary and mandibular arches. These variables were selected due to their availability in both datasets and their clinical relevance to cognitive and systemic health in older adults.

MMSE scores are known to vary within individuals over time. Research indicates that changes of up to 3 points may occur without representing a clinically meaningful cognitive change, especially in older populations [28]. To reduce misclassification due to such variability, only individuals with MMSE scores of ≤26 or exactly 30 were included in the dataset. Based on this analogy, the MMSE ≤26 and the MMSE 30 score groups were designated and labeled as "1" and "0," respectively. No normalization, mean-centering, or outlier filtering was performed prior to model training. Tree-based models like RF and CB are scale-invariant, and for consistency, unscaled features were also used with SVM.

XSL•FO
RenderX

Table . List of features used for the study.

Parameter	Description	Index/Categories
Age	Participant age	• Number
Education	Level of education	• Elementary School • Secondary School • Higher education
PI[a]	Number of tooth surfaces in % with dental plaque of the total number of surfaces	• Percentage
PPD[b] 4mm	The number of PPD 4 mm in % of the total number of surfaces	• Percentage
Use of dental hygiene tools for approximal cleaning	How often do you use approximal dental hygiene tools?	• Rarely/never • Once a week • Daily • Several times daily
Gender	Gender	• Male, female
A feeling of dry mouth	Do you experience a sensation of dry mouth?	• Yes, often • Yes sometimes • No never
Number of teeth	Number of teeth	• Number
PPD 5mm	The number of PPD 5 mm in % of the total number of surfaces	• Percentage
Mirror test	Mirror test	• Glides easily • Sliding • Getting stuck
BOP[c]	The number of surfaces with BOP in % of the total number of surfaces.	• Percentage
PPD≥6mm	The number of PPD ≥ 6 mm in % of the total number of surfaces	• Percentage
Mandibular denture	Mandibular denture	• Yes, No
Maxillary denture	Maxillary denture	• Yes, No
Mandibular partial denture	Mandibular partial denture	• Yes, No
Maxillary partial denture	Maxillary partial denture	• Yes, No

[a]PI: Plaque Index.

[b]PPD: probing pocket depth.

[c]BOP: bleeding on probing.

Classification Experiment

Several well-known classifiers, RF, CB, and SVM, were used for the classification experiment. The dataset was split into 2 subgroups: a training set comprising 80% of the data (554/693 samples) and a test set containing 20% (139/693 samples). To ensure an unbiased estimation of model performance and to reduce the risk of overfitting during hyperparameter tuning, nested cross-validation (nCV) was applied within the training data.

The parameter grid for hyperparameter tuning was defined as follows:

- For Random Forest:{'n_estimators': [50, 100, 200],'max_depth': [None, 10, 20], 'min_samples_split': [2,5,10]}
- For SVM: {'C': [0.1, 1, 10],'kernel': ['linear', 'rbf,' 'poly'], 'degree': [2, 3, 4]}
- For CatBoost:{'iterations': [100, 200, 300], 'learning_rate': [0.01, 0.1, 0.2], 'depth': [4, 6, 8], 'l2_leaf_reg': [1, 3, 5]}

nCV is particularly appropriate in ML pipelines that involve hyperparameter optimization or model selection. It separates the parameter tuning step from the performance evaluation step, which prevents information leakage between training and test data and avoids optimistically biased performance estimates. This methodological rigor is especially important in

XSL•FO
RenderX

moderate-sized datasets where variance due to overfitting can significantly affect the results [29-31].

Model performance was assessed using a 10 × 10 nCV framework. The outer 10-fold loop was used to evaluate generalization performance, while the inner loop was used solely for hyperparameter optimization. This design avoids information leakage and produces unbiased performance estimates, allowing for a robust assessment of model performance under varying fold configurations and providing a stable basis for comparison across classifiers.

Performance Evaluation

To evaluate the performance of each ML classifier, multiple metrics were used, including accuracy, precision, recall, and F_1-score. To enhance clinical interpretability, the following definitions were used: true positives (TP) represent correctly identified positive cases; false positives (FPs) refer to negative cases incorrectly classified as positive; true negatives (TN) are correctly identified negative cases; and false negatives (FN) denote positive cases that were incorrectly classified as negative. Box plots, which illustrate the distribution of accuracy scores for the respective models and additional statistical information, were used for the data visualization. Subsequently, the classifier with the highest scores was further analyzed for its feature importance. The examination of the most essential features relied on Shapley Additive Explanation (SHAP) summary plots, providing visualizations of the influence of parameter groups on the output, organized by their importance. This importance is based on SHAP values, offering insights into features' effects on the ML model's decision-making process [32].

Experimental Setup

The experiment was conducted on a Dell Precision 7920 MT desktop, and all models were implemented using Python (version 3.9; Python Software Foundation) with Scikit-learn (version 1.2.2) and CB (version 1.2). Visualization was supported via Seaborn (version 0.12.2).

Results

Experimental Results

The dataset, comprising 693 observations, each containing 16 features in its feature vector, underwent experimentation using 3 different ML models to discriminate between MMSE ≤26 and MMSE 30 score groups. Figure 1 displays the accuracy of each model for all nCV combinations. The box plot analysis reveals that the CB model outperforms the RF and SVM models in accuracy. Specifically, the CB model achieves the highest median accuracy of 0.760, the highest mean accuracy of 0.752, and the highest maximum accuracy of 0.810. Additionally, the CB model shows the smallest variability in accuracy scores, as evidenced by the lowest IQR of 0.020. The RF model demonstrates a solid performance with a median and mean accuracy of 0.740, but it does not reach the same maximum accuracy as the CB model, peaking at 0.780. The RF model also has a moderate IQR of 0.030, indicating some variability in its performance. While still competitive, the SVM model shows the lowest median accuracy of 0.730 and the lowest mean accuracy of 0.721 among the 3 models. It also has a maximum accuracy of 0.760, which is lower than both RF and CB. The IQR of 0.030 is comparable to that of RF, indicating a similar level of performance variability.

The performance of the 3 ML models (CB, RF, and SVM) was evaluated using accuracy, precision, recall, and F_1-score on both the training and test datasets. Table 2 summarizes these results. On the training set, RF achieved the highest scores across all metrics, followed closely by CB. However, on the test set, CB demonstrated the most balanced and generalizable performance, with an accuracy of 80.6%, precision of 77.4%, recall of 78.7%, and an F_1-score of 78.0%. In contrast, RF showed signs of overfitting, indicated by a decline in test precision and accuracy despite maintaining high recall. SVM yielded moderate but consistent results across both datasets. These results suggest that CB is better suited for generalization in this context, likely due to its regularization features. RF, while highly effective on the training set, may have captured dataset-specific patterns that did not generalize well. SVM demonstrated stable but lower overall performance.

Table 3 shows the confusion matrix results associated with all models. The performance of 3 ML models, CB, RF, and SVM, was evaluated on both training and test datasets in terms of TP, FP, TN, and FN. Rather than focusing on raw counts, the interpretation emphasizes overall performance patterns. CB maintained a strong balance between correctly identifying both positive and negative cases. RF achieved high recall but also produced more FPs on the test set, which may limit its clinical precision. SVM showed more balanced errors, though with generally lower performance.

The hyperparameters and nCV combinations associated with each and the best-performing model are as follows:

- CB: 3X3nCV, ('depth': 4, 'iterations': 200, 'l2_leaf_reg': 5, 'learning rate': 0.1).
- RF: 4X7nCV, ('max depth: 20, 'min samples split': 5, 'n estimators': 50).
- SVM: 8X5nCV, ('C': 10, 'degree': 3, 'kernel': 'poly').

XSL•FO
RenderX

Figure 1. Box plot-based accuracy comparison of each machine learning model. CB: CatBoost; RF: random forests; SVM: support vector machine.

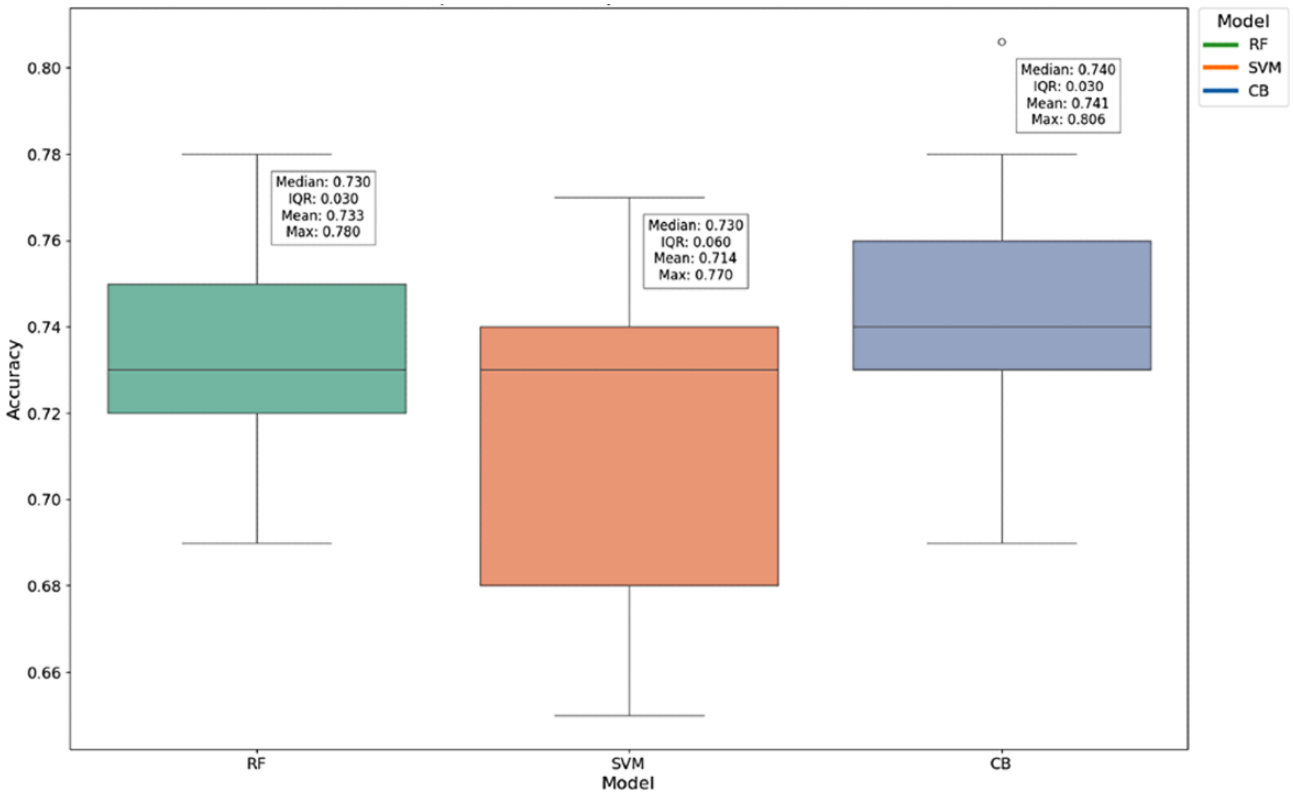


Table . The average performance metric scores for each machine learning model are displayed for the training and test sets.

Model	Precision (%)	Recall (%)	Accuracy (%)	F_1-score (%)
Training set				
CB[a]	90.2	87.4	88.6	88.8
RF[b]	90.4[c]	92.6[c]	91.2[c]	91.5[c]
SVM[d]	75.8	69.1	72.7	72.3
Test set				
CB	77.4[c]	78.7	80.6[c]	78.0[c]
RF	68.5	82.0[c]	75.6	74.6
SVM	75.3	68.4	72.2	71.7

[a]CB: CatBoost.

[b]RF: random forests.

[c]Top-performing values.

[d]SVM: support vector machine.

XSL•FO
RenderX

Table . The confusion matrix outcomes for every machine learning classifier on both the validation and test sets.

	CB[a]		RF[b] Predictedd)		SVM[c]	
	+	–	+	–	+	–
Training set						
Actual						
Positive (+)	249	36	264	21	195	90
Negative (–)	27	242	28	241	64	205
Test set						
Actual						
Positive (+)	48	13	50	11	46	15
Negative (–)	14	64	23	55	17	61

[a]CB: CatBoost.

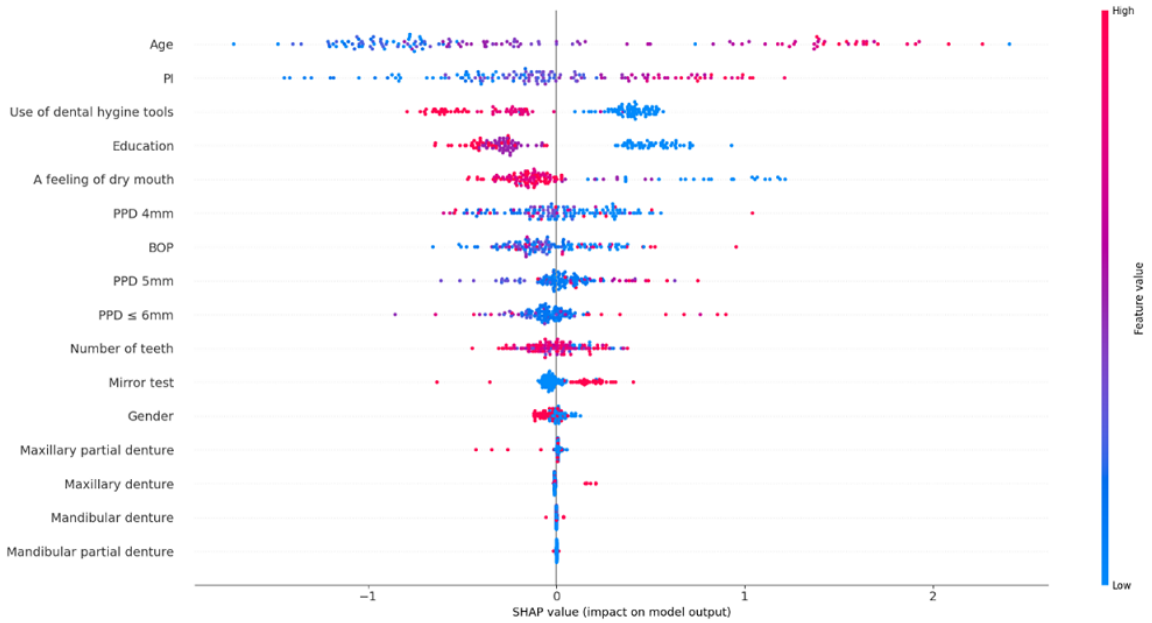
[b]RF: random forests.

[c]SVM: support vector machine.

Feature Importance

The SHAP summary plot in Figure 2 illustrates the impact of various features on the model's output. Each dot represents a Shapley value for a feature for an individual instance, and the color denotes the feature value, ranging from low (blue) to high (red). The SHAP summary plot reveals that age, PI, dental hygiene devices, education, a feeling of dry mouth, and PPD are critical in influencing the model's predictions. The balance of these features, along with others like BOP and the number of teeth, determines the overall outcome predicted by the model. These findings indicate that age, PI, and PPD are significant predictors, with older age and higher PI correlating with an increased likelihood of having an MMSE score ≤26. Education appears to inversely affect the prediction, suggesting that higher education levels may be associated with better oral health practices. The number of teeth shows an inverse relationship, where having more teeth is linked to a lower risk of MMSE ≤26. Additionally, the presence of dental prosthetics and feelings of dry mouth positively influence the prediction, indicating a higher likelihood of MMSE ≤26. Gender shows a minimal impact, with the female gender slightly reducing the predicted MMSE ≤26 risk.

Figure 2. SHAP summary plot for model features. The plot illustrates the impact of each feature on the model's output. BOP: bleeding on probing; PI: Plaque Index; PPD: probing pocket depth; SHAP: Shapley Additive Explanation.



XSL•FO
RenderX

Discussion

Principal Findings

This study explored the potential of using ML technologies using oral health and demographic examination data to predict the probability of having MMSE scores of 30 or ≤26 in Swedish individuals older than 60 years. The main findings of the study were that all CB, RF, and SVM classifiers achieved high classification accuracies, but the CB classifier outperformed both RF and SVM classifiers with an average accuracy of 80.6%. Acceptable accuracy levels vary across studies [33-35], but it can be argued that all CB, RF, and SVM classifiers demonstrate strong performance, each exceeding 72% accuracy. This indicates that with specific nCV combinations and hyperparameter tuning, all classifiers can indicate whether the individual belongs to ≤26 MMSE scores or higher MMSE score (score=30) groups with varying grades of accuracy [36]. These findings hold the potential to identify individuals in need of support and treatment, benefiting not only them but also health care professionals and systems by optimizing treatment with fewer resources.

The performance evaluation based on the training and test set results is a common indicator of finding the unexpected accuracy relation of ML models [37]. The evaluation of the models reveals distinct differences in performance and generalization capabilities. On the training set, RF showed a well-balanced performance with strong metrics across the board, reflected in its Precision, Recall, Accuracy, and F_1-score and its TP, TN, FP, and FN counts. The classifier CB performs better in the test set regarding the average performance metric, and SVM lagged significantly behind in both training and test sets. However, the general performance evaluation might differ from a clinical point of view when the higher recall is considered a more important parameter. In that case, RF with the highest TP values becomes the best classifier. FP could lead to unnecessary clinical evaluations or interventions, while FN could result in missed diagnoses, delaying treatment for cognitive impairment. When the goal of ML models is early detection and ensuring no cases of cognitive impairment are missed, minimizing FN is essential [38]. However, if the focus of these models is on reducing unnecessary interventions and managing health care resources efficiently, minimizing FP should be prioritized [39]. From a generalizability perspective, SVM shows the lowest performance drop between training and test, and CB indicates a second strong generalizability with a low-performance drop compared with the training and test set results. On the other hand, RF showed a decline in performance between the training and test sets. This suggests that SVM and CB are more suitable than RF for handling new, unseen data. Hyperparameter tuning was conducted through nCV using model-specific grids. For RF, parameters included the number of estimators, tree depth, and minimum samples per split. Despite this rigorous tuning, RF exhibited overfitting, reflected by its high training accuracy and reduced performance on the test set. This behavior suggests that RF, with its tendency to create deep and complex trees, may have captured noise or sample-specific patterns. In contrast, CB's built-in regularization mechanisms, including L2-leaf regularization, contributed to more stable generalization. To address overfitting in future implementations, simpler models or additional regularization techniques such as pruning, reduced tree depth, or feature selection could be explored.

Oral health and demographic factors vary across different regions globally, and this method's applicability is specific to Swedish conditions, which poses a limitation. However, a study from Taiwan [24], using oral health biomarkers and CB for cognitive decline classification predictions, yielded results akin to those presented in this study. In their model [24], crucial features included daily social interaction, oral diadochokinesis, PI, saliva protein, and age. In contrast, this study benefits from a more extensive and balanced dataset, presenting absolute average values rather than weighted results. Additionally, to mitigate overfitting risks, nCV was used to train ML classifiers across various k-fold combinations to mitigate overfitting risks in ML classifiers across various k-fold combinations. Furthermore, these studies collectively highlight oral health and demographic factors that vary across different regions globally, and this method's applicability is specific to Swedish conditions. Additionally, while the use of 10 × 10 nCV ensures an unbiased estimate of generalization performance within the dataset, the importance of validating models on external data is well recognized. Internal validation alone cannot capture the variability introduced by different clinical environments, geographic regions, or data acquisition protocols. External validation on independent cohorts or through integration into routine dental examinations would be required to evaluate robustness. Such efforts would help assess the model's applicability under real-world variability and determine its readiness for broader clinical use.

The implications drawn from the SHAP summary plot underscore critical insights into feature relevance concerning cognitive health assessments via ML models. The clear demarcation between the groups of MMSE scores ≤26 and 30 across influential variables like age suggests that such demographic factors hold substantial weight in predictive analytics. Notably, age emerges as a pivotal factor, with higher age correlating strongly with lower cognitive health scores. This correlation is also highlighted in other studies that consistently demonstrated that MMSE scores tend to be lower for older individuals and decline over time [40]. The SHAP summary plot highlights age, PI, and use of dental hygiene tools as the most influential predictors of MMSE classification. Older age and higher plaque levels were associated with increased likelihood of MMSE ≤26, suggesting that both biological aging and reduced oral hygiene maintenance contribute to cognitive risk [20,41]. In particular, individuals with lower use of interdental hygiene tools exhibited stronger SHAP effects, indicating a potential interaction between age-related decline in motor or cognitive function and oral hygiene behaviors. This aligns with findings that individuals with cognitive impairment often experience challenges in maintaining oral hygiene due to reduced executive functioning and manual dexterity [7,42]. Features such as dry mouth and education also showed moderate predictive strength, consistent with their known associations with polypharmacy and cognitive reserve, respectively [41]. In contrast, features like BOP, gender, and presence of dentures showed minimal SHAP influence, suggesting weaker or less

XSL•FO
RenderX

consistent relationships within this sample. These findings suggest that age-related decline may act synergistically with deteriorating oral hygiene habits, offering further evidence for behaviorally anchored early risk screening in clinical practice.

Given that MCI resides on the border between healthy aging and neurocognitive illness, individuals with MCI may fluctuate between MMSE scores ≤26 and 30 [43]. About 50% of individuals with MCI receive a neurocognitive diagnosis within 3 years, with a 2-step decrease in MMSE score within 12 months indicating disease onset. Recommended thresholds for the MMSE can be expressed as 0 - 22, indicating dementia; 23 - 26, MCI [44]; and 27 - 30, indicating normal cognitive function [7,42]. In this study, the threshold MMSE≤26 was used. This criterion was adopted in the study, resulting in the exclusion of MMSE scores of 27, 28, and 29 from calculations. This limit has been chosen as 2 different studies have found that changes of 2 to 3 points indicate reliable changes in the MMSE test value at the 90% confidence level [28,45]. However, it is important to note that this regulatory threshold may limit the study, potentially leading to missed indications. The exclusion of MMSE scores of 27, 28, and 29 may also affect generalizability. One of the strengths of this study is the use of ML as the methodology. Recent studies in ML have shown significant promise in predicting various disorders, such as dementia [46,47], chronic obstructive pulmonary disease [48], cancer [49], and Parkinson disease [50]. The used tree-based models, CB and RF, and the distance-based model SVM allow comparability in the case of possible effects of outliers in the dataset, where the tree-based models are known to be more resistant to imbalance in the dataset than the distance-based models [51-53]. Despite this study seeking a balanced data set, there is a heterogeneity regarding ages represented in the dataset where some ages might be overrepresented, which can be seen as a limitation in this study. Another limitation is the low number of participants and the recruitment that took place in a small county in southern Sweden, which is an obstacle to making conclusions from a broader perspective that represents more variety in demographic and regional differences. However, in relation to previous research, this study includes a larger number of participants, thereby increasing the generalizability of the findings. Another notable difference concerns the threshold used to distinguish between the MMSE ≤26 and MMSE 30 groups; in this study, a higher threshold was applied. Since the dataset of 693 observations is relatively small and may not be representative of a larger population, it may affect generalizability. In addition, even if the groups are relatively balanced, small differences in group size (339/693, 49% vs 354/693, 51%) can affect model performance and bias. These limitations can be overcome by expanding the data set by including divergent and wider participants' data from larger geographical areas in upcoming studies. Future research may also address the performance of capturing changes over time for monitoring purposes, highlighting the need for longitudinal studies. Although the findings demonstrate strong internal performance, several practical challenges constrain the model's readiness for clinical use. These include variability in oral health assessment protocols, limited interpretability of model outputs for nontechnical users, and the absence of integration pathways with existing clinical information systems. SHAP plots provide valuable transparency but may need adaptation for clinician-facing use. Implementation would require standardization of input data, compatibility with electronic health records, and interdisciplinary development efforts. Further investigation is needed to evaluate clinical usability and workflow alignment.

Other limitations of the study are that only baseline data were used from longitudinal studies, meaning that potential changes over time may be missed. Only 16 parameters were selected, which means that other important parameters that could affect the results may have been omitted. The oral health features used in the models were selected based on their consistent availability across both datasets and their previously reported clinical relevance to cognitive function. These features, such as PI, number of teeth, and dry mouth, may reflect both localized oral conditions and systemic factors, including frailty, polypharmacy, and reduced self-care capacity. Such conditions have been associated with cognitive impairment in older adults. Other potentially relevant features, like microbial profiles or periodontal attachment levels, were not included due to data limitations, but future work could incorporate these variables in extended datasets.

Conclusion

This study suggests that oral health parameters, demographic data, and ML techniques offer a potential tool for screening MMSE scores for individuals aged 60 years and older. The data used as inputs for ML classifiers contains sufficient information to differentiate between MMSE scores ≤26 and 30.

It is important to include both demographic and oral health-related factors in predictive models. Despite some limitations, the study offers valuable insights for future research and potential clinical applications. To ensure the robustness and generalizability of the model, further external validation and adaptation to different clinical settings are required.

Acknowledgments

We want to express our greatest appreciation to the participants and staff of the Swedish National Study on Aging and Care and Support Monitoring and Reminder Technology for Mild Dementia studies. The Blekinge Institute of Technology funded this study.

XSL•FO
RenderX

Data Availability

The datasets analyzed during this study are not publicly available due to licensing restrictions from Blekinge Institute of Technology, Department of Health, but are available from the corresponding author upon reasonable request and with permission from Blekinge Institute of Technology. The Python code can be found on [54].

Authors' Contributions

AI and JF conducted the experiment and analyzed the data. AI and JF drafted the paper, and then SNG, EMM, HD, AA, and ALD critically revised the text regarding intellectually important content. All authors have given final approval for publication and take public responsibility for all its parts.

Conflicts of Interest

None declared.

References

1. World population prospects 2024. United Nations Population Division. URL: https://population.un.org/wpp/ [accessed 2025-04-02]
2. Prince M, Bryce R, Albanese E, Wimo A, Ribeiro W, Ferri CP. The global prevalence of dementia: a systematic review and metaanalysis. Alzheimers Dement 2013 Jan;9(1):63. [doi: 10.1016/j.jalz.2012.11.007]
3. Yiannopoulou KG, Papageorgiou SG. Current and future treatments in Alzheimer disease: an update. J Cent Nerv Syst Dis 2020;12:1179573520907397. [doi: 10.1177/1179573520907397] [Medline: 32165850]
4. Long JM, Holtzman DM. Alzheimer disease: an update on pathobiology and treatment strategies. Cell 2019 Oct 3;179(2):312-339. [doi: 10.1016/j.cell.2019.09.001] [Medline: 31564456]
5. Park KW. Anti-amyloid antibody therapies for Alzheimer's disease. Nucl Med Mol Imaging 2024 Jun;58(4):227-236. [doi: 10.1007/s13139-024-00848-3] [Medline: 38932758]
6. Syrjälä AH, Ylöstalo P, Ruoppi P, et al. Dementia and oral health among subjects aged 75 years or older. Gerodontology 2012 Mar;29(1):36-42. [doi: 10.1111/j.1741-2358.2010.00396.x]
7. Gil-Montoya JA, Sánchez-Lara I, Carnero-Pardo C, et al. Oral hygiene in the elderly with different degrees of cognitive impairment and dementia. J Am Geriatr Soc 2017 Mar;65(3):642-647. [doi: 10.1111/jgs.14697] [Medline: 28024093]
8. Flyborg J, Renvert S, Sanmartin Berglund J, Anderberg P. Use of a powered toothbrush to improve oral health in individuals with mild cognitive impairment. Gerodontology 2023 Mar;40(1):74-82. [doi: 10.1111/ger.12619] [Medline: 35064682]
9. Guo H, Chang S, Pi X, et al. The effect of periodontitis on dementia and cognitive impairment: a meta-analysis. Int J Environ Res Public Health 2021 Jun 25;18(13):34202071. [doi: 10.3390/ijerph18136823] [Medline: 34202071]
10. Folstein MF, Folstein SE, McHugh PR. "Mini-mental state". a practical method for grading the cognitive state of patients for the clinician. J Psychiatr Res 1975 Nov;12(3):189-198. [doi: 10.1016/0022-3956(75)90026-6] [Medline: 1202204]
11. Roshanzamir A, Aghajan H, Soleymani Baghshah M. Transformer-based deep neural network language models for Alzheimer's disease risk assessment from targeted speech. BMC Med Inform Decis Mak 2021 Mar 9;21(1):92. [doi: 10.1186/s12911-021-01456-3] [Medline: 33750385]
12. Parsapoor Parsa MM, Alam MR, Mihailidis A. Performance of machine learning algorithms for dementia assessment: impacts of language tasks, recording media, and modalities. BMC Med Inform Decis Mak 2023 Mar 3;23(1):45. [doi: 10.1186/s12911-023-02122-6] [Medline: 36869377]
13. Vyas A, Aisopos F, Vidal ME, Garrard P, Paliouras G. Identifying the presence and severity of dementia by applying interpretable machine learning techniques on structured clinical records. BMC Med Inform Decis Mak 2022 Oct 17;22(1):271. [doi: 10.1186/s12911-022-02004-3] [Medline: 36253849]
14. Kang MJ, Kim SY, Na DL, et al. Prediction of cognitive impairment via deep learning trained with multi-center neuropsychological test data. BMC Med Inform Decis Mak 2019 Nov 21;19(1):231. [doi: 10.1186/s12911-019-0974-x] [Medline: 31752864]
15. Twait EL, Andaur Navarro CL, Gudnason V, Hu YH, Launer LJ, Geerlings MI. Dementia prediction in the general population using clinically accessible variables: a proof-of-concept study using machine learning. the AGES-Reykjavik study. BMC Med Inform Decis Mak 2023 Aug 28;23(1):168. [doi: 10.1186/s12911-023-02244-x] [Medline: 37641038]
16. Luo S, Yao X, Yuan Z, Zhou L. Prediction of mini-mental state examination scores via machine learning for Alzheimer's disease. In: You P, Li H, Chen Z, editors. Proceedings of International Conference on Image, Vision and Intelligent Systems 2022 (ICIVIS 2022): Springer Nature; 2023:878-883. [doi: 10.1007/978-981-99-0923-0_87]
17. Wang J, Wang Z, Liu N, et al. Random forest model in the diagnosis of dementia patients with normal mini-mental state examination scores. J Pers Med 2022 Jan 4;12(1):37. [doi: 10.3390/jpm12010037] [Medline: 35055352]
18. Qiu S, Chang GH, Panagia M, Gopal DM, Au R, Kolachalama VB. Fusion of deep learning models of MRI scans, mini–mental state examination, and logical memory test enhances diagnosis of mild cognitive impairment. Alz & Dem Diag Ass & Dis Mo 2018 Jan;10(1):737-749. [doi: 10.1016/j.dadm.2018.08.013]

XSL•FO
RenderX

19. Zeng LN, Zong QQ, Xu SW, et al. Oral health in patients with dementia: a meta-analysis of comparative and observational studies. Int J Geriatr Psychiatry 2021 Apr;36(4):467-478. [doi: 10.1002/gps.5453] [Medline: 33105039]
20. Hamza SA, Asif S, Bokhari SAH. Oral health of individuals with dementia and Alzheimer's disease: a review. J Indian Soc Periodontol 2021;25(2):96-101. [doi: 10.4103/jisp.jisp_287_20] [Medline: 33888939]
21. Wei T, Du Y, Hou T, et al. Association between adverse oral conditions and cognitive impairment: a literature review. Front Public Health 2023;11:1147026. [doi: 10.3389/fpubh.2023.1147026] [Medline: 37089515]
22. Inamochi Y, Ogino Y, Harada K, et al. Do oral care and rehabilitation improve cognitive function? a systematic review of clinical studies. J Evid Based Dent Pract 2024 Mar;24(1):101948. [doi: 10.1016/j.jebdp.2023.101948]
23. Zuluaga DJM, Montoya JAG, Contreras CI, Herrera RR. Association between oral health, cognitive impairment and oral health-related quality of life. Gerodontology 2012 Jun;29(2):e667-e673. [doi: 10.1111/j.1741-2358.2011.00542.x] [Medline: 21883423]
24. Chung PC, Chan TC. Digital oral health biomarkers for early detection of cognitive decline. BMC Public Health 2023 Oct 9;23(1):1952. [doi: 10.1186/s12889-023-16897-w] [Medline: 37814231]
25. Support, monitoring and reminder technology for mild dementia. SMART4MD project. European Commission. URL: https://cordis.europa.eu/project/id/643399 [accessed 2021-10-01]
26. Lagergren M, Fratiglioni L, Hallberg IR, et al. A longitudinal study integrating population, care and social services data. the Swedish national study on Aging and Care (SNAC). Aging Clin Exp Res 2004 Apr;16(2):158-168. [doi: 10.1007/BF03324546] [Medline: 15195992]
27. Flyborg J, Renvert S, Anderberg P, Sanmartin-Berglund J. The long-term effect on oral health and quality of life using a powered toothbrush in individuals with mild cognitive impairment. an intervention trial. Spec Care Dentist 2024;44(6):1700-1708. [doi: 10.1111/scd.13040] [Medline: 38994574]
28. Stein J, Luppa M, Maier W, et al. Assessing cognitive changes in the elderly: reliable change indices for the mini-mental state examination. Acta Psychiatr Scand 2012 Sep;126(3):208-218. [doi: 10.1111/j.1600-0447.2012.01850.x] [Medline: 22375927]
29. Varma S, Simon R. Bias in error estimation when using cross-validation for model selection. BMC Bioinformatics 2006 Feb 23;7(1):91. [doi: 10.1186/1471-2105-7-91] [Medline: 16504092]
30. Cawley GC, Talbot NLC. On over-fitting in model selection and subsequent selection bias in performance evaluation. J Mach Learn Res 2010 Aug 1;11:2079-2107 [FREE Full text]
31. Arlot S, Celisse A. A survey of cross-validation procedures for model selection. Statist Surv 2010 Jan;4(none):40-79. [doi: 10.1214/09-SS054]
32. Marcilio WE, Eler DM. From explanations to feature selection: assessing SHAP values as feature selection mechanism. 2020 Presented at: 2020 33rd SIBGRAPI Conference on Graphics, Patterns and Images (SIBGRAPI); Nov 7-10, 2020; Porto de Galinhas, Brazil p. 340-347. [doi: 10.1109/SIBGRAPI51738.2020.00053]
33. Cabitza F, Campagner A, Del Zotti F, Verona N, Ravizza A, Sternini F. All you need is higher accuracy? on the quest for minimum acceptable accuracy for medical artificial intelligence. 2020 Presented at: E-Health Procedings 12th International Conference on e-Health; Sep 23-25, 2020.
34. Ebrahim M, Sedky AAH, Mesbah S. Accuracy assessment of machine learning algorithms used to predict breast cancer. Data (Basel) 2023 Feb;8(2):35. [doi: 10.3390/data8020035]
35. Agliata A, Giordano D, Bardozzo F, Bottiglieri S, Facchiano A, Tagliaferri R. Machine learning as a support for the diagnosis of type 2 diabetes. Int J Mol Sci 2023 Apr 5;24(7):6775. [doi: 10.3390/ijms24076775] [Medline: 37047748]
36. How to know if your machine learning model has good performance. Obviously AI. URL: https://www.obviously.ai/post/machine-learning-model-performance [accessed 2024-05-29]
37. Yoon H. Finding unexpected test accuracy by cross validation in machine learning. Int J Comput Sci Netw Secur 2021;21(12spc):549-555. [doi: 10.22937/IJCSNS.2021.21.12.76]
38. Petticrew MP, Sowden AJ, Lister-Sharp D, Wright K. False-negative results in screening programmes: systematic review of impact and implications. Health Technol Assess 2000;4(5). [doi: 10.3310/hta4050]
39. Dresselhaus TR, Luck J, Peabody JW. The ethical problem of false positives: a prospective evaluation of physician reporting in the medical record. J Med Ethics 2002 Oct;28(5):291-294. [doi: 10.1136/jme.28.5.291] [Medline: 12356955]
40. Piccinin AM, Muniz-Terrera G, Clouston S, et al. Coordinated analysis of age, sex, and education effects on change in MMSE scores. J Gerontol B Psychol Sci Soc Sci 2013 May 1;68(3):374-390. [doi: 10.1093/geronb/gbs077]
41. Ghezzi EM, Ship JA. Dementia and oral health. Oral Surg Oral Med Oral Pathol Oral Radiol Endod 2000 Jan;89(1):2-5. [doi: 10.1016/s1079-2104(00)80003-7] [Medline: 10630932]
42. Marchini L, Ettinger R, Caprio T, Jucan A. Oral health care for patients with Alzheimer's disease: an update. Spec Care Dentist 2019 May;39(3):262-273. [doi: 10.1111/scd.12375] [Medline: 30964560]
43. Overton M, Pihlsgård M, Elmståhl S. Diagnostic stability of mild cognitive impairment, and predictors of reversion to normal cognitive functioning. Dement Geriatr Cogn Disord 2020. [doi: 10.1159/000506255]
44. Delavaran H, Jönsson AC, Lövkvist H, et al. Cognitive function in stroke survivors: a 10-year follow-up study. Acta Neurol Scand 2017 Sep;136(3):187-194. [doi: 10.1111/ane.12709]

XSL•FO
RenderX

45. Hensel A, Angermeyer MC, Riedel-Heller SG. Measuring cognitive change in older adults: reliable change indices for the mini-mental state examination. J Neurol Neurosurg Psychiatry 2007 Dec;78(12):1298-1303. [doi: 10.1136/jnnp.2006.109074] [Medline: 17442763]
46. Nyholm J, Ghazi AN, Ghazi SN, Sanmartin Berglund J. Prediction of dementia based on older adults' sleep disturbances using machine learning. Comput Biol Med 2024 Mar;171:108126. [doi: 10.1016/j.compbiomed.2024.108126] [Medline: 38342045]
47. Javeed A, Dallora AL, Berglund JS, et al. Early prediction of dementia using feature extraction battery (FEB) and optimized support vector machine (SVM) for classification. Biomedicines 2023 Feb 2;11(2):439. [doi: 10.3390/biomedicines11020439] [Medline: 36830975]
48. Idrisoglu A, Dallora AL, Cheddad A, Anderberg P, Jakobsson A, Sanmartin Berglund J. COPDVD: automated classification of chronic obstructive pulmonary disease on a new collected and evaluated voice dataset. Artif Intell Med 2024 Oct;156:102953. [doi: 10.1016/j.artmed.2024.102953] [Medline: 39222579]
49. Cheddad A. Machine learning in healthcare: breast cancer and diabetes cases. In: Reis T, Bornschlegl MX, Angelini M, Hemmje ML, editors. Advanced Visual Interfaces Supporting Artificial Intelligence and Big Data Applications 2021:125-135. [doi: 10.1007/978-3-030-68007-7_8]
50. Saleh S, Cherradi B, El Gannour O, Hamida S, Bouattane O. Predicting patients with Parkinson's disease using machine learning and ensemble voting technique. Multimed Tools Appl 2024;83(11):33207-33234. [doi: 10.1007/s11042-023-16881-x]
51. Breiman L. Random forests. Mach Learn 2001 Oct;45(1):5-32. [doi: 10.1023/A:1010933404324]
52. Prokhorenkova L, Gusev G, Vorobev A, Dorogush AV, Gulin A. CatBoost: unbiased boosting with categorical features. 2018 Presented at: Advances in Neural Information Processing Systems 31 (NeurIPS 2018); Dec 3-8, 2018; Montréal, Canada URL: https://proceedings.neurips.cc/paper_files/paper/2018/hash/14491b756b3a51daac41c24863285549-Abstract.html [accessed 2024-09-11]
53. Baldomero-Naranjo M, Martínez-Merino LI, Rodríguez-Chía AM. A robust SVM-based approach with feature selection and outliers detection for classification problems. Expert Syst Appl 2021 Sep;178:115017. [doi: 10.1016/j.eswa.2021.115017]
54. AIITPlanet/code. GitHub. URL: https://github.com/AIITPlanet/Code/blob/main/ClassificationOfMMSE.py [accessed 2025-06-24]

Abbreviations

AD: Alzheimer Disease
BOP: bleeding on probing
CB: CatBoost
FN: false negative
FP: false positive
MCI: mild cognitive impairment
ML: machine learning
MMSE: Mini-Mental State Examination
nCV: nested cross-validation
PI: Plaque Index
PPD: probing pocket depth
RF: random forest
SHAP: Shapley additive explanation
SMART4MD: Support Monitoring and Reminder Technology for Mild Dementia
SNAC-B: Swedish National Study on Aging and Care
SVM: support vector machine
TN: true negative
TP: true positive

Edited by A Benis; submitted 27.03.25; peer-reviewed by KA Obisesan Olawuni, S Kavuluri, Z Xiang; revised version received 24.06.25; accepted 15.07.25; published 25.08.25.

Please cite as:
Idrisoglu A, Flyborg J, Nauman Ghazi S, Mikaelsson Midlöv E, Dellkvist H, Axén A, Dallora AL
Prediction of Mini-Mental State Examination Scores for Cognitive Impairment and Machine Learning Analysis of Oral Health and Demographic Data Among Individuals Older Than 60 Years: Cross-Sectional Study
JMIR Med Inform 2025;13:e75069
URL: https://medinform.jmir.org/2025/1/e75069
doi:10.2196/75069

XSL•FO
RenderX

© Alper Idrisoglu, Johan Flyborg, Sarah Nauman Ghazi, Elina Mikaelsson Midlöv, Helén Dellkvist, Anna Axén, Ana Luiza Dallora. Originally published in JMIR Medical Informatics (https://medinform.jmir.org), 25.8.2025. This is an open-access article distributed under the terms of the Creative Commons Attribution License (https://creativecommons.org/licenses/by/4.0/), which permits unrestricted use, distribution, and reproduction in any medium, provided the original work, first published in JMIR Medical Informatics, is properly cited. The complete bibliographic information, a link to the original publication on https://medinform.jmir.org/, as well as this copyright and license information must be included.

XSL•FO
RenderX

Experience of Cardiovascular and Cerebrovascular Disease Surgery Patients: Sentiment Analysis Using the Korean Bidirectional Encoder Representations from Transformers (KoBERT) Model

Hocheol Lee[1], PhD; Yu Seong Hwang[2], PhD; Ye Jun Kim[3], BS; Yukyung Park[2,4], MD, MPH, PhD; Heui Sug Jo[2,4], MD, MPH, PhD

[1]Department of AI Health Information Management, Software Digital Healthcare Convergence College, Yonsei University, Wonju, Republic of Korea

[2]Department of Health Policy and Management, School of Medicine, Kangwon National University, 510 School of Medicine Building #1 (N414), 1, Kangwondaehak-gil, Chuncheon, Gangwon-do, Republic of Korea

[3]Division of Data Science, Yonsei University, Wonju, Republic of Korea

[4]Department of Preventive Medicine, Kangwon National University Hospital, Chuncheon, Republic of Korea

Corresponding Author:
Heui Sug Jo, MD, MPH, PhD
Department of Health Policy and Management, School of Medicine, Kangwon National University, 510 School of Medicine Building #1 (N414), 1, Kangwondaehak-gil, Chuncheon, Gangwon-do, Republic of Korea

Abstract

Background: Cardiovascular and cerebrovascular diseases significantly contribute to global mortality and disability. The shift to outpatient postoperative care, accelerated by the COVID-19 pandemic, emphasizes the need for effective management of postoperative outcomes. The high rates of cardiovascular and cerebrovascular diseases in Korea necessitate focused transitional care during patient discharge periods. However, limited research exists on the postoperative experiences of discharged patients, underscoring the necessity of establishing evidence-based services to optimize transitional care.

Objective: The objective of this paper was to analyze the emotional experiences of patients who underwent cardiovascular and cerebrovascular surgeries using data from Naver, a major South Korean web portal.

Methods: Posts were collected using specific keywords and processed with the Korean Bidirectional Encoder Representations from Transformers (KoBERT) model based on Transformer, which classified sentiments into positive, neutral, and negative categories. Model performance was validated according to precision, recall, F_1-score, and support. Sentiment analysis was conducted within the Transitional Care Model (TCM) framework, divided into 5 domains: health status, care resources, care demand, interaction, and mental state.

Results: The KoBERT model demonstrated high classification performance, achieving a precision of 96%, recall of 94%, and an F_1-score of 94%. Sentiment analysis revealed that compared with cardiovascular surgery patients, cerebrovascular surgery patients experienced higher negative emotions regarding health status, whereas cardiovascular surgery patients expressed more negative sentiments in care demands.

Conclusions: Different patient groups experience distinct emotional and practical challenges postdischarge. Particularly, keywords within the TCM framework highlight that cerebrovascular surgery patients require robust rehabilitation and caregiver support, whereas cardiovascular surgery patients need better cost management. These findings underscore the importance of personalized transitional care strategies tailored for cardiovascular and cerebrovascular diseases. The insights derived from this study can guide health care policymakers in designing more targeted and patient-centered interventions to improve postdischarge care and patient-centered transitional care, ensuring continuous and effective postoperative management.

(JMIR Med Inform 2025;13:e65127) doi:10.2196/65127

KEYWORDS

cardiovascular; cerebrovascular; KoBERT; artificial intelligence; TCM; transitional care model; hospitalization; care model; surgery; emotional experiences; emotion; South Korea; Asia; web portal; transformer; sentiment analysis; health status; rehabilitation; caregiver support; cost management; Korean Bidirectional Encoder Representations from Transformers

XSL•FO
RenderX

Introduction

Cardiovascular and cerebrovascular diseases are among the leading causes of mortality worldwide, causing 17.5 million deaths annually. Ischemic heart disease and stroke rank as the second and fourth leading contributors to the global disease burden, respectively. Furthermore, the disability-adjusted life years (ie, years lost due to premature death and years lived with disability) related to ischemic heart disease and stroke are projected to increase progressively [1,2]. In addition, with increases in life expectancy owing to advancements in medical technology and improved health care access, the number of older patients undergoing cardiac and neurological surgeries also continues to increase [3,4]. Although postoperative prognostic monitoring has traditionally been conducted in hospital settings, the COVID-19 pandemic has accelerated a shift toward outpatient treatment for prognosis, facilitated by advancements in surgical techniques and improved success rates [5]. This transition offers several benefits, including reduced medical costs and a quicker return to normal life. However, it also underscores the need for further research on the management of postoperative outcomes in outpatient settings. There have been reports of patients experiencing deterioration or death owing to inadequate management or reduced continuity of care following a transition from inpatient to outpatient treatment [6,7]. Considering these concerns, patients often experience anxiety and uncertainty regarding the appropriateness of postoperative discharge decisions during transitional periods during transitional periods.

These transitional periods refer to the change among health care providers, medical staff, or the health service environment. The period during which patients are discharged from hospitals to their homes or other facilities is critical. During this time, patients face a higher risk of medical complications, management failures, and adverse drug reactions because of potential interruptions in treatment, care, and information flow [8-10]. “Transitional care services” refer to interventions provided to high-risk patients with multiple vulnerabilities to mitigate risk during critical transition periods and ensure continuous care, enabling them to effectively manage and recover from illnesses [8]. This extends beyond medical management and focuses on providing services tailored to the unique lives and needs of patients with specific conditions.

Numerous studies have demonstrated the health-promoting and economic benefits of transitional care services [11]. The Transitional Care Model (TCM) comprises several core components, namely, screening, staffing, relationship maintenance, patient and family caregiver engagement, risk and symptom assessment and management, education and self-management promotion, collaboration, continuity promotion, and coordination fostering [12]. Extensive research shows that TCM provides a validated structure for analyzing postdischarge challenges by integrating components such as health status monitoring, care resource coordination, patient-provider interaction, and mental health support [13]. Many Organisation for Economic Cooperation and Development (OECD) countries, including the United States with its Hospital Readmission Reduction Program, incentivize hospitals to provide transitional care services to reduce readmissions. However, in Korea, transitional care services remain at the pilot stage and have not yet been implemented for the general public. By analyzing the emotional experiences encountered during the transitional period of patients who have undergone hospitalization and surgery for cardiovascular and cerebrovascular diseases, valuable insights may be gained regarding the need for transitional care services in a patient-centered care design and further improvements in the care system.

Recently, artificial intelligence (AI)–driven sentiment analysis has enhanced personalized health care and improved postoperative care. Through sentiment analysis using large language models (LLMs), patient emotions extracted from clinical records and nursing diaries have provided insights into emotional well-being and its impact on recovery from cardiovascular disease [14]. In addition, LLMs have been used to assist health care providers in developing more patient-centered treatment strategies by identifying sentiment-based patterns in medical documentation [15]. The Bidirectional Encoder Representations from Transformers (BERT) model, introduced in 2018, has shown outstanding capabilities in natural language processing and has been applied to various emotional analyses [16]. This has led to a growing body of research that uses the BERT model for emotional analysis in the health care sector. South Korea is among the most rapidly advancing countries in information technology within the OECD, boasting exceptionally high rates of smartphone adoption and social media engagement [17]. Particularly, patients who have undergone brain or cardiac surgery often share their postoperative progress, physical condition, and psychological well-being with fellow patients who have undergone similar procedures. With South Korea’s advanced digital infrastructure and high levels of internet use, an increasing number of discharged patients share status updates through online support groups or online communities. This information is continuously accumulated as unstructured data on various websites, and there is a growing trend of analyzing these posts to study patients’ emotional states and experiences [18]. However, existing research on the postoperative experiences of patients undergoing cardiovascular and cerebrovascular disease surgery remains limited, leading to a lack of empirical evidence necessary for developing effective transitional care strategies. In particular, comprehensive investigations into the challenges and needs of patients during their recovery period are scarce, emphasizing the urgent need for evidence-based, tailored support services. The objectives of this study were as follows: (1) to analyze the emotional states of patients who have undergone cerebrovascular and cardiovascular surgeries, (2) to categorize these emotional states based on TCM, (3) to identify scores and keywords in each field related to the patients, and (4) to provide policy recommendations for the management of surgical patients based on these findings. Toward this goal, the Korean Bidirectional Encoder Representations from Transformers (KoBERT) model was applied for sentiment analysis of postdischarge cardiovascular and cerebrovascular surgery patients. Data were integrated with the TCM framework to categorize patient emotions across 5 key domains, identify disease-specific

XSL•FO
RenderX

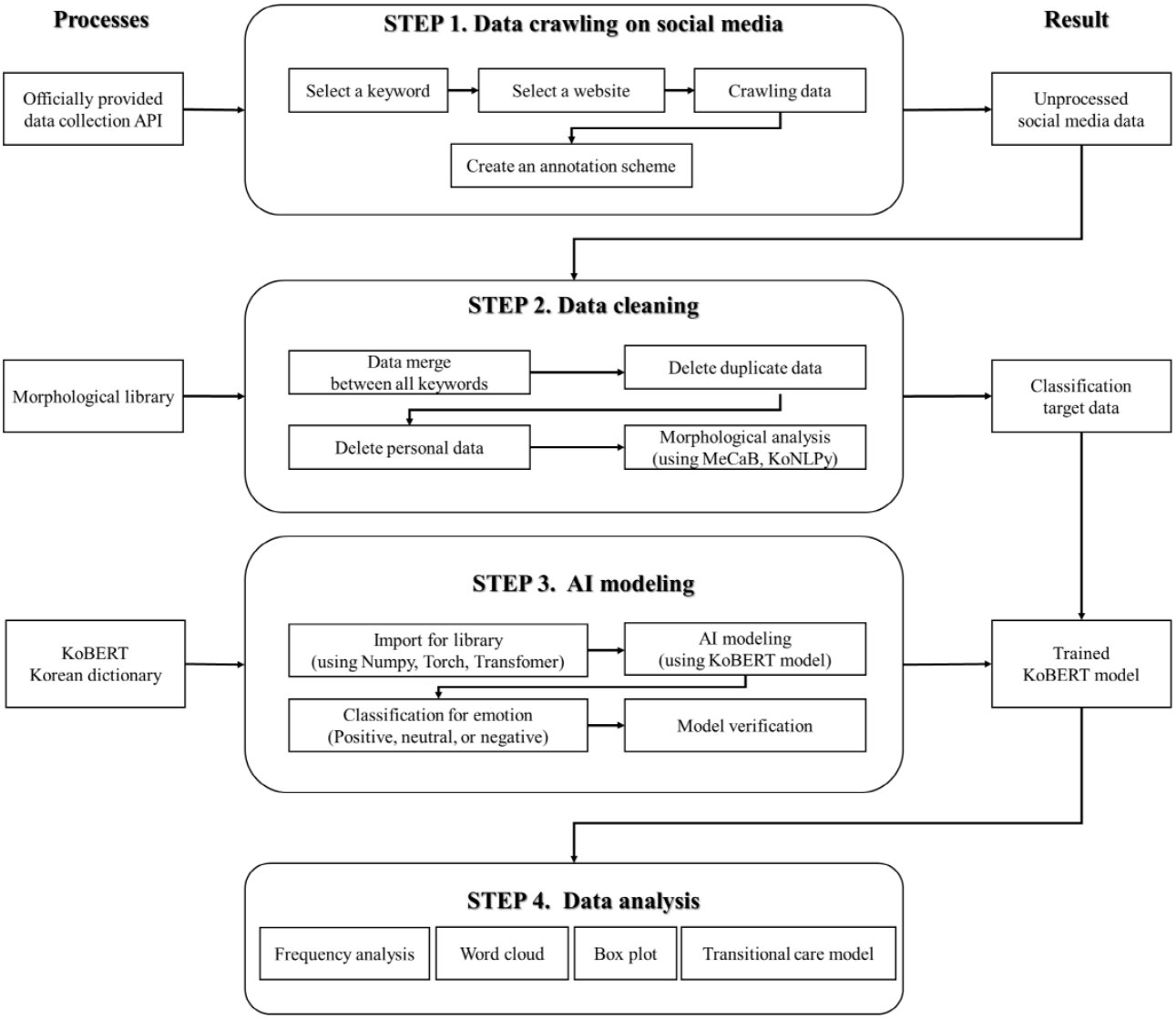
emotional trends, and provide practical insights for personalized transitional care and health care policy improvements.

Methods

Study Design

This study investigated the emotional experiences of patients who underwent cerebrovascular or cardiovascular surgery and were subsequently discharged from the hospital. The research methodology used a four-step process: (1) data crawling, (2) data cleaning, (3) AI modeling, and (4) data analysis. Figure 1 shows a schematic of the workflow.

Figure 1. Research framework. API: application programming interface; MeCaB: yet another part-of-speech and morphological analyzer; KoNLPy: Korean natural language processing in Python; AI: artificial intelligence; KoBERT: Korean Bidirectional Encoder Representations from Transformers.



Ethical Considerations

Institutional review board approval was not sought, as the study did not involve human subjects. All websites were publicly accessible, and only archived versions were reviewed. No identifiable private information was accessed or recorded.

Data Collection

This study used data collected from Naver [19], South Korea's premier search engine, and web portals. Naver offers a comprehensive suite of services, including search engines, portals, blogging platforms, discussion forums, and e-commerce solutions, and has the largest user base in Korea. As of November 2024, Naver's search engine usage rate in South Korea stands at 77.4%, significantly higher than that of Google, the second most used search engine, at 34.1%. In addition, Naver grants crawling application programming interface (API) access exclusively to researchers, whereas other search engines and social media platforms have restrictions on API access. As such, only Naver was included in this study [20]. In addition, it was selected for this study because of its diverse user demographics, particularly the broad age range of the blog contributors. Data were collected using Naver's API in Python (Python Software Foundation), targeting posts published over the past decade. The keywords used for data crawling included "stroke," "cerebral hemorrhage," "cerebrovascular," "cardiovascular

XSL•FO
RenderX

disease," "surgery review," "inpatient review," and "discharge review," resulting in a total of 10 distinct subsets. Each subset was limited to a maximum of 1000 posts, yielding a comprehensive corpus of 9393 blog posts for analysis (see Table 1).

Table . Keywords for crawling data.

Patient group and subset		Posts collected (N=9393), n (%)	Crawling keywords	
			Keyword 1	Keyword 2
Cerebrovascular disease				
	1	872 (9.28)	Surgery review	Stroke
	2	990 (10.53)	Surgery review	Cerebral hemorrhage
	3	951 (10.12)	Surgery review	Cerebrovascular
	4	850 (9.05)	Inpatient review	Stroke
	5	970 (10.33)	Inpatient review	Cerebral hemorrhage
	6	930 (9.90)	Discharge review	Stroke
	7	960 (10.22)	Discharge review	Cerebral hemorrhage
	8	910 (9.69)	Discharge review	Cerebrovascular
Cardiovascular disease				
	9	1000 (10.65)	Surgery review	Cardiovascular
	10	960 (10.22)	Discharge review	Cardiovascular

Data Cleaning

The collected data were preprocessed for analysis. All posts were initially consolidated into a single dataset (data merging), and then 787 duplicate posts were subsequently eliminated along with posts related to animals. Redundant content was removed, and personal information (eg, names, phone numbers, and addresses) was redacted. Preprocessing was conducted using a MeCab morphological analyzer from the Korean Natural Language Processing in Python library. MeCab was selected for its high accuracy, efficient part-of-speech recognition, high processing speed, multilingual support, and ease of installation. From the 9393 posts, 575,505 words were extracted for analysis.

Data Training

For the sentiment analysis of crawled posts, this study used the KoBERT model. Briefly, KoBERT is a deep learning model for Korean natural language processing and is based on Google's BERT model. It is widely used in applications such as chatbots, search engines, and machine translations. In this study, the model was trained using the Korean Sentiment Dictionary from the Emotional Dialogue Corpus. This corpus is a comprehensive natural-language sentiment dictionary comprising 15,700 sentences from 1500 Korean speakers and 270,000 sentences encompassing 60 detailed sentences [21]. The Emotional Dialogue Corpus served as a sentiment dictionary for training the KoBERT model. For model training, the dataset was split into 216,000 samples (80%) for the training set and 54,000 samples (20%) for the test set (see Table 2).

The KoBERT model was trained to classify the sentiment of the data (posts) into 3 sentiment score categories: "positive," "neutral," and "negative." Relevant documentation is available on GitHub [22]. We used KoBERT as the base model for sentiment classification. The input text was first tokenized using the MeCab morphological analyzer with a maximum sequence length of 64 tokens. The tokenized input was then processed through the KoBERT transformer encoder, followed by a fully connected classification layer to predict the sentiment as positive, neutral, or negative. For training, we used the Adam optimizer with a learning rate of 5×10^{-5}, a warmup ratio of 0.1, and gradient clipping with a max norm of 1 to stabilize learning. The model was trained for 3 epochs with a batch size of 64. To evaluate computational performance, the training and inference times were measured. The total training time per epoch was approximately 4.15 minutes, while the inference time per batch was approximately 233 ms. A summary table of hyperparameters and a diagram illustrating the model architecture are included for clarity.

XSL•FO
RenderX

Table . Model training and analysis parameters.

Parameter	Value	Description
Model	KoBERT[a]	Korean Bidirectional Encoder Representations from Transformers–based sentiment classification model.
Pretrained dataset	Korean Sentiment Corpus	Used for initial model training.
Optimizer	Adam	Optimizer for gradient descent.
Learning rate	5×10^{-5}	Initial learning rate for model training.
Log_interval	200	Gradient clipping value.
Batch size, n	64	Number of samples per batch
Epochs, n	3	Number of training iterations.
Max_len, n	64	Maximum token length per input text.
Max_Grad_norm	1	Logging interval during training.
Train split, n (%)	216,000 (80)	Rate of train set.
Test split, n (%)	54,000 (20)	Rate of test set.
Evaluation metrics	Precision, recall, and F_1-score	Performance measures for sentiment classification.

[a]KoBERT: Korean Bidirectional Encoder Representations from Transformers.

Data Validation

The performance of the AI deep learning model was assessed according to 4 key metrics: precision, recall, F_1-score, and support. The operational definitions of these metrics are provided in the subsections below.

Precision

Precision indicated the percentage of actual positive samples among cases predicted to be positive by the machine learning (ML) model. Particularly, it referred to the percentage of the actual sentiment classes relative to the predicted sentiment classes. Precision was calculated as follows:

Precision (%)=(tptp+fp)×100

Recall

Recall showed the percentage of sentiment classes predicted by the ML models relative to the actual sentiment classes. Specifically, it is the percentage predicted to show the risk group among the actual sentiment classes. Recall was calculated as follows:

Recall (%)=(tptp+fn)×100

F_1-score

The F_1-score represented the harmonic mean of precision and recall. The mathematical formula was as follows:

F1score%=2tp2tp+fp+fn×100

Support

Support represented the number of occurrences of each class in an actual dataset. It was not included in the calculation of any score but provided additional information about the distribution of classes in the dataset. Support is often used to identify class imbalance.

Data Analysis

Sentiment analysis was performed based on the data collected using the KoBERT model, and a more detailed analysis was conducted using the TCM framework divided into 5 domains. The TCM framework was used as the analytical framework and was restructured from the patient's perspective into the following 5 domains: health status, care resources, care demand, interaction (with medical staff), and mental state. Detailed information is provided in Multimedia Appendix 1. A detailed analysis of the following 4 focus areas was conducted. First, word clouds were generated to analyze keywords related to the emotions of patients discharged after heart and brain surgery. Second, the postdischarge sentiment scores (calculated as percentages) of the patients who underwent cardiovascular and cerebrovascular surgeries were classified into 3 score categories: positive, neutral, or negative. Each category is presented with its minimum, maximum, 95% CI, median, mean, and variance. Third, patient distribution according to the 5 domains of patient-centered TCM was identified. Finally, the "positive" score category for the emotional state was presented as 5 mean scores (%) based on the TCM framework and presented as box plots. These plots displayed the frequency, quartiles, and minimum and maximum values. All analyses were conducted using GraphPad Prism 10.2.2.

Results

Model Verification

The AI KoBERT model used in this study was trained using the Korean Sentiment Dictionary derived from the Emotional Dialogue Corpus. The trained model achieved satisfactory performance. The precision, recall, and F_1-scores exceeded 0.8, indicating a high level of accuracy and reliability in sentiment classification (see Table 3).

XSL•FO
RenderX

Table . Korean Bidirectional Encoder Representations from Transformers (KoBERT) model verification.

Class	Precision	Recall	F_1-score	Support, n
Positive	0.96	0.89	0.92	1217
Neutral	0.93	0.93	0.93	318
Negative	0.98	0.99	0.98	6054
Average	0.96	0.94	0.94	2529

Word Cloud

Data pertaining to cerebrovascular and cardiovascular surgeries were visualized and analyzed using word clouds (Multimedia Appendix 2). For cerebrovascular surgery patients, the prominent keywords were “surgery,” “hospital,” “test,” “receive,” and “symptom.” For cardiovascular surgery patients, the key terms that emerged were “surgery,” “hospital,” “receive,” “eat,” “admission,” and “symptom.”

Sentiment Scores by Patient Type

The patients’ emotional states were categorized as positive, neutral, or negative, and their respective distributions were analyzed. The results revealed a lower proportion of patients with “neutral” emotional state among cerebrovascular surgery patients than among cardiovascular surgery patients (62,896/84,100,74.8% vs 12,456/16,000, 77.9%). Conversely, the proportion of patients with “positive” (16,839/84,100, 20.0% vs 3072/16,000, 19.2%) and “negative” (4364/84,100, 5.2% vs 471/16,000, 2.9%) emotional states was higher among cerebrovascular surgery patients than their cardiovascular surgery counterparts (see Table 4).

Table . Rates of emotions by patient type.

Patient type and emotional state		Min, %	Max, %	Mean (SD), %	Variance	Range
Total						
	Positive	0	68.8	19.9 (11)	121.0	68.8
	Neutral	0	36.4	4.8 (4.9)	23.9	36.4
	Negative	25	100	75.3 (12)	143.9	75.0
Cerebrovascular						
	Positive	0	68.8	20 (11.2)	126.3	68.8
	Neutral	25	100	74.8 (12.3)	150.7	75.0
	Negative	0	36.4	5.2 (5)	25.2	36.4
Cardiovascular						
	Positive	0	53.3	19.2 (9.7)	93.3	53.3
	Neutral	40	100	77.9 (10)	100.8	60.0
	Negative	0	24	2.9 (3.6)	13.3	24.0

Keyword Analysis Related to the Transitional Care Model

We analyzed 575,505 words from 9393 posts. The data were classified into 5 domains within the TCM framework and restructured based on the patient’s perspective (see Table 5). For cerebrovascular surgery patients, the top 3 keywords in each domain were as follows: (1) “health status:” sick (n=1860), symptom (n=1819), and sleep disturbance (n=881); (2) “care resources:” mom (n=1792), transfer (n=1774), and caregiver (n=890); (3) “care demand:” rehab (n=1323), postcare (n=689), and check (n=647); (4) “interaction:” hospital (n=5623), test (n=4215), and therapy (n=3117); and (5) “mental state:” good (n=2406), confirm (n=828), and tough (n=716). For cardiovascular surgery patients, the top 3 keywords in each domain were as follows: (1) “health status:” ache (n=410), symptom (n=297), and sick (n=294); (2) “care resources:” counseling (n=205), visit (n=125), and cost (n=104); (3) “care demand:” medication (n=193), preparation (n=108), and check (n=108); (4) “interaction:” hospital (n=898), procedure (n=321), and doctor (n=223); and (5) “mental state:” void (n=625), good (n=410), and confirm (n=313).

XSL•FO
RenderX

Table . Keywords ranked by occurrence in each component of the Transitional Care Model (TCM) for cerebrovascular and cardiovascular surgery patients.

Rank	Cerebrovascular surgery patients (n=483,922)					Cardiovascular surgery patients (n=75,765)				
	Health status[a]	Care resource[a]	Care demand[a]	Interaction[a]	Mental state[a]	Health status[a]	Care resources[a]	Care demand[a]	Interaction[a]	Mental state[a]
1	Sick (1860)	Mom (1792)	Rehab (1323)	Hospital (5623)	Good (2406)	Ache (410)	Counseling (205)	Medication (193)	Hospital (898)	Void (625)
2	Symptom (1819)	Transfer (1774)	Post-care (689)	Test (4215)	Confirm (828)	Symptom (297)	Visit (125)	Prep (109)	Procedure (321)	good (410)
3	Sleep disturbance (881)	Caregiver (890)	Check (647)	Therapy (3117)	Tough (716)	Sick (294)	Cost (104)	Check (108)	Doctor (223)	Confirm (313)
4	Not sure (878)	Ambulance (844)	Cause (558)	Procedure (1592)	Worry (698)	Side effect (252)	Insurance (94)	Post-care (98)	Teacher (137)	Problem (178)
5	Severe (669)	Visit (645)	Prep (501)	Teacher (1427)	Problem (687)	Severe (211)	Transfer (91)	Workout (94)	Diagnosis (130)	Worry (176)
6	Recovery (650)	Aid (598)	Counseling (443)	Consult (1421)	Prayer (607)	Swelling (185)	Mom (87)	Control (75)	Decision (130)	Stress (128)
7	Alright (622)	Cost (510)	Medication (426)	Professor (1301)	Gratitude (576)	Inflammation (133)	Caregiver (86)	Cause (62)	Prescription (104)	Tough (103)
8	Headache (593)	Insurance (469)	Disability (424)	Nurse (1174)	Scary (407)	Discomfort (113)	Provide (67)	Living (62)	Professor (104)	Prayer (58)
9	Breathing (584)	Counseling (443)	Control (205)	Doctor (887)	Relaxed (349)	Complication (86)	Family (53)	Recovery (59)	Nurse (103)	Complex (57)
10	Side effect (581)	Care (390)	Recovery (127)	Explanation (726)	Tough (286)	Breathing (83)	Premium (23)	Safety (59)	Specialist (82)	Relaxed (49)

[a]Keyword (n)

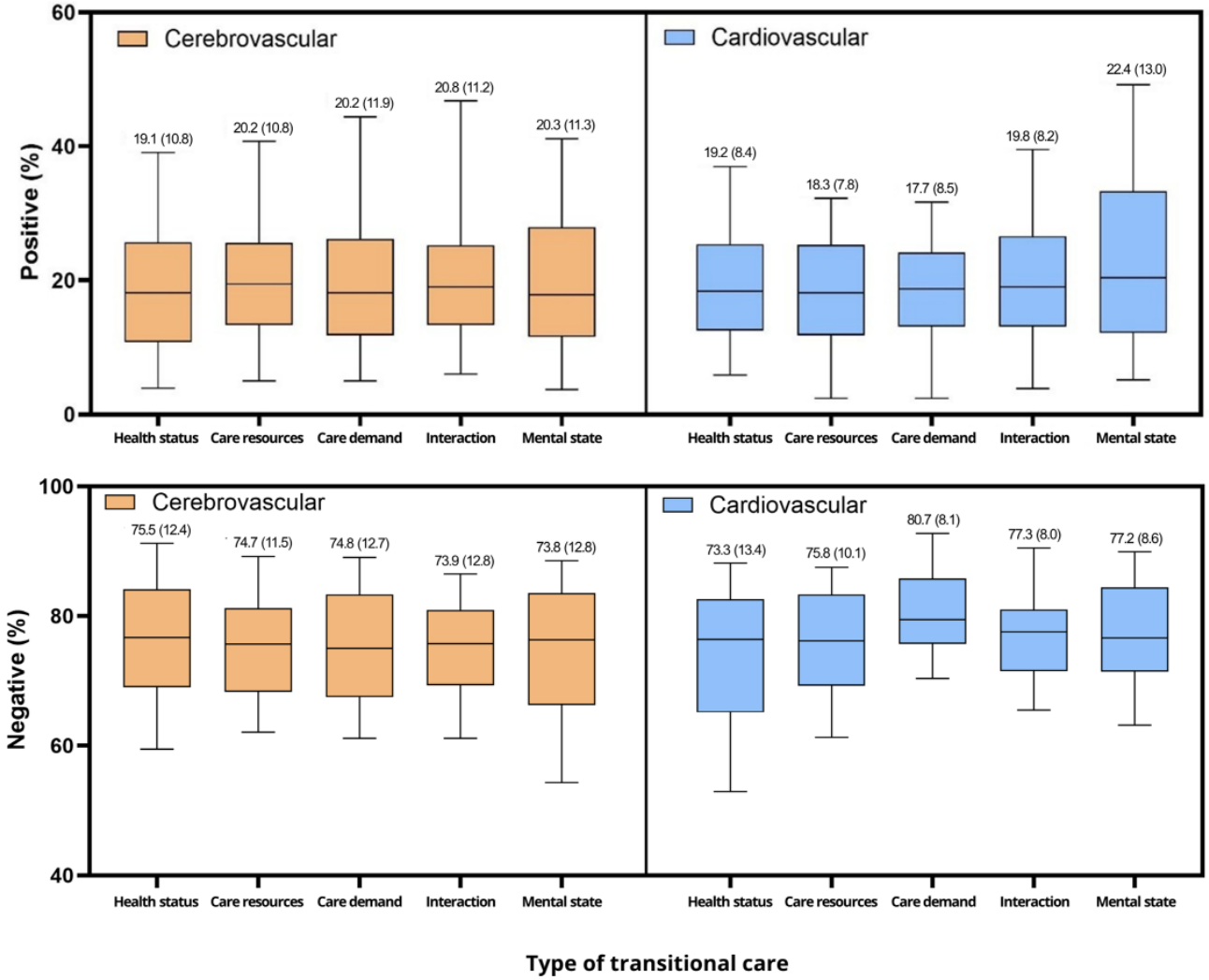
Sentiment Scores by Patient Type

Figure 2 shows the box plots of the distribution of the sentiment scores (%) for the 5 domains within the TCM framework (health status, care resources, care demands, patient-provider interactions, and mental state).

Compared with cardiovascular surgery patients, cerebrovascular surgery patients demonstrated higher mean postdischarge positive sentiment scores in 3 domains: care resources (3,765/18,600, 20.2% vs 292/1600, 18.3%), care demand (4465/22,100, 20.2% vs 1280/7200, 17.7%), and interaction (2107/10,100, 20.8% vs 575/2900, 19.8%). Conversely, cardiovascular surgery patients exhibited higher mean postdischarge positive sentiment scores in 2 domains: health status (267/1400, 19.2% vs 4467/23,300, 19.1%) and mental state (674/3000, 22.4% vs 2034/10,000, 20.3%). With respect to negative sentiment scores, there was a higher level of dissatisfaction with their health status among patients with cerebrovascular disease than among patients with cardiovascular disease (17,594/23,300, 75.5% vs 2199/3000, 73.3%). Meanwhile, compared with their cerebrovascular counterparts, patients with cardiovascular disease expressed more negative emotions regarding care resources (2198/2900, 75.8% vs 13,898/18,600, 74.7%), care demand (5817/7200, 80.7% vs 16,551/22,100, 74.8%), interactions (1236/1600, 77.3% vs 7467/10,100, 73.9%), and mental state (2316/3000, 77.2% vs 7384/10,000, 73.8%).

XSL•FO
RenderX

Figure 2. Box plot of sentiment scores by patient type; values are mean (SD).



Discussion

Principal Findings

This study addresses the critical gap in understanding the postoperative experiences of patients who have undergone cardiovascular and cerebrovascular disease surgery. The sentiment analysis revealed significant challenges faced by patients during their recovery, underscoring the need for evidence-based, tailored support services to enhance transitional care strategies. The KoBERT model used for sentiment analysis demonstrated high performance, achieving a precision of 0.96, recall of 0.94, and F_1-score of 0.94.

These results are consistent with those of previous studies that used KoBERT. For instance, a BERT model trained on clinical notes from Korean doctors achieved a precision of 0.99, recall of 0.97, and F_1-score of 0.93. Another KoBERT model trained on sentiments from Korean Internet posts showed precision, recall, and F_1-scores of 0.86 across all metrics. Previous studies have evaluated models using mean squared error, root mean squared error, mean absolute error, and R^2. However, this study focused on classification rather than continuous variables, and thus, these metrics were not used [23].

The performance level of the KoBERT model used in this study is closely similar with that of existing models [24,25], validating its effectiveness in classifying sentiments as positive, neutral, or negative. Furthermore, the model's capability to identify emotional trends in real time during consultations presents opportunities for its expanded use in relevant research fields. The analysis revealed that the proportion of patients who experienced more negative emotions was higher among those who had underwent cerebrovascular surgery (5.2%) than among those who had undergone cardiovascular surgery (2.9%). This finding is consistent with previous research demonstrating that patients with cerebrovascular disease tend to experience higher levels of anxiety and worry relative to those with other diseases [26]. In a study involving 3200 surgical patients, 40.5% experienced negative postoperative emotions, such as depression, anxiety, and fear. The lower levels of negative emotions observed in our study may be attributed to various factors, including advanced medical technology in Korea leading to high surgical success rates, improved patient management owing to high medical accessibility, and a relatively low financial burden owing to comprehensive health insurance coverage [27-29]. However, it is important to note that the data in this study were obtained by crawling internet posts made by patients after surgery. That is, the patients had access to the internet, potentially indicating a lesser severity of illness,

XSL•FO
RenderX

younger age, and relatively good overall physical health. Furthermore, the lower prevalence of negative emotions among cardiovascular surgery patients than among cerebrovascular surgery patients may be explained by the nature of cardiovascular disease treatment in Korea. Most hospitalizations and surgeries related to cardiovascular issues involve ischemic heart disease, which is often treated with percutaneous coronary intervention rather than major surgery. This less invasive approach typically leads to quicker discharge and a lower risk of long-term disability in cardiovascular diseases than in cerebrovascular diseases [30].

TCM is designed to provide continuous care for patients transitioning postoperatively from the hospital to home or another care facility. This study analyzed keywords and sentiment scores (calculated as percentages) across 5 TCM domains classified from the patient's perspective: health status, care resources, care demand, interaction, and mental state. Across all conditions, keywords indicating physical pain and side effects, such as pain, sickness, and severe, were frequently mentioned in relation to health status. Regarding mental state, negative emotional keywords, such as tough, worry, and problems, were frequently mentioned. This highlights the impact of hospitalization and surgery on patients with severe conditions, such as cardiovascular and cerebrovascular diseases, as well as the need for related care. The interaction-related keywords mainly involved medical care and treatment, including hospitals, procedures, and doctors. This highlights the absence of elements crucial for transitional care services in the Korean health care setting, such as coordination, education, consultation, and explanations. Disease-specific differences were also observed, especially in the domains of care resources and demand, indicating that postdischarge care resources and needs varied according to disease type. For patients with cerebrovascular disease, the highlighted keywords were mother, caregiver, transfer, ambulance (care resources), rehabilitation, and postcare (care demand). This indicated a high demand for postsurgery or postdischarge rehabilitation and related transfers. In contrast, for patients with cardiovascular diseases, the keywords were insurance and cost (care resources) and medication and workout (care demand), indicating a high demand for cost-related items. These disease-specific differences in TCM domain keywords reflect varying patient needs during transition periods. This information is crucial and should be incorporated when modeling patient-centered transitional care services.

When comparing the sentiment scores of patient-centered TCM domains for cardiovascular and cerebrovascular diseases, the positive score categories for health status were similar, accounting for 19.1% and 19.2% of the total scores, respectively. However, in the domains of care resources, care demand, and interaction, the cerebrovascular surgery patients exhibited higher positive sentiment scores than did the cardiovascular surgery patients. This disparity may be due to the fact that cerebrovascular diseases often involve longer postsurgery or postdischarge processes and are more likely to involve additional care services such as rehabilitation, leading to more positive keywords being mentioned during the recovery process. Regarding mental state, cardiovascular surgery patients showed a higher positive score than did cerebrovascular surgery patients (22.4% vs 20.3%). This difference may be attributed to the typically shorter hospital stay of cardiovascular surgery patients and the fact that their immediate problems are often resolved through procedures. These factors can potentially contribute to a more positive average sentiment score among cardiovascular surgery patients than among cerebrovascular surgery patients.

For cerebrovascular diseases, the positive sentiment score category related to interaction (20.8%) was notably higher than that related to other areas, with health status scoring the lowest (19.1%). In contrast, for cardiovascular diseases, the positive sentiment score category was the highest for mental state (22.4%), whereas it was the lowest for care demand (17.7%). These findings may be attributed to the nature of cerebrovascular diseases in which prolonged interactions with medical staff, rehabilitation specialists, and caregivers are crucial during the transition period. Conversely, for cardiovascular diseases, despite the recognized importance of postdischarge cardiac rehabilitation, it appears to be underdeveloped, as reflected by lower scores. This finding is consistent with previous findings showing that only 44.2% of stroke patients discharged from university hospitals continue outpatient rehabilitation and that only 17% of cardiovascular surgery patients discharged from regional cardiovascular centers pursue outpatient cardiac rehabilitation [31,32]. This analysis of sentiment scores for each disease type suggests which components of transitional care are lacking and require improvement, as determined based on patients' reported experiences that highlight positive or negative sentiments.

Negative sentiment analysis revealed the highest score for health status (75.5%) for cerebrovascular diseases, surpassing that for cardiovascular diseases. This finding aligns with the lower positive sentiment score in this category, likely because of the high risk of postdischarge sequelae. Postdischarge sequelae are closely associated with physical and mental health challenges and result in increased negative sentiment scores. Conversely, among cardiovascular surgery patients, negative sentiment scores were the highest for care demands (80.7%), followed by those for care resources (75.8%), interactions (77.3%), and mental state (77.2%). These scores were higher than those among cerebrovascular surgery patients. This suggests that although cardiovascular diseases significantly affect patient lives, the relatively underdeveloped infrastructure and resources for postdischarge transitional care services may still contribute to the higher negative scores. Patients experience an ongoing need for care, such as cardiac rehabilitation, which can be burdensome and may exacerbate negative sentiments.

Consequently, the keywords and sentiments analyzed within the TCM framework encompass the experiences of surgery or hospitalization and are not restricted to postdischarge transitional care. Therefore, these results should be interpreted with caution. A combination of quantitative and qualitative research methods is essential to gain a comprehensive understanding of patients' emotional states. Future research can enhance these findings by incorporating focus group interviews with discharged patients and integrating clinical data.

XSL•FO
RenderX

Limitations

This study had some limitations. First, access to primary data is restricted by South Korea's Personal Information Protection Act, particularly by the Medical Care Act. Future research can address this limitation by conducting analyses of primary data under strict protocols and anonymization procedures in collaboration with medical research institutions, allowing for the inclusion of detailed clinicodemographic variables. Second, we analyzed posts from patients who shared their health status on the online community. Considering that internet users are likely to have better physical health, information from patients with more severe conditions may have been underrepresented, potentially introducing sample bias. Third, the keywords used as search terms pertained to surgical and inpatient experiences, making it challenging to distinguish between experiences during hospitalization and those during the postdischarge transition period. Fourth, this research classified emotions into only 3 categories. Emotions can be defined in various ways, and we acknowledge the limitations in classifying emotions into more detailed categories due to accuracy concerns. Future research should aim to classify emotions in a more exhaustive manner.

Conclusions

The sentiment analysis results demonstrated that the KoBERT model had comparable performance levels to those of previous models. For sentiment analysis, the TCM components was categorized into 5 patient-centered domains: health status, care resources, care demand, interaction, and mental state. The sentiment analysis revealed that cardiovascular surgery patients expressed fewer negative sentiments than did cerebrovascular surgery patients, likely because of the relatively simpler procedures generally used in treating cardiovascular conditions. Conversely, patients with cerebrovascular disease who typically required long-term rehabilitation had higher negative sentiment scores. Notably, cerebrovascular surgery patients showed high positive sentiment scores in the "interaction" domain (relating to medical staff) but high negative sentiment scores in the "health status" domain. In contrast, cardiovascular surgery patients exhibited high positive sentiment scores for mental states and high negative sentiment scores for care demands. Collectively, these results suggest that a one-size-fits-all approach is not applicable for managing cardiovascular and cerebrovascular diseases. Instead, considering the differences in sentiment scores for each TCM domain, health care providers should provide personalized patient care during the transition from surgery to postdischarge care.

Acknowledgments

This work was supported by the National Research Foundation of Korea (NRF) grant funded by the Korean government (Ministry of Science and ICT [MSIT]; RS-2023- ‐ 00279534).

Conflicts of Interest

None declared.

Multimedia Appendix 1
A total of 5 domains were classified from the patient's perspective based on Transitional Care Model (TCM) components, with examples of related terms.
[DOCX File, 15 KB - medinform_v13i1e65127_app1.docx]

References

1. Tsao CW, Aday AW, Almarzooq ZI, et al. Heart disease and stroke statistics-2023 update: a report from the American Heart Association. Circulation 2023 Feb 21;147(8):e93-e621. [doi: 10.1161/CIR.0000000000001123] [Medline: 36695182]
2. Global Burden of Disease 2021: findings from the GBD 2021 study. : Institute for Health Metrics and Evaluation; 2024.
3. Hao L, Xu X, Dupre ME, et al. Adequate access to healthcare and added life expectancy among older adults in China. BMC Geriatr 2020 Apr 9;20(1):129. [doi: 10.1186/s12877-020-01524-9] [Medline: 32272883]
4. Kim Y, Byon YJ, Yeo H. Enhancing healthcare accessibility measurements using GIS: a case study in Seoul, Korea. PLoS ONE 2018;13(2):e0193013. [doi: 10.1371/journal.pone.0193013] [Medline: 29462194]
5. Shariq OA, Bews KA, Etzioni DA, Kendrick ML, Habermann EB, Thiels CA. Performance of general surgical procedures in outpatient settings before and after onset of the COVID-19 pandemic. JAMA Netw Open 2023 Mar 1;6(3):e231198. [doi: 10.1001/jamanetworkopen.2023.1198] [Medline: 36862412]
6. Dencker EE, Bonde A, Troelsen A, Varadarajan KM, Sillesen M. Postoperative complications: an observational study of trends in the United States from 2012 to 2018. BMC Surg 2021 Nov 6;21(1):393. [doi: 10.1186/s12893-021-01392-z] [Medline: 34740362]
7. Walker-Smith T, Joyce K, Maishman R, et al. Outcome Monitoring After Cardiac Surgery (OMACS): a single-centre prospective cohort study of cardiac surgery patients. BMJ Open 2022 Dec 19;12(12):e063268. [doi: 10.1136/bmjopen-2022-063268] [Medline: 36535713]
8. Naylor MD, Hirschman KB, Toles MP, Jarrín OF, Shaid E, Pauly MV. Adaptations of the evidence-based Transitional Care Model in the U.S. Soc Sci Med 2018 Sep;213:28-36. [doi: 10.1016/j.socscimed.2018.07.023] [Medline: 30055423]

XSL•FO
RenderX

9. Buurman BM, Hoogerduijn JG, de Haan RJ, et al. Geriatric conditions in acutely hospitalized older patients: prevalence and one-year survival and functional decline. PLoS One 2011;6(11):e26951. [doi: 10.1371/journal.pone.0026951] [Medline: 22110598]
10. Forster AJ, Asmis TR, Clark HD, et al. Ottawa Hospital Patient Safety Study: incidence and timing of adverse events in patients admitted to a Canadian teaching hospital. CMAJ 2004 Apr 13;170(8):1235-1240. [doi: 10.1503/cmaj.1030683] [Medline: 15078845]
11. Naylor MD, Aiken LH, Kurtzman ET, Olds DM, Hirschman KB. The importance of transitional care In achieving health reform. Health Aff (Millwood) 2011 Apr;30(4):746-754. [doi: 10.1377/hlthaff.2011.0041] [Medline: 21471497]
12. Hirschman KB, Shaid E, McCauley K, Pauly MV, Naylor MD. Continuity of care: the transitional care model. Online J Issues Nurs 2015 Sep 30;20(3):1. [Medline: 26882510]
13. Naylor MD, Sochalski JA. Scaling up: bringing the transitional care model into the mainstream. Issue Brief (Commonw Fund) 2010 Nov;103:1-12. [Medline: 21053533]
14. Zhuang Y, Zhang J, Li X, et al. Autonomous international classification of diseases coding using pretrained language models and advanced prompt learning techniques: evaluation of an automated analysis system using medical text. JMIR Med Inform 2025 Jan 6;13:e63020. [doi: 10.2196/63020] [Medline: 39761555]
15. Ferrario A, Sedlakova J, Trachsel M. The role of humanization and robustness of large language models in conversational artificial intelligence for individuals with depression: a critical analysis. JMIR Ment Health 2024 Jul 2;11:e56569. [doi: 10.2196/56569] [Medline: 38958218]
16. Devlin J, Chang MW, Lee K, Toutanova K. BERT: pre-training of deep bidirectional transformers for language understanding. arXiv. Preprint posted online on Oct 11, 2018. [doi: 10.48550/arXiv.1810.04805]
17. Cha JH, Choi YJ, Ryu S, Moon JH. Association between smartphone usage and health outcomes of adolescents: A propensity analysis using the Korea youth risk behavior survey. PLoS One 2023;18(12):e0294553. [doi: 10.1371/journal.pone.0294553] [Medline: 38055658]
18. Zhang D, Yin C, Zeng J, Yuan X, Zhang P. Combining structured and unstructured data for predictive models: a deep learning approach. BMC Med Inform Decis Mak 2020 Oct 29;20(1):280. [doi: 10.1186/s12911-020-01297-6] [Medline: 33121479]
19. NAVER. URL: https://www.naver.com/ [accessed 2023-11-11]
20. Websites with the highest reach on PC in South Korea as of november 2024. Statistica. URL: https://www.statista.com/statistics/989367/south-korea-reach-rate-websites-pc/ [accessed 2024-02-08]
21. Emotional conversation corpus. AI Hub. URL: https://www.aihub.or.kr/aihubdata/data/view.do?currMenu=115&topMenu=100&dataSetSn=86 [accessed 2024-02-02]
22. Repository of python code, trained KOBERT model. GitHub. URL: https://github.com/lhc0104/KoBERT_CC/ [accessed 2024-04-13]
23. Abdel Hady DA, Abd El-Hafeez T. Predicting female pelvic tilt and lumbar angle using machine learning in case of urinary incontinence and sexual dysfunction. Sci Rep 2023 Oct 20;13(1):17940. [doi: 10.1038/s41598-023-44964-0] [Medline: 37863988]
24. An J, Kim J, Sunwoo L, Baek H, Yoo S, Seunggeun L. De-identification of clinical notes with pseudo-labeling using regular expression rules and pre-trained BERT. BMC Med Inform Decis Mak 2025 Feb;25(1):82. [doi: 10.21203/rs.3.rs-2672115/v1] [Medline: 39962485]
25. Lee MA, Park YJ, Na JY, Sohn CB. Implementation of review sentiment analysis application using KoBERT, KoGPT-2, and KoBART optimized hyperparameters. dcs 2023 Nov 30;24(11):2831-2840. [doi: 10.9728/dcs.2023.24.11.2831]
26. Hart T, Cicerone K. Emotional problems after traumatic brain injury. Brainline. URL: https://www.brainline.org/article/emotional-problems-after-traumatic-brain-injury [accessed 2024-01-22]
27. Yang GZ, Jiang TZ, editors. Medical Imaging and Augmented Reality: Medical Imaging and Augmented Reality: Second International Workshop, MIAR 2004, Beijing, China, August 19-20, 2004 Proceedings, 1st edition: Springer Berlin Heidelberg; 2004.
28. Chae W, Kim J, Park EC, Jang SI. Comparison of patient satisfaction in inpatient care provided by hospitalists and nonhospitalists in South Korea. Int J Environ Res Public Health 2021 Jul 30;18(15):8101. [doi: 10.3390/ijerph18158101] [Medline: 34360394]
29. Shin J. Private health insurance in South Korea: an international comparison. Health Policy 2012 Nov;108(1):76-85. [doi: 10.1016/j.healthpol.2012.08.011] [Medline: 22958939]
30. The state of heart disease care [Web page in Korean]. Health Insurance Review & Assessment Service. 2023. URL: https://www.hira.or.kr/bbsDummy.do?pgmid=HIRAA020041000100&brdScnBltNo=4&brdBltNo=11037&pageIndex=1#none [accessed 2024-05-01]
31. Kim WS, Jung YS, Paik NJ, et al. Multidimensional approach for rehabilitation status and social adaptation in stroke patients after discharge – interim analysis. Weekly Health Illness 2020;13:3009-3026 [FREE Full text]
32. Kim C, Sung J, Han JY, et al. Current status of cardiac rehabilitation in the regional cardiocerebrovascular centers in Korea. J Clin Med 2021 Oct 29;10(21):5079. [doi: 10.3390/jcm10215079] [Medline: 34768598]

XSL•FO
RenderX

Abbreviations

AI: artificial intelligence
API: application programming interface
BERT: Bidirectional Encoder Representations from Transformers
KoBERT: Korean Bidirectional Encoder Representations from Transformers
LLM: large language model
ML: machine learning
OECD: Organisation for Economic Cooperation and Development
TCM: Transitional Care Model

Edited by A Benis; submitted 06.08.24; peer-reviewed by F Shah-Mohammadi, R Chen, TA El-Hafeez; revised version received 05.03.25; accepted 24.03.25; published 30.05.25.

Please cite as:
Lee H, Hwang YS, Kim YJ, Park Y, Jo HS
Experience of Cardiovascular and Cerebrovascular Disease Surgery Patients: Sentiment Analysis Using the Korean Bidirectional Encoder Representations from Transformers (KoBERT) Model
JMIR Med Inform 2025;13:e65127
URL: https://medinform.jmir.org/2025/1/e65127
doi:10.2196/65127

© Hocheol Lee, Yu Seong Hwang, Ye Jun Kim, Yukyung Park, Heui Sug Jo. Originally published in JMIR Medical Informatics (https://medinform.jmir.org), 30.5.2025. This is an open-access article distributed under the terms of the Creative Commons Attribution License (https://creativecommons.org/licenses/by/4.0/), which permits unrestricted use, distribution, and reproduction in any medium, provided the original work, first published in JMIR Medical Informatics, is properly cited. The complete bibliographic information, a link to the original publication on https://medinform.jmir.org/, as well as this copyright and license information must be included.

XSL•FO
RenderX

Enhancing Antidiabetic Drug Selection Using Transformers: Machine-Learning Model Development

Hisashi Kurasawa[1,2*], PhD; Kayo Waki[1*], MD, MPH, PhD; Tomohisa Seki[1], MD, PhD; Eri Nakahara[1,2], MS; Akinori Fujino[2], PhD; Nagisa Shiomi[2], MS; Hiroshi Nakashima[2], PhD; Kazuhiko Ohe[1], MD, PhD

[1]The University of Tokyo Hospital, 7-3-1 Hongo, Bunkyo-ku, Tokyo, Japan

[2]Nippon Telegraph and Telephone Corporation, Japan

[*]these authors contributed equally

Corresponding Author:
Kayo Waki, MD, MPH, PhD
The University of Tokyo Hospital, 7-3-1 Hongo, Bunkyo-ku, Tokyo, Japan

Abstract

Background: Diabetes affects millions worldwide. Primary care physicians provide a significant portion of care, and they often struggle with selecting appropriate medications.

Objective: This study aimed to develop a model that accurately predicts what drug an endocrinologist would prescribe based on the current measurements. The goal was to create a system that would assist nonspecialists in choosing medications, thereby potentially improving diabetes treatment outcomes. Based on the performance of previous studies, we set a performance target of achieving a receiver operating characteristic area under the curve (ROC-AUC) above 0.95.

Methods: A transformer-based encoder-decoder model predicts whether 44 types of diabetes drugs will be prescribed. The model uses sequences of age, sex, history for 12 laboratory tests, and prescribed drug history as inputs. We assessed the model using the electronic health records from 7034 patients with diabetes seeing endocrinologists between 2012 and 2022 at the University of Tokyo Hospital. We assessed model performance trained on data subsets spanning different time periods (2, 5, and 10 years) using micro- and macro-averaged ROC-AUC on a hold-out test set comprising data solely from 2022. The model's performance was compared against LightGBM.

Results: The model trained on data from the past 5 years (2017 - 2021) yielded the best predictive performance, achieving a microaverage (95% CI) ROC-AUC of 0.993 (0.992-0.994) and a macroaverage (95% CI) ROC-AUC of 0.988 (0.980-0.993). The model achieved an ROC-AUC above 0.95 for 43 out of 44 drugs. These results surpassed the predefined performance target and outperformed both previous studies and the LightGBM model's microaverage ROC-AUC of 0.988 (0.985-0.990) in terms of prediction accuracy. Furthermore, training the model with short-term data from the past 5 years yielded high accuracy compared to using data from the past 10 years, suggesting that learning from more recent prescribing patterns might be advantageous.

Conclusions: The proposed model demonstrates the feasibility of accurately predicting the next prescribed drugs. This model, trained from the past prescriptions of endocrinologists, has the potential to provide information that can assist nonspecialists in making diabetes-treatment decisions. Future studies will focus on incorporating important factors such as prescription contraindications and constraints to enhance safety, as well as leveraging large-scale clinical data across multiple hospitals to improve the generalizability of the model.

(JMIR Med Inform 2025;13:e67748) doi:10.2196/67748

KEYWORDS

AI; diabetes; drug selection; machine learning; transformer; artificial intelligence

Introduction

Diabetes affects 529 million people worldwide, with 1 in every 10 adults experiencing the condition [1]. Patients with diabetes receive care from primary care physicians, not endocrinologists, in many areas including the United States, Europe [2], and Japan [3]. This is particularly concerning in the United States, where the endocrinologist shortage is significant: the population-to-endocrinologist ratio within 20 miles was 29,887:1 for adults aged 18 - 64. Rural areas face even greater disparities, with only 55.5% of adults having access to at least 1 endocrinologist within that distance [4]. Japan also faces a similar problem. Japan has 11 million patients with diabetes but only about 7000 specialists, and two-thirds of people with type 2 diabetes (T2D) receive care from primary care physicians [3]. These nonspecialists may struggle to predict a patient's glycemic control. Approximately 60% of surveyed patients with T2D treated by nonspecialists experienced poor glycemic control

XSL•FO
RenderX

(hemoglobin A_{1c} [HbA_{1c}] ≥8%), with around 30% seeing worsened levels the following year, according to a survey on T2D treatment practices by primary care physicians [3].

One of the difficulties in diabetes treatment for primary care physicians is drug selection [5,6]. Medications are prescribed either as monotherapy or in combination. Medications need to be chosen [7] considering insulin secretion and insulin resistance [8], age [9,10], degree of obesity [11], severity of chronic complications [12], liver function, and kidney function [13]. New diabetes treatments continue to be developed, expanding the options for medication selection. For example, in Japan, sodium–glucose cotransporter 2 [14], imeglimin [15], and tirzepatide [16] were introduced in 2014, 2021, and 2023, respectively. The selection of diabetes medications depends on individual patient factors, with guidelines [17] and treatment tendencies [18] that vary from country to country. A tool supporting drug selection could enhance treatment outcomes. It could provide early warning to physicians and potentially improve treatment outcomes for patients who are being examined by nonspecialized physicians.

Clinical decision support systems (CDSS) provide physicians with safety tools for drug selection [19]. By adopting a knowledge-based approach aligned with clinical guidelines, CDSS help to prevent medication errors such as overdosing, incomplete, or unclear orders [20,21]. However, replicating the ability of endocrinologists to select drugs for individual patient conditions in a CDSS is complex and challenging for knowledge-based approaches.

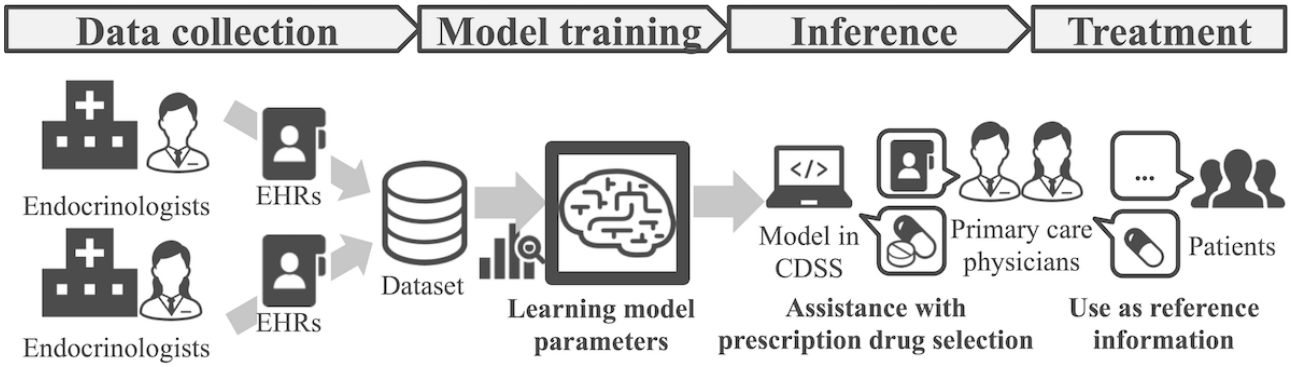
Machine learning (ML) has demonstrated success in predicting patient symptoms, including forecasting the onset of T2D [22] and predicting complications [23]. Several studies have applied ML to the problem of drug selection for patients with diabetes [24]. A study predicting the next prescribed diabetes drugs for 161,497 patients with diabetes using sequential pattern mining demonstrated an accuracy of 89.1% - 90.5% in guessing from 37 drug classes (eg, DPP-4 inhibitor) and 63.5% - 64.9% accuracy in guessing from 43 drugs (eg, algliptin) [25]. Another study predicted 7 drug classes with an ROC-AUC of 90.6% - 94.3% using recurrent neural networks (RNN) [26]. There are also proposed methods for predicting treatment outcomes after selecting diabetes medications [27].

The field of ML has undergone significant advancement since the introduction of the transformer approach in 2017 [28,29]. Transformers enable contextual interactions for natural language processing tasks and have become a core technology across diverse domains [30-32]. The transformer model incorporates an attention mechanism and has shown remarkable performance in tasks involving the extraction of temporal and semantic relationships, leading to success in tasks such as generation and classification [33]. Generally, transformers enhance predictive performance through two types of training: pretraining via self-supervised learning and fine-tuning via supervised learning. For example, large language models like GPT and bidirectional encoder representations from transformers (BERT) were pretrained on a task predicting the next or masked word and then fine-tuned on a task generating responses to an instruction [34]. Several studies in health care have already used this scheme of 2 types of learning. TransformEHR improved performance on the fine-tuned task of predicting the onset of pancreatic cancer and intentional self-harm among patients with posttraumatic stress disorder by pretraining on the task of predicting randomly-masked diseases and outcomes in time series of 6.5 million patients [35]. A deep neural sequence transduction model for electronic health records (BEHRT) [36] was pretrained using an electronic health records (EHR) dataset of 1.6 million patients and was fine-tuned to predict diagnosis codes. Recent transformers have also made advancements in learning by combining different modalities of information such as images, audio, and text. Foresight [37] was trained with structured data such as laboratory results as well as unstructured data such as free text from 1.5 million patients across three EHR datasets. The transformer approach has not previously been applied to the task of selecting diabetes medications. In addition, while efforts have been made to train models with large amounts of data to improve accuracy [38], the impact of the training data period on predictions is largely unexplored.

Diabetes drug selection involves deciding to prescribe one or more drugs from among many candidates. This selection can be handled by ML as a multichoice task. This study aimed to develop an ML tool that accurately predicts the next prescribed drugs using the patient's medical condition and prescription history over the past year. The objective is to enhance diabetes treatment outcomes for nonspecialists through improved support in drug selection (Figure 1). Based on the performance of previous studies [24-26], our goal was to achieve an ROC-AUC above 0.95 when predicting the next prescribed drugs. Drawing on our team's previous work in self-management support for T2D treatment [39] and predicting treatment discontinuations [40,41], we designed this task with the hope of overcoming barriers to nonspecialist diabetes treatment in clinical practice, believing it could significantly improve diabetes treatment outcomes.

XSL•FO
RenderX

Figure 1. System image of prescription drug selection assistant.



Methods

Datasets

All data were collected from the EHRs at the University of Tokyo Hospital, which included 7034 patients who visited the hospital, had diagnostic codes, and were registered to the Japan diabetes comprehensive database project based on an advanced electronic medical record system (J-DREAMS) cohort [42]. The data were recorded in the EHRs between January 1, 2011 and December 31, 2022. The data, including treatment decisions and outcomes, were reflective of care by endocrinologists. Variables extracted from the EHRs included sex, age, 12 kinds of diabetes-related laboratory tests, and drugs. The laboratory tests included numerical values of HbA_{1c}, glucose, triacylglycerol, high density lipoprotein cholesterol, total cholesterol [43], urinary albumin creatinine ratio, creatinine [44], alanine transaminase, aspartate transaminase, and γ-glutamyltransferase [45], and categorical values of proteins [45] and glycogen. Drugs were identified using the list of drug price standards [46] provided by the Ministry of Health, Labour and Welfare of Japan, and 44 types prescribed in 2021 were selected.

Training and Test Data

The records used for training were not used for testing to ensure that the same patients were not included in both groups. A total of 80% (5627/7034) of patients were included in the training group, and the remaining 20% (1407/7034) of patients were included in the testing group.

In order to examine the size of the training data needed to achieve the target prediction accuracy, we extracted three different subsets of training data from the sequences of the 5627 patients in the training group: 2 years from 2020 to 2021 (3013 patients and their 25484 subsequences), 5 years from 2017 to 2021 (4009 patients and their 78,020 subsequences), and 10 years from 2012 to 2021 (4524 patients and their 168,595 subsequences). For testing, we further identified a subset of the testing data that was solely data from 2022 (637 patients and their 2988 subsequences). Thus, there was no overlap in patients or time periods between training and testing. Table 1 shows the characteristics of the patients. The drugs in the table are the top 5 and bottom 5 in terms of number of prescriptions in the 2-year training data. All characteristics are provided in Multimedia Appendix 1.

XSL•FO
RenderX

Table . Characteristics of patients with diabetes included in the training and testing datasets. Characteristics are presented separately for the patient groups belonging to the different training datasets defined by period: 2 years (2020-2021), 5 years (2017-2021), 10 years (2012-2021) and the independent test dataset (data exclusively from 2022).

	2 years of training data		5 years of training data		10 years of training data		1 year of test data	
	Records (n=25484)	Patient (n=3013)	Records (n=78020)	Patient (n=4009)	Records (n=168595)	Patient (n=4524)	Records (n=2988)	Patient (n=637)
Sex								
Male, n (%)	16224 (63.66)	1915 (63.56)	49348 (63.25)	2543 (63.43)	106782 (63.34)	2869 (63.42)	1793 (60.01)	381 (59.81)
Female, n (%)	9260 (36.34)	1098 (36.44)	28672 (36.75)	1466 (36.57)	61813 (36.66)	1655 (36.58)	1195 (39.99)	256 (40.19)
Age, mean (SD)	67.62 (12.59)	69.06 (12.50)	67.25 (12.56)	69.17 (12.87)	66.41 (12.30)	68.98 (13.10)	68.80 (12.31)	69.68 (12.26)
HbA1c[a]								
Mean (SD)	7.37 (1.08)	—[b]	7.31 (1.06)	—	7.25 (1.03)	—	7.31 (1.02)	—
<6, n (%)	920 (3.61)	323 (10.72)	3046 (3.90)	754 (18.81)	7286 (4.32)	1345 (29.73)	96 (3.21)	49 (7.69)
6 - 7, n (%)	8874 (34.82)	1865 (61.90)	29030 (37.21)	3027 (75.51)	66470 (39.43)	3835 (84.77)	1113 (37.25)	370 (58.08)
7 - 8, n (%)	10177 (39.93)	2135 (70.86)	30493 (39.08)	3157 (78.75)	64355 (38.17)	3830 (84.66)	1189 (39.79)	404 (63.42)
≥8, n (%)	5513 (21.63)	1224 (40.62)	15451 (19.80)	2008 (50.09)	30484 (18.08)	2725 (60.23)	590 (19.75)	200 (31.40)
missing, n (%)	0 (0.00)	0 (0.00)	0 (0.00)	0 (0.00)	0 (0.00)	0 (0.00)	0 (0.00)	0 (0.00)
HDL-C[c]								
Mean (SD)	60.99 (18.23)	—	60.07 (17.94)	—	59.81 (17.80)	—	63.76 (19.79)	—
<40, n (%)	1943 (7.62)	512 (16.99)	6633 (8.50)	964 (24.05)	14694 (8.72)	1374 (30.37)	158 (5.29)	67 (10.52)
40 - 120, n (%)	21304 (83.60)	2737 (90.84)	63249 (81.07)	3644 (90.90)	134924 (80.03)	4195 (92.73)	2564 (85.81)	577 (90.58)
≥120, n (%)	195 (0.77)	59 (1.96)	494 (0.63)	100 (2.49)	966 (0.57)	137 (3.03)	44 (1.47)	11 (1.73)
missing, n (%)	2042 (8.01)	178 (5.91)	7644 (9.80)	243 (6.06)	18011 (10.68)	219 (4.84)	222 (7.43)	40 (6.28)
Cre[d]								
Mean (SD)	0.97 (0.69)	—	0.96 (0.75)	—	0.95 (0.72)	—	1.04 (1.08)	—
Male								
Mean (SD)	1.08 (0.71)	—	1.07 (0.74)	—	1.05 (0.74)	—	1.18 (1.23)	—
<0.65, n (%)	758 (2.97)	191 (6.34)	2675 (3.43)	405 (10.10)	5783 (3.43)	566 (12.51)	111 (3.71)	37 (5.81)
0.65 - 1.09, n (%)	10672 (41.88)	1482 (49.19)	32766 (42.00)	2057 (51.31)	71870 (42.63)	2456 (54.29)	1145 (38.32)	290 (45.53)
≥1.09, n (%)	4543 (17.83)	750 (24.89)	13140 (16.84)	1093 (27.26)	27001 (16.02)	1337 (29.55)	516 (17.27)	129 (20.25)
missing, n (%)	251 (0.98)	6 (0.20)	767 (0.98)	5 (0.12)	2128 (1.26)	7 (0.15)	21 (0.70)	1 (0.16)
Female								
Mean (SD)	0.78 (0.60)	—	0.78 (0.72)	—	0.77 (0.65)	—	0.82 (0.74)	—
<0.46, n (%)	357 (1.40)	89 (2.95)	1160 (1.49)	175 (4.37)	2616 (1.55)	282 (6.23)	28 (0.94)	11 (1.73)
0.46 - 0.82, n (%)	6596 (25.88)	895 (29.70)	20561 (26.35)	1224 (30.53)	44130 (26.18)	1428 (31.56)	825 (27.61)	194 (30.46)
≥0.82, n (%)	2133 (8.37)	372 (12.35)	6370 (8.16)	596 (14.87)	13572 (8.05)	730 (16.14)	326 (10.91)	93 (14.60)

XSL•FO
RenderX

	2 years of training data		5 years of training data		10 years of training data		1 year of test data	
	Records (n=25484)	Patient (n=3013)	Records (n=78020)	Patient (n=4009)	Records (n=168595)	Patient (n=4524)	Records (n=2988)	Patient (n=637)
missing, n (%)	174 (0.68)	11 (0.37)	581 (0.74)	11 (0.27)	1495 (0.89)	16 (0.35)	16 (0.54)	2 (0.31)
Glu[e]								
Mean (SD)	147.68 (51.19)	—	147.00 (51.31)	—	144.12 (50.77)	—	145.47 (48.67)	—
<70, n (%)	302 (1.19)	169 (5.61)	979 (1.25)	403 (10.05)	2709 (1.61)	743 (16.42)	28 (0.94)	22 (3.45)
70 - 110, n (%)	4230 (16.60)	1389 (46.10)	13604 (17.44)	2483 (61.94)	33633 (19.95)	3403 (75.22)	555 (18.57)	260 (40.82)
≥110, n (%)	20863 (81.87)	2924 (97.05)	63201 (81.01)	3907 (97.46)	131586 (78.05)	4418 (97.66)	2394 (80.12)	609 (95.60)
missing, n (%)	89 (0.35)	7 (0.23)	236 (0.30)	5 (0.12)	667 (0.40)	6 (0.13)	11 (0.37)	2 (0.31)
Prescribed drug (top 5)								
Metformin hydrochloride, n (%)	11257 (44.17)	1390 (46.13)	33442 (42.86)	1952 (48.69)	72337 (42.91)	2376 (52.52)	1361 (45.55)	297 (46.62)
Sitagliptin phosphate hydrate, n (%)	4963 (19.47)	693 (23.00)	15420 (19.76)	1148 (28.64)	37438 (22.21)	1808 (39.96)	425 (14.22)	101 (15.86)
Insulin aspart (genetical recombination), n (%)	3212 (12.60)	377 (12.51)	10039 (12.87)	603 (15.04)	20149 (11.95)	833 (18.41)	403 (13.49)	85 (13.34)
Glimepiride, n (%)	2885 (11.32)	398 (13.21)	10387 (13.31)	690 (17.21)	28855 (17.11)	1141 (25.22)	358 (11.98)	76 (11.93)
Pioglitazone hydrochloride, n (%)	2731 (10.72)	354 (11.75)	9450 (12.11)	592 (14.77)	24305 (14.42)	910 (20.11)	244 (8.17)	53 (8.32)
Prescribed drug (buttom 5)								
Saxagliptin hydrate, n (%)	158 (0.62)	17 (0.56)	586 (0.75)	41 (1.02)	960 (0.57)	52 (1.15)	30 (1.00)	6 (0.94)
Anagliptin, n (%)	142 (0.56)	17 (0.56)	528 (0.68)	34 (0.85)	986 (0.58)	51 (1.13)	5 (0.17)	1 (0.16)
Insulin lispro (genetical recombination) [Insulin lispro Biosimilar 1], n (%)	59 (0.23)	19 (0.63)	59 (0.08)	19 (0.47)	59 (0.03)	19 (0.42)	58 (1.94)	13 (2.04)
Insulin glargine (genetical recombination) [Insulin glargin biosimilar 2], n (%)	39 (0.15)	9 (0.30)	86 (0.11)	14 (0.35)	86 (0.05)	14 (0.31)	1 (0.03)	1 (0.16)
Glibenclamide, n (%)	33 (0.13)	5 (0.17)	280 (0.36)	24 (0.60)	1722 (1.02)	87 (1.92)	11 (0.37)	3 (0.47)

[a]HbA_{1c}: hemoglobin A_{1c}.

[b]not applicable.

[c]HDL-C: high density lipoprotein cholesterol.

[d]Cre: creatinine..

[e]Glu: glucose.

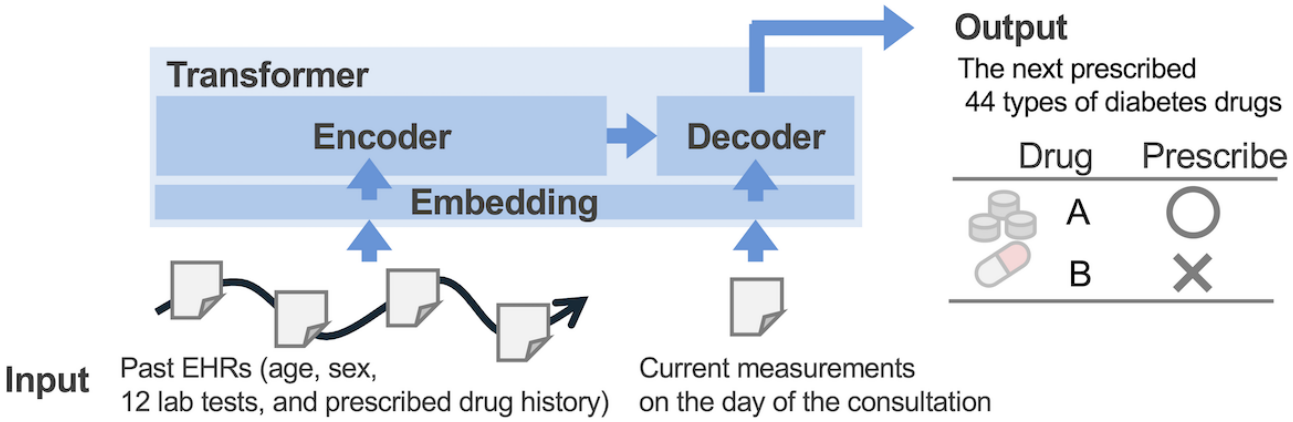
XSL•FO
RenderX

ML Models

Patients' medical conditions and prescription histories are in general irregularly spaced, reflecting variability in patient care appointment dates, with updates to outpatient EHR occurring before and after clinical visits. We organized the data into Monday-to-Sunday weeks and quantized the data to a single value per week, using the average in the case of multiple measurements and treating weeks with no values as having missing values [47]. This approach allowed the ML model to treat irregularly spaced data spanning Y (a natural number) years as regularly spaced data consisting of (Y×365)/7 (rounded up to the nearest integer) values, that is we treated all data as weekly data. We did not perform preprocessing, including interpolation, on missing values in the regularly spaced data. No normalization, outlier removal, or dimensionality reduction was performed.

We designed a transformer-based encoder-decoder model (Figure 2) that takes as input a time series of drugs prescribed and laboratory tests over the past 1 year, sex, and age. The model approaches drug selection as a multichoice task. With N types of drugs, there are 2^N potential prescription combinations. By setting the number of units in the output layer of the transformer decoder to N, we implemented N binary classifications. The model outputs a set of scores representing the probability of each drug being prescribed on that day and, for each drug and day, a binary prescription decision based on whether the prescription probability is greater than or equal to 0.5.

Figure 2. Architecture of the transformer-based encoder-decoder model for predicting the next-prescribed diabetes medications. EHRs: electronic health records.



We treated age and HbA_{1c} values as numerical data, sex as a categorical label, and prescription history as a set of categorical labels. In addition, a time series representing the presence or absence of missing data, called an attention mask, was simultaneously generated. Each data type was transformed into a uniform-dimensional vector using an embedding layer specific to that data type, which was then handled by the transformer model. Time information was converted to a uniform-dimensional vector using a positional embedding layer with a periodic function and added to the output value of the embedding layers.

The model incorporates two types of attention layers: self-attention in the encoder, designed to extract relationships in time and meaning from the time series of drugs prescribed and laboratory tests, and cross-attention in the decoder, used to predict the next prescribed drugs based on these relationships. Times in the time series that contain missing data are ignored in the self-attention and mutual attention calculation process using the attention mask. This makes it easy to handle without additional processing for missing data completion. The self-attention weights were optimized through self-supervised learning. This involves the task of predicting both the next laboratory test values and drugs prescribed using a time series of past laboratory tests and drugs prescribed. The cross-attention weights were optimized through supervised learning involving the task of predicting a set of scores representing the probability of each drug being prescribed on that day.

The model consisted of four transformer-encoder layers including four multihead self-attention blocks and four transformer-decoder layers including four multihead cross-attention blocks, along with a hidden layer of dimension 256. Compared to the text data handled by the language model, the prescription drug selection data has a smaller vocabulary (number of drug types) and a shorter time series, so these hyperparameters were set to about one-third the size of the BERT model [34]. The parameters were optimized by Adam with a learning rate of 1e-4, a batch size of 256, and 100 epochs. The loss functions for numerical and categorical data were mean squared error and focal loss [48], respectively. All implementations were written in Python 3.11 (Python Software Foundation) and PyTorch 2.2 (Meta AI).

The model was trained using prescription records from endocrinologists at the University of Tokyo Hospital. As a result, the model generates outputs aligned with the treatment approaches of these specialists.

Statistical Methods

We analyzed the characteristics of patients in the dataset using means, SD, and frequency counts. We calculated 95% CI using the bootstrap method where applicable. We performed all statistical analyses using custom Python code.

We compared our model with an established ML method recognized for high accuracy. There were validations on similar T2D prediction tasks favored LightGBM [49,50], making it our chosen reference for comparisons. We compared the predictive

XSL•FO
RenderX

accuracy of the two methods with the three different training dataset for the prescription prediction of 44 drugs using both macro- and microaverages [51] of the receiver operating characteristic area under the curve (ROC-AUC) as metrics. The macroaverage is a measure of the average performance across all classes independently. The method computes the metrics of ROC-AUC for each individual drug, then averages them to obtain an overall score. This analysis method gives equal weight to each drug, regardless of its size or imbalance in the dataset. On the other hand, the microaverage is a measure of the aggregate performance that weights all instances in the dataset equally. This analysis method first aggregates the true positives, false positives, true negatives, and false negatives across all drugs, and then computes each metric using these aggregated values. The microaverage treats every prediction equally, without considering the kinds of drugs.

The predictive performance of each drug was also evaluated using ROC-AUC.

Ethical Considerations

This study was approved by the institutional review board of the University of Tokyo School of Medicine (approval number: 10705-(4)) and was conducted in accordance with the Declaration of Helsinki. This was a retrospective, noninterventional database study without patient involvement. Confidentiality was safeguarded by the University of Tokyo Hospital. According to the Guidelines for Epidemiological Studies of the Ministry of Health, Labour and Welfare of Japan, written informed consent was not required. Information about the current study was available to patients on a website, and patients have the right to cease registration of their data at any time [52].

Results

Prediction Performance for Various Sizes of Training Data

We assessed different sizes of training data (Table 2). The best prediction performance was obtained from training with the 5 years of data from 2017 to 2021. This version achieved a microaverage (95% CI) ROC-AUC of 0.993 (0.992-0.994) and a macroaverage (95% CI) ROC-AUC of 0.988 (0.980-0.993), and we selected it as our model. Performance was similar when trained using the full range of 10 years of data, from 2012 to 2021, producing somewhat worse results. For all sizes of training data, we met the study's objectives of achieving an ROC-AUC above 0.95 from our macro- and microaverage evaluations. The prediction accuracy of LightGBM with the 5 years of data had a microaverage ROC AUC of 0.988 (0.985-0.990), and the transformer outperformed LightGBM.

Table . Overall prediction performance of models for the next-prescribed diabetes drugs, stratified by the training data period. This table compares the overall accuracy of the developed transformer model against a LightGBM model.

	Transformer		LightGBM	
	Microaverage (95% CI)	Macroaverage (95% CI)	Microaverage (95% CI)	Macroaverage (95% CI)
2 years of training data	0.991 (0.990-0.992)	0.981 (0.975-0.988)	0.987 (0.984-0.989)	0.970 (0.941-0.992)
5 years of training data	0.993 (0.992-0.994)	0.988 (0.980-0.993)	0.988 (0.985-0.990)	0.962 (0.916-0.993)
10 years of training data	0.992 (0.990-0.993)	0.987 (0.976-0.994)	0.984 (0.981-0.986)	0.959 (0.921-0.987)

Prediction Performance for Each Drug

We examined the prediction performance for each of the 44 drugs (Table 3). The drugs in the table are the top 5 and bottom 5 in terms of the number of prescriptions in the 2 years of training data. All results are provided in the supplemental file (Multimedia Appendix 2). We achieved an ROC-AUC above our target of 0.95 for 43 of the 44 drugs when trained with the 5 years of data.

XSL•FO
RenderX

Table . Prediction performance for drugs when trained with various sizes of training data. The table shows results for the top 5 and bottom 5 most frequently prescribed drugs, showing a comparison of performance between specific drugs and the impact of the data period of the training data on the prediction accuracy of individual drugs.

	Number of prescriptions in 1 year of test data, n (%)	Number of prescriptions in 2 years of training data		Number of prescriptions in 5 years of training data		Number of prescriptions in 10 years of training data	
		ROC-AUC (95% CI)	Accuracy (95% CI)	ROC-AUC (95% CI)	Accuracy (95% CI)	ROC-AUC (95% CI)	Accuracy (95% CI)
Prescribed drug (top 5)							
Metformin hydrochloride, n (%)	1361 (45.55)	0.992 (0.989-0.995)	0.977 (0.971-0.982)	0.992 (0.989-0.995)	0.982 (0.978-0.987)	0.993 (0.990-0.996)	0.980 (0.975-0.985)
Sitagliptin phosphate hydrate, n (%)	425 (14.22)	0.991 (0.985-0.996)	0.988 (0.985-0.992)	0.994 (0.990-0.997)	0.990 (0.987-0.994)	0.996 (0.994-0.998)	0.992 (0.989-0.995)
Insulin aspart (genetical recombination), n (%)	403 (13.49)	0.993 (0.989-0.997)	0.985 (0.981-0.989)	0.996 (0.993-0.998)	0.985 (0.981-0.989)	0.995 (0.991-0.999)	0.993 (0.990-0.996)
Glimepiride, n (%)	358 (11.98)	0.988 (0.979-0.995)	0.991 (0.988-0.994)	0.991 (0.984-0.996)	0.994 (0.991-0.996)	0.995 (0.990-0.999)	0.992 (0.989-0.995)
Pioglitazone hydrochloride, n (%)	244 (8.17)	0.989 (0.978-0.998)	0.993 (0.990-0.996)	0.990 (0.979-0.999)	0.993 (0.990-0.996)	0.995 (0.992-0.997)	0.985 (0.981-0.989)
Prescribed drug (buttom 5)							
Saxagliptin hydrate, n (%)	30 (1.00)	0.978 (0.944-1.000)	0.998 (0.996-0.999)	0.999 (0.999-1.000)	0.999 (0.998-1.000)	0.999 (0.999-1.000)	0.999 (0.998-1.000)
Anagliptin, n (%)	5 (0.17)	0.999 (0.998-1.000)	0.998 (0.996-0.999)	0.999 (0.999-1.000)	0.999 (0.998-1.000)	0.999 (0.998-1.000)	1.000 (0.999-1.000)
Insulin lispro (genetical recombination) [Insulin lispro Biosimilar 1], n (%)	58 (1.94)	0.945 (0.910-0.972)	0.986 (0.981-0.990)	0.848 (0.784-0.904)	0.981 (0.976-0.986)	0.799 (0.735-0.860)	0.981 (0.975-0.986)
Insulin glargine (genetical recombination) [Insulin glargin biosimilar 2], n (%)	1 (0.03)	0.938 (0.500-0.945)	0.996 (0.994-0.998)	0.990 (0.500-0.993)	0.999 (0.998-1.000)	0.938 (0.500-0.945)	1.000 (0.999-1.000)
Glibenclamide, n (%)	11 (0.37)	0.999 (0.999-1.000)	0.999 (0.997-1.000)	0.999 (0.999-1.000)	0.999 (0.997-1.000)	0.973 (0.935-0.999)	0.996 (0.994-0.998)

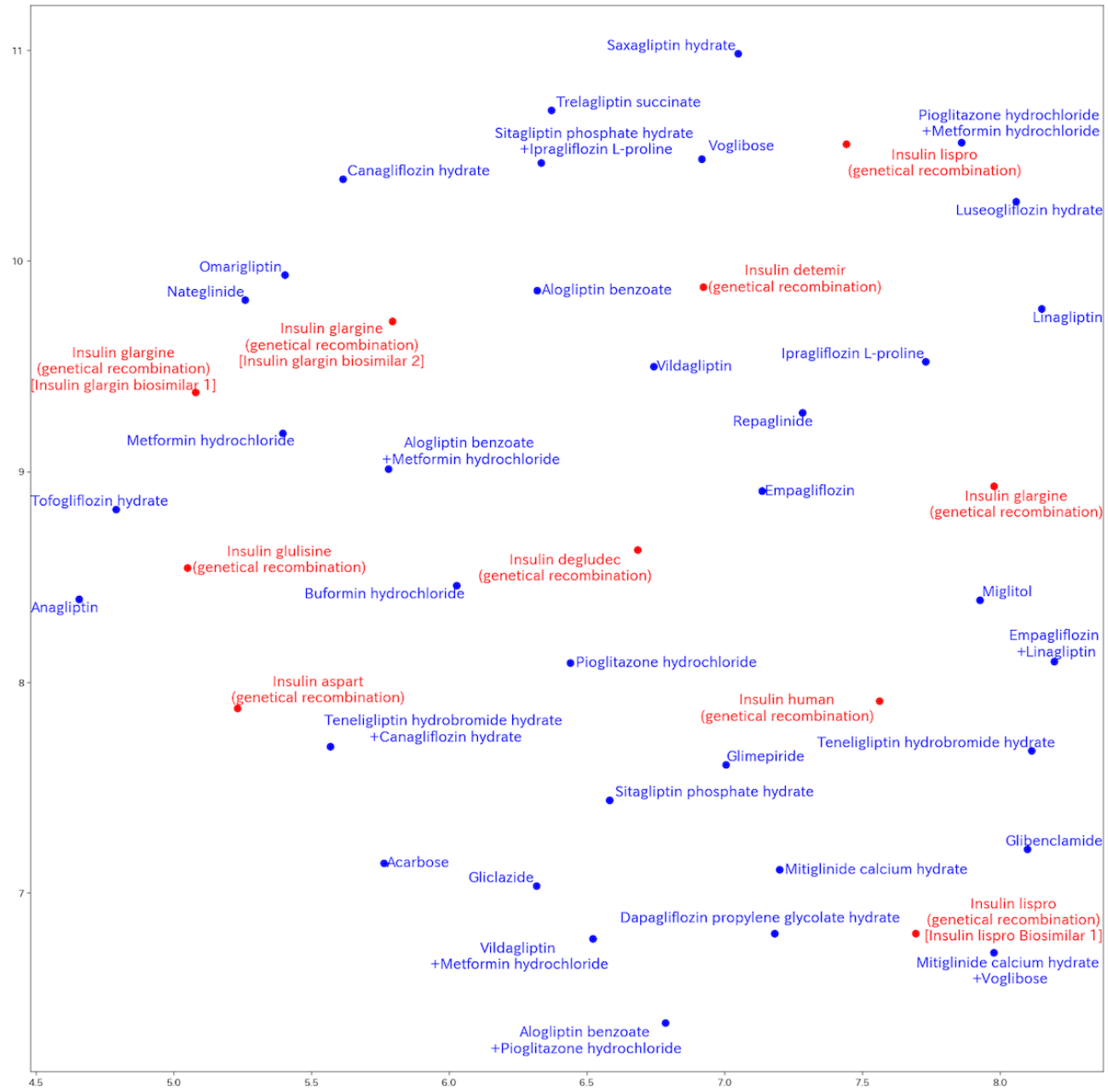
The only drug that did not achieve the target value was "Insulin lispro (genetical recombination) [Insulin lispro Biosimilar 1]." The prescription of this drug began in 2020. Therefore, the same instances of prescription were present in all three training data periods. For this drug, the model trained on just 2 years of data had the highest ROC-AUC.

Interpretability

The proposed model performed as well as other transformer-based models considering the ability for extracting relationships in time and meaning [53]. The embedding vectors obtained through training represent the closeness of relationships between vectors as proximity. The embedding vectors in this experiment were the same 256 dimensions as the transformer hidden size. Projecting onto two dimensions using uniform manifold approximation and projection [54] allows visualization (Figure 3). While we did not observe a strong tendency for clustering, several biosimilar drugs, such as insulin glargine (genetical recombination, ie, insulin glargin biosimilar 1), were positioned close to the biosimilar drug.

XSL•FO
RenderX

Figure 3. Visualization of learned drug embedding vectors using uniform manifold approximation and projection. This plot displays a 2D representation of the relationships between 44 different diabetes drugs, as learned by the transformer model's encoder component. Each point corresponds to a specific diabetes drug. Proximity between points suggests that the model identified similarities in how these drugs were used or in the patient contexts associated with their prescription within the training dataset.



Discussion

Evaluation of the Predictive Accuracy

The proposed model achieved impressive predictive accuracy, with macroaverages (95% CI) of ROC-AUC of 0.988 (0.980-0.993). In previous studies [11,12], the ROC-AUC for drugs was less than 0.95, and our model represents a significant improvement relative to this previous work.

The prediction accuracy was higher when trained with short-term data from 5 years than when trained using data from the past 10 years. We suspect that changes in the treatment environment, such as the introduction of new prescription drugs, are responsible for this difference in prediction accuracy. When training on data from the past N years, the model uniformly learns the prescription selection trends for the past N years. Therefore, when N is large, the model is heavily influenced by the trends of older prescription selections. This suspicion is supported by our results that the prescription drug that did not reach target accuracy, "Insulin lispro (genetical recombination) [Insulin lispro Biosimilar 1]," was only recently approved and prescribed. Introduced in 2020, this drug has remained relatively rare in the dataset, as demonstrated in Table 1. Even when expanding the training data period from 2 to 10 years, the number of prescriptions for this drug has remained stagnant at 59, and its proportion within the overall dataset has decreased from 0.23% to a mere 0.03%. This low frequency and temporal bias in the data have rendered learning this specific drug's patterns challenging. Although ML models generally perform better with more data, for this application it may be better to

XSL•FO
RenderX

gather data from more hospitals rather than a longer time span, since it is desirable to learn more fresh data, including new prescription drugs. Transformer models, known for power-law characteristics, benefit from scale-ups [38], and expanding the study to multiple hospitals could explore potential performance enhancements and test the applicability of the power-law in the medical field.

Physicians select drugs considering insulin secretion and insulin resistance, age, obesity, severity of chronic complications, and liver and kidney function. In this experiment, we used age, sex, 12 kinds of diabetes-related laboratory tests, and past prescription history. By adding comprehensive items likely used in medication selection to the model input, performance may be improved.

Our ultimate goal is to improve the treatment outcomes of diabetes. Merely predicting drug selection alone cannot achieve this goal. Expanding the scope to predict the impact of prescribed drugs could further enhance the model's utility in diabetes treatment.

Limitations

Our study has notable limitations. First, the model uses only age, sex, 12 kinds of diabetes-related laboratory tests, and past prescription history as inputs. It is desirable to fully account for the various constraints and contraindications that physicians consider in real-world clinical practice. For example, when considering patient characteristics, factors such as age (older adults or pediatric), pregnancy, lactation, BMI, type of diabetes, c-peptide, renal and hepatic function, comorbidities, allergies, urinary tract infection history, diabetic ketoacidosis history, cardiac history, and hypoglycemia must be considered. Regarding medications, considerations include adverse effects, drug resistance, and cost. However, despite these limitations, this study demonstrates that it is possible to narrow down treatment options to some extent using a limited set of variables. We believe that this result holds promise for providing primary care physicians with some guidance and direction. Regarding warnings of constraints and contraindications in drug selection, CDSS have traditionally excelled in this [20,21] and can effectively complement this model. In addition, recent advancements in natural language processing within ML models [33,34] have enabled the extraction of important information on constraints and contraindications from fresh sources such as research papers published daily. We believe there is substantial potential for future research to integrate these important factors into ML models, and we intend to work on this improvement.

Second, the data were sourced from a single hospital, limiting generalizability. Potential biases in the results include the race and geography of the patients and the prescribing tendencies of a limited number of endocrinologists at the hospital. ML models tend to learn biases present in the training data, resulting in predictions that reflect those biases. Prediction accuracy is significantly degraded when different biases exist between the training data and the test data. Therefore, in order to generalize the prediction results of the model, a large dataset of data from multiple hospitals containing data on patients with diverse backgrounds is required. However, in reality, it is difficult to build an ideal dataset due to constraints such as privacy protection and data collection costs. As one solution, we believe that it is good to collect training data that resembles the patterns of patients treated by the primary care physicians who are the users of the model, thereby eliminating biase differences between the training data and the test data as much as possible. Specifically, we collect EHRs of patients who have been involved in prescriptions by endocrinologists at multiple hospitals in a specific region, and use this to build the model that selects prescription drugs for patients treated by primary care physicians in the same region. We believe that this approach will reduce the bias differences in regional characteristics between the training data and the test data, and improve generalization performance with realistic data collection. We would like to verify the validity of this solution in the future.

Third, ML reflects majority characteristics, potentially limiting applicability to diverse patient populations. In the dataset used in the experiment, over 40% (297/637) of patients were prescribed metformin hydrochloride, and patient characteristics are biased. There is a risk that truly effective treatments may not be prescribed correctly to a minority of patients. Prediction failure analysis needs to be further scrutinized, including versus patient characteristics. We should examine this issue by comparing prediction accuracy for each patient cluster.

Fourth, this was a backward-looking study, using past data, and the essential next phase is to assess the model's predictive capabilities in clinical practice. There is a need for a careful exploration of the model's effectiveness in real clinical scenarios.

Fifth, while the proposed model requires hyperparameters, we determined these values based on previous studies. Although fine-tuning hyperparameters is generally desirable, transformer models are typically computationally expensive to train, and many previous studies have likewise not fully tuned their parameters. There is potential for performance improvement through hyperparameter tuning, and we intend to investigate this further in future work.

Sixth, the model has poor interpretability. We investigated the proximity relationship between embedding vectors, but no strong tendency was found. It would be better to use other information obtained from the transformer, such as attention weights, to further improve interpretability.

These limitations raise important ethical considerations in the development and application of medical artificial intelligence. Physicians who use the model must be aware of these limitations and exercise appropriate clinical judgment. Obtaining appropriate informed consent from patients is important.

Conclusions

The proposed model addresses the challenge of predicting the next prescribed drugs. This model, trained using past prescriptions of endocrinologists, has the potential to improve treatment outcomes for nonspecialists by assisting them in making prescription decisions. Future efforts should focus on improving accuracy by incorporating disease state information beyond current inputs and validating the model on large clinical datasets across multiple hospitals.

XSL•FO
RenderX

Acknowledgments

We thank Daniel Lane for his support in manuscript editing and scientific discussions. We made no use of generative AI in the development of this paper.

This work was funded by The University of Tokyo and Nippon Telegraph and Telephone Corporation in a joint research program at the University of Tokyo Center of Innovation, Sustainable Life Care, and the Ageless Society dedicated to Self-managing Healthcare in the Aging Society of Japan. The funding source had no role in the design and conduct of the study; collection, management, analysis, and interpretation of the data; preparation, review, or approval of the manuscript; and decision to submit the manuscript for publication. The content is solely the responsibility of the authors and does not necessarily represent the official views of the University of Tokyo Center of Innovation.

Data Availability

The datasets analyzed during this study are not publicly available due the restrictions imposed by the research ethics committees that approved this study.

Conflicts of Interest

HK, EN, AF, NS, and NN are employees of Nippon Telegraph and Telephone Corporation (NTT), Tokyo, Japan.

Multimedia Appendix 1
Characteristics of patients with diabetes included in the training and testing datasets. Characteristics are presented separately for the patient groups belonging to the different training datasets defined by period: 2 years (2020-2021), 5 years (2017-2021), 10 years (2012-2021) and the independent test dataset (data exclusively from 2022). Variables shown include patient counts, age, sex distribution, laboratory values, and prescription frequencies of 44 drugs.
[DOCX File, 54 KB - medinform_v13i1e67748_app1.docx]

Multimedia Appendix 2
Prediction performance for drugs when trained with various sizes of training data. The table shows results for the 44 prescribed drugs, showing a comparison of performance between specific drugs and the impact of the data period of the training data on the prediction accuracy of individual drugs.
[DOCX File, 36 KB - medinform_v13i1e67748_app2.docx]

References

1. GBD 2021 Diabetes Collaborators. Global, regional, and national burden of diabetes from 1990 to 2021, with projections of prevalence to 2050: a systematic analysis for the Global Burden of Disease Study 2021. Lancet 2023 Jul 15;402(10397):203-234. [doi: 10.1016/S0140-6736(23)01301-6] [Medline: 37356446]
2. Davies MJ, Aroda VR, Collins BS, et al. Management of hyperglycaemia in type 2 diabetes, 2022. A consensus report by the American Diabetes Association (ADA) and the European Association for the Study of Diabetes (EASD). Diabetologia 2022 Dec;65(12):1925-1966. [doi: 10.1007/s00125-022-05787-2] [Medline: 36151309]
3. Primary care physicians' practices in diabetes treatment. 2024. URL: https://www.jdome.jp/doc/jdome-2021-64jds.pdf [accessed 2025-05-29]
4. Lu H, Holt JB, Cheng YJ, Zhang X, Onufrak S, Croft JB. Population-based geographic access to endocrinologists in the United States, 2012. BMC Health Serv Res 2015 Dec 7;15(1):541. [doi: 10.1186/s12913-015-1185-5] [Medline: 26644021]
5. Bolen S, Feldman L, Vassy J, et al. Systematic review: comparative effectiveness and safety of oral medications for type 2 diabetes mellitus. Ann Intern Med 2007 Sep 18;147(6):386-399. [doi: 10.7326/0003-4819-147-6-200709180-00178] [Medline: 17638715]
6. Bolen S, Tseng E, Hutfless S, et al. Diabetes medications for adults with type 2 diabetes: an update [internet]. : Rockville (MD): Agency for Healthcare Research and Quality (US); 2016 16-EHC013-EF. [Medline: 27227214]
7. American Diabetes Association Professional Practice Committee. Erratum. 9. Pharmacologic approaches to glycemic treatment: standards of care in diabetes-2024. Diabetes Care 2024;47(Suppl. 1):S158-S178. Diabetes Care 2024 Jul 1;47(7):S158-S178. [doi: 10.2337/dc24-er07a] [Medline: 38696224]
8. Wilcox G. Insulin and insulin resistance. Clin Biochem Rev 2005 May;26(2):19-39. [Medline: 16278749]
9. American Diabetes Association Professional Practice Committee. 13. Older adults: standards of care in diabetes-2024. Diabetes Care 2024 Jan 1;47(Suppl 1):S244-S257. [doi: 10.2337/dc24-S013] [Medline: 38078580]
10. Babiker A, Al Dubayee M. Anti-diabetic medications: How to make a choice? Sudan J Paediatr 2017;17(2):11-20. [doi: 10.24911/SJP.2017.2.12] [Medline: 29545660]

XSL•FO
RenderX

11. American Diabetes Association Professional Practice Committee. 8. Obesity and weight management for the prevention and treatment of type 2 diabetes: standards of care in diabetes-2024. Diabetes Care 2024 Jan 1;47(Suppl 1):S145-S157. [doi: 10.2337/dc24-S008] [Medline: 38078578]
12. Steiger K, Herrin J, Swarna KS, Davis EM, McCoy RG. Disparities in acute and chronic complications of diabetes along the U.S. rural-urban continuum. Diabetes Care 2024 May 1;47(5):818-825. [doi: 10.2337/dc23-1552] [Medline: 38387066]
13. American Diabetes Association Professional Practice Committee. 11. Chronic kidney disease and risk management: standards of care in diabetes-2024. Diabetes Care 2024 Jan 1;47(Suppl 1):S219-S230. [doi: 10.2337/dc24-S011] [Medline: 38078574]
14. Vasilakou D, Karagiannis T, Athanasiadou E, et al. Sodium-glucose cotransporter 2 inhibitors for type 2 diabetes: a systematic review and meta-analysis. Ann Intern Med 2013 Aug 20;159(4):262-274. [doi: 10.7326/0003-4819-159-4-201308200-00007] [Medline: 24026259]
15. Hallakou-Bozec S, Vial G, Kergoat M, et al. Mechanism of action of Imeglimin: a novel therapeutic agent for type 2 diabetes. Diabetes Obes Metab 2021 Mar;23(3):664-673. [doi: 10.1111/dom.14277] [Medline: 33269554]
16. Karagiannis T, Avgerinos I, Liakos A, et al. Management of type 2 diabetes with the dual GIP/GLP-1 receptor agonist tirzepatide: a systematic review and meta-analysis. Diabetologia 2022 Aug;65(8):1251-1261. [doi: 10.1007/s00125-022-05715-4] [Medline: 35579691]
17. American Diabetes Association. Standards of Care in Diabetes-2023 Abridged for Primary Care Providers. Clin Diabetes 2022;41(1):4-31. [doi: 10.2337/cd23-as01] [Medline: 36714254]
18. Bouchi R, Sugiyama T, Goto A, et al. Retrospective nationwide study on the trends in first-line antidiabetic medication for patients with type 2 diabetes in Japan. J Diabetes Investig 2022 Feb;13(2):280-291. [doi: 10.1111/jdi.13636] [Medline: 34309213]
19. Sutton RT, Pincock D, Baumgart DC, Sadowski DC, Fedorak RN, Kroeker KI. An overview of clinical decision support systems: benefits, risks, and strategies for success. NPJ Digit Med 2020;3:17. [doi: 10.1038/s41746-020-0221-y] [Medline: 32047862]
20. Helmons PJ, Suijkerbuijk BO, Nannan Panday PV, Kosterink JGW. Drug-drug interaction checking assisted by clinical decision support: a return on investment analysis. J Am Med Inform Assoc 2015 Jul;22(4):764-772. [doi: 10.1093/jamia/ocu010] [Medline: 25670751]
21. Koutkias V, Bouaud J, Section Editors for the IMIA Yearbook Section on Decision Support. Contributions from the 2017 literature on clinical decision support. Yearb Med Inform 2018 Aug;27(1):122-128. [doi: 10.1055/s-0038-1641222] [Medline: 30157515]
22. Zou Q, Qu K, Luo Y, Yin D, Ju Y, Tang H. Predicting diabetes mellitus with machine learning techniques. Front Genet 2018;9:515. [doi: 10.3389/fgene.2018.00515] [Medline: 30459809]
23. Dagliati A, Marini S, Sacchi L, et al. Machine learning methods to predict diabetes complications. J Diabetes Sci Technol 2018 Mar;12(2):295-302. [doi: 10.1177/1932296817706375] [Medline: 28494618]
24. Fujihara K, Sone H. Machine learning approach to drug treatment strategy for diabetes care. Diabetes Metab J 2023 May;47(3):325-332. [doi: 10.4093/dmj.2022.0349] [Medline: 36631990]
25. Wright AP, Wright AT, McCoy AB, Sittig DF. The use of sequential pattern mining to predict next prescribed medications. J Biomed Inform 2015 Feb;53:73-80. [doi: 10.1016/j.jbi.2014.09.003] [Medline: 25236952]
26. Mei J, Zhao S, Jin F, et al. Deep diabetologist: learning to prescribe hypoglycemic medications with recurrent neural networks. Stud Health Technol Inform 2017;245(1277):29295362. [Medline: 29295362]
27. Tarumi S, Takeuchi W, Chalkidis G, et al. Leveraging artificial intelligence to improve chronic disease care: methods and application to pharmacotherapy decision support for type-2 diabetes mellitus. Methods Inf Med 2021 Jun;60(S 01):e32-e43. [doi: 10.1055/s-0041-1728757] [Medline: 33975376]
28. Vaswani A, Shazeer N, Parmar N, et al. Attention is all you need. 2017 Presented at: Proceedings of the 31st Annual Conference on Neural Information Processing Systems (NIPS'17); Dec 4-9, 2017; Long Beach, California, USA p. 6000-6010 URL: https://dl.acm.org/doi/10.5555/3295222.3295349
29. Bommasani R, Hudson DA, Adeli E, et al. On the opportunities and risks of foundation models. arXiv. Preprint posted online on 2021. [doi: 10.48550/arXiv.2108.07258]
30. Lakew SM, Cettolo M, Federico M. A comparison of transformer and recurrent neural networks on multilingual neural machine translation. Presented at: Proceedings of the 27th International Conference on Computational Linguistics (COLING 2018); Aug 20-26, 2018; Santa Fe, New Mexico, USA p. 641-652 URL: https://aclanthology.org/C18-1054/
31. Zerveas G, Jayaraman S, Patel D, Bhamidipaty A, Eickhoff C. A transformer-based framework for multivariate time series representation learning. Presented at: KDD '21: Proceedings of the 27th ACM SIGKDD Conference on Knowledge Discovery & Data Mining; Aug 14, 2021; Virtual Event Singapore p. 2114-2124. [doi: 10.1145/3447548.3467401]
32. Zhou H, Zhang S, Peng J, et al. Informer: beyond efficient transformer for long sequence time-series forecasting. AAAI 2021;35(12):11106-11115. [doi: 10.1609/aaai.v35i12.17325]
33. Lin T, Wang Y, Liu X, Qiu X. A survey of transformers. AI Open 2022;3:111-132. [doi: 10.1016/j.aiopen.2022.10.001]
34. Devlin J, Chang MW, Lee K, Toutanova K. Bert: pre-training of deep bidirectional transformers for language understanding. arXiv. Preprint posted online on 2018. [doi: 10.48550/arXiv.1810.04805]

XSL•FO
RenderX

35. Yang Z, Mitra A, Liu W, Berlowitz D, Yu H. TransformEHR: transformer-based encoder-decoder generative model to enhance prediction of disease outcomes using electronic health records. Nat Commun 2023 Nov 29;14(1):7857. [doi: 10.1038/s41467-023-43715-z] [Medline: 38030638]
36. Li Y, Rao S, Solares JRA, et al. BEHRT: transformer for electronic health records. Sci Rep 2020;10(1):7155. [doi: 10.1038/s41598-020-62922-y]
37. Kraljevic Z, Bean D, Shek A, et al. Foresight-a generative pretrained transformer for modelling of patient timelines using electronic health records: a retrospective modelling study. Lancet Digit Health 2024 Apr;6(4):e281-e290. [doi: 10.1016/S2589-7500(24)00025-6] [Medline: 38519155]
38. Henighan T, Kaplan J, Katz M, et al. Scaling laws for autoregressive generative modeling. arXiv. Preprint posted online on 2020. [doi: 10.48550/arXiv.2010.14701]
39. Waki K, Fujita H, Uchimura Y, et al. DialBetics: a novel smartphone-based self-management support system for type 2 diabetes patients. J Diabetes Sci Technol 2014 Mar;8(2):209-215. [doi: 10.1177/1932296814526495] [Medline: 24876569]
40. Kurasawa H, Hayashi K, Fujino A, et al. Machine-learning-based prediction of a missed scheduled clinical appointment by patients with diabetes. J Diabetes Sci Technol 2016 May;10(3):730-736. [doi: 10.1177/1932296815614866] [Medline: 26555782]
41. Kurasawa H, Waki K, Chiba A, et al. Treatment discontinuation prediction in patients with diabetes using a ranking model: machine learning model development. JMIR Bioinform Biotechnol 2022 Sep 23;3(1):e37951. [doi: 10.2196/37951] [Medline: 38935955]
42. Sugiyama T, Miyo K, Tsujimoto T, et al. Design of and rationale for the Japan diabetes comprehensive database project based on an advanced electronic medical record system (J-DREAMS). Diabetol Int 2017 Nov;8(4):375-382. [doi: 10.1007/s13340-017-0326-y] [Medline: 30603343]
43. Mooradian AD. Dyslipidemia in type 2 diabetes mellitus. Nat Clin Pract Endocrinol Metab 2009 Mar;5(3):150-159. [doi: 10.1038/ncpendmet1066] [Medline: 19229235]
44. Thomas MC, Brownlee M, Susztak K, et al. Diabetic kidney disease. Nat Rev Dis Primers 2015 Jul 30;1:15018. [doi: 10.1038/nrdp.2015.18] [Medline: 27188921]
45. El-Serag HB, Tran T, Everhart JE. Diabetes increases the risk of chronic liver disease and hepatocellular carcinoma. Gastroenterology 2004 Feb;126(2):460-468. [doi: 10.1053/j.gastro.2003.10.065] [Medline: 14762783]
46. List of drugs covered by the drug price standards and information on generic pharmaceuticals [Website in Japanese]. 2024. URL: https://www.mhlw.go.jp/topics/2023/04/tp20230401-01.html [accessed 2025-05-29]
47. Kazijevs M, Samad MD. Deep imputation of missing values in time series health data: A review with benchmarking. J Biomed Inform 2023 Aug;144:104440. [doi: 10.1016/j.jbi.2023.104440] [Medline: 37429511]
48. Lin TY, Goyal P, Girshick R, He K, Dollar P. Focal loss for dense object detection. IEEE Trans Pattern Anal Mach Intell 2020 Feb;42(2):318-327. [doi: 10.1109/TPAMI.2018.2858826] [Medline: 30040631]
49. Seto H, Oyama A, Kitora S, et al. Author Correction: Gradient boosting decision tree becomes more reliable than logistic regression in predicting probability for diabetes with big data. Sci Rep 2022 Dec 30;12(1):22599. [doi: 10.1038/s41598-022-27052-7] [Medline: 36585468]
50. Rufo DD, Debelee TG, Ibenthal A, Negera WG. Diagnosis of diabetes mellitus using gradient boosting machine (LightGBM). Diagnostics (Basel) 2021 Sep 19;11(9):1714. [doi: 10.3390/diagnostics11091714] [Medline: 34574055]
51. Grandini M, Bagli E, Visani G. Metrics for multi-class classification: an overview. arXiv. Preprint posted online on 2020. [doi: 10.48550/arXiv.2008.05756]
52. Information about the current study. 2024. URL: https://www.h.u-tokyo.ac.jp/patient/depts/taisha/pdf/pa_md_md_info-04.pdf [accessed 2025-05-29]
53. Dar G, Geva M, Gupta A, Berant J. Analyzing transformers in embedding space. arXiv. Preprint posted online on 2022. [doi: 10.48550/arXiv.2209.02535]
54. McInnes L. Umap: uniform manifold approximation and projection for dimension reduction. arXiv. Preprint posted online on 2018. [doi: 10.48550/arXiv.1802.03426]

Abbreviations

CDSS: clinical decision support system
EHR: electronic health record
LightGBM: light gradient boosting machine
ML: machine learning
RNN: recurrent neural network
ROC-AUC: area under the receiver operating characteristic curve
T2D: type 2 diabete

XSL•FO
RenderX

Edited by A Coristine; submitted 20.10.24; peer-reviewed by A Victor, LP Mahali; revised version received 21.04.25; accepted 21.04.25; published 02.06.25.

Please cite as:
Kurasawa H, Waki K, Seki T, Nakahara E, Fujino A, Shiomi N, Nakashima H, Ohe K
Enhancing Antidiabetic Drug Selection Using Transformers: Machine-Learning Model Development
JMIR Med Inform 2025;13:e67748
URL: https://medinform.jmir.org/2025/1/e67748
doi:10.2196/67748

© Hisashi Kurasawa, Kayo Waki, Tomohisa Seki, Eri Nakahara, Akinori Fujino, Nagisa Shiomi, Hiroshi Nakashima, Kazuhiko Ohe. Originally published in JMIR Medical Informatics (https://medinform.jmir.org), 2.6.2025. This is an open-access article distributed under the terms of the Creative Commons Attribution License (https://creativecommons.org/licenses/by/4.0/), which permits unrestricted use, distribution, and reproduction in any medium, provided the original work, first published in JMIR Medical Informatics, is properly cited. The complete bibliographic information, a link to the original publication on https://medinform.jmir.org/, as well as this copyright and license information must be included.

XSL•FO
RenderX

Transformer-Based Language Models for Group Randomized Trial Classification in Biomedical Literature: Model Development and Validation

Elaheh Aghaarabi, MSc; David Murray, PhD

Office of Disease Prevention, National Institutes of Health, 6705 Rockledge Dr, Bethesda, MD, United States

Corresponding Author:
Elaheh Aghaarabi, MSc
Office of Disease Prevention, National Institutes of Health, 6705 Rockledge Dr, Bethesda, MD, United States

Abstract

Background: For the public health community, monitoring recently published articles is crucial for staying informed about the latest research developments. However, identifying publications about studies with specific research designs from the extensive body of public health publications is a challenge with the currently available methods.

Objective: Our objective is to develop a fine-tuned pretrained language model that can accurately identify publications from clinical trials that use a group- or cluster-randomized trial (GRT), individually randomized group-treatment trial (IRGT), or stepped wedge group- or cluster-randomized trial (SWGRT) design within the biomedical literature.

Methods: We fine-tuned the BioMedBERT language model using a dataset of biomedical literature from the Office of Disease Prevention at the National Institute of Health. The model was trained to classify publications into three categories of clinical trials that use nested designs. The model performance was evaluated on unseen data and demonstrated high sensitivity and specificity for each class.

Results: When our proposed model was tested for generalizability with unseen data, it delivered high sensitivity and specificity for each class as follows: negatives (0.95 and 0.93), GRTs (0.94 and 0.90), IRGTs (0.81 and 0.97), and SWGRTs (0.96 and 0.99), respectively.

Conclusions: Our work demonstrates the potential of fine-tuned, domain-specific language models to accurately identify publications reporting on complex and specialized study designs, addressing a critical need in the public health research community. This model offers a valuable tool for the public health community to directly identify publications from clinical trials that use one of the three classes of nested designs.

(JMIR Med Inform 2025;13:e63267) doi:10.2196/63267

KEYWORDS

document classification; machine learning; natural language processing; randomized trials; transformer; AI; artificial intelligence; clinical trials; language model; development; dataset; biomedical; model; tool; trial; public health

Introduction

Researchers need to identify publications from trials that use nested designs to access evidence relevant to community-level interventions and make informed decisions about public health strategies, as well as to understand the effectiveness of these interventions in improving health outcomes and reducing health disparities within populations. Additionally, they may require these publications to conduct meta-analyses and systematic reviews.

There are three important classes of nested designs widely used in clinical trials [1,2]. The parallel group- or cluster-randomized trial (GRT) involves the randomization of groups or clusters to study arms with observations taken using members of those groups or clusters [3-8]. This design is widely used to evaluate interventions that are delivered to groups or clusters that modify the physical or social environment, or that cannot be delivered to individuals without the substantial risk of contamination. The stepped wedge group or cluster-randomized trial (SWGRT) involves the randomization of groups or clusters to sequences; all groups or clusters begin in the control arm and transition to the intervention arm on a schedule determined by their sequence so that by the end of the trial, all groups or clusters are in the intervention arm [9]. The individually randomized group-treatment (IRGT) trial involves the random assignment of individuals to study arms but delivery of the intervention in a group-based format or using shared intervention agents [10,11]. All three nested designs have design, analytic, and sample size challenges not found in the traditional randomized clinical trial [1,2].

XSL•FO
RenderX

Currently, most public health researchers, including ourselves, use manual searches to identify GRTs, IRGTs, or SWGRTs, because, so far as we are aware, there are no automated methods for identifying published papers using these designs. However, manual searches can easily miss many qualifying publications due to the complexity of search parameters and the lack of consistent reporting. Document classification using machine learning and natural language processing techniques offers a more promising approach for categorizing documents into predefined groups.

Garcia et al [12] enhanced automatic document classification in the biomedical domain by leveraging Wikipedia knowledge to create bag-of-concepts representations, resulting in performance gains over traditional bag-of-words approaches in both single-label and multi-label classification tasks. Cohen [13] also proposed a biomedical text classifier, which integrates document words, MeSH terms, and normalized biological entity identifiers.

Previous studies have demonstrated the utility of machine learning approaches in identifying randomized controlled trials (RCTs) from biomedical literature databases. Marshal et al [14] used machine learning models, including convolutional neural networks, support vector machines, and ensemble models to identify RCT publications. Al-Jaishi et al [15] addressed the challenge of accurately identifying GRTs reports from bibliographic citations by leveraging static embedding techniques, developing and validating machine learning algorithms for information retrieval.

While these studies have focused on identifying specific types of RCTs, such as conventional RCTs and GRTs, our research aims to extend this approach to the identification of diverse categories of randomized trials, including GRTs, IRGTs, and SWGRTs. To achieve this, we propose a novel approach leveraging fine-tuned language models, specifically the pretrained BioMedBERT model, trained on a dataset of biomedical literature curated by the Office of Disease Prevention at the National Institute of Health.

Large language models represent an ideal choice for the development of biomedical text classifiers due to their capacity to grasp the contextual nuances within the data. Pretrained transformer language models, like bidirectional encoder representations from transformers (BERT) [16-18], have outperformed the existing deep neural network models, including convolutional neural networks and recurrent neural networks. Examples of transformer-based models trained on biomedical data include BioBERT [19], BioLinkBERT [20], BlueBERT [21], and BioMedBERT [22], which are pretrained on biomedical literature and clinical text.

While these pretrained models are readily applicable to common tasks due to their training on biomedical data, classifying scientific literature presents a unique challenge because scientific literature encompasses a diverse range of topics, writing styles, and research fields. Identifying and categorizing clinical trials into highly specialized categories is especially challenging, even for human coders. Leveraging transfer learning and fine-tuning a pretrained language model allows the machine learning platform to learn and adapt to the particular context and vocabulary of these types of documents, enhancing its effectiveness in tasks such as document classification, information extraction, and summarization [18].

To our knowledge, there is currently no transformer-based language model fine-tuned to identify clinical trial publications based on nested designs. In our method, we leverage BioMedBERT [22], a model that has been pretrained from scratch using abstracts from PubMed and full-text articles from PubMedCentral. We fine-tuned BioMedBERT using labeled clinical trials, with a specific focus on distinguishing various types of clinical trial publications, including GRTs, IRGTs, and SWGRTs. The fine-tuning process involved training on a carefully curated dataset comprising a substantial number of GRTs, IRGTs, and SWGRTs. The outcome of this fine-tuning process is a model that provides a high level of sensitivity and specificity in classifying and differentiating various types of randomized trial publications.

Methods

Traditional Machine Learning Models (Baseline Model)

In our study, we initially established a baseline model for classifying publications using traditional machine learning and word embedding techniques to demonstrate the effectiveness of employing a transformer-based model in identifying publications based on nested designs. To create the baseline model, we employed FastText (Facebook AI Research) to generate word embeddings, followed by a logistic regression model. Logistic regression has been widely recognized in the literature as an effective classifier for text data due to its simplicity, interpretability, and robust performance across various domains [23]. To enhance the model's capability to process biomedical text data, we leveraged pretrained FastText embeddings specifically trained on PubMed and MIMIC-III data, known as BioWordVec [24], to extract meaningful features from titles and abstracts of publications. Subsequently, we used these extracted embeddings to train a logistic regression model for the classification of publications.

Evaluation Metrics

There are various metrics available to evaluate the performance of a classifier. While the area under the curve is commonly used in binary classifiers, accuracy can be helpful for balanced evaluation datasets. However, in our case, where the model serves as a multiclass classifier with imbalanced data, the F_1-score emerges as the most reliable metric [25]. Our primary objective was to fine-tune an existing pretrained language model to maximize the F_1-score on a validation dataset.

The F_1-score is the harmonic mean of precision and recall. Precision is the ratio of correctly predicted positive observations to the total predicted positives. It measures the accuracy of the positive predictions made by the model. High precision ensures that when our model predicts an article belongs to a nested design group, it is highly likely to be accurate. This is crucial in applications where precision contributes to the trustworthiness of the classification outcomes, such as systemically classifying research publications. Recall, which is the same as sensitivity,

XSL•FO
RenderX

is vital when the cost of false negatives is high. A high recall ensures that our model effectively captures a comprehensive set of articles within each predefined group.

The F_1-score is particularly useful in situations where there is an imbalance between the classes or when there is an equal importance placed on precision and recall. It is a metric that balances the trade-off between precision and recall, providing a single value that reflects the overall performance of the model.

Our dataset is imbalanced with fewer examples in the IRGT and SWGRT classes, and accuracy alone can be misleading. Precision, recall, and F1-score provide a more nuanced view of a model's effectiveness, especially in identifying the strengths and weaknesses associated with false positives and false negatives.

$$\text{Precision} = \frac{\text{True Positives}}{\text{True Positives} + \text{False Positives}}$$

$$\text{Recall} = \frac{\text{True Positives}}{\text{True Positives} + \text{False Negatives}}$$

$$\text{F1 Score} = 2 \times \frac{\text{Precision} \times \text{Recall}}{\text{Precision} + \text{Recall}}$$

Specificity serves as a crucial metric for assessing the number of false positives within a model. It measures the ability of the model to correctly identify negative instances, thus providing insight into the model's performance in avoiding false-positive predictions. Although it was not initially used as an evaluation metric during our experimental phase and model development, it was calculated to provide a comprehensive assessment of performance, particularly in gauging the rate of false positives.

$$\text{Specificity} = \frac{\text{True Negatives}}{\text{True Negatives} + \text{False Positives}}$$

The weighted average considers the class imbalance in the dataset by considering the contribution of each class proportional to the number of instances in that class. In other words, classes with more instances have a greater impact on the overall metric than classes with fewer instances.

$$\text{WeightedAverage} = \sum_{i=1}^{C} m_i \cdot \frac{n_i}{N}$$

Where

m_i is the metric value (eg, precision, recall, F1-score) for class, n_i is the number of instances in class i, C is the number of classes, and *N* is the total number of instances in the dataset

BioMedBERT

We chose BioMedBERT as the initial pretrained model due to its superior performance compared to other existing models on our gold standard data, publications published prior to 2021 that were identified as GRT, IRGT, and SWGRT papers using search queries. BioMedBERT is a pretrained language model developed by Microsoft Research for biomedical text processing using abstracts from PubMed and full-text articles from PubMedCentral [22]. It is a specialized variant of the BERT architecture [16], designed to capture domain-specific nuances in biomedical literature. The architecture of BioMedBERT enables it to learn contextualized representations of words and phrases bidirectionally and understand the contextual relationships within biomedical texts. The BERT model used in our study was downloaded from Hugging Face's Transformers library, configured as a classifier. In this framework, the tokenizer automatically manages special tokens such as [CLS] and [SEP], ensuring proper preprocessing for input sequences.

For the classification task, the [CLS] token's embedding from the final layer of BERT serves as a representation of the input sequence's contextual information. A multilayer perceptron is applied to this embedding to perform the classification. This multilayer perceptron consists of fully connected layers that map the [CLS] token's representation to the output space, followed by the softmax activation for probability distribution over classes.

The pretrained BioMedBERT uses a bidirectional transformer architecture with several layers of self-attention mechanisms. The model embeddings, including word embeddings and positional embeddings, contribute to encoding patterns in biomedical language.

During the pretraining phase, BioMedBERT was initialized with weights obtained from training on a domain-specific corpus: 14 million abstracts, 3.2 billion words, and 21 gigabytes [22]. This large-scale training ensures that the model captures a wide range of biomedical concepts, terminology, and contextual relationships. BERT-BASE [16] with 12 transformer layers and 100 million parameters was used to pretrain BioMedBERT.

A pooling layer was introduced atop the transformer's final layer, known as the embedding layer. This embedding layer underwent pooling to derive a fixed-size representation of the entire input sequence. To capture nonlinearity and intricate patterns within the data, a feedforward layer was incorporated. This layer is linked to the output layer, responsible for computing logits.

Fine-Tuning BioMedBERT

For this study, we fine-tuned BioMedBERT to adapt the model to the specific nuances of our dataset related to publications from clinical trials that use nested designs. By leveraging the contextual information encoded in BioMedBERT, we aimed to enhance the accuracy and efficiency of our machine learning model in identifying and distinguishing various types of clinical trial publications. In particular, our goal was for BioMedBERT to serve as a multiclass classifier that can categorize biomedical publications into four distinct categories: GRT, IRGT, SWGRTs, and the broader category of publications based on studies that used other designs, which we refer to as negatives (Multimedia Appendix 1).

Data

The National Institute of Health Office of Disease Prevention provided a labeled dataset consisting of publications from PubMed, published prior to 2021, with each publication categorized into one of the three classes: GRT, IRGT, and SWGRT. We selected nonclinical trial publications from a list of 120 journals that published most of the nested clinical trial publications; we will refer to those publications as negative publications. The original dataset consisted of 891 GRT publications, 59 IRGT publications, 109 SWGRT publications, and 996 negative publications. The first version of the fine-tuned

XSL•FO
RenderX

language model underwent training on titles and abstracts from this dataset. The best-performing model was subsequently employed to classify unlabeled publications published in 2021. After thorough verification of predictions by domain experts, a complementary set of 299 GRT, 40 IRGT, 65 SWGRT, and 1200 negative examples from 2021 was added to the original training, validation, and test sets.

The new dataset served as the foundation for tuning the model hyperparameters to predict labels for publications published in 2022. With the improved training data, the model demonstrated higher accuracy and F1-score, enabling precise classification of publications from the subsequent year, 2022. The same strategy as above was employed to add 2022 verified data to our training dataset, which resulted in the addition of 461 GRT, 195 IRGT, and 93 SWGRT, and 539 negative publications to the training, validation, and test datasets to prepare the classifier to predict labels for publications published in 2023. The Results section describes the final performance of the model trained and evaluated on this dataset.

Tokenization

To process the textual data, we utilized the Hugging Face Trainer API in conjunction with the BioMedBERT tokenizer. The BioMedBERT tokenizer is trained on a corpus of biomedical text to tokenize and segment text into subwords using the WordPiece algorithm, just like the original BERT tokenizer. Therefore, the tokenizer is tailored to handle biomedical terminology and language patterns [22]. For instance, when tokenizing the title "Comparison of different intervention methods to reduce the incidence of venous thromboembolism: study protocol for a cluster-randomized, crossover trial" from a 2023 publication, the tokens are segmented as follows: ["comparison," "of," "different," "intervention," "methods," "to," "reduce," "the," "incidence," "of,' "venous," "thromboembolism," ":," "study," "protocol," "for," "a," "cluster," "-," "randomized," ",", "crossover," "trial," "."]. The tokenization process was carried out separately for the titles and abstracts of the publications. In order to maintain computational efficiency and manage memory constraints, we imposed a length limit on the tokenized text. Titles were truncated to a maximum length of 30 tokens, which was the maximum title length in the data, while abstracts were truncated to 256 tokens from the start of the text, ensuring that majority of abstracts in our dataset fit within this allocation. Shorter sequences were padded with zeros. Based on the length distribution of titles and abstracts, we adjusted the allocation to align with actual usage patterns, ensuring that all instances remain within the supported range while optimizing model efficiency.

Addressing Class Imbalance

An imbalanced dataset refers to any dataset where there is an unequal distribution among classes, with one or more classes having significantly fewer instances than others. When trained on imbalanced datasets, models may exhibit a bias towards predicting the majority class more frequently, resulting in poor generalization for the minority class. Therefore, selecting the appropriate evaluation metric becomes crucial in such scenarios. A model might achieve high accuracy by predominantly predicting the majority class while displaying poor performance on the minority class. Various strategies exist to address class imbalance, including selecting appropriate performance metrics, such as precision-recall or the F_1-score, to accurately reflect model performance. Techniques like undersampling the majority class, oversampling the minority class, employing synthetic data generation methods like SMOTE (synthetic minority over-sampling technique), leveraging algorithms designed to handle class imbalance robustly, and incorporating cost-sensitive learning by assigning costs to the loss function are among the approaches commonly employed [26-28]. Given the observed class imbalance within the dataset, we implemented a customized loss function to mitigate the impact of this imbalance during the training phase. To achieve this, inverse class weights were calculated based on the number of examples in each class within the training dataset. These weights were then utilized in the weighted categorical cross-entropy loss function, assigning varying levels of importance to each class during model training.

The weighted categorical cross-entropy loss function is defined as follows:

$$\text{Weighted Categorical Cross-Entropy Loss} = -\sum_{i=1}^{N}\sum_{j=1}^{C} w_j \cdot y_{i,j} \cdot \log(P_{i,j})$$

- where C is the number of classes, N is the number of samples in the dataset, yi is the true probability distribution (one-hot encoded vector) for class i, Pi is the predicted probability distribution for class i, and wi is the weight assigned to class i

The inverse class frequency method is used to assign higher weights to classes with fewer examples. The rationale is to give higher weights to classes that are under-represented, making the model more sensitive to minority classes and potentially improving performance on imbalanced datasets.

$$w_i = \frac{\text{Total Number of Examples}}{\text{Number of Examples in class } i}$$

Hyperparameter Tuning

To evaluate the model's performance, we split our dataset into three subsets: a training set, a validation set, and a test set. The test set comprised 20% of the total dataset and was created by stratified random sampling from the labeled data. To assess the generalizability of our model to unseen data and to ensure a robust and unbiased evaluation of our model, a stratified k-fold cross-validation technique was used by splitting the remaining 80% of the dataset into subsets to train and validate the model iteratively, k times. In this technique, the dataset is divided into k folds while maintaining the same class distribution in each fold as the original dataset. We chose k=5 for a 5-fold cross-validation. Each fold maintained the proportion of class labels similar to that in the overall dataset. This helped prevent the model from being biased toward the majority class [29].

We conducted a series of experiments to determine the optimal hyperparameters for our model. These included exploring various values for learning rates, weight decay, batch sizes, and the number of training epochs [22]. Our goal was to identify the combination of hyperparameters that produced the best model performance with the highest F1-score. The initial hyperparameters were selected based on the pretrained

XSL•FO
RenderX

BioMedBERT model, and they were changed during the training process iteratively. The final model hyperparameters include a batch size of 32 and a learning rate of 0.00003098.

A regularization term is added to the loss function during training to penalize large weights and prevent overfitting [29]. The modified loss function with weight decay is calculated as follows:

$$\text{Total Loss} = \text{Original Loss} + \lambda 2 \sum i \parallel \theta i \parallel 2$$

Where original loss is the loss without regularization, λ is the weight decay hyperparameter, and Σi ‖ θi ‖ 2 represents the sum of squared weights across all layers of the model.

The value of the weight decay hyperparameter is a crucial aspect of training. It determines the strength of the regularization effect. Too small a value may not prevent overfitting, while too large a value may penalize weights too much and stop the learning process. Moreover, early stopping was applied to the classifier head to prevent overfitting and improve efficiency with a patience of 5 epochs.

By following these steps, we developed a fine-tuned BioMedBERT model capable of classifying publications into the specified categories. This model was rigorously trained, validated, and optimized to maximize the classification accuracy and F_1-score.

Results

To assess each model for generalizability, we evaluated its performance on the test set containing 20% of the final dataset that was randomly stratified and had not been introduced to the model previously.

Baseline Model Performance

After generating features using a FastText model and training the logistic regression model, we evaluated its performance across all classes. While the model demonstrated good performance on the majority class, indicating its efficacy in capturing prevalent patterns within the dataset, its performance on the minority class, IRGT, and SWGRT is suboptimal. Table 1 presents the baseline model's performance across all classes, while Table 2 depicts the confusion matrix of the baseline model. The weighted average for precision, recall or sensitivity, specificity, and F_1-score is 0.85.

Table . Performance metrics of logistic regression model across all classes.

Class	Accuracy	Precision	Recall or sensitivity	Specificity	F_1-score
Negative	0.85	0.87	0.93	0.90	0.90
GRT[a]		0.83	0.81	0.90	0.82
IRGT[b]		0.65	0.45	0.96	0.53
SWGRT[c]		1	0.70	0.98	0.82

[a]GRT: group- or cluster-randomized trial.

[b]IGRT: individually randomized group-treatment.

[c]SWGRT: stepped wedge group or cluster-randomized trial.

Table . Confusion matrix.

Actual	Predicted			
Classes	Negative	GRT	IRGT	SWGRT
Negative	508	27	12	0
GRT[a]	60	269	2	2
IRGT[b]	17	15	26	0
SWGRT[c]	2	14	0	37

[a]GRT: group- or cluster-randomized trial.

[b]IGRT: individually randomized group-treatment.

[c]SWGRT: stepped wedge group or cluster-randomized trial.

Pretrained Versus Fine-Tuned Performance

The low performance of the pretrained BioMedBERT classifier on all classes justifies the fine-tuning of the transformer-based model. Following the fine-tuning process using a training set that was curated by domain experts iteratively, the model's performance exhibited noticeable enhancement in all performance metrics. The inclusion of domain expertise in the data curation process contributed to refining the model's understanding and, consequently, improving its predictive capabilities.

Table 3 shows the performance of the latest version of the fine-tuned model on our test set, which was not seen by the model during training and validation. The confusion matrix, depicted in Table 4, provides a breakdown of the model's predictions against the actual values. The weighted average for precision, recall or sensitivity, specificity, and F_1-score are 0.94.

XSL•FO
RenderX

Table . Performance metrics of fine-tuned BioMedBERT across all classes.

Class	Accuracy	Precision	Recall or sensitivity	Specificity	F_1-score
Negative	0.94	0.96	0.95	0.93	0.95
GRT[a]		0.95	0.94	0.90	0.94
IRGT[b]		0.69	0.81	0.97	0.75
SWGRT[c]		0.96	0.96	0.99	0.96

[a]GRT: group- or cluster-randomized trial.

[b]IGRT: individually randomized group-treatment.

[c]SWGRT: stepped wedge group or cluster-randomized trial.

Table . Confusion matrix.

Actual	Predicted			
Classes	Negative	GRT	IRGT	SWGRT
Negative	518	12	17	0
GRT[a]	14	311	4	2
IRGT[b]	8	3	47	0
SWGRT[c]	0	2	0	51

[a]GRT: group- or cluster-randomized trial.

[b]IGRT: individually randomized group-treatment.

[c]SWGRT: stepped wedge group or cluster-randomized trial.

Discussion

Principal Results

The model developed in this research used data provided by the Office of Disease Prevention at the National Institute of Health and leveraged a transformer-based pretrained language model, BioMedBERT, to identify publications of clinical trials that used one of three nested designs. The model outperformed the baseline model developed using features generated by BioWordVec and logistic regression. Compared to our baseline model, the recall and specificity for each class demonstrated improvements as follows: 2 points for recall and 3 points for specificity in non-randomized class; 13 points for recall and 0 points for specificity in GRT; 36 points for recall and 1 point for specificity in IRGT; 26 points for recall and 1 point for specificity in SWGRT. The IRGT class exhibited the lowest sensitivity compared to other classes, due to fewer examples in the training data and the inherent difficulty in identifying such publications by only processing titles and abstracts. Even for human curators, labeling these publications is challenging, often necessitating meticulous examination of the whole paper's content. Since the fine-tuned model was trained solely on titles and abstracts, it had limited information available for predicting IRGT publications.

Comparison With Prior Work

While machine learning and natural language processing techniques have been utilized to identify RCTs in the medical literature [15], there have been fewer models specifically designed to identify special categories of group randomized clinical trials. Existing models for biomedical document classification predominantly rely on static embedding techniques, such as Word2Vec or FastText, although recent approaches have increasingly adopted nonstatic embedding methods, particularly transformer-based models like BERT and BioBERT, for more dynamic and context-aware text representations [30-32]. Our model leverages attention mechanisms and dynamic embedding techniques to capture the varying importance of words within the context of each document. By dynamically adjusting the embedding representations based on the context of the input sequence, our model can better capture the nuances and semantic relationships within the text, leading to improved classification performance.

Future Work

Moving forward, future research endeavors may focus on refining the model to distinguish between subcategories within each main category, such as the method, protocol, and results [33]. Tailoring the model to address these distinctions could further enhance its utility in biomedical text classification tasks, facilitating more precise and comprehensive literature analysis.

Conclusions

Our study presents a robust framework leveraging transformer-based language models to effectively identify distinct categories of clinical trial publications within the biomedical literature. Through fine-tuning the pretrained BioMedBERT model, we achieved high accuracy and F_1-score metrics across three categories: GRTs, IRGTs, and SWGRTs. The developed framework outperforms conventional search queries, providing advanced language understanding capabilities for discerning a broader spectrum of publications.

XSL•FO
RenderX

Our findings underscore the significance of transformer-based models in biomedical text classification, offering improved performance compared to traditional machine learning approaches and static embedding techniques. By continually updating and refining our model with new training data, we anticipate ongoing improvements in performance and adaptability over time. This iterative approach ensures the model remains up to date on the latest developments in the biomedical field, contributing to more efficient literature exploration, information retrieval, and knowledge discovery.

Conflicts of Interest

None declared.

Multimedia Appendix 1
Python code
[DOCX File, 26 KB - medinform_v13i1e63267_app1.docx]

References

1. Murray DM. Influential methods reports for group-randomized trials and related designs. Clin Trials 2022 Aug;19(4):353-362. [doi: 10.1177/17407745211063423] [Medline: 34991379]
2. Murray DM, Taljaard M, Turner EL, George SM. Essential ingredients and innovations in the design and analysis of group-randomized trials. Annu Rev Public Health 2020 Apr 2;41(1-19):1-19. [doi: 10.1146/annurev-publhealth-040119-094027] [Medline: 31869281]
3. Campbell MJ, Walters SJ. How to Design, Analyse and Report Cluster Randomised Trials in Medicine and Health Related Research: John Wiley & Sons Ltd; 2014. [doi: 10.1002/9781118763452]
4. Donner A, Klar N. Design and Analysis of Cluster Randomization Trials in Health Research: Arnold; 2000:178.
5. Eldridge S, Kerry S. A practical guide to cluster randomised trials in health services research. 2012. URL: https://onlinelibrary.wiley.com/doi/book/10.1002/9781119966241 [doi: 10.1002/9781119966241]
6. Hayes RJ, Moulton LH. Cluster Randomised Trials, 1st edition: CRC Press; 2009. [doi: 10.1201/9781584888178]
7. Hayes RJ, Moulton LH. Cluster Randomised Trials: CRC Press; 2017.
8. Murray DM. Design and Analysis of Group-Randomized Trials: Oxford University Press; 1998:467.
9. Hussey MA, Hughes JP. Design and analysis of stepped wedge cluster randomized trials. Contemp Clin Trials 2007 Feb;28(2):182-191. [doi: 10.1016/j.cct.2006.05.007] [Medline: 16829207]
10. Pals SL, Murray DM, Alfano CM, Shadish WR, Hannan PJ, Baker WL. Individually randomized group treatment trials: a critical appraisal of frequently used design and analytic approaches. Am J Public Health 2008 Aug;98(8):1418-1424. [doi: 10.2105/AJPH.2007.127027] [Medline: 18556603]
11. Moyer JC, Li F, Cook AJ, et al. Evaluating analytic models for individually randomized group treatment trials with complex clustering in nested and crossed designs. Stat Med 2024 Nov 10;43(25):4796-4818. [doi: 10.1002/sim.10206] [Medline: 39225281]
12. Antonio Mouriño García M, Pérez Rodríguez R, Anido Rifón L. Leveraging Wikipedia knowledge to classify multilingual biomedical documents. Artif Intell Med 2018 Jun;88:37-57. [doi: 10.1016/j.artmed.2018.04.007] [Medline: 29730047]
13. Cohen AM. An effective general purpose approach for automated biomedical document classification. AMIA Annu Symp Proc 2006;2006(161-5):161-165. [Medline: 17238323]
14. Marshall IJ, Noel-Storr A, Kuiper J, Thomas J, Wallace BC. Machine learning for identifying randomized controlled trials: an evaluation and practitioner's guide. Res Synth Methods 2018 Dec;9(4):602-614. [doi: 10.1002/jrsm.1287] [Medline: 29314757]
15. Al-Jaishi AA, Taljaard M, Al-Jaishi MD, et al. Machine learning algorithms to identify cluster randomized trials from MEDLINE and EMBASE. Syst Rev 2022 Oct 25;11(1):229. [doi: 10.1186/s13643-022-02082-4] [Medline: 36284336]
16. Devlin J, Chang M, Lee K, Toutanova K. BERT: pre-training of deep bidirectional transformers for language understanding. arXiv. URL: https://arxiv.org/abs/1810.04805 [accessed 2025-04-25] [doi: 10.48550/arXiv.1810.04805]
17. Yang Z, Dai Z, Yag Y, Carbonell J, Salakhutdinov R, Le Q. XLNet: generalized autoregressive pretraining for language understanding. arXiv. URL: https://arxiv.org/abs/1906.08237 [accessed 2025-04-25] [doi: 10.48550/arXiv.1906.08237]
18. Liu Y, Ott M, Goyal N, Du J, Joshi M, Chen D, et al. RoBERTa: A robustly optimized BERT pretraining approach. arXiv. URL: https://arxiv.org/abs/1907.11692 [accessed 2025-04-25] [doi: 10.48550/arXiv.1907.11692]
19. Lee J, Yoon W, Kim S, et al. BioBERT: a pre-trained biomedical language representation model for biomedical text mining. Bioinformatics 2020 Feb 15;36(4):1234-1240. [doi: 10.1093/bioinformatics/btz682] [Medline: 31501885]
20. Yasunaga M, Leskovec J, Liang P. LinkBERT: pretraining language models with document links. . URL: https://aclanthology.org/2022.acl-long [doi: 10.18653/v1/2022.acl-long.551]
21. Peng Y, Yan S, Lu Z. Transfer learning in biomedical natural language processing: an evaluation of BERT and elmo on ten benchmarking datasets. . Preprint posted online on 2019 URL: https://www.aclweb.org/anthology/W19-50 [doi: 10.18653/v1/W19-5006]

XSL•FO
RenderX

22. Gu Y, Tinn R, Cheng H, et al. Domain-specific language model pretraining for biomedical natural language processing. ACM Trans Comput Healthcare 2022 Jan 31;3(1):1-23. [doi: 10.1145/3458754]
23. Shah K, Patel H, Sanghvi D, Shah M. A comparative analysis of logistic regression, random forest and KNN models for the text classification. Augment Hum Res 2020 Dec;5(1):12. [doi: 10.1007/s41133-020-00032-0]
24. Zhang Y, Chen Q, Yang Z, Lin H, Lu Z. BioWordVec, improving biomedical word embeddings with subword information and MeSH. Sci Data 2019 May 10;6(1):52. [doi: 10.1038/s41597-019-0055-0] [Medline: 31076572]
25. Sokolova M, Lapalme G. A systematic analysis of performance measures for classification tasks. Inf Process Manag 2009 Jul;45(4):427-437. [doi: 10.1016/j.ipm.2009.03.002]
26. Christen P, Hand DJ, Kirielle N. A review of the f-measure: its history, properties, criticism, and alternatives. ACM Comput Surv 2024 Mar 31;56(3):1-24. [doi: 10.1145/3606367]
27. Sun Y, Kamel MS, Wong AKC, Wang Y. Cost-sensitive boosting for classification of imbalanced data. Pattern Recognit DAGM 2007 Dec;40(12):3358-3378. [doi: 10.1016/j.patcog.2007.04.009]
28. Chawla NV, Bowyer KW, Hall LO, Kegelmeyer WP. SMOTE: synthetic minority over-sampling technique. jair 2002;16:321-357. [doi: 10.1613/jair.953]
29. Hastie T, Tibshirani R, Friedman J. The Elements of Statistical Learning: Data Mining, Inference, and Prediction, 2nd edition: Springer; 2009. [doi: 10.1007/978-0-387-84858-7]
30. Li P, Jiang X, Zhang G, et al. Utilizing image and caption information for biomedical document classification. Bioinformatics 2021 Jul 12;37(Suppl_1):i468-i476. [doi: 10.1093/bioinformatics/btab331] [Medline: 34252939]
31. Kesiku CY, Chaves-Villota A, Garcia-Zapirain B. Natural language processing techniques for text classification of biomedical documents: a systematic review. Information 2022;13(10):499. [doi: 10.3390/info13100499]
32. Syriopoulos PG, Andriopoulos AD, Koutsomitropoulos DA. Evaluation of language models for multilabel classification of biomedical texts. Presented at: Artificial Intelligence Applications and Innovations; Jun 21, 2024 p. 68-78. [doi: 10.1007/978-3-031-63211-2_6]
33. Walwyn R, Roberts C. Therapist variation within randomised trials of psychotherapy: implications for precision, internal and external validity. Stat Methods Med Res 2010 Jun;19(3):291-315. [doi: 10.1177/0962280209105017] [Medline: 19608603]

Abbreviations

GRT: group- or cluster-randomized trial
IGRT: individually randomized group-treatment
SMOTE: synthetic minority over-sampling technique
SWGRT: stepped wedge group or cluster-randomized trial

Edited by C Lovis; submitted 14.06.24; peer-reviewed by H Yu, M Lan; revised version received 02.02.25; accepted 06.02.25; published 09.05.25.

Please cite as:
Aghaarabi E, Murray D
Transformer-Based Language Models for Group Randomized Trial Classification in Biomedical Literature: Model Development and Validation
JMIR Med Inform 2025;13:e63267
URL: https://medinform.jmir.org/2025/1/e63267
doi:10.2196/63267

© Elaheh Aghaarabi, David Murray. Originally published in JMIR Medical Informatics (https://medinform.jmir.org), 9.5.2025. This is an open-access article distributed under the terms of the Creative Commons Attribution License (https://creativecommons.org/licenses/by/4.0/), which permits unrestricted use, distribution, and reproduction in any medium, provided the original work, first published in JMIR Medical Informatics, is properly cited. The complete bibliographic information, a link to the original publication on https://medinform.jmir.org/, as well as this copyright and license information must be included.

XSL•FO
RenderX

A Risk Warning Model for Anemia Based on Facial Visible Light Reflectance Spectroscopy: Cross-Sectional Study

Yahan Zhang[1*], MS; Yi Chun[1*], MD; Hongyuan Fu[1*], MD; Wen Jiao[2], PhD; Jizhang Bao[3], PhD; Tao Jiang[4], PhD; Longtao Cui[4], PhD; Xiaojuan Hu[4], PhD; Ji Cui[4], PhD; Xipeng Qiu[5], PhD; Liping Tu[4], PhD; Jiatuo Xu[1], PhD

[1]Traditional Chinese Medicine College, Shanghai University of Traditional Chinese Medicine, No. 1200 Cailun Road, Pudong New Area, Shanghai, China

[2]Clinical Research Unit, Shanghai Municipal Hospital of Traditional Chinese Medicine, Shanghai, China

[3]Department of Hematology, Shanghai Municipal Hospital of Traditional Chinese Medicine, Shanghai, China

[4]Collaborative Innovation Center for Traditional Chinese Medicine Health Services, Shanghai University of Traditional Chinese Medicine, Shanghai, China

[5]School of Computer Science and Technology, Fudan University, Shanghai, China

[*]these authors contributed equally

Corresponding Author:
Jiatuo Xu, PhD
Traditional Chinese Medicine College, Shanghai University of Traditional Chinese Medicine, No. 1200 Cailun Road, Pudong New Area, Shanghai, China

Abstract

Background: Anemia is a global public health issue causing symptoms such as fatigue, weakness, and cognitive decline. Furthermore, anemia is associated with various diseases and increases the risk of postoperative complications and mortality. Frequent invasive blood tests for diagnosis also pose additional discomfort and risks to patients.

Objective: This study aims to assess the facial spectral characteristics of patients with anemia and to develop a predictive model for anemia risk using machine learning approaches.

Methods: Between August 2022 and September 2023, we collected facial image data from 78 anemic patients who met the inclusion criteria from the Hematology Department of Shanghai Hospital of Traditional Chinese Medicine. Between March 2023 and September 2023, we collected data from 78 healthy adult participants from Shanghai Jiading Community Health Center and Shanghai Gaohang Community Health Center. A comprehensive statistical analysis was performed to evaluate differences in spectral characteristics between the anemic patients and healthy controls. Then, we used 10 different machine learning algorithms to create a predictive model for anemia. The least absolute shrinkage and selection operator was used to analyze the predictors. We integrated multiple machine learning classification models to identify the optimal model and developed Shapley additive explanations (SHAP) for personalized risk assessment.

Results: The study identified significant differences in facial spectral features between anemic patients and healthy controls. The support vector machine classifier outperformed other classification models, achieving an accuracy of 0.875 (95% CI 0.825-0.925) for distinguishing between the anemia and healthy control groups. In the SHAP interpretation of the model, forehead-570 nm, right cheek-520 nm, right zygomatic-570 nm, jaw-570 nm, and left cheek-610 nm were the features with the highest contributions.

Conclusions: Facial spectral data demonstrated clinical significance in anemia diagnosis, and the early warning model for anemia risk constructed based on spectral information demonstrated a high accuracy rate.

(JMIR Med Inform 2025;13:e64204) doi:10.2196/64204

KEYWORDS

anemia; hemoglobin; spectroscopy; machine learning; risk warning model; Shapley additive explanation

Introduction

Background

Anemia is a condition characterized by a decrease in red blood cell count or hemoglobin concentration below a certain threshold, thereby reducing the blood's oxygen-carrying capacity throughout the body. It serves as an indicator of poor nutritional and health status [1]. A study conducted from 1990 to 2019 reported that more than 1.7 billion people worldwide were anemic [2]. Typical symptoms include fatigue, drowsiness, weakness, tachycardia, shortness of breath, increased heart rate, decreased appetite, hypotension, and dizziness [3]. According

XSL•FO
RenderX

to the results of China's fourth nutritional survey, the prevalence of anemia among Chinese residents is 20.1%, and the global prevalence of anemia in all ages is 22.8% in 2019 [4], indicating it has become an important public health issue. In a survey of 13,175 Chinese adults aged >50 years, the prevalence of anemia is 31%, indicating that anemia is particularly prevalent in China's middle-aged and older adult population [5]. Especially among older adults, anemia has been identified as one of the independent risk factors for poor patient outcomes [6]. Studies have found that older adults with anemia were more than twice as likely to suffer from frailty [7], and the survival rate of older adult patients with anemia was significantly lower than that of the nonanemic older adult population [8]. Hemoglobin (Hb) concentration is a reliable indicator for diagnosing anemia [9]. Specifically, a low hemoglobin concentration is strongly correlated with disability, poor physical performance, and declining cognitive ability and strength in aging individuals [10,11], especially so for the oldest individuals [12]. Anemia is associated with a variety of diseases for which there is a negative impact on the patient's prognosis [13]. Additionally, preoperative anemia has been identified as an independent correlation factor of increased postoperative complications and mortality rates [14]. Anemia is often diagnosed by an invasive blood specimen collection method that patients may find uncomfortable, especially for those who are sensitive and fearful of invasive blood tests. Bateman et al [15] conducted a prospective, multicenter, epidemiological, and observational study with 977 children enrolled and found that blood draws accounted for 73% of daily blood loss, and that 96.5% of the children lost blood as a result of blood draws. In fact, frequent drawing of blood can lead to medical anemia.

Current Research on Noninvasive Hemoglobin Detection

Current noninvasive testing methods being explored include photoelectric volumetric pulse wave, spectroscopy, and hyperspectral techniques. For diagnosis via photoelectric volumetric pulse wave, Acharya et al [16] developed a multimodel stacking regressor and estimate the total Hb using noninvasively acquired photoplethysmogram. Spectroscopic techniques explore material properties through the interaction between matter and electromagnetic waves of different frequencies [17]. Hyperspectral imaging techniques provide a more detailed segmentation in spectral dimensions and contain much more information than red, green, and blue [18]. Color measurement in Chinese medicine color diagnosis by visible reflectance spectroscopy is similar to clinical color diagnosis, reflecting the accuracy, authenticity, and reliability of color diagnosis results [19]. Raman spectroscopy can be used to analyze the distribution of metabolite, lipid, protein, water, and blood content in tissues by detecting the skin[20]. Hyperspectral imaging can estimate Hb concentration and blood oxygen saturation by diffuse reflection of tissues [21]. Spectral imaging of sublingual microcirculation was proven to be able to detect anemia [22]. Research on noninvasive Hb measurement using spectroscopy predominantly focuses on areas such as the palm, fingernails, and conjunctiva. Kesarwani et al [23] proposed a noninvasive palm pallor–based anemia detection system, which utilizes a smartphone app to estimate Hb levels by monitoring changes in palm pallor. The system achieved a sensitivity of 0.93, mean squared error of 0.701, and root mean squared error of 0.698. Liu et al [24] used a fingertip measurement method, constructed partial least squares and back propagation artificial neural network models, and developed a portable prototype for their noninvasive Hb detection system. Mannino et al [25] used the color of patients' nail beds from smartphone photos to estimate Hb levels, defining anemia as 11.0 g dL<threshold. The model for the study had a sensitivity and specificity of 0.92 and 0.76 in the classification of anemia versus healthy individuals. Bevilacqua et al [26] proposed an alternative method for noninvasive Hb estimation based on image analysis of specific regions of the conjunctiva; in total, 77 patients with anemia and healthy individuals were studied and modeled using a binary support vector machine (SVM) classifier with a resulting accuracy of 0.844, specificity of 0.824, and sensitivity of 1.000. Kalantri et al [27] conducted a blind, independent comparison of the presence and absence of pallor in physical features (including conjunctiva, tongue, palms, and nail beds) and a reference standard (Hb estimated by an electronic cell counter). Diagnostic accuracy was measured by calculating likelihood ratios, 95% confidence intervals for different Hb thresholds, and the area under the characteristic curve of the subjects. The area under the characteristic curve was 0.84 and 0.71 for Hb of 7 g/dL and 9 g/dL as cutoffs. Wang et al [28] developed HemaApp, which uses a smartphone camera and different light sources to noninvasively monitor Hb concentration based on photoelectric volumetric pulse wave techniques. HemaApp was evaluated on 31 patients, with a light source passing through the patient's finger for chromatic analysis to estimate the Hb concentration by blood color. Regression analysis of Hb concentration was performed in the paper for different light sources: when white +970 nm LEDs were used, R=0.69; when white +970 nm LEDs + incandescent were used, R=0.74; when white + 880 nm and 970 nm LEDs + incandescent were used, R=0.82.

Facial diagnosis is an important and intuitive method of traditional Chinese medicine (TCM). The facial features of patients with anemia always differ from those of healthy persons, usually showing a pale complexion [27]. Pallor of the conjunctiva, palms, nail beds, or any part of the body is associated with significantly lower Hb concentrations [29]. The continuous development of intelligent diagnostic methods has provided classification models for recognizing facial complexions, which to some extent avoids the subjective limitations of the traditional facial diagnosis that are qualitative and experience-based [30]. An increasing number of experts are integrating color optical theories and modern instrumentation into the modern research field of TCM diagnosis, making the research more scientific and objective, and avoiding biases caused by human factors [31]. However, there is currently a lack of formal studies focusing on noninvasive, spectral Hb monitoring of the facial region [32].

Goals

Based on this, we collected data from patients with anemia and healthy controls, analyzed the spectral reflectance and image features of their faces, and built an anemia classification model based on machine learning (ML) methods. The results showed

XSL•FO
RenderX

that patients with anemia generally have a paler complexion, with the most noticeable differences located in the nose, right cheek, right zygomatic, and jaw.

Methods

General Description of Participants

To control for variables such as age, locale, and gender, we implemented rigorous matching criteria. Between March 2023 and September 2023, we collected data on people who underwent routine physical examinations at the Shanghai Jiading and Gaohang Community Health Centers, from which we randomly selected 78 healthy individuals, consisting of 38 males (49%) and 40 females (51%), aged 45 to 85 years, with a mean age of 68 years. Additionally, from August 2022 to September 2023, we gathered data from patients admitted to the hematology ward at the Shanghai Hospital of Traditional Chinese Medicine, ultimately analyzing 78 patients with anemia consisting of 38 males (49%) and 40 females (51%) aged 45 to 85 years, with a mean age of 67 years. This anemia group contained 26 mild (33%), 26 moderate (33%), and 26 severe cases (33%) of anemia.

Diagnostic Criteria

According to the diagnostic criteria established by Chinese hematologists [33], in China, anemia can be diagnosed in adult males with a Hb level ≤120 g/L and in adult females (nonpregnant) with Hb ≤110 g/L. Within this range, Hb ≥90 g/L is considered mild anemia, 60 g/L≤ Hb ≤89 g/L is considered moderate anemia, and 30 g/L≤Hb ≤59 g/L is considered severe anemia.

Inclusion and Exclusion Criteria

The inclusion criteria for the healthy control group is as follows: (1) the absence of any acute or chronic diseases according to clinical diagnostic criteria (no diagnosis of any acute disease within 3 months, and no diagnosis of any chronic disease within 6 months), (2) no current medication use or other irregularity found in the blood, and (3) regular urine, liver, and kidney functions.

The inclusion criteria for the anemia group is as follows: (1) the patient's Hb value must meet the diagnostic criteria for anemia [33]; (2) the patient exhibits symptoms of anemia, such as pale complexion, lips, or nails, fatigue, weakness, shortness of breath, and resting tachycardia [3,34]; and (3) the patient's age is between 45 and 85 years. Both male and female patients were included.

The exclusion criteria for the anemia group is as follows: (1) the patient requests to withdraw informed consent; (2) the patient is unable to meet the inclusion criteria; (3) presence of severe cardiovascular, cerebrovascular, endocrine, motor, autoimmune, or infectious diseases; (4) presence of mental illnesses or disorders of consciousness and communication; (5) patients undergoing blood transfusion; and (6) pregnant and breastfeeding women, or those preparing for pregnancy.

Observation Methods

Facial spectroscopic data of the healthy controls and patients with anemia were collected using a CS-600CG spectrophotometric colorimeter (Figure 1).

Figure 1. CS-600CG Spectrophotometer



To obtain more comprehensive facial information, we selected 8 points on the subjects' faces: the forehead, glabellum, nose, jaw, right zygomatic, left zygomatic, right cheek, and left cheek. It should be noted that subjects were required to be free of cosmetics and maintain a natural facial complexion during data collection. The following specific steps were taken: (1) calibrate the spectrometer and adjust the parameters to standard values; (2) instruct subjects to keep their faces clean; (3) sterilize the instrument with 75% medical alcohol; (4) position the collection port against the subject's skin and collect data at the following locations in the order specified: forehead, glabellum, nose, jaw, right zygomatic, left zygomatic, right cheek, and left cheek; and (5) verify the consistency of the collected data and minimize excessive variability between each facial area.

XSL•FO
RenderX

Statistical Analysis

We used SPSS (version 25.0; IBM Corp) for statistical analysis. Data satisfying normality were expressed as mean (SD), whereas data not satisfying normality were expressed as median (IQR). The significance level was set at α=.05. To compare the 2 groups, independent samples *t* tests were used for data that were normally distributed and demonstrated homogeneity of variance; otherwise, Mann-Whitney *U* tests were applied. All tests were 2-tailed, and a P<.05 was considered to indicate statistical significance. To compare the 4 groups, 1-way ANOVAs were used for data that were normally distributed and exhibited homogeneity of variance; Kruskal-Wallis tests were applied for data that were not normally distributed or exhibited inhomogeneity of variance. All tests were 2-tailed, and a P<.05 was considered to indicate statistical significance.

Model Selection

After selecting feature factors from all independent variables, we divided patients with anemia and healthy controls into training and test sets. Multiple ML classification models were then applied for a comprehensive analysis to compare the discriminative performance of different models. Additionally, we evaluated and validated the results using the optimized model. A SHAP demonstration model was also developed. The specific steps are as follows:

1. Feature selection: Initially, we conducted the least absolute shrinkage and selection operator (LASSO) regression analysis in R to adjust variable selection and complexity. Subsequently, the results from the LASSO regression analysis were utilized as feature variables for machine learning.

2. Data division: To prevent randomness in modeling results, we classified patients with mild, moderate, and severe anemia according to the diagnostic criteria established by Chinese hematologists. Using average random sampling, we divided the data proportionally for training and validating the classification model: 108 cases (70%) for the training set and 48 cases (30%) for the test set.

3. Comprehensive analysis of multiple classification models: We utilized an open-source version of Python 3.7 for our analysis. Subsequently, we used various functions from the scikit-learn library via Python 3.7, applying LASSO regression to extract different spectral bands as feature bands. We constructed a risk warning model for anemia using 10 ML algorithms: logistic regression, decision tree, SVM, random forest, k-nearest neighbor (KNN), artificial neural network (ANN), Bayesian classifier, extreme gradient boosting (XGBoost), adaptive boosting (AdaBoost), and light gradient boosting machine (LightGBM).

Logistic regression is used for binary and multiclass classification, using maximum likelihood for parameter estimation [35]. Decision tree uses tree diagrams for decision-making, handling classification and regression without data standardization [36]. SVMs find optimal hyperplanes for classification, using kernel tricks for complex issues [37]. Random forest uses multiple trees for better stability and accuracy, ideal for high-dimensional datasets [38]. KNN predicts by nearest categories, which is best for simple, small-scale datasets [39]. ANNs learn complex data relationships through neural connections, great for nonlinear and large datasets [40]. Bayesian classifiers use Bayes' theorem for probabilistic outputs, suitable for medical diagnostics [41]. XGBoost optimizes boosting trees for performance and efficiency, excelling in large or feature-rich datasets [42]. AdaBoost improves classification by adjusting for misclassified samples, using multiple weak classifiers [43]. LightGBM focuses on efficient learning with high precision and speed, and it is optimized for distributed environments [44]. We then trained and tested the above parameterized models, analyzed the importance of the training set and testing set indicators in different models, and selected the optimal one. Python 3.7 was used to construct the area under the receiver operating characteristic curve (AUROC), which is often used to describe tools for diagnostic testing or the identification accuracy of predictive models [45]. Python 3.7 was used to plot precision-recall (PR) curves, which were widely used to evaluate the performance of models. PR and the area under the PR (average precision [AP]) curve can provide a valuable complement to existing model evaluation methods [46]. Python 3.7 was used to plot the decision curve analysis (DCA), essentially the decision analysis. Thus, with these evaluations, it was possible to determine the viability of a given model, as well as which of several models was optimal, with significant advantages in assessing the clinical applicability of the model [47]. Also, we evaluated the performance of the classification models using a range of metrics, including accuracy, sensitivity, specificity, F_1-score, AUROC, positive predictive value (PPV), and negative predictive value (NPV). The formulas for accuracy, sensitivity, specificity, precision, F_1-score, PPV, and NPV are as follows:

(1)Accuracy=TP+TNTP+TN+FP+FN

(2)Sensitivity=TPTP+FN

(3)Specificity=TNTP+FP

(4)Precision=TPTP+FP

(5)F1=2×Precision×SensitivityPrecision+Sensitivity

(6)PPV=TPTP+FP

(7)NPV=TNTN+FN

4. We used SHAP library via Python 3.7 to plot the SHAP interpretation of importance and contribution to the model and interpreted the model results by calculating the contribution of each feature to the prediction results.

Ethical Considerations

The studies involving human participants were reviewed and approved by the Ethics Committee of Shanghai Municipal Hospital of Traditional Chinese Medicine affiliated to Shanghai University of Traditional Chinese Medicine (registration number 2021SHL-KY-03-01) and the institutional review board of Shuguang Hospital affiliated with Shanghai University of Traditional Chinese Medicine (registration number 2018-626-55-03). Informed consent was obtained from all subjects involved in the study. The privacy and confidentiality of patients' personal information were strictly protected throughout the research process. All patient data were anonymized and stored securely.

XSL•FO
RenderX

Results

Participant Characteristics

The baseline characteristics of the first 2 healthy and patient groups are shown in Table 1 and the baseline characteristics of the latter healthy and patient groups classified by severity group are shown in Table 2.

Table . Baseline comparison of 2 groups (n=156).

Characteristics	Healthy controls (n=78)	Patients with anemia (n=78)	*P* value
Gender, n (%)			
Male	38 (49)	38 (49)	1.00
Female	40 (51)	40 (51)	
Age (years), mean (SD)	67.03 (10.62)	68.24 (4.68)	.94

Table . Baseline comparison of 4 groups (n=104).

Characteristics	Healthy controls (n=26)	Anemia patients (n=78)			*P* value
		Mild (n=26)	Moderate (n=26)	Severe (n=26)	
Gender, n (%)					
Male	13 (50)	12 (46)	14 (54)	12 (46)	.94
Female	13 (50)	14 (54)	12 (46)	14 (54)	
Age (years), mean (SD)	67.03 (10.62)	70.35 (11.03)	65.19 (11.14)	65.54 (9.19)	.11

The results indicate that there were no statistically significant differences in gender and age distribution among the 2 or 4 groups (χ^2 test for gender, Kruskal-Wallis test for age).

Statistical Analysis of Facial Spectral Data

The results (Multimedia Appendix 1) showed statistically significant differences in spectral reflectance at specific wavelength ranges between the 2 groups ($P<.05$), including the forehead (400 - 600 nm), glabellum (400 - 700 nm), nose (400 - 700 nm), jaw (400 - 610 nm), right zygomatic (400 - 700 nm), left zygomatic (400 - 470 nm and 500 - 610 nm), and right cheek (400 - 700 nm). Additionally, significant differences were noted at the forehead (400 - 420 nm, 520 - 590 nm, 690 - 700 nm), glabellum (400 - 700 nm), nose (400 - 700 nm), jaw (470 - 500 nm), right zygomatic (400 - 700 nm), left zygomatic (440 - 700 nm), right cheek (400 - 700 nm), and left cheek (400 - 600 nm, 650 - 700 nm) between the 4 groups ($P<.05$).

To directly observe and understand the differences in facial spectral images between the anemia group and the healthy group, we plotted the average spectra at 8 locations for both the anemic and healthy groups, as depicted in Figure 2. The red line represents the average spectral reflectance of the anemic group, while the green line represents that of the healthy control group. It is evident that at the glabellum, nose, right zygomatic, and right cheek locations, the spectral reflectance of the anemic group is significantly higher than that of the healthy control group. Similarly, at the forehead, jaw, left zygomatic, and left cheek locations, the spectral reflectance of the anemic group remained significantly higher, particularly in the 480 - 630 nm range.

XSL•FO
RenderX

Figure 2. Comparison between 2 groups of spectral lines for 8 positions: (**A**) the spectral reflectance of the forehead, (**B**) the spectral reflectance of the glabellum, (**C**) the spectral reflectance of the nose, (**D**) the spectral reflectance of the jaw, (**E**) the spectral reflectance of the right zygomatic, (**F**) the spectral reflectance of the left zygomatic, (**G**) the spectral reflectance of the right cheek, and (**H**) the spectral reflectance of the left cheek.

XSL•FO
RenderX

Furthermore, to directly observe and understand the differences in facial spectral images between the anemia group and the healthy control group, we plotted the average spectra of the healthy control group and the mild, moderate, and severe anemia groups across a total of 4 groups at 8 positions, as shown in Figure 3. The red line represents the average spectral reflectance of the moderate anemia group, the yellow line represents that of the severe anemia group, the blue line represents the spectral reflectance of the mild anemia group, and the green line represents the average spectral reflectance of the healthy control group.

We observed that the spectral reflectance of both the healthy control group and the severe anemia group is significantly different from that of the other groups at all 8 positions. Moreover, a gradual decrease in spectral reflectance is noted from the severe anemia group to the moderate anemia group, then to the mild anemia group, and finally to healthy individuals across the 400 - 630 nm wavelength interval. This gradient of decrease was particularly pronounced at the nose.

XSL•FO
RenderX

Figure 3. Comparison between 4 groups of spectral lines for 8 positions: (**A**) the spectral reflectance of the forehead, (**B**) the spectral reflectance of the glabellum, (**C**) the spectral reflectance of the nose, (**D**) the spectral reflectance of the jaw, (**E**) the spectral reflectance of the right zygomatic, (**F**) the spectral reflectance of the left zygomatic, (**G**) the spectral reflectance of the right cheek, and (**H**) the spectral reflectance of the left cheek.

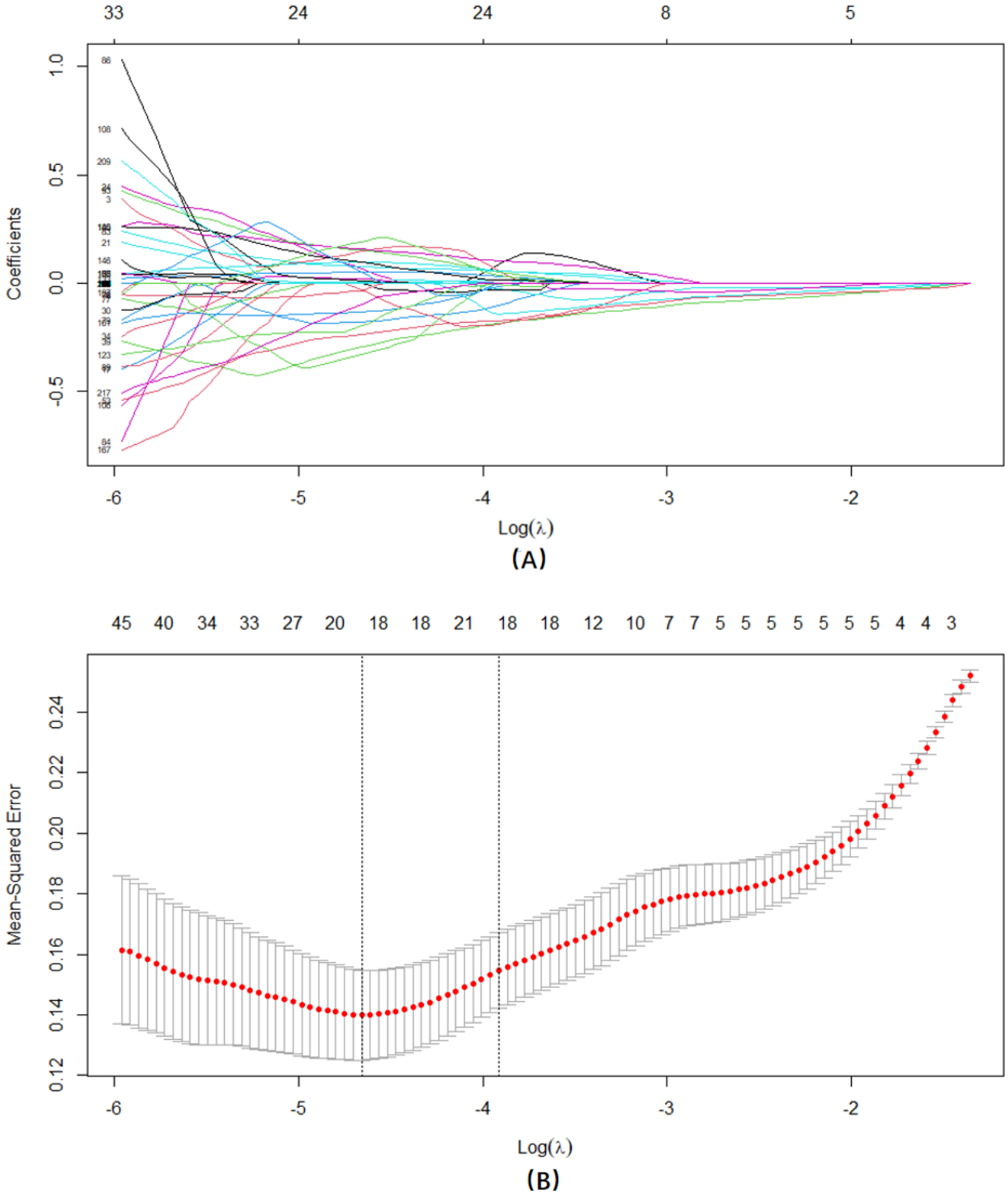
XSL•FO
RenderX

Screening of Characteristic Factors for Risk of Patients With Anemia

Using the presence or absence of anemia as the dependent variable, we performed LASSO regression analysis on 217 independent variables exhibiting statistical differences (Figure 4). LASSO can compress variable coefficients to prevent overfitting and address severe collinearity issues [48]. The results showed that (lambda with minimum mean square error=0.009) 217 independent variables were reduced to 20 (20/217, 9%). The selected variables included glabellum-570 nm, right cheek-520 nm, right zygomatic-570 nm, jaw-570 nm, left cheek-610 nm, left cheek-700 nm, nose-700 nm, jaw-490 nm, nose-490 nm, left zygomatic-500 nm, jaw-610 nm, left cheek-420 nm, forehead-420 nm, nose-400 nm, right cheek-640 nm, right zygomatic-670 nm, glabellum-660 nm, glabellum-670 nm, jaw-420 nm, and glabellum-420 nm.

XSL•FO
RenderX

Figure 4. LASSO regression analysis was used to select characteristic factors. (**A**) The use of 10-fold cross-validation to draw vertical lines at selected values, where the optimal lambda produces 20 nonzero coefficients. (**B**) In the LASSO model, the coefficient profiles of 217 features were drawn from the log (λ) sequence. Vertical dotted lines are drawn at the minimum mean square error (λ=0.009) and the standard error of the minimum distance (λ=0.020). LASSO: least absolute shrinkage and selection operator.



Comprehensive Analysis of Classified Multimodel

We included locations and bands that exhibited statistically significant differences as identified in our statistical analyses and used these to construct various models. Specifically, we used logistic regression, decision tree, SVM, random forest, KNN, ANN, Bayesian classifier, XGBoost, AdaBoost, and LightGBM algorithms.

By using both the anemia group and the healthy control group as evaluation test sets, we evaluated the performance of the 10 ML methods, with the results summarized in Table 3.

XSL•FO
RenderX

Table . Classification model results of each model (95% CIs).

Classifier	Precision	Specificity	Sensitivity	F_1-score	PPV[a]	NPV[b]	Accuracy	AUC[c]	AP[d]
LR[e]	0.836-0.924	0.831-0.919	0.871-0.962	0.853-0.943	0.836-0.924	0.867-0.959	0.846-0.946	0.889-0.983	0.874-0.966
DT[f]	0.887-0.980	0.910-1.000	0.554-0.613	0.682-0.754	0.887-0.980	0.662-0.732	0.721-0.821	0.835-0.922	0.758-0.838
SVM[g]	0.864-0.955	0.871-0.963	0.792-0.875	0.826-0.913	0.864-0.955	0.804-0.888	0.825-0.925	0.925-1.000	0.916-1.000
RF[h]	0.867-0.959	0.870-0.963	0.831-0.919	0.849-0.938	0.867-0.959	0.836-0.924	0.846-0.946	0.879-0.972	0.798-0.882
KNN[i]	0.897-0.992	0.910-1.000	0.673-0.744	0.783-0.833	0.897-0.992	0.728-0.805	0.783-0.883	0.871-0.963	0.825-0.912
ANN[j]	0.809-0.894	0.792-0.875	0.910-1.000	0.846-0.946	0.809-0.894	0.905-1.000	0.846-0.946	0.905-1.000	0.890-0.983
NB[k]	0.769.-0.850	0.792-0.875	0.673-0.744	0.718-0.793	0769.-0.850	0.704-0.778	0.721-0.821	0.811-0.897	0.775-0.856
XGBoost[l]	0.855-0.945	0.871-0.963	0.712-0.788	0.777-0.859	0.855-0.945	0.746-0.825	0.783-0.883	0.849-0.939	0.774-0.855
AdaBoost[m]	0.774-0.856	0.752-0.831	0.871-0.963	0.820-0.906	0.774-0.856	0.860-0.950	0.804-0.904	0.902-0.997	0.869-0.960
LightGBM[n]	0.712-0.788	0.712-0.788	0.712-0.788	0.712-0.788	0.712-0.788	0.712-0.788	0.700-0.800	0.833-0.921	0.806-0.891

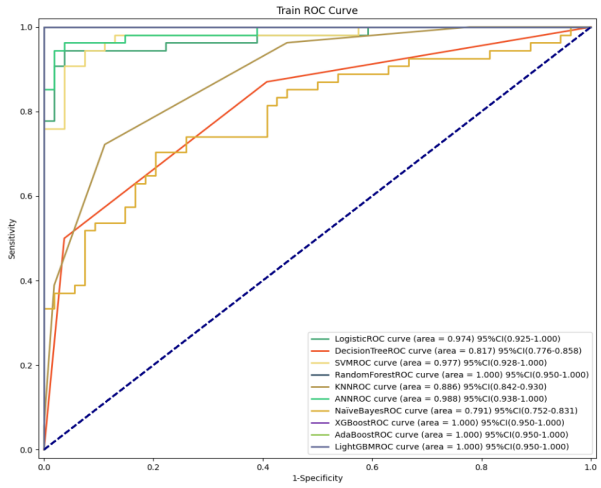
[a]PPV: positive predictive value.
[b]NPV: negative predictive value.
[c]AUC: area under the curve.
[d]AP: average precision.
[e]LR: logistic regression.
[f]DT: decision tree.
[g]SVM: support vector machine.
[h]RF: random forest.
[i]KNN: k-nearest neighbor.
[j]ANN: artificial neural network.
[k]NB: naive Bayes.
[l]XGBoost: extreme gradient boosting.
[m]AdaBoost: adaptive boosting.
[n]LightGBM: light gradient boosting machine.

To ensure that we considered both the precision and clinical applicability of our predictive models, we plotted the receiver operating characteristic (ROC) curve (Figure 5A and B), the PR curve (Figure 5C and D), and the DCA curve (Figure 5E). A comprehensive comparison indicated that the SVM prediction model demonstrated superior performance, with an accuracy of 0.875 (95% CI 0.825-0.925), an AUC of 0.974 (95% CI 0.925-1.000), and an AP of 0.964 (95% CI 0.916-1.000).

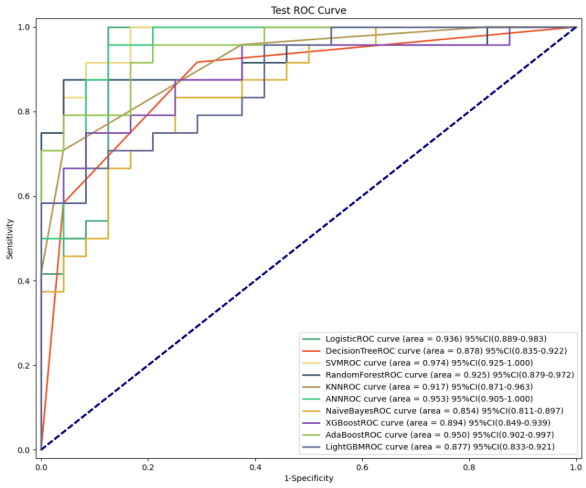
XSL•FO
RenderX

Figure 5. Comprehensive analysis of 10 machine learning models. (**A**) Training set ROC curve and (AUC), (**B**) test set ROC and AUC, (**C**) training set PR curves and AP, (**D**) test set PR curves and AP. The y-axis is the precision axis and the x-axis is the recall axis. If the PR curve of one model is completely covered by the PR curve of another model, the latter can be considered superior to the former; the higher the AP value, the better the model performance. (**E**) Test set DCA, where the black dashed line represents the hypothesis that all subjects are anemic, and the red dashed and thin black lines represent the hypothesis that all subjects are healthy. The remaining solid lines represent different models. The different colors in the pictures represent the corresponding models and the values are expressed as mean and 95% CI. AP: average precision; AUC: area under the curve; DCA: decision curve analysis; PR: precision-recall; ROC: receiver operating characteristic.

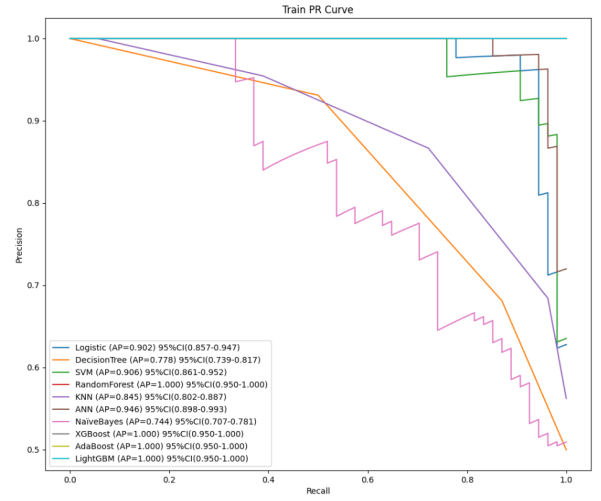
XSL•FO
RenderX



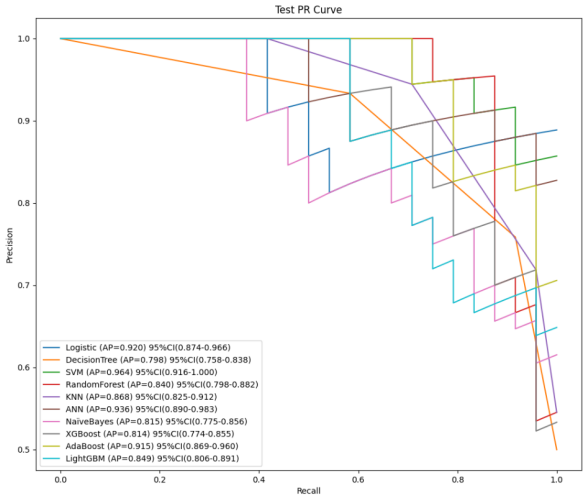
(A)



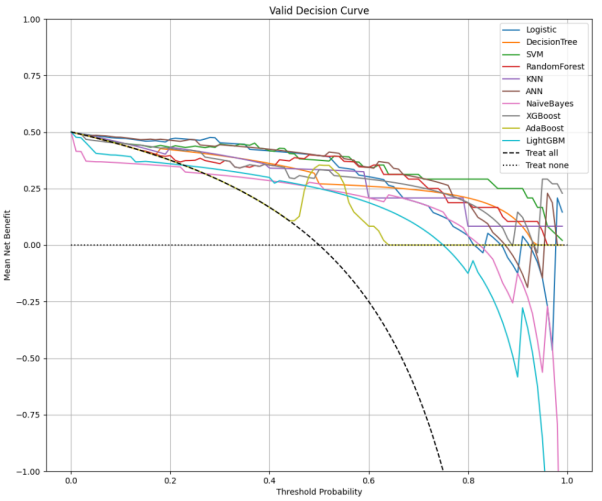
(B)



(C)



(D)



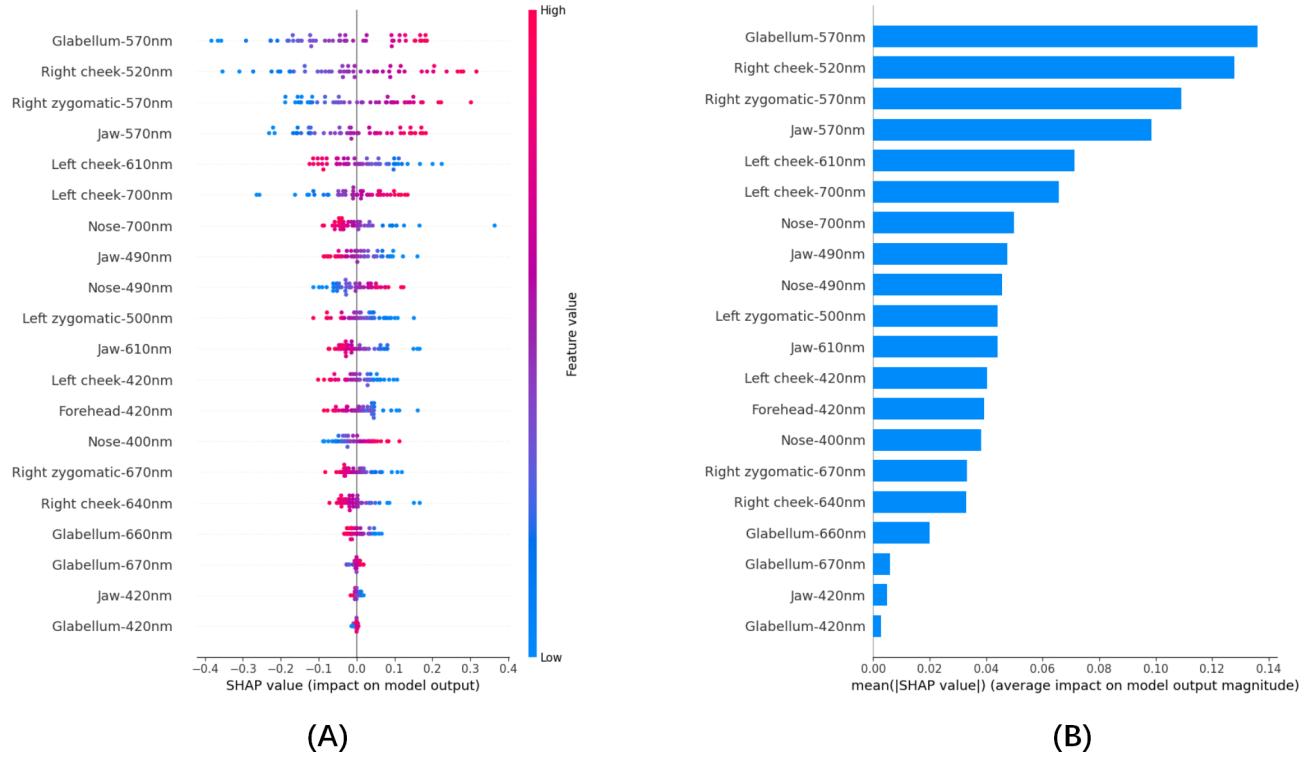
(E)

XSL•FO
RenderX

The SHAP to the Test Model Interpretation

Since the SVM classification produced the best results, to intuitively interpret the selected variables, we used SHAP to illustrate how these variables contribute to the diagnosis of anemia within the SVM algorithm [49]. Figure 6A displays the 20 features extracted by LASSO regression. The vertical axis orders the features according to the sum of SHAP values for all samples, and the horizontal axis represents the SHAP values (the distribution of the feature's impact on the model's output); each point represents a sample, with the sample size stacked vertically. In each feature importance line, the corresponding results for all subjects are plotted with points of different colors, where red points denote high-risk values and blue points denote low-risk values. The results indicate that glabellum-570 nm, right cheek-520 nm, right zygomatic-570 nm, jaw-570 nm, left cheek-700 nm, nose-490 nm, nose-400 nm, glabellum-670 nm, and glabellum-420 nm positively impacted the diagnosis of anemia, while left cheek-610 nm, nose-700 nm, jaw-490 nm, left zygomatic-500 nm, jaw-610 nm, left cheek-420 nm, forehead-420 nm, right zygomatic-670 nm, right cheek-640 nm, glabellum-660 nm, and jaw-420 nm negatively impacted the diagnosis of anemia. Figure 6B shows the ranking of the 20 risk factors assessed by the average absolute SHAP values, with the x-axis representing SHAP values that indicate the importance of the predictive model.

Figure 6. SHAP interprets the model. (**A**) Attributes of characteristics in SHAP. Each line represents a feature, and the abscissa is the SHAP value. Red dots represent higher eigenvalues and blue dots represent lower eigenvalues. (**B**) Feature importance ranking as indicated by SHAP. The matrix diagram describes the importance of each covariate in the development of the final prediction model. SHAP: Shapley additive explanations.



Discussion

Principal Results

The findings of this study revealed that the spectral reflectance at most characteristic facial sites and bands was significantly higher in the anemia group than in the healthy control group, with particularly notable increases at some specific sites and bands. Incorporating facial spectral data into the modeling dataset facilitates the creation of an improved classification model, building upon previous studies.

As depicted in Figure 2, reflectance at forehead 410 - 600 nm is higher in patients with anemia than in healthy controls. For the glabellum, nose, right zygomatic, right cheek, and left cheek, the spectral reflectance of patients with anemia from 400 - 700 nm is higher than that of healthy controls. Reflectance at jaw 430 - 610 nm, left zygomatic 400 - 540 nm, and 510 - 600 nm are higher than that of healthy controls. This study reveals a statistically significant increase in facial spectral reflectance among individuals with anemia compared to healthy controls. Several physiological mechanisms may contribute to the observed increase in reflectance.

First, changes in Hb concentration are a critical factor [50]. Hemoglobin, a light-absorbing component of blood, has a decrease in concentration with anemia, potentially enhancing light reflectance through tissues at specific wavelengths. This is particularly noticeable in the nose region. Second, alterations in blood oxygen saturation could play a role [51]. Reduced oxygen binding to Hb in anemic conditions could diminish the light absorption capacity, thereby increasing reflectance at certain wavelengths. It is feasible to use spectroscopy to detect skin oxygen saturation [52]. Additionally, anemia may induce changes in tissue moisture content, which in turn can modulate the optical behavior of tissues and influence light reflectance. The intensity of the absorption spectrum is proportional to the moisture content of the skin [53].

XSL•FO
RenderX

We used LASSO regression analysis to identify the 217 independent variables that showed statistically significant differences. This approach allowed us to compress variable coefficients and address collinearity issues, ultimately reducing the number of independent variables to 20. The selected variables, such as glabellum-570 nm, right cheek-520 nm, and left cheek-700 nm, highlight specific facial regions and wavelength bands that are associated with anemia risk. These findings suggest that certain spectral characteristics of the face may serve as indicators of anemia, warranting further investigation into the underlying physiological mechanisms.

To comprehensively analyze the classifiers in a multimodel comparison, we used 10 different ML algorithms, including logistic regression, decision tree, SVM, random forest, KNN, ANN, Bayesian classifier, XGBoost, adaptive boosting, and LightGBM. The performance of these models was evaluated using 2 distinct test sets, and the results indicated that the SVM prediction model demonstrated the best overall performance.

Within the SVM algorithm, we used the SHAP method to further explain the selected variables and their contribution to the diagnosis of anemia. The SHAP values provided intuitive insights into the impact of each feature on the model's output. For instance, glabellum-420 nm, 570 nm, and 670 nm; nose-400 nm and 490 nm; jaw-570 nm; right cheek-520 nm; right zygomatic-570 nm; and left cheek-700 nm positively impacted the diagnosis of anemia, while glabellum-660nm; forehead-420nm; jaw-420, 490, and 610 nm; nose-700 nm; right zygomatic-670 nm; left zygomatic-500nm; right cheek-640 nm; and left cheek-420 and 610 nm negatively impacted the diagnosis. These findings suggested that specific spectral characteristics may play a crucial role in distinguishing between anemic and healthy individuals.

Application and Advantages of Noninvasive Spectral Techniques in Anemia Diagnosis

According to the final model of this study, anemia was found to be strongly correlated with facial spectral reflectance at specific locations and bands. Therefore, incorporating facial spectral information into the modeling dataset can create a better classification model based on previous studies.

A plethora of studies have integrated advanced ML algorithms with spectral data, resulting in the development of predictive models that not only diagnose anemia but also predict the risk of disease onset in vulnerable populations. Noninvasive Hb measurement techniques have been developed to assess various sites on the human body, including fingers, palpebral conjunctiva, nail beds, bulbar conjunctiva, and other localized skin [32]. The ability to monitor Hb levels without the need for invasive procedures or complex equipment is expected to greatly enhance health care delivery in various settings, thereby contributing to the global effort to reduce the burden of anemia.

The face is not only the most exposed and conveniently assessable part of the human body but also holds significant importance in TCM diagnostics, where facial diagnosis plays a crucial role.

This study has unique advantages when targeting specific populations and environments. For particular groups, such as patients with anemia with low Hb levels, frequent invasive testing methods can lead to additional blood loss, therefore, using noninvasive spectroscopic detection technology can reduce the risk of blood loss. In specific environmental conditions, such as health check-ups for older individuals in the community, noninvasive spectral detection methods demonstrate their convenience and speed, with lower skill requirements for operators. Furthermore, in environments with a high incidence of infectious diseases, the implementation of noninvasive testing methods can significantly reduce the risk of group infections compared to traditional invasive testing techniques.

Based on the model of this study, strong correlations exist for facial spectral reflectance at specific locations and bands. Consequently, incorporating facial spectral information into the modeling dataset, building upon previous research, allows for the creation of an improved classification model. Given that pallor is often a common symptom of anemia [29,54-56], and the face is the most directly exposed part of the body, it serves as an important diagnostic tool. It is an important and intuitive diagnostic method. Therefore, it is necessary to establish a predictive model for anemia risk based on facial visible light reflection spectra. Future research will explore transitioning from contact spectroscopy to noncontact hyperspectral devices.

Limitations

This study possesses several limitations. First, the sample size is small, necessitating future studies to use larger, multicenter cohorts. Second, the study's focus on the middle-aged and older adult population suggests a need for future research to broaden the age range to enhance generalizability. Last, while facial coloration is influenced by various factors, this study controlled for common medical research variables. For the anemia group, additional physiological and biochemical markers that could affect facial coloration have not been considered. Future studies should aim to exclude the influence of such markers, including bilirubin, to provide a more comprehensive understanding of anemia-related facial spectral reflectance.

Conclusion

Facial spectral data of patients with anemia showed distinctive features and correlations. These indicators were of greater significance for the differential diagnosis of anemia, including specific bands such as the glabellum at 570 nm, the nose at 400 nm, the right zygomatic at 400 nm, the right cheek at 530 nm, the left zygomatic at 400 nm, and the left cheek at 700 nm. They emphasized the subtle differences in light absorption and reflection associated with different degrees of anemia. In conclusion, this study constructed a predictive model based on the ML model, and the SVM model demonstrated superior performance in this study. In addition, we provided a personalized risk assessment for the development of patients with anemia explained by SHAP. This effective computer-aided approach can help first-line clinicians and patients identify and intervene early in the case of anemia. It holds promise for future applications in noninvasive diagnosis and population screening for anemia-related conditions.

XSL•FO
RenderX

Acknowledgments

We thank our organization colleagues from Shanghai Jiading Community Health Center, Shanghai Gaohang Community Health Center, and Shanghai Hospital of Traditional Chinese Medicine. This research was funded by the National Natural Science Foundation of China (82104738, 82004255, and 82004258); General Program of China Postdoctoral Science Foundation (2023M732337); The Shanghai 2023 "Science and Technology Innovation Action Plan" Medical Innovation Research Special Project (number 23Y11921300); and The Shanghai 2022 “Science and Technology Innovation Action Plan” Medical Innovation Research Special Project (number 22Y11921100).

Data Availability

Data are contained within the article. The data presented in this study are available upon request from the corresponding author.

Authors' Contributions

YZ contributed to the conceptualization, methodology, validation, formal analysis, data curation, investigation, writing of the original draft, writing - review & editing, and visualization of the study. YC was involved in the conceptualization, methodology, validation, software development, data curation, investigation, writing of the original draft, writing - review & editing, and visualization. HF participated in the conceptualization, methodology, formal analysis, writing of the original draft, and writing - review & editing. WJ provided resources and acquired funding. JB provided resources. TJ contributed to the methodology. LC was responsible for project administration. XH was in charge of project administration. JC handled project administration. XQ provided resources. LT contributed to the methodology and provided resources. JX was involved in the methodology and provided resources. XQ, LT, and JX are the cocorresponding authors of this manuscript.

Conflicts of Interest

None declared.

Multimedia Appendix 1
Three-line table for all subjects.
[DOCX File, 32 KB - medinform_v13i1e64204_app1.docx]

References

1. World Health Organization. Metas mundiales de nutrición 2025: documento normativo sobre anemia [Website in Spanish]. 2017. URL: https://www.who.int/es/publications/i/item/WHO-NMH-NHD-14.4 [accessed 2024-09-25]
2. Safiri S, Kolahi AA, Noori M, et al. Burden of anemia and its underlying causes in 204 countries and territories, 1990-2019: results from the Global Burden of Disease Study 2019. J Hematol Oncol 2021 Nov 4;14(1):185. [doi: 10.1186/s13045-021-01202-2] [Medline: 34736513]
3. World Health Organization. Anaemia. 2023. URL: https://www.who.int/news-room/fact-sheets/detail/ANAEMIA [accessed 2024-09-26]
4. Gardner W, Kassebaum N. Global, regional, and national prevalence of anemia and its causes in 204 countries and territories, 1990–2019. Current Developments in Nutrition 2020 Jun;4:nzaa053. [doi: 10.1093/cdn/nzaa053_035]
5. Ruan Y, Guo Y, Kowal P, et al. Association between anemia and frailty in 13,175 community-dwelling adults aged 50 years and older in China. BMC Geriatr 2019 Dec 4;19(1):327. [doi: 10.1186/s12877-019-1342-5] [Medline: 31796000]
6. Balducci L. Epidemiology of anemia in the elderly: information on diagnostic evaluation. J Am Geriatr Soc 2003 Mar;51(3 Suppl):S2-S9. [doi: 10.1046/j.1532-5415.51.3s.4.x] [Medline: 12588565]
7. Palmer K, Vetrano DL, Marengoni A, et al. The relationship between anaemia and frailty: a systematic review and meta-analysis of observational studies. J Nutr Health Aging 2018;22(8):965-974. [doi: 10.1007/s12603-018-1049-x] [Medline: 30272101]
8. Kikuchi M, Inagaki T, Shinagawa N. Five-year survival of older people with anemia: variation with hemoglobin concentration. J Am Geriatr Soc 2001 Sep;49(9):1226-1228. [doi: 10.1046/j.1532-5415.2001.49241.x] [Medline: 11559383]
9. Morris SS, Ruel MT, Cohen RJ, Dewey KG, de la Brière B, Hassan MN. Precision, accuracy, and reliability of hemoglobin assessment with use of capillary blood. Am J Clin Nutr 1999 Jun;69(6):1243-1248. [doi: 10.1093/ajcn/69.6.1243] [Medline: 10357746]
10. Penninx B, Pahor M, Cesari M, et al. Anemia is associated with disability and decreased physical performance and muscle strength in the elderly. J Am Geriatr Soc 2004 May;52(5):719-724. [doi: 10.1111/j.1532-5415.2004.52208.x] [Medline: 15086651]
11. Roy CN. Anemia in frailty. Clin Geriatr Med 2011 Feb;27(1):67-78. [doi: 10.1016/j.cger.2010.08.005] [Medline: 21093723]

XSL•FO
RenderX

12. Astorga RS. Haemoglobin sensing with optical spectroscopy during minimally invasive procedures. J Biomed Opt 2015 Feb;20(2):021113. [doi: 10.1117/1.JBO.20.2.021113] [Medline: 25947829]
13. Robinson B. Cost of anemia in the elderly. J Am Geriatr Soc 2003 Mar;51(3 Suppl):S14-S17. [doi: 10.1046/j.1532-5415.51.3s.5.x] [Medline: 12588567]
14. Fowler AJ, Ahmad T, Phull MK, Allard S, Gillies MA, Pearse RM. Meta-analysis of the association between preoperative anaemia and mortality after surgery. Br J Surg 2015 Oct;102(11):1314-1324. [doi: 10.1002/bjs.9861] [Medline: 26349842]
15. Bateman ST, Lacroix J, Boven K, et al. Anemia, blood loss, and blood transfusions in North American children in the intensive care unit. Am J Respir Crit Care Med 2008 Jul 1;178(1):26-33. [doi: 10.1164/rccm.200711-1637OC] [Medline: 18420962]
16. Acharya S, Swaminathan D, Das S, et al. Non-invasive estimation of hemoglobin using a multi-model stacking regressor. IEEE J Biomed Health Inform 2020 Jun;24(6):1717-1726. [doi: 10.1109/JBHI.2019.2954553] [Medline: 31751256]
17. Yuan B, Yang Q. Spectroscopic Techniques and Applications Hangzhou: Zhejiang University Press; 2019.
18. Zhang Y, Wu X, He L, et al. Applications of hyperspectral imaging in the detection and diagnosis of solid tumors. Transl Cancer Res 2020 Feb;9(2):1265-1277. [doi: 10.21037/tcr.2019.12.53] [Medline: 35117471]
19. Zeng CC, Yang L, Xu Y, Liu PP, Guo SJ, Liu SH. Colorimetric investigation of normal tongue and lip colors from 516 healthy adults by visible reflection spectrum. Zhong Xi Yi Jie He Xue Bao 2011 Sep;9(9):948-954. [doi: 10.3736/jcim20110905] [Medline: 21906519]
20. Lunter D, Klang V, Kocsis D, Varga-Medveczky Z, Berkó S, Erdő F. Novel aspects of Raman spectroscopy in skin research. Exp Dermatol 2022 Sep;31(9):1311-1329. [doi: 10.1111/exd.14645] [Medline: 35837832]
21. Zuzak KJ, Schaeberle MD, Lewis EN, Levin IW. Visible reflectance hyperspectral imaging: characterization of a noninvasive, in vivo system for determining tissue perfusion. Anal Chem 2002 May 1;74(9):2021-2028. [doi: 10.1021/ac011275f] [Medline: 12033302]
22. Nadeau RG, Groner W. The role of a new noninvasive imaging technology in the diagnosis of anemia. J Nutr 2001 May;131(5):1610S-1614S. [doi: 10.1093/jn/131.5.1610S] [Medline: 11340126]
23. Kesarwani A, Das S, Dalui M, et al. Non-invasive anaemia detection by examining palm pallor: a smartphone-based approach. Biomed Signal Process Control 2023 Jan;79:104045. [doi: 10.1016/j.bspc.2022.104045]
24. Liu H, Peng F, Hu M, et al. Development and validation of a photoplethysmography system for noninvasive monitoring of hemoglobin concentration. Journal of Electrical and Computer Engineering 2020 Jan 18;2020:1-9. [doi: 10.1155/2020/3034260]
25. Mannino RG, Myers DR, Tyburski EA, et al. Smartphone app for non-invasive detection of anemia using only patient-sourced photos. Nat Commun 2018 Dec 4;9(1):4924. [doi: 10.1038/s41467-018-07262-2] [Medline: 30514831]
26. Bevilacqua V, Dimauro G, Marino F, et al. A novel approach to evaluate blood parameters using computer vision techniques. Presented at: 2016 IEEE International Symposium on Medical Measurements and Applications (MeMeA); May 15-18, 2016; Benevento, Italy p. 1-6. [doi: 10.1109/MeMeA.2016.7533760]
27. Kalantri A, Karambelkar M, Joshi R, Kalantri S, Jajoo U. Accuracy and reliability of pallor for detecting anaemia: a hospital-based diagnostic accuracy study. PLoS One 2010 Jan 1;5(1):e8545. [doi: 10.1371/journal.pone.0008545] [Medline: 20049324]
28. Wang EJ, Li W, Hawkins D, Gernsheimer T, Norby-Slycord C, Patel SN. HemaApp: noninvasive blood screening of hemoglobin using smartphone cameras. GetMobile: Mobile Comp and Comm 2017;21(2):26-30. [doi: 10.1145/3131214.3131223]
29. Stoltzfus RJ, Edward-Raj A, Dreyfuss ML, et al. Clinical pallor is useful to detect severe anemia in populations where anemia is prevalent and severe. J Nutr 1999 Sep;129(9):1675-1681. [doi: 10.1093/jn/129.9.1675] [Medline: 10460203]
30. Zhao C, Li GZ, Li F, Wang Z, Liu C. Qualitative and quantitative analysis for facial complexion in traditional Chinese medicine. Biomed Res Int 2014;2014:207589. [doi: 10.1155/2014/207589] [Medline: 24967342]
31. Lu LM, Chen X, Xu JT. Determination methods for inspection of the complexion in traditional Chinese medicine: a review. Zhong Xi Yi Jie He Xue Bao 2009 Aug;7(8):701-705. [doi: 10.3736/jcim20090801] [Medline: 19671406]
32. Kumar Y, Dogra A, Kaushik A, Kumar S. Progressive evaluation in spectroscopic sensors for non-invasive blood haemoglobin analysis-a review. Physiol Meas 2022 Mar 7;43(2). [doi: 10.1088/1361-6579/ac41b7] [Medline: 34883473]
33. Ge JB, Xu YJ, Wang C. Internal Medicine, 9th edition: People's Health Publishing House; 2018.
34. Cascio MJ, DeLoughery TG. Anemia: evaluation and diagnostic tests. Med Clin North Am 2017 Mar;101(2):263-284. [doi: 10.1016/j.mcna.2016.09.003] [Medline: 28189170]
35. Wang QQ, Yu SC, Qi X, et al. Overview of logistic regression model analysis and application. Zhonghua Yu Fang Yi Xue Za Zhi 2019 Sep 6;53(9):955-960. [doi: 10.3760/cma.j.issn.0253-9624.2019.09.018] [Medline: 31474082]
36. Kotsiantis SB. Decision trees: a recent overview. Artif Intell Rev 2013 Apr;39(4):261-283. [doi: 10.1007/s10462-011-9272-4]
37. Cervantes J, Garcia-Lamont F, Rodríguez-Mazahua L, Lopez A. A comprehensive survey on support vector machine classification: applications, challenges and trends. Neurocomputing 2020 Sep;408:189-215. [doi: 10.1016/j.neucom.2019.10.118]
38. Rigatti SJ. Random forest. J Insur Med 2017;47(1):31-39. [doi: 10.17849/insm-47-01-31-39.1] [Medline: 28836909]
39. Acito F. Predictive Analytics with KNIME: Analytics for Citizen Data Scientists: Waltham Press; 2023, Vol. 1st.

XSL•FO
RenderX

40. Štuikys V, Burbaitė R. Introduction to artificial neural networks and machine learning. In: Evolution of STEM-Driven Computer Science Education: The Perspective of Big Concepts: Springer Nature Switzerland; 2024:311-346 URL: https://link.springer.com/chapter/10.1007/978-3-031-48235-9_11 [accessed 2024-09-27] [doi: 10.1007/978-3-031-48235-9_11]
41. Xu S, Li Y, Wang Z, editors. Bayesian Multinomial Naïve Bayes Classifier to Text Classification Advanced Multimedia and Ubiquitous Engineering: Springer Singapore; 2017, Vol. 448:347-352. [doi: 10.1007/978-981-10-5041-1_57]
42. Ahmetoglu H, Das R. A comprehensive review on detection of cyber-attacks: data sets, methods, challenges, and future research directions. Internet of Things 2022 Nov;20:100615. [doi: 10.1016/j.iot.2022.100615]
43. Walker KW. Exploring adaptive boosting (AdaBoost) as a platform for the predictive modeling of tangible collection usage. The Journal of Academic Librarianship 2021 Dec;47(6):102450. [doi: 10.1016/j.acalib.2021.102450]
44. Fan J, Ma X, Wu L, Zhang F, Yu X, Zeng W. Light gradient boosting machine: an efficient soft computing model for estimating daily reference evapotranspiration with local and external meteorological data. Agric Water Manag 2019 Nov;225:105758. [doi: 10.1016/j.agwat.2019.105758]
45. Obuchowski NA, Bullen JA. Receiver operating characteristic (ROC) curves: review of methods with applications in diagnostic medicine. Phys Med Biol 2018 Mar 29;63(7):07TR01. [doi: 10.1088/1361-6560/aab4b1] [Medline: 29512515]
46. Li W, Guo Q. Plotting receiver operating characteristic and precision-recall curves from presence and background data. Ecol Evol 2021 Aug;11(15):10192-10206. [doi: 10.1002/ece3.7826] [Medline: 34367569]
47. Vickers AJ, Holland F. Decision curve analysis to evaluate the clinical benefit of prediction models. Spine J 2021 Oct;21(10):1643-1648. [doi: 10.1016/j.spinee.2021.02.024] [Medline: 33676020]
48. Sauerbrei W, Royston P, Binder H. Selection of important variables and determination of functional form for continuous predictors in multivariable model building. Stat Med 2007 Dec 30;26(30):5512-5528. [doi: 10.1002/sim.3148] [Medline: 18058845]
49. Lundberg SM, Lee SI. A unified approach to interpreting model predictions. Presented at: Proceedings of the 31st International Conference on Neural Information Processing Systems; Dec 4-9, 2017; Long Beach, California, USA.
50. Lister T, Wright PA, Chappell PH. Optical properties of human skin. J Biomed Opt 2012 Sep;17(9):90901-90901. [doi: 10.1117/1.JBO.17.9.090901] [Medline: 23085902]
51. Pothisarn W, Chewpraditkul W, Yupapin PP. Noninvasive hemoglobin-measurement-based pulse oximetry. SPIE/COS Photonics Asia. 2002. URL: https://api.semanticscholar.org/CorpusID:71998624 [accessed 2024-10-10]
52. van Manen L, Birkhoff WAJ, Eggermont J, et al. Detection of cutaneous oxygen saturation using a novel snapshot hyperspectral camera: a feasibility study. Quant Imaging Med Surg 2021 Sep;11(9):3966-3977. [doi: 10.21037/qims-21-46] [Medline: 34476182]
53. Gidado IM, Qassem M, Triantis IF, Kyriacou PA. Review of advances in the measurement of skin hydration based on sensing of optical and electrical tissue properties. Sensors (Basel) 2022 Sep 21;22(19):7151. [doi: 10.3390/s22197151] [Medline: 36236250]
54. Adeyemo TA, Adeyemo WL, Adediran A, Akinbami AJA, Akanmu AS. Orofacial manifestations of hematological disorders: anemia and hemostatic disorders. Indian J Dent Res 2011;22(3):454-461. [doi: 10.4103/0970-9290.87070] [Medline: 22048588]
55. Rojas Hernandez CM, Oo TH. Advances in mechanisms, diagnosis, and treatment of pernicious anemia. Discov Med 2015 Mar;19(104):159-168. [Medline: 25828519]
56. Mansour M, Donmez TB, Kutlu M, Mahmud S. Non-invasive detection of anemia using lip mucosa images transfer learning convolutional neural networks. Front Big Data 2023;6:1291329. [doi: 10.3389/fdata.2023.1291329] [Medline: 38025943]

Abbreviations

AdaBoost: adaptive boosting
ANN: artificial neural network
AP: average precision
AUC: area under the receiver operating characteristic curve
DCA: decision curve analysis
DT: decision tree
Hb: hemoglobin
KNN: k-nearest neighbor
LASSO: least absolute shrinkage and selection operator
LightGBM: light gradient boosting machine
LR: logistic regression
ML: machine learning
NPV: negative predictive value
PPV: positive predictive value
PR: precision-recall
RF: random forest

XSL•FO
RenderX

ROC: receiver operating characteristic
SHAP: Shapley additive explanations
SVM: support vector machine
TCM: traditional Chinese medicine
XGBoost: Extreme Gradient Boosting

Edited by A Benis; submitted 12.07.24; peer-reviewed by B Pei, P Zhang; revised version received 30.12.24; accepted 05.01.25; published 14.02.25.

Please cite as:
Zhang Y, Chun Y, Fu H, Jiao W, Bao J, Jiang T, Cui L, Hu X, Cui J, Qiu X, Tu L, Xu J
A Risk Warning Model for Anemia Based on Facial Visible Light Reflectance Spectroscopy: Cross-Sectional Study
JMIR Med Inform 2025;13:e64204
URL: https://medinform.jmir.org/2025/1/e64204
doi:10.2196/64204

© Yahan Zhang, Yi Chun, Hongyuan Fu, Wen Jiao, Jizhang Bao, Tao Jiang, Longtao Cui, Xiaojuan Hu, Ji Cui, Xipeng Qiu, Liping Tu, Jiatuo Xu. Originally published in JMIR Medical Informatics (https://medinform.jmir.org), 14.2.2025. This is an open-access article distributed under the terms of the Creative Commons Attribution License (https://creativecommons.org/licenses/by/4.0/), which permits unrestricted use, distribution, and reproduction in any medium, provided the original work, first published in JMIR Medical Informatics, is properly cited. The complete bibliographic information, a link to the original publication on https://medinform.jmir.org/, as well as this copyright and license information must be included.

XSL•FO
RenderX

Predicting Agitation-Sedation Levels in Intensive Care Unit Patients: Development of an Ensemble Model

Pei-Yu Dai[1], MS; Pei-Yi Lin[2], MS; Ruey-Kai Sheu[3], PhD; Shu-Fang Liu[2], MS; Yu-Cheng Wu[4], MD; Chieh-Liang Wu[4,5], PhD; Wei-Lin Chen[2,3], BS; Chien-Chung Huang[6], MS; Guan-Yin Lin[2], MS; Lun-Chi Chen[7], PhD

[1]Department of Digital Medicine, Taichung Veterans General Hospital, Taichung, Taiwan

[2]Department of Nursing, Taichung Veterans General Hospital, 1650 Taiwan Boulevard Sect. 4, Taichung, Taiwan

[3]Department of Computer Science, Tunghai University, Taichung, Taiwan

[4]Department of Critical Care Medicine, Taichung Veterans General Hospital, No 1650, Section 4, Taiwan Boulevard, Xitan District, Taichung City, Taiwan

[5]Department of Post-Baccalaureate Medicine, College of Medicine, National Chung Hsing University, Taichung, Taiwan

[6]Computer & Communications Center, Taichung Veterans General Hospital, Taichung, Taiwan

[7]College of Engineering, Tunghai University, Taichung, Taiwan

Corresponding Author:
Chieh-Liang Wu, PhD
Department of Critical Care Medicine, Taichung Veterans General Hospital, No 1650, Section 4, Taiwan Boulevard, Xitan District, Taichung City, Taiwan

Abstract

Background: Agitation and sedation management is critical in intensive care as it affects patient safety. Traditional nursing assessments suffer from low frequency and subjectivity. Automating these assessments can boost intensive care unit (ICU) efficiency, treatment capacity, and patient safety.

Objectives: The aim of this study was to develop a machine-learning based assessment of agitation and sedation.

Methods: Using data from the Taichung Veterans General Hospital ICU database (2020), an ensemble learning model was developed for classifying the levels of agitation and sedation. Different ensemble learning model sequences were compared. In addition, an interpretable artificial intelligence approach, SHAP (Shapley additive explanations), was employed for explanatory analysis.

Results: With 20 features and 121,303 data points, the random forest model achieved high area under the curve values across all models (sedation classification: 0.97; agitation classification: 0.88). The ensemble learning model enhanced agitation sensitivity (0.82) while maintaining high AUC values across all categories (all >0.82). The model explanations aligned with clinical experience.

Conclusions: This study proposes an ICU agitation-sedation assessment automation using machine learning, enhancing efficiency and safety. Ensemble learning improves agitation sensitivity while maintaining accuracy. Real-time monitoring and future digital integration have the potential for advancements in intensive care.

(JMIR Med Inform 2025;13:e63601) doi:10.2196/63601

KEYWORDS

intensive care units; ICU; agitation; sedation; ensemble learning; machine learning; ML; artificial intelligence; AI; patient safety; efficiency; automation; ICU care; ensemble model; learning model; explanatory analysis

Introduction

Patients admitted to intensive care units (ICUs) often experience various clinical problems, such as pain, agitation, and delirium. Agitation refers to physical restlessness due to treatment discomfort or delirium; this condition cannot be self-controlled [1]. Agitation is common in patients in ICUs; most of these patients (71%) exhibit agitation on approximately 58% of their total inpatient days [2-4]. Agitation can lead to the accidental removal of tubes and catheters, compromising patient safety, extending ICU stays, and causing complications [5]. Throughout the treatment period, nurses must regularly evaluate the levels of agitation and sedation and titrate the dosages of sedatives accordingly for patient care.

Various scales have been developed for measuring sedation effects. Among them, the Richmond Agitation-Sedation Scale (RASS) is the most reliable and effective [6]. This scale was developed by a multidisciplinary team at Virginia Commonwealth University in Richmond. It employs a simple and clearly defined scoring system with distinct standards for

XSL•FO
RenderX

measuring the levels of sedation and agitation. Agitation and sedation levels are represented by positive and negative scores, respectively. The RASS assessment is performed by nurses every few hours, which consumes their significant work time. Reducing the time required for RASS evaluations could increase ICU treatment capacity, thereby improving care quality and patient safety.

However, this scale has some disadvantages, such as low evaluation frequency and high subjectivity, due to variations in patient evaluation standards among medical personnel. Occasionally, nurses may have insufficient knowledge about delirium, which can increase the risk of incorrect evaluations by 20 times [7]. Furthermore, errors in evaluation of patient conditions may result in excessive or insufficient sedation. These issues can be attributed to the subjectivity and uncertainties in the RASS evaluation process, which relies on patients' audiovisual responses, making it is unsuitable for those with severe audiovisual impairment [8]. The RASS facilitates intermittent measurement of agitation levels and assessment of patient behavior; however, unlike activity monitors, it cannot assist in the continuous monitoring of agitation levels [9].

The study's aim was to develop an ensemble learning model for the continuous evaluation of agitation and sedation levels in patients admitted to ICUs. The model is expected to facilitate patient monitoring, provide early warnings about patient behavior, increase assessment frequency, and enable automatic evaluation of patient conditions with treatment suggestions. We believe that this novel design could improve the clinical monitoring of agitation and sedation levels in patients in ICUs, enhance the quality of medical care, and reduce the wastage of medical resources.

Methods

Setting

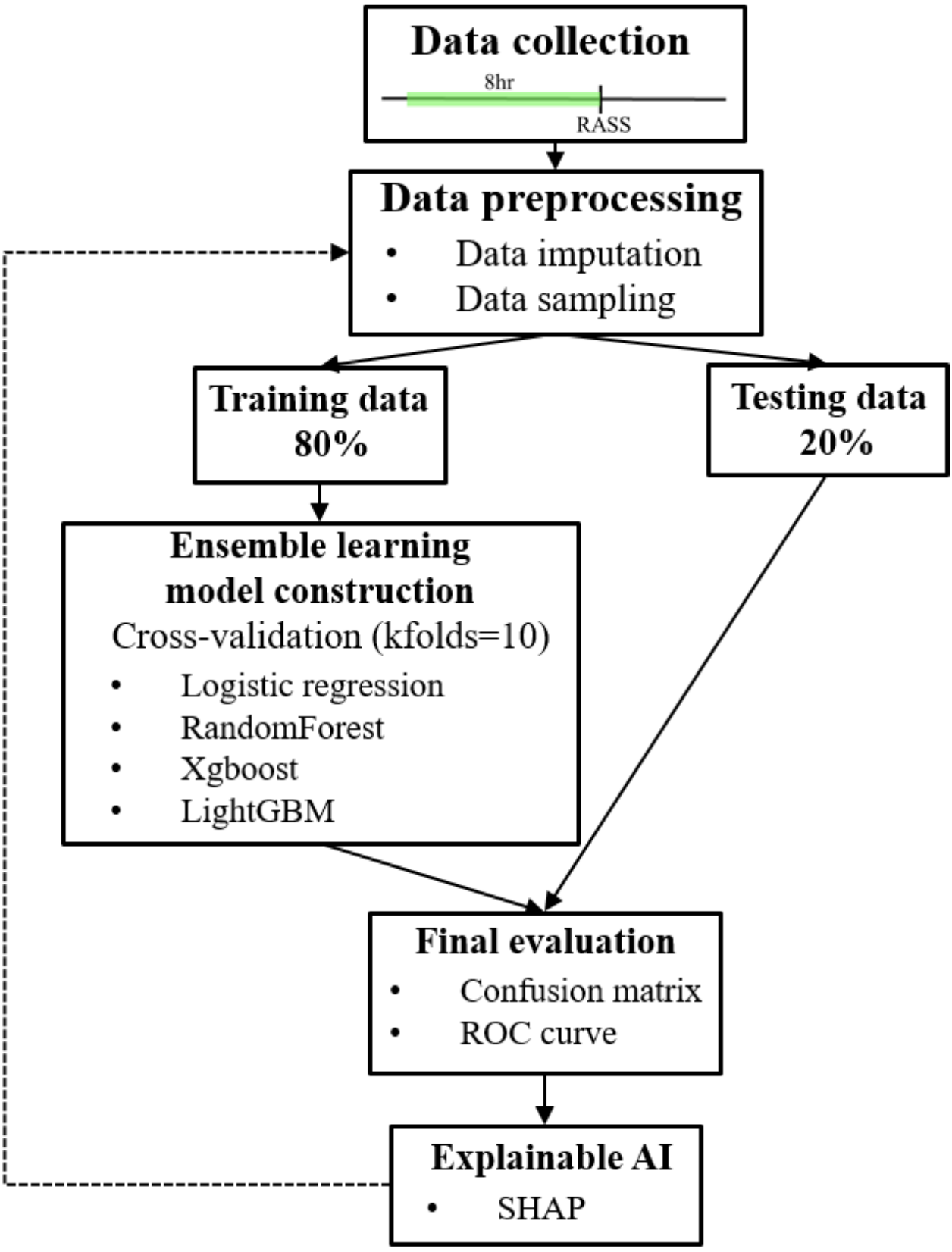
Taichung Veterans General Hospital (TCVGH) is a 1530-bed medical center in central Taiwan with 7 ICUs comprising a total of 138 beds. We obtained access to the critical care database (AI-111010) of the AI Center of TCVGH. The following data were collected: basic information, disease severity, ventilator use, blood biochemistry, vital signs, catheter types, and medication records.

Research Framework

The study consisted of five major steps: (1) data collection in the ICU, (2) data preprocessing (data imputation and data sampling), (3) ensemble learning model construction, (4) final evaluation, and (5) implementation of explainable AI (Figure 1).

XSL•FO
RenderX

Figure 1. Research framework consisted of 5 steps: (1) data collection in the ICU, (2) data preprocessing (data imputation, data sampling), (3) ensemble learning model construction, (4) final evaluation, (5) explainable AI. AI: artificial intelligence; RASS: Richmond Agitation–Sedation scale; ROC: receiver operating characteristic; SHAP: Shapley additive explanations.



XSL•FO
RenderX

Data Preprocessing

Data Imputation

Basic information includes patients' age. Predicting RASS in older patients is more challenging. Regarding disease severity, patients' acute physiology and chronic health evaluation (APACHE II) scores may impact their predicted RASS scores [6,10]. Missing data were imputed using average values.

In addition, the use of ventilators was considered. Ventilator modes were categorized into 3 conditions: no ventilator use, noninvasive ventilator use, and invasive ventilator use. Invasive ventilators may cause discomfort, indirectly affecting RASS scores [8,10-12]. Furthermore, PAW (average airway pressure) values, a ventilator parameter, were estimated accordingly. For patients on ventilators, the average value from all ventilator-wearing patients was used to impute missing data, whereas patients without ventilators were assigned normal random values.

In the category of blood biochemistry, features such as creatinine, lactate, and glucose were included. These were directly associated with patients' physiological conditions [10]. Typically, blood tests were conducted weekly within a 7-day data window. When no blood test data were available within this timeframe, indicating stable patient condition, normal random values were used for imputation.

Vital signs, including blood pressure, pulse rate, and respiratory rate, were indirectly associated with changes in patients' RASS scores [13]. Since vital signs were densely and continuously monitored features, adjacent values were used to fill in missing data directly.

Medication records included the type and dosage of sedatives and analgesics administered to patients, such as benzodiazepine sedatives, muscle relaxants, opioid-related analgesics, antipsychotics, hypnotics, and anesthetics. These drugs can directly or indirectly influence patients' consciousness levels and RASS score changes. Due to the varying recording methods for drug dosage across different types of medications, establishing a consistent standard was challenging. Therefore, in this study, the presence or absence of records indicating the use of muscle relaxants or sedative-hypnotics within the past 8 hours was used as a feature for RASS assessment.

Data Sampling

To address severe data imbalance issues (oversedation: 43,199 cases, maintain range: 77,290 cases, agitation: 814 cases), this study employed data oversampling and undersampling techniques to enhance model learning effectiveness. In addition, discussions with clinical experts were conducted to determine the most suitable sampling approach.

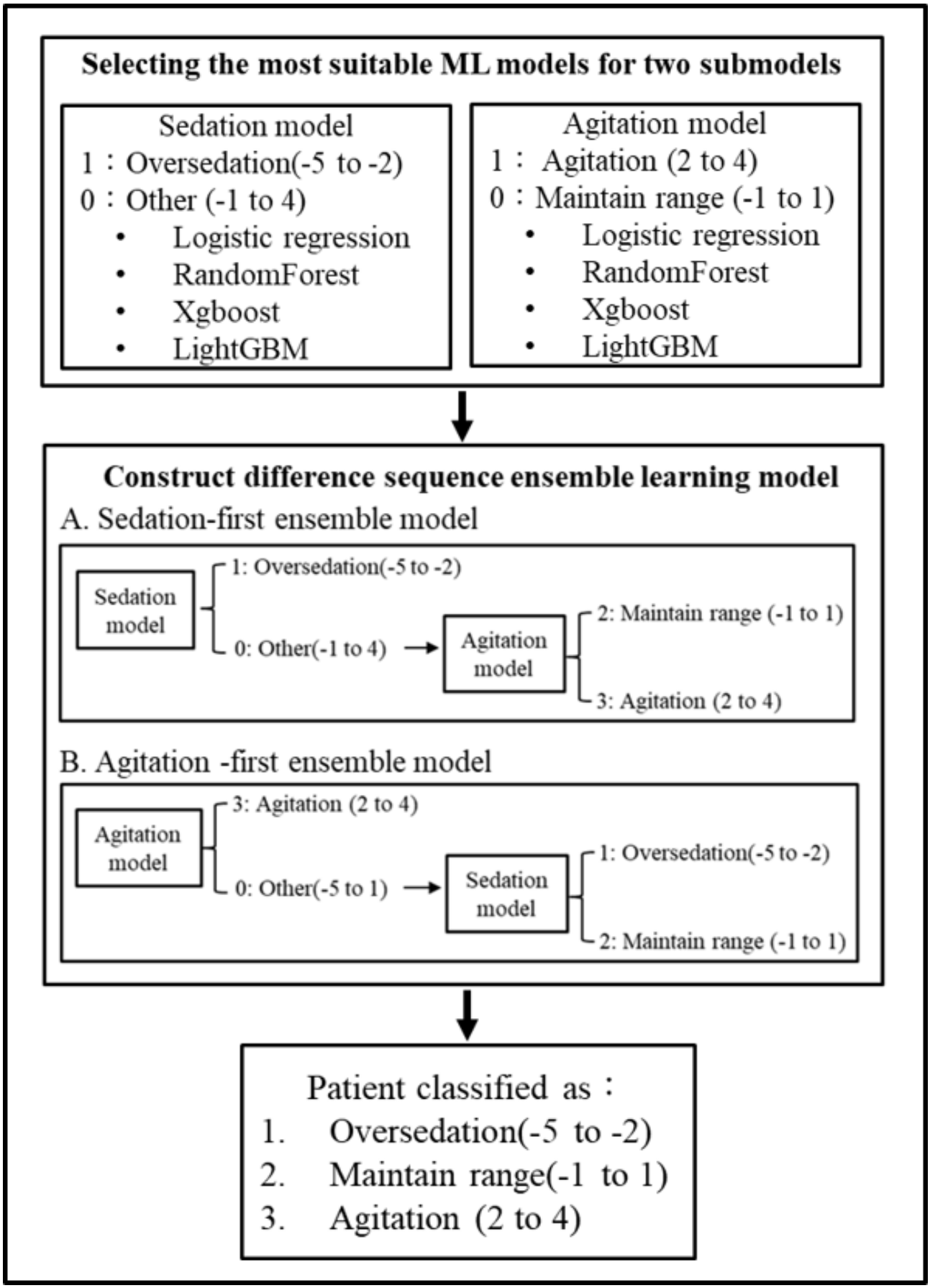
Model Construction

Based on clinical care experience, this study proposed an ensemble learning model that integrates two submodels—sedation and agitation—to classify events into oversedation (RASS -5 to -2), maintain range (clinically expected maintenance RASS -1 to 1), and agitation (RASS 2 to 4).

First, the sedation and agitation models were constructed using 4 ML algorithms: logistic regression, random forest, XGBoost, and LightGBM. The algorithm with the best performance was selected as the foundation for both the sedation and agitation models. Subsequently, the two submodels were combined into 2 sequential ensemble learning models: the sedation-first ensemble model and the agitation-first ensemble model. In the sedation-first model, the sedation model was first used to distinguish "oversedation" from "other," and the remaining categories were then input into the agitation model to further differentiate between "maintain range" and "agitation." Conversely, in the agitation-first model, the agitation model was first applied to separate "agitation" from "other," and the remaining categories were then passed into the sedation model to classify "oversedation" and "maintain range." (Figure 2).

XSL•FO
RenderX

Figure 2. Ensemble model construction consisted of 3 steps: (1) Choose a more suitable ML model, (2) Construct difference sequence ensemble learning model, (3) Classify patient into three categories. ML: machine learning



XSL•FO
RenderX

Final Evaluation

We used confusion matrices and the receiver operating characteristic (ROC) curves as indicators to evaluate model accuracy, precision, recall, F1-score, and area under the curve. The ROC curves helped to compare sensitivity with specificity. Effective models exhibited high sensitivity and specificity, resulting in high area under the curve values.

Explainable AI

Explainable Artificial Intelligence (XAI) was applied, making the ML system transparent. The top 20 features were selected, and Shapley additive explanations and partial dependence plots were used to visualize their contributions, aiding in understanding the model's decision-making process. Clinical personnel could use this information to offer patient-specific evaluations or decision-making suggestions.

Statistics

This study used statistical methods, including mean (SD) and *t*-test, for numerical data analysis and observation. These methods were used to describe dataset central tendencies, assess variability, and compare group differences. Proportions of each category were also calculated for categorical data. They helped to extract meaningful information and interpret research results.

Ethical Considerations

This study was approved by the TCVGH Institutional Review Board (CE22484A). Informed consent was obtained, with participants given the option to withdraw at any time. For secondary analyses, original consent covered data reuse without additional approval. Data were anonymized to protect privacy, and strict security measures were applied.

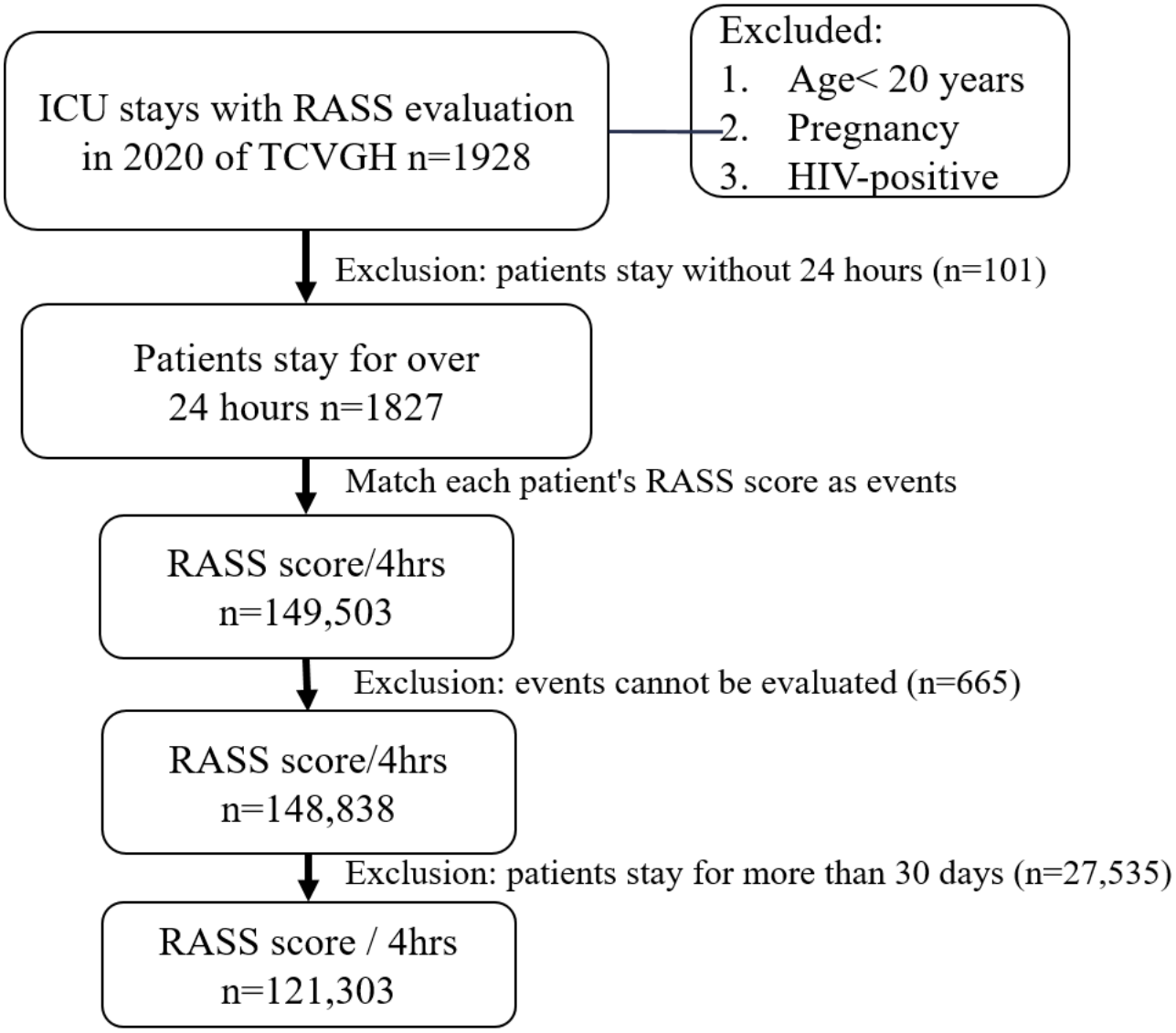
Results

Data Collection

This study collected data from adult patients (aged≥20 years) admitted to the ICU at TCVGH between January 1 and December 31, 2020, with an ICU stay lasting more than 24 hours. Every 4-hour RASS assessment (with increased frequency depending on the patient's condition) was considered as a classification event, with events marked as not assessable excluded due to concurrent procedures. Since the average ICU stay did not exceed 30 days, events from ICU stays longer than 30 days were also excluded. A total of 121,306 events were collected, with an average of 108 events per patient (range: 6 to 186). The machine learning (ML) model was trained using data from the 8 hours prior to each event, including ventilator parameters, vital signs, and medication records, along with laboratory biochemical data from the previous week (Figure 3).

XSL•FO
RenderX

Figure 3. Flowchart of subject enrollment. ICU: intensive care unit; RASS: Richmond Agitation–sedation scale; TCVGH: Taichung Veterans General Hospital.



Feature Selection

Based on the literature and clinical experience, the feature selection process in this study involved in-depth discussions with physicians and nurses. During this process, the missing rate of each feature was considered, and features with a missing rate exceeding 20% were excluded. Finally, 23 features were selected, and appropriate imputation methods were applied (Table 1). Categorical features (eg, ventilator modes and medications) were defined based on the presence of recorded events within the past 8 hours. Continuous features such as vital signs and ventilator parameters were calculated as the average values over the past 8 hours, while laboratory test features were based on the most recent record within the past week.

XSL•FO
RenderX

Table . All features used in model training, including their respective units, missing rates, and data imputation methods aligned with clinical requirements.

Projects and features	Unit	Missing rate (%)	Imputation method
Basic Information			
Age	years	0.0	None
Disease severity			
APACHE[a] II	score	2.4	Average
Use of ventilator	__[b]	0.0	None
Ventilation Mode	—		
No ventilation (0)	—		
Noninvasive ventilation (1)	—		
Invasive ventilation (2)	—		
Average airway pressure (Paw)	cmH_2O	5.0	Average/Normal Range (Random)
Blood biochemical test data			Normal Range (Random)
BUN[c]	mg/dL	4.8	
Creatinine	mg/dL	2.0	
Glucose (One touch)	mg/dL	2.7	
Bicarbonate (HCO_3)	mmol/L	11.8	
Hematocrit (Hct)	%	12.7	
Hemoglobin (Hgb)	g/dL	0.2	
Potassium (K)	mEq/L	0.2	
Lactate	mg/dl	17.3	
Phytohemagglutinin (PH_A)	value	12.7	
Sodium (Na)	mEq/L	12.7	
Platelets (PLT)	thou/mm^3	0.2	
Partial pressure of oxygen (PO_2)	mmHg	4.1	
White blood cells (WBC)	thou/mm^3	0.3	
Vital signs			Pre and post values
Systolic blood pressure (SBP)	mmHg	0.1	
Diastolic blood pressure (DBP)	mmHg	0.1	
Respiratory rate (RR)	bpm	0.1	
Blood oxygen saturation (SPO_2)	%	0.0	
Pulse	bpm	0.0	
Medication records		0.0	None
Medicine	—		
No (0)			
Yes (1)			

[a]APACHE: acute physiology and chronic health evaluation.

[b]Not applicable.

[c]BUN: blood urea nitrogen.

Description of the Study Population

Statistical analysis indicated that nearly all features significantly affect the level of agitation-sedation. Patients with oversedation typically exhibited higher disease severity, lower blood oxygen levels, and a higher proportion of invasive ventilator use. In contrast, patients with agitation showed higher vital sign values and a greater proportion of sedative medication usage (Table 2).

XSL•FO
RenderX

Table . Statistical analysis of datasets used to train the two models. Proportion: Percentage of Population

	Overall (N=121,303)	Oversedation (n=43,199)	Maintain range (n=77,290)	Agitation (n=814)	*P* value
Numerical features, mean (SD)					
Age	67.5 (14.9)	68.21 (5.2)	67.2 (14.8)	66.1 (15.3)	<.001
APACHE[a] II	23.9 (7)	26.4 (6.6)	22.5 (6.8)	23.2 (6.2)	<.001
Average airway pressure (Paw)	22.0 (5.7)	23.6 (6.2)	21.1 (5.1)	21.3 (4.9)	<.001
BUN[b]	39.8 (30.6)	45.1 (33.7)	36.8 (28.4)	34.7 (26.7)	<.001
Creatinine	2.0 (2.2)	2.1 (2.2)	1.9 (2.2)	1.9 (2.2)	<.001
Glucose (One touch)	168.8 (49.4)	175.5 (53.1)	165.2 (46.8)	162.9 (46.9)	<.001
Bicarbonate (HCO_3)	24.1 (4.7)	23.4 (5.1)	24.5 (4.4)	24.8 (4.7)	<.001
Hematocrit (Hct)	30.9 (7.1)	30.9 (7.6)	30.9 (6.8)	32.2 (7)	.14
Hemoglobin (Hgb)	9.7 (1.9)	9.6 (2)	9.8 (1.8)	10.1 (1.9)	<.001
Potassium (K)	3.9 (0.6)	4.0 (0.6)	3.9 (0.5)	3.9 (0.6)	<.001
Lactate	17.7 (16.6)	22.4 (21.4)	15.1 (12.4)	18.0 (20.4)	<.001
Phytohemagglutinin (PH_A)	7.4 (0.1)	7.4 (0.1)	7.4 (0.1)	7.4 (0.1)	<.001
Sodium (NA)	140.3 (6.5)	141.0 (6.9)	139.9 (6.2)	141.4 (6.4)	<.001
Platelets (PLT)	187.8 (114.5)	175.3 (108.2)	194.7 (117.3)	201.1 (115.5)	<.001
Partial pressure of oxygen (PO_2)	124.2 (50.2)	120.4 (49.6)	126.3 (50.4)	121.5 (53.7)	<.001
White blood cells (WBC)	12394.1 (12277)	13764.4 (15679.1)	11636.5 (9854)	11601.5 (6364.6)	<.001
Systolic blood pressure (SBP)	123.2 (19.4)	119.5 (19.7)	125.2 (18.9)	126.2 (18.5)	<.001
Diastolic blood pressure (DBP)	70.1 (12.7)	67.4 (13)	71.6 (12.2)	73.7 (11.8)	<.001
Respiratory rate (RR)	18.8 (4.2)	19.7 (4.9)	18.2 (3.7)	19.1 (3.9)	<.001
SPO_2	97.2 (7.2)	95.9 (10.9)	97.9 (3.7)	97.2 4)	<.001
Pulse	88.7 (17.8)	90.4 (19.3)	87.7 (16.8)	93.2 (18.5)	<.001
Categorical features, n (%)					
Medicine (Yes)	26,787 (22%)	8,601 (20%)	17,658 (23%)	528 (65%)	<.001
Invasive ventilation	92,257 (76%)	40,168 (93%)	51,505 (67%)	584 (72%)	<.001
Noninvasive ventilation	5937 (5%)	587 (1%)	5295 (7%)	55 (7%)	<.001
No ventilation	23,109 (19%)	2444 (6%)	20,490 (26%)	175 (21%)	<.001

[a]APACHE: acute physiology and chronic health evaluation.

[b]BUN: blood urea nitrogen.

Model Development and Validation

Data Sampling of Agitation Classification

Given the significant class imbalance observed (Table 2), we explored various data sampling methods to enhance the model's sensitivity (recall) for detecting agitated patients. Among these methods, the undersampling approach demonstrated the most notable performance, achieving a sensitivity of 0.82 (Table 3). Consequently, we selected the undersampling method as the data processing strategy.

XSL•FO
RenderX

Table . Random forest model performance of different sampling methods for agitation category patients.

Classification	Sampling method (number of patients)	Precision	Recall	F1 score
Agitation Model	Non (n=77288, 814)	0.81	0.26	0.39
	Undersampling (n=642,642)	0.03	0.82	0.06
	SMOTE[a] (n=61834, 61834)	0.28	0.24	0.26

[a]SMOTE: synthetic minority oversampling technique

Performance Comparison of Two Submodels in ML Models

The results of the confusion matrices and ROC curves for the 4 ML models (as shown in Table 4) indicate that the random forest model outperformed the others in both the sedation prediction (accuracy: 0.92, AUC: 0.96) and agitation prediction (accuracy: 0.80, AUC: 0.88). Additionally, the random forest model exhibited superior sensitivity (recall) for detecting agitated patients. Consequently, we selected the random forest model as the foundation for constructing various ensemble learning frameworks to facilitate further analysis and applications.

Table . Four different ML models performance comparison of sedation classification and agitation classification.

Classification and models	Accuracy	Precision	Recall	AUC[a]	Cross-validation Avg-ACC[b] (kfold=10)
Sedation					
Logistic regression	0.72	0.71	0.65	0.71	0.71
Random forest	0.92	0.91	0.91	0.96	0.92
XGBoost[c]	0.92	0.91	0.91	0.94	0.90
LGBM[d]	0.83	0.81	0.83	0.90	0.84
Agitation					
Logistic regression	0.64	0.51	0.61	0.72	0.66
Random forest	0.80	0.03	0.82	0.88	0.77
XGBoost	0.76	0.51	0.76	0.84	0.73
LGBM	0.75	0.51	0.77	0.85	0.75

[a]AUC: area under the curve.

[b]ACC: accuracy.

[c]XGBoost: extreme gradient boosting.

[d]LGBM: light gradient-boosting machine.

Ensemble Learning Model Performance Comparison

The performance results of different sequences of ensemble learning models indicate that prioritizing the identification of agitated patients is more effective in improving sensitivity (recall: 0.82) compared to strategies that first identify oversedated patients. Furthermore, the AUC for all 3 states remained above 0.82 (as shown in Table 5. Given the higher immediate risk associated with agitated patients, the agitation-first ensemble model was selected as the most suitable approach.

XSL•FO
RenderX

Table . Comparison of performance in classifying the three categories among ensemble learning models with different sequences.

Classification sequence and categories	Accuracy	Precision	Recall	AUC[a]
Sedation-first ensemble model	0.79			
Oversedation		0.91	0.84	0.90
Maintain range		0.92	0.84	0.82
Agitation		0.03	0.76	0.81
Agitation-first ensemble model	0.75			
Oversedation		0.92	0.73	0.85
Maintain range		0.92	0.76	0.82
Agitation		0.03	0.82	0.82

[a]AUC: area under the curve.

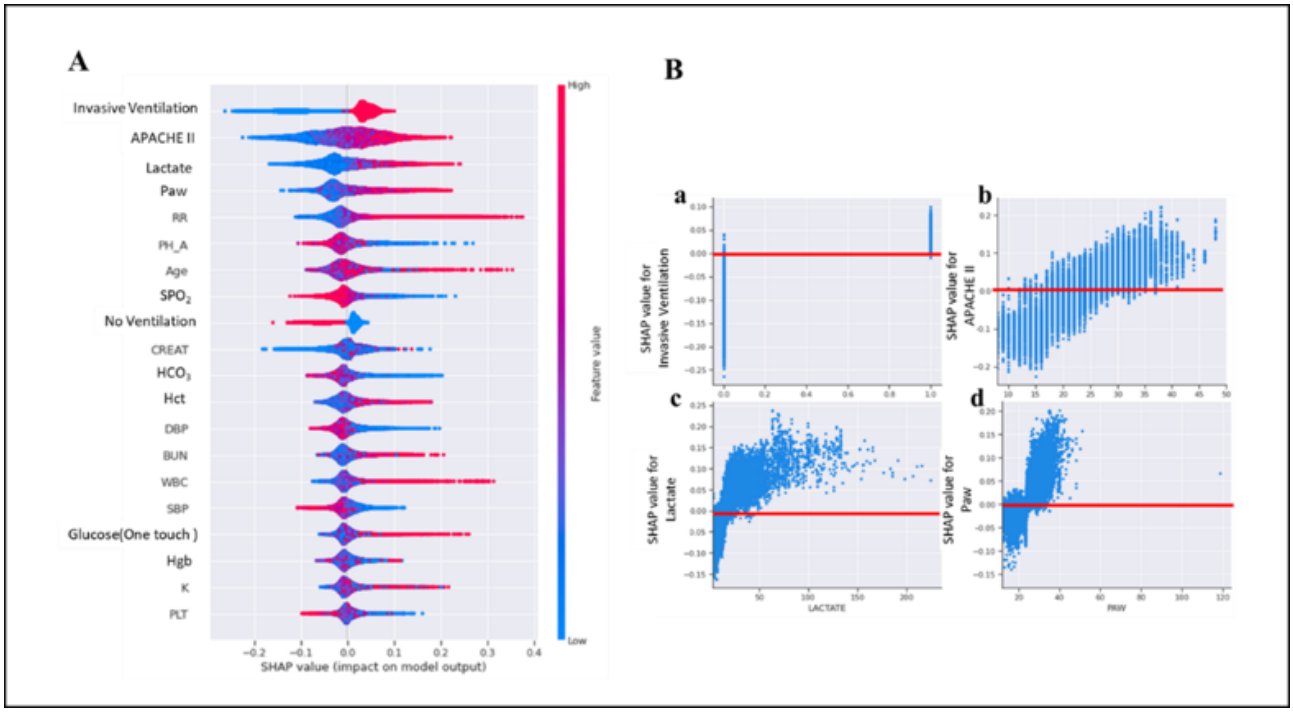
Explainable AI (XAI)

The top 4 features that contribute the most to sedation classification are the use of an invasive ventilator (invasive ventilation), APACHE II score, lactate level (LACTATE), and average airway pressure (PAW). A high APACHE II score indicates a high likelihood of oversedation (Figure 4A). The dependency graph of the first 4 features represents how each feature affects the classification results. In most cases, an APACHE II score>29 was positively associated with oversedation (Figure 4B).

Patients who used sedatives were more likely to experience agitation. Patients with a high hemoglobin level were more likely to experience agitation. The dependence plots of the top 4 features indicated that sedative use was positively correlated with agitation. Hemoglobin levels >10 g/dL and≤10 g/dL were positively correlated with agitation and maintained sedation range, respectively (Figure 5).

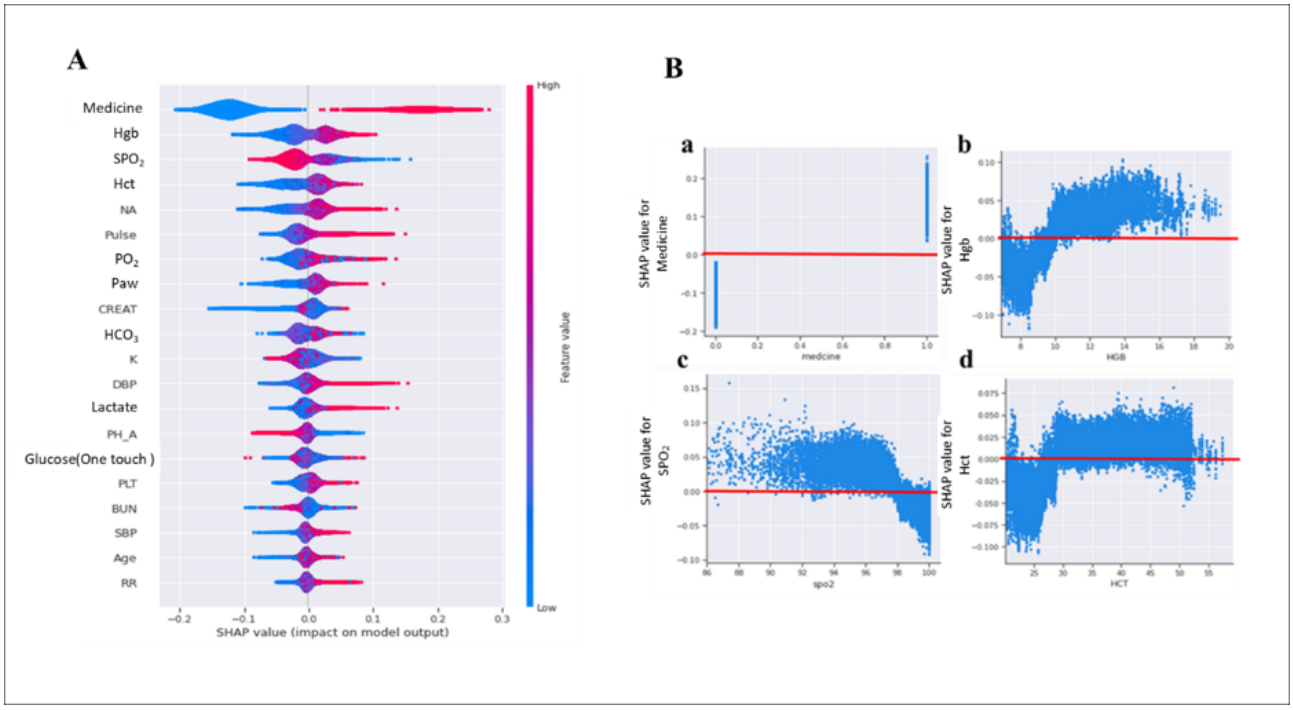
Overall, patients on mechanical ventilation were mostly sedated, with those in the maintain range exhibiting more stable blood test results and vital signs compared to oversedated or agitated patients.

Figure 4. The explanations of features contribution to sedation classification. (A) The attributes of the features in the model. Each line represents a feature, and the abscissa is the SHAP value. Red dots represent higher feature values, and blue dots represent lower feature values. (B) SHAP dependence plot for the top 4 clinical features contributing to the model. APACHE: acute physiology and chronic health evaluation; Paw: average airway pressure.



XSL•FO
RenderX

Figure 5. The explanations of features contribution to agitation classification. (A) The attributes of the features in the model. Each line represents a feature, and the abscissa is the SHAP value. Red dots represent higher feature values, and blue dots represent lower feature values. (B) SHAP dependence plot for the top 4 clinical features contributing to the model. HCT: hematocrit; Hgb: hemoglobin; SpO_2: blood oxygen saturation.



Discussion

Principal findings

This study successfully developed a model for automating RASS-like agitation-sedation evaluation. Automated agitation-sedation evaluation could be an alternative to RASS and play a crucial role in enhancing ICU efficiency, ultimately improving health care outcomes, care quality, and patient safety.

Machine learning aids ICU personnel in the early detection of high-risk events [14]. Previous studies have used ML to predict mortality rates in ICU patients with acute kidney injury, predict postoperative sepsis mortality rates, and forecast extubation failure in the ICU [15-17]. However, studies on ML for agitation-sedation evaluation in ICU patients are limited.

Zhang et al [18] ensemble 4 machine-learning methods for predicting agitation in ventilated patients under light sedation for 24 hours. However, their ensemble model was limited to predicting agitation in patients with invasive ventilator support under light sedation for 24 hours. Other researchers have proposed using patient body and facial image monitoring for agitation detection [19,20]. However, image monitoring faces challenges such as data acquisition, clinical environment influences, workflow integration, and system installation. Therefore, in addition to the imaging model developed by our research team [21], we have created another model using commonly available feature data in most hospitals, serving as an alternative solution when image monitoring is not feasible.

The study employs 2 ML models for ensemble learning to automate RASS assessment. By using undersampling and adjusting the classification sequence, the sensitivity for detecting agitation is enhanced. Although models with higher sensitivity may reduce the accuracy of classifying over-sedated patients, they perform better in mitigating immediate risks. Traditional methods, which involve manual assessments every 4 hours, result in insufficient monitoring, especially for patients who may experience multiple episodes of agitation within a short period. In contrast, our health care information system can transmit data in real time, perform inference every hour, and adjust inference frequency based on clinical needs, enabling more intensive monitoring. This allows clinicians to track patient conditions and respond promptly to changes continuously.

Understanding algorithmic predictions is crucial in clinical practice. Due to the lack of explanations in the decision-making process, clinicians often distrust black-box models. Explainable artificial intelligence enhances transparency, aiding in the development of reliable decision models [22-24]. Continuous analgesics and sedatives ensure optimal gas exchange between patients and ventilators, making deep sedation important during this period [25]. For patients with stable parameters such as hemoglobin, hematocrit, blood oxygen saturation, and creatinine, the goal is maintaining light sedation (RASS score 0 to −2) [26]. It has been demonstrated that the interpretability of the model aligns with clinical experience.

This study acknowledges its limitations, particularly the imbalance in case numbers due to the high risk of agitation in patients. Especially for agitated individuals, the model's precision of 0.03 suggests there is room for improvement. In future clinical applications, we plan to adjust the decision threshold based on specific needs to balance sensitivity and specificity and reduce false positives. Additionally, the study lacks observations of potential drug overdoses at different sedation levels. Future efforts will focus on integrating this model with digital imaging monitoring and a comprehensive drug dosage system. Real-time monitoring will help identify

XSL•FO
RenderX

patient conditions, guide prescription adjustments, and accelerate recovery, ultimately supporting early intervention, ensuring patient safety, and improving the quality of intensive care.

Conclusions

This study proposes using ML technology to achieve automated RASS-based assessments in ICU settings, enhancing clinical efficiency, and patient safety. Our integrated learning model, combined with the hospital information system, enables real-time data transmission, supports intensive monitoring, and facilitates continuous tracking of patient conditions. The system automatically categorizes patients into three groups, significantly improving sensitivity in detecting agitation categories. This innovative approach not only alleviates the workload of health care professionals but also advances the precision and intelligence of critical care management.

Acknowledgments

This study was supported by Taichung Veterans General Hospital (TCVGH-1114404C) and the National Science and Technology Council (112-2634-F-A49-003-1,NSTC 113-2634-F-A49-003-1). The funders had no role in the study design, data collection and analysis, decision to publish, or preparation of the manuscript.

Data Availability

All data generated or analyzed during this study are included in this published article.

Authors' Contributions

Conceptualization: PD
Data Curation: PD
Formal Analysis: PD
Investigation: YW
Methodology: YW
Supervision: RS, CW
Validation: RS, CW, SL, PL
Writing – Original Draft: PD, YW
Writing – Review & Editing: PL, WC, GL, CH, LC

Conflicts of Interest

None declared.

References

1. Jacobi J, Fraser GL, Coursin DB, Task force of the American College of Critical Care Medicine (ACCM) of the Society of Critical Care Medicine (SCCM), American Society of Health-System Pharmacists (ASHP), American College of Chest Physicians, et al. Clinical practice guidelines for the sustained use of sedatives and analgesics in the critically ill adult. Crit Care Med 2002;30:119-141. [doi: 10.1097/00003246-200201000-00020] [Medline: 11902253]
2. Chanques G, Jaber S, Barbotte E, et al. Impact of systematic evaluation of pain and agitation in an intensive care unit. Crit Care Med 2006 Jun;34(6):1691-1699. [doi: 10.1097/01.CCM.0000218416.62457.56] [Medline: 16625136]
3. Fraser GL, Prato BS, Riker RR, Berthiaume D, Wilkins ML. Frequency, severity, and treatment of agitation in young versus elderly patients in the ICU. Pharmacotherapy 2000 Jan;20(1):75-82. [doi: 10.1592/phco.20.1.75.34663] [Medline: 10641977]
4. Fraser GL, Riker RR. Sedation and analgesia in the critically ill adult. Curr Opin Anaesthesiol 2007 Apr;20(2):119-123. [doi: 10.1097/ACO.0b013e32808255b4] [Medline: 17413394]
5. Cohen IL, Gallagher TJ, Pohlman AS, Dasta JF, Abraham E, Papadokos PJ. Management of the agitated intensive care unit patient. Crit Care Med 2002 Jan;30(1):S97-S123. [doi: 10.1097/00003246-200201002-00001] [Medline: 11852874]
6. Ely EW, Truman B, Shintani A, et al. Monitoring sedation status over time in ICU patients: reliability and validity of the Richmond Agitation-Sedation Scale (RASS). JAMA 2003 Jun 11;289(22):2983-2991. [doi: 10.1001/jama.289.22.2983] [Medline: 12799407]
7. Guenther U, Weykam J, Andorfer U, et al. Implications of objective vs subjective delirium assessment in surgical intensive care patients. Am J Crit Care 2012 Jan;21(1):e12-e20. [doi: 10.4037/ajcc2012735] [Medline: 22210705]
8. Sessler CN, Gosnell MS, Grap MJ, et al. The Richmond Agitation-Sedation Scale: validity and reliability in adult intensive care unit patients. Am J Respir Crit Care Med 2002 Nov 15;166(10):1338-1344. [doi: 10.1164/rccm.2107138] [Medline: 12421743]
9. Grap MJ, Hamilton VA, McNallen A, et al. Actigraphy: analyzing patient movement. Heart Lung 2011;40(3):e52-e59. [doi: 10.1016/j.hrtlng.2009.12.013] [Medline: 20723984]

XSL•FO
RenderX

10. Woods JC, Mion LC, Connor JT, et al. Severe agitation among ventilated medical intensive care unit patients: frequency, characteristics and outcomes. Intensive Care Med 2004 Jun;30(6):1066-1072. [doi: 10.1007/s00134-004-2193-9] [Medline: 14966671]
11. Pun BT, Badenes R, Calle G, et al. COVID-19 Intensive Care International Study Group. Prevalence and risk factors for delirium in critically ill patients with COVID-19 (COVID-D): a multicentre cohort study. Lancet Respir Med 2021 Mar;9(3):239-250. [doi: 10.1016/S2213-2600(21)00047-3] [Medline: 33428871]
12. Jauk S, Kramer D, Großauer B, et al. Risk prediction of delirium in hospitalized patients using machine learning: an implementation and prospective evaluation study. J Am Med Inform Assoc 2020 Jul 1;27(9):1383-1392. [doi: 10.1093/jamia/ocaa113] [Medline: 32968811]
13. Wong A, Young AT, Liang AS, Gonzales R, Douglas VC, Hadley D. Development and validation of an electronic health record-based machine learning model to estimate delirium risk in newly hospitalized patients without known cognitive impairment. JAMA Netw Open 2018 Aug 3;1(4):e181018. [doi: 10.1001/jamanetworkopen.2018.1018] [Medline: 30646095]
14. Syed M, Syed S, Sexton K, et al. Application of machine learning in intensive care unit (ICU) settings using MIMIC dataset: systematic review. Informatics (MDPI) 2021 Mar;8(1):16. [doi: 10.3390/informatics8010016] [Medline: 33981592]
15. Lin K, Hu Y, Kong G. Predicting in-hospital mortality of patients with acute kidney injury in the ICU using random forest model. Int J Med Inform 2019 May;125:55-61. [doi: 10.1016/j.ijmedinf.2019.02.002] [Medline: 30914181]
16. Yao RQ, Jin X, Wang GW, et al. A machine learning-based prediction of hospital mortality in patients with postoperative sepsis. Front Med ;7:445. [doi: 10.3389/fmed.2020.00445] [Medline: 32903618]
17. Zhao QY, Wang H, Luo JC, et al. Development and validation of a machine-learning model for prediction of extubation failure in intensive care units. Front Med (Lausanne) 2021;8:676343. [doi: 10.3389/fmed.2021.676343] [Medline: 34079812]
18. Zhang Z, Liu J, Xi J, Gong Y, Zeng L, Ma P. Derivation and validation of an ensemble model for the prediction of agitation in mechanically ventilated patients maintained under light sedation. Crit Care Med 2021 Mar 1;49(3):e279-e290. [doi: 10.1097/CCM.0000000000004821] [Medline: 33470778]
19. Chase JG, Agogue F, Starfinger C, et al. Quantifying agitation in sedated ICU patients using digital imaging. Comput Methods Programs Biomed 2004 Nov;76(2):131-141. [doi: 10.1016/j.cmpb.2004.03.005] [Medline: 15451162]
20. Becouze P, Hann CE, Chase JG, Shaw GM. Measuring facial grimacing for quantifying patient agitation in critical care. Comput Methods Programs Biomed 2007 Aug;87(2):138-147. [doi: 10.1016/j.cmpb.2007.05.005] [Medline: 17574701]
21. Dai PY, Wu YC, Sheu RK, et al. An automated ICU agitation monitoring system for video streaming using deep learning classification. BMC Med Inform Decis Mak 2024 Mar 18;24(1):77. [doi: 10.1186/s12911-024-02479-2] [Medline: 38500135]
22. Watson DS, Krutzinna J, Bruce IN, et al. Clinical applications of machine learning algorithms: beyond the black box. BMJ 2019 Mar 12;364:l886. [doi: 10.1136/bmj.l886] [Medline: 30862612]
23. Cabitza F, Rasoini R, Gensini GF. Unintended consequences of machine learning in medicine. JAMA 2017 Aug 8;318(6):517-518. [doi: 10.1001/jama.2017.7797] [Medline: 28727867]
24. Yang G, Ye Q, Xia J. Unbox the black-box for the medical explainable AI via multi-modal and multi-centre data fusion: a mini-review, two showcases and beyond. Inf Fusion 2022 Jan;77:29-52. [doi: 10.1016/j.inffus.2021.07.016] [Medline: 34980946]
25. Ng SY, Phua J, Wong YL, et al. Singapore SPICE: sedation practices in intensive care evaluation in Singapore - a prospective cohort study of the public healthcare system. Singapore Med J 2020 Jan;61(1):19-23. [doi: 10.11622/smedj.2019055] [Medline: 31197381]
26. Bose S, Kelly L, Shahn Z, Novack L, Banner-Goodspeed V, Subramaniam B. Sedative polypharmacy mediates the effect of mechanical ventilation on delirium in critically ill COVID-19 patients: a retrospective cohort study. Acta Anaesthesiol Scand 2022 Oct;66(9):1099-1106. [doi: 10.1111/aas.14119] [Medline: 35900078]

Abbreviations

APACHE: acute physiology and chronic health evaluation
AUC: area under the curve
ICU: intensive care unit
ML: machine learning
RASS: Richmond Agitation-Sedation Scale
ROC: Receiver Operating Characteristic
TCVGH: Taichung Veterans General Hospital

XSL•FO
RenderX

Edited by A Benis; submitted 25.06.24; peer-reviewed by A Maach, KA Ansari, P Wu; revised version received 27.12.24; accepted 29.01.25; published 26.02.25.

Please cite as:
Dai PY, Lin PY, Sheu RK, Liu SF, Wu YC, Wu CL, Chen WL, Huang CC, Lin GY, Chen LC
Predicting Agitation-Sedation Levels in Intensive Care Unit Patients: Development of an Ensemble Model
JMIR Med Inform 2025;13:e63601
URL: https://medinform.jmir.org/2025/1/e63601
doi:10.2196/63601

© Pei-Yu Dai, Pei-Yi Lin, Ruey-Kai Sheu, Shu-Fang Liu, Yu-Cheng Wu, Chieh-Liang Wu, Wei-Lin Chen, Chien-Chung Huang, Guan-Yin Lin, Lun-Chi Chen. Originally published in JMIR Medical Informatics (https://medinform.jmir.org), 26.2.2025. This is an open-access article distributed under the terms of the Creative Commons Attribution License (https://creativecommons.org/licenses/by/4.0/), which permits unrestricted use, distribution, and reproduction in any medium, provided the original work, first published in JMIR Medical Informatics, is properly cited. The complete bibliographic information, a link to the original publication on https://medinform.jmir.org/, as well as this copyright and license information must be included.

XSL•FO
RenderX

Development and Validation of a Machine Learning Algorithm for Predicting Diabetes Retinopathy in Patients With Type 2 Diabetes: Algorithm Development Study

Sunyoung Kim[1,2*], MD, PhD; Jaeyu Park[2,3*], PhD; Yejun Son[2,4], PhD; Hojae Lee[2,3], BS; Selin Woo[2], PhD; Myeongcheol Lee[2,3], BS; Hayeon Lee[2], PhD; Hyunji Sang[2,5], MD; Dong Keon Yon[2,3,4,6], MD, PhD; Sang Youl Rhee[2,5], MD, PhD

[1]Department of Family Medicine, Kyung Hee University Medical Center, Kyung Hee University College of Medicine, Seoul, Republic of Korea

[2]Center for Digital Health, Medical Science Research Institute, Kyung Hee University College of Medicine, 23 Kyungheedae–ro, Dongdaemun–gu, Seoul, Republic of Korea

[3]Department of Regulatory Science, Kyung Hee University, Seoul, Republic of Korea

[4]Department of Precision Medicine, Kyung Hee University College of Medicine, Seoul, Republic of Korea

[5]Department of Endocrinology, Kyung Hee University Medical Center, Kyung Hee University College of Medicine, Seoul, Republic of Korea

[6]Department of Pediatrics, Kyung Hee University Medical Center, Kyung Hee University College of Medicine, Seoul, Republic of Korea

[*]these authors contributed equally

Corresponding Author:
Sang Youl Rhee, MD, PhD
Center for Digital Health, Medical Science Research Institute, Kyung Hee University College of Medicine, 23 Kyungheedae–ro, Dongdaemun–gu, Seoul, Republic of Korea

Abstract

Background: Diabetic retinopathy (DR) is the leading cause of preventable blindness worldwide. Machine learning (ML) systems can enhance DR in community-based screening. However, predictive power models for usability and performance are still being determined.

Objective: This study used data from 3 university hospitals in South Korea to conduct a simple and accurate assessment of ML-based risk prediction for the development of DR that can be universally applied to adults with type 2 diabetes mellitus (T2DM).

Methods: DR was predicted using data from 2 independent electronic medical records: a discovery cohort (one hospital, n=14,694) and a validation cohort (2 hospitals, n=1856). The primary outcome was the presence of DR at 3 years. Different ML-based models were selected through hyperparameter tuning in the discovery cohort, and the area under the receiver operating characteristic (ROC) curve was analyzed in both cohorts.

Results: Among 14,694 patients screened for inclusion, 348 (2.37%) were diagnosed with DR. For DR, the extreme gradient boosting (XGBoost) system had an accuracy of 75.13% (95% CI 74.10 - 76.17), a sensitivity of 71.00% (95% CI 66.83 - 75.17), and a specificity of 75.23% (95% CI 74.16 - 76.31) in the original dataset. Among the validation datasets, XGBoost had an accuracy of 65.14%, a sensitivity of 64.96%, and a specificity of 65.15%. The most common feature in the XGBoost model is dyslipidemia, followed by cancer, hypertension, chronic kidney disease, neuropathy, and cardiovascular disease.

Conclusions: This approach shows the potential to enhance patient outcomes by enabling timely interventions in patients with T2DM, improving our understanding of contributing factors, and reducing DR-related complications. The proposed prediction model is expected to be both competitive and cost-effective, particularly for primary care settings in South Korea.

(JMIR Med Inform 2025;13:e58107) doi:10.2196/58107

KEYWORDS

type 2 diabetes; diabetes retinopathy; algorithm; machine learning; prediction; comorbidities; retinal; ophthalmology

Introduction

The global prevalence of diabetes mellitus (DM) in 2019 was estimated to be 463 million and is expected to reach 700 million by 2045 [1]. Diabetic retinopathy (DR) is the most common complication of DM and a leading cause of preventable blindness in adults [2-4]. The longer the period of diabetes and the lower the blood sugar control, the higher the risk of DR. Particularly, in patients with diabetes for >10 and >15 years, the prevalence of DR was 46.2% and 66.7%, respectively [5]. Additionally, the risk of DR increases by 1.4-fold for each 1% increase in glycated hemoglobin (HbA_{1c}) levels. Moreover,

XSL•FO
RenderX

alongside well-established risk factors, such as poor glycemic control and prolonged diabetes duration, it is important to acknowledge that DR can also manifest in patients with a relatively lower BMI.

DR progression risk factors include both correctable and noncorrectable factors [6,7]. Although DR can be continuously examined and prevented from the beginning, by the time a patient with diabetes experiences symptoms, such as decreased vision due to DR, the disease has already progressed significantly, and serious complications have occurred. Accordingly, the US Centers for Disease Control and Prevention recommends that patients undergo regular tests for DR, even those without symptoms, and receive appropriate management for any identified abnormalities [8,9]. Therefore, patients with diabetes are widely recommended to undergo routine testing annually to prevent DR progression [9].

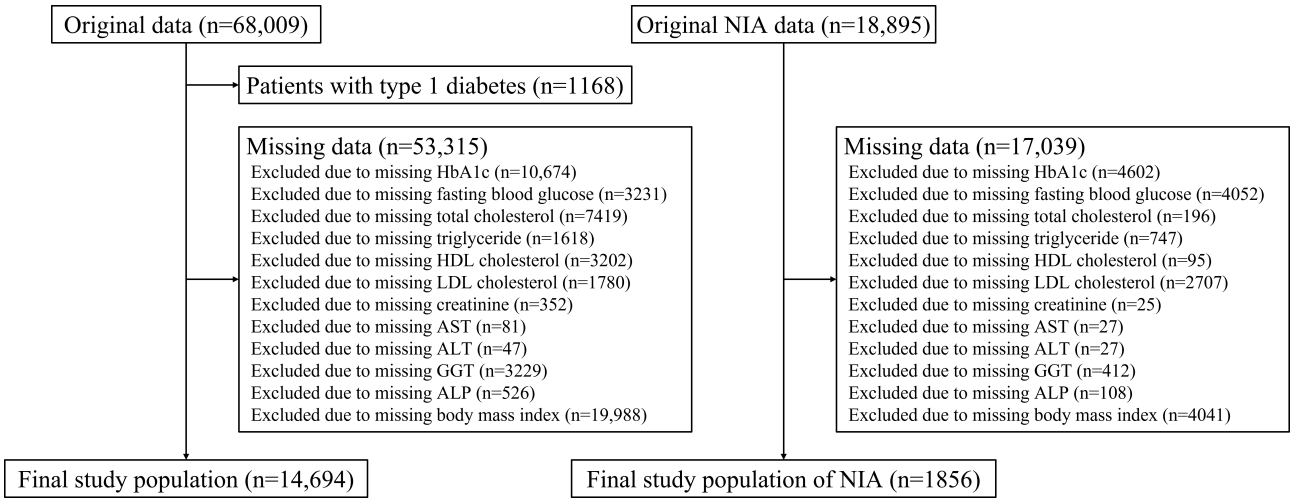
DR testing requires significant time and effort. However, shortages in trained professionals have been reported. According to a 2022 survey, only 46% of patients with DM in South Korea underwent fundus examination, with examination rates in the mid to high 30% for patients in their 30s to 50s [10]. Effective DR management requires individualized risk models and tools to predict and identify the cause of disease onset. Developing these models can allow for a better prediction of DR risk and improved screening efficiency. DR progression can be prevented using a DR management strategy that focuses on high-risk individuals.

Methods

Study Population and Data Collection

This retrospective study used data from 2 independent longitudinal cohorts as part of an observational study. Data were collected from a hospital between January 1, 2008, and December 31, 2022. Appropriate participants were selected from patients with type 2 diabetes mellitus (T2DM), excluding those with type 1DM (T1DM) and prior cases of DR. Finally, 14,694 patients from a tertiary hospital at Kyung Hee University Medical Center were included in the discovery cohort. Extravalidation data were acquired from a retrospective dataset from Kyung Hee University Hospital at Gangdong and Gachon University Gil Hospital, which included 1856 suitable patients (Figure 1).

Figure 1. Study workflow. ALP: alkaline phosphatase; ALT: alanine transaminase; AST: aspartate transaminase; GGT: γ-glutamyl transferase; HbA_{1c}: glycated hemoglobin; HDL: high-density lipoprotein; LDL: low-density lipoprotein; NIA: National Information Society Agency.



Input Variables

The model encompasses an exhaustive set of 57 variables, including demographic variables such as age, sex, and BMI [11]. Medical history included comorbidities (hypertension and dyslipidemia), macrovascular complications (cardiovascular disease [CVD], dementia, Parkinson disease, and microangiopathic disease), microvascular complications (chronic kidney disease [CKD] and neuropathy), end-stage renal disease, and cancer.

The medication history variables considered the types of drugs used to treat DM (metformin, sulfonylurea, dipeptidyl peptidase-4 inhibitors, meglitinide, thiazolidinedione, α-glucosidase inhibitors, insulin, glucagon-like peptide-1 receptor agonists, and sodium-glucose cotransporter 2 inhibitors), hypertension (angiotensin II receptor blockers, angiotensin-converting enzyme inhibitors, calcium channel blockers, diuretics, and β-blockers), and dyslipidemia (statin, fibrate, and ezetimibe), as well as antiplatelet drugs (aspirin, clopidogrel, cilostazol, and glycoprotein IIb/IIIa antagonists). Blood tests were performed to measure HbA_{1c}, fasting blood glucose, total cholesterol, triglyceride, high-density lipoprotein cholesterol, low-density lipoprotein cholesterol, serum creatinine, aspartate aminotransferase, alanine aminotransferase, γ-glutamyl transferase, and alkaline phosphatase. The median and SD of each parameter were used as input variables for the BMI and blood test results. Demographic variables such as age, sex, and BMI were collected at the patient's initial visit to the clinic. Blood tests (HbA_{1c}, fasting blood glucose, and total cholesterol) were conducted during regular follow-up visits, with the last recorded value before the onset of DR used for analysis.

Identification of New DR Cases

New-onset DR in patients with T2DM was identified using the *ICD-10* (*International Statistical Classification of Diseases,*

XSL•FO
RenderX

Tenth Revision) codes for retinopathy (E11.3-E14.3). T2DM was diagnosed as an anchoring event, and subsequent data collection, including DR identification, was based on the patient's first recorded diagnosis of diabetes. As relying solely on electronic health record data to identify conditions has inherent limitations in terms of accuracy, *ICD-10* codes were used to confirm whether the patients were diagnosed with retinopathy. This approach allowed for more reliable identification of retinopathy cases in this cohort.

Data Preprocessing

The data were preprocessed in 3 steps. First, individuals with T1DM were excluded to focus on those with T2DM using electronic health record data and identifying patients with T1DM via the *ICD-10* code (E10). Second, patients with a prior diagnosis of DR were excluded and identified using the *ICD-10* codes for retinopathy (E11.3-E14.3). Thirdly, patients with missing data in categories such as demographics, physical examination results, blood test results, medication history, or comorbidities were excluded from the analysis. Data from physical examinations and blood tests conducted before the onset of DR were analyzed. The most recent values recorded before DR onset were used and averaged across the study period for each patient. Covariates, including medication history and comorbidities, were collected at the patient's first visit and incorporated into the analysis. The final dataset represents variables as means (SD) or numbers (percentages), as appropriate.

Model Training and Validation

The conventional machine learning (ML) methodology for prediction tasks requires splitting the data into training and testing sets. However, the available data on the 3-year incidence of DR are insufficient in the context of this study. Therefore, the model was trained on the complete dataset rather than dividing it for internal validation. A separate external dataset, the National Information Society Agency, was used to assess the model's generalizability. This method was vital for confirming the robustness of the model for new unencountered data.

Model Development

This study applied decision-tree-based ensemble models, including AdaBoost, CatBoost, light gradient-boosting machine (LightGBM), random forest, and extreme gradient boosting (XGBoost). To optimize each model's performance, hyperparameter tuning was conducted using GridSearchCV to achieve the highest area under the receiver operating characteristic (ROC) curve (AUROC) and determine the most practical combination of hyperparameters.

ML Analysis

Tree-based and linear classification models were used to establish AUROC scores to predict the occurrence of DR. After determining the optimal hyperparameters, the model was trained to ensure accurate prediction. Given the class imbalance in the data, a synthetic minority oversampling technique was used to generate synthetic samples. The model's performance was evaluated using various metrics, such as AUROC, accuracy, sensitivity, specificity, and balanced accuracy, which were calculated based on the probability predictions generated by the model. A 10-fold stratified cross-validation was used to assess the model's ability to process new data, and the Youden Index was used within each stratification to pinpoint the optimal threshold [12]. The mean and 95% CIs for each performance metric were calculated to determine the average performance and variability of the model. The model performance was graphically represented by an ROC curve supplemented by the mean ROC curve and SD within that range, illustrating the model performance distribution. The XGBoost model, which provided the highest AUROC score among the various decision-tree models examined, was selected to determine the most crucial features for predicting DR. The significance of each feature was extracted by leveraging the important attributes of the XGBoost model. The top 15 features with the most significant impacts on the model were identified and plotted to visualize their effects on the predictions.

Performance Metrics

Five metrics were used to evaluate the performance of the proposed model: AUROC, accuracy, sensitivity, specificity, and balance accuracy. The AUROC is a resilient performance measure that assesses a model's ability to distinguish between classes across all potential thresholds. Resilience stems from the consideration of both sensitivity and specificity, making it the preferred metric, particularly in scenarios where classes are imbalanced. Accuracy is a simple and intuitive performance metric that denotes the ratio of accurate results (both true positives and negatives) to the total number of cases examined. However, when used alone, the accuracy can be misleading, particularly for unbalanced datasets, thereby necessitating additional performance metrics. The sensitivity and specificity were used to evaluate the ability of the model to correctly identify positive and negative cases, respectively. Sensitivity measures the ability of a model to identify positive cases correctly. By contrast, specificity measures the ability of the model to correctly identify negative cases, indicating its ability to avoid false-positive findings. Finally, balanced accuracy was included to provide a more balanced view of the model performance, particularly when dealing with class imbalances. Balanced accuracy is an excellent alternative to accuracy for unbalanced datasets because it assigns equal weights to sensitivity and specificity. Combining these metrics enabled an assessment of the performance of the model from different perspectives, ensuring a more comprehensive evaluation [13,14].

Software and Libraries

All data preprocessing, model creation, and analyses were performed using Python (version 3.9.16; Python Software Foundation). The libraries used to execute the ML algorithms and manipulate the data included Scikit-learn 1.2.2, NumPy 1.23.5, and Pandas 1.5.3. For data visualization, Matplotlib 3.7.1 and Seaborn 0.12.2 were used.

Ethical Considerations

This study was approved as exempt by the institutional review board of Kyung Hee University Hospital because of the use of deidentified patient data in a secure environment (approval number KHSIRB-22-473(EA)).

XSL•FO
RenderX

Results

Cohort Baseline Characteristics

Among the 14,694 patients in the discovery cohort, the mean age was 62.8 (11.24) years with 7730 (52.61%) males, and the mean BMI was 25.1 (3.58) kg/m^2. The discovery cohort identified 348 (2.37%) patients as having DR. For additional validation, 1856 patients were included, of which 1053 (56.73%) patients were male, and the mean age was 57.7 (11.88) years. A total of 137 patients (7.38%) were identified as having DR within this validation cohort (Table 1 and Figure 1).

XSL•FO
RenderX

Table . Baseline characteristics of the study and extra-validation datasets.

	Study dataset			Extra-validation dataset		
	Total (N=14,694)	Control (n=14,346)	Case[a] (n=348)	Total (n=1856)	Control (n=1719)	Case (n=137)
Age (years), mean (SD)	62.8 (11.24)	62.9 (11.26)	60.2 (10.15)	57.7 (11.74)	57.6 (11.88)	58.4 (9.92)
Male, n (%)	7730 (52.61)	7555 (52.66)	175 (50.29)	1053 (56.73)	976 (56.78)	77 (56.20)
Female, n (%)	6964 (47.39)	6791 (47.34)	173 (49.71)	803 (43.27)	743 (43.22)	60 (43.80)
BMI (kg/m^2), mean (SD)	25.1 (3.58)	25.1 (3.58)	24.6 (3.29)	25.2 (3.45)	25.2 (3.49)	24.6 (2.84)
Blood test, mean (SD)						
HbA_{1c}[b] (%)	6.9 (0.90)	6.9 (0.89)	7.3 (0.91)	7.2 (1.07)	7.2 (1.08)	7.3 (0.94)
Fasting blood glucose (mg/dL)	146.6 (38.12)	146.4 (38.08)	154.8 (39.09)	141.8 (38.06)	142.1 (38.05)	138.1 (38.12)
Total cholesterol (mg/dL)	155.7 (30.16)	155.8 (30.17)	150.3 (29.30)	158.1 (29.82)	158.2 (29.96)	156.9 (28.04)
Triglyceride (mg/dL)	140.8 (63.09)	141.1 (63.28)	130.9 (53.97)	145.0 (63.33)	145.4 (63.90)	141.1 (55.78)
HDL[c] cholesterol (mg/dL)	47.5 (11.34)	47.5 (11.35)	47.6 (10.80)	44.7 (9.78)	44.7 (9.76)	44.9 (10.03)
LDL[d] cholesterol (mg/dL)	88.1 (24.22)	88.2 (24.24)	84.1 (22.94)	88.2 (27.70)	88.6 (27.82)	83.9 (25.77)
Creatinine (mg/dL)	0.9 (0.45)	0.9 (0.45)	1.0 (0.59)	1.1 (1.00)	1.1 (1.02)	1.1 (0.72)
AST[e] (U/L)	26.3 (11.19)	26.3 (11.25)	23.8 (8.19)	24.3 (8.12)	24.4 (8.16)	23.2 (7.50)
ALT[f] (U/L)	23.7 (12.13)	23.8 (12.19)	20.7 (9.11)	24.9 (12.55)	25.1 (12.77)	21.9 (8.81)
GGT[g] (U/L)	37.6 (33.86)	37.7 (33.97)	32.6 (28.37)	37.9 (32.24)	38.4 (32.68)	31.8 (25.39)
ALP[h] (U/L)	77.9 (23.03)	77.9 (23.05)	77.7 (22.02)	148.5 (88.93)	147.2 (89.21)	164.4 (83.97)
Comorbid conditions, n (%)						
Hypertension	8522 (58.00)	8367 (58.32)	155 (44.54)	1209 (65.14)	1138 (66.20)	71 (51.82)
Dyslipidemia	9343 (63.58)	9217 (64.25)	126 (36.21)	1004 (54.09)	946 (55.03)	58 (42.34)

XSL•FO
RenderX

	Study dataset			Extra-validation dataset		
	Total (N=14,694)	Control (n=14,346)	Case[a] (n=348)	Total (n=1856)	Control (n=1719)	Case (n=137)
Macrovascular complications, n (%)						
Cardiovascular disease[i]	7343 (49.97)	7216 (50.30)	127 (36.49)	785 (42.30)	747 (43.46)	38 (27.74)
Dementia	14,515 (98.78)	178 (1.24)	1 (0.29)	83 (4.47)	82 (4.77)	1 (0.73)
Parkinson disease	279 (1.90)	279 (1.94)	N/A	13 (0.70)	13 (0.76)	N/A[j]
Microangiopathic disease[k]	102 (0.69)	99 (0.69)	3 (0.86)	336 (18.10)	321 (18.67)	15 (10.95)
Microvascular complications, n (%)						
ESRD[l]	135 (0.92)	132 (0.92)	3 (0.86)	155 (8.35)	151 (8.78)	4 (2.92)
Neuropathy	4657 (31.69)	4564 (31.81)	93 (26.72)	543 (29.26)	508 (29.55)	35 (25.55)
Cancer	2755 (18.75)	2734 (19.06)	21 (6.03)	249 (13.42)	246 (14.31)	3 (2.19)
Medication use, n (%)						
Diabetes mellitus[m]						
Metformin	8374 (56.99)	8147 (56.79)	227 (65.23)	558 (30.06)	503 (29.26)	55 (40.15)
Sulfonylurea	5186 (35.29)	5029 (35.06)	157 (45.11)	218 (11.75)	191 (11.11)	27 (19.71)
DPP-4[n] inhibitor	3226 (21.95)	3150 (21.96)	76 (21.84)	94 (5.06)	88 (5.12)	6 (4.38)
Meglitinide	802 (5.46)	763 (5.32)	39 (11.21)	78 (4.20)	65 (3.78)	13 (9.49)
Thiazolidinedione	1062 (7.23)	1012 (7.05)	50 (14.37)	17 (0.92)	15 (0.87)	2 (1.46)
α-glucosidase inhibitor	763 (5.19)	735 (5.12)	28 (8.05)	64 (3.45)	51 (2.97)	13 (9.49)
Insulin	5186 (35.29)	5029 (35.06)	157 (45.11)	N/A	N/A	N/A
GLP-1[o] agonist	19 (0.13)	19 (0.13)	N/A	N/A	N/A	N/A
SGLT2[p] inhibitor	340 (2.31)	331 (2.31)	9 (2.59)	N/A	N/A	N/A
Hypertension[q]						
Angiotensin II receptor blockers	6501 (44.24)	6328 (44.11)	173 (49.71)	116 (6.25)	105 (6.11)	11 (8.03)

XSL•FO
RenderX

	Study dataset			Extra-validation dataset		
	Total (N=14,694)	Control (n=14,346)	Case[a] (n=348)	Total (n=1856)	Control (n=1719)	Case (n=137)
ACE[r] inhibitor	1314 (8.94)	1273 (8.87)	41 (11.78)	69 (3.72)	61 (3.55)	8 (5.84)
Calcium-channel blocker	6507 (44.28)	6343 (44.21)	164 (47.13)	282 (15.19)	255 (14.83)	27 (19.71)
Diuretics	4499 (30.62)	4392 (30.61)	107 (30.75)	104 (5.60)	94 (5.47)	10 (7.30)
Beta-blocker	4007 (27.27)	3925 (27.36)	82 (23.56)	1 (0.05)	1 (0.06)	N/A
Dyslipidemia[s]						
Statin	8248 (56.13)	8043 (56.06)	205 (58.91)	453 (24.41)	407 (23.68)	46 (33.58)
Fibrate	653 (4.44)	640 (4.46)	13 (3.74)	31 (1.67)	22 (1.28)	9 (6.57)
Ezetimibe	804 (5.47)	794 (5.53)	10 (2.87)	41 (2.21)	37 (2.15)	4 (2.92)
Antiplatelet[t]						
Aspirin	6218 (42.32)	6048 (42.16)	170 (48.85)	358 (19.29)	324 (18.85)	34 (24.82)
Clopidogrel	4174 (28.41)	4078 (28.43)	96 (27.59)	156 (8.41)	133 (7.74)	23 (16.79)
Cilostazol	1898 (12.92)	1813 (12.64)	85 (24.43)	74 (3.99)	60 (3.49)	14 (10.22)
Glycoprotein IIb/IIIa antagonist	197 (1.34)	193 (1.35)	4 (1.15)	N/A	N/A	N/A

[a]Group of patients with newly developed neurodegenerative disease within 3 years.

[b]HbA_{1c}: glycated hemoglobin.

[c]HDL: high-density lipoprotein.

[d]LDL: low-density lipoprotein.

[e]AST: aspartate transaminase.

[f]ALT: alanine transaminase.

[g]GGT: gamma-glutamyl transferase.

[h]ALP: alkaline phosphatase.

[i]Ischemic heart disease, myocardial infarction, heart failure, atrial fibrillation, stroke, and cerebrovascular disease.

[j]N/A: not available.

[k]Peripheral vascular disease and amputation.

[l]ESRD: end-stage renal disease.

[m]Metformin, sulfonylurea, DPP-4 inhibitor, meglitinide, thiazolidinedione, α-glucosidase inhibitor, insulin, GLP-1 receptor agonist, and SGLT2 inhibitor.

[n]DPP-4: dipeptidyl peptidase-4.

[o]GLP-1: glucagon-like peptide-1.

[p]SGLT2: sodium-glucose cotransporter 2.

[q]Angiotensin II receptor blockers, ACE inhibitors, calcium channel blockers, diuretics, and beta-blockers.

[r]ACE: angiotensin-converting enzyme.

[s]Statin, fibrate, ezetimibe, and omega-3.

[t]Aspirin, clopidogrel, cilostazol, and glycoprotein IIb/IIIa antagonist.

XSL•FO
RenderX

Comparisons of Prediction Model Performance

The XGBoost model performed well on the discovery set (AUROC 82.36 [95% CI 80.48 - 84.25]; accuracy 75.13% [95% CI 74.10 - 76.17]; sensitivity 71.00% [95% CI 66.83 - 75.17]; specificity 75.23% [95% CI 74.16 - 76.31]; balanced accuracy 73.12% [95% CI 71.06 - 75.17]; precision 6.51% [95% CI 6.09 - 6.94]; F1-score 11.93% [95% CI 11.18 - 12.68]; and AUPRC 22.08 [95% CI18.04 - 26.13]) (Table 2). When these models were applied to an external validation set, the XGBoost model achieved an AUROC of 71.67 (Table 2). Consequently, with consistent results in both independent datasets, the XGBoost model emerged as the best predictor of DR development within 3 years among patients with T2DM (Figure 2).

Table . Performance metrics of 5 different machine learning algorithms on the original and validation NIA[a] datasets.

Model	AUROC[b]	Accuracy	Sensitivity	Specificity	Balanced accuracy	Precision	F_1-score	AUPRC[c]
Original dataset, mean (95% CI)								
XGBoost[d]	82.36 (80.48 - 84.25)[e]	75.13 (74.10-76.17)[e]	71.00 (66.83-75.17)[e]	75.23 (74.16-76.31)[e]	73.12 (71.06-75.17)[e]	6.51 (6.09-6.94)[e]	11.93 (11.18-12.68)[e]	22.08 (18.04-26.13)[e]
CatBoost	82.12 (80.24-84.00)	73.51 (70.31-76.72)	73.01 (70.03-75.99)	73.53 (70.32-76.73)	73.27 (70.18-76.36)	6.45 (5.50-7.40)	11.84 (10.19-13.48)	21.70 (18.80-24.60)
LightGBM[f]	82.25 (79.83-84.67)	77.73 (76.95-78.50)	69.55 (65.03-74.06)	77.92 (77.09-78.76)	73.74 (71.63-75.84)	7.10 (6.69-7.52)	12.88 (12.14-13.63)	22.09 (18.85-25.33)
Random forest	80.84 (79.03-82.65)	73.55 (70.97-76.12)	73.01 (70.95-75.07)	73.56 (70.97-76.15)	73.28 (70.98-75.59)	6.39 (5.66-7.12)	11.74 (10.48-13.00)	18.91 (15.45-22.37)
AdaBoost	79.99 (76.32-83.67)	73.15 (69.06-77.23)	72.68 (69.20-76.17)	73.16 (69.05-77.26)	72.92 (69.21-76.63)	6.44 (5.33-7.54)	11.80 (9.88-13.72)	20.74 (16.62-24.87)
Validation dataset, mean								
XGBoost	71.67[e]	65.14[e]	64.96[e]	65.15[e]	65.06[e]	12.94[e]	21.58[e]	16.57[e]
CatBoost	71.43	65.95	65.69	65.97	65.83	13.33	22.17	21.49
LightGBM	70.87	64.98	64.96	64.98	64.97	12.88	21.50	17.84
Random forest	68.12	62.39	62.04	62.42	62.23	11.63	19.59	15.89
AdaBoost	65.35	61.42	61.31	61.43	61.37	11.24	19.00	14.70

[a]NIA: National Information Society Agency.

[b]AUROC: area under the receiver operating characteristic.

[c]AUPRC: area under the precision-recall curve.

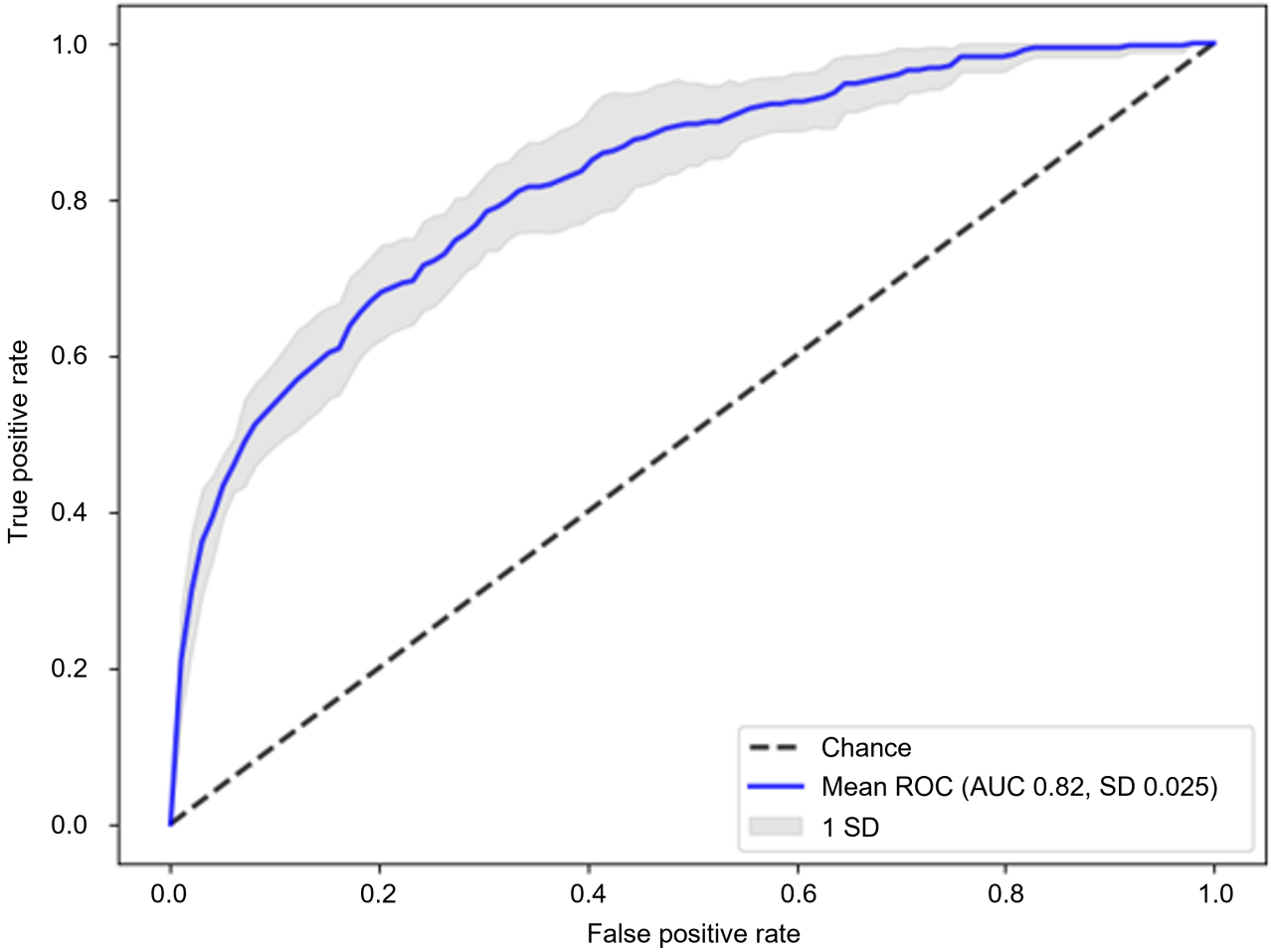
[d]XGBoost: extreme gradient boosting.

[e]Best-performing model.

[f]LightGBM: light gradient-boosting machine.

XSL•FO
RenderX

Figure 2. ROC curve of the XGBoost model. Mean ROC curve from 10-fold cross-validation on the original dataset. AUC: area under the ROC curve; ROC: receiver operating characteristic; XGBoost: extreme gradient boosting.

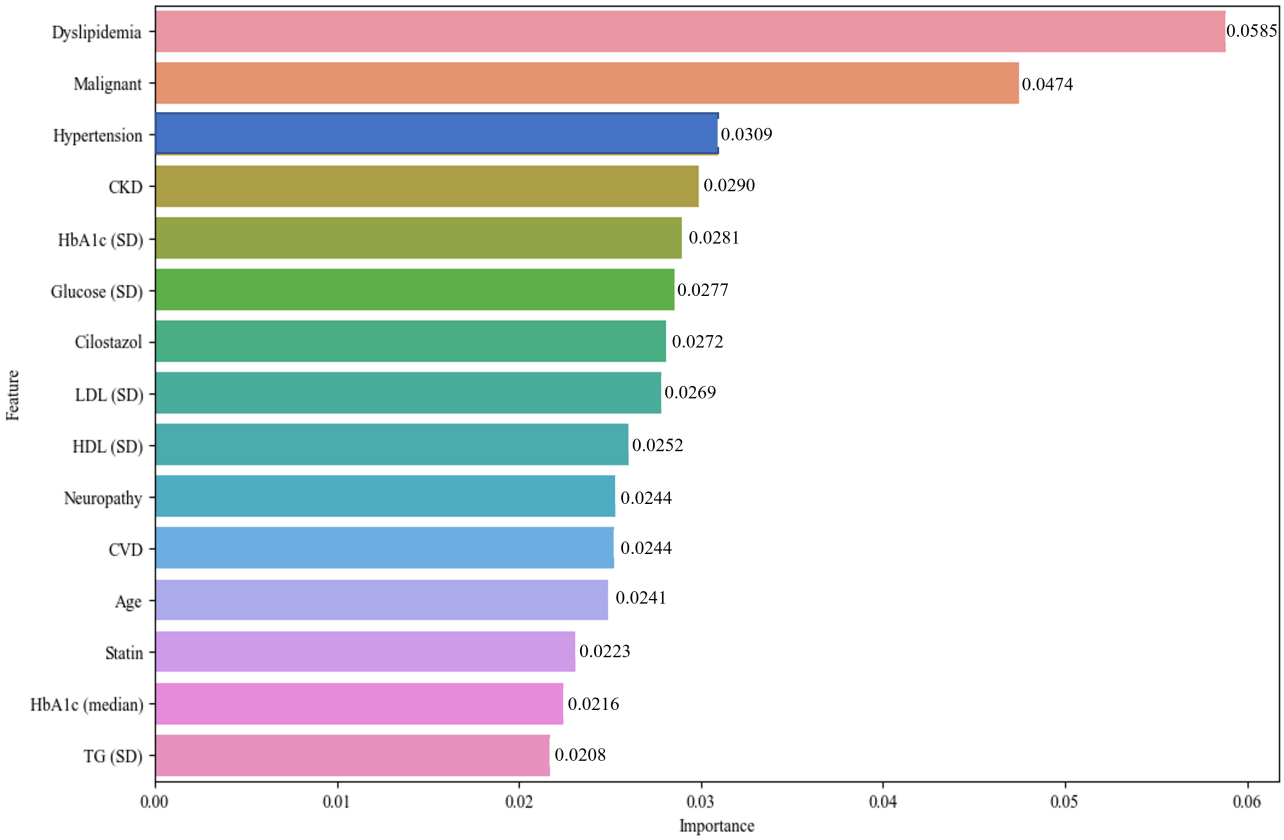


Feature Importance

The XGBoost model identified dyslipidemia (0.0585) as the most significant factor in predicting the development of DR within 3 years in patients with T2DM (Figure 3). Following dyslipidemia, the most critical factors included malignancy (0.0474), hypertension (0.0309), CKD (0.0290), HbA_{1c} variability (SD) (0.0281), glucose variability (SD) (0.0277), cilostazol use (0.0272), low-density lipoprotein variability (SD) (0.0269), high-density lipoprotein variability (SD) (0.0252), neuropathy (0.0244), CVD (0.0244), age (0.0241), statin use (0.0223), median HbA_{1c} (0.0216), and triglyceride variability (SD) (0.0208). These factors were ranked in descending order based on their importance in predicting DR.

XSL•FO
RenderX

Figure 3. Top 15 important features in the XGBoost model. CVD: cardiovascular disease; CKD: chronic kidney disease; DDP: Dipeptidyl Peptidase; HbA_{1c}: glycated hemoglobin; HDL: high-density lopoprotein; LDL: low-density lipoprotein; TG: triglyceride; XGBoost: extreme gradient boosting.



Discussion

Principal Findings

This study used data from 3 university hospitals in South Korea to conduct a simple and accurate assessment of ML-based risk prediction for DR development that can be universally applied to adults with T2DM. The AdaBoost, LightGBM, Random Forest, and XGBoost ensemble models performed well, with AUROC values of 82.36% (95% CI 80.48‐84.25). Dyslipidemia and cancer were the most important factors influencing the predictive model.

Several studies have investigated vision-threatening DR using deep learning (DL) approaches. Gulshan et al [15] used 9963 fundus images, achieving an AUROC of 0.999. Similarly, Ting et al [16] validated a DL system using 71,896 images, reporting an AUROC of 0.958 (95% CI 0.956‐0.961). Li et al [17] also validated a DL system with 35,201 images, obtaining an AUROC of 0.955. These studies reported a more robust performance of DL systems than human testing in various patient populations [15,18]. However, it is important to note that these investigations primarily focused on patients with severe vision-threatening DR, diagnosed through specialized ophthalmological care. Furthermore, a direct end-to-end training approach links the fundus image to the DR grade labels and may overlook critical lesion features due to the inherent black-box nature of DR classification models [19]. This limitation underscores the need for more comprehensive methodologies that can effectively capture and encode relevant lesion characteristics in the context of DR diagnosis.

This study offers the advantage of identifying the strong predictive performance of previously unseen data using a decision tree–based ensemble model that optimizes the combination of hyperparameters. Specifically, the findings suggest that DR can be reliably predicted in patients with T2DM using simple medical information obtained in primary care settings before ophthalmologist consultation and at the onset of visual symptoms. This approach can significantly reduce health care costs by enabling early detection and intervention. Gayathri et al [20] introduced a DR classification system based on various MLs, including multipath convolutional neural networks, random forests, and support vector machines. Similarly, Math et al [21] developed a DR classification system based on adaptive ML and obtained an AUC of 0.963.

This study proposed a new selection method for predicting DR with high accuracy and minimal predictors. The final dataset comprised 15 independent variables, and to identify the most significant risk factors of DR, ensemble models including the AdaBoost, LightGBM, Random Forest, and XGBoost were used to reduce the number of features among the numerous risk factors. The findings indicate that DR exhibited the strongest correlation with dyslipidemia, followed by cancer, hypertension, CKD, neuropathy, and CVD. These results are consistent with previously reported correlations between dyslipidemia [22,23], cancer [24], hypertension [25,26], CKD [27], neuropathy [28], and CVD [29]. This study underscores the importance of these correlations in understanding the multifactorial nature of DR.

XSL•FO
RenderX

It highlights the necessity for comprehensive risk assessments in patients with DM to effectively mitigate the risk of developing DR. In addition, a higher BMI is commonly associated with an increased risk of complications in patients with DM, and studies have shown that DR can develop even in individuals with a BMI of approximately 25, as observed in the study cohort. This suggests that a lower BMI does not necessarily protect against DR and highlights the need for comprehensive risk assessment in all patients with DM, regardless of BMI.

The findings demonstrated that DR in patients with diabetes can be predicted using simple medical information in the primary care setting before the onset of visual impairment and before ophthalmological treatment, thus potentially dramatically reducing medical costs. Furthermore, this study highlights the generalizability of ML systems and their feasibility in scaling up screening programs while maintaining the standards of care. ML systems offer reasonably accurate predictions that can significantly improve settings where additional testing may take weeks or months.

Artificial intelligence (AI)–based technologies support testing for DR, which is an unmet public health concern [30,31]. The results demonstrated that AI-based personalized testing intervals can be incorporated to improve the efficiency, equity, and accessibility of DR testing [32]. In particular, the findings of this study could improve patient outcomes by enabling timely intervention, improving the understanding of contributing variables, and reducing the burden of DR complications in patients with T2DM. The use of AI in the new DR classification is promising and there is optimism regarding future guideline revisions for the use of AI in the management of DR [33].

Limitations

First, as a cohort study conducted in hospitals in urban areas of a single ethnic group, the findings may not represent the entire population. Second, the diagnosis of DR relied on disease codes, which may lead to underestimation. Third, obtaining accurate information was difficult as a retrospective study based on hospital medical records. As no systematic referral tracking exists for the review of electronic medical records, a customized tracking process was implemented within the study. Fourth, the performance of this prediction model cannot be directly compared with existing prediction models. Additionally, the severity of DR was not reflected in the results. Fifth, this study could not confirm a causal relationship between the predictors used in the model and the occurrence of DR. Additional studies are needed to accurately identify the pathophysiological pathways and demonstrate the mechanisms of interaction between variables associated with DR and their impact on DR development. Finally, because the model operates over a wide range of retrospective scenarios, it may not work well if an unexpected situation occurs, such as the outbreak of a new infectious disease such as COVID-19, or if medical records are inconsistent or insufficient. Future studies should use additional models to reduce the dependence of supervised feature selection techniques on a wide range of training data.

This study is the first to apply an ML-based DR prediction system to a nationwide population with diabetes. The results indicate that the implementation of evidence-based, individualized preventive interventions can reduce the burden of DR in Korean patients with diabetes.

Conclusions

This study used a hospital-based cohort to develop an ML-based prediction model to accurately predict the DR risk in a Korean population with T2DM. These results may improve patient outcomes by enabling timely interventions to prevent DR in patients with T2DM, enhancing the understanding of contributing variables, and reducing the burden of DR complications in patients with T2DM. The prediction model proposed in this study is expected to be competitive and cost-effective in preventing DR in patients with T2DM in South Korea and is expected to be widely used, especially in primary care settings.

Acknowledgments

This study will be expanded to include data collected by the National Information Society Agency in South Korea and multicenter research associated with the Korean Diabetes Association and the Korea Disease Control and Prevention Agency. This study was supported by the National Institute of Health Research Project of South Korea (2022-ER1102-01). This research was supported by the Bio&Medical Technology Development Program of the National Research Foundation (NRF) funded by the Korean government (MSIT; RS-2023-00262002). Also, this work was supported by the Institute of Information & communications Technology Planning & Evaluation (IITP) grant funded by the Korea government (MSIT; RS-2022-00143911, AI Excellence Global Innovative Leader Education Program and RS-2024-00509257, Global AI Frontier Lab). The funders had no role in the study design, data collection, data analysis, data interpretation, or manuscript writing.

Data Availability

The datasets generated or analyzed during this study are not publicly available due to human subjects' approval to protect patient privacy but are available from the corresponding author on reasonable request.

Authors' Contributions

Drs DKY and SYR had full access to all data in the study and took responsibility for the integrity of the data and the accuracy of the data analysis. All authors have approved the final version of the manuscript before submission. DKY and SYR conceptualized and designed the study. JP, YS, and ML acquired, analyzed, and interpreted the data. All the authors drafted and revised the

XSL•FO
RenderX

manuscript. All authors discussed the results and contributed to the final manuscript. SK and JP contributed equally to this study as the first authors. DKY and SYR contributed equally to this study as corresponding authors. The corresponding author attests that all listed authors meet the authorship criteria and that no others meeting the criteria have been omitted.

Conflicts of Interest

None declared.

References

1. Saeedi P, Petersohn I, Salpea P, et al. Global and regional diabetes prevalence estimates for 2019 and projections for 2030 and 2045: results from the International Diabetes Federation Diabetes Atlas, 9th edition. Diabetes Res Clin Pract 2019 Nov;157:107843. [doi: 10.1016/j.diabres.2019.107843] [Medline: 31518657]
2. Khalil H. Diabetes microvascular complications—a clinical update. Diabetes Metab Syndr Clin Res Rev 2017 Nov;11:S133-S139. [doi: 10.1016/j.dsx.2016.12.022]
3. Teo ZL, Tham YC, Yu M, et al. Global prevalence of diabetic retinopathy and projection of burden through 2045: systematic review and meta-analysis. Ophthalmology 2021 Nov;128(11):1580-1591. [doi: 10.1016/j.ophtha.2021.04.027] [Medline: 33940045]
4. Wong TY, Cheung CMG, Larsen M, Sharma S, Simó R. Diabetic retinopathy. Nat Rev Dis Primers 2016 Mar 17;2(1):16012. [doi: 10.1038/nrdp.2016.12] [Medline: 27159554]
5. Lima VC, Cavalieri GC, Lima MC, Nazario NO, Lima GC. Risk factors for diabetic retinopathy: a case-control study. Int J Retina Vitreous 2016;2(1):21. [doi: 10.1186/s40942-016-0047-6] [Medline: 27847639]
6. Jenkins AJ, Joglekar MV, Hardikar AA, Keech AC, O'Neal DN, Januszewski AS. Biomarkers in diabetic retinopathy. Rev Diabet Stud 2015;12(1-2):159-195. [doi: 10.1900/RDS.2015.12.159] [Medline: 26676667]
7. Stratton IM, Kohner EM, Aldington SJ, et al. UKPDS 50: risk factors for incidence and progression of retinopathy in type II diabetes over 6 years from diagnosis. Diabetologia 2001 Feb;44(2):156-163. [doi: 10.1007/s001250051594] [Medline: 11270671]
8. Daskivich LP, Vasquez C, Martinez C Jr, Tseng CH, Mangione CM. Implementation and evaluation of a large-scale teleretinal diabetic retinopathy screening program in the Los Angeles County Department of Health Services. JAMA Intern Med 2017 May 1;177(5):642-649. [doi: 10.1001/jamainternmed.2017.0204] [Medline: 28346590]
9. Alali NM, Albazei A, Alotaibi HM, et al. Diabetic retinopathy and eye screening: diabetic patients standpoint, their practice, and barriers; a cross-sectional study. J Clin Med 2022 Oct 27;11(21):6351. [doi: 10.3390/jcm11216351] [Medline: 36362578]
10. Choi JH, Lee KA, Moon JH, et al. 2023 clinical practice guidelines for diabetes mellitus of the Korean Diabetes Association. Diabetes Metab J 2023 Sep;47(5):575-594. [doi: 10.4093/dmj.2023.0282]
11. Eum S, Son JW, Min C, et al. Ethnic and sex differences in the distributions of body mass index and waist circumference among adults: a binationally representative study in South Korea and the United States. Eur Rev Med Pharmacol Sci 2023 Mar;27(5):1889-1903. [doi: 10.26355/eurrev_202303_31555] [Medline: 36930486]
12. Wacker C, Prkno A, Brunkhorst FM, Schlattmann P. Procalcitonin as a diagnostic marker for sepsis: a systematic review and meta-analysis. Lancet Infect Dis 2013 May;13(5):426-435. [doi: 10.1016/S1473-3099(12)70323-7] [Medline: 23375419]
13. Lee SW. Regression analysis for continuous independent variables in medical research: statistical standard and guideline of life cycle committee. Life Cycle 2022;2:e3. [doi: 10.54724/lc.2022.e3]
14. Kim J, Kim SC, Kang D, Yon DK, Kim JG. Classification of Alzheimer's disease stage using machine learning for left and right oxygenation difference signals in the prefrontal cortex: a patient-level, single-group, diagnostic interventional trial. Eur Rev Med Pharmacol Sci 2022 Nov;26(21):7734-7741. [doi: 10.26355/eurrev_202211_30122] [Medline: 36394721]
15. Gulshan V, Rajan RP, Widner K, et al. Performance of a deep-learning algorithm vs manual grading for detecting diabetic retinopathy in India. JAMA Ophthalmol 2019 Sep 1;137(9):987-993. [doi: 10.1001/jamaophthalmol.2019.2004] [Medline: 31194246]
16. Ting DSW, Cheung CYL, Lim G, et al. Development and validation of a deep learning system for diabetic retinopathy and related eye diseases using retinal images from multiethnic populations with diabetes. JAMA 2017 Dec 12;318(22):2211-2223. [doi: 10.1001/jama.2017.18152] [Medline: 29234807]
17. Li Z, Keel S, Liu C, et al. An automated grading system for detection of vision-threatening referable diabetic retinopathy on the basis of color fundus photographs. Diabetes Care 2018 Dec;41(12):2509-2516. [doi: 10.2337/dc18-0147] [Medline: 30275284]
18. Ruamviboonsuk P, Krause J, Chotcomwongse P, et al. Erratum: author correction: deep learning versus human graders for classifying diabetic retinopathy severity in a nationwide screening program. NPJ Digit Med 2019;2(1):68. [doi: 10.1038/s41746-019-0146-5] [Medline: 31341955]
19. Papernot N, McDaniel P, Goodfellow I, Jha S, Celik ZB, Swami A. Practical black-box attacks against machine learning. 2017 Apr 2 Presented at: ASIA CCS '17; Abu Dhabi United Arab Emirates URL: https://dl.acm.org/doi/proceedings/10.1145/3052973 [doi: 10.1145/3052973.3053009]
20. Gayathri S, Gopi VP, Palanisamy P. Diabetic retinopathy classification based on multipath CNN and machine learning classifiers. Phys Eng Sci Med 2021 Sep;44(3):639-653. [doi: 10.1007/s13246-021-01012-3] [Medline: 34033015]

XSL•FO
RenderX

21. Math L, Fatima R. Adaptive machine learning classification for diabetic retinopathy. Multimed Tools Appl 2021 Feb;80(4):5173-5186. [doi: 10.1007/s11042-020-09793-7]
22. Jeng CJ, Hsieh YT, Yang CM, Yang CH, Lin CL, Wang IJ. Diabetic retinopathy in patients with dyslipidemia: development and progression. Ophthalmol Retina 2018 Jan;2(1):38-45. [doi: 10.1016/j.oret.2017.05.010] [Medline: 31047300]
23. Zhou Y, Wang C, Shi K, Yin X. Relationship between dyslipidemia and diabetic retinopathy: a systematic review and meta-analysis. Medicine (Balt) 2018 Sep;97(36):e12283. [doi: 10.1097/MD.0000000000012283] [Medline: 30200172]
24. Park S, Rhee SY, Jeong SJ, et al. Features of long-standing Korean type 2 diabetes mellitus patients with diabetic retinopathy: a study based on standardized clinical data. Diabetes Metab J 2017;41(5):393. [doi: 10.4093/dmj.2017.41.5.393]
25. Lopes de Faria JB, Silva KC, Lopes de Faria JM. The contribution of hypertension to diabetic nephropathy and retinopathy: the role of inflammation and oxidative stress. Hypertens Res 2011 Apr;34(4):413-422. [doi: 10.1038/hr.2010.263] [Medline: 21228783]
26. Chatziralli IP, Sergentanis TN, Keryttopoulos P, Vatkalis N, Agorastos A, Papazisis L. Risk factors associated with diabetic retinopathy in patients with diabetes mellitus type 2. BMC Res Notes 2010 Jun 1;3:1-4. [doi: 10.1186/1756-0500-3-153] [Medline: 20515457]
27. Hong J, Surapaneni A, Daya N, et al. Retinopathy and risk of kidney disease in persons with diabetes. Kidney Med 2021;3(5):808-815. [doi: 10.1016/j.xkme.2021.04.018] [Medline: 34693260]
28. Rasheed R, Pillai GS, Kumar H, Shajan AT, Radhakrishnan N, Ravindran GC. Relationship between diabetic retinopathy and diabetic peripheral neuropathy - neurodegenerative and microvascular changes. Indian J Ophthalmol 2021 Nov;69(11):3370-3375. [doi: 10.4103/ijo.IJO_1279_21] [Medline: 34708808]
29. Hsu CY, Lee CM, Chou KY, et al. The association of diabetic retinopathy and cardiovascular disease: a 13-year nationwide population-based cohort study. Int J Environ Res Public Health 2021 Jul 30;18(15):8106. [doi: 10.3390/ijerph18158106] [Medline: 34360398]
30. Dai L, Wu L, Li H, et al. A deep learning system for detecting diabetic retinopathy across the disease spectrum. Nat Commun 2021;12(1):3242. [doi: 10.1038/s41467-021-23458-5]
31. Wong TY, Sabanayagam C. The war on diabetic retinopathy: where are we now? Asia Pac J Ophthalmol (Phila) 2019;8(6):448-456. [doi: 10.1097/APO.0000000000000267] [Medline: 31789647]
32. Liu H, Li R, Zhang Y, et al. Economic evaluation of combined population-based screening for multiple blindness-causing eye diseases in China: a cost-effectiveness analysis. Lancet Glob Health 2023 Mar;11(3):e456-e465. [doi: 10.1016/S2214-109X(22)00554-X] [Medline: 36702141]
33. Yang Z, Tan TE, Shao Y, Wong TY, Li X. Classification of diabetic retinopathy: past, present and future. Front Endocrinol 2022;13:1079217. [doi: 10.3389/fendo.2022.1079217]

Abbreviations

AI: artificial intelligence
AUROC: area under the receiving operating characteristic
CKD: chronic kidney disease
CVD: cardiovascular disease
DL: deep learning
DM: diabetes mellitus
DR: diabetic retinopathy
HbA_{1c}: glycated hemoglobin
***ICD-10*:** *International Statistical Classification of Diseases, Tenth Revision*
LightGBM: light gradient-boosting machine
ML: machine learning
ROC: receiver operating characteristic
T1DM: type 1 diabetes mellitus
T2DM: type 2 diabetes mellitus
XGBoost: extreme gradient boosting

XSL•FO
RenderX

Edited by A Benis; submitted 06.03.24; peer-reviewed by DR Mazzotti, M Elfiky, YH Kim; revised version received 02.12.24; accepted 03.12.24; published 07.02.25.

Please cite as:
Kim S, Park J, Son Y, Lee H, Woo S, Lee M, Lee H, Sang H, Yon DK, Rhee SY
Development and Validation of a Machine Learning Algorithm for Predicting Diabetes Retinopathy in Patients With Type 2 Diabetes: Algorithm Development Study
JMIR Med Inform 2025;13:e58107
URL: https://medinform.jmir.org/2025/1/e58107
doi:10.2196/58107

© Sunyoung Kim, Jaeyu Park, Yejun Son, Hojae Lee, Selin Woo, Myeongcheol Lee, Hayeon Lee, Hyunji Sang, Dong Keon Yon, Sang Youl Rhee. Originally published in JMIR Medical Informatics (https://medinform.jmir.org), 7.2.2025. This is an open-access article distributed under the terms of the Creative Commons Attribution License (https://creativecommons.org/licenses/by/4.0/), which permits unrestricted use, distribution, and reproduction in any medium, provided the original work, first published in JMIR Medical Informatics, is properly cited. The complete bibliographic information, a link to the original publication on https://medinform.jmir.org/, as well as this copyright and license information must be included.

XSL•FO
RenderX

Predicting Readmission Among High-Risk Discharged Patients Using a Machine Learning Model With Nursing Data: Retrospective Study

Eui Geum Oh[1,2,3*], PhD, RN; Sunyoung Oh[4], MSN, RN; Seunghyeon Cho[5], MAI; Mir Moon[3,6,7*], PhD, RN

[1]College of Nursing, Yonsei University, Seoul, Republic of Korea

[2]Mo-Im Kim Nursing Research Institute, Yonsei University, Seoul, Republic of Korea

[3]Institute for Innovation in Digital Healthcare, Yonsei University, Seoul, Republic of Korea

[4]School of Nursing, Yale University, New Haven, CT, United States

[5]Digital & Technology Group, CJ CheilJedang, Suwon, Republic of Korea

[6]Department of Nursing, Graduate School, Yonsei University, Seoul, Republic of Korea

[7]Department of Nursing, Daejeon University, 62, Daehak-ro, Dong-gu, Daejeon, Republic of Korea

[*]these authors contributed equally

Corresponding Author:
Mir Moon, PhD, RN
Institute for Innovation in Digital Healthcare, Yonsei University, Seoul, Republic of Korea

Abstract

Background: Unplanned readmissions increase unnecessary health care costs and reduce the quality of care. It is essential to plan the discharge care from the beginning of hospitalization to reduce the risk of readmission. Machine learning–based readmission prediction models can support patients' preemptive discharge care services with improved predictive power.

Objective: This study aimed to develop a readmission early prediction model utilizing nursing data for high-risk discharge patients.

Methods: This retrospective study included the electronic medical records of 12,977 patients with 1 of the top 6 high-risk readmission diseases at a tertiary hospital in Seoul from January 2018 to January 2020. We used demographic, clinical, and nursing data to construct a prediction model. We constructed unplanned readmission prediction models by dividing them into Model 1 and Model 2. Model 1 used early hospitalization data (up to 1 day after admission), and Model 2 used all the data. To improve the performance of the machine learning method, we performed 5-fold cross-validation and utilized adaptive synthetic sampling to address data imbalance. The 6 algorithms of logistic regression, random forest, decision tree, XGBoost, CatBoost, and multiperceptron layer were employed to develop predictive models. The analysis was conducted using Python Language Reference, version 3.11.3. (Python Software Foundation).

Results: In Model 1, among the 6 prediction model algorithms, the random forest model had the best result, with an area under the receiver operating characteristic (AUROC) curve of 0.62. In Model 2, the CatBoost model had the best result, with an AUROC of 0.64. BMI, systolic blood pressure, and age consistently emerged as the most significant predictors of readmission risk across Models 1 and 2. Model 1, which enabled early readmission prediction, showed a higher proportion of nursing data variables among its important predictors compared to Model 2.

Conclusions: Machine learning–based readmission prediction models utilizing nursing data provide basic data for evidence-based clinical decision support for high-risk discharge patients with complex conditions and facilitate early intervention. By integrating nursing data containing diverse patient information, these models can provide more comprehensive risk assessment and improve patient outcomes.

(JMIR Med Inform 2025;13:e56671) doi:10.2196/56671

KEYWORDS

machine learning; EHR; electronic health record; electronic medical record; EMR; artificial intelligence; readmission; nursing data; clinical decision support; prediction; predictive; discharge; admission; hospitalization

XSL•FO
RenderX

Introduction

Readmission is an unintended outcome that occurs in patients discharged from the hospital. In South Korea, the 30-day readmission rate in tertiary general hospitals in 2020 was approximately 30%, increasing yearly along with readmission cost statistics [1]. According to a Center for Medicare and Medicaid Services report in the United States, readmission rates for patients reach 2 million yearly, with readmissions costing $26 billion [2]. Despite the growing interest and literature on readmissions, unplanned readmission rates still need to be managed.

It is essential to accurately predict and select high-risk discharge patients to reduce readmission costs and improve the quality of medical care. Predictive modeling is an efficient way to stratify patient readmission risk and optimize the allocation of clinical resources by providing preventive interventions to high-risk patients [3]. Traditional statistical methods for creating predictive models have focused on inference, which involves creating a mathematical model of a data-generating process to formalize an understanding of how it works or to test hypotheses. The problem is that as the sample size of the data grows and the number of input variables increases, the possible associations between variables increase, making the model more complex and the statistical inference less accurate [4]. In particular, traditional risk prediction models, such as regression analysis, show limited predictive power [5]. In response to these challenges, machine learning methodologies have emerged as a powerful alternative. These approaches employ diverse algorithms to systematically process complex and voluminous datasets, identifying patterns and generating predictions. This capability proves particularly advantageous when dealing with "big data" characterized by numerous input variables and complex nonlinear interactions [6]. However, it is crucial to note that the application of machine learning in medical contexts presents certain challenges. In the absence of robust predictors and comprehensive domain-specific knowledge, establishing direct correlations between machine learning outcomes and existing medical information can be problematic. Despite these limitations, recent advancements have led to the development of machine learning–based high-prediction models. These models function as advanced predictive analysis technologies, capable of identifying and processing diverse patient information and conditions. Through the analysis of high-dimensional medical data, these sophisticated models generate hierarchical predictive frameworks with enhanced prognostic capabilities. This approach effectively addresses the inherent limitations of conventional statistical methods, thereby facilitating the implementation of personalized treatment strategies tailored to individual patients [7].

Treatment of high-risk discharged patients with high readmission is focused only at discharge, mainly by providing postdischarge care interventions [8]. Additionally, most existing readmission prediction models only utilize medical information data such as the patient's diagnostic tests [9]. Although nursing data in the early stages of a patient's hospitalization include comprehensive and direct information on physical and functional health factors, psychosocial characteristics, and socioeconomic status, studies have yet to be conducted on developing predictive models utilizing the usefulness of this nursing assessment information [10]. Predicting a patient's readmission should be done from the beginning of hospitalization so that a patient-tailored discharge plan can be established and reflected in treatment. It is necessary to actively utilize nursing data containing comprehensive information [11,12].

Therefore, this study aimed to develop a readmission early prediction model utilizing nursing data, including physical, mental, and social information for high-risk discharge patients.

Methods

Study Design and Setting

Our article follows the guidelines of the Transparent Reporting of a Multivariable Prediction Model for Individual Prognosis (TRIPOD) consensus document. This study is a retrospective electronic health record (EHR) data analysis. This retrospective observational study used EHR data collected at a tertiary acute care hospital with over 2500 medical conditions in Seoul, Republic of Korea. To develop a readmission early prediction model for readmission of high-risk discharge patients, we employed a retrospective study design utilizing nursing data.

Data Sources

We extracted medical record data of 12,977 patients at S Hospital in Seoul, Korea, for 25 months from January 2018 to January 2020. As a study to confirm the EHR data from the time of admission to the time of discharge of the patient, the information collected until January 31, 2021, was used to track readmission within 30 days. Data were requested from S University Hospital via the SOBIG data portal using subject inclusion criteria. The big data team extracted and received data from the first hospitalization of adult patients hospitalized for 6 major disease groups (chronic obstructive pulmonary disease, liver disease, diabetes mellitus, lung disease, heart failure, and chronic kidney disease) for 2 years. Hospital S is a high-level general hospital with about 2500 beds, with approximately 2000 to 3000 surgeries per month and more than 10,000 outpatient visits per day. We secured medical records of medical institutions where many patients are frequently hospitalized and readmitted and used them to develop a prediction model.

We used various types of EHR data from the participants, including during hospitalization and follow-up data within 30 days of discharge point. Analysis in this study included general, clinical, and nursing data recorded after the direct assessment of patients.

Data Inclusion and Exclusion Criteria

The data inclusion criteria are as follows: patients were older than 18 years at admission. The disease group selection of the subjects was based on the most recent 2021 HIRA (Health Insurance Review and Assessment Service) data, and the discharged patients from the top 6 main diagnosis groups with high readmission rates were selected. One patient had only one record.

XSL•FO
RenderX

The data exclusion criteria are as follows: patients who died during hospitalization. Data resulting in death were excluded from discharge records.

Data Preprocessing

Data Extraction

Of the initial 12,977 pieces of data, 388 duplicates were excluded, and 10,076 pieces of data were confirmed. Of these, 9536 medical records were analyzed, excluding data from 540 patients who died and data from 2513 patients with diagnoses who did not meet the inclusion criteria. Records with more than 65% missing values or records with missing values in categorical variables were deleted, and the final 9028 medical records were used to develop a prediction model.

To predict early readmissions at the same time as the patient's admission, we built two models, Model 1 using the initial data up to the first day of admission and Model 2 using the data from the entire hospital stay to just before discharge, with different data extraction times.

Data Imputation

Category and continuous variables with missing values were handled differently. For categorical variables, we excluded data by deleting missing values, and for continuous variables, we had about 25% missing values for BMI and ward severity, and less than 5% missing values for all other variables. For BMI, the proportion of missing values was higher than for other variables due to the large number of cases where only weight was entered among the patient's height and weight measurements. For ward severity, there were missing values due to the patient's room change, but there was no difference in predictive power based on missing values when training the model. These missing values were imputed using KNN imputation (K=5). Finally, we constructed a readmission prediction model using 9028 data.

Data Imbalance

The observed readmission rate for all data used in this study was 16.5%. To solve the data imbalance problem when building readmission prediction models, we compared four sampling methods: ADASYN, under-sampling, SMOTE, and random over-sampling. The ADASYN method was ultimately selected among the four sampling methods to resolve the data imbalance issue because the ADASYN method showed the highest possible model performance results.

Ethical Considerations

The ethics review committee of Severance Hospital approved this retrospective data analysis study (DRB approval number 4-2021-1334). Severance Medical Center's guidelines for using EHRs require the data to be provided in Excel format with patient identification information removed. Data analysis was performed based on this data.

Variables

EHR data were analyzed to predict patient readmissions. Readmissions, the primary outcome of interest in the study, were assessed as unplanned readmissions within 30 days [13]. The study aimed to determine a patient's likelihood of readmission to develop an early discharge care plan. To determine the likelihood of patient readmission, we classified the target variable Y as yes (1) or no (0). Predictor variables (X) necessary to confirm the presence or absence of rehospitalization, which is the target variable of the patient, including sex, age, admission days, diagnosis group, number of ICD-10 codes, admission and discharge medications, state of consciousness, BMI, falls and pressure ulcer risk, vital signs, literacy, economic status, functional and emotional evaluation, number of nursing diagnosis records, presence of the caregiver, admission via the emergency room, health behavior habits (smoking, drinking, regular exercise, sleep disorder, and nutritional status), blood test values (levels of sodium, hemoglobin, potassium, aspartate aminotransferase, glucose, and creatinine; and white blood cell counts) were included in the analysis. Utilizing coefficient of variation (CV) values, Model 2 incorporated patient data from admission to discharge to capture data variability.

Among the various variables, the following are included as nursing data: falls and pressure ulcer risks, vital signs, literacy, economic status, functional and emotional evaluation, number of nursing diagnosis records, presence of the caregiver, health behavior habits (eg, smoking, drinking, regular exercise, sleep disorder, and nutritional status), and ward severity. The ward severity score is a score given by the nurse in charge of the ward to each patient by identifying the number of interventions in the areas of hygiene, nutrition, elimination, exercise and activity, education and counselling, emotional support, measurement and observation, communication and alertness, treatment and testing, medication, interdepartmental coordination of patient care, discharge, and power management. The modified Barthel index scale is an ordinal scale that measures an individual's ability to complete activities of daily living. It consists of 10 items and has a total score of 100. However, the organization that collected the data evaluated 11 items by adding an item on the ability to use walking aids other than wheelchairs, and the total score was 105. All of these nursing data variables include information recorded by the nurse during the patient's admission to the hospital to indicate the patient's condition. We built a model to predict unexpected readmissions, divided into Model 1 and Model 2. Model 1 entered possible variables based on data from the first day of hospitalization, and Model 2 selected variables based on data from the entire period of hospitalization. All variables were selected based on prior literature and entered through stepwise feature selection [14,15].

Table 1 displays all the input variables according to Models 1 and 2.

XSL•FO
RenderX

Table . An overview of the input variables.

Variable name	Type	Value (range)	Model
General data			
Sex	Nominal	Male or Female	1, 2
Patient age	Ordinal	(19, 102)	1, 2
Diagnosis group	Nominal	0, 1, 2, 3, 4, 5	1, 2
Length of stay	Ordinal	(0, 532)	2
BMI	Ordinal	(10.63, 51.54)	1, 2
Emergency room visits	Nominal	Yes or No	1, 2
Admission to the intensive care unit	Nominal	Yes or No	2
Clinical data			
ICD-10 code	Ordinal	(1, 29)	1, 2
Medicine	Ordinal	(0, 37)	1
Discharge medication	Ordinal	(0, 33)	2
Number of surgeries	Ordinal	(0, 6)	2
Mental status	Nominal	Alert or Non-Alert	1, 2
SBP[a]	Ordinal	(48, 255)	1
SBP_CV[b]	Ordinal	(0, 0.31)	2
DBP[c]	Ordinal	(20, 156)	1
Heart rate	Ordinal	(22, 195)	1
Heart rate_CV	Ordinal	(0, 0.52)	2
Body temperature	Ordinal	(34.5, 40.8)	1
Body temperature_CV	Ordinal	(0, 0.03)	2
Respiration	Ordinal	(8, 52)	1
Saturation	Ordinal	(62, 100)	1
Whole blood test[d]	Ordinal	(0, 5)	1
Chemistry test[e]	Ordinal	(0, 5)	1
Electrolyte test[f]	Ordinal	(0, 5)	1
WBC_CV	Ordinal	(0, 1.75)	2
Hemoglobin_CV	Ordinal	(0, 0.62)	2
Na_CV	Ordinal	(0, 0.09)	2
AST_CV	Ordinal	(0, 3.28)	2
Glucose_CV	Ordinal	(0, 1.66)	2
K_CV	Ordinal	(0, 0.42)	2
Creatinine_CV	Ordinal	(0, 1.32)	2
Nursing data			
Number of nursing diagnosis	Ordinal	(0, 15)	1, 2
Ward severity	Ordinal	(9, 48)	1
Ward severity_CV	Ordinal	(0, 0.71)	2
Caregiver	Nominal	Yes or No	1, 2
Health behavior habits[g]	Ordinal	(0, 8)	1, 2
Fall risk assessment	Ordinal	(0, 20)	1
Fall risk assessment_CV	Ordinal	(0, 3.06)	2

XSL•FO
RenderX

Variable name	Type	Value (range)	Model
Braden scale	Ordinal	(10, 26)	1
Braden scale_CV	Ordinal	(0, 0.33)	2
Literacy	Nominal	Adequate or Inadequate	1, 2
Financial problem	Nominal	Yes or No	1, 2
Emotional assessment	Ordinal	(0, 6)	1, 2
Modified Barthel index	Ordinal	(0, 105)	1, 2

[a]SBP: systolic blood pressure.

[b]CV: coefficient of variation.

[c]DBP: diastolic blood pressure.

[d]Whole blood test: The sum of the normal items of the white blood cell count, hemoglobin, hematocrit, platelet count, and lymphocyte tests among the complete blood count tests.

[e]Chemistry test: The sum of the normal items of blood urea nitrogen, creatinine, aspartate aminotransferase, alanine transaminase, and albumin tests among routine chemistry serum tests.

[f]Electrolyte test: The sum of the normal items of calcium, inorganic P, Na, K, and Cl tests among electrocyte serum tests.

[g]Health behavior habits: smoking history, drinking history, sleep disorder, regular exercise, and nutritional status.

Machine Learning-Based Predictive Models

Machine learning is a field of artificial intelligence that studies the development of computer algorithms and techniques that automatically improve through experience [16]. Machine learning is divided into supervised learning and unsupervised learning and predicts outcomes through supervised learning. There are various types of machine learning. A representative example is a decision tree, a graph representing a selection and its result in the form of a tree. The nodes of the graph represent events or selections, and the edges of the graph represent decision rules or conditions. Each tree consists of nodes and branches. Each node represents an attribute of a group to be classified, and each branch represents a value that the node can take. It is an algorithm suitable for a rehospitalization prediction model that mainly predicts the presence or absence of rehospitalization. The boosting algorithm is a family of algorithms that transform weak learners into strong learners. Boosting is an ensemble learning technique used to reduce bias and variance. A weak learner is defined as a classifier, and a strong learner is a classifier that is randomly correlated with the actual classification. Many algorithms with high accuracy and predictive power are being developed in prediction algorithms. Bagging is applied where the accuracy and stability of machine learning algorithms must be increased, and it can be applied to classification and regression and helps reduce variance and handle overfitting. The random forest algorithm is an algorithm that creates a decision tree using this bagging method. It is an algorithm that can solve the overfitting problem that a single decision tree can have by creating various subdatasets through bootstrapping and having multiple decision trees learn each dataset and collate the results [6]. In this study, we used a supervised learning method through 6 algorithms that are considered most suitable for predicting readmission among machine learning algorithms: logistic regression, decision tree, random forest, CatBoost, XGBoost (extreme gradient boosting), and multilayer perceptron, and developed a readmission prediction model for high-risk patients. The dataset was split into 60% for training, 20% for validation, and 20% for testing, with all models trained 5 times and model performance evaluated using layered 5-fold cross-validation. We performed a grid search to find the most suitable hyperparameters for the model while training and evaluating the model, and then performed model fine tuning.

According to the data inclusion and exclusion criteria and missing value processing, data from 9028 patients were available for analysis. We constructed unexpected readmission prediction models by dividing them into Model 1 and Model 2. Model 1 implemented an early readmission prediction model based on data from the first day of hospitalization to predict readmission early. Model 2 implemented a model to supplement data that should have been included in Model 1 based on all the data. All machine learning–based predictive model development processes were conducted with the participation of artificial intelligence experts, who conducted the procedures together, provided advice, and reviewed them. The analysis in this study was performed using Python Language Reference, version 3.11.3. (Python Software Foundation).

Evaluation of Prediction Performance

After implementing 6 models, we selected the final model and evaluated each model's confusion matrix, accuracy, precision, recall, F1-score, and area under the receiver operating characteristic (AUROC) curve.

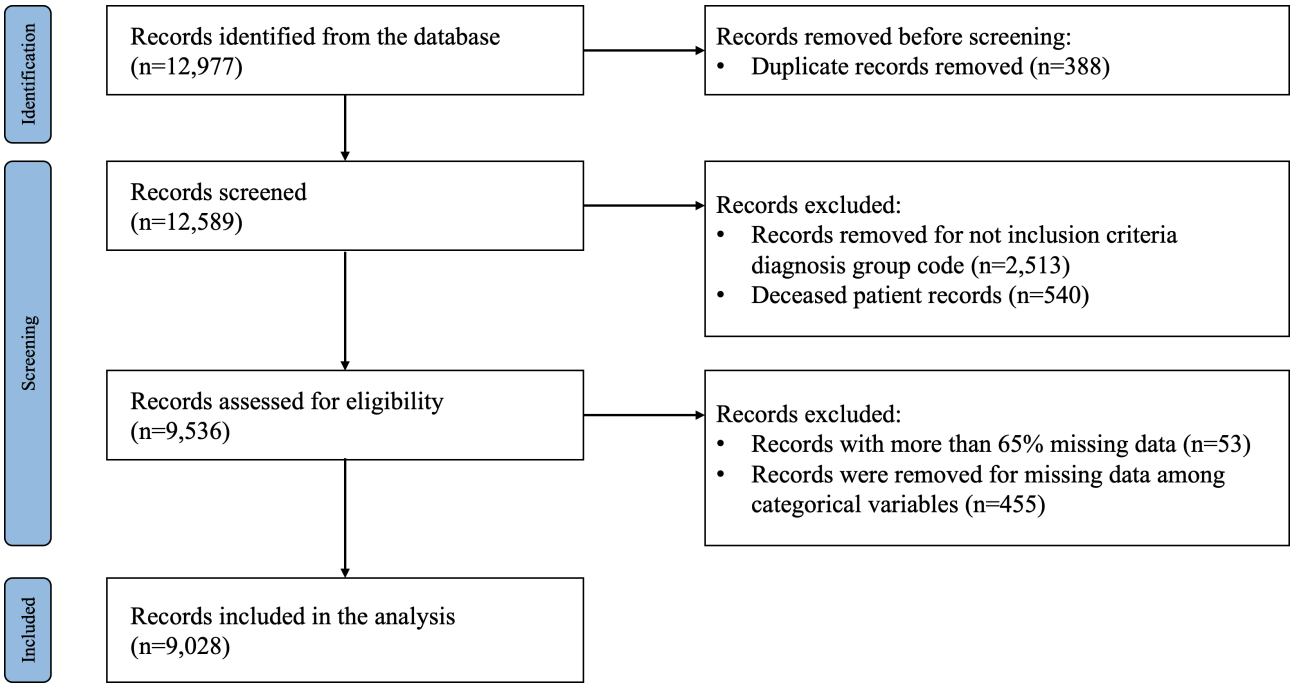
We compared techniques using performance measures of different models. Confusion matrices were used to determine accuracy, recall, precision, and F1-score. True positive, true negative, false positive, and false negative were used to determine the performance of each model. True positive refers to cases where the model predicted yes, and the patient was actually readmitted. In contrast, true negative refers to cases where the model predicted no, and the patient was not readmitted. Conversely, false positive refers to cases where the model predicted yes, but the patient was not actually readmitted, and false negative refers to cases where the model predicted no, but the patient was not actually readmitted.

XSL•FO
RenderX

Results

Figure 1 shows the flow of data extraction. Of the initial 12,589 data, we analyzed a final of 9536 medical records, excluding 2513 duplicates and 540 deceased patient data. Of the 9028 participants, 1493 experienced an unplanned readmission within 30 days; the rate of unplanned readmissions within 30 days was 16.5%. Table 2 shows the essential characteristics of the study participants. There were 3186 (35.29%) patients under the age of 60 years, 1194 (13.23%) patients over the age of 80 years, and 4648 (51.48%) patients between the ages of 60 and 80 years. In terms of sex, there were 3309 (36.65%) men and 5719 (63.35%) women in the study, and by diagnosis, 4725 (52.34%) patients had liver disease, followed by 1612 (17.86%) patients with pulmonary disease, 1309 (14.50%) with chronic kidney disease, 1004 (11.12%) with heart failure, 279 (3.09%) with diabetes, and 99 (1.10%) with chronic obstructive pulmonary disease. A total of 3237 (35.86%) patients were admitted unplanned via the emergency department, while 5791 (64.14%) were planned via the outpatient department.

Figure 1. Flow chart showing data extraction.



XSL•FO
RenderX

Table . Demographic information of the dataset.

Patient characteristics	n (%) (N=9028)
Sex	
Male	3312 (36.69)
Female	5716 (63.31)
Age (years)	
<60	3185 (35.28)
60-79	4650 (51.51)
≥80	1193 (13.21)
Diagnosis group	
COPD[a]	99 (1.10)
Liver disease	4728 (52.36)
Diabetes mellitus	278 (3.08)
Pulmonary disease	1612 (17.86)
Heart failure	1004 (11.12)
CKD[b]	1307 (14.48)
Admission route	
Emergency room	3238 (35.87)
Outpatient	5790 (64.13)
Readmission	
Yes	1492 (16.53)
No	7536 (83.47)

[a]COPD: chronic obstructive pulmonary disease

[b]CKD: chronic kidney disease

In this study, we developed 2 prediction models to enable the early prediction of high-risk patient readmissions when admitted to the hospital: one using early hospitalization data and the other using complete data that can compensate for the initial lack of information. Model 1 was a high-risk patient readmission prediction model developed using initial data up to the first day of hospitalization. Model 2 was a prediction model developed based on complete patient hospitalization data. The performance evaluation results of the 5-fold cross-validation test of the 6 candidate model algorithms in Model 1 and Model 2 are shown in Table 3.

XSL•FO
RenderX

Table . Comparison of the performance of the predictive models of Model 1 and Model 2.

Algorithm	Set	Accuracy	Precision	Recall	F1-score	AUROC[a] curve
Model 1						
LR[b]	Train	0.59	0.58	0.62	0.60	0.61
	Test	0.83	0.20	0	0	0.60
DT[c]	Train	0.84	0.98	0.70	0.82	0.88
	Test	0.83	0.21	0	0	0.55
RF[d]	Train	0.89	0.99	0.78	0.87	0.95
	Test	0.79	0.25	0.57	0.33	0.62
CatBoost	Train	0.89	0.99	0.78	0.88	0.93
	Test	0.83	0.28	0	0	0.62
XGB[e]	Train	0.85	0.94	0.76	0.84	0.92
	Test	0.83	0.25	0	0	0.60
MLP[f]	Train	0.62	0.68	0.55	0.55	0.72
	Test	0.83	0.21	0.01	0.02	0.60
Model 2						
LR	Train	0.60	0.59	0.61	0.60	0.63
	Test	0.83	0	0	0	0.62
DT	Train	0.83	0.93	0.72	0.81	0.88
	Test	0.83	0	0	0	0.61
RF	Train	0.83	0.95	0.70	0.80	0.90
	Test	0.59	0.22	0.59	0.10	0.63
CatBoost	Train	0.86	0.98	0.73	0.84	0.92
	Test	0.83	0	0	0	0.64
XGB	Train	0.99	1	0.99	0.99	1
	Test	0.82	0.24	0.05	0.08	0.62
MLP	Train	0.76	0.75	0.78	0.76	0.84
	Test	0.83	0.45	0.03	0.06	0.64

[a]AUROC: area under a receiver operating characteristic.

[b]LR: logistic regression.

[c]DT: decision tree.

[d]RF: Random forest.

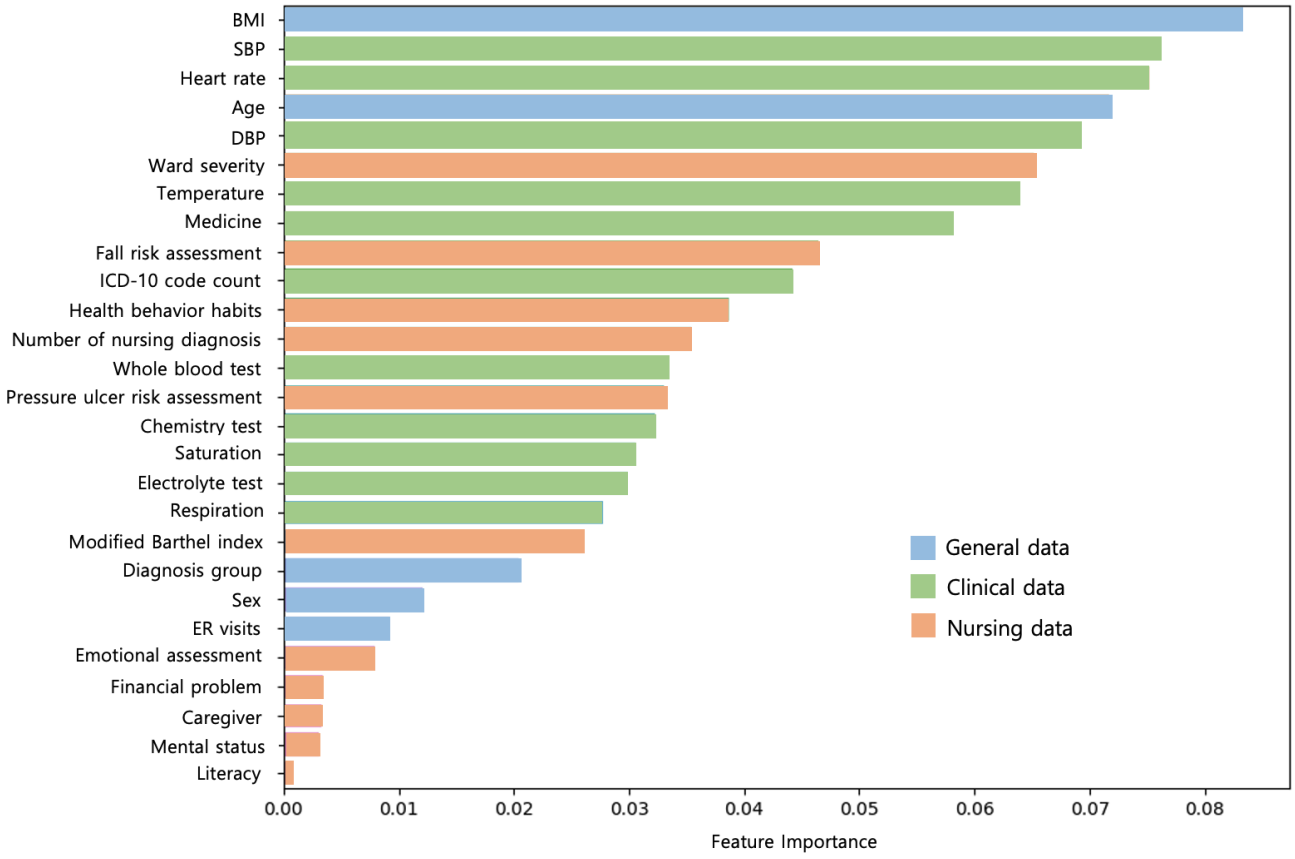
[e]XGBoost: extreme gradient boosting.

[f]MLP: multilayer perceptron.

For Model 1, the random forest model had the highest AUROC curve of 0.62 compared to all other models, while the decision tree model performed the worst with an AUROC curve of 0.55. The feature importance of the best-performing random forest model in Model 1 is shown in Figure 2. In Model 2, the CatBoost model had the highest AUROC curve of 0.64 compared to all other models, while the decision tree model had the lowest performance with an AUROC curve of 0.61. The feature importance of the best-performing CatBoost model in Model 2 is shown in Figure 3. Ultimately, the best-performing prediction models were the random forest model for Model 1 and the CatBoost model for Model 2. Although the random forest model and CatBoost model have the same AUROC curve value, when comparing the performance values of all models including the training data, the random forest model was not overfitted and performed evenly well, so after statistical discussion with AI experts, it was selected as the Model 1 final model.

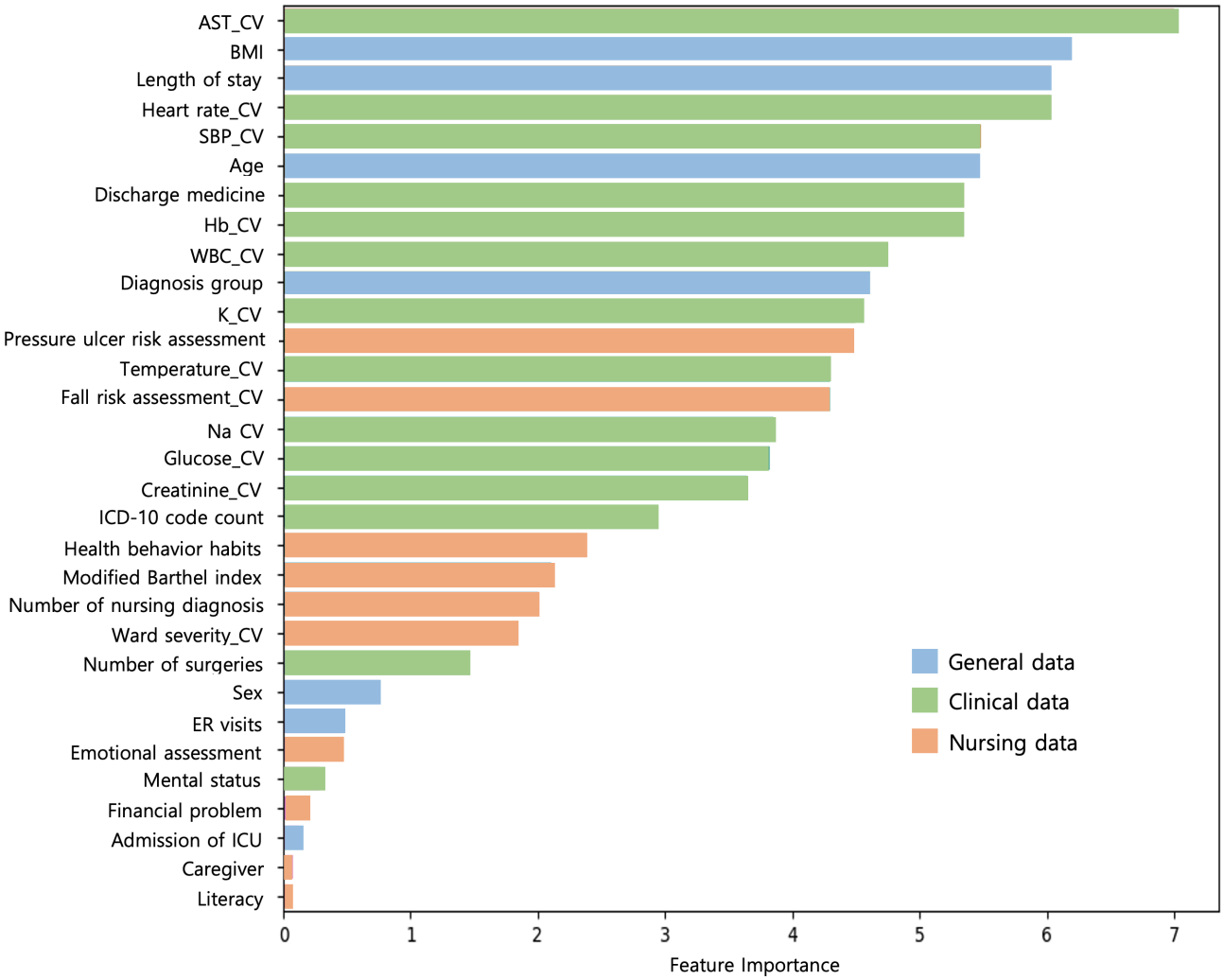
XSL•FO
RenderX

Figure 2. Feature importance of the random forest model in Model 1. SBP: systolic blood pressure; DBP: diastolic blood pressure; ER: emergency room.



XSL•FO
RenderX

Figure 3. Feature importance of the CatBoost model in Model 2. AST: aspartate transaminase; CV: coefficient of variation; SBP: systolic blood pressure; Hb: hemoglobin; WBC: white blood cell; ER: emergency room; ICU: intensive care unit.



As a result of analyzing the feature importance of Model 1 and Model 2, the three variables of BMI, systolic blood pressure, and age were commonly found to be important predictors of readmission risk. According to Figure 2, Model 1, which enabled the early prediction of readmission, had a higher proportion of nursing data among the important predictors than Model 2. In Model 1, constructed using early hospitalization data, 45% of the nursing data variables (ward severity, fall risk assessment, health behavior habits, number of nursing diagnoses, and pressure ulcer risk assessment) were ranked within the top 50% of important variables. This finding suggests the potential significance of incorporating nursing data in early readmission prediction models.

Discussion

Principal Findings and Comparison With Previous Works

In predicting unplanned readmission within 30 days using data from 9028 high-risk discharged patients, machine learning methods (random forest and CatBoost models) showed better predictive power than traditional logistic regression methods, similar to other previous studies [17,18]. While previous studies have focused on developing a prediction model for a specific condition for a specific group of patients with a specific diagnosis [19], this study is significant in that it is a prediction model development study that focuses on the generalization process of predicting unplanned readmissions within 30 days by incorporating the top 6 diagnosis groups of high-risk discharged patients suggested by the Health Insurance Review and Assessment Service to predict the potential of readmission.

Many interventions aimed at reducing patients' unplanned readmissions are often initiated just before or after inpatient discharge, which has little impact on improving the inpatient quality of care [20]. Providing early interventions related to readmissions during hospitalization with early discharge planning can reduce readmissions [21]. However, most readmission prediction models are built on posthospitalization data, often including information about the patient's physical and diagnostic tests. Because clinically essential variables such as the length of stay, diagnosis codes, laboratory test results, and medications are usually entered just before discharge, readmission prediction models are primarily built on patient data immediately before or after discharge. The most widely used measures of readmission risk in US health care settings are the HOSPITAL score [22] and the LACE index [23], but both have the limitation that they are only available at the end of a hospital stay. When creating a prediction model that

XSL•FO
RenderX

includes all variables, its prediction performance is good. However, it needs to be applied for more time to actual patients, making it challenging to support effective clinical decision-making. In this study, to overcome these limitations, we implemented two patient readmission prediction models, Model 1 and Model 2, to predict the readmission rate from the time of hospitalization and plan discharge care. Model 1, implemented based on the patient's initial hospitalization data, and Model 2, implemented by adding variables that can complement Model 1, can help clinical decision-making by predicting the patient's readmission rate earlier. Model 1, which utilized data from the first day of hospitalization, had an AUROC curve of 0.62 in our study. Although this performance is not exceptionally high, it is consistent with most previous studies that developed readmission prediction models using initial hospitalization data, which reported results of less than an AUROC curve of 0.75 [5,17,24,25]. Importantly, it enables the proactive identification of high-risk patients and the provision of timely and preventive therapeutic interventions early in their hospital stay.

Unplanned readmissions cause a heavy burden on individuals and society through unnecessary health care costs and resource use, and readmission management has been recognized as an essential issue in improving patient quality of care [26]. To reduce the cost of unnecessary readmissions and improve the quality of care for patients, the Korea Health Insurance Review and Assessment Service conducts a national risk-based readmission cost appropriateness assessment, and the US government has implemented the Hospital Readmission Reduction Program (HRRP) since 2012 to encourage the reduction of hospital readmissions by involving patients and caregivers in discharge planning [27]. However, limited health care resources make it challenging to provide discharge interventions to all patients, and screening high-risk patients for early discharge planning is essential. Evidence suggests that focusing interventions on high-risk patients can reduce the risk of hospital readmission within 30 days by 11 - 28% [28-30], and it is essential to utilize nursing data that include holistic information from the patient's initial hospitalization to develop a preventive care plan for high-risk patients. A previous study found the potential importance of utilizing nursing variables to identify risk factors for readmission [31]. The BMI variable at the top of the feature importance of Model 1 is the same as the result that it was highly related to the patient's obesity level, cardiovascular problems, and readmission, similar to the previous study [32]. This study is significant in that it proved that BMI is the most simple and important screening variable related to the patient's readmission in the early stage of hospitalization. In the future, it is necessary to recognize the importance of BMI screening and collect information related to the probability of early patient readmission [32].

Information collected directly about patients' physical, mental, and social aspects by nurses, who interact most closely with patients in the hospital and provide care, is essential in predictive models for the early identification of high-risk discharges. In this study, we developed an early prediction model for unplanned readmissions using nursing data from patients in the early stage of hospitalization. In particular, we found that many nursing data variables were included in the high rankings among the important predictors in Model 1 developed using early hospitalization data. The high representation of nursing variables among the most influential predictors underscores the potential value of integrating nursing-specific information into risk assessment tools for hospital readmission. Further investigation into the specific contributions of these nursing variables may provide valuable insights for enhancing the accuracy and clinical utility of early readmission prediction models. Although most predictions of high-risk discharged patients are based on data at discharge, identifying high-risk patients should ideally be performed early enough to allow for therapeutic interventions during hospitalization, which was attempted in this study.

Limitations

This study has several limitations. First, our prediction model, designed for adults aged over 18 years, does not apply to pediatric patients aged less than 18 years. Second, the model's development was based on data from a single hospital in a specific region. Consequently, its applicability to readmission scenarios in different health care settings or countries may be limited. Furthermore, tracking patient readmissions poses a challenge, especially in cases where patients admitted to our hospital could have subsequent readmissions to different facilities. This potential for cross-hospital readmissions might not be fully captured in our model.

Additionally, as this was a retrospective study utilizing deidentified data, it limited our ability to validate the relationships between our findings and factors identified in other studies. Finally, there were limitations in implementing perfectly standardized data, as the data were manually entered as part of the medical and nursing data.

Clinical Implications

Our readmission prediction model can be used to predict and continuously monitor a patient's risk of readmission during the entire hospital stay. It can be used as an early screening tool to assess the risk associated with a patient's readmission.

Conclusions

This study developed two prediction models, Model 1 using initial hospitalization data and Model 2 reflecting the variability of variables from admission to discharge, for the early prediction of unplanned readmission within 30 days in high-risk discharged patients. Model 1 showed the best performance of the random forest model, with an AUROC curve of 0.95 for the training data and 0.62 for the test data. For Model 2, the CatBoost model performed the best, with an AUROC curve of 0.92 for the training data and an AUROC curve of 0.64 for the test data. The Model 1 and Model 2 predictive models allow us to predict the likelihood of readmission from the beginning of a patient's hospitalization and proactively plan for early discharge. In addition, this study identified various significant predictors of unplanned readmission and identified changes in patients over time. The predictive model was developed and validated using data from 9028 discharged patients and can be applied to adult patients who represent the high-risk discharge population in tertiary care hospitals. However, further research and experimentation are necessary to implement the developed

XSL•FO
RenderX

predictive models in clinical practice within an EHR environment for predicting early readmission and monitoring readmission risk. In particular, additional studies must be conducted to address the limitations of this monocentric study, consider the characteristics of medical data with numerous missing values, and validate the data sources for each variable. Based on this study, future development of a systematic clinical decision support system that utilizes machine learning–based readmission prediction models with nursing data could enable real-time early risk prediction of patient readmission. This approach would facilitate the provision of preventive discharge services for high-risk patients and improve the quality of health care services.

Acknowledgments

This work was supported by the National Research Foundation (NRF) grant funded by the Korean government (No. 2022R1A2C201229411).

Conflicts of Interest

None declared.

References

1. Health insurance review & assessment service. (3rd) risk-standardized readmission cost adequacy assessment results. 2020. URL: https://www.hira.or.kr/ra/eval/asmWrptPopup.do?evlCd=29&pgmid=HIRAA030004000000#none [accessed 2025-02-24]
2. Betancourt JR, Tan-McGrory A, Kenst KS. Guide to preventing readmissions among racially and ethnically diverse Medicare beneficiaries.: Prepared by the Disparities Solutions Center, Mongan Institute for Health Policy at Massachusetts General Hospital. Baltimore, MD: Centers for Medicare & Medicaid Services Office of Minority Health; 2015 Sep. URL: https://eldercarebroker.com/pub/OMH_Readmissions_Guide.pdf [accessed 2025-02-21]
3. Zhou H, Della PR, Roberts P, Goh L, Dhaliwal SS. Utility of models to predict 28-day or 30-day unplanned hospital readmissions: an updated systematic review. BMJ Open 2016 Jun 27;6(6):e011060. [doi: 10.1136/bmjopen-2016-011060] [Medline: 27354072]
4. Bzdok D, Altman N, Krzywinski M. Statistics versus machine learning. Nat Methods 2018 Apr;15(4):233-234. [doi: 10.1038/nmeth.4642] [Medline: 30100822]
5. Artetxe A, Beristain A, Graña M. Predictive models for hospital readmission risk: a systematic review of methods. Comput Methods Programs Biomed 2018 Oct;164:49-64. [doi: 10.1016/j.cmpb.2018.06.006] [Medline: 30195431]
6. Mahesh B. Machine learning algorithms - a review. IJSR 2020 Jan 5;9(1):381-386. [doi: 10.21275/ART20203995]
7. Parikh RB, Kakad M, Bates DW. Integrating predictive analytics into high-value care: the dawn of precision delivery. JAMA 2016 Feb 16;315(7):651-652. [doi: 10.1001/jama.2015.19417] [Medline: 26881365]
8. Hansen LO, Young RS, Hinami K, Leung A, Williams MV. Interventions to reduce 30-day rehospitalization: a systematic review. Ann Intern Med 2011 Oct 18;155(8):520-528. [doi: 10.7326/0003-4819-155-8-201110180-00008] [Medline: 22007045]
9. Huang Y, Talwar A, Chatterjee S, Aparasu RR. Application of machine learning in predicting hospital readmissions: a scoping review of the literature. BMC Med Res Methodol 2021 May 6;21(1):96. [doi: 10.1186/s12874-021-01284-z] [Medline: 33952192]
10. Kansagara D, Englander H, Salanitro A, et al. Risk prediction models for hospital readmission: a systematic review. JAMA 2011 Oct 19;306(15):1688-1698. [doi: 10.1001/jama.2011.1515] [Medline: 22009101]
11. Kim YM, Lee T, Lee HJ, Yang YL, Oh EG. Readmission of high-risk discharged patients at a tertiary hospital in Korea. J Healthc Qual 2019;41(4):e30-e37. [doi: 10.1097/JHQ.0000000000000151] [Medline: 30362997]
12. Lee HJ, Kim Y, Oh EG. A systematic review on nurse-led transitional care programs for discharged patients from hospital to home. Journal of Korean Clinical Nursing Research 2017;23(3):376-387. [doi: 10.22650/JKCNR.2017.23.3.376] [Medline: 28649855]
13. Stefan MS, Pekow PS, Nsa W, et al. Hospital performance measures and 30-day readmission rates. J Gen Intern Med 2013 Mar;28(3):377-385. [doi: 10.1007/s11606-012-2229-8] [Medline: 23070655]
14. Zuckerman RB, Sheingold SH, Orav EJ, Ruhter J, Epstein AM. Readmissions, observation, and the hospital readmissions reduction program. N Engl J Med 2016 Apr 21;374(16):1543-1551. [doi: 10.1056/NEJMsa1513024] [Medline: 26910198]
15. Oh EG, Sung JH, Park YS, Lee HJ, Kim YK. Physiological functional status and the levels of unmet care needs after discharge in patients with chronic pulmonary disease, colorectal cancer, and strokes. Journal of Korean clinical nursing research 2016;22(2):194-204. [doi: 10.22650/JKCNR.2016.22.2.194]
16. Holzinger A. From machine learning to explainable AI. Presented at: 2018 World Symposium on Digital Intelligence for Systems and Machines (DISA); Aug 23-25, 2018; Kosice p. 55-66. [doi: 10.1109/DISA.2018.8490530]

XSL•FO
RenderX

17. Lo YT, Liao JC, Chen MH, Chang CM, Li CT. Predictive modeling for 14-day unplanned hospital readmission risk by using machine learning algorithms. BMC Med Inform Decis Mak 2021 Oct 20;21(1):288. [doi: 10.1186/s12911-021-01639-y] [Medline: 34670553]
18. Mohanty SD, Lekan D, McCoy TP, Jenkins M, Manda P. Machine learning for predicting readmission risk among the frail: explainable AI for healthcare. Patterns 2022 Jan 14;3(1). [doi: 10.1016/j.patter.2021.100395] [Medline: 100395]
19. Garcia-Arce A, Rico F, Zayas-Castro JL. Comparison of machine learning algorithms for the prediction of preventable hospital readmissions. J Healthc Qual 2018;40(3):129-138. [doi: 10.1097/JHQ.0000000000000080] [Medline: 28857931]
20. Zhao P, Yoo I, Naqvi SH. Early prediction of unplanned 30-day hospital readmission: model development and retrospective data analysis. JMIR Med Inform 2021 Mar 23;9(3):e16306. [doi: 10.2196/16306] [Medline: 33755027]
21. Fox M. Nurse-led early discharge planning for chronic disease reduces hospital readmission rates and all-cause mortality. Evid Based Nurs 2016 Apr;19(2):62. [doi: 10.1136/eb-2015-102197] [Medline: 26701748]
22. Donzé J, Aujesky D, Williams D, Schnipper JL. Potentially avoidable 30-day hospital readmissions in medical patients: derivation and validation of a prediction model. JAMA Intern Med 2013 Apr 22;173(8):632-638. [doi: 10.1001/jamainternmed.2013.3023] [Medline: 23529115]
23. van Walraven C, Dhalla IA, Bell C, et al. Derivation and validation of an index to predict early death or unplanned readmission after discharge from hospital to the community. CMAJ 2010 Apr 6;182(6):551-557. [doi: 10.1503/cmaj.091117] [Medline: 20194559]
24. Schiltz NK, Dolansky MA, Warner DF, Stange KC, Gravenstein S, Koroukian SM. Impact of instrumental activities of daily living limitations on hospital readmission: an observational study using machine learning. J Gen Intern Med 2020 Oct;35(10):2865-2872. [doi: 10.1007/s11606-020-05982-0] [Medline: 32728960]
25. Aldhoayan MD, Khayat AM. Leveraging advanced data analytics to predict the risk of all-cause seven-day emergency readmissions. Cureus 2022 Aug;14(8):e27630. [doi: 10.7759/cureus.27630] [Medline: 36127978]
26. Bahrami MA, Kharazmi E, Ghalehgolab F, Farhadi P, Ahmadi F. Interventions to reduce hospital readmissions: a scoping review. Health Scope 2024 Jul 28;13(3). [doi: 10.5812/healthscope-143235]
27. NEJM Catal. Hospital readmissions reduction program (HRRP). URL: https://catalyst.nejm.org/doi/full/10.1056/CAT.18.0194 [accessed 2025-02-25]
28. Naylor MD, Brooten D, Campbell R, et al. Comprehensive discharge planning and home follow-up of hospitalized elders: a randomized clinical trial. JAMA 1999 Feb 17;281(7):613-620. [doi: 10.1001/jama.281.7.613] [Medline: 10029122]
29. Koehler BE, Richter KM, Youngblood L, et al. Reduction of 30-day postdischarge hospital readmission or emergency department (ED) visit rates in high-risk elderly medical patients through delivery of a targeted care bundle. J Hosp Med 2009 Apr;4(4):211-218. [doi: 10.1002/jhm.427] [Medline: 19388074]
30. Evans RL, Hendricks RD. Evaluating hospital discharge planning: a randomized clinical trial. Med Care 1993 Apr;31(4):358-370. [doi: 10.1097/00005650-199304000-00007] [Medline: 8464252]
31. Lodhi MK, Ansari R, Yao Y, Keenan GM, Wilkie DJ, Khokhar AA. Predicting Hospital Re-admissions from Nursing Care Data of Hospitalized Patients. Adv Data Min 2017;2017:181-193. [doi: 10.1007/978-3-319-62701-4_14] [Medline: 29104962]
32. Ram P, Shah M, Lo KBU, et al. Etiologies and predictors of readmission among obese and morbidly obese patients admitted with heart failure. Heart Fail Rev 2021 Jul;26(4):829-838. [doi: 10.1007/s10741-020-09920-4] [Medline: 32002731]

Abbreviations

AUROC: area under a receiver operating characteristic
CV: coefficient of variation
EHR: electronic health record
F1: harmonic mean of precision and recall
HRRP: Hospital Readmission Reduction Program

Edited by C Lovis; submitted 23.01.24; peer-reviewed by B Ryu, E Manuela, MJ Roulin; revised version received 14.01.25; accepted 06.02.25; published 05.03.25.

Please cite as:
Oh EG, Oh S, Cho S, Moon M
Predicting Readmission Among High-Risk Discharged Patients Using a Machine Learning Model With Nursing Data: Retrospective Study
JMIR Med Inform 2025;13:e56671
URL: https://medinform.jmir.org/2025/1/e56671
doi:10.2196/56671

XSL•FO
RenderX

© Eui Geum Oh, Sunyoung Oh, Seunghyeon Cho, Mir Moon. Originally published in JMIR Medical Informatics (https://medinform.jmir.org), 5.3.2025. This is an open-access article distributed under the terms of the Creative Commons Attribution License (https://creativecommons.org/licenses/by/4.0/), which permits unrestricted use, distribution, and reproduction in any medium, provided the original work, first published in JMIR Medical Informatics, is properly cited. The complete bibliographic information, a link to the original publication on https://medinform.jmir.org/, as well as this copyright and license information must be included.

XSL•FO
RenderX

Performance of Artificial Intelligence Chatbots on Ultrasound Examinations: Cross-Sectional Comparative Analysis

Yong Zhang[1], MSc; Xiao Lu[1], BSc; Yan Luo[1], MSc; Ying Zhu[2], BSc; Wenwu Ling[1], PhD

[1]Department of Medical Ultrasound, West China Hospital of Sichuan University, 37 Guoxue Alley, Chengdu, China

[2]Department of Thoracic Surgery, West China Hospital of Sichuan University, Chengdu, China

Corresponding Author:
Wenwu Ling, PhD
Department of Medical Ultrasound, West China Hospital of Sichuan University, 37 Guoxue Alley, Chengdu, China

Abstract

Background: Artificial intelligence chatbots are being increasingly used for medical inquiries, particularly in the field of ultrasound medicine. However, their performance varies and is influenced by factors such as language, question type, and topic.

Objective: This study aimed to evaluate the performance of ChatGPT and ERNIE Bot in answering ultrasound-related medical examination questions, providing insights for users and developers.

Methods: We curated 554 questions from ultrasound medicine examinations, covering various question types and topics. The questions were posed in both English and Chinese. Objective questions were scored based on accuracy rates, whereas subjective questions were rated by 5 experienced doctors using a Likert scale. The data were analyzed in Excel.

Results: Of the 554 questions included in this study, single-choice questions comprised the largest share (354/554, 64%), followed by short answers (69/554, 12%) and noun explanations (63/554, 11%). The accuracy rates for objective questions ranged from 8.33% to 80%, with true or false questions scoring highest. Subjective questions received acceptability rates ranging from 47.62% to 75.36%. ERNIE Bot was superior to ChatGPT in many aspects (P<.05). Both models showed a performance decline in English, but ERNIE Bot's decline was less significant. The models performed better in terms of basic knowledge, ultrasound methods, and diseases than in terms of ultrasound signs and diagnosis.

Conclusions: Chatbots can provide valuable ultrasound-related answers, but performance differs by model and is influenced by language, question type, and topic. In general, ERNIE Bot outperforms ChatGPT. Users and developers should understand model performance characteristics and select appropriate models for different questions and languages to optimize chatbot use.

(JMIR Med Inform 2025;13:e63924) doi:10.2196/63924

KEYWORDS

chatbots; ChatGPT; ERNIE Bot; performance; accuracy rates; ultrasound; language; examination

Introduction

With the rapid development of artificial intelligence (AI) technology, deep learning models are being increasingly and widely used in various fields, especially in natural language processing and computer vision [1,2]. In the field of natural language processing, several large pretrained models, such as OpenAI's ChatGPT and Baidu's ERNIE Bot [3,4], have demonstrated strong text generation and understanding capabilities. These models acquire rich semantic knowledge and language patterns through pretraining on large-scale corpora, which enables them to handle various complex natural language tasks [5,6]. In recent years, researchers have explored new algorithms and frameworks to optimize the performance of models and improve their accuracy and efficiency in handling complex tasks. In these studies, model selection, training, evaluation, and performance in practical applications have become the focus of research [7,8]. The proportion of medical health–related knowledge obtained through the internet is large, and chatbots are also used to answer various medical questions [9,10]. Researchers have performed many evaluations and studies on chatbots to answer medical questions, including ophthalmology, pediatric, urology, dentistry, and other professional directions, involving myopia, cirrhosis, hypertension, obesity, and other diseases and medical examination questions [11,12].

With the rapid development of ultrasound medicine, the demand for ultrasound examination is increasing, and the teaching and popularization of ultrasound is limited. An increasing number of junior ultrasound doctors, students, and patients have begun to use chatbots to obtain ultrasound-related consultation and answers. However, current research shows that chatbot performance is uneven; in some areas or tasks, chatbot performance can reach more than 90% of the accuracy rate or satisfaction, and chatbot performance can even exceed that of some doctors; however, in some tasks, the answer provided is

XSL•FO
RenderX

not valid or even wrong [13,14]. There are performance differences among different models, which are also affected by many factors, such as language, question type, and topic [15]. An in-depth understanding of how models perform in various domains and under various conditions is necessary and valuable for both users and developers [16,17].

ChatGPT is a large-scale language model based on the transformer architecture developed by OpenAI, an American AI research laboratory. It simulates the process of human language generation and understanding through deep learning technology and adopts an autoregressive language modeling method to predict the next word or phrase in the text sequence to generate coherent text [18,19]. ChatGPT training data are derived from massive amounts of text data on the internet, including news reports, academic articles, and social media content. After the data are cleaned and labeled, the data are used to train the parameters of the model so that it can capture the complex patterns and semantic relationships of natural language [20,21]. ChatGPT's powerful language generation and context understanding capabilities enable it to automatically generate relevant and coherent responses based on the input text content, enabling natural interaction with human users and completing multiple linguistic tasks, such as questions and answers, text summaries, and sentiment analysis [6,20,22].

ERNIE Bot is an intelligent question-and-answer system based on deep learning technology created by China's Baidu. Its basic principle is to analyze and understand the questions raised by users by natural language processing technology, convert the questions of users into a form that computers can understand, and extract relevant information from massive amounts of data [23,24]. Natural language generation models are then used to transform the extracted information into a form that humans can understand, generate answers, and return them to the user. ERNIE Bot has a large amount of data, including trillions of web data, billions of search data and image data, billions of daily voice call data, and 550 billion facts in the knowledge graph [25]. ERNIE Bot uses advanced natural language processing algorithms to accurately understand user questions and provide precise answers. Furthermore, it supports personalized customization according to different scenarios and needs and can continue to learn and accumulate knowledge to improve intelligence.

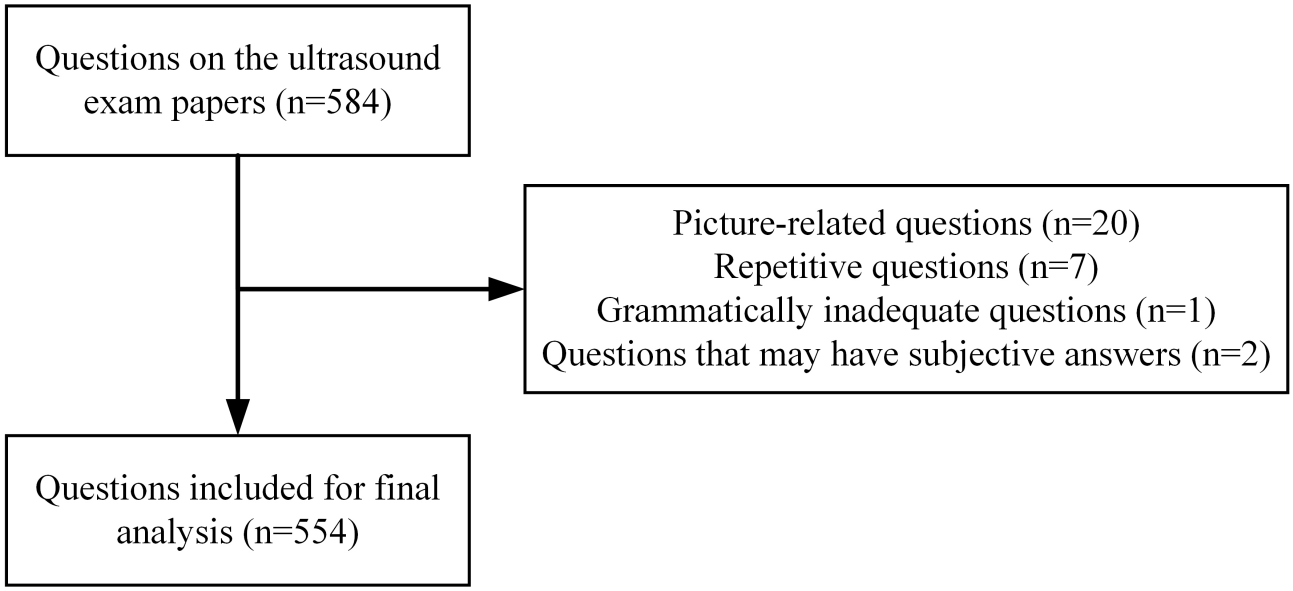
The purpose of this cross-sectional study is (1) to evaluate and compare the performance of ChatGPT and ERNIE Bot in answering questions in ultrasound examination papers; (2) to comprehensively analyze and compare the performance differences of the models in different question types, topics, and input language environments; and (3) to explore the reasons for these differences. This study is expected to provide insight for chatbot users and developers so that we can better understand the performance of various models in different fields. For more complex medical problems and fields, we can attempt to combine the advantages of multiple models to make an objective comprehensive judgment and consider the results. Chatbots can provide better services while constantly improving their own performance.

Methods

Question Curation

We used questions from ultrasound examination papers as a data set. The questions, from the West China Clinical College of Medicine of Sichuan University, covered basic knowledge of ultrasound medicine, the digestive system, the urinary system, superficial organs, blood vessels, and the heart. The question types included single-choice, multiple-choice, true or false questions; noun explanations; and short answers. With a total of 584 questions, we excluded picture-related questions, repetitive questions, questions with poor grammar, and questions with subjective answers from this cross-sectional study. Finally, a total of 554 questions were included, and the flowchart of the questions suitable for inclusion in the study is shown in Figure 1.

Figure 1. Flowchart of the questions included in the study.



XSL•FO
RenderX

Response Generation and Grading

Each question was entered into GPT-3.5 Turbo (GPT-3.5) and ERNIE Bot-3.5 (Bot-3.5) in both English and Chinese, and the responses were recorded. For each input question, the background definition of the question, and the explanation of the question type are given, such as the noun explanation of the undergraduate superficial organ ultrasound examination. An example of the questioning methods for different types of questions is shown in Textbox 1. The subjective questions in this cross-sectional study included noun interpretation questions and short answer questions. All the subjective questions were scored by 5 experts in the field of ultrasound medicine who are fluent in both Chinese and English and have more than 20 years of experience in the fields of ultrasound diagnosis and ultrasound teaching. The experts rated the comprehensive quality of the responses in both languages on a Likert scale [26-28], which is an effective, objective, and fair evaluation method for quantifying and grading answers. The evaluation of subjective responses in this study includes completeness, logical clarity, accuracy, depth and breadth, creativity, and so on. A higher score indicates higher quality (1 point: very poor, the answer content seriously deviates from the requirements of the question, the logic is confused, and there is basically no correct content; 2 points: poor, part of the answer deviates from the requirements of the question, contains some correct content, but the logic is not clear enough, and there are some mistakes or omissions; 3 points: acceptable, the answers basically meet the requirements of the question, the content is relatively complete, the logic is relatively clear, but some details or explanations are not accurate or in depth; 4 points: good, the answer fully meets the requirements of the question, and the content is accurate, complete, and logical; and 5 points: very good, the answers fully meet the requirements of the question, the content is accurate and in depth, comprehensive, logical and rigorous, and even new insights or solutions are proposed). The experiments were completed in October 2024.

XSL•FO
RenderX

Textbox 1. Examples of how to ask questions, including the content of the question, background, and question type description.

Example A

- The following is a single-choice question for the ultrasound examination. Please select the most appropriate one from the options given.
- Which of the following is true about ultrasound?
- Ultrasound is an electromagnetic wave with a strong penetrating force.
- The commonly used frequency range of medical ultrasound is 2.5-12 MHz.
- Ultrasound wave is a wave with a frequency greater than 2000 Hz.
- The form of ultrasound wave propagation in the human body is mainly shear wave.
- Ultrasound is not easily affected by gas and bone.

Example B

- The following is a multiple-choice question for the superficial organ ultrasound examination. Please select two or more of the correct answers from the options given.
- To which layers is the mammary gland subdivided by the fascia layer?
- Skin layer
- Subcutaneous fat layer
- Glandular (parenchymal) layer
- Fat layer in the retromammary space
- Chest wall layer

Example C

- The following is a judgment question for the ultrasound imaging examination. Please judge whether the following description is correct or not.
- An infective endocarditis patient can definitely detect growth on ultrasound.

Example D

- The following is a noun explanation question for the superficial organ ultrasound examination. Please make an appropriate explanation of the following nouns.
- Acoustic impedance

Example E

- The following is a short answer question for the ultrasound examination.
- Please briefly describe the common etiology and typical ultrasound features of cirrhosis.

Statistical Analysis

For statistical analysis purposes, all the questions were grouped into categories: basic knowledge, disease and etiology, ultrasound examination, ultrasound diagnosis, ultrasound signs, case analysis, etc. We used Microsoft Excel to conduct statistical analyses (version 2019; Microsoft Corporation).

Ethical Considerations

Ethics approval was not required since the research did not involve human subjects or animals.

Results

All the questions included in this cross-sectional study are from real ultrasound examination papers, and the proportions of question types and categories are highly representative. The types and categories of all the questions included in this study are shown in Tables 1 and 2. Among the 554 eligible questions included in this study, according to the classification of question types, single-choice answers accounted for the highest proportion (354/554, 64%), followed by short-choice answers (69/554, 12%) and noun explanations (63/554, 11%), and the rest were multiple-choice and true or false questions. According to the classification of topics, the greatest proportion of topics were basic knowledge (181/554, 33%), followed by disease and etiology (106/554, 19%) and ultrasound signs (96/554, 17%), and the rest were ultrasound examination, ultrasound diagnosis, and ultrasound case analysis.

XSL•FO
RenderX

Table . Questions types and categories included in this study.

Categories	Basics, n	Examinations, n	Diagnosis, n	Cases, n	Disease, n	Signs, n	Total, n
Single choice	124	49	41	26	63	51	354
Multiple choice	13	8	6	—[a]	12	9	48
True or false	10	7	3	—	—	—	20
Noun explanation	21	8	3	—	24	7	63
Short answer	13	10	10	—	7	29	69
Total	181	82	63	26	106	96	554

[a]Not applicable.

Table . Study results for each question category, stratified by question style (single-choice, multiple-choice, and true or false questions), language (English and Chinese), and artificial intelligence model (GPT-3.5 Turbo [GPT-3.5] and ERNIE Bot-3.5 [Bot-3.5]).

Categories	Model	Basics, %	Examination, %	Diagnosis, %	Cases, %	Disease, %	Signs, %	Total, %
Single choice (English)	GPT-3.5	58.87	59.18	58.54	57.69	50.79	58.82	57.34
Correct (%)	Bot-3.5	57.26	61.22	58.54	61.54	63.49	60.78	59.89
Single choice (Chinese)	GPT-3.5	60.48	61.22	63.41	57.69	53.97	60.78	59.6
Correct (%)	Bot-3.5	58.06	65.31	56.1	65.38	68.25	70.59	62.99
Multiple choice (English)	GPT-3.5	7.69	0	16.67	—[a]	8.33	11.11	8.33
Correct (%)	Bot-3.5	46.15	12.5	16.67	—	25.0	66.67	35.42
Multiple choice (Chinese)	GPT-3.5	7.69	0	16.67	—	16.67	11.11	10.42
Correct (%)	Bot-3.5	53.85	12.5	16.67	—	33.33	66.67	39.58
True or false (English)	GPT-3.5	50	57.14	100	—	—	—	60
Correct (%)	Bot-3.5	60	85.71	100	—	—	—	75
True or false (Chinese)	GPT-3.5	50	71.43	100	—	—	—	65
Correct (%)	Bot-3.5	70	85.71	100	—	—	—	80

[a]Not applicable.

We collected the accuracy rate results of the 2 AI models, GPT-3.5 and Bot-3.5, for single-choice, multiple-choice, and true or false questions in English and Chinese. When the models were asked questions in Chinese (the original language of the test paper), the overall accuracy rate was as follows (GPT-3.5 vs Bot-3.5): single-choice (59.6% vs 62.99%), multiple-choice (10.42% vs 39.58%), and true or false questions (65% vs 80%). When the test paper was translated into English for questioning, the overall accuracy rates were as follows (GPT-3.5 vs Bot-3.5): single-choice (57.34% vs 59.89%), multiple-choice (8.33% vs 35.42%), and true or false questions (60% vs 75%). All translations are performed manually by experts who are proficient in English. It can be clearly seen that Bot-3.5 is superior to GPT-3.5 in all question types and languages. Furthermore, we calculated classified statistics according to the accuracy rates of different categories of questions, and the statistical results are shown in Table 2.

We collected the scores of the GPT-3.5 and Bot-3.5 AI models for noun interpretation and short answers in both Chinese and English. A total of 63 noun explanation questions and 69 short answer questions were included in this cross-sectional study. The scoring criteria were divided into 5 levels—1 point=very poor, 2 points=poor, 3 points=acceptable, 4 points=good, and 5 points=very good. We take the average score of 5 experts, round the average score to the nearest whole number, and finally calculate classification statistics according to the score values. When asked questions in Chinese (the original language of the test paper), the most common scores were as follows (GPT-3.5 vs Bot-3.5): noun explanation (3 points vs 5 points) and short answer (3 points vs 4 points). When the test paper was translated

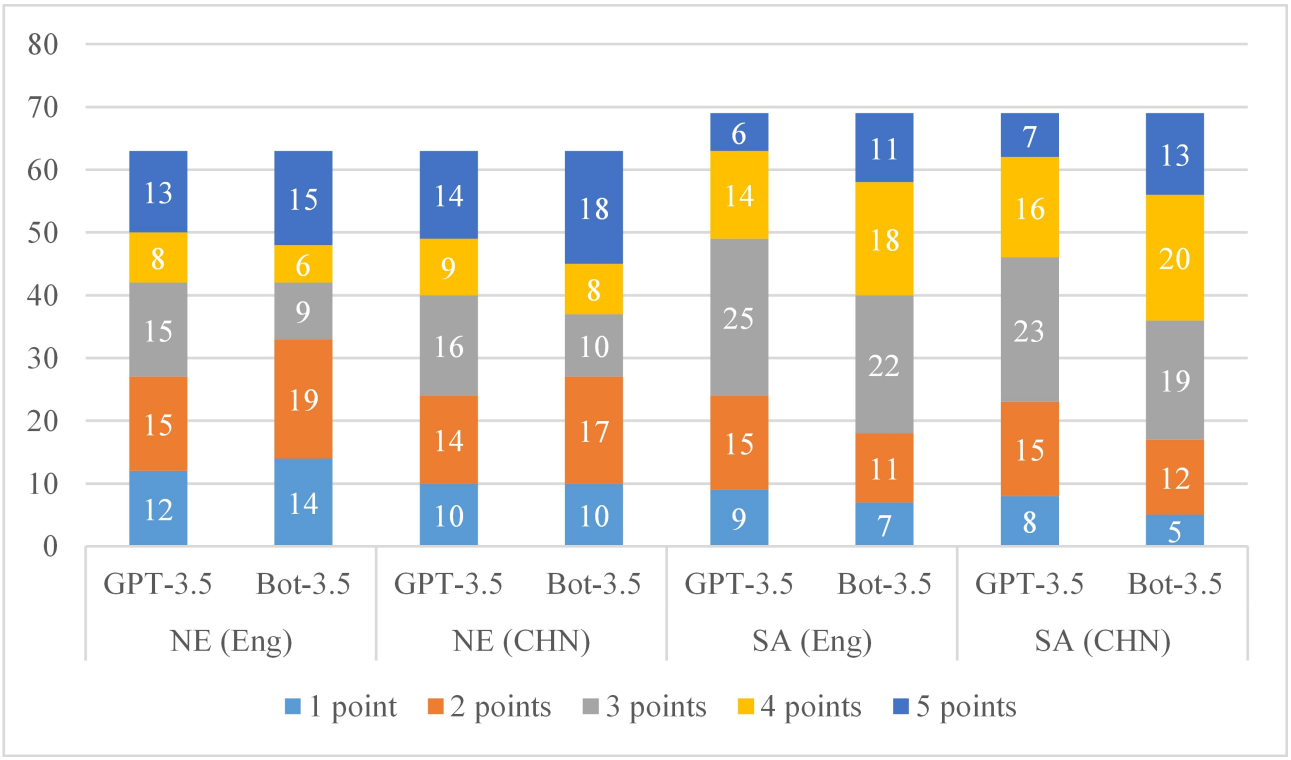
XSL•FO
RenderX

into English for questions, the most points were scored (GPT-3.5 vs Bot-3.5): noun explanation (2 points vs 2 points) and short answer (3 points vs 4 points). The detailed frequency tables are shown in Table 3 and Figure 2.

Table . Comparison of the distribution of scores stratified by question type (no explanation, short answer), language (English and Chinese), and artificial intelligence model (GPT-3.5 Turbo [GPT-3.5] and ERNIE Bot-3.5 [Bot-3.5]).

Categories and model	1 point	2 points	3 points	4 points	5 points	Total
Noun explanation (English)						
GPT-3.5	12	15	15	8	13	63
Bot-3.5	14	19	9	6	15	63
Noun explanation (Chinese)						
GPT-3.5	10	14	16	9	14	63
Bot-3.5	10	17	10	8	18	63
Short answer (English)						
GPT-3.5	9	15	25	14	6	69
Bot-3.5	7	11	22	18	11	69
Short answer (Chinese)						
GPT-3.5	8	15	23	16	7	69
Bot-3.5	5	12	19	20	13	69

Figure 2. The distribution of scores. Bot-3.5: ERNIE Bot-3.5; CHN: Chinese; Eng: English; GPT-3.5: GPT-3.5 Turbo; NE: noun explanation; SA: short answer.



We conducted a quantitative statistical analysis of noun explanations and short answer scores, including minimum, maximum, IQR, median, mean, sum, and SD scores. We compared the quantitative statistics of the GPT-3.5 and Bot-3.5 scores in the Chinese language environment. For noun interpretation, the maximum, minimum, and median values were equal for GPT-3.5 versus Bot-3.5; other statistics were as follows: IQR 2 - 4 vs 2 - 5, mean 2.86 vs 3.37, sum 180 vs 212, and SD 1.4 vs 1.37. There was a significant difference between the 2 models in terms of the quality of answers to noun interpretation (P<.05). For short answers, the maximum, minimum, and median values were equal (IQR 2 - 4 vs 2.5 - 4, mean 2.93 vs 3.36, sum 202 vs 232, and SD 1.15 vs 1.19), and there was a significant difference between the 2 models in terms of the quality of answers to short answers (P<.05). The statistical results are shown in Table 4.

XSL•FO
RenderX

Table . Quantitative statistical results of noun interpretation and short answer scores for 2 artificial intelligence models (GPT-3.5 Turbo [GPT-3.5] and ERNIE Bot-3.5 [Bot-3.5]).

Categories	Noun explanations (n=63)		Short answers (n=69)	
	GPT-3.5	Bot-3.5	GPT-3.5	Bot-3.5
Minimum	1	1	1	1
Maximum	5	5	5	5
IQR	2 - 4	2 - 5	2 - 4	2.5 - 4
Median	3	3	3	3
Mean	2.86	3.37	2.93	3.36
Sum	180	212	202	232
SD	1.40	1.37	1.15	1.19

To compare and analyze the performance of the 2 AI models (GPT-3.5 and Bot-3.5) in the Chinese language environment when noun explanations and short answers are classified according to different topics, we calculated the number of scores for each type of topic in the Chinese language environment. For noun interpretation, the highest percentage scores were obtained for GPT-3.5 vs Bot-3.5, basic knowledge (4 points vs 4 points), ultrasound examinations (5 points vs 5 points), disease and etiology (1 point vs 2 points), and ultrasound signs (1 point vs 1 point). For short answers, those with the highest percentage of points (3.5 points vs Bot-3.5), basic knowledge (3 points vs 5 points), ultrasound examinations (2 points vs 3 points), ultrasound diagnosis (3 points vs 5 points), disease and etiology (3 points vs 2 points), and ultrasound signs (3 points vs 3 points) were included. The statistical results are shown in Table 5.

Table 5 also shows the differences in scores between the 2 models on different subject categories. Based on the above results, the most important finding is that Bot-3.5 performs better than GPT-3.5 in the Chinese environment, both objectively and subjectively. Bot-3.5 is representative of the localization model, and GPT-3.5 is representative of the internationalization model. The excellent performance of Bot-3.5 is due to its comprehensiveness and depth in the Chinese training data set. The discovery of this performance difference has implications for both users and developers of chatbot systems, and it is necessary for users to have a deeper understanding of the model's data set background, language, and performance to better use them. Developers can also improve and optimize robot models according to performance differences.

XSL•FO
RenderX

Table . The score distributions of noun interpretations and short answers in different topic categories for 2 artificial intelligence models (GPT-3.5 Turbo [GPT-3.5] and ERNIE Bot-3.5 [Bot-3.5]).

Categories	Noun explanations			Short answers		
	Total	GPT-3.5	Bot-3.5	Total	GPT-3.5	Bot-3.5
Basic knowledge	21			13		
1 point		5	3		3	1
2 points		4	0		1	1
3 points		4	4		4	2
4 points		5	8		2	4
5 points		3	6		3	5
Examinations	8			10		
1 point		0	1		2	0
2 points		2	1		4	3
3 points		1	1		1	3
4 points		2	1		2	3
5 points		3	4		1	1
Diagnosis	3			10		
1 point		0	1		1	2
2 points		1	0		2	1
3 points		1	1		5	2
4 points		0	0		2	2
5 points		1	1		0	3
Disease and etiology	24			7		
1 point		6	0		0	0
2 points		5	9		2	3
3 points		6	6		3	1
4 points		6	3		1	2
5 points		1	6		1	1
Ultrasound signs	7			29		
1 point		3	2		2	2
2 points		2	2		8	4
3 points		0	1		10	10
4 points		0	1		7	10
5 points		2	1		2	3

Discussion

Preliminary Findings

Since the public release of ChatGPT, its convenience has made AI more accessible than ever before. It has demonstrated its ability to provide answers even to knowledgeable and experienced professors, and its numerous advantages have quickly made it a hot topic and the focus of research. Many technology companies around the world are also developing chatbot systems [4,29,30]. Industries are also exploring how to integrate these AI technologies with their own work and learning to improve quality and efficiency [31,32]. In the medical field, chatbot systems can be used as learning and consulting assistants to answer a variety of medical-related questions, but the accuracy and quality of their information must be carefully evaluated [33,34].

In this cross-sectional study, we analyzed 554 actual examination paper questions from the field of ultrasound medicine and evaluated the performance of an AI chatbot system in answering these medical paper questions. Medical examination papers are often used to evaluate chatbot performance, mainly because of their wide coverage,

XSL•FO
RenderX

representativeness, and reference answers [35-37]. Alessandri et al [35] used the Residency Admission National Examination to evaluate ChatGPT. Humar et al [22] evaluated ChatGPT with questions from the plastic surgery in-service examination. The main advantage of our study is that the questions are from actual ultrasound medical examinations, and its content is broad and representative. The question types included single-choice, multiple-choice, true or false questions; noun explanations; short answers; basic knowledge; ultrasound examination; ultrasound diagnosis; ultrasound case analysis; disease and etiology; and ultrasound signs. We conducted a quantitative comparative analysis of the performance of two of the most representative free chatbots (GPT-3.5 and Bot-3.5). Samaan et al [16] demonstrated that chatbot performance is affected by the language environment. We use both English and Chinese to ask questions and analyze the quality of the answers provided by the 2 models in different linguistic environments.

Regardless of whether the input language is English or Chinese, the GPT-3.5 and Bot-3.5 models perform somewhat well on different types of questions in the field of ultrasound medicine. For objective questions (including single-choice, multipl-choice, and true or false questions in this cross-sectional study), we took the accuracy rate as the evaluation index, and a score of ≥60% is acceptable, which is also the passing score of medical students. The best performance was true or false questions (accuracy rate: 60%-80%), followed by single-choice questions (accuracy rate: 57.34%-62.99%), and the worst performance was multiple-choice questions (accuracy rate: 8.33%-39.58%). For subjective questions (including noun explanations and short answers in this cross-sectional study ≥3 points, considered to be acceptable answers, also the assessment criteria), the performance was better for short answers, with acceptable answers (≥3 points) accounting for 65.22%-75.36%, whereas the performance for noun explanations was lower, with acceptable answers accounting for 47.62%-61.9%.

The reasons behind these differences are worth exploring and analyzing. For objective questions, the difficulty and complexity of the questions may be important factors. Branum and Schiavenato [14] reported that chatbots sometimes provide plausible but incorrect answers to complex clinical questions [38]. True or false questions usually involve only the truth or falsity of a statement and are the least difficult. Although multiple options are provided in a single choice, the answer is unique, and the model needs to identify only the correct answer from a limited number of options, with moderate difficulty. The research results of Lai et al [32] indicate that chatbots have high accuracy in single-choice selection. However, multiple choice requires the model to identify the correctness of multiple options at the same time, which significantly increases the difficulty and complexity of information processing. Mihalache et al [3] demonstrated that substantial progress has not been made in multiple-choice chatbots. Furthermore, the processing of multiple-choice questions in the process of model training may be less common than that of other types of questions, and most of the multiple-choice answers are more flexible. For subjective questions, differences in openness, flexibility, and scoring criteria may be the reasons for differences in performance. Short answer questions often require the model to provide a short paragraph of explanation or description, which allows the model to show more flexibility and depth in its responses. On the other hand, noun interpretation is more focused on the precise interpretation of specific terms, which requires higher accuracy and professionalism of the model. When short answers are graded, the grading criteria may be more flexible, allowing a degree of freedom. Other studies have asked questions about diseases similar to the short-answer questions in this study. Yun et al [33] demonstrated the effectiveness of chatbots when short-answer questions are answered. Noun interpretation, on the other hand, can be more rigorous, requiring the model to provide a precise and professional interpretation [39]. Therefore, the differences in the performance of the models on different question types can be attributed to the differences in the difficulty of the questions, the complexity of information processing, the training data, and the scoring criteria. As a user, it is necessary to understand the performance differences of models of different types in advance, and as a developer, adjusting the distribution of the training data set and optimizing the model are important.

When comparing the performance of the GPT-3.5 and Bot-3.5 AI models in the field of ultrasound medicine, we found some significant differences. Table 2 reported that the accuracy rate of GPT-3.5 for multiple-choice and true or false questions is lower than that of Bot-3.5, suggesting that Bot-3.5 may be more capable of handling problems that require deep understanding and reasoning. Tang and Yang [23] demonstrated that Bot-3.5 shows greater participation and enthusiasm in teaching applications. This difference may be related to the differences in training data and algorithm architecture between the 2 models. Bot-3.5 may have been exposed to more diverse and complex data from the medical field during training to be better able to handle these types of problems. From Tables 4,5 and 5, we further analyze the scores of the 2 models on different question types. In terms of noun interpretation and short answers, Bot-3.5 scores are generally higher than GPT-3.5 scores, especially in the Chinese context. This result suggested that Bot-3.5 may have greater accuracy in understanding and interpreting medical terms and concepts. In addition, from the comparison of the score statistics, we can observe that Bot-3.5 is more concentrated in the score distribution, which implies that it has greater stability and consistency in dealing with similar problems.

When the test paper was translated into English for questioning, the performance of both models declined, but Bot-3.5 maintained its advantage in terms of multiple-choice and true or false questions. This finding reveals the limitations of both models in cross-language processing. Zhu et al [25] compared the performance of large language models developed in different countries, highlighting the necessity for localized models. Although both models claim to support multilingual processing, in practice, the model's ability to process across languages is affected by various aspects, such as architecture, algorithms, or training data, and when the model switches from 1 language to another, it may need to readjust to new language features. This adaptation process can lead to performance degradation, especially when dealing with complex tasks. During the training of the model, there may be differences in the distribution and scale of the Chinese and English data, and if the model is trained

XSL•FO
RenderX

more fully on the Chinese data, it may perform better on the Chinese input. Bot-3.5 was developed and trained in China and has a large Chinese corpus. During the design and training process, Chinese language features were deeply optimized. This optimization allows Bot-3.5 to perform well in terms of Chinese semantic understanding and context grasp.

Biswas et al [26] conducted a categorical assessment analysis of these problems. In terms of noun interpretation and short answer questions, both models scored highly in basic knowledge, ultrasonography, disease, and cause, which may be related to the importance of these topics in the medical field and their richness in the training data. However, in areas such as ultrasound signs and ultrasound diagnosis, both models scored relatively low, which may reflect the complexity and challenge of these topics in the medical field, requiring more in-depth reasoning and understanding of complex issues [40].

Although chatbots are not yet able to provide perfect answers in all aspects of medicine, chatbots have great potential for answering medical questions. Because the performance of chatbots is not static, with the continuous enrichment of training data and the continuous improvement and optimization of algorithms, chatbot performance will continue to improve. The results of this cross-sectional study have implications for both users and developers of chatbot systems. To improve the quality and efficiency of chatbot use, users need to deeply understand the performance and characteristics of different models and carefully study the performance differences and evaluation results of different models on different topics or task types to select the appropriate model according to actual needs [24]. Moreover, users should set clear expectations and establish appropriate evaluation criteria based on the model's actual performance to conduct objective and comprehensive evaluations in practical applications. For complex tasks or tasks requiring high accuracy, users can attempt to combine the advantages of multiple models, adopt the method of ensemble learning, and weight the prediction results of multiple models to obtain more accurate prediction results. Specific feedback and suggestions are provided to developers in appropriate ways and channels when the model is used. For developers, the results of the study can be used to optimize the model for performance issues on a particular topic or task. For example, training data in related fields can be increased, or more advanced training algorithms can be used to improve the performance of the model in the medical field. The user feedback and suggestions are actively collected, and the model is constantly iterated and improved. Everyone needs to recognize that no chatbot is omnipotent. We need to understand it, use it correctly rather than contradict or abuse it, treat it as a judge, let it grow healthily, and create more and better value for human beings.

Limitations

Our study has several limitations. First, the original language of all the questions in this cross-sectional study was Chinese, and the questions were asked in Chinese or translated from Chinese to English, which may not represent the performance of the model in other languages. Second, the sample size of our study was not large and focused only on text-related topics related to ultrasound medicine. Experts also have potential bias in the scoring. The universality of the results of this study in other medical specialties needs further research. Finally, chatbot versions are constantly being updated, and the results of this study may not be representative of the performance of the most recent version of the model at the time of publication [41]. However, GPT-3.5 and Bot-3.5 are the best-performing versions of the current free versions, as well as the largest number of users, and it is meaningful to study the performance comparison of the latest free versions of each model over the same period.

Conclusions

The results show that the AI chatbots represented by GPT-3.5 have a certain ability to answer questions in ultrasound medical examination papers, but there are varying degrees of performance differences across chatbot models, input languages, question types. and topics. For the Chinese ultrasound medical questions in this study, Bot-3.5 was superior to GPT-3.5 in terms of both accuracy and quality in many aspects. These findings suggest that users need to thoroughly understand the performance characteristics of various models and their applicability to different types of problems. For complex problems, multiple models are needed for comprehensive analysis. This finding also suggests that developers need to continuously optimize models to enrich training data, especially in medical specialties. In this way, chatbots can be continuously optimized, their performance consistently improved, and their ability to provide high-quality services enhanced.

Acknowledgments

The authors would like to acknowledge the assistance provided by Dr Lu from West China Hospital for data collection and validation. This research was supported by the 1.3.5 project for disciplines of excellence, West China Hospital, Sichuan University.

Data Availability

The data presented in this study are available upon request from the corresponding author. The data are not publicly available due to privacy restrictions.

Conflicts of Interest

None declared.

References

XSL•FO
RenderX

1. Deiana G, Dettori M, Arghittu A, Azara A, Gabutti G, Castiglia P. Artificial intelligence and public health: evaluating ChatGPT responses to vaccination myths and misconceptions. Vaccines (Basel) 2023 Jul 7;11(7):1217. [doi: 10.3390/vaccines11071217] [Medline: 37515033]
2. Hoch CC, Wollenberg B, Lüers JC, et al. ChatGPT's quiz skills in different otolaryngology subspecialties: an analysis of 2576 single-choice and multiple-choice board certification preparation questions. Eur Arch Otorhinolaryngol 2023 Sep;280(9):4271-4278. [doi: 10.1007/s00405-023-08051-4] [Medline: 37285018]
3. Mihalache A, Popovic MM, Muni RH. Performance of an artificial intelligence chatbot in ophthalmic knowledge assessment. JAMA Ophthalmol 2023 Jun 1;141(6):589-597. [doi: 10.1001/jamaophthalmol.2023.1144] [Medline: 37103928]
4. Cakir H, Caglar U, Yildiz O, Meric A, Ayranci A, Ozgor F. Evaluating the performance of ChatGPT in answering questions related to urolithiasis. Int Urol Nephrol 2024 Jan;56(1):17-21. [doi: 10.1007/s11255-023-03773-0] [Medline: 37658948]
5. Luykx JJ, Gerritse F, Habets PC, Vinkers CH. The performance of ChatGPT in generating answers to clinical questions in psychiatry: a two-layer assessment. World Psychiatry 2023 Oct;22(3):479-480. [doi: 10.1002/wps.21145] [Medline: 37713576]
6. Samaan JS, Yeo YH, Rajeev N, et al. Assessing the accuracy of responses by the language model ChatGPT to questions regarding bariatric surgery. Obes Surg 2023 Jun;33(6):1790-1796. [doi: 10.1007/s11695-023-06603-5] [Medline: 37106269]
7. Tariq R, Malik S, Khanna S. Evolving landscape of large language models: an evaluation of ChatGPT and Bard in answering patient queries on colonoscopy. Gastroenterology 2024 Jan;166(1):220-221. [doi: 10.1053/j.gastro.2023.08.033] [Medline: 37634736]
8. Danesh A, Pazouki H, Danesh K, Danesh F, Danesh A. The performance of artificial intelligence language models in board-style dental knowledge assessment: a preliminary study on ChatGPT. J Am Dent Assoc 2023 Nov;154(11):970-974. [doi: 10.1016/j.adaj.2023.07.016] [Medline: 37676187]
9. Walker HL, Ghani S, Kuemmerli C, et al. Reliability of medical information provided by ChatGPT: assessment against clinical guidelines and patient Information quality instrument. J Med Internet Res 2023 Jun 30;25:e47479. [doi: 10.2196/47479] [Medline: 37389908]
10. Chervenak J, Lieman H, Blanco-Breindel M, Jindal S. The promise and peril of using a large language model to obtain clinical information: ChatGPT performs strongly as a fertility counseling tool with limitations. Fertil Steril 2023 Sep;120(3 Pt 2):575-583. [doi: 10.1016/j.fertnstert.2023.05.151] [Medline: 37217092]
11. Kao HJ, Chien TW, Wang WC, Chou W, Chow JC. Assessing ChatGPT's capacity for clinical decision support in pediatrics: A comparative study with pediatricians using KIDMAP of Rasch analysis. Medicine (Balt) 2023 Jun 23;102(25):e34068. [doi: 10.1097/MD.0000000000034068] [Medline: 37352054]
12. Cocci A, Pezzoli M, Lo Re M, et al. Quality of information and appropriateness of ChatGPT outputs for urology patients. Prostate Cancer Prostatic Dis 2024 Mar;27(1):103-108. [doi: 10.1038/s41391-023-00705-y] [Medline: 37516804]
13. Yeo YH, Samaan JS, Ng WH, et al. Assessing the performance of ChatGPT in answering questions regarding cirrhosis and hepatocellular carcinoma. Clin Mol Hepatol 2023 Jul;29(3):721-732. [doi: 10.3350/cmh.2023.0089] [Medline: 36946005]
14. Branum C, Schiavenato M. Can ChatGPT accurately answer a PICOT question? Assessing AI response to a clinical question. Nurse Educ 2023;48(5):231-233. [doi: 10.1097/NNE.0000000000001436] [Medline: 37130197]
15. Gencer A, Aydin S. Can ChatGPT pass the thoracic surgery exam? Am J Med Sci 2023 Oct;366(4):291-295. [doi: 10.1016/j.amjms.2023.08.001] [Medline: 37549788]
16. Samaan JS, Yeo YH, Ng WH, et al. ChatGPT's ability to comprehend and answer cirrhosis related questions in Arabic. Arab J Gastroenterol 2023 Aug;24(3):145-148. [doi: 10.1016/j.ajg.2023.08.001] [Medline: 37673708]
17. Cohen A, Alter R, Lessans N, Meyer R, Brezinov Y, Levin G. Performance of ChatGPT in Israeli Hebrew OBGYN national residency examinations. Arch Gynecol Obstet 2023 Dec;308(6):1797-1802. [doi: 10.1007/s00404-023-07185-4] [Medline: 37668790]
18. Fergus S, Botha M, Ostovar M. Evaluating academic answers generated using ChatGPT. J Chem Educ 2023 Apr 11;100(4):1672-1675. [doi: 10.1021/acs.jchemed.3c00087]
19. Friederichs H, Friederichs WJ, März M. ChatGPT in medical school: how successful is AI in progress testing? Med Educ Online 2023 Dec;28(1):2220920. [doi: 10.1080/10872981.2023.2220920] [Medline: 37307503]
20. Aburumman R, Al Annan K, Mrad R, Brunaldi VO, Gala K, Abu Dayyeh BK. Assessing ChatGPT vs. standard medical resources for endoscopic sleeve gastroplasty education: a medical professional evaluation study. Obes Surg 2024 Jul;34(7):2718-2724. [doi: 10.1007/s11695-024-07283-5] [Medline: 38758515]
21. Deebel NA, Terlecki R. ChatGPT performance on the American Urological Association Self-Assessment Study Program and the potential influence of artificial intelligence in urologic training. Urology 2023 Jul;177:29-33. [doi: 10.1016/j.urology.2023.05.010] [Medline: 37209880]
22. Humar P, Asaad M, Bengur FB, Nguyen V. ChatGPT is equivalent to first-year plastic surgery residents: evaluation of ChatGPT on the plastic surgery in-service examination. Aesthet Surg J 2023 Nov 16;43(12):1085-NP1089. [doi: 10.1093/asj/sjad130] [Medline: 37140001]
23. Tang X, Yang X. Applying large language models in teaching business English writing: a case study of business proposal writing. SHS Web Conf 2024;181:01052. [doi: 10.1051/shsconf/202418101052]

XSL•FO
RenderX

24. He W, Zhang W, Jin Y, Zhou Q, Zhang H, Xia Q. Physician versus large language model chatbot responses to web-based questions from autistic patients in Chinese: cross-sectional comparative analysis. J Med Internet Res 2024 Apr 30;26:e54706. [doi: 10.2196/54706] [Medline: 38687566]
25. Zhu L, Mou W, Lai Y, Lin J, Luo P. Language and cultural bias in AI: comparing the performance of large language models developed in different countries on Traditional Chinese Medicine highlights the need for localized models. J Transl Med 2024 Mar 29;22(1):319. [doi: 10.1186/s12967-024-05128-4] [Medline: 38553705]
26. Biswas S, Logan NS, Davies LN, Sheppard AL, Wolffsohn JS. Assessing the utility of ChatGPT as an artificial intelligence‐based large language model for information to answer questions on myopia. Ophthalmic Physiol Opt 2023 Nov;43(6):1562-1570. [doi: 10.1111/opo.13207]
27. Madrid-García A, Rosales-Rosado Z, Freites-Nuñez D, et al. Harnessing ChatGPT and GPT-4 for evaluating the rheumatology questions of the Spanish access exam to specialized medical training. Sci Rep 2023;13(1):22129. [doi: 10.1101/2023.07.21.23292821]
28. Potapenko I, Malmqvist L, Subhi Y, Hamann S. Artificial intelligence-based ChatGPT responses for patient questions on Optic Disc Drusen. Ophthalmol Ther 2023 Dec;12(6):3109-3119. [doi: 10.1007/s40123-023-00800-2] [Medline: 37698823]
29. Haver HL, Ambinder EB, Bahl M, Oluyemi ET, Jeudy J, Yi PH. Appropriateness of breast cancer prevention and screening recommendations provided by ChatGPT. Radiology 2023 May;307(4):e230424. [doi: 10.1148/radiol.230424] [Medline: 37014239]
30. Kusunose K, Kashima S, Sata M. Evaluation of the accuracy of ChatGPT in answering clinical questions on the Japanese Society of Hypertension Guidelines. Circ J 2023 Jun 23;87(7):1030-1033. [doi: 10.1253/circj.CJ-23-0308] [Medline: 37286486]
31. Hong D, Huang C, Chen X, Chen L. ChatGPT's responses to gout-related questions. Asian J Surg 2023 Dec;46(12):5935-5936. [doi: 10.1016/j.asjsur.2023.08.217] [Medline: 37696697]
32. Lai UH, Wu KS, Hsu TY, Kan JKC. Evaluating the performance of ChatGPT-4 on the United Kingdom Medical Licensing Assessment. Front Med 2023;10:1240915. [doi: 10.3389/fmed.2023.1240915]
33. Yun JY, Kim DJ, Lee N, Kim EK. A comprehensive evaluation of ChatGPT consultation quality for augmentation mammoplasty: A comparative analysis between plastic surgeons and laypersons. Int J Med Inform 2023 Nov;179:105219. [doi: 10.1016/j.ijmedinf.2023.105219] [Medline: 37776670]
34. Das D, Kumar N, Longjam LA, et al. Assessing the capability of ChatGPT in answering first- and second-order knowledge questions on microbiology as per competency-based medical education curriculum. Cureus 2023 Mar;15(3):e36034. [doi: 10.7759/cureus.36034] [Medline: 37056538]
35. Alessandri Bonetti M, Giorgino R, Gallo Afflitto G, De Lorenzi F, Egro FM. How does ChatGPT perform on the Italian Residency Admission National Exam compared to 15,869 medical graduates? Ann Biomed Eng 2024 Apr;52(4):745-749. [doi: 10.1007/s10439-023-03318-7] [Medline: 37490183]
36. Gupta R, Herzog I, Park JB, et al. Performance of ChatGPT on the Plastic Surgery Inservice Training Examination. Aesthet Surg J 2023 Nov 16;43(12):1078-NP1082. [doi: 10.1093/asj/sjad128] [Medline: 37128784]
37. Oztermeli AD, Oztermeli A. ChatGPT performance in the medical specialty exam: An observational study. Medicine (Baltimore) 2023 Aug 11;102(32):e34673. [doi: 10.1097/MD.0000000000034673] [Medline: 37565917]
38. Javid M, Bhandari M, Parameshwari P, Reddiboina M, Prasad S. Evaluation of ChatGPT for patient counseling in kidney stone clinic: a prospective study. J Endourol 2024 Apr;38(4):377-383. [doi: 10.1089/end.2023.0571] [Medline: 38411835]
39. Laukamp KR, Terzis RA, Werner JM, et al. Monitoring patients with glioblastoma by using a large language model: accurate summarization of radiology reports with GPT-4. Radiology 2024 Jul;312(1):e232640. [doi: 10.1148/radiol.232640] [Medline: 39041936]
40. Tian Tran J, Burghall A, Blydt-Hansen T, et al. Exploring the ability of ChatGPT to create quality patient education resources about kidney transplant. Patient Educ Couns 2024 Dec;129:108400. [doi: 10.1016/j.pec.2024.108400] [Medline: 39232336]
41. Brin D, Sorin V, Vaid A, et al. Comparing ChatGPT and GPT-4 performance in USMLE soft skill assessments. Sci Rep 2023 Oct 1;13(1):16492. [doi: 10.1038/s41598-023-43436-9] [Medline: 37779171]

Abbreviations

AI: artificial intelligence
Bot-3.5: ERNIE Bot-3.5
GPT-3.5: GPT-3.5 Turbo

XSL•FO
RenderX

Edited by A Castonguay; submitted 03.07.24; peer-reviewed by B Thies, C Wang, J Kufel, M Chatzimina; revised version received 23.10.24; accepted 19.11.24; published 09.01.25.

Please cite as:
Zhang Y, Lu X, Luo Y, Zhu Y, Ling W
Performance of Artificial Intelligence Chatbots on Ultrasound Examinations: Cross-Sectional Comparative Analysis
JMIR Med Inform 2025;13:e63924
URL: https://medinform.jmir.org/2025/1/e63924
doi:10.2196/63924

© Yong Zhang, Xiao Lu, Yan Luo, Ying Zhu, Wenwu Ling. Originally published in JMIR Medical Informatics (https://medinform.jmir.org), 9.1.2025. This is an open-access article distributed under the terms of the Creative Commons Attribution License (https://creativecommons.org/licenses/by/4.0/), which permits unrestricted use, distribution, and reproduction in any medium, provided the original work, first published in JMIR Medical Informatics, is properly cited. The complete bibliographic information, a link to the original publication on https://medinform.jmir.org/, as well as this copyright and license information must be included.

XSL•FO
RenderX

Robust Automated Harmonization of Heterogeneous Data Through Ensemble Machine Learning: Algorithm Development and Validation Study

Doris Yang[1]; Doudou Zhou[2], PhD; Steven Cai[3]; Ziming Gan[4], PhD; Michael Pencina[5], PhD; Paul Avillach[1], MD, PhD; Tianxi Cai[1*], SCD; Chuan Hong[5*], PhD

[1]Department of Biomedical Informatics, Harvard Medical School, Boston, MA, United States

[2]Department of Statistics and Data Science, National University of Singapore, Singapore, Singapore

[3]Department of Computer Science, Rensselaer Polytechnic Institute, Rochester, NY, United States

[4]Department of Statistics, University of Chicago, Chicago, IL, United States

[5]Department of Biostatistics & Bioinformatics, Duke University, Durham, NC, United States

[*]these authors contributed equally

Corresponding Author:
Chuan Hong, PhD
Department of Biostatistics & Bioinformatics, Duke University, Durham, NC, United States

Abstract

Background: Cohort studies contain rich clinical data across large and diverse patient populations and are a common source of observational data for clinical research. Because large scale cohort studies are both time and resource intensive, one alternative is to harmonize data from existing cohorts through multicohort studies. However, given differences in variable encoding, accurate variable harmonization is difficult.

Objective: We propose SONAR (Semantic and Distribution-Based Harmonization) as a method for harmonizing variables across cohort studies to facilitate multicohort studies.

Methods: SONAR used semantic learning from variable descriptions and distribution learning from study participant data. Our method learned an embedding vector for each variable and used pairwise cosine similarity to score the similarity between variables. This approach was built off 3 National Institutes of Health cohorts, including the Cardiovascular Health Study, the Multi-Ethnic Study of Atherosclerosis, and the Women's Health Initiative. We also used gold standard labels to further refine the embeddings in a supervised manner.

Results: The method was evaluated using manually curated gold standard labels from the 3 National Institutes of Health cohorts. We evaluated both the intracohort and intercohort variable harmonization performance. The supervised SONAR method outperformed existing benchmark methods for almost all intracohort and intercohort comparisons using area under the curve and top-*k* accuracy metrics. Notably, SONAR was able to significantly improve harmonization of concepts that were difficult for existing semantic methods to harmonize.

Conclusions: SONAR achieves accurate variable harmonization within and between cohort studies by harnessing the complementary strengths of semantic learning and variable distribution learning.

(JMIR Med Inform 2025;13:e54133) doi:10.2196/54133

KEYWORDS

ensemble learning; semantic learning; distribution learning; variable harmonization; machine learning; cardiovascular health study; intracohort comparison; intercohort comparison; gold standard labels

Introduction

Data harmonization, the process that ensures the compatibility of diverse datasets for their cogent integration, is an indispensable tool in today's data-driven research environment [1-3]. The power of data harmonization lies in its capacity to enhance the statistical robustness of studies, thereby enabling the investigation of intricate research questions unattainable within a single dataset's limits. This ability to pool data from existing sources expedites research processes, reduces associated costs, and accelerates the translation of knowledge into practical applications [4,5]. However, despite the advantages of pooling data, the path to effective data harmonization is laden with challenges [6-9]. The most pronounced among these is the discrepancies in how individual datasets document and measure similar concepts [10-12]. Even within datasets, documentation

XSL•FO
RenderX

for analogous concepts is not consistent, thereby further complicating data integration.

Current data harmonization techniques mainly depend on manual curation [10,13,14]. In spite of its widespread use, manual curation is time-intensive, prone to human error, and often constrained in scope, focusing predominantly on a single disease or condition. These drawbacks limit the applicability and efficacy of manual curation in broader, more complex contexts and highlight the need for advanced harmonization methodologies [12,15-17]. Recently, there has been a shift towards automated techniques, like freely available mapping tools [18-20] and algorithms based on corpora or lexicons [21-23]. These tools aim to map terminologies across varied clinical domains. Yet, such methods might still necessitate significant domain expertise and depend on benchmark labels. Furthermore, many of these methods cater to only one kind of medical code, for instance, drug or lab codes.

Another promising approach for data harmonization is through semantic learning. In a study by Zhou et al [24], an automated harmonization algorithm was proposed to cotrain embeddings for electronic health record codes from multiple institutions by combining both electronic health record co-occurrence information and textual information from the code descriptions. As a technique that uses machine learning to infer meaning from data, semantic learning presents a promising avenue for enhancing data harmonization. However, semantic learning's applicability is limited by its demand for extensive, high-quality training data, its sensitivity to noisy or unreliable data, and the complexity involved in manually crafting semantic features.

In this paper, we propose SONAR (Semantic and Distribution-Based Harmonization), an innovative data harmonization approach that synthesizes the strengths of semantic learning with patient data learning. Patient data offers an alternative, unexplored source of learning for data harmonization purposes. The patient-level values for each variable provide information about the underlying concept that a variable measures, separate from the textual information in variable descriptions. By harnessing the context comprehension and inferential power of semantic learning and augmenting it with the capacity of patient data learning to capture concept-specific trends and nuances, we propose a more robust and accurate data harmonization strategy. We demonstrate the implementation and advantages of the proposed approach through its application across 3 major National Institutes of Health cohort studies: the Multi-Ethnic Study of Atherosclerosis (MESA) [25], the Cardiovascular Health Study (CHS) [26], and the Women's Health Initiative (WHI) [27]. Our aspiration is that the method proposed here will provide a valuable foundation for future studies aiming to tackle the multifaceted challenges of data harmonization between heterogeneous datasets.

Methods

Ethical Considerations

The data used in this study were obtained from 3 well-established cohort studies, namely CHS, MESA, and WHI. Ethics approval (IRB17-2059) was granted by the Institutional Review Board of the Harvard Faculty of Medicine. Institutional Review Board approval was secured for access to all studies' retrospective data. De-identified data was accessed through a secure cloud storage platform. Participants were not compensated for the use of their data in this study.

Data Sources

The CHS was a population-based longitudinal study initiated to determine the risk factors for the development and progression of clinically validated cardiovascular disease in adults aged 65 years and older. Beginning in 1989, the study enrolled 5888 participants from 4 US communities: Forsyth County, NC; Sacramento County, CA; Washington County, MD; and Pittsburgh, PA. The cohort consisted of two recruitment waves: the original cohort (1989-1990) and the African American cohort (1992-1993). Comprehensive baseline examinations were conducted, including medical history, physical examinations, laboratory tests, and others, with annual follow-ups to ascertain cardiovascular events [26].

The WHI was a long-term national health study that focused on strategies for preventing heart disease, breast and colorectal cancer, and osteoporotic fractures in postmenopausal women. Launched in 1991, the WHI involved multiple clinical trials and an observational study, enrolling a total of 161,808 women aged 50-79 years across 40 clinical centers throughout the United States. The participants were ethnically diverse, reflecting the demographic composition of the US population. Extensive data on lifestyle, health, and medical history were collected at baseline and at regular intervals throughout the study, creating a rich source of information for a variety of research endeavors [27].

The MESA study was a prospective cohort designed to delve into the prevalence and progression of subclinical cardiovascular disease among community-dwelling adults. MESA assessed a diverse, population-based sample of 6814 asymptomatic men and women aged between 45 and 84 years from 2000 to 2018. The participants were recruited from 6 field centers across the United States, including Wake Forest University, Columbia University, Johns Hopkins University, University of Minnesota, Northwestern University, and University of California – Los Angeles. The MESA cohort was made up of 38% White, 28% African-American, 22% Hispanic, and 12% Asian (primarily Chinese) individuals. Since its inception in July 2000, the study conducted 6 examinations, each occurring every 18 to 24 months [25].

Data Extraction

The process of data extraction necessitated the gathering of documentation for variables within the CHS, MESA, and WHI studies. This information was procured from the Database of Genotypes and Phenotypes (dbGaP) [28]. We used dbGaP metadata to procure the following salient information for each variable within the study: (1) variable accession, (2) variable name, (3) variable description, and (4) dataset accession. While the variable name and variable description were not necessarily unique within or between studies, the variable accession was a unique identifier across all studies. We used the variable description strings as the semantic data in our model. From the

XSL•FO
RenderX

raw variable description strings, we further extracted and removed the temporal period during which the variables were measured by parsing for key temporal terms, such as visit and exam. This data extraction process facilitated a comprehensive understanding of the variables' conceptual characteristics, thereby providing the foundation for the subsequent data harmonization efforts.

We used the dataset accession and variable accession identifiers to access (1) variable metadata and (2) the patient-level data for the set of variables already extracted from dbGaP. To allow for relevant distribution comparisons between variables, we kept only continuous data by filtering variables using the continuous flag in the metadata.

Data Preprocessing

Our study scope was primarily focused on the harmonization of continuous variables at the conceptual level. A "concept" in this context was defined as the underlying notion or theme that a variable represents, independent of the specific unit or time point of measurement. For example, a biomarker such as C-reactive protein, despite being reported in different units across different visits, was treated as having the same concept. Moreover, concepts were sometimes encoded in natural language or questionnaire form, rather than standard medical terms. We focused on conceptual level harmonization for several reasons. Researchers conducting multicohort studies are often interested in identifying all variables corresponding to a concept. Depending on the application, they might be interested in further refining this concept-level harmonization or also harmonizing the variable values across different units or collection time periods. Removing temporal information and units allowed us to focus on the essential meaning or theme underlying the variable, thereby facilitating the primary task of concept-level harmonization, which is manually challenging and resource intensive, paving the way for further data harmonization. Moreover, doing so enhanced comparability across studies, as variables with the same concept were treated as equivalent, irrespective of the units used. During the initial phase of data preprocessing, we streamlined variable descriptions by eliminating temporal information phrases. This practice not only simplified the descriptions but also augmented their comparability.

We also applied filters to variables according to their values. First, we removed variables with incomplete patient data. To preserve a significant portion of variables, we considered incomplete patient data at the subgroup level rather than the individual patient level. We defined patient subgroups using the anchor variables of age, race, and sex. Per the characteristics of the study populations and data availability, we defined 4 age buckets (≤59 years, 60 to 69 years, 70 to 79 years, and ≥80 years). For the categorical anchor variables, we used 2 predefined race categories (White and Black) and 2 predefined sex categories (female and male), yielding a total of 16 possible patient subgroups (calculated as 4×2×2). For each study, we removed variables that had no patient data for one or more subgroups, considering only patient subgroups that were represented in the cohort.

Second, we purged variables that had uniformly zero values across all patients. This removal was necessary as variables without variability do not offer predictive power and thus, contribute little to subsequent analyses. Subsequently, we identified variables within the same study with identical descriptions and treated them as a single entity. Rather than maintaining these as separate variables, we amalgamated their distribution vectors by computing their element-wise mean. This consolidation concurrently reduced redundancy and bolstered the statistical power and robustness of downstream analyses. The underlying principle driving these measures was the emphasis on the core conceptual content encapsulated within variables, a focus that lays the groundwork for a more efficient and meaningful process of data harmonization.

Creation of Gold Standard Labels

To assess the harmonization accuracy of SONAR, we manually created a set of gold standard labels. The process began with the curation of a concept list, consisting of common diseases, laboratory results, and medications, consistent with the goal of harmonization at the conceptual level (details in Multimedia Appendix 1, Section 4). With the concept list in hand, each of the 3 independent reviewers assigned raw variables from all 3 studies to the corresponding concepts based on their descriptions. Not all variables had labels, since the curated concept list was not comprehensive of all underlying concepts present in the studies. To ensure consistency and accuracy, we adopted a consensus-based approach for handling any discrepancies among the reviewers. In cases of disagreements, the reviewers discussed their rationales for their assignments, and through a process of discussion, literature review, and majority vote, they reached a consensus on the appropriate concept assignment. This rigorously prepared set of annotations, backed by consensus, formed our gold standard labels. In particular, each pair of variables corresponding to the same underlying concept formed a gold standard pair (ie, a pair of variables that a harmonization algorithm should map to each other). Such pairs consisted of variables from two different datasets (intercohort) or the same dataset (intracohort), since multiple variables from a single dataset could correspond to the same underlying concept. These labels offered a reliable standard against which we could validate our semantic learning and patient data learning techniques.

SONAR (Semantic and Distribution-Based Harmonization)

The proposed SONAR approach had 4 steps, including semantic learning, distribution learning, concatenation of the two learnings, and supervised training. Underpinning both semantic learning and distribution learning was the idea that variables with similar textual descriptions and patient-level value distributions were more likely to encode the same underlying concept.

Step 1: Semantic Learning

We combined two existing pretrained large language models (LLMs) for semantic learning, CODER (Crosslingual Knowledge-Infused Medical Term Embedding) [29] and SapBERT (Self-Alignment Pretraining for Biomedical Entity

XSL•FO
RenderX

Representations) [30]. CODER, a semantic representation learning tool, is a type of pretrained language model using a contrastive learning framework [30,31]. It is particularly suited to the biomedical terms and descriptions found in clinical studies because it was trained on terms, concepts, and their relations in the Unified Medical Language System (UMLS) [32] knowledge graph. SapBERT is a pretrained, masked learning model also trained on synonyms in the UMLS knowledge graph. Both CODER and SapBERT create embedding vector representations from textual input, which were the variable description strings in our method. Combining CODER and SapBERT, which use different pretraining algorithms and training sets within the same knowledge graph, allowed us to increase the robustness of our semantic embeddings. The advantage of using these existing language models pretrained was a balance between saved training time and specificity to the domain and task. The output of this step was a CODER embedding vector (*VAR_coder*) and a SapBERT embedding vector (*VAR_sapbert*) for each variable. The goal of this process was to transform the variable descriptions into a uniform, computable format that captured their semantic essence.

Step 2: Distribution Learning

In order to conduct comparisons of patient-level values for pairs of variables, we constructed vectors encoding the distributions of variables. For each study, we aggregated patients into the previously defined 16 subgroups, using the anchor variables of age, race, and sex. These anchor variables were present in all studies and clinically relevant to most of the other study variables. It was possible and permissible that the number of anchor groups varied across different cohorts. For instance, in the WHI cohort that consisted only of women, the number of anchor groups was reduced to 8 (4×1×2). Then, we computed the subgroup quartiles (ie, the 25th, 50th, and 75th percentiles), thus yielding a numerical distribution vector for each variable (*VAR_dist*) of up to length 48 (16×3). This process was designed to capture the distribution characteristics of each variable within defined anchor groups, thereby adding a computationally efficient layer of contextual understanding to our harmonization strategy. Moreover, the quartile distribution encoding strategy allowed for greater flexibility in data handling by preserving patient confidentiality.

Step 3: Concatenation

This stage combined the insights gained from semantic learning and distribution learning. Specifically, for each variable, we concatenated its *VAR_coder*, *VAR_sapbert*, and *VAR_dist* vectors into a single *VAR_concat* vector. In order to ensure standardized comparisons with *VAR_concat* vectors of the same length, we kept only the variable distribution dimensions in *VAR_dist* corresponding to anchor groups present in both cohorts in each interdataset harmonization. We kept all available variable distribution dimensions for intradataset harmonization. Prior to concatenation, we also normalized the *VAR_coder*, *VAR_sapbert*, and *VAR_dist* vectors separately to ensure they operated on the same scale. In particular, we took the absolute magnitude of each element in a vector, selected the maximum value among these values, then divided the original vector by the maximum absolute value. After normalization in this manner, the elements in each vector were bound to the −1 to 1 range. This was crucial because it ensured that no vector's magnitude dominated during the concatenation process, thereby preserving the integrity of the information they conveyed. We then concatenated the normalized *VAR_coder*, *VAR_sapbert*, and *VAR_dist* vectors, resulting in a vector for each variable that we denoted as *VAR_concat* with dimension *d*. This concatenated vector, containing both semantic and distribution information, formed the foundation of our automated harmonization strategy.

Step 4: Supervised Training

We further refined the SONAR method through supervised training of a d×d rotation matrix *M* through gradient descent of a loss function (details in Multimedia Appendix 1, Section 1). The supervised embeddings were then the cross product of the unsupervised SONAR embeddings and *M*. Overall, this 4-step process served to capture the nuances and complexities of variable-concept relationships in a computationally efficient and robust manner. The systematic integration of semantic learning with distribution learning offered an innovative approach to data harmonization, promising to enhance accuracy, efficiency, and overall applicability of harmonization strategies.

Evaluation Metrics

We assessed the performance of the proposed SONAR approach both within individual cohorts (intracohort) and between different cohorts (intercohort). We considered the area under the curve (AUC) of the receiver operating characteristic curve as the overall metric for harmonization accuracy. Specifically, for each underlying concept, we first computed the cosine similarity of the embedding vectors for known concept pairs (true positives) and an equal number of randomly selected concept pairs (false positives), where the cosine similarity measured the cosine of the angle between 2 vectors in a multidimensional space, effectively quantifying how similar they are. The AUC was then calculated, summarizing the overall accuracy of our method across varying decision thresholds for a given underlying concept. The overall AUC was the average of the concept-level AUC values. To reduce the effect of outliers within the sampled negative pairs, we averaged the 3 overall AUC values calculated for 3 sets of sampled negative pairs.

We also evaluated the performance of SONAR on hard concepts, defined to be concepts for which the benchmark SapBERT AUC was below the threshold of 0.900. The hard AUC was the average of the concept-level AUC values for the hard concepts. This was an important metric for demonstrating the added value of distribution learning and more broadly the complementary effects of the two forms of learning.

To further scrutinize the performance of our method, we reported the top-*k* accuracy (acc@*k*) for mapping of codes from Cohort A to Cohort B, where the cohorts were identical for intradataset mapping. For variable a in Cohort A, we let Ba be the set of variables within Cohort B with embeddings that had the largest cosine similarity with variable a, and we let Ga be the set of variables within Cohort B that were in a positive gold standard pair with variable a. Then, the acc@*k* for an underlying concept for the mapping from Cohort A to Cohort B was the

XSL•FO
RenderX

number of codes a such that Ba∩Ga≠0 divided by the total number of gold standard variables in Cohort A corresponding to the underlying concept. The acc@*k* for the mapping from Cohort A to Cohort B was then the average of the acc@*k* across all underlying concepts. This prevented dominance by underlying concepts with many corresponding gold standard variables. To calculate the intracohort acc@*k*, we first computed the intracohort acc@*k* for each underlying concept by averaging the acc@*k* for that underlying concept across all 3 intracohort comparisons (intra-CHS, intra-MESA, and intra-WHI). Underlying concepts were only averaged over the comparisons for which they were relevant, so the intracohort acc@*k* for a concept that had gold standard pairs in only CHS and MESA was be the average of the CHS acc@*k* and the MESA acc@*k* for the concept in question. Then, the intracohort acc@*k* was the average of the acc@k across all underlying concepts. The intercohort acc@*k* was calculated similarly, except across the 6 intercohort mappings (CHS to MESA, CHS to WHI, MESA to CHS, MESA to WHI, WHI to CHS, WHI to MESA). Finally, the overall acc@*k* was calculated across the 9 total mappings for each underlying variable. We obtained acc@*k* values for *k* values of 1, 3, 5, 10, 20 in order to provide additional insight into SONAR's effectiveness at capturing true positives at different thresholds. These rigorous evaluations allowed us to confidently assert the efficacy of our harmonization method in both intracohort and intercohort settings.

For the supervised portion of our method, we used 2-fold cross-validation. We pooled cosine similarity values from both rounds of training before AUC calculations and averaged the 2 resulting cosine similarity values for non–gold standard pairs before acc@*k* calculations. To provide a comprehensive understanding of our method's performance, we compared the AUC and other accuracy metrics obtained by SONAR with those obtained when using semantic learning (BioBERT [Bidirectional Encoder Representations from Transformers for Biomedical Text Mining], CODER, SapBERT) or distribution learning alone. We also obtained metrics for the concatenated semantic portion of SONAR (ie, CODER concatenated with SapBERT) to further highlight the added value of distribution learning. This comparative approach allowed us to illuminate the relative strengths and contributions of the individual components of our method and the added value achieved by their combination.

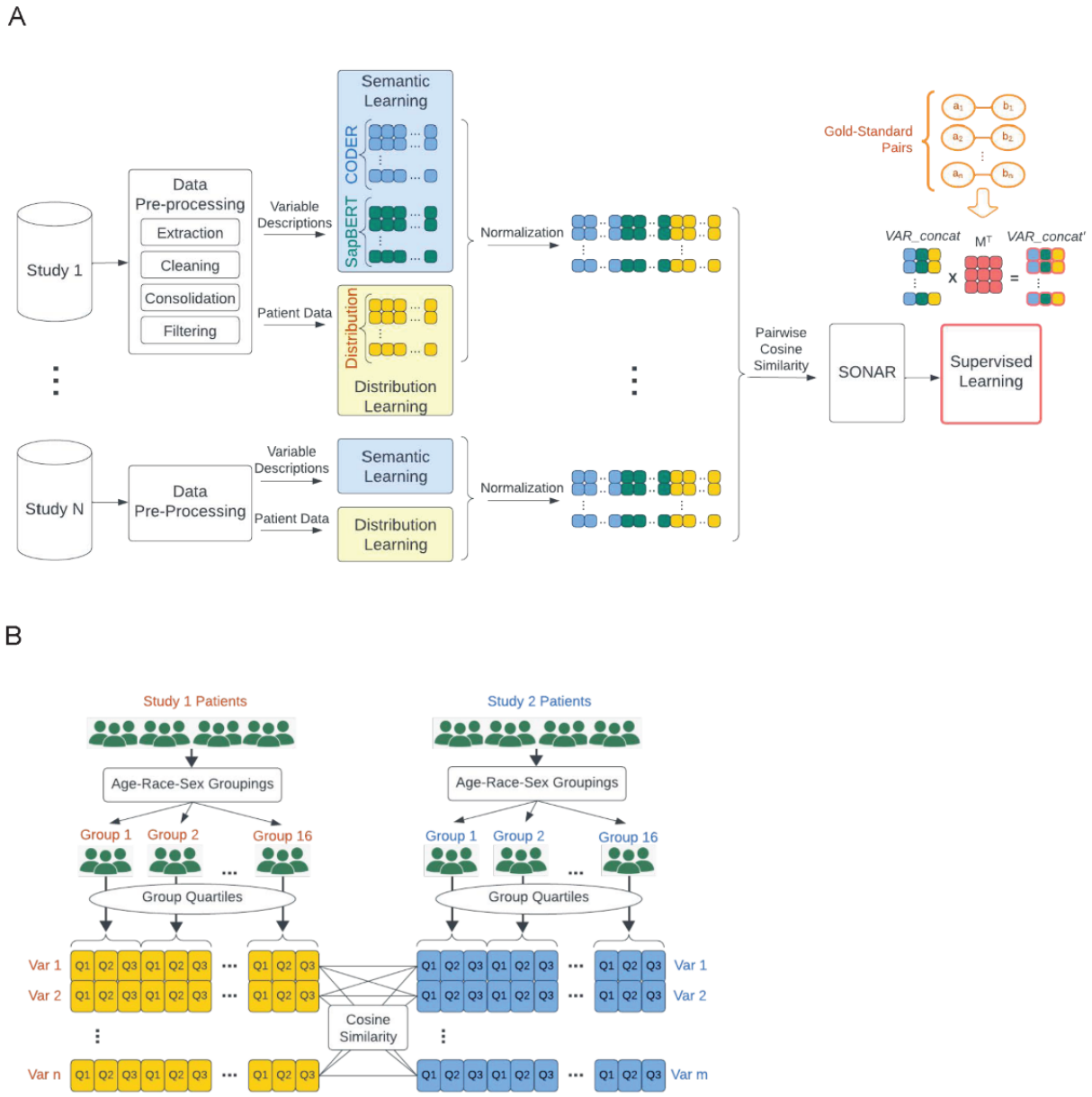
Results

Data Extraction and Preprocessing

The proposed SONAR approach had 4 steps, including semantic learning, distribution learning, concatenation of the two learnings, and supervised training (Figure 1). We extracted metadata and semantic data from the dbGaP for 14,717 CHS variables, 22,147 MESA variables, and 6207 WHI variables. Filtering for continuous, complete, and nonzero variables using metadata and patient-level data from Service WorkBench, as well as consolidating variables with identical semantic descriptions yielded 2076 CHS variables, 2525 MESA variables, and 1328 WHI variables. Patient data was available for 12 subgroups, 16 subgroups, and 6 subgroups for CHS, MESA, and WHI, respectively. This yielded distribution vectors of length 36, 48, and 18 for intra-CHS, intra-MESA, and intra-WHI harmonization, respectively. Based on overlapping patient subgroups between the cohorts, we used distribution vectors of length 36, 12, and 18 for intercohort CHS-MESA, CHS-WHI, and MESA-WHI harmonization, respectively.

XSL•FO
RenderX

Figure 1. Workflow of semantic and distribution based harmonization. (A) Overall workflow of semantic and distribution based harmonization. (B) Workflow of the distribution learning step. CODER: Crosslingual Knowledge-Infused Medical Term Embedding; SapBERT: Self-Alignment Pretraining for Biomedical Entity Representations; SONAR: Semantic and Distribution-Based Harmonization. Var: variable.



Gold Standard Labels

We identified a total of 123 concepts with continuous data, consisting of 112 laboratory test concepts, 6 disease concepts, and 5 medication concepts. A total of 531 variables across all cohorts were identified as gold standard representations of these concepts. These yielded 606, 318, and 89 gold standard concept pairs for intradataset harmonization evaluation within the CHS, MESA, and WHI, respectively. For interdataset harmonization evaluation, we had 352, 325, and 133 gold standard concept pairs for CHS-MESA, CHS-WHI, and MESA-WHI, respectively. Detailed numerical summaries of gold standard labels are provided in Table 1.

XSL•FO
RenderX

Table . Data preprocessing and gold standard labels.

Variables	Intracohort, n			Intercohort, n		
	CHS[a]	MESA[b]	WHI[c]	CHS-MESA	CHS-WHI	MESA-WHI
dbGaP[d] variables	14,717	22,147	6207	36,864	51,581	28,354
Preprocessed variables	2076	2525	1328	4601	3404	3853
Distribution dimensions	36	48	18	36	12	18
Gold standard concepts	53	39	32	53	54	48
Gold standard variables	204	125	86	242	229	146
Gold standard pairs	606	318	89	352	325	133

[a]CHS: Cardiovascular Health Study.

[b]MESA: Multi-Ethnic Study of Atherosclerosis.

[c]WHI: Women's Health Initiative.

[d]dbGaP: Database of Genotypes and Phenotypes.

Intracohort Evaluation

Supervised SONAR achieved a strong performance across all intracohort AUC (Figure 2 and Table S1 in Multimedia Appendix 1) and acc@*k* (Figure 3 and Table S2 in Multimedia Appendix 1) measures, exceeding or meeting all benchmark comparisons. The number of hard concepts for each intracomparison was 13 concepts, 5 concepts, and 5 concepts for intra-CHS, intra-MESA, and intra-WHI, respectively. It is notable that the distribution-only AUC was significantly higher than the semantic-only methods for the intra-CHS and intra-WHI hard concepts, illustrating the advantage of incorporating both semantic and distribution learning in SONAR. While the addition of supervised training only improved overall AUC performance for the intra-WHI comparison, it improved intracohort AUC performance on hard concepts for all 3 intracohort comparisons, exceeding all benchmark methods. The addition of supervised training also improved acc@*k* performance of SONAR across different values of *k*. Across intracohort evaluations, distribution learning provided a clear added value to semantic learning, in spite of a weaker distribution-only performance in comparison to the semantic components of SONAR (CODER only, SapBERT only, CODER + SapBERT). Moreover, there was not a single best semantic learning method between CODER and SapBERT using the various AUC and acc@*k* metrics, providing support for the use of both semantic learning methods in SONAR.

XSL•FO
RenderX

Figure 2. Comparison of areas under the curve for different methods in intracohort comparisons. AUC: area under the curve; BioBERT: Bidirectional Encoder Representations from Transformers for Biomedical Text Mining; CHS: Cardiovascular Health Study; CODER: Crosslingual Knowledge-Infused Medical Term Embedding; MESA: Multi-Ethnic Study of Atherosclerosis; SapBERT: Self-Alignment Pretraining for Biomedical Entity Representations; SONAR: Semantic and Distribution-Based Harmonization; WHI: Women's Health Initiative.

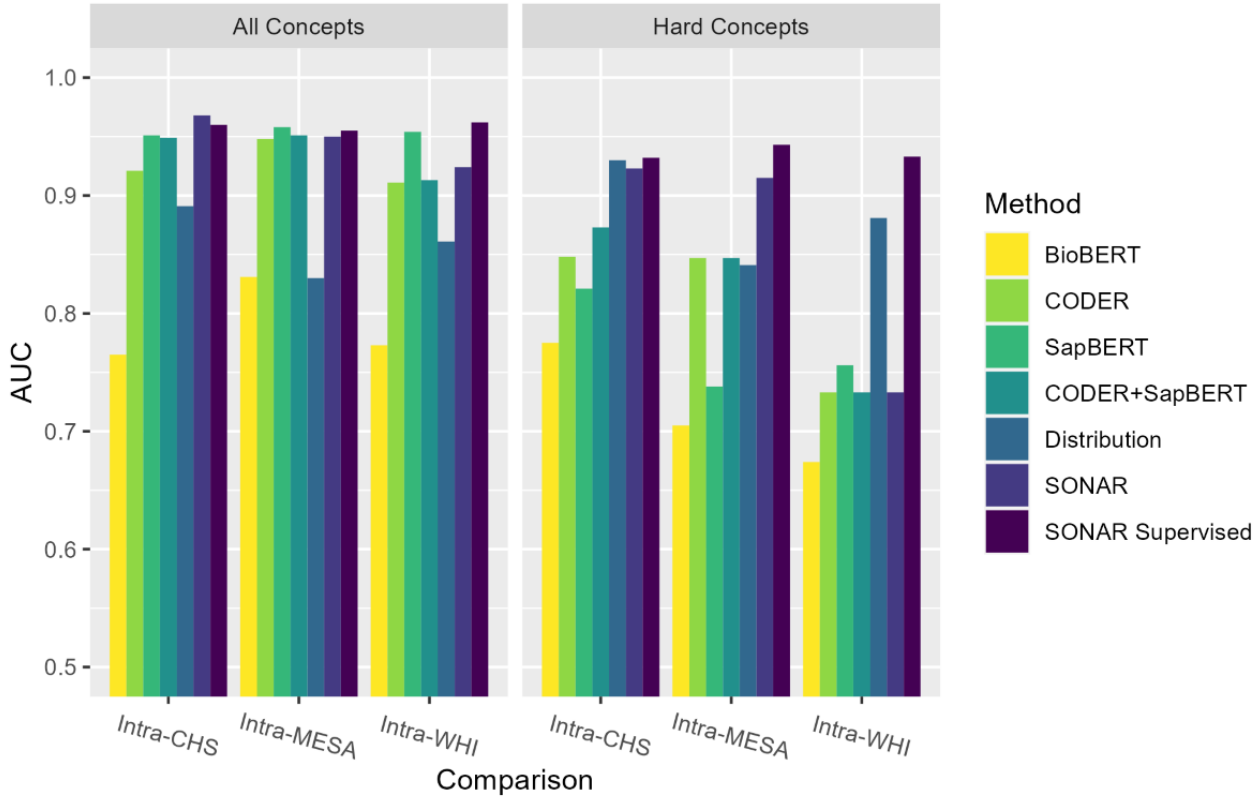
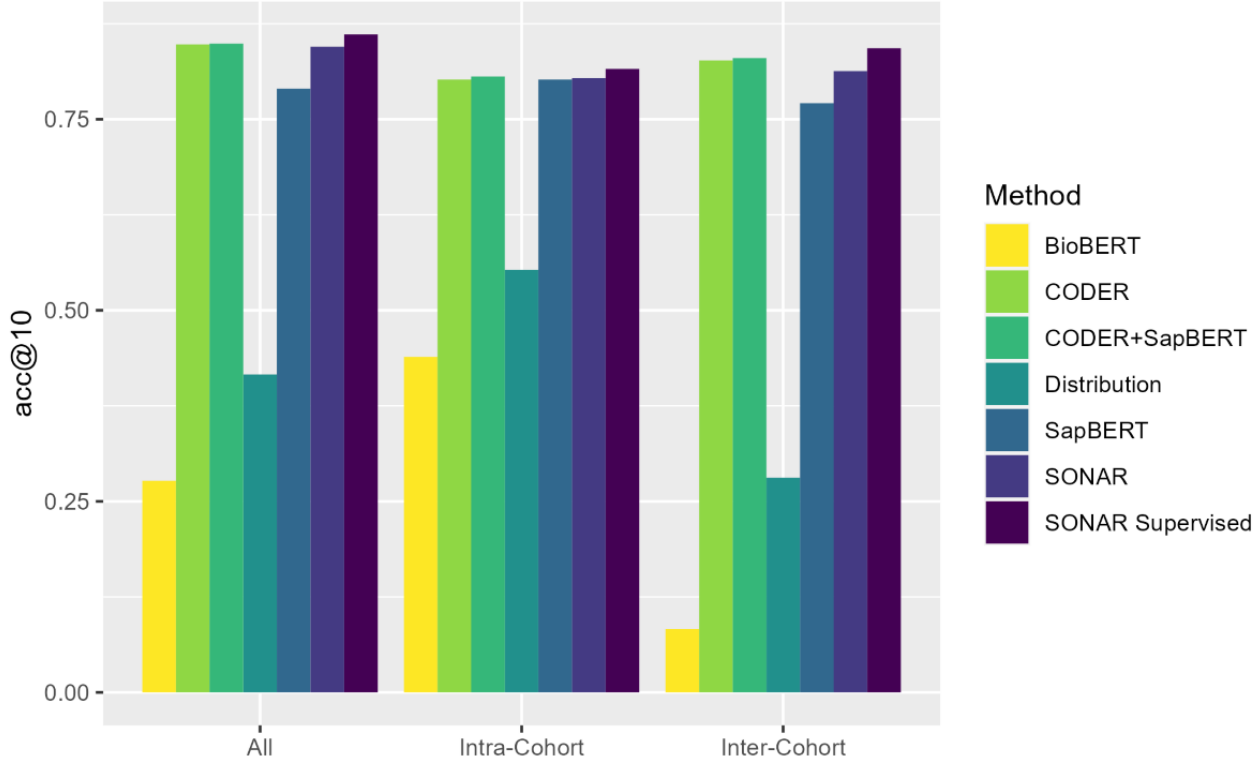


Figure 3. Comparison of top-10 sensitivities for different methods in both intracohort and intercohort comparisons. acc@10: top-10 accuracy; BioBERT: Bidirectional Encoder Representations from Transformers for Biomedical Text Mining; CODER: Crosslingual Knowledge-Infused Medical Term Embedding; SapBERT: Self-Alignment Pretraining for Biomedical Entity Representations; SONAR: Semantic and Distribution-Based Harmonization.

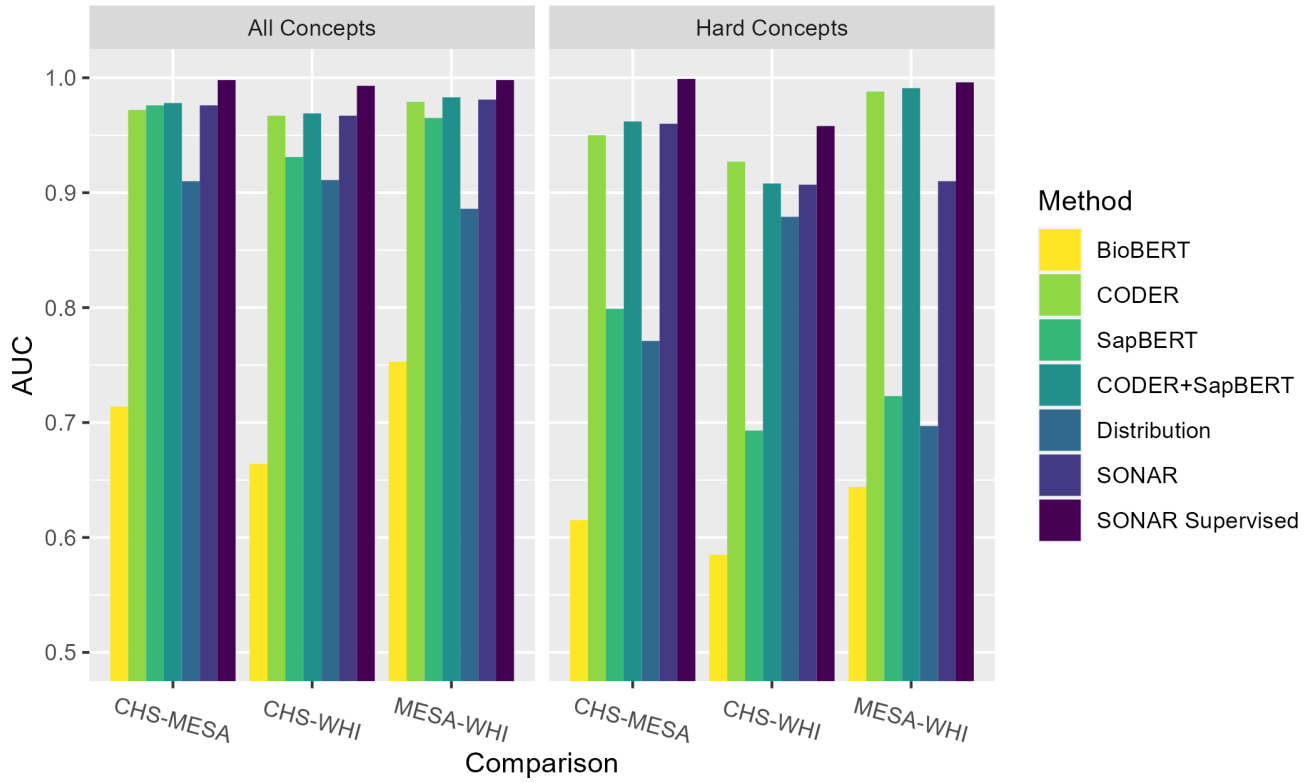


XSL•FO
RenderX

Intercohort Evaluation

Supervised SONAR also achieved a consistently high performance in intercohort harmonization evaluation, exceeding or meeting all benchmark comparisons except for acc@3 and acc@20 (Figure 3). The number of hard concepts for each intracomparison was 4 concepts, 11 concepts, and 5 concepts for the CHS-MESA, CHS-WHI, and MESA-WHI comparisons, respectively. Similar to intracohort harmonization, supervised training improved AUC performance on hard concepts for all 3 comparisons, exceeding all benchmark methods. In contrast with intracohort harmonization, supervised training also improved AUC performance on all concepts to above 0.99 for all 3 intercohort comparisons (Figure 4). Notably, the CODER only and SapBERT only AUC values were higher for intercohort harmonization as compared to intracohort harmonization because identical variable descriptions were allowed for intercohort semantic learning.

Figure 4. Comparison of areas under the curve for different methods in the intercohort comparisons. AUC: area under the curve; BioBERT: Bidirectional Encoder Representations from Transformers for Biomedical Text Mining; CHS: Cardiovascular Health Study; CODER: Crosslingual Knowledge-Infused Medical Term Embedding; MESA: Multi-Ethnic Study of Atherosclerosis; SapBERT (Self-Alignment Pretraining for Biomedical Entity Representations); SONAR: Semantic and Distribution-Based Harmonization; WHI: Women's Health Initiative.



Discussion

The SONAR method provides a robust method for concept-level data harmonization across and within longitudinal cohort studies by efficiently constructing variable embeddings from longitudinal cohort study variable descriptions and data. We used a supervised algorithm to refine the concatenated embeddings built from normalized distribution and semantic vectors. When applied to harmonization within and between 3 National Institutes of Health cohort studies, SONAR achieved enhanced performance compared to benchmark methods, with notable improvements over semantic-only and distribution-only methods. These results demonstrate the effectiveness of learning from both semantic and patient-level data. Our method is able to conduct this learning with relatively low training costs by taking advantage of the one-time pretraining of biomedical entity representation–based language models using domain-specific UMLS terms.

There are some limitations to this study. We focused only on continuous variables with complete data, excluding categorical variables and variables with incomplete data. Future studies can expand variable distribution learning to categorical variables and develop methodologies for comparing distribution vectors of differing lengths in the case of variables with incomplete data, allowing for harmonization of a greater range of variables. Moreover, we focused on concept-level variable harmonization, which may be inappropriate for certain applications that require more granular harmonization, such as at the unit level or comparisons between different temporal periods. SONAR already drastically reduces the resources needed for concept-level harmonization, which is a crucial first step for more granular harmonization. Future studies could also automate the manual process of unit and temporal harmonization across variables corresponding to the same concept. Another direction for future research is automating the underlying concept identification process, perhaps by variable clustering using the newest generation of LLMs such as GPT-4. While powerful LLMs like GPT-4 could further improve the semantic learning aspect of our model, future research would need to adapt these generally trained models to the biomedical domain and control for the monetary costs associated with GPT-4 use. Additionally,

XSL•FO
RenderX

although the current implementation of intercohort SONAR involves harmonization of 2 studies, it can be adapted to harmonize 3 or more studies.

SONAR paves the way for multicohort studies through high-quality and efficient variable harmonization. Harmonization at the concept-level is the crucial first step for researchers seeking to identify all variables corresponding to a disease, medication, or laboratory test of interest. Manual curation of or simple keyword searches for such variables are resource intensive and error-prone. The automation provided by SONAR is particularly helpful for harmonization of thousands of variables between large-scale cohort studies with heterogeneous variable encoding of underlying concepts. Multicohort studies that draw upon existing cohort studies are a resource-efficient method for studying risk factors associated with diseases and their pathogenesis. By effectively expanding the study population, multicohort studies also allow for greater statistical power and diversity in the study population, leading to greater generalizability of results and an enhanced ability to study health disparities. Beyond variable harmonization between cohorts, the variable embeddings generated through SONAR can be used for downstream analyses within multicohort studies, including for feature selection and the construction of knowledge graphs.

In conclusion, SONAR provides an approach for investigators to integrate semantic and patient data for multicohort variable harmonization. We demonstrate the robust added value of distribution learning when combined with existing semantic learning methods in variable mapping between cohorts. This innovation will facilitate and expedite multicohort studies by building upon existing data from decades-long cohort studies.

Acknowledgments

CH and MP's contributions to this work were partially funded by National Institute of Neurological Disorders and Stroke grant number R61-NS120246-02.

Conflicts of Interest

None declared.

Multimedia Appendix 1
Revised supplementary material.
[DOCX File, 3457 KB - medinform_v13i1e54133_app1.docx]

References

1. Curran PJ, Hussong AM. Integrative data analysis: the simultaneous analysis of multiple data sets. Psychol Methods 2009 Jun;14(2):81-100. [doi: 10.1037/a0015914] [Medline: 19485623]
2. Sansone SA, Rocca-Serra P, Field D, et al. Toward interoperable bioscience data. Nat Genet 2012 Jan 27;44(2):121-126. [doi: 10.1038/ng.1054] [Medline: 22281772]
3. Shaw DL, Ross JS. US federal government efforts to improve clinical trial transparency with expanded trial registries and open data sharing. AMA J Ethics 2015 Dec 1;17(12):1152-1159. [doi: 10.1001/journalofethics.2015.17.12.pfor1-1512] [Medline: 26698589]
4. Thompson A. Thinking big: large-scale collaborative research in observational epidemiology. Eur J Epidemiol 2009;24(12):727-731. [doi: 10.1007/s10654-009-9412-1] [Medline: 19967428]
5. Walport M, Brest P. Sharing research data to improve public health. Lancet 2011 Feb 12;377(9765):537-539. [doi: 10.1016/S0140-6736(10)62234-9] [Medline: 21216456]
6. Bennett SN, Caporaso N, Fitzpatrick AL, et al. Phenotype harmonization and cross-study collaboration in GWAS consortia: the GENEVA experience. Genet Epidemiol 2011 Apr;35(3):159-173. [doi: 10.1002/gepi.20564] [Medline: 21284036]
7. Jovicich J, Barkhof F, Babiloni C, et al. Harmonization of neuroimaging biomarkers for neurodegenerative diseases: a survey in the imaging community of perceived barriers and suggested actions. Alzheimers Dement (Amst) 2019 Dec;11:69-73. [doi: 10.1016/j.dadm.2018.11.005] [Medline: 31673595]
8. Tratwal J, Labella R, Bravenboer N, et al. Reporting guidelines, review of methodological standards, and challenges toward harmonization in bone marrow adiposity research. Report of the Methodologies Working Group of the International Bone Marrow Adiposity Society. Front Endocrinol (Lausanne) 2020;11:65. [doi: 10.3389/fendo.2020.00065] [Medline: 32180758]
9. Ohmann C, Banzi R, Canham S, et al. Sharing and reuse of individual participant data from clinical trials: principles and recommendations. BMJ Open 2017 Dec 14;7(12):e018647. [doi: 10.1136/bmjopen-2017-018647] [Medline: 29247106]
10. Pan H, Bakalov V, Cox L, et al. Identifying datasets for cross-study analysis in dbGaP using PhenX. Sci Data 2022 Sep 1;9(1):532. [doi: 10.1038/s41597-022-01660-4] [Medline: 36050327]
11. Simko LC, Chen L, Amtmann D, et al. Challenges to the standardization of trauma data collection in burn, traumatic brain injury, spinal cord injury, and other trauma populations: a call for common data elements for acute and longitudinal trauma databases. Arch Phys Med Rehabil 2019 May;100(5):891-898. [doi: 10.1016/j.apmr.2018.10.004] [Medline: 31030731]

XSL•FO
RenderX

12. Stilp AM, Emery LS, Broome JG, et al. A system for phenotype harmonization in the National Heart, Lung, and Blood Institute Trans-Omics for Precision Medicine (TOPMed) program. Am J Epidemiol 2021 Oct 1;190(10):1977-1992. [doi: 10.1093/aje/kwab115] [Medline: 33861317]
13. Tudur Smith C, Nevitt S, Appelbe D, et al. Resource implications of preparing individual participant data from a clinical trial to share with external researchers. Trials 2017 Jul 17;18(1):319. [doi: 10.1186/s13063-017-2067-4] [Medline: 28712359]
14. Fortier I, Raina P, Van den Heuvel ER, et al. Maelstrom Research guidelines for rigorous retrospective data harmonization. Int J Epidemiol 2017 Feb 1;46(1):103-105. [doi: 10.1093/ije/dyw075] [Medline: 27272186]
15. Burns NS, Miller PW. Learning what we didn't know - the SPRINT data analysis challenge. N Engl J Med 2017 Jun 8;376(23):2205-2207. [doi: 10.1056/NEJMp1705323] [Medline: 28445656]
16. Meeuws S, Yue JK, Huijben JA, et al. Common data elements: critical assessment of harmonization between current multi-center traumatic brain injury studies. J Neurotrauma 2020 Jun 1;37(11):1283-1290. [doi: 10.1089/neu.2019.6867] [Medline: 32000562]
17. Budin-Ljøsne I, Isaeva J, Knoppers BM, et al. Data sharing in large research consortia: experiences and recommendations from ENGAGE. Eur J Hum Genet 2014 Mar;22(3):317-321. [doi: 10.1038/ejhg.2013.131] [Medline: 23778872]
18. Kim H, El-Kareh R, Goel A, Vineet FNU, Chapman WW. An approach to improve LOINC mapping through augmentation of local test names. J Biomed Inform 2012 Aug;45(4):651-657. [doi: 10.1016/j.jbi.2011.12.004] [Medline: 22210167]
19. Kopanitsa G. Application of a Regenstrief RELMA V.6.6 to map Russian laboratory terms to LOINC. Methods Inf Med 2016;55(2):177-181. [doi: 10.3414/ME15-01-0068] [Medline: 26666563]
20. Zunner C, Bürkle T, Prokosch HU, Ganslandt T. Mapping local laboratory interface terms to LOINC at a German university hospital using RELMA V.5: a semi-automated approach. J Am Med Inform Assoc 2013;20(2):293-297. [doi: 10.1136/amiajnl-2012-001063] [Medline: 22802268]
21. Peters L, Kapusnik-Uner JE, Bodenreider O. Methods for managing variation in clinical drug names. AMIA Annu Symp Proc 2010 Nov 13;2010:637-641. [Medline: 21347056]
22. Zhou L, Plasek JM, Mahoney LM, Chang FY, DiMaggio D, Rocha RA. Mapping Partners Master Drug Dictionary to RxNorm using an NLP-based approach. J Biomed Inform 2012 Aug;45(4):626-633. [doi: 10.1016/j.jbi.2011.11.006] [Medline: 22142948]
23. Fidahussein M, Vreeman DJ. A corpus-based approach for automated LOINC mapping. J Am Med Inform Assoc 2014;21(1):64-72. [doi: 10.1136/amiajnl-2012-001159] [Medline: 23676247]
24. Zhou D, Gan Z, Shi X, et al. Multiview Incomplete Knowledge Graph Integration with application to cross-institutional EHR data harmonization. J Biomed Inform 2022 Sep;133:104147. [doi: 10.1016/j.jbi.2022.104147] [Medline: 35872266]
25. Bild DE, Bluemke DA, Burke GL, et al. Multi-ethnic study of atherosclerosis: objectives and design. Am J Epidemiol 2002 Nov 1;156(9):871-881. [doi: 10.1093/aje/kwf113] [Medline: 12397006]
26. Fried LP, Borhani NO, Enright P, et al. The cardiovascular health study: design and rationale. Ann Epidemiol 1991 Feb;1(3):263-276. [doi: 10.1016/1047-2797(91)90005-w] [Medline: 1669507]
27. The Women's Health Initiative Study Group. Design of the Women's Health Initiative Clinical Trial and Observational Study. Cont Clin Trials 1998 Feb;19(1):61-109. [doi: 10.1016/S0197-2456(97)00078-0] [Medline: 9492970]
28. Mailman MD, Feolo M, Jin Y, et al. The NCBI dbGaP database of genotypes and phenotypes. Nat Genet 2007 Oct;39(10):1181-1186. [doi: 10.1038/ng1007-1181] [Medline: 17898773]
29. Yuan Z, Zhao Z, Sun H, Li J, Wang F, Yu S. CODER: knowledge-infused cross-lingual medical term embedding for term normalization. J Biomed Inform 2022 Feb;126:103983. [doi: 10.1016/j.jbi.2021.103983] [Medline: 34990838]
30. Liu F, Shareghi E, Meng Z, Basaldella M, Collier N. Self-alignment pretraining for biomedical entity representations. Presented at: Conference of the North American Chapter of the Association for Computational Linguistics; Jun 6-11, 2021 p. 4228-4238. [doi: 10.18653/v1/2021.naacl-main.334]
31. Wang H, Li J, Wu H, Hovy E, Sun Y. Pre-trained language models and their applications. Eng (Beijing) 2023 Jun;25:51-65. [doi: 10.1016/j.eng.2022.04.024]
32. Unified medical language system (UMLS). National Library of Medicine. URL: https://www.nlm.nih.gov/research/umls/index.html [accessed 2025-01-07]

Abbreviations

acc@k: top-*k* accuracy
AUC: area under the curve
BioBERT: Bidirectional Encoder Representations from Transformers for Biomedical Text Mining
CHS: Cardiovascular Health Study
CODER: Crosslingual Knowledge-Infused Medical Term Embedding
dbGaP: Database of Genotypes and Phenotypes
LLM: large language models
MESA: Multi-Ethnic Study of Atherosclerosis
SapBERT: Self-Alignment Pretraining for Biomedical Entity Representations

XSL•FO
RenderX

SONAR: Semantic and Distribution-Based Harmonization
UMLS: Unified Medical Language System
WHI: Women's Health Initiative

Edited by C Lovis; submitted 30.10.23; peer-reviewed by F Alam, L Wang; revised version received 26.11.24; accepted 30.11.24; published 22.01.25.

Please cite as:
Yang D, Zhou D, Cai S, Gan Z, Pencina M, Avillach P, Cai T, Hong C
Robust Automated Harmonization of Heterogeneous Data Through Ensemble Machine Learning: Algorithm Development and Validation Study
JMIR Med Inform 2025;13:e54133
URL: https://medinform.jmir.org/2025/1/e54133
doi:10.2196/54133

©Doris Yang, Doudou Zhou, Steven Cai, Ziming Gan, Michael Pencina, Paul Avillach, Tianxi Cai, Chuan Hong. Originally published in JMIR Medical Informatics (https://medinform.jmir.org), 22.1.2025. This is an open-access article distributed under the terms of the Creative Commons Attribution License (https://creativecommons.org/licenses/by/4.0/), which permits unrestricted use, distribution, and reproduction in any medium, provided the original work, first published in JMIR Medical Informatics, is properly cited. The complete bibliographic information, a link to the original publication on https://medinform.jmir.org/, as well as this copyright and license information must be included.

XSL•FO
RenderX

Development and Validation of a Machine Learning Method Using Vocal Biomarkers for Identifying Frailty in Community-Dwelling Older Adults: Cross-Sectional Study

Taehwan Kim[1*], PhD; Jung-Yeon Choi[2*], MD, PhD; Myung Jin Ko[1], MD; Kwang-il Kim[2,3], MD, PhD

[1]Silvia Health Inc., Seoul, Republic of Korea

[2]Department of Internal Medicine, Seoul National University College of Medicine, Seoul, Republic of Korea

[3]Department of Internal Medicine, Seoul National University Bundang Hospital, Gyeonggi-do, Seongnam-si, Republic of Korea

[*]these authors contributed equally

Corresponding Author:
Kwang-il Kim, MD, PhD
Department of Internal Medicine, Seoul National University College of Medicine, Seoul, Republic of Korea

Abstract

Background: The two most commonly used methods to identify frailty are the frailty phenotype and the frailty index. However, both methods have limitations in clinical application. In addition, methods for measuring frailty have not yet been standardized.

Objective: We aimed to develop and validate a classification model for predicting frailty status using vocal biomarkers in community-dwelling older adults, based on voice recordings obtained from the picture description task (PDT).

Methods: We recruited 127 participants aged 50 years and older and collected clinical information through a short form of the Comprehensive Geriatric Assessment scale. Voice recordings were collected with a tablet device during the Korean version of the PDT, and we preprocessed audio data to remove background noise before feature extraction. Three artificial intelligence (AI) models were developed for identifying frailty status: SpeechAI (using speech data only), DemoAI (using demographic data only), and DemoSpeechAI (combining both data types).

Results: Our models were trained and evaluated on the basis of 5-fold cross-validation for 127 participants and compared. The SpeechAI model, using deep learning–based acoustic features, outperformed in terms of accuracy and area under the receiver operating characteristic curve (AUC), 80.4% (95% CI 76.89% - 83.91%) and 0.89 (95% CI 0.86 - 0.92), respectively, while the model using only demographics showed an accuracy of 67.96% (95% CI 67.63% - 68.29%) and an AUC of 0.74 (95% CI 0.73 - 0.75). The SpeechAI model outperformed the model using only demographics significantly in AUC (t_4=8.705 [2-sided]; P<.001). The DemoSpeechAI model, which combined demographics with deep learning–based acoustic features, showed superior performance (accuracy 85.6%, 95% CI 80.03% - 91.17% and AUC 0.93, 95% CI 0.89 - 0.97), but there was no significant difference in AUC between the SpeechAI and DemoSpeechAI models (t_4=1.057 [2-sided]; P=.35). Compared with models using traditional acoustic features from the openSMILE toolkit, the SpeechAI model demonstrated superior performance (AUC 0.89) over traditional methods (logistic regression: AUC 0.62; decision tree: AUC 0.57; random forest: AUC 0.66).

Conclusions: Our findings demonstrate that vocal biomarkers derived from deep learning–based acoustic features can be effectively used to predict frailty status in community-dwelling older adults. The SpeechAI model showed promising accuracy and AUC, outperforming models based solely on demographic data or traditional acoustic features. Furthermore, while the combined DemoSpeechAI model showed slightly improved performance over the SpeechAI model, the difference was not statistically significant. These results suggest that speech-based AI models offer a noninvasive, scalable method for frailty detection, potentially streamlining assessments in clinical and community settings.

(JMIR Med Inform 2025;13:e57298) doi:10.2196/57298

KEYWORDS

frailty; cross-sectional study; vocal biomarkers; older adults; artificial intelligence; machine learning; classification model; self-supervised

Introduction

Global population aging is undergoing a profound transformation as the number of older adults continues to rise at an unprecedented rate. South Korea is undergoing an accelerated aging trend coupled with one of the world's most dwindling birth rates. By 2025, South Korea is predicted to become a superaged society, with the proportion of people aged

XSL•FO
RenderX

≥65 years making up 20% of the population. This demographic shift is expected to continue, with estimates indicating that nearly 44% of South Korea's population will be older than 65 years expected by 2050 [1].

Among the older population, frailty is a very common and significantly important geriatric condition because it affects health-related status, quality of life, place of residence, and mortality [2]. Frailty is a common geriatric syndrome characterized by a decline in physiological reserves and increased vulnerability to stressors. Early diagnosis and management of frailty are important not only for tailoring care plans and predicting adverse health outcomes at the individual level but also for strategizing public health initiatives that meet the distinct requirements of the rapidly growing older population [3].

Although the concept of frailty is universally recognized, methods for measuring frailty have not yet been standardized. The two most commonly used methods to identify frailty are the frailty phenotype and the frailty index [4,5]. However, these two methods have limitations in clinical application as they require measuring the frailty phenotype through a predetermined methodology or collecting various variables, making them not easily adaptable and usable in clinical settings. Another method for assessing frailty is the use of questionnaires [6]. As measuring frailty involves time, cost, and labor, it is necessary to develop a simplified, universally implantable, and convenient methodology to screen for frailty.

A recent study explored the integration of machine learning to enhance frailty detection, demonstrating that the choice of classifier and feature selection significantly impacted model performance, particularly when combining clinical and nonclinical data [7]. Voice biomarkers have been successfully used to identify acute diseases such as COVID-19, cognitive dysfunction, Parkinson disease, and psychiatric disorders [8-11]. Early research on detecting frailty using voice biomarkers often relied on simple methods, such as brief, predetermined vocal tasks [12]. Rosen-Lang et al [13] demonstrated the feasibility of using more sophisticated voice biomarkers for frailty classification, highlighting their potential for improving diagnostic accuracy in this population. Furthermore, the applicability of vocal biomarkers extends beyond frailty detection. Kaufman et al [14] demonstrated that acoustic analysis could effectively predict type 2 diabetes using voice segments, highlighting the versatility of voice biomarkers in noninvasive health diagnostics across various conditions.

The aim of this study was to develop and validate a classification model for predicting frailty status using vocal biomarkers in community-dwelling older people based on the voice recordings obtained from a picture description task (PDT) conducted for 2 minutes via a tablet and modeling with a machine learning algorithm.

Methods

Study Design

In this prospective cross-sectional study for developing and validating an artificial intelligence (AI) model to predict frailty status from vocal biomarkers, we recruited participants aged ≥50 years. We posted research promotion posters at Seoul National University Bundang Hospital to recruit participants. We enrolled those patients or their caregivers who expressed interest after seeing the posters and consented to participate in our study. Exclusion criteria were patients who (1) were diagnosed with dysarthria; (2) had a score of ≥10 on the Korean version of the Short Form Geriatric Depression Scale (SGDS-K) score of ≥10; (3) had a history of uncontrolled sleep disorders, anxiety, or behavioral disorders within 3 months; and (4) were deemed unable to comply with the study at the discretion of the researcher.

Ethical Considerations

This study received ethics review and approval from the Institutional Review Board of Seoul National University Bundang Hospital (approval number B-2107-698-302) for the collection of data from participants in the clinical study. All data used in the study were collected and processed in accordance with the institutional review board guidelines. Informed consent was obtained from all participants for the collection of voice data. Participants were informed that their data would be anonymized or deidentified to protect their privacy and confidentiality.

Data Collection

Voices were recorded in an academic tertiary hospital. The voice recording device, a Galaxy Tablet A7 LTE (SM-T505; Samsung Electronics Co, Ltd), was located between the participant and clinician at a distance of approximately 100 cm. The recordings were performed using an application developed for the PDT by Silvia Health, Inc. The recorded speech signals were digitized at a 48 kHz sampling rate. Audacity (version 3.3.3; Audacity Team) was used to remove noise other than participants' voices.

Development of the Korean Version of the PDT

We conducted experiments to estimate the frailty status from speech signals. We used the PDT, which is commonly used for screening cognitive function impairments, to collect speech data. In the PDT process, a picture is shown, and the participants are asked to describe everything visible and explainable in the picture for 2 minutes [15]. The participant's cognitive function is assessed based on which part of the picture the participant observes and how they express the situations in syntactic and semantic terms. The PDT is usually used as a screening tool for Alzheimer disease, one of the types of degenerative brain disease, and we adopted the PDT as a tool to collect voice data for developing an AI model to evaluate frailty status [16,17].

The Boston Cookie Theft picture has been commonly used in the PDT to assess cognitive function; however, it does not fit South Korea's culture [18]. For this reason, we developed a Korean version of the PDT, which contains Korean cultural references and could thus feel familiar to Koreans. The illustration was designed according to the following principles [19]: (1) salience of information, (2) semantic categories, (3) referential cohesion, (4) causal and temporal relations, (5) mental state language, (6) structural language, and (7) general cognition and perception. Detailed descriptions for each principle are represented in Multimedia Appendix 1.

XSL•FO
RenderX

The picture shown in Multimedia Appendix 2 was developed on the basis of these principles for the Korean version of the PDT. In our data acquisition phase, the picture was provided to the participants through an app developed for a tablet, and they were asked to describe it for 2 minutes. While they explained the picture, the participants' voices were recorded using the application.

Short Form of the Comprehensive Geriatric Assessment

The participants completed a short form of the Comprehensive Geriatric Assessment (SF-CGA) to identify comorbidities, functional status, cognitive function, and depressive symptoms. Medical history, including hypertension, diabetes, heart failure, atrial fibrillation, chronic kidney disease, chronic liver disease, respiratory disease, cerebrovascular disease, myocardial infection, Parkinson disease, dementia, and depression, was assessed. Cognitive function was assessed using the Korean version of the Mini-Mental State Examination-2 (K-MMSE-2) [20]. In addition, the Clinical Dementia Rating scale (CDR), a numerical scale used to quantify the severity of dementia symptoms, was assessed [21]. Functional status, including activities of daily living (ADLs) and instrumental ADLs (IADLs), were assessed using the Barthel index and the Lawton and Brody index, respectively [22,23]. Depressive symptoms of the participants were evaluated with the SGDS-K [24].

Outcomes and Definition of Frailty and Prefrailty

Frailty status was defined using the Korean version of the Fatigue, Resistance, Ambulation, Illnesses, and Loss of Weight Scale (K-FRAIL) questionnaire [6]. We considered K-FRAIL scale scores with ≥3 positive items to indicate frailty. K-FRAIL scores of 1 or 2 were classified as prefrail, and a K-FRAIL score of 0 was categorized as robust. In this study, since the prefrail group is considered to exhibit some physiological deficits, the prefrail and frail groups were combined and compared with the robust group, which is consistent with previous research [25-27].

Acoustic Features

Recent AI technologies have been used in speech recognition, generation, and analysis. However, few studies have used speech signals as biomarkers to evaluate frailty using machine learning techniques. In our experiments, we considered using voice recordings to evaluate the frailty. Specifically, we converted raw speech data into acoustic features expressed in the frequency domain for the input of an AI model. The spectral characteristics of speech signals can be expressed using mel-frequency cepstral coefficients (MFCCs) and are well suited for various deep-learning methodologies [28].

In preprocessing using MFCCs, the audio signals are transformed from the time domain to the frequency domain via a Fourier transform after quantization to time-windowing segments. Subsequently, the mel scale is applied to the spectrum to reflect the sensitivity of the frequency band. The first "n" coefficients are then gathered after transforming the mel spectrum through the discrete cosine transform. The gathered coefficients are called MFCCs and represent the unique characteristics of the audio signal. In general, studies using MFCCs have considered not only the coefficients but also their first- or second-order derivatives. In our study, to develop an AI model for identifying frailty using speech signals, we set the number of coefficients "n" to 20 and used the first- and second-order derivatives. Consequently, the acoustic features constructed using the MFCC technique comprised 60 dimensions. To convert the speech signals into acoustic features, we used Python 3.8 (Python Software Foundation) and the Librosa library (Python Software Foundation).

Prediction Model Development and Validation

AI models using demographic and speech data were trained and validated to predict the frailty status. Among the machine learning methods, we trained the models using a supervised learning scheme, and the dataset collected from the prospective cohort was used for training and validation. The entire collected dataset was separated for training and validation purposes; there was no overlap between the training and validation datasets.

We explored and compared three types of machine learning models to predict frailty. The first model, SpeechAI, was constructed to predict the frailty status using only the acoustic features of speech signals. In the second model, DemoAI, demographic data were used to predict the frailty status, and in the third model, DemoSpeechAI, demographic data and acoustic features were combined to predict the frailty status. A total of 3 primary modules were designed to construct these models. One was designed as a classifier to identify frailty status from the data represented in the embedding space. The others were designed to represent demographics and speech data as embedding vectors.

The SpeechAI model was organized to predict frailty using acoustic features extracted from voice signals and was constructed with two modules: speech embedding and classifier. The Transformer structure was used in the speech-embedding module to express the acoustic features in the vector space [29]. The vector expressed via the Transformer model is passed to the classifier module, which consists of one hidden layer to predict the frailty status. The SpeechAI model shown in Figure S1 of Multimedia Appendix 3 had approximately 612,000 deep-learning network parameters to be trained. Among the parameters, approximately 96% (587,520/612,000) belonged to the Transformer architecture, and the classifier module had approximately 25,000 parameters.

The DemoAI model consists of a demographically embedded module that projects demographic information provided as a categorical type in an embedding space and a classifier module that predicts frailty based on the information expressed in the embedding space, as shown in Figure S2 of Multimedia Appendix 3. The demographic embedding module receives chronological age categorized into 10-year intervals and sex as the input among demographic information. They are projected onto 2D and 4D continuous embedding spaces, and the embedding vectors are concatenated to express a joint vector. The classifier module, which consists of one hidden layer, receives the joint vector expressed by the demographically embedded module, and serves as a binary classifier that distinguishes between frailty and robustness. The DemoAI model had approximately 26,000 entire network parameters for training.

XSL•FO
RenderX

The DemoSpeechAI model shown in Figure S3 of Multimedia Appendix 3 was constructed using demographics, speech-embedding modules, and a classifier module. The demographics and acoustic features were projected onto each embedding space through the embedding modules and then combined as a joint embedding vector. Subsequently, the joint embedding vector was passed to the classifier module to estimate frailty. The embedding modules used in the DemoSpeechAI model have the same structure as those used in the DemoAI and SpeechAI models. The parameters of the DemoSpeechAI model were approximately 621,000, consisting of approximately 34,000 for the classifier and 587,000 for the embedding module.

To build and train the deep-learning model, we used the PyTorch (version 2.0.1; PyTorch Team) library for Python, and an early stopping technique was used to prevent overfitting of the models in the training phase [30]. The dataset was split into five folds for 5-fold cross-validation; 4 sets were used for training, and 1 set was used to analyze the performance of the models. Each fold was divided into a balanced number of robust and frail labels.

Pretraining Strategy Using Self-Supervised Learning

We designed and modularized three types of models to predict the frailty status of the participants using deep neural networks. Among the modules constructing each model, the speech-embedding module contained a significant number of parameters to be trained compared with the amount of data collected from participants, accounting for approximately 95% of the parameters in the SpeechAI and DemoSpeechAI models. To address the risk of overfitting due to the limited data, we used a self-supervised learning (SSL) strategy [31,32]. In the SSL strategy, an AI model is pretrained on a different task before being fine-tuned for the primary task. This involves pretraining the model on a different dataset, which helps establish a robust parameter foundation. As a result, there is no need to train the parameters from scratch, allowing effective training with a relatively small dataset. To implement the SSL technique, we used the AIHub dataset from the Open AI Dataset Project (AIHub) for public purposes [33]. The AIHub dataset includes voice recordings of 1002 Korean participants, which we used for pretraining the speech embedding module of the SpeechAI and DemoSpeechAI models. Consequently, only about 5% of the parameters in these models, specifically those in the classifier and demographics embedding modules, were trained using the dataset collected from our prospective cohort.

Results

A total of 127 Korean participants aged ≥50 years were recruited to collect data at Seoul National University Bundang Hospital from June to December 2022. We acquired demographics, SF-CGA results, and voice recordings and developed an AI model for predicting frailty status. Among the participants, 43 out of 127 participants (34%) were female, the average number of years of education was 11.787 (SD 4.732) years, and the mean age was 69.2 (SD 10.9) years.

Among the 65 participants in the frail group (prefrail and frail), 6 out of 65 (9%) had dependent ADLs, and 7 out of 65 (11%) had dependent IADLs. The mean scores for the K-MMSE-2, standard total T-score, and CDR-Sum of Boxes were 25.874 (SD 4.53), 44.748 (SD 13.4), and 0.591 (SD 1.3), respectively. In the CDR, 87 out of 127 participants (68%) had 0 points, 37 out of 127 participants (29%) had 0.5 points, and 3 out of 127 participants (2%) had 1 point or higher. The mean SGDS-K scores were 2.945 (SD 2.89).

According to the K-FRAIL results, 65 out of 127 participants (51%) belonged to the frail group. The participants in the prefrail to frail group were older (73.4 vs 64.9 years; $P<.001$), had lower education levels (10.2 vs 13.5 years; $P<.001$), lower cognitive function (K-MMSE-2, 23.9 vs 27.9; $P<.001$), more depressive symptoms (SGDS-K, 4.1 vs 1.7; $P<.001$), and dependent ADL and IADL levels (Table 1).

XSL•FO
RenderX

Table . Clinical characteristics of the study population.

Characteristics	All (N=127)	Groups		*P* value
		Robust (n=62)	Prefrail and frail (n=65)	
Sex, n (%)				
Female	43 (33.9)	17 (27.4)	26 (40)	.19
Age (years), mean (SD)	69.2 (10.95)	64.9 (9.26)	73.4 (10.84)	<.001
Education (years), mean (SD)	11.8 (4.73)	13.5 (3.33)	10.2 (5.28)	<.001
K-MMSE-2 [a] (points), mean (SD)				
Total score	25.9 (4.53)	27.9 (2.07)	23.9 (5.31)	<.001
Standardized T-score	44.7 (13.40)	49.5 (10.24)	40.3 (14.47)	<.001
SGDS-K[b] (points), mean (SD)	2.95 (2.89)	1.7 (2.27)	4.1 (2.93)	<.001
ADL[c] independency, n (%)	121 (95.3)	62 (100)	59 (90.8)	.04
IADL[d] independency, n (%)	120 (90.5)	62 (100)	58 (89.2)	.02
CDR[e], n (%)				.003
0.0	87 (68.5)	51 (82.3)	36 (55.4)	
0.5	37 (29.1)	11 (17.7)	26 (40)	
≥1.0	3 (2.4)	0 (0)	3 (4.6)	
CDR-SOB[f] (points), mean (SD)	0.59 (1.30)	0.15 (0.32)	1.02 (1.68)	<.001

[a]K-MMSE-2: Korean version of the Mini-Mental State Examination-2.

[b]SGDS-K: Korean version of the Short Form Geriatric Depression Scale.

[c]ADL: activities of daily living.

[d]IADL: instrumental activities of daily living.

[e]CDR: Clinical Dementia Rating scale.

[f]SOB: sum of boxes.

We explored and compared 3 AI models for predicting the frailty status using speech only (SpeechAI), demographics only (DemoAI), and a combination of speech and demographics (DemoSpeechAI). In this study, we used 5-fold cross-validation to train and evaluate our models using a dataset corresponding to 127 participants. The entire dataset was randomly divided into 5 subsets, with each fold containing approximately 20% of the total samples. Each fold was used once as the validation set, while the remaining 80% of the samples were combined to form the training set. This process was repeated 5 times so that each fold served as the validation set exactly once. Consequently, all data points were used for validation once, and the performance metrics reported are the average results from these 5 validation runs. This approach ensures that the model's performance is robust and generalizable, avoiding overfitting and clearly defining the proportion of samples used in the validation phase. The accuracy, area under the receiver operating characteristic (ROC) curve (AUC), sensitivity, and specificity were used to analyze the performance of the model.

The mean accuracy of the SpeechAI model for the 5 validation results was 80.4% (95% CI 76.89% - 83.91%), with minimum and maximum values of 75.05% and 86.93%, respectively. The mean AUC was 0.89 (95% CI 0.86 - 0.92), with minimum and maximum values of 0.86 and 0.94, respectively. Furthermore, the average sensitivity and specificity of the SpeechAI model for 5-fold validation results were 0.75 (95% CI 0.67 - 0.83) and 0.86 (95% CI 0.84 - 0.88), respectively (Table 2). ROC curves were observed for 5-fold cross-validation, and the results and means are shown in Figure 1.

XSL•FO
RenderX

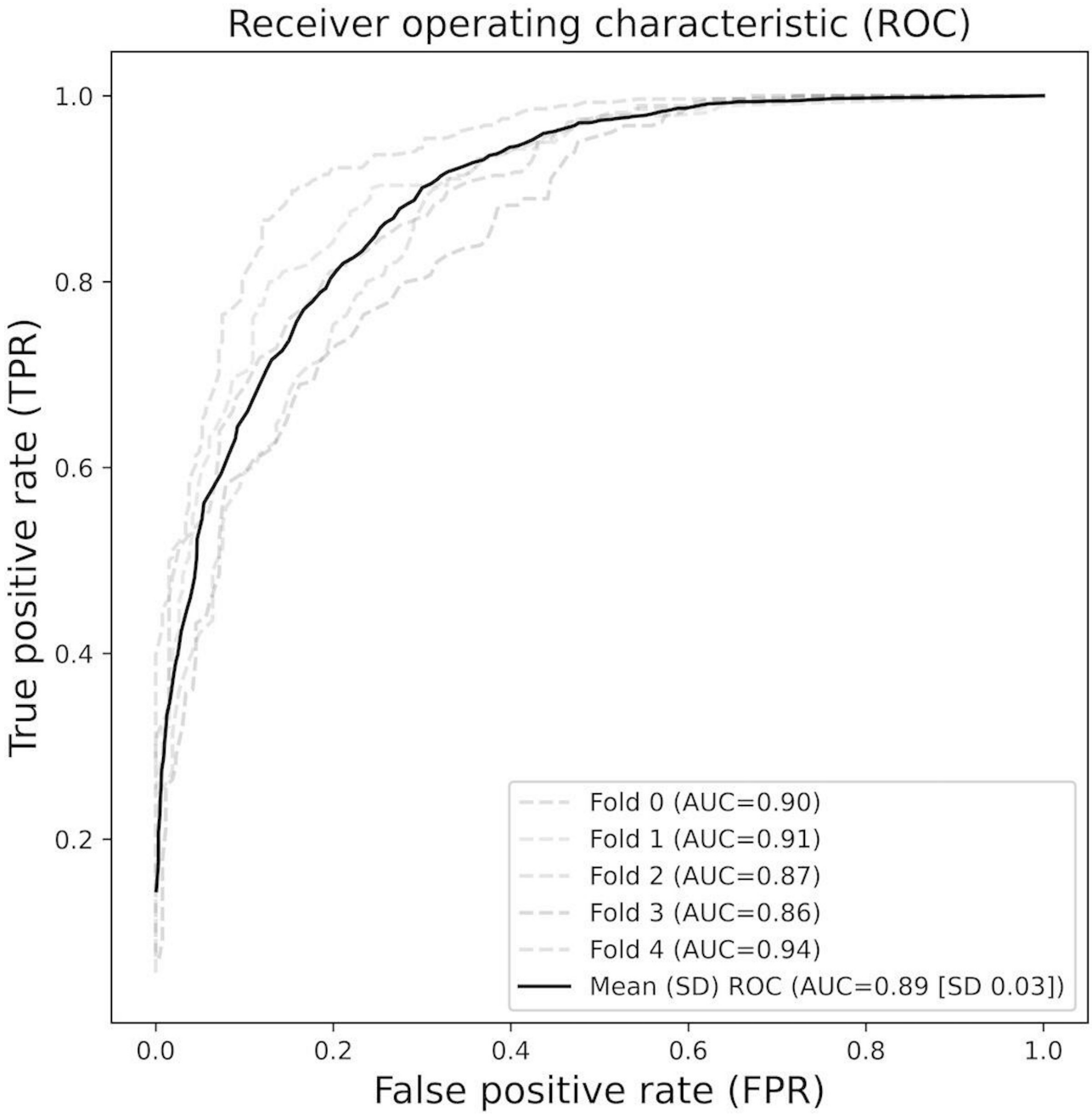
Table . The performance of the SpeechAI, DemoAI, and DemoSpeechAI models by 5-fold cross-validation.

		Accuracy (%)	AUC[a]	Sensitivity	Specificity
SpeechAI					
	Mean (95% CI)	80.40 (76.89 - 83.91)	0.89 (0.86 - 0.92)	0.75 (0.67 - 0.83)	0.86 (0.84 - 0.88)
	Minimum	75.05	0.86	0.62	0.83
	Maximum	86.93	0.94	0.88	0.88
DemoAI					
	Mean (95% CI)	67.96 (67.63 - 68.29)	0.74 (0.73 - 0.75)	0.65 (0.61 - 0.69)	0.71 (0.68 - 0.74)
	Minimum	67.51	0.73	0.60	0.66
	Maximum	68.44	0.75	0.71	0.75
DemoSpeechAI					
	Mean (95% CI)	85.60 (80.03 - 91.17)	0.93 (0.89 - 0.97)	0.89 (0.83 - 0.95)	0.83 (0.77 - 0.89)
	Minimum	74.31	0.83	0.75	0.73
	Maximum	92.29	0.98	0.95	0.91

[a]AUC: area under the receiver operating characteristic curve.

XSL•FO
RenderX

Figure 1. ROC curves for each fold demonstrating the performance of the SpeechAI model. AUC: area under the receiver operating characteristic curve; ROC: receiver operating characteristic.

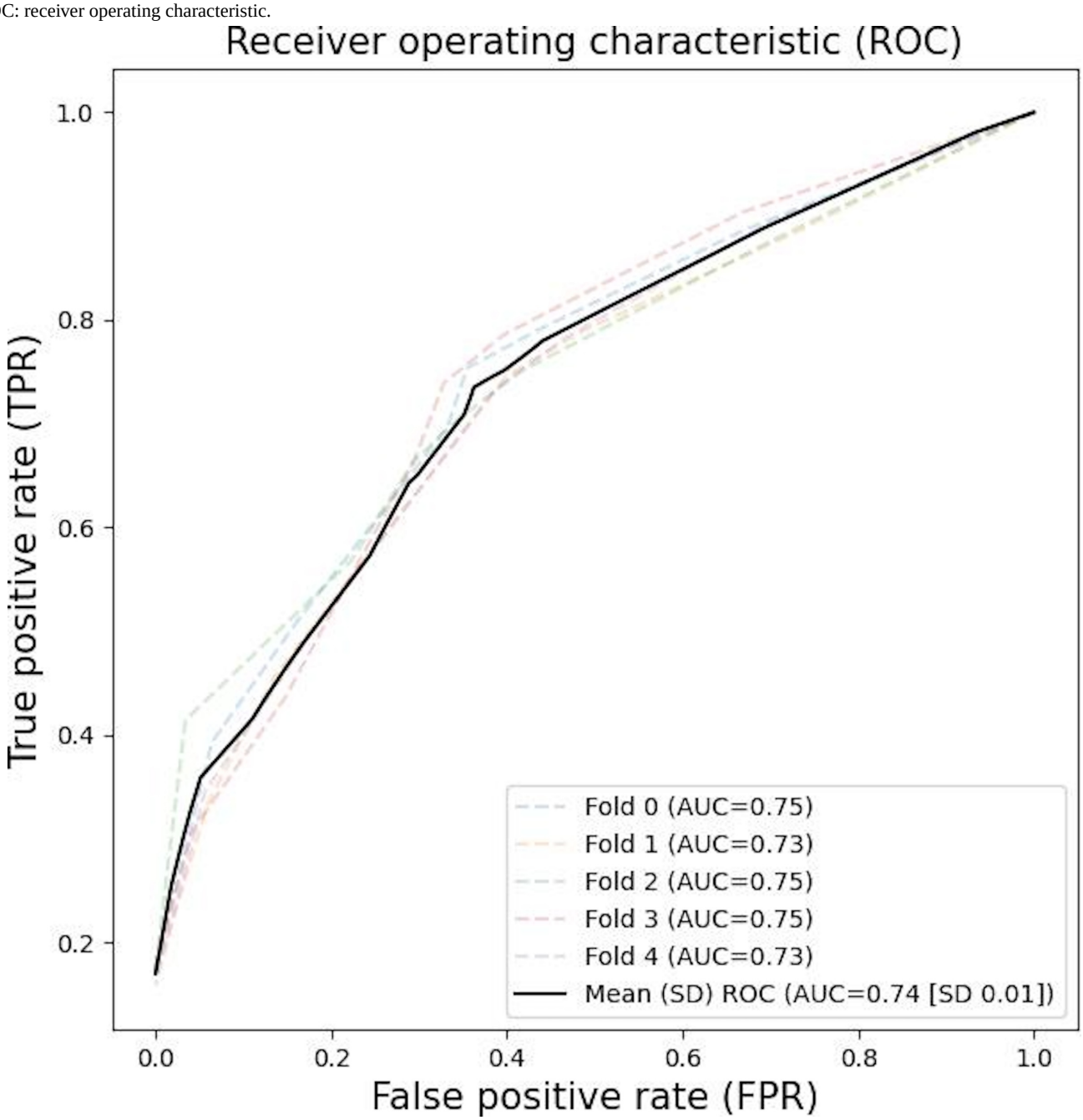


The curves represent the trade-off between true positive and false positive rates across different threshold values. The AUC values reflect the ability to distinguish between indviduals who were and were not frail.

On the other hand, the performance of the DemoAI model using the validation dataset, which was equal to that used for the SpeechAI model validation, was 67.96% (95% CI 67.63% - 68.29%) for the mean accuracy, and its minimum and maximum values were 67.51% and 68.44%, respectively. The ROC curves of each fold by 5-fold cross-validation are shown in Figure 2, and the mean AUC was 0.74 (95% CI 0.73 - 0.75), along with 0.73 and 0.75 for minimum and maximum values, respectively. Moreover, the mean sensitivity and specificity of the DemoAI model elicited from 5-fold cross-validation results were 0.65 (95% CI 0.61 - 0.69) and 0.71 (95% CI 0.68 - 0.74), respectively (Table 2).

XSL•FO
RenderX

Figure 2. ROC curves for each fold demonstrating the performance of the DemoAI model. AUC: area under the receiver operating characteristic curve; ROC: receiver operating characteristic.

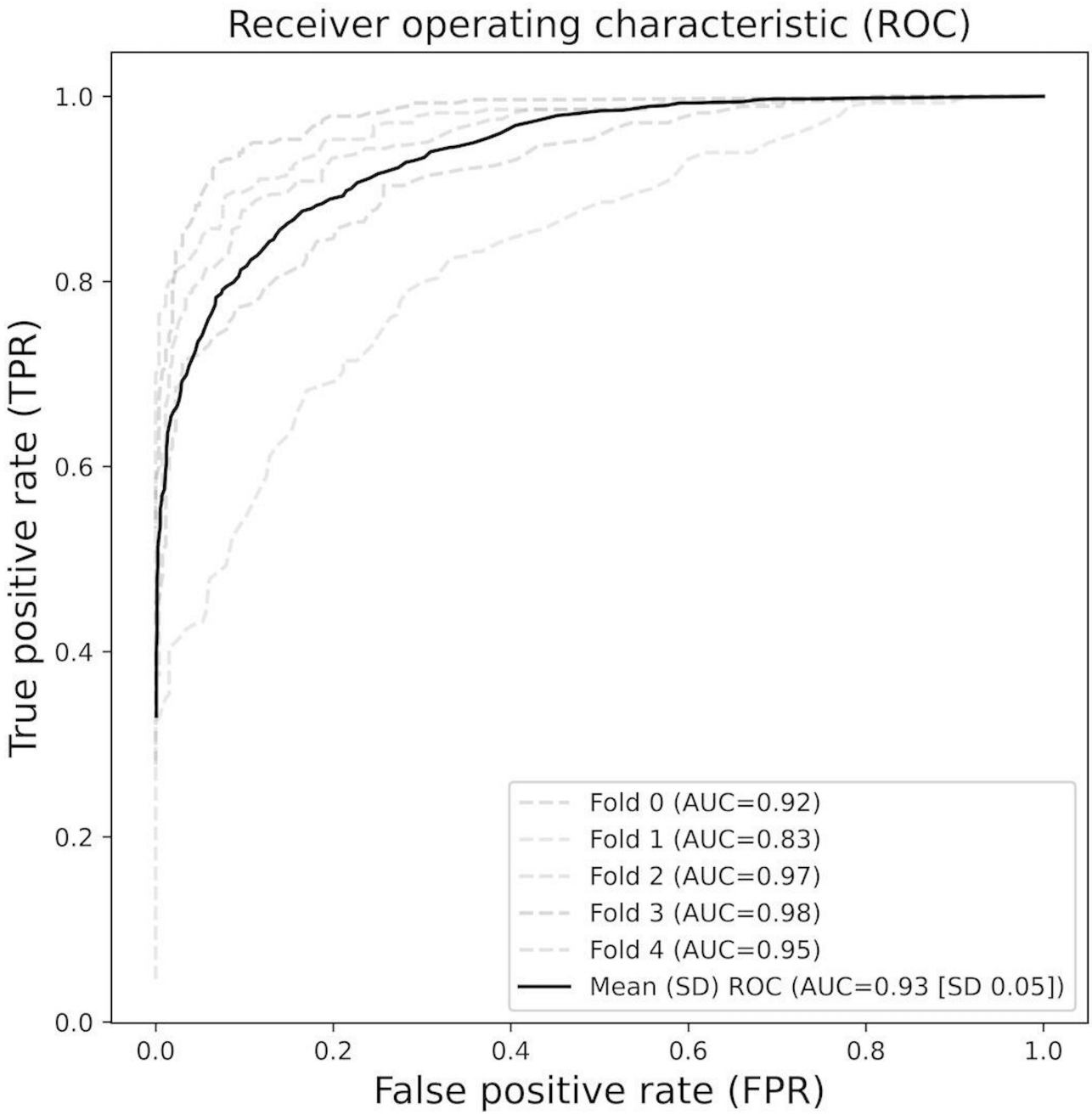


The curves represent the trade-off between true positive and false positive rates across different threshold values. The AUC values reflect the ability to distinguish between individuals who were and were not frail.

The mean accuracy of the DemoSpeechAI model for 5-fold cross-validation was 85.6% (SD 6.35%, 95% CI 80.03% - 91.17%), and the minimum and maximum values were 74.31% and 92.29%, respectively. Furthermore, the mean AUC values of the DemoSpeechAI model elicited from 5-fold cross-validation were 0.93 (SD 0.05, 95% CI 0.89 - 0.97), and the mean sensitivity and specificity were 0.89 (SD 0.07, 95% CI 0.83 - 0.95) and 0.83 (SD 0.07, 95% CI 0.77 - 0.89), respectively (Table 2). Figure 3 shows the ROC curves obtained from 5-fold cross-validation and their mean.

XSL•FO
RenderX

Figure 3. ROC curves for each fold demonstrating the performance of the DemoSpeechAI model. AUC: area under the receiver operating characteristic curve; ROC: receiver operating characteristic.



In the comparison between the SpeechAI and DemoAI models, the SpeechAI (AUC 0.89, 95% CI 0.86 - 0.92) model showed superior performance to the DemoAI model (AUC 0.74, 95% CI 0.73 - 0.75) in AUC values (t_4=8.705 [2-tailed]; P<.001), and the DemoSpeechAI model (AUC 0.93, 95% CI 0.89 - 0.97) was superior to the DemoAI model in AUC values (t_4=7.978 [2-tailed]; P<.001). However, there was no significant difference between the SpeechAI and DemoSpeechAI models (t_4=1.057 [2-tailed]; P=.35).

To evaluate the effectiveness of our models using deep learning–based acoustic features, we conducted a comparative analysis with simpler machine learning models, specifically logistic regression, random forest, and decision tree. For this comparison, we used acoustic features extracted using the openSMILE toolkit [34], a commonly used tool for extracting audio features. The extracted features included frequency domain characteristics such as MFCCs, pitch, and loudness.

We trained logistic regression, random forest, and decision tree models using these acoustic features and compared their performance with our model, which use a transformer-based architecture for feature extraction. The results of this comparison are summarized in Table 3.

XSL•FO
RenderX

Table . Performance metrics for machine learning methods using acoustic features extracted by the openSMILE toolkit.

Model	Accuracy (%), mean (95% CI)	AUC[a], mean (95% CI)	Sensitivity, mean (95% CI)	Specificity, mean (95% CI)
Logistic regression	61.45 (46.54 - 76.35)	0.62 (0.47 - 0.77)	0.62 (0.52 - 0.71)	0.62 (0.36 - 0.87)
Decision tree	57.48 (40.11 - 74.84)	0.57 (0.40 - 0.75)	0.59 (0.31 - 0.86)	0.56 (0.41 - 0.72)
Random forest	66.09 (57.69 - 74.50)	0.66 (0.58 - 0.75)	0.69 (0.58 - 0.81)	0.63 (0.42 - 0.84)

[a]AUC: area under the receiver operating characteristic curve.

The results in Table 3 compare with our model, SpeechAI, which uses the deep neural network–based feature extractor. SpeechAI significantly outperforms these traditional features-based models. The performance metrics for SpeechAI are as follows: accuracy: 80.40%, AUC: 0.89, sensitivity: 0.75, and specificity: 0.86. This demonstrates the superiority of our deep-learning approach, particularly in handling the complex and high-dimensional nature of acoustic features. The advanced feature extraction capabilities of the SpeechAI model enable it to capture intricate patterns and nuances in the voice data, which simpler models fail to exploit fully.

While traditional models provide a baseline performance, the deep learning–based model's ability to leverage large-scale pretraining and complex feature extraction processes leads to improved predictive accuracy. These results underscore the effectiveness of deep-learning techniques for this application and highlight their potential for broader adoption in related research fields.

Discussion

Principal Findings

In recent years, several studies have investigated the use of voice data to predict frailty among older adults. One study explored the application of vocal biomarkers for frailty classification, finding significant associations between specific voice parameters and frailty levels [12]. Our study builds on this by using advanced deep-learning techniques to extract more nuanced features from voice data, potentially improving the accuracy and reliability of frailty predictions. In addition, a study demonstrated the feasibility of using voice biomarkers to classify frailty, focusing on various acoustic parameters such as formant frequencies and spectral energy ratios [13]. Our findings align with these results, further validating the effectiveness of voice biomarkers in predicting frailty. However, our approach differs by incorporating a more extensive set of acoustic features and using robust cross-validation methods to ensure generalizability. Our study aligns with the growing body of research that leverages vocal biomarkers to predict cognitive and functional decline. Notably, a study demonstrated the effectiveness of using spontaneous speech analysis to identify cognitive function decline among older adults in a multilanguage cross-sectional study [35]. Their findings highlighted that specific acoustic features could discriminate between healthy individuals and those with mild to severe cognitive impairment with high accuracy, supporting the viability of voice as a noninvasive diagnostic tool.

Using acoustic features to predict frailty is promising, particularly in the context we have adopted, where participants describe and explain a picture. Recent studies have demonstrated that transformer models yield superior results in various speech-related tasks, such as speech recognition, speech synthesis, and speech classification, surpassing traditional methods. Transformer architectures significantly improve the ability to capture complex patterns and long-range dependencies in sequential data, which are crucial for accurate speech processing [36].

In our study, we compared the performance of our transformer-based SpeechAI model with machine learning models that use acoustic features extracted by the openSMILE toolkit, which does not rely on deep neural networks. The openSMILE toolkit is widely used for extracting features such as pitch, loudness, and MFCCs. Our experiments showed that the deep neural network–based model outperformed simpler models using acoustic features, demonstrating the effectiveness of the transformer architecture in extracting and leveraging high-level acoustic features for predicting frailty.

The ability of the transformer architecture to model long-range dependencies and process sequences in parallel contributes to its enhanced performance [37]. This capability allows the transformer-based SpeechAI model to capture intricate patterns and nuances in the voice data, which extractors that do not rely on deep neural networks fail to exploit fully. The abilities can be experimentally observed by the superior performance metrics of SpeechAI, such as higher accuracy and better sensitivity and specificity, compared with models based on traditional acoustic feature extraction methods.

Through this study, the picture, Silvia Train Station, was developed for the Korean version of the PDT. It was designed according to the appropriate principles, containing Korean cultural references that would feel familiar to Koreans. We recruited a prospective cohort that included various clinical, medical, and demographic information and voice data encompassing the frailty status of 127 individuals. We developed and validated a model to predict frailty using AI techniques in conjunction with voice data from a prospective cohort and public AIHub dataset. Our study showed that 3 modularized models can be used to predict the participants' frailty status using deep neural networks, which showed excellent performance.

Evaluation With Imbalanced Validation Set

In our study, we investigated whether speech data could be used to classify frailty and observed meaningful results. We conducted experiments to classify between robust individuals and a combined group of individuals with prefrailty and frailty.

XSL•FO
RenderX

We trained the model using a balanced class distribution between the two groups to ensure effective learning and avoid bias toward the majority class. Balancing the dataset during training is crucial, as it prevents the model from favoring the majority class, leading to improved performance across both classes and enhancing the model's generalization capability. However, recognizing that the real-world prevalence of frailty is approximately 20%, we conducted an additional sensitivity analysis with the SpeechAI model to better reflect real-world conditions by using a validation set where the frailty group constituted 20% of the data. The results showed an accuracy of 74.80% (95% CI 69.36% - 80.25%), an AUC of 0.79 (95% CI 0.71 - 0.88), a sensitivity of 0.77 (95% CI 0.67 - 0.87), and a specificity of 0.63 (95% CI 0.39 - 0.88). These results indicate that the model maintained strong predictive accuracy with the imbalanced validation set, demonstrating its robustness. While this approach provides meaningful insights, future research should aim to include more diverse and representative cohorts to fully validate the model's applicability to real-world scenarios.

Strengths and Limitations

Our study had several strengths. First, we developed and validated a model that successfully estimated the frailty state by showing a picture and obtaining voice recordings that freely described the picture using a tablet. Previous methods to diagnose frailty consumed a lot of time, space, and manpower or required much effort to process existing medical data. According to the methodology used in this study, older adults can check their risk of frailty in a way that can be performed on their own without having to visit a hospital or research institution. Second, voice data predicted frailty well, and it was experimentally confirmed that the acoustic features extracted from the voice recordings played an important role in predicting frailty. Based on these results, we demonstrated the possibility of developing many acoustic feature–derived models that can identify many health-related characteristics of older people, such as cognitive function, certain disease status, morbidity, and mortality. Third, despite statistical challenges, the model was developed and validated using a limited dataset, providing effective performance, even with a small sample size. The model efficiently leveraged voice data, omitted frailty-related variables, and demonstrated robust predictive capability while avoiding unnecessary complexity.

Our study had several limitations. First, in research using voice data, there are inevitable limitations in noise processing. The data collected for this study contained various noises as they were collected in a routine hospital environment. To remove noise, it was necessary to remove sounds other than the participants' voices. So, it is necessary to provide an automatic noise removal process using technologies such as noise canceling, speaker recognition, and voice activity detection in further studies. Second, in the PDT, which was performed in our study, cognitive function could be assessed by the participants' understanding of the causal relationship or the importance of the PDT. However, during the PDT, the participants had some difficulty explaining the given picture for 2 minutes, which made it difficult to collect complete and diverse sound characteristics from the participants. Therefore, if the PDT can be developed to be more specialized and suitable for the older population and to extract acoustic features, the accuracy of AI technology will further increase. Third, the relatively small sample size may not fully represent the diversity of each group, and biases introduced during participant selection could have affected the generalizability of the results. In addition, the study involved only Korean participants, thus caution should be taken in generalizing the results to populations from different regions or ethnicities. Furthermore, there is a significant age difference between the robust and prefrail and frail groups in our cohort. Due to this existing significant difference in age between the two groups, the DemoAI model, which was trained using only age and sex, also showed relatively high performance. Nevertheless, the model using speech data demonstrated statistically superior performance compared with the DemoAI model, highlighting the effectiveness of incorporating vocal biomarkers in frailty prediction. Future work should include more diverse participants to address these limitations and ensure the broader applicability of the findings. In addition, developing advanced noise processing techniques to improve the clarity of voice data collected in natural environments is essential. Expanding the use of vocal biomarkers to predict various health conditions and integrating these models into mobile health apps will make health monitoring more accessible. This approach could lead to noninvasive, efficient, and widely applicable health assessment tools for older adults.

Conclusions

We developed and evaluated 3 types of models, DemoAI, SpeechAI, and DemoSpeechAI, to predict participants' frailty status using deep neural networks with SSL techniques based on voice recordings collected via a tablet during the PDT. This was successfully developed using voice data collected from the recruited participants, assisted by an independently released voice database (AIHub). The next possible step would include applying the model to electronic health records, which can assist in decision-making, additional perioperative evaluation, and supportive care to prevent adverse outcomes after surgery.

Acknowledgments

This work was supported by a Korea Planning & Evaluation institute of Industrial Technology (KEIT) grant funded by the Korea government (Ministry of Trade, Industry and Energy [MOTIE]; project name: Development and validation of a digital phenotype based platform for the treatment and prevention of MCI using a multidisciplinary approach to decrease dementia risk/project number: 20024263) and by a Korea Health Industry Development Institute (KHIDI) grant funded by the Korea government (Ministry of Health and Welfare [MOHW]; project name: Development of an at-home "cognitive monitoring" application equipped

XSL•FO
RenderX

with the Korean version of the picture description task). The funders had no role in the study design, data collection and analysis, decision to publish, or manuscript preparation.

Conflicts of Interest

TK and MJK are employees and CEO of Silvia Health Inc, respectively.

Multimedia Appendix 1
Detailed descriptions of principles to build the illustrations for the picture description task.
[PDF File, 36 KB - medinform_v13i1e57298_app1.pdf]

Multimedia Appendix 2
Silvia Train Station (Copyright 2022. Silvia Health Inc.), an image used in the Korean version of the PDT.
[PDF File, 1783 KB - medinform_v13i1e57298_app2.pdf]

Multimedia Appendix 3
Architecture of the three artificial intelligence models used for predicting frailty.
[PDF File, 678 KB - medinform_v13i1e57298_app3.pdf]

References

1. The Lancet Regional Health-Western Pacific. South Korea's population shift: challenges and opportunities. Lancet Reg Health West Pac 2023 Jul 31;36:100865. [doi: 10.1016/j.lanwpc.2023.100865] [Medline: 37621310]
2. Buckinx F, Rolland Y, Reginster JY, Ricour C, Petermans J, Bruyère O. Burden of frailty in the elderly population: perspectives for a public health challenge. Arch Public Health 2015;73(1):19. [doi: 10.1186/s13690-015-0068-x] [Medline: 25866625]
3. Boreskie KF, Hay JL, Boreskie PE, Arora RC, Duhamel TA. Frailty-aware care: giving value to frailty assessment across different healthcare settings. BMC Geriatr 2022 Jan 3;22(1):13. [doi: 10.1186/s12877-021-02722-9] [Medline: 34979966]
4. Fried LP, Tangen CM, Walston J, et al. Frailty in older adults: evidence for a phenotype. J Gerontol A Biol Sci Med Sci 2001 Mar;56(3):M146-M156. [doi: 10.1093/gerona/56.3.m146] [Medline: 11253156]
5. Rockwood K, Song X, MacKnight C, et al. A global clinical measure of fitness and frailty in elderly people. CMAJ 2005 Aug 30;173(5):489-495. [doi: 10.1503/cmaj.050051] [Medline: 16129869]
6. Jung HW, Yoo HJ, Park SY, et al. The Korean version of the FRAIL scale: clinical feasibility and validity of assessing the frailty status of Korean elderly. Korean J Intern Med 2016 May;31(3):594-600. [doi: 10.3904/kjim.2014.331] [Medline: 26701231]
7. Pan C, Luo H, Cheung G, et al. Identifying frailty in older adults receiving home care assessment using machine learning: longitudinal observational study on the role of classifier, feature selection, and sample size. JMIR AI 2024 Jan 31;3:e44185. [doi: 10.2196/44185] [Medline: 38875533]
8. Kranthi Kumar L, Alphonse PJA. COVID-19 disease diagnosis with light-weight CNN using modified MFCC and enhanced GFCC from human respiratory sounds. Eur Phys J Spec Top 2022;231(18-20):3329-3346. [doi: 10.1140/epjs/s11734-022-00432-w] [Medline: 35096278]
9. Martínez-Nicolás I, Llorente TE, Martínez-Sánchez F, Meilán JJG. Ten years of research on automatic voice and speech analysis of people with Alzheimer's disease and mild cognitive impairment: a systematic review article. Front Psychol 2021;12:620251. [doi: 10.3389/fpsyg.2021.620251] [Medline: 33833713]
10. Tracy JM, Özkanca Y, Atkins DC, Hosseini Ghomi R. Investigating voice as a biomarker: deep phenotyping methods for early detection of Parkinson's disease. J Biomed Inform 2020 Apr;104:103362. [doi: 10.1016/j.jbi.2019.103362] [Medline: 31866434]
11. Guidi A, Salvi S, Ottaviano M, et al. Smartphone application for the analysis of prosodic features in running speech with a focus on bipolar disorders: system performance evaluation and case study. Sensors (Basel) 2015 Nov 6;15(11):28070-28087. [doi: 10.3390/s151128070] [Medline: 26561811]
12. Lin YC, Yan HT, Lin CH, Chang HH. Predicting frailty in older adults using vocal biomarkers: a cross-sectional study. BMC Geriatr 2022 Jul 1;22(1):549. [doi: 10.1186/s12877-022-03237-7] [Medline: 35778699]
13. Rosen-Lang Y, Zoubi S, Cialic R, Orenstein T. Using voice biomarkers for frailty classification. Geroscience 2024 Feb;46(1):1175-1179. [doi: 10.1007/s11357-023-00872-9] [Medline: 37480417]
14. Kaufman JM, Thommandram A, Fossat Y. Acoustic analysis and prediction of type 2 diabetes mellitus using smartphone-recorded voice segments. Mayo Clin Proc Dig Health 2023 Dec;1(4):534-544. [doi: 10.1016/j.mcpdig.2023.08.005]
15. Goodglass H, Kaplan E, Barresi B. Boston diagnostic aphasia examination: stimulus cards. In: Sarno MT, editor. Acquired Aphasia, 3rd edition: Academic Press; 2001.

XSL•FO
RenderX

16. Gómez-Gómez ME, Zapico SC. Frailty, cognitive decline, neurodegenerative diseases and nutrition interventions. Int J Mol Sci 2019 Jun 11;20(11):2842. [doi: 10.3390/ijms20112842] [Medline: 31212645]
17. Mefford JA, Zhao Z, Heilier L, et al. Varied performance of picture description task as a screening tool across MCI subtypes. PLOS Dig Health 2023 Mar;2(3):e0000197. [doi: 10.1371/journal.pdig.0000197] [Medline: 36913425]
18. Kaplan E, Gallagher RE, Glosser G. Aphasia-related disorders. In: Sarno MT, editor. Acquired Aphasia, 3rd edition: Academic Press; 2001.
19. Cummings L. Describing the Cookie Theft picture. PS (Wash DC) 2019 Jul 5;10(2):153-176 [FREE Full text] [doi: 10.1075/ps.17011.cum]
20. Baek MJ, Kim K, Park YH, Kim S. The validity and reliability of the Mini-Mental State Examination-2 for detecting mild cognitive impairment and Alzheimer's disease in a Korean population. PLoS One 2016;11(9):e0163792. [doi: 10.1371/journal.pone.0163792] [Medline: 27668883]
21. Morris JC. Clinical dementia rating: a reliable and valid diagnostic and staging measure for dementia of the Alzheimer type. Int Psychogeriatr 1997;9 Suppl 1:173-176. [doi: 10.1017/s1041610297004870] [Medline: 9447441]
22. Mahoney FI, Barthel DW. Functional evaluation: the Barthel Index. Md State Med J 1965 Feb;14:61-65. [Medline: 14258950]
23. Lawton MP, Brody EM. Assessment of older people: self-maintaining and instrumental activities of daily living. Gerontol 1969 Sep 1;9(3 Part 1):179-186. [doi: 10.1093/geront/9.3_Part_1.179]
24. Bae JN, Cho MJ. Development of the Korean version of the Geriatric Depression Scale and its short form among elderly psychiatric patients. J Psychosom Res 2004 Sep;57(3):297-305. [doi: 10.1016/j.jpsychores.2004.01.004] [Medline: 15507257]
25. Yu R, Tong C, Woo J. Effect of an integrated care model for pre-frail and frail older people living in community. Age Ageing 2020 Oct 23;49(6):1048-1055. [doi: 10.1093/ageing/afaa087] [Medline: 32479591]
26. Cano-Escalera G, Graña M, Irazusta J, Labayen I, Gonzalez-Pinto A, Besga A. Mortality risks after two years in frail and pre-frail older adults admitted to hospital. J Clin Med 2023 Apr 24;12(9):3103. [doi: 10.3390/jcm12093103] [Medline: 37176544]
27. Haider S, Grabovac I, Dorner TE. Effects of physical activity interventions in frail and prefrail community-dwelling people on frailty status, muscle strength, physical performance and muscle mass-a narrative review. Wien Klin Wochenschr 2019 Jun;131(11-12):244-254. [doi: 10.1007/s00508-019-1484-7] [Medline: 30941525]
28. Abdul Z, Al-Talabani AK. Mel frequency cepstral coefficient and its applications: a review. IEEE Access 2022;10:122136-122158. [doi: 10.1109/ACCESS.2022.3223444]
29. Vaswani A, Shazeer N, Parmar N, et al. Attention is all you need. Presented at: 31st Conference on Neural Information Processing Systems (NIPS 2017); Dec 4-9, 2017; Long Beach, California. [doi: 10.48550/arxiv.1706.03762]
30. Ying X. An overview of overfitting and its solutions. J Phys Conf Ser 2019 Mar 1;1168:022022. [doi: 10.1088/1742-6596/1168/2/022022]
31. Ericsson L, Gouk H, Loy CC, Hospedales TM. Self-supervised representation learning: introduction, advances, and challenges. IEEE Signal Process Mag 2022;39(3):42-62. [doi: 10.1109/MSP.2021.3134634]
32. Nguyen TD, Le DT, Bum J, Kim S, Song SJ, Choo H. Self-FI: Self-supervised learning for disease diagnosis in fundus images. Bioeng (Basel) 2023 Sep 16;10(9):1089. [doi: 10.3390/bioengineering10091089] [Medline: 37760191]
33. AI-Hub. URL: http://www.aihub.or.kr/ [accessed 2024-12-10]
34. Eyben F, Wöllmer M, Schuller B. OpenSMILE: the Munich versatile and fast open-source audio feature extractor. Presented at: 18th ACM International Conference on Multimedia; Oct 25-29, 2010; Firenze, Italy p. 1459-1462. [doi: 10.1145/1873951.1874246]
35. Ambrosini E, Giangregorio C, Lomurno E, et al. Automatic spontaneous speech analysis for the detection of cognitive functional decline in older adults: multilanguage cross-sectional study. J Aging 2024 Apr 29;7:e50537. [doi: 10.2196/50537] [Medline: 38386279]
36. Li J, Su R, Xie X, Wang L, Yan N. A multi-level acoustic feature extraction framework for transformer based end-to-end speech recognition. arXiv. Preprint posted online on Aug 18, 2021. [doi: 10.48550/arXiv.2108.07980]
37. Latif S, Zaidi A, Cuayahuitl H, Shamshad F, Shoukat M, Qadir J. Transformers in speech processing: a survey. arXiv. Preprint posted online on Mar 21, 2023. [doi: 10.48550/arXiv.2303.11607]

Abbreviations

ADL: activities of daily living
AI: artificial intelligence
AUC: area under the receiver operating characteristic curve
CDR: Clinical Dementia Rating scale
IADL: instrumental activities of daily living
K-FRAIL: Korean version of the Fatigue, Resistance, Ambulation, Illnesses, and Loss of Weight Scale
K-MMSE-2: Korean version of the Mini-Mental State Examination-2
MFCC: mel-frequency cepstral coefficient
PDT: picture description task

XSL•FO
RenderX

ROC: receiver operating characteristic
SF-CGA: short form of the Comprehensive Geriatric Assessment
SGDS-K: Korean version of the Short Form Geriatric Depression Scale
SSL: self-supervised learning

Edited by A Benis; submitted 11.02.24; peer-reviewed by C Ochoa-Zezzatti, C Bai; revised version received 29.10.24; accepted 12.11.24; published 16.01.25.

Please cite as:
Kim T, Choi JY, Ko MJ, Kim KI
Development and Validation of a Machine Learning Method Using Vocal Biomarkers for Identifying Frailty in Community-Dwelling Older Adults: Cross-Sectional Study
JMIR Med Inform 2025;13:e57298
URL: https://medinform.jmir.org/2025/1/e57298
doi:10.2196/57298

© Taehwan Kim, Jung-Yeon Choi, Myung Jin Ko, Kwang-il Kim. Originally published in JMIR Medical Informatics (https://medinform.jmir.org), 16.1.2025. This is an open-access article distributed under the terms of the Creative Commons Attribution License (https://creativecommons.org/licenses/by/4.0/), which permits unrestricted use, distribution, and reproduction in any medium, provided the original work, first published in JMIR Medical Informatics, is properly cited. The complete bibliographic information, a link to the original publication on https://medinform.jmir.org/, as well as this copyright and license information must be included.

XSL•FO
RenderX

Interpretable Machine Learning Model for Predicting Postpartum Depression: Retrospective Study

Ren Zhang[1,2*], MD; Yi Liu[3*], MD; Zhiwei Zhang[2*], MD; Rui Luo[4], MEng; Bin Lv[1], MD

[1]Department of Gynecology and Obstetrics, West China Second University Hospital, Sichuan University, Key Laboratory of Birth Defects and Related Diseases of Women and Children (Sichuan University), Ministry of Education, Chengdu, China

[2]West China School of Medicine, Sichuan University, Chengdu, China

[3]Department of Thoracic Surgery and Institute of Thoracic Oncology, West China Hospital, Sichuan University, Chengdu, China

[4]College of Engineering, University of California, Berkeley, CA, United States

[*]these authors contributed equally

Corresponding Author:
Bin Lv, MD
Department of Gynecology and Obstetrics, West China Second University Hospital, Sichuan University, Key Laboratory of Birth Defects and Related Diseases of Women and Children (Sichuan University), Ministry of Education, Chengdu, China

Abstract

Background: Postpartum depression (PPD) is a prevalent mental health issue with significant impacts on mothers and families. Exploring reliable predictors is crucial for the early and accurate prediction of PPD, which remains challenging.

Objective: This study aimed to comprehensively collect variables from multiple aspects, develop and validate machine learning models to achieve precise prediction of PPD, and interpret the model to reveal clinical implications.

Methods: This study recruited pregnant women who delivered at the West China Second University Hospital, Sichuan University. Various variables were collected from electronic medical record data and screened using least absolute shrinkage and selection operator penalty regression. Participants were divided into training (1358/2055, 66.1%) and validation (697/2055, 33.9%) sets by random sampling. Machine learning–based predictive models were developed in the training cohort. Models were validated in the validation cohort with receiver operating curve and decision curve analysis. Multiple model interpretation methods were implemented to explain the optimal model.

Results: We recruited 2055 participants in this study. The extreme gradient boosting model was the optimal predictive model with the area under the receiver operating curve of 0.849. Shapley Additive Explanation indicated that the most influential predictors of PPD were antepartum depression, lower fetal weight, elevated thyroid-stimulating hormone, declined thyroid peroxidase antibodies, elevated serum ferritin, and older age.

Conclusions: This study developed and validated a machine learning–based predictive model for PPD. Several significant risk factors and how they impact the prediction of PPD were revealed. These findings provide new insights into the early screening of individuals with high risk for PPD, emphasizing the need for comprehensive screening approaches that include both physiological and psychological factors.

(JMIR Med Inform 2025;13:e58649) doi:10.2196/58649

KEYWORDS

postpartum depression; machine learning; predictive model; risk factors; XGBoost; extreme gradient boosting; PPD

Introduction

Postpartum depression (PPD) is a common mental disorder characterized by low mood, loss of pleasure, and sleep disturbance during the postpartum period [1]. The prevalence of PPD ranges from 3% to 38% in different nations and is higher in limited-income countries [2,3]. PPD leads to adverse consequences for the mother and family members, such as emotional strain and increased caregiving burden. Women with PPD may experience prolonged periods of distress and are more vulnerable to recurrent depressive episodes [4]. Previous studies revealed that PPD can impair a mother's parenting ability, such as breastfeeding, potentially resulting in enduring adverse effects on the child's development across emotional, cognitive, and physical domains [5,6]. Moreover, PPD can strain family relationships and impose economic burdens due to increased health care needs and reduced productivity [6].

With such a profound impact, mothers should be routinely screened for PPD, and early interventions should be implemented. However, current screening for PPD is mainly based on existing depressive symptoms such as fatigue and sleep disturbance, which are believed to be overlooked due to

XSL•FO
RenderX

overlap with normal physiological manifestations after delivery [7,8]. In addition, the diagnosis of PPD depends on patients' subjective reporting of personal health conditions [9]. It is urgent to identify individuals with high risk for PPD before clinical symptoms appear, while no effective and validated screening tools are currently available [7,10].

Previous studies have identified several risk factors of PPD such as unplanned pregnancy, lack of social support, and family history of mental disorders [11,12]. However, limited variables in such studies led to a lack of integrity. Machine learning algorithms provide support for the development of predictive models to prevent and intervene adverse health outcomes, offering avenues for personalized prediction and intervention strategies [13,14]. Several studies have adapted machine learning into the prediction of PPD risk in the last few years and achieved impressive performance [15-17]. However, insufficient model explanations leave obstacles for actual implementation. Besides, mental disorders are strongly associated with cultural backgrounds and study populations. Thus, the challenge remains to develop more nuanced and culturally adaptable machine learning models for the early detection and effective management of PPD, bridging the gap in current research and practice.

Given the importance of early screening for PPD and the limitations mentioned earlier, we conducted a retrospective study at our institution. This study comprehensively collected variables from multiple aspects, adopted machine learning algorithms to identify risk factors, and aimed to achieve precise prediction of PPD.

Methods

Participants

Pregnant women who underwent perinatal examinations and delivered at West China Second University Hospital, Sichuan University, from January 2017 to December 2020 were invited to participate in this study. The study cohort was divided into training and validation sets by random sampling. Participants were screened for eligibility. The inclusion criteria were as follows: (1) participants who completed regular examinations and delivered at our institution, (2) participants with a gestational age of ≥28 weeks, and (3) participants who gave consent to participation and be followed up. The exclusion criteria were (1) participants with a psychiatric history in the 6 months before conception and (2) participants with missing data.

Outcome

Participants were assessed for PPD 3 months post partum with the Edinburgh Postnatal Depression Scale [18]. The Edinburgh Postnatal Depression Scale has 10 items concerning depressive symptoms, and each item is evaluated using scores ranging from 0 to 3, constituting a total score of 30. Participants who scored 13 or more were regarded as having PPD [18]. The diagnosis of PPD was confirmed by 2 experienced senior psychiatrists using the Structured Clinical Interview for *Diagnostic and Statistical Manual of Mental Disorders, Fifth Edition* (*DSM-5*) [19] and the *Chinese Classification and Diagnostic Criteria of Mental Disorders, Third Edition* (*CCMD-3*) [20].

Variable Screening

Demographic variables were collected from the electronic medical record system of our institution. Clinical variables were assessed and documented by qualified clinicians. Relevant laboratory indicators were collected at 28 weeks of gestation from the medical laboratory system of the institution.

Participants were assessed for antepartum depression before delivery with the Zung Self-Rating Depression Scale [21]. The Self-Rating Depression Scale is a self-reported scale with 20 items concerning depressive symptoms, and each item is evaluated with scores ranging from 0 to 4, according to the severity of symptoms. All participants with more than 53 points were regarded as having antepartum depression [22].

Social variables, including education, income, exposure to suspected adverse factors, and family and social relations, were collected using scales and self-administered questionnaires. Income level was assessed using the local minimum income standard. Suspected adverse factors included alcohol consumption and smoking. Family and social relations comprised spouses in good health, only child, planned pregnancy, social support, family satisfaction, adverse marital status, and family history of mental illness. The level of social support was measured using the Social Support Rating Scale, which is widely used to assess social support with great reliability [23]. Scores higher than 35 are considered normal; scores of 35 or lower indicate low levels of social support [24]. Family satisfaction was assessed using the Family Adaptation, Partnership, Growth, Affection, Resolve index [25]. The Family Adaptation, Partnership, Growth, Affection, Resolve index consists of 5 items, each with a score ranging from 0 to 2. It systematically evaluates the level of family care a pregnant woman receives. A total score of 0 - 3 represents a low level of family satisfaction, and a score higher than 4 represents a normal level.

To avoid the potential bias of multicollinearity and overfitting, least absolute shrinkage and selection operator (LASSO) regression was performed to select and filter the variables in the training set. LASSO is a regression-based methodology that can reduce model complexity; multicollinearity and overfitting are avoided by constructing a penalty function [26]. LASSO regression is applied to filter a large number of variables and remove those that are insignificant [27,28]. The 5-fold cross-validation method was used to calculate the optimal λ values, and variables with nonzero coefficients were selected as the final predictive factors. After LASSO regression, the variance inflation factor (VIF) was calculated among the included variables to assess multicollinearity. The VIF was introduced to understand the impact of collinearity in regression models and has since been widely applied in various fields, including medical research [29-31]. VIF helps ensure that machine learning models or statistical models are not adversely affected by collinear predictors [32]. Typically, a VIF value greater than 10 is considered indicative of high multicollinearity, which may necessitate removing or adjusting variables to improve model stability [29,33].

XSL•FO
RenderX

Model Development

We used the following 3 machine learning algorithms to develop the PPD prediction model: extreme gradient boosting (XGBoost), random forest (RF), and gradient boosting machine (GBM). XGBoost is a powerful and efficient machine learning algorithm known for its exceptional performance in regression, classification, and ranking problems. It is an extension of the traditional gradient boosting method that combines multiple weak classifiers to create a strong classifier that minimizes the loss function [34]. RF is an ensemble machine learning algorithm based on decision trees. It creates multiple decision trees, each based on a randomly sampled subset of the training data to create a more accurate and robust output [35]. GBM is a popular machine learning algorithm that combines the principles of boosting and gradient descent to create a powerful predictive model [36]. Additionally, logistic regression, a traditional method, was implemented to predict PPD as a control.

Machine learning models were developed in the training set. To mitigate overfitting and achieve ideal model performance, hyperparameters for each machine learning model were tuned by grid search. In each session of hyperparameter tuning, 3-fold cross-validation was implemented, and the area under the receiver operating characteristic curve (AUC) was the criterion to assess model performance [37]. The combination of hyperparameters with the largest AUC value was further evaluated in the validation set.

Model Evaluation

Predictive models were evaluated with the receiver operating characteristic curve (ROC) and decision curve analysis (DCA) in the validation set. ROC reflects the ability of a model to discriminate PPD [38]. DCA is used to evaluate and compare the clinical utility of different diagnostic or predictive models. It provides a framework for assessing the net benefit of a model by taking into account the potential harms and benefits associated with different decision thresholds [39]. Additionally, accuracy, sensitivity, specificity, positive predictive value (PPV), and negative predictive value (NPV) of each model were calculated for comprehensive evaluation. Based on ROC, the predictive model with the greatest AUC value was considered as the optimal model, which would be further explored for interpretation.

Model Interpretation

We performed variable importance, partial dependence plot (PDP), and Shapley Additive Explanation (SHAP) to interpret the optimal predictive model. Variable importance assesses the contribution of each input variable by calculating the decrease in error when split by a variable [40]. PDPs calculate the partial dependence of a variable by fixing the values of other variables and observing the variation in the outcome [41]. It helps to explain how the outcome changes with changes in input variables. SHAP measures the contribution of variables in each individual sample [42]. The SHAP values show how much each variable contributes, either positively or negatively, to the outcome.

Statistical Software

All statistical analyses were performed with R software (version 4.3.1; R Foundation for Statistical Computing). LASSO regression was performed using the R package *glmnet*. Logistic regression model was implemented using the R package *glm*. XGBoost, RF, and GBM models were developed and assessed with R package *mlr3*. Model interpretation was performed with R packages *fastshap* and *pdp*. Other involved packages include *xgboost*, *randomForest*, *gbm*, *pROC*, *ggplot2*, and their various dependencies.

Ethical Considerations

This study was approved by the ethics committee of West China Second University Hospital, Sichuan University (approval 2021-186). Informed consent was obtained from all individual participants involved in the study. The original informed consent covered the secondary use of the data without the need for additional consent. All participant data were anonymized to protect privacy and confidentiality. No compensation was provided for participation in this study.

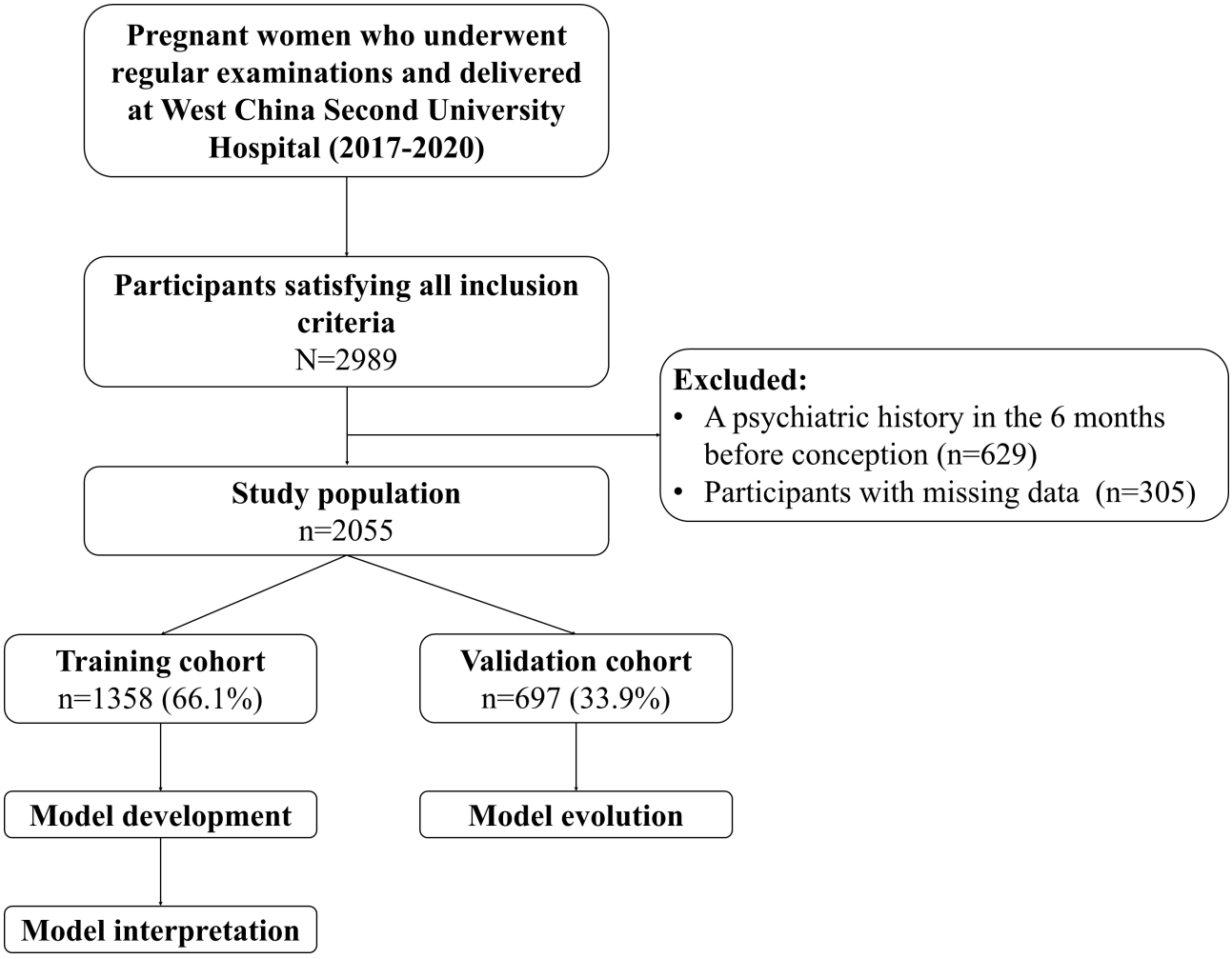
Results

Participant Characteristics

The overall procedure of this study is shown in Figure 1. After eligibility screening, 2055 participants were included in the study cohort. A total of 78 variables were incorporated in our study including 16 psychosocial characteristics, 43 obstetric characteristics, and 19 laboratory indicators. The baseline characteristics were analyzed by χ^2 test and Wilcoxon test for category variables and continuous variables, respectively. The detailed characteristics are shown in Tables 1-3. Of these participants, 697 (33.9%) participants were diagnosed with PPD, 621 (30.2%) participants had antepartum depression, 101 (4.9%) were unemployed, 187 (9.1%) had an income below the local minimum income standard, 1947 (94.7%) pregnant women were the only child of the family, and 45 (2.2%) reported low family satisfaction; the median age of participants was 32 (IQR 29-35) years.

XSL•FO
RenderX

Figure 1. The flow chart of the study design.



XSL•FO
RenderX

Table . Psychosocial characteristics of participants.

Psychosocial characteristics		Non-PPD[a] (n=1358)	PPD (n=697)	*P* value	Method
Age (years), median (IQR)		31 (29-35)	32 (29-35)	.03	Wilcoxon
Antepartum depression, n (%)				<.001	χ^2 test
	No	1170 (86.2)	264 (37.9)		
	Yes	188 (13.8)	433 (62.1)		
Ethnics, n (%)				.15	χ^2 test
	Han	1326 (97.6)	673 (96.6)		
	Others	32 (2.4)	24 (3.4)		
Work status, n (%)				.002	χ^2 test
	Employed	1277 (94)	677 (97.1)		
	Unemployed	81 (6)	20 (2.9)		
Season of delivery, n (%)				.51	χ^2 test
	Spring	343 (25.3)	193 (27.7)		
	Summer	350 (25.8)	165 (23.7)		
	Autumn	411 (30.3)	217 (31.1)		
	Winter	254 (18.7)	122 (17.5)		
Education, n (%)				.63	χ^2 test
	Below higher education	459 (33.8)	243 (34.9)		
	Higher education	899 (66.2)	454 (65.1)		
Income, n (%)				.46	χ^2 test
	Below normal level	119 (8.8)	68 (9.8)		
	At or above normal level	1239 (91.2)	629 (90.2)		
Smoking, n (%)				.69	Yates' correction
	No	1355 (99.8)	694 (99.6)		
	Yes	3 (0.2)	3 (0.4)		
Drinking, n (%)				>.99	Yates' correction
	No	1355 (99.8)	695 (99.7)		
	Yes	3 (0.2)	2 (0.3)		
Spouse in good health, n (%)				.95	χ^2 test
	Yes	1339 (98.6)	687 (98.6)		
	No	19 (1.4)	10 (1.4)		
Only child, n (%)				.17	χ^2 test
	Yes	1280 (94.3)	667 (95.7)		
	No	78 (5.7)	30 (4.3)		
Planned pregnancy, n (%)				.31	χ^2 test
	Yes	1310 (96.5)	666 (95.6)		
	No	48 (3.5)	31 (4.4)		
Social support, n (%)				.52	χ^2 test
	Normal	1329 (97.9)	679 (97.4)		
	Low	29 (2.1)	18 (2.6)		
Family satisfaction, n (%)				.13	χ^2 test

XSL•FO
RenderX

Psychosocial characteristics		Non-PPD[a] (n=1358)	PPD (n=697)	*P* value	Method
	Normal	1333 (98.2)	677 (97.1)		
	Low	25 (1.8)	20 (2.9)		
Adverse marital status, n (%)				.006	χ^2 test
	No	1349 (99.3)	683 (98)		
	Yes	9 (0.7)	14 (2)		
Family history of mental illness, n (%)				.04	Yates' correction
	No	1356 (99.9)	691 (99.1)		
	Yes	2 (0.1)	6 (0.9)		

[a]PPD: postpartum depression.

XSL•FO
RenderX

Table . Obstetric characteristics of participants.

Obstetric characteristics		Non-PPD[a] (n=1358)	PPD (n=697)	*P* value	Method
Weight gain during pregnancy, median (IQR)		12.5 (9.425 - 15)	12.5 (9.7 - 16)	.39	Wilcoxon
BMI, median (IQR)		20.83 (19.43 - 22.68)	20.83 (19.36 - 23.01)	.63	Wilcoxon
Age of menarche (years), median (IQR)		13 (12-13)	13 (12-14)	.30	Wilcoxon
Gestational days, median (IQR)		274 (268-280)	274 (267-278)	.05	Wilcoxon
Bleeding volume, median (IQR)		400 (300-400)	400 (300-400)	.07	Wilcoxon
Fetal weight, median (IQR)		3.28 (2.94 - 3.57)	3.23 (2.8 - 3.53)	.001	Wilcoxon
Fetal height, median (IQR)		50 (48-51)	49 (48-51)	.03	Wilcoxon
Apgar[b] 1 minute, median (IQR)		10 (10-10)	10 (10-10)	<.001	Wilcoxon
Apgar 5 minutes, median (IQR)		10 (10-10)	10 (10-10)	<.001	Wilcoxon
Apgar 10 minutes, median (IQR)		10 (10-10)	10 (10-10)	<.001	Wilcoxon
Length of stay, median (IQR)		4 (4-6)	4 (4-6)	.79	Wilcoxon
Gravidity				.19	χ^2 test
	1, n (%)	471 (22.9)	217 (10.6)		
	2, n (%)	370 (18)	207 (10.1)		
	3, n (%)	265 (12.9)	136 (6.6)		
	4, n (%)	160 (7.8)	79 (3.8)		
	≥5, n (%)	92 (4.5)	58 (2.8)		
	Median (IQR)	2 (1-3)	2 (1-3)		
Abortions, n (%)				.38	χ^2 test
	0	624 (45.9)	301 (43.2)		
	1	409 (30.1)	207 (29.7)		
	2	207 (15.2)	115 (16.5)		
	≥3	118 (8.7)	74 (10.6)		
Parity, n (%)				.89	Yates' correction
	0	831 (40.4)	434 (21.1)		
	1	497 (24.2)	246 (12)		
	2	29 (1.4)	16 (0.8)		
	≥3	1 (0)	1 (0)		
Conception method, n (%)				.93	χ^2 test
	Normal	1169 (86.1)	599 (85.9)		
	Assisted reproduction	189 (13.9)	98 (14.1)		
Fetal malformation, n (%)				.02	χ^2 test
	No	1308 (96.3)	656 (94.1)		
	Yes	50 (3.7)	41 (5.9)		
Amniotic fluid volume disorder, n (%)				.35	χ^2 test
	No	1284 (94.6)	652 (93.5)		
	Yes	74 (5.4)	45 (6.5)		
Renal disease, n (%)				.58	χ^2 test
	No	1334 (98.2)	687 (98.6)		
	Yes	24 (1.8)	10 (1.4)		
Systemic lupus erythematosus, n (%)				.69	Yates' correction

XSL•FO
RenderX

Obstetric characteristics		Non-PPD[a] (n=1358)	PPD (n=697)	*P* value	Method
	No	1351 (99.5)	695 (99.7)		
	Yes	7 (0.5)	2 (0.3)		
Gestational diabetes mellitus, n (%)				.92	χ^2 test
	No	1030 (75.8)	530 (76)		
	Yes	328 (24.2)	167 (24)		
Gestational hypertension, n (%)				.25	χ^2 test
	No	1290 (95)	670 (96.1)		
	Yes	68 (5)	27 (3.9)		
Threatened premature labor, n (%)				.002	χ^2 test
	No	1183 (87.1)	571 (81.9)		
	Yes	175 (12.9)	126 (18.1)		
Hepatitis B, n (%)				.49	χ^2 test
	No	72 (5.3)	42 (6)		
	Yes	1286 (94.7)	655 (94)		
Twin pregnancy, n (%)				.07	χ^2 test
	No	1247 (91.8)	623 (89.4)		
	Yes	111 (8.2)	74 (10.6)		
Placenta previa, n (%)				.45	χ^2 test
	No	1281 (94.3)	663 (95.1)		
	Yes	77 (5.7)	34 (4.9)		
Heart disease, n (%)				.29	χ^2 test
	No	1344 (99)	693 (99.4)		
	Yes	14 (1)	4 (0.6)		
Scarred uterus, n (%)				.81	χ^2 test
	No	342 (25.2)	179 (25.7)		
	Yes	1016 (74.8)	518 (74.3)		
Rh blood type, n (%)				.01	χ^2 test
	Positive	1350 (99.4)	685 (98.3)		
	Negative	8 (0.6)	12 (1.7)		
ABO blood type, n (%)				.63	χ^2 test
	O	491 (36.2)	241 (34.6)		
	B	335 (24.7)	179 (25.7)		
	A	423 (31.1)	211 (30.3)		
	AB	109 (8)	66 (9.5)		
Abnormal fetal position, n (%)				.92	χ^2 test
	No	1206 (88.8)	618 (88.7)		
	Yes	152 (11.2)	79 (11.3)		
Uterine myoma, n (%)				.94	χ^2 test
	No	1227 (90.4)	629 (90.2)		
	Yes	131 (9.6)	68 (9.8)		
Ovarian cyst, n (%)				>.99	Yates' correction
	No	1349 (99.3)	693 (99.4)		

XSL•FO
RenderX

Obstetric characteristics		Non-PPD[a] (n=1358)	PPD (n=697)	*P* value	Method
	Yes	9 (0.7)	4 (0.6)		
Umbilical cord encirclements, n (%)				.65	χ^2 test
	No	869 (64)	453 (65)		
	Yes	489 (36)	244 (35)		
Hypothyroidism, n (%)				.40	χ^2 test
	No	1130 (83.2)	590 (84.6)		
	Yes	228 (16.8)	107 (15.4)		
Pelvic anomaly, n (%)				.56	χ^2 test
	No	1346 (99.1)	689 (98.9)		
	Yes	12 (0.9)	8 (1.1)		
Intrauterine death, n (%)				<.001	Yates' correction
	No	1358 (100)	684 (98.1)		
	Yes	0 (0)	13 (1.9)		
Macrosomia, n (%)				.84	χ^2 test
	No	1295 (95.4)	666 (95.6)		
	Yes	63 (4.6)	31 (4.4)		
Fetal growth restriction, n (%)				.34	χ^2 test
	No	1335 (98.3)	681 (97.7)		
	Yes	23 (1.7)	16 (2.3)		
Premature labor, n (%)				<.001	χ^2 test
	No	1207 (88.9)	579 (83.1)		
	Yes	151 (11.1)	118 (16.9)		
Mode of delivery, n (%)				.45	Yates' correction
	Vaginal delivery	842 (62)	433 (62.1)		
	Cesarean section	506 (37.3)	262 (37.6)		
	Assisted delivery	10 (0.7)	2 (0.3)		
Fetal sex, n (%)				.96	χ^2 test
	Male	668 (49.2)	342 (49.1)		
	Female	690 (50.8)	355 (50.9)		
Fetal distress, n (%)				.001	χ^2 test
	No	1333 (98.2)	667 (95.7)		
	Yes	25 (1.8)	30 (4.3)		
Breastfeeding, n (%)				.61	χ^2 test
	No	32 (2.4)	19 (2.7)		
	Yes	1326 (97.6)	678 (97.3)		

[a]PPD: postpartum depression.

[b]Apgar: appearance, pulse, grimace, activity, and respiration.

XSL•FO
RenderX

Table . Laboratory indicators.

Laboratory indicators	Non-PPD[a] (n=1358), median (IQR)	PPD (n=697), median (IQR)	*P* value	Method
Hemoglobin (g/L)	111 (104 - 117.75)	111 (104-118)	.893	Wilcoxon
Serum ferroprotein (ng/nL)	18.15 (12.4 - 25.9)	18.9 (11.9 - 27.2)	.400	Wilcoxon
International normalized ratio	0.97 (0.92 - 1.01)	0.96 (0.91 - 1.01)	.325	Wilcoxon
Alanine aminotransferase (U/L)	17 (12.25 - 28)	18 (12-31)	.170	Wilcoxon
Aspartate aminotransferase (U/L)	21 (18-27)	21 (17-28)	.263	Wilcoxon
Total bile acid (μmol/L)	2.3 (1.6 - 3.5)	2.5 (1.6 - 3.7)	.091	Wilcoxon
Direct bilirubin (μmol/L)	2.1 (1.6 - 2.8)	2.1 (1.7 - 2.7)	.771	Wilcoxon
Albumin (g/L)	38.7 (36.3 - 41.2)	38.7 (36.3 - 41.4)	.627	Wilcoxon
Globulin (g/L)	27.6 (25.4 - 30.1)	27.3 (25.2 - 29.9)	.207	Wilcoxon
Lactate dehydrogenase (U/L)	179 (163-201)	181 (164-204)	.161	Wilcoxon
Alkaline phosphatase (U/L)	84 (55-121)	87 (55-128)	.423	Wilcoxon
Urea nitrogen (μmol/L)	3.5 (3.07 - 4.3475)	3.48 (3.08 - 4.35)	.787	Wilcoxon
Creatinine (μmol/L)	44 (40-48)	44 (40-48)	.561	Wilcoxon
Cystatin C (μmol/L)	0.77 (0.64 - 0.97)	0.77 (0.64 - 0.99)	.725	Wilcoxon
Uric acid (μmol/L)	259 (217-309)	254 (218-305)	.250	Wilcoxon
Thyroid-stimulating hormone (mIU/L)	1.9695 (1.277 - 2.8878)	1.847 (1.176 - 2.776)	.183	Wilcoxon
Free thyroxine (pmol/L)	14.56 (13.29 - 16.22)	14.55 (13.21 - 16.02)	.522	Wilcoxon
Thyroid peroxidase antibody (U/mL)	40.65 (30.4 - 56.1)	40.1 (30.2 - 55.3)	.425	Wilcoxon
Vitamin D (nmol/L)	23.9 (17.3 - 31.3)	22.9 (16.1 - 29.8)	.011	Wilcoxon

[a]PPD: postpartum depression.

Variable Screening

After LASSO regression, 18 variables with nonzero coefficients were identified as potential predictors of PPD. Among these variables, the 5-minute Apgar (appearance, pulse, grimace, activity, and respiration) score and the 10-minute Apgar score had VIF values over 10, indicating multicollinearity between them. Of these 2 variables, the 5-minute Apgar score had a lower coefficient in absolute value in the LASSO regression, suggesting its lower contribution to the outcome; therefore, it was excluded. Another round of VIF analysis was performed after excluding the 5-minute Apgar score, and the results showed that all remaining variables had a VIF below 10, indicating low multicollinearity. Finally, 17 variables including prenatal depression, ethnics, occupation, income, only child, family satisfaction, adverse marital status, amniotic fluid volume disorder, Rh negative, intrauterine death, fetal distress, age, fetal weight, 10-minute Apgar score, serum ferroprotein, thyroid-stimulating hormone (TSH), and thyroid peroxidase antibody (TPOAb) were identified as features to develop predictive models. The detailed results of the LASSO regression and VIF analyses are presented in Table 4.

XSL•FO
RenderX

Table . LASSO[a] coefficients and VIF[b] of screened variables after LASSO regression.

Variable	Coefficient	VIF	VIF (second round)
Prenatal depression	2.245	1.014	1.013
Ethnics	0.055	1.008	1.008
Occupation	−0.215	1.047	1.045
Income	0.015	1.043	1.043
Only child	0.081	1.013	1.012
Family satisfaction	0.134	1.287	1.286
Adverse marital status	0.422	1.296	1.293
Amniotic fluid volume disorder	0.416	1.011	1.011
Rh negative	−0.163	1.012	1.011
Intrauterine death	1.042	1.487	1.486
Fetal distress	0.339	1.034	1.034
Age	0.002	1.035	1.034
Fetal weight	−0.17	1.472	1.347
Apgar[c] 5 minutes	−0.002	44.005	N/A[d]
Apgar 10 minutes	−0.155	42.777	1.860
Serum ferroprotein	0.001	1.043	1.043
TSH[e]	−0.001	1.003	1.003
TPOAb[f]	0.001	1.008	1.008

[a]LASSO: least absolute shrinkage and selection operator.

[b]VIF: variance inflation factor.

[c]Apgar: appearance, pulse, grimace, activity, and respiration.

[d]N/A: not applicable.

[e]TSH: thyroid-stimulating hormone.

[f]TPOAb: thyroid peroxidase antibody.

Model Development and Evaluation

Predictive models were established in the training set. With optimal hyperparameters, models were evaluated in the validation set. The AUC values obtained in the validation set of all 4 models were above 0.75 (Table 5 and Figure 2A). The XGBoost model outperformed other models with the highest AUC of 0.849 (95% CI 0.828 - 0.871). GBM had the poorest performance with an AUC value of 0.779 (95% CI 0.738 - 0.820). Detailed results of model evaluation were shown in Table 5.

XSL•FO
RenderX

Table . Model evaluation metrics.

	AUC[a] (95% CI)	Accuracy (95% CI)	Sensitivity (95% CI)	Specificity (95% CI)	PPV[b] (95% CI)	NPV[c] (95% CI)
XGBoost[d]	0.849 (0.828 - 0.871)	0.813 (0.772 - 0.854)	0.718 (0.646 - 0.790)	0.862 (0.807 - 0.917)	0.718 (0.646 - 0.790)	0.855 (0.805 - 0.905)
RF[e]	0.781 (0.740 - 0.821)	0.782 (0.750 - 0.815)	0.656 (0.591 - 0.720)	0.848 (0.813 - 0.883)	0.688 (0.624 - 0.753)	0.827 (0.791 - 0.864)
GBM[f]	0.779 (0.738 - 0.820)	0.786 (0.753 - 0.818)	0.675 (0.611 - 0.738)	0.843 (0.807 - 0.878)	0.688 (0.624 - 0.751)	0.835 (0.799 - 0.870)
LR[g]	0.788 (0.754 - 0.822)	0.779 (0.739 - 0.816)	0.685 (0.615 - 0.748)	0.823 (0.782 - 0.858)	0.646 (0.577 - 0.710)	0.848 (0.808 - 0.881)

[a]AUC: area under the receiver operating characteristic curve.

[b]PPV: positive predictive value.

[c]NPV: negative predictive value.

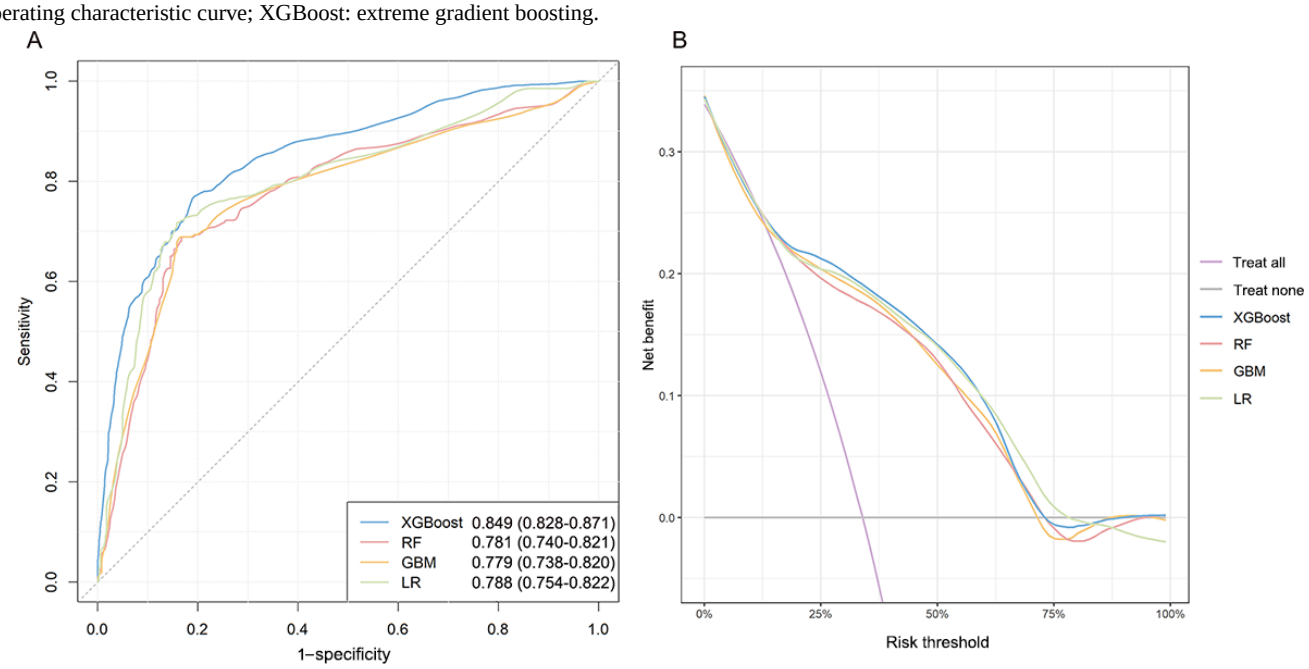
[d]XGBoost: extreme gradient boosting.

[e]RF: random forest.

[f]GBM: gradient boosting machine.

[g]LR: logistic regression.

Figure 2. (**A**) The ROC and (**B**) the DCA of predictive models. The area under the curve and the corresponding 95% CI for each model are shown in the legend of Figure 2A. DCA: decision curve analysis; GBM: gradient boosting machine; LR: logistic regression; RF: random forest; ROC: receiver operating characteristic curve; XGBoost: extreme gradient boosting.



DCA (Figure 2B) was performed for 4 models in the validation set to compare the net benefit of the best model and alternative approaches for clinical decision-making. Treatment strategies informed by any of the 4 models are superior to the default strategies of treating all or no patients. The net benefit of the XGBoost model exceeded those of the other models at 20%-60% threshold probabilities.

Model Interpretation

The XGBoost model, identified as the optimal model in terms of AUC value, was further explored for interpretation. Table 6 demonstrates the variable importance of the XGBoost model. Antepartum depression, TSH, fetal weight, serum ferritin, TPOAb, and age were the 6 variables that most influenced the outcome of the model.

PDPs illustrate a visual representation of the relationship between the most influential variables and the predicted response while accounting for the average effect of the other predictors in the model (Figure 3). As our predictive outcome is a binary categorical variable, the impacts of variables on the outcome were presented in the form of predictive probability ranging from 0 to 1. These plots indicate that the probability of PPD increases when participants have antepartum depression, higher TSH, higher serum ferritin, and older age. Likewise, the probability descends when participants have higher fetal weight and higher TPOAb.

XSL•FO
RenderX

Table . Variable importance for extreme gradient boosting model.

Variable	Importance
Prenatal depression	0.268
Fetal weight	0.169
TSH[a]	0.162
TPOAb[b]	0.132
Serum ferritin	0.131
Age	0.063
Apgar[c] 10 minutes	0.024
Income	0.014
Occupation	0.012
Amniotic fluid volume disorder	0.011
Fetal distress	0.010
Family satisfaction	0.009
Only child	0.009
Intrauterine death	0.007
Rh negative	0.005
Adverse marital status	0.002
Ethnics	0.002

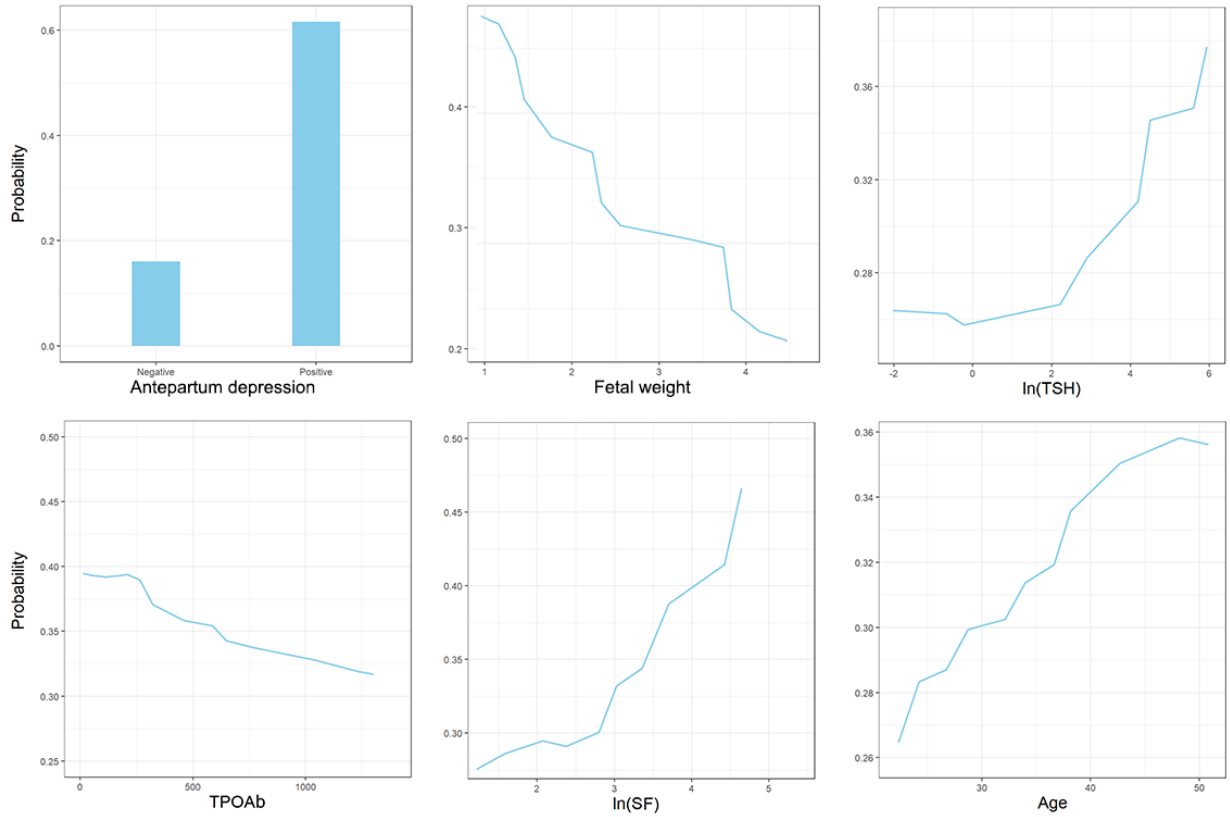
[a]TSH: thyroid-stimulating hormone.

[b]TPOAb: thyroid peroxidase antibody.

[c]Apgar: appearance, pulse, grimace, activity, and respiration.

XSL•FO
RenderX

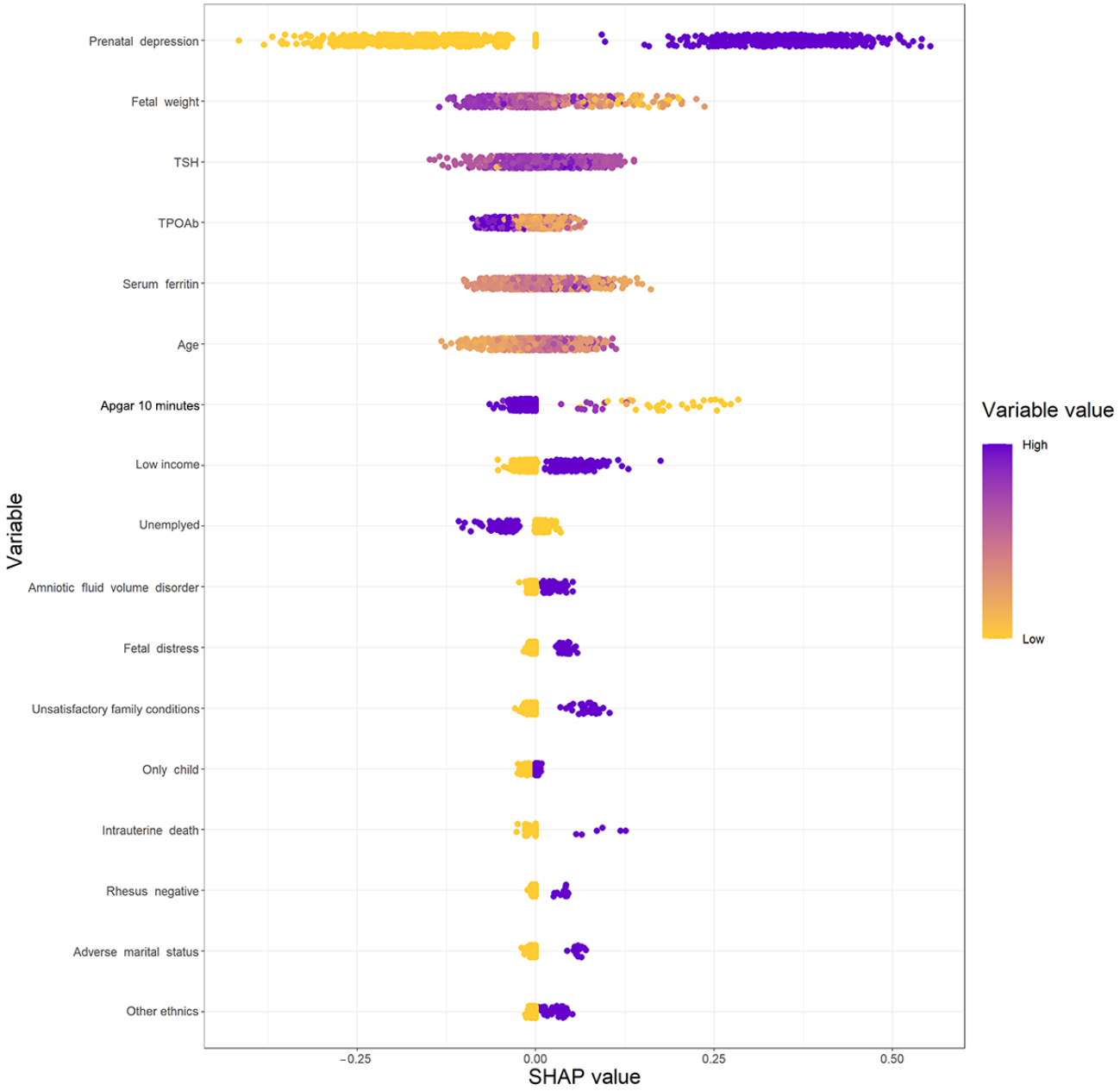
Figure 3. Partial dependence plots for the 6 most influential variables in the extreme gradient boosting model. The y-axis is set on a probability scale since our model was a binary classification model; the values of TSH and SF were on a logarithmic scale to present more pronounced trends in predicted probability as the values of the variables change. SF: serum ferritin; TPOAb: thyroid peroxidase antibody; TSH: thyroid-stimulating hormone.



SHAP provides an insight into how variables influence the prediction in each single sample (Figure 4). It can be concluded that the risk of PPD increases for participants with antepartum depression, lower fetal weight, lower level of TPOAb, elevated serum ferritin, and older age. The overall impact of TSH is not obvious. The interpretation of SHAP was mostly consistent with the interpretation of PDP. A higher risk of PPD is also associated with lower Apgar scores at 10 minutes, low income, amniotic fluid volume disorder, fetal distress, unsatisfactory family conditions, only child in the family, intrauterine death, Rh negative blood type, adverse marital status, and other ethnics.

XSL•FO
RenderX

Figure 4. The SHAP values for the extreme gradient boosting model. Each dot in the figure represents a variable for a single participant. The horizontal position indicates whether that variable has a positive or negative impact on the predictive probability. Greater absolute values of SHAP represent a greater predictive probability of postpartum depression. The color shows the value of the variable for that observation. Purple indicates a higher value, representing the positive contribution of predictive outcome; and yellow indicates a lower value, representing the negative contribution of predictive outcome. A larger absolute value means that the variable has a greater impact on the result. For example, lower fetal weight (yellow dots) caused a negative impact on the predictive outcome. Since the SHAP system only accepts numeric input, binary categorical variables are converted to 0 (negative) and 1 (positive). In this case, low income and fetal distress are associated with a greater probability of postpartum depression. Apgar: appearance, pulse, grimace, activity, and respiration; SHAP: Shapley Additive Explanation; TPOAb: thyroid peroxidase antibody; TSH: thyroid-stimulating hormone.



Discussion

Principal Findings

This study developed and validated a machine learning–based model for prediction of PPD with an AUC of 0.849. Through the model interpretation of our optimal XGBoost model, several significant predictors of PPD were identified. These findings derived from the XGBoost model provide insightful contributions to the understanding of PPD.

Based on variable importance, antepartum depression was the most influential predictor of PPD in our analysis. Women with antepartum depression are likely to extend depressive symptoms into the postpartum period. In an epidemiology study, more than 54% of women with PPD reported depressive symptoms during pregnancy [5]. Several studies excluded participants with antepartum depression to focus on newly diagnosed PPD [16,43]. This might avoid the bias associated with chronic depression but neglect the impact of maternal prenatal mental status on PPD.

In addition, our study identified key biochemical markers of PPD including TSH, TPOAb, and serum ferritin. According to the result of the PDP interpretation, women with elevated serum ferritin levels were prone to PPD. Ferritin serves a critical role

XSL•FO
RenderX

in the synthesis of monoamine neurotransmitters including dopamine [44]. With excessive ferritin, neurotransmitter dysregulation might play a part in the onset of PPD [45]. This finding warns the risks of excessive iron supplementation during pregnancy. Apart from that, elevated TSH and declined TPOAb were associated with a higher risk of PPD in our model interpretation. Elevated TSH often indicates hypothyroidism, whose clinical manifestation includes depression [46]. TPOAb is an autoantibody against the enzyme thyroid peroxidase and is commonly associated with autoimmune thyroid diseases such as Hashimoto thyroiditis [47,48]. A systematic review reported that the association between TPOAb and PPD remains controversial [49]. The specific mechanism of how TPOAb affects PPD requires more investigation.

Additionally, women with older age and lower infant weight were prone to PPD in our findings. This aligns with existing literature [49]. Other commonly recognized predictors like lack of social support, gestational diabetes, and overweight were excluded in the LASSO regression due to potential multicollinearity. These results not only validate some of the existing hypotheses about the pathophysiology of PPD but also open new avenues for research, particularly in the context of developing more effective, holistic screening methods.

Our study offers several advancements over previous research on PPD prediction. Earlier studies predominantly focused on clinical factors, such as obstetric history and comorbidities during pregnancy [50-52]. Our research comprehensively collected variables from multiple domains, including clinical, psychosocial, and biochemical markers. This broader scope allows for a more holistic view of the potential risk factors contributing to PPD, addressing the multifactorial nature of the condition. In addition, many previous studies were limited by relatively small sample sizes, often involving fewer than 1000 participants, which may have restricted the generalizability of their findings [50,51,53]. In contrast, our study included a larger cohort of over 2000 participants, providing greater statistical power and a more reliable basis for identifying significant risk factors. This larger sample size also enhances the model's ability to detect more subtle associations between variables and PPD, which might have been overlooked in studies with smaller sample size. Moreover, previous research has often been limited to populations in Western countries [54,55]. Our study focuses on a Chinese cohort, offering insights that are culturally specific and potentially more relevant for addressing PPD in non-Western settings. This regional focus helps fill a critical gap in the literature, as the risk factors and prevalence of PPD may vary significantly between different cultural and geographical populations. Finally, our inclusion of biochemical markers, such as thyroid function and serum ferritin levels, adds a novel dimension to PPD research. These physiological indicators have rarely been incorporated in prior studies; yet, they may play a crucial role in understanding the biological underpinnings of PPD. By integrating these markers with traditional clinical and psychosocial factors, our study provides a more comprehensive framework for early detection and intervention.

Although our study was conducted on a specific population from Southwestern China, the comprehensive nature of the variables included in the model suggests that it could be adapted to other populations with similar characteristics. Future studies could explore the model's applicability in different regions and cultural contexts, potentially leading to a robust, universally applicable tool for PPD prediction.

Our study offers significant insights into the clinical application of machine learning models for PPD. By integrating a broad spectrum of both biochemical and psychosocial factors, our models offer a more nuanced and accurate prediction compared to traditional methods. Incorporating often-overlooked indicators such as thyroid function and iron metabolism provides insight into the early screening of PPD. The XGBoost model, which demonstrated the highest performance, is particularly valuable for its ability to manage complex interactions between variables, making it universally applicable in a clinical setting where multiple risk factors are at play. This comprehensive approach enhances the understanding risk factors for PPD and supports more effective early interventions. Future research can build on these findings by validating them in larger, more diverse populations, integrating these predictive factors into routine prenatal care, and exploring interventions targeting these risks to reduce the incidence of PPD.

Limitations

This work is not without limitations. First, our analysis is constrained by the retrospective nature of the data, which may introduce biases such as recall bias or selection bias. Additionally, during the process of variable screening, removing variables with collinearity ensured the independence of final predictors, but also eliminated substantial amounts of variables, leading to loss of information. Furthermore, the study's reliance on a specific population from a single institution may limit the generalizability of our findings to broader, more diverse populations.

Conclusions

This study developed and validated several machine learning–based models for predicting PPD, integrating a comprehensive set of clinical, psychosocial, and biochemical factors, and incorporating a larger sample size. The XGBoost model was considered as the optimal model with an AUC of 0.849. Interpretation derived from the predictive model revealed significant predictors of PPD, encompassing antepartum depression, elevated TSH, declined TPOAb, elevated serum ferritin, older age, and lower infant weight. These identified risk factors could be implemented to the early screening of PPD for individuals at high risk. These findings underscore the advantages of integrating diverse predictors and advanced machine learning techniques to improve early screening for PPD. This approach not only enhances prediction accuracy but also provides valuable insights for future research and clinical applications.

XSL•FO
RenderX

Acknowledgments

The authors would like to express their gratitude to all colleagues and individuals at West China Second University Hospital, Sichuan University, who contributed to this research. Their insights and support were invaluable to the completion of this work.

Authors' Contributions

RZ and YL conceptualized the research. RZ, BL, and YL conducted the data acquisition, data analysis, and writing of the manuscript. RZ, ZZ, and RL performed the statistical analyses and created the figures. RZ and ZZ conducted the image optimization. BL revised the manuscript and supervised the project. All authors contributed to and have approved the final manuscript.

Conflicts of Interest

None declared.

References

1. Stewart DE, Vigod S. Postpartum depression. N Engl J Med 2016 Dec;375(22):2177-2186. [doi: 10.1056/NEJMcp1607649]
2. Howard LM, Molyneaux E, Dennis CL, Rochat T, Stein A, Milgrom J. Non-psychotic mental disorders in the perinatal period. Lancet 2014 Nov 15;384(9956):1775-1788. [doi: 10.1016/S0140-6736(14)61276-9] [Medline: 25455248]
3. Hahn-Holbrook J, Cornwell-Hinrichs T, Anaya I. Economic and health predictors of national postpartum depression prevalence: a systematic review, meta-analysis, and meta-regression of 291 studies from 56 countries. Front Psychiatry 2017;8:248. [doi: 10.3389/fpsyt.2017.00248] [Medline: 29449816]
4. Cooper PJ, Murray L, Wilson A, Romaniuk H. Controlled trial of the short- and long-term effect of psychological treatment of post-partum depression. I. Impact on maternal mood. Br J Psychiatry 2003 May;182:412-419. [Medline: 12724244]
5. Gelaye B, Rondon MB, Araya R, Williams MA. Epidemiology of maternal depression, risk factors, and child outcomes in low-income and middle-income countries. Lancet Psychiatry 2016 Oct;3(10):973-982. [doi: 10.1016/S2215-0366(16)30284-X] [Medline: 27650773]
6. O'Hara MW, McCabe JE. Postpartum depression: current status and future directions. Annu Rev Clin Psychol 2013;9:379-407. [doi: 10.1146/annurev-clinpsy-050212-185612] [Medline: 23394227]
7. US Preventive Services Task Force, Curry SJ, Krist AH, et al. Interventions to prevent perinatal depression: US Preventive Services Task Force recommendation statement. JAMA 2019 Feb 12;321(6):580-587. [doi: 10.1001/jama.2019.0007] [Medline: 30747971]
8. Mukherjee S, Trepka MJ, Pierre-Victor D, Bahelah R, Avent T. Racial/ethnic disparities in antenatal depression in the United States: a systematic review. Matern Child Health J 2016 Sep;20(9):1780-1797. [doi: 10.1007/s10995-016-1989-x] [Medline: 27016352]
9. Dennis C, Chung‐Lee L. Postpartum depression help‐seeking barriers and maternal treatment preferences: a qualitative systematic review. Birth 2006 Dec;33(4):323-331. [doi: 10.1111/j.1523-536X.2006.00130.x]
10. O'Connor E, Senger CA, Henninger ML, Coppola E, Gaynes BN. Interventions to prevent perinatal depression: evidence report and systematic review for the US Preventive Services Task Force. JAMA 2019 Feb 12;321(6):588-601. [doi: 10.1001/jama.2018.20865] [Medline: 30747970]
11. Cheng D, Schwarz EB, Douglas E, Horon I. Unintended pregnancy and associated maternal preconception, prenatal and postpartum behaviors. Contraception 2009 Mar;79(3):194-198. [doi: 10.1016/j.contraception.2008.09.009] [Medline: 19185672]
12. Stone SL, Diop H, Declercq E, Cabral HJ, Fox MP, Wise LA. Stressful events during pregnancy and postpartum depressive symptoms. J Womens Health (Larchmt) 2015 May;24(5):384-393. [doi: 10.1089/jwh.2014.4857]
13. Austin PC, Tu JV, Ho JE, Levy D, Lee DS. Using methods from the data-mining and machine-learning literature for disease classification and prediction: a case study examining classification of heart failure subtypes. J Clin Epidemiol 2013 Apr;66(4):398-407. [doi: 10.1016/j.jclinepi.2012.11.008] [Medline: 23384592]
14. Bidoki NH, Zera KA, Nassar H, et al. Machine learning models of plasma proteomic data predict mood in chronic stroke and tie it to aberrant peripheral immune responses. Brain Behav Immun 2023 Nov;114:144-153. [doi: 10.1016/j.bbi.2023.08.002] [Medline: 37557961]
15. Shin D, Lee KJ, Adeluwa T, Hur J. Machine learning-based predictive modeling of postpartum depression. J Clin Med 2020 Sep 8;9(9):2899. [doi: 10.3390/jcm9092899] [Medline: 32911726]
16. Hochman E, Feldman B, Weizman A, et al. Development and validation of a machine learning-based postpartum depression prediction model: a nationwide cohort study. Depress Anxiety 2021 Apr;38(4):400-411. [doi: 10.1002/da.23123] [Medline: 33615617]
17. Amit G, Girshovitz I, Marcus K, et al. Estimation of postpartum depression risk from electronic health records using machine learning. BMC Pregnancy Childbirth 2021 Sep 17;21(1):630. [doi: 10.1186/s12884-021-04087-8] [Medline: 34535116]
18. Cox JL, Holden JM, Sagovsky R. Detection of postnatal depression. Development of the 10-item Edinburgh Postnatal Depression Scale. Br J Psychiatry 1987 Jun;150:782-786. [doi: 10.1192/bjp.150.6.782] [Medline: 3651732]
19. Diagnostic and Statistical Manual of Mental Disorders, 5th edition: American Psychiatric Association; 2013.

XSL•FO
RenderX

20. The Chinese Classification and Diagnostic Criteria of Mental Disorders, 3rd edition: Chinese Society of Psychiatry; 2001:184-188.
21. Zung WW. A self-rating depression scale. Arch Gen Psychiatry 1965 Jan;12:63-70. [doi: 10.1001/archpsyc.1965.01720310065008] [Medline: 14221692]
22. Wang Y, Di Y, Ye J, Wei W. Study on the public psychological states and its related factors during the outbreak of coronavirus disease 2019 (COVID-19) in some regions of China. Psychol Health Med 2021 Jan 2;26(1):13-22. [doi: 10.1080/13548506.2020.1746817]
23. Yi J, Zhong B, Yao S. Health-related quality of life and influencing factors among rural left-behind wives in Liuyang, China. BMC Womens Health 2014 May 14;14:67. [doi: 10.1186/1472-6874-14-67] [Medline: 24886024]
24. Tang X, Lu Z, Hu D, Zhong X. Influencing factors for prenatal stress, anxiety and depression in early pregnancy among women in Chongqing, China. J Affect Disord 2019 Jun 15;253:292-302. [doi: 10.1016/j.jad.2019.05.003] [Medline: 31077972]
25. Smilkstein G, Ashworth C, Montano D. Validity and reliability of the Family APGAR as a test of family function. J Fam Pract 1982 Aug;15(2):303-311. [Medline: 7097168]
26. Tibshirani R. Regression shrinkage and selection via the lasso. J R Stat Soc Ser B 1996 Jan 1;58(1):267-288. [doi: 10.1111/j.2517-6161.1996.tb02080.x]
27. Efron B, Hastie T, Johnstone I, Tibshirani R. Least angle regression. Ann Statist 2004;32(2):407-451. [doi: 10.1214/009053604000000067]
28. Bickel PJ, Ritov Y, Tsybakov AB. Simultaneous analysis of lasso and Dantzig selector. Ann Statist 2009;37(4):1705-1732. [doi: 10.1214/08-AOS620]
29. Mason CH, Perreault WD. Collinearity, power, and interpretation of multiple regression analysis. J Market Res 1991 Aug;28(3):268-280. [doi: 10.1177/002224379102800302]
30. Quah Y, Jung S, Chan JYL, et al. Predictive biomarkers for embryotoxicity: a machine learning approach to mitigating multicollinearity in RNA-Seq. Arch Toxicol 2024 Dec;98(12):4093-4105. [doi: 10.1007/s00204-024-03852-w] [Medline: 39242367]
31. Musmar B, Adeeb N, Gendreau J, et al. Creation of a predictive calculator to determine adequacy of occlusion of the woven endobridge (WEB) device in intracranial aneurysms—a retrospective analysis of the WorldWide WEB Consortium database. Interv Neuroradiol 2024 Aug 10:15910199241267320. [doi: 10.1177/15910199241267320] [Medline: 39127463]
32. O'brien RM. A caution regarding rules of thumb for variance inflation factors. Qual Quant 2007 Sep 11;41(5):673-690. [doi: 10.1007/s11135-006-9018-6]
33. Ozata IH, Tufekci T, Karahan SN, et al. Reliability and validity of the Turkish version of the New Cleveland Clinic Colorectal Cancer Quality of Life Questionnaire. Int J Colorectal Dis 2023 Dec 27;39(1):10. [doi: 10.1007/s00384-023-04572-w] [Medline: 38150157]
35. Chen TQ, Guestrin C, Comp MA. XGBoost: a scalable tree boosting system. Presented at: 22nd ACM SIGKDD International Conference on Knowledge Discovery and Data Mining (KDD); Aug 13-17, 2016; San Francisco, CA, United States.
35. Breiman L. Random forests. Mach Learn 2001;45(1):5-32. [doi: 10.1023/A:1010933404324]
36. Friedman JH. Greedy function approximation: a gradient boosting machine. Ann Statist 2001;29(5):1189-1232. [doi: 10.1214/aos/1013203451]
37. Muraoka K, Sada Y, Miyazaki D, Chaikittisilp W, Okubo T. Linking synthesis and structure descriptors from a large collection of synthetic records of zeolite materials. Nat Commun 2019 Oct 1;10(1):4459. [doi: 10.1038/s41467-019-12394-0] [Medline: 31575862]
38. Park SH, Goo JM, Jo CH. Receiver operating characteristic (ROC) curve: practical review for radiologists. Korean J Radiol 2004;5(1):11-18. [doi: 10.3348/kjr.2004.5.1.11] [Medline: 15064554]
39. Lee C, Light A, Alaa A, Thurtle D, van der Schaar M, Gnanapragasam VJ. Application of a novel machine learning framework for predicting non-metastatic prostate cancer-specific mortality in men using the Surveillance, Epidemiology, and End Results (SEER) database. Lancet Digit Health 2021 Mar;3(3):e158-e165. [doi: 10.1016/S2589-7500(20)30314-9] [Medline: 33549512]
40. Fisher A, Rudin C, Dominici F. All models are wrong, but many are useful: learning a variable's importance by studying an entire class of prediction models simultaneously. J Mach Learn Res 2019;20:20. [Medline: 34335110]
41. Goldstein A, Kapelner A, Bleich J, Pitkin E. Peeking inside the black box: visualizing statistical learning with plots of individual conditional expectation. J Comput Graph Stat 2015 Jan 2;24(1):44-65. [doi: 10.1080/10618600.2014.907095]
42. Lundberg SM, Lee SI. A unified approach to interpreting model predictions. Presented at: 31st Annual Conference on Neural Information Processing Systems (NIPS); Dec 4-9, 2017; Long Beach, CA, United States.
43. Yang ST, Yang SQ, Duan KM, et al. The development and application of a prediction model for postpartum depression: optimizing risk assessment and prevention in the clinic. J Affect Disord 2022 Jan 1;296:434-442. [doi: 10.1016/j.jad.2021.09.099] [Medline: 34606808]
44. Larsen B, Olafsson V, Calabro F, et al. Maturation of the human striatal dopamine system revealed by PET and quantitative MRI. Nat Commun 2020 Feb 12;11(1):846. [doi: 10.1038/s41467-020-14693-3] [Medline: 32051403]

XSL•FO
RenderX

45. Hare BD, Duman RS. Prefrontal cortex circuits in depression and anxiety: contribution of discrete neuronal populations and target regions. Mol Psychiatry 2020 Nov;25(11):2742-2758. [doi: 10.1038/s41380-020-0685-9] [Medline: 32086434]
46. Chaker L, Bianco AC, Jonklaas J, Peeters RP. Hypothyroidism. Lancet 2017 Sep 23;390(10101):1550-1562. [doi: 10.1016/S0140-6736(17)30703-1] [Medline: 28336049]
47. Ralli M, Angeletti D, Fiore M, et al. Hashimoto's thyroiditis: an update on pathogenic mechanisms, diagnostic protocols, therapeutic strategies, and potential malignant transformation. Autoimmun Rev 2020 Oct;19(10):102649. [doi: 10.1016/j.autrev.2020.102649] [Medline: 32805423]
48. De Leo S, Lee SY, Braverman LE. Hyperthyroidism. Lancet 2016 Aug 27;388(10047):906-918. [doi: 10.1016/S0140-6736(16)00278-6] [Medline: 27038492]
49. Zhao XH, Zhang ZH. Risk factors for postpartum depression: an evidence-based systematic review of systematic reviews and meta-analyses. Asian J Psychiatr 2020 Oct;53:102353. [doi: 10.1016/j.ajp.2020.102353] [Medline: 32927309]
50. Chen JJ, Chen XJ, She QM, Li JX, Luo QH. Clinical risk factors for preterm birth and evaluating maternal psychology in the postpartum period. World J Psychiatry 2024 May 19;14(5):661-669. [doi: 10.5498/wjp.v14.i5.661] [Medline: 38808088]
51. Eriksson A, Kimmel MC, Furmark T, et al. Investigating heart rate variability measures during pregnancy as predictors of postpartum depression and anxiety: an exploratory study. Transl Psychiatry 2024 May 14;14(1):203. [doi: 10.1038/s41398-024-02909-9] [Medline: 38744808]
52. Gomora D, Kene C, Embiale A, et al. Health related quality of life and its predictors among postpartum mother in Southeast Ethiopia: a cross-sectional study. Heliyon 2024 Apr 15;10(7):e27843. [doi: 10.1016/j.heliyon.2024.e27843] [Medline: 38560152]
53. Lilhore UK, Dalal S, Varshney N, et al. Prevalence and risk factors analysis of postpartum depression at early stage using hybrid deep learning model. Sci Rep 2024 Feb 24;14(1):4533. [doi: 10.1038/s41598-024-54927-8] [Medline: 38402249]
54. Hiraoka D, Kawanami A, Sakurai K, Mori C. Within-individual relationships between mother-to-infant bonding and postpartum depressive symptoms: a longitudinal study. Psychol Med 2024 Jun;54(8):1749-1757. [doi: 10.1017/S0033291723003707] [Medline: 38173095]
55. Power J, Watson S, Chen W, Lewis A, van IJzendoorn M, Galbally M. The trajectory of maternal perinatal depressive symptoms predicts executive function in early childhood. Psychol Med 2023 Dec;53(16):7953-7963. [doi: 10.1017/S0033291723002118] [Medline: 37781906]

Abbreviations

Apgar: appearance, pulse, grimace, activity, and respiration
AUC: area under the receiver operating characteristic curve
***CCMD-3*:** *Chinese Classification and Diagnostic Criteria of Mental Disorders, Third Edition*
DCA: decision curve analysis
***DSM-5*:** *Diagnostic and Statistical Manual of Mental Disorders, Fifth Edition*
GBM: gradient boosting machine
LASSO: least absolute shrinkage and selection operator
PDP: partial dependence plot
PPD: postpartum depression
RF: random forest
ROC: receiver operating characteristic curve
SHAP: Shapley Additive Explanation
TPOAb: thyroid peroxidase antibody
TSH: thyroid-stimulating hormone
VIF: variance inflation factor
XGBoost: extreme gradient boosting

Edited by Q Chen; submitted 21.03.24; peer-reviewed by F Xie, SN Mohanty, Y Cao; revised version received 11.09.24; accepted 21.11.24; published 20.01.25.

Please cite as:
Zhang R, Liu Y, Zhang Z, Luo R, Lv B
Interpretable Machine Learning Model for Predicting Postpartum Depression: Retrospective Study
JMIR Med Inform 2025;13:e58649
URL: https://medinform.jmir.org/2025/1/e58649
doi:10.2196/58649

XSL•FO
RenderX

© Ren Zhang, Yi Liu, Zhiwei Zhang, Rui Luo, Bin Lv. Originally published in JMIR Medical Informatics (https://medinform.jmir.org), 20.1.2025. This is an open-access article distributed under the terms of the Creative Commons Attribution License (https://creativecommons.org/licenses/by/4.0/), which permits unrestricted use, distribution, and reproduction in any medium, provided the original work, first published in JMIR Medical Informatics, is properly cited. The complete bibliographic information, a link to the original publication on https://medinform.jmir.org/, as well as this copyright and license information must be included.

XSL•FO
RenderX

Original Paper

The Social Construction of Categorical Data: Mixed Methods Approach to Assessing Data Features in Publicly Available Datasets

Theresa Willem[1,2], MA; Alessandro Wollek[3], Dr rer nat; Theodor Cheslerean-Boghiu[3], MSc; Martha Kenney[4], PhD; Alena Buyx[1], Dr med

[1]Institute of History and Ethics in Medicine, School of Medicine and Health, Technical University of Munich, Munich, Germany

[2]Helmholtz AI, Helmholtz Munich, Munich, Germany

[3]Munich Institute of Biomedical Engineering, School of Computation, Information, and Technology, Technical University of Munich, Munich, Germany

[4]Women & Gender Studies, San Francisco State University, San Francisco, CA, United States

Corresponding Author:
Theresa Willem, MA
Institute of History and Ethics in Medicine
School of Medicine and Health
Technical University of Munich
Ismaningerstraße 22
Munich, 81675
Germany
Phone: 49 89 4140 4041
Email: theresa.willem@tum.de

Abstract

Background: In data-sparse areas such as health care, computer scientists aim to leverage as much available information as possible to increase the accuracy of their machine learning models' outputs. As a standard, categorical data, such as patients' gender, socioeconomic status, or skin color, are used to train models in fusion with other data types, such as medical images and text-based medical information. However, the effects of including categorical data features for model training in such data-scarce areas are underexamined, particularly regarding models intended to serve individuals equitably in a diverse population.

Objective: This study aimed to explore categorical data's effects on machine learning model outputs, rooted the effects in the data collection and dataset publication processes, and proposed a mixed methods approach to examining datasets' data categories before using them for machine learning training.

Methods: Against the theoretical background of the social construction of categories, we suggest a mixed methods approach to assess categorical data's utility for machine learning model training. As an example, we applied our approach to a Brazilian dermatological dataset (Dermatological and Surgical Assistance Program at the Federal University of Espírito Santo [PAD-UFES] 20). We first present an exploratory, quantitative study that assesses the effects when including or excluding each of the unique categorical data features of the PAD-UFES 20 dataset for training a transformer-based model using a data fusion algorithm. We then pair our quantitative analysis with a qualitative examination of the data categories based on interviews with the dataset authors.

Results: Our quantitative study suggests scattered effects of including categorical data for machine learning model training across predictive classes. Our qualitative analysis gives insights into how the categorical data were collected and why they were published, explaining some of the quantitative effects that we observed. Our findings highlight the social constructedness of categorical data in publicly available datasets, meaning that the data in a category heavily depend on both how these categories are defined by the dataset creators and the sociomedico context in which the data are collected. This reveals relevant limitations of using publicly available datasets in contexts different from those of the collection of their data.

Conclusions: We caution against using data features of publicly available datasets without reflection on the social construction and context dependency of their categorical data features, particularly in data-sparse areas. We conclude that social scientific, context-dependent analysis of available data features using both quantitative and qualitative methods is helpful in judging the utility of categorical data for the population for which a model is intended.

XSL•FO
RenderX

(JMIR Med Inform 2025;13:e59452) doi:10.2196/59452

KEYWORDS

machine learning; categorical data; social context dependency; mixed methods; dermatology; dataset analysis

Introduction

Background

Artificial intelligence (AI) promises to transform medical diagnostics and treatment; however, this paradigm change comes with social and ethical challenges [1,2]. One particular challenge is the persistent unreliability of medical machine learning models for diverse populations [3-7]. The variation in performance reliability across populations stems, among other factors, from data scarcity in medical datasets. Publicly available datasets to train medical models, compared to those in other disciplines, are small or have little variation, often featuring populations from a specific area of the world in which the data were collected. When a machine learning model is trained on such a dataset, the results can have limited generalizability to a more diverse population seeking medical care, having disadvantaging or discriminatory effects [8].

Computer scientists increasingly turn to innovative multimodal computational methods to counter data scarcity and leverage the full potential of the limited available information. Recently, (deep) multimodal data fusion algorithms (ie, algorithms incorporating available categorical data such as a patient's medical history and demographics in addition to a main data category such as a medical image) have been developed and successfully used in, for example, dermatology and radiology [9-14]. However, the effects of including categorical data for machine learning training are understudied, particularly regarding models such as medical image classifiers intended to equitably serve individuals from diverse populations. However, understanding the impacts of categorical data on machine learning outcomes is crucial for the development of fairer and more accurate machine learning models.

From a social science perspective, using categorical data for machine learning training is controversial. Categorization, by definition, clusters individuals in groups based on their attributes. Many categories, such as gender, socioeconomic status, and skin color, are used broadly to structure everyday communication and facilitate scientific research. However, these categories are socially constructed, meaning that they are the result of artificial definitions that go beyond biological facts [15]. As a result, socially constructed categories are unstable and can be too broad or narrow for the context they are used in or simply inadequate shorthands [3]. When rendered statistically, such as in a machine learning model, the inexactitude of such categories becomes materially significant and can introduce biases.

This paper proposes a mixed methods approach to assess the qualitative utility of available categorical data before machine learning model training. We first assess data categories' social construction as a major reason behind their context dependency. We then report an exploratory, quantitative examination of the effects of data features from a specific dermatological dataset's [16] unique categorical data features on a vision transformer model. We square the quantitative findings with a qualitative study of the data collection process and inclusion and exclusion logics of the dataset's categorical data for publication.

Our results suggest how data collection practices and publication decisions are roots for the observable effects of categorical data on machine learning model training. This study practically exemplifies how insights into the social construction and context dependency of available categorical data can be derived and used for inclusion or exclusion decision-making during training. This demonstrates how integrating quantitative and qualitative insights to decide on the inclusion or exclusion of categorical data can help incorporate health equity considerations into machine learning–based medical imaging workflows, such as considering who is served or neglected when certain data categories are used or disregarded during training. Such interdisciplinary results, we argue, are pertinent to inform model training accounting for the unavoidable performance differences of machine learning models for different groups.

The Dermatological and Surgical Assistance Program at the Federal University of Espírito Santo 20 Dataset

In dermatology, the primary data category typically consists of images of skin lesions. Additional data often collected include the patient's age, sex or gender, and dermatologically relevant factors such as skin type or the location of the lesion on the body. We base our work on experiments with and analyses of the Brazilian Dermatological and Surgical Assistance Program at the Federal University of Espírito Santo (PAD-UFES) 20 dermatological dataset [16]. The dataset contains 2298 entries in total labeled for 6 skin lesion classes: 3 malignant (basal cell carcinoma [BCC], nevus [NEV], and melanoma [MEL]) and 3 benign (seborrheic keratosis [SEK], actinic keratosis [ACK], and squamous cell carcinoma [SCC]).

The PAD-UFES 20 dataset has a unique combination and a comparatively high number of 21 patient-focused data features. These features are leverageable for machine learning model training. The dataset's data cover the patients' medical information and history (eg, *skin_cancer_history*), medical details about the skin lesion not captured by the image (eg, *itch*, *grew*, *bleed*, and *elevation*), demographics (eg, *age*, *gender*, *background_father*, and *background_mother*), environmental determinants (eg, *pesticide*, *has_piped_water*, and *has_sewage_system*), and lifestyle (eg, *smoke* or *drink*), with many of the data types being categorical (ie, the assignment of individual patients to a category is a matter of definition; Table 1 [15]). This unique combination of data features for each entry, its comparably small sample size for a machine learning context, and its public availability that makes PAD-UFES 20 accessible for researchers worldwide were significant criteria for choosing this dataset for exploring the implications of using categorical data for machine learning training.

XSL•FO
RenderX

Examining the PAD-UFES 20 dataset's categorical data features illuminates its theoretical limitations. Most of the samples in the dataset originate from Brazilian patients of central European ancestry. Prevalent characteristics of this group include a White phenotype and a dominantly disadvantaged socioeconomic status. The combined characteristics of lighter skin tones typical of the White phenotype and their heightened sun exposure during various activities common among those of a disadvantaged socioeconomic status in Brazil, such as fieldwork and domestic labor, make this subgroup particularly susceptible to skin lesions induced by the intense Brazilian sun. While the resulting high prevalence of skin cancer in the dataset renders the PAD-UFES 20 dataset effective for training a skin lesion classifier, especially for skin cancer, it is crucial to recognize that the dataset's population is notably specific and, thus, introduces significant biases. Because the dataset is skewed toward lighter skin tones and a particular socioeconomic status, a model trained using this dataset might, even when trained on image data alone, limitedly generalize to other populations. In the following section, we will consider how data categories are socially constructed and, thus, context dependent, calling their utility for the model training process into question.

Table 1. Description of (categorical) data attributes available with the PAD-UFES 20 dataset (in the metadata CSV file).

Attribute	Description
patient_id	A string representing the patient ID – example: PAT_1234
lesion_id	A string representing the lesion ID – example: 123
image_id	A string representing the image ID, which is a composition of the patient ID, lesion ID, and a random number – example: PAT_1234_123_000
smoke	A Boolean to map if the patient smokes cigarettes
drink	A Boolean to map if the patient consumes alcoholic beverages
background_father and background_mother	A string representing the country in which the patient's father and mother descends. Note: many patients descend from Pomerania, a region between Poland and Germany. Although it is not a country, we decided to keep the nomenclature, since they identify themselves as Pomeranian descendants.
age	An integer representing the patient's age
pesticide	A Boolean to map if the patient uses pesticides
gender	A string representing the patient's gender
skin_cancer_history	A Boolean to map if the patient or someone in their family has had skin cancer in the past
cancer_history	A Boolean to map if the patient or someone in their family has had any type of cancer in the past
has_piped_water	A Boolean to map if the patient or someone in their family has had any type of cancer in the past
has_sewage_system	A Boolean to map if the patient has access to a sewage system in their home
fitspatrick	An integer representing the Fitspatrick skin type
region	A string representing one of the 15 macro-regions previously described
diameter_1 and diameter_2	A float representing the skin lesions' horizontal and vertical diameters
diagnostic	A string representing the skin lesion diagnostic – BCC, SCC, ACK, SEK, MEL, or NEV
itch	A Boolean to map if the skin lesion itches
grew	A Boolean to map if the skin lesion has recently grown
hurt	A Boolean to map if the skin lesion hurts
changed	A Boolean to map if the skin lesion has recently changed
bleed	A Boolean to map if the skin lesion has bled
elevation	A Boolean to map if the skin lesion has an elevation
biopsed	A Boolean to map if the diagnostic comes from clinical consensus or biopsy

The Social Construction of Categorical Data

Data categories featured in publicly available datasets such as the PAD-UFES 20 and used to train medical imaging machine learning models are often assigned to someone or something as biological despite being "socially constructed." Socially constructed categories are historically produced, reproduced, and changed within institutions or cultures [15]. Many demographics, for example, age, race, or gender, are examples of socially constructed categories. They play a key role in shaping and structuring human communication as well as the beliefs we hold about the world, but they are also loaded with meanings that go beyond their biological bases or initial definitions and depend on the working definitions of these categories in a specific assessment setting [15]. Hence, while sometimes appearing universally applicable and comparable, socially constructed categories harbor underlying ambiguities that make them context dependent. When such

XSL•FO
RenderX

context-dependent data are used for machine learning training, their ambiguities create biases and can disadvantage population groups, often those already marginalized [3,5].

In the early nineties, Suchman [17], building on the analysis by Winner [18] of how artifacts have politics, described how categories have politics. The works by both Winner [18] and Suchman [17] drew attention to how moral values are inscribed in human-made constructs, be they artifacts made of concrete, such as bridges that disallow a specific population from entering a public beach [18], or categorial classifications, such as racial categories that group specific individuals and bestow upon these groups value-laden associations [17] that have tangible, measurable impacts on aspects of their lives, such as income, access to health care, and education [19-21]. The category "race" and its experienced disparities constitute an illustrative example of how categories are socially constructed and create social and political struggles for those classified under them. To elucidate, we can juxtapose the official "race" categories used in the census of countries such as the United States, Brazil, and Germany. In the United States, the collection of racial categories has undergone much change since the establishment of racial categories in the country's census in 1790 [22]. Today, the US Office of Management and Budget "requires five minimum categories (White, Black or African American, American Indian or Alaska Native, Asian, and Native Hawaiian or Other Pacific Islander) for race [and] permits the Census Bureau to also use a sixth category - Some Other Race" [23]. Following Statistical Policy Directive 15 in October 1997, "the option to choose multiple racial categories was introduced as part of the U.S. government's routine data-collection mission" [24]. For census data collection in Brazil, on the other hand, "white, brown, black, yellow (amarelo, i.e., of some Asian descent), and...the Indigenous (indígena) category [which was added] in the 1991 census" [25] constitute the "official" racial categories. In Germany, as another contrasting example, the census systematically omitted data collection of ethnic and racial categories after World War II. Instead, the German census collects "related data on foreigners, migrants and their descendants" [26], such as individuals' "migration background."

Note how the different handling of racial categories in a census creates subtle classification differences. Foremost, the categories collected are different. As a result, a single person could be classified differently depending on whether they live in the United States, Brazil, or Germany. Second, the categories themselves are based on different features. For example, "[u]nlike the USA, color or race in Brazil refers primarily to appearance rather than descent" [25]. Third, the approach to collecting the data is notably different. While, in the United States, the categorization was conducted by an authority employee until 1970 [22], "[s]elf-identification has been the official method for recording racial category membership in Brazil since 1950" [25]. Finally, Germany applies a "color blind" approach, collecting neither appearance-based nor self-identified racial data in its official census [26]. The decisions (not) to collect and how to collect the data shape the potential applications of the data on a country-by-country basis and influence the local medical data collection practices. The resulting differences hamper cross-national comparison and complexify the transfer of publicly available datasets that include such categories to different national contexts (it is important to note that the categories used for assessments in the official census do not always translate to the medical sector; for example, in the United States, the census categories are being challenged for the context of medical use by the Agency for Healthcare Research and Quality [27]). In addition to national differences in handling racial data categories, the inexactitude of racial categories and their intertwining with proxies such as skin color have been criticized [28]. In increasingly diverse populations, classifying someone as belonging to a single or even multiple races becomes increasingly complex and, thus, inaccurate. Because assessment strategies and categories can never be defined in a fine granular enough way, the categories are, by default, more descriptive of some than others classified within the same category. Following a recent controversy on a published paper that distinctly depicted human ancestry [29], a coauthor of the paper said that their "analysis reaffirms that race and ethnicity are social constructs that do not have a basis in genetics" [30].

In the context of machine learning models, the nuanced effects of using social constructs as categories can impact performance. Computer scientists who build machine learning and other statistical models "work every day on the design delegation, and choice of classification systems and standards" [24]. Thus, they have immense decision-making power over the specifications of the classification systems implemented. However, as Bowker and Star [24] note, "few see them as artifacts embodying moral and aesthetic choices that in turn craft people's identities, aspirations, and dignity." When, as a result, machine learning models process multiple individuals as classified under a single data category, subtle distinctions crucial for the model's intended use might be overlooked, manifesting inaccuracies and biases. The resulting models will tend to perform better for those who align closely with the mean of their assigned category and less reliably for individuals who fall between or outside of the categories or are placed within a category that is too broad. Famous examples of the effects that the incautious consideration of racial categories can have in practice are the "racist soap dispenser" [31], which would not identify darker-skinned hands and, thus, not dispense soap for them; Google Photo's facial recognition software, which identified darker-skinned individuals in photo postings as gorillas [32]; the perpetuation of discriminatory biases through search engines [33]; and the worrisome automation of decisions on whether someone is worthy of help, for example, when triggering child abuse investigations [34].

In health care, studies accounting for racial differences have reified categorial differences of inexact, socially constructed categories. For example, the hypertension medication BiDil was granted Food and Drug Administration approval after showing efficacy for Americans of African ancestry, whereas earlier, when tested on Americans of European ancestry, it was believed to be ineffective. Duster, a social scientist and critic of using socially constructed categories in genomic research, criticized the parties involved in both the study and its approval for insufficiently accounting for the "complex feedback loop and interaction effect between phenotype and social practices

XSL•FO
RenderX

related to that phenotype" [35]. His work contributed to a large body of science studies scrutinizing the utility of assessing and using race, ancestry, gender, and other data categories in different areas of medical research [36-42]. For example, in precision medicine, scholars claimed that the absence of biomedical significance of categorizations creates shorthands, which are, at most, unhelpful for meaningful statistical inference [43,44]. Despite potentially providing clues for correlations, data categories used in health care are frequently proxies for other factors that matter in the context of diagnosis or treatment. In dermatology, health and its categorial social determinants are particularly intertwined as different skin types have different susceptibilities to skin lesions [45].

Feature Selection: The Current State of the Art to Assess Data Feature Utility for Machine Learning

The fact that data features have different utility for different contexts is well established in the data science community. Hence, so-called feature selection methods have followed the introduction of techniques that use multiple, possibly multimodal (ie, various data types) data features in a single medical machine learning model [46]. Using feature selection in developing a machine learning model, computer scientists test which data features make sense to include for training. To do so, feature selection methods render available data features statistically and rank them regarding their relevance for the intended use of a particular model. In addition to helping choose which data to include for a model, data feature selection methods have been used to create new insights about certain statistical connections of variables and, thus, strengthen the explainability of a model [47] or find clues about the root causes of certain diseases [48].

The feature selection approach effectively provides insights into the statistical relevance of the data features of a particular dataset and its corresponding machine learning model. However, available feature selection methods fail to provide qualitative insights into why a specific data category contributes to a model's reliability, explainability, and performance. An additional limitation of currently used feature selection methods is that they usually look at the relevance of a data category across the entire model and fail to investigate performance increases or decreases due to the inclusion or exclusion of certain data features per class. As a result, the effects of irrelevant data features, or those reducing the performance of a particular class, might be balanced out if another class does correlate with the same data features.

Methods

The methods for this work were a mix of applied computing and qualitative investigations based on grounded theory [49]. For the claims we make, it is necessary to incorporate both computer scientific findings from experimenting with the dataset and qualitative accounts that can shed light on some of the effects we observed in more detail than numbers can.

Quantitative Analysis

The quantitative analysis aimed to investigate the effect that each available data feature, including categorical data, has on a skin lesion classifier model to provide insights into the utility of each data feature. Therefore, we trained multiple similar transformer-based models using the PAD-UFES 20 dataset while randomizing one of the data categories in each case. We then compared the performance of the obtained models per class. Coauthors AW and TC-B led the method and implementation of the quantitative analysis.

For preprocessing, duplicates and entries with 2 images or lacking data were excluded. A total of 64.14% (1474/2298) of the entries remained. Patient data were first converted to categorical data (numerical data entries [age and lesion size] were binned) and encoded into soft one-hot vectors.

We trained identical multi-classifier vision transformer models (with a training, validation, and testing data split of 70%-15%-15%) based on the architecture published in the study by Cheslerean-Boghiu et al [13]. As the feature extractor, we used the "vit_small_patch16_224" vision transformer, which comprises 12 transformer encoder layers and a classification head operating on embedding vectors with 384 elements. The model, loaded via the PyTorch Image Models library [50] with ImageNet-1K (Standford Vision Lab) pretrained weights, operates at an input resolution of 224 × 224 pixels. Positional embeddings were also derived from ImageNet pretraining, and we performed fine-tuning across the entire model without any layer freezing. The framework used for this implementation was PyTorch.

One model was trained using all available data, and one model was trained using randomized values for all data features. For the other 16 models, we randomized the input for 1 data feature in each case: *Fitzpatrick*, *background_father*, *background_mother*, *gender*, *hurt*, *region*, *age*, *smoke*, *drink*, *pesticide*, *has_piped_water*, *has_sewage_system*, *cancer_history*, and *skin_cancer_history*. The data features we tested were selected based on an internal discussion about the potential utility of the data features for the model. These decisions were made before having spoken to the authors of the PAD-UFES 20 dataset.

To solidify our results, all models were trained in 5 separate runs each; the randomized values of the models were set differently in each training run. The seed was set differently in every run. The fixed input dimensions of our vision transformer model constituted the rationale for this process. Feature randomization has been successfully applied in other studies [51]. Leaving out data features instead of randomizing them would alter the model and, thus, impair our analysis of the effects of each data feature.

For the result presentation, we concatenated all runs per model (one model with all data features included, one model with randomized values for all data features, and one model for each randomized data feature). We created receiver operating characteristic (ROC) curve plots for each of the 6 classes (NEV, BCC, MEL, ACK, SCC, and SEK). Each ROC plot shows the performance of all models for one of the classes in color-coded graphs. For each performance representation, we included area under the ROC curve values and CIs calculated using the nonparametric bootstrap method with 10,000-fold resampling at the image level.

XSL•FO
RenderX

The quantitative part of our analysis is an exploratory study; needs replication to substantiate it, including reproduction with combinations of data features included or excluded; and is naturally limited by the small sample size of the dataset, particularly in combination with the transformer model architecture used. This setup was selected not to develop a robust skin lesion classifier but to simulate a real-world application of this dataset [13], highlighting the realistic limitations and implications associated with its use.

Qualitative Analysis

The qualitative analysis featured in this work is based on one-on-one interviews with 3 of the authors of the PAD-UFES 20 dataset. The interviews aimed to gain (unpublished) insights into the dataset and the data therein.

The first author of this paper (TW) approached André Pacheco, assistant professor at the Federal University of Espírito Santo, lead of the PAD-UFES project, corresponding author of the dataset, and presenter of multiple (publicly available) talks on the PAD-UFES 20 dataset, via email, establishing first contact, explaining the context of the study, discussing participation in an interview for the study at hand, leading to the first interview in October 2023. After the initial interview, 2 other authors of the dataset publication were recruited via snowballing: Gabriel Giorisatto, a machine learning student working in André Pacheco's research laboratory when the PAD-UFES project started and who helped gain skin cancer domain knowledge facilitating dialogues with medical colleagues, and Breno Krohling, a machine engineer who was working as an undergraduate student in the laboratory facilitating the PAD-UFES project by helping with data collection. The second and third interviews were conducted in October 2024.

An initial interview was conducted with André Pacheco in October 2023. To solidify the findings, 2 additional interviews were conducted in October 2024 (Breno Krohling and Gabriel Giorisatto). All interviews were conducted by TW via Zoom (Zoom Video Communications) and followed the peer-to-peer interview method [52] using a semistructured interview guide to structure the conversation. The interviews lasted between 40 minutes and 1.5 hours and covered the genesis of the PAD-UFES 20 project; the context in which the dataset was created; the authors' rationale for collecting the data; their rationales for collecting each of the data features; the initial intended use of the dataset; how access to the community centrally featured in the dataset was established; how the dataset was created; and how the authors of the dataset reflected on the public use of the dataset, which, at least in some instances, includes the data features for analysis.

Initial interview transcripts were created with AI assistance [53]. TW double-checked and corrected the transcripts while relistening to the interview audio files. The interview transcripts were analyzed using a grounded theory–inspired coding process that included line-by-line coding and axial coding with sensitizing concept clusters according to initial findings [49]. Initial codes were selectively recoded to inform our analysis and condition our findings. TW created memos based on the codes that later formed the basis for the qualitative accounts in this work. The quotes used in this manuscript have been edited for readability and were returned to the interviewees to double-check that the correctness of meaning stayed intact before publication. The interview data showed strong consistency across participants, suggesting a high level of theoretical saturation.

We followed the COREQ (Consolidated Criteria for Reporting Qualitative Research) checklist for reporting the qualitative part of this study (Multimedia Appendix 1).

Ethical Considerations

Before each interview, TW explained the reservations about participating in the study, including the interviewees' ability to opt out of the study at any time and the impossibility of granting them pseudonymization. All interviewees gave their written informed consent to participate in the interviews and to be referred to by their real names throughout this manuscript. Interviewees did not receive any compensation for participating in the interviews.

Results

Overview

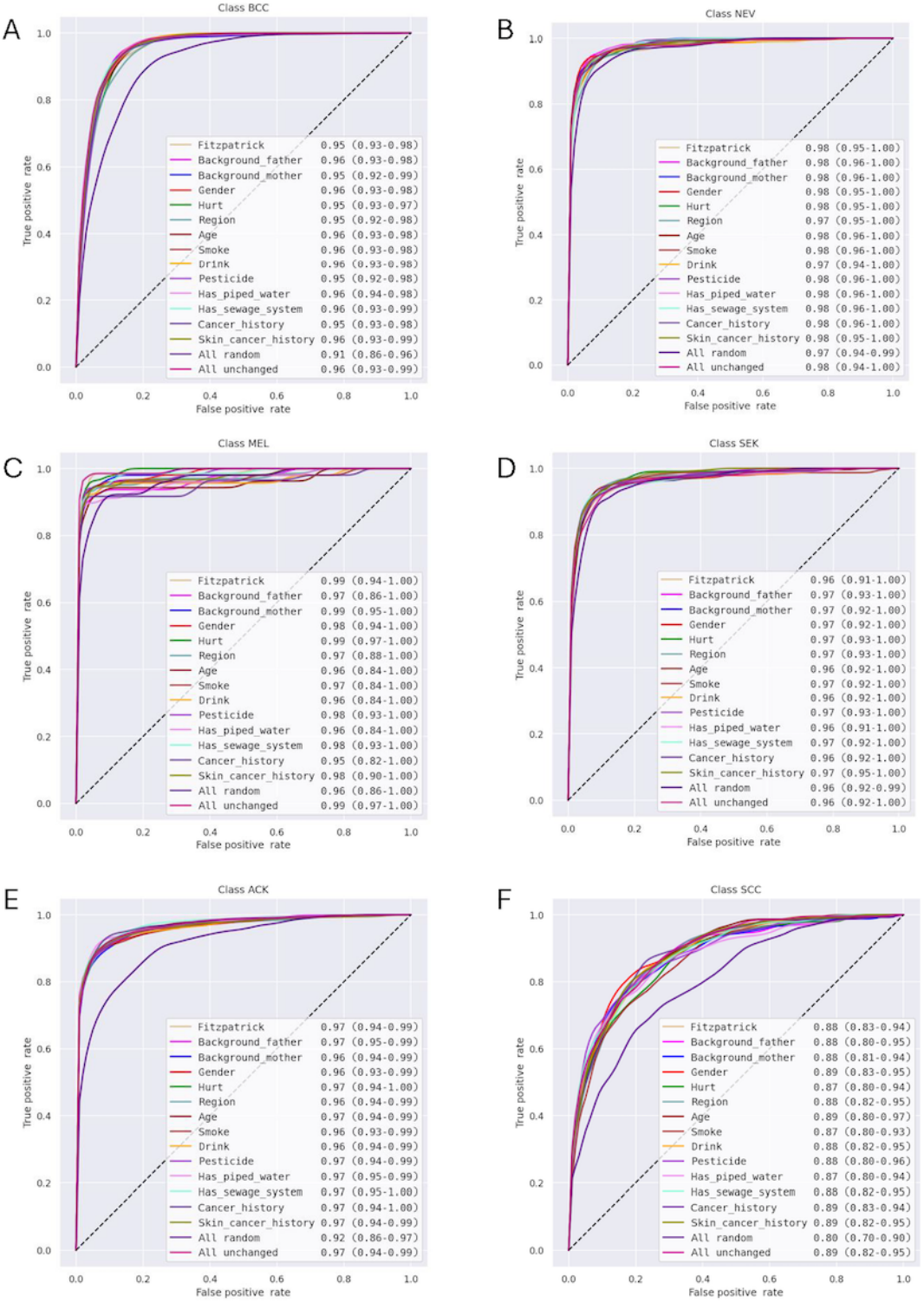
In the following sections, we present our findings of the experimental inclusion or exclusion of the data features of the Brazilian PAD-UFES 20 dermatological dataset for training a vision transformer multi-classifier and the pairing of these quantitative findings with a qualitative investigation. We observed scattered effects in the quantitative analysis and interpreted them regarding the creation and use practices of publicly available medical datasets. However, combined with our qualitative analysis, the observed scattered effects provide insights into how data collected in or for a particular social context can have adverse effects when used to train models intended for different or broader contexts. On the other hand, our data solidify evidence that the optimization of a model for a social context such as the dataset's by including categorical metadata for training can make the model more precise if data categories are not too broad, narrow, or ambiguous or shorthands. However, there is reason to believe that, in these cases, the precision of the model overfits the dataset's context and, hence, the resulting model might impede the ability of health care professionals to decide whether a particular model will work for a new patient. Our insights advise for interdisciplinary dialogue to assess the data or context fit before model training.

Changes in Model Performance Through Data Feature Randomization

The juxtaposition of the performance of the models, which were trained using all available data features (model 1), using randomized values for all available data features in training (model 2), or randomizing 1 data feature in each case (models 3-16), showed scattered effects for each class (Figure 1).

XSL•FO
RenderX

Figure 1. Performance of the vision transformer models trained on the Dermatological and Surgical Assistance Program at the Federal University of Espírito Santo 20 dataset per class—(A) basal cell carcinoma (BCC), (B) nevus (NEV), (C) melanoma (MEL), (D) seborrheic keratosis (SEK), (E) actinic keratosis (ACK), and (F) squamous cell carcinoma (SCC). Each graph represents the mean performance of 5 similar concatenated models; the color of each graph corresponds to the metadata feature that was randomized for this model's training (see the legend in each of the images) except for the "all random" and "all unchanged" graphs. The "all random" graph represents the model performance when all metadata features were randomized, and the "all unchanged" graph represents the model performance when all metadata features were included in the training as per the dataset.



Randomizing All Data Features

Across all classes, the performance of the models decreased when all data features were randomized for training compared to the model for which we included all data feature values according to the PAD-UFES 20 dataset ("all unchanged"), indicating the predictive utility of the data features for the classes.

XSL•FO
RenderX

The magnitude of the performance drop from the "all unchanged" to the "all random" model varied notably across classes. For example, for SCC (Figure 1F), the performance decreased from 0.89 to 0.80 by 0.09. For other classes, the performance difference was only very slight (eg, 0.01; Figure 1B), or the performance even stayed the same (eg, 0.00 for SEK; Figure 1D) when all data features were randomized. This indicates that the data are more relevant to some classes than others.

Randomizing Individual Data Features

Randomizing individual data features impacted the models. In some instances, the model's performance decreased when a data feature was randomized, indicating that the randomized data feature had predictive utility for the model's performance. For example, randomizing the "cancer history" data feature reduced the average predictive performance for the melanoma class (Figure 1C) by 0.04. Considering the breadth of some confidence intervals (CIs), this effect seems even more pronounced for some of the models created in our experiment. In other cases, the model's performance increased when a data feature was randomized, indicating that the randomized data feature hampered the model's predictive power. For example, when "background father" was randomized, the performance for the SEK class increased by 0.01 compared to that of the "all unchanged" model.

The effects observed in our quantitative analysis coincide with the qualitatively contextualized expectations regarding the relevance of data features to the overall model and some classes (detailed analysis in the following sections). As a general trend, the randomization of data features considered highly medically relevant by the dataset's authors, on average, also decreased the model's performance, indicating that the data features have predictive power. The performance variance varied per class and randomized data feature across those expected to be highly medically relevant (eg, *itch*, *bleed*, and *elevation*) and those expected to be confounded through their social context dependency to the envisaged prediction (eg, *background_mother* and *background_father*, *has_sewage_system*, or *has_piped_water*).

Comparative Analysis of the Randomization of Individual and All Data Features

When all data features were randomized, the model in some cases performed better than a model for which we randomized only 1 data category during training. This suggests that a model trained using all random data features ignored the meta data and took only the image data into account. The fact that the CI reaches (close to) 1.00 in most models supports this hypothesis and further shows that, in our experiment, relatively well-performing models were obtainable even when one or all data features were randomized. Note that, in our experiment, we validated the performance of the models on a split from the training dataset. The performance increased for some models when data were included, which can partially be explained by the heterogeneity of the PAD-UFES 20 dataset, which is largely biased toward a lighter-skinned immigrant population. The model likely overfits this population.

Overall, the quantitative analysis of the models showed a scattered impact of the available data features in the PAD-UFES 20 dataset, making it difficult to quantitatively evaluate the usefulness of including individual data features. However, medical data appeared slightly more pertinent to the model than other categories serving as proxies, whereas demographic, context-dependent variables showed uneven relevance per model class. However, note that the empirical evidence exploratively derived from our quantitative analysis can only provide limited (stand-alone) information about specific impacts of the inclusion and exclusion of data features from the PAD-UFES 20 dataset and is rather meant to showcase the potential of quantitative analysis for the evaluation of data features. Checking whether the results are consistent across other feature selection methods would exceed the scope of this exploratory study. Still, it would be highly relevant to future work to provide further insights into the utility of the PAD-UFES 20 data.

Qualitative Contextualization

Overview

This section features qualitative data from interviews with the authors of the PAD-UFES 20 dataset to show an example contextualization of the quantitative findings using qualitative analysis. The accounts presented provide insights into how the dataset was created and why certain data categories were included in and excluded from the publicly available version. Thus, they provide insights into the quality of the publicly available PAD-UFES 20 data features.

Inclusion: How Data Categories Were Chosen

First, it is essential to understand how the team decided which data categories to include for data collection. Our interlocutors told us that one purpose of the PAD-UFES project was to digitize the university's dermatological data collection process that, at the time, was still conducted manually by medical students. Therefore, an initial set of data categories to collect originated from formerly institutionally established data collection practices. The refinement of the data collection specifications for the PAD-UFES 20 dataset specifically was established while aiming to satisfy multiple actors' interests at the same time:

> *They [the medical colleagues] wanted to have this data to make research on this data, so, for example, the geographic location of the patient, if the patient has clean water, the income of the patient per month...they wanted relevant data for their research about the demography of the patients. This information was initially not relevant to us, we wanted specific information about the lesion. So, we had these two types of data to collect.* [Gabriel]

Hence, some data categories were defined independently by medical students and scholars, whereas the computer scientists leading the data collection were less interested in these.

To determine which data categories would be relevant for machine learning, André and his colleagues referred to the "reporting standard in most medical data sets" (Breno) and consulted additional medical experts. André explained that their

XSL•FO
RenderX

selections of which data features to collect were ultimately related to the following:

> *...specific questions [dermatologists ask their patients], like "does this lesion itch" or "has it bled in the past"..."has this been growing"...this kind of questions. Because they [doctors] try to simulate the algorithm that they have in their head.* [André]

On the basis of the factors that dermatologists reported working with to diagnose a lesion, André and his colleagues created a combination of data categories to potentially accompany the dermatological images. They ran the categories by the dermatologists again before starting the data collection process, asking the following:

> *If you have only this information, can you classify or...provide a diagnosis from this lesion for this lesion? And most doctors said "okay, now I have enough information.*" [André]

Re-Exclusion: Medically Irrelevant Data

Despite basing the choice of which data categories to collect on dermatological clinical practice, it became clear during data collection that not all data categories seemed reasonable to include for analysis:

> *[For the dataset creation] we asked people if they had contact with chemicals. Most of them work on farms. They are peasants...and some doctors say chemicals, you know, when you put them in the food [on the fields], they may have an impact on skin lesions. So, we have this in the data set. But most doctors don't ask [their] patients [about chemicals during skin assessments] because they don't think this is relevant.* [André]

The "pesticide" category serves as a representative example here. Gabriel and Breno shared similar insights regarding the categories "has_sewage_system" and "has_piped_water." They reported that these categories were initially collected for medical students to analyze demographic factors and skin cancer or explore potential causal links between these features and skin cancer that could not be established in a subsequent analysis [54]. Notably, they still chose to publish these data categories despite excluding them from their machine learning analysis after deeming them medically irrelevant:

> *We left this information there [in the dataset] because we thought something like "maybe someone in the world wants to have this information to do something with it," right?* [André]

Re-Exclusion: Unreliable Answers

Some other data categories available in the dataset were unreliable due to ambiguous internal definitions or varying degrees of patient honesty, such as the following:

> *If the patient uses cigarettes or drinks...if they consume alcohol. Those are general questions most people don't like to answer.... Most of them say no, but sometimes they use that.* [André]

André explained that the resulting vagueness of the data features "smoke" and "drink" caused them to disregard these categories in the version of the dataset that they used for training algorithms. However, again, they held onto these features for publication of the dataset in case "someone wants to do some analysis with it," as Breno said. This highlights the importance of critically reflecting on the available data features for their applicability for the intended use of a new model and the integrity of the categories.

Re-Exclusion: "Purposeful" Shorthands

Particularly striking data categories in the PAD-UFES 20 dataset are "background_father" and "background_mother." André and his colleagues included these data categories for data collection for the following reason:

> *...many people in Brazil are descendants from Europe. Immigration. So, you know, this is a complicated feature because if I ask [a patient about their background and they say] "Oh, I'm descended from Germany," we know that they are very white. They probably have Fitzpatrick skin type 1 or 2...because they work on a farm in the sun.... [Sun] exposure and being white is a very, very, um, you know, predisposition for skin cancer.* [André]

Hence, the categories referring to the patients' parents' background are conscious shorthands to assess their skin color. When asked why they collected both the patients' parents' backgrounds and their Fitzpatrick skin type, André answered the following:

> *Because sometimes people don't know from which part of the world they descend. And at the office, they use that for statistics...just to see which region [the patients come from]. And in Brazil, there is a very high miscegenation. It doesn't mean if people descend from, I don't know, Italy, for example, [some might be] very white and [others], they have, you know, Fitzpatrick skin type 3 or 4 because of miscegenation, right? So, it tells us some part of the history, but not the whole history.* [André]

Several noteworthy observations emerge from this and similar accounts that we obtained from our interlocutors. First, it is interesting to highlight the decision to assess the migration background instead of racial categories. The rationale for including the background categories seems closely related to race-related concepts. However, the team hoped to assess who migrated from countries in which lighter skin tones are more prevalent. Second, while race or family origin appears to be an intuitive category to ask about to assess skin tone, its medical relevance in the context of a dermatological classifier seems questionable under closer scrutiny. Individuals descending from a specific region may have a higher likelihood of a particular skin type, yet their actual skin characteristics could deviate significantly, especially if their parents themselves underwent migration. Finally, including the background categories served multiple purposes: assessing the skin type, potentially including genetically important information that goes beyond skin type, and delivering statistics. The assessment of the patients' parents' backgrounds is a shorthand to fulfill all these goals

XSL•FO
RenderX

simultaneously; however, not asking these questions separately compromises the exactitude of the categories.

These nuances suggest that the "fitzpatrick_skin_type" variable might offer greater reliability in assessing the intended parameters of the background data categories. However, according to André, the team included the variable "fitzpatrick_skin_type" only as a backup to the background categories. They did so because they expected that some patients might be unable to provide satisfactory answers regarding their backgrounds or migration history. Furthermore, he argued, "Fitzpatrick is subjective. You know, maybe a doctor may say this person is type two, and another doctor says this person is type three." Moreover, the Fitzpatrick skin type scale, being a social construct in itself, harbors numerous limitations regarding its suitability to assess the intended parameters. For example, the scale has recently been criticized for having a Eurocentric bias toward lighter skin tones [55] and for incorrectly and inadequately reflecting sunburn and tanning risks for skins of color [56]. A useful data category would assess a cause factor of the classes the dataset is used to predict. For example, assessing how much melanin a patient's skin holds might be more expedient in the case at hand.

Therefore, it was not surprising that all interviewees told us that the project team ultimately did not use some of the categorical data features for their analyses. This shows, once again, how limited the utility of some of the data categories included in the publicly available dataset can be. The fact that, in their qualitative analysis, they "didn't find [some features] that useful when compared to the other data features" (André) is in line with the scattered effects of our quantitative results, in which the utility of other data features was much more visible compared to that of the background categories (Figure 1). Again, this emphasizes the necessity for thoroughly scrutinizing the available data categories in publicly available datasets.

Another purposeful shorthand that André and his colleagues used can be found in the categories "has_piped_water" and "has_sewage_system." The team told us that they collected these data for the following reason:

> *...most people [in the dataset] are very poor. They work in farms, you know, this kind of thing. Right? When you collect "has_piped_water" and "has_sewage_system," you can draw some correlations to family income. Usually, people with low family income don't have piped water and don't have a sewage system. And they usually have more skin lesions.* [André]

Our other interlocutors seconded this, and Breno added that "the age was also important because, as...they were farmers, the older they were, the more sun-exposed they were, so they have an increased risk of skin cancer," showing how sometimes combinations of categorical data features were believed to have statistical importance for assessing skin cancer using predictive machine learning models.

However, as André noted, "this is a correlation, not causation.... They [poorer people] usually have more skin lesions because they don't have money to afford the private treatment." While it seems meaningful to assess social determinants of health, such as socioeconomic status, our aforementioned quantitative analysis did not show a particularly pronounced utility of this data feature across classes. In addition, André told us that these categories are not used in their model. Furthermore, because of the specific population in the dataset, correlations between the data categories are expected. For example, during data collection, André and his colleagues recruited heavily among the European immigrant population, creating a dataset predominantly of individuals with lighter skin tones and who were socioeconomically disadvantaged and prone to skin lesions because of their high sun exposure. While the research group is still grappling with mitigating the resulting biases, André pointed out that "it's very hard to see how it could generalize to other groups here in Brazil." When taken into consideration in isolation, some biases of a skin lesion classifier trained using the PAD-UFES 20 dataset might be productive for the accuracy of diagnoses in a population with similar characteristics to those of the population included in the PAS-UFES 20. According to André, the population they use their current model with—which is similar to the population of the dataset—is "98%...skin types under four."

These Fitzpatrick skin types (1 to 3) are very well represented in the dataset; hence, the model they use regarding this aspect presumably works well for the vast majority of the patients they diagnose with the help of the model. This shows how a machine learning model might be locally helpful but hardly transferable to another context, in this case, a more diverse population, providing yet another reason for a context-sensitive assessment of data categories before their inclusion in training. However, what this leaves open is how the remaining 2% of patients in the Brazilian case can be granted fair access to dermatological care, how high the number of individuals who do not have access to this dermatological workflow is, and what skin types they have.

Renomination: Missing Categories Create Missing Values

André and his colleagues not only omitted specific data features from their model during analysis, but in other instances, they also discovered during the data collection process that specific data categories are indeed pertinent yet they had overlooked assessing them:

> *For example, the "elevation" data...one year after the [data] collection started, some doctors said to us, "Oh, the elevation is important, because if the lesion has elevation...it's probably not a melanoma." And we said, "Oh my God, this is very important information. Why haven't any doctors here said that to us before." Right. So, if you check the data set, you will see that elevation is missing for many samples in the dataset.* [André]

When the data features that result from the late inclusion of categories in data collection are included for training a machine learning model, the missing values must be accounted for; otherwise, they could distort the results. We did not explicitly test for the impact of missing values; however, because they are relatively many in the case of the PAD-UFES 20 dataset's

XSL•FO
RenderX

"elevation" category, it seems best to exclude this data category for training or wait for a new version of the dataset, which, according to André at the time of this writing, will be published shortly.

Publication: Making the Data Available to the Public

Our qualitative analysis showed that the authors of the PAD-UFES 20 dataset were aware of the caveats of the dataset. André and his colleagues carefully considered which data to include for the training of their model based on the quantitative analysis they performed and, importantly, the contextual knowledge they had about the population; the ways in which the data were assessed; and the quality of the data features they produced regarding unreliable answers, shorthands, medically irrelevant data, or missing values. However, when prompted about whether they had concerns about how their publicly available dataset might be decontextualized when used in other areas of the world by other developers with less contextual knowledge or applied to different population groups, André answered the following:

> *No, we don't have concerns about that. We just released the data set to, you know, to help the research community. You know, when we started to work in this field, we felt like, "oh, the data, there are just a few open [publicly available] datasets, and it would be great if we could release a data set that people from any part of the world could use." Right. But, of course, that can be used for good or bad. Of course, we cannot control what people do with this data set.* [André]

This account brings together several arguments. Again, it highlights that the team's motivation to publish the PAD-UFES 20 dataset was to counter the frustration within the medical machine learning community regarding the challenge of accessing datasets just above the quantitative threshold for being effective for machine learning applications. While emphasizing the pervasive scarcity of data in health care and the urgent need for comprehensive datasets, all interviewees underscored the dual use potential of datasets—the obtained results can either be advantageous or detrimental for individual patients or society at large depending on the decisions made by those using the dataset.

On the basis of our analysis, the potential damages that uncontextualized datasets might result in are not necessarily due to adverse decision-making of developers but can stem from a challenging-to-bridge gap in contextual knowledge. The significant gap between the pressing need for publicly available data to pursue the promised benefits of AI in health care and the potential for unintended harms highlights the need to exercise caution when dealing with unfamiliar, publicly available categorical data. It prompts important questions about responsible data publication practices.

Discussion

Principal Findings

For this study, we conducted a quantitative analysis and interpreted it regarding the creation and use practices of publicly available datasets. Our results showed that vague data categories, which are medically irrelevant, unreliable, shorthands for other categories, or otherwise distorted (eg, by missing values), can impair the quality of a machine learning model either overall or for specific predictive classes. The second part of our study—a qualitative analysis of an interview with authors of the dataset—provided evidence that the effects observed in the quantitative study are due to the social context dependency of the data categories chosen for a dataset and the medico-social context in which the data were collected.

Our results suggest that the uncritical use of context-dependent categorical data from publicly available datasets can introduce significant biases. These biases are particularly challenging to detect and mitigate because, under current machine learning standards, performance tests—even subgroup-specific performance tests—are typically conducted on a test split derived from the same dataset used for training. As this test split shares its context-dependent categorizations with the training split, these biases can go unnoticed. Such biases pose a particular risk in sensitive fields such as health care, which are challenged by scarce data landscapes combined with high-stakes decision-making in which every false negative and false positive can be detrimental to individual patients. As we demonstrated, a qualitative examination of how categorical data features are defined and an assessment of where categories may be vague, unreliable, oversimplified, or otherwise unsuitable for the model's intended application can help detect these biases.

Limitations

It is important to note that the magnitude of the observed effects of data categories on a machine learning model's performance likely varies depending on the dataset used. We expect, for example, that, if a similar study to ours were conducted using a larger dataset, the impacts of the data categories and washout effects would make the results more challenging to quantify. Conversely, in our experiment, the washout was less pronounced, and thus, the impact of the data categories became visible. However, the fact that we worked with a publicly available medical imaging dataset positions our results to raise significant concerns, particularly for domains such as medicine in which data scarcity frequently results in particularly small datasets being used for machine learning training. However, other studies should replicate our findings and investigate the impact of data categories in different settings.

An established limitation of case-sensitive research is limited generalizability. We would like to highlight that the phenomena observed in this study might not immediately lend themselves to generalization. This work intended to explore the interplay among data collection practices, the social construction of categories, and current use practices of publicly available datasets for machine learning model training in high-risk areas such as health care. While offering insights that might apply to similar cases or broader trends, this work, instead of deriving generalizable claims, exemplifies our research approach. We recommend conducting additional analyses when applying the approach to other scenarios. We made corresponding remarks throughout the manuscript. In line with the trend toward structured assessment of data categories [9-14], our data suggest

XSL•FO
RenderX

that including well-defined and contextually relevant data features in machine learning training can increase the accuracy of a model. However, this renders overfitting likely, and the translation to a more diverse population likely holds potential for harm because the accuracy of a model for any given patient and, therefore, the reliability of the model's outputs become more complex to assess. Further investigations are required to validate these hypotheses.

Relationship to Prior Work and Outlook

Our results deepen concerns raised by scholars about the social construction of attributes and intersectionality, for example, that machine learning puts specific, already marginalized groups at risk of medical under- or overtreatment [3,5-7]. Following the idea that categories have politics [17,18,24], our analysis of the politics of data categories extended established risks of the use of image data [7] and cautions against the inconsiderate use of categorical data accompanying image data in medical machine learning settings and beyond. In light of the context dependency and social constructedness of categorical attributes, such as racial categories used in the official censuses of individual countries [22,23,25-28], our results highlight the need for sociomedical studies to identify more precise data categories tailored to each of the diverse contexts in which medical machine learning models are applied. We believe that an increase in data category quality is essential to fulfill the potential of enhancing machine learning algorithms by incorporating relevant data categories during training. To achieve this, interdisciplinary research that establishes context-dependent data category definitions is needed. Context-dependent definitions should account for the, as Duster [35] put it, "complex feedback loop and the interaction effect between phenotype and social practices related to that phenotype."

As we have pointed out in this paper, the trend toward structured assessment of data categories in medical imaging is accompanied by an increase in data fusion algorithms. Both practices follow a sublime "more data is better" narrative previously reported in the context of publicly available image databases such as ImageNet [57]. This logic incentivizes those collecting data to include categories that fulfill multiple purposes simultaneously and those who develop machine learning models to include more of these potentially vague or too specific data features for training. Feature selection methods [46], the insights of which are based on statistics leveraged from the training dataset and lack qualitative contextualization, seem to be toothless against the context-sensitive limitations of data inclusion and exclusion for training. Additional mechanisms are needed to investigate the suitability of data categories for a new model, its context, and the population to which it will be applied. Consequently, this work advocates for deepening transdisciplinary collaborations in high-risk areas such as machine learning for medical images. We believe that the combination of applied computing and qualitative assessment is pertinent to assessing the contextual dependencies of data assessments and data applications and providing analytical insights into relevant gaps. As demonstrated in this research, considering quantitative and qualitative evaluations together can yield valuable recommendations for using or refraining from using data categories.

Conclusions

This work case-sensitively explored the effects of including categorical data features for training in data-scarce and community-serving areas such as medical imaging. We suggested a mixed methods approach, a blend of quantitative and qualitative analysis, to draw contextual conclusions about the social construction and context dependency of categorical data in publicly available datasets before using them for machine learning training. We exemplified our approach by applying it to the PAD-UFES 20 dermatological dataset, for which we quantitatively observed scattered effects on model performance when comparing scenarios in which we included all available data features for training, randomized all data features, or randomized a single data feature at a time. A qualitative analysis of the genesis of the dataset revealed root causes for the futility of some of the available data features.

Highlighting the nuanced and complex relationship between categorical data features and model performance, our observations suggest the need for an overall cautious use of publicly available categorical data for machine learning training. Our findings showed that data collection and categorization practices are not always intentional (enough) and that data categories' social constructedness and context dependency limit their transferability to new models. This underscores the importance of conducting qualitative, context-dependent analyses when considering integrating categorical data features into model training, particularly in domains in which the impact on diverse populations is paramount.

We further deduce from these findings that, first, interdisciplinary social science and health care scholarship is needed to create more purposeful and context-dependent definitions of data categories to guide data collection. Second, dataset creators should include detailed descriptions of the collection context of each data category. Finally, those using publicly available datasets should assume that more features may be available than are necessarily useful to include in training. Machine learning scientists should further institute robust practices to test available categorical data for their integrity within the context of the intended model application to prevent the perpetuation of biases when too narrow or vague data categories translate to their model. Importantly, the absence of reliable methods to assess and mitigate the adverse effects of context-sensitive data features creates an ethical imperative of refraining from including categorical data features unless proven safe for use in a diverse population related to the model's intended use.

We believe our findings to be particularly relevant for fields such as medicine, where sample sizes are often limited, demanding meticulous scrutiny of available data features for suitability before incorporation into model training. We advocate for an interdisciplinary approach that combines technical rigor with sociological understanding, ensuring that machine learning models are developed with the complexity of categorial attributes in mind. This collaborative effort is essential for

XSL•FO
RenderX

advancing the ethical and effective deployment of AI in a manner that respects the complexities of human societies.

Acknowledgments

This work was supported in part by the German Federal Ministry of Health's program for digital innovations for the improvement of patient-centered care in health care (grant agreement 2520DAT920).

Data Availability

The datasets generated during and analyzed during this study are not publicly available to protect the confidentiality and privacy of the participants but are available from the corresponding author on reasonable request. The Dermatological and Surgical Assistance Program at the Federal University of Espírito Santo 20 dataset analyzed during this study is available in the GitHub repository [58]. The architecture used to perform the analysis is available as a preprint [13].

Conflicts of Interest

None declared.

Multimedia Appendix 1
COREQ (Consolidated Criteria for Reporting Qualitative Research) checklist for reporting the qualitative part of this study.
[PDF File (Adobe PDF File), 500 KB - medinform_v13i1e59452_app1.pdf]

References

1. Čartolovni A, Tomičić A, Lazić Mosler E. Ethical, legal, and social considerations of AI-based medical decision-support tools: a scoping review. Int J Med Inform 2022 May;161:104738. [doi: 10.1016/j.ijmedinf.2022.104738] [Medline: 35299098]
2. Chen IY, Pierson E, Rose S, Joshi S, Ferryman K, Ghassemi M. Ethical machine learning in healthcare. Annu Rev Biomed Data Sci 2021 Jul 20;4(1):123-144 [FREE Full text] [doi: 10.1146/annurev-biodatasci-092820-114757] [Medline: 34396058]
3. Buolamwini J, Gebru T. Gender shades: intersectional accuracy disparities in commercial gender classification. In: Proceedings of the 1st Conference on Fairness, Accountability and Transparency. 2018 Presented at: FAT* '18; February 23-24, 2018; New York, NY.
4. O'Neil C. Weapons of Math Destruction: How Big Data Increases Inequality and Threatens Democracy. New York, NY: Crown Publishing Group; 2016.
5. Benjamin R. Race After Technology: Abolitionist Tools for the New Jim Code. Cambridge, UK: Polity Press; 2019.
6. Broussard M. More Than a Glitch: Confronting Race, Gender, and Ability Bias in Tech. Cambridge, MA: The MIT Press; 2023.
7. Obermeyer Z, Powers B, Vogeli C, Mullainathan S. Dissecting racial bias in an algorithm used to manage the health of populations. Science 2019 Oct 25;366(6464):447-453. [doi: 10.1126/science.aax2342] [Medline: 31649194]
8. Azar AK, Draghi B, Rotalinti Y, Myles P, Tucker A. The impact of bias on drift detection in AI health software. In: Proceedings of the 21st International Conference on Artificial Intelligence in Medicine. 2023 Presented at: AIME 2023; June 12-15, 2023; Portorož, Slovenia. [doi: 10.1007/978-3-031-34344-5_37]
9. Cui C, Yang H, Wang Y, Zhao S, Asad Z, Coburn LA, et al. Deep multimodal fusion of image and non-image data in disease diagnosis and prognosis: a review. Prog Biomed Eng (Bristol) 2023 Apr 11;5(2):022001 [FREE Full text] [doi: 10.1088/2516-1091/acc2fe] [Medline: 37360402]
10. Kline A, Wang H, Li Y, Dennis S, Hutch M, Xu Z, et al. Multimodal machine learning in precision health: a scoping review. NPJ Digit Med 2022 Nov 07;5(1):171 [FREE Full text] [doi: 10.1038/s41746-022-00712-8] [Medline: 36344814]
11. Praveen Kumar S, Sridevi S. Image fusion algorithm for medical images using DWT and SR. In: Proceedings of the International Conference on Artificial Intelligence and Smart Systems. 2021 Presented at: ICAIS 2021; March 25-27, 2021; Coimbatore, India URL: https://ieeexplore.ieee.org/document/9396001 [doi: 10.1109/icais50930.2021.9396001]
12. Zhang Y, Sheng M, Liu X, Wang R, Lin W, Ren P, et al. A heterogeneous multi-modal medical data fusion framework supporting hybrid data exploration. Health Inf Sci Syst 2022 Dec 26;10(1):22 [FREE Full text] [doi: 10.1007/s13755-022-00183-x] [Medline: 36039096]
13. Cheslerean-Boghiu T, Fleischmann ME, Willem T, Lasser T. Transformer-based interpretable multi-modal data fusion for skin lesion classification. arXiv. Preprint posted online on April 3, 2023 2024 [FREE Full text]
14. Kharazmi P, Kalia S, Lui H, Wang ZJ, Lee TK. A feature fusion system for basal cell carcinoma detection through data-driven feature learning and patient profile. Skin Res Technol 2018 May 22;24(2):256-264. [doi: 10.1111/srt.12422] [Medline: 29057507]
15. Kang M, Lessard D, Heston L, Nordmarken S. Social constructionism. In: Introduction to Women, Gender, Sexuality Studies. Amherst, MA: University of Massachusetts Amherst Libraries; 2017.

XSL•FO
RenderX

16. Pacheco AG, Lima GR, Salomão AS, Krohling B, Biral IP, de Angelo GG, et al. PAD-UFES-20: a skin lesion dataset composed of patient data and clinical images collected from smartphones. Data Brief 2020 Oct;32:106221 [FREE Full text] [doi: 10.1016/j.dib.2020.106221] [Medline: 32939378]
17. Suchman L. Do categories have politics? The language/action perspective reconsidered. Comput Supported Coop Work 2013 Aug 23;2(3):177-190. [doi: 10.1007/bf00749015]
18. Winner L. Do artifacts have politics? Daedalus 1980;109(1):36 [FREE Full text] [doi: 10.4324/9781315259697-21]
19. Bailey SR, Saperstein A, Penner A. Race, color, and income inequality across the Americas. Demogr Res 2014 Sep 19;31:735-756. [doi: 10.4054/demres.2014.31.24]
20. Ohlson M. Effects of socioeconomic status and race on access to healthcare in the United States. Perspectives 2020;12(2) [FREE Full text]
21. Budig MJ, Lim M, Hodges MJ. Racial and gender pay disparities: the role of education. Soc Sci Res 2021 Aug;98:102580. [doi: 10.1016/j.ssresearch.2021.102580] [Medline: 34247725]
22. Strmic-Pawl HV, Jackson BA, Garner S. Race counts: racial and ethnic data on the U.S. census and the implications for tracking inequality. Sociol Race Ethnicity 2017 Dec 04;4(1):1-13. [doi: 10.1177/2332649217742869]
23. Race. U.S. Census Bureau. URL: https://www.census.gov/quickfacts/fact/note/US/RHI625222 [accessed 2023-11-21]
24. Bowker GC, Star SL. Sorting Things Out: Classification and Its Consequences. Cambridge, MA: MIT Press; 2000.
25. Bailey SR, Telles EE. Multiracial versus collective Black categories: examining census classification debates in Brazil. Ethnicities 2006 Mar 01;6(1):74-101. [doi: 10.1177/1468796806061080]
26. Will AK. The German statistical category “migration background”: historical roots, revisions and shortcomings. Ethnicities 2019 Mar 06;19(3):535-557. [doi: 10.1177/1468796819833437]
27. Race, ethnicity, and language data: standardization for health care quality improvement. Agency for Healthcare Research and Quality. URL: https://www.ahrq.gov/research/findings/final-reports/iomracereport/reldatasum.html [accessed 2023-11-22]
28. Jablonski NG. Skin color and race. Am J Phys Anthropol 2021 Jun 29;175(2):437-447. [doi: 10.1002/ajpa.24200] [Medline: 33372701]
29. All of Us Research Program Genomics Investigators. Genomic data in the All of Us Research Program. Nature 2024 Mar 19;627(8003):340-346 [FREE Full text] [doi: 10.1038/s41586-023-06957-x] [Medline: 38374255]
30. Kozlov M. ‘All of Us’ genetics chart stirs unease over controversial depiction of race. Nature. 2024 Feb 23. URL: https://www.nature.com/articles/d41586-024-00568-w [accessed 2024-04-09]
31. This 'Racist soap dispenser' at Facebook office does not work for Black people. YouTube. URL: https://www.youtube.com/watch?v=YJjv_OeiHmo [accessed 2023-11-21]
32. Grant N, Hill K. Google’s photo app still can’t find gorillas. And neither can Apple’s. The New York Times. 2023 May 22. URL: https://www.nytimes.com/2023/05/22/technology/ai-photo-labels-google-apple.html [accessed 2023-11-21]
33. Noble SU. Algorithms of Oppression: How Search Engines Reinforce Racism. New York, NY: New York University Press; 2018.
34. Eubanks V. Automating Inequality: How High-Tech Tools Profile, Police, and Punish the Poor. New York, NY: St. Martin's Publishing Group; 2018.
35. Duster T. Medicine. Race and reification in science. Science 2005 Feb 18;307(5712):1050-1051. [doi: 10.1126/science.1110303] [Medline: 15718453]
36. Duster T. A post-genomic surprise. The molecular reinscription of race in science, law and medicine. Br J Sociol 2015 Mar 18;66(1):1-27. [doi: 10.1111/1468-4446.12118] [Medline: 25789799]
37. Epstein S. Inclusion The Politics of Difference in Medical Research: (Chicago Studies in Practices of Meaning). Chicago, IL: The University of Chicago Press; 2010.
38. Caulfield T, Fullerton SM, Ali-Khan SE, Arbour L, Burchard EG, Cooper RS, et al. Race and ancestry in biomedical research: exploring the challenges. Genome Med 2009 Jan 21;1(1):8 [FREE Full text] [doi: 10.1186/gm8] [Medline: 19348695]
39. Reardon J. The Postgenomic Condition: Ethics, Justice, & Knowledge after the Genome. Chicago, IL: The University of Chicago Press; 2017.
40. Collins FS. What we do and don't know about 'race', 'ethnicity', genetics and health at the dawn of the genome era. Nat Genet 2004 Nov 26;36(11 Suppl):S13-S15. [doi: 10.1038/ng1436] [Medline: 15507997]
41. Kowal E, Llamas B. Race in a genome: long read sequencing, ethnicity-specific reference genomes and the shifting horizon of race. J Anthropol Sci 2019 Dec 31;96:91-106 [FREE Full text] [doi: 10.4436/JASS.97004] [Medline: 31589588]
42. Osborne NG, Feit MD. The use of race in medical research. JAMA 1992 Jan 08;267(2):275-279. [doi: 10.1001/jama.1992.03480020085037]
43. Kenney M, Mamo L. The imaginary of precision public health. Med Humanit 2020 Sep 16;46(3):192-203. [doi: 10.1136/medhum-2018-011597] [Medline: 31420373]
44. Lee S. Waiting on the promise of prescribing precision: race in the era of pharmacogenomics. In: Wailoo K, Nelson A, Lee C, editors. Genetics and the Unsettled Past: The Collision of DNA, Race, and History. Ithaca, NY: Rutgers University Press; 2012.

XSL•FO
RenderX

45. Adamson AS, Smith A. Machine learning and health care disparities in dermatology. JAMA Dermatol 2018 Nov 01;154(11):1247-1248. [doi: 10.1001/jamadermatol.2018.2348] [Medline: 30073260]
46. Remeseiro B, Bolon-Canedo V. A review of feature selection methods in medical applications. Comput Biol Med 2019 Sep;112:103375. [doi: 10.1016/j.compbiomed.2019.103375] [Medline: 31382212]
47. Singh A, Sengupta S, Lakshminarayanan V. Explainable deep learning models in medical image analysis. J Imaging 2020 Jun 20;6(6):52 [FREE Full text] [doi: 10.3390/jimaging6060052] [Medline: 34460598]
48. Strobl E, Lasko T. Identifying patient-specific root causes of disease. In: Proceedings of the 13th ACM International Conference on Bioinformatics, Computational Biology and Health Informatics. 2022 Presented at: BCB '22; August 7-10, 2022; Northbrook, IL URL: https://doi.org/10.1145/3535508.3545553 [doi: 10.1145/3535508.3545553]
49. Charmaz K. Constructing Grounded Theory. Thousand Oaks, CA: Sage Publications; 2006.
50. Ross Wightman. GitHub. URL: https://github.com/rwightman [accessed 2024-11-01]
51. Adebayo J, Gilmer J, Muelly M, Goodfellow I, Hardt M, Kim B. Sanity checks for saliency maps. arXiv. Preprint posted online on October 8, 2018 2024 [FREE Full text]
52. Müller R, Kenney M. Agential conversations: interviewing postdoctoral life scientists and the politics of mundane research practices. Sci Culture 2014 May 29;23(4):537-559. [doi: 10.1080/09505431.2014.916670]
53. Amberscript homepage. Amberscript. URL: https://www.amberscript.com/en/ [accessed 2022-02-17]
54. Pacheco AG, Krohling RA. The impact of patient clinical information on automated skin cancer detection. Comput Biol Med 2020 Jan;116:103545 [FREE Full text] [doi: 10.1016/j.compbiomed.2019.103545] [Medline: 31760271]
55. Lasisi T. The constraints of racialization: how classification and valuation hinder scientific research on human variation. Am J Phys Anthropol 2021 Jun;175(2):376-386 [FREE Full text] [doi: 10.1002/ajpa.24264] [Medline: 33675042]
56. Goon P, Banfield C, Bello O, Levell NJ. Skin cancers in skin types IV-VI: does the Fitzpatrick scale give a false sense of security? Skin Health Dis 2021 Sep 08;1(3):e40 [FREE Full text] [doi: 10.1002/ski2.40] [Medline: 35663142]
57. Denton E, Hanna A, Amironesei R, Smart A, Nicole H. On the genealogy of machine learning datasets: a critical history of ImageNet. Big Data Soc 2021 Sep 24;8(2). [doi: 10.1177/20539517211035955]
58. labcin-ufes / PAD-UFES-20. GitHub. URL: https://github.com/labcin-ufes/PAD-UFES-20 [accessed 2025-01-12]

Abbreviations

AI: artificial intelligence
COREQ: Consolidated Criteria for Reporting Qualitative Research
PAD-UFES: Dermatological and Surgical Assistance Program at the Federal University of Espírito Santo
ROC: receiver operating characteristic
SCC: squamous cell carcinoma
SEK: seborrheic keratosis

Edited by C Lovis; submitted 12.04.24; peer-reviewed by GK Gupta, R Kaczmarczyk; comments to author 26.09.24; revised version received 14.11.24; accepted 17.11.24; published 28.01.25.

Please cite as:
Willem T, Wollek A, Cheslerean-Boghiu T, Kenney M, Buyx A
The Social Construction of Categorical Data: Mixed Methods Approach to Assessing Data Features in Publicly Available Datasets
JMIR Med Inform 2025;13:e59452
URL: https://medinform.jmir.org/2025/1/e59452
doi:10.2196/59452
PMID:

©Theresa Willem, Alessandro Wollek, Theodor Cheslerean-Boghiu, Martha Kenney, Alena Buyx. Originally published in JMIR Medical Informatics (https://medinform.jmir.org), 28.01.2025. This is an open-access article distributed under the terms of the Creative Commons Attribution License (https://creativecommons.org/licenses/by/4.0/), which permits unrestricted use, distribution, and reproduction in any medium, provided the original work, first published in JMIR Medical Informatics, is properly cited. The complete bibliographic information, a link to the original publication on https://medinform.jmir.org/, as well as this copyright and license information must be included.

XSL•FO
RenderX

Original Paper

Machine Learning–Based Risk Factor Analysis and Prediction Model Construction for the Occurrence of Chronic Heart Failure: Health Ecologic Study

Qian Xu[1], BSN; Xue Cai[2], PhD; Ruicong Yu[1], BSN; Yueyue Zheng[3], BSN; Guanjie Chen[4], MSN; Hui Sun[1], BSN; Tianyun Gao[1], BSN; Cuirong Xu[5], MSN; Jing Sun[6], Prof Dr

[1]School of Medicine, Southeast University, Nanjing, China

[2]Department of Respiratory and Critical Care, Zhongda Hospital Southeast University, Nanjing, China

[3]Department of Geriatrics, Zhongda Hospital Southeast University, Nanjing, China

[4]Department of Intensive Care, Zhongda Hospital Southeast University, Nanjing, China

[5]Department of Nursing, Zhongda Hospital Southeast University, Nanjing, China

[6]Rural Health Research Institute, Charles Sturt University, Orange, Australia

Corresponding Author:
Cuirong Xu, MSN
Department of Nursing
Zhongda Hospital Southeast University
No.87 Dingjiaqiao
Nanjing, 210009
China
Phone: 86 13912990156
Fax: 86 02583272077
Email: xucuirong67@126.com

Abstract

Background: Chronic heart failure (CHF) is a serious threat to human health, with high morbidity and mortality rates, imposing a heavy burden on the health care system and society. With the abundance of medical data and the rapid development of machine learning (ML) technologies, new opportunities are provided for in-depth investigation of the mechanisms of CHF and the construction of predictive models. The introduction of health ecology research methodology enables a comprehensive dissection of CHF risk factors from a wider range of environmental, social, and individual factors. This not only helps to identify high-risk groups at an early stage but also provides a scientific basis for the development of precise prevention and intervention strategies.

Objective: This study aims to use ML to construct a predictive model of the risk of occurrence of CHF and analyze the risk of CHF from a health ecology perspective.

Methods: This study sourced data from the Jackson Heart Study database. Stringent data preprocessing procedures were implemented, which included meticulous management of missing values and the standardization of data. Principal component analysis and random forest (RF) were used as feature selection techniques. Subsequently, several ML models, namely decision tree, RF, extreme gradient boosting, adaptive boosting (AdaBoost), support vector machine, naive Bayes model, multilayer perceptron, and bootstrap forest, were constructed, and their performance was evaluated. The effectiveness of the models was validated through internal validation using a 10-fold cross-validation approach on the training and validation sets. In addition, the performance metrics of each model, including accuracy, precision, sensitivity, F_1-score, and area under the curve (AUC), were compared. After selecting the best model, we used hyperparameter optimization to construct a better model.

Results: RF-selected features (21 in total) had an average root mean square error of 0.30, outperforming principal component analysis. Synthetic Minority Oversampling Technique and Edited Nearest Neighbors showed better accuracy in data balancing. The AdaBoost model was most effective with an AUC of 0.86, accuracy of 75.30%, precision of 0.86, sensitivity of 0.69, and F_1-score of 0.76. Validation on the training and validation sets through 10-fold cross-validation gave an AUC of 0.97, an accuracy of 91.27%, a precision of 0.94, a sensitivity of 0.92, and an F_1-score of 0.94. After random search processing, the accuracy and AUC of AdaBoost improved. Its accuracy was 77.68% and its AUC was 0.86.

XSL•FO
RenderX

Conclusions: This study offered insights into CHF risk prediction. Future research should focus on prospective studies, diverse data, advanced techniques, longitudinal studies, and exploring factor interactions for better CHF prevention and management.

(JMIR Med Inform 2025;13:e64972) doi:10.2196/64972

KEYWORDS

machine learning, chronic heart failure, risk of occurrence; prediction model, health ecology

Introduction

Heart failure is a complex clinical syndrome where the ventricular filling or ejection capacity is compromised due to any structural or functional abnormality of the heart [1]. Chronic heart failure (CHF) is a severe manifestation or advanced stage of various cardiovascular diseases. It features high mortality and rehospitalization rates, thus constituting the ultimate battlefield for cardiovascular disease prevention and control [2]. According to the World Health Organization, the global prevalence of heart failure in adults is 1% to 2%, with 25,000-30,000 new cases expected each year [3]. The multiple physical and psychological symptoms endured by patients with CHF not only intensify the burden of the patients and caregivers but also diminish their quality of life [4,5]. Therefore, it has become an inevitable trend to identify risk factors for those who have not developed CHF and patients with CHF, to prevent the occurrence of CHF in a timely manner, and to strengthen the health management of patients with CHF.

Preventive management in current guidelines and practice is mostly based on comprehensive cardiovascular interventions [6]. However, within the framework of the goals of "health for all" and "personalized medicine," early and precise risk stratification takes precedence in cardiovascular prevention and control [7]. Risk factors for heart failure are the primary concern in suspected diagnoses, and the control of risk factors is the top priority in the primary prevention of patients with heart failure. Diagnosis, treatment, and management are based on this. Risk assessment, as the initiating link of precise health management of CHF, particularly needs to recognize the significance of risk factor identification in the face of the disease characteristics of CHF, such as complex etiology, severe condition, rapid progression, and poor prognosis. With the in-depth research of precision medicine and the change in residents' living behaviors, the update of important risk factors and cardiovascular markers is a crucial element in the development of risk assessment programs and the improvement of assessment tools.

The accuracy and comprehensiveness of identifying the risk factors of CHF, as well as the advancement and scientific nature of the modeling techniques, are the keys to guaranteeing the smooth implementation of risk assessment. As for the risk factors, they mainly include personal factors (such as gender, age, weight, etc) [8] and disease-related factors (such as ejection fraction, biomarkers, myocardial imaging, cardiac ultrasound parameters, etc). For instance, Salvioni et al [9] developed a method for integrating Metabolic Exercise Test data combined with Cardiac and Kidney Indexes (MECKI) scores from 2715 patients. It was demonstrated that the MECKI score is a highly efficient tool for facilitating risk stratification and therapeutic decision-making for patients with heart failure. Klimczak-Tomaniak et al [10] conducted repeated measurements of 92 biomarkers that optimally predict adverse clinical events in heart failure and can be used for dynamic risk assessment in clinical practice. However, these risk factor identifications focus only on individual and disease treatment–related factors, ignoring broader social factors that affect health. In terms of modeling techniques, traditional modeling methods such as Cox and logistic regressions cannot well deal with the complex relationships that may exist between variables, and researchers have begun to introduce digital technology into model construction to obtain a large amount of data information in the database after multidimensional interactions. Angraal et al [11] used a random forest (RF) model to predict mortality and hospitalization rates for heart failure in outpatients with preserved ejection fraction. Wang et al [12] used a machine learning model to accurately predict the risk of heart failure in older patients with prediabetes or diabetes using data from the National Health and Nutrition Examination Survey. Although risk assessment models based on big data and artificial intelligence exist, the mainstay of current risk assessment approaches remains the risk factor itself. Moreover, most of the models are predicated on the patient's medical record information from the initial diagnosis and hospitalization, intended for medical and nursing professional evaluations, as well as checks of objective data such as those from laboratories, and a dynamic prediction model that changes with the condition has not been established.

In summary, in the face of the incomplete coverage of clinical risk factors of CHF and the low accuracy of risk prediction modeling, constructing an accurate and convenient heart failure risk prediction model is an important pathway and tool for the identification of accurate risk factors, and fully using the big data resources for the refinement of risk factors and completing the digital modeling is an important guarantee for the effectiveness of the final risk assessment.

Methods

Data Source

This study applied to the Jackson Heart Study (JHS) database through the National Heart Lung and Blood Institute. The database contains data on 3883 individuals. The participants were African American adults aged 35-84 years. Data were collected at baseline (V1: 2000-2004), first follow-up (V2: 2005-2008), and second follow-up (V3: 2009-2013). There were 489 patients with CHF at baseline and 3394 without CHF. The first follow-up V2 (2005-2008) lost 777 cases, leaving 3106 cases; the second follow-up V3 (2009-2013) lost 462 cases, leaving 2644 cases.

XSL•FO
RenderX

Study Population

Patients who did not have heart failure at baseline (V1) of the JHS database were selected for this study (Textbox 1).

Textbox 1. Inclusion and exclusion criteria.

Inclusion criteria

- Those who did not have chronic heart failure at baseline
- Those who participated in the first and second follow-up visits, or those who had electronic medical records

Exclusion criteria

- Patients who met the Framingham heart failure diagnostic criteria [13]

Study Variables

The inclusion of study variables was carried out at 5 levels of health ecology. A total of 53 variables were finally included. Among them, the individual trait level, including general information, biological indicators, disease history, family history, and symptoms, had a total of 28 variables; the individual behavioral trait level, including diet, exercise, sleep, and psychology, had a total of 12 variables; the interpersonal relationship level, including family relationship, social relationship, neighborhood relationship, had a total of 4 variables; the work and life level, including working conditions, living conditions, access to health care, had a total of 8 variables; and the macropolicy level had only 1 variable, being health insurance policy. All the variables can be seen in Table S1 in Multimedia Appendix 1.

Statistical Analyses

The study encompassed several crucial steps. In the data preprocessing stage, 2 primary operations were undertaken. First, for data proofreading, a check was made to determine if there were any missing values within the data. In the case of categorized data, values were assigned if necessary. Second, with regard to missing value processing, data with missing values exceeding 30% were directly eliminated. Concurrently, for data with missing values less than 30%, Monte Carlo multiple interpolation was used for interpolation.

Proceeding to the data analysis phase, SPSS 22.0 (IBM Corp) was used for data statistical analysis. For measurement data, if they adhered to a normal distribution, a *t* test (2-tailed) was used for comparison between groups. The *t* test (2-tailed) was a statistical test designed to determine if there was a significant difference between the means of the two groups. In the event that the measurement data did not follow a normal distribution, they were represented as median (IQR). Count data were described by frequency and percentage. Regarding the measured information in the influencing factors, if it satisfied the normal distribution, the independent samples *t* test (2-tailed) was used for testing. The independent samples *t* test (2-tailed) was a method for comparing the means of two independent groups. If the measured information in the influencing factors did not conform to the normal distribution, the Mann-Whitney *U* rank sum test was used. The Mann-Whitney *U* rank sum test was a nonparametric test used for comparing two independent groups. This study consisted entirely of count data, frequency and percentage were used for statistical description, and the chi-square test was used for statistical analysis. The chi-square test was a statistical test designed to determine if there was a significant association between two categorical variables.

Next, in the delineation of the dataset step, this study used randomized splitting to divide the dataset into a training set (70%), a test set (15%), and a validation set (15%).

In the feature selection process, before feature selection, the data were standardized. Then, after the completion of the standardization process, feature selection was carried out. Pycharm (JetBrains Corp) was used. Principal component analysis (PCA) and RF were two methods used to screen the variables, respectively. PCA was a statistical procedure that used an orthogonal transformation to convert a set of correlated variables into a set of uncorrelated variables known as principal components [14]. RF was an ensemble learning method for classification, regression, and other tasks that operated by constructing a multitude of decision trees during training and outputting the class that was the mode of the classes of the individual trees [15]. The two feature selection methods were compared, the importance of the features was ranked, and the visualization of feature importance was also performed.

In the imbalance data handling stage, this study used 5 methods for processing unbalanced datasets. These methods included oversampling, undersampling, Adaptive Synthetics Sampling, Synthetic Minority Over-sampling Technique (SMOTE), and Synthetic Minority Over-sampling Technique and Edited Nearest Neighbors (SMOTE-ENN). Models constructed using the original dataset were compared with models constructed from datasets that had been processed by these 5 methods.

Finally, in the model construction stage, 7 models were constructed in this study. They were decision tree, RF, support vector machine, extreme gradient boosting, adaptive boosting (AdaBoost), naive Bayes model, multilayer perceptron, and bootstrap forest. The decision tree was a flowchart-like structure where each internal node represented a test on an attribute, each branch represented the outcome of a test, and each leaf node represented a class or a value [16]. The RF was an ensemble learning method as previously mentioned [17]. The support vector machine was a supervised learning algorithm that analyzed data for classification and regression analysis [18]. Extreme gradient boosting was an efficient implementation of gradient boosting for large datasets [19]. AdaBoost was an iterative algorithm that combined multiple weak classifiers to form a strong classifier [20]. The naive Bayes model was a probabilistic classifier based on applying Bayes' theorem with

XSL•FO
RenderX

strong independence assumptions between the features [16]. The multilayer perceptron was a type of artificial neural network with multiple layers of neurons [21]. The bootstrap forest was an ensemble method that combined multiple bootstrap samples to build a forest of trees. The accuracy, precision, sensitivity, F_1-score, and area under the curve (AUC) of each model were compared, and receiver operating characteristic (ROC) curves of each model were drawn. After selecting the optimal model, a 10-fold cross-validation was performed using the training and validation set. In order to construct a better model, we used hyperparameter optimization to find the best combination of parameters that makes the model perform best on the training set and achieve better results on the test set.

Ethical Considerations

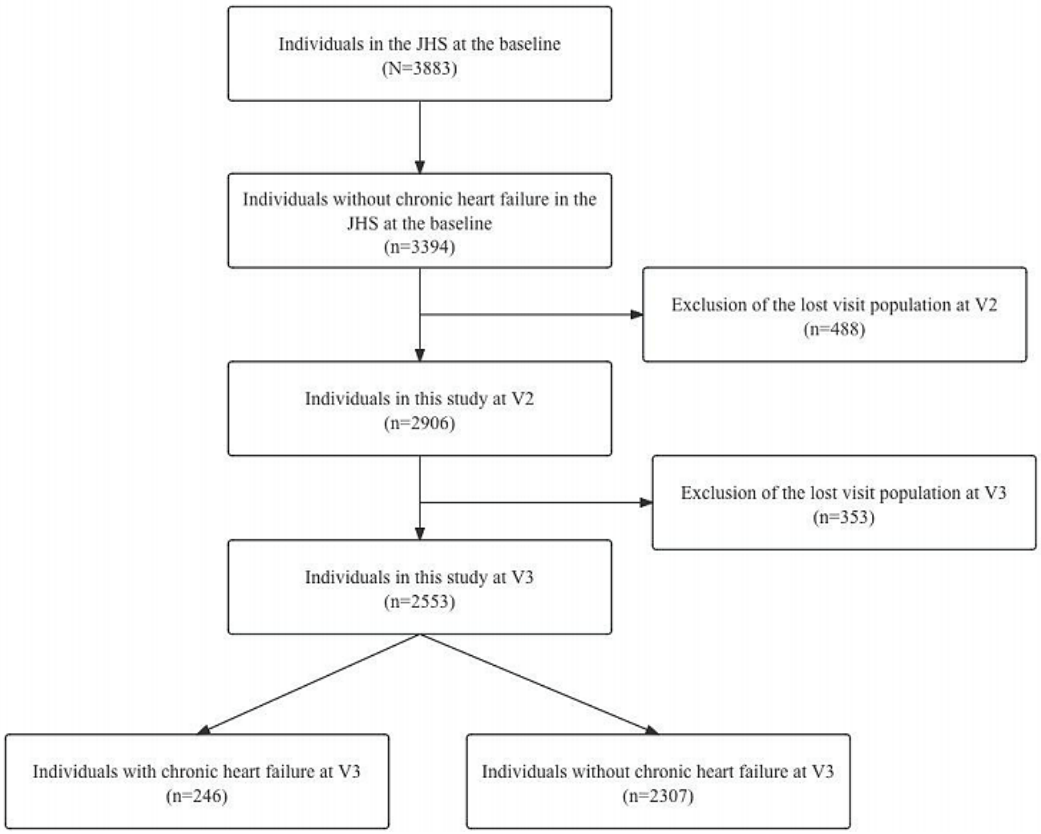
The study was approved by the Ethics Committee of Zhongda Hospital, Southeast University (2022ZDSYLL401-Y01).

Results

Patient Characteristics

Among the 3883 individuals in the JHS, 489 had CHF at baseline and 3394 did not have CHF. Excluding patients who were lost to visit and did not have any electronic medical records, 2553 people did not have CHF at baseline. The mean age of this population was 57.84 (13.45) years, with 1590 female participants (62.2% of the population) and 963 male participants (37.7% of the population). The screening process is shown in Figure 1. The dataset (n=2553) was randomly divided into three parts: 70% (n=1787) of the data for model training, 15% (n=383) for model test and 15% (n=383) for model validation. The amount of missing data for the predictors left ventricular diastolic diameter, left ventricular systolic diameter, left ventricular mass, depression, vitamin D_2, vitamin D_3 derivatives, shortness of breath, walking 100 m with wheezing, and loneliness was greater than 30%, so these predictors were not included in the analysis.

Figure 1. Study flowchart. CHF: chronic heart failure; JHS: Jackson Heart Study; V2: first follow-up; V3: second follow-up.



Univariate Analysis of Variables Influencing the Occurrence of CHF

Alcohol, smoking, health insurance, income, occupation, education, minutes of walking or running, nocturnal sleep dyspnea, ever had swelling of feet or ankles, chest ever sound wheezy without cold, left ventricular regional wall motion, cardiac disease, age, BMI, systolic blood pressure, glycosylated hemoglobin, triglycerides, ultrasensitive C-reactive protein, glomerular filtration rate, heart rate, stress, regional poverty population ratio, the status of favorite food stores within 3 km, status of sports facilities within 3 km, and the ratio of early maximal ventricular filling velocity to atrial maximal ventricular filling velocity were statistically significantly different in the population without heart failure (P<.05). A one-way analysis of the baseline characteristics of the included patients is shown in Tables 1-3.

XSL•FO
RenderX

Table 1. One-way analysis of the baseline characteristics (part 1).

Variables	People without heart failure (n=2307), n (%)	People with heart failure (n=264), n (%)	Chi-square (*df*)	*P*
Gender			0.3 (1)	.56
Woman	1441 (56.4)	149 (5.84)		
Man	866 (33.92)	97 (3.8)		
Alcohol			26.2 (1)	<.001
Yes	1114 (43.63)	76 (2.98)		
No	1183 (46.34)	167 (6.54)		
Smoking			11.1 (1)	<.001
Yes	680 (2.66)	98 (3.84)		
No	1621 (63.49)	148 (5.8)		
Health insurance			9.5 (1)	.002
Yes	1972 (77.24)	192 (7.52)		
No	335 (13.12)	54 (2.12)		
Threats or harassment			12.1 (6)	.06
Several times a day	15 (0.59)	3 (0.12)		
Almost every day	15 (0.59)	3 (0.12)		
At least once a week	45 (1.76)	3 (0.12)		
A few times a month	42 (1.65)	4 (0.16)		
A few times a year	102 (4)	3 (0.12)		
Less than a few times a year	351 (13.75)	27 (1.06)		
Never	1704 (66.75)	196 (7.68)		
Income			47.5 (3)	<.001
Poor	198 (7.76)	42 (1.65)		
Lower-middle	431 (16.88)	71 (2.78)		
Upper-middle	632 (24.76)	56 (2.19)		
Affluent	707 (27.69)	39 (1.53)		
Occupation			31.6 (10)	<.001
Management or Professional	903 (35.37)	71 (2.78)		
Service	515 (20.17)	81 (3.17)		
Sales	441 (17.27)	30 (1.18)		
Farming	2 (0.08)	0 (0)		
Construction	119 (4.66)	19 (0.74)		
Production	311 (12.18)	44 (1.72)		
Military	3 (0.12)	0 (0)		
Sick	2 (0.08)	0 (0)		
Unemployed	2 (0.08)	1 (0.04)		
Retired	3 (0.12)	0 (0)		
Student	2 (0.08)	0 (0)		
Education			100.5 (2)	<.001
Less than high school	300 (11.75)	91 (3.56)		
High-school graduate or General Educational Development	459 (17.98)	45 (1.76)		
Attended vocational school, trade school, or college	1543 (60.43)	110 (4.31)		

XSL•FO
RenderX

Table 2. One-way analysis of the baseline characteristics (part 2).

Variables	People without heart failure (n=2307), n (%)	People with heart failure (n=264), n (%)	Chi-square (*df*)	*P*
Stress living in neighborhood			2.1 (3)	.56
Not stressful	1708 (6.66)	188 (7.36)		
Mildly stressful	348 (13.63)	31 (1.21)		
Moderately stressful	148 (5.80)	12 (0.59)		
Very stressful	91 (3.56)	11 (4.31)		
Minutes of walking or running			10.1 (4)	.04
Less than 5 minutes	1069 (41.87)	133 (5.21)		
At least 5 but less than 15 minutes	405 (15.87)	44 (1.72)		
At least 15 but less than 30 minutes	331 (12.97)	22 (0.86)		
At least 30 but less than 45 minutes	200 (7.83)	24 (0.94)		
At least 45 minutes	298 (11.67)	23 (0.90)		
Place they usually go to for health care			11.4 (8)	.18
Walk-in clinic	180 (7.05)	11 (0.43)		
Health Maintenance Organization clinic	16 (0.63)	0 (0)		
Hospital clinic	242 (9.48)	30 (1.18)		
Neighborhood health center	115 (4.5)	18 (0.71)		
Hospital emergency room	66 (2.59)	10 (0.39)		
Public health department clinic	23 (0.9)	2 (0.08)		
Company or industry clinic	63 (2.47)	4 (0.16)		
Doctor’s office	1334 (52.25)	155 (6.07)		
Other	12 (0.47)	0 (0)		
Difficulty in obtaining health service			6.2 (3)	.10
Very hard	85 (3.33)	13 (0.51)		
Fairly hard	114 (4.47)	20 (0.78)		
Not too hard	395 (15.47)	42 (1.65)		
Not hard at all	1694 (66.35)	171 (6.7)		
Satisfied with doctor			1.7 (4)	.79
Very satisfied	1524 (59.69)	173 (6.78)		
Somewhat satisfied	595 (23.31)	60 (2.35)		
Somewhat dissatisfied	56 (2.19)	5 (0.2)		
Very dissatisfied	21 (0.82)	2 (0.08)		
Not sure	38 (1.49)	3 (0.12)		
Ever awakened by trouble breathing			102.4 (1)	<.001
Yes	78 (3.06)	44 (1.72)		
No	2204 (86.33)	200 (7.83)		
Rate your sleep quality overall			7.5 (4)	.68
Excellent	232 (9.09)	23 (0.9)		
Fair	514 (20.13)	52 (2.04)		
Good	796 (31.18)	77 (3.02)		
Poor	190 (7.44)	31 (1.21)		
Very good	562 (22.01)	52 (2.04)		

XSL•FO
RenderX

Variables	People without heart failure (n=2307), n (%)	People with heart failure (n=264), n (%)	Chi-square (*df*)	*P*
Ever had swelling of feet or ankles			27.1 (1)	<.001
Yes	956 (37.45)	144 (5.64)		
No	1328 (52.02)	99 (3.88)		
Chest ever sound wheezy without cold			21.8 (1)	<.001
Yes	156 (6.11)	37 (1.45)		
No	2131 (83.47)	207 (8.11)		
Marriage			37.5 (4)	<.001
Divorced	342 (13.4)	31 (1.21)		
Married	1356 (53.11)	118 (4.62)		
Unmarried	258 (10.11)	26 (1.02)		
Separate	92 (3.6)	11 (0.43)		
Widowed	249 (9.75)	59 (2.31)		
LV[a] regional wall motion			29.7 (3)	<.001
Abnormal	7 (2.74)	4 (0.16)		
Border	7 (2.74)	6 (0.24)		
Normal	2179 (85.35)	222 (8.7)		
Can’t assess	13 (0.51)	1 (0.04)		
Cardiac disease			66.6 (1)	<.001
Yes	168 (6.58)	56 (2.19)		
No	2139 (83.78)	190 (7.44)		
Family history of cardiovascular disease, n (%)			0.0 (1)	.87
Yes	748 (29.30)	81 (3.17)		
No	1559 (61.07)	165 (6.46)		

[a]LV: left ventricle.

XSL•FO
RenderX

Table 3. One-way analysis of the baseline characteristics (part 3).

Variables	People without heart failure, median (IQR)	People with heart failure, median (IQR)	Mann-Whitney *U* test	*P*
Age (years)	54 (45-63)	67 (58.75-73)	–11.9	
BMI (kg/m^2)	30.29 (26.74-35)	31.58 (28.06-42.61)	–3.59	<.001
Systolic blood pressure (mm Hg)	123.83 (114.66-134.83)	132.08 (122.91-145.38)	–7.83	<.001
Glycosylated hemoglobin (%)	5.6 (5.3-6.1)	6 (5.5-7.3)	–7.39	<.001
Low-density lipoprotein (mg/dL)	126 (102-149)	120.5 (99.75-147.25)[c]	–1.16	.25
High-density lipoprotein (mg/dL)	50 (42-60)	49 (40-58)[c]	–1.66	.10
Fasting triglycerides (mg/dL)	87 (63-124)	98 (74-141)[c]	–4.35	<.001
Fasting total cholesterol (mg/dL)	197 (173-223)	193 (170-220)[c]	–0.97	.33
Ultrasensitive C-Reactive protein (mg/dL)	0.25 (0.1-0.54)	0.31 (0.14-0.65)	–2.73	.01
Glomerular filtration rate (mL/min)	87.09 (76.97-97.78)	80.16 (64.43-91.9)	–6.65	<.001
Ejection fraction (%)	65 (55-65)	65 (55-65)	–1.18	.24
Heart rate (beats/min)	63 (56-70)	66 (57-73)	–3.37	<.001
Vitamin D_3 (ng/mL)	12.2 (8.7-16.9)	11.7 (8.75-15.45)	–1.29	.20
Dark-colored green vegetables (ng/mL)	0.26 (0.15-0.42)	0.24 (0.15-0.39)	–1.14	.25
Stress	4 (2-8)	4 (1-7)	–2.69	.01
Egg (ng/mL)	0.32 (0.91-0.66)	0.32 (0.84-0.8)	–0.07	.94
Fish (ng/mL)	0.86 (0-0.17)	0.86 (0-0.2)	–1.53	.13
Proportion of the population living in poverty in the area (%)	0.22 (0.1-0.32)	0.31 (0.21-0.36)	–5.24	<.001
Status of favorite food stores within 3 km	0.24 (0.06-0.44)	0.34 (0.16-0.49)	–4.43	<.001
Status of sports facilities within 3 km	0.37 (0.18-0.63)	0.4 (0.23-0.71)	–2.24	.03
Peak early diastolic velocity of mitral annulus (cm/s)	0.83 (0.71-0.96)	0.8 (0.67-0.97)	–1.10	.27
Ratio of early maximal ventricular filling velocity to atrial maximal ventricular filling velocity	1.06 (0.87-1.27)	0.92 (0.76-1.35)	–6.37	<.001
Hours of actual sleep at night	6 (6-7)	6 (5-8)	–1.04	.30

Machine Learning Analysis of the Occurrence of CHF

Feature Selection

This study made use of PCA and the RF method for feature selection. The model was trained using root mean square error (RMSE) as a criterion. The principle is that each step includes an additional feature with the highest variance as a basis for classification [22]. The number of selected features was used as the horizontal axis and the predicted RMSE score for each fitted model was used as the vertical axis.

PCA offers the advantage of transforming a set of correlated variables into a set of uncorrelated principal components, thereby reducing dimensionality and enhancing interpretability. After feature selection by PCA, a total of 15 features were incorporated. The initial eigenvalues, percentage of variance, and accumulation of these features are presented in Table 4. RMSE results are presented in Figure 2.

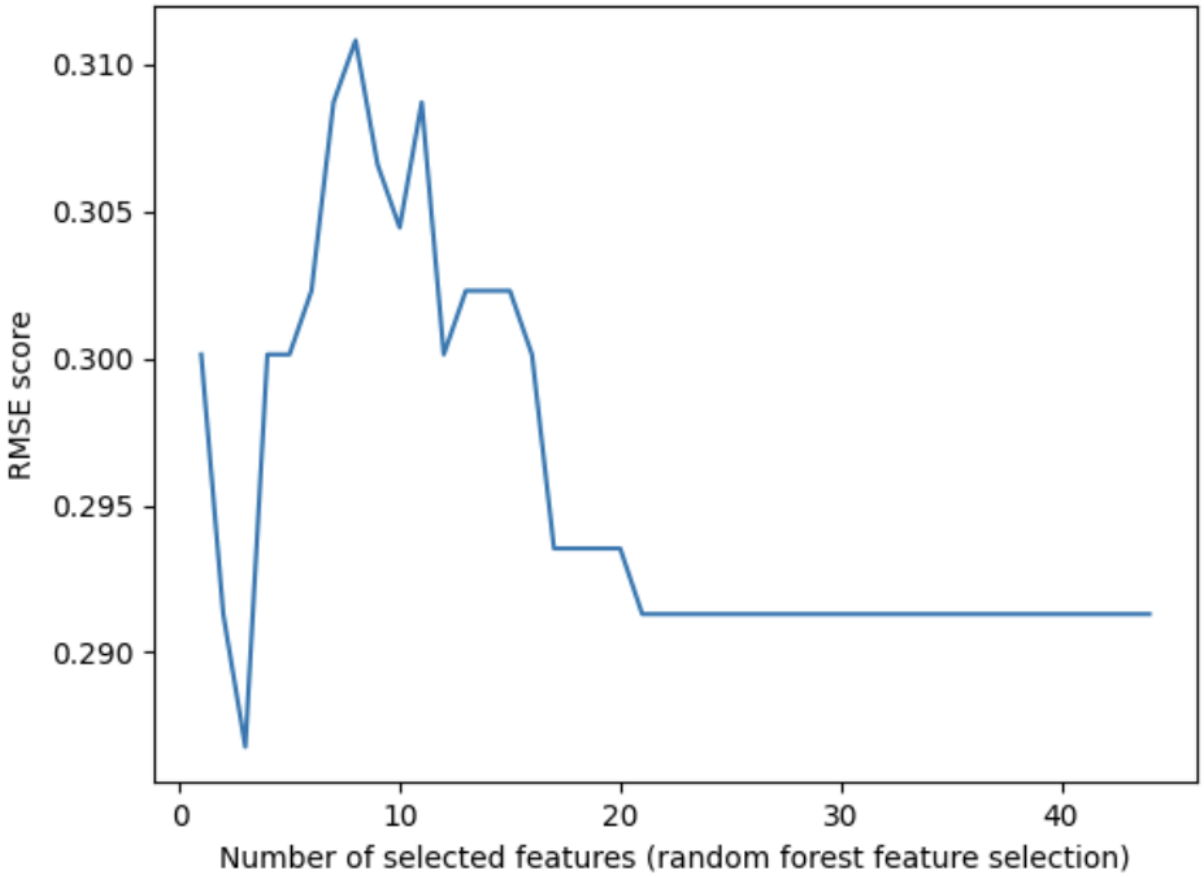
XSL•FO
RenderX

Table 4. The result of these features selected by principal component analysis.

Feature	Initial eigenvalue	Percentage of variance (%)	Accumulation (%)
Age (years)	3.27	7.42	7.42
Gender	2.47	5.61	13.03
Fasting total cholesterol (mg/dL)	2.21	5.02	18.04
High-density lipoprotein (mg/dL)	1.95	4.44	22.48
Status of favorite food stores within 3 km	1.78	4.03	26.52
Income	1.72	3.90	30.41
Peak early diastolic velocity of mitral annulus	1.48	3.36	33.77
LV[a] regional wall motion	1.36	3.09	36.86
Smoke	1.26	2.85	39.71
Dark-colored green vegetables	1.22	2.78	42.49
Minutes of walking or running	1.17	2.67	45.16
Cardiac disease	1.11	2.52	47.68
Threats or harassment	1.08	2.45	50.13
Rate your sleep quality overall	1.05	2.4	52.54
Systolic blood pressure (mm Hg)	1.03	74	54.88

[a]LV: left ventricle.

Figure 2. Root mean square error (RMSE) results of the principal component analysis.



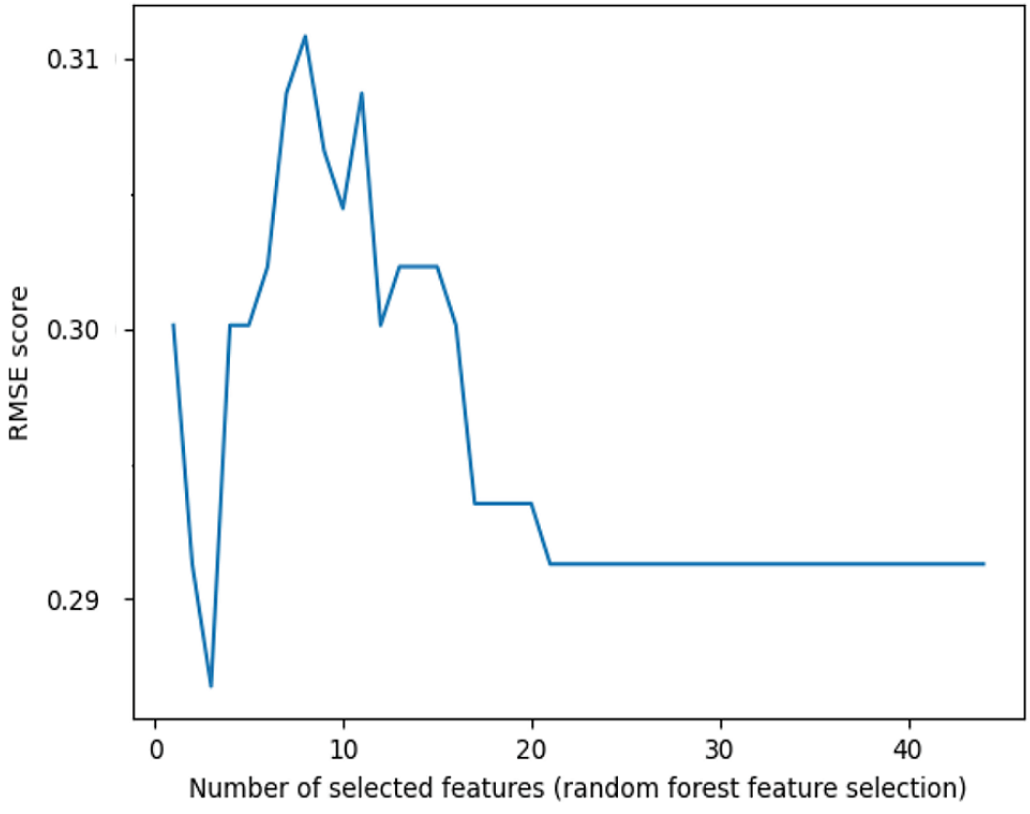
On the other hand, the RF method is known for its robustness and ability to handle high-dimensional data. After feature selection by RF, a total of 21 features were included. The importance of these features is shown in Table 5. RMSE results are presented in Figure 3.

XSL•FO
RenderX

Table 5. Characteristic importance of feathers selected by random forest.

Feature	Characteristic importance
Age	0.07
Glomerular filtration rate	0.07
Glycosylated hemoglobin	0.06
Systolic blood pressure	0.05
BMI	0.04
Ratio of early maximal ventricular filling velocity to atrial maximal ventricular filling velocity	0.04
Eggs	0.04
Dark-colored green vegetables	0.04
Heart rate	0.03
Peak early diastolic velocity of mitral annulus	0.03
Fasting total cholesterol	0.03
Vitamin D_3	0.03
Proportion of the population living in poverty in the area	0.03
Ultrasensitive C-reactive protein	0.03
Status of sports facilities within 3 km	0.03
Low-density lipoprotein	0.03
Ever awakened by trouble breathing	0.03
Status of favorite food stores within 3 km	0.03
Fasting triglycerides	0.03
High-density lipoprotein	0.03
Ejection fraction	0.03

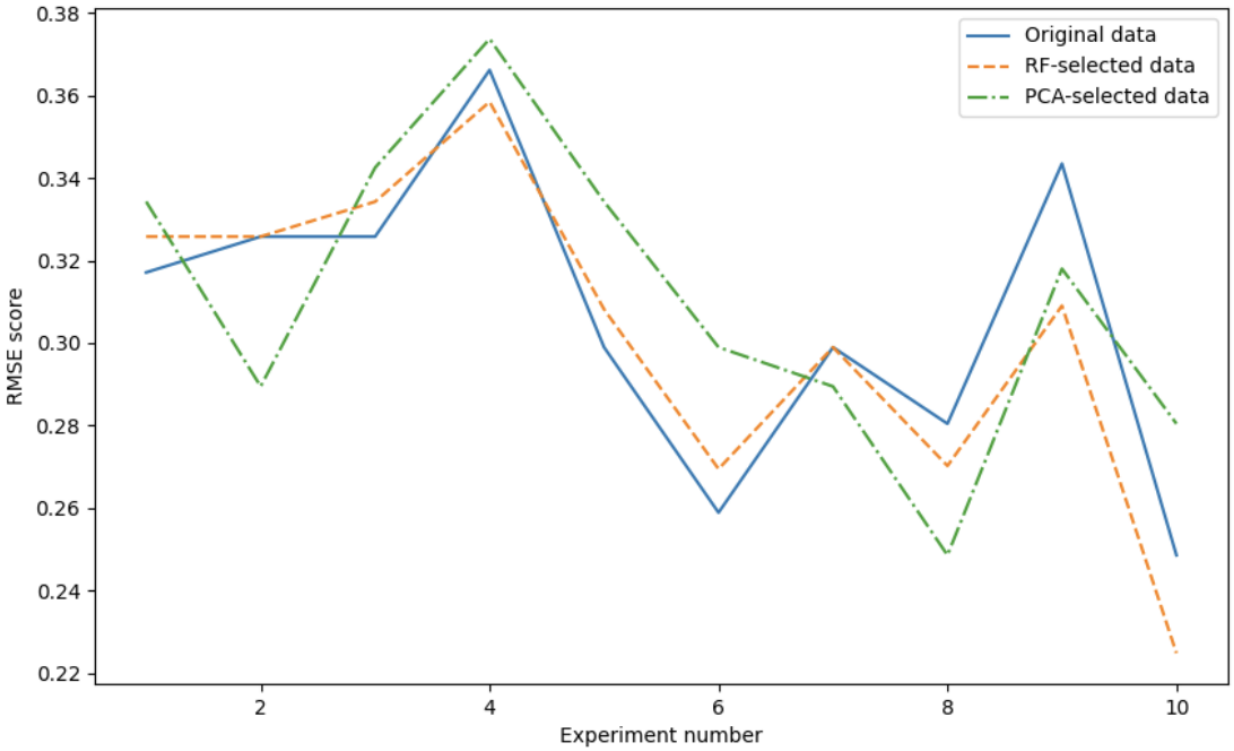
Figure 3. Root mean square error (RMSE) results of the random forest method.



XSL•FO
RenderX

To compare the feature selection methods, this study used 10-fold cross-validation. After calculating the mean RMSE and plotting the image as shown in Figure 4, the results demonstrated that the outcomes after feature selection by RF outperformed those after feature selection by PCA. The average RMSE mean of RF was 0.30. The average RMSE mean of both RF and original data was 0.31. This highlights the superiority of the RF method in terms of providing more accurate and reliable feature selection results.

Figure 4. Root mean square error (RMSE) results of the original data and different feather selection. PCA: principal component analysis; RF: random forest.



Data Balance

This study's analysis of machine learning algorithms using diverse data balancing techniques is presented in Table 6. The result indicated that, in contrast to other data balancing strategies used in this study, SMOTE-ENN consistently surpassed all evaluated models in terms of accuracy.

XSL•FO
RenderX

Table 6. Comparison of imbalanced data handling techniques across each machine learning algorithm.

Algorithms and performance metrics	Unbalanced data	Undersampling	Oversampling	ADASYN[a]	SMOTE[b]	SMOTE-ENN[c]
Decision tree						
Accuracy	88.51%	56.06%	55.43%	59.30%	61.86%	68.14%
AUC[d]	0.66	0.56	0.55	0.60	0.62	0.71
Random forest						
Accuracy	91.38%	68.18%	54.43%	55.06%	67.86%	69.33%
AUC	0.81	0.83	0.77	0.80	0.80	0.85
XGBoost[e]						
Accuracy	90.86%	69.70%	59.71%	59.44%	70.57%	68.68%
AUC	0.80	0.76	0.77	0.81	0.79	0.81
AdaBoost[f]						
Accuracy	87.73%	71.21%	67.43%	76.76%	71.71%	75.30%
AUC	0.67	0.83	0.68	0.85	0.82	0.86
SVM[g]						
Accuracy	91.38%	72.73%	63.86%	63.24%	62.71%	66.78%
AUC	0.71	0.80	070	0.66	0.67	0.75
NBM[h]						
Accuracy	86.42%	78.79%	74.00%	72.11%	73%	77.17%
AUC	0.78	0.84	0.79	0.76	0.75	0.80
MLP[i]						
Accuracy	87.73%	65.16%	56%	59.15%	58.86%	62.86%
AUC	0.61	0.66	0.63	0.67	0.66	0.71

[a]ADASYN: adaptive synthetics sampling.

[b]SMOTE: Synthetic Minority Oversampling Technique.

[c]SMOTE-ENN: Synthetic Minority Oversampling Technique and Edited Nearest Neighbors.

[d]AUC: area under the curve.

[e]XGBoost: extreme gradient boosting.

[f]AdaBoost: adaptive boosting.

[g]SVM: support vector machine.

[h]NBM: naïve Bayes model.

[i]MLP: multilayer perceptron.

Development and Performance Comparisons of Machine Learning Models

This study used SMOTE-ENN for oversampling and model construction. The evaluation of each performance metric of the model is presented in Table 7, and the ROC curve of the model is shown in Figure 5. Among the models, the AdaBoost model exhibited the greatest effectiveness, boasting an AUC of 0.86, an accuracy of 75.3%, a precision of 0.86, a sensitivity of 0.69, and an F_1-score of 0.76. Simultaneously, to validate the model's efficacy, the training and validation data in this study were used to carry out validation of the model through 10-fold cross-validation. The results showed an AUC of 0.97, an accuracy of 91.27%, a precision of 0.94, a sensitivity of 0.92, an F_1-score of 0.94, and the ROC curve is presented in Figure 6. We used grid search and random search on the test set to make a better model. Comparing these two methods, random search performed better on the AdaBoost model. The data processed by grid search had an accuracy of 74.79% with an AUC of 0.84. After random search processing, the accuracy and AUC of AdaBoost improved. Its accuracy was 77.68% and its AUC was 0.86.

XSL•FO
RenderX

Table 7. Performance comparison of different models.

Algorithms	AUC[a] (95% CI)	Accuracy	Precision	Sensitivity	F_1-score
Decision tree	0.71 (0.7-0.71)	68.14%	0.84	0.57	0.68
Random forest	0.85 (0.84-0.85)	69.33%	0.90	0.54	0.68
XGBoost[b]	0.81 (0.8-0.81)	68.68%	0.87	0.57	0.69
AdaBoost[c]	0.86 (0.85-0.86)	75.30%	0.86	0.69	0.77
SVM[d]	0.75 (0.75-0.76)	66.78%	0.87	0.52	0.65
NBM[e]	0.80 (0.79-0.8)	77.17%	0.83	0.77	0.8
MLP[f]	0.71 (0.7-0.71)	62.86%	0.83	0.47	0.6

[a]AUC: area under the curve.

[b]XGBoost: extreme gradient boosting.

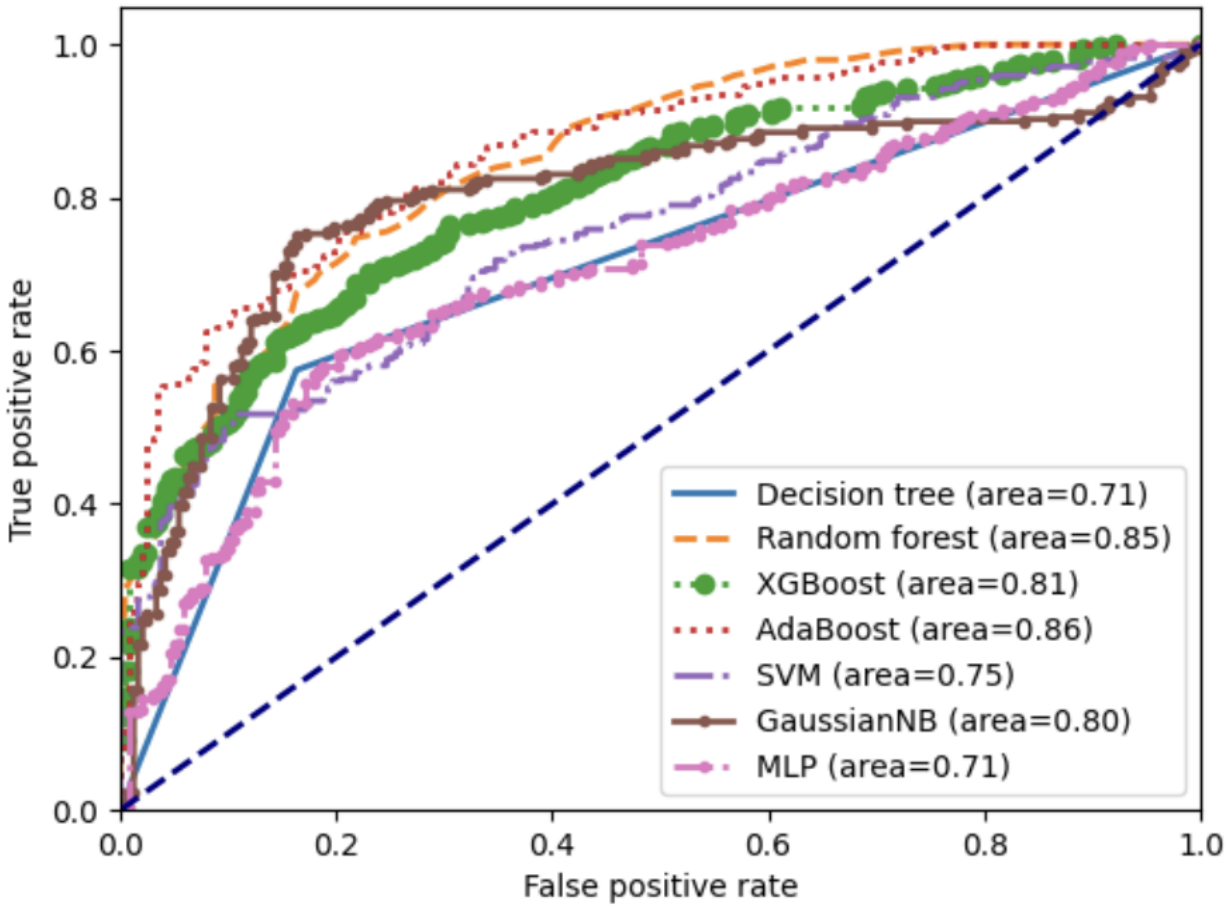
[c]AdaBoost: adaptive boosting.

[d]SVM: support vector machine.

[e]NBM: naïve Bayes model.

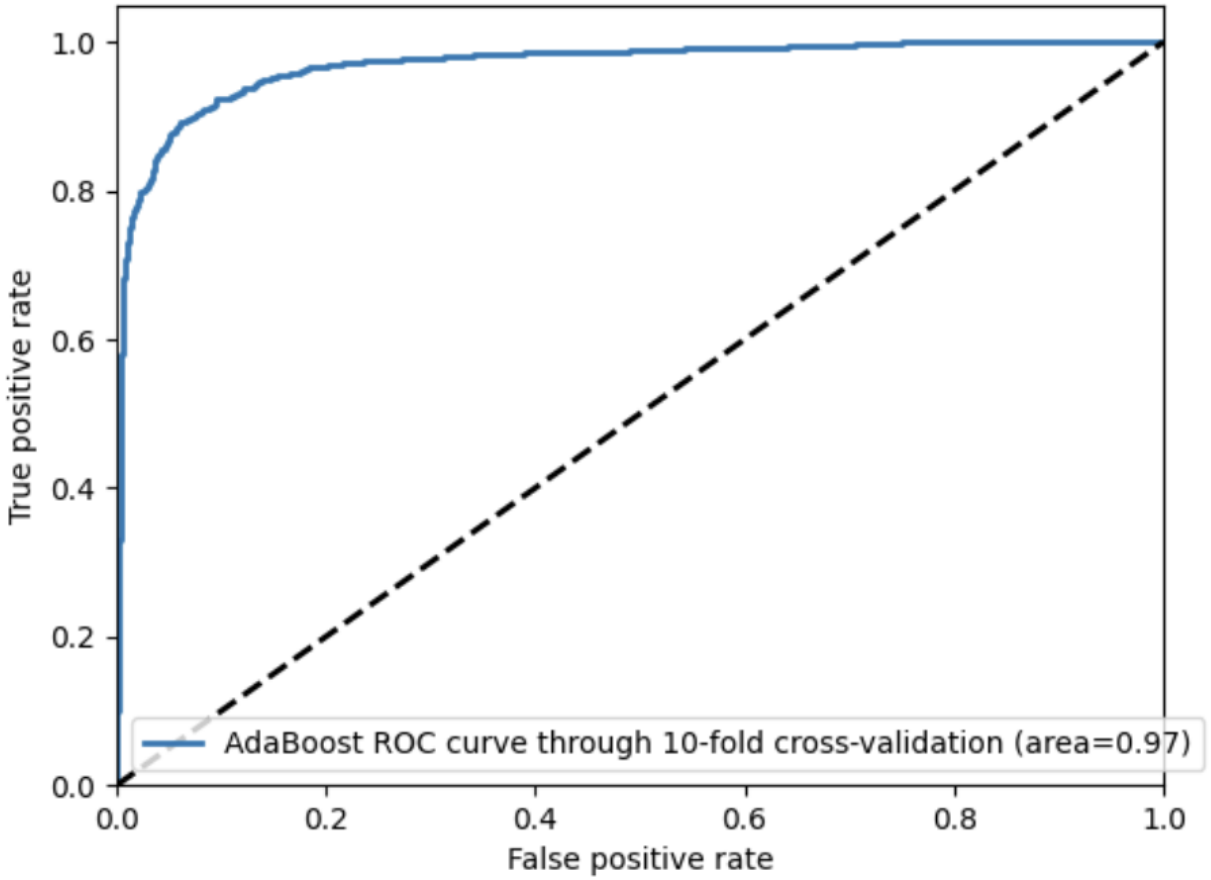
[f]MLP: multilayer perceptron.

Figure 5. Comparison of ROC curves of different models. AdaBoost: adaptive boosting; GaussianNB: Gaussian naïve Bayes; MLP: multilayer perceptron; ROC: receiver operating characteristic; SVC: support vector classifier; XGBoost: extreme gradient boosting.



XSL•FO
RenderX

Figure 6. ROC curves of AdaBoost on the whole data through 10-fold cross-validation. AdaBoost: adaptive boosting; ROC: receiver operating characteristic.



Discussion

Analysis of Risk Factor Analysis for the Occurrence of CHF Based on the Health Ecology

This study found that 22 risk factors predicting the occurrence of CHF were identified through a machine learning algorithm and hierarchically classified in accordance with the health ecology theory, with the objective of offering a comprehensive perspective for the prevention and intervention of CHF in the future. Health ecology not only takes into account the influence of individual disease factors on health but also conducts an all-round and holistic management of health from aspects such as individual traits, behavior and lifestyle, family and social interpersonal networks, and macropolicies [23].

At the individual trait level, this study identified age, glomerular filtration rate, glycosylated hemoglobin, systolic blood pressure, BMI, the ratio of early maximal ventricular filling velocity to atrial maximal ventricular filling velocity, ever awakened by trouble breathing, fasting triglycerides, heart rate, high-density lipoprotein, peak early diastolic velocity of mitral annulus, ejection fraction, fasting total cholesterol, ultrasensitive C-reactive protein, and low-density lipoprotein, for a total of 14 risk factors. Results from existing population-based cohort studies [24] suggest that despite the lower incidence and absolute risk of heart failure in younger people compared with older people, the associations of modifiable risk factors were stronger, and attributable risks were greater in younger participants, consistent with age factors. Systolic blood pressure, glycated hemoglobin, heart rate, high-density lipoprotein, low-density lipoprotein, ejection fraction, fasting total cholesterol, and ratio of early maximal ventricular filling velocity to atrial maximal ventricular filling velocity are important indicators for evaluating cardiac systolic-diastolic function, blood glucose levels, and glomerular filtration function, along with hypertension, diabetes mellitus, and comorbidities as the traditional independent risk factors for CHF [25-27]. Ever awakened by trouble breathing is used as a typical symptom of nocturnal paroxysmal dyspnea and edema in heart failure [28,29].

At the behavioral and lifestyle level, this study identified vitamin D_3, eggs, and dark-colored green vegetables, a total of 3 risk factors. Diet has a great influence on the development of CHF and is one of the important risk factors for the development of CHF [30].

In the living and working conditions stratum, this study identified the proportion of the population living in poverty in the area, the status of sports facilities within 3 km, and the status of favorite food stores within 3 km, for a total of 3 risk factors. The status of favorite food stores within 3 km reflects the impact of dietary nutrition in at-risk populations; nutrition has been shown to be an important factor in the prevention of heart failure [31]. The status of sports facilities within 3 km could reflect the exercise situation. Studies have shown a strong association between physical inactivity, low fitness, and heart failure and have emphasized the importance of regular physical activity in

XSL•FO
RenderX

the prevention and treatment of heart failure [32], which is consistent with the exercise and activity index factors identified in this study. The proportion of the population living in poverty in the area reflects income and wealth. Yusuf et al [33] conducted a study to explore the risk factors for cardiovascular events and showed that each risk factor varied according to the economic level of the country.

The above risk factor analyses based on the health ecology perspective not only make up for the limitations of the individual factor level of CHF but also provide a researchable direction for the future health management of heart failure.

Analysis of Prediction Model Construction for the Occurrence of CHF Based on Machine Learning

At present, traditional regression methods are mainly used in clinical practice to screen for high-risk factors of CHF, and no conventional prediction methods have been found for the occurrence of CHF. Although traditional regression methods can provide effective prediction results, they still cannot effectively solve the problem of deviation between predicted and actual values, and more advanced technologies are needed to solve it. With the advent of the big data era, the application of machine learning in the medical and health field is becoming increasingly widespread, especially in disease prediction and prognosis evaluation [34]. This study compares different methods for processing unbalanced datasets. SMOTE-ENN is the optimal processing method. SMOTE-ENN combines the SMOTE and ENN methods. SMOTE is first used to generate new synthetic samples, and then the ENN method is used to clean the synthetic dataset to remove the noisy samples and outliers to improve the quality of the dataset and the classification performance of the model [35].

This study found that AdaBoost has a better ability to handle the problem of CHF occurrence, with better performance. Many studies have shown that AdaBoost is able to achieve high accuracy in solving various classification problems [36,37]. AdaBoost focuses on hard-to-classify samples by constantly adjusting the sample weights, allowing the classifier to better learn the features of these samples, thus improving overall accuracy. Currently, AdaBoost has been used in the area of heart disease. Rath et al [38] conducted a study demonstrating that the proposed AdaBoost algorithm has been shown to have an advantage over other algorithms in terms of accuracy when solving the electrocardiogram quality assessment problem. Therefore, AdaBoost is an efficient machine learning algorithm that is particularly suitable for processing large-scale datasets. Its efficient computational performance, excellent prediction accuracy, and flexible model configuration give it natural advantages in the construction of cross-domain models in medical engineering.

Limitations

This study has certain limitations. First, due to the limitations of retrospective research attributes, there are inevitably issues such as insufficient variable collection, missing data, and anomalies. Second, there is a lack of external datasets to further test the generalization ability of the model. Finally, due to some missing data obtained from the National Heart, Lung and Blood Institute in this research database, there is a lack of biological indicators that are highly correlated with CHF, such as N-terminal pro-B-type natriuretic peptide.

Conclusion

In this study, we endeavored to construct a predictive model for CHF occurrence using machine learning and analyze CHF risk from a health ecology perspective. Through a series of comprehensive procedures, including data preprocessing to handle missing values and standardize data, and applying feature selection methods like PCA and RF, we identified relevant factors associated with CHF. The analysis of risk factors based on health ecology provided a holistic understanding. At the individual trait level, multiple factors were recognized, along with several at the behavioral and lifestyle level and the living and working conditions level. Among the machine learning models evaluated, the AdaBoost model showed relatively high effectiveness. However, the study had limitations. The retrospective design led to issues such as incomplete variable collection and missing data, and the lack of external datasets affected the assessment of model generalization.

For future research, prospective studies should be considered to improve data quality and collection. Incorporating more diverse data sources and advanced machine learning techniques could enhance the model’s performance and generalizability. Longitudinal studies could track the changes in risk factors over time to better understand CHF development. In addition, further exploration of the interactions between different levels of health ecology factors could provide deeper insights into CHF prevention and management strategies. By addressing these areas, future research can build on the current work and contribute to more effective approaches to dealing with CHF.

Acknowledgments

Funding from the 2022 Key Medical Research Project of the Jiangsu Provincial Health Commission of Jiangsu Province is gratefully acknowledged (ZD2022057).

Authors' Contributions

QX, CRX, XC, YYZ, and JS developed and designed the study. QX and RCY drafted the manuscript. QX and TYG conducted data analysis and figure drawing. QX, HS, JS, GJC, and TYG critically reviewed and edited the manuscript. CRX and JS guided and supervised the writing of the manuscript, and all authors participated in the review and editing of the manuscript.

XSL•FO
RenderX

Conflicts of Interest

None declared.

Multimedia Appendix 1
Predictor variables.
[DOCX File , 15 KB - medinform_v13i1e64972_app1.docx]

References

1. Lloyd-Jones D, Adams RJ, Brown TM, Carnethon M, Dai S, de Simone G, et al. Heart disease and stroke statistics—2010 Update. Circulation 2010;121(7):e46-e215. [doi: 10.1161/circulationaha.109.192667]
2. Wu Q, Zhang Q, Li Y, Yu L, Zhang Y, Ao M. A systematic review and meta-analysis of high-frequency prescription of zhigancao decoction combined with conventional western medicine in the treatment of chronic heart failure. Evid Based Complement Alternat Med 2021;2021:7140044 [FREE Full text] [doi: 10.1155/2021/7140044] [Medline: 34795787]
3. Liang M, Bian B, Yang Q. Characteristics and long-term prognosis of patients with reduced, mid-range, and preserved ejection fraction: a systemic review and meta-analysis. Clin Cardiol 2022;45(1):5-17 [FREE Full text] [doi: 10.1002/clc.23754] [Medline: 35043472]
4. Xu J, Sun Y, Gong D, Fan Y. Association between disease-specific health-related quality of life and all-cause mortality in patients with heart failure: a meta-analysis. Curr Probl Cardiol 2023;48(4):101592. [doi: 10.1016/j.cpcardiol.2023.101592] [Medline: 36632931]
5. Hafkamp FJ, Tio RA, Otterspoor LC, de Greef T, van Steenbergen GJ, van de Ven ART, et al. Optimal effectiveness of heart failure management - an umbrella review of meta-analyses examining the effectiveness of interventions to reduce (re)hospitalizations in heart failure. Heart Fail Rev 2022;27(5):1683-1748 [FREE Full text] [doi: 10.1007/s10741-021-10212-8] [Medline: 35239106]
6. Dongfeng GU, Jianping WENG, Xiangfeng LU. Guidelines for the prevention of cardiovascular and metabolic diseases by healthy lifestyles in China. Chinese Circulation Journal 2020 Mar 24;35(03):209-230 [FREE Full text]
7. Lin YH, Zhou ZHOU. [Cardiovascular biomarkers improve precise risk assessment for cardiovascular diseases]. Zhonghua Yi Xue Za Zhi 2022;102(35):2731-2733. [doi: 10.3760/cma.j.cn112137-20220726-01626] [Medline: 36124345]
8. Aimo A, Vergaro G, Barison A, Maffei S, Borrelli C, Morrone D, et al. Sex-related differences in chronic heart failure. Int J Cardiol 2018;255:145-151. [doi: 10.1016/j.ijcard.2017.10.068] [Medline: 29425552]
9. Salvioni E, Bonomi A, Re F, Mapelli M, Mattavelli I, Vitale G, et al. The MECKI score initiative: development and state of the art. Eur J Prev Cardiol 2020;27(2_suppl):5-11 [FREE Full text] [doi: 10.1177/2047487320959010] [Medline: 33238744]
10. Klimczak-Tomaniak D, de Bakker M, Bouwens E, Akkerhuis KM, Baart S, Rizopoulos D, et al. Dynamic personalized risk prediction in chronic heart failure patients: a longitudinal, clinical investigation of 92 biomarkers (Bio-SHiFT study). Sci Rep 2022;12(1):2795 [FREE Full text] [doi: 10.1038/s41598-022-06698-3] [Medline: 35181700]
11. Angraal S, Mortazavi BJ, Gupta A, Khera R, Ahmad T, Desai NR, et al. Machine learning prediction of mortality and hospitalization in heart failure with preserved ejection fraction. JACC Heart Fail 2020;8(1):12-21 [FREE Full text] [doi: 10.1016/j.jchf.2019.06.013] [Medline: 31606361]
12. Wang Y, Hou R, Ni B, Jiang Y, Zhang Y. Development and validation of a prediction model based on machine learning algorithms for predicting the risk of heart failure in middle-aged and older US people with prediabetes or diabetes. Clin Cardiol 2023;46(10):1234-1243 [FREE Full text] [doi: 10.1002/clc.24104] [Medline: 37519220]
13. Emmons-Bell S, Johnson C, Roth G. Prevalence, incidence and survival of heart failure: a systematic review. Heart 2022;108(17):1351-1360 [FREE Full text] [doi: 10.1136/heartjnl-2021-320131] [Medline: 35042750]
14. Chen X, Chen H, Nan S, Kong X, Duan H, Zhu H. Dealing with missing, imbalanced, and sparse features during the development of a prediction model for sudden death using emergency medicine data: machine learning approach. JMIR Med Inform 2023;11:e38590 [FREE Full text] [doi: 10.2196/38590] [Medline: 36662548]
15. Zhang W, Liu H, Silenzio VMB, Qiu P, Gong W. Machine learning models for the prediction of postpartum depression: application and comparison based on a cohort study. JMIR Med Inform 2020;8(4):e15516 [FREE Full text] [doi: 10.2196/15516] [Medline: 32352387]
16. Maheswari S, Pitchai R. Heart disease prediction system using decision tree and naive bayes algorithm. Curr Med Imaging Rev 2019;15(8):712-717. [doi: 10.2174/1573405614666180322141259] [Medline: 32008540]
17. Lee H, Cho JK, Park J, Lee H, Fond G, Boyer L, et al. Machine learning-based prediction of suicidality in adolescents with allergic rhinitis: derivation and validation in 2 independent nationwide cohorts. J Med Internet Res 2024;26:e51473 [FREE Full text] [doi: 10.2196/51473] [Medline: 38354043]
18. Akbarian S, Ghahjaverestan NM, Yadollahi A, Taati B. Noncontact sleep monitoring with infrared video data to estimate sleep apnea severity and distinguish between positional and nonpositional sleep apnea: model development and experimental validation. J Med Internet Res 2021;23(11):e26524 [FREE Full text] [doi: 10.2196/26524] [Medline: 34723817]

XSL•FO
RenderX

19. Subha Ramakrishnan M, Ganapathy N. Extreme gradient boosting based improved classification of blood-brain-barrier drugs. Stud Health Technol Inform 2022;294:872-873. [doi: 10.3233/SHTI220612] [Medline: 35612231]
20. Vlasák A, Gerla V, Skalický P, Mládek A, Sedlák V, Vrána J, et al. Boosting phase-contrast MRI performance in idiopathic normal pressure hydrocephalus diagnostics by means of machine learning approach. Neurosurg Focus 2022;52(4):E6. [doi: 10.3171/2022.1.FOCUS21733] [Medline: 35364583]
21. Yu H, Liu Y, Zhou G, Peng M. Multilayer perceptron algorithm-assisted flexible piezoresistive PDMS/Chitosan/cMWCNT sponge pressure sensor for sedentary healthcare monitoring. ACS Sens 2023;8(11):4391-4401. [doi: 10.1021/acssensors.3c01885] [Medline: 37939316]
22. Kouadri S, Pande CB, Panneerselvam B, Moharir KN, Elbeltagi A. Prediction of irrigation groundwater quality parameters using ANN, LSTM, and MLR models. Environ Sci Pollut Res Int 2022;29(14):21067-21091. [doi: 10.1007/s11356-021-17084-3] [Medline: 34748181]
23. Summary of the China Cardiovascular Health and Disease Report 2020. Chinese Circulation Journal. 2021. URL: https://med.wanfangdata.com.cn/Paper/Detail?id=PeriodicalPaper_zgxhzz202106001 [accessed 2025-01-13]
24. Age dependent associations of risk factors with heart failure: pooled population based cohort study. BMJ. 2021. URL: https://www.bmj.com/lookup/pmidlookup?view=long&pmid=33795254 [accessed 2025-01-13]
25. Di Palo KE, Barone NJ. Hypertension and heart failure: prevention, targets, and treatment. Heart Fail Clin 2020;16(1):99-106. [doi: 10.1016/j.hfc.2019.09.001] [Medline: 31735319]
26. Triposkiadis F, Xanthopoulos A, Parissis J, Butler J, Farmakis D. Pathogenesis of chronic heart failure: cardiovascular aging, risk factors, comorbidities, and disease modifiers. Heart Fail Rev 2022;27(1):337-344. [doi: 10.1007/s10741-020-09987-z] [Medline: 32524327]
27. D'Elia JA, Bayliss GP, Weinrauch LA. The diabetic cardiorenal nexus. Int J Mol Sci 2022;23(13):7351 [FREE Full text] [doi: 10.3390/ijms23137351] [Medline: 35806355]
28. Abassi Z, Khoury EE, Karram T, Aronson D. Edema formation in congestive heart failure and the underlying mechanisms. Front Cardiovasc Med 2022;9:933215 [FREE Full text] [doi: 10.3389/fcvm.2022.933215] [Medline: 36237903]
29. deSouza IS, Martindale JL. Dyspnea due to acute heart failure syndrome. Am Fam Physician 2019;99(3):201-209 [FREE Full text]
30. Kerley CP. Nutritional interventions in heart failure: challenges and opportunities. Curr Heart Fail Rep 2018;15(3):131-140. [doi: 10.1007/s11897-018-0388-6] [Medline: 29623529]
31. Billingsley HE, Hummel SL, Carbone S. The role of diet and nutrition in heart failure: a state-of-the-art narrative review. Prog Cardiovasc Dis 2020;63(5):538-551 [FREE Full text] [doi: 10.1016/j.pcad.2020.08.004] [Medline: 32798501]
32. Lindgren M, Börjesson M. The importance of physical activity and cardiorespiratory fitness for patients with heart failure. Diabetes Res Clin Pract 2021;176:108833 [FREE Full text] [doi: 10.1016/j.diabres.2021.108833] [Medline: 33895194]
33. Yusuf S, Joseph P, Rangarajan S, Islam S, Mente A, Hystad P, et al. Modifiable risk factors, cardiovascular disease, and mortality in 155 722 individuals from 21 high-income, middle-income, and low-income countries (PURE): a prospective cohort study. The Lancet 2020;395(10226):795-808. [doi: 10.1016/s0140-6736(19)32008-2]
34. Ngiam KY, Khor IW. Big data and machine learning algorithms for health-care delivery. The Lancet Oncology 2019;20(5):e262-e273. [doi: 10.1016/s1470-2045(19)30149-4]
35. Kumari M, Subbarao N. A hybrid resampling algorithms SMOTE and ENN based deep learning models for identification of marburg virus inhibitors. Future Med Chem 2022;14(10):701-715. [doi: 10.4155/fmc-2021-0290] [Medline: 35393862]
36. Wenbo W, Yang S, Guici C. Blood glucose concentration prediction based on VMD-KELM-AdaBoost. Med Biol Eng Comput 2021;59(11-12):2219-2235. [doi: 10.1007/s11517-021-02430-x] [Medline: 34510372]
37. Zuo D, Yang L, Jin Y, Qi H, Liu Y, Ren L. Machine learning-based models for the prediction of breast cancer recurrence risk. BMC Med Inform Decis Mak 2023;23(1):276 [FREE Full text] [doi: 10.1186/s12911-023-02377-z] [Medline: 38031071]
38. Rath A, Mishra D, Panda G. Imbalanced ECG signal-based heart disease classification using ensemble machine learning technique. Front Big Data 2022;5:1021518 [FREE Full text] [doi: 10.3389/fdata.2022.1021518] [Medline: 36299660]

Abbreviations

AdaBoost: adaptive boosting
AUC: area under the curve
CHF: chronic heart failure
JHS: Jackson Heart Study
MECKI: Metabolic Exercise Test data combined with Cardiac and Kidney Indexes
ML: machine learning
PCA: principal component analysis
RF: random forest
RMSE: root mean square error
SMOTE-ENN: Synthetic Minority Oversampling Technique and Edited Nearest Neighbors

XSL•FO
RenderX

Edited by C Lovis; submitted 31.07.24; peer-reviewed by J Nalepa; comments to author 13.11.24; revised version received 04.12.24; accepted 25.12.24; published 31.01.25.

Please cite as:
Xu Q, Cai X, Yu R, Zheng Y, Chen G, Sun H, Gao T, Xu C, Sun J
Machine Learning–Based Risk Factor Analysis and Prediction Model Construction for the Occurrence of Chronic Heart Failure: Health Ecologic Study
JMIR Med Inform 2025;13:e64972
URL: https://medinform.jmir.org/2025/1/e64972
doi:10.2196/64972
PMID:

©Qian Xu, Xue Cai, Ruicong Yu, Yueyue Zheng, Guanjie Chen, Hui Sun, Tianyun Gao, Cuirong Xu, Jing Sun. Originally published in JMIR Medical Informatics (https://medinform.jmir.org), 31.01.2025. This is an open-access article distributed under the terms of the Creative Commons Attribution License (https://creativecommons.org/licenses/by/4.0/), which permits unrestricted use, distribution, and reproduction in any medium, provided the original work, first published in JMIR Medical Informatics, is properly cited. The complete bibliographic information, a link to the original publication on https://medinform.jmir.org/, as well as this copyright and license information must be included.

XSL•FO
RenderX

Original Paper

Identification of Clusters in a Population With Obesity Using Machine Learning: Secondary Analysis of The Maastricht Study

Maik JM Beuken[1], MEd; Melanie Kleynen[2], PhD; Susy Braun[2], PhD; Kees Van Berkel[1,3], PhD; Carla van der Kallen[4,5], PhD; Annemarie Koster[6,7], PhD; Hans Bosma[6,7], PhD; Tos TJM Berendschot[8], PhD; Alfons JHM Houben[4,5], PhD; Nicole Dukers-Muijrers[9,10], PhD; Joop P van den Bergh[4,11], PhD; Abraham A Kroon[4,5], PhD; Maastricht Study Management[12]; Iris M Kanera[2], PhD

[1]Faculty of Financial Management, Research Center for Statistics & Data Science, Zuyd University of Applied Sciences, Sittard, Netherlands

[2]Faculty of Health, School of Physiotherapy, Research Center for Nutrition, Lifestyle and Exercise, Zuyd University of Applied Sciences, Heerlen, Netherlands

[3]Department of Data Collection, Research and Innovation, Statistics Netherlands, Heerlen, Netherlands

[4]Department of Internal Medicine, Maastricht University Medical Center+, Maastricht, Netherlands

[5]Cardiovascular Research Institute Maastricht, Maastricht University, Maastricht, Netherlands

[6]Department of Social Medicine, Maastricht University, Maastricht, Netherlands

[7]Care and Public Health Research Institute, Maastricht University, Maastricht, Netherlands

[8]University Eye Clinic Maastricht, Maastricht University, Maastricht, Netherlands

[9]Department of Health Promotion, Care and Public Health Research Institute, Maastricht University, Maastricht, Netherlands

[10]Department of Sexual Health, Infectious Diseases and Environmental Health, Living Lab Public Health Mosa, Public Health Service South Limburg, Heerlen, Netherlands

[11]Department of Internal Medicine, VieCuri Medical Center, Venlo, Netherlands

[12]See Acknowledgments

Corresponding Author:
Maik JM Beuken, MEd
Faculty of Financial Management
Research Center for Statistics & Data Science
Zuyd University of Applied Sciences
Ligne 1
Sittard, 6131 MT
Netherlands
Phone: 31 682243809
Email: maik.beuken@zuyd.nl

Abstract

Background: Modern lifestyle risk factors, like physical inactivity and poor nutrition, contribute to rising rates of obesity and chronic diseases like type 2 diabetes and heart disease. Particularly personalized interventions have been shown to be effective for long-term behavior change. Machine learning can be used to uncover insights without predefined hypotheses, revealing complex relationships and distinct population clusters. New data-driven approaches, such as the factor probabilistic distance clustering algorithm, provide opportunities to identify potentially meaningful clusters within large and complex datasets.

Objective: This study aimed to identify potential clusters and relevant variables among individuals with obesity using a data-driven and hypothesis-free machine learning approach.

Methods: We used cross-sectional data from individuals with abdominal obesity from The Maastricht Study. Data (2971 variables) included demographics, lifestyle, biomedical aspects, advanced phenotyping, and social factors (cohort 2010). The factor probabilistic distance clustering algorithm was applied in order to detect clusters within this high-dimensional data. To identify a subset of distinct, minimally redundant, predictive variables, we used the statistically equivalent signature algorithm. To describe the clusters, we applied measures of central tendency and variability, and we assessed the distinctiveness of the clusters through the emerged variables using the *F* test for continuous variables and the chi-square test for categorical variables at a confidence level of α=.001

XSL•FO
RenderX

Results: We identified 3 distinct clusters (including 4128/9188, 44.93% of all data points) among individuals with obesity (n=4128). The most significant continuous variable for distinguishing cluster 1 (n=1458) from clusters 2 and 3 combined (n=2670) was the lower energy intake (mean 1684, SD 393 kcal/day vs mean 2358, SD 635 kcal/day; *P*<.001). The most significant categorical variable was occupation (*P*<.001). A significantly higher proportion (1236/1458, 84.77%) in cluster 1 did not work compared to clusters 2 and 3 combined (1486/2670, 55.66%; *P*<.001). For cluster 2 (n=1521), the most significant continuous variable was a higher energy intake (mean 2755, SD 506.2 kcal/day vs mean 1749, SD 375 kcal/day; *P*<.001). The most significant categorical variable was sex (*P*<.001). A significantly higher proportion (997/1521, 65.55%) in cluster 2 were male compared to the other 2 clusters (885/2607, 33.95%; *P*<.001). For cluster 3 (n=1149), the most significant continuous variable was overall higher cognitive functioning (mean 0.2349, SD 0.5702 vs mean –0.3088, SD 0.7212; *P*<.001), and educational level was the most significant categorical variable (*P*<.001). A significantly higher proportion (475/1149, 41.34%) in cluster 3 received higher vocational or university education in comparison to clusters 1 and 2 combined (729/2979, 24.47%; *P*<.001).

Conclusions: This study demonstrates that a hypothesis-free and fully data-driven approach can be used to identify distinguishable participant clusters in large and complex datasets and find relevant variables that differ within populations with obesity.

(JMIR Med Inform 2025;13:e64479) doi:10.2196/64479

KEYWORDS

Maastricht Study; participant clusters; cluster analysis; factor probabilistic distance clustering; FPDC algorithm; statistically equivalent signature; SES feature selection; unsupervised machine learning; obesity; hypothesis free; risk factor; physical inactivity; poor nutrition; physical activity; chronic disease; type 2 diabetes; diabetes; heart disease; long-term behavior change

Introduction

Overwhelming evidence shows that modern unhealthy lifestyle behaviors (eg, physical inactivity, poor nutrition, tobacco consumption) in many parts of the world increase the prevalence and incidence of obesity and chronic illnesses such as type 2 diabetes mellitus (T2DM), coronary heart disease, and some forms of cancer [1]. Prevention of (secondary) diseases and health promotion have been proposed as important solutions to ensure a sustainable health care system for the future [2,3]. Dutch national programs aiming at promoting a healthy lifestyle in a large number of people have, however, not yet led to a decrease in the prevalence of the abovementioned diseases or a decrease in health care consumption [4].

Obesity needs to be considered a complex system problem, influenced by a combination of genetic, biological, behavioral, social, economic, and environmental factors. These factors are intertwined and can reinforce each other. An unhealthy diet can be influenced by, for example, personal factors, cultural habits, the availability of healthy food, and economic conditions. To better understand the multifaceted nature of obesity, a systems approach is needed [5,6].

Research indicates that personalized interventions appear to be more effective than general programs in achieving long-term lifestyle behavior change among various populations [7-9]. Personalized treatment takes the variability among patients into account, considering, for example, genetic, environmental, disease-related, behavioral, and lifestyle-related factors to optimize treatment outcomes. In recent years, growing experience has been gained in applying advanced data analytics and machine learning (ML) in the context of public health [10]. Processing large amounts of data by including ML enables the recognition of patterns and the identification of variables that might play an important role in personalizing programs and interventions, due to the possibility to identify persons in a certain cluster or possibilities in exploring mechanisms underlying the distinctiveness between the different clusters. Moreover, emerging hypotheses may lead to additional opportunities. Recently, data-driven approaches are increasingly being explored on large datasets. ML algorithms can detect patterns in large and complex datasets, which would be difficult to find by more simple, conventional analyses. Clustering algorithms can organize similar data points into groups, uncovering patterns that may not be obvious with traditional statistical methods. Conventional statistical models, which require a priori information, often struggle with these complex systems; this restriction requires thorough data analysis and clear modeling, which can be challenging to manage in large datasets [11]. Interestingly, this kind of exploratory data analysis can be conducted without a predefined hypothesis. With regard to obesity, hypothesis-driven methods may be less suitable for understanding the complexity of this problem because they focus on isolated variables, might miss interactions, overlook broader contexts, and may not capture the multifaceted influences on obesity. Such a hypothesis-free approach provides the chance for exploration and discovery of patterns and relationships in the data without being limited or biased by a priori–defined expectations. In general, emerging patterns may be meaningful in describing complex phenomena; discovering cross-links between different variables; and identifying possible, distinct clusters within a population. Due to recent progress in processing large amounts of intricate and unorganized data, contemporary ML techniques are becoming ever more essential in the realm of personalized medicine [12].

Recently, various data clustering approaches have been applied among different populations. Nagamine et al [13] used a hypothesis-free approach to find patterns within the symptom range mentioned by patients with heart failure (n=25,861) and characterized these clusters in terms of their distinguishing variables in order to generate characteristics and progression patterns of heart failure. Nicolet et al [14] identified clusters for clinical practice to investigate the patient multimorbidity and complexity of Swiss residents aged ≥50 years (n=18,732) in claims data. Elbattah and Molloy [15] clustered older adult

XSL•FO
RenderX

participants in Ireland after a hip fracture into subgroups, in order to better predict the most beneficial care strategy for each patient. Takeshita et al [16] identified 7 clusters of obesity (BMI ≥35 kg/m^2) in order to tailor interventions based on the data in a health care claims database (n=9494). The abovementioned studies show that using unsupervised ML techniques offers unique opportunities to uncover unexpected insights, identify novel patterns, and elucidate previously unknown connections within large data by taking the approach of exploratory, data-driven, and hypothesis-free analysis. All these studies use the k-means clustering technique. Given these promising results and developments in the field of unsupervised ML techniques, we chose to include new developments in this study.

In particular, we explore in this paper the clustering of a large multidimensional dataset provided by The Maastricht Study. The Maastricht Study is an observational, prospective, population-based, cohort study [17]. Contrary to the aforementioned studies, which rely mainly on health care data, The Maastricht Study data include a broader range of potential variables, including etiology, pathophysiology, complications, and comorbidities of T2DM and other chronic diseases, and are featured by a comprehensive phenotyping approach. This dataset is complex due to the high number of variables, which implies high mathematical dimensionality, including noisy data and outliers. To handle these mathematical characteristics of the data, we choose to apply factor probabilistic distance clustering (FPDC) in this study [18].

The main aim of this study is a methodological exploration to identify potential clusters and relevant variables among individuals with obesity among participants in The Maastricht Study, using a data-driven and hypothesis-free ML approach.

Methods

Ethical Considerations

We used cross-sectional data from The Maastricht Study, an observational, prospective, population-based, cohort study. The rationale and methodology were described previously by Schram et al [19]. The Maastricht Study was approved by the institutional medical ethical committee (NL31329.068.10) and the Minister of Health, Welfare, and Sports of the Netherlands (Permit 131088-105234-PG). All participants gave written informed consent.

Study Population

Eligible for inclusion into this study were participants of The Maastricht Study with obesity. Within The Maastricht Study context, individuals were enlisted through widespread media outreach efforts and by sending invitations through postal mail to those registered in municipal records as well as the regional Diabetes Patient Registry. Recruitment was structured based on the known status of T2DM, with a deliberate emphasis on selecting more individuals with T2DM to ensure operational efficiency as part of The Maastricht Study.

Measurements

The Maastricht Study dataset includes a wide range of variables disaggregated in various general and disease-specific measurements comprising, for example, questionnaire data, physical examinations, and blood and urine examinations. For a detailed description of all measurements, see Schram et al [19].

In this study, data were included from all measured variables (2971 variables) of the cross-sectional data from the first 9188 participants who were included in the baseline survey between November 2010 and October 2020. For the specific purpose of our study, data from individuals with obesity were selected for our data analysis within this dataset based on the waist circumference variable. Men with a waist circumference higher than 102 cm (about 3.35 ft) and women with a waist circumference higher than 88 cm (about 2.89 ft) can be defined as being abdominal obese [20,21]. For a detailed description of the variables included, we refer to The Maastricht Study Dictionary [20]. This dictionary provides an overview of the variables included in our study.

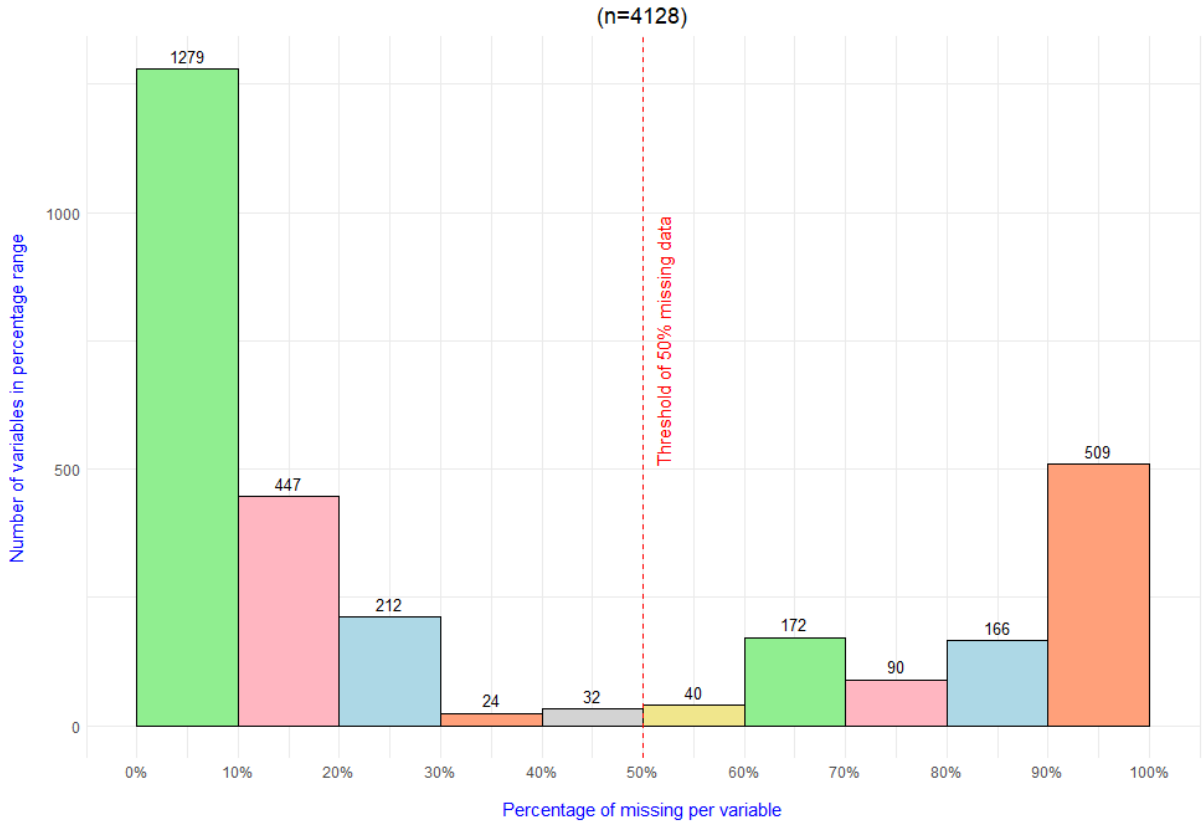
Statistical Analysis

Overview

All data were assessed for aberrant measurement data and missing data. One of the steps to prepare the data before clustering was to remove variables with more than 50% missing data from the dataset. To provide more detail on the amount of missing data, an overview of the missingness is given in Figure 1. To impute the missing data in the remaining variables, we used the chained random forests (CRF) method [22,23] from the *missRanger* package in R. This package allows the use of predictive mean matching. Predictive mean matching ensures an imputed value that (1) occurs in the variables of interest in the case of categorical values and (2) attempts to bring the variance to a realistic size. In this research, all remaining variables were used to fill in the missing values in the data. Random forests have properties that allow them to impute heterogeneous data, unlike most standard methods, and can handle complex, nonlinear relationships in the data automatically [24], with high imputation accuracy [22]. The strength of the ensemble approach, by using random forest, lies in combining the predictions of multiple trees, which ensures a more reliable usage of the patterns underneath the data. Linear or distance-based methods struggle to capture this data structure and these underlying patterns. This feature of CRF makes the clustering, based on the decomposition into factors, more reflective of the actual data structure and underlying patterns. Another important feature of CRF is the ability to handle high-dimensional data, without overfitting [25]. This is in contrast to methods like k-nearest neighbors, which suffer in high dimensional space [26], and work well when no assumptions are made regarding the different types of missingness [27]. These properties led to the conviction that CRF is a suitable choice to impute this high-dimensional dataset when keeping the aim—to cluster the data—in mind. Further handling of missing data including data imputation is described in Multimedia Appendix 1. Data were standardized before inclusion.

XSL•FO
RenderX

Figure 1. Histogram of the amount of missing data.



Software

R Studio (version 4.3.0 {2023-04-21}; R Foundation for Statistical Computing) was used as an integrated development environment for the R programming language. R has been used including the packages in Textbox 1.

Textbox 1. List of R packages used in this study

- *missRanger*: An approach using random forests in sequence to fill in missing values within datasets containing a mix of different data types [22,28].
- *FPDclustering*: Factor probabilistic distance clustering is a factor clustering method that involves linear transformation of variables and clusters that optimize the probabilistic distance clustering criterion [18,29,30].
- *MXM*: Many feature selection methods for a wide range of response variables, including minimal, statistically equivalent, and equally predictive feature subsets [31,32].
- *uwot*: The uniform manifold approximation and projection method for dimensionality reduction [33].
- *vtable*: Variable table for variable documentation [34].

Identification of Participant Clusters

A novel unsupervised ML technique developed to handle high-dimensional and complex data was used to identify clusters in data from people with obesity. We applied the FPDC algorithm with the *FPDclustering* package in R. The FPDC algorithm was used to cluster individual cases into *k* clusters after preparing the data as described in Multimedia Appendices 2 and 3. The parameter *k* is required to be established within the algorithm framework. Subsequently, clustering was conducted across a range from 2 to 30 clusters, in line with previous research [13,35]. Followed by the identification of the optimal number of clusters through evaluation criteria, the number of clusters was determined by choosing an adequate number for the practice, but also by aiming for the highest possible average silhouette coefficient (SC) score. In addition, the uniform manifold approximation and projection (UMAP) plot provides insight into the actual distinctiveness of the clustering through visualization.

This algorithm executes a linear transformation of the original variables to reduce the number of variables into orthogonal factors, the so-called Tucker-3 decomposition [36]. Thereafter, these orthogonal factors are clustered with probabilistic distance (PD) clustering [18,30]. PD clustering assigns units to a cluster according to their probability of membership. Different

XSL•FO
RenderX

connections between probabilities and distances can be postulated, leading to diverse methods of clustering the data. In this study, the assumption holds that the product of the probability and the distance from each point to any cluster's center is a constant; thus, it is more probable that a data point is assigned to a cluster when this point is closer to the cluster's center [37,38]. The probabilistic nature of FPDC and its ability to handle transformed data (ie, Tucker-3 decomposition) allow it to be more robust to outliers [18]. Unlike some traditional deterministic methods, FPDC does not rigidly assign outliers to clusters, which can help maintain the integrity of the main clusters. This robustness is particularly useful in real-world applications where data can be noisy or contain anomalies. To overcome unstable results due to a large number of variables and correlated variables, which is a problem with PD clustering, the transformation into orthogonal factors is important. This combination results in a clustering algorithm suitable for high-dimensional datasets [39]. Besides being suited for high-dimensional datasets with correlating variables, the FPDC algorithm is also considered in this study because of the advantages it offers: (1) being a distribution-free clustering method. It outperforms models relying on k-means clustering (eg, factorial k-means) when dealing with non–Gaussian-shaped clusters or when (2) dealing with noisy data. This is due to the probabilistic approach that is more flexible and robust in handling noise in the data. Next to these advantages, the FPDC algorithm is (3) robust to outliers [18], as mentioned before. We believe that in this study the FPDC algorithm is suitable to handle outliers and noisy data, which is an important feature because of the complexity of the data used. Next to this, the FPDC algorithm is also considered because of the vast amount of variables and the amount of correlating variables, which is also a property of this dataset.

Evaluation of the Clustering Algorithm

To assess the outcome of the FPDC algorithm (ie, definition and number of clusters), we used the average SC, which provides a measure of both the cohesion and segregation of each data point [40]. This SC is derived from the probability matrix generated by the FPDC algorithm, which assigns a probability to each point in a cluster. To achieve this, a density-based SC is used [41]. In addition, apart from computing the SC, we depicted the data in 2 dimensions using UMAP. As the SC value approaches 1, the cohesion among data points within one cluster strengthens, while the segregation between data points within that cluster, relative to those in other clusters, increases. In conjunction with this metric, UMAP offers visualization of the data in 2D space, aiding in assessing the effectiveness of the clusters and their separation.

Description of Participant Clusters

In an attempt to take a data-driven and hypothesis-free approach to find and characterize the patterns in the large and complex The Maastricht Study dataset (ie, clusters), a feature selection technique was used to find the most distinguishing variables for each cluster separately. To understand each cluster's unique combination of variables separately, after the FPDC algorithm assigned participants to clusters, we applied a feature selection model (the statistically equivalent signature [SES] algorithm [42]) for cluster C_j with fixed j {1,…,k} based on binary logistic regression as a conditional independence test [32].

The cluster assignment is decoded in such a way that



With this, a binary classification problem was thus created. The data used in this feature selection model consists of N_j data points in C_j and randomly selected data points from cluster subsets other than C_j. To ensure that no class imbalance arises, we drew a simple random sample from the data points in the other clusters, where the ratio of the number of data points from the clusters other than cluster C_j was maintained and the sum of the sampled data points equaled the number of data points in C_j. Refer to Multimedia Appendix 4 for a deeper explanation. By studying the variable importance with the SES algorithm, we can make statements about which variables have a greater impact on the classification performance (ie, which variables can better distinguish C_j from the other clusters). Since we used sampling, we sampled the data points 8 times and thus used the SES algorithm 8 times for each cluster separately to select the variables. We sampled 8 times so that (1) we could capture the loss of information as much as possible and (2) the randomness in selecting variables could be counteracted by being sampled.

Variable Selection

The SES algorithm attempts to identify predictive variables grouped into subsets, which are called signatures of the target variable, while avoiding a high degree of redundancy; it aims for a minimum size of these variable subsets and to maximize the predictive power of the variable subsets over the target variable, that is, trying to predict the binary outcome variable introduced in the previous section. The algorithm identifies multiple predictive variable subsets whose performance, in terms of predictive power, is statistically equivalent [32]. It does this by using conditional independence tests (α=.01) to assess the relationship between variables and the target variable (ie, being in a certain cluster or not) [43]. By applying these statistical tests, with an iterative forward-backward filtering technique on every variable, it will add variables that are significantly related to the target variable, conditional on already selected variables, to the subset of variables (ie, the signature) in the forward phase. It will also remove variables, after selecting a new variable, that have become redundant in their information in the subset by testing whether these variables are still significantly associated with the target variable given all other selected variables. Initially, each variable is selected in its own group. If variables seem to be interchangeable in predicting the target variable, then they will be combined into one group. The SES algorithm will pick one variable from each group to form this so-called signature. By following these steps, the SES algorithm aims to provide a minimal subset of variables that contains all the information needed to predict the target variable without adding variables that do not provide unique information to the subset of variables, considering the variables already in the subset [32,43].

In this algorithm, the use of a conditional independence test, suitable for heterogeneous data and a binary target variable,

XSL•FO
RenderX

makes it possible to extend the SES algorithm to meet the specific requirements of the dataset used in this study. Therefore, we used a conditional independence test, provided in the algorithm, that is characterized by the binary target variable and the heterogeneous predictor variables it can handle, by using the binary logistic regression model to predict the target variable. Variables emerged by the SES algorithm, in terms of differences between the clusters, can be considered as a set of variables that are selected in such a way that the variables are minimally redundant in their predictive information within the subset of variables and that, as a set of variables, have maximum predictive power toward the binary classification of the outcome variable. This property is useful in terms of the aim of this study because it will return a subset of variables that is strongly related to the cluster number without providing redundant information in the subset of variables. When using a conventional statistical test for comparison between the variables in each cluster (eg, the Mann-Whitney *U* test) on all variables, it is difficult to select variables that are very distinguishable under the condition that we do not only report on variables that provide similar information. This would lead to an unsuitable interpretation of the clusters in an attempt to find cross-links between a variety of variables within the clusters. These considerations led to the use of the SES algorithm, which was introduced by Tsamardinos et al [42], on the data used in this study.

Description of Results

We used descriptive statistics to describe the variables of the identified clusters (mean, 5-number summary, SD, and the number and percentages) to indicate whether there is distinctiveness between participants, whether they belonging to a certain cluster or not, and the outcomes in a variable of interest. We used the group differences *F* test for continuous variables and the chi-square test of independence for categorical variables at a confidence level of α=.001. To compute these measures, we used the *sumtable* function from the *vtable* package (version 1.4.4) [34]. To ensure that it is easy to compare statistics, we created separate tables for continuous and categorical variables, resulting in 6 tables. These tables are presented in Multimedia Appendices 5-10. Although all *P* values are denoted as <.001, these values are actually all less than or equal to 1.13×10^{-9}. All these variables were extracted from The Maastricht Study dataset; their explanations are available on the web [20].

Results

Overview of the study population

In total, we included 4128 eligible participants from The Maastricht Study who were obese in our data analysis (Table 1). In total, 1586 variables were included after the data preparation and thus used in the FPDC algorithm.

XSL•FO
RenderX

Table 1. General description of the sample (n=4128)

Variable and category	Value
Sex, n (%)	
Female	2246 (54.41)
Age (years), mean (SD)	60.92 (8.39)
Marital status, n (%)	
Divorced	345 (8.36)
Living together	202 (4.89)
Married	3031 (73.43)
Other marital status	22 (0.53)
Single (not necessarily never married)	308 (7.46)
Widowed	220 (5.33)
Educational level, n (%)	
Higher professional education or university education	1335 (32.34)
Intermediate vocational education, higher secondary education, or higher vocational education	1878 (45.49)
No education or primary education or lower vocational education.	915 (22.17)
Employment status, n (%)	
Employed	1672 (40.5)
Unemployed	2389 (57.87)
Other	67 (1.62)
Do or did you have a paid job? n (%)	
No	285 (6.9)
Yes	3843 (93.1)
Occupational category, n (%)	
High occupational class	496 (12.02)
Intermediate occupational class	208 (5.04)
Low occupational class	247 (5.98)
Not working	2722 (65.94)
Self-employed	446 (10.8)
Other	9 (0.22)
Waist circumference (cm), mean (SD)	
Female	99.65 (9.69)
Male	112 (8.52)
Diabetes status, n (%)	
No diabetes	1868 (45.25)
Type 2 diabetes	1434 (34.74)
Prediabetes	804 (19.48)
Other types of diabetes	22 (0.53)
Assigned numbering cluster, n (%)	
Cluster 1	1458 (35.32)
Cluster 2	1521 (36.85)
Cluster 3	1149 (27.83)

XSL•FO
RenderX

Identification of Participant Clusters

The SC in Multimedia Appendix 11 shows that 2 and 3 clusters were identified as the most optimal clustering number by the FPDC algorithm. Figure 2 shows the results of the FPDC algorithm by a UMAP projection that displays 3 distinct clusters, each with different characteristics.

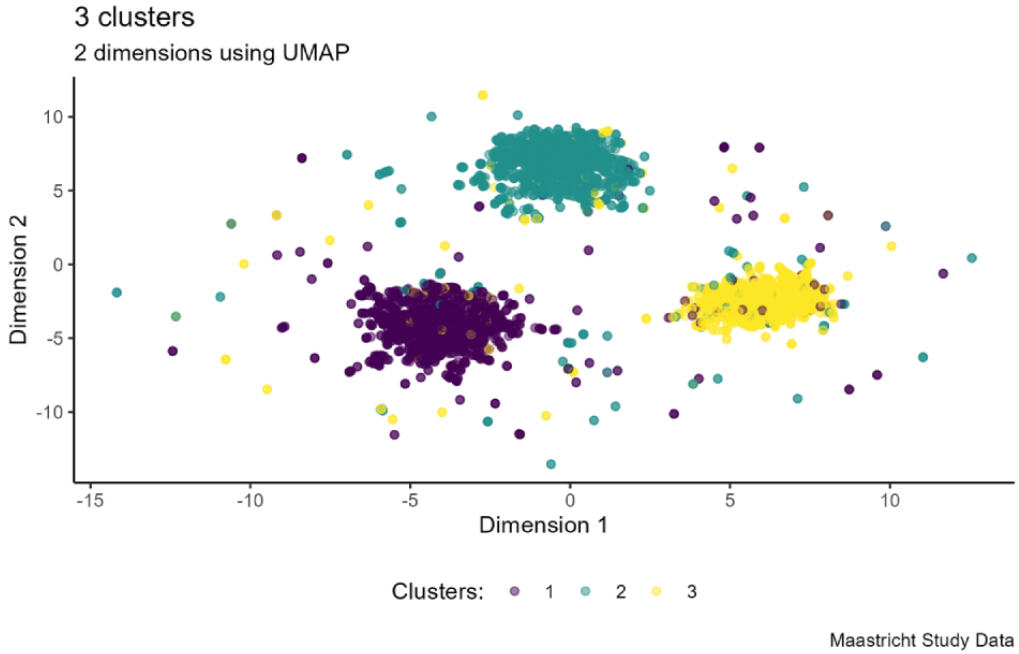
A comprehensive overview of all selected variables and how the clusters differ from the other two clusters is displayed in Multimedia Appendices 5-10. Pictured next here, a description is given of the 2 variables of each cluster with the highest *F* statistic, for continuous variables, and the highest chi-square statistic, for categorial variables, by which a cluster differed from the other 2 clusters. For more information about these variables, we refer to the online dictionary of The Maastricht Study [20].

Cluster 1 (1458/4128, 35.32%) reported on average a significantly lower energy intake (mean 1684, SD 393 kcal/day; *P*<.001) than the average kilocalorie intake for clusters 2 and 3 combined (mean 2358, SD 635 kcal/day). The most significant (*P*<.001) categorical variable was occupation. A larger proportion of cluster 1 (1236/1458, 84.77%) did not work compared with clusters 2 and 3 (1486/2670, 55.66%); in cluster 1, the proportion of high occupational category (76/1458, 5.21%) was smaller than that in clusters 2 and 3 (420/2670, 15.73%). A similar picture can be seen for the proportion of intermediate occupational class; of the 1458 participants in cluster 1, a total of 31 (2.13%) participants report being in an intermediate occupational class, against 177 (6.63%) of 2670 participants in clusters 2 and 3. Of all participants in cluster 1, 54 (3.7%) out of 1458 reported a low occupational class, against 193 (7.23%) of 2670 participants in cluster 2 and 3. Of 1458 participants in cluster 1, a total of 57 (3.91%) were self-employed; in the other 2 clusters, 389 (14.57%) out of 2670 participants were self-employed. In Figure 3, these results are visualized.

Cluster 2 (1521/4128, 36.85%) included predominantly male participants. Sex was in this cluster the most significant (*P*<.001) categorical variable. A total of 997 (65.55%) of all 1521 participants in cluster 2 were male; this was in contrast to clusters 1 and 3, where 885 (33.95%) of 2607 participants were male. Looking at the most significant continuous variable, cluster 2 reported a significantly higher energy intake (mean 2755, SD 506.2 kcal/day; *P*<.001) than clusters 1 and 3 (mean 1749, SD 375 kcal/day). In Figure 4, these results are visualized.

Cluster 3 (1149/4128, 27.83%) reported significantly higher overall cognitive functioning (mean 0.2349, SD 0.5702; *P*<.001)) than clusters 1 and 2 combined (mean –0.3088, SD 0.7212). Educational level was the most significant categorical variable (*P*<.001). A higher proportion of cluster 3 participants received higher vocational or university education (475/1149, 41.34%) compared with the other 2 clusters combined (729/2979, 24.47%). A substantially lower proportion of cluster 3 attended no education, did not complete primary education, completed only primary education, or had lower vocational education. Of 1149 participants in cluster 3, a total of 281 (24.46%) reported this low educational level. In cluster 1 and 2 combined, 1515 (50.86%) out of 2979 participants reported the same educational level. Participants in cluster 3 received, relatively more often, intermediate vocational education or higher secondary education (393/1149, 34.2%) than the other 2 clusters combined (735/2979, 24.67%). In Figure 5, these results are visualized.

Figure 2. Uniform manifold approximation and projection (UMAP) on 2D of the 3 clusters.



XSL•FO
RenderX

Figure 3. Visualization of the most significant (A) continuous and (B) categorical variable of cluster 1 versus clusters 2 and 3 combined.

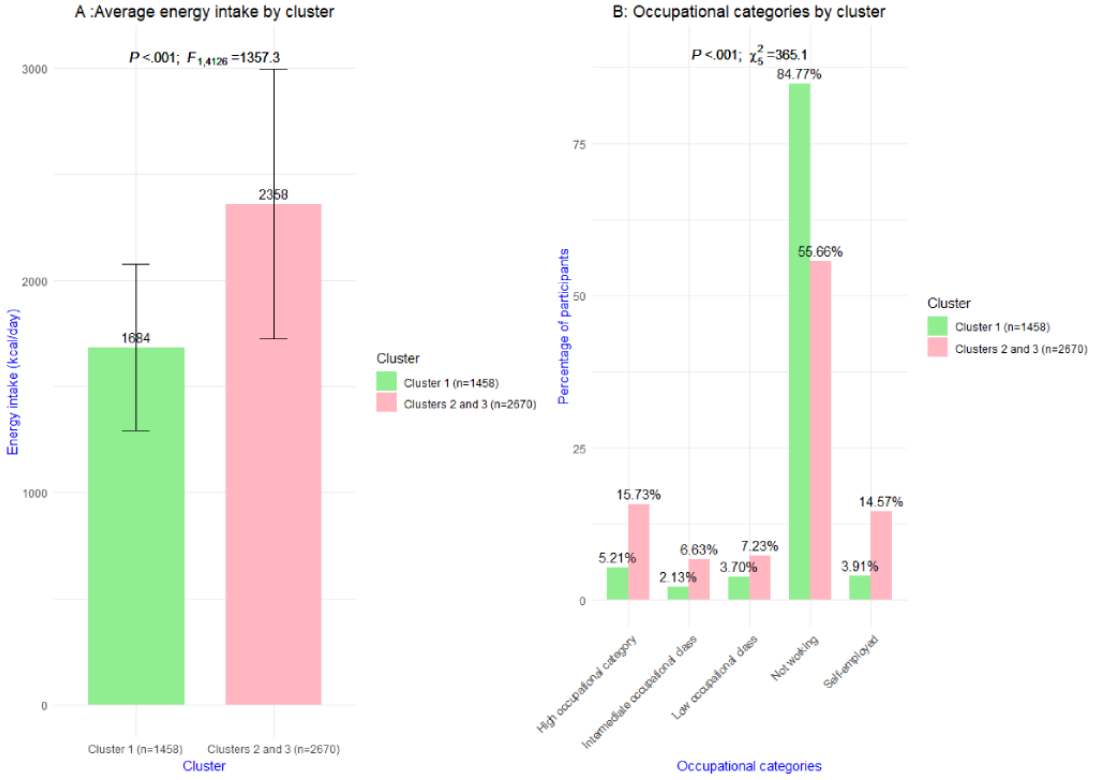
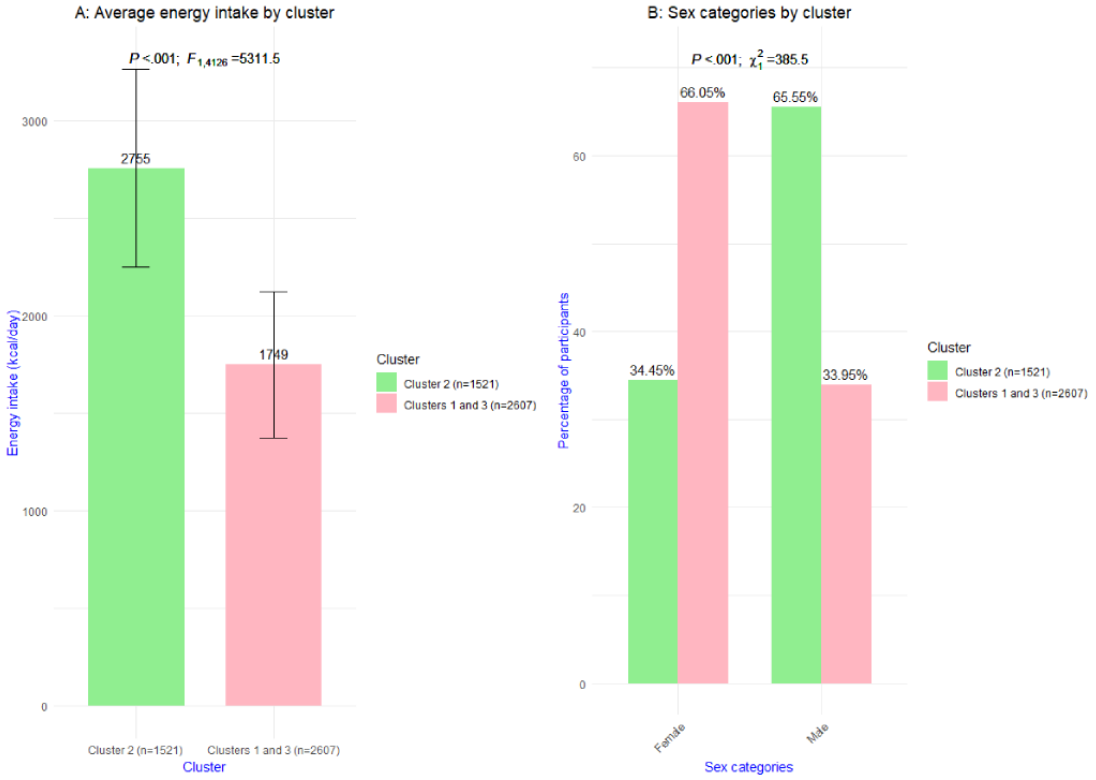
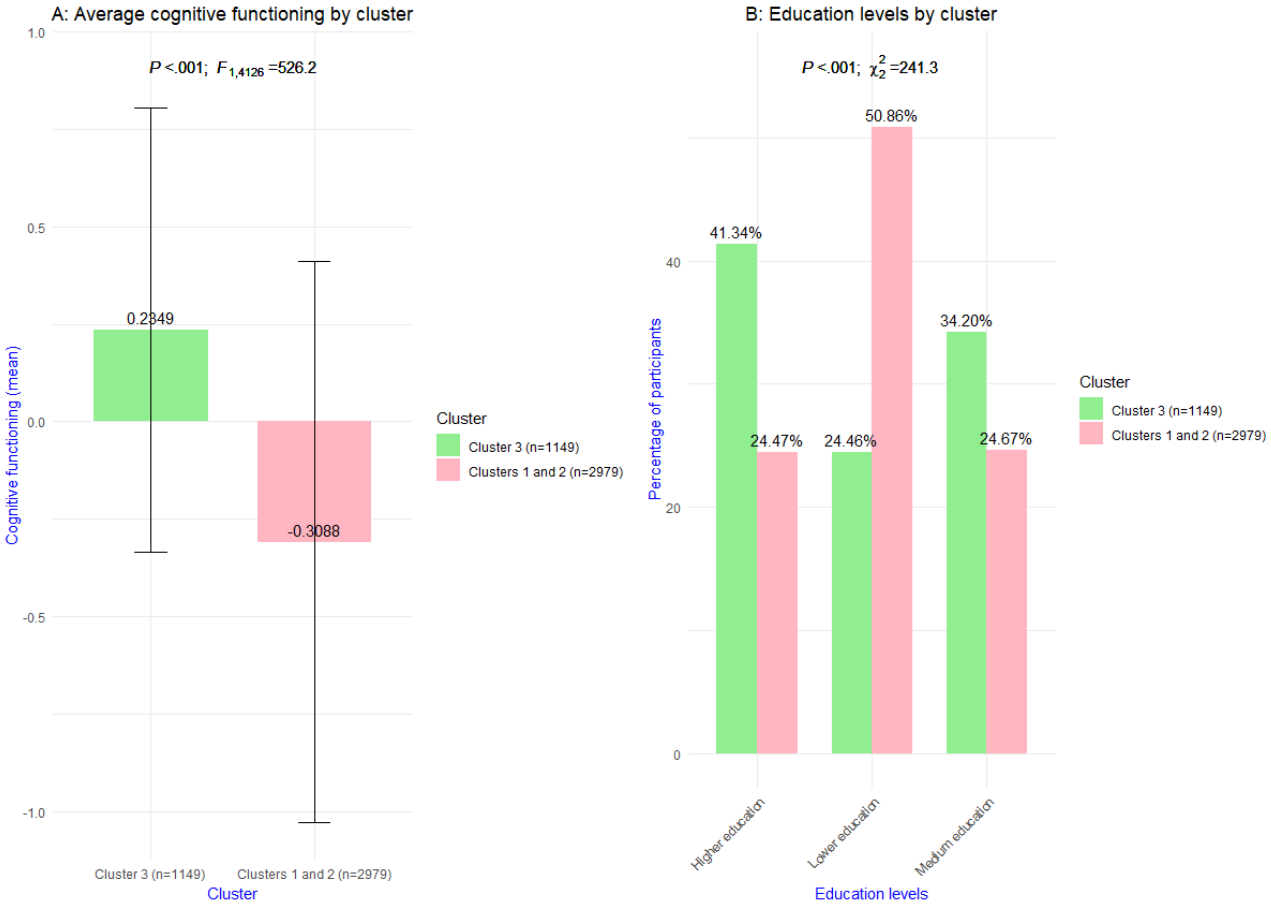


Figure 4. Visualization of the most significant (A) continuous and (B) categorical variable of cluster 2 versus clusters 1 and 3 combined.



XSL•FO
RenderX

Figure 5. Visualization of the most significant (A) continuous and (B) categorical variable of cluster 3 versus clusters 1 and 2 combined.



Discussion

Principal Findings

This study aimed to identify distinct clusters and relevant variables on which the clusters differ within a large population of individuals with obesity (n=4128) by applying an unsupervised ML algorithm. We included all available and eligible personal-level variables (2971 variables) from a population-based rich dataset of The Maastricht Study and used a hypothesis-free approach to group the data into clusters, analyzing the variables for their clustered association with obesity, without any previous human selection-based on established hypotheses.

Our novel data analysis strategy, which included (1) the FPDC algorithm, (2) SES feature selection, and (3) statistical testing, appeared valuable and successful for identifying distinct clusters within a population. This conclusion is based on the highly significant *F* and chi-square statistics observed for the selected variables across the clusters (refer to Multimedia Appendices 5-10). In this study, we chose to describe 3 clusters. This choice was based on the results of the SC and the UMAP. In this analysis strategy, we see particular strength in the use of an algorithm, specifically designed to cluster high dimensional data, in combination with the selection of a subset of minimally redundant predictive variables; this subset does not include variables that do not provide unique information in predicting the cluster numbers and has maximum predictive power over the cluster numbers generated by the clustering algorithm. This approach offers the opportunity to find relationships between the most proximate variables for obesity included in the dataset (eg, nutrition and physical activity) and the more distal variables (eg, occupation and education) that come into play in the background. This provides the opportunity to not only address the more proximal factors but also to learn about the importance of the more distal variables within the 3 different clusters. In each cluster, the root of the obesity problem might be a different one.

It should be noted, however, that the extent to which these 3 clusters could be relevant to clinical practice was not investigated in this study. To provide a meaningful interpretation and translate the findings to practical advice and programs, expert researchers, health care professionals, and representatives of those with obesity must be involved as well in field testing.

In comparison with the study of Takeshita et al [16], who also used unsupervised ML, we can point out some differences. The differences in results (eg, 7 clusters) within a population with morbid obesity may be explained by differences in the study population, type of data, and statistical analysis approach. In our study, we included individuals with obesity based on waist circumference, while Takeshita et al [16] included individuals with class 2 obesity (BMI≥35 kg/m^2). We chose not to use BMI as a measure of obesity because BMI does not take into account fat distribution throughout the body. Waist circumference is a measure of visceral fat and is strongly associated with all-cause morbidity and mortality [44]. Even though both studies used unsupervised ML, there are differences in the statistical

XSL•FO
RenderX

approach. We used the SES algorithm to identify the subset of variables that has the strongest predictive power toward the cluster number, resulting in a set of substantial distinguishing variables that are minimally redundant in their predictive information. Despite using the SES algorithm, we report variables that provide similar information (eg, energy intake reported as kilocalorie intake and kilojoule intake). This is due to using this algorithm 8 times and thus creating 8 subsets of variables for each cluster. This approach ensured the clusters were interpreted such that cross-links could be made between a variety of distinct variables within the clusters. Takeshita et al [16], on the other hand, performed a chi-square test to identify clinical variables. Nevertheless, some of our findings seem to be in line with Takeshita et al [16]. In particular, the findings of Takeshita et al [16] indicate that ocular diseases are a significant factor in differentiating cluster 4 from the other 6 obesity subgroups. In our study, we found that ocular measurements were contributing factors in the difference between cluster 1 and the other 2 clusters. In the study of Takeshita et al [16], age and sex are likely among several factors that contribute to the differences observed between the clusters. We see a similar picture in our clustering output. In Takeshita et al [16], cluster 6 is identified with the lowest hemoglobin A_{1c} (HbA_{1c}) level among the clusters. In our study, we found that cluster 3 has a significantly lower HbA_{1c} level in comparison with the other 2 clusters. This suggests that HbA_{1c} is a critical factor in differentiating these clusters from others in both studies. These findings indicate a certain similarity in the cluster characteristics. However, because The Maastricht Study offers more broadly varied data, compared to Takeshita et al [16], we can report on other potential differentiating factors such as dietary intake and energy consumption, and we also can offer insights into factors like cognitive functioning, aggression, and socioeconomic status.

This study primarily centered on the data analysis strategy. In future research, the content of the clusters should be interpreted by experts in the field of obesity and the clinical relevance should be assessed.

Limitations

Even though we used a hypothesis-free approach, data preparation was needed to apply the FPDC algorithm. For instance, The Maastricht Study data collected from participants lacked clear differentiation across all variables due to indistinguishable answer options in some variables. Essentially, these variables had significant overlap, rendering them ineffective for distinguishing between clusters. For example, the variable for ethnicity is divided into 2 categories (Caucasian or other); however, since almost 99% of the participants with obesity reported to be Caucasian, this variable is not useful to cluster on. The use of the FPDC algorithm is subject to some limitations. This algorithm can be computationally intensive, which leads to long processing times on high-dimensional data. Furthermore, this algorithm is sensitive to the choice of the initial parameters used, for example, the choice of the number of factors. In our study, we applied hyperparameter tuning to ensure a valid choice of these parameters. In addition, due to its flexibility with outliers, the FPDC algorithm may have difficulty detecting clustering structures if there is a significant size difference between clusters and the 2 clusters are not far apart. For example, if one cluster has a much larger number of units than another cluster and the clusters are not far apart, the FPDC algorithm may fail to identify the smaller cluster. Given the absence of significant differences in the number of data points across clusters in this study, we anticipate that this issue does not adversely affect our results. In our dataset, individuals diagnosed with T2D were overrepresented. In the Dutch general population, the prevalence with T2D is about 7%, but in this study, the prevalence is almost 35%. We chose not to correct for oversampling of patients with T2D in this study, because we have come to the belief that (1) this study is methodological in nature, (2) the loss of information cannot be compensated for, and (3) the objective of this study does not involve the generalization to T2D patients.

Conclusions

This study illustrates that using a hypothesis-free approach using the FPDC algorithm successfully identified 3 distinct clusters within a complex and extensive dataset concerning a population with obesity. The SES algorithm proved to be adept at uncovering highly discriminative variables that highlight differences between the clusters identified by the FPDC algorithm. Further research and collaboration with clinical experts are needed to interpret the content of the clusters and to assess potential clinical relevance.

Acknowledgments

The authors thank the owners of the data for their contribution to the conversations about the variables that are presented in the results, as their views have highly enriched our study. In particular, we thank Dr. Martijn Zoet, SB, and the Maastricht Study Management Team for their contribution to the beginning of this project. The following respondents opted to have their names acknowledged as members of the Maastricht Study Management Team:

Pieter C Dagnelie, CARIM School for Cardiovascular Diseases, Maastricht University/Department of Internal Medicine, Maastricht University Medical Center, Maastricht, the Netherlands; Marleen van Greevenbroek, Cardiovascular Research Institute Maastricht (CARIM), Maastricht University/ Department of Internal Medicine, Maastricht University, Maastricht, The Netherlands; Sebastian Köhler, School for Mental Health and Neuroscience (MHeNS) Maastricht University/Alzheimer Centrum Limburg Maastricht University Medical Center+ (MUMC+)/Department of Psychiatry and Neuropsychology, Faculty of Health, Medicine & Life Sciences Maastricht University, Maastricht, The Netherlands; Miranda T Schram, School for Mental Health and Neurosciences (MHeNs), Maastricht University/Department of Internal Medicine, Maastricht University Medical Centre/School for Cardiovascular

XSL•FO
RenderX

Disease (CARIM), Maastricht University/Heart and Vascular Centre, Maastricht University Medical Centre, Maastricht, The Netherlands; and Anke Wesselius, Department of Epidemiology Maastricht University, Maastricht, The Netherlands.

This study was supported by the European Regional Development Fund through OP-Zuid, the Province of Limburg, the Dutch Ministry of Economic Affairs (grant 31O.041), Stichting De Weijerhorst (Maastricht, The Netherlands), the Pearl String Initiative Diabetes (Amsterdam, The Netherlands), the Cardiovascular Center (CVC, Maastricht, the Netherlands), CARIM School for Cardiovascular Diseases (Maastricht, The Netherlands), CAPHRI Care and Public Health Research Institute (Maastricht, The Netherlands), NUTRIM School for Nutrition and Translational Research in Metabolism (Maastricht, the Netherlands), Stichting Annadal (Maastricht, The Netherlands), Health Foundation Limburg (Maastricht, The Netherlands), and unrestricted grants from Janssen-Cilag BV (Tilburg, The Netherlands), Novo Nordisk Farma BV (Alphen aan den Rijn, the Netherlands), and Sanofi-Aventis Netherlands BV (Gouda, the Netherlands).

Data Availability

The dataset analyzed in this study is not publicly available due to the availability of these data, which were used under license for this study but are available from the corresponding author on reasonable request and with permission of the Maastricht Study Management Team.

Authors' Contributions

MJMB and MK took responsibility for the acquisition of the data from The Maastricht Study in close consultation with CvdK and AK. MJMB and KVB designed the study. MJMB conducted a quantitative study. MK, IMK, and MJMB conducted conversations with several owners of the data. MJMB wrote the script for the data cleaning, the factor probabilistic distance clustering (FPDC) algorithm, the statistically equivalent signature (SES) algorithm, and the statistical analysis. IMK, SB, and MK discussed and took the choice for the inclusion criteria (ie, using the waist circumference) and discussed the variables in the analyses. IMK and MJMB drafted the manuscript, and MK, SB, and KVB reviewed all versions of the manuscript. All authors read and contributed to editing the manuscript for final submission.

Conflicts of Interest

None declared.

Multimedia Appendix 1
Handling missing data including imputation.
[DOC File , 33 KB - medinform_v13i1e64479_app1.doc]

Multimedia Appendix 2
Preparing data for clustering.
[DOC File , 29 KB - medinform_v13i1e64479_app2.doc]

Multimedia Appendix 3
Flowchart: dataset preparation.
[DOC File , 195 KB - medinform_v13i1e64479_app3.doc]

Multimedia Appendix 4
Sampling data for the use of the SES algorithm. SES: statistically equivalent signature.
[DOC File , 235 KB - medinform_v13i1e64479_app4.doc]

Multimedia Appendix 5
Table with cluster 1 (n=1458) compared to clusters 2 and 3 combined (n=2670), continuous variables.
[DOC File , 288 KB - medinform_v13i1e64479_app5.doc]

Multimedia Appendix 6
Table with cluster 1 (n=1458) compared to clusters 2 and 3 combined (n=2670), categorical variables.
[DOC File , 121 KB - medinform_v13i1e64479_app6.doc]

Multimedia Appendix 7
Table with cluster 2 (n=1521) compared to clusters 1 and 3 combined (n=2607), continuous variables.
[DOC File , 226 KB - medinform_v13i1e64479_app7.doc]

XSL•FO
RenderX

Multimedia Appendix 8
Table with cluster 2 (n=1521) compared to clusters 1 and 3 combined (n=2607), categorical variables.
[DOC File , 50 KB - medinform_v13i1e64479_app8.doc]

Multimedia Appendix 9
Table with cluster 3 (n=1149) against clusters 1 and 2 combined (n=2979), continuous variables.
[DOC File , 323 KB - medinform_v13i1e64479_app9.doc]

Multimedia Appendix 10
Table with cluster 3 (n=1149) against clusters 1 and 2 combined (n=2979), categorical variables.
[DOC File , 96 KB - medinform_v13i1e64479_app10.doc]

Multimedia Appendix 11
Silhouette coefficient per number of clusters.
[PNG File , 12 KB - medinform_v13i1e64479_app11.png]

References

1. Khoury MJ, Gwinn M, Ioannidis JPA. The emergence of translational epidemiology: from scientific discovery to population health impact. Am J Epidemiol 2010;172(5):517-524 [FREE Full text] [doi: 10.1093/aje/kwq211] [Medline: 20688899]
2. Fischer M. Fit for the future? A new approach in the debate about what makes healthcare systems really sustainable. Sustainability 2014;7(1):294-312. [doi: 10.3390/su7010294]
3. (RIVM) RvVeM. Ministerie van Volksgezondheid, Welzijn en Sport. Sustainable care and prevention (SPR 2019-2022). 2019. URL: https://www.rivm.nl/en/about-rivm/knowledge-and-expertise/strategic-programme-rivm/2019-2022/sustainable-care-and-prevention [accessed 2024-04-02]
4. Eykelenboom M, Boer J, ten DJ, Sanderman-Nawijn E, Hoekstra J, Bogaardt L, et al. Worden de ambities voor 2040 bereikt? Calculating the impact of the National Prevention Agreement ? subagreement on overweight Will the 2040 ambitions be reached?: Rijksinstituut voor Volksgezondheid en Milieu. Doorrekening Impact Nationaal Preventieakkoord: Deelakkoord Overgewicht. URL: https://www.rivm.nl/publicaties/doorrekening-impact-nationaal-preventieakkoord-deelakkoord-overgewicht-worden-ambities [accessed 2024-01-17]
5. Luna Pinzon A, Stronks K, Dijkstra C, Renders C, Altenburg T, den Hertog K, et al. The ENCOMPASS framework: a practical guide for the evaluation of public health programmes in complex adaptive systems. Int J Behav Nutr Phys Act 2022;19(1):33 [FREE Full text] [doi: 10.1186/s12966-022-01267-3] [Medline: 35346233]
6. Lee BY, Bartsch SM, Mui Y, Haidari LA, Spiker ML, Gittelsohn J. A systems approach to obesity. Nutr Rev 2017;75(suppl 1):94-106 [FREE Full text] [doi: 10.1093/nutrit/nuw049] [Medline: 28049754]
7. Noar SM, Benac CN, Harris MS. Does tailoring matter? Meta-analytic review of tailored print health behavior change interventions. Psychol Bull 2007;133(4):673-693. [doi: 10.1037/0033-2909.133.4.673] [Medline: 17592961]
8. Lustria MLA, Noar SM, Cortese J, Van Stee SK, Glueckauf RL, Lee J. A meta-analysis of web-delivered tailored health behavior change interventions. J Health Commun 2013;18(9):1039-1069. [doi: 10.1080/10810730.2013.768727] [Medline: 23750972]
9. Broekhuizen K, Kroeze W, van Poppel NM, Oenema A, Brug J. A systematic review of randomized controlled trials on the effectiveness of computer-tailored physical activity and dietary behavior promotion programs: an update. Ann Behav Med 2012;44(2):259-286 [FREE Full text] [doi: 10.1007/s12160-012-9384-3] [Medline: 22767052]
10. Benke K, Benke G. Artificial intelligence and big data in public health. Int J Environ Res Public Health 2018;15(12):2796 [FREE Full text] [doi: 10.3390/ijerph15122796] [Medline: 30544648]
11. Burk H. Learning from Data: Artificial Intelligence and Statistics V. New York: Springer; 1996.
12. Zhang S, Bamakan SMH, Qu Q, Li S. Learning for personalized medicine: a comprehensive review from a deep learning perspective. IEEE Rev Biomed Eng 2019;12:194-208. [doi: 10.1109/RBME.2018.2864254] [Medline: 30106692]
13. Nagamine T, Gillette B, Kahoun J, Burghaus R, Lippert J, Saxena M. Data-driven identification of heart failure disease states and progression pathways using electronic health records. Sci Rep 2022;12(1):17871 [FREE Full text] [doi: 10.1038/s41598-022-22398-4] [Medline: 36284167]
14. Nicolet A, Assouline D, Le Pogam MA, Perraudin C, Bagnoud C, Wagner J, et al. Exploring patient multimorbidity and complexity using health insurance claims data: a cluster analysis approach. JMIR Med Inform 2022;10(4):e34274 [FREE Full text] [doi: 10.2196/34274] [Medline: 35377334]
15. Elbattah M, Molloy O. Data-driven patient segmentation using k-means clustering: the case of hip fracture care in Ireland. 2017 Presented at: Proceedings of the Australasian Computer Science Week Multiconference; 2017 January 30; Australia. [doi: 10.1145/3014812.3014874]

XSL•FO
RenderX

16. Takeshita S, Nishioka Y, Tamaki Y, Kamitani F, Mohri T, Nakajima H, et al. Novel subgroups of obesity and their association with outcomes: a data-driven cluster analysis. BMC Public Health 2024;24(1):124 [FREE Full text] [doi: 10.1186/s12889-024-17648-1] [Medline: 38195492]
17. Vogelzangs N, van der Kallen CJH, van Greevenbroek MMJ, van der Kolk BW, Jocken JWE, Goossens GH, et al. Metabolic profiling of tissue-specific insulin resistance in human obesity: results from the Diogenes Study and the Maastricht Study. Int J Obes (Lond) 2020;44(6):1376-1386. [doi: 10.1038/s41366-020-0565-z] [Medline: 32203114]
18. Tortora C, Summa MG, Marino M, Palumbo F. Factor probabilistic distance clustering (FPDC): a new clustering method. Adv Data Anal Classif 2015;10(4):441-464. [doi: 10.1007/s11634-015-0219-5]
19. Schram MT, Sep SJS, van der Kallen CJ, Dagnelie PC, Koster A, Schaper N, et al. The Maastricht Study: an extensive phenotyping study on determinants of type 2 diabetes, its complications and its comorbidities. Eur J Epidemiol 2014;29(6):439-451. [doi: 10.1007/s10654-014-9889-0] [Medline: 24756374]
20. Data dictionary. The Maastricht Study. 2024. URL: https://demaastrichtstudie.app/data-dictionary/ [accessed 2023-04-15]
21. Klein S, Romijn JA. Williams Textbook of Endocrinology (Thirteenth Edition). Philadelphia. In: Melmed S, Polonsky KS, Larsen PR, Kronenberg HM, editors. Chapter 36 - Obesity. Netherlands: Elsevier; 2016.
22. Stekhoven DJ, Bühlmann P. MissForest--non-parametric missing value imputation for mixed-type data. Bioinformatics 2012;28(1):112-118. [doi: 10.1093/bioinformatics/btr597] [Medline: 22039212]
23. Buuren S, Groothuis-Oudshoorn K. Multivariate imputation by chained equations in. J. Stat. Soft 2011;45(3). [doi: 10.18637/jss.v045.i03]
24. Biau G, Scornet E. A random forest guided tour. TEST 2016;25(2):197-227. [doi: 10.1007/s11749-016-0481-7]
25. Tang F, Ishwaran H. Random forest missing data algorithms. Stat Anal Data Min 2017;10(6):363-377 [FREE Full text] [doi: 10.1002/sam.11348] [Medline: 29403567]
26. Pestov V. Is the-NN classifier in high dimensions affected by the curse of dimensionality? Computers & Mathematics with Applications 2013;65(10):1427-1437. [doi: 10.1016/j.camwa.2012.09.011]
27. Kokla M, Virtanen J, Kolehmainen M, Paananen J, Hanhineva K. Random forest-based imputation outperforms other methods for imputing LC-MS metabolomics data: a comparative study. BMC Bioinformatics 2019;20(1):492 [FREE Full text] [doi: 10.1186/s12859-019-3110-0] [Medline: 31601178]
28. Mayer M. missRanger: fast imputation of missing values. 2023. URL: https://cran.r-project.org/web/packages/missRanger/index.html [accessed 2023-04-28]
29. Tortora C, Vidales N, Palumbo F, Kalra T, McNicholas P. FPDclustering. 2022. URL: https://CRAN.R-project.org/package=FPDclustering [accessed 2022-08-31]
30. Tortora C, Summa M, Palumbo F. Factor PD-clustering. Cham: Springer International Publishing; 2013.
31. Biza K, Tsamardinos I, Lagani V, Athineou G, Tsagris M, Borboudakis G. MXM: feature selection (including multiple solutions) and Bayesian networks. URL: https://CRAN.R-project.org/package=MXM [accessed 2023-01-12]
32. Lagani V, Athineou G, Farcomeni A, Tsagris M, Tsamardinos I. Feature selection with the package discovering statistically equivalent feature subsets. J. Stat. Soft 2017;80(7):1-25. [doi: 10.18637/jss.v080.i07]
33. Melville J, Lun A, Djekidel M, Hao Y, Eddelbuettel D. uwot: the uniform manifold approximation and projection (UMAP) method for dimensionality reduction. URL: https://CRAN.R-project.org/package=uwot [accessed 2022-08-22]
34. Huntington-Klein N. vtable: variable table for variable documentation. URL: https://CRAN.R-project.org/package=vtable [accessed 2023-04-29]
35. Nagamine T, Gillette B, Pakhomov A, Kahoun J, Mayer H, Burghaus R, et al. Multiscale classification of heart failure phenotypes by unsupervised clustering of unstructured electronic medical record data. Sci Rep 2020;10(1):21340 [FREE Full text] [doi: 10.1038/s41598-020-77286-6] [Medline: 33288774]
36. Tsuchida J, Yadohisa H. Tucker-3 decomposition with sparse core array using a penalty function based on Gini-index. Jpn J Stat Data Sci 2022;5(2):675-700. [doi: 10.1007/s42081-022-00179-7]
37. Ben-Israel A, Iyigun C. Probabilistic D-Clustering. J Classif 2008;25(1):5-26. [doi: 10.1007/s00357-008-9002-z]
38. Tortora C, Palumbo F. FPDclustering: a comprehensive R package for probabilistic distance clustering based methods. Comput Stat 2024. [doi: 10.1007/s00180-024-01490-5]
39. Tortora C, Marino M. Robustness and stability analysis of factor PD-clustering on large social datasets. In: Vicari D, Okada A, Ragozini G, Weihs C, editors. Analysis and Modeling of Complex Data in Behavioral and Social Sciences. Cham: Springer; 2014.
40. Rousseeuw PJ. Silhouettes: a graphical aid to the interpretation and validation of cluster analysis. Journal of Computational and Applied Mathematics 1987;20:53-65. [doi: 10.1016/0377-0427(87)90125-7]
41. Menardi G. Density-based silhouette diagnostics for clustering methods. Stat Comput 2010;21(3):295-308. [doi: 10.1007/s11222-010-9169-0]
42. Tsamardinos I, Lagani V, Pappas D. Discovering multiple, equivalent biomarker signatures. 2012 Presented at: Proc 7th Conf Hellenic Soc Comput Biol Bioinf; 2012 October 6; Hellas.
43. Tsagris M, Lagani V, Tsamardinos I. Feature selection for high-dimensional temporal data. BMC Bioinformatics 2018;19(1):17 [FREE Full text] [doi: 10.1186/s12859-018-2023-7] [Medline: 29357817]

XSL•FO
RenderX

44. Ross R, Neeland IJ, Yamashita S, Shai I, Seidell J, Magni P, et al. Waist circumference as a vital sign in clinical practice: a consensus statement from the IAS and ICCR working group on visceral obesity. Nat Rev Endocrinol 2020;16(3):177-189 [FREE Full text] [doi: 10.1038/s41574-019-0310-7] [Medline: 32020062]

Abbreviations

CRF: chained random forests
FPDC: factor probabilistic distance clustering
HbA1c: hemoglobin A1c
ML: machine learning
PD: probabilistic distance
SC: silhouette coefficient
SES: statistically equivalent signature
T2DM: type 2 diabetes mellitus
UMAP: uniform manifold approximation and projection

Edited by J Klann; submitted 18.07.24; peer-reviewed by S Koks, M Elbattah, X Zou; comments to author 07.10.24; revised version received 28.11.24; accepted 09.12.24; published 05.02.25.

Please cite as:
Beuken MJM, Kleynen M, Braun S, Van Berkel K, van der Kallen C, Koster A, Bosma H, Berendschot TTJM, Houben AJHM, Dukers-Muijrers N, van den Bergh JP, Kroon AA, Maastricht Study Management, Kanera IM
Identification of Clusters in a Population With Obesity Using Machine Learning: Secondary Analysis of The Maastricht Study
JMIR Med Inform 2025;13:e64479
URL: https://medinform.jmir.org/2025/1/e64479
doi:10.2196/64479
PMID:

©Maik JM Beuken, Melanie Kleynen, Susy Braun, Kees Van Berkel, Carla van der Kallen, Annemarie Koster, Hans Bosma, Tos TJM Berendschot, Alfons JHM Houben, Nicole Dukers-Muijrers, Joop P van den Bergh, Abraham A Kroon, Maastricht Study Management, Iris M Kanera. Originally published in JMIR Medical Informatics (https://medinform.jmir.org), 05.02.2025. This is an open-access article distributed under the terms of the Creative Commons Attribution License (https://creativecommons.org/licenses/by/4.0/), which permits unrestricted use, distribution, and reproduction in any medium, provided the original work, first published in JMIR Medical Informatics, is properly cited. The complete bibliographic information, a link to the original publication on https://medinform.jmir.org/, as well as this copyright and license information must be included.

XSL•FO
RenderX

Original Paper

An Interpretable Model With Probabilistic Integrated Scoring for Mental Health Treatment Prediction: Design Study

Anthony Kelly[1,2], PhD; Esben Kjems Jensen[3], MSc; Eoin Martino Grua[1], PhD; Kim Mathiasen[4,5], PhD; Pepijn Van de Ven[1,2], PhD

[1]Department of Electronic and Computer Engineering, University of Limerick, Limerick, Ireland

[2]Health Research Institute, University of Limerick, Limerick, Ireland

[3]Center for Digital Psykiatri, Forskningsenhed, Denmark

[4]Department of Psychology and Behavioural Sciences, Aarhus University, Aarhus, Denmark

[5]Department of Clinical Research, University of Southern Denmark, Odense, Denmark

Corresponding Author:
Anthony Kelly, PhD
Department of Electronic and Computer Engineering
University of Limerick
Castletroy
Limerick, V94 T9PX
Ireland
Phone: 353 087545973
Email: anthony.kelly@ul.ie

Abstract

Background: Machine learning (ML) systems in health care have the potential to enhance decision-making but often fail to address critical issues such as prediction explainability, confidence, and robustness in a context-based and easily interpretable manner.

Objective: This study aimed to design and evaluate an ML model for a future decision support system for clinical psychopathological treatment assessments. The novel ML model is inherently interpretable and transparent. It aims to enhance clinical explainability and trust through a transparent, hierarchical model structure that progresses from questions to scores to classification predictions. The model confidence and robustness were addressed by applying Monte Carlo dropout, a probabilistic method that reveals model uncertainty and confidence.

Methods: A model for clinical psychopathological treatment assessments was developed, incorporating a novel ML model structure. The model aimed at enhancing the graphical interpretation of the model outputs and addressing issues of prediction explainability, confidence, and robustness. The proposed ML model was trained and validated using patient questionnaire answers and demographics from a web-based treatment service in Denmark (N=1088).

Results: The balanced accuracy score on the test set was 0.79. The precision was ≥0.71 for all 4 prediction classes (depression, panic, social phobia, and specific phobia). The area under the curve for the 4 classes was 0.93, 0.92, 0.91, and 0.98, respectively.

Conclusions: We have demonstrated a mental health treatment ML model that supported a graphical interpretation of prediction class probability distributions. Their spread and overlap can inform clinicians of competing treatment possibilities for patients and uncertainty in treatment predictions. With the ML model achieving 79% balanced accuracy, we expect that the model will be clinically useful in both screening new patients and informing clinical interviews.

(JMIR Med Inform 2025;13:e64617) doi:10.2196/64617

KEYWORDS

machine learning; mental health; Monte Carlo dropout; explainability; explainable AI; XAI; artificial intelligence; AI

XSL•FO
RenderX

Introduction

Overview

As in most areas of human activity, mental health care has seen an increase in the application of artificial intelligence (AI), particularly in assisting the diagnosis and treatment of mental disorders [1]. While the debate between clinical judgment and statistical methods is longstanding in the field of clinical psychology [2], under appropriate conditions, statistical tools can perform as well as—or better than—clinical judgment in diagnosing psychopathologies [3]. To be effective, these statistical tools should be context-based and simple for clinicians to use [3,4].

When assessing patients for treatment in a mental health setting, clinicians consider various screening instruments in addition to demographic and medical information, assessing the scores related to possible diagnoses and treatments based on the patient's answers to questions [5]. Patients with complex clinical scenarios present a challenge for clinicians in assessing the various possible symptoms to arrive at a most likely diagnosis [6]. In diagnosing depression, for example, comorbidity with anxiety disorders and other factors was found to lead to uncertainty in diagnosis in as many as 40% of cases [7]. The consequences of an uncertain diagnosis may be high rates of treatment-resistant depression [7,8].

Early correct intervention may reduce the burden of disease for the individual as well as the society. The global costs of mental disorders were estimated to be US $2493 billion in 2010 and are expected to more than double by 2030 [9]. Wittchen et al [10] deemed mental disorders "the core health challenge of the 21st century." In their key recommendations for future research, they state that "clinically sensitive and economically feasible decision algorithms could be explored to determine what types of interventions should be assigned to which type of patient." Therefore, insight into the underlying factors that characterize a psychopathological diagnosis and the factors that discriminate between alternative diagnoses is valuable and a contribution to solving a larger and urgent health need.

Mental health care has benefited from the ability of AI technologies to analyze data, infer classifications from new data, and communicate insights from data [11]. AI has been recognized as an important tool in clinical decision-making for mental health [12]. In assessment, AI technologies offer the potential to complement the role of clinicians with diagnostic decision support technologies [13,14]. Such diagnostic tools require the AI models to be explainable and interpretable [15], both in terms of the model itself (global) and the individual model predictions (local). Interpretability refers to how a model arrives at a decision, and explainability refers to why the decision is reached [16]. While explainability in AI has been a topic of interest since the 1980s, the recent accelerations in the widespread use of AI have resulted in guidelines on the responsible use of AI. Responsible AI requires a robust model that conveys the confidence and degree of uncertainty in prediction [16-18]. Although confidence and uncertainty estimation are considered a necessity for medical AI models to enable safe clinical deployment [19], it has been claimed that most machine learning (ML) methods in the recent medical literature neglect the important issue of model uncertainty [19].

This paper presents the design of an ML model for psychopathological mental health treatment tailored to the omnipresent questionnaire-type screening instruments. The AI model described here is based on a novel hierarchical structure that aims to meet the needs of clinical interpretability while accounting for decision confidence and uncertainty. The presented approach facilitates the questionnaire instruments that are typically used in mental health care to assess symptom severity, but in a data-driven way [13], while leveraging any other information known about respondents.

This paper first lays out the rationale for explainable AI (XAI) methods in medical models, introducing the important issues of model confidence and uncertainty. Typical ways in which model confidence and uncertainty can be quantified are introduced with an emphasis on Monte Carlo dropout (MCD), the method used in this paper. The model structure is then introduced and shown to provide interpretability by design with confidence and uncertainty estimation provided through the use of MCD. Next, model training and validation on clinical data from a Danish web-based mental health treatment service are detailed and results presented. Finally, the implications of the work are discussed.

Background

After initial interest in the explainability of AI models in the 1980s and 1990s, recent advances in AI and ML, and the increased use of such technologies in safety-critical, socioeconomically and medically impactful applications have driven a renewed interest in XAI [20]. The explainability of AI models is generally understood as the ability for a wider range of users to understand the outputs of a given AI or ML model [21]. The concept of interpretability is closely related and refers to the ability of a person to understand how a given set of inputs results in a model output [22].

As an extension to the explainability of ML models, recent endeavors have put more emphasis on responsible or trustworthy AI [23], with confidence and robustness being important technical prerequisites. The confidence of an ML algorithm is defined as the model's own assessment that the provided inferences are correct. Robustness is defined as the ability of a model to yield consistent results in the presence of uncertainty [16]. In practice, robustness can be evaluated by perturbing the model structure to induce distribution shifts [24], introducing epistemic uncertainty. According to XAI frameworks, robustness extends explainability while increasing stability and user satisfaction [16]. Such measures of confidence and robustness are important for a model aimed at medical decision support systems (DSSs), such as the one presented in this paper [25].

ML Methods in Relation to XAI

Logistic regression is a classification model used in ML that applies a linear combination of the data X, with weights W, to discriminate between classes of the dependent variable Y. It models the probability of an outcome using a logistic (sigmoid) function:

XSL•FO
RenderX



(1)

Since the equation consists of a linear combination of the features transformed by a sigmoid function, each weight of the model directly corresponds to the weight of a feature in determining the output. Because of this linear nature, XAI deems logistic regression to be a white-box model [16,18]. White-box models are also referred to as having the property of transparency [18]. In contrast, gray-box models and black-box models are categories of AI models with less ability to inspect the inner workings of the model (less interpretability and less transparency), but typically with more power to discriminate, and are often used in complex applications such as computer vision. This property of powerful models being black-box is often referred to as the interpretability-performance trade off [26]. Other common white-box ML models include decision trees and K-nearest neighbor models [18]. Deep neural networks are an example of a black-box model due to their many stacked nonlinear layers, typically consisting of millions of weights, which make their operation uninterpretable. Post hoc techniques add interpretability as an additional method or algorithm to the AI model [16]. One such approach is to add an additional, surrogate model that simplifies relevant sections of the AI model to be explained. Local interpretable model-agnostic explanations (LIME) [27] is a method that can explain the prediction of any classifier by building a local model that aims to approximate the original model and its predictions. The new model is chosen to be an interpretable model (such as logistic regression). This allows the user to better understand the relationship between a single input and the corresponding output prediction by providing a local explanation and is, therefore, an explanation by simplification. However, LIME has some drawbacks: it does not inherently provide global explanations of the dataset as a whole and it can experience inconsistency because it requires multiple perturbations of input data and retraining local surrogate models [28]. An alternative XAI method that ranks the importance of features used by the model is Shapley additive explanations (SHAP) [29]. SHAP is a method that calculates an additive feature importance score, which can provide local explanations for individual predictions as well as global explanations for the whole dataset. However, SHAP may experience sensitivity to feature perturbations and to feature correlations and interactions [30]. As a whole, a drawback of post hoc explainability techniques is that they approximate the model's decision-making rather than directly reflecting its internal structure.

Since explaining black-box models requires post hoc techniques, SHAP and LIME have been applied to deep learning models in medical applications, for example, to aid the explainability of complex convolutional neural network medical diagnostic models for chest X-ray classification for COVID-19 infection [31]. SHAP has also been applied as a backend explanation module for a neural network predictor of COVID-19 infection diagnosis in eHealth record data [32], providing both local and global explanations. Post hoc XAI techniques, such as these, represent the vast majority of XAI use cases in health care [33]. To overcome the drawbacks of post hoc methods, our new approach offers an inherently interpretable model for predicting mental health treatment outcomes. Its transparency stems from a logistic regression framework, which, as described earlier, is interpretable as it is possible to make a direct link between the value of an input parameter, its associated weight, and the prediction made by the model. Moreover, by using a hierarchical structure that moves from questions to scores to classification predictions, this design enables users to understand how and why the model makes decisions, both at the questionnaire score level and the individual question level.

Responsible AI

As previously stated, responsible AI requires an understanding of its own confidence and robustness in inferences. The advent of deep learning has resulted in a step change in the performance of models and the associated practical use of AI. However, this has come with disadvantages. Deep learning models can be confidently wrong, especially in case of a shift in the input data, and in recent years, such overconfidence in incorrect inferences has proved fatal, as illustrated by serious accidents caused by machine vision models in cars [34]. Most ML algorithms provide point-estimate predictions, meaning they provide an inference with, at best, a scalar estimate of the model's confidence in the inference. More recently, methods based on the application of Bayesian statistics have been proposed [35]. In such methods, rather than estimating a point estimate, the models provide a probabilistic inference modeled by a probability distribution. This distribution can then be used for a point-estimate inference (eg, by taking the mode of the distribution as the inference) and can also be used to assess the model's uncertainty in this inference by considering the shape of the probability distribution. Distributions strongly peaked around the inference indicate low uncertainty; very wide and flat distributions around the inference indicate high uncertainty.

These models often also provide probabilistic information on the effect of model predictions in the face of perturbations in the input features. For example, Cardelli et al [36] showed that for Bayesian inference with Gaussian processes, a class of algorithms overlapping with deep neural networks that have inherent uncertainty estimates [19], the model's uncertainty in response to perturbations in the input space can be upper-bounded, thus providing a measure for the model's robustness.

If a full Bayesian probability distribution is established for all parameters in the model, with statistics either learned from data or based on existing knowledge, it can then be used to investigate the confidence and robustness of the model. However, a significant drawback of this approach is that it can be compute-intensive [37].

An alternative method called MCD is inspired by using the dropout layers in deep neural networks to improve the ability of a network to "generalize," or provide good quality predictions on yet unseen data [38]. When used to allow the model to generalize well, dropout sets weights of the model to 0 randomly during training only [38]. The result is that the trained model does not become overreliant on any one (potentially spurious) characteristic of the data. In contrast, MCD also uses dropout when new predictions are made. It does so by obtaining repeated

XSL•FO
RenderX

inferences from the trained model, but with different weights dropped out in every iteration of the inference. The result is a distribution of inferences rather than a point-estimate. Such inference distributions can be shown to be equivalent to those obtained by a fully Bayesian model for an important family of probabilistic models, called Gaussian process models, when dropout is applied before every weight layer [39]. Consequently, MCD results in a Bayesian approximation by randomly switching off connections in the network during inference.

MCD has been applied to estimate uncertainty in medical imaging AI convolutional neural network models where the model perturbations allow the estimation of epistemic uncertainty in the prediction of potentially cancerous skin lesions [17] and brain tumors [40]. Using this method, the model is sampled N times with dropout elements set to 0 randomly according to Bernoulli random variables. Given a prediction s^*, the model is sampled N times, with model parameters  at each iteration, to yield the sample distribution y^*. The mean value of class c (μ_c) of the sample is the prediction probability of the class, while the variance of class c (σ_c^2) is the uncertainty measure:



(2)



(3)

Methods

Overview

This paper presents a methodology to obtain explainable, interpretable models that are robust and provide a reliable confidence score for use with an important class of data in mental health, namely that of sum-score questionnaires. The model uses the answers to individual questions as inputs, but also explicitly represents the traditionally used sum-scores of such questionnaires in the model. Hence, explainability and interpretability are provided both at the question level and at the sum-score level. To also provide robustness and a measure of model confidence in its predictions, MCD is applied as described in the previous section.

The ability of the proposed model to provide interpretable predictions as well as estimates of confidence is demonstrated with a use case aimed at providing clinicians with treatment recommendations for several mental disorders.

Metrics

Precision, recall, F_1-score, balanced accuracy score, weighted F_1-score, and area under the curve (AUC) are relevant metrics for evaluating the predictive model's classification performance. Precision measures the proportion of correctly predicted treatment decisions among all predictions for a given class. A high precision score ensures that the model minimizes incorrect treatment assignments. Recall (or sensitivity) assesses the proportion of correctly predicted treatments among all actual instances of that class, reflecting the model's ability to identify the correct treatment when needed. F_1-score is the harmonic mean of precision and recall, balancing both metrics to provide a single performance measure, particularly useful in cases of class imbalance. The balanced accuracy score is the average of recall across all classes, accounting for imbalanced class distributions by ensuring each class contributes equally to the overall performance evaluation. Weighted F_1-score adjusts the F_1-score by considering class frequencies, preventing minority classes from being overshadowed in imbalanced datasets. The AUC measures the model's ability to distinguish between different treatment classes, with higher values indicating better discrimination. During validation these metrics ensure reliable treatment predictions, minimize incorrect classifications, and balance performance across all treatment options, reducing potential clinical risks.

Data

A dataset comprising patient questionnaire answers and demographics was used to train and validate the model. The data were gathered between November 14, 2019, and December 31, 2022, from patients of the "Internetpsykiatrien" web-based treatment services delivered by the Centre for Digital Psychiatry, Denmark. The center delivers routine care internet-delivered cognitive behavioral therapy with nationwide coverage [41]. The data consisted of answers to the Patient Health Questionnaire-9 (PHQ-9) [42], the Generalized Anxiety Disorder Questionnaire-7 (GAD-7) [43], the Social Interaction Anxiety Scale (SIAS) [44], the Panic Disorder Severity Scale (PDSS) [45], and the Fear Questionnaire [46]. Additional features included demographic information and a brief medical history, such as previously diagnosed conditions.

The ground truth of the dataset was the choice of treatment selected by the psychologists in the clinic for each patient. The treatment decision was reached using multiple steps. First, clinical psychologists or psychologists under the supervision of a clinical psychologist, assessed patients using questionnaires to determine the optimal treatment. This assessment used the same questionnaire and demographic data that was used by the model, except for free text data, which were available to the psychologists, but not to the model. Second, they performed a clinical assessment interview, including the use of the semistructured interview, Mini Neuropsychiatric Interview. Any ambiguities were discussed at a clinical conference.

A total of 91 input features were selected for inclusion in the models (Table 1), with data completeness as the primary inclusion criterion. The dataset (N=1068) was randomly split into a training set (n=801, 75%) and a test set (n=267, 25%). The training data consisted of 4 prediction class categories as follows: (1) depression (n=269, 33.6%); (2) panic (n=269, 33.6%); (3) social phobia (n=193, 24.1%); and (4) specific phobia (n=70, 8.7%). The test set class categories were stratified to match the training set in proportion: 33.7% (90/267); 33.3% (89/267); 24% (64/267); and 9% (24/267) for the 4 classes, respectively.

XSL•FO
RenderX

The percentages of training or test set data per class were: 34% (269/801); 34% (269/801); 24% (193/801); and 9% (70/801) (rounded), respectively. Given this class distribution, we opted against upsampling the underrepresented classes (social phobia and specific phobia) or downsampling the overrepresented classes (depression and panic). While upsampling could mitigate class imbalance, it risks introducing synthetic patterns that may not generalize well to real-world data. In addition, given the relatively small sample size of the latter category (70/801, 9% in training), aggressive upsampling could lead to overfitting, where the model learns artifacts of the duplicated instances rather than underlying patterns in the data.

Conversely, downsampling depression and panic would reduce the total available training data and potentially discard valuable information, impairing the model's ability to capture the full variation within these classes. Furthermore, since the dataset represents naturally occurring clinical distributions, artificial class balancing could distort the real-world relevance of model predictions. Instead, we opted to maintain the original class distribution and address class imbalance using performance metrics robust to class imbalance, such as balanced accuracy, weighted F_1-score, and AUC, ensuring that model evaluation accounts for differences in class representation.

XSL•FO
RenderX

Table 1. Dataset features.

ID	Feature	Description	Feature type and values
1	Education	Years of education	• Ordinal • 0: primary school (0 to 9th grade) • 1: high school (10th to 12th grade) • 2: vocational education • 3: short further education (≤3 years) • 4: intermediate further education (4 or 5 years) • 5: long further education (≥5 years) • 6: other
2	AlcoholIntake	Weekly alcohol use (units)	• Ordinal • 0: 0 • 1: 1-5 or 1-7 • 2: 6-10 or 8-13 • 3: 11-20 or 14-20 • 4: 21-30 • 5: >30
3	UseOfDrugs	Use of euphoric drugs or pills	• Categorical • 0: no • 1: yes
4	CurrentMedication	Current psychopharmacological treatment	• Ordinal: • 0: none • 1: <1 month • 2: 1 to 2 months • 3: ≥2 months
5-13	Phq{One: Nine}	All 9 questions of PHQ-9[a] [42] over the previous 2 weeks scored on a 4-point Likert scale	• Ordinal • 0: not at all • 1: several days • 2: more than half the days • 3: nearly every day
14	PhqTen	Assessing to what extent the symptoms reported using PHQ-9 have affected work, household tasks, and relationships scored on a 4-point Likert scale	• Ordinal • 0: not difficult at all • 1: somewhat difficult • 2: very difficult • 3: extremely difficult
15-21	Gad{One:Seven)	All 7 questions of GAD-7[b] [43] scored on a 4-point Likert scale	• Ordinal • 0: not at all • 1: several days • 2: more than half the days • 3: nearly every day
22	HasPhobia	Binary categorical variable of self-reported previous phobia diagnosis	• Categorical • 0: no previous phobia • 1: previous phobia

XSL•FO
RenderX

ID	Feature	Description	Feature type and values

23-46	Fq{One:TwentyFour}	All 24 questions of the Fear Questionnaire [46] Items 1-17 assess avoidance. Item 18 assesses phobic symptom severity. Items 19-24 assess how reported phobia affects the respondent.	• Items 1-17:
			  • ordinal
			  • 0: would not avoid it
			  • 2: slightly avoid it
			  • 4: definitely avoid it
			  • 6: markedly avoid it
			  • 8: always avoid it
			• Item 18:
			  • ordinal
			  • 0: no phobias present
			  • 2: slightly disturbing or not really disabling
			  • 4: definitely disturbing or disabling
			  • 6: markedly disturbing or disabling
			  • 8: very severely disturbing or disabling
			• Items 19-24:
			  • ordinal
			  • 0: hardly at all
			  • 2: slightly troublesome
			  • 4: definitely troublesome
			  • 6: markedly troublesome
			  • 8: very severely troublesome

47-66	Sias{One:Twenty}	SIAS[c] questionnaire [44] assesses the respondent's social interaction anxiety using 20 statements, which the respondent indicates agreement with ("... characteristic or true of me") on a 5-item Likert scale	• Ordinal • 0: not at all • 1: slightly • 2: moderately • 3: very • 4: extremely

67-73	Pdss{One:Seven}	PDSS[d] questionnaire [45]	• Separate ordinal answer key for each item with severity of responses rated as follows:
			  • 0: no or not
			  • 1: mild, occasional, or slight
			  • 2: moderate or significant
			  • 3: severe, very often, or substantial
			  • 4: extreme or nearly constantly

74,75,76	MansaTen, MansaTwentyFour, MansaTwentyFive	Questions 10, 24, and 25 of the 25-item MANSA[e] questionnaire [47]	• Ordinal • 1: could not be worse • 2: displeased • 3: mostly dissatisfied • 4: mixed • 5: mostly satisfied • 6: pleased • 7: couldn't be better
77-80	DAD	Previous diagnosis one-hot encoded using dummy variables DAD0-DAD3	• One-hot encoded • DAD0: not previously diagnosed with anxiety or depression • DAD1: previously diagnosed with depression • DAD2: previously diagnosed with anxiety • DAD3: previously diagnosed with anxiety and depression
81-87	INC	Describing source of income of the respondent. One-hot encoded using dummy variables INC_1 to INC_7	• One-hot encoded • INC_1: employed • INC_2: social security • INC_3: sickness benefit or pay • INC_4: unemployment benefit • INC_5: stipend • INC_6: pension • INC_7: other

XSL•FO
RenderX

ID	Feature	Description	Feature type and values
88-91	APP	Treatment applied for one-hot encoded using dummy variables APP_1 to APP_4	• One-hot encoded • APP_1: applied for anxiety treatment • APP_2: applied for depression treatment • APP_3: applied for both anxiety and depression treatment • APP_4: does not know what treatment to apply for
GT	TreatmentType	Treatment decision (ground truth)	• Categorical • 1: depression • 2: panic • 3: social anxiety • 4: specific phobia

[a]PHQ-9: Patient Health Questionnaire-9.

[b]GAD-7: Generalized Anxiety Disorder Questionnaire-7.

[c]SIAS: Social Interaction Anxiety Scale.

[d]PDSS: Panic Disorder Severity Scale.

[e]MANSA: Manchester Short Assessment of Quality of Life.

Ethical Considerations

Data were extracted from Internetpsykiatrien after approval from The Regional Council in Southern Denmark. Since this was a secondary data analysis, separate informed consent was not required. However, the Regional Committees on Health Research Ethics for Southern Denmark were informed about the study and were provided with the case number S-20232000-65. In accordance with Danish national ethical guidelines, no additional ethics approval was needed. The study was reported to the Danish Data Protection Agency. Data was anonymized before being provided to the researchers. No compensation was provided.

Model

The proposed model was designed to interpret the traditional sum-score questionnaires used in mental health treatment in a data-driven, explainable fashion. Sum-score questionnaires offer several prespecified answers to each question, with each answer associated with a numeric, typically integer, score. These scores are then summed and in many cases a threshold is then applied, which indicates whether the respondent demonstrates clinically significant symptoms for the disorders tested by the instrument. Hence, such sum-scores play an important role in clinical decision-making. ML models such as logistic regression strongly align with this principle while also offering inherent interpretability due to the nature of the output activation being related to a weighted sum of the inputs. Such inherent explainability is appealing; however, the complexity of the information conveyed when models contain many weights can lead to cognitive overload, hampering decision-making [15] and explainability [16].

To improve the model's explainability while also retaining its inherent interpretability, a hierarchical model was proposed. As can be seen in Figure 1, this model mimics the sum-score models in the hidden layer of the model, in which the responses of each individual instrument are multiplied by their respective weight and then summed to yield pseudosum scores. These scores differ from normal sum-scores by applying a learned weighting to each answer before summing. These pseudosum scores incorporate a rectified linear unit activation function to ensure a linear sum while also ensuring the sum cannot be negative (due to the model learning negative weights during training). These scores and their weights allow inherent interpretability on a per-score basis, which will be familiar to clinical users of traditional questionnaire instruments. These pseudosum scores are then weighted before being combined in the output layer with the weighted sum-score of all other used instruments. In addition to the pseudosum scores, any other features with potentially discriminative power, such as sociodemographical information, can be added. All weights have dropout applied during prediction, consistent with the use of MCD as described previously. A softmax-type activation function is used in the output layer. The softmax activation function ensures that the sum of all the outputs of the model equals 1. Hence, each of the outputs can be interpreted as the probability that the corresponding treatment should be recommended. This output probability is illustrated as p(depression), as shown in Figure 1. Note that the output layer will typically contain 1 output node for each of the treatments considered by the model and that this number is not necessarily the same as the number of screening instruments used as inputs to the model.

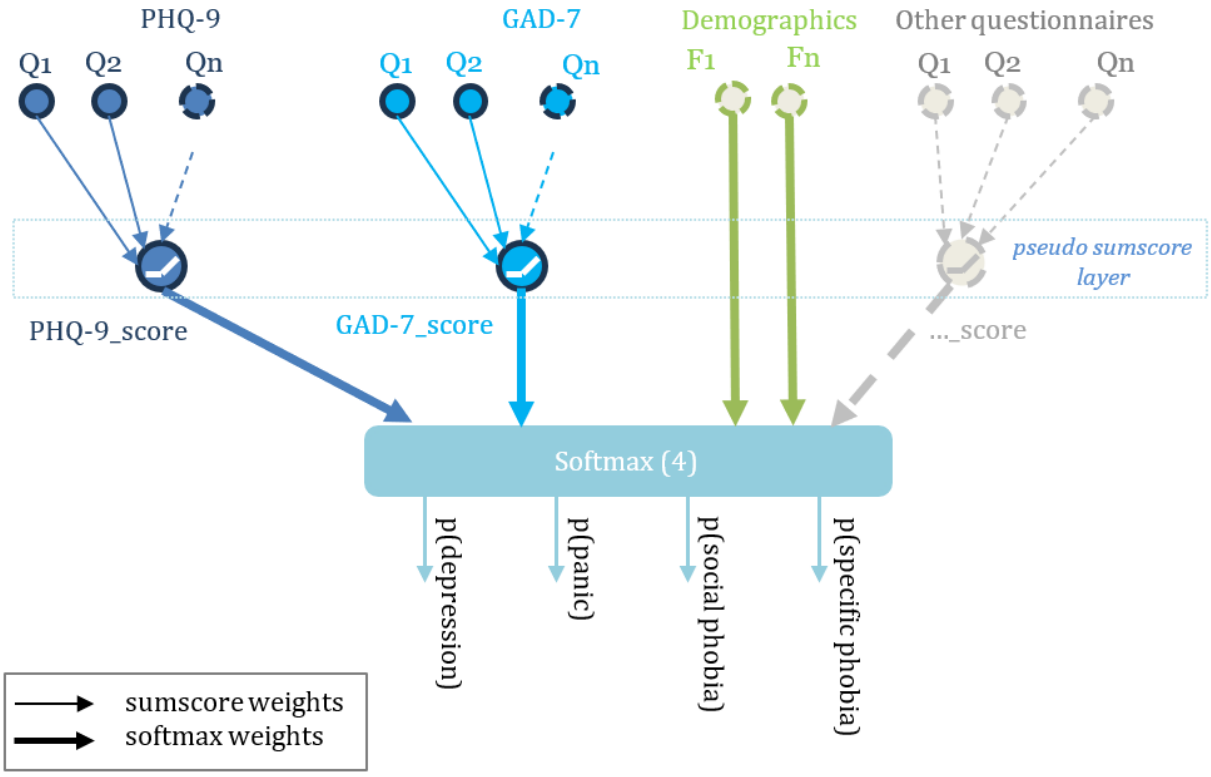
With this specific architecture, the model achieved three important goals as follows: (1) the model allows the nonlinear combination of multiple instruments to achieve a treatment prediction, (2) the model allows the explanation of its predictions based on pseudosum score results and thus provides score-level explainability and trust in the model, and (3) at the same time, the model allows for the analysis of model predictions based on the input features, enabling users to understand which particular responses to each questionnaire drive the model predictions. These insights may provide therapists with valuable information on how to personalize the therapy.

The model's structure inherited its interpretability from its foundation in logistic regression, while confidence and robustness of the model were addressed using the

XSL•FO
RenderX

aforementioned MCD. As previously stated, MCD can be shown to approximate the probabilistic results obtained by Bayesian approaches for a class of models called Gaussian Processes. The latter are a generalization of generalized linear models, one of which is the logistic regression model chosen in our approach for its explainability. The hierarchical logistic regression model has dropout applied before every weight layer, since the Bayesian properties of MCD apply for neural networks of arbitrary depth and nonlinearities, as long as dropout is applied in this way [39]. While it is usual for dropout to be applied to neural networks to fulfill the function of regularization during training time [38], as explained, MCD also applies dropout during inference. The probability of a node being dropped, the dropout rate, is a parameter of the dropout layers. In MCD, the dropout rate is typically set heuristically. Extensions to the technique, such as learnable Bernoulli dropout [48], allows the dropout rate to be jointly optimized in the model training phase. When MCD is used in this way, to approximate a Bayesian network, it should not be seen as a regularization method [49]. Therefore, L1 regularization is applied during training to reduce overfitting. L1 regularization attempts to achieve good generalization (ie, good performance on yet unseen data) by forcing the influence of unimportant features to 0. L2 regularization can be applied as an alternative, fulfilling the regularization function without enforcing sparsity in the weights. Further justification for the choice of L1 regularization is provided in the Results section. Multimedia Appendix 1 shows the model details.

Figure 1. Model structure. The structure of the hierarchical model shows the questionnaire input features (Q) being passed to the pseudosum score layer and then to the output layer. The pseudosum layer incorporates a rectified linear unit activation function to ensure the pseudosum scores cannot be negative. The output layer performs a softmax function, predicting the probabilities of the 4 classes. The weights are represented by the arrows, with the thicker arrows representing the weights in the softmax layer. The demographic features (f) pass directly to the output layer with softmax weightings. GAD-7: Generalized Anxiety Disorder Questionnaire-7; PHQ-9: Patient Health Questionnaire-9.



Prediction Explainability and Confidence

The distribution of the softmax output classes over the N samples , are visualized using Violin plots of the output class probability distribution over the N samples of a single patient prediction. A prediction for a single patient is shown in Figures 2 and 3. The outer, colored, “violin” shape visualizes the probability distributions over the N samples of the single patient example, while the embedded box-plots illustrate the medians and IQR of the model’s predictions. The confidence and uncertainty of the prediction can be understood by observing the shape and overlapping of the violin plots. Figure 2 provides an example of depression being predicted with high likelihood and nonoverlapping with the other 3 classes, whereas the predictions for all 3 other disorders have a low median probability. Predictions with low confidence (ie, low probabilities) and high uncertainty (ie, large probability variation), where more than 1 class may credibly be predicted, resulted in outputs, such as shown in Figure 3. This is an example of the relation between XAI concepts [16], using visualization to enhance explainability, contributing to improved interpretability, and the interpretability of the model leading to validation of the explanation.

XSL•FO
RenderX

Figure 2. A representation of the output class distribution. A violin plot showing the probability distribution of the 4 treatment classes for a single example over N runs (samples) of Monte Carlo dropout. The separation of the probabilities (x-axis) indicates high model confidence in the prediction of depression compared to the other classes. The low dispersion in the predictions indicates low uncertainty.

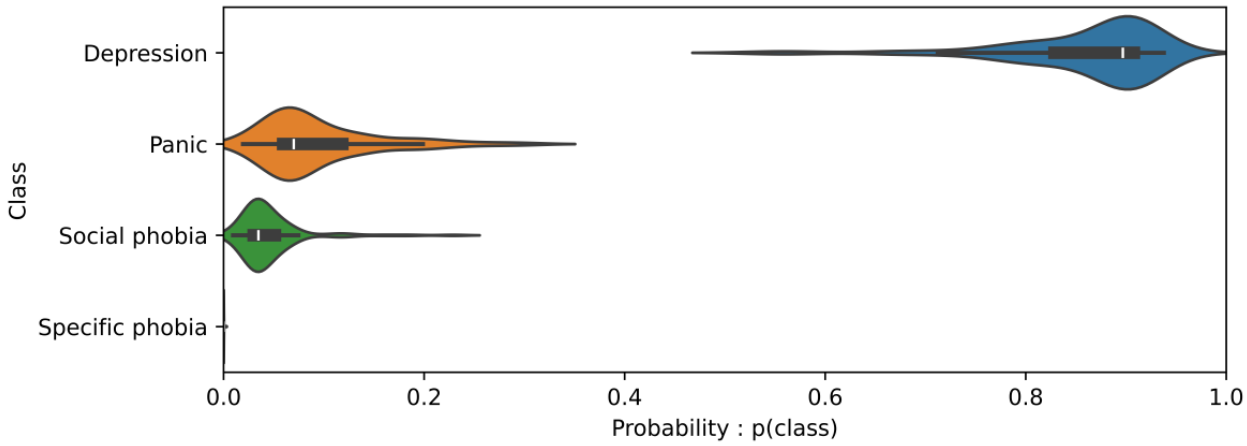
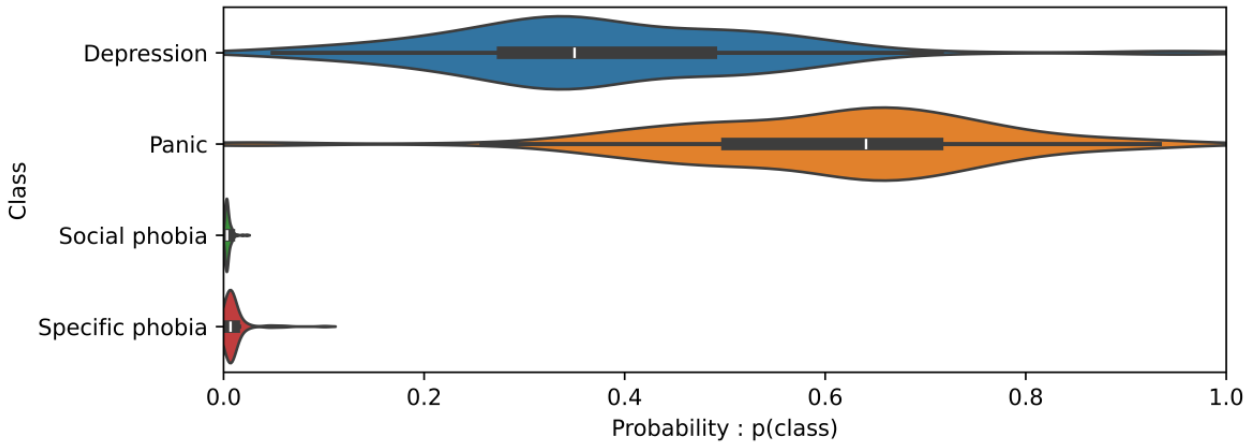


Figure 3. Class distribution of high uncertainty and low confidence. A violin plot showing the probability distribution of the 4 treatment classes for a single example over N runs (samples) of Monte Carlo dropout. The overlap of the probabilities (x-axis) indicates low model confidence in the prediction of panic compared to depression. The high dispersion in the predictions indicates high uncertainty.



Prediction Interpretability and Robustness

Interpretability at the model level is aided by examining the learned weights after training. Since the scores are weighted linear sums of the question inputs W^TX, the learned weights (W) are informative of the importance of each of the question features in determining the score used in the output class predictions in the softmax layer. The softmax layer implements a multiclass logistic regression function for each class (subscript c) and score (subscript s):



(4)

Where σ represents the sigmoid (or logistic) function, X_s is the input coming from the score layer or demographic features, W_c represents the weights in the softmax layer for class c, and B_c represents a bias value for each class.

Determining feature importance is an important aspect of explainability. At the model level, applying L1 regularization to logistic regression tends to force the weights of unimportant features to zero, leaving more important features as nonzero [50]. However, it is important to be aware that collinear features may not be equally important for a model since they can be accounted for by just one of the collinear features, with the others set to 0. Constraining trained weights to be nonnegative in the score layer aids interpretability since traditionally, questions are summed to produce a score. Therefore, the relative weights play a useful role in determining feature importance, provided that the inputs have been normalized to the same scale during training and prediction.

At the model level, standardized coefficients obtained by multiplying the original coefficients by the SD of the corresponding feature, provides a scale-free measure of influence, allowing the comparison of the relative importance of different features [51].

At the prediction level, for a specific patient record, the weights can be interpreted as the feature importance, given the normalized input range and positive weight constraint.

XSL•FO
RenderX

Results

Overview

The model was constructed using the TensorFlow library for Python (Python Software Foundation) and trained over 2000 epochs with a batch size of 32. The Adam optimizer was used at default setting, with L1 regularization of 0.001 and a dropout rate of 0.05 [52].

During development, both L1 and L2 regularization were considered, with evaluations involving 5-fold cross-validation on the training set. The optimal balanced accuracy score for both L1 and L2 corresponded to a regularization factor of 0.001 for both, with L1 and L2 achieving similar cross-validated mean balanced accuracy scores. Since L1 regularization tends to lead to a sparse solution by forcing unrequired weights to 0, it may be favored over L2 for transparent interpretability. However, when there are multiple near-equivalent predictors (eg, correlated measures), small fluctuations in initialization can lead the model to "select" a slightly different subset of features for its nonzero coefficients, eliminating one correlated feature, for example, while retaining the other. In consistency tests over 30 training runs, consistency in the top features was observed, although the order of importance may switch the top positive weight. In the depression class, for example, the top positive feature was PHQ-9 in 70% (21/30) of the runs and DAD_1.0 (previously diagnosed with depression) in 30% (9/30) of the runs. In the panic class, PDSS was always the top positive feature, with GAD-7 taking second place in 40% (12/30) of the runs and fq_total in 30% (9/30) of the runs. Examining the softmax weights, 80% (24/30) of the cumulative sum of the weights for each class were represented in the top 6 factors for L1 regularization, whereas for L2, up to 11 factors were required to represent the 80% (24/30). Therefore, L1 regularization was adopted for interpretability since: (1) both L1 and L2 regularization demonstrated similar accuracy; (2) L1 regularization enforces sparsity, requiring fewer weights to explain the top 80% (24/30); (3) the top weights are consistently in the top 3; and (4) the model transparency ensures the same weights are used in both prediction and explanation.

Following training, the model was evaluated on the held-out test set, achieving a balanced accuracy score of 0.79, indicating good generalization. The validation metrics (Table 2) indicate strong predictive performance across all 4 classes, with F_1-scores ranging from 0.71 to 0.86, which indicates a balanced trade off between precision and recall. Specific phobia achieved the highest precision (0.84) and the highest recall (0.88), suggesting that the model is highly accurate in predicting this class when it does make a prediction. However, social phobia had the lowest recall (0.70) compared to other classes, indicating some difficulty in correctly identifying all cases of this condition. The AUC values, all >0.90, suggest strong discrimination between classes. The aggregated metrics demonstrate an overall balanced accuracy score of 0.79 and a weighted F_1-score of 0.78, confirming that class imbalance did not severely impact overall model performance. The use of these weighted metrics ensures that smaller classes, such as specific phobia, contribute proportionally without distorting the results.

The confusion matrix (Table 3) details the number of treatment recommendations proposed by the model, with correct classifications appearing on the main diagonal of the table. Off-diagonal elements quantify the number of cases in which the model chose a different treatment than the clinician.

Patients assessed with social phobia were misclassified as depression in 4.9% (13/267) cases and as panic disorder in 1.9% (5/267) cases, suggesting that the model struggles to distinguish social phobia from other anxiety-related conditions. This was consistent with the lower recall observed for social phobia in Table 2, indicating that some patients with social phobia were incorrectly classified into other categories.

For specific phobia, the model correctly identified 7.9% (21/267) cases, but 1.1% (3/267) cases were misclassified as panic disorder (2/267, 0.7% cases) or social phobia (1/267, 0.4% case). Given that specific phobia was the least represented category in the dataset, the model's relatively strong performance in this class may be influenced by its high specificity (0.98, Table 2), which suggests that when the model does predict specific phobia, it does so with a high degree of accuracy. However, the smaller sample size in this class may also lead to performance variability.

The model generally performed well in classifying depression and panic disorder, with high agreement between model predictions and clinician labels (72/267, 27% and 69/267, 25.8% correct classifications, respectively). However, 3.7% (10/267) panic disorder cases were misclassified as depression, indicating some overlap in how these conditions were represented in the feature space or possible comorbidities.

Table 2. Validation metrics on the test set.

Treatment	Precision	Recall (sensitivity)	F_1-score	Specificity	Per-class balanced accuracy	AUC[a]
Depression	0.76	0.81	0.78	0.87	0.84	0.93
Panic	0.82	0.77	0.79	0.91	0.84	0.92
Social phobia	0.71	0.70	0.71	0.91	0.81	0.91
Specific phobia	0.84	0.88	0.86	0.98	0.93	0.98

[a]AUC: area under the curve.

XSL•FO
RenderX

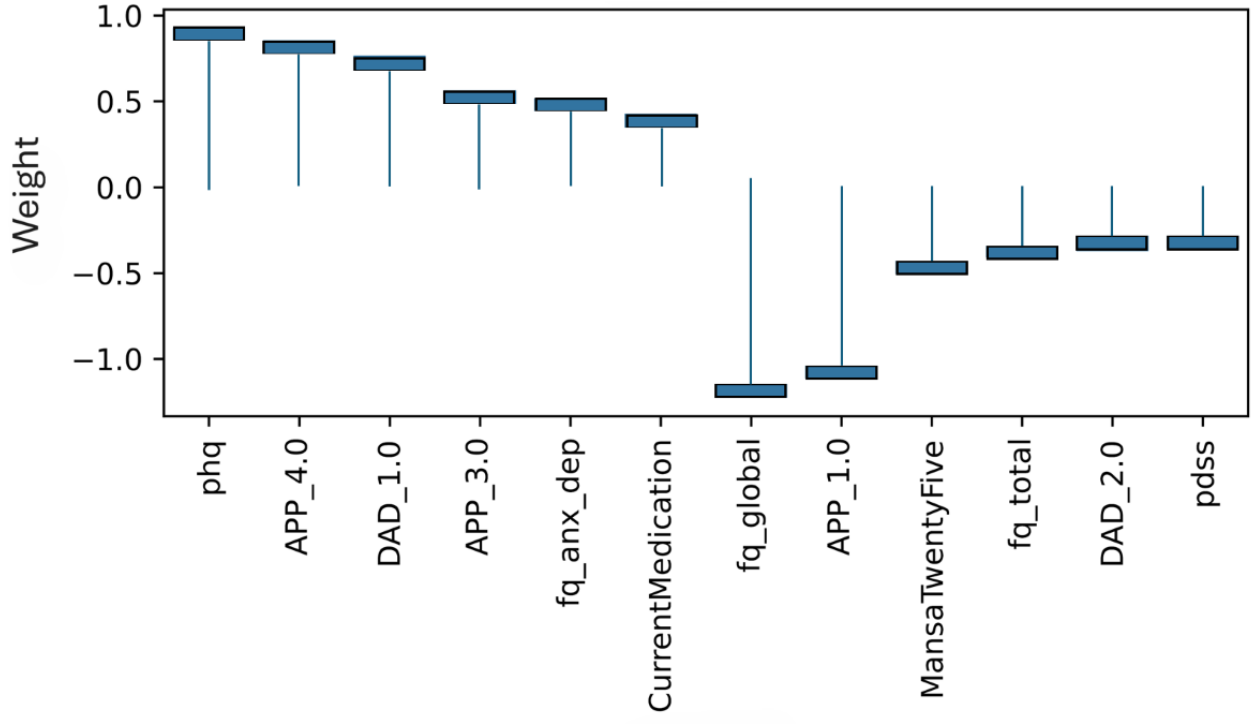
Table 3. Confusion matrix on the test set.

Clinician proposed treatment (ground truth)	Model proposed treatment, n (%)			
	Depression	Panic disorder	Social phobia	Specific phobia
Depression	72 (27)	8 (3)	9 (3.4)	0 (0)
Panic	10 (3.7)	69 (25.8)	8 (3)	3 (1.1)
Social phobia	13 (4.9)	5 (1.9)	45 (16.8)	1 (0.4)
Specific phobia	0 (0)	2 (0.7)	1 (0.4)	21 (7.9)

Model Level (Global) Explainability of Classes From Score Totals and Demographics

Examining the learned weights of the softmax layer that predicts the class probabilities from the score and demographic features is informative to interpret their relative importance at the model level. Positive weights contribute toward a more probable class prediction, while negative weights detract. Examining the top 6 positive and negative contributions, the depression class (Figure 4), is mostly influenced by the PHQ-9 score, application-related variables (APP_4.0, APP_3.0), and the previous diagnosis of depression (DAD_1.0). The Fear Questionnaire Global Phobia rating (question 18) detracts from this class prediction. The panic class (Figure 5) is most influenced positively by the PDSS score and the Fear Questionnaire total score (fq_total) and most negatively by the use of euphoric drugs or pills (UseOfDrugs), so drug use detracts from this class probability. The social phobia class (Figure 6) is most influenced by the SIAS score and the Fear Questionnaire Global Phobia rating (fq_global). Having been previously diagnosed with depression (DAD_1.0) works against this class. The specific phobia class (Figure 7) is most influenced by the Fear Questionnaire main level of avoidance (item 1), and the Global Phobia rating (fq_global), while having applied for both anxiety and depression treatment (APP_3.0) counts against this class.

Figure 4. Weights of the softmax depression class node (top 6 positive and negative). The chart shows the top 6 positive and negative weights of the softmax output layer with respect to the depression class. The relative magnitude and sign indicate the importance of the feature for the prediction. Positive weights contribute to the class prediction probability. Negative weights detract from it. The chart indicates that the Patient Health Questionnaire (PHQ-9) score (phq), and application-related variables (APP_4.0, APP_3.0) have the most influence on the prediction of the depression class, while the Fear Questionnaire Global Phobia rating (fq_global) has the strongest negative influence.



XSL•FO
RenderX

Figure 5. Weights of the softmax panic class node (top 6 positive and negative). The chart shows the top 6 positive and negative weights of the softmax output layer with respect to the panic class. The relative magnitude and sign indicate the importance of the feature for the prediction. Positive weights contribute to the class prediction probability. Negative weights detract from it. The chart indicates that the Panic Disorder Severity Scale (PDSS) score (pdss), and the fear questionnaire total score (fq_total) have the most influence on the prediction of the panic class, while the use of euphoric drugs or pills (UseOfDrugs) has the strongest negative influence.

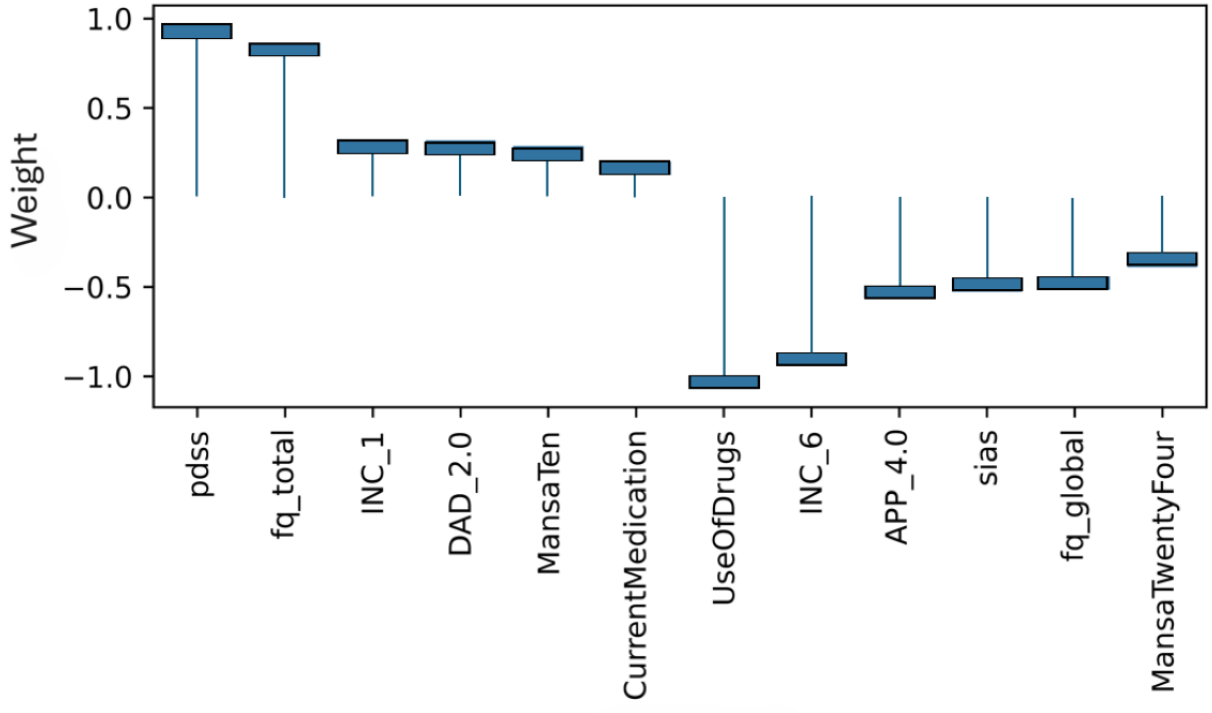
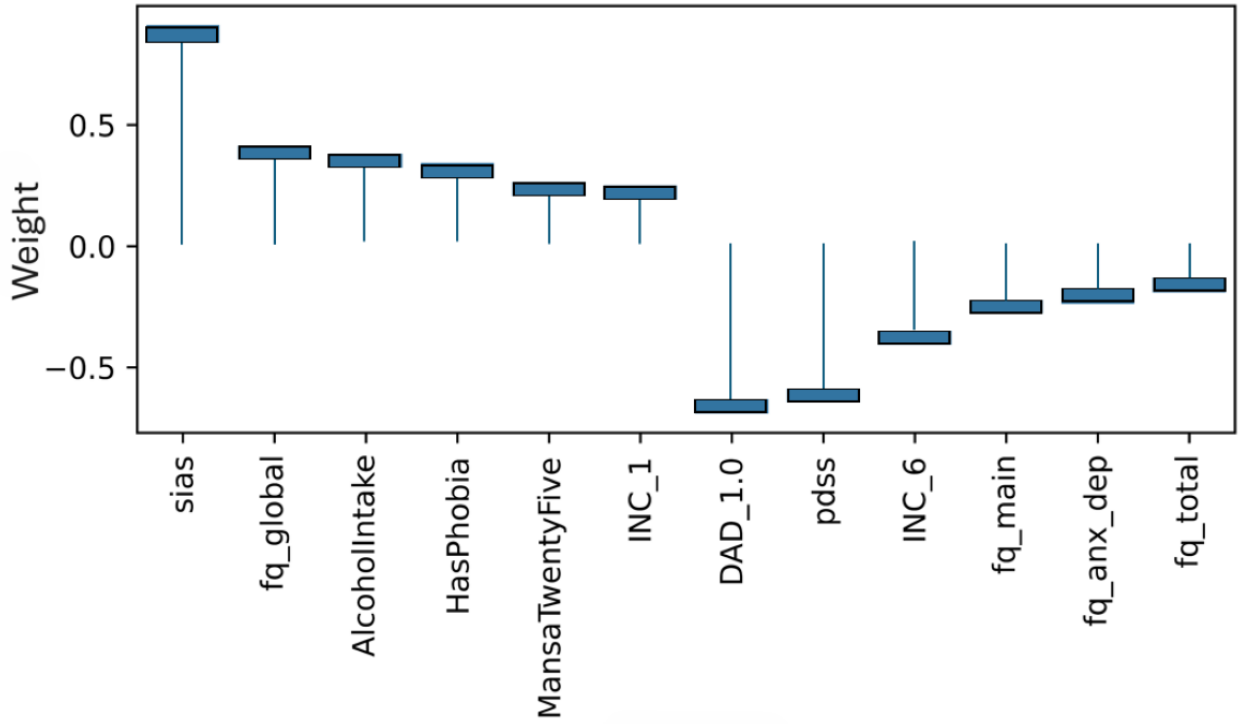
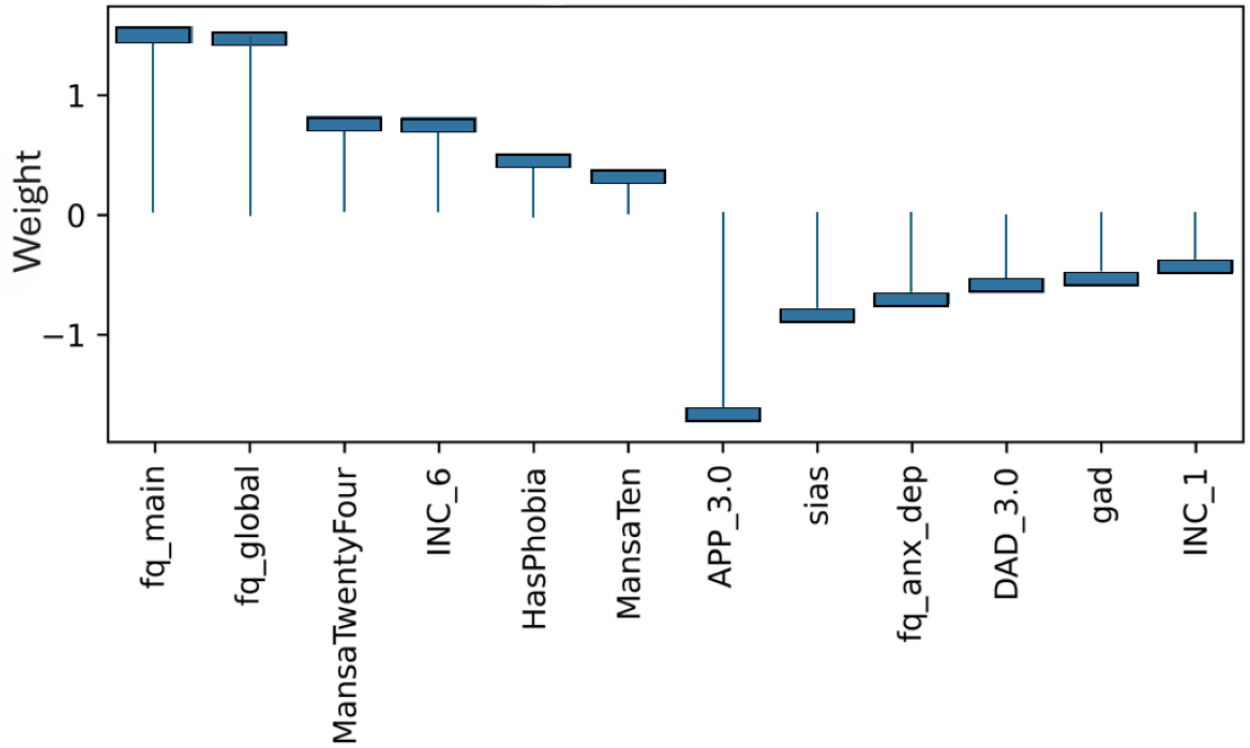


Figure 6. Weights of the softmax social phobia class node (top 6 positive and negative). The chart shows the top 6 positive and negative weights of the softmax output layer with respect to the social phobia class. The relative magnitude and sign indicate the importance of the feature for the prediction. Positive weights contribute to the class prediction probability. Negative weights detract from it. The chart indicates that the SIAS score (sias) and the Fear Questionnaire Global Phobia rating (fq_global) have the most influence on the prediction of the social phobia class. Having been previously diagnosed with depression (DAD_1.0) has the strongest negative influence.



XSL•FO
RenderX

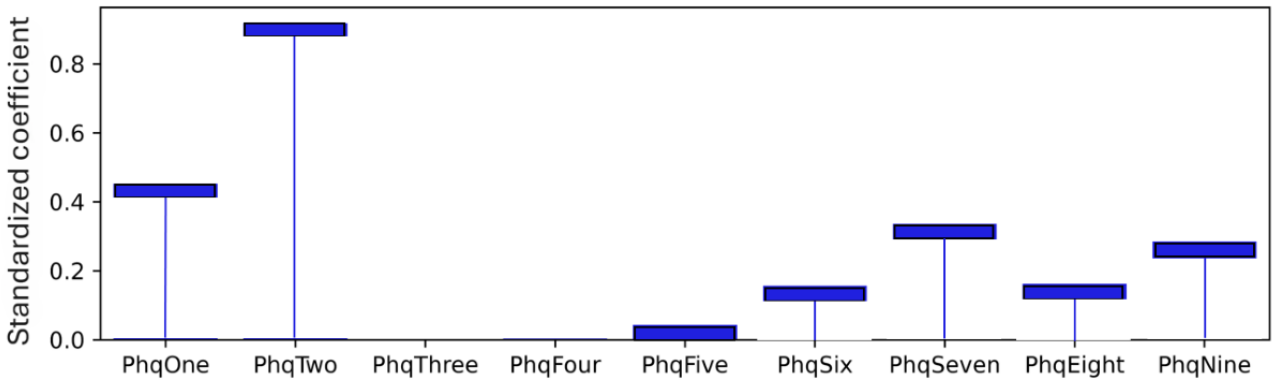
Figure 7. Weights of the softmax specific phobia class node (top 6 positive and negative). The chart shows the top 6 positive and negative weights of the softmax output layer with respect to the specific phobia class. The relative magnitude and sign indicate the importance of the feature for the prediction. Positive weights contribute to the class prediction probability. Negative weights detract from it. The chart indicates that the Fear Questionnaire has the most influence on the prediction of the panic class. The main Phobia Level of Avoidance score (fq_main), and Global Phobia rating (fq_global) are the top 2 positive weights. Having applied for both anxiety and depression treatment, (APP_3.0) has the strongest negative influence.



Model Level (Global) Explainability of Score Totals

As explained, standardized coefficients obtained by multiplying the original coefficients by the SD of the corresponding feature in the dataset provide a scale-free measure of influence, allowing the comparison of the relative importance of different features. The standardized coefficients are shown in Figures 8-12. Examining the PHQ-9 standardized coefficients (Figure 8), questions 1 and 2, the main cognitive factors of the questionnaire [53] are the most important, with all the 5 cognitive factors being represented. The importance of the GAD-7 (Figure 9) is almost exclusively represented by questions 4 (“Trouble relaxing”) and 2 (“Not being able to stop or control worrying”). The most important SIAS questions (Figure 10) were 6 and 1. Question 3, (“How often do you feel anxious about the possibility of having a panic attack?”) was the most important in the PDSS (Figure 11). In the Fear Questionnaire anxiety or depression subscale (Figure 12), question 23, “Feeling you or your surroundings are strange or unreal,” was the most important. The Total Phobia Score from the Fear Questionnaire was defined as the sum of the subscale scores for agoraphobias, blood injury phobia, and social phobia. In this case, only the learned agoraphobia subscore was weighted at nonzero (Figure 13). Question 5 was the most relevant question in the Fear Questionnaire agoraphobia subscale (Figure 14).

Figure 8. Patient Health Questionnaire-9 (PHQ-9) question standardized coefficients. This chart illustrates the relative importance of the PHQ-9 questions with respect to the pseudosum score for the PHQ-9 (phq) after model training.



XSL•FO
RenderX

Figure 9. Generalized Anxiety Disorder Questionnaire-7 (GAD-7) question standardized coefficients. This chart illustrates the relative importance of the GAD-7 questions with respect to the pseudosum score for the GAD-7 (gad) after model training. GAD question 4 “Trouble relaxing” and GAD question 2 “Not being able to stop or control worrying,” are the main nonzero standardized coefficient after L1 regularization pushes unimportant weights to zero.

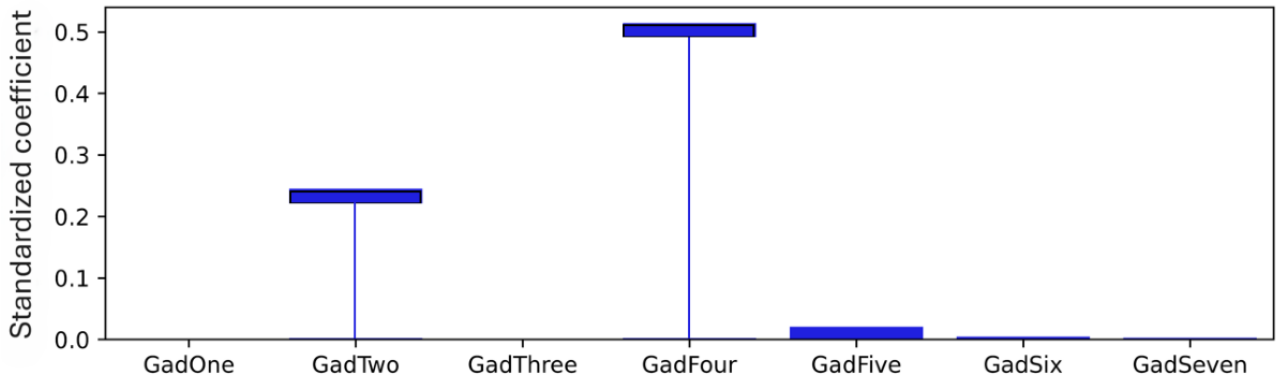


Figure 10. Social Interaction Anxiety Scale (SIAS) question standardized coefficients. This chart illustrates the relative importance of the SIAS questions with respect to the pseudosum score for the SIAS (sias) after model training. Reverse scored features have an R suffix, for example, Sias5R.

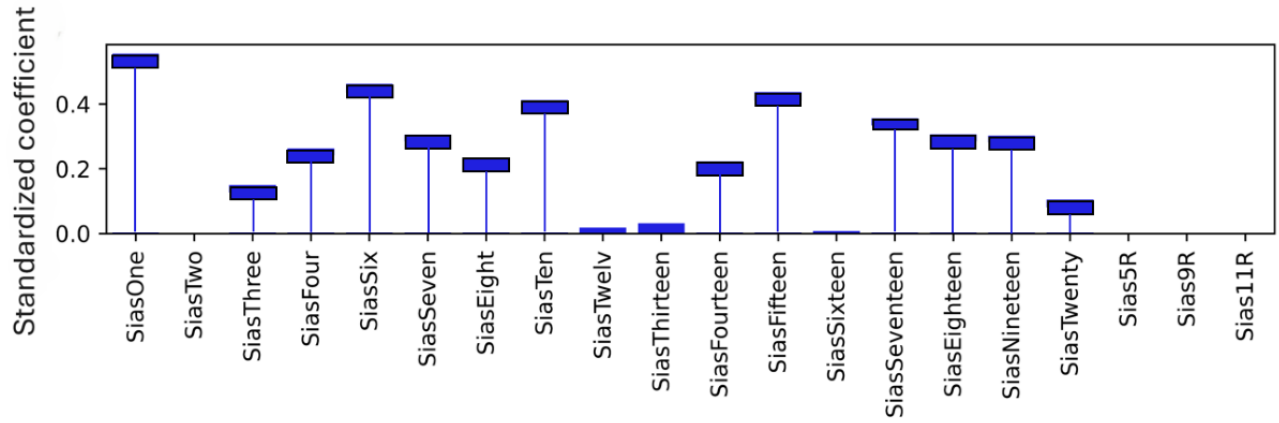
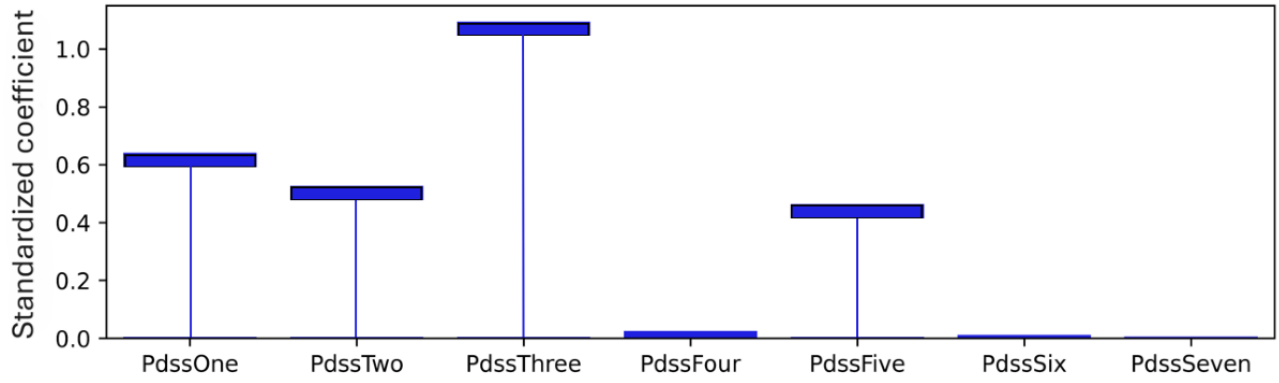


Figure 11. PDSS question standardised coefficients. This chart illustrates the relative importance of the PDSS questions with respect to the pseudo-sum score for the PDSS (pdss) after model training.



XSL•FO
RenderX

Figure 12. Fear Questionnaire (FQ) anxiety depression subscale question standardized coefficients. This chart illustrates the relative importance of the Fear Questionnaire Total Phobia Score questions with respect to the pseudosum score (fq) after model training. Question 23, "Feeling you or your surroundings are strange or unreal." is the largest standardized coefficient after L1 regularization pushes unimportant weights to 0.

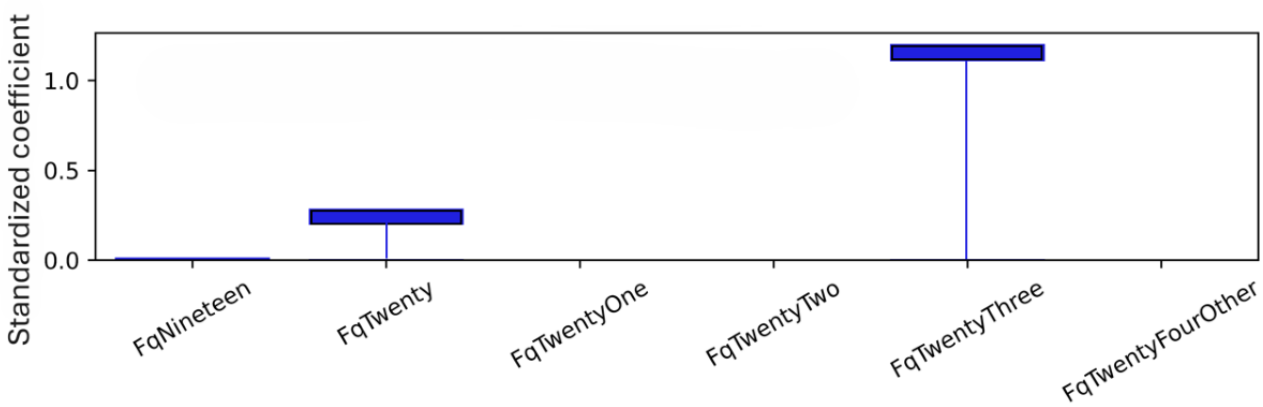


Figure 13. Fear Questionnaire (FQ) total score weighting of the FQ subscales. This chart illustrates how the Fear Questionnaire subscales are weighted in relation to the fear questionnaire total score fq_total. Only the agoraphobia subscale (fq_ago) was learned as being relevant. This is likely to be due to L1 regularization of correlated factors.

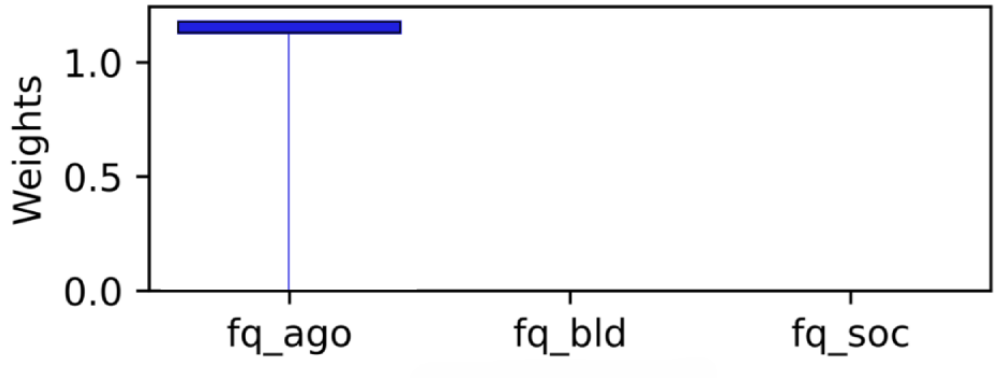
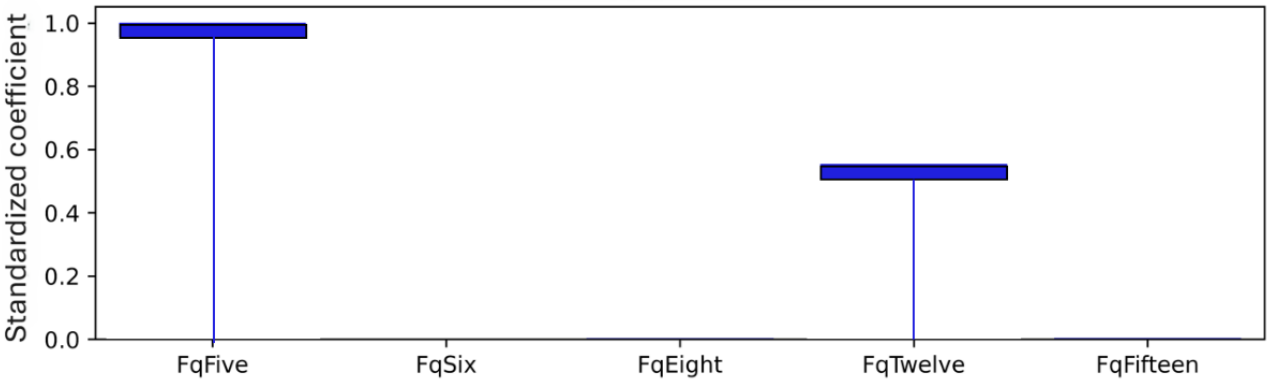


Figure 14. Fear Questionnaire (FQ) agoraphobia subscale question standardized coefficients. This chart illustrates the relative importance of the FQ agoraphobia subscore questions.



Patient Level (Local) Explainability

The relevant questionnaire total score summaries of a test patient (patient 1) are provided here. The PHQ-9 (15) score indicated moderately severe depression [42]. The PDSS score (13) indicated "moderately ill" panic disorder [54]. The GAD-7 score (17) indicated severe anxiety [55]. The SIAS score (22) was lower than the threshold for an indication of social phobia [56]. The clinical assessment (ground truth) of an appropriate treatment was panic. Other scores included Fear Questionnaire total score (6), global score (0), and main score (0).

Examining a local explanation at the individual patient level for patient 1 (Figure 15), the predicted probability distribution of panic (the prescribed treatment), overlapped with depression. The importance was determined from the weighted inputs to the softmax layer, combining both the patient record and the learned weights. Examining the importance associated with the prediction in the softmax layer for the panic class shows the top 6 positive factors (Figure 16), and the top 6 negative factors (Figure 17). Positive values make the class more probable, while negative values make the class less probable. It should be noted that the positive and negative y-values for each class are derived

XSL•FO
RenderX

from the same weight layer and, therefore, are suitable for comparative analysis. In the patient 1 example, the PDSS questionnaire score explained most of the probability for the panic class, while the SIAS questionnaire detracted from the probability of the panic class, but to a lesser degree.

The model can also be used to explain any of the class probabilities. It is not limited to explaining the highest probability prediction. Hence, the class prediction for depression can be examined in the same way. This showed the PHQ-9 score as the most important (Figure 18), followed by APP_3 (the patient applied for both anxiety and depression treatment). The PDSS score showed a negative influence on this class (Figure 19), which was important but lower than the positive importance of PHQ-9. It is interesting to note that the negative importances for the depression class (Figure 19) were larger than the negative importances for panic, the highest probability class (Figure 17). This goes some way to explain why panic was predicted to be more probable than depression.

The hierarchical model also allowed a closer examination of the individual questions. For example, an examination of the PHQ-9 questions that contributed to the probability of the depression class (Figure 20), showed PHQ-9 questions 1 and 2 as having the most influence on the model prediction for this class, for this patient.

Figure 15. Prediction for patient 1. A violin plot showing the probability distribution of the 4 treatment classes for the data of patient 1. Although panic has the highest probability, the overlap of the probabilities (x-axis) indicates low model confidence in the prediction of panic compared to depression. The high dispersion in the predictions indicate high uncertainty. Overall, this plot indicates to a clinical user that both panic and depression are credible treatments according to the model.

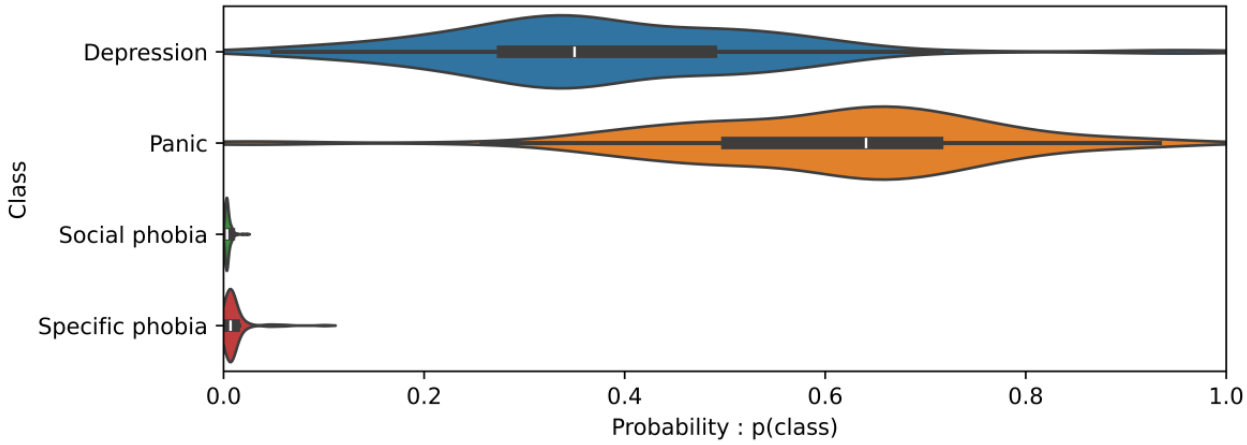
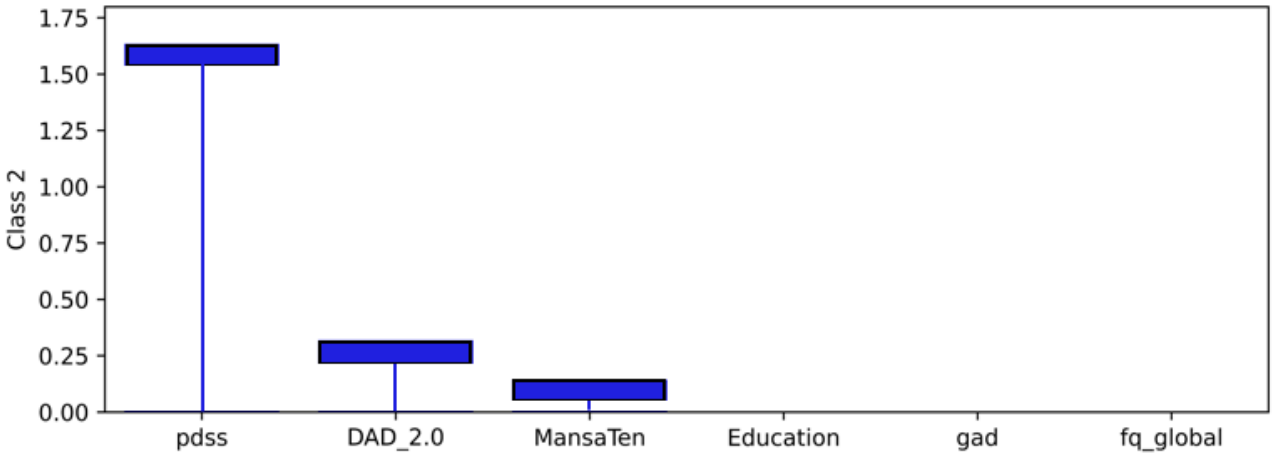


Figure 16. Patient 1 explainability for panic prediction (positive weightings). The product of the weights and the pseudosum score data or demographic data explains the importance of those features in determining the local prediction from a patient record. These positive values contribute to the class probability. The Panic Disorder Severity Scale (PDSS) score (pdss) is the most significant contributor to the probability of the panic class for patient 1.



XSL•FO
RenderX

Figure 17. Patient 1 explainability for panic (class 2) prediction (negative weightings). The product of the weights and the pseudosum score data or demographic data explains the importance of those features in determining the local prediction from a patient record. These negative values detract from the class probability. The Social Interaction Anxiety Scale (SIAS) score (sias) is the most significant detractor from the probability of the panic class for patient 1, but at approximately −0.5, it has less contribution than the comparative positive scores.

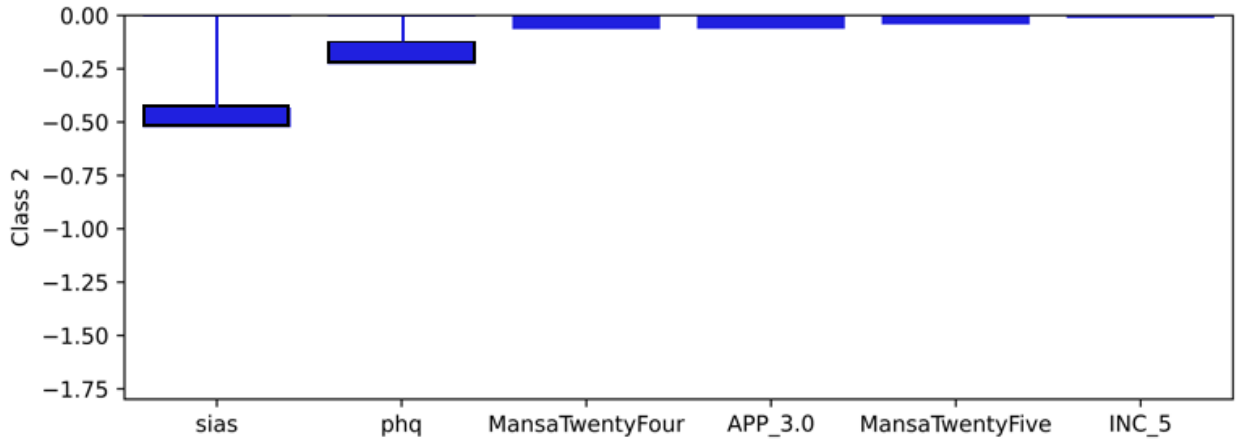
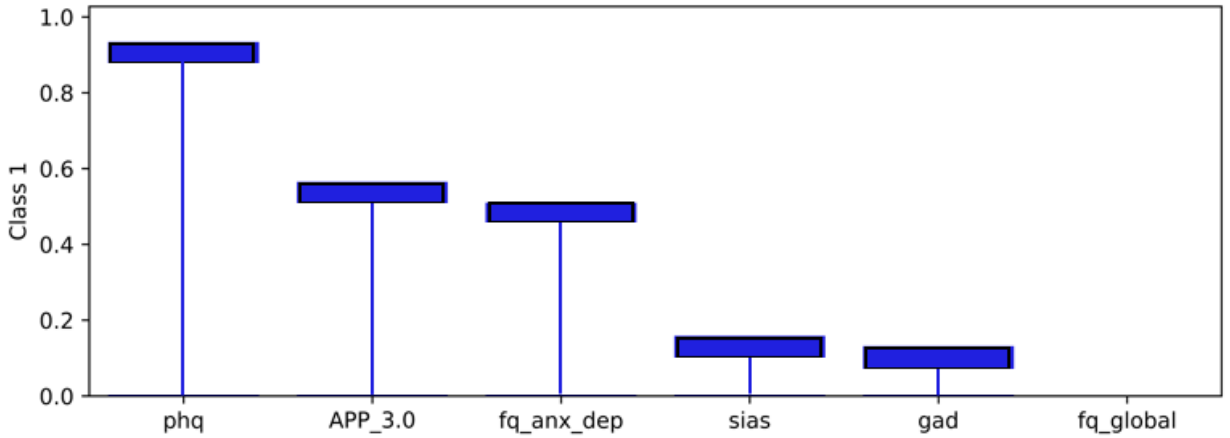


Figure 18. Patient 1 explainability for depression prediction (positive weightings). The product of the weights and the pseudosum score data or demographic data explains the importance of those features in determining the local prediction from a patient record. These positive values contribute to the class probability. The Patient Health Questionnaire-9 (PHQ-9) score (phq) is the most significant contributor to the probability of the depression class for patient 1.



XSL•FO
RenderX

Figure 19. Patient 1 explainability for depression prediction (negative weightings). The product of the weights and the pseudosum score data or demographic data explains the importance of those features in determining the local prediction from a patient record. These negative values detract from the class probability. The Panic Disorder Severity Scale (PDSS) score (pdss) is the most significant detractor from the probability of the depression class for patient 1.

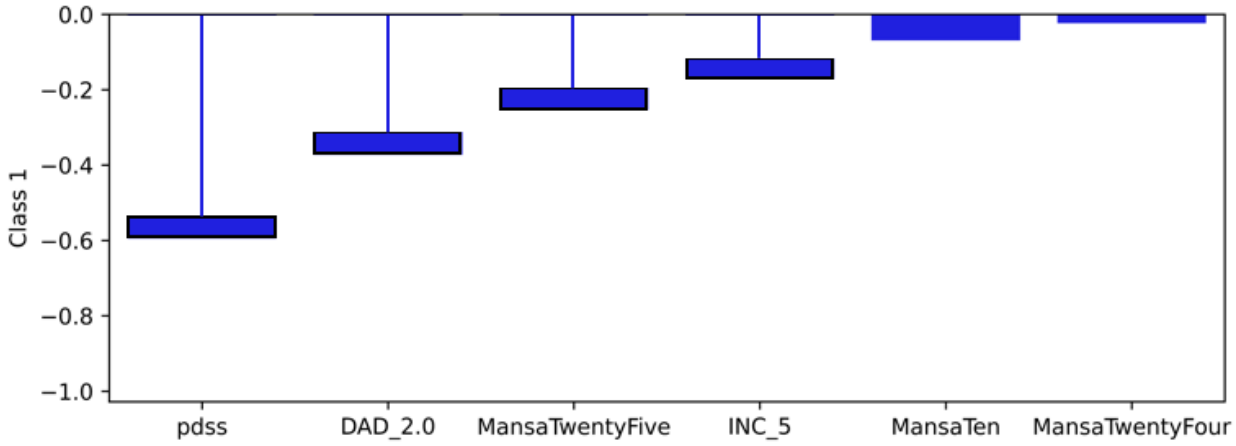
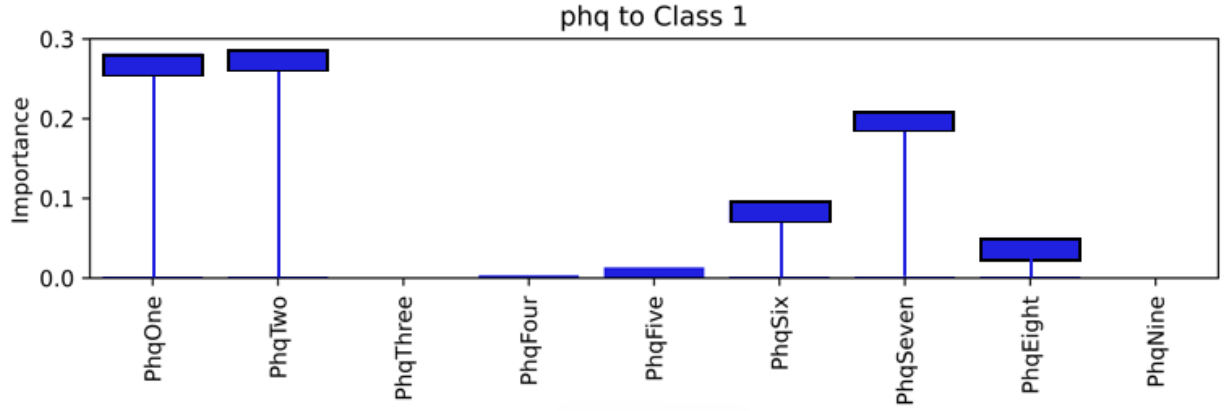


Figure 20. Patient 1 explainability for the Patient Health Questionnaire-9 (PHQ-9) questions in the depression prediction. The product of the weights and the question data explains the importance of the questions in determining the local prediction from a patient record. The PHQ-9 questions 1 and 2 score are the most significant contributors to the phq pseudosum score of depression class for patient.



Discussion

Overview

Uncertainty and lack of confidence in diagnosing psychopathological conditions can present a considerable challenge due to comorbidities and overlapping symptoms [6]. The diagnosis of social anxiety disorder, for example, must be differentiated from major depression, panic disorder, agoraphobia, and generalized anxiety disorder [7,57]. Furthermore, maintaining human involvement in patient assessments involving AI is critical [58]. Therefore, explaining predictions and enabling clinicians to explore the clinical factors associated with the predictions, has been a central aspect of this work.

Principal Findings

We have demonstrated the design and quantitative evaluation of a hierarchical model that aims to aid diagnosis and meet the requirements of providing explainable predictions that are context-based and easy for clinicians to use in questionnaire-based assessments [4]. Issues of confidence and robustness that are important for ML models aimed at medical DSSs [25] have been addressed.

As the model achieved a balanced accuracy score of 0.79 and AUC >0.90, it is expected that it will be clinically useful in both screening a new patient and informing a clinical interview. In patient screening, for example, the graphical interpretation of the class probabilities, their spread, and their overlap can inform the clinician of competing treatment possibilities for the patient. Even in the case where the treatment prediction is unambiguous and agrees with the clinician's assessment, the model may serve as a confirmatory second opinion. At the clinical interview stage, the specific questions that are deemed important for the class prediction may inform the clinician of which areas to probe further in the clinical interview.

Limitations

ML models extract knowledge from data, limiting their applicability to use in scenarios that are statistically similar to the training scenario. The models reported in this study were trained on data obtained from the Internetpsykiatrien web-based treatment with nationwide coverage in Denmark [41]. Hence,

XSL•FO
RenderX

while similar performance for individuals presenting to this service in Denmark can be expected, performance in a different country or otherwise different setting cannot be guaranteed. This can be seen as a limitation of ML models, but also as a strength; retraining the model described in this study is cheap. Hence, it is relatively straightforward for any regional mental health service to train this model on local data and obtain predictions that are sensitive to regional sociodemographics and patient characteristics. Moreover, patient characteristics may well change over time, and such temporal changes can be addressed by retraining the model periodically.

The ground truth is based on clinical judgment and is, therefore, influenced by the subjectivity of the clinicians, interrater variability, and possibly by group dynamics in decision-making clinical conferences. Clinicians have access to free-text provided by the patient, which the model does not have. A future direction may involve the development of a hybrid model that makes use of all the relevant questionnaire and demographic and free-text data for each patient. An additional limitation of the ground truth is that the assessment relies on structured questionnaires and the Mini Neuropsychiatric Interview, which may not capture all relevant patient characteristics, leading to potential gaps in the ground truth.

During training, L1 regularization adjusts the standardized coefficients and model weights toward 0 for features deemed unimportant or redundant, for example, due to having a high correlation with another feature. Consequently, features that clinicians consider relevant may be excluded by the model and thus do not appear in the explanations of predictions. However, it is common for clinicians to prioritize the importance of certain features over others in a diagnostic context [59]. It is anticipated that clinicians will find the specificity of the explanations at the question level to be clarifying and informative, complementing their own clinical judgment. Moreover, L1 regularization may result in model instability in the sense that small changes in the training set may result in a different selection of nonzero coefficients (and thus important features). Hence, a retrained model may yield different explanations to the original model for similar individuals, and this could be confusing to clinicians. However, it should be emphasized that the feature weights that explain the predictions are the same feature weights that the model uses to make the predictions, due to the model's transparency. However, using L1 regularization is not a prerequisite for the use of the proposed approach. L2 regularization, which attempts to achieve good generalization by keeping model weights small (rather than forcing a subset to 0 such as in L1 regularization) can also be used. The result would be that the model contains mostly nonzero weights, and thus, the explainability of model decisions becomes more complex. However, clinicians could choose to focus on the most important features (ie, those with the highest influence on the model). Visualizations, such as those in Figures 16-19, could be constrained to the N most important features with N chosen by the clinician.

The clinical use of the ML model would require the development of a DSS so that clinicians can view and explore the model predictions and explanations when provided with patient records. The lack of such a DSS may be seen as a limitation in demonstrating the clinical effectiveness of the model. While this study does not empirically demonstrate that the aims of clinical interpretability have been met, further work is planned to develop the DSS and study the clinical usefulness of the system incorporating the model.

Overall, the results highlight the key challenges in differentiating social phobia from other anxiety disorders and suggests that future improvements could focus on enhancing feature differentiation for overlapping categories, particularly social phobia and panic disorder.

Future Work

The incorporation of this model into a DSS for mental health treatment prediction will be an important future step for this work. Once developed, assessing its use in a clinical setting will help to validate it for future clinical use. The model itself could be extended to use more input features, especially those that have a potential to enhance feature differentiation for overlapping categories (particularly social phobia and panic disorder). Additional hybrid features may include free-text data input for each patient. Output enhancements can also be foreseen to further build on the model's explainability. For example, a text output of the model's prediction, competing predictions, and explanations in written form could form an important input to clinical notes and provide material for clinical conferences.

Conclusions

This paper presents the design of a model aimed at a DSS for psychopathological mental health treatment. Its basis in standard screening questionnaires will allow seamless adoption in a clinical setting in the future. The AI model incorporated in the system is based on a novel hierarchical structure that aims to meet the needs of clinical interpretability while accounting for decision confidence and uncertainty that are lacking in previous work.

Acknowledgments

This work has been supported by the Innovation Fund, Denmark. The authors wish to thank the clinical staff, administrative staff, and patients at the Centre for Digital Psychiatry, Denmark.

Authors' Contributions

AK conceived the probabilistic model; designed, trained, and verified the models; and drafted the paper. PVdV conceived the hierarchical score model, made significant contributions to the paper's Introduction and Methods sections, and improved all sections of the paper. EMG made contributions to the explainable artificial intelligence literature description. EKJ and KM made

XSL•FO
RenderX

contributions to the Data and Introduction sections as well as provided the clinical input, data, infrastructure, and support for the project. All authors reviewed the completed paper.

Conflicts of Interest

None declared.

Multimedia Appendix 1
Details of the model layers and structure.
[DOCX File , 21 KB - medinform_v13i1e64617_app1.docx]

References

1. Minerva F, Giubilini A. Is AI the future of mental healthcare? Topoi (Dordr) 2023 May 31;42(3):1-9 [FREE Full text] [doi: 10.1007/s11245-023-09932-3] [Medline: 37361723]
2. Meehl PE. Clinical Versus Statistical Prediction: A Theoretical Analysis and a Review of the Evidence. Brattleboro, VT: Echo Point Books and Media; 2013.
3. Ægisdóttir S, White MJ, Spengler PM, Maugherman AS, Anderson LA, Cook RS, et al. The meta-analysis of clinical judgment project: fifty-six years of accumulated research on clinical versus statistical prediction. Counsel Psychol 2006 May 01;34(3):341-382 [FREE Full text] [doi: 10.1177/0011000005285875]
4. Katsikopoulos K, Machery E, Pachur T, Wallin A. The search for models of clinical judgment: fast, frugal, and friendly in Paul Meehl's spirit. J Behav Decis Mak 2004 [FREE Full text]
5. Makivić I, Kragelj A, Lasalvia A. Quantitative needs assessment tools for people with mental health problems: a systematic scoping review. Curr Psychol 2024 Mar 12;43(22):19996-20013 [FREE Full text] [doi: 10.1007/s12144-024-05817-9]
6. Morrison J. Diagnosis Made Easier: Principles and Techniques for Mental Health Clinicians. New York, NY: Guilford Press; 2024.
7. Mogi T, Toda H, Yoshino A. Clinical characteristics of patients with diagnostic uncertainty of major depressive disorder. Asian J Psychiatr 2017 Dec;30:159-162 [FREE Full text] [doi: 10.1016/j.ajp.2017.10.001] [Medline: 29055250]
8. Souery D, Papakostas GI, Trivedi MH. Treatment-resistant depression. J Clin Psychiatry 2006;67 Suppl 6:16-22. [Medline: 16848672]
9. Bloom DE, Cafiero ET, Jané-Llopis E, Abrahams-Gessel S, Bloom LR, Fathima S, et al. The global economic burden of noncommunicable diseases. World Economic Forum. 2011. URL: https://www3.weforum.org/docs/WEF_Harvard_HE_GlobalEconomicBurdenNonCommunicableDiseases_2011.pdf [accessed 2024-05-30]
10. Wittchen HU, Jacobi F, Rehm J, Gustavsson A, Svensson M, Jönsson B, et al. The size and burden of mental disorders and other disorders of the brain in Europe 2010. Eur Neuropsychopharmacol 2011 Sep;21(9):655-679 [FREE Full text] [doi: 10.1016/j.euroneuro.2011.07.018] [Medline: 21896369]
11. D'Alfonso S. AI in mental health. Curr Opin Psychol 2020 Dec;36:112-117 [FREE Full text] [doi: 10.1016/j.copsyc.2020.04.005] [Medline: 32604065]
12. Graham S, Depp C, Lee EE, Nebeker C, Tu X, Kim HC, et al. Artificial intelligence for mental health and mental illnesses: an overview. Curr Psychiatry Rep 2019 Nov 07;21(11):116 [FREE Full text] [doi: 10.1007/s11920-019-1094-0] [Medline: 31701320]
13. Martin-Key NA, Spadaro B, Funnell E, Barker EJ, Schei TS, Tomasik J, et al. The current state and validity of digital assessment tools for psychiatry: systematic review. JMIR Ment Health 2022 Mar 30;9(3):e32824 [FREE Full text] [doi: 10.2196/32824] [Medline: 35353053]
14. Thakkar A, Gupta A, De Sousa A. Artificial intelligence in positive mental health: a narrative review. Front Digit Health 2024;6:1280235 [FREE Full text] [doi: 10.3389/fdgth.2024.1280235] [Medline: 38562663]
15. Ghassemi M, Oakden-Rayner L, Beam A. The false hope of current approaches to explainable artificial intelligence in health care. Lancet Digit Health 2021 Nov;3(11):e745-e750 [FREE Full text] [doi: 10.1016/s2589-7500(21)00208-9]
16. Ali S, Abuhmed T, El-Sappagh S, Muhammad K, Alonso-Moral JM, Confalonieri R, et al. Explainable Artificial Intelligence (XAI): what we know and what is left to attain Trustworthy Artificial Intelligence. Inf Fusion 2023 Nov;99:101805 [FREE Full text] [doi: 10.1016/j.inffus.2023.101805]
17. Singh RK, Gorantla R, Allada SG, Narra P. SkiNet: a deep learning framework for skin lesion diagnosis with uncertainty estimation and explainability. PLoS One 2022;17(10):e0276836 [FREE Full text] [doi: 10.1371/journal.pone.0276836] [Medline: 36315487]
18. Barredo Arrieta A, Díaz-Rodríguez N, Del Ser J, Bennetot A, Tabik S, Barbado A, et al. Explainable Artificial Intelligence (XAI): concepts, taxonomies, opportunities and challenges toward responsible AI. Inf Fusion 2020 Jun;58:82-115 [FREE Full text] [doi: 10.1016/j.inffus.2019.12.012]
19. Kompa B, Snoek J, Beam AL. Second opinion needed: communicating uncertainty in medical machine learning. NPJ Digit Med 2021 Jan 05;4(1):4 [FREE Full text] [doi: 10.1038/s41746-020-00367-3] [Medline: 33402680]

XSL•FO
RenderX

20. Gunning D, Vorm E, Wang JY, Turek M. DARPA's explainable AI (XAI) program: a retrospective. Appl AI Letters 2021 Dec 16;2(4):e61 [FREE Full text] [doi: 10.1002/ail2.61]
21. Explainable AI: the basics. The Royal Society. 2019 Nov. URL: https://royalsociety.org/-/media/policy/projects/explainable-ai/AI-and-interpretability-policy-briefing.pdf [accessed 2024-05-30]
22. TechDispatch #2/2023 - explainable artificial intelligence. European Data Protection Supervisor. 2023. URL: https://www.edps.europa.eu/data-protection/our-work/publications/techdispatch/2023-11-16-techdispatch-22023-explainable-artificial-intelligence_en [accessed 2024-05-30]
23. Ethics guidelines for trustworthy AI. European Commission. 2019 Apr 8. URL: https://digital-strategy.ec.europa.eu/en/library/ethics-guidelines-trustworthy-ai [accessed 2024-05-30]
24. Subbaswamy A, Adams R, Saria S. Evaluating model robustness and stability to dataset shift. arXiv Preprint posted online on October 28, 2020 [FREE Full text]
25. Begoli E, Bhattacharya T, Kusnezov D. The need for uncertainty quantification in machine-assisted medical decision making. Nat Mach Intell 2019 Jan 07;1(1):20-23 [FREE Full text] [doi: 10.1038/s42256-018-0004-1]
26. Wanner J, Herm LV, Heinrich K, Janiesch C. Stop ordering machine learning algorithms by their explainability! An empirical investigation of the tradeoff between performance and explainability. In: Proceedings of the Conference on e-Business, e-Services and e-Society. 2021 Presented at: I3E 2021; September 1-3, 2021; Galway, Ireland URL: https://doi.org/10.1007/978-3-030-85447-8_22/FIGURES/3 [doi: 10.1007/978-3-030-85447-8_22]
27. Ribeiro MT, Singh S, Guestrin C. "Why should I trust you?": explaining the predictions of any classifier. In: Proceedings of the 22nd ACM SIGKDD International Conference on Knowledge Discovery and Data Mining. 2016 Presented at: KDD '16; August 13-17, 2016; San Francisco, CA URL: https://doi.org/10.1145/2939672.2939778 [doi: 10.1145/2939672.2939778]
28. Zhang Y, Song K, Sun Y, Tan S, Udell M. "Why should you trust my explanation?" Understanding uncertainty in lime explanations. arXiv Preprint posted online on April 29, 2019 [FREE Full text]
29. Lakkaraju H, Kamar E, Caruana R, Leskovec J. Interpretable and explorable approximations of black box models. arXiv Preprint posted online on July 4, 2017 [FREE Full text]
30. Alvarez-Melis D, Jaakkola TS. On the robustness of interpretability methods. arXiv Preprint posted online on June 21, 2018 [FREE Full text]
31. Abeyagunasekera SH, Perera Y, Chamara K, Kaushalya U, Sumathipala P, Senaweera O. LISA : enhance the explainability of medical images unifying current XAI techniques. In: Proceedings of the IEEE 7th International conference for Convergence in Technology. 2022 Presented at: I2CT 2022; April 07-09, 2022; Mumbai, India URL: https://doi.org/10.1109/I2CT54291.2022.9824840 [doi: 10.1109/i2ct54291.2022.9824840]
32. Singh Dhaliwal B, Imran R, Leung CK, Evan EW. Trustworthy explanations for knowledge discovered from e-health records. In: Proceedings of the IEEE International Conference on E-health Networking, Application & Services. 2022 Presented at: HealthCom 2022; October 17-19, 2022; Genoa, Italy URL: https://doi.org/10.1109/HEALTHCOM54947.2022.9982786 [doi: 10.1109/healthcom54947.2022.9982786]
33. Chaddad A, Peng J, Xu J, Bouridane A. Survey of explainable AI techniques in healthcare. Sensors (Basel) 2023 Jan 05;23(2):634 [FREE Full text] [doi: 10.3390/s23020634] [Medline: 36679430]
34. Ovadia Y, Fertig E, Ren J, Nado Z, Sculley D, Nowozin S, et al. Can you trust your model's uncertainty? Evaluating predictive uncertainty under dataset shift. arXiv Preprint posted online on June 6, 2019 [FREE Full text]
35. Ghahramani Z. Probabilistic machine learning and artificial intelligence. Nature 2015 May 28;521(7553):452-459 [FREE Full text] [doi: 10.1038/nature14541] [Medline: 26017444]
36. Cardelli L, Kwiatkowska M, Laurenti L, Patane A. Robustness guarantees for Bayesian inference with gaussian processes. Proc AAAI Conf Artif Intell 2019 Jul 17;33(01):7759-7768 [FREE Full text] [doi: 10.1609/aaai.v33i01.33017759]
37. Winter S, Campbell T, Lin L, Srivastava S, Dunson DB. Machine learning and the future of Bayesian computation. arXiv Preprint posted online on April 21, 2023 [FREE Full text]
38. Srivastava N, Hinton G, Krizhevsky A, Sutskever I, Salakhutdinov R. Dropout: a simple way to prevent neural networks from overfitting. J Mach Learn Res 2014;15(1):1929-1958.
39. Gal Y, Ghahramani Z. Dropout as a Bayesian approximation: representing model uncertainty in deep learning. arXiv Preprint posted online on June 6, 2015 [FREE Full text]
40. Wang G, Li W, Aertsen M, Deprest J, Ourselin S, Vercauteren T. Aleatoric uncertainty estimation with test-time augmentation for medical image segmentation with convolutional neural networks. Neurocomputing (Amst) 2019 Sep 03;335:34-45 [FREE Full text] [doi: 10.1016/j.neucom.2019.01.103] [Medline: 31595105]
41. Mathiasen K, Riper H, Andersen TE, Roessler KK. Guided internet-based cognitive behavioral therapy for adult depression and anxiety in routine secondary care: observational study. J Med Internet Res 2018 Nov 28;20(11):e10927 [FREE Full text] [doi: 10.2196/10927] [Medline: 30487118]
42. Kroenke K, Spitzer RL, Williams JB. The PHQ-9: validity of a brief depression severity measure. J Gen Intern Med 2001 Sep;16(9):606-613 [FREE Full text] [doi: 10.1046/j.1525-1497.2001.016009606.x] [Medline: 11556941]
43. Spitzer RL, Kroenke K, Williams JB, Löwe B. A brief measure for assessing generalized anxiety disorder: the GAD-7. Arch Intern Med 2006 May 22;166(10):1092-1097 [FREE Full text] [doi: 10.1001/archinte.166.10.1092] [Medline: 16717171]

XSL•FO
RenderX

44. Mattick RP, Clarke JC. Development and validation of measures of social phobia scrutiny fear and social interaction anxiety. Behav Res Ther 1998 Apr;36(4):455-470 [FREE Full text] [doi: 10.1016/s0005-7967(97)10031-6] [Medline: 9670605]
45. Houck PR, Spiegel D, Shear M, Rucci P. Reliability of the self-report version of the panic disorder severity scale. Depress Anxiety 2002;15(4):183-185 [FREE Full text] [doi: 10.1002/da.10049] [Medline: 12112724]
46. Marks I, Mathews A. Brief standard self-rating for phobic patients. Behav Res Ther 1979;17(3):263-267. [doi: 10.1016/0005-7967(79)90041-x] [Medline: 526242]
47. Priebe S, Huxley P, Knight S, Evans S. Application and results of the Manchester Short Assessment of Quality of Life (MANSA). Int J Soc Psychiatry 1999;45(1):7-12 [FREE Full text] [doi: 10.1177/002076409904500102] [Medline: 10443245]
48. Boluki S, Ardywibowo R, Dadaneh SZ, Zhou M, Qian X. Learnable bernoulli dropout for Bayesian deep learning. arXiv Preprint posted online on February 12, 2020 [FREE Full text]
49. Jospin LV, Laga H, Boussaid F, Buntine W, Bennamoun M. Hands-on Bayesian neural networks—a tutorial for deep learning users. IEEE Comput Intell Mag 2022 May;17(2):29-48 [FREE Full text] [doi: 10.1109/mci.2022.3155327]
50. Saarela M, Jauhiainen S. Comparison of feature importance measures as explanations for classification models. SN Appl Sci 2021 Feb 03;3(2):1 [FREE Full text] [doi: 10.1007/s42452-021-04148-9]
51. Menard S. Six approaches to calculating standardized logistic regression coefficients. Am Stat 2004 Aug;58(3):218-223 [FREE Full text] [doi: 10.1198/000313004x946]
52. Forsell E, Jernelöv S, Blom K, Kaldo V. Clinically sufficient classification accuracy and key predictors of treatment failure in a randomized controlled trial of internet-delivered cognitive behavior therapy for insomnia. Internet Interv 2022 Sep;29:100554 [FREE Full text] [doi: 10.1016/j.invent.2022.100554] [Medline: 35799973]
53. Boothroyd L, Dagnan D, Muncer S. PHQ-9: one factor or two? Psychiatry Res 2019 Jan;271:532-534 [FREE Full text] [doi: 10.1016/j.psychres.2018.12.048] [Medline: 30553100]
54. Keough ME, Porter E, Kredlow MA, Worthington JJ, Hoge EA, Pollack MH, et al. Anchoring the panic disorder severity scale. Assessment 2012 Jun;19(2):257-259 [FREE Full text] [doi: 10.1177/1073191112436668] [Medline: 22327206]
55. Sapra A, Bhandari P, Sharma S, Chanpura T, Lopp L. Using generalized anxiety disorder-2 (GAD-2) and GAD-7 in a primary care setting. Cureus 2020 May 21;12(5):e8224 [FREE Full text] [doi: 10.7759/cureus.8224] [Medline: 32582485]
56. Peters L. Discriminant validity of the Social Phobia and Anxiety Inventory (SPAI), the Social Phobia Scale (SPS) and the Social Interaction Anxiety Scale (SIAS). Behav Res Ther 2000 Sep;38(9):943-950. [doi: 10.1016/s0005-7967(99)00131-x] [Medline: 10957828]
57. Moutier CY, Stein MB. The history, epidemiology, and differential diagnosis of social anxiety disorder. J Clin Psychiatry 1999;60 Suppl 9:4-8. [Medline: 10335673]
58. Olawade DB, Wada OZ, Odetayo A, David-Olawade AC, Asaolu F, Eberhardt J. Enhancing mental health with artificial intelligence: current trends and future prospects. J Med Surg Public Health 2024 Aug;3:100099 [FREE Full text] [doi: 10.1016/j.glmedi.2024.100099]
59. Arroll B, Goodyear-Smith F, Crengle S, Gunn J, Kerse N, Fishman T, et al. Validation of PHQ-2 and PHQ-9 to screen for major depression in the primary care population. Ann Fam Med 2010;8(4):348-353 [FREE Full text] [doi: 10.1370/afm.1139] [Medline: 20644190]

Abbreviations

AI: artificial intelligence
AUC: area under the curve
DSS: decision support system
GAD-7: Generalized Anxiety Disorder Questionnaire-7
LIME: local interpretable model-agnostic explanations
MCD: Monte Carlo dropout
ML: machine learning
PDSS: Panic Disorder Severity Scale
PHQ-9: Patient Health Questionnaire-9
SHAP: Shapley additive explanations
SIAS: Social Interaction Anxiety Scale
XAI: explainable artificial intelligence

XSL•FO
RenderX

Edited by C Lovis; submitted 22.07.24; peer-reviewed by P Bjurner, A Peimankar, A Dasgupta; comments to author 25.01.25; revised version received 08.02.25; accepted 16.02.25; published 26.03.25.

Please cite as:
Kelly A, Jensen EK, Grua EM, Mathiasen K, Van de Ven P
An Interpretable Model With Probabilistic Integrated Scoring for Mental Health Treatment Prediction: Design Study
JMIR Med Inform 2025;13:e64617
URL: https://medinform.jmir.org/2025/1/e64617
doi:10.2196/64617
PMID:

©Anthony Kelly, Esben Kjems Jensen, Eoin Martino Grua, Kim Mathiasen, Pepijn Van de Ven. Originally published in JMIR Medical Informatics (https://medinform.jmir.org), 26.03.2025. This is an open-access article distributed under the terms of the Creative Commons Attribution License (https://creativecommons.org/licenses/by/4.0/), which permits unrestricted use, distribution, and reproduction in any medium, provided the original work, first published in JMIR Medical Informatics, is properly cited. The complete bibliographic information, a link to the original publication on https://medinform.jmir.org/, as well as this copyright and license information must be included.

XSL•FO
RenderX

Original Paper

Identification of Patients With Congestive Heart Failure From the Electronic Health Records of Two Hospitals: Retrospective Study

Daniel Sumsion[1,2], BS; Elijah Davis[1,2], BS; Marta Fernandes[3], PhD; Ruoqi Wei[1,4], MD, PhD; Rebecca Milde[1,5], BS; Jet Malou Veltink[1,6], BS; Wan-Yee Kong[1], MD; Yiwen Xiong[1,7], BS; Samvrit Rao[1], HS; Tara Westover[1], HS; Lydia Petersen[1,2], BS; Niels Turley[1], BS; Arjun Singh[3], MD; Stephanie Buss[1], MD; Shibani Mukerji[3], MD, PhD; Sahar Zafar[3], MD; Sudeshna Das[3], PhD; Valdery Moura Junior[1,3], PhD; Manohar Ghanta[1,3], MSc; Aditya Gupta[1,3], MSc; Jennifer Kim[8], MD, PhD; Katie Stone[9,10], PhD; Emmanuel Mignot[11], MD, PhD; Dennis Hwang[12], MD; Lynn Marie Trotti[13], MSc, MD; Gari D Clifford[13,14], DPhil; Umakanth Katwa[15], MD; Robert Thomas[16], MD; M Brandon Westover[1,3], MD, PhD; Haoqi Sun[1,3], PhD

[1]Department of Neurology, Beth Israel Deaconess Medical Center, Boston, MA, United States
[2]Brigham Young University, Provo, UT, United States
[3]Department of Neurology, Massachusetts General Hospital, Boston, MA, United States
[4]Department of Health Outcomes and Biomedical Informatics, College of Medicine, University of Florida, Gainesville, FL, United States
[5]Northeastern University, Boston, MA, United States
[6]Utrecht University, Utrecht University, Utrecht, The Netherlands
[7]Boston College, Boston, MA, United States
[8]Yale School of Medicine, New Haven, CT, United States
[9]California Pacific Medical Center Research Institute, San Francisco, CA, United States
[10]Department of Epidemiology and Biostatistics, University of California, San Francisco, CA, United States
[11]Stanford University, Stanford, CA, United States
[12]Kaiser Permanente, Fontana, CA, United States
[13]Emory University, Atlanta, GA, United States
[14]Georgia Institute of Technology, Atlanta, GA, United States
[15]Boston Children's Hospital, Boston, MA, United States
[16]Division of Pulmonary, Critical Care and Sleep Medicine, Department of Medicine, Beth Israel Deaconess Medical Center, Boston, United States

Corresponding Author:
Haoqi Sun, PhD
Department of Neurology
Beth Israel Deaconess Medical Center
DA-0815, 330 Brookline Avenue
Boston, MA, 02215
United States
Phone: 1 781 539 9402
Email: hsun3@bidmc.harvard.edu

Abstract

Background: Congestive heart failure (CHF) is a common cause of hospital admissions. Medical records contain valuable information about CHF, but manual chart review is time-consuming. Claims databases (using *International Classification of Diseases* [*ICD*] codes) provide a scalable alternative but are less accurate. Automated analysis of medical records through natural language processing (NLP) enables more efficient adjudication but has not yet been validated across multiple sites.

Objective: We seek to accurately classify the diagnosis of CHF based on structured and unstructured data from each patient, including medications, *ICD* codes, and information extracted through NLP of notes left by providers, by comparing the effectiveness of several machine learning models.

Methods: We developed an NLP model to identify CHF from medical records using electronic health records (EHRs) from two hospitals (Mass General Hospital and Beth Israel Deaconess Medical Center; from 2010 to 2023), with 2800 clinical visit

XSL•FO
RenderX

notes from 1821 patients. We trained and compared the performance of logistic regression, random forests, and RoBERTa models. We measured model performance using area under the receiver operating characteristic curve (AUROC) and area under the precision-recall curve (AUPRC). These models were also externally validated by training the data on one hospital sample and testing on the other, and an overall estimated error was calculated using a completely random sample from both hospitals.

Results: The average age of the patients was 66.7 (SD 17.2) years; 978 (54.3%) out of 1821 patients were female. The logistic regression model achieved the best performance using a combination of *ICD* codes, medications, and notes, with an AUROC of 0.968 (95% CI 0.940-0.982) and an AUPRC of 0.921 (95% CI 0.835-0.969). The models that only used *ICD* codes or medications had lower performance. The estimated overall error rate in a random EHR sample was 1.6%. The model also showed high external validity from training on Mass General Hospital data and testing on Beth Israel Deaconess Medical Center data (AUROC 0.927, 95% CI 0.908-0.944) and vice versa (AUROC 0.968, 95% CI 0.957-0.976).

Conclusions: The proposed EHR-based phenotyping model for CHF achieved excellent performance, external validity, and generalization across two institutions. The model enables multiple downstream uses, paving the way for large-scale studies of CHF treatment effectiveness, comorbidities, outcomes, and mechanisms.

(JMIR Med Inform 2025;13:e64113) doi:10.2196/64113

KEYWORDS

electronic health record; machine learning; artificial intelligence; phenotype; congestive heart failure; medication; claims database; International Classification of Diseases; effectiveness; natural language processing; model performance; logistic regression; validity

Introduction

Congestive heart failure (CHF) and all types of heart disease are the primary causes of hospital admissions and the leading cause of death in the United States [1-3]. The prevalence of CHF in the United States is estimated to be 7% for men and 4.2% for women [4]. As a result, it is important to diagnose CHF early and accurately, which is difficult given the diversity of CHF and the lack of definitive, universally applicable diagnostic tests [5]. This underscores the need for research on improving diagnosis and predicting patient outcomes. The heterogeneity of CHF makes it hard to design clinical trials that can accurately and uniformly diagnose CHF [6]. In this context, accurate classification is crucial for the reliability of epidemiological and outcomes research. Traditionally, the identification of CHF is a labor-intensive process. Local sites identify potential cases and forward medical records to a Central Clinical Events Committee, comprised of physician experts, who manually review each case against established standards [7-9]. While this method is considered the gold standard, it is impractical for large observational studies, where *International Classification of Diseases* (*ICD*) codes are typically used. However, sole reliance on *ICD* codes is problematic due to their imprecision; it is estimated that approximately 40% of hospitalizations labeled with primary *ICD* codes for CHF do not hold up upon detailed medical record review [9]. Consequently, there is a growing interest in automated methods for adjudicating CHF hospitalizations from medical records that could streamline the process; reduce reliance on physician-based Central Clinical Events Committee reviews; foster the development of large, cost-effective clinical trials; and help gather more accurate data for research [9].

In this context, electronic health records (EHRs) have become invaluable. Encompassing millions of patient profiles, these records are stored across various hospitals and institutions as structured and unstructured data. Much of the data exists as unstructured natural language in physicians' notes, documenting symptoms, conditions, and diagnoses. Natural language processing (NLP) approaches present an opportunity to harness this rich source of data, enabling high-throughput identification and phenotyping of patients directly from hospital databases [10-13]. Some applications of these models in inpatient fall detection [14], emergency triage notes [15], and inpatient fall risk assessment [16] have already achieved a high level of effectiveness using a variety of modeling methods, including large language models such as Bidirectional Encoder Representations from Transformers, showing the need for further development in other medical applications.

Here, we address these gaps by introducing a comprehensive approach to EHR-based phenotyping of CHF within a large multihospital cohort, based on clinical notes, *ICD* codes, and medications, contributing to the growing body of knowledge in automated medical record review and phenotyping of patients with CHF, as well as ensuring reproducible and reliable clinical use [17,18].

Methods

Cohort

We retrospectively obtained EHR data from two sites: Beth Israel Deaconess Medical Center (BIDMC) and Massachusetts General Hospital (MGH), from 2010 to 2023. The EHR data contain clinical notes written by the clinician, *ICD* diagnosis codes (*ICD-9* and *ICD-10*) assigned during encounters, and prescribed medications. To enable initial cohort selection and maximize the chance of including patients with CHF from this large pool of inpatient and outpatient encounters, we divided patients into groups based on the presence of prespecified *ICD* codes ("*ICD*+" or "*ICD*–") related to CHF and prespecified medications ("MED+" or "MED–"), creating four groups: "*ICD*+/MED+," "*ICD*–/MED+," "*ICD*+/MED–," and "*ICD*–/MED–." We then randomly sampled a total of 1400 notes with keywords (such as heart, CHF, etc) from the four groups at each site to undergo manual annotation (described

XSL•FO
RenderX

below) to provide labels for model training. This sample size was selected to enable appropriate training and to not overwhelm the available computing power.

Ethical Considerations

The retrospective data were obtained under Beth Israel Deaconess Medical Center's institutional review board that waived the need for informed consent (BIDMC IRB# 2022P000481).

CHF-Related Keywords, ICD Codes, and Medications for Initial Cohort Selection

ICD codes and medications related to CHF were specified as a part of the model input. *ICD* codes included 428 (*ICD-9*) for "Congestive Heart Failure, unspecified" and I50 (*ICD-10*) for "Heart Failure." The medications are shown in Table 1. We also specified CHF-related keywords to be highlighted during manual note review, to facilitate the annotation of ground-truth CHF status and to include them as classifying features (see below). The keywords were determined using two approaches. The first was the knowledge-driven approach: we obtained as many keywords as possible from medical doctors and by manually reviewing published papers. This was done by simply reading papers and selecting words that appeared frequently and were related to CHF and then presenting them to physicians to check for accuracy (see references for links to papers). The second was the data-driven approach: we listed all unique words (1-gram), consecutive two-word sequences (2-gram), and consecutive three-word sequences (3-gram) in all notes. Then, using the associated, CHF-related *ICD* codes as a rough approximation of ground-truth CHF status, for each n-gram, we conducted a Mann-Whitney *U* test to compare the median number of occurrences in the groups with and without CHF. Words that occurred with significantly different frequencies between groups were included in the keyword list. We further expanded the set of potentially classifying features by augmenting keywords and phrases with their negations.

Table 1. Medications related to congestive heart failure.

Medication generic name	Medication description
Lisinopril	Angiotensin-converting enzyme inhibitor
Furosemide	Diuretic
Bumetanide	Diuretic
Propranolol	Beta-blocker
Amlodipine	Calcium channel blocker
Hydrochlorothiazide	Diuretic
Omeprazole	Proton pump inhibitor
Isosorbide mononitrate	Vasodilator
Enalapril	Angiotensin-converting enzyme inhibitor

Annotation of the Ground-Truth CHF Status

Ground-truth CHF status was based on having human annotators read through clinical notes and make a yes-or-no decision for each note as to whether the note author affirmed a diagnosis of CHF in the note. To ease annotation, we displayed each clinical note with keywords highlighted so that the annotator could more quickly determine CHF status by reading the note. Notes were randomly assigned to 5 independent annotators. We followed a standard operating procedure to ensure consistency between raters. Notes were randomly split between 5 annotators without overlap. Patients who were said to have CHF or a "history of CHF" were labeled as "positive" cases. All others were labeled as "negative" cases. This included patients noted as being "unlikely [to have] CHF," patients with a family history but no personal diagnosis of CHF, and patients with no indication of CHF given in the note.

Feature Matrix Construction

Features constructed to train the NLP model included three subsets: features based on keywords and/or phrases in the notes; features based on *ICD* codes; and features based on medications. To construct features based on notes, we applied stemming and lemmatization. The number of occurrences for each keyword or phrase in the note was then defined as the feature value. Features based on *ICD* codes and medications were identified as the number of occurrences in the medical record dated within 18 months before or after the note's date.

Model Development: Logistic Regression, Random Forests, and RoBERTa

We developed models based on different subsets of information and with different model architectures. The first model was a logistic regression model. The training was done using nested, 5-fold cross-validation with an elastic-net penalty, using Bayesian optimization to fine-tune the hyperparameters (penalty strength and L1 ratio) to achieve the maximum average area under the receiver operating characteristic curve (AUROC) across all inner validation sets. For each outer fold, a model was fitted with the best hyperparameters, and a receiver operating characteristic curve was obtained using the outer testing set. Using the Youden index, we determined a probability cutoff value for binary classification in each outer fold. The final performance metric was calculated as the average of the 5 AUROCs from the outer folds. We also trained a random forests classifier using the same approach with nested, 5-fold cross-validation, using Bayesian optimization to fine-tune the hyperparameters (minimum leaves per sample, number of

XSL•FO
RenderX

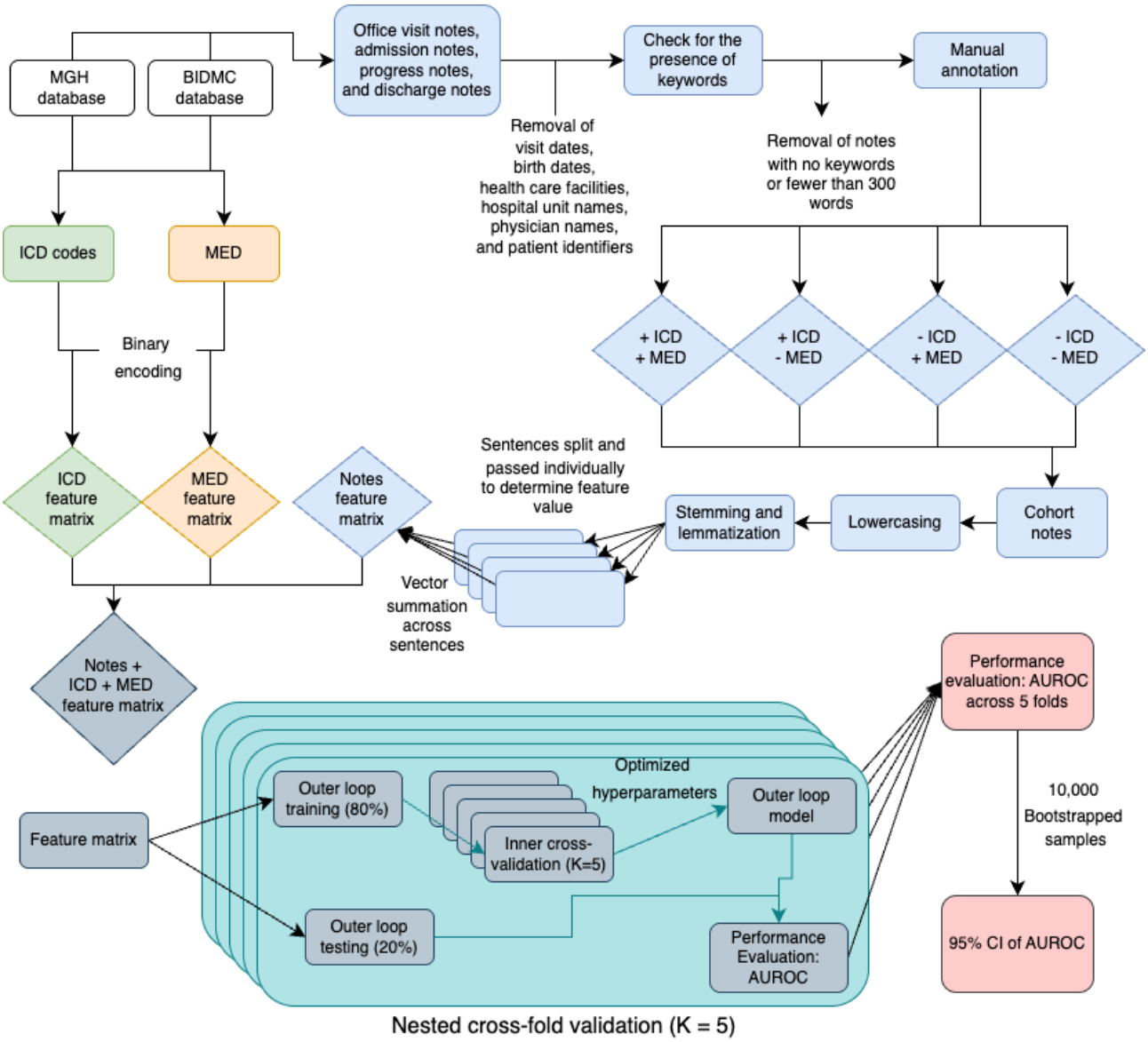
estimators, maximum depth, and cost-complexity pruning coefficient) to incorporate ensemble methods because of their robustness to reduce bias [19]. We finally trained a deep learning model based on RoBERTa followed by logistic regression. We used the embeddings from RoBERTa as our feature matrix with no additional pretraining, as previous studies have shown that RoBERTa has already been optimized [20]. We did this in three different ways. First, we split the note into sections of up to 512 tokens with each section having a one-sentence overlap. We then took the vector representations of these segments and took the elementwise average to get a feature matrix. Second, we took 250 tokens forward and backward from the keywords "CHF" or "congestive heart failure" and found the embeddings from these sections. Third, if multiple keywords were found, then the elementwise average was taken. If no keywords were found, then all columns were set to zero.

For model type, we tested logistic regression, random forests, and RoBERTa, spanning linear and nonlinear models, as well as simple statistical and deep learning models. While large language models are powerful tools, they are not always necessary, nor are they always the best approach. Simpler approaches often demonstrate that excellent results can be achieved without the additional complexity.

Feature Importance

All models used to derive feature importance were trained using median hyperparameters across the 5 outer cross-validation folds and trained on the entire dataset. For logistic regression, feature importance was given by model coefficients. For random forests, feature importance was measured by the total reduction of the Gini impurity associated with that feature, normalized to sum up to 1 across all features. We did not investigate feature importance from RoBERTa since it did not achieve better performance than logistic regression or random forests (see the *Results* section). Figure 1 summaries the methods into a visual aid.

Figure 1. Flowchart demonstrating the data collection, methods of feature matrix construction, and model usage. AUROC: area under the receiver operating characteristic curve; BIDMC: Beth Israel Deaconess Medical Center; ICD: International Classification of Diseases; MED: medications; MGH: Mass General Hospital.



XSL•FO
RenderX

Statistical Analysis

Statistical significance was set at $P<.05$. Further, 95% CIs were determined using 10,000 rounds of bootstrapping. All analyses were performed using Python (version 3.10.13; Python Software Foundation).

Results

Cohort Characteristics

The final cohort included 1821 patients with 2800 notes (Table 2). The average age was 66.7 (SD 17.2) years; 978 (54.3%) out of 1821 patients were female. The racial and ethnic composition of the sample was 3.8% (69/1821) Black or African American, 6.3% (115/1821) Hispanic, 1.9% (35/1821) Asian, and 80.7% (1471/1821) White. The three most common medications used were omeprazole, furosemide, and lisinopril. The most common *ICD* code stem was I50. In terms of institutions, of the 2800 notes, 1440 (50%) came from BIDMC and 1400 (50%) came from MGH. CHF prevalence in our cohort was 425 (15.9%) out of 1400 notes in the BIDMC dataset and 445 (15.2%) out of 1400 notes in the MGH dataset. Note length varied from 1907 to 60,870 characters.

Table 2. Cohort characteristics.

Characteristics	Site and group classification									
	Mass General Hospital					Beth Israel Deaconess Medical Center				
	ICD[a]+ /MED[b]+	*ICD*+ /MED–	*ICD*– /MED+	*ICD*– /MED–	Total	*ICD*+ /MED+	*ICD*+ /MED–	*ICD*+ /MED+	*ICD*+ /MED–	Total
Patients, n	347	348	348	350	1398	41	0	220	167	428
Notes, n	350	350	350	350	1400	350	—[c]	700	350	1400
Positive cases based on manual annotation, n (%)[d]	151 (43.1)	184 (52.6)	44 (12.6)	46 (13.1)	—	135 (38.6)	—	192 (27.4)	118 (33.7)	—
Age (years), mean (SD)	73.8 (12.3)	74.5 (13.1)	65.4 (15.2)	57.3 (23.4)	67.7 (18.0)	71.2 (11.9)	—	63.8 (13.1)	65.0 (14.1)	65.0 (13.8)
Sex, n (%)[e]										
Female	175 (50.4)	178 (51.1)	196 (56.3)	214 (61.1)	763 (54.8)	20 (48.8)	—	110 (50)	85 (50.9)	215 (50.2)
Male	172 (49.6)	170 (48.9)	152 (43.7)	136 (38.9)	630 (45.2)	21 (51.2)	—	110 (50)	82 (49.1)	213 (49.8)
Race and ethnicity, n (%)[d]										
Black or African American	22 (6.3)	15 (4.3)	17 (4.9)	15 (4.3)	69 (4.9)	0 (0)	—	0 (0)	0 (0)	0 (0)
Hispanic	14 (4.0)	22 (6.3)	25 (7.2)	19 (5.4)	80 (5.7)	2 (4.9)	—	20 (9.1)	13 (7.8)	35 (8.2)
Asian	7 (2)	4 (1.1)	4 (1.1)	7 (2)	22 (1.6)	0 (0)	—	8 (3.6)	5 (3)	13 (3)
White	295 (85)	305 (87.6)	289 (83)	296 (84.6)	1185 (85.1)	29 (70.7)	—	141 (64.1)	116 (69.5)	286 (66.8)

[a]ICD: International Classification of Diseases.

[b]MED: medications.

[c]Not applicable.

[d]Percentages are based on the number of notes as the denominators.

[e]Percentages are based on the number of patients as the denominators.

Model Performance

Table 3 shows performances from all three models and four input modalities (9 models in total). Models that used *ICD* codes, medications, and notes from both hospitals combined performed the best, followed by models that used notes only. Models that used *ICD* codes or medications only performed substantially worse. Meanwhile, logistic regression models performed the best, followed by random forests models, and then RoBERTa models. The receiver operating characteristic and precision-recall curves for the best-performing model and input modalities are shown in Figure 2.

XSL•FO
RenderX

Table 3. AUROC[a] and AUPRC[b] on the combined MGH[c] and BIDMC[d] test data for the logistic regression, random forests, and RoBERTa embeddings models, using different types of model input (ICD[e] codes, medications, and notes). The best performances are italicized.

Input	Logistic regression		Random forests		RoBERTa	
	AUROC (95% CI)	AUPRC (95% CI)	AUROC (95% CI)	AUPRC (95% CI)	AUROC (95% CI)	AUPRC (95% CI)
ICD codes, medications, and notes	*0.968 (0.940-0.982)*	*0.921 (0.835-0.969)*	0.962 (0.719-0.991)	0.894 (0.720-0.985)	0.866 (0.821-0.904)	0.766 (0.632-0.853)
Notes only	0.964 (0.942-0.975)	0.901 (0.805-0.956)	0.963 (0.916-0.976)	0.899 (0.659-0.968)	—[f]	—
ICD codes only	0.646 (0.580-0.826)	0.557 (0.486-0.716)	0.646 (0.595-0.835)	0.557 (0.492-0.720)	—	—
Medications only	0.639 (0.338-0.875)	0.428 (0.235-0.651)	0.644 (0.326-0.936)	0.459 (0.320-0.779)	—	—

[a]AUROC: area under the receiver operating characteristic curve.

[b]AUPRC: area under the precision-recall curve.

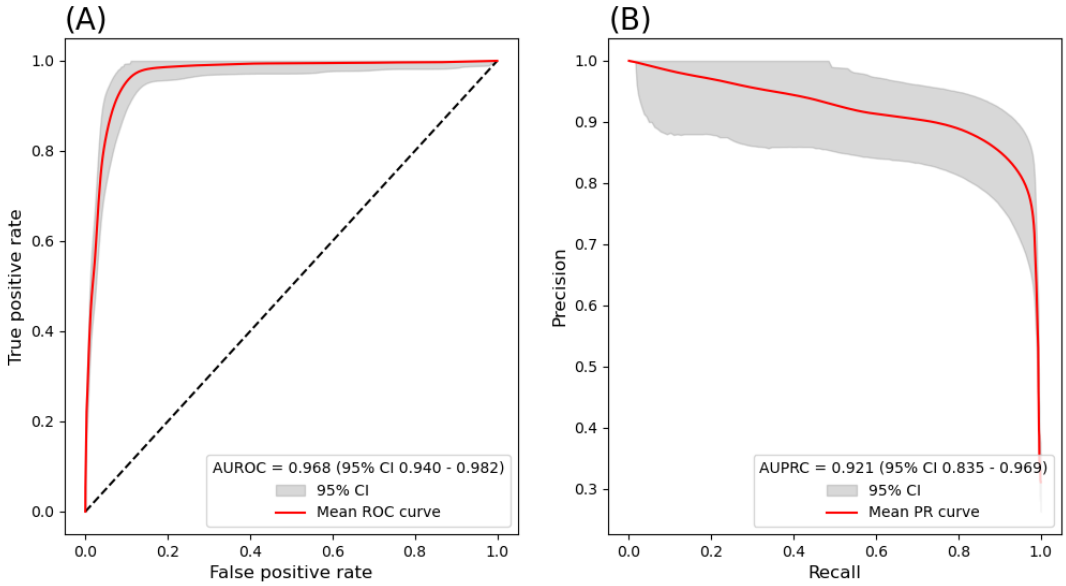
[c]MGH: Mass General Hospital.

[d]BIDMC: Beth Israel Deaconess Medical Center.

[e]ICD: International Classification of Diseases.

[f]Not applicable.

Figure 2. Model performance using the combined MGH and BIDMC test data. (A) Receiver operating characteristic (ROC) curve using logistic regression with notes, ICD codes, and medications as input. The area under the ROC curve (AUROC) was 0.968 (95% CI 0.940-0.982). The optimal cutoff (according to the Youden index) achieved a false positive rate of 11.9% (230/1903; ie, specificity at 88.1%) and a true positive rate of 97.7% (852/870; ie, sensitivity at 97.7%). (B) Precision-recall (PR) curve using logistic regression with notes, ICD codes, and medications as input. The area under the PR curve (AUPRC) was 0.921 (95% CI 0.835-0.969). The optimal cutoff achieved a recall of 96.78% (842/870; ie, sensitivity at 96.78%) and a precision of 80.88% (842/1081). BIDMC: Beth Israel Deaconess Medical Center; ICD: International Classification of Diseases; MGH: Mass General Hospital.



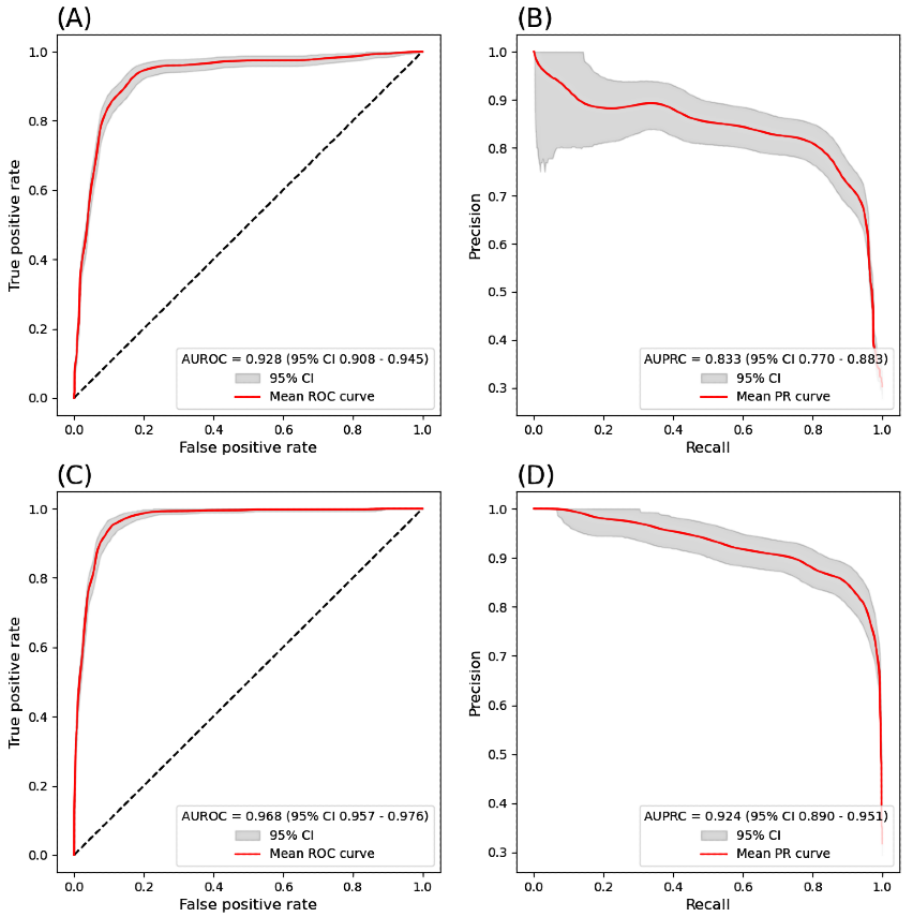
External Validity

To investigate how the model generalizes, we also obtained the performance when training on data from one site and testing on data from the other site (Figure 3 and Table 4). Training on BIDMC data and testing on MGH data showed significantly higher performance than training on MGH data and testing on BIDMC data. The performance of training on BIDMC data and testing on MGH data was similar to the cross-validated performance shown in Figure 2.

The results in Figure 3 show high external validity of the model due to its ability to perform well with training on one hospital dataset and subsequent testing on the other hospital dataset.

XSL•FO
RenderX

Figure 3. Model performance of training exclusively on one hospital's data and testing on the other's data. (A) and (B) Performance of training on MGH data and testing on BIDMC data. (C) and (D) Performance of training on BIDMC data and testing on MGH data. AUPRC: area under the precision-recall curve; AUROC: area under the receiver operating characteristic curve; BIDMC: Beth Israel Deaconess Medical Center; MGH: Mass General Hospital; PR: precision-recall; ROC: receiver operating characteristic.



XSL•FO
RenderX

Table 4. Logistic regression coefficients from using the model trained with notes, ICD[a] codes, and medications. Unexpected results are discussed in the Error Analysis section. Small coefficients for some input variables were expected and removed at the time of model deployment.

Features	Logistic regression coefficients
CHF[b]	2.39
Congestive heart failure	1.89
With CHF	1.34
CHF father	–1.15
Histori congestive heart failure	0.94
CHF mother	–0.80
No CHF	–0.72
I50	0.68
Dx[c] CHF	0.64
Exacerb CHF	0.61
With congestive heart failure	–0.60
[] CHF	–0.54
Ascites	0.54
() Congestive heart failure	0.52
Diagnosis congestive heart failure	0.49

[a]ICD: International Classification of Diseases.

[b]CHF: congestive heart failure.

[c]Dx: diagnosis.

Feature Importance

Feature importance for the best-performing model (logistic regression) is shown in Table 4. The top-3 positive predictors were the words and phrases "CHF," "congestive heart failure," and "with CHF." The top-3 negative predictors were "CHF father," "CHF mother," and "no CHF."

In Table 4, the negative weights of "CHF father" and "CHF mother" came from clinicians' discussion of family history in the note. Brackets such as those in "[] CHF" or "() CHF" were purposely left in each note as they were often part of a medical questionnaire to obtain the medical history for new patients. Coefficients of "with CHF" and "with congestive heart failure" were given negative and positive weights, respectively, possibly due to the high collinearity between them.

Error Analysis

We investigated reasons for misclassification in cases where the model output disagreed with manual labels. For false positives, reasons included patients with symptoms typical for CHF who had not been given a formal diagnosis of CHF, patients with a family medical history of CHF, cases where negation was expressed unusually (eg, "I do not feel like this is consistent with congestive heart failure"), and notes that had templated preoperative instructions or medication descriptions (eg, "tell your doctor if you have CHF"). For false negatives, reasons included notes explaining a noncardiac medical visit but mentioning a history of CHF, and patients with a diagnosis of CHF no longer experiencing symptoms.

Performance in Unselected or Random EHR Samples

The sample used for training and testing was, by construction, enriched for "positive" cases; that is, there were more "*ICD*+/MED+," "*ICD*–/MED+," and "*ICD*+/MED–" cases and fewer "*ICD*–/MED–" cases than would be present in a random sample. To estimate the expected performance in a general hospital population, we randomly sampled an additional 500 patients from BIDMC and 500 patients from MGH. Using our final fitted model from logistic regression methods (explained in detail above), we classified these 1000 patients as per Table 5. Using the prevalence values (p+/+, p+/–, p–/+, and p–/–) along with the corresponding overall model error rate (P_e+/+, P_e+/–, P_e–/+, and P_e–/–), the estimated performance within the overall hospital population was calculated as follows:

$$P(E) = (P_e+/+ \times p+/+) + (P_e+/- \times p+/-) + (P_e-/+ \times p-/+) + (P_e-/- \times p-/-)$$

$$= (0.074 \times 0.1) + (0.074 \times 0.098) + (0.079 \times 0.0088) + (0.094 \times 0.0021)$$

$$= 0.016$$

$$= 1.6\%$$

Thus, the overall error rate in the general hospital population was estimated to be 1.6%.

XSL•FO
RenderX

Table 5. The statistics used to derive the overall error rate in the general hospital population, stratified by the four groups.

Statistics	Group classification			
	ICD[a]+/MED[b]+	*ICD*+/MED–	*ICD*–/MED+	*ICD*–/MED–
Error rate in the original samples for model training and testing (P_e), n/N (%)	52/700 (7.4)	26/350 (7.4)	83/1050 (7.9)	66/700 (9.4)
Prevalence in additional random samples (p), n/N (%)	14/140 (10)	4/41 (9.8)	3/342 (0.9)	1/477 (0.21)

[a]*ICD*: *International Classification of Diseases*.

[b]MED: medications.

Discussion

Principal Findings

In this work, we present a highly accurate machine learning model that uses NLP to identify patients diagnosed with CHF in EHRs. The simple modeling technique demonstrated excellent discrimination for the presence or absence of CHF. Testing across two hospitals demonstrated the generalization of our model. This model provides a strong foundation for automated, scalable phenotyping of CHF at singular hospitals with big data and enable large-scale, EHR-based, epidemiological outcomes research. This work also provides the groundwork for future clinical applications, with the potential for improving clinical decision-making and patient outcomes by providing classification for diseases overlooked by clinicians. Such models could be incorporated into the current clinical workflow by inputting structured and unstructured data from visit notes by providers and comparing inconsistencies between providers' interpretation of patients' problems and what the model predicts could be an issue. This would ensure greater patient care and better use of technological advancements. The best-performing model was also simplistic, ensuring greater interpretability, computational efficiency, scalability, and cost-effectiveness of implementation of these methods.

In a previous study, EHR-based phenotyping of CHF was performed by comparing a deep learning model's predictions against *ICD* code–based diagnoses using a large cohort from a single hospital [10]. This work, however, did not address the common issues of *ICD* codes being an inaccurate representation of the true diagnosis and the generalizability of the model. Other studies have used inductive logic programming to create helpful rules for phenotyping patients with several diagnoses [8]. These studies, however, did not address how such approaches can be scaled to larger and noisier data as found in clinical databases.

Differences in generalizability between the two hospital cohorts need future research. When comparing training on a single hospital cohort and testing on the other, training on BIDMC data and subsequent testing on MGH data had a slight improvement compared to the reverse. This could be due to different hospitals or clinicians classifying CHF in different ways (such as heart failure with preserved ejection fraction, heart failure with reduced ejection fraction, etc), as well as inconsistencies of information provided in unstructured text (history of present illness, family history, etc) between hospitals.

The performance of the notes-only models was not significantly different from models using notes, *ICD* codes, and medications, suggesting future avenues of research comparing the necessity of obtaining such information for model improvement. Much of the information presented by medication lists and *ICD* codes is already found within clinical notes and could be redundant information.

Our work has important limitations. First, data used for training and testing were collected exclusively from two large hospitals in Boston, Massachusetts. Generalizability to other hospital and health care systems needs to be explored, understanding that these results are biased toward the Massachusetts population and use data from primarily top academic institutions. Second, echocardiography reports were not used. Future models that incorporate echocardiography records may have even better performance for CHF [17]. Third, the lack of racial and ethnic diversity in the saturated sample with CHF may inhibit generalizability.

Conclusion

We developed and validated a highly accurate NLP model for identifying patients with CHF from EHRs. This provides a foundation for large-scale, automated phenotyping of patients with CHF, enabling more efficient and scalable epidemiologic and outcomes research compared to manual chart review.

Acknowledgments

This work was supported by grants from the National Institutes of Health (R01NS102190, R01NS102574, R01NS107291, RF1AG064312, RF1NS120947, R01AG073410, R01HL161253, R01NS126282, and R01NS130119) awarded to MBW. SM is supported by the National Institute of Mental Health (R01MH131194 and R01MH134823) and the Claflin Distinguished Scholar award (Massachusetts General Hospital).

Data Availability

The deidentified electronic health record dataset is available upon reasonable request from the corresponding author. The code and intermediate results are available on GitHub [16].

XSL•FO
RenderX

Conflicts of Interest

KLS has grant funding from Eli Lilly, unrelated to this work. MBW is a cofounder, scientific advisor, and consultant to Beacon Biosignals and has a personal equity interest in the company. SB receives royalties from UpToDate that are unrelated to this work. All other authors declare no other conflicts of interest.

References

1. Armstrong PW, Pieske B, Anstrom KJ, Ezekowitz J, Hernandez AF, Butler J, et al. Vericiguat in patients with heart failure and reduced ejection fraction. N Engl J Med 2020 Mar 28;382(20):1883-1893 [FREE Full text]
2. Leading causes of death. Centers for Disease Control and Prevention. 2024. URL: https://www.cdc.gov/nchs/fastats/leading-causes-of-death.htm [accessed 2025-02-27]
3. Congestive heart failure symptoms and diagnosis. Brigham and Women's Hospital. URL: https://www.brighamandwomens.org/heart-and-vascular-center/resources/congestive-heart-failure [accessed 2024-02-20]
4. Heart disease prevalence - health, United States. Centers for Disease Control and Prevention. 2024 Aug 5. URL: https://www.cdc.gov/nchs/hus/topics/heart-disease-prevalence.htm [accessed 2025-02-27]
5. Common tests for heart failure. American Heart Association. 2023. URL: https://www.heart.org/en/health-topics/heart-failure/diagnosing-heart-failure/common-tests-for-heart-failure [accessed 2025-02-27]
6. Marantz PR, Alderman MH, Tobin JN. Diagnostic heterogeneity in clinical trials for congestive heart failure. Ann Intern Med 1988 Jul 01;109(1):55-61. [doi: 10.7326/0003-4819-109-1-55] [Medline: 3288033]
7. Carson P, Teerlink JR, Komajda M, Anand I, Anker SD, Butler J, et al. Comparison of investigator-reported and centrally adjudicated heart failure outcomes in the EMPEROR-Reduced trial. JACC Heart Fail 2023 Apr;11(4):407-417 [FREE Full text] [doi: 10.1016/j.jchf.2022.11.017] [Medline: 36881400]
8. Peissig P, Santos Costa V, Caldwell MD, Rottscheit C, Berg RL, Mendonca EA, et al. Relational machine learning for electronic health record-driven phenotyping. J Biomed Inform 2014 Dec;52:260-270 [FREE Full text] [doi: 10.1016/j.jbi.2014.07.007] [Medline: 25048351]
9. Yang J, Soltan AAS, Clifton DA. Machine learning generalizability across healthcare settings: insights from multi-site COVID-19 screening. NPJ Digit Med 2022 Jun 07;5(1):69 [FREE Full text] [doi: 10.1038/s41746-022-00614-9] [Medline: 35672368]
10. Cheng Y, Wang F, Zhang P, Hu J. Risk prediction with electronic health records: a deep learning approach. 2016 Presented at: Proceedings of the 2016 SIAM International Conference on Data Mining; May 5-7, 2016; Miami, FL p. 432-440 URL: https://epubs.siam.org/doi/10.1137/1.9781611974348.49 [doi: 10.1137/1.9781611974348.49]
11. Cunningham JW, Singh P, Reeder C, Claggett B, Marti-Castellote PM, Lau ES, et al. Natural language processing for adjudication of heart failure in a multicenter clinical trial: a secondary analysis of a randomized clinical trial. JAMA Cardiol 2024 Feb 01;9(2):174-181 [FREE Full text] [doi: 10.1001/jamacardio.2023.4859] [Medline: 37950744]
12. Khurshid S, Reeder C, Harrington LX, Singh P, Sarma G, Friedman SF, et al. Cohort design and natural language processing to reduce bias in electronic health records research. NPJ Digit Med 2022 Apr 08;5(1):47 [FREE Full text] [doi: 10.1038/s41746-022-00590-0] [Medline: 35396454]
13. Minaee S, Kalchbrenner N, Cambria E, Nikzad N, Chenaghlu M, Gao J. Deep learning based text classification: a comprehensive review. arXiv Preprint posted online on April 6, 2020 [FREE Full text]
14. Cheligeer C, Wu G, Lee S, Pan J, Southern DA, Martin EA, et al. BERT-based neural network for inpatient fall detection from electronic medical records: retrospective cohort study. JMIR Med Inform 2024 Jan 30;12:e48995 [FREE Full text] [doi: 10.2196/48995] [Medline: 38289643]
15. Fantuzzo J, Manz PH, McDermott P. Preschool version of the Social Skills Rating System. J Sch Psychol 1998;36(2):199-214 [FREE Full text] [doi: 10.1016/s0022-4405(98)00005-3]
16. Sumsion D. dsumsio / CHF_phenotyping. GitHub. 2024. URL: https://github.com/dsumsio/CHF_phenotyping [accessed 2025-02-27]
17. Heart failure - diagnosis and treatment. Mayo Clinic. 2024. URL: https://www.mayoclinic.org/diseases-conditions/heart-failure/diagnosis-treatment/drc-20373148 [accessed 2024-02-20]
18. McDermott MBA, Wang S, Marinsek N, Ranganath R, Foschini L, Ghassemi M. Reproducibility in machine learning for health research: still a ways to go. Sci Transl Med 2021 Mar 24;13(586):eabb1655 [FREE Full text] [doi: 10.1126/scitranslmed.abb1655] [Medline: 33762434]
19. Breiman L. Random forests. UC Berkeley. 2001 Jan. URL: https://www.stat.berkeley.edu/~breiman/randomforest2001.pdf [accessed 2025-02-27]
20. Liu Y, Ott M, Goyal N, Du J, Joshi M, Chen D, et al. RoBERTa: a robustly optimized BERT pretraining approach. arXiv Preprint posted online on July 26, 2019 [FREE Full text] [doi: 10.48550/arXiv.1907.11692]

Abbreviations

AUPRC: area under the precision-recall curve
AUROC: area under the receiver operating characteristic curve

XSL•FO
RenderX

BIDMC: Beth Israel Deaconess Medical Center
CHF: congestive heart failure
EHR: electronic health record
ICD: International Classification of Diseases
MGH: Mass General Hospital
NLP: natural language processing

Edited by C Lovis; submitted 11.07.24; peer-reviewed by H Rajaguru, S Mao, D Chrimes, M Elbattah; comments to author 22.09.24; revised version received 11.11.24; accepted 17.11.24; published 10.04.25.

Please cite as:
Sumsion D, Davis E, Fernandes M, Wei R, Milde R, Veltink JM, Kong WY, Xiong Y, Rao S, Westover T, Petersen L, Turley N, Singh A, Buss S, Mukerji S, Zafar S, Das S, Junior VM, Ghanta M, Gupta A, Kim J, Stone K, Mignot E, Hwang D, Trotti LM, Clifford GD, Katwa U, Thomas R, Westover MB, Sun H
Identification of Patients With Congestive Heart Failure From the Electronic Health Records of Two Hospitals: Retrospective Study
JMIR Med Inform 2025;13:e64113
URL: https://medinform.jmir.org/2025/1/e64113
doi:10.2196/64113
PMID:40208662

©Daniel Sumsion, Elijah Davis, Marta Fernandes, Ruoqi Wei, Rebecca Milde, Jet Malou Veltink, Wan-Yee Kong, Yiwen Xiong, Samvrit Rao, Tara Westover, Lydia Petersen, Niels Turley, Arjun Singh, Stephanie Buss, Shibani Mukerji, Sahar Zafar, Sudeshna Das, Valdery Moura Junior, Manohar Ghanta, Aditya Gupta, Jennifer Kim, Katie Stone, Emmanuel Mignot, Dennis Hwang, Lynn Marie Trotti, Gari D Clifford, Umakanth Katwa, Robert Thomas, M Brandon Westover, Haoqi Sun. Originally published in JMIR Medical Informatics (https://medinform.jmir.org), 10.04.2025. This is an open-access article distributed under the terms of the Creative Commons Attribution License (https://creativecommons.org/licenses/by/4.0/), which permits unrestricted use, distribution, and reproduction in any medium, provided the original work, first published in JMIR Medical Informatics, is properly cited. The complete bibliographic information, a link to the original publication on https://medinform.jmir.org/, as well as this copyright and license information must be included.

XSL•FO
RenderX

Original Paper

Daily Automated Prediction of Delirium Risk in Hospitalized Patients: Model Development and Validation

Kendrick Matthew Shaw[1,2], MD, PhD; Yu-Ping Shao[3], MS; Manohar Ghanta[3,4], MS; Valdery Moura Junior[3,4], MS; Eyal Y Kimchi[5], MD, PhD; Timothy T Houle[1,2], PhD; Oluwaseun Akeju[1,2], MD; Michael Brandon Westover[3,4], MD, PhD

[1]Department of Anesthesia, Pain, and Critical care Medicine, Massachusetts General Hospital, Boston, MA, United States

[2]Harvard Medical School, Boston, MA, United States

[3]Department of Neurology, Massachusetts General Hospital, Boston, MA, United States

[4]Department of Neurology, Beth Israel Deaconess Medical Center, Boston, MA, United States

[5]Ken & Ruth Davee Department of Neurology, Feinberg School of Medicine, Northwestern University, Chicago, IL, United States

Corresponding Author:
Kendrick Matthew Shaw, MD, PhD
Department of Anesthesia, Pain, and Critical care Medicine
Massachusetts General Hospital
55 Fruit Street
Boston, MA, 02114
United States
Phone: 1 6177262000
Email: kmshaw@mgh.harvard.edu

Abstract

Background: Delirium is common in hospitalized patients and is correlated with increased morbidity and mortality. Despite this, delirium is underdiagnosed, and many institutions do not have sufficient resources to consistently apply effective screening and prevention.

Objective: This study aims to develop a machine learning algorithm to identify patients at the highest risk of delirium in the hospital each day in an automated fashion based on data available in the electronic medical record, reducing the barrier to large-scale delirium screening.

Methods: We developed and compared multiple machine learning models on a retrospective dataset of all hospitalized adult patients with recorded Confusion Assessment Method (CAM) screens at a major academic medical center from April 2, 2016, to January 16, 2019, comprising 23,006 patients. The patient's age, gender, and all available laboratory values, vital signs, prior CAM screens, and medication administrations were used as potential predictors. Four machine learning approaches were investigated: logistic regression with L1-regularization, multilayer perceptrons, random forests, and boosted trees. Model development used 80% of the patients; the remaining 20% was reserved for testing the final models. Laboratory values, vital signs, medications, gender, and age were used to predict a positive CAM screen in the next 24 hours.

Results: The boosted tree model achieved the greatest predictive power, with an area under the receiver operator characteristic curve (AUROC) of 0.92 (95% CI 0.913-9.22), followed by the random forest (AUROC 0.91, 95% CI 0.909-0.918), multilayer perceptron (AUROC 0.86, 95% CI 0.850-0.861), and logistic regression (AUROC 0.85, 95% CI 0.841-0.852). These AUROCs decreased to 0.78-0.82 and 0.74-0.80 when limited to patients who currently do not or never have had delirium, respectively.

Conclusions: A boosted tree machine learning model was able to identify hospitalized patients at elevated risk for delirium in the next 24 hours. This may allow for automated delirium risk screening and more precise targeting of proven and investigational interventions to prevent delirium.

(JMIR Med Inform 2025;13:e60442) doi:10.2196/60442

KEYWORDS

delirium; prediction model; machine learning; boosted trees; model development; validation; AI; artificial intelligence; screening; prevention; develop; logistic regression; vitals; vital signs; gender; age; prevent

XSL•FO
RenderX

Introduction

Delirium is a common condition in hospitalized patients and has been recognized as an independent risk factor for poor clinical outcomes, including mortality, institutionalization, and cognitive impairment following hospital discharge [1-3]. The US annual national costs attributable to delirium have been estimated to be as high as US $152 billion, rivaling costs attributable to diabetes and falls [4]. As a result, a basic assessment for delirium is recommended for all hospitalized patients aged 65 years or older [5], and formal screening for delirium is recommended for critically ill patients [6].

Despite these recommendations, delirium frequently remains undiagnosed [7]. An automated delirium prediction tool could help address this, by alerting clinicians to at-risk patients so that they could be more carefully assessed for delirium. Such screening tools could also help focus interventions aimed at the prevention of delirium (eg, components of the hospital elder life program [8]) and provide an enriched patient sample for future delirium prevention studies.

In particular, we intend to use an automated tool to identify hospitalized patients at our institution who are at high risk of delirium in the next 24 hours. These patients will then be visited by a member of a delirium service for further evaluation and identification of interventions that may reduce the patient's risk of delirium. For this purpose, near-term risk (24-h risk) is more useful than the risk of delirium at some point during this hospitalization, and any history of prior or current delirium is relevant to identifying the patients at risk of ongoing delirium who should be seen (as reducing the duration of ongoing delirium is still likely to benefit the patient).

Although multiple prior delirium prediction tools have been described [9-12] (for a recent systematic review, see [13]) most have properties that have limited their use as a tool to be applied daily to every patient in the hospital. Most prediction tools are designed to allow a risk score to be easily calculated by a clinician by hand, limiting the model's performance compared to larger models with more features and favoring features that are easy for a human to produce over those easily extracted from the medical record. In addition, most prior models were developed using datasets of only a few hundred to a few thousand patients, limiting the complexity of the models that could be developed without overfitting.

To address these limitations, we have developed a model that can provide automated delirium screening based on data readily available from the electronic health record, emphasizing predictive power over ease of manual computation or ease of interpretation. Because current and prior delirium are known risk factors for future delirium, we also explore the performance of the model in patients without these risk factors. This tool achieves state-of-the-art accuracy for delirium prediction in this automated setting and maintains good performance even when restricted to patients without current or prior delirium.

Methods

Ethical Considerations

This study was reviewed and approved by the Mass General Brigham institutional review board (approval 2013P001024). The institutional review board determined that informed consent was not required for this retrospective study. This study adheres to the applicable TRIPOD (Transparent Reporting of a multivariable prediction model for Individual Prognosis Or Diagnosis) guidelines.

Study Cohort

Data were obtained for all patients who received any variation of a Confusion Assessment Method (CAM) screen [14] (eg, the CAM-ICU) [15]) in our hospital between April 2, 2016, and January 16, 2019, for a total of 23,006 patients. No specific exclusion criteria were used, as we wished the results to be applicable to the typical population of the hospital. Approximately 20% (n=4511) of patients were randomly selected and set aside for the final evaluation of the model (the "test dataset"); we remained blind to this dataset until after all model choices and parameters had been fixed in preparation for publication. The remaining 80% of patients (the "training dataset") were used for model selection, model training, and hyperparameter tuning.

Model Development Overview

We provide an overview of the model development here; additional details can be found in Multimedia Appendix 1.

For the outcome to be predicted, we used the presence of at least one positive CAM screen within a given day where CAM screens were performed. The CAM screen is a validated and widely used tool for assessing delirium where an observer assesses for a change in cognition with an acute onset and fluctuating course involving inattention and either disorganized thinking or an altered level of consciousness. [14] For each patient, we first identified all 24-hour intervals from 5 AM to 5 AM during which at least one CAM screen or CAM screen variation had been performed. For each such interval, the model was required to predict whether at least one CAM screen variant would be positive during that interval (vs all negative CAM screens).

As model inputs, we used the patient's age, gender, and all prior recorded vital signs, laboratory values, medications, and prior CAM assessments present in the medical record at 5 AM before the 24 hours in which delirium was to be predicted. Categorical values were converted to integers (eg, "1" for "Positive," "0" for "Negative"). These data were reduced to summary statistics for each measurement (eg, minimum, maximum, and mean systolic blood pressure in the past 24 h), which were used to form fixed-length feature vectors for each prediction interval. These feature vectors were then normalized by subtracting the median and dividing by the interquartile interval, with both the median and the quartiles estimated by the P2 algorithm [16]. Because the P2 algorithm provides only an approximation of the quantiles, the resulting values were generally not exact integers even for categorical values (eg, a binary measure that was mostly negative would have an estimated median that was

XSL•FO
RenderX

slightly above 0). Features that were missing in more than 95% of the patients were discarded. The remaining missing values were imputed to be the (P2-estimated) median value for the feature. To provide a consistent basis of comparison, we used these imputed values for all the models, including those (such as boosted trees) that do not strictly require imputation. Because of the sparsity of these features, this implies that most features for a patient will be at the median (imputed) value, especially for the first patient snapshot. Of note, however, because the P2-estimated median is a unique value that is otherwise infrequent in the data, nonlinear models can use this as a marker for missing data (and this missingness itself may have predictive value).

In effect, we are asking the model to produce a single prediction each morning of whether the patient will have delirium later that day using all of the information available that morning (including prior CAM screens). In this study, we do not train or test the performance of the model when used on a rolling basis throughout the day (eg, to generate a new prediction at 4 PM incorporating data from 3 PM that day).

The XGBoost library [17] was used to fit boosted tree models [18] for the cleaned and normalized training datasets. For comparison, random forest models [19] and logistic regression models using L1 regularization [20] were also fit to the data using scikit-learn [21]. In addition, a deep neural network model was developed using TensorFlow (Google) [22]. The final network had a 32-node rectified linear unit [23] input layer, 2 hidden layers of 16 and 8 rectified linear unit nodes, respectively, and an output layer with a single sigmoidal node. All layers were fully connected, and a 50% dropout [24] was used between layers. For the logistic regression and random forest models, Platt scaling was used to improve the calibration of the model. We used 10-fold cross-validation [25] for hyperparameter tuning to minimize overfitting. Hyperparameters (such as lambda for L1 regularization) were tuned using a grid search.

All development was done using the Ubuntu 18.04 distribution of Gnu-Linux. Data processing and analysis were performed using the Python [26] and Julia [27] programming languages. The code used to generate the models and figures is publicly available [28]. The datasets used to develop and test the model contain personally identifiable health information, and thus, are not publicly available; the authors can be contacted for more information.

Statistical Analysis

We provide an overview of the statistical analysis here; additional details can be found in Multimedia Appendix 2. The receiver operator characteristic curve and the area underneath the receiver operating characteristic curve (AUROC) were used to evaluate the performance of each model. To capture the effects of population prevalence on performance, we also used precision-recall curves and the area under the precision-recall curves (AUPRC). Calibration curves were used to qualitatively evaluate model calibration, and the expected calibration error (ECE) and maximum calibration error (MCE) were used to quantify the degree of calibration. CIs were calculated in Python using bootstrapping with 1000 rounds, and resampling by prediction day. To interpret the final behavior of the models, we used Shapley Additive Explanations (SHAP) value estimation methods as described by Lundberg et al [29,30].

The final models were trained on the full training dataset (80% of patients). Once the final models were trained, the test dataset was unblinded and the model performance was measured on the test dataset. The performance of the cross-validated version of the models on the training dataset was similar to the performance of the final models on the test dataset and is not reported here.

Although current and prior delirium are useful predictors for our intended use of the model, these are well-known risk factors for delirium and it is thus useful to explore how the model performs on patients without these risk factors. To test the model performance of these populations with a lower initial probability of delirium, versions of the final models were trained and tested on only snapshots of patients who did not have delirium (ie, no positive CAM screens in the past 24 h) or never had delirium (no prior positive CAM screens). Conceptually, all patients start in the "never delirious" state, and then potentially transition to a "currently delirious" state and then potentially between this state and a "previously but not currently delirious" state. For a summary of the assignment of patient snapshots to these groups, please see Multimedia Appendix 3.

Results

Of the 20,006 patients in the dataset, 4583 (19.9%) patients had at least one positive CAM screen (Table 1). The average age of the patients was 65 (SD 17) years and slightly higher in patients with a positive CAM screen (mean 70, SD 16 years). Approximately, 54% (n=12,502) of patients were male and 46% (n=10,500) of patients were female; no other genders were recorded in this dataset. The fraction of male patients was slightly higher (2614/4582, 57%) in patients with a positive CAM screen. An average of 12.6 (SD 17.9) CAM screens were recorded per patient, with more (mean 24.8, SD 29) recorded for patients with a positive CAM screen than for patients with no positive CAM screens (mean 9.5, SD 12). An average of 8.3% (SD 22%) of CAM screens per patient were positive, which rose to an average of 42% (SD 33%) of CAM screens per patient that were positive in patients who had at least one positive CAM screen. CAM screens were performed on an average of 8.1 (SD 11) days per patient, of which 8.1% (SD 21%) of days with CAM screens had at least one positive CAM screen.

All models provided significant predictive power for delirium (a positive CAM screen in the next 24 h) when applied to all hospitalized patients in the dataset (Figure 1). The boosted tree model had the highest AUROC (0.92, 95% CI 0.913-9.22). This was followed by the random forest model, the multilayer perceptron, and the logistic regression model with L1-regularization (AUROC 0.85, 95% CI 0.841-0.852).

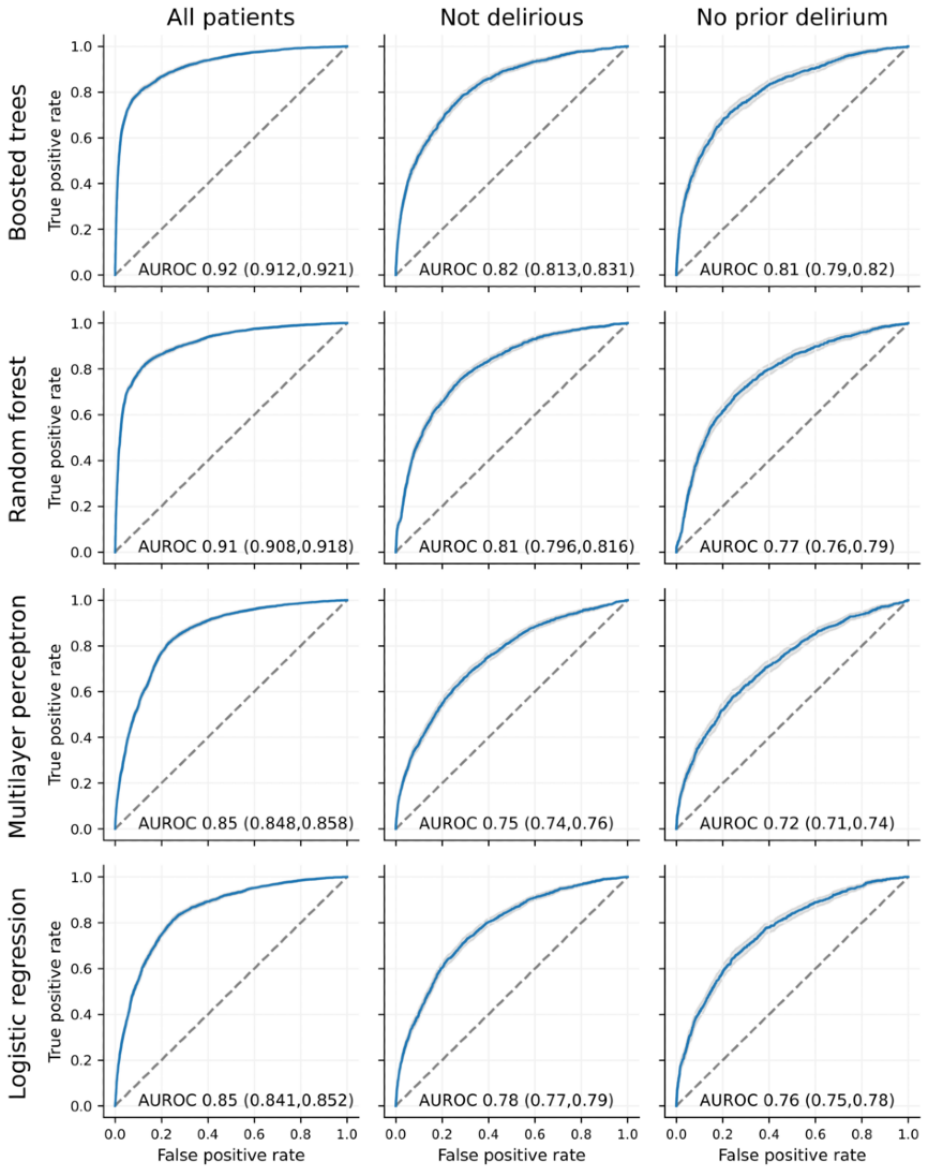
XSL•FO
RenderX

Table 1. Patient demographics.

Measure	All patients (n=23,006)	Training set (n=18,495)	Testing set (n=4511)	One or more positive CAM[a] (n=4583)	All CAM negative (n=18,423)
Age (years), mean (SD)	65.5 (17.3)	65.5 (17.3)	65.5 (17.2)	69.8 (16.1)	64.4 (17.4)
Male, n (%)	12,502 (54.3)	10,037 (54.3)	2465 (54.6)	2614 (57)	9888 (53.7)
Female, n (%)	10,500 (45.6)	8455 (45.7)	2045 (45.3)	1968 (42.9)	8532 (46.3)
Patients with at least one positive CAM screen, n (%)	4583 (19.9)	3656 (19.8)	927 (20.5)	4583 (100)	0 (0)
CAM evaluations per patient, mean (SD)	12.6 (17.9)	12.5 (18.0)	12.9 (17.6)	24.8 (29.0)	9.5 (12.0)
Percent of positive CAM screens per patient, mean (SD)	8.3 (22)	8.3 (22)	8.3 (22)	42 (33)	0 (0)
CAM evaluation days per patient, mean (SD)	8.1 (11.1)	8.1 (11.3)	8.3 (10.5)	15.6 (18.0)	6.2 (7.6)
Percent positive CAM days, mean (SD)	8.1 (21)	8.1 (21)	8.2 (21)	40.8 (31)	0 (0)

[a]CAM: Confusion Assessment Method.

Figure 1. Receiver operator characteristic curves for different model types (rows) and patient subsets (columns) showing the true positive rate (ie, recall) as a function of the false positive rate. The thin light gray region around the line shows the bootstrap 95% CI. AUROC: area under the receiver operator characteristic curve.

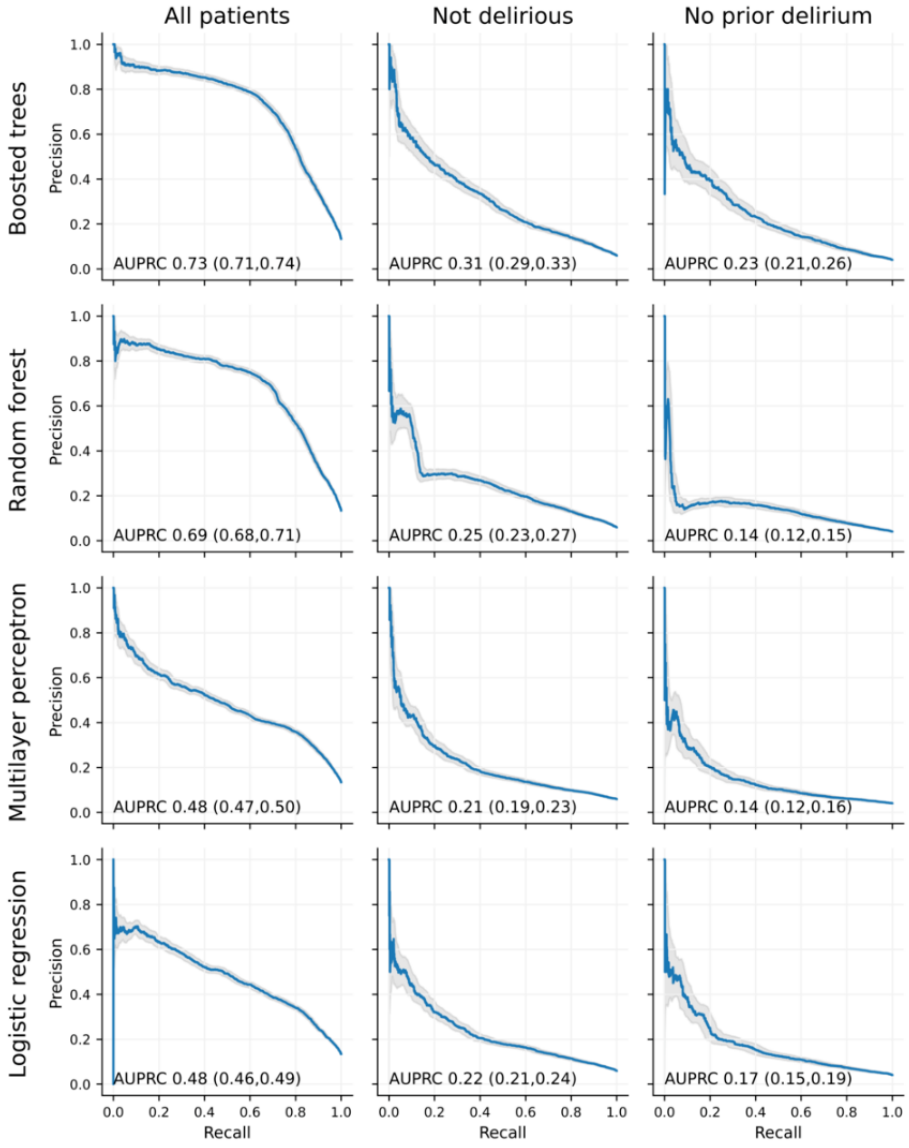


XSL•FO
RenderX

The models were then retrained and evaluated with patients who did not currently have delirium (most recent CAM screen was negative) and with patients who had no history of delirium (no prior positive CAM screens). Although the models did not perform as well on these more difficult subsets, they still provided good predictive power. The boosted tree model declined from an AUROC of 0.92 to an AUROC of 0.82 (95% CI 0.815-0.834) and 0.80 (95% CI 0.79-0.81) when limited to patients who did not currently have delirium and patients with no prior delirium, respectively. The other models showed a similar decrement, with the AUROC decreasing to 0.77-0.81 and 0.74-0.77 when limited to patients who do not currently have delirium and those who never have had delirium, respectively. The boosted tree model outperformed the other models in all three patient groups.

The models significantly varied in their ability to maintain a high positive predictive value as sensitivity was increased (Figure 2). The boosted tree model performed well (AUPRC 0.73, 95% CI 0.72-0.75), its performance declining significantly (AUPRC 0.32, 95% CI 0.30-0.34) for patients who do not currently have delirium and (0.22, 95% CI 0.20-0.25) those with no prior delirium. The incidence of delirium in all patients was 13%, those with no current delirium 6%, and those who never have had delirium 4%; thus, the decrement in AUPRC appears to be largely driven by the decreased incidence in these subgroups. While the random forest model performs relatively (AUPRC 0.70, 95% CI 0.68-0.71), it also experiences significant decrements in performance with patients who do not currently have delirium (AUPRC 0.25) or have no history of delirium (AUPRC 0.14). The multilayer perceptron models perform somewhat worse than the tree-based models, with AUPRCs of 0.50, 0.23, and 0.15 in all patients, those who do not currently have delirium, and those with no prior delirium groups. Logistic regression performed similarly to the multilayer perceptron with AUPRCs of 0.48, 0.22, and 0.17.

Figure 2. Precision-recall curves for different model types (rows) and patient subsets (columns) showing precision (ie, positive predictive value) as a function of recall (ie, true positive rate). The gray region indicates the bootstrap 95% CI.

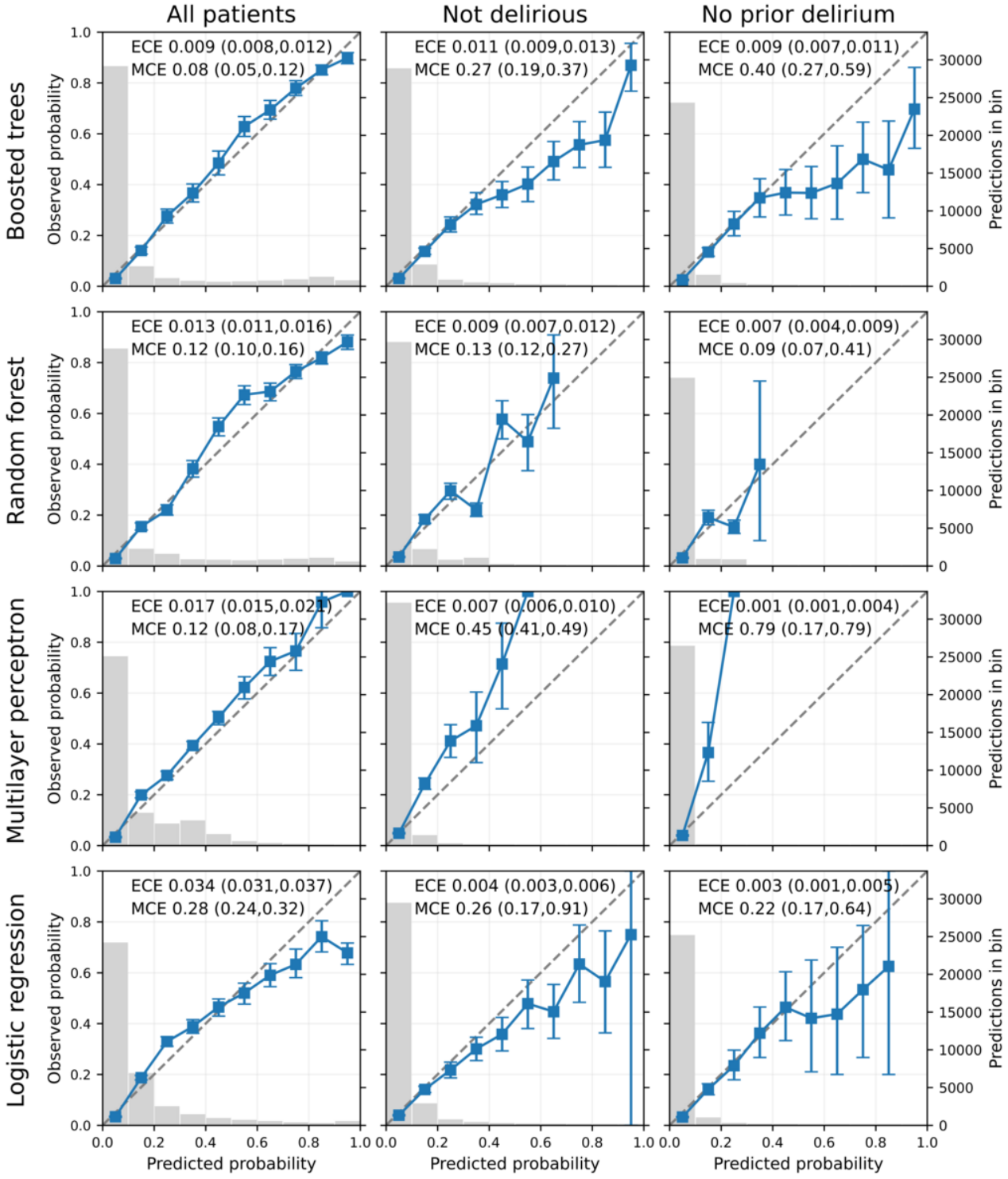


We next investigated the calibration of the prediction models. All the models were well calibrated (ECE≤0.02; MCE≤0.11) when applied to all hospitalized patients (Figure 3), with the exception of the logistic regression model which overestimated

XSL•FO
RenderX

the risk of delirium in the highest-scored group (ECE 0.03; MCE 0.28). The boosted tree model and the random forest model both identified a larger number of high-risk patients while still maintaining good calibration in this higher-risk group. When restricted to patients who do not currently have delirium or to patients with no prior delirium, all models classified very few patients as high risk (consistent with the earlier precision-recall curves), and the random forest did not assign higher probabilities to any patients in these subgroups.

Figure 3. Reliability diagrams for different model types (rows) and patient subsets (columns) showing the actual fraction of patient snapshots with delirium for groups with a given predicted risk of delirium (blue squares, left y-axis). Error bars show the bootstrap 95% CI. The gray bars in the background show the number of patient snapshots in each predicted probability bin (y-axis on the right). ECE and MCE are with a 95% CI. ECE: expected calibration error; MCE: maximum calibration error.

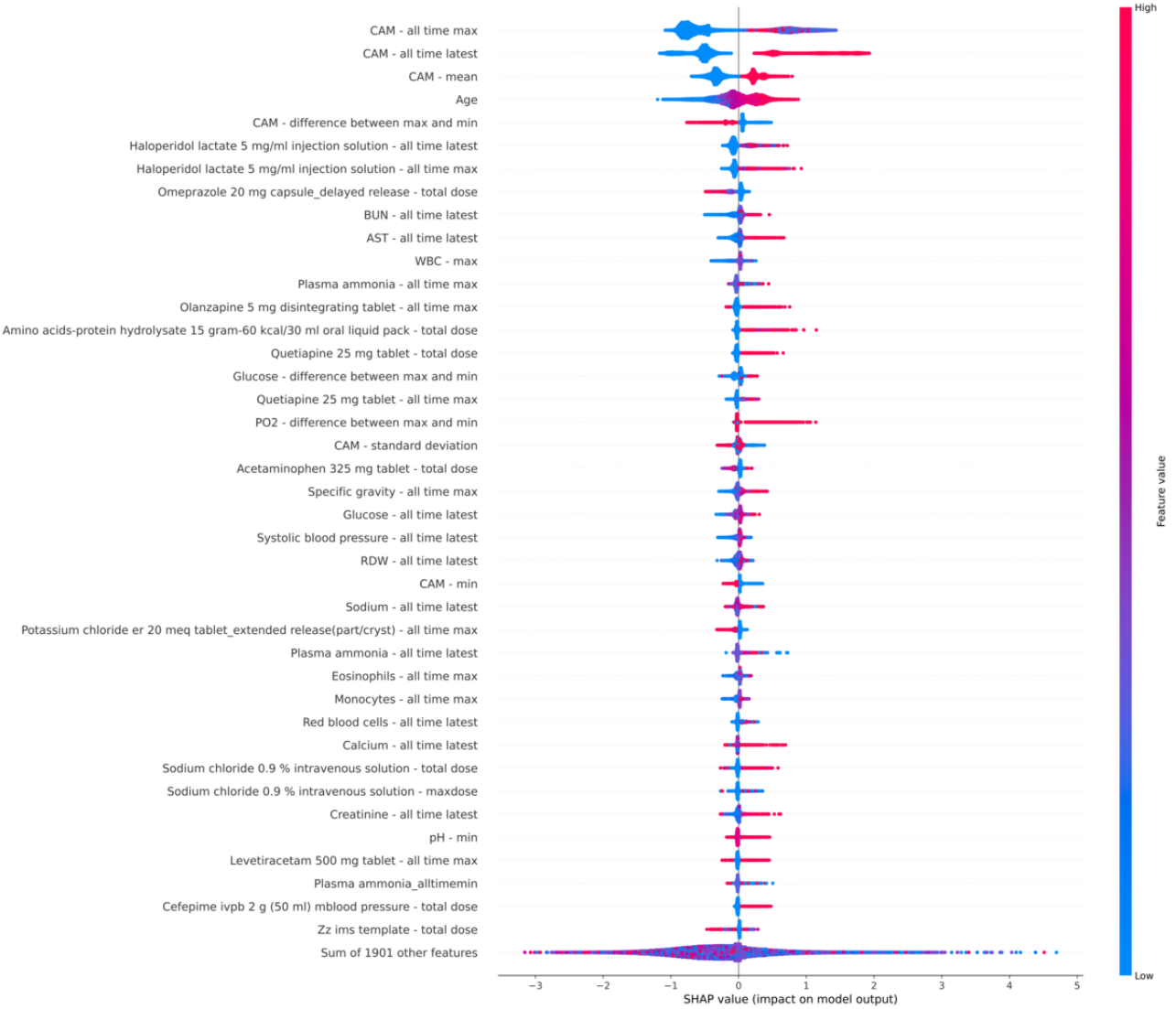


We finally turn to an examination of the features influencing the predictions of the most successful model (the boosted tree model). Ordering the features by average SHAP magnitude (Figure 4 [29,30]), we first note that the range of SHAP values

XSL•FO
RenderX

for any of the top 40 features is smaller than the range of SHAP values for the sum of the remaining 1901 features; thus, the predictions of the model across cannot easily be simplified to a small number of driving features that are the same for all patients. The features with the highest average SHAP magnitude appear to fall into several known risk factors for delirium. Current and prior delirium is a known predictor of future delirium, and 6 of the top 40 features relate to the prior CAM screen (including 4 of the top 5 features). Of note, the model considers a patient with no prior CAM screens to be at higher risk than a patient with prior negative CAM screens, and this feature remains important even for the "no prior delirium" case (not shown). Antipsychotic administration is also as expected a risk-predicting feature, as it is often used to convert hyperactive delirium to hypoactive delirium. The majority of the top 40 risk features fall into other categories, however, which include known risk factors such as age, liver failure (eg, aspartate transferase levels, ammonia levels, and hepatitis C virus levels), infection (eg, white blood cells, monocytes, and cefepime [which is also neurotoxic]), and malnutrition or frailty (amino acid supplementation, albumin levels).

Figure 4. SHAP beeswarm plots [28,29] of the 40 features with the highest SHAP magnitude for patients in the holdout dataset. Each dot shows a single prediction for a patient, the color of the dot indicates how high (red) or low (blue) the feature was for this patient, and the horizontal position of the dot indicates the relative effect of this feature on the predicted risk for the given patient.



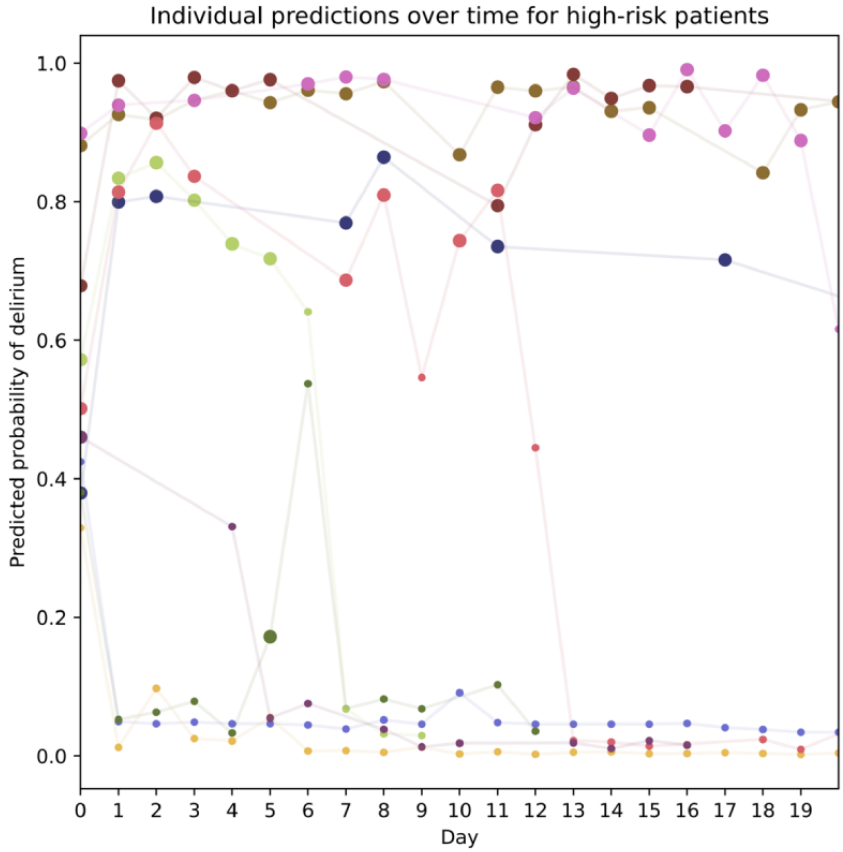
Of note, many of the top features had missing values in the majority of patients (Multimedia Appendix 4). These often-included values such as neutrophil counts from cerebrospinal fluid, where the presence of the measurement itself suggests a high risk of delirium. This is again consistent with what is seen with the SHAP plot, where the models are able to use a constellation of low-frequency features of each patient to determine delirium risk (eg, laboratories reflecting concern for meningitis) rather than being limited to a few broad risk factors such as age.

To explore the dynamics of delirium predictions in individual patients over time, we examine the predicted risk and actual occurrence of positive CAM screens over time for a small number of patients with an elevated initial risk of delirium using delirium predictions from the boosted tree model (Figure 5). Of note, the prediction for the next day was strongly correlated with the delirium status of the previous day (as expected), but

XSL•FO
RenderX

the first day without delirium usually had a lower predicted risk of delirium than the last day with delirium, suggesting that the model had identified changes correlated with resolution of the delirium.

Figure 5. Predicted versus actual delirium incidence for ten patients with elevated (>30%) initial risk of delirium using predictions from the boosted tree model. Each patient is plotted in a different color, with a large dot reflecting at least one positive CAM screen that day and a small dot reflecting all negative CAM screens that day. The vertical axis shows the predicted risk for delirium that day (ie, for a perfect predictor, all large dots would be at the top of the plot and all small dots at the bottom). The horizontal axis shows the time (in days) from the first delirium screen, with day 0 being the day of the first delirium screen. CAM: Confusion Assessment Method.



Discussion

Principal Results

We have described the development of a prediction model that can provide automated daily predictions of the risk of delirium for a general population of hospitalized patients. We found that a boosted tree model performed best for this dataset and was able to identify a group of high-risk patients even when limited to patients who did not have delirium or had no prior history of delirium. However, the random forest, multilayer perceptron, and logistic regression models, while less effective, still provided substantial predictive power. All of the models showed good calibration on the full dataset but showed poorer MCE when applied to subsets of the data where delirium was less common—patients who did not currently have delirium and patients with no prior history of delirium.

The relative performance of the various models may reflect the relative match between the flexibility of each of the types of models and the size of the dataset we used. Although the L1 regularization used for the logistic regression model allowed for some tuning of flexibility by adjusting how many features were used, the logistic model can only capture monotonic relationships. Both boosted tree models and random forest models can better capitalize on nonmonotonic relationships which likely underlies their better performance on this dataset. In contrast, it was difficult to prevent overfitting with the multilayer perceptron model; preventing this overfitting would likely require either a larger dataset or additional methods of regularization.

Limitations

All of the models showed a decrement in performance when restricted to patients who did not currently have delirium and a further decrement when restricted without prior delirium. Except for the multilayer perceptron in the no prior delirium case; however, the AUROC of all of the models remained greater than 0.75, which many would consider the threshold for “good” performance of a clinical test [31]. The boosted tree model, in particular, maintained an AUROC of 0.80, which compares very favorably to commonly used diagnostic tests such as D-dimer levels in the setting of a suspected pulmonary embolism (with a reported AUROC of 0.71 [32]). The decrement of performance in these subgroups likely reflects the increased difficulty of the task—those patients with significant risk factors are likely to have had delirium on prior days or hospitalizations and most of those who remain are relatively unlikely to become delirious in the next 24 hours. Even within the patients with no

XSL•FO
RenderX

prior delirium, however, the boosted tree model was able to identify high-risk patients who would likely warrant further evaluation and interventions—for example, from the precision-recall curves (Figure 2), we can see that even if one were to demand a 50% true-positive threshold for an intervention, the model would correctly identify over 10% of the patients who have never had delirium who would become delirious as candidates for that intervention.

An additional limitation is the potential selection bias of the training and evaluation dataset used by this study. During the time period used, CAM screening was used universally on some inpatient units in the study hospital (eg, orthopedics) but not others (eg, general surgery), and thus, the study population is more reflective of these units than of the hospital as a whole. Thus, the generalizability of these results to other institutions will depend on how similar their patient population is to these units, rather than to the patient population of the study hospital. In addition, the results reported reflect this population where serial screens are performed and prior delirium screens are often present, which may not be applicable in many settings. One would expect the model's performance to be worse in this setting (similar to what is seen in the results reported for patients with no prior delirium).

As with many machine learning models, more complex models such as the boosted tree model may trade accuracy for interpretability, for example, for a clinician trying to understand why a particular patient is at risk for delirium. While this can be partially addressed by including the relative contributions of each input to the model to a given patient's risk (eg, using Shapley values [29,30]) as part of the delirium risk report for each patient, this still can hide complex interactions between risk factors that may be important.

We have chosen to leave the predictions of the model in the form of a percentage risk, rather than simplifying the result to a binary prediction as is more familiar for many clinical tests. To the limits of calibration of the model, the predicted percentage of delirium can be interpreted as the positive predictive value of the test for that particular patient (and 100% minus the predicted percentage as the negative predictive value). For given interventions, it may make sense to set a threshold predicted risk based on a cost or benefit analysis of the intervention (thus reducing the prediction to a binary value with a single positive predictive value and negative predictive value for all patients); examinations of specific thresholds for specific interventions may be addressed in future work.

While we have included many potential input features in our prediction model, there are many additional features in the medical record that we have not attempted to use, such as flowsheet data, length of stay, and unstructured data such as clinical notes. In addition, we have not exhaustively explored the types of models available in the literature, including many regularization techniques (such as early stopping and L2 normalization). While future models incorporating these predictors and techniques may perform even better than the models described here, this work provides a lower bound for their performance.

Comparison With Prior Work

Multiple prior prediction models for delirium have been developed for use in intensive care unit patients [11,12,33] and in hospitalized older patients [9]. In general, these models use a small number of predictors (4-11) identified using logistic regression, including such predictors as age, history of cognitive impairment, history of alcohol abuse, respiratory failure, blood urea nitrogen, mean arterial pressure, use of corticosteroids, admission category, admission urgency, and vision impairment. Our prediction goal (predicting a positive CAM screen within the next 24 h) is somewhat different than the existing models we are aware of, as it is aimed at the specific task of helping determine which hospitalized patients should be seen by a delirium service that day. With that caveat, the performance of our model appears to compare well with other models on similar tasks. Chua et al [13] provide a good review of similar models; reported AUROCs in this review range from 0.71 to 0.91 (compared to 0.92 for the boosted tree model we report). As delirium is an infrequent event, however, the AUPRC may provide a better estimate of the model's performance as a screening tool. Comparing our model to the best-performing models in the review by Chua et al [13], only the model described by Corradi et al [34] (one of the two models with an AUROC of 0.91) reported an AUPRC, which was 0.60 (compared to 0.73 for the boosted tree model we report).

One of the challenges machine learning has faced in medicine is translating predictions into improvements in patient outcomes [35]. We plan to use this model to screen all of the patients in a 1000-bed hospital (which would be prohibitively labor-intensive to do by hand) and identify a set of high-risk patients to be visited by a delirium service. The members of this delirium service will then evaluate patients and provide recommendations to the team caring for the patient on how to reduce that patient's risk of delirium. By focusing this additional clinical effort and possible interventions on the patients who would most likely benefit from them, we hope to use this tool to improve care at a lower cost per patient than providing the same interventions to every patient (including those at much lower risk of delirium).

Because of this intended use, we have made trade-offs that may limit the use of this model in other contexts. For example, our focus was on maximizing the ability of the model to identify high-risk hospitalized patients rather than on identifying the causal mechanism for a given patient's delirium. Thus, for example, an arterial blood gas showing mild hyperoxia might be used for prediction by the model because it is correlated with intubation, sedation, and critical illness rather than because it is directly increasing the patient's risk for delirium, and blindly attempting to correct this laboratory value may not decrease the patient's risk of delirium. In addition, some features, such as administering an antipsychotic medication, may happen to treat an agitated delirium that has not been documented in the medical record; while this may still be quite useful for a delirium service, it may be less useful for a responding clinician who is treating the agitation who likely already knows he or she is treating a symptom of delirium. This is an example of a "shortcut feature" as described by Bellamy et al [36], where a causal connection is present in the training data (eg, the use of an antipsychotic

XSL•FO
RenderX

for a patient the clinician has already decided has delirium) may not be present in a desired use-case of the model (eg, a clinician trying to decide whether a patient is at risk of delirium). Thus, while the model works well for finding high-risk patients, interpreting these risk factors and identifying appropriate interventions will still require clinical expertise.

Although our model can be applied in its current form, there are limitations that a user will need to be mindful of. For some machine learning models, such as logistic regression, it can be relatively easy to understand a prediction from the model in terms of the individual features contributing to the prediction. For many others, however, including boosted tree models such as our best-performing model, the nonlinear interaction of many features can make it difficult to understand why a given patient was assigned a high or low-risk score. Providing interpretability for these more complex, nonlinear models is an active area of research in machine learning, and while tools such as SHAP can provide some insight into a model, for some uses, a less accurate but more interpretable model (such as logistic regression) may be preferred.

Another limitation of our model is that many of the risk factors such as sleep disruption may only be documented in clinical notes and not in the structured data we have used, and thus high-risk patients may be missed by the model. We hope to address this in future work by integrating natural language processing techniques into the model.

The dataset used for the development and validation of the model is another potential source of bias in this study. Because the patients from this study are only those patients from a single academic medical center who received delirium screens, they may not be reflective of patients in other settings, and potentially not even representative of patients at the same institution who did not receive delirium screens. Although this could raise concerns that this would bias our dataset toward patients with delirium, this does not appear to have been the case. Only 4583 of the 23,006 patients (Table 1), or about 20%, of the patients in our dataset had one or more positive CAM screens. This is consistent with the 23% (95% CI 19%-26%) incidence of delirium reported in the meta-analysis of estimates of delirium occurrence reported by Gibb et al [37]. Although this is reassuring, future studies will be needed to provide external validation of the model at other institutions and on other patient populations.

Conclusions

In this paper, we have described a method for predicting delirium in hospitalized patients given the information already present in the electronic medical record. A large dataset of over 23,000 patients allowed us to consider a larger number of candidate features while still allowing for rigorous validation with a blinded test dataset. The resulting model provides both good accuracy and good calibration and can be run in an automated fashion on data in the electronic patient record without requiring additional human effort. We believe this model can be of use in guiding clinicians and researchers in focusing on patients at greatest risk of delirium in hopes of mitigating the morbidity and mortality associated with this disease.

Acknowledgments

KMS was supported by NIH (T32-GM007592). MBW was supported by the Glenn Foundation for Medical Research and American Federation for Aging Research (Breakthroughs in Gerontology Grant); American Academy of Sleep Medicine (AASM Foundation Strategic Research Award); Football Players Health Study at Harvard University; Department of Defense through a subcontract from Moberg ICU Solutions, Inc; NIH (R01NS102190, R01NS102574, R01NS107291, RF1AG064312, and R01AG062989); and NSF (award SCH-2014431).

Authors' Contributions

KMS helped with study design, data preparation, implementation of the models, analysis, and drafting of the manuscript. YPS helped with data acquisition, preparation, and review of the manuscript. MG and VMJ helped with data acquisition, preparation, and review of the manuscript. EYK helped with the study design and review of the manuscript. TTH and OA helped with the study design, interpretation, and review of the manuscript. MBW helped with the conception of the work, study design, interpretation, and review of the manuscript.

Conflicts of Interest

MBW is a cofounder of Beacon Biosignals, which had no role in this work.

Multimedia Appendix 1
Details of the model development.
[DOCX File , 23 KB - medinform_v13i1e60442_app1.docx]

Multimedia Appendix 2
Details of the analysis.
[DOCX File , 18 KB - medinform_v13i1e60442_app2.docx]

XSL•FO
RenderX

Multimedia Appendix 3
Flowchart showing assignment of delirium status.
[DOCX File , 134 KB - medinform_v13i1e60442_app3.docx]

Multimedia Appendix 4
Missing fraction of top 100 features from boosted tree model.
[DOCX File , 19 KB - medinform_v13i1e60442_app4.docx]

References

1. Siddiqi N, House AO, Holmes JD. Occurrence and outcome of delirium in medical in-patients: a systematic literature review. Age Ageing 2006;35(4):350-364. [doi: 10.1093/ageing/afl005] [Medline: 16648149]
2. Witlox J, Eurelings LSM, de Jonghe JFM, Kalisvaart KJ, Eikelenboom P, van Gool WA. Delirium in elderly patients and the risk of postdischarge mortality, institutionalization, and dementia: a meta-analysis. JAMA 2010;304(4):443-451. [doi: 10.1001/jama.2010.1013] [Medline: 20664045]
3. Wilson JE, Mart MF, Cunningham C, Shehabi Y, Girard TD, MacLullich AMJ, et al. Delirium. Nat Rev Dis Primers 2020;6(1):90 [FREE Full text] [doi: 10.1038/s41572-020-00223-4] [Medline: 33184265]
4. Leslie DL, Marcantonio ER, Zhang Y, Leo-Summers L, Inouye SK. One-year health care costs associated with delirium in the elderly population. Arch Intern Med 2008;168(1):27-32 [FREE Full text] [doi: 10.1001/archinternmed.2007.4] [Medline: 18195192]
5. Delirium: Prevention, Diagnosis and Management in Hospital and Long-Term Care. London: National Institute for Health and Care Excellence (NICE); 2023.
6. Barr J, Fraser GL, Puntillo K, Ely EW, Gélinas C, Dasta JF, et al. Clinical practice guidelines for the management of pain, agitation, and delirium in adult patients in the intensive care unit. Crit Care Med 2013;41(1):263-306. [doi: 10.1097/CCM.0b013e3182783b72] [Medline: 23269131]
7. Patel RP, Gambrell M, Speroff T, Scott TA, Pun BT, Okahashi J, et al. Delirium and sedation in the intensive care unit: survey of behaviors and attitudes of 1384 healthcare professionals. Crit Care Med 2009;37(3):825-832 [FREE Full text] [doi: 10.1097/CCM.0b013e31819b8608] [Medline: 19237884]
8. Hshieh TT, Yang T, Gartaganis SL, Yue J, Inouye SK. Hospital elder life program: systematic review and meta-analysis of effectiveness. Am J Geriatr Psychiatry 2018;26(10):1015-1033 [FREE Full text] [doi: 10.1016/j.jagp.2018.06.007] [Medline: 30076080]
9. Inouye SK, Viscoli CM, Horwitz RI, Hurst LD, Tinetti ME. A predictive model for delirium in hospitalized elderly medical patients based on admission characteristics. Ann Intern Med 1993;119(6):474-481. [doi: 10.7326/0003-4819-119-6-199309150-00005] [Medline: 8357112]
10. van den Boogaard M, Schoonhoven L, Maseda E, Plowright C, Jones C, Luetz A, et al. Recalibration of the delirium prediction model for ICU patients (PRE-DELIRIC): a multinational observational study. Intensive Care Med 2014;40(3):361-369. [doi: 10.1007/s00134-013-3202-7] [Medline: 24441670]
11. Wassenaar A, van den Boogaard M, van Achterberg T, Slooter AJC, Kuiper MA, Hoogendoorn ME, et al. Multinational development and validation of an early prediction model for delirium in ICU patients. Intensive Care Med 2015;41(6):1048-1056 [FREE Full text] [doi: 10.1007/s00134-015-3777-2] [Medline: 25894620]
12. Chen Y, Du H, Wei BH, Chang XN, Dong CM. Development and validation of risk-stratification delirium prediction model for critically ill patients: a prospective, observational, single-center study. Medicine (Baltimore) 2017;96(29):e7543 [FREE Full text] [doi: 10.1097/MD.0000000000007543] [Medline: 28723773]
13. Chua SJ, Wrigley S, Hair C, Sahathevan R. Prediction of delirium using data mining: a systematic review. J Clin Neurosci 2021;91:288-298. [doi: 10.1016/j.jocn.2021.07.029] [Medline: 34373042]
14. Inouye SK, van Dyck CH, Alessi CA, Balkin S, Siegal AP, Horwitz RI. Clarifying confusion: the confusion assessment method. A new method for detection of delirium. Ann Intern Med 1990;113(12):941-948. [doi: 10.7326/0003-4819-113-12-941] [Medline: 2240918]
15. Ely EW, Inouye SK, Bernard GR, Gordon S, Francis J, May L, et al. Delirium in mechanically ventilated patients: validity and reliability of the confusion assessment method for the intensive care unit (CAM-ICU). JAMA 2001;286(21):2703-2710. [doi: 10.1001/jama.286.21.2703] [Medline: 11730446]
16. Jain R, Chlamtac I. The P2 algorithm for dynamic calculation of quantiles and histograms without storing observations. Commun. ACM 1985;28(10):1076-1085. [doi: 10.1145/4372.4378]
17. Chen T, Guestrin C. XGBoost: a scalable tree boosting system. : Association for Computing Machinery; 2016 Presented at: KDD '16: The 22nd ACM SIGKDD International Conference on Knowledge Discovery and Data Mining; August 13-17, 2016; San Francisco California USA p. 785-794. [doi: 10.1145/2939672.2939785]
18. Friedman JH. Greedy function approximation: a gradient boosting machine. Ann Stat 2001;29(5):1189-1232. [doi: 10.1214/aos/1013203451]

XSL•FO
RenderX

19. Breiman L. Random forests. Mach Learn 2011;45:5-32 [FREE Full text] [doi: 10.1023/A:1010933404324] [Medline: 21816105]
20. Tibshirani R. Regression shrinkage and selection via the lasso. J R Stat Soc: Ser B (Methodological) 2018;58(1):267-288. [doi: 10.1111/j.2517-6161.1996.tb02080.x]
21. Pedregosa F, Varoquaux G, Gramfort A, Michel V, Thirion B, Grisel O, et al. Scikit-learn: machine learning in python. J Mach Learn Res 2015 Jun;12:2825-2830. [doi: 10.5555/1953048.2078195]
22. Abadi M, Barham P, Chen J, Chen Z, Davis A, Dean J, et al. TensorFlow: a system for large-scale machine learning. USA: USENIX Association; 2016 Presented at: OSDI'16: Proceedings of the 12th USENIX conference on Operating Systems Design and Implementation; November 2-4, 2016; Savannah GA USA p. 265-283. [doi: 10.1145/3190508.3190551]
23. Krizhevsky A, Sutskever I, Hinton GE. ImageNet classification with deep convolutional neural networks. Commun ACM 2017;60(6):84-90. [doi: 10.1145/3065386]
24. Srivastava N, Hinton G, Krizhevsky A, Sutskever I, Salakhutdinov R. Dropout: a simple way to prevent neural networks from overfitting. J Mach Learn Res 2014;15(1):1929-1958. [doi: 10.5555/2627435.2670313]
25. Stone M. Cross-validatory choice and assessment of statistical predictions. Journal of the Royal Statistical Society: Series B (Methodological) 2018;36(2):111-133. [doi: 10.1111/j.2517-6161.1974.tb00994.x]
26. Rossum GV, Boer JD. Linking a stub generator (AIL) to a prototyping language (Python). 1991 Presented at: Proceedings of the Spring EurOpen Conference; 1991; Troms, Norway p. 229-247.
27. Bezanson J, Edelman A, Karpinski S, Shah VB. Julia: a fresh approach to numerical computing. SIAM Rev 2017;59(1):65-98. [doi: 10.1137/141000671]
28. Shaw KM, Shao YP, Ghanta M, Junior VM, Kimchi EY, Houle TT, et al. DeliriumPredictor2023a: code for models and figures. GitHub. 2023. URL: https://github.com/kms15/DeliriumPredictor2023a [accessed 2025-04-03]
29. Lundberg SM, Lee SI. Lee S-I. In: A Unified Approach to Interpreting Model Predictions.: Curran Associates Inc; 2017 Presented at: NIPS'17: Proceedings of the 31st International Conference on Neural Information Processing Systems; December 4-9, 2017; Long Beach California USA p. 4768-4777.
30. Lundberg SM, Erion G, Chen H, DeGrave A, Prutkin JM, Nair B, et al. From local explanations to global understanding with explainable AI for trees. Nat Mach Intell 2020;2(1):56-67 [FREE Full text] [doi: 10.1038/s42256-019-0138-9] [Medline: 32607472]
31. Jones CM, Athanasiou T. Summary receiver operating characteristic curve analysis techniques in the evaluation of diagnostic tests. Ann Thorac Surg 2005;79(1):16-20. [doi: 10.1016/j.athoracsur.2004.09.040] [Medline: 15620907]
32. Fu Z, Zhuang X, He Y, Huang H, Guo W. The diagnostic value of D-dimer with simplified Geneva score (SGS) pre-test in the diagnosis of pulmonary embolism (PE). J Cardiothorac Surg 2020;15(1):176 [FREE Full text] [doi: 10.1186/s13019-020-01222-y] [Medline: 32690039]
33. van den Boogaard M, Pickkers P, Slooter AJC, Kuiper MA, Spronk PE, van der Voort PHJ, et al. Development and validation of PRE-DELIRIC (PREdiction of DELIRium in ICu patients) delirium prediction model for intensive care patients: observational multicentre study. BMJ 2012;344:e420 [FREE Full text] [doi: 10.1136/bmj.e420] [Medline: 22323509]
34. Corradi JP, Thompson S, Mather JF, Waszynski CM, Dicks RS. Prediction of incident delirium using a random forest classifier. J Med Syst 2018;42(12):261. [doi: 10.1007/s10916-018-1109-0] [Medline: 30430256]
35. Marwaha JS, Kvedar JC. Crossing the chasm from model performance to clinical impact: the need to improve implementation and evaluation of AI. NPJ Digital Med 2022;5(1):25 [FREE Full text] [doi: 10.1038/s41746-022-00572-2] [Medline: 35241790]
36. Bellamy D, Hernán MA, Beam A. A structural characterization of shortcut features for prediction. Eur J Epidemiol 2022;37(6):563-568 [FREE Full text] [doi: 10.1007/s10654-022-00892-3] [Medline: 35792990]
37. Gibb K, Seeley A, Quinn T, Siddiqi N, Shenkin S, Rockwood K, et al. The consistent burden in published estimates of delirium occurrence in medical inpatients over four decades: a systematic review and meta-analysis study. Age Ageing 2020;49(3):352-360 [FREE Full text] [doi: 10.1093/ageing/afaa040] [Medline: 32239173]

Abbreviations

AUPRC: area under the precision-recall curve
AUROC: area under the receiver operator characteristic curve
CAM: Confusion Assessment Method
ECE: expected calibration error
MCE: maximum calibration error
SHAP: Shapley Additive Explanations
TRIPOD: Transparent Reporting of a multivariable prediction model for Individual Prognosis Or Diagnosis

XSL•FO
RenderX

Edited by C Lovis; submitted 15.05.24; peer-reviewed by MS Abusamaan, BJ Marafino; comments to author 06.08.24; revised version received 01.12.24; accepted 25.12.24; published 18.04.25.

Please cite as:
Shaw KM, Shao YP, Ghanta M, Junior VM, Kimchi EY, Houle TT, Akeju O, Westover MB
Daily Automated Prediction of Delirium Risk in Hospitalized Patients: Model Development and Validation
JMIR Med Inform 2025;13:e60442
URL: https://medinform.jmir.org/2025/1/e60442
doi:10.2196/60442
PMID:39721068

©Kendrick Matthew Shaw, Yu-Ping Shao, Manohar Ghanta, Valdery Moura Junior, Eyal Y Kimchi, Timothy T Houle, Oluwaseun Akeju, Michael Brandon Westover. Originally published in JMIR Medical Informatics (https://medinform.jmir.org), 18.04.2025. This is an open-access article distributed under the terms of the Creative Commons Attribution License (https://creativecommons.org/licenses/by/4.0/), which permits unrestricted use, distribution, and reproduction in any medium, provided the original work, first published in JMIR Medical Informatics, is properly cited. The complete bibliographic information, a link to the original publication on https://medinform.jmir.org/, as well as this copyright and license information must be included.

XSL•FO
RenderX

Original Paper

Prediction of Snacking Behavior Involving Snacks Having High Levels of Saturated Fats, Salt, or Sugar Using Only Information on Previous Instances of Snacking: Survey- and App-Based Study

Shaima Dammas[1], PhD; Tillman Weyde[2], PhD; Katy Tapper[3], PhD; Gerasimos Spanakis[4], PhD; Anne Roefs[5], PhD; Emmanuel M Pothos[3], PhD

[1]Department of Health Services and Hospitals Administration, King AbdulAziz University, Jeddah, Saudi Arabia

[2]Department of Computer Science, City, University of London, London, United Kingdom

[3]Department of Psychology, City, University of London, London, United Kingdom

[4]Department of Advanced Computing Sciences, Maastricht University, Maastricht, The Netherlands

[5]Faculty of Psychology & Neuroscience, Maastricht University, Maastricht, The Netherlands

Corresponding Author:
Shaima Dammas, PhD
Department of Health Services and Hospitals Administration
King AbdulAziz University
PO Box 80200
67 Administration Street
Jeddah, 21589
Saudi Arabia
Phone: 966 126952951
Email: smalghamdi2@kau.edu.sa

Abstract

Background: Consuming high amounts of foods or beverages with high levels of saturated fats, salt, or sugar (HFSS) can be harmful for health. Many snacks fall into this category (HFSS snacks). However, the palatability of these snacks means that people can sometimes struggle to reduce their intake. Machine learning algorithms could help in predicting the likely occurrence of HFSS snacking so that just-in-time adaptive interventions can be deployed. However, HFSS snacking data have certain characteristics, such as sparseness and incompleteness, which make snacking prediction a challenge for machine learning approaches. Previous attempts have employed several potential predictor variables and have achieved considerable success. Nevertheless, collecting information from several dimensions requires several potentially burdensome user questionnaires, and thus, this approach may be less acceptable for the general public.

Objective: Our aim was to consider the capacity of standard (unmodified in any way; to tailor to the specific learning problem) machine learning algorithms to predict HFSS snacking based on the following minimal data that can be collected in a mostly automated way: day of the week, time of the day (divided into time bins), and location (divided into work, home, and other).

Methods: A total of 111 participants in the United Kingdom were asked to record HFSS snacking occurrences and the location category over a period of 28 days, and this was considered the UK dataset. Data collection was facilitated by a purpose-specific app (Snack Tracker). Additionally, a similar dataset from the Netherlands was used (Dutch dataset). Both datasets were analyzed using machine learning methods, including random forest regressor, Extreme Gradient Boosting regressor, feed forward neural network, and long short-term memory. We additionally employed 2 baseline statistical models for prediction. In all cases, the prediction problem was the time to the next HFSS snack from the current one, and the evaluation metric was the mean absolute error.

Results: The ability of machine learning methods to predict the time of the next HFSS snack was assessed. The quality of the prediction depended on the dataset, temporal resolution, and machine learning algorithm employed. In some cases, predictions were accurate to as low as 17 minutes on average. In general, machine learning methods outperformed the baseline models, but no machine learning method was clearly better than the others. Feed forward neural network showed a very marginal advantage.

XSL•FO
RenderX

Conclusions: The prediction of HFSS snacking using sparse data is possible with reasonable accuracy. Our findings offer a foundation for further exploring how machine learning methods can be used in health psychology and provide directions for further research.

(JMIR Med Inform 2025;13:e57530) doi:10.2196/57530

KEYWORDS

high fats, salt, or sugar snacks; machine learning algorithms; internet data collection; just-in-time interventions

Introduction

General Background

Noncommunicable diseases, such as cardiovascular disease, cancer, and chronic respiratory disease, are currently the biggest threats to health [1]. These are greatly influenced by behaviors, such as poor diet, physical inactivity, and smoking (eg, [2,3]). Modification of the obesogenic environment would be most effective at bringing about change on a large scale [4]. However, such an environmental change is unlikely to occur in a short period. Therefore, most related interventions seek to change people's responses to their environments. Approaches to achieve these changes have ranged from mass media campaigns at the population level to group-based and individual healthy lifestyle coaching. Over the last decade, digital technologies for supporting a healthy lifestyle have been on the rise, but there is still room for improvement [5-7].

A potential avenue for improving the effectiveness of technology-assisted interventions is providing just-in-time adaptive interventions (JITAIs). JITAIs are designed to predict the points at which a person is likely to be in most need of and most receptive to reminders or assistance for changing a target behavior [8]. For example, a person engaged in an effort to quit smoking could be reminded of their goal at the point at which they are most likely to lapse [9,10]. This may be effective because motivation for a particular behavior can vary over time [11]. Additionally, health-related behaviors may be elicited by cues in the environment (eg, a certain time of the day or walking past a bakery store) and be largely habitual [12-15]. This can make change difficult unless behaviors elicited by these cues are disrupted. Helping a person identify those cues may reduce the undesired behavior in a number of ways, for example, by helping the person avoid the cues, adjust their behavior, or respond to the cues in a different way [15,16]. JITAIs could help people achieve such goals.

There is increasing research into the use of JITAIs (eg, [17,18]). Their development has been greatly boosted by the widespread adoption of powerful personal smartphones. For example, in 2021, 88% of all adults (aged 16 years or older) possessed a smartphone in the United Kingdom [19], with similar statistics throughout Western Europe and North America. Modern smartphones allow increasingly complex data collection from their owners, including date, time, ambient temperature, and location. Furthermore, owing to the high computational capabilities of modern smartphones, many of the required computations (eg, for prediction) can be carried out locally, without the need for distant servers and an active internet connection.

Snacking on foods and drinks that have high saturated fats, salt, or sugar (HFSS) is the focus of this research. Snacking can be defined as "food and beverage intake between meals, including products, such as potato chips, chocolate, and soft beverages" [20]. HFSS foods contribute to poor health [21], and many snacks fall into this category. Indeed, a previous study found that people who are overweight or obese eat an average of 1.3 snacks per day, with 79% of these snacks being high in either fat or sugar [12]. However, reducing HFSS snacking poses many challenges, particularly because it can be triggered by emotional or environmental factors [22]. It can also occur in an automatized (reflexive) way, making it less amenable to conscious control efforts [12-14]. Additionally, snacks that are high in sugar may make a person crave more sugary foods, because consumption of these snacks can lead to a spike and subsequent dip in blood sugar levels [23,24]. Indeed, feelings of hunger and food preoccupation are key reasons cited for snacking [12].

Several sophisticated approaches to predict aspects of maladaptive eating behavior have already been proposed, using ecological momentary assessments (EMAs). For example, Arend et al [25] studied binge eating episodes in clinical participants. The authors reported excellent predictive accuracy based on an EMA protocol with 36 items, including emotional and environmental variables. Based on initial testing, they were subsequently able to identify a smaller subset (n=5-9) of highly valid individualized predictors (EMA items), thereby reducing the need for an extensive EMA protocol. Forman et al [26] similarly investigated the predictive adequacy of a large number of variables concerning dietary lapses. Some questions, such as those relating to cravings or affect, were answered as many as 4 times a day, and others were answered only once. Kaiser et al [27] used data from 2 weeks of EMAs on stress and emotion, together with sensor data, to predict (reasonable accuracy) food cravings. Finally, Spanakis et al [28] tracked several individual states, such as emotions and cravings, which might predict "unhealthy eating events," including unhealthy snacking and other events, such as consumption of high-calorie food as part of a meal, in people who were overweight or obese. Participants were questioned as many as 10 times a day. Based on the collected data, a bottom-up clustering algorithm was used to arrive at 6 different subgroups of participants characterized by a specific pattern of eating behavior (eg, eating in the evening at home), to enable tailoring the intervention to a specific profile, which was implemented in a randomized controlled trial [29].

Research based on EMAs is valuable because the prediction of a behavior as complex as eating can potentially only be accomplished by considering a multitude of variables, including

XSL•FO
RenderX

environmental, psychological, and physiological variables. Moreover, the assessment of these variables takes place in daily life, contributing to ecological validity. However, health interventions based on EMAs typically require long periods to train the machine learning (ML) algorithms for prediction, as well as considerable commitment and motivation from participants. There is therefore interest in exploring whether the prediction of a particular behavior can proceed based on information that is both minimal and easily available, without much effort from participants.

In the domain of mental health, research on so-called digital phenotyping has recently started to develop. Digital phenotyping uses a smartphone as a tool for objective and ecologically valid measurements. This method includes passively obtained data, without needing input from the user. Digital biomarkers, such as sensor technology, geolocation, characteristics of voice and speech, and human-computer interaction, are obtained [30-33]. Through this method, a pattern might be discovered over several weeks (ie, the user is taking too long to respond to messages, is browsing online until late at night, and is mostly at home). This can lead to suspicion that things are not going particularly well for the user, and the suspicion may be increased by the tone, timing, and content of the user's social media posts. Research has shown that mood states in mood disorders can be predicted using digital biomarkers based on the circadian rhythm [34].

Prediction of HFSS Snacking Using ML

This research project takes a step in the direction of digital phenotyping for the prediction of unhealthy eating behavior. Specifically, to what extent can HFSS snacking be predicted only based on prior HFSS snacking combined with information that can be automatically or easily collected from a smartphone (date, time, and location)? However, this endeavor might fail due to temporal resolution requirements. If high precision is needed, failure will be inevitable owing to the intrinsic stochasticity of the eating behavior. Another problem is the degree of accuracy that can be achieved after a modest training period, because participants may not have the patience for extended training (eg, Tulu et al [35]), and even with mostly passively collected data, participants still need to indicate instances of HFSS snack consumption.

On the positive side, ML has progressed to such an extent that modern algorithms have many characteristics desirable for the present application, including the capacity to deal with sparse data and efficient learning of time series. For example, as an alternative to recurrent neural networks, which are well suited to time series data, ensemble methods have a good ability to deal with sparse data by reducing the impact of noise and outliers [36]. Therefore, our aim was to compare a selection of ML algorithms, with a view to identify a good algorithm for predicting instances of HFSS snacking based on only prior instances, which were coded in terms of time, day, and location (the latter was encoded in terms of broad categories). The algorithms were chosen to reflect complementary characteristics and be representative of the range of good options currently available. Random forest regressor (RFreg), Extreme Gradient Boosting regressor (XGBreg), feed forward neural network (FFNN), and long short-term memory (LSTM) were considered.

RFreg is a tree-based ensemble method that trains many decision trees simultaneously with bootstrapping followed by aggregation, collectively referred to as bagging. Bootstrapping involves the training of several individual decision trees (between 100 and 300 in the present case) on several subsets of the dataset, using various subsets of available features [36]. Aggregation means that the outputs from the distinct decision trees are combined into a single decision. RFreg is considered to generalize well and be resistant to overfitting, as well as produce high prediction accuracy, because of ensemble learning [37].

XGBreg is another tree-based ensemble method, which uses a form of gradient boosting, relying on the idea that correcting the model's earlier errors and learning from them can help to improve performance in the future. This is a sequential ensemble learning method where the model tries to improve performance with each iteration [38]. Both RFreg and XGBreg are ensemble learning techniques, but the former builds multiple trees in parallel and then employs an average for prediction, while the latter constructs 1 tree at a time, in a way that is informed from the errors of the previous tree [39].

FFNN is a relatively simple type of artificial neural network, in which information is processed in 1 direction, from input units to units in one or more hidden layers to output units, such that there are no cycles in the connections between the nodes. Hidden layer units apply nonlinear functions to their input, enabling an FFNN to learn complex associations between input and output [40]. An FFNN is trained using gradient descent methods, specifically error backpropagation [41].

Finally, the LSTM model is a kind of recurrent neural network with an architecture designed for learning long-term dependencies in time series [42]. A recurrent neural network includes cycles that feed network activations from earlier time steps as inputs to determine predictions at the present time step. As a result of these recurrent connections, the model creates an implicit recollection of past occurrences, stored in its hidden layer [43]. Recurrent models can process contexts of arbitrary length; the LSTM model has a specific structure designed to store values for longer compared to standard recurrent neural networks. The LSTM model is the only recurrent model that was employed, with the other models operating on a fixed context.

Summary of the Purpose and Aims

Despite much interest in predicting eating behavior, there has been less work on prediction involving minimal data. Therefore, the feasibility of predicting HFSS snacking using only previous instances of snacking collected across a "practical" length of time (practical in the sense of participant recruitment and engagement) is unclear. Additionally, there is a wide range of ML algorithms. It is of interest to explore the quality of prediction against the assumed characteristics of HFSS snacking behavior, such as sparseness and high noise.

With these considerations in mind, this study aimed to (1) develop an app, which would enable data collection on HFSS

XSL•FO
RenderX

snacking with minimum effort from participants; (2) define a sensible problem for characterizing HFSS snacking behavior (prediction of HFSS snacking using previous instances of snacking and limited information [time, location, and day of the week]); (3) apply a range of standard and unmodified ML algorithms to the problem; (4) compare the performance of these algorithms to each other and to some baseline statistical models; and (5) consider whether the task of predicting HFSS snacking from minimal information is feasible and suggest some directions for future work.

Methods

Outline of Data Collection

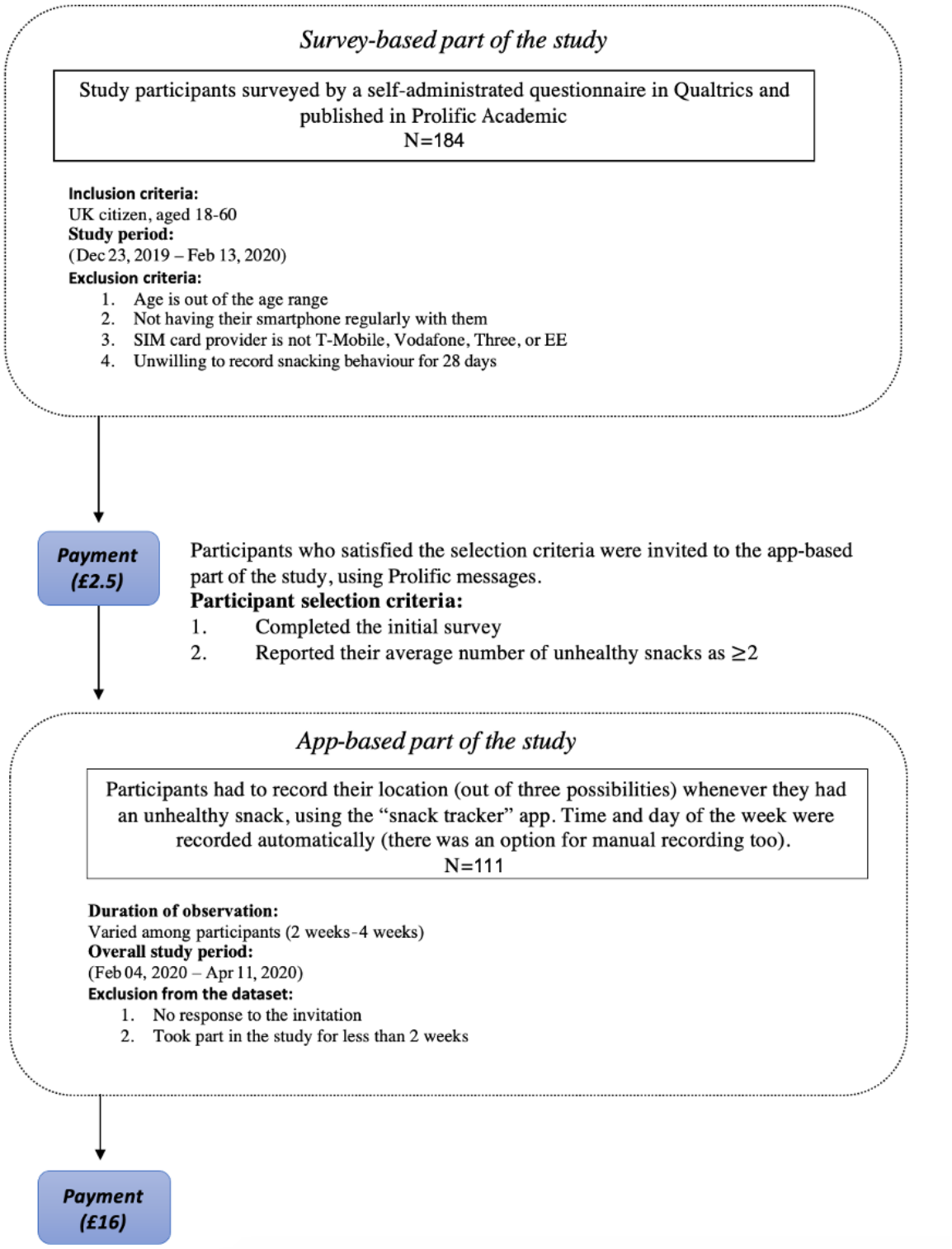
Data on HFSS snacking were collected to examine which ML algorithm was best able to predict such behavior based on only previous instances and minimal information (time, location, and day of the week). We first describe the procedures employed to collect the data.

Data were collected in 2 parts. First, a survey was created to explore various assumptions about the target behavior of interest. Second, we implemented an app to obtain data on HFSS snacking. Participants who reported having 2 or more HFFS snacks daily in the first part were invited for the app-based second part of the study. The second part of the study involved monitoring participants' snacking behaviors for 28 days. The 2 parts of the study are outlined in Figure 1. This dataset is referred to as the "UK dataset." To increase the ecological validity of our work, we also employed a cleaned version of a similar dataset collected in the Netherlands, which has been described by Spanakis et al [28]. The dataset in the report by Spanakis et al [28] is referred to as the "Dutch dataset."

The data collection details below concern the UK dataset; corresponding details for the Dutch dataset can be found in the report by Spanakis et al [28].

XSL•FO
RenderX

Figure 1. Screening and data collection processes for the UK dataset. Initially, demographic and lifestyle (weight/diet) surveys were used to determine eligibility for the trial. In part 2 (app-based part of the study), participants were asked to record snacking habits for a target period of 4 weeks.



Ethical Considerations

For the UK dataset, ethics approval was granted by the Psychology Research Ethics Committee at City, University of London (reference: PSYETH (S/L) 17/18 87). The informed consent form for the first study part (survey part) informed participants that the study was about snacks that are high in sugar, salt, and fat and that the study would be conducted in 2 parts (a brief first part concerning some general questions about eating behavior and a 28-day second part, which would involve participants recording occasions of snacking on their smartphones via an app). The informed consent form for the second part (app-based part) explained in detail about HFSS snacks and informed participants that they would have to record their HFSS snack consumption on an app for 28 days. The informed consent form provided some information about the

XSL•FO
RenderX

next steps, if the individual agreed to participate, and the amount of compensation.

All data were collected anonymously. To protect participant anonymity, the Data Protection Office at City, University of London, which is registered with the Information Commissioner's Office (registration number: Z8947127), was engaged to confirm that any personally identifiable information (PII) was securely collected. Data collection involved 3 companies external to City, University of London: Dev Technosys implemented the app, Linode provided virtual private servers, and Twillo provided programmable messaging services. It was ensured that these companies were compliant with the General Data Protection Regulation (GDPR) and used encrypted communication.

Participants were compensated £2.50 (US $3.13) for their time for the survey part of the study and £16 (US $20.00) for the app-based part.

For the Dutch dataset, ethics approval for the study was provided by the Faculty of Psychology and Neuroscience of Maastricht University in 2013. While the data were not open access, the principal investigators of the study stated availability of the data upon reasonable request [28].

UK Dataset: Survey-Based Part of the Study

Data for the first part of the study were collected using a self-administered survey designed using Qualtrics [44]. The survey was run on the crowdsourcing platform Prolific Academic [45]. The study was made available on Prolific Academic, and prospective participants decided whether to take part. The study had a target sample of 200 participants on December 23, 2019, and recruitment was closed on February 13, 2020, when this participant number had been reached.

There are no established guidelines for the minimum sample size required for an ML assessment, and a particular ML algorithm can work effectively up to a certain error threshold [46] for a promising but still experimental proposal. Based on previous related research (Spanakis et al [28] recruited 100 participants for an ML study broadly similar to our study), the expected time to train all 4 ML models for each participant, and our budget for paying participants to take part for 28 days, we aimed for approximately 100 participants for the ML assessment. The target of 200 participants for the survey part of the study was an estimate of how many participants would be needed to identify enough participants with a reasonably high intake of HFSS snacks, who would be willing to take part in the app-based part of the study across 4 weeks. The survey part had no inferential value.

Only UK citizens between the ages of 18 and 60 years were allowed to participate in the study. Participants were excluded if they did not have a smartphone or stated that they were unwilling to participate in the follow-up study (ie, the app-based part). Additionally, we only recruited participants having a T-Mobile, O2, Vodafone, Three, or EE mobile phone service, since at the time of running the study, these were the only SIM card providers in the United Kingdom providing services compatible with the Twillo messaging service, which we employed in the second part of the study. After these exclusions, there were 184 participants for the first part of the study.

The survey consisted of questions concerning basic demographics and motivation for healthy eating (Tables S1 and S2 in Multimedia Appendix 1). Specifically, there were 10 questions covering gender, ethnicity, employment status, weight, height, HFSS snacking habit, whether the person is trying to lose weight (2 questions), and whether the person is trying to eat in a healthy way. Participants were not allowed to skip questions. The duration of the survey was about 15 minutes.

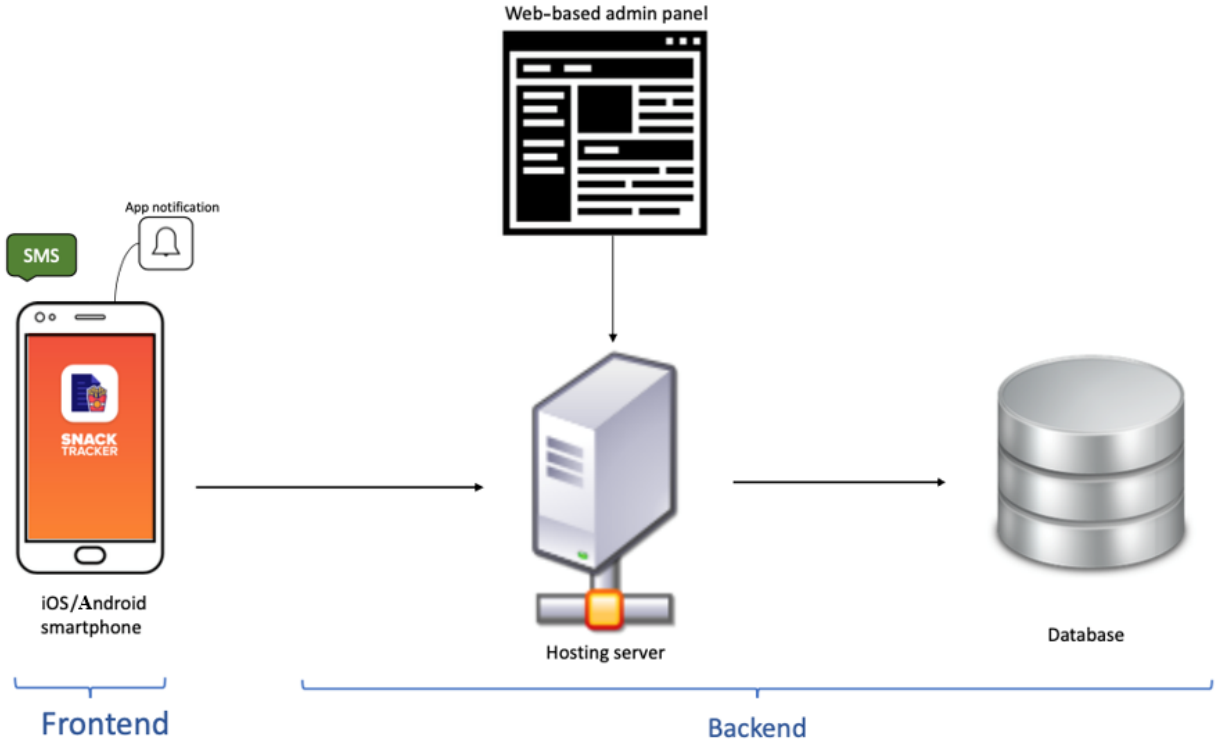
UK Dataset: App-Based Part of the Study – Snack Tracker App

We developed the Snack Tracker app to record unhealthy snacking for this project. The app was designed by SD, and the coding was undertaken by Dev Technosys [47], a company specializing in app development. We created versions of the app for both Android and iOS devices. However, the app is no longer available for use.

Mobile app development is usually divided into 2 main components: frontend and backend (Figure 2). Regarding the frontend (the user interface), the app was designed to be easy to use, with a simple sequence of screens (Figure 3 and Figure S1 in Multimedia Appendix 1). The current date and day of the week were automatically captured for each recording to minimize user effort. The app worked online, allowing users to log in and record any snacks they had eaten. In the case of connection loss, the app allowed users to save their records, and the app transmitted the data to the server once the mobile device was connected to the internet.

XSL•FO
RenderX

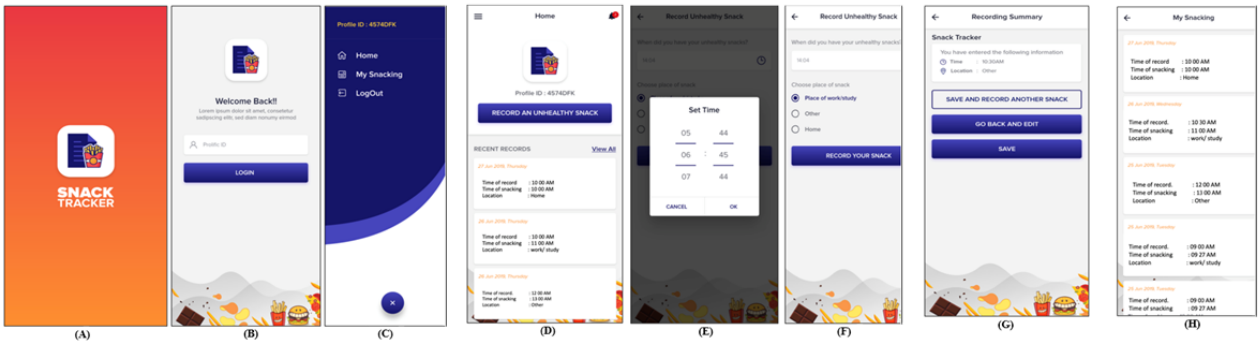
Figure 2. The frontend (user interface) and backend (data storage) of the Snack Tracker app used for participants in the second part of the study to record their intake of snacks with high saturated fats, salt, or sugar over a period of 4 weeks.



The app frontend was coded using React Native, which is an open-source JavaScript framework for writing iOS and Android apps. All operations performed by app users and project admins were handled by Rest Application Programming Interfaces (APIs) created in Node JS, which allows running JavaScript on the server side. Rest APIs were used to communicate with the database of participant data (MongoDB) for store and retrieve operations (ie, these APIs acted as a bridge between the app frontend and the database where participant data were stored). The server used in this project was a cloud-based server (Linode), which controlled all operations and allowed the management of the app environment.

The backend part of the app concerned storing the data and user credentials, as well as offering a web-based admin panel to manage the project. Participants accepting the invitation to the app-based part of the study were registered manually using the admin panel to prevent random users from recording data on the app. The backend also handled initial user login and user requests to save and record another snack, go back and edit, or just save an entry (Figure 3).

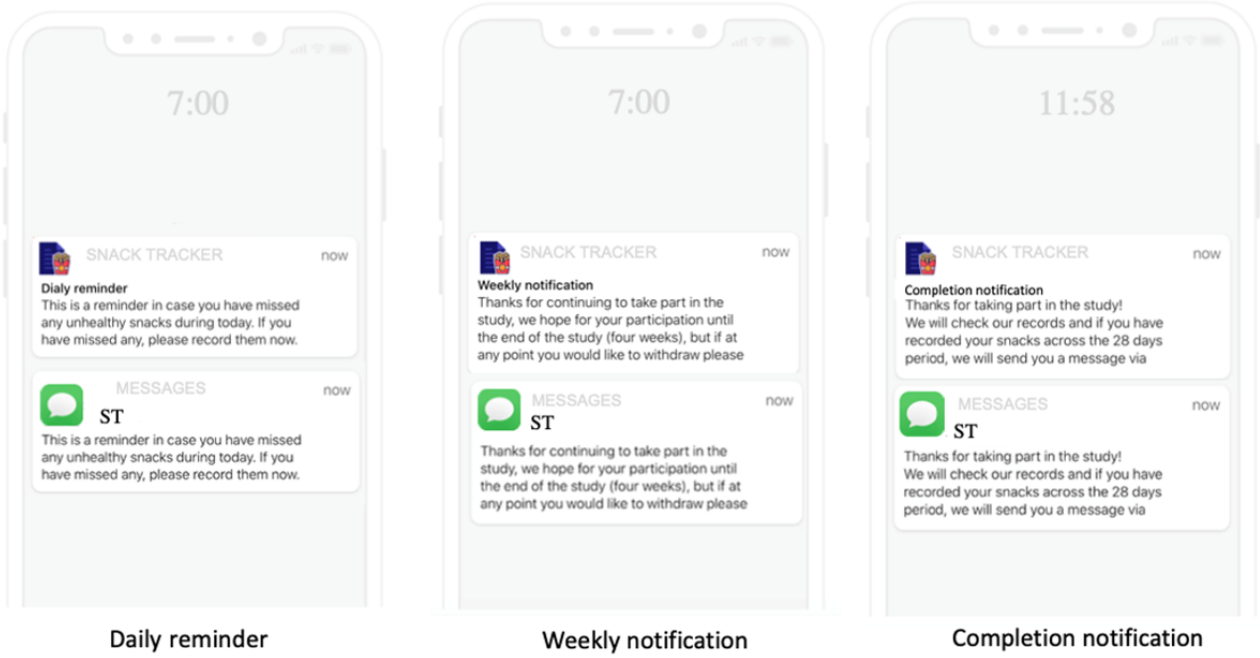
Figure 3. The frontend of the Snack Tracker app: (A) splash screen, (B) login screen, (C) home screen, (D) new snack screen, (E) time recording screen (time picker), (F) location recording screen, (G) recording save screen, and (H) review recording summary.



The app development included designing and delivering messages as SMS text messages and app push notifications to keep users engaged and remind them to record snacks (Figure 4). Push notifications could be offered even if participants had no internet access. For automated SMS text messages, Twilio was used, which is a cloud communication tool. The software could programmatically send SMS text messages using Twillo's web service APIs. For more information, see [48].

XSL•FO
RenderX

Figure 4. Examples of reminders sent to participants to "nudge" them to record their intake of snacks with high saturated fats, salt, or sugar during the second part of the study (app-based part).



UK Dataset: App-Based Part of the Study – Data Collection

Among the 184 participants who completed the survey-based part of the study, participants were further excluded if they reported consuming fewer than two HFSS snacks per day, leaving 170 participants. We initially invited 100 of these participants to participate in the app-based part of the study, with the invitations sent in 3 stages between February and March 2020. Initially, only 68 participants accepted the invitation, and in the second and third invitation stages, 45 and 25 participants, respectively, were invited, with 27 and 16, respectively, accepting the invitation, resulting in an overall sample of 111.

Participants were instructed to participate for 28 days. However, exact start and end dates of the study differed between participants, as was expected.

During the study, participants were messaged via Prolific if they made only 1 recording or no recordings on any day and if they had made multiple recordings (two or more) each day for a period but then abruptly made a reduced number of recordings. These messages were sent in part to ensure that there were no technical problems with the Snack Tracker app. Additionally, a few Prolific messages were sent to randomly selected participants to check that the reminders regarding snack recording (Figure 4) were received as intended. Informal feedback from participants throughout the study did not indicate any technical problems.

For the purpose of the study, an HFSS snack was defined as any food eaten between the main meals, which was high in either saturated fat, salt, or sugar. Specifically, participants were informed that we are interested in "snacks high in sugar, salt, or fat, which includes… sugary snacks… salty and fatty snacks." For each of these categories, several examples common in the United Kingdom were provided (eg, biscuits, cake, chocolate, crisps, salted nuts, and salted popcorn). Multimedia Appendix 1 shows exactly how HFSS snacks were explained to the participants. Considering the instructions and several examples of typical items provided, it is likely that participants did not have difficulty with the definition of HFSS snacks. There was no poststudy feedback of any such difficulties. In addition, in keeping with the broad aim of the study (to help people manage their own behavior), there were no strict criteria on what participants should or should not define as an HFSS snack. It was not considered that the app needed to be independently validated, which is in line with similar work, including the study by Spanakis et al [28].

Whenever participants had an HFSS snack, they were asked to record it in the Snack Tracker app. In this mode, they only had to mention the location (coded as home, place of work, and other; although a GPS-based method would aid in this process, this method was not possible in our app) as the time and day of the week were saved automatically. If participants had 2 HFSS snacks at the same time, this would be recorded as a single snacking instance. Throughout the study, participants received 3 kinds of notifications (Figure 4). Daily reminders were sent at 7 PM, asking participants to record any instances of HFSS snacking that they missed. In this mode of the Snack Tracker app, participants had to manually indicate the time and day of the week as well as the location. Additionally, at the end of each week, participants were sent a notification (instead of the daily notification) to keep them engaged and provide information or ask questions (eg, to ask about any technical problems; Multimedia Appendix 1). The final notification was sent at the end of the 28-day period (from the first app recording) to instruct the participants that the study had ended, thank them for their participation, and offer them a completion code for Prolific Academic.

XSL•FO
RenderX

Dutch Dataset: Brief Notes

The Dutch dataset was collected by a research group at the Faculty of Psychology and Neuroscience at Maastricht University (Study I in the report by Spanakis et al [28]). The dataset was collected with an app called Think Slim. The sample consisted of 57 participants who were overweight and 43 participants with a healthy weight in the Netherlands. This study employed EMAs. Data on 15 variables were collected (eg, mood, activity, and location), and the variables were monitored across 8 to 10 measurements per day depending on the participants' waking and sleeping times. Spanakis et al [28] aimed to study eating behavior in general (including main meals and snacks, both unhealthy and otherwise), with a view to identify participant clusters and provide adaptive feedback for improving eating behavior. Accordingly, we extracted measurements corresponding to HFSS snacks from the general eating behavior data [28] to create the Dutch dataset. Only "eating moments" were used from the original dataset [28]. Eating moments were event contingent (ie, they were initiated by users whenever they were about to eat something). Therefore, users were not prompted or reminded to record their eating behavior.

The Dutch dataset was already present when the data collection for the UK dataset was planned, and there is a reasonable question as to why we did not adopt a sampling approach similar to that used for the Dutch dataset. In brief, the purpose of the UK dataset was different from that of the Dutch dataset. For the UK dataset, the priority was to collect snacking information in a way that was as nonintrusive as possible. Moreover, we wanted to focus on individuals with some snacking behavior in the first place, since sparsity of data would complicate the application of ML. On the other hand, the purpose of the Dutch dataset was to explore prediction using a range of variables, with a focus on eating behavior in general and not just snacking, and it aimed to understand differences in daily lifestyle between people with a healthy weight and people who are overweight. Accordingly, the extent of snacking behavior was less relevant.

Data Preprocessing

Regarding the UK dataset, it was decided to exclude participants who did not remain in the study for its intended duration.

Some basic operations were carried out to remove erroneous entries and ensure consistency between the UK and Dutch datasets. In the UK dataset, we removed missing and duplicate entries and ensured that measurement units for height and weight were the same across participants. In the Dutch dataset, we translated data from Dutch to English and manually reclassified 950 locations, originally in free text, into the 3 categories employed in the UK dataset. Finally, HFSS snacks were extracted from the general information about meals or snacks. This involved focusing on data concerning food items, such as burgers, chocolate bars, strawberries, and pasta, and identifying the items considered as snacks. Each snack was manually categorized as healthy or unhealthy (HFSS).

Data were coded in terms of the following 3 features: location (home, place of work, and other), day of the week (Monday to Sunday), and time. A time bin feature was constructed, and there were 4 large and 12 small time bins. A regular day was divided into 4 or 12 time bins. In the former case, the time bins were early morning (midnight to 05:59 AM), morning (6:00 AM to 11:59 AM), afternoon (noon to 4:59 PM), and evening (5:00 PM to 11:59 PM). In the latter case, the first time bin started at midnight and had a 2-hour duration, and every subsequent time bin had a 2-hour duration, resulting in a total of 12 time bins. Models were trained and evaluated for these 2 encodings of the time variable.

As is common in ML, for the 2 nominal variables in the datasets (location and day of the week), one-hot encoding was used, converting each variable to separate variables that take the value 1 or 0 to indicate the presence or absence of different levels of the variable [49]. The time bin variable was kept in its numerical format.

Finally, although additional data were collected from participants in the United Kingdom, including motivation for healthy eating, these additional variables were not considered in this study for practical reasons and for meeting the focus of snacking prediction using minimal information.

Computational Methods

We employed 3 fixed context models (RFreg, XGBreg, and FFNN) and 1 recurrent model (LSTM). Fixed context models require a fixed input size, which can be achieved by windowing a longer sequence. Windowing is a technique used to divide a longer sequence into smaller, fixed-length sequences. Due to the sparseness of our data, we decided to treat each individual data point as a separate window for prediction, rather than grouping them into larger sequences. This approach is often used when the data are not abundant enough to create longer sequences, and it can simplify the modeling process for the algorithms. Recurrent models can process an input sequence of arbitrary length. They function in cycles, during which the activation from the previous time step is used as input (together with other information) for the current time step. For the single recurrent model in the study, we used the observation sequences of 4 time steps. In our study, the day was divided into different time bins, including a case of 4 time bins (early morning, morning, afternoon, and evening). While the 4 time steps in this model do not directly correspond to the day time divisions, they broadly align with it, and this was sufficient for our analysis.

Some models can benefit from standardization, normalization, and dropout regularization more than others, and these techniques were explored accordingly. Feature scaling (such as standardization or normalization) was considered for the FFNN and LSTM models. Neural networks often benefit from having consistent scales across features. This is because neural networks learn complex relationships and patterns among features, which can be influenced by the differing scales of features, if not appropriately managed [50,51]. On the other hand, tree-based models, such as RFreg and XGBreg, operate by splitting nodes based on feature thresholds and thus are less sensitive to feature scaling. For the FFNN model, we standardized features using the formula $z_i = (x_i - \mu) / \sigma$, where μ and σ are the mean and SD values of the variable, respectively; z_i indicates the standardized value; and x_i is the original value. For the LSTM model, we

XSL•FO
RenderX

employed the normalization $y_i = x_i - \min(X) / (\max(X) \cdot \min(X))$.

Dropout was also explored. It is a regularization technique that randomly sets to zero (drops out) a percentage of the features during training [52]. Dropout regularization introduces randomness during training and prevents overspecialization of units, which can improve generalization. This is important for neural networks, as they can overfit the training data. Accordingly, we evaluated and ended up retaining dropout regularization for the FFNN and LSTM models. Tree-based models use other (inherently incorporated) mechanisms, such as feature selection, bootstrapping, and ensemble aggregation, to manage overfitting.

We executed a total of 5 experiments for each model (5-fold cross-validation) to evaluate their performance. In each experiment, the models were evaluated based on their predefined configurations (Table 1). Both random forest and XGBoost are based on decision trees, and Figure 5 illustrates their differences as well as some of the main parameters.

Table 1. Hyperparameters for each of the machine learning algorithms used to analyze the data collected about consumption of snacks with high saturated fats, salt, or sugar during the app-based part of the study.

Model and hyperparameter	Value or range
RFreg[a]	
n_E, number of estimators (trees in the forest)	150
Min_{ss}, minimum number of samples an internal node must cover to consider splitting (when a node has fewer samples than this value, it is regarded as final and called a terminal node or leaf)	2
Max_{depth}, maximum number of splits that each tree is permitted to execute	Not user specified (nodes are expanded until leaves are pure or contain less than Min_{ss})
XGBreg[b]	
n_E, number of boosting rounds (estimators)	100
Min_{SS}	2
Max_{depth}	6
LR, learning rate (step size for each boosting iteration)	0.3
Gamma[c] (how much the loss must be decreased by a split in order for that split to occur)	0.05
FFNN[d]	
Number of hidden layers	4
Dropout regularization[e]	0.5, after the 2nd and 4th hidden layers
Number of neurons at the hidden layer (NHL)	1st hidden layer: 32; 2nd hidden layer: 32; 3rd hidden layer: 8; 4th hidden layer: 8
Activation function	ReLU[f], in the dense and output layers
LSTM[g]	
Number of neurons in the LSTM layer (NLL)	128
Number of hidden layers	3
Dropout regularization[e]	0.5, after the 3rd hidden layer
NHL	64
Activation function	ReLU, in the dense and output layers

[a]RFreg: random forest regressor.

[b]XGBreg: Extreme Gradient Boosting regressor.

[c]In relation to gamma, loss is the function minimized during model training. It is based on the difference between the current output of the machine learning model and the target (ie, the true value).

[d]FFNN: feed forward neural network.

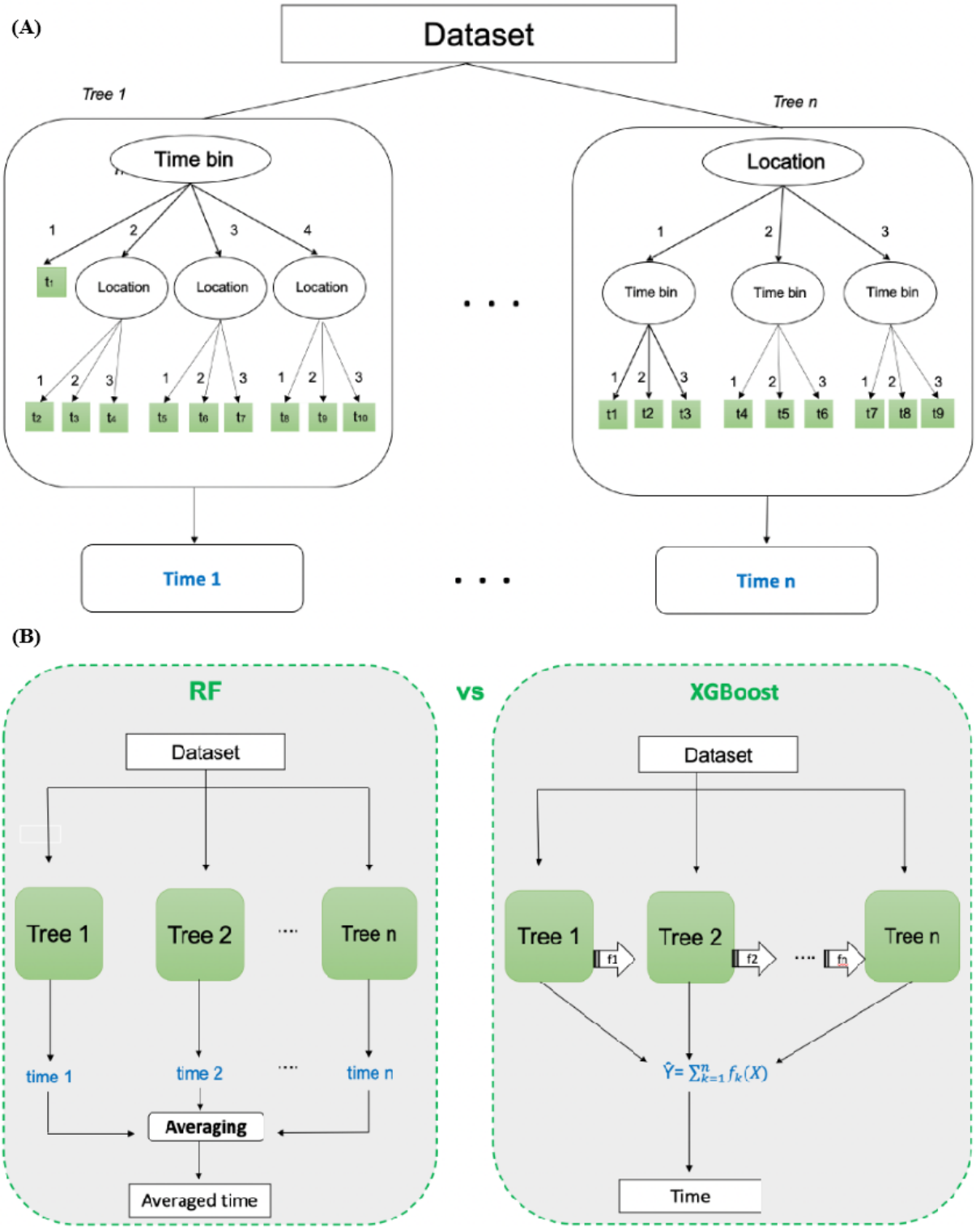
[e]Dropout regularization is a technique that randomly switches off neurons in a neural network during training to avoid overfitting. The number given refers to the fraction of neurons switched off.

[f]ReLU: rectified linear unit.

[g]LSTM: long short-term memory.

XSL•FO
RenderX

Figure 5. The 2 panels of the figure illustrate the differences between the 2 random forest machine learning algorithms in the study. (A) Both random forest regressor (RFreg) and Extreme Gradient Boosting regressor (XGBreg) are based on the same building block, a decision tree, which is a set of rules built from the dataset. In our case, the aim is to predict the time until the next snack having high saturated fats, salt, or sugar in minutes. n is the number of trees in the model, selected based on cross-validation performance. Time k is the expected time until the final unhealthy snack is predicted using Tree k. (B) For RFreg (on the left), the model creates several different trees and then averages predictions. For XGRreg (on the right), there is a sequence of trees, which progressively refine the prediction. Splits in a decision tree correspond to the data points associated with a node being divided and the parts assigned to child nodes. RF: random forest; XGBoost: Extreme Gradient Boosting.



All algorithms had the same objective, which was to predict the time until the next HFSS snack (in minutes), given the current time bin, location (work, home, and other), and day of the week. Specifically, given the presence of an HFSS snack in a time bin, the ML algorithms attempted to predict the number of minutes to the next HFSS snack (snack to snack interval). ML algorithms were applied separately to the snacking data from each participant to take into account individual differences in

XSL•FO
RenderX

how the available predictors can be related to snacking behavior. In ML terms, the question is whether there is structure in the data to predict the density of snacking instances, based on the available predictors, location, time bin, and day of the week. To summarize the main approach, we used an input of fixed size, comprising current location, current day of the week, and current time bin, for RFreg, XGBreg, and FFNN. The LSTM model processed data as a sequence of inputs.

To appreciate the capacity of the ML models to extract regularities from the data, 2 baseline models were explored. The first was a simple linear regression model, which attempted to predict snacking instances based on a linear combination of available features, which were suitably weighted. The second was a basic baseline model corresponding to prediction based on the grand mean of snacking (computed separately for each participant) across the time bins.

Five-fold cross-validation was applied on all fixed-context models. In each data split, the datasets were divided into 2 parts (80% for training and 20% for testing). That is, 20% of the data reserved for testing constitutes out-of-sample validation of the models. The error (mean absolute error [MAE]) values were computed on the part of the dataset left for testing (20%). This procedure was repeated 5 times, with each iteration corresponding to a different, randomly determined partition of the data into training and test parts. Reported MAE values were averaged across these 5 iterations. We ensured that data distributions in the training and testing data subsets were similar to those in the whole dataset, using stratified data sampling [53]. Regarding the choice of using 5-fold cross-validation, there is a question of whether it would make sense to have more "folds." However, each different "fold" increases the number of simulations that must be run and leads to more unbalanced training and testing subsets. Five-fold cross-validation is a fairly standard approach.

For the LSTM, a time series cross-validation was employed. Time series cross-validation is more suitable for temporal data modeling, because the training set only includes the observations occurring before those in the testing set. It begins with a small subset of data for training that is successively extended to generate new predictions [54]. Because of the sparseness of the data, it was decided to use time series cross-validation with only 2 splits.

MAE is the main evaluation metric for the models. MAEs were computed as differences in minutes between the time of the current snack and the predicted time for the next snack. This is because our research focus was the time difference between the prediction and the actual time until the next HFSS snack occurrence. Additionally, residuals allow quantification of positive and negative errors, which were employed in a further analysis (related to the creation of hypothetical interventions). Residuals were calculated as true values minus predicted values. Thus, positive residuals indicate that the predicted time is earlier than the observed time, and negative residuals indicate that the predicted time is later than the observed time. It is important to note that the MAE is computed as the average of the absolute values of the residuals. Residuals were examined as standard, and corresponding plots are provided in Multimedia Appendix 2.

Results

Preliminary Notes

Regarding the UK dataset, as expected, some participants did not stay in the study for its intended duration (4 participants). Majority of the participants (107/111) recorded their HFSS snacks for the full 28 days or more. Among these participants, there were 34 female and 73 male participants, with an average age of 32.85 (SD 10.10) years. Some participants continued recording snacking for an additional 6 to 11 days after reaching the 28-day target and after receiving the completion message. These additional data were used in the analyses. Overall, the total number of recordings across all participants was 5391, which reduced to 4978 data points after data cleaning. There were some positive comments about the study in general. For example, participants mentioned that recording their snacks made them aware of the amount consumed daily and helped them reduce food intake.

There were 413 missing and duplicate entries in the UK dataset. Regarding duplicates in the UK dataset, when participants recorded their snacking instances, they might have pressed the submit button twice, which resulted in 2 instances of the same event. However, such duplicate instances were few (approximately 7.7%). In each participant, the total number of recorded snack instances ranged from 7 to 157.

The Dutch dataset included 3705 data points. In each participant, the number of recorded snack instances ranged from 6 to 348. Demographic and other characteristics of the Dutch dataset can be found in the original publication [28].

The sizes of the training and testing sets were 3982 and 996, respectively, in the UK dataset and 2778 and 927, respectively, in the Dutch dataset.

We noted that normalization slightly enhanced the results from the LSTM model but not the FFNN model.

Model Results

Table 2 and Figure 6 show the MAEs for the 4 models using all input features. In brief, the RFreg model performed very poorly with the UK dataset using 4 time bins. In contrast, the XGBreg, FFNN, and LSTM models all demonstrated reasonable performance with the UK dataset using 4 time bins, achieving lower MAE values and indicating better predictive ability compared to the RFreg and baseline (grand mean) models. When using 12 time bins for the UK dataset, all 4 models performed relatively similarly and demonstrated satisfactory performance. It is not possible to compute significance values from MAE differences in such an ML analysis. This is because to compute statistical significance, some knowledge of the sampling distribution of MAE differences is needed if the null hypothesis (there is no structure in the time series) is true, which is not possible. The best guide for the interpretation of MAE values is the MAE of the baseline (grand mean) model.

XSL•FO
RenderX

Table 2. Performance of the machine learning algorithms for predicting consumption of snacks with high saturated fats, salt, or sugar in the UK and Dutch datasets.

Dataset and model	Training set with 4 time bins (MAE[a,b])	Testing set with 4 time bins (MAE[b])	Training set with 12 time bins (MAE[b])	Testing set with 12 time bins (MAE[b])
UK dataset				
Grand mean	29.2	47.3	29.2	47.1
LR[c]	9.3	56.3	6.8	60.3
RFreg[d]	14.7	52.3	6.2	16.2
XGBreg[e]	4.8	17.8	2.3	17.5
FFNN[f]	15.3	15.8	15.3	16.3
LSTM[g]	14.7	15.9	14.8	16.5
Dutch dataset				
Grand mean	1049.0	1397.3	1049.0	1400.1
LR	116.1	816.1	99.2	914.6
RFreg	306.9	309.9	311.5	239.1
XGBreg	3.2	238.9	4.1	229.9
FFNN	690.3 (133.8[h])	151.5 (130.0[h])	723.3 (133.7[h])	154.0 (129.8[h])
LSTM	1271.5	171.0	1330.0	174.2

[a]MAE: mean absolute error.

[b]MAEs for predicting the time of the next snack having high saturated fats, salt, or sugar in minutes using all features (fractional part of a minute is indicated as decimals). A lower MAE is better. The average across participants is provided.

[c]LR: linear regression.

[d]RFreg: random forest regressor.

[e]XGBreg: Extreme Gradient Boosting regressor.

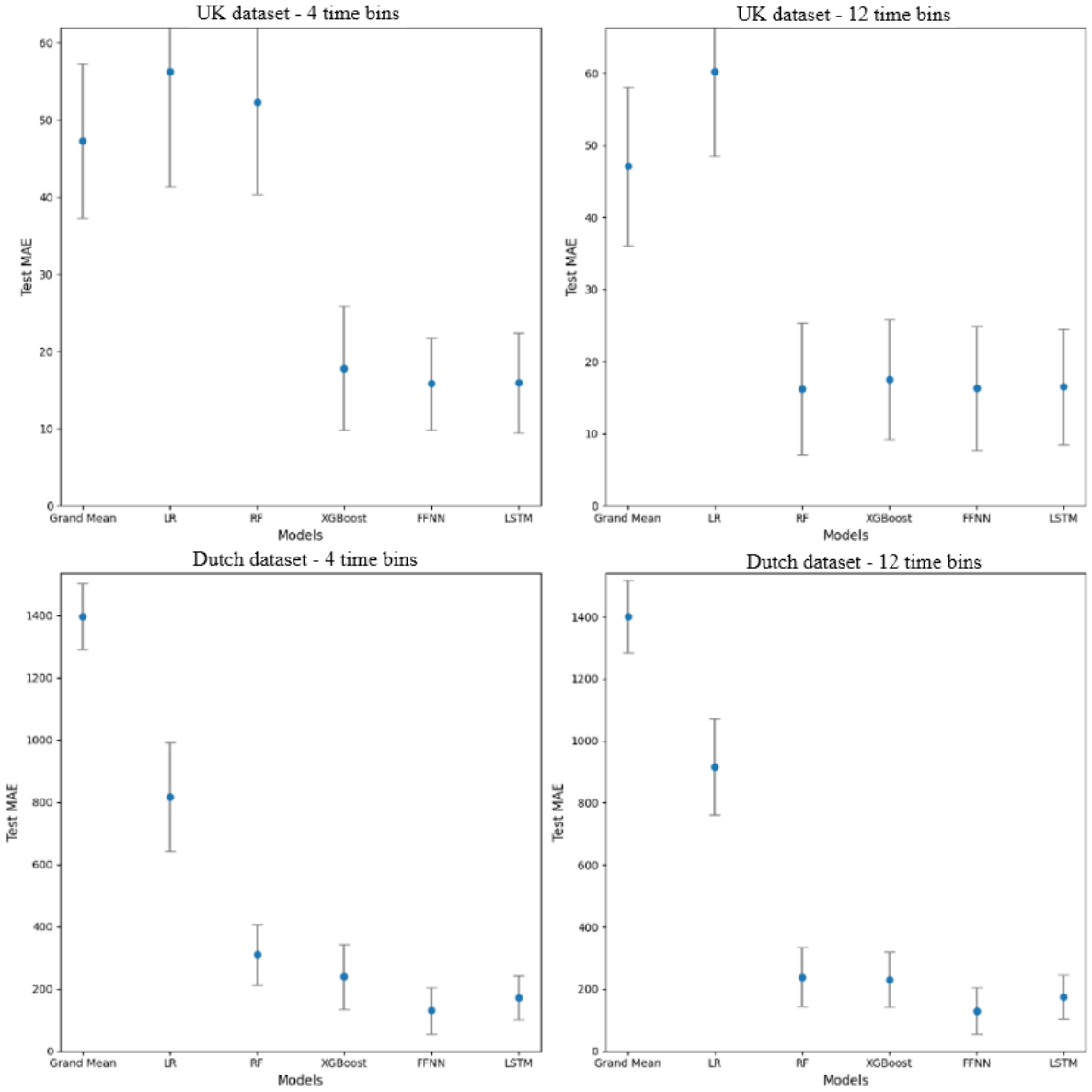
[f]FFNN: feed forward neural network.

[g]LSTM: long short-term memory.

[h]The numbers in parentheses refer to model performance after applying regularization and early stopping.

XSL•FO
RenderX

Figure 6. A graphical illustration of the relative performance of the machine learning algorithms (random forest regressor [RFreg], Extreme Gradient Boosting regressor [XGBreg], feed forward neural network [FFNN], and long short-term memory [LSTM]) for predicting consumption of snacks with high saturated fats, salt, or sugar in the UK and Dutch datasets and using 2 different approaches for partitioning time. Performance is quantified using the average mean absolute error (MAE) values from Table 2 (lower values are better). The error bars indicate the IQR. LR: logistic regression; RF: random forest; XGBoost: Extreme Gradient Boosting.



For the Dutch dataset, errors were high. The FFNN model was the best performing model when using both 4 and 12 time bins. The training MAE for the FFNN model was much higher than the testing MAE, suggesting underfitting of data but good generalization. To assess whether the training MAE can be reduced, regularization and early stopping with the FFNN model were employed for the Dutch dataset.

The results can be explored in 2 ways. First, the scatter plots of residuals can be considered for the best performing version of each model. For most noisy processes, the default expectation is that residuals should be evenly distributed around zero, with the spread of the residuals dependent on the amount of noise and the quality of the model. A narrow spread of residuals around zero is generally indicative of good quality predictions [55]. Model residuals with scatter plots are presented in Multimedia Appendix 2. Overall, nonlinear models, particularly random forest, XGBoost, and FFNN, show the most potential for accurately predicting the time until the next HFSS snack, with the predominance of positive residuals being advantageous for just-in-time interventions (since positive residuals indicate that the prediction is earlier than the actual event).

Second, feature importance can be examined in the prediction task. Although there were only 3 features for prediction (time bin, location, and day of the week) and all of them appeared important, there might be enough information for prediction after eliminating day of the week or location. Feature importance analysis is one way to proceed in this case, but because of the approach used for model fit (individually for each participant), this was deemed impractical. Therefore, instead, we carried out 2 feature ablation analyses, one for location and another for day

XSL•FO
RenderX

of the week. For the UK dataset, both these features appeared essential for the prediction task, since eliminating either one of them reduced model performance quite substantially (without either of the features, model performance became equivalent to that of the grand mean model) (Tables 3 and 4). On the other hand, for the Dutch dataset, the reduction in model performance in the ablation analyses was milder, indicating that prediction could be based on a subset of the available features.

Table 3. Location ablation analysis of the machine learning algorithms for predicting consumption of snacks with high saturated fats, salt, or sugar in the UK and Dutch datasets.

Dataset and model	Training set with 4 time bins (MAE[a,b])	Testing set with 4 time bins (MAE[b])	Training set with 12 time bins (MAE[b])	Testing set with 12 time bins (MAE[b])
UK dataset				
Grand mean	29.2	47.3	29.2	47.1
LR[c]	17.1	>10,000[d]	13.8	>10,000[d]
RFreg[e]	15.3	52.2	12.1	42.5
XGBreg[f]	10.2	49.9	4.2	46.6
FFNN[g]	26.0	45.9	26.0	45.9
LSTM[h]	23.4	55.4	23.5	55.4
Dutch dataset				
Grand mean	1049.0	1397.3	1049.0	1398.0
LR	132.4	>10,000[d]	76.1	>10,000[d]
RFreg	370.4	267.6	341.6	276.3
XGBreg	73.4	222.5	23.1	258.8
FFNN	690.3	151.5	690.3	151.5
LSTM	1271.5	171.0	1271.5	171.0

[a]MAE: mean absolute error.

[b]MAEs for predicting the time of the next snack having high saturated fats, salt, or sugar in minutes using all features (fractional part of a minute is indicated as decimals). A lower MAE is better. The average across participants is provided. Values are based on time bin and day of the week only.

[c]LR: linear regression.

[d]Extremely poor performance with a very high error.

[e]RFreg: random forest regressor.

[f]XGBreg: Extreme Gradient Boosting regressor.

[g]FFNN: feed forward neural network.

[h]LSTM: long short-term memory.

XSL•FO
RenderX

Table 4. Day of the week ablation analysis of the machine learning algorithms for predicting consumption of snacks with high saturated fats, salt, or sugar in the UK and Dutch datasets.

Dataset and model	Training set with 4 time bins (MAE[a,b])	Testing set with 4 time bins (MAE[b])	Training set with 12 time bins (MAE[b])	Testing set with 12 time bins (MAE[b])
UK dataset				
Grand mean	29.2	47.3	29.2	47.1
LR[c]	21.1	>10,000[d]	15.2	>10,000[d]
RFreg[e]	21.1	45.9	16.9	39.9
XGBreg[f]	20.2	46.2	13.8	46.4
FFNN[g]	26.0	45.8	26.0	45.9
LSTM[h]	23.5	55.4	23.5	55.5
Dutch dataset				
Grand mean	1049.0	1397.3	1049.0	1398.0
LR	152.7	>10,000[d]	96.2	>10,000[d]
RFreg	416.0	284.4	360.9	229.3
XGBreg	135.3	212.2	73.5	197.6
FFNN	690.3	151.5	690.3	151.5
LSTM	1271.5	171.0	1271.5	171.0

[a]MAE: mean absolute error.

[b]MAEs for predicting the time of the next snack having high saturated fats, salt, or sugar in minutes using all features (fractional part of a minute is indicated as decimals). A lower MAE is better. The average across participants is provided. Values are based on time bin and location only.

[c]LR: linear regression.

[d]Extremely poor performance with a very high error.

[e]RFreg: random forest regressor.

[f]XGBreg: Extreme Gradient Boosting regressor.

[g]FFNN: feed forward neural network.

[h]LSTM: long short-term memory.

An alternative, exploratory analysis is presented in Multimedia Appendix 3, which illustrates a different way to use the present data. This involved a sensitivity/specificity analysis, and the focus was to predict unhealthy snacks within windows of a certain size. This analysis was arguably better suited to the specific goal of building JITAIs. It was framed as a timing analysis for the delivery of a hypothetical intervention, which involved testing whether predicted snacking times fell within time windows of 120, 60, and 30 minutes before the actual HFSS snack time. This analysis was carried out only for the FFNN model, because FFNN residuals were notably positive and thus indicated early predictions, which is a desirable property for JITAIs. We briefly summarize the results from this analysis on individual behavior. Assuming the delivery of an intervention 45 minutes before a predicted snack, 90% of predictions would occur within a 1-hour window before the actual snack for the UK dataset and the Dutch dataset. If the acceptable window between the intervention and snack is reduced to 30 minutes (and the intervention is delivered 20 minutes before the prediction), the accuracy would be 75% and 74% for the UK dataset and the Dutch dataset, respectively.

Discussion

Principal Findings

Interventions can be made more effective by delivering messages at the right time before the target behavior is performed, as is the case with JITAIs (eg, [17,18]). ML can in principle help. The goal of this study was to design an app to collect data on HFSS snacking behavior in order to explore the capacity of well-known ML methods to capture the underlying statistical structure.

Over a period of 4 weeks, 111 participants provided data on HFSS snacking, using our Snack Tracker app, and this was considered the UK dataset. In addition, we analyzed an analogous dataset from the Netherlands (100 participants with a varying weight status), which was considered the Dutch dataset. In both cases, a number of preprocessing steps were carried out. We considered dividing a regular day into 4 and 12 time bins. We explored 4 established ML models, namely RFreg, XGBreg, FFNN, and LSTM, in the 2 datasets for predicting the number of minutes to the next HFSS snack (given the time bin in which HFSS snacking occurred) in each participant separately. The models were able to predict the time until the next HFSS snack with reasonable accuracy (the MAE was low

XSL•FO
RenderX

at about 17 minutes in the UK dataset and was 130 minutes in the Dutch dataset). Although errors of 130 minutes (more than 2 hours) may appear large, this finding should be evaluated in the context of behaviors that themselves might occur only once every several hours. In many cases, prediction on the basis of the grand mean was inferior, demonstrating that the models were able to extract some regularity from the data. The residual analysis revealed reasonably narrow distributions, with desirable (in most cases) properties, such as positive residuals. Positive residuals mean that the prediction of the next HFSS snack is before the actual event, making them preferable (compared to negative residuals) for JITAIs. It would have been nice to offer a simple summary conclusion regarding which model performed better. Although there was some evidence that the FFNN model was overall superior, this was based mostly on the Dutch dataset. It makes sense to be cautious about overall model adequacy, and more analyses like the present ones are needed.

Strengths

A strength of the study is the use of 2 datasets involving different populations, sampling approaches, and data collection methods. However, there is concern regarding the difference in MAE values between the UK and Dutch datasets. This may be attributed to differences in participant selection criteria between the 2 datasets. In the UK dataset, participants were selected based on their reported frequency of unhealthy snacking, and specifically, those who consumed two or more unhealthy snacks daily were considered. This likely led to a more homogeneous group in terms of snacking behavior, contributing to the lower MAE values. On the other hand, the Dutch dataset had a broader participant base without prior assessment of the snacking habit. The Dutch dataset included both people with a healthy weight and those who were overweight, but the UK dataset did not select participants based on BMI and instead included participants who consumed two or more unhealthy snacks daily. There were also differences in methodology and sampling techniques, which might have led to differences in the variability of snacking behavior and thus the capacity of the ML algorithms to perform well. Another point concerns the difference in the cultural context and how this might impact snacking behavior. For example, people in the United Kingdom (vs those in the Netherlands) eat less fruit (295 g vs 461 g per day; Food and Agriculture Organization of the United Nations, 2023) and are more likely to experience obesity (30% vs 23% of adults) [56].

Overall, there were several potential differences between the Dutch and UK datasets, and examining the performance of the ML algorithms separately for each dataset was an interesting exercise. Conversely, considering the range of differences mentioned above, there was little justification for combining the 2 datasets into a single analysis.

A major difference between the UK and Dutch datasets was related to the dependence on the additional features of location and day of the week over and above the main prediction feature of time bin. While prediction dropped substantially after eliminating either of these 2 additional features in the UK dataset, this was not the case in the Dutch dataset (prediction was equivalent with and without the 2 features). It is possible that location coding in the Dutch dataset was less accurate than that in the UK dataset. In the UK dataset, we specifically asked for location in terms of home, work, or other, which corresponded exactly to the feature coding in the analyses, but in the Dutch dataset, the location variable had to be derived from other data. However, this is a fairly weak reason (there is reasonable confidence in how the location variable was coded in the Dutch dataset), and in any case, this argument does not apply to the day of the week feature. More generally, there might have been more variation in the contextual cues that drive HFSS behavior between the 2 countries. At a preliminary level, it could be argued that the food environments between the 2 countries are broadly similar, but clearly, this is a possibility that cannot be addressed without further work.

From a technical point of view, a feature of the present approach is that the choice of methods represents relevant ML models for this type and size of dataset, without an attempt to develop a customized approach. Our emphasis was on how good prediction can be with standard ML algorithms. It is therefore interesting that the selected models mostly outperformed the baseline grand mean model. Models based on decision trees (XGBoost and random forest) performed competitively in predicting the next HFSS snack, but overall, neural networks (FFNN and LSTM) performed somewhat better. This finding may change with an increase in the number of data points, as neural networks, particularly deep ones, benefit greatly from large datasets. Moreover, there are alternative neural network models that merit examination, such as the Gated Recurrent Unit network, which is fast, requires little memory, and sometimes has better performance than LSTM [57]. One direction for future work is to determine how to use the characteristics of the present modeling challenge (such as sparsity) to fine-tune learning algorithms.

Limitations

There are several technical challenges that need to be mentioned. First, behaviorally, for many users, it is difficult to commit to providing data for a long time, before interesting predictions are made. Even if most information is passively obtained, there would still be a small burden to record snacks. Therefore, it is worth exploring online ML, whereby data streams are used to continuously update a model. Another approach is to entirely obviate the need for user input through the use of sensor data combined with ML (digital phenotyping work mentioned earlier, eg, [30,31]). For example, Bangamuarachchi et al [58] reported some promising results concerning the identification of eating and noneating events, using only passive smartphone data (also see the study by Chen et al [59]). An important future direction would be to compare the quality of prediction from data collected actively versus passively, though the 2 approaches should not necessarily be seen in competition (eg, sensor data could be employed to validate active data entry).

The issue of recording snacks has another facet in terms of the change potential stemming from awareness of a behavior [11]. While this is a desirable effect of data collection (and indeed consistent with other research, eg, research in alcohol abuse; see the study by Pimpini et al [11]), it is a complicating factor regarding the validity of the dataset in that observation of the behavior impacts the behavior itself. However, it is very

XSL•FO
RenderX

difficult, if not impossible, to disentangle such factors from the general variability in behaviors, such as HFSS snacking, which are inherently stochastic and subject to change from random environmental changes (eg, periods of stress or going on holiday). There is a profound challenge here, which goes beyond current standard practice in ML.

Second, a related challenge is that of data sparseness. ML models work better with more data. With a larger sample, it might be possible to examine whether there are natural groupings in HFSS snacking behavior, defined by, for example, demographic characteristics, personality traits, physiological differences, or eating behavior traits (eg, [60-63]). Different groups of this kind might display higher regularity in the HFSS eating behavior. Thus, categorizing a new participant against a pre-existing classification of individuals might inform our confidence of how well one can predict the behavior of that participant (eg, see Study II in the report by Spanakis et al [28]). Currently, the form of such a classification is unclear. Researchers could rely on ML to identify appropriate aspects and then attempt to interpret them against eating behavior characteristics.

Third, there is a question of whether the sample size was adequate. We have already mentioned the lack of established guidelines on sample size to achieve particular levels of sensitivity in ML work [46], as well as noted research similar to ours with similar sample sizes (eg, Spanakis et al [28]). Nonetheless, given the limitations in sampling, it can be questioned whether the present sample is sufficiently representative of the general population. Participants were recruited through Prolific Academic, which is one of the most widely employed crowd-sourcing platforms for behavioral experiments. Their age characteristics and gender balance revealed no peculiarities. The recruited participants were biased toward those who consume more HFSS snacks and those with enough technology familiarity to use our app. Nonetheless, they represent participants who would take part in future interventions, based on the kind of HFSS snacking prediction considered here.

Fourth, in this work, we only employed day of the week, time, and location (coarsely coded). In contrast, the studies by Arend et al [25], Forman et al [26], and Spanakis et al [28] are all sophisticated examples of similar predictive modeling but based on more information. The use of a greater number of features has the potential for more accurate prediction. Regarding HFSS snacks, the times of meals and drinks are particularly pertinent. However, we wanted to explore the predictive potential based on information that would be as straightforward as possible for participants to provide. The motivation for such an approach is that any scheme suitable for roll-out to the general population would benefit from being as unobtrusive as possible in terms of requests for information. In our app, location required participant input, but in future iterations, this feature could be automated through simple look-up tables involving geolocation data and the prerecorded locations of particular users for work, home, etc. Additional information that could be recorded automatically include sensor data from sophisticated smartwatches, such as heart rate, blood pressure, and possibly blood sugar, or whether the individual is alone or with company. There could be a tradeoff here among predictive power, usability, and participant fatigue, which will require more work before clarification.

A related point is whether an autoregressive approach might be more fruitful. Our analyses were based on taking all time bins in which there were snacks and trying to predict the time (minutes) to the next snack (given the time bin, location, and day of the week). What if *all* time bins are considered as input for the models, regardless of whether there is a snack, and the presence of a snack is used as an additional feature? In brief, such an approach does not work with the present data. The likely problem is the sparseness of snacking bins relative to no-snacking bins, and thus, the dataset is skewed toward the latter. This kind of data skew is a recognized problem in ML, leading to poor performance of ML models [64]. Such problems from undersampling of snacking instances might be mitigated in larger datasets.

Fifth, the possibility of using more extensive sensor data goes hand in hand with the intriguing suggestion to individualize the ML approach [65]. There are merits and demerits for both collecting more data per participant (to allow, for example, individualization) and adopting a more general approach with minimal data collection per participant (Spanakis et al [28] provide a discussion of the tradeoff between individualization and generality). It is worth noting, however, that even with the present minimal data collection and a general approach to ML, it was possible to achieve reasonably low prediction errors.

Sixth, HFSS snacking behavior is not necessarily stable and might vary depending on factors such as the time of the year. Accordingly, an ML approach would need to be able to adapt to any changes in behavior. The difficulty then is how to distinguish between routine deviations in baseline behavior and changes in the behavior itself. Online ML might again offer promise in addressing such a challenge [66]. These considerations also challenge a perception that perhaps it would be more appropriate to base predictions on stationary data.

Challenges like those mentioned above are not independent of the goal of the prediction. Arguably, if the purpose of prediction is to carry out an intervention, it may be valuable to know not only the time of an HFSS snacking event, but also additional variables, such as whether particular emotions preceded a snacking event. Currently, for the reasons outlined above, it seems unlikely that a practical method (ie, beyond research) based on multiple variables or EMAs can be developed, but future personal electronic devices may make the collection of the data possible. Participants are likely to engage with intensive data-collection procedures if they are sufficiently motivated to accomplish goals related to dietary change, weight reduction, etc.

Conclusions

The examination of standard ML algorithms produced promising findings concerning the prediction of HFSS snacking based on sparse data involving only previous occasions of such snacking behavior. There are promising behavioral implications given that a reasonable degree of predictive accuracy was possible even with limited data (in terms of both features and the window

XSL•FO
RenderX

for data collection). One direction for application concerns using prediction data to deliver behavior change techniques for HFSS snacking behavior (eg, [16,67]). These behavior change techniques could be delivered in several different ways (eg, by text or audio messages) to increase engagement and could also be selected and personalized for the individual. Additionally, the ML work by itself could be applied to other behaviors targeted for reduction, such as smoking and alcohol consumption.

The present results offer a foundation for further exploring how ML methods can be used in health psychology and provide directions for further research, which can be both more technically oriented and focused on behavioral applications and extensions.

Acknowledgments

SD received funding from the Saudi Arabian Cultural Bureau (SACB) in London. Additionally, the SACB provided further funds for the data collection part of this research. No generative AI was used in any portion of the manuscript.

Data Availability

The data and code in this study are publicly available through an Open Science Foundation page [68].

Authors' Contributions

Conceptualization: TW, KT, EMP
Data curation: SD, KT, GS, AR, EMP
Formal analysis: SD, TW, EMP
Funding acquisition: SD, TW
Investigation: SD
Methodology: SD, TW, KT, EMP
Project administration: SD, TW, EMP
Software: SD, TW
Resources: SD, TW, EMP
Supervision: TW, EMP
Validation: All authors
Visualization: SD
Writing – original draft: SD, KT, EMP
Writing – review and editing: All authors

Conflicts of Interest

None declared.

Multimedia Appendix 1
Additional information on the study methods.
[DOC File , 655 KB - medinform_v13i1e57530_app1.doc]

Multimedia Appendix 2
Model residuals concerning the objective of predicting the time until the next unhealthy snack.
[DOCX File , 410 KB - medinform_v13i1e57530_app2.docx]

Multimedia Appendix 3
An alternative predictive objective.
[DOCX File , 478 KB - medinform_v13i1e57530_app3.docx]

References

1. GBD Compare Data Visualization. Institute for Health Metrics and Evaluation (IHME). URL: http://vizhub.healthdata.org/gbd-compare [accessed 2024-03-06]
2. Bolnick HJ, Bui AL, Bulchis A, Chen C, Chapin A, Lomsadze L, et al. Health-care spending attributable to modifiable risk factors in the USA: an economic attribution analysis. The Lancet Public Health 2020 Oct;5(10):e525-e535. [doi: 10.1016/s2468-2667(20)30203-6]
3. The Heavy Burden of Obesity. OECD. 2019. URL: https://www.oecd.org/en/publications/the-heavy-burden-of-obesity_67450d67-en.html [accessed 2025-04-10]

XSL•FO
RenderX

4. Marteau TM, Fletcher PC, Munafò MR, Hollands GJ. Beyond choice architecture: advancing the science of changing behaviour at scale. BMC Public Health 2021 Aug 10;21(1):1531 [FREE Full text] [doi: 10.1186/s12889-021-11382-8] [Medline: 34376159]
5. Lau Y, Chee DGH, Chow XP, Cheng LJ, Wong SN. Personalised eHealth interventions in adults with overweight and obesity: A systematic review and meta-analysis of randomised controlled trials. Prev Med 2020 Mar;132:106001. [doi: 10.1016/j.ypmed.2020.106001] [Medline: 31991155]
6. Myers-Ingram R, Sampford J, Milton-Cole R, Jones GD. Effectiveness of eHealth weight management interventions in overweight and obese adults from low socioeconomic groups: a systematic review. Syst Rev 2023 Mar 30;12(1):59 [FREE Full text] [doi: 10.1186/s13643-023-02207-3] [Medline: 36998094]
7. O'Boyle J, Davidson P. The effects of mHealth versus eHealth on weight loss in adults: a systematic review. Topics in Clinical Nutrition 2022;37(1):69-84 [FREE Full text]
8. Nahum-Shani I, Smith SN, Spring BJ, Collins LM, Witkiewitz K, Tewari A, et al. Just-in-time adaptive interventions (JITAIs) in mobile health: key components and design principles for ongoing health behavior support. Ann Behav Med 2018 May 18;52(6):446-462 [FREE Full text] [doi: 10.1007/s12160-016-9830-8] [Medline: 27663578]
9. Naughton F, Hopewell S, Lathia N, Schalbroeck R, Brown C, Mascolo C, et al. A context-sensing mobile phone app (Q Sense) for smoking cessation: a mixed-methods study. JMIR Mhealth Uhealth 2016 Sep 16;4(3):e106 [FREE Full text] [doi: 10.2196/mhealth.5787] [Medline: 27637405]
10. Naughton F, Cooper S, Foster K, Emery J, Leonardi-Bee J, Sutton S, et al. Large multi-centre pilot randomized controlled trial testing a low-cost, tailored, self-help smoking cessation text message intervention for pregnant smokers (MiQuit). Addiction 2017 Jul 02;112(7):1238-1249 [FREE Full text] [doi: 10.1111/add.13802] [Medline: 28239919]
11. Pimpini L, Franssen S, Reber P, Jansen A, Roefs A. Effects of a health versus hedonic mindset on daily-life snacking behaviour. J Hum Nutr Diet 2023 Oct 06;36(5):2085-2098. [doi: 10.1111/jhn.13221] [Medline: 37545043]
12. Cleobury L, Tapper K. Reasons for eating 'unhealthy' snacks in overweight and obese males and females. J Hum Nutr Diet 2014 Aug;27(4):333-341. [doi: 10.1111/jhn.12169] [Medline: 24134077]
13. Neal DT, Wood W, Wu M, Kurlander D. The pull of the past: when do habits persist despite conflict with motives? Pers Soc Psychol Bull 2011 Nov 22;37(11):1428-1437. [doi: 10.1177/0146167211419863] [Medline: 21859902]
14. Verhoeven AAC, Adriaanse MA, Evers C, de Ridder DTD. The power of habits: unhealthy snacking behaviour is primarily predicted by habit strength. Br J Health Psychol 2012 Nov;17(4):758-770. [doi: 10.1111/j.2044-8287.2012.02070.x] [Medline: 22385098]
15. Gardner B. A review and analysis of the use of 'habit' in understanding, predicting and influencing health-related behaviour. Health Psychol Rev 2015 Jan 21;9(3):277-295 [FREE Full text] [doi: 10.1080/17437199.2013.876238] [Medline: 25207647]
16. Jenkins KT, Tapper K. Resisting chocolate temptation using a brief mindfulness strategy. Br J Health Psychol 2014 Sep 17;19(3):509-522. [doi: 10.1111/bjhp.12050] [Medline: 23678870]
17. Hardeman W, Houghton J, Lane K, Jones A, Naughton F. A systematic review of just-in-time adaptive interventions (JITAIs) to promote physical activity. Int J Behav Nutr Phys Act 2019 Apr 03;16(1):31 [FREE Full text] [doi: 10.1186/s12966-019-0792-7] [Medline: 30943983]
18. Perski O, Hébert ET, Naughton F, Hekler EB, Brown J, Businelle MS. Technology-mediated just-in-time adaptive interventions (JITAIs) to reduce harmful substance use: a systematic review. Addiction 2022 May 11;117(5):1220-1241 [FREE Full text] [doi: 10.1111/add.15687] [Medline: 34514668]
19. UK mobile phone statistics. Uswitch. URL: https://www.uswitch.com/mobiles/studies/mobile-statistics/ [accessed 2025-04-12]
20. Almoraie NM, Saqaan R, Alharthi R, Alamoudi A, Badh L, Shatwan IM. Snacking patterns throughout the life span: potential implications on health. Nutr Res 2021 Jul;91:81-94. [doi: 10.1016/j.nutres.2021.05.001] [Medline: 34144310]
21. GBD 2017 Diet Collaborators. Health effects of dietary risks in 195 countries, 1990-2017: a systematic analysis for the Global Burden of Disease Study 2017. Lancet 2019 May 11;393(10184):1958-1972 [FREE Full text] [doi: 10.1016/S0140-6736(19)30041-8] [Medline: 30954305]
22. McArthur LH, Holbert D, Forsythe W. Is field of study or location associated with college students' snacking patterns? J Obes 2012;2012:297195-297110 [FREE Full text] [doi: 10.1155/2012/297195] [Medline: 22288006]
23. Ehrampoush E, Nazari N, Homayounfar R, Ghaemi A, Osati S, Tahamtan S, et al. Association between dietary patterns with insulin resistance in an Iranian population. Clinical Nutrition ESPEN 2020;36:45-52 [FREE Full text] [doi: 10.1016/j.clnesp.2020.02.011]
24. Wyatt P, Berry SE, Finlayson G, O'Driscoll R, Hadjigeorgiou G, Drew DA, et al. Author Correction: Postprandial glycaemic dips predict appetite and energy intake in healthy individuals. Nat Metab 2021 Jul 13;3(7):1032-1032. [doi: 10.1038/s42255-021-00436-1] [Medline: 34253908]
25. Arend A, Kaiser T, Pannicke B, Reichenberger J, Naab S, Voderholzer U, et al. Toward individualized prediction of binge-eating episodes based on ecological momentary assessment data: item development and pilot study in patients with bulimia nervosa and binge-eating disorder. JMIR Med Inform 2023 Feb 23;11:e41513 [FREE Full text] [doi: 10.2196/41513] [Medline: 36821359]

XSL•FO
RenderX

26. Forman E, Goldstein SP, Zhang F, Evans BC, Manasse SM, Butryn ML, et al. OnTrack: development and feasibility of a smartphone app designed to predict and prevent dietary lapses. Transl Behav Med 2019 Mar 01;9(2):236-245 [FREE Full text] [doi: 10.1093/tbm/iby016] [Medline: 29617911]
27. Kaiser T, Butter B, Arzt S, Pannicke B, Reichenberger J, Ginzinger S, et al. Time-lagged prediction of food craving with qualitative distinct predictor types: an application of BISCWIT. Front Digit Health 2021 Sep 20;3:694233. [doi: 10.3389/fdgth.2021.694233]
28. Spanakis G, Weiss G, Boh B, Lemmens L, Roefs A. Machine learning techniques in eating behavior e-coaching. Pers Ubiquit Comput 2017 Jun 8;21(4):645-659. [doi: 10.1007/s00779-017-1022-4]
29. Boh B, Lemmens LHJM, Jansen A, Nederkoorn C, Kerkhofs V, Spanakis G, et al. An Ecological Momentary Intervention for weight loss and healthy eating via smartphone and Internet: study protocol for a randomised controlled trial. Trials 2016 Mar 22;17(1):154 [FREE Full text] [doi: 10.1186/s13063-016-1280-x] [Medline: 27000058]
30. Brietzke E, Hawken ER, Idzikowski M, Pong J, Kennedy SH, Soares CN. Integrating digital phenotyping in clinical characterization of individuals with mood disorders. Neurosci Biobehav Rev 2019 Sep;104:223-230. [doi: 10.1016/j.neubiorev.2019.07.009] [Medline: 31330197]
31. Insel TR. Digital phenotyping: a global tool for psychiatry. World Psychiatry 2018 Oct 07;17(3):276-277 [FREE Full text] [doi: 10.1002/wps.20550] [Medline: 30192103]
32. Oudin A, Maatoug R, Bourla A, Ferreri F, Bonnot O, Millet B, et al. Digital phenotyping: data-driven psychiatry to redefine mental health. J Med Internet Res 2023 Oct 04;25:e44502 [FREE Full text] [doi: 10.2196/44502] [Medline: 37792430]
33. Prakash J, Chaudhury S, Chatterjee K. Digital phenotyping in psychiatry: When mental health goes binary. Ind Psychiatry J 2021;30(2):191-192 [FREE Full text] [doi: 10.4103/ipj.ipj_223_21] [Medline: 35017799]
34. Cho C, Lee T, Kim M, In HP, Kim L, Lee H. Mood prediction of patients with mood disorders by machine learning using passive digital phenotypes based on the circadian rhythm: prospective observational cohort study. J Med Internet Res 2019 Apr 17;21(4):e11029 [FREE Full text] [doi: 10.2196/11029] [Medline: 30994461]
35. Tulu B, Ruiz C, Allard J, Acheson J, Busch A, Roskuski A, et al. SlipBuddy: a mobile health intervention to prevent overeating. ScholarSpace. 2017. URL: https://scholarspace.manoa.hawaii.edu/items/7a174a16-00ce-4ba9-8a5f-6c86cccb51c5 [accessed 2025-04-10]
36. Lee TH, Ullah A, Wang R. Bootstrap Aggregating and Random Forest. In: Fuleky P, editor. Macroeconomic Forecasting in the Era of Big Data. Advanced Studies in Theoretical and Applied Econometrics, vol 52. Cham: Springer; 2020:389-429.
37. Fawagreh K, Gaber MM, Elyan E. Random forests: from early developments to recent advancements. Systems Science & Control Engineering 2014 Oct 06;2(1):602-609. [doi: 10.1080/21642583.2014.956265]
38. Brownlee J. XGBoost With Python: Gradient Boosted Trees with XGBoost and scikit-learn. San Juan, PR: Machine Learning Mastery; 2016.
39. Li Y, Li M, Li C, Liu Z. Forest aboveground biomass estimation using Landsat 8 and Sentinel-1A data with machine learning algorithms. Sci Rep 2020 Jun 19;10(1):9952 [FREE Full text] [doi: 10.1038/s41598-020-67024-3] [Medline: 32561836]
40. Ojha VK, Abraham A, Snášel V. Metaheuristic design of feedforward neural networks: A review of two decades of research. Engineering Applications of Artificial Intelligence 2017 Apr;60:97-116. [doi: 10.1016/j.engappai.2017.01.013]
41. Rumelhart DE, McClelland JL. Parallel Distributed Processing, Volume 1: Explorations in the Microstructure of Cognition: Foundations. Cambridge, MA: The MIT Press; 1986.
42. Hochreiter S, Schmidhuber J. Long short-term memory. Neural Comput 1997 Nov 15;9(8):1735-1780. [doi: 10.1162/neco.1997.9.8.1735] [Medline: 9377276]
43. Van Houdt G, Mosquera C, Nápoles G. A review on the long short-term memory model. Artif Intell Rev 2020 May 13;53(8):5929-5955. [doi: 10.1007/s10462-020-09838-1]
44. Qualtrics. URL: https://www.qualtrics.com/ [accessed 2025-04-12]
45. Prolific. URL: https://www.prolific.com/ [accessed 2025-04-12]
46. Goldenholz DM, Sun H, Ganglberger W, Westover MB. Sample size analysis for machine learning clinical validation studies. Biomedicines 2023 Feb 23;11(3):685 [FREE Full text] [doi: 10.3390/biomedicines11030685] [Medline: 36979665]
47. Dev Technosys. URL: https://devtechnosys.com/ [accessed 2025-04-12]
48. Twillo. URL: https://www.twilio.com/en-us [accessed 2025-04-12]
49. Berry KJ, Mielke PW, Iyer HK. Factorial designs and dummy coding. Percept Mot Skills 1998 Dec 01;87(3):919-927. [doi: 10.2466/pms.1998.87.3.919]
50. Albon C. Machine Learning with Python Cookbook. Sebastopol, CA: O'Reilly Media, Inc; 2018.
51. Pagan M, Zarlis M, Candra A. Investigating the impact of data scaling on the k-nearest neighbor algorithm. Comput Sci Inf Technol 2023 Jul 01;4(2):135-142. [doi: 10.11591/csit.v4i2.p135-142]
52. Salehin I, Kang D. A review on dropout regularization approaches for deep neural networks within the scholarly domain. Electronics 2023 Jul 17;12(14):3106. [doi: 10.3390/electronics12143106]
53. Reitermanova Z. Data Splitting. 2010 Presented at: 19th Annual Conference of Doctoral Students; June 1-4, 2010; Prague, Czech Republic.
54. Hyndman RJ, Athanasopoulos G. Forecasting: Principles and Practice (3rd ed). Melbourne, Australia: OTexts; 2015.

XSL•FO
RenderX

55. Fuller WA. Measurement Error Models. Hoboken, NJ: John Wiley & Sons, Inc; 2009.
56. Obesity in adults. Our World in Data. URL: https://ourworldindata.org/grapher/share-of-adults-defined-as-obese [accessed 2024-03-06]
57. ArunKumar K, Kalaga DV, Mohan Sai Kumar C, Kawaji M, Brenza TM. Comparative analysis of Gated Recurrent Units (GRU), long Short-Term memory (LSTM) cells, autoregressive Integrated moving average (ARIMA), seasonal autoregressive Integrated moving average (SARIMA) for forecasting COVID-19 trends. Alexandria Engineering Journal 2022 Oct;61(10):7585-7603. [doi: 10.1016/j.aej.2022.01.011]
58. Bangamuarachchi W, Chamantha A, Meegahapola L, Ruiz-Correa S, Perera I, Gatica-Perez D. Sensing eating events in context: a smartphone-only approach. IEEE Access 2022;10:61249-61264. [doi: 10.1109/access.2022.3179702]
59. Chen F, Wang R, Zhou X, Campbell AT. My smartphone knows i am hungry. In: WPA '14: Proceedings of the 2014 workshop on physical analytics. 2014 Presented at: 12th Annual International Conference on Mobile Systems, Applications, and Services; June 16, 2014; Bretton Woods, NH. [doi: 10.1145/2611264.2611270]
60. Cifuentes L, Ghusn W, Feris F, Campos A, Sacoto D, De la Rosa A, et al. Phenotype tailored lifestyle intervention on weight loss and cardiometabolic risk factors in adults with obesity: a single-centre, non-randomised, proof-of-concept study. EClinicalMedicine 2023 Apr;58:101923 [FREE Full text] [doi: 10.1016/j.eclinm.2023.101923] [Medline: 37007741]
61. Tapper K, Baker L, Jiga-Boy G, Haddock G, Maio GR. Sensitivity to reward and punishment: Associations with diet, alcohol consumption, and smoking. Personality and Individual Differences 2015 Jan;72:79-84. [doi: 10.1016/j.paid.2014.08.025]
62. Pentikäinen S, Arvola A, Karhunen L, Pennanen K. Easy-going, rational, susceptible and struggling eaters: A segmentation study based on eating behaviour tendencies. Appetite 2018 Jan 01;120:212-221. [doi: 10.1016/j.appet.2017.09.001] [Medline: 28888729]
63. Dakin CA, Finlayson G, Horgan G, Palmeira AL, Heitmann BL, Larsen SC, et al. Exploratory analysis of reflective, reactive, and homeostatic eating behaviour traits on weight change during the 18-month NoHoW weight maintenance trial. Appetite 2023 Oct 01;189:106980 [FREE Full text] [doi: 10.1016/j.appet.2023.106980] [Medline: 37495176]
64. Branco P, Torgo L, Ribeiro R. A Survey of Predictive Modelling under Imbalanced Distributions. arXiv. 2015. URL: https://arxiv.org/abs/1505.01658 [accessed 2025-04-10]
65. Schneidergruber T, Blechert J, Arzt S, Pannicke B, Reichenberger J, Arend A, et al. Predicting food craving in everyday life through smartphone-derived sensor and usage data. Front Digit Health 2023 Jun 26;5:1163386 [FREE Full text] [doi: 10.3389/fdgth.2023.1163386] [Medline: 37435352]
66. He J, Mao R, Shao Z, Zhu F. Incremental Learning in Online Scenario. 2020 Presented at: 2020 IEEE/CVF Conference on Computer Vision and Pattern Recognition (CVPR); June 13-19, 2020; Seattle, WA. [doi: 10.1109/CVPR42600.2020.01394]
67. Wilson E, Senior V, Tapper K. The effect of visualisation and mindfulness-based decentering on chocolate craving. Appetite 2021 Sep 01;164:105278. [doi: 10.1016/j.appet.2021.105278] [Medline: 33905790]
68. Unhealthy Snacking Predictions. OSF. URL: https://osf.io/xkz4n/?view_only=7b1a3be89080432db8973d9ac35b43db [accessed 2025-04-12]

Abbreviations

API: application programming interface
EMA: ecological momentary assessment
FFNN: feed forward neural network
HFSS: high saturated fats, salt, or sugar
JITAI: just-in-time adaptive intervention
LSTM: long short-term memory
MAE: mean absolute error
ML: machine learning
RFreg: random forest regressor
XGBreg: Extreme Gradient Boosting regressor

XSL•FO
RenderX

Edited by A Coristine; submitted 20.02.24; peer-reviewed by LN Laan, A Hassan, AK Arend; comments to author 06.04.24; revised version received 31.07.24; accepted 28.03.25; published 23.04.25.

Please cite as:
Dammas S, Weyde T, Tapper K, Spanakis G, Roefs A, Pothos EM
Prediction of Snacking Behavior Involving Snacks Having High Levels of Saturated Fats, Salt, or Sugar Using Only Information on Previous Instances of Snacking: Survey- and App-Based Study
JMIR Med Inform 2025;13:e57530
URL: https://medinform.jmir.org/2025/1/e57530
doi:10.2196/57530
PMID:

©Shaima Dammas, Tillman Weyde, Katy Tapper, Gerasimos Spanakis, Anne Roefs, Emmanuel M Pothos. Originally published in JMIR Medical Informatics (https://medinform.jmir.org), 23.04.2025. This is an open-access article distributed under the terms of the Creative Commons Attribution License (https://creativecommons.org/licenses/by/4.0/), which permits unrestricted use, distribution, and reproduction in any medium, provided the original work, first published in JMIR Medical Informatics, is properly cited. The complete bibliographic information, a link to the original publication on https://medinform.jmir.org/, as well as this copyright and license information must be included.

XSL•FO
RenderX

Original Paper

Prediction of Spontaneous Breathing Trial Outcome in Critically Ill-Ventilated Patients Using Deep Learning: Development and Verification Study

Hui-Chiao Yang[1], MSc; Angelica Te-Hui Hao[2,3], MSc; Shih-Chia Liu[2,4], PhD; Yu-Cheng Chang[5], MSc; Yao-Te Tsai[6], PhD; Shao-Jen Weng[4], PhD; Ming-Cheng Chan[7], MD, PhD; Chen-Yu Wang[7], MD, PhD; Yeong-Yuh Xu[8], PhD

[1]Department of Chest Medicine, Division of Respiratory Therapy, Taichung Veterans General Hospital, Taichung, Taiwan

[2]Department of Nursing, Hungkuang University, Taichung, Taiwan

[3]Department of Information Management, National Central University, Taoyuan, Taiwan

[4]Department of Industrial Engineering and Enterprise Information, Tunghai University, Taichung, Taiwan

[5]Department of Computer and Communications Center, Taichung Veterans General Hospital, Taichung, Taiwan

[6]Department of Information Management, National Kaohsiung University of Science and Technology, Kaohsiung, Taiwan

[7]Department of Critical Care Medicine, Taichung Veterans General Hospital, Taichung, Taiwan

[8]Department of Artificial Intelligence and Computer Engineering, National Chin-Yi University of Technology, Taichung, Taiwan

Corresponding Author:
Yeong-Yuh Xu, PhD
Department of Artificial Intelligence and Computer Engineering
National Chin-Yi University of Technology
No.57, Sec. 2, Zhongshan Rd., Taiping Dist.
Taichung, 41170
Taiwan
Phone: 886 4 2392 4505 ext 8501
Fax: 886 4 2391 7331
Email: yyxu@ncut.edu.tw

Abstract

Background: Long-term ventilator-dependent patients often face problems such as decreased quality of life, increased mortality, and increased medical costs. Respiratory therapists must perform complex and time-consuming ventilator weaning assessments, which typically take 48-72 hours. Traditional disengagement methods rely on manual evaluation and are susceptible to subjectivity, human errors, and low efficiency.

Objective: This study aims to develop an artificial intelligence–based prediction model to predict whether a patient can successfully pass a spontaneous breathing trial (SBT) using the patient's clinical data collected before SBT initiation. Instead of comparing different SBT strategies or analyzing their impact on extubation success, this study focused on establishing a data-driven approach under a fixed SBT strategy to provide an objective and efficient assessment tool. Through this model, we aim to enhance the accuracy and efficiency of ventilator weaning assessments, reduce unnecessary SBT attempts, optimize intensive care unit resource usage, and ultimately improve the quality of care for ventilator-dependent patients.

Methods: This study used a retrospective cohort study and developed a novel deep learning architecture, hybrid CNN-MLP (convolutional neural network–multilayer perceptron), for analysis. Unlike the traditional CNN-MLP classification method, hybrid CNN-MLP performs feature learning and fusion by interleaving CNN and MLP layers so that data features can be extracted and integrated at different levels, thereby improving the flexibility and prediction accuracy of the model. The study participants were patients aged 20 years or older hospitalized in the intensive care unit of a medical center in central Taiwan between January 1, 2016, and December 31, 2022. A total of 3686 patients were included in the study, and 6536 pre-SBT clinical records were collected before each SBT of these patients, of which 3268 passed the SBT and 3268 failed.

Results: The model performed well in predicting SBT outcomes. The training dataset's precision is 99.3% (2443/2460 records), recall is 93.5% (2443/2614 records), specificity is 99.3% (2597/2614 records), and F_1-score is 0.963. In the test dataset, the model maintains accuracy with a precision of 89.2% (561/629 records), a recall of 85.8% (561/654 records), a specificity of 89.6%

XSL•FO
RenderX

(586/654 records), and an F_1-score of 0.875. These results confirm the reliability of the model and its potential for clinical application.

Conclusions: This study successfully developed a deep learning–based SBT prediction model that can be used as an objective and efficient ventilator weaning assessment tool. The model's performance shows that it can be integrated into clinical workflow, improve the quality of patient care, and reduce ventilator dependence, which is an important step in improving the effectiveness of respiratory therapy.

(JMIR Med Inform 2025;13:e64592) doi:10.2196/64592

KEYWORDS

ventilator; ventilator weaning; respiratory therapy; intensive care unit; artificial intelligence; deep learning; neural networks; spontaneous breathing trial

Introduction

According to statistics from the National Health Insurance Administration, Taiwan saw an increase of 175,148 patients dependent on ventilators in 2017, with 70% of intensive care unit (ICU) patients requiring ventilator support. This significant trend in ventilator usage persists in Taiwan, irrespective of its impact on ongoing health crises. The current medical practice requirements involving ventilator use include initiating ventilator support, conducting spontaneous breathing tests, and assessing readiness for ventilator weaning. In practical terms, respiratory therapists must perform a ventilator weaning assessment before a spontaneous breathing trial (SBT). This process is complex, meticulous, time-consuming, and spans a period of 48-72 hours. In other words, successful weaning from a ventilator for patients depends on passing an SBT.

In retrospective studies [1,2], confirming whether all patients receive the same SBT strategy is essential based on the specific study design. SBT strategies typically include fixed pressure support (PS) and positive end-expiratory pressure (PEEP). In this paper, the study's SBT strategy was set at a PS of 10 cm H_2O and a PEEP of 5 cm H_2O, lasting 2 hours. A successful SBT is generally defined as the patient's ability to maintain a stable respiratory state during the trial without mechanical ventilation support and be safely extubated at the end of the trial. An unsuccessful SBT is defined as a patient experiencing respiratory distress, hypoxemia, hypercapnia, or other conditions requiring the reinitiation of mechanical ventilation during the trial.

Conventional weaning criteria often involve manual selection, with therapists assessing patients based on their responses to a ventilator weaning assessment form to determine if they are eligible for an SBT. However, previous studies have explored the use of information systems to automate ventilator weaning assessments, revealing that this approach can reduce ventilator usage time and enhance the efficiency of respiratory therapists [3]. Research also suggests that automated weaning protocols may decrease the weaning period, theoretically surpassing the need for manual weaning [4,5]. Studies have investigated consciousness status, oxygenation, ventilation modes, and airway protection strategies [6]. Reducing ventilator usage time, weaning time, and ICU stay has been discussed [7]. At the same time, certain elements that cannot be automated in the weaning process have been pointed out [8]. Daily screening methods have effectively decreased dependence on ventilators [9].

Recently, numerous studies have investigated the impact of SBT, including assessing the relationship between end-expiratory lung volumes during SBT and successful ventilator weaning [10]. Some studies have suggested considering respiratory rate (RR) and ventilation time in patients intubated in the ICU for more than 72 hours before extubation after passing an SBT [11]. In different populations, research has cautioned against using an SBT to assess the appropriate timing of extubation for premature infants [12]. Additionally, studies have proposed methods for evaluating extubation in neonates through minimal pressure SBTs [13], by measuring diaphragmatic electrical activity in premature infants to predict extubation success [14], and investigating optimal duration and reasons for failure in pediatric SBTs, noting that a 30-minute SBT may be too brief for pediatric acute respiratory distress syndrome patients in the recovery phase [15]. The impact of SBT on extubation success and prognosis in patients diagnosed with acute exacerbation of chronic obstructive pulmonary disease has been evaluated [16]. On another note, some studies have used oxygen saturation as a crucial indicator for predicting SBT success or failure [17].

However, the factors affecting SBTs and ventilator weaning are diverse and include age [18-20], weaning prediction parameters, sputum volume, cough strength, and consciousness status [21-23], as well as ventilator usage time, disease severity (acute physiology and chronic health evaluation II), and patient nutritional status. Patients experiencing difficult or delayed weaning are often presented with a combination of factors, thus requiring careful assessment by health care professionals. Due to the complexity of patient weaning from ventilators, numerous studies have explored various aspects. For instance, the impact of adding different doses of sedatives (ketamine) on spontaneous breathing patients [24], the correlation between microcirculation during SBTs and successful extubation [25], and for patients passing an SBT, a spontaneous awakening trial could serve as a predictive factor for extubation on the same day. It has also been noted that a higher Richmond Agitation Sedation Scale, no sedative administration on the previous day, no infections, and the absence of neurological diseases or hemodynamic instability increase the chances of extubation on the same day [26].

XSL•FO
RenderX

Using varied SBT strategies can affect outcomes in different studies [27,28]. These differences primarily manifest in several aspects, such as the level of PS, PEEP settings, continuous positive airway pressure (CPAP) use, and the T-piece trial. The level of PS directly impacts the patient's ability to breathe spontaneously. Higher PS, such as 10 cm H_2O, reduces the patient's breathing effort, potentially leading to a higher SBT success rate. However, this may not fully reflect the patient's breathing capacity at lower support levels. The setting of PEEP affects alveolar stability and airway pressure. Different PEEP settings, such as 5 cm H_2O, can have varying impacts on a patient's oxygenation and respiratory dynamics, thereby altering the outcomes of the SBT. CPAP provides continuous positive PS, helping to reduce the work of breathing. Conducting an SBT with CPAP at 5 cm H_2O may make it easier for patients to pass the trial. However, compared to PS strategies, this might offer a different assessment of the patient's respiratory muscle function. The T-piece trial provides no PS, relying entirely on the patient's spontaneous breathing ability. This strategy more accurately reflects the patient's autonomous breathing capacity but may result in a lower SBT success rate due to higher demands on the patient.

Given these differences, it is crucial to recognize how varying SBT strategies can influence the interpretation and comparison of study outcomes. The choice of SBT strategy can significantly affect clinical decisions and patient management. Therefore, understanding the potential impacts of different strategies is essential for improving patient care and optimizing treatment protocols.

Different SBT strategies will lead to varying SBT success rates. Higher PS or the use of CPAP might result in higher success rates, while the T-piece trial might lead to lower success rates. Variations in SBT strategy might also affect postextubation outcomes. If an SBT strategy makes it easier for patients to pass the trial, it could increase the risk of postextubation respiratory distress or the need for reintubation. Due to the different SBT strategies used in various studies, caution is needed when directly comparing study results. The potential impacts of strategy differences on outcomes should be considered.

Artificial intelligence (AI) integrated with health care aims to predict disease diagnosis or prevention through medical alerts. In the current trend of AI applications, incorporating physician expertise into the training of predictive models can provide appropriate treatment for high-risk patients [29]. AI applications in health care include medical robots, AI intelligent diagnosis and image recognition, intelligent drug development, and intelligent health management. Intelligent health management applies AI technology to daily health management, focusing on risk identification, virtual nurses, mental health, web-based consultations, and precision medicine-based health management. Certain studies have used deep learning combined with random forest for risk prediction. One study constructed and validated machine learning models to predict unplanned extubation in ICU patients using electronic health record (EHR) data [30]. Another study developed machine learning algorithms to predict the likelihood of successful weaning from mechanical ventilation using clinical and laboratory data obtained before or shortly after intubation [31]. Recent developments have also explored using reinforcement learning to optimize ventilator management. Using real-world ICU data, a reinforcement learning–based model, EZ-Vent, was proposed to dynamically adjust ventilator settings such as PEEP, FiO_2 (fraction of inspired oxygen), and tidal volume [32]. A broader review further emphasized the potential of reinforcement learning as a clinical decision support tool in the ICU, highlighting its application in optimizing mechanical ventilation and predicting outcomes related to SBTs [33]. By way of explanation, the introduction of AI can process more significant amounts of data faster, achieve higher accuracy, and assist in decision-making without medical staff experiencing fatigue, thereby implementing intelligent health care models.

The main objective of this study was to develop an AI-based prediction model to predict the outcome of an SBT under a specific SBT strategy using a pre-SBT clinical record gathered just before a patient's SBT. The proposed model is trained and validated based on pre-SBT clinical records to ensure that the model can predict whether an SBT will succeed under a fixed SBT strategy. The proposed model can provide clinicians with an objective and reliable decision-making aid to reduce the subjectivity and errors of traditional manual judgment. The ultimate goal is to facilitate timely and effective clinical decision-making, optimize the weaning process from the ventilator, and improve ICU management efficiency.

Methods

Data Source

The respiratory information system database of Taichung Veterans General Hospital served as the data source for this study. We covered the research period from January 1, 2016, to December 31, 2022. We conducted a retrospective case review, including patients aged 20 and older admitted to the ICU during this period. The data were accessed on April 7, 2023, for research purposes. The clinical data were collected from 3686 patients, comprising 6536 pre-SBT clinical records gathered just before each SBT of patients. Among these records, 3268 passed the SBT, while the other 3268 did not pass. Each clinical record includes 2 demographic variables, 7 respiratory parameters, and 5 vital signs, as detailed below (Textbox 1).

The pre-SBT clinical records serve as input features for model training and prediction. These input features comprehensively represent the patient's respiratory and physiological status, providing critical information for the model to assess SBT outcomes effectively. In total, 80% (5228/6536 records) were allocated for training, while the remaining 20% (1308/6536 records) were reserved for testing. In addition, the division process of the training and test datasets follows a random split strategy to ensure that the proportions of different categories (those who passed and failed SBT) remain balanced to avoid bias in the model.

XSL•FO
RenderX

Textbox 1. Details of clinical record.

- Age—Patient's age
- Gender—Patient's gender
- FiO_2 (%)—Fraction of inspired oxygen, indicating the percentage of oxygen the patient is inhaling
- PaO_2 (mm Hg)—Partial pressure of oxygen in arterial blood
- VTe (exhaled VT) (mL)—Exhaled tidal volume per breath
- Measured respiratory rate (bpm)—Measured respiratory rate, defined as breaths per minute
- Paw (cm H_2O)—Peak airway pressure, the highest pressure reached during inhalation
- MAP (cm H_2O)—Mean airway pressure, representing the average pressure in the airways over the respiratory cycle
- MVe (exhaled MV)—Minute ventilation, the total volume of air exhaled per minute
- Heart rate (bpm)—Number of heart beats per minute
- Systolic blood pressure (mm Hg)—Blood pressure during heart contraction
- Diastolic blood pressure (mm Hg)—Blood pressure during heart relaxation
- SpO_2 (%)—Oxygen saturation, indicating the percentage of oxygenated hemoglobin in the blood
- Body temperature (°C)—Core body temperature of the patient

Ethical Considerations

This study was reviewed and approved by the institutional review board (IRB) of Taichung Veterans General Hospital (IRB number: CE23123A), in accordance with institutional and national ethical standards for human subjects research.

The study involved a retrospective analysis of clinical data. All patient data were fully anonymized prior to access and analysis to ensure privacy and confidentiality.

Given the study's retrospective nature and the anonymization of all data, the IRB waived the requirement for informed consent.

No compensation was provided, as no direct contact with participants occurred, and no new data were collected.

Spontaneous Breathing Test and Ventilator Weaning Assessment

The successful determination of an SBT was defined as a patient undergoing a spontaneous breathing test for 2 hours with the ventilator mode PS level set at 10 cm H_2O and PEEP set at 5 cm H_2O. Additionally, the patient had to meet the Wean Score criteria to be considered a successful SBT. Therefore, this study included model analysis based on the following inclusion criteria (Textbox 2).

Textbox 2. Inclusion and exclusion criteria.

Inclusion criteria

- Pressure support (PS) level set at 10 cm H_2O and positive end-expiratory pressure (PEEP) set at 5 cm H_2O.

Exclusion criteria

- PS level greater or PS level less than 10 cm H_2O, and PEEP greater or less than 5 cm H_2O.

Model Design

Given the constant advancements in technology, machine learning has now become widely used, primarily due to the effectiveness of information products. As a subset of data science, machine learning is now being further extended through the branch of deep learning. Therefore, we can generate models from extensive data through machine learning and develop predictions for various outcomes using existing data.

Deep learning is an algorithm centered within machine learning that focuses on representation learning from data. Several deep learning architectures exist, including deep belief networks, recurrent neural networks, and convolutional neural networks (CNNs). CNNs, a highly representative data-driven architecture, require large, high-quality datasets for effective model training. Data augmentation, transfer learning from pretrained models, and semi-automatic annotation are often used to address this issue. In the training phase of this study, multiple training datasets were prepared, each including the status feature inputs and corresponding outputs from various investigations of the study cases. CNNs succeed in image recognition and object detection because they can automatically extract spatial hierarchical features from images. Although this study does not include direct visual data, the characteristics of CNNs make it suitable for processing structured nonvisual data [34]. For instance, the convolutional layers of CNNs excel at capturing local patterns and correlations within the data, irrespective of whether these patterns come from spatial features in images,

XSL•FO
RenderX

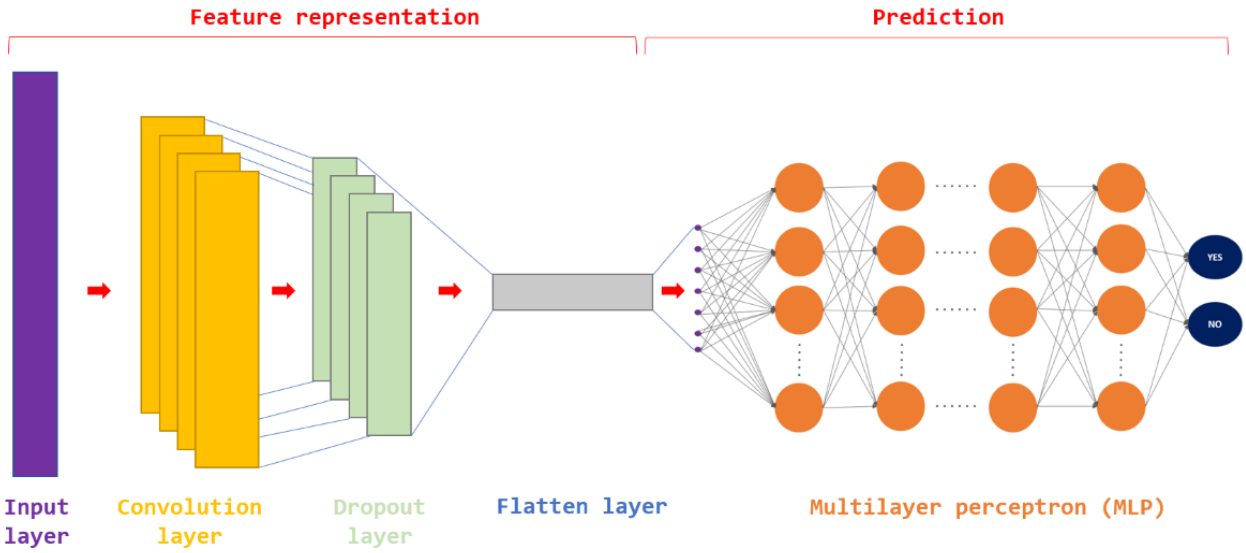
structural features in time-series data, or multidimensional matrices. We used a deep CNN to learn the features of older adults' mental health before storing them in the network. Challenges in this process include preparing training data and designing learning algorithms. Subsequently, we tailor a learning algorithm suitable for the characteristics of the training data [35,36].

At the initial stage, the neural network is assigned random weight values, with its output differing significantly from the standard answer. After multiple learning iterations, the weights gradually adjust in the correct direction, resulting in a better or more accurate prediction. Given the multitude of feature factors influencing the prediction results of ventilator weaning, finding appropriate or correct features amongst the numerous characteristics is highly challenging.

Using the learning characteristics of deep learning, the model can autonomously deduce the characteristics of feature factors from the training data, thereby establishing a highly accurate prediction model. Figure 1 illustrates the architectural layout of the traditional CNN-MLP (convolutional neural network–multilayer perceptron) model. The model design begins with the input layer having the same number of neurons as the dimensions of the dataset. Subsequently, it connects to multiple convolutional layers, with pooling layers interspersed between them. Their primary function is to extract key features from the training data autonomously. Finally, the network concludes with a fully connected multilayer perceptron (MLP), transforming these features into 2 outputs. Selecting appropriate model initialization parameters is crucial for both the stability and convergence of training.

The optimization of the CNN model's ideal architecture is influenced by the task's complexity and the dataset's features. Since deep learning is primarily based on empirical learning methods, the efficiency of CNN models often stems from practical testing and iterative adjustments. The results of preliminary models can also serve as reference points for measuring performance improvements.

Figure 1. Architecture diagram of traditional CNN-MLP model. CNN: convolutional neural network.

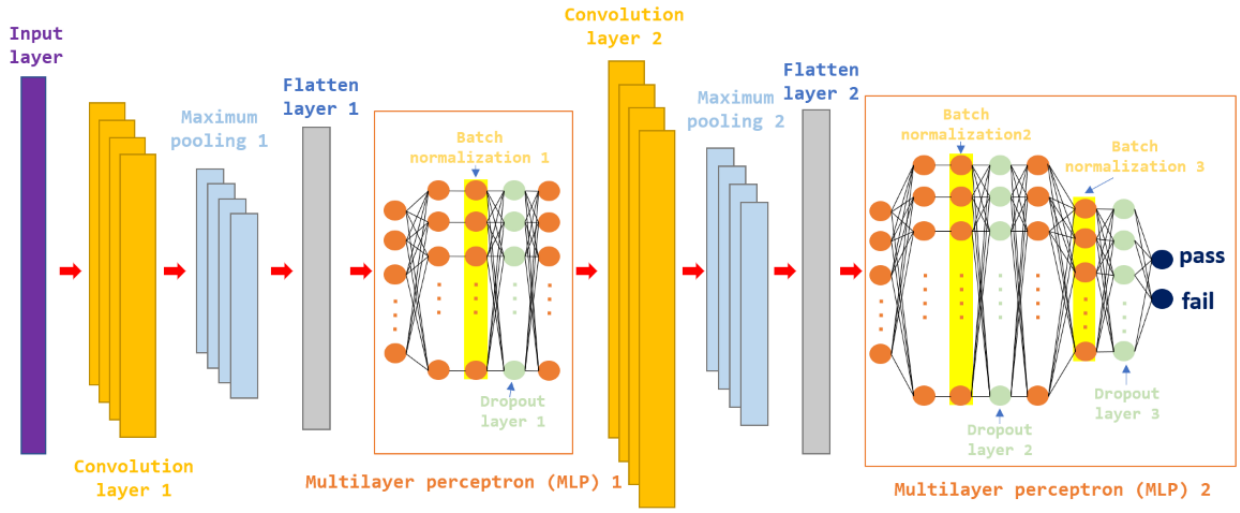


In this study, we proposed a novel deep learning architecture, hybrid CNN-MLP, to predict the outcome of an SBT. Figure 2 depicts the proposed hybrid CNN-MLP model architecture in this study. Unlike the traditional CNN-MLP classification method, hybrid CNN-MLP performs feature learning and fusion by interleaving CNN and MLP layers so that data features can be extracted and integrated at different levels, thereby improving the flexibility and prediction accuracy of the model.

This study begins with a simple framework for the hybrid CNN-MLP design, gradually increasing its complexity by adjusting the number of layers and neurons. Starting with a straightforward structure accelerates training and evaluation, streamlining the continuous refinement of the hybrid CNN-MLP model. The hybrid CNN-MLP model architecture is explained as follows (Textbox 3).

XSL•FO
RenderX

Figure 2. Architecture diagram of the hybrid CNN-MLP model. CNN: convolutional neural network.



Textbox 3. Hybrid CNN-MLP (convolutional neural network–multilayer perceptron) model architecture.

The first CNN module

- Convolutional layer (14×64): the input channels are 14, the output channels are 64, and convolutional feature extraction is performed.
- Maximum pooling layer (kernel_size=2, stride=2): dimensionality reduction to retain the main features and reduce the amount of computation.

MLP (fully connected layer)

- Flatten layer: flatten the features extracted by CNN so that they can be input into the fully connected layer.
- Linear layer (64×128): fully connected layer with output dimensions of 128.
- Batch normalization layer (128): Stabilizes the training process.
- Dropout layer (*P*=.50): randomly inactivate 50% of neurons to prevent overfitting.
- Linear layer (128×128): fully connected, keeping the same dimension.

The second CNN module

- Convolutional layer (128×64): performs the convolution operation again.
- Maximum pooling layer (kernel_size=2, stride=2): reduces the dimension again to improve the generalization ability of the model.

The second phase of MLP

- Flatten layer: flatten into a vector for feeding into the MLP layer.
- Linear layer (64×256): fully connected layer with output dimensions of 256.
- Batch normalization layer (256): batch normalization to improve training stability.
- Dropout layer (*P*=.50): prevent overfitting.
- Linear layer (256×64): fully connected layer, reducing the dimension to 64.
- Batch normalization layer (64): batch normalization.
- Dropout layer (*P*=.30): reduce overfitting by inactivating 30% of neurons.
- Linear layer (64×2): output layer, the final output is 2-dimensional (probably representing a binary classification problem).

In the network used in this study, the Xavier Glorot initialization method [1] was used to assign weights. This method mitigates potential issues, particularly gradient vanishing or exploding problems in deep networks, by adjusting weights based on the quantity of input and output units. This ensures a smoother and more effective training process.

To avoid overfitting, we adopt multiple strategies to ensure the stability and generalization ability of the model. First, we use L2 regularization (weight decay) to discourage overly complex models from memorizing too much training data. Second, during the model training process, we applied the dropout technology to randomly deactivate some neurons to reduce the overadaptation (coadaptation) between neurons and improve the model's generalization ability. We also adopt the early

XSL•FO
RenderX

stopping strategy to monitor the loss changes of the validation set during training. When the validation loss fails to decrease within several consecutive training cycles, training is stopped to prevent the model from overfitting to the training data. In addition, to ensure that the model is not too complex, we control the number of layers and neurons in the neural network to balance learning and generalization abilities.

Regarding hyperparameter tuning, we conducted multiple experiments to optimize the model performance. First, in terms of learning rate adjustment, we initially set it to 0.001 and used learning rate decay to gradually reduce the learning rate during training to improve convergence stability. For batch size, we tested different values, such as 32, 64, and 128, and finally chose 64 to balance training efficiency and model stability. Regarding the activation function, the hidden layer uses Rectified Linear Unit to solve the gradient disappearance problem, and the output layer uses Softmax for classification. For the optimizer, we tested Adam and Stochastic Gradient Descent and finally chose Adam because it performed best regarding convergence speed and stability. Finally, in terms of network architecture, we tested different numbers of layers and neuron configurations to ensure that the model can effectively learn data features while avoiding overfitting problems caused by excessive complexity.

During the training of the deep learning network model, this study inputs labeled data into the network, uses backpropagation and the Adam optimization algorithm, and adjusts the network weights based on the loss calculated using the binary cross-entropy function. On the other hand, the batch size used in this study is 64, with the model undergoing training for 6000 iterations. Of the dataset, 80% (5228/6536 records) is used as the training dataset, while the remaining 20% (1308/6536 records) is designated as the testing dataset to evaluate the model's performance on previously unseen data. Regular checkpoints and an early stopping mechanism ensure that the model used in this study does not overfit and retains its optimal performance architecture.

This study aims to develop a neural network model suitable for predicting respiratory outcomes. It aims to serve as an assessment standard and prediction tool for respiratory care, thus helping health care professionals provide higher quality health care. In establishing this study's intelligent respiratory care model, the prediction variable is based on the success or failure of the SBT, with relevant respiratory information incorporated into the model training.

Evaluation Indexes

This study aims to develop an AI-based model to predict whether patients can successfully pass an SBT. Since SBT is a key test for whether mechanically ventilated patients can breathe spontaneously, and its prediction results directly affect clinical decision-making, it is crucial to evaluate the model's accuracy. This study adopted a variety of evaluation indicators to ensure the reliability and stability of the model in clinical applications.

When we try to predict whether a patient will successfully pass the SBT, accuracy alone may not be sufficient to evaluate the model's performance fully. Accuracy represents the proportion of all participants correctly predicted and is applicable when the proportion of SBT passes and fails is equal. However, if the data's ratio of successes to failures is unbalanced, focusing only on accuracy may lead to falsely optimistic estimates. For example, if most patients can successfully pass the SBT, and the model only predicts that “all patients will succeed,” although the accuracy may be high, it cannot effectively assist clinical decision-making. Therefore, we use precision and recall to evaluate the model's effectiveness.

Precision measures the proportion of patients predicted by the model to pass the SBT who did. This is crucial to avoid unnecessary SBTs. If the model's precision is too low, it means that among the successful cases it predicts, many patients actually cannot pass the SBT, which may lead to initiating SBT too early, resulting in respiratory muscle fatigue, hypoxemia, and even acute respiratory failure in patients. Therefore, a higher precision ensures that the model has a higher credibility when recommending the initiation of SBT.

Recall (also known as sensitivity) measures how many of the patients who successfully passed the SBT were correctly identified by the model. This has a critical impact on avoiding erroneous prolongation of mechanical ventilation. If the recall rate is too low, it means that many patients who should be able to be successfully weaned are incorrectly predicted to be unable to pass the SBT, causing them to continue to be maintained on mechanical ventilation, which may increase the risk of lung infection or muscle atrophy. Therefore, the higher recall ensures that no patients who can pass the SBT are missed.

In addition to precision and recall, this study also calculates the F_1-score, which is a comprehensive indicator used to balance the trade-off between precision and recall. In clinical decision-making, we hope to ensure that the SBT is successfully passed (high precision) while not missing patients who should be able to pass the SBT (high recall), so the F_1-score can be used as a measure of the overall effectiveness of the model.

Specificity is also an important evaluation indicator, measuring whether the model can correctly identify patients who cannot pass SBT. High specificity indicates that the model is effective in avoiding erroneous attempts to start SBTs in patients who cannot pass SBT. Finally, we also considered the false positive rate (FPR) and false negative rate (FNR) to analyze the model's error prediction pattern further and help clinicians understand the model's performance in different scenarios.

Based on the predictive results of the proposed model, we can obtain the following parameters: true positive, false positive, false negative, and true negative. Details of the evaluation metric formulas are available in Multimedia Appendix 1. The receiver operating characteristic (ROC) curve is an important tool for evaluating the classification ability of a model. It describes the changes in the true positive rate (TPR; recall rate) and FPR of the model at different decision thresholds. When the threshold is lower, the model is more likely to predict positive cases; TPR will increase, but FPR may also increase. When the threshold is higher, the model becomes more conservative, and FPR decreases, but some true positive cases may be missed. The closer the ROC curve is to the upper left corner, the better the classification ability of the model, while the ROC curve on the

XSL•FO
RenderX

diagonal indicates that the classification effect of the model is no different from random guessing.

Area under the curve (AUC) is the area under the ROC curve, with a value range of 0-1, representing the overall classification ability of the model. The closer the AUC is to 1, the more stable the model is at different thresholds and the more effective it is in distinguishing different categories. In the SBT prediction model, a high AUC value means that the model can more accurately distinguish which patients can successfully pass the SBT and which patients still need mechanical ventilation support.

Results

Table 1 presents the study cases' demographic variables, respiratory parameters, and vital signs. Among the cases, the average age of patients is around 67.5 (SD 16.3) years. In the successful SBT group, the average age is 68.5 (SD 15.3) years, while in the failure group, it is 66.5 (SD 17.2) years. Regarding gender distribution, 4091 out of 6536 (62.6%) patients are male. Among them, 1178 of 3268 (36%) patients were in the successful SBT group, while 2913 of 3268 (89.1%) patients were in the failure group.

Table 1. Characteristics of intubated patients in the intensive care unit.

	Case group		
	Successful SBT[a] (n=3268)	Failure of SBT (n=3268)	Total (N=6536)
Demographic			
Age (years), mean (SD)	68.5 (15.3)	66.5 (17.2)	67.5 (16.3)
Gender, n (%)			
Male	1178 (36.0)	2913 (89.1)	4091 (62.6)
Female	2090 (64.0)	355 (10.9)	2445 (37.4)
Mechanical ventilator settings and respiratory function, mean (SD)			
FiO_2[b] (%)	32.9 (6.2)	37.5 (11.8)	35.2 (9.7)
PaO_2[c] (mm Hg)	107.4 (20.2)	109.6 (27.9)	108.5 (24.4)
VTe[d] (exhaled VT; mL)	0.6 (1.7)	0.9 (2.9)	0.8 (2.4)
Measured RR[e] (bpm)	19 (8)	21 (10)	20 (9)
Paw[f] (cm H_2O)	16.3 (1.9)	22.5 (5.2)	19.4 (5.0)
MAP[g] (cm H_2O)	8.3 (1.2)	11.3 (3.2)	9.8 (2.8)
MVe[h] (exhaled MV; Lpm)	8.0 (3.0)	7.9 (2.4)	7.9 (2.7)
Vital signs, mean (SD)			
Heart rate (bpm)	84.9 (16.7)	87.6 (18.9)	86.2 (17.9)
Systolic blood pressure (mm Hg)	126.5 (20.2)	122.7 (22.5)	124.6 (21.5)
Diastolic blood pressure (mm Hg)	71.7 (14.4)	68.1 (15.4)	69.9 (15.0)
SpO_2[i] (%)	99 (2)	98 (3)	98 (2)
Body temperature (°C)	36.5 (0.5)	36.5 (0.6)	36.5 (0.5)

[a]SBT: spontaneous breathing trial.

[b]FiO_2: fraction of inspired oxygen.

[c]PaO_2: partial pressure of oxygen.

[d]VTe: exhaled tidal volume.

[e]RR: respiratory rate.

[f]Paw: peak airway pressure.

[g]MAP: mean airway pressure.

[h]MVe: minute ventilation.

[i]SpO_2: oxygen saturation.

For respiratory parameters, the average FiO_2 is 35.2%, with the successful group at 32.9% and the failure group at 37.5%. The partial pressure of oxygen levels are similar across all groups, with slight variations. The failure group has a higher exhaled tidal volume and measured RR. The peak airway pressure and mean airway pressure are also higher in the failure group than

XSL•FO
RenderX

in the successful group. Minute ventilation shows minimal difference between the groups.

Vital signs indicate that the heart rate is slightly higher in the failure group (87.6 bpm) compared to the successful group (84.9 bpm). Systolic and diastolic blood pressure are lower in the failure group. Oxygen saturation remains high across all groups, with minimal variation. Body temperature is consistent, averaging around 36.5 °C across all groups.

The PyTorch framework in Python is used to construct the proposed model.

In order to present the prediction results of the model more intuitively, this study uses the confusion matrix to show the classification of the model on the training and test datasets. The confusion matrix of the model's prediction results is shown in Figures 3 and 4. The results show that the model performs well on the training data, and the classification ability on the test data remains stable. Although the number of misclassifications increases slightly, it is still within an acceptable range.

Table 2 illustrates the performance metrics of a model for predicting successful and failed SBT across both training and testing datasets.

Figure 3. Confusion matrices for training data.

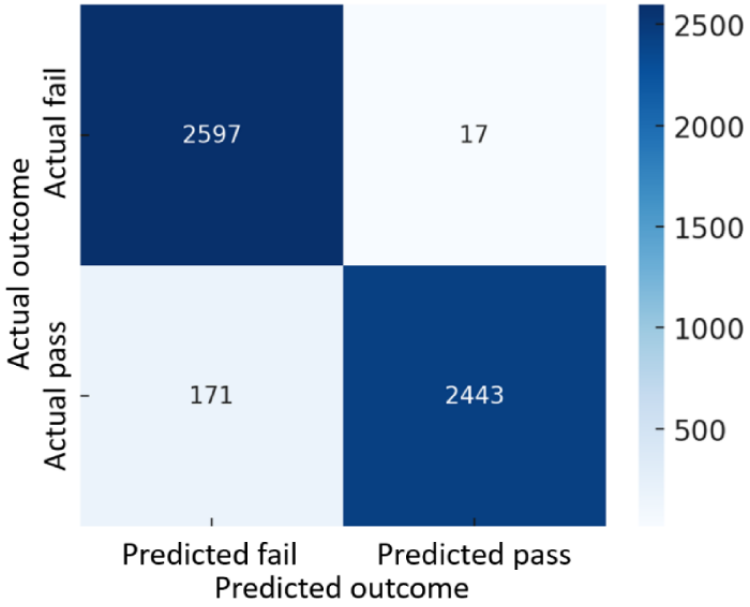
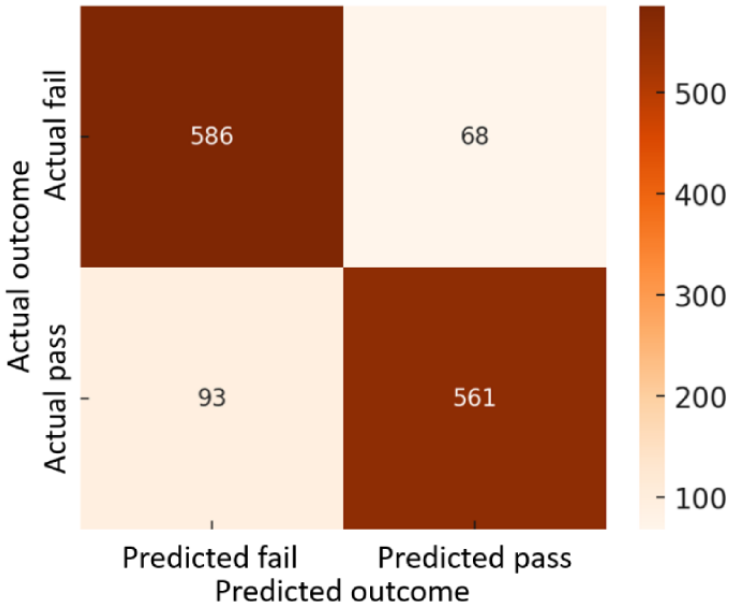


Figure 4. Confusion matrices for testing data.



XSL•FO
RenderX

Table 2. Performance metrics of the spontaneous breathing trial prediction model.

Metric	Training value	Testing value
Accuracy	96.4% (5040/5228)	87.7% (1147/1308)
Precision	99.3% (2443/2460)	89.2% (561/629)
Recall (sensitivity)	93.5% (2443/2614)	85.8% (561/654)
Specificity	99.3% (2597/2614)	89.6% (586/654)
FPR[a]	0.7% (17/2614)	10.4% (68/654)
FNR[b]	6.5% (171/2614)	14.2% (93/654)
F_1-score	0.963	0.875

[a]FPR: false positive rate.

[b]FNR: false negative rate.

Overall, the model's accuracy is 96.4% (5040/5228 records) in the training data and 87.7% (1147/1308 records) in the test data. Although the test results are slightly lower than the training results, they can still maintain a high accuracy, indicating that the model has good generalization ability and no overfitting problem.

Further analysis of the model's performance showed that the precision was 99.3% (2443/2460 records) in the training data and 89.2% (561/629 records) in the test data, indicating that the model had a slightly higher FPR on the test data but was still able to identify patients who could successfully pass an SBT effectively. In other words, in clinical applications, when the model predicts that a patient can pass the SBT, the likelihood of their actual success is still quite high, reducing the risk of unnecessary weaning failure.

However, in terms of recall (sensitivity), the recall rate in the training data was 93.5% (2443/2614 records), while it dropped to 85.8% (561/654 records) in the test data, indicating that some patients who should have passed the SBT in the test data were still not correctly identified. This may result in some patients being wrongly judged as unable to pass the SBT and continuing to receive unnecessary mechanical ventilation, thereby increasing the risk of lung infection or other complications.

In addition, the specificity was 99.3% (2597/2614 records) in the training data and 89.6% (586/654 records) in the test data, indicating that the model can still maintain good recognition ability for patients who cannot pass the SBT without significant deviation. This means that when the model predicts that a patient will not be able to pass the SBT, its judgment is correct in most cases, reducing the risk of the patient failing the SBT.

The F_1-score, which is a comprehensive measure of precision and recall, is 0.963 in the training data and 0.875 in the test data, indicating that the model has achieved a certain balance between precision and recall and is suitable as a clinical decision-making aid.

Figures 5 and 6 display the ROC curve of the SBT prediction model for both training and test data, with the AUC used to assess the model's classification ability. Figure 5 is the ROC curve of the training data, and Figure 6 is the ROC curve of the test data. Both are used to measure the changes in the TPR and FPR of the model at different decision thresholds, and the AUC value is used to quantify the overall effectiveness of the model in distinguishing between successful and failed patients.

XSL•FO
RenderX

Figure 5. ROC curves for training data. AUC: area under the ROC curve.

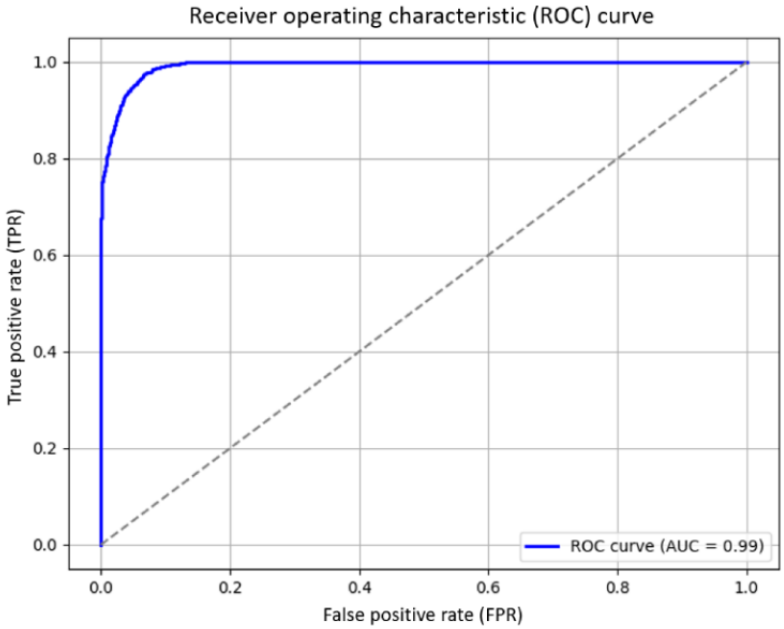
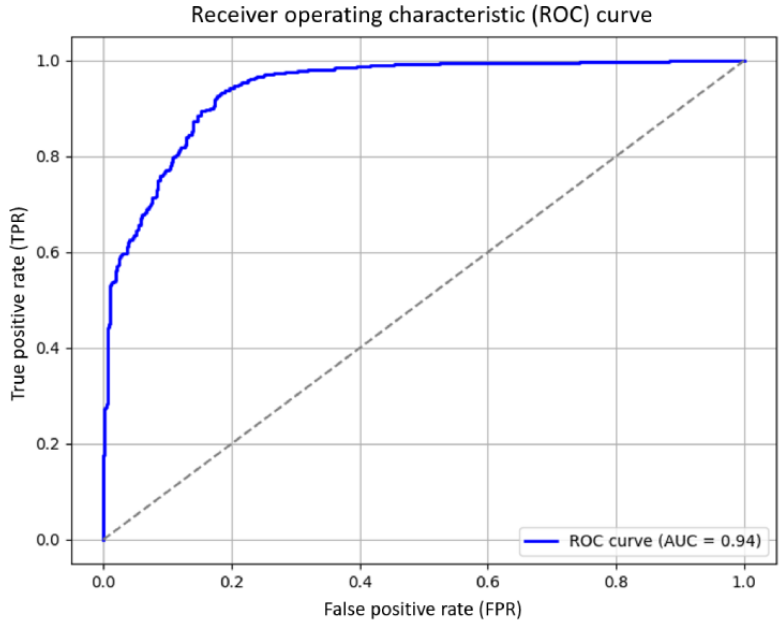


Figure 6. ROC curves for testing data. AUC: area under the ROC curve.



The results showed that the AUC for the training data was 0.99, indicating that the model could almost perfectly distinguish between successful and failed SBT patients during training, showing extremely high predictive ability. However, when the model was applied to the test data, the AUC dropped to 0.94, which is slightly lower than the training data but still within the excellent range, indicating that the model still has a good discrimination ability for unseen data. This means that although the model has a certain degree of generalization ability decline on the test data, it can still effectively distinguish which patients can successfully pass the SBT and which still need mechanical ventilation support.

This study successfully developed an AI-based SBT prediction model that can effectively assist clinicians in determining whether patients can successfully pass the SBT. Through evaluation metric analysis, including accuracy, precision, recall, specificity, F_1-score, FPR, FNR, ROC curve, and AUC, we verified the robust performance of the model on both training and test data. Overall, the accuracy and reliability of the model in clinical applications have reached a high level and can provide strong support for clinical decision-making.

Discussion

Overview

This study demonstrates the potential of deep learning technology in evaluating SBT, which can effectively improve the accuracy and efficiency of managing mechanically ventilated patients. Traditional SBT assessment methods rely on simple threshold settings, which cannot fully reflect the patient's

XSL•FO
RenderX

complex physiological state. The deep learning model developed in this study can integrate multidimensional clinical data to provide more precise prediction results that conform to actual physiological conditions.

A major innovation of this study is the design of the hybrid CNN-MLP architecture. Compared with the traditional deep learning model that only relies on CNN for feature extraction and MLP for classification, this study uses CNN and MLP layers alternately to form a novel feature learning and fusion method. This design helps capture features at different levels, making the model more flexible and efficient when processing data with complex feature structures. The research results show that the model achieves high accuracy in the training phase and maintains stable performance in the testing phase. The final F_1-score on the test dataset is about 0.875, which proves its feasibility and reliability in predicting SBT results. These findings are consistent with previous studies [37,38], showing that AI technology can improve clinical decision-making accuracy and patient outcomes in critically ill patient care.

This study aimed to establish a model to predict whether a patient can successfully pass an SBT. The data division does not necessarily lead to data leakage in our research setting because our model learns the relationship between pre-SBT clinical parameters and SBT outcomes. That means the model does not track a patient's historical SBT trials but makes independent predictions based on the patient's current state before each SBT trial. We treat each SBT trial as an independent sample rather than linking multiple records from the same patient. Even if a patient has undergone multiple SBTs at different time points, each trial is considered a separate instance for training and prediction. Therefore, within-patient clustering does not significantly impact the model's learning process, and even if records of the same patient at different time points appear in the training and test sets, the model still learns the pattern that determines a patient's likelihood of passing the SBT, rather than focusing on individual patient characteristics.

Regarding patients who have undergone multiple SBT attempts with varying outcomes, the model learns to predict each SBT outcome independently based on pre-SBT clinical records of that specific attempt rather than being influenced by previous trials. Therefore, it does not distinguish between patients who succeeded on their first attempt and those who required multiple attempts; instead, it evaluates each instance based on its pre-SBT clinical record.

This study did not specifically adjust the time variables since the time factor has a limited impact on the model based on the following considerations. The SBT implementation standards of the research institutions were consistent with the clinical operation procedures throughout the study period. Therefore, data from different years can be regarded as homogeneous and will not significantly impact the model training and prediction results. In addition, during the data partitioning process, we used random sampling to ensure that the data distribution between the training and test sets was balanced to reduce the possible impact of time variability.

Strengths and Limitations

The innovation of this study is to develop an AI-based prediction model to evaluate the outcome of an SBT under a specific SBT strategy using clinical parameters collected before an SBT begins. Traditionally, clinicians must comprehensively assess multiple physiological parameters to determine whether a patient is suitable for SBT. However, this process is highly subjective, experience-dependent, and has a high risk of misjudgment. This study uses AI technology to develop an objective and efficient prediction model to reduce the error of traditional manual evaluation and improve the accuracy of predicting whether an SBT will be successful.

The model in this study is built on pre-SBT clinical data to identify the relationship between these variables and SBT outcomes and to make predictions under a fixed SBT strategy. Unlike traditional approaches, this study does not compare different SBT strategies or analyze their impact on extubation success rates. Instead, it focuses on developing a data-driven method within a specific SBT strategy's framework to accurately predict whether patients can successfully pass SBT, providing clinicians with an objective and reliable decision-making aid.

Furthermore, the AI prediction model in this study focuses on predicting SBT success and highlights the clinical value of identifying patients who may fail SBT in advance. In current clinical practice, the SBT evaluation process typically takes 48-72 hours, and initiating SBT too early can result in respiratory muscle fatigue, hypoxemia, and even acute respiratory failure in patients. The proposed model can predict whether an SBT will be successful in advance and assist clinicians in identifying patients who may not be ready yet, which would prevent unnecessary testing, reduce the physiological burden on patients, and enhance the efficiency of ICU resource management.

The main advantage of this study lies in its innovative CNN-MLP hybrid architecture, which enables the model to effectively learn and fuse feature information at different levels and improve the prediction ability of SBT results. Compared with traditional deep learning models, the method of this study can not only extract features from image and time series data through CNN but also further enhance the understanding of high-dimensional features through MLP, thereby improving the accuracy and applicability of the model. In addition, by integrating multidimensional physiological data, the model of this study can more comprehensively assess the patient's clinical condition and provide more accurate and personalized extubation decision support compared with traditional threshold-based indicators.

The final F_1-score on the test dataset is about 0.875, which proves its feasibility and reliability in predicting SBT results. The AUC for the test data was 0.94, indicating that the model has a good discrimination ability for unseen data. The study showed that the model maintained stable predictive performance during the testing phase and exhibited an excellent F_1-score, confirming its potential in clinical applications.

The contributions of this study are summarized as follows:

XSL•FO
RenderX

1. Enhancing clinical decision support and prediction accuracy: Traditionally, clinicians assess whether patients are suitable for SBT by comprehensively analyzing multiple physiological parameters. This process relies heavily on experience and is subjective, which can easily lead to errors in judgment. This study uses AI technology to develop a prediction model based on pre-SBT clinical data, providing more accurate prediction results, reducing manual evaluation errors, and enhancing SBT prediction accuracy.
2. Identifying patients who may fail in advance: In current clinical practice, SBT evaluation typically takes 48-72 hours. If SBT is conducted too early, it may lead to respiratory muscle fatigue, hypoxemia, and even acute respiratory failure in patients. The AI prediction model introduced in this study can identify patients who may not successfully pass the SBT beforehand, preventing unnecessary trials, reducing the physiological burden on patients, and effectively managing ICU resources to enhance overall medical efficiency.
3. Innovative hybrid CNN-MLP model design: This study's methodological innovation proposes a hybrid deep learning architecture called hybrid CNN-MLP. This architecture differs from the traditional CNN-MLP classification method since it uses a unique approach to feature learning and fusion through the interlaced combination of CNN and MLP layers, where the data features can be extracted and integrated at various levels, making the model more flexible and efficient in processing complex data structures and enhancing the accuracy and applicability of SBT predictions.

However, this study still has some limitations. First, the data in this study came from a single medical institution, which may affect the model's generalization ability and limit its applicability in different clinical settings. Therefore, its robustness needs to be verified through multicenter data in the future. Second, although the model shows high accuracy at the technical level, in practical application, it is still necessary to consider how to integrate it with the clinical workflow to ensure that medical staff can adopt the technology smoothly. In addition, in the test dataset, the model’s performance decreased slightly compared to the training stage, indicating that there is still room for further optimization. These challenges can be overcome in the future through multicenter data expansion, improved model training strategies, and enhanced AI interpretation capabilities.

Future Perspectives

In order to enhance the influence and application value of this study, the data scope should be further expanded in the future, and model training and verification should be carried out with multicenter data to ensure its applicability in different medical institutions and diverse patient groups. By introducing data from different medical environments, not only can the model's generalization ability be increased, but its adaptability to patients from different groups can also be improved. In addition, prospective clinical trials should be conducted to evaluate the impact of this model in actual clinical decision-making, such as whether it can effectively reduce the duration of mechanical ventilation, improve the success rate of extubation, and further analyze its impact on the clinical prognosis of patients.

In addition to increasing the breadth of data and validating real-world applications, the model in this study can be further optimized to improve its performance and interpretability. Although the deep learning model used in this study has strong predictive capabilities, it is a “black box model” with low interpretability. Hence, to ensure that the model applies to different health care systems, we pay special attention to the availability and variability of the input features. The characteristics used in this study are key indicators in clinical diagnosis and monitoring. These variables were selected primarily based on clinical relevance and availability. However, there may be variations in equipment and data collection methods between different medical systems. For example, the type of ventilator or blood oxygen monitor used in different wards may affect the measurement of certain values. Therefore, when the model is applied to different medical institutions in the future, it is recommended to first conduct a feature distribution analysis to evaluate the input data's adaptability and reduce heterogeneity's impact on model performance through transfer learning or regularization techniques.

By improving the model's training strategy, such as applying transfer learning or reinforcement learning, the model can be helped to learn feature patterns from different environments more effectively, thereby improving its adaptability. In addition, the interpretability of the model is also an important direction for future development. By designing a more transparent AI model architecture, medical staff can understand the decision-making logic of the model, which will help enhance clinical users' trust in AI-assisted decision-making systems and further promote their application in the medical field.

Finally, future attention should be paid to the model's actual deployment and clinical integration and the possibility of embedding it into the EHR system. Through seamless integration with existing medical information systems, the model can be ensured to be immediately available in clinical decision-making and enhance its auxiliary value to medical staff. In addition, when designing the user interface, the user-centered design principles should be considered so that medical staff can operate and understand the system more intuitively, ensuring that it can truly become an effective tool in the clinical decision-making. Through these efforts, deep learning–based SBT assessment technology will be able to be more widely used in clinical fields, improve the efficiency of mechanical ventilation management, and ultimately improve patients' treatment and rehabilitation outcomes.

Conclusions

This study demonstrates the potential of deep learning technology to predict whether a patient can successfully pass an SBT, improving the accuracy and efficiency of mechanically ventilated patient management. Traditional SBT evaluation methods rely on simple threshold settings and are difficult to fully reflect the patient's complex physiological state. This study's AI prediction model integrates multidimensional clinical data to provide more accurate prediction results that meet actual clinical needs.

The main innovation of this study is the proposed hybrid CNN-MLP architecture, which uses CNN and MLP layers

XSL•FO
RenderX

alternately for feature learning and fusion. Compared with traditional deep learning models, this method can more flexibly capture features at different levels and improve the model's ability to handle complex data structures. The results showed that the model achieved an F_1-score of 0.875 on the test dataset, confirming its feasibility and reliability in predicting the success of SBT, which is consistent with previous research results on the application of AI technology in critical care.

In addition, this study highlights the value of AI prediction models in clinical decision support, especially in identifying patients who may not pass the SBT in advance, thereby reducing unnecessary trials, reducing the physiological burden on patients, and improving the management efficiency of ICU resources. However, the study's limitations are that the research data came from a single medical institution and, as a consequence, may affect the generalization ability of the model. In the future, it should be verified through multicenter data. In addition, integrating this technology seamlessly into clinical workflow and increasing the acceptance of medical staff are challenges that need to be addressed in the future.

In the future, this study recommends further expanding the data scope and evaluating the model's applicability in different medical institutions and patient groups through multicenter clinical trials. In addition, the model can be optimized through transfer learning or reinforcement learning to make it more adaptable to data patterns in different environments. Besides, the model's interpretability will be improved to enhance the trust of medical staff, and its integration into the EHR system will be explored to ensure that it can provide real-time support for clinical decision-making.

In summary, the hybrid CNN-MLP proposed in this study can improve the accuracy and efficiency of SBT assessment and provide a more reliable auxiliary tool for clinical decision-making. The ultimate goal is to optimize the mechanical ventilation weaning process, improve patient prognosis, and enhance the quality of ICU care.

Acknowledgments

This work was supported by Taichung Veterans General Hospital (grant TCVGH-1124101B). We sincerely thank the medical and administrative staff for their invaluable support and contributions throughout this study.

Conflicts of Interest

None declared.

Multimedia Appendix 1
Detailed mathematical formulas used in model construction and evaluation.
[DOCX File , 16 KB - medinform_v13i1e64592_app1.docx]

References

1. Xavier G, Yoshua B. Understanding the difficulty of training deep feedforward neural networks. 2010 Presented at: Proceedings of the Thirteenth International Conference on Artificial Intelligence and Statistics; May 13-15, 2010; Sardinia, Italy p. 13-15 URL: https://proceedings.mlr.press/v9/glorot10a.html
2. Boles JM, Bion J, Connors A, Herridge M, Marsh B, Melot C, et al. Weaning from mechanical ventilation. Eur Respir J 2007;29(5):1033-1056 [FREE Full text] [doi: 10.1183/09031936.00010206] [Medline: 17470624]
3. Yang HC, Liu SC, Tsai YT, Weng SJ, Huang SC, Chan MC. Benefits of a respiratory care-ventilator weaning information system. J Respir Ther 2021;20(2):1-9. [doi: 10.6269/JRT.202107_20(2).0001]
4. Holets SR, Marini JJ. Is automated weaning superior to manual spontaneous breathing trials? Respir Care 2016;61(6):749-760. [doi: 10.4187/respcare.04329] [Medline: 27235311]
5. Burns KEA, Meade MO, Lessard MR, Hand L, Zhou Q, Keenan SP, et al. Wean earlier and automatically with new technology (the WEAN study). A multicenter, pilot randomized controlled trial. Am J Respir Crit Care Med 2013;187(11):1203-1211. [doi: 10.1164/rccm.201206-1026OC] [Medline: 23525929]
6. Ramachandran V, Grap MJ, Sessler CN. Protocol-directed weaning: a process of continuous performance improvement. Crit Care 2005;9(2):138-140 [FREE Full text] [doi: 10.1186/cc3053] [Medline: 15774063]
7. Blackwood B, Alderdice F, Burns K, Cardwell C, Lavery G, O'Halloran P. Use of weaning protocols for reducing duration of mechanical ventilation in critically ill adult patients: Cochrane systematic review and meta-analysis. Br Med J 2011;342:c7237 [FREE Full text] [doi: 10.1136/bmj.c7237] [Medline: 21233157]
8. Taniguchi C, Victor ES, Pieri T, Henn R, Santana C, Giovanetti E, et al. Smart Care™ versus respiratory physiotherapy-driven manual weaning for critically ill adult patients: a randomized controlled trial. Crit Care 2015;19(1):246 [FREE Full text] [doi: 10.1186/s13054-015-0978-6] [Medline: 26580673]
9. Ely EW, Baker AM, Dunagan DP, Burke HL, Smith AC, Kelly PT, et al. Effect on the duration of mechanical ventilation of identifying patients capable of breathing spontaneously. N Engl J Med 1996;335(25):1864-1869. [doi: 10.1056/NEJM199612193352502] [Medline: 8948561]

XSL•FO
RenderX

10. Cheng JC, Chen HC, Jerng JS, Kuo PH, Wu HD. End-expiratory lung volumes during spontaneous breathing trials in tracheostomized subjects on prolonged mechanical ventilation. Respir Care 2021;66(11):1704-1712. [doi: 10.4187/respcare.08957] [Medline: 34465570]
11. Haruna J, Tatsumi H, Kazuma S, Sasaki A, Masuda Y. Frequent tracheal suctioning is associated with extubation failure in patients with successful spontaneous breathing trial: a single-center retrospective cohort study. JA Clin Rep 2022;8(1):5 [FREE Full text] [doi: 10.1186/s40981-022-00495-7] [Medline: 35024978]
12. Nakato AM, Ribeiro DDF, Simão AC, Da Silva RP, Nohama P. Impact of spontaneous breathing trials in cardiorespiratory stability of preterm infants. Respir Care 2021;66(2):286-291. [doi: 10.4187/respcare.07955] [Medline: 32994356]
13. Fiatt M, Bosio AC, Neves D, Symanski da Cunha R, Fonseca LT, Celeste RK. Accuracy of a spontaneous breathing trial for extubation of neonates. J Neonatal Perinatal Med 2021;14(3):375-382. [doi: 10.3233/NPM-200573] [Medline: 33337394]
14. Williams EE, Arattu Thodika FMS, Chappelow I, Chapman-Hatchett N, Dassios T, Greenough A. Diaphragmatic electromyography during a spontaneous breathing trial to predict extubation failure in preterm infants. Pediatr Res 2022;92(4):1064-1069 [FREE Full text] [doi: 10.1038/s41390-022-02085-w] [Medline: 35523885]
15. Knox KE, Hotz JC, Newth CJL, Khoo MCK, Khemani RG. A 30-minute spontaneous breathing trial misses many children who go on to fail a 120-minute spontaneous breathing trial. Chest 2023;163(1):115-127 [FREE Full text] [doi: 10.1016/j.chest.2022.08.2212] [Medline: 36037984]
16. Liu W, Guo H, Wang J, Ding F. Effect of spontaneous breathing trial on extubation in patients with acute exacerbation of chronic obstructive pulmonary disease under mechanical ventilation. BMC Emerg Med 2022;22(1):112 [FREE Full text] [doi: 10.1186/s12873-022-00672-y] [Medline: 35729524]
17. Louvaris Z, Van Hollebeke M, Poddighe D, Meersseman P, Wauters J, Wilmer A, et al. Do cerebral cortex perfusion, oxygen delivery, and oxygen saturation responses measured by near-infrared spectroscopy differ between patients who fail or succeed in a spontaneous breathing trial? A prospective observational study. Neurocrit Care 2023;38(1):105-117 [FREE Full text] [doi: 10.1007/s12028-022-01641-w] [Medline: 36450970]
18. Bezanson J. Respiratory care of older adults after cardiac surgery. J Cardiovasc Nurs 1997;12(1):71-83. [doi: 10.1097/00005082-199710000-00008] [Medline: 9315963]
19. Epstein SK, Ciubotaru RL, Wong JB. Effect of failed extubation on the outcome of mechanical ventilation. Chest 1997;112(1):186-192. [doi: 10.1378/chest.112.1.186] [Medline: 9228375]
20. Epstein CD, El-Mokadem N, Peerless JR. Weaning older patients from long-term mechanical ventilation: a pilot study. Am J Crit Care 2002;11(4):369-377. [Medline: 12102438]
21. Coplin WM, Pierson DJ, Cooley KD, Newell DW, Rubenfeld GD. Implications of extubation delay in brain-injured patients meeting standard weaning criteria. Am J Respir Crit Care Med 2000;161(5):1530-1536. [doi: 10.1164/ajrccm.161.5.9905102] [Medline: 10806150]
22. Khamiees M, Raju P, DeGirolamo A, Amoateng-Adjepong Y, Manthous CA. Predictors of extubation outcome in patients who have successfully completed a spontaneous breathing trial. Chest 2001;120(4):1262-1270. [doi: 10.1378/chest.120.4.1262] [Medline: 11591570]
23. Namen AM, Ely EW, Tatter SB, Case LD, Lucia MA, Smith A, et al. Predictors of successful extubation in neurosurgical patients. Am J Respir Crit Care Med 2001;163(3 Pt 1):658-664. [doi: 10.1164/ajrccm.163.3.2003060] [Medline: 11254520]
24. Suleiman A, Santer P, Munoz-Acuna R, Hammer M, Schaefer MS, Wachtendorf LJ, et al. Effects of ketamine infusion on breathing and encephalography in spontaneously breathing ICU patients. J Intensive Care Med 2023;38(3):299-306. [doi: 10.1177/08850666221119716] [Medline: 35934953]
25. Shin MH, Hsu HS, Chien JY, Huang CK, Kuo LC, Shun TM, et al. Association between microcirculation in spontaneous breathing trial and extubation success. Microvasc Res 2023;148:104552. [doi: 10.1016/j.mvr.2023.104552] [Medline: 37207721]
26. Patel S, Stollings JL, Casey JD, Wang L, Rice TW, Semler MW. Identifying predictors of extubation on the day of passing an SBT in critically ill adults. J Intensive Care Med 2023;38(6):529-533. [doi: 10.1177/08850666221149370] [Medline: 36648173]
27. Brochard L, Rauss A, Benito S, Conti G, Mancebo J, Rekik N, et al. Comparison of three methods of gradual withdrawal from ventilatory support during weaning from mechanical ventilation. Am J Respir Crit Care Med 1994;150(4):896-903. [doi: 10.1164/ajrccm.150.4.7921460] [Medline: 7921460]
28. Esteban A, Alía I, Gordo F, Fernández R, Solsona JF, Vallverdú I, et al. Extubation outcome after spontaneous breathing trials with T-tube or pressure support ventilation. The Spanish Lung Failure Collaborative Group. Am J Respir Crit Care Med 1997;156(2 Pt 1):459-465. [doi: 10.1164/ajrccm.156.2.9610109] [Medline: 9279224]
29. Verghese A, Shah NH, Harrington RA. What this computer needs is a physician: humanism and artificial intelligence. J Am Med Assoc 2018;319(1):19-20. [doi: 10.1001/jama.2017.19198] [Medline: 29261830]
30. Hur S, Min JY, Yoo J, Kim K, Chung CR, Dykes PC, et al. Development and validation of unplanned extubation prediction models using intensive care unit data: retrospective, comparative, machine learning study. J Med Internet Res 2021;23(8):e23508 [FREE Full text] [doi: 10.2196/23508] [Medline: 34382940]

XSL•FO
RenderX

31. Kim J, Kim YK, Kim H, Jung H, Koh S, Kim Y, et al. Machine learning algorithms predict successful weaning from mechanical ventilation before intubation: retrospective analysis from the medical information mart for intensive care IV database. JMIR Form Res 2023;7:e44763 [FREE Full text] [doi: 10.2196/44763] [Medline: 37962939]
32. Liu S, Xu Q, Xu Z, Liu Z, Sun X, Xie G, et al. Reinforcement learning to optimize ventilator settings for patients on invasive mechanical ventilation: retrospective study. J Med Internet Res 2024;26:e44494 [FREE Full text] [doi: 10.2196/44494] [Medline: 39219230]
33. Liu S, See KC, Ngiam KY, Celi LA, Sun X, Feng M. Reinforcement learning for clinical decision support in critical care: comprehensive review. J Med Internet Res 2020;22(7):e18477. [doi: 10.2196/18477] [Medline: 32706670]
34. Kiranyaz S, Ince T, Gabbouj M. Real-time patient-specific ECG classification by 1-D convolutional neural networks. IEEE Trans Biomed Eng 2016;63(3):664-675. [doi: 10.1109/TBME.2015.2468589] [Medline: 26285054]
35. Xu YY. Multiple-instance learning based decision neural networks for image retrieval and classification. Neurocomputing 2016;171:826-836. [doi: 10.1016/j.neucom.2015.07.024]
36. Xu YY, Tseng CL, Fu HC. Texture recognition by generalized probabilistic decision-based neural networks. Expert Syst Appl 2011;38(5):6184-6189. [doi: 10.1016/j.eswa.2010.11.051]
37. Topol EJ. High-performance medicine: the convergence of human and artificial intelligence. Nat Med 2019;25(1):44-56. [doi: 10.1038/s41591-018-0300-7] [Medline: 30617339]
38. Komorowski M, Celi LA, Badawi O, Gordon AC, Faisal AA. The artificial intelligence clinician learns optimal treatment strategies for sepsis in intensive care. Nat Med 2018;24(11):1716-1720 [FREE Full text] [doi: 10.1038/s41591-018-0213-5] [Medline: 30349085]

Abbreviations

AI: artificial intelligence
AUC: area under the curve
CNN: convolutional neural network
CPAP: continuous positive airway pressure
EHR: electronic health record
FiO2: fraction of inspired oxygen
FNR: false negative rate
FPR: false positive rate
ICU: intensive care unit
IRB: institutional review board
MLP: multilayer perceptron
PEEP: positive end-expiratory pressure
PS: pressure support
ROC: receiver operating characteristic
RR: respiratory rate
SBT: spontaneous breathing trial
TPR: true positive rate

Edited by A Benis; submitted 21.07.24; peer-reviewed by E Ayan, MA Ilani, A Tan, WC Shia; comments to author 24.10.24; revised version received 17.03.25; accepted 20.04.25; published 21.05.25.

Please cite as:
Yang HC, Hao ATH, Liu SC, Chang YC, Tsai YT, Weng SJ, Chan MC, Wang CY, Xu YY
Prediction of Spontaneous Breathing Trial Outcome in Critically Ill-Ventilated Patients Using Deep Learning: Development and Verification Study
JMIR Med Inform 2025;13:e64592
URL: https://medinform.jmir.org/2025/1/e64592
doi:10.2196/64592
PMID:

©Hui-Chiao Yang, Angelica Te-Hui Hao, Shih-Chia Liu, Yu-Cheng Chang, Yao-Te Tsai, Shao-Jen Weng, Ming-Cheng Chan, Chen-Yu Wang, Yeong-Yuh Xu. Originally published in JMIR Medical Informatics (https://medinform.jmir.org), 21.05.2025. This is an open-access article distributed under the terms of the Creative Commons Attribution License (https://creativecommons.org/licenses/by/4.0/), which permits unrestricted use, distribution, and reproduction in any medium,

XSL•FO
RenderX

provided the original work, first published in JMIR Medical Informatics, is properly cited. The complete bibliographic information, a link to the original publication on https://medinform.jmir.org/, as well as this copyright and license information must be included.

XSL•FO
RenderX

Original Paper

Machine Learning for the Prediction of Acute Kidney Injury in Critically Ill Patients With Coronary Heart Disease: Algorithm Development and Validation

Yike Li[1], MM; Mingyang Xiao[1], MM; Yaqian Li[1], MM; Lulu Lv[1], MM; Shanshan Zhang[1], MM; Yuhui Liu[1], MM; Juan Zhang[1], MM

The Second Clinical Medical School, Zhengzhou University, Zhengzhou, China

Corresponding Author:
Juan Zhang, MM
The Second Clinical Medical School
Zhengzhou University
No 2 Jingba Road, Jinshui District
Zhengzhou
China
Phone: 86 15038180882
Email: zj78420@163.com

Abstract

Background: Acute kidney injury (AKI) frequently occurs in critically ill patients with coronary heart disease (CHD), and its development markedly elevates mortality rates and prolongs hospitalization duration. Early AKI prediction is crucial for timely intervention and amelioration of patient outcomes.

Objective: This study aimed to develop and verify a clinical prediction model for the occurrence of AKI upon admission in the critically ill population with CHD through machine learning (ML).

Methods: Data from the MIMIC-IV (Medical Information Mart for Intensive Care IV) version 2.2 database were gathered and included information about critically ill individuals with CHD in the intensive care unit (ICU). The dataset was randomized into a training set (70%) and a testing set (30%). Least absolute shrinkage and selection operator (LASSO) regression was used for feature variable selection. ML models, including logistic regression (LR), decision tree (DT), naive Bayes (NB), random forest (RF), extreme gradient boosting (XGBoost), and support vector machine (SVM), were constructed using 13 variables in the training set. The 6 models were compared in the testing set to identify the best-performing model. Subsequently, the model was assessed using calibration curve analysis and decision curve analysis (DCA). External validation was conducted using data from the Second Affiliated Hospital of Zhengzhou University. Ultimately, the predictive model was interpreted via Shapley Additive Explanation (SHAP) values.

Results: In total, 2711 patients with CHD admitted to the ICU were selected, with 1809 (66.7%) having AKI. XGBoost exhibited the best performance regarding discrimination (area under the receiver operating characteristic curve [AUROC]=0.765, 95% CI 0.731-0.800), accuracy (0.725), and sensitivity (0.759). External validation using a cohort of 226 patients confirmed the strong generalizability of the XGBoost model (AUROC=0.835, 95% CI 0.782-0.887). Feature importance analyses derived from SHAP values, DT, RF, and XGBoost consistently identified 5 key predictors associated with the development of AKI: mechanical ventilation, use of antiplatelet agents, age, N-terminal pro–B-type natriuretic peptide (NT-proBNP) levels, and acute physiology score III (APSIII).

Conclusions: ML models can serve as reliable tools for forecasting AKI in the critically ill population with CHD. The XGBoost model is highly accurate and may aid doctors in identifying high-risk individuals for early intervention to lower mortality.

(JMIR Med Inform 2025;13:e72349) doi:10.2196/72349

KEYWORDS

coronary heart disease; coronary artery disease; acute kidney injury; machine learning; MIMIC-IV database

XSL•FO
RenderX

Introduction

Acute kidney injury (AKI) is a frequent complication in people admitted to the intensive care unit (ICU), particularly in the coronary care unit (CCU). The incidence of AKI in the CCU is 28.5% [1]. In patients in the ICU, the onset of AKI is linked to significantly longer hospital stays and higher in-hospital death rates in contrast to the population without AKI, resulting in a worse overall prognosis [2]. However, with timely intervention and effective treatment, AKI can be reversed early, thereby reducing mortality related to AKI [3]. Therefore, early AKI identification is essential for critically ill individuals with coronary heart disease (CHD) in the ICU. To better manage critically ill patients with CHD, an accurate predictive model is required to find high-risk individuals, enabling early intervention to ameliorate their prognosis.

In recent years, several cardiac disease–related AKI prediction models have been created. For instance, Ma et al [4] used nomograms to develop a prediction model for contrast-induced AKI in individuals with non–ST elevation acute coronary syndrome (ACS), and Peng et al [5] developed a machine learning (ML)-based predictive model for AKI in patients with congestive heart failure. Existing predictive models are primarily designed for patients with isolated risk factors, such as acute myocardial infarction (AMI) or those undergoing percutaneous coronary intervention (PCI). However, critically ill patients admitted to the ICU often present with complex conditions and multiple comorbidities, rendering current models less applicable to this population. Therefore, it is important to establish a more widely applicable predictive model for AKI in the critically ill cohort with CHD. As statistical theory and computational technologies advance, artificial intelligence (AI) is beginning to play a vital role in medicine. AI can learn to recognize large datasets from databases, enabling precise disease prediction, which helps clinicians develop appropriate treatment plans [6,7]. ML approaches have been extensively used in the construction of predictive models for multiple illnesses, exhibiting higher performance in comparison to conventional models, such as logistic regression (LR) or Cox regression analysis [8,9].

This study endeavored to assess the incidence of AKI following hospital admission in critically ill patients with CHD, as well as to identify potential influencing factors. Using a range of ML algorithms, we aimed to develop a generalizable predictive model for postadmission AKI in this patient population, identify the model with the best predictive performance, evaluate its accuracy and generalizability, and conduct interpretability analyses. Our model is designed to operate within an electronic health record (EHR) system to continuously monitor and analyze patient data in real time, automatically calculate the risk score for AKI, and issue early warnings in high-risk cases. This approach may assist clinicians in implementing timely preventive measures or initiating early interventions.

Methods

Study Design and Population

The Medical Information Mart for Intensive Care IV (MIMIC-IV) database, a single-center ICU dataset of the Laboratory for Computational Physiology at the Massachusetts Institute of Technology (MIT), has gained approval from the Institutional Review Boards (IRBs) of MIT and the Beth Israel Deaconess Medical Center (BIDMC). The patient information within the database is anonymized, obviating the need for informed consent from patients [10,11]. MIMIC-IV version 2.2 includes medical data from 73,181 patients in the ICU from 2008 to 2019 [12]. Our study cohort consisted of patients diagnosed with CHD upon admission. The inclusion criteria were (1) age of 18 years or more; (2) hospitalization duration exceeding 24 hours; (3) patients diagnosed with CHD according to the *International Classification of Diseases, 9th Revision* (ICD-9: 41401, 41402, 41404, 41405, 41407) and *International Classification of Diseases, 10th Revision* (ICD-10: I2101, I2102, I2109, I2111, I2119, I2121, I240, I251). In total, 30,136 patients with CHD were found in the MIMIC-IV database. Patients were excluded if they (1) were not admitted to the ICU (n=13,461); (2) had missing outcome variables (n=1); (3) had missing categorical variables, such as gender, marital status, and ethnicity (n=2420); (4) had missing N-terminal pro–B-type natriuretic peptide (NT-proBNP) or neutrophil count data (n=11,430); (5) had a history of pre-existing renal disease (n=99); or (6) had a lymphocyte count of 0 (n=14).

Additionally, clinical data were collected from 226 critically ill patients with CHD admitted to the Second Affiliated Hospital of Zhengzhou University from January 1, 2021, to August 1, 2024, as an external validation cohort. A retrospective analysis was performed using the hospital's EHR system. The eligibility criteria were consistent with those for the training and internal validation cohorts.

Outcome

Our research team was granted access to the MIMIC-IV database on July 12, 2024, and subsequently extracted data on 2711 critically ill patients with CHD admitted to the ICU. As of March 30, 2025, we had also collected external validation data from 226 patients at the Second Affiliated Hospital of Zhengzhou University. A total of 7 investigators participated in this study.

Data Extraction and Processing

Data extraction was completed via structured query language (SQL) and the PostgreSQL tool (version 16.0). The extracted data consisted of the first recorded vital signs and laboratory parameters following ICU admission, as well as medications administered within the first 7 days of hospitalization. The study extracted the following variables:

- Demographic characteristics: gender, age, race, blood pressure, and BMI
- Comorbidities: AMI, history of previous myocardial infarction (MI), diabetes mellitus, hypertension, heart failure, and atrial fibrillation
- Vital signs: systolic blood pressure, diastolic blood pressure, heart rate, and respiratory rate
- Laboratory parameters: white blood cells (WBCs), red blood cells (RBCs), platelets, albumin, hemoglobin, aspartate aminotransferase (AST), alanine aminotransferase (ALT), lymphocyte percentage, lymphocyte count, neutrophil

XSL•FO
RenderX

percentage, neutrophil count, neutrophil-to-lymphocyte ratio (NLR), anion gap, bicarbonate, total bilirubin, serum potassium, serum sodium, NT-proBNP, blood urea nitrogen (BUN), serum chloride, creatine kinase isoenzymes (CKMB), international normalized ratio (INR), lactate dehydrogenase (LDH), prothrombin time (PT), activated partial thromboplastin time (PTT), RBC distribution width (RDW), and serum creatinine (SCr)
- Medication use and treatment: antiplatelet agents, antihypertensive drugs, statins, vasopressors, heparin, diuretics, coronary angiography (CAG), or PCI
- Simplified acute physiology score III (APSIII) and sequential organ failure assessment (SOFA)

Variables having more than 20% missing values were eliminated from the final cohort in order to reduce bias brought on by missing data. Other variables with missing data were imputed via multiple imputation, a widely used and effective technique to handle missing data [13] estimating multiple plausible values for each missing entry [14]. Additionally, to enhance the accuracy and reliability of data and models, outliers were identified using box plots [15], and extreme values were mitigated through winsorization [16], wherein data points above the 99th percentile were substituted with the value at the 99th percentile and those below the 1st percentile were replaced with the value at the 1st percentile.

Outcome Variables

Our study cohort comprised adult patients diagnosed with AKI following hospital admission. The diagnosis of AKI was based on the guidelines published in 2012 by the organization called Kidney Disease: Improving Global Outcomes (KDIGO) [17]. AKI was defined by the presence of any one of the following criteria: (1) an increase in SCr by ≥26.5 μmol/L (≥0.3 mg/dL) within 48 hours; (2) an increase in SCr to >1.5 times the baseline value, which is known or presumed to have occurred within the prior 7 days; or (3) a urine output of <0.5 mL/kg/hour for more than 6 hours.

Variable Selection

To minimize the potential bias of multicollinearity and model overfitting, we used the least absolute shrinkage and selection operator (LASSO) regression to select and filter variables in the training dataset. LASSO is a regression-based method that reduces model complexity through the construction of a penalty function. The optimal regularization parameter (λ) was determined using tenfold cross-validation, and variables with nonzero coefficients were retained as the final predictors. Following LASSO regression, the variance inflation factor (VIF) was calculated for the included variables to assess multicollinearity. The VIF values for all predictors are presented in Table S1 in Multimedia Appendix 1.

Model Development and Evaluation

The sample was randomized into a training set and a testing set in a 7:3 ratio. Six ML models were established in the training set: LR, decision tree (DT), naive Bayes (NB), random forest(RF), extreme gradient boosting (XGBoost), and support vector machine (SVM). To minimize overfitting and achieve optimal model performance, the hyperparameters of the ML models were tuned using a grid search. In contrast, the LR model was implemented using its conventional parameter settings. Detailed parameter configurations for each model are presented in Table S2 in Multimedia Appendix 1.

The models' predictive performances were evaluated on the testing dataset by comparing the area under the receiver operating characteristic curve (AUROC), accuracy, precision, sensitivity, and specificity. Among these, AUROC was considered the primary performance metric. The model demonstrating the highest predictive performance was selected as the optimal model for this study. A calibration curve was subsequently plotted to assess the agreement between observed outcomes and predicted probabilities. In addition, decision curve analysis (DCA) was conducted to evaluate the clinical utility of the model. Finally, external validation was performed using data from the Second Affiliated Hospital of Zhengzhou University to assess the model's generalizability and applicability in an independent cohort.

Model Interpretation

To interpret the predictive models, feature importance was visualized for 3 tree-based models (DT, RF, and XGBoost) and interpreted using Shapley Additive Explanation (SHAP) values. Feature importance, quantified through each model's intrinsic evaluation mechanism, directly reflects the contribution of individual input variables to the model's predictive output, thereby elucidating the practical relevance of each feature in the decision-making process. SHAP has been widely leveraged to explain the contribution of predictive variables [18,19] to model output by offering consistent, locally accurate attribution values for every characteristic in the model. Higher values would suggest an elevated likelihood of AKI. SHAP dependence plots for the top 5 feature variables were generated to illustrate the relationship between the SHAP values and feature values, as well as to demonstrate feature interactions. In addition, to visually illustrate the decision-making logic of the model, a SHAP force plot for individual samples was generated to demonstrate the contribution of each variable to the model's prediction.

Statistical Analysis

All analyses were conducted in R version 4.3.1 (R Foundation for Statistical Computing). For continuous variables, the Shapiro-Wilk test was performed to evaluate the normality of the data. The mean (SD) was used for expressing variables having a normal distribution, and the independent samples *t* test was performed for comparison. The Wilcoxon rank-sum test was applied to compare non-normally distributed variables, which were displayed as medians (IQRs). The chi-square or the Fisher exact test was carried out to compare categorical variables, which were presented as numbers and percentages. $P<.05$ suggested statistical significance.

Ethical Considerations

The MIMIC-IV database was approved by the IRBs of the MIT(0403000206) and the BIDMC(2011-P-001418). As all patient data contained within the database are deidentified, individual informed consent was not required. This study has obtained access authorization to the MIMIC-IV database through

XSL•FO
RenderX

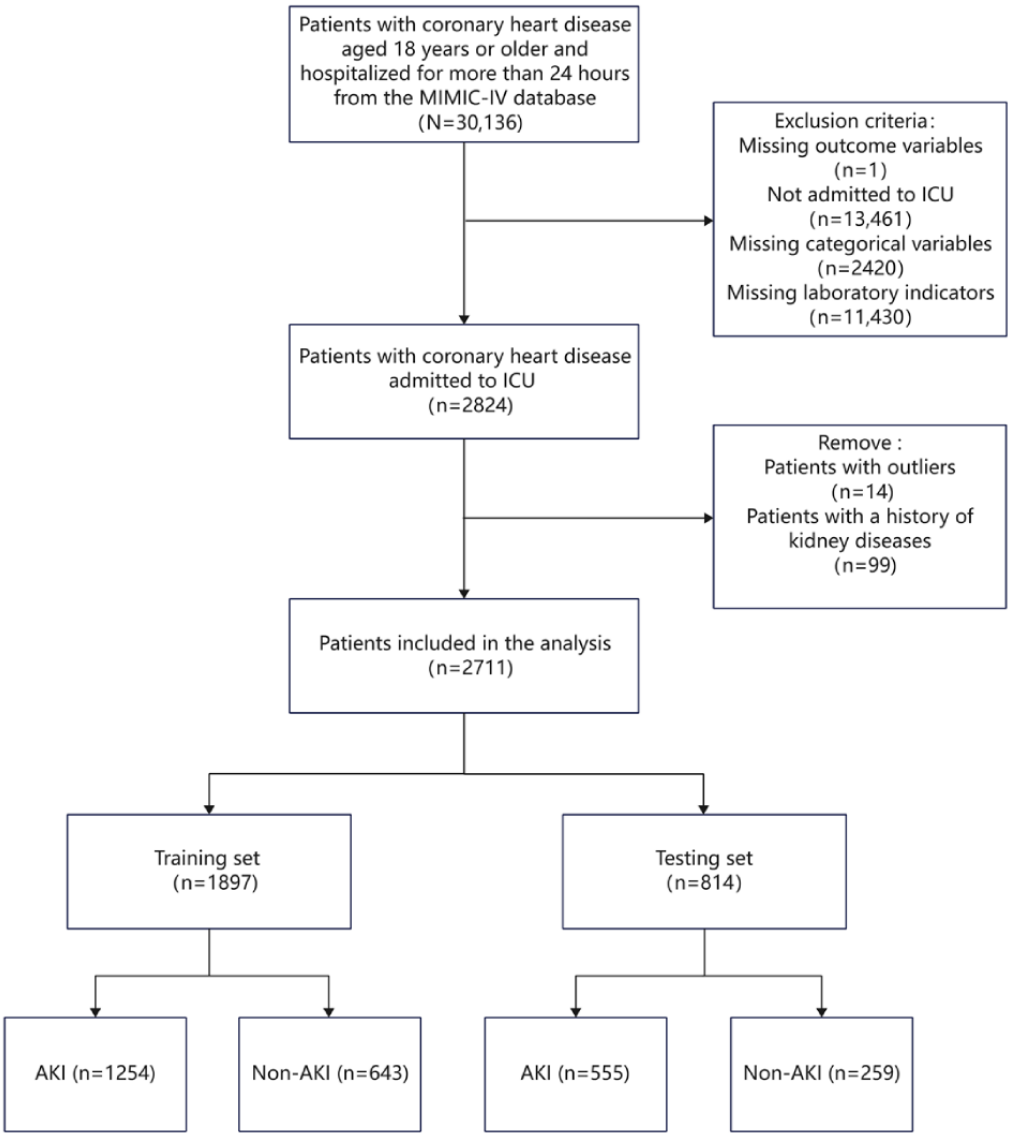
PhysioNet approval (ID: 13470927). In addition, the study protocol was approved by the Ethics Committee of the Second Affiliated Hospital of Zhengzhou University (approval numer: KY2024215). Informed consent was obtained from all patients enrolled at this institution, and all data were fully deidentified. Given that the study did not involve direct interaction with participants, no compensation was provided.

Results

Patient Characteristics

The inclusion process is illustrated in Figure 1. Of the 2711 patients included whose median age was 71 years, 1629 (60.1%) were males, 1985 (73.2%) White, and 1809 (66.7%) cases of AKI. After randomly splitting the dataset into a 7:3 ratio, the training group had 1897 (70%) patients, with a median age of 71 years, 1139 (60%) males, 1386 (73.1%) White, and 1254 (66.1%) cases of AKI. The testing group comprised 814 (30%) patients, with a median age of 71 years, 490 (60.2%) males, 599 (73.6%) White, and 555 (68.2%) cases of AKI. In the training set, 37 variables, including age, race, mechanical ventilation, albumin, and potassium levels, were statistically significant (P<.05). Table 1 presents the baseline characteristics of the patients in the training set, while the baseline characteristics of the testing set can be found in Table S3 in Multimedia Appendix 2.

Figure 1. Participant-screening process diagram. AKI: acute kidney injury; ICU: intensive care unit; MIMIC-IV: Medical Information Mart for Intensive Care IV.



XSL•FO
RenderX

Table 1. Baseline characteristics of the training cohort (n=1897).

Characteristics	Total patients (N=2711)	Training set (n=1897)		
		Non-AKI[a] (n=643)	AKI (n=1254)	*P* value
Age (years), median (IQR)	71.0 (62.0-79.0)	69.0 (60.0-79.0)	71.0 (62.0-78.0)	.02
BMI (kg/m^2), median (IQR)	29.1 (25.5-34.0)	29.0 (25.2-34.4)	29.0 (25.4-34.0)	.96
Gender, n (%)				.08
Male	1629 (60.1)	354 (55.1)	785 (62.6)	—[b]
Female	1082 (39.9)	289 (44.9)	469 (37.4)	—
Marital status, n (%)				.45
Single	661 (24.4)	170 (26.4)	307 (24.5)	—
Divorced/widowed	615 (22.7)	151 (23.5)	281 (22.4)	—
Married	1435 (52.9)	322 (50.1)	666 (53.1)	—
Race, n (%)				.02
White	1985 (73.2)	448 (69.7)	938 (74.8)	—
Non-White	726 (26.8)	195 (30.3)	316 (25.2)	—
Heart rate (beats/minute), median (IQR)	83.0 (73.0-96.0)	83.0 (73.0-97.0)	82.5 (73.0-95.0)	.35
Mechanical ventilation, n (%)	1517 (55.9)	263 (40.9)	809 (64.5)	<.001
Respiratory rate (beats/minute), median (IQR)	18.0 (15.0-22.0)	19.0 (15.0-23.0)	18.0 (15.0-22.0)	.05
Laboratory values, median (IQR)				
Albumin (g/dL)	3.50 (3.00-4.00)	3.60 (3.10-4.10)	3.45 (3.00-3.90)	.001
ALT[c] (IU/L)	22.0 (14.0-38.0)	23.0 (14.0-38.0)	22.0 (14.0-37.0)	.44
Anion gap (mmol/L)	14.0 (12.0-170)	14.0 (12.0-17.0)	14.0 (12.0-17.0)	.32
AST[d] (IU/L)	29.0 (20.0-51.0)	27.0 (19.5-47.0)	29.0 (20.0-54.0)	.08
Bicarbonate (mmol/L)	23.0 (21.0-26.0)	23.0 (21.0-26.0)	23.0 (20.0-25.0)	.01
Bilirubin total (mg/dL)	0.5 (0.3-0.9)	0.5 (0.3-0.8)	0.5 (0.4-0.8)	.12
Potassium (mEq/L)	4.2 (3.8-4.6)	4.1 (3.8-4.6)	4.2 (3.9-4.7)	.01
Sodium (mEq/L)	138 (136-141)	138 (136-141)	138 (135-141)	.50
NT-proBNP[e] (pg/mL)	2422 (720-6896)	1612 (470-4696)	3096 (936-8121)	<.001
BUN[f] (mg/dL)	22.0 (15.0-35.0)	21.0 (14.0-32.0)	23.0 (16.0-37.0)	<.001
Chloride (mEq/L)	103 (100-108)	104 (99.0-107)	103 (99.0-108)	.63
CKMB[g] (ng/mL)	4.0 (2.0-7.0)	3.00 (2.0-6.0)	4.0 (2.0-8.0)	<.001
Hemoglobin (g/dL)	10.3 (8.70-11.9)	10.4 (8.70-12.1)	10.3 (8.70-11.8)	.43
INR[h]	1.3 (1.1-1.5)	1.2 (1.1-1.5)	1.3 (1.1-1.5)	.13
Lactate (mmol/L)	1.6 (1.2-2.4)	1.7 (1.2-2.4)	1.6 (1.2-2.4)	.26
Lymphocyte count (10^9/L)	1.28 (0.84-1.88)	1.32 (0.90-1.94)	1.30 (0.83-1.89)	.14
Lymphocytes (%)	14.1 (8.60-21.7)	15.5 (9.45-22.8)	13.6 (8.30-21.2)	.002
Neutrophil count (10^9/L)	6.41 (4.34-9.74)	5.94 (4.09-8.94)	6.58 (4.51-10.1)	<.001
Neutrophils (%)	75.6 (67.0-83.1)	73.8 (65.8-81.7)	76.1 (67.5-83.2)	.003
Platelets (K/uL)	185 (138-240)	187 (136-246)	185 (137-239)	.79
NLR[i]	4.90 (2.90-9.10)	4.50 (2.70-7.30)	5.20 (2.90-9.57)	<.001
PT[j] (seconds)	13.9 (12.3-16.5)	13.8 (12.2-16.3)	13.9 (12.4-16.5)	.16

XSL•FO
RenderX

Characteristics	Total patients (N=2711)	Training set (n=1897)		
		Non-AKI[a] (n=643)	AKI (n=1254)	*P* value
PTT[k] (seconds)	31.3 (27.6-38.5)	30.9 (27.5-37.8)	31.5 (27.7-39.7)	.09
RBC[l] (m/uL)	3.50 (2.97-4.03)	3.53 (3.01-4.08)	3.46 (2.96-4.01)	.18
RDW[m] (%)	14.6 (13.6-15.9)	14.6 (13.6-15.9)	14.4 (13.5-15.9)	.28
SCr[n] (mg/dL)	1.1 (0.8-1.6)	1.0 (0.8-1.5)	1.1 (0.9-1.7)	<.001
WBC[o] (K/uL)	10.1 (7.40-14.0)	9.50 (7.00-13.4)	10.5 (7.70-14.2)	<.001
Comorbidities, n (%)				
AMI[p]	1105 (40.8)	169 (26.3)	590 (47)	<.001
Atrial fibrillation	1538 (56.7)	315 (49)	747 (59.6)	<.001
Diabetes	1561 (57.6)	346 (53.8)	759 (60.5)	.006
Heart failure	2252 (83.1)	497 (77.3)	1078 (86)	<.001
Hypertension	2558 (94.4)	609 (94.7)	1185 (94.5%)	.93
Old MI[q]	1254 (46.3)	213 (33.1)	656 (52.3)	<.001
Drugs, n (%)				
Angiotensin-converting enzyme (ACE) inhibitor–angiotensin receptor blocker (ACEI-ARB)	1262 (46.6)	281 (43.7)	611 (48.7)	.04
Antibiotic	1928 (71.1)	388 (60.3)	935 (74.6)	<.001
Antiplatelet drug	2148 (79.2)	407 (63.3)	1087 (86.7)	<.001
Aspirin	1747 (64.4)	319 (49.6)	894 (71.3)	<.001
Clopidogrel	602 (22.2)	78 (12.1)	350 (27.9)	<.001
Dual-antiplatelet therapy	504 (18.6)	64 (10)	293 (23.4)	<.001
Dobutamine	121 (4.5)	17 (2.6)	74 (5.9)	.002
Dopamine	144 (5.31)	30 (4.7)	78 (6.2)	.20
Epinephrine	332 (12.2)	44 (6.8)	189 (15.1)	<.001
Heparin	947 (34.9)	149 (23.2)	519 (41.4)	<.001
Hydragogue	2172 (80.1)	451 (70.1)	1065 (84.9)	<.001
Noradrenaline	865 (31.9)	132 (20.5)	476 (38)	<.001
Two vasoactive drugs	258 (9.5)	32 (5)	140 (11.2)	<.001
Three vasoactive drugs	63 (2.3)	7 (1.1)	42 (3.3)	.005
Tatin	2138 (78.9)	429 (66.7)	1064 (84.8)	<.001
CAG[r], n (%)	152 (5.6)	30 (4.7)	78 (6.2)	.20
PCI[s], n (%)	76 (2.8)	7 (1.1)	48 (3.8)	.001
APSIII[t], mean (SD)	43.5 (17.0)	40.3 (16.1)	45.2 (17.4)	<.001

XSL•FO
RenderX

Characteristics	Total patients (N=2711)	Training set (n=1897)		
		Non-AKI[a] (n=643)	AKI (n=1254)	*P* value
SOFA[u], median (IQR)	4.00 (2.00-6.00)	4.00 (2.00-6.00)	4.00 (2.00-7.00)	<.001

[a]AKI: acute kidney injury.
[b]Not applicable.
[c]ALT: alanine aminotransferase.
[d]AST: aspartate aminotransferase.
[e]NT-proBNP: N-terminal pro–B-type natriuretic peptide.
[f]BUN: blood urea nitrogen.
[g]CKMB: creatine kinase isoenzymes.
[h]INR: international normalized ratio.
[i]NLR: neutrophil-to-lymphocyte ratio.
[j]PT: prothrombin time.
[k]PTT: partial thromboplastin time.
[l]RBC: red blood cell.
[m]RDW: red blood cell distribution width.
[n]SCr: serum creatinine.
[o]WBC: white blood cell.
[p]AMI: acute myocardial infarction.
[q]MI: myocardial infarction.
[r]CAG: coronary angiography.
[s]PCI: percutaneous coronary intervention.
[t]APSIII: acute physiology score III.
[u]SOFA: sequential organ failure assessment.

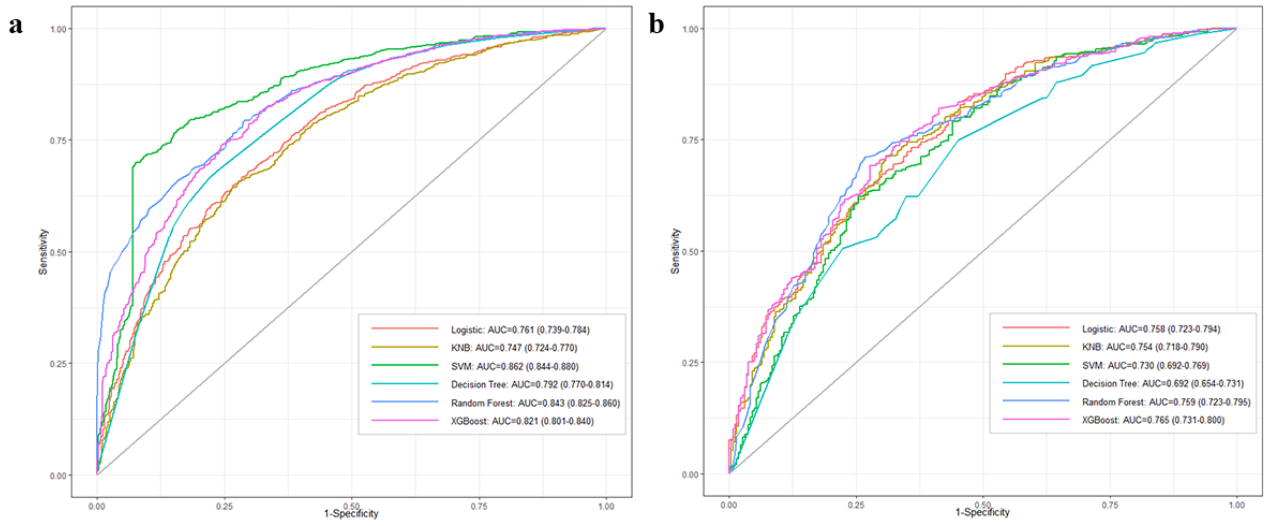
Variable Selection

Based on the feature selection results from the LASSO regression (Figure S1 in Multimedia Appendix 3), 13 features were included: age, mechanical ventilation, NT-proBNP, NLR, AMI, history of prior MI, antiplatelet therapy, dual-antiplatelet therapy, heparin, diuretics, norepinephrine, statins, and APSIII.

ML Model Performance

Six ML models were created to forecast AKI occurrence. Figure 2 illustrates the ROC performance of these models in both training and testing cohorts. In the testing cohort, the XGBoost model (AUROC=0.765) demonstrated the best forecasting performance, followed by LR (AUROC=0.758), NB (AUROC=0.754), RF (AUROC=0.759), SVM (AUROC=0.731), and DT (AUROC=0.692). Table 2 presents detailed performance metrics for all 6 models. The XGBoost model demonstrated superior discriminative ability, with accuracy (0.725) and sensitivity (0.759) higher than those of the other 5 models, indicating that XGBoost is the optimal model.

Figure 2. Comparison of AUC values across 6 models: (a) training set and (b) testing set. AUC: area under the curve; KNB: kernel naive Bayes; SVM: support vector machine; XGBoost: extreme gradient boosting.



XSL•FO
RenderX

Table 2. Performance indicators of 6 models.

Model and datasets	AUROC[a]	Accuracy	Precision	Sensitivity	Specificity
LR[b]					
Training set	0.761	0.687	0.817	0.679	0.703
Testing set	0.758	0.720	0.795	0.537	0.840
External validation set	0.823	0.801	0.775	0.782	0.816
NB[c]					
Training set	0.747	0.679	0.822	0.658	0.722
Testing set	0.754	0.706	0.832	0.714	0.691
External validation set	0.780	0.761	0.753	0.693	0.816
SVM[d]					
Training set	0.862	0.775	0.947	0.699	0.924
Testing set	0.731	0.661	0.839	0.622	0.745
External validation set	0.786	0.761	0.733	0.733	0.784
DT[e]					
Training set	0.792	0.709	0.849	0.681	0.764
Testing set	0.692	0.686	0.780	0.750	0.548
External validation set	0.771	0.770	0.747	0.733	0.800
RF[f]					
Training set	0.843	0.766	0.843	0.794	0.711
Testing set	0.759	0.717	0.851	0.710	0.734
External validation set	0.771	0.752	0.747	0.673	0.816
XGBoost[g]					
Training set	0.821	0.769	0.845	0.796	0.715
Testing set	0.765	0.725	0.824	0.759	0.653
External validation set	0.835	0.788	0.757	0.772	0.800

[a]AUROC: area under the receiver operating characteristic curve.

[b]LR: logistic regression.

[c]NB: naive Bayes.

[d]SVM: support vector machine.

[e]DT: decision tree.

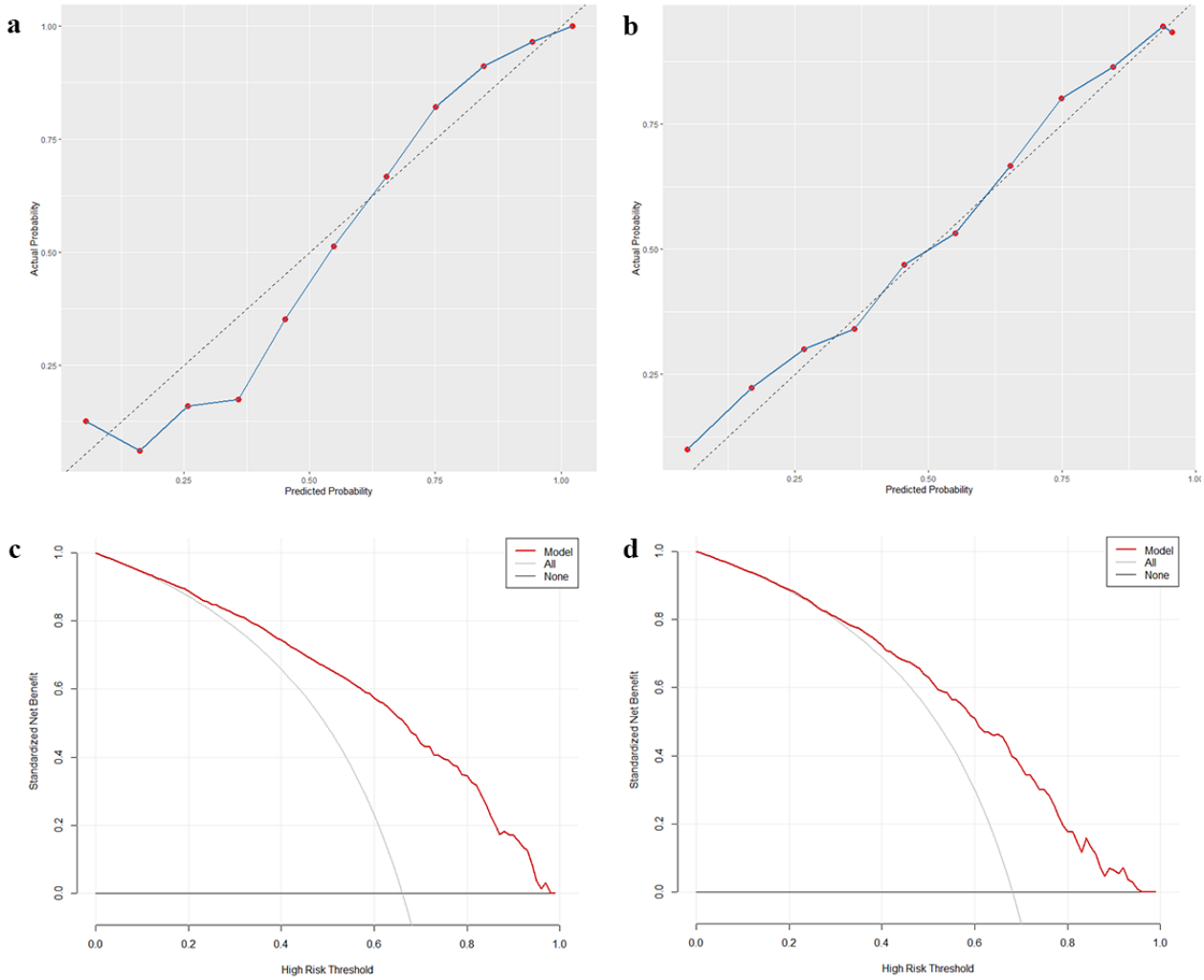
[f]RF: random forest.

[g]XGBoost: extreme gradient boosting.

Calibration curves and DCA were used to further assess the ideal model (Figure 3). The calibration curve is an important tool for assessing the performance of predictive models, as it compares the predicted probabilities with actual observed outcomes to measure accuracy and reliability. Clinical DCA evaluates the practical value of a clinical prediction model by comparing the net benefit of different decision thresholds. Based on the results, the calibration curve of the testing set demonstrated excellent calibration of the model, while DCA indicated that the model provides clinical net benefit across a threshold probability range of 0.20-0.95, suggesting that the model has outstanding clinical applicability.

XSL•FO
RenderX

Figure 3. Calibration curve of the XGBoost model: (a) training set and (b) testing set. DCA of the XGBoost model: (c) training set and (d) testing set. DCA: decision curve analysis; XGBoost: extreme gradient boosting.

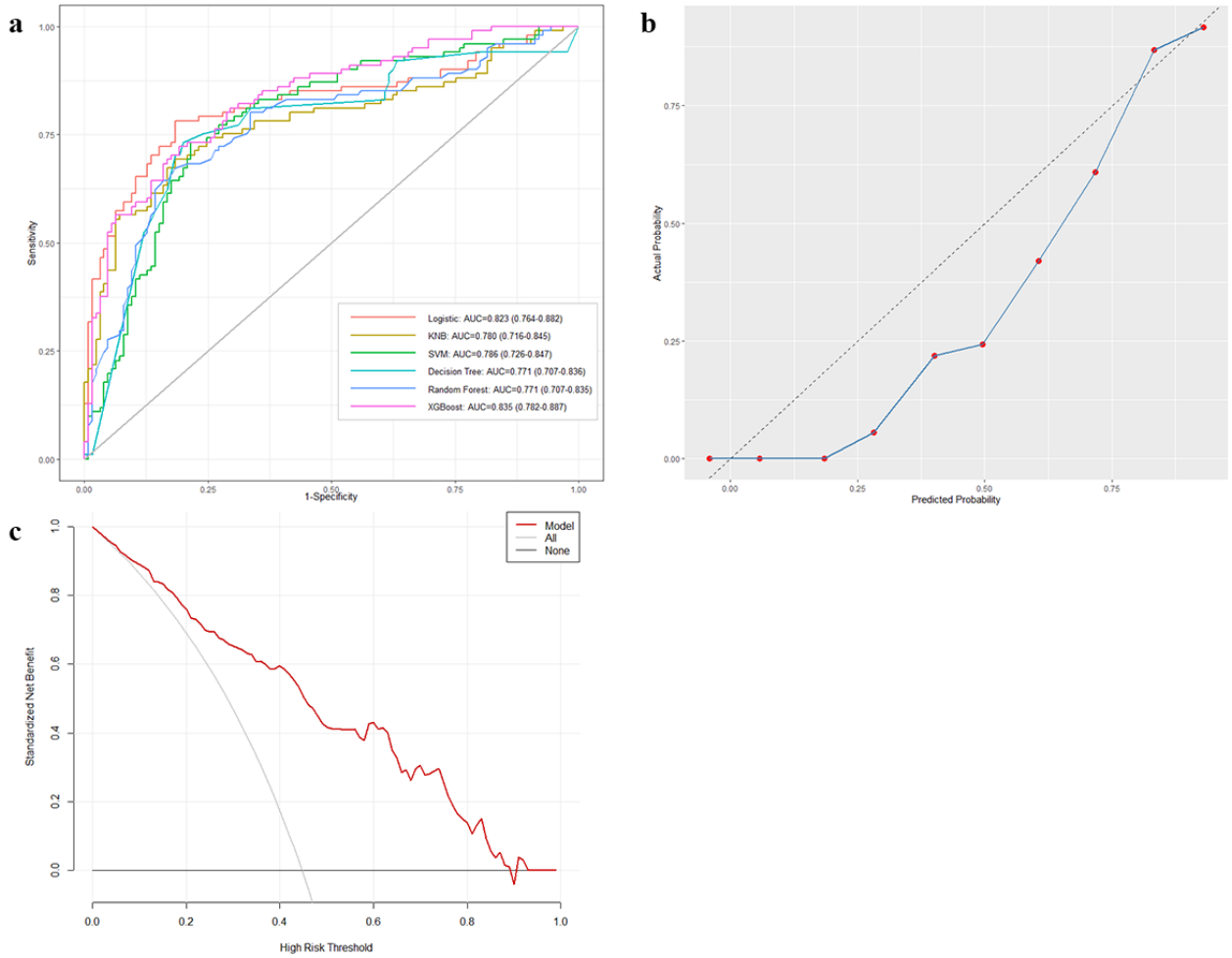


External Validation

Clinical data from 226 critically ill individuals with CHD, admitted to the Second Affiliated Hospital of Zhengzhou University between January 1, 2021, and August 1, 2024, were collected and the patients included in the external validation group. Their baseline characteristics are provided in Table S4 in Multimedia Appendix 2. As shown in Figure 4a, the XGBoost model in the external validation set exhibited the highest AUROC of 0.835, similar to its performance in the testing cohort. Furthermore, the calibration curve demonstrated good calibration (Figure 4b), and the DCA curve indicated net benefit at threshold probabilities lower than 0.9 (Figure 4c), indicating that the XGBoost model has superior generalizability and can be reliably applied to external data.

XSL•FO
RenderX

Figure 4. (a) Comparison of AUC values of the 6 models in the external validation set and (b) the calibration curve and (c) the DCA curve of the XGBoost model. AUC: area under the curve; DCA: decision curve analysis; KNB: kernel naive Bayes; SVM: support vector machine; XGBoost: extreme gradient boosting.

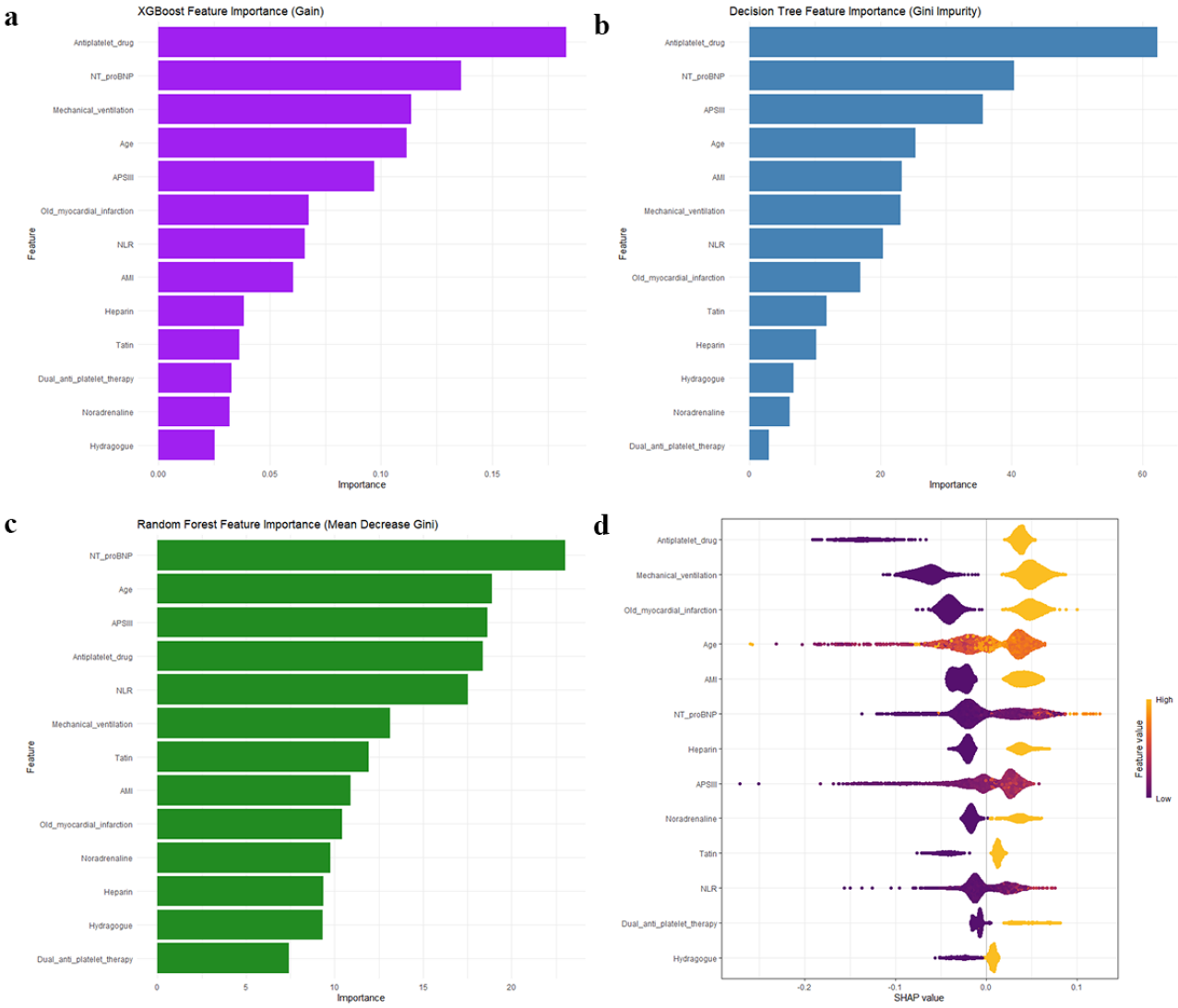


Model Interpretation

Our study compared the feature importance rankings of XGBoost (Figure 5a), DT (Figure 5b), and RF (Figure 5c) models, and provided global and local explanations of the predictions using SHAP values (Figure 5d), to comprehensively assess the contribution of each clinical feature to the risk of AKI. NT-proBNP ranked among the top 3 predictors in XGBoost, RF, and DT models, and its global contribution was also significant according to SHAP analysis. The SHAP dependence plot (Figure S2 in Multimedia Appendix 3) shows that as the NT-proBNP value increased, the incidence of AKI also rose, which is highly consistent with the clinical significance of NT-proBNP as a biomarker for heart failure and renal dysfunction, thereby confirming its predictive value for AKI. Age ranked high in XGBoost (fourth in gain importance) and RF models, with SHAP values indicating a positive contribution to the prediction, aligning with the clinical consensus that elderly patients are at a higher risk for AKI. Antiplatelet drugs ranked first in gain importance in the XGBoost model and in Gini impurity in the DT model; the SHAP value for high feature importance was 0.05, the SHAP value for low feature importance reached –0.2. This suggests that the use of antiplatelet drugs has a limited contribution to the promotion of AKI, while patients not using them have a lower risk of AKI. Mechanical ventilation ranked third in the XGBoost model, with its global SHAP contribution indicating a significant positive correlation with AKI risk, which supports the potential mechanisms of iatrogenic renal injury in critically ill patients. APSIII ranked third in both RF and DT models, and its SHAP dependence plot (Multimedia Appendix 3) suggests that when APSIII exceeds 40, the incidence of AKI significantly increases, reflecting the stable predictive value of composite physiological indices in AKI risk prediction.

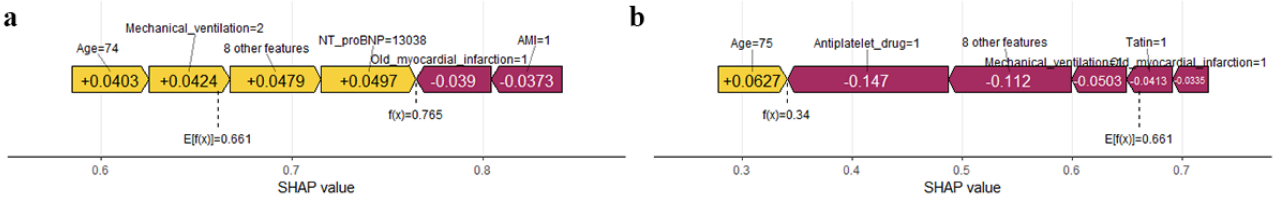
XSL•FO
RenderX

Figure 5. Feature importance derived from (a) XGBoost, (b) DT, and (c) RF models, along with (d) SHAP analysis summary diagram based on XGBoost. Each row represents a feature; a point represents a sample; yellow represents a high feature value; and purple represents a low feature value. A further distance from a point to the baseline SHAP value of 0 indicates a greater impact on the output. AMI: acute myocardial infarction; APSIII: acute physiology score III; NLR: neutrophil-to-lymphocyte ratio; NT-proBNP: N-terminal pro–B-type natriuretic peptide.



To intuitively demonstrate the consistency between the model's decision logic and clinical-pathological mechanisms, this study selected 2 typical AKI risk prediction cases for SHAP force plot analysis (Figure 6). The SHAP analysis of individual samples reveals how each variable influences the model's decision-making. As shown in Figure 6a, age, NT-proBNP, and mechanical ventilation usage contributed the highest positive predictive values, while the absence of AMI and old MI reduced the risk of AKI. In Figure 6b, the age of 75 years increased the risk of AKI, and the absence of antiplatelet drugs and mechanical ventilation usage significantly reduced the risk of AKI. These variables are all among the top 6 predictive features for AKI in the XGBoost model.

Figure 6. SHAP force plot of (a) a patient with AKI and (b) a patient without AKI. Features contributing to an increase in the predicted value are shown in yellow, whereas those contributing to a decrease are shown in red. The length of the arrows represents the magnitude of each feature's influence on the model output. The scale on the x-axis indicates the extent to which each feature increases or decreases the predicted value. AKI: acute kidney injury; AMI: acute myocardial infarction; NT-proBNP: N-terminal pro–B-type natriuretic peptide; SHAP: Shapley Additive Explanation.



XSL•FO
RenderX

Discussion

Principal Findings

This study, based on data from the MIMIC-IV database and the Second Affiliated Hospital of Zhengzhou University, is the first to develop and externally validate an ML model for predicting AKI in critically ill patients with CHD. By incorporating 13 clinical variables, 6 ML algorithms were systematically compared. The results demonstrated that the XGBoost model exhibited superior predictive performance in both the internal testing set (AUROC=0.765, 95% CI 0.731-0.800) and the external validation cohort (AUROC=0.850, 95% CI 0.731-0.800). Calibration curve analysis and DCA further confirmed the model's excellent calibration and wide range of clinically beneficial threshold probabilities (0.20-0.95). External validation also confirmed the model's net clinical benefit across threshold probabilities below 0.9, underscoring its strong generalizability.

In model development, we used a feature selection strategy that combined LASSO regression with VIF analysis, consistent with methodologies adopted in previous studies [20]. We ultimately included13 variables and applied tree-based feature importance rankings, along with SHAP analysis, to enhance model interpretability. Our findings identified antiplatelet therapy, NT-proBNP, age, mechanical ventilation, and APSIII as the 5 most influential predictors, all of which were clinically plausible. Notably, NT-proBNP ranked among the top 3 variables in importance across the XGBoost, RF, and DT models and contributed significantly to AKI prediction, as indicated by SHAP values—an observation well aligned with its known pathophysiological role. As a sensitive biomarker of cardiorenal syndrome, NT-proBNP is cleared by glomerular filtration and can reflect early declines in the glomerular filtration rate (GFR) during the initial stages of AKI [21,22]. This finding supports the mechanistic evidence reported by Wang et al [23], who observed elevated NT-proBNP levels in patients with postoperative AKI following cardiac surgery. In addition, Liu et al [24] reported that preoperative NT-proBNP levels can more effectively predict postoperative AKI in patients undergoing noncardiac surgery, further corroborating the prognostic utility of NT-proBNP.

Given that our study cohort consisted of patients with CHD, we included relevant pharmacological agents in the predictive model. Results revealed that antiplatelet therapy ranks first in importance in both the XGBoost and DT models. SHAP analysis indicated that the risk of AKI is lowest among patients not receiving antiplatelet agents. Although monotherapy did not significantly increase AKI risk, dual-antiplatelet therapy was associated with a markedly elevated probability of AKI. Concerning how antiplatelet medications affect renal function, a Cochrane systematic review [25] showed that the risk of renal dysfunction in users of antiplatelet drugs is not high. Another systematic review indicated that in patients with chronic kidney disease (CKD), antiplatelet medication did not reduce the eGFR drop rate (−0.15 mL/1.73m²/year, 95% CI −0.89 to 1.20, I^2=40.8%) and affected renal failure events (odds ratio [OR] 0.87, 95% CI 0.32-1.55) [26]. However, retrospective case-control research by Fored et al [27] on the correlation of analgesic use with renal function revealed that in subjects who rarely used acetaminophen, frequent aspirin use was linked to a 2.5-fold increase in the likelihood of chronic renal failure compared to nonusers, with the relative risk increasing as the cumulative lifetime dose increased. Similarly, Bonet-Monné et al [28] noted a decrease in renal function associated with the use of nonsteroidal anti-inflammatory drugs (NSAIDs), analgesics, and antiplatelet drugs, which aligns with our findings.

As a core indicator for assessing disease severity in critically ill patients, APSIII systematically quantifies the extent of systemic pathophysiological derangements by integrating 12 acute physiological parameters, thereby revealing its close association with the risk of AKI. In this study, the SHAP dependence plot demonstrated a marked increase in AKI incidence when the APSIII exceeded 40. This threshold effect may be attributable to the severe hemodynamic instability reflected by high APSIII values [29]. In addition, the SOFA score, a commonly used tool in ICUs, has also been widely applied for predicting AKI in critically ill patients [30]. Although originally developed for sepsis, the SOFA score has been adopted by numerous cardiovascular studies as a quantitative measure of organ dysfunction [31-33]. In our cohort, the median SOFA score was 4.00 (IQR 2.00-6.00), suggesting that a considerable proportion of patients may have been at risk for infection. Notably, although the SOFA score was not selected as a feature variable in the modeling process, NLR, an established inflammatory marker, was selected by LASSO regression and incorporated into the model. This highlights the potential role of infection in the development of AKI among critically ill patients. For example, systemic inflammatory responses may lead to tubular epithelial injury and hemodynamic disturbances that impair renal perfusion, thereby triggering the onset of AKI.

Furthermore, our study revealed that advancing age and the use of mechanical ventilation also contribute to a higher incidence of AKI. Elderly adults represent a particularly vulnerable population for AKI, as the GFR naturally declines with age and the renal functional reserve diminishes, rendering them more susceptible to AKI under stress conditions. According to the SHAP dependence plot, patients between the ages of 70 and 80 years are at the highest risk for developing AKI. Retrospective studies have shown that younger females are less likely to develop postoperative AKI; however, the incidence increases progressively with age [34]. An ML model designed for predicting postoperative AKI similarly identified age as a critical predictor [35]. The use of mechanical ventilation has likewise been associated with an elevated risk of AKI, a finding consistently supported by many studies. Patients who need invasive mechanical ventilation have a threefold higher risk of AKI, according to a high-quality systematic review and meta-analysis, with no decrease in risk despite adjustments in the tidal volume or positive end-expiratory pressure (PEEP) settings [36].

XSL•FO
RenderX

Comparison With Previous Work

Forecasting AKI in individuals in the ICU has long been a focus in intensive care medicine. In recent years, multiple studies have developed ML models for AKI prediction. For example, Yue et al [37] developed a predictive model for AKI in patients with sepsis, Cho et al [38] established an AKI prediction model applicable to patients in general wards, and Zhou et al [39] established a forecasting model for AKI in the cohort with acute respiratory distress syndrome (ARDS) [39], incorporating 12 predictive variables, with XGBoost emerging as the ideal model, which aligns with our findings. Tseng et al [40] used 94 preoperative and intraoperative features to create a prediction model for cardiac surgery–associated AKI (CSA-AKI), where the RF model realized the highest AUROC (0.839, 95% CI 0.772-0.898) and was identified as the best model. They also used SHAP summary and dependence plots to explain the model, a similar approach to ours. Some AKI-forecasting models have been constructed for cardiovascular disease, but these primarily focus on predicting AKI following cardiac surgery. For instance, Kuno et al [41] built one for AKI after PCI [41], and Sun et al [42] predicted contrast-induced kidney injury in patients with AMI. However, patients with severe CHD in the ICU typically receive conservative treatment rather than surgical intervention. Thus, existing predictive models do not apply to these patients. At present, no forecasting models are designed for AKI in the patients with CHD in the ICU. Accordingly, we developed a dedicated predictive model for AKI among patients with CHD in the ICU, using the MIMIC-IV database. To the best of our knowledge, this is the first model specifically designed for the entire population of critically ill patients with CHD. Compared with previously established models limited to single clinical scenarios, our tool offers improved support for clinicians in identifying high-risk patients within complex clinical settings.

Strengths

The strength of ML is in integrating diverse data types and providing personalized treatment recommendations for patients. This study included data from 2 centers: the BIDMC and the Second Affiliated Hospital of Zhengzhou University. The data were rich and multidimensional, providing a meaningful representation of real-world clinical practice. Additionally, new variables not included in previous models, such as NT-proBNP and NLR, along with additional categorical variables, were incorporated with the aim of improving the model's performance. Moreover, the feature variables in our study differ from those in previous research. We used 13 feature variables to construct the model, including 4 continuous variables and 9 categorical variables. Categorical variables predominated in our model; however, in existing AKI prediction models, most selected variables are continuous. This discrepancy may be attributed to the fact that in addition to laboratory indicators, 25 binary categorical variables were incorporated, whereas previous studies have predominantly focused on laboratory indicators and other continuous variables, often lacking detailed data on comorbidities and medication use. Our results suggest that these categorical variables may have higher predictive value, indicating that future predictive models incorporating more categorical variables could potentially enhance predictive performance.

Limitations

First, as a retrospective study based on the MIMIC-IV database, the substantial missing data for several key variables, such as contrast agent dosage, infection markers (eg, procalcitonin and C-reactive protein), and cardiac biomarkers, may have led to the loss of potentially valuable predictive information related to contrast-induced nephropathy, AMI, and sepsis-associated AKI. This feature selection bias could have adversely impacted the model's ability to accurately identify AKI. Second, although hyperparameters were optimized using a grid search approach, the inclusion of 13 feature variables may have contributed to overfitting in certain models, such as the SVM and DT classifiers. Third, the external validation dataset was small, which may impact the external validity of the model. Therefore, further research involving larger sample sizes and multiple centers is necessary. Fourth, multiple imputation was used to estimate variables with less than 20% missing data, which may have introduced deviations from the true values. Additionally, this study aimed to provide a broadly applicable AKI risk assessment model for all critically ill patients with CHD—a clinical context in which the etiology of AKI is often initially unclear. However, due to the limited size of the external validation cohort, we did not perform more refined subgroup analyses to develop prediction models tailored to patients with specific comorbidities, which may have obscured potential heterogeneity across subpopulations with CHD.

Future Work

This study established the first predictive model for AKI encompassing the entire population of critically ill patients with CHD. However, its generalizability requires further confirmation through external validation in multicenter settings. We plan to integrate multicenter data from both CCUs and general ICUs to expand the sample size of the external validation cohort, thereby providing adequate statistical power for subsequent subgroup analyses. In the future, we intend to conduct collaborative multicenter studies and perform more granular stratification of the target population, for instance, critically ill patients with CHD complicated by MI and those undergoing PCI. These efforts aim to develop tailored AKI prediction models specific to different comorbid conditions, further addressing current gaps in our research. Moreover, we will develop an interactive explanatory interface to enable a closed-loop decision support system—from risk alerting to intervention recommendations. In parallel, we will design a user-friendly interface, formulate detailed implementation guidelines, and initiate pilot projects to evaluate the model's practical performance and user experience.

Conclusion

In conclusion, ML models can be a trustworthy tool for forecasting AKI in individuals with severe CHD. Across tested models, the XGBoost model demonstrated the best performance. It can help physicians identify patients with CHD who are at risk of AKI early, allowing for prompt therapies to lower mortality and enhance prognosis.

XSL•FO
RenderX

Acknowledgments

This study was supported by the Henan Province Medical Science and Technology Research Plan Joint Construction Project (grant number: LHGJ20220438).

Conflicts of Interest

None declared.

Multimedia Appendix 1
Variance inflation factors (VIFs) of variables and model parameters.
[DOCX File , 14 KB - medinform_v13i1e72349_app1.docx]

Multimedia Appendix 2
Baseline characteristics of the test set and the external validation set.
[DOCX File , 34 KB - medinform_v13i1e72349_app2.docx]

Multimedia Appendix 3
Variable selection based on least absolute shrinkage and selection operator (LASSO) regression and Shapley Additive Explanation (SHAP) dependence plot of the extreme gradient boosting (XGBoost) model.
[DOCX File , 222 KB - medinform_v13i1e72349_app3.docx]

References

1. Chang C, Fu C, Yang C, Fan P, Li P, Hsu G, et al. Society of Thoracic Surgeons score predicts kidney injury in patients not undergoing bypass surgery. Ann Thorac Surg 2015 Jan;99(1):123-129. [doi: 10.1016/j.athoracsur.2014.07.072] [Medline: 25440280]
2. Bagur R, Webb JG, Nietlispach F, Dumont E, De Larochellière R, Doyle D, et al. Acute kidney injury following transcatheter aortic valve implantation: predictive factors, prognostic value, and comparison with surgical aortic valve replacement. Eur Heart J 2010 Apr;31(7):865-874 [FREE Full text] [doi: 10.1093/eurheartj/ehp552] [Medline: 20037180]
3. Schiefer J, Bernardi MH, Lichtenegger P, Schak G, Atallah L, Ristl R, et al. Incidence and outcomes of AKI in postoperative patients admitted to ICU using full KDIGO criteria - a cohort study. J Clin Anesth 2023 Oct;89:111156 [FREE Full text] [doi: 10.1016/j.jclinane.2023.111156] [Medline: 37356195]
4. Ma K, Li J, Shen G, Zheng D, Xuan Y, Lu Y, et al. Development and validation of a risk nomogram model for predicting contrast-induced acute kidney injury in patients with non-ST-elevation acute coronary syndrome undergoing primary percutaneous coronary intervention. Clin Interv Aging 2022;17:65-77 [FREE Full text] [doi: 10.2147/CIA.S349159] [Medline: 35115770]
5. Peng X, Li L, Wang X, Zhang H. A machine learning-based prediction model for acute kidney injury in patients with congestive heart failure. Front Cardiovasc Med 2022 Mar 4;9:842873 [FREE Full text] [doi: 10.3389/fcvm.2022.842873] [Medline: 35310995]
6. Baek S, Jeong YJ, Kim Y, Kim JY, Kim JH, Kim EY, et al. Development and validation of a robust and interpretable early triaging support system for patients hospitalized with COVID-19: predictive algorithm modeling and interpretation study. J Med Internet Res 2024 Jan 11;26:e52134 [FREE Full text] [doi: 10.2196/52134] [Medline: 38206673]
7. Trinkley KE, Simon ST, Rosenberg MA. Impact of an alert-based inpatient clinical decision support tool to prevent drug-induced long QT Syndrome: large-scale, system-wide observational study. J Med Internet Res 2025 Apr 14;27:e68256 [FREE Full text] [doi: 10.2196/68256] [Medline: 40228236]
8. Guan C, Gong A, Zhao Y, Yin C, Geng L, Liu L, et al. Interpretable machine learning model for new-onset atrial fibrillation prediction in critically ill patients: a multi-center study. Crit Care 2024 Oct 29;28(1):349 [FREE Full text] [doi: 10.1186/s13054-024-05138-0] [Medline: 39473013]
9. Peng J, Lu Y, Chen L, Qiu K, Chen F, Liu J, et al. The prognostic value of machine learning techniques versus Cox regression model for head and neck cancer. Methods 2022 Sep;205:123-132. [doi: 10.1016/j.ymeth.2022.07.001] [Medline: 35798257]
10. Goldberger AL, Amaral LA, Glass L, Hausdorff JM, Ivanov PC, Mark RG, et al. PhysioBank, PhysioToolkit, and PhysioNet: components of a new research resource for complex physiologic signals. Circulation 2000 Jun 13;101(23):E215-E220. [doi: 10.1161/01.cir.101.23.e215] [Medline: 10851218]
11. Oweira H, Schmidt J, Mehrabi A, Kulaksiz H, Schneider P, Schöb O, et al. Comparison of three prognostic models for predicting cancer-specific survival among patients with gastrointestinal stromal tumors. Future Oncol 2018 Feb;14(4):379-389. [doi: 10.2217/fon-2017-0450] [Medline: 29318911]

XSL•FO
RenderX

12. Johnson AEW, Bulgarelli L, Shen L, Gayles A, Shammout A, Horng S, et al. MIMIC-IV, a freely accessible electronic health record dataset. Sci Data 2023 Jan 03;10(1):1 [FREE Full text] [doi: 10.1038/s41597-022-01899-x] [Medline: 36596836]
13. Zhang Z. Multiple imputation with multivariate imputation by chained equation (MICE) package. Ann Transl Med 2016 Jan;4(2):30 [FREE Full text] [doi: 10.3978/j.issn.2305-5839.2015.12.63] [Medline: 26889483]
14. Lee KJ, Simpson JA. Introduction to multiple imputation for dealing with missing data. Respirology 2014 Feb;19(2):162-167 [FREE Full text] [doi: 10.1111/resp.12226] [Medline: 24372814]
15. Pirson M, Dramaix M, Leclercq P, Jackson T. Analysis of cost outliers within APR-DRGs in a Belgian general hospital: two complementary approaches. Health Policy 2006 Mar;76(1):13-25. [doi: 10.1016/j.healthpol.2005.04.008] [Medline: 15921818]
16. Yang L, Zhang X, Chen J. Winsorization greatly reduces false positives by popular differential expression methods when analyzing human population samples. Genome Biol 2024 Oct 30;25(1):282 [FREE Full text] [doi: 10.1186/s13059-024-03230-w] [Medline: 39478636]
17. Khwaja A. KDIGO clinical practice guidelines for acute kidney injury. Nephron Clin Pract 2012;120(4):c179-c184 [FREE Full text] [doi: 10.1159/000339789] [Medline: 22890468]
18. Xu L, Li C, Gao S, Zhao L, Guan C, Shen X, et al. Personalized prediction of long-term renal function prognosis following nephrectomy using interpretable machine learning algorithms: case-control study. JMIR Med Inform 2024 Sep 20;12:e52837 [FREE Full text] [doi: 10.2196/52837] [Medline: 39303280]
19. Lv Z, Cui F, Zou Q, Zhang L, Xu L. Anticancer peptides prediction with deep representation learning features. Brief Bioinform 2021 Sep 02;22(5):bbab008. [doi: 10.1093/bib/bbab008] [Medline: 33529337]
20. Zhang R, Liu Y, Zhang Z, Luo R, Lv B. Interpretable machine learning model for predicting postpartum depression: retrospective study. JMIR Med Inform 2025 Jan 20;13:e58649 [FREE Full text] [doi: 10.2196/58649] [Medline: 39864955]
21. Dutta A, Saha S, Bahl A, Mittal A, Basak T. A comprehensive review of acute cardio-renal syndrome: need for novel biomarkers. Front Pharmacol 2023 May 23;14:1152055 [FREE Full text] [doi: 10.3389/fphar.2023.1152055] [Medline: 37288107]
22. Bansal N, Zelnick L, Shlipak MG, Anderson A, Christenson R, Deo R, CRIC Study Investigators. Cardiac and stress biomarkers and chronic kidney disease progression: the CRIC Study. Clin Chem 2019 Nov;65(11):1448-1457 [FREE Full text] [doi: 10.1373/clinchem.2019.305797] [Medline: 31578216]
23. Wang C, Gao Y, Tian Y, Wang Y, Zhao W, Sessler DI, et al. Prediction of acute kidney injury after cardiac surgery from preoperative N-terminal pro-B-type natriuretic peptide. Br J Anaesth 2021 Dec;127(6):862-870 [FREE Full text] [doi: 10.1016/j.bja.2021.08.015] [Medline: 34561052]
24. Liu X, Pang K, Tang Y, Le Y. Corrigendum: The predictive value of pre-operative N-terminal pro-B-type natriuretic peptide in the risk of acute kidney injury after non-cardiac surgery. Front Med (Lausanne) 2022;9:1010604 [FREE Full text] [doi: 10.3389/fmed.2022.1010604] [Medline: 36186773]
25. Natale P, Palmer SC, Saglimbene VM, Ruospo M, Razavian M, Craig JC, et al. Antiplatelet agents for chronic kidney disease. Cochrane Database Syst Rev 2022 Feb 28;2(2):CD008834 [FREE Full text] [doi: 10.1002/14651858.CD008834.pub4] [Medline: 35224730]
26. Su X, Yan B, Wang L, Lv J, Cheng H, Chen Y. Effect of antiplatelet therapy on cardiovascular and kidney outcomes in patients with chronic kidney disease: a systematic review and meta-analysis. BMC Nephrol 2019 Aug 7;20(1):309 [FREE Full text] [doi: 10.1186/s12882-019-1499-3] [Medline: 31390997]
27. Fored CM, Ejerblad E, Lindblad P, Fryzek JP, Dickman PW, Signorello LB, et al. Acetaminophen, aspirin, and chronic renal failure. N Engl J Med 2001 Dec 20;345(25):1801-1808. [doi: 10.1056/NEJMoa010323] [Medline: 11752356]
28. Bonet-Monné S, Urgell CV, Sáez MJP, Puertolás OC, Baena-Díez JM, Pascual J, et al. NSAIDs, analgesics, antiplatelet drugs, and decline in renal function: a retrospective case-control study with SIDIAP database. BMC Pharmacol Toxicol 2024 Aug 28;25(1):58 [FREE Full text] [doi: 10.1186/s40360-024-00771-5] [Medline: 39198874]
29. Yang J, Peng H, Luo Y, Zhu T, Xie L. Explainable ensemble machine learning model for prediction of 28-day mortality risk in patients with sepsis-associated acute kidney injury. Front Med 2023 May 18;10:1165129 [FREE Full text] [doi: 10.3389/fmed.2023.1165129] [Medline: 37275353]
30. Hua Y, Ding N, Jing H, Xie Y, Wu H, Wu Y, et al. Association between SOFA score and risk of acute kidney injury in patients with diabetic ketoacidosis: an analysis of the MIMIC-IV database. Front Endocrinol (Lausanne) 2024;15:1462330 [FREE Full text] [doi: 10.3389/fendo.2024.1462330] [Medline: 39764255]
31. Gu Y, Han X, Liu J, Li Y, Li Z, Zhang W, et al. Prognostic significance of the estimated pulse wave velocity in critically ill patients with coronary heart disease: analysis from the MIMIC-IV database. Eur Heart J Qual Care Clin Outcomes 2024 Sep 14:qcae076. [doi: 10.1093/ehjqcco/qcae076] [Medline: 39277781]
32. Kim YK, Seo W, Lee SJ, Koo JH, Kim GC, Song HS, et al. Early prediction of cardiac arrest in the intensive care unit using explainable machine learning: retrospective study. J Med Internet Res 2024 Sep 17;26:e62890 [FREE Full text] [doi: 10.2196/62890] [Medline: 39288404]

XSL•FO
RenderX

33. Lin X, Pan X, Yang Y, Yang W, Wang X, Zou K, et al. Machine learning models to predict 30-day mortality for critical patients with myocardial infarction: a retrospective analysis from MIMIC-IV database. Front Cardiovasc Med 2024;11:1368022 [FREE Full text] [doi: 10.3389/fcvm.2024.1368022] [Medline: 39371393]
34. Privratsky JR, Fuller M, Raghunathan K, Ohnuma T, Bartz RR, Schroeder R, et al. Postoperative acute kidney injury by age and sex: a retrospective cohort association study. Anesthesiology 2023 Feb 01;138(2):184-194 [FREE Full text] [doi: 10.1097/ALN.0000000000004436] [Medline: 36512724]
35. Min JW, Min J, Chang S, Chung BH, Koh ES, Kim YS, et al. A risk prediction model (CMC-AKIX) for postoperative acute kidney injury using machine learning: algorithm development and validation. J Med Internet Res 2025 Apr 09;27:e62853 [FREE Full text] [doi: 10.2196/62853] [Medline: 40203303]
36. van den Akker JPC, Egal M, Groeneveld ABJ. Invasive mechanical ventilation as a risk factor for acute kidney injury in the critically ill: a systematic review and meta-analysis. Crit Care 2013 May 27;17(3):R98 [FREE Full text] [doi: 10.1186/cc12743] [Medline: 23710662]
37. Yue S, Li S, Huang X, Liu J, Hou X, Zhao Y, et al. Machine learning for the prediction of acute kidney injury in patients with sepsis. J Transl Med 2022 May 13;20(1):215 [FREE Full text] [doi: 10.1186/s12967-022-03364-0] [Medline: 35562803]
38. Cho N, Jeong I, Ahn S, Gil H, Kim Y, Park J, et al. Machine learning to assist in managing acute kidney injury in general wards: multicenter retrospective study. J Med Internet Res 2025 Mar 18;27:e66568 [FREE Full text] [doi: 10.2196/66568] [Medline: 40101226]
39. Zhou Y, Feng J, Mei S, Zhong H, Tang R, Xing S, et al. Machine learning models for predicting acute kidney injury in patients with sepsis-associated acute respiratory distress syndrome. Shock 2023 Mar 01;59(3):352-359. [doi: 10.1097/SHK.0000000000002065] [Medline: 36625493]
40. Tseng P, Chen Y, Wang C, Chiu K, Peng Y, Hsu S, et al. Prediction of the development of acute kidney injury following cardiac surgery by machine learning. Crit Care 2020 Jul 31;24(1):478 [FREE Full text] [doi: 10.1186/s13054-020-03179-9] [Medline: 32736589]
41. Kuno T, Mikami T, Sahashi Y, Numasawa Y, Suzuki M, Noma S, et al. Machine learning prediction model of acute kidney injury after percutaneous coronary intervention. Sci Rep 2022 Jan 14;12(1):749 [FREE Full text] [doi: 10.1038/s41598-021-04372-8] [Medline: 35031637]
42. Sun L, Zhu W, Chen X, Jiang J, Ji Y, Liu N, et al. Machine learning to predict contrast-induced acute kidney injury in patients with acute myocardial infarction. Front Med (Lausanne) 2020;7:592007 [FREE Full text] [doi: 10.3389/fmed.2020.592007] [Medline: 33282893]

Abbreviations

ACS: acute coronary syndrome
AI: artificial intelligence
AKI: acute kidney injury
ALT: alanine aminotransferase
AMI: acute myocardial infarction
APSIII: acute physiology score III
AST: aspartate aminotransferase
AUROC: area under the receiver operating characteristic curve
BIDMC: Beth Israel Deaconess Medical Center
BUN: blood urea nitrogen
CAG: coronary angiography
CCU: coronary care unit
CHD: coronary heart disease
CKMB: creatine kinase isoenzymes
DCA: decision curve analysis
DT: decision tree
EHR: electronic health record
GFR: glomerular filtration rate
ICD-10: International Classification of Diseases, 10th Revision
ICD-9: International Classification of Diseases, 9th Revision
ICU: intensive care unit
INR: international normalized ratio
IRB: Institutional Review Board
LASSO: least absolute shrinkage and selection operator
LR: logistic regression
MI: myocardial infarction
MIMIC-IV: Medical Information Mart for Intensive Care IV

XSL•FO
RenderX

MIT: Massachusetts Institute of Technology
ML: machine learning
NB: naive Bayes
NLR: neutrophil-to-lymphocyte ratio
NT-proBNP: N-terminal pro–B-type natriuretic peptide
PCI: percutaneous coronary intervention
PT: prothrombin time
PTT: partial thromboplastin time
RBC: red blood cell
RDW: red blood cell distribution width
RF: random forest
ROC: receiver operating characteristic
SCr: serum creatini
SHAP: Shapley Additive Explanation
SOFA: sequential organ failure assessment
SVM: support vector machine
VIF: variance inflation factor
WBC: white blood cell
XGBoost: extreme gradient boosting

Edited by A Benis; submitted 08.02.25; peer-reviewed by A Li, JMI Arockiasamy; comments to author 20.03.25; revised version received 28.04.25; accepted 18.05.25; published 28.05.25.

Please cite as:
Li Y, Xiao M, Li Y, Lv L, Zhang S, Liu Y, Zhang J
Machine Learning for the Prediction of Acute Kidney Injury in Critically Ill Patients With Coronary Heart Disease: Algorithm Development and Validation
JMIR Med Inform 2025;13:e72349
URL: https://medinform.jmir.org/2025/1/e72349
doi:10.2196/72349
PMID:

©Yike Li, Mingyang Xiao, Yaqian Li, Lulu Lv, Shanshan Zhang, Yuhui Liu, Juan Zhang. Originally published in JMIR Medical Informatics (https://medinform.jmir.org), 28.05.2025. This is an open-access article distributed under the terms of the Creative Commons Attribution License (https://creativecommons.org/licenses/by/4.0/), which permits unrestricted use, distribution, and reproduction in any medium, provided the original work, first published in JMIR Medical Informatics, is properly cited. The complete bibliographic information, a link to the original publication on https://medinform.jmir.org/, as well as this copyright and license information must be included.

XSL•FO
RenderX

Original Paper

Intelligent Prediction Platform for Sepsis Risk Based on Real-Time Dynamic Temporal Features: Design Study

Mingwei Zhang[1], PhD; Ming Zhong[2], MD; Yunzhang Cheng[1,3], PhD; Tianyi Zhang[1], PhD

[1]School of Health Sciences and Engineering, University of Shanghai for Science and Technology, Shanghai, China

[2]Department of Critical Care Medicine, Zhongshan Hospital Affiliated to Fudan University, Shanghai, China

[3]Lin-gang Medical Device Innovation Center, Shanghai, China

Corresponding Author:
Tianyi Zhang, PhD
School of Health Sciences and Engineering
University of Shanghai for Science and Technology
Jungong road 334
Shanghai, 200093
China
Phone: 86 19117192540
Email: 19117192540@163.com

Abstract

Background: The development of sepsis in the intensive care unit (ICU) is rapid, the golden rescue time is short, and the effective way to reduce mortality is rapid diagnosis and early warning. Therefore, real-time prediction models play a key role in the clinical diagnosis and management of sepsis. However, the existing sepsis prediction models based on artificial intelligence still have limitations, such as poor real-time performance and insufficient interpretation.

Objective: Our objective is to develop a real-time sepsis prediction model that integrates high timeliness and clinical interpretability. The model is designed to dynamically predict the risk of sepsis in ICU patients and establish a practical, tailored sepsis prediction platform.

Methods: Within a retrospective analysis framework, the model comprises a real-time prediction module and an interpretability module. The real-time prediction module leverages 3-hour dynamic temporal features derived from 8 noninvasive, real-time physiological indicators: heart rate, respiratory rate, blood oxygen saturation, mean arterial pressure, systolic blood pressure, diastolic blood pressure, body temperature, and blood glucose. Three linear parameters (mean, SD, and endpoint value) were calculated to construct the prediction model using multiple ML algorithms. The interpretability module uses the TreeSHAP (Tree-Based Shapley Additive Explanations) method to enhance model transparency through both individual prediction and global explanations. Further, it added a link between the output interpretation of the explainable artificial intelligence method and its potential physiological or pathophysiological significance, including the relationship among the output interpretation and the patient's hemodynamics, thermoregulatory response, and the balance between oxygen delivery and oxygen consumption. Finally, a web-based platform was developed to integrate prediction and interpretability functions.

Results: The sepsis prediction model demonstrated robust performance in the test cohort (224 patients), achieving an accuracy of 0.7 (95% CI 0.68-0.71), precision of 0.69 (95% CI 0.68-0.71), F_1-score of 0.69 (95% CI 0.67-0.70), and area under the receiver operating characteristic curve of 0.76 (95% CI 0.74-0.77). The TreeSHAP method effectively visualized feature contributions, enabling clinicians to interpret the model's prediction logic and identify anomalies. The link between the output interpretation of the model and its potential physiological or pathophysiological significance improved the interpretability and credibility of the explainable artificial intelligence method. The web-based platform significantly enhanced clinical utility by providing real-time risk assessment, statistical summaries, trend analysis, and actionable insights.

Conclusions: This platform provides real-time dynamic warnings for sepsis risk in critically ill ICU patients, supporting timely clinical decision-making.

(JMIR Med Inform 2025;13:e74940) doi:10.2196/74940

KEYWORDS

sepsis; real-time dynamic warnings; machine learning; interpretability; web-based platform

XSL•FO
RenderX

Introduction

Sepsis, a life-threatening clinical syndrome triggered by infection, continues to impose a significant global burden due to its persistently high incidence and mortality rates. In the United States, approximately 750,000 individuals are diagnosed with sepsis annually, with a mortality rate exceeding 30%; Europe reports 150,000 sepsis-related deaths yearly [1,2]. The economic impact is staggering, with annual US health care costs exceeding US $20.3 billion [3]. Patients with sepsis experience hospital stays twice as long as those with other conditions, and the incidence of severe sepsis continues to rise by 13% annually [4]. Early detection is critical to reducing mortality; yet, current diagnostic methods lack accuracy and real-time capability [5]. The multifactorial characteristics of sepsis increase the difficulty of early diagnosis, and the specificity of its diagnostic indicators is relatively low, which is prone to cause misdiagnosis [6]. Timely initiation of protocolized treatment bundles significantly improves survival [7], with evidence suggesting that a 1-hour resuscitation bundle may become the cornerstone of septic shock management [8]. However, sepsis pathophysiology is complex, microbiological confirmation is time-consuming, and existing scoring systems (eg, Mortality in Emergency Department Sepsis or Sequential Organ Failure Assessment) have limitations [9]. Thus, establishing a real-time sepsis prediction system is imperative to reduce clinical mortality.

Current research has leveraged artificial intelligence (AI) to develop sepsis prediction models using dynamic physiological and laboratory data. Machine learning has gained traction in critical care for disease diagnosis [10], outcome prediction [11-13], and clinical decision support [14]. Recent AI models for sepsis prediction outperform traditional methods [15-18], but reliance on non–real-time laboratory data and the "black-box" nature of AI models hinder clinical adoption [19,20]. These models often fall short in real-time performance and interpretability, limiting their clinical utility. Intensive care unit (ICU) clinicians require transparent, medically logical AI tools to preserve decision-making autonomy, aligning with evidence-based principles. Current sepsis prediction models also lack integration into practical platforms, further limiting clinical utility.

This study addresses these gaps by developing ML models based on dynamic features from real-time, noninvasive physiological indicators. We use local and global interpretability methods to enhance clinical trust and establish a web-based sepsis prediction platform.

Methods

Data Source

Data were extracted from the MIMIC-IV (Medical Information Mart for Intensive Care IV) database, developed by the MIT (Massachusetts Institute of Technology) Laboratory for Computational Physiology. This deidentified database includes clinical and waveform data from ICU and emergency department patients at Beth Israel Deaconess Medical Center (2008-2019) [21,22]. The physiological indicators were obtained from patient monitors. Blood oxygen saturation (SpO_2), heart rate (HR), and respiratory rate (RES) were collected 1-10 times per hour. Blood glucose (GLU) and body temperature (TEM) were measured once every 1 to 5 hours, depending on the patient's condition. Other indicators were collected hourly.

Study Cohort and Variable Selection

Patients with sepsis were identified per the 2018 Chinese Guidelines for Sepsis or Septic Shock Management (positive blood culture + antibiotic use + Sequential Organ Failure Assessment score ≥2). A control cohort included ICU patients without sepsis. Among 1118 patients (550 with sepsis and 568 controls), 8 real-time physiological indicators were selected: HR, systolic blood pressure (SP), diastolic blood pressure (DP), mean arterial pressure (MP), RES, TEM, SpO_2, and GLU. Stratified sampling divided the cohort into training (n=894) and test (n=224) groups. Baseline characteristics showed no significant differences (Table 1).

Table 1. *t* test analysis of characteristics between training and test groups[a].

Parameter	Training (n=894), median (IQR)	Test (n=224), median (IQR)	*P* value
Heart rate (bpm)	86.1 (30.5-157)	86.5 (43-137.5)	.81
Systolic BP[b] (mm Hg)	119.6 (48-191)	115.5 (36.8-187)	.08
Diastolic BP (mm Hg)	61.5 (10-116)	61.9 (19-121)	.67
Mean arterial pressure (mm Hg)	77.8 (24.3-149)	75.7 (8-127)	.08
Respiratory rate (bpm)	19.8 (5-44)	19.6 (6-52)	.60
Temperature (°C)	36.8 (31.7-40.4)	36.8 (33.1-39.9)	.74
SpO_2[c] (%)	96 (28.4-100)	95.6 (23-100)	.42
Blood glucose (mg/dL)	140.6 (42-309)	139.3 (63-326)	.75

[a]*P*<.05 indicates statistical significance.

[b]BP: blood pressure.

[c]SpO_2: blood oxygen saturation.

XSL•FO
RenderX

Data Preprocessing

First, the data underwent outlier removal. Since part of the MIMIC-IV data was manually entered by health care providers, potential input errors or anomalies were addressed. Clinical knowledge was applied to define valid physiological ranges and filter absolute outliers (for instance, TEM: 20 °C-50 °C; SpO_2: 21%-100%; HR: 0-300 bpm). Data points outside these ranges were deemed invalid and removed. Next, missing data imputation was performed to address gaps in the cleaned dataset. A hybrid approach combining multiple interpolation methods was applied:

1. Mean imputation: Replacing missing values with the overall mean of the feature.

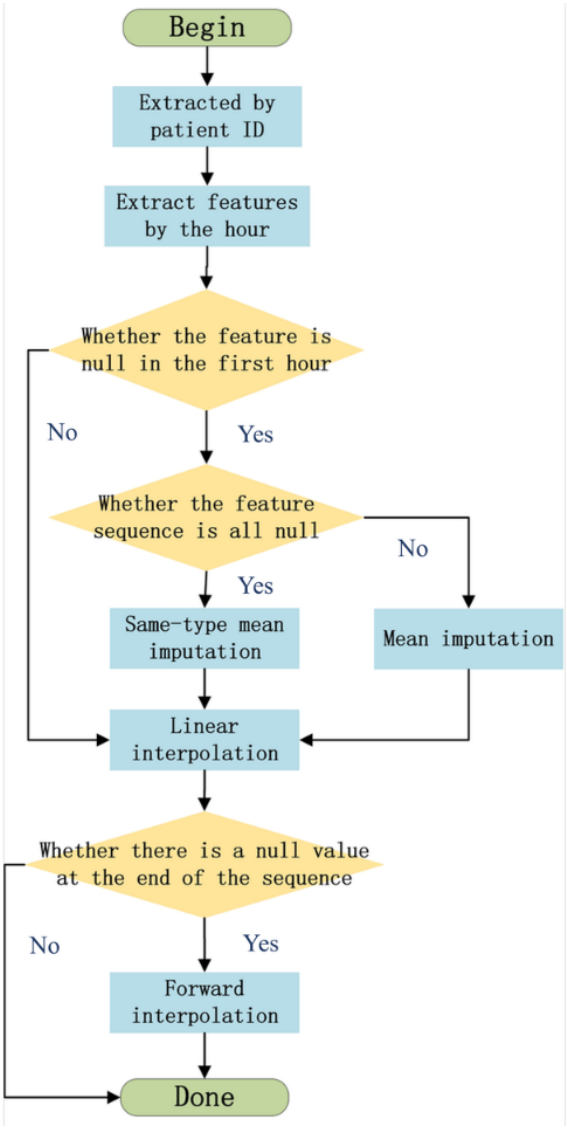
2. Class-specific mean imputation: Using mean values from subgroups (eg, sepsis vs nonsepsis cohorts).

3. Linear interpolation: Filling gaps using linear trends between adjacent valid data points.

4. Forward-fill imputation: Propagating the last valid observation forward.

The entire preprocessing workflow is illustrated in Figure 1.

Figure 1. The entire preprocessing workflow.



To minimize reliance on long-term temporal dependencies, the prediction model was designed to operate on a 3-hour sliding window of real-time physiological data. This allows the model to initiate sepsis risk prediction immediately after 3 hours of monitoring. A 3-hour window allows sufficient time for sign monitoring and subsequent sepsis prediction, providing doctors with ample time for intervention. From the 3-hour time series of each physiological indicator, 3 linear parameters were computed: mean value over the 3-hour window, fluctuation coefficient (SD within the window), and endpoint value (the last recorded value in the window).

This generated a 24-dimensional feature vector for each patient, structured as follows:

- Endpoint values: HR, SP, DP, MP, RES, TEM, SpO_2, and GLU.
- Mean values: mean-HR, mean-SP, mean-DP, mean-MP, mean-RES, mean-TEM, mean-SpO_2, and mean-GLU.

XSL•FO
RenderX

- Fluctuation coefficients (SDs): var-HR (variation in heart rate), var-SP (variation in systolic blood pressure), var-DP, var-MP (variation in mean arterial pressure), var-RES (variation in respiratory rate), var-TEM (variation in body temperature), var-SpO_2 (variation in blood oxygen saturation), and var-GLU (variation in blood glucose).

All features were standardized (*z* score normalization) to ensure consistent scaling before model training. This preprocessing pipeline ensures robust, clinically meaningful inputs for the subsequent machine learning workflow.

Sepsis Prediction Model

We developed and evaluated the sepsis prediction model for actual ICU sign monitoring to achieve a model with greater generality in a broader clinical setting. Critically ill patients in the ICU have different needs for GLU monitoring frequency. The incidence of glucose metabolism disorders in critically ill patients is high, and the incidence increases in turn in sepsis, severe sepsis and septic shock [23], which not only reflects the abnormal secretion of hormones and the severity of the disease, but is also closely related to the increase of mortality and complications [24]. High or low GLU is one of the causes of organ dysfunction. Therefore, it is necessary to increase the frequency of GLU monitoring in the face of the clinical background of insufficient energy intake, high catabolism, impaired GLU regulation mechanism, or the implementation of insulin treatment. At the same time, it is also necessary to increase the frequency of GLU monitoring in critically ill patients with diabetes or hypoglycemia. Whereas in most other ICU patients, GLU is usually measured only once or twice a day.

Therefore, to improve the generalization of sepsis prediction models, we developed and evaluated 2 sepsis prediction models, one based on high-frequency glucose monitoring and the other based on routine vital signs monitoring without glucose. By combining the 2 models, a model with greater generality in a wider range of clinical settings was achieved.

This study used 6 machine learning algorithms—support vector machine, random forest, ExtraTrees, XGBoost (Extreme Gradient Boosting), AdaBoost, and Logistic—to construct real-time sepsis prediction models. Model performance was evaluated and compared using metrics including accuracy, precision, recall, F_1-score, and area under the receiver operating characteristic curve (AUROC).

Model Interpretation

The TreeSHAP (Tree-Based Shapley Additive Explanations) method was used to provide both local (individual prediction) and global explanations for the sepsis prediction model. TreeSHAP, grounded in cooperative game theory, constructs an additive explanation model that treats all features as “contributors” to the prediction outcome. For each sample, TreeSHAP generates a Shapley value for each feature, quantifying its marginal contribution to the model’s decision. For the sepsis prediction model with 24 features, let the original model be f, trained using AdaBoost. The explanation model g in SHAP (Shapley Additive Explanations) is defined as:



$x=(x_1,x_2\ldots x_{24})$ represents the feature vector of a single patient. f(x) is the prediction from the original model. g(x) is the prediction from the explanation model. $ø_i$ is the Shapley value for the ith feature.





S is a subset of {1,2,3…24}, with 2^{24-1} possible combinations. |S| is the number of features in subset S. f_x (S ∪ i) and f_x(S) are model predictions with and without feature i, respectively. Global interpretation aggregates local explanations by averaging the absolute Shapley values across all samples.

Ethical Considerations

Our study was conducted in accordance with the guidelines of the Helsinki Declaration. The Review Committee of the Massachusetts Institute of Technology and Beth Israel Deaconess Medical Center approved access to the MIMIC-IV database. Authors fulfilled the database access request. All these data were deidentified; therefore, the study was exempt from ethical approval and informed consent requirements.

Results

Model Prediction Performance

The performances of the sepsis prediction models based on high-frequency glucose monitoring are summarized in Figure 2 and Table 2. Among all models, AdaBoost achieved the highest accuracy of 0.70 (95% CI 0.68-0.71), precision of 0.69 (95% CI 0.68-0.71), F_1-score of 0.69 (95% CI 0.67-0.70), and AUROC of 0.76 (95% CI 0.74-0.77), demonstrating superior real-time prediction capability. The performances of the sepsis prediction models based on routine vital signs monitoring without glucose are summarized in Figure 3 and Table 3. Among all models, AdaBoost achieved the highest accuracy of 0.67 (95% CI 0.66-0.69), precision of 0.67 (95% CI 0.65-0.68), and AUROC of 0.75 (95% CI 0.74-0.77). The experimental results show that the sepsis prediction model based on high-frequency monitoring of GLU has better prediction performance, and the sepsis prediction model based on routine vital signs monitoring has a wider application scenario.

XSL•FO
RenderX

Figure 2. Receiver operating characteristic curves of machine learning models based on high-frequency glucose monitoring. AUC: area under the curve; ROC: receiver operating characteristic; SVM: support vector machine; XGBoost: Extreme Gradient Boosting.

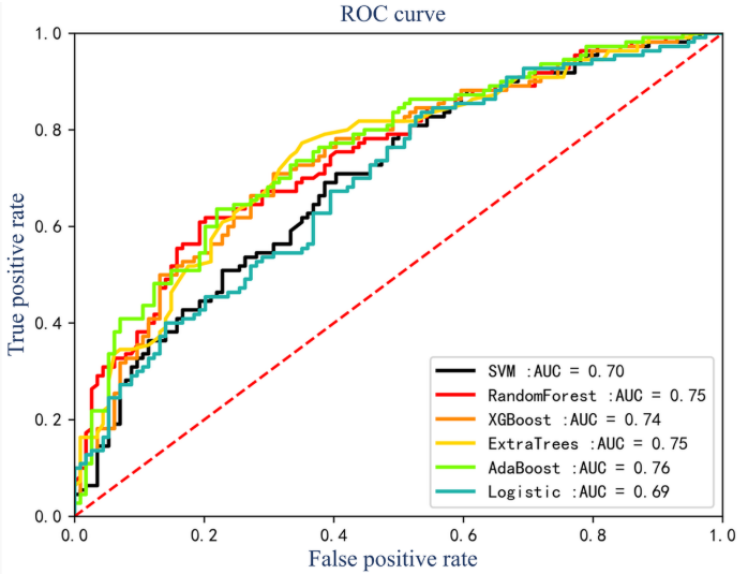


Table 2. Models' performance comparison of machine learning models based on high-frequency glucose monitoring.

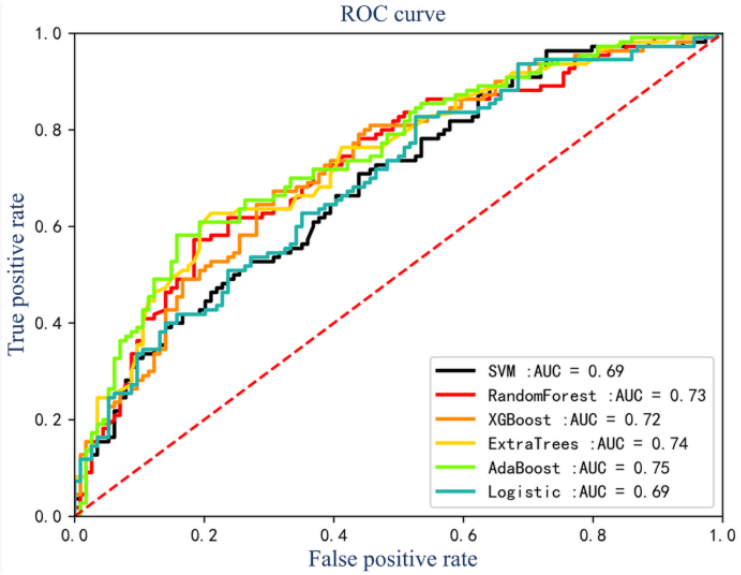
Models	Accuracy, median (IQR)	Precision, median (IQR)	Recall, median (IQR)	F_1-score, median (IQR)	AUROC[a], median (IQR)
SVM[b]	0.64 (0.61-0.66)	0.64 (0.62-0.67)	0.6 (0.59-0.61)	0.62 (0.6-0.65)	0.7 (0.69-0.72)
Random forest	0.68 (0.65-0.7)	0.65 (0.62-0.67)	0.7 (0.68-0.73)	0.67 (0.65-0.69)	0.75 (0.74-0.77)
ExtraTrees	0.69 (0.67-0.71)	0.69 (0.67-0.71)	0.66 (0.65-0.68)	0.67 (0.65-0.7)	0.75 (0.72-0.78)
XGBoost[c]	0.7 (0.68-0.72)	0.68 (0.68-0.69)	0.71 (0.7-0.72)	0.69 (0.68-0.69)	0.74 (0.73-0.75)
AdaBoost	0.7 (0.68-0.71)	0.69 (0.68-0.71)	0.67 (0.66-0.69)	0.69 (0.67-0.7)	0.76 (0.74-0.77)
Logistic	0.63 (0.62-0.63)	0.62 (0.61-0.62)	0.62 (0.61-0.63)	0.62 (0.62-0.63)	0.69 (0.67-0.7)

[a]AUROC: area under the receiver operating characteristic curve.

[b]SVM: support vector machine.

[c]XGBoost: Extreme Gradient Boosting.

Figure 3. Receiver operating characteristic curves of machine learning models based on routine vital signs monitoring without glucose. AUC: area under the curve; ROC: receiver operating characteristic; SVM: support vector machine; XGBoost: Extreme Gradient Boosting.



XSL•FO
RenderX

Table 3. Models' performance comparison of machine learning models based on routine vital signs monitoring without glucose.

Models	Accuracy, median (IQR)	Precision, median (IQR)	Recall, median (IQR)	F_1-score, median (IQR)	AUROC[a], median (IQR)
SVM[b]	0.61 (0.59-0.64)	0.61 (0.59-0.63)	0.57 (0.55-0.6)	0.59 (0.57-0.61)	0.69 (0.67-0.71)
Random forest	0.66 (0.65-0.68)	0.65 (0.62-0.67)	0.68 (0.66-0.71)	0.66 (0.64-0.69)	0.73 (0.72-0.74)
ExtraTrees	0.67 (0.65-0.7)	0.65 (0.63-0.67)	0.66 (0.65-0.68)	0.66 (0.65-0.67)	0.74 (0.72-0.76)
XGBoost[c]	0.67 (0.66-0.69)	0.65 (0.63-0.67)	0.73 (0.71-0.74)	0.68 (0.66-0.7)	0.72 (0.7-0.73)
AdaBoost	0.67 (0.66-0.69)	0.67 (0.65-0.68)	0.66 (0.64-0.68)	0.66 (0.65-0.67)	0.75 (0.74-0.77)
Logistic	0.64 (0.63-0.65)	0.63 (0.62-0.64)	0.63 (0.61-0.64)	0.63 (0.62-0.63)	0.69 (0.67-0.7)

[a]AUROC: area under the receiver operating characteristic curve.

[b]SVM: support vector machine.

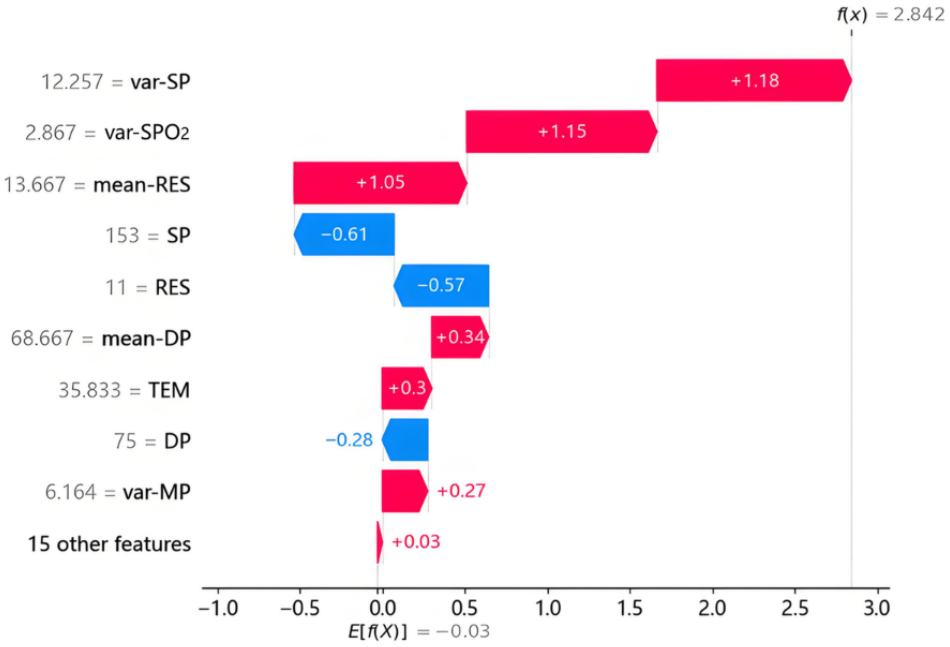
[c]XGBoost: Extreme Gradient Boosting.

Interpretability Analysis Using TreeSHAP

Individual Prediction Explanation

The TreeSHAP method was used to generate local explanations for individual cases to elucidate the contribution of dynamic features to model predictions. Figure 4 illustrates the interpretability analysis for a patient predicted as having sepsis, where features are color-coded to reflect their impact: red denotes a positive contribution (increasing sepsis risk) and blue indicates a negative contribution (reducing sepsis risk). The baseline value E[f(x)], representing the model's average prediction across the dataset, serves as the reference point. Key findings include: SP fluctuation coefficient (var-SP=12.257) exerted the strongest positive influence (+1.18), followed by SpO_2 fluctuation (var-SpO_2=2.867), mean RES (mean-RES=3.667), mean DP (mean-DP=68.667), TEM (TEM=35.833), and MP fluctuation (var-MP=6.164). Negative contributors included SP (SP=15), RES (RES=11), and DP (DP=75). These results basically align with clinical intuition, where elevated variability in hemodynamic parameters (eg, var-SP or var-MP), hypothermia, and reduced RES correlate with sepsis pathophysiology. The interpretability framework enables clinicians to validate model logic against established diagnostic criteria and identify anomalous predictions.

Figure 4. Individual prediction explanation. DP: diastolic blood pressure; MP: mean arterial pressure; RES: respiratory rate; SP: systolic blood pressure; SpO_2: blood oxygen saturation; TEM: body temperature.



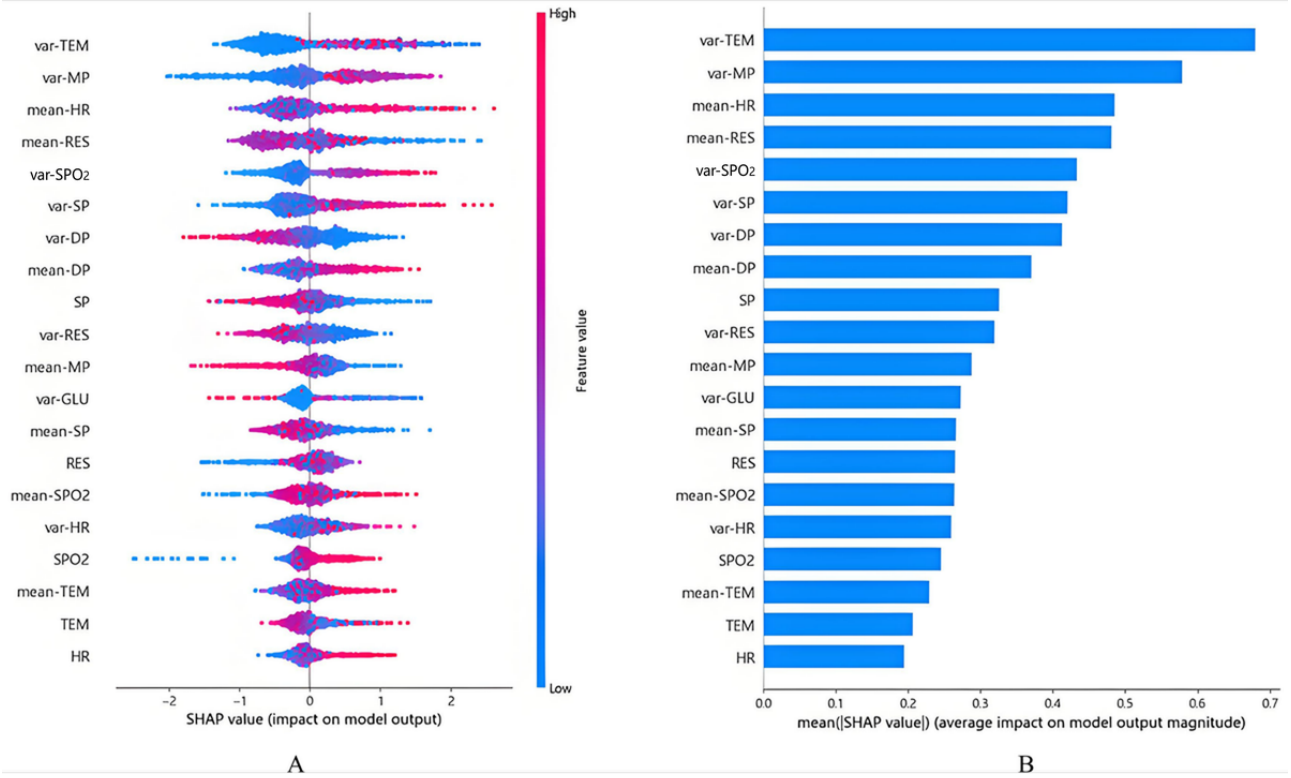
Global Interpretation

Global interpretability analysis aggregated Shapley values across all samples to reveal the model's overarching decision logic and feature importance rankings (Figure 5). As illustrated in Figure 5A, the model demonstrated associations between decreased SP and elevated sepsis risk (row 9), increased SP fluctuation (var-SP) and elevated sepsis risk (row 6), and increased MP fluctuation (var-MP) with elevated sepsis risk (row 2). These interpretations align closely with existing clinical evidence and provide clinically meaningful insights that are of particular interest to clinicians. For instance, increased var-SP is more likely to elevate the probability of sepsis compared to increased var-MP. The Surviving Sepsis Campaign 2021

XSL•FO
RenderX

guidelines emphasize the importance of SP in the diagnostic criteria for sepsis and recommend using SP<90 mm Hg after adequate fluid resuscitation as one of the indicators for evaluating septic shock [25]. Additionally, studies have shown that blood pressure variability in sepsis patients correlates with disease severity [26].

Figure 5. Global interpretation of the model and feature importance based on mean Shapley values. DP: diastolic blood pressure; GLU: blood glucose; HR: heart rate; MP: mean arterial pressure; RES: respiratory rate; SHAP: Shapley Additive Explanations; SP: systolic blood pressure; SpO_2: blood oxygen saturation; TEM: body temperature.



The connection between the parasympathetic nervous system and inflammation suggests interdependence between autonomic nervous system function and inflammatory responses [27]. Furthermore, physiological systems exhibit nonlinear patterns of complexity, including fractal self-similarity across time scales [28]. Previous research has documented an association between the complexity of autonomic nervous system control and hemodynamic instability, indicating that such complexity may serve as a potential window into understanding hemodynamic confusion. However, the relevance of these measures of complexity in sepsis remains unclear [26].

High temperature fluctuations (var-TEM) were strongly associated with increased sepsis probability, while stable temperatures reduced the risk (row 1). Notably, extreme TEMs, whether hyperthermia or hypothermia, were linked to elevated risks, whereas normal-range temperatures exhibited protective effects (row next-to-last). This interpretation of the model aligns with the clinical presentation of sepsis.

Both hypothermia and hyperthermia are generally associated with elevated lactate levels, and patients with severe sepsis often develop either hypothermia or, more commonly, a febrile response. Hypothermia in some patients with sepsis is well-documented and forms part of the definition of systemic inflammatory response syndrome [29]. There is variable thermoregulatory response in sepsis, and the definition of systemic inflammatory response syndrome in sepsis-1 includes both fever and hypothermia. The impact of thermoregulatory response on sepsis prognosis remains controversial. Studies have shown that hypothermia or fever can have either protective or detrimental effects in animal models of severe infection or inflammation [30]. Fever is a physiological response to infection that inhibits bacterial growth, prevents fungal proliferation, and enhances immune cell activity against pathogens [31]. Pathogens detected in blood cultures and elevated procalcitonin levels, both associated with high fever, indicate robust immune resistance to pathogen challenges [32].

The model revealed an association between increased variability in oxygen saturation (var-SpO_2) and elevated sepsis risk (row 5). This finding underscores the necessity of maintaining SpO_2 levels within a reasonable range for ICU patients during hospitalization, which is consistent with existing clinical evidence. Studies have demonstrated a U-shaped relationship between SpO_2 levels and in-hospital all-cause mortality in patients with sepsis, where both hyperoxia and hypoxia are associated with increased mortality risk. The optimal SpO_2 range is determined to be 0.96-0.98 [33]. Under normal physiological conditions, oxygen supply and consumption remain relatively stable, with SpO_2 fluctuating within a normal range without extreme variation. During shock, however, the imbalance between oxygen supply and consumption leads to deviations in SpO_2 values, resulting in increased var-SpO_2. A multicenter observational study involving over 600 patients with sepsis confirmed that abnormal SpO_2 levels (either

XSL•FO
RenderX

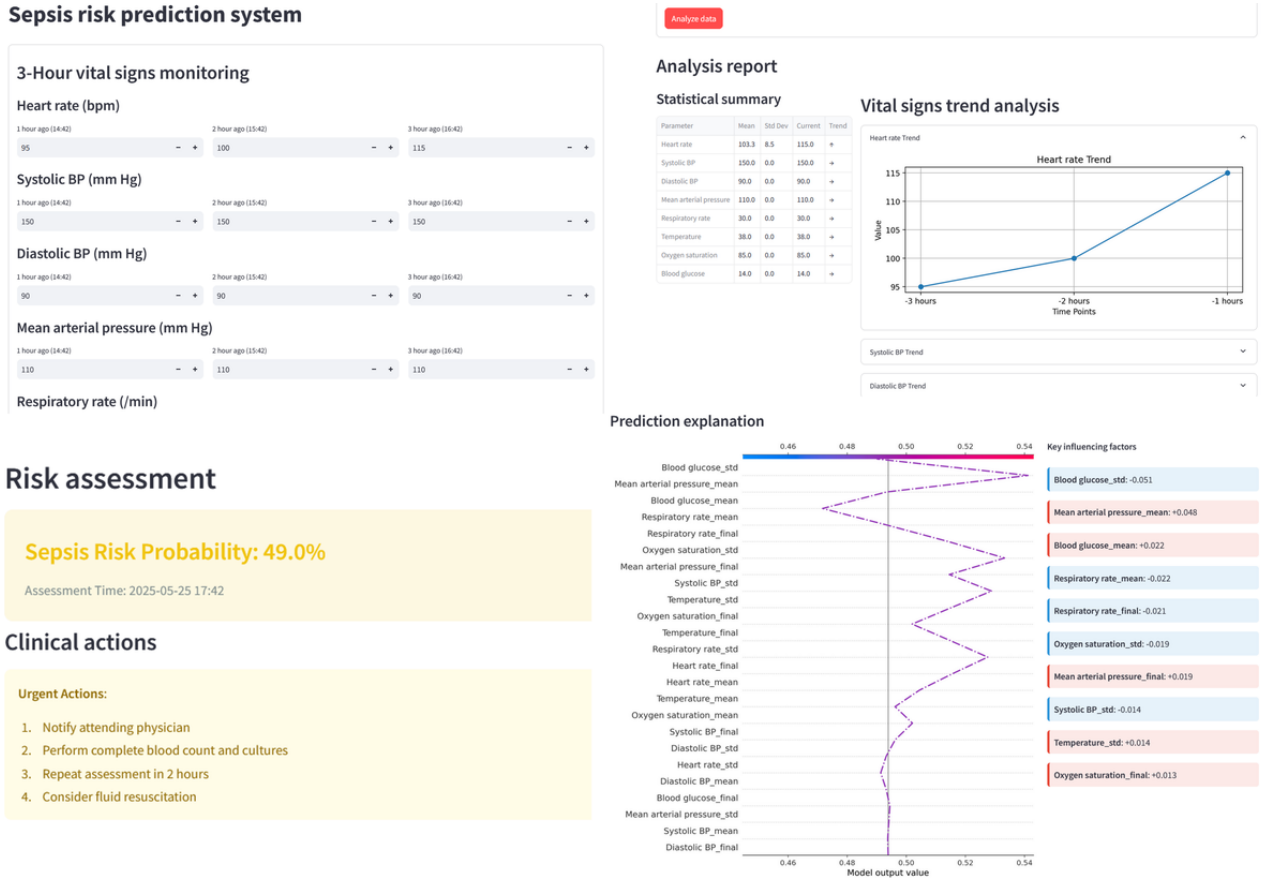
abnormally high or low) were associated with increased mortality [34].

Figure 5B ranks feature mean absolute Shapley values, identifying the top 6 determinants of sepsis risk: temperature fluctuation (var-TEM), MP fluctuation (var-MP), mean HR (mean-HR), mean RES (mean-RES), SpO_2 fluctuation (var-SpO_2), and SP fluctuation (var-SP). These findings underscore the critical role of hemodynamic and thermoregulatory instability in sepsis onset, consistent with clinical biomarkers. The global analysis also highlights potential outliers, guiding model refinement and clinical vigilance.

Implementation of the Practical and Efficient Sepsis Risk Prediction Platform

We developed a practical and intelligent sepsis risk prediction platform using a web-based tool [35] (Figure 6). By monitoring 3-hour dynamic temporal features of ICU patients—including HR, SP, DP, MP, RES, TEM, SpO_2, and GLU—the platform automatically generates a graphical analysis report comprising:

Figure 6. Practical and efficient sepsis risk prediction platform. BP: blood pressure.



Statistical summary: quantitative analysis of dynamic temporal features (mean, SD, and endpoint values).

Vital signs trend analysis: visualization of physiological trends via time-series curves.

- Risk assessment: sepsis risk prediction using the trained model, based on calculated linear parameters.
- Clinical actions: automated recommendations (for reference only) tailored to risk stratification.
- Prediction explanation: visual display of key influencing factors using Shapley values to interpret model decisions.

This platform, built on real-time dynamic temporal features, enables personalized sepsis risk prediction for ICU patients, enhances clinical utility by integrating interpretable AI insights, and streamlines decision-making through intuitive data visualization and actionable outputs.

Discussion

Principal Findings

Our study developed a real-time sepsis prediction model that integrates high timeliness and clinical interpretability based on 3-hour dynamic temporal sequences of 8 rapidly accessible physiological indicators. The real-time sepsis prediction model demonstrated robust performance. The output interpretation of explainable artificial intelligence (XAI) enhanced model transparency through both individual prediction and global explanations, and it linked the potential physiological or pathophysiological significance, including the patient's hemodynamics, thermoregulatory response, and the balance between oxygen delivery and oxygen consumption. Although current consensus emphasizes early intervention for sepsis management, the optimal predictors guiding intervention and markers of early sepsis severity remain unclear. In this study, we further elucidated the model's output results, explored the potential relationships between relevant sign parameters and

XSL•FO
RenderX

sepsis, and discussed their potential physiological or pathophysiological significance. This enhances the interpretability and credibility of the XAI method, supporting the model's applicability in real-world clinical practice. Finally, the web-based platform significantly enhanced clinical utility by providing real-time risk assessment, statistical summaries, trend analysis, and actionable insights.

Limitations

However, as a retrospective study, potential biases may exist in this study. Future efforts should prioritize multicenter validation and large-scale prospective studies to strengthen the robustness of these results. XAI holds immense promise in sepsis diagnosis and treatment, yet its development and clinical application face significant challenges [36]. Data quality remains a critical bottleneck. Heterogeneous hospital databases, inconsistent data collection and storage standards, and poor interoperability between health care information systems have led to fragmented "data silos," hindering the application of large-scale clinical feature datasets. Additionally, the reliance on limited public or institution-specific databases in research settings restricts generalizability. In clinical practice, clinicians must integrate XAI predictions with laboratory findings (eg, lactate or procalcitonin), imaging results, and patient-specific symptoms to ensure accurate diagnosis and treatment planning.

Conclusions

In ICU settings, real-time physiological indicators—such as HR, RES, and SpO_2—are typically used to monitor symptom fluctuations rather than generate objective diagnostic reports. This limitation stems from the significant variability in individual physiological data, the complexity of multiparameter interactions, and the diverse clinical implications of these metrics. This study demonstrates that XAI can bridge this gap by synthesizing real-time physiological data into actionable insights. By analyzing dynamic trends and providing interpretable explanations, XAI uncovers the diagnostic potential of these data. Our model, focused on sepsis risk prediction, leverages real-time physiological features to generate predictions while emphasizing the interpretability of results. In the future, XAI systems could deliver intelligent diagnostic reports integrating disease prediction, anomaly detection, and causal analysis of abnormal indicators, empowering clinicians to navigate complex physiological data with precision.

Acknowledgments

This work was supported by Shanghai Engineering Technology Research Center (18DZ2250900).

Data Availability

The data used in this study are publicly available from the Medical Information Mart for Intensive Care IV (MIMIC-IV) database. As a result of patient privacy concerns, the raw EHR (electronic health records) text data cannot be shared publicly but can be accessed through a compliant application to MIMIC-IV.

Authors' Contributions

M Zhang conceptualized the study and carried out the formal analysis, investigation, and writing and editing of the original draft. M Zhong conceptualized the study and carried out the formal analysis, investigation, and validation. YC carried out the formal analysis, investigation, and validation. TZ assisted with the conceptualization, investigation, analysis, project administration, and paper review and editing.

Conflicts of Interest

None declared.

References

1. Angus D, Linde-Zwirble WT, Lidicker J, Clermont G, Carcillo J, Pinsky MR. Epidemiology of severe sepsis in the United States: analysis of incidence, outcome, and associated costs of care. Crit Care Med 2001;29(7):1303-1310. [doi: 10.1097/00003246-200107000-00002] [Medline: 11445675]
2. Stevenson EK, Rubenstein AR, Radin GT, Wiener RS, Walkey AJ. Two decades of mortality trends among patients with severe sepsis: a comparative meta-analysis*. Crit Care Med 2014;42(3):625-631 [FREE Full text] [doi: 10.1097/CCM.0000000000000026] [Medline: 24201173]
3. Moore B, Levit K, Elixhause A. Costs for hospital stays in the United States, 2012: statistical brief #181. In: Cancer Drug Discovery & Development. Rockville: Agency for Healthcare Research and Quality; 2014:265-284.
4. Gaieski D, Edwards J, Kallan MJ, Carr BG. Benchmarking the incidence and mortality of severe sepsis in the United States. Crit Care Med 2013;41(5):1167-1174. [doi: 10.1097/CCM.0b013e31827c09f8] [Medline: 23442987]
5. Zea-Vera A, Ochoa TJ. Challenges in the diagnosis and management of neonatal sepsis. J Trop Pediatr 2015;61(1):1-13 [FREE Full text] [doi: 10.1093/tropej/fmu079] [Medline: 25604489]
6. Fernando S, Rochwerg B, Seely AJE. Clinical implications of the third international consensus definitions for sepsis and septic shock (Sepsis-3). CMAJ 2018;190(36):E1058-E1059 [FREE Full text] [doi: 10.1503/cmaj.170149] [Medline: 30201611]

XSL•FO
RenderX

7. Fernando S, Tran A, Taljaard M, Cheng W, Rochwerg B, Seely AJE, et al. Prognostic accuracy of the quick sequential organ failure assessment for mortality in patients with suspected infection: a systematic review and meta-analysis. Ann Intern Med 2018;168(4):266-275. [doi: 10.7326/M17-2820] [Medline: 29404582]
8. Hiensch R, Poeran J, Saunders-Hao P, Adams V, Powell CA, Glasser A, et al. Impact of an electronic sepsis initiative on antibiotic use and health care facility-onset clostridium difficile infection rates. Am J Infect Control 2017;45(10):1091-1100. [doi: 10.1016/j.ajic.2017.04.005] [Medline: 28602274]
9. Subbe CP, Kruger M, Rutherford P, Gemmel L. Validation of a modified Early Warning Score in medical admissions. QJM 2001;94(10):521-526. [doi: 10.1093/qjmed/94.10.521] [Medline: 11588210]
10. Chen Z, Li X, Jin F, Shi Y, Zhang L, Yin H, et al. Diagnosis of sarcopenia using convolutional neural network models based on muscle ultrasound images: prospective multicenter study. J Med Internet Res 2025;27:e70545 [FREE Full text] [doi: 10.2196/70545] [Medline: 40327860]
11. Rubulotta F, Marshall J, Ramsay G, Nelson D, Levy M, Williams M. Predisposition, insult/infection, response, and organ dysfunction: a new model for staging severe sepsis. Crit Care Med 2009;37(4):1329-1335. [doi: 10.1097/CCM.0b013e31819d5db1] [Medline: 19242329]
12. Howell M, Talmor D, Schuetz P, Hunziker S, Jones AE, Shapiro NI. Proof of principle: the predisposition, infection, response, organ failure sepsis staging system. Crit Care Med 2011;39(2):322-327. [doi: 10.1097/CCM.0b013e3182037a8e] [Medline: 21099424]
13. Etholén A, Roos T, Hänninen M, Bouri I, Kulmala J, Rahkonen O, et al. Forecasting subjective cognitive decline: AI approach using dynamic Bayesian networks. J Med Internet Res 2025;27:e65028 [FREE Full text] [doi: 10.2196/65028] [Medline: 40327854]
14. Macdonald SPJ, Arendts G, Fatovich DM, Brown SGA. Comparison of PIRO, SOFA, and MEDS scores for predicting mortality in emergency department patients with severe sepsis and septic shock. Acad Emerg Med 2014;21(11):1257-1263 [FREE Full text] [doi: 10.1111/acem.12515] [Medline: 25377403]
15. Su L, Xu Z, Chang F, Ma Y, Liu S, Jiang H, et al. Early prediction of mortality, severity, and length of stay in the intensive care unit of sepsis patients based on sepsis 3.0 by machine learning models. Front Med (Lausanne) 2021;8:664966 [FREE Full text] [doi: 10.3389/fmed.2021.664966] [Medline: 34291058]
16. Bedoya AD, Futoma J, Clement ME, Corey K, Brajer N, Lin A, et al. Machine learning for early detection of sepsis: an internal and temporal validation study. JAMIA Open 2020;3(2):252-260 [FREE Full text] [doi: 10.1093/jamiaopen/ooaa006] [Medline: 32734166]
17. Fohner AE, Greene JD, Lawson BL, Chen JH, Kipnis P, Escobar GJ, et al. Assessing clinical heterogeneity in sepsis through treatment patterns and machine learning. J Am Med Inform Assoc 2019;26(12):1466-1477 [FREE Full text] [doi: 10.1093/jamia/ocz106] [Medline: 31314892]
18. Scott H, Colborn K, Sevick CJ, Bajaj L, Deakyne Davies SJ, Fairclough D, et al. Development and validation of a model to predict pediatric septic shock using data known 2 hours after hospital arrival. Pediatr Crit Care Med 2021;22(1):16-26 [FREE Full text] [doi: 10.1097/PCC.0000000000002589] [Medline: 33060422]
19. Robnik-Šikonja M, Štrumbelj E, Kononenko I. Efficiently explaining the predictions of a probabilistic radial basis function classification network. IDA 2013;17(5):791-802 [FREE Full text] [doi: 10.3233/ida-130607]
20. Ribeiro MT, Singh S, Guestrin C. 'Why should I trust you?' explaining the predictions of any classifier. 2016 Presented at: KDD '16: Proceedings of the 22nd ACM SIGKDD International Conference on Knowledge Discovery and Data Mining; 2016 August 13 - 17; San Francisco California USA p. 1135-1144 URL: https://doi.org/10.1145/2939672.2939778 [doi: 10.1145/2939672.2939778]
21. Johnson A, Pollard T, Shen L, Lehman LWH, Feng M, Ghassemi M, et al. MIMIC-III, a freely accessible critical care database. Sci Data 2016;3:160035 [FREE Full text] [doi: 10.1038/sdata.2016.35] [Medline: 27219127]
22. Goldberger AL, Amaral LA, Glass L, Hausdorff JM, Ivanov PC, Mark RG, et al. PhysioBank, PhysioToolkit, and PhysioNet: components of a new research resource for complex physiologic signals. Circulation 2000;101(23):E215-E220. [doi: 10.1161/01.cir.101.23.e215] [Medline: 10851218]
23. Preechasuk L, Suwansaksri N, Ipichart N, Vannasaeng S, Permpikul C, Sriwijitkamol A. Hyperglycemia and glycemic variability are associated with the severity of sepsis in nondiabetic subjects. J Crit Care 2017;38:319-323. [doi: 10.1016/j.jcrc.2016.12.005] [Medline: 28107738]
24. Magee F, Bailey M, Pilcher DV, Mårtensson J, Bellomo R. Early glycemia and mortality in critically ill septic patients: interaction with insulin-treated diabetes. J Crit Care 2018;45:170-177. [doi: 10.1016/j.jcrc.2018.03.012] [Medline: 29544173]
25. Evans L, Rhodes A, Alhazzani W, Antonelli M, Coopersmith CM, French C, et al. Surviving sepsis campaign: international guidelines for management of sepsis and septic shock 2021. Crit Care Med 2021 Nov 01;49(11):e1063-e1143. [doi: 10.1097/CCM.0000000000005337] [Medline: 34605781]
26. Tang Y, Sorenson J, Lanspa M, Grissom CK, Mathews V, Brown SM. Systolic blood pressure variability in patients with early severe sepsis or septic shock: a prospective cohort study. BMC Anesthesiol 2017;17(1):82 [FREE Full text] [doi: 10.1186/s12871-017-0377-4] [Medline: 28623891]

XSL•FO
RenderX

27. Huston JM, Tracey KJ. The pulse of inflammation: heart rate variability, the cholinergic anti-inflammatory pathway and implications for therapy. J Intern Med 2011;269(1):45-53 [FREE Full text] [doi: 10.1111/j.1365-2796.2010.02321.x] [Medline: 21158977]
28. Goldberger AL, Amaral LAN, Hausdorff JM, Ivanov PC, Peng C, Stanley HE. Fractal dynamics in physiology: alterations with disease and aging. Proc Natl Acad Sci U S A 2002;99 Suppl 1(Suppl 1):2466-2472 [FREE Full text] [doi: 10.1073/pnas.012579499] [Medline: 11875196]
29. Bone RC, Balk RA, Cerra FB, Dellinger RP, Fein AM, Knaus WA, et al. Definitions for sepsis and organ failure and guidelines for the use of innovative therapies in sepsis. The ACCP/SCCM Consensus Conference Committee. American College of Chest Physicians/Society of Critical Care Medicine. Chest 1992;101(6):1644-1655. [doi: 10.1378/chest.101.6.1644] [Medline: 1303622]
30. Ganeshan K, Nikkanen J, Man K, Leong YA, Sogawa Y, Maschek JA, et al. Energetic trade-offs and hypometabolic states promote disease tolerance. Cell 2019;177(2):399-413.e12 [FREE Full text] [doi: 10.1016/j.cell.2019.01.050] [Medline: 30853215]
31. Walter EJ, Hanna-Jumma S, Carraretto M, Forni L. The pathophysiological basis and consequences of fever. Crit Care 2016;20(1):200 [FREE Full text] [doi: 10.1186/s13054-016-1375-5] [Medline: 27411542]
32. Thomas-Rüddel DO, Hoffmann P, Schwarzkopf D, Scheer C, Bach F, Komann M, MEDUSA study group. Fever and hypothermia represent two populations of sepsis patients and are associated with outside temperature. Crit Care 2021;25(1):368 [FREE Full text] [doi: 10.1186/s13054-021-03776-2] [Medline: 34674733]
33. Ye Y, Li F, Yang B. Exploring the optimal range of pulse oxygen saturation in patients with sepsis: a retrospective study based on MIMIC- IV dataJ. Zhonghua Wei Zhong Bing Ji Jiu Yi Xue 2024;36(8):813-820.
34. Pope JV, Jones AE, Gaieski DF, Arnold RC, Trzeciak S, Shapiro NI, Emergency Medicine Shock Research Network (EMShockNet) Investigators. Multicenter study of central venous oxygen saturation (ScvO(2)) as a predictor of mortality in patients with sepsis. Ann Emerg Med 2010;55(1):40-46.e1 [FREE Full text] [doi: 10.1016/j.annemergmed.2009.08.014] [Medline: 19854541]
35. Sepsis Risk Prediction System. Streamlit Community Cloud. URL: https://sepsis-vision-explanation.streamlit.app/ [accessed 2025-05-23]
36. Wang G, Bennamoun H, Kwok WH, Quimbayo JPO, Kelly B, Ratajczak T, et al. Investigating protective and risk factors and predictive insights for aboriginal perinatal mental health: explainable artificial intelligence approach. J Med Internet Res 2025;27:e68030 [FREE Full text] [doi: 10.2196/68030] [Medline: 40306634]

Abbreviations

AI: artificial intelligence
AUROC: area under the receiver operating characteristic curve
DP: diastolic blood pressure
GLU: blood glucose
HR: heart rate
ICU: intensive care unit
MIMIC-IV: Medical Information Mart for Intensive Care IV
MIT: Massachusetts Institute of Technology
MP: mean arterial pressure
RES: respiratory rate
SHAP: Shapley Additive Explanations
SP: systolic blood pressure
SpO_2: blood oxygen saturation
TEM: body temperature
TreeSHAP: Tree-Based Shapley Additive Explanations
var-GLU: variation in blood glucose
var-HR: variation in heart rate
var-MP: variation in mean arterial pressure
var-RES: variation in respiratory rate
var-SP: variation in systolic blood pressure
var-SpO_2: variation in blood oxygen saturation
var-TEM: variation in body temperature
XAI: explainable artificial intelligence
XGBoost: Extreme Gradient Boosting

XSL•FO
RenderX

Edited by M Focsa; submitted 25.03.25; peer-reviewed by E Kawamoto, Z Peng; comments to author 25.04.25; revised version received 15.05.25; accepted 17.05.25; published 30.05.25.

Please cite as:
Zhang M, Zhong M, Cheng Y, Zhang T
Intelligent Prediction Platform for Sepsis Risk Based on Real-Time Dynamic Temporal Features: Design Study
JMIR Med Inform 2025;13:e74940
URL: https://medinform.jmir.org/2025/1/e74940
doi:10.2196/74940
PMID:

©Mingwei Zhang, Ming Zhong, Yunzhang Cheng, Tianyi Zhang. Originally published in JMIR Medical Informatics (https://medinform.jmir.org), 30.05.2025. This is an open-access article distributed under the terms of the Creative Commons Attribution License (https://creativecommons.org/licenses/by/4.0/), which permits unrestricted use, distribution, and reproduction in any medium, provided the original work, first published in JMIR Medical Informatics, is properly cited. The complete bibliographic information, a link to the original publication on https://medinform.jmir.org/, as well as this copyright and license information must be included.

XSL•FO
RenderX

Original Paper

Trajectory-Ordered Objectives for Self-Supervised Representation Learning of Temporal Healthcare Data Using Transformers: Model Development and Evaluation Study

Ali Amirahmadi[1], MSc; Farzaneh Etminani[2,3], PhD; Jonas Björk[4], PhD; Olle Melander[5], MD, PhD; Mattias Ohlsson[2,6], PhD

[1]Center for Applied Intelligent Systems Research in Health, Halmstad University, Halmstad, Sweden

[2]Center for Applied Intelligent Systems Research, Halmstad University, Halmstad, Sweden

[3]Department of research and development (FoU), Region Halland, HALMSTAD, Sweden

[4]Division of Occupational and Environmental Medicine, Lund University, Lund, Sweden

[5]Department of Clinical Sciences, Lund University, Lund, Sweden

[6]Centre for Environmental and Climate Science, Lund University, Lund, Sweden

Corresponding Author:
Ali Amirahmadi, MSc
Center for Applied Intelligent Systems Research in Health
Halmstad University
Kristian IV:s väg 3
Halmstad, 30118
Sweden
Phone: 46 03516 7100
Email: ali.amirahmadi@hh.se

Abstract

Background: The growing availability of electronic health records (EHRs) presents an opportunity to enhance patient care by uncovering hidden health risks and improving informed decisions through advanced deep learning methods. However, modeling EHR sequential data, that is, patient trajectories, is challenging due to the evolving relationships between diagnoses and treatments over time. Significant progress has been achieved using transformers and self-supervised learning. While BERT-inspired models using masked language modeling (MLM) capture EHR context, they often struggle with the complex temporal dynamics of disease progression and interventions.

Objective: This study aims to improve the modeling of EHR sequences by addressing the limitations of traditional transformer-based approaches in capturing complex temporal dependencies.

Methods: We introduce Trajectory Order Objective BERT (Bidirectional Encoder Representations from Transformers; TOO-BERT), a transformer-based model that advances the MLM pretraining approach by integrating a novel TOO to better learn the complex sequential dependencies between medical events. TOO-Bert enhanced the learned context by MLM by pretraining the model to distinguish ordered sequences of medical codes from permuted ones in a patient trajectory. The TOO is enhanced by a conditional selection process that focus on medical codes or visits that frequently occur together, to further improve contextual understanding and strengthen temporal awareness. We evaluate TOO-BERT on 2 extensive EHR datasets, MIMIC-IV hospitalization records and the Malmo Diet and Cancer Cohort (MDC)—comprising approximately 10 and 8 million medical codes, respectively. TOO-BERT is compared against conventional machine learning methods, a transformer trained from scratch, and a transformer pretrained on MLM in predicting heart failure (HF), Alzheimer disease (AD), and prolonged length of stay (PLS).

Results: TOO-BERT outperformed conventional machine learning methods and transformer-based approaches in HF, AD, and PLS prediction across both datasets. In the MDC dataset, TOO-BERT improved HF and AD prediction, increasing area under the receiver operating characteristic curve (AUC) scores from 67.7 and 69.5 with the MLM-pretrained Transformer to 73.9 and 71.9, respectively. In the MIMIC-IV dataset, TOO-BERT enhanced HF and PLS prediction, raising AUC scores from 86.2 and 60.2 with the MLM-pretrained Transformer to 89.8 and 60.4, respectively. Notably, TOO-BERT demonstrated strong performance in HF prediction even with limited fine-tuning data, achieving AUC scores of 0.877 and 0.823, compared to 0.839 and 0.799 for the MLM-pretrained Transformer, when fine-tuned on only 50% (442/884) and 20% (176/884) of the training data, respectively.

XSL•FO
RenderX

Conclusions: These findings demonstrate the effectiveness of integrating temporal ordering objectives into MLM-pretrained models, enabling deeper insights into the complex temporal relationships inherent in EHR data. Attention analysis further highlights TOO-BERT's capability to capture and represent sophisticated structural patterns within patient trajectories, offering a more nuanced understanding of disease progression.

(JMIR Med Inform 2025;13:e68138) doi:10.2196/68138

KEYWORDS

patient trajectories; disease prediction; representation learning; masked language mode; deep learning; BERT; electronic health record; language mode; transformer; heart failure; alzheimer disease; prolonged health of stay; effectiveness; temporal

Introduction

In modern health care, electronic health records (EHRs) are crucial as comprehensive repositories encompassing a wide range of patient data, including diagnoses, medications, treatments, laboratory data, and demographic information. The accumulation of EHR data longitudinally builds EHR trajectories, sometimes called patient trajectories. This information serves as an important resource for assessing a patient's current health status and predicting potential health risks. Using advanced deep learning (DL) models with this extensive data opens the possibility of making predictions, such as disease risks, treatment outcomes, and patient prognoses. This possibility equips health care providers with the tools to make informed decisions, ultimately improving patient care, optimizing interventions, and reducing health care costs.

However, developing DL methods for modeling EHR data is full of challenges. Effectively addressing the complexity of the heterogeneous data extracted from patients' EHR [1-4], capturing short- and long-term relationships between medical codes across various visits, contending with the scarcity of publicly available EHR sources, and navigating the vast diversity of diseases pose significant hurdles. In addition, ensuring transparency and explainability in the predictions made by DL techniques demands substantial effort [5-7].

Current state-of-the-art models for EHR trajectory data are based on transformer architecture [8], in particular, models inspired by the Bidirectional Encoder Representations from Transformers (BERT) [9] architecture [10-14]. Such models aim to capture short- and long-term relationships through a task-agnostic representation learning (RL) approach, where the masked language model (MLM) pretraining objective is very common.

The BERT-inspired models for EHR trajectory data can be examined from various perspectives: data and model size, used data modalities, architecture, and pretraining objectives. Within this context, we focus on the primary and auxiliary pretraining objective functions designed to enhance the capabilities of the learned representation.

The primary objective typically takes the form of a generative task, benefiting from its enhanced ability to grasp intricate relationships. MLM objectives have found widespread application in EHR trajectory prediction tasks, largely owing to the capabilities of BERT models to learn the context (both past and future simultaneously) [10,11,15-22]. The autoregressive pretraining objective [23,24] serves as the other approach for RL of EHR trajectory data. It accomplishes this by predicting upcoming medical events, such as the codes for the next day or the subsequent visit, leveraging the patient's historical data [25-27].

A range of auxiliary pretraining objectives has been proposed to enhance the RL performance, incorporating either external knowledge or using contrastive learning. Examples of the former include Shang et al [15] and Amirahmadi et al [28] that predicted medications based on diagnoses and diagnoses based on medication to induce relationships within the diagnoses and interventions in the learned representation. Med-BERT [11] introduced a length of stay auxiliary prediction task to enrich contextual information about the severity of patients' health conditions. CEHRT-BERT [16] and Claim-PT [27] incorporated visit type predictions (eg, inpatient and outpatient visits) to represent external domain knowledge into the model, mitigating the effect of sparse codes based on the observation that different medical concepts are associated with different visit types.

RareBERT [19] introduced a 1-class classification objective to improve model performance for rare disease prediction. Similarly, AdaDiag [18] added a domain classifier to distinguish data from different institutes and enhance the generalizability and robustness of the learned representation against dataset shifts.

From the contrastive learning category, we find Hierarchical BEHRT (Hi-BEHRT) [17] that used bootstrap your own latent (BYOL) [29] similarity learning, operating under the assumption that varying augmentations of the same input yield similar representations, thereby enhancing the latent representation of the network. Rapt [21] trained the transformer to differentiate between different patient trajectories, relying on the Euclidean distance between their last visits to enrich the RL's understanding of their health condition. In addition, Rapt used another auxiliary objective, like the next sentence prediction, to discern whether a trajectory belongs to a specific patient or constitutes a fusion of various patient trajectories, facilitating the learning of trends within health trajectories. Generative Adversarial Networks Enhanced Pretraining (GRACE) [22], addressing the EHR data insufficiency challenge, incorporated a real or fake contrastive learning objective to distinguish authentic EHR data from generative adversarial network (GAN)–generated EHR data within the MLM framework.

Instances of medical events can influence the likelihood of other medical events, shaping the trajectory of patients toward more or less severe health conditions. Moreover, numerous medical events exhibit semicausal relationships through chains of probability paths that have not been extensively studied [30-33].

XSL•FO
RenderX

The relative intervals between medical events play a pivotal role in adjusting a patient's trajectory and are a key factor for the RL model. In pretrained language models, similar concepts are applied to comprehend the global coherence of data. BERT [9] used a next-sentence prediction (NSP) to capture the global relations between sentences. However, Liu et al [34] showed that NSP does not generate a positive impact, and Lan et al [35] speculate that the reason lies in the simplicity of NSP and its overlap with the MLM loss. Consequently, they replaced NSP with sentence order prediction, prioritizing coherence prediction over topic prediction [36,37]. Before the mentioned studies, researchers improved their machine translation, constituency parsing models, and object detection by altering the order of input [38-40]. Vinyals et al [41] delved into the problem that, while in theory incorporating the order of sequences should not have a significant impact when using complex encoders due to their nature as universal approximators, in practice, it does matter due to underlying nonconvex optimization and more fitting priors.

Furthermore, EHR trajectories encompass a history of abnormal health conditions, including diseases, laboratory data, and prescribed interventions like medications and procedures. The occurrence of certain diseases can alter a person's health trajectory and increase the probability of other illnesses. Similarly, interventions often mitigate the severity of conditions at the cost of raising other health risks. Thus, every medical event, whether it involves diseases or medications, can serve as a cause, complication, or early symptom of the recorded codes [42]. This study will demonstrate that order objectives, besides the context, enhance the model performance by learning more structural information. In summary, the contributions are mentioned in Textbox 1.

Textbox 1. Overview of the study's main contributions.

- We have examined the ability of Bidirectional Encoder Representations from Transformers–inspired models to capture the representation of sequential information of medical codes. Our findings indicate that although transformers and language models excel at identifying global dependencies based on contextual information, learning the order of diseases and medications can be challenging, especially for patients with long trajectories.
- We introduced a novel "trajectory order objective" self-supervised auxiliary task to the masked language model (MLM). This new objective was applied at both the single code and visit levels, and we demonstrated its efficacy in enhancing the original MLM by evaluating it on heart failure, Alzheimer disease, and prolonged length of stay downstream prediction tasks on 2 distinct datasets.
- We introduced the conditional code swapping and conditional visit swapping functions built on the "conditional-based order of medical codes." This function allows swapping more frequent consecutive repetitions, enabling the model to systematically learn the patterns of transitions at both the single code and visit levels.
- We demonstrated how adding the new objective reshapes the attention behavior of the transformer model and encourages the model to attend to relations between 2 sets rather than 2 individual codes, enabling the learning of more complex structural relationships.

Methods

Data

In this study, we extracted medical diagnoses and medication histories from 2 distinct (EHR) trajectory datasets, namely the Medical Information Mart for Intensive Care IV (MIMIC-IV) hosp module [43] and the Malmo Diet and Cancer Cohort (MDC) [44]. These 2 datasets have unique characteristics that suit our research objectives.

The MIMIC-IV hosp module encompasses a rich, detailed collection of inpatient EHR trajectories, comprising a total of approximately 173,000 patient records recorded during 407,000 visits. The data spans from 2008 to 2019, offering a comprehensive view of patient journeys within the hospital setting. MIMIC-IV hosp module contains approximately 10.6 million medical codes associated with a large volume of patients. The MDC data is a prospective cohort from Sweden. It consists of approximately 30,000 individuals residing in the municipality of Malmo (southern Sweden) between 1991 and 1996. The cohort was recruited from a total population of about 74,000 individuals, encompassing all men born between 1923 and 1945 and all women born between 1923 and 1950. All inpatient and outpatient visits between 1992 and 2020 have been recorded, resulting in a total of 531,000 visits. Although the MDC dataset has fewer overall samples, it excels in providing a more extensive patient history, averaging 257 codes per patient compared to MIMIC-IV's 61 (for more details, refer to Multimedia Appendix 1).

Diseases and medications in both datasets are classified using the *ICD* (*International Classification of Diseases and Related Health Problems*) and Anatomical Therapeutic Chemical Code (ATC), respectively. These coding systems follow a hierarchical format, providing granular details about diseases or medications based on code length.

To facilitate our self-supervised pre-training, supervised fine-tuning, and final testing, we randomly partitioned the extracted cohort into 3 subsets: 70%, 20%, and 10%, respectively. For further details on the specifications of the MIMIC-IV and MDC datasets, refer to Tables 1 and 2.

XSL•FO
RenderX

Table 1. Summary statistics of the Medical Information Mart for Intensive Care IV (MIMIC-IV) dataset.

	Pretraining dataset	Fine-tuning dataset	Test dataset	Total dataset
Patients, n	121,000	36,000	16,000	173,000
Visits, n	285,000	86,000	37,000	408,000
ICD-9[a] codes, n	1,940,000	579,000	248,000	2,767,000
ATC[b] codes, n	5,511,000	1,655,000	688,000	7,854,000
All codes, n	7,451,000	2,234,000	937,000	10,622,000

[a]ICD-9: International Classification of Diseases, Ninth Revision.

[b]ATC: Anatomical Therapeutic Chemical Code.

Table 2. Summary statistics of the Malmo Diet and Cancer Cohort (MDC) dataset.

	Pretraining dataset	Fine-tuning dataset	Test dataset	Total dataset
Patients, n	21,000	6000	3000	30,000
Visits, n	373,000	107,000	52,000	531,000
ICD-10[a] codes, n	1,155,000	331,000	161,000	1,647,000
ATC[b] codes, n	4,185,000	1,223,000	580,000	5,988,000
All codes, n	5,339,000	1,554,000	741,000	7,634,000

[a]ICD-10: International Statistical Classification of Diseases, Tenth Revision.

[b]ATC: Anatomical Therapeutic Chemical Code.

Ethical Considerations

The use of the MDC dataset for this study was approved by the Ethics Review Board of Sweden (Dnr 2023-00503-01). Regarding the MIMIC-IV dataset, all protected health information (PHI) is officially deidentified. It means that the deletion of PHI from structured data sources (eg, database fields that provide age, genotypic information, and past and current diagnosis and treatment categories) is performed in compliance with the HIPAA (Health Insurance Portability and Accountability Act) standards in order to facilitate public access to the datasets.

Data Processing and Problem Formulation

Each dataset D comprises a set of patients P, $D = \{P^1, P^2, ..., P^{|D|}\}$. In our study, we considered a total of |D|= 172,980 patients for MIMIC-IV and |D|= 29,664 patients for the MDC cohort. We represent each patient's longitudinal medical trajectory through a structured set of visit encounters. Given the continuous recording of medical codes in the MDC cohort, we define a visit entity V for each code and all previous subsequent codes occurring within a 6-month time window. For the MIMIC-IV, we used the predefined visits. This representation is denoted as P, $P^i = \{V^i_1, V^i_2, \ldots, V^i_O\}$, where O represents the total number of visit encounters for patient I. For each visit, $V^i_j = I_j \cup M_j$ is the union of all diagnoses codes $I_j \subset I$ and prescribed medications $M_j \subset M$ that are recorded for the P^i at visit V^i_j. To reduce the sparsity, we excluded less frequently occurring medical codes and retained only the initial 4 digits of *ICD* and ATC codes (refer to Multimedia Appendix 1). This process resulted in 2195 *ICD-9* (*International Classification of Diseases, Ninth Revision*) and 137 ATC-5 unique codes for the MIMIC-IV dataset and 1558 *ICD-10* (*International Statistical Classification of Diseases, Tenth Revision*) and 111 ATC-5 unique codes for the MDC dataset. In addition, for the MIMIC-IV, we converted medication data from National Drug Code (NDC format to ATC format to benefit from its hierarchical structure and improve comparability.

To guide the model in understanding changes in encounter times and the structure of each patient's trajectory, like BERT, we used special tokens. A CLS token is placed at the beginning of each patient's trajectory, while a SEP token is inserted between visits. Consequently, each patient trajectory is represented as $P^i = \{CLS, V_1^i, SEP, V_2^i, SEP, \ldots, V_0^i, SEP\}$, providing the model with valuable context for analysis and prediction.

Heart Failure Prediction

The primary downstream task is heart failure (HF) prediction, where the model predicts the incidence of the first HF *ICD* codes $I_{N=HF}$ on the Nth visit, given the patient's previous history of diagnosis and medication intervention:



For each patient's trajectory, if there were no occurrences of the target disease, it is considered a negative case; otherwise, we excluded the first visit with target codes and all subsequent visits and considered it a positive case. Furthermore, all ATC codes related to HF treatment are excluded. To mitigate trajectory length bias, trajectories with fewer than 10 and 30 visits are excluded from MIMIC IV and the MDC dataset, respectively, ensuring an equal average number of visits within positive and negative cases. Following these preprocessing steps, we obtained Cohorts with a history of 5 visits for

XSL•FO
RenderX

MIMIC-IV and 20 visits for the MDC dataset on average. As a remark, in the MDC Cohort, this task is equivalent to predicting HF in the next 6 months, as per the preprocessing design.

Alzheimer Disease Prediction

The next downstream task is Alzheimer disease (AD) prediction. Similar to the HF prediction downstream task, the model predicts the occurrence of the first AD *ICD* codes $I_{N=AD}$ on the Nth visit, considering the patient's previous history of diagnoses and medication interventions:



We followed the HF prediction preprocessing steps. The AD downstream prediction task was tested on the MDC dataset.

Prolonged Length of Stay Prediction

To explore the adaptability of pretrained models to a distinct task from the one they were initially trained on (code prediction), we used the prediction of prolonged length of stay (PLS) as a binary classification downstream task. In this task, the model is assigned the objective of predicting the PLS in the Nth visit based on a patient's diagnoses and medications in previous visits in the MIMIC-IV dataset:



Consistent with [45], patients with a stay longer than 5 days were considered positive cases for PLS. To maintain consistency with the HF prediction task, trajectories with fewer than 3 visits were excluded, and the average number of visits was equalized between positive and negative cases. Following these steps, we obtained a Cohort with an average history of 5 visits (refer to Multimedia Appendix 1).

Methods

Recent studies have underscored the effectiveness of using multihead transformer architecture and MLM self-supervised learning in the domain of EHR trajectory modeling. While these methods have exhibited superior performance in various contexts, we focus on investigating their limitations related to sequential order learning and propose enhancements to address this issue.

A fundamental aspect of EHR trajectory modeling is the critical role of the sequential order of medical events in guiding patients' trajectories. For instance, the timely administration of appropriate medical interventions can significantly alter a patient's trajectory, either improving the severity of their condition or, conversely, leading to unintended side effects.

Models Objective

Our approach involves pretraining a transformer model on 2 distinct generative and contrastive self-supervised learning objectives: MLM and Trajectory-Order Objective (TOO). The MLM is crafted to learn the context, while TOO is designed to capture relations between local contexts. By simultaneously training the model on both of these objectives, we aim to leverage the entire set of patient trajectories and acquire a more comprehensive data representation.

MLM

The MLM generative task is used to learn the contextual dependencies among medical codes. In this paper, we corrupt the input by randomly masking the medical codes in each patient's trajectory, denoted as $P^i_{corrupted}$, and train the model to maximize the likelihood of the masked codes, denoted as x^k:



where is the conditional probability modeled by a deep neural network with parameter . We used a sliding window approach across patients' trajectories to generate additional samples for the MLM objective (refer to Multimedia Appendix 1).

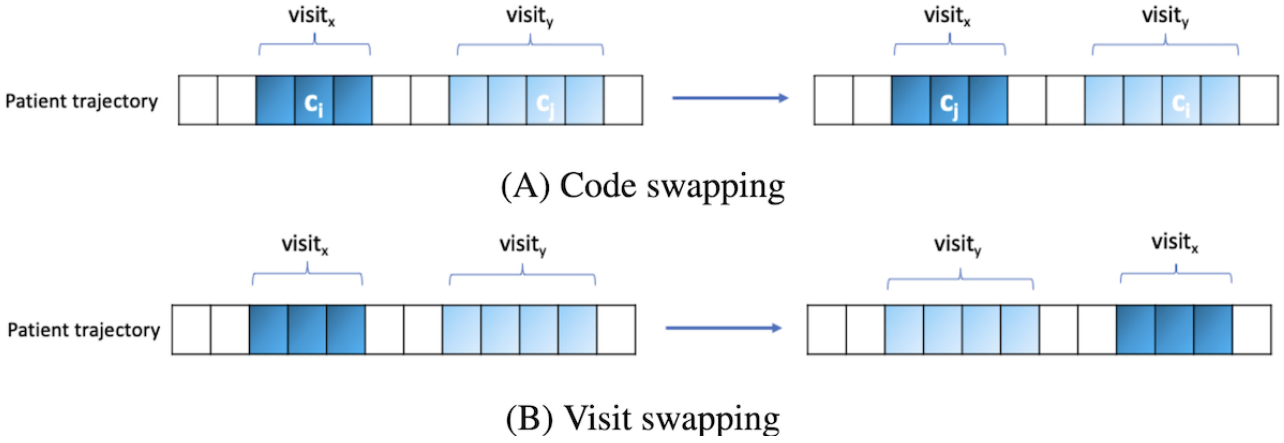
In the trajectory order objective, we train the transformer model to learn the relative positions of local features across 2 hierarchical levels, visits and medical codes. The TOO task helps the model gain insights into both causal and noncausal relationships within medical codes and visits. We achieved this by permuting each patient's trajectory, using them as negative samples, while the unpermuted sequences served as positive examples for the TOO self-supervised contrastive learning task.



In this equation, state ∈ {permutated, ordered} denotes whether the trajectory P^i is ordered or permutated, and $y_{state} \in \{0,1\}$ is the corresponding label. We implemented the TOO task at the code level and visit level, by code swapping and visit swapping, respectively (refer to Figure 1).

XSL•FO
RenderX

Figure 1. Code versus visits swapping. (A) Code swapping does not alter the visit structures of patient trajectories and only substitutes one medical code with another medical code in a different visit. (B) Visits swapping substitutes one visit, along with all its contents, with another visit, further disrupting the relative-time-wise dependencies between diagnoses and medications.



Code swapping: We initiated code swapping by swapping codes between different visits of a patient's trajectory. Given the complexity, especially for long trajectories, we designed and implemented 2 distinct methods. First, we randomly selected and swapped a subset of code pairs c_i and c_j with uniform probability, called random code swapping (RCS).

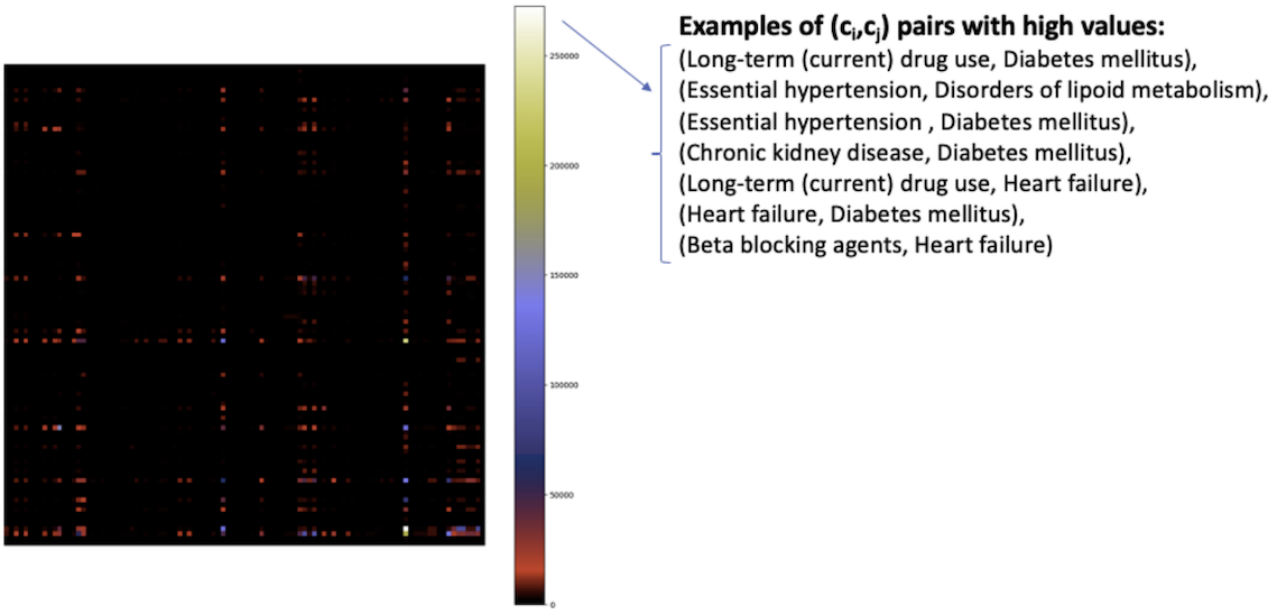
Second, to further facilitate the learning process for the transformer model and guide it toward more meaningful patterns, we introduced a conditional code swapping function (CCS; c_i, c_j). The idea is to prioritize code pairs that show a temporal dependency. The CCS function will provide a numerical estimate for such temporal relations, and in practice, code pairs (c_i, c_j) with large CCS (c_i, c_j) values are sampled more often than pairs with smaller values. We defined the CCS function as follows:



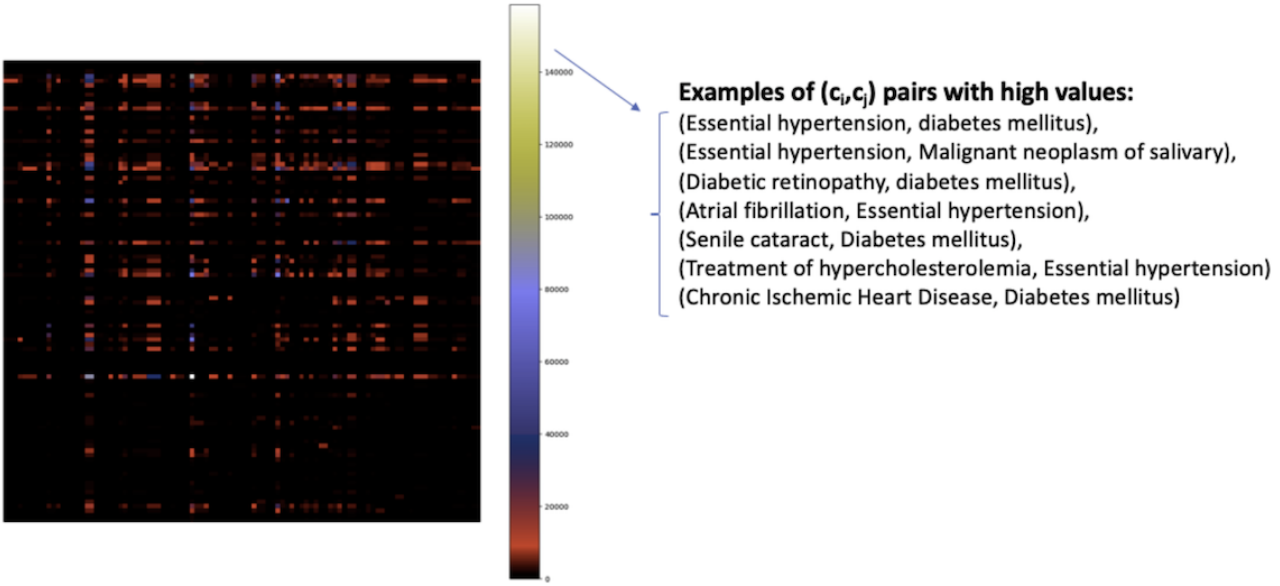
Here, CCnt(c_i, c_j) is the count of all occurrences of code pairs (c_i, c_j) with the condition that code c_i appears after code c_j and that they are located in different visits. The count is performed over all patient trajectories in the pretraining dataset. The max operator in the nominator forces the CCS function to only consider the simple temporal dependencies that code c_i follows code c_j. In other words, the maximum operator transforms the bidirectional transition graph between 2 medical codes into a unidirectional graph based on observations in the pretraining dataset. To account for a possible difference in the number of diagnoses and the number of medications, the CCS function was adjusted with a scaling factor $S_{i,j}$ (refer to Multimedia Appendix 1, for more details). Finally, ε is a small number added to allow for a nonzero probability of selecting code pairs regardless of the relation between CCnt(c_i, c_j) and CCnt(c_j, c_i). Figure 2 show the CCS values, as a heatmap, for a selection of code pairs (c_i, c_j) for both datasets used in this study.

XSL•FO
RenderX

Figure 2. The conditional code swapping matrix heat map for a subset of medical codes in the medical information mart for Intensive Care IV and Malmo Diet cohort datasets.



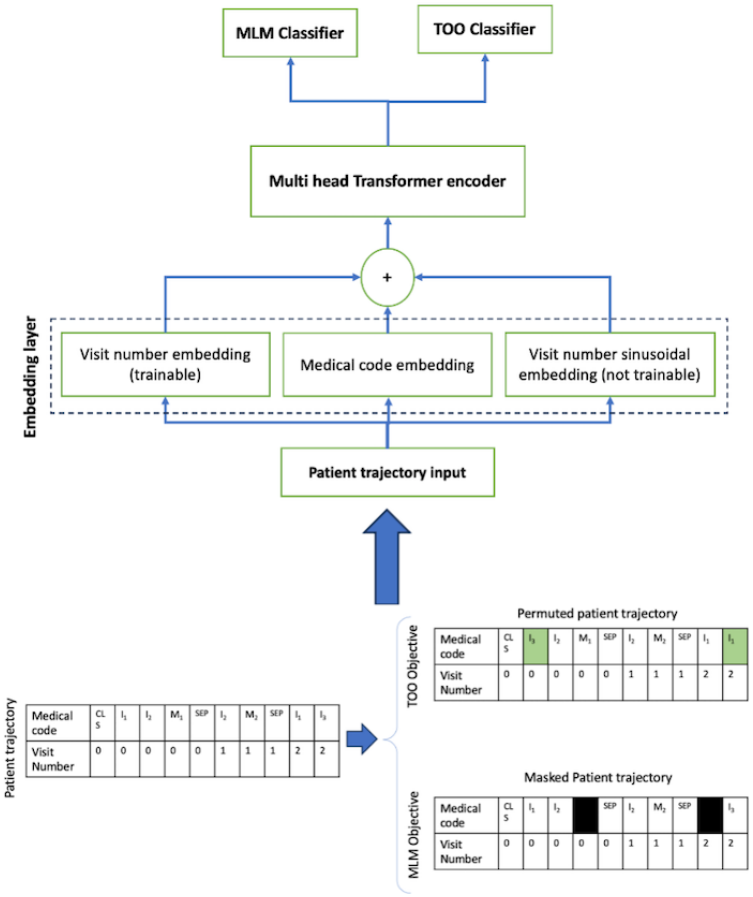
(A) The CCS heat-map for the MIMIC IV



(B) The CCS heat-map for the MDC

XSL•FO
RenderX

Figure 3. Trajectory order objective-Bidirectional Encoder Representations from Transformers architecture and example patient trajectory input. MLM: masked language modeling; TOO: trajectory-order objective.



Visits Swapping

Visit swapping aims to teach the model the coherence between different levels of local features in the global context. Instead of swapping positions of individual c_i and c_j codes, this method involves swapping the positions of all medical codes in visit x with those in visit y. Similar to code swapping, we implemented 2 methods for swapping visits. In the first method, we randomly sampled 2 visits x and y, with a uniform probability, and swapped them, denoted random visit swapping (RVS).

Second, we introduced the conditional visit swapping (CVS) function to prioritize among the visits to swap. This prioritization is based on the presence of codes within the visits that exhibited the simple temporal relation from the CCS approach as expressed by the CCS function above. To that end, the CVS function is calculated as the sum of CCS scores for all medical codes within visits x and y:



Similar to the way the CCS function was used for code swapping, pairs of visits with large $CVS(v_x,v_y)$ values are sampled more often than visit pairs with lower values.

Figure 2 shows the CCS matrix heat map for a subset of medical codes in the MIMIC-IV and MDC datasets. Each row and column represents a medical code, and the heat map indicates the CCS score for all combinations of medical codes. Pairs with higher scores (indicated by lighter colors here) are more likely to be swapped with each other. Due to the long-tail distribution of medical codes and the predominance of less frequent codes, only a subset of the more frequent codes is displayed here. Examples of medical code pairs with the highest CCS scores are printed on the right side. For instance, in the MIMIC-IV dataset, “chronic kidney disease” and “diabetes mellitus” exhibit one of the highest CCS scores, suggesting that kidney disease frequently follows diabetes (but not vice versa). Similarly, in the MDC dataset, “atrial fibrillation” and “essential hypertension” have a high CCS score, indicating that atrial fibrillation often appears after hypertension. Training the model explicitly on such relationships allows it to learn more relevant connections between diseases and medications.

Model Architecture

In this study, we used a multihead attention transformer encoder, drawing inspiration from BERT [8,9]. The model architecture, illustrated in Figure 3, includes an embedding module, a multihead attention transformer encoder, a feed-forward layer, and 2 classifier heads. The embedding module integrates medical codes with their associated temporal information. To capture the temporal dynamics, each medical code is paired with a visit sequence number, represented by 2 types of embeddings: a trainable visit number embedding and a nontrainable sinusoidal embedding, added together. These embeddings are summed with the medical code embeddings to form the input tensor X_0, which is then passed through a standard transformer encoder to obtain the transformed representation X_1:

XSL•FO
RenderX



The learned representation is then passed to both the MLM and TOO classifier heads. The MLM classifier is a large softmax applied along the vocabulary dimension, used for predicting masked tokens. The TOO classifier is a binary classifier responsible for predicting the correct temporal order of the medical codes.

Pretraining TOO-BERT

In the pretraining phase, we adopted a multitask learning approach to train the transformer network on both the MLM and TOO tasks simultaneously. For each batch, we alternated between these 2 objectives and performed gradient descent-based optimization on the weighted sum of their respective losses. This strategy allowed the model to learn both tasks cohesively, mitigating the risk of catastrophic forgetting that could occur if the objectives were trained sequentially [46,47] (ie, training on MLM first and then on TOO).

The total loss function for pretraining was defined as follows.

Each patient trajectory consists of a sequence of diagnoses, medications, and their associated visit sequence numbers, which are processed as input to TOO-BERT. The model includes an embedding layer, a multihead transformer encoder, and 2 classifier heads. First, all medical codes and their temporal information are embedded in the embedding layer. The combined embeddings are then passed through the multihead transformer encoder, followed by the MLM and TOO classifiers.



where W_{MLM} and W_{TOO} represent the weights assigned to each loss.

For the MLM objective, we randomly masked 15% [9] of the medical codes (equation 4). Similar to BERT and Med-BERT, during the masking process, each code had an 80% (n/N) chance of being replaced by [Mask], 10% (n/N) by a random code, and 10% (n/N) remained unchanged.

In the TOO task, we trained the model to classify the permuted trajectories using RCS, CCS, RVS, and CVS methods. We initially evaluated the model's capability on the TOO task across various permutations.

Fine-Tuning for Downstream Task

Following the pretraining phases for trajectory representation learning, we added a Bidirectional Gated Recurrent Unit (Bi-GRU) classifier head on top of the pretrained network, similar to Med-BERT, and finetuned it using the fine-tuning split for each specific downstream task. To enhance the fine-tuning process, we incorporated a layer-wise learning rate decay strategy [48,49] with gradient descent to decrease the weight changes in the initial layers compared with the later layers, thereby retaining the basic knowledge acquired during pretraining. In the final step, we compared the performance of our models against Logistic Regression, Random Forest, MLP, Bi-GRU, and a pretrained transformer with only the MLM objective.

Implementation Details

We set aside 10% (12000/121000 in the MIMIC-IV and 2000/21000 in the MDC dataset) of the pretraining dataset for monitoring the transformer's performance on the MLM and TOO pretraining objectives. The fine-tuning dataset was divided into 5 splits. For each iteration, we fine-tuned the pretrained models and trained the baseline models on 4 splits, using the remaining portion for early stopping. The reported results represent the average and SD of the performance across the 5 trained models on the isolated test dataset.

For the pretraining phase, we used a neural network featuring 5 self-attention heads and one transformer encoder with a $d_k = d_v = d_x = 36$ (refer to Multimedia Appendix 1), comprising approximately 300,000 learnable parameters. In each dataset, we computed the length of the trajectory for all patients and considered the 0.7 quantiles of the trajectory lengths as the maximum sequence length. For trajectories exceeding this length, we applied a moving window to generate additional augmented pretraining samples. We used the Adam optimizer with a learning rate of 7e-5, a weight decay of 0.015, and a dropout rate of 0.1, and trained the model until the loss curve stabilized. The MLP network comprises 2 hidden layers with 250 and 100 nodes, and the Bi-GRU network features one bidirectional GRU layer with 64 hidden nodes.

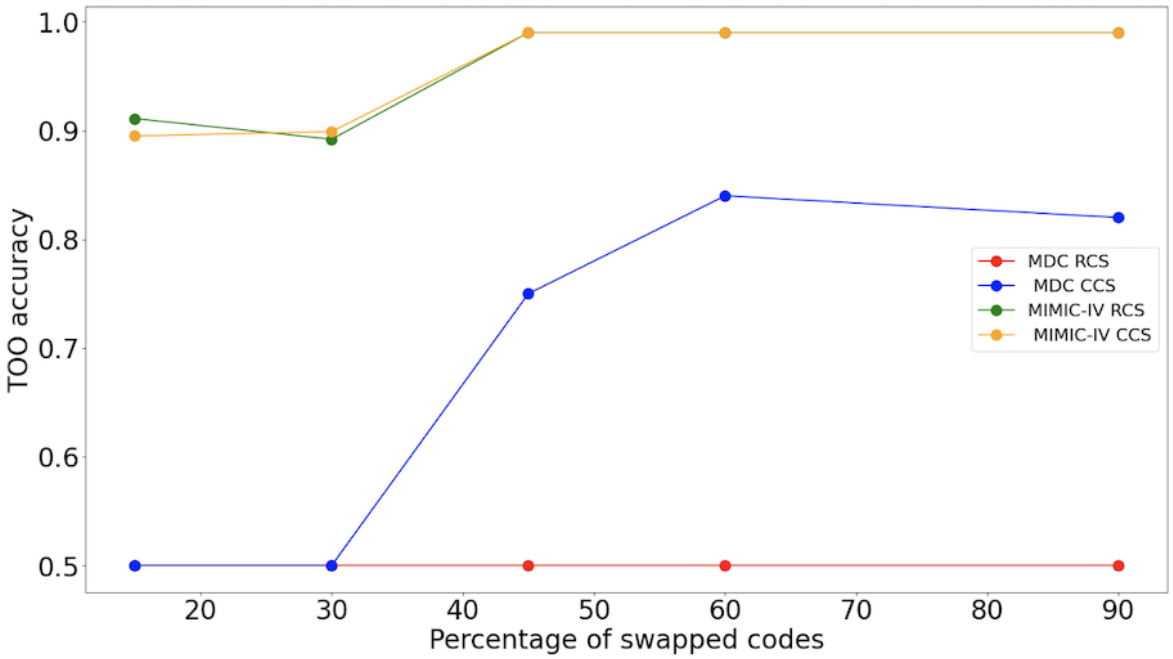
Results

Evaluation of Pretraining on the TOO Auxiliary Task

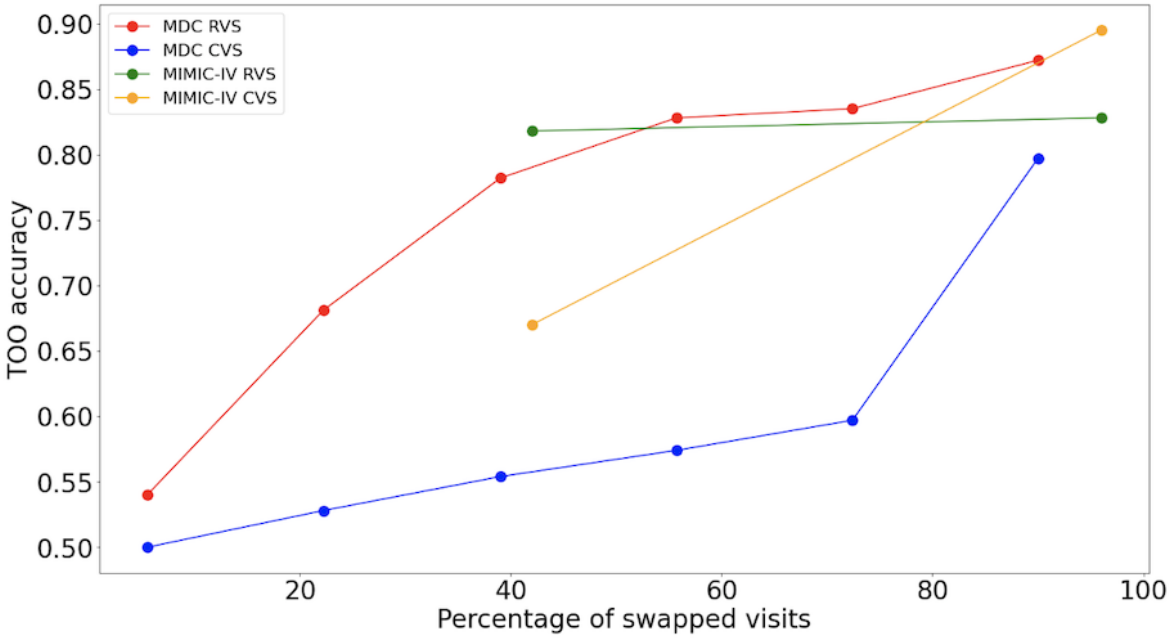
We assessed the effectiveness of the transformer models in learning the proposed TOO auxiliary objectives through a series of experiments conducted on the MDC and MIMIC-IV datasets. The four proposed swapping methods (RCS, CCS, RVS, and CVS) were applied with different amounts of swapped code or visit pairs, and the models' performance in detecting whether a trajectory contained swapped codes or visits was evaluated under varying amounts of swapping. Figure 4 illustrates the impact of increasing the percentage of swaps on classification performance for each dataset and swapping method.

XSL•FO
RenderX

Figure 4. The accuracy of the transformer model in classifying various types of swapping during the pretraining phase on the 10% unseen data from the pretraining split is shown for MDC and MIMIC-IV datasets. (A) The pretrained model can classify permuted samples with even a very low percentage of swapping on the MIMIC-IV dataset. On the other hand, classifying the permuted samples on the MDC was quite challenging. (B) The classification accuracy of the visits-swapped samples increases by raising the number of swapped visits for both methods and both datasets. MDC: Malmo Diet and Cancer Cohort; MIMIC-IV: Medical Information Mart for Intensive Care IV.



(A) The pretraining accuracy of the transformer models for different percentages of medical code swapping.



(B) The pretraining accuracy of the transformer models for different percentages of visit swapping.

As shown in Figure 4A, for the MIMIC-IV dataset, the transformer model could easily detect swapped trajectories using RCS and CCS methods for swap percentages above 40% (25/62). In contrast, the MDC dataset presented a different challenge. MDC trajectories are, on average, approximately 8 times longer (in terms of visits per patient) than those in MIMIC-IV. Here, the model struggled with the RCS, failing to find solutions effectively across any percentage of swapped pairs. In the CCS task, the model began to classify swapped trajectories more accurately only when the percentage of swaps exceeded 45% (102/254).

XSL•FO
RenderX

The results for the visit-swapping tasks (RVS and CVS) are presented in Figure 4B. These tasks proved more challenging for the models, especially at lower percentages of swaps. For the CVS task in the MDC dataset, the model required over 80% (14/18) of visits to be swapped before achieving satisfactory classification performance. Conversely, in the RVS task, the model achieved 0.8 accuracy with just 40% (7/18) of swapped visits.

For the MIMIC-IV dataset, the CVS task remained difficult for the transformer models, with only a single visit swap (1/2, 42%). However, in the RVS task, the model successfully classified trajectories with only one visit swap, demonstrating greater ease in learning visit-level temporal disruptions in this dataset.

To improve the pretraining performance on the MDC cohort with the RCS swapping method, we used a transfer learning approach. Initial weights from the transformer using the CCS method were used for the RCS task with 45% (102/254) code swapping, and this resulted in an accuracy of 0.684. This approach was also applied during the fine-tuning step for MLM+TOO$_{RCS}$ on the MDC dataset.

Evaluation of Downstream Tasks

We evaluated the prediction performance of HF and PLS for the MIMIC-IV dataset, while for the MDC dataset, we evaluated the HF and AD prediction performance. The datasets' specifications and the downstream tasks definitions are described in the section data. The percentages of swapping used for RCS, CCS, RVS, and CVS during pretraining are shown in Multimedia Appendix 1, Table S2 in Multimedia Appendix 1, and the selection was based on the performance on the validation performance within the fine-tuning dataset.

Table 3 shows the performance of Logistic Regression, Random Forest, MLP, Bi-GRU, the transformer pretrained with the MLM auxiliary task, and the 4 variations of the MLM+TOO auxiliary tasks. Consistent with the results of the Med-BERT model [11], the transformer pretrained with only MLM outperformed almost all other conventional methods in all downstream tasks for both datasets.

Table 3. Average AUC[a] values (%) and SD for different methods for the HF[b] prediction, AD[c] prediction, and PLS[d] prediction downstream tasks on the test datasets.

Model or dataset	HF prediction (MDC[e])	AD prediction (MDC)	HF prediction (MIMIC-IV[f])	PLS prediction (MIMIC-IV)
Logistic regression	62.4 (1.1)	56.4 (1.1)	83.8 (1.1)	54.2 (0.4)
Random forest	60.7 (0.5)	51.8 (0.3)	78.6 (1.6)	51.1 (0.3)
MLP	67.9 (3.0)	68.0 (1.5)	86.0 (0.5)	59.3 (1.9)
Bi-GRU	62.3 (1.2)	60.4 (1.1)	85.0 (1.3)	55.9 (1.0)
MLM[g]	67.7 (2.6)	69.5 (1.6)	86.2 (0.9)	60.2 (1.2)
MLM+TOO[h]$_{RCS}$[i]	65.1 (1.2)	65.6 (0.7)	88.1 (0.7)	58.4 (0.9)
MLM+TOO$_{CCS}$[j]	64.6 (2.7)	67.2 (1.3)	89.8 (0.8)	60.4 (1.2)
MLM+TOO$_{RVS}$[k]	72.8 (3.1)	70.4 (0.2)	87.9 (1.7)	57.3 (0.8)
MLM+TOO$_{CVS}$[l]	73.9 (1.9)	71.9 (1.6)	87.2 (1.8)	58.8 (1.6)

[a]AUC: area under the receiver operating characteristic curve.
[b]HF: heart failure.
[c]AD: Alzheimer disease.
[d]PLS: prolonged length of stay.
[e]MDC: Malmo Diet and Cancer Cohort.
[f]MIMIC-IV: Medical Information Mart for Intensive Care IV.
[f]gLM: masked language modelling.
[h]TOO: trajectory-order objective.
[i]RCS: random code swapping.
[j]CCS: code swapping function.
[j]RVS: random visit swapping.
[l]CVS: conditional visit swapping.

The visit-level TOO objective methods yielded the best HF and AD prediction performance on the MDC dataset, which features much longer patient trajectories. Using the CVS for the TOO objective achieved the highest area under the receiver operating characteristic curve (AUC) of 0.739 and 0.719 for HF and AD prediction, respectively. Moreover, since the model pretrained with random code swapping exhibited weak performance on the MDC dataset (Figure 4A), we initialized the model with the weights of the CCS pretrained model. We achieved approximately 0.74 accuracy on the TOO objective and subsequently fine-tuned this model for HF prediction, increasing

XSL•FO
RenderX

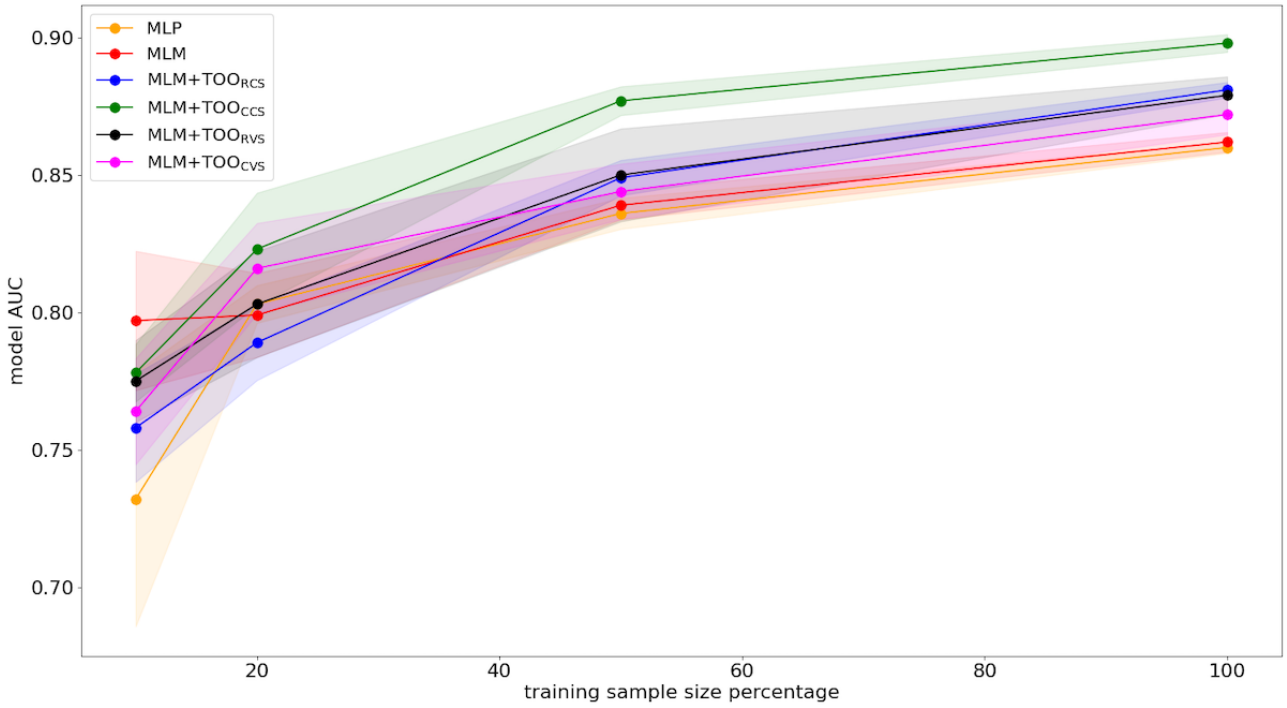
the AUC to 0.65.9. However, this result remained lower than that of the transformer pretrained solely on MLM.

For HF prediction on the MIMIC-IV dataset, the TOO auxiliary task with code swapping improved performance more than other methods. Applying the CCS over the TOO objective achieved the best AUC of 0.89.8. Although predicting the PLS on the next visit is challenging for all models, adding the CCS objective led to the best AUC.

Performance Boost on Data Insufficiency

We further evaluated the impact of combining the proposed TOO with the MLM, using varying fine-tuning sample sizes for predicting HF on the MIMIC-IV test dataset, and compared its performance to the transformer pretrained on MLM and MLP, the most successful conventional method. Fine-tuning sample sizes was reduced to 50% (442/884), 20% (176/884), and 10% (88/884). Figure 5 presents the performance of the MLP (orange line), the transformer pretrained with only MLM (red line), and transformers pretrained with MLM combined with RCS (blue line), CCS (green line), RVS (black line), and CVS (pink line). As the sample size decreased, the transformer pretrained with MLM+TOO_{CCS} achieved higher AUC scores, highlighting its effectiveness in handling data insufficiency.

Figure 5. Comparison of HF prediction AUC values for the test sets by fine-tuning on different data sizes on the MIMIC-IV dataset. The shadows represent the 90% CI. AUC: area under the receiver operating characteristic curve; HF: heart failure; MIMIC-IV: Medical Information Mart for Intensive Care IV. MLM: masked language modeling; MLP: multilayer perceptron; TOO: trajectory-order objective.

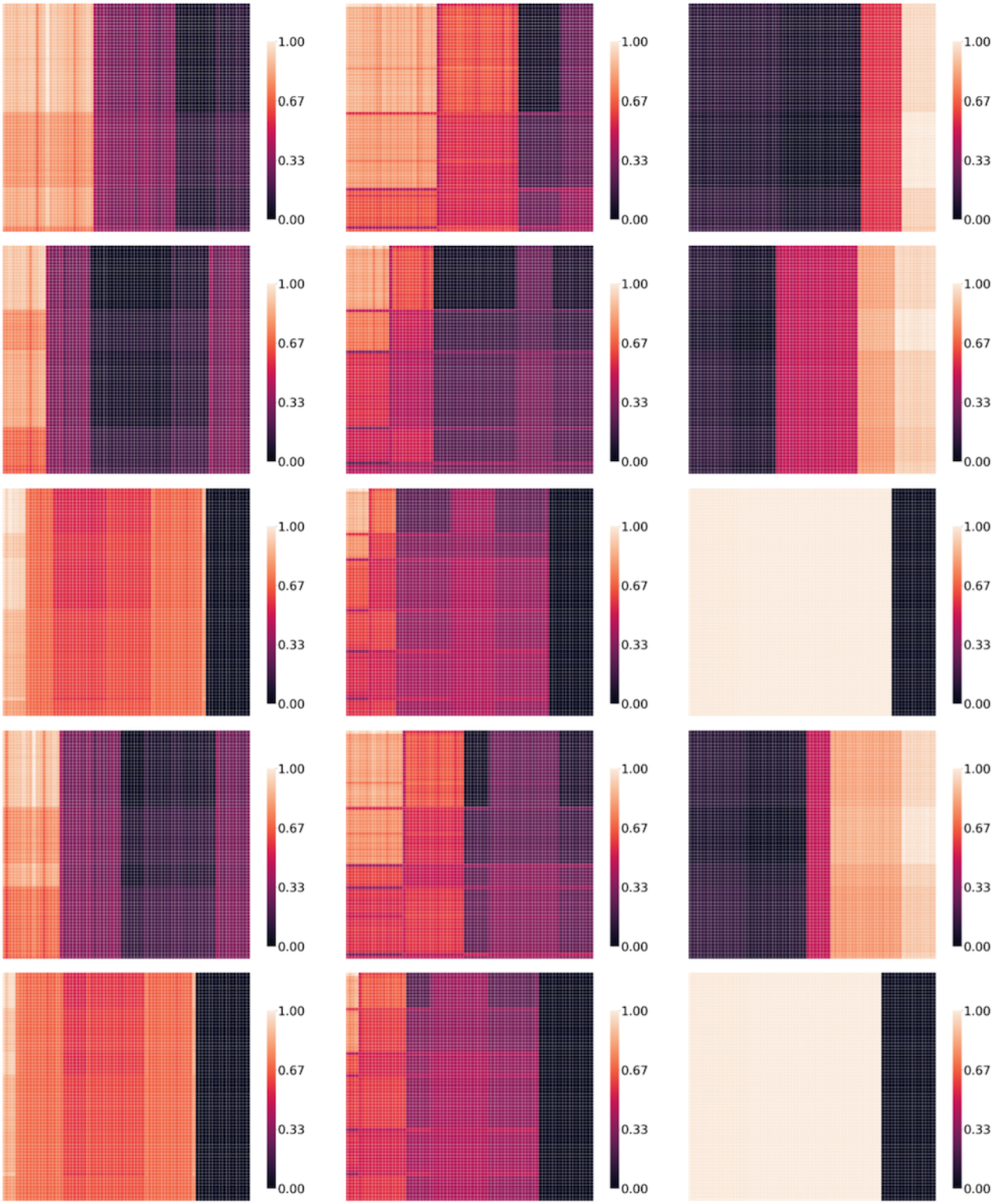


The Effect of TOO on Attention Weights

Visualizing the attention scores, A_h, of the transformer provides valuable insights into the model's decision-making process and its representation learning capabilities. More capable models can learn and attend to more complex patterns. Figure 6 shows attention scores for the fine-tuned models based on only MLM, MLM+TOO_{RVS}, and MLM+TOO_{CCS} pretraining. The attention scores come from a single patient trajectory for the HF prediction task on the MIMIC-IV dataset. Attention scores for all TOO-BERT variants can be found in Multimedia Appendix 1. In the rightmost column, the attention scores of the model pretrained solely with MLM show a primary focus on the latest codes in the trajectory. In contrast, models pretrained with the TOO objective (shown in the first and second columns) exhibit more diverse attention patterns, capturing more complex and structured relationships across the trajectory. In addition, models pretrained with the visit-level TOO objective (RVS) demonstrated an increased focus on the interactions between sets of consecutive codes (ie, segment-level attention). In contrast, the model pretrained with the CCS objective tended to exhibit attention at the individual code level.

XSL•FO
RenderX

Figure 6. The attention scores (5 heads) for 3 fine-tuned models on HF prediction for the MIMIC-IV dataset, shown for a specific sample from the test set. HF: heart failure; MIMIC-IV: Medical Information Mart for Intensive Care IV.



In Figure 6, lighter colors in the heatmap indicate higher attention weights, while darker colors represent lower attention weights. The variations within each model's attention heads are meaningful, reflecting how the model allocates attention to specific medical codes within the trajectory. The attention scores of the model pretrained on MLM+CCS demonstrate a greater ability to learn complex patterns. For better interpretability, the attention scores for each head are normalized between 0 and 1, though the original values range from 0 to 0.033, with slight variations across different models.

Discussion

Principal Findings

The sequential order of the medical codes and their interactions within a patient's EHR trajectory is crucial for understanding

XSL•FO
RenderX

and modeling their health status. While BERT-inspired methods have shown good results in this domain, the challenge lies in capturing the intricate relationships between diseases and prescribed interventions. TOO-BERT enhances the performance of BERT-inspired models by simultaneously learning the order of medical codes and the context of the EHR trajectory. Our approach involves pretraining these models explicitly on the sequential information within a patient's EHR trajectory, aiming to enhance their learning capability by using the temporal structure. In addition, the introduction of 2 novel weighting methods, CCS and CVS, within the TOO objective enables the models to learn more relevant and frequent causal and correlation dependencies with a data-driven approach.

The pretraining results highlight the differences in learning sequential information between the MIMIC-IV and MDC datasets. The MDC dataset, characterized by an average of approximately 18 visits per patient, presented more challenges in learning single code level sequential information compared to the MIMIC-IV dataset, which has an average of about 2.5 visits per patient (Figure 4A). This discrepancy could stem from the tendencies of transformers to learn the global dependencies and might require additional strategies to capture local patterns as well [50-53]. In addition, the performance of the model initialized with weights from the CCS task in the MDC dataset on the RCS task demonstrated that the proposed conditional probability approach can effectively help the model converge (section Evaluation of pretraining on the TOO auxiliary task).

Combining the proposed TOO with the MLM improved estimated AUC values for all downstream tasks on both datasets. Interestingly, in longer trajectories, visit-level swapping seemed more informative than code-level swapping, suggesting that the TOO auxiliary pretraining objective may improve the efficacy of the transformer in modeling long EHR trajectory data, in addition to suggested architectural improvements [54,55]. Moreover, code-level TOO-BERT reduced the performance of MLM in the MDC dataset, possibly due to the increase in MLM loss associated with adding the TOO auxiliary task during pretraining. Transformers trained solely on MLM demonstrated similar performance to MLP, indicating the complexity of EHR trajectories and data insufficiency in pretraining these models. The addition of the TOO task leveraged the MLM, potentially compensating for data insufficiency in complex models.

Predicting PLS from previous visits based on diagnoses and medications proved to be a particularly challenging task for all models. In addition, while previous research has indicated that BERT-inspired models are excellent few-shot learners [11,24,56], the addition of the TOO auxiliary task showed superior performance with reduced fine-tuning sample sizes for HF prediction in the MIMIC-IV dataset.

The CCS and CVS weighting function enhances the learning process by prioritizing more frequent transitional patterns. This prioritization helps the model focus on meaningful dependencies, such as transitions where the occurrence of one event strongly predicts the occurrence of another. By emphasizing these strong correlations, the model can converge more efficiently and avoid learning from rare or noisy transitions that may not represent meaningful relationships.

This approach is particularly beneficial in the context of small datasets. CCS and CVS ensure the model concentrates on the most informative patterns early in training, which not only facilitates convergence but also helps reduce overfitting to spurious relationships. While larger datasets and highly expressive models may eventually learn such relationships without CCS, the function remains valuable for guiding the model toward robustness in more resource-constrained settings. The other way to conceptualize CCS and CVS is the resemblance to first-order and higher-order Markov chains. CCS amplifies the probability weight of swapping a code pair based on the observation that the occurrence of one code increases the probability of observing the other in future visits. Similarly, CVS approximates a higher-order Markov chain by considering a set of conditions [57].

An interesting finding in our study was that training transformers on sequential information enables them to learn more intricate structures. The variability in the size and number of tiles in the attention weights (Figure 6) suggests that the TOO-objective enabled the transformers to learn a wide range of patterns. However, a quantitative analysis approach would be more suitable for gaining a more concrete understanding of the attention behaviors.

Limitations

This study has several limitations. The TOO task only considers the order of the medical codes and skips the time irregularity of visits in the EHR [58-60]. Extending the investigation of the new TOO-BERT variant to other datasets with larger sample sizes and longer visit trajectories would enhance our understanding of the differences between code and visit-level swapping pretraining objectives. Furthermore, the inclusion of additional EHR data sources with various modalities, such as test result values and demographic information, with continuous and categorical data types, in TOO-BERT requires further exploration.

Future Directions

Future research directions may involve a more comprehensive investigation of the challenges associated with the lack of locality in transformers and the exploration of more sample-efficient techniques to enhance the performance of TOO-BERT methods in data-limited scenarios. Enhanced positional encoding techniques and transformer architectures could prove beneficial. The impact of history length, influenced by code and visit level swapping, could be examined by pretraining TOO-BERT on larger datasets with longer visit histories. Furthermore, assessing the performance of pretrained TOO-BERT on other types of downstream tasks or tasks subject to dataset shifts would be valuable.

Conclusion

In this study, we explored the potential of incorporating the relative positions of medical codes to improve the learned representation of intricate disease-intervention dependencies, especially in scenarios involving lengthy sequences and limited data. Our introduction of TOO-BERT extends the capabilities of the MLM by focusing on the sequential information within patients' trajectories at both the single code and visit levels. In

XSL•FO
RenderX

addition, to enhance the TOO objective, we introduced condition-based code and swapped self-supervised tasks. The outcomes highlight TOO-BERT's superior performance in predicting PLS, AD, and HF across different sample sizes. Our analysis of attention weights reveals that the TOO task equips transformers to grasp more intricate structural patterns. Future research might involve exploring more sample-efficient pretraining methods and refining transformer architecture and positional encoding to enhance TOO-BERT's representation learning capabilities further.

Acknowledgments

This study was conducted as part of the AIR Lund (Artificially Intelligent use of Registers at Lund University) research environment and was funded by the Swedish Research Council (VR, grant 2019-00198). Additional support was provided by CAISR Health, funded by the Knowledge Foundation (KK-stiftelsen) in Sweden (grant 20200208 01 H).

We shared the Trajectory Order Objective Bidirectional Encoder Representations from Transformers (TOO-BERT) source code on TOO-BERT [61]. The pre-trained models are available from the authors upon request and with permission from the Medical Information Mart for Intensive Care IV (MIMIC-IV) and the Malmo Population-Based Cohorts Joint Database.

Data Availability

The MIMIC-IV dataset is publicly available from the PhysioNet repository [62]. The Malmo Diet and Cancer Cohort data that support the findings of this study are not publicly available due to data access restrictions imposed by the Malmo Population-Based Cohorts Joint Database. However, the data are available from the corresponding author upon reasonable request and with permission from the Malmo Population-Based Cohorts Joint Database [63].

Authors' Contributions

All persons who meet authorship criteria are listed as authors, and all authors certify that they have participated sufficiently in the work to take public responsibility for the content, including participation in the concept, design, analysis, writing, or revision of the manuscript. AA managed conceptualization, methodology, data curation, validation, formal analysis, writing-original draft, writing-review, editing, and visualization.

FE contributed to the investigation, conceptualization, methodology, validation, supervision, and writing—review and editing. JB was involved in validation, supervision, and writing—review and editing. OM contributed to validation, supervision, and writing—review and editing. MO contributed to the investigation, conceptualization, methodology, validation, supervision, writing—review and editing, as well as project administration.

Conflicts of Interest

None declared.

Multimedia Appendix 1
Additional material.
[PDF File (Adobe PDF File), 7441 KB - medinform_v13i1e68138_app1.pdf]

References

1. Miotto R, Li L, Kidd BA, Dudley JT. Deep patient: An unsupervised representation to predict the future of patients from the electronic health records. Sci Rep 2016;6:26094 [FREE Full text] [doi: 10.1038/srep26094] [Medline: 27185194]
2. Choi E, Bahadori M, Sun J, Kulas J, Schuetz A, Stewart W, et al. RETAIN: an interpretable predictive model for healthcare using reverse time attention mechanism. 2016 Presented at: NIPS'16: Proceedings of the 30th International Conference on Neural Information Processing Systems; 2016 December 05; Red Hook, NY, United States p. 3512-3520.
3. Ma F, Chitta R, Zhou J, You Q, Sun T, Gao J. Dipole: Diagnosis prediction in healthcare via attention-based bidirectional recurrent neural networks. 2017 Presented at: KDD '17: Proceedings of the 23rd ACM SIGKDD International Conference on Knowledge Discovery and Data Mining; 2017 August 13; NS, Halifax, Canada p. 1903-1911.
4. Luo J, Ye M, Xiao C, Ma F. HiTANet: Hierarchical time-aware attention networks for risk prediction on electronic health records. 2020 Presented at: KDD '20: Proceedings of the 26th ACM SIGKDD International Conference on Knowledge Discovery & Data Mining; 2020 August 20; CA, Virtual Event, USA p. 647-656.
5. Xiao C, Choi E, Sun J. Opportunities and challenges in developing deep learning models using electronic health records data: a systematic review. J Am Med Inform Assoc 2018;25(10):1419-1428 [FREE Full text] [doi: 10.1093/jamia/ocy068] [Medline: 29893864]
6. Amirahmadi A, Ohlsson M, Etminani K. Deep learning prediction models based on EHR trajectories: a systematic review. J Biomed Inform 2023;144:104430 [FREE Full text] [doi: 10.1016/j.jbi.2023.104430] [Medline: 37380061]

XSL•FO
RenderX

7. Si Y, Du J, Li Z, Jiang X, Miller T, Wang F, et al. Deep representation learning of patient data from Electronic Health Records (EHR): A systematic review. J Biomed Inform 2021;115:103671 [FREE Full text] [doi: 10.1016/j.jbi.2020.103671] [Medline: 33387683]
8. Vaswani A, Shazeer N, Parmar N, Uszkoreit J, Jones L, Gomez AN, et al. Attention is all you need. 2017 Presented at: NIPS'17: Proceedings of the 31st International Conference on Neural Information Processing Systems; 2017 December 04; Red Hook, NY, United States p. 6000-6010.
9. Devlin J, Chang MW, Lee K, Toutanova K. Bert: Pre-training of deep bidirectional transformers for language understanding. arXiv:1810.04805 2018.
10. Li Y, Rao S, Solares JRA, Hassaine A, Ramakrishnan R, Canoy D, et al. BEHRT: Transformer for electronic health records. Sci Rep 2020;10(1):7155 [FREE Full text] [doi: 10.1038/s41598-020-62922-y] [Medline: 32346050]
11. Rasmy L, Xiang Y, Xie Z, Tao C, Zhi D. Med-BERT: pretrained contextualized embeddings on large-scale structured electronic health records for disease prediction. NPJ Digit Med 2021;4(1):86 [FREE Full text] [doi: 10.1038/s41746-021-00455-y] [Medline: 34017034]
12. Meng Y, Speier W, Ong MK, Arnold CW. Bidirectional representation learning from transformers using multimodal electronic health record data to predict depression. IEEE J Biomed Health Inform 2021;25(8):3121-3129 [FREE Full text] [doi: 10.1109/JBHI.2021.3063721] [Medline: 33661740]
13. Chen YP, Lo YH, Lai F, Huang CH. Disease concept-embedding based on the self-supervised method for medical information extraction from electronic health records and disease retrieval: Algorithm development and validation study. J Med Internet Res 2021;23(1):e25113 [FREE Full text] [doi: 10.2196/25113] [Medline: 33502324]
14. Wamil M, Hassaine A, Rao S, Li Y, Mamouei M, Canoy D, et al. Stratification of diabetes in the context of comorbidities, using representation learning and topological data analysis. Sci Rep 2023;13(1):11478 [FREE Full text] [doi: 10.1038/s41598-023-38251-1] [Medline: 37455284]
15. Shang J, Ma T, Xiao C, Sun J. Pre-training of graph augmented transformers for medication recommendation. arXiv:1906.00346 2019.
16. Pang C, Jiang X, Kalluri KS, Spotnitz M, Chen R, Perotte A, et al. CEHR-BERT: Incorporating temporal information from structured EHR data to improve prediction tasks. Proceedings of Machine Learning for Health, PMLR 2021;158:239-260.
17. Li Y, Mamouei M, Salimi-Khorshidi G, Rao S, Hassaine A, Canoy D, et al. Hi-BEHRT: Hierarchical transformer-based model for accurate prediction of clinical events using multimodal longitudinal electronic health records. IEEE J Biomed Health Inform 2023;27(2):1106-1117 [FREE Full text] [doi: 10.1109/JBHI.2022.3224727] [Medline: 36427286]
18. Zhang T, Chen M, Bui AAT. AdaDiag: Adversarial domain adaptation of diagnostic prediction with clinical event sequences. J Biomed Inform 2022;134:104168 [FREE Full text] [doi: 10.1016/j.jbi.2022.104168] [Medline: 35987449]
19. Prakash P, Chilukuri S, Ranade N, Viswanathan S. RareBERT: Transformer architecture for rare disease patient identification using administrative claims. Proc. AAAI Conf. Artif. Intell 2021;35(1):453-460. [doi: 10.1609/aaai.v35i1.16122]
20. Agarwal K, Choudhury S, Tipirneni S, Mukherjee P, Ham C, Tamang S, et al. Preparing for the next pandemic via transfer learning from existing diseases with hierarchical multi-modal BERT: a study on COVID-19 outcome prediction. Sci Rep 2022;12(1):10748 [FREE Full text] [doi: 10.1038/s41598-022-13072-w] [Medline: 35750878]
21. Ren H, Wang J, Zhao W, Wu N. RAPT: Pre-training of time-aware transformer for learning robust healthcare representation. 2021 Presented at: KDD '21: Proceedings of the 27th ACM SIGKDD Conference on Knowledge Discovery & Data Mining; 2021 August 14; Virtual Event, Singapore p. 3503-3511.
22. Ren H, Wang J, Zhao W. Generative adversarial networks enhanced pre-training for insufficient electronic health records modeling. 2022 Presented at: KDD '22: Proceedings of the 28th ACM SIGKDD Conference on Knowledge Discovery and Data Mining; 2022 August 14; Washington DC, USA p. 3810-3818.
23. Radford A, Wu J, Child R, Luan D, Amodei D, Sutskever I. Language models are unsupervised multitask learners. OpenAI blog 2019;1(8):9.
24. Brown TB, Mann B, Ryder N, Subbiah M, Kaplan J, Dhariwal P, et al. Language models are few-shot learners. 2020 Presented at: NIPS'20: Proceedings of the 34th International Conference on Neural Information Processing Systems; 2020 December 06; Red Hook, NY, United States p. 1877-1901.
25. Guo LL, Steinberg E, Fleming SL, Posada J, Lemmon J, Pfohl SR, et al. EHR foundation models improve robustness in the presence of temporal distribution shift. Sci Rep 2023;13(1):3767 [FREE Full text] [doi: 10.1038/s41598-023-30820-8] [Medline: 36882576]
26. Steinberg E, Jung K, Fries JA, Corbin CK, Pfohl SR, Shah NH. Language models are an effective representation learning technique for electronic health record data. J Biomed Inform 2021;113:103637 [FREE Full text] [doi: 10.1016/j.jbi.2020.103637] [Medline: 33290879]
27. Zeng X, Linwood SL, Liu C. Pretrained transformer framework on pediatric claims data for population specific tasks. Sci Rep 2022;12(1):3651 [FREE Full text] [doi: 10.1038/s41598-022-07545-1] [Medline: 35256645]
28. Amirahmadi A, Ohlsson M, Etminani K, Melander O, Bjork J. A Masked language model for multi-source EHR trajectories contextual representation learning. arXiv:2402.06675 2023.

XSL•FO
RenderX

29. Grill JB, Strub F, Altché F, Tallec C, Richemond P, Buchatskaya E, et al. Bootstrap your own latent a new approach to self-supervised learning. 2020 Presented at: NIPS'20: Proceedings of the 34th International Conference on Neural Information Processing Systems; 2020 December 06; Red Hook, NY, United States p. 33-84.
30. Vo TH, Nguyen NTK, Kha QH, Le NQK. On the road to explainable AI in drug-drug interactions prediction: a systematic review. Comput Struct Biotechnol J 2022;20:2112-2123 [FREE Full text] [doi: 10.1016/j.csbj.2022.04.021] [Medline: 35832629]
31. Doherty MJ. Algorithms for assessing the probability of an adverse drug reaction. Respiratory Medicine CME 2009;2(2):63-67. [doi: 10.1016/j.rmedc.2009.01.004]
32. Khan LM, Al-Harthi SE, Osman AM, Sattar MAAA, Ali AS. Dilemmas of the causality assessment tools in the diagnosis of adverse drug reactions. Saudi Pharm J 2016;24(4):485-493 [FREE Full text] [doi: 10.1016/j.jsps.2015.01.010] [Medline: 27330379]
33. Rizzoli R, Reginster J, Boonen S, Bréart G, Diez-Perez A, Felsenberg D, et al. Adverse reactions and drug-drug interactions in the management of women with postmenopausal osteoporosis. Calcif Tissue Int 2011;89(2):91-104 [FREE Full text] [doi: 10.1007/s00223-011-9499-8] [Medline: 21637997]
34. Liu Y, Ott M, Goyal N, Du J, Joshi M, Chen D. Roberta: A robustly optimized bert pretraining approach. arXiv:1907.11692 2019.
35. Lan Z, Chen M, Goodman S, Gimpel K, Sharma P, Soricut R. Albert: A lite bert for self-supervised learning of language representations. arXiv:1909.11942 2019.
36. Liu X, Zhang F, Hou Z, Mian L, Wang Z, Zhang J, et al. Self-supervised Learning: Generative or Contrastive. IEEE Trans. Knowl. Data Eng 2021;35(01):857-876. [doi: 10.1109/tkde.2021.3090866]
37. Kalyan KS, Rajasekharan A, Sangeetha S. AMMU: A survey of transformer-based biomedical pretrained language models. J Biomed Inform 2022;126:103982 [FREE Full text] [doi: 10.1016/j.jbi.2021.103982] [Medline: 34974190]
38. Sutskever I, Vinyals O, Le QV. Sequence to sequence learning with neural networks. 2014 Presented at: NIPS'14: Proceedings of the 28th International Conference on Neural Information Processing Systems - Volume 2; 2014 December 08; Cambridge, MA, United States.
39. Vinyals O, Kaiser ?, Koo T, Petrov S, Sutskever I, Hinton G. Grammar as a foreign language. 2015 Presented at: NIPS'15: Proceedings of the 29th International Conference on Neural Information Processing Systems - Volume 2; 2015 December 07; Cambridge, MA, United States p. 2773-2781.
40. Noroozi M, Favaro P. Unsupervised learning of visual representations by solving jigsaw puzzles. In: Leibe B, Matas J, Sebe N, Welling M, editors. Computer Vision – ECCV 2016. ECCV 2016. Lecture Notes in Computer Science(), vol 9910. Switzerland: Springer, Cham; 2016.
41. Vinyals O, Bengio S, Kudlur M. Order mattersquence to sequence for sets. arXiv:1511.06391 2015.
42. Sun C, Dui H, Li H. Interpretable time-aware and co-occurrence-aware network for medical prediction. BMC Med Inform Decis Mak 2021;21(1):305 [FREE Full text] [doi: 10.1186/s12911-021-01662-z] [Medline: 34727940]
43. Johnson A, Bulgarelli L, Pollard T, Horng S, Celi L, Mark R. PhysioNet. Mimic-iv. URL: https://physionet org/content/mimiciv/10 [accessed 2021-08-23]
44. Berglund G, Elmstähl S, Janzon L, Larsson SA. The malmo diet and cancer study. Design and feasibility. J Intern Med 1993;233(1):45-51. [doi: 10.1111/j.1365-2796.1993.tb00647.x] [Medline: 8429286]
45. Gentimis T, Alnaser AJ, Durante A, Cook K, Steele R. Predicting hospital length of stay using neural networks on mimic iii data. 2017 Presented at: IEEE 15th Intl Conf on Dependable, Autonomic and Secure Computing, 15th Intl Conf on Pervasive Intelligence and Computing, 3rd Intl Conf on Big Data Intelligence and Computing and Cyber Science and Technology Congress(DASC/PiCom/DataCom/CyberSciTech); 2017 November 06-10; Orlando, FL, USA p. 1194-1201.
46. Farajtabar M, Azizan N, Mott A, Li A. Orthogonal gradient descent for continual learning. 2020 Presented at: Proceedings of the Twenty Third International Conference on Artificial Intelligence and Statistics, PMLR; 2020 JAN 01; Palermo, Italy p. 3762-7373.
47. Mirzadeh S, Farajtabar M, Gorur D, Pascanu R, Ghasemzadeh H. Linear mode connectivity in multitask and continual learning. arXiv:2010.04495 2020. [doi: 10.48550/arXiv.2010.04495]
48. Bao H, Dong L, Piao S, Wei F. Beit: Bert pre-training of image transformers. arXiv:2106.08254 2021.
49. Dong X, Bao J, Zhang T, Chen D, Gu S, Zhang W. CLIP itself is a strong fine-tuner: Achieving 85.7% and 88.0% top-1 accuracy with ViT-B and ViT-L on ImageNet. arXiv:2212.06138 2022.
50. Liu Y, Sangineto E, Bi W, Sebe N, Lepri B, Nadai M. Efficient training of visual transformers with small datasets. arXiv:2106.03746 2021:-30.
51. Cao YH, Yu H, Wu J. Training vision transformers with only 2040 images. Berlin: Springer; 2022 Presented at: Computer Vision – ECCV 2022: 17th European Conference, Tel Aviv, Israel; 2022 October 23; Berlin, Heidelberg p. 220-237.
52. Clark K, Luong MT, Le QV, Manning CD. Electra: Pre-training text encoders as discriminators rather than generators. arXiv:2003.10555 2020.
53. Gulati A, Qin J, Chiu CC, Parmar N, Zhang Y, Yu J, et al. Conformer: Convolution-augmented transformer for speech recognition. arXiv:2005.08100 2020.

XSL•FO
RenderX

54. Zaheer M, Guruganesh G, Dubey K, Ainslie J, Alberti C, Ontanon S. Big bird: Transformers for longer sequences. 2020 Presented at: NIPS'20: Proceedings of the 34th International Conference on Neural Information Processing Systems; 2020 December 06; Red Hook, NY, United States p. 17283-17297.
55. Zhou H, Zhang S, Peng J, Zhang S, Li J, Xiong H, et al. Informer: Beyond efficient transformer for long sequence time-series forecasting. Proc. AAAI Conf. Artif. Intell 2021;35(12):11106-11115.
56. Schick T, Schutze H. It?s not just size that mattersmall language models are also few-shot learners. arXiv:2009.07118 2020.
57. Lundström J, Järpe E, Verikas A. Detecting and exploring deviating behaviour of smart home residents. Expert Syst. Appl 2016;55:429-440. [doi: 10.1016/j.eswa.2016.02.030]
58. Ahmed N, Schmidt-Thieme L. Sparse self-attention guided generative adversarial networks for time-series generation. Int J Data Sci Anal 2023;16(4):1-14. [doi: 10.1007/s41060-023-00416-6]
59. Pham T, Tran T, Phung D, Venkatesh S. Predicting healthcare trajectories from medical records: A deep learning approach. J Biomed Inform 2017;69:218-229 [FREE Full text] [doi: 10.1016/j.jbi.2017.04.001] [Medline: 28410981]
60. Men L, Ilk N, Tang X, Liu Y. Multi-disease prediction using LSTM recurrent neural networks. Expert Syst. Appl 2021;177:114905. [doi: 10.1016/j.eswa.2021.114905]
61. Amirahmadii A. ali-amirahmadii. URL: https://github.com/ali-amirahmadii/ [accessed 2025-05-16]
62. PhysioNet repository. URL: https://physionet.org/content/mimiciv/ [accessed 2025-05-16]
63. Malmo population-based Cohorts joint database. URL: https://www.malmo-kohorter.lu.se/malmo-cohorts [accessed 2025-05-16]

Abbreviations

AD: Alzheimer disease
ATC: Anatomical Therapeutic Chemical Code
AUC: area under the receiver operating characteristic curve
BERT: Bidirectional Encoder Representations from Transformers
Bi-GRU: Bidirectional Gated Recurrent Unit
BYOL: Bootstrap Your Own Latent
CCS: conditional code swapping
CVS: Conditional Visit Swapping
DL: deep learning
EHR: electronic health record
GAN: generative adversarial network
GRACE: Generative Adversarial Networks Enhanced Pretraining
HF: heart failure
Hi-BEHRT: Hierarchical BEHRT
HIPAA: Health Insurance Portability and Accountability Act
ICD: International Classification of Diseases and Related Health Problems
ICD-9: International Classification of Diseases, Ninth Revision
ICD-10: International Statistical Classification of Diseases, Tenth Revision
MDC: Malmo Diet and Cancer Cohort
MIMIC-IV: Medical Information Mart for Intensive Care IV
MLM: masked language modeling
NDC: National Drug Code
NSP: next-sentence prediction
PHI: protected health information
PLS: prolonged length of stay
RCS: random code swapping
RL: representation learning
RVS: random visit swapping
TOO: trajectory-order objective
TOO-BERT: Trajectory Order Objective Bidirectional Encoder Representations from Transformers

XSL•FO
RenderX

Edited by A Coristine; submitted 29.10.24; peer-reviewed by H Turbe, CC Hung; comments to author 13.12.24; revised version received 26.01.25; accepted 28.03.25; published 04.06.25.

Please cite as:
Amirahmadi A, Etminani F, Björk J, Melander O, Ohlsson M
Trajectory-Ordered Objectives for Self-Supervised Representation Learning of Temporal Healthcare Data Using Transformers: Model Development and Evaluation Study
JMIR Med Inform 2025;13:e68138
URL: https://medinform.jmir.org/2025/1/e68138
doi:10.2196/68138
PMID:40465350

©Ali Amirahmadi, Farzaneh Etminani, Jonas Björk, Olle Melander, Mattias Ohlsson. Originally published in JMIR Medical Informatics (https://medinform.jmir.org), 04.06.2025. This is an open-access article distributed under the terms of the Creative Commons Attribution License (https://creativecommons.org/licenses/by/4.0/), which permits unrestricted use, distribution, and reproduction in any medium, provided the original work, first published in JMIR Medical Informatics, is properly cited. The complete bibliographic information, a link to the original publication on https://medinform.jmir.org/, as well as this copyright and license information must be included.

XSL•FO
RenderX

Original Paper

A Machine Learning Model for Predicting Sarcopenia Among Middle-Aged Adults: Development and External Validation

Hye Jin Chong[1], Prof Dr, PhD, RN

Department of Nursing, Sunchon National University, Suncheon-si, Republic of Korea

Corresponding Author:
Hye Jin Chong, Prof Dr, PhD, RN
Department of Nursing
Sunchon National University
255 Joongang-ro
Suncheon-si, 57922
Republic of Korea
Phone: 82 61 750 3882
Fax: 82 61 750 3880
Email: hyejin@scnu.ac.kr

Abstract

Background: Sarcopenia is a common muscle disorder in older adults, and its early identification and management in middle-aged populations are essential for ensuring a healthier later life. Detecting sarcopenia at an earlier stage may reduce the future burden on health care systems and enhance the quality of life in older adults. Machine learning (ML) models can evaluate large datasets, identify essential variables, and find complicated correlations between input variables. However, using ML models to detect sarcopenia remains an unsatisfied need.

Objective: This study aimed to develop and externally validate an ML model to predict sarcopenia risk among middle-aged adults using a nationally representative dataset.

Methods: We analyzed data from 1926 participants aged 40 to 64 years and enrolled in the 2022 Korea National Health and Nutrition Examination Survey (KNHANES). Sarcopenia was diagnosed and defined based on the 2019 Asian Working Group for Sarcopenia criteria, which incorporate both low muscle mass and reduced muscle strength. Muscle mass was assessed using bioelectrical impedance analysis with cutoffs of <7.0 kg/m² for men and <5.7 kg/m² for women. Muscle strength was measured via handgrip strength using a digital dynamometer with thresholds of <28 kg for men and <18 kg for women. Participants meeting both criteria were classified as those with sarcopenia. Four ML algorithms, random forest, support vector machine, extreme gradient boosting, and logistic regression, were used to identify risk factors of sarcopenia and predict its likelihood. The top-performing model was subsequently validated in an external cohort of 2247 middle-aged adults from the 2023 KNHANES. Model performance was assessed using the F_2-score, area under the curve of a receiver operating characteristic curve, and sensitivity. All analyses were conducted using Python 3.13.2 (Python Software Foundation).

Results: Among the 4 models, the logistic regression model demonstrated the strongest performance, yielding an area under the curve of 0.85, a sensitivity of 0.92, and an F_2-score of 0.66. External validation using the 2023 KNHANES dataset confirmed the model's robust performance, indicating its potential for widespread applications.

Conclusions: This study developed and externally validated an ML model that accurately identified sarcopenia in middle-aged adults. Leveraging data from a comprehensive national survey, our findings underscore the significance of early detection and customized interventions in midlife to mitigate sarcopenia risk and optimize long-term health outcomes.

(JMIR Med Inform 2025;13:e75760) doi:10.2196/75760

KEYWORDS

machine learning; predictive model; risk factors; sarcopenia; middle aged adults

XSL•FO
RenderX

Introduction

Sarcopenia is increasingly recognized as a significant muscle disease characterized by progressive and generalized loss of skeletal muscle mass and function, resulting in an elevated susceptibility to falls, fractures, infections, cardiovascular diseases, disability, and mortality [1].

In 2019, both the European Working Group on Sarcopenia in Older People [2] and the Asian Working Group for Sarcopenia (AWGS) [1] updated their definitions to emphasize the clinical importance of low muscle strength and function and reduced muscle mass.

Various causes for early-life sarcopenia have been identified, and the gap between sarcopenia progression and normal processes starts early in life [3-5]. The loss of muscle mass occurs as early as age 55 years in men and 45 years in women [6]. Midlife is also a period commonly associated with the emergence or escalation of chronic diseases and metabolic syndrome, which can further exacerbate muscle loss and functional decline. Skeletal muscle mass declines by about 6% every decade beyond middle age. Sarcopenia has a prevalence of up to 29% in middle-aged adults depending on the diagnostic criteria used [7]. Increased hospitalization expenditures due to sarcopenia are considerably greater in patients younger than 65 years than in those older than 65 years [8]. In addition, sarcopenia develops gradually and without obvious signs until a substantial decrease in muscle function occurs. Therefore, it is critical to detect risk factors for early sarcopenia in middle-aged adults. Nevertheless, the majority of risk prediction models for sarcopenia have been created to work for older adults because sarcopenia is a severe form of senescence that only affects older people [3,7]. Thus, these prediction models have restricted use in midlife populations. This gap emphasizes the importance of developing and validating new, data-driven models for early detection and intervention, promoting healthier trajectories into retirement and beyond.

Machine learning (ML) models can evaluate large datasets, identify essential variables, and find complicated correlations between input variables, making them practical tools for predicting health outcomes [9]. Clinical prediction models that use ML allow for integrating many elements to predict individual outcomes, providing deeper insights into disease risk determinants and enhancing prognosis precision [10]. Leveraging data from a population-based Korea National Health and Nutrition Examination Survey (KNHANES), this study aimed to provide a reliable, generalizable ML-based tool that can be integrated into clinical or public health settings for early detection and intervention in sarcopenia for middle-aged adults. The findings of this study could help develop approaches for improving the management and treatment of sarcopenia.

This direction is substantiated by growing evidence indicating that the risk factors for sarcopenia vary meaningfully across different age groups [4,11]. Specifically, our findings suggest that low body weight and insufficient protein intake are more influential in middle-aged adults, whereas sarcopenic obesity patterns are more frequently reported in older adults [12,13]. These distinctions highlight the need for age-specific prediction models throughout the course of life.

Methods

Datasets

The data for this study were obtained from the KNHANES, a nationwide dataset compiled by the Korea Ministry of Health and Welfare to investigate the nutritional and overall health status of the general public since 1998. Since 2007, cross-sectional datasets of around 10,000 people have been produced annually by stratified multilevel cluster sampling to ensure the representativeness of samples and allow the findings of research to be combined [14]. In this study, we categorized all selected variables into four domains to improve clarity and interpretability: (1) demographic variables (eg, age, gender, education level, marital status, and residence), (2) clinical variables (eg, BMI category, hypertension, diabetes mellitus, hypercholesterolemia, high-sensitivity C-reactive protein (hs-CRP), number of comorbid conditions, and subjective health perception), (3) health behavioral variables (eg, current smoking, current alcohol use, average sitting time per day, protein intake, and weekly aerobic and strength exercise participation), and (4) psychological variables (eg, perceived stress and generalized anxiety) based on the Generalized Anxiety Disorder-7 (GAD-7) score. A complete list of these variables and their distributions is provided in Table 1. Feature selection was guided by a combination of theory-driven rationale and data-driven evaluation. Initially, variables were selected based on their clinical relevance to sarcopenia as supported by existing literature. Subsequently, model-based methods, including L1-regularized logistic regression (LR) and recursive feature elimination, were used to refine the feature set based on contribution to model performance. To refine variable selection beyond theoretical rationale, we applied L1-regularized LR and recursive feature elimination as supplementary strategies. These approaches helped identify variables that consistently contributed to model performance while maintaining interpretability. Because KNHANES measurement items differ slightly from year to year, we only used datasets from years that included measurements of all relevant features (2022: test and training set; 2023: external validation set). We examined data of middle-aged adults (aged 19-64 years) from 1926 participants in 2022 and 2247 in 2023 in this study. After excluding participants who were missing variables, 1119 participants in 2022 and 1359 in 2023 were included in the final analysis (Multimedia Appendix 1).

XSL•FO
RenderX

Table 1. Baseline population characteristics of middle-aged adults from the 2022 Korea National Health and Nutrition Examination Surveys (N=1119).

Variables	Nonsarcopenia, n=894	Sarcopenia, n=135	*P*
Age (years), mean (SD)	54.85 (5.70)	56.61 (5.46)	<.001
Protein intake (g/day), mean (SD)	69.94 (32.54)	61.76 (27.12)	.002
hs-CRP[a] (mg/L), mean (SD)	1.30 (3.79)	1.84 (7.99)	.44
Sitting time per day (hours), mean (SD)	8.42 (5.24)	8.29 (3.27)	.69
BMI category, n (%)			<.001
Low weight	3 (0.3)	14 (10.4)	
Normal	277 (28.2)	110 (81.5)	
Preobesity	247 (25.1)	9 (6.7)	
Obesity	457 (46.4)	2 (1.5)	
Subjective health perception[b], n (%)			.59
1	33 (3.4)	7 (5.2)	
2	279 (28.4)	33 (24.4)	
3	498 (50.6)	66 (48.9)	
4	160 (16.3)	27 (20)	
5	14 (1.4)	2 (1.5)	
Current smoking, n (%)			.68
No	813 (82.6)	109 (80.7)	
Yes	171 (17.4)	26 (19.3)	
Current alcohol use, n (%)			.007
No	457 (46.4)	80 (59.3)	
Yes	527 (53.6)	55 (40.7)	
Anxiety, n (%)			.74
Low	945 (96)	131 (97)	
High	39 (4)	4 (3)	
Perceived stress, n (%)			.50
Low	752 (76.4)	99 (73.3)	
High	232 (23.6)	36 (26.7)	
Hypercholesterolemia, n (%)			.63
No	623 (63.3)	82 (60.7)	
Yes	361 (36.7)	53 (39.3)	
Hypertriglyceridemia, n (%)			.46
No	824 (83.7)	117 (86.7)	
Yes	160 (16.3)	18 (13.3)	
Hypertension, n (%)			<.001
Normal	381 (38.7)	78 (57.8)	
Caution stage	73 (7.4)	10 (7.4)	
Prehypertension	179 (18.2)	24 (17.8)	
Hypertension	351 (35.7)	23 (17)	
Diabetes, n (%)			.01
Normal	435 (44.2)	78 (57.8)	
Prediabetes	405 (41.2)	40 (29.6)	

XSL•FO
RenderX

Variables	Nonsarcopenia, n=894	Sarcopenia, n=135	*P*
Diabetes	144 (14.6)	17 (12.6)	
Number of comorbid conditions, n (%)			.07
0	403 (41)	67 (49.6)	
1-2	465 (47.3)	59 (43.7)	
≥3	116 (11.8)	9 (6.7)	
Marital status, n (%)			.80
Married	928 (94.3)	126 (93.3)	
Single	56 (5.7)	9 (6.7)	
Gender, n (%)			.001
Male	430 (43.7)	38 (28.1)	
Female	554 (56.3)	97 (71.9)	
Residence, n (%)			.55
City	783 (79.6)	111 (82.2)	
Rural	201 (20.4)	24 (17.8)	
Education level, n (%)			.29
Under elementary school	65 (6.6)	15 (11.1)	
Middle school	85 (8.6)	10 (7.4)	
High school	411 (41.8)	55 (40.7)	
College or above	423 (43)	55 (40.7)	
Weekly aerobic exercise participation, n (%)			.27
No	522 (53)	79 (58.5)	
Yes	462 (47)	56 (41.5)	
Weekly strength exercise participation, n (%)			.11
No	760 (77.2)	113 (83.7)	
Yes	224 (22.8)	22 (16.3)	

[a]hs-CRP: high-sensitivity C-reactive protein.

[b]Ranked on a 5-point scale from 1 (very good) to 5 (very bad).

Variables

For the diagnosis of sarcopenia, AWGS 2019 maintained the original cutoffs in a sarcopenia diagnosis as a bioelectrical impedance analysis <7.0 kg/m^2 in men and <5.7 kg/m^2 in women [15]. Predictable variables included the following 4 categories: demographic variables, clinical variables, health behavioral variables, and psychological variables. Demographic variables included age, gender, level of education, marital status, and residence. Clinical variables included hypertension, diabetes mellitus, hypercholesterolemia, hypertriglyceridemia, anemia by diagnosis or medication, hs-CRP, number of comorbid conditions, BMI categories, and subjective health perception. For clinical variables, BMI was included as an important predictor of sarcopenia. BMI categories were classified according to the World Health Organization Asia-Pacific criteria adopted by the KNHANES as underweight (<18.5 kg/m²), normal (18.5-22.9 kg/m²), overweight (23-24.9 kg/m²), and obese (≥25 kg/m²). Subjective health perception, often measured via a single self-rated health question, is a key indicator in KNHANES and internationally. This variable was recorded as 1 (very good) to 5 (very bad). Health behavioral variables included current smoking, rate of alcohol drinking per month (under 1 cup, 0; over 1 cup, 1), sitting time per day, amount of protein intake, aerobic exercise participation, and strength exercise participation. Psychological variables included perceived stress and generalized anxiety disorder evaluated using the GAD-7 scale. Perceived stress assessed how strongly respondents feel stress in daily life from 1 (very high) to 4 (none). For reporting purposes, when analyzing the data, KNHANES typically collapses 1 and 2 together as a high-stress group and 3 and 4 as a low-stress group, deriving the variable high perceived stress (yes or no) for analysis. The GAD-7 is a self-report questionnaire with 7 items. Each item is scored on a 4-point Likert scale from 0 (not at all) to 3 (nearly every day), yielding a total possible score from 0 to 21. Researchers commonly create a binary variable for anxiety disorder (yes or no) by using a cutoff of ≥10 on the total GAD-7 scale [16].

Model Development

We sought to predict sarcopenia by first randomly partitioning our dataset into training (75%) and test (25%) subsets using the

XSL•FO
RenderX

2022 dataset and a stratified method to preserve the original class distribution of sarcopenia. To enhance generalizability and minimize overfitting, we applied 5-fold stratified cross-validation during model training. This approach preserved class distribution in each fold and ensured robust performance evaluation across splits. Furthermore, to counteract class imbalance in the training data, we applied the synthetic minority over-sampling technique (SMOTE). Unlike simple random oversampling, which merely duplicates existing minority-class instances, SMOTE generates synthetic data points by interpolating between similar minority samples, resulting in a more generalized representation of the positive class. Following SMOTE, the number of sarcopenia-positive cases in the training set achieved a balanced 1:1 ratio between positive and negative classes. To prevent data leakage and ensure fair evaluation, SMOTE was applied exclusively to the training dataset. The test and external validation sets were left unaltered to reflect real-world class distribution during evaluation.

Model Evaluation and External Validation

We independently evaluated the predictive performance of 4 models using area under the curve (AUC), accuracy, precision, recall, specificity, F_1-score, and F_2-score as the primary metrics. For external validation, the same 4 models were subsequently tested on the 2023 dataset, and their predictive performances were assessed and compared using the same evaluation criteria. This approach facilitated a robust comparison of model effectiveness across the original and external validation datasets. Then, we conducted an original variable importance analysis to evaluate each predictor's contribution to the model's performance because assessing the significance of input features is critical in ML models [17]. In addition, a confusion matrix–based comparison was conducted for the test set and the external validation set. This method offers a detailed view of each model's classification performance by explicitly displaying true positives, false positives, true negatives, and false negatives. By applying it to both data partitions, we could directly assess the consistency of model predictions and identify misclassification patterns. This approach complements standard summary metrics (eg, accuracy and precision) by illuminating where errors occur, thereby enhancing the overall interpretability and validating the generalizability of the models [18].

Data Analysis

All statistical analyses were performed with Python 3.9.13 (Python Software Foundation). All continuous variables were standardized using z-score normalization, and categorical variables were 1-hot encoded. To address extreme values, particularly in hs-CRP, which exhibited high skewness, we applied percentile-based trimming by capping values at the 99th percentile. This preprocessing strategy ensured comparability across variables, mitigated the impact of outliers, and enhanced model stability. All continuous variables were normalized via z-score standardization, and categorical variables were coded as dummy features. A *t* test was performed to compare the characteristics of the sarcopenia and nonsarcopenia groups. Variables with *P* values of <.05 were defined as statistically significant.

To achieve our research objective of developing a fast and accurate predictive model for sarcopenia diagnosis in middle-aged adults, we conducted analyses as follows. Several different ML models were selected and applied to determine the model with the best accuracy and speed. We implemented LR, a traditional statistical model, to compare its performance with the relatively recently introduced ML models. Hyperparameter tuning was performed using GridSearchCV for LR and RandomizedSearchCV for tree-based models, namely, random forest (RF) and extreme gradient boosting (XGBoost). The tuning process aimed to optimize parameters such as regularization strength, tree depth, and learning rate based on validation performance. Moreover, we used several ML algorithms, including support vector machine (SVM), RF, and XGBoost. To support reproducibility, all data preprocessing and modeling steps have been documented in Multimedia Appendix 1. A deidentified version of the analysis code will be made publicly available via GitHub upon manuscript acceptance.

Ethical Considerations

This study was approved by the Ethics Committee of Sunchon National University (1040173-202503-HR-010-02).

Results

Population Characteristics

The study analyzed 1119 middle‐aged adults, comprising 984 (88%) individuals in the group without sarcopenia (nonsarcopenia group) and 135 (12%) in the group with sarcopenia (sarcopenia group). As shown in Table 1, the mean age was significantly higher in the sarcopenia group (mean 56.61, SD 5.46 years) than in the nonsarcopenia group (mean 54.85, SD 5.70 years; *P*<.001); protein levels differed significantly between the groups (sarcopenia group: mean 61.76, SD 27.12 g/day; nonsarcopenia group: mean 69.94, SD 32.54 g/day; *P*=.002). Obesity was more prevalent in the nonsarcopenia group (n=457, 46.4%) than in the sarcopenia group (n=2, 1.5%; *P*<.001). Conversely, the proportion of low weight individuals was much higher in the sarcopenia group (n=14, 10.4%) than in the nonsarcopenia group (n=3, 0.3%). Health behavioral and psychosocial factors, such as current smoking (*P*=.68) and stress (*P*=.50) did not differ significantly between the 2 groups; however, drinking status did (*P*=.007). Gender showed a notable association (*P*=.001), with individuals with sarcopenia more likely to be female (n=97, 71.9%) than male (n=38, 28.1%). Hypertension (*P*<.001) and diabetes status (*P*=.011) also differed significantly between the 2 groups. Other variables, including hs‐CRP, sitting time, anxiety, hypercholesterolemia, and hypertriglyceridemia, were not significantly different between the 2 groups. Marriage status (*P*=.80), residence (*P*=.55), aerobic exercise participation (*P*=.27), and strength exercise participation (*P*=.11) similarly showed no statistical differences between the sarcopenia and nonsarcopenia groups.

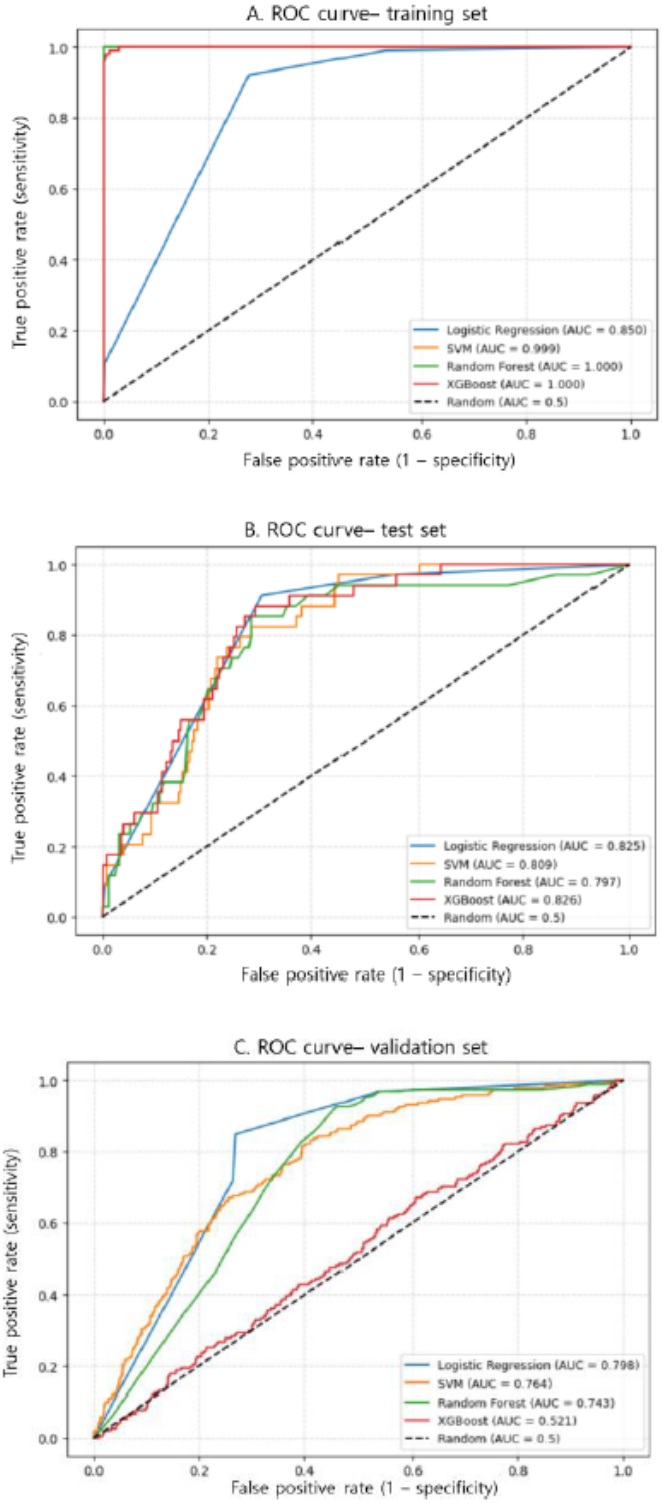
Model Evaluation and External Validation

Figure 1 and Table 2 show that in comparing 4 ML models for predicting sarcopenia, LR demonstrated the most stable performance in the test set, with an AUC of 0.82, an F_2-score

XSL•FO
RenderX

of 0.64, and a sensitivity of 91%. Notably, its high sensitivity and F_2-score for the minority class (patients with sarcopenia) suggest a strong potential for clinical application. In contrast, SVM, RF, and XGBoost exhibited extremely high performance on the training set but significant drops in F_2-score in the test set, indicating a risk of overfitting. Their sensitivities ranged from 24% to 29% in the test set, reflecting limited practical utility in detecting sarcopenia. Given its consistent performance across the training and test sets, along with advantages in identifying the minority class, LR was selected as the final predictive model in this study.

Figure 1. The receiver operating characteristic (ROC) curves of the predictive models. AUC: area under the curve; SVM: support vector machine; XGBoost: extreme gradient boosting.



XSL•FO
RenderX

Table 2. Model evaluation metrics.

Metric	Logistic regression (training)	Random forest (training)	SVM[a] (training)	XGBoost[b] (training)	Logistic regression (evaluation)	Random forest (evaluation)	SVM (evaluation)	XGBoost(evaluation)	Logistic regression (validation)	Random forest (validation)	SVM (validation)	XGBoost(validation)
AUC[c]	0.850	1.0	0.999	1.000	0.825	0.797	0.809	0.826	0.798	0.743	0.764	0.521
Accuracy	0.746	1.0	0.995	0.993	0.721	0.864	0.839	0.825	0.748	0.141	0.840	0.141
F_1-score	0.466	1.0	0.981	0.970	0.443	0.321	0.262	0.290	0.486	0.246	0.264	0.246
F_2-score	0.662	1.0	0.992	0.970	0.640	0.283	0.245	0.292	0.653	0.450	0.225	0.450
Precision	0.312	1.0	0.962	0.970	0.292	0.409	0.296	0.286	0.340	0.141	0.375	0.141
Recall (sensitivity)	0.921	1.0	1.000	0.970	0.912	0.265	0.235	0.294	0.848	1.000	0.204	1.000
Specificity	0.722	1.0	0.995	0.996	0.695	0.947	0.923	0.898	0.731	0.000	0.944	0.0000

[a]SVM: support vector machine.

[b]XGBoost: extreme gradient boosting.

[c]AUC: area under the curve.

In external validation, LR exhibited stable and consistent results across the training, test, and external validation sets. Notably, it achieved an AUC of 0.80, sensitivity of 0.85, and F_2-score of 0.65 in the validation dataset, indicating the most balanced capability for detecting the clinically significant minority class. In contrast, RF and XGBoost showed extremely high performance in the training set (AUC 1.00), yet demonstrated severe overfitting during validation, with a sensitivity of 1.00 but a specificity of 0.00, predicting all cases as patients. Although SVM achieved a high specificity of 0.94, its sensitivity was only 0.20 in the validation set, revealing limited utility for actual patient detection. These observations support that LR should be selected as the final predictive model in this study.

Model Interpretation

Table 3 shows the top ten important variables. Using the LR coefficients, we evaluated each predictor's importance by aggregating dummy-coded levels into the original variable units and calculating the mean absolute coefficient values. Obesity emerged as the most critical predictor, indicating the strongest association with sarcopenia risk in this model. Age and protein intake were also identified as influential factors.

Table 3. Top10 important variables based on the mean of absolute logistic regression coefficients across dummy-coded variables. This table represents the relative contribution of predictors to the model.

Variable	|Coefficient|, mean (SD)
Obesity	0.84, 0.41 (0.50)
Age	0.44, 55.06 (5.70)
Protein	0.39, 68.95 (32.04)
Drinking	0.14, 0.52 (0.50)
Hypercholesterolemia	0.14, 0.37 (0.48)
Gender	0.12, 0.42 (0.49)
Subjective health perspective	0.12, 2.85 (0.79)
Comorbidity	0.08, 0.58 (0.49)
Anxiety	0.08, 0.04 (0.19)
Hypertension	0.08, 0.33 (0.47)

Figure 2 presents the confusion matrices for the LR model in the test set (left panel) and external validation set (right panel). In the test set, a sensitivity (recall) of 91.2% (true positives=31, false negatives=3) and a specificity of 69.5% (true negatives=171, false positives=75) were achieved, suggesting that the model correctly identifies a high proportion of sarcopenia cases and maintains reasonable accuracy in classifying nonsarcopenia instances. A similar pattern was observed in the validation set, with a sensitivity of 84.8% (true positives=162, false negatives=29) and a specificity of 73.1% (true negatives=854, false positives=314). These results indicate that the model generalizes well, maintaining stable classification performance when applied to external data. Although SMOTE was applied only to the training set, we acknowledge that class imbalance remained in the test and validation datasets. Nonetheless, the LR model maintained high sensitivity and a

XSL•FO
RenderX

stable AUC, suggesting good generalizability even under imbalanced evaluation conditions.

Table 4 provides a critical comparison of sarcopenia incidence across predicted risk categories (low, medium, high) in the test set and the external validation set, visually demonstrating the consistent classification performance and clinical applicability of the LR model. In the high-risk group, sarcopenia incidence was 29.2% in the test set and 30.8% in the validation set, reflecting a high degree of consistency and underscoring that the risk stratification threshold effectively functions in a clinically meaningful way.

Figure 2. Confusion matrix for the logistic regression model.

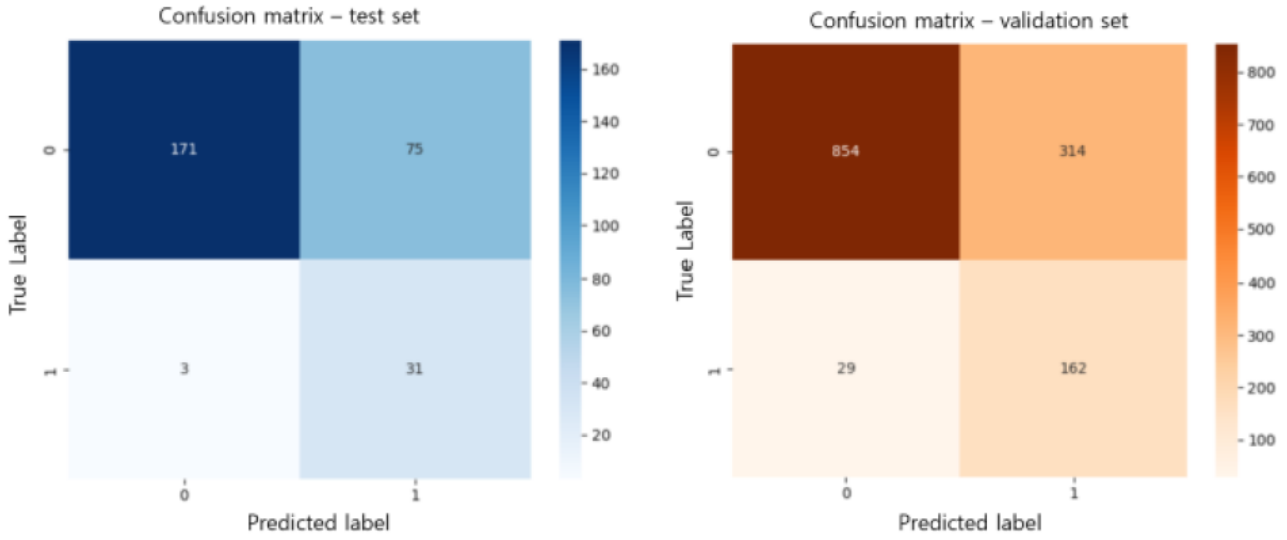


Table 4. Observed sarcopenia incidence rate by risk group in the logistic regression model.

Predicted risk group	Test set	Validation set
Low	1.7	0.0
Medium	0.0	5.9
High	29.2	30.8

Discussion

Principal Findings

The primary objective of this study was to develop an ML-based model for predicting sarcopenia in middle-aged adults and to identify the optimal model among various algorithms. As a result, our study demonstrated that an ML-based risk prediction model, particularly using LR, can reliably identify sarcopenia in middle-aged adults. The LR model showed strong and consistent performance in internal testing and external validation (AUC range 0.80-0.85), underscoring its clinical applicability for early detection. One notable strength of this model is that its coefficients allow us to discern both the direction (positive or negative) and the relative magnitude of each variable's impact, thereby providing more than just strong predictive capabilities. While interpretation tools, such as Shapley additive explanations and local interpretable model agnostic explanation, are valuable for complex models, they were not applied in this study because LR, our final model, is inherently interpretable. The model coefficients provide both direction and magnitude of each predictor's impact, making additional posthoc interpretability tools unnecessary. This preserves clarity and enhances clinical applicability.

By elucidating how individual variables contribute to sarcopenia risk, the model offers enhanced explanatory power and actionable insights into clinical and public health interventions. Moreover, the high generalizability and strong clinical applicability of the model are evident in its consistently superior performance relative to a random classifier (AUC=0.5) across the training, test, and external validation sets. This robust and stable performance, maintained regardless of the dataset used, underscores the model's potential for broad clinical implementation. Although direct comparisons are challenging due to a lack of research on predicting models for middle-aged adults, we were successful in developing a sarcopenia prediction model for middle-aged adults that might serve as a valuable diagnostic tool in clinical settings.

Our findings that obesity, age, and protein intake are key predictors highlight the importance of addressing modifiable risk factors before substantial muscle function decline sets in. By leveraging a large, population-based dataset, our work provides robust evidence that targeted interventions and screening in midlife can potentially mitigate the burden of sarcopenia in later life. Our findings indicate that, among middle-aged adults, lower body mass, rather than obesity, was associated with an increased risk of sarcopenia. This observation contrasts with several prior studies conducted in older populations where obesity, particularly sarcopenic obesity, has been frequently cited as a contributing factor for poor muscle function and outcomes [12,13]. However, our findings,

XSL•FO
RenderX

comprising individuals in midlife, may reflect a different trajectory of muscle decline, wherein low body weight, often indicative of inadequate nutritional reserves or underlying muscle wasting, emerges as a more salient predictor [19]. Previous evidence suggests that body composition plays a distinct role depending on life stage: in older adults, excess fat mass may exacerbate functional limitations, while in younger or middle-aged adults, insufficient muscle and fat mass (as seen in underweight individuals) may indicate early sarcopenic changes [20]. Our findings thus support a life course perspective on sarcopenia, emphasizing that underweight status in midlife is not benign and may serve as a precursor to more severe muscle dysfunction in later life. This underscores the need for early lifestyle interventions aiming at maintaining healthy muscle mass and adequate protein intake before the onset of significant age-related musculoskeletal decline [21]. On the other hand, age and protein intake emerged as key predictive factors, aligning with a robust body of evidence, indicating that advancing age is a primary risk factor for sarcopenia due to age-related muscle mass decline and that insufficient protein intake significantly contributes to muscle loss and functional impairment [19,22]. Conversely, factors such as strength training, urban versus rural residence, and anemia demonstrated comparatively lower variable importance in the model, which further highlights the central role of obesity, age, and nutritional intake in sarcopenia pathogenesis and prediction [21-24].

When contextualized within prior research, our study offers several distinct advancements in the domain of sarcopenia prediction. First, while much of the existing literature has predominantly focused on older adults and has frequently relied on conventional analytical techniques, such as LR, without incorporating robust sampling strategies, our research addresses a gap by targeting middle-aged populations and using state-of-the-art ML algorithms in conjunction with SMOTE to mitigate class imbalance, an approach shown to enhance classification performance in imbalanced biomedical datasets [25,26]. Prior studies have recognized the significance of age and nutritional status in sarcopenia etiology [3], but they have often lacked external validation. In contrast, our 2-step validation strategy comprising internal cross-validation and external dataset testing strengthens the model's generalizability and clinical utility, in line with recent calls for more rigorous validation frameworks in predictive modeling [27]. Second, conventional sarcopenia prediction tools often rely on limited indicators, such as grip strength alone. Our model adheres to the updated AWGS 2019 guidelines, integrating both handgrip strength and bioelectrical impedance analysis to provide a more comprehensive diagnostic foundation [28]. This alignment with contemporary clinical standards enhances the translational potential of our findings. Third, although muscle deterioration is known to begin in midlife, especially from the mid-40s onward [11], few studies have systematically investigated the interplay of obesity, protein intake, and age within this demographic. Our findings identify obesity and low protein intake as significant risk factors for sarcopenia in middle-aged adults, thereby extending earlier work on modifiable lifestyle components in muscle preservation [21,23]. Lastly, we demonstrate the utility of ML-based variable importance analyses, offering refined insights into the predictive strength of individual risk factors. This granularity supports the development of personalized interventions, such as tailored dietary strategies and exercise programs, for an often-overlooked age group [29].

Limitations and Future Directions

This study has several limitations and offers opportunities for future research. First, although the large national dataset strengthens generalizability, the cross-sectional design precludes establishing causal relationships among variables. A longitudinal cohort study would be beneficial to determine temporal patterns and causation in sarcopenia onset. Second, certain lifestyle and dietary variables relied on self-reported data, which may introduce recall bias. Due to limitations in the KNHANES dataset, which lacked harmonized continuous measures of physical activity across the 2022 and 2023 waves, we adopted a categorical representation to ensure consistency and comparability across cohorts. This methodological choice is acknowledged as a limitation. Future research should integrate more objective measures, such as wearable device data, to improve accuracy. Third, while our model performed robustly overall, additional tuning or integration with newer ML techniques could further enhance prediction metrics. Larger, multicountry cohorts and diverse populations are recommended for validating and extending the applicability of our findings.

Conclusions

Our ML-based prediction model offers a valuable framework for the early identification of sarcopenia risk in middle-aged adults, addressing a gap left by previous studies that have predominantly focused on older populations. These findings underscore the significance of proactive, personalized interventions targeting key modifiable risk factors, particularly obesity and nutrition, to mitigate muscle decline and related morbidities. By advocating for earlier detection and tailored preventive strategies, this study paves the way for improved midlife health care protocols, contributing to healthier aging trajectories globally.

Data Availability

All data supporting the findings of this study are available from the Korea National Health and Nutrition Examination Survey

Conflicts of Interest

None declared.

Multimedia Appendix 1

XSL•FO
RenderX

Detailed dataset, variable definitions, and data preprocessing procedures for machine learning model development and external validation.
[DOCX File , 21 KB - medinform_v13i1e75760_app1.docx]

References

1. Hanna JS. Sarcopenia and critical illness: a deadly combination in the elderly. JPEN J Parenter Enteral Nutr 2015 Mar;39(3):273-281. [doi: 10.1177/0148607114567710] [Medline: 25591973]
2. Cruz-Jentoft AJ, Sayer AA. Sarcopenia. Lancet 2019 Jun 29;393(10191):2636-2646. [doi: 10.1016/S0140-6736(19)31138-9] [Medline: 31171417]
3. Cruz-Jentoft AJ, Bahat G, Bauer J, Boirie Y, Bruyère O, Cederholm T, Writing Group for the European Working Group on Sarcopenia in Older People 2 (EWGSOP2),the Extended Group for EWGSOP2. Sarcopenia: revised European consensus on definition and diagnosis. Age Ageing 2019 Jan 01;48(1):16-31 [FREE Full text] [doi: 10.1093/ageing/afy169] [Medline: 30312372]
4. Sayer AA, Syddall H, Martin H, Patel H, Baylis D, Cooper C. The developmental origins of sarcopenia. J Nutr Health Aging 2008;12(7):427-432 [FREE Full text] [doi: 10.1007/BF02982703] [Medline: 18615224]
5. Thomas DR. Loss of skeletal muscle mass in aging: examining the relationship of starvation, sarcopenia and cachexia. Clin Nutr 2007 Aug;26(4):389-399. [doi: 10.1016/j.clnu.2007.03.008] [Medline: 17499396]
6. Krzymińska-Siemaszko R, Fryzowicz A, Czepulis N, Kaluźniak-Szymanowska A, Dworak LB, Wieczorowska-Tobis K. The impact of the age range of young healthy reference population on the cut-off points for low muscle mass necessary for the diagnosis of sarcopenia. Eur Rev Med Pharmacol Sci 2019 May;23(10):4321-4332 [FREE Full text] [doi: 10.26355/eurrev_201905_17938] [Medline: 31173305]
7. Jung HN, Jung CH, Hwang Y. Sarcopenia in youth. Metabolism 2023 Jul;144:155557. [doi: 10.1016/j.metabol.2023.155557] [Medline: 37080353]
8. Sousa AS, Guerra RS, Fonseca I, Pichel F, Ferreira S, Amaral TF. Financial impact of sarcopenia on hospitalization costs. Eur J Clin Nutr 2016 Sep;70(9):1046-1051. [doi: 10.1038/ejcn.2016.73] [Medline: 27167668]
9. Nevin L, PLOS Medicine Editors. Advancing the beneficial use of machine learning in health care and medicine: toward a community understanding. PLoS Med 2018 Nov;15(11):e1002708 [FREE Full text] [doi: 10.1371/journal.pmed.1002708] [Medline: 30500811]
10. Watson DS, Krutzinna J, Bruce IN, Griffiths CE, McInnes IB, Barnes MR, et al. Clinical applications of machine learning algorithms: beyond the black box. BMJ 2019 Mar 12;364:l886 [FREE Full text] [doi: 10.1136/bmj.l886] [Medline: 30862612]
11. Mitchell WK, Williams J, Atherton P, Larvin M, Lund J, Narici M. Sarcopenia, dynapenia, and the impact of advancing age on human skeletal muscle size and strength; a quantitative review. Front Physiol 2012;3:260 [FREE Full text] [doi: 10.3389/fphys.2012.00260] [Medline: 22934016]
12. Han SJ, Boyko EJ. The evidence for an obesity paradox in type 2 diabetes mellitus. Diabetes Metab J 2018 Jun;42(3):179-187 [FREE Full text] [doi: 10.4093/dmj.2018.0055] [Medline: 29885111]
13. Zamboni M, Mazzali G, Fantin F, Rossi A, Di Francesco V. Sarcopenic obesity: a new category of obesity in the elderly. Nutr Metab Cardiovasc Dis 2008 Jun;18(5):388-395. [doi: 10.1016/j.numecd.2007.10.002] [Medline: 18395429]
14. Kweon S, Kim Y, Jang M, Kim Y, Kim K, Choi S, et al. Data resource profile: the Korea National Health and Nutrition Examination Survey (KNHANES). Int J Epidemiol 2014 Feb;43(1):69-77 [FREE Full text] [doi: 10.1093/ije/dyt228] [Medline: 24585853]
15. Chen L, Liu L, Woo J, Assantachai P, Auyeung T, Bahyah KS, et al. Sarcopenia in Asia: consensus report of the Asian Working Group for Sarcopenia. J Am Med Dir Assoc 2014 Feb;15(2):95-101. [doi: 10.1016/j.jamda.2013.11.025] [Medline: 24461239]
16. Spitzer RL, Kroenke K, Williams JBW, Löwe B. A brief measure for assessing generalized anxiety disorder: the GAD-7. Arch Intern Med 2006 May 22;166(10):1092-1097. [doi: 10.1001/archinte.166.10.1092] [Medline: 16717171]
17. Zheng J, Li X, Zhu J, Guan S, Zhang S, Wang W. Interpretable machine learning for predicting chronic kidney disease progression risk. Digit Health 2024;10:20552076231224225 [FREE Full text] [doi: 10.1177/20552076231224225] [Medline: 38235416]
18. Alabi RO, Almangush A, Elmusrati M, Leivo I, Mäkitie AA. An interpretable machine learning prognostic system for risk stratification in oropharyngeal cancer. Int J Med Inform 2022 Dec;168:104896 [FREE Full text] [doi: 10.1016/j.ijmedinf.2022.104896] [Medline: 36279655]
19. Sehouli J, Mueller K, Richter R, Anker M, Woopen H, Rasch J, et al. Effects of sarcopenia and malnutrition on morbidity and mortality in gynecologic cancer surgery: results of a prospective study. J Cachexia Sarcopenia Muscle 2021 Apr;12(2):393-402 [FREE Full text] [doi: 10.1002/jcsm.12676] [Medline: 33543597]
20. Woo J, Leung J, Morley JE. Validating the SARC-F: a suitable community screening tool for sarcopenia? J Am Med Dir Assoc 2014 Sep;15(9):630-634. [doi: 10.1016/j.jamda.2014.04.021] [Medline: 24947762]
21. Houston DK, Nicklas BJ, Ding J, Harris TB, Tylavsky FA, Newman AB, Health ABC Study. Dietary protein intake is associated with lean mass change in older, community-dwelling adults: the Health, Aging, and Body Composition (Health ABC) Study. Am J Clin Nutr 2008 Jan;87(1):150-155 [FREE Full text] [doi: 10.1093/ajcn/87.1.150] [Medline: 18175749]

XSL•FO
RenderX

22. Park JE, Lee S, Kim K. The effect of combining nutrient intake and physical activity levels on central obesity, sarcopenia, and sarcopenic obesity: a population-based cross-sectional study in South Korea. BMC Geriatr 2023 Mar 03;23(1):119 [FREE Full text] [doi: 10.1186/s12877-023-03748-x] [Medline: 36869315]
23. Beaudart C, Dawson A, Shaw SC, Harvey NC, Kanis JA, Binkley N, IOF-ESCEO Sarcopenia Working Group. Nutrition and physical activity in the prevention and treatment of sarcopenia: systematic review. Osteoporos Int 2017 Jun;28(6):1817-1833 [FREE Full text] [doi: 10.1007/s00198-017-3980-9] [Medline: 28251287]
24. Beberashvili I, Azar A, Khatib A, Abu Hamad R, Neheman A, Efrati S, et al. Sarcopenic obesity versus nonobese sarcopenia in hemodialysis patients: differences in nutritional status, quality of life, and clinical outcomes. J Ren Nutr 2023 Jan;33(1):147-156. [doi: 10.1053/j.jrn.2022.05.003] [Medline: 35597322]
25. Chawla N, Bowyer K, Hall L, Kegelmeyer W. SMOTE: synthetic minority over-sampling technique. J Artif Intell Res 2002 Jun 01;16:321-357 [FREE Full text] [doi: 10.1613/jair.953]
26. Buda M, Maki A, Mazurowski MA. A systematic study of the class imbalance problem in convolutional neural networks. Neural Netw 2018 Oct;106:249-259. [doi: 10.1016/j.neunet.2018.07.011] [Medline: 30092410]
27. Collins GS, Reitsma JB, Altman DG, Moons KGM, TRIPOD Group. Transparent reporting of a multivariable prediction model for individual prognosis or diagnosis (TRIPOD): the TRIPOD statement. The TRIPOD Group. Circulation 2015 Jan 13;131(2):211-219 [FREE Full text] [doi: 10.1161/CIRCULATIONAHA.114.014508] [Medline: 25561516]
28. Chen L, Woo J, Assantachai P, Auyeung T, Chou M, Iijima K, et al. Asian Working Group for Sarcopenia: 2019 consensus update on sarcopenia diagnosis and treatment. J Am Med Dir Assoc 2020 Mar;21(3):300-307.e2. [doi: 10.1016/j.jamda.2019.12.012] [Medline: 32033882]
29. Leong DP, Teo KK, Rangarajan S, Lopez-Jaramillo P, Avezum A, Orlandini A, Prospective Urban Rural Epidemiology (PURE) Study investigators. Prognostic value of grip strength: findings from the Prospective Urban Rural Epidemiology (PURE) study. Lancet 2015 Jul 18;386(9990):266-273. [doi: 10.1016/S0140-6736(14)62000-6] [Medline: 25982160]

Abbreviations

AUC: area under the curve
AWGS: Asian Working Group for Sarcopenia
GAD-7: Generalized Anxiety Disorder-7
hs-CRP: high-sensitivity C-reactive protein
KNHANES: Korea National Health and Nutrition Examination Survey
LR: logistic regression
ML: machine learning
RF: random forest
SMOTE: synthetic minority over-sampling technique
SVM: support vector machine
XGBoost: extreme gradient boosting

Edited by A Benis; submitted 10.04.25; peer-reviewed by MJ Kim, HK Kim, J Kim; comments to author 06.06.25; revised version received 21.07.25; accepted 11.08.25; published 27.08.25.

Please cite as:
Chong HJ
A Machine Learning Model for Predicting Sarcopenia Among Middle-Aged Adults: Development and External Validation
JMIR Med Inform 2025;13:e75760
URL: https://medinform.jmir.org/2025/1/e75760
doi:10.2196/75760
PMID:40864499

©Hye Jin Chong. Originally published in JMIR Medical Informatics (https://medinform.jmir.org), 27.08.2025. This is an open-access article distributed under the terms of the Creative Commons Attribution License (https://creativecommons.org/licenses/by/4.0/), which permits unrestricted use, distribution, and reproduction in any medium, provided the original work, first published in JMIR Medical Informatics, is properly cited. The complete bibliographic information, a link to the original publication on https://medinform.jmir.org/, as well as this copyright and license information must be included.

XSL•FO
RenderX

Original Paper

A Machine Learning Algorithm With an Oversampling Technique in Limited Data Scenarios for the Prediction of Present and Future Restorative Treatment Need: Development and Validation Study

Elina Väyrynen[1], DDS; Otso Tirkkonen[1], BDS; Henna Tiensuu[2], PhD; Jaakko Suutala[2], Prof Dr; Vuokko Anttonen[1], Prof Dr, DDS; Marja-Liisa Laitala[1,3], Prof Dr, DDS; Katri Kukkola[4], MSci; Saujanya Karki[1], BDS, MPH, PhD

[1]Research Unit of Population Health, Faculty of Medicine, University of Oulu, Oulu, Finland

[2]Biomimetics and Intelligent Systems Group, Faculty of Information Technology and Electrical Engineering, University of Oulu, Oulu, Finland

[3]Oulu University Hospital, Oulu, Finland

[4]Optoelectronics and Measurement techniques, Faculty of Information Technology and Electrical Engineering, University of Oulu, Oulu, Finland

Corresponding Author:
Saujanya Karki, BDS, MPH, PhD
Research Unit of Population Health
Faculty of Medicine
University of Oulu
Aapistie 3
Oulu, 90220
Finland
Phone: 358 294485643
Fax: 358 358 294485643
Email: Saujanya.Karki@oulu.fi

Abstract

Background: Untreated dental caries is the most common health condition worldwide. Therefore, new strategies need to be developed to reduce the manifestations of dental caries.

Objective: This study aimed to develop and test a machine learning (ML) algorithm for detecting present and predicting future carious lesions in the adolescent population using a set of easy-to-collect predictive variables. In addition, this study aimed to deal with an imbalanced and small dataset using an oversampling method.

Methods: This population-based study was conducted among secondary schoolchildren, aged between 13 and 17 years, from the northern parts of Finland in 2022. After meeting the inclusion criteria, a total of 218 participants were included in this study. The inclusion criteria consisted of participants having completed a web-based risk assessment questionnaire and having undergone a clinical examination at public health care services. Dental caries (International Caries Detection and Assessment System [ICDAS] scores of 4, 5, and 6; ie, ICDAS 4-6) and active initial caries (ICDAS 2+, 3+) were considered as outcomes. Several predictors, such as behavioral and dietary habits, were included. An extreme gradient boosting model was developed, tested, and assessed for its predictive performance. A 4-fold cross-validation was performed using the nested resampling technique. The random oversampling examples method and the k-nearest neighbors classifiers were used for all 4 folds. The mean (SD) performance of all the folds was computed.

Results: Dental caries (ICDAS 2+,3+,4-6) were prevalent in 65.6% (143/218) of the participants. The mean area under the curve was 0.77 (SD 0.04) and the mean F_1-score was 0.82 (SD 0.06) for the extreme gradient boosting model. Similarly, the mean area under the curve and mean F_1-scores after oversampling were 0.74 (SD 0.05) and 0.79 (SD 0.04), respectively. The Shapley additive explanation values were calculated for all 4 folds to assess feature importance, revealing that previous dental fillings were the feature most strongly associated with the need for restorative treatment.

Conclusions: On the basis of the performance metrics, the ML algorithm developed and tested in this study can be considered good. The ML algorithm could serve as a cost-effective screening tool for dental professionals to identify the risk of future restorative treatment needs. However, future studies with longitudinal cohorts and longitudinal data, along with external validation for generalizability, are needed to validate our model.

XSL•FO
RenderX

(JMIR Med Inform 2025;13:e75117) doi:10.2196/75117

KEYWORDS

oral health; machine learning; dentistry; dental caries; caries management

Introduction

Background

Dental caries is the most common dietary-microbial disease, requiring regular exposure to fermentable carbohydrates. Enrichment of acid-producing and acid-tolerating microorganisms in dental plaque leads to a demineralized tooth structure, which, in turn, can lead to loss of tooth structure, ultimately resulting in cavities [1]. The risks of dental caries include physical, biological, environmental, behavioral, and lifestyle-related factors [2]. The balance between pathological and protective factors, such as insufficient exposure to fluoride or irregular brushing of teeth, influences the initiation and progression of dental caries [3].

Individual-level risk recognition is of utmost importance, since recent dental caries management protocol prioritizes early prevention and minimal intervention at an individual level [4]. The availability of caries risk assessment tools (CRATs) has assisted clinicians in risk identification, as well as in risk minimization. However, most existing CRATs require either dental visits or measurements of salivary parameters at dental clinics (face-to-face methods). A systematic review [5] considered the possibility of using a reduced Cariogram (without saliva parameters), one of the CRATs, due to its better performance when compared to a full Cariogram. The use of artificial intelligence (AI) and machine learning (ML) in the medical field is gaining attention worldwide. The possibility of an automated dental caries risk prediction method using ML algorithms needs to be explored. A recent study by Xiong et al [6] highlighted the possibility of using ML algorithms and easy-to-collect predictors in screening active dental caries and urgent treatment needs in school-age children. However, the questionnaire mainly consisted of predictors covering physical, mental, and social aspects, missing important predictors, such as dietary habits and oral health-related behaviors. As the development and progression of carious lesions are multifactorial, such information is important to consider.

AI can be defined as the nonbiological ability of a computer to try to imitate human intelligence to accomplish complex tasks, such as problem-solving and decision-making [7]. ML is a subset of AI designed to identify patterns or make predictions based on the data used. ML algorithms can model nonlinear and high-dimensional characteristics, such as health data [8]. In addition to being the latest and often the most popular technology, ML algorithms have the ability to learn themselves and improve over time when exposed to more data [9]. The use of ML models can improve patient care by providing individualized outcome predictions and by reducing standardized processes, allowing clinicians to spend more time with patients [10]. In dentistry, the literature showed that various ML algorithms, such as logistic regression, decision trees, random forest, and extreme gradient boosting (XGBoost), are used in predicting dental caries. However, these studies are in their early stages, and more research needs to be conducted to validate these methods [11]. Furthermore, the ground truth in the above-mentioned studies is based only on clinical examinations (visual-tactile), even though it is recommended to perform both clinical and radiographic examinations to minimize the risk of misdiagnosis in caries evaluation [12]. In this regard, the severity and activity of carious lesions are crucial when deciding on the treatment path [13,14]. It is important to include real-life clinical environment observations when training and testing ML algorithms.

However, there are some challenges, such as high costs, data security, and legal restrictions in dentistry, making the acquisition of individual-level comprehensive data more difficult [15,16]. Studies have used electronic health records and national registries for training ML algorithms [17]. However, in dentistry, the availability of extensive electronic health record data or national registries is scarce [18]. Therefore, to overcome the challenges associated with small datasets, oversampling techniques can be explored. Oversampling is a data augmentation technique that aims to rebalance the training data distribution by amplifying the volume of instances that belong to the underrepresented class, helping to correct the imbalance between minority and majority examples [19,20]. Another challenge in dentistry is also related to class imbalance. When the number of patients with a target disease differs from the healthy population, the situation is referred to as the imbalanced data problem. The accuracy of ML models can be affected by these imbalances.

Objectives

Therefore, this study aimed to (1) develop and test an ML algorithm in detecting present and predicting future carious lesions among adolescents using a set of easy-to-collect predictive variables; and (2) deal with challenges due to the imbalanced and small dataset in cariology with the use of the oversampling method.

Methods

Study Population and Data Sources

This cross-sectional study used data collected for the Digileap project, conducted among secondary school children aged 13 to 17 years from the northern parts of Finland in 2022. Before the study, the sample size (N=246) was calculated based on the prevalence of dental caries from a previous study by Suominen-Taipale et al [21] with 95% CIs and a precision set at 0.05, assuming that the total population of children aged 13 to 15 years is 100,000 [22]. Participants completed a web-based risk assessment questionnaire within their school premises, and their oral health records were registered at public health care services from 2022 to 2023, from where they were later requested through Findata services [23]. Findata is the Finnish Social and Health Data Permit authority, which grants permits for the secondary use of social and health care data, improving

XSL•FO
RenderX

data protection for individuals. The inclusion criteria for this study included the following: (1) aged 13 to 17 years with signed informed consent, (2) completion of a web-based risk assessment questionnaire, and (3) completion of a dental examination performed at public dental clinics during 2022 to 2023. After meeting the inclusion criteria, a total of 218 participants were included in this study.

Ethical Considerations

The study was conducted in full accordance with the World Medical Association Declaration of Helsinki. The ethical committee of Northern Ostrobothnia Hospital District approved the study protocol (EETTMK 62/2021), and the Finnish Medicines Agency [24] also issued the Medical Device Permit (2022/007715). In addition, study permissions were also obtained from the public health care services in Kuusamo, Ylivieska, Oulu, and Liminka. Oral health records (dental caries registered at the public dental services) were obtained from the Finnish Social and Health Data Permit Authority, Findata [25], with a data permit (THL/6268/14.02.00/2021). All the schools were contacted before the study via an official email requesting the participation of schoolchildren and their parents. Participants aged ≥15 years signed the informed consent, and informed consent was obtained from the parents of participants aged <15 years. Participation was completely voluntary, privacy and confidentiality were secured, and the participants had the right to withdraw their participation at any given phase of the study.

Study Variables

Outcome Variables

Initial active carious lesions (enamel and dentin caries) and all cavitated lesions were considered as the main outcome variable for this study. The carious lesions were diagnosed using the International Caries Detection and Assessment System (ICDAS) criteria with the aim to differentiate between different stages of dental caries. ICDAS stands for the assessment of the caries process by stage (noncavitated or cavitated) and activity (active or arrested or inactive). The "+" symbol indicates a caries lesion that is active and progressing. The "–" symbol indicates an inactive lesion with no active progression, and the tooth surface is considered sound [26].

To describe the transition of caries lesions in this study, the ICDAS score of 0 or ICDAS scores of 2− and 3− were considered as sound in contrast to the ICDAS scores of 2+, 3+, 4, 5, and 6 being considered as diseased. The ICDAS 2+ and 3+ codes were merged into 1 category (ICDAS 2+, 3+) to represent noncavitated lesions or microcavitated active lesions, and the ICDAS 4, 5, and 6 codes were used as 1 category (ICDAS 4-6) to represent cavitated lesions. A study by Abdalla et al [27] concluded that the active caries lesions were more likely to progress to more severe conditions than inactive lesions; active noncavitated (ICDAS 2+) and active microcavitated or shadow lesions (ICDAS 3+) had a 2-fold progression rate compared to noncavitated inactive lesions. In a nutshell, any initial active carious lesion (enamel and dentin caries) and all cavitated lesions were considered as the main outcome variable for this study (ICDAS 2+,3+,4-6) [13]. ICDAS 1 was not found in our study population due to challenges in diagnostics; these lesions were characterized by the first visual changes in enamel, often appearing as white spots or lines that were only visible when the tooth was carefully air-dried for 5 seconds.

Caries assessment with surface-by-surface evaluation was conducted by a licensed dentist following the Finnish Current Care Guidelines [28]. All teeth of the participants were examined with halogen light with a surface reflecting mirror and explorer and a fiberoptic transilluminator, followed by radiographic examination, if needed. A radiographic examination was suggested if (1) one localized enamel breakdown lesion was found, (2) the patient had several initial caries lesions, (3) the patient had dental caries risk factors or suspicion that the patient might have hidden dental caries lesions, or (4) radiographs had not been taken in the past few years [29]. Previously, data collected from the Finnish public health care records were shown not to be inferior to the calibrated examiners [30].

Predictors

For this study, age, sex, and oral health-related behaviors (such as frequency of toothbrushing, toothbrush type, toothpaste type, frequency of fluoride toothpaste use, interdental cleaning frequency, frequency of xylitol use, additive sugar consumption, and smoking habits) were considered as independent variables. The questionnaire consisted of information about the food and drink consumption of the participants. Participants were asked to report the amounts and frequencies. The average daily consumption was calculated for each product and multiplied by the quantity consumed. The additive sugar consumption was calculated using the Fineli database, a Finnish national food consumption database maintained by the Finnish Institute for Health and Welfare [31]. Using the Fineli database, total sugar content was matched to the food items, and the amount of sugar (g) in each item was calculated. Finally, the total daily sugar intake was calculated for each food item consumed per day (daily added sugar intake). Similarly, local factors, such as recent restorations, extracted teeth, bleeding when brushing, and the dry mouth index, were considered as predictors. To complement the self-reported survey, clinical data on missing teeth and dental fillings were also included as predictors. The dry mouth index included questions, such as "Does your mouth feel dry when you eat?" "Do you have difficulties swallowing some food?" and "Do you have to drink in order to make it easier to swallow dry food?" Participants responded yes or no, and answers were combined as one continuous variable, achieving values from 0 to 3.

Model Development and Training

In this study, the XGBoost algorithm was applied to predict the outcome variable. The model was trained using the R software (version 4.3.1; R Foundation for Statistical Computing) [32].

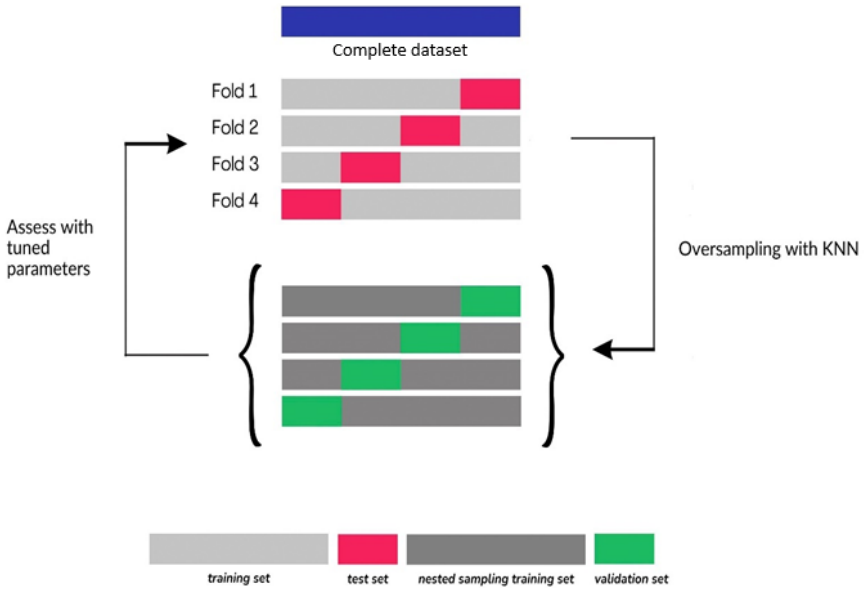
Model Fitting (Training and Testing)

The training and testing of the ML models were performed using the nested resampling technique with 4-fold cross-validation. In a typical k-fold cross-validation, the dataset is randomly and evenly split into k parts. The model is built using k−1 parts of the dataset, called the training set, and

XSL•FO
RenderX

evaluated based on the remaining part, known as the test set. This process is repeated k times so that each part is used as a test set once [33]. Four folds were created, each containing 75% of the data as a training set and 25% of the unseen data as a test set. These 4 folds are seen in Figure 1.

Figure 1. The model training protocol: The training and testing of machine learning algorithms were performed using 4-fold cross-validation, the nested resampling technique, and hyperparameter tuning. The tuned model was evaluated by a separate validation set, which was distinct from the nested sampling testing set. The oversampling technique was applied to all 4 folds. The oversampling fold included both the original training set and the nested sampling training set. Finally, the performance of the optimized model was assessed on each fold's test set. This entire training protocol was repeated for all 4 folds. KNN: k-nearest neighbor.



Model Training Protocol

For each 4 folds, the ML models were built by using the mlr package [34]. During the training, hyperparameter tuning was conducted separately for all 4 folds. The grid search method was used for hyperparameter tuning, allowing the model to identify the optimal combination from a predefined set of hyperparameters. Detailed information on these predefined hyperparameters is provided in the Multimedia Appendix 1. The tuned model was evaluated based on a validation set, which was independent of the nested sampling testing set. Finally, the optimized model's performances were evaluated on each fold's completely unseen test set. For all 4 folds, the model training protocol was then repeated using the new oversampled training dataset. The model training protocol is shown in Figure 1.

Oversampling

As the total sample was 218, the oversampling technique was used as suggested by previous studies [35,36]. The oversampling technique was applied exclusively to each training dataset, while the respective test sets remained untouched to ensure the absence of data leakage. The random oversampling examples (ROSE) method and the k-nearest neighbors classifier were used for all folds [37]. Oversampling simulated 2000 new synthetic participants to the training dataset (P=.05). In the context of oversampling techniques, "P" refers to the proportion or percentage of the minority class instances that are to be oversampled. In the complete dataset, the number of participants with carious lesions was 143. The training sets consisted of 75% of the data, and the average number of participants with carious lesions in the training set was 0.75×143=107. Using the oversampling method, 2000×0.95=1900 new participants with carious lesions were created. As a result, the total number of participants with carious lesions increased on average to 107+1900=2007. Likewise, in the complete dataset, the number of participants with sound teeth was 75. The training set included 75% of the complete data, and the average number of participants with sound teeth in the training set was 0.75×75=56. Using the oversampling method, a total of 100 (2000×0.05=100) new synthetic participants with sound teeth were created. This resulted in an average total of 156 participants with sound teeth.

Model Evaluation

To assess the predictive performance of the ML models, the area under the curve (AUC), accuracy, sensitivity, specificity, positive predictive value, negative predictive value, no information rate, precision, recall, and F_1-score for each predictive model were calculated. The mean (SD) performance of all folds was computed.

Shapley additive explanations (SHAP) values were computed for all folds and also after oversampling. The SHAP values were computed to determine the importance of each variable in predicting the dental caries outcomes of this study. The SHAP values are an additive feature importance measure that represents the responsibility of each feature in pushing the model output away from its base value [38]. This study was reported in accordance with the TRIPOD+AI (Transparent Reporting of a multivariable prediction model for Individual Prognosis Or Diagnosis–Artificial Intelligence) statement for developing or evaluating the performance of prediction models [39].

XSL•FO
RenderX

Results

The demographic characteristics and descriptive analysis of the categorical independent variables are shown in Table 1. In this study group, 143 out of 218 (65.6%) participants had carious lesions (enamel and dental caries, ICDAS 2+, 3+, 4-6). More than half of the study participants were female (118/218, 54.1%), and more than half (124/218, 56.9%) had a habit of toothbrushing twice daily. Most of the participants (158/218, 72.5%) reported using fluoride toothpaste, while less than half of the participants (106/218, 48.6%) reported using an electronic toothbrush. Most of the participants (198/218, 90.8%) did not smoke, and the mean daily added sugar intake was 50.6 (SD 81.3) g. In addition, more than half of the participants (122/218, 56%) had dental restorations as seen in Table 1.

The performance metrics of all folds of the XGBoost model before and after oversampling are shown in Table 2. In addition, the mean performance across all folds is presented. The mean AUC value, which evaluates the model's ability to discriminate between carious and sound teeth, was good after oversampling (before oversampling: 0.77, SD 0.04; after oversampling: 0.74, SD 0.05). The mean accuracy, which evaluates the performance of the models, was also high (before oversampling: 0.75, SD 0.06; after oversampling: 0.73, SD 0.03). The AUC and accuracy values were complemented by the F_1-scores. The F_1-score is the harmonic mean of precision and recall, and it provides a comprehensive evaluation of a model with an imbalanced dataset. The mean F_1-score was 0.82 (SD 0.06) before oversampling and 0.79 (SD 0.04) after oversampling. The ability of the model to predict carious lesions (true positive cases), expressed as a mean sensitivity, was 0.85 (SD 0.12) before oversampling and 0.78 (SD 0.09) after oversampling. These values were considered high. The ability to predict sound teeth (true negative cases), expressed as mean specificity, was 0.56 (SD 0.13) before oversampling, and it slightly increased to 0.61 (SD 0.15) after oversampling. These values, in turn, were considered low, as seen in Table 2.

XSL•FO
RenderX

Table 1. Demographic characteristics and descriptive analysis of the categorical independent variables (N=218).

Characteristics	Values
Fillings, n (%)	
No	96 (44)
Yes	122 (56)
Missing	0 (0)
Missing tooth, n (%)	
No	168 (77.1)
Yes	50 (22.9)
Missing	0 (0)
Smoking frequency, n (%)	
Not smoking	198 (90.8)
Smoking	20 (9.2)
Missing	0 (0)
Interdental cleaning frequency, n (%)	
At least twice a day	7 (3.2)
Once a day	18 (8.3)
2-6 times per week	47 (21.6)
Once a week	78 (35.8)
Never	68 (31.2)
Missing	0 (0)
Tooth extracted, n (%)	
No	174 (79.8)
Yes	44 (20.2)
Missing	0 (0)
Recent restoration, n (%)	
No	115 (52.8)
Yes	103 (47.2)
Missing	0 (0)
Bleeding while brushing, n (%)	
No bleeding	169 (77.5)
I do not know	26 (11.9)
Yes	23 (10.6)
Missing	0 (0)
Toothbrush type, n (%)	
Electric toothbrush	106 (48.6)
Variability both	48 (22)
Manual toothbrush	64 (29.4)
Missing	0 (0)
Toothbrushing frequency, n (%)	
At least twice a day	124 (56.9)
Once a day	67 (30.7)
2-6 times a week	22 (10.1)
Less often	5 (2.3)

XSL•FO
RenderX

Characteristics	Values
Missing	0 (0)
Xylitol use frequency, n (%)	
Never	15 (6.9)
Once a month	9 (4.1)
1-3 times a month	15 (6.9)
Once a week	24 (11)
2-4 times a week	42 (19.3)
5-6 times a week	23 (10.6)
Once a day	17 (7.8)
2-3 times a day	48 (22)
>3 times a day	25 (11.5)
Missing	0 (0)
Toothpaste type, n (%)	
Fluoride	158 (72.5)
I do not know or fluoride-free	60 (27.5)
Missing	0 (0)
Fluoride paste use frequency, n (%)	
Daily	140 (64.2)
Few times a week	18 (8.3)
No or unsure of fluoride	60 (27.5)
Missing	0 (0)
Dry mouth index, n (%)	
0	104 (47.7)
1	51 (23.4)
2	9 (4.1)
Missing	54 (24.8)
Sex, n (%)	
Female	118 (54.1)
Male	100 (45.9)
Missing	0 (0)
Age (y), mean (SD)	15.5 (1.11)
Daily added sugar intake[a], mean (SD)	50.6 (81.3)
Caries status, n (%)	
Healthy	64 (29.4)
Inactive enamel caries	11 (5)
Active enamel caries	125 (57.3)
Dentine caries	18 (8.3)

[a]The sugars from each food item that the person consumed per day (g).

XSL•FO
RenderX

Table 2. Performance metrics of machine learning (ML) models before and after oversampling.

Fold and ML model	AUC[a], mean (95% CI)	Accuracy, mean (95% CI)	NIR[b]	Sensitivity	Specificity	PPV[c]	NPV[d]	Precision	Recall	F_1-score
First fold										
XGBoost[e]	0.73 (0.59-0.87)	0.67 (0.53-0.79)	0.64	0.71	0.58	0.76	0.52	0.76	0.71	0.74
XGBoost with oversampling	0.74 (0.56-0.88)	0.70 (0.56-0.82)	0.65	0.77	0.58	0.77	0.58	0.77	0.77	0.77
Second fold										
XGBoost	0.82 (0.70-0.94)	0.80 (0.67-0.90)	0.62	0.97	0.52	0.77	0.92	0.77	0.97	0.86
XGBoost with oversampling	0.80 (0.68-0.93)	0.76 (0.63-0.87)	0.62	0.79	0.71	0.82	0.68	0.82	0.79	0.81
Third fold										
XGBoost	0.79 (0.66-0.92)	0.78 (0.65-0.88)	0.67	0.81	0.72	0.86	0.65	0.86	0.81	0.83
XGBoost with oversampling	0.73 (0.59-0.87)	0.69 (0.55-0.81)	0.67	0.68	0.72	0.83	0.52	0.83	0.68	0.75
Fourth fold										
XGBoost	0.74 (0.58-0.89)	0.76 (0.62-0.87)	0.69	0.92	0.41	0.77	0.70	0.77	0.92	0.84
XGBoost with oversampling	0.70 (0.53-0.86)	0.74 (0.60-0.85)	0.69	0.89	0.41	0.77	0.64	0.77	0.89	0.83
Performance across all folds[f]										
XGBoost	0.77 (0.04)	0.75 (0.06)	0.66 (0.03)	0.85 (0.12)	0.56 (0.13)	0.79 (0.05)	0.70 (0.16)	0.79 (0.04)	0.85 (0.10)	0.82 (0.06)
XGBoost with oversampling	0.74 (0.05)	0.73 (0.03)	0.66 (0.03)	0.78 (0.09)	0.61 (0.15)	0.80 (0.54)	0.60 (0.07)	0.80 (0.03)	0.78 (0.08)	0.79 (0.04)

[a]AUC: area under the curve.

[b]NIR: no information rate.

[c]PPV: positive predictive value.

[d]NPV: negative predictive value.

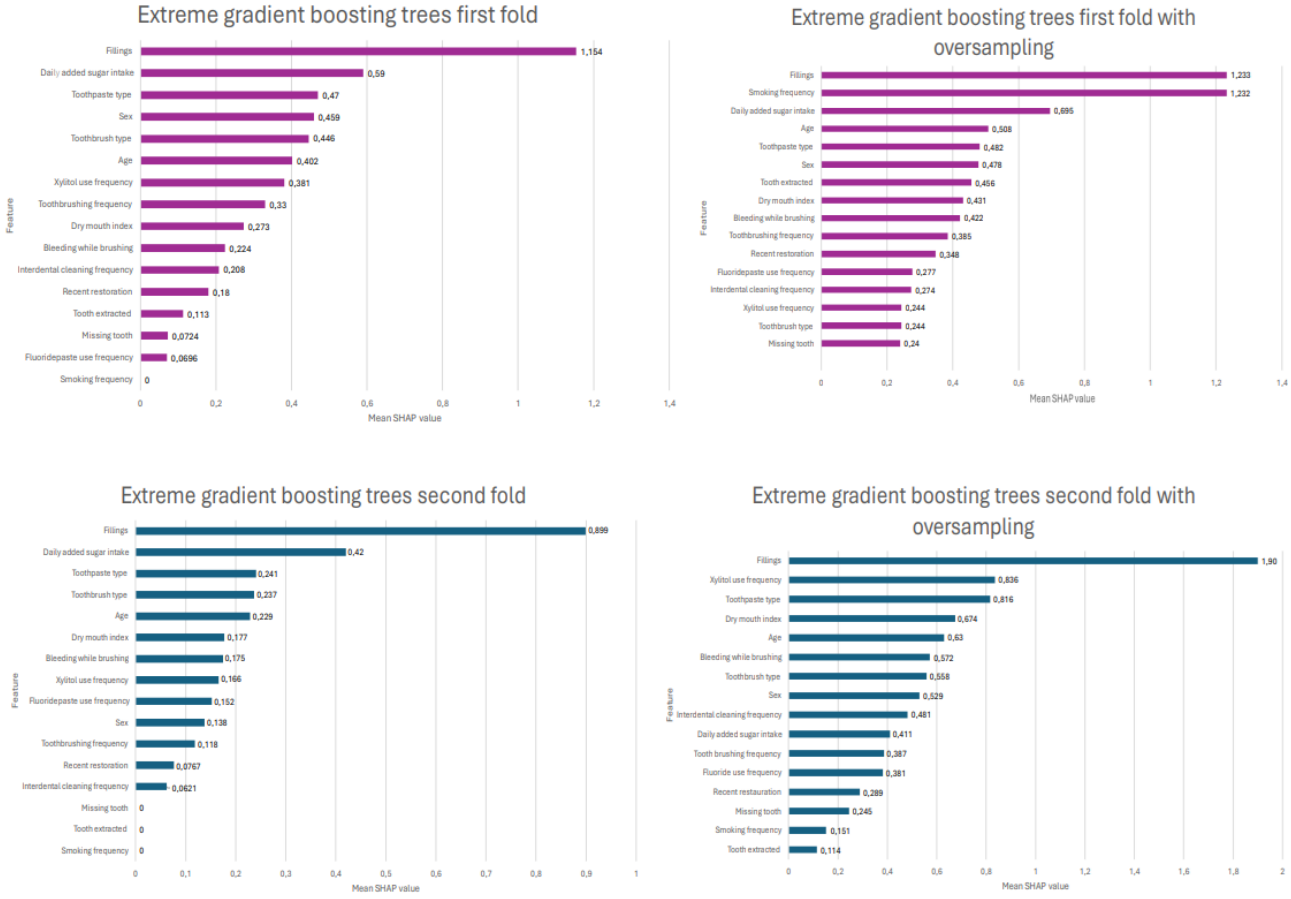
[e]XGBoost: extreme gradient boosting.

[f]The performance across all folds is presented as mean (SD).

After evaluating the performance of each model, the SHAP values were computed for all 4 folds and after oversampling. The SHAP values for each of the 4 folds of the XGBoost model before and after oversampling are shown in Figures 2 and 3. The feature that most strongly predicted the need for present and future restorative treatment was previous fillings in all folds, followed by the total added sugar intake, frequency of smoking, toothpaste type, and frequency of toothbrushing, varying between 4 folds, as seen in Figures 2 and 3. Interestingly, the importance of minor predictors slightly increased after the oversampling method was applied in all folds. Fillings and total added sugar intake were in the top 4 most important features in every fold before oversampling. There was more variation in the folds after oversampling, but clearly, fillings remained the most important feature.

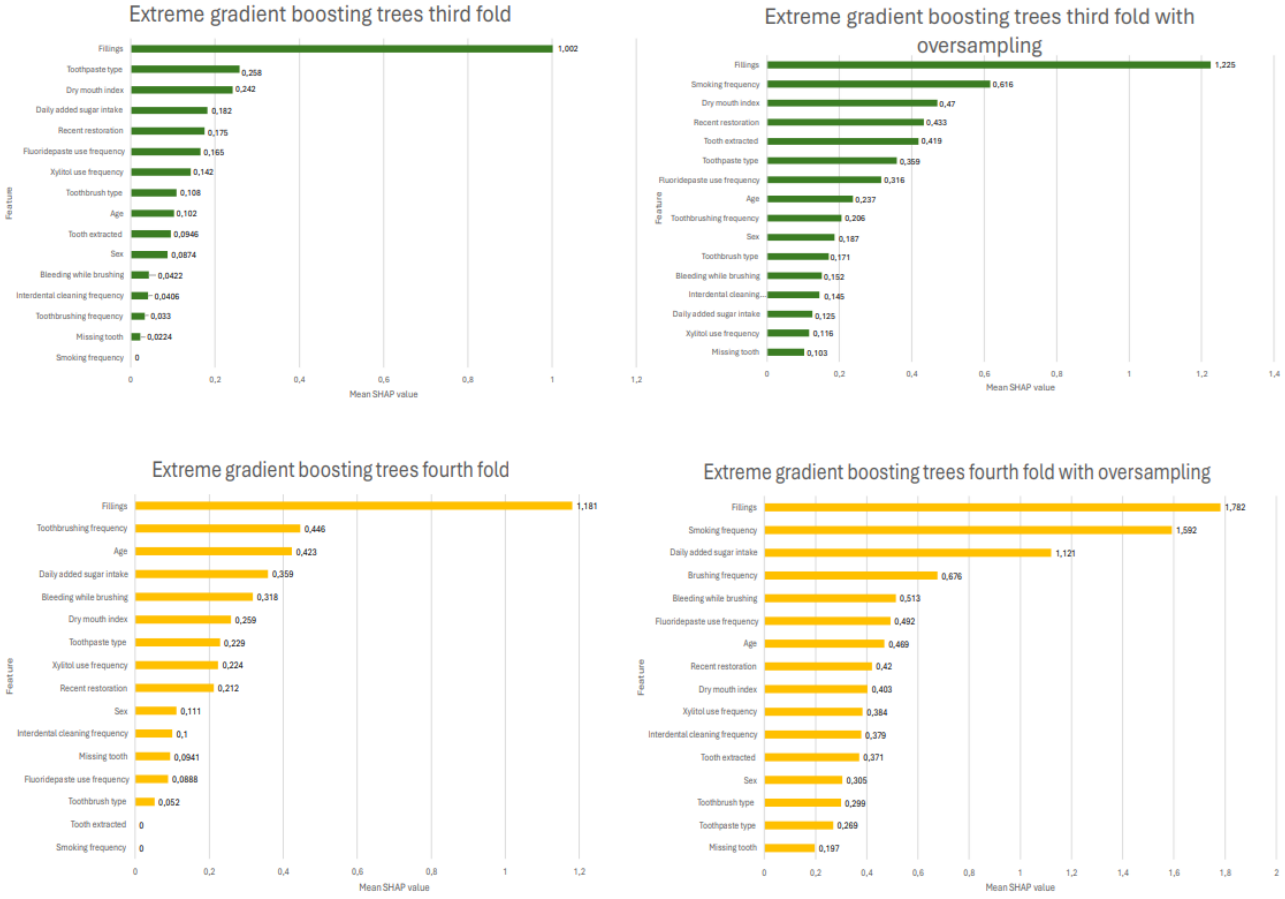
XSL•FO
RenderX

Figure 2. Shapley additive explanation (SHAP) values from folds 1 and 2, before and after oversampling. The absolute SHAP value shows how much a single feature affected the prediction of dental caries. The higher the SHAP value of a feature, the more likely it is to influence the prediction.



XSL•FO
RenderX

Figure 3. Shapley additive explanation (SHAP) values from folds 3 and 4, before and after oversampling. The absolute SHAP value shows how much a single feature affected the prediction of dental caries. The higher the SHAP value of a feature, the more likely it is to influence the prediction.



Discussion

Principal Findings

The main aim of this study was to develop and test an ML algorithm for predicting carious lesions among the adolescent population using a set of easy-to-collect predictors and to evaluate the importance of each predictor. Another aim was to use a novel oversampling approach in cariology research to deal with and improve the imbalance of a small dataset. The ML models developed and tested in this study performed well in predicting present and future restorative treatment needs among adolescents. Despite the drop in performance metrics after oversampling, the parameters were within the acceptable range, supporting the positive performance of the ML algorithm in this study. The XGBoost algorithm used in this study performed well. This is comparable with previous studies by Toledo et al [40] and Bomfim [41] from Brazil. In both studies, the XGBoost model outperformed other ML algorithms, such as logistic regression and decision tree. Both studies used socioeconomic variables, such as income and parents' employment, as predictors for carious lesions. However, these variables were not considered in this study, because in Finland, all individuals aged ≤18 years are entitled to free dental care. This study aimed to use easy-to-collect predictors. A recent study by Xiong et al [6] also used ML algorithms and easy-to-collect information when screening active dental caries and urgent treatment needs in adolescents and concluded that the naïve Bayes model outperformed other models. However, that study particularly considered physical, mental, and social factors rather than behavioral factors. Furthermore, both clinical and radiographic examinations were performed in this study to minimize the risk of over- or underdiagnosis. In a real-life clinical environment, the use of radiographic methods is considered advantageous when deciding the need for operative care, especially when a patient was presented with an ICDAS score of 3 [29]. The drop in performance after oversampling in this study is comparable to a previous study [6] from the United States. Xiong et al [6] considered the synthetic minority oversampling technique for oversampling in their studies. However, the ROSE was used in this study for oversampling. The ROSE technique created synthetic examples by drawing from a smoothed bootstrap distribution in the feature space around the minority class, thus producing more balanced datasets with better generalization properties [42]. This method is particularly suitable for datasets containing categorical or binary variables, which were prominent in our study. In contrast, the synthetic minority oversampling technique was primarily designed for a continuous feature space and might not perform optimally with categorical or binary variables. In addition, the k-nearest neighbors classifier cleaning method was used in this study to further enhance the data quality after oversampling. In this study, the ability of the model to predict carious lesions (sensitivity) was high before and after oversampling. For dental caries screening, high sensitivity is vital to ensure that diseased individuals are correctly identified with the disease. However, the ability to predict sound teeth

XSL•FO
RenderX

(specificity) was lower, which might be subject to overdiagnosis; therefore, cautious explanation is necessary. Therefore, oral health care professionals are encouraged to carefully examine those with high dental caries risk.

Dental caries is a multifactorial disease influenced by individual, biological, behavioral, and environmental factors [43]. In the literature, past caries experience was found to be the most powerful caries predictor [44]. High consumption of carbohydrates increased the chance of developing dental caries [45], and xylitol-containing products significantly prevented caries when compared with other nonxylitol products [46]. These findings from previous literature are in line with the results of this study, as delivered by the feature importance SHAP values. The past caries experience, nonuse of fluoridated toothpaste, socioeconomic level, and a higher frequency of sugar consumption were predictors that influenced caries progression the most in a previous longitudinal study that aimed to predict dental caries in primary and permanent teeth among children aged 1 to 5 years [40]. Similarly, the use of dental floss, unhealthy food consumption, self-declared race, and exposure to fluoridated water were the most predictive variables in another study by Bomfim [41]. The previous fillings (explaining past caries experience) and total added sugar intake (explaining high consumption of carbohydrates) were the most predictive variables in this study.

The application of SHAP values in this study enhanced the interpretability of the ML model, providing a transparent understanding of how each feature contributed to the predictions. Interpretability was a key element of explainable AI, which played a critical role in ensuring that the ML models were not only accurate but also transparent and reliable for real-world applications. In contrast to black-box models, explainable AI makes the model's decisions more comprehensible and trustworthy. Understanding the rationale behind predictions helps in validating the model's clinical relevance.

Strengths and Limitations

One of the strengths of this study is that the outcome variable, carious lesions, was recorded by a licensed dentist based on both clinical and radiographic evaluations, following the Finnish Current Care Guidelines [29]. Another strength is the absence of missing values, which was ensured by the strict inclusion criteria of this study. Selection bias due to voluntary participation in this study can be considered a limitation. Another limitation is the potential for response bias due to the use of a self-reported questionnaire; self-reported data can be biased due to respondents' subjective perceptions, memory recall issues, or intentional misreporting. However, the aim was to keep the questionnaire short and simple to minimize response bias. Finally, the generalizability of the ML algorithm might be questionable, as the model did not undergo external validation. Future studies with longitudinal cohorts are needed both to validate our models and to perform external validation in socioeconomically diverse or racially varied populations. In ML, validation provides evidence that a model is reliable and performs sufficiently with new data. External validation also requires testing the model on independent populations to assess its applicability [47]. Before clinical use, external validation is necessary [48]. However, this was beyond the scope of this study. For the external validation to be successful, dental caries categorization needs to be synchronized using ICDAS in both study populations.

Clinical Implications

Rising health care costs associated with restorative treatment require justification in early prevention and control of dental caries. New strategies need to be developed to reduce social impacts, such as aesthetic and functional disturbances, on both the individual and societal levels. A potential application of ML algorithms in dental caries prognostic studies enables evidence - based personalized dental care that could assist in decreasing dental caries prevalence globally. The ML model developed and tested in this study has the potential to identify possible risk factors of dental caries before the onset of actual dental caries lesions. In this study, each SHAP indicated the importance of each feature in dental caries progression, and the information gained can be transformed into a deeper dental caries risk assessment. Algorithm-based risk assessment tools can be integrated into electronic health records and used in electronic preassessment forms. Information about dental caries risk is valuable for both patients and dental professionals, influencing treatment and prevention plans, follow-up, and patient education [49]. Linking ML algorithms to intraoral images using deep learning algorithms is expected to increase dental screening potential. Individuals encounter unique challenges in adhering to behavioral changes. To overcome these obstacles, behavioral change interventions need to be both multifaceted and personalized. Health behavior factors, such as unhealthy food consumption, can be modified by health promotion policies and strategies. This study is unique and innovative because it is the first study to use ML models in dental caries prediction in adolescents using easy-to-collect predictors. In the future, after further development and external validation, this ML model could be used as a risk assessment tool and even be integrated into health record systems, which would be beneficial for the patient and the health care professionals in saving time and resources [50]. For the CRAT to be successful, it needs to be inexpensive, user-friendly, and open for everyone, even in low-income countries. SHAP values include participants' dental caries risk profile and can be used for personalized behavioral change interventions in which patients themselves can alter their overall risk.

Conclusions

Despite the small and imbalanced dataset, XGBoost performed well in predicting restorative treatment among adolescents with and without the oversampling method in this study. The results from this study suggest the potential feasibility of the ML models in caries risk assessment, enabling easier, cost-effective, less time-consuming, and more effective decision-making. However, future studies with longitudinal data and external validation are needed to validate our models.

XSL•FO
RenderX

Acknowledgments

The authors would like to acknowledge all the participants and the project partners of this study. The authors would also like to acknowledge Ville Kaikkonen, Eero Molkoselka, and Laura Pentti for their contributions to the data collection.

This project was financially supported by the European Regional Development Fund (project: *Digileap of Oral Health Toward Virtual Reception*; A76934), the Minerva Foundation, the Finnish Dental Society Apollonia, and the Finnish Medical Foundation. EV also received a personal research grant from the Finnish Cultural Foundation, the Terttu Foundation, and the Minerva Foundation.

Data Availability

Due to national legislation, restrictions apply to the availability of clinical data at the individual level, which were used with the Finnish Social and Health Data Permit Authority (Findata). Findata was responsible for the pseudonymization of the data and ensuring the anonymity of the results (THL/6268/14.02.00/2021).

Authors' Contributions

EV, OT, HT, and SK were responsible for conceptualization, data curation, and visualization. EV and OT were responsible for writing the original draft. OT, HT, and SK were responsible for the formal analysis. HT and SK were responsible for supervision. HT, JS, VA, MLL, KK, and SK were responsible for writing, reviewing, and editing the manuscript.

Conflicts of Interest

None declared.

Multimedia Appendix 1
Hyperparameter tuning using the grid search method.
[DOCX File , 15 KB - medinform_v13i1e75117_app1.docx]

References

1. Tanner AC, Kressirer CA, Faller LL. Understanding caries from the oral microbiome perspective. J Calif Dent Assoc 2023 Mar 09;44(7):437-446. [doi: 10.1080/19424396.2016.12221036]
2. Selwitz RH, Ismail AI, Pitts NB. Dental caries. The Lancet 2007 Jan;369(9555):51-59 [FREE Full text] [doi: 10.1016/s0140-6736(07)60031-2]
3. Pitts NB, Zero DT, Marsh PD, Ekstrand K, Weintraub JA, Ramos-Gomez F, et al. Dental caries. Nat Rev Dis Primers 2017 May 25;3:17030 [FREE Full text] [doi: 10.1038/nrdp.2017.30] [Medline: 28540937]
4. Innes NP, Chu CH, Fontana M, Lo EC, Thomson WM, Uribe S, et al. A century of change towards prevention and minimal intervention in cariology. J Dent Res 2019 Jun;98(6):611-617. [doi: 10.1177/0022034519837252] [Medline: 31107140]
5. Su N, Lagerweij MD, van der Heijden GJ. Assessment of predictive performance of caries risk assessment models based on a systematic review and meta-analysis. J Dent 2021 Jul;110:103664 [FREE Full text] [doi: 10.1016/j.jdent.2021.103664] [Medline: 33984413]
6. Xiong D, Marcus M, Maida CA, Lyu Y, Hays RD, Wang Y, et al. Development of short forms for screening children's dental caries and urgent treatment needs using item response theory and machine learning methods. PLoS One 2024 Mar 22;19(3):e0299947 [FREE Full text] [doi: 10.1371/journal.pone.0299947] [Medline: 38517846]
7. Ahuja AS. The impact of artificial intelligence in medicine on the future role of the physician. PeerJ 2019 Oct 04;7:e7702 [FREE Full text] [doi: 10.7717/peerj.7702] [Medline: 31592346]
8. Krois J, Graetz C, Holtfreter B, Brinkmann P, Kocher T, Schwendicke F. Evaluating modeling and validation strategies for tooth loss. J Dent Res 2019 Sep;98(10):1088-1095 [FREE Full text] [doi: 10.1177/0022034519864889] [Medline: 31361174]
9. Sarker IH. Machine learning: algorithms, real-world applications and research directions. SN Comput Sci 2021;2(3):160 [FREE Full text] [doi: 10.1007/s42979-021-00592-x] [Medline: 33778771]
10. Pfob A, Lu SC, Sidey-Gibbons C. Machine learning in medicine: a practical introduction to techniques for data pre-processing, hyperparameter tuning, and model comparison. BMC Med Res Methodol 2022 Nov 01;22(1):282 [FREE Full text] [doi: 10.1186/s12874-022-01758-8] [Medline: 36319956]
11. Reyes LT, Knorst JK, Ortiz FR, Ardenghi TM. Scope and challenges of machine learning-based diagnosis and prognosis in clinical dentistry: a literature review. J Clin Transl Res 2021;7(4):12. [doi: 10.18053/jctres.07.202104.012]
12. Reyes LT, Knorst JK, Ortiz FR, Ardenghi TM. Machine learning in the diagnosis and prognostic prediction of dental caries: a systematic review. Caries Res 2022;56(3):161-170 [FREE Full text] [doi: 10.1159/000524167] [Medline: 35636386]
13. Ekstrand KR, Gimenez T, Ferreira FR, Mendes FM, Braga MM. The international caries detection and assessment system - ICDAS: a systematic review. Caries Res 2018;52(5):406-419. [doi: 10.1159/000486429] [Medline: 29518788]

XSL•FO
RenderX

14. Ismail AI, Pitts NB, Tellez M. The international caries classification and management system (ICCMS™) an example of a caries management pathway. BMC Oral Health 2015 Sep 15;15(Suppl 1):S9. [doi: 10.1186/1472-6831-15-s1-s9]
15. Schwendicke F, Krois J. Data dentistry: how data are changing clinical care and research. J Dent Res 2022 Jan;101(1):21-29 [FREE Full text] [doi: 10.1177/00220345211020265] [Medline: 34238040]
16. Ducato R. Data protection, scientific research, and the role of information. Comput Law Secur Rev 2020 Jul;37:105412 [FREE Full text] [doi: 10.1016/j.clsr.2020.105412]
17. Swinckels L, Bennis FC, Ziesemer KA, Scheerman JF, Bijwaard H, de Keijzer A, et al. The use of deep learning and machine learning on longitudinal electronic health records for the early detection and prevention of diseases: scoping review. J Med Internet Res 2024 Aug 20;26:e48320 [FREE Full text] [doi: 10.2196/48320] [Medline: 39163096]
18. Tiwari T, Patel JS, Nascimento GG. Big data and oral health disparities: a critical appraisal. J Dent Res 2025 Feb;104(2):119-130. [doi: 10.1177/00220345241285847] [Medline: 39629938]
19. Fujiwara K, Huang Y, Hori K, Nishioji K, Kobayashi M, Kamaguchi M, et al. Over- and under-sampling approach for extremely imbalanced and small minority data problem in health record analysis. Front Public Health 2020 May 19;8:178 [FREE Full text] [doi: 10.3389/fpubh.2020.00178] [Medline: 32509717]
20. Alkhawaldeh IM, Albalkhi I, Naswhan AJ. Challenges and limitations of synthetic minority oversampling techniques in machine learning. World J Methodol 2023 Dec 20;13(5):373-378 [FREE Full text] [doi: 10.5662/wjm.v13.i5.373] [Medline: 38229946]
21. Suominen-Taipale AL, Widström E, Sund R. Association of examination rates with children's national caries indices in Finland. Open Dent J 2009 Apr 16;3:59-67 [FREE Full text] [doi: 10.2174/1874210600903010059] [Medline: 19543545]
22. Population structure [e-publication]. Official Statistics of Finland (OSF). Helsinki: Statistics Finland URL: https://stat.fi/til/vaerak/index_en.html [accessed 2025-08-16]
23. Data. Finnish Social and Health Data Permit Authority Findata. Helsinki URL: https://findata.fi/en/data/ [accessed 2025-08-16]
24. Medical devices. Fimea. Helsinki URL: https://fimea.fi/en/medical-devices [accessed 2025-08-16]
25. Permits. Finnish Social and Health Data Permit Authority Findata. Helsinki URL: https://findata.fi/en/permits/ [accessed 2025-08-16]
26. Ismail AI, Sohn W, Tellez M, Amaya A, Sen A, Hasson H, et al. The International Caries Detection and Assessment System (ICDAS): an integrated system for measuring dental caries. Community Dent Oral Epidemiol 2007 Jun;35(3):170-178 [FREE Full text] [doi: 10.1111/j.1600-0528.2007.00347.x] [Medline: 17518963]
27. Abdalla H, Allison PJ, Madathil SA, Veronneau JE, Pustavoitava N, Tikhonova S. Caries lesions progression in adults: a prospective 2-year cohort study. Community Dent Oral Epidemiol 2025 Feb;53(1):33-41 [FREE Full text] [doi: 10.1111/cdoe.13005] [Medline: 39160698]
28. Working group set up by the Finnish Medical Society Duodecim and the Finnish Dental Society Apollonia. Tooth Restoration Treatment. Current Care Guidelines. Helsinki: The Finnish Medical Society Duodecim; 2023. URL: https://www.kaypahoito.fi/hoi50117 [accessed 2025-08-16]
29. Working group set up by the Finnish Medical Society Duodecim and the Finnish Dental Society Apollonia. Dental Caries management. Current Care Guidelines. Helsinki: The Finnish Medical Society Duodecim; 2023 Jan 10. URL: https://www.kaypahoito.fi/hoi50127 [accessed 2025-08-16]
30. Hausen H, Kärkkäinen S, Seppä L. Caries data collected from public health records compared with data based on examinations by trained examiners. Caries Res 2001;35(5):360-365. [doi: 10.1159/000047475] [Medline: 11641572]
31. Food Items. Fineli -The National Food Composition Database in Finland.: Finnish Institute of Health and Welfare URL: https://fineli.fi/fineli/fi/elintarvikkeet [accessed 2025-08-16]
32. R Core Team. R: a language and environment for statistical computing. R Foundation for Statistical Computing. 2022. URL: https://www.r-project.org [accessed 2025-08-16]
33. Nematzadeh S, Kiani F, Torkamanian-Afshar M, Aydin N. Tuning hyperparameters of machine learning algorithms and deep neural networks using metaheuristics: a bioinformatics study on biomedical and biological cases. Comput Biol Chem 2022 Apr;97:107619 [FREE Full text] [doi: 10.1016/j.compbiolchem.2021.107619] [Medline: 35033837]
34. Bischl B, Lang M, Kotthoff L, Schiffner J, Richter J, Studerus E, et al. mlr: machine learning in R. J Mach Learn Res 2016;17:1-5 [FREE Full text] [doi: 10.32614/cran.package.mlr]
35. Guan H, Zhang Y, Xian M, Cheng HD, Tang X. SMOTE-WENN: solving class imbalance and small sample problems by oversampling and distance scaling. Appl Intell 2020 Sep 25;51:1394-1409. [doi: 10.1007/s10489-020-01852-8]
36. Lunardon N, Menardi G, Torelli N. Package 'ROSE': random over-sampling examples. The Comprehensive R Archive Network. 2021. URL: https://cran.r-project.org/web/packages/ROSE/ROSE.pdf [accessed 2025-08-16]
37. Wang Y, Pan Z, Pan Y. A training data set cleaning method by classification ability ranking for the k-nearest neighbor classifier. IEEE Trans Neural Netw Learning Syst 2020 May;31(5):1544-1556. [doi: 10.1109/tnnls.2019.2920864]
38. Lundberg S, Lee SI. A unified approach to interpreting model predictions. ArXiv. Preprint posted online on May 22, 2017 2025. [doi: 10.48550/arXiv.1705.07874]
39. Collins GS, Dhiman P, Andaur Navarro CL, Ma J, Hooft L, Reitsma JB, et al. Protocol for development of a reporting guideline (TRIPOD-AI) and risk of bias tool (PROBAST-AI) for diagnostic and prognostic prediction model studies based

XSL•FO
RenderX

on artificial intelligence. BMJ Open 2021 Jul 09;11(7):e048008 [FREE Full text] [doi: 10.1136/bmjopen-2020-048008] [Medline: 34244270]
40. Toledo Reyes L, Knorst JK, Ortiz FR, Brondani B, Emmanuelli B, Saraiva Guedes R, et al. Early childhood predictors for dental caries: a machine learning approach. J Dent Res 2023 Aug;102(9):999-1006. [doi: 10.1177/00220345231170535] [Medline: 37246832]
41. Bomfim RA. Machine learning to predict untreated dental caries in adolescents. BMC Oral Health 2024 Mar 09;24(1):316 [FREE Full text] [doi: 10.1186/s12903-024-04073-4] [Medline: 38461227]
42. Selamat NA, Abdullah A, Mat Diah N. Association features of smote and rose for drug addiction relapse risk. J King Saud Univ Comput Inf Sci 2022 Oct;34(9):7710-7719. [doi: 10.1016/j.jksuci.2022.06.012]
43. Pitts NB, Twetman S, Fisher J, Marsh PD. Understanding dental caries as a non-communicable disease. Br Dent J 2021 Dec;231(12):749-753 [FREE Full text] [doi: 10.1038/s41415-021-3775-4] [Medline: 34921271]
44. Cagetti MG, Bontà G, Cocco F, Lingstrom P, Strohmenger L, Campus G. Are standardized caries risk assessment models effective in assessing actual caries status and future caries increment? A systematic review. BMC Oral Health 2018 Jul 16;18(1):123 [FREE Full text] [doi: 10.1186/s12903-018-0585-4] [Medline: 30012136]
45. Teshome A, Muche A, Girma B. Prevalence of dental caries and associated factors in East Africa, 2000-2020: systematic review and meta-analysis. Front Public Health 2021 Apr 29;9:645091 [FREE Full text] [doi: 10.3389/fpubh.2021.645091] [Medline: 33996722]
46. ALHumaid J, Bamashmous M. Meta-analysis on the effectiveness of Xylitol in caries prevention. J Int Soc Prev Community Dent 2022 Apr 08;12(2):133-138 [FREE Full text] [doi: 10.4103/jispcd.JISPCD_164_21] [Medline: 35462747]
47. Cabitza F, Campagner A, Soares F, García de Guadiana-Romualdo L, Challa F, Sulejmani A, et al. The importance of being external methodological insights for the external validation of machine learning models in medicine. Comput Methods Programs Biomed 2021 Sep;208:106288 [FREE Full text] [doi: 10.1016/j.cmpb.2021.106288] [Medline: 34352688]
48. Ramspek CL, Jager KJ, Dekker FW, Zoccali C, van Diepen M. External validation of prognostic models: what, why, how, when and where? Clin Kidney J 2020 Nov 24;14(1):49-58 [FREE Full text] [doi: 10.1093/ckj/sfaa188] [Medline: 33564405]
49. Ng TC, Luo BW, Lam WY, Baysan A, Chu CH, Yu OY. Updates on caries risk assessment-a literature review. Dent J (Basel) 2024 Sep 29;12(10):312 [FREE Full text] [doi: 10.3390/dj12100312] [Medline: 39452440]
50. Chen S, Guo X, Ju X. The design of personalized artificial intelligence diagnosis and the treatment of health management systems simulating the role of general practitioners. In: Proceedings of the International Conference on Smart Health. 2018 Presented at: ICSH 2018; July 1-3, 2018; Wuhan, China. [doi: 10.1007/978-3-030-03649-2_3]

Abbreviations

AI: artificial intelligence
AUC: area under the curve
CRAT: caries risk assessment tool
ICDAS: International Caries Detection and Assessment System
ML: machine learning
ROSE: random oversampling examples
SHAP: Shapley additive explanations
TRIPOD+AI: Transparent Reporting of a multivariable prediction model for Individual Prognosis or Diagnosis–Artificial Intelligence
XGBoost: extreme gradient boosting

Edited by A Benis; submitted 04.04.25; peer-reviewed by RT Potla, S Mohamed Shaffi, V Alemede; comments to author 16.06.25; revised version received 30.06.25; accepted 15.07.25; published 28.08.25.

Please cite as:
Väyrynen E, Tirkkonen O, Tiensuu H, Suutala J, Anttonen V, Laitala ML, Kukkola K, Karki S
A Machine Learning Algorithm With an Oversampling Technique in Limited Data Scenarios for the Prediction of Present and Future Restorative Treatment Need: Development and Validation Study
JMIR Med Inform 2025;13:e75117
URL: https://medinform.jmir.org/2025/1/e75117
doi:10.2196/75117
PMID:40778806

©Elina Väyrynen, Otso Tirkkonen, Henna Tiensuu, Jaakko Suutala, Vuokko Anttonen, Marja-Liisa Laitala, Katri Kukkola, Saujanya Karki. Originally published in JMIR Medical Informatics (https://medinform.jmir.org), 28.08.2025. This is an open-access

XSL•FO
RenderX

article distributed under the terms of the Creative Commons Attribution License (https://creativecommons.org/licenses/by/4.0/), which permits unrestricted use, distribution, and reproduction in any medium, provided the original work, first published in JMIR Medical Informatics, is properly cited. The complete bibliographic information, a link to the original publication on https://medinform.jmir.org/, as well as this copyright and license information must be included.

XSL•FO
RenderX

Original Paper

An Artificial Intelligence–Based Framework for Predicting Emergency Department Overcrowding: Development and Evaluation Study

Orhun Vural[1], MSc; Bunyamin Ozaydin[2,3], PhD; Khalid Y Aram[4], PhD; James Booth[5], MD; Brittany Freeman Lindsey[6], MPA; Abdulaziz Ahmed[2,3], PhD

[1]Department of Electrical and Computer Engineering, School of Engineering, University of Alabama at Birmingham, Birmingham, AL, United States

[2]Department of Health Services Administration, School of Health Professions, University of Alabama at Birmingham, Birmingham, AL, United States

[3]Department of Biomedical Informatics and Data Science, Heersink School of Medicine, University of Alabama at Birmingham, Birmingham, AL, United States

[4]School of Business & Technology, Emporia State University, Emporia, United States

[5]Department of Emergency Medicine, Heersink School of Medicine, University of Alabama at Birmingham, Birmingham, AL, United States

[6]Department of Patient Throughput, University of Alabama at Birmingham Hospital, Birmingham, AL, United States

Corresponding Author:
Abdulaziz Ahmed, PhD
Department of Health Services Administration
School of Health Professions
University of Alabama at Birmingham
1716 9th Ave S
Birmingham, AL, 35233
United States
Phone: 1 205 975 1083
Email: aahmed2@uab.edu

Abstract

Background: Emergency department (ED) overcrowding remains a critical challenge, leading to delays in patient care and increased operational strain. Current hospital management strategies often rely on reactive decision-making, addressing congestion only after it occurs. However, effective patient flow management requires early identification of overcrowding risks to allow timely interventions. Machine learning (ML)–based predictive modeling offers a solution by forecasting key patient flow measures, such as waiting count, enabling proactive resource allocation and improved hospital efficiency.

Objective: The aim of this study is to develop ML models that predict ED waiting room occupancy (waiting count) at 2 temporal resolutions. The first approach is the hourly prediction model, which estimates the waiting count exactly 6 hours ahead at each prediction time (eg, a 1 PM prediction forecasts 7 PM). The second approach is the daily prediction model, which forecasts the average waiting count for the next 24-hour period (eg, a 5 PM prediction estimates the following day's average). These predictive tools support resource allocation and help mitigate overcrowding by enabling proactive interventions before congestion occurs.

Methods: Data from a partner hospital's ED in the southeastern United States were used, integrating internal and external sources. Eleven different ML algorithms, ranging from traditional approaches to deep learning architectures, were systematically trained and evaluated on both hourly and daily predictions to determine the models that achieved the lowest prediction error. Experiments optimized feature combinations, and the best models were tested under high patient volume and across different hours to assess temporal accuracy.

Results: The best hourly prediction performance was achieved by time series vision transformer plus (TSiTPlus) with a mean absolute error (MAE) of 4.19 and a mean squared error (MSE) of 29.36. The overall hourly waiting count had a mean of 18.11 and a SD (σ) of 9.77. Prediction accuracy varied by time of day, with the lowest MAE at 11 PM (2.45) and the highest at 8 PM (5.45). Extreme case analysis at (mean + 1σ), (mean + 2σ), and (mean + 3σ) resulted in MAEs of 6.16, 10.16, and 15.59, respectively. For daily predictions, an explainable convolutional neural network plus (XCMPlus) achieved the best results with an MAE of 2.00 and a MSE of 6.64. The daily waiting count had a mean of 18.11 and a SD of 4.51. Both models outperformed traditional forecasting approaches across multiple evaluation metrics.

XSL•FO
RenderX

Conclusions: The proposed prediction models effectively forecast ED waiting count at both hourly and daily intervals. The results demonstrate the value of integrating diverse data sources and applying advanced modeling techniques to support proactive resource allocation decisions. The implementation of these forecasting tools within hospital management systems has the potential to improve patient flow and reduce overcrowding in emergency care settings. The code is available in our GitHub repository.

(JMIR Med Inform 2025;13:e73960) doi:10.2196/73960

KEYWORDS

emergency overcrowding; time series prediction; patient flow forecasting; hospital resource management; reactive and proactive full capacity protocol

Introduction

Background

Emergency departments (EDs) are the primary source of hospital admissions, even though most individuals seen in the ED are ultimately discharged [1]. In 2021, there were more than 140 million visits to American EDs [2], of which 14.5 million (10.4%) led to hospital inpatient admissions, and 2 million (1.4%) led to admission to critical care units [3]. Several factors lead to ED overcrowding, including complexity of complaints and injuries [4,5], resource limitations [6], large patient volumes [7], and inefficient flow of patients [8]. ED overcrowding is associated with poor health care outcomes. It can lead to delays in diagnosis and treatment, which can result in poorer patient outcomes, higher comorbidities, and increased patient illness [9,10]. For instance, it was found that patients with acute coronary syndrome who presented to overcrowded EDs had a significantly higher rate of serious complications compared with those who presented to noncrowded EDs (6% vs 3%). The complications include death, late myocardial infarction, cardiac arrest, arrhythmias, heart failure, stroke, and hypotension [11]. Treatment delays also lead to serious complications, including death [12]. Sprivulis et al [13] observed a significant linear relationship between ED overcrowding and patient mortality based on 3 years of data from 3 large hospital systems.

The Emergency Medicine Practice Committee of the American College of Emergency Physicians reported that ED overcrowding is a hospital-wide patient flow problem rather than an isolated ED problem [1,2]. The full capacity protocol (FCP), a key approach recommended by the American College of Emergency Physicians to improve patient flow across the entire hospital, is an internationally recognized communication tool between the ED and inpatient units [8]. It contains a set of interventions that can be tailored to the severity levels of ED overcrowding [14]. A set of criteria triggers each intervention level. The criteria are based on different patient flow measures (PFMs), such as the number of patients waiting to be admitted to an inpatient unit (boarded patients) [14,15].

In the current FCP practice, the unit responsible for managing patient flow relies on near real-time PFM values to activate different FCP levels, which is a reactive approach. Specifically, at our partner hospital—an urban, university-affiliated academic medical center in the southeastern United States—this unit is referred to as the patient flow coordination team (PFCT). Implementing FCP interventions (eg, creating hallway treatment spaces or activating on-call personnel) requires preparation time, forcing PFCT to prepare and act simultaneously when the ED is already overcrowded, significantly increasing their stress. Therefore, accessing the predicted PFM values before overcrowding can provide the PFCT enough time to prepare before they implement FCP interventions. Given the critical role of timely and accurate information in driving FCP interventions, it is essential to develop prediction models to forecast PFMs used by the FCP criteria, transforming FCP from reactive to proactive. Proactive FCP can help in planning and implementing interventions at different crowding severity levels proactively before the ED is already overcrowded. Predicted PFMs built into a proactive FCP can help the PFCT anticipate future FCP level escalation and prepare for interventions, such as coordinating staffing needs and creating additional hallway treatment spaces.

There are many PFMs that can be used to determine the FCP level, such as ED hourly waiting count, ED boarding count, ED arrival count, and the number of patients by Emergency Severity Index (ESI), among others. For this study, the advisory board of the project recommended that we start with building a prediction model for the ED waiting count, as it is one of the most important PFMs. The ED waiting count represents the number of patients who have arrived at the ED but have not yet been moved to a treatment room or started their clinical care. The advisory board members represent different ED units at the partner hospital. The members include the chair of Emergency Medicine, the chief medical information officer, the associate principals of the Office of Clinical Practice Transformation, the associate vice president of clinical operations at the center of patient flow, the senior director of Emergency Services, and the nurse director for Emergency Services. Based on the feedback from the advisory board, the goal of this paper is to build deep learning models to predict the ED waiting count at two time points: (1) In the hourly basis, in which the prediction models forecast the waiting count in the next 6 hours; (2) In daily basis where the models predict the average waiting count for next working day. The prediction information allows PFCT to prepare ED resources to improve patient flow and consequently mitigate ED overcrowding. This study is part of a larger funded ED improvement project, and the models presented in this study will be integrated into a decision support system to be used by our partner hospital.

As part of a broader effort to build a data-driven decision support system for ED operations, this paper focuses on the critical metric of ED waiting room count. This predictive model represents a foundational component of the broader effort to operationalize proactive FCP. Using real-world operational and contextual data, we assess the utility of multiple time-series

XSL•FO
RenderX

algorithms and dataset variations to inform timely, data-driven predictions in ED management. The contributions of this study are as follows:

- We proposed an improvement for the current reactive FCP to make it proactive based on prediction models.
- This study was based on a real-world dataset and was conducted in collaboration with key decision makers from the ED.
- We developed predictive models that integrate multiple predictors from various sources to provide a comprehensive understanding of patient flow dynamics and improve forecasting performance.
- We introduced 2 complementary prediction approaches—hourly and daily—that provide actionable insights at different time scales.

Prior Work

Numerous studies in the literature have focused on predicting different ED PFMs or outcomes. Traditional models have been developed to predict hospital admissions at ED triage, often relying on a limited set of demographic, administrative, and clinical variables [16-18]. For example, Parker et al [17] used variables such as age group, race, postal code, day of the week, time of day, triage category, mode of arrival, and fever status in a logistic regression model to predict hospital admissions with an area under the curve of 0.825. Similarly, Sun et al [18] developed a model to predict immediate hospital admission at the time of ED triage using routine administrative data, including age, patient acuity category, arrival mode, and coexisting chronic diseases like diabetes, hypertension, and dyslipidemia, achieving an area under the curve of 0.849. However, because these models focus on only individual patient-level triage outcome predictions, they offer limited utility for administrative management in addressing ED crowding, as they do not provide a comprehensive view of overall patient flow or resource utilization.

In one of the earlier studies that focused on predicting ED PFMs at the aggregate patient level, Schweigler et al [19] developed a baseline model to predict ED overcrowding using historical averages and compared its performance to more advanced time series models, including seasonal autoregressive integrated moving average (ARIMA) and a sinusoidal model with an autoregressive error term. However, these models relied solely on historical averages to predict ED crowding based on bed occupancy, without considering any other predictors, limiting their utility for comprehensive ED crowding management. A subsequent time series modeling study by Kadri et al [20] also developed an ARIMA model to predict daily pediatric ED attendances using only historical attendance data, without external predictors.

Recent studies have leveraged advanced machine learning (ML) models to predict ED PFMs, which are generally the number of patients arriving [21-23] or waiting time [24,25], across different prediction horizons. Our study targets waiting count prediction, which measures the number of patients present in the ED waiting room during each time interval by cumulatively adding patients for every hour they remain. Arrival count and waiting count are fundamentally different PFMs: arrival count records each patient once, at the moment they enter the ED, whereas waiting count tracks each patient for every hour they remain in the waiting area. For example, if a patient arrives at 1:05 PM and leaves at 3:35 PM, they are counted for 1-2 PM in the arrival count but are included in the waiting count for 1-2 PM, 2-3 PM, and 3-4 PM. To the best of our knowledge, no published studies have focused on predicting waiting count in US EDs using deep learning models. Since the literature on waiting count prediction is lacking, we summarize key studies on arrival count prediction, which most closely align with our research objective. For example, Harrou et al [6] developed deep learning models to predict hourly and daily ED arrival counts, comparing the performance of a variational autoencoder with 7 others: recurrent neural networks (RNNs), long short-term memory (LSTM), bidirectional long short-term memory (BiLSTM), convolutional LSTM, restricted Boltzmann machine, gated recurrent units, and convolutional neural networks (CNN). Tuominen et al [26] used advanced ML models, including probabilistic forecasting with autoregressive recurrent networks (DeepAR) [27], neural basis expansion analysis for interpretable time series forecasting (N-BEATS) [28], temporal fusion transformer, and light gradient boosting machine (LightGBM) [29], with multivariable inputs such as bed availability in catchment area hospitals, traffic data, and weather variables to predict daily ED occupancy. Similarly, Giunta et al [30] developed a multivariable predictive model based on the National Emergency Department Overcrowding Study score to predict sustained critical ED overcrowding lasting 8 or more hours, incorporating weather, patient flow, and bed occupancy variables. However, despite their advanced methodologies and multivariable approaches, none of these studies examined their predictions within the context of a proactive FCP.

Although these studies advance ED overcrowding prediction, each has limitations that reduce practical use in high-volume EDs. Many models have relied on a narrow set of inputs, such as patient arrivals or historical bed occupancy, without incorporating a broader range of operational, staffing, or environmental variables. In our study, we focus on forecasting the ED waiting count rather than the arrival count, as the arrival count only captures new patient entries and does not reflect ongoing congestion in the waiting area. In contrast, waiting count directly measures the number of patients present at any given time, providing a more accurate assessment of real-time crowding. Additionally, most studies have focused exclusively on daily metrics, failing to capture both hourly and daily fluctuations needed for real-time resource planning. To address these gaps, this study integrates hourly and daily predictions for more granular, actionable forecasting.

Methods

Ethical Considerations

This study was reviewed and approved by the Institutional Review Board (IRB) at the University of Alabama at Birmingham, with IRB# IRB-300011584.

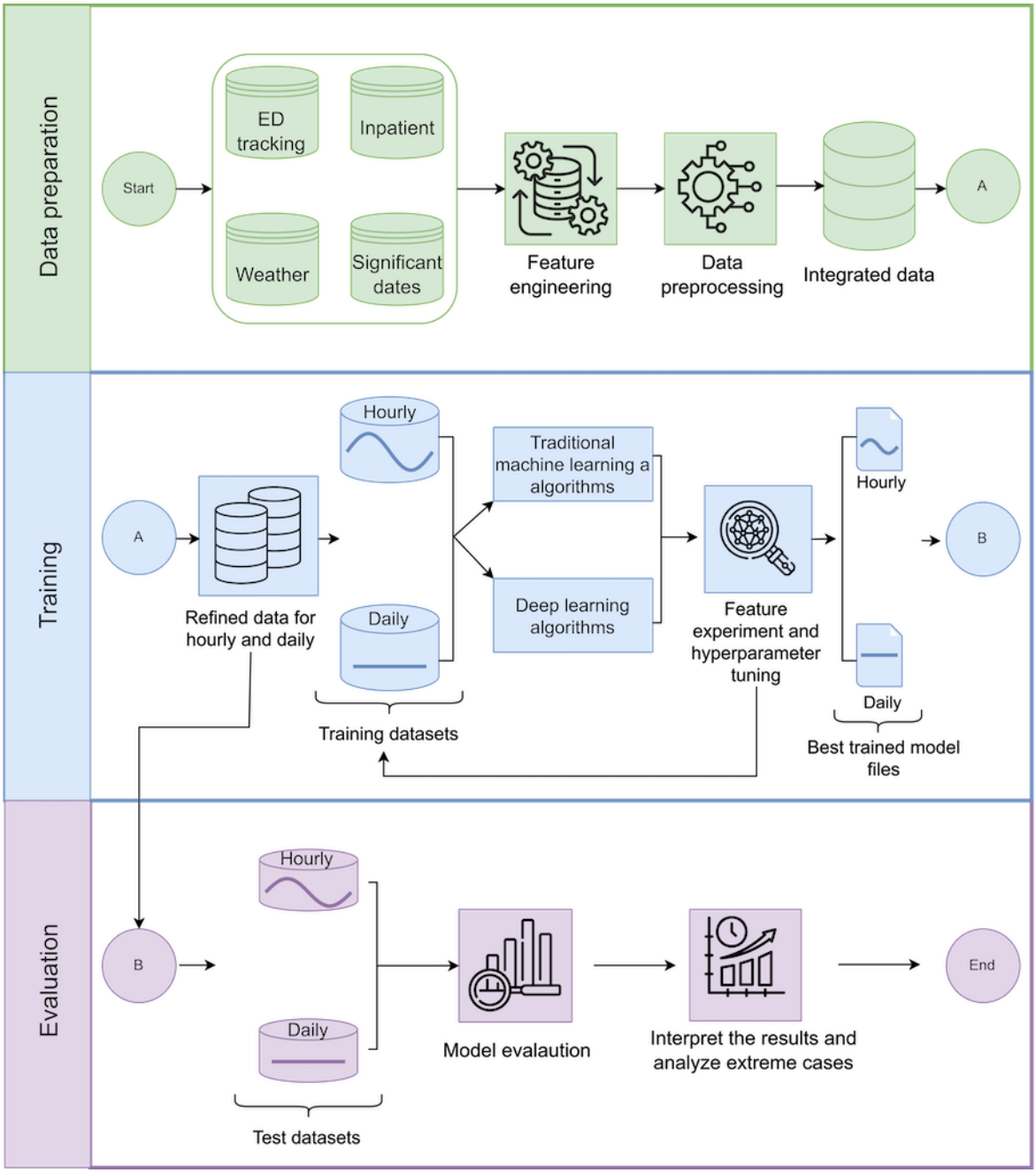
Research Framework

Figure 1 shows our proposed framework, which has 3 main phases: data preparation, training, and evaluation. The

XSL•FO
RenderX

framework includes 2 prediction approaches. The first provides hourly predictions, estimating the number of patients in the waiting room 6 hours ahead to support intraday resource management. The second provides daily predictions, estimating the average waiting count for the next 24 hours to help anticipate ED conditions for the following day. In this paper, patient counts in the waiting room are referred to as "waiting counts," and their 24-hour average as "average waiting count."

Figure 1. Proposed research framework. ED: emergency department.



The data preparation phase involves processing data from 4 sources: the ED tracking system, inpatient records, weather information, and significant dates. After obtaining data from different sources, feature engineering and data preprocessing are applied separately to each source before creating the integrated final data. Following this, data preprocessing focuses on cleaning, scaling, and recategorizing certain categorical variables to prepare datasets for use in predictive modeling. After completing feature engineering and data preprocessing for each data source, all sources are integrated on an hourly basis into a single comprehensive dataset. The mathematical calculation of all features, including the target variable waiting count, along with all preprocessing and feature engineering steps, is described in detail in Multimedia Appendix 1 [31-56]. Table 1 includes descriptive statistics: numerical features show mean (SD), min, and max; categorical features indicate dataset percentages; and temporal features specify the time range used.

XSL•FO
RenderX

Table 1. Summary of the overcrowding dataset.

Features	Hourly	Daily
Date range[a]		
Number of years	4	4
Number of months	12	12
Days of a month	1-31	1-31
Days of a week	7	7
Time (hours)	24	24
Waiting count (target variable)		
Average (SD)	18.11 (9.77)	18.11 (4.51)
Range	0-59	7-35
Waiting count by ESI[b] **levels (%)**		
ESI levels 1 and 2	26.38	26.38
ESI level 3	58.34	58.34
ESI levels 4 and 5	14.69	14.69
Average waiting time (minutes)		
Average (SD)	90.98 (62.85)	90.98 (32.24)
Range	0-425	9-170
Average waiting time by ESI levels (minutes)		
ESI levels 1 and 2		
Average (SD)	62.81 (69.98)	62.81 (31.69)
Range	0-538	5-162
ESI level 3		
Average (SD)	106.9 (76.13)	106.9 (38.92)
Range	0-526	8-193
ESI levels 4 and 5		
Average (SD)	56.03 (66.79)	56.03 (28.53)
Range	0-536	8-166
Treatment count		
Average (SD)	68.29 (23.69)	68.29 (22.64)
Range	9-139	31-123
Average treatment time (minutes)		
Average (SD)	52.93 (3.11)	52.93 (2.07)
Range	28-60	46-57
Boarding count		
Average (SD)	46.78 (29.60)	46.78 (29.30)
Range	3-121	8-115
Average boarding time (minutes)		
Average (SD)	54.06 (4.45)	54.06 (3.15)
Range	12-60	42-58
Extreme case indicator (%)	3.1	28.77[c]
Hospital census		
Average (SD)	794.23 (71.88)	794.23 (61.50)

XSL•FO
RenderX

Features	Hourly	Daily
Range	584-1017	610-931
Temperature (°F)		
Average (SD)	64.06 (15.36)	64.06 (13.60)
Range	9-100	15-87
Wind speed (m/s)		
Average (SD)	2.26 (1.97)	2.26 (1.22)
Range	0-15	0-7
Humidity (%)		
Average (SD)	73.38 (19.08)	73.38 (11.97)
Range	15-100	40-97
Weather status (%)		
Clouds	57.67	57.67
Clear	22.89	22.89
Rain	15.12	15.12
Mist	2.55	2.55
Thunderstorm	1.27	1.27
Drizzle	0.16	0.16
Fog	0.13	0.13
Haze	0.12	0.12
Snow	0.06	0.06
Smoke	0.03	0.03
Number of football games	40	40
Number of federal holidays	34	34

[a]Data from January 1, 2020, to May 1, 2021, was excluded due to COVID-19.

[b]ESI: Emergency Severity Index.

[c]28.77% of rows have nonzero values, indicating days that experienced extreme patient volumes during at least some portion of the day.

During the training phase, the integrated data from the data preparation stage is used to generate 2 refined datasets: one for the hourly prediction approach and another for the daily prediction approach. Subsequently, 16 different dataset variations are created to be used by both approaches, each with distinct feature combinations, as detailed in Table S2 in Multimedia Appendix 2. A total of 11 ML algorithms, in Table S1 in Multimedia Appendix 1 [31-56], are used to train and evaluate models on both hourly and daily datasets to identify the best-performing models. These algorithms are categorized into four groups: (1) traditional machine learning (random forest [RF] [31] and extreme gradient boosting [XGBoost] [32]); (2) RNN-based models (LSTM) [33], BiLSTM [34], and sequence to sequence learning with neural networks [Seq2Seq] [35]; (3) CNN-based architectures (fully convolutional network plus [FCNPlus] [36], residual network plus [ResNetPlus] [37], XceptionTimePlus [38], and explainable convolutional neural network plus [XCMPlus] [39]); and (4) transformer-based models (time series transformer plus [TSTPlus] [40] and time series vision transformer plus [TSiTPlus] [41]). The architectures of all algorithms are explained in detail in Multimedia Appendix 1 [31-56]. Each combination of an algorithm and a dataset is considered a separate model in this study. To improve performance, different hyperparameter configurations are tested across the 16 dataset variations.

In the evaluation phase, performances of the trained models are evaluated. The best-performing models, selected for both hourly and daily prediction tasks, are tested using evaluation metrics detailed in the Model Evaluation section of Multimedia Appendix 1 [31-56]. The evaluation is primarily based on 4 different metrics: mean absolute error (MAE), mean squared error (MSE), root mean squared error (RMSE), and the coefficient of determination (R^2). To further assess model effectiveness, the best-performing hourly prediction model is evaluated under extreme case scenarios, representing periods of exceptionally high patient volumes, with the results presented in Table 2. Additionally, the performance of the best hourly model is analyzed across the hour-of-day, capturing variations and trends in predictive accuracy at different times, as illustrated in Figure S3 in Multimedia Appendix 3.

XSL•FO
RenderX

Table 2. Performance of the time series vision transformer plus (TSiTPlus) in predicting extreme cases across different datasets.

Dataset	MAE[a]		
	Extreme (≥28) (mean + 1σ[b])	Very extreme (≥38) (mean + 2σ)	Highly extreme (≥48) (mean + 3σ)
DS0	6.86	11.61	17.90
DS1	7.07	12.13	19.30
DS2	7.08	12.06	19.21
DS3	6.98	11.61	18.10
DS4	6.85	11.36	17.77
DS5	6.88	11.78	18.75
DS6	6.84	11.61	18.41
DS7	6.63	11.21	17.54
DS8	6.59	11.07	17.14
DS9	6.57	11.13	17.35
DS10	6.58	11.11	17.15
DS11	6.31	10.69	16.76
DS12	6.31	10.70	16.82
DS13	6.18	10.44	16.78
DS14	6.16[c]	10.16[c]	15.59[c]
DS15	6.31	10.45	16.16

[a]MAE: mean absolute error.

[b]σ: SD.

[c]Lowest MAE.

Data Sources

The data sources in this study cover the period from January 2019 to July 2023 and are categorized into hospital data, including ED tracking system and inpatient records, and external data, consisting of weather information and significant dates for football games and federal holidays.

The ED tracking data provides detailed records of patient arrivals and departures within the ED waiting and treatment rooms of our partner hospital. This data also includes ESI levels indicating acuity, patient classifications, room types, event status (eg, complete, request, and cancel), and other ED-related information. Both waiting room and treatment room identifiers are recorded, enabling comprehensive tracking of patient movements from arrival to discharge or inpatient admission through unique patient and visit identifiers. The data contains 161,477 unique patients and 308,196 unique visits.

The inpatient data contains time-stamped records of patient admissions to and discharges from inpatient units. These records enable the hourly calculation of the hospital-wide patient census feature, as shown in Table 1. The dataset comprises 293,716 unique inpatient visits for 180,589 unique patients, representing hospital-wide admissions encompassing the study period.

The external data includes weather data and significant events, which are federal holidays and local football game event data. The weather data provides hourly weather information collected from a nearby weather station located close to the partner hospital. This data is sourced from the historical data archive of the OpenWeatherMap History Bulk [57] and includes numerical variables such as temperature, humidity, and wind speed, as well as a categorical variable indicating categories of clear skies, clouds, rain, mist, thunderstorm, snow, drizzle, haze, fog, and smoke. The significant dates consist of 2 external datasets: federal holidays and football game dates for a major team near the hospital. On average, there are 13 football games and 10 federal holidays each year. Federal holidays were obtained from the United States Office of Personnel Management Government website [58], and football game dates were sourced from the team's official website [59].

Problem Modeling

To predict waiting counts in the ED waiting room at a time point h steps into the future (eg, predicting 6 hours from now, or any other chosen future time point), we model this problem as a time series ML problem. We set up the problem as a direct single-step forecast targeting y_{t+h} from the current time t. Let:

- y_t represent the waiting count at the current time t.
- h be the prediction horizon (ie, the number of time steps ahead for the forecast (eg, h=6 for 6 hours ahead).
- k denote the number of past observations (lags) included in the model.
- $(l_1, l_2,\ldots, l_N)$ represent variables that do not require lagging (eg, weather conditions, holidays).
- $x_t, x_{t-1},\ldots, x_{t-k+1}$ represent any feature other than the waiting count that has a lag.

XSL•FO
RenderX

- $g(.)$ be the function learned by the ML model, trained using historical data.

The model can be expressed as follows:



Where:

- y_{t+h} is the predicted waiting count at time $t+h$.
- y_t, y_{t-1},…, $y_{t-k+1}$are waiting count lag features to capture temporal dependencies.
- M is the total number of observations and the training dataset size is $M-k-h+1$.

Model Design

Model design involves selecting the relevant feature combinations for prediction. With a total of 34 main features, excluding lag and rolling mean features, determining the optimal feature set is an essential step in improving model performance. Therefore, numerous experiments were conducted initially to refine feature combinations, scaling methods, COVID-19 date exclusion ranges, weather categorizations, and hyperparameter ranges. Based on the outcomes of these experiments, a total of 16 datasets were generated, as shown in Table S2 in Multimedia Appendix 2, each containing different combinations of features. These combinations were selected through a manual but systematic approach guided by domain knowledge and performance feedback. Specifically, we varied key dimensions such as lag lengths, rolling window sizes, weather encodings, temporal coverage, and the inclusion of engineered variables like the extreme case indicator. Each dataset was crafted to test how individual or grouped feature categories (eg, ED tracking, inpatient census, weather, significant dates) influence model generalization and forecasting accuracy. To evaluate these combinations, 11 different algorithms, as detailed in Table S1 in Multimedia Appendix 1 [31-56], were applied to train models on each dataset. The primary objective was to identify the most effective combination of features and algorithms for achieving optimal performance. For both hourly and daily prediction models, a total of 8800 experiments (11 algorithms × 16 datasets × 50 trials) were conducted separately to evaluate these combinations and determine the best-performing model and feature set.

Hourly and Daily Time Horizons

To address the varying forecasting needs in ED, this study uses 2 types of predictive models: hourly and daily, as illustrated in Figure S4 in Multimedia Appendix 3. These models were developed to handle different prediction horizons, allowing for more comprehensive management of patient flow in the ED.

The hourly model predicts the waiting count 6 hours ahead. As shown by the red arcs in Figure S4 in Multimedia Appendix 3, this model provides flexibility by not being restricted to specific times of the day. Instead, it generates forecasts for 6 hours into the future whenever it runs, enabling it to be applied at any time when updated predictions are needed.

The daily model predicts the average waiting count for the next 24-hour period, running each day at 5 PM and using data from the previous 24 hours (5 PM the previous day to 5 PM today). At each run, it provides a single estimate for the upcoming 24-hour window (5 PM today to 5 PM tomorrow), offering insights that aid in planning for the next day. Figure S4 in Multimedia Appendix 3 shows the daily model's prediction timeline, represented by the orange elements, where forecasts are generated once per day to estimate the average waiting count in the waiting room for the next 24-hour period.

The selection of the 2 prediction horizons—6 hours ahead and daily—was informed by consultations with hospital operational leadership and the clinical advisory board to align with real-world decision-making workflows. The 6-hour-ahead forecast supports intrashift planning by enabling proactive resource allocation for anticipated short-term crowding. The daily forecast facilitates long-range planning, including staffing, bed coordination, and potential FCP activation based on projected 24-hour patient volumes. Together, these models address both immediate and next-day operational needs.

Results

Overview

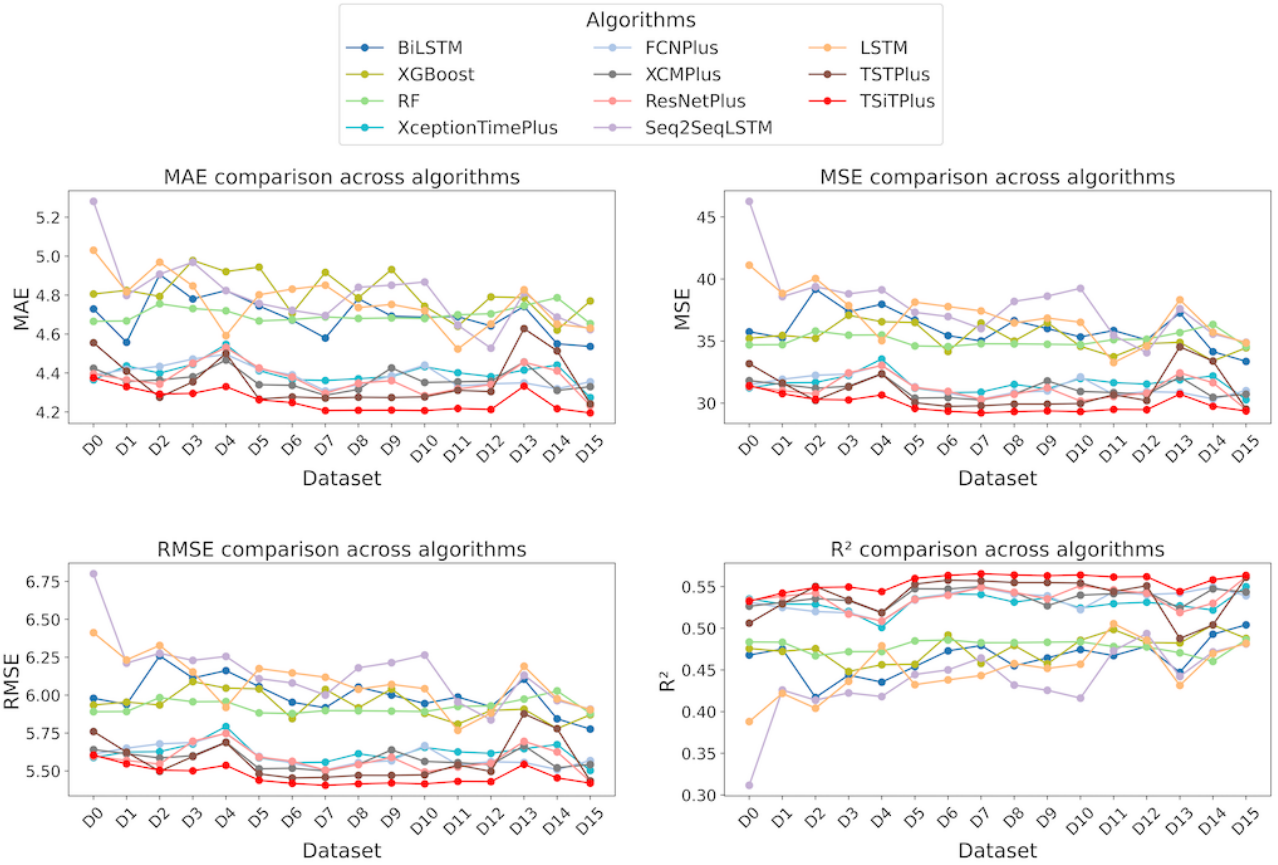
We present and analyze the evaluation results of 11 ML algorithms (listed in Table S1 in Multimedia Appendix 1 [31-56]) applied to 16 different datasets (described in Table S2 in Multimedia Appendix 2). The results cover 2 separate prediction approaches: one focuses on forecasting the waiting count 6 hours ahead, and the other estimates the average waiting count over the next 24-hour period.

Performances of Hourly Prediction Models

The target variable waiting count, which represents the number of patients in the waiting room during a given hourly interval, has a mean value of 18.11 and a SD of 9.77, as shown in Table 1. Figure 2 presents the performance analysis of ML models in predicting waiting counts 6 hours ahead across 16 different datasets (DS0 to DS15). In Figure 2, the x-axis in all subplots represents the datasets, while the y-axis corresponds to each evaluation metric. Among the evaluated models, the TSiTPlus algorithm demonstrated the best overall performance, achieving an MAE of 4.19, an MSE of 29.36, an RMSE of 5.42, and an R^2 of 0.56 on dataset DS15.

XSL•FO
RenderX

Figure 2. Comparison of hourly model performances across 16 datasets and 11 algorithms based on different evaluation metrics. BiLSTM: bidirectional long short-term memory; FCNPlus: fully convolutional network plus; LSTM: long short-term memory; MAE: mean absolute error; MSE: mean squared error; ResNetPlus: residual network plus; RF: random forest; RMSE: root mean squared error; Seq2Seq: sequence to sequence learning with neural networks; TSiTPlus: time series vision transformer plus; TSTPlus: time series transformer plus; XCMPlus: explainable convolutional neural network plus.



As shown in Figure 2, traditional ML algorithms, RF and XGB, displayed similar performance patterns, with RF achieving its best results on dataset DS15 and XGB on dataset DS14. Specifically, RF's performance on DS15 yielded an MAE of 4.65, an MSE of 34.56, an RMSE of 5.87, and an R^2 of 0.48, using 100 estimators, a maximum depth of 30, and 4 samples per leaf, with bootstrapping enabled. Across all datasets, RF's MAE varied between 4.65, its best performance, and 4.78, its worst performance. On the other hand, XGB achieved slightly better values on dataset DS14, with an MAE of 4.62, an MSE of 33.40, an RMSE of 5.78, and an R^2 of 0.50, with a maximum depth of 15, a learning rate of 0.02, a subsample ratio of 0.8, and a column sampling rate of 0.3. These results highlight the limitations of traditional algorithms, which treat each observation independently and lack the ability to capture the long-term dependencies and complex sequential patterns inherent in time-series data.

RNN-based models, including Seq2Seq, LSTM, and BiLSTM, delivered better results than traditional ML algorithms for predicting waiting counts 6 hours ahead. Among these, Seq2Seq achieved its best performance on dataset DS12, with an MAE of 4.52, an MSE of 34.06, an RMSE of 5.83, and an R^2 of 0.49. This result was obtained using a batch size of 32, a learning rate of 0.01, a weight decay of 0.2, a dropout rate of 0.1, and Adam as the optimization function. The Seq2Seq model's performance, based on MAE, ranged from its worst result of 5.28 on dataset DS0 to its best result of 4.52 on dataset DS12. LSTM demonstrated consistent results across datasets, delivering its best performance on dataset DS11, with an MAE of 4.52, an MSE of 33.26, an RMSE of 5.76, and an R^2 score of 0.505. This result was achieved using a batch size of 32, a learning rate of 0.01, a dropout rate of 0.2, a weight decay of 0.1, and stochastic gradient descent as the optimization algorithm [60]. The LSTM model's performance, based on MAE, ranged from its worst result of 5.03 on dataset DS0 to its best result of 4.52 on dataset DS11. BiLSTM, which leverages its bidirectional architecture, achieved its best results on dataset DS15, with an MAE of 4.54, an MSE of 34.67, an RMSE of 5.89, and an R^2 score of 0.48. However, it encountered higher errors on datasets such as DS2, where the MAE was 4.91.

The CNN-based algorithms, including ResNetPlus, XceptionTimePlus, FCNPlus, and XCMPlus, demonstrated better performance than both traditional ML and RNN-based algorithms across multiple datasets in this study. Among these, ResNetPlus achieved the best overall performance, particularly on dataset DS15, with an MAE of 4.23, an MSE of 29.93, an RMSE of 5.47, and an R^2 of 0.555. XceptionTimePlus achieved its best results on dataset DS15 as well, with an MAE of 4.274, an MSE of 30.279, an RMSE of 5.503, and an R^2 of 0.55. FCNPlus performed best on dataset DS7, with an MAE of 4.3081, an MSE of 30.3208, an RMSE of 5.5064, and an R^2 of 0.5491. Finally, XCMPlus delivered its best results on dataset

XSL•FO
RenderX

DS7, with an MAE of 4.285, an MSE of 30.254, an RMSE of 5.5, and an R^2 of 0.55. These results suggest that CNN-based models generally provided more accurate predictions than traditional and RNN-based algorithms.

The transformer-based models, TSiTPlus and TSTPlus, delivered better results compared with other algorithm categories in this study, with TSiTPlus being the best-performing model based on MAE. TSiTPlus achieved its best performance on dataset DS15, with an MAE of 4.19, an MSE of 29.36, an RMSE of 5.41, and an R^2 of 0.56. In comparison, TSTPlus showed good performance but had slightly higher errors. Its best results were on dataset DS15, with an MAE of 4.24, an MSE of 29.52, an RMSE of 5.43, and an R^2 of 0.561. DS15 incorporated a range of features, including waiting count lags, rolling averages, patient flow indicators, weather conditions, hospital census data, and significant event markers. Across other datasets, TSTPlus achieved MAE values such as 4.27 on DS7 and 4.27 on DS8. The performance of TSiTPlus indicates that it was the most accurate model in this study for predicting waiting counts. To examine the impact of including the COVID-19 period, TSiTPlus was evaluated on DS15, the best-performing model and dataset combination. The results indicated noticeably higher prediction errors (MAE: 4.82 vs 4.19; MSE: 40.22 vs 29.32), suggesting that patient flow anomalies during the pandemic adversely affected model performance.

TSiTPlus demonstrated superior performance over all other models in hourly predictions. Specifically, it achieved a 9.8% reduction in mean MAE compared with RF (MAE=4.65), a 7.3% reduction compared with the best-performing RNN-based model, Seq2Seq (MAE=4.52), and a 0.9% improvement over the best CNN-based model, ResNetPlus (MAE=4.23). Although the performance gap between TSiTPlus (MAE=4.19) and the best traditional ML model, XGBoost (MAE=4.62), may initially appear modest, its operational significance becomes clear when scaled to the continuous nature of ED operations. Given that predictions are generated hourly—24 times each day—this 0.43 improvement in MAE results in approximately 10.3 (0.43 × 24 hours), more accurate waiting count forecasts per day. When extended over an entire year, this translates to 3767 waiting counts (10.3 × 365 days), more accurate predictions, each representing a more informed decision point for hospital staff.

To estimate uncertainty around our model's point estimates, we applied a bootstrap resampling approach [61], which repeatedly samples from the original test data to approximate the sampling distribution of evaluation metrics. Specifically, we used block bootstrapping with our best-performing model, TSiTPlus, on DS15. A block size of 24 was chosen to match the 24-hour lag window, preserving local temporal dependencies inherent in hourly hospital data. For each iteration, blocks of 24 consecutive hours were resampled with replacement from the test dataset to form a new evaluation set, and performance metrics were computed. This method yielded robust IQRs for each metric. As shown in Table 3, MAE reaches 4.19 with an IQR of 4.16-4.25, varying by only 0.09 across samples—indicating highly consistent model performance. MSE reaches 29.36 (IQR 28.65-30.20), RMSE reaches 5.42 (IQR 5.35-5.49), and R^2 reaches 0.56 (IQR 0.55-0.57); all similarly demonstrate narrow IQRs, further supporting the stability and reliability of the model's predictions. These narrow IQRs suggest that the model is not only accurate but also reliable under different test-time conditions.

Table 3. Bootstrap-based uncertainty estimates for model performance metrics using Time Series Vision Transformer Plus (TSiTPlus) on dataset DS15.

Model and metric	Median (IQR)
TSiTPlus	
MAE[a]	4.19 (4.16-4.25)
MSE[b]	29.36 (28.65-30.20)
RMSE[c]	5.42 (5.35-5.49)
R^2	0.56 (0.55-0.57)

[a]MAE: mean absolute error.

[b]MSE: mean squared error.

[c]RMSE: root mean squared error.

The strong performance of TSiTPlus in this study can be attributed to its ability to capture complex patterns in multivariate time series data. As a transformer-based model, it is well-suited for recognizing relationships and trends over time. TSiTPlus divides the time series into smaller segments, treating them as input tokens—similar to words in a sentence—which allows the model to capture both short- and long-term patterns. This design enables it to learn from multiple timeframes, making it particularly effective for datasets with complex temporal dynamics.

Analysis of Extreme Case and Hour-of-Day

Table 2 presents the performance of TSiTPlus, the best-performing algorithm, in predicting extreme cases across various datasets. For "Extreme Cases" (mean + 1σ), MAE ranged from 6.16 on DS14 to 7.08 on DS2. In "Very Extreme Cases" (mean + 2σ), MAE ranged from 10.16 on DS14 to 12.13 on DS1. For "Highly Extreme Cases" (mean + 3σ), TSiTPlus achieved its best result on DS14 with an MAE of 15.59. When averaging errors across all 3 categories, DS14 performed best, followed by DS15, demonstrating strong predictive capabilities under high patient volume. DS14's superior performance is

XSL•FO
RenderX

likely due to its 48-hour lag features, which incorporate data from the past 2 days (Table S2 in Multimedia Appendix 2).

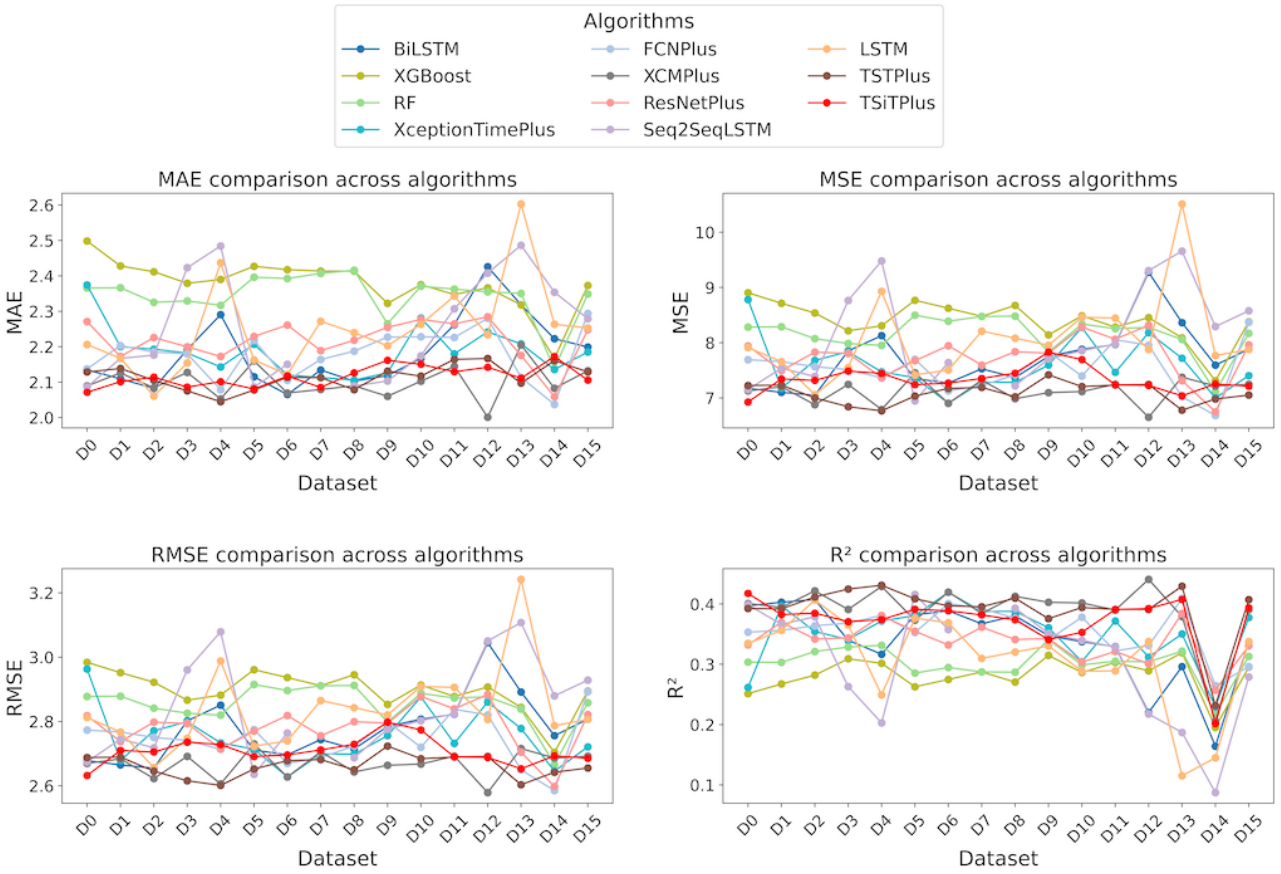
Our best-performing model not only predicts typical waiting counts accurately but also performs well under extreme crowding. Compared with traditional models, such as RF (MAE: 14.0 for Very Extreme, 20.0 for Highly Extreme) and XGBoost (MAE: 13.9 for Very Extreme, 19.6 for Highly Extreme), TSiTPlus consistently shows lower error rates during critical situations. This reduction in prediction error during peak periods allows for earlier, more accurate interventions, improving ED responsiveness and resource coordination. When evaluating the cumulative effect of prediction performance over time, the difference becomes even more meaningful. For example, in very extreme scenarios, TSiTPlus achieves an MAE of 10.16 compared with XGBoost's 13.9—an improvement of 3.74. This translates to approximately 90 (3.74 × 24 hours) more accurate waiting count predictions per day. When applied year-round, this provides a clear operational advantage for anticipating and managing ED overcrowding.

Figure S3 in Multimedia Appendix 3 shows the TSiTPlus model's performance by hour of day. It performs best between 10 PM and 6 AM, with MAE under 4 and RMSE between 3 and 5.25, reflecting more stable patient volumes. Error metrics increase between 6 PM and 8 PM, where MAE nears 5 and RMSE exceeds 6, likely due to higher variability in waiting counts during this time.

Performance of Daily Prediction Models

As shown in Figure S4 in Multimedia Appendix 3, daily prediction is conducted at 5 PM each day to estimate the next day's average waiting count. The target variable has a mean of 18.11 and an SD of 4.51 (Table 1). Daily prediction errors are lower than hourly due to smoother target values and a smaller dataset. Using the same 11 ML algorithms (Table S1 in Multimedia Appendix 1 [31-56]) across 16 datasets (Multimedia Appendix 2), the best performance was achieved by XCMPlus with an MAE of 2.00, MSE of 6.64, RMSE of 2.57, and R^2 of 0.44, as shown in Figure 3.

Figure 3. Comparison of daily model performance across 16 datasets based on different evaluation metrics. BiLSTM: bidirectional long short-term memory; FCNPlus: fully convolutional network plus; LSTM: long short-term memory; MAE: mean absolute error; MSE: mean squared error; ResNetPlus: residual network plus; RF: random forest; RMSE: root mean squared error; Seq2Seq: sequence to sequence learning with neural networks; TSiTPlus: time series vision transformer plus; TSTPlus: time series transformer plus; XCMPlus: explainable convolutional neural network plus.



Traditional ML algorithms, RF and XGBoost, demonstrated similar performance across all 16 dataset configurations for daily predictions, as illustrated in Figure 3. Both algorithms achieved their best results on dataset DS14, with RF slightly outperforming XGBoost. Specifically, RF recorded the lowest MAE of 2.13, MSE of 7.10, RMSE of 2.66, and an R^2 of 0.217, while XGBoost followed closely with an MAE of 2.16, MSE of 7.31, RMSE of 2.70, and an R^2 of 0.195. The performance gap between the best and worst configurations for both algorithms, with RF ranging from 2.13 to 2.41 MAE and XGBoost from 2.16 to 2.49 MAE, indicates consistent behavior across different feature combinations. RF achieved its optimal performance with 200 estimators, a maximum depth of 40, a minimum sample split of 10, and 8 samples per leaf with

XSL•FO
RenderX

bootstrapping enabled. Similarly, XGBoost's best configuration used a dart booster with a maximum depth of 12, learning rate of 0.02, subsample ratio of 0.8, column sampling rate of 0.4, and weighted sampling with a rate drop of 0.2.

The analysis of the RNN-based models, including LSTM, BiLSTM, and Seq2Seq, shows varying performance across datasets. The LSTM model performs consistently, with MAE values between 2.06 and 2.60 and RMSE between 2.65 and 3.24, achieving the lowest MAE on dataset DS2 and the highest on dataset DS13. BiLSTM performs slightly better, with MAE ranging from 2.06 to 2.42 and RMSE from 2.65 to 3.07, showing the best performance on dataset DS6 and the highest error on dataset DS12. Seq2Seq provides competitive results, with MAE between 2.08 and 2.48 and RMSE from 2.63 to 3.10, performing best on dataset DS5 and worst on dataset DS13. The R^2 values indicate that all models exhibit moderate predictive power, with the highest values around 0.41 and the lowest around 0.11. Among the 3 models, BiLSTM offers the best balance between low MAE and stable R^2 values, while Seq2Seq shows more consistent performance across datasets.

The analysis of CNN-based models, including FCNPlus, ResNetPlus, XceptionTimePlus, and XCMPlus, shows varying performance across datasets. FCNPlus has MAE values from 2.03 to 2.44 and RMSE between 2.58 and 3.01, performing best on dataset DS14 and worst on dataset DS11, with R^2 values ranging from 0.26 to 0.23. ResNetPlus shows slightly better performance, with MAE values between 2.05 and 2.40, RMSE from 2.59 to 3.02, and R^2 values between 0.25 and 0.22. XceptionTimePlus provides competitive performance, with MAE between 2.10 and 2.33 and RMSE from 2.71 to 2.88, achieving its best results on dataset DS8 and the highest error on dataset DS11. XCMPlus outperforms the other models, with the lowest MAE (2.00 to 2.28) and RMSE (2.57 to 2.92), showing the best performance on dataset DS12 and the highest error on dataset DS0. DS12 incorporated waiting count by ESI levels, treatment and boarding counts, and weather conditions, with rolling means and lag features enhancing trend detection. These features contributed to its strong predictive performance, especially for XCMPlus. It also has the highest R^2 values, ranging from 0.44 to 0.28, indicating better predictive accuracy. Overall, XCMPlus demonstrates the best performance among all algorithms, not just CNN-based models, achieving the lowest MAE and highest R^2 values, making it the most effective model for predicting daily waiting counts across datasets.

The analysis of the transformer-based models, TSiTPlus and TSTPlus, highlights differences in their performance across datasets. TSiTPlus demonstrates MAE values ranging from 2.08 to 2.17 and RMSE values between 2.63 and 2.80, with the best performance observed on dataset DS5 and the highest error on dataset DS14. The R^2 values for TSiTPlus vary from 0.41 to 0.20, indicating moderate predictive accuracy. TSTPlus achieves slightly lower MAE values compared with TSiTPlus, ranging from 2.04 to 2.18, and RMSE values between 2.57 and 2.70. The best results

are observed for dataset DS4, while the highest error occurs on dataset DS11. The R^2 values range from 0.42 to 0.27, showing slightly better predictive power compared with TSiTPlus. Overall, TSTPlus shows slightly better performance than TSiTPlus in terms of lower MAE and higher R^2 values across datasets, making it the more effective transformer-based model for predicting waiting counts.

Discussion

Principal Findings

This study developed time series ML models to forecast ED waiting room counts using real-world operational and contextual data. TSiTPlus achieved the best 6-hour-ahead prediction performance (MAE: 4.19, RMSE: 5.42, R^2: 0.56 on DS15), while XCMPlus performed best for daily forecasts (MAE: 2.00, RMSE: 2.57, R^2: 0.44 on DS12). MAE differences across datasets for TSiTPlus and XCMPlus were minimal in hourly predictions; however, the extreme case analysis revealed greater variation, underscoring the importance of feature engineering. For the hourly prediction models, comparing datasets highlights the incremental impact of added features. For example, the MAE for TSiTPlus decreased from 4.29 in DS2 to 4.26 in DS5 with the inclusion of weather status and ESI-based waiting counts. Incorporating significant dates such as football games and federal holidays further improved performance, reducing the MAE to 4.24 in DS6. Additional operational features—like treatment count, boarding count, and related time metrics—lowered the MAE to 4.21 in DS8. Further adjustments, such as different lagged features and rolling means, resulted in only minor MAE changes across DS8 to DS14. Ultimately, the best performance was achieved with DS15, where TSiTPlus reached an MAE of 4.19 after integrating all available features. For the daily prediction models, the best accuracy was achieved using DS14, which shares the same feature combination as the best hourly dataset, DS15, except that DS14 does not include temperature, humidity, wind speed, or football match variables. This suggests these variables do not significantly impact long-term average waiting count predictions. These results demonstrate the potential of deep learning–based time series models to support proactive FCP implementation through accurate, time-sensitive predictions. Additionally, we evaluated the impact of including COVID-19 period data for TSiTPlus on DS15. Contrary to some findings in the literature [62], which reported improved results for arrival count prediction when COVID-19 data was included, our results showed that adding the pandemic period to our training data negatively affected model performance for waiting count prediction (MAE increased from 4.19 to 4.82; MSE increased from 29.32 to 40.22). This suggests that the atypical patient flow patterns during the COVID-19 pandemic introduced additional variability, making it harder for the model to accurately capture or reflect standard ED operations.

Managerial Impact

EDs often face overcrowding due to challenges such as limited resources [6], high patient volumes [7], and inefficient patient flow management [8]. This represents an initiative to transform reactive FCP to be proactive by developing predictive models that forecast a key PFM, which is ED waiting counts. The prediction is done at two distinct time scales—6 hours ahead and 24 hours in advance—allowing for both hourly operational

XSL•FO
RenderX

adjustments and daily planning. The selection of these prediction horizons was based on input from the hospital's PFCT and the project advisory board. The 6-hour window was identified as a critical lead time for initiating immediate operational responses such as surge staffing, bed reassignments, and overflow room activation. In contrast, the 24-hour forecast was designed to inform daily planning activities, including staff scheduling, diversion decisions, and intensive care unit (ICU) bed coordination. Predictions with longer windows can provide a greater margin for operational adjustments, making it easier for hospitals to mobilize resources and take proactive action when surges are anticipated. However, evidence is still lacking as to which prediction window offers the most sustainable and actionable foundation for managing real-world ED surges, since practical constraints and response capabilities can vary significantly between institutions.

The hourly prediction model, which predicts the total waiting count in the next 6 hours, enables real-time resource allocation by giving hospital managers enough time (eg, 6 hours) to proactively implement FCP interventions and resources that help mitigate ED crowding, such as adjusting staffing, mobilizing overflow spaces, and ensuring the availability of critical equipment before surges occur. For example, if the model predicts a peak in patient volume during the evening shift, managers can activate a surge plan, offering voluntary short-term shifts to nurses or physicians who opt in to alleviate crowding. Additionally, they can offer overtime to extend staff hours, call in additional clinical staff, or reassign staff to the ED ahead of anticipated crowding. These proactive measures help prevent bottlenecks, ensuring adequate coverage during peak times while minimizing unnecessary overtime costs. This capability minimizes understaffing during peak times while reducing unnecessary overtime costs. Additionally, FCP interventions—such as coordinating with inpatient units to expedite bed turnover or opening additional inpatient surge capacity, such as unstaffed beds or hallways, to absorb some of the ED boarding patients and relieve crowding—can be activated before crowding worsens, improving compliance with key performance indicators such as Centers for Medicare & Medicaid Services door-to-provider times and reducing "left without being seen" rates, which impact hospital revenue and reputation. These FCP interventions are not reserved for rare or exceptional circumstances but are routinely needed in everyday ED operations due to the persistent and dynamic nature of crowding.

The daily prediction model, which estimates the average patient waiting count over the next 24 hours (ie, from 5 PM on the current day to 5 PM the following day), supports broader decision-making processes. By forecasting average daily patient volumes, managers can optimize next-day staffing schedules and implement strategic interventions such as placing the hospital on diversion to temporarily halt nonessential incoming transfers, thereby preserving ED and inpatient capacity for critical cases. These predictions also enhance cross-departmental collaboration by facilitating proactive ICU bed reservations for anticipated ED admissions or diverting nonurgent cases to alternative care settings, such as urgent care clinics, to alleviate ED congestion. Over time, insights from daily predictions inform long-term capacity planning, such as adjusting seasonal budgets for flu surges or expanding ED infrastructure to accommodate growth trends.

The ability to act in advance is supported by the model's predictive accuracy, particularly under extreme crowding scenarios. This is critical because the most impactful decisions—such as activating surge capacity, reallocating staff, or adjusting admissions—are typically required when the ED is under the most pressure. Having reliable forecasts during these peak periods ensures that hospital managers can make timely, confident decisions that reduce overcrowding and maintain the quality of patient care.

The practical implications of this study go beyond forecasting accuracy, offering direct support for real-world hospital operations. By leveraging both internal operational features—such as patient flow metrics, boarding counts, treatment activity, and hospital census—and external contextual features—including weather conditions, federal holidays, and major local events—the models provide actionable insights tailored to each facility's environment. For example, if the 6-hour-ahead model forecasts a surge in ED waiting counts during an upcoming evening shift, hospital managers can proactively deploy surge nurses, call in backup physicians, prepare overflow treatment areas, or expedite inpatient bed turnover hours in advance. In parallel, daily forecasts indicating above-average volumes can be used during morning planning meetings to revise staffing levels, reserve ICU beds, or activate diversion protocols for nonurgent cases. In cases of anticipated extreme crowding, hospitals may also delay elective admissions, accelerate discharge rounds, or mobilize unstaffed bed capacity. Embedding these forecasts into hospital dashboards or integrating them with electronic health record systems enables timely alerts and streamlined workflows. By incorporating both operational and external drivers of demand, the system supports proactive, risk-informed decision-making that improves patient throughput, reduces waiting times, and enhances overall ED efficiency.

Limitations and Future Work

A key limitation of this study is that we did not evaluate how the predictions directly support proactive FCP implementation. While our models can anticipate patient surges, their real-world impact on operational decision-making remains untested. In a future study, we will address this by using discrete event simulation to compare reactive versus proactive FCP strategies, assessing how prediction-driven interventions influence resource allocation, patient flow, and ED performance metrics.

Short-notice staffing adjustments can be challenging in ED settings, and a 6-hour notice may be insufficient for several reasons. Many clinical staff may be unable to respond to requests for additional coverage with such limited advance notice, particularly during nights or weekends. Longer-term forecasting horizons—such as 24-hour, weekly, or monthly predictions—may provide a more practical foundation for surge planning. While many studies have adopted daily or multiday horizons [21,22,26,63,64], the literature does not provide clear evidence about which prediction window is most effective in real-world practice. Given these constraints, future work will

XSL•FO
RenderX

include a systematic evaluation of prediction windows across both short and long horizons to identify the most practical and operationally relevant timeframes for ED staffing.

Refinement of model adaptability and incorporation of more external data sources could further enhance predictive performance and real-world applicability. Another important consideration is the potential for data drift, including both covariate drift [65] and concept drift [66] over time. As clinical workflows, hospital policies, and external conditions evolve, model performance may degrade. To mitigate this risk, future deployments should incorporate drift detection mechanisms and model monitoring systems to ensure consistent forecast accuracy and trigger retraining when necessary.

The proposed system is designed for real-time operation, and a key direction for future work is its pilot deployment in a live clinical environment. This will be accompanied by a simulation-based evaluation to assess how the system integrates into operational workflows and influences decision-making. This study represents one component of a larger project, specifically focusing on the development of a predictive model for one of the PFMs—the waiting count. The broader project includes additional modules to predict other PFMs, such as boarding count and average waiting time, which will collectively support a comprehensive decision-support system for ED operations. Building on this, our future work will extend beyond standard ML workflows by implementing a real-time deployment architecture tailored for hospital operations. The planned deployment pipeline will run within the partner hospital's internal supercomputing infrastructure, ingesting hourly data streams from the ED tracking system, inpatient units, weather application programming interfaces, and event calendars. We will consider technologies such as columnar storage formats (eg, Apache Parquet [67]) and embedded analytical engines (eg, DuckDB [68]) to enable low-latency access to recent data. A containerized preprocessing pipeline using Docker [69] is envisioned to ensure consistent and reproducible real-time data cleaning and feature engineering. Model lifecycle management, including data versioning and experiment tracking, will be managed by tools such as MLflow [70], enabling continuous preprocessing, inference, and updates as new data arrives. Predictions will ultimately feed into a decision support module to provide early warnings for crowding, with results visualized on an internal dashboard to enhance operational planning. Additionally, future efforts will address key implementation steps such as ensuring data privacy, developing user-facing interfaces aligned with clinical workflows, and conducting usability testing. The goal is to build a fully automated infrastructure for continuous monitoring, model retraining, and maintenance, supporting long-term reliability and clinical utility.

Conclusions

The results of this study show that advanced ML approaches are effective in predicting ED waiting counts based on real-world data from our collaborating hospital. By integrating multiple datasets—ED tracking, inpatient data, weather, and significant dates—the research developed hourly and daily prediction models. The hourly model provides real-time, 6-hour-ahead forecasts, enhancing decision-making and resource allocation. The daily models offer insights into patient volumes at daily averages, aiding in operational planning.

A comprehensive evaluation was conducted by testing 11 different ML algorithms on 16 distinct datasets, each generated through careful feature engineering and hyperparameter optimization to explore optimal feature combinations. The results revealed that for the hourly prediction approach (6-hour-ahead prediction), the TSiTPlus algorithm consistently delivered the best performance, with DS15 emerging as the most effective dataset. DS15 incorporated a diverse range of features, including waiting count lags, rolling averages, patient flow indicators, weather conditions, hospital census data, and significant event markers. This combination enabled the model to achieve an MAE of 4.19, MSE of 29.36, RMSE of 5.42, and R^2 of 0.56, outperforming all other datasets. For the daily prediction approach (predicting the next 24-hour average waiting count), the best performance was achieved by the XCMPlus model using DS12, with an MAE of 2.00, MSE of 6.64, RMSE of 2.57, and an R^2 of 0.44. Through the creation and analysis of multiple feature sets, we identified the most effective feature combinations for improving prediction accuracy, demonstrating the critical role of feature engineering in model optimization.

This study also incorporated detailed extreme case and hour-of-the-day analyses to better understand prediction performance under various conditions. Extreme case analysis specifically evaluated how well the model predicts waiting counts during periods of severe overcrowding, defined as values exceeding the mean by 1, 2, or 3 SDs. The hour-of-the-day analysis further highlighted performance variations throughout the day, providing actionable insights into periods of higher prediction uncertainty and variability. This research paper represents one component of a larger decision support system initiative; in the future, hourly and daily prediction models—alongside additional PFMs such as boarding count and treatment count—will be integrated and operated together as part of a comprehensive, real-world decision-support system for ED management. Such a system can improve resource allocation, optimize staffing, and enhance overall operational efficiency. By leveraging the hourly model's real-time forecasts and the daily model's planning insights, ED administrators can make data-driven decisions to better handle patient flow, reduce overcrowding, and ensure timely care delivery.

Acknowledgments

This project was supported by the Agency for Healthcare Research and Quality (AHRQ) under grant number 1R21HS029410-01A1.

XSL•FO
RenderX

Data Availability

The data used in this study were obtained through a formal collaboration with our partner hospital and are subject to strict confidentiality agreements, institutional review board regulations, and institutional data protection policies. Access is limited to authorized personnel for research purposes under the approved ethical framework. As such, we are unable to share the dataset outside the terms of this agreement to ensure compliance with privacy and institutional standards. However, deidentified data may be shared under a data-use agreement upon reasonable request and institutional approval. The source code and model implementation are available in our GitHub repository [71].

Conflicts of Interest

None declared.

Multimedia Appendix 1
Summary of methods covering feature engineering, data integration, model training, and evaluation.
[DOCX File , 35 KB - medinform_v13i1e73960_app1.docx]

Multimedia Appendix 2
Features and their combinations for dataset variants.
[DOCX File , 28 KB - medinform_v13i1e73960_app2.docx]

Multimedia Appendix 3
Distribution of hourly waiting counts with extreme thresholds, hourly mean and standard deviation of ED waiting room counts, model performance by hour, and the design of hourly and daily prediction models.
[DOCX File , 271 KB - medinform_v13i1e73960_app3.docx]

References

1. Moore BJ, Stocks C, Owens PL. Trends in emergency department visits, 2006–2014. HCUP Statistical Brief 2017;227:-20.
2. Cairns C, Ashman JJ, King JM. Emergency department visit rates by selected characteristics: United States, 2021. NCHS Data Brief 2023(478):1-8 [FREE Full text] [Medline: 37642973]
3. Rui P, Kang K. National Hospital Ambulatory Medical Care Survey: 2017 Emergency Department Summary Tables. Hyattsville, MD: National Center for Health Statistics; 2017.
4. Ashour OM, Okudan Kremer GE. Dynamic patient grouping and prioritization: a new approach to emergency department flow improvement. Health Care Manag Sci 2016;19(2):192-205. [doi: 10.1007/s10729-014-9311-1] [Medline: 25487711]
5. Chonde SJ, Ashour OM, Nembhard DA, Kremer GEO. Model comparison in emergency severity index level prediction. Expert Syst Appl 2013;40(17):6901-6909. [doi: 10.1016/j.eswa.2013.06.026]
6. Harrou F, Dairi A, Kadri F, Sun Y. Forecasting emergency department overcrowding: a deep learning framework. Chaos Solitons Fractals 2020;139:110247 [FREE Full text] [doi: 10.1016/j.chaos.2020.110247] [Medline: 32982079]
7. Cowan RM, Trzeciak S. Clinical review: emergency department overcrowding and the potential impact on the critically ill. Crit Care 2005;9(3):291-295 [FREE Full text] [doi: 10.1186/cc2981] [Medline: 15987383]
8. Emergency Department Crowding: High Impact Solutions. Irving, TX: Emergency Medicine Practice Committee; 2016.
9. Huang Y, Ortiz SS, Rowe BH, Rosychuk RJ. Emergency department crowding negatively influences outcomes for adults presenting with Asthma: a population-based retrospective cohort study. BMC Emerg Med 2022;22(1):209 [FREE Full text] [doi: 10.1186/s12873-022-00766-7] [Medline: 36566194]
10. Salway RJ, Valenzuela R, Shoenberger JM, Mallon WK, Viccellio A. Emergency department (Ed) overcrowding: evidence-based answers to frequently asked questions. Revista Médica Clínica Las Condes 2017;28(2):213-219. [doi: 10.1016/j.rmclc.2017.04.008]
11. Pines JM, Hollander JE. Emergency department crowding is associated with poor care for patients with severe pain. Ann Emerg Med 2008;51(1):1-5. [doi: 10.1016/j.annemergmed.2007.07.008] [Medline: 17913299]
12. Pines JM. Emergency department crowding in California: a silent killer? Ann Emerg Med 2013;61(6):612-614. [doi: 10.1016/j.annemergmed.2012.12.016] [Medline: 23374418]
13. Sprivulis PC, Da Silva J, Jacobs IG, Frazer ARL, Jelinek GA. The association between hospital overcrowding and mortality among patients admitted via western Australian emergency departments. Med J Aust 2006;184(5):208-212. [doi: 10.5694/j.1326-5377.2006.tb00416.x] [Medline: 16515429]
14. Alishahi Tabriz A, Birken SA, Shea CM, Fried BJ, Viccellio P. What is full capacity protocol, and how is it implemented successfully? Implement Sci 2019;14(1):73 [FREE Full text] [doi: 10.1186/s13012-019-0925-z] [Medline: 31319857]
15. Villa-Roel C, Guo X, Holroyd BR, Innes G, Wong L, Ospina M, et al. The role of full capacity protocols on mitigating overcrowding in EDs. Am J Emerg Med 2012;30(3):412-420. [doi: 10.1016/j.ajem.2010.12.035] [Medline: 21367554]

XSL•FO
RenderX

16. Ahmed A, Ashour O, Ali H, Firouz M. An integrated optimization and machine learning approach to predict the admission status of emergency patients. Expert Syst Appl 2022;202:117314. [doi: 10.1016/j.eswa.2022.117314]
17. Parker CA, Liu N, Wu SX, Shen Y, Lam SSW, Ong MEH. Predicting hospital admission at the emergency department triage: a novel prediction model. Am J Emerg Med 2019;37(8):1498-1504. [doi: 10.1016/j.ajem.2018.10.060] [Medline: 30413365]
18. Sun Y, Heng B, Tay SY, Seow E. Predicting hospital admissions at emergency department triage using routine administrative data. Acad Emerg Med 2011;18(8):844-850 [FREE Full text] [doi: 10.1111/j.1553-2712.2011.01125.x] [Medline: 21843220]
19. Schweigler LM, Desmond JS, McCarthy ML, Bukowski KJ, Ionides EL, Younger JG. Forecasting models of emergency department crowding. Acad Emerg Med 2009;16(4):301-308 [FREE Full text] [doi: 10.1111/j.1553-2712.2009.00356.x] [Medline: 19210488]
20. Kadri F, Harrou F, Chaabane S, Tahon C. Time series modelling and forecasting of emergency department overcrowding. J Med Syst 2014;38(9):107. [doi: 10.1007/s10916-014-0107-0] [Medline: 25053208]
21. Porto BM, Fogliatto FS. Enhanced forecasting of emergency department patient arrivals using feature engineering approach and machine learning. BMC Med Inform Decis Mak 2024;24(1):377 [FREE Full text] [doi: 10.1186/s12911-024-02788-6] [Medline: 39696224]
22. Ming C, Lee GJ, Teo YN, Teo YH, Zhou X, Ho ES, et al. Deep learning modelling to forecast emergency department visits using calendar, meteorological, internet search data and stock market price. Comput Methods Programs Biomed 2025;267:108808. [doi: 10.1016/j.cmpb.2025.108808] [Medline: 40315688]
23. Asheim A, Bache-Wiig Bjørnsen LP, Næss-Pleym LE, Uleberg O, Dale J, Nilsen SM. Real-time forecasting of emergency department arrivals using prehospital data. BMC Emerg Med 2019;19(1):42 [FREE Full text] [doi: 10.1186/s12873-019-0256-z] [Medline: 31382882]
24. Kuo YH, Chan NB, Leung JMY, Meng H, So AMC, Tsoi KKF, et al. An integrated approach of machine learning and systems thinking for waiting time prediction in an emergency department. Int J Med Inform 2020;139:104143. [doi: 10.1016/j.ijmedinf.2020.104143] [Medline: 32330853]
25. Benevento E, Aloini D, Squicciarini N. Towards a real-time prediction of waiting times in emergency departments: a comparative analysis of machine learning techniques. Int J Forecast 2023;39(1):192-208. [doi: 10.1016/j.ijforecast.2021.10.006]
26. Tuominen J, Pulkkinen E, Peltonen J, Kanniainen J, Oksala N, Palomäki A, et al. Forecasting emergency department occupancy with advanced machine learning models and multivariable input. Int J Forecast 2024;40(4):1410-1420. [doi: 10.1016/j.ijforecast.2023.12.002]
27. Salinas D, Flunkert V, Gasthaus J, Januschowski T. DeepAR: probabilistic forecasting with autoregressive recurrent networks. Int J Forecast 2020 Jul;36(3):1181-1191. [doi: 10.1016/j.ijforecast.2019.07.001]
28. Oreshkin BN, Carpov D, Chapados N, Bengio Y. N-BEATS: neural basis expansion analysis for interpretable time series forecasting. arXiv preprint 2019. [doi: 10.48550/arXiv.1905.10437]
29. Ke G, Meng Q, Finley T, Wang T, Chen W, Ma W, et al. LightGBM: a highly efficient gradient boosting decision tree. 2017 Presented at: Proceedings of the 31st International Conference on Neural Information Processing Systems; December 2017; Long Beach, CA, USA p. 3149-3157.
30. Giunta DH, Thomas DS, Bustamante L, Ratti MFG, Martinez BJ. Development and validation of a multivariable predictive model for emergency department overcrowding based on the national emergency department overcrowding study (NEDOCS) score. Intern Emerg Med 2024:03848-5. [doi: 10.1007/s11739-024-03848-5] [Medline: 39739295]
31. Breiman L. Random forests. Mach Learn 2001;45(1):5-32. [doi: 10.1023/a:1010933404324]
32. Chen T, He T, Benesty M, Khotilovich V, Tang Y, Cho H. Xgboost: extreme gradient boosting. R Package Version 04-2. 2015. URL: https://cran.r-project.org/web/packages/xgboost/index.html [accessed 2025-08-12]
33. Hochreiter S, Schmidhuber J. Long short-term memory. Neural Comput 1997;9(8):1735-1780. [doi: 10.1162/neco.1997.9.8.1735] [Medline: 9377276]
34. Schuster M, Paliwal K. Bidirectional recurrent neural networks. IEEE Trans Signal Process 1997;45(11):2673-2681. [doi: 10.1109/78.650093]
35. Sutskever I, Vinyals O, Le QV. Sequence to sequence learning with neural networks. Adv Neural Inf Process Syst 2014:27.
36. Oguiza I. FCNPlus. Github. 2023. URL: https://timeseriesai.github.io/tsai/models.fcnplus.html [accessed 2025-08-09]
37. Oguiza I. ResNetPlus. Github. 2023. URL: https://timeseriesai.github.io/tsai/models.resnetplus.html [accessed 2025-08-09]
38. Oguiza I. XceptionTimePlus. Githu. 2023. URL: https://timeseriesai.github.io/tsai/models.xceptiontimeplus.html [accessed 2025-08-09]
39. Oguiza I. XCMPlus. Github. 2023. URL: https://timeseriesai.github.io/tsai/models.xcmplus.html [accessed 2025-08-09]
40. Oguiza I. TSTPlus. Github. 2023. URL: https://timeseriesai.github.io/tsai/models.tstplus.html [accessed 2025-08-09]
41. Oguiza I. TSiT. Github. 2023. URL: https://timeseriesai.github.io/tsai/models.tsitplus.html [accessed 2025-08-09]
42. MinMaxScaler. Python Scikit Learn. URL: https://scikit-learn.org/stable/modules/generated/sklearn.preprocessing.MinMaxScaler.html [accessed 2025-08-09]
43. Oguiza I. Tsai - a state-of-the-art deep learning library for time series and sequential data. Github. 2023. URL: https://github.com/timeseriesAI/tsai [accessed 2025-08-09]

XSL•FO
RenderX

44. Paszke A, Gross S, Massa F, Lerer A, Bradbury J, Chanan G, et al. Pytorch: an imperative style, high-performance deep learning library. Adv Neural Inf Process Syst 2019;32. [doi: 10.7551/mitpress/11474.003.0014]
45. Howard J, Gugger S. Fastai: a layered API for deep learning. Information 2020;11(2):108. [doi: 10.3390/info11020108]
46. A superpower for ML developers. Keras. 2015. URL: https://keras.io/ [accessed 2025-08-09]
47. Long J, Shelhamer E, Darrell T. Fully convolutional networks for semantic segmentation. 2015 Presented at: Proceedings of the IEEE Conference on Computer Vision and Pattern Recognition; 2022 June 22; Seattle, WA, USA. [doi: 10.1109/cvpr.2015.7298965]
48. Wang Z, Yan W, Oates T. Time series classification from scratch with deep neural networks: a strong baseline. 2017 Presented at: 2017 International Joint Conference on Neural Networks (IJCNN); 2017 May 14 - 19; Anchorage, AK, USA. [doi: 10.1109/ijcnn.2017.7966039]
49. He K, Zhang X, Ren S, Sun J. Deep residual learning for image recognition. 2016 Presented at: Proceedings of the IEEE Conference on Computer Vision and Pattern Recognition; 2016 June 27-30; Las Vegas, NV, USA. [doi: 10.1109/cvpr.2016.90]
50. Chollet F. Xception: Deep learning with depthwise separable convolutions. 2017 Presented at: Proceedings of the IEEE Conference on Computer Vision and Pattern Recognition; 2017 July 21-26; Honolulu, HI, USA. [doi: 10.1109/cvpr.2017.195]
51. Fauvel K, Lin T, Masson V, Fromont ?, Termier A. XCM: an explainable convolutional neural network for multivariate time series classification. Mathematics 2021;9(23):3137. [doi: 10.3390/math9233137]
52. Zerveas G, Jayaraman S, Patel D, Bhamidipaty A, Eickhoff C. A transformer-based framework for multivariate time series representation learning. 2021 Presented at: Proceedings of the 27th ACM SIGKDD Conference on Knowledge Discovery & Data mining; 2021 August 14-18; New York, NY, United States. [doi: 10.1145/3447548.3467401]
53. Dosovitskiy A, Beyer L, Kolesnikov A, Weissenborn D, Zhai X, Unterthiner T, et al. An image is worth 16x16 words: transformers for image recognition at scale. arXiv preprint arXiv:201011929 2020. [doi: 10.48550/arXiv.2010.11929]
54. Vaswani A, Shazeer N, Parmar N, Uszkoreit J, Jones L, Gomez AN. Attention is all you need. Adv Neural Inf Process Syst 2017;30. [doi: 10.5860/choice.189890]
55. StandardScaler. Scikit-learn. URL: https://scikit-learn.org/stable/modules/generated/sklearn.preprocessing.StandardScaler.html [accessed 2025-08-29]
56. Pedregosa F, Varoquaux G, Gramfort A, Michel V, Thirion B, Grisel O. Scikit-learn: machine learning in python. J Mach Learn Res 2011;12:2825-2830 [FREE Full text] [doi: 10.5555/1953048.2078195]
57. History bulk. OpenWeatherMap. URL: https://openweathermap.org/history#historybulk [accessed 2025-08-09]
58. Federal Holidays. Government USOoPM. URL: https://www.opm.gov/policy-data-oversight/pay-leave/federal-holidays/ [accessed 2025-08-09]
59. Football schedule. Rolltide. URL: https://rolltide.com/sports/football [accessed 2025-08-09]
60. Bottou L. Large-scale machine learning with stochastic gradient descent. : Springer; 2010 Presented at: Proceedings of COMPSTAT'2010: 19th International Conference on Computational Statistics; 2010 August 22-27; Paris France p. 22-27. [doi: 10.1007/978-3-7908-2604-3]
61. Tibshirani RJ, Efron B. An introduction to the bootstrap. Monogr Stat Appl Probab 1993;57(1):1-436. [doi: 10.1007/978-1-4899-4541-9_1]
62. Akbasli IT, Birbilen AZ, Teksam O. Artificial intelligence-driven forecasting and shift optimization for pediatric emergency department crowding. JAMIA Open 2025;8(2):ooae138. [doi: 10.1093/jamiaopen/ooae138] [Medline: 40124532]
63. Zhang Y, Zhang J, Tao M, Shu J, Zhu D. Forecasting patient arrivals at emergency department using calendar and meteorological information. Appl Intell (Dordr) 2022;52(10):11232-11243 [FREE Full text] [doi: 10.1007/s10489-021-03085-9] [Medline: 35079202]
64. Rostami-Tabar B, Browell J, Svetunkov I. Probabilistic forecasting of hourly emergency department arrivals. Health Syst (Basingstoke) 2024;13(2):133-149 [FREE Full text] [doi: 10.1080/20476965.2023.2200526] [Medline: 38800601]
65. Shimodaira H. Improving predictive inference under covariate shift by weighting the log-likelihood function. J Stat Plan Inference 2000;90(2):227-244. [doi: 10.1016/s0378-3758(00)00115-4]
66. Widmer G, Kubat M. Learning in the presence of concept drift and hidden contexts. Mach Learn 1996;23(1):69-101. [doi: 10.1023/a:1018046501280]
67. Vohra D. Practical hadoop ecosystem. In: Apache Parquet. Berkeley, CA: Apress; 2016:325-335.
68. Raasveldt M, Mühleisen H. Duckdb: an embeddable analytical database. 2019 Presented at: Proceedings of the 2019 International Conference on Management of Data; 2019 July 05; Amsterdam, The Netherlands. [doi: 10.1145/3299869.3320212]
69. Merkel D. Docker: lightweight linux containers for consistent development and deployment. Linux J 2014;239(2):2.
70. Zaharia M, Chen A, Davidson A, Ghodsi A, Hong S, Konwinski A, et al. Accelerating the machine learning lifecycle with MLflow. IEEE Data Eng Bull 2018;41(4):39-45.
71. Vural O. ED overcrowding predictions. GitHub. URL: https://github.com/drorhunvural/ED_OverCrowding_Predictions [accessed 2025-08-29]

XSL•FO
RenderX

Abbreviations

ARIMA: autoregressive integrated moving average
BiLSTM: bidirectional long short-term memory
CNN: convolutional neural network
ED: emergency department
ESI: Emergency Severity Index
FCNPlus: fully convolutional network plus
FCP: full capacity protocol
ICU: intensive care unit
IRB: Institutional Review Board
LSTM: long short-term memory
MAE: mean absolute error
ML: machine learning
MSE: mean squared error
N-BEATS: neural basis expansion analysis for interpretable time series forecasting
PFCT: patient flow coordination team
PFM: patient flow measure
ResNetPlus: residual network plus
RF: random forest
RMSE: root mean squared error
RNN: recurrent neural network
Seq2Seq: sequence to sequence learning with neural networks
TSiTPlus: time series vision transformer plus
TSTPlus: time series transformer plus
XCMPlus: explainable convolutional neural network plus
XGBoost: extreme gradient boosting

Edited by A Benis; submitted 14.03.25; peer-reviewed by M Saban, T Abd El-Hafeez, IT Akbasli; comments to author 28.05.25; revised version received 18.06.25; accepted 04.08.25; published 17.09.25.

Please cite as:
Vural O, Ozaydin B, Aram KY, Booth J, Lindsey BF, Ahmed A
An Artificial Intelligence–Based Framework for Predicting Emergency Department Overcrowding: Development and Evaluation Study
JMIR Med Inform 2025;13:e73960
URL: https://medinform.jmir.org/2025/1/e73960
doi:10.2196/73960
PMID:

©Orhun Vural, Bunyamin Ozaydin, Khalid Y Aram, James Booth, Brittany Freeman Lindsey, Abdulaziz Ahmed. Originally published in JMIR Medical Informatics (https://medinform.jmir.org), 17.09.2025. This is an open-access article distributed under the terms of the Creative Commons Attribution License (https://creativecommons.org/licenses/by/4.0/), which permits unrestricted use, distribution, and reproduction in any medium, provided the original work, first published in JMIR Medical Informatics, is properly cited. The complete bibliographic information, a link to the original publication on https://medinform.jmir.org/, as well as this copyright and license information must be included.

XSL•FO
RenderX

Original Paper

Synthetic Tabular Data Generation Under Horizontal Federated Learning Environments in Acute Myeloid Leukemia: Case-Based Simulation Study

Imanol Isasa[1,2], MSc; Mikel Catalina[1], MSc; Gorka Epelde[1,3], PhD; Naiara Aginako[2], PhD; Andoni Beristain[1,2,3], PhD

[1]Digital Health & Biomedical Technologies Department, Vicomtech Foundation (BRTA), Donostia-San Sebastián, Spain

[2]Computer Science and Artificial Intelligence Department, University of the Basque Country UPV/EHU, Donostia-San Sebastián, Spain

[3]eHealth Group, Biogipuzkoa Health Research Institute, Donostia-San Sebastián, Spain

Corresponding Author:
Imanol Isasa, MSc
Digital Health & Biomedical Technologies Department
Vicomtech Foundation (BRTA)
Mikeletegi Pasealekua 57
Donostia-San Sebastián, 20009
Spain
Phone: 34 943309230
Fax: 34 943309393
Email: iisasa@vicomtech.org

Abstract

Background: Data scarcity and dispersion pose significant obstacles in biomedical research, particularly when addressing rare diseases. In such scenarios, synthetic data generation (SDG) has emerged as a promising path to mitigate the first issue. Concurrently, federated learning is a machine learning paradigm where multiple nodes collaborate to create a centralized model with knowledge that is distilled from the data in different nodes, but without the need for sharing it. This research explores the combination of SDG and federated learning technologies in the context of acute myeloid leukemia, a rare hematological disorder, evaluating their combined impact and the quality of the generated artificial datasets.

Objective: This study aims to evaluate the privacy- and fidelity-related impact of horizontally federating SDG models in different data distribution scenarios and with different numbers of nodes, comparing them with centralized baseline SDG models.

Methods: Two state-of-the-art generative models, conditional tabular generative adversarial network and FedTabDiff, were trained considering four different scenarios: (1) a nonfederated baseline with all the data available, (2) a federated scenario where the data were evenly distributed among different nodes, (3) a federated scenario where the data were unevenly and randomly distributed (imbalanced data), and (4) a federated scenario with nonindependent and identically distributed data distributions. For each of the federated scenarios, a fixed set of node quantities (3, 5, 7, 10) was considered to assess its impact, and the generated data were evaluated, attending to a fidelity-privacy trade-off.

Results: The computed fidelity metrics exhibited statistically significant deteriorations (P<.001) up to 21% in the conditional tabular generative adversarial network and up to 62% in the FedTabDiff model due to the federation process. When comparing federated experiments trained with diverse numbers of nodes, no strong tendencies were observed, even if specific comparisons resulted in significative differences. Privacy metrics were mainly maintained while obtaining maximum improvements of 55% and maximum deteriorations of 26% between both models, although they were not statistically significant.

Conclusions: Within the scope of the use case scenario in this paper, the act of horizontally federating SDG algorithms results in a loss of data fidelity compared to the nonfederated baseline while maintaining privacy levels. However, this deterioration does not significantly increase as the number of nodes used to train the models grows, even though significative differences were found in specific comparisons. The different data partition distribution configurations had no significant effect on the metrics, as similar tendencies were found for all scenarios.

(JMIR Med Inform 2025;13:e74116) doi:10.2196/74116

XSL•FO
RenderX

KEYWORDS

rare diseases; privacy; machine learning; federated learning; synthetic data generation; leukemia; data fidelity; trade-off

Introduction

Overview

Acute myeloid leukemia (AML) is a group of bone marrow stem cell cancers that causes an extreme proliferation of clonal hematopoietic cells. This abnormal growth is caused by multiple cytogenetic and genetic malformations, resulting in a poorly differentiated myeloid cell accumulation in the bone marrow and the consequent spread to the blood [1].

Despite the latest scientific advances and at least 10 recently approved therapies, it is still causing 250,000 deaths yearly worldwide [2]. Moreover, even if AML accounts for about 80% of all diagnosed leukemias in adults, there are just 4.2 new cases per 100,000 people in the United States yearly, which makes it classifiable as a rare hematological disease [3]. On top of that, the proportion of AML cases among all the diagnosed leukemias worldwide increased from 18% in 1990 to 23.1% in 2017, augmenting their incidence and suggesting a potential upcoming major global public health concern [4].

According to the World Health Organization (WHO), AML can be classified into several categories: those that are derived from (1) genetic abnormalities, (2) myelodysplasia-related changes, those that are related to (3) previous chemotherapy or radiation therapies, (4) myeloid sarcomas, (5) myeloid proliferations related to Down syndrome, (6) undifferentiated and biphenotypic leukemias, and those that (7) are not otherwise specified [5,6]. In them, symptoms include bleeding, bruising, infections, fatigue, and bone pain.

The rarity of AML as a prevalent form of leukemia brings with it inherent limitations with regard to the data exploitation and consequent improvement in terms of artificial intelligence (AI) models and their application in real-world environments. First, the necessity of data is leading to the emergence of various repositories that encompass information of the disease [7], but it is important to highlight that these are often limited in size [8,9], revealing an underlying problem of data scarcity. Besides, the data protection legislation, such as the General Data Protection Regulation in Europe or the Health Insurance Portability and Accountability Act in the United States, adds a layer of complexity to the process of data sharing due to the sensitive nature of health data, as it typically consists of electronic health records (EHRs) that may contain extensive clinical or even genomic data. As a consequence, even if AML data records exist, they are unevenly distributed across different institutions, hindering any intention to make use of large amounts of data. This uneven distribution not only refers to the amount of data points available in each data silo but also to biases in them, such as racial and ethnic disparities in AML prevalence statistics [10], especially in pediatric patients [11]. This makes it even more difficult to access quality data that can be used to infer knowledge using AI.

Synthetic data (SD) is defined as artificial information that is generated from original data and a model that is trained to reproduce its characteristics and structure [12]. Thus, SD generation (SDG) is a widely used tool for creating data that mimics real-world datasets, which has been found to be helpful for augmentation tasks, as a class balancing tool, and as a privacy-enhancing technology [13]. Therefore, SD is often evaluated in terms of its fidelity with respect to the real data, its utility for downstream applications, and the privacy that it offers, the last one being one of the main topics of research in literature. In light of the current situation regarding the AML use case, SD can be considered a suitable approach for improving the current paradigm by increasing the quantity of data institution-wise. However, while SD aims to replicate real-world distributions by capturing the same range and structure as the input data, its primary focus is on addressing data scarcity rather than mitigating the problem of scattering. In this regard, SDG would be able to learn based on the local distributions and attending to the data variability found within an institution, possibly limiting the learning process and not being able to sufficiently represent a global population [14].

To mitigate the challenges related to data fragmentation and governance in distributed environments, federated learning (FL) offers a decentralized machine learning (ML) framework that enables collaborative model training across multiple institutions, ensuring that raw patient data remains local and is never transferred or shared externally. [15]. In a canonical FL environment, a model is trained in a central server using the weights each client shares after training local models on local real data [16]. Even if that local real data does not leave the node, the learned information is shared, and a global model is created, covering all the local distributions among the federated nodes and better adapting to a theoretical global distribution. That said, the type of data distributions found within a federated network directly impacts models' behaviors, affecting communication efficiency, model convergence, and FL accuracy. Nonindependent and identically distributed (non-IID) data are currently being widely explored, as they may pose performance and privacy-related difficulties in FL contexts [17,18]. When data are distributed such that clients share the same feature space but contain distinct sets of records, the FL setting is referred to as horizontal federated learning (HFL). Conversely, when clients hold different feature subsets corresponding to the same set of records, the setting is known as vertical FL. The results presented in this work belong to HFL and may not generalize to other FL settings, like vertical FL. Hereafter, the term FL will be used analogously to HFL for the sake of clarity.

However, the adoption of technologies that combine both elements and the posterior validation of those should go hand in hand with thorough prior analyses. To do that, the contributions of this paper are:

- An evaluation of the impact of federating SDG algorithms with respect to having a model trained on all data available on the same site (centralized).

XSL•FO
RenderX

- An evaluation of the impact of the number of federated nodes on the performance of SDG models.
- An evaluation of the impact of having a randomly sampled imbalanced quantity of data in each federated node.
- An evaluation of the impact of having an imbalanced quantity of data that constitutes non-IID distributions in each federated node.

The remainder of this paper is organized as follows: the Methods section provides information about the materials used and the methodology, describing the dataset that was used, the generative model, the evaluation metrics that were implemented, and the FL setup. The next section presents the Results, while the Discussion section shows the principal results, the limitations of this work, a comparison with prior existing work, and final conclusions.

Background

Over the last few years, the use of SD has gained momentum in several contexts. In health care, simulations and prediction research, educational and training content creation, and investigation, including the release of data, have benefited from SD use [19]. In this sense, SDG must be understood as a spectrum of possibilities regarding model selection, parameter tuning, and use case-specific contextualization. However, generating data inevitably involves sophisticated techniques, which may include generative adversarial networks (GANs), variational autoencoders (VAEs), or diffusion models, among other AI approaches.

One of the most promising uses of SD, as was mentioned previously, is the generation of artificial information that does not compromise patient privacy while maintaining its fidelity to the original counterpart. Therefore, the assessment and analyses of SD are expanding to such an extent that the expectations are surpassing those of traditional anonymization techniques, which are algorithms that typically reduce the quality of the data in terms of fidelity and utility, even attempting to combine them. In this sense, it is important to mention differential privacy (DP), which is a technique that ensures the privacy of individuals by adding random noise to the data, making it nearly impossible to determine whether any individual's data is included in a dataset or not. DP is the most widely used privacy-enhancing technology that is being implemented in generative models to enhance data privacy, and its implementation in them depends on the intended use for the resulting SD [20-22], aligning it with the fidelity of the data. Privacy preservation of real data trades directly off with the fidelity and the utility of the generated SD, which must be maintained to ensure its suitability for downstream applications.

Regarding AI models, a GAN is composed of two networks, a generator and a discriminator, working in an adversarial manner. While the former one is supposed to minimize the loss function by generating samples that are as similar as possible to the training set, the latter is tasked with differentiating original samples from synthetic ones, trying to maximize the loss. GANs were first presented by Goodfellow et al [23] in 2014, and since then, several modifications have been proposed in order to cover a wide range of use cases. The work developed by Zhao et al [24], for example, represents the latest generation of GAN architectures, named CTAB-GAN+, which includes state-of-the-art features such as conditional generation of samples, improved loss functions, the possibility to handle both categorical and continuous data simultaneously, and DP. Narrowing down to tabular data generation for health care–related use cases, GANs were identified to be the most widely used architectures [25]. Additionally, several recent publications have addressed various unresolved questions within the field. For instance, Ramachandranpillai et al [26] introduced the bias-transforming GAN, which addresses the challenge of biased data generation in the health care domain by incorporating several information constraints inside the generation process. Moreover, various GANs are currently being experimentally tested for several use cases, as demonstrated by Akiya et al [27] in oncological clinical trials, Khan et al [28] in cardiovascular disease mortality predictions, or Dhawan and Nijhawan [29] in brain magnetic resonance imaging and chest x-ray data.

As for VAEs in the context of SDG, they are also composed of two fundamental components: the encoder and the decoder. In this context, the encoder is responsible for mapping the input training data into a latent space with a lower dimensionality, while the decoder samples new values from this latent space to reconstruct data that imitates the original inputs. Starting from the original architecture, VAEs have also undergone several modifications that help cover diverse use cases [30]. As for the latest research, Biswas and Talukdar [31] researched the enhancement of clinical documentation using both GAN and VAE-generated SD with the aim of improving patient care. Li et al [32] implemented the causal recurrent VAE, aiming to generate medical time series data. Other applications that are being investigated and include VAEs are drug dosing determinants, such as in Titar and Ramanathan [33].

Finally, diffusion models create SD by gradually transforming simple, noise-like data into complex data structures that were used during the training process. Even if this type of generative model has mostly been focused on image generation, currently, they are able to support different data types, too [34,35]. For example, Naseer et al [36] presented ScoEHR, a continuous-time diffusion model able to generate artificial EHRs. Digital pathology data was also generated with diffusion models by Pozzi et al [37].

As for generative modeling applied to rare hematological diseases, recently, D'Amico et al [38] trained a conditional tabular generative adversarial network (CTGAN) with the aim of generating myelodysplastic syndromes and AML data. Additionally, Eckardt et al [39] made their synthetic AML dataset publicly available after having considered both utility and privacy thresholds. The published synthetic dataset comprises 1606 patients generated using a CTAB-GAN+ [24]. Licandro et al [40] used a Wasserstein GAN for two distinct scenarios where differently sized datasets were used. In their research, the primary objective was to discern the embeddings of the data, enabling subsequent differentiation between blast and nonblast cells. The results show that using the generator model to learn embeddings outperforms the results obtained with baseline models, improving the area under the curve (AUC) for both dataset sizes. The study carried out by Rupapara et al

XSL•FO
RenderX

[41] made use of the ADASYN [42] SD generator to balance the dataset and enhance prediction outcomes. The dataset encompassed data from various blood-related cancers, including AML. By using the ADASYN resampler, the classification models demonstrated improved accuracy.

Regarding FL-related studies, several experiments have been conducted to overcome the data scattering issue. For example, the study carried out by Linardos et al [43] simulates a federated environment consisting of four nodes. The study aimed to help diagnose hypertrophic cardiomyopathy diseases, the results supporting the effectiveness of FL by achieving better AUC results than with a collaborative data-sharing framework. The work presented by Liu et al [44] focused on using FL to achieve a deep learning model that makes use of EHRs to predict patient mortality, which they called FADL. The work presented by Azizi et al [45] also used EHR information scattered among 50 nodes, each of which contained 560 patients, to predict mortality. However, in this case, they used a clustering method and used community-based FL, surpassing the performance of the canonical FL environment across various scenarios.

Both techniques, SDG and FL, have demonstrated their effectiveness in various sectors and use cases. The combination of both is being investigated to such an extent that inherently federated generative models are being published in the literature, such as the private FL-GAN model [46]. Focusing on health care–related topics, in Azizi et al [45], a framework for cardiovascular data based on an FL architecture of two nodes and a generative model using sequential trees is shown. The study presented by Behera et al [47] demonstrates the implementation of a GAN within a federated environment, called FedSyn. In addition to applying DP, thereby enhancing data protection, the researchers used the CIFAR10 and Modified National Institute of Standards and Technology datasets for their analyses. The research outlined by Xin et al [48] uses a federated GAN augmented with DP, trained on both Modified National Institute of Standards and Technology and CelebA datasets. The authors analyzed the privacy of the generated data offered against the original one, concluding an improved privacy against membership inference attacks (MIA). However, despite the combination of both SDG and FL explored in different studies, many aspects of this mixture still require evaluation.

Methods

AML Dataset

The AML dataset used to perform the research of this paper was accessed from the work developed by Tazi et al [49] and its associated GitHub repository [50].

Among the available datasets in the repository, the paper_full_data_validation dataset was chosen for this research. All the genetic mutation-related variables were discarded, preserving clinical, demographic, and disease-related information. Multimedia Appendix 1 includes a description of the variables used in the experiments. The variable selection was carried out to maintain acceptable sample-to-feature ratios across various federated configurations regarding node quantities, as the original dataset comprised 130 features. Having a low number of samples and too many variables would have limited the experiments in this regard, as highly overfitted models would appear. The resulting dataset consisted of 1540 samples and 12 features, from which the categorical ones were label encoded in the preprocessing stage. All these preprocessing steps were applied before the data were split into different client nodes for the sake of simplicity. Applying these specific preprocessing steps to our federated experiments would entail just an additional preliminary step in the training process, which was omitted by manually preprocessing the data.

Ethical Considerations

That study was conducted following the completion of informed consent forms by all the included participants. In addition, all the relevant ethical guidelines were followed, and necessary Institutional Review Board and ethics committee approvals were obtained. The trial was conducted in accordance with the tenets of the Helsinki Declaration, and it was sponsored by Cardiff University and approved by the Wales research ethics committee (protocol 08/MRE09/29). The analysis of the data in the original study was approved by the Memorial Sloan Kettering Cancer Center Institutional Review Board (protocol x20-064). All the raw data were deposited in the European Genome Phenome Archive (reference EGAS00001000570). In this paper, all the information that allows the identification of any of the participants was omitted in accordance with privacy and confidentiality standards. The authors in Tazi et al [49] and Tazi [50], who performed the original analysis on the data, do not bear any responsibility for the further research reported in this work.

Generative Models

The first generative model that was selected for this experiment is the CTGAN [51], as it was recently reported to have one of the most appropriate generators among different GAN and VAE architectures [52]. Additionally, it is implemented in a way that models the relationships between imbalanced variable distributions [53]. The Synthetic Data Vault [54] CTGAN implementation was used in this work, even if some modifications had to be implemented for the correct use of the model in a federated environment.

Regarding the model parameters used on the CTGAN, the default parameters presented in the Synthetic Data Vault (v0.18.0) implementation were used. The same architecture was set for both the discriminator and the generator with a two-layer hidden structure, both containing 256 units each. The learning rates of both objects were set to 2×10^{-4}, with the decay fixed to 1×10^{-6}. A batch size of 500 samples was defined along with an embedding dimension of 128 samples. The discriminator was updated along with the generator at every training step, and a 10-sample group (pac parameter) was introduced into the discriminator each time it was applied.

On the other hand, a diffusion model was also included. Diffusion models [55] are a newer class of generative models that have demonstrated superior performance compared to other tabular generative models [56,57]. The implementation used in this work is the one presented by Sattarov et al [58], where the

XSL•FO
RenderX

authors claim high fidelity and privacy metrics were obtained in their experiments.

As for the FedTabDiff model parameters, default values were also chosen. Specifically, the number of diffusion steps was set to 500, and the multilayer perceptron layers were configured as {512,512}. To ensure comparability across models, a consistent batch size of 500 was used, and the learning rate for the deep learning models was fixed to 1×10^{-4}, with a linear scheduler. Additionally, the diffusion beta start was set to 1×10^{-4}, and the beta end was set to 0.02. It is worth mentioning that the model was slightly modified in order for it to interact multiple times with similar data, with the idea of the results being comparable among experiments.

As mentioned previously, in order for each participant node to transform the data in the same manner and to avoid averaging mismatches, one-hot encoding for discrete columns and Gaussian mixture transformations for continuous variables were fit using the whole dataset, also being able to avoid unseen classes in federated nodes. The objects were then included in each client with the aim of transforming each data partition in situ and using the same mapping.

Regarding the number of epochs to be performed during the training process of the models, different experiments were empirically conducted on the baseline model with 500, 1000, 1500, 2000, and 3000 epochs. The optimal configuration was proven to be 500 epochs, as increasing the iterations did not show any significant improvement in the generated synthetic sample quality. All the federated models were trained for 500 epochs for the experiments to be comparable. In addition, the number of federation rounds was set to 500.

Evaluation Metrics

The generated SD was analyzed to gauge its fidelity and privacy with respect to the real data. In the scope of this work, fidelity is defined as the degree to which the generated SD replicates the characteristics, patterns, correlations, and distributions of the real data. While a high fidelity means the SD resembles the real data well, a low fidelity would indicate poor learning by the model generators. On the other hand, privacy is defined as the extent to which the generated data protects sensitive information from being disclosed in the original dataset. In this section, the methods and metrics to evaluate the SD are described.

Considering a simulated FL scenario, the comparison was performed against the whole real data, thus being able to compare the performance of each setup against the nonfederated scenario as a baseline. Inspired by usual ML cross-validation, 10 different synthetic datasets were generated with each model, allowing a separate evaluation for each of them. The results were then averaged to provide a more robust perspective on their generalizability. The set of metrics calculated in each fold also enabled the execution of statistical tests for significance.

In order to assess intervariable correlations, the φ_k coefficient [59] and the Vendi Score (VS) [60] metrics were implemented. On the one hand, the φ_k coefficient is based on the refinement of Pearson hypothesis tests. However, unlike Pearson hypothesis, φ_k can calculate correlations with both numerical and categorical variables, the higher the values, suggesting better intervariable relations. Moreover, φ_k can capture nonlinear relationships. Correlation matrices were generated for both real and synthetic versions of the datasets using the φ_k coefficient, and the cosine similarity (CS) metric was used to obtain a quantitative measure that compares them, which is defined as $1-d_{cos}$:



Where x_i is a real sample and x_i' is a synthetic counterpart. A low CS metric suggests the two matrices do not look alike, while higher values imply higher similarities between them.

On the other hand, the VS is a novel metric that computes the diversity of a given dataset without the need to compare it against another set of data. This score requires defining a positive semidefinite similarity function, which was set to be the CS in this case [61]. Accordingly, the VS of just the numerical attributes was computed due to the CS only being applicable to numerical features. In the following equation, the mathematical expression for the VS can be observed.



Where k is a given similarity function and λ_n are the eigenvalues of K/n, and K is the kernel matrix.

Furthermore, a data labeling analysis (DLA) was performed. In this procedure, an ML classifier is trained to ascertain its ability to differentiate between synthetic and real samples, mimicking the functionality of a GAN discriminator. Due to the characteristics of the analysis, the classification process was evaluated using the F_1-score metric since it is sensitive to the class distributions, making it a reliable metric when labels are imbalanced, and the recall score, as it returns the number of correctly identified synthetic samples. On top of that, the AUC curve was calculated. Regarding the trained ML models for the DLA, the LazyPredict classifier [62] object was used to train various models per iteration. The best classifier was chosen for each fold to account for the most restrictive case, while the mean and standard deviation were calculated in the process.

On top of those, the Hellinger distance was chosen to quantify the similarity between two probability distributions, offering a bounded metric that is interpretable and less sensitive to outliers than other distance calculations, such as the Wasserstein one [63]. Finally, the depth versus depth plot (DD-plot) was used, which is a nonparametric method that can evaluate the multivariate distributional similarity between two distributions (real and synthetic, in this case). While the DD-plot aims to represent the depth of a real distribution with respect to the associated synthetic depth in a graphical way, the coefficient of determination (R^2) is proposed in the literature to obtain an analytical value from it. Both the real and SD depths are more similar when R^2 is higher, meaning that the DD-plot better fits a theoretical optimal function $x=y$.

XSL•FO
RenderX

With respect to privacy metrics, four types of attacks were conducted: MIAs, attribute inference attacks (AIAs), linkability attacks, and singling out attacks. MIA and AIA assessments were conducted using the Anonymeter tool [64]. In MIAs, an adversary is simulated to assess whether a specific data point was part of the training dataset used to train a generative model, thereby posing potential privacy risks. The attack methodology involves computing distance measures between pairs of records and applying a threshold to distinguish between high-risk matches and those considered safe. In the context of this experiment and following the work of Hernandez et al [63], a Gower distance of 0.05 was defined, which is a similarity measure that may be used to handle multitype data within the same dataset.

In contrast, AIAs occur when an adversary attempts to infer sensitive information that was not originally disclosed with the dataset. AIAs seek to extract additional private information about individuals, even if their membership is already known or assumed. In this case, risks are calculated variable-wise as each one may pose differently ranked sensitivities. For numerical variables, an AIA is considered successful if the predicted value falls within a predefined confidence interval of the true value, which is defined to 0.05 in the scope of this work. For categorical variables, a correct prediction requires an exact match. This evaluation is conducted across all variables individually, and the average success rate is used to compute the overall attribute inference risk.

Regarding linkability attacks, their goal is to associate attributes from two or more records with the same individual or group, either using a single dataset or multiple ones. If the known attributes and a synthetic dataset allow the linkage to the real dataset, revealing sensitive information, the attack is considered successful. Singling out attacks, on the other hand, occurs when unique data records can be identified based on a distinct combination of attributes within the real data. In the scope of this work, the most stringent approach was adopted, using the conjunction of all attributes to perform the attacks (multivariate singling out).

Experimental Setup

In this experiment, a comparison between nonfederated and federated generative models was performed for three different federated scenarios. In the first one, the data quantity was assumed to be evenly distributed across the participant nodes (from now on, B scenario, for balanced), while for the second, the data points were randomly split, creating partitions with uneven sample quantities (from now on, IB scenario). In the third federated scenario, non-IID distributions (Figure 1) were built depending on the age variable (from now on, $IB_{non\text{-}iid}$ scenario).

For the three scenarios, the data were partitioned prior to the model training phase, allowing for traceability and higher result reproducibility. The partitions for the B scenario were created by randomly selecting n/N samples for each of the nodes, being the total number of samples in the original dataset and being the number of nodes that participate in a specific federated experiment. On the other hand, the IB scenario partitions were created so that for a specific N, N–1 nodes were trained on 5% of the data that was chosen randomly, and the th node was trained on the remaining samples. The $IB_{non\text{-}iid}$ scenario was created by sampling age-dependent data points from Dirichlet (α=10) distributions [65]. The distribution of categorical variable labels across the partitions, as well as the exact number of samples per scenario, can be consulted in Multimedia Appendix 2, showing bias among scenarios. In this analysis, the federation was evaluated for a set of $N \in \{3,5,7,10\}$.

Regarding the aggregation method selection, a preliminary study was performed using the federated average (FedAvg), the adaptive federation optimization (FedOpt), and the federated optimization for heterogeneous networks (FedProx) algorithms. The most challenging experiment scenarios (10 nodes and non-IID scenarios) were tested with the three algorithms, evaluating the models using the metrics that were presented in the previous section. The results either demonstrated that FedAvg was the best-performing algorithm or showed no statistically significant improvement when comparing to FedOpt or FedProx algorithms. Therefore, the experiments intended to evaluate the contributions defined in the introduction section of this paper were trained by averaging the model weights coming from each node and attending to the number of samples each one contained (FedAvg). The results of the preliminary analysis can be found in Multimedia Appendix 3.

The Flower 1.7.0 Framework [66] was used in order to federate the models using the simulation module. The experiments were performed in a high-performance computing cluster, and they were allocated for 10 central processing unit and 2 graphics processing unit jobs, having initiated a Ray actor cluster prior to executing federation rounds. Figure 2 represents the workflow that was carried out during the experiment execution, where data partition, model training, and evaluation phases are shown.

XSL•FO
RenderX

Figure 1. Generated non-IID age-dependent distribution plots. The top left shows the scenario with 3 nodes, the top right shows the 7-node scenario, the bottom left shows the 10-node scenario, and the bottom right shows the 5-node one. KDE: kernel density estimate; non-IID: nonindependent and identically distributed.

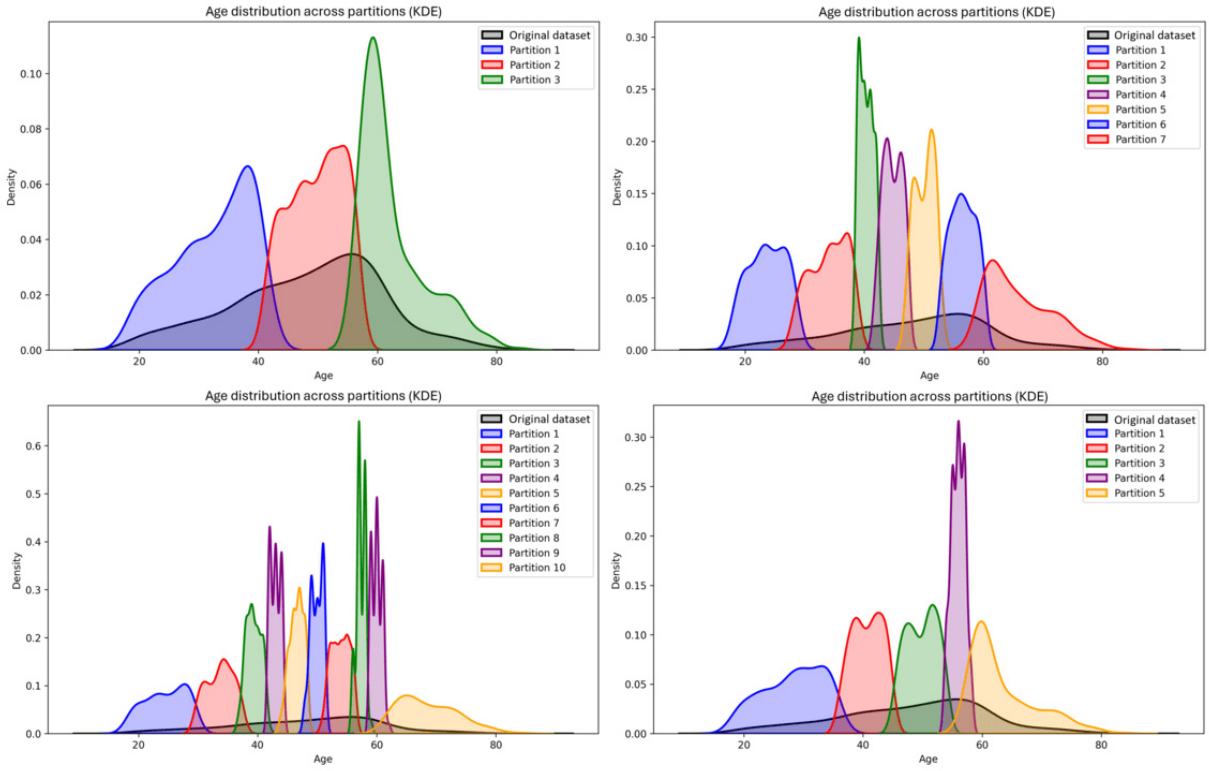
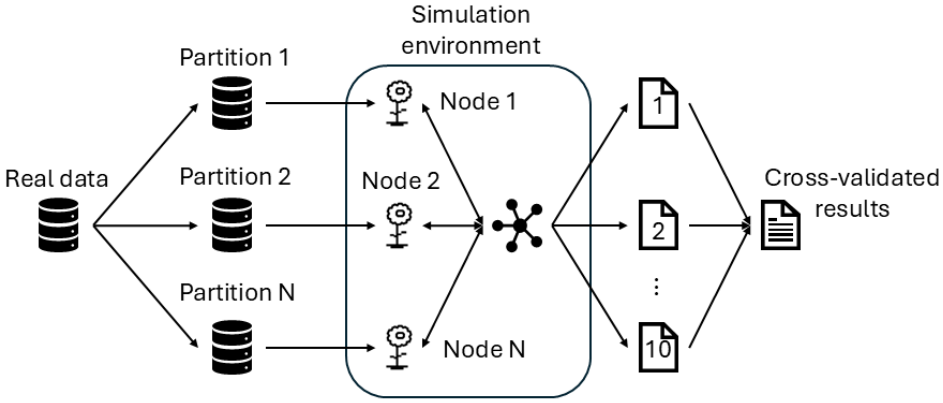


Figure 2. Experiment execution framework, including data partitioning, model training, and synthetic data evaluation processes.



Results

Overview

The results of the study are presented in this section, comparing the three presented federated scenarios with the baseline model, both for the CTGAN and the FedTabDiff. All statistical tests were performed for a significance level of .05 using the averaged results, while some variable-specific metrics can be checked in Multimedia Appendices 4 and 5.

CTGAN

Starting with the baseline nonfederated CTGAN model fidelity evaluation, the coefficient results showed a mean CS of 0.930 (standard deviation 0.002). Regarding the DLA execution, the obtained AUC was 0.796 (standard deviation 0.026), the F_1-score was 0.872 (standard deviation 0.015), and the recall metric was 0.958 (standard deviation 0.009). The VS resulted in a mean value of 1.405 (standard deviation 0.004) in the SD, compared to the VS obtained in the real dataset of 1.406. To finish, the average Hellinger distance was 0.223 (standard deviation 0.002). Regarding the privacy evaluation, the MIA demonstrated no significant membership inference risk, while the averaged AIA resulted in a 5% risk for attribute information to be inferred.

Regarding the federated models that were trained with balanced datasets (the B scenario), most of the performed experiments showed statistically significant differences in fidelity metrics with respect to the baseline scenario (P<.001), even with variations in the number of nodes (Table 1). Statistical significance was found in singling out attack metrics, while the rest of the privacy measures did not significantly vary from the baseline.

XSL•FO
RenderX

Table 1. Fidelity and privacy metric results of the CTGAN[a] for the B scenario[b].

Metric	Baseline	3N	5N	7N	10N
Fidelity					
CS[c] φ_k					
μ	0.930	0.842	0.846	0.845	0.849
σ	0.002	0.005	0.003	0.003	0.003
t test (*df*)	—[d]	45.525 (18)	67.770 (18)	74.556 (18)	78.915 (18)
P value	—	<.001	<.001	<.001	<.001
DLA[e] AUC [f]					
μ	0.796	0.965	0.962	0.946	0.965
σ	0.026	0.008	0.008	0.008	0.009
t test (*df*)	—	19.818 (18)	19.333 (18)	17.391 (18)	19.402 (18)
P value	—	<.001	<.001	<.001	<.001
DLA F_1-score					
μ	0.872	0.965	0.961	0.945	0.964
σ	0.015	0.007	0.008	0.008	0.009
t test (*df*)	—	17.940 (18)	16.931 (18)	13.853 (18)	16.935 (18)
P value	—	<.001	<.001	<.001	<.001
DLA recall					
μ	0.958	0.969	0.948	0.940	0.968
σ	0.009	0.012	0.009	0.012	0.010
t test (*df*)	—	2.402 (18)	2.644 (18)	3.791 (18)	2.316 (18)
P value	—	.02	.02	.001	.03
VS[g]					
μ	1.405	1.437	1.442	1.337	1.251
σ	0.004	0.002	0.001	0.004	0.006
t test (*df*)	—	24.969 (18)	31.451 (18)	39.839 (18)	66.590 (18)
P value	—	<.001	<.001	<.001	<.001
μ	0.223	0.229	0.223	0.220	0.221
σ	0.002	0.010	0.002	0.002	0.002
t test (*df*)	—	1.767 (18)	0.165 (18)	2.930 (18)	2.517 (18)
P value	—	.09	.87	.009	.02
Depth versus depth-plot R^2					
μ	0.948	0.950	0.668	0.828	0.619
σ	0.011	0.007	0.006	0.007	0.005
t test (*df*)	—	0.525 (18)	71.176 (18)	29.506 (18)	86.088 (18)
P value	—	.61	<.001	<.001	<.001
Privacy					
MIA[h]					
μ	0	0[i]	0[i]	0[i]	0[i]
σ	0	0	0	0	0
t test (*df*)	—	—	—	—	—

XSL•FO
RenderX

Metric	Baseline	3N	5N	7N	10N
P value	—	—	—	—	—
AIA[j]					
μ	0.045	0.038	0.055	0.038	0.039
σ	0.025	0.018	0.031	0.019	0.009
t test (*df*)	—	1.496 (18)	1.000 (18)	1.414 (18)	1.667 (18)
P value	—	.15	.33	.17	.11
Linkability					
μ	0.001	0.001[k]	0.001[k]	0.001[k]	0[i]
σ	0.003	0.003	0.003	0.003	0
t test (*df*)	—	—	—	—	—
P value	—	—	—	—	—
Singling out					
μ	0.123	0.048	0.018	0.048	0.046
σ	0.045	0.016	0.018	0.025	0.025
t test (*df*)	—	4.954 (18)	6.785 (18)	4.548 (18)	4.645 (18)
P value	—	<.001	<.001	<.001	<.001

[a]CTGAN: conditional tabular generative adversarial network.

[b]*t* tests were performed between the baseline and each federated experiment. Significance level is .05 for all statistical tests.

[c]CS: cosine similarity.

[d]Not applicable.

[e]DLA: data labeling analysis.

[f]AUC: area under the curve.

[g]VS: Vendi Score.

[h]MIA: membership inference attack.

[i]*t* tests were not performed for these due to the standard deviation being zero.

[j]AIA: attribute inference attack.

[k]*t* tests were not performed for these due to the results being the same as the ones found in the baseline metrics.

Specifically, intervariable correlations were shown to be more distorted than the ones presented by the baseline model, and the DLA suggested that the synthetic samples that were generated by federated models are prone to being detected more easily than the ones generated by the baseline model, although variable-wise metrics such as the Hellinger distance did not demonstrate too different results.

In the IB scenario, most of the performed experiments showed high statistical significances ($P<.001$) with respect to the baseline, too (Table 2). Intervariable correlations, DLA metrics, and VS values were shown to be quite different from the baseline model, attending the statistical tests, while the Hellinger distances did not show too big a difference. In this case, the 10N experiment showed statistically significant differences with the AIA metric obtained in the baseline, suggesting an improvement in privacy while deteriorating the fidelity values. All the experiments in this scenario supported the privacy improvement suggestion, as all the multivariate singling out attacks proved to perform better in federated setups. However, no specific tendency can be observed while increasing the number of nodes in this sense.

The $IB_{non\text{-}iid}$ scenario followed the same overall patterns found in the previous two scenarios, showing statistically significant differences in fidelity metrics but with no difference in the performed privacy metrics other than those found for multivariate singling out attacks (Table 3).

XSL•FO
RenderX

Table 2. Fidelity and privacy metric results of the CTGAN[a] for the IB scenario[b].

Metric	Baseline	3N	5N	7N	10N
Fidelity					
CS [c] φ_k					
μ	0.930	0.848	0.841	0.839	0.847
σ	0.002	0.002	0.003	0.005	0.001
t test (*df*)	—[d]	87.050	84.898	56.581	110.235
P value	—	<.001	<.001	<.001	<.001
DLA[e] AUC[f]					
μ	0.796	0.983	0.993	0.968	0.938
σ	0.026	0.004	0.004	0.005	0.009
t test (*df*)	—	23.187 (18)	23.700 (18)	20.550 (18)	16.342 (18)
P value	—	<.001	<.001	<.001	<.001
DLA F_1-score					
μ	0.872	0.988	0.993	0.968	0.938
σ	0.015	0.004	0.004	0.005	0.008
t test (*df*)	—	24.086 (18)	25.109 (18)	19.405 (18)	12.136 (18)
P value	—	<.001	<.001	<.001	<.001
DLA recall					
μ	0.958	0.979	0.986	0.964	0.928
σ	0.009	0.007	0.008	0.008	0.014
t test (*df*)	—	5.749 (18)	7.472 (18)	1.581 (18)	5.666 (18)
P value	—	<.001	<.001	.13	<.001
VS[g]					
μ	1.405	1.360	1.424	1.436	1.360
σ	0.004	0.011	0.003	0.003	0.011
t test (*df*)	—	27.714 (18)	11.833 (18)	21.772 (18)	12.155 (18)
P value	—	<.001	<.001	<.001	<.001
μ	0.223	0.222	0.216	0.223	0.217
σ	0.002	0.001	0.002	0.002	0.002
t test (*df*)		0.976 (18)	7.892 (18)	0.119 (18)	5.931 (18)
P value		.34	<.001	.90	<.001
Depth versus depth-plot R^2					
μ	0.948	0[h]	0[h]	0.737	0[h]
σ	0.011	0	0	0	0
t test (*df*)	—	—	—	56.069 (18)	—
P value	—	—	—	<.001	—
Privacy					
MIA[i]					
μ	0	0[h]	0[h]	0[h]	0[h]
σ	0	0	0	0	0
t test (*df*)	—	—	—	—	—

XSL•FO
RenderX

Metric	Baseline	3N	5N	7N	10N
P value	—	—	—	—	—
AIA[j]					
μ	0.045	0.052	0.061	0.041	0.029
σ	0.025	0.019	0.029	0.016	0.017
t test (*df*)	—	0.076 (18)	0.768 (18)	1.400 (18)	2.437 (18)
P value	—	.94	.45	.27	.03
Linkability					
μ	0.001	0.001[k]	0[h]	0.002	0.002
σ	0.003	0.003	0	0.004	0.004
t test (*df*)	—	—	—	0.600 (18)	0.600 (18)
P value	—	—	—	.56	.56
Singling out					
μ	0.123	0.024	0.025	0.030	0.060
σ	0.045	0.022	0.015	0.014	0.025
t test (*df*)	—	6.181 (18)	6.457 (18)	6.189 (18)	3.798 (18)
P value	—	<.001	<.001	<.001	.001

[a]CTGAN: conditional tabular generative adversarial network.

[b]*t* tests were performed between the baseline and each federated experiment. Significance level is .05 for all statistical tests.

[c]CS: cosine similarity.

[d]Not applicable.

[e]DLA: data labeling analysis.

[f]AUC: area under the curve.

[g]VS: Vendi Score.

[h]*t* tests were not performed for these due to the standard deviation being zero.

[i]MIA: membership inference attack.

[j]AIA: attribute inference attack.

[k]*t* tests were not performed for these due to the results being the same as the ones found in the baseline metrics.

XSL•FO
RenderX

Table 3. Fidelity and privacy metric results of the CTGAN[a] for the IBnon-iid scenario[b].

Metric	Baseline	3N	5N	7N	10N
Fidelity					
$CS^{c}\varphi_k$					
μ	0.930	0.848	0.842	0.841	0.842
σ	0.002	0.003	0.001	0.004	0.003
t test (*df*)	__[d]	82.533 (18)	111.330 (18)	69.045 (18)	83.862 (18)
P value	—	<.001	<.001	<.001	<.001
DLA[e] AUC[f]					
μ	0.796	0.977	0.948	0.983	0.950
σ	0.026	0.006	0.010	0.005	0.006
t test (*df*)	—	21.572 (18)	17.233 (18)	22.408 (18)	18.339 (18)
P value	—	<.001	<.001	<.001	<.001
DLA F_1-score					
μ	0.872	0.976	0.947	0.982	0.950
σ	0.015	0.005	0.010	0.005	0.006
t test (*df*)	—	21.033 (18)	13.353 (18)	22.724 (18)	15.602 (18)
P value	—	<.001	<.001	<.001	<.001
DLA recall					
μ	0.958	0.960	0.938	0.985	0.952
σ	0.009	0.010	0.019	0.009	0.013
t test (*df*)	—	0.383 (18)	3.039 (18)	6.891 (18)	1.195 (18)
P value	—	.71	.007	<.001	.25
VS[g]					
μ	1.405	1.440	1.445	1.198	1.367
σ	0.004	0.001	0.001	0.010	0.004
t test (*df*)	—	28.834 (18)	33.888 (18)	62.753 (18)	21.978 (18)
P value	—	<.001	<.001	<.001	<.001
μ	0.223	0.214	0.214	0.215	0.213
σ	0.002	0.002	0.003	0.002	0.002
t test (*df*)	—	8.801 (18)	8.147 (18)	8.333 (18)	11.928 (18)
P value	—	<.001	<.001	<.001	<.001
Depth versus depth-plot R^2					
μ	0.948	0.708	0.809	0[h]	0.847
σ	0.011	0.021	0.006	0	0.004
t test (*df*)	—	32.423 (18)	35.585 (18)	—	27.404 (18)
P value	—	<.001	<.001	—	<.001
Privacy					
MIA[i]					
μ	0	0[h]	0[h]	0[h]	0[h]
σ	0	0	0	0	0
t test (*df*)	—	—	—	—	—

XSL•FO
RenderX

Metric	Baseline	3N	5N	7N	10N
P value	—	—	—	—	—
AIA[j]					
μ	0.045	0.048	0.044	0.049	0.057
σ	0.025	0.022	0.023	0.024	0.032
t test (*df*)	—	0.366 (18)	0.799 (18)	0.325 (18)	0.362 (18)
P value	—	.72	.44	.75	.72
Linkability					
μ	0.001	0.002	0.001[k]	0.001[k]	0[h]
σ	0.003	0.006	0.003	0.003	0
t test (*df*)	—	0.447 (18)	—	—	—
P value	—	.66	—	—	—
Singling out					
μ	0.123	0.030	0.029	0.033	0.021
σ	0.045	0.020	0.021	0.019	0.021
t test (*df*)	—	5.877 (18)	5.900 (18)	5.768 (18)	6.136 (18)
P value	—	<.001	<.001	<.001	<.001

[a]CTGAN: conditional tabular generative adversarial network.

[b]*t* tests were performed between the baseline and each federated experiment. Significance level is .05 for all statistical tests.

[c]CS: cosine similarity.

[d]Not applicable.

[e]DLA: data labeling analysis.

[f]AUC: area under the curve.

[g]VS: Vendi Score.

[h]*t* tests were not performed for these due to the standard deviation being zero.

[i]MIA: membership inference attack.

[j]AIA: attribute inference attack.

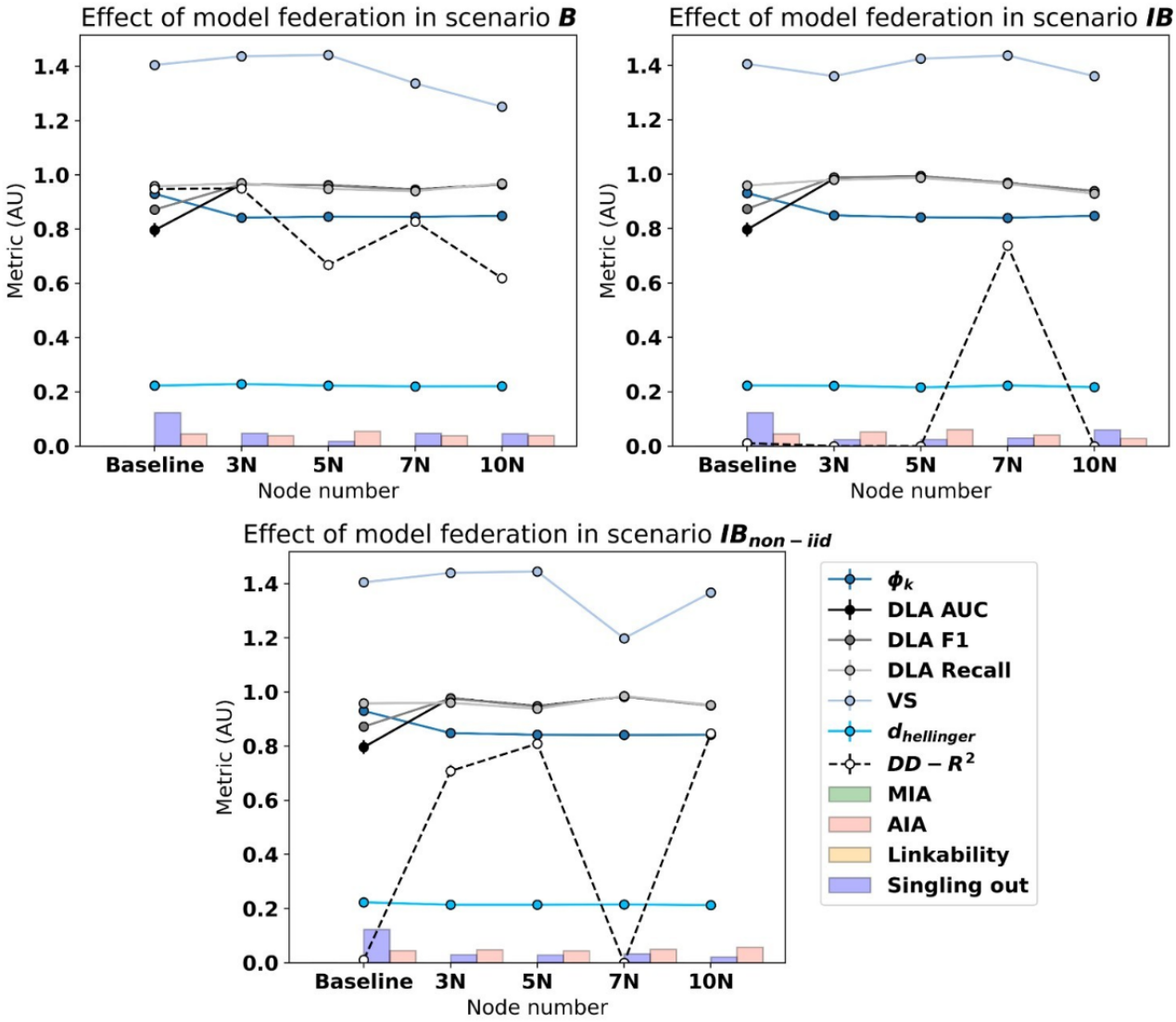
[k]*t* tests were not performed for these due to the results being the same as the ones found in the baseline metrics.

Gathering all the results in a single figure, similar tendencies can be observed in the three scenarios, where lower correlation values and higher DLA-related metrics can be found among the federated models with respect to the baseline model. The VS metric fluctuated most among the scenarios along with the DD-plot R^2, offering insight regarding the variability of each generated SD. Hellinger distances were found not to fluctuate even when comparing centralized and federated models, while a difference in privacy protection measures is observable in singling out attacks (Figure 3).

Now, considering federated experiment pairs (ie, comparing 3N experiments with 5N, 5N with 7N, and 7N with 10N) to evaluate if additional federated nodes impact the SD quality in terms of fidelity and privacy, no clear tendencies can be observed in either scenario (Table 4). Privacy metrics did not show statistical significance; therefore, assuming no improvement was achieved in terms of privacy, even though the baseline centralized model offered good results already. Among the fidelity metrics, the CS of the was found to differ between pairs of experiments in some cases, but no specific trend was detected. The same occurred for the DLA-related metrics, where some pairs pointed out significant differences. All the VS metrics were found to be different, even if no improvement or deterioration trend was found, and the Hellinger distance metric varied depending on the scenario, just as the DD-plot R^2.

XSL•FO
RenderX

Figure 3. Graphical comparison of federated scenarios regarding fidelity and privacy metrics using the CTGAN model. AIA: attribute inference attack; AUC: area under the curve; CTGAN: conditional tabular generative adversarial network; DD: depth versus depth; DLA: data labeling analysis; MIA: membership inference attack; non-IID: nonindependent and identically distributed; VS: Vendi Score.



XSL•FO
RenderX

Table 4. *t* test results for CTGAN[a] experiment pairs[b].

Metric	3N-5N		5N-7N		7N-10N	
	t test (*df*)	*P* value	*t* test (*df*)	*P* value	*t* test (*df*)	*P* value
B scenario						
Fidelity						
CS[c] φ_k	1.858 (18)	.08	0.522 (18)	.61	2.939 (18)	.008
DLA[d] AUC[e]	0.895 (18)	.38	4.522 (18)	<.001	4.944 (18)	<.001
DLA F_1-score	0.875 (18)	.39	4.495 (18)	<.001	4.951 (18)	<.001
DLA Recall	4.612 (18)	<.001	1.621 (18)	.12	5.553 (18)	<.001
VS[f]	7.949 (18)	<.001	82.267 (18)	<.001	36.200 (18)	<.001
$d_{\text{hellinger}}$	1.704 (18)	.11	2.815 (18)	.01	0.714 (18)	.48
DD-plot[g] R^2	98.714 (18)	<.001	55.822 (18)	<.001	77.093 (18)	<.001
Privacy						
MIA[h,i]	—[j]	—	—	—	—	—
AIA[k]	1.000 (18)	.33	1.000 (18)	.33	0.045 (18)	.96
Linkability[i,l]	—	—	—	—	—	—
Singling out	3.702 (18)	.002	2.898 (18)	.01	0.120 (18)	.91
IB scenario						
Fidelity						
CS φ_k	6.296 (18)	<.001	1.447 (18)	.16	5.676 (18)	<.001
DLA AUC	2.165 (18)	.04	11.306 (18)	<.001	9.083 (18)	<.001
DLA F_1-score	2.192 (18)	.04	11.485 (18)	<.001	9.026 (18)	<.001
DLA Recall	2.088 (18)	.051	6.129 (18)	<.001	6.967 (18)	<.001
VS	14.629 (18)	<.001	9.680 (18)	<.001	21.062 (18)	<.001
$d_{\text{hellinger}}$	8.239 (18)	<.001	7.517 (18)	<.001	5.708 (18)	<.001
DD-plot R^2[i]	—	—	—	—	—	—
Privacy						
MIA[i]	—	—	—	—	—	—
AIA	0.743 (18)	.47	1.796 (18)	.09	1.592 (18)	.13
Linkability[i,l]	—	—	—	—	—	—
Singling out	0.192 (18)	.85	0.719 (18)	.48	3.074 (18)	.007
$IB_{\text{non-iid}}$ scenario						
Fidelity						
CS φ_k	7.211 (18)	<.001	0.985 (18)	.34	0.476 (18)	.64
DLA AUC	7.895 (18)	<.001	9.805 (18)	<.001	14.043 (18)	<.001
DLA F_1-score	7.705 (18)	<.001	9.718 (18)	<.001	14.039 (18)	<.001
DLA Recall	3.192 (18)	.005	7.086 (18)	<.001	6.784 (18)	<.001
VS	15.145 (18)	<.001	79.749 (18)	<.001	50.058 (18)	<.001
$d_{\text{hellinger}}$	0.120 (18)	.91	0.585 (18)	.57	2.085 (18)	.054
DD-plot R^2[i]	14.916 (18)	<.001	—	—	—	—
Privacy						

XSL•FO
RenderX

Metric	3N-5N		5N-7N		7N-10N	
	t test (*df*)	*P* value	*t* test (*df*)	*P* value	*t* test (*df*)	*P* value
MIA[i]	—	—	—	—	—	—
AIA	0.435 (18)	.67	0.441 (18)	.66	0.615 (18)	.54
Linkability[i,l]	0.447 (18)	.66	—	—	—	—
Singling out	0.131 (18)	.90	0.457 (18)	.65	1.577 (18)	.13

[a]CTGAN: conditional tabular generative adversarial network.

[b]Significance level is .05 for all statistical tests.

[c]CS: cosine similarity.

[d]DLA: data labeling analysis.

[e]AUC: area under the curve.

[f]VS: Vendi Score.

[g]DD-plot: depth versus depth plot.

[h]MIA: membership inference attack.

[i]*t* tests were not performed for these due to the standard deviation being zero.

[j]Not applicable.

[k]AIA: attribute inference attack.

[l]*t* tests were not performed for these due to the results being the same as the ones found in the baseline metrics.

FedTabDiff

Regarding the baseline FedTabDiff model, a CS φ_k value of 0.866 was obtained, while results above 0.990 were obtained for all DLA-related metrics. The VS was 1.417, while the Hellinger distance was 0.339, and the DD-plot R^2 was 0.971. The privacy analyses demonstrated there was no membership inference risk, while the linkability risk was minimal. Values of 0.031 for the AIA and 0.156 for the singling out were obtained.

The FedTabDiff models that were trained with balanced datasets (the B scenario) showed statistical significance in most of the fidelity metrics when compared to the baseline scenario ($P<.001$), while the tests carried out with the privacy metrics were found to be nonsignificant. Therefore, fidelity metrics worsened while the number of nodes augmented, but privacy seemed not to be affected (Table 5).

XSL•FO
RenderX

Table 5. Fidelity and privacy metric results of FedTabDiff for the B scenario[a].

Metric	Baseline	3N	5N	7N	10N
Fidelity					
CS[b] φ_k					
μ	0.866	0.854	0.674	0.873	0.645
σ	0.010	0.011	0.185	0.008	0.168
t test (*df*)	—[c]	2.489 (18)	3.121 (18)	1.588 (18)	3.931 (18)
P value	—	.02	.006	.13	<.001
DLA[d] AUC[e]					
μ	0.992	0.981	0.989	0.994	0.997
σ	0.001	0.001	0.001	0.001	0.003
t test (*df*)	—	19.152 (18)	5.594 (18)	5.965 (18)	14.631 (18)
P value	—	<.001	<.001	<.001	<.001
DLA F_1-score					
μ	0.997	0.994	0.999	1	0.999
σ	0.003	0.002	0.001	0	0.001
t test (*df*)	—	2.642 (18)	1.886 (18)	2.899 (18)	2.612 (18)
P value	—	.02	.08	.009	.02
DLA recall					
μ	0.999	0.997	0.999	1	1
σ	0.002	0.003	0.002	0	0
t test (*df*)	—	1.470 (18)	0.306 (18)	1.409 (18)	1.409 (18)
P value	—	.16	.76	.18	.18
VS[f]					
μ	1.417	1.407	1.387	1.395	1.372
σ	0.002	0.003	0.003	0.003	0.003
t test (*df*)	—	9.729 (18)	24.385 (18)	19.278 (18)	34.668 (18)
P value	—	<.001	<.001	<.001	<.001
d **hellinger**					
μ	0.339	0.363	0.380	0.381	0.360
σ	0.009	0.008	0.018	0.011	0.018
t test (*df*)	—	6.589 (18)	6.375 (18)	9.481 (18)	3.217 (18)
P value	—	<.001	<.001	<.001	.005
DD-plot [g] R^2					
μ	0.971	0.980	0.955	0.956	0.983
σ	0.005	0.003	0.004	0.003	0.002
t test (*df*)	—	4.767 (18)	7.413 (18)	7.505 (18)	7.101 (18)
P value	—	<.001	<.001	<.001	<.001
Privacy					
MIA[h]					
μ	0	0[i]	0[i]	0[i]	0[i]
σ	0	0	0	0	0

XSL•FO
RenderX

Metric	Baseline	3N	5N	7N	10N
t test (*df*)	—	—	—	—	—
P value	—	—	—	—	—
AIA[j]					
μ	0.031	0.031	0.028	0.031	0.027
σ	0.015	0.013	0.009	0.016	0.018
t test (*df*)		0.063 (18)	0.422 (18)	0.024 (18)	0.559 (18)
P value		.95	.68	.98	.58
Linkability					
μ	0.002	0.004	0.001	0.002[k]	0.003
σ	0.004	0.005	0.003	0.004	0.006
t test (*df*)	—	0.949 (18)	0.600 (18)	—	0.397 (18)
P value	—	.35	.55	—	.70
Singling out					
μ	0.156	0.149	0.132	0.134	0.138
σ	0.040	0.031	0.040	0.031	0.044
t test (*df*)	—	0.425 (18)	1.287 (18)	1.344 (18)	0.922 (18)
P value	—	.68	.21	.20	.37

[a]*t* tests were performed between the baseline and each federated experiment. Significance level is .05 for all statistical tests.

[b]CS: cosine similarity.

[c]Not applicable.

[d]DLA: data labeling analysis.

[e]AUC: area under the curve.

[f]VS: Vendi Score.

[g]DD-plot: depth versus depth plot.

[h]MIA: membership inference attack.

[i]*t* tests were not performed for these due to the standard deviation being zero.

[j]AIA: attribute inference attack.

[k]*t* tests were not performed for these due to the results being the same as the ones found in the baseline metrics.

In this scenario, the intervariable correlation metric, φ_k, was the measure that most varied among the fidelity metrics, while the DLA metrics showed a similar tendency to the one found within the CTGAN results. The DD-plot R^2 value, the VS, and the Hellinger distance, although statistically significant, did not show any relevant tendency linked to the number of nodes.

Regarding privacy measures, no membership inference risk was found among the generated SD in scenario B, while calculated linkability risks were minimal. Privacy risks did not significantly vary linked to the number of nodes.

In the IB scenario, the results were found to be similar to the ones found in scenario B, most of the fidelity metrics showing statistically significant differences between experiments with different numbers of nodes (P<.001), and no significance in privacy-related metrics (Table 6). In this scenario, the DLA metrics varied slightly more, even if no clear tendency is observable. In addition, the intervariable correlations seemed to be better maintained within this experiment, even if no tendency was found either.

XSL•FO
RenderX

Table 6. Fidelity and privacy metric results of FedTabDiff for the IB scenario[a].

Metric	Baseline	3N	5N	7N	10N
Fidelity					
CS[b] φ_k					
μ	0.866	0.632	0.838	0.857	0.531
σ	0.010	0.014	0.008	0.007	0.088
t test (*df*)	—[c]	41.539 (18)	6.657 (18)	2.318 (18)	11.294 (18)
P value	—	<.001	<.001	.03	<.001
DLA[d] AUC[e]					
μ	0.992	0.994	0.986	0.977	0.997
σ	0.001	0.001	0.001	0.001	0.002
t test (*df*)	—	6.063 (18)	10.205 (18)	35.140 (18)	15.540 (18)
P value	—	<.001	<.001	<.001	<.001
DLA F_1-score					
μ	0.997	0.999	0.995	0.992	0.999
σ	0.003	0.001	0.002	0.003	0.001
t test (*df*)	—	2.612 (18)	1.787 (18)	3.765 (18)	2.612 (18)
P value	—	.02	.09	.001	.02
DLA recall					
μ	0.999	0.999	0.996	0.995	1[f]
σ	0.002	0.001	0.004	0.004	0
t test (*df*)	—	0.833 (18)	1.686 (18)	2.241 (18)	—
P value	—	.42	.11	.04	—
VS[g]					
μ	1.417	1.422	1.408	1.404	1.394
σ	0.002	0.002	0.002	0.002	0.002
t test (*df*)	—	4.744 (18)	9.942 (18)	12.669 (18)	22.485 (18)
P value	—	<.001	<.001	<.001	<.001
d **hellinger**					
μ	0.339	0.374	0.319	0.370	0.361
σ	0.009	0.029	0.003	0.003	0.013
t test (*df*)	—	3.525 (18)	6.849 (18)	10.258 (18)	4.280 (18)
P value	—	.002	<.001	<.001	<.001
DD-plot[h] R^2					
μ	0.971	0.973	0.936	0.988	0.931
σ	0.005	0.005	0.007	0.001	0.005
t test (*df*)	—	0.739 (18)	11.702 (18)	9.648 (18)	17.166 (18)
P value	—	.47	<.001	<.001	<.001
Privacy					
MIA[i]					
μ	0	0[f]	0[f]	0[f]	0[f]
σ	0	0	0	0	0

XSL•FO
RenderX

Metric	Baseline	3N	5N	7N	10N
t test (*df*)	—	—	—	—	—
P value	—	—	—	—	—
AIA[j]					
μ	0.031	0.021	0.019	0.020	0.024
σ	0.015	0.008	0.013	0.006	0.012
t test (*df*)	—	1.668 (18)	1.750 (18)	1.605 (18)	1.140 (18)
P value	—	.11	.10	.13	.27
Linkability					
μ	0.002	0.004	0.001	0	0[f]
σ	0.004	0.010	0.003	0	0
t test (*df*)		0.638 (18)	0.600 (18)	0.939 (18)	—
P value		.53	.56	.36	—
Singling out					
μ	0.156	0.156	0.133	0.134	0.142
σ	0.040	0.038	0.056	0.041	0.033
t test (*df*)	—	0.032 (18)	0.988 (18)	1.122 (18)	0.830 (18)
P value	—	.97	.34	.28	.42

[a]*t* tests were performed between the baseline and each federated experiment. Significance level is .05 for all instances.

[b]CS: cosine similarity.

[c]Not applicable.

[d]DLA: data labeling analysis.

[e]AUC: area under the curve.

[f]*t* tests were not performed for these due to the standard deviation being zero.

[g]VS: Vendi Score.

[h]DD-plot: depth versus depth plot.

[i]MIA: membership inference attack.

[j]AIA: attribute inference attack.

Regarding the privacy metrics, no statistical significance was detected among the results. No membership inference risk was found in any of the experiments, while the linkability risk was minimal, as it was in scenario B.

The $IB_{non\text{-}iid}$ scenario followed the same pattern as those of the B and IB scenarios, with the difference of some singling out risk differences were statistically significant in this case. No membership inference risk was found in this scenario, and the linkability risks were also found to be minimal (Table 7).

XSL•FO
RenderX

Table 7. Fidelity and privacy metric results of FedTabDiff for the IBnon-iid scenario[a].

Metric	Baseline	3N	5N	7N	10N
Fidelity					
CS[b] φ_k					
μ	0.866	0.613	0.529	0.570	0.545
σ	0.010	0.009	0.084	0.084	0.026
t test (*df*)	—[c]	56.766 (18)	12.014 (18)	10.579 (18)	34.233 (18)
P value	—	<.001	<.001	<.001	<.001
DLA[d] AUC[e]					
μ	0.992	0.995	0.998	0.997	0.998
σ	0.001	0.001	0.001	0.001	0.001
t test (*df*)	—	8.232 (18)	16.336 (18)	15.255 (18)	19.792 (18)
P value	—	<.001	<.001	<.001	<.001
DLA F_1-score					
μ	0.997	0.999	1[f]	0.999	1[f]
σ	0.003	0.001	0	0.001	0
t test (*df*)	—	2.612 (18)	—	2.612 (18)	—
P value	—	.02	—	.02	—
DLA recall					
μ	0.999	1[f]	1[f]	1[f]	1[f]
σ	0.002	0	0	0	0
t test (*df*)	—	—	—	—	—
P value	—	—	—	—	—
VS[g]					
μ	1.417	1.426	1.432	1.422	1.398
σ	0.002	0.002	0.001	0.001	0.002
t test (*df*)	—	9.581 (18)	18.524 (18)	5.557 (18)	19.534 (18)
P value	—	<.001	<.001	<.001	<.001
$d_{\text{hellinger}}$					
μ	0.339	0.363	0.385	0.384	0.381
σ	0.009	0.006	0.018	0.014	0.003
t test (*df*)	—	6.171 (18)	7.107 (18)	8.471 (18)	15.022 (18)
P value	—	<.001	<.001	<.001	<.001
DD-plot $^{h}R^2$					
μ	0.971	0.947	0.578	0.931	0.913
σ	0.005	0.005	0.041	0.008	0.002
t test (*df*)	—	9.549 (18)	28.846 (18)	12.677 (18)	32.593 (18)
P value	—	<.001	<.001	<.001	<.001
Privacy					
MIA[i]					
μ	0	0[f]	0[f]	0[f]	0[f]
σ	0	0	0	0	0

XSL•FO
RenderX

Metric	Baseline	3N	5N	7N	10N
t test (*df*)	—	—	—	—	—
P value	—	—	—	—	—
AIA[j]					
μ	0.031	0.028	0.020	0.027	0.038
σ	0.015	0.010	0.008	0.009	0.016
t test (*df*)	—	0.443 (18)	1.988 (18)	0.721 (18)	0.953 (18)
P value	—	.66	.06	.48	.35
Linkability					
μ	0.002	0[f]	0.002[k]	0.001	0.005
σ	0.004	0	0.004	0.003	0.009
t test (*df*)	—	—	—	0.532 (18)	0.898 (18)
P value	—	—	—	.60	.38
Singling out					
μ	0.156	0.099	0.101	0.087	0.091
σ	0.040	0.034	0.037	0.030	0.026
t test (*df*)	—	3.332 (18)	3.099 (18)	4.229 (18)	4.194 (18)
P value	—	.003	.006	<.001	<.001

[a]*t* tests were performed between the baseline and each federated experiment. Significance level is .05 for all statistical tests.

[b]CS: cosine similarity.

[c]Not applicable.

[d]DLA: data labeling analysis.

[e]AUC: area under the curve.

[f]*t* tests were not performed for these due to the standard deviation being zero.

[g]VS: Vendi Score.

[h]DD-plot: depth versus depth plot.

[i]MIA: membership inference attack.

[j]AIA: attribute inference attack.

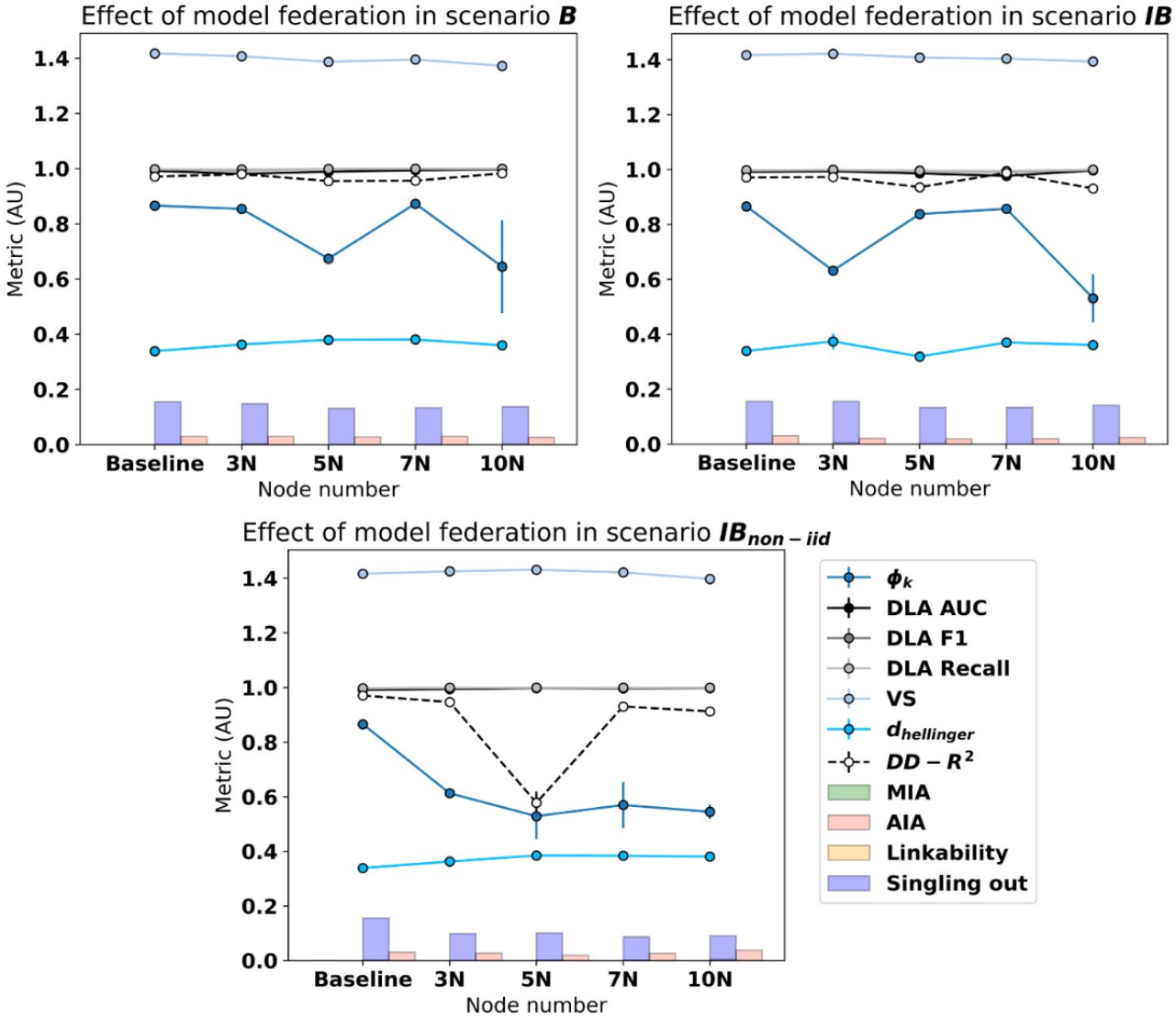
[k]*t* tests were not performed for these due to the results being the same as the ones found in the baseline metrics.

Fidelity metrics specifically showed a kind of worsening tendency in terms of the CS φ_k metric along with the increase in the number of nodes. In addition, the Hellinger distance seemed to increase accordingly. The DLA did not show any significant change, nor did the DD-plot R^2.

Now, gathering all the results in a single figure (Figure 4) to find all the information in a graphical manner, it can be observed that the singling out and attribute inference risks prevail over the membership and the linkability ones. Saying that, either a neutral tendency to maintain the privacy levels on the federated experiments, or an improvement of it (mostly in scenario $IB_{non\text{-}iid}$), is observable with respect to the centralized baseline metrics.

XSL•FO
RenderX

Figure 4. Graphical comparison of federated scenarios regarding fidelity and privacy metrics using the FedTabDiff model. AIA: attribute inference attack; AUC: area under the curve; DD: depth versus depth; DLA: data labeling analysis; MIA: membership inference attack; non-IID: nonindependent and identically distributed; VS: Vendi Score.



As it was pointed out in the CTGAN results, the fidelity metric tendency can be found to kind of worsen once the FedTabDiff model is federated, but the effect seems to be mostly maintained across experimentation with different numbers of nodes.

Now, to finish with the result explanation and considering federated experiment pairs as previously (ie, comparing 3N experiments with 5N, 5N with 7N, and 7N with 10N), no statistically significant differences were observed in terms of the privacy metrics in any of the scenarios. Statistical significance was found in some of the comparisons across fidelity metrics and different scenarios (Table 8).

XSL•FO
RenderX

Table 8. *t* test results for FedTabDiff experiment pairs[a].

Metric	3N-5N		5N-7N		7N-10N	
	t test (*df*)	*P* value	*t* test (*df*)	*P* value	*t* test (*df*)	*P* value
B scenario						
Fidelity						
CS[b] φ_k	2.917 (18)	.009	3.230 (18)	.005	4.051 (18)	<.001
DLA[c] AUC[d]	14.827 (18)	<.001	13.258 (18)	<.001	13.524 (18)	<.001
DLA F_1-score[e]	5.701 (18)	<.001	—[f]	—	—	—
DLA recall[g]	1.849 (18)	.08	—	—	—	—
VS[h]	14.140 (18)	<.001	5.787 (18)	<.001	16.078 (18)	<.001
$d_{\text{hellinger}}$	2.780 (18)	.01	0.202 (18)	.84	3.176 (18)	.005
DD-plot[i] R^2	15.341 (18)	<.001	0.469 (18)	.64	21.397 (18)	<.001
Privacy						
MIA[g,j]	—	—	—	—	—	—
AIA[k]	0.560 (18)	.58	0.356 (18)	.73	0.508 (18)	.62
Linkability	1.567 (18)	.13	0.600 (18)	.56	0.397 (18)	.70
Singling out	0.985 (18)	.34	0.094 (18)	.93	0.234 (18)	.82
IB scenario						
Fidelity						
CS φ_k	39.051 (18)	<.001	5.080 (18)	<.001	11.001 (18)	<.001
DLA AUC	16.701 (18)	<.001	18.768 (18)	<.001	80.136 (18)	<.001
DLA F_1-score	6.293 (18)	<.001	2.528 (18)	.02	7.400 (18)	<.001
DLA recall[g]	2.472 (18)	.02	0.617 (18)	.54	—	—
VS	14.454 (18)	<.001	3.620 (18)	.002	8.573 (18)	<.001
$d_{\text{hellinger}}$	5.667 (18)	<.001	32.574 (18)	<.001	2.082 (18)	.05
DD-plot R^2	11.921 (18)	<.001	20.719 (18)	<.001	34.050 (18)	<.001
Privacy						
MIA[a]	—	—	—	—	—	—
AIA	0.400 (18)	.69	0.072 (18)	.94	0.873 (18)	.39
Linkability[g]	0.946 (18)	.36	—	—	—	—
Singling out	1.016 (18)	.32	0.153 (18)	.88	0.686 (18)	.50
$IB_{\text{non-iid}}$ scenario						
Fidelity						
CS φ_k	3.011 (18)	.007	1.036 (18)	.31	0.834 (18)	.42
DLA AUC	10.399 (18)	<.001	2.494 (18)	.02	7.239 (18)	<.001
DLA F_1-score[g]	—	—	—	—	—	—
DLA recall[g]	—	—	—	—	—	—
VS	8.510 (18)	<.001	16.032 (18)	<.001	27.498 (18)	<.001
$d_{\text{hellinger}}$	3.310 (18)	.004	0.221 (18)	.83	0.446 (18)	.66
DD-plot R^2[g]	27.073 (18)	<.001	25.599 (18)	<.001	7.204 (18)	<.001

XSL•FO
RenderX

Metric	3N-5N		5N-7N		7N-10N	
	t test (*df*)	*P* value	*t* test (*df*)	*P* value	*t* test (*df*)	*P* value
Privacy						
MIA[g]	—	—	—	—	—	—
AIA	2.029 (18)	.06	1.702 (18)	.11	1.788 (18)	.09
Linkability[e,g]	—	—	0.532 (18)	.60	0.898 (18)	.38
Singling out	0.082 (18)	.94	1.224 (18)	.24	0.736 (18)	.47

[a]Significance level is .05 for all statistical tests.

[b]CS: cosine similarity.

[c]DLA: data labeling analysis.

[d]AUC: area under the curve.

[e]*t* tests were not performed for these due to the results being the same as the ones found in the baseline metrics.

[f]Not applicable.

[g]*t* tests were not performed for these due to the standard deviation being zero.

[h]VS: Vendi Score.

[i]DD-plot: depth versus depth plot.

[j]MIA: membership inference attack.

[k]AIA: attribute inference attack.

Discussion

Principal Results

In these experiments, a comparison between centralized SDG models and federated implementations of them was performed using AML data with the aim of evaluating the SD fidelity and privacy in each of the scenarios, assessing the SD generation techniques over an FL approach to address the data scattering issue while addressing data scarcity. Three different scenarios were considered for the federated models: the one in which the number of samples in each node was evenly distributed (B), the one where the node-wise data quantity was randomly and unevenly distributed (IB), and the one where non-IID data distributions were created ($IB_{non\text{-}iid}$).

In the case of the CTGAN model, in the B scenario, the φ_k metric deteriorated to a maximum of 9% with respect to the baseline, while the DLA showed an average difference of 17% in the AUC, a difference of 9% for the F_1-score, and a difference of 0.21% for the recall metric. The VS showed a difference between 2% and 12% showing that the diversity of the generated samples varied among experiments. For this scenario, the Hellinger distance varied to a maximum of 3%, and the DD-plot R^2 to a maximum of 35%. The most privacy-preserving experiments in terms of the AIA were 3N and 7N, with a risk reduction of 18% with respect to the baseline, while the worst one (5N) performed 18% below, although not statistically significant. Privacy against singling out attacks improved between 46% and 61%, while no difference was found for MIAs and linkability attacks.

In the IB scenario, the maximum deterioration of the φ_k metric was 11%, and the DLA showed average values of 17% in the case of the AUC, 10% for the F_1-score, and 1% for the recall metric. The VS showed that numerical variables are diversely generated, achieving differences between 1% and 3%, while the Hellinger distances varied to a maximum of 3%. DD-plot R^2 values varied by about 22%. AIA analyses showed a maximum improvement of 55% on data privacy, while the maximum deterioration was 26%, although not statistically significant. Singling out attacks showed differences between 51% and 80%, while the linkability ones varied minimally.

Finally, the $IB_{non\text{-}iid}$ scenario showed a maximum deterioration of 11% in the φ_k metric, while DLA AUC scores showed average differences of 21%, the F_1-score varied 10%, and the recall varied minimally. The VS showed maximum variations of 17%, and the Hellinger distance varied to 5%. Regarding privacy metrics, the AIA showed a maximum improvement of 2% and a maximum deterioration of 21%, although neither was statistically significant in this case either. In this case, singling out attack risk differences varied between 73% and 83% with respect to the baseline, and the linkability measure differences were again minimal.

Now talking about the principal results of the FedTabDiff model in scenario B, the metric varied between 26% and 81%, the VS between 1% and 3%, and the Hellinger distance between 6% and 12%. In the DLA, the AUC value varied to a maximum of 1% while both the recall and the F_1-score matched the baseline results. To finish with the fidelity metrics, the DD-plot R^2 results varied between 1% and 2% with respect to the baseline. In terms of privacy, no membership inference risk was detected, while the linkability risk difference was minimal. The AIA results varied between 10% and 13%, while the singling out ones varied between 4% and 15%.

Talking about scenario IB, the φ_k metric varied between 1% and 27%, and the DLA-related AUC metric varied by 2% at most, matching the baseline results for both the recall and the F_1-score, just as in the B scenario. The VS variation was neither high, reaching 2% differences at most. While the Hellinger

XSL•FO
RenderX

distance oscillated between 6% and 10%, the DD-plot R^2 varied to a maximum of 4%. Regarding the privacy metrics, no membership inference risk was found, and the linkability varied minimally with respect to the baseline results. While the attribute inference risk difference oscillated between 23% and 39%, the singling out risk difference varied to a maximum of 15%.

To finish, the $IB_{non\text{-}iid}$ scenario showed an oscillation between 29% and 39% for the φ_k metric, while all the DLA AUC changes were minimal and the recall- and F_1-score-related results matched those of the baseline. For the VS, the variation reached 22% at maximum, and the Hellinger distance varied between 7% and 62%. The DD-plot R^2 varied between 2% and 40%. To finish, the privacy metrics in this scenario followed the previous tendencies by showing no membership inference risk and minimal linkability risks. Attribute inference risk differences oscillated between 10% and 35%, while the singling out ones varied between 35% and 44%.

Limitations

As it was pointed out in the beginning, this work aims to provide insight into a specific use case of federated SDG for an AML dataset, both with a GAN-type model and a diffusion-type model. However, extending the analysis by using upcoming SDG models and more extensive aggregation functions for the FL framework may result in more generalizable conclusions, which will be prioritized in future work. Linked with that, models incorporating more novel tools like DP and the implementation of advanced FL security frameworks should be covered in future extensions of this research. Parameter tuning for model optimization remains a considerable path for analyzing the combination of both SDG and FL.

Furthermore, the three scenarios resulted in similar overall tendencies for all the calculated metrics and both models, suggesting the scenario proposals in this work may not have that much of an impact on the results. Further research may uncover differences for various data dispersion schemas and non-IID distribution types, which may have a much greater impact on the calculated metrics and the methodology to be followed. In addition, extremely imbalanced approaches may show different tendencies in the analyses.

Finally, the generative aspect of this research should be taken into account for future research, as expanding the calculations to a higher number of datasets may result in more robust and scalable optimizations on federated SDG. Related to the issue, a more extensive set of metrics could also be considered in the future, as literature is rapidly evolving and novel metrics could be introduced in upcoming publications. Our metric selection, however, is intended to be comparable to other state-of-the-art works.

Comparison With Prior Work

While there are a few studies that analyze the combination of both FL and SDG, this is, to the best of the authors' knowledge, the first research work that tries to quantify the impact of generative model federation over fidelity and privacy metrics, using different numbers of nodes, and considering different real-world data distribution scenarios in AML.

Expanding the literature search, incorporating DP to federated SDG models has been widely investigated, as well as successfully integrated into several use cases, improving privacy metrics under those conditions [46-48]. Our research, however, has shown reasonable privacy guarantees both for centralized and federated scopes without the need for using DP, suggesting the incorporation of it may depend on the final use case, as it deteriorates SD fidelity, even though more extensive evaluations should be performed. In addition, the latest research shows DP may not have statistically significant differences in terms of privacy, suggesting that applications with no need to implement it exist [63].

Furthermore, in the scope of FL, previous works on classification and regression models have hardly shown any deterioration due to the federation process with regard to a centralized model [67]. Instead, when SDG models were compared to centralized results in this AML use case, statistically significant differences appeared, suggesting that SDG models may be more sensible to the federation step than usual ML cases, such as classification or regression.

To finish, the data distribution scenarios considered for this research demonstrated robustness against non-IID distributions, which is in line with other experiments performed in the literature [68].

Conclusions

The results for both models and the three scenarios showed considerable data fidelity losses after the model federation process, while no significant deterioration or improvement tendency was found in the respective privacy metrics. The number of federated nodes did not show any significant trend, even though specific comparisons resulted in statistically relevant differences in some cases.

Acknowledgments

Funded by the European Union's Horizon Europe Research and Innovation Program under project SYNTHEMA (grant 101095530). Views and opinions expressed are, however, those of the authors only and do not necessarily reflect those of the European Health and Digital Executive Agency. Neither the European Union nor the granting authority can be held responsible for them.

Data Availability

The original datasets analyzed during this study are available in the Tazi_NatureC_AML repository [49,50].

XSL•FO
RenderX

Conflicts of Interest

None declared.

Multimedia Appendix 1
Description of the variables that were included in this study.
[PDF File (Adobe PDF File), 97 KB - medinform_v13i1e74116_app1.pdf]

Multimedia Appendix 2
Categorical variable distributions and number of samples per node and scenario.
[PDF File (Adobe PDF File), 841 KB - medinform_v13i1e74116_app2.pdf]

Multimedia Appendix 3
Aggregation algorithm comparison.
[PDF File (Adobe PDF File), 175 KB - medinform_v13i1e74116_app3.pdf]

Multimedia Appendix 4
Variable-wise metric results using the CTGAN model.
[PDF File (Adobe PDF File), 1383 KB - medinform_v13i1e74116_app4.pdf]

Multimedia Appendix 5
Variable-wise metric results using the FedTabDiff model.
[PDF File (Adobe PDF File), 1497 KB - medinform_v13i1e74116_app5.pdf]

References

1. Dozzo A, Galvin A, Shin J, Scalia S, O Driscoll CM, Ryan KB. Modelling acute myeloid leukemia (AML): what's new? A transition from the classical to the modern. Drug Deliv Transl Res 2023;13(8):2110-2141 [FREE Full text] [doi: 10.1007/s13346-022-01189-4] [Medline: 35930221]
2. Dhall A, Zee BM, Yan F, Blanco MA. Intersection of epigenetic and metabolic regulation of histone modifications in acute myeloid leukemia. Front Oncol 2019;9:432 [FREE Full text] [doi: 10.3389/fonc.2019.00432] [Medline: 31192132]
3. Vakiti A, Mewawalla P. Acute Myeloid Leukemia. Florida: StatPearls Publishing; 2024.
4. Dong Y, Shi O, Zeng Q, Lu X, Wang W, Li Y, et al. Leukemia incidence trends at the global, regional, and national level between 1990 and 2017. Exp Hematol Oncol 2020;9:14 [FREE Full text] [doi: 10.1186/s40164-020-00170-6] [Medline: 32577323]
5. Arber DA, Orazi A, Hasserjian R, Thiele J, Borowitz MJ, Le Beau MM, et al. The 2016 revision to the World Health Organization classification of myeloid neoplasms and acute leukemia. Blood 2016;127(20):2391-2405 [FREE Full text] [doi: 10.1182/blood-2016-03-643544] [Medline: 27069254]
6. Acute myeloid leukemia (AML) subtypes and prognostic factors. American Cancer Society. 2018. URL: https://www.cancer.org/cancer/types/acute-myeloid-leukemia/detection-diagnosis-staging/how-classified.html [accessed 2024-01-31]
7. Benard B, Gentles AJ, Köhnke T, Majeti R, Thomas D. Data mining for mutation-specific targets in acute myeloid leukemia. Leukemia 2019;33(4):826-843 [FREE Full text] [doi: 10.1038/s41375-019-0387-y] [Medline: 30728456]
8. Abhishek A, Jha RK, Sinha R, Jha K. Automated classification of acute leukemia on a heterogeneous dataset using machine learning and deep learning techniques. Biomed Signal Process Control 2022;72:103341. [doi: 10.1016/j.bspc.2021.103341]
9. Karami K, Akbari M, Moradi M, Soleymani B, Fallahi H. Survival prognostic factors in patients with acute myeloid leukemia using machine learning techniques. PLoS One 2021;16(7):e0254976 [FREE Full text] [doi: 10.1371/journal.pone.0254976] [Medline: 34288963]
10. Dong S, Premnath N, Sadeghi N, Kainthla R, Chung SS, Collins RH, et al. Racial and ethnic disparities in acute myeloid leukemia: 15-year experience at a safety net hospital system. Leuk Res 2024;141:107503. [doi: 10.1016/j.leukres.2024.107503] [Medline: 38676993]
11. Winestone LE, Getz KD, Li Y, Burrows E, Scheurer ME, Tam V, et al. Racial and ethnic disparities in acuity of presentation among children with newly diagnosed acute leukemia. Pediatr Blood Cancer 2024;71(1):e30726 [FREE Full text] [doi: 10.1002/pbc.30726] [Medline: 37856154]
12. Synthetic data. European Data Protection Supervisor. 2024. URL: https://www.edps.europa.eu/press-publications/publications/techsonar/synthetic-data [accessed 2025-09-09]
13. Hernandez M, Epelde G, Alberdi A, Cilla R, Rankin D. Synthetic data generation for tabular health records: a systematic review. Neurocomputing 2022;493:28-45. [doi: 10.1016/j.neucom.2022.04.053]

XSL•FO
RenderX

14. Van BB, Qian Z, Van DSM. Synthetic data, real errors: how (not) to publish and use synthetic data. 2023 Presented at: Proceedings of the 40th International Conference on Machine Learning; July 23–29, 2023; Honolulu, Hawaii, USA p. 34793-34808 URL: https://proceedings.mlr.press/v202/van-breugel23a.html
15. McMahan H, Moore E, Ramage D, Hampson S. Communication-efficient learning of deep networks from decentralized data. ArXiv. Preprint posted online on February 17, 2016 2016. [doi: 10.48550/arXiv.1602.05629]
16. Shouval R, Labopin M, Unger R, Giebel S, Ciceri F, Schmid C, et al. Prediction of hematopoietic stem cell transplantation related mortality—lessons learned from the in-silico approach: a European society for blood and marrow transplantation acute leukemia working party data mining study. PLoS One 2016;11(3):e0150637 [FREE Full text] [doi: 10.1371/journal.pone.0150637] [Medline: 26942424]
17. Lu Z, Pan H, Dai Y, Si X, Zhang Y. Federated learning with non-IID data: a survey. IEEE Internet Things J 2024;11(11):19188-19209. [doi: 10.1109/jiot.2024.3376548]
18. Luo G, Chen N, He J, Jin B, Zhang Z, Li Y. Privacy-preserving clustering federated learning for non-IID data. Future Gener Comput Syst 2024;154:384-395. [doi: 10.1016/j.future.2024.01.005]
19. Gonzales A, Guruswamy G, Smith SR. Synthetic data in health care: a narrative review. PLOS Digital Health 2023;2(1):e0000082 [FREE Full text] [doi: 10.1371/journal.pdig.0000082] [Medline: 36812604]
20. Hu J, Du J, Wang Z, Pang X, Zhou Y, Sun P, et al. Does differential privacy really protect federated learning from gradient leakage attacks? IEEE Trans Mobile Comput 2024;23(12):12635-12649. [doi: 10.1109/tmc.2024.3417930]
21. Shenoy D, Bhat R, Prakasha KK. Exploring privacy mechanisms and metrics in federated learning. Artif Intell Rev 2025;58(8):223. [doi: 10.1007/s10462-025-11170-5]
22. Zhu L, Han S. Deep leakage from gradients. In: Federated Learning. Cham: Springer; 2019:17-31.
23. Goodfellow I, Pouget-Abadie J, Mirza M. Generative adversarial networks. Commun ACM 2020;63(11):139-144 [FREE Full text] [doi: 10.1145/3422622]
24. Zhao Z, Kunar A, Birke R, Van der Scheer H, Chen LY. CTAB-GAN+: enhancing tabular data synthesis. Front Big Data 2023;6:1296508 [FREE Full text] [doi: 10.3389/fdata.2023.1296508] [Medline: 38260053]
25. Osorio-Marulanda PA, Epelde G, Hernandez M, Isasa I, Reyes NM, Iraola AB. Privacy mechanisms and evaluation metrics for synthetic data generation: a systematic review. IEEE Access 2024;12:88048-88074. [doi: 10.1109/access.2024.3417608]
26. Ramachandranpillai R, Sikder MF, Bergström D, Heintz F. Bt-GAN: generating fair synthetic healthdata via bias-transforming generative adversarial networks. J Artif Intell Res 2024;79:1313-1341. [doi: 10.1613/jair.1.15317]
27. Akiya I, Ishihara T, Yamamoto K. Comparison of synthetic data generation techniques for control group survival data in oncology clinical trials: simulation study. JMIR Med Inform 2024;12:e55118 [FREE Full text] [doi: 10.2196/55118] [Medline: 38889082]
28. Khan SA, Murtaza H, Ahmed M. Utility of GAN generated synthetic data for cardiovascular diseases mortality prediction: an experimental study. Health Technol 2024;14(3):557-580. [doi: 10.1007/s12553-024-00847-6]
29. Dhawan K, S Nijhawan S. Cross-modality synthetic data augmentation using GANs: enhancing brain MRI and chest X-ray classification. medRxiv. Preprint posted online on June 10, 2024 2024. [doi: 10.1101/2024.06.09.24308649]
30. Pezoulas VC, Zaridis DI, Mylona E, Androutsos C, Apostolidis K, Tachos NS, et al. Synthetic data generation methods in healthcare: a review on open-source tools and methods. Comput Struct Biotechnol J 2024;23:2892-2910 [FREE Full text] [doi: 10.1016/j.csbj.2024.07.005] [Medline: 39108677]
31. Biswas A, Talukdar W. Enhancing clinical documentation with synthetic data: leveraging generative models for improved accuracy. Int J Innovative Sci Res Technol 2024:1553-1566. [doi: 10.38124/ijisrt/ijisrt24may2085]
32. Li H, Yu S, Principe J. Causal recurrent variational autoencoder for medical time series generation. AAAI 2023;37(7):8562-8570. [doi: 10.1609/aaai.v37i7.26031]
33. Titar RR, Ramanathan M. Variational autoencoders for generative modeling of drug dosing determinants in renal, hepatic, metabolic, and cardiac disease states. Clin Transl Sci 2024;17(7):e13872 [FREE Full text] [doi: 10.1111/cts.13872] [Medline: 38949489]
34. Saragih DG, Hibi A, Tyrrell PN. Using diffusion models to generate synthetic labeled data for medical image segmentation. Int J Comput Assist Radiol Surg 2024;19(8):1615-1625. [doi: 10.1007/s11548-024-03213-z] [Medline: 38900372]
35. Yang Y, Jin M, Wen H. A survey on diffusion models for time series and spatio-temporal data. ArXiv. Preprint posted online on April 29, 2024 2024. [doi: 10.48550/arXiv.2404.18886]
36. Naseer AA, Walker B, Landon C. ScoEHR: generating synthetic electronic health records using continuous-time diffusion models. 2023 Presented at: Proceedings of the 8th Machine Learning for Healthcare Conference, PMLR; July 11–12, 2023; Cham, Switzerland p. 489-508 URL: https://proceedings.mlr.press/v219/naseer23a.html
37. Pozzi M, Noei S, Robbi E, Cima L, Moroni M, Munari E, et al. Generating and evaluating synthetic data in digital pathology through diffusion models. Sci Rep 2024;14(1):28435 [FREE Full text] [doi: 10.1038/s41598-024-79602-w] [Medline: 39557989]
38. D'Amico S, Dall'Olio D, Sala C, Dall'Olio L, Sauta E, Zampini M, et al. Synthetic data generation by artificial intelligence to accelerate research and precision medicine in hematology. JCO Clin Cancer Inform 2023;7:e2300021 [FREE Full text] [doi: 10.1200/CCI.23.00021] [Medline: 37390377]

XSL•FO
RenderX

39. Eckardt J, Hahn W, Röllig C, Stasik S, Platzbecker U, Müller-Tidow C, et al. Mimicking clinical trials with synthetic acute myeloid leukemia patients using generative artificial intelligence. NPJ Digital Med 2024;7(1):76 [FREE Full text] [doi: 10.1038/s41746-024-01076-x] [Medline: 38509224]
40. Licandro R, Schlegl T, Reiter M. WGAN latent space embeddings for blast identification in childhood acute myeloid leukaemia. : IEEE; 2018 Presented at: 24th International Conference on Pattern Recognition (ICPR); August 20-24, 2018; Beijing, China p. 3868-3873. [doi: 10.1109/icpr.2018.8546177]
41. Rupapara V, Rustam F, Aljedaani W, Shahzad HF, Lee E, Ashraf I. Blood cancer prediction using leukemia microarray gene data and hybrid logistic vector trees model. Sci Rep 2022;12(1):1000 [FREE Full text] [doi: 10.1038/s41598-022-04835-6] [Medline: 35046459]
42. He H, Bai Y, Garcia E, Li S. ADASYN: adaptive synthetic sampling approach for imbalanced learning. : IEEE; 2008 Presented at: IEEE International Joint Conference on Neural Networks (IEEE World Congress on Computational Intelligence); June 01-08, 2008; Hong Kong p. 1322-1328. [doi: 10.1109/ijcnn.2008.4633969]
43. Linardos A, Kushibar K, Walsh S, Gkontra P, Lekadir K. Federated learning for multi-center imaging diagnostics: a simulation study in cardiovascular disease. Sci Rep 2022;12(1):3551 [FREE Full text] [doi: 10.1038/s41598-022-07186-4] [Medline: 35241683]
44. Liu D, Miller T, Sayeed R, Mandl K. ADL:federated-autonomous deep learning for distributed electronic health record. ArXiv. Preprint posted online on November 28, 2018 2018. [doi: 10.48550/arXiv.1811.11400]
45. Azizi Z, Lindner S, Shiba Y, Raparelli V, Norris CM, Kublickiene K, et al. A comparison of synthetic data generation and federated analysis for enabling international evaluations of cardiovascular health. Sci Rep 2023;13(1):11540 [FREE Full text] [doi: 10.1038/s41598-023-38457-3] [Medline: 37460705]
46. Xin B, Yang W, Geng Y, Chen S, Wang S, Huang L. Private FL-GAN: differential privacy synthetic data generation based on federated learning. : IEEE; 2020 Presented at: ICASSP 2020—2020 IEEE International Conference on Acoustics, Speech and Signal Processing (ICASSP); May 04-08, 2020; Barcelona, Spain p. 2927-2931. [doi: 10.1109/icassp40776.2020.9054559]
47. Behera MR, Upadhyay S, Shetty S, Priyadarshini S, Patel P, Lee K. FedSyn: synthetic data generation using federated learning. ArXiv. Preprint posted online on March 11, 2022 2022. [doi: 10.48550/arXiv.2203.05931]
48. Xin B, Geng Y, Hu T, Chen S, Yang W, Wang S, et al. Federated synthetic data generation with differential privacy. Neurocomputing 2022;468:1-10. [doi: 10.1016/j.neucom.2021.10.027]
49. Tazi Y, Arango-Ossa JE, Zhou Y, Bernard E, Thomas I, Gilkes A, et al. Unified classification and risk-stratification in acute myeloid leukemia. Nat Commun 2022;13(1):4622 [FREE Full text] [doi: 10.1038/s41467-022-32103-8] [Medline: 35941135]
50. Tazi Y. yanistazi/Tazi_NatureC_AML: nature paper release. Zenodo. URL: https://zenodo.org/records/6878209 [accessed 2025-09-12]
51. Xu L, Skoularidou M, Cuesta-Infante A, Veeramachaneni K. Modeling tabular data using conditional GAN. 2019 Presented at: Advances in Neural Information Processing Systems (NeurIPS); December 8–14, 2019; Vancouver, Canada p. 5541-5551 URL: https://proceedings.neurips.cc/paper_files/paper/2019/hash/254ed7d2de3b23ab10936522dd547b78-Abstract.html
52. Kiran A, Kumar SS. A methodology and an empirical analysis to determine the most suitable synthetic data generator. IEEE Access 2024;12:12209-12228. [doi: 10.1109/access.2024.3354277]
53. Fössing E, Drechsler J. An evaluation of synthetic data generators implemented in the python library synthcity. In: Privacy in Statistical Databases. Cham: Springer; 2024:178-193.
54. Patki N, Wedge R, Veeramachaneni K. The synthetic data vault. : IEEE; 2016 Presented at: IEEE International Conference on Data Science and Advanced Analytics (DSAA); October 17-19, 2016; Montreal, QC, Canada p. 399-410. [doi: 10.1109/dsaa.2016.49]
55. Sohl-Dickstein J, Weiss E, Maheswaranathan N, Ganguli S. Deep unsupervised learning using nonequilibrium thermodynamics. : Proceedings of the 32nd International Conference on Machine Learning. PMLR; 2015 Presented at: 32nd International Conference on Machine Learning (ICML 2015); July 6–11, 2015; Lille, France p. 2256-2265 URL: https://proceedings.mlr.press/v37/sohl-dickstein15.html
56. Zhang H, Zhang J, Srinivasan B. Mixed-type tabular data synthesis with score-based diffusion in latent space. ArXiv. Preprint posted online on October 14, 2023 2023. [doi: 10.48550/arXiv.2310.09656]
57. Kotelnikov A, Baranchuk D, Rubachev I, Babenko A. TabDDPM: modelling tabular data with diffusion models. 2023 Presented at: 40th International Conference on Machine Learning (ICML 2023); July 23–29, 2023; Honolulu, Hawaii, USA p. 17564-17579 URL: https://proceedings.mlr.press/v202/kotelnikov23a.html
58. Sattarov T, Schreyer M, Borth D. FedTabDiff: federated learning of diffusion probabilistic models for synthetic mixed-type tabular data generation. ArXiv. Preprint posted online on January 11, 2024 2024. [doi: 10.48550/arXiv.2401.06263]
59. Baak M, Koopman R, Snoek H, Klous S. A new correlation coefficient between categorical, ordinal and interval variables with Pearson characteristics. Comput Stat Data Anal 2020;152:107043. [doi: 10.1016/j.csda.2020.107043]
60. Friedman D, Dieng AB. The vendi score: a diversity evaluation metric for machine learning. Trans Mach Learn Res 2023;5:1-16. [doi: 10.1162/tmlr_a_00474]

XSL•FO
RenderX

61. Hernadez M, Epelde G, Alberdi A, Cilla R, Rankin D. Synthetic tabular data evaluation in the health domain covering resemblance, utility, and privacy dimensions. Methods Inf Med 2023;62(S 01):e19-e38 [FREE Full text] [doi: 10.1055/s-0042-1760247] [Medline: 36623830]
62. Pandala SR. LazyPredict. GitHub. 2024. URL: https://github.com/shankarpandala/lazypredict [accessed 2024-09-04]
63. Hernandez M, Osorio-Marulanda PA, Catalina M, Loinaz L, Epelde G, Aginako N. Comprehensive evaluation framework for synthetic tabular data in health: fidelity, utility and privacy analysis of generative models with and without privacy guarantees. Front Digital Health 2025;7:1576290 [FREE Full text] [doi: 10.3389/fdgth.2025.1576290] [Medline: 40343213]
64. Giomi M, Boenisch F, Wehmeyer C, Tasnádi B. A unified framework for quantifying privacy risk in synthetic data. Proc Priv Enhanc Technol 2023:312-328. [doi: 10.56553/popets-2023-0055]
65. Li Q, Diao Y, Chen Q, He B. Federated learning on non-IID data silos: an experimental study. 2021 Presented at: 2022 IEEE 38th International Conference on Data Engineering (ICDE); May 09-12, 2022; Kuala Lumpur, Malaysia p. 965-978. [doi: 10.1109/icde53745.2022.00077]
66. Beutel DJ, Topal T, Mathur A. Flower: A friendly federated learning research framework. ArXiv. Preprint posted online on July 28, 2020 2020 [FREE Full text]
67. Rodríguez-Barroso N, Stipcich G, Jiménez-López D, Ruiz-Millán JA, Martínez-Cámara E, González-Seco G, et al. Federated learning and differential privacy: software tools analysis, the sherpa.ai FL framework and methodological guidelines for preserving data privacy. Inf Fusion 2020;64:270-292. [doi: 10.1016/j.inffus.2020.07.009]
68. Apellániz PA, Parras J, Zazo S. Improving synthetic data generation through federated learning in scarce and heterogeneous data scenarios. BDCC 2025;9(2):18. [doi: 10.3390/bdcc9020018]

Abbreviations

AI: artificial intelligence
AIA: attribute inference attack
AML: acute myeloid leukemia
AUC: area under the curve
CS: cosine similarity
CTGAN: conditional tabular generative adversarial network
DD-plot: depth versus depth plot
DLA: data labeling analysis
DP: differential privacy
EHR: electronic health record
FL: federated learning
GAN: generative adversarial network
HFL: horizontal federated learning
MIA: membership inference attack
ML: machine learning
Non-IID: nonindependent and identically distributed
SD: synthetic data
SDG: synthetic data generation
VAE: variational autoencoder
VS: Vendi Score
WHO: World Health Organization

Edited by A Benis; submitted 20.03.25; peer-reviewed by A Ortuzar, MB Kaabachi, G Santangelo; comments to author 20.04.25; revised version received 10.06.25; accepted 04.09.25; published 29.09.25.

Please cite as:
Isasa I, Catalina M, Epelde G, Aginako N, Beristain A
Synthetic Tabular Data Generation Under Horizontal Federated Learning Environments in Acute Myeloid Leukemia: Case-Based Simulation Study
JMIR Med Inform 2025;13:e74116
URL: https://medinform.jmir.org/2025/1/e74116
doi:10.2196/74116
PMID:

XSL•FO
RenderX

©Imanol Isasa, Mikel Catalina, Gorka Epelde, Naiara Aginako, Andoni Beristain. Originally published in JMIR Medical Informatics (https://medinform.jmir.org), 29.09.2025. This is an open-access article distributed under the terms of the Creative Commons Attribution License (https://creativecommons.org/licenses/by/4.0/), which permits unrestricted use, distribution, and reproduction in any medium, provided the original work, first published in JMIR Medical Informatics, is properly cited. The complete bibliographic information, a link to the original publication on https://medinform.jmir.org/, as well as this copyright and license information must be included.

XSL•FO
RenderX

Original Paper

Evaluation of Machine Learning Model Performance in Diabetic Foot Ulcer: Retrospective Cohort Study

Veerle Y van Velze[1,2*], MD; Hendrico L Burger[3*], BSc; Tim J van der Steenhoven[1,4], MD, PhD; Hani Al-Ers[3], PhD; Lauren N Goncalves[1], MD; Daniël Eefting[1,4,5], MD, PhD; Willem-Jan J de Jong[1,4], MD; Harm J Smeets[1,4], MD, PhD; Janna C Specken Welleweerd[1,4], MD, PhD; Joost R van der Vorst[4,5], MD, PhD; Sandy Uchtmann[1], MSc; Robert Rissmann[2,6,7], Prof Dr, PhD; Jaap F Hamming[4,5], Prof Dr Med, MD, PhD; Lampros Stergioulas[3], Prof Dr, PhD; Koen EA van der Bogt[1,4,5], MD, PhD

[1]Department of Surgery, Haaglanden Medical Center, The Hague, The Netherlands

[2]Centre for Human Drug Research, Leiden, The Netherlands

[3]The Hague University of Applied Sciences, The Hague, Zoetermeer, The Netherlands

[4]University Vascular Centre West, Leiden, The Hague, Delft, The Netherlands

[5]Department of Vascular Surgery, Leiden University Medical Center, Leiden, The Netherlands

[6]Department of Dermatology, Leiden University Medical Center, Leiden, The Netherlands

[7]Leiden Academic Center for Drug Research, Leiden, The Netherlands

[*]these authors contributed equally

Corresponding Author:
Koen EA van der Bogt, MD, PhD
Department of Surgery
Haaglanden Medical Center
Lijnbaan 32
The Hague, 2512 VA
The Netherlands
Phone: 31 88 979 7900
Email: kvdb@haaglandenmc.nl

Abstract

Background: Machine learning (ML) has shown great potential in recognizing complex disease patterns and supporting clinical decision-making. Diabetic foot ulcers (DFUs) represent a significant multifactorial medical problem with high incidence and severe outcomes, providing an ideal example for a comprehensive framework that encompasses all essential steps for implementing ML in a clinically relevant fashion.

Objective: This paper aims to provide a framework for the proper use of ML algorithms to predict clinical outcomes of multifactorial diseases and their treatments.

Methods: The comparison of ML models was performed on a DFU dataset. The selection of patient characteristics associated with wound healing was based on outcomes of statistical tests, that is, ANOVA and chi-square test, and validated on expert recommendations. Imputation and balancing of patient records were performed with MIDAS (Multiple Imputation with Denoising Autoencoders) Touch and adaptive synthetic sampling, respectively. Logistic regression, support vector machine (SVM), k-nearest neighbors, random forest (RF), extreme gradient boosting (XGBoost), Bayesian additive regression trees, and artificial neural network were trained, cross-validated, and optimized using random sampling on the patient dataset. To evaluate model calibration and clinical utility, calibration curves, Brier scores, and decision curve analysis (DCA) were performed.

Results: The exploratory dataset consisted of 700 patient records with 199 variables. After dataset cleaning, the variables used for model training included age, smoking status, toe systolic pressure, blood pressure, oxygen saturation, hemoglobin, hemoglobin A_{1c}, estimated glomerular filtration rate, wound location, diabetes type, Texas wound classification, neuropathy, and wound area measurement. The SVM obtained a stable accuracy of 0.853 (95% CI 0.810-0.896) with an area under the receiver operating characteristic curve of 0.922 (95% CI 0.889-0.955). The RF and XGBoost acquired an accuracy of 0.838 (95% CI 0.793-0.883) and 0.815 (95% CI 0.768-0.862), respectively, with areas under the receiver operating characteristic curve of 0.917 (95% CI 0.883-0.951) for RF and 0.889 (95% CI 0.849-0.929) for XGBoost. SVM, RF, and XGBoost were well-calibrated, with average

XSL•FO
RenderX

Brier scores around 0.127 (SD 0.013). DCA showed that the SVM provided the highest net clinical benefit across relevant risk thresholds.

Conclusions: Handling missing values, feature selection, and addressing class imbalance are critical components of the key steps in developing ML applications for clinical research. Seven models were selected for comparing their predictive power regarding complete wound healing, and each model representing a different branch in ML. In this initial DFU dataset used as an example, the SVM achieved the best performance in predicting clinical outcomes, followed by RF and XGBoost. The model's calibration and clinical utility were determined through calibration curves, Brier scores, and DCA, demonstrating its potential relevance in clinical decision-making.

(JMIR Med Inform 2025;13:e71994) doi:10.2196/71994

KEYWORDS

machine learning; diabetic foot ulcer; complete wound healing; logistic regression; k-nearest neighbor; support vector machine; random forest; extreme gradient boosting; Bayesian additive regression trees; artificial neural network

Introduction

Machine learning (ML) has demonstrated remarkable efficacy in recognizing complex disease patterns and informing clinical decision-making, where conventional methods do not provide sufficient insights [1-4]. ML algorithms have been applied in various medical conditions, including cardiovascular diseases and diabetic foot ulcer (DFU) research. Previous papers have either provided an overview of potential ML models through a review or applied ML in data analyses [5]. However, there seems to be no prior medical study that has created a clear and detailed overview including examples of all the key steps generally involved in applying ML to datasets: data preprocessing, model selection, hyperparameter optimization, evaluation and comparison of model performance, and interpretation of results. Certain critical aspects of data analysis, such as addressing missing values and class imbalance, are frequently left out of the literature [6-11]. While a wide range of models can be used and compared, heavily imbalanced classes can still result in low area under the receiver operating characteristic curve (AUC) scores and accuracy [12]. Furthermore, previous studies compare at most 6 ML models, and no paper was found that explores the full spectrum of common ML models [6].

DFUs represent a complex and significant multifactorial medical problem, making these highly suitable for the application of ML. According to estimates from the International Diabetes Federation, in 2021, 537 million adults worldwide (10.5%) were living with diabetes mellitus, a number projected to escalate to 642 million by 2030. On average, 1 in 4 diabetics will experience a DFU in their lifetime, of which 22.3% (95% CI 15.3-29.2) eventually undergo a lower extremity amputation [13,14]. The personal and societal costs of DFUs and amputations are enormous, and as such, it is of utmost importance to correctly identify predictors of treatment response to optimize targeted interventions and prevent unnecessary treatments [15-18].

This study evaluates the use of 7 distinct ML models: logistic regression (LR), support vector machine (SVM), k-nearest neighbors (KNN), random forest (RF), extreme gradient boosting (XGBoost), Bayesian additive regression trees (BART), and artificial neural network (ANN). These models accommodate a wide range of regression, tree-based, probabilistic, and neural network methods, addressing higher complexity data. Moreover, LR, tree-based models, and BART provide a level of transparency that offers clear insights into the decision-making process.

Despite notable progress and research in ML, challenges persist in fully implementing all necessary steps. The multifactorial nature of DFU makes it a demanding and challenging case for evaluating the performance of ML models. By elucidating these methodologies, this paper aims to provide a framework for the proper use of ML algorithms to predict clinical outcomes of multifactorial diseases and their treatments, thereby assisting decision-making for clinicians.

Methods

Data Acquisition and Contextual Analysis

This study made use of a dataset containing records from 700 patients with a DFU due to neuropathy, ischemia, or both, who were treated at the Haaglanden Medical Center in The Hague, The Netherlands, between October 1, 2013, and October 1, 2021. Patients with a wound resulting from trauma, a surgical procedure, venous insufficiency, unguis incarnatus, or a wound located proximal to the malleoli were excluded. Structured into 71 unique categories, the dataset encapsulated 199 features per patient, reflecting a detailed record of each patient's medical journey. These features spanned from generally available information to data acquired through medical examinations and posttreatment outcomes, all extracted from the electronic patient record, Healthcare Information Exchange. General demographic information was obtained from the cover page of the record, while medical history was retrieved from referral letters, outpatient reports, hospitalization records, and discharge summaries. Substance use was assessed through records from the departments of surgery, internal medicine, pulmonology, cardiology, and anesthesiology. Vital sign measurements and laboratory results were extracted from designated Healthcare Information Exchange sections, with averages calculated for the period in which the DFU was present. Medication use was determined based on prescription records, pharmacy verifications conducted during hospital admissions, and data from the National Exchange Point (ie, LSP). Information regarding the DFU was extracted from wound care center reports and hospitalization records.

XSL•FO
RenderX

A subset of the collected features was selected for analysis (see Feature Selection section). The patient's age at the onset of the DFU was recorded in the database. Smoking encompassed the use of cigarettes, cigars, or other tobacco products. Wound location was categorized according to the angiosome concept [19]. Diabetes type was classified as type 1, noninsulin-dependent, and insulin-dependent diabetes. Neuropathy was defined as peripheral impairment of gnostic sensory function. Wound area was calculated by multiplying the average length by the average width of the DFU. Complete wound healing was defined as full closure of the DFU, with an intact epithelium and no signs of infection, necrosis, or fluid.

A key criterion for the inclusion of patient data in this retrospective cohort study was the completeness of the feature set. Patient data were included for analysis if it was entirely complete or if any missing values could be reliably imputed (see Handling Missing Values section). A significant proportion of patients did not undergo any form of treatment (ie, other than wound care or offloading), resulting in systematic presence of missing values in treatment-related features. To accommodate this and enhance the model's predictive power, the selection of features for model training and application was intentionally restricted to those that are obtainable early in the patient's care pathway (see Feature Selection section). In preparing the dataset for analysis, meticulous cleaning processes were used, which involved the exclusion of features based on redundancy in information, insufficiency in example frequency (eg, features related to rare treatments), and duplication of information through inverse representation.

Handling Missing Values

Addressing missing values was paramount for the effective use of patient data in ML models. Imputation of missing values was used to mitigate substantial information loss (Table 1) [20,21]. Numerical variables necessitating imputation, such as average systolic and diastolic blood pressure, O_2 saturation level, serum hemoglobin A_{1c} (HbA_{1c}), hemoglobin (Hb), and estimated glomerular filtration rate (eGFR), were predominantly missing due to unmeasured instances rather than systemic bias. As such, to ensure statistical validity, a multiple imputation technique was applied to preserve the integrity of the data distribution. The technique used was matching imputation, specifically the MIDAS (Multiple Imputation with Denoising Autoencoders) Touch algorithm, due to its effectiveness in handling both numerical and categorical data gaps [22-24]. This algorithm identified data patterns to infer missing values through a linear regression model, with coefficients randomly selected from the feature distribution, and the process was iteratively refined to enhance imputation accuracy. Additionally, a weighted mean imputation strategy was incorporated that adopted 50 repetitions to ensure realistic and generalized imputation. Weight determination was based on the absolute difference between the median of the imputation and its vector value, followed by calculating the reciprocal of this difference. Weight values were capped at 2.0 to prevent excessive weighting.

Table 1. Features selected and transformed for model training and testing.

Feature name	Missing amount prior to imputation, n (%)	Data type	Transformation
Age	0 (0)	Numerical	$x \rightarrow \sqrt{\max(x)-x}$
Smoking	0 (0)	Categorical	N/A[a]
Systolic blood pressure	113 (16.1)	Numerical	N/A
Diastolic blood pressure	113 (16.1)	Numerical	N/A
Oxygen saturation level	154 (22)	Numerical	$x \rightarrow \sqrt{\max(x)-x}$
HbA_{1c}[b]	82 (11.7)	Numerical	$x \rightarrow \log(x)$
Hemoglobin	0 (0)	Numerical	N/A
eGFR[c]	21 (3)	Numerical	$x \rightarrow \sqrt{x}$
Wound location	0 (0)	Categorical	N/A
Toe systolic blood pressure	264 (37.7)	Numerical	N/A
Diabetes type	0 (0)	Categorical	N/A
Texas wound classification	0 (0)	Categorical	N/A
Neuropathy	0 (0)	Categorical	N/A
Wound area	80 (11.3)	Numerical	$x \rightarrow \log(x)$
Complete wound healing	0 (0)	Categorical	N/A

[a]N/A: not applicable.

[b]HbA_{1c}: hemoglobin A_{1c}.

[c]eGFR: estimated glomerular filtration rate.

XSL•FO
RenderX

Feature Selection

In the preprocessing phase, feature selection played a crucial role in managing model complexity and ensuring adequate patient representation across different scenarios. This process relied on both statistical analysis and validation through literature to identify influential features, thus streamlining the model while preserving its predictive capability. Normalization of numerical values to approximate normal distributions was performed as a preliminary step to enhance statistical validity and facilitate effective feature selection. Normalization proved beneficial, where the normal distribution's statistical properties were leveraged for analysis. Transformations were applied to nonnormally distributed variables, such as age, HbA_{1c}, wound area, and eGFR, to align them with normal distribution characteristics. This helps the model recognize possible nonlinear correlations. To prevent imposing normality on the data, only common transformations such as lognormal, Box-Cox, and inverse transformations were applied. The selection of transformation depended on the form of skewness. Log and inverse transformations were applied to right-skewed data, while the Box-Cox transformation was used to address left-skewed data. Each transformation was based on visual inspection of the distribution and skewness prior to transformation. To check whether the distribution aids the transformation to normality, the Shapiro-Wilk test was performed after transformation with a threshold of 0.05. Feature selection was carried out using a 2-fold approach. First, relevant features were identified statistically. For each numeric feature, the group means were compared using ANOVA for normally distributed variables and Kruskal-Wallis for nonnormally distributed data. Chi-square tests were used for categorical variables. For both approaches, the 5% threshold was used to evaluate whether the feature should be included in the model. To prevent multicollinearity, only variables with a variance inflation factor below 5 were included. In the second time, expert recommendations (TJS, DE, WJJJ, JCSW, and KEAB) contributed to a second round of selection in the feature set, to include the role of clinical judgment in the final selection for context, and to resolve conflicting results, supported by literature on known predictors of DFU outcomes [25-32]. Age, smoking history, toe systolic pressure, blood pressure, oxygen saturation, Hb, HbA_{1c}, eGFR, wound location, diabetes type, Texas wound classification, neuropathy, and wound area measurement were ultimately the features used to train the models.

Addressing Class Imbalance

The balance of datasets is crucial for ML models, especially in medical diagnostics, where accurate identification of rare instances such as hemodialysis is significant despite their lower incidence in patient populations. Imbalanced datasets, with predominance of one class over another, can lead to bias in ML models by undervaluing the minority class, adversely affecting the model's predictive performance on critical, less common outcomes [33,34]. A balanced dataset ensures equitable representation of all classes, mitigating bias and enhancing the model's ability to capture the nuances of each category. To address class imbalance, sampling methods were used to adjust the class distribution within the dataset. The adaptive synthetic (ADASYN) oversampling method, a weighted variant of a synthetic minority oversampling technique, was used to balance the dataset between patients exhibiting full healing and those not, thereby correcting the initial skewness [35]. ADASYN focuses on oversampling in regions where the minority class is sparse, essentially making the algorithm focus on harder cases to predict. Furthermore, it improves on usual oversampling methods, as it uses a combination of KNN and linear interpolation, which helps preserve the statistical properties of the dataset. It was shown that ADASYN can improve the accuracy of a classifier in clinical trials [36]. Oversampling is a common practice in handling imbalanced classification problems. In numerous cases, it helps improve the accuracy of the model. However, in some studies, oversampling has shown no significant improvement in the performance of the classifier [37]. In oversampling, it is crucial that the original data are accurate, as any existing bias can be amplified through the oversampling process. Moreover, the smaller the number of minority class examples, the greater the risk of overfitting to synthetic patterns. Oversampling may also lead to the generation of illogical cases, which is why it is important to carefully inspect the synthetic data for such issues. To ensure the validity of synthetic patients with a nonhealing ulcer, logical tests were applied to detect any illogical oversampling instances. For example, when synthetic patient data fell outside of their respective prior distribution, this patient was deemed illogical and was then resampled. Validations included the ratio of systolic to diastolic blood pressure, the limitation to a single wound location, and the correct use of the Texas wound classification.

Model Selection

This study evaluated 7 widely adopted, distinct ML models, LR, KNN, SVM, RF, XGBoost, BART, and ANN, for their efficacy in predicting DFU healing outcomes within 1 year. With these 7 models, an attempt was made to apply ML across the broadest range of possibilities. Specifically, the following range represents all ML models for the prediction of a (binary) classification.

LR, the baseline model, is widely recognized for its simplicity and effectiveness in medical binary classification tasks, although it may struggle with capturing nonlinear data relationships. LR is most appropriate when the relationship between features and the outcome is linear and when model interpretability and simplicity are prioritized. It performs effectively with smaller datasets and under conditions of minimal multicollinearity.

SVM excels in handling high-dimensional spaces through its capability to perform both linear and nonlinear classification; yet, it faces challenges with large datasets. Its capacity to handle nonlinear relationships via kernel functions makes it a robust choice for small- to medium-sized datasets where interpretability is less critical than accuracy.

KNN introduces flexibility by predicting outcomes based on the majority outcome of the most similar patients, adapting well to complex datasets at the cost of sensitivity to the number of patients and the distance metric. The KNN algorithm is well-suited for applications where no strong assumptions about the data distribution can be made. It is particularly effective for nonlinear decision boundaries and is most efficient on small-

XSL•FO
RenderX

to medium-sized datasets due to its computational overhead during inference.

RF, an ensemble method, is praised for its ability to manage nonlinear data and variable interactions, offering insights into feature importance despite its comparatively lower interpretability. RF is a preferred method when dealing with datasets containing a large number of features or where overfitting is a concern. It effectively reduces variance and is versatile for both classification and regression tasks while also handling missing values well.

XGBoost stands out for its speed, performance, and robustness against overfitting through gradient boosted decision trees, although it demands meticulous hyperparameter tuning. XGBoost is highly effective for large-scale datasets with complex interactions and structured noise, particularly when computational efficiency and predictive performance are paramount. Its built-in handling of missing data and regularization makes it especially suitable for imbalanced datasets and high-stakes prediction tasks.

BART leverages probabilistic relationships to model dependencies between variables, making them useful for interpretative insights in complex datasets. Although BART can handle uncertainty effectively, it may require extensive domain knowledge and computational resources for accurate structure learning in large datasets. BART is recommended for problems requiring flexible nonparametric modeling with integrated uncertainty quantification and automatic variable selection.

ANN is powerful for capturing complex, nonlinear patterns in high-dimensional data, often outperforming other models in prediction accuracy for intricate tasks. However, their "black-box" nature limits transparency, making it difficult to interpret specific decision pathways, and they typically require substantial, highly varied data and computational power for optimal performance.

Hyperparameter Optimization

The configuration of the hyperparameters affects the performance of the model, as the structure of the model and its capacity to generalize from the training data are significantly altered. These hyperparameters are configured independently of the data on which the model is trained, but the inherent meaning of the data does affect the predictive power of the configuration. Therefore, identifying the optimal configuration is crucial. A grid search was used to identify the best hyperparameter combination based on model accuracy. The grid search method iterated 1000 times over the model training and testing, recording the results of each iteration along with its hyperparameter setup and the prediction accuracy. In the event of missing values, class imbalance, or lack of data, it is essential to measure all performance metrics (see Evaluation and Comparison of Model Performance section). Only accuracy was ultimately used, as other metrics did not yield additional insight, and the other factors have been addressed. In cases where the hyperparameter range is large or computational time is a concern, heuristic search methods offer a more efficient alternative. For grid search specifically, each possibility of the configuration is included at least once. Visual confirmation was used to determine whether convergence toward the best hyperparameter combination was incidental or deterministic.

For LR, only the model weights were adjusted to reflect feature importance. For KNN, the k-number of neighbors was optimized to balance flexibility and overfitting. In SVM, cost and γ controlled the margin and kernel function, while degree and kernel type shaped the function itself.

In tree-based models like RF and XGBoost, hyperparameters such as the number of trees, maximum tree depth, and features per split regulated complexity and diversity of the ensemble trees. XGBoost further required learning rate η for convergence, split thresholds γ to prune weak splits, and regularization terms λ and α to reduce overfitting. BART retained default prior distributions for simplicity, although they can be adjusted when data-specific insights deem them unfit. For ANN, the number of hidden layers and neurons per layer was prioritized for their impact on model capacity and complexity.

Evaluation and Comparison of Model Performance

As random variation in dataset partitioning can influence model outcomes, steps were taken to ensure that the results reflected both robustness and representativeness rather than chance. To address this challenge, repeated random split cross-validation was used by iteratively splitting the dataset and training the hyperparameter-optimized model 1000 times, ensuring that each possible configuration was included at least once in the grid search. In each iteration, the dataset was randomly divided into a unique training (70%) and testing (30%) set, which were kept separate to prevent data leakage. This iterative process allowed the model to be evaluated on different combinations of training and testing data, enhancing the reliability of its predictions. For each split, the model, configured with optimal hyperparameters, was then trained on the training set and evaluated on the testing set, both using patient characteristics. Following the prediction, the results were compared to the true values and fitted into a confusion matrix, with performance further quantified by average accuracy, specificity, precision, recall, and AUC. Finally, the iterative process provided not only a look into the average performance but also the variance. Low variance indicates the model's ability to generalize well for patients outside of the training and testing data. Noteworthy indicators of model performance included accuracy for average performance, specificity for predictive power on patients with a nonhealing ulcer, and the considered balance between specificity and recall.

For the BART model, uncertainty quantification was enhanced through a density plot, providing greater transparency in the decision-making process. The density plot visualizes the probability distribution of wound healing. The peak of the plot indicates where the model is most confident in its classification. A red line marks the threshold, the probability level used to distinguish between healing and nonhealing outcomes. Predicted probabilities exceeding this threshold are classified as healing, while those falling below it are classified as nonhealing.

A calibration curve was used to ensure that the predicted probabilities reflect true outcome likelihoods. This curve

XSL•FO
RenderX

compares predicted probabilities to observed outcomes to detect systematic over- or underestimation. To quantitatively evaluate calibration, Brier scores were calculated. The Brier score, ranging from 0 to 1, reflects the model's ability to estimate true outcome probabilities with high certainty, with lower values indicating better calibration.

Decision curve analysis (DCA) was used to evaluate the clinical use of the ML models (see Model Selection section) [38]. DCA measures the net benefit of a model dependent on risk threshold probability. It displays the most beneficial decision-making strategy corresponding to a patient risk probability. For instance, in a patient with a DFU who receives a predicted 85% risk of nonhealing, a clinical decision rule that recommends amputation for any risk exceeding 80% would lead to an amputation. If, in reality, the DFU would have healed without surgical intervention, this decision would constitute overtreatment. DCA allows such trade-offs to be visualized and quantified across a range of thresholds, thereby supporting the selection of a decision threshold that yields the highest overall clinical benefit.

Dataset Size

A common challenge in ML training is the need for a sufficiently large dataset to effectively train a classification model. In practical applications, obtaining such data is difficult and time-consuming. Hence, the improvement in model performance relative to dataset size was measured. The selected ML models were trained with randomly sampled, evenly classified train and test datasets. The performance results were visualized together with a learning curve illustrating the dataset size expansion required to achieve the anticipated performance level. Learning curves are a practical tool for evaluating the relationship between model performance and dataset size. These curves help determine the extent to which additional training data might enhance model performance.

Ethical Considerations

The study was conducted in accordance with the principles of the World Medical Association Declaration of Helsinki. The independent Medical Ethics Review Committee Southwest Holland reviewed the study and determined that it does not fall within the scope of the Medical Research Involving Human Subjects Act (approval number 18-038), as it does not constitute scientific research as defined in article 1, paragraph 1, subsection b of the Medical Research Involving Human Subjects Act. The study consists of a retrospective chart review rather than research in which individuals are subjected to interventions or imposed behavioral regulations. Additionally, the scientific and general board of directors of the Haaglanden Medical Center approved the execution of the study and granted an exemption from obtaining informed consent due to the retrospective nature of data collection and the exclusive use of anonymized data. This decision was based on the minimal risk to patients, the impracticality of contacting patients, and the strict safeguards implemented to protect privacy. The data were derived from electronic patient records and documented anonymously within the Castor medical web application. All data handling was conducted in compliance with the General Data Protection Regulation. Access to the dataset was restricted to authorized members of the research team, which was stored on a protected hospital server with controlled access. No identifiable information was used in the analyses or presented in the results. As the study relied exclusively on retrospective and anonymized data, no patients were contacted, and no financial or other compensation was provided.

Results

The final dataset used for prediction and analysis contained information from 900 patients. After applying imputation and oversampling techniques for incomplete patient records, 308 (44%) patients were recovered for model training (Table 2). The original dataset comprised 700 patients, with 427 (61%) representing cases of complete wound healing. Through ADASYN, approximately 200 synthetic patient records with a nonhealing ulcer were generated, equalizing the representation of both classes to 450 (50%) patients.

Table 2. Statistical validity before and after imputation of empty values.

Feature	Before imputation, mean (SD)	After imputation, mean (SD)
Diastolic blood pressure (mm Hg)	69 (12)	70 (12)
O_2 saturation (%)	97 (2)	97 (2)
Serum eGFR[a] (mL/min/1.73 m^2)	66 (33)	66 (33)
Serum hemoglobin (mmol/L)	7.8 (1.2)	7.8 (1.1)
Serum HbA_{1c}[b] (mmol/mol)	69 (19)	69 (18)
Systolic blood pressure (mm Hg)	137 (18)	137 (16)
Toe systolic blood pressure (mm Hg)	77 (46)	76 (39)
Wound area measurement (cm^2)	4.1 (11.6)	3.8 (11.0)

[a]eGFR: estimated glomerular filtration rate.

[b]HbA_{1c}: hemoglobin A_{1c}.

Feature selection of the dataset yielded the features that are linearly correlated with wound healing (α=.05) and used in the prediction of DFU healing (see Feature Selection section). Only wound location contained variance inflation factor values greater than 5 due to the wide variety of locations. Seven models, LR, KNN, SVM, RF, XGBoost, BART, and ANN, were optimized

XSL•FO
RenderX

with a grid search set within the most commonly used boundaries (see Table 3 for hyperparameters) [39]. These models were trained and tested, resulting in the following outcomes. The validation of model training demonstrated a high predictive power with an average accuracy of 0.794 (SD 0.023). However, notable performance differences existed when comparing models against their respective baselines. Feature importance measured by both the RF and XGBoost models revealed critical predictors for DFU healing outcomes. These predictors were determined by their use in decision-making. Key predictors highlighted by both models included toe systolic pressure on the affected side, Hb, wound area, age, systolic blood pressure, and diastolic blood pressure. Furthermore, BART offered enhanced insights into uncertainty quantification through a density plot, contributing to greater transparency in the decision-making process. The density plot represents the probability of wound healing for a randomly selected patient, with a 69% likelihood that healing will occur (Figure 1). Table 4 shows the model performance averaged over 1000 iterations in terms of accuracy, specificity, precision, recall, and AUC metrics. SVM achieved the highest performance with an accuracy of 0.853, followed by RF (accuracy=0.838) and XGBoost (accuracy=0.815). KNN (accuracy=0.789) and ANN (accuracy=0.789) scored lower, followed by BART (accuracy=0.748), with LR (accuracy=0.725) scoring the least in overall performance. The reliability of the predicted probabilities was assessed using calibration curves (Figure 2). The ideal calibration is represented by the diagonal dotted black line, indicating perfect alignment between predicted and actual probabilities. Deviations from this line indicate miscalibration. Curves below the diagonal suggest overconfidence (ie, predicted probabilities are too high), while curves above the diagonal indicate underconfidence (ie, predicted probabilities are too low). The Brier scores indicate that SVM, RF, and XGBoost are better at class discrimination, whereas LR, KNN, and ANN exhibit less reliable probability estimates (Table 4).

Table 3. Results of the model hyperparameter tuning.

Model	Hyperparameters (lower bound-upper bound)
Logistic regression	
—[a]	—
Support vector machine	
Gamma	0.1 (0.1-10)
Cost	7.1 (0.1-100)
Degree	3 (1-5)
Kernel	Radial basis
K-nearest neighbor	
K	1 (1-10)
Random forest	
Number of trees	230 (10-300)
Depth	90 (10-100)
Features	3 (1-25)
Extreme gradient boosting	
Number of trees	30 (10-300)
Depth	16 (10-100)
Eta	0.23 (0.01-0.4)
Gamma	0.19 (0.01-0.2)
Lambda	1.60 (0.1-2)
Alpha	0.30 (0.1-2)
Bayesian additive regression trees	
Number of trees	30 (10-100)
Depth	90 (10-100)
Artificial neural network	
Layers	2 (1-5)
Neurons	16. 8 (64.2-32.2)
Threshold	0.001 (0.1-0.001)

[a]Not available.

XSL•FO
RenderX

Figure 1. Density plot for uncertainty quantification of a Bayesian additive regression trees model prediction.

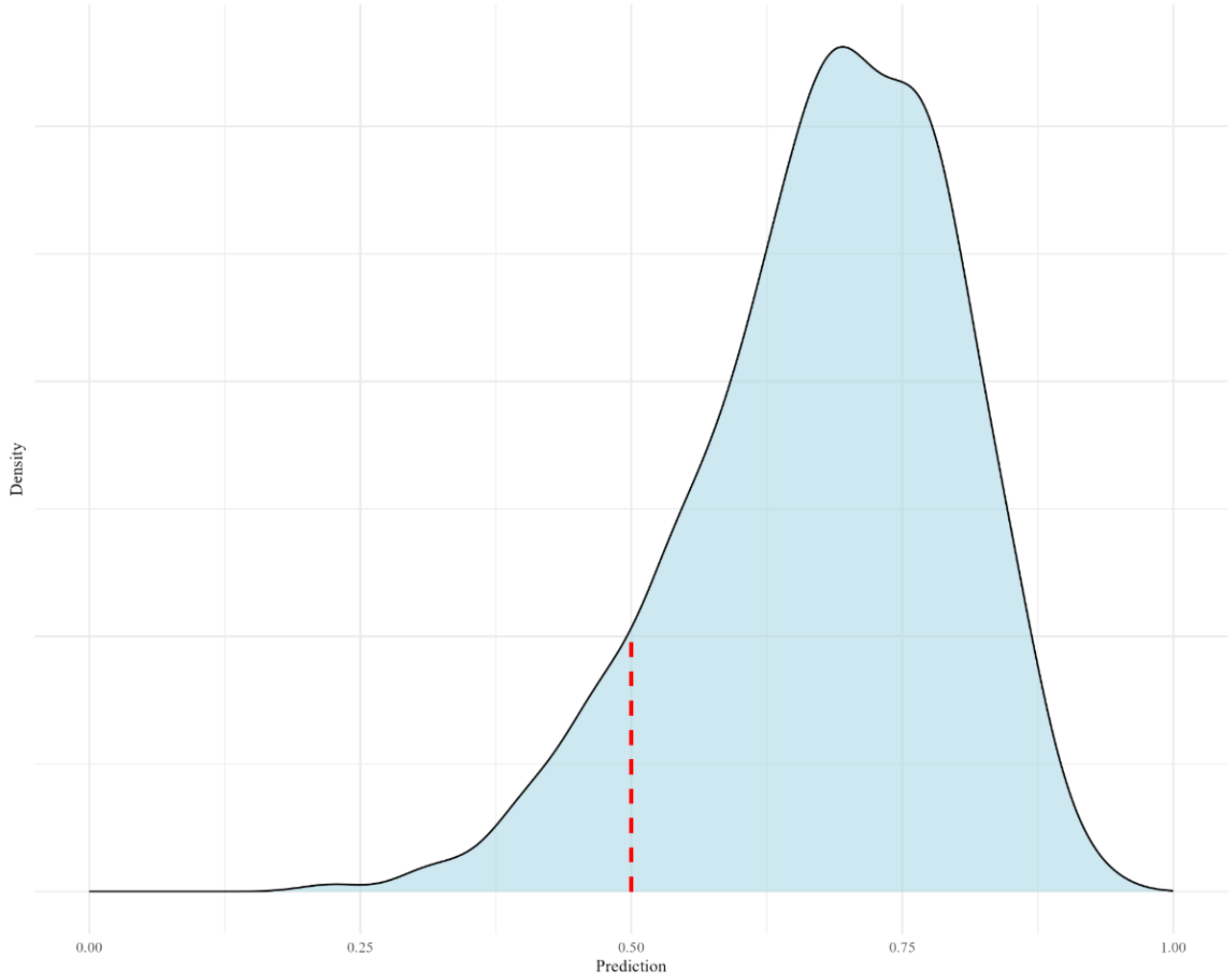


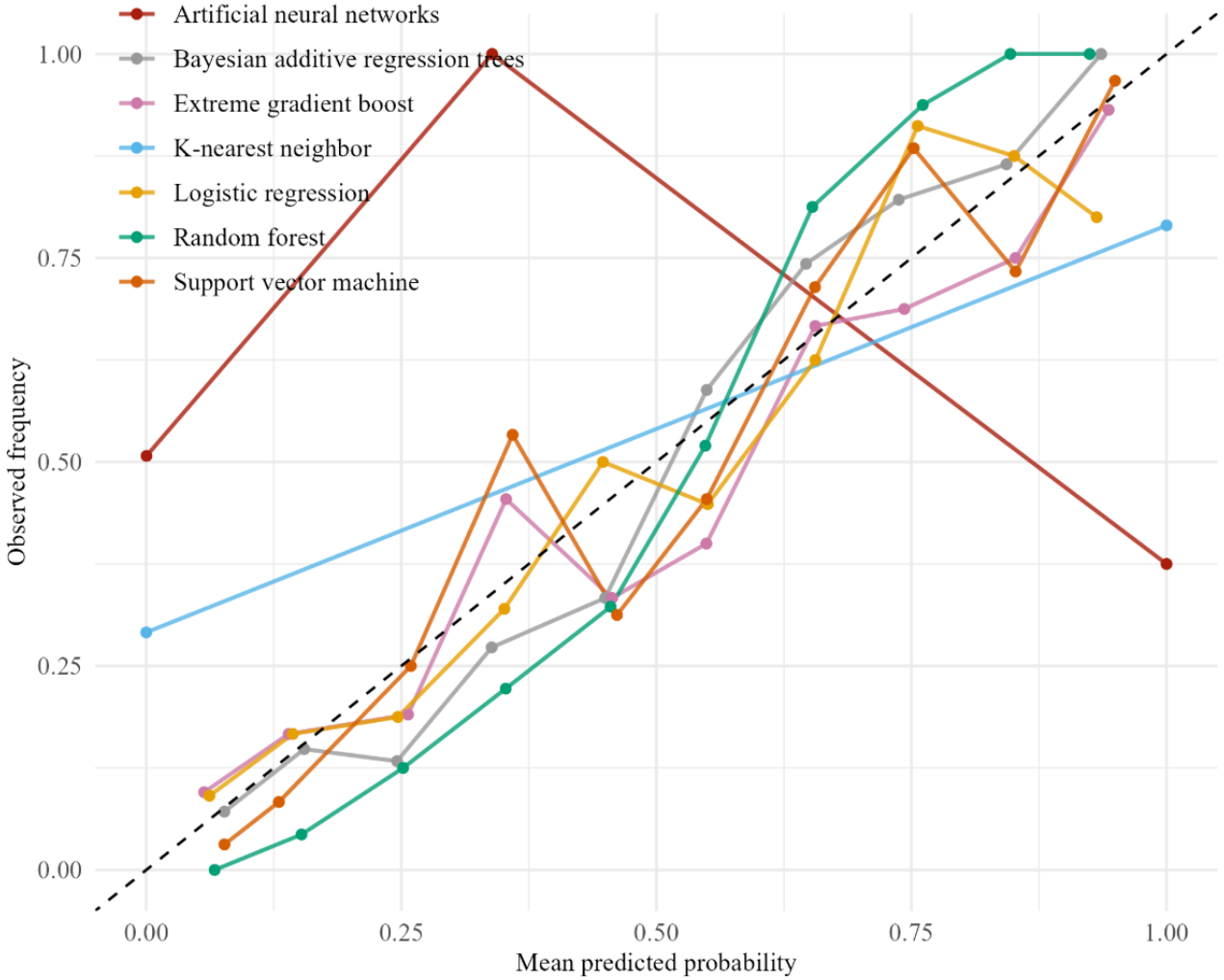
Table 4. Model performance metrics with 95% CI.

Model	Accuracy (95% CI)	Specificity (95% CI)	Precision (95% CI)	Recall (95% CI)	AUC[a] (95% CI)	Brier score (95% CI)
Logistic regression	0.725 (0.679-0.771)	0.711 (0.628-0.794)	0.723 (0.669-0.793)	0.739 (0.666-0.812)	0.794 (0.751-0.837)	0.179 (0.156-0.202)
Support vector machine	0.853 (0.810-0.896)	0.846 (0.772-0.920)	0.851 (0.792-0.910)	0.860 (0.799-0.921)	0.922 (0.889-0.955)	0.111 (0.087-0.135)
K-nearest neighbor	0.789 (0.744-0.834)	0.891 (0.831-0.951)	0.870 (0.808-0.932)	0.692 (0.620-0.764)	0.792 (0.747-0.837	0.131 (0.131-0.131)
Random forest	0.838 (0.793-0.883)	0.850 (0.781-0.919)	0.853 (0.793-0.910)	0.826 (0.761-0.891)	0.917 (0.883-0.951)	0.133 (0.115-0.151)
Extreme gradient boosting	0.815 (0.768-0.862)	0.822 (0.747-0.897)	0.827 (0.768-0.886)	0.809 (0.742-0.876)	0.889 (0.849-0.929)	0.138 (0.105-0.171)
Bayesian additive regression trees	0.748 (0.701-0.795)	0.736 (0.661-0.811)	0.746 (0.692-0.800)	0.762 (0.688-0.836)	0.749 (0.702-0.796)	0.169 (0.129-0.190)
Artificial neural network	0.789 (0.736-0.842)	0.770 (0.703-0.837)	0.761 (0.654-0.868)	0.811 (0.730-0.892)	0.793 (0.744-0.842)	0.202 (0.153-0.251)

[a]AUC: area under the receiver operating characteristic curve.

XSL•FO
RenderX

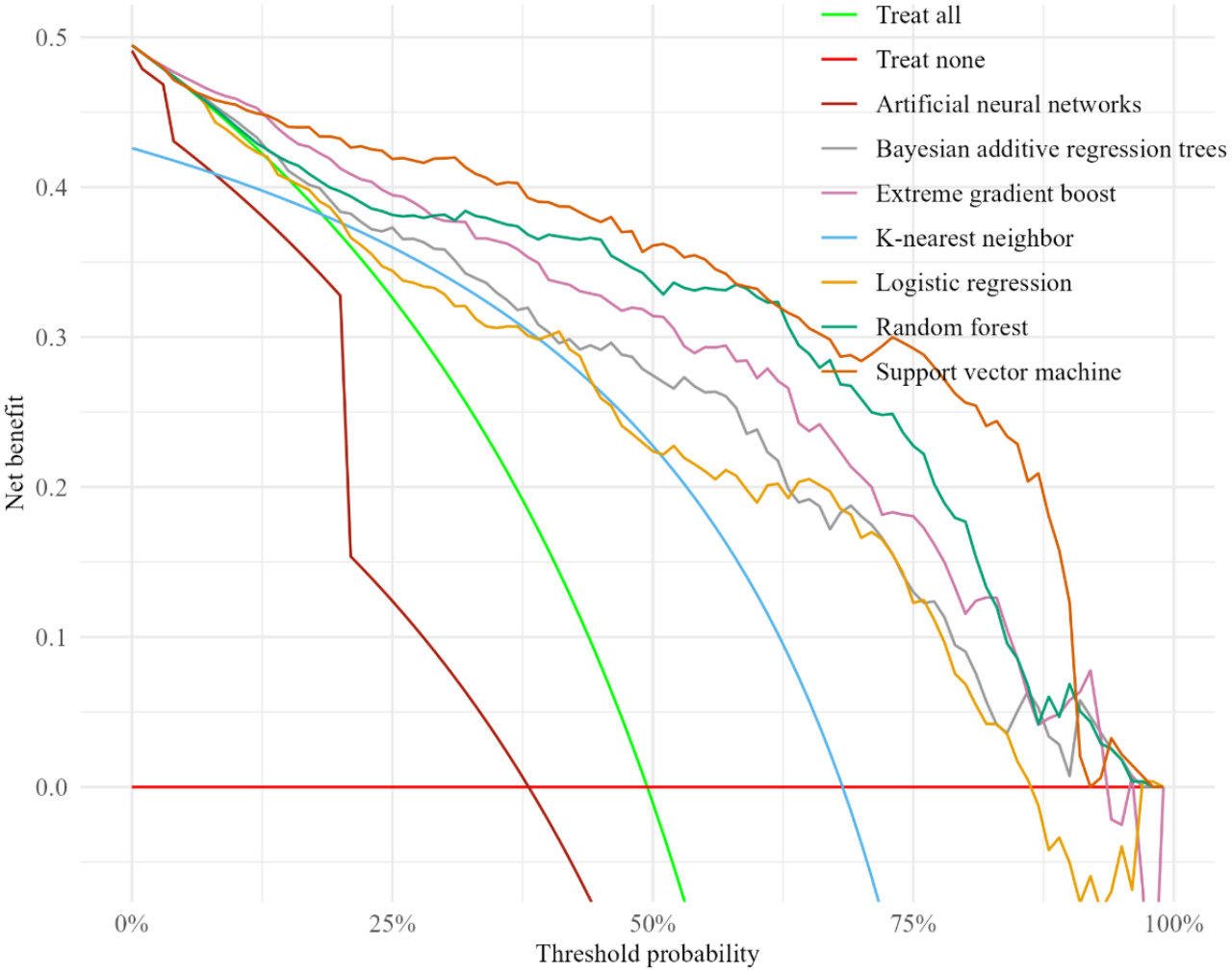
Figure 2. Calibration curves: calibration performance of the machine learning models compared to the ideal calibration represented by the diagonal dotted black line.



The DCA showed the benefit of each ML model in the application of complete wound healing within 1 year (Figure 3). To facilitate interpretation, the threshold probability was modeled to the estimated risk of patients not achieving complete wound healing within 1 year. Overall, the SVM consistently outperformed both the treat all and treat none strategies, as well as the other ML models evaluated. This advantage was particularly evident at the 75% risk threshold, where the SVM demonstrated the highest net benefit. With the exception of the ANN, the curves remained distant from the extremes of treating all or no patients, demonstrating clear clinical benefit. The ANN curve remained close to the treat all baseline, indicating limited net benefit compared to the other models. The analysis highlighted the potential of ML to support and enhance clinical decision-making in DFU care, especially between the higher risk threshold values (0.2-1.0).

XSL•FO
RenderX

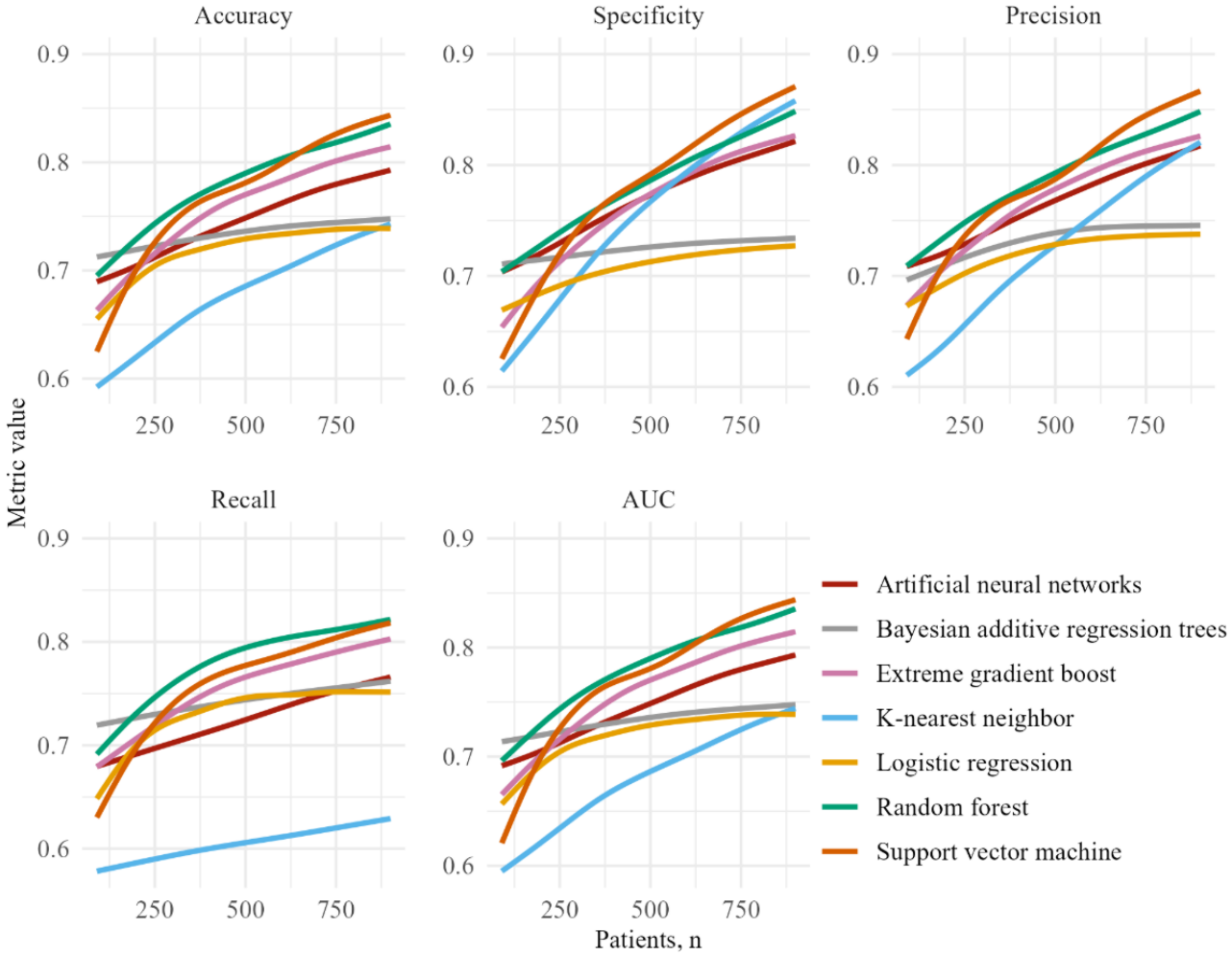
Figure 3. Decision curve analysis: correlation between net benefit and patient risk threshold probability of model predictions.



Finally, the model's performance in relation to the dataset size provided valuable insights into potential improvements in average performance (Figure 4). While the baseline LR reached its peak accuracy at approximately 73%, the SVM, RF, XGBoost, and ANN exhibited promising signs of improvement with increasing dataset size.

XSL•FO
RenderX

Figure 4. Learning curves: correlation between model performance metrics and dataset size. AUC: area under the receiver operating characteristic curve.



Discussion

Principal Findings

This paper offered a structured framework for applying ML models in clinical research. Using ML in a dataset necessitated several fundamental steps: data acquisition, contextual analysis, handling missing values, feature selection, addressing class imbalance, model selection, hyperparameter optimization, evaluation and comparison of model performance, and interpretation of results. As ML models become more accurate with more examples in a database, developing a good model requires significant computational power. The choice of different statistical methods was related to the number of available variables, the size of the studied population, and the outcomes of interest. This study demonstrated that SVM, RF, and XGBoost achieved the best performance in predicting outcomes from a dataset related to a multifactorial disease.

Imputation with low variance in feature distribution ensured statistical coherence, which is essential in medical research. This coherence supports the accuracy of patient representation and validates the reliability of the results, providing a statistically coherent foundation for model training.

Preprocessing and feature selection resulted in a clean dataset with features that were linearly correlated with complete wound healing within a year. These features included age, smoking status, toe systolic pressure, blood pressure, oxygen saturation, Hb, HbA_{1c}, eGFR, wound location, diabetes type, Texas wound classification, neuropathy, and wound area measurement. These features aligned with findings reported in prior literature [40,41]. Seven models were selected for comparing their predictive power regarding complete wound healing, and each model representing a different branch in ML [42,43]. Each model provided distinct characteristics and unique insights, suggesting that combining multiple models could be a valuable approach to enhance predictive accuracy and interpretability. This study's comparative approach sought not only to discern the optimal models for predicting DFU healing but also endeavored to deepen the understanding of the underlying factors influencing these outcomes. Feature importance therefore played a pivotal role in understanding the relative significance of features within each algorithm. To achieve this, the influence of features on model predictions was explored. Specifically, the feature importance of the RF and XGBoost models was taken into account due to their ability to measure nonlinear correlations. Upon comparing overall predictive scores, SVM performed best. While the baseline LR model and BART plateaued at 0.75

XSL•FO
RenderX

accuracy, KNN, RF, XGBoost, ANN, and even SVM itself continued to show signs of improvement when trained on an increasing dataset size. Although BART did not achieve high accuracy, it demonstrated value by providing predictive certainty, which is essential for supporting informed decision-making, assessing risk, and enhancing transparency in complex scenarios, where achieving complete accuracy is not feasible. The Brier scores, which quantify overall model calibration quality, supported the results observed in model performance. SVM achieved the lowest Brier score, indicating that the predicted probabilities were also well-calibrated and were able to discriminate between classes. These findings are further reinforced by the DCA, which demonstrated that ML models, especially SVM, consistently yielded the highest net benefit across the full range of threshold probabilities, validating clinical usability. The limited performance of the ANN likely stems from its inclination to predict predominantly a single class, reflecting both insufficient training data and difficulty in capturing complex patterns within the dataset. To realize improved model performances for KNN, RF, XGBoost, ANN, and SVM, we aim to include more patients before moving toward clinical applicability.

Imperative Steps in Clinical ML

The fundamental steps necessary for applying ML to a dataset are elaborated on in the Methods section. Each step serves a distinct purpose, and omitting any of them may lead to detrimental consequences. For instance, handling missing values is imperative, as ignoring them can result in an inaccurate representation of the patient population, distorting the model's output and leading to incorrect predictions that fail to reflect the true clinical situation. Similarly, neglecting class imbalance can cause the model to perform poorly in predicting the rarer class, which may lead to incorrect treatment decisions in clinical practice. Additionally, choosing the wrong model or failing to optimize hyperparameters can prevent the model from generalizing well to new data, ultimately undermining its clinical applicability.

Comparison with Prior Work

In other DFU-related studies, 1 or a combination of up to 6 different ML models were used to predict disease outcomes [6,11,25,44-49]. In addition to the 7 models selected for this paper, various papers proposed the use of specialized model variants, ensembles, or hybrids. Some examples are stacking C, bagging, Adaboost, and light gradient boosting machine [42,45,50]. We chose to exclude these models to uphold the simplicity and clarity of our application.

Transferability Across Clinical Domains

The methodological framework outlined in this paper is intended to be broadly applicable across a wide range of clinical domains and is particularly well-suited for multifactorial diseases, such as cardiovascular diseases, oncology, autoimmune disorders, neurodegenerative diseases, and psychiatric conditions. These disorders are often characterized by complex, nonlinear interactions between numerous variables. ML models offer a distinct advantage over conventional analytical approaches by effectively identifying and prioritizing relevant features. Moreover, there is growing recognition that environmental and geographical factors significantly influence disease outcomes, contributing to an increasing number of relevant variables in datasets. To ensure optimal model performance and enhance clinical applicability, it is crucial to ensure that a database comprises a sufficiently large cohort with an adequate number of variables. Potential challenges in applying the framework to other clinical conditions include the presence of variables with many distinct classes or free-text fields, rare outcomes occurring in only a small subset of the population, a dataset with a large proportion of imaging data, and structurally missing or incomplete data. In certain domains, temporal dynamics play a critical role, which may necessitate the use of more advanced modeling techniques to appropriately capture and analyze time-dependent patterns.

Strengths and Limitations

For this paper, a near-complete dataset was compiled, encompassing all consecutive patients from one of the largest hospitals in the Netherlands regarding DFU management, comprising 199 variables. Substantial effort was dedicated to collecting and curating the data to ensure its completeness and quality. Additionally, 7 different ML models were applied, making this paper a strong representation of the current capabilities of ML in this domain.

Leveraging this extensive dataset and the application of multiple ML models, this study highlights the advantages of ML over conventional statistical methods in DFU management. Besides their ability to process large amounts of data, these ML models offer several key benefits. First, the models can identify complex, nonlinear relationships between variables that may be overlooked by conventional methods. In complex datasets such as the one used in this paper, interactions between different factors can be subtle. Second, the ML models used provided alternative methods to extract relevant features from data, helping researchers identify important predictive factors that might have otherwise been overlooked. Certain variables may unexpectedly prove important, as manually identifying the most relevant features in high-dimensional datasets can be challenging. Unlike traditional approaches, which rely on human intuition and domain knowledge, both of which can introduce bias, ML models use data-driven techniques to determine feature importance objectively. Third, the models effectively handled missing data through imputation, enhancing data usability and improving predictive accuracy. It is important to note, however, that imputation should only be applied when a small proportion of data is missing. Applying imputation to a large number of missing values can significantly distort the dataset, introduce bias, and compromise the validity and reliability of the resulting predictive models. ML models can adapt and improve, as more data become available, continuously refining and optimizing predictions. Integrating ML models into clinical decision support systems can offer objective, data-driven insights for health care providers and patients, allowing informed personalized decisions, such as the option to wait longer for wound healing or to pursue a different path in DFU treatment such as amputation and early revalidation when muscle mass is not yet decreased because of prolonged immobilization.

XSL•FO
RenderX

The retrospective nature of this database presents a limitation for this study, as some data were not recorded for a portion of the patient cohort. In this regard, it would have been ideal to analyze a prospective dataset. Furthermore, clinical applicability would be more profound with a larger database. This could not have been anticipated prior to the analysis, as the learning curves demonstrate an increase in performance up to at least 900 patients (Figure 4). Learning curves provide valuable insights into how much the model's performance might improve with additional training data, helping to determine whether collecting more data is beneficial or if the model has reached its performance plateau. When there is still room for improvement, one must be cautious of overfitting, where models overly adapt to training data, performing well on training data but poorly generalizing to new, unseen data. This can result in inaccurate predictions and decision-making in practice. This limitation may be overcome by providing sufficient training data, reducing the likelihood that unseen data will yield a different outcome. In addition, implementing cross-validation helps assess generalizable performance, while avoiding data leakage, ensuring balanced class distributions, and minimizing the number of features further contribute to reducing overfitting. Moreover, there was limited availability of specific variables, such as having a rare condition. These variables could not be included in the feature selection, as their absence can lead to biases in the models and inaccurate predictions. Therefore, clinical applicability needs to be validated in an extended database.

To ensure the added value of ML models in clinical practice, it is an important role of computer data scientists to formulate quality standards for clinical decision models. In addition, a careful collaboration between the computer scientists, statisticians, and clinicians is necessary to identify suitable outcomes in clinical, imaging, and biochemical parameters. For example, one would be most interested in factors that can be clinically modified or that strongly predict good or absolutely worst outcomes. Moreover, clinical interpretation of findings from ML models is clearly needed. For example, Hb levels showed a strong relationship with wound healing outcomes in this study. However, while poor wound healing could be a direct result of anemia, anemia may also be a consequence of a generally ill patient because of a chronic wound.

Future Research

The next step will focus on obtaining more than 1000 complete patient records in the DFU dataset to provide clinically relevant features and develop a combined ML prediction model with an accuracy exceeding 90%.

Conclusions

This study aimed to provide a framework for using ML models to investigate factors influencing a multifactorial disease. Taken together, the steps involved in the process include data acquisition, contextual analysis, handling missing values, feature selection, addressing class imbalance, model selection, hyperparameter optimization, evaluation and comparison of model performance, and interpretation of results. By using 7 different ML models, we have shown quality control for each method. In the pilot DFU dataset used as an example, the SVM performed the best, followed by RF and XGBoost. By incorporating our framework, explanations to model behavior can be structurally approached, providing better insights compared to metric values alone.

Acknowledgments

The authors are grateful to Dr Mathis JF Mourey for his assistance with the editing phase. Funding for VYV and HLB was provided by Stichting Researchfonds Bronovo. This study was supported by the Haaglanden Medical Center Scientific Fund and RULER (real time multimodal and multidisciplinary perfusion imaging) project.

Data Availability

The dataset generated and analyzed during this study is not publicly available due to the protection of patient privacy but are available from the corresponding author on reasonable request. All analyses were performed on the Windows 11 operating system using RStudio (version 4.4.1; Posit PBC) and open-source packages. The complete code and workflow are available on GitHub, ensuring full reproducibility [51].

Authors' Contributions

Conceptualization: VYV, HA-E, LS, KEAB
Data curation: VYV, HLB
Formal analysis: HLB
Funding acquisition: RR, KEAB
Investigation: VYV, TJS, LNG, DE, WJJJ, HJS, JCSW, JRV, SU, JFH, KEAB
Methodology: VYV, HLB, TJS, HA-E, KEAB
Project administration: HA-E, LS, KEAB
Software: HLB
Supervision: RR, LS, KEAB
Writing—original draft: VYV, HLB, KEAB
Writing—review and editing: VYV, HLB, TJS, HA-E, LNG, DE, WJJJ, HJS, JCSW, JRV, SU, RR, JFH, LS, KEAB

XSL•FO
RenderX

Conflicts of Interest

None declared.

References

1. Premsagar P, Aldous C, Esterhuizen TM, Gomes BJ, Gaskell JW, Tabb DL. Comparing conventional statistical models and machine learning in a small cohort of South African cardiac patients. Inform Med Unlocked 2022;34:101103. [doi: 10.1016/j.imu.2022.101103]
2. Desai RJ, Wang SV, Vaduganathan M, Evers T, Schneeweiss S. Comparison of machine learning methods with traditional models for use of administrative claims with electronic medical records to predict heart failure outcomes. JAMA Netw Open 2020 Jan 03;3(1):e1918962 [FREE Full text] [doi: 10.1001/jamanetworkopen.2019.18962] [Medline: 31922560]
3. Shin S, Austin PC, Ross HJ, Abdel-Qadir H, Freitas C, Tomlinson G, et al. Machine learning vs. conventional statistical models for predicting heart failure readmission and mortality. ESC Heart Fail 2021 Feb;8(1):106-115 [FREE Full text] [doi: 10.1002/ehf2.13073] [Medline: 33205591]
4. Churpek MM, Yuen TC, Winslow C, Meltzer DO, Kattan MW, Edelson DP. Multicenter comparison of machine learning methods and conventional regression for predicting clinical deterioration on the wards. Crit Care Med 2016 Feb;44(2):368-374 [FREE Full text] [doi: 10.1097/CCM.0000000000001571] [Medline: 26771782]
5. Basu S, Johnson KT, Berkowitz SA. Use of machine learning approaches in clinical epidemiological research of diabetes. Curr Diab Rep 2020 Dec 03;20(12):80. [doi: 10.1007/s11892-020-01353-5] [Medline: 33270183]
6. Du C, Li Y, Xie P, Zhang X, Deng B, Wang G, et al. The amputation and mortality of inpatients with diabetic foot ulceration in the COVID-19 pandemic and postpandemic era: a machine learning study. Int Wound J 2022 Oct;19(6):1289-1297 [FREE Full text] [doi: 10.1111/iwj.13723] [Medline: 34818691]
7. Lin C, Yuan Y, Ji L, Yang X, Yin G, Lin S. The amputation and survival of patients with diabetic foot based on establishment of prediction model. Saudi J Biol Sci 2020 Mar;27(3):853-858 [FREE Full text] [doi: 10.1016/j.sjbs.2019.12.020] [Medline: 32127762]
8. Lopez-de-Andres A, Hernandez-Barrera V, Lopez R, Martin-Junco P, Jimenez-Trujillo I, Alvaro-Meca A, et al. Predictors of in-hospital mortality following major lower extremity amputations in type 2 diabetic patients using artificial neural networks. BMC Med Res Methodol 2016 Nov 22;16(1):160 [FREE Full text] [doi: 10.1186/s12874-016-0265-5] [Medline: 27876006]
9. Luo Y, Tang Z, Hu X, Lu S, Miao B, Hong S, et al. Machine learning for the prediction of severe pneumonia during posttransplant hospitalization in recipients of a deceased-donor kidney transplant. Ann Transl Med 2020 Feb;8(4):82 [FREE Full text] [doi: 10.21037/atm.2020.01.09] [Medline: 32175375]
10. Manilich E, Remzi FH, Fazio VW, Church JM, Kiran RP. Prognostic modeling of preoperative risk factors of pouch failure. Dis Colon Rectum 2012 Apr;55(4):393-399. [doi: 10.1097/DCR.0b013e3182452594] [Medline: 22426262]
11. Ferreira ACBH, Ferreira DD, Oliveira HC, Resende ICD, Anjos A, Lopes MHBDM. Competitive neural layer-based method to identify people with high risk for diabetic foot. Comput Biol Med 2020 May;120:103744. [doi: 10.1016/j.compbiomed.2020.103744] [Medline: 32421649]
12. Awan SE, Bennamoun M, Sohel F, Sanfilippo FM, Dwivedi G. Machine learning-based prediction of heart failure readmission or death: implications of choosing the right model and the right metrics. ESC Heart Fail 2019 Apr;6(2):428-435 [FREE Full text] [doi: 10.1002/ehf2.12419] [Medline: 30810291]
13. Armstrong DG, Boulton AJM, Bus SA. Diabetic foot ulcers and their recurrence. N Engl J Med 2017 Jun 15;376(24):2367-2375. [doi: 10.1056/NEJMra1615439] [Medline: 28614678]
14. Rodrigues BT, Vangaveti VN, Urkude R, Biros E, Malabu UH. Prevalence and risk factors of lower limb amputations in patients with diabetic foot ulcers: a systematic review and meta-analysis. Diabetes Metab Syndr 2022 Feb;16(2):102397. [doi: 10.1016/j.dsx.2022.102397] [Medline: 35085918]
15. Costa IG, Camargo-Plazas P. The impact of diabetic foot ulcer on individuals' lives and daily routine: a qualitative study informed by social constructivism and symbolic interactionism frameworks. J Wound Ostomy Continence Nurs 2023;50(1):73-77. [doi: 10.1097/WON.0000000000000941] [Medline: 36640167]
16. Khunkaew S, Fernandez R, Sim J. Health-related quality of life among adults living with diabetic foot ulcers: a meta-analysis. Qual Life Res 2019 Jun;28(6):1413-1427. [doi: 10.1007/s11136-018-2082-2] [Medline: 30565072]
17. Rice JB, Desai U, Cummings AKG, Birnbaum HG, Skornicki M, Parsons NB. Burden of diabetic foot ulcers for medicare and private insurers. Diabetes Care 2014;37(3):651-658. [doi: 10.2337/dc13-2176] [Medline: 24186882]
18. Guest JF, Fuller GW, Vowden P. Diabetic foot ulcer management in clinical practice in the UK: costs and outcomes. Int Wound J 2018 Feb;15(1):43-52 [FREE Full text] [doi: 10.1111/iwj.12816] [Medline: 29243399]
19. Taylor G, Palmer J. The vascular territories (angiosomes) of the body: experimental study and clinical applications. Br J Plast Surg 1987 Mar;40(2):113-141. [doi: 10.1016/0007-1226(87)90185-8] [Medline: 3567445]
20. Rubin DB. Multiple imputation after 18+ years. J Am Stat Assoc 1996 Jun;91(434):473-489. [doi: 10.1080/01621459.1996.10476908]

XSL•FO
RenderX

21. Jakobsen JC, Gluud C, Wetterslev J, Winkel P. When and how should multiple imputation be used for handling missing data in randomised clinical trials—a practical guide with flowcharts. BMC Med Res Methodol 2017 Dec 06;17(1):162 [FREE Full text] [doi: 10.1186/s12874-017-0442-1] [Medline: 29207961]
22. Hong S, Lynn HS. Accuracy of random-forest-based imputation of missing data in the presence of non-normality, non-linearity, and interaction. BMC Med Res Methodol 2020 Jul 25;20(1):199 [FREE Full text] [doi: 10.1186/s12874-020-01080-1] [Medline: 32711455]
23. van Buuren S, Groothuis-Oudshoorn K. mice: Multivariate imputation by chained equations in R. J Stat Soft 2011;45(3):1-67. [doi: 10.18637/jss.v045.i03]
24. Gaffert P, Meinfelder F, Bosch V. Towards an MI-proper predictive mean matching. 2018 Presented at: 2018 JSM Proceedings; July 28-August 2, 2018; Vancouver, Canada URL: https://ww2.amstat.org/meetings/proceedings/2018/data/assets/pdf/867081.pdf
25. Wang Y, Jiang C, Xing YQ, Zou L, Song M, Qu X, et al. Establishing a clinical prediction model for diabetic foot ulcers in type 2 diabetic patients with lower extremity arteriosclerotic occlusion using machine learning. Sci Rep 2025 Apr 05;15(1):11737 [FREE Full text] [doi: 10.1038/s41598-025-96502-9] [Medline: 40188298]
26. Fan Z, Huang J, Liu Y, Xie H, Yang Q, Liang Y, et al. Multifactorial analysis of risk factors for foot ulcers in patients with neurovascular complications of diabetes. Front Endocrinol (Lausanne) 2024;15:1399924 [FREE Full text] [doi: 10.3389/fendo.2024.1399924] [Medline: 39464185]
27. Jeon B, Choi HJ, Kang JS, Tak MS, Park ES. Comparison of five systems of classification of diabetic foot ulcers and predictive factors for amputation. Int Wound J 2017 Jun;14(3):537-545 [FREE Full text] [doi: 10.1111/iwj.12642] [Medline: 27723246]
28. Margolis DJ, Mitra N, Malay DS, Mirza ZK, Lantis JC, Lev-Tov HA, et al. Further evidence that wound size and duration are strong prognostic markers of diabetic foot ulcer healing. Wound Repair Regen 2022 Jul;30(4):487-490 [FREE Full text] [doi: 10.1111/wrr.13019] [Medline: 35470507]
29. Pickwell KM, Siersma VD, Kars M, Holstein PE, Schaper NC, Eurodiale Consortium. Diabetic foot disease: impact of ulcer location on ulcer healing. Diabetes Metab Res Rev 2013 Jul;29(5):377-383. [doi: 10.1002/dmrr.2400] [Medline: 23390115]
30. Monteiro-Soares M, Martins-Mendes D, Vaz-Carneiro A, Sampaio S, Dinis-Ribeiro M. Classification systems for lower extremity amputation prediction in subjects with active diabetic foot ulcer: a systematic review and meta-analysis. Diabetes Metab Res Rev 2014 Oct;30(7):610-622. [doi: 10.1002/dmrr.2535] [Medline: 24523130]
31. Oyibo SO, Jude EB, Tarawneh I, Nguyen HC, Harkless LB, Boulton AJ. A comparison of two diabetic foot ulcer classification systems: the Wagner and the University of Texas wound classification systems. Diabetes Care 2001 Jan;24(1):84-88. [doi: 10.2337/diacare.24.1.84] [Medline: 11194247]
32. Brownrigg JRW, Hinchliffe RJ, Apelqvist J, Boyko EJ, Fitridge R, Mills JL, et al. Performance of prognostic markers in the prediction of wound healing or amputation among patients with foot ulcers in diabetes: a systematic review. Diabetes Metab Res Rev 2016 Jan;32 Suppl 1:128-135. [doi: 10.1002/dmrr.2704] [Medline: 26342129]
33. Fernández A, García S, Galar M, Prati R, Krawczyk B, Herrera F. Learning from Imbalanced Data Sets. Cham: Springer; 2018:19-46.
34. Kaur H, Pannu HS, Malhi AK. A systematic review on imbalanced data challenges in machine learning. ACM Comput Surv 2019 Aug 30;52(4):1-36. [doi: 10.1145/3343440]
35. He H, Bai Y, Garcia E, Li S. ADASYN: adaptive synthetic sampling approach for imbalanced learning. 2008 Presented at: IEEE International Joint Conference on Neural Networks (IEEE World Congress on Computational Intelligence); June 1-8, 2008; Hong Kong p. 1322-1328. [doi: 10.1109/ijcnn.2008.4633969]
36. Zhu J, Pu S, He J, Su D, Cai W, Xu X, et al. Processing imbalanced medical data at the data level with assisted-reproduction data as an example. BioData Min 2024 Sep 04;17(1):29 [FREE Full text] [doi: 10.1186/s13040-024-00384-y] [Medline: 39232851]
37. Beinecke J, Heider D. Gaussian noise up-sampling is better suited than SMOTE and ADASYN for clinical decision making. BioData Min 2021 Nov 29;14(1):49 [FREE Full text] [doi: 10.1186/s13040-021-00283-6] [Medline: 34844620]
38. Vickers AJ, Elkin EB. Decision curve analysis: a novel method for evaluating prediction models. Med Decis Making 2006;26(6):565-574 [FREE Full text] [doi: 10.1177/0272989X06295361] [Medline: 17099194]
39. Yang L, Shami A. On hyperparameter optimization of machine learning algorithms: theory and practice. Neurocomputing 2020 Nov;415:295-316. [doi: 10.1016/j.neucom.2020.07.061]
40. Burgess JL, Wyant WA, Abdo Abujamra B, Kirsner RS, Jozic I. Diabetic wound-healing science. Medicina (Kaunas) 2021 Oct 08;57(10):1072 [FREE Full text] [doi: 10.3390/medicina57101072] [Medline: 34684109]
41. Armstrong DG, Tan T, Boulton AJM, Bus SA. Diabetic foot ulcers: a review. JAMA 2023 Jul 03;330(1):62-75 [FREE Full text] [doi: 10.1001/jama.2023.10578] [Medline: 37395769]
42. Sarker IH. Machine learning: algorithms, real-world applications and research directions. SN Comput Sci 2021;2(3):160 [FREE Full text] [doi: 10.1007/s42979-021-00592-x] [Medline: 33778771]
43. Kumari R, Kr. S. Machine learning: a review on binary classification. Int J Comput Appl 2017 Feb 15;160(7):11-15. [doi: 10.5120/ijca2017913083]

XSL•FO
RenderX

44. Nanda R, Nath A, Patel S, Mohapatra E. Machine learning algorithm to evaluate risk factors of diabetic foot ulcers and its severity. Med Biol Eng Comput 2022 Aug;60(8):2349-2357. [doi: 10.1007/s11517-022-02617-w] [Medline: 35751828]
45. Xie P, Li Y, Deng B, Du C, Rui S, Deng W, et al. An explainable machine learning model for predicting in-hospital amputation rate of patients with diabetic foot ulcer. Int Wound J 2022 May;19(4):910-918 [FREE Full text] [doi: 10.1111/iwj.13691] [Medline: 34520110]
46. Liu S, Zhang R, Shang X, Li W. Analysis for warning factors of type 2 diabetes mellitus complications with Markov blanket based on a Bayesian network model. Comput Methods Programs Biomed 2020 May;188:105302. [doi: 10.1016/j.cmpb.2019.105302] [Medline: 31923820]
47. Shi L, Wei H, Zhang T, Li Z, Chi X, Liu D, et al. A potent weighted risk model for evaluating the occurrence and severity of diabetic foot ulcers. Diabetol Metab Syndr 2021 Aug 31;13(1):92 [FREE Full text] [doi: 10.1186/s13098-021-00711-x] [Medline: 34465375]
48. Jian Y, Pasquier M, Sagahyroon A, Aloul F. A machine learning approach to predicting diabetes complications. Healthcare (Basel) 2021 Dec 09;9(12):1712 [FREE Full text] [doi: 10.3390/healthcare9121712] [Medline: 34946438]
49. Tao H, You L, Huang Y, Chen Y, Yan L, Liu D, et al. An interpreting machine learning models to predict amputation risk in patients with diabetic foot ulcers: a multi-center study. Front Endocrinol (Lausanne) 2025;16:1526098 [FREE Full text] [doi: 10.3389/fendo.2025.1526098] [Medline: 40201760]
50. Buchlak QD, Esmaili N, Bennett C, Wang YY, King J, Goldschlager T. Predictors of improvement in quality of life at 12-month follow-up in patients undergoing anterior endoscopic skull base surgery. PLoS One 2022;17(7):e0272147 [FREE Full text] [doi: 10.1371/journal.pone.0272147] [Medline: 35895728]
51. Coding for ML model implementations in a diabetic foot ulcer database. GitHub. URL: https://github.com/HLBurger/dfu-ml-framework-code [accessed 2025-04-22]

Abbreviations

ADASYN: adaptive synthetic
ANN: artificial neural network
AUC: area under the receiver operating characteristic curve
BART: Bayesian additive regression trees
DCA: decision curve analysis
DFU: diabetic foot ulcer
eGFR: estimated glomerular filtration rate
Hb: hemoglobin
HbA1c: hemoglobin A1c
KNN: k-nearest neighbor
LR: logistic regression
MIDAS: Multiple Imputation with Denoising Autoencoders
ML: machine learning
RF: random forest
SVM: support vector machine
XGBoost: extreme gradient boosting

Edited by A Coristine; submitted 06.02.25; peer-reviewed by H Zhang, C Udensi; comments to author 17.03.25; revised version received 22.04.25; accepted 25.04.25; published 10.10.25.

Please cite as:
van Velze VY, Burger HL, van der Steenhoven TJ, Al-Ers H, Goncalves LN, Eefting D, de Jong WJJ, Smeets HJ, Welleweerd JCS, van der Vorst JR, Uchtmann S, Rissmann R, Hamming JF, Stergioulas L, van der Bogt KEA
Evaluation of Machine Learning Model Performance in Diabetic Foot Ulcer: Retrospective Cohort Study
JMIR Med Inform 2025;13:e71994
URL: https://medinform.jmir.org/2025/1/e71994
doi:10.2196/71994
PMID:

©Veerle Y van Velze, Hendrico L Burger, Tim J van der Steenhoven, Hani Al-Ers, Lauren N Goncalves, Daniël Eefting, Willem-Jan J de Jong, Harm J Smeets, Janna C Specken Welleweerd, Joost R van der Vorst, Sandy Uchtmann, Robert Rissmann, Jaap F Hamming, Lampros Stergioulas, Koen EA van der Bogt. Originally published in JMIR Medical Informatics (https://medinform.jmir.org), 10.10.2025. This is an open-access article distributed under the terms of the Creative Commons

XSL•FO
RenderX

Attribution License (https://creativecommons.org/licenses/by/4.0/), which permits unrestricted use, distribution, and reproduction in any medium, provided the original work, first published in JMIR Medical Informatics, is properly cited. The complete bibliographic information, a link to the original publication on https://medinform.jmir.org/, as well as this copyright and license information must be included.

XSL•FO
RenderX

Original Paper

Prediction of Postoperative Venous Thromboembolism in Patients With Traumatic Brain Injury: Model Development and Validation Study

Jiang Zheng[1*], MD; Qiling Jiang[1*], MD; Yusheng Zhan[2*], BS; Yanming Tang[1*], BS; Xiaohui Du[1], MD; Guangrong Xiang[1], BS; Yufang Ouyang[1], BS; Hong Fu[1*], MD

[1]Department of Anesthesiology, Chongqing Emergency Medical Center, Chongqing University Central Hospital, School of Medicine, Chongqing University, Chongqing, China, Chongqing, China

[2]The First People's Hospital of Chongqing High-Tech Zone, Chongqing, China

[*]these authors contributed equally

Corresponding Author:
Hong Fu, MD
Department of Anesthesiology, Chongqing Emergency Medical Center, Chongqing University Central Hospital, School of Medicine, Chongqing University, Chongqing, China
No 1, JianKang Road, Yuzhong District
Chongqing, 400014
China
Phone: 86 13018396185
Email: fuhong1974@cqu.edu.cn

Abstract

Background: Venous thromboembolism (VTE) remains a critical cause of mortality among patients who are hospitalized. Patients with traumatic brain injury (TBI) are particularly susceptible to VTE due to coagulation abnormalities and immobilization. Despite this elevated risk, no validated predictive model currently exists for postoperative VTE in populations with TBI.

Objective: This study aims to develop machine learning (ML)–based predictive models for VTE in patients with TBI undergoing surgical procedures, with a focus on clinical translatability.

Methods: Data were collected from patients with TBI who underwent surgical treatment at Chongqing University Central Hospital (from October 2016 to December 2024). The dataset was randomly partitioned into a training set and an internal test set in a 7:3 ratio. The recursive feature elimination algorithm was applied for feature selection, followed by the synthetic minority oversampling technique to address class imbalance. Six ML models, including logistic regression (LR), random forest, gradient boosting decision tree, extreme gradient boosting, support vector machine, and categorical boosting, were trained and validated. Model performance was evaluated using receiver operating characteristic analysis, calibration curves (assessing probability-observation alignment), and decision curve analysis to quantify clinical net benefit. For the LR model, clinical utility was enhanced through nomogram construction, with Shapley additive explanation values providing interpretability.

Results: A total of 1806 participants were enrolled in this study, and 257 (14.2%) experienced VTE events. All ML models demonstrated strong predictive performance, with area under the receiver operating characteristic curve values ranging from 0.79 to 0.83. The LR model exhibited the highest discriminatory power (area under the receiver operating characteristic curve 0.83; accuracy 0.80; specificity 0.83). Calibration curves confirmed that the LR model provided well-calibrated probability estimates. Shapley additive explanations analysis identified key contributors to VTE risk and transformed model outputs into individualized risk predictions. A user-friendly postoperative VTE risk prediction nomogram was developed for patients with TBI.

Conclusions: This study successfully developed and validated multiple ML models for postoperative VTE prediction in patients with TBI. The LR-based nomogram, supported by calibration and decision curve validation, offers a clinically actionable tool to guide thromboprophylaxis strategies. Future external validation across diverse populations is warranted to confirm generalizability.

(JMIR Med Inform 2025;13:e78655) doi:10.2196/78655

KEYWORDS

venous thromboembolism; traumatic brain injury; machine learning; postoperative; predictive model

XSL•FO
RenderX

Introduction

Venous thromboembolism (VTE), encompassing deep vein thrombosis (DVT) and pulmonary embolism (PE), is a critical clinical syndrome associated with high morbidity and mortality among hospitalized patients [1]. Globally, an estimated 10 million individuals experience VTE annually. In the United States, PE ranks among the leading causes of cardiovascular death, accounting for up to 300,000 fatalities per year [2]. Patients with VTE experience severe complications, including adverse effects of long-term anticoagulation (eg, hemorrhage risk), prolonged hospitalization, elevated 30-day readmission rates, and delayed adjuvant therapies (eg, chemotherapy or radiotherapy) [3]. VTE significantly contributes to extended hospital stays and increased mortality [4,5]. Notably, patients with traumatic brain injury (TBI) who develop VTE exhibit prolonged intensive care unit stays and extended mechanical ventilation duration [6].

TBI affects approximately 50 million individuals globally each year, with epidemiological models suggesting that nearly half of the global population may sustain at least 1 TBI during their lifetime [7]. TBI is an independent risk factor for VTE, elevating the risk through multifactorial pathophysiological mechanisms [6]. Studies indicate that patients with multitrauma and TBI face significantly higher VTE risk than those without TBI, attributable to disease complexity and delayed early interventions [8]. Coagulopathy is prevalent in this population; 67% of the patients with severe TBI exhibit coagulation abnormalities upon emergency presentation, which often progress during hospitalization [9,10]. In addition, cohorts of patients who underwent surgical procedures demonstrate elevated VTE incidence due to venous stasis from general anesthesia and intraoperative immobilization, postoperative mobility restrictions, and tissue injury–induced inflammation and coagulation pathway activation [11].

Severe TBI is strongly associated with coagulopathy, substantially elevating the risk of VTE, particularly in cohorts of patients who underwent surgical procedures. Identifying patients at high risk for postoperative VTE is thus critically imperative. Despite this established clinical need, current literature lacks dedicated studies developing VTE predictive models tailored to patients with surgical TBI. Machine learning (ML) has demonstrated significant efficacy in perioperative risk prediction across diverse surgical contexts [12]. Therefore, the objective of our study is to develop an ML-based risk assessment model for VTE in patients with TBI undergoing surgical procedures.

Methods

Recruitment

This retrospective study consecutively enrolled patients hospitalized with TBI who underwent surgical intervention at Chongqing University Central Hospital between October 2016 and December 2024.

Ethical Considerations

This study was approved by the Institutional Review Board of Chongqing University Central Hospital (2024-66). The requirement of obtaining written informed consent was waived owing to the retrospective study design. All visual representations in this manuscript, including feature importance diagrams, contain only aggregated or anonymized data. No personally identifiable information of research participants is displayed in any figures or supplementary materials.

Data Collection

Overview

This study collected comprehensive clinical data from patients with TBI who underwent surgery, encompassing 6 core domains.

Demographics

Demographic data included age, sex, weight, height, American Society of Anesthesiologists (ASA) physical status classification, and history of smoking and alcohol use.

Preoperative Comorbidities

Preoperative comorbidities included hypertension, coronary heart disease, diabetes mellitus, atrial fibrillation, chronic renal insufficiency, myocardial infarction, pulmonary infection, and malignant tumors.

Injury Characteristics

The following variables were recorded: Glasgow Coma Scale (GCS) score, Rotterdam computed tomography score, injury mechanism (falls, traffic accidents, or assaults), Injury Severity Score, Abbreviated Injury Scale (AIS), head injury types (eg, concussion, cerebral contusion, diffuse axonal injury, subdural or epidural hematoma, subarachnoid hemorrhage, or skull fracture), and injury-to-admission interval.

Biochemical Parameters

Biochemical parameters included complete blood count, liver function tests, comprehensive metabolic panel, and coagulation profiles.

Preoperative Interventions

Information on medications and supportive measures included the following: anticoagulants and antiplatelets (eg, rivaroxaban, clopidogrel, and aspirin), hemostatic agents (eg, tranexamic acid, vitamin K, and etamsylate), and supportive therapies (eg, pneumatic compression therapy, mechanical ventilation, blood transfusion, endotracheal intubation or tracheostomy, and mannitol administration).

Surgical and Anesthesia Details

Data included surgical site (intracranial or extracranial), emergency status, multiple surgeries (≥2 procedures), anesthesia method (general or regional), surgery duration, intraoperative fluid balance, blood loss volume, vasopressor use, invasive monitoring (central venous), and intraoperative hypotension (systolic blood pressure <90 mm Hg).

Missing data were imputed using the K-nearest neighbors algorithm for continuous variables and the mode for categorical variables.

XSL•FO
RenderX

Outcome

The diagnosis of VTE, encompassing DVT and PE, relies on confirmatory imaging studies integrated with clinical presentation. The first-line imaging modality for DVT is Doppler ultrasonography, which identifies noncompressible veins with hypoechoic thrombi and abnormal blood flow patterns. Symptoms of PE typically present acutely and include respiratory and cardiovascular manifestations. The diagnosis of PE is commonly established using computed tomography pulmonary angiography. Clinical signs suggestive of DVT in the lower limbs include edema, discomfort, tenderness, the presence of a palpable cord, and erythema or cyanosis.

Inclusion and Exclusion Criteria

The inclusion and exclusion criteria are presented in Textbox 1.

Textbox 1. Inclusion and exclusion criteria.

Inclusion Criteria

- Patients with traumatic brain injury (including concussion, cerebral contusion, diffuse axonal injury, subarachnoid hemorrhage, and epidural or subdural hemorrhage of traumatic origin)
- Patients undergoing surgical management during the current hospitalization
- Patients aged 18 years or older at the time of enrollment

Exclusion Criteria

- Patients aged younger than 18 years
- No surgical intervention performed during the study period, surgery performed before admission to the study institution, or surgery conducted during previous hospitalizations
- Missing more than 20% of essential study variables
- Length of hospital stay shorter than 72 hours after admission
- Venous thromboembolism diagnosed before surgery

Model Development and Explanation

The comprehensive dataset was stratified randomly and partitioned into a training set (1264/1806, 70%) and an internal validation set (542/1806, 30%) while preserving class distribution. Feature selection was performed using the recursive feature elimination algorithm followed by application of the synthetic minority oversampling technique to mitigate class imbalance [13,14]. A total of 6 ML algorithms were evaluated for predictive performance: logistic regression (LR), support vector machine (SVM), random forest (RF), gradient boosting decision tree (GBDT), extreme gradient boosting (XGBoost), and categorical boosting (CatBoost).

Model performance was comprehensively evaluated through a suite of discriminative, calibrated, and clinically interpretable metrics. For discriminative capacity, we assessed receiver operating characteristic analysis with area under the curve, alongside precision-recall metrics (including F_1-score—the harmonic mean of precision and recall), sensitivity, specificity, positive predictive values (PPVs), and negative predictive values (NPVs). Calibration was quantified using the Brier score and visualized via calibration curves that compared predicted probabilities against observed outcomes across risk deciles to ensure reliable probability estimates. In terms of clinical interpretability, Shapley additive explanations (SHAP) were applied to quantify feature contributions to individual predictions, elucidating both global feature importance and local decision logic, while a nomogram was developed based on LR coefficients to translate model outputs into clinically actionable risk stratification categories. Advanced validation further strengthened the robustness of findings. Decision curve analysis was performed to evaluate net clinical benefit across threshold probabilities (0%-100%), comparing model-guided interventions against “treat-all” or baseline strategies.

Statistical Analysis

Continuous variables were presented as medians (IQRs), and categorical variables were presented as numbers and percentages. All analyses were performed using PyCharm (version 2023.3.4; JetBrains), SPSS (version 26.0; IBM Corp), and R (version 4.2.1; R Foundation for Statistical Computing).

Results

Overview

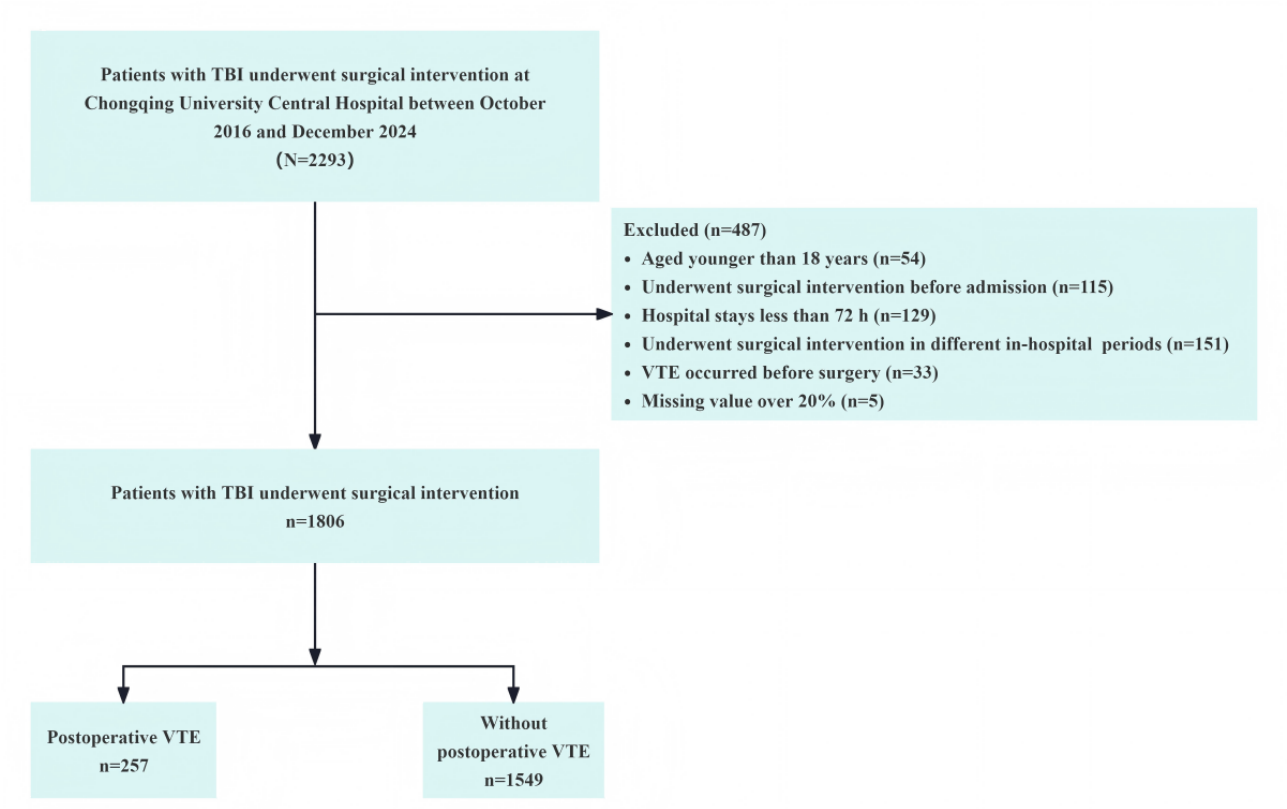
From October 2016 to December 2024, a total of 1806 patients with TBI who underwent surgical intervention were enrolled in this study (Figure 1). Among these patients, 257 (14.2%) experienced VTE, including 254 (14.1%) cases of DVT and 3 (0.2%) cases of PE (Figure S1 in Multimedia Appendix 1). Table 1 presents the demographic and clinical characteristics of the study population. The median age of the patients was 51 (IQR 37-62) years. A total of 1324 (73.4%) patients were male. The most common cause of injury was traffic accidents, affecting 1033 (57.2%) patients. Cerebral contusion was diagnosed in 1017 (56.3%) patients, subdural or epidural hematoma in 967 (53.5%) patients, and subarachnoid hemorrhage in 910 (50.4%) patients (Figures S2 and S3 in Multimedia Appendix 1). Regarding the severity of head injury based on the GCS scores, 1022 (56.6%) patients had mild head injury (GCS score 13-15), 226 (12.5%) had moderate head injury (GCS score 9-12), and 558 (30.9%) had severe head injury (GCS score 3-8; Table 1 and Figure S4 in Multimedia

XSL•FO
RenderX

Appendix 1). For the modeling dataset, 1806 cases were included, with 1264 (70%) assigned to the training set and 541 (30%) to the internal validation set (Table 1).

The top 7 variables selected for inclusion in the models based on the recursive feature elimination were as follows: age, Barthel index (BI), ASA class, multiple surgeries, anesthesia types, serum magnesium (Mg^{2+}) levels, and limb AIS score (Figure 2).

Figure 1. The flowchart of the study population. TBI: traumatic brain injury; VTE: venous thromboembolism.



XSL•FO
RenderX

Table 1. Baseline characteristics of the patients in the training set and test set.

Variables	Total (N=1806)	Training set (n=1264)	Test set (n=542)
Age (y), median (IQR)	51 (37-62)	52 (37-61)	51 (36-62)
Weight (kg), median (IQR)	62 (55-70)	63 (55-70)	62 (55-70)
Barthel index, median (IQR)	0 (10-30)	10 (0-30)	10 (0-30)
Male, n (%)	1324 (73.3)	935 (74)	389 (71.8)
ASA[a] physical status classification≥3, n (%)	1133 (62.7)	800 (63.2)	333 (61.4)
Delayed admission, n (%)	278 (15.4)	197 (15.6)	82 (15.1)
Smoking, n (%)	539 (29.8)	384 (30.4)	155 (28.6)
Drinking, n (%)	288 (15.9)	201 (15.9)	87 (16.1)
Hypertension, n (%)	236 (13.1)	166 (13.1)	70 (12.9)
Coronary heart disease, n (%)	35 (1.9)	22 (1.7)	13 (2.4)
Diabetes, n (%)	112 (6.2)	83 (6.6)	29 (5.4)
Pulmonary infection, n (%)	66 (3.7)	45 (3.6)	21 (3.9)
Chronic kidney disease, n (%)	10 (0.6)	7 (0.6)	3 (0.6)
Cancer, n (%)	14 (0.8)	11 (0.9)	3 (0.6)
Atrial fibrillation, n (%)	16 (0.9)	12 (0.9)	4 (0.7)
Estrogen or progestin, n (%)	16 (0.9)	8 (0.6)	8 (1.5)
Shock, n (%)	189 (10.5)	127 (10)	62 (11.4)
Preoperative treatment, n (%)			
Admission to the ICU[b]	861 (47.7)	593 (46.9)	268 (49.4)
Anticoagulation and antiplatelet therapy	474 (26.2)	429 (33.9)	145 (26.8)
Hemostatic drugs	173 (9.6)	109 (8.6)	64 (11.8)
Mannitol	485 (26.9)	353 (27.9)	133 (24.5)
Trachea intubation	154 (8.5)	106 (8.4)	48 (8.9)
Tracheotomy	66 (3.7)	41 (3.2)	25 (4.6)
Limb pressure therapy	80 (4.4)	64 (5.1)	17 (3.1)
Mechanical ventilation	136 (7.5)	92 (7.3)	44 (8.1)
Blood transfusion	116 (6.4)	75 (5.9)	42 (7.7)
Mechanism of injury, n (%)			
Fall	293 (16.2)	211 (16.7)	82 (15.1)
Traffic accident	1033 (57.2)	706 (55.9)	326 (60.1)
Fall from height	354 (19.6)	256 (20.3)	98 (18.1)
Assault	85 (4.7)	67 (5.3)	18 (3.3)
Attack	41 (2.3)	23 (1.8)	18 (3.3)
Type of head injury			
Concussion, n (%)	403 (22.3)	287 (22.7)	116 (21.4)
Contusion, n (%)	1017 (56.3)	712 (56.3)	305 (56.3)
Subdural or extradural hematoma, n (%)	967 (53.5)	676 (53.5)	291 (53.7)
Diffuse axonal injury, n (%)	87 (4.8)	64 (5.1)	23 (4.2)
Subarachnoid hemorrhage, n (%)	910 (50.4)	643 (50.9)	267 (49.3)
Skull fracture, n (%)	684 (37.9)	469 (37.1)	215 (39.7)
ISS[c], median (IQR)	16 (11-22)	16 (10-22)	16 (11-22)

XSL•FO
RenderX

Variables	Total (N=1806)	Training set (n=1264)	Test set (n=542)
Head AIS[d] score, median (IQR)	3 (3-3)	3 (2-3)	3 (2-3)
Limb AIS score, median (IQR)	0 (0-3)	0 (0-2)	0 (0-2)
GCS[e] score, median (IQR)	13 (7-15)	13 (7-15)	13 (8-15)
Mild, n (%)	1022 (56.6)	711 (56.3)	311 (57.4)
Moderate, n (%)	226 (12.5)	158 (12.5)	68 (12.5)
Severe, n (%)	558 (30.9)	395 (31.3)	163 (30.1)
Rotterdam CT[f] score, median (IQR)	2 (1-2)	2 (1-2)	2 (1-2)
Intraoperative events, n (%)			
Vasoconstrictor	984 (54.5)	693 (54.8)	292 (53.9)
Transfusion	336 (18.6)	239 (18.9)	98 (18.1)
Invasive monitoring	1156 (64)	825 (65.3)	332 (61.3)
Emergency	949 (52.5)	686 (54.3)	263 (48.5)
General anesthesia	1589 (88)	1124 (88.9)	466 (86)
Hypotension	743 (41.1)	508 (40.2)	235 (43.4)
Surgical site, n (%)			
Head	831 (46)	598 (47.3)	245 (45.2)
Thorax	360 (19.9)	239 (18.9)	121 (22.3)
Limbs	452 (25)	313 (24.8)	139 (25.6)
Abdomen	88 (4.9)	68 (5.4)	21 (3.9)
Body surface	74 (4.1)	58 (4.6)	15 (2.8)
Multiple surgeries, n (%)	489 (27.1)	347 (27.5)	143 (26.4)
Intracranial surgery, n (%)	674 (37.3)	480 (38)	194 (35.8)
Extracranial surgery, n (%)	1268 (70.2)	880 (69.6)	389 (71.8)
Operation duration (min), median (IQR)	158 (109-215)	157 (106-210)	160 (110-220)
Bleeding (mL), median (IQR)	200 (50-500)	200 (50-500)	200 (93-400)
Intraoperative fluid volume (mL), median (IQR)	1800 (1200-2600)	1800 (1200-2600)	1700 (1200-2500)

[a]ASA: American Society of Anesthesiologists.

[b]ICU: intensive care unit.

[c]ISS: Injury Severity Score.

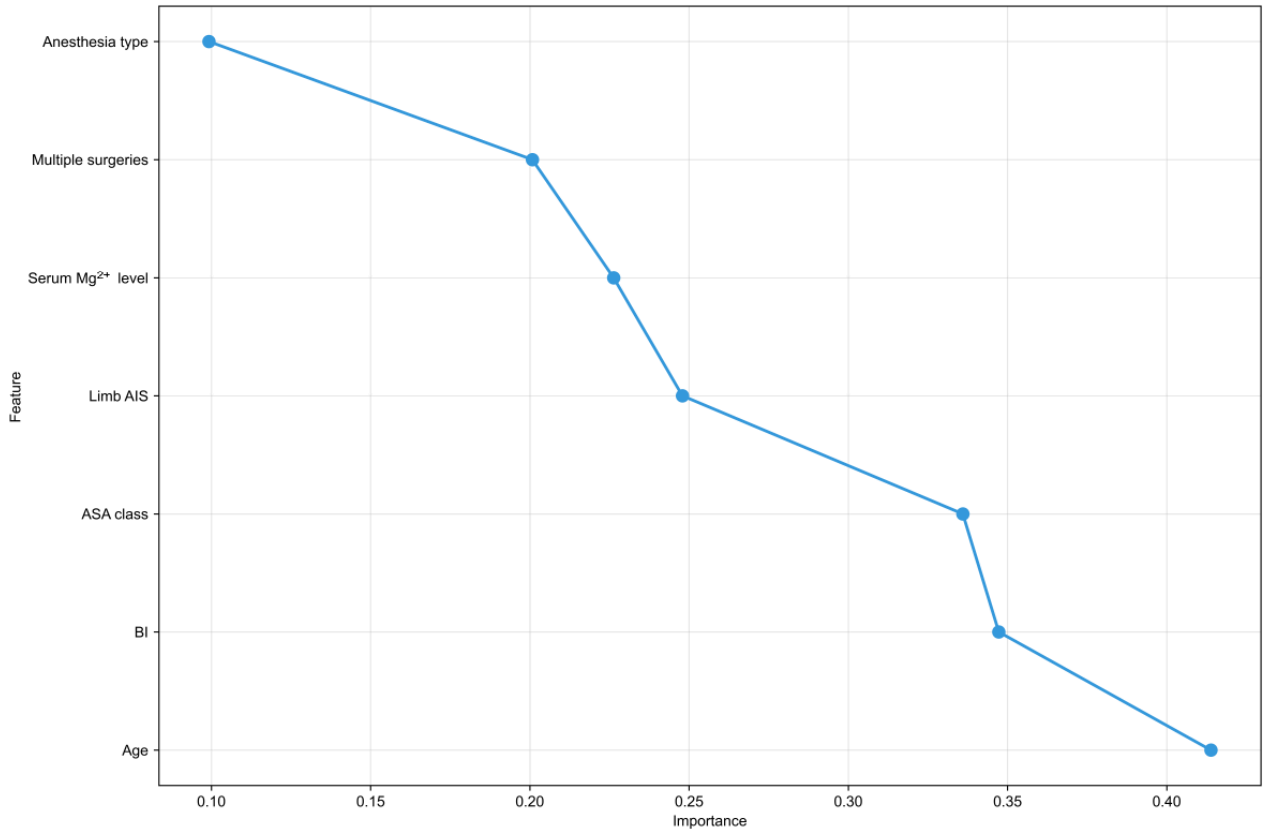
[d]AIS: Abbreviated Injury Scale.

[e]GCS: Glasgow Coma Scale.

[f]CT: computed tomography.

XSL•FO
RenderX

Figure 2. Selected features by recursive feature elimination. AIS: Abbreviated Injury Scale; ASA: American Society of Anesthesiologists; BI: Barthel index; Mg: magnesium.



Model Performance

Figure 3 displays the area under the receiver operating characteristic curve (AUC-ROC) for the 6 models in the internal validation set. Table 2 and Figure S5 in Multimedia Appendix 1 present the additional evaluation metrics, including accuracy, sensitivity, specificity, PPV, and NPV for each model.

XSL•FO
RenderX

Figure 3. Area under the receiver operating characteristic curves (AUC-ROC) of 6 machine learning models in the internal validation dataset. CatBoost: categorical boosting; GBDT: gradient boosting decision tree; SVM: support vector machine; XGBoost: extreme gradient boosting.

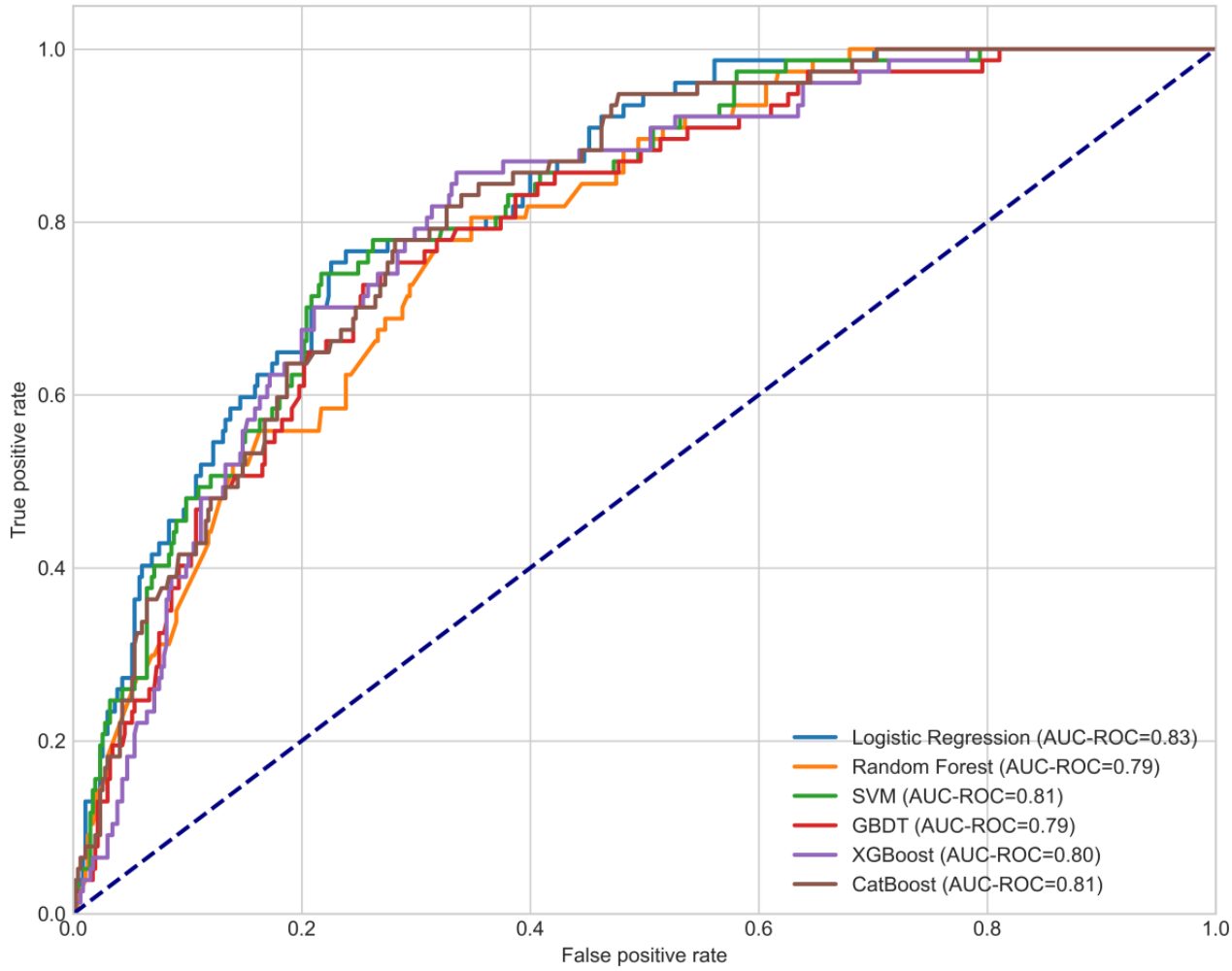


Table 2. Model performance in predicting venous thromboembolism in the validation set.

Model	AUC-ROC[a]	Accuracy	Sensitivity	Specificity	PPV[b]	NPV[c]	F_1-score
Logistic regression	0.83	0.80	0.62	0.83	0.37	0.93	0.47
Random forest	0.79	0.72	0.69	0.72	0.29	0.92	0.41
SVM[d]	0.81	0.78	0.74	0.78	0.36	0.95	0.49
GBDT[e]	0.80	0.77	0.65	0.79	0.34	0.93	0.44
XGBoost[f]	0.80	0.80	0.58	0.84	0.38	0.92	0.45
CatBoost[g]	0.81	0.79	0.57	0.83	0.36	0.92	0.44

[a]AUC-ROC: area under the receiver operating characteristic curve.

[b]PPV: positive predictive value.

[c]NPV: negative predictive value.

[d]SVM: support vector machine.

[e]GBDT: gradient boosting decision tree.

[f]XGBoost: extreme gradient boosting.

[g]CatBoost: categorical boosting.

Among the evaluated models, LR demonstrated superior performance in the internal validation set, achieving the highest AUC-ROC of 0.83, with an accuracy of 0.80 and specificity of 0.83, consistently generating reliable predictions and accurately identifying true negative cases. Although other models showed merit, they fell short in key performance domains. RF had an AUC-ROC of 0.78 (lower than LR), accuracy of 0.72, and specificity of 0.82, but its sensitivity of 0.69 (relatively low)

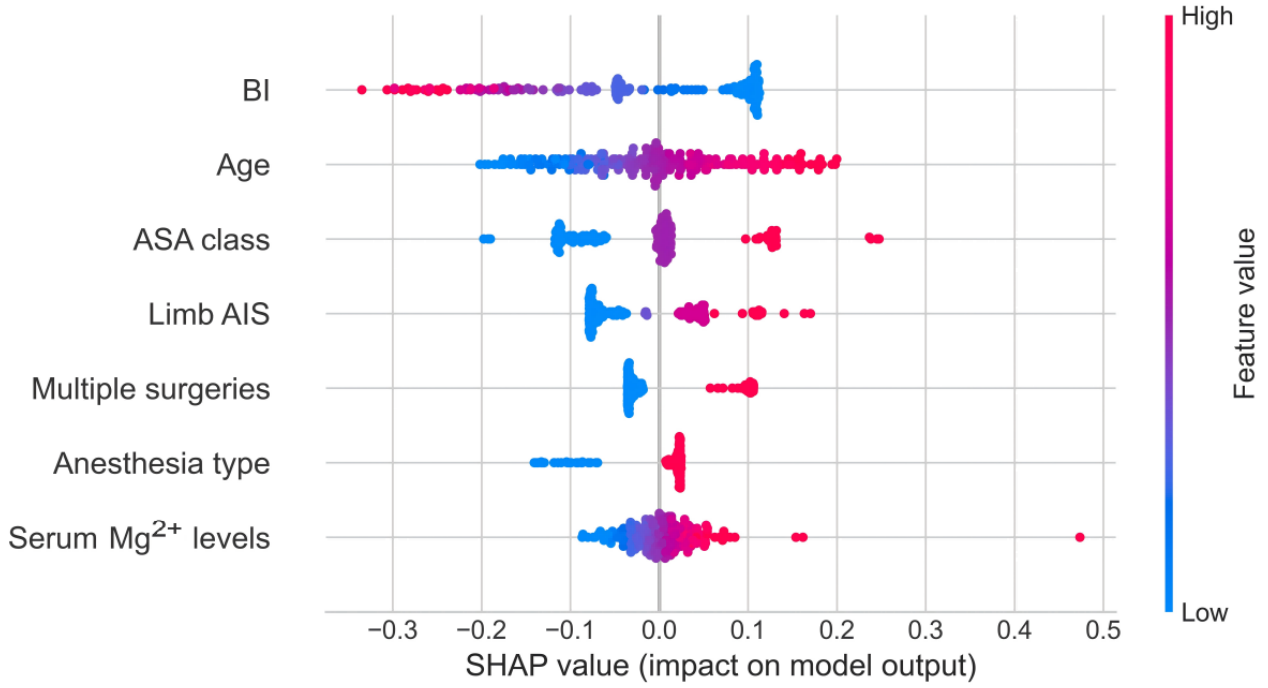
XSL•FO
RenderX

led to more false negatives. SVM had an AUC-ROC of 0.81 (close to LR) but underperformed in sensitivity (0.74) and PPV (0.36). GBDT and XGBoost both achieved an AUC-ROC of 0.80 (respectable but trailing LR), with GBDT's sensitivity (0.65) slightly better than LR and XGBoost, despite the highest accuracy (0.80) among non-LR models, suffering from suboptimal PPV (0.38) and lower sensitivity (0.58). CatBoost, with an AUC-ROC of 0.81, had a low sensitivity (0.57) despite a high NPV (0.92; still lower than LR's NPV of 0.93). These results underscore LR's balanced performance across discriminative, calibration, and clinical utility metrics, making it the most robust choice for VTE prediction in this cohort of patients with TBI undergoing surgical procedures.

Model Explanation Results and Nomogram

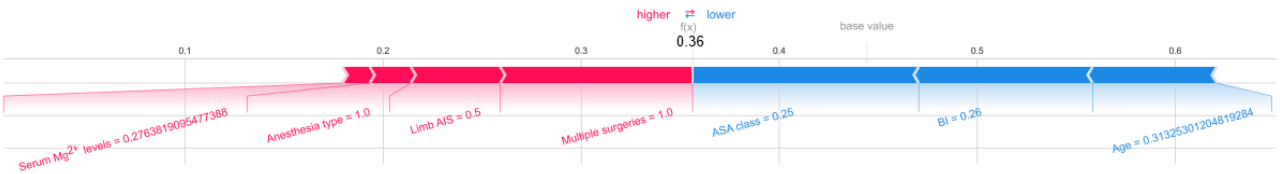
The SHAP algorithm enabled interpretable insights at both global and instance-specific levels. Figure 4 visualizes the relative importance and directional impact of 7 key features on the LR model's predictions, as derived from SHAP's interpretation of the model's output. These features were identified as critical predictors: BI, age, limb AIS, ASA Class, multiple surgeries, serum magnesium (Mg^{2+}) levels, and anesthesia type.

Figure 4. Global feature importance on the logistic regression model. AIS: Abbreviated Injury Scale; ASA: American Society of Anesthesiologists; BI: Barthel Index; Mg: magnesium; SHAP: Shapley additive explanations.



Subsequently, we linked SHAP values to their directional impact on VTE risk (ie, the probability of a feature increasing or decreasing the likelihood of VTE) and visualized these relationships using data from 1 patient with VTE and 1 patient without VTE in the internal validation dataset (Figure 5). Figure 6 specifically illustrates a case of a patient with VTE, where red segments denote features with positive SHAP values (indicating they contributed to an increased predicted VTE risk) and blue segments represent features with negative SHAP values (indicating they reduced the predicted VTE risk). This visualization clarified how individual features collectively modulate the model's risk stratification for VTE.

Figure 5. Local explanation for a non–venous thromboembolism sample. AIS: Abbreviated Injury Scale; ASA: American Society of Anesthesiologists; BI: Barthel index; Mg: magnesium.



XSL•FO
RenderX

Figure 6. Local explanation for a venous thromboembolism sample. AIS: Abbreviated Injury Scale; ASA: American Society of Anesthesiologists; BI: Barthel index; Mg: magnesium.

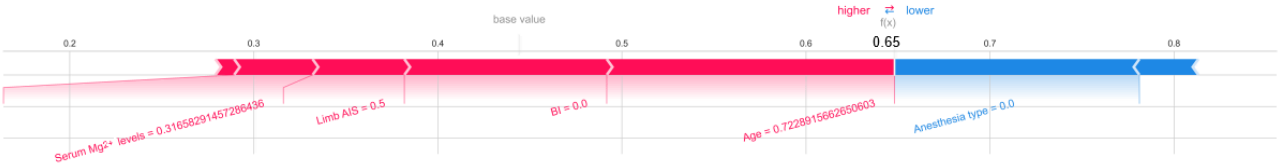
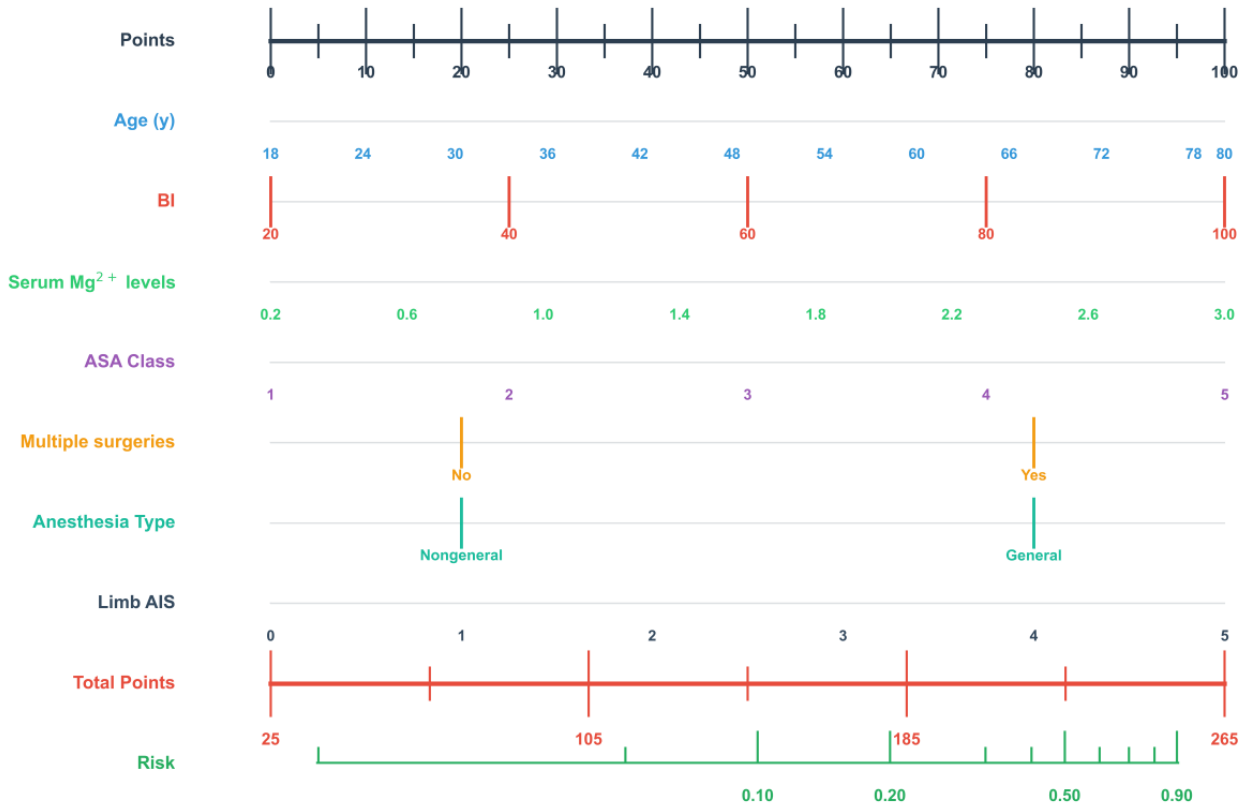


Figure 7 presents a user-friendly nomogram for rapid risk quantification, where feature scores are weighted by regression coefficients, allowing clinicians to sum points and visualize risk thresholds. This aligned with SHAP-derived feature importance, bridging statistical rigor with clinical decision-making. The calibration curve illustrated the calibration performance of the LR model in the internal validation set, with the x-axis representing predicted probabilities (0-1) and the y-axis depicting observed risks (0-1). Key curves included the bias-corrected curve (derived from 1000 bootstrap resamples), which aligned closely with the ideal reference line in the moderate-risk range (0.2-0.7), indicating strong predictive accuracy and the apparent curve, reflecting raw data fit with minor deviations at extreme probabilities (<0.2 and >0.8; Figure S6 in Multimedia Appendix 1). Further evaluation of clinical utility using the decision curve analysis demonstrated that the nomogram provided superior net benefits on the validation set (Figure S7 in Multimedia Appendix 1).

Collectively, the LR model's balanced performance (AUC-ROC=0.83; NPV=0.93), robust calibration, and actionable interpretability—coupled with the nomogram's clinical utility—establish it as a reliable tool for VTE prediction in TBI surgical cohorts.

Figure 7. Postoperative venous thromboembolism risk prediction nomogram for patients with traumatic brain injury. AIS: Abbreviated Injury Scale; ASA: American Society of Anesthesiologists; BI: Barthel index; Mg: magnesium.



Discussion

Principal Findings

The prevention of VTE remains a cornerstone in the management of patients with TBI, particularly those undergoing surgical intervention, due to their heightened thrombotic risk driven by prolonged immobilization, hypercoagulability, and endothelial injury. Although pharmacological thromboprophylaxis (eg, low-molecular-weight heparin) and mechanical methods (eg, sequential compression devices) are widely implemented, balancing efficacy with safety remains challenging due to the risk of intracranial hemorrhage associated with these agents [15]. Current guidelines lack consensus on optimal dosing protocols, timing of initiation, and patient selection criteria, further complicating clinical decision-making [16].

XSL•FO
RenderX

In this study, we documented a postoperative VTE incidence of 14.2% among patients with TBI, markedly exceeding the 3.9% reported in a 2019 national registry study [17]. This disparity underscores the urgent need for improved risk assessment tools to identify high-risk patients and guide targeted thromboprophylactic interventions.

Previous studies have used various risk-scoring systems to assess PE risk in patients who were hospitalized, including the Caprini and Padua scores [18-20]. The Caprini score, while simple and widely adopted, has significant limitations, such as its overreliance on subjective historical data (eg, previous VTE and obesity), omission of objective biomarkers (eg, D-dimer dynamics), and failure to account for anatomical factors (eg, craniotomy type) or anticoagulation therapy risks. For instance, in Asian cohorts, where patients with TBI frequently undergo prolonged surgeries (>45 min) and present with comorbid conditions (eg, hypertension), the Caprini score often overestimates VTE risk by classifying excessive numbers of patients as high risk. This has led to unnecessary anticoagulation therapy, increasing bleeding risks and health care costs [21,22].

To address these challenges and more accurately identify patients with TBI at high risk of postoperative VTE, we used 6 ML algorithms (including LR, RF, SVM, XGBoost, GBDT, and CatBoost) to develop predictive models and created a postoperative VTE risk prediction nomogram specifically for patients with TBI. These models aim to enhance risk assessment precision, enabling more targeted and effective thromboprophylactic interventions. ML has demonstrated efficacy in VTE prediction across various patient populations. Wang et al [23] and Liu et al [24] validated the RF model for VTE risk assessment in Chinese inpatients and patients who have experienced stroke, respectively.

Comparison With Prior Work

The morphology and influence of most features on the predictions are consistent with clinical practice and previous evidence. LR-based global feature importance analysis identified several critical VTE risk factors. BI scores, a validated measure of activities of daily living, emerged as the strongest predictor, with poorer functional status (lower BI scores) substantially increasing VTE risk—likely due to immobility and venous stasis—with moderate-certainty evidence supporting this association [25,26]. Advanced age was another key determinant of VTE risk, as older patients exhibited heightened susceptibility to VTE, attributed to age-related coagulation changes, increased comorbidity burden, and potential immobilization—all well-documented VTE risk factors consistent with previous epidemiological studies. Severe limb injuries (eg, pelvic fractures) were significantly associated with elevated VTE risk, aligning with findings by Hereford et al [27]. Higher ASA scores, reflecting greater comorbidity burden and poorer physiological reserve, strongly correlated with increased VTE risk, consistent with the American College of Chest Physicians' guidelines, which emphasize ASA status in VTE risk assessment for patients undergoing major surgeries [28].

Our study further demonstrated that lower serum magnesium (Mg^{2+}) levels are associated with higher VTE risk, potentially mediated by endothelial dysfunction (eg, slowed endothelial cell proliferation, stimulated monocyte adhesion, and impaired synthesis of vasoregulatory molecules) and myocardial instability (eg, altered intracellular calcium handling, prolonged QT intervals, and increased arrhythmia risk) [29-31]. However, a prospective cohort study conducted by Kunutsor and Laukkanen [32] among middle-aged Caucasian men (n=2361) reported no significant association between serum magnesium (Mg^{2+}) levels and VTE risk (adjusted hazard ratio 1.38, 95% CI 0.48-3.96), with discrepancies potentially attributed to population heterogeneity (eg, age, sex, and comorbidities). Therefore, future studies are warranted to validate the association between serum magnesium levels and VTE risk in more diverse populations encompassing varying age groups, sexes, and comorbid conditions. Although other factors (eg, multiple surgeries and anesthesia type) also influenced VTE risk to a lesser extent, these findings collectively provide critical insights for developing targeted preventive strategies and enhancing patient-specific risk assessment in clinical practice. This study investigated potential VTE predictors in patients with TBI after undergoing surgery and compared the performance of multiple machine learning algorithms. Nonetheless, the model's reliance solely on preoperative and intraoperative variables, excluding postoperative data such as laboratory tests and therapeutic interventions, potentially constrained its predictive power. Abbasi et al [33] successfully predicted postoperative bleeding events, VTE, and stroke risk in cardiac surgery by integrating preoperative, intraoperative, and postoperative variables, achieving high performance (AUC-ROC=0.92-0.97). Their study demonstrated that including postoperative variables significantly enhanced model performance, with prediction accuracy critically dependent on these data. Thus, future studies should integrate postoperative laboratory tests and therapeutic interventions as key variables to enhance the predictive capability of VTE risk models in populations with TBI.

Limitations

Several limitations of this study warrant acknowledgment. First, the dataset was derived from a single medical center for an 8-year period, which may have introduced data heterogeneity and unavoidable selection bias. Second, although this study included 1806 cases with a notably high VTE incidence, the number of VTE-positive events remained relatively small. Therefore, larger sample sizes are critical for future studies to enable more precise analyses and the development of robust predictive models. Third, postoperative laboratory tests and treatment regimens were not integrated into the analysis, which may have affected the study outcomes. Finally, given that all data originated from a single center, external validation of the developed model across multiple centers over time is necessary to confirm its generalizability.

Conclusions

This study successfully developed and validated ML models for VTE risk prediction in patients with TBI undergoing surgery, with a specific focus on clinical translatability. Leveraging the LR model's robust performance, we constructed a practical nomogram that enables bedside VTE risk assessment using

XSL•FO
RenderX

routinely collected preoperative and intraoperative data. This user-friendly tool empowers clinicians to rapidly quantify individualized VTE risk and guide targeted thromboprophylactic decisions at the point of care. Future external validation across diverse clinical settings and patient populations is warranted to confirm the model's generalizability and ensure its broader applicability in real-world practice.

Acknowledgments

This work was supported by Chongqing Municipal Studios for Young and Middle-aged Top Medical Talents (ZQNYXGDRCGZS2019006) and the Wu Jieping Medical Foundation (320.6750.2024-5-69).

Data Availability

The datasets generated or analyzed during this study are not publicly available due to patient privacy concerns and the ethical restrictions imposed by the Institutional Review Board, but are available from the corresponding author on reasonable request.

Conflicts of Interest

None declared.

Multimedia Appendix 1
Overview of study population characteristics, head injury profiles, and model performance for predicting venous thromboembolism.
[DOCX File , 145 KB - medinform_v13i1e78655_app1.docx]

References

1. Buchanan IA, Lin M, Donoho DA, Patel A, Ding L, Amar AP, et al. Predictors of venous thromboembolism after nonemergent craniotomy: a nationwide readmission database analysis. World Neurosurg 2019 Feb;122:e1102-e1110 [FREE Full text] [doi: 10.1016/j.wneu.2018.10.237] [Medline: 30465948]
2. Wendelboe AM, Raskob GE. Global burden of thrombosis: epidemiologic aspects. Circ Res 2016 Apr 29;118(9):1340-1347 [FREE Full text] [doi: 10.1161/CIRCRESAHA.115.306841] [Medline: 27126645]
3. Shah MN, Stoev IT, Sanford DE, Gao F, Santiago P, Jaques DP, et al. Are readmission rates on a neurosurgical service indicators of quality of care? J Neurosurg 2013 Oct;119(4):1043-1049 [FREE Full text] [doi: 10.3171/2013.3.JNS121769] [Medline: 23621593]
4. Geerts WH, Bergqvist D, Pineo GF, Heit JA, Samama CM, Lassen MR, et al. Prevention of venous thromboembolism: American College of Chest Physicians Evidence-Based Clinical Practice Guidelines (8th Edition). Chest 2008 Jun;133(6 Suppl):381S-453S. [doi: 10.1378/chest.08-0656] [Medline: 18574271]
5. Fernandez MM, Hogue S, Preblick R, Kwong WJ. Review of the cost of venous thromboembolism. Clinicoecon Outcomes Res 2015;7:451-462 [FREE Full text] [doi: 10.2147/CEOR.S85635] [Medline: 26355805]
6. Denson K, Morgan D, Cunningham R, Nigliazzo A, Brackett D, Lane M, et al. Incidence of venous thromboembolism in patients with traumatic brain injury. Am J Surg 2007 Mar;193(3):380-383. [doi: 10.1016/j.amjsurg.2006.12.004] [Medline: 17320539]
7. Maas AI, Menon DK, Adelson PD, Andelic N, Bell MJ, Belli A, InTBIR ParticipantsInvestigators. Traumatic brain injury: integrated approaches to improve prevention, clinical care, and research. Lancet Neurol 2017 Dec;16(12):987-1048 [FREE Full text] [doi: 10.1016/S1474-4422(17)30371-X] [Medline: 29122524]
8. Chen D, Luo J, Zhang C, Tang L, Deng H, Chang T, et al. Venous thrombus embolism in polytrauma: special attention to patients with traumatic brain injury. J Clin Med 2023 Feb 21;12(5):1716 [FREE Full text] [doi: 10.3390/jcm12051716] [Medline: 36902502]
9. Hoyt DB. A clinical review of bleeding dilemmas in trauma. Semin Hematol 2004 Jan;41(1 Suppl 1):40-43. [doi: 10.1053/j.seminhematol.2003.11.009] [Medline: 14872420]
10. Harhangi BS, Kompanje EJ, Leebeek FW, Maas AI. Coagulation disorders after traumatic brain injury. Acta Neurochir (Wien) 2008 Feb;150(2):165-175. [doi: 10.1007/s00701-007-1475-8] [Medline: 18166989]
11. Agnelli G. Prevention of venous thromboembolism in surgical patients. Circulation 2004 Dec 14;110(24 Suppl 1):IV4-I12. [doi: 10.1161/01.CIR.0000150639.98514.6c] [Medline: 15598646]
12. Zhu Y, Liu X, Li Y, Yi B. The applications and prospects of big data in perioperative anesthetic management. Anesthesiol Perioper Sci 2024 Aug 26;2(3):30. [doi: 10.1007/S44254-024-00068-0]
13. Guyon I, Elisseeff A. An introduction to variable and feature selection. J Mach Learn Res 2003;3:82 [FREE Full text]
14. Zhu T, Lin Y, Liu Y. Synthetic minority oversampling technique for multiclass imbalance problems. Pattern Recognit 2017 Dec;72:327-340 [FREE Full text] [doi: 10.1016/j.patcog.2017.07.024]

XSL•FO
RenderX

15. Skrifvars MB, Bailey M, Presneill J, French C, Nichol A, Little L, EPO-TBI investigatorsthe ANZICS Clinical Trials Group. Venous thromboembolic events in critically ill traumatic brain injury patients. Intensive Care Med 2017 Mar;43(3):419-428. [doi: 10.1007/s00134-016-4655-2] [Medline: 28028552]
16. Rappold JF, Sheppard FR, Carmichael Ii SP, Cuschieri J, Ley E, Rangel E, et al. Venous thromboembolism prophylaxis in the trauma intensive care unit: an American Association for the Surgery of Trauma Critical Care Committee clinical consensus document. Trauma Surg Acute Care Open 2021;6(1):e000643 [FREE Full text] [doi: 10.1136/tsaco-2020-000643] [Medline: 33718615]
17. Hoffman H, Jalal MS, Chin LS. The risk factors, outcomes, and costs associated with venous thromboembolism after traumatic brain injury: a nationwide analysis. Brain Inj 2019;33(13-14):1671-1678. [doi: 10.1080/02699052.2019.1667536] [Medline: 31526026]
18. Hou L, Hu L, Gao W, Sheng W, Hao Z, Chen Y, et al. Construction of a risk prediction model for hospital-acquired pulmonary embolism in hospitalized patients. Clin Appl Thromb Hemost 2021;27:10760296211040868 [FREE Full text] [doi: 10.1177/10760296211040868] [Medline: 34558325]
19. Wang L, Wei S, Zhou B, Wu S. A nomogram model to predict the venous thromboembolism risk after surgery in patients with gynecological tumors. Thromb Res 2021 Jun;202:52-58 [FREE Full text] [doi: 10.1016/j.thromres.2021.02.035] [Medline: 33735691]
20. Zhou H, Hu Y, Li X, Wang L, Wang M, Xiao J, et al. Assessment of the risk of venous thromboembolism in medical inpatients using the padua prediction score and caprini risk assessment model. J Atheroscler Thromb 2018 Nov 01;25(11):1091-1104 [FREE Full text] [doi: 10.5551/jat.43653] [Medline: 29540637]
21. Bahl V, Hu HM, Henke PK, Wakefield TW, Campbell DA, Caprini JA. A validation study of a retrospective venous thromboembolism risk scoring method. Ann Surg 2010 Feb;251(2):344-350. [doi: 10.1097/SLA.0b013e3181b7fca6] [Medline: 19779324]
22. Kim MH, Jun KW, Hwang JK, Kim SD, Kim JY, Park SC, et al. Venous thromboembolism following abdominal cancer surgery in the Korean population: incidence and validation of a risk assessment model. Ann Surg Oncol 2019 Nov;26(12):4037-4044. [doi: 10.1245/s10434-019-07633-z] [Medline: 31489552]
23. Wang X, Yang YQ, Liu SH, Hong XY, Sun XF, Shi JH. Comparing different venous thromboembolism risk assessment machine learning models in Chinese patients. J Eval Clin Pract 2020 Feb;26(1):26-34. [doi: 10.1111/jep.13324] [Medline: 31840330]
24. Liu L, Li L, Zhou J, Ye Q, Meng D, Xu G. Machine learning-based prediction model of lower extremity deep vein thrombosis after stroke. J Thromb Thrombolysis 2024 Oct;57(7):1133-1144. [doi: 10.1007/s11239-024-03010-0] [Medline: 39068348]
25. Mahoney FI, BAarthel DW. Functional evaluation: the Barthel index. Md State Med J 1965 Feb;14:61-65. [Medline: 14258950]
26. Kelly J, Rudd A, Lewis RR, Coshall C, Moody A, Hunt BJ. Venous thromboembolism after acute ischemic stroke: a prospective study using magnetic resonance direct thrombus imaging. Stroke 2004 Oct;35(10):2320-2325. [doi: 10.1161/01.STR.0000140741.13279.4f] [Medline: 15322298]
27. Hereford T, Thrush C, Kimbrough MK. Using injury severity score and abbreviated injury score to determine venous thromboembolism risk. Cureus 2019 Oct 23;11(10):e5977 [FREE Full text] [doi: 10.7759/cureus.5977] [Medline: 31803559]
28. Kearon C, Akl EA, Comerota AJ, Prandoni P, Bounameaux H, Goldhaber SZ, et al. Antithrombotic therapy for VTE disease: antithrombotic therapy and prevention of thrombosis, 9th ed: American College of Chest Physicians evidence-based clinical practice guidelines. Chest 2012 Feb;141(2 Suppl):e419S-e496S [FREE Full text] [doi: 10.1378/chest.11-2301] [Medline: 22315268]
29. Swaminathan R. Magnesium metabolism and its disorders. Clin Biochem Rev 2003 May;24(2):47-66 [FREE Full text] [Medline: 18568054]
30. Kostov K, Halacheva L. Role of magnesium deficiency in promoting atherosclerosis, endothelial dysfunction, and arterial stiffening as risk factors for hypertension. Int J Mol Sci 2018 Jun 11;19(6):1724 [FREE Full text] [doi: 10.3390/ijms19061724] [Medline: 29891771]
31. Chakraborti S, Chakraborti T, Mandal M, Mandal A, Das S, Ghosh S. Protective role of magnesium in cardiovascular diseases: a review. Mol Cell Biochem 2002 Sep;238(1-2):163-179. [doi: 10.1023/a:1019998702946] [Medline: 12349904]
32. Kunutsor SK, Laukkanen JA. Circulating serum magnesium and the risk of venous thromboembolism in men: a long-term prospective cohort study. Pulse (Basel) 2021 Jun;8(3-4):108-113 [FREE Full text] [doi: 10.1159/000515409] [Medline: 34307207]
33. Abbasi A, Li C, Dekle M, Bermudez CA, Brodie D, Sellke FW, et al. Interpretable machine learning-based predictive modeling of patient outcomes following cardiac surgery. J Thorac Cardiovasc Surg 2025 Jan;169(1):114-23.e28. [doi: 10.1016/j.jtcvs.2023.11.034] [Medline: 38040328]

Abbreviations

AIS: Abbreviated Injury Scale
ASA: American Society of Anesthesiologists

XSL•FO
RenderX

AUC-ROC: area under the receiver operating characteristic curve
BI: Barthel index
CatBoost: categorical boosting
DVT: deep vein thrombosis
GBDT: gradient boosting decision tree
GCS: Glasgow Coma Scale
LR: logistic regression
ML: machine learning
NPV: negative predictive value
PE: pulmonary embolism
PPV: positive predictive value
RF: random forest
SHAP: Shapley additive explanations
SVM: support vector machine
TBI: traumatic brain injury
VTE: venous thromboembolism
XGBoost: extreme gradient boosting

Edited by A Benis; submitted 06.06.25; peer-reviewed by S Xia, SAM Shah; comments to author 11.08.25; revised version received 25.08.25; accepted 13.10.25; published 17.11.25.

Please cite as:
Zheng J, Jiang Q, Zhan Y, Tang Y, Du X, Xiang G, Ouyang Y, Fu H
Prediction of Postoperative Venous Thromboembolism in Patients With Traumatic Brain Injury: Model Development and Validation Study
JMIR Med Inform 2025;13:e78655
URL: https://medinform.jmir.org/2025/1/e78655
doi:10.2196/78655
PMID:

©Jiang Zheng, Qiling Jiang, Yusheng Zhan, Yanming Tang, Xiaohui Du, Guangrong Xiang, Yufang Ouyang, Hong Fu. Originally published in JMIR Medical Informatics (https://medinform.jmir.org), 17.11.2025. This is an open-access article distributed under the terms of the Creative Commons Attribution License (https://creativecommons.org/licenses/by/4.0/), which permits unrestricted use, distribution, and reproduction in any medium, provided the original work, first published in JMIR Medical Informatics, is properly cited. The complete bibliographic information, a link to the original publication on https://medinform.jmir.org/, as well as this copyright and license information must be included.

XSL•FO
RenderX

Original Paper

Risk Prediction of Major Adverse Cardiovascular Events Within One Year After Percutaneous Coronary Intervention in Patients With Acute Coronary Syndrome: Machine Learning–Based Time-to-Event Analysis

Hong-Jae Choi[1], PhD; Changhee Lee[2], PhD; Hack-Lyoung Kim[3], MD, PhD; Youn-Jung Son[4], PhD

[1]Department of Thoracic and Cardiovascular Surgery, Seoul Metropolitan Government-Seoul National University Boramae Medical Center, Seoul National University College of Medicine, Seoul, Republic of Korea

[2]Department of Artificial Intelligence, Korea University, Seoul, Republic of Korea

[3]Division of Cardiology, Department of Internal Medicine, Seoul Metropolitan Government-Seoul National University Boramae Medical Center, Seoul National University College of Medicine, Seoul, Republic of Korea

[4]Red Cross College of Nursing, Chung-Ang University, Seoul, Republic of Korea

Corresponding Author:
Youn-Jung Son, PhD
Red Cross College of Nursing, Chung-Ang University
84 Heukseok ro, Dongjak-gu
Seoul, 06974
Republic of Korea
Phone: 82 2 820 5198
Email: yjson@cau.ac.kr

Abstract

Background: Patients with acute coronary syndrome (ACS) who undergo percutaneous coronary intervention (PCI) remain at high risk for major adverse cardiovascular events (MACE). Conventional risk scores may not capture dynamic or nonlinear changes in postdischarge MACE risk, whereas machine learning (ML) approaches can improve predictive performance. However, few ML models have incorporated time-to-event analysis to reflect changes in MACE risk over time.

Objective: This study aimed to develop a time-to-event ML model for predicting MACE after PCI in patients with ACS and to identify the risk factors with time-varying contributions.

Methods: We analyzed electronic health records of 3159 patients with ACS who underwent PCI at a tertiary hospital in South Korea between 2008 and 2020. Six time-to-event ML models were developed using 54 variables. Model performance was evaluated using the time-dependent concordance index and Brier score. Variable importance was assessed using permutation importance and visualized with partial dependence plots to identify variables contributing to MACE risk over time.

Results: During a median follow-up of 3.8 years, 626 (19.8%) patients experienced MACE. The best-performing model achieved a time-dependent concordance index of 0.743 at day 30 and 0.616 at 1 year. Time-dependent Brier scores increased and remained stable across all ML models. Key predictors included contrast volume, age, medication adherence, coronary artery disease severity, and glomerular filtration rate. Contrast volume ≥300 mL, age ≥60 years, and medication adherence score ≥30 were associated with early postdischarge risk, whereas coronary artery disease severity and glomerular filtration rate became more influential beyond 60 days.

Conclusions: The proposed time-to-event ML model effectively captured dynamic risk patterns after PCI and identified key predictors with time-varying effects. These findings may support individualized postdischarge management and early intervention strategies to prevent MACE in high-risk patients.

(JMIR Med Inform 2025;13:e81778) doi:10.2196/81778

KEYWORDS

acute coronary syndrome; machine learning; major adverse cardiovascular events; percutaneous coronary intervention; predictive models; survival analysis

XSL•FO
RenderX

Introduction

Acute coronary syndrome (ACS) is a critical and sudden presentation of underlying coronary artery disease (CAD); it requires timely intervention to reduce the risk of adverse outcomes and mortality [1-5]. The primary method of revascularization used in the management of ACS is percutaneous coronary intervention (PCI) because it promptly improves coronary blood flow and minimizes myocardial damage [4,6]. Although timely PCI enhances acute survival, patients often face challenges such as poor medication adherence, insufficient lifestyle modification, and residual psychosocial stress following discharge [7,8]. They also remain at substantial risk for major adverse cardiovascular events (MACE), particularly within the first year after PCI [9-12]. MACE are typically defined as the composite outcome of cardiovascular death, nonfatal myocardial infarction, stroke, or unplanned revascularization [4,13]. Approximately 14.8% to 34.4% of patients who have ACS and undergo PCI experience MACE within the first year [14,15]. The MACE risk arises from the combined influence of multiple contributing factors, including demographic characteristics, lifestyle-related factors, comorbidities, and medication-related factors such as polypharmacy and medication use patterns [2,11].

Several risk stratification tools have been developed to estimate the MACE risk in patients with ACS; among them, the Thrombolysis in Myocardial Infarction Risk Score and the Global Registry of Acute Coronary Events Risk Score are the most widely used [16]. Although these tools provide valuable support for initial triage and decision-making, they have several critical limitations. First, they are based on a limited set of clinical variables; as such, they fail to capture the multifactorial nature of the MACE risk [7,16]. Second, they do not reflect temporal variations in MACE risk after discharge; instead, they rely on static, single timepoint assessments [1,16]. Additionally, these traditional models are built on simplified linear statistical assumptions, which may inadequately reflect the complex, nonlinear relationships between risk factors [1,16]. Moreover, when risk stratification scores are used, manual data entry is required, thereby reducing practicality and limiting routine use in real-world clinical settings; it also lacks adaptability to incorporate emerging clinical guidelines [17,18].

Some of these limitations have been addressed by recent advances in machine learning (ML). For instance, ML models have improved the ability to capture complex nonlinear relationships, automate risk prediction without manual data entry, and facilitate faster updates consistent with evolving clinical knowledge [19,20]. Despite these improvements, most ML models developed for predicting MACE in patients with ACS who undergo PCI continue to rely on a limited set of clinical variables and fail to incorporate time-to-event information [21-23]. As a result, they overlook the dynamic nature of MACE risk over time. Particularly, most existing ML studies have framed MACE prediction as a binary classification problem [21-23] and focused solely on whether an event will occur within a fixed time frame. With this approach, right-censored patients are often excluded, thereby introducing a potential risk of bias in the prediction model because of the underlying covariate shift [24]. Moreover, such models have a limited ability to estimate the probability of event occurrence across clinically relevant time intervals [25]. Consequently, their applications are limited in guiding temporally informed clinical interventions.

Time-to-event ML models that combine the strengths of survival analysis and ML offer a compelling solution to overcome the limitations of traditional methods. They can be used to estimate event occurrence probabilities over time without requiring the proportional hazards assumption of traditional Cox models; consequently, they provide greater flexibility for modeling complex real-world scenarios [24,25]. Accordingly, we aimed to develop a time-to-event ML model for predicting MACE in patients who had ACS and underwent PCI. Our model incorporated clinical, demographic, and medication-related variables and used time-to-event information to enable dynamic risk estimation. Furthermore, we aimed to identify how key risk factors contributed to MACE at different time intervals by evaluating the time-varying importance of predictive variables, thereby supporting personalized and time-sensitive clinical decision-making.

Methods

Study Design

This retrospective cohort study followed the Transparent Reporting of a Multivariable Prediction Model for Individual Prognosis or Diagnosis + Artificial Intelligence (TRIPOD+AI) checklist to uphold methodological rigor and ensure transparent reporting of the ML–based predictive model [26]. In addition, we adhered to the Strengthening the Reporting of Observational Studies in Epidemiology (STROBE) checklist [27]. Details of the TRIPOD+AI checklist are provided in Multimedia Appendix 1, and the STROBE reporting items are presented in Multimedia Appendix 2.

Data Sources and Patients

This study was conducted using electronic medical record (EMR) data from a single tertiary hospital in Seoul, South Korea. Patients diagnosed with ACS and subjected to PCI between January 1, 2008, and December 31, 2020, were identified. The EMR data included demographic, lifestyle, clinical, and medication-related information. The extracted data were fully anonymized to protect patient privacy. PCI procedures were performed in accordance with current guideline recommendations [4,6,27].

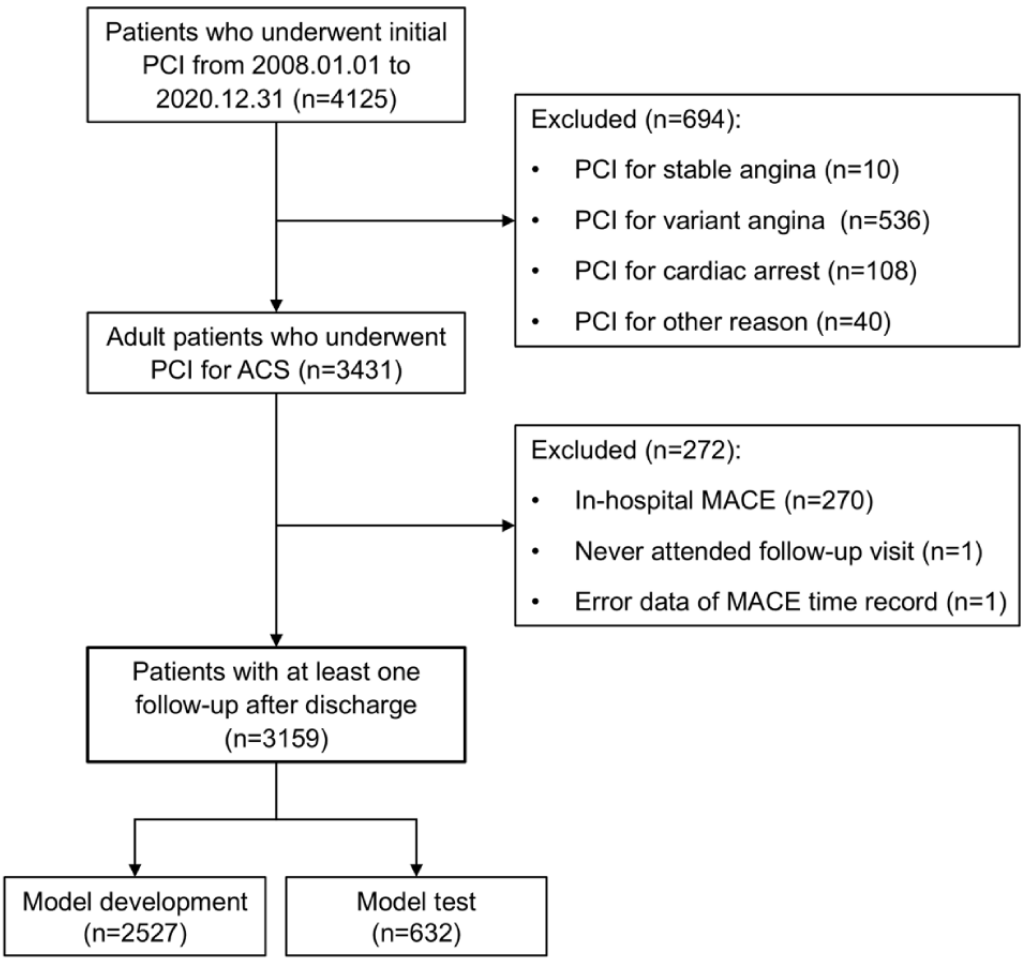
The patients were eligible for inclusion if they met the following criteria (1) aged 19 years or older and (2) underwent PCI for the first time. The exclusion criteria were as follows (1) patients who experienced MACE during the index hospitalization, (2) patients without follow-up records after discharge, and (3) patients with missing or erroneous outcome records for MACE after discharge.

The required sample size was determined on the basis of the number of predictors and the incidence of 1-year MACE, following the established recommendations for prediction model development [28]. An estimated 1-year MACE incidence ranging from 14.8% to 34.4% was considered [14,15]. The

XSL•FO
RenderX

minimum required sample size calculated using the lowest event rate (14.8%) to ensure adequate statistical power was 3006 patients. The final analytical cohort was composed of 3159 patients who satisfied all eligibility criteria (Figure 1).

Figure 1. Flowchart of the study population. ACS: acute coronary syndrome; MACE: major adverse cardiovascular events; PCI: percutaneous coronary intervention.



Data Collection

Based on an extensive review of the literature and the clinical expertise of the cardiology and cardiovascular nursing team participating in the study, 54 variables were selected as potential predictors of MACE. These variables covered a broad range of patient characteristics, including demographic variables, lifestyle-related variables, comorbidities, PCI-related variables, laboratory tests, medication status, and medication adherence. The predictor variables and measurement methods are described in detail in Multimedia Appendix 3.

Predictors

The final set of predictors included 54 variables classified into 7 categories: demographic variables (eg, age, sex, and insurance type), lifestyle-related variables (eg, smoking status and alcohol consumption), comorbidities (eg, presence of hypertension, renal impairment, or diabetes mellitus), PCI-related variables (eg, contrast volume, catheterization status, and left ventricular ejection fraction), laboratory tests (eg, troponin I and glomerular filtration rate [GFR]), medication status (eg, use of antiplatelets, statins, and beta blockers), and medication adherence indicators (eg, medication regimen complexity index [MRCI]).

The nutrition risk index was used to assess nutritional status, where low values indicate a high nutritional risk [29]. The catheterization status was categorized as elective, urgent, emergent, or salvage procedures based on the clinical context [30]. The MRCI was used to quantify the complexity of each patient's medication regimen; high scores reflected increased regimen complexity and potentially poor medication adherence [31,32]. Changes in the MRCI between admission and discharge (MRCI changed) were evaluated as a dynamic indicator of medication adjustment during hospitalization. Laboratory test values were collected on the basis of the most unfavorable results on the day of admission, reflecting the worst clinical status likely to influence outcomes. A complete list of all predictors and their detailed definitions is available in Multimedia Appendix 3.

Outcome Variable: MACE

The primary outcome of this study was the time to the first occurrence of MACE after hospital discharge as identified through EMRs. MACE was defined as a composite outcome comprising cardiovascular death, myocardial infarction, stroke, or revascularization according to standardized definitions from prior consensus guidelines [4,33]. The final date for data

XSL•FO
RenderX

collection was December 31, 2021, and survival time was calculated from the date of hospital discharge.

Statistical Analysis

Means and SDs were used to summarize continuous data; categorical data were reported as counts and percentages. Groups were statistically compared using 2-tailed *t* tests and chi-square tests.

For the time-to-event analysis, patients who did not experience MACE during follow-up were treated as censored cases, and MACE occurrence was coded as a binary outcome (1=event, 0=no event). Statistical analyses were performed using SPSS (version 25.0; IBM Corp), and the time-to-event ML model was developed in Python (version 3.9.13; Python Software Foundation). All tests were 2-tailed, and the significance level was set at $P<.05$.

Model Development

The valid ranges of all variables were reviewed and confirmed by the cardiology and cardiovascular nursing team involved in this study. Missing values were assumed to follow a missing-at-random pattern and handled using standard imputation techniques; specifically, the mode was used for binary and categorical variables, and the mean was used for continuous variables. Continuous variables were normalized using minimum–maximum scaling, and categorical variables were processed using one-hot encoding.

The dataset was stratified by MACE occurrence and randomly split into a training set (80%) and a test set (20%) to preserve the event-to-censoring ratio across sets. Five-fold cross-validation within the training set was applied to evaluate model discrimination and calibration and to minimize the risk of overfitting. Among the time-to-event ML models evaluated, Survival Quilts served as the primary algorithm. Survival Quilts is an open-source AutoML framework (implemented from Survival Quilts GitHub [34]) that constructs an ensemble of baseline time-to-event models and adaptively adjusts their weights across time horizons to optimize discriminative performance while maintaining calibration constraints [24].

In total, six time-to-event ML models were developed and compared: Survival Quilts, ensemble-based survival models including Random Survival Forest and CoxBoost (implemented with *scikit-survival* v0.23.0); parametric accelerated failure time models including LogNormal and Weibull (implemented with *lifelines* v0.30.0), and the Cox proportional hazards model (implemented with *scikit-survival* v0.23.0).

Model development was conducted using the training set, with 20% of this training data reserved as a validation subset for hyperparameter optimization. Hyperparameters were tuned through an exhaustive grid search. For ensemble models (Random Survival Forest and CoxBoost), the number of estimators was varied across (50, 100, 200, 300, 400, 500). For accelerated failure time models (LogNormal and Weibull) and the Cox model, 10 regularization coefficients logarithmically spaced between 10e-3 and 1 were tested. For Survival Quilts, time horizons were defined as (30, 60, 90, 180, 270, 365), while all other parameters were set to default values. Random seeds were fixed (seed=1234) across all analyses to ensure reproducibility.

Model Performance

The performance of the time-to-event ML models was evaluated on the basis of discrimination and calibration, which are essential factors for assessing the clinical use of time-to-event ML models [24]. Model performance was examined using the metrics tailored for right-censored data: the time-dependent concordance index (C-index) for discrimination and the time-dependent Brier score for overall prediction accuracy. The time-dependent C-index measures the effectiveness of the model in distinguishing individual risks at different time points, particularly in the presence of censored observations [35]. The time-dependent Brier score assesses the accuracy of predicted survival probabilities by comparing them with the actual distribution of observed events across multiple time points [36].

Permutation-based variable importance scores were calculated to assess the contribution of individual predictors to model performance. Through this method, the decrease in model performance is quantified when the values of a specific variable are randomly permuted, thereby disrupting its relationship with the outcome [37]. The greater the reduction in model performance, the greater the importance of that variable. The time-dependent C-index was used as the reference metric for assessing the effect of each permutation; a large drop indicated a strong influence on the model's discriminative power.

Partial dependence plots were used to show the effect of changes in each predictor on the model's predicted risk. For continuous variables, predictor values varied from minimum to maximum, and the corresponding changes in the predicted risk were plotted [25]. For binary variables, predictions were compared between 0 and 1. For categorical variables, predictions were calculated for each category.

Ethical Considerations

The study was conducted in accordance with the ethical principles outlined in the Declaration of Helsinki. This study was approved by the institutional review board of Seoul Metropolitan Government-Seoul National University Boramae Medical Center, Seoul, Korea (IRB No 30-2024-31).

Results

Baseline Characteristics

The baseline characteristics of the study participants are summarized in Multimedia Appendix 4. The median follow-up duration for the total cohort (N=3159) was 3.8 (IQR 1.6-6.7) years; during follow-up, 626 (19.8%) patients experienced MACE. The mean age of the total patient population was 66.8 years, and 2084 (66%) patients were male. The MACE group was significantly older than the censored group (68.33, SD 11.29 vs 66.42, SD 11.77 years; $P<.001$).

Comorbidities were more common in the MACE group than in the censored group. The prevalence of hypertension was significantly higher in the MACE group (420/626, 67.1%) than in the censored group (1573/2533, 62.1%; $P=.02$). Similarly, higher proportions were observed for peripheral artery disease

XSL•FO
RenderX

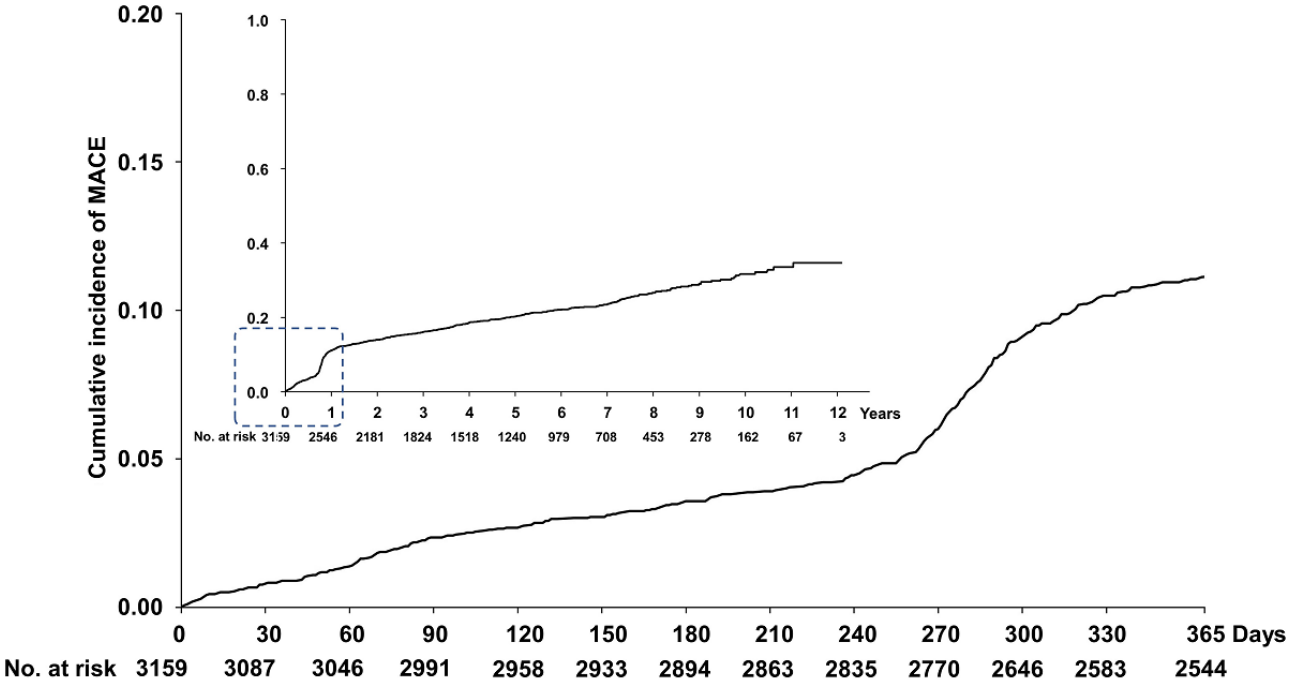
(23/626, 3.7% vs 41/2533, 1.6%; *P*=.002), atrial fibrillation (39/626, 6.2% vs 90/2533, 3.6%; *P*=.004), heart failure (50/626, 8% vs 81/2533, 3.2%; *P*<.001), chronic kidney disease (63/626, 10.1% vs 126/2533 5.0%; *P*<.001), and dialysis-dependent renal failure (32/626, 5.1% vs 49/2533, 1.9%; *P*<.001). The prevalence of diabetes mellitus differed significantly between the MACE and censored groups (χ^2_3=39.7, *P*<.001). Patients without diabetes were less common in the MACE group (361/626, 57.7%) than in the censored group (1718/2533, 67.8%).

Unstable angina was the most frequent ACS subtype (1703/3159, 53.9%) among patients who underwent PCI, and 50.4% (1592/3159) were admitted via the emergency department. Overall, 40.5% (1281/3159) of patients had three-vessel disease, and 7.3% (230/3159) had left main disease. The MACE group received a significantly larger contrast volume during PCI than the censored group (300.66, SD 140.38 mL vs 256.10, SD 125.98 mL; *P*<.001). The severity of CAD was also greater in the MACE group, with three-vessel disease observed in 53.7% (336/626) patients compared with 37.3% (945/2533) patients in the censored group (*P*<.001).

In general, patients who experienced MACE had lower lipid profiles and higher C-reactive protein levels than those without MACE. GFR was also lower in the MACE group (70.68, SD 28.73 mL/min/1.73 m² vs 77.25, SD 26.26 mL/min/1.73 m²; *P*<.001). Among baseline medications, the most frequently prescribed were antiplatelets (2932/3159, 92.8%), followed by nitrates (1992/3159, 63.1%) and statins (1706/3159, 54%). MRCI at discharge was significantly higher in the MACE group (26.14, SD 12.68 vs 24.91, SD 11.20; *P*=.03).

Figure 2 shows the Kaplan–Meier curve of the cumulative MACE rate after hospital discharge. The main graph presents the 1-year survival curve. Within 1 year, the incidence of MACE increased gradually over time; after approximately 270 days, it increased more sharply. The cumulative MACE rates were 0.8%, 3.6%, and 11.1% after 30 days, 180 days, and 1 year, respectively. Our analysis primarily focused on the first year following discharge because most MACE occur, and early intervention is likely to be the most effective during this period.

Figure 2. Incidence of major adverse cardiac events (MACE) after percutaneous coronary intervention (PCI) in patients with acute coronary syndrome ACS.

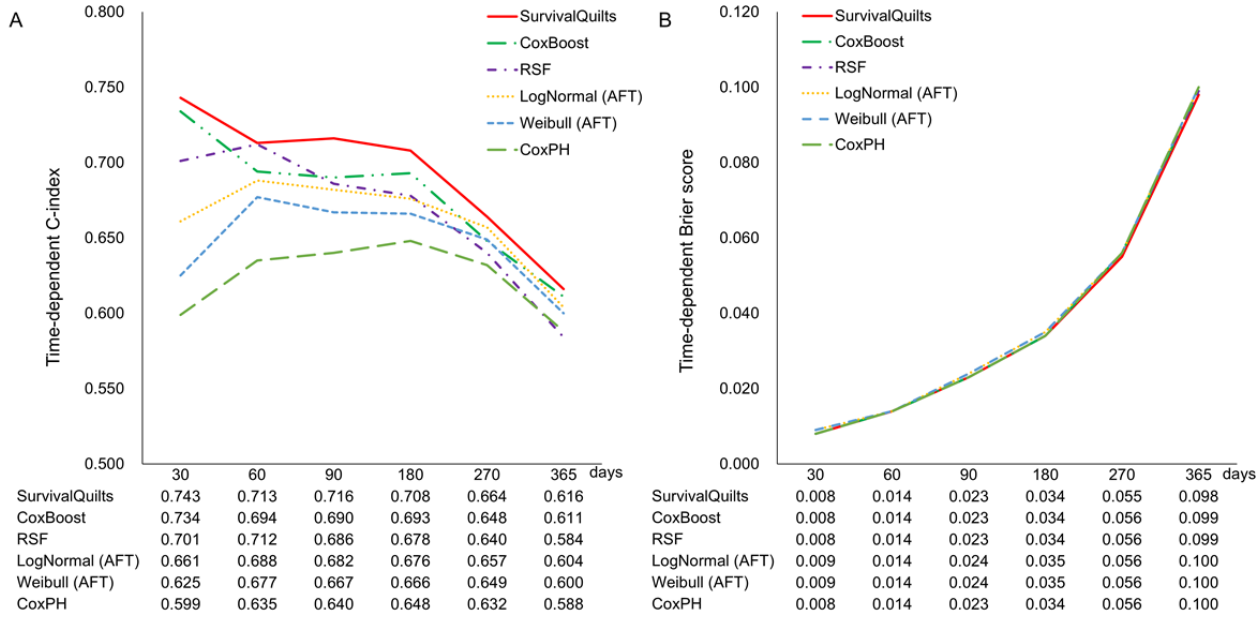


Model Performance

We evaluated the predictive performance of the models for MACE by using the time-dependent C-index and the time-dependent Brier score (Figure 3). Figure 3A presents the time-dependent C-index of multiple models, including Survival Quilts, CoxBoost, Random Survival Forest, LogNormal, Weibull, and Cox proportional hazards model. We compared the model performance on days 30, 60, 90, 180, 270, and 365. Although the time-dependent C-index values decreased over time across all models, the Survival Quilts model consistently demonstrated the highest discriminative performance at each time point. It also showed the highest C-index of 0.743 on day 30, but this index gradually declined to 0.616 on day 365. Figure 3B displays the time-dependent Brier scores for the same models. Overall, the Brier scores increased over time. All models demonstrated comparable and stable Brier scores in the observed time points.

XSL•FO
RenderX

Figure 3. Comparison of the time-dependent model performance for major adverse cardiac events (MACE) prediction. (A) Time-dependent concordance index (C-index) from 30 days to 365 days. (B) Time-dependent Brier scores from 30 days to 365 days. AFT: accelerated failure time; CoxPH: Cox proportional hazards model; RSF: Random Survival Forest.



	30	60	90	180	270	365 days
SurvivalQuilts	0.743	0.713	0.716	0.708	0.664	0.616
CoxBoost	0.734	0.694	0.690	0.693	0.648	0.611
RSF	0.701	0.712	0.686	0.678	0.640	0.584
LogNormal (AFT)	0.661	0.688	0.682	0.676	0.657	0.604
Weibull (AFT)	0.625	0.677	0.667	0.666	0.649	0.600
CoxPH	0.599	0.635	0.640	0.648	0.632	0.588

	30	60	90	180	270	365 days
SurvivalQuilts	0.008	0.014	0.023	0.034	0.055	0.098
CoxBoost	0.008	0.014	0.023	0.034	0.056	0.099
RSF	0.008	0.014	0.023	0.034	0.056	0.099
LogNormal (AFT)	0.009	0.014	0.024	0.035	0.056	0.100
Weibull (AFT)	0.009	0.014	0.024	0.035	0.056	0.100
CoxPH	0.008	0.014	0.023	0.034	0.056	0.100

Among the 6 time-to-event ML models compared, Survival Quilts exhibited the best overall performance based on the time-dependent C-index and Brier score. Therefore, Survival Quilts was defined as the best model in this study, and subsequent analyses, including predictor importance and time-varying risk contribution, were conducted using this model. A web-based demonstrator of the best-performing model is available at Streamlit [38], where individualized MACE risk predictions based on the Survival Quilts algorithm can be interactively explored.

Variable Importance in the Best Model

Table 1 presents the permutation-based variable importance of the best model at different time points. At 30 days post discharge, contrast volume emerged as the strongest predictor, followed by age and the MRCI at discharge. On day 60, the most important predictor was CAD severity, followed by GFR. Conversely, the importance of age and MRCI at discharge decreased. After day 60, CAD severity and GFR remained the most important predictors throughout the follow-up.

Table 1. Top 10 predictor variables for major adverse cardiovascular events (MACE) over time in the best machine learning model.

Rank	30 days	60 days	90 days	180 days	270 days	365 days
1	Contrast volume	CAD[a] severity	CAD severity	CAD severity	CAD severity	CAD severity
2	Age	GFR[b]	GFR	CRP[c]	GFR	GFR
3	MRCI[d] on discharge	CRP	Uric acid	GFR	IABP[e] used	Uric acid
4	LVEF[f]	Uric acid	Age	Uric acid	Atrial fibrillation	IABP used
5	LDL[g]	LDL	CRP	Contrast volume	Uric acid	Creatinine
6	Severity CAD	Creatinine	Atrial fibrillation	IABP used	LVEF	LVEF
7	Uric acid	LVEF	LVEF	Atrial fibrillation	Insurance type	Total cholesterol
8	Fluoro duration	Age	IABP used	LVEF	Contrast volume	Dialysis
9	CRP	Dialysis	Insurance type	HbA_{1c}	Dialysis	Fluoro duration
10	Hemoglobin	MRCI on discharge	Creatinine	Insurance type	Hemoglobin	Insurance type

[a]CAD: coronary artery disease.

[b]GFR: glomerular filtration rate.

[c]CRP: C-reactive protein.

[d]MRCI: medication regimen complexity index.

[e]IABP: intra-aortic balloon pump.

[f]LVEF: left ventricular ejection fraction.

[g]LDL: low density lipoprotein.

XSL•FO
RenderX

Figure 4 shows the partial dependence plots of the top predictors in the best model: contrast volume, age, MRCI at discharge, CAD severity, and GFR. An increase in contrast volume was associated with a high risk of MACE occurrence, particularly when the contrast volume exceeded 300 mL (Figure 4A). Age showed similar predicted risks of MACE occurrence among patients aged 40-49 years and 60-69 years; however, the risk increased sharply in patients aged >60 years (Figure 4B). The MRCI at discharge minimally influenced the MACE occurrence risk up to a score of 20, but the risk progressively increased above this threshold; it showed a steep rise beyond 30 points (Figure 4C). The MACE occurrence risk of patients with three-vessel disease was higher than that of patients with single- or two-vessel disease (Figure 4D). A high GFR was associated with a low MACE occurrence risk, while the risk increased sharply in patients with GFR below 80 mL/min/1.73 m^2 (Figure 4E).

Figure 4. Partial dependence plots of key predictors of major adverse cardiovascular events (MACE) based on the best machine learning (ML) model. (A) Contrast volume and predicted risk of MACE. (B) Age and predicted risk of MACE. (C) The medication regimen complexity index (MRCI) at discharge and predicted risk of MACE. (D) Severity of coronary artery disease (CAD) and predicted MACE. (E) The glomerular filtration rate (GFR) and predicted risk of MACE. VD: vessel disease.

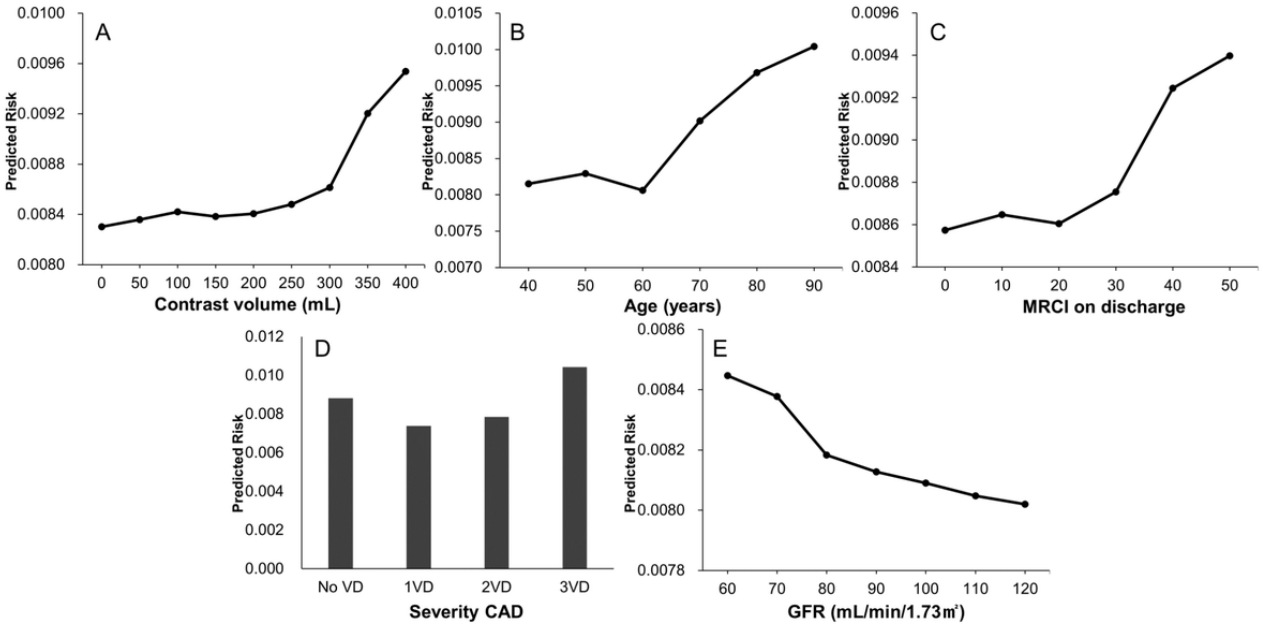
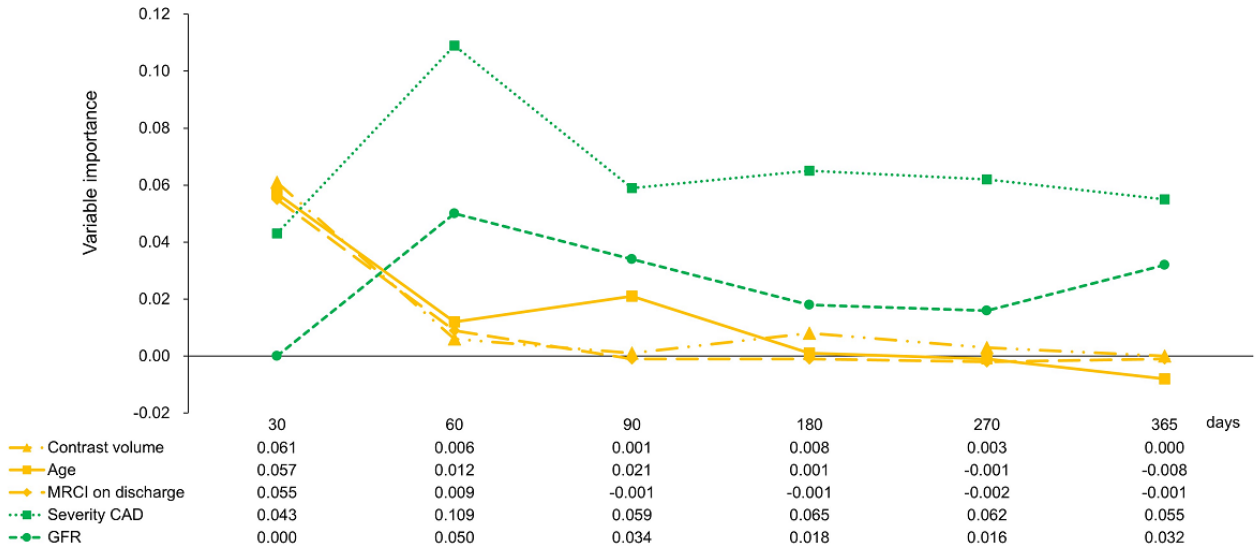


Figure 5 illustrates the time-varying patterns of variable importance for the key predictors based on permutation analysis. Contrast volume, age, and MRCI at discharge showed the highest importance on day 30, but they gradually declined over time. Conversely, CAD severity and GFR became more important after day 60 and maintained high importance throughout the follow-up.

Figure 5. Temporal variation in the importance of key variables in the best machine learning (ML) model. CAD: coronary artery disease; GFR: glomerular filtration rate; MRCI: medication regimen complexity index.



XSL•FO
RenderX

Discussion

Overview

We identified 5 key predictors, namely, contrast volume, age, medication adherence (measured by MRCI at discharge), severity of CAD, and GFR, which showed time-varying importance in predicting MACE after PCI in patients with ACS. The risk of MACE occurrence exhibited nonlinear patterns; specifically, abrupt changes were observed at specific thresholds rather than a steady increase or decrease. Furthermore, the temporal patterns of predictor importance revealed 2 distinct trends. First, contrast volume, age, and medication adherence were the most influential predictors within the first 30 days after hospital discharge; however, their importance diminished over time. Our findings highlighted the importance of optimizing care during the early postdischarge period to prevent early adverse events. Second, CAD severity and renal function emerged as the dominant predictors after 60 days and remained consistently important throughout the follow-up. These insights were obtained through the application of a time-to-event ML framework. This framework could be used to identify nonlinear risk patterns and temporal changes in predictor importance, which are difficult to achieve using traditional statistical methods. By focusing on the first year after discharge, the period of the highest clinical vulnerability could be determined. Thus, actionable insights into timely intervention could be provided.

Early Hospital Discharge Period: Within 30 Days

In this study, the risk of MACE increased sharply when the contrast volume exceeded 300 mL. Contrast volume was identified as the most important variable in the early hospital discharge period, particularly within the first 30 days. The sharp increase in MACE risk above the 300 mL threshold suggests a nonlinear relationship; thus, contrast volume was an important early determinant of MACE after PCI. This finding highlighted the relevance of minimizing contrast exposure during the procedure to reduce MACE early after hospital discharge.

Our results were consistent with previous studies reporting the association between a higher contrast volume and the increased risk of contrast-induced nephropathy and MACE [39,40]. Saito and Kobayashi [41] examined patients with ACS who received PCI and found that those treated for multivessel disease received a higher average contrast volume (295 mL) than those with single-vessel disease (180 mL); they also exhibited a significantly increased MACE incidence. Similarly, Yao et al [40] reported that contrast volumes exceeding 300 mL are a strong independent risk factor for kidney injury, which in turn increases MACE incidence. Notably, Ng et al [39] showed that contrast-induced nephropathy is associated with an approximately 82% increase in MACE risk within the first 30 days after discharge; however, they also demonstrated that this risk decreased to 13% between 30 days and 1 year and was no longer statistically significant beyond 12 months.

This time-varying importance of contrast volume may be explained by the transient effect of contrast-induced renal injury occurring in the early post-PCI period. The early increase in MACE risk is attributed to the occurrence of acute kidney injury shortly after PCI; however, its effect decreases as renal function stabilizes over time [42]. Therefore, targeted efforts to minimize contrast use are crucial, particularly in the periprocedural and early period after hospital discharge.

From a clinical perspective, the health care team should work collaboratively to reduce contrast use during PCI. After PCI, information regarding contrast volume should be clearly communicated to the ward team to facilitate ongoing monitoring of renal function, particularly in patients who receive more than 300 mL of contrast and may require closer follow-up. Previous quality improvement initiatives established that interdisciplinary collaboration could reduce the incidence of contrast-induced renal impairment by up to 21% [43]. In patients who had ACS treated with PCI and received a large contrast volume, outcome improvement may depend on effective interdisciplinary communication and coordinated care efforts. In addition, emerging technologies such as the dynamic coronary roadmap, which provides real-time vascular guidance without the need for repeated contrast injections, show potential for applications in further reducing contrast volume during PCI [44]. The adoption of such innovations in clinical practice may help prevent contrast-related complications and reduce the incidence of MACE following PCI.

In this study, age was identified as an important predictor of MACE, particularly in the early period after hospital discharge. The risk of MACE remained relatively stable among patients aged 40-60 years but increased sharply in those older than 60 years. The importance of age as a predictor was highest at 30 days after discharge and decreased over time. This finding suggested that older patients are at a greater risk of early MACE following PCI and may benefit from closer monitoring during this period. These results were consistent with prior evidence suggesting that age is a recognized contributor to an increased MACE risk [45-47]. The increased vulnerability associated with advancing age may be explained by the cumulative effects of vascular degeneration, increased prevalence of comorbidities, and reduced medication adherence [45,47]. Helber et al [48] reported that patients aged 75 years and older who underwent PCI for ST-elevation myocardial infarction (STEMI) have higher risks of in-hospital complications, including bleeding, cardiogenic shock, and mortality, than younger patients. However, Chen et al [49] found that MACE incidence does not significantly differ between older and younger groups at 6 months post-PCI. This result supports the interpretation that the influence of age on MACE risk diminishes over time as the effect of acute complications decreases. These findings indicate that management immediately after the hospital discharge of older patients with ACS subjected to PCI may help reduce the risk of early MACE through enhanced surveillance and tailored interventions.

A key finding of this study is that lower medication adherence, as reflected by higher MRCI at discharge, was notably related to a higher likelihood of MACE occurrence, particularly during the early period after hospital discharge. In our cohort, the mean MRCI score at discharge was approximately 25, which typically indicated that patients were prescribed 2 or more additional medications beyond standard PCI-related medications because of comorbid conditions.

XSL•FO
RenderX

Further subgroup analysis based on MRCI component scores, namely, dosage forms, dosing frequency, and additional user instructions, revealed that the patients with MRCI scores of 20, 25, and 30 exhibited a progressively higher MACE risk (Multimedia Appendix 5). Differences in dosage forms were significant only between the lowest (20) and highest (30) score groups; conversely, dosing frequency and additional user instructions significantly differed across all 3 groups. These findings indicated that all components of medication adherence—namely, dosage forms, dosing frequency, and additional user instructions—play a meaningful role in influencing MACE risk; therefore, comprehensive strategies should be developed to simplify medication regimens. This finding is consistent with earlier research, which indicated that the increased regimen complexity reduces medication adherence and consequently raises MACE risk [50,51]. In this study, the predictive importance of medication adherence was also the highest within the first 30 days during the early period after hospital discharge and declined thereafter. Therefore, early intervention strategies should be developed to simplify medication regimens and improve adherence, particularly during the early period after hospital discharge, to reduce the risk of MACE.

Later Hospital Discharge Period: From 60 Days to 1 Year

In this study, CAD severity and renal function, measured by GFR, emerged as the most important predictors of MACE during the later period after hospital discharge, particularly beyond 60 days. Patients with more severe CAD, especially those with three-vessel disease, showed a consistently higher risk of MACE over time. Similarly, reduced GFR was related to an increased risk of MACE, independent of acute kidney injury related to contrast exposure.

These findings were consistent with prior research, which demonstrated that the extent of CAD reflects the burden of atherosclerosis, which increases the likelihood of new lesion development or restenosis over time [52]. Three-vessel disease has been well established as a predictor of long-term MACE because of factors such as persistent myocardial ischemia, plaque instability, and progression of atherosclerosis [4,45,47]. Regarding renal function, our findings highlight that lower GFR remained a significant independent risk factor for MACE even beyond the early period of PCI. This finding was consistent with previous studies showing that reduced GFR, reflecting chronic kidney dysfunction, independently contributes to increased MACE regardless of contrast-induced acute kidney injury [53]. Decreased GFR reflects the progression of chronic kidney disease, which is closely associated with the increased long-term MACE incidence [54].

Time-to-Event ML for Risk Prediction

The application of a time-to-event ML framework enabled the identification of time-varying predictor importance and nonlinear risk patterns for MACE following PCI in patients with ACS. Through this approach, risk estimation can be performed to reflect the changes over time at different hospital discharge periods, which is difficult to achieve using traditional statistical models, such as the Cox proportional hazards model. These findings were consistent with previous studies that demonstrated the utility of time-to-event ML models in various clinical contexts. For example, Choi et al [25] applied a time-to-event ML approach to patients who experienced cardiac arrest and showed that temporal changes in predictor importance can guide the optimal timing of reperfusion therapies. Similarly, Lee et al [24] highlighted that incorporating time-to-event ML improves prediction accuracy and supports more informed clinical decision-making.

The ability of time-to-event ML models to determine changes in risk over time and nonlinear relationships provides meaningful advantages in long-term risk prediction. In patients with ACS undergoing PCI, this approach offers the potential to inform the timing of tailored interventions based on changes in risk over time. Future studies are warranted to validate these methods in larger and more diverse patient populations and to explore their integration into real-time clinical decision support systems.

Strengths and Implications

This study has several key strengths. First, we developed a ML model specifically for patients with ACS undergoing PCI; thus, MACE could be more accurately predicted by incorporating time-to-event information. Second, we identified nonlinear risk patterns and specific thresholds for key predictors using permutation-based variable importance and partial dependence plots, providing deeper insights into risk dynamics. Third, our approach could estimate how risk changes over time, which can support the planning of tailored interventions at different time points after hospital discharge.

Limitations

This study is subject to several limitations. First, because the model was developed and internally validated using data from a single center, there remains a potential risk of overfitting and optimistic performance estimates despite the use of 5-fold cross-validation. External validation using multicenter data is required to confirm generalizability. Second, missing values were handled under a missing-at-random assumption using simple imputation. However, this approach may underestimate variability and does not fully capture the uncertainty associated with missing data. More advanced strategies, such as multiple imputation or the k-fold cross validation, could be explored in future work to reduce potential bias. Third, as this study relied on EMR data, the available predictors were limited; some potential risk factors, such as psychosocial variables including stress, were also not considered. Fourth, all patient data were collected prior to PCI, and laboratory values were represented using either maximum values or averaged results from multiple measurements. Thus, temporal changes in patient condition after PCI were not reflected in the model. Fifth, medication adherence was indirectly assessed using the MRCI, which measures regimen complexity rather than actual adherence behavior. Although MRCI demonstrated good reliability in this population, future studies should incorporate the direct measures of medication adherence to improve predictive accuracy. Sixth, although the study identified a nonlinear relationship between contrast volume and MACE risk, particularly beyond 300 mL, factors such as body weight and renal function ratio were not

XSL•FO
RenderX

considered; results should be carefully interpreted, and further investigation should be performed. Finally, because of the nature of secondary data analysis, there may have been data entry errors or missing values, which could have influenced the results. Despite these limitations, this study provides meaningful contributions by demonstrating the utility of time-to-event ML in predicting MACE in patients with ACS undergoing PCI and by identifying key risk factors that may inform clinical practice.

Conclusions

We developed a time-to-event ML model to predict MACE in patients with ACS undergoing PCI. This model incorporated time-dependent risk estimation during the entire follow-up; thus, nonlinear risk patterns and temporal changes in predictor importance could be identified, thereby enhancing interpretability and clinical applicability. Notably, contrast volume, age, and medication adherence exhibited the greatest influence within the first 30 days after hospital discharge; conversely, the severity of CAD and GFR became more influential in the later period, particularly beyond 60 days. Although the model was trained using full follow-up data, our findings highlighted that the first year after discharge was a critical window for intervention. During this period, targeted strategies, such as minimizing contrast use, closely monitoring renal function, and improving medication adherence, might provide the most clinical benefit. These insights might help health care providers implement time-informed, personalized strategies to improve patient outcomes.

Acknowledgments

We would like to acknowledge the contributions of individuals who supported this work but did not meet the criteria for authorship.

The authors declare that generative AI tools were not used in the preparation of this manuscript.

Funding

This work was supported by grants from the National Research Foundation of Korea (NRF), funded by the Korean government (MSIT; grant RS-2025-00562535), and from the Institute of Information and Communications Technology Planning & Evaluation (IITP), funded by the Korean government (MSIT; grant RS-2019-II190079, Artificial Intelligence Graduate School Program, Korea University).

Data Availability

The datasets generated or analyzed during this study are available from the corresponding author on reasonable request.

Authors' Contributions

Conceptualization: HJC (lead), HLK (equal), YJS (equal)
Data curation: HJC (lead), CL (supporting)
Formal analysis: HJC (lead), CL (supporting)
Funding acquisition: YJS
Methodology: HJC (lead), CL (supporting), HLK (supporting), YJS (equal)
Project administration: YJS
Supervision: YJS (lead), HLK (Supporting)
Validation: YJS (lead)
Visualization: HJC
Software: HJC
Writing – original draft: HJC (lead), YJS (supporting)
Writing – review & editing: HJC (lead), CL (supporting), HLK (supporting), YJS (equal)

Conflicts of Interest

None declared.

Multimedia Appendix 1
TRIPOD+AI checklist.
[DOCX File , 2015 KB - medinform_v13i1e81778_app1.docx]

Multimedia Appendix 2
STROBE statement.
[DOCX File , 25 KB - medinform_v13i1e81778_app2.docx]

Multimedia Appendix 3

XSL•FO
RenderX

Predictors used in the time-to-event machine learning (ML) model.
[DOCX File , 30 KB - medinform_v13i1e81778_app3.docx]

Multimedia Appendix 4
Baseline characteristics of patients who underwent percutaneous coronary intervention (PCI) for acute coronary syndrome (ACS; N= 3159).
[DOCX File , 43 KB - medinform_v13i1e81778_app4.docx]

Multimedia Appendix 5
Three medication regimen complexity index (MRCI) components across score-based subgroups and the total cohort.
[DOCX File , 146 KB - medinform_v13i1e81778_app5.docx]

References

1. Knuuti J, Wijns W, Saraste A, Capodanno D, Barbato E, Funck-Brentano C, ESC Scientific Document Group. 2019 ESC guidelines for the diagnosis and management of chronic coronary syndromes. Eur Heart J 2020;41(3):407-477 [FREE Full text] [doi: 10.1093/eurheartj/ehz425] [Medline: 31504439]
2. Virani SS, Newby LK, Arnold SV, Bittner V, Brewer LC, Demeter SH, Peer Review Committee Members. 2023 AHA/ACC/ACCP/ASPC/NLA/PCNA guideline for the management of patients with chronic coronary disease: a report of the American Heart Association/American College of Cardiology Joint Committee on Clinical Practice Guidelines. Circulation 2023;148(9):e9-e119 [FREE Full text] [doi: 10.1161/CIR.0000000000001168] [Medline: 37471501]
3. Vrints C, Andreotti F, Koskinas KC, Rossello X, Adamo M, Ainslie J, ESC Scientific Document Group. 2024 ESC guidelines for the management of chronic coronary syndromes. Eur Heart J 2024;45(36):3415-3537. [doi: 10.1093/eurheartj/ehae177] [Medline: 39210710]
4. Byrne RA, Rossello X, Coughlan JJ, Barbato E, Berry C, Chieffo A, ESC Scientific Document Group. 2023 ESC guidelines for the management of acute coronary syndromes. Eur Heart J 2023;44(38):3720-3826 [FREE Full text] [doi: 10.1093/eurheartj/ehad191] [Medline: 37622654]
5. Jia S, Liu Y, Yuan J. Evidence in guidelines for treatment of coronary artery disease. Adv Exp Med Biol 2020;1177:37-73. [doi: 10.1007/978-981-15-2517-9_2] [Medline: 32246443]
6. Writing Committee Members, Lawton JS, Tamis-Holland JE, Bangalore S, Bates ER, Beckie TM, et al. 2021 ACC/AHA/SCAI guideline for coronary artery revascularization: executive summary: a report of the American College of Cardiology/American Heart Association Joint Committee on Clinical Practice Guidelines. J Am Coll Cardiol 2022;79(2):197-215 [FREE Full text] [doi: 10.1016/j.jacc.2021.09.005] [Medline: 34895951]
7. Qin H, Mayer H, Öztürk B, Badr Eslam R. Patients' perspectives with acute coronary syndrome after percutaneous coronary intervention. J Nurse Pract 2021;17(5):588-593 [FREE Full text] [doi: 10.1016/j.nurpra.2021.02.006]
8. Pietrzykowski, Michalski P, Kosobucka A, Kasprzak M, Fabiszak T, Stolarek W, et al. Medication adherence and its determinants in patients after myocardial infarction. Sci Rep 2020;10(1):12028 [FREE Full text] [doi: 10.1038/s41598-020-68915-1] [Medline: 32694522]
9. Giustino G, Colombo A, Camaj A, Yasumura K, Mehran R, Stone GW, et al. Coronary in-stent restenosis: JACC state-of-the-art review. J Am Coll Cardiol 2022;80(4):348-372 [FREE Full text] [doi: 10.1016/j.jacc.2022.05.017] [Medline: 35863852]
10. Kumar R, Shah JA, Solangi BA, Ammar A, Kumar M, Khan N, et al. The burden of short-term major adverse cardiac events and its determinants after emergency percutaneous coronary revascularization: a prospective follow-up study. J Saudi Heart Assoc 2022;34(2):100-109 [FREE Full text] [doi: 10.37616/2212-5043.1302] [Medline: 36237223]
11. Okkonen M, Havulinna AS, Ukkola O, Huikuri H, Pietilä A, Koukkunen H, et al. Risk factors for major adverse cardiovascular events after the first acute coronary syndrome. Ann Med 2021;53(1):817-823 [FREE Full text] [doi: 10.1080/07853890.2021.1924395] [Medline: 34080496]
12. Kalyoncuoğlu M, Katkat F, Biter HI, Cakal S, Tosu AR, Can MM. Predicting one-year deaths and major adverse vascular events with the Controlling Nutritional Status Score in elderly patients with non-ST-elevated myocardial infarction undergoing percutaneous coronary intervention. J Clin Med 2021;10(11):2247 [FREE Full text] [doi: 10.3390/jcm10112247] [Medline: 34067233]
13. Bosco E, Hsueh L, McConeghy KW, Gravenstein S, Saade E. Major adverse cardiovascular event definitions used in observational analysis of administrative databases: a systematic review. BMC Med Res Methodol 2021;21(1):241 [FREE Full text] [doi: 10.1186/s12874-021-01440-5] [Medline: 34742250]
14. Murphy A, Hamilton G, Andrianopoulos N, Yudi MB, Farouque O, Duffy SJ, Melbourne Interventional Group. One-year outcomes of patients with established coronary artery disease presenting with acute coronary syndromes. Am J Cardiol 2019;123(9):1387-1392. [doi: 10.1016/j.amjcard.2019.01.037] [Medline: 30797559]

XSL•FO
RenderX

15. Choi H, Kim C, Lee D, Joo J, Kim H. Participation and prognostic impact of cardiac rehabilitation after acute coronary syndrome: big-data study of the Korean National Health Insurance Service. J Korean Med Sci 2023;38(15):e119 [FREE Full text] [doi: 10.3346/jkms.2023.38.e119] [Medline: 37069813]
16. Bauer D, Toušek P. Risk stratification of patients with acute coronary syndrome. J Clin Med 2021;10(19):4574 [FREE Full text] [doi: 10.3390/jcm10194574] [Medline: 34640592]
17. Lu Y, Melnick ER, Krumholz HM. Clinical decision support in cardiovascular medicine. BMJ 2022;377:e059818. [doi: 10.1136/bmj-2020-059818] [Medline: 35613721]
18. Sherazi SWA, Bae J, Lee JY. A soft voting ensemble classifier for early prediction and diagnosis of occurrences of major adverse cardiovascular events for STEMI and NSTEMI during 2-year follow-up in patients with acute coronary syndrome. PLoS One 2021;16(6):e0249338 [FREE Full text] [doi: 10.1371/journal.pone.0249338] [Medline: 34115750]
19. Ryu L, Han K. Machine learning vs. statistical model for prediction modelling: application in medical imaging research. J Korean Soc Radiol 2022;83(6):1219-1228 [FREE Full text] [doi: 10.3348/jksr.2022.0111] [Medline: 36545410]
20. Rajula HSR, Verlato G, Manchia M, Antonucci N, Fanos V. Comparison of conventional statistical methods with machine learning in medicine: diagnosis, drug development, and treatment. Medicina (Kaunas) 2020;56(9):455 [FREE Full text] [doi: 10.3390/medicina56090455] [Medline: 32911665]
21. Aziz F, Malek S, Ibrahim KS, Raja Shariff RE, Wan Ahmad WA, Ali RM, et al. Short- and long-term mortality prediction after an acute ST-elevation myocardial infarction (STEMI) in Asians: a machine learning approach. PLoS One 2021;16(8):e0254894 [FREE Full text] [doi: 10.1371/journal.pone.0254894] [Medline: 34339432]
22. Bai Z, Lu J, Li T, Ma Y, Liu Z, Zhao R, et al. Clinical feature-based machine learning model for 1-year mortality risk prediction of st-segment elevation myocardial infarction in patients with hyperuricemia: a retrospective study. Comput Math Methods Med 2021;2021:7252280 [FREE Full text] [doi: 10.1155/2021/7252280] [Medline: 34285708]
23. Chopannejad S, Sadoughi F, Bagherzadeh R, Shekarchi S. Predicting major adverse cardiovascular events in acute coronary syndrome: a scoping review of machine learning approaches. Appl Clin Inform 2022;13(3):720-740 [FREE Full text] [doi: 10.1055/a-1863-1589] [Medline: 35617971]
24. Lee C, Zame W, Alaa A, Schaar M. Temporal quilting for survival analysis. Proceedings of Machine Learning Research 2019;89:596-605 [FREE Full text]
25. Choi H, Lee C, Chun J, Seol R, Lee YM, Son Y. Development of a predictive model for survival over time in patients with out-of-hospital cardiac arrest using ensemble-based machine learning. Comput Inform Nurs 2024;42(5):388-395. [doi: 10.1097/CIN.0000000000001145] [Medline: 39248449]
26. Collins GS, Moons KGM, Dhiman P, Riley RD, Beam AL, Van Calster B. TRIPOD+AI statement: updated guidance for reporting clinical prediction models that use regression or machine learning methods. BMJ 2024;385:e078378 [FREE Full text] [doi: 10.1136/bmj.q902] [Medline: 38636956]
27. Collet J, Thiele H, Barbato E, Barthélémy O, Bauersachs J, Bhatt DL, ESC Scientific Document Group. 2020 ESC guidelines for the management of acute coronary syndromes in patients presenting without persistent ST-segment elevation. Eur Heart J 2021;42(14):1289-1367. [doi: 10.1093/eurheartj/ehaa575] [Medline: 32860058]
28. Riley RD, Snell KI, Ensor J, Burke DL, Harrell FE, Moons KG, et al. Minimum sample size for developing a multivariable prediction model: part II – binary and time-to-event outcomes. Stat Med 2019;38(7):1276-1296 [FREE Full text] [doi: 10.1002/sim.7992] [Medline: 30357870]
29. Kang SH, Song HN, Moon JY, Kim S, Sung J, Kim IJ, et al. Prevalence and prognostic significance of malnutrition in patients with acute coronary syndrome treated with percutaneous coronary intervention. Medicine (Baltimore) 2022;101(34):e30100 [FREE Full text] [doi: 10.1097/MD.0000000000030100] [Medline: 36042595]
30. Seto AH, Shroff A, Abu-Fadel M, Blankenship JC, Boudoulas KD, Cigarroa JE, et al. Length of stay following percutaneous coronary intervention: an expert consensus document update from the Society for Cardiovascular Angiography and Interventions. Catheter Cardiovasc Interv 2018;92(4):717-731. [doi: 10.1002/ccd.27637] [Medline: 29691963]
31. George J, Phun Y, Bailey MJ, Kong DCM, Stewart K. Development and validation of the medication regimen complexity index. Ann Pharmacother 2004;38(9):1369-1376. [doi: 10.1345/aph.1D479] [Medline: 15266038]
32. Lee S, Jang J, Yang S, Hahn J, Min KL, Jung EH, et al. Development and validation of the Korean version of the medication regimen complexity index. PLoS One 2019;14(5):e0216805 [FREE Full text] [doi: 10.1371/journal.pone.0216805] [Medline: 31095602]
33. Hicks KA, Mahaffey KW, Mehran R, Nissen SE, Wiviott SD, Dunn B, Standardized Data Collection for Cardiovascular Trials Initiative (SCTI). 2017 cardiovascular and stroke endpoint definitions for clinical trials. Circulation 2018;137(9):961-972. [doi: 10.1161/CIRCULATIONAHA.117.033502] [Medline: 29483172]
34. Survival Quilts. URL: https://github.com/chl8856/SurvivalQuilts [accessed 2025-11-17]
35. Gerds TA, Kattan MW, Schumacher M, Yu C. Estimating a time-dependent concordance index for survival prediction models with covariate dependent censoring. Stat Med 2013;32(13):2173-2184. [doi: 10.1002/sim.5681] [Medline: 23172755]
36. Mogensen UB, Ishwaran H, Gerds TA. Evaluating random forests for survival analysis using prediction error curves. J Stat Softw 2012;50(11):1-23 [FREE Full text] [doi: 10.18637/jss.v050.i11] [Medline: 25317082]

XSL•FO
RenderX

37. Molnar C, Freiesleben T, König G, Herbinger J, Reisinger T, Casalicchio G. Relating the partial dependence plotpermutation feature importance to the data generating process. 1901 Presented at: First World Conference, xAI 2023; July 26-28, 2023; Lisbon p. 456-479 URL: https://doi.org/10.1007/978-3-031-44064-9_24 [doi: 10.1007/978-3-031-44064-9_24]
38. Streamlit. URL: https://survival-calculato-mace.streamlit.app/ [accessed 2025-11-17]
39. Ng AK, Ng PY, Ip A, Lam LT, Ling IW, Wong AS, et al. Impact of contrast-induced acute kidney injury on long-term major adverse cardiovascular events and kidney function after percutaneous coronary intervention: insights from a territory-wide cohort study in Hong Kong. Clin Kidney J 2022;15(2):338-346 [FREE Full text] [doi: 10.1093/ckj/sfab212] [Medline: 35145648]
40. Yao Z, Shen H, Tang M, Yan Y, Ge J. A novel risk assessment model of contrast-induced nephropathy after percutaneous coronary intervention in patients with diabetes. Basic Clin Pharmacol Toxicol 2021;128(2):305-314 [FREE Full text] [doi: 10.1111/bcpt.13501] [Medline: 32991776]
41. Saito Y, Kobayashi Y. Percutaneous coronary intervention strategies in patients with acute myocardial infarction and multivessel disease: completeness, timing, lesion assessment, and patient status. J Cardiol 2019;74(2):95-101 [FREE Full text] [doi: 10.1016/j.jjcc.2019.04.001] [Medline: 31053505]
42. Yang Y, George KC, Luo R, Cheng Y, Shang W, Ge S, et al. Contrast-induced acute kidney injury and adverse clinical outcomes risk in acute coronary syndrome patients undergoing percutaneous coronary intervention: a meta-analysis. BMC Nephrol 2018;19(1):374. [doi: 10.1186/s12882-018-1161-5] [Medline: 30577763]
43. Lambert P, Chaisson K, Horton S, Petrin C, Marshall E, Bowden S, Northern New England Cardiovascular Disease Study Group. Reducing acute kidney injury due to contrast material: how nurses can improve patient safety. Crit Care Nurse 2017;37(1):13-26 [FREE Full text] [doi: 10.4037/ccn2017178] [Medline: 28148611]
44. Hennessey B, Danenberg H, De Vroey F, Kirtane AJ, Parikh M, Karmpaliotis D, et al. Dynamic coronary roadmap versus standard angiography for percutaneous coronary intervention: the randomised, multicentre DCR4Contrast trial. EuroIntervention 2024;20(3):e198-e206 [FREE Full text] [doi: 10.4244/EIJ-D-23-00460] [Medline: 38343370]
45. Jalali A, Hassanzadeh A, Najafi MS, Nayebirad S, Dashtkoohi M, Karimi Z, et al. Predictors of major adverse cardiac and cerebrovascular events after percutaneous coronary intervention in older adults: a systematic review and meta-analysis. BMC Geriatr 2024;24(1):337 [FREE Full text] [doi: 10.1186/s12877-024-04896-4] [Medline: 38609875]
46. Jenab Y, Hedayat B, Karimi A, Taaghi S, Ghorashi SM, Ekhtiari H. Effects of opium use on one-year major adverse cardiovascular events (MACE) in the patients with ST-segment elevation MI undergoing primary PCI: a propensity score matched - machine learning based study. BMC Complement Med Ther 2023;23(1):16 [FREE Full text] [doi: 10.1186/s12906-023-03833-z] [Medline: 36658513]
47. Ulvenstam A, Graipe A, Irewall A, Söderström L, Mooe T. Incidence and predictors of cardiovascular outcomes after acute coronary syndrome in a population-based cohort study. Sci Rep 2023;13(1):3447 [FREE Full text] [doi: 10.1038/s41598-023-30597-w] [Medline: 36859606]
48. Helber I, Alves CMR, Grespan SM, Veiga ECA, Moraes PIM, Souza JM, et al. The impact of advanced age on major cardiovascular events and mortality in patients with ST-elevation myocardial infarction undergoing a pharmaco-invasive strategy. Clin Interv Aging 2020;15:715-722 [FREE Full text] [doi: 10.2147/CIA.S218827] [Medline: 32546989]
49. Chen P, Wang D, Chen K, Liang C, Reng Y, Yang J, et al. Outcomes of percutaneous coronary intervention in patients ≥ 75 years: one-center study in a Chinese patient group. J Geriatr Cardiol 2015;12(6):626-633 [FREE Full text] [doi: 10.11909/j.issn.1671-5411.2015.06.004] [Medline: 26788039]
50. Franchi C, Ludergnani M, Merlino L, Nobili A, Fortino I, Leoni O, et al. Multiple medication adherence and related outcomes in community-dwelling older people on chronic polypharmacy: a retrospective cohort study on administrative claims data. Int J Environ Res Public Health 2022;19(9):5692 [FREE Full text] [doi: 10.3390/ijerph19095692] [Medline: 35565087]
51. Kuo SZ, Haftek M, Lai JC. Factors associated with medication non-adherence in patients with end-stage liver disease. Dig Dis Sci 2017;62(2):543-549 [FREE Full text] [doi: 10.1007/s10620-016-4391-z] [Medline: 27933471]
52. Ralapanawa U, Sivakanesan R. Epidemiology and the magnitude of coronary artery disease and acute coronary syndrome: a narrative review. J Epidemiol Glob Health 2021;11(2):169-177 [FREE Full text] [doi: 10.2991/jegh.k.201217.001] [Medline: 33605111]
53. Murugan R, Boudreaux-Kelly MY, Kellum JA, Palevsky PM, Weisbord S. Contrast-associated acute kidney injury and cardiovascular events: a secondary analysis of the PRESERVE cohort. Clin Kidney J 2023;16(12):2626-2638 [FREE Full text] [doi: 10.1093/ckj/sfad214] [Medline: 38046040]
54. Caracciolo A, Scalise RFM, Ceresa F, Bagnato G, Versace AG, Licordari R, et al. Optimizing the outcomes of percutaneous coronary intervention in patients with chronic kidney disease. J Clin Med 2022;11(9):2380 [FREE Full text] [doi: 10.3390/jcm11092380] [Medline: 35566504]

Abbreviations

ACS: acute coronary syndrome
CAD: coronary artery disease

XSL•FO
RenderX

C-index: concordance index
EMR: electronic medical record
GFR: glomerular filtration rate
MACE: major adverse cardiovascular events
ML: machine learning
MRCI: medication regimen complexity index
PCI: percutaneous coronary intervention
STEMI: ST-elevation myocardial infarction
STROBE: Strengthening the Reporting of Observational Studies in Epidemiology
TRIPOD+AI: Transparent Reporting of a Multivariable Prediction Model for Individual Prognosis or Diagnosis + Artificial Intelligence

Edited by A Benis; submitted 03.08.25; peer-reviewed by M Tsiknakis; comments to author 27.10.25; revised version received 03.11.25; accepted 11.11.25; published 27.11.25.

Please cite as:
Choi HJ, Lee C, Kim HL, Son YJ
Risk Prediction of Major Adverse Cardiovascular Events Within One Year After Percutaneous Coronary Intervention in Patients With Acute Coronary Syndrome: Machine Learning–Based Time-to-Event Analysis
JMIR Med Inform 2025;13:e81778
URL: https://medinform.jmir.org/2025/1/e81778
doi:10.2196/81778
PMID:

©Hong-Jae Choi, Changhee Lee, Hack-Lyoung Kim, Youn-Jung Son. Originally published in JMIR Medical Informatics (https://medinform.jmir.org), 27.11.2025. This is an open-access article distributed under the terms of the Creative Commons Attribution License (https://creativecommons.org/licenses/by/4.0/), which permits unrestricted use, distribution, and reproduction in any medium, provided the original work, first published in JMIR Medical Informatics, is properly cited. The complete bibliographic information, a link to the original publication on https://medinform.jmir.org/, as well as this copyright and license information must be included.

XSL•FO
RenderX

Original Paper

Identifying Key Variances in Clinical Pathways Associated With Prolonged Hospital Stays Using Machine Learning and ePath Real-World Data: Model Development and Validation Study

Saori Tou[1], MS; Koutarou Matsumoto[1], MPH, PhD; Asato Hashinokuchi[2], MD; Fumihiko Kinoshita[2], MD, PhD; Yasunobu Nohara[3], PhD; Takanori Yamashita[4], PhD; Yoshifumi Wakata[5], MD, PhD; Tomoyoshi Takenaka[2], MD, PhD; Hidehisa Soejima[6], MD, PhD; Tomoharu Yoshizumi[2], MD, PhD; Naoki Nakashima[4,7], MD, PhD; Masahiro Kamouchi[1,8], MD, PhD

[1]Department of Health Care Administration and Management, Graduate School of Medical Sciences, Kyushu University, Fukuoka, Japan

[2]Department of Surgery and Science, Graduate School of Medical Sciences, Kyushu University, Fukuoka, Japan

[3]Big Data Science and Technology, Faculty of Advanced Science and Technology, Kumamoto University, Kumamoto, Japan

[4]Medical Information Center, Kyushu University Hospital, Fukuoka, Japan

[5]Department of Medical Informatics, Tokushima University Hospital, Tokushima, Japan

[6]Institute for Medical Information Research and Analysis, Saiseikai Kumamoto Hospital, Kumamoto, Japan

[7]Department of Medical Informatics, Graduate School of Medical Sciences, Kyushu University, Fukuoka, Japan

[8]Center for Cohort Studies, Graduate School of Medical Sciences, Kyushu University, Fukuoka, Japan

Corresponding Author:
Koutarou Matsumoto, MPH, PhD
Department of Health Care Administration and Management, Graduate School of Medical Sciences, Kyushu University
3-1-1 Maidashi, Higashi-ku
Fukuoka, 812-8582
Japan
Phone: 81 92 642 6960
Email: matsumoto.kotaro.251@m.kyushu-u.ac.jp

Abstract

Background: Prolonged hospital stays can lead to inefficiencies in health care delivery and unnecessary consumption of medical resources.

Objective: This study aimed to identify key clinical variances associated with prolonged length of stay (PLOS) in clinical pathways using a machine learning model trained on real-world data from the ePath system.

Methods: We analyzed data from 480 patients with lung cancer (age: mean 68.3, SD 11.2 years; n=263, 54.8% men) who underwent video-assisted thoracoscopic surgery at a university hospital between 2019 and 2023. PLOS was defined as a hospital stay exceeding 9 days after video-assisted thoracoscopic surgery. The variables collected between admission and 4 days after surgery were examined, and those that showed a significant association with PLOS in univariate analyses (P<.01) were selected as predictors. Predictive models were developed using sparse linear regression methods (Lasso, ridge, and elastic net) and decision tree ensembles (random forest and extreme gradient boosting). The data were divided into derivation (earlier study period) and testing (later period) cohorts for temporal validation. The model performance was assessed using the area under the receiver operating characteristic curve, Brier score, and calibration plots. Counterfactual analysis was used to identify key clinical factors influencing PLOS.

Results: A 3D heatmap illustrated the temporal relationships between clinical factors and PLOS based on patient demographics, comorbidities, functional status, surgical details, care processes, medications, and variances recorded from admission to 4 days after surgery. Among the 5 algorithms evaluated, the ridge regression model demonstrated the best performance in terms of both discrimination and calibration. Specifically, it achieved area under the receiver operating characteristic curve values of 0.84 and 0.82 and Brier scores of 0.16 and 0.17 in the derivation and test cohorts, respectively. In the final model, a range of variables, including blood tests, care, patient background, procedures, and clinical variances, were associated with PLOS. Among these, particular emphasis was placed on clinical variances. Counterfactual analysis using the ridge regression model identified 6 key

XSL•FO
RenderX

variables strongly linked to PLOS. In order of impact, these were abnormal respiratory sounds, postoperative fever, arrhythmia, impaired ambulation, complications after drain removal, and pulmonary air leaks.

Conclusions: A machine learning–based model using ePath data effectively identified critical variances in the clinical pathways associated with PLOS. This automated tool may enhance clinical decision-making and improve patient management.

(JMIR Med Inform 2025;13:e71617) doi:10.2196/71617

KEYWORDS

clinical pathway; hospital stay; machine learning; video-assisted thoracoscopic surgery; artificial intelligence; AI

Introduction

Prolonged length of stay (PLOS) remains a persistent challenge in modern health care, contributing to inefficient resource use, increased health care costs, and delayed recovery [1]. To address these concerns, hospitals have adopted strategies such as standardized clinical pathways designed to streamline care and promote timely discharge [2,3]. Despite these efforts, PLOS remains common, particularly among surgical patients, due to factors such as postoperative complications, functional decline, and comorbidities.

Identifying patients at high risk of PLOS is crucial for enabling timely and targeted interventions. However, predicting PLOS in routine clinical settings remains challenging due to the complex and dynamic nature of patient conditions and the multidimensional nature of clinical data. Recent advancements in electronic clinical pathways have enabled systematic, real-time recording of deviations from expected recovery trajectories—referred to as “variances” [2]. These variances may reflect meaningful clinical events and could provide valuable insights for predicting outcomes such as PLOS. Nevertheless, predictive systems that fully leverage variance data remain underdeveloped.

To address this gap, we developed a novel electronic clinical pathway system called “ePath,” which records outcomes, outcome assessments, and associated tasks in a structured format known as the outcomes-assessments-tasks (OAT) unit. ePath integrates seamlessly with electronic medical records via a custom data conversion interface and provides a standardized data model for pathway-based care [4-6].

In this study, we applied machine learning algorithms to real-world ePath data from patients undergoing video-assisted thoracoscopic surgery (VATS) for lung cancer, aiming to develop a robust model to predict PLOS risk. VATS has become widely adopted as a minimally invasive alternative to traditional open thoracotomy and is associated with shorter hospital stays and lower health care costs [7-14]. These cost savings are largely attributed to a reduction in PLOS [11,14]. However, a considerable proportion of patients still experience prolonged hospitalization, highlighting the need for more advanced predictive tools.

The objective of this study was to develop an accurate and clinically actionable PLOS prediction model using machine learning applied to variance data captured by ePath. Establishing such a system could enable timely interventions and support clinical decision-making to reduce PLOS.

Methods

Ethical Considerations

The study design was approved by the Certified Review Board of the Clinical Research Network Fukuoka (M23082-00). The requirement for informed consent was waived, as this was a retrospective study using anonymized records. No compensation or incentives were provided to participants because this retrospective study used anonymized data and did not involve direct contact with individuals.

Study Design

This study included patients with lung cancer hospitalized at Kyushu University Hospital in Fukuoka, Japan, who received treatment via the VATS electronic clinical pathway. The ePath system implemented at Kyushu University Hospital in 2018 has been described in previous publications [4-6]. Inpatient clinical data were electronically collected through ePath and compiled into a dataset for outcome prediction using machine learning models.

Clinical Outcomes

The clinical outcome of interest, PLOS, was defined as a postoperative hospital stay exceeding 9 days based on the target length of stay outlined in the clinical pathway at Kyushu University Hospital.

Clinical Variables

Data collected during routine inpatient care were comprehensively recorded in the ePath system and used as variables. ePath is an electronic clinical pathway platform developed to standardize and share clinical pathways across multiple electronic medical record systems [4-6]. It facilitates the systematic collection and analysis of related clinical data, thereby supporting the application of artificial intelligence in routine clinical practice. The variables included baseline patient characteristics, functional status, pharmacotherapy, surgical procedures, care processes, variance, and laboratory results.

Baseline patient characteristics, functional status, care procedures, and pharmacotherapy were obtained from the Diagnosis Procedure Combination database, Japan’s medical billing data system, which comprises forms 1, H, and EF files. Form 1 contains demographic information, diagnoses, and disease severity. The H file provides daily records of physical condition, patient care, and activities of daily living. The EF file details daily pharmacotherapy, surgeries, and other clinical activities.

XSL•FO
RenderX

Care processes, outcomes, and variances were embedded in the electronic clinical pathway and collected using the ePath system. The clinical pathway data comprised OAT and variances for each care process during hospitalization; these were collectively referred to as OAT units [4-6]. The OAT units included expected outcomes, assessments of outcomes, and tasks required for assessments, all of which are interlinked. Deviations from predefined care processes were recorded as variances in the OAT units.

Laboratory results were obtained from the laboratory database using the Standardized Structured Medical Information eXchange, a standardized clinical data export system.

The number of discharges began to increase on postoperative day 5. To minimize the impact of missing values due to discharge and to reduce the risk of reverse causality, we limited the candidate explanatory variables to those available by postoperative day 4. From these, we first excluded variables with high overall missingness or outcome-related missingness, as these could introduce substantial bias. Although regularization methods are designed to mitigate overfitting, our previous research showed that including a large number of variables improved apparent prediction accuracy in the derivation cohort but reduced performance in the validation cohort, likely because of high-dimensional noise. To optimize model performance while maintaining generalizability, we used a 2-step variable selection process that combined the exclusion of variables with high missingness and univariate screening. This hybrid approach enabled us to retain clinically important predictors, reduce noise, and enhance the robustness of the final model [15].

Study Participants

Between July 2019 and May 2023, a total of 577 patients with lung cancer at Kyushu University Hospital underwent VATS treatment. Daily patient data were collected using the ePath system, resulting in 1562 variables. To reduce potential bias, the selection of both the explanatory variables and patients was based on the method described above. We excluded 18 variables with significant differences in PLOS status and 106 with a missing rate of >10%. Of the remaining variables, from those with a univariate significance level of $P<.01$ between the PLOS groups, 63 variables from the day with the lowest P values (from admission to postoperative day 4) were chosen as explanatory variables. Patients with missing data for any of these 63 key variables were excluded, resulting in a final cohort of 480 patients for complete case analysis. Figure S1 in Multimedia Appendix 1 shows the flowchart detailing the variables and patient selection process.

Machine Learning–Based Model

The PLOS prediction model was developed using machine learning algorithms, including sparse linear regression models (Lasso [16], ridge [17], and elastic net [18]) and decision tree ensemble models (random forest [19] and extreme gradient boosting [XGBoost] [20]), following previous research [15]. These algorithms include L1, L2, and mixed regularization techniques for linear models; random forest as a bagging-based decision tree ensemble model using parallel trees; and XGBoost as a boosting-based decision tree model using sequential trees.

The algorithms used in this study were selected considering their complementary strengths. Real-world clinical datasets often contain variables with multicollinearity. To address this issue, we used regularized regression models (ie, Lasso, ridge, and elastic net), which incorporate penalty terms (based on the absolute values, squares, or both) into their loss functions to suppress variance inflation caused by multicollinearity. We also used tree-based ensemble models (ie, random forest and XGBoost), which are inherently robust to multicollinearity because they do not rely on regression coefficients or the inversion of a design matrix. Additionally, sparse regression models offer interpretable, coefficient-based outputs and perform well with high-dimensional clinical data, whereas tree-based models are capable of capturing nonlinear interactions and assessing variable importance.

For each algorithm, hyperparameters were optimized using grid search with 5-fold cross-validation within the derivation cohort (refer to Multimedia Appendix 2 for details). This process was designed to maximize predictive performance while minimizing the risk of overfitting.

The study period was divided into early and late phases, with April 2022 constituting the boundary due to reimbursement revisions and staff turnover in Japan. To assess the generalizability of the predictive model, we used a temporal validation approach. For temporal validation, patients admitted during the early phase (July 2019 to March 2022) were included in the derivation cohort, whereas those admitted during the late phase (April 2022 to May 2023) were included in the test cohort. The model was developed using data from July 2019 to March 2022 and validated with data from April 2022 to May 2023.

To evaluate model performance, we used the area under the receiver operating characteristic curve (AUROC) to assess discrimination and both calibration plots and Brier scores to evaluate calibration (ie, the agreement between predicted probabilities and observed outcomes). AUROC provides a threshold-independent measure of a model's ability to distinguish between positive and negative cases. The Brier score quantifies the accuracy of probabilistic predictions, while calibration plots visually assess the alignment between predicted and observed probabilities. These metrics are widely used in clinical prediction research and offer complementary perspectives on model performance.

For internal validation, the derivation data underwent 5-fold cross-validation, and the AUROC was calculated. For external validation, the model developed using the derivation data was applied to the test data to calculate the AUROC. Calibration plots were created by dividing the predicted PLOS probabilities into 10 groups and plotting the average predicted PLOS probability against the observed PLOS rate for each group.

Variable importance was assessed using standardized regression coefficients in sparse regression models, MeanDecreaseAccuracy in a random forest, and Gain in XGBoost. All the variables in each predictive model were ranked by importance, with percentages calculated relative to the highest value. These percentages were then averaged across all machine learning algorithms to determine the top-ranking variables, and the values across the models were compared.

XSL•FO
RenderX

The algorithm and variables with the best predictive performance were selected as the final models. Using this final model, differences in PLOS probabilities were estimated for the test cohort based on the presence or absence of variance within OAT units. Variance variables were selected from the highest-ranking variables in the final model based on their importance. This estimation involved comparing PLOS probabilities, assuming that all patients had variances, with actual variance values.

Statistical Analysis

Differences in frequency based on PLOS presence were tested using the χ^2 test or Fisher exact test, while continuous variables were used for the Mann-Whitney *U* test. Differences in the predicted PLOS probabilities (assuming all variances vs actual variances) were evaluated using the Wilcoxon signed-rank test. Machine learning model development and statistical analyses were performed using the R statistical package (version 4.0.5; R Foundation for Statistical Computing). Statistical significance was defined as a 2-sided $P<.05$. The detailed R code is provided in Multimedia Appendix 2.

Results

Baseline Characteristics of the Patients

The study included 480 patients with lung cancer, with a mean age of 68.3 (SD 11.2) years, of whom 263 (54.8%) were men. Of the 480 patients, 141 (29.4%) had PLOS (Figure S2 in Multimedia Appendix 1). The baseline characteristics were compared according to the PLOS status (Table 1). The patients with PLOS were older, included a higher proportion of men, and had a higher smoking index. In addition, a lower proportion of patients underwent wedge resection in the PLOS group.

Table 1. Baseline characteristics of patients with and without prolonged length of stay (PLOS; n=480).

	Without PLOS (n=339)	With PLOS (n=141)	*P* value
Age (y), mean (SD)	67.0 (11.4)	71.5 (9.8)	<.001
Male, n (%)	173 (51)	90 (63.8)	.01
BMI (kg/m^2), median (IQR)	23.3 (21.0-25.2)	22.6 (20.9-25.8)	.45
Diabetes mellitus, n (%)	43 (12.7)	22 (15.6)	.48
Smoking index, median (IQR)	0 (0-600)	400 (0-900)	<.001
Type of surgery, n (%)			.005
Lobectomy	134 (39.5)	77 (54.6)	
Segmentectomy	45 (13.3)	19 (13.5)	
Wedge resection	160 (47.2)	45 (31.9)	

Time Course Changes in Variables Related to PLOS

A heatmap was created to visualize the relationship between daily clinical variables and PLOS, highlighting specific variables associated with an increased risk of PLOS. The heatmap provided temporal information on the timing since admission, measurement frequency of each variable, and their association with PLOS. Various factors, including the occurrence of variances (Figure S3 in Multimedia Appendix 1), activities of daily living (Figure S4 in Multimedia Appendix 1), treatments (Figure S5 in Multimedia Appendix 1), medications (Figure S6 in Multimedia Appendix 1), and laboratory results (Figure S7 in Multimedia Appendix 1), were significantly associated with PLOS at different time points.

Machine Learning–Based Prediction Models for PLOS

Five machine learning algorithms were used to develop prediction models in the derivation cohort. The ridge, elastic net, and random forest models showed high discrimination (Figure 1; Multimedia Appendix 3), with calibration plots indicating a good fit (Figure 2) and low Brier scores (Multimedia Appendix 3). These models were validated in the test cohort. Among the models, ridge regression demonstrated the best performance with high discrimination (Figure 3; Multimedia Appendix 4), good calibration (Figure 4), and a low Brier score (Multimedia Appendix 4). Consequently, it was selected as the final model, and the importance of the individual variables was assessed.

XSL•FO
RenderX

Figure 1. Discriminative performance of the prolonged length of stay (PLOS) prediction model in the derivation cohort. This figure demonstrates the predictive performance of the PLOS prediction model for the derivation cohort of patients admitted in the earlier phase. Variables were selected as predictors from each day between 2 days before VATS and 4 days after surgery based on the lowest *P* value in univariate analysis for each day by PLOS status. The model was developed with 5 machine learning algorithms: Lasso (green), ridge (orange), elastic net (gray), random forest (yellow), and extreme gradient boosting (XGBoost; blue). A 5-fold cross-validation was conducted, and the receiver operating characteristic curve is shown.

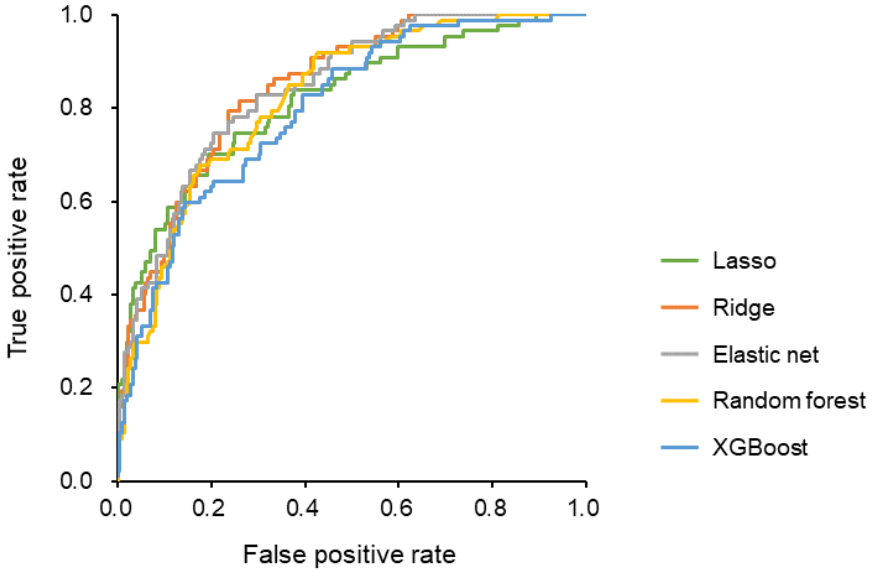
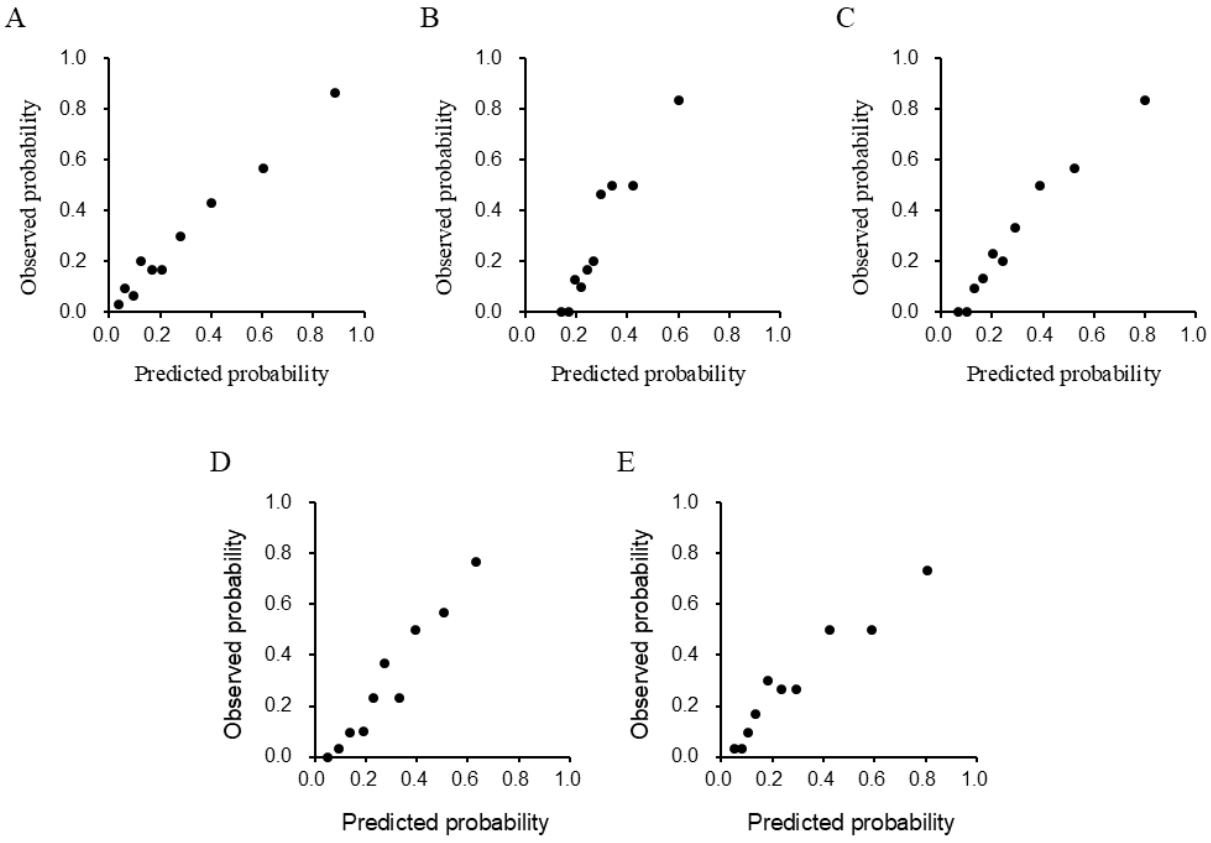


Figure 2. Calibration of the prolonged length of stay (PLOS) prediction model in the derivation cohort. This figure shows the calibration performance of the PLOS prediction model for the derivation cohort of patients admitted in the earlier phase. The model, constructed using 5 machine learning algorithms, namely, Lasso (A), ridge (B), elastic net (C), random forest (D), and extreme gradient boosting (XGBoost; E). The calibration plot divided patients into 10 groups based on predicted PLOS probabilities, with the mean predicted probability on the x-axis and the observed probability on the y-axis.



XSL•FO
RenderX

Figure 3. Discriminative performance of the prolonged length of stay (PLOS) prediction model in the test cohort. This figure demonstrates the predictive performance of the PLOS prediction model, initially developed in the derivation cohort, when applied to the temporally validated test cohort of patients admitted in the later phase. The model was developed with 5 machine learning algorithms: Lasso (green), ridge (orange), elastic net (gray), random forest (yellow), and extreme gradient boosting (XGBoost; blue).

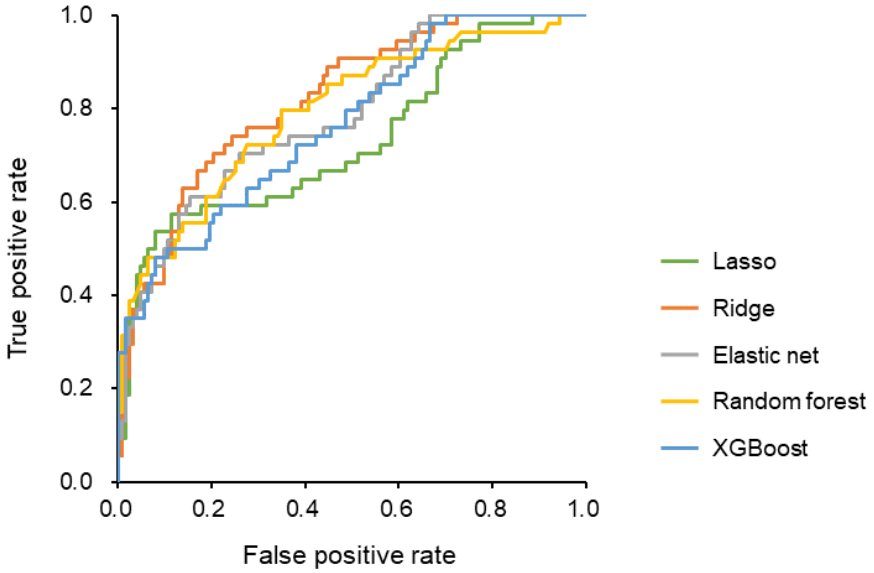
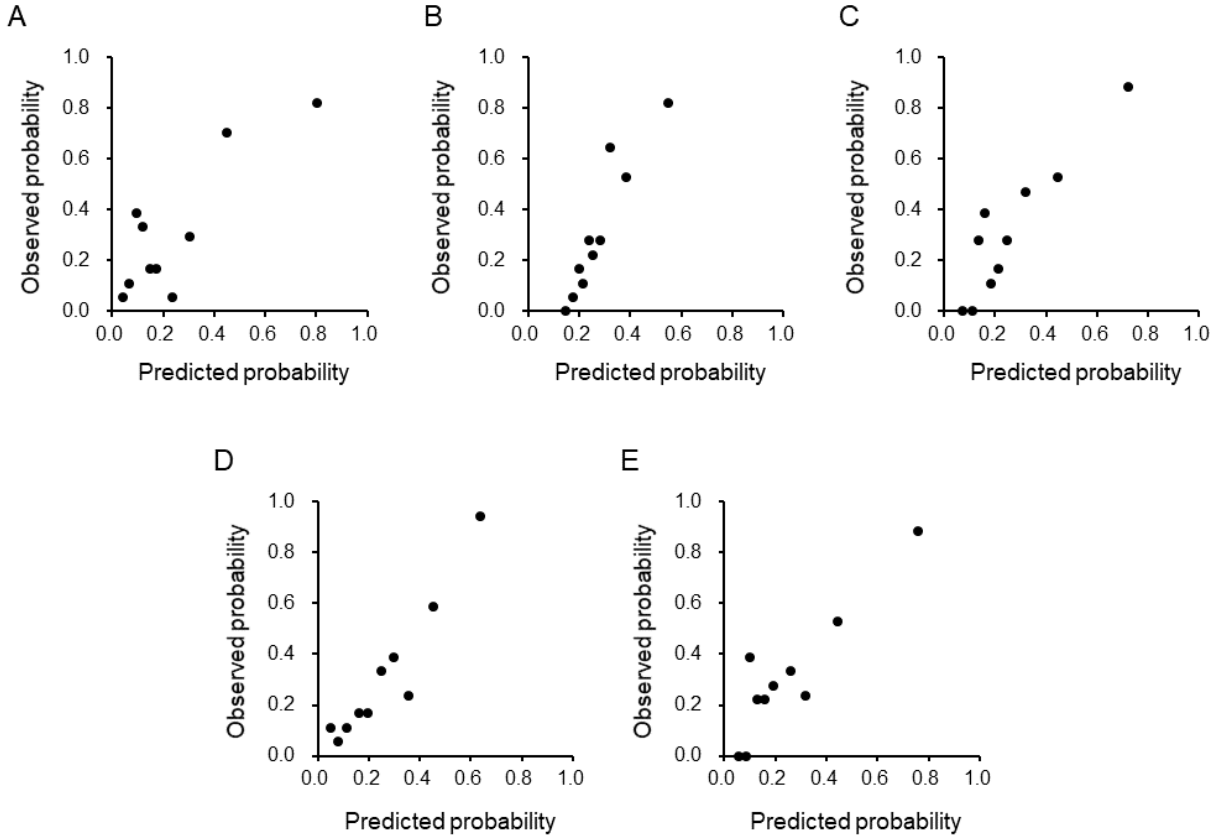


Figure 4. Calibration of the prolonged length of stay (PLOS) prediction model in the test cohort. This figure shows the calibration performance of the PLOS prediction model, initially developed in the derivation cohort, when applied to the temporally validated test cohort of patients admitted in the later phase. The model constructed using 5 machine learning algorithms, namely, Lasso (A), ridge (B), elastic net (C), random forest (D), and extreme gradient boosting (XGBoost; E). The calibration plot divided patients into 10 groups based on predicted PLOS probabilities, with the mean predicted probability on the x-axis and the observed probability on the y-axis.



XSL•FO
RenderX

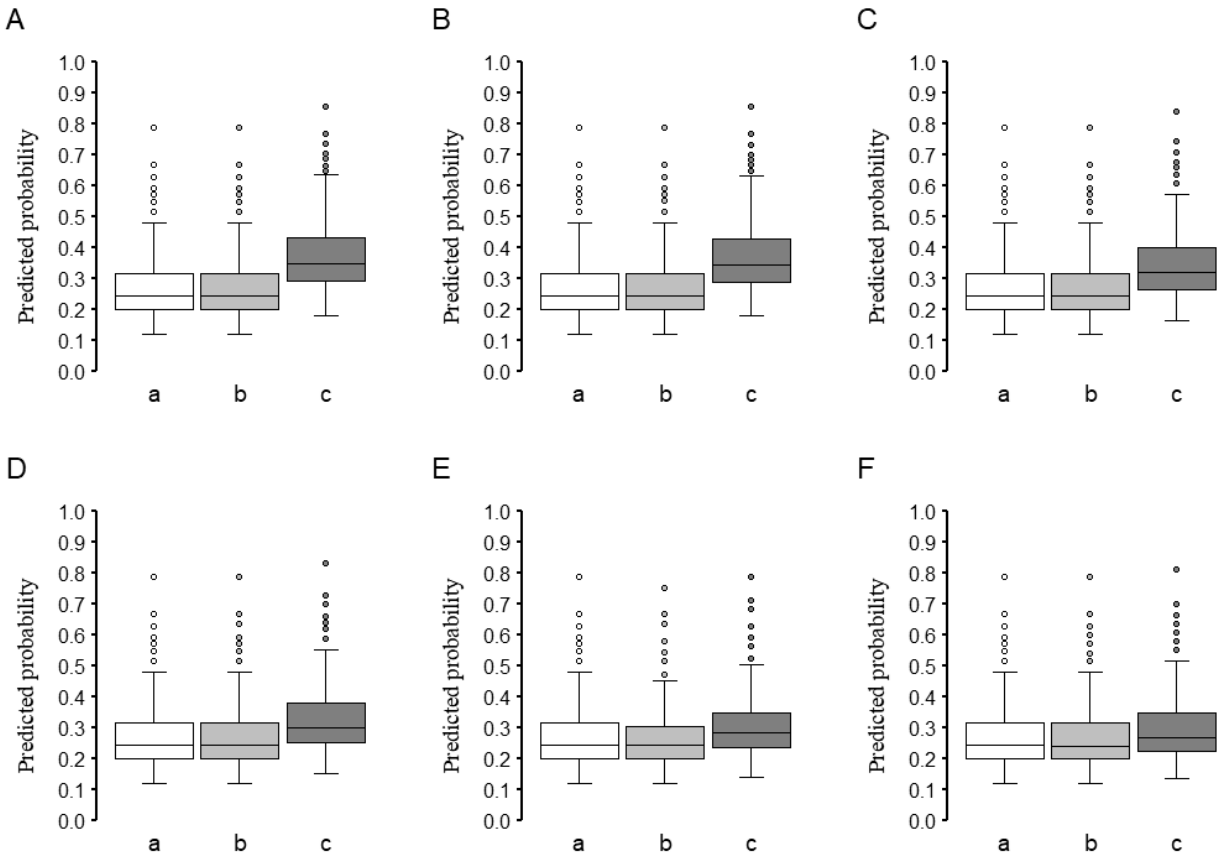
Variable Importance in Machine Learning–Based Prediction Models

We comprehensively analyzed the variable importance identified by the final ridge regression model (Figures S8 and S9 in Multimedia Appendix 1). The ridge regression analysis highlighted several key predictors, such as drain management, respiratory care, use of fibrin sealants, wedge resection, smoking index, age, and levels of C-reactive protein and albumin. Multimedia Appendix 5 shows the importance of the predictors identified by the final model.

Key Variances Influencing PLOS

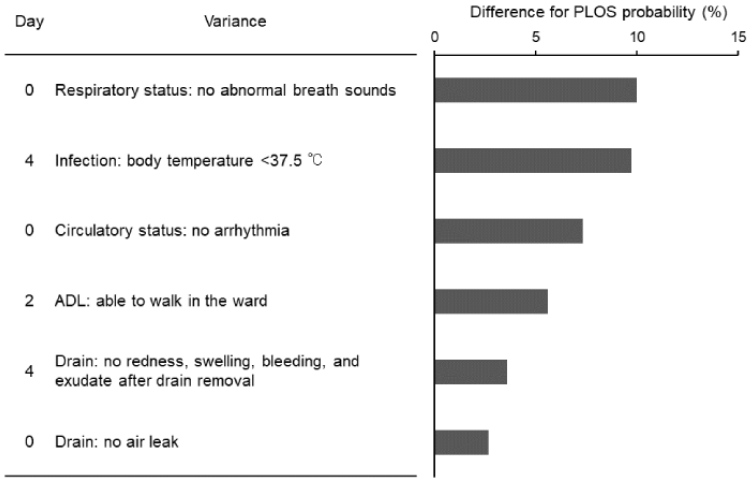
The frequency of clinical variance differed between patients with and without PLOS (Multimedia Appendix 6). Using the final ridge model, we calculated the predicted probability of PLOS for each patient by comparing scenarios assuming a specific variance to be present in all patients with its actual occurrence in individual patients (Figure 5). This analysis identified 6 key postoperative variables whose presence significantly increased the predicted probability of PLOS: abnormal respiratory sounds (P<.001), fever (P<.001), arrhythmia (P<.001), inability to ambulate (P<.001), abnormal drain characteristics (P<.001), and air leak (P=.005; Figure 6). These were identified as critical variances associated with a higher risk of PLOS in this patient population.

Figure 5. Variance presence and changes in prolonged length of stay (PLOS) probability. This figure shows predicted PLOS probability distributions under different variance conditions: (a) assuming all patients exhibit specific variances ([A] respiratory status: no abnormal breathing sounds; [B] infection: body temperature <37.5 ˚C; [C] circulatory status: no arrhythmia; [D] activities of daily living (ADL): able to walk in the ward; [E] drain: no redness, swelling, bleeding, and exudate after drain removal; and [F] drain: no air leak), (b) under actual variance values, and (c) assuming each patient has variances. Box plots show PLOS probabilities for each condition per patient.



XSL•FO
RenderX

Figure 6. Change in prolonged length of stay (PLOS) probability based on the presence or absence of variances. This figure shows the percentage difference in predicted PLOS probabilities when the PLOS prediction model, developed in the derivation cohort, was applied to the temporally validated test cohort under 2 scenarios: assuming all patients had variances or using the actual presence or absence of variances. The final model was constructed using ridge regression, and the figure illustrates the estimated change in PLOS probability for each variance, assuming all patients exhibit them compared to actual values.



Discussion

Principal Findings

In this study, we successfully collected comprehensive real-world data using the ePath system from routine clinical practice. A heatmap was used to visualize the timing and emergence of factors potentially associated with PLOS. The importance of the variables, except the top-ranked ones, varied across machine learning algorithms. Temporal validation in the test cohort demonstrated that the ridge regression model performed well in both cohorts. Using this data-driven ridge model, we identified 6 key variances in the clinical pathway that significantly influenced the PLOS risk. Applying machine learning to real-world data allowed us to identify the variances contributing to PLOS, providing a foundation for potential mitigation strategies. This system is promising as a data-driven support tool that leverages electronic information to improve patient care in clinical practice.

Factors Related to PLOS

Compared with open surgery, VATS is associated with fewer postoperative complications and thus preferred for early-stage lung cancer [7-10,12,13,21]. However, postoperative complications can still arise, leading to potential PLOS [22-24]. Previous studies have identified various factors contributing to PLOS in patients undergoing VATS [25-37]. Many of these factors, such as age [25,27,31,32,34,36,37], male sex [25], BMI [25,31], functional status [25,31], smoking history [25,36], pulmonary function [25,28,31-34], comorbidities [25,26,30-32], tumor status [29,36], and the American Society of Anesthesiologists score [25,32,36], are challenging to modify after admission. Additionally, surgical factors [27-29,31,37], postoperative complications [28,29,37], and chest tube duration [29,30,32] are contributing factors that require further optimization from a surgical perspective.

In real-world settings, addressing modifiable factors before and after VATS is critical for effectively predicting and reducing PLOS. In this study, a heatmap was used to visualize the timing of the relevant factors and their associations with PLOS in the patient cohort. We assessed variable importance in machine learning–based models to identify the key contributors to PLOS risk. The identified factors are consistent with previously reported ones, such as age, smoking history, and surgical techniques (lobectomy and wedge resection), as well as laboratory results indicative of inflammation and malnutrition. Furthermore, we identified additional daily fluctuating factors, described as variances in clinical pathways, that may be associated with postoperative complications. These factors underscore the importance of close monitoring and targeted intervention to enable early and accurate prediction of PLOS and mitigate its impact.

Key Variances Influencing PLOS

Previous studies on PLOS-related factors have primarily focused on patient characteristics that are not easily modifiable during hospitalization, leading to a lack of clarity regarding specific in-hospital conditions associated with an increased PLOS risk. Moreover, many factors are interrelated, highlighting the need for a comprehensive assessment of how in-hospital conditions affect PLOS risk while adjusting for baseline patient characteristics. Clinical pathways capture variances or deviations from the expected course, enabling the identification of atypical patient trajectories. Recognizing the variances linked to higher PLOS risk can help identify at-risk patients early, optimizing patient care.

Although numerous factors influencing PLOS have been reported in previous studies, their impacts may vary across populations [25-37]. In our cohort, several variables significantly altered the PLOS risk, including postoperative abnormal respiratory sounds, arrhythmia, air leaks, fever, reduced mobility, and abnormal drain characteristics. These variances reflect underlying issues such as pulmonary air leaks, arrhythmias (eg, atrial fibrillation), postoperative infections, and functional impairments.

The emergence of variances may contribute to PLOS through these underlying causes. For instance, a prolonged air leak may

XSL•FO
RenderX

delay drain removal, arrhythmias and related complications may necessitate prolonged treatment, infections may require extended use of antibiotics and additional testing, and decreased activities of daily living may slow rehabilitation progress. Although these variances may also be interrelated, identifying and addressing the underlying causes of the 6 key variances may help reduce the risk of PLOS.

Once a variance occurs, prompt clinical intervention is essential. Evaluation of potential causes may include chest x-rays, blood tests (eg, arterial blood gas analysis, inflammatory markers, and electrolyte panels), and inspection of the drainage system. Interventions may include oxygen therapy, postural adjustments, enforced rest, infection control (eg, wound irrigation, disinfection, and dressing changes), administration of antiarrhythmic medications, early mobilization, antibiotic therapy for infections, or pleurodesis for persistent air leaks. Implementing a structured, variance-specific response protocol that integrates timely assessment and targeted intervention may be critical in minimizing PLOS.

Nonmodifiable factors during hospitalization, such as age and comorbidities, are beyond the scope of immediate interventions. However, by understanding how deviations from typical recovery (ie, variance) impact PLOS risk, we can target these specific variances for early intervention. By quantifying changes in the predicted PLOS probability under hypothetical scenarios of variance, we can objectively assess their impact on patient outcomes. Counterfactual analyses simulating changes in outcome probabilities may help estimate population-level effects, paving the way for clinical improvements using the ePath system.

When key variances associated with PLOS are identified, feedback should be provided to the medical team, followed by discussions and consideration of potential improvements. Wherever possible, the underlying causes of each variance should be addressed to prevent recurrence. For variances with significant clinical impact or those amenable to effective intervention, specific management strategies should be developed. Strengthening interprofessional collaboration, providing staff education on early response protocols, and evaluating outcomes can all contribute to continuous improvement. In this context, ePath can facilitate a sustainable plan-do-check-act or plan-do-study-act cycle.

In real-world clinical practice, the variances identified through our approach may help reduce PLOS if managed with appropriate clinical responses. For example, a variance response bundle or an actionable protocol triggered by the model could provide a formal structure for these interventions. Assessing whether such structured approaches reduce PLOS is an important next step.

Clinical Implications

Machine learning and deep learning are being increasingly applied in health care to uncover hidden patterns in complex datasets and generate predictive insights [38-40]. One of their most promising clinical applications is the automated prediction and visualization of outcomes such as PLOS, which can support clinical decision-making and enhance operational efficiency. However, predicting outcomes using real-world clinical data remains challenging due to its unstructured and heterogeneous nature [41].

To address these challenges, we developed the ePath system—an electronic clinical pathway system designed to systematically collect patient-level and care process data through an integrated workflow. In this study, we adopted a data-driven approach to explore potential causes of PLOS. As a result, we were able to confirm several clinical risk factors. Moreover, we provide novel insights by visualizing when and how specific changes in patient status contribute to the risk of PLOS. This was achieved by integrating a prediction model into the ePath system, enabling real-time, patient-specific visualization of PLOS risk. The structured nature of ePath facilitates robust, data-driven analysis and model development. Recently, tools using clustering techniques on real-world clinical data have been developed to support the design of clinical pathways for patients with lung cancer [42]. The integration of real-world data with pathway analysis via electronic health information systems may mark a new era in data-driven health care.

The novelty of our study lies in leveraging the ePath to capture real-time postoperative clinical variances and applying machine learning techniques to identify key factors associated with PLOS. By embedding the predictive models into a dashboard system, clinicians can visualize each patient's risk and corresponding clinical variances. When high-risk patterns are detected, the system can generate alerts that prompt timely interventions. Early and appropriate responses may help reduce unnecessary hospitalization and improve patient outcomes. In this way, the system has the potential to serve as an effective clinical decision support tool.

Beyond its clinical utility, ePath also offers managerial value. Hospitals can monitor the occurrence of variances and predicted PLOS risks across patient populations in real time. This enables data-driven decision-making for care delivery and supports the implementation of quality improvement initiatives. By tracking length of stay metrics before and after protocol modifications, institutions can assess the effectiveness of interventions and refine care pathways accordingly. Once validated, such interventions can be standardized and scaled across the organization.

It is important to note that factors contributing to PLOS can vary by institution and patient population [25,31] and may include not only clinical indicators but also social and operational factors [34]. Therefore, models developed using an institution's data—as enabled by ePath—may be particularly valuable for generating context-specific insights and designing tailored interventions.

Nonetheless, several barriers must be addressed to implement such a system effectively. First, a structured data collection infrastructure, such as ePath, must be established and integrated into clinical workflows. Second, model transparency is essential for clinicians' trust. While many machine learning models are often perceived as "black boxes," we selected ridge regression (L2 regularization) as our final model due to its strong performance and interpretability. This model effectively handles multicollinearity and provides coefficients with clear direction

XSL•FO
RenderX

and magnitude, which are easily interpretable in clinical contexts.

To further enhance interpretability, we used visualization techniques such as standardized coefficients and variable importance heatmaps. These tools can assist clinicians in understanding model outputs and recognizing the clinical relevance of key variances. Ultimately, the integration of predictive outputs into actionable clinical workflows—through protocols linked to specific alerts—will be essential for translating data insights into meaningful improvements in patient care.

Limitations

This study has several limitations. Because it used real-world data, issues such as missing values persisted even after dataset preprocessing. In this study, 97 patients were excluded from the complete case analysis (Multimedia Appendix 7), which may have introduced potential selection bias. Additionally, the misclassification of variables cannot be ruled out, which may introduce bias. Given the use of machine learning models, caution is required to address potential overfitting, which may reduce the generalizability of the results. Although we used methods such as 5-fold cross-validation to enhance generalizability and conducted temporal validation, the developed model may not be fully applicable to other patient populations. Moreover, to minimize overfitting from excessive noise, we performed initial variable selection by excluding potentially noncontributory variables. However, this approach may have excluded predictors that were not significant in univariate analyses but could become significant in a multivariate context, potentially reducing predictive accuracy. Further research is warranted to refine variable selection methods that address this methodological trade-off. Differences in health care systems, especially with Japan's universal health insurance system leading to longer hospital stays than international standards, could also affect the defined outcomes. The postoperative length of stay following VATS varies across countries. Numerous studies have reported a median hospital stay of 4 to 6 days after VATS [25-37]. Although the definition of PLOS differs in the literature—ranging from 2 to 14 days after surgery—it is most commonly set at 4 to 7 days. In this study, the median length of stay was 8 (IQR 7-10) days, and we defined PLOS as 9 days or more based on our institutional clinical pathway target. This threshold may be longer than those used in other countries, and therefore, cross-national comparisons should be interpreted with caution. Hospital length of stay is influenced by a wide range of factors that vary across hospitals, regions, and countries. In addition to patient-level clinical characteristics, institutional and systemic factors can significantly impact length of stay. These include health care financing and reimbursement systems, the availability of regional health care resources, hospital size and function, clinical staff expertise, adherence to clinical guidelines, the robustness of discharge planning infrastructure, access to postacute care services, and the presence of family support systems. This study was based on data from one university hospital, which may not be representative of the general hospital population. To enhance the generalizability of our findings, future research should include model retraining and validation using multicenter datasets, the incorporation of health care system–related variables into the models, and the development of customizable models that can be adapted to specific institutional or regional contexts.

Conclusions

Using the ePath system, we systematically collected real-world data and developed machine learning models to predict PLOS in a data-driven manner. Successful implementation of data-driven PLOS prediction for specific patient populations could serve as a valuable tool for evidence-based quality improvement in health care. However, additional validation is necessary to implement and operationalize these prediction systems in real-world clinical environments.

Acknowledgments

This study was supported by the Japan Society for the Promotion of Science KAKENHI (grant JP25H01083).

Data Availability

The datasets analyzed during this study are not publicly available due the confidential nature of the data but are available from the corresponding author on reasonable request.

Authors' Contributions

ST had full access to all the study data and takes responsibility for study data integrity and the accuracy of the data analysis. The study concept and design were handled by ST, KM, MK, NN, and HS; acquisition, analysis, and interpretation of data were undertaken by KM, YN, TT, and YW; the paper was drafted by TS, KM, and MK, with MK carrying out critical revision of the paper for important intellectual content; statistical analysis was conducted by ST, KM, and YN; funding was obtained by KM; administrative, technical, and material support was provided by AH, FK, TT, and TY; and the project was supervised by MK, HS, TY, and NN.

Conflicts of Interest

None declared.

XSL•FO
RenderX

Multimedia Appendix 1
Supplementary figures.
[DOCX File , 927 KB - medinform_v13i1e71617_app1.docx]

Multimedia Appendix 2
Supplementary information on methods.
[DOCX File , 25 KB - medinform_v13i1e71617_app2.docx]

Multimedia Appendix 3
Area under the receiver operating characteristic curve and Brier score of prolonged length of stay prediction models in derivation cohorts.
[DOCX File , 24 KB - medinform_v13i1e71617_app3.docx]

Multimedia Appendix 4
Area under the receiver operating characteristic curve and Brier score of prolonged length of stay prediction models in test cohort.
[DOCX File , 25 KB - medinform_v13i1e71617_app4.docx]

Multimedia Appendix 5
Variable importance for predicting prolonged length of stay in the ridge regression model.
[DOCX File , 29 KB - medinform_v13i1e71617_app5.docx]

Multimedia Appendix 6
Frequency of variance by prolonged length of stay.
[DOCX File , 33 KB - medinform_v13i1e71617_app6.docx]

Multimedia Appendix 7
Baseline characteristics of included and excluded patients.
[DOCX File , 25 KB - medinform_v13i1e71617_app7.docx]

References

1. Stone K, Zwiggelaar R, Jones P, Mac Parthaláin N. A systematic review of the prediction of hospital length of stay: towards a unified framework. PLOS Digit Health 2022 Apr 14;1(4):e0000017 [FREE Full text] [doi: 10.1371/journal.pdig.0000017] [Medline: 36812502]
2. Aspland E, Gartner D, Harper P. Clinical pathway modelling: a literature review. Health Syst (Basingstoke) 2019 Sep 11;10(1):1-23 [FREE Full text] [doi: 10.1080/20476965.2019.1652547] [Medline: 33758656]
3. Siddique SM, Tipton K, Leas B, Greysen SR, Mull NK, Lane-Fall M, et al. Interventions to reduce hospital length of stay in high-risk populations: a systematic review. JAMA Netw Open 2021 Sep 01;4(9):e2125846 [FREE Full text] [doi: 10.1001/jamanetworkopen.2021.25846] [Medline: 34542615]
4. Yamashita T, Flanagan B, Wakata Y, Hamai S, Nakashima Y, Iwamoto Y, et al. Visualization of key factor relation in clinical pathway. Procedia Comput Sci 2015;60:342-351. [doi: 10.1016/j.procs.2015.08.139]
5. Yamashita T, Wakata Y, Hamai S, Nakashima Y, Iwamoto Y, Franagan B, et al. Temporal relation extraction in outcome variances of clinical pathways. Stud Health Technol Inform 2015;216:1077. [Medline: 26262376]
6. Yamashita T, Wakata Y, Nakaguma H, Nohara Y, Hato S, Kawamura S, et al. Machine learning for classification of postoperative patient status using standardized medical data. Comput Methods Programs Biomed 2022 Feb;214:106583 [FREE Full text] [doi: 10.1016/j.cmpb.2021.106583] [Medline: 34959156]
7. Cattaneo SM, Park BJ, Wilton AS, Seshan VE, Bains MS, Downey RJ, et al. Use of video-assisted thoracic surgery for lobectomy in the elderly results in fewer complications. Ann Thorac Surg 2008 Jan;85(1):231-235. [doi: 10.1016/j.athoracsur.2007.07.080] [Medline: 18154816]
8. Whitson BA, Groth SS, Duval SJ, Swanson SJ, Maddaus MA. Surgery for early-stage non-small cell lung cancer: a systematic review of the video-assisted thoracoscopic surgery versus thoracotomy approaches to lobectomy. Ann Thorac Surg 2008 Dec;86(6):2008-2016. [doi: 10.1016/j.athoracsur.2008.07.009] [Medline: 19022040]
9. Flores RM, Park BJ, Dycoco J, Aronova A, Hirth Y, Rizk NP, et al. Lobectomy by video-assisted thoracic surgery (VATS) versus thoracotomy for lung cancer. J Thorac Cardiovasc Surg 2009 Jul;138(1):11-18 [FREE Full text] [doi: 10.1016/j.jtcvs.2009.03.030] [Medline: 19577048]
10. Swanson SJ, Meyers BF, Gunnarsson CL, Moore M, Howington JA, Maddaus MA, et al. Video-assisted thoracoscopic lobectomy is less costly and morbid than open lobectomy: a retrospective multiinstitutional database analysis. Ann Thorac Surg 2012 Apr;93(4):1027-1032. [doi: 10.1016/j.athoracsur.2011.06.007] [Medline: 22130269]

XSL•FO
RenderX

11. Farjah F, Backhus LM, Varghese TK, Mulligan MS, Cheng AM, Alfonso-Cristancho R, et al. Ninety-day costs of video-assisted thoracic surgery versus open lobectomy for lung cancer. Ann Thorac Surg 2014 Jul;98(1):191-196. [doi: 10.1016/j.athoracsur.2014.03.024] [Medline: 24820393]
12. Klapper J, D'Amico TA. VATS versus open surgery for lung cancer resection: moving toward a minimally invasive approach. J Natl Compr Canc Netw 2015 Feb 17;13(2):162-164. [doi: 10.6004/jnccn.2015.0023] [Medline: 25691607]
13. Nwogu CE, D'Cunha J, Pang H, Gu L, Wang X, Richards WG, Alliance for Clinical Trials in Oncology. VATS lobectomy has better perioperative outcomes than open lobectomy: CALGB 31001, an ancillary analysis of CALGB 140202 (Alliance). Ann Thorac Surg 2015 Feb;99(2):399-405 [FREE Full text] [doi: 10.1016/j.athoracsur.2014.09.018] [Medline: 25499481]
14. Watson TJ, Qiu J. The impact of thoracoscopic surgery on payment and health care utilization after lung resection. Ann Thorac Surg 2016 Apr;101(4):1271-1979. [doi: 10.1016/j.athoracsur.2015.10.104] [Medline: 26872730]
15. Tou S, Matsumoto K, Hashinokuchi A, Kinoshita F, Nakaguma H, Kozuma Y, et al. Data-driven prediction of prolonged air leak after video-assisted thoracoscopic surgery for lung cancer: development and validation of machine-learning-based models using real-world data through the ePath system. Learn Health Syst 2025 Apr 11;9(2):e10469 [FREE Full text] [doi: 10.1002/lrh2.10469] [Medline: 40247901]
16. Tibshirani R. Regression shrinkage and selection via the Lasso. J R Stat Soc Ser B Stat Methodol 1996;58(1):267-288. [doi: 10.1111/j.2517-6161.1996.tb02080.x]
17. Hoerl AE, Kennard RW. Ridge regression: biased estimation for nonorthogonal problems. Technometrics 1970 Feb;12(1):55-67. [doi: 10.1080/00401706.1970.10488634]
18. Zou H, Hastie T. Regularization and variable selection via the Elastic Net. J R Stat Soc Ser B Stat Methodol 2005;67(2):301-320. [doi: 10.1111/j.1467-9868.2005.00503.x]
19. Breiman L. Random forests. Mach Learn 2001 Oct;45(1):5-32. [doi: 10.1023/A:1010933404324]
20. Chen T, Guestrin C. XGBoost: a scalable tree boosting system. In: Proceedings of the 22nd ACM SIGKDD International Conference on Knowledge Discovery and Data Mining. 2016 Presented at: KDD '16; August 13-17, 2016; San Francisco, CA p. 785-794 URL: https://dl.acm.org/doi/10.1145/2939672.2939785 [doi: 10.1145/2939672.2939785]
21. Villamizar NR, Darrabie MD, Burfeind WR, Petersen RP, Onaitis MW, Toloza E, et al. Thoracoscopic lobectomy is associated with lower morbidity compared with thoracotomy. J Thorac Cardiovasc Surg 2009 Aug;138(2):419-425 [FREE Full text] [doi: 10.1016/j.jtcvs.2009.04.026] [Medline: 19619789]
22. Imperatori A, Rotolo N, Gatti M, Nardecchia E, De Monte L, Conti V, et al. Peri-operative complications of video-assisted thoracoscopic surgery (VATS). Int J Surg 2008;6 Suppl 1:S78-S81 [FREE Full text] [doi: 10.1016/j.ijsu.2008.12.014] [Medline: 19186114]
23. Berfield KS, Farjah F, Mulligan MS. Video-assisted thoracoscopic lobectomy for lung cancer. Ann Thorac Surg 2019 Feb;107(2):603-609. [doi: 10.1016/j.athoracsur.2018.07.088] [Medline: 30278164]
24. Lim E, Batchelor TJ, Dunning J, Shackcloth M, Anikin V, Naidu B, et al. Video-assisted thoracoscopic or open lobectomy in early-stage lung cancer. NEJM Evid 2022 Mar;1(3):EVIDoa2100016. [doi: 10.1056/EVIDoa2100016] [Medline: 38319202]
25. Wright CD, Gaissert HA, Grab JD, O'Brien SM, Peterson ED, Allen MS. Predictors of prolonged length of stay after lobectomy for lung cancer: a society of thoracic surgeons general thoracic surgery database risk-adjustment model. Ann Thorac Surg 2008 Jun;85(6):1857-1865. [doi: 10.1016/j.athoracsur.2008.03.024] [Medline: 18498784]
26. Matsuoka K, Kuroda A, Kang A, Imanishi N, Nagai S, Ueda M, et al. Surgical results of video-assisted thoracic surgery and risk factors for prolonged hospitalization for secondary pneumothorax in elderly patients. Ann Thorac Cardiovasc Surg 2013;19(1):18-23 [FREE Full text] [doi: 10.5761/atcs.oa.12.01909] [Medline: 22971717]
27. Rogers LJ, Bleetman D, Messenger DE, Joshi NA, Wood L, Rasburn NJ, et al. The impact of enhanced recovery after surgery (ERAS) protocol compliance on morbidity from resection for primary lung cancer. J Thorac Cardiovasc Surg 2018 Apr;155(4):1843-1852 [FREE Full text] [doi: 10.1016/j.jtcvs.2017.10.151] [Medline: 29352586]
28. Zhang Z, Mostofian F, Ivanovic J, Gilbert S, Maziak DE, Shamji FM, et al. All grades of severity of postoperative adverse events are associated with prolonged length of stay after lung cancer resection. J Thorac Cardiovasc Surg 2018 Feb;155(2):798-807 [FREE Full text] [doi: 10.1016/j.jtcvs.2017.09.094] [Medline: 29103816]
29. Dumitra TC, Molina JC, Mouhanna J, Nicolau I, Renaud S, Aubin L, et al. Feasibility analysis for the development of a video-assisted thoracoscopic (VATS) lobectomy 23-hour recovery pathway. Can J Surg 2020 Jul 31;63(4):E349-E358 [FREE Full text] [doi: 10.1503/cjs.002219] [Medline: 32735430]
30. Forster C, Doucet V, Perentes JY, Abdelnour-Berchtold E, Zellweger M, Marcucci C, et al. Impact of compliance with components of an ERAS pathway on the outcomes of anatomic VATS pulmonary resections. J Cardiothorac Vasc Anesth 2020 Jul;34(7):1858-1866. [doi: 10.1053/j.jvca.2020.01.038] [Medline: 32139340]
31. Linden PA, Perry Y, Worrell S, Wallace A, Argote-Greene L, Ho VP, et al. Postoperative day 1 discharge after anatomic lung resection: a society of thoracic surgeons database analysis. J Thorac Cardiovasc Surg 2020 Feb;159(2):667-78.e2 [FREE Full text] [doi: 10.1016/j.jtcvs.2019.08.038] [Medline: 31606175]
32. Forster C, Perentes JY, Ojanguren A, Abdelnour-Berchtold E, Zellweger M, Bouchaab H, et al. Early discharge after thoracoscopic anatomical pulmonary resection for non-small-cell lung cancer. Interact Cardiovasc Thorac Surg 2021 Nov 22;33(6):892-898 [FREE Full text] [doi: 10.1093/icvts/ivab187] [Medline: 34279040]

XSL•FO
RenderX

33. Forster C, Doucet V, Perentes JY, Abdelnour-Berchtold E, Zellweger M, Faouzi M, et al. Impact of an enhanced recovery after surgery pathway on thoracoscopic lobectomy outcomes in non-small cell lung cancer patients: a propensity score-matched study. Transl Lung Cancer Res 2021 Jan;10(1):93-103 [FREE Full text] [doi: 10.21037/tlcr-20-891] [Medline: 33569296]
34. Huang L, Kehlet H, Petersen RH. Reasons for staying in hospital after video-assisted thoracoscopic surgery lobectomy. BJS Open 2022 May 02;6(3):zrac050 [FREE Full text] [doi: 10.1093/bjsopen/zrac050] [Medline: 35511502]
35. Gómez-Hernández MT, Forcada C, Fuentes M, Novoa N, Aranda JL, Rivas C, et al. Variables influencing hospital stay and 10-year staying trending after anatomical lung resection. Arch Bronconeumol 2023 Mar;59(3):180-182. [doi: 10.1016/j.arbres.2022.09.018] [Medline: 36272835]
36. Zheng YL, Huang RS, Liang XY. Identification of preoperative risk factors associated with prolonged length of stay after lobectomy. Heliyon 2023 May;9(5):e16061 [FREE Full text] [doi: 10.1016/j.heliyon.2023.e16061] [Medline: 37206051]
37. Zini J, Dayan G, Têtu M, Kfouri T, Maqueda LB, Abdulnour E, et al. Intersurgeon variations in postoperative length of stay after video-assisted thoracoscopic surgery lobectomy. JTCVS Open 2024 Apr;18:253-260 [FREE Full text] [doi: 10.1016/j.xjon.2024.01.003] [Medline: 38690406]
38. Rajkomar A, Dean J, Kohane I. Machine learning in medicine. N Engl J Med 2019 Apr 04;380(14):1347-1358. [doi: 10.1056/nejmra1814259]
39. Kline A, Wang H, Li Y, Dennis S, Hutch M, Xu Z, et al. Multimodal machine learning in precision health: a scoping review. NPJ Digit Med 2022 Nov 07;5(1):171 [FREE Full text] [doi: 10.1038/s41746-022-00712-8] [Medline: 36344814]
40. Zhang A, Xing L, Zou J, Wu JC. Shifting machine learning for healthcare from development to deployment and from models to data. Nat Biomed Eng 2022 Dec 04;6(12):1330-1345. [doi: 10.1038/s41551-022-00898-y] [Medline: 35788685]
41. de Hond AA, Leeuwenberg AM, Hooft L, Kant IM, Nijman SW, van Os HJ, et al. Guidelines and quality criteria for artificial intelligence-based prediction models in healthcare: a scoping review. NPJ Digit Med 2022 Jan 10;5(1):2 [FREE Full text] [doi: 10.1038/s41746-021-00549-7] [Medline: 35013569]
42. Aspland E, Harper PR, Gartner D, Webb P, Barrett-Lee P. Modified Needleman-Wunsch algorithm for clinical pathway clustering. J Biomed Inform 2021 Mar;115:103668 [FREE Full text] [doi: 10.1016/j.jbi.2020.103668] [Medline: 33359110]

Abbreviations

AUROC: area under the receiver operating characteristic curve
XGBoost: extreme gradient boosting
OAT: outcomes-assessments-tasks
PLOS: prolonged length of stay
VATS: video-assisted thoracoscopic surgery

Edited by J Klann; submitted 22.01.25; peer-reviewed by D Gartner, JMI Arockiasamy, LR Guo; comments to author 11.07.25; revised version received 20.08.25; accepted 08.10.25; published 01.12.25.

Please cite as:
Tou S, Matsumoto K, Hashinokuchi A, Kinoshita F, Nohara Y, Yamashita T, Wakata Y, Takenaka T, Soejima H, Yoshizumi T, Nakashima N, Kamouchi M
Identifying Key Variances in Clinical Pathways Associated With Prolonged Hospital Stays Using Machine Learning and ePath Real-World Data: Model Development and Validation Study
JMIR Med Inform 2025;13:e71617
URL: https://medinform.jmir.org/2025/1/e71617
doi:10.2196/71617
PMID:

©Saori Tou, Koutarou Matsumoto, Asato Hashinokuchi, Fumihiko Kinoshita, Yasunobu Nohara, Takanori Yamashita, Yoshifumi Wakata, Tomoyoshi Takenaka, Hidehisa Soejima, Tomoharu Yoshizumi, Naoki Nakashima, Masahiro Kamouchi. Originally published in JMIR Medical Informatics (https://medinform.jmir.org), 01.12.2025. This is an open-access article distributed under the terms of the Creative Commons Attribution License (https://creativecommons.org/licenses/by/4.0/), which permits unrestricted use, distribution, and reproduction in any medium, provided the original work, first published in JMIR Medical Informatics, is properly cited. The complete bibliographic information, a link to the original publication on https://medinform.jmir.org/, as well as this copyright and license information must be included.

XSL•FO
RenderX

Original Paper

Unsupervised Characterization of Temporal Dataset Shifts as an Early Indicator of AI Performance Variations: Evaluation Study Using the Medical Information Mart for Intensive Care-IV Dataset

David Fernández-Narro[1], MSc; Pablo Ferri[1], PhD; Alba Gutiérrez-Sacristán[2], PhD; Juan M García-Gómez[1], PhD; Carlos Sáez[1], PhD

[1]Biomedical Data Science Lab, Instituto Universitario de Tecnologías de la Información y Comunicaciones, Universitat Politècnica de València, Valencia, Valencia, Spain

[2]Department of Biomedical Informatics, Harvard Medical School, Harvard University, Boston, MA, United States

Corresponding Author:
David Fernández-Narro, MSc
Biomedical Data Science Lab
Instituto Universitario de Tecnologías de la Información y Comunicaciones
Universitat Politècnica de València
Camino de Vera s/n
Valencia, Valencia, 46022
Spain
Phone: 34 96 387 70 00 ext 75278
Email: dfernar@upv.es

Abstract

Background: Reusing long-term data from electronic health records is essential for training reliable and effective health artificial intelligence (AI). However, intrinsic changes in health data distributions over time—known as dataset shifts, which include concept, covariate, and prior shifts—can compromise model performance, leading to model obsolescence and inaccurate decisions.

Objective: In this study, we investigate whether unsupervised, model-agnostic characterization of temporal dataset shifts using data distribution analyses through Information Geometric Temporal (IGT) projections is an early indicator of potential AI performance variations before model development.

Methods: Using the real-world Medical Information Mart for Intensive Care-IV (MIMIC-IV) electronic health record database, encompassing data from over 40,000 patients from 2008 to 2019, we characterized its inherent dataset shift patterns through an unsupervised approach using IGT projections and data temporal heatmaps. We trained and evaluated annually a set of random forests and gradient boosting models to predict in-hospital mortality. To assess the impact of shifts on model performance, we checked the association between the temporal clusters found in both IGT projections and the intertime embedding of model performances using the Fisher exact test.

Results: Our results demonstrate a significant relationship between the unsupervised temporal shift patterns, specifically covariate and concept shifts, identified using the IGT projection method and the performance of the random forest and gradient boosting models (P<.05). We identified 2 primary temporal clusters that correspond to the periods before and after *ICD-10* (*International Statistical Classification of Diseases, Tenth Revision*) implementation. The transition from *ICD-9* (*International Classification of Diseases, Ninth Revision*) to *ICD-10* was a major source of dataset shift, associated with a performance degradation.

Conclusions: Unsupervised, model-agnostic characterization of temporal shifts via IGT projections can serve as a proactive monitoring tool to anticipate performance shifts in clinical AI models. By incorporating early shift detection into the development pipeline, we can enhance decision-making during the training and maintenance of these models. This approach paves the way for more robust, trustworthy, and self-adapting AI systems in health care.

(JMIR Med Inform 2025;13:e78309) doi:10.2196/78309

KEYWORDS

AI; artificial intelligence; data quality; machine learning; temporal variability

XSL•FO
RenderX

Introduction

Leveraging trustworthy artificial intelligence (AI) and machine learning (ML) in health critically depends on reusing data from diverse sources collected over extended periods. However, the inherent variability in medical data and their acquisition processes often results in significant shifts in data distributions [1-3]. At the population level, data-generating processes are generally nonstationary, leading to shifting statistical patterns over time. These shifts can arise from changes in clinical protocols, environmental or seasonal variations, inherent biological and social behaviors, or unexpected biases caused by systematic or random errors [4,5]. Such variability between training and test datasets, whether temporal or site-specific, can severely undermine the development and performance of ML models in health [6-10]. These variations in data distributions are classified as dataset shifts [11,12] and are especially relevant in a nonstationary environment, such as real-world health data [2,13]. Addressing dataset shifts proactively is crucial to ensure the reliability and effectiveness of the training and prospective continual use of health AI.

In classification problems involving input (x) and output (y) variables, a dataset shift occurs when the joint probability distribution of the data differs between training and test datasets. This can happen, for instance, when translating a model to a different site or during the AI's use or adaptation over time (equation 1).



In this work, we considered 3 primary sources of dataset shift: covariate shift, prior probability shift, and concept shift [11], as described next.

Covariate shifts refer to changes in the marginal features distribution over time, such as changes in the distribution of the population (equation 2) [14].



Prior probability shifts refer to changes in the distribution of each class p(y) over time (equation 3) [15].



Concept shifts refer to changes in the posterior distribution p(y|x) [11] over time (equation 4).



Approaches to identifying dataset shifts can be broadly classified into supervised and unsupervised methods. Supervised methods, such as progressive error and external holdout [16], require evaluation of the target model to detect shifts. Progressive error involves tracking the performance of the model over time to identify deviations, while external retention evaluates the model's performance on a held-out dataset collected over different periods [11]. Additionally, domain adaptation methods like transfer component analysis and domain-adversarial neural networks help in adapting models to new domains by aligning feature representations across different distributions [17,18]. These techniques can be effective but are often model-dependent and require labeled data, limiting their applicability and flexibility.

On the other hand, unsupervised methods do not rely on model performance and can be applied directly to the data. Techniques such as computing statistical distances (eg, Kullback-Leibler divergence, Wasserstein distance) between distributions, novelty detectors, and discriminative distance measures are commonly used [4,16,19]. Change detection algorithms, such as the Page-Hinkley test and the cumulative sum algorithm, detect changes in the statistical properties of data streams in real time, making them particularly useful for online monitoring of data shifts [20]. Reconstruction-based methods, such as autoencoders, detect shifts by measuring reconstruction error on new data, where high reconstruction error can indicate a distribution shift [21].

Among these unsupervised methods, the Information Geometric Temporal (IGT) projection proposed by Sáez et al [4] provides an unsupervised approach to characterization and exploratory visualization of distributional changes over time. The IGT methodology estimates the statistical distributions of data over time and projects their temporal evolution through nonparametric statistical manifolds. This method presents a robust, straightforward, and model-agnostic way to characterize dataset shifts. It excels in its ability to capture the dynamic nature of data distributions, making it highly sensitive to subtle changes that other techniques might miss. Furthermore, its nonparametric nature ensures flexibility and applicability across various datasets and AI models, enhancing its utility in diverse health settings.

In this study, we investigate how temporal changes in the Medical Information Mart for Intensive Care-IV (MIMIC-IV) health record repository [22] influence the performance of AI models, aiming to develop more reliable and robust health AI applications. Through early, unsupervised characterization of dataset shifts, we seek to identify early indicators that can predict performance variations before they impact clinical outcomes. To detect these shifts, we used the IGT projection method implemented in the *EHRTemporalVariability* package using R software (version 1.2.1; R Foundation for Statistical Computing) [3,4], previously validated in health care data studies [3,23,24]. The combination of temporal heatmaps and IGT projections provided actionable insights into the underlying dynamics of the data. By training AI models in annual data batches, we were able to link these temporal shifts with changes in performance metrics. Our findings demonstrate the potential of early characterization of temporal dataset shifts as a proactive monitoring tool to anticipate performance shifts over time. This proactive identification of dataset shifts paves the way for the development of reliable AI systems, leading to improved health outcomes and increased reliability in clinical settings.

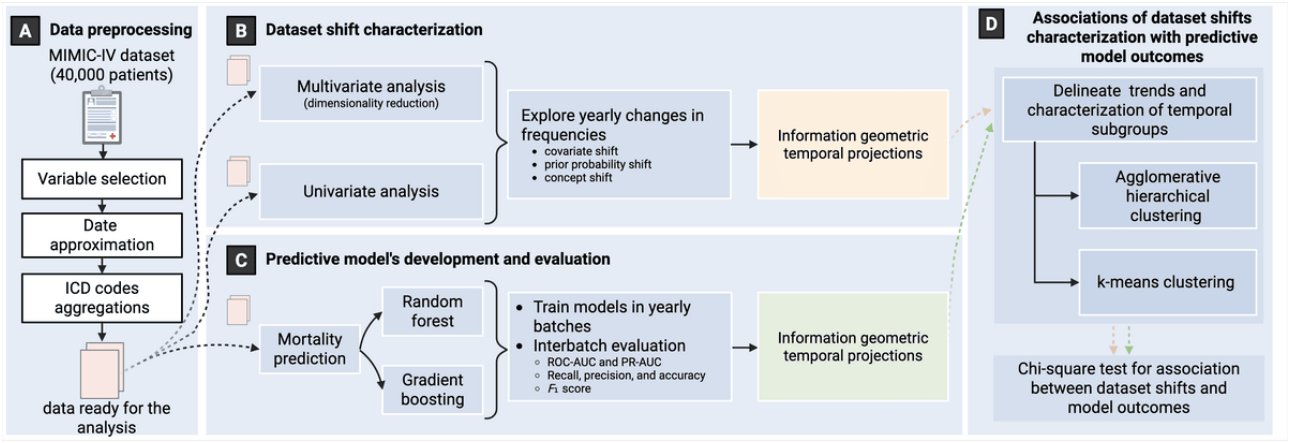
XSL•FO
RenderX

Methods

Overview

Our study comprised 4 phases, including the MIMIC-IV data preparation, the characterization of temporal dataset shifts, the characterization of changes in predictive models' performance metrics, and the test for association between the dataset shifts and model performance metrics (Figure 1). Next, we describe each of the phases of the methodology.

Figure 1. Workflow of the study phases to assess the relationship between the temporal dataset shift characterization of the Medical Information Mart for Intensive Care-IV (MIMIC-IV) database and the machine learning models developed to predict the mortality of the patients. (A) Data preprocessing steps. (B) Dataset shift characterization. (C) Predictive model's development and evaluation. (D) Association of dataset shifts characterization with predictive models outcome process. ICD: International Classification of Diseases; PR-AUC: precision recall area under the curve; ROC-AUC: receiver operating characteristic area under the curve.



MIMIC-IV Dataset

The MIMIC-IV dataset contains electronic health records (EHRs) of more than 40,000 patients from the Beth Israel Deaconess Medical Center (BIDMC) [22]. The MIMIC-IV dataset contains information sourced from the intensive care unit, which is known for its abundance of data and its use in other AI-related works [9]. This modern EHR dataset spans a decade of admissions from 2008 to 2019 and includes precise digital records, such as the electronic medicine administration record. The data are organized modularly, allowing for easy linking to external departments.

For our aim of in-hospital mortality prediction, we included adult patients (age ≥18 years) with at least one hospital admission in the MIMIC-IV dataset. The input features include, on one hand, characteristics of each patient, such as the gender, age, or ethnic group, and on the other hand, the *ICD* (*International Classification of Diseases*) codes of the diagnoses and procedures of each admission in the versions 9 (*ICD-9* [*International Classification of Diseases, Ninth Revision*], from 2008 to 2015) and 10 (*ICD-10* [*International Statistical Classification of Diseases, Tenth Revision*], from 2016 to 2019). Each admission can be linked with multiple *ICD* codes for procedures and diagnoses.

Data Preprocessing

Since we aim to evaluate dataset shifts and model performance over time, the temporal identifier of data is of utmost importance. In MIMIC-IV, admission dates are anonymized and grouped into 3-year cohorts spanning 2008-2019. To approximate the admission year for each record, we applied the date preprocessing method developed by Yao et al [9], which assigns each admission to a specific year within its cohort (see Section 1.1 in Multimedia Appendix 1 for details). This process allows for yearly analysis but introduces a possible deviation of up to ±1 year for any given admission. Consequently, some admissions from, for example, 2015 or 2016 may be labeled as 2014.

To reduce the dimensionality of the dataset and the effect that updating the codes could have on temporal variability, all the *ICD-9* and *ICD-10* codes have been grouped and mapped into common chapters [25] using information from the Chronic Condition Indicator from the Healthcare Cost and Utilization Group [26]. Despite the increased number of codes between *ICD-9* (13,000 codes) and *ICD-10* (68,000 codes), both keep a hierarchical structure that allows the aggregation of the codes at higher levels. In both systems, codes are organized into chapters or categories, representing a broader group of diseases. Regarding diagnosis codes, the *ICD-9* codes are aggregated into 19 chapters (Table S1 in Multimedia Appendix 1), while the *ICD-10* codes are aggregated into 21 (Table S2 in Multimedia Appendix 1) [27]. Furthermore, we created some final chapters by merging the corresponding chapters from both *ICD-9* and *ICD-10* versions (Table S3 in Multimedia Appendix 1). Regarding procedure codes, we aggregated them into 18 chapters for the *ICD-9* version (Table S4 in Multimedia Appendix 1) and 17 for the *ICD-10* version (Table S5 in Multimedia Appendix 1). Then, these chapters were merged into 17 final chapters (Table S6 in Multimedia Appendix 1). Most of the *ICD-9* procedure chapters were merged into a single final chapter, Medical and Surgical, linked to only 1 *ICD-10* chapter based on the merging method used. This could reduce the degree of detail in our study. We decided to expand this final chapter into 13 different subchapters to provide a more detailed mapping of the *ICD-9* chapters into the *ICD-10* ones. (Table S7 in Multimedia Appendix 1). Lastly, given the multiplicity in the number of *ICD* codes per patient, the final groups were coded

XSL•FO
RenderX

using one-hot encoding to allow a richer, unordered input for the predictive models regarding the *ICD* codes.

Dataset Shift Characterization

To characterize dataset shifts, we used the unsupervised approach by Sáez et al [3,4]. This method enables an exploratory characterization and quantification of temporal changes using data temporal heatmaps (DTHs) and IGT projections [5]. The DTHs allow users to dynamically explore changes in absolute and relative frequencies of the variables over time and simultaneously at multiple variable values. The IGT projections embed time batches as a series of points in a latent information space, namely a geometric statistical manifold of nonparametric information from the temporal batches. The IGT projection is obtained, first, by calculating the dissimilarity matrix of the probability distribution functions in temporal batches and, second, by embedding the batches through their dissimilarity matrix with multidimensional scaling in a reduced dimensional space of 2 or 3 dimensions. Consequently, the data batches are represented as temporally indexed points in a latent information space where distances between them correspond to the dissimilarity of their statistical distributions. The IGT projection allows for delineating trends as continuously flowing time batches, abrupt changes as gaps between groups of batches, temporal subgroups as clusters of batches, and seasonality as temporal cycles [3]. Additionally, the IGT projection enables the empirical characterization of conceptually related temporal subgroups using unsupervised machine-learning techniques on the projected temporal points.

We characterized covariate and prior probability shifts using the DTHs and IGT projections provided by the *EHRTemporalVariability* package. To capture concept shifts, we extended the library to compute both class-conditional feature distributions p(x|y) and posterior probabilities p(y|x) and then visualized their temporal evolution with corresponding DTHs and IGT plots.

To explore temporal relationships and patterns in both categorical (eg, *ICD* codes) and numerical variables (eg, age), we conducted a multivariate analysis. This approach allowed us to examine how variables evolve collectively over time, revealing trends, cycles, or structural shifts in the data. We applied factorial analysis of mixed data (FAMD) [28], a dimensionality reduction technique suitable for datasets with mixed data types. Unlike t-distributed Stochastic Neighbor Embedding or Uniform Manifold Approximation and Projection (UMAP), FAMD is a linear technique that preserves the global relationships and variance, which aids with the interpretability [29]. We retained the first 3 FAMD dimensions, which together explained 15.16% of the total variance, striking a balance between meaningful representation for our exploratory analysis and computational efficiency. This reduced space enabled clearer visualization of latent patterns while minimizing the computational load, especially for resource-intensive steps like kernel density estimation (KDE), which scales poorly with higher dimensionality. Finally, to determine whether the low variance retained by the first 3 components of the FAMD was adequate for capturing temporal variability, we conducted the same unsupervised characterization analysis using UMAP as the dimensionality reduction method.

Then, we separated the FAMD coordinates into 2 datasets, one for deceased patients and one for nondeceased patients. This allowed us to study how concepts might change over time using conditional probability p(x|y). We derived probability distributions from the FAMD dimensions to obtain the DTHs, which helped us spot shifts in probabilities linked to covariate or concept shifts. Next, we applied a KDE by year on the first 3 FAMD dimensions for the full and conditioned datasets. Then, for the conditioned datasets, we combined their KDE probability maps into a single map. This map was renormalized to calculate the IGT projection for conditional probabilities, using the *EHRTemporalVariability* package [3]. This step helped us identify shifts in concepts and temporal trends. Finally, we calculated the IGT for the entire FAMD dataset to examine covariate shifts and broader temporal trends.

Next, we conducted a univariate analysis to pinpoint which features drive temporal variability. We began by estimating each feature's marginal distribution in the overall dataset, p(x), to detect covariate shifts, and the class prior, p(y), to detect prior probability shifts. We then estimated the class-conditional feature distributions, p(x|y), for each outcome. Applying Bayes' theorem (equation 5),



we derived the posterior probability p(y|x) for each feature, thereby isolating concept shifts. Finally, we embedded each of these univariate distributions into an IGT projection. This IGT projection for each distribution allowed us to visualize each feature's temporal trajectory and systematically identify covariate, prior, and concept shifts over time.

Predictive Models' Development and Evaluation

The models developed to predict the in-hospital mortality of the patients in the dataset were based on ensemble learning methods, including random forest and gradient boosting. These methods are at the state of the art for the classification of tabular data [30,31]. Random forest is an ensemble learning method that builds multiple decision trees during training and then combines their predictions to improve overall accuracy and reduce overfitting. Gradient boosting is an ensemble learning technique that iteratively combines weak predictive models, typically decision trees, to create a robust predictive model. Through sequential optimization of an objective function, this method progressively reduces errors, demonstrating significant efficacy in diverse classification and regression tasks within high-dimensional data spaces.

To analyze the performance of the models over time, the initial dataset was batched on a yearly basis from 2008 to 2019. Thus, we used 12 subsets to train and validate the yearly models. We divided each subset following a criterion of 80% for training and 20% for testing. Of the 80% of the training data, 70% was for pure training, and the remaining 30% was used for validation.

We trained each model on the training set and tuned hyperparameters using grid search on the validation set. For

XSL•FO
RenderX

random forest and gradient boosting, we predefined values for the number of trees and maximum depth. To reduce computation time, we ran a grid search in parallel. We validated models on data from the same year as training, using the receiver operating characteristic area under the curve (ROC-AUC) as the metric for its robustness to class imbalance and threshold independence [32]. Finally, we averaged ROC-AUC scores across 12 models for each hyperparameter set and selected the configuration with the highest mean score.

Once the hyperparameters were defined, we studied each model's performance over time, evaluating them on the test sets from all 12 temporal batches. The metrics used to evaluate a more detailed performance of the models, in this case, included the ROC-AUC, precision recall area under the curve, recall (or sensitivity) of the positive class, precision, accuracy, and macro F_1-score. However, due to the high class imbalance (Figure S2 in Multimedia Appendix 1), we used a prediction threshold other than the default 0.5. To determine this threshold, we ranked possible values using the Youden index (equation 6) and selected the one with the highest score using the validation data from the most recent temporal batch. We then applied this optimal threshold to binarize the test data predictions.



Association of Dataset Shift Characterization With Predictive Model Outcomes

To prove our objective of determining whether an early unsupervised exploratory characterization of dataset shifts can explain prospective changes in the performance of predictive models, we compared the patterns from the dataset shift characterization, those in the IGT projections, with equivalent embeddings from the interbatch evaluation of AI performance metrics over time. These embeddings, leading to a characterization of the patterns in AI performance metrics, were calculated by applying multidimensional scaling to the interbatch evaluation matrices evaluated year by year and representing the batches in a 3-dimensional space. This procedure is equivalent to the obtention of the IGT for the predictive models' metrics.

We applied agglomerative hierarchical clustering to identify temporal clusters in both the IGT projection and interbatch model evaluation embeddings. We aimed to delineate temporal subgroups, thus elucidating patterns of similarity in the data and the behavior of the models over time [5]. This allowed us to identify groups of conceptually related time periods in which probability distributions are similar within a group but dissimilar between groups. We used a complete linkage and the Manhattan distance, which, according to Strauss and Maltitz [33], is less sensitive to outliers. To justify the number of clusters to be performed on each case, we applied the elbow method [34] and the analysis of the dendrogram distances, joined to the results extracted from the exploratory unsupervised characterization.

Additionally, we implemented a k-means clustering process to reinforce the results obtained in the hierarchical clustering process. To do so, we initialized the k-means with 2 centroids in the data of the first and last years to follow the natural temporal trend, as it was the optimal number of clusters obtained in the hierarchical clustering.

Finally, to statistically determine the existence of a significant association between the clusters from the dataset shift characterization and the interbatch model evaluation embeddings, we applied the Fisher exact test with a significance level of .05.

Ethical Considerations

This study used the MIMIC-IV dataset, which is a publicly available deidentified dataset of EHRs from the BIDMC. The dataset was obtained in accordance with the guidelines set forth by the Massachusetts Institute of Technology and the BIDMC Institutional Review Board. Access to the dataset was granted upon completion of the required Collaborative Institutional Training Initiative program course on data use and privacy for researchers, ensuring compliance with ethical standards for using health data. To ensure patient privacy, all data collected at BIDMC as part of routine clinical care are deidentified and transformed before being made available to researchers who have completed human research training and signed a data use agreement [22]. As the data are fully deidentified and publicly accessible, patient consent was not required.

Results

Data Preprocessing Results

The final dataset comprised 61 features and 239,246 admissions, of which 232,276 belonged to nondeceased patients and the remaining 6970 (2.91%) to deceased ones. After batching data on a yearly basis, the average number of patients per year was 35,781, with a standard deviation of 27,610 (Figure S1 in Multimedia Appendix 1 shows the amount of data per year).

Dataset Shifts Characterization

As an overall representation of the data changes over time, Figure 2A shows the first 2 components of the FAMD divided by class and 2 time periods, previous and after 2014, the year the update of *ICD-9* to *ICD-10* took place. These results show that both survivors' and nonsurvivors' positions and class-conditional layouts change over time. The nondeceased patients show a wider variance over the first dimension. The magnitude and impact of these changes on AI are further explored.

XSL•FO
RenderX

Figure 2. Results of the multivariate dataset shift characterization. (A) Scatter plot of the first 2 dimensions of the studied Medical Information Mart for Intensive Care-IV (MIMIC-IV) dataset's factorial analysis of mixed data (FAMD). Dim 1 is the largest variance dimension, and Dim 2 is the second largest variance dimension. The data are divided by classes (green and red) and time (darker and lighter colors). (B) Information Geometric Temporal (IGT) projection of the entire dataset after applying the FAMD and the kernel density estimation to the first 3 dimensions. Temporal subgroups are highlighted by red circles. (C) Heatmap of the probability distribution of the first 2 dimensions of the FAMD over time. (D) Heatmap of the conditional probability distribution of each class in the second dimension of the FAMD.

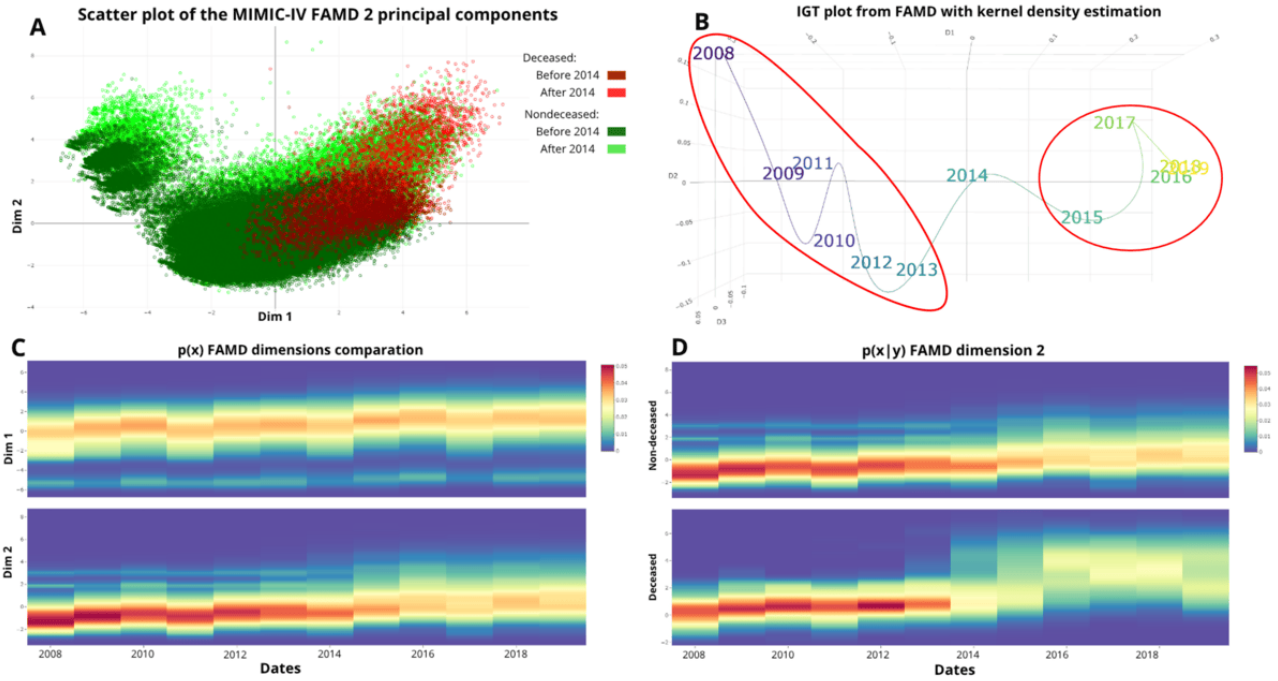


Figure 2B shows the IGT of the data after applying the FAMD and the KDE to the principal 3 dimensions. The colors in the IGT projection plot represent a gradient that distinguishes different yearly temporal batches. Subsequently, Figures 2C and 2D present temporal heatmaps depicting the temporal variability derived from the first 2 dimensions of the FAMD applied to the entire dataset and the second dimension when segmented by class, respectively. In Figure 2D, we chose the second dimension of the FAMD over the first one because it better represents the presence of the temporal discriminative variability of the classes. The contribution of the variables to the principal components of the FAMD can be examined in Figure S16 in Multimedia Appendix 1. Figure S17 in Multimedia Appendix 1 displays the results of the unsupervised characterization of temporal variability based on the UMAP-reduced data. It is evident that the IGT projection reflects the same trend previously observed with FAMD. Specifically, there are 2 distinct temporal groups, one comprising data from 2008 to 2013 and the other from 2015 to 2019, along with a transition year in between. The rest of the results are obtained for the FAMD dimensionality-reduced data.

A notable increase in the variability of the data's probability distribution occurs after 2014, coinciding with the adoption of the *ICD-10* coding system, leading to enhanced dispersion across the temporal spectrum. Specifically, 2014, 2015, and 2016 exhibited pronounced shifts in the conditional probability distribution, characterized by significant variations in distribution trends and increased dispersion, which is indicative of concept shifts. Additionally, a distinct covariate shift was detected in 2015, marked by a notable dispersion in data and an ascending trend. The IGT analysis, as depicted in Figure 2, corroborated these phenomena, affirming the initial observations. In the IGT plot, we identified 2 distinguished groups, one from 2009 to 2013 and the other from 2016 to 2019. In the middle, there are some transition years. Thus, the presence of covariate shift and concept shift is justified.

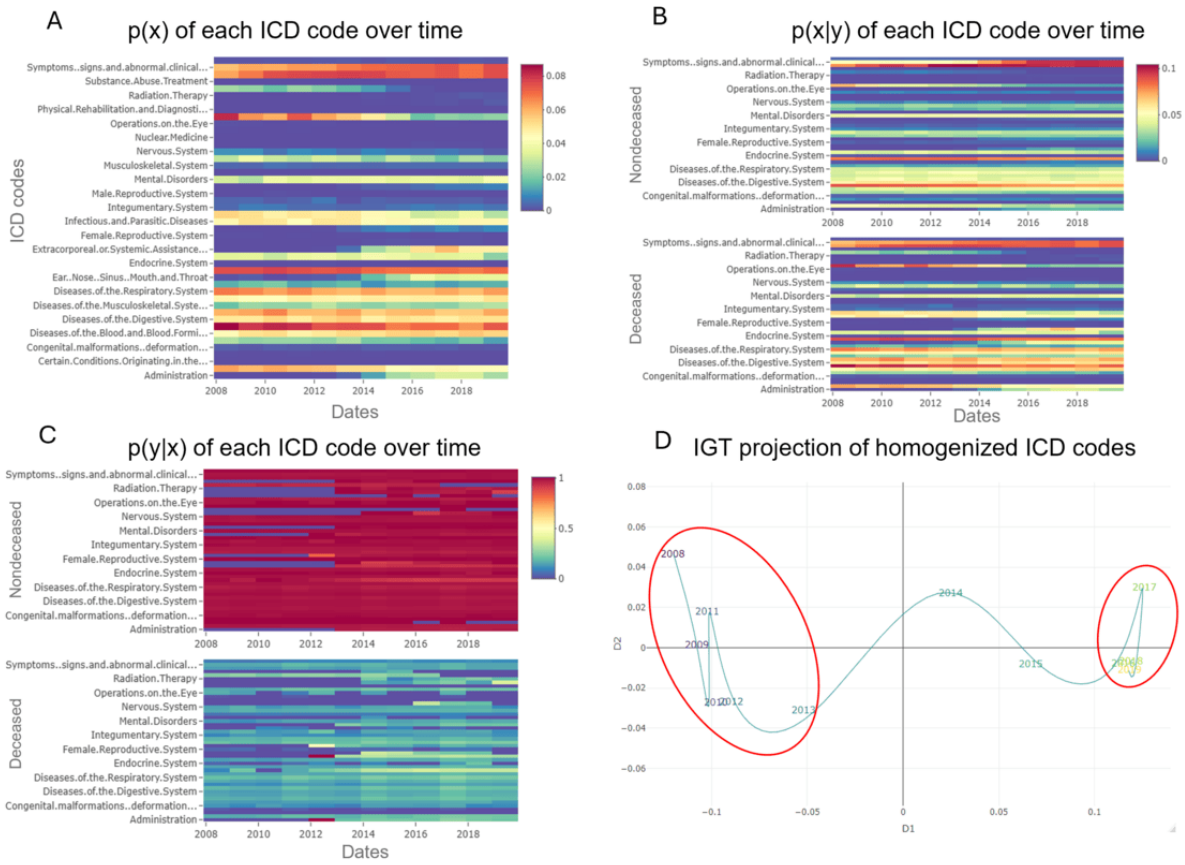
Figure 3 shows the results of the univariate analysis regarding the homogenized *ICD* codes. Figure 3A shows each chapter's overall prevalence from 2008 to 2019. Notably, "Other procedures" code diminishes its distribution over time, as it is much more present between 2008 and 2015 than in the following years. It happened similarly in the "Cardiovascular system" code. These are 2 of the most frequent chapters, both exceeding 70,000 entries. This means that variations in their distributions have a high relevance in the total variability of the dataset. The diagnosis chapters "Diseases of the circulatory system" and "Endocrine nutritional and metabolic diseases and immunity disorders" also show a diminution in the probability distribution over time. As before, these are very frequent chapters. The common fact between these chapters is that their probability distribution is higher when only *ICD-9* codes were used. This means that some of the procedures and diagnosis codes related to these chapters have been redistributed into others with the implementation of the *ICD-10*. This may have happened with the diagnoses chapter "Symptoms signs and abnormal clinical and laboratory findings not elsewhere classified" and the procedures chapters "Imaging" and "Extracorporeal or systemic assistance and performance administration," which increased their probability distribution over time. Again, these variations are clear evidence of a covariate shift. Both the DTHs for p(x|y)

XSL•FO
RenderX

and p(y|x), shown in Figures 3B and 3C, reveal synchronous changes in key chapters, such as "Administration" or "Extracorporeal or systemic assistance." These parallel shifts in feature prevalence and their link to mortality confirm a genuine concept shift, where the relationship between certain codes and the outcome evolves over time. Figure 3D shows the IGT projection of the features' marginal distribution, yielding 2 clear temporal subgroups (2008-2013 and 2015-2019), with a transition year.

Finally, Figure S2 in Multimedia Appendix 1 shows a stable probability for the mortality class over time, indicating no prior probability shift.

Figure 3. Results of the dataset shift characterization of each International Classification of Diseases (*ICD*) code, homogenized between *ICD-9* (*International Classification of Diseases, Ninth Revision*) and *ICD-10* (*International Statistical Classification of Diseases, Tenth Revision*) versions (Tables S1-S7 in Multimedia Appendix 1). (A) Heatmap of the probability distribution p(x) of each homogenized ICD code over time, sorted alphabetically. (B) Heatmap of the conditional probability distribution p(x|y) of each class for each homogenized ICD code sorted alphabetically. (C) Heatmap of the posterior probability distribution p(y|x) for each class of homogenized ICD codes, sorted alphabetically, with a square root transformation for improved visualization. (D) Information Geometric Temporal (IGT) projection of the p(x) of ICD codes. Temporal subgroups are highlighted by red circles.



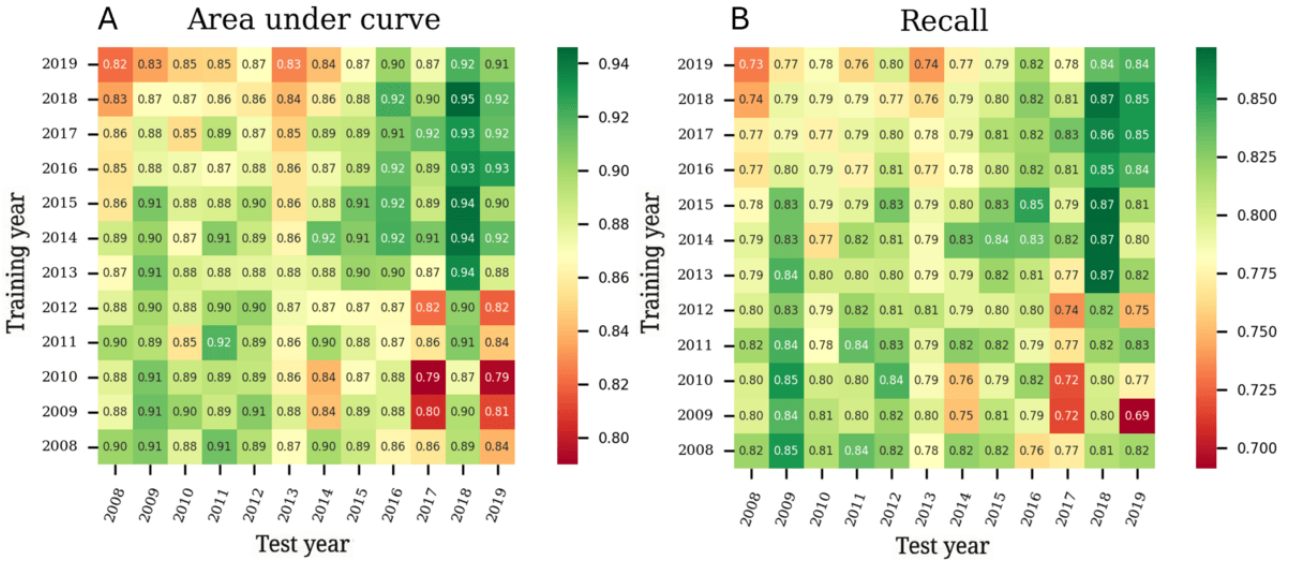
Assessment of Models' Performance Over Time

After applying grid search for the hyperparameter tuning, the number of trees selected for the random forest models was 500 with a maximum depth of 9. In the case of gradient boosting models, the number of estimators was 100 with a maximum depth of 2. Figure 4 shows the matrices of resulting metrics from training, representing how the trained models perform when validated with data from different years. This provides insight into their behavior across temporal variations for random forest. Almost every metric described the same trend. The best results were in the lower left and upper right quadrants. These areas belonged to the models trained and tested with data batches preinstauration of *ICD-10* codes and post instauration, respectively. The remaining metrics for random forest are in Figure S3 in Multimedia Appendix 1.

As with the random forest, for gradient boosting models, every metric except precision showed better results when the models were trained and tested with pre–*ICD-10* and post–*ICD-10* data (Figure S4 in Multimedia Appendix 1). The precision metric showed very similar results in every temporal batch. Both techniques performed similarly, with slightly better results in the random forest.

XSL•FO
RenderX

Figure 4. Interyear evaluation of the random forest (RF) machine learning models using the test datasets for (A) area under the receiver operating characteristic curve and (B) recall of the positive class metrics. The selected hyperparameters for the RF model were 500 trees and a maximum depth of 9.



Relationship Between Temporal Variability and ML Models' Performance

Figure 5 presents the exploratory results of hierarchical clustering applied to the IGT of both the dataset shift (covariate shift) characterization of the FAMD data and the recall metric from the random forest models. The remaining metrics are detailed in Figures S5-S15 in Multimedia Appendix 1. For the covariate shift (Figures 5B and 5C), the clustering results reveal 2 distinct groups (one covering 2008-2014 and the other 2015-2019), indicating similar probability distributions within these periods. These clusters suggest periods with consistent covariate characteristics, while also highlighting the presence of shifts between them. Figure 5D shows the IGT for the recall metric over time, reflecting fluctuations in model performance. The clustering results (Figures 5E and 5F) reveal 2 distinct clusters as well, with one corresponding to 2008-2013 and the other to 2014-2019. These findings illustrate how both dataset shifts and model performance evolve over time, identifying similar temporal patterns in both the data and the model behavior.

Table 1 shows the results of the Fisher exact tests comparing groups formed by hierarchical and k-means clustering of temporal variability against the metrics of random forest models for 2 clusters. All metrics registered *P* values of <.05 for both clustering methods, indicating statistically significant differences between the clusters. Specifically, these *P* values suggest that the likelihood of observing such differences by chance is less than 5%, allowing us to confidently reject the null hypothesis of independence between clusters and model performance metrics.

Similarly, Table 2 presents the results of the Fisher exact tests comparing groups formed by hierarchical and k-means clustering of temporal variability with the performance metrics of gradient boosting models across 2 clusters. In the hierarchical clustering scenario, all performance metrics except for recall exhibited *P* values <.05, indicating statistically significant differences between the clusters. This allows us to reject the null hypothesis of independence, suggesting a significant association between temporal variability and the performance metrics of gradient boosting models. For the k-means clustering, every metric recorded a *P* value of <.05. To minimize the type 1 error rate after conducting multiple statistical tests and to ensure the robustness of our results, we adjusted the *P* values using the false discovery rate method (Tables S8 and S9 in Multimedia Appendix 1). The adjusted *P* values yielded the same statistically significant results. Furthermore, the findings from the gradient boosting analysis reinforce the association between temporal variability and model performance, which aligns with the patterns observed in the random forest results. The significant *P* values for key metrics in both hierarchical and k-means clustering reinforce the conclusion that temporal variability is an important factor influencing AI model performance outcomes. These results highlight the necessity of monitoring temporal shifts in datasets to maintain and enhance the reliability and accuracy of AI models in clinical settings.

XSL•FO
RenderX

Figure 5. Exploratory results of comparing dataset shift characterization of factor analysis of mixed data (FAMD), data covariate shift, and random forest model evaluation matrices of recall. (A) Information Geometric Temporal (IGT) of the initial 3 dimensions of the FAMD after applying a kernel density estimation. (B) Dendrogram depicting the hierarchical clustering of the IGT for the initial 3 dimensions derived from the FAMD, following the application of kernel density estimation. (C) Representation of the hierarchical clustering of the IGT from the FAMD following the application of kernel density estimation. (D) IGT of the evaluation matrix for the recall metric of the random forest model. (E) Dendrogram depicting the hierarchical clustering of the IGT for the evaluation matrix for the recall metric on the random forest model. (F) Representation of the hierarchical clustering of the IGT from the evaluation matrix for the recall metric on the random forest model.

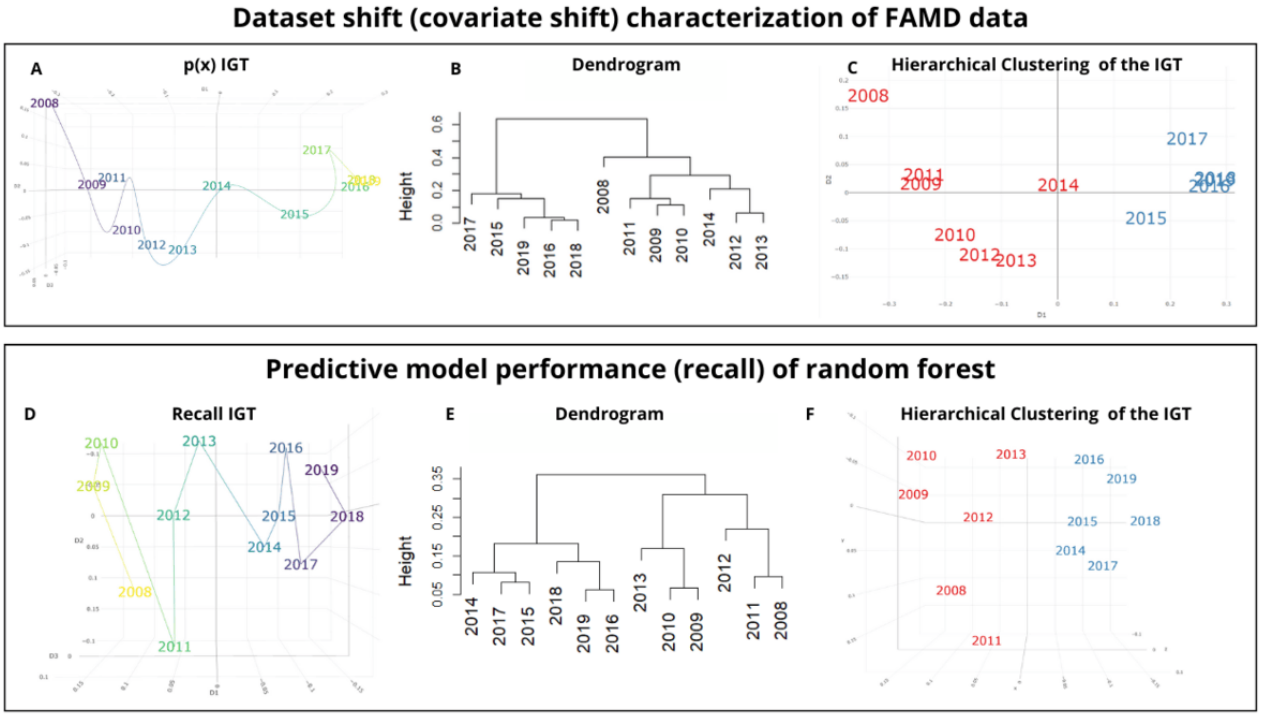


Table 1. Results of the Fisher exact test to compare 2 clustering methods for the random forest models (hierarchical clustering and k-means), both for *k*=2. Clustering was applied to the Information Geometric Temporal (IGT) obtained from the metrics of the random forest model and the IGT from the 3 principal dimensions of the factorial analysis of mixed data after applying the kernel density estimation. This comparison aimed to test the hypothesis of independence of both clusters (α=.05). All *P* values of <.05 are statistically significant.

Metric	*P* value for hierarchical clustering	*P* value for k-means
ROC-AUC[a]	.03	.03
PR-AUC[b]	.02	.03
Precision	.02	.03
Recall	.02	.02
Accuracy	.02	.02
F_1-score	.03	.03

[a]ROC-AUC: receiver operating characteristic area under the curve.

[b]PR-AUC: precision recall area under the curve.

XSL•FO
RenderX

Table 2. Results of the Fisher exact test to compare 2 clustering methods for the gradient boosting model (hierarchical clustering and k-means), both for *k*=2. Clustering was applied to the Information Geometric Temporal (IGT) obtained from the metrics of the gradient boosting model and the IGT from the 3 principal dimensions of the factorial analysis of mixed data after applying the kernel density estimation. This comparison aimed to test the hypothesis of independence of both clusters (α=.05). All *P* values of <.05 are statistically significant.

Metric	*P* value for hierarchical clustering	*P* value for k-means
ROC-AUC[a]	.03	.03
PR-AUC[b]	.03	.03
Precision	.03	.02
Recall	.08	.02
Accuracy	.02	.02
F_1-score	.02	.02

[a]ROC-AUC: receiver operating characteristic area under the curve.

[b]PR-AUC: precision recall area under the curve.

Discussion

Overview

Our study reveals a strong link between temporal dataset shifts in the MIMIC-IV dataset and the observed variations in ML performance. By using an unsupervised exploratory method to detect these shifts before model training, we can offer actionable insights regarding data curation or learning strategies (eg, domain adaptation or continual learning techniques). This early characterization not only enhances the robustness and reliability of AI models but also sets the stage for future work on online dataset shift detection. Such real-time monitoring could dynamically adjust training processes, ensuring optimal performance without frequent retraining.

When considering approaches for detecting dataset shift, there are important trade-offs between unsupervised and supervised methods. Unsupervised methods, like the one used in our study, since they are based only on data, do not require any model training nor, in the case of covariate shift analyses, labeled data. This makes them scalable and relatively cost-effective for large and dynamic clinical datasets. In contrast, supervised methods such as progressive error tracking or evaluation on external holdout sets provide direct insights into performance changes but require training particular models and computational resources. This may limit their feasibility for continuous or real-time monitoring when no labeled data are still available, as well as the inherent limitations of the selected model. Ultimately, combining both approaches may offer the most comprehensive strategy for maintaining robust AI performance in the face of evolving health data.

Our analysis of the MIMIC-IV dataset provides crucial information for understanding its characteristics and potential applications in AI. We have observed both gradual and abrupt changes in the dataset's probability distribution over time, primarily due to variations in *ICD* codes. The transition from *ICD-9* to *ICD-10* has been the main factor contributing to this temporal variability. Even after standardizing the values, we found that this transition can significantly impact data analysis. Although mapping *ICD-9* codes to *ICD-10* codes helps reduce dimensionality and facilitates longitudinal analysis, it may not fully account for changes in coding practices or semantic shifts between the 2 versions. This issue is particularly important for chapters that have undergone significant restructuring. It has opened up new avenues for investigation, such as a thorough fidelity assessment for all chapters. Although this assessment is currently beyond the scope of this work, it may lay the groundwork for future research.

We have also discovered that the optimal number of clusters aligns with the number of *ICD* code versions. The data years are typically grouped based on the *ICD* versions used during the clustering process. Although the transition year from *ICD-9* to *ICD-10* was 2015, this study's cutoff point was 2014. This is because the data deidentification process is not entirely precise, which is the biggest limitation in this paper, and the obtained year falls within a 3-year group. Therefore, data from 2015 may be labeled as from 2014. For this reason, we have established 2014 as the cutoff point for our association analysis (more information about the deidentification process in Section 1.1 in Multimedia Appendix 1).

It is important to note that small differences between years may arise from variations in available data, deidentification procedures, and the approximate date assignment. By following the annual extraction approach of Yao et al [9], we achieve better temporal granularity, but we must recognize that the assigned admission year may be offset by up to 1 year due to the 3-year cohort structure. As a result, the timing of observed transitions, such as the shift to *ICD-10*, should be interpreted as occurring within a 3-year window rather than as a precise annual event. This limitation may artificially sharpen the observed temporal break and exaggerate the separation between clusters in our analysis. Therefore, some of the distinct clustering observed around the *ICD* system transition could reflect this methodological artifact rather than a purely organic change in the underlying data distribution. To assess the impact of this limitation, we repeated our analysis using the original 3-year cohort groups instead of annual assignments and observed that our main conclusions regarding dataset shifts and their effects on model performance remained unchanged. This suggests that our findings are robust to the temporal aggregation method.

Importantly, we showed that both linear (FAMD) and nonlinear (UMAP) dimensionality reduction techniques produce consistent

XSL•FO
RenderX

temporal clusters, supporting the robustness of our findings despite FAMD capturing only 15.16% of total variance. This robustness underscores the value of unsupervised characterization for understanding temporal variability. It suggests that, despite the relatively low explained variance of the FAMD approach, our main conclusions regarding temporal dataset shifts remain stable across both linear and nonlinear dimensionality reduction techniques.

Recent studies have further emphasized the importance of considering temporal shifts in health AI. Peracchio et al [35] and Nicora et al [36] focused on performing an online detection of temporal changes in clinical settings during the deployment phase of AI models, highlighting how these shifts impact AI model performance, which aligns with our findings. Saurav et al [37] contributed to this field by performing an anomaly detection methodology using recurrent neural networks to make multistep time series predictions and using the prediction errors to detect shifts and rapidly adapt the model to changes. Furthermore, Koch et al [38] have shown that detecting dataset shifts is crucial for monitoring AI-based medical products during postmarket surveillance, implementing 3 different methods to do it. While Guo et al [39] also used an unsupervised approach to investigate dataset shifts in the MIMIC-IV dataset, our study differs by focusing on a model-agnostic and exploratory characterization of these shifts. Our approach is computationally simpler and offers enhanced flexibility and scalability. Additionally, our study explores how unsupervised methods can interact with supervised approaches, offering complementary insights into the identification of temporal variability.

Overall, our work builds upon existing literature on the impact of temporal variability and dataset shifts on ML models. By adopting an unsupervised, model-agnostic approach based on information geometry, we contribute to a growing body of research seeking to address the challenges posed by temporal shifts in clinical AI. Our findings enhance the understanding of how these shifts influence model robustness and performance.

This approach not only optimizes decision-making in clinical practice but also enhances the adaptability of AI systems. By enabling early characterization of dataset shifts, our work can guide clinicians and developers in identifying emerging trends and anticipating potential risks. Ultimately, this work lays the groundwork for the development of continuously learning, self-adaptive AI models that are better equipped to handle the dynamic nature of health data.

Conclusions

This work demonstrates that early identification of changes in data statistical distributions through unsupervised dataset shift characterization is a potential indicator of performance variations in prospective ML models. The association between variations in data distributions and the model's performance has been statistically demonstrated in the MIMIC-IV dataset as a significant benchmark. Noteworthy, the implementation of *ICD-10* coding resulted in significant temporal variability in covariates and outcome-conditional distributions. This translates into the presence of covariate and concept shift, but not prior probability shift in the dataset.

Our findings underscore the importance of characterizing and adjusting for dataset shifts when developing AI models in health. By integrating temporal variability analysis, such as IGT projection data, with the development of AI models, we pave the way to the creation of trustworthy and self-adaptive AI systems. Our research sets the stage for building more resilient and adaptable AI solutions, which will help enhance patient safety and increase the applicability of AI in the ever-evolving health industry.

Funding

This study was funded by the project PID2022-138636OA-I00 (KINEMAI) by Agencia Estatal de Investigación-Proyectos de Generación de Conocimiento 2022.

Authors' Contributions

DFN, PF, and CS conceived and designed the work. DFN performed data collection, processing, and analysis. CS, PF, AGS, JMGG, and DFN reviewed and interpreted the results. DFN drafted the study. CS, PF, AGS, and JMGG provided critical revision of the study. All authors approved the final version to be published.

Conflicts of Interest

None declared.

Multimedia Appendix 1
Additional information, tables, and figures.
[DOCX File , 7653 KB - medinform_v13i1e78309_app1.docx]

References

1. Balahur-Dobrescu A, Jenet A, Hupont T, Charisi V, Ganesh A, Griesinger C, et al. Data Quality Requirements for Inclusive, Non-Biased Trustworthy AI. Luxembourg: European Union (Joint Research Centre - JRC Publications Repository); 2022.
2. Nestor B, McDermott M, Boag W, Berner G, Naumann T, Hughes M, et al. Feature robustness in non-stationary health records: caveats to deployable model performance in common clinical machine learning tasks. In: PMLR. 2019 Presented

XSL•FO
RenderX

at: Proceedings of the 4th Machine Learning for Healthcare Conference; 2019 August 9-10; Michigan p. 381-405 URL: https://proceedings.mlr.press/v106/nestor19a.html
3. Sáez C, Gutiérrez-Sacristán A, Kohane I, García-Gómez JM, Avillach P. EHRtemporalVariability: delineating temporal data-set shifts in electronic health records. Gigascience 2020;9(8):giaa079 [FREE Full text] [doi: 10.1093/gigascience/giaa079] [Medline: 32729900]
4. Sáez C, Rodrigues PP, Gama J, Robles M, García-Gómez JM. Probabilistic change detection and visualization methods for the assessment of temporal stability in biomedical data quality. Data Min Knowl Disc 2014;29(4):950-975. [doi: 10.1007/s10618-014-0378-6]
5. Sáez C, García-Gómez JM. Kinematics of big biomedical data to characterize temporal variability and seasonality of data repositories: functional data analysis of data temporal evolution over non-parametric statistical manifolds. Int J Med Inform 2018;119:109-124 [FREE Full text] [doi: 10.1016/j.ijmedinf.2018.09.015] [Medline: 30342679]
6. Ferri P, Lomonaco V, Passaro LC, Félix-de Castro A, Sánchez-Cuesta P, Sáez C, et al. Deep continual learning for medical call incidents text classification under the presence of dataset shifts. Comput Biol Med 2024;175:108548 [FREE Full text] [doi: 10.1016/j.compbiomed.2024.108548] [Medline: 38718666]
7. Guo LL, Pfohl SR, Fries J, Posada J, Fleming SL, Aftandilian C, et al. Systematic review of approaches to preserve machine learning performance in the presence of temporal dataset shift in clinical medicine. Appl Clin Inform 2021;12(4):808-815 [FREE Full text] [doi: 10.1055/s-0041-1735184] [Medline: 34470057]
8. Sáez C, Romero N, Conejero J, García-Gómez JM. Potential limitations in COVID-19 machine learning due to data source variability: a case study in the nCov2019 dataset. J Am Med Inform Assoc 2021;28(2):360-364 [FREE Full text] [doi: 10.1093/jamia/ocaa258] [Medline: 33027509]
9. Yao H, Choi C, Cao B, Lee Y, Koh P, Finn C. Wild-time: a benchmark of in-the-wild distribution shift over time. Wild-Time: A Benchmark of in-the-Wild Distribution Shift over Time. arXiv; 2022 Presented at: 36th Conference on Neural Information Processing Systems (NeurIPS 2022) Track on Datasets and Benchmarks; 2022 Nov 28-Dec 9; New Orleans URL: https://proceedings.neurips.cc/paper_files/paper/2022/file/43119db5d59f07cc08fca7ba6820179a-Paper-Datasets_and_Benchmarks.pdf [doi: 10.48550/arXiv.2211.14238]
10. Zhang A, Xing L, Zou J, Wu JC. Shifting machine learning for healthcare from development to deployment and from models to data. Nat Biomed Eng 2022;6(12):1330-1345. [doi: 10.1038/s41551-022-00898-y] [Medline: 35788685]
11. Moreno-Torres JG, Raeder T, Alaiz-Rodríguez R, Chawla NV, Herrera F. A unifying view on dataset shift in classification. Pattern Recognit 2012;45(1):521-530. [doi: 10.1016/j.patcog.2011.06.019]
12. Quiñonero-Candela J. Dataset Shift in Machine Learning. Cambridge, Mass: MIT Press; 2009.
13. Sáez C, Ferri P, García-Gómez JM. Resilient artificial intelligence in health: synthesis and research agenda toward next-generation trustworthy clinical decision support. J Med Internet Res 2024;26:e50295 [FREE Full text] [doi: 10.2196/50295] [Medline: 38941134]
14. Kelly MG, Hand DJ, Adams NM. The impact of changing populations on classifier performance. USA: Association for Computing Machinery; 1999 Presented at: KDD '99: Proceedings of the fifth ACM SIGKDD international conference on Knowledge discovery and data mining; 1999 August 15-18; San Diego California USA p. 367-371. [doi: 10.1145/312129.312285]
15. Alaiz R, Japkowicz N. Assessing the impact of changing environments on classifier performance. : Springer; 2008 Presented at: 21st Conference of the Canadian Society for Computational Studies of Intelligence, Canadian AI 2008; 2008 May 28-30; Windsor, Canada p. 13-24. [doi: 10.1007/978-3-540-68825-9_2]
16. Stewart M. Understanding dataset shift. Towards Data Science. 2020. URL: https://towardsdatascience.com/understanding-dataset-shift-f2a5a262a766 [accessed 2024-03-08]
17. Ganin Y, Ustinova E, Ajakan H, Germain P, Larochelle H, Laviolette F, et al. Domain-adversarial training of neural networks. JMLR 2016;17(59):1-35 [FREE Full text] [doi: 10.1007/978-3-319-58347-1_10]
18. Pan SJ, Tsang IW, Kwok JT, Yang Q. Domain adaptation via transfer component analysis. IEEE Trans Neural Netw 2011;22(2):199-210. [doi: 10.1109/tnn.2010.2091281]
19. Raeder T, Hoens T, Chawla N. Consequences of variability in classifier performance estimates. 2010 Presented at: IEEE International Conference on Data Mining; 2010 December 13-17; Sydney, NSW, Australia p. 421-430. [doi: 10.1109/icdm.2010.110]
20. Ikonomovska E, Gama J, Sebastião R, Gjorgjevik D. Regression trees from data streams with drift detection. Discov Sci Berlin, Heidelberg: Springer; 2009 Presented at: 12th International Conference, DS 2009; 2009 October 3-5; Porto, Portugal p. 121-135. [doi: 10.1007/978-3-642-04747-3_12]
21. Zong B, Song Q, Min MR, Cheng W, Lumezanu C, Cho D, et al. Deep autoencoding Gaussian mixture model for unsupervised anomaly detection. 2018 Presented at: The Sixth International Conference on Learning Representations (ICLR 2018); 2018 Apr 30-May 3; Vancouver URL: https://openreview.net/forum?id=BJJLHbb0-
22. Johnson AEW, Bulgarelli L, Shen L, Gayles A, Shammout A, Horng S, et al. MIMIC-IV, a freely accessible electronic health record dataset. Sci Data 2023;10(1):1 [FREE Full text] [doi: 10.1038/s41597-022-01899-x] [Medline: 36596836]

XSL•FO
RenderX

23. Ferri P, Sáez C, Félix-de Castro A, Juan-Albarracín J, Blanes-Selva V, Sánchez-Cuesta P, et al. Deep ensemble multitask classification of emergency medical call incidents combining multimodal data improves emergency medical dispatch. Artif Intell Med 2021;117:102088 [FREE Full text] [doi: 10.1016/j.artmed.2021.102088] [Medline: 34127234]
24. Sáez C, Zurriaga O, Pérez-Panadés J, Melchor I, Robles M, García-Gómez JM. Applying probabilistic temporal and multisite data quality control methods to a public health mortality registry in Spain: a systematic approach to quality control of repositories. J Am Med Inform Assoc 2016;23(6):1085-1095 [FREE Full text] [doi: 10.1093/jamia/ocw010] [Medline: 27107447]
25. Nestor B, McDermott M, Chauhan G, Naumann T, Hughes M, Goldenberg A, et al. Rethinking clinical prediction: Why machine learning must consider year of care and feature aggregation. 2018 Presented at: NeurIPS 2018 (32nd Conference on Neural Information Processing Systems); 2018 Dec 7; Montreal. [doi: 10.48550/arXiv.1811.12583]
26. HCUP-US home page. 2025. URL: https://hcup-us.ahrq.gov/ [accessed 2025-03-12]
27. Cartwright D. ICD-9-CM to ICD-10-CM Codes: what? Why? How? Adv Wound Care (New Rochelle) 2013;2(10):588-592 [FREE Full text] [doi: 10.1089/wound.2013.0478] [Medline: 24761333]
28. Pagès J. Multiple Factor Analysis by Example Using R. New York: Chapman and Hall/CRC; 2014.
29. Hou CKJ, Behdinan K. Dimensionality reduction in surrogate modeling: a review of combined methods. Data Sci Eng 2022;7(4):402-427 [FREE Full text] [doi: 10.1007/s41019-022-00193-5] [Medline: 36345394]
30. Shwartz-Ziv R, Armon A. Tabular data: deep learning is not all you need. Inf Fusion 2022;81:84-90. [doi: 10.1016/j.inffus.2021.11.011]
31. Ghimire B, Rogan J, Galiano VR, Panday P, Neeti N. An evaluation of bagging, boosting, and random forests for land-cover classification in cape cod, Massachusetts, USA. GIScience Remote Sens 2013;49(5):623-643. [doi: 10.2747/1548-1603.49.5.623]
32. Brabec J, Komárek T, Franc V, Machlica L. On model evaluation under non-constant class imbalance. Cham: Springer International Publishing; 2020 Presented at: The 20th International Conference on Computational Science (ICCS 2020); 2020 June 3-5; Amsterdam, The Netherlands p. 74-87. [doi: 10.1007/978-3-030-50423-6_6]
33. Strauss T, von Maltitz MJ. Generalising ward's method for use with manhattan distances. PLoS One 2017;12(1):e0168288 [FREE Full text] [doi: 10.1371/journal.pone.0168288] [Medline: 28085891]
34. Syakur MA, Khotimah BK, Rochman EMS, Satoto BD. Integration integration k-means clustering method and elbow method for identification of the best customer profile cluster. IOP Conf Ser Mater Sci Eng 2018;336:012017. [doi: 10.1088/1757-899x/336/1/012017]
35. Peracchio L, Nicora G, Parimbelli E, Buonocore TM, Tavazzi E, Bergamaschi R, et al. RelAI: an automated approach to judge pointwise ML prediction reliability. Int J Med Inform 2025;197:105857 [FREE Full text] [doi: 10.1016/j.ijmedinf.2025.105857] [Medline: 40037268]
36. Nicora G, Rios M, Abu-Hanna A, Bellazzi R. Evaluating pointwise reliability of machine learning prediction. J Biomed Inform 2022;127:103996 [FREE Full text] [doi: 10.1016/j.jbi.2022.103996] [Medline: 35041981]
37. Saurav S, Malhotra P, Gugulothu N, Vig L, Agarwal P, Shroff G. Online anomaly detection with concept drift adaptation using recurrent neural networks. USA: Association for Computing Machinery; 2018 Presented at: The ACM India Joint International Conference; 2025 December 17-20; Pune, India p. 78-87. [doi: 10.1145/3152494.3152501]
38. Koch L, Baumgartner C, Berens P. Distribution shift detection for the postmarket surveillance of medical AI algorithms: a retrospective simulation study. NPJ Digit Med 2024;7(1):120 [FREE Full text] [doi: 10.1038/s41746-024-01085-w] [Medline: 38724581]
39. Guo LL, Pfohl SR, Fries J, Johnson AEW, Posada J, Aftandilian C, et al. Evaluation of domain generalization and adaptation on improving model robustness to temporal dataset shift in clinical medicine. Sci Rep 2022;12(1):2726 [FREE Full text] [doi: 10.1038/s41598-022-06484-1] [Medline: 35177653]

Abbreviations

AI: artificial intelligence
BIDMC: Beth Israel Deaconess Medical Center
DTH: data temporal heatmaps
EHR: electronic health record
FAMD: factorial analysis of mixed data
ICD: International Classification of Diseases
ICD-9: International Classification of Diseases, Ninth Revision
ICD-10: International Statistical Classification of Diseases, Tenth Revision
IGT: Information Geometric Temporal
KDE: kernel density estimation
MIMIC-IV: Medical Information Mart for Intensive Care-IV
ML: machine learning
ROC-AUC: receiver operating characteristic area under the curve

XSL•FO
RenderX

UMAP: Uniform Manifold Approximation and Projection

Edited by A Sen; submitted 30.05.25; peer-reviewed by B Bhasuran, S Sivarajkumar; comments to author 19.07.25; revised version received 10.09.25; accepted 18.10.25; published 03.12.25.

Please cite as:
Fernández-Narro D, Ferri P, Gutiérrez-Sacristán A, García-Gómez JM, Sáez C
Unsupervised Characterization of Temporal Dataset Shifts as an Early Indicator of AI Performance Variations: Evaluation Study Using the Medical Information Mart for Intensive Care-IV Dataset
JMIR Med Inform 2025;13:e78309
URL: https://medinform.jmir.org/2025/1/e78309
doi:10.2196/78309
PMID:

©David Fernández-Narro, Pablo Ferri, Alba Gutiérrez-Sacristán, Juan M García-Gómez, Carlos Sáez. Originally published in JMIR Medical Informatics (https://medinform.jmir.org), 03.12.2025. This is an open-access article distributed under the terms of the Creative Commons Attribution License (https://creativecommons.org/licenses/by/4.0/), which permits unrestricted use, distribution, and reproduction in any medium, provided the original work, first published in JMIR Medical Informatics, is properly cited. The complete bibliographic information, a link to the original publication on https://medinform.jmir.org/, as well as this copyright and license information must be included.

XSL•FO
RenderX

Original Paper

Automated Speech Analysis for Screening and Monitoring Bipolar Depression: Machine Learning Model Development and Interpretation Study

Sooyeon Min[1*], MSc, MD, PhD; Tae-Sung Yeum[2*], MD; Daun Shin[3], MD, PhD; Sang Jin Rhee[1], MD, PhD; Hyunju Lee[1], MD, PhD; Han-Sung Lee[1], MD; Seongmin Park[4], MSc; Jihwa Lee[4], MSc; Yong Min Ahn[1,2], MD, PhD

[1]Department of Neuropsychiatry, Seoul National University Hospital, Seoul, Republic of Korea

[2]Department of Psychiatry and Behavioral Science, College of Medicine, Seoul National University, Seoul, Republic of Korea

[3]Department of Psychiatry, Korea University Medical Center, Seoul, Republic of Korea

[4]ActionPower Corp., Seoul, Republic of Korea

[*]these authors contributed equally

Corresponding Author:
Yong Min Ahn, MD, PhD
Department of Psychiatry and Behavioral Science
College of Medicine
Seoul National University
103 Daehak-ro, Jongno-gu
Seoul
Republic of Korea
Phone: 82 2 740 8114
Email: aym@snu.ac.kr

Abstract

Background: Depressive episodes in bipolar disorder are frequent, prolonged, and contribute substantially to functional impairment and reduced quality of life. Therefore, early and objective detection of bipolar depression is critical for timely intervention and improved outcomes. Multimodal speech analyses hold promise for capturing psychomotor, cognitive, and affective changes associated with bipolar depression.

Objective: This study aims to develop between- and within-person classifiers to screen for bipolar depression and monitor longitudinal changes to detect depressive recurrence in patients with bipolar disorder. A secondary objective was to compare the predictive performance across speech modalities.

Methods: We collected 304 voice audio recordings obtained during semistructured interviews with 92 patients diagnosed with bipolar disorder over a 1-year period. Depression severity was assessed using the Hamilton Depression Rating Scale. Acoustic features were extracted using the openSMILE toolkit, and linguistic features were extracted using the Linguistic Inquiry and Word Count frameworks following automatic speech recognition and machine translation. Mixed-effects multivariate linear regression evaluated the associations between speech markers and Hamilton Depression Rating Scale scores adjusting for demographic variables, diagnosis, and feature-specific covariates. Extreme gradient boosting and light gradient boosting were used as base learners. We developed a between-person classifier to detect moderate to severe depression and a within-person classifier to detect recurrence. Hyperparameter tuning and 95% CI estimation were performed using a bootstrap bias-corrected cross-validation (k=5) approach combined with a grid search. Feature contributions were interpreted using Shapley additive explanations.

Results: Patients with depression showed reduced energy modulation, prolonged monotony, and more frequent use of words related to death and negative emotions. The between-person classifier combining acoustic and linguistic features detected moderate to severe depression with an area under the curve of 0.76 compared to 0.54 for the demographic model. The within-person classifier based on speech features detected depression recurrence with an area under the curve of 0.70 compared to 0.55 for the demographic model.

Conclusions: Between- and within-person comparisons of speech markers can be leveraged in detecting and monitoring bipolar depression. We demonstrate the feasibility of applying Linguistic Inquiry and Word Count–based psycholinguistic analysis to

XSL•FO
RenderX

machine–transcribed and translated speech, supporting the replicability of this approach across languages. Automated multimodal voice analysis can be integrated into digital health platforms, providing a scalable and effective approach for accessing mental health monitoring and care.

(JMIR Med Inform 2025;13:e79093) doi:10.2196/79093

KEYWORDS

depression; voice analysis; speech modalities; bipolar disorder; artificial intelligence; AI; natural language processing

Introduction

Depression affects more than 280 million individuals worldwide and is a leading contributor to the global burden of disease [1,2]. As diagnosis relies entirely on symptomatology without the support of laboratory tests or imaging, clinicians must depend on subjective evaluations of patients' reported experiences and observable behaviors [3], which poses challenges for accurate and timely diagnosis.

Clinicians have long observed speech changes in depression, such as reduced pitch variation, slower speech rate, and diminished output [4,5]. Speech has acoustic features (eg, lower pitch and narrower pitch range) [5,6], which may reflect psychomotor or autonomic alterations, and linguistic features (eg, increased use of first-person singular pronouns and negative-sentiment words) [7], which may reflect cognitive and affective disturbances. Voice data offer several advantages: they are noninvasive, low cost, and suitable for repeated assessments even in remote or resource-limited settings. Furthermore, voice is also sensitive to within-person mood fluctuations, making it well suited for longitudinal monitoring [8]. Recent advances have increased sophistication in voice-based depression detection, with growing adoption of multimodal approaches [9-11] and application of deep learning–based models [12].

A recent systematic review highlighted the promising potential of voice markers in the detection of depression [13], reporting classification performance with an area under the receiver operating characteristic curve (AUC) ranging from 0.71 to 0.93. However, substantial methodological heterogeneity was identified across the studies, including patient selection and diagnosis based on clinician- or self-rated symptom scales. Many studies have not validated models using cross-validation or an independent test set. Some studies have explored changes in speech patterns associated with changes in depression severity [14] or clinical outcomes after treatment [15-17], but they are limited in modality—primarily acoustic—and duration, typically involving 4 to 6 weeks of follow-up. To the best of our knowledge, no previous study has systematically compared the cross-sectional and longitudinal performance of acoustic and linguistic speech markers in a clinically diagnosed sample and assessed their utility for ongoing symptom monitoring in real-world practice.

While much of this research has focused on major depressive disorder (MDD), depressive episodes are also the predominant and most debilitating feature of bipolar disorder. Although bipolar disorder is defined by the presence of manic or hypomanic episodes, longitudinal studies have consistently shown that patients spend most of their illness course in depressive states rather than manic or hypomanic phases [18-20]. These depressive episodes are frequent and prolonged and contribute disproportionately to functional impairment, suicide risk, and reduced quality of life. Accordingly, developing objective methods for detecting and monitoring bipolar depression is of high clinical importance.

In this prospective study, we collected voice recordings from 92 individuals with a psychiatrist-confirmed diagnosis of bipolar disorder over a 1-year period. The main objective of this study was to develop machine learning–based classification models for detecting and monitoring bipolar depression using voice recordings. A between-person classifier that compared the severity of depression between individual recordings and a within-person classifier that compared changes in severity within the same individual were developed. The secondary objective was to compare the acoustic, linguistic, and combined speech features to detect and monitor depressive symptoms.

Methods

Study Participants and Clinical Assessments

Adult patients (aged ≥19 years) diagnosed with bipolar disorder (type 1, type 2, and not otherwise specified) attending the Mood and Anxiety Clinic at Seoul National University Hospital were recruited through convenience sampling. Board-certified psychiatrists confirmed the psychiatric diagnoses. The exclusion criteria included major psychiatric disorders other than bipolar disorder, laryngeal conditions or surgeries that could impair voice production, and psychiatric symptoms attributable to organic brain diseases or previous intracranial surgery.

Clinical evaluations were conducted at baseline and repeated at 2, 4, 8, and 12 months. Demographic and clinical data, including age, sex, height, weight, comorbidities, and prescribed medications, were collected at baseline, and changes were tracked at each follow-up visit. Cumulative antipsychotic dosages were standardized to the equivalent dose of aripiprazole [21,22], which was the predominant antipsychotic prescribed in the study sample. Depressive symptom severity was assessed using the Korean adaptation of the 17-item Hamilton Depression Rating Scale (HAM-D) [23,24], administered by trained raters. Each HAM-D item is scored from 0 (not present) to 4 (severe), yielding total scores ranging from 0 to 68. Standard clinical cutoffs classify scores of ≤7 as minimal depression, scores of 8 to 16 as mild depression, scores of 17 to 23 as moderate depression, and scores of ≥24 as severe depression [25]. The patients also self-rated suicidality, depression, and anxiety symptoms using the Korean version of the Beck Scale for Suicide Ideation, Patient Health Questionnaire-9 items, and

XSL•FO
RenderX

Beck Anxiety Inventory. A more detailed study protocol has been published previously [22].

Preprocessing of Voice Data and Speech Feature Extraction

Study participants' voices were recorded during semistructured psychiatric interviews conducted by 1 of the 2 research nurses using a Sony ICD-SX813 voice recorder in a standardized interview room setting [22]. While interview structure ensured consistency across participants, interviewers were encouraged to use open-ended prompts. Segments with the interviewer's voice, overlapping speech or background noise, and utterances shorter than 3 seconds were excluded. Audio files were transcribed using the Daglo application programming interface (ActionPower Corp), a conformer-based automatic speech recognition engine [26-28] recognized for its superior accuracy in Korean speech recognition tasks. We manually reviewed 2% of the automatically generated transcripts and compared them to their corresponding audio recordings to verify transcription accuracy and calculate the character error rate (CER). CER quantifies transcription errors as the percentage of incorrectly transcribed characters (including substitutions, deletions, and insertions) normalized by the total character count [29].

The acoustic features were extracted using the INTERSPEECH 2016 Computational Paralinguistics Challenge (ComParE 2016) feature set, the largest available set in the openSMILE toolkit (audEERING GmbH) [30-32], which is widely used for depression detection because of its well-documented and standardized feature extraction process [31,33-35]. A total of 6373 features were extracted per recording, covering functionals derived from low-level descriptors such as pitch (F0), loudness, mel-frequency cepstral coefficients, jitter, shimmer, and spectral features.

Linguistic features were extracted using a Linguistic Inquiry and Word Count (LIWC) framework (Pennebaker Conglomerates, Inc). The LIWC framework calculates the frequency of words within psychologically relevant categories serving as proxies for various social, cognitive, and affective processes. It is one of the most widely used psycholinguistic dictionaries in natural language processing tasks [36,37]. For this analysis, we used the LIWC and the LIWC Extension framework (Receptiviti) [38]. As the Korean LIWC library was unavailable at the time of our study, we machine translated texts using the DeepL application programming interface (DeepL SE) from Korean to English and then assigned words to categories using the LIWC frameworks in English [39,40]. LIWC scores range between 0 and 1 and denote the proportion of words in a specific category relative to the total word count in the text.

Statistical Analyses and Development of Machine Learning Classifiers

Given the repeated-measurement structure, we applied mixed-effects multivariate linear regression models to identify the speech features associated with the HAM-D score after applying an inverse normal transformation. Features that were constant across all recordings (such as the "parentheses" LIWC category) were excluded from analysis. Covariates included age, sex, BMI, diagnosis, and antipsychotic dosage for acoustic feature analysis and age, sex, years of education, and diagnosis for linguistic analysis. The significance level was set at $P<.05$, and the Benjamini-Hochberg test was conducted to correct for multiple hypotheses. All statistical analyses were conducted using R (version 4.1.0; R Foundation for Statistical Computing).

All acoustic and linguistic features were used for classifier development. Decision tree classifiers were selected for their robustness and established performance in previous studies [22,41,42]. We used extreme gradient boosting (XGB) and light gradient boosting (LGB) as the base learner algorithms. XGB and LGB are both gradient boosting frameworks. LGB is noted for its computational efficiency, whereas XGB is renowned for its fast convergence speed.

To address class imbalance at both the data and algorithmic levels, we combined the synthetic minority oversampling technique (SMOTE) with the focal loss function. SMOTE was applied exclusively to the training set within each cross-validation fold to generate synthetic samples of the minority class while preventing data leakage. In parallel, focal loss was implemented in both the LGB and XGB models to further mitigate imbalance during model optimization. The α parameter of focal loss was automatically calculated based on class ratios to balance positive and negative samples, and the γ parameter was fixed at 2.0 to emphasize harder-to-classify samples.

Hyperparameter tuning and 95% CIs were estimated using a bootstrap bias-corrected cross-validation (BBCV; k=5) approach. BBCV involves nonparametric bootstrapping with 1000 iterations on the out-of-sample predictions from the validation folds combined with a grid search for hyperparameter optimization [43]. BBCV provides unbiased and conservative estimates of model performance, particularly in studies with small sample sizes, and it may outperform alternatives such as nested cross-validation. The model performance was evaluated using the AUC. The accuracy, sensitivity, specificity, and positive predictive value at the optimal threshold defined by the Youden index (sensitivity + specificity − 1) were also reported.

The participants were categorized as having moderate to severe depression if their HAM-D score was ≥17 [25]. The HAM-D is the gold-standard instrument for evaluating antidepressant treatment efficacy, with a ≥50% reduction in score considered a conventional criterion for treatment response [44]. Although there is no established consensus regarding the operational definition of relapse or recurrence in depression, we defined recurrence as a transition from minimal or mild depression (HAM-D<17) to moderate or severe depression (HAM-D≥17) between consecutive visits. In this paper, we use the term *recurrence* to refer to such worsening without formally distinguishing it from *recurrence* as defined in the *Diagnostic and Statistical Manual of Mental Disorders, Fifth Edition* [3]. The following two models were developed: (1) a between-person model to classify patients with moderate to severe depression and (2) a within-person model to detect recurrence since the last visit. All recordings were treated as individual data points with the goal of cross-sectional screening for severe depression.

XSL•FO
RenderX

Within-person models used changes in voice features between time intervals to predict recurrence. Five-fold GroupKFold cross-validation was used to perform cross-validation at the participant level and prevent data leakage. To evaluate multimodal integration, we tested the following five feature sets: (1) age and sex variables only (referred to as "demographic"); (2) acoustic features only (referred to as "acoustic"); (3) linguistic features only (referred to as "linguistic"); (4) acoustic and linguistic features combined (referred to as "speech"); and (5) age, sex, and speech features (referred to as "speech+demographic"). Shapley additive explanation (SHAP) analysis was conducted to interpret feature contributions for each prediction task [45].

Machine learning experiments were conducted on a computing cluster with Intel Xeon Gold 6138 central processing units, NVIDIA RTX A6000 graphics processing units (48-GB video RAM), and 128-GB RAM. Analyses used Python (version 3.9.6; Python Software Foundation) with the scikit-learn (version 1.6.1; Google Summer of Code project), *lightgbm* (version 4.6.0), and *xgboost* (version 3.0.2) packages.

Ethical Considerations

This study was approved by the institutional review board of Seoul National University Hospital (1812-081-995) and conducted in accordance with the ethical standards of the 1964 Declaration of Helsinki and its later amendments. Written informed consent was obtained from all participants during their initial visit, which included information about the study purpose, data use, and the right to withdraw at any time. All audio files were anonymized and securely stored and are not to be used for any purpose beyond the scope of consent. No identifiable information appears in the manuscript or supplementary materials, and participants are not recognizable in any shared data or figures. Participants received approximately US $20 per visit as reimbursement for transportation and time in line with standard research practices.

All participants in our study were receiving ongoing care at our outpatient psychiatric clinic throughout the study period, ensuring continuous clinical monitoring and appropriate treatment independent of the research protocol. Given that bipolar disorder is associated with high suicide risk [46], the research nurses were instructed to immediately notify the attending psychiatrist if a participant appeared to be at high risk during the interview.

Results

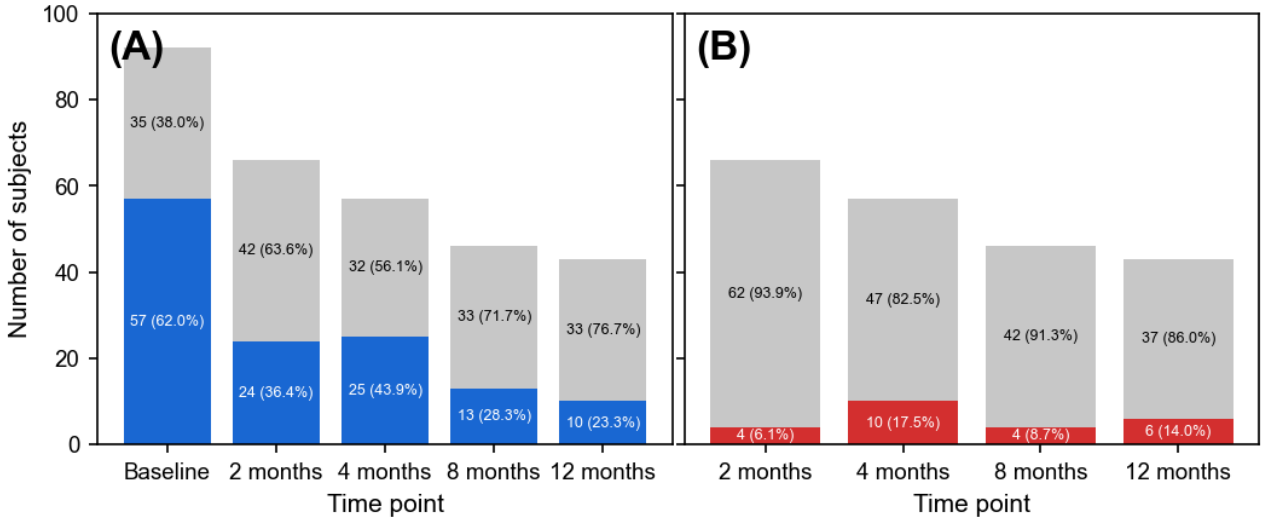
Study Participants and Speech Recordings

Participants (N=92; 70/92, 76% female) were outpatients visiting the Mood and Anxiety Clinic at Seoul National University Hospital for mild to severe depressive symptoms. After the baseline interview, 72% (66/92) of the participants attended the 2-month follow-up, 62% (57/92) attended at 4 months, 50% (46/92) attended 8 months, and 47% (43/92) attended at 12 months. In total, we collected 304 recordings, and the study participants collectively spoke for approximately 55 hours (197,081 seconds) and said 323,280 words. The average length of the concatenated patients' voice segments at each interview session was 648.69 (SD 486.4) seconds and included 1063 (SD 833.5) words. The average sentence was 15.91 (SD 5.9) words. When manually reviewing 2% of the randomly selected machine-generated transcripts against their corresponding audio recordings, we identified a CER below 1% (range 0.02%-1.08%). There was no significant correlation between CER and HAM-D scores (r=0.10; P=.83). In total, 6373 acoustic features and 105 linguistic features were extracted.

At baseline, 62% (57/92) of the participants had moderate to severe depression. A total of 36% (24/66) at 2 months, 44% (25/57) at 4 months, 28% (13/46) at 8 months, and 23% (10/43) at 12 months were moderately to severely depressed (Figure 1A). At baseline, there were no statistically significant differences in sex (P=.54), BMI (P=.84), psychiatric diagnosis (P=.54), socioeconomic status (P=.64), years of education (P=.61), antipsychotic dosage (P=.40), and medical comorbidities (P=.20) between patients with bipolar disorder with moderate to severe depression and their counterparts with minimal to mild depression (Table 1). Patients with more severe depressive symptoms had greater self-reported depressive, anxiety, and suicidal symptoms (P<.001 in all cases). At baseline, 89% (82/92) of the participants were prescribed antipsychotics; 94% (86/92) were prescribed mood stabilizers; 30% (28/92) were prescribed antidepressants; 67% (62/92) were prescribed benzodiazepines; and 46% (42/92) were prescribed other medications, such as propranolol and benztropine. The type and dosage of medications were modified by the attending psychiatrist at each visit. Of the 92 participants, 14 (15%) completed only 1 visit, 13 (14%) completed 2 visits, 22 (24%) completed 3 visits, 17 (19%) completed 4 visits, and 26 (28%) completed all 5 visits. In 11.3% (24/212) of cases, participants had recurrence at follow-up (Figure 1B).

XSL•FO
RenderX

Figure 1. Distribution of depression severity and change in depressive symptoms over time. (A) The blue bars represent participants with moderate to severe depression, whereas the gray bars represent participants with minimal to mild depression. (B) The red bars represent participants who had recurrence, and the gray bars represent those whose symptoms remained the same or improved since their last visit.



XSL•FO
RenderX

Table 1. Baseline characteristics of the groups with moderate to severe depression and minimal to mild depression.

Characteristic	Moderate to severe depression (n=57)	Minimal to mild depression (n=35)	*P* value
Age (y), mean (SD)	29.28 (9.53)	31.97 (12.45)	.25
Sex, n (%)			.54
Male	11 (19)	10 (29)	
Female	46 (81)	25 (71)	
BMI (kg/m^2), mean (SD)	24.63 (4.99)	24.85 (4.95)	.84
Diagnosis, n (%)			.54
Bipolar disorder type 1	8 (14)	6 (17)	
Bipolar disorder type 2	39 (68)	26 (74)	
Bipolar disorder NOS[a]	10 (18)	3 (9)	
Marital status, n (%)			.69
Single	43 (75)	27 (77)	
Married	12 (21)	7 (20)	
Divorced or widowed	2 (4)	1 (3)	
Household income (KRW), median (IQR)	2,300,000 (1,978,147-5,000,000)[b]	2,272,500 (2,036,911-5,000,000)[c]	.92
SES[d], n (%)			.64
Very low	1 (2)	2 (6)	
Low	10 (18)	7 (20)	
Middle	31 (54)	15 (43)	
High	8 (14)	4 (11)	
Very high	7 (12)	7 (20)	
Years of education, mean (SD)	13.89 (2.14)	14.14 (2.21)	.61
Antipsychotic dosage (mg)[e], median (IQR)	7.50 (5-15)	5.00 (2.25-12.7)	.40
Medical comorbidity, n (%)			.20
None	43 (75)	28 (80)	
Mild	10 (18)	3 (9)	
Moderate	2 (4)	4 (11)	
Severe	2 (4)	0 (0)	
History of suicide attempts, n (%)	10 (18)	3 (9)	.36
HAM-D[f] score (range 0-68), mean (SD)	20.63 (2.21)	12.97 (2.92)	<.001
SSI[g] score (range 0-38), mean (SD)	22.17 (8.01)	13.06 (8.01)	<.001
PHQ-9[h] score (range 0-27), mean (SD)	18.39 (5.01)	12.68 (6.17)	<.001
BAI[i] score (range 0-63), mean (SD)	28.89 (15.11)	17.40 (14.39)	<.001

[a]NOS: not otherwise specified.

[b]US $1769 (US $1522-$3846).

[c]US $1748 (US $1567-$3846).

[d]SES: socioeconomic status; based on the Hollingshead-Redlich index.

[e]Antipsychotic dosage converted into the equivalent dose of aripiprazole.

[f]HAM-D: Hamilton Depression Rating Scale.

[g]SSI: Beck Scale for Suicide Ideation.

[h]PHQ-9: Patient Health Questionnaire-9 items.

[i]BAI: Beck Anxiety Inventory.

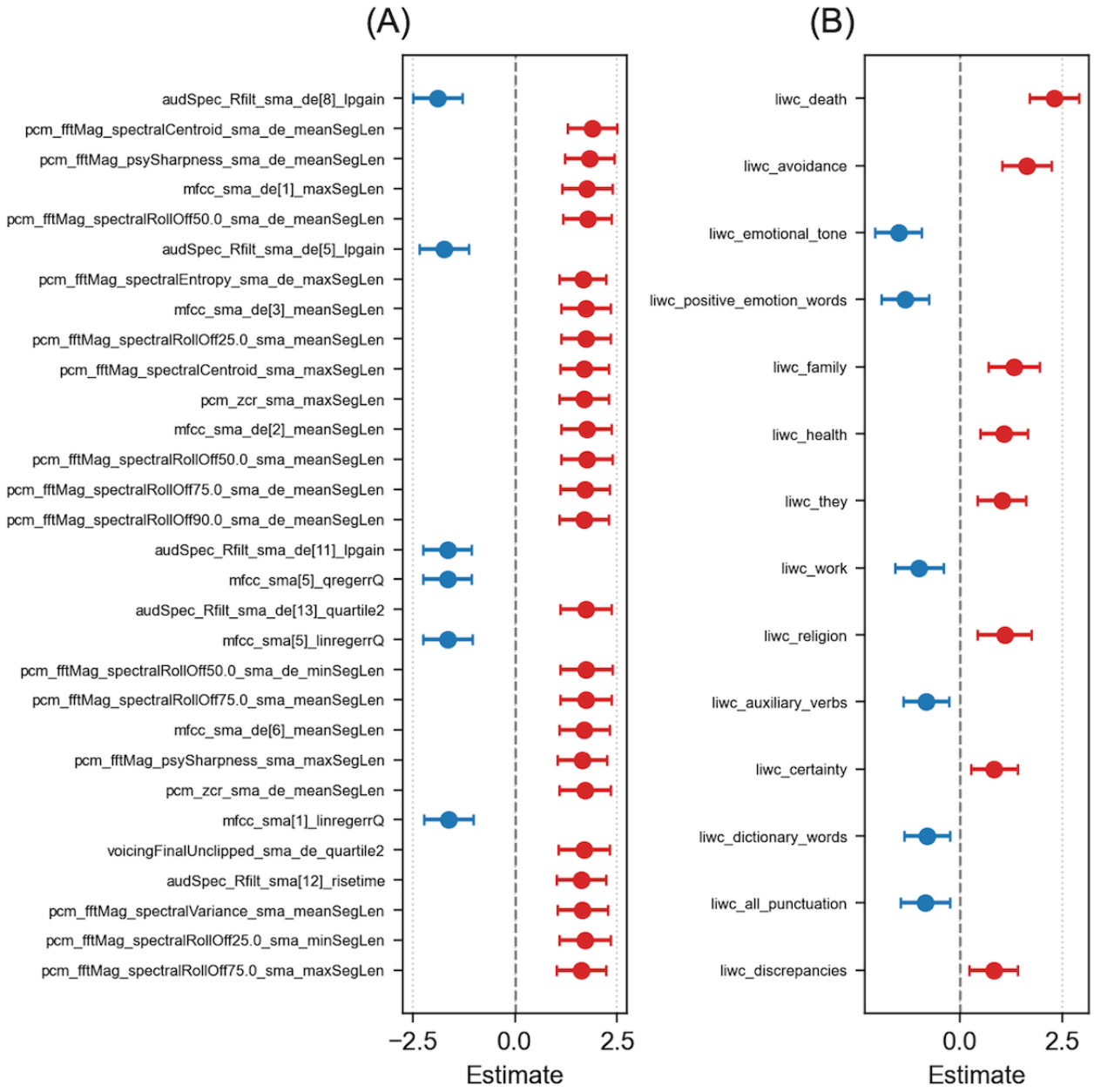
XSL•FO
RenderX

Acoustic and Linguistic Features Associated With Depression Severity

After adjusting for age, sex, BMI, and antipsychotic dosage and correcting for multiple testing, 1709 acoustic features were significantly associated with depression severity. The 5 most strongly associated acoustic features were audSpec_Rfilt_sma_de(8)_lpgain (linear prediction gain computed from the delta (first derivative) of the smoothed 8th RASTA-filtered auditory spectral band; β=−1.89; SE 0.31; Benjamini-Hochberg adjusted $P<.001$), pcm_fftMag_spectralCentroid_sma_de_meanSegLen (mean segment length of the time-derivative (delta) of the smoothed spectral centroid computed from the FFT-magnitude spectrum of the PCM signal; β=1.89, SE 0.31; adjusted $P<.001$), pcm_fftMag_psySharpness_sma_de_meanSegLen (mean segment length of the time-derivative (delta) of the smoothed psychoacoustic sharpness computed from the FFT-magnitude spectrum of the PCM signal; β=1.819, SE 0.31; adjusted $P<.001$), mfcc_sma_de(1)_maxSegLen (maximum segment length of the time-derivative (delta) of the smoothed first MFCC coefficient; β=1.765, SE 0.31; adjusted $P<.001$), and pcm_fftMag_spectralRollOff50.0_sma_de_meanSegLen (mean segment length of the time-derivative (delta) of the smoothed 50% spectral roll-off computed from the FFT-magnitude spectrum of the PCM signal; β=1.77, SE 0.30; adjusted $P<.001$; Multimedia Appendix 1). Participants with greater depression severity exhibited a reduced gain in relative spectral transform–filtered bands, which is related to speech clarity. The spectral centroid reflects the brightness of sound, whereas spectral roll-off measures the frequency below which 50% of the spectral energy is concentrated. Psychoacoustic sharpness captures the perceived clarity or harshness of the sound. Increased segment lengths in their temporal derivatives suggest prolonged periods of relatively unchanging frequency distribution, energy concentration, and perceptual sharpness (Figure 2A) [31].

XSL•FO
RenderX

Figure 2. Forest plots displaying the results (β estimate) of mixed-effects multivariate linear regression between depression severity and (A) acoustic and (B) linguistic features. Only 30 acoustic features with the lowest *P* values are depicted for brevity. Red represents a positive association, whereas blue represents a negative association.



After adjusting for age, sex, and years of education, 14 linguistic features were significantly associated with depression severity. The top 5 psycholinguistic categories associated with depression severity were "death" (β=2.307; SE 0.31; adjusted *P*<.001), "avoidance" (β=1.641; SE 0.30; adjusted *P*<.001), "emotional tone" (β=−1.50; SE 0.29; adjusted *P*<.001), "positive emotion" (β=−1.356; SE 0.30; adjusted *P*<.001), and "family" (β=1.32; SE 0.32; adjusted *P*<.001; Multimedia Appendix 2). Participants with depression more frequently used words related to death, avoidance, family, health, religion, negative emotions, and discrepancies and less frequently used words related to positive emotions and reward than their counterparts with minimal to mild depression (Figure 2B).

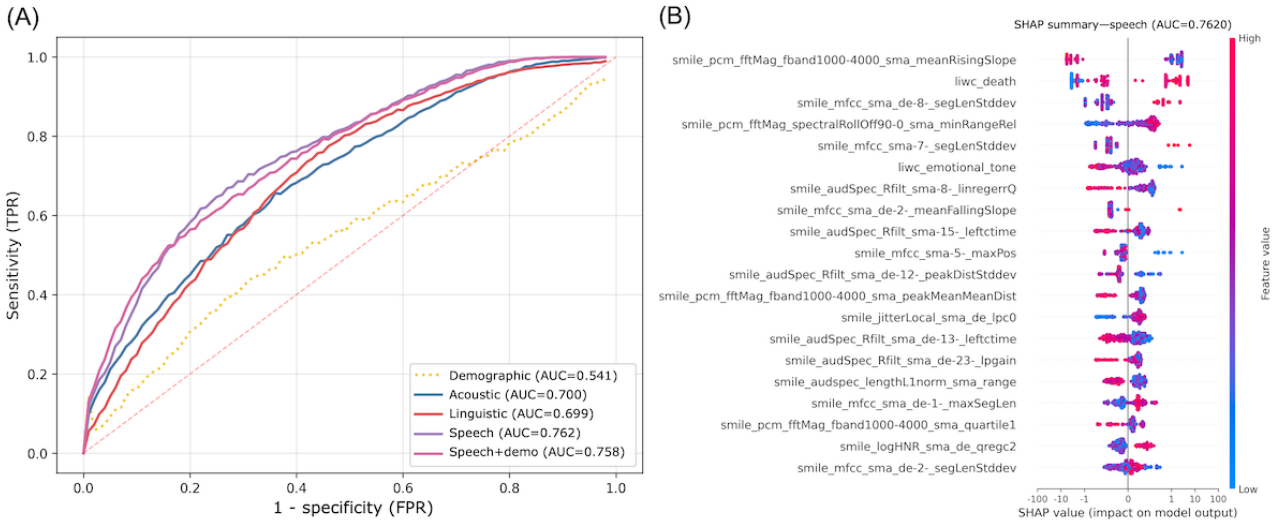
Machine Learning Classification

Between-Person Classifier

Of 304 audio recordings, 129 (42.4%) were from patients with moderate to severe depression. Overall, LGB outperformed XGB. The best-performing classifier was the speech model (mean AUC 0.762, SD 0.002), followed by the speech+demographic model (mean AUC 0.758, SD 0.002). At the cutoff determined by the Youden index (0.30), the speech model achieved 72.5% sensitivity, 67.4% specificity, 69.6% accuracy, and a positive predictive value of 62%. Both acoustic and linguistic models outperformed the demographic model (AUC=0.700 and 0.699, respectively, vs AUC=0.541; Figure 3A).

XSL•FO
RenderX

Figure 3. Between-person classification models for detecting moderate to severe depression: (A) receiver operating characteristic curves for light gradient boosting models (yellow line: demographic model [age and sex]; blue line: acoustic model; green line: linguistic model; purple line: speech model [acoustic+linguistic]; pink line: speech+demographic model) and (B) Shapley additive explanation (SHAP) summary plot for feature contributions for the best-performing model. AUC: area under the receiver operating characteristic curve; FPR: false positive rate; TPR: true positive rate.

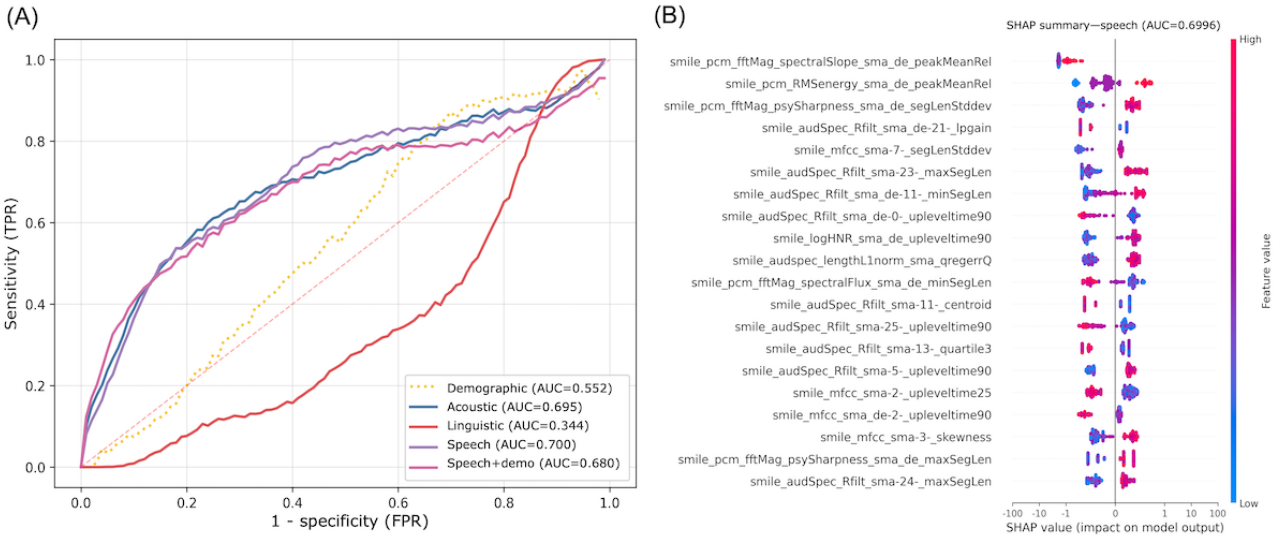


SHAP analysis indicated that both acoustic and linguistic features contributed meaningfully to the inference of bipolar depression. Among linguistic features, a higher frequency of words related to death and lower emotional tone were associated with an increased likelihood of a positive (depressive) prediction. Acoustic predictors such as reduced variation in spectral slope and temporal instability increased the likelihood of a positive prediction (Figure 3B). To verify that the predictive importance of the LIWC "death" category was not driven by a small number of extreme cases, we examined its distribution (mean 0.00238, SD 0.00282). After excluding the recordings that exceeded the 3 SD cutoff (>0.01084; z=+3.04 to +5.55), the between-person model performance remained comparable or slightly improved (linguistic AUC=0.678 vs 0.699 before exclusion; acoustic AUC=0.781 vs 0.700; speech AUC=0.800 vs 0.762). These results confirm that the association between the "death" category and depression severity was not driven by outlier effects.

Within-Person Classifier for Predicting Recurrence

The change in features from 212 paired audio recordings from consecutive visits was used, among which 24 (11.3%) follow-ups corresponded to recurrence events. XGB outperformed LGB. The best performance was achieved by the speech model, with a mean AUC of 0.700 (SD 0.003), accuracy of 80.6%, sensitivity of 49.3%, and specificity of 84.6% at the optimal cutoff of 0.10. The acoustic model achieved a comparable performance, with an AUC of 0.695 and accuracy of 0.835 (Figure 4). All performance metrics can be found in Multimedia Appendix 3.

Figure 4. Within-person classification models for detecting recurrence: (A) receiver operating characteristic curves for extreme gradient boosting models (yellow line: demographic model [age and sex]; blue line: acoustic model; green line: linguistic model; purple line: speech model [acoustic+linguistic]; pink line: speech+demographic model) and (B) Shapley additive explanation (SHAP) summary plot for feature contributions for the best-performing model. AUC: area under the receiver operating characteristic curve; FPR: false positive rate; TPR: true positive rate.



XSL•FO
RenderX

SHAP analysis of the speech model suggests that the model relied primarily on acoustic features of reduced vocal energy, prosodic flattening, and articulatory slowing to infer depressive recurrence in bipolar disorder.

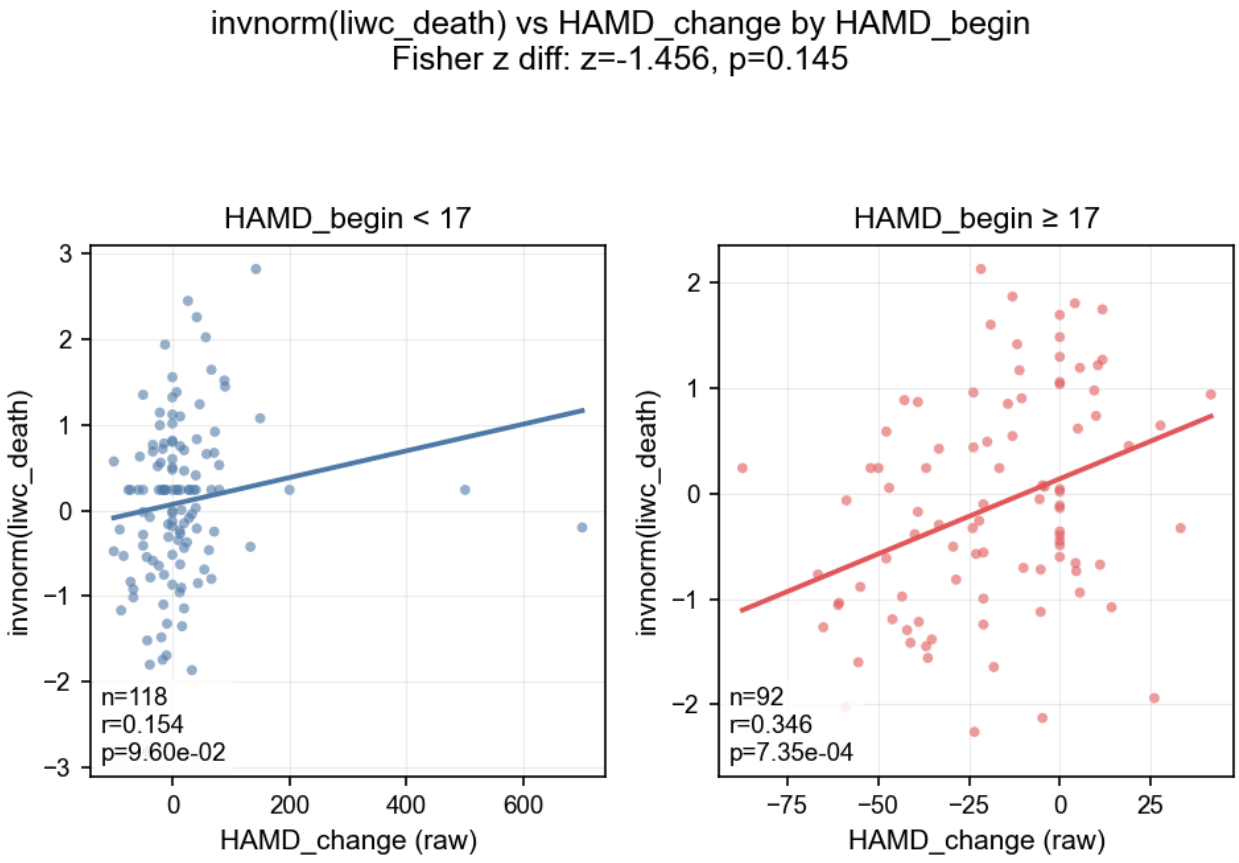
Discussion

Principal Findings

In this prospective longitudinal study of individuals with bipolar disorder, we demonstrated that both the acoustic and linguistic features of voice are strongly associated with depression severity and can be leveraged to accurately detect and monitor depressive states. In both between- and within-person analyses, models combining acoustic and linguistic speech features achieved the highest performance for identifying moderate to severe depression and predicting recurrence. In the between-person analysis, single-modality models using either acoustic or linguistic features outperformed the demographic-only (null) model, whereas in the within-person analysis, only the acoustic model showed superior performance over the null model. Incorporating demographic variables did not improve model performance in either task.

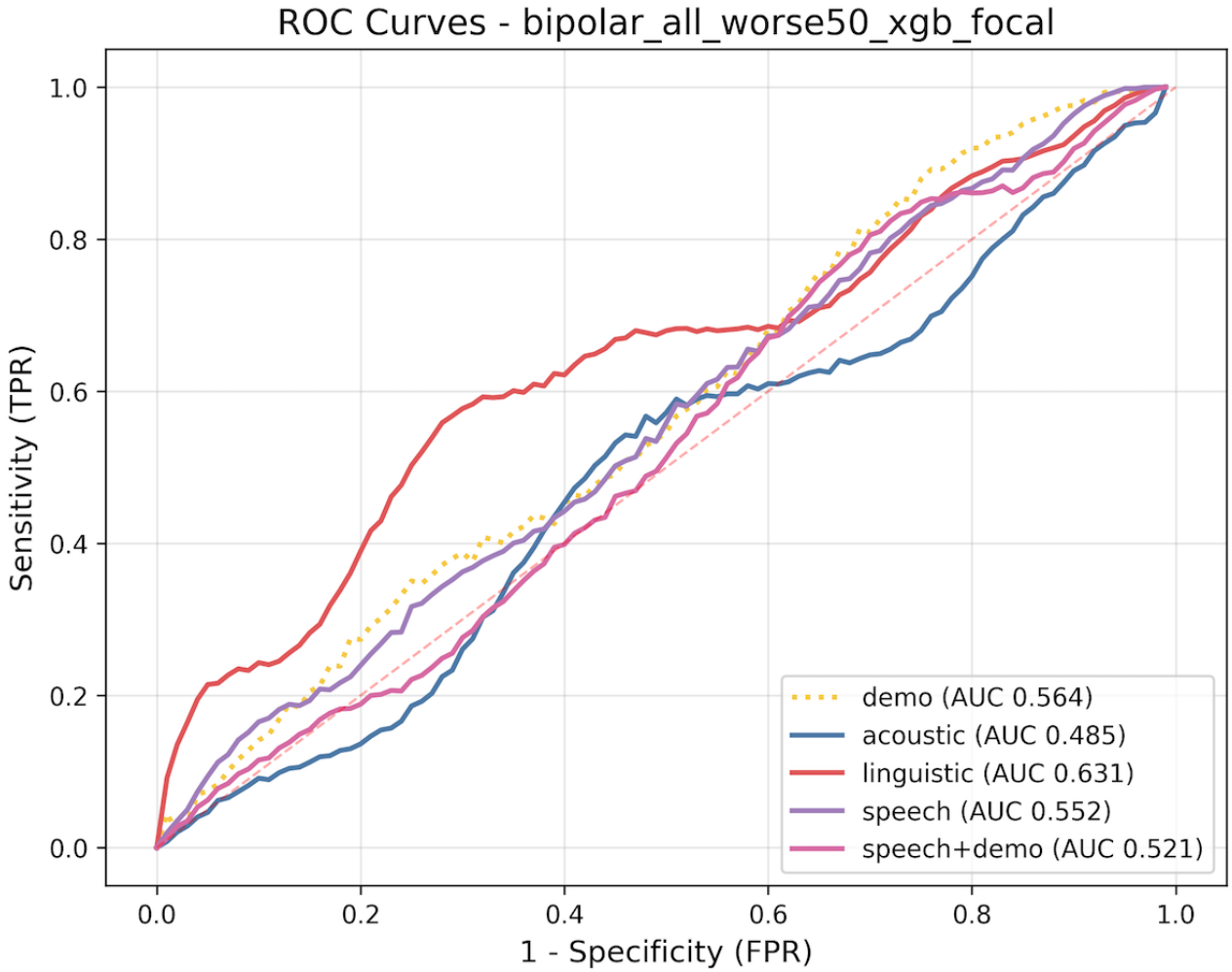
The within-person models did not outperform the between-person models. A major challenge was the substantial class imbalance, with recurrence occurring in only 11.3% (24/212) of follow-up visits. We addressed this by applying SMOTE to the training set within each cross-validation fold. Because participants who completed more visits contributed more paired samples to model training, these individuals may have exerted a greater influence on model learning. If attrition was nonrandom—if participants with sudden worsening were more likely to drop out—the within-person models may have been biased toward patterns characteristic of participants with better clinical course. We further examined the unexpected negative finding of the linguistic-only model. Changes in linguistic content were more pronounced among participants already in a severe depressive state where suicidal ideation and negative appraisals were more likely. For instance, the correlation between changes in death-related word use and HAM-D score change was stronger in those with a baseline HAM-D score of ≥17 than in those below the threshold (r=0.346 vs 0.154; Figure 5). Therefore, in many cases, the model would have predicted that greater increases in HAM-D scores were associated with worsening mood, yet these instances were labeled as negative because recurrence was defined as crossing the threshold from HAM-D<17 to ≥17. When recurrence was defined as a ≥50% increase in HAM-D score, thereby including the cases showing further worsening within the range of HAM-D≥17, the linguistic model's performance improved (AUC=0.631; Figure 6), supporting our hypothesis.

Figure 5. Correlation between changes in the Linguistic Inquiry and Word Count "death" category and changes in depression severity (Hamilton Depression Rating Scale) stratified by baseline severity. HAM-D: Hamilton Depression Rating Scale.



XSL•FO
RenderX

Figure 6. Receiver operating characteristic curves for the within-person classification models predicting recurrence defined as a ≥50% increase in Hamilton Depression Rating Scale score. The yellow line represents the demographic model (age and sex), the blue line represents the acoustic model, the green line represents the linguistic model, the purple line represents the speech model (acoustic+linguistic features), and the pink line represents the speech+demographic model. AUC: area under the receiver operating characteristic curve; FPR: false positive rate; ROC: receiver operating characteristic curve; TPR: true positive rate.



Among the most important acoustic markers distinguishing depressed speech, we identified a reduced gain in the relative spectral transform–filtered spectral bands and longer continuous segments exhibiting changes in the spectral centroid, roll-off, and sharpness. These findings suggest that individuals with more severe depression display greater temporal monotony in the key spectral properties of their speech, which is consistent with the clinical observation of monotonous or less modulated vocal output in depression [5,8]. Numerous studies and meta-analyses have highlighted pitch-related features as one of the most robust acoustic markers of depression [5,6,8,15]. Changes in the fundamental frequency (F0), including reductions in mean pitch, pitch range, and pitch variability, have consistently been reported as characteristics of depressed speech. In our analysis, various pitch-related features were significantly associated with depression severity (Multimedia Appendix 1). Several metrics reflecting the temporal variability, range, and distributional characteristics of pitch change (ΔF0) were strongly associated with higher HAM-D scores.

Linguistically, individuals with depression used words related to death, avoidance, family, health, religion, negative emotions, and discrepancies more frequently, whereas positive emotions and reward-related words were less common. These linguistic features reflect the cognitive and affective themes of depressive states. Our findings closely align with meta-analytic results showing that depression is associated with increased use of negative emotion words and decreased use of positive emotion words [7]. Notably, although previous studies have highlighted increased first-person singular pronoun use as a linguistic marker of depression, no significant association between the use of first-person singular pronouns and depression severity was observed in our analysis. One explanation is that our study sample consisted of patients already diagnosed with bipolar disorder, which may have attenuated the discriminatory power of this marker. Additionally, the Korean language is known as one of the “pro-drop languages,” where pronouns are often omitted within sentences, especially when the subject, such as “I,” remains unchanged throughout the discourse [47]. Increased use of words related to death and health may reflect suicidal and somatic symptoms in patients with depression, whereas increased use of words related to avoidance and discrepancies and decreased use of reward-related words may reflect cognitive changes.

XSL•FO
RenderX

Comparisons to Prior Work

While similar designs have demonstrated the potential for applying LIWC to automatically transcribed speech, this study implemented LIWC-based psycholinguistic analysis on automatically transcribed and machine-translated speech derived from psychiatric patient interviews. Previous research has applied LIWC to manually transcribed psychiatric interviews [36,48] or examined its use in artificial intelligence–generated transcripts in nonclinical populations [49]. However, none have used a fully automated pipeline combining both automatic speech recognition and machine translation in psychiatric populations. By advancing this methodology, our findings highlight the feasibility of scalable, cross-linguistic, multimodal speech-based digital biomarkers for depression.

Our study also included age, sex, antipsychotic dosage, and years of education as covariates in speech analysis. Previously, we have reported how antipsychotic medication can act as a confounder when analyzing changes in voice features associated with psychiatric symptoms, especially when drug-naïve individuals were used as controls [22,50]. Clinicians commonly prescribe or increase the dosage of antipsychotics when psychiatric symptoms worsen. Studies have reported that atypical antipsychotics affect vocal pitch and spectral features in a dose-dependent manner [50,51]. Years of education and speech content are also strongly associated with each other; individuals with fewer years of education produce less lexical and semantic content than those with higher levels of education [52]. Our covariate adjustments strengthened the robustness of our findings regarding the speech characteristics of patients with depression.

We implemented several strategies to mitigate overfitting, including BBCV with patient-level 5-fold cross-validation and 1000 iterations [43]. For linguistic analysis, we used the LIWC framework to quantify changes in the use of different psycholinguistic classes instead of counting the lexicons themselves. We considered the risk of overfitting by using a purely lexical approach, particularly when multiple recordings were collected from each participant. Previous studies have illustrated this limitation: Cohen et al [53] reported “yeah,” “very,” and “at” as top text model features, and Shin et al [54] reported “admission” as the single most important feature for detecting current depression, which is a finding unlikely to be replicated outside the tertiary hospital setting. To further assess the stability of our linguistic predictors, sensitivity analyses excluding recordings with extreme “death”-related word frequencies (>+3 SD) showed that between-person model performance remained comparable or slightly improved. This indicates that, rather than reflecting isolated outliers, the predictive contribution of death-related language represents a consistent and generalizable linguistic marker of depressive severity across participants.

Limitations

This study has several limitations. First, all participants were diagnosed with bipolar disorder, which may limit the generalizability of our findings to other mood disorders. To assess the impact of diagnostic composition, we repeated all analyses after including patients with MDD. Including participants with MDD (44 recordings) did not substantially affect the between-person model performance (speech model AUC=0.751) but reduced the performance of the within-person model (speech model AUC=0.505; Multimedia Appendix 3). This finding suggests that consistent with the clinical distinction between bipolar and unipolar depression, their acoustic and linguistic patterns may diverge more prominently in the context of longitudinal recurrence prediction. The increased class imbalance introduced by including patients with MDD (from 7.83:1 to 8.38:1) may have also hindered classifier learning.

Second, because there is no established consensus on defining recurrence based on HAM-D scores, we adopted an operational definition of recurrence as a change from HAM-D<17 to 17 across 2 consecutive visits. This definition may have missed clinically meaningful fluctuations within the same severity range (eg, from 1 to 16 or from 17 to 24). We also tested an alternative definition of recurrence as a ≥50% increase in HAM-D scores; however, this approach did not improve classification performance (speech model AUC=0.552). Interestingly, the linguistic model was better trained at predicting 50% increase (AUC=0.631) than at predicting recurrence based on threshold crossing (AUC=0.344). This suggests that linguistic changes may be more sensitive to relative shifts in symptom severity than to categorical transitions in depression status.

Third, all interviews were conducted in a controlled environment, which may not reflect the variability in speech quality, background noise, or recording conditions encountered in real-world settings such as telemedicine or mobile apps.

Fourth, although participants were regularly followed up on in outpatient clinics and received appropriate care, we did not collect objective measures of hypomanic or manic symptoms, which may have influenced speech patterns.

Fifth, although antipsychotic dosage was included as a covariate in acoustic analyses, other psychotropic medications were not. Benzodiazepines can theoretically affect voice due to their muscle relaxation properties [55], and an early study reported that they can influence the modulation of the fundamental frequency of speech [56]. We found no empirical evidence that mood stabilizers affect voice acoustics. Although these medications were not included as covariates due to the limited evidence base, they may nonetheless represent potential confounding factors that warrant consideration in future work.

Sixth, the sample size was relatively small compared with the large number of features used in the classifiers. Nonetheless, a post hoc DeLong test incorporating the observed sample size, label distribution, and AUCs indicated statistical power exceeding 0.95 for feature comparisons against the demographic (null) model. We also applied BBCV to reduce overfitting. However, no independent external validation set was available at the time of our study.

Seventh, the sample was restricted to Korean-speaking individuals, which may constrain cross-cultural and cross-linguistic applicability. Given that acoustic and linguistic markers of depression may vary across languages and cultures, model performance may differ in more diverse populations.

XSL•FO
RenderX

Finally, we did not perform a manual validation of the translation accuracy. Therefore, potential translation bias may have influenced the distribution of specific LIWC categories, and this limitation should be considered when interpreting the linguistic results.

Future Work

Replication in larger, independent samples—including different demographic groups, languages, and clinical settings—will be essential before widespread clinical implementation. While our study demonstrated the feasibility of applying LIWC-based analysis to machine–transcribed and translated speech, the impact of linguistic and cultural nuances on model accuracy can be further explored. Cross-cultural validation studies or fine-tuning of large language models on domain-specific corpora—such as annotated clinical interview transcripts—could enhance the accuracy and contextual relevance of linguistic feature extraction. Future studies should also compare speech-based biomarkers with other digital biomarkers and traditional clinical assessments to establish their relative utility and optimal integration strategies for comprehensive mental health monitoring platforms. Moreover, privacy and data security concerns are paramount when implementing such monitoring platforms in the real world based on biomarkers such as speech as voice can contain sensitive biometric information. With secure data pipelines, ethical governance frameworks, and clear clinical decision support protocols, speech-based mood monitoring can be effectively deployed across a spectrum of digital mental health tools, from virtual care services to AI-driven therapeutic platforms.

Conclusions

Our findings provide evidence that both acoustic and linguistic features of speech serve as digital biomarkers of depression. By leveraging multimodal voice analysis and longitudinal modeling, we demonstrated the feasibility of scalable, automated, and noninvasive monitoring of depressive symptoms in real-world clinical practice. These results provide the groundwork for the future integration of speech-based tools into digital health platforms, offering new opportunities for personalized and continuous mental health care.

Acknowledgments

This study was supported by the Basic Science Research Program of the National Research Foundation of Korea funded by the Ministry of Education (grant NRF-2018R1D1A1A02086027), the Seoul Business Agency (CY140170), and Seoul National University Hospital (032022230). The funders played no role in the study design; data collection, analysis, or interpretation; or writing of the manuscript. The authors would like to thank Editage for editing and reviewing this manuscript for the English language.

Data Availability

The datasets generated or analyzed during this study are not publicly available due to the consent that did not cover public sharing of data, but the processed data are available from the corresponding author on reasonable request. Raw audio recordings could not be made available because of their sensitivity. Both the principal investigator (YMA) and first authors (SM and TY) had complete access to the data and took responsibility for their integrity.

Authors' Contributions

SM and TY conducted the data analysis, prepared the figures and tables, and drafted the manuscript. SP and JL contributed to machine learning. SM, DS, HL, HSL, SJR, and YMA contributed to the conceptualization and design of the study, including data collection. YMA supervised this study. All authors have reviewed and approved the final manuscript.

Conflicts of Interest

SP was an employee and JL is the chief technology officer of ActionPower Corp, which commercializes the automatic speech recognition tool used in this study. Unrelated to this work, YMA has received research support from or served as a speaker for Janssen Korea Ltd and Korea Otsuka Pharmaceutical. All other authors declare no other conflicts of interest.

Multimedia Appendix 1
Associations between acoustic features and depression severity after adjusting for age, sex, BMI, and antipsychotic dosage.
[XLSX File (Microsoft Excel File), 432 KB - medinform_v13i1e79093_app1.xlsx]

Multimedia Appendix 2
Associations between linguistic features and depression severity after adjusting for age, sex, and years of education.
[XLSX File (Microsoft Excel File), 19 KB - medinform_v13i1e79093_app2.xlsx]

Multimedia Appendix 3
Performance metrics of all classification models.

XSL•FO
RenderX

[XLSX File (Microsoft Excel File), 19 KB - medinform_v13i1e79093_app3.xlsx]

References

1. GBD results. Institute for Health Metrics and Evaluation. URL: https://vizhub.healthdata.org/gbd-results [accessed 2025-06-07]
2. Depressive disorder (depression). World Health Organization. URL: https://www.who.int/news-room/fact-sheets/detail/depression [accessed 2025-03-28]
3. Diagnostic and Statistical Manual of Mental Disorders (DSM-5). Washington, DC: American Psychiatric Association; 2013.
4. Kraepelin E. Manic-depressive insanity and paranoia. JAMA 1921 Aug 20;77(7):572. [doi: 10.1001/jama.1921.02630330070026]
5. Low DM, Bentley KH, Ghosh SS. Automated assessment of psychiatric disorders using speech: a systematic review. Laryngoscope Investig Otolaryngol 2020 Feb 31;5(1):96-116 [FREE Full text] [doi: 10.1002/lio2.354] [Medline: 32128436]
6. Di Y, Rahmani E, Mefford J, Wang J, Ravi V, Gorla A, et al. Unraveling the associations between voice pitch and major depressive disorder: a multisite genetic study. Mol Psychiatry 2025 Jun;30(6):2686-2695. [doi: 10.1038/s41380-024-02877-y] [Medline: 39741179]
7. Tølbøll KB. Linguistic features in depression: a meta-analysis. J Lang Works 2019 Dec 15;4(2):39-59 [FREE Full text]
8. Cummins N, Scherer S, Krajewski J, Schnieder S, Epps J, Quatieri TF. A review of depression and suicide risk assessment using speech analysis. Speech Commun 2015 Jul;71:10-49. [doi: 10.1016/j.specom.2015.03.004]
9. Sadeghi M, Richer R, Egger B, Schindler-Gmelch L, Rupp LH, Rahimi F, et al. Harnessing multimodal approaches for depression detection using large language models and facial expressions. Npj Ment Health Res 2024 Dec 23;3(1):66 [FREE Full text] [doi: 10.1038/s44184-024-00112-8] [Medline: 39715786]
10. Menne F, Dörr F, Schräder J, Tröger J, Habel U, König A, et al. The voice of depression: speech features as biomarkers for major depressive disorder. BMC Psychiatry 2024 Nov 12;24(1):794 [FREE Full text] [doi: 10.1186/s12888-024-06253-6] [Medline: 39533239]
11. Ghosh D, Karande H, Gite S, Pradhan B. Psychological disorder detection: a multimodal approach using a transformer-based hybrid model. MethodsX 2024 Sep 24;13:102976 [FREE Full text] [doi: 10.1016/j.mex.2024.102976] [Medline: 39430783]
12. Xu Z, Gao Y, Wang F, Zhang L, Zhang L, Wang J, et al. Depression detection methods based on multimodal fusion of voice and text. Sci Rep 2025 Jul 01;15(1):21907 [FREE Full text] [doi: 10.1038/s41598-025-03524-4] [Medline: 40593978]
13. Briganti G, Lechien JR. Speech and voice quality as digital biomarkers in depression: a systematic review. J Voice 2025 May 22:S0892-1997(25)00187-0. [doi: 10.1016/j.jvoice.2025.05.002] [Medline: 40410060]
14. Wasserzug Y, Degani Y, Bar-Shaked M, Binyamin M, Klein A, Hershko S, et al. Development and validation of a machine learning-based vocal predictive model for major depressive disorder. J Affect Disord 2023 Mar 15;325:627-632. [doi: 10.1016/j.jad.2022.12.117] [Medline: 36586600]
15. Mundt JC, Vogel AP, Feltner DE, Lenderking WR. Vocal acoustic biomarkers of depression severity and treatment response. Biol Psychiatry 2012 Oct 01;72(7):580-587 [FREE Full text] [doi: 10.1016/j.biopsych.2012.03.015] [Medline: 22541039]
16. Mundt JC, Snyder PJ, Cannizzaro MS, Chappie K, Geralts DS. Voice acoustic measures of depression severity and treatment response collected via interactive voice response (IVR) technology. J Neurolinguistics 2007 Jan;20(1):50-64 [FREE Full text] [doi: 10.1016/j.jneuroling.2006.04.001] [Medline: 21253440]
17. Wang Y, Liang L, Zhang Z, Xu X, Liu R, Fang H, et al. Fast and accurate assessment of depression based on voice acoustic features: a cross-sectional and longitudinal study. Front Psychiatry 2023 Jun 21;14:1195276 [FREE Full text] [doi: 10.3389/fpsyt.2023.1195276] [Medline: 37415683]
18. Judd LL, Schettler PJ, Akiskal HS, Maser J, Coryell W, Solomon D, et al. Long-term symptomatic status of bipolar I vs. bipolar II disorders. Int J Neuropsychopharmacol 2003 Jun;6(2):127-137 [FREE Full text] [doi: 10.1017/S1461145703003341] [Medline: 12890306]
19. Judd LL, Akiskal HS, Schettler PJ, Endicott J, Maser J, Solomon DA, et al. The long-term natural history of the weekly symptomatic status of bipolar I disorder. Arch Gen Psychiatry 2002 Jun;59(6):530-537. [doi: 10.1001/archpsyc.59.6.530] [Medline: 12044195]
20. Judd LL, Akiskal HS, Schettler PJ, Coryell W, Endicott J, Maser JD, et al. A prospective investigation of the natural history of the long-term weekly symptomatic status of bipolar II disorder. Arch Gen Psychiatry 2003 Mar;60(3):261-269. [doi: 10.1001/archpsyc.60.3.261] [Medline: 12622659]
21. Gardner DM, Murphy AL, O'Donnell H, Centorrino F, Baldessarini RJ. International consensus study of antipsychotic dosing. Am J Psychiatry 2010 Jun;167(6):686-693. [doi: 10.1176/appi.ajp.2009.09060802] [Medline: 20360319]
22. Min S, Shin D, Rhee SJ, Park CH, Yang JH, Song Y, et al. Acoustic analysis of speech for screening for suicide risk: machine learning classifiers for between- and within-person evaluation of suicidality. J Med Internet Res 2023 Mar 23;25:e45456 [FREE Full text] [doi: 10.2196/45456] [Medline: 36951913]
23. Yi JS, Bae SO, Ahn YM, Park DB, Noh KS, Shin HK, et al. Validity and reliability of the Korean version of the Hamilton Depression Rating Scale(K-HDRS). J Korean Neuropsychiatr Assoc 2005 Jul;44(4):456-465 [FREE Full text]

XSL•FO
RenderX

24. Hamilton M. Development of a rating scale for primary depressive illness. Br J Soc Clin Psychol 1967 Dec;6(4):278-296. [doi: 10.1111/j.2044-8260.1967.tb00530.x] [Medline: 6080235]
25. Zimmerman M, Martinez JH, Young D, Chelminski I, Dalrymple K. Severity classification on the Hamilton Depression Rating Scale. J Affect Disord 2013 Sep 05;150(2):384-388. [doi: 10.1016/j.jad.2013.04.028] [Medline: 23759278]
26. Kim J, Lee J. Generalizing RNN-transducer to out-domain audio via sparse self-attention layers. 2022 Presented at: INTERSPEECH '22: Proceedings of the 23rd Annual Conference of the International Speech Communication Association; September 18-22; Incheon, Korea p. 4123-4127 URL: https://www.isca-archive.org/interspeech_2022/kim22f_interspeech.pdf [doi: 10.21437/interspeech.2022-581]
27. Gulati A, Qin J, Chiu CC, Parmar N, Zhang Y, Yu J, et al. Conformer: convolution-augmented transformer for speech recognition. In: Proceedings of the 21st Annual Conference of the International Speech Communication Association. 2020 Presented at: INTERSPEECH '20; October 25-29; Shanghai, China p. 5036-5040 URL: https://www.isca-archive.org/interspeech_2020/gulati20_interspeech.pdf [doi: 10.21437/interspeech.2020-3015]
28. Shin D, Mun H, Kim G, Park S, Lee J. End-to-end speech recognition using grapheme-level information [Article in Korean]. In: Proceedings of the Korean Information Science Society Academic Conference. 2022 Presented at: Korea Computer Congress 2022; June 29-July 1; Seoul, South Korea p. 801-803 URL: https://www.dbpia.co.kr/journal/articleDetail?nodeId=NODE11113479
29. Park C, Kang H, Hain T. Character error rate estimation for automatic speech recognition of short utterances. In: Proceedings of the 32nd European Signal Processing Conference. 2024 Presented at: EUSIPCO '24; August 26-30; Lyon, France. [doi: 10.23919/eusipco63174.2024.10715433]
30. Schuller B, Steidl S, Batliner A, Hirschberg J, Burgoon JK, Baird A, et al. he INTERSPEECH 2016 Computational Paralinguistics Challenge: Deception, Sincerity and Native Language. In: Proceedings of the 17th Annual Conference of the International Speech Communication Association. 2016 Presented at: INTERSPEECH '16; September 8-12; San Francisco, CA p. 2001-2005 URL: https://www.isca-archive.org/interspeech_2016/schuller16_interspeech.pdf [doi: 10.21437/interspeech.2016-129]
31. Eyben F. Real-time Speech and Music Classification by Large Audio Feature Space Extraction. Cham, Switzerland: Springer; Dec 24, 2015.
32. Eyben F, Weninger F, Wöllmer M, Schuller B. openSMILE Python. audEERING. URL: https://audeering.github.io/opensmile-python/ [accessed 2025-03-31]
33. Syed ZS, Schroeter J, Sidorov K, Marshall D. Computational paralinguistics: automatic assessment of emotions, mood and behavioural state from acoustics of speech. In: Proceedings of the 19th Annual Conference of the International Speech Communication Association. 2018 Presented at: INTERSPEECH '18; September 2-6; Hyderabad, India p. 511-515 URL: https://www.isca-archive.org/interspeech_2018/syed18_interspeech.pdf [doi: 10.21437/interspeech.2018-2019]
34. Afshan A, Guo J, Park SJ, Ravi V, Flint J, Alwan A. Effectiveness of voice quality features in detecting depression. In: Proceedings of the 19th Annual Conference of the International Speech Communication Association. 2018 Presented at: INTERSPEECH '18; September 2-6; Hyderabad, India p. 1676-1680 URL: https://www.isca-archive.org/interspeech_2018/afshan18_interspeech.pdf [doi: 10.21437/interspeech.2018-1399]
35. Weninger F, Eyben F, Schuller BW, Mortillaro M, Scherer KR. On the acoustics of emotion in audio: what speech, music, and sound have in common. Front Psychol 2013 May 27;4:292 [FREE Full text] [doi: 10.3389/fpsyg.2013.00292] [Medline: 23750144]
36. Corbin L, Griner E, Seyedi S, Jiang Z, Roberts K, Boazak M, et al. A comparison of linguistic patterns between individuals with current major depressive disorder, past major depressive disorder, and controls in a virtual, psychiatric research interview. J Affect Disord Rep 2023 Dec;14:100645. [doi: 10.1016/j.jadr.2023.100645]
37. Burkhardt HA, Alexopoulos GS, Pullmann MD, Hull TD, Areán PA, Cohen T. Behavioral activation and depression symptomatology: longitudinal assessment of linguistic indicators in text-based therapy sessions. J Med Internet Res 2021 Jul 14;23(7):e28244. [doi: 10.2196/28244] [Medline: 34259637]
38. Receptiviti. URL: https://docs.receptiviti.com/the-receptiviti-api [accessed 2025-03-31]
39. Lee J, Choi H. Machine translation of Korean statutes examined from the perspective of quality and productivity. In: Proceedings of the 19th Machine Translation Summit. 2023 Presented at: MTS '23; September 4-8; Macau, China p. 143-151 URL: https://aclanthology.org/2023.mtsummit-users.13.pdf
40. Boot P. Machine-translated texts as an alternative to translated dictionaries for LIWC. OSF Preprint posted online on January 12, 2021 [FREE Full text] [doi: 10.31219/osf.io/tsc36]
41. Belouali A, Gupta S, Sourirajan V, Yu J, Allen N, Alaoui A, et al. Acoustic and language analysis of speech for suicidal ideation among US veterans. BioData Min 2021 Feb 02;14(1):11 [FREE Full text] [doi: 10.1186/s13040-021-00245-y] [Medline: 33531048]
42. Li TM, Chen J, Law FO, Li CT, Chan NY, Chan JW, et al. Detection of suicidal ideation in clinical interviews for depression using natural language processing and machine learning: cross-sectional study. JMIR Med Inform 2023 Dec 01;11:e50221 [FREE Full text] [doi: 10.2196/50221] [Medline: 38054498]

XSL•FO
RenderX

43. Tsamardinos I, Greasidou E, Borboudakis G. Bootstrapping the out-of-sample predictions for efficient and accurate cross-validation. Mach Learn 2018;107(12):1895-1922 [FREE Full text] [doi: 10.1007/s10994-018-5714-4] [Medline: 30393425]
44. Israel JA. Remission in depression: definition and initial treatment approaches. J Psychopharmacol 2006 May;20(3 Suppl):5-10. [doi: 10.1177/1359786806064306] [Medline: 16644766]
45. Lundberg S, Lee SI. A unified approach to interpreting model predictions. ArXiv Preprint posted online on May 22, 2017. [doi: 10.48550/arXiv.1705.07874]
46. Kim H, Jung JH, Han K, Jeon HJ. Risk of suicide and all-cause death in patients with mental disorders: a nationwide cohort study. Mol Psychiatry 2025 Jul;30(7):2831-2839. [doi: 10.1038/s41380-025-02887-4] [Medline: 39843548]
47. Jung S, Lee C. Deep neural architecture for recovering dropped pronouns in Korean. ETRI J 2018 Apr 11;40(2):257-265. [doi: 10.4218/etrij.2017-0085]
48. Weintraub MJ, Posta F, Arevian AC, Miklowitz DJ. Using machine learning analyses of speech to classify levels of expressed emotion in parents of youth with mood disorders. J Psychiatr Res 2021 Apr;136:39-46 [FREE Full text] [doi: 10.1016/j.jpsychires.2021.01.019] [Medline: 33549901]
49. Naffah A, Pfeifer VA, Mehl MR. Spoken language analysis in aging research: the validity of AI-generated speech to text using OpenAI's Whisper. Gerontology 2025;71(5):417-424. [doi: 10.1159/000545244] [Medline: 40552848]
50. Sinha P, Vandana VP, Lewis NV, Jayaram M, Enderby P. Predictors of effect of atypical antipsychotics on speech. Indian J Psychol Med 2015;37(4):429-433 [FREE Full text] [doi: 10.4103/0253-7176.168586] [Medline: 26702176]
51. Kim H, Kim S, Lee S, Lee K, Kim E. Exploring the relationships between antipsychotic dosage and voice characteristics in relation to extrapyramidal symptoms. Psychiatry Investig 2024 Aug;21(8):822-831 [FREE Full text] [doi: 10.30773/pi.2023.0417] [Medline: 39111750]
52. Le Dorze G, Bédard C. Effects of age and education on the lexico-semantic content of connected speech in adults. J Commun Disord 1998;31(1):53-70. [doi: 10.1016/s0021-9924(97)00051-8] [Medline: 9421767]
53. Cohen J, Richter V, Neumann M, Black D, Haq A, Wright-Berryman J, et al. A multimodal dialog approach to mental state characterization in clinically depressed, anxious, and suicidal populations. Front Psychol 2023 Sep 11;14:1135469 [FREE Full text] [doi: 10.3389/fpsyg.2023.1135469] [Medline: 37767217]
54. Shin D, Kim K, Lee SB, Lee C, Bae YS, Cho WI, et al. Detection of depression and suicide risk based on text from clinical interviews using machine learning: possibility of a new objective diagnostic marker. Front Psychiatry 2022 May 24;13:801301 [FREE Full text] [doi: 10.3389/fpsyt.2022.801301] [Medline: 35686182]
55. Edinoff AN, Nix CA, Hollier J, Sagrera CE, Delacroix BM, Abubakar T, et al. Benzodiazepines: uses, dangers, and clinical considerations. Neurol Int 2021 Nov 10;13(4):594-607 [FREE Full text] [doi: 10.3390/neurolint13040059] [Medline: 34842811]
56. Smith GA. Voice analysis of the effects of benzodiazepine tranquillizers. Br J Clin Psychol 1982 Jun;21(2):141-142. [doi: 10.1111/j.2044-8260.1982.tb00542.x] [Medline: 6127129]

Abbreviations

AUC: area under the receiver operating characteristic curve
BBCV: bootstrap bias-corrected cross-validation
CER: character error rate
HAM-D: Hamilton Depression Rating Scale
LGB: light gradient boosting
LIWC: Linguistic Inquiry and Word Count
MDD: major depressive disorder
SHAP: Shapley additive explanation
SMOTE: synthetic minority oversampling technique
XGB: extreme gradient boosting

Edited by A Coristine; submitted 15.06.25; peer-reviewed by F Sundram, A Mohammed, J Oghuan, WI Cho, A Belouali, D Manamalage; comments to author 10.07.25; revised version received 03.11.25; accepted 03.11.25; published 04.12.25.

Please cite as:
Min S, Yeum TS, Shin D, Rhee SJ, Lee H, Lee HS, Park S, Lee J, Ahn YM
Automated Speech Analysis for Screening and Monitoring Bipolar Depression: Machine Learning Model Development and Interpretation Study
JMIR Med Inform 2025;13:e79093
URL: https://medinform.jmir.org/2025/1/e79093
doi:10.2196/79093
PMID:

XSL•FO
RenderX

©Sooyeon Min, Tae-Sung Yeum, Daun Shin, Sang Jin Rhee, Hyunju Lee, Han-Sung Lee, Seongmin Park, Jihwa Lee, Yong Min Ahn. Originally published in JMIR Medical Informatics (https://medinform.jmir.org), 04.12.2025. This is an open-access article distributed under the terms of the Creative Commons Attribution License (https://creativecommons.org/licenses/by/4.0/), which permits unrestricted use, distribution, and reproduction in any medium, provided the original work, first published in JMIR Medical Informatics, is properly cited. The complete bibliographic information, a link to the original publication on https://medinform.jmir.org/, as well as this copyright and license information must be included.

XSL•FO
RenderX

Original Paper

A Machine Learning Approach to Predicting Mortality Risk in Chemotherapy-Treated Lung Cancer: Machine Learning Model Development and Validation

Jianjun Zou[1,2,3*], MD; Jinyi Huang[4*], MD; Katie Lu[5*], BD; Ao Lin[4,6,7], MD, PhD; Chen Xie[4], MD; Jinrong Zhang[4], MD; Boqi Rao[4,6,8], MD, PhD; Zhi Li[4], MD; Dongming Xie[4], MD; Ling Lu[4], MD; Feng Luo[4], BD; Jinbin Chen[9], MD, PhD; Lei Yang[4,10,11], MD, PhD; Fuman Qiu[4], MD, PhD; Xin Zhang[6,7,12], MD, PhD; Yibin Deng[13], MD, PhD; Jiachun Lu[4,10,11], MD, PhD

[1]Institute of Tuberculosis, Guangzhou Medical University, Guangzhou, Guangdong, China

[2]Guangzhou Key Laboratory of Tuberculosis Research, Guangzhou Chest Hospital, Guangzhou, Guangdong, China

[3]Department of General Medicine, Guangzhou Chest Hospital, Guangzhou, Guangdong, China

[4]School of Public Health, Guangzhou Medical University, Guangzhou, Guangdong, China

[5]School of Medicine, University of Arizona, Tucson, AZ, United States

[6]State Key Laboratory of Respiratory Disease, Guangzhou Medical University, Guangzhou, Guangdong, China

[7]Department of Thoracic Surgery, The First Affiliated Hospital of Guangzhou Medical University, Guangzhou, Guangdong, China

[8]Emergency Department, The Second Affiliated Hospital of Guangzhou Medical University, Guangzhou, China

[9]KingMed School of Laboratory Medicine, Guangzhou Medical University, Guangzhou, China

[10]The Key Laboratory of Advanced Interdisciplinary Studies, The First Affiliated Hospital of Guangzhou Medical University, Guangzhou, Guangdong, China

[11]The Institute for Chemical Carcinogenesis, Guangzhou Medical University, Guangzhou, Guangdong, China

[12]Guangzhou Institute of Respiratory Health, Guangzhou Medical University, Guangzhou, China

[13]Centre for Medical Laboratory Science, The Affiliated Hospital of Youjiang Medical University for Nationalities, Baise, China

[*]these authors contributed equally

Corresponding Author:
Jiachun Lu, MD, PhD
School of Public Health
Guangzhou Medical University
Xinzao, Panyu District
Guangzhou, 511436
China
Phone: 86 20 37103043
Email: jclu@gzhmu.edu.cn

Abstract

Background: Accurately predicting the survival outcomes of patients with lung cancer receiving chemotherapy remains challenging.

Objective: To improve clinical management of this population, this study developed a multivariate machine learning (ML) model to assess all-cause mortality risk in chemotherapy-treated patients with lung cancer.

Methods: This study retrospectively recruited 1278 postchemotherapy patients with lung cancer from Guangzhou Chest Hospital between 2017 and 2019. Candidate features such as demographic characteristics, environmental exposures, clinical information, and patient-reported symptoms were collected via questionnaires and the electronic medical record system. The survival status and the deceased date were investigated twice a year. A total of 84 predictive models were constructed on the training set using 5 ML algorithms either individually or in pairwise combinations. The concordance index was used to identify the optimal model on the testing set, with performance validated via receiver operating characteristic curves, calibration curves, and decision curve analysis. Additionally, Shapley Additive Explanations and restricted cubic splines were applied for feature attribution analysis.

Results: The optimal model ultimately retained 21 prognosis-association features, including age, sex, BMI, smoking status, environmental smoke, the MD Anderson Symptom Inventory for Lung Cancer total score trajectories, cluster of differentiation

XSL•FO
RenderX

56, TNM stage, histology, and prechemotherapy blood biomarkers. On the testing set, the model acquired a concordance index of 0.702 (95% CI 0.652-0.753). The decision curves demonstrated positive clinical benefit when the risk thresholds were 0.40-0.69, 0.62-0.99, and 0.72-0.99 for 1-, 3-, and 5-year mortality predictions, respectively. The calibration curves showed that the predicted mortality probabilities fluctuated around the observed probabilities, and the Brier scores for 1-, 3-, and 5-year predictions were 0.20, 0.18, and 0.11, respectively. The area under the curve of the model was 0.740, 0.777, and 0.915 for 1-, 3-, and 5-year mortality predictions, respectively. Interpretability feature attribution analysis revealed that the significant features could predict all-cause mortality risk in chemotherapy-treated patients with lung cancer.

Conclusions: Our ML models exhibited acceptable discrimination, calibration, and clinical benefit in predicting the mortality risk of chemotherapy-treated patients with lung cancer, which could help clinicians in personalized prognostic management.

(JMIR Med Inform 2025;13:e72424) doi:10.2196/72424

KEYWORDS

lung cancer; chemotherapy; mortality; machine learning; prediction model

Introduction

Lung cancer is the leading cause of cancer-related deaths globally. Lung cancer claimed approximately 1.8 million lives in 2022 alone, accounting for 18.7% of global cancer deaths [1]. With the advancements in medicine, the emergence of targeted and immune drugs introduces new options for lung cancer treatment. Personalized treatment strategies combining surgery, radiotherapy, chemotherapy, targeted therapy, and immunotherapy demonstrate significant efficacy in improving the living quality and long-term survival rates of patients with lung cancer. However, for some advanced lung cancers lacking driver mutations and with negative immune checkpoint expression, chemotherapy remains the primary treatment modality [2,3]. Thus, accurately predicting the mortality risk of chemotherapy-treated lung cancers to optimize treatment planning and patient care is of significant public health importance.

Machine learning (ML) models have become increasingly important tools for predicting the mortality risk of patients with lung cancer treated with chemotherapy, offering new insights and improved accuracy over traditional methods. While demographic and clinical characteristics are important, recent research has highlighted the potential benefits of incorporating additional data sources to enhance model performance [4-6]. For example, although the TNM stage is a recognized factor associated with the prognosis, it explains just less than 30% of the prognostic differences [7,8]. It is noted that genomic biomarkers present a means of refining prognosis assessment models, but the expensive genetic testing restricts the clinical application [9-11]. The above situation underscores the requirement for a more effective and interpretable mortality risk stratification model for postchemotherapy patients with lung cancer.

The biopsychosocial framework advocates dissecting disease from diverse angles, including symptom burden. The MD Anderson Symptom Inventory for Lung Cancer (MDASI-LC), a patient-reported outcome (PRO) tool, offers key perspectives into the self-reported symptom experience of patients receiving chemotherapy [12]. Integrating longitudinal PRO information into prognostic models has notable value in refining the prediction of patient outcomes [13-16].

This study adheres to the transparent reporting of a multivariable prediction model for individual prognosis or diagnosis guidelines as much as possible to ensure the transparent and accurate reporting of our predictive model development and validation [17]. This study developed a multivariable ML model that integrated demographic characteristics, clinical features, environmental factor exposure, immunohistochemical indicators, and total PRO score to predict the mortality risk of chemotherapy-treated patients with lung cancer. The model aims to provide clinicians with an effective tool for predicting the risk of death in patients with lung cancer after chemotherapy, assisting clinicians in customizing treatment plans, optimizing patient care plans, and improving patient prognosis.

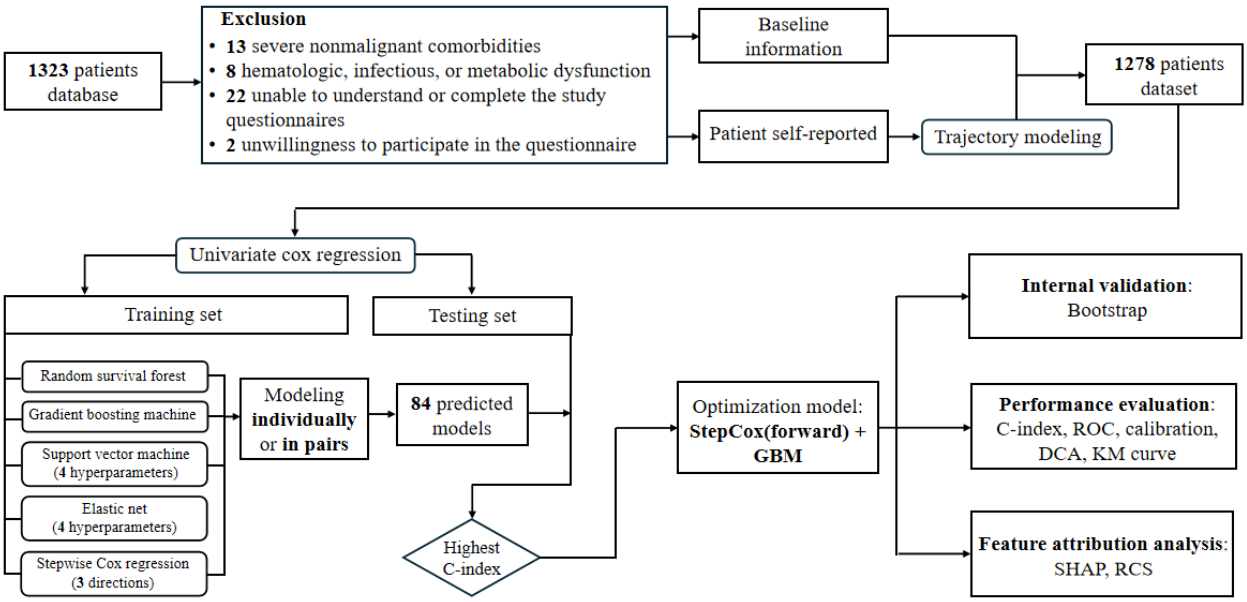
Methods

Overview

An overview of the entire study design and ML framework is provided in Figure 1.

XSL•FO
RenderX

Figure 1. The flowchart of this study. This study provided a comprehensive framework for building machine learning models to predict mortality risk for patients with lung cancer after chemotherapy. C-index: concordance index; DCA: decision curve analysis; GBM: gradient boosting machine; KM: Kaplan-Meier; RCS: restricted cubic spline; ROC: receiver operating characteristic curve; SHAP: Shapley Additive Explanations.



Study Population

This retrospective and semilongitudinal investigation included 1278 patients with lung cancer who received platinum-based chemotherapy at Guangzhou Chest Hospital between November 2017 and 2019. Demographic characteristics, environmental exposures, clinical information, and patient-reported symptoms were collected using questionnaires and the electronic medical record system. Patients' TNM stage was identified by the seventh edition of the classification system.

Patients who met the following inclusion criteria were included (1) histologically confirmed diagnosis of primary lung cancer, (2) absence of prior chemotherapy for lung carcinoma, and (3) demonstrated ability to comprehend and complete study questionnaires with clear consciousness.

Patients with the following presentations that would bias their symptom reporting or outcome were excluded: (1) severe nonmalignant comorbidities; (2) hematopoietic, infectious, or metabolic dysfunction; and (3) preexisting psychological disorders. The specific number of excluded participants is presented in the flowchart of Figure 1.

Patient-Reported Symptom

Patients completed self-report questionnaires at admission and the first 4 chemotherapy cycles. The professional questionnaires included (1) the MDASI-LC: this is a validated PRO tool specifically designed to assess symptom severity in patients with lung cancer. It consists of 22 items divided into 3 parts: core symptoms, lung cancer-specific symptoms, and additional symptoms. Each item is scored on a scale from 0 to 10, with higher scores indicating more severe symptoms [18]. (2) The Karnofsky Performance Status (KPS): this is a widely used tool for assessing the overall health status and functional state of patients. The KPS score ranges from 0 to 100, with higher scores indicating better functional status. It is commonly used in clinical practice to evaluate patient prognosis and treatment response, and it has been validated in various studies [19]. (3) The Zubrod Performance Score (ZPS): this tool assesses the physical condition of patients, with scores ranging from 0 to 5. Higher scores indicate worse physical status. ZPS is another widely used tool in clinical practice, providing valuable insights into patients' daily living abilities and overall health [20].

The Primary End Point

All-cause mortality served as the primary end point in this study. The professionals monitored the patients biannually by telephone. The death date was recorded if the patients had died; otherwise, they would be followed until death. The time horizon for this outcome is defined as 1-, 3-, and 5-year posttreatment initiation. The follow-up period in this research ranged from 1 month to 11 years.

Statistical Analysis Methods

The normality of continuous variables was assessed using the Shapiro-Wilk test, and the group comparisons were made using the 2-tailed *t* test or the Mann-Whitney *U* test. Categorical variables were analyzed using the chi-square or the Fisher exact test. Survival curves were generated using Kaplan-Meier and compared using the log-rank test. Hazard ratio and 95% CI were estimated using Cox regression. Statistical significance was defined when $P<.05$ (2-tailed). Missing data imputation was performed using the missForest algorithm, which accommodated mixed data types and handled nonlinearities and outliers.

The reliability of the scales was assessed using Cronbach α to measure internal consistency. Pearson correlation coefficients were calculated to examine the correlations between the 3 scales, assessing their validity. Longitudinal symptom burden trajectories were identified using group-based trajectory modeling (GBTM), with data from the 3 scales assessed across 5 separate time points [21]. GBTM criteria were odds of correct

XSL•FO
RenderX

classification >5, average posterior probability (Avepp) >0.7, posterior probability of group membership (P_j) >5%, correspondence between P_j and probability of group membership (π_j), relative entropy (E_k) >0.7, and a minimized Bayesian information criterion value.

ML Methods

Random survival forest (RSF), gradient boosting machine (GBM), survival support vector machine (survival-SVM), elastic net (Enet), and stepwise Cox regression were used to develop a prognostic model [22-25]. For the RSF and GBM models, the best hyperparameters for these 2 models were determined by constructing separate base models on the training set and performing preliminary cross-validation and performance evaluation. For the hyperparameter γ of the survival-SVM model, the hyperparameter α of the Enet model, and the 3 directions of the stepwise Cox regression model, a grid search method was used. The specific parameters of the five algorithms are as follows: (1) RSF: ntree=1000, nodesize=32, mtry=10; (2) GBM: ntrees=3750, interaction.depth=2, n.minobsinnode=20; (3) survival-SVM: γ in 0.25, 0.5, 1, 2, 4; (4) Enet: α in 0.1, 0.2, 0.3, 0.4; and (5) stepwise Cox regression: direction in both, backward, forward. Five separate ML models with a total of 13 models (different hyperparameter models of the same algorithm are considered as different models) were first constructed: RSF (1 model), GBM (1 model), survival-SVM (4 hyperparameters and 4 models), Enet (4 hyperparameters and 4 models), and stepwise Cox regression (3 directions and 3 models). Second, two-by-two combinations of the above 13 models in sequential order totaled 71 models, for a total of 84 models being constructed.

Continuous features were not binarized or split-boxed during the modeling process in order to maximize the amount of information retained in the data, and for categorical features, such as sex, smoking status, and tumor staging, the modeling process used discrete values.

Model discrimination, accuracy, and clinical benefit were evaluated using the concordance index (C-index), decision curve analysis, calibration curves, and the area under the curve (AUC). Internal validation of the models was performed using the bootstrap method. Feature attribution analysis was conducted using Shapley Additive Explanations and restricted cubic splines (RCSs).

Ethical Considerations

The protocol for this study was approved by the ethics review board of Guangzhou Medical University. All patients were informed of the data collection methods and privacy protection measures. All patient identifiers were removed after data collection and replaced with unique nonidentifiable serial numbers, and deidentified data were stored in a password-protected electronic database, with access restricted to the core research team. The deidentified data were only used for this study without sharing with third parties without additional approval.

Results

Baseline Characteristics of the Patients

This study enrolled 1278 eligible patients, with a median age of 61 (IQR 54-68) years, comprising 946 (74%) male and 332 (26%) female patients. Among 1278 enrolled patients with lung cancer undergoing chemotherapy, 408, 94, and 19 cases were alive at the 1-, 3-, and 5-year follow-ups, yielding overall survival rates of 31.9% (95% CI 29.4%-34.6%), 7.4% (95% CI 6%-9%), and 1.5% (95% CI 0.9%-2.4%), respectively. The specific distribution of histological types in our study population is as follows: adenocarcinoma (876/1274, 68.8%), squamous cell carcinoma (247/1274, 19.4%), small cell lung cancer (SCLC; 125/1274, 9.8%), and other types (26/1274, 2%). Some of the more important characteristics can be found in Table 1, and the complete Table 1 can be found in Multimedia Appendix 1.

XSL•FO
RenderX

Table 1. Baseline characteristics of chemotherapy-treated patients with lung cancer.

Variable	Missing, n (%)	Baseline data (N=1278)		Statistics	*P* value
		Living (n=758)	Deceased (n=520)		
Sex, n (%)	0 (0)			χ^2_1=0.6	.43
Male		555 (73.2)	391 (75.2)		
Female		203 (26.8)	129 (24.8)		
Age (years), median (IQR)	0 (0)	60.0 (53.0-66.0)	63.0 (57.0-70.0)	*z*=5.5	<.01[a]
BMI (kg/m^2), median (IQR)	48 (3.8)	20.8 (18.9-23.0)	20.6 (18.4-22.6)	*z*=–2.1	.03[a]
Education, n (%)	80 (6.3)			7.1 (2)	.03
Never attended school or primary school		377 (53.4)	294 (59.8)		
Junior high school or high school		304 (43.1)	175 (35.6)		
University and above		25 (3.5)	23 (4.7)		
WBC[b] (10^9 per liter), median (IQR)	150 (11.7)	8 (6-10)	8 (7-11)	*z*=2.9	<.01[a]
HGB[c] (g/L), median (IQR)	150 (11.7)	125.0 (111.0-136.0)	121.0 (107.0-134.0)	*z*=–3.4	<.01[a]
D-dimer (mg/L), median (IQR)	150 (11.7)	0.69 (0.34-1.87)	0.91 (0.44-2.52)	*z*=3.7	<.01[a]
CEA[d] (ng/mL), median (IQR)	150 (11.7)	5 (2-20)	7 (3-52)	*z*=4.6	<.01[a]
CA12-5[e] (U/mL), median (IQR)	150 (11.7)	31.2 (14.7-100.8)	52.9 (19.3-145.7)	*z*=4.1	<.01[a]
CA19-9[f] (U/mL), median (IQR)	150 (11.7)	13.0 (7.0-26.3)	16.3 (7.2-44.9)	*z*=2.8	<.01[a]
CYFRA21-1[g] (ng/mL), median (IQR)	150 (11.7)	5 (3-11)	8 (4-18)	*z*=7.1	<.01[a]
Histology, n (%)	4 (0.3)			χ^2_3=1.0	.79
LUAD[h]		522 (69.1)	354 (68.2)		
LUSC[i]		149 (19.7)	98 (18.9)		
SCLC[j]		69 (9.1)	56 (10.8)		
Others		15 (2.1)	11 (2.1)		
Tumor stage, n (%)	31 (2.4)			χ^2_1=1.5	.22
T1+T2		281 (38)	176 (34.7)		
T3+T4		458 (62)	332 (65.4)		
Nodal stage, n (%)	68 (5.3)			χ^2_3=16.7	<.01
N1		85 (11.9)	30 (6.1)		
N2		69 (9.6)	34 (6.9)		
N3		296 (41.3)	212 (42.9)		
N4		266 (37.2)	218 (44.1)		
Metastasis stage, n (%)	156 (12.2)			χ^2_1=28.3	<.01
M1		174 (26.1)	59 (13)		
M2		493 (73.9)	396 (87)		

[a]Using the Mann-Whitney *U* test.
[b]WBC: white blood cell.
[c]HGB: hemoglobin.
[d]CEA: carcinoembryonic antigen.
[e]CA12-5: carbohydrate antigen 12-5.
[f]CA19-9: carbohydrate antigen 19-9.

XSL•FO
RenderX

[g]CYFRA21-1: recombinant cytokeratin fragment antigen 21-1.

[h]LUAD: lung adenocarcinoma.

[i]LUSC: lung squamous cell carcinoma.

[j]SCLC: small cell lung cancer.

Patient Report Outcomes Trajectory Modeling

GBTM was applied to characterize PRO trajectories. Table 2 presents detailed information on the GBTM evaluation indicators and trajectory groups. A comprehensive evaluation process is described in Tables S1-S6 in Multimedia Appendix 2. In particular, following a rigorous evaluation of model fit indices and clinical interpretability, 3 distinct trajectory groups were identified for the MDASI-LC total score (group A: high burden, group B: medium burden, and group C: low burden), 3 for the KPS score (group A: high burden, group B: medium burden, and group C: low burden), and 2 for the ZPS score (group A: high burden and group B: low burden). All equation coefficients showed significant differences (P<.001; Figure S1 in Multimedia Appendix 2).

Table 2. The number of each scale trajectory groups, classification counts, and results of various evaluation indicators for the scale[a].

Scales	Group number	OCC[b]	Avepp[c] (%)	P_j[d] (%)	π_j[e] (%)	E_k[f]	BIC[g]
MDASI-LC[h]	3 (3 0 3)	33.2/33.4/81.1	98.24/90.83/93.18	62.82/22.89/14.29	62.71/22.87/14.42	0.91	–9140.61
KPS[i]	3 (0 0 0)	943.70/43.10/60.80	98.03/95.25/99.05	4.76/32.60/62.67	5.01/31.74/63.25	0.95	–6565.35
ZPS[j]	2 (0 2)	5.60/538.10	93.74/98.94	90.84/9.16	85.26/14.74	0.77	–376.79

[a]Optimization model criteria: The odds of correct classification should surpass a value of 5, reflecting a high likelihood of accurate classification. Each group should exhibit an Avepp exceeding the threshold of 0.7, indicating a high degree of confidence in the classification. The P_j should be greater than 5%, signifying that the probability of an entity belonging to a particular group is statistically significant. There should be a close alignment between P_j and the π_j, ensuring that the posterior probabilities are congruent with the a priori probabilities. The E_k should be greater than 0.7, indicating a substantial degree of differentiation between the groups in terms of information content.

[b]OCC: odds of correct classification.

[c]Avepp: average posterior probability.

[d]P_j: posterior probability of group membership.

[e]π_j: probability of group membership.

[f]E_k: relative entropy.

[g]BIC: Bayesian information criterion.

[h]MDASI-LC: MD Anderson Symptom Inventory for Lung Cancer.

[i]KPS: Karnofsky Performance Status.

[j]ZPS: Zubrod Performance Score.

Univariate Cox Regression Analysis of Feature Selection

The missForest algorithm did not induce statistically significant changes in the data distribution after baseline imputation. A detailed comparison of the baseline data distribution before and after imputation is reported in Table S7 in Multimedia Appendix 2.

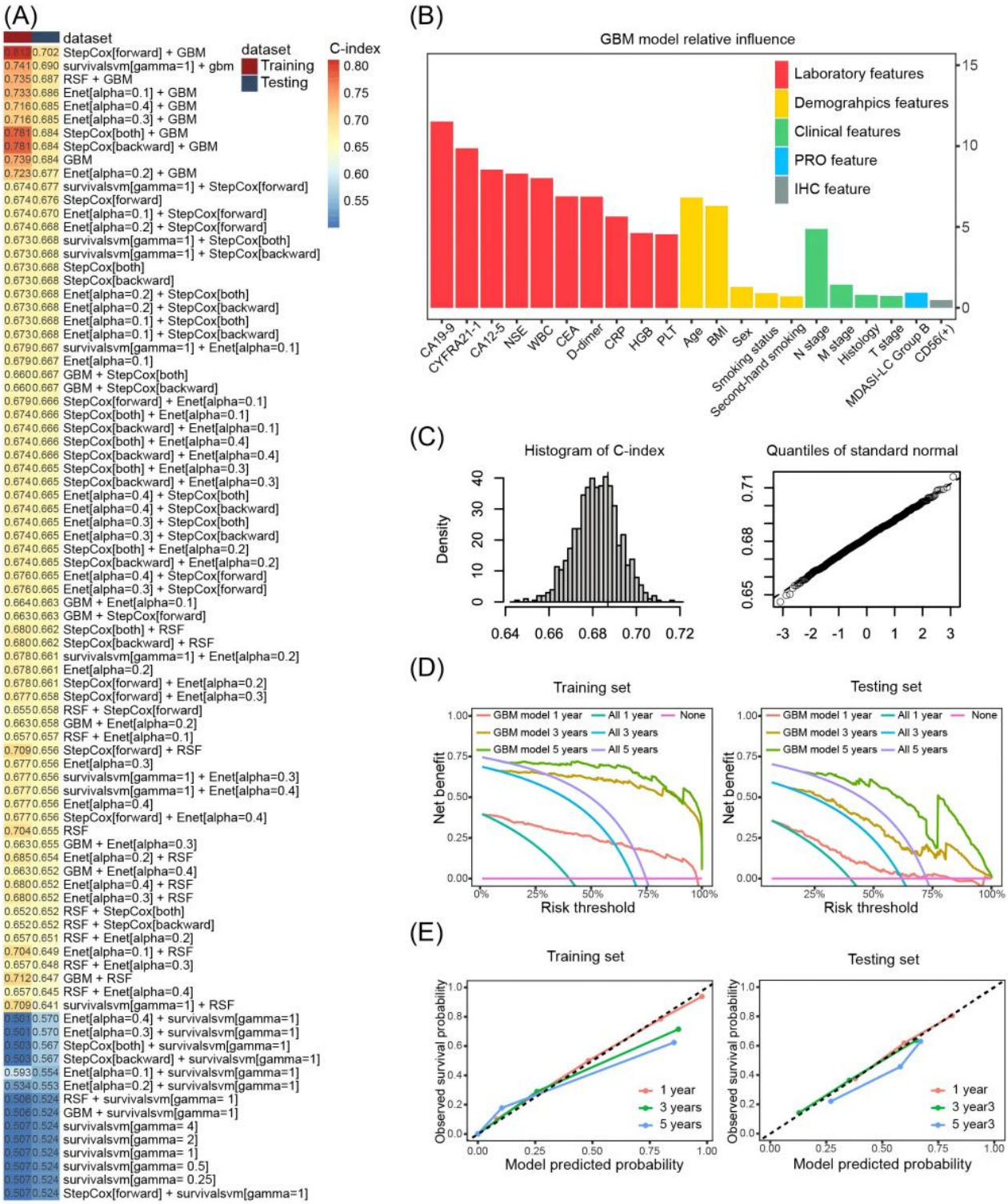
Univariate Cox regression analysis (P value of <.05 is statistically significant) identified 27 features significantly associated with prognosis in patients with lung cancer receiving chemotherapy, which served as an initial feature selection step. A comprehensive summary of the univariate analysis is available in Table S8 in Multimedia Appendix 2. Beyond statistically significant findings, an additional 10 features with perceived prognostic relevance, such as a family history of respiratory disease, were included in feature selection despite their lack of statistical significance in the univariate analysis. These features were retained to ensure a comprehensive evaluation of potential prognostic factors and to allow the ML models to capture complex interactions between features. Finally, 37 features were retained for the ML model development.

Models Development and Internal Validation

The dataset of 1278 observations was randomly split into a training dataset (n=895) and a testing dataset (n=383) at a 7:3 ratio. Table S9 in Multimedia Appendix 2 shows that there is no difference between the distributions of the main baseline features of the patients in the training and testing sets. On the training set, a total of 84 predicted models were built with 5 ML algorithms individually or binately 5 ML models were trained and then tested both individually and in all possible combinations of pairs, yielding a total of 84 predictive models (Figure 2A).

XSL•FO
RenderX

Figure 2. Illustration of the machine learning procedure for prediction model development and validation. (A) displays a ranking of 84 predictive models from highest to lowest based on their C-index calculated on the testing set. These models resulted from all possible 2-way combinations of 5 machine learning models. (B) presents the ranked feature importance identified by the GBM model, with the y-axis indicating the relative importance. (C) displays the C-index distribution along with results of a Shapiro-Wilk normality test, obtained during an internal validation using bootstrap resampling. (D) and (E) display DCA curves and calibration plots, respectively, for predicting 1-, 3-, and 5-year mortality risk using the optimal model on both the training and the testing set. CA12-5: carbohydrate antigen 12-5; CA19-9: carbohydrate antigen 19-9; CD56: cluster of differentiation 56; CEA: carcinoembryonic antigen; C-index: concordance index; CRP: C-reactive protein; CYFRA21-1: recombinant cytokeratin fragment antigen 21-1; DCA: decision curve analysis; Enet: elastic net; GBM: gradient boosting machine; HGB: hemoglobin; IHC: immunohistochemistry; MDASI-LC: MD Anderson Symptom Inventory for Lung Cancer; NSE: neuron-specific enolase; PLT: platelet count; PRO: patient-reported outcome; RSF: random survival forest; WBC: white blood cell.



On the testing set, we calculated the C-index of the 84 predicted models to identify the optimal predictive model. We found that the optimal predictive model was a combination of forward stepwise Cox regression and GBM and demonstrated the highest

XSL•FO
RenderX

C-index of 0.702 (95% CI 0.652-0.753; Figure 2A). The final feature set of the optimal predictive model comprised 5 demographic features, 10 prechemotherapy laboratory features, 1 PRO feature, 4 clinical features, and 1 immunohistochemical feature (Figure 2B).

In total, 1000 bootstrap resamplings were performed and yielded an average C-index of 0.682 (95% CI 0.676-0.689) on the testing dataset. Shapiro-Wilk test indicated that the distribution of the C-index was normal (P=.86; Figure 2C). The evidence suggested a reasonable robustness of the optimal predictive model.

Performance Evaluation of the Model

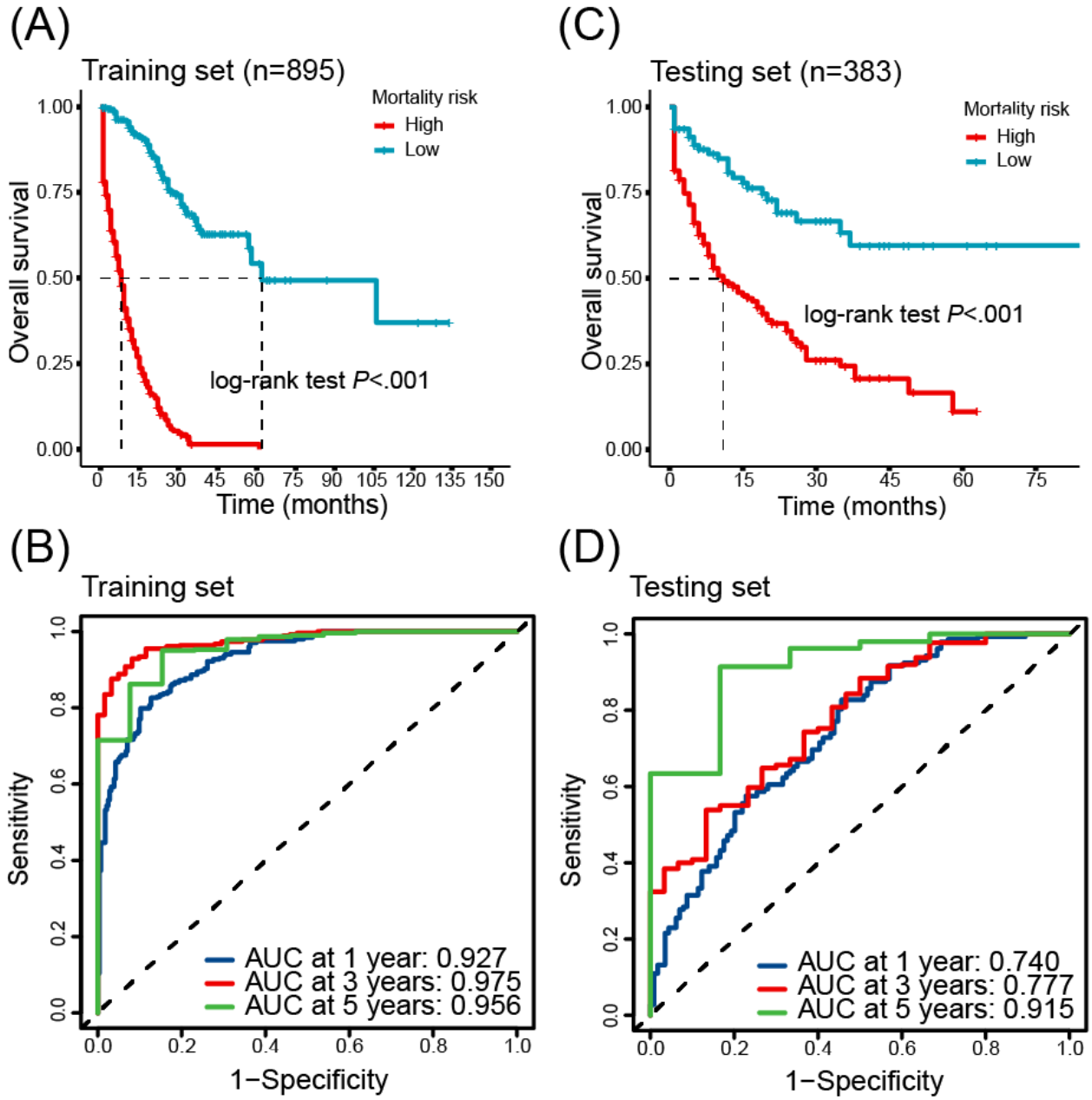
Performance evaluation of the model was implemented on both the training and testing sets. The decision curve analysis demonstrated that the predicted model had a net benefit over the strategies of predicting all deaths or all survivals when the risk thresholds were 0.40-0.97, 0.68-0.99, and 0.75-0.99 for 1-, 3-, and 5-year mortality predictions, respectively, on the training set, while 0.40-0.69, 0.62-0.99, and 0.72-0.99 on the testing set (Figure 2D).

In addition, the calibration curves displayed strong agreement between model predictions and observed outcomes (Figure 2E). The Brier scores for 1-, 3-, and 5-year mortality predictions were 0.11, 0.07, and 0.08, respectively, on the training set, while 0.20, 0.18, and 0.11 on the testing set.

Furthermore, we determined an optimal risk score cutoff point by the *survminer* package to stratify patients into high-risk and low-risk groups. Kaplan-Meier survival analysis showed a significant difference in survival curves between the 2 groups, indicating that the model could well stratify patients when predicting 1-, 3-, or 5-year survival (P<.01; Figures 3A and C). The time-dependent receiver operating characteristic curve analysis found that the model demonstrated AUC values of 0.927, 0.975, and 0.956 for 1-, 3-, and 5-year mortality predictions, respectively, on the training set, while 0.740, 0.777, and 0.915 on the testing set, which exhibited robust predictive accuracy for both short-term and long-term mortality risk (Figures 3B and D).

XSL•FO
RenderX

Figure 3. Evaluation of the mortality risk prediction model's prognostic performance. (A) and (C) show the Kaplan-Meier curve for high- and low-risk patients, generated from the training and testing set, respectively, illustrating significant differences in survival. (B) and (D) present the time-dependent receiver operating characteristic curves assessing 1-, 3-, and 5-year mortality prediction in the training and testing data, respectively. AUC: area under the curve.

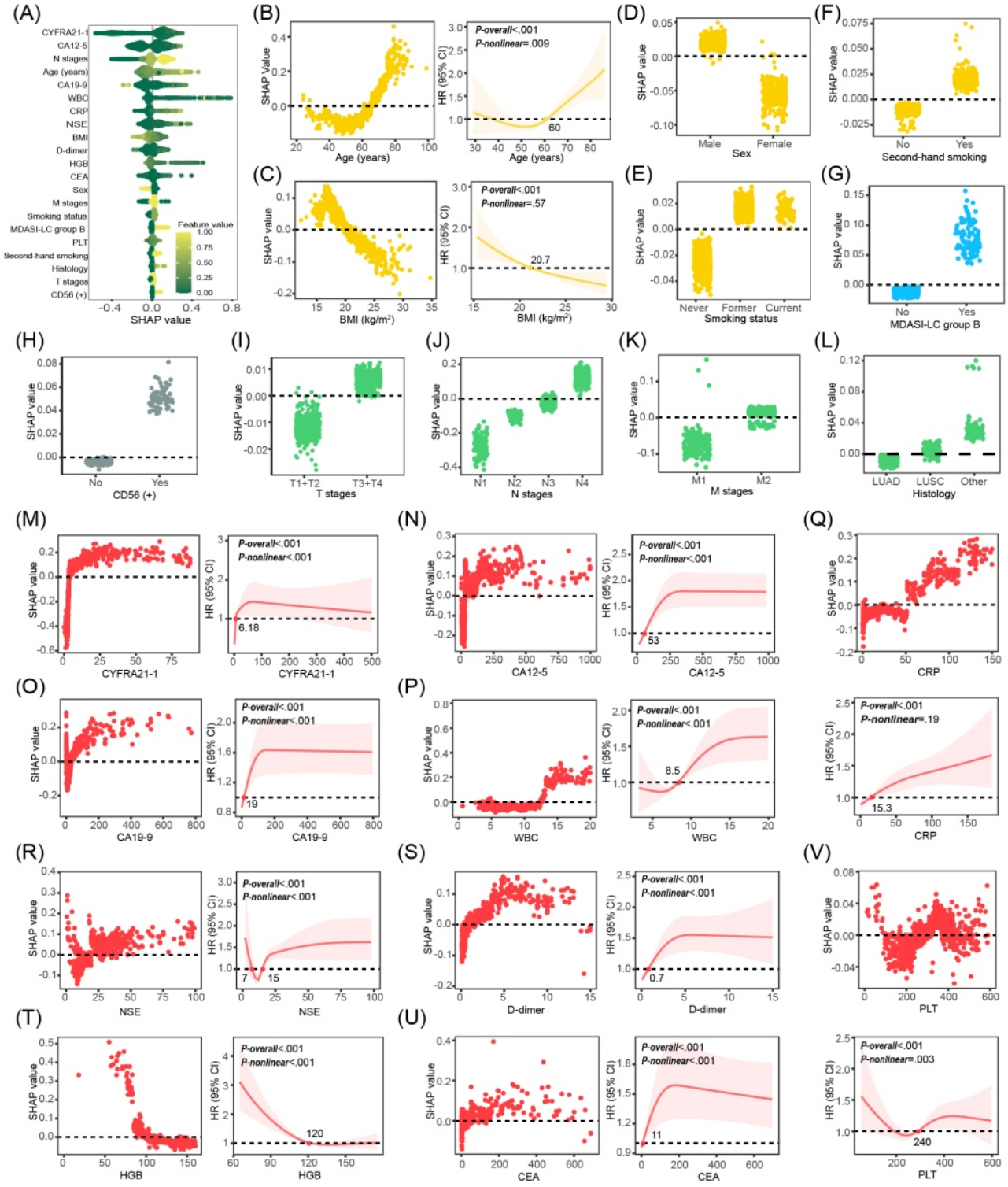


Feature Attribution Analysis

Figure 4A provides insights into the most significant features influencing the model's prediction of mortality risk in this study. These insights facilitate an improved understanding of the biological basis of risk and the identification of potential targets to optimize clinical care. The visualization of these influential features highlights their importance in guiding clinical decisions and the development of personalized treatment approaches grounded in individual patient risk profiles.

XSL•FO
RenderX

Figure 4. Visualization of feature importance and variable relationships influencing mortality risk. (A) displays the global feature importance. (B-F) illustrate partial dependence plots for demographic characteristics and RCS analyses for continuous variables. (G and H) and (I-L) show partial dependence plots for symptom burden PRO trajectories, immunohistochemical indicators, and tumor biological indicators, respectively. (M-V) provide partial dependence plots and RCS analysis results for prechemotherapy blood biomarkers. All partial dependence plots are annotated with the zero-SHAP value position, while the RCS plots show the points where changes in mortality risk occur. CA12-5: carbohydrate antigen 12-5; CA19-9: carbohydrate antigen 19-9; CD56: cluster of differentiation 56; CEA: carcinoembryonic antigen; CRP: C-reactive protein; CYFRA21-1: recombinant cytokeratin fragment antigen 21-1; HGB: hemoglobin; HR: hazard ratio; LUAD: lung adenocarcinoma; LUSC: lung squamous cell carcinoma; MDASI-LC: MD Anderson Symptom Inventory for Lung Cancer; NSE: neuron-specific enolase; PLT: platelet count; RCS: restricted cubic spline; SHAP: Shapley Additive Explanations; WBC: white blood cell.



The use of RCS in this study facilitated the detection of key inflection points within continuous variables, thereby providing valuable insights into the intricate relationships among factors that contribute to mortality risk in patients with lung cancer. This refined understanding can support clinical decision-making and provide personalized approaches to patient management.

XSL•FO
RenderX

Age emerged as a significant predictor of mortality risk, with a key threshold at 60 years. Individuals younger than 60 years of age presented with a lower and less prominent mortality risk, while the risk accelerated beyond this age (Figure 4B). BMI demonstrated an inverse relationship with mortality, with a critical value of 20.7 kg/m^2, below which mortality risk was diminished (Figure 4C). Furthermore, male sex, smoking history (inclusive of both former and current smoking), and passive smoke exposure were all linked to an increased mortality risk (Figures 4D and F).

Patients in the MDASI-LC relatively high-symptom burden group exhibited a higher mortality risk, with a median symptom score of 45.4 (IQR 36.2-51.4), while the other group had a score of 8.2 (IQR 5.2-19.8; Figure 4G). A higher chemotherapy symptom burden was associated with reduced survival.

Key clinical features, including the presence of cluster of differentiation 56 (CD56) positivity, T3 or T4 stage, N2, N3, and N4 stages, and M2 stage, were associated with a significantly higher relative risk of mortality. No significant difference in mortality risk was observed between patients with lung squamous cell carcinoma and lung adenocarcinoma, while patients with SCLC or other less frequently occurring lung cancers demonstrated decreased survival times (Figures 4H-L).

Prechemotherapy levels of laboratory markers recombinant cytokeratin fragment antigen 21-1, carbohydrate antigen 12-5, carbohydrate antigen 19-9, white blood cell count, D-dimer, and carcinoembryonic antigen showed a nonlinear increase in mortality risk, with respective critical values identified at 6.18 ng/mL, 53 U/mL, 19 U/mL, 8.5×10^9/L, 0.7 mg/L, and 11 ng/mL, respectively. Mortality risk was significantly higher beyond these thresholds. Hemoglobin exhibited a distinct pattern, with mortality risk increasing significantly at levels below 120 g/L. In contrast, C-reactive protein was associated with a linear increase in mortality risk, with a risk inflection point at 15.3 mg/L. Prechemotherapy neuron-specific enolase levels exhibited a nonlinear relationship with mortality, where risk increased both below 7 ng/mL and above 15 ng/mL. Platelet counts also had a nonlinear relationship with mortality risk, displaying an initial decrease followed by an increase, with a turning point at 240×10^9 per liter (Figures 4M-V).

The observed relationships are visually depicted in Shapley Additive Explanations partial dependence plots and through RCS analyses (Figures 4B-V). Subgroup analyses further confirmed these observations, demonstrating statistically significant differences in mortality risk associated with the described characteristics (P<.05), except for prechemotherapy platelet levels (Figure S2 in Multimedia Appendix 2 illustrating subgroup analysis validation performed after determining key values via feature attribution analysis).

Discussion

Principal Findings

This study developed a combined ML prediction model by integrating multisource data to assess the all-cause mortality risk of patients with lung cancer receiving chemotherapy. It identified key prognosis-related factors, including demographic characteristics, prechemotherapy laboratory indicators, longitudinal symptom burden, and clinical features, and analyzed the correlation patterns between each factor and mortality risk. The model exhibited favorable performance in discriminative ability, predictive accuracy, and clinical utility, with overall satisfactory effectiveness.

Demographic and Lifestyle Impacts on Lung Cancer Prognosis

Age is a core factor influencing the chemotherapy outcomes of patients with lung cancer. Aging is accompanied by decreased genomic and transcriptomic stability, leading to the accumulation of mutations and abnormal gene expression, which promotes the development of malignant tumor phenotypes and reduces treatment sensitivity. Meanwhile, aging-induced metabolic disorders (such as abnormal glucose metabolism and insulin resistance) provide a favorable environment for tumor growth; the decline in immune function weakens the body's antitumor capacity; and the reduction in tissue repair ability increases the risk of chemotherapy side effects, ultimately affecting survival [26-28]. The impact of sex on prognosis may be related to the regulation of tumor progression and chemotherapy response by sex hormones (especially estrogen), but the specific mechanism requires further research [29-31]. BMI showed a negative correlation with mortality risk, with a critical value of 20.7 kg/m^2, and the risk increased when BMI was below this value. This finding is consistent with the "obesity paradox"—individuals with mild overweight may gain survival advantages due to the secretion of cardioprotective adipokines by adipose tissue [32-34]. In addition, smoking history (including former and current smoking) and second-hand smoke exposure significantly increased mortality risk, emphasizing the importance of smoking cessation and reducing second-hand smoke exposure for improving treatment efficacy and survival [34]. These results suggest that chemotherapy regimens should be formulated based on individual patient characteristics; nutritional status should be closely monitored during treatment with targeted support provided; and research on sex-specific treatment differences needs to be strengthened.

The Prognostic Significance of Tumor Biological Characteristics

SCLC is often diagnosed at an advanced stage and is typically more aggressive. Tumors at T3/T4 stages (locally advanced or invasive tumors) are closely associated with increased tumor burden and local invasion, which may lead to chemotherapy resistance and elevated all-cause mortality risk [35]. The N stage reflects the spread of cancer cells to lymph nodes, leading to increased drug resistance. Patients with advanced metastatic stages (M2) frequently lose the opportunity for curative surgery, making platinum-based chemotherapy the main palliative treatment modality. However, metastatic disease, especially distant organ metastasis, is associated with inherent chemotherapy resistance, resulting in an unfavorable prognosis [36].

XSL•FO
RenderX

Potential Prognostic Value of CD56

The association between CD56 positivity and lung cancer prognosis remains controversial. Some studies have found a correlation with poor prognosis [37,38], while others have not observed a significant association [39]. This discrepancy may be related to sample size and patient population heterogeneity, and larger-scale multicenter studies are needed to clarify the relationship between the two.

Prognostic Value of PRO

This study suggested that the symptom burden reflected by the MDASI-LC score is related to survival time, with patients in the high-symptom burden group having a significantly increased mortality risk. This is consistent with previous research conclusions on the prognostic value of health-related quality of life [40]; incorporating MDASI-LC into routine follow-up can timely capture symptom changes and provide a basis for individualized prognostic management.

Clinical Application Value of Biomarkers

Blood biomarkers directly reflect tumor burden and biological characteristics. Elevated prechemotherapy biomarker levels have been associated with unfavorable chemotherapy outcomes in patients with lung cancer [41-44]. For patients with abnormal biomarkers, early interventions, such as anti-inflammatory and anti-infective treatments, can improve prognosis.

Limitations

This study has several limitations, which need to be taken into account when interpreting the results. The study used retrospective single-center data, which might limit the external validity and universality of the constructed model. Although the sample size of 1278 patients is relatively large for a single-center study, the complexity of the ML framework increases the risk of overfitting. We did not adjust the performance estimates using optimistic correction or penalty methods, which might overestimate the model's predictive ability. The robustness of the feature attribution results was not verified under different model parameter settings, so the stability of these key prognostic thresholds still needs to be further confirmed.

Among the 1278 enrolled patients with lung cancer undergoing chemotherapy, the survival rates at 1-, 3-, and 5-year follow-ups were 31.9% (95% CI 29.4%-34.6%), 7.4% (95% CI 6.0%-9.0%), and 1.5% (95% CI 0.9%-2.4%), respectively. A smaller sample size may increase the variability of the AUC statistic. This might be part of the reason why the 5-year AUC (0.915) is higher than the 1-year (0.740) and 3-year (0.777) AUC, which needs to be taken into account when interpreting the long-term predictive performance of the model.

In this study, 84 models were constructed on the training set, and then, the C-index was used on the test set to determine the best model. This process may violate the principle that the test set should only be used once to evaluate the performance of the final, prespecified model, which may lead to an overestimation of the model's C-index. In future research, model selection and hyperparameter tuning can be attempted to be accomplished solely through cross-validation of the training set, with the test set reserved only for evaluating the prespecified final model performance.

Conclusions

This study developed an innovative ML model to predict all-cause mortality risk in patients with lung cancer receiving chemotherapy. The model demonstrates acceptable discrimination, accuracy, and clinical efficacy, offering clinicians an interpretable tool for mortality risk assessment. By enabling personalized risk stratification, this model can guide targeted postchemotherapy care for patients with high risk, ultimately supporting the development of individualized treatment plans.

Acknowledgments

The authors are sincerely grateful to Professor Charles S Cleeland and Professor Shelley X Wang of The University of Texas MD Anderson Cancer Center and Professor Qiuling Shi from Chongqing Medical University, who provided the MD Anderson Symptom Inventory for Lung Cancer questionnaire and other assistance for this study.

Data Availability

The datasets generated or analyzed during this study are not publicly available due patient privacy but are available from the corresponding author on reasonable request.

Funding

This study was supported by the National Natural Science Foundation of China Grant (82173609, 82373678, 82574198, 81673267), Tertiary Education Scientific Research Project of Guangzhou Municipal Education Bureau (202235407), Key Research Fund for colleges and universities of Guangdong Education Department (2023ZDZX2049), Guangzhou Science and Technology Plan Project (2025A03J3605), Guangzhou Science and Technology Plan Project (2025A03J4485), and Guangdong Provincial Medical Science and Technology Research Fund Project (A2023352).

Authors' Contributions

Conceptualization: J Zou
Data curation: AL

XSL•FO
RenderX

Validation: ZL (lead), BR (supporting)
Formal analysis: JH (lead), CX (supporting)
Investigation: J Zou (lead), J Zhang (supporting), LL (supporting), FL (supporting)
Methodology: JH (lead), CX (equal)
Project administration: JL (lead), YD (equal), JC (supporting), FQ (supporting), LY (supporting)
Funding acquisition: JL (lead), LY (supporting), JC (supporting), XZ (supporting)
Visualization: JH (lead), DX (equal)
Writing—original draft: JH (lead), J Zou (equal)
Writing—review and editing: KL (lead), JH (supporting), J Zou (supporting)

Conflicts of Interest

None declared.

Multimedia Appendix 1
Complete baseline characteristics of chemotherapy-treated patients with lung cancer.
[DOCX File , 47 KB - medinform_v13i1e72424_app1.docx]

Multimedia Appendix 2
The evaluation of trajectory model fitting for the MD Anderson Symptom Inventory for Lung Cancer, Karnofsky Performance Status, and Zubrod Performance Score scales, the comparison of baseline data distribution before and after missForest interpolation, the results of univariate Cox regression, the comparison of baseline characteristics between the training and test sets, and the subgroup analysis of key values for feature attribution.
[DOCX File , 253 KB - medinform_v13i1e72424_app2.docx]

References

1. Bray F, Laversanne M, Sung H, Ferlay J, Siegel RL, Soerjomataram I, et al. Global cancer statistics 2022: GLOBOCAN estimates of incidence and mortality worldwide for 36 cancers in 185 countries. CA Cancer J Clin 2024;74(3):229-263 [FREE Full text] [doi: 10.3322/caac.21834] [Medline: 38572751]
2. Zhao Y, Mei T, Na F, Tian X, Ao R, Long X, et al. First-line treatment of driver gene-negative metastatic lung adenocarcinoma with malignant pleural effusion: should chemotherapy be combined with an immune checkpoint inhibitor or bevacizumab? Invest New Drugs 2024;42(2):196-206 [FREE Full text] [doi: 10.1007/s10637-024-01424-4] [Medline: 38386170]
3. Wu K, House L, Liu W, Cho WCS. Personalized targeted therapy for lung cancer. Int J Mol Sci 2012;13(9):11471-11496 [FREE Full text] [doi: 10.3390/ijms130911471] [Medline: 23109866]
4. Pei Q, Luo Y, Chen Y, Li J, Xie D, Ye T. Artificial intelligence in clinical applications for lung cancer: diagnosis, treatment and prognosis. Clin Chem Lab Med 2022;60(12):1974-1983 [FREE Full text] [doi: 10.1515/cclm-2022-0291] [Medline: 35771735]
5. Huang Z, Hu C, Chi C, Jiang Z, Tong Y, Zhao C. An artificial intelligence model for predicting 1-year survival of bone metastases in non-small-cell lung cancer patients based on XGBoost algorithm. Biomed Res Int 2020;2020:3462363 [FREE Full text] [doi: 10.1155/2020/3462363] [Medline: 32685470]
6. Sibille L, Seifert R, Avramovic N, Vehren T, Spottiswoode B, Zuehlsdorff S, et al. 18F-FDG PET/CT uptake classification in lymphoma and lung cancer by using deep convolutional neural networks. Radiology 2020;294(2):445-452. [doi: 10.1148/radiol.2019191114] [Medline: 31821122]
7. Goldstraw P, Crowley J, Chansky K, Giroux DJ, Groome PA, Rami-Porta R, et al. The IASLC Lung Cancer Staging Project: proposals for the revision of the TNM stage groupings in the forthcoming (seventh) edition of the TNM Classification of malignant tumours. J Thorac Oncol 2007;2(8):706-714 [FREE Full text] [doi: 10.1097/JTO.0b013e31812f3c1a] [Medline: 17762336]
8. López-Encuentra A, López-Ríos F, Conde E, García-Luján R, Suárez-Gauthier A, Mañes N, et al. Composite anatomical-clinical-molecular prognostic model in non-small cell lung cancer. Eur Respir J 2011;37(1):136-142 [FREE Full text] [doi: 10.1183/09031936.00028610] [Medline: 20817702]
9. Zhang R, Chen C, Dong X, Shen S, Lai L, He J, et al. Independent validation of early-stage non-small cell lung cancer prognostic scores incorporating epigenetic and transcriptional biomarkers with gene-gene interactions and main effects. Chest 2020;158(2):808-819 [FREE Full text] [doi: 10.1016/j.chest.2020.01.048] [Medline: 32113923]
10. Chen YX, Chen J, Yin JY, Zhou HH, He BM, Liu ZQ. Non-coding RNA polymorphisms (rs2910164 and rs1333049) associated with prognosis of lung cancer under platinum-based chemotherapy. Front Pharmacol 2021;12:709528 [FREE Full text] [doi: 10.3389/fphar.2021.709528] [Medline: 34603024]

XSL•FO
RenderX

11. Rudin CM, Durinck S, Stawiski EW, Poirier JT, Modrusan Z, Shames DS, et al. Comprehensive genomic analysis identifies SOX2 as a frequently amplified gene in small-cell lung cancer. Nat Genet 2012;44(10):1111-1116 [FREE Full text] [doi: 10.1038/ng.2405] [Medline: 22941189]
12. Cleeland CS, Mendoza TR, Wang XS, Chou C, Harle MT, Morrissey M, et al. Assessing symptom distress in cancer patients: the M.D. Anderson Symptom Inventory. Cancer 2000;89(7):1634-1646. [doi: 10.1002/1097-0142(20001001)89:7<1634::aid-cncr29>3.0.co;2-v] [Medline: 11013380]
13. Wei X, Yu H, Dai W, Mu Y, Wang Y, Liao J, et al. Patient-reported outcomes of video-assisted thoracoscopic surgery versus thoracotomy for locally advanced lung cancer: a longitudinal cohort study. Ann Surg Oncol 2021;28(13):8358-8371. [doi: 10.1245/s10434-021-09981-1] [Medline: 33880671]
14. Calvert M, Kyte D, Mercieca-Bebber R, Slade A, Chan A, King MT, et al. Guidelines for inclusion of patient-reported outcomes in clinical trial protocols: the SPIRIT-PRO Extension. JAMA 2018;319(5):483-494 [FREE Full text] [doi: 10.1001/jama.2017.21903] [Medline: 29411037]
15. Efficace F, Bottomley A, Smit E, Lianes P, Legrand C, Debruyne C, et al. Is a patient's self-reported health-related quality of life a prognostic factor for survival in non-small-cell lung cancer patients? A multivariate analysis of prognostic factors of EORTC study 08975. Ann Oncol 2006;17(11):1698-1704 [FREE Full text] [doi: 10.1093/annonc/mdl183] [Medline: 16968876]
16. Deliu N, Cottone F, Collins GS, Anota A, Efficace F. Evaluating methodological quality of Prognostic models Including Patient-reported HeAlth outcomes iN oncologY (EPIPHANY): a systematic review protocol. BMJ Open 2018;8(10):e025054 [FREE Full text] [doi: 10.1136/bmjopen-2018-025054] [Medline: 30361409]
17. Collins GS, Reitsma JB, Altman DG, Moons KGM. Transparent reporting of a multivariable prediction model for individual prognosis or diagnosis (TRIPOD): the TRIPOD statement. BMJ 2015;350:g7594 [FREE Full text] [doi: 10.1136/bmj.g7594] [Medline: 25569120]
18. Mendoza TR, Wang XS, Lu C, Palos GR, Liao Z, Mobley GM, et al. Measuring the symptom burden of lung cancer: the validity and utility of the lung cancer module of the M. D. Anderson Symptom Inventory. Oncologist 2011;16(2):217-227 [FREE Full text] [doi: 10.1634/theoncologist.2010-0193] [Medline: 21285393]
19. Mor V, Laliberte L, Morris JN, Wiemann M. The Karnofsky Performance Status Scale. An examination of its reliability and validity in a research setting. Cancer 1984;53(9):2002-2007. [doi: 10.1002/1097-0142(19840501)53:9<2002::aid-cncr2820530933>3.0.co;2-w] [Medline: 6704925]
20. Oken MM, Creech RH, Tormey DC, Horton J, Davis TE, McFadden ET, et al. Toxicity and response criteria of the Eastern Cooperative Oncology Group. Am J Clin Oncol 1982;5(6):649-655. [Medline: 7165009]
21. Nagin DS. Group-based trajectory modeling: an overview. Ann Nutr Metab 2014;65(2-3):205-210. [doi: 10.1159/000360229] [Medline: 25413659]
22. Ishwaran H, Kogalur UB, Blackstone EH, Lauer MS. Random survival forests. Ann Appl Stat 2008;2(3):841-860. [doi: 10.1214/08-aoas169]
23. Friedman JH. Greedy function approximation: a gradient boosting machine. Ann Stat 2001 Oct 1;29(5):1189-1232. [doi: 10.1214/aos/1013203451]
24. Van Belle V, Pelckmans K, Van Huffel S, Suykens JAK. Support vector methods for survival analysis: a comparison between ranking and regression approaches. Artif Intell Med 2011;53(2):107-118. [doi: 10.1016/j.artmed.2011.06.006] [Medline: 21821401]
25. Zou H, Hastie T. Addendum: regularization and variable selection via the elastic net. J R Stat Soc Series B Stat Methodol 2005;67(5):768 [FREE Full text] [doi: 10.1111/j.1467-9868.2005.00527.x]
26. Ianniello A, Sansovini M, Severi S, Nicolini S, Grana CM, Massri K, et al. Peptide receptor radionuclide therapy with (177)Lu-DOTATATE in advanced bronchial carcinoids: prognostic role of thyroid transcription factor 1 and (18)F-FDG PET. Eur J Nucl Med Mol Imaging 2016;43(6):1040-1046. [doi: 10.1007/s00259-015-3262-8] [Medline: 26611427]
27. Li S, Wang W, Yu H, Zhang S, Bi W, Sun S, et al. Characterization of genomic instability-related genes predicts survival and therapeutic response in lung adenocarcinoma. BMC Cancer 2023;23(1):1115 [FREE Full text] [doi: 10.1186/s12885-023-11580-0] [Medline: 37974107]
28. Feng J, Lan Y, Liu F, Yuan Y, Ge J, Wei S, et al. Combination of genomic instability score and TP53 status for prognosis prediction in lung adenocarcinoma. NPJ Precis Oncol 2023;7(1):110 [FREE Full text] [doi: 10.1038/s41698-023-00465-x] [Medline: 37907595]
29. Wisnivesky JP, Halm EA. Sex differences in lung cancer survival: do tumors behave differently in elderly women? J Clin Oncol 2007;25(13):1705-1712. [doi: 10.1200/JCO.2006.08.1455] [Medline: 17470862]
30. Skuladottir H, Olsen JH. Can reproductive pattern explain better survival of women with lung cancer? Acta Oncol 2006;45(1):47-53. [doi: 10.1080/02841860500374455] [Medline: 16464795]
31. Moore KA, Mery CM, Jaklitsch MT, Estocin AP, Bueno R, Swanson SJ, et al. Menopausal effects on presentation, treatment, and survival of women with non-small cell lung cancer. Ann Thorac Surg 2003;76(6):1789-1795. [doi: 10.1016/s0003-4975(03)01024-5] [Medline: 14667585]
32. Johnston EM, McIntyre LM, Hoff JA, Bepler G. The effect of orchiectomy on lung cancer survival. Anticancer Res 1999;19(6C):5567-5570. [Medline: 10697618]

XSL•FO
RenderX

33. Antonopoulos AS, Tousoulis D. The molecular mechanisms of obesity paradox. Cardiovasc Res 2017;113(9):1074-1086. [doi: 10.1093/cvr/cvx106] [Medline: 28549096]
34. Caan BJ, Cespedes Feliciano EM, Kroenke CH. The importance of body composition in explaining the overweight paradox in cancer-counterpoint. Cancer Res 2018;78(8):1906-1912 [FREE Full text] [doi: 10.1158/0008-5472.CAN-17-3287] [Medline: 29654153]
35. Bergman M, Fountoukidis G, Smith D, Ahlgren J, Lambe M, Valachis A. Effect of smoking on treatment efficacy and toxicity in patients with cancer: a systematic review and meta-analysis. Cancers (Basel) 2022;14(17):4117 [FREE Full text] [doi: 10.3390/cancers14174117] [Medline: 36077654]
36. Wu Y, Yuan M, Wang C, Chen Y, Zhang Y, Zhang J. T lymphocyte cell: a pivotal player in lung cancer. Front Immunol 2023;14:1102778. [doi: 10.3389/fimmu.2023.1102778] [Medline: 36776832]
37. Feng J, Sheng H, Zhu C, Qian X, Wan D, Su D, et al. Correlation of neuroendocrine features with prognosis of non-small cell lung cancer. Oncotarget 2016;7(44):71727-71736 [FREE Full text] [doi: 10.18632/oncotarget.12327] [Medline: 27687592]
38. Wang X, Zhang Y, Hu M, Wang R, Liu L, Qian K, et al. Prognostic and predictive value of thyroid transcription factor-1, CD56, P40 and other clinical characteristics in small cell lung cancer patients. Zhongguo Fei Ai Za Zhi 2017;20(8):522-527 [FREE Full text] [doi: 10.3779/j.issn.1009-3419.2017.08.04] [Medline: 28855032]
39. Georgakopoulou V, Zygouris E, Damaskos C, Pierrakou A, Papalexis P, Garmpis N, et al. Prognostic value of the immunohistochemistry markers CD56, TTF-1, synaptophysin, CEA, EMA and NSE in surgically resected lung carcinoid tumors. Mol Clin Oncol 2022;16(2):31 [FREE Full text] [doi: 10.3892/mco.2021.2464] [Medline: 34984102]
40. Wang XS, Shi Q, Lu C, Basch EM, Johnson VE, Mendoza TR, et al. Prognostic value of symptom burden for overall survival in patients receiving chemotherapy for advanced nonsmall cell lung cancer. Cancer 2010;116(1):137-145 [FREE Full text] [doi: 10.1002/cncr.24703] [Medline: 19852033]
41. Barlési F, Gimenez C, Torre J, Doddoli C, Mancini J, Greillier L, et al. Prognostic value of combination of Cyfra 21-1, CEA and NSE in patients with advanced non-small cell lung cancer. Respir Med 2004;98(4):357-362 [FREE Full text] [doi: 10.1016/j.rmed.2003.11.003] [Medline: 15080079]
42. Mandrekar SJ, Schild SE, Hillman SL, Allen KL, Marks RS, Mailliard JA, et al. A prognostic model for advanced stage nonsmall cell lung cancer. Pooled analysis of North Central Cancer Treatment Group trials. Cancer 2006;107(4):781-792 [FREE Full text] [doi: 10.1002/cncr.22049] [Medline: 16847887]
43. Kanoh Y, Abe T, Masuda N, Akahoshi T. Progression of non-small cell lung cancer: diagnostic and prognostic utility of matrix metalloproteinase-2, C-reactive protein and serum amyloid A. Oncol Rep 2013;29(2):469-473. [doi: 10.3892/or.2012.2123] [Medline: 23135313]
44. Albain KS, Crowley JJ, LeBlanc M, Livingston RB. Survival determinants in extensive-stage non-small-cell lung cancer: the Southwest Oncology Group experience. J Clin Oncol 1991;9(9):1618-1626. [doi: 10.1200/JCO.1991.9.9.1618] [Medline: 1651993]

Abbreviations

AUC: area under the curve
CD56: cluster of differentiation 56
C-index: concordance index
Enet: elastic net
GBM: gradient boosting machine
GBTM: group-based trajectory modeling
KPS: Karnofsky Performance Status
MDASI-LC: MD Anderson Symptom Inventory for Lung Cancer
ML: machine learning
PRO: patient-reported outcome
RCS: restricted cubic spline
RSF: random survival forest
SCLC: small cell lung cancer
Survival-SVM: survival support vector machine
ZPS: Zubrod Performance Score

XSL•FO
RenderX

Edited by A Coristine, A Castonguay; submitted 10.02.25; peer-reviewed by C Wu, W Fu, D Surian; comments to author 28.04.25; accepted 18.11.25; published 18.12.25.

Please cite as:
Zou J, Huang J, Lu K, Lin A, Xie C, Zhang J, Rao B, Li Z, Xie D, Lu L, Luo F, Chen J, Yang L, Qiu F, Zhang X, Deng Y, Lu J
A Machine Learning Approach to Predicting Mortality Risk in Chemotherapy-Treated Lung Cancer: Machine Learning Model Development and Validation
JMIR Med Inform 2025;13:e72424
URL: https://medinform.jmir.org/2025/1/e72424
doi:10.2196/72424
PMID:41411039

©Jianjun Zou, Jinyi Huang, Katie Lu, Ao Lin, Chen Xie, Jinrong Zhang, Boqi Rao, Zhi Li, Dongming Xie, Ling Lu, Feng Luo, Jinbin Chen, Lei Yang, Fuman Qiu, Xin Zhang, Yibin Deng, Jiachun Lu. Originally published in JMIR Medical Informatics (https://medinform.jmir.org), 18.12.2025. This is an open-access article distributed under the terms of the Creative Commons Attribution License (https://creativecommons.org/licenses/by/4.0/), which permits unrestricted use, distribution, and reproduction in any medium, provided the original work, first published in JMIR Medical Informatics, is properly cited. The complete bibliographic information, a link to the original publication on https://medinform.jmir.org/, as well as this copyright and license information must be included.

XSL•FO
RenderX

Original Paper

A Machine Learning Model Based on Clinical Factors to Predict the Efficacy of First-Line Immunochemotherapy for Patients With Advanced Gastric Cancer: Retrospective Study

Xu Cheng[1,2], MSc; Ping Li[1,2], PhD; Enqing Meng[1,2], MSc; Xinyi Wu[1,2], MBS; Hao Wu[1,2], PhD

[1]Gastric Cancer Center, The First Affiliated Hospital of Nanjing Medical University, Nanjing, China

[2]Department of Oncology, The First Affiliated Hospital of Nanjing Medical University, Nanjing, China

Corresponding Author:
Hao Wu, PhD
Department of Oncology
The First Affiliated Hospital of Nanjing Medical University
No. 300, Guangzhou Road, Gulou District, Nanjing City, Jiangsu Province
Nanjing, 210029
China
Phone: 86 13913855335
Email: whdactor@njmu.edu.cn

Abstract

Background: The development of immunotherapy has provided new hope for patients with advanced gastric cancer (AGC). However, due to the high heterogeneity of the disease, the efficacy of first-line immunochemotherapy varies among patients. There is still a lack of simple and effective models to predict the efficacy of immunochemotherapy in this setting.

Objective: This study aimed to identify critical factors and develop predictive models to evaluate the efficacy of first-line immunochemotherapy in patients with AGC using clinically available data. The goal was to offer evidence-based guidance for clinical practice and enable personalized treatment strategies.

Methods: To evaluate the effectiveness of first-line immunochemotherapy in AGC, we retrospectively collected clinical data from The First Affiliated Hospital of Nanjing Medical University between January 2018 and October 2023. The data collected were divided into a training set (168/240, 70%) and an internal validation set (72/240, 30%). Additionally, a temporal validation cohort of 76 patients recruited from November 2023 to September 2024 was assembled to further evaluate the predictive performance of the models. We used univariate and multivariate Cox regression analyses, along with the least absolute shrinkage and selection operator (LASSO) regression, and integrated clinical expertise to identify key predictors of treatment efficacy and to construct the LASSO-Cox model. We developed 4 models (LASSO-Cox, random survival forest [RSF], extreme gradient boosting, and survival support vector machine) and evaluated their performance using the C-index, area under the curve (AUC), calibration curves, and decision curve analysis. The optimal model was interpreted using Shapley additive explanations, and its risk scores were used to stratify patients for Kaplan-Meier survival analysis.

Results: Among the 4 prognostic models developed in this study, the RSF model demonstrated superior predictive accuracy and discrimination for progression-free survival, as evidenced by its higher AUC, concordance index, continuous AUC curves, and calibration curves compared with the other 3 models. Additionally, decision curve analysis showed that the RSF model offered greater net clinical benefit. The Shapley additive explanations results identified that age, histological subtype, the proportion of $CD19^+$ B cells, $CD16^+CD56^+$ natural killer cells, and the presence of liver metastasis were key prognostic factors influencing patient outcomes. Patients in the low-risk group, as determined by the RSF model's risk score, exhibited a significantly higher progression-free survival rate than those in the high-risk group, further validating the value of the RSF model for risk stratification.

Conclusions: This study is the first to use machine learning algorithms to develop a predictive model for the efficacy of first-line immunochemotherapy in AGC, and to identify key predictors of treatment outcome. The results indicate that the RSF model not only enables precise stratification of patients likely to benefit but, more importantly, provides quantifiable decision support for individualized clinical strategies, underscoring its potential value in clinical decision-making.

(JMIR Med Inform 2025;13:e82533) doi:10.2196/82533

XSL•FO
RenderX

KEYWORDS

advanced gastric cancer; immunochemotherapy; machine learning; random survival forest; prognostic models

Introduction

Gastric cancer (GC) ranks as the fifth most common malignancy worldwide and is the fourth leading cause of cancer-related mortality [1]. In 2022, there were over 968,000 new cases of GC, resulting in nearly 660,000 deaths [2]. Due to the delayed onset of clinical symptoms and the absence of effective diagnostic methods for early-stage GC, 40% of patients are diagnosed at an advanced stage, where surgical intervention is typically not feasible [3]. Among patients undergoing radical resection, over two-thirds experience recurrence or metastasis [4,5]. Consequently, chemotherapy remains the cornerstone of treatment for advanced gastric cancer (AGC), yet the prognosis for advanced or metastatic cases remains dismal, with an overall survival (OS) of only 9-14 months [6]. Therefore, a comprehensive upfront assessment of prognosis is essential for guiding clinical decisions in multidisciplinary treatment approaches [7].

The advent of immune checkpoint inhibitors (ICIs), particularly those targeting programmed cell death protein 1 (PD-1) and programmed death-ligand 1 (PD-L1), has revolutionized cancer therapy, yielding robust and durable responses in GC. Clinical trials, such as CheckMate-649 and KEYNOTE-062, have demonstrated that combining immunochemotherapy significantly improves OS and progression-free survival (PFS) in patients with PD-L1–positive tumors [8,9]. However, the high heterogeneity of GC leads to variations in the efficacy of immunochemotherapy among different patients [10]. Identifying individuals who are likely to respond to immunochemotherapy is therefore critical for providing personalized treatment.

Nowadays, numerous biomarkers, including tumor mutation burden (TMB), PD-L1 expression, microsatellite instability (MSI), and Epstein-Barr virus infection status, have been proposed to predict responsiveness to PD-1 and PD-L1 inhibitors [11,12]. Additionally, circulating tumor DNA positivity has been associated with relapse and poorer prognosis [13]. However, given the highly heterogeneous nature of GC, relying on a single factor for prognostic prediction is often insufficient [14]. For instance, only 45% of patients with high TMB (≥20 mutations per megabase [mut/Mb]) respond to immunotherapy, while approximately 5% of patients with low TMB exhibit significant therapeutic responses to ICIs [15,16]. Furthermore, the predictive utility of single biomarkers is undermined by the dynamic alteration of the tumor microenvironment following therapeutic interventions (eg, chemotherapy or radiotherapy), as well as inconsistencies in detection methodologies and threshold definitions—such as the varying PD-L1 scoring systems (tumor proportion score, combined positive score, immune cell score, and H-score) and platform-dependent criteria for MSI and TMB. While recent studies have developed prognostic models based on transcriptomics or targeted metabolomics [17-19], the clinical translation of these omics-based signatures is severely constrained by their high costs, complex data processing, and reliance on specialized laboratory infrastructure [20,21]. This creates a clear and unmet need for prognostic tools built on more accessible, cost-effective, and routinely collected data. Although recent studies have made progress in applying machine learning (ML) algorithms to clinical data for postoperative patients with GC or to predict immunotherapy-related adverse events in AGC [22,23], a critical gap remains, as robust predictive models for the efficacy of first-line immunochemotherapy in the advanced setting are notably lacking. Therefore, this study was designed to address this specific gap. We aimed to develop and validate a robust prognostic model based only on readily available baseline clinical parameters. The objective of this tool is to effectively predict first-line immunochemotherapy outcomes, identify patients most likely to benefit, and thereby advance personalized therapy for AGC. Furthermore, understanding the key risk factors derived from such a model is crucial for devising appropriate follow-up strategies.

The Cox proportional hazards model has long been the standard for quantifying the impact of clinical indicators on survival outcomes [24,25]. However, its reliance on linear assumptions often fails to capture the intricate, nonlinear patterns characteristic of heterogeneous diseases like GC. Consequently, there is a need for more adaptive modeling strategies to maximize predictive performance. To this end, we used a comprehensive ML framework comprising random survival forest (RSF), extreme gradient boosting (XGBoost), and survival support vector machine (SVM). These algorithms were selected for their specific strengths in handling complex survival data: RSF is robust in ranking variable importance [26,27]; XGBoost offers superior efficiency and the ability to model complex feature interactions; and survival-SVM excels in distinguishing risk stratifications in high-dimensional spaces [28,29]. Our primary objective was not merely to compare these methodologies, but to leverage their combined strengths to select the best-performing model. This approach ensures the development of a clinically practical and highly accurate prognostic instrument for first-line immunochemotherapy [30-32].

Given the poor prognosis and high recurrence rate of AGC, as well as the urgent need for individualized treatment strategies, the ability to predict risk factors associated with prognosis and survival rates before treatment could enable more targeted therapeutic adjustments, ultimately improving patient outcomes and quality of life. This study aims to retrospectively analyze the clinical and pathological data of patients with AGC who received first-line immunochemotherapy. By identifying key prognostic factors that predict the efficacy of immunochemotherapy, 4 prognostic models will be developed and compared in terms of discrimination, calibration, stability, and clinical net benefit. The optimal model will be selected for clinical application, providing a reference for personalized treatment strategies and ultimately improving the prognosis of patients with AGC.

XSL•FO
RenderX

Methods

Data Source and Study Population

Clinical data of patients for the model development cohort were collected retrospectively from January 1, 2018, to October 31, 2023, at The First Affiliated Hospital of Nanjing Medical University, China. Additionally, a temporal validation cohort between November 1, 2023, and September 13, 2024, was included from the same hospital. Patients were enrolled in this study based on the following inclusion criteria: (1) aged 18 years or older, (2) histologically or cytologically confirmed gastric adenocarcinoma, (3) received ICIs as first-line treatment for advanced disease, (4) presence of at least 1 measurable lesion according to the Response Evaluation Criteria in Solid Tumors (RECIST) version 1.1. (lesions in hollow viscera, such as the esophagus and stomach, were not considered measurable; lesions situated in a previously irradiated area were considered measurable only if progression had been demonstrated), and (5) Eastern Cooperative Oncology Group performance status of 0 or 1. The exclusion criteria were (1) discontinuation of treatment due to intolerance to immunotherapy or combination agents, (2) receiving fewer than 2 treatment cycles, precluding efficacy assessment, (3) presence of concurrent malignancies of other origins, and (4) incomplete baseline clinical data or lost to follow-up.

Data Collection and Outcomes

Baseline characteristics were assessed, including age, sex, BMI, presence of underlying comorbidities, Eastern Cooperative Oncology Group performance status, smoking history, drinking history, tumor location (including cardia and esophagogastric junction, fundus, body, antrum, and pylorus of the stomach), Lauren classification (including intestinal type, mixed type, diffuse type, and unknown), tumor differentiation (including G3, G2, G2-G3, and unknown), histopathological type (including gastric adenocarcinoma and signet ring cell carcinoma), intraperitoneal chemotherapy (with or without), type of PD-1 or PD-L1 inhibitor (including sintilimab, nivolumab, tislelizumab, camrelizumab, and others), radiotherapy (with or without), targeted therapy (with or without), use of antiangiogenic drugs (including anlotinib, apatinib, others, and none), pretreatment levels of alpha-fetoprotein (AFP; <1.9 or ≥1.9 ng/μL), the pretreatment percentage of $CD16^+CD56^+$ natural killer (NK) cell (<27.41 or ≥27.41), the pretreatment percentage of the ratio of $CD4^+$ to $CD8^+$ T cell (<2.66 or ≥2.66), the pretreatment percentage of $CD19^+$ B cell (<12.04 or ≥12.04), human epidermal growth factor receptor 2 (HER2) expression status (including positive, negative, and unknown), PD-L1 expression status (including positive, negative, and unknown), microsatellite stability (including microsatellite stability, high MSI, and unknown), TMB status (including low, high, and unknown), presence of liver metastasis (with or without), peritoneal metastasis (with or without), bone metastasis (with or without), and distant organ metastasis (with or without).

To ensure data consistency and reliability, all data collection adhered to strict standards. Tumor location, differentiation grade, Lauren classification, and histopathological type were categorized based on the 2024 guidelines of the Chinese Society of Clinical Oncology. BMI was classified according to the World Health Organization criteria, with a BMI ≥25 considered overweight. Continuous numerical variables, including age, pretreatment levels of AFP, and pretreatment lymphocyte subset percentages, were subsequently categorized into discrete groups by determining optimal cutoff values in order to enhance analytical convenience and effectiveness. HER2 expression status was determined through immunohistochemistry or fluorescence in situ hybridization: 0 to 1+ was classified as negative; 2+ was considered equivocal, requiring confirmation via fluorescence in situ hybridization; and 3+ was classified as positive. PD-L1 expression status was assessed following the standards of the US Food and Drug Administration: PD-L1 combined positive score <1 was classified as negative; PD-L1 combined positive score ≥1 was classified as positive. Microsatellite stability status was defined as follows: microsatellite stability indicated no significant difference in microsatellite length between tumor and normal tissue; high MSI was defined as the presence of insertion or deletion mutations in at least 2 microsatellite loci. TMB≥10 mut/Mb was classified as high expression; TMB<10 mut/Mb was categorized as low expression. AFP and lymphocyte subset data were obtained from peripheral blood samples collected before first-line immunochemotherapy in patients with AGC. Distant metastasis and disease progression were evaluated through contrast-enhanced computed tomography scans of the chest and entire abdomen. Progressive disease was determined based on the RECIST version 1.1. The primary end points of this study were the predictive capability, validity, and clinical utility of the developed prognostic model. The primary time-to-event outcome was PFS, defined as the interval from the initiation of first-line immunochemotherapy to the date of radiologically confirmed disease progression. The model development cohort was followed up until March 13, 2024, while the temporal validation cohort was followed up until September 13, 2024. Progressive disease was assessed via imaging evaluations conducted every 2 treatment cycles, ensuring that all outcome assessments were supported by radiographic evidence. This methodology ensures the robustness and clinical applicability of the prognostic models developed in this study.

Statistical Analysis

The dataset for the model development cohort was split into a training cohort (168/240, 70%) and a validation cohort (72/240, 30%). The training cohort was used for model construction, while the training cohort and the internal validation cohort were used for model assessment. Additionally, a temporal validation cohort was used to further assess model performance over time as an external validation set. Categorical variables are presented as frequencies and percentages, with group comparisons made using the chi-square test or Fisher exact test. Normally distributed continuous variables are expressed as the mean and SD, and between-group comparisons are performed using the 2-tailed *t*-test. Nonnormally distributed continuous variables are reported as the median and IQR, with between-group comparisons conducted using the Wilcoxon rank-sum test. Statistical significance is defined as $P<.05$.

XSL•FO
RenderX

All baseline clinical characteristics were incorporated into the construction of the prognostic model. Patients with missing data rates ≥10% for baseline characteristics were excluded from the analysis. For cases with missing values <10%, we used multiple imputation by chained equations, implemented with the "mice" R package. The multiple imputation by chained equations procedure was configured to generate five imputed datasets (m=5), with a fixed random seed to ensure reproducibility. The imputation model included predictor variables (the pretreatment proportions of $CD16^+CD56^+$ NK cells, $CD19^+$ B cells, and $CD4^+/CD8^+$ T cells) and the outcome variable (PFS and event status) to preserve prognostic correlations. For continuous variables, the default predictive mean matching method was used, which is robust to nonnormality. This advanced approach iteratively generates multiple imputed datasets through observed data patterns while appropriately accounting for the uncertainty inherent in the imputation process. After imputation, we generate diagnostic plots to examine the distribution of the imputed data (Multimedia Appendix 1). The results indicated that, for most variables, the imputed values aligned well with the original data distribution. Because missing data patterns may influence study outcomes, we conducted 2-tailed *t*-tests and Kolmogorov-Smirnov (KS) tests on both the imputed and original complete datasets to assess any significant differences. The pretreatment proportion of $CD16^+CD56^+$ NK cells had 2-tailed *t*-test and KS test *P* values of .73 and .98, respectively, before and after imputation; the pretreatment proportion of $CD19^+$ B cells showed 2-tailed *t*-test and KS test *P* values of .51 and .99, respectively; and the pretreatment proportion of $CD4^+/CD8^+$ T cells had 2-tailed *t*-test and KS test *P* values of .60 and .99, respectively. None of these variables demonstrated a statistically significant difference ($P>.05$), suggesting that the chosen imputation method had minimal impact on the overall analysis. Furthermore, to assess the robustness of our results and rule out potential bias introduced by the imputation of missing values, a sensitivity analysis was performed. We reconstructed and re-evaluated all 4 models using a complete-case cohort (excluding all patients with missing data). The results from this analysis were consistent with those derived from the imputed dataset, indicating that the imputation procedure introduced negligible bias to the model performance (Multimedia Appendix 2).

In this study, important predictive features were identified through a combination of univariate analysis, least absolute shrinkage and selection operator (LASSO) regression, multivariate analysis, and the clinical expertise of 2 experienced clinicians, which served as the foundation for constructing a LASSO-Cox model. In parallel, ML was used to develop RSF, XGBoost, and survival-SVM models, with parameter tuning carried out for each. The performance of these 4 models was systematically evaluated and compared using metrics such as area under the curve (AUC), concordance index (C-index), receiver operating characteristic (ROC) curves, continuous AUC curves, calibration curves, and decision curve analysis (DCA) to identify the optimal predictive model. Patients were then stratified into high- and low-risk groups based on the risk scores derived from this optimal model, and Kaplan-Meier (KM) analysis was performed to assess survival differences. Finally, Shapley additive explanations (SHAP) analysis was conducted to interpret the optimal model and to pinpoint the key predictive variables. All statistical analyses were performed using R version 4.4.1 (R Foundation for Statistical Computing).

Ethical Considerations

This study was approved by the Ethics Committee of The First Affiliated Hospital of Nanjing Medical University (approval 2024-SR-453). No personally identifiable information was involved in this study. Due to the retrospective nature of the research, the requirement for informed consent was waived.

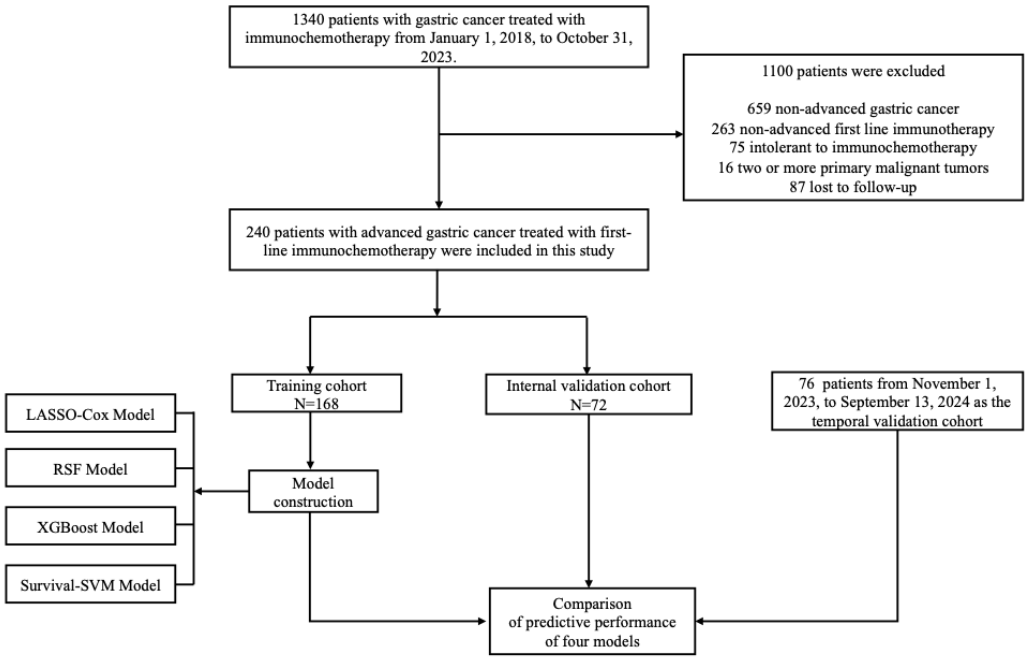
Results

The Clinical Characteristics of Patients With AGC

The workflow of the study is illustrated in Figure 1. Ultimately, 316 eligible patients were included in the study. Among them, 240 patients were enrolled between January 1, 2018 and October 31, 2023, forming the model development cohort, while the remaining 76 patients, recruited between November 1, 2023 and September 13, 2024, comprised the temporal validation cohort for further assessment of the model's predictive performance. The median follow-up duration for the model development cohort was 16 (95% CI 13.1-18.9) months, with a median progression-free survival (mPFS) of 8.97 (95% CI 7.9-11.1) months. In the temporal validation cohort, the median follow-up time was 10.3 (95% CI 9.5-upper limit not reached) months. Patients in the model development cohort were randomly divided into a training set (n=168, 70%) and an internal validation set (n=72, 30%). Baseline clinical characteristics of all patients are summarized in Multimedia Appendix 3. The mPFS was 8.83 (95% CI 7.43-11.4) months in the training cohort and 10 (95% CI 7.77-15.6) months in the internal validation cohort. In the temporal validation cohort, the mPFS was 6.8 (95% CI 6.4-8.03) months. The 6-month, 12-month, and 18-month PFS rates in the training set were 61%, 25%, and 11%, respectively, while in the internal validation set, they were 57%, 26%, and 13%, respectively. In the temporal validation cohort, the 6-month, 9-month, and 12-month PFS rates were 53%, 17%, and 8%, respectively. Due to the limited follow-up period in the temporal validation cohort, the 18-month PFS rate was not determined.

XSL•FO
RenderX

Figure 1. Study flow chart. LASSO: least absolute shrinkage and selection operator; SVM: support vector machine; RSF: random survival forest; XGBoost: extreme gradient boosting.

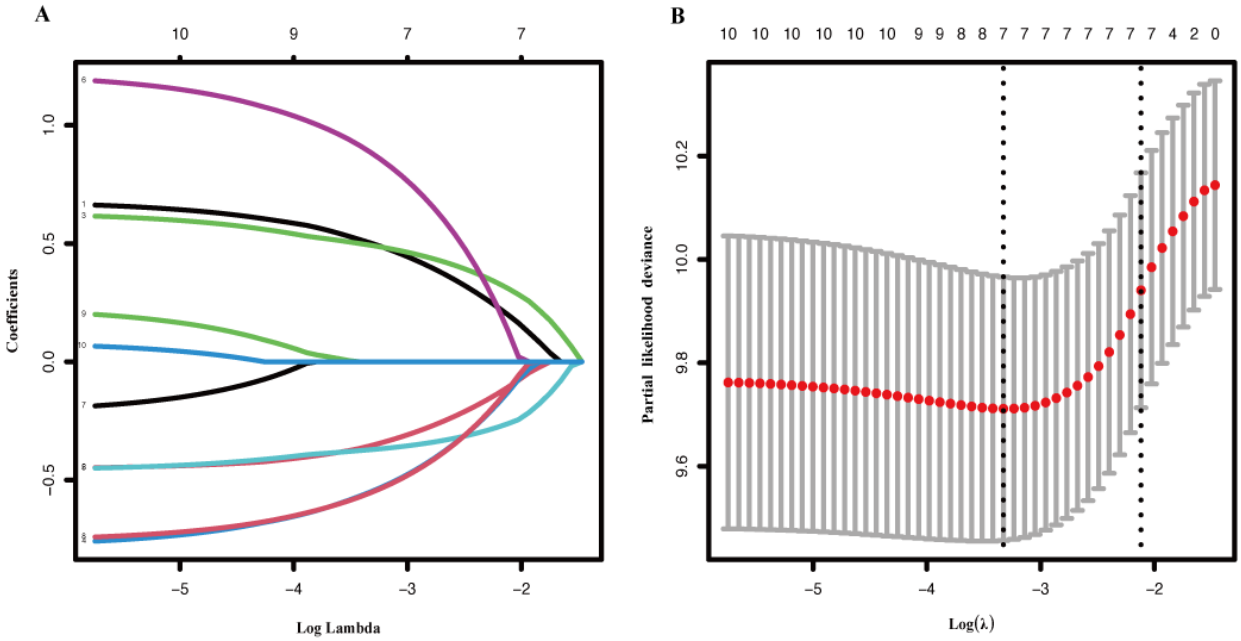


Construction of the LASSO-Cox Model and Nomogram

The prognostic value of various factors for predicting PFS was assessed using the training cohort. In univariate analysis, age, histological subtype, pretreatment levels of AFP, pretreatment proportion of $CD19^+$ B cell, $CD16^+CD56^+$ NK cell, $CD4^+/CD8^+$ T cell, TMB expression, and the presence of liver metastases were all found to be statistically significant ($P<.05$) (Multimedia Appendix 4). Recognizing that reliance solely on univariate analysis might introduce bias, 2 experienced clinicians reviewed these results and manually incorporated additional clinically relevant variables that, although not significant in the univariate analysis, have been linked to treatment efficacy, for example, PD-L1 expression, HER2 status, and MSI. This approach ensured that the model encompassed variables that are both clinically relevant and biologically meaningful. Subsequently, the significant factors from the univariate analysis were combined with clinically pertinent variables to form a LASSO regression. The LASSO algorithm was applied to identify the variables most strongly associated with PFS (Figure 2A). Through cross-validation, the optimal regularization parameter (λ) was determined to be 0.043, corresponding to the minimum partial likelihood deviance. Ultimately, 7 variables with nonzero coefficients were retained, that is, age, histological subtype, pretreatment levels of AFP, pretreatment proportion of $CD19^+$ B cell, $CD16^+CD56^+$ NK cell, $CD4^+/CD8^+$ T cell, and the presence of liver metastases (Figure 2B).

XSL•FO
RenderX

Figure 2. Feature selection using the least absolute shrinkage and selection operator regression. (A) The variation characteristics of the coefficient of variables; and (B) the selection process of the optimum value of the parameter λ in the least absolute shrinkage and selection operator regression model by cross-validation method.



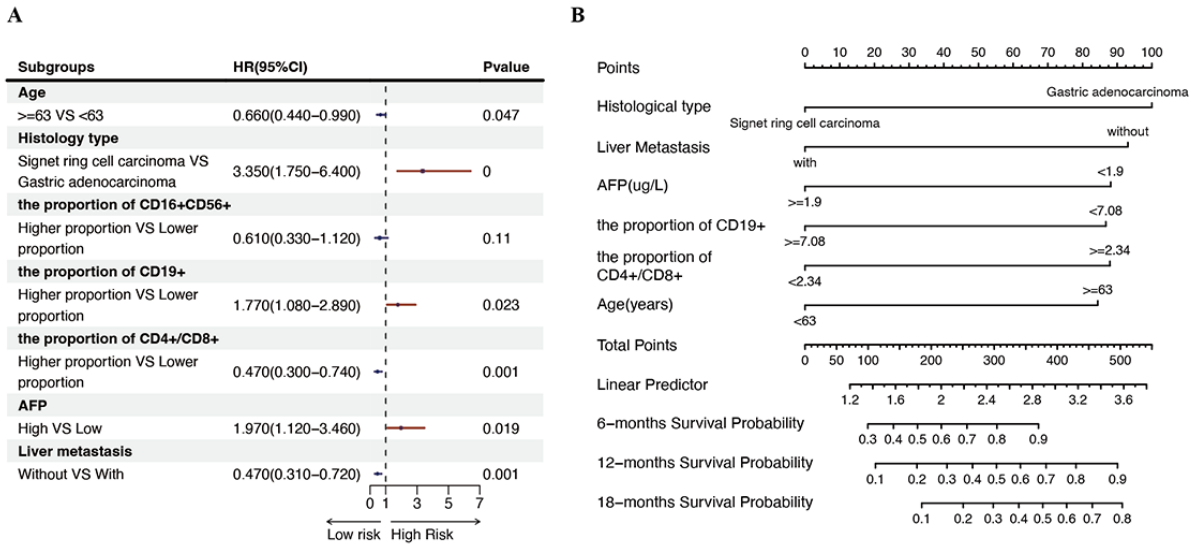
To further evaluate the independent impact of the selected variables on the prognosis of AGC, a multivariate Cox regression analysis was performed based on the 7 variables identified through LASSO regression. Among these, age (*P*=.047), histological subtype (*P*<.001), pretreatment levels of AFP (*P*=.02), pretreatment proportion of $CD19^+$ B cells (*P*=.02), $CD4^+/CD8^+$ T cells (*P*=.001), and liver metastasis (*P*=.001) were identified as independent predictors of PFS in patients with AGC (Table 1). The forest plot of the multivariate Cox regression analysis is illustrated in Figure 3A. Subsequently, the 6 independent predictors determined by the multivariate analysis were incorporated into a nomogram model for visual representation. In the nomogram, each variable is assigned a specific weight, and scores for individual predictors are projected onto a total points axis. The cumulative score is then used to estimate the 6-, 12-, and 18-month PFS rates by drawing a vertical line from the total points to the outcome axis (Figure 3B).

Table 1. Results of multivariate Cox proportional hazards regression analysis for progression-free survival in the training set.

Characteristics	Multivariable Cox regression, hazard ratio (95% CI)	*P* value
Age (years)		
≥63 vs <63	0.660 (0.44-0.99)	.047
Histological type		
Signet ring cell carcinoma vs gastric adenocarcinoma	3.35 (1.75-6.40)	<0.001
AFP (ng/μL)		
≥1.9 vs <1.9	1.97 (1.12-3.46)	.02
The proportion of $CD16^+CD56^+$T cell		
≥27.41 vs <27.41	0.61 (0.33-1.12)	.110
The proportion of $CD19^+$B cell		
≥12.04 vs <12.04	1.77 (1.08-2.89)	.02
The proportion of $CD4^+/CD8^+$T cell		
≥2.66 vs <2.66	0.47 (0.30-0.74)	.001
Liver metastasis		
Without vs with	0.47 (0.31-0.72)	.001

XSL•FO
RenderX

Figure 3. (A) Forest plot showing hazard ratios for different factors. (B) Nomogram for predicting progression-free survival of patients with advanced gastric cancer receiving first-line treatment with immunochemotherapy. AFP: alpha-fetoprotein.



Construction of Prognostic Models Based on ML

To establish a robust predictive model, PFS was categorized into short-PFS and long-PFS groups based on the cut point value determined in the training cohort. A decision tree (DT) model was first developed using the training cohort and validated on the internal validation cohort. However, the DT model demonstrated suboptimal performance (accuracy=0.5278). Given the limitations of the DT model described above, we turned to a more robust ML method—the RSF model. In the training cohort, we used 5-fold cross-validation and grid search to optimize the model's hyperparameters. The grid search spanned a range of values for "mtry" (1 to 30) and "nodesize" (1 to 50), and the number of trees ("ntree") was ultimately fixed at 1000. When "mtry" (the number of variables considered at each split) was set to 9 and "nodesize" (the minimum sample size in terminal nodes) was set to 6, the model achieved an out-of-bag error rate of 37%. At this configuration, the model reached its maximum AUC, while the error rate remained low and stable (Multimedia Appendix 5). The RSF model presents the relationship between the trees and error rate, and the variable importance rankings and grid search process. The top 9 variables significantly influencing the model were age, pretreatment proportion of $CD19^+$ B cells, liver metastasis, pretreatment proportion of $CD16^+CD56^+$ NK cells, histological subtype, pretreatment proportion of $CD4^+/CD8^+$ T cells, pretreatment levels of AFP, sex, and PD-L1 expression (Multimedia Appendix 6).

In addition, we developed XGBoost and survival-SVM models based on ML methods to comprehensively evaluate the performance of different algorithms for predicting prognosis in patients with AGC. For the XGBoost model, grid search and cross-validation were used to determine the optimal hyperparameters, and the model was constructed and fine-tuned on the training cohort. In contrast, the survival-SVM model leveraged the strengths of SVMs in handling survival data by optimizing kernel parameters to capture nonlinear relationships among samples. Subsequently, the predictive performance of these 4 models was compared to assess their robustness and practical applicability.

Comparison of Predictive Performance of 4 Models

To evaluate the predictive performance of the models, we assessed their discrimination, calibration, and robustness at different time points (Table 2). The RSF and XGBoost models exhibit higher C-index values, suggesting stronger predictive capabilities. In both the internal validation cohort and the temporal validation cohort, the RSF model demonstrated significantly superior AUC values compared with the other 3 models, indicating its superior discriminatory power.

XSL•FO
RenderX

Table 2. The concordance index and area under the curve values for the 4 models in both the internal validation cohort and the temporal validation cohort.

Model	C-index[a]	AUC[b]					
		Internal validation cohort (n=72)			Temporal validation cohort (n=76)		
		6 months	12 months	18 months	6 months	9 months	12 months
RSF[c]	0.828	0.887	0.943	0.945	0.896	0.930	0.950
LASSO[d]-Cox	0.719	0.660	0.756	0.778	0.724	0.720	0.728
XGBoost[e]	0.836	0.743	0.634	0.605	0.771	0.792	0.663
Survival-SVM[f]	0.740	0.789	0.808	0.711	0.802	0.825	0.697

[a]C-index: concordance index.

[b]AUC: area under the curve.

[c]RSF: random survival forest.

[d]LASSO: least absolute shrinkage and selection operator.

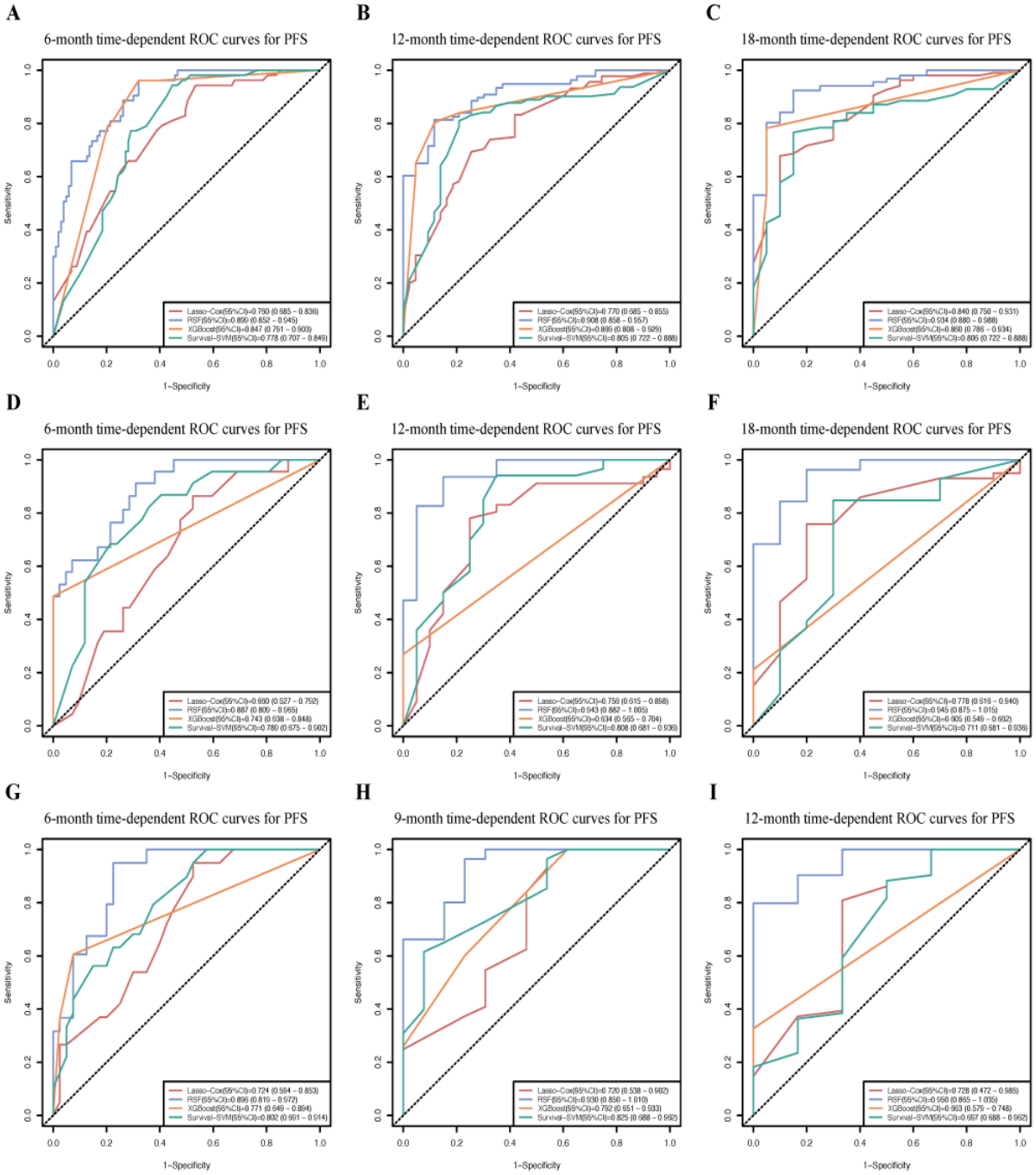
[e]XGBoost: extreme gradient boosting.

[f]SVM: support vector machine.

Figures 4A-4F illustrate the ROC curves for predicting 6-, 12-, and 18-month PFS rates using 4 models in both the training and internal validation cohorts, while Figures 4G-4I display the ROC curves for predicting 6-, 9-, and 12-month PFS rates in the temporal validation cohort. To compare the performance of these models, we analyzed the differences in AUC values using the DeLong test. The results confirmed that the RSF model significantly outperformed the other 3 models at all time points (P<.05). Notably, the RSF model exhibited higher AUC values for 12- and 18-month PFS predictions across all cohorts, suggesting its strong potential in long-term survival prediction.

XSL•FO
RenderX

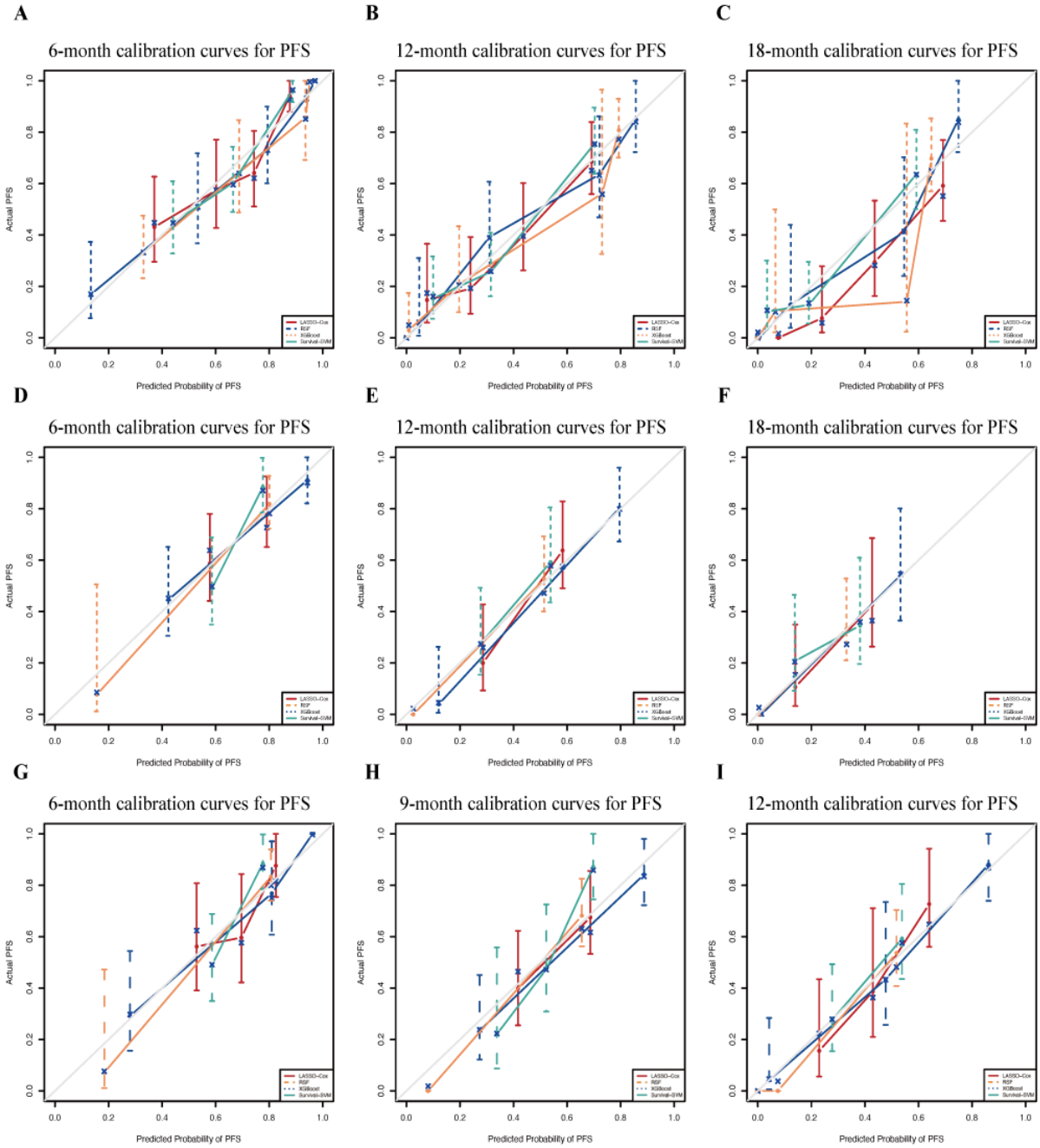
Figure 4. Comparison of time-dependent receiver operating characteristic curves of 4 models for predicting progression-free survival. (A-C) Receiver operating characteristic curves in the training cohort; (D-F) receiver operating characteristic curve in the internal validation cohort; and (G-I) receiver operating characteristic curves in the temporal validation cohort. Lasso: least absolute shrinkage and selection operator; PFS: progression-free survival; RFS: random survival forest; ROC: receiver operating characteristic; SVM: support vector machine; XGBoost: extreme gradient boosting.



To assess the accuracy of the predictive models for PFS rates, we generated calibration curves. The x-axis represents the predicted PFS values, while the y-axis shows the actual PFS. The calibration curves for the training, internal validation, and temporal validation cohorts were all close to the ideal line, demonstrating that all 4 models are well-calibrated and that there is strong concordance between the predicted and observed outcomes. This further supports the predictive accuracy of the RSF model (Figures 5A-5I).

XSL•FO
RenderX

Figure 5. Calibration curves for the 4 models. (A-C) Calibration curves for the training cohort; (D-F) calibration curves for the internal validation cohort; and (G-I) calibration curves for the temporal validation cohort. LASSO: least absolute shrinkage and selection operator; PFS: progression-free survival; RFS: random survival forest; SVM: support vector machine; XGBoost: extreme gradient boosting.

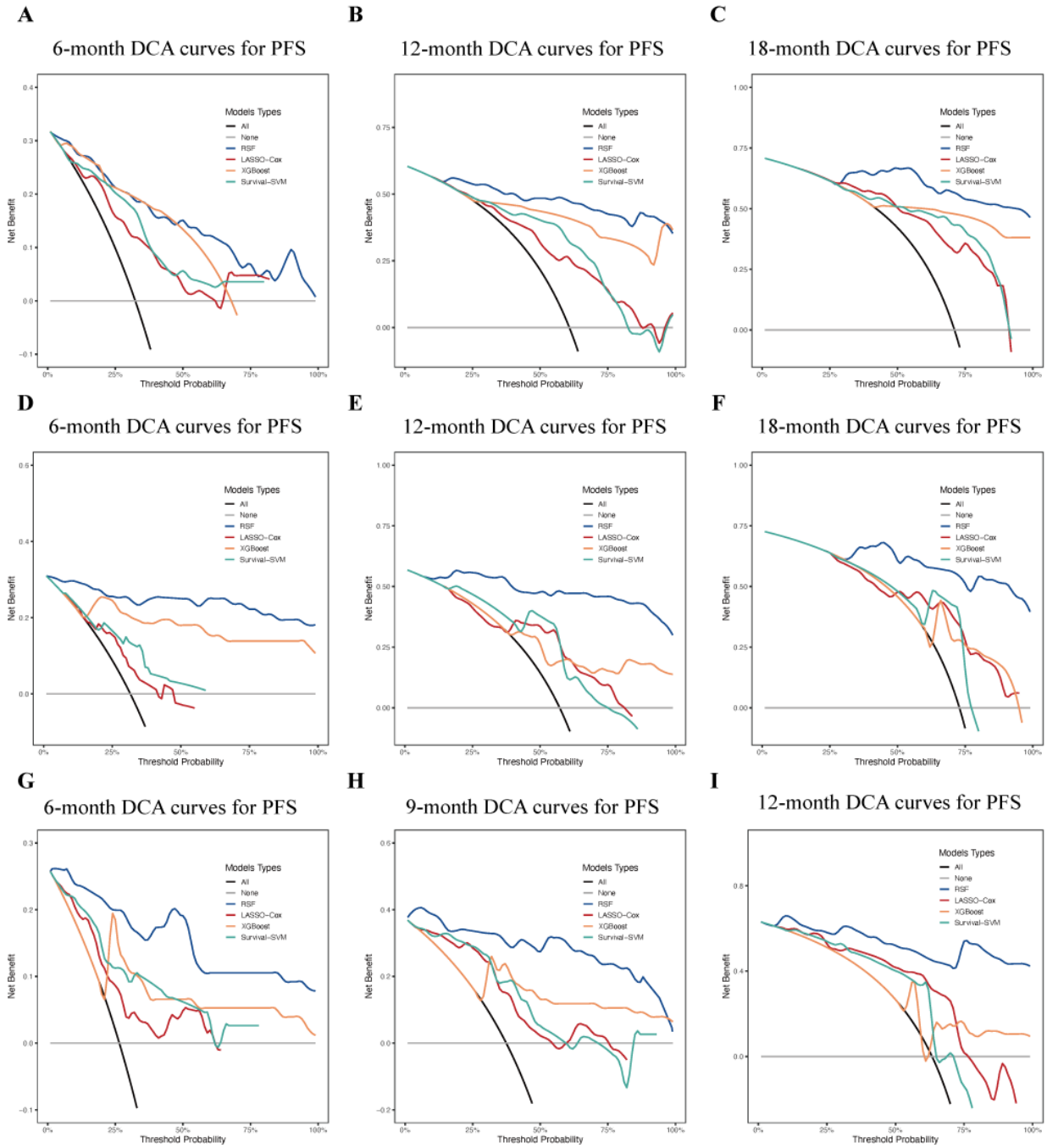


Furthermore, the continuous AUC curves for the RSF model at different time points were consistently higher, further confirming its excellent and long-term discriminatory power in both the internal validation and temporal validation cohorts (Multimedia Appendix 7).

DCA, which evaluates the clinical utility of models by calculating net benefits across various threshold probabilities, demonstrated that higher net benefits correspond to greater clinical decision-making value. The DCA curves of the 4 models revealed that the RSF model exhibited consistently superior net benefits compared with the other 3 models in all datasets, including the training set, internal validation set, and temporal validation cohort (Figure 6A-I).

XSL•FO
RenderX

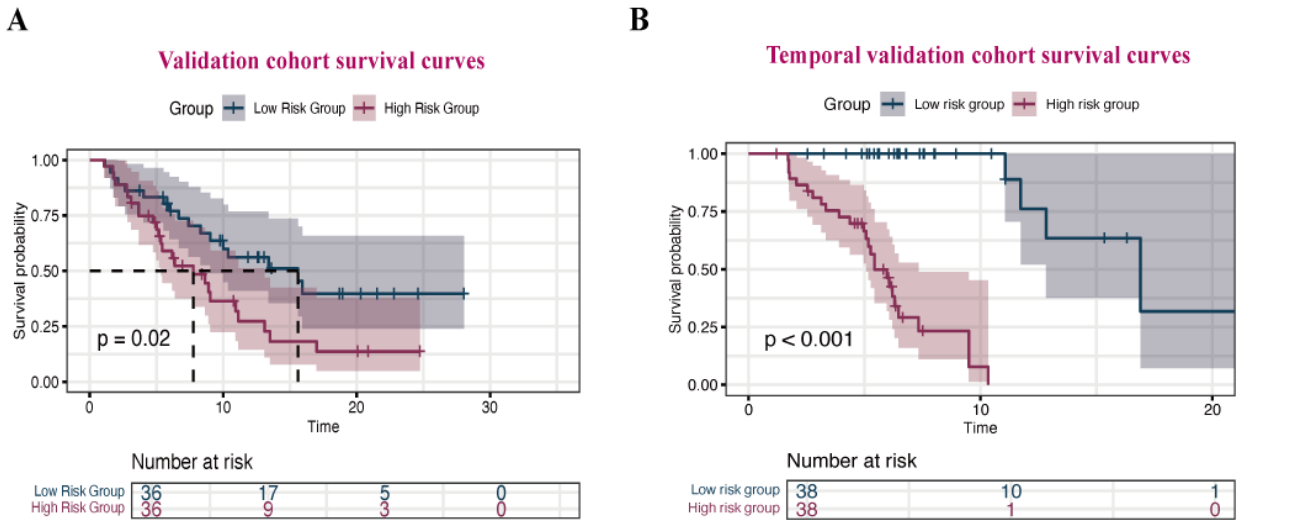
Figure 6. Decision curve analyses for the 4 models. (A-C) Calibration curves for the training cohort; (D-F) calibration curves for the internal validation cohort; and (G-I) calibration curves for the temporal validation cohort. DCA: decision curve analysis; LASSO: least absolute shrinkage and selection operator; PFS: progression-free survival; RFS: random survival forest; SVM: support vector machine; XGBoost: extreme gradient boosting.



Based on comprehensive comparisons of the 4 models in discrimination, calibration, consistency, and clinical net benefit, our findings indicate that the RSF model demonstrates superior predictive performance compared with the other 3 models. Patient risk stratification constitutes a critical component in guiding clinical management decisions. Using risk scores calculated by the RSF model, the optimal cutoff value for stratifying the cohort into high-risk and low-risk groups was determined as 55.42. Subsequent stratification revealed distinct survival outcomes, as illustrated by risk score distribution plots and KM survival curves. The KM analysis demonstrated significantly higher survival rates in the low-risk group compared with the high-risk group across both internal validation and temporal validation cohorts (Figure 7). These findings were statistically consistent regardless of the evaluation time frame.

XSL•FO
RenderX

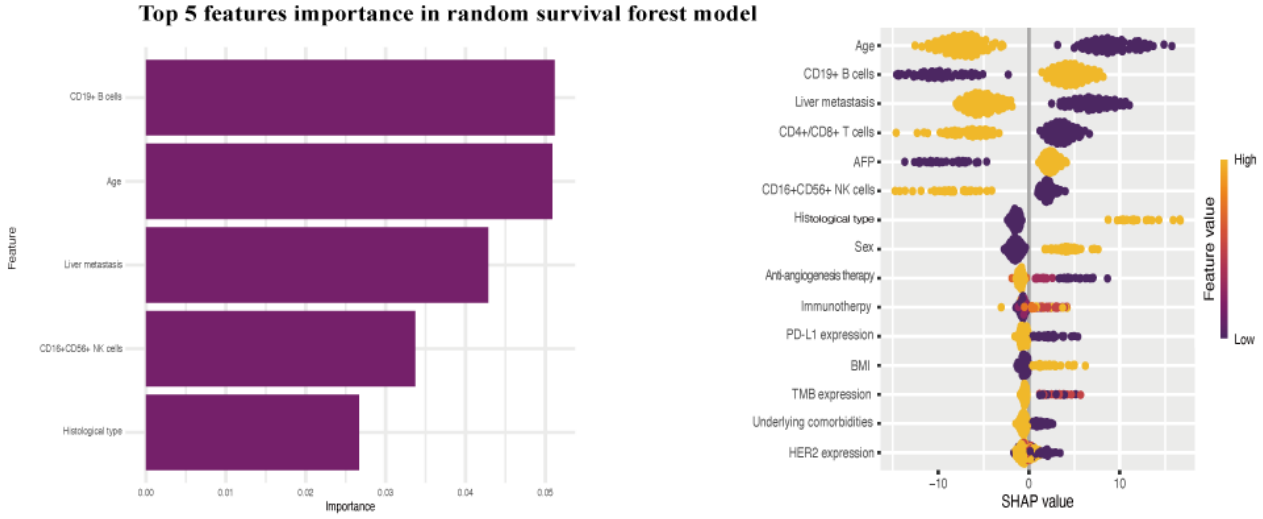
Figure 7. Kaplan-Meier survival curves of the high and low risk groups in internal validation cohort (*P*=.02) and temporal validation cohort (*P*<.001).



Feature Importance Analysis

To elucidate the decision-making rationale of the RSF model in predicting PFS for patients with AGC receiving first-line immunochemotherapy, interpretability analysis was performed using SHAP. Figure 8 displays the feature importance bar plot and SHAP value bee swarm plot for the RSF model. The analysis revealed that features including age, histological subtype, pretreatment proportion of CD19 B cells, pretreatment proportion of CD16 CD56 NK cells, and presence of liver metastasis exhibited broad value ranges and substantial positive and negative effects in SHAP distributions, identifying them as pivotal predictors of PFS. Subsequent KM analysis of these 5 key predictors demonstrated that patients aged <63 years, those with signet ring cell carcinoma histology, elevated pretreatment proportion of CD19 B cells, reduced pretreatment proportion of CD16 CD56 NK cells, or presence of liver metastasis experienced significantly worse prognosis (Multimedia Appendix 8).

Figure 8. Feature importance ranking bar plot and Shapley Additive Explanations beeswarm plot of the random survival forest model. AFP: alpha-fetoprotein; HER2: human epidermal growth factor receptor 2; NK: natural killer; PD-L1: programmed death-ligand 1; TMB: tumor mutation burden.



Discussion

Principal Results

In this study, we developed and compared 4 prognostic models using a comprehensive set of baseline parameters to predict PFS in patients with AGC receiving first-line immunochemotherapy. Our principal finding is that an ML model based on the RSF algorithm exhibited superior predictive performance over the LASSO-Cox, XGBoost, and survival-SVM models. Specifically, the RSF model exhibited the highest discriminatory power (as measured by C-index and AUC) and the greatest clinical utility (as determined by DCA) across both internal and temporal validation cohorts. Furthermore, the RSF-derived risk stratification system effectively stratified patients into distinct high- and low-risk prognostic groups, underscoring its potential utility in guiding individualized therapeutic decisions. Interpretability analysis

XSL•FO
RenderX

subsequently identified 5 key predictors driving the model's performance: age, histological subtype, pretreatment proportion of CD19 B cells, pretreatment proportion of CD16 CD56 NK cells, and the presence of liver metastasis. Collectively, these findings establish a robust and clinically applicable tool for personalized prognostic assessment in this patient population.

In-depth analysis of these predictors revealed that tumor-infiltrating lymphocytes and liver metastasis status significantly influenced prognosis. Our study observed that patients with an elevated pretreatment proportion of CD19 B cells exhibited poorer outcomes. Analysis of the cohort demonstrated a mPFS of 7.4 (95% CI 6.67-8.9) months in the high CD19 B cells subgroup compared with 15.9 (95% CI 10.9-upper limit not reached) months in the low CD19 B cells subgroup. The function of B cells in cancer is highly heterogeneous, with distinct subsets capable of exerting either protumorigenic or antitumorigenic effects [33,34]. While the presence of B cells organized in tertiary lymphoid structure is often correlated with improved clinical outcomes and response to immunotherapy in many cancers [35], a substantial body of evidence also points to a protumorigenic B cell function. This negative role is frequently mediated by regulatory B cells (Bregs), which suppress antitumor immunity through the secretion of inhibitory cytokines like IL-10, IL-35, and TGF-β [36,37]. Our observation is consistent with studies specifically in GC, which have identified intratumoral Bregs (eg, $CD19^{+}CD24^{hi}CD38^{hi}$ or $CD19^{+}CD24^{hi}CD27^{+}$) that produce IL-10 [38]. Furthermore, IL-35-secreting B cells have been found to be elevated in patients with AGC and correlate with an accumulation of other immunosuppressive populations, such as regulatory T cells [39]. Therefore, it is plausible that the high $CD19^{+}$ B cell population identified in our poor-prognosis cohort represents a dominance of these immunosuppressive Breg subsets, which dampen T cell effector function and contribute to therapeutic resistance. Conversely, other B cell subsets in the tumour microenvironment (TME) function as potent antigen-presenting cells to prime T cell responses or differentiate into plasma cells that produce tumor-specific antibodies [40]. The continued development and application of advanced analytical approaches, such as single-cell and spatial omics, are essential for comprehensively dissecting B cell heterogeneity and elucidating the precise mechanisms by which B cells modulate the immune response in GC.

NK cells are cytotoxic innate-like lymphocytes essential for tumor immunosurveillance, hardwired to recognize and kill stressed or malignant cells [41]. Evidence from mouse models confirms this, as long-term NK cell depletion results in increased tumor incidence and severity, demonstrating their fundamental role in suppressing tumor development [42]. NK cells deploy multiple antitumor mechanisms. Their activity is often perforin-dependent, highlighting the importance of direct cytotoxicity. Furthermore, NK cells express activating receptors like the high-affinity Fc receptor CD16, enabling them to mediate antibody-dependent cell-mediated cytotoxicity [43]. This function, critical for many antibody-based therapies, triggers the killing of antibody-coated cells and cytokine release. Beyond direct killing, recent work reveals a crucial "sentinel" function: NK cells detect nascent tumors and recruit dendritic cells to the TME, thereby mobilizing the adaptive immune response [44,45]. Clinically, numerous studies from The Cancer Genome Atlas correlate high NK cell infiltration with improved OS outcomes in diverse cancers, including melanoma, breast cancer, and GC [46-48].

Additionally, liver metastasis emerged as an independent adverse prognostic factor for the efficacy of first-line immunochemotherapy in AGC. KM curve analysis confirmed that patients with liver metastasis responded poorly to immunochemotherapy compared with those with distant metastases in other organs. Mechanistically, this is attributed to the formation of a highly immunosuppressive TME within the liver [49]. Numerous studies support this, revealing an increased presence of cancer-associated fibroblasts, myeloid-derived suppressor cell-like macrophages, tumor-associated macrophage-like macrophages, and naive T cells in liver metastasis. Conversely, conventional dendritic cells and effector $CD8^{+}$ T cells were diminished [50,51]. This aligns with existing literature. Liver metastasis is known to upregulate immune checkpoint molecules like PD-1 or PD-L1, which can induce systemic exhaustion of tumor-specific $CD8^{+}$ T cells and attenuate immunotherapy efficacy [52].

In summary, this study is the first to develop and rigorously validate an ML-based prognostic model specifically for patients with AGC receiving first-line immunochemotherapy. A key advantage of this model is its foundation on readily available, baseline clinical variables, offering a cost-effective and easily implementable prognostic tool in contrast to more complex omics-based assays. We demonstrated that the RSF model provides superior predictive performance and clinical utility, effectively stratifying patients into distinct high- and low-risk groups. This model is driven by key predictors identified in our analysis, including baseline immune cell proportions ($CD19^{+}$ B cells and $CD16^{+}CD56^{+}$ NK cells) and the presence of liver metastasis. Consequently, the RSF model represents a robust tool that offers quantifiable decision support, holding significant potential for guiding individualized therapeutic strategies and enhancing clinical decision-making in this setting.

Limitations and Future Work

Despite successful validation of the RSF model's performance in predicting outcomes for patients with AGC receiving first-line immunochemotherapy via internal and temporal validation cohorts, several limitations warrant acknowledgment. First, the single-center, retrospective design is a primary constraint that may introduce selection bias. Our cohorts were derived from a single institution with specific patient demographics, referral patterns, and clinical management protocols. Consequently, the model may be overfit to these local characteristics, and its external validity remains to be determined. Second, the high prevalence of missing values for established biomarkers, notably PD-L1, MSI status, and TMB, presented a significant limitation. This data sparsity precluded a direct comparative analysis of the prognostic accuracy of our RSF model against these established biologically based predictors. Furthermore, it inhibited our ability to investigate whether the integration of these potent biomarkers could have further augmented the

XSL•FO
RenderX

model's predictive performance. Third, our findings are based on a multiple imputation approach, which assumes that data are missing at random, a potential source of bias if violated. However, the robustness of our main conclusions was confirmed by a sensitivity analysis, mitigating this concern.

Future research will focus on a multistage approach designed to rigorously validate, enhance, and ultimately translate our RSF model into clinical practice. The most immediate priority is to address the current limitation of generalizability. This requires rigorously testing the model's performance and robustness in independent, prospective, and multicenter cohorts to definitively establish its external validity. Following successful validation, the next phase will involve enhancing the model's predictive power by incorporating broader multiomics data, such as genomic, transcriptomic, or proteomic profiles. This integration not only promises to refine prognostic accuracy but may also uncover deeper biological insights into the mechanisms of immunochemotherapy response. Contingent upon this robust validation and enhancement, the final objective is the translation of the optimized model into an accessible clinical decision support tool. We envision the development of a user-friendly platform, such as a web-based calculator or a simplified score system. This would provide clinicians with a practical means to generate real-time, individualized predictions for prognosis and recurrence risk, thereby advancing personalized treatment strategies for patients with AGC.

Conclusions

In conclusion**,** this study draws the following findings. First, 4 prognostic models were developed in this study, with comparative analyses demonstrating that the RSF model outperformed others in discriminative ability, calibration, and clinical utility. Second, SHAP analysis of the RSF model identified age, liver metastasis, histological subtype, and tumor-infiltrating lymphocytes as critical prognostic predictors for patients with AGC undergoing first-line immunochemotherapy. Third, this study is the first to use ML to construct a prognostic model for assessing treatment efficacy in patients with AGC receiving first-line immunochemotherapy. The results underscore the model's significant clinical value in prognostic evaluation and therapeutic decision-making. This study provides methodological innovation and evidence-based medical rationale for advancing precision therapy in AGC, offering substantial potential for clinical translation.

Acknowledgments

The authors thank the researchers from The First Affiliated Hospital of Nanjing Medical University for their help with data recording and collection.

Funding

This study was supported by the Health Development Promotion Project (BJHA-CRP-071), Beijing Xisike Clinical Oncology Research Foundation (sy2018-249), and the Clinical Ability Improvement Project (JSPH-MB-2020-3).

Authors' Contributions

XC designed the study, collected and analyzed the data, and wrote the paper as the first author. EM contributed to data collection. XC contributed to the statistical analysis of the results. PL and HW verified the analytical methods. HW investigated and supervised the findings of this work and assisted with language editing. XW contributed to the data collection of the temporal validation cohort and reviewed the paper. HW was in charge of the overall direction of the study as the corresponding author. All authors gave final approval of the paper for submission.

Conflicts of Interest

None declared.

Multimedia Appendix 1
Diagnostic plots of each variable after multiple imputation.
[PNG File , 4377 KB - medinform_v13i1e82533_app1.png]

Multimedia Appendix 2
Sensitivity analysis evaluating the predictive performance in the complete-case cohort.
[PNG File , 367 KB - medinform_v13i1e82533_app2.png]

Multimedia Appendix 3
Demographics and clinicopathologic characteristics of the training, internal validation and temporal validation cohorts.
[DOCX File , 26 KB - medinform_v13i1e82533_app3.docx]

Multimedia Appendix 4

XSL•FO
RenderX

Results of univariable Cox proportional hazards regression analysis for progression-free survival in the training set.
[DOCX File , 21 KB - medinform_v13i1e82533_app4.docx]

Multimedia Appendix 5
Hyperparameter tuning.
[PNG File , 233 KB - medinform_v13i1e82533_app5.png]

Multimedia Appendix 6
RSF model and ranking of variable importance.
[PNG File , 102 KB - medinform_v13i1e82533_app6.png]

Multimedia Appendix 7
Continuous AUC curves for the four models: A represents the internal validation cohort, while B represents the temporal validation cohort.
[PNG File , 66 KB - medinform_v13i1e82533_app7.png]

Multimedia Appendix 8
Kaplan–Meier survival analysis based on age, pathological histological subtype, pre-treatment proportion of CD19 B cells, pre-treatment proportion of CD16 CD56 NK cells, and presence of liver metastasis.
[PNG File , 79 KB - medinform_v13i1e82533_app8.png]

References

1. Bray F, Laversanne M, Sung H, Ferlay J, Siegel RL, Soerjomataram I, et al. Global cancer statistics 2022: GLOBOCAN estimates of incidence and mortality worldwide for 36 cancers in 185 countries. CA Cancer J Clin 2024;74(3):229-263 [FREE Full text] [doi: 10.3322/caac.21834] [Medline: 38572751]
2. Chia N, Tan P. Molecular classification of gastric cancer. Ann Oncol 2016;27(5):763-769 [FREE Full text] [doi: 10.1093/annonc/mdw040] [Medline: 26861606]
3. Guan W, He Y, Xu R. Gastric cancer treatment: recent progress and future perspectives. J Hematol Oncol 2023;16(1):57 [FREE Full text] [doi: 10.1186/s13045-023-01451-3] [Medline: 37245017]
4. Li GZ, Doherty GM, Wang J. Surgical management of gastric cancer: a review. JAMA Surg 2022;157(5):446-454. [doi: 10.1001/jamasurg.2022.0182] [Medline: 35319717]
5. Cai J, Tan X, Hu Q, Pan H, Zhao M, Guo C, et al. Flavonoids and gastric cancer therapy: from signaling pathway to therapeutic significance. Drug Des Devel Ther 2024;18:3233-3253 [FREE Full text] [doi: 10.2147/DDDT.S466470] [Medline: 39081701]
6. Selim JH, Shaheen S, Sheu W, Hsueh C. Targeted and novel therapy in advanced gastric cancer. Exp Hematol Oncol 2019;8:25 [FREE Full text] [doi: 10.1186/s40164-019-0149-6] [Medline: 31632839]
7. Yamada Y, Higuchi K, Nishikawa K, Gotoh M, Fuse N, Sugimoto N, et al. Phase III study comparing oxaliplatin plus S-1 with cisplatin plus S-1 in chemotherapy-naïve patients with advanced gastric cancer. Ann Oncol 2015;26(1):141-148 [FREE Full text] [doi: 10.1093/annonc/mdu472] [Medline: 25316259]
8. Janjigian YY, Shitara K, Moehler M, Garrido M, Salman P, Shen L, et al. First-line nivolumab plus chemotherapy versus chemotherapy alone for advanced gastric, gastro-oesophageal junction, and oesophageal adenocarcinoma (CheckMate 649): a randomised, open-label, phase 3 trial. Lancet 2021;398(10294):27-40 [FREE Full text] [doi: 10.1016/S0140-6736(21)00797-2] [Medline: 34102137]
9. Shitara K, Van Cutsem E, Bang Y, Fuchs C, Wyrwicz L, Lee K, et al. Efficacy and safety of pembrolizumab or pembrolizumab plus chemotherapy vs chemotherapy alone for patients with first-line, advanced gastric cancer: The KEYNOTE-062 phase 3 randomized clinical trial. JAMA Oncol 2020;6(10):1571-1580 [FREE Full text] [doi: 10.1001/jamaoncol.2020.3370] [Medline: 32880601]
10. Marusyk A, Janiszewska M, Polyak K. Intratumor heterogeneity: the Rosetta Stone of therapy resistance. Cancer Cell 2020;37(4):471-484. [doi: 10.1016/j.ccell.2020.03.007] [Medline: 32289271]
11. Kim ST, Cristescu R, Bass AJ, Kim K, Odegaard JI, Kim K, et al. Comprehensive molecular characterization of clinical responses to PD-1 inhibition in metastatic gastric cancer. Nat Med 2018;24(9):1449-1458. [doi: 10.1038/s41591-018-0101-z] [Medline: 30013197]
12. Hou W, Zhao Y, Zhu H. Predictive biomarkers for immunotherapy in gastric cancer: current status and emerging prospects. Int J Mol Sci 2023;24(20):15321 [FREE Full text] [doi: 10.3390/ijms242015321] [Medline: 37895000]
13. Yang J, Gong Y, Lam VK, Shi Y, Guan Y, Zhang Y, et al. Deep sequencing of circulating tumor DNA detects molecular residual disease and predicts recurrence in gastric cancer. Cell Death Dis 2020;11(5):346 [FREE Full text] [doi: 10.1038/s41419-020-2531-z] [Medline: 32393783]

XSL•FO
RenderX

14. Duan Y, Xu Y, Dou Y, Xu D. Helicobacter pylori and gastric cancer: mechanisms and new perspectives. J Hematol Oncol 2025;18(1):10 [FREE Full text] [doi: 10.1186/s13045-024-01654-2] [Medline: 39849657]
15. Chan T, Yarchoan M, Jaffee E, Swanton C, Quezada S, Stenzinger A, et al. Development of tumor mutation burden as an immunotherapy biomarker: utility for the oncology clinic. Ann Oncol 2019;30(1):44-56 [FREE Full text] [doi: 10.1093/annonc/mdy495] [Medline: 30395155]
16. Palmeri M, Mehnert J, Silk A, Jabbour S, Ganesan S, Popli P, et al. Real-world application of tumor mutational burden-high (TMB-high) and microsatellite instability (MSI) confirms their utility as immunotherapy biomarkers. ESMO Open 2022;7(1):100336 [FREE Full text] [doi: 10.1016/j.esmoop.2021.100336] [Medline: 34953399]
17. Greener JG, Kandathil SM, Moffat L, Jones DT. A guide to machine learning for biologists. Nat Rev Mol Cell Biol 2022;23(1):40-55. [doi: 10.1038/s41580-021-00407-0] [Medline: 34518686]
18. Toh TS, Dondelinger F, Wang D. Looking beyond the hype: applied AI and machine learning in translational medicine. EBioMedicine 2019;47:607-615 [FREE Full text] [doi: 10.1016/j.ebiom.2019.08.027] [Medline: 31466916]
19. Yosefian I, Farkhani EM, Baneshi M. Application of random forest survival models to increase generalizability of decision trees: a case study in acute myocardial infarction. Comput Math Methods Med 2015;2015:576413 [FREE Full text] [doi: 10.1155/2015/576413] [Medline: 26858773]
20. Li F, Li J, Yu J, Pan T, Yu B, Sang Q, et al. Identification of ARGLU1 as a potential therapeutic target for gastric cancer based on genome-wide functional screening data. EBioMedicine 2021;69:103436 [FREE Full text] [doi: 10.1016/j.ebiom.2021.103436] [Medline: 34157484]
21. Chen Y, Wang B, Zhao Y, Shao X, Wang M, Ma F, et al. Metabolomic machine learning predictor for diagnosis and prognosis of gastric cancer. Nat Commun 2024;15(1):1657 [FREE Full text] [doi: 10.1038/s41467-024-46043-y] [Medline: 38395893]
22. Wei T, Yuan X, Gao R, Johnston L, Zhou J, Wang Y, et al. Survival prediction of stomach cancer using expression data and deep learning models with histopathological images. Cancer Sci 2023;114(2):690-701 [FREE Full text] [doi: 10.1111/cas.15592] [Medline: 36114747]
23. He X, Du B, Wu T, Shen H. Prognostic analysis of related factors of adverse reactions to immunotherapy in advanced gastric cancer and establishment of a nomogram model. World J Gastrointest Oncol 2024;16(4):1268-1280 [FREE Full text] [doi: 10.4251/wjgo.v16.i4.1268] [Medline: 38660670]
24. Yang Y, Shao Y, Wang J, Cheng Q, Yang H, Li Y, et al. Development and validation of novel immune-inflammation-based clinical predictive nomograms in HER2-negative advanced gastric cancer. Front Oncol 2023;13:1185240 [FREE Full text] [doi: 10.3389/fonc.2023.1185240] [Medline: 37746295]
25. Balachandran VP, Gonen M, Smith JJ, DeMatteo RP. Nomograms in oncology: more than meets the eye. Lancet Oncol 2015;16(4):e173-e180 [FREE Full text] [doi: 10.1016/S1470-2045(14)71116-7] [Medline: 25846097]
26. Yu D, Yang J, Wang B, Li Z, Wang K, Li J, et al. New genetic insights into immunotherapy outcomes in gastric cancer via single-cell RNA sequencing and random forest model. Cancer Immunol Immunother 2024;73(6):112 [FREE Full text] [doi: 10.1007/s00262-024-03684-8] [Medline: 38693422]
27. Huang Y, Li J, Li M, Aparasu RR. Application of machine learning in predicting survival outcomes involving real-world data: a scoping review. BMC Med Res Methodol 2023;23(1):268 [FREE Full text] [doi: 10.1186/s12874-023-02078-1] [Medline: 37957593]
28. D'Antonio M, G Gonzalez Rivera W, Greenes RA, Gymrek M, Frazer KA. A highly accurate risk factor-based XGBoost multiethnic model for identifying patients with skin cancer. Nat Commun 2025;16(1):9542 [FREE Full text] [doi: 10.1038/s41467-025-64556-y] [Medline: 41162377]
29. Zhang Y, Shen Y, Huang Q, Wu C, Zhou L, Ren H. Predicting survival of advanced laryngeal squamous cell carcinoma: comparison of machine learning models and Cox regression models. Sci Rep 2023;13(1):18498 [FREE Full text] [doi: 10.1038/s41598-023-45831-8] [Medline: 37898687]
30. Wang F, Wang J. Establishment and validation of a prognostic risk early-warning model for retinoblastoma based on XGBoost. Am J Cancer Res 2025;15(1):99-112. [doi: 10.62347/WHUQ1208] [Medline: 39949950]
31. Hu X, Dong H, Qin W, Bin Y, Huang W, Kang M, et al. Machine learning-based identification of a consensus immune-derived gene signature to improve head and neck squamous cell carcinoma therapy and outcome. Front Pharmacol 2024;15:1341346 [FREE Full text] [doi: 10.3389/fphar.2024.1341346] [Medline: 38666027]
32. Vollmer A, Hartmann S, Vollmer M, Shavlokhova V, Brands RC, Kübler A, et al. Multimodal artificial intelligence-based pathogenomics improves survival prediction in oral squamous cell carcinoma. Sci Rep 2024;14(1):5687 [FREE Full text] [doi: 10.1038/s41598-024-56172-5] [Medline: 38453964]
33. Kim S, Shen S, Miyauchi S, Sanders PD, Franiak-Pietryga I, Mell L, et al. B cells improve overall survival in hpv-associated squamous cell carcinomas and are activated by radiation and PD-1 blockade. Clin Cancer Res 2020;26(13):3345-3359 [FREE Full text] [doi: 10.1158/1078-0432.CCR-19-3211] [Medline: 32193227]
34. Shalapour S, Font-Burgada J, Di Caro G, Zhong Z, Sanchez-Lopez E, Dhar D, et al. Immunosuppressive plasma cells impede T-cell-dependent immunogenic chemotherapy. Nature 2015;521(7550):94-98 [FREE Full text] [doi: 10.1038/nature14395] [Medline: 25924065]

XSL•FO
RenderX

35. Fristedt R, Borg D, Hedner C, Berntsson J, Nodin B, Eberhard J, et al. Prognostic impact of tumour-associated B cells and plasma cells in oesophageal and gastric adenocarcinoma. J Gastrointest Oncol 2016;7(6):848-859 [FREE Full text] [doi: 10.21037/jgo.2016.11.07] [Medline: 28078109]
36. Poznansky SA, Yu M, Deng K, Fu Q, Markmann JF, LeGuern C. Leveraging the tolerogenic potential of TNF-α and regulatory B cells in organ transplantation. Front Immunol 2023;14:1173672 [FREE Full text] [doi: 10.3389/fimmu.2023.1173672] [Medline: 37180165]
37. Andreu P, Johansson M, Affara NI, Pucci F, Tan T, Junankar S, et al. FcRgamma activation regulates inflammation-associated squamous carcinogenesis. Cancer Cell 2010;17(2):121-134 [FREE Full text] [doi: 10.1016/j.ccr.2009.12.019] [Medline: 20138013]
38. Sarvaria A, Madrigal JA, Saudemont A. B cell regulation in cancer and anti-tumor immunity. Cell Mol Immunol 2017;14(8):662-674 [FREE Full text] [doi: 10.1038/cmi.2017.35] [Medline: 28626234]
39. Lindner S, Dahlke K, Sontheimer K, Hagn M, Kaltenmeier C, Barth TFE, et al. Interleukin 21-induced granzyme B-expressing B cells infiltrate tumors and regulate T cells. Cancer Res 2013;73(8):2468-2479. [doi: 10.1158/0008-5472.CAN-12-3450] [Medline: 23384943]
40. Arbogast F, Arnold J, Hammann P, Kuhn L, Chicher J, Murera D, et al. ATG5 is required for B cell polarization and presentation of particulate antigens. Autophagy 2019 Feb;15(2):280-294 [FREE Full text] [doi: 10.1080/15548627.2018.1516327] [Medline: 30196744]
41. Maskalenko NA, Zhigarev D, Campbell KS. Harnessing natural killer cells for cancer immunotherapy: dispatching the first responders. Nat Rev Drug Discov 2022;21(8):559-577 [FREE Full text] [doi: 10.1038/s41573-022-00413-7] [Medline: 35314852]
42. Ma W, Morris S, Jamieson C. Reprogramming natural killer cells in the tumor microenvironment: challenges and therapeuticopportunities. Cytokine Growth Factor Rev 2025;86:71-82 [FREE Full text] [doi: 10.1016/j.cytogfr.2025.10.001] [Medline: 41092888]
43. Pinto S, Pahl J, Schottelius A, Carter PJ, Koch J. Reimagining antibody-dependent cellular cytotoxicity in cancer: the potential of natural killer cell engagers. Trends Immunol 2022;43(11):932-946 [FREE Full text] [doi: 10.1016/j.it.2022.09.007] [Medline: 36306739]
44. Si C, Gao J, Ma X. Natural killer cell-derived exosome-based cancer therapy: from biological roles to clinical significance and implications. Mol Cancer 2024;23(1):134 [FREE Full text] [doi: 10.1186/s12943-024-02045-4] [Medline: 38951879]
45. Ghaedrahmati F, Esmaeil N, Abbaspour M. Targeting immune checkpoints: how to use natural killer cells for fighting against solid tumors. Cancer Commun (Lond) 2023;43(2):177-213 [FREE Full text] [doi: 10.1002/cac2.12394] [Medline: 36585761]
46. Choi WS, Kwon H, Yi E, Lee H, Kim JM, Park HJ, et al. HPK1 dysregulation-associated NK cell dysfunction and defective expansion promotes metastatic melanoma progression. Adv Sci (Weinh) 2024;11(29):e2400920. [doi: 10.1002/advs.202400920] [Medline: 38828677]
47. Ben-Shmuel A, Gruper Y, Halperin C, Levi-Galibov O, Rosenberg-Fogler H, Barki D, et al. Cancer-associated fibroblasts serve as decoys to suppress NK cell anticancer cytotoxicity in breast cancer. Cancer Discov 2025;15(6):1247-1269. [doi: 10.1158/2159-8290.CD-24-0131] [Medline: 40052789]
48. Cui J, Xu X, He T, Liu J, Xie T, Tian W, et al. L-kynurenine induces NK cell loss in gastric cancer microenvironment via promoting ferroptosis. J Exp Clin Cancer Res 2023;42(1):52 [FREE Full text] [doi: 10.1186/s13046-023-02629-w] [Medline: 36855135]
49. Zhu C, Liao J, Liu Y, Chen Z, Chang R, Chen X, et al. Immune dynamics shaping pre-metastatic and metastatic niches in liver metastases: from molecular mechanisms to therapeutic strategies. Mol Cancer 2024;23(1):254 [FREE Full text] [doi: 10.1186/s12943-024-02171-z] [Medline: 39543660]
50. Deng J, Gou Q, Yang L, Chen Z, Yang M, Yang X, et al. Immune suppressive microenvironment in liver metastases contributes to organ-specific response of immunotherapy in advanced non-small cell lung cancer. J Immunother Cancer 2023;11(7):e007218 [FREE Full text] [doi: 10.1136/jitc-2023-007218] [Medline: 37463790]
51. Yu J, Green MD, Li S, Sun Y, Journey SN, Choi JE, et al. Liver metastasis restrains immunotherapy efficacy via macrophage-mediated T cell elimination. Nat Med 2021;27(1):152-164 [FREE Full text] [doi: 10.1038/s41591-020-1131-x] [Medline: 33398162]
52. Gao Y, Chen S, Wang H, Wu C, An R, Li G, et al. Liver metastases across cancer types sharing tumor environment immunotolerance can impede immune response therapy and immune monitoring. J Adv Res 2024;61:151-164 [FREE Full text] [doi: 10.1016/j.jare.2023.08.011] [Medline: 37619932]

Abbreviations

AFP: alpha-fetoprotein
AGC: advanced gastric cancer
AUC: area under the curve
Breg: regulatory B cell

XSL•FO
RenderX

C-index: concordance index
DCA: decision curve analysis
DT: decision tree
GC: gastric cancer
HER2: human epidermal growth factor receptor 2
ICI: immune checkpoint inhibitor
KM: Kaplan-Meier
KS: Kolmogorov-Smirnov
LASSO: the least absolute shrinkage and selection operator
ML: machine learning
mPFS: median progression-free survival
MSI: microsatellite instability
mut/Mb: mutations per megabase
NK: natural killer
OS: overall survival
PD-1: programmed cell death protein 1
PD-L1: programmed death-ligand 1
PFS: progression-free survival
RECIST: Response Evaluation Criteria in Solid Tumors
ROC: receiver operating characteristic
RSF: random survival forest
SHAP: Shapley additive explanations
SVM: support vector machine
TMB: tumor mutation burden
TME: tumour microenvironment
XGBoost: extreme gradient boosting

Edited by M Focsa; submitted 17.08.25; peer-reviewed by L Liang, J Wang; comments to author 08.10.25; revised version received 30.11.25; accepted 02.12.25; published 22.12.25.

Please cite as:
Cheng X, Li P, Meng E, Wu X, Wu H
A Machine Learning Model Based on Clinical Factors to Predict the Efficacy of First-Line Immunochemotherapy for Patients With Advanced Gastric Cancer: Retrospective Study
JMIR Med Inform 2025;13:e82533
URL: https://medinform.jmir.org/2025/1/e82533
doi:10.2196/82533
PMID:

©Xu Cheng, Ping Li, Enqing Meng, Xinyi Wu, Hao Wu. Originally published in JMIR Medical Informatics (https://medinform.jmir.org), 22.12.2025. This is an open-access article distributed under the terms of the Creative Commons Attribution License (https://creativecommons.org/licenses/by/4.0/), which permits unrestricted use, distribution, and reproduction in any medium, provided the original work, first published in JMIR Medical Informatics, is properly cited. The complete bibliographic information, a link to the original publication on https://medinform.jmir.org/, as well as this copyright and license information must be included.

XSL•FO
RenderX

Original Paper

Predicting Left Ventricular Ejection Fraction Recovery After Percutaneous Coronary Intervention in Patients With Chronic Coronary Syndrome by Using Interpretable Machine Learning Models: Retrospective Study

Jiayi Ding[1], MSc; Guanqi Lyu[1], MPH; Masaharu Nakayama[1], MD, PhD; Kotaro Nochioka[2], MD, PhD; Jun Takahashi[2], MD, PhD; Satoshi Yasuda[2], MD, PhD; Tetsuya Matoba[3], MD, PhD; Takahide Kohro[4], MD, PhD; Naoyuki Akashi[5], MD, PhD; Hideo Fujita[5], MD, PhD; Yusuke Oba[6], MD, PhD; Tomoyuki Kabutoya[6], MD, PhD; Kazuomi Kario[6], MD, PhD; Yasushi Imai[7], MD, PhD; Arihiro Kiyosue[8], MD, PhD; Yoshiko Mizuno[9], MD, PhD; Takamasa Iwai[10], MD, PhD; Yoshihiro Miyamoto[11], MD, PhD; Masanobu Ishii[12], MPH, MD, PhD; Kenichi Tsujita[12], MD, PhD; Taishi Nakamura[13], MD, PhD; Hisahiko Sato[14], MD, PhD; Ryozo Nagai[15], MD, PhD

[1]Department of Medical Informatics, Graduate School of Medicine, Tohoku University, Sendai, Japan
[2]Division of Cardiovascular Medicine, Tohoku University Hospital, Sendai, Japan
[3]Department of Cardiovascular Medicine, Graduate School of Medical Sciences, Kyushu University, Fukuoka, Japan
[4]Department of Clinical Informatics, School of Medicine, Jichi Medical University, Tochigi, Japan
[5]Division of Cardiovascular Medicine, Jichi Medical University Saitama Medical Center, Saitama, Japan
[6]Department of Medicine, School of Medicine, Jichi Medical University, Tochigi, Japan
[7]Department of Pharmacology, Division of Clinical Pharmacology, Jichi Medical University, Tochigi, Japan
[8]Department of Cardiovascular Medicine, University of Tokyo Hospital, Tokyo, Japan
[9]Development Bank of Japan, Tokyo, Japan
[10]Department of Cardiovascular Medicine, National Cerebral and Cardiovascular Center, Suita, Japan
[11]Open Innovation Center, National Cerebral and Cardiovascular Center, Suita, Japan
[12]Department of Cardiovascular Medicine, Graduate School of Medical Sciences, Kumamoto University, Kumamoto, Japan
[13]Department of Medical Information Science, Graduate School of Medical Sciences, Kumamoto University, Kumamoto, Japan
[14]Precision Inc., Tokyo, Japan
[15]School of Medicine, Jichi Medical University, Tochigi, Japan

Corresponding Author:
Masaharu Nakayama, MD, PhD
Department of Medical Informatics
Graduate School of Medicine
Tohoku University
2-1 Seiryo-machi, Aoba-ku
Sendai
Japan
Phone: 81 22 717 7572
Email: masaharu.nakayama.a2@tohoku.ac.jp

Abstract

Background: Accurately predicting left ventricular ejection fraction (LVEF) recovery after percutaneous coronary intervention (PCI) in patients with chronic coronary syndrome (CCS) is crucial for clinical decision-making.

Objective: This study aimed to develop and compare multiple machine learning (ML) models to predict LVEF recovery and identify key contributing features.

Methods: We retrospectively analyzed 520 patients with CCS from the Clinical Deep Data Accumulation System database. Patients were categorized into 4 binary classification tasks based on baseline LVEF (≥50% or <50%) and degree of recovery: (1) good recovery, defined as an LVEF increase of >10% compared with ≤0%; and (2) normal recovery, defined as an LVEF increase

XSL•FO
RenderX

of 0% to 10% compared with ≤0%. For each task, 3 feature selection strategies (all features, least absolute shrinkage and selection operator [LASSO] regression, and recursive feature elimination [RFE]) were combined with 4 ML algorithms (extreme gradient boosting [XGBoost], categorical boosting, light gradient boosting machine, and random forest), resulting in 48 models. Models were evaluated using 10-fold cross-validation and assessed by the area under the curve (AUC), decision curve analysis, and calibration plots.

Results: The highest AUCs were achieved by RFE combined with XGBoost (AUC=0.93) for preserved LVEF with good recovery, LASSO combined with XGBoost (AUC=0.79) for preserved LVEF with normal recovery, LASSO combined with XGBoost (AUC=0.88) for reduced LVEF with good recovery, and RFE combined with XGBoost (AUC=0.84) for reduced LVEF with normal recovery. Shapley Additive Explanation analysis identified uric acid, platelets, hematocrit, brain natriuretic peptide, glycated hemoglobin, glucose, creatinine, baseline LVEF, left ventricular end-diastolic internal diameter, heart rate, R wave amplitude in V5, and R wave amplitude in V6 as important predictive factors of LVEF recovery.

Conclusions: ML models incorporating feature selection strategies demonstrated strong predictive performance for LVEF recovery after PCI. These interpretable models may support clinical decision-making and can improve the management of patients with CCS after PCI.

(JMIR Med Inform 2025;13:e77839) doi:10.2196/77839

KEYWORDS

chronic coronary syndrome; left ventricular ejection fraction; percutaneous coronary intervention; machine learning; prognostic modeling

Introduction

With changing lifestyle habits and aging populations, coronary artery disease (CAD) has emerged as a leading global threat to health and mortality. It is projected that CAD will cause 7.8 million deaths worldwide by 2025 [1-4]. CAD is generally categorized into acute coronary syndrome (ACS) or chronic coronary syndrome (CCS) [5]. Among these, CCS is characterized by stable but progressive myocardial ischemia, presenting substantial challenges in long-term management and risk stratification [6].

Percutaneous coronary intervention (PCI), a mainstay treatment for CAD, aims to restore myocardial perfusion and is extensively used in patients with CCS [7]. However, despite successful revascularization, not all patients experience improved cardiac function, leading to poor long-term prognosis [8,9]. Recovery and remodeling of ventricular function critically influence PCI outcomes, and left ventricular ejection fraction (LVEF) is a key metric for assessing these changes [10-12]. Dynamic changes in LVEF are closely associated with myocardial recovery, heart failure incidence, hospital readmission, and cardiovascular mortality [13-15]. Therefore, identifying patients with varying degrees of LVEF recovery after PCI is essential for early risk stratification and personalized clinical management.

Traditionally, research on post-PCI recovery has focused primarily on patients with reduced LVEF, while those with preserved baseline LVEF have received less attention [16,17]. However, several studies have shown that a large proportion patient with preserved LVEF progress to reduced LVEF during follow-up, and this transition is usually associated with a worse clinical prognosis [14,18]. Thus, stratified modeling based on baseline LVEF is essential to capture the heterogeneity of post-PCI recovery and to enable early identification of potential high-risk patients.

In recent years, machine learning (ML) has been increasingly applied to PCI outcome prediction. However, most existing studies have focused on ACS populations and short-term events, such as major adverse cardiovascular events, mortality, or readmission [19-23]. By contrast, limited studies and datasets exist for the CCS population, in which post-PCI myocardial recovery plays a central role in long-term prognosis. Moreover, few studies have addressed the heterogeneity across baseline LVEF subgroups or incorporated interpretable ML approaches to elucidate the determinants of ventricular recovery. Therefore, this study aimed to develop and validate ML-based predictive frameworks to assess LVEF recovery within 6 to 12 months after PCI in patients with CCS with different baseline LVEF levels. Furthermore, we aimed to identify key factors influencing LVEF recovery to optimize post-PCI follow-up and treatment strategies, ultimately enhancing the long-term prognosis of patients with CCS.

Methods

Data Source

This study used the Clinical Deep Data Accumulation System (CLIDAS) database. Briefly, CLIDAS involves 6 university hospitals and 1 national center hospital in Japan, namely, Tohoku University, Jichi Medical University, Jichi Medical University Saitama Medical Center, University of Tokyo, National Cerebral and Cardiovascular Center Hospital, Kyushu University, and Kumamoto University [24,25]. The database includes data on patients' backgrounds, blood test results, medication prescriptions, echocardiography data, electrocardiogram data, long-term prognosis, and information on cardiac catheterization [26].

Ethical Considerations

This retrospective study was reviewed and approved by the Institutional Review Board of Jichi Medical University Hospital, Jichi Medical University, Tochigi, Japan (reference 23-158), and was conducted in accordance with the Declaration of Helsinki. The requirement for written informed consent was waived owing to the retrospective study design. All patient

XSL•FO
RenderX

information was anonymized before analysis. JD and GL had full access to all the data in the study and take responsibility for its integrity and the data analysis.

Study Population

We retrospectively analyzed patients with CCS who underwent PCI between April 2013 and December 2018 and were registered in the CLIDAS database. The inclusion criteria were as follows: (1) patients diagnosed with CCS and undergoing PCI for reasons other than ACS; (2) at least one echocardiogram showing LVEF within 30 days before PCI, that is, baseline LVEF (including day 30 before PCI and the day of PCI); (3) at least one echocardiogram showing LVEF during follow-up (180-365 days after PCI), that is, follow-up LVEF (including days 180 and 365 after PCI); and (4) available blood test data, demographics, electrocardiogram records, echocardiography examination records, cardiac catheterization insertion reports within 1 month before PCI (including day 30 before PCI and the day of PCI), and medication records within 10 days of PCI and before PCI. In total, 520 patients were included.

Group Classification and Definition

The patients were grouped according to the change in their LVEF values (ΔLVEF; ΔLVEF=follow-up LVEF−baseline LVEF) to specifically characterize the improvement or deterioration of LVEF after PCI. For baseline and follow-up LVEF, only values closest to days 0 and 180, respectively, were considered. Good LVEF recovery was defined as ΔLVEF>10%, normal recovery as ΔLVEF>0% to ≤10%, and nonrecovery as ΔLVEF≤0%. Although the most recent European Society of Cardiology guidelines have introduced a new subtype of heart failure with a mild reduction in ejection fraction (ie, LVEF 40%-49%), this subtype is uncertain and is underrepresented in many clinical trials. In addition, owing to observer variability during echocardiographic procedures, this subtype is more difficult to differentiate and can lead to serious misclassifications.

Both American and Australian heart failure guidelines prefer to categorize heart failure with preserved ejection fraction and heart failure with reduced ejection fraction using a 50% LVEF threshold [27]. Therefore, in this study, the 50% baseline LVEF threshold was used to classify the patients into the preserved LVEF group (ie, LVEF≥50%) and the reduced LVEF group (ie, LVEF<50%). Subsequently, different degrees of LVEF recovery were combined with the 2 aforementioned groups, resulting in 4 distinct groups. These groups were used for model development and validation, with the aim of investigating the similarities and differences in factors influencing the varying degrees of LVEF recovery in these patients.

Predictive Variables

A total of 131 predictor variables were analyzed. These included blood test data, demographic data, electrocardiogram recordings, echocardiogram recordings, cardiac catheterization reports within 30 days before PCI, and medication records within 10 days before PCI. Given that the same patient may have multiple measurements for each predictor variable, except for medication records, the one closest to the date of PCI was used. The number of medications was very large; thus, the medications were divided into categories to narrow them down, and the categories were converted into categorical variables using one-hot encoding. As the vascular locations of PCI implementation vary in cardiac catheterization reports, namely, the right coronary artery (RCA), left main trunk (LMT), left anterior descending artery (LAD), and left circumflex artery (LCX), 4 new binary variables were created to indicate the PCI implementation site: site_RCA, site_LMT, site_LAD, and site_LCX.

Data Preprocessing

We first examined the distribution of missing data across the entire cohort and found no apparent systematic pattern. Therefore, data processing was conducted under an approximately missing at random assumption.

Variables with more than 30% missing data were removed. For variables with 10% to 30% data missingness, multivariate imputation by chained equations was applied, while variables with <10% data missingness were imputed using the median and mode value [28].

Feature Selection

Three feature selection strategies were applied: all 131 variables (no selection), least absolute shrinkage and selection operator (LASSO) regression, and recursive feature elimination (RFE). LASSO selects features by penalizing the coefficients of less important variables, whereas RFE iteratively removes the least important features based on model performance. Both LASSO and RFE were implemented with embedded cross-validation to ensure the robustness and stability of feature selection across data partitions.

Model Development and Evaluation

We constructed predictive models for each task using 4 ML algorithms: extreme gradient boosting (XGBoost), CatBoost, LightGBM, and random forest. Models were trained using 10-fold cross-validation to mitigate overfitting. Hyperparameters were optimized using the Optuna Bayesian optimization framework (Preferred Networks). Model performance was primarily evaluated by the receiver operating characteristic (ROC) and area under the curve (AUC), complemented by decision curve analysis (DCA) and calibration plots.

Model Interpretability

To interpret and visualize model predictions, we used Shapley Additive Explanation (SHAP), which quantifies the contribution of each feature to the model's predictions, facilitating clinical interpretability.

Statistical Analysis

For baseline characteristics, categorical variables were expressed as percentages and compared between the groups using the chi-square test. The Kolmogorov-Smirnov test was used to assess the normality of the distribution of continuous variables. Normally distributed continuous variables were presented as the mean (SD) and compared using 2-tailed Student *t* test. Nonnormally distributed continuous variables were presented as the median (IQR) and compared using the Mann-Whitney *U* test. All statistical analyses and the model construction process were performed using Jupyter Notebook 6.4.8 (Project Jupyter)

XSL•FO
RenderX

and Anaconda Navigator 2.3.2 (Anaconda Inc). The programming language used was Python 3.9.12. Statistical significance was set at $P<.05$, and it refers to the predefined threshold.

Results

Baseline Characteristics

We included 520 patients from the CLIDAS database. The average age of the total population was 71 (SD 10.49) years, and 401 (77.1%) patients were male. Diabetes mellitus and hypertension were present in 200 (38.5%) patients and 431 (82.9%) patients, respectively. According to the baseline LVEF, 418 (80.38%) patients belonged to the preserved LVEF group and 102 (19.61%) to the reduced LVEF group. The distribution of patients across baseline LVEF and recovery categories is presented in Table 1. The baseline characteristics of the preserved and reduced LVEF groups are summarized in Tables S1 and S2 in Multimedia Appendix 1, respectively. Owing to the large number of clinical variables, representative variables from each category are presented here. In the preserved LVEF group, hemoglobin, hematocrit (Hct), left ventricular end-systolic internal diameter, and baseline LVEF were substantially different between patients with and without functional recovery. In the reduced LVEF group, serum creatinine (Cre) and glucose (GLU) demonstrated sizable differences between recovery and nonrecovery patients.

Table 1. Group inclusion (N=520).

Group	Recovery, n (%)	Nonrecovery, n (%)
Baseline LVEF[a] ≥50%		
Preserved LVEF with good recovery[b] (n=229)	43 (8.26)	186 (35.77)
Preserved LVEF with normal recovery[c] (n=375)	189 (36.35)	186 (35.77)
Baseline LVEF<50%		
Reduced LVEF with good recovery (n=68)	44 (8.46)	24 (4.61)
Reduced LVEF with normal recovery (n=58)	34 (6.54)	24 (4.61)

[a]LVEF: left ventricular ejection fraction.

[b]Good recovery: an LVEF increase of >10% compared with ≤0%.

[c]Normal recovery: an LVEF increase of 0% to 10% compared with ≤0%.

Predictive Performance of the Models

A total of 48 predictive models were developed by combining 3 feature selection strategies (all features, LASSO, and RFE) with 4 ML algorithms (XGBoost, CatBoost, LightGBM, and random forest) across 4 prediction tasks. Model performance evaluated using the AUC score is summarized in Table 2. Additional details, including task-specific feature selection, ROC curves, calibration, and DCA plots of all models, as well as other performance metrics for the best-performing models are presented in Figures S1-S3 and Table S3 in Multimedia Appendix 1.

XSL•FO
RenderX

Table 2. The area under the curve score of each model.

	XGBoost[a]	CatBoost[b]	LightGBM[c]	RF[d]
pG[e]				
All features	0.90	0.89	0.87	0.86
LASSO[f]	0.89	0.90	0.87	0.87
RFE[g]	0.93	0.92	0.90	0.88
pN[h]				
All features	0.76	0.75	0.75	0.70
LASSO	0.79	0.77	0.75	0.72
RFE	0.77	0.74	0.75	0.72
rG[i]				
All features	0.83	0.81	0.76	0.60
LASSO	0.88	0.81	0.80	0.82
RFE	0.85	0.82	0.83	0.74
rN[j]				
All features	0.81	0.83	0.77	0.66
LASSO	0.82	0.81	0.78	0.72
RFE	0.84	0.83	0.77	0.68

[a]XGBoost: extreme gradient boosting.

[b]CatBoost: categorical boosting.

[c]LightGBM: light gradient boosting machine.

[d]RF: random forest.

[e]pG: preserved left ventricular ejection fraction with good recovery.

[f]LASSO: least absolute shrinkage and selection operator.

[g]RFE: recursive feature elimination.

[h]pN: preserved left ventricular ejection fraction with normal recovery.

[i]rG: reduced left ventricular ejection fraction with good recovery.

[j]rN: reduced left ventricular ejection fraction with normal recovery.

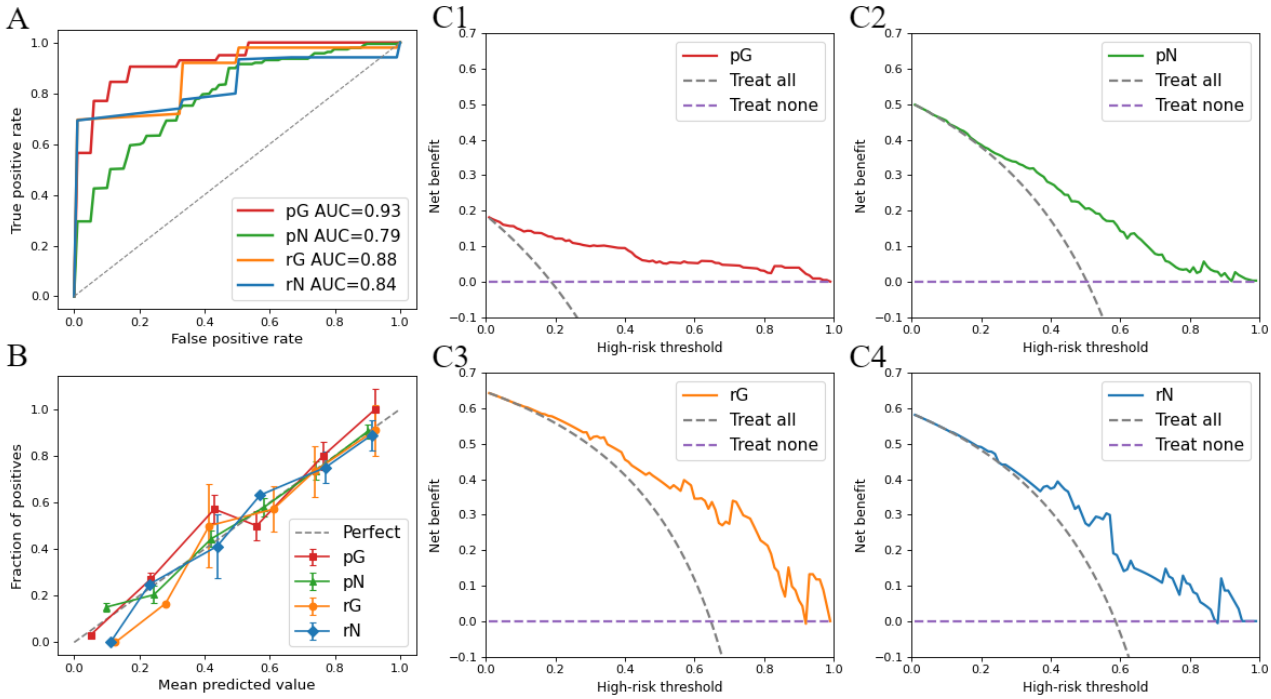
The best-performing models for each task were as follows:

- Preserved LVEF with good recovery: RFE+XGBoost (AUC=0.93)
- Preserved LVEF with normal recovery: LASSO+XGBoost (AUC=0.79)
- Reduced LVEF with good recovery: LASSO+XGBoost (AUC=0.88)
- Reduced LVEF with normal recovery: RFE+XGBoost (AUC=0.84)

Figure 1 shows the performance of the optimal models for each task. ROC curves demonstrated strong discriminative power across tasks, especially in predicting patient with good recovery tasks. Calibration plots showed the alignment of predicted probabilities with observations for different risk levels, providing a visual assessment of how well each model's predicted risk fits with actual event rates. DCA plots revealed substantial clinical net benefit of the optimal models compared to treat-all and treat-none strategies across a wide range of threshold probabilities, supporting their potential clinical applicability.

XSL•FO
RenderX

Figure 1. Model performance of each task: (A) receiver operating characteristic curves for optimal models in each task, (B) calibration curve of the 4 optimal models, and (C1-C4) clinical decision curves of the optimal models for each task. AUC: area under the curve; pG: preserved left ventricular ejection fraction with good recovery task; pN: preserved left ventricular ejection fraction with normal recovery task; rG: reduced left ventricular ejection fraction with good recovery task; rN: reduced left ventricular ejection fraction with normal recovery task.



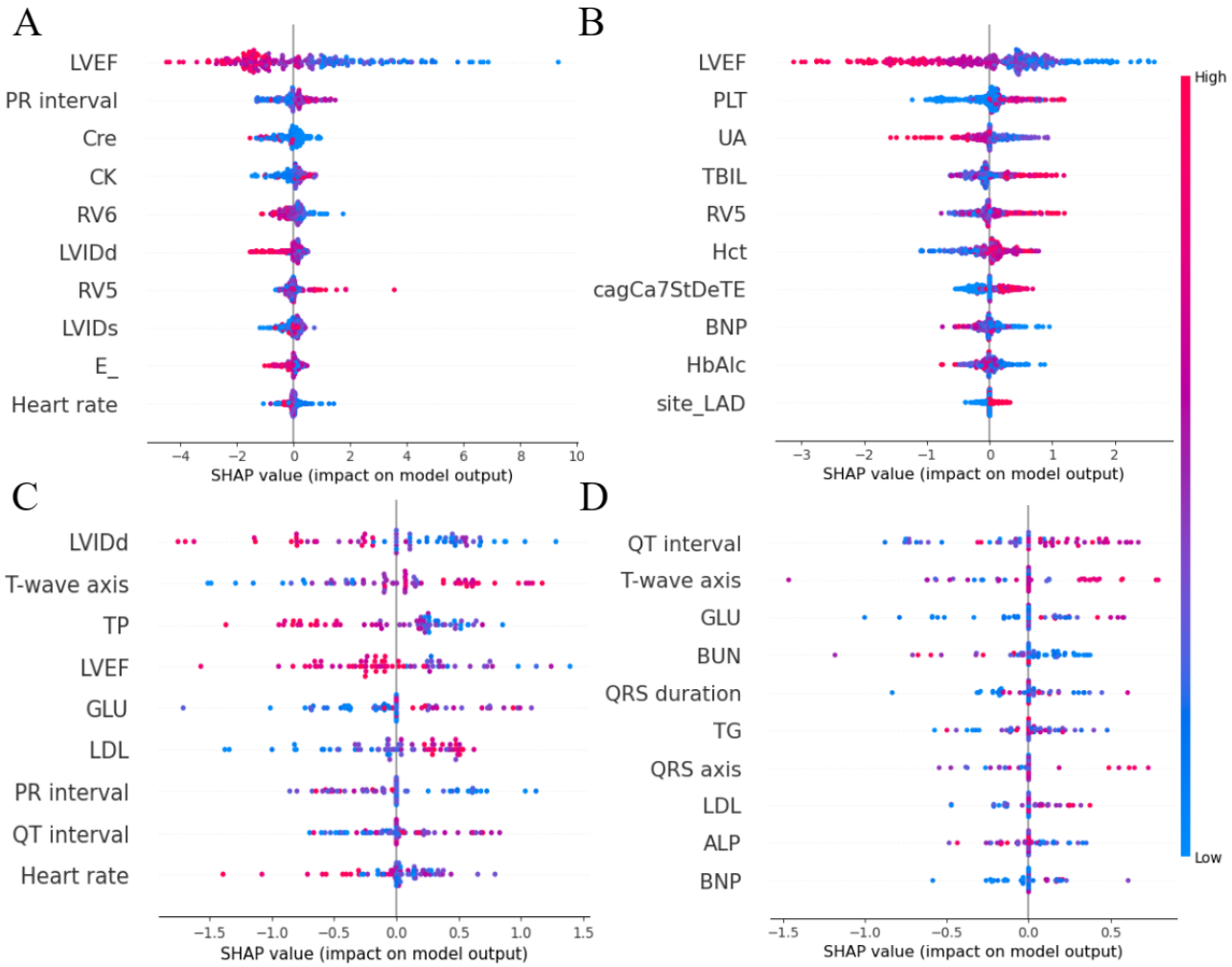
Subgroup analyses stratified by sex, age, and comorbidities demonstrated consistent model performance across clinically relevant patient groups (Table S4 in Multimedia Appendix 1).

SHAP Summary Plot

SHAP is a graphical method for interpreting ML models based on the concept of Shapley values in game theory. Each line in the SHAP summary plot represents a predictor variable, with variables that have a greater impact on the model output being closer to the top. The SHAP summary plots for the 4 optimal models are shown in Figure 2. Overall, some cardiac function–related parameters were identified as important. These included baseline LVEF; left ventricular end-diastolic internal diameter (LVIDd); R wave amplitude in V5 (RV5) or R wave amplitude in V6 (RV6); heart rate; and some laboratory parameters, including uric acid (UA), platelets (PLTs), Hct, brain natriuretic peptide (BNP), glycated hemoglobin (HbA_{1c}), GLU, and Cre.

XSL•FO
RenderX

Figure 2. Top important features identified by Shapley Additive Explanations (SHAP): (A) important features in the preserved left ventricular ejection fraction with good recovery task, (B) important features in the preserved left ventricular ejection fraction with normal recovery task, (C) important features in the reduced left ventricular ejection fraction with good recovery task, and (D) important features in the reduced left ventricular ejection fraction with normal recovery task. ALP: alkaline phosphatase; BNP: brain natriuretic peptide; BUN: blood urea nitrogen; cagCa7StDeTE: stenosis degree of coronary artery segment 7; CK: creatine kinase; Cre: creatinine; E_: mitral E wave velocity; GLU: glucose; HbA_{1c}: glycated hemoglobin; Hct: hematocrit; LAD: left anterior descending artery; LDL: low-density lipoprotein; LVEF: left ventricular ejection fraction; LVIDd: left ventricular end-diastolic internal diameter; LVIDs: left ventricular end-systolic internal diameter; PLT: platelet; RV5: R wave amplitude in V5; RV6: R wave amplitude in V6; TBIL: total bilirubin; TG: triglycerides; TP: total protein; UA: uric acid.



Discussion

Principal Findings

In this study, our models showed satisfactory performance across all groups after hyperparameter optimization and 10-fold cross-validation. The results indicated the strong discriminatory ability of ML models in predicting the recovery status of LVEF within 6 months to 1 year after PCI in patients with CCS. The application of feature selection strategies, such as RFE and LASSO, effectively improved model performance. Furthermore, UA, PLTs, Hct, BNP, HbA_{1c}, GLU, Cre, baseline LVEF, LVIDd, heart rate, RV5, and RV6 were identified as important predictors of post-PCI LVEF recovery in patients with CCS with different baseline LVEF levels. These findings can help clinicians better understand the factors influencing LVEF recovery, thereby supporting timely adjustments in treatment and follow-up strategies to improve patient outcomes.

Compared with previous studies, our work presents several methodological and clinical advancements. From a clinical perspective, our study moves beyond the traditional focus on adverse end points. Previous ML-based PCI studies have primarily focused on ACS populations and short-term event outcomes such as major adverse cardiovascular events or mortality [19-23], which capture only terminal prognostic states. In contrast, post-PCI LVEF recovery reflects the intermediate phase of cardiac repair, serving as a mechanistically meaningful and clinically actionable indicator of long-term prognosis. We focused on the 6- to 12-month post-PCI period, which captures the critical window of myocardial remodeling while minimizing interference from immediate or distant postoperative events. As most improvement or decline in LVEF occurs within this period [12,17], early prediction of recovery potential during this phase enables timely adjustment of medical therapy and secondary prevention strategies, providing a more proactive framework for improving patient outcomes [29]. Furthermore, our study addresses the real-world heterogeneity of CCS by

XSL•FO
RenderX

uniquely including patients across both reduced and preserved LVEF subgroups [30,31], thereby covering a broader clinical spectrum that was often overlooked in previous research. Methodologically, we used a more rigorous and transparent framework. Earlier post-PCI studies mainly relied on single statistical models or isolated ML algorithms, often neglecting subgroup variability and the robustness of feature selection [16,32,33]. In contrast, our framework systematically compared different feature selection methods (RFE and LASSO) and integrated SHAP analysis to enhance interpretability. This combination improved model robustness clarified the contribution of individual predictors, and strengthened clinical transparency and trust.

Interestingly, models generally perform better with larger, more balanced datasets [34]. However, in our study, the best-performing task was predicting good recovery in preserved LVEF, rather than the task with the largest and most balanced sample size. The results remained consistent after accounting for class imbalance through category weighting sensitivity analysis (Table S5 in Multimedia Appendix 1). In addition, the good recovery task was superior to the normal recovery task across different baseline LVEF groups, indicating that patients with substantial LVEF improvement after PCI may have more defined potential patterns and clinical characteristics. This phenomenon is consistent with previous studies, suggesting that clear patient characteristics typically yield higher prediction accuracy even with smaller datasets [35,36]. Identifying these unique clinical trajectories and patterns can accurately stratify patients, leading to targeted interventions and improved clinical management.

Currently, clinical practice and research in post-PCI management focus on patients with reduced LVEF due to their substantial myocardial dysfunction, while largely ignoring patients with preserved LVEF. However, a *normal* LVEF does not necessarily reflect normal myocardial function. Previous studies have shown that patients with preserved LVEF may exhibit abnormal myocardial strain, elevated ventricular filling pressures, and an increased risk of adverse outcomes [37-39]. Yoshihisa et al [18] reported that approximately 30% of patients with preserved LVEF had a reduction in LVEF to ≤50% within 6 months, which was associated with poorer clinical outcomes. Similarly, another longitudinal study showed that a significant proportion of patients with preserved LVEF converted to reduced LVEF during a 3-year follow-up [40]. These results highlight the importance of promptly and accurately predicting LVEF trends in patients with preserved LVEF after PCI. Our model provides a practical tool for the early detection of potentially high-risk patients with preserved LVEF, which can improve their long-term prognosis through close monitoring of key factors and timely intervention.

In this study, SHAP analysis identified several key predictors of LVEF recovery, including laboratory parameters (UA, PLT, Hct, BNP, HbA_{1c}, GLU, Cre), cardiac function–related variables (baseline LVEF, LVIDd, and heart rate), and electrocardiogram parameters such as RV5 and RV6. Among laboratory and metabolic indicators, higher UA levels were associated with predicted nonrecovery, consistent with the role of hyperuricemia in promoting oxidative stress, endothelial dysfunction, and inflammation that drive adverse ventricular remodeling [41,42]. This aligns with the findings of Akashi et al [25], who identified hyperuricemia as a risk factor for heart failure after PCI in patients with CCS. Low Hct impairs oxygen delivery, and Wang et al [43] found that Hct levels were significantly lower in patients with CAD than in healthy controls. Interestingly, higher PLT counts were positively associated with recovery probability. This finding may reflect the reparative function of PLTs beyond thrombosis, as they release bioactive mediators, including growth factors and cytokines, that promote myocardial repair, angiogenesis, and inflammatory resolution [44]. Beyond these hematologic and metabolic markers, cardiovascular and systemic biomarkers also aid in risk stratification. Elevated BNP reflects neurohormonal activation and ventricular wall stress and has been linked to adverse outcomes even in patients with preserved LVEF after revascularization [45,46]. Increased HbA_{1c} indicates chronic metabolic stress and impaired myocardial recovery potential, consistent with studies showing that poor glycemic control limits functional improvement after PCI in both diabetic and nondiabetic populations [47,48]. Elevated Cre, as a marker of renal dysfunction [49], was also correlated with impaired cardiac functional recovery [50]. GLU also emerged as an important predictor in some subgroups. As the myocardium relies predominantly on GLU oxidation for energy, moderate elevations in GLU may reflect adequate metabolic substrate availability, consistent with the positive association observed in our model [51].

Regarding cardiac structural and functional parameters, an enlarged LVIDd was negatively associated with recovery, reflecting impaired ventricular compliance and chronic remodeling, as also shown by Chen et al [52]. Higher resting heart rate predicted poorer recovery, plausibly because increased sympathetic activation elevates myocardial oxygen demand and exacerbates ischemic stress, consistent with the findings of Lei et al [2].

For electrocardiographic parameters, the SHAP analysis indicated that higher RV6 amplitudes and lower RV5 amplitudes were predictive of nonrecovery. These voltage patterns are typical of left ventricular hypertrophy and electrical remodeling, both of which reduce compliance and delay reverse remodeling after revascularization [42]. Repolarization features, such as longer QT intervals and greater T-wave axis deviations, were positively associated with recovery in the reduced LVEF group, possibly reflecting adaptive electrical remodeling during functional improvement.

Importantly, lesion-specific variables, such as stenosis degree of coronary artery segment 7 (cagCa7StDeTE) and site_LAD, were positively associated with predicted recovery in the preserved LVEF with normal recovery group. This positive association does not imply a beneficial effect of severe stenosis but rather reflects the efficacy of complete and timely revascularization in critical myocardial territory. Proximal LAD lesions compromise a large myocardial territory and are critical determinants of left ventricular function; therefore, successful PCI in these segments can lead to substantial recovery [45]. Patients in our cohort with severe LAD stenosis who underwent

XSL•FO
RenderX

PCI demonstrated superior LVEF recovery. This suggests that anatomically targeted revascularization meaningfully contributes to reverse remodeling, even in the preserved function group. The inclusion of these lesion-level features underscores our dataset's unique strength. It shows that the model captures not only systemic and biochemical predictors but also procedural and anatomical factors. This provides an additional layer of interpretability that has been rarely addressed in prior studies.

Limitations

First, the relatively small sample size and the inclusion of only patients with complete echocardiographic follow-up data may have introduced selection bias, although this was necessary to ensure outcome accuracy. Second, although the dataset was derived from a multicenter real-world cohort in Japan, external validation was not conducted due to the specificity of included variables, limiting generalizability. Third, as a real-world cohort, unavoidable data missingness existed. Removing variables with a high proportion of missing data may have affected model performance. Furthermore, if some variables were missing not at random, this could affect feature selection or model performance.

Future work should expand the cohort and include external datasets for validation, while prospectively collecting standardized data to allow a more rigorous evaluation of missingness mechanisms and model generalizability. Moreover, developing dynamic models to predict continuous changes in LVEF and integrating additional modalities, such as imaging and biomarkers, may further enhance predictive accuracy and clinical utility.

Conclusions

Our ML models, which integrated feature selection strategies, demonstrated strong predictive performance for LVEF recovery after PCI. SHAP analysis identified UA, PLT, Hct, BNP, HbA_{1c}, GLU, Cre, baseline LVEF, LVIDd, heart rate, RV5, and RV6 as key factors of post-PCI LVEF recovery.

Acknowledgments

The authors thank the Kowa Company for funding Clinical Deep Data Accumulation System (CLIDAS) and all members of the CLIDAS research group for their contributions. The authors also thank Yuri Matoba (Precision Inc, Tokyo, Japan) for her support.

Funding

This work was supported by Kowa Company, Ltd; the Health Labour Sciences Research Grant (22FA1016); and the Cross-Ministerial Strategic Innovation Promotion Program on "Integrated Health Care System" (JPJ012425).

Authors' Contributions

JD, GL, and MN contributed to the conception and design of the study. JD performed feature selection, developed the models, and drafted the original manuscript. GL conducted data processing and statistical analysis. TM, T Kohro, NA, T Kabutoya, MI, TN, and HS collected data and organized the database. All authors contributed to the critical revision of the manuscript and approved the final version.

Conflicts of Interest

The authors declare the following financial interests or personal relationships that may be considered as potential competing interests. TK has received scholarship funding from Abbott. KK has received a research grant from Otsuka Pharmaceutical, Sanwa Kagaku Kenkyusho, Daiichi-Sankyo, MSD, Astellas Pharma, Eisai, Taisho Pharmaceutical, Sumitomo Dainippon Pharma, Takeda Pharmaceutical, Mitsubishi Tanabe Pharma, Teijin Pharma, Boehringer Ingelheim Japan, Bristol-Myers Squibb, and Mochida Pharmaceutical; consulting fees from Kyowa Kirin, Sanwa Kagaku Kenkyusho, and Mochida Pharmaceutical; honoraria from Otsuka Pharmaceuticals, Daiichi-Sankyo, Novartis Pharma, and Mylan European Pharmaceutical Distribution; and served on the advisory boards of Daiichi-Sankyo and Novartis Pharma. HF received scholarship funds from Abbott Vascular and speaking honoraria from Novartis and Otsuka Pharmaceutical Co, Ltd and served as a consultant for Mehergen Group Holdings, Inc. KT has received personal fees from Abbott Medical Co, Ltd, Amgen KK, AstraZeneca KK, Bayer Yakuhin, Ltd, Daiichi Sankyo Co, Ltd, Medtoronic Japan Co, Ltd, Kowa Pharmaceutical Co, Ltd, Novartis Pharma KK, Otsuka Pharmaceutical Co, Ltd, Pfizer Japan Inc, and Janssen Pharmaceutical K.K.; grants from PPD-Shin Nippon Biomedical Laboratories K.K, Alexion Pharmaceuticals, Inc, Abbott Medical Co, Ltd, Bayer Yakuhin, Ltd, Boehringer Ingelheim Japan, Daiichi Sankyo Co, Ltd, ITI Co, Ltd, ONO Pharmaceutical Co, Ltd, Otsuka Pharmaceutical Co, Ltd, and Takeda Pharmaceutical Co, Ltd; and other funds from Abbott Japan Co, Ltd, Boston Scientific Japan KK, Fides-One, Inc, GM Medical Co, Ltd, ITI Co, Ltd, Kaneka Medix Co, Ltd, NIPRO CORPORATION, TERUMO Co, Ltd, Abbott Medical Co, Ltd, Boston Scientific Japan KK, Cardinal Health Japan, Fukuda Denshi Co, Ltd, Japan Lifeline Co, Ltd, Medical Appliance Co, Ltd, and Medtronic Japan Co, Ltd outside the submitted work. SY reports remuneration for lectures from Takeda, Daiichi-Sankyo, and Bristol-Myers Squibb and trust research or joint research funds from Takeda and Daiichi-Sankyo. TM has received lecture fees from Abbott, Bayer Yakuhin, and MSD and research funding from Amgen, Bayer Yakuhin, and Kowa. YM received research funds from Kowa Company, Ltd within the submitted work and from Tokyo Marine and Nichido Fire Insurance Co, Ltd, Fujitsu Co, Ltd, Softbank Co, Ltd, Saraya Co, Ltd, and Meiji Yasuda Life Insurance Company outside of the submitted work.

XSL•FO
RenderX

Multimedia Appendix 1
Additional results of various analyses.
[DOCX File , 27300 KB - medinform_v13i1e77839_app1.docx]

References

1. Benjamin EJ, Virani SS, Callaway CW, Chamberlain AM, Chang AR, Cheng S, et al. Heart disease and stroke statistics-2018 update: a report from the American Heart Association. Circulation 2018 Mar 20;137(12):e67-492 [FREE Full text] [doi: 10.1161/CIR.0000000000000558] [Medline: 29386200]
2. Lei Z, Li B, Li B, Peng W. Predictors and prognostic impact of left ventricular ejection fraction trajectories in patients with ST-segment elevation myocardial infarction. Aging Clin Exp Res 2022 Jun;34(6):1429-1438 [FREE Full text] [doi: 10.1007/s40520-022-02087-y] [Medline: 35147922]
3. Mortensen MB, Falk E. Primary prevention with statins in the elderly. J Am Coll Cardiol 2018 Jan 02;71(1):85-94 [FREE Full text] [doi: 10.1016/j.jacc.2017.10.080] [Medline: 29301631]
4. Roth GA, Nguyen G, Forouzanfar MH, Mokdad AH, Naghavi M, Murray CJ. Estimates of global and regional premature cardiovascular mortality in 2025. Circulation 2015 Sep 29;132(13):1270-1282. [doi: 10.1161/CIRCULATIONAHA.115.016021] [Medline: 26408271]
5. Knuuti J, Wijns W, Saraste A, Capodanno D, Barbato E, Funck-Brentano C, et al. 2019 ESC Guidelines for the diagnosis and management of chronic coronary syndromes. Eur Heart J 2020 Jan 14;41(3):407-477 [FREE Full text] [doi: 10.1093/eurheartj/ehz425] [Medline: 31504439]
6. Jing T, Wang Y, Li Y, Cui L, Liu X, Liu D, et al. Diagnosis, treatment, and management for chronic coronary syndrome: a systematic review of clinical practice guidelines and consensus statements. Int J Clin Pract 2023;2023:9504108 [FREE Full text] [doi: 10.1155/2023/9504108] [Medline: 38146345]
7. Coerkamp CF, Hoogewerf M, van Putte BP, Appelman Y, Doevendans PA. Revascularization strategies for patients with established chronic coronary syndrome. Eur J Clin Invest 2022 Aug;52(8):e13787 [FREE Full text] [doi: 10.1111/eci.13787] [Medline: 35403216]
8. Guo S, Luo X, Huang L, Wang C, Yang Y, Yang L. Hot spots and trends in PCI prognostic research: a bibliometric analysis with CiteSpace. Medicine (Baltimore) 2023 Oct 27;102(43):e35599 [FREE Full text] [doi: 10.1097/MD.0000000000035599] [Medline: 37904392]
9. Kim DH, Park CB, Jin EH, Hwang HJ, Sohn IS, Cho JM, et al. Predictors of decreased left ventricular function subsequent to follow-up echocardiography after percutaneous coronary intervention following acute ST-elevation myocardial infarction. Exp Ther Med 2018 May;15(5):4089-4096 [FREE Full text] [doi: 10.3892/etm.2018.5962] [Medline: 29725361]
10. Pfeffer MA, Braunwald E. Ventricular remodeling after myocardial infarction. Experimental observations and clinical implications. Circulation 1990 Apr;81(4):1161-1172. [doi: 10.1161/01.cir.81.4.1161] [Medline: 2138525]
11. Passino C, Vergaro G. Left ventricular ejection fraction and coronary artery disease in the era of precision medicine. Eur J Prev Cardiol 2019 Aug;26(12):1271-1272. [doi: 10.1177/2047487319847546] [Medline: 31053050]
12. Batra MK, Malik MA, Khan KA, Rai L, Kumar R, Shah JA, et al. Left ventricular functional remodeling after primary percutaneous coronary intervention. J Cardiovasc Echogr 2022;32(1):12-16 [FREE Full text] [doi: 10.4103/jcecho.jcecho_64_21] [Medline: 35669137]
13. Levi A, Bental T, Assali AR, Lev EI, Vaknin Assa H, Shaul AA, et al. Dynamic changes in left ventricular function after a percutaneous coronary intervention: prevalence, predictors, and prognosis. Coron Artery Dis 2016 May;27(3):199-206. [doi: 10.1097/MCA.0000000000000351] [Medline: 26848535]
14. Aoyanagi H, Nochioka K, Sakata Y, Miura M, Shiroto T, Abe R, CHART-2 Investigators. Temporal changes in left ventricular ejection fraction and their prognostic impacts in patients with Stage B heart failure. Int J Cardiol 2020 May 01;306:123-132. [doi: 10.1016/j.ijcard.2020.02.040] [Medline: 32113664]
15. Miller RJ, Nabipoor M, Youngson E, Kotrri G, Fine NM, Howlett JG, et al. Heart failure with mildly reduced ejection fraction: retrospective study of ejection fraction trajectory risk. ESC Heart Fail 2022 Jun;9(3):1564-1573 [FREE Full text] [doi: 10.1002/ehf2.13869] [Medline: 35261203]
16. Khaled S, Shalaby G. Myocardial recovery after percutaneous coronary intervention in coronary artery disease patients with impaired systolic function- predictive utility of global longitudinal strain. Indian Heart J 2022;74(6):488-493 [FREE Full text] [doi: 10.1016/j.ihj.2022.11.004] [Medline: 36372350]
17. Yee NP, Siu AM, Davis J, Kao J. Recovery of left ventricular function after percutaneous coronary intervention compared to coronary artery bypass grafting in patients with multi-vessel coronary disease and left ventricular dysfunction. Hawaii J Med Public Health 2016 Sep;75(9):273-277 [FREE Full text] [Medline: 27688953]
18. Yoshihisa A, Sato Y, Kanno Y, Takiguchi M, Yokokawa T, Abe S, et al. Prognostic impacts of changes in left ventricular ejection fraction in heart failure patients with preserved left ventricular ejection fraction. Open Heart 2020;7(1):e001112 [FREE Full text] [doi: 10.1136/openhrt-2019-001112] [Medline: 32341787]
19. Deng W, Wang D, Wan Y, Lai S, Ding Y, Wang X. Prediction models for major adverse cardiovascular events after percutaneous coronary intervention: a systematic review. Front Cardiovasc Med 2023;10:1287434 [FREE Full text] [doi: 10.3389/fcvm.2023.1287434] [Medline: 38259313]

XSL•FO
RenderX

20. Zaka A, Mutahar D, Gorcilov J, Gupta AK, Kovoor JG, Stretton B, et al. Machine learning approaches for risk prediction after percutaneous coronary intervention: a systematic review and meta-analysis. Eur Heart J Digit Health 2025 Jan;6(1):23-44. [doi: 10.1093/ehjdh/ztae074] [Medline: 39846069]
21. Tofighi S, Poorhosseini H, Jenab Y, Alidoosti M, Sadeghian M, Mehrani M, et al. Comparison of machine-learning models for the prediction of 1-year adverse outcomes of patients undergoing primary percutaneous coronary intervention for acute ST-elevation myocardial infarction. Clin Cardiol 2024 Jan;47(1):e24157 [FREE Full text] [doi: 10.1002/clc.24157] [Medline: 37721426]
22. Aziz F, Malek S, Ibrahim KS, Raja Shariff RE, Wan Ahmad WA, Ali RM, et al. Short- and long-term mortality prediction after an acute ST-elevation myocardial infarction (STEMI) in Asians: a machine learning approach. PLoS One 2021;16(8):e0254894 [FREE Full text] [doi: 10.1371/journal.pone.0254894] [Medline: 34339432]
23. Kunadian V, Pugh A, Zaman AG, Qiu W. Percutaneous coronary intervention among patients with left ventricular systolic dysfunction: a review and meta-analysis of 19 clinical studies. Coron Artery Dis 2012 Nov;23(7):469-479. [doi: 10.1097/MCA.0b013e3283587804] [Medline: 22960383]
24. Oba Y, Kabutoya T, Kohro T, Imai Y, Kario K, Sato H, et al. Relationships among heart rate, β-blocker dosage, and prognosis in patients with coronary artery disease in a real-world database using a multimodal data acquisition system. Circ J 2023 Jan 25;87(2):336-344 [FREE Full text] [doi: 10.1253/circj.CJ-22-0314] [Medline: 36216562]
25. Akashi N, Kuwabara M, Matoba T, Kohro T, Oba Y, Kabutoya T, et al. Hyperuricemia predicts increased cardiovascular events in patients with chronic coronary syndrome after percutaneous coronary intervention: a nationwide cohort study from Japan. Front Cardiovasc Med 2022;9:1062894 [FREE Full text] [doi: 10.3389/fcvm.2022.1062894] [Medline: 36704454]
26. Akashi N, Matoba T, Kohro T, Oba Y, Kabutoya T, Imai Y, et al. Sex differences in long-term outcomes in patients with chronic coronary syndrome after percutaneous coronary intervention - insights from a Japanese real-world database using a storage system. Circ J 2023 May 25;87(6):775-782 [FREE Full text] [doi: 10.1253/circj.CJ-22-0653] [Medline: 36709982]
27. Palazzuoli A, Beltrami M. Are HFpEF and HFmrEF so different? The need to understand distinct phenotypes. Front Cardiovasc Med 2021;8:676658 [FREE Full text] [doi: 10.3389/fcvm.2021.676658] [Medline: 34095263]
28. Zhang Z. Multiple imputation with multivariate imputation by chained equation (MICE) package. Ann Transl Med 2016 Jan;4(2):30 [FREE Full text] [doi: 10.3978/j.issn.2305-5839.2015.12.63] [Medline: 26889483]
29. Wennberg E, Abualsaud AO, Eisenberg MJ. Patient management following percutaneous coronary intervention. JACC Adv 2025 Jan;4(1):101453 [FREE Full text] [doi: 10.1016/j.jacadv.2024.101453] [Medline: 39801818]
30. Shah SJ. Matchmaking for the optimization of clinical trials of heart failure with preserved ejection fraction: no laughing matter. J Am Coll Cardiol 2013 Oct 08;62(15):1339-1342 [FREE Full text] [doi: 10.1016/j.jacc.2013.07.010] [Medline: 23916923]
31. Hwang SJ, Melenovsky VM, Borlaug BA. Implications of coronary artery disease in heart failure with preserved ejection fraction. J Am Coll Cardiol 2014 Jul 01;63(25 Pt A):2817-2827 [FREE Full text] [doi: 10.1016/j.jacc.2014.03.034] [Medline: 24768876]
32. Yang Y, Dong YZ, Hou AX, Liu DP, He JW, Chen JY, et al. Establishment and validation of a prediction model for nonrecovery of left ventricular ejection fraction in acute myocardial infarction patients combined with decreased left ventricular ejection fraction. Clin Cardiol 2024 Feb;47(2):e24212 [FREE Full text] [doi: 10.1002/clc.24212] [Medline: 38402553]
33. Sammour YM, Bou Chaaya RG, Kharsa C, Philip J, Hatab T, Samimi S, et al. Assessment of left ventricular function after percutaneous coronary intervention for chronic total occlusion. J Soc Cardiovasc Angiogr Interv 2025 Jan;4(1):102460 [FREE Full text] [doi: 10.1016/j.jscai.2024.102460] [Medline: 40061410]
34. Rajput D, Wang WJ, Chen CC. Evaluation of a decided sample size in machine learning applications. BMC Bioinformatics 2023 Feb 14;24(1):48 [FREE Full text] [doi: 10.1186/s12859-023-05156-9] [Medline: 36788550]
35. Robinson GA, Peng J, Dönnes P, Coelewij L, Naja M, Radziszewska A, et al. Disease-associated and patient-specific immune cell signatures in juvenile-onset systemic lupus erythematosus: patient stratification using a machine-learning approach. Lancet Rheumatol 2020 Aug;2(8):e485-e496 [FREE Full text] [doi: 10.1016/S2665-9913(20)30168-5] [Medline: 32818204]
36. Suresh S, Newton DT, Everett TH, Lin G, Duerstock BS. Feature selection techniques for a machine learning model to detect autonomic dysreflexia. Front Neuroinform 2022;16:901428 [FREE Full text] [doi: 10.3389/fninf.2022.901428] [Medline: 36033642]
37. Dimond MG, Ibrahim NE, Fiuzat M, McMurray JJ, Lindenfeld J, Ahmad T, et al. Left ventricular ejection fraction and the future of heart failure phenotyping. JACC Heart Fail 2024 Mar;12(3):451-460 [FREE Full text] [doi: 10.1016/j.jchf.2023.11.005] [Medline: 38099892]
38. Ma C, Luo H, Fan L, Liu X, Gao C. Heart failure with preserved ejection fraction: an update on pathophysiology, diagnosis, treatment, and prognosis. Braz J Med Biol Res 2020;53(7):e9646 [FREE Full text] [doi: 10.1590/1414-431X20209646] [Medline: 32520204]

XSL•FO
RenderX

39. Obokata M, Reddy YN, Borlaug BA. Diastolic dysfunction and heart failure with preserved ejection fraction: understanding mechanisms by using noninvasive methods. JACC Cardiovasc Imaging 2020 Jan;13(1 Pt 2):245-257 [FREE Full text] [doi: 10.1016/j.jcmg.2018.12.034] [Medline: 31202759]
40. Ueda T, Kawakami R, Nishida T, Onoue K, Soeda T, Okayama S, et al. Left ventricular ejection fraction (EF) of 55% as cutoff for late transition from heart failure (HF) with preserved EF to HF with mildly reduced EF. Circ J 2015;79(10):2209-2215 [FREE Full text] [doi: 10.1253/circj.CJ-15-0425] [Medline: 26227392]
41. Doehner W, Anker SD, Butler J, Zannad F, Filippatos G, Ferreira JP, et al. Uric acid and sodium-glucose cotransporter-2 inhibition with empagliflozin in heart failure with reduced ejection fraction: the EMPEROR-reduced trial. Eur Heart J 2022 Sep 21;43(36):3435-3446 [FREE Full text] [doi: 10.1093/eurheartj/ehac320] [Medline: 35788657]
42. Yang Y, Zhang X, Jin Z, Zhao Q. Association of serum uric acid with mortality and cardiovascular outcomes in patients with hypertension: a meta-analysis. J Thromb Thrombolysis 2021 Nov;52(4):1084-1093. [doi: 10.1007/s11239-021-02453-z] [Medline: 33966143]
43. Wang H, Li H, Wang Y, Zhao C, Tian Q, Wang Q, et al. Hematological parameters and early-onset coronary artery disease: a retrospective case-control study based on 3366 participants. Ther Adv Chronic Dis 2023;14:20406223221142670 [FREE Full text] [doi: 10.1177/20406223221142670] [Medline: 36699111]
44. Walsh TG, Poole AW. Do platelets promote cardiac recovery after myocardial infarction: roles beyond occlusive ischemic damage. Am J Physiol Heart Circ Physiol 2018 May 01;314(5):H1043-H1048 [FREE Full text] [doi: 10.1152/ajpheart.00134.2018] [Medline: 29547023]
45. Zhang C, Huang D, Shen D, Zhang L, Wang Y, Sun H, et al. Brain natriuretic peptide as the long-term cause of mortality in patients with cardiovascular disease: a retrospective cohort study. Int J Clin Exp Med 2015;8(9):16364-16368 [FREE Full text] [Medline: 26629158]
46. Manola S, Pavlović N, Radeljić V, Delić Brkljacić D, Pintarić H, Stambuk K, et al. B-type natriuretic peptide as predictor of heart failure in patients with acute ST elevation myocardial infarction, single-vessel disease, and complete revascularization: follow-up study. Croat Med J 2009 Oct;50(5):449-454 [FREE Full text] [doi: 10.3325/cmj.2009.50.449] [Medline: 19839068]
47. Çiçek G, Korkmaz A. Two-year prognosis of admission hemoglobin A1c following a primary percutaneous coronary intervention. Coron Artery Dis 2016 Dec;27(8):673-681. [doi: 10.1097/MCA.0000000000000411] [Medline: 27433996]
48. Cavero-Redondo I, Peleteiro B, Álvarez-Bueno C, Rodriguez-Artalejo F, Martínez-Vizcaíno V. Glycated haemoglobin A1c as a risk factor of cardiovascular outcomes and all-cause mortality in diabetic and non-diabetic populations: a systematic review and meta-analysis. BMJ Open 2017 Jul 31;7(7):e015949 [FREE Full text] [doi: 10.1136/bmjopen-2017-015949] [Medline: 28760792]
49. Demir M, Kahraman F, Sen T, Astarcioglu MA. The relationship of the hemoglobin to serum creatinine ratio with long-term mortality in patients with acute coronary syndrome: a retrospective study. Medicine (Baltimore) 2023 Oct 13;102(41):e35636 [FREE Full text] [doi: 10.1097/MD.0000000000035636] [Medline: 37832061]
50. Beldhuis IE, Lam CS, Testani JM, Voors AA, Van Spall HG, Ter Maaten JM, et al. Evidence-based medical therapy in patients with heart failure with reduced ejection fraction and chronic kidney disease. Circulation 2022 Mar;145(9):693-712 [FREE Full text] [doi: 10.1161/CIRCULATIONAHA.121.052792] [Medline: 35226558]
51. Lopaschuk GD, Karwi QG, Tian R, Wende AR, Abel ED. Cardiac energy metabolism in heart failure. Circ Res 2021 May 14;128(10):1487-1513 [FREE Full text] [doi: 10.1161/CIRCRESAHA.121.318241] [Medline: 33983836]
52. Chen YC, Hsing SC, Chao YP, Cheng YW, Lin CS, Lin C, et al. Front Med (Lausanne) 2022;9:846361 [FREE Full text] [doi: 10.3389/fmed.2022.846361] [Medline: 35646999]

Abbreviations

ΔLVEF: change in left ventricular ejection fraction value
ACS: acute coronary syndrome
AUC: area under the curve
BNP: brain natriuretic peptide
CAD: coronary artery disease
CatBoost: categorical boosting
CCS: chronic coronary syndrome
CLIDAS: Clinical Deep Data Accumulation System
Cre: creatinine
DCA: decision curve analysis
GLU: glucose
HbA_{1c}: glycated hemoglobin
Hct: hematocrit
LAD: left anterior descending artery
LASSO: least absolute shrinkage and selection operator
LightGBM: light gradient boosting machine

XSL•FO
RenderX

LMT: left main trunk
LVEF: left ventricular ejection fraction
LVIDd: left ventricular end-diastolic internal diameter
ML: machine learning
PCI: percutaneous coronary intervention
PLT: platelet
RCA: right coronary artery
RFE: recursive feature elimination
ROC: receiver operating characteristic
RV5: R wave amplitude in V5
RV6: R wave amplitude in V6
SHAP: Shapley Additive Explanation
UA: uric acid
XGBoost: extreme gradient boosting

Edited by A Benis; submitted 26.05.25; peer-reviewed by VV Khanna, Y Si; comments to author 06.10.25; revised version received 26.11.25; accepted 30.11.25; published 29.12.25.

Please cite as:
Ding J, Lyu G, Nakayama M, Nochioka K, Takahashi J, Yasuda S, Matoba T, Kohro T, Akashi N, Fujita H, Oba Y, Kabutoya T, Kario K, Imai Y, Kiyosue A, Mizuno Y, Iwai T, Miyamoto Y, Ishii M, Tsujita K, Nakamura T, Sato H, Nagai R
Predicting Left Ventricular Ejection Fraction Recovery After Percutaneous Coronary Intervention in Patients With Chronic Coronary Syndrome by Using Interpretable Machine Learning Models: Retrospective Study
JMIR Med Inform 2025;13:e77839
URL: https://medinform.jmir.org/2025/1/e77839
doi:10.2196/77839
PMID:

©Jiayi Ding, Guanqi Lyu, Masaharu Nakayama, Kotaro Nochioka, Jun Takahashi, Satoshi Yasuda, Tetsuya Matoba, Takahide Kohro, Naoyuki Akashi, Hideo Fujita, Yusuke Oba, Tomoyuki Kabutoya, Kazuomi Kario, Yasushi Imai, Arihiro Kiyosue, Yoshiko Mizuno, Takamasa Iwai, Yoshihiro Miyamoto, Masanobu Ishii, Kenichi Tsujita, Taishi Nakamura, Hisahiko Sato, Ryozo Nagai. Originally published in JMIR Medical Informatics (https://medinform.jmir.org), 29.12.2025. This is an open-access article distributed under the terms of the Creative Commons Attribution License (https://creativecommons.org/licenses/by/4.0/), which permits unrestricted use, distribution, and reproduction in any medium, provided the original work, first published in JMIR Medical Informatics, is properly cited. The complete bibliographic information, a link to the original publication on https://medinform.jmir.org/, as well as this copyright and license information must be included.

XSL•FO
RenderX

Authors' Reply: Involving Health, Technology, and Financial Stakeholders in Co-Designing Digital Pathways for Value-Based Care

Jinsong Chen[1,2,3], BHSc, MPH, PhD; Christopher Bullen[1], MBChB, MPH, PhD; Lan Zhang[3], BEng, MM, PhD

[1]University of Auckland, Auckland, New Zealand

[2]Zhejiang University, Hangzhou, China

[3]Hangzhou City University, 51 Huzhou Street, Gongshu District, Hangzhou, China

Corresponding Author:
Lan Zhang, BEng, MM, PhD
Hangzhou City University, 51 Huzhou Street, Gongshu District, Hangzhou, China

Related Articles:

https://medinform.jmir.org/2025/1/e57385

https://medinform.jmir.org/2025/1/e84885

(JMIR Med Inform 2025;13:e86837) doi:10.2196/86837

KEYWORDS

digital health; value-based health care; VBHC; patient-reported outcome measures; PROM; digital transformation; health care innovation; patient-centric care; health technology; patient-reported outcome; PRO; outcome measure; telehealth; telemedicine; eHealth; personalized; customized; engagement; patient-centered care; standardization; implementation

We appreciate the thoughtful comments shared in response to our viewpoint, "Digital Health Innovations to Catalyze the Transition to Value-Based Health Care" [1]. The correspondents have highlighted several critical dimensions that must be addressed for value-based health care (VBHC) to move from theory to real-world practice [2].

We agree that realizing VBHC requires much more than the adoption of digital technologies—it calls for a systemic reorientation of how health systems deliver, measure, and fund care. The points raised regarding patient co-design, digital equity, data interoperability, and integration into workflows align strongly with our original arguments [1]. As we noted, digital transformation must go beyond digitization and instead support participatory, patient-centered models that meaningfully engage patients and clinicians in decision-making processes.

We also concur that trust is foundational to successful adoption. As health systems increasingly rely on patient-reported outcome measures (PROMs) and patient-reported experience measures, transparent governance and ethical data practices will be key to building confidence among both patients and providers. Similar to prior recommendations in the literature [3], we view trust-building as integral to ensuring that patient-generated data are used responsibly to inform care decisions and improve outcomes.

The correspondents' emphasis on education and training for health care professionals is also well taken. As we continue to study digital PROM implementation in clinical settings, we are exploring structured capacity-building initiatives to strengthen clinicians' digital literacy and analytic skills—ensuring they can interpret and act upon PROM and patient-reported experience measure data in a timely, patient-centered manner.

Moreover, we appreciate the thoughtful expansion on sustainable financing and business models. We fully agree that aligning payment systems with outcomes is central to sustaining VBHC reforms. As highlighted in recent research on alternative payment models [4,5], outcome-linked incentives and cross-sector collaboration are essential to support the infrastructure, workforce, and long-term viability of value-based initiatives.

In conclusion, we share the correspondents' vision for a holistic and equitable transformation of health systems. Realizing the promise of digital health for VBHC requires concurrent progress in technology, governance, education, and financing. We echo their call for further empirical research across diverse health system contexts to identify actionable pathways for scaling digital innovations that deliver measurable value for patients, providers, and society.

XSL•FO
RenderX

Acknowledgments

The authors would like to acknowledge that in line with JMIR's policy on generative artificial intelligence (AI) usage, we used a generative language model (ChatGPT-5) solely to perform grammar checking and improve the expression of the manuscript text. No content was generated by the AI tool beyond refining wording, and all substantive ideas, analyses, and interpretations remain the responsibility of the authors. The use of the tool is disclosed here for transparency, consistent with JMIR's requirement for full disclosure of any generative AI usage.

Conflicts of Interest

None declared.

References

1. Zhang L, Bullen C, Chen J. Digital health innovations to catalyze the transition to value-based health care. JMIR Med Inform 2025 Jan 20;13:e57385. [doi: 10.2196/57385] [Medline: 39864959]
2. Vandekerckhove P, Harris BHL, Koizia LJ, Howard S. Involving health, technology, and financial stakeholders in co-designing digital pathways for value-based care. JMIR Med Inform 2025;13:e84885. [doi: 10.2196/84885]
3. Snyder CF, Aaronson NK, Choucair AK, et al. Implementing patient-reported outcomes assessment in clinical practice: a review of the options and considerations. Qual Life Res 2012 Oct;21(8):1305-1314. [doi: 10.1007/s11136-011-0054-x] [Medline: 22048932]
4. Howard SW, Bradford N, Belue R, et al. Building alternative payment models in health care. Front Health Serv 2024;4:1235913. [doi: 10.3389/frhs.2024.1235913] [Medline: 38948085]
5. Teisberg E, Wallace S, O'Hara S. Defining and implementing value-based health care: a strategic framework. Acad Med 2020 May;95(5):682-685. [doi: 10.1097/ACM.0000000000003122] [Medline: 31833857]

Abbreviations

PROM: patient-reported outcome measure
VBHC: value-based health care

Edited by A Iannaccio; submitted 30.10.25; this is a non–peer-reviewed article;accepted 21.11.25; published 04.12.25.

Please cite as:
Chen J, Bullen C, Zhang L
Authors' Reply: Involving Health, Technology, and Financial Stakeholders in Co-Designing Digital Pathways for Value-Based Care
JMIR Med Inform 2025;13:e86837
URL: https://medinform.jmir.org/2025/1/e86837
doi:10.2196/86837

© Jinsong Chen, Christopher Bullen, Lan Zhang. Originally published in JMIR Medical Informatics (https://medinform.jmir.org), 4.12.2025. This is an open-access article distributed under the terms of the Creative Commons Attribution License (https://creativecommons.org/licenses/by/4.0/), which permits unrestricted use, distribution, and reproduction in any medium, provided the original work, first published in JMIR Medical Informatics, is properly cited. The complete bibliographic information, a link to the original publication on https://medinform.jmir.org/, as well as this copyright and license information must be included.

XSL•FO
RenderX

Involving Health, Technology, and Financial Stakeholders in Co-Designing Digital Pathways for Value-Based Care

Pieter Vandekerckhove[1,2], PhD; Benjamin H L Harris[3,4,5,6,7], MD, MBA, PhD; Louis J Koizia[5], MBBS, MD; Steven Howard[8], MBA, PhD

[1]Delft Centre for Entrepreneurship, Delft University of Technology, Jaffalaan 5, Delft, The Netherlands

[2]Erasmus School of Health Policy & Management, Erasmus University Rotterdam, Rotterdam, The Netherlands

[3]Department of Oncology, University of Oxford, Oxford, United Kingdom

[4]St. Catherine's College, University of Oxford, Oxford, United Kingdom

[5]Department of Bioengineering, Cutrale Perioperative and Ageing Group, Imperial College London, London, United Kingdom

[6]Division of Medicine, Institute for Liver and Digestive Health, University College London, London, United Kingdom

[7]Department of Psychosocial Rehabilitation, Faculty of Health Sciences, Medical University of Lodz, Lodz, Poland

[8]Department of Health Services Administration, School of Health Professions, University of Alabama at Birmingham, Birmingham, AL, United States

Corresponding Author:
Pieter Vandekerckhove, PhD
Delft Centre for Entrepreneurship, Delft University of Technology, Jaffalaan 5, Delft, The Netherlands

Related Articles:

https://medinform.jmir.org/2025/1/e57385

Comment in: https://medinform.jmir.org/2025/1/e86837

(JMIR Med Inform 2025;13:e84885) doi:10.2196/84885

KEYWORDS

digital health; value-based health care; VBHC; patient-reported outcome measures; PROM; digital transformation; health care innovation; patient-centric care; health technology; patient-reported outcome; PRO; outcome measure; telehealth; telemedicine; eHealth; personalized; customized; engagement; patient-centered care; standardization; implementation

Dear editor,

We read with great interest the recent viewpoint by Zhang et al [1] on leveraging digital technologies to integrate patient-reported experience measures and patient-reported outcome measures (PROMs) into value-based health care (VBHC). As researchers, practitioners, and educators committed to advancing VBHC, we share their enthusiasm and believe that digital tools have transformative potential.

However, this discussion is part of a longstanding struggle to operationalize VBHC in real-world practice. A fundamental shift is needed in how patient input is considered to both improve and innovate care delivery. Evidence suggests that survey-based approaches alone are insufficient; what is required is a more value-sensitive methodology that truly integrates the perspectives and needs of all stakeholders [2,3].

Such an approach demands horizontal and vertical engagement across the health system, embedding values through co-design processes. The example presented by Zhang et al illustrates this well: the collection of PROMs alone was not enough, but the oncology team's subsequent actions to adapt care pathways led to more personalized care. Importantly, contrary to common assumptions, this did not result in greater complexity or reduced efficiency, but instead in more patient-centered care and higher levels of engagement.

The promise of digital tools will only be realized if challenges around digital access, health literacy, and inclusivity are addressed. Without careful attention, technology risks amplifying inequities rather than reducing them. Sustainable implementation also depends on overcoming barriers such as data interoperability, integration into clinical workflows, and building trust among clinicians and patients in the use of patient-reported data. Embedding patient-reported experience measures and PROMs into routine care further requires equipping health professionals with the skills to interpret and act on these measures, highlighting the central role of education and training in driving meaningful change.

In addition, the business models and revenue streams that underpin value-based transformations remain underexplored. Value-based care is only viable through sustainable financial reforms, which require adaptive strategies. Provider organizations' legacy financial systems and processes are deeply rooted in fee-for-service payment, and it is difficult for them to transition to more advanced forms of alternative payment [4], supporting the need for incorporating strong financial incentives into VBHC and digital technology reforms. Previous studies

XSL•FO
RenderX

have also demonstrated that diverse stakeholders are crucial for the design and implementation of sustainable VBHC business models [5]. Psychological and behavioral mechanisms underlying financial incentives may stand as barriers to VBHC and digital technology adoption. We therefore echo Zhang et al's call for stakeholder involvement and argue that dynamic, participatory approaches to business model development are essential to achieving sustainable improvements in care quality and value.

In conclusion, digital technologies hold great promise in advancing VBHC, but realizing this potential requires more than technological adoption. It demands systemic reorientation toward value-sensitive design, stakeholder collaboration, equitable implementation, education and training of health professionals, and adaptive business modeling. We encourage future research that not only evaluates outcomes but also tests models for scaling and sustaining these approaches across diverse health systems.

Acknowledgments

We used the generative artificial intelligence tool ChatGPT by OpenAI to make minor copyedits to parts of the manuscript for conciseness and clarity, which were further reviewed and revised by the authors.

Conflicts of Interest

None declared.

References

1. Zhang L, Bullen C, Chen J. Digital health innovations to catalyze the transition to value-based health care. JMIR Med Inform 2025 Jan 20;13:e57385. [doi: 10.2196/57385] [Medline: 39864959]
2. Vandekerckhove P, Harris BHL, Koizia LJ, Handa A, Brainard C, Howard S. Why we need a patient-centered innovation renaissance: a horizontal and vertical integration of knowledge to transform care pathways. Patient Exp J 2025;12(2):9-13. [doi: 10.35680/2372-0247.2023]
3. Glover WJ, Hendricks-Sturrup R. Ethics and equity-centred perspectives in engineering systems design. In: Handbook of Engineering Systems Design: Springer; 2023:1-24. [doi: 10.1007/978-3-030-46054-9_34-3]
4. APM framework report. HCPLAN. 2017. URL: https://hcp-lan.org/apm-framework/
5. Howard SW, Bradford N, Belue R, et al. Building alternative payment models in health care. Front Health Serv 2024;4:1235913. [doi: 10.3389/frhs.2024.1235913] [Medline: 38948085]

Abbreviations

PROM: patient-reported outcome measure
VBHC: value-based health care

Edited by A Iannaccio; submitted 26.09.25; this is a non–peer-reviewed article;accepted 21.11.25; published 04.12.25.

Please cite as:
Vandekerckhove P, Harris BHL, Koizia LJ, Howard S
Involving Health, Technology, and Financial Stakeholders in Co-Designing Digital Pathways for Value-Based Care
JMIR Med Inform 2025;13:e84885
URL: https://medinform.jmir.org/2025/1/e84885
doi:10.2196/84885

© Pieter Vandekerckhove, Benjamin H L Harris, Louis J Koizia, Steven Howard. Originally published in JMIR Medical Informatics (https://medinform.jmir.org), 4.12.2025. This is an open-access article distributed under the terms of the Creative Commons Attribution License (https://creativecommons.org/licenses/by/4.0/), which permits unrestricted use, distribution, and reproduction in any medium, provided the original work, first published in JMIR Medical Informatics, is properly cited. The complete bibliographic information, a link to the original publication on https://medinform.jmir.org/, as well as this copyright and license information must be included.

XSL•FO
RenderX

Code Error in "Diagnostic Classification and Prognostic Prediction Using Common Genetic Variants in Autism Spectrum Disorder: Genotype-Based Deep Learning"

Catriona Miller, BSc; Theo Portlock, PhD; Denis M Nyaga, PhD; Greg D Gamble, PhD; Justin M O'Sullivan, PhD

Liggins Institute, University of Auckland, 85 Park Road, Private Bag 92019, Auckland, New Zealand

Corresponding Author:
Justin M O'Sullivan, PhD
Liggins Institute, University of Auckland, 85 Park Road, Private Bag 92019, Auckland, New Zealand

Related Articles:

https://medinform.jmir.org/2021/4/e24754/

https://medinform.jmir.org/2025/1/e76833

(JMIR Med Inform 2025;13:e66556) doi:10.2196/66556

KEYWORDS

autism prediction; machine learning; data leakage

Wang and Avillach [1] developed a convolutional neural network (CNN)–based diagnostic classifier for autism spectrum disorder (ASD). After preprocessing the genomics data from the Simons Simplex Collection (SSC) [2], common variants that may be protective or pathogenic for autism were extracted based on a χ^2 test. The authors then designed a CNN-based diagnostic classifier for ASD with an accuracy and area under the receiver operating characteristic curve of 88% and 0.955, respectively. The predictor in Wang and Avillach [1] is currently considered the exemplar in the field, giving much more accurate predictions for autism than other studies [3].

However, when inspecting the code and repeating the analyses, we contend that the method used is flawed and leads to an approximately 30% overestimation of predictive ability.

Wang and Avillach [1] did not provide a GitHub link to the code that was used in their paper. However, code can be found in Dr Wang's GitHub repository [4] that matches the results and figures in the manuscript.

An error occurred in the data split for training and test sets. The methods state "...the SSC samples were partitioned into two sets based on random sampling of individuals into a training set (80%) and a hold-out test set (20%). There was no overlap of individuals across the two partitions" [1]. However, the code uses different indexing methods for the test and training sets (Multimedia Appendix 1). Because there appears to be no random seed in Wang and Avillach [1], we cannot reproduce the exact overlap that was mentioned in the manuscript. However, simulations (N=100) using the code identified an average of 80% (SD 1%) of the test dataset being represented in the training dataset.

We corrected this error in the code [5] and generated new models using the 100 features that were identified in Wang and Avillach [1] and the genomics data from the SSC [2]. Simulations (N=100) with these models result in an area under the receiver operating characteristic curve of 0.61 (SD 0.02) and an accuracy of 60% (SD 2%; Multimedia Appendix 1). This is 0.34 and 28% lower than the reported metrics, respectively, in Wang and Avillach [1].

The accuracy of the CNN-based diagnostic classifier for ASD presented in Wang and Avillach [1] is overestimated by ~28%. We contend that Wang and Avillach [1] should be retracted according to the Committee on Publication Ethics (COPE) guidelines.

Acknowledgments

We acknowledge Simons Simplex Collection project number 15286.1.1.

Data Availability

The code used for Wang and Avillach [1] is available on GitHub [4]. The clone of the code and corrected code are also available on GitHub [5]. Simons Simplex Collection is accessible at [6].

XSL•FO
RenderX

Conflicts of Interest

None declared.

Editorial Notice

The corresponding author of "Diagnostic Classification and Prognostic Prediction Using Common Genetic Variants in Autism Spectrum Disorder: Genotype-Based Deep Learning" did not submit a reply to this letter.

Multimedia Appendix 1
Walkthrough of the steps that were taken and the results of our attempt to reproduce the work of Wang and Avillach (2021).
[PPTX File, 417 KB - medinform_v13i1e66556_app1.pptx]

References

1. Wang H, Avillach P. Diagnostic classification and prognostic prediction using common genetic variants in autism spectrum disorder: genotype-based deep learning. JMIR Med Inform 2021 Apr 7;9(4):e24754 Retracted inJMIR Med Inform 2025;13:e76833. [doi: 10.2196/76833]
2. Fischbach GD, Lord C. The Simons Simplex Collection: a resource for identification of autism genetic risk factors. Neuron 2010 Oct 21;68(2):192-195. [doi: 10.1016/j.neuron.2010.10.006] [Medline: 20955926]
3. Alowais SA, Alghamdi SS, Alsuhebany N, et al. Revolutionizing healthcare: the role of artificial intelligence in clinical practice. BMC Med Educ 2023 Sep 22;23(1):689. [doi: 10.1186/s12909-023-04698-z] [Medline: 37740191]
4. Wang H. Hms-dbmi/haishuai. GitHub. 2020. URL: https://github.com/hms-dbmi/Haishuai [accessed 2024-09-12]
5. Miller C. Catriona-miller/sfari_paper_clone. GitHub. 2024. URL: https://github.com/Catriona-Miller/SFARI_paper_clone [accessed 2024-09-12]
6. Simons Simplex Collection. Simons Foundation Autism Research Initiative. URL: https://www.sfari.org/resource/simons-simplex-collection/ [accessed 2025-04-24]

Abbreviations

ASD: autism spectrum disorder
CNN: convolutional neural network
COPE: Committee on Publication Ethics
SSC: Simons Simplex Collection

Edited by JMIREO ; submitted 21.09.24; this is a non–peer-reviewed article;accepted 12.04.25; published 06.05.25.

Please cite as:
Miller C, Portlock T, Nyaga DM, Gamble GD, O'Sullivan JM
Code Error in "Diagnostic Classification and Prognostic Prediction Using Common Genetic Variants in Autism Spectrum Disorder: Genotype-Based Deep Learning"
JMIR Med Inform 2025;13:e66556
URL: https://medinform.jmir.org/2025/1/e66556
doi:10.2196/66556

© Catriona Miller, Theo Portlock, Denis M Nyaga, Greg D Gamble, Justin M O'Sullivan. Originally published in JMIR Medical Informatics (https://medinform.jmir.org), 6.5.2025. This is an open-access article distributed under the terms of the Creative Commons Attribution License (https://creativecommons.org/licenses/by/4.0/), which permits unrestricted use, distribution, and reproduction in any medium, provided the original work, first published in JMIR Medical Informatics, is properly cited. The complete bibliographic information, a link to the original publication on https://medinform.jmir.org/, as well as this copyright and license information must be included.

XSL•FO
RenderX

Letter to the Editor

The Anemia Risk Warning Model Based on a Noninvasive Method: Key Insights and Clarifications

Jiaqi Wei[1,2*], MS; Nana Zheng[1,2*], PhD; Depei Wu[1,2], Prof Dr Med

[1]Jiangsu Institute of Hematology, National Clinical Research Center for Hematologic Diseases, The First Affiliated Hospital of Soochow University, Suzhou, China

[2]Institute of Blood and Marrow Transplantation, Collaborative Innovation Center of Hematology, Soochow University, Suzhou, China

[*]these authors contributed equally

Corresponding Author:
Depei Wu, Prof Dr Med
Jiangsu Institute of Hematology
National Clinical Research Center for Hematologic Diseases
The First Affiliated Hospital of Soochow University
188 Shizi Street
Suzhou, 215006
China
Phone: 86 139 5110 2021
Email: wudepei@suda.edu.cn

Related Articles:

Comment on: https://medinform.jmir.org/2025/1/e64204

Comment in: https://medinform.jmir.org/2025/1/e74333/

(JMIR Med Inform 2025;13:e73297) doi:10.2196/73297

KEYWORDS

anemia; hemoglobin; spectroscopy; machine learning; risk warning model; Shapley Additive Explanation

We recently read with great interest the article by Zhang et al [1], which presents a noninvasive technique for diagnosing anemia using facial visible light reflectance spectroscopy, combined with machine learning (ML) algorithms for predictive modeling. Anemia is a widespread public health issue affecting over 1.7 billion people, with symptoms including fatigue and cognitive decline [2]. The study focuses on using facial spectral data to develop a risk warning model for anemia, providing a reliable alternative to conventional methods and holding promise for future clinical applications in noninvasive anemia diagnosis. Having perused the article, we wish to recommend some insights and clarifications to enhance the robustness of the results.

Anemia is affected by various factors, including physiological, nutritional, genetic, environmental, and socioeconomic factors. Zhang et al [1] applied stringent matching criteria for age, location, and gender. However, other factors, such as smoking and nutrient intake, can also impact anemia severity, which should be taken into careful consideration. Additionally, skin types in various regions and lighting conditions at different times can also affect spectral reflectance measurements. When light enters human skin, the epidermis and dermis along with the light-absorbing chromophores, such as water, lipid, hemoglobin, and melanin, constitute the scattering medium and determine the skin's spectral reflectance [3]. Thus, individual variations in skin moisture, temperature, and melanin levels can also significantly alter reflectance. To minimize these effects, standardized protocols for controlling environmental factors should be strictly enforced, and data from a broader range of skin types could be incorporated to enhance the generalizability of the results.

Application of ML methods in medical fields aims to enhance the reliability and predictability of disease diagnosis for future development. Zhang et al [1] used 10 ML algorithms to thoroughly analyze the classifiers, with the support vector machine (SVM) algorithm demonstrating the best performance. However, despite its superior performance, the SVM model may still be prone to overfitting due to the relatively small sample size. Additionally, the lack of external validation using independent datasets raises concerns about the model's actual performance. Future studies should incorporate cross-validation with larger datasets to enhance predictive accuracy and generalizability.

Noninvasive diagnostic methods are currently advancing rapidly. By analyzing facial light reflectance, this study pinpoints

XSL•FO
RenderX

specific facial regions and wavelengths strongly correlated with anemia risk. However, it would be beneficial to compare its diagnostic performance with that of other noninvasive hemoglobin measurements, such as the microwave resonant system [4] and photoplethysmography signal sensors [5]. A comparative study could help assess whether spectral reflectance provides higher accuracy and clinical utility than these methods or when combined with them.

In conclusion, the study identifies significant differences in the facial spectral characteristics of patients with anemia and develops a high-accuracy warning model for predicting anemia risk. This noninvasive technique provides valuable opportunities to analyze facial signs of anemia and offers a more affordable approach to facilitate diagnosis. Undoubtedly, this research reveals a promising direction for personalized patient management and lays the foundation for potential applications in community-based health screenings.

Conflicts of Interest

None declared.

References

1. Zhang Y, Chun Y, Fu H, Jiao W, Bao J, Jiang T, et al. A risk warning model for anemia based on facial visible light reflectance spectroscopy: cross-sectional study. JMIR Med Inform 2025 Feb 14;13:e64204 [FREE Full text] [doi: 10.2196/64204] [Medline: 39952235]
2. Safiri S, Kolahi A, Noori M, Nejadghaderi SA, Karamzad N, Bragazzi NL, et al. Burden of anemia and its underlying causes in 204 countries and territories, 1990-2019: results from the Global Burden of Disease Study 2019. J Hematol Oncol 2021 Nov 04;14(1):185 [FREE Full text] [doi: 10.1186/s13045-021-01202-2] [Medline: 34736513]
3. Svenskaya YI, Verkhovskii RA, Zaytsev SM, Lademann J, Genina EA. Current issues in optical monitoring of drug delivery via hair follicles. Adv Drug Deliv Rev 2025 Feb;217:115477. [doi: 10.1016/j.addr.2024.115477] [Medline: 39615632]
4. Basey-Fisher TH, Guerra N, Triulzi C, Gregory A, Hanham SM, Stevens MM, et al. Microwaving blood as a non-destructive technique for haemoglobin measurements on microlitre samples. Adv Healthc Mater 2014 Apr;3(4):536-542 [FREE Full text] [doi: 10.1002/adhm.201300169] [Medline: 24002989]
5. Lakshmi M, Manimegalai P. Non-invasive estimation of haemoglobin level using PCA and artificial neural networks. TOBEJ 2019 Dec 17;13(1):114-119. [doi: 10.2174/1874120701913010114]

Abbreviations

ML: machine learning
SVM: support vector machine

Edited by A Iannaccio; submitted 01.03.25; this is a non–peer-reviewed article;accepted 31.03.25; published 22.04.25.

Please cite as:
Wei J, Zheng N, Wu D
The Anemia Risk Warning Model Based on a Noninvasive Method: Key Insights and Clarifications
JMIR Med Inform 2025;13:e73297
URL: https://medinform.jmir.org/2025/1/e73297
doi:10.2196/73297
PMID:

©Jiaqi Wei, Nana Zheng, Depei Wu. Originally published in JMIR Medical Informatics (https://medinform.jmir.org), 22.04.2025. This is an open-access article distributed under the terms of the Creative Commons Attribution License (https://creativecommons.org/licenses/by/4.0/), which permits unrestricted use, distribution, and reproduction in any medium, provided the original work, first published in JMIR Medical Informatics, is properly cited. The complete bibliographic information, a link to the original publication on https://medinform.jmir.org/, as well as this copyright and license information must be included.

XSL•FO
RenderX

Letter to the Editor

Authors' Reply: The Anemia Risk Warning Model Based on a Noninvasive Method: Key Insights and Clarifications

Yahan Zhang[1], MS; Yi Chun[1], MD; Liping Tu[1], PhD; Jiatuo Xu[1], PhD

Traditional Chinese Medicine College, Shanghai University of Traditional Chinese Medicine, Shanghai, China

Corresponding Author:
Jiatuo Xu, PhD
Traditional Chinese Medicine College
Shanghai University of Traditional Chinese Medicine
No.1200 Cailun Road, Pudong New Area
Shanghai, 201203
China
Phone: 86 021 51322143
Email: xjt@fudan.edu.cn

Related Articles:

Comment on: https://medinform.jmir.org/2025/1/e73297/

Comment on: https://medinform.jmir.org/2025/1/e64204

(JMIR Med Inform 2025;13:e74333) doi:10.2196/74333

KEYWORDS

anemia; hemoglobin; spectroscopy; machine learning; risk warning model; Shapley Additive Explanation

We sincerely appreciate your thoughtful and constructive comments on our recent paper exploring noninvasive anemia diagnosis through facial visible light reflectance spectroscopy and machine learning [1,2]. Your attention and insightful suggestions greatly guide our efforts to enhance this work. We address your key points below, offering clarifications as needed. You noted that uncontrolled factors like smoking and nutrition might influence anemia severity and spectral data. While our initial focus was validating this approach by controlling core variables (eg, age and gender), we plan to broaden future data collection to include these factors, analyze their effects, and integrate them into our model to improve reliability. You also emphasized how skin types, lighting, and individual variations could affect reflectance. We standardized conditions and preparation to minimize variability yet acknowledge our sample's limited diversity. Given hemoglobin's specific absorption peaks, we hypothesize that certain wavelength bands may be less skin tone–dependent. To explore this, we intend to collect data from diverse regions and skin types, aiming to identify such bands and enhance model applicability.

We value your recognition of our SVM model's performance and your concern about overfitting due to sample size. Though it outperformed other algorithms, we are addressing this limitation by gathering more data via multicenter collaboration, applying 10-fold cross-validation, and validating with external datasets to boost accuracy and robustness. Our study focused on establishing facial spectral imaging's potential for anemia detection, but comparative analysis could better assess its clinical utility. We are particularly intrigued by multimodal integration, such as combining spectroscopy with photoplethysmography (PPG) to improve diagnostic precision. Future work will involve comparative experiments to evaluate metrics like sensitivity and specificity, exploring whether synergy yields superior results. However, PPG indirectly reflects hemoglobin via light intensity changes, suiting routine monitoring, whereas spectroscopy directly measures hemoglobin concentration through reflectance spectra, fitting clinical diagnosis and research. Thus, stand-alone spectroscopy for noninvasive hemoglobin measurement holds significant promise, which we aim to further investigate.

We are encouraged by your recognition of this technique's potential for community screening and personalized care. Thank you again for your rigorous review and profound insights. We look forward to further discussion and sharing progress or collaboration opportunities as our research advances.

XSL•FO
RenderX

Conflicts of Interest

None declared.

References

1. Zhang Y, Chun Y, Fu H, Jiao W, Bao J, Jiang T, et al. A risk warning model for anemia based on facial visible light reflectance spectroscopy: cross-sectional study. JMIR Med Inform 2025 Feb 14;13:e64204 [FREE Full text] [doi: 10.2196/64204] [Medline: 39952235]
2. Wei J, Zheng N, Wu D. The anemia risk warning model based on a noninvasive method: key insights and clarifications. JMIR Med Inform 2025:e73297 [FREE Full text] [doi: 10.2196/73297]

Abbreviations

PPG: photoplethysmography

Edited by A Iannaccio; submitted 22.03.25; this is a non–peer-reviewed article;accepted 31.03.25; published 22.04.25.

Please cite as:
Zhang Y, Chun Y, Tu L, Xu J
Authors' Reply: The Anemia Risk Warning Model Based on a Noninvasive Method: Key Insights and Clarifications
JMIR Med Inform 2025;13:e74333
URL: https://medinform.jmir.org/2025/1/e74333
doi:10.2196/74333
PMID:

©Yahan Zhang, Yi Chun, Liping Tu, Jiatuo Xu. Originally published in JMIR Medical Informatics (https://medinform.jmir.org), 22.04.2025. This is an open-access article distributed under the terms of the Creative Commons Attribution License (https://creativecommons.org/licenses/by/4.0/), which permits unrestricted use, distribution, and reproduction in any medium, provided the original work, first published in JMIR Medical Informatics, is properly cited. The complete bibliographic information, a link to the original publication on https://medinform.jmir.org/, as well as this copyright and license information must be included.

XSL•FO
RenderX

Letter to the Editor

Data Contamination in AI Evaluation

Alaeddin Acar[1], MD

Department of Neurosurgery, Kulu State Hospital, Konya, Turkey

Corresponding Author:
Alaeddin Acar, MD
Department of Neurosurgery, Kulu State Hospital
No 4, 139518 Street, Dinek, Kulu
Konya, 42770
Turkey
Phone: 90 542 472 37 23
Email: alaeacar@gmail.com

Related Articles:

Comment on: https://medinform.jmir.org/2025/1/e68409/

Comment in: http://medinform.jmir.org/2025/1/e82057/

(JMIR Med Inform 2025;13:e80987) doi:10.2196/80987

KEYWORDS

artificial intelligence; large language model; ChatGPT; emergency medicine; clinical performance examination; history taking; clinical reasoning; empathy; patient experience

This letter is regarding the recent publication of the article titled "Clinical Performance and Communication Skills of ChatGPT Versus Physicians in Emergency Medicine: Simulated Patient Study" by Park et al [1]. The study makes a significant contribution to the growing field of artificial intelligence (AI) evaluation in medicine, and I congratulate the authors on their valuable work. However, I would like to highlight a potential methodological limitation in the written examination portion of the study. The authors state that their examination questions were taken from a 2018 textbook, *100 Cases in Emergency Medicine and Critical Care* [2]. The AI model they tested, ChatGPT (OpenAI), was trained on huge amounts of public text from the internet, which likely included this textbook. This means ChatGPT may have seen exactly the same questions and answers during its training.

This problem is known as "data contamination." If the AI has already seen the test questions, its high scores might show good memory, not good medical reasoning. This makes the comparison to human doctors, who were seeing the questions for the first time, unfair. The study found that ChatGPT performed much better than doctors on this written test, but this result could be due to this methodological limitation.

Other researchers in the field are aware of this problem and take steps to avoid it. For example, a study by Busch et al [3] on radiology used private, members-only cases that were not likely in the AI's training data to minimize this risk. Another study by Noda et al [4] on a Japanese medical examination used questions from an examination that took place after the AI's training data cut-off date.

These studies show the importance of using new and unseen questions when testing AI. Because the study by Park et al [1] did not use this approach, I believe the results of their written examination should be viewed with caution. Future studies must use methods like those in the Busch et al [3] and Noda et al [4] papers to ensure a fair and valid test of AI's abilities.

Acknowledgments

Google Gemini was used for language editing.

Conflicts of Interest

None declared.

References

XSL•FO
RenderX

1. Park C, An MH, Hwang G, Park RW, An J. Clinical performance and communication skills of ChatGPT versus physicians in emergency medicine: simulated patient study. JMIR Med Inform 2025 Jul 17;13:e68409 [FREE Full text] [doi: 10.2196/68409] [Medline: 40674718]
2. Shamil E, Ravi P, Mistry D. 100 Cases in Emergency Medicine and Critical Care. Boca Raton, FL: CRC Press; 2018.
3. Busch F, Han T, Makowski MR, Truhn D, Bressem KK, Adams L. Integrating text and image analysis: exploring GPT-4V's capabilities in advanced radiological applications across subspecialties. J Med Internet Res 2024 May 01;26:e54948. [doi: 10.2196/54948] [Medline: 38691404]
4. Noda M, Ueno T, Koshu R, Takaso Y, Shimada MD, Saito C, et al. Performance of GPT-4V in answering the Japanese otolaryngology board certification examination questions: evaluation study. JMIR Med Educ 2024 Mar 28;10:e57054 [FREE Full text] [doi: 10.2196/57054] [Medline: 38546736]

Abbreviations

AI: artificial intelligence

Edited by A Iannaccio; submitted 20.07.25; this is a non–peer-reviewed article;accepted 20.08.25; published 29.09.25.

Please cite as:
Acar A
Data Contamination in AI Evaluation
JMIR Med Inform 2025;13:e80987
URL: https://medinform.jmir.org/2025/1/e80987
doi:10.2196/80987
PMID:

©Alaeddin Acar. Originally published in JMIR Medical Informatics (https://medinform.jmir.org), 29.09.2025. This is an open-access article distributed under the terms of the Creative Commons Attribution License (https://creativecommons.org/licenses/by/4.0/), which permits unrestricted use, distribution, and reproduction in any medium, provided the original work, first published in JMIR Medical Informatics, is properly cited. The complete bibliographic information, a link to the original publication on https://medinform.jmir.org/, as well as this copyright and license information must be included.

XSL•FO
RenderX

Letter to the Editor

Author's Reply: "Data Contamination in AI Evaluation"

ChulHyoung Park[1,2,3*], MD; Min Ho An[1,2,3*], MD; Gyubeom Hwang[1,2,3*], MD; Rae Woong Park[1,2,3,4], MD, PhD; Juho An[5], MD

[1]Department of Biomedical Informatics, School of Medicine, Ajou University, Suwon, Republic of Korea
[2]Center for Biomedical Informatics Research, Ajou University Medical Center, Suwon, Republic of Korea
[3]Department of Medical Sciences, Graduate School of Ajou University, Suwon, Republic of Korea
[4]BK21 R&E Initiative for Advanced Precision Medicine, Suwon, Republic of Korea
[5]Department of Emergency Medicine, School of Medicine, Ajou University, Suwon, Republic of Korea
[*]these authors contributed equally

Corresponding Author:
Juho An, MD
Department of Emergency Medicine
School of Medicine
Ajou University
164 Worldcup-ro
Yeongtong-gu
Suwon, 16499
Republic of Korea
Phone: 82 0312195016
Email: ermd.jh@gmail.com

Related Articles:

Comment on: https://medinform.jmir.org/2025/1/e68409/

Comment on: http://medinform.jmir.org/2025/1/e80987/

(JMIR Med Inform 2025;13:e82057) doi:10.2196/82057

KEYWORDS

artificial intelligence; large language model; ChatGPT; emergency medicine; clinical performance examination; history taking; clinical reasoning; empathy; patient experience

We sincerely thank the author for the constructive commentary on our recent publication. Our study evaluated ChatGPT's performance across multiple dimensions—including history taking, diagnostic accuracy, communication skills, and empathic expression—through a clinical performance examination using simulated patients combined with written examinations [1].

In our study, the written examination was not intended to solely serve as a direct comparison of performance between ChatGPT and human physicians. Rather, it was included to support the interpretation of ChatGPT's communication skills and empathic responses observed during simulated patient interactions by providing additional context regarding the model's underlying clinical knowledge. A previous study has shown that patients may perceive ChatGPT's responses as empathic or trustworthy, even when those responses are clinically inappropriate [2]. However, effective clinical communication is not merely about verbal fluency or emotional tone; it must be grounded in adequate medical knowledge. For this reason, earlier studies evaluating artificial intelligence empathy have also assessed the clinical appropriateness of responses and compared them to those of human physicians [2,3].

Consistent with prior work, we also assessed the simulated patient conversations in terms of both clinical accuracy and empathic engagement, as evaluated by an emergency medicine professor. However, we recognize that physicians vary in their diagnostic styles and communication approaches. Subjective judgment from the evaluator may have influenced the ratings, especially given that the evaluated outputs were full conversations rather than single responses. To provide a complementary and more structured assessment, we incorporated a written test focused on 3 key domains: diagnosis, investigation, and treatment planning. Performance on this test may serve as a supporting element to help ensure that ChatGPT's interpersonal strengths were not misaligned with clinical reasoning.

As the author correctly pointed out, the questions in the written examination were adapted from a publicly available textbook

XSL•FO
RenderX

published in 2018 [4]. We cannot rule out the possibility that ChatGPT was exposed to this material or similar content during pretraining, due to the limited transparency regarding its training data. Therefore, part of the model's performance on the written test may have been influenced by data contamination. We fully acknowledge this methodological limitation and agree that the results from the written examination should be interpreted with caution.

We are truly grateful for the author's thoughtful engagement, which raises important considerations for future studies regarding the assessment of AI in clinical settings.

Acknowledgments

During the preparation of this manuscript, the authors used ChatGPT to assist with improving readability and correcting grammatical errors. After using this tool, the authors reviewed and edited the content as needed and take full responsibility for the content of the publication.

Conflicts of Interest

None declared.

References

1. Park C, An MH, Hwang G, Park RW, An J. Clinical performance and communication skills of ChatGPT versus physicians in emergency medicine: simulated patient study. JMIR Med Inform 2025 Jul 17;13:e68409 [FREE Full text] [doi: 10.2196/68409] [Medline: 40674718]
2. Armbruster J, Bussmann F, Rothhaas C, Titze N, Grützner PA, Freischmidt H. "Doctor ChatGPT, can you help me?" The patient's perspective: cross-sectional study. J Med Internet Res 2024 Oct 01;26:e58831 [FREE Full text] [doi: 10.2196/58831] [Medline: 39352738]
3. Ayers JW, Poliak A, Dredze M, Leas EC, Zhu Z, Kelley JB, et al. Comparing physician and artificial intelligence chatbot responses to patient questions posted to a public social media forum. JAMA Intern Med 2023 Jun 01;183(6):589-596 [FREE Full text] [doi: 10.1001/jamainternmed.2023.1838] [Medline: 37115527]
4. Shamil E, Ravi P, Mistry D. 100 Cases in Emergency Medicine and Critical Care. Boca Raton, FL: CRC Press; 2018.

Edited by A Iannaccio; submitted 15.08.25; this is a non–peer-reviewed article;accepted 20.08.25; published 29.09.25.

Please cite as:
Park C, An MH, Hwang G, Park RW, An J
Author's Reply: "Data Contamination in AI Evaluation"
JMIR Med Inform 2025;13:e82057
URL: https://medinform.jmir.org/2025/1/e82057
doi:10.2196/82057
PMID:

©ChulHyoung Park, Min Ho An, Gyubeom Hwang, Rae Woong Park, Juho An. Originally published in JMIR Medical Informatics (https://medinform.jmir.org), 29.09.2025. This is an open-access article distributed under the terms of the Creative Commons Attribution License (https://creativecommons.org/licenses/by/4.0/), which permits unrestricted use, distribution, and reproduction in any medium, provided the original work, first published in JMIR Medical Informatics, is properly cited. The complete bibliographic information, a link to the original publication on https://medinform.jmir.org/, as well as this copyright and license information must be included.

XSL•FO
RenderX

Correction: Patients' Experienced Usability and Satisfaction With Digital Health Solutions in a Home Setting: Instrument Validation Study

Susan J Oudbier[1,2,3,4], MD; Ellen M A Smets[2,4,5], PhD; Pythia T Nieuwkerk[2,6], PhD; David P Neal[3,7], PhD; S Azam Nurmohamed[8], MD, PhD; Hans J Meij[1,9], PhD; Linda W Dusseljee-Peute[7], PhD

[1]Outpatient Division, Amsterdam University Medical Center, Meibergdreef 9, Amsterdam, The Netherlands
[2]Department of Medical Psychology, Amsterdam University Medical Center, University of Amsterdam, Amsterdam, The Netherlands
[3]Digital Health, Amsterdam Public Health Research Institute, Amsterdam, The Netherlands
[4]Quality of Care, Amsterdam Public Health Research Institute, Amsterdam, The Netherlands
[5]Personalized Medicine, Amsterdam Public Health Research Institute, Amsterdam, The Netherlands
[6]Amsterdam Institute for Infection and Immunity, Amsterdam, The Netherlands
[7]Department of Medical Informatics, Amsterdam University Medical Center, University of Amsterdam, Amsterdam, The Netherlands
[8]Department of Nephrology, Amsterdam University Medical Center, Amsterdam, The Netherlands
[9]Yong Loo Lin School of Medicine, National University of Singapore, Singapore, Singapore

Corresponding Author:
Susan J Oudbier, MD
Outpatient Division, Amsterdam University Medical Center, Meibergdreef 9, Amsterdam, The Netherlands

Related Article:

Correction of: https://medinform.jmir.org/2025/1/e63703

(JMIR Med Inform 2025;13:e73416) doi:10.2196/73416

KEYWORDS

digital health solution; questionnaire development; usability instruments; self-management; home setting; validation; reliability

In "Patients' Experienced Usability and Satisfaction With Digital Health Solutions in a Home Setting: Instrument Validation Study" (JMIR Med Inform 2025 Jan 8:13:e63703) the authors noted two errors.

The ORCID for author David P Neal was changed from:

000-0002-5531-9962

To the following:

0000-0001-7916-3299

Additionally, the author "Ellen MA Smets" was changed to "Ellen M A Smets."

The correction will appear in the online version of the paper on the JMIR Publications website on March 27, 2025, together with the publication of this correction notice. Because this was made after submission to PubMed, PubMed Central, and other full-text repositories, the corrected article has also been resubmitted to those repositories.

Submitted 04.03.25; this is a non–peer-reviewed article;accepted 10.03.25; published 27.03.25.

Please cite as:
Oudbier SJ, Smets EMA, Nieuwkerk PT, Neal DP, Nurmohamed SA, Meij HJ, Dusseljee-Peute LW
Correction: Patients' Experienced Usability and Satisfaction With Digital Health Solutions in a Home Setting: Instrument Validation Study
JMIR Med Inform 2025;13:e73416
URL: https://medinform.jmir.org/2025/1/e73416
doi:10.2196/73416

XSL•FO
RenderX

© Susan J Oudbier, Ellen M A Smets, Pythia T Nieuwkerk, David P Neal, S Azam Nurmohamed, Hans J Meij, Linda W Dusseljee-Peute. Originally published in JMIR Medical Informatics (https://medinform.jmir.org), 27.3.2025. This is an open-access article distributed under the terms of the Creative Commons Attribution License (https://creativecommons.org/licenses/by/4.0/), which permits unrestricted use, distribution, and reproduction in any medium, provided the original work, first published in JMIR Medical Informatics, is properly cited. The complete bibliographic information, a link to the original publication on https://medinform.jmir.org/, as well as this copyright and license information must be included.

XSL•FO
RenderX

Correction: Distributed Statistical Analyses: A Scoping Review and Examples of Operational Frameworks Adapted to Health Analytics

Félix Camirand Lemyre[1,2*], PhD; Simon Lévesque[1,2,3*], MSc; Marie-Pier Domingue[1,2,4], BSc; Klaus Herrmann[2], PhD; Jean-François Ethier[1,3,5], MD, PhD

[1]GRIIS, Université de Sherbrooke, 2500, boul. de l'Université, Sherbrooke, QC, Canada

[2]Département de mathématiques, Faculté des sciences, Université de Sherbrooke, Sherbrooke, QC, Canada

[3]Health Data Research Network Canada, Vancouver, BC, Canada

[4]Chaire MEIE Québec - Le numérique au service des systèmes de santé apprenants, Université de Sherbrooke, Sherbrooke, QC, Canada

[5]Département de médecine, Faculté de médecine et des sciences de la santé, Université de Sherbrooke, Sherbrooke, QC, Canada

[*]these authors contributed equally

Corresponding Author:
Jean-François Ethier, MD, PhD
GRIIS, Université de Sherbrooke, 2500, boul. de l'Université, Sherbrooke, QC, Canada

Related Article:

Correction of: https://medinform.jmir.org/2024/1/e53622

(JMIR Med Inform 2025;13:e71249) doi:10.2196/71249

In "Distributed Statistical Analyses: A Scoping Review and Examples of Operational Frameworks Adapted to Health Analytics" (JMIR Med Inform 2024;12:e53622) the authors noted four errors.

In subsection "Results Related to Objective 3," paragraph "Simple Averaging," three mathematical formulas have been corrected to include a matrix inversion as follows:

In "Textbox 1 . Algorithm 1 —simple averaging inference procedure,"

$\Sigma\hat{}SA=\varphi\hat{}SA\sum k=1Knw(k)2n(k)VMLE(k)$ *has been corrected to* $\Sigma\hat{}SA=\varphi\hat{}SA\sum k=1Knw(k)2n(k)(VMLE(k))-1$.

In the text below Textbox 1, $\Sigma SA=\varphi\sum k=1Kw(k)2p(k)T\beta(k)$ *was changed to* $\Sigma SA=\varphi\sum k=1Kw(k)2p(k)(T\beta(k))-1$ *and* $\Sigma\hat{}SA=\varphi\hat{}SA\sum k=1Knw(k)2n(k)VMLE(k)$ *has been corrected to* $\Sigma\hat{}SA=\varphi\hat{}SA\sum k=1Knw(k)2n(k)(VMLE(k))-1$.

Finally, in Multimedia Appendix 2,

$\Sigma SA=\varphi\sum k=1Kw(k)2p(k)T\beta(k)$ *has been corrected to* $\Sigma SA=\varphi\sum k=1Kw(k)2p(k)(T\beta(k))-1$. *Please note that the revised version has been attached here as Multimedia Appendix 1.*

The correction will appear in the online version of the paper on the JMIR Publications website on February 11, 2025, together with the publication of this correction notice. Because this was made after submission to PubMed, PubMed Central, and other full-text repositories, the corrected article has also been resubmitted to those repositories.

Multimedia Appendix 1
Revised version of Multimedia Appendix 2: Mathematical derivations pertaining to objective 3.
[DOCX File, 100 KB - medinform_v13i1e71249_app1.docx]

Submitted 13.01.25; this is a non–peer-reviewed article;accepted 17.01.25; published 11.02.25.

Please cite as:
Camirand Lemyre F, Lévesque S, Domingue MP, Herrmann K, Ethier JF
Correction: Distributed Statistical Analyses: A Scoping Review and Examples of Operational Frameworks Adapted to Health Analytics
JMIR Med Inform 2025;13:e71249
URL: https://medinform.jmir.org/2025/1/e71249
doi:10.2196/71249

XSL•FO
RenderX

© Félix Camirand Lemyre, Simon Lévesque, Marie-Pier Domingue, Klaus Herrmann, Jean-François Ethier. Originally published in JMIR Medical Informatics (https://medinform.jmir.org), 11.2.2025. This is an open-access article distributed under the terms of the Creative Commons Attribution License (https://creativecommons.org/licenses/by/4.0/), which permits unrestricted use, distribution, and reproduction in any medium, provided the original work, first published in JMIR Medical Informatics, is properly cited. The complete bibliographic information, a link to the original publication on https://medinform.jmir.org/, as well as this copyright and license information must be included.

XSL•FO
RenderX

Correction: Relationship Between Stroke Knowledge, Health Information Literacy, and Health Self- Management Among Patients With Stroke: Multicenter Cross-Sectional Study

Mengxue Zeng[1,2*], MNS; Yanhua Liu[2*], MNS; Ying He[2*], MNS; Wenxia Huang[1], MD

[1]Health Management Center, General Practice Medical Center, West China Hospital, Sichuan University, 37 Guoxue Lane, Wuhou District, Chengdu, China

[2]West China School of Nursing, Sichuan University, Chengdu, China

[*]these authors contributed equally

Corresponding Author:
Wenxia Huang, MD
Health Management Center, General Practice Medical Center, West China Hospital, Sichuan University, 37 Guoxue Lane, Wuhou District, Chengdu, China

Related Article:

Correction of: https://medinform.jmir.org/2025/1/e63956/

Abstract

(JMIR Med Inform 2025;13:e80547) doi:10.2196/80547

In "Relationship Between Stroke Knowledge, Health Information Literacy, and Health Self- Management Among Patients with Stroke: Multicenter Cross-Sectional Study" (JMIR Med Inform 2025;13:e63956) the authors made one correction.

The affiliations for the first author have been changed from:

1. West China School of Nursing, Sichuan University, Chengdu, China

To the following, which has swapped the order of affiliations:

1. Health Management Center, General Practice Medical Center, West China Hospital, Sichuan University, Chengdu, China

2. West China School of Nursing, Sichuan University, Chengdu, China

The correction will appear in the online version of the paper on the JMIR Publications website, together with the publication of this correction notice, and the numeration of the other author affiliations have been adjusted sequentially. Because this was made after submission to PubMed, PubMed Central, and other full-text repositories, the corrected article has also been resubmitted to those repositories.

Submitted 12.07.25; this is a non–peer-reviewed article;accepted 16.07.25; published 29.07.25.

Please cite as:
Zeng M, Liu Y, He Y, Huang W
Correction: Relationship Between Stroke Knowledge, Health Information Literacy, and Health Self- Management Among Patients With Stroke: Multicenter Cross-Sectional Study
JMIR Med Inform 2025;13:e80547
URL: https://medinform.jmir.org/2025/1/e80547
doi:10.2196/80547

© Mengxue Zeng, Yanhua Liu, Ying He, Wenxia Huang. Originally published in JMIR Medical Informatics (https://medinform.jmir.org), 29.7.2025. This is an open-access article distributed under the terms of the Creative Commons Attribution License (https://creativecommons.org/licenses/by/4.0/), which permits unrestricted use, distribution, and reproduction in any medium, provided the original work, first published in JMIR Medical Informatics, is properly cited. The complete

XSL•FO
RenderX

bibliographic information, a link to the original publication on https://medinform.jmir.org/, as well as this copyright and license information must be included.

XSL•FO
RenderX

Corrigenda and Addenda

Correction: Toward a Domain-Overarching Metadata Schema for Making Health Research Studies FAIR (Findable, Accessible, Interoperable, and Reusable): Development of the NFDI4Health Metadata Schema

Haitham Abaza[1], PhD; Aliaksandra Shutsko[2], MLIS; Sophie A I Klopfenstein[3], MD; Carina N Vorisek[3], MD, PhD; Carsten Oliver Schmidt[4], Prof Dr; Claudia Brünings-Kuppe[5], Dipl Dok (FH); Vera Clemens[2], MSc; Johannes Darms[2], MSc; Sabine Hanß[6], Dipl Inf; Timm Intemann[5], Dr rer nat; Franziska Jannasch[7], PhD; Elisa Kasbohm[4], MSc; Birte Lindstädt[2], MLIS; Matthias Löbe[8], Dipl Inf; Katharina Nimptsch[9], DrScHum; Ute Nöthlings[10], Prof Dr; Marisabel Gonzalez Ocanto[2], MA; Tracy Bonsu Osei[9], MPhil; Ines Perrar[10], Dr troph; Manuela Peters[5], PhD; Tobias Pischon[9], Prof Dr; Ulrich Sax[6], Prof Dr; Matthias B Schulze[7], DrPH; Florian Schwarz[7], PhD; Carolina Schwedhelm[9], DrPH; Sylvia Thun[3], Prof Dr; Dagmar Waltemath[4], Prof Dr; Atinkut A Zeleke[4], PhD; Wolfgang Müller[1], Priv Doz Dr; Martin Golebiewski[1], MSc

[1]Scientific Databases and Visualization, Heidelberg Institute for Theoretical Studies (HITS), Heidelberg, Germany
[2]Information Centre for Life Sciences, German National Library of Medicine (ZB MED), Cologne, Germany
[3]Core Facility Digital Medicine and Interoperability, Universitätsmedizin Berlin, Berlin Institute of Health at Charité, Berlin, Germany
[4]Institute for Community Medicine, University Medicine Greifswald, Greifswald, Germany
[5]Department of Biometry and Data Management, Leibniz Institute for Prevention Research and Epidemiology - BIPS, Bremen, Germany
[6]Department of Medical Informatics, University Medical Center Göttingen, Georg-August-University, Göttingen, Germany
[7]Department of Molecular Epidemiology, German Institute of Human Nutrition Potsdam-Rehbruecke, Nuthetal, Germany
[8]Institute for Medical Informatics, Statistics and Epidemiology, University Leipzig, Leipzig, Germany
[9]Molecular Epidemiology Research Group, Max-Delbrück-Center for Molecular Medicine in the Helmholtz Association (MDC), Berlin, Germany
[10]Department of Nutrition and Food Science, University of Bonn, Bonn, Germany

Corresponding Author:
Haitham Abaza, PhD
Scientific Databases and Visualization
Heidelberg Institute for Theoretical Studies (HITS)
Schloss-Wolfsbrunnenweg 35
Heidelberg, 69118
Germany
Phone: 49 6221533231
Email: haithamabaza@gmail.com

Related Article:

Correction of: https://medinform.jmir.org/2025/1/e63906/

(JMIR Med Inform 2025;13:e78151) doi:10.2196/78151

In "Toward a Domain-Overarching Metadata Schema for Making Health Research Studies FAIR (Findable, Accessible, Interoperable, and Reusable): Development of the NFDI4Health Metadata Schema" (JMIR Med Inform 2025;13:e63906) the following corrections have been made.

Author Hannes Wünsche was erroneously included in the authorship list. Hence, their name and affiliation have been removed.

In addition, the following affiliation has been changed from:

Department of Molecular Epidemiology, German Institute of Human Nutrition, Potsdam-Rehbruecke, Nuthetal, Germany

to:

Department of Molecular Epidemiology, German Institute of Human Nutrition Potsdam-Rehbruecke, Nuthetal, Germany

The corrections will appear in the online version of the paper on the JMIR Publications website, together with the publication

XSL•FO
RenderX

of this correction notice. Because this was made after submission to PubMed, PubMed Central, and other full-text repositories, the corrected article has also been resubmitted to those repositories.

Submitted 27.05.25; this is a non–peer-reviewed article;accepted 27.05.25; published 04.06.25.

Please cite as:
Abaza H, Shutsko A, Klopfenstein SAI, Vorisek CN, Schmidt CO, Brünings-Kuppe C, Clemens V, Darms J, Hanß S, Intemann T, Jannasch F, Kasbohm E, Lindstädt B, Löbe M, Nimptsch K, Nöthlings U, Ocanto MG, Osei TB, Perrar I, Peters M, Pischon T, Sax U, Schulze MB, Schwarz F, Schwedhelm C, Thun S, Waltemath D, Zeleke AA, Müller W, Golebiewski M
Correction: Toward a Domain-Overarching Metadata Schema for Making Health Research Studies FAIR (Findable, Accessible, Interoperable, and Reusable): Development of the NFDI4Health Metadata Schema
JMIR Med Inform 2025;13:e78151
URL: https://medinform.jmir.org/2025/1/e78151
doi:10.2196/78151
PMID:

©Haitham Abaza, Aliaksandra Shutsko, Sophie A I Klopfenstein, Carina N Vorisek, Carsten Oliver Schmidt, Claudia Brünings-Kuppe, Vera Clemens, Johannes Darms, Sabine Hanß, Timm Intemann, Franziska Jannasch, Elisa Kasbohm, Birte Lindstädt, Matthias Löbe, Katharina Nimptsch, Ute Nöthlings, Marisabel Gonzalez Ocanto, Tracy Bonsu Osei, Ines Perrar, Manuela Peters, Tobias Pischon, Ulrich Sax, Matthias B Schulze, Florian Schwarz, Carolina Schwedhelm, Sylvia Thun, Dagmar Waltemath, Atinkut A Zeleke, Wolfgang Müller, Martin Golebiewski. Originally published in JMIR Medical Informatics (https://medinform.jmir.org), 04.06.2025. This is an open-access article distributed under the terms of the Creative Commons Attribution License (https://creativecommons.org/licenses/by/4.0/), which permits unrestricted use, distribution, and reproduction in any medium, provided the original work, first published in JMIR Medical Informatics, is properly cited. The complete bibliographic information, a link to the original publication on https://medinform.jmir.org/, as well as this copyright and license information must be included.

XSL•FO
RenderX

Corrigenda and Addenda

Correction: The Roles of Electronic Health Records for Clinical Trials in Low- and Middle-Income Countries: Scoping Review

JMIR Publications Editorial Office

Related Article:

Correction of: https://medinform.jmir.org/2023/1/e47052

(JMIR Med Inform 2025;13:e84394) doi:10.2196/84394

Following the publication of "The Roles of Electronic Health Records for Clinical Trials in Low- and Middle-Income Countries: Scoping Review" [1], concerns were raised regarding the author Jiancheng Ye's rate of self-citation within the article's reference list. Further investigation into this matter identified that numerous self-citations were added to the manuscript following acceptance of the article without adequate disclosure.

All authors were contacted for a response regarding this matter. Authors Shangzhi Xiong, Tengyi Wang, Jingyi Li, Nan Cheng, Maoyi Tian, and Yang Yang indicated that they were unaware of the addition of references post acceptance. They did not consent to such changes and believed a number of the additions to be irrelevant to the content of the article and requested their removal. Author Jiancheng Ye responded with a scientific justification for each added self-citation within the published article.

Following review of these responses, the JMIR Publications Editorial Office determined that several of the added references were not relevant to the article or were used to support a generic statement where another reference could have been used instead of self-citation. Therefore, the JMIR Publications Editorial Office is issuing this corrigendum to remove the following references:

- Reference 13: Ye J, Wang Z, Hai J. Social networking service, patient-generated health data, and population health informatics: national cross-sectional study of patterns and implications of leveraging digital technologies to support mental health and well-being. J Med Internet Res 2022 Apr 29;24(4):e30898 [doi: 10.2196/30898] [Medline: 35486428]
- Reference 14: Ye J. The role of health technology and informatics in a global public health emergency: practices and implications from the COVID-19 pandemic. JMIR Med Inform 2020 Jul 14;8(7):e19866 [doi: 10.2196/19866] [Medline: 32568725]
- Reference 48: Ye J, Orji IA, Baldridge AS, Ojo TM, Shedul G, Ugwuneji EN, et al. Characteristics and patterns of retention in hypertension care in primary care settings from the hypertension treatment in Nigeria program. JAMA Netw Open 2022 Sep 01;5(9):e2230025 [doi: 10.1001/jamanetworkopen.2022.30025] [Medline: 36066896]
- Reference 49: Ye J, Li N, Lu Y, Cheng J, Xu Y. A portable urine analyzer based on colorimetric detection. Anal Methods 2017;9(16):2464-2471 [doi: 10.1039/C7AY00780A]
- Reference 51: Ye J, Ren Z. Examining the impact of sex differences and the COVID-19 pandemic on health and health care: findings from a national cross-sectional study. JAMIA Open 2022 Sep 28;5(3):ooac076 [doi: 10.1093/jamiaopen/ooac076] [Medline: 36177395]
- Reference 52: Ye J, Yao L, Shen J, Janarthanam R, Luo Y. Predicting mortality in critically ill patients with diabetes using machine learning and clinical notes. BMC Med Inform Decis Mak 2020 Dec 30;20(Suppl 11):295 [doi: 10.1186/s12911-020-01318-4] [Medline: 33380338]
- Reference 53: Ye J. Pediatric mental and behavioral health in the period of quarantine and social distancing with COVID-19. JMIR Pediatr Parent 2020 Jul 28;3(2):e19867 [doi: 10.2196/19867] [Medline: 32634105]
- Reference 54: Ye J. Advancing mental health and psychological support for health care workers using digital technologies and platforms. JMIR Form Res 2021 Jun 30;5(6):e22075 [doi: 10.2196/22075] [Medline: 34106874]
- Reference 55: Ye J, Hai J, Wang Z, Wei C, Song J. Leveraging natural language processing and geospatial time series model to analyze COVID-19 vaccination sentiment dynamics on Tweets. JAMIA Open 2023 Apr 12;6(2):ooad023 [doi: 10.1093/jamiaopen/ooad023] [Medline: 37063408]
- Reference 59: Ye J. Patient safety of perioperative medication through the lens of digital health and artificial intelligence. JMIR Perioper Med 2023 May 31;6:e34453 [doi: 10.2196/34453] [Medline: 37256663]
- Reference 62: Ye J, Woods D, Bannon J, Bilaver L, Kricke G, McHugh M, et al. Identifying contextual factors and strategies for practice facilitation in primary care quality improvement using an informatics-driven model: framework development and mixed methods case study. JMIR Hum Factors 2022 Jun 24;9(2):e32174 [doi: 10.2196/32174] [Medline: 35749211]

The JMIR Publications Editorial Office regrets that these issues were not identified prior to publication.

The correction will appear in the online version of the paper on the JMIR Publications website together with the publication of this correction notice. Because this was made after submission to PubMed, PubMed Central, and other full-text repositories,

XSL•FO
RenderX

the corrected article has also been resubmitted to those repositories.

Reference

1. Ye J, Xiong S, Wang T, Li J, Cheng N, Tian M, et al. The roles of electronic health records for clinical trials in low- and middle-income countries: scoping review. JMIR Med Inform 2023 Nov 22;11:e47052 [FREE Full text] [doi: 10.2196/47052] [Medline: 37991820]

Submitted 18.09.25; this is a non–peer-reviewed article;accepted 18.09.25; published 08.10.25.

Please cite as:
JMIR Publications Editorial Office
Correction: The Roles of Electronic Health Records for Clinical Trials in Low- and Middle-Income Countries: Scoping Review
JMIR Med Inform 2025;13:e84394
URL: https://medinform.jmir.org/2025/1/e84394
doi:10.2196/84394
PMID:

©JMIR Publications Editorial Office. Originally published in JMIR Medical Informatics (https://medinform.jmir.org), 08.10.2025. This is an open-access article distributed under the terms of the Creative Commons Attribution License (https://creativecommons.org/licenses/by/4.0/), which permits unrestricted use, distribution, and reproduction in any medium, provided the original work, first published in JMIR Medical Informatics, is properly cited. The complete bibliographic information, a link to the original publication on https://medinform.jmir.org/, as well as this copyright and license information must be included.

XSL•FO
RenderX

Prescription Refill Adherence Before and After Patient Portal Registration in Among General Practice Patients in England Using the Clinical Practice Research Datalink: Longitudinal Observational Study

Abrar Alturkistani[1], MPH, PhD; Thomas Beaney[1], MBBS, MSc, PhD; Geva Greenfield[1], PhD; Ceire E Costelloe[1,2], MSc, PhD, CStat

[1]Department of Primary Care and Public Health, Imperial College, Reynolds Building, London, United Kingdom

[2]Division of Clinical Studies, Institute of Cancer Research, London, United Kingdom

Corresponding Author:
Abrar Alturkistani, MPH, PhD
Department of Primary Care and Public Health, Imperial College, Reynolds Building, London, United Kingdom

Abstract

Background: Patient portal use has been associated with improved patient health and improved adherence to medications, including statins. However, there is limited research on the association between patient portal registration and outcomes such as statin prescription refill adherence in the context of the National Health Service of England, where patient portals have been widely available since 2015.

Objective: We aimed to explore statin prescription refill adherence among general practice patients in England.

Methods: This study was approved by the Clinical Practice Research Datalink Independent Scientific Advisory Committee (ID: 21_000411). We used patient-level general practice data from the Clinical Practice Research Datalink in England. The data included patients with cardiovascular disease, diabetes, and chronic kidney disease, who were registered on the patient portal. The primary aim was to investigate whether statin prescription refill adherence, defined as ≥80% adherence based on the medication possession ratio, improved after patient portal registration. We used a multilevel logistic regression model to compare aggregate adherence 12 months before and 12 months after patient portal registration.

Results: We included 44,141 patients in the study. The analysis revealed a 16% reduction in the odds of prescription refill adherence 12 months after patient portal registration (odds ratio [OR]: 0.84, 95% CI 0.81-0.86) compared to 12 months before registration in the fully adjusted model for patient- and practice-level variables.

Conclusions: This study evaluated prescription refill adherence after patient portal registration. Registering to the portal does not fully explain the mechanisms underlying the relationship between patient portal use and health-related outcomes such as medication adherence. Although a small reduction in prescription refill adherence was observed, this reduction disappeared when the follow up time was reduced to 6 months. Given the limitations of the study, reduction in prescription refill adherence cannot be entirely attributable to patient portal registration. However, there may be potential confounding factors influencing this association which should be explored through future research.

(JMIR Med Inform 2025;13:e50294) doi:10.2196/50294

KEYWORDS

patient portals; personal health records; general practice; delivery of health care; medication ordering; health care; medication adherence; clinical practice research; patient portal; England; longitudinal analysis; patient health; medication; cardiovascular disease; diabetes; chronic kidney disease

Introduction

Patient portals are online websites or applications that are tethered to the health care system's electronic health record and typically offer services such as online appointment booking and repeat prescription ordering. It is suggested that patient portal use may improve patients' health through factors such as improving patients' efficiency, information access, and continuity of care. The mechanisms involved in patient portal use can facilitate communication and could help improve patients' health. For example, in a large integrated health care system in the United States, patients who found the use of patient portals to be more convenient than in-person care were more likely to report improved health as a result of using patient portals [1]. Patient portals provide access to medical record data on information such as diagnoses and test results and may

XSL•FO
RenderX

include patient education information on managing specific health conditions or general health advice. Furthermore, information access could also include collation of patients' information such as medications and consultations in one place, allowing patients to better manage their care [1], engage in shared decision-making, and understand their treatments [2]. Additionally, simple functionalities such as appointment booking and access to appointment records may help patients avoid missing appointments and enabling continuity of care [3].

It is hypothesised that patient portal use could improve medication adherence. A study among patients with diabetes reported that time without medication was reduced for those who exclusively used the refill function of the portal compared to those who did not use it [4]. Nonadherence to statins reduced by 6% (95% CI 4% - 7%) among patients with diabetes exclusively using the refill function compared to nonusers of the portal [5]. However, this relationship has not been studied within the National Health Service (NHS) in England, where all patient portals have been required to be offered in all General Practice (GP) practices since 2015 [6]. Studies reporting the relationship between patient portal use and medication adherence usually focus on specific functionalities of the portal. For example, studies may report the relationship between access to medical records, ordering medication through the patient portal (mainly repeat prescriptions), receiving reminder text messages, or booking appointments online. Studies also reported outcomes of patient portal use when coupled with another intervention such as telemedicine (technologies that enable remote medical consultations) or other digital interventions such as health monitoring devices or educational materials [7,8]. For example, a study found that digital technologies used for telemonitoring (which can be a feature of patient portals) that included monitoring patient health metrics and helping patients remember the time and type of medication improved medication adherence among patients with hypertension [7]. Additionally, telemonitoring may offer more accurate information on blood pressure values among patients with hypertension, which has been linked to improve therapeutic adherence to prescribed medications [7]. The digital technologies referenced in this study included apps, wearable decides, telemedicine, and digital monitoring tools (which include recording and reporting of health metrics to the health care system), and digital rehabilitation [7]. While the intervention considered in this study only includes access to medical records (Multimedia Appendix 1), descriptions of patient portals in the NHS (also known as online services) may also include features such as telemedicine, access to patient education materials, ability to book appointments, and ordering repeat prescriptions [6,9-11].

Statins are prescribed to patients both for primary prevention or secondary prevention of cardiovascular events; they are typically taken once a day and mostly continued for life, once prescribed to the patient [12]. Statin adherence could lower the risk of mortality [13]. Conversely, low adherence to statins increases the risk of death in the second year after a myocardial infraction and is also associated with increased risk of cardiovascular and cancer mortality [14-16]. A systematic review on factors associated with statin adherence for primary prevention of cardiovascular disease (CVD), included age, gender, or sex, diabetes status, hypertension, socioeconomic status, level of education, geographical region, race, and marital status [17]. This review also added that factors such as presence of dyslipidemia (high cholesterol), smoking status, work status, and comorbidity are either not associated or have mixed associations with statin adherence [17]. In this study we aimed to determine whether adherence to prescription refill statins improved after registering to patient portals among general practice patients using the Clinical Practice Research Datalink (CPRD), focusing on patients with adverse cardiovascular events, chronic kidney disease (CKD), CVD, and diabetes. This article is based on Chapter 4 of the author's PhD thesis [18].

Methods

Ethical Considerations

The study protocol was approved by CPRD's Independent Scientific Advisory Committee (ID: 21_000411). In the context of CPRD data usage, informed consent is not required for the anonymized data provided to CPRD from participating GP practices. The data is anonymized to the extent that individual patients cannot be identified. Participants have the option to opt out of having their health records shared for research purposes [19]. The original study approval covers secondary analyses, eliminating the need for additional consent from participants. No compensation was provided to participants in this study. Approved researchers could gain access to the data after submitting a study protocol.

Study Design

This was an observational study using longitudinal data on prescribed medication (statins) extracted from electronic health record data to compare patient-level aggregate adherence 12 months before and 12 months after patient portal registration, Adherence was measured using the medication possession ratio (MPR) with a threshold of 80% as an indicator of adherence. The data source, CPRD Aurum, comprises electronic health record data from GPs in England, where GPs are the gatekeepers of the health care system, and almost all of the population is registered with a GP [20]. The study period varied by patient and ranged from January 1, 2014, to August 15, 2021.

Study Population

To determine our population, we first included all patients in CPRD Aurum who had a patient portal registration code (available in Multimedia Appendix 1) recorded on or after January 1, 2015, when online services were required to be offered by all GPs in England [6]. Eligible patients had a diagnosis of at least one of the following conditions: adverse cardiovascular event, CKD, CVD, or diabetes, using codes in the study by Davidson et al [21]. These patient groups were chosen because they may be prescribed statins according to National Institute for Health and Care Excellence (NICE) guidelines for CVD prevention [22]. Although not all patients with diabetes will be prescribed statins, we included them due to the interest in the literature on the association between patient portal use and diabetes-related outcomes, including statin adherence [23].

XSL•FO
RenderX

Variables

Outcome Variable

The statin prescription refill adherence was determined through several steps. First, we extracted the codes of statin prescriptions using the codes provided in the study by Davidson et al [21], and aggregated the duration variable (defined as duration of treatment in days)for the period of one year before and one year after patient portal registration [24]. We assumed that if a patient duration was recorded as equal to zero, it was either entered by error or that it did not represent an actual statin prescription, as medication cannot be prescribed for zero days; therefore these observations were removed. Next, we calculated the MPR, which is a measure created by dividing the number of days of supply of the prescribed medication for all prescriptions within a time interval by the time interval [25]. In our study, we divided the aggregated duration by 365 (ie, 1 yr-period). The MPR was calculated twice for each patient for each time-period—one year before and one year after patient portal registration. We assumed that patients who did not have any record of statin prescriptions either before or after patient portal registration, to have an adherence of zero for that period. The MPR was then categorized into a binary variable of prescription refill adherence, with an 80% threshold by considering all values of ≥80% as adherent, and those <80% as nonadherent. The 80% cut off point was chosen to create easy-to-interpret binary variable for adherence following the same measure used in a previous CPRD study [26], as recommended research that determined 80% MPR to be a reasonable cut off point for categorizing the patient as adherent or nonadherent [27]. However, we have considered other cut off points, including 50% and 65% to compare the differences between these measures. The same logic was applied for adherence values of 65% and 50%. The various adherence values only indicate a change in the level of MPR that is considered adherent. Patients were considered adherent at the 80% threshold if they had an MPR ≥80%, at 65% if they had an MPR ≥65%, and at 50% if they had an MPR ≥50%. Patients having an MPR of ≥80% were considered adherent at all lower thresholds.

Predictors

The description of other variables included in the study including the predictor variable (ie, patient portal registration status) are described in Table 1. While multiple factors are associated with statin adherence, the research team decided to use the same variables included in our previous studies on at factors associated with patient portal use in NHS GP practice settings [28]. We also included all of the factors that are essential to the model such as gender, age group, ethnicity, and level of deprivation, which are associated with both patient portal use and medication refill adherence [17,28]. Hearing loss was added as a predictor because it can be associated with patient portal use and has been included in other studies on patient portal use in NHS GP settings [28-30].

XSL•FO
RenderX

Table . Description of study variables, their categories, and sources. Adapted from [18], under CC BY-NC license [31].

Variables	Description and categories
Gender	Gender is provided by Clinical Practice Research Datalink (CPRD) and consists of 3 categories including male, female, and indeterminate [24]. However, there were no patients with the indeterminate gender category in this cohort.
Patient portal registration status	We identified 6 codes that indicated registration or access to patients' online medical record and used them as a proxy for patient portal registration in CPRD to search patients' observation files for identifying the codes that indicate patient portal registration (Multimedia Appendix 1). We used registration to patient portals as a proxy for patient portal use due to lack of data in CPRD on the actual usage of patient portals.
Date of patient portal registration	The date of patient portal registration was determined as the observation date of the patient portal registration code. As patients only needed to register to the portal once, most patients only had one observation for patient portal registration. For those that had more than one code and therefore more than one observation date, we maintained the latest observation date as the patient portal registration date.
Age at registration age groups	CPRD provided only birth-year record of patients over 16 years. To calculate age, we assumed all patients were born on July 1 and calculated their age in reference to their patient portal registration date. We categorized age into 6 age groups: 16-44, 45-54, 55-64, 65-74, 75-84, and >85 years.
Self-reported ethnicity	Self-reported ethnicity was extracted from the observation files of patients using code list for ethnicity provided in the study by Davidson et al [32]. Ethnicity was categorized into 5 Office for National Statistics groups: White, Black, Mixed, South Asian, and other. Patients who did not have a code for ethnicity were placed in the 6th category "unknown." Patients who had more than one code for ethnicity were categorized into the ethnicity that had the majority of codes. If patients had multiple ethnicities with an equal number of codes for each ethnicity category, we assigned them the most recent ethnicity category as their ethnicity.
Index of multiple deprivation (IMD) quintiles	IMD 2019 was calculated using patients' postcodes and was provided by CPRD as linkage data on request.
Hearing loss	Hearing loss codes were extracted from the study by Head et al [33] using patients' observation files, and a binary variable was created to indicate whether the patient had hearing loss.
General practice rurality	2011 rural-urban classification at lower layer super output area level.

Statistical Methods

All analyses were performed using RStudio software (version 2023.06.0+421; R Foundation for Statistical Computing). We compared statin prescription refill adherence (measured by MPR ≥80%) 12 months before and 12 months after patient portal registration using multilevel logistic regression. We assumed that once patients were prescribed statins they would be for long-term use, indicating that they should have ordered statins consistently over the 12-month period before and after patient portal registration. The multilevel logistic regression was performed in three major steps:

1. First, we created a null model with only the outcome variable and added GP practice as the grouping variable. This step helped observe if clustering by GP was present. We checked the interclass correlation coefficient (ICC), which ranged from 0 - 1. A value of 0 ICC indicates no clustering at the group level and a value of 1 indicates perfect clustering at the group level.
2. At step 2, we added patient-level characteristics, as multilevel modeling requires separate steps for variables from two different levels (in this case, patients at level 1 and GP practices at level 2) [34]. Therefore, step we added all the predictor variables that were at the patient-level, including gender (male, female), age group (16-44, 45-54, 55-64, 65-74, 75-84, >85 years), self-reported ethnicity (White, Black, mixed, South Asian, and other), Index of Multiple Deprivation (IMD) quintiles (1-5), and hearing loss (yes, no).
3. At step three, we added rurality of the GP practice as the GP practice-level variable.

Sensitivity Analysis

We reduced the follow up time to 6 months instead of 12 months before and after patient portal registration to examine potential differences in association. Additionally, we performed a sensitivity analysis including all patients that were initially excluded from the study due to missing IMD measure data.

XSL•FO
RenderX

Results

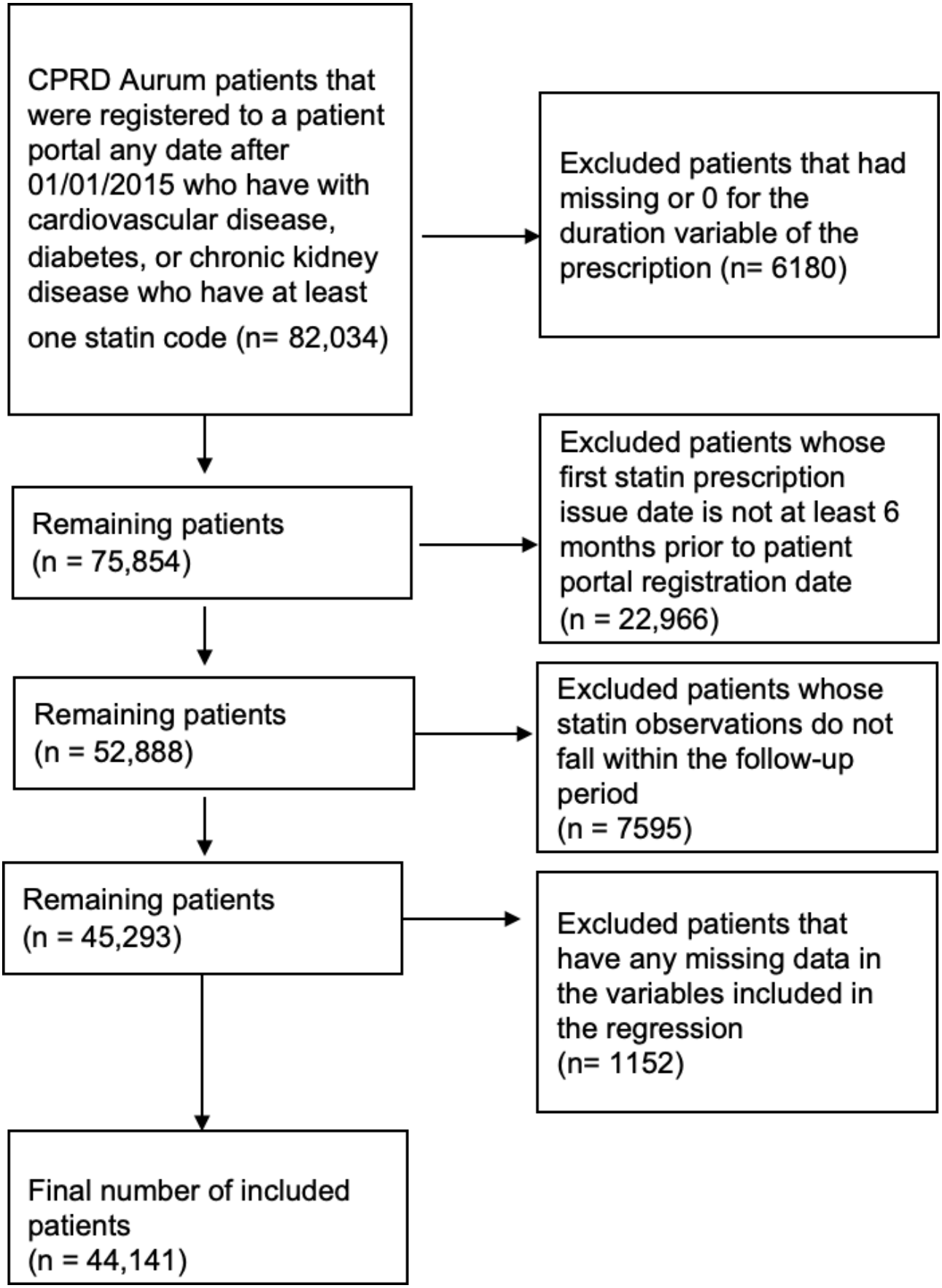
Study Size

Patients who had missing duration or 0-duration prescriptions were excluded (n=6180) (Figure 1). We excluded all patients whose first statin prescription was recorded at least 12 months before patient portal registration date (n=22,966) (Figure 1) to ensure that patients had at least 12 months of follow-up before patient portal registration. All patients whose statin observations did not fall within the required follow-up period (12 months before and 12 months after patient portal registration date) were excluded (n=7595) (Figure 1). Finally, we only included patients with complete data in the analysis, and excluded all patients that had missing IMD quintile data (n=44,141) (Figure 1). There were no missing data in any other variable except ethnicity, which was included as a separate category in the analysis.

Figure 1 is reused from PhD Thesis by Alturkistani [18].

XSL•FO
RenderX

Figure 1. Flow chart of the study population and excluded patients.



XSL•FO
RenderX

Summary Statistics

A total of 44,141 patients were included in the study. The majority (n=13,812) of the patients were men aged 65 - 74 years at the time of patient portal registration and had a prescription refill adherence of 80% or higher (n=27,208) (Table 2).

Table . Summary statistics of the study population. Reused from Alturkistani [18] under CC BY-NC license [31].

Characteristics	Patients (N=44,141), n (%)
Gender	
Men	26,620 (60.3)
Women	17,521 (39.7)
Age groups (years)	
16-44	1787 (4)
45-54	5550 (12.6)
55-64	11,308 (25.6)
65-74	13,812 (31.3)
75-84	8755 (19.8)
>85	2929 (6.6)
Prescription refill adherence (medication possession ratio ≥80%)	
No	16,933 (38.4)
Yes	27,208 (61.6)
Ethnicity	
White	32,547 (73.7)
South Asian	4664 (10.6)
Black	1601 (3.6)
Mixed	340 (0.8)
Other	436 (1)
Unknown	4553 (10.3)
IMD[a] quintile (1-5)[b]	
1	8041 (18.2)
2	9507 (21.5)
3	8697 (19.7)
4	9288 (21)
5	8608 (19.5)
Location of GP[c]	
Urban	38,054 (86.2)
Rural	6087 (13.8)
Hearing loss condition	
No	25,198 (57.1)
Yes	18,943 (42.9)

[a]IMD: Index of Multiple Deprivation.

[b]Quintiles: 1 (most deprived) to 5 (least deprived).

[c]GP: General practice.

Adherence Summary Statistics

The mean MPR 12 months before patient portal registration was 87% and ranged from 0%-183%, while the mean MPR 12 months after patient portal registration was 81%, ranging from 0%-164%. The median MPR was 92%, both before and after patient portal registration.

XSL•FO
RenderX

Association Between Patient Portal Registration and Statin Prescription Refill Adherence

Table 2 presents the results of the fully adjusted, multilevel logistic regression for the outcome variable (statin prescription refill adherence of ≥50%, ≥65%, and ≥80%). The odds ratio (OR) for statin prescription refill adherence of ≥80% was 0.84 (95% CI 0.81-0.86), indicating a 16% reduction in the odds of statin prescription refill adherence at this threshold after patient portal registration, compared to 12 months before registration (Table 3). The OR for adherence at 50% and 65% thresholds also indicated a reduction in adherence after patient portal registration, indicating that even patients with lower baseline adherence were less likely to remain adherent after patient portal registration (Table 3). The ICC varied for different levels of adherence but were generally 15% or lower, indicating the proportion of adherence variance that can be attributable to practice-level factors. For example, an ICC of 15% can be interpreted as 15% of the total variance in adherence by patients can be explained by differences at the GP practice level.

Table . Results of the fully-adjusted multilevel logistic regression model of patient portal registration status on statin prescription refill adherence of ≥50%, ≥65%, and ≥80% (level 1, N=88,282 observations of 44,141 patients; level 2, n=1190 general practices) 12 months before and 12 months after patient portal registration. Reused from [18] under CC BY-NC license [31].

Predictors	Adherence ≥50%		Adherence ≥65%		Adherence ≥80%	
	OR (95% CI)	*P* value	OR (95% CI)	*P* value	OR (95% CI)	*P* value
Patient portal registration status (after registration)	0.79 (0.77-0.82)	<.001	0.83 (0.81- 0.86)	<.001	0.84 (0.81-0.86)	<.001
Gender- (Ref: Male)						
Women	0.96 (0.93-0.99)	0.01	0.98 (0.95-1.01)	0.30	1.00 (0.97-1.03)	0.85
Age group, years (Ref: 65 - 74)						
16 - 44	0.46 (0.42-0.49)	<.001	0.43 (0.39-0.46)	<.001	0.40 (0.37-0.43)	<.001
45 - 54	0.67 (0.64-0.71)	<.001	0.65 (0.62-0.68)	<.001	0.60 (0.58-0.63)	<.001
55 - 64	0.84 (0.80-0.87)	<.001	0.84 (0.81-0.88)	<.001	0.78 (0.75-0.81)	<.001
75 - 84	1.08 (1.03-1.13)	0.002	1.08 (1.04-1.13)	<.001	1.08 (1.04-1.13)	<.001
>85	0.82 (0.77-0.88)	<.001	0.89 (0.83-0.95)	<.001	0.95 (0.90-1.02)	0.14
Ethnicity (Ref: White)						
Asian	0.88 (0.83-0.94)	<.001	0.90 (0.84-0.96)	<.001	0.89 (0.84-0.94)	<.001
Black	0.62 (0.56-0.68)	<.001	0.59 (0.54-0.65)	<.001	0.60 (0.55-0.65)	<.001
Mixed	0.77 (0.65-0.92)	0.003	0.72 (0.61-0.85)	<.001	0.72 (0.61-0.84)	<.001
Other	0.81 (0.70-0.95)	0.01	0.85 (0.74-0.99)	0.04	0.82 (0.71-0.95)	0.01
Unknown	1.08 (1.02-1.15)	0.01	1.10 (1.04-1.17)	<.001	1.09 (1.04-1.15)	<.001
IMD[a] quintile[b] (Ref: 5)						
1	0.93 (0.87-0.99)	0.03	0.93 (0.87-0.99)	0.02	0.95 (0.89-1.00)	0.07
2	0.90 (0.85-0.96)	0.001	0.90 (0.85-0.95)	0.00	0.91 (0.86-0.96)	0.001
3	0.91 (0.85-0.96)	0.001	0.91 (0.86-0.96)	0.001	0.92 (0.87-0.97)	0.002
4	0.97 (0.91-1.02)	0.23	0.94 (0.90-1.00)	0.03	0.94 (0.89-0.99)	0.01
Hearing loss (Ref: No)						
Yes	1.01 (0.98-1.05)	0.48	1.03 (0.99-1.06)	0.10	1.00 (0.97-1.03)	0.78
General practice location(Ref: Urban)						
Rural	1.02 (0.88-1.17)	0.82	1.04 (0.88-1.22)	0.65	1.00 (0.86-1.16)	0.99
Interclass correlation coefficient	0.10		0.15		0.13	

[a]IMD: Index of Multiple Deprivation.

[b]Quintiles 1 (most deprived) to 5 (least deprived).

XSL•FO
RenderX

Results of the Sensitivity Analysis

When the time of follow up was reduced to 6 months, the OR for statin prescription refill adherence of ≥80% was 1.01 (95% CI 0.98-1.04) in the fully-adjusted model, indicating no difference in statin prescription refill adherence 6 months after patient portal registration compared to the 6 months before patient portal registration (Multimedia Appendix 2).

The OR differed by only 0.01 - 0.02 of sensitivity analyses, which included patients who had missing IMD quintiles data (results not shown).

Discussion

Main Findings of the Study

After registering to the patient portal, patients had lower odds of achieving adherence of 50%, 65%, and 80% thresholds. However, this relationship was attenuated when the follow-up time was reduced to 6 months before and after patient portal registration and indicated no change in adherence after registration. This study found a reduction in prescription refill adherence after patient portal registration, which may be due to several reasons. Patients in this study were only registered to the portal once, and it is likely that may have enrolled at a time of high health care utilization. This could lead to increased medication requests prior to patient portal registration, compared to after registration. Additionally, patients may have overall reduced adherence to statins after using it for some time due to factors such as side effects, continuity of care, disease severity, or socioeconomic factors, which could all affect adherence to ordering prescriptions [26,27].

Comparison to Prior Work

Previous studies revealed that factors such as experiencing side effects, CVD severity, continuity of care and income, or other indicators of deprivation may influence adherence to statins [26,27]. Other factors that could be associated with statin adherence but were not examined in this study include the type of statin, intensity of the dose, timing of prescribing statins (eg, before or after puberty) [17]. Given that statin adherence reduced when patients were followed up for one year but not over 6 months, it is possible that statin adherence naturally reduced over time. Since the codes used for patient portal registration in this study indicated to access medical records, we could not explore potential mechanisms involved between accessing medical records and medication adherence. We acknowledge this as a limitation of the study, as registration to the patient portal does not necessarily mean continued use of the patient portal, discussed further in the limitations and strengths subsection [35].

Among features of patient portals, the ability to order prescriptions through the portal is most strongly associated with medication adherence. For example, one study reported that when medication is ordered through a patient portal, it can have less errors and more clear instructions (compared to hand-written prescriptions), which in turn improves adherence to treatment [36]. Having a higher supply of statin (eg, a supply of 60 d vs 30 d) was associated with improved adherence, which can be achieved by using a patient portal (by providing instant access to ordering medication) [17].

Limitations and Strengths of the Study

This study is relevant in the wake of increased popularity of using patient portals and other remote or digital health care services, particularly during and post-COVID-19 pandemic, both in England and other countries. Although widely offered within the NHS, this technology is rarely studied. We were unable to study active or continuous patient portal use, as this information was not recorded in CPRD, despite it being a rich source of data for clinical patient records. This study highlights the need to improve recording of the use of technologies to enable research in this field. To the authors' knowledge, this is the first study using CPRD data to examine patient portal use. Although the study was only able to capture registration to patient portals, the records of registration were obtained from an objective source (ie, electronic health records), which is a reliable method.

A strength of this study was that it controlled for clustering of patients within GP practices by using a multilevel model and including GP practices as a fixed effect, using a model which controls for the hierarchy of the data [37]. This could be attributed to patients from the same practice being more similar to each other, patient portals varying in functionalities, and knowledge and encouragement of their staff including GPs in using the patient portal [9].

One limitation in our study was that we could not measure or report the differences in patient portal functionalities that were included in the study, as our study included more than 1000 GP practices. Despite this, by including a large number of practices, we were able to analyze a more representative sample. We attempted to account for the differences between practices by running a multilevel model, recognizing that patients from the same GP practice may have more similar outcomes due to various factors including the type of patient portal offered in the practice and type of education and training available to both staff and patients [9].

While registration to the patient portal is the first step needed to benefit from its functionalities, studies show that without continuous or active use, patients cannot benefit from the technology. Registering to the portal does not guarantee continuous use of the portal, [38] which is essential to observe benefits associated with patient portal use [39]. A major limitation of this study was only using codes that indicated registration for accessing medical record as a proxy for patient portal use. This limited our study in two ways. First, access to medical records may have a minimal impact on prescription refill adherence. Second, patient portals offered through the NHS GPs, typically offer various functionalities beyond access to medical records, including online appointment booking and repeat prescription ordering [40]. However, as described in Multimedia Appendix 1, our search for codes that indicate patient portal use in CPRD Aurum only identified codes that indicate access to the medical records. This presented a challenge as patients using other portal functionalities, such as online appointment booking and prescription ordering, were not reflected in their electronic health records. Consequently,

XSL•FO
RenderX

we could not determine if patients without these specific codes (codes in Multimedia Appendix 1) were indeed nonusers of patient portals and therefore, suitable as controls for our study. While we recognize that this limitation reduces the robustness of the results, it was the most suitable approach to examine this relationship that remains unexplored within the NHS, despite a wide availability of patient portals for nearly a decade. Further information about the use of patient portals such as prescription refill requests or appointment bookings made through the portal could better inform the relationship between patient portal use and medication adherence. Additionally, our study population included patients with chronic diseases including CVD, CKD, and diabetes, who may be less likely to use patient portals and more likely to enroll or register to patient portals [41]. According to a study conducted in the United States, patients with certain circulatory diseases such as heart failure, myocardial infraction, peripheral vascular disease, and those with diabetes and renal disease were less likely to use the patient portal of the health care system [42]. Given that patients included in this study included those with CVD, CKD, and diabetes, it is possible that although they were registered to the patient portal, these patients may not have been active users. Therefore, we cannot conclude whether the patient experienced reduced adherence to refilling their prescriptions due to the patient portal use based solely on the findings from this study.

Conclusion

In this study, patients had a slightly reduced adherence one year after patient portal registration, although adherence did not change after a 6 months follow up. This could be attributed to other mechanisms, including those mentioned above, that could influence medication adherence and were not included in this study. Registration to the portal alone does not influence health-related behaviors such as medication adherence. Future studies on recording of patient portal use in electronic health records such as log files of functionality use in patient portals (eg, appointment booking, messaging health care providers, or requesting medications) could enable studying health related outcomes and explain mechanisms involved between patient portal use and health outcomes.

Acknowledgments

This article presents independent research commissioned by the National Institute for Health Research (NIHR) under the Applied Health Research (ARC) programme for Northwest London. TB acknowledges support from the Wellcome Trust. The views expressed in this publication are those of the authors and not necessarily those of the NHS, the NIHR, the Wellcome Trust or the Department of Health.

Authors' Contributions

Conceptualization: AA, CAC, GG, TB
Data curation: AA
Methodology: AA, CAC, GG, TB
Formal analysis: AA
Validation: TB
Writing – original draft – AA
Writing – review & editing – AA, CAC, GG, TB

Conflicts of Interest

None declared.

Multimedia Appendix 1
Patient portal registration codes used to extract patient records from CPRD Aurum.
[DOCX File, 15 KB - medinform_v13i1e50294_app1.docx]

Multimedia Appendix 2
Results of the fully adjusted multilevel logistic regression model of patient portal registration status on statin ordering adherence (medication possession ratio) of 50% or more, 65% or more, and 80% or more (level 1, N= 89,064 observations of 44,532 patients; level 2, N=1188 general practices) with 6 months before and 6 months after patient portal registration.
[DOCX File, 17 KB - medinform_v13i1e50294_app2.docx]

Checklist 1
The reporting of studies conducted using observational routinely collected health data checklist.
[DOCX File, 22 KB - medinform_v13i1e50294_app3.docx]

References

1. Reed ME, Huang J, Millman A, et al. Portal use among patients with chronic conditions: patient-reported care experiences. Med Care 2019 Oct;57(10):809-814. [doi: 10.1097/MLR.0000000000001178] [Medline: 31415340]

XSL•FO
RenderX

2. van der Vaart R, Drossaert CHC, Taal E, Drossaers-Bakker KW, Vonkeman HE, van de Laar MAFJ. Impact of patient-accessible electronic medical records in rheumatology: use, satisfaction and effects on empowerment among patients. BMC Musculoskelet Disord 2014 Mar 26;15:102. [doi: 10.1186/1471-2474-15-102] [Medline: 24673997]
3. Wildenbos GA, Maasri K, Jaspers M, Peute L. Older adults using a patient portal: registration and experiences, one year after implementation. Digit Health 2018;4:2055207618797883. [doi: 10.1177/2055207618797883] [Medline: 30186619]
4. Lyles CR, Sarkar U, Schillinger D, et al. Refilling medications through an online patient portal: consistent improvements in adherence across racial/ethnic groups. J Am Med Inform Assoc 2016 Apr;23(e1):e28-e33. [doi: 10.1093/jamia/ocv126] [Medline: 26335983]
5. Sarkar U, Lyles CR, Parker MM, et al. Use of the refill function through an online patient portal is associated with improved adherence to statins in an integrated health system. Med Care 2014 Mar;52(3):194-201. [doi: 10.1097/MLR.0000000000000069] [Medline: 24374412]
6. Patient online communications pack. NHS England. 2015. URL: https://www.england.nhs.uk/wp-content/uploads/2015/11/po-comms-toolkit-15.pdf [accessed 2024-02-23]
7. Minuz P, Albini FL, Imbalzano E, et al. Telemedicine and digital medicine in the clinical management of hypertension and hypertension-related cardiovascular diseases: a position paper of the Italian Society of Arterial Hypertension (SIIA). High Blood Press Cardiovasc Prev 2023;30(5):387-399. [doi: 10.1007/s40292-023-00595-0]
8. Deng L, Wu Q, Ding F, et al. The effect of telemedicine on secondary prevention of atherosclerotic cardiovascular disease: A systematic review and meta-analysis. Front Cardiovasc Med 2022;9:1020744. [doi: 10.3389/fcvm.2022.1020744] [Medline: 36440018]
9. NHS England. GP online services case studies. 2023 URL: https://www.england.nhs.uk/gp-online-services/learning-so-far/case-studies/ [accessed 2025-02-23]
10. Online access to GP health records – what's in it for patients? The Patient Association. URL: https://www.patients-association.org.uk/recording-webinar-online-access-to-gp-health-records [accessed 2025-02-23]
11. Online access to GP health records. NHS Digital. 2023. URL: https://digital.nhs.uk/services/nhs-app/nhs-app-guidance-for-gp-practices/guidance-on-nhs-app-features/online-access-to-gp-health-records [accessed 2025-02-23]
12. Statins to reduce the risk of CHD and stroke: patient decision aid. National Institute for Health and Care Excellence. 2014. URL: http://www.nice.org.uk/guidance/cg181/resources/cg181-lipid-modification-update-patient-decision- aid2 [accessed 2025-02-23]
13. Rodriguez F, Maron DJ, Knowles JW, Virani SS, Lin S, Heidenreich PA. Association of statin adherence with mortality in patients with atherosclerotic cardiovascular disease. JAMA Cardiol 2019 Mar 1;4(3):206-213. [doi: 10.1001/jamacardio.2018.4936] [Medline: 30758506]
14. Khalaf K, Johnell K, Austin PC, et al. Low adherence to statin treatment during the 1st year after an acute myocardial infarction is associated with increased 2nd-year mortality risk-an inverse probability of treatment weighted study on 54 872 patients. Eur Heart J Cardiovasc Pharmacother 2021 Mar 15;7(2):141-147. [doi: 10.1093/ehjcvp/pvaa010] [Medline: 32058542]
15. Brown R, Lewsey J, Wild S, Logue J, Welsh P. Associations of statin adherence and lipid targets with adverse outcomes in myocardial infarction survivors: a retrospective cohort study. BMJ Open 2021 Sep;11(9):e054893. [doi: 10.1136/bmjopen-2021-054893]
16. Lee YR, Oh SS, Jang SI, Park EC. Statin adherence and risk of all-cause, cancer, and cardiovascular mortality among dyslipidemia patients: a time-dependent analysis. Nutr Metab Cardiovasc Dis 2020 Nov 27;30(12):2207-2214. [doi: 10.1016/j.numecd.2020.07.024] [Medline: 32912787]
17. Hope HF, Binkley GM, Fenton S, Kitas GD, Verstappen SMM, Symmons DPM. Systematic review of the predictors of statin adherence for the primary prevention of cardiovascular disease. PLoS One 2019;14(1):e0201196. [doi: 10.1371/journal.pone.0201196] [Medline: 30653535]
18. Alturkistani A. Patient portals in the national health service general practice (GP) practices: a systematic review and analysis of GP patient surveys and clinical practice research datalink (in-press). PhD Thesis.: Department of Primary Care and Public Health. Imperial College.Custom; 2024 URL: https://www.thelancet.com/journals/landig/article/PIIS2589-7500(21)00203-X/fulltext [accessed 2025-02-23]
19. Safeguarding patient data. CPRD. 2023. URL: https://cprd.com/safeguarding-patient-data [accessed 2025-02-23]
20. Time series comparing the number of patients registered at a GP to the ONS mid-year population estimate - NDRS. NHS Digital. 2023. URL: https://digital.nhs.uk/data-and-information/publications/statistical/patients-registered-at-a-gp-practice/april-2021/spotlight-report-april-2021 [accessed 2025-02-23]
21. Davidson JA, Banerjee A, Smeeth L, et al. Risk of acute respiratory infection and acute cardiovascular events following acute respiratory infection among adults with increased cardiovascular risk in England between 2008 and 2018: a retrospective, population-based cohort study. Lancet Digit Health 2021 Dec;3(12):e773-e783. [doi: 10.1016/S2589-7500(21)00203-X] [Medline: 34823706]
22. Cardiovascular disease: risk assessment and reduction, including lipid modification. : (Clinical guideline [CG181]); 2014.

XSL•FO
RenderX

23. Alturkistani A, Qavi A, Anyanwu PE, Greenfield G, Greaves F, Costelloe C. Patient portal functionalities and patient outcomes among patients with diabetes: systematic review. J Med Internet Res 2020 Sep 22;22(9):e18976. [doi: 10.2196/18976] [Medline: 32960182]
24. CPRD Aurum data specification. Medicines & healthcare products regulatory agency. 2022. URL: https://cprd.com/sites/default/files/2022-02/CPRD%20Aurum%20Data%20Specification%20v2.7%20%28002%29.pdf [accessed 2025-02-23]
25. Sperber CM, Samarasinghe SR, Lomax GP. An upper and lower bound of the medication possession ratio. Patient Prefer Adherence 2017;11:1469-1478. [doi: 10.2147/PPA.S136890] [Medline: 28919719]
26. Tammes P, Payne RA, Salisbury C. Association between continuity of primary care and both prescribing and adherence of common cardiovascular medications: a cohort study among patients in England. BMJ Open 2022 Sep 13;12(9):e063282. [doi: 10.1136/bmjopen-2022-063282] [Medline: 36100300]
27. Karve S, Cleves MA, Helm M, Hudson TJ, West DS, Martin BC. Good and poor adherence: optimal cut-point for adherence measures using administrative claims data. Curr Med Res Opin 2009 Sep;25(9):2303-2310. [doi: 10.1185/03007990903126833] [Medline: 19635045]
28. Alturkistani A, Greenfield G, Beaney T, Norton J, Costelloe CE. Cross-sectional analyses of online appointment booking and repeat prescription ordering user characteristics in general practices of England in the years 2018-2020. BMJ Open 2023 Oct 12;13(10):e068627. [doi: 10.1136/bmjopen-2022-068627] [Medline: 37827735]
29. Gomez-Cano M, Atherton H, Campbell J, et al. Awareness and use of online appointment booking in general practice: analysis of GP Patient Survey data. Br J Gen Pract 2020 Jun;70(suppl 1):bjgp20X711365. [doi: 10.3399/bjgp20X711365] [Medline: 32554662]
30. Gomez-Cano M, Atherton H, Campbell J, et al. Awareness and use of online appointment booking in general practice: analysis of GP Patient Survey data. Br J Gen Pract 2020 Jun;70(suppl 1):bjgp20X711365. [doi: 10.3399/bjgp20X711365]
31. Creative Commons. Attribution-NonCommercial 40 International - Creative Commons. URL: https://creativecommons.org/licenses/by-nc/4.0/ [accessed 2025-02-27]
32. Davidson J, Banerjee A, Mathur R, et al. Ethnic differences in the incidence of clinically diagnosed influenza: an England population-based cohort study 2008-2018. Wellcome Open Res 2021;6:49. [doi: 10.12688/wellcomeopenres.16620.3] [Medline: 34056137]
33. Head A, Fleming K, Kypridemos C, Schofield P, Pearson-Stuttard J, O'Flaherty M. Inequalities in incident and prevalent multimorbidity in England, 2004-19: a population-based, descriptive study. Lancet Healthy Longev 2021 Aug;2(8):e489-e497. [doi: 10.1016/S2666-7568(21)00146-X] [Medline: 36097998]
34. Sommet N, Morselli D. Keep calm and learn multilevel linear modeling: a three-step procedure using SPSS, Stata, R, and Mplus. Int Rev Soc Psychol 2021 Sep 9;34(1):24. [doi: 10.5334/irsp.555]
35. Fraccaro P, Vigo M, Balatsoukas P, Buchan IE, Peek N, van der Veer SN. Patient portal adoption rates: a systematic literature review and meta-analysis. Stud Health Technol Inform 2017;245:79-83 [FREE Full text] [Medline: 29295056]
36. Kamath S, Jawdekar AM. A comparison of innovative app-based prescriptions with conventional prescriptions for children by general dentists: a mixed methods study. Cureus 2023 Jan;15(1):e33583. [doi: 10.7759/cureus.33583] [Medline: 36788825]
37. What are multilevel models and why should I use them? Centre for Multilevel Modelling. 2023. URL: https://www.bristol.ac.uk/cmm/learning/multilevel-models/what-why.html [accessed 2025-02-23]
38. Tuan WJ, Mellott M, Arndt BG, Jones J, Simpson AN. Disparities in use of patient portals among adults in family medicine. J Am Board Fam Med 2022;35(3):559-569. [doi: 10.3122/jabfm.2022.03.210486] [Medline: 35641056]
39. Holder K, Ukoha E, Feinglass J, Yee LM. Relationship between patient portal utilization and glycemic control outcomes during pregnancy. J Diabetes Sci Technol 2021 Jul;15(4):970-971. [doi: 10.1177/1932296821998742] [Medline: 33736473]
40. GP online services for GP practices. NHS England. URL: https://www.england.nhs.uk/gp-online-services/about-the-prog/services-for-gps/ [accessed 2025-02-23]
41. Antonio MG, Petrovskaya O, Lau F. The state of evidence in patient portals: umbrella review. J Med Internet Res 2020 Nov 11;22(11):e23851. [doi: 10.2196/23851] [Medline: 33174851]
42. Liu SK, Osborn AE, Bell S, Mecchella JN, Hort S, Batsis JA. Patient characteristics and utilization of an online patient portal in a rural academic general internal medicine practice. BMC Med Inform Decis Mak 2022 Feb 16;22(1):42. [doi: 10.1186/s12911-022-01778-w] [Medline: 35172805]

Abbreviations:

CKD: chronic kidney disease
CPRD: Clinical Practice Research Datalink
CVD: cardiovascular disease
GP: general practice
IMD: index of multiple deprivation
MPR: medication possession ratio
NHS: National Health Service
NICE: The National Institute for Health and Care Excellence

XSL•FO
RenderX

OR: odds ratio

Edited by C Lovis; submitted 26.06.23; peer-reviewed by E Ukoha, M Lee; revised version received 15.01.25; accepted 23.01.25; published 11.03.25.

Please cite as:
Alturkistani A, Beaney T, Greenfield G, Costelloe CE
Prescription Refill Adherence Before and After Patient Portal Registration in Among General Practice Patients in England Using the Clinical Practice Research Datalink: Longitudinal Observational Study
JMIR Med Inform 2025;13:e50294
URL: https://medinform.jmir.org/2025/1/e50294
doi:10.2196/50294

© Abrar Alturkistani, Thomas Beaney, Geva Greenfield, Ceire E Costelloe. Originally published in JMIR Medical Informatics (https://medinform.jmir.org), 11.3.2025. This is an open-access article distributed under the terms of the Creative Commons Attribution License (https://creativecommons.org/licenses/by/4.0/), which permits unrestricted use, distribution, and reproduction in any medium, provided the original work, first published in JMIR Medical Informatics, is properly cited. The complete bibliographic information, a link to the original publication on https://medinform.jmir.org/, as well as this copyright and license information must be included.

XSL•FO
RenderX

Innovative Integration of 4D Cardiovascular Reconstruction and Hologram: Framework Development of a New Visualization Tool for Coronary Artery Bypass Grafting Planning

Shuo Wang[1*], PhD; Tong Ren[2*], MM; Nan Cheng[2], MD; Li Zhang[1], MM; Rong Wang[1], MD

[1]Department of Engineering Physics, Key Laboratory of Particle and Radiation Imaging, Ministry of Education, Tsinghua University, 30 Shuangqing Road, Haidian District, Beijing, China

[2]Department of Adult Cardiac Surgery, Senior Department of Cardiology, The Six Medical Center of People's Liberation Army General Hospital, 6 Fucheng Road,, Haidian District, Beijing, China

[*]these authors contributed equally

Corresponding Author:
Rong Wang, MD
Department of Engineering Physics, Key Laboratory of Particle and Radiation Imaging, Ministry of Education, Tsinghua University, 30 Shuangqing Road, Haidian District, Beijing, China

Abstract

Background: Planning for coronary artery bypass grafting (CABG) necessitates advanced spatial visualization skills and consideration of multiple factors, including the depth of coronary arteries within the subepicardium, calcification levels, and pericardial adhesions.

Objective: This study aimed to address these requirements by reconstructing a dynamic cardiovascular model, displaying it as a naked-eye hologram, and evaluating the clinical utility of this innovative visualization tool for preoperative CABG planning.

Methods: We used preoperative 4D cardiac computed tomography angiography (4D-CCTA) data from 14 patients scheduled for CABG to develop a semiautomated workflow. This workflow enabled time-resolved segmentation of the heart chambers, epicardial adipose tissue (EAT), and coronary arteries, complete with calcium scoring. Methods for segmenting cardiac structures, quantifying coronary calcification, visualizing coronary depth within EAT, and assessing pericardial adhesions via motion analysis were incorporated. These dynamic reconstructions captured spatial relationships, coronary stenosis, calcification, and depth in EAT, as well as pericardial adhesions. Dynamic cardiovascular holograms were then generated and displayed using the Looking Glass platform (Looking Glass Factory Inc). Thirteen cardiac surgeons assessed the utility of the holographic visualization tool on a Likert scale. In addition, a surgeon visually scored pericardial adhesions using the holograms of all 21 patients (including 7 undergoing secondary cardiac surgeries) and compared these scores with actual intraoperative findings.

Results: Cardiac surgeons highly rated the visualization tool for its utility in preoperative planning, with a mean Likert score of 4.57/5.0 (SD 0.5). The hologram-based scoring of pericardial adhesions showed a strong correlation with intraoperative findings (correlation coefficient r=0.786; P<.001).

Conclusions: This study delineates the structural framework of a visualization tool specifically designed for preoperative CABG planning. It produces high-quality, clinically relevant, dynamic holograms from patient-specific volumetric data, with clinical feedback confirming its practicality and effectiveness for preoperative surgical planning.

(JMIR Med Inform 2025;13:e72237) doi:10.2196/72237

KEYWORDS

hologram; 4D cardiovascular modeling; 4D cardiac CT angiogram; CABG; preoperative planning; coronary artery bypass graft

Introduction

Coronary artery disease (CAD) is one of the leading causes of death worldwide [1]. Coronary artery bypass grafting (CABG) is the most frequently performed cardiac surgery globally [2]. Compared with percutaneous interventions or medication therapy alone, CABG provides a survival advantage for patients with complex coronary artery disease [3]. Accurate identification of the coronary arteries and careful selection of the anastomotic site are critical for surgical success. If the chosen anastomosis site is located too deep within the thoracic cavity, the limited operating space may hinder surgical maneuverability. Furthermore, when a coronary artery lies deep within epicardial adipose tissue (EAT) or within the myocardium, intraoperative localization becomes challenging. This can lead to longer operative times, increased tissue trauma, and a reduction in the morphological quality of the anastomosis. In addition, plaque may obstruct suturing, and pericardial adhesions can increase

XSL•FO
RenderX

the risk of injury to the heart or major vessels, further prolonging the procedure and raising its overall risk. Therefore, collecting detailed information on pericardial adhesions, spatial orientation, coronary artery depth within EAT, stenosis, and calcification is crucial for preoperative CABG planning.

Enhanced 3D cardiac models that incorporate multiple functional imaging modalities provide more comprehensive insights [4]. A practical strategy to realize precision medicine in cardiovascular care is through the digital twinning of the cardiovascular system, using coronary angiography, echocardiography, and coronary computed tomography angiography (CTA) data [5]. Compared with ultrasound and magnetic resonance imaging (MRI), CTA offers superior spatial resolution and is widely used for reconstructing patient-specific 3D models. While MRI techniques such as 4D cardiac MRI and cine multislice MRI offer excellent temporal resolution along with good spatial resolution and are well-established in clinical practice, 4D cardiac computed tomography (CT) imaging offers sufficient spatial and temporal resolution to support advanced visualization. This enables dynamic and functional assessments of cardiovascular conditions. Although 3D and 4D visualization technologies with effective depth cues are already established in clinical practice, enabled by robust 3D viewers that allow simultaneous multiview display and free-angle reformatting of volumetric datasets, our study hypothesizes that holographic displays may provide additional benefits for specific surgical planning tasks, warranting further investigation.

Building upon the established foundation of clinical 3D visualization, our research explores whether holographic displays can provide complementary benefits for CABG planning. Rather than suggesting limitations in current clinical displays, we aim to explore whether the stereoscopic nature of holography offers added value for specific surgical planning scenarios. Effective communication among health care team members can be hindered by individual differences in spatial visualization abilities. Researchers have made significant progress in representing medical 3D images through virtual and augmented reality (VR and AR) technologies, as well as various stereoscopic display systems. In recent years, holographic display technology has made notable advances in the fields of surgical planning and intraoperative navigation, with the Microsoft HoloLens emerging as the leading AR and MR headset [6-10]. Holography is widely considered the most advanced form of display technology, as it incorporates all human visual cues, including stereopsis and accommodation, allowing for naked-eye visualization [9]. Although modern head-mounted devices have become more lightweight and support networked multiuser viewing, they still present significant limitations. One persistent issue with VR is “cybersickness”—a condition marked by symptoms such as headaches, nausea, and vomiting [11]. In addition, these devices often fall short in providing true depth perception [10]. The HOLOSCOPE is the world’s first medical-grade holographic system. Bruckheimer et al [10] demonstrated the creation of real-time, internet-based 3D digital holograms without the need for headgear, using actual patient voxel data from 3D rotational angiography and intraoperative real-time 3D transesophageal echocardiography in patients with structural heart disease for preoperative assessment [12]. Looking Glass Factory has introduced the world’s first group-viewable holographic displays [13], offering a significantly more affordable alternative to the RealView HOLOSCOPE, which typically costs hundreds of thousands of dollars. In contrast, entry-level Looking Glass devices are priced at just a few thousand dollars. These displays offer substantial advantages for simultaneous multiuser viewing, collaborative discussion, and cost-effectiveness, making them particularly valuable for surgical planning in procedures like CABG, which often require input from multidisciplinary teams.

Building on a strong medical-industrial collaboration, our study addresses critical challenges in preoperative CABG planning by designing a 4D cardiovascular hologram based on 4D-CCTA data and evaluating the feasibility of using this holographic visualization tool for surgical planning.

Methods

Study Design and Overview

A total of 21 patients scheduled for cardiac surgery were evaluated using 4D-CCTA before the procedure. This cohort included 14 patients with complex coronary artery lesions who were candidates for CABG, with a mean age of 53.6 (SD 8.9) years; 13 of them were male. Because pericardial adhesions are common in patients undergoing repeat cardiac surgery, we selected 7 patients undergoing secondary procedures as a control group for evaluating pericardial adhesions. These patients had a mean age of 55.5(SD 11.5)years , and 6 were male. Operative reports confirmed extensive pericardial adhesions in all patients undergoing reoperation and the absence of adhesions in all patients undergoing first-time surgery. All reoperations involved heart valve procedures, with the interval between the initial and repeat surgeries ranging from 1 to 35 years. Among these patients, 3 had valve dysfunction following corrective surgery for congenital heart defects; 1 had infective endocarditis after left ventricular outflow tract unblocking, mitral valve replacement, and CABG; 1 developed infective endocarditis following mechanical valve replacement; 1 experienced tricuspid insufficiency after left heart valve surgery; 1 had mitral valve insufficiency after mitral valve plasty; and 1 had mitral valve insufficiency following prior left heart valve surgery. Inclusion criteria for the study were: (1) patients with complex coronary lesions meeting the clinical indications for CABG and no history of previous cardiac surgery; (2) patients undergoing secondary surgery in whom the autologous pericardium had been closed during the initial procedure. Exclusion criteria included poor-quality imaging data.

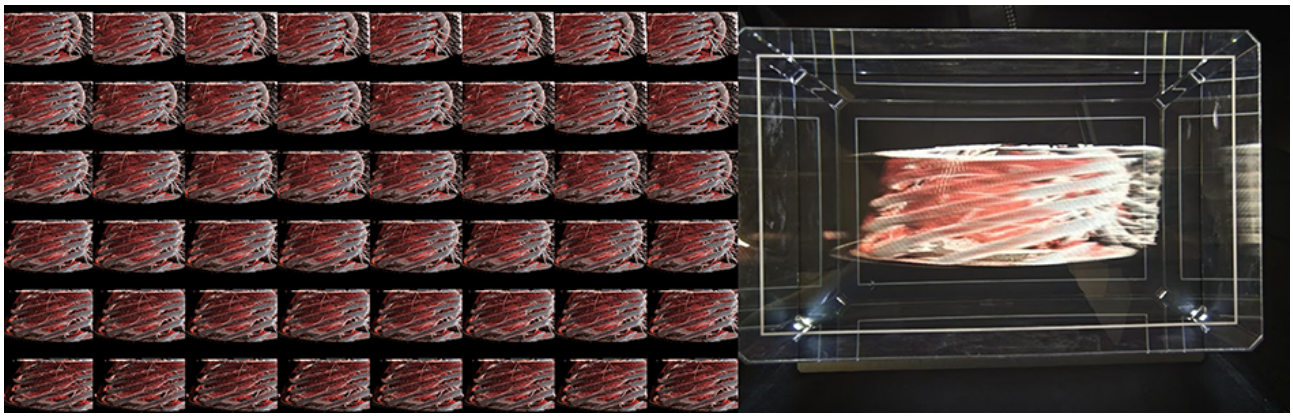
Our study aimed to construct a 4D cardiovascular hologram using individualized patient imaging to address key challenges in the preoperative planning of CABG. Clinicians will evaluate the effectiveness of the holographic visualization tool by comparing it with patients’ preoperative and intraoperative data, in order to assess the system’s practical utility for surgical planning. The surgeon will not use the holograms to guide the procedure or make clinical decisions based on these images.

XSL•FO
RenderX

Hologram Visualization System

The holographic display used in this study is the 8.9-inch Dev Kit from Looking Glass Factory Inc, which leverages advanced light field technology to produce highly realistic 3D visualizations of cardiovascular structures. This system generates true volumetric imagery by projecting 48 distinct horizontal perspectives of the same visual content through calibrated lenticular arrays, allowing multiple observers to simultaneously view and interact with the 3D cardiac models from various angles without positional restrictions (Figure 1).

Figure 1. Holographic display system consisting of 48 viewing angles.



The dynamic cardiac hologram is displayed at 60 frames per second, closely replicating the visual fluidity of normal cardiac cycles. The system provides a horizontal viewing angle of 58°, enabling up to 5 observers to simultaneously view the same holographic image from different perspectives without distortion. Depth perception is significantly enhanced by the system's ability to render between 45 and 100 discrete depth planes along the z-axis, producing a seamless sense of depth that is crucial for interpreting complex cardiac anatomy. These complementary features—multiple horizontal perspectives and discrete depth planes—combine to deliver a truly immersive 3D visualization experience.

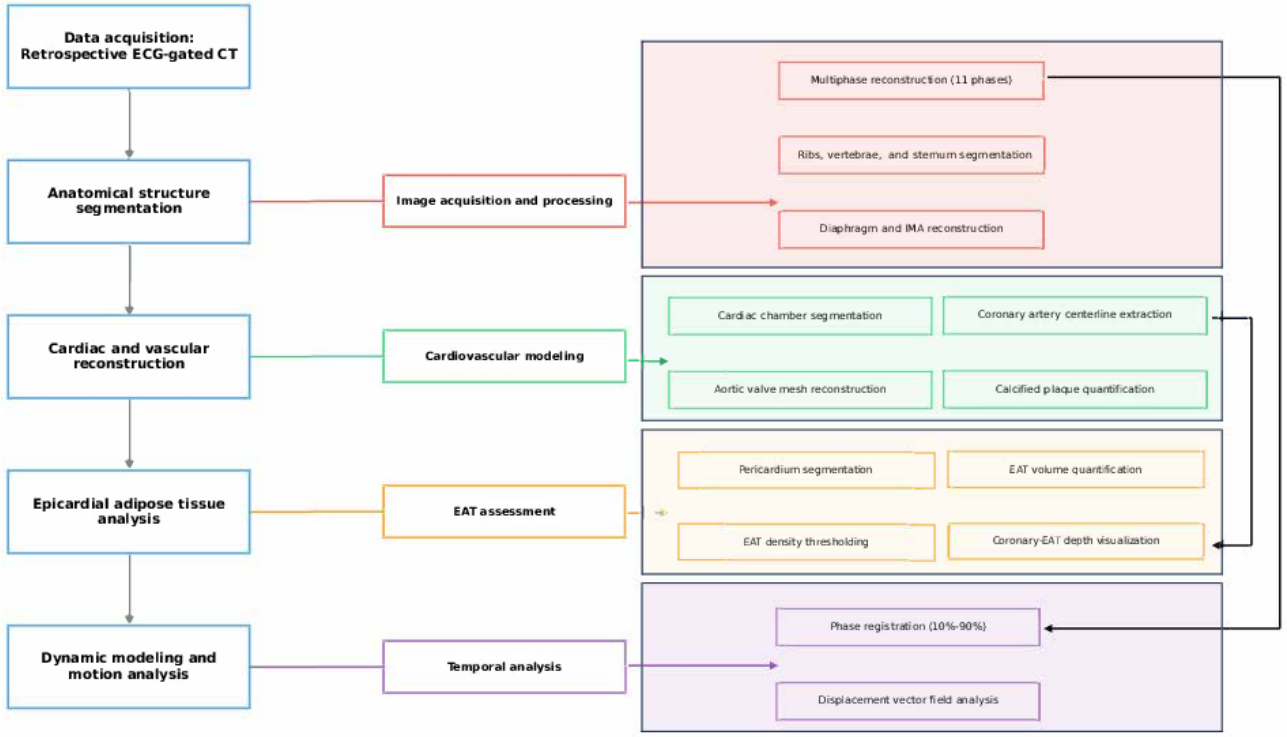
Unlike conventional VR or AR solutions, this technology does not require head-mounted displays or specialized eyewear, allowing surgical teams to communicate naturally while examining patient-specific anatomy. Interaction with the holographic model is enabled via a Leap Motion controller (Ultraleap Ltd), which supports intuitive, gesture-based manipulation. Users can rotate the model along any axis, zoom into regions of interest, adjust the playback speed of the cardiac cycle, and selectively display or hide specific tissue layers—including epicardial fat, coronary vessels, and calcification sites—using natural hand movements. This gesture control system is particularly valuable during preoperative planning sessions, where multiple specialists can collaboratively examine and manipulate complex anatomical structures while maintaining full situational awareness and unimpeded lines of communication.

Images and Processing

CT images were acquired during end-expiratory breath-hold and in sinus rhythm using a GE APEX CT scanner (Revolution Apex; GE Healthcare) with a retrospective electrocardiogram-gated protocol to optimize cardiac motion compensation. An iodinated contrast agent (Iohexol, 350 mg I/mL) was administered at a volume of 70 mL, followed by a 40 mL saline chaser at a flow rate of 5.5 mL/s via antecubital venous access. SmartPrep bolus tracking (GE Healthcare) was used to ensure optimal contrast timing. The z-axis coverage was 157.5 mm, encompassing the entire heart from above the carina to below the diaphragmatic surface. A noncontrast scan was performed before contrast-enhanced CCTA to allow for coronary calcium scoring. Images were reconstructed across 11 temporal phases, each corresponding to a range of R-R interval values from −5% to 106%. Slice thickness was 0.625 mm with matching intervals, and the in-plane resolution was 0.23 × 0.23 mm. The mean effective radiation dose, calculated according to European guidelines for multislice CT, was 14.93 mSv (DLP: 1066.66 mGy·cm, using a conversion factor of 0.014 mSv/mGy·cm). Coronary plaque quantification and Agatston scoring were performed using GE's cardiac analysis software (AW VolumeShare 7), specifically the SmartScore module. As illustrated in Figure 2, our processing pipeline for cardiac CT data follows a sequential workflow beginning with retrospective electrocardiogram-gated image acquisition. The methodology proceeds through 4 key analytical stages. First, anatomical structure segmentation is performed, including multiphase reconstruction and skeletal structure delineation. Second, cardiac and vascular reconstruction is conducted with detailed cardiovascular modeling of chambers, vessels, and pathological features. Third, the EAT assessment quantifies the distribution and characteristics of pericardial fat deposits. Finally, dynamic modeling and motion analysis are achieved through temporal registration and displacement vector field analysis. This integrated approach enables a comprehensive evaluation of cardiac anatomy, function, and associated tissue characteristics, supporting both advanced clinical applications and research objectives.

XSL•FO
RenderX

Figure 2. Comprehensive cardiac computed tomography imaging pipeline for cardiovascular analysis. CT: computed tomography; EAT: epicardial adipose tissue; ECG: electrocardiogram; IMA: internal mammary artery.

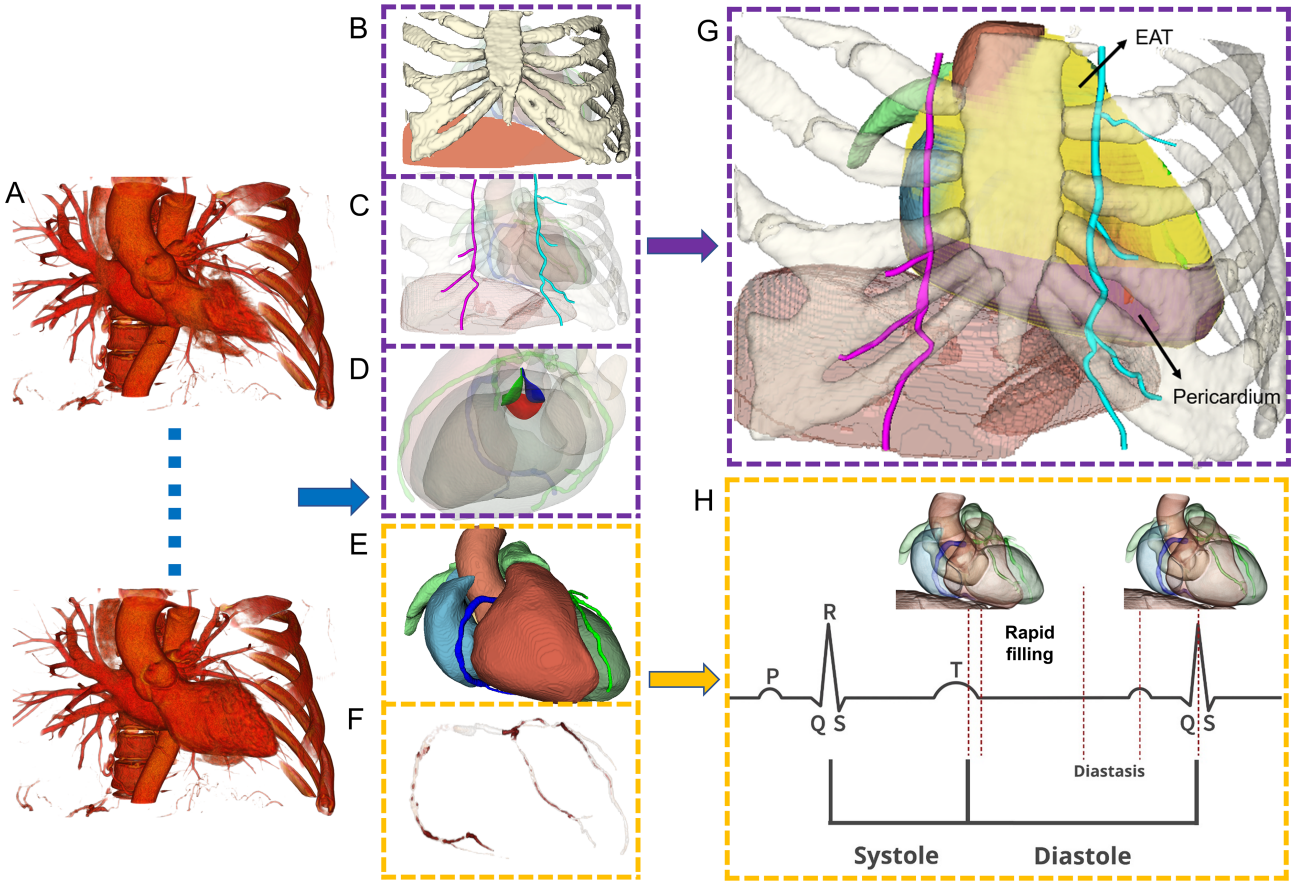


First, we implemented our approach using MONAI [14] (Medical Open Network for Artificial Intelligence; NVIDIA), an open-source framework for deep learning in health care imaging, using its Auto3DSeg project (a component of the MONAI framework) for automated 3D segmentation. We segmented and reconstructed the ribs, vertebrae, sternum, diaphragm, and internal mammary artery from end-diastolic phase (70% R-R interval) CT images (Figure 3B-C). Next, we applied HeartDeformNet [15] to automatically segment the left ventricle, right ventricle, left atrium, right atrium, left ventricular myocardium, aorta, and pulmonary artery across all phases of the cardiac cycle (Figure 3A,E). A slightly modified version of DeepCarve [16] was used for aortic valve mesh reconstruction (Figure 3D). The primary modification involved using a template from an end-diastolic segmented left ventricle model, which contained fewer distorted elements. An experienced cardiologist manually marked and recorded arterial contours on planes perpendicular to the vessel centerline using SimVascular-v2023.03.27 [17], thus achieving segmentation of the coronary arteries from the 70% phase image (Figure 3F). Subsequently, we imported 9 cardiac phases (10% - 90%) and registered them to the selected 70% phase. This registration provided the transformations needed to adjust the 3D surface model points of the coronary arteries. These transformations were then used to generate a time-dependent sequence of 3D coronary artery models (Figure 3G,H), completing the process of dynamic modeling.

Second, for the visualization of calcified plaques, we followed the Agatston method [18]. We first identified contiguous calcium voxels within the 3D space of the binarized calcium image (Figure 4A). Three quantitative indices—Agatston score, mass score, and volume score—were calculated for the major branches of the coronary arteries (Figure 4B,C). In the calcified regions, medium and heavily calcified plaques were highlighted in red (Figure 4D). Fiz et al [19] classified plaque calcium density into tertiles: light (130 - 210 HU), medium (211 - 510 HU), and heavy (>510 HU) (Figure 4).

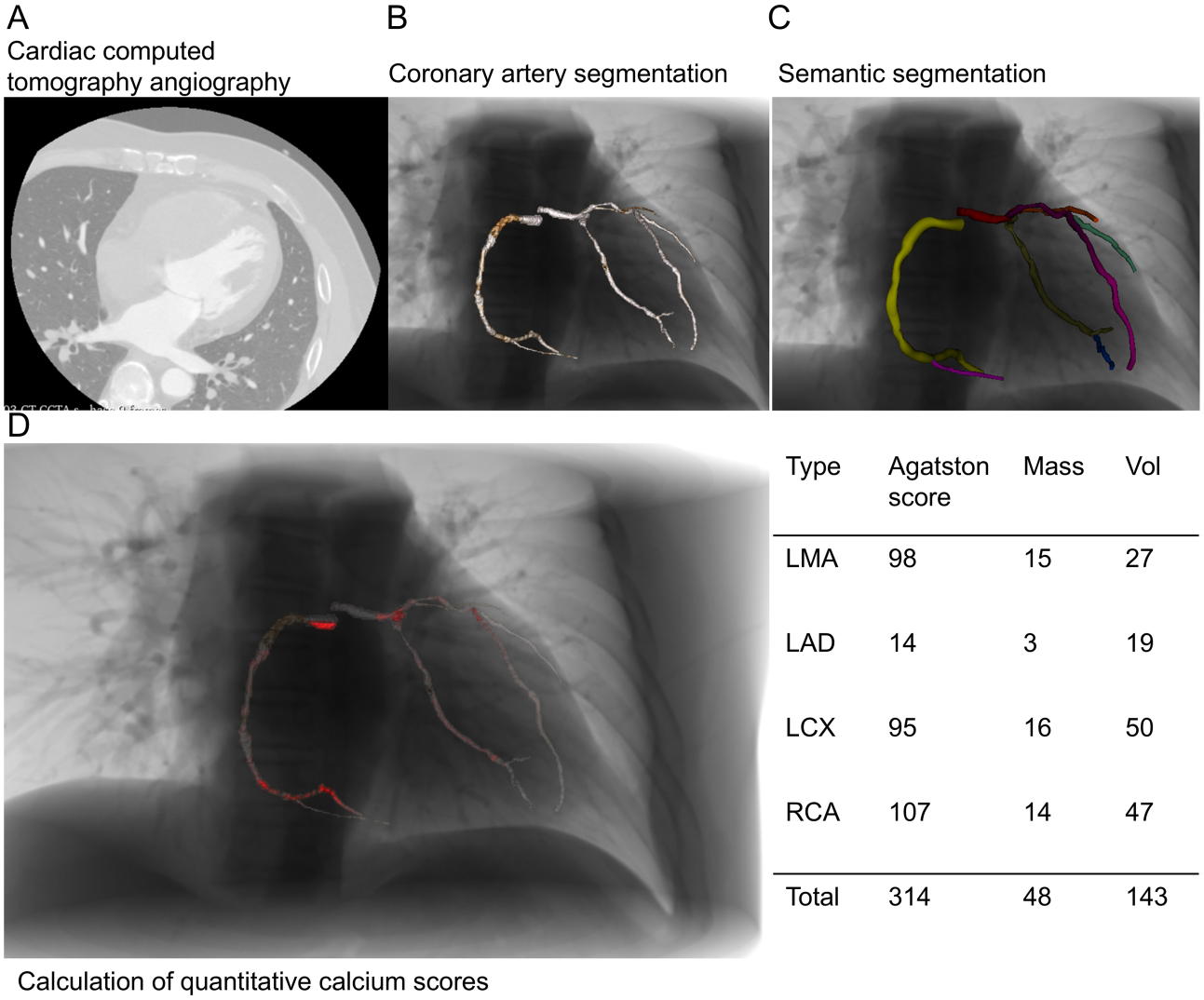
XSL•FO
RenderX

Figure 3. Technical visualization of cardiac computed tomography analysis results. (A) Electrocardiogram-gated sequential cardiac images showing the heart at different phases of the cardiac cycle. (B) 3D reconstruction of the thoracic cage and diaphragm. (C) Internal mammary artery visualization and anatomical relationships. (D) Detailed aortic valve structural analysis. (E) Complete heart mesh model displaying chambers and great vessels. (F) 3D reconstruction of coronary arteries. (G) Complete scene view with labeled epicardial adipose tissue and pericardium. (H) Model sequence of the cardiac cycle correlated with electrocardiogram waveform. EAT: epicardial adipose tissue.



XSL•FO
RenderX

Figure 4. Calculation and visualization of quantitative indices for coronary artery calcification. (A) Original cardiac computed tomography angiography image. (B) Coronary artery segmentation showing the contours of major coronary vessels. (C) Semantic segmentation with different coronary artery branches marked in distinct colors. (D) Quantitative analysis of calcified plaques, with visualization of calcification areas (marked in red) on the left, and a table on the right showing quantitative results including Agatston score, calcium mass, and volume for each coronary artery branch. CCTA: cardiac computed tomography angiography; LAD: left anterior descending artery; LCX: left circumflex artery; LMA: left main artery; RCA: right coronary artery.

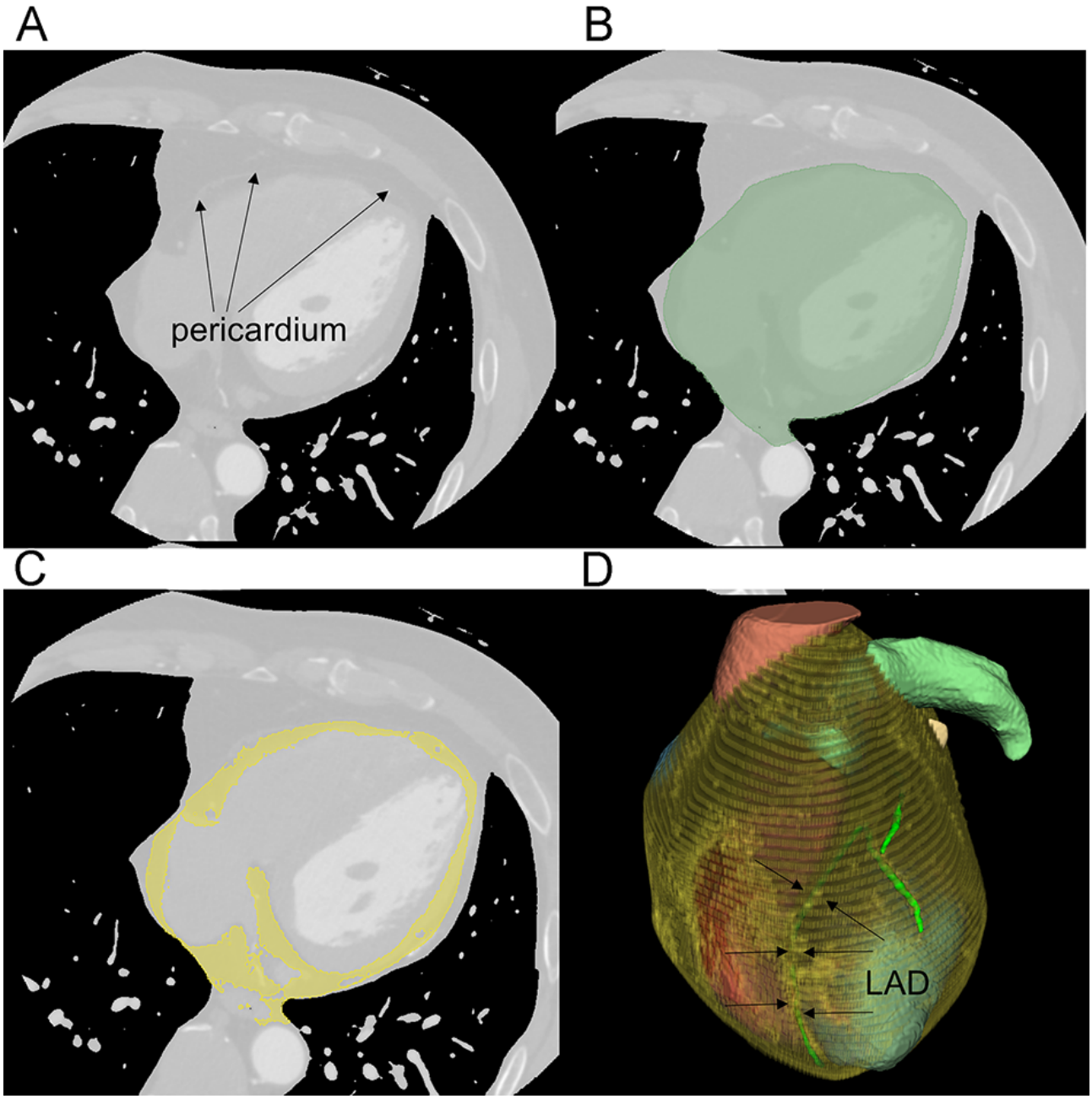


Type	Agatston score	Mass	Vol
LMA	98	15	27
LAD	14	3	19
LCX	95	16	50
RCA	107	14	47
Total	314	48	143

Third, to visualize the depth of coronary artery travel, we modeled EAT to assess how deeply the coronary arteries are embedded within it. EAT measurements were performed using a semiautomated procedure (Figure 5A). Expert analysts segmented the pericardium using 3D Slicer v5.2.2 [20] in a sequential, slice-by-slice manner. EAT was measured from the bifurcation of the pulmonary trunk to the apex of the heart. Manual pericardial contours were drawn on every 5 - 10 slices (Figure 5B), followed by interpolation and corrections where necessary. Contiguous voxels with attenuation values between −190 and −30 Hounsfield units were used to define and quantify EAT (Figure 5C) [21]. A fusion display combining EAT and coronary artery models was used to present depth information, visualized through variations in coronary artery fluoroscopy (Figure 5D).

XSL•FO
RenderX

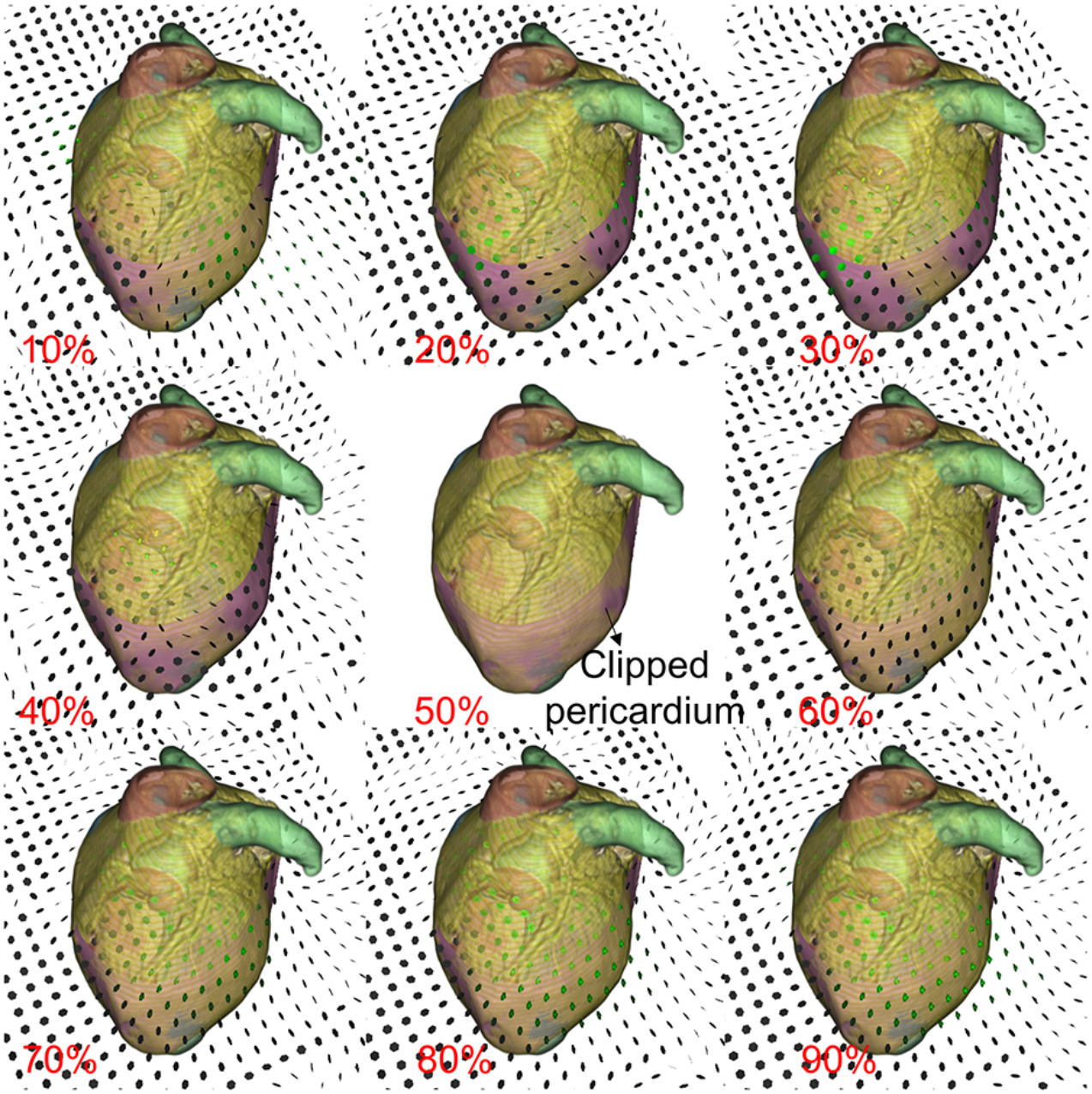
Figure 5. Proposed epicardial adipose tissue segmentation method. (A) The pericardium appears as a thin white line in the coronary computed tomography angiography image. (B) The region encompassing the pericardium is first segmented by manual labeling (green region). (C) The threshold method is used to segment the adipose tissue within the pericardial mask (yellow region). (D) The volume rendering result of the segmented epicardial adipose tissue. LAD: left anterior descending artery.



Finally, when adhesions exist between the pericardium and the heart, the motion of the 2 structures tends to be synchronized. In contrast, the absence of adhesions results in noticeable differences in their relative motion. To observe this, we dynamically reconstructed both the pericardium and the outer cardiac tissue. Nine cardiac phases (10% - 90%) were imported and registered to the selected 50% phase. This registration used the symmetric diffeomorphic algorithm proposed by Avants et al [22], generating a sequence of transformations represented as a time-varying 3D displacement field. This sequence was then applied to deform the pericardium and EAT (Figure 6). The pericardium is cut open to help observe the inner EAT structures. The corresponding deformation field of the cutting plane is visualized using arrows, where each arrow represents the displacement vector, indicating the direction and magnitude of displacement originating from its starting point on the plane.

XSL•FO
RenderX

Figure 6. Relative motion of the pericardium and epicardial adipose tissue.



Evaluation of Outcomes

Evaluation of Naked-Eye Holographic Display

The outcome parameters were assessed qualitatively. Thirteen cardiac surgery clinicians evaluated various aspects of the holographic display, including display quality, realism of 3D spatial positioning, identification of calcified plaques, perception of coronary artery alignment depth, realism of dynamic visualization, and detection of pericardial adhesions. Evaluations were conducted using a Likert scale, based on preoperative and intraoperative data from 14 patients scheduled for CABG. In addition, the researchers evaluated participants' attitudes toward the system's usefulness in preoperative planning and clinical education, as well as their willingness to adopt the system in practice. A score of 5 represented the most positive evaluation, while a score of 1 indicated the least favorable response (see Questionnaire 1 in Multimedia Appendix 1).

Evaluation of Pericardial Adhesions

Pericardial adhesions were classified as either 0 or 1, where 0 indicated no adhesions and 1 indicated significant adhesions requiring the removal of a substantial portion of the pericardium. The intraoperative score was derived from the patient's operative report. Adhesion severity in the holograms was visually assessed by an experienced cardiovascular surgeon trained in interpreting holographic representations of pericardial adhesions, including the significance of the color schemes. The surgeon was blinded to all patient information. To assess intrarater reliability, the same evaluator performed a second blinded evaluation of the same hologram samples 2 months later.

XSL•FO
RenderX

Statistical Analysis

The Spearman rank correlation test was conducted using SPSS version 25 for Windows (SPSS Inc) to evaluate the correlation between hologram-based adhesion scores and intraoperative adhesion scores. Statistical analysis of the holographic display evaluation scores was performed using Microsoft Excel (version 2021 MSO). All statistical analyses were descriptive. Continuous variables were summarized using the mean, standard deviation, minimum, median, and maximum values, while categorical variables were reported as counts and percentages.

Ethical Considerations

Ethics approval was granted by the Ethics Committee of the General Hospital of the Chinese People's Liberation Army (approval number: S2024-580). This study was conducted in accordance with the Declaration of Helsinki. Informed consent was obtained from all individual participants included in the study. No compensation was provided to the participants of the study.

Results

All 13 cardiac surgery professionals who tested the hologram system were male. The group consisted of 6 attending physicians and 7 senior doctors, with ages ranging from 34 to 54 years (median: 37 years).

When viewing the holograms from various angles (see Figure 7A-D; Video 1 in Multimedia Appendix 2), all participants—regardless of their level of expertise—agreed that the system offered a realistic visualization and allowed for accurate identification of the major coronary artery branches, the locations of severe stenosis, and calcified plaques. In addition, by zooming and rotating the model, users could clearly view the spatial relationships among the heart, coronary arteries, and internal mammary artery within the thoracic cavity (median rating: 5/5, Table 1). However, 2 experts assigned scores of 2 and 3, respectively, for the identification of coronary stenosis and calcified plaques. They expressed concern that CCTA data may not reliably discriminate coronary stenosis and noted that intravascular contrast enhancement could impact plaque identification, potentially leading to inaccurate results. To assess interrater reliability, Fleiss κ coefficients were calculated for each evaluation item. The results indicated substantial to almost perfect agreement among evaluators across all assessment criteria (κ ranging from 0.68 to 0.85). The highest agreement was observed for comparisons with traditional 2D displays (κ=0.85) and dynamic display fidelity (κ=0.82), reflecting strong consensus regarding the system's superiority over conventional visualization methods. While all criteria demonstrated substantial agreement, coronary calcified plaque visualization received the relatively lowest κ score (κ=0.68), suggesting some variability in expert perception of this feature. Overall, the high κ values confirm the reliability of the evaluation results and strengthen the validity of the positive assessments across all measured dimensions.

XSL•FO
RenderX

Figure 7. Typical scenarios on a holographic viewing system. (A) Dynamic 3D coronary artery scene segmented from computed tomography data, medium and heavily calcified plaques are marked in red. (B) A 4D chest scene including the heart, coronary artery, internal mammary artery, ribs, vertebrae, sternum, and diaphragm. (C) Scenes demonstrating coronary depth. (D) Dynamic pericardium and cardiac motion scene.

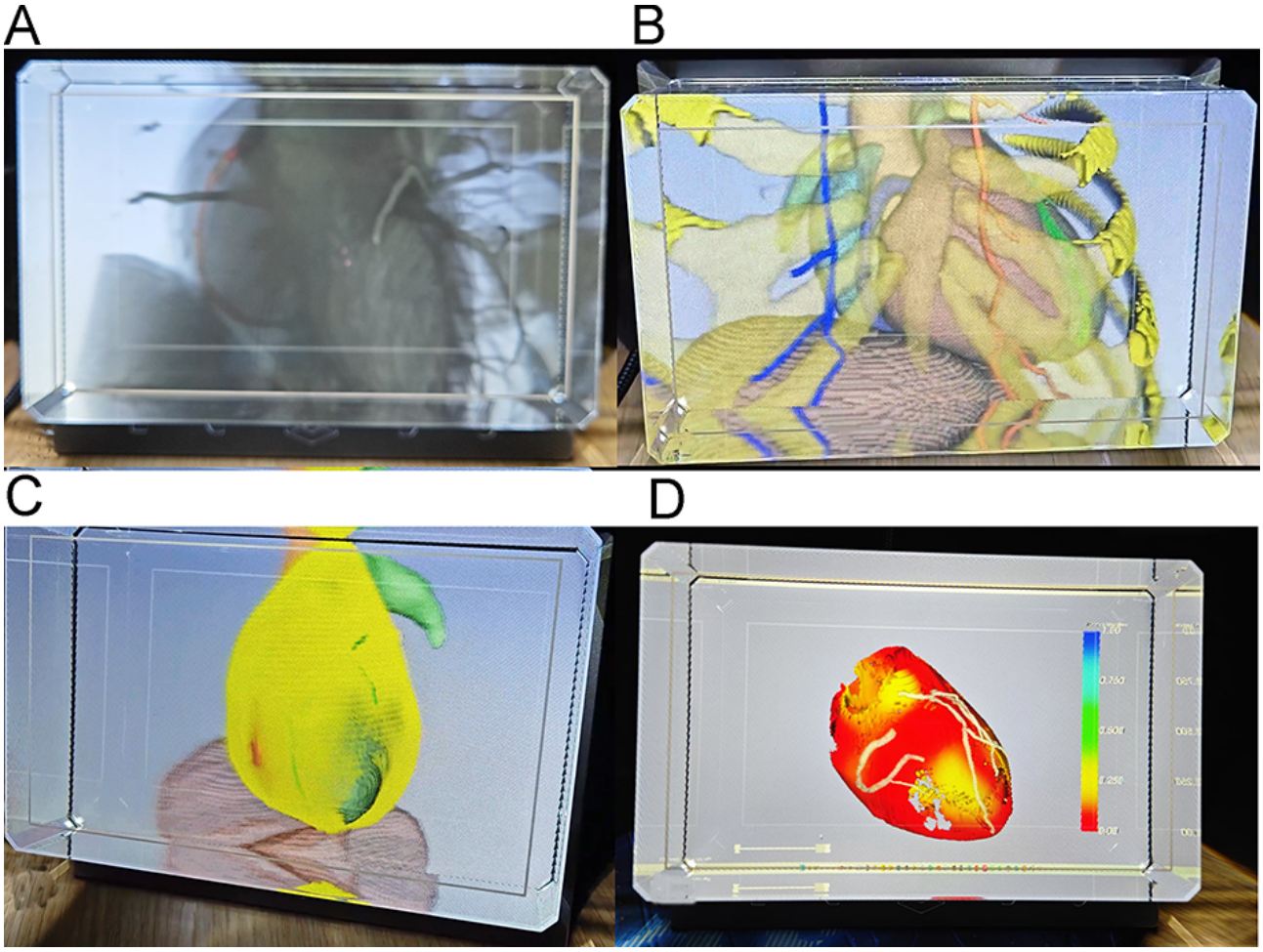


Table . Holographic experience reviews and attitude toward (future) use of holographic imaging system.

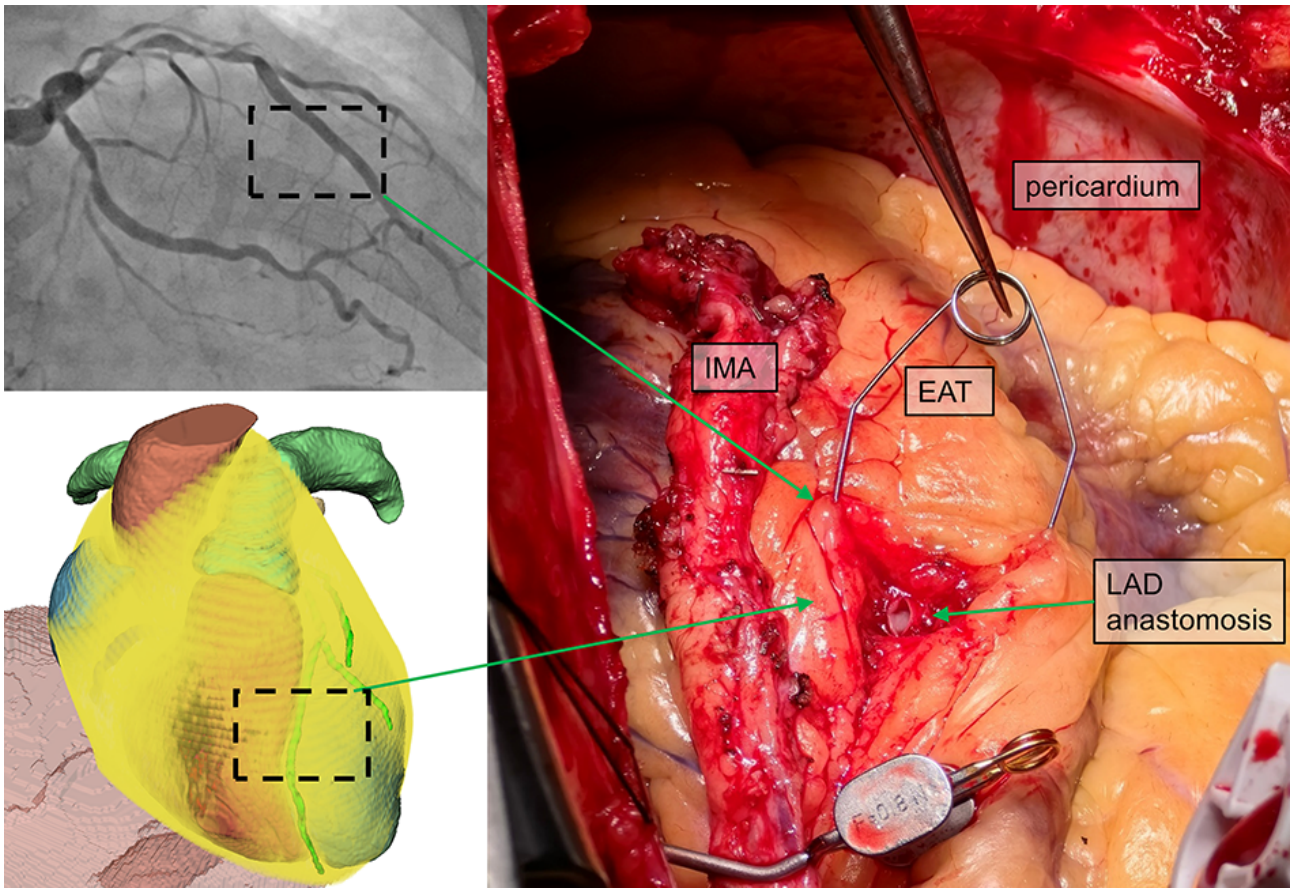
Assessment items	Mean (SD)	Median rating (1–5)	Interrater agreement (κ)
Spatial perception	4.78 (0.4)	5	0.79
Coronary calcified plaque	4.28 (1.0)	5	0.68
Coronary depth	4.71 (0.5)	5	0.76
Dynamic display fidelity	4.78 (0.4)	5	0.82
Pericardial adhesions	4.64 (0.6)	5	0.73
Basic tools (rotate, zoom)	4.71 (0.5)	5	0.79
Compared to traditional 2D screens	4.85 (0.4)	5	0.85
Overall evaluation	4.71 (0.5)	5	0.74
Helpful for preoperative planning	4.57 (0.5)	5	0.71
Beneficial for clinical teaching	4.78 (0.4)	5	0.81
Useful for patient education	4.64 (0.5)	5	0.72

Anterior descending superficial myocardial bridges were observed in 2 of the 14 CABG patients based on CTA images. Evaluators perceived the depth trajectory of the coronary arteries within the EAT by noting a progressive transition in the holograms, from a blurred proximal segment to a clearer mid-to-distal segment. This trend corresponded with intraoperative findings, where anastomotic selection could not avoid the bridged region due to limitations in internal mammary artery length (Figure 8). Depth perception scores for the coronary arteries were consistently rated as “agree” or “strongly agree,” with a median score of 5/5. As demonstrated in patient number 9, the anterior descending branch anastomosis proposed before surgery was located deep in the EAT, with the anterior descending branch alignment appearing straight in preoperative

XSL•FO
RenderX

coronary angiography, implying potential myocardial bridges. The hologram produced results consistent with both the intraoperative situation and the diagnostic results of preoperative imaging.

Figure 8. Figure 8. The intraoperative situation of patient number 9. EAT: epicardial adipose tissue; IMA: internal mammary artery; LAD: left anterior descending artery.

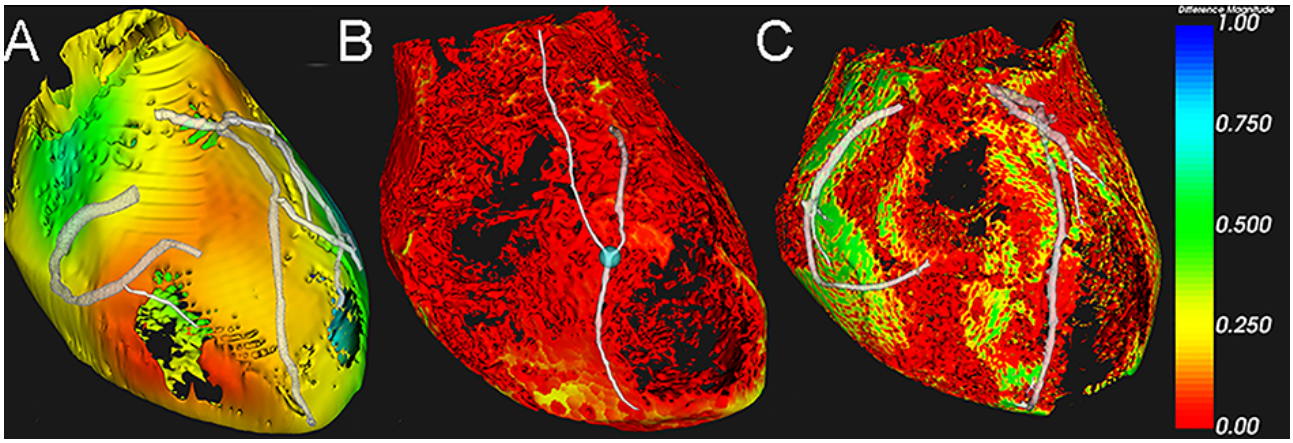


Conventionally, images are viewed on a 2D screen following 3D reconstruction of the heart and coronary arteries using 3D Slicer software. To compare approaches, we asked evaluators to respond to assessment item 7 “Compared to traditional 2D screens”: in obtaining the information needed for preoperative evaluation, it provides more intuitive and comprehensive insights compared to observing static 3D cardiovascular CT images on a 2D screen. The mean score was 4.85 (SD 0.4), with 5 representing the most positive evaluation and 1 the least. Cardiac surgeons who participated in the evaluation agreed that the visualization method used in this study provided superior insights compared with traditional techniques. Key advantages included enhanced depth perception and more detailed cardiac modeling, particularly in representing coronary artery travel depth and pericardial adhesions.

The hologram-based adhesion score showed a strong correlation with the intraoperative adhesion score (r=0.786; P<.001; 95% CI 0.53 - 0.92), confirming the validity of the data. All participants acknowledged the effective visualization of pericardial adhesions (median score: 5/5; Figure 9), and noted that the holographic display provided a more intuitive and 3D representation than traditional ultrasound images. For example, patients without prior cardiac surgery showed clear relative motion between pericardium and epicardial adipose tissue (Figure 9A), while those with previous operations demonstrated restricted motion, indicating adhesions (Figure 9B). Notably, one case showed discordance between operative findings and holographic assessment (Figure 9C). The dynamic visualization of pericardial motion and adhesion patterns can be further observed in the supplementary video demonstration (Video 2 in Multimedia Appendix 3). The hologram-based adhesion score showed a strong correlation with intraoperative findings. Among the 20 cases evaluated, 14 cases with hologram score 0 corresponded to intraoperative score 0, while 6 cases with hologram score 1 matched intraoperative score 1, demonstrating excellent agreement (r=0.786; P<.001; 95% CI 0.53-0.92). A second blinded evaluation was conducted two months later to assess repeatability. The intrarater reliability, measured by the κ coefficient, was 0.85, indicating strong consistency in the evaluation results.

XSL•FO
RenderX

Figure 9. Visualization images of pericardial adhesions. (A) Patient number 6, scheduled for first-time CABG, exhibits significant relative motion between the pericardium and EAT, suggesting the absence of pericardial adhesions. (B) Patient number 7, who underwent left ventricular outflow tract unblocking, mitral valve replacement, and CABG one year ago, demonstrates poor relative motion between the pericardium and EAT, indicating the presence of pericardial adhesions, consistent with intraoperative findings. (C) Patient number 2, who had an aortic valve replacement one year prior, shows extensive pericardial adhesions in the operative report, but the hologram pericardial adhesion score is rated as 0, suggesting no adhesions. CABG: coronary artery bypass graft; EAT: epicardial adipose tissue.



Discussion

Principal Findings

Holograms have demonstrated the ability to provide realistic depth perception, enhancing the intuitive understanding of a patient's 3D anatomy. However, the complexity of current hologram production methods has limited the widespread adoption of this technology in routine clinical practice. In addition, existing head-mounted display devices are often uncomfortable and can hinder effective communication among health care team members. This study presents an approach to use real patient volumetric data—specifically 4D-CCTA—to generate high-quality, naked-eye–viewable, 3D, color dynamic holograms relevant to CABG surgery. This visualization tool eliminates the need for clinicians to rely on personal spatial imagination to synthesize relevant anatomical information. Instead, it offers a more intuitive, comprehensive, and vivid representation of the data required for preoperative CABG planning. The holograms can be simultaneously viewed and discussed by multiple surgeons or with patients, without the need for headgear. Unlike most existing cardiac and coronary models, this study introduces a specialized modeling framework tailored for CABG preoperative planning. It includes a dynamic representation of the pericardium, heart, and coronary arteries, all derived from the patient's 4D-CCTA data. Presenting volumetric patient data as dynamic, multicolor, and internet-based holograms represents a potential advancement in cardiac medical imaging. This study outlines the fabrication process, structural framework, and preliminary feasibility assessment.

The preprocessing time for each patient dataset requires approximately 15 min, making it clinically feasible for use in preoperative planning. However, coronary artery segmentation remains the most time-consuming and technically challenging component—especially in patients with advanced CAD. In cases of significant vessel occlusion or calcification, which are common among CABG candidates, automated segmentation methods often require manual refinement to ensure clinical accuracy. This limitation is well recognized in the field and represents a key area for future algorithmic development.

In this study, the EAT, pericardium, and coronary arteries were segmented to characterize their relative motion and structural features in order to extract clinically relevant information regarding coronary artery depth and pericardial adhesions. Pericardial adhesions increase both the difficulty and risk of minimally invasive or median sternotomy procedures and must be identified preoperatively. Currently, pericardial adhesions are typically evaluated using ultrasonography, which detects motion discrepancies between the pericardium and outer myocardium, or CT imaging, which assesses changes in pericardial density [23]. However, thickening of the pericardium on CT does not reliably correlate with adhesions, and although ultrasonography can reveal relative motion, it lacks 3D detail and fails to provide a comprehensive view of adhesion location relative to the coronary arteries. Another significant challenge is assessing the depth of coronary artery travel within the EAT. This is clinically important because intraoperative identification of deeply embedded coronary arteries can be difficult. Accurately obtaining this anatomical information preoperatively can significantly inform the selection of an anastomotic site during surgery. CCTA is currently the preferred modality for evaluating EAT [24]. Traditionally, EAT has been studied in terms of its volume or composition to explore its relationship with the progression of CAD [25]; however, these approaches offer limited insight into spatial relationships relevant for surgical planning. In this study, we dynamically fused models of epicardial fat and coronary arteries to represent their positional relationship and visualize the depth trends of the coronary arteries. Combined with a holographic display, this approach achieved the intended visualization effect. The accuracy of coronary artery depth representation was supported by comparison with intraoperative findings. Furthermore, the strong correlation between preoperative holographic assessments of pericardial adhesions and intraoperative scores provides preliminary validation of the system's clinical reliability.

XSL•FO
RenderX

Comparison With Previous Work

Several research teams have explored the application of holographic imaging technology in the medical field. Our work shares some commonalities with these studies but also presents significant innovations.

Tanwani et al [26] developed a head-mounted holographic needle guidance system for enhanced ultrasound-guided neuraxial anesthesia. They used the Microsoft HoloLens mixed reality headset to project a hologram of the ideal needle path, helping operators replicate the correct needle angulation. While this work demonstrated the value of holographic technology in surgical navigation, its primary focus was on visualizing a single surgical path, whereas our system provides a dynamic holographic representation of the complete cardiac anatomy, including the complex spatial relationships between coronary arteries and surrounding tissues. Liu et al [27] demonstrated in a randomized controlled trial how 3D holograms with mixed reality techniques can improve medical professionals' understanding of pulmonary lesions caused by COVID-19. Their study showed that holographic visualization significantly enhanced physicians' ability to identify lung lesions compared to traditional 2D CT, especially for medical students and nonspecialist doctors. This aligns with our findings that holographic visualization can bridge gaps in specialist knowledge, but our work further extends this concept by transforming static anatomical structures into dynamic visualizations that capture anatomical changes throughout the cardiac cycle. Parekh et al [28] developed a method for depth estimation and visualization of dermatological lesions, using neural networks and explainable AI for lesion classification, and holographic projection to display lesion depth. Their work focused on generating 3D holograms from 2D images, while our approach directly uses 4D CT data to capture the dynamic nature of the heart, providing surgeons with more comprehensive anatomical information.

Compared with these previous works, our research demonstrates innovation in several key areas: (1) dynamic visualization: our system not only displays static anatomical structures but captures the dynamic changes of coronary arteries throughout the cardiac cycle, which is crucial for CABG surgical planning. (2) Naked-eye holographic technology: unlike solutions requiring specialized headsets, our system allows multiple clinicians to simultaneously view and interact with the same anatomical structure, facilitating collaborative discussion among the surgical team. (3) Enhanced depth perception: we specifically focus on the depth variations of coronary arteries within epicardial fat tissue, critical information that traditional imaging methods struggle to adequately display and which has significant value for CABG surgical planning. These innovations make our holographic system a powerful tool not only for assisting surgeons in CABG surgical planning but also as a bridge for doctor-patient communication, helping patients and their families better understand the necessity and potential risks of surgery.

Limitations

First, our initial assessments were subjective and qualitative in nature and, therefore, not amenable to rigorous statistical analysis. Although clinician feedback was generally positive, we did not use validated quantitative metrics to compare the utility of the holographic visualization with conventional imaging techniques. Future studies should incorporate standardized assessment tools and objective performance measures to quantitatively evaluate the impact of holographic visualization on surgical planning and clinical outcomes.

Second, we did not perform quantitative analyses of calcified plaques, coronary artery travel depth, or pericardial–cardiac motion differentials. While we strived to maintain data fidelity throughout the visualization pipeline, it is important to recognize that the segmentation process inherently introduces variability and potential distortion. This may be influenced by factors such as the choice of segmentation algorithms, parameter settings, and manual corrections. Although experienced radiologists reviewed all segmentations to ensure clinical accuracy, this oversight does not entirely eliminate the risk of error. These limitations may have affected the accuracy of the spatial relationships depicted in our holograms.

Third, we did not quantify segmentation error or validate the geometric accuracy of our models against the original source data, which represents a significant limitation of the current methodology. Future work should include rigorous validation of segmentation accuracy and quantification of model fidelity relative to the source CT data to better understand clinical reliability.

Fourth, due to the limitations of current CT imaging, coronary stenosis still requires coronary angiography as the clinical "gold standard." While our approach integrates information from both CCTA and angiography, it does not yet match the diagnostic accuracy of invasive angiography for stenosis assessment. Future iterations could address this limitation by incorporating computational fluid dynamics to better evaluate the functional severity of stenosis.

Fifth, this study represents only a preliminary feasibility assessment of holographic visualization. We did not conduct quantitative or comparative studies of procedures performed using conventional imaging alone versus those supported by holographic assistance. Such comparative studies are essential to determine the practical utility, effectiveness, and broader applicability of holographic imaging in real-world clinical settings.

Future Perspectives

The potential impact of holographic technology on medical imaging is substantial, particularly in the context of minimally invasive surgery. These procedures involve small incisions and a limited field of view, making a clear understanding of patient-specific spatial anatomy crucial. In future studies, we plan to further investigate the use of holographic imaging systems for preoperative planning in minimally invasive cardiac surgery. This includes integrating internet-based tools and hemodynamic analyses and exploring the possibility of overlaying holograms onto the real intraoperative environment with internet-based manipulation for real-time surgical guidance.

XSL•FO
RenderX

Conclusions

This study presents a structural framework for a visualization tool specifically designed for preoperative planning of CABG procedures. By leveraging patient-derived volumetric data, the system generates potentially clinically relevant, dynamic holograms that provide depth perception, detailed coronary stenosis and calcification information, alignment depth data, and 4D spatial insights. Clinician feedback was positive, supporting the tool's potential utility for preoperative planning. The system also shows promise for applications in medical education, including surgical demonstrations for interns and preoperative education for patients. While further development and validation are needed, this work represents an important step toward enhancing visualization capabilities in cardiac surgical planning.

Authors' Contributions

SW and TR contributed equally to this work, both as the first authors. LZ is the co-corresponding author and can be reached via email at ZZhanggLi@hotmail.com or by phone at +86 13910686306.

Conflicts of Interest

None declared.

Multimedia Appendix 1
Holographic experience reviews.
[DOC File, 47 KB - medinform_v13i1e72237_app1.doc]

Multimedia Appendix 2
Dynamic display of typical application scenarios of the holographic viewing system. Contains 4D chest scenes of the heart, coronary arteries, internal mammary arteries, aortic valves, ribs, spine, sternum, and diaphragm.
[MP4 File, 194255 KB - medinform_v13i1e72237_app2.mp4]

Multimedia Appendix 3
Dynamic demonstration of typical different pericardial adhesions.
[MP4 File, 40975 KB - medinform_v13i1e72237_app3.mp4]

References

1. GBD 2021 Forecasting Collaborators. Burden of disease scenarios for 204 countries and territories, 2022-2050: a forecasting analysis for the Global Burden of Disease Study 2021. Lancet 2024 May 18;403(10440):2204-2256. [doi: 10.1016/S0140-6736(24)00685-8] [Medline: 38762325]
2. Baibhav B, Gedela M, Moulton M, et al. Role of invasive functional assessment in surgical revascularization of coronary artery disease. Circulation 2018 Apr 17;137(16):1731-1739. [doi: 10.1161/CIRCULATIONAHA.117.031182] [Medline: 29661951]
3. Lawton JS, Tamis-Holland JE, Bangalore S, et al. 2021 ACC/AHA/SCAI guideline for coronary artery revascularization: executive summary: a report of the American College of Cardiology/American Heart Association Joint Committee on Clinical Practice Guidelines. Circulation 2022 Jan 18;145(3). [doi: 10.1161/CIR.0000000000001039] [Medline: 34895951]
4. Niederer SA, Lumens J, Trayanova NA. Computational models in cardiology. Nat Rev Cardiol 2019 Feb;16(2):100-111. [doi: 10.1038/s41569-018-0104-y] [Medline: 30361497]
5. Corral-Acero J, Margara F, Marciniak M, et al. The "Digital Twin" to enable the vision of precision cardiology. Eur Heart J 2020 Dec 21;41(48):4556-4564. [doi: 10.1093/eurheartj/ehaa159] [Medline: 32128588]
6. Bindschadler M, Buddhe S, Ferguson MR, Jones T, Friedman SD, Otto RK. HEARTBEAT4D: an open-source toolbox for turning 4D cardiac CT into VR/AR. J Digit Imaging 2022 Dec;35(6):1759-1767. [doi: 10.1007/s10278-022-00659-y] [Medline: 35614275]
7. Tsai TY, Kageyama S, He X, et al. Feasibility and accuracy of real-time 3D-holographic graft length measurements. Eur Heart J Digit Health 2024 Jan;5(1):101-104. [doi: 10.1093/ehjdh/ztad071] [Medline: 38264694]
8. Sadeghi AH, Taverne Y, Bogers A, Mahtab EAF. Immersive virtual reality surgical planning of minimally invasive coronary artery bypass for Kawasaki disease. Eur Heart J 2020 Sep 7;41(34):3279-3279. [doi: 10.1093/eurheartj/ehaa518] [Medline: 32637982]
9. Blinder D, Ahar A, Bettens S, et al. Signal processing challenges for digital holographic video display systems. Signal Processing: Image Communication 2019 Feb;70:114-130. [doi: 10.1016/j.image.2018.09.014]
10. Bruckheimer E, Rotschild C, Dagan T, et al. Computer-generated real-time digital holography: first time use in clinical medical imaging. Eur Heart J Cardiovasc Imaging 2016 Aug;17(8):845-849. [doi: 10.1093/ehjci/jew087] [Medline: 27283456]

XSL•FO
RenderX

11. Jung C, Wolff G, Wernly B, et al. Virtual and augmented reality in cardiovascular care: state-of-the-art and future perspectives. JACC Cardiovasc Imaging 2022 Mar;15(3):519-532. [doi: 10.1016/j.jcmg.2021.08.017] [Medline: 34656478]
12. Bruckheimer E, Rotschild C. Holography for imaging in structural heart disease. EuroIntervention 2016 May 17;12 Suppl X(X):X81-X84. [doi: 10.4244/EIJV12SXA15] [Medline: 27174119]
13. Deliver the best 3D experience. Looking Glass Factory. URL: https://lookingglassfactory.com/ [accessed 2025-04-18]
14. Cardoso MJ, Li W, Brown R, et al. MONAI: an open-source framework for deep learning in healthcare. arXiv. Preprint posted online on Nov 4, 2022. [doi: 10.48550/arXiv.2211.02701]
15. Kong F, Shadden SC. Learning whole heart mesh generation from patient images for computational simulations. IEEE Trans Med Imaging 2023 Feb;42(2):533-545. [doi: 10.1109/TMI.2022.3219284] [Medline: 36327186]
16. Pak DH, Liu M, Kim T, et al. Patient-specific heart geometry modeling for solid biomechanics using deep learning. IEEE Trans Med Imaging 2024 Jan;43(1):203-215. [doi: 10.1109/TMI.2023.3294128] [Medline: 37432807]
17. Updegrove A, Wilson NM, Merkow J, Lan H, Marsden AL, Shadden SC. SimVascular: an open source pipeline for cardiovascular simulation. Ann Biomed Eng 2017 Mar;45(3):525-541. [doi: 10.1007/s10439-016-1762-8] [Medline: 27933407]
18. Agatston AS, Janowitz WR, Hildner FJ, Zusmer NR, Viamonte M, Detrano R. Quantification of coronary artery calcium using ultrafast computed tomography. J Am Coll Cardiol 1990 Mar 15;15(4):827-832. [doi: 10.1016/0735-1097(90)90282-t] [Medline: 2407762]
19. Fiz F, Morbelli S, Piccardo A, et al. 18F-NaF uptake by atherosclerotic plaque on PET/CT imaging: Inverse correlation between calcification density and mineral metabolic activity. J Nucl Med 2015 Jul;56(7):1019-1023. [doi: 10.2967/jnumed.115.154229] [Medline: 25952737]
20. Fedorov A, Beichel R, Kalpathy-Cramer J, et al. 3D Slicer as an image computing platform for the Quantitative Imaging Network. Magn Reson Imaging 2012 Nov;30(9):1323-1341. [doi: 10.1016/j.mri.2012.05.001] [Medline: 22770690]
21. Nerlekar N, Baey YW, Brown AJ, et al. Poor correlation, reproducibility, and agreement between volumetric versus linear epicardial adipose tissue measurement: a 3D computed tomography versus 2D echocardiography comparison. JACC Cardiovasc Imaging 2018 Jul;11(7):1035-1036. [doi: 10.1016/j.jcmg.2017.10.019] [Medline: 29361482]
22. Avants BB, Tustison NJ, Song G, Cook PA, Klein A, Gee JC. A reproducible evaluation of ANTs similarity metric performance in brain image registration. Neuroimage 2011 Feb 1;54(3):2033-2044. [doi: 10.1016/j.neuroimage.2010.09.025] [Medline: 20851191]
23. Lin J, Li M, Huang Y, et al. Evaluation of pericardial thickening and adhesion using high-frequency ultrasound. J Am Soc Echocardiogr 2023 Aug;36(8):841-848. [doi: 10.1016/j.echo.2023.03.010] [Medline: 37019343]
24. Guglielmo M, Lin A, Dey D, et al. Epicardial fat and coronary artery disease: role of cardiac imaging. Atherosclerosis 2021 Mar;321:30-38. [doi: 10.1016/j.atherosclerosis.2021.02.008] [Medline: 33636676]
25. Iacobellis G. Epicardial adipose tissue in contemporary cardiology. Nat Rev Cardiol 2022 Sep;19(9):593-606. [doi: 10.1038/s41569-022-00679-9] [Medline: 35296869]
26. Tanwani J, Alam F, Matava C, et al. Development of a head-mounted holographic needle guidance system for enhanced ultrasound-guided neuraxial anesthesia: system development and observational evaluation. JMIR Form Res 2022 Jun 23;6(6):e36931. [doi: 10.2196/36931] [Medline: 35737430]
27. Liu S, Xie M, Zhang Z, et al. A 3D hologram with mixed reality techniques to improve understanding of pulmonary lesions caused by COVID-19: randomized controlled trial. J Med Internet Res 2021 Sep 10;23(9):e24081. [doi: 10.2196/24081] [Medline: 34061760]
28. Parekh P, Oyeleke R, Vishwanath T. The depth estimation and visualization of dermatological lesions: development and usability study. JMIR Dermatol 2024 Dec 18;7(PMID):e59839. [doi: 10.2196/59839] [Medline: 39693616]

Abbreviations

4D-CCTA: 4D cardiac computed tomography angiography
CABG: coronary artery bypass grafting
CAD: coronary artery disease
CCTA: cardiac computed tomography angiography
CT: computed tomography
CTA: computed tomography angiography
EAT: epicardial adipose tissue
MONAI: Medical Open Network for Artificial Intelligence
MRI: magnetic resonance imaging
VR: virtual reality

XSL•FO
RenderX

Edited by A Coristine; submitted 06.02.25; peer-reviewed by M Stanuch, O Wieben, R Motta; revised version received 26.05.25; accepted 27.05.25; published 30.09.25.

Please cite as:
Wang S, Ren T, Cheng N, Zhang L, Wang R
Innovative Integration of 4D Cardiovascular Reconstruction and Hologram: Framework Development of a New Visualization Tool for Coronary Artery Bypass Grafting Planning
JMIR Med Inform 2025;13:e72237
URL: https://medinform.jmir.org/2025/1/e72237
doi:10.2196/72237

© Shuo Wang, Tong Ren, Nan Cheng, Li Zhang, Rong Wang. Originally published in JMIR Medical Informatics (https://medinform.jmir.org), 30.9.2025. This is an open-access article distributed under the terms of the Creative Commons Attribution License (https://creativecommons.org/licenses/by/4.0/), which permits unrestricted use, distribution, and reproduction in any medium, provided the original work, first published in JMIR Medical Informatics, is properly cited. The complete bibliographic information, a link to the original publication on https://medinform.jmir.org/, as well as this copyright and license information must be included.

XSL•FO
RenderX

Assessment of a Digital Platform for Routine Outcome Monitoring in Psychotherapy: Usability Study and Thematic Analysis

Mattia Vincenzo Olive[1], PhD; Antonino La Tona[2], PhD; Gianluca Lo Coco[3], PhD; Angelo Compare[2], PhD; Joseph Antony Cafazzo[4,5], PhD; Cristina Masella[1], MS

[1]Department of Management, Economics and Industrial Engineering, Politecnico di Milano, Via Raffaele Lambruschini 4B, Milano, Italy

[2]Department of Human and Social Sciences, University of Bergamo, Bergamo, Italy

[3]Department of Psychology, Educational Science and Human Movement, University of Palermo, Palermo, Italy

[4]Healthcare Human Factors; Centre for Digital Therapeutics, University Health Network, Toronto, ON, Canada

[5]Institute of Health Policy, Management and Evaluation, University of Toronto, Toronto, ON, Canada

Corresponding Author:
Mattia Vincenzo Olive, PhD
Department of Management, Economics and Industrial Engineering, Politecnico di Milano, Via Raffaele Lambruschini 4B, Milano, Italy

Abstract

Background: The integration of digital tools into psychotherapy has gained increasing attention, particularly for practices such as routine outcome monitoring (ROM), which involves the regular collection of patient-reported data to inform treatment decisions. However, despite the potential benefits, the adoption of digital platforms remains limited, partly due to usability concerns and workflow misalignment.

Objective: This study aimed to assess the usability of a digital platform, Mindy, designed to support psychotherapists in implementing ROM and to explore broader challenges associated with the integration of digital tools into psychotherapeutic practice.

Methods: This study adopted a qualitative, 2-stage approach. Sixteen psychotherapists participated in semistructured interviews, which included task-based usability testing and reflective discussions. Participants interacted with Mindy by performing typical clinical tasks, such as creating patient profiles, managing session data, and sending questionnaires. The first stage of analysis used a deductive thematic approach focused on predefined platform functionalities. The second stage followed an inductive methodology to identify broader themes related to the integration of digital tools in psychotherapy.

Results: The usability assessment identified strengths in the platform's appointment scheduling, questionnaire delivery, and dashboard functionalities, which were perceived as intuitive and supportive of ROM practices. However, limitations were reported in areas such as documentation flexibility, interoperability with other systems, and control over information sharing with patients. Broader thematic analysis revealed three main challenges: (1) the tension between standardized documentation and the need for narrative and implicit information; (2) difficulties in embedding digital platforms into existing therapeutic workflows, especially for clinicians less familiar with technology; and (3) concerns about confidentiality and the potential for misinterpretation when sharing therapeutic notes with patients.

Conclusions: These findings underscore the importance of considering both technical and contextual dimensions when developing and implementing digital platforms in mental health care. Tailoring digital tools to the needs and practices of psychotherapists may improve adoption and ultimately enhance the quality of care.

(JMIR Med Inform 2025;13:e75885) doi:10.2196/75885

KEYWORDS

digital mental health; psychotherapy; routine outcome monitoring; usability; digital tools

Introduction

Digital technologies, such as electronic health records (EHRs) and digital mental health platforms (DMHPs), have become increasingly relevant in psychotherapy [1-3]. These technologies offer several benefits, such as improved documentation and legibility, enhanced information sharing and communication among providers, timely information retrieval, and increased accountability [4]. However, their implementation also presents several challenges, including issues with standardization and codification, the time burden placed on clinicians, potential negative impacts on therapeutic relationships, usability and learning curve difficulties, and privacy concerns [4]. Certain practices and approaches in psychotherapy are notably enhanced

XSL•FO
RenderX

by digital technologies, with routine outcome monitoring (ROM) being a prime example [5]. ROM has been studied and implemented under different names, including "progress monitoring" [6], "feedback-informed treatment" [7], and "outcome monitoring feedback" [8,9], "measurement-based care" [10], and "outcome feedback" [11]. ROM consists of the systematic collection and analysis of patient progress and outcome data throughout therapy sessions, using standardized self-report measures at regular intervals to provide valuable insights to optimize treatment strategies. The information derived from these measurements is typically presented in graphical form and provided to the therapist and possibly the patient to facilitate monitoring of the patient's improvement trajectory over time. Historically, implementing ROM has been hindered by challenges such as the continuous monitoring of patients and the timely delivery of feedback to therapists [5]. The adoption of digital solutions, however, has been shown to significantly mitigate these obstacles, facilitating a more efficient process [5]. Before these innovations, the collection of patient data was predominantly based on paper-based practices, which were often incomplete, lacked comprehensiveness, and were prone to memory bias [5,12]. The advent of digital technologies has enabled real-time collection of more detailed and objective patient data, allowing therapists to assess information both before and after the visit and thereby reducing reliance on patient memory [13].

The American Psychological Association (APA) has long advocated the use of ROM and feedback practices in psychological therapy [14]. A recent advisory committee appointed by APA governance further recommended the creation of comprehensive guidelines regarding the integration of outcome and process monitoring systems into therapeutic practice. These guidelines state that therapists should undertake regular evaluations of the treatment process and outcomes, integrating this evidence-based practice into clinical practice [12].

Despite substantial scientific evidence supporting the clinical benefits of ROM, its adoption remains limited in certain contexts. This hesitation can be attributed to several factors, such as the lack of tailored validation studies, insufficient technological infrastructure, and cultural resistance within clinical practice. Moreover, there is a broader challenge of translating evidence-based approaches into actionable practices in health care systems that may be underresourced or overly reliant on traditional methods [15].

This research is part of the broader OutProFeed project, which is conducting the first randomized controlled trial in Italy focused on ROM.

Within the framework of this larger initiative, the paper addresses 2 specific objectives. The first is to assess the usability of Mindy, an integrated EHR-DMHP platform, designed to support ROM implementation. This usability assessment aims to evaluate how effectively the platform aligns with clinicians' workflows [16,17].

The second objective stems from a broader reflection on the current state of research on digital platforms in mental health. While the effectiveness of these tools for data collection and patient monitoring is widely addressed in the literature [18], often focusing on their technical functionalities, advantages, disadvantages, and impacts on clinical outcomes [18], there is limited evidence on how psychotherapists integrate such platforms into their daily routines [2,19,20]. As a result, adopting a holistic and integrated approach to the design and implementation of digital tools in mental health appears increasingly important. Through the specific case of Mindy's use of ROM, this research aims to contribute to this underexplored area by analyzing the challenges involved in integrating digital platforms into psychotherapeutic practice.

Methods

Overview

This study used a single dataset but followed a 2-pronged data analysis approach to address distinct objectives. The research began by assessing the usability [16,17] of the Mindy digital platform, focusing on its features and collecting feedback from psychotherapists. A deductive thematic analysis [21-23] was applied to organize the data into predefined categories aligned with the platform's features, such as appointment scheduling, patient profile management, and session data entry. The findings were synthesized into actionable recommendations for improving the platform, which were communicated to Mindy's technical and development teams during 2 feedback stages: after a preliminary usability testing phase and following the main evaluation.

However, during this usability analysis, recurring patterns emerged that extended beyond platform features, pointing to broader challenges in integrating digital tools into psychotherapeutic workflows. Recognizing the significance of these themes, the research team conducted a second round of data analysis using an inductive approach [21,23,24]. This phase revisited the data without predefined categories, identifying emerging themes, grouping them into broader concepts, and ultimately into aggregate dimensions. This 2-stage analysis allowed the study to address both the usability of the platform and the deeper, systemic challenges faced by psychotherapists when incorporating digital tools into their daily practice.

The following sections provide a detailed description of the Mindy platform's features, outline the data collection process, and explain the 2-stage data analysis approach.

Key Features of the Platform Under Assessment

Mindy is the digital platform under assessment, and its functionalities include a calendar for scheduling appointments, a document management system for tasks such as handling informed consent forms, session reports, and patient management. It also features an integrated system for administering questionnaires, which provides automatic and standardized scoring of copyright-free measures. In addition, the platform includes a dashboard for monitoring patient progress and the therapeutic alliance, based on patient responses to predefined, validated questionnaires. An overview of the features is provided in Table 1, while screenshots of the main interface for these features are available in Multimedia Appendix 1.

XSL•FO
RenderX

Table . Main features of the "Mindy" platform.

Feature	Description
Agenda and appointment booking	The platform provides therapists with access to a calendar in monthly or weekly views, enabling the scheduling of patient appointments in both in-person and remote modes. Upon booking, an email reminder is automatically sent to both the patient and therapist. For remote appointments, the system also sends the patient a link to the virtual meeting room.
Patient profile creation	Therapists can use the platform to register new patients, collect their personal information, and create a dedicated folder for each individual. Following registration, an informed consent form is automatically emailed to the patient, who must download, sign, and return it electronically or in paper format.
Management of session data with the patient	The platform includes a section for recording details of patient visits, with fields available for annotations and attachments (free-text notes); mandatory fields (eg, current symptoms, examination findings, and preliminary diagnosis) that must be completed to finalize the visit and generate a report; detailed data (optional fields for lifestyle recommendations, observations, or care plans); and questionnaires (predefined forms that can be automatically delivered to patients, with timing specified by the therapist and responses viewable in a dedicated section).
Report delivery to patients	The platform enables therapists to generate and send reports to patients, primarily containing information recorded in the mandatory fields
Dashboard to monitor patient progress and the therapeutic alliance	The platform includes a dashboard where therapists can track patient progress and assess the therapeutic relationship. For instance, therapists can send predefined questionnaires to patients to monitor their condition over time. The results are automatically processed by the platform and presented graphically for review.
Online session system	The platform facilitates online therapy sessions by allowing therapists to initiate video calls directly from the system. A link to the virtual meeting is automatically sent to the patient before the session begins.

Data Collection Process

The data collection process involved semistructured interviews with psychotherapists (refer to Multimedia Appendix 1 for the interview outline), conducted remotely via Microsoft Teams to ensure flexibility and allow direct observation of participants interacting with the platform.

Each session lasted 30 - 45 minutes and followed a 2-part structure. In the first part, participants were asked to complete tasks simulating typical psychotherapeutic activities, such as creating a patient profile, scheduling an appointment, filling out a session report, and sending a questionnaire. These tasks were selected to range from relatively straightforward but essential for basic platform use to more complex tasks critical for implementing ROM through the platform. This progression was designed to reflect both the importance of these activities in psychotherapeutic workflows and their potential to highlight areas where users might encounter challenges.

During these tasks, the thinking-aloud approach [25-27] was used, encouraging participants to verbalize their thoughts while navigating the platform. This approach provided insights into how participants interacted with the system and identified any usability challenges. Interviewers intervened only when participants struggled to articulate their thoughts, using prompts such as, "What are you thinking?" or "What are you trying to do?" In the second part, participants stopped screen sharing to respond to questions exploring their experiences with the platform and its potential integration into their clinical workflow. These questions sought feedback on specific features and how the platform could fit into daily practice.

To ensure familiarity, participants were given 3 days before the interview to explore the platform independently, performing activities such as creating patient profiles or scheduling appointments. Before each session, interviewers clarified that the study aimed to evaluate the platform, not the digital skills of the participants, fostering a noncritical and supportive environment. The choice of a qualitative methodology to assess usability was driven by its capacity to provide detailed insights regarding the usability of Mindy, emphasizing the reasons behind observed behaviors and the contextual factors shaping them [26,28]. Unlike quantitative approaches, which prioritize measurable metrics such as task completion times or error rates [16,17,29], the qualitative method allows for a richer analysis of user interactions [28]. This approach was considered most appropriate for the objectives of the study, as it facilitated the identification of usability issues while simultaneously offering a deeper understanding of how the platform could be integrated into psychotherapists' daily workflows.

All interviews were recorded with consent to capture verbal and nonverbal data for later analysis. Informed written consent was obtained from all participants before their inclusion in the study.

Sample

Among those who participated in the broader OutProFeed project, 16 psychotherapists were recruited for this study using a convenience sampling approach. Recruitment and interviews

XSL•FO
RenderX

were conducted from June 15, 2024, to July 20, 2024. No maximum number of interviews was predefined, as the focus was on reaching data saturation [30], ensuring that additional interviews would not yield new insights. However, a minimum number of 15 participants was established based on Food and Drug Administration (FDA) guidelines [31], which emphasize the importance of collecting sufficient data to identify usability issues and gather comprehensive feedback.

A preusability testing phase was conducted with 3 therapists to pilot the initial methodology, which involved only semistructured interviews without direct interaction with the platform. This phase highlighted the limitations of the initial approach, as the lack of hands-on interaction made it difficult to obtain detailed and actionable feedback. Consequently, the methodology was revised to include a user testing phase using the thinking-aloud method, enabling therapists to interact directly with the platform while verbalizing their thoughts.

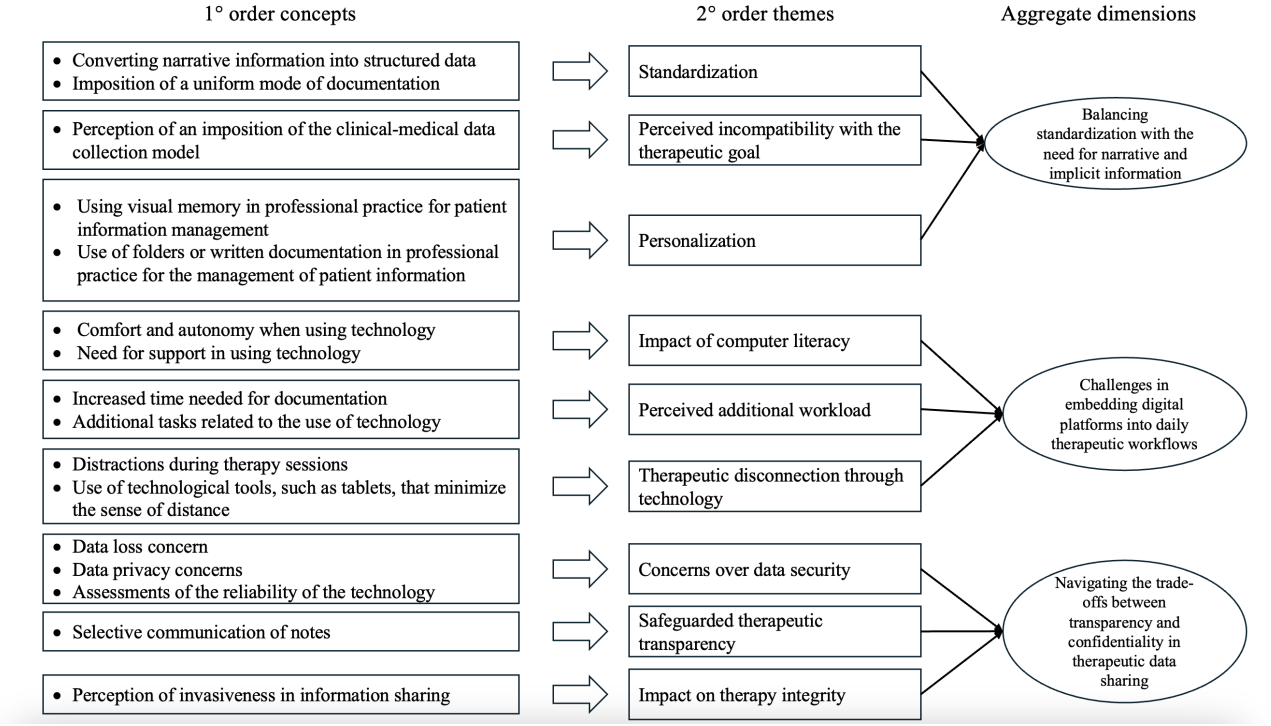
The psychotherapists who participated in the study had varying levels of professional experience, with the majority (n=8) reporting 1 - 4 years of practice, followed by those with 5 - 9 years (n=6), and a smaller group with over 10 years (n=1). The sample was predominantly female, with 15 of 16 participants (94%) identifying as women and only 1 of 16 (6%) as a man. In terms of specialization, most participants practiced cognitive behavioral therapy (n=8), while others specialized in transactional analysis (n=4) and integrated approaches (n=4). This distribution reflects a diverse sample in terms of experience and therapeutic orientation, providing a well-rounded perspective for the study.

Two-Round Data Analysis

The data analysis followed a 2-stage approach. In the first stage, a deductive approach was used [21-23], guided by Braun and Clarke's [32] thematic analysis methodology. This phase involved coding the data and organizing it into themes directly linked to the predefined features of the Mindy platform, such as appointment scheduling, patient profile creation, and session data management. This structured approach ensured that participants' feedback was systematically categorized according to the platform's functionalities, allowing for a targeted assessment of usability issues and areas for improvement.

The second stage used an inductive approach [21,23,24], based on the Gioia methodology [33], to explore broader themes that emerged from the data. Open coding was used to identify first-order concepts, which were subsequently grouped into second-order themes and finally into aggregate dimensions. The data structure is provided in Figure 1.

Figure 1. Data structure.



Ethical Considerations

This study received ethical approval from the Comitato per l'Integrità e l'etica della ricerca of the University of Bergamo (reference no 2024_04_08) during the meeting held on April 15, 2024 (minutes no 04/2024). The committee issued a favorable opinion without identifying significant critical issues regarding the study design or execution. All procedures were conducted in accordance with institutional and national ethical standards and adhered to the Declaration of Helsinki. Informed written consent was obtained from all participants before their inclusion in the study. Participants were provided comprehensive information regarding the study's nature, purpose, procedures, and data usage. The privacy and confidentiality of all participants were rigorously protected. Video interviews were conducted, and all recordings are securely stored in the institutional archives of Politecnico di Milano in compliance with European privacy regulations, General Data Protection Regulation (GDPR), and ethical committee requirements, with access restricted to authorized research personnel only. No

XSL•FO
RenderX

financial or material compensation was offered or provided to the participants in this study.

Results

Overview

The results are presented and discussed in 2 parts. The first part focuses on the usability study, outlining the issues identified and linking them to specific functionalities of the Mindy platform. The second part explores broader themes that emerged from the data, highlighting the challenges of integrating digital platforms into psychotherapeutic practice.

Results From the Usability Study

To organize the feedback collected, a summary table was created (Table 2), which groups usability evaluations by platform functionality. The rows of the table represent the various functionalities of the platform, while the columns are divided into 3 categories: positive evaluations, negative evaluations, and suggestions for improvement.

Each intersection between a functionality and a category includes detailed descriptions:

- “Positive evaluations” highlight aspects of the functionality that therapists found effective or beneficial.
- “Negative evaluations” describe elements identified as problematic or inadequate.
- “Suggestions for improvement” provide recommendations for enhancing the usability of the functionality.

XSL•FO
RenderX

Table . Results from usability assessment.

Functionality	Positive evaluation	Negative evaluation	Suggestions for improvement
Agenda and appointment booking	Intuitive and easy-to-navigate layout; automatic reminders sent 24 hours before appointments streamline scheduling	Limited flexibility: no integration with external calendars; restricts comprehensive appointment management across platforms	Consider integrating with external calendars (eg, Google Calendar) to provide a unified view of schedules; this feature would enhance organization and reduce scheduling conflicts
Patient profile creation	Comprehensive data collection aligns with therapists' practices; quick and clear data entry ensures ease of use	Gender options are restricted to male and female; inability to attach identity document scans complicates work, especially for minors	Add an "Other" option for gender selection to accommodate diverse patient identities; enable attachment of scanned identity documents for compliance and better record-keeping
Automatic sending of the informed consent form	Easy-to-use feature that automatically sends forms after patient data is entered; customizable templates allow personalization for different therapists	Requires physical printing, signing, and scanning of consent forms, reducing digital efficiency	Enable patients to upload signed forms directly via a secure link; add support for digital signatures to allow seamless consent management; facilitate secure digital storage of signed forms to eliminate paper documentation
Annotations and attachments section	Flexible, unstructured format allows personalized and spontaneous note-taking; supports diverse documentation needs during or after sessions	Requires a laptop, which can distract therapists during sessions; incompatible with tablets or digital pens, limiting usability for many practitioners; online-only access risks data inaccessibility during connection issues	Enable uploading of scanned handwritten notes or photos; ensure compatibility with tablets and support digital pen input for flexible note-taking; introduce an offline mode or a synchronization feature to maintain access during outages
Mandatory fields and detailed data sections	Helps therapists remember to document important details during sessions	Requires frequent updates to rarely changing data (eg, medical history), leading to inefficiencies; overly medicalized structure does not align with all therapy needs	Make certain fields permanent for stable information, avoiding repeated updates; add a feature for incremental updates, enabling therapists to log changes only when necessary
Dashboard to monitor patient progress and therapeutic alliance	Graphical progress display is intuitive and provides a clear visual overview; it helps therapists quickly identify patient progress or regression	Graphs lack dates, limiting the ability to contextualize progress over time	Add dates to the horizontal axis of graphs, linking progress to specific sessions or events; this improvement would enhance trend analysis and treatment planning
Sending questionnaires	Fast and efficient process that allows results to be stored directly in the patient's file; simplifies data collection and organization	No option to include custom questionnaires, reducing flexibility for therapists	Allow therapists to upload and manage custom questionnaires in a dedicated section; this would increase adaptability to specific patient needs
Sending reports to patients	Automatic report generation is quick and easy to use	Therapists cannot control what content is shared in the report; reports are sent automatically after each session, limiting flexibility in timing; lack of control can cause confusion if all details are not relevant for immediate discussion	Allow therapists to customize which information is shared in the report; make report sending optional, giving therapists control over the timing and content; this flexibility would improve communication and align report sharing with therapeutic goals

Challenges of Integrating Digital Platforms Into Psychotherapeutic Practice

Three main themes emerged from the inductive analysis of the data, offering insights into the challenges of integrating a digital platform such as Mindy into psychotherapeutic practice: (1) balancing standardization with the need for narrative and implicit information; (2) embedding digital platforms into daily therapeutic workflows; and (3) navigating the trade-offs between transparency and confidentiality in therapeutic data sharing.

With respect to ROM practices, the feedback gathered on dashboards to monitor patient progress and questionnaire management (Table 1) was particularly relevant. These features are central in ROM practices enabled by digital systems, as they allow easy and intuitive management of clinical data on outcomes and therapeutic processes. These tools increase the therapist's responsiveness [34], which in turn can impact patient change from one session to the next [35]. The literature has shown that ROM data, especially those managed by digital systems, can increase therapists' awareness of how they have affected patients, improve their humility and empathy, increase patients' understanding of themselves, and involve them more

XSL•FO
RenderX

actively in treatment [36]—aspects that influence the quality of therapy [8]. The perceived importance and usefulness of ROM methods by therapists will influence their adoption [37]. Therefore, any implementation efforts should seek to improve awareness and understanding by providing data on the empirical basis and clinical efficacy of ROM as an evidence-based practice, which enables personalization of therapy, improves outcomes even in the most difficult cases, and reduces patient drop-out rates [34].

Balancing Standardization With the Need for Narrative and Implicit Information

The Mindy platform introduces a structured system for psychotherapeutic documentation that promotes uniformity and consistency. However, this shift has raised concerns about the loss of flexibility and personalization that are central to psychotherapeutic practice. Traditionally, therapists relied on free-text notes to capture nuanced details such as tone, body language, and contextual observations. In contrast, Mindy requires the use of structured fields, drop-down menus, and predefined scales, which some therapists find limiting. One therapist commented:

> *Instead of having a window with options for the objective examination, it would be more effective to use an open-ended question. That way, after formulating a diagnostic hypothesis, I would have the opportunity to add arguments and details to support that initial diagnosis.*

The rigidity of standardized documentation risks oversimplifying therapeutic interactions and reducing the richness needed to fully understand a patient's unique case. A therapist observed:

> *This section, in my opinion, is completely useless unless one works exactly with DCA and decides to use this questionnaire. I, for example, would not use it.*

While some therapists appreciate the structured fields for reminding them to cover key aspects during sessions, others emphasize the importance of flexibility. One explained:

> *Sometimes one leaves room for the flow, not the free association of the patient, and forgets to ask determined things.*

To address these concerns, introducing customizable templates and free-text options could help Mindy balance standardization with the flexibility therapists require. Such changes would allow therapists to retain the depth and personalization critical to effective documentation without compromising consistency.

Challenges in Embedding Digital Platforms Into Daily Therapeutic Workflows

Integrating Mindy into psychotherapists' daily workflows presents challenges, particularly for those accustomed to paper-based methods. Many therapists perceive the transition as requiring significant effort and time, which they already find scarce. One therapist noted:

> *Compared to what I need, it asks me for a major effort, so I don't do it.*

Computer literacy also plays a role in adoption resistance, especially among experienced therapists less familiar with digital tools. Despite some willingness to adapt, as one therapist stated:

> *It might be useful, but I would have to change my way of working a little bit, being very paper-based.*

Therapists also expressed concerns about how the use of digital tools during sessions might create a barrier between them and their patients. For instance, one therapist remarked:

> *When I do the examination, I don't keep the desk in front. I stand in the chairs in front of the patient, so I don't have anything technological in front of me.*

Another added:

> *Using the PC unhooks me too much. I tried it, but it creates too much of a boundary between me and the patient.*

Data security is another significant concern, as therapists are responsible for safeguarding highly sensitive information. Any perceived vulnerabilities in the platform's security could deter adoption. Addressing these challenges requires a user-centered design approach, targeted training, and direct engagement with therapists to ensure that the platform aligns with their workflows and supports, rather than disrupts, their practice.

Navigating the Trade-Offs Between Transparency and Confidentiality in Therapeutic Data Sharing

Mindy's secure environment for managing therapeutic data offers significant advantages, but sharing session notes with patients raises concerns about misinterpretation. Traditionally, therapists' notes were intended for personal use, containing preliminary observations and reflections that could be misunderstood if taken out of context. One therapist explained:

> *I never send notes to the patient unless they specifically ask me. Otherwise, they might misunderstand what I'm writing.*

Unmediated sharing of notes risks undermining the therapeutic alliance by introducing confusion or unnecessary anxiety. A reflective comment, for example, might be mistaken for a definitive diagnosis, potentially straining the trust between therapist and patient. Another therapist elaborated:

> *Sometimes I write things that are hypotheses, ideas to explore further, and I wouldn't want the patient to think those are fixed conclusions. It could create unnecessary worry.*

To mitigate these risks, Mindy should include customizable sharing options that allow therapists to control what information is shared with patients and when. This would preserve the confidentiality and trust essential to effective therapy while enabling transparency where appropriate.

Discussion

Overview

This study aimed to evaluate the usability of the Mindy platform and explore broader challenges in integrating digital tools into psychotherapeutic workflows. Usability has long been

XSL•FO
RenderX

recognized as a critical factor in the adoption and effectiveness of digital health technologies [16,17]. By combining a usability evaluation with an exploration of systemic challenges, the study builds on existing research emphasizing the importance of human-centered design and contextual integration [37,38]. Platforms such as Mindy hold significant potential to enhance therapeutic practices, particularly in supporting ROM, but the integration of such tools often encounters barriers related to design, workflow alignment, and therapist adoption. Addressing these challenges is essential for maximizing the benefits of digital health technologies in psychotherapy.

On the Usability of Digital Platforms in Psychotherapy

The usability evaluation of the Mindy platform identified a range of strengths and weaknesses in its design, offering valuable insights for broader considerations in developing and implementing DMHPs. Although this study focused on Mindy, many of the observed usability issues reflect challenges that are likely to arise with similar platforms, emphasizing the importance of prioritizing user-centered design to address clinicians' needs [16,17].

One of the platform's key strengths lies in its intuitive and easy-to-navigate interface, particularly its scheduling and appointment booking functionality. Features such as appointment scheduling and automatic email reminders facilitate streamlined workflows and reduce the risk of missed sessions. However, the lack of integration with external calendars limits the platform's broader utility, as therapists often manage their schedules across multiple systems. This aligns with previous findings highlighting how insufficient interoperability can hinder workflow efficiency in digital health tools [39]. Incorporating calendar interoperability could make digital platforms more adaptable to real-world practices, enhancing usability and reducing scheduling conflicts.

The patient profile creation feature demonstrated another usability strength, offering a comprehensive approach to data collection and ensuring quick and clear data entry. Nevertheless, certain limitations restrict its inclusivity and functionality. The binary gender options fail to accommodate diverse patient identities, and the inability to attach scanned identification documents complicates the process of working with certain patient groups, such as minors. These issues reflect a broader need for platforms to adopt inclusive design principles, such as customizable gender fields and support for uploading supporting documentation, to enhance usability and accessibility for diverse users [40].

Similarly, the system for handling informed consent forms reflects a mix of strengths and weaknesses. While the automatic sending of consent forms is valuable, the reliance on physical printing, signing, and scanning introduces inefficiencies, reducing the platform's potential to streamline administrative tasks. Supporting digital signatures and enabling secure uploads of signed forms would align the platform with modern standards for digital efficiency, as observed in previous studies advocating for the use of technology to minimize manual processes [38].

The annotations and attachments section, which allows for flexible note-taking, underscores the importance of accommodating diverse practitioner preferences. While the unstructured format supports various documentation needs, requiring a laptop for note-taking can distract therapists during sessions and limit functionality for those who prefer using tablets or digital pens. Such device limitations reflect broader issues of compatibility that must be addressed to ensure platforms are adaptable to different clinical settings [39]. Adding offline functionality and synchronization features would further enhance accessibility, ensuring that therapists can work even in environments with limited connectivity.

The mandatory fields and detailed data sections illustrate the tension between standardization and flexibility. While mandatory fields ensure essential information is documented consistently, the frequent updating of rarely changing data, such as medical histories, creates inefficiencies. In addition, the overly medicalized structure of these fields may not align with therapeutic needs, particularly for less diagnostic-focused approaches. Simplifying data entry by introducing permanent fields for stable information and incremental updates could address these inefficiencies and improve alignment with diverse therapeutic approaches.

The dashboard for monitoring patient progress represents a key strength, offering an intuitive graphical display to visualize patient trajectories. However, the lack of dates on progress graphs limits therapists' ability to contextualize changes over time, an important feature for treatment planning and trend analysis. Including time-stamped data would enhance the dashboard's utility and align it with therapists' needs for precision and longitudinal tracking [38,39].

The functionality for sending questionnaires highlights the platform's potential to simplify data collection, but is constrained by its inability to include custom questionnaires. Allowing therapists to upload and manage custom questionnaires would increase adaptability to specific therapeutic needs. Similarly, the feature for generating and sending reports to patients, while efficient, lacks flexibility in controlling content and timing. Offering greater control over report customization and dissemination would align the platform's functionalities with therapeutic goals and minimize potential patient confusion.

These findings underscore the need for usability improvements that extend beyond individual features to address how digital tools integrate into broader clinical workflows. The challenges identified reflect broader systemic issues noted in previous research, including the need for flexibility, inclusivity, and integration [39,40].

On the Integration of Digital Platforms Into Psychotherapeutic Practices

The introduction of a structured digital system for documentation, such as Mindy, has raised significant tensions between the need for standardization and the inherent flexibility required in psychotherapeutic practice (first theme—"balancing standardization with the need for narrative and implicit information"). While structured fields and predefined scales facilitate consistency and quantitative analysis, they risk oversimplifying or omitting critical narrative details, such as tone, body language, and contextual observations. This issue

XSL•FO
RenderX

aligns with previous literature, which suggests that EHRs in mental health care often interfere with the richness of documentation required for effective treatment [38]. The rigidity of standardized fields may constrain therapists' ability to adapt documentation to individual patients, reducing the depth necessary to fully capture therapeutic dynamics [41]. This concern is particularly pronounced in psychoanalytic approaches, where patient narratives and nonverbal cues play a crucial role in treatment [40]. Addressing this challenge requires a balance between standardization for uniformity and flexibility to accommodate the personalized nature of psychotherapy. Looking forward, the emergence and popular use of artificial intelligence–based scribes [42] present an intriguing development that may reshape perceptions of platforms such as Mindy. AI scribes, which automatically transcribe and summarize clinical interactions, have the potential to reduce the documentation burden on clinicians while preserving the richness of narrative and implicit information. These technologies could complement platforms such as Mindy by enabling therapists to focus more on patient interaction rather than manual data entry. However, their widespread adoption raises new questions about data security, integration with existing systems, and the ethical implications of AI-mediated documentation.

The adoption of digital platforms presents both technical and operational challenges for psychotherapists, particularly regarding their integration into daily workflows (second theme—"challenges in embedding digital platforms into daily therapeutic workflows"). The study highlighted difficulties related to time management, computer literacy, and resistance to change. Experienced therapists, in particular, expressed reluctance to move away from established practices, perceiving digital tools as an additional workload rather than a resource for streamlining processes. Similar issues are noted in the literature, where the adaptation to EHRs has been shown to demand significant cognitive and operational adjustments [40]. Moreover, the study revealed concerns about how using digital tools, even in face-to-face sessions, can create a perceived barrier between therapist and patient, potentially disrupting the therapeutic alliance—a phenomenon also discussed in telehealth contexts [43]. In addition, concerns about data security were prevalent, with therapists emphasizing the importance of robust protections against unauthorized access, echoing findings by Golz et al [39]. To overcome these barriers, platforms such as Mindy must prioritize user-centered design, offering clear training and flexible integration strategies to minimize disruption to professional routines.

The final theme ("navigating the trade-offs between transparency and confidentiality in therapeutic data sharing") revolves around the management of transparency and confidentiality in sharing sensitive therapeutic data. While transparency can strengthen the therapeutic alliance [44], unmediated sharing of session notes poses risks of misinterpretation and patient distress. For example, preliminary observations or speculative diagnoses might be misunderstood as definitive, leading to unnecessary anxiety or erosion of trust. This study supports previous literature advocating for selective and context-sensitive sharing of documentation [45]. In particular, therapeutic notes may be better suited for selective disclosure, depending on the stage of treatment and the specific needs of the patient. Digital platforms must, therefore, incorporate customizable sharing options to ensure communication is adapted to the therapeutic context while maintaining the foundation of trust essential to effective psychotherapy.

Conclusions

This study examined the integration of digital technologies into psychotherapy [1,15,38], focusing on usability and broader implementation challenges associated with platforms such as Mindy. While EHRs and DMHPs offer benefits such as improved documentation, enhanced communication, and timely information retrieval [38], their adoption in psychotherapeutic practice is hindered by challenges related to standardization, workload, usability, and impacts on the therapeutic relationship [38]. These challenges are particularly relevant in the context of ROM, a practice that digital platforms are intended to support but that also introduces specific constraints [5].

The usability analysis of Mindy revealed that while its structured fields and predefined formats facilitate consistency and support ROM implementation, they limit therapists' ability to personalize documentation. This lack of flexibility affects the capacity to capture the complexity and depth of therapeutic interactions, which is essential for tailoring treatments to individual patients. In addition, the inductive analysis identified 3 main dimensions that represent broader challenges of incorporating digital platforms into psychotherapeutic workflows.

Understanding how digital tools can be effectively integrated into clinical practice necessitates approaches that focus on the human-computer interaction, as emphasized by usability studies [17,26,27,27,28]. These studies, which observe how users interact with technology in real-world settings, provide valuable insights into the challenges faced by professionals. By capturing both immediate usability issues and broader themes emerging from these interactions, the study demonstrated how usability methods are critical not only for identifying technical barriers but also for uncovering contextual factors that influence the adoption of digital tools in psychotherapy.

In contributing to the broader goals of the OutProFeed project, this study highlighted the importance of a multidisciplinary approach to improving Mindy's usability and integrating it into professional workflows. The findings underscore the need for collaboration between clinicians, software engineers, and researchers, each bringing distinct expertise and perspectives. While these groups often approach the design and implementation of digital tools with different priorities and terminologies, fostering a shared understanding is essential to ensure that technical features align with clinical needs.

XSL•FO
RenderX

Acknowledgments

We thank Edoardo Forestiero and Kamila Daka for their contribution to this research and wish them a successful career ahead.

This study was supported by PRIN 2022 (CUP:2022Z4BB82), funded by the Italian Ministry of University and Research under call D.D. 1409 (14/09/2022).

Data Availability

The datasets generated and analyzed during the current study are not publicly available due to the need to protect participant anonymity, but are available from the corresponding author on reasonable request.

Conflicts of Interest

None declared.

Multimedia Appendix 1
Mindy's interface.
[DOCX File, 3052 KB - medinform_v13i1e75885_app1.docx]

References

1. Bond RR, Mulvenna MD, Potts C, O'Neill S, Ennis E, Torous J. Digital transformation of mental health services. Npj Ment Health Res 2023 Aug 22;2(1):13. [doi: 10.1038/s44184-023-00033-y] [Medline: 38609479]
2. Salomon RM, Blackford JU, Rosenbloom ST, et al. Openness of patients' reporting with use of electronic records: psychiatric clinicians' views. J Am Med Inform Assoc 2010;17(1):54-60. [doi: 10.1197/jamia.M3341] [Medline: 20064802]
3. Schiller B, Kuska M, Becher-Urbaniak S, Wimmer E, Reisinger M, Mörtl K. Online psychotherapy as a first clinical experience during the Covid-19 pandemic: a new generation of psychotherapists in the digital age. Heliyon 2024 Apr 30;10(8):e29464. [doi: 10.1016/j.heliyon.2024.e29464] [Medline: 38638950]
4. Menachemi N, Collum TH. Benefits and drawbacks of electronic health record systems. Risk Manag Healthc Policy 2011;4:47-55. [doi: 10.2147/RMHP.S12985] [Medline: 22312227]
5. Gual-Montolio P, Martínez-Borba V, Bretón-López JM, Osma J, Suso-Ribera C. How are information and communication technologies supporting routine outcome monitoring and measurement-based care in psychotherapy? A systematic review. Int J Environ Res Public Health 2020 May 2;17(9):3170. [doi: 10.3390/ijerph17093170] [Medline: 32370140]
6. Lambert MJ, Hansen NB, Finch AE. Patient-focused research: using patient outcome data to enhance treatment effects. J Consult Clin Psychol 2001 Apr;69(2):159-172. [doi: 10.1037/0022-006X.69.2.159] [Medline: 11393594]
7. Miller SD, Hubble MA, Chow D, Seidel J. Beyond measures and monitoring: realizing the potential of feedback-informed treatment. Psychotherapy (Chic) 2015 Dec;52(4):449-457. [doi: 10.1037/pst0000031] [Medline: 26641375]
8. De Jong K, Timman R, Hakkaart-Van Roijen L, et al. The effect of outcome monitoring feedback to clinicians and patients in short and long-term psychotherapy: a randomized controlled trial. Psychother Res 2014;24(6):629-639. [doi: 10.1080/10503307.2013.871079] [Medline: 24386975]
9. Bickman L, Douglas SR, De Andrade ARV, et al. Implementing a measurement feedback system: a tale of two sites. Adm Policy Ment Health 2016 May;43(3):410-425. [doi: 10.1007/s10488-015-0647-8] [Medline: 25876736]
10. Lewis CC, Boyd M, Puspitasari A, et al. Implementing measurement-based care in behavioral health: a review. JAMA Psychiatry 2019 Mar 1;76(3):324-335. [doi: 10.1001/jamapsychiatry.2018.3329] [Medline: 30566197]
11. Delgadillo J, Overend K, Lucock M, et al. Improving the efficiency of psychological treatment using outcome feedback technology. Behav Res Ther 2017 Dec;99:89-97. [doi: 10.1016/j.brat.2017.09.011] [Medline: 29024821]
12. Boswell JF, Hepner KA, Lysell K, et al. The need for a measurement-based care professional practice guideline. Psychotherapy (Chic) 2023 Mar;60(1):1-16. [doi: 10.1037/pst0000439] [Medline: 35771518]
13. Hegland PA, Aasprang A, Hjelle Øygard S, et al. A review of systematic reviews on the effects of patient-reported outcome monitoring with clinical feedback systems on health-related quality of life-implications for a novel technology in obesity treatment. Clin Obes 2018 Dec;8(6):452-464. [doi: 10.1111/cob.12277] [Medline: 30208266]
14. Wright CV, Goodheart C, Bard D, et al. Promoting measurement-based care and quality measure development: the APA mental and behavioral health registry initiative. Psychol Serv 2020 Aug;17(3):262-270. [doi: 10.1037/ser0000347] [Medline: 31021113]
15. Wainberg ML, Gouveia L, McKinnon K. Generating better implementation evidence to improve mental health care everywhere. Lancet Psychiatry 2024 May;11(5):317-319. [doi: 10.1016/S2215-0366(24)00090-7] [Medline: 38552664]
16. Fernandez A, Insfran E, Abrahão S. Usability evaluation methods for the web: a systematic mapping study. Inf Softw Technol 2011 Aug;53(8):789-817. [doi: 10.1016/j.infsof.2011.02.007]
17. Jaspers MWM. A comparison of usability methods for testing interactive health technologies: methodological aspects and empirical evidence. Int J Med Inform 2009 May;78(5):340-353. [doi: 10.1016/j.ijmedinf.2008.10.002] [Medline: 19046928]

XSL•FO
RenderX

18. Bauer S, Moessner M. Technology-enhanced monitoring in psychotherapy and e-mental health. J Ment Health 2012 Aug;21(4):355-363. [doi: 10.3109/09638237.2012.667886] [Medline: 22548363]
19. Atik E, Schückes M, Apolinário-Hagen J. Patient and therapist expectations for a blended cognitive behavioral therapy program for depression: qualitative exploratory study. JMIR Ment Health 2022 Dec 30;9(12):e36806. [doi: 10.2196/36806] [Medline: 36583934]
20. Derman YD, Arenovich T, Strauss J. Speech recognition software and electronic psychiatric progress notes: physicians' ratings and preferences. BMC Med Inform Decis Mak 2010 Aug 25;10:44. [doi: 10.1186/1472-6947-10-44] [Medline: 20738875]
21. Yin RK. Case Study Research: Design and Methods: SAGE Publications; 2013.
22. Fife ST, Gossner JD. Deductive qualitative analysis: evaluating, expanding, and refining theory. Int J Qual Methods 2024 Jan;23:16094069241244856. [doi: 10.1177/16094069241244856]
23. Bryman A. Social Research Methods: Oxford University Press; 2016.
24. Eisenhardt KM. Building theories from case study research. Acad Manage Rev 1989 Oct;14(4):532. [doi: 10.2307/258557]
25. Boren T, Ramey J. Thinking aloud: reconciling theory and practice. IEEE Trans Profess Commun 2000;43(3):261-278. [doi: 10.1109/47.867942]
26. Nielsen J. Estimating the number of subjects needed for a thinking aloud test. Int J Hum Comput Stud 1994 Sep;41(3):385-397. [doi: 10.1006/ijhc.1994.1065]
27. Krahmer E, Ummelen N. Thinking about thinking aloud: a comparison of TwoVerbal protocols for usability testing. IEEE Trans Profess Commun 2004 Jun;47(2):105-117. [doi: 10.1109/TPC.2004.828205]
28. Paz F, Pow-Sang JA. Usability evaluation methods for software development: a systematic mapping review. Presented at: 2015 8th International Conference on Advanced Software Engineering & Its Applications (ASEA); Nov 25-28, 2015; Jeju p. 1-4. [doi: 10.1109/ASEA.2015.8]
29. Lewis JR. IBM computer usability satisfaction questionnaires: psychometric evaluation and instructions for use. Int J Hum Comput Interact 1995 Jan;7(1):57-78. [doi: 10.1080/10447319509526110]
30. Guest G, Namey E, Chen M. A simple method to assess and report thematic saturation in qualitative research. PLOS ONE 2020;15(5):e0232076. [doi: 10.1371/journal.pone.0232076] [Medline: 32369511]
31. Applying human factors and usability engineering to medical devices. US Food and Drug Administration. 2019. URL: https://www.fda.gov/regulatory-information/search-fda-guidance-documents/applying-human-factors-and-usability-engineering-medical-devices [accessed 2024-11-21]
32. Braun V, Clarke V. Using thematic analysis in psychology. Qual Res Psychol 2006 Jan;3(2):77-101. [doi: 10.1191/1478088706qp063oa]
33. Gioia DA, Corley KG, Hamilton AL. Seeking qualitative rigor in inductive research: notes on the Gioia methodology. Organ Res Methods 2012;16:15-31. [doi: 10.1177/1094428112452151]
34. Delgadillo J, McMillan D, Gilbody S, et al. Cost-effectiveness of feedback-informed psychological treatment: evidence from the IAPT-FIT trial. Behav Res Ther 2021 Jul;142:103873. [doi: 10.1016/j.brat.2021.103873] [Medline: 33945983]
35. Barkham M, De Jong K, Delgadillo J, Lutz W. Routine outcome monitoring (ROM) and feedback: research review and recommendations. Psychother Res 2023 Sep;33(7):841-855. [doi: 10.1080/10503307.2023.2181114] [Medline: 36931228]
36. Låver J, McAleavey A, Valaker I, Castonguay LG, Moltu C. Therapists' and patients' experiences of using patients' self-reported data in ongoing psychotherapy processes-A systematic review and meta-analysis of qualitative studies. Psychother Res 2024 Mar;34(3):293-310. [doi: 10.1080/10503307.2023.2222896] [Medline: 37322037]
37. Mackrill T, Sørensen KM. Implementing routine outcome measurement in psychosocial interventions – a systematic review. Eur J Soc Work 2020 Sep 2;23(5):790-808. [doi: 10.1080/13691457.2019.1602029]
38. Kariotis TC, Prictor M, Chang S, Gray K. Impact of electronic health records on information practices in mental health contexts: scoping review. J Med Internet Res 2022 May 4;24(5):e30405. [doi: 10.2196/30405] [Medline: 35507393]
39. Golz C, Peter KA, Müller TJ, Mutschler J, Zwakhalen SMG, Hahn S. Technostress and digital competence among health professionals in Swiss psychiatric hospitals: cross-sectional study. JMIR Ment Health 2021 Nov 4;8(11):e31408. [doi: 10.2196/31408] [Medline: 34734840]
40. Dobson R, Variava R, Douglas M, Reynolds LM. Digital competency of psychologists in Aotearoa New Zealand: a cross-sectional survey. Front Digit Health 2022;4:951366. [doi: 10.3389/fdgth.2022.951366] [Medline: 36158995]
41. Stanhope V, Matthews EB. Delivering person-centered care with an electronic health record. BMC Med Inform Decis Mak 2019 Aug 22;19(1):168. [doi: 10.1186/s12911-019-0897-6] [Medline: 31438960]
42. Buckley P, Wang Y, Gopalan P. Artificial intelligence scribes in psychiatry. Focus (Am Psychiatr Publ) 2025 Jan;23(1):44-48. [doi: 10.1176/appi.focus.20240024] [Medline: 39776453]
43. Banbury A, Nancarrow S, Dart J, Gray L, Parkinson L. Telehealth interventions delivering home-based support group videoconferencing: systematic review. J Med Internet Res 2018 Feb 2;20(2):e25. [doi: 10.2196/jmir.8090] [Medline: 29396387]
44. Ardito RB, Rabellino D. Therapeutic alliance and outcome of psychotherapy: historical excursus, measurements, and prospects for research. Front Psychol 2011;2(270):270. [doi: 10.3389/fpsyg.2011.00270] [Medline: 22028698]

XSL•FO
RenderX

45. Chimowitz H, O'Neill S, Leveille S, Welch K, Walker J. Sharing psychotherapy notes with patients: therapists' attitudes and experiences. Soc Work 2020 Apr 1;65(2):159-168. [doi: 10.1093/sw/swaa010] [Medline: 32236447]

Abbreviations

APA: American Psychiatric Association
DMHP: digital mental health platform
EHR: electronic health record
FDA: Food and Drug Administration
GDPR: General Data Protection Regulation
ROM: routine outcome monitoring

Edited by A Benis; submitted 12.04.25; peer-reviewed by F Zoccarato, P Bjurner; revised version received 12.08.25; accepted 15.08.25; published 30.09.25.

Please cite as:
Olive MV, La Tona A, Lo Coco G, Compare A, Cafazzo JA, Masella C
Assessment of a Digital Platform for Routine Outcome Monitoring in Psychotherapy: Usability Study and Thematic Analysis
JMIR Med Inform 2025;13:e75885
URL: https://medinform.jmir.org/2025/1/e75885
doi:10.2196/75885

© Mattia Vincenzo Olive, Antonino La Tona, Gianluca Lo Coco, Angelo Compare, Joseph Antony Cafazzo, Cristina Masella. Originally published in JMIR Medical Informatics (https://medinform.jmir.org), 30.9.2025. This is an open-access article distributed under the terms of the Creative Commons Attribution License (https://creativecommons.org/licenses/by/4.0/), which permits unrestricted use, distribution, and reproduction in any medium, provided the original work, first published in JMIR Medical Informatics, is properly cited. The complete bibliographic information, a link to the original publication on https://medinform.jmir.org/, as well as this copyright and license information must be included.

XSL•FO
RenderX

A Unique Way to Axe the Fax Through Using Business Automation Workflow to Expedite eReferral Adoption, Bridging eReferral, and Fax: Proof-of-Concept Study

Zhigang Tian[1,2], MD, MHI; Kayla Wierts[1], MHE; Lirije Hyseni[1], MSc; Beth Gerritsen[1], MHI, MSCN; Kim Lynch[1]; Russell Buchanan[1], BA; Mohamed Alarakhia[1,3], MD, MSc

[1]Amplify Care, 235 The Boardwalk, Suite 301, Kitchener, ON, Canada

[2]Institute of Health Policy, Management and Evaluation, Dalla Lana School of Public Health, University of Toronto, Toronto, ON, Canada

[3]Department of Family Medicine, McMaster University, Hamilton, ON, Canada

Corresponding Author:
Zhigang Tian, MD, MHI
Amplify Care, 235 The Boardwalk, Suite 301, Kitchener, ON, Canada

Abstract

Background: It is estimated that 88% of Ontario physicians still use fax technology to share patient information. Transitioning to electronic referral (eReferral) has been shown to have numerous benefits, but the major barrier to adoption of eReferral is the need for both sending and receiving clinicians on the same platform to enable information sharing. The traditional onboarding process takes time and effort. An innovative method is required to improve eReferral adoption by bridging the gap between eReferral senders and fax referral receivers.

Objective: This study aimed to explore the technological feasibility of leveraging a business automation workflow (BAW) platform to connect the digital (eReferral) and nondigital referral platform (fax), enabling eReferral senders to send referrals to fax receivers, thereby improving the clinician experience.

Methods: An eReferral via eFax solution was developed and evaluated on the BAW platform to connect the eReferral platform and the clinicians using fax. A selected number of fax receivers were identified and enabled on the eReferral platform as eFax receivers. Sending clinicians initiated eFaxes through the familiar eReferral workflow, with eFaxes transmitted to BAW and delivered to the target receiver via fax. Retry and reminder logic were built to improve the user experience. If the eFax failed after all retries, a message was sent to the sending clinician through the eReferral platform explaining the failure reason. The appointment information was entered into the eReferral platform by the sending clinicians to trigger patient email notifications. Surveys and focused interviews were conducted to collect clinicians' feedback.

Results: From May 2022 to December 2023, 224 eFax receivers were enabled on the platform, processing 4504 eFaxes for 4132 unique patients and 843 unique senders across the province. Nearly 70% (3137/4504) of patients consented and received email notifications; 19% (875/4504) received appointment details after manual entry in the eReferral platform. On average, eFax referrals contained 5.6 pages, with a minimal 0.7% exceeding 30 pages. Initially, fax service retries were disabled to observe delivery error rates. This resulted in a 37.7% (1023/2712) fax failure. However, after implementing new retry logic in March 2023, the failure rate dropped significantly to 9.9% (304/3082), and 98.7% (2770/2806) of eFaxes were successfully delivered after automatic retries. Clinician feedback revealed a positive impact on sending clinicians' experience, maintaining their familiar workflow while accommodating fax-reliant receivers who can gradually transition to eReferral at their own pace.

Conclusions: This project demonstrates the potential of the BAW platform to bridge the gap between fax and eReferral systems. It minimizes disruption for sending clinicians while allowing fax receivers to incrementally adopt the new platform. This technology can significantly expedite eReferral adoption by reducing the reliance on receiving clinics to adopt eReferral, ultimately enhancing the experience for both clinicians and patients.

(JMIR Med Inform 2025;13:e62983) doi:10.2196/62983

KEYWORDS

eReferral; business automation workflow; fax; referral; electronic referral; electronic fax; fax failure; interoperability; axe the fax

XSL•FO
RenderX

Introduction

When a medical referral is necessary in the Canadian health care system, the sending clinician selects the most appropriate receiving clinician and forwards the patient's relevant information through fax or other digital technologies, like an electronic referral (eReferral) system [1]. eReferral simplifies the referral process by enhancing communication between primary care clinicians and specialists or organizations, enabling quick and secure referrals to be sent and received through an electronic platform. The eReferral system has been proven to be more secure, can reduce wait times, improve tracking, and lower costs [2,3]. eReferral has also demonstrated the ability to improve patients' experience [4]. To relieve physician burnout, the Ontario Medical Association recommended enabling electronic information sharing between clinicians to reduce the administrative burden and free up more time to provide patient care [5].

Surprisingly, fax machines are still widely used in health care globally. Fax technology is the lowest common denominator when it comes to physicians who are not working on the same electronic medical record (EMR) systems to share information. It is estimated that around 75% of medical institutions in the United States still rely on faxing for communication [6]. In the United Kingdom, despite the National Health Service's (NHS) call in 2018 for a complete phase-out of fax use by April 2020 [7], 1 in 6 NHS trusts was found still using fax machines in 2023 [8,9].

The 2021 National Survey of Canadian Physicians indicated Ontario ranked the first in the percentage of physicians sharing information electronically, with 39.9% of the respondents using eReferral to request or receive care from specialists or other physicians for their patients [10]. Although significant progress has been made with eReferral in Ontario, 88% of doctors still have to use fax technology to share patient information [5]. Doctors who already adopted eReferral technology cannot completely move away from the fax technology and have to maintain duplicate workflows to be able to refer to receivers who have not adopted eReferral yet. This has resulted in a significant admin workload for the sending clinicians. In 2023, the Ontario government announced that fax machines would be phased out with digital communication alternatives at all Ontario health care clinicians within the next 5 years in the document, entitled Your Health- A Plan for Connected and Convenient Care [11].

One of the key barriers to eReferral adoption is peers not using eReferrals, the need for both sending and receiving clinicians to have a linked health information system through a shared EMR or an independent eReferral platform [1,2], sometimes also referred to as a "chicken-and-egg" problem. Onboarding the sending and receiving clinicians to the same platform takes time and requires enormous change management support [12]. In a hybrid environment where some receivers adopted the eReferral platform and others are still using fax machines, sending clinicians have reported experiencing frustration over the management of a duplicate workflow in selecting appropriate technologies to prepare and submit the referrals to support patient care.

A new and innovative solution was designed using the business automation workflow (BAW) platform as middleware to bridge the gap between the eReferral senders and the fax receivers. This helps explore the technological feasibility of leveraging the BAW platform to connect digital and nondigital (fax) referral platforms to improve the current referral experience, especially for the sending clinicians. The Amplify Care team (previously eHealth Centre of Excellence) started a Proof-of-Concept (PoC) project in 2022 called eReferral via eFax to better understand using a BAW platform to support managing fax-based referrals by leveraging the existing digital referral platform, to measure fax failure risks and to improve the short-term fax failures and retries management, and in the long term, to support migrating away from fax-based referrals. Eventually, the solution will help expedite the eReferral adoption.

Methods

Overview

The design of the solution tried to minimize the impact on the existing workflow for both referral senders and receiving sites so that senders can manage their referrals on one single referral platform, with no need to switch between eReferral and fax workflow and have a seamless experience. At the same time, the receivers can maintain their current workflow to receive the referral on their fax machines. With the new technology implementation, senders should be able to send referrals to a larger group of receivers including those who are still using fax machines, while the fax receivers will start to be exposed to the eReferral technology and this should accelerate their eReferral adoption.

Platform

The BAW platform has the key capability to receive and deliver information through standard Application Programming Interfaces and it also supports workflow customization based on clinical needs to help automate the tasks and gain insight [13]. This is essential when handling the complex fax failures in daily practices that usually require human intervention.

To bridge the gap, we developed and configured the BAW platform as the middleware to connect the digital referral platform and the fax receivers. Through integration with the eReferral platform using Health Level Seven (HL7) Fast Healthcare Interoperability Resources (FHIR), the BAW platform will receive the pdf package, including the referral details and the required fax number [14-16]. The BAW platform will then automate the process following a predefined workflow and deliver information to the fax-based receiving clinician through the second integration with the fax service platform. Retry or reminder logic is built into the workflow to increase the success rate of fax delivery.

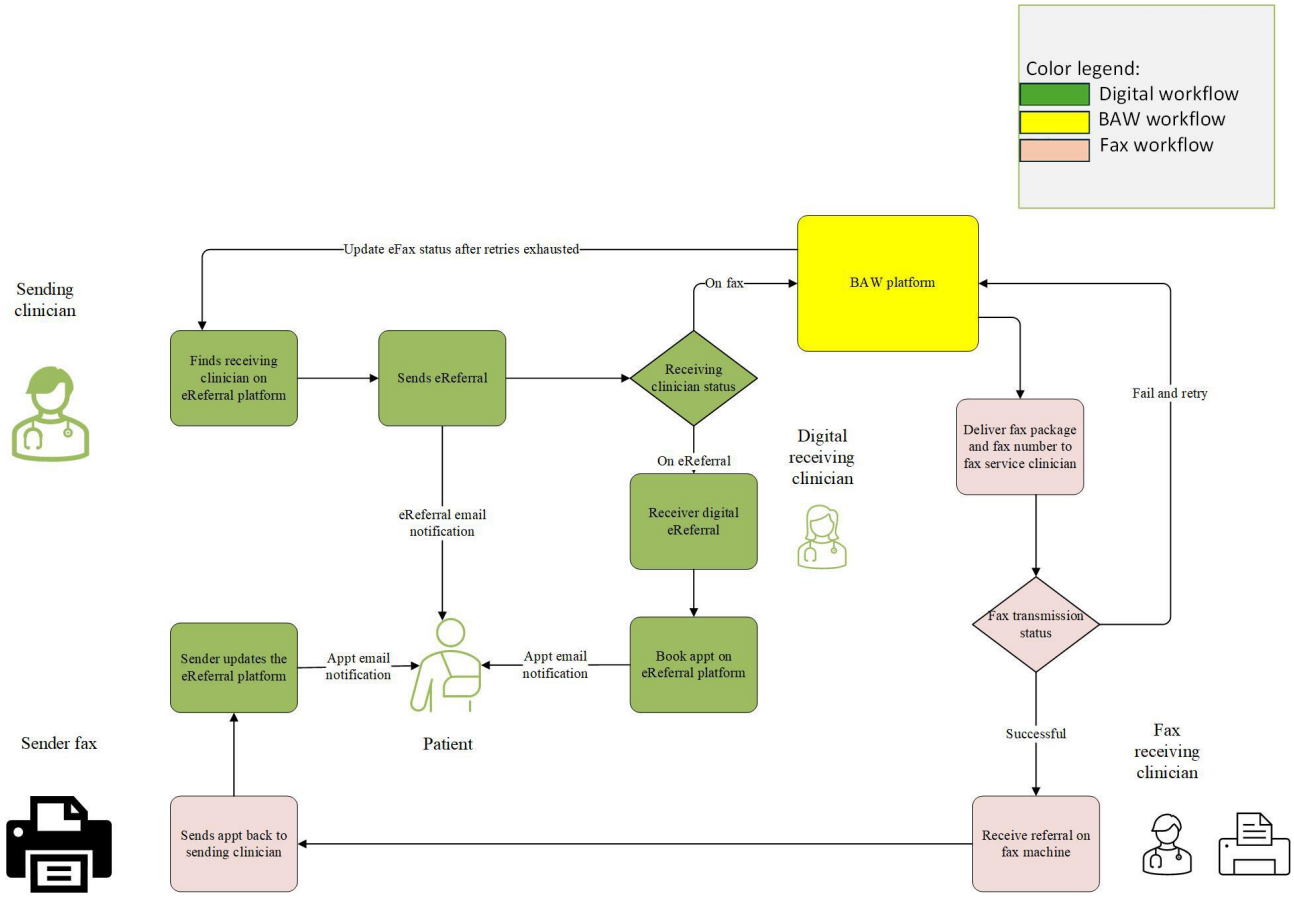
The Privacy Impact Assessment and Threat Risk Assessment were conducted to ensure the solution complies with Ontario's Personal Health Information Protection Act and met all privacy and security requirements.

XSL•FO
RenderX

Workflow Configuration

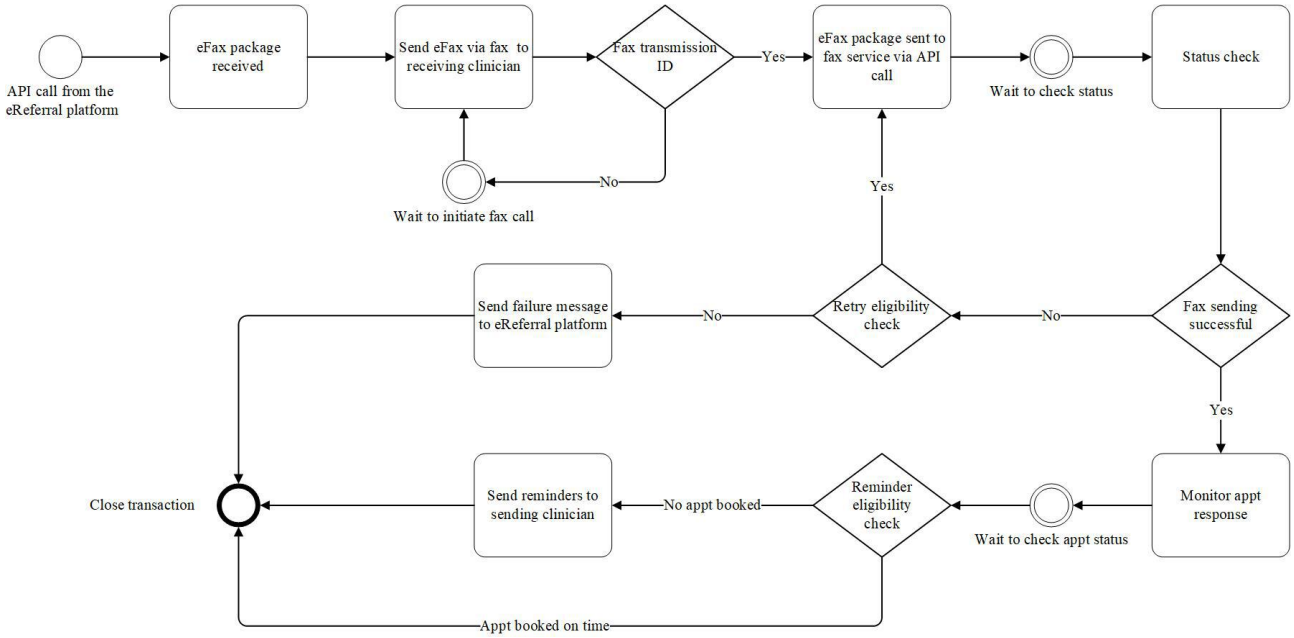
The workflow is configured on the BAW platform using business process model and Notation 2.0 to allow the BAW platform to comprehend and follow the defined clinical workflow (Figures 1 and 2). First, the sender starts the eFax using the same workflow directly within the eReferral platform as other digital referrals. Second, the eReferral platform packages the eFax into a PDF document with a cover page and sends it to the BAW platform together with the fax number through the Application Programming Interface. Third, the BAW platform receives the package or correct fax number and passes the information to the fax service following the defined process. Fourth, the fax service will deliver the pdf package to the fax number provided and provide a status update to the BAW platform once the task is completed or failed. Fifth, if the transaction failed, a notification message will be sent to the clinician via the existing eReferral platform to remind the clinician for further action or resubmission according to their discretion. Sixth, retry or reminder logic is included in the workflow to reduce the human interventions required. Seventh, when the patient is booked, the sender receives the response from the receiver using traditional means (fax machine). The appointment details can be entered digitally into the eReferral platform to enable patient notifications so the patient can enjoy the benefits of eReferral technology. Finally, a reminder message will be triggered to the sending clinician if no appointment is booked after a certain period (7 days for an urgent eFax, 30 days for a routine eFax).

Figure 1. eReferral via eFax workflow diagram. Appt: appointment; BAW: business automation workflow; eFax: eReferral via eFax transaction; eReferral: electronic referral.



XSL•FO
RenderX

Figure 2. Business automation workflow platform workflow diagram (illustrating retry and reminder logic). API: Application Programming Interface; Appt: appointment; eFax: eReferral via eFax transaction; eReferral: electronic referral.



Receiving Clinician Recruitment

The PoC started with a select number of clinicians. Working with multiple Ontario Health Teams, the team identified 229 high-volume receivers in the region who have not yet adopted eReferral technology in their practices. Communications were distributed through fax to the identified receivers, and they were provided the choice to "opt-out" if the receiver had concerns about the PoC. A total of 5 receivers reached out and were removed from the list since they were retiring and no longer accepting medical referrals. The rest (224) were successfully added to the referral platform.

Fax Retry Logic

The PoC was broken into 2 phases to better understand the current fax performance in the Ontario health care system and how the BAW platform can help address the issue. When the fax system communicates with the receiver's fax system, a status code is generated. The BAW platform then receives this status code and determines if a retry is necessary. The fax failure rate was used to track the fax service performance, which is defined as how often the BAW needs to trigger the retry after the eFax delivery fails. During phase 1 (10 mo, May 2022 to March 2023), the fax-service level retry functionality was disabled to observe the fax performance and understand how frequently the fax process will encounter errors. The BAW platform monitored and tracked every error encountered and the result was analyzed to inform the second phase enhancements. Furthermore, 7 of the most common error codes will trigger automatic retries, including "line busy", "no answer", "unexpected disconnect", "device timeout", "device busy", "canceled", and "no channels available". The BAW retries once every 30 minutes, up to 10 times, for routine referrals and once every 10 minutes, up to 10 times, for urgent referrals. After all the retries are exhausted, the BAW will mark the referral status as "declined", attach the reason for the errors encountered, and send the information back to the eReferral platform so the senders can review it for consideration of resubmission.

During phase 2 (March 2023 to December 2023), a new enhanced error handling logic was developed and deployed to retry all error codes and combine the BAW retries with the fax service's built-in retries to simplify the workflow. The fax service's built-in retries (every 5 min with total 5 attempts) were enabled to reduce the need for BAW intervention. BAW receives the last status code from the fax service and will trigger a retry during the 5-hour period if the status code is not "no errors." If the eFax is still not delivered within a 5-hour period, the eFax will be marked as "declined" and returned to the sender for further resubmission.

The retry logic for routine referrals has been updated to retry every 30 minutes during the 5-hour period. For urgent referrals, the BAW system will trigger a retry every 12 minutes.

Generic Referral Form Development

A working group led by the physician champions was created to discuss the referral forms and templates. Multiple review meetings were held with local clinicians to collect feedback, and a generic eFax referral form template was created and assigned to all eFax referral receivers. The generic form included the option to use a unique form if required by the receiving clinic, which could be included as an attachment[17].

Evaluation

Solution-generated data were collected from all 3 platforms, including the Business Automation Insights tool (IBM Corp), the eReferral solution, and the fax service portal. The solution-generated data included elements such as fax failure or success rates, page counts, sending and receiving clinician information, referral details like health service offering, referral processing details like status and time stamps, patient email inclusion, and appointment information (if included).

XSL•FO
RenderX

A combination of surveys and interviews collected qualitative data to understand the impact of the eReferral via eFax solution.

Surveys were sent out to all users who have sent or received at least 1 eFax between May 20, 2022 and September 30, 2022. Senders received the survey by email, and receivers received information on how to access the survey by fax. Due to low response rates, the top 10 receivers were contacted by phone to ask if they would participate in the survey. The Ontario Health Teams conducted focus group interviews to gather feedback from eFax senders and receivers. Patient survey data were monitored to see if the satisfaction rate was positively or negatively impacted. Focused interviews were conducted with the eReferral deployment team members to gather their experience onboarding the receivers who transitioned away from eFax to eReferral.

Ethical Considerations

This study does not require ethics approval as it is quality improvement in nature and uses both publicly available information and secondary analysis with nonidentifiable data as per the Tri-Council Policy Statement from the Government of Canada Panel on Research Ethics [18].

Results

eFax Receivers Information

A total of 224 receivers from Ontario Health Regions of Central, Toronto, and West were identified and enabled during the PoC. Of the total, 8 receivers (3.6%) are specialists practicing in academic institutions and hospital clinics, 11 receivers (4.9%) are from specialist group clinics, and the rest (91.5%) are independent specialists. As of December 26, 2023, 14 receivers (6.3%) converted to the eReferral platform (Table S1 in Multimedia Appendix 1). The receiver specialties are primarily in surgical pathways (Table S2 in Multimedia Appendix 1).

eFax Transaction Information

From May 2022 to December 2023 (as of December 26, 2023), a total of 4504 eFaxes were processed using the eReferral via the eFax platform for 4132 unique patients from 843 unique senders all over the province. Throughout the PoC, 3137 (69.6%) patients received notification emails about the referral details. In total, 875 (19.4%) appointment details were entered into the eReferral platform to support the wait 1 time calculation (Table 1). The receivers declined 158 (3.5%) eFaxes, and the sender entered the decline reason in the eReferral platform with the patient notification message.

XSL•FO
RenderX

Table . eFax referrals processed by sender region (May 2022-December 2023).

Sender Ontario Health Region	Sender region (historical Local Health Integration Network area)	Referrals, n	Unique referrers, n	Unique patients, n	Referral targets, n	Referrals with patient email notification, n (%)	Referrals with appointment booked, n (%)[a]
Central							
	Central	449	110	410	68	337 (75.1)	39 (8.7)
	Central West	152	26	137	56	126 (82.9)	6 (3.9)
	Mississauga Halton	99	33	94	51	62 (62.6)	4 (4)
	North Simcoe Muskoka	16	11	14	14	11 (68.8)	0 (0)
East							
	Central East	92	92	85	51	68 (73.9)	2 (2.2)
	Champlain	6	6	6	6	4 (66.7)	1 (16.7)
	South East	7	6	6	7	4 (57.1)	0 (0)
North							
	North East	8	7	7	8	5 (62.5)	0 (0)
	North West	3	1	3	3	3 (100)	0 (0)
Toronto							
	Toronto Central	448	147	412	93	370 (82.6)	47 (10.5)
West							
	Erie St. Clair	112	36	105	47	57 (50.9)	19 (17)
	Hamilton Niagara Haldimand Brant	1478	107	1361	114	987 (66.8)	453 (30.6)
	South West	1211	164	1114	113	824 (68)	246 (20.3)
	Waterloo Wellington	271	131	247	98	197 (72.7)	40 (14.8)
Total		4504	200	4132	224	3137 (69.6)	875 (19.4)

[a]Appointment status as of December 26, 2023.

Fax Performance

The fax performance report is broken into 2 phases.

Phase 1

From May 20, 2022, to March 20, 2023, 1706 eFaxes were initiated and processed. As illustrated in Table 2, if the status code indicates “no errors,”, it means the eFax was successfully delivered. If there is a code other than “no errors,” the system counts it as a failure and will start the retry following the retry logic described in the method section. In total, 1658 eFaxes (97.2%) were sent successfully after 0 - 10 retries without manual resubmission, and 48 (2.8%) were marked as declined and required manual resubmission from the senders. Among the declined or failed eFaxes, 31 were resubmitted and delivered successfully. The other 17 eFaxes remained in the “declined” folder on the eReferral platform and required sending clinicians’ further attention or resubmission. During phase 1, senders submitted 1706 eFaxes, while BAW made 2712 delivery attempts due to the error codes encountered during the delivery process. Out of these, 1689 (99%) attempts successfully delivered the eFaxes, resulting in an average of 1.59 attempts per successful delivery. The overall fax failure rate was 37.7%. The most common error code is “line busy” (381/2712, 14%), followed by “unexpected disconnect”(224/2712, 8.3%).

XSL•FO
RenderX

Table . eFax status codes (May 2022-March 2023).

eFax status code	Count, n (%)
Success (no errors)	1689 (62.3)
Line busy	381 (14)
Unexpected disconnect	224 (8.3)
Invalid or missing number[a]	183 (6.7)
No answer	150 (5.5)
Error	63 (2.3)
Line failure	10 (0.4)
No dial tone	9 (0.3)
Incompatible fax machine	3 (0.1)
Total	2712 (100)

[a]This is a system-generated status code indicating there was no valid fax number recognized when communicating with the receiver's fax machine, although the fax numbers do exist.

Phase 2

After March 20, 2023, the new retry logic was deployed to simplify the workflow. From March 21, 2023, to December 26, 2023, a total of 2806 eFaxes were initiated and processed. Of these, 2778 (99%) were successfully delivered to the receivers. Among the delivered eFaxes, 2770 (98.7%) were sent successfully without requiring resubmission, while 36 (1.3%) were marked as declined and required manual resubmission by the senders. Out of the declined eFaxes, 8 were resubmitted and delivered successfully. In contrast, the remaining 28 eFaxes stayed in the "declined" folder on the eReferral platform, needing further attention or resubmission by the sending clinicians.

As illustrated in Table 3, during phase 2, the BAW attempted to deliver 2806 eFaxes, making 3082 attempts in total. Out of these, 2778 (90.1%) attempts successfully delivered the eFaxes, resulting in an average of 1.11 attempts per successful delivery. Under the new retry logic, the fax failure rate, which is the number of times the BAW needs to trigger the retry, decreased to 9.9%. The top error during this period changed to "remote end did not answer" (107/3082, 3.5%), followed by "remote end busy" (89/3082, 2.9%).

Table . eFax status codes (March 2023- December 2023, post new retry logic deployment).

eFax status code	Count, n (%)
No errors	2778 (90.1)
Remote end did not answer	107 (3.5)
Remote end busy	89 (2.9)
Unexpected error	72 (2.3)
No fax was detected	25 (0.8)
Unable to negotiate fax session with remote terminal	7 (0.2)
An error occurred during the file rasterization process	2 (0.1)
Failure to confirm page reception by remote terminal	1 (0)
Remote terminal terminated the fax session unexpectedly	1 (0)
Total	3082 (100)

Referral Pages Count

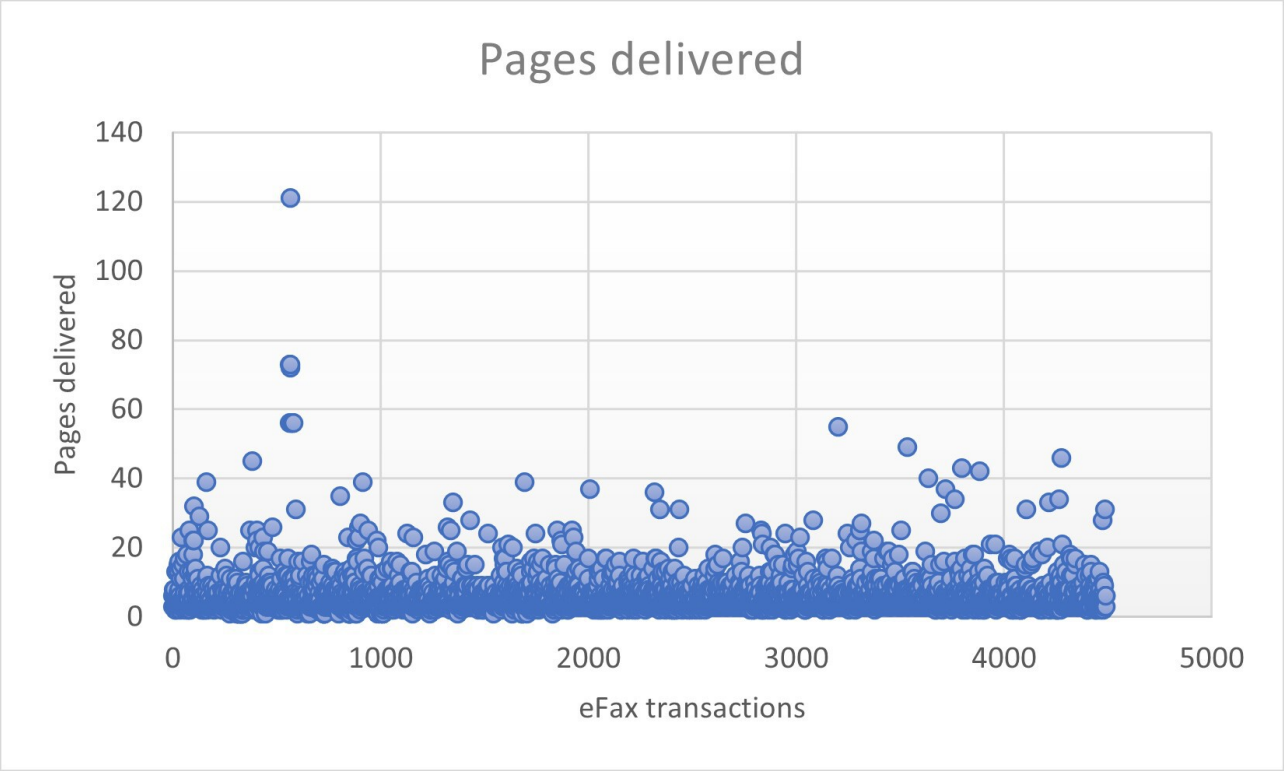
The majority of eFaxes processed during the PoC were between 1 and 10 pages long (4115/4504, 91.4%), with the most common number of pages being 3 (1951/4504, 43.3%), and an overall average of 5.6 pages per eFax. A few outliners were observed, such as 32 eFaxes (0.7%) having more than 30 pages in the packages, with a maximum of 121 pages (Table 4 and Figure 3).

XSL•FO
RenderX

Table . eFax pages processed count.

Pages delivered	Transactions count, n (%)
1	38 (0.8)
2	151 (3.4)
3	1951 (43.3)
4	416 (9.2)
5	517 (11.5)
6	335 (7.4)
7	281 (6.2)
8	201 (4.5)
9	138 (3.1)
10	87 (1.9)
11 - 20	307 (6.8)
21 - 30	50 (1.1)
31+	32 (0.7)
Total	4504 (100)

Figure 3. eFax pages delivered scatter plot diagram.



Clinician and Patient Experience

During the PoC, the primary care sender survey was sent to 147 unique sending clinicians, and responses were received from 18 (12% response rate). Of the 18 responses, 72% (n=13) were satisfied with the eFax workflow, and 72% (n=13) felt the eFax has improved their ability to track or follow the referrals (Multimedia Appendix 2).

Multiple senders still noted that there were not enough receivers on the map. Furthermore, 4 out of the top 10 receiver clinics were able to answer a phone call from the PoC team, but none of them were aware of the eFax PoC work, although they did receive the most eFaxes during the PoC and multiple faxes were sent to their clinics. They did not notice the difference between the eFaxes and their regular fax-based referrals. The findings from the focus group interviews illustrated that the primary care senders felt that the new solution improved their workflow, helped them track the referral status, and that patients were more involved in the process. On the other hand, receivers noticed the eReferral platform logo, but there was no positive or negative

XSL•FO
RenderX

impact on their existing workflow. Patient experience data related explicitly to the eFax referrals processed over the evaluation period could not be segmented from the eReferral dataset. However, patient satisfaction rates remained consistently high during the PoC time, similar to those seen before the PoC was implemented, which could be an indicator that from patient perspective, satisfaction with the referrals made via eFax was high and similar to the satisfaction with eReferral. However, more data will need to be collected to prove this assumption. Feedback from interviews with 4 different deployment team members indicated that there was no significant difference in engaging the eFax receivers as compared with the routine flow when onboarding as an eReferral receiver.

Discussion

Study Rationale

Ontario has made several efforts to improve patient information sharing in clinical settings. The Ontario Medical Association has recommended transitioning from fax technology to the eReferral system to enhance efficiency and patient experience [5]. The Ontario eServices program was established to provide change management support and expedite the adoption of eReferral technology. Digital standards, such as the digital health information exchange framework and eReferral HL7 FHIR specifications, have been established to improve interoperability and secure information sharing [16]. In addition, the government has initiated a plan to phase out fax machines by 2028, promoting the adoption of digital communication alternatives [11]. While transitioning to eReferral offers numerous benefits, a significant barrier to its adoption is the requirement for both sending and receiving clinicians to be on the same platform for effective information sharing. The traditional onboarding process is time-consuming and labor-intensive. Therefore, an innovative method is essential to bridge the gap between digital eReferral senders and fax-based referral receivers, thereby expediting eReferral adoption.

This PoC study investigated the feasibility of using the BAW platform as a temporary solution to support eReferral adoption by connecting the eReferral platform and select fax services, enabling them on the eReferral platform as eFax receivers. This solution aimed to improve the sending clinicians' experience by expanding the available receiving clinicians on the platform, reducing workflow redundancy and leveraging the BAW platform to facilitate the senders' transition to eReferral. The solution is designed to provide a seamless user experience and can be used as a temporary bridging technology while the onboarding process is underway.

Clinician Experience Improvement

The solution design principle focused on minimizing the impact on the current workflow for both senders and receivers. Senders can reduce the need to maintain 2 separate workflows for eReferral and non-eReferral receivers, accessing an expanded list of eReferral receivers. eFax receivers can keep their current workflow with no alterations, as the referrals made to them look the same as fax referrals and do not require any workflow changes. The survey findings reflected that the clinicians felt the solution achieved the goals of the design principle; the senders were satisfied and they felt it improved their workflow while receivers' workflows were not interrupted and they noticed minimal changes throughout the PoC. The only behavioral change required was the need for senders to manually enter the appointment information back into the eReferral platform so that the patient can be notified through emails. Due to the extra tasks required, the entry percentage was 19.4% for the eFaxes booked (Table 1) with appointment dates documented in the eReferral platform, as compared with 57% of eReferrals within that same time period. As such, there is an opportunity for future enhancements to better capture the appointment information for eFaxes sent. Although this was lower than the automatic collection via the traditional eReferral workflow, this still presented an opportunity to calculate the wait time information so it can be published for eFax receivers, supporting clinician informed decision-making when initiating a referral for a patient.

In the current hybrid workflow, a sender needs to go back to the fax referral workflow if the receiver is not on the eReferral platform. Senders either need to maintain the duplicate workflow or prompt the receivers to adopt the eReferral technology, which usually takes a few weeks after the receivers agree to participate. By bridging the gap with the BAW platform, senders can ensure that they take advantage of the benefits of eReferral without experiencing any significant disruptions or delays. The enabled eReferral via eFax receivers list was expanded to allow eReferral to flow to the receivers unavailable through the traditional eReferral workflows. This solution allows for the eReferral platform to have more transactions flow through the solution reducing the need for eReferral users to maintain more than one referral pathway in order to provide care to their patient population. The more receivers are enabled through this solution, the less the need for senders to fax referrals, with the optimal goal to have senders send all referrals through a similar workflow, electronically.

Patient Experience Improvement

It is reported that eReferral can improve patients' experience with the referral process, and more specifically that 80% of patients felt they were more informed during the referral process [4]. The eReferral via eFax technology enables the patients to experience the benefits of eReferral even though the receivers were not onboarded to eReferral. Throughout the PoC, 3137 (69.6%) patients had their email included in their referral and received notification emails about the referral progress and updates. eFax specific patient experience survey results could not be segmented from the eReferral data set during the same period and therefore could not be assessed. However, the overall patient satisfaction rate remained consistently high throughout the PoC period.

This technology enables the option of patients being included in the communication loop on their referrals, regardless of whether the receiver of their referral is on fax or eReferral, as the solution enabled email notifications, keeping patients informed surrounding referral status updates, throughout the referral journey. This technology reduces the known issue for patients, as traditional fax referrals can never send an email notification to patient. This can contribute to fulfilling the

XSL•FO
RenderX

commitment of patient-centered care, even during this migration phase.

Cost Saving

The new bridging technology also helps to save costs. First, the technology reduces senders' need for paper usage, as they no longer need to print and fax documents. This can lead to significant cost savings. During the PoC, the average number of pages sent was 5.6 pages, translating to about 11 pages for both senders and receivers combined. It is reported that primary care clinicians send a median of 26 referrals per month [19]. The bridging technology can reduce half of that cost through the adoption of eFax and eventually remove all the paper costs when all the senders and receivers are onboarded to the eReferral platform. In addition, costs related to fax maintenance and printing ink would significantly be reduced over time.

Second, as part of the eReferral technology benefits, the eFax technology triggers email communication for patients, which can help avoid staff calls to the primary care clinic and reduce the time patients and clinical staff spend hunting down information [20-23]. This can lead to significant time savings for both patients and clinical staff. The new bridging technology is a step toward a more efficient and cost-effective health care system.

Third, the built-in BAW retry logic helped to reduce the human effort required to track the fax status and resend if the fax fails. The data from both phases illustrated in real practice when using the fax technology to communicate, the clinicians still need to manually monitor and resend the fax if the fax fails. Failures occurred in 37.7% (1023/2712) of transmissions without the fax service retry enabled (phase 1), compared with 9.9% (304/3082) with the retry enabled (phase 2). During phase 1, the BAW platform automatically retried failed eFax transactions to improve the delivery successful rate to 97.2%, avoided 37.5% (1017/2712) manual resubmission, and only 2.8% (48/1706) eFaxes required manual intervention. During phase 2, after the fax service automatic retry setting was enabled, the fax failure rate was reduced to 9.9%, which still required the built in BAW retry logic to automatically resend the failed eFaxes. The new updated retry logic improved the delivery success rate to 98.7% and further reduced the manual monitoring and resubmission to 1.3%.

There were improvements made in the eFax technology, and the BAW retry logic that reduced the failure rate but there is still increased value in transitioning to eReferral. eReferral requires extremely few retires, if any, due to the digital nature of the system. Unless there is a system or internet connectivity disruption, the eReferral will be delivered to the receiver immediately upon sending. There will be less failures and improved connectivity between the senders and receivers, limiting the risk of lost or failed referrals and decreasing the negative outcomes for the patient that might occur due to failures or lost transmissions.

System-Level Benefits

The eReferral via eFax platform provides system-level benefits that are only available using the eReferral platform and are otherwise unavailable in traditional nondigital workflows. In the fax referral workflow, transaction data are often recorded on paper, making tracking the referral flow from senders to receivers difficult. In addition, the wait times of receivers are generally not publicly available since it is challenging to track when and how appointments are booked. By leveraging the BAW platform, transactional data can be accessed earlier, and insights into the referral process can be gained that would otherwise be impossible. By providing visibility into the referral flow, the BAW platform can help optimize the referral workflows and improve the patient's experience. The BAW platform can also help identify bottlenecks in the referral process and take corrective action to improve the efficiency of the process. When the senders make referrals, essential factors like wait times and distance can be reviewed to support a more informative decision-making process, supporting better outcomes for patients.

The traditional onboarding process of an eReferral receiver includes multiple steps, such as the initiation of the discussion, referral form review and customization, EMR integration deployment, and end user training. Based on the learnings from the Ontario eServices Program, this process usually takes 6 - 8 weeks of change management support and sometimes even longer. Compared with the traditional receiver onboarding process, enabling the eFax workflow only includes receiver identification and validation, which usually takes a few minutes. The new process can drastically reduce the time required for the receiver onboarding process. The senders can start having a broader receiver list on the eReferral platform without disrupting the regular receiver onboarding process. It is very common for the senders to send referrals across regions (Table 1), and enabling the receivers through the proposed technology has the great potential to allow a large number of receivers enabled across the regions. Meaning, more receivers (as well as their wait times) will be visible on the eReferral platform to support the senders' decision making. It is beneficial to use relatively less effort to allow the maximum benefits that both senders and patients can start to experience. At the same time, the normal eReferral onboarding process can still take its own pace while increasing the number of receiving sites to support increased usage by those senders already within the eReferral network. The senders and their adoption of eReferral are currently restricted by the number of receivers present on the eReferral platform and users note that expanding the receiver list increases their usage of the tool. The lack of having a sufficient number of receivers that eReferrals can be sent to could lead to less opportunities to send eReferrals for clinicians and thus become a risk of discontinuing eReferral use by maintaining one workflow via faxing. This may lead to the need of re-engaging of clinicians to promote active use of eReferral, which in turn presents a monetary loss for the health system.

Future Work

There are more than 17,800 specialists registered in Ontario that might receive referrals [24]. With other hospital service providers and independent Health Facilities, Ontario's total possible medical referral receivers are likely more than 19,000. The Ontario eServices Program (previously System Coordinated Access) started to onboard clinicians to the eReferral platform in 2017. Using an approach that focused on both the onboarding

XSL•FO
RenderX

of primary care clinicians as well as receiving specialists, in just over 6 years, in Ontario 2000 receivers and 11000 senders were onboarded with change management supports, accounting for over 2 million referrals processed. There is still significant progress to be made. The eServices Program has been working on multiple strategies to increase the speed of adoption, such as exploring the use of the central intake models. A more innovative solution may be required to support eReferral adoption compared to the number of possible receivers.

The BAW platform could be used to bridge the gap between the fax system, that is widely used in the Canadian health care system, and the new eReferral systems, allowing minimal disruption of the sender's workflow while receivers using the fax system can take their pace being onboarded to the new platform. This approach presents a significant value for senders to adopt the eReferral solution, as it can provide access to a large number of referral receivers from the start of the initiative, which it can be difficult to attain through eReferral onboarding and change management initiatives alone. Senders may not wish to adopt the solution if it does not allow them access to a large number of receiving specialists, and specialists may not want to adopt the solution and introduce another workflow in their clinic as there may not be a sufficient number of primary care clinician senders onboarded on eReferral to send eReferrals to them. This presents a challenging dilemma on which to focus first, that can be minimized with the BAW platform allowing access to large number of receivers with minimal effort, presenting a favorable context for sender onboarding, followed by receivers.

The current evaluation demonstrates the effectiveness of expediting eReferral usage through the eReferral via eFax platform, while also highlighting the potential to further increase utilization by including additional receivers. In addition, there is a future opportunity to conduct a time-saving study to illustrate further the cost savings achieved by implementing this methodology.

Acknowledgments

The authors would like to thank Dr. Scott Laing for his efforts in creating the generic referral form to support the eReferral via eFax project. Our gratitude to Middlesex London Ontario Health Team (OHT), Northwestern Toronto OHT and Burlington OHT, for their support during the receiver identification and solution implementation. The authors appreciate Paul Sulker for his expertise and knowledge on digital health transformation strategies.

Funding for this project was provided by the Ontario Ministry of Health and Ontario Health. The funders were not involved in the study design, data collection, data analysis, or manuscript preparation, or in the decision to publish the results. The views expressed do not necessarily reflect those of the Province of Ontario.

Conflicts of Interest

None declared.

Multimedia Appendix 1
eFax receivers distribution.
[DOCX File, 16 KB - medinform_v13i1e62983_app1.docx]

Multimedia Appendix 2
Primary care sender clinician survey results.
[JPG File, 122 KB - medinform_v13i1e62983_app2.jpg]

References

1. Keely E, Liddy C. Transforming the specialist referral and consultation process in Canada. CMAJ 2019 Apr 15;191(15):E408-E409. [doi: 10.1503/cmaj.181550] [Medline: 30988040]
2. Hughes CA, Allen P, Bentley M. eReferrals: Why are we still faxing? Aust J Gen Pract 2018;47(1-2):50-57. [doi: 10.31128/AFP-07-17-4285] [Medline: 29429313]
3. Adetunji A, Aremu A(, Wong A, et al. Alberta netcare ereferral evaluation report. : Alberta Health Services; 2019 URL: https://www.albertanetcare.ca/documents/Netcare-eReferral-Evaluation-Report_2019.pdf [accessed 2024-01-15]
4. Mohammed HT, Huebner LA. Assessing patient satisfaction and experience with an electronic referral process. Qual Manag Health Care 2020;29(1):20-29. [doi: 10.1097/QMH.0000000000000235] [Medline: 31855932]
5. Prescription for Ontario: doctors' 5-point plan for better health care. : Ontario Medical Association; 2021 URL: https://www.oma.org/siteassets/oma/media/public/prescription-for-ontario-doctors-5-point-plan-for-better-health-care.pdf
6. Must-know fax machine usage statistics. Gitnux. 2023 Dec 25. URL: https://gitnux.org/fax-machine-usage-statistics/ [accessed 2024-05-08]
7. NHS banned from buying any more fax machines. The Guardian.: Guardian News and Media Limited; 2018. URL: https://www.theguardian.com/society/2018/dec/09/nhs-banned-from-buying-any-more-fax-machines [accessed 2024-05-08]

XSL•FO
RenderX

8. NHS is using 800 fax machines despite government vowing to phase them out almost four years ago. Daily Mail Online.: Daily Mail and General Trust; 2022 Aug 6. URL: https://www.dailymail.co.uk/news/article-11088377/NHS-using-800-fax-machines-despite-government-vowing-phase-four-years-ago.html [accessed 2024-05-08]
9. Hundreds of NHS hospitals still using archaic fax machines despite orders to bin them. The Sun. 2023 May. URL: https://www.thesun.co.uk/health/22431913/nhs-hospitals-still-using-fax-machines/ [accessed 2024-05-08]
10. Taking the pulse: a snapshot of canadian health care, 2023. Canadian Institute for Health Information. 2023. URL: https://www.cihi.ca/en/taking-the-pulse-a-snapshot-of-canadian-health-care-2023/better-access-to-electronic-health [accessed 2024-05-08]
11. Your health: a plan for connected and convenient care. OntarioMD. 2023. URL: https://www.ontario.ca/page/your-health-plan-connected-and-convenient-care [accessed 2024-05-08]
12. Tuot DS, Leeds K, Murphy EJ, et al. Facilitators and barriers to implementing electronic referral and/or consultation systems: a qualitative study of 16 health organizations. BMC Health Serv Res 2015 Dec 19;15(568):568. [doi: 10.1186/s12913-015-1233-1] [Medline: 26687507]
13. Business automation workflow product overview. IBM. URL: https://www.ibm.com/docs/en/baw/23.x?topic=2301-product-overview [accessed 2024-05-08]
14. FHIR integration: ocean FHIR API documentation. OceanMD. URL: https://ocean.cognisantmd.com/public/fhirApiDocs.html#section/API-Principles [accessed 2024-05-08]
15. Pan-Canadian eReferral-eConsult (CA:eReC) 1.0.3-DFT. Simplifier. URL: https://simplifier.net/guide/pan-canadian-ereferral-econsult-ca-erec-iguide/Index/Home/Introduction?version=1.0.3-DFT [accessed 2025-03-31]
16. Ontario eReferral eConsult HL7® FHIR® Implementation Guide - Draft v0.11.1. Simplifier. URL: https://simplifier.net/guide/ca-on-ereferral-r4-iguide/Index/Home/Introduction?version=0.11.1 [accessed 2025-03-31]
17. Laing S, Jarmain S, Elliott J, et al. Codesigned standardised referral form: simplifying the complexity. BMJ health & care informatics 2024 Jun 19;31(1):e100926. [doi: 10.1136/bmjhci-2023-100926] [Medline: 38901862]
18. Tri-Council Policy Statement: Ethical Conduct for Research Involving Humans – TCPS 2. Canadian Institutes of Health Research, Natural Sciences and Engineering Research Council of Canada, and Social Sciences and Humanities Research Council of Canada. 2022. URL: https://ethics.gc.ca/eng/policy-politique_tcps2-eptc2_2022.html [accessed 2025-05-08]
19. Liddy C, Arbab-Tafti S, Moroz I, Keely E. Primary care physician referral patterns in Ontario, Canada: a descriptive analysis of self-reported referral data. BMC Fam Pract 2017 Aug 22;18(1):81. [doi: 10.1186/s12875-017-0654-9] [Medline: 28830380]
20. Mohammed HT, Payson LA, Alarakhia M. The impact of integrating electronic referral within a musculoskeletal model of care on wait time to receive orthopedic care in Ontario. PLoS ONE 2020;15(11):e0241624. [doi: 10.1371/journal.pone.0241624] [Medline: 33141866]
21. Azamar-Alonso A, Costa AP, Huebner LA, Tarride JE. Electronic referral systems in health care: a scoping review. Clinicoecon Outcomes Res 2019;11:325-333. [doi: 10.2147/CEOR.S195597] [Medline: 31190925]
22. Cannaby S, Westcott D, Pedersen CD, Voss H, Wanscher CE. The cost benefit of electronic patient referrals in Denmark: summary report. Stud Health Technol Inform 2004;100:238-245. [Medline: 15718585]
23. Patient electronic messaging: 12 tips to save time. American Academy of Family Physicians. URL: https://www.aafp.org/pubs/fpm/issues/2022/1100/electronic-messaging-tips.html [accessed 2025-05-30]
24. Physicians in Ontario Longitudinal Overview. Ontario Physician Reporting Centre (OPRC). 2023 Oct 5. URL: https://physicianreporting.org/data-visuals/pio-overview/ [accessed 2024-05-08]

Abbreviations

BAW: business automation workflow
EMR: electronic medical record
eReferral: electronic referral
FHIR: Fast Healthcare Interoperability Resources
HL7: Health Level Seven
NHS: National Health Service
PoC: Proof-of-Concept

XSL•FO
RenderX

Edited by J Klann; submitted 14.06.24; peer-reviewed by C Wu, MV Ebrahim; revised version received 15.04.25; accepted 25.04.25; published 30.06.25.

Please cite as:
Tian Z, Wierts K, Hyseni L, Gerritsen B, Lynch K, Buchanan R, Alarakhia M
A Unique Way to Axe the Fax Through Using Business Automation Workflow to Expedite eReferral Adoption, Bridging eReferral, and Fax: Proof-of-Concept Study
JMIR Med Inform 2025;13:e62983
URL: https://medinform.jmir.org/2025/1/e62983
doi:10.2196/62983

© Zhigang Tian, Kayla Wierts, Lirije Hyseni, Beth Gerritsen, Kim Lynch, Russell Buchanan, Mohamed Alarakhia. Originally published in JMIR Medical Informatics (https://medinform.jmir.org), 30.6.2025. This is an open-access article distributed under the terms of the Creative Commons Attribution License (https://creativecommons.org/licenses/by/4.0/), which permits unrestricted use, distribution, and reproduction in any medium, provided the original work, first published in JMIR Medical Informatics, is properly cited. The complete bibliographic information, a link to the original publication on https://medinform.jmir.org/, as well as this copyright and license information must be included.

XSL•FO
RenderX

Incorporating Generative AI Into a Health Informatics Curriculum to Build 21st Century Competencies: Multisite Pre-Post Study

Freddie Seba[1,2], MBA, MIPS; Miriam Isola[3], DrPH, CPHIMS; Laura Mills[3], MA, PCOE; Mohan Zalake[3], PhD; Jacob Krive[3], PhD, MBA, CPHIMS

[1]Masters of Science in Digital Health Informatics School of Nursing and Health Professions, University of San Francisco, 2130 Fulton Street, San Francisco, CA, United States

[2]School of Education, Leadership Studies Program, University of San Francisco, 2350 Turk Blvd., San Francisco, CA, United States

[3]Department of Biomedical and Health Information Sciences, University of Illinois Chicago, Chicago, IL, United States

Corresponding Author:
Freddie Seba, MBA, MIPS
Masters of Science in Digital Health Informatics School of Nursing and Health Professions, University of San Francisco, 2130 Fulton Street, San Francisco, CA, United States

Abstract

Background: We designed learning assignments for students to develop knowledge, skills, and professional attitudes about generative artificial intelligence (AI) in 2 different Master's level courses in health informatics. Our innovative approach assumed that the students had no technical background or experience in using generative AI tools.

Objective: This study aims to offer generalizable methods and experiences on integration and assessment of generative AI content into the higher education's health informatics curricula. The study's central driver is the preparation of graduate students with generative AI tools, skills, ethical discernment, and critical thinking capacities aligned with the rapidly shifting job-market requirements, independent of graduate students' backgrounds and technical expertise.

Methods: During the semester, students completed a pretest and posttest to assess knowledge about generative AI. Reflections explored their expectations and experiences using generative AI to complete their assignments and projects during the semester. Strong emphasis was placed on building skills and professional attitudes by using generative AI. Student engagement in behavioral, emotional, and cognitive domains was explored via detailed analysis of student reflections by faculty.

Results: Students at the University of Illinois Chicago increased their knowledge about generative AI from 81% to 93% through research of the basic generative AI concepts, as evidenced from outcomes of the open-book pre-and posttests given at the beginning and end of the capstone course. University of San Francisco students also improved from 77% to 80% by the end of the semester. Faculty analysis of student reflections upon completion of the course revealed primary interests in the essentials of generative AI, AI transformations to information and knowledge, and organizational changes influenced by AI adoption in the health care organizations, with ethics being a primary driver of students' interests and engagement.

Conclusions: Data from student reflections provided insight into generative AI skills that students developed and that health informatics programs can consider incorporating into their curricula. Building competencies in generative AI will prepare students for the 21st century workforce and enable them to build skills employers are seeking in the new digital health environment.

(JMIR Med Inform 2025;13:e76507) doi:10.2196/76507

KEYWORDS

generative artificial intelligence; student engagement; capstone experience; generative AI ethics; pedagogical innovation; generative AI; artificial intelligence; AI

Introduction

The current decade has seen much technological progress, but one of the most impactful and controversial areas has been generative artificial intelligence (AI). Since AI was first discussed in the 1950s [1] and especially since it exploded onto the technological scene in the 2020s, it has been a source of both wonder and fear about how it might help, hinder, and otherwise permanently alter human life. Today, in 2025, AI is a household term and a daily topic of news and discussion. It is easy to imagine a future in which AI is even more ubiquitous than it already is, but two of the most talked-about areas of AI incorporation today are education and health care.

AI use has both supporters and detractors in education and health care. Proponents of AI in education tout its potential to individualize learning experiences and thereby increase student engagement; they also advocate for AI's many supportive functions such as analyzing and managing various student data

XSL•FO
RenderX

and streamlining administrative tasks [2]. Meanwhile, AI has been used in health care since the development of a glaucoma consultation program at Rutgers University in 1976 [1]. Since then, exponential advancements in AI system design have led to a proliferation of clinical uses. ChatGPT, a popular tool developed by Open AI, for example, is being used in applications such as answering patient questions; assisting in clinical data analysis and decision making; responding to emergencies; assisting in practice management; and assisting in data management and other aspects of medical research [3].

Along with the advantages and benefits of generative AI's educational and health care applications, each presents specific challenges and raises questions. Detractors of generative AI in education cite the potential for students to cheat with AI. Some also warn against students leaning too heavily on AI to the diminishment of their own critical thinking abilities [2]. In both education and health care, questions arise about output accuracy plus such ethical issues as data privacy and output bias, among others.

Health informatics lies at the intersection of technology and health care, and as health informatics educators, we realize that whether we welcome it or fear it, AI will play a large role in our students' futures. In August of 2024, 28% of the US population aged 18 - 64 years reported using AI at work, with 1 in 9 using it on a daily basis [4]. More precisely, our students will graduate into a health care profession that is already regularly using AI, and they will work for employers who expect that they are well prepared to use it in their jobs. In fact, employers already prioritize AI competencies over prior non-AI experience [5] in the job candidates' profiles and believe AI skill sets are more important than many others [6]. Employers want graduates who can design, implement, and then manage needs-based AI systems; they also want graduates equipped with the specialized knowledge and skills to monitor and maintain those systems [7]. Job seekers need proficiency in using AI for data cleaning and management, performance management, and predictive analytics, among other knowledge and skills, to compete for positions in the most AI-advanced companies [8] Knowing that technology, including AI, advances vastly more quickly than official university curricula, we felt it imperative to transition some of our assignments so our students could begin using AI in a health informatics context now.

Let us first define what we mean by AI literacy. AI literacy is the critical ability to understand and mindfully interact with AI. It is more than just understanding how AI applications operate at a technical level. It is about understanding their functional level, benefits, challenges, and limitations [8]. AI literacy encompasses understanding the technical aspects of how it operates but also involves using critical thinking to assess its impact on humans, systems, society, and the environment [9]. AI literacy extends beyond a conceptual understanding of the theory behind it to also encompass the ability to ethically and responsibly use it to address problems, conduct research, or enhance productivity and growth. It is about actively using AI tools to solve problems and, in doing so, feeling engaged and interested in the process [10]. According to recent research, developing AI literacy involves 3 integrated skills: understanding fundamental AI concepts, evaluating the broader societal impacts of AI, and effectively using AI technologies in everyday contexts [9].

We represent two very distinct Master's in Health Informatics programs. University of Illinois Chicago (UIC) is an all-online, asynchronous program founded in 1999 and has been completely online since 2010. Many of our students are returning to school after time spent working; thus, they are older than traditional graduate students, and many already possess significant experience in health care, business, or technical fields. The UIC program has an overall focus on population-level social informatics and offers students courses and specialization options in data science, mHealth, and leadership.

University of San Francisco (USF) is a hybrid program. Students spend over half their time in-person on campus and the remainder of their time online. The USF's Master of Science in Digital Health Informatics is a young, dynamic program designed for small cohorts of approximately ≤20 students, offering personalized education through a combination of hybrid and in-person formats. Many students are recent bachelor's degree recipients with backgrounds in public health, business, health professions, nursing, medicine, and technology. The USF program focuses on data analytics, digital health, and clinical informatics, as well as offering course options in public health informatics, clinical leadership, and nursing informatics. The Master of Science in Digital Health Informatics program equips students with essential skills in health care, data science, and technology, emphasizing practical and project-based learning. Graduates typically pursue careers in hospitals, digital health startups, health care analytics companies, pharmaceutical companies, nonprofit organizations, and clinical research institutions, leveraging their specialized training to improve health care outcomes and informatics solutions.

In our endeavor to rapidly infuse AI into our curricula, we focused on 4 knowledge domains of AI competencies for health informatics education: essentials of AI; applications of AI to health informatics; AI transformations to information and knowledge; and organizational change and adoption of AI within the health care organization. We based these categories on prior work done in the development of a health data science concentration within a health informatics curriculum [11]. As part of that work, a list of 50 skills and competencies, categorized into 4 knowledge domains, was developed based on input from health informatics professionals and industry experts, health informatics faculty, and analysis of the health informatics labor market. We modeled the 4 knowledge domains of AI competencies for health informatics education on the original 4 knowledge domains for health data science. Within each of these AI competency categories, we listed knowledge, skills, and attitudes we believed our programs would need to provide for our students, leaving room for future ideas. Our new work builds on the previous work, incorporating generative AI skills and competencies into the same knowledge domains. The domains, skills, and competencies then enabled us to develop generative AI assignments.

During the fall 2024 semester, each program incorporated a generative AI assignment into a course, assessing each student's preliminary knowledge of AI, their knowledge of AI at the

XSL•FO
RenderX

conclusion of the assignment, and then each student's reflections on AI. UIC students participated in this study during BHIS 593, their capstone experience, the culminating course in the Master's in Health Informatics. This course requires students to research a topic of interest over the 16-week semester, delivering a paper or project at the end. The goal is for students to synthesize their learnings from their degree program and demonstrate competency as health informaticians.

USF students participated in this study during HS 633, *Exploring Generative AI Ethics: Intersection of Education and Health Ecosystems*, which they took approximately half-way through their master's program. This course, a hands-on workshop, incorporates the latest AI literature and tools and focuses on generative AI, AI ethics and governance concepts, AI applications, use cases, frameworks, and AI policies with special emphasis on health care. The goal is to equip students with foundational knowledge and practical skills in generative AI, preparing them to navigate the Silicon Valley tech ecosystem and the traditional health care landscape [11]. USF's generative AI Ethics course (HS 633) was conceived not as a technical deep dive into generative AI models and methods but as a framework-building course that foregrounds ethics and governance. This course was offered for the first time in Fall 2024 to coincide with this research study.

Our research questions for this multisite study were:

1. Did students learn (develop knowledge) about generative AI by doing the assignments?
2. Did students say they developed generative AI skills and professional attitudes by completing the assignments?

Methods

Design, Setting, and Participant Recruitment

This was a multisite study of assessment of assignments completed by Master of Health Informatics students at UIC and USF campuses in the fall of 2024. Across both sites, a total of 17 students participated in the research.

Ethical Considerations

The institutional review boards (IRB) of the UIC and USF approved this study under the exempt research determination under the UIC ID STUDY2024-0927 and USF's ID 2167. This was a multisite study of the assessment of assignments completed by Master of Health Informatics students at UIC and USF campuses in the fall of 2024. Across both sites, a total of 17 students participated in the research.

UIC Program

At UIC, the research was implemented in the online health informatics curricula for Biomedical Health Information Sciences in the capstone course required to complete the Master of Science in Health Informatics (MSHI) program. There were 10 (59%) participants from UIC. Students chose from the 4 areas of generative AI practice and developed their specific topics working with faculty to define the scope and deliverables for their project. Topics explored real-world questions of interest for which students developed a blueprint or prototype solution or a use case. Table 1 contains information about the 4 topic areas.

XSL•FO
RenderX

Table . Generative artificial intelligence (AI) topics.

Topics	Focusing questions	Description
Clinical uses	• How is generative AI being used to augment provider and clinician workflows? • What is the potential for generative AI to assist in improving health outcomes?	The information needed to make medical decisions (eg, medical history, laboratory and imaging results, and unstructured clinical notes) can be scattered across multiple records that exist in myriad formats and locations. Generative AI could be used to compile and organize this information—and put it into a format that is accessible and clinician-friendly—to accelerate and augment critical thinking. In addition, generative AI–enabled ambient documentation could pull information from clinician conversations and generate natural-sounding notes. Technology could also be trained to identify patterns that are too subtle for a human to recognize.
Patients or consumers	• What is the consumer or patient perspective on using generative AI for health care? • In what ways can generative AI improve the patient experience or patient engagement to manage chronic conditions?	Accurate real-time audio and SMS text messaging could be generated instantly, and in different languages, as frontline workers interact with people for health care and social services. Generative AI also could translate documents, websites, laws, regulations, and policies. Health advisories could make essential information accessible to a diverse population. Generative AI could also play a central role in optimizing and mitigating health and safety risks by generating worksite-specific safety training that replicates real-world settings and critical scenarios.
Frontline or first responders and public health, community social services use of AI	• How might generative AI be used to improve patient engagement (from the public health perspective)? • In what ways can generative AI be used to streamline emergency response in the field, urgent care, or the hospital emergency department?	Operational inefficiencies or limited capacity in the call center can translate to decreased customer satisfaction. Generative AI could help to create hyperpersonalized experiences with customers and patients. It could also help efficiently support customers and reduce call volume handled by associates. The technology might also assist human staff in generating responses to customer questions, insurance coverage, and other plan details. The customer service experience can have a direct impact on patient perception, even without any change in charged costs or appointment wait times.
Ethical use of generative AI	• How can organizations create an ethical framework for generative AI in health care (consider bias and hallucinations)? How can they use an ethical framework and still support team science and innovation? • What are the data governance policies and steps needed for quality control and validation of a generative AI model?	Set up an experiment that identifies and examines these issues. Recommendations for how organizations should proceed to build this into governance policies for generative AI and how it should be considered in building capabilities for using generative AI to increase AI literacy in the workforce.

All students enrolled in the course were given the opportunity to participate in the research at the beginning of the semester. Participation was voluntary, and students who chose not to do the research were still able to complete the course.

All data were collected via the Blackboard Learning Management System (Anthology Inc). In Blackboard, students completed a pretest to assess their baseline knowledge of generative AI. The same questions were given as a posttest at the end of the course to assess student learning. The purpose of the pre-post test was to determine any familiarity or knowledge of basic AI concepts. The questions were adapted from LinkedIn Learning courses available to UIC students. Questions were also generated by using ChatGPT with this prompt (Textbox 1):

XSL•FO
RenderX

Textbox 1. Prompt and sample questions

Provide 12 questions about generative AI that can be used as a pretest to assess health informatics graduate students' current understanding of generative AI. Make the questions multiple choice, true or false, and make 2 of them short answer. Provide the answer key and any citations that support the questions and that students can go to for more detailed information on the question.

Sample questions were as follows:

1. What is generative AI?

a. A type of AI that focuses on generating new data similar to existing data

b. A method for organizing data

c. A technique for visualizing data

d. A process for analyzing big data

Answer: a

2. Which of the following is a common application of generative AI in health care?

a. Predicting stock market trends

b. Generating synthetic medical images for training purposes

c. Analyzing social media trends

d. Managing electronic health records

Answer: b

3. Generative AI can only be used for creating images and text. True False

Answer: False

4. Describe one way generative AI can be used to improve health care outcomes.

In addition, students completed self-reflections about skills developed and their attitudes toward using generative AI and how they thought it might impact their health informatics work and careers. The reflections were also completed at the beginning and at the end of the semester (Table 2).

XSL•FO
RenderX

Table . Student reflections.

Reflection	Questions
Reflection 1	• As you look to the future, to what degree do you think generative AI[a] will be useful to your work in health informatics? To what degree do you think it might become part of your work process? • What generative AI skills do you think will be most valuable to you in your health informatics career? To what extent do you think generative AI has the potential to enhance your ability to do health informatics work or enhance your productivity? • What concerns do you have about using generative AI in your professional work? Are there aspects of generative AI that you anticipate might be problematic? What do you see as some of the drawbacks or challenges of generative AI use?
Reflection 2	• Describe how using generative AI for your capstone impacted your satisfaction with the work you produced. Do you think you were more or less satisfied with your results than you would have been without using generative AI? • Did you experience disappointment, worry, or anxiety about using generative AI to augment your capstone project? Describe any way in which using generative AI was disappointing or led to worry for you. Did this change over the course of the semester? • What impact did using generative AI have on your critical thinking as you worked on your capstone? Did it enhance your critical thinking? Did you experience reduced critical thinking due to overreliance on AI technology? • Overall, what was the best thing (the thing you enjoyed the most) about using generative AI for your capstone project? What was the worst thing (thing you enjoyed the least) about using generative AI for your capstone? • Please add any additional comments you would like to make about your learning experience and the use of generative AI.

[a]AI: artificial intelligence.

Student Assignments and Projects

For their projects, UIC students completed foundational readings. They conducted additional research exploring their chosen topic and developed prompts to use generative AI to assist in their research, brainstorm, and synthesize information. Students then drafted a 1-page description of the project scope and deliverables (final end-products) along with references that support their ideas for approval and feedback. For the rest of the semester, student projects were submitted at defined checkpoints during the semester and faculty provided feedback to guide the projects' development.

The generative AI projects in the capstone course were individualized, and faculty mentors guided students to do work that would explore their topic and use generative AI specifically for tasks such as brainstorming, research, policy and tool development, and prototype design. For example, for a project on *Ethical Implementation of Generative AI in Primary Care*, the student used a generative AI tool to generate a list of policies that the organization would need to revise or develop to establish organizational governance for using generative AI in primary care. This student then used generative AI to generate a list of roles and job titles that should be considered to participate in a subcommittee for generative AI governance. The student developed a governance structure diagram based on this research. Finally, a clinic-wide training program was developed with generative AI assistance that included basic awareness, role-based training, and ongoing support.

At USF, HS 633 introduces students to generative AI in digital health informatics through a scaffolded blend of technical foundations and applied ethical inquiry. Students are not expected to have prior coding or AI experience; instead, we begin with accessible primers on transformer architectures, natural language processing pipelines, and prompt engineering, grounding each concept in real-world health and ethical use cases. Alongside this, students engage in critical discussions about bias, transparency, and the societal impacts of large language models in clinical and public health contexts. Some of the classroom learning activities include conducting a literature review, interrogating deployment case studies, and prototyping generative AI–informed interventions and workflows.

The capstone assignment asks each student to design a credible generative AI deployment for a real-world clinical or operational problem—one that not only demonstrates feasibility but also foregrounds ethics, equity, and sustainability. Students articulate the problem space, quantify the opportunity, and craft a value-aligned solution that fits into existing health care infrastructures. The major components include market sizing using Total Addressable Market, Serviceable Available Market, and Serviceable Obtainable Market frameworks to assess reach and adoption pathways; ethical charter that explicitly addresses risks around privacy, bias, transparency, and Health Insurance

XSL•FO
RenderX

Portability and Accountability Act (HIPAA) compliance—with a mitigation plan for each dimension; evidence-based value proposition detailing projected outcomes, cost savings, and a 5-feature comparison against both legacy workflows and rival technologies; quality measurement strategy, including a 10-item Likert survey aligned to interoperability standards like Fast Healthcare Interoperability Resources, Health Level Seven International, or Systematized Nomenclature of Medicine—Clinical Terms; technical blueprint and product requirements document describing integration touchpoints with electronic medical records, mobile apps, and telehealth systems; scenario analysis exploring best- and worst-case implementation paths, resilience under public health emergencies, and tailored strategies for historically underserved populations; and scenario analysis exploring best- and worst-case implementation paths, resilience under public health emergencies, and tailored strategies for historically underserved populations.

- Technical blueprint and product requirements document describing integration touchpoints with electronic medical records, mobile apps, and telehealth systems
- Scenario analysis exploring best- and worst-case implementation paths, resilience under public health emergencies, and tailored strategies for historically underserved populations

Final deliverables include a written paper, a concise pitch deck, and a 10-minute oral defense. At the core of the assignment is an ethical charter that addresses privacy, bias, transparency, security, and HIPAA compliance, accompanied by a mitigation plan for each identified risk. Deliverables comprise a 15-to-20-page American Psychological Association–formatted concept paper, a 12 to 15 slide pitch deck with an appendix dossier, and a live scholarly defense. Assessment emphasizes the clarity of the argument, the rigor of ethical analysis, and practical feasibility, equipping graduates to articulate and implement responsible generative AI innovations in contemporary health informatics practice. Students are not only conversant in generative AI's capabilities and limits, but they are equipped to lead conversations at the intersection of innovation, governance, and health equity.

Knowledge was assessed using multiple choice and short answer tests. A pretest was given at the start of the semester, and an identical posttest was completed at the end of the semester. The tests were open book, administered on a learning management system with unlimited attempts. However, students were advised that these tests had no bearing on their grade for the course but were only for research purposes to get a baseline of what students know about generative AI.

An important part of this study was to identify skills that students will need in the workforce. AI skills and attitudes were identified using student reflections on student engagement topics exploring how they would use generative AI in their future career, concerns with using generative AI, and their satisfaction with the end product for their courses [12] At UIC, reflections were given at the beginning and end of the semester.

USF

The USF participants for this study are 7 out of 8 students who took the *Generative AI Ethics* course in the fall of 2024. A student absent from the initial survey distribution at the beginning of the fall 2024 semester was excluded from this study. The participants are in their second year of the Master's degree program in digital health informatics. USF students were introduced in class to the UIC+USF study and explained the purpose, inclusion criteria, privacy, and harm risk per the IRB-approved documentation. The 2 components of the survey (pre- or posttest and reflections) were explained to students. Students were told that participation was voluntary and would not affect their grades.

The initial USF pretest was distributed during in-person class time. Students were given ample time, up to 1 hour, to complete their surveys. Surveys identical to those used at UIC were delivered using the Google Survey app. The USF results were deidentified and remained in Google Cloud until the end of the semester. At the end of the semester, a second survey was administered via Google. This survey had 2 sections. The first section was identical to the pretest at the beginning of the semester. The additional second section was for the reflections of students who completed generative AI semester-long projects. USF's IRB approved the second test before distribution to the study participants.

The second USF survey, like the first, was distributed during in-person class time, their last before students presented their final semester-long *Generative AI Ethics* projects. Participants were given ample time, up to 1 hour in class to answer and reflect on their semester. The USF participants in the second survey were 6 out of 7 students who took the *Generative AI Ethics* course in the fall of 2024. The student absent from the initial study was excluded from the second survey for consistency. Once USF students completed the second survey, deidentified survey results were uploaded to UIC's secure box system for analysis.

The UIC capstone experience is a culmination of learning throughout the MSHI program. In their capstone, students personalize their project by pursuing an area of interest to them. This has the advantage of incorporating real-world scenarios and teaches critical divergent thinking and active learning. The USF's *Generative AI Ethics* course equips students with foundational AI knowledge that they can then bring into their work at the intersection of technology and health care. In both programs, assignment instructions included use of generative AI to support the creation of a final product.

Applying Established Frameworks

Prior to this study, we examined knowledge domains for health informatics education used in previous work by Krive and Isola [11] to create a data science concentration within the MSHI program, and we adapted the following knowledge domains for AI competencies:

1. Essentials of AI
2. Application of AI to health informatics
3. AI transformations to information and knowledge

XSL•FO
RenderX

4. Organizational change and adoption of AI within the health care organization

We developed a preliminary list of 33 competencies (Multimedia Appendix 1) as part of an effort to capture knowledge and skills employers would be looking for in health informatics graduates. The competencies came from multiple sources, including literature, job market analysis, input from industry experts, and our professional experience.

The current study was a first attempt to actually bring generative AI into the curriculum. We used Lo et al [12] as a framework to explore student reactions to using generative AI and also explore the 3 domains of students' emotional, cognitive, and behavioral engagement and disengagement with regards to ChatGPT use. Lo et al [13] conducted a systematic review that examined indicators of engagement and disengagement in each domain; they found that much remains to be researched about ChatGPT as a learning tool but that current research shows it leads to both beneficial and concerning emotional, cognitive, and behavioral outcomes [12].

The 23 pre-post test questions were foundational knowledge questions about generative AI that would be used in an introductory course assuming no prior knowledge of generative AI. The reflection prompts were based on Lo et al [13], exploring student engagement with generative AI. Using short answer prompts enabled us to gather qualitative data on student reactions to and experiences with using generative AI. Student responses were then examined against the list of AI competencies (Multimedia Appendix 1) for analysis in seeing what changes in knowledge, skills, and attitudes had taken place. These data can inform programs about key domains and concepts to consider when bringing generative AI into their curricula.

Main Measures

We collected data about developing student competencies in generative AI (knowledge, skills, and professional attitudes). The research questions were as follows:

1. Did students learn (develop knowledge) about generative AI by doing the assignments?

Regarding knowledge, students completed a pre- and posttest survey with 23 items each worth 1 point. Final scores for pretest and posttest were compared to see if students demonstrated higher scores on the posttest.

2. Did students say they developed generative AI skills and professional attitudes by completing the assignments?

Regarding skills and professional attitudes, student reflection data were collected.

Categorization of student responses was completed by 2 faculty members from UIC and 1 from USF. Each student response was evaluated to select the 1 primary element it contained and then was assigned to 1 competency category. Responses that were not related to the subject received no assignment (eg, "thank you" and "happy I took the class"). Due to this variety of the responses we received in terms of the content, depth, and clarity, we evaluated and counted all applicable student reflections across all domains. This method of evaluating all eligible responses (and excluding the most basic ones) from students explains why our numbers presented in the results exceed the number of students in the UIC and USF cohorts. Differences in faculty categorization were examined together in a work session to develop a consensus. To help us come to a consensus, we used some basic rules, that is, reflections related to ethics or accuracy were assigned to the AI transformations to the information and knowledge domain; and for longer student responses with multiple perspectives, raters assigned the knowledge domain that they agreed was the predominant domain. In most instances, such basic rules enabled us to arrive at an easy consensus with a higher degree of reliability, while in a smaller number of instances, we needed a larger discussion around the real meaning behind student reflections. The latter discussion component introduced minor variability to the qualitative outcomes of our work, since some student reflections were comprehensive and could be interpreted in more than one way.

Results

Pre-Post Test: Quantitative

Students completed a pretest survey of 23 multiple choice and short answer questions. Students demonstrated an improvement in knowledge from pretest to posttest in both courses, with UIC students improving from 81% to 93% at the end of the capstone course. USF students also improved from 77% to 80% by the end of the *Generative AI Ethics* course.

Reflections: Qualitative

To inform revisions to the preliminary list of skills, reflections were rated by 3 faculty members individually followed by a group review and consensus-building session using the knowledge domain definitions and preliminary list of skills (Multimedia Appendix 1). Results of the faculty classifications of student responses into the 4 knowledge domains are summarized in Table 3.

XSL•FO
RenderX

Table . Faculty classifications of emerging generative themes from student reflections.

Knowledge domain	UIC[a] faculty 1	USF[b] faculty	UIC faculty 2
Essentials of AI[c]	28	28	27
Application of AI to health informatics	14	14	14
AI transformations to information and knowledge	38	38	38
Organizational change and adoption of AI within the health care organization	23	23	23

[a]UIC: University of Illinois Chicago.

[b]USF: University of San Francisco.

[c]AI: artificial intelligence.

Discussion

Generative AI in Health Professions Education and Comparisons With Prior Work

The latest generative AI technologies are forging ahead and aim to change the ways students in health professions are educated [13] and medicine is practiced by emphasizing personalized care delivery based on individual characteristics of each patient derived from a wide variety of sources [14]. These technologies have already entered the medical field, whether educators are ready to address their impacts or not. So, despite faculty concerns over ethics, cheating in classrooms, and adjusting assignments to the current realities of the knowledge sources available to students, educators must ensure that generative AI is incorporated into the classroom. AI-assisted medical offices are already a reality for many health professions, and employers will have an expectation of this knowledge. The dialog about skills to be taught in the classroom, which is typically the combination of technical, medical application, and ethics perspectives [15] has already started via surveys of educators and practitioners [16], and analysis of the existing and upcoming programs and courses in clinical informatics [17].

Academic leadership in several fields of medicine has initiated inquiries into potential curriculum updates to embed AI, whether as a single course dedicated to AI or as modules embedded into existing courses to infuse AI competencies into curriculum [15,18, 19 20]. Research has explored how AI changes exam taking by comparing the performance of AI versus students on structured multiple-choice tests in medical specialties, subspecialties, and even a basic medical informatics course [20, 21]. These are interesting and valid perspectives for inquiry that will inevitably result in a solid basis for embedding generative AI into curricula and understanding how it will change classrooms of the future. However, educators have a more immediate task at hand—how do we prepare our graduates to face the realities of professional practice and employer expectations today, when the job market already requires generative AI skills? A productive dialogue among educators leading to future methods and models of education will not prepare current students for market realities. Therefore, while today's methodological efforts will result in strong foundations and understanding of the generative AI role in the classroom in the longer-term future, we assessed what could be done now to prepare our students for AI realities of the present day.

Principal Results

Differences between pre- and post-tests were noted, with higher scores achieved on the posttest. However, due to the open-book nature of the tests, performance increases may reflect the use of resources or research skills. The UIC capstone course is a research course, and students may have done research on the subject prior to and during the initial testing, despite instructions to use their existing knowledge for pretesting. Higher scores on the majority of the tests do indicate a high level of student engagement and interest in the subject, and if nothing else, these tests may have served to create interest in generative AI research among students. Because HS 633 is a novel course at USF that introduced students to generative AI concepts, emphasizing ethical frameworks rather than the technical details covered by the knowledge test, its content aligned less directly with the test domains, resulting in a smaller score gain for USF students.

A variety of perspectives was observed in the responses to the student reflection questions. Student reflection questions were developed to capture a broad range of potential reactions to using generative AI tools and asked about various dimensions of student engagement in behavioral, emotional, and cognitive domains as defined by Lo et al [13]. Students reported both satisfactions and dissatisfactions with using generative AI. Satisfaction can support creativity and innovation, build enthusiasm for the subject, and stimulate emergence in learning. This feature makes it worthwhile for educators to incorporate it into assignments. Responses included statements such as:

> *Excitement about building something and feeling empowered to build it. In the past, I would have "big" ideas that felt impossible to see through or felt like it was "just a dream." Now, with Generative AI, it's like building it can be a reality.*
>
> *Being able to experiment! I felt like keep on writing more and more prompts and keep reading the answers, that way I invested more time in the project and was able to dive in deeper in my project.*

Satisfactions were related to (1) the process of using generative AI, that is, "it helped me get the ball rolling with my project," and (2) satisfaction with results, that is, writing a paper with a

XSL•FO
RenderX

higher degree of confidence. There are several other observations of satisfaction, as follows:

- Generative AI helped to brainstorm and be more creative ("it brought the best side of me").
- Generative AI allowed me to focus on critical analysis while minimizing time spent on tedious tasks. It helped me to evaluate the analysis, improve the quality ("this is doing it better, not simply faster").
- Saved time and efficiency ("the point of using Generative AI is NOT just so you can do it faster, but it is so you can do it better-saving time allows you to do it better"). This must be explicitly conveyed to students and be part of the design of the assignments.
- Just to be trying it out ("as something new, it deserves exploration; it is a gift to be in on something exciting and new").

Dissatisfactions were more prominent early in the use of generative AI, and with experience and time, concerns decreased as students developed ways to cope with and address these concerns. Some examples of dissatisfaction were:

1. Using generative AI will be seen as cheating. Faculty should address this concern with students directly upfront, to clarify their requirements and expectations for using generative AI as a research tool in the learning process.
2. Concern about the impact on critical thinking, how to keep generative AI in the augmenting rather than dominating role. This was not a shared concern mentioned by most students, yet it is a legitimate and important one to bring up.
3. Lose originality of my work, become too reliant on generative AI. This is where students need help from faculty to understand the dividing line between using generative AI for background research versus becoming fully reliant on it to do the work and simply regurgitate and synthesize commonly available knowledge available on the Internet.
4. Inconsistency in generative AI's outputs, trusting the output. This aspect is good to address at the formative stage for building the initial generative AI skills, such as prompt engineering, or coming up with the right questions, so students feel empowered to use generative AI with confidence and to the best of their technical ability.
5. AI causing harm to patients, which is an ethical concern over the validity of the information provided by generative AI and the safety of patient information made available to generative AI.
6. Decreased anxiety, which is ultimately a positive factor in supporting student learning.

We also observed the following differences and similarities between UIC and USF student cohorts:

1. UIC students were more focused on clinical applications and process or ethics knowledge domains 2 and 3.
2. USF students were more focused on the technical and process or ethics knowledge domains 1 and 3.
3. Domain 3 (process or ethics) is the common domain of interest between students from both institutions.
4. USF students have a distinct technical focus, in addition to concerns over ethics and validity of the outcomes or information.
5. UIC students have a distinct clinical application and process focus, in addition to concerns over ethics and validity of the outcomes or information.

These differences could be attributed to variances in demographics and professional orientations of students, with USF graduates interested in positions in technology and consulting, and UIC students primarily expecting to be employed by health care providers, community, and public health organizations.

Student reflections were open format, allowing them to reflect on topics of their choice, and they frequently commented on more than one knowledge domain in a single response. This made reflections open to interpretation, and the evaluating faculty differed in how they categorized them. Using basic rules and the process of coming to a consensus among the three faculty who evaluated reflections helped us minimize the differences between faculty perceptions and normalize the numbers, leaving few differences between faculty classifications. We pursued this normalization process to be able to report on the top knowledge domains of interest by students together and on behalf of both USF and UIC institutions, as quantified by faculty based on which topics students focused on in their course reflections.

Table 3 shows the distribution of student responses across the domains. The data reveals that students responded more often to the topics of ethics, knowledge generation, organizational efficiency, and technology essentials, making them a high priority or area of interest or concern for our students. These interests consequently fall under domain knowledge 1 (essentials of generative AI) and domain knowledge 3 (ethics and knowledge of generative AI), followed closely by domain knowledge 4 (organizational change and efficiency). These choices by students indicate a high level of concern over proper technology selection and accuracy or appropriateness, compared to clinical applications, with organizational applicability and driving efficiencies as a secondary area of interest. A lower level of concern over application to health informatics is interesting, given that students are engaged in the informatics dialog and pursuing graduate education in health informatics. However, this might be explained by higher concern over proper selection and implementation of these technologies, which must be solved before medical applications are pursued with provider and patient safety in mind.

The competencies taught in accredited health informatics programs were examined recently by El-Gayar et al [22]. This group looked at the gaps in CAHIIM-accredited HI curricula competencies compared to skills/competencies employers are seeking in actual jobs posted on Indeed.com. They found that educational programs tended to focus on foundational competencies, while the job market demands were more focused on practical applications. Forty-six specific competencies were identified as gaps needed to prepare the health informatics workforce.

XSL•FO
RenderX

This analysis raises some questions about how well programs' stated competencies capture exactly what we are teaching in the courses at the assignment level. Competencies for the program may be defined more broadly and do not capture regular updates faculty make to courses and assignments. Programs may already be teaching some of the competencies El-Gayar et al [22] identify as gaps. However, this analysis also points out that areas of expectations between programs and employers may be disconnected. It is a useful starting point to inform further research and discussions about curriculum, with the goal of aligning Commission on Accreditation for Health Informatics and Health Information Management Education accreditation competencies, employers' needs with regards to AI and other knowledge and skills, and what instructors are actually teaching.

Limitations

This work was a collaboration between 2 distinctly different institutions of higher education in Illinois and California based on the common interest of swiftly bringing generative AI into the classroom. Our programs differ by student demographics, goals, and mode of education (hybrid vs online attendance). This allowed us to test various methods in 2 different academic environments. The cohorts of students were relatively small, and the courses were offered for one academic term, with plans for expanded offerings informed by these findings. We derive strengths by having two distinctly different academic environments and speed of innovation (summarizing results to quickly share with faculty colleagues around the world) and face limitations with our approach (small cohorts not allowing advanced statistical analysis, lack of identical course offerings, different student cohort characteristics). Demographic differences between our student cohorts introduce challenges to group comparisons and influence outcomes, making comparison methods potentially inaccurate. The knowledge test was foundational and may not equally reflect learning in both courses. Due to differences between the programs, we must be careful in making direct comparisons of outcomes between UIC and USF. However, these differences also represent opportunities to widen the scope of our work and generalize it to more schools and faculty looking to learn from our experience of introducing generative AI in various health informatics learning settings and to a wider audience of students. These factors could be excellent subjects of future scholarly inquiry.

Attrition of two UIC students at posttest indicates that they did not choose to complete the posttest. Even with a reminder message, those 2 students did not complete the posttest. We agree that this could also skew any reported improvement. One USF student was absent during the proctored, in-person posttest session and later requested to take the survey; this student's request was declined to avoid introducing uncontrolled variables. Both USF's before and after surveys were completed on students' laptops under faculty supervision, making it reasonable to assume they did not consult external materials while responding.

These 2 programs share a common goal of embedding generative AI into curriculum by teaching students to use cutting-edge technologies in a safe academic space where experimentation is both acceptable and highly encouraged. Thus, we demonstrate a practical approach for bringing generative AI into the classroom to prepare students to meet employer needs and the realities of future practice of health informatics. Therefore, implementation of generative AI assignments into the curriculum is beneficial to students immediately by building competencies, and it can inform faculty in the further development of the health informatics curriculum.

Our assessment of the students' first foray into generative AI was achieved through a combination of measurements and the subsequent dialog. Therefore, we report knowledge assessments as data and reflection responses in this discussion. More research would be necessary to study the introduction of additional assignments and measuring outcomes of their work, as generative AI curriculum continues to develop. However, this initial work to introduce practical generative AI curriculum in the graduate health informatics programs arms faculty with a glimpse into the potential successes and challenges of teaching generative AI and provides information on student perspectives which can further inform curriculum updates.

We did not formally calculate an interrater reliability statistic before engaging in dialog about the student reflections. Our faculty dialog and normalization of student reflections analyses to reach near-consensus on outcomes in identifying areas of interest and concern introduced a bias resulting from the ability to see each other's classifications by knowledge domain. This being an initial attempt to rapidly infuse AI into our curriculum and a first exploration of our qualitative findings, we contemplated this bias and ultimately decided that faculty dialog offered the greatest opportunity to arrive at usable results. We chose this bias as a better form of dialog to enhance usability and generalizability of our academic project and its reported outcomes. Still, we acknowledge that this bias may have influenced our results toward preestablished expectations and produced inaccurate overall ratings of student responses. Future research could include interrater reliability and blind ratings of student reflections to strengthen the rigor of the qualitative findings.

Implications of This Work on Building the Future Health Informatics Curriculum

Our success in implementing a modular approach to introducing generative AI within a larger health informatics context, and considering other AI implications in health care, has implications for health informatics education. Our work shows that health informatics programs may adopt generative AI competencies into their existing curriculum and then use them as guidelines in designing competency-building learning experiences in generative AI [7]. Existing courses can be modernized by rapidly infusing generative AI (and the overall AI) curriculum into the existing lectures and assignments, thus reducing the administrative overhead associated with a major effort to revamp the curriculum. Limited faculty time can be spent rapidly introducing generative AI to students as a hot-market skill. Major program revisions could also have implications for health informatics accreditation standards. To address employer desires for application skills, a next-level accreditation might ultimately require programs to go further into "doing" on the Miller Level

XSL•FO
RenderX

of Competence, perhaps reaching an 80 - 20 ratio of Doing to Knowing [22].

We propose rapid targeted curriculum updates as a productive form of delivering high-demand knowledge to students. Moreover, such a targeted approach may be the optimal route for all health professions educators to use when updating curriculum with generative AI content, due to limited resources within those programs which must also adhere to their accredited standards of education.

Taking a modular approach to updating the health informatics curriculum would also enable programs to assess the impacts of the changes from results received from small cohorts of students, because they would be able to introduce updates more rapidly and engage more students. Consequently, sample sizes for curriculum research studies would rise beyond a pilot in this initial study and provide deeper understanding of how generative AI, and AI education overall, impacts student satisfaction and preparedness to enter the job market upon graduation.

Implications of This Work on the Health Professions Curriculum

While we focused our efforts on the cohorts of health informatics students, our experiences and findings are generalizable to wider student populations preparing for careers in several health professions, particularly nursing, public health, pharmacy, and medicine, but also applicable to other health professions. The entire health care delivery system worldwide will be transformed by generative AI, and all programs are interested in updating their curriculum to include AI and prepare their students to face technological realities of the digital health care workplace. Some programs may decide to create entire courses dedicated to AI, while others will adopt modular approaches by embedding applicable AI topics across multiple courses. We presented 2 distinct ways of embedding generative AI content into the curriculum, so programs looking for a modular approach could learn from USF experience, while those looking for a deeper dive into the generative AI topic may learn from UIC experience of running a dedicated generative AI laboratory. Our 4 knowledge domains and skills-based approach to learning can be adopted by any health professions programs, while introducing clinical use cases and examples which are more unique to the subjects they teach.

Conclusions

Proliferation of generative AI and digital health education in the health professions curricula is in the early stages and is poised to grow into a large-scale academic debate about implementation, with consensus on the need to embed elements of AI expected from professional societies and graduate education commissions. Therefore, the need to define AI competencies and include them among educational outcomes stretches beyond informatics programs, expanding into the existing health professions [23] as well as emerging specialties such as Master of Digital Health [24,25]. There are ongoing attempts to define a clear set of skills to be taught in such digital health programs, with many of the grassroots efforts originating from experiences of the faculty [23]. By beginning with the AI competencies and designing learning experiences based on them, we innovatively addressed a gap in generative AI education in a health informatics program, tested 2 distinct cohorts of students in both online and hybrid content delivery programs, and shared our experiences and recommendations for rapidly infusing generative AI into the curriculum. These recommendations are generalizable to a wide variety of informatics and health professions education programs, to address the growing need for academia to update programs with the latest technology developments in clinical care and life sciences [24,25].

Acknowledgments

The authors want to thank their colleagues, students, and leadership at the University of Illinois Chicago (UIC) and the University of San Francisco (USF), whose enthusiasm for exploring generative AI in health informatics education inspired and enriched this work. All authors made significant contributions to the development of the methods described as well as the production and editing of this manuscript. MI, JK, and FS worked with students in the aforementioned courses at UIC and USF, collected student data and reflections, and organized student responses into spreadsheets for analysis. Additionally, JK and FS served as co-pricinpalprincipal investigators on the multi-institutional inistitutionalinstitutional review board submitted and approved to conduct this study.

At the time of the study, Freddie Seba served as Program Director and faculty in the MS in Digital Health Informatics program (School of Nursing and Health Professions) at the University of San Francisco (until May 2025). He was concurrently pursuing a Doctor of Education (EdD) degree in the School of Education at the University of San Francisco, with a dissertation focused on generative AI ethics and governance in higher education, which he successfully defended in December 2025.

Data Availability

All available data were deidentified and provided as part of this manuscript.

Conflicts of Interest

JK is an associate editor of *Online Journal of Public Health Informatics* (OJPHI), a JMIR Publications journal, at the time of this publication.

XSL•FO
RenderX

Multimedia Appendix 1
Generative artificial intelligence (AI) competencies.
[DOCX File, 19 KB - medinform_v13i1e76507_app1.docx]

References

1. Kaul V, Enslin S, Gross SA. History of artificial intelligence in medicine. Gastrointest Endosc 2020 Oct;92(4):807-812. [doi: 10.1016/j.gie.2020.06.040] [Medline: 32565184]
2. Wills C. Artificial intelligence usage in higher education: influence on online learning. Pinnacle 2024;2(3) [FREE Full text] [doi: 10.61643/c40097]
3. Neha F, Bhati D, Shukla DK, Amiruzzaman M. ChatGPT: Transforming healthcare with AI. AI 2024;5(4):2618-2650. [doi: 10.3390/ai5040126]
4. Bick A, Blandin A, Deming DJ. The rapid adoption of generative AI. : NBER Working Paper Series; 2024 URL: https://doi.org/10.3386/w32966 [accessed 2025-11-24]
5. Wells R. 71% of employers prefer AI skills above experience in 2024. Forbes. 2024 Nov 5. URL: https://www.forbes.com/sites/rachelwells/2024/11/05/71-of-employers-prefer-ai-skills-above-experience-in-2024 [accessed 2025-04-17]
6. Machuel M. Leveraging generative AI for job augmentation and workforce productivity. : World Economic Forum; 2024 Jan URL: https://reports.weforum.org/docs/WEF_Leveraging_Generative_AI_for_Job_Augmentation_and_Workforce_Productivity_2024.pdf [accessed 2025-04-17]
7. National Academy of Medicine. An Artificial Intelligence Code of Conduct for Health and Medicine: Essential Guidance for Aligned Action: The National Academies Press; 2025. [doi: 10.17226/29087] [Medline: 40674514]
8. Solis B. How AI-first companies are outpacing rivals and redefining the future of work. Forbes. 2024 Aug 7. URL: https://www.forbes.com/sites/briansolis/2024/08/07/how-ai-first-companies-are-outpacing-rivals-and-redefining-the-future-of-work [accessed 2025-04-17]
9. Nguyen T, Carberry A, Tsingos-Lucas C. AI literacy: Understanding artificial intelligence in higher education. Coll Res Libr News 2024;85(1):5-9 [FREE Full text]
10. AI literacy: A framework to understand, evaluate, and use emerging technology. Digital Promise. 2024 Jun 18. URL: https://digitalpromise.org/2024/06/18/ai-literacy-a-framework-to-understand-evaluate-and-use-emerging-technology [accessed 2025-04-17]
11. Isola M, Krive J. Innovation of health data science curricula. JAMIA Open 2022 Oct;5(3):ooac073. [doi: 10.1093/jamiaopen/ooac073] [Medline: 36042919]
12. Fera B. From fax machines to Gen AI: Are hospitals/health systems ready? Deloitte Health Forward Blog. 2023 Oct 19. URL: https://www2.deloitte.com/us/en/blog/health-care-blog/2023/from-fax-machines-to-gen-ai-are-hospitals-health-systems-ready.html [accessed 2025-04-17]
13. Lo CK, Hew KF, Jong MY. The influence of ChatGPT on student engagement: a systematic review and future research agenda. Comput Educ 2024 Oct;219:105100. [doi: 10.1016/j.compedu.2024.105100]
14. Boscardin CK, Gin B, Golde PB, Hauer KE. ChatGPT and generative artificial intelligence for medical education: potential impact and opportunity. Acad Med 2024 Jan 1;99(1):22-27. [doi: 10.1097/ACM.0000000000005439] [Medline: 37651677]
15. Almansour M, Alfhaid FM. Generative artificial intelligence and the personalization of health professional education: a narrative review. Medicine (Baltimore) 2024 Aug 2;103(31):e38955. [doi: 10.1097/MD.0000000000038955] [Medline: 39093806]
16. Karabacak M, Ozkara BB, Margetis K, Wintermark M, Bisdas S. The advent of generative language models in medical education. JMIR Med Educ 2023 Jun 6;9:e48163. [doi: 10.2196/48163] [Medline: 37279048]
17. Singla R, Pupic N, Ghaffarizadeh SA, et al. Developing a Canadian artificial intelligence medical curriculum using a Delphi study. NPJ Digit Med 2024 Nov 18;7(1):323. [doi: 10.1038/s41746-024-01307-1] [Medline: 39557985]
18. Krive J, Isola M, Chang L, Patel T, Anderson M, Sreedhar R. Grounded in reality: Artificial intelligence in medical education. JAMIA Open 2023 Jul;6(2):ooad037. [doi: 10.1093/jamiaopen/ooad037] [Medline: 37273962]
19. Min H, Jing X, Gong Y, Yu P. Perspectives on enhancing clinical informatics education in the artificial intelligence era. J Clin Inform 2024;1(1):4496. [Medline: 40051784]
20. Southworth J, Migliaccio K, Glover J, et al. Developing a model for AI across the curriculum: transforming the higher education landscape via innovation in AI literacy. Comput Educ AI 2023;4:100127. [doi: 10.1016/j.caeai.2023.100127]
21. Hersh W, Fultz Hollis K. Results and implications for generative AI in a large introductory biomedical and health informatics course. NPJ Digit Med 2024 Sep 13;7(1):247. [doi: 10.1038/s41746-024-01251-0] [Medline: 39271955]
22. El-Gayar O, Wahbeh A, Al-Ramahi M, Elnoshokaty A. Highlighting competency gaps in health informatics education using advanced text-embedding models. 2025 Presented at: Hawaii International Conference on System Sciences; Jan 7-10, 2025 URL: https://scholarspace.manoa.hawaii.edu/items/abae724a-16aa-4086-b70c-557ad314b9b7 [accessed 2025-11-24] [doi: 10.24251/HICSS.2025.600]
23. Ramani S, Leinster S. AMEE Guide no. 34: Teaching in the clinical environment. Med Teach 2008;30(4):347-364. [doi: 10.1080/01421590802061613] [Medline: 18569655]

XSL•FO
RenderX

24. Car J, Ong QC, Erlikh Fox T, et al. The digital health competencies in medical education framework: an international consensus statement based on a Delphi study. JAMA Netw Open 2025 Jan 2;8(1):e2453131. [doi: 10.1001/jamanetworkopen.2024.53131] [Medline: 39888625]
25. Car J, Topol EJ. Advocating for a master of digital health degree. JAMA 2025 Mar 4;333(9):753-754. [doi: 10.1001/jama.2024.27365] [Medline: 39821005]

Abbreviations

AI: artificial intelligence
HIPAA: Health Insurance Portability and Accountability Act
IRB: institutional review board
MSHI: Master of Science in Health Informatics
UIC: University of Illinois Chicago
USF: University of San Francisco

Edited by A Benis; submitted 24.04.25; peer-reviewed by C Obianyo, G Adewumi, S Sivarajkumar; revised version received 04.08.25; accepted 17.09.25; published 16.12.25.

Please cite as:
Seba F, Isola M, Mills L, Zalake M, Krive J
Incorporating Generative AI Into a Health Informatics Curriculum to Build 21st Century Competencies: Multisite Pre-Post Study
JMIR Med Inform 2025;13:e76507
URL: https://medinform.jmir.org/2025/1/e76507
doi:10.2196/76507

© Freddie Seba, Miriam Isola, Laura Mills, Mohan Zalake, Jacob Krive. Originally published in JMIR Medical Informatics (https://medinform.jmir.org), 16.12.2025. This is an open-access article distributed under the terms of the Creative Commons Attribution License (https://creativecommons.org/licenses/by/4.0/), which permits unrestricted use, distribution, and reproduction in any medium, provided the original work, first published in JMIR Medical Informatics, is properly cited. The complete bibliographic information, a link to the original publication on https://medinform.jmir.org/, as well as this copyright and license information must be included.

XSL•FO
RenderX

AI Scribes in Health Care: Balancing Transformative Potential With Responsible Integration

Tiffany I Leung[1,2], MPH, MD; Andrew J Coristine[1,3], MSc, PhD; Arriel Benis[4], PhD

[1]JMIR Publications, 130 Queens Quay East, Unit 1100, Toronto, ON, Canada

[2]Department of Internal Medicine (adjunct), Southern Illinois University School of Medicine, Springfield, IL, United States

[3]Division of Cardiology (affiliate), Department of Medicine, McGill University, Montreal, QC, Canada

[4]Department of Digital Medical Technologies, Holon Institute of Technology, Holon, Israel

Corresponding Author:
Tiffany I Leung, MPH, MD
JMIR Publications, 130 Queens Quay East, Unit 1100, Toronto, ON, Canada

Abstract

The administrative burden of clinical documentation contributes to health care practitioner burnout and diverts valuable time away from direct patient care. Ambient artificial intelligence (AI) scribes—also called “digital scribes” or “AI scribes”—are emerging as a promising solution, given their potential to automate clinical note generation and reduce clinician workload, and those specifically built on a large language model (LLM) are emerging as technologies for facilitating real-time clinical documentation tasks. This potentially transformative development has a foundation on longer-standing, AI-based transcription software, which uses automated speech recognition and/or natural language processing. Recent studies have highlighted the potential impact of ambient AI scribes on clinician well-being, workflow efficiency, documentation quality, user experience, and patient interaction. So far, limited evidence indicates that ambient AI scribes are associated with reduced clinician burnout, lower cognitive task load, and significant time savings in documentation, particularly in after-hours electronic health record (EHR) work. One consistently reported benefit is the improvement in the patient-physician interaction, as physicians feel more present during a clinical encounter. However, these benefits are counterbalanced by persisting concerns regarding the accuracy, consistency, language use, and style of AI-generated notes. Studies noting errors, omissions, or hallucinations caution that diligent clinician oversight is necessary. The user experience is also heterogeneous, with benefits varying by specialty and individual workflow. Further, there are concerns about ethical and legal issues, algorithmic bias, the potential for long-term “cognitive debt” from overreliance on AI, and even the potential loss of physician autonomy. Additional pragmatic concerns include security, privacy, integration, interoperability, user acceptance and training, and the cost-effectiveness of adoption at scale. Finally, limited studies describe adoption or evaluation of these technologies by nonphysician clinicians and health professionals. Although ambient AI scribes and AI-driven documentation technologies are promising as potentially practice-changing tools, there are many questions remaining. Key issues persist, including responsible deployment with the goal of ensuring that ambient AI scribes produce clinical documentation that supports more efficient, equitable, and patient-centered care. To advance our collective understanding and address key issues, *JMIR Medical Informatics* is launching a call for papers for a new section on “Ambient AI Scribes and AI-Driven Documentation Technologies.” As editors, we look forward to the opportunity to advance the science and understanding of these fields through publishing high-quality and rigorous scholarly work in this new section of *JMIR Medical Informatics*.

(JMIR Med Inform 2025;13:e80898) doi:10.2196/80898

KEYWORDS

ambient AI scribe; digital scribe; AI scribe; virtual scribe; documentation assistant; ambient listening technology; AI assistant; artificial intelligence; clinical documentation; electronic health records; administrative burden

Introduction

Administrative burdens associated with widespread electronic health record (EHR) adoption are well documented, as are the associated clinician burnout and negative consequences for direct patient care and the patient experience. In response, ambient artificial intelligence (AI) scribes have emerged as promising transformative technologies. These technologies aim to listen to patient-practitioner conversations during clinic visits or other synchronous encounters; then, they generate clinical notes for health care practitioner review, revision, and approval. AI scribes are still in the early stages of adoption and evaluation; however, they are already seen operationally as powerful tools that could combat administrative burdens and clinician burnout. Accelerating efforts to install AI scribes in clinical practices are taking place, with a backdrop of long-standing efforts to automate all aspects of documentation workload, which typically includes clinical note generation and other forms of administrative burden, such as preparation of computerized order entry, prior authorization forms, and medical assessments

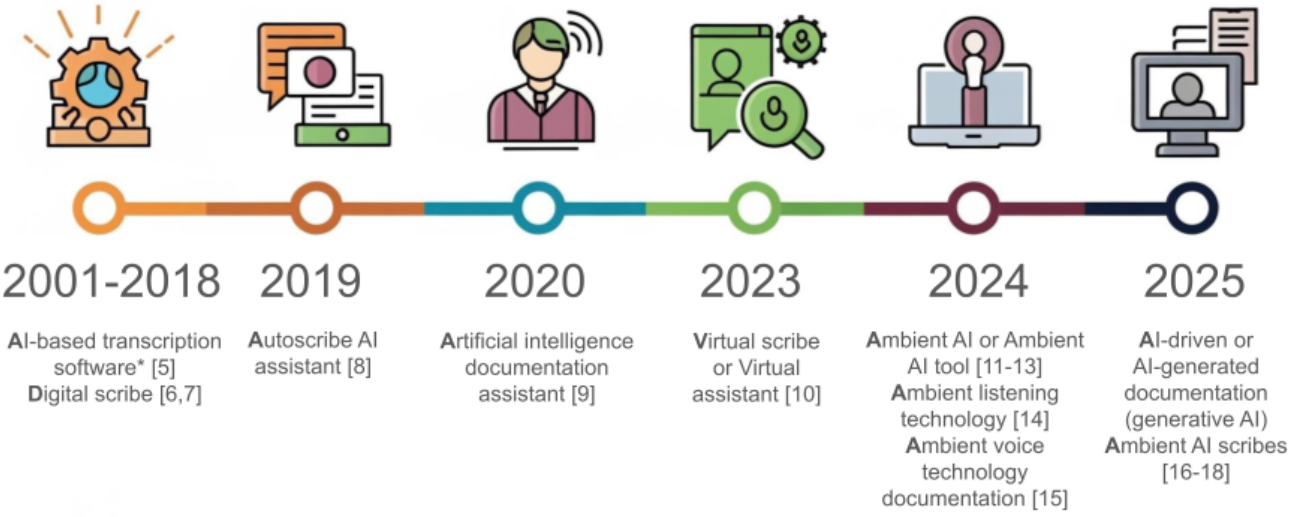
XSL•FO
RenderX

according to structured requirements, as well as coding and billing [1]. In this editorial, we describe our interpretations of the current landscape of ambient AI scribe technology and opportunities for further research and publication, as a part of the *JMIR Medical Informatics* call for papers on "Ambient AI Scribes and AI-Driven Documentation Technologies" [2].

Hype and Hope of Ambient AI Scribes

The conceptualization of ambient clinical documentation has evolved in parallel with the technology over the past several years (Figure 1), with a clear bibliometric trend of increasing research on the subject. There is no taxonomy of AI scribe technologies, although one appears to be emerging. One general operating definition of "digital scribe" is the use of automatic speech recognition technology or natural language processing to support clinical documentation [3]. Although the digital scribe concept does not explicitly exclude the use of AI technology, it is only in more recent years that AI has been explicitly labeled as a component of clinical documentation tools. One published literature review subdivided AI-driven documentation systems into generative AI and ambient AI, even if ambient AI may also make use of architecture comparable to that of generative AI [4].

Figure 1. Terminology used for artificial intelligence (AI)–based documentation technologies, based on published literature over the past decade [5-18]. *Transcription software in this period was based on different types of AI models, including one or more of the following: automated speech recognition, natural language processing, probabilistic graphical models (conditional random field), or logistic regression models [5].



Coiera et al [19] envisioned a progression through the following three stages: (1) human-led systems augmented by tools like dictation and templates (2); mixed-initiative systems where AI assists in converting conversations into summaries; and (3) computer-led systems that autonomously handle documentation, seeking human input only for exceptions. It would seem that in the last 3 years, health care organizations and physicians have been firmly shifting into the second stage, driven by the increasingly advanced technologies available and the salient burdens on clinical and patient care time, particularly in the United States, which has generated the largest proportion of published original research studies on ambient AI scribes. Professional societies and physician groups around the world are also engaged in the global dialogue on the role and promise of AI scribes in medical practice [20-22]. Ultimately, intelligent clinical environments, which capture and integrate data into the EHR, offer the promise of off-loading human-led documentation tasks onto a machine and doing so with an ability to integrate multimodal data from various sources, thereby freeing up the human in the loop and allowing them to focus cognitive efforts on clinical and medical decision-making. So far, initial evaluations have come from small-scale, short-term pilot studies [12,13] that often have volunteer participants who may be biased toward technology.

This excitement has no doubt been spurred by the introduction and widespread availability of large language models (LLMs), which, in terms of development and adoption, have rapidly outpaced other AI technologies underlying documentation support. Numerous industry products [1,23] and a rapidly increasing number of publications have emerged regarding ambient AI scribes using LLMs, even though other AI technologies for documentation tasks have been studied and used for the last 2 decades. A simple PubMed literature search on June 1, 2025, resulted in the retrieval of 940 potentially relevant articles published in the last 10 years (Multimedia Appendix 1); of the most relevant articles (ie, based on their titles), 7 have been published in 2025 (as of the search date) [12,13,17,18,23-25], 8 were published in 2024 [14,15,26-31], and 3 were published in 2023 [10,32,33]. Since this search, further studies have been published to guide ambient digital scribe evaluation [5,34]. During the course of preparing this editorial, authors identified more peer-reviewed literature on ambient AI scribes every few days. Undoubtedly, additional research is forthcoming as hype, hope, and operational needs coincide to drive further adoption.

Despite the rapidly growing published literature on ambient AI scribes and AI-driven documentation, we found that many still focus on similar objectives and evaluation metrics. Consequently, we felt that a call for papers on the topic in *JMIR Medical Informatics* would be valuable for collecting and publishing scientific studies and evidence-based perspectives on broader aspects of ambient AI scribe technologies. As a

XSL•FO
RenderX

starting point, we synthesized recent literature about their impact on clinical workflows, well-being, note quality, user experience, patient interaction, and medicolegal aspects, identifying opportunities for further investigation in this field (Multimedia Appendices 2-4).

Ambient AI Scribe Opportunities

The enthusiasm surrounding AI scribes is tempered by caution. An initial focus of evaluating the outputs of AI scribes is the quality of the note [4], which is assessed by using instruments such as the Physician Documentation Quality Instrument (PDQI-9) [35] or Sheffield Assessment Instrument for Letters (SAIL) [36]; usability is assessed with the NASA Task Load Index (NASA-TLX) [37], and burnout is assessed with various inventories. Results suggest that there is risk for hallucinations or fictitious information [4]. Other evaluations of stand-alone tools for audio recordings suggest potentially high rates of errors, including incorrect information, omissions, and hallucinations [11,29,38]. The high rates of omissions and hallucinations found in some studies underscore the need to evaluate for potential diagnostic errors or other long-term safety risks stemming from AI-generated content [4,10,29-32,39-42]. Others express caution regarding the potential for security risks or risks to medical decision-making in cases where LLMs can access and modify sensitive patient data [31]. Overviews on the topic emphasize the need for careful consideration of the ethical and practical integration of LLMs into clinical practice [1,4], cautioning about potential risks, such as automation bias, privacy concerns, and medicolegal implications [19].

Another major unexamined area is the impact on tangible clinical outcomes and patient safety. Although efficiency, time savings, and productivity are important, there are other measures that are also important. Assessments of note quality, accuracy, and impact on patient safety are essential; Gellert [32] raised a crucial point—there is currently no systematic data collection for evaluating the extent to which clinical errors or negative patient outcomes can be attributed to the use of medical scribes. More comprehensive evaluations of the safe and effective implementation of ambient AI scribe technologies (eg, along the dimensions of the seminal sociotechnological model of health information technology) are still lacking [43]. Additional diversity of clinical specialty applications, clinical disciplines, and practice settings also would be insightful. We identified studies published in a dermatology and urology journal but were unable to retrieve the full-text articles. One pediatrics application indicated positive outcomes during a digital AI scribe pilot in an outpatient pediatric setting [44]. Further, two conference proceeding papers described LLM applications in nursing documentation [27,45], as did a position paper from the Nursing and Artificial Intelligence Leadership Collaborative regarding multimodal LLM support for nursing documentation [46], although these stopped short of discussing AI scribe applications.

The most frequently mentioned gap is the limited study of patients' or caregivers' perspectives regarding AI scribes. Most studies rely on clinicians' perceptions of the patient experience, with very few directly capturing patient viewpoints. Additional research could directly measure patients' experiences, preferences, and patient-reported outcomes [4,47], especially given recent studies solely examining physicians' experiences of the patient-physician visit. Pelletier et al [44] incorporated the assessment of caregiver satisfaction in pediatrics, with the sole statistically significant finding being that caregivers' "provider-specific likelihood to recommend" was higher after the pilot digital scribe implementation. There are also potential patient benefits that remain unexplored. AI scribes may prove useful in providing rapid, patient-friendly visit summaries; outlining the diagnosis and management plan; scheduling appointments; and providing reasons to seek follow-up care [31]. They might also help to bridge communication gaps by highlighting misunderstandings or discrepancies between patient-reported details and those documented in EHRs [45].

The downstream effects of AI-generated notes on clinical communication and reasoning are also unknown. Note bloat—the well-established phenomenon of creating lengthy clinical documentation, which is most often attributed to the copy-paste phenomenon of digitizing documentation [42,48,49]—may also result from AI scribe use; whether large quantities of text redundancy change as a result of AI scribe use is unknown. With regard to clinical reasoning and cognition, as per preliminary evidence from nonmedical studies, such as a study by Kosmyna et al [50], one potential consequence of using generative AI for a writing task is "cognitive debt," where repeated reliance on AI for cognitive tasks may lead to the atrophy of critical thinking and memory skills. The study found that LLM use impaired memory recall and reduced the brain's neural engagement with the studied task. Although potentially dull, the documentation process may have beneficial effects on retention and memory. Learner experiences and consequences on expertise development, such as the formative diagnostic process for trainees, are underexplored [51].

Finally, system-level and economic outcomes require more rigorous investigation. Studies call for comprehensive cost-benefit analyses to justify the significant expense of AI scribe technologies [17]. On a broader scale, Gellert [32] cautioned about a largely unstudied systemic risk—the widespread adoption of scribes may decouple physicians from their EHRs and thereby impede the user-driven feedback necessary for the long-term evolution of next-generation clinical AI. In clinical informatics networks, user engagement in the co-design and development of AI scribes is seen as an essential component of the appropriate advancement and adoption of the technology, yet only one study has taken steps to pursue this ideal in evaluating primary care physician needs [9].

Conclusions

Ambient AI scribes, particularly with the widespread availability of LLMs, offer potential solutions to a previously difficult-to-bridge technological gap in clinical documentation. Although many health systems and physicians are welcoming this potentially practice-changing technology, there are many questions and areas that remain to be fully understood. Substantial clinical documentation also occurs adjacent to or outside of a clinical visit, and the applications of ambient AI

XSL•FO
RenderX

scribes and AI-driven documentation technologies in these areas are yet to be explored. Such areas involve various clinician types and health professionals, clinical settings, or community settings. As editors, we look forward to the opportunity to advance the science and understanding of these fields through publishing high-quality and rigorous scholarly work in the *JMIR Medical Informatics* call for papers on "Ambient AI Scribes and AI-Driven Documentation Technologies" [2].

Acknowledgments

Gemini 2.5 Pro and NotebookLM (Google) were used to help with article summarization and synthesis tasks during manuscript preparation. The prompts and responses used for the summarization tasks are available in Multimedia Appendices 2 and 3. Limited reuse of summarized text has been incorporated into portions of the manuscript, with manual editing and revisions by authors for clarity and style. Authors manually verified all claims and citations and are accountable for the content of this manuscript.

Data Availability

Data sharing is not applicable as no datasets were generated or analyzed during the preparation of this manuscript.

Authors' Contributions

Conceptualization: TIL, AJC
Supervision: TIL, AB
Writing – original draft: TIL, AJC
Writing – review & editing: TIL, AJC, AB

Conflicts of Interest

TIL is the scientific editorial director at JMIR Publications and a director on the Board of Directors, American Medical Informatics Association. AJC is a scientific editor at JMIR Publications and the editor in chief of *JMIR Cardio*. AB is the editor in chief of *JMIR Medical Informatics*.

Multimedia Appendix 1
PubMed search and Gemini 2.5 Pro prompts and responses.
[DOCX File, 24 KB - medinform_v13i1e80898_app1.docx]

Multimedia Appendix 2
NotebookLM prompts and responses.
[DOCX File, 28 KB - medinform_v13i1e80898_app2.docx]

Multimedia Appendix 3
NotebookLM mind map: challenges and limitations.
[PNG File, 1069 KB - medinform_v13i1e80898_app3.png]

Multimedia Appendix 4
NotebookLM mind map: future directions and recommendations.
[PNG File, 1152 KB - medinform_v13i1e80898_app4.png]

References

1. Kunze KN, Bepple J, Bedi A, Ramkumar PN, Pean CA. Commercial products using generative artificial intelligence include ambient scribes, automated documentation and scheduling, revenue cycle management, patient engagement and education, and prior authorization platforms. Arthroscopy 2025 May 24:S0749-8063(25)00397-4. [doi: 10.1016/j.arthro.2025.05.021] [Medline: 40419172]
2. Call for papers - Theme Issue: Ambient AI Scribes and AI-Driven Documentation Technologies. JMIR Medical Informatics. URL: https://medinform.jmir.org/announcements/601 [accessed 2025-07-11]
3. van Buchem MM, Boosman H, Bauer MP, Kant IMJ, Cammel SA, Steyerberg EW. The digital scribe in clinical practice: a scoping review and research agenda. NPJ Digit Med 2021 Mar 26;4(1):57. [doi: 10.1038/s41746-021-00432-5] [Medline: 33772070]
4. Bracken A, Reilly C, Feeley A, Sheehan E, Merghani K, Feeley I. Artificial intelligence (AI) - powered documentation systems in healthcare: a systematic review. J Med Syst 2025 Feb 18;49(1):28. [doi: 10.1007/s10916-025-02157-4] [Medline: 39966286]

XSL•FO
RenderX

5. Ng JJW, Wang E, Zhou X, et al. Evaluating the performance of artificial intelligence-based speech recognition for clinical documentation: a systematic review. BMC Med Inform Decis Mak 2025 Jul 1;25(1):236. [doi: 10.1186/s12911-025-03061-0] [Medline: 40598136]
6. Quiroz JC, Laranjo L, Kocaballi AB, Berkovsky S, Rezazadegan D, Coiera E. Challenges of developing a digital scribe to reduce clinical documentation burden. NPJ Digit Med 2019 Nov 22;2(1):114. [doi: 10.1038/s41746-019-0190-1] [Medline: 31799422]
7. Coiera E, Liu S. Evidence synthesis, digital scribes, and translational challenges for artificial intelligence in healthcare. Cell Rep Med 2022 Dec 20;3(12):100860. [doi: 10.1016/j.xcrm.2022.100860] [Medline: 36513071]
8. Lin SY, Shanafelt TD, Asch SM. Reimagining clinical documentation with artificial intelligence. Mayo Clin Proc 2018 May;93(5):563-565. [doi: 10.1016/j.mayocp.2018.02.016] [Medline: 29631808]
9. Kocaballi AB, Ijaz K, Laranjo L, et al. Envisioning an artificial intelligence documentation assistant for future primary care consultations: A co-design study with general practitioners. J Am Med Inform Assoc 2020 Nov 1;27(11):1695-1704. [doi: 10.1093/jamia/ocaa131] [Medline: 32845984]
10. Yim WW, Fu Y, Ben Abacha A, Snider N, Lin T, Yetisgen M. Aci-bench: a novel ambient clinical intelligence dataset for benchmarking automatic visit note generation. Sci Data 2023 Sep 6;10(1):586. [doi: 10.1038/s41597-023-02487-3] [Medline: 37673893]
11. Balloch J, Sridharan S, Oldham G, et al. Use of an ambient artificial intelligence tool to improve quality of clinical documentation. Future Healthc J 2024 Jun 26;11(3):100157. [doi: 10.1016/j.fhj.2024.100157] [Medline: 39371531]
12. Misurac J, Knake LA, Blum JM. The effect of ambient artificial intelligence notes on provider burnout. Appl Clin Inform 2025 Mar;16(2):252-258. [doi: 10.1055/a-2461-4576] [Medline: 39500346]
13. Stults CD, Deng S, Martinez MC, et al. Evaluation of an ambient artificial intelligence documentation platform for clinicians. JAMA Netw Open 2025 May 1;8(5):e258614. [doi: 10.1001/jamanetworkopen.2025.8614] [Medline: 40314951]
14. Owens LM, Wilda JJ, Hahn PY, Koehler T, Fletcher JJ. The association between use of ambient voice technology documentation during primary care patient encounters, documentation burden, and provider burnout. Fam Pract 2024 Apr 15;41(2):86-91. [doi: 10.1093/fampra/cmad092] [Medline: 37672297]
15. Galloway JL, Munroe D, Vohra-Khullar PD, et al. Impact of an artificial intelligence-based solution on clinicians' clinical documentation experience: initial findings using ambient listening technology. J Gen Intern Med 2024 Oct;39(13):2625-2627. [doi: 10.1007/s11606-024-08924-2] [Medline: 38980463]
16. Ma SP, Liang AS, Shah SJ, et al. Ambient artificial intelligence scribes: utilization and impact on documentation time. J Am Med Inform Assoc 2025 Feb 1;32(2):381-385. [doi: 10.1093/jamia/ocae304] [Medline: 39688515]
17. Shah SJ, Devon-Sand A, Ma SP, et al. Ambient artificial intelligence scribes: physician burnout and perspectives on usability and documentation burden. J Am Med Inform Assoc 2025 Feb 1;32(2):375-380. [doi: 10.1093/jamia/ocae295] [Medline: 39657021]
18. Shah SJ, Crowell T, Jeong Y, et al. Physician perspectives on ambient AI scribes. JAMA Netw Open 2025 Mar 3;8(3):e251904. [doi: 10.1001/jamanetworkopen.2025.1904] [Medline: 40126477]
19. Coiera E, Kocaballi B, Halamka J, Laranjo L. The digital scribe. NPJ Digit Med 2018 Oct 16;1:58. [doi: 10.1038/s41746-018-0066-9] [Medline: 31304337]
20. Guidance on the use of AI-enabled ambient scribing products in health and care settings. NHS England. URL: https://www.england.nhs.uk/long-read/guidance-on-the-use-of-ai-enabled-ambient-scribing-products-in-health-and-care-settings/ [accessed 2025-07-12]
21. Shemtob L, Majeed A, Beaney T. Regulation of AI scribes in clinical practice. BMJ 2025 Jun 20;389:r1248. [doi: 10.1136/bmj.r1248] [Medline: 40541424]
22. AI scribes. OntarioMD. URL: https://www.ontariomd.ca/pages/ai-scribe-overview.aspx [accessed 2025-07-12]
23. Blaseg E, Huffstetler A. Artificial intelligence scribes shape health care delivery. Am Fam Physician 2025 Apr;111(4):304-305. [Medline: 40238969]
24. Schaye V, DiTullio D, Guzman BV, et al. Large language model-based assessment of clinical reasoning documentation in the electronic health record across two institutions: development and validation study. J Med Internet Res 2025 Mar 21;27:e67967. [doi: 10.2196/67967] [Medline: 40117575]
25. Duggan MJ, Gervase J, Schoenbaum A, et al. Clinician experiences with ambient scribe technology to assist with documentation burden and efficiency. JAMA Netw Open 2025 Feb 3;8(2):e2460637. [doi: 10.1001/jamanetworkopen.2024.60637] [Medline: 39969880]
26. Bundy H, Gerhart J, Baek S, et al. Can the administrative loads of physicians be alleviated by AI-facilitated clinical documentation? J Gen Intern Med 2024 Nov;39(15):2995-3000. [doi: 10.1007/s11606-024-08870-z] [Medline: 38937369]
27. Chen CJ, Liao CT, Tung YC, Liu CF. Enhancing healthcare efficiency: integrating ChatGPT in nursing documentation. Stud Health Technol Inform 2024 Aug 22;316:851-852. [doi: 10.3233/SHTI240545] [Medline: 39176926]
28. Huang TY, Hsieh PH, Chang YC. Performance comparison of junior residents and ChatGPT in the Objective Structured Clinical Examination (OSCE) for medical history taking and documentation of medical records: development and usability study. JMIR Med Educ 2024 Nov 21;10(1):e59902. [doi: 10.2196/59902] [Medline: 39622713]

XSL•FO
RenderX

29. Kernberg A, Gold JA, Mohan V. Using ChatGPT-4 to create structured medical notes from audio recordings of physician-patient encounters: comparative study. J Med Internet Res 2024 Apr 22;26:e54419. [doi: 10.2196/54419] [Medline: 38648636]
30. Seo J, Choi D, Kim T, et al. Evaluation framework of large language models in medical documentation: development and usability study. J Med Internet Res 2024 Nov 20;26:e58329. [doi: 10.2196/58329] [Medline: 39566044]
31. Tripathi S, Sukumaran R, Cook TS. Efficient healthcare with large language models: optimizing clinical workflow and enhancing patient care. J Am Med Inform Assoc 2024 May 20;31(6):1436-1440. [doi: 10.1093/jamia/ocad258] [Medline: 38273739]
32. Gellert GA. Medical scribes: symptom or cause of impeded evolution of a transformative artificial intelligence in the electronic health record? Perspect Health Inf Manag 2023 Jan 10;20(1):1d. [Medline: 37215336]
33. Socrates V, Gilson A, Lopez K, Chi L, Taylor RA, Chartash D. Predicting relations between SOAP note sections: the value of incorporating a clinical information model. J Biomed Inform 2023 May;141:104360. [doi: 10.1016/j.jbi.2023.104360] [Medline: 37061014]
34. Wang H, Yang R, Alwakeel M, et al. An evaluation framework for ambient digital scribing tools in clinical applications. NPJ Digit Med 2025 Jun 13;8(1):358. [doi: 10.1038/s41746-025-01622-1] [Medline: 40514413]
35. Stetson PD, Bakken S, Wrenn JO, Siegler EL. Assessing electronic note quality using the Physician Documentation Quality Instrument (PDQI-9). Appl Clin Inform 2012;3(2):164-174. [doi: 10.4338/aci-2011-11-ra-0070] [Medline: 22577483]
36. Crossley GM, Howe A, Newble D, Jolly B, Davies HA. Sheffield Assessment Instrument for Letters (SAIL): performance assessment using outpatient letters. Med Educ 2001 Dec;35(12):1115-1124. [doi: 10.1046/j.1365-2923.2001.01065.x] [Medline: 11895235]
37. Hart SG, Staveland LE. Development of NASA-TLX (Task Load Index): results of empirical and theoretical research. Advances in Psychology 1988;52:139-183. [doi: 10.1016/S0166-4115(08)62386-9]
38. Biro J, Handley JL, Cobb NK, et al. Accuracy and safety of AI-enabled scribe technology: instrument validation study. J Med Internet Res 2025 Jan 27;27:e64993. [doi: 10.2196/64993] [Medline: 39869899]
39. Chelli M, Descamps J, Lavoué V, et al. Hallucination rates and reference accuracy of ChatGPT and Bard for systematic reviews: comparative analysis. J Med Internet Res 2024 May 22;26:e53164. [doi: 10.2196/53164] [Medline: 38776130]
40. Metz C. Chatbots may 'hallucinate' more often than many realize. The New York Times. 2023 Nov 6. URL: https://www.nytimes.com/2023/11/06/technology/chatbots-hallucination-rates.html [accessed 2025-07-07]
41. Hatem R, Simmons B, Thornton JE. A call to address AI “hallucinations” and how healthcare professionals can mitigate their risks. Cureus 2023 Sep 5;15(9):e44720. [doi: 10.7759/cureus.44720] [Medline: 37809168]
42. Liu J, Capurro D, Nguyen A, Verspoor K. “Note bloat” impacts deep learning-based NLP models for clinical prediction tasks. J Biomed Inform 2022 Sep;133:104149. [doi: 10.1016/j.jbi.2022.104149] [Medline: 35878821]
43. Sittig DF, Singh H. A new sociotechnical model for studying health information technology in complex adaptive healthcare systems. Qual Saf Health Care 2010 Oct;19 Suppl 3(Suppl 3):i68-i74. [doi: 10.1136/qshc.2010.042085] [Medline: 20959322]
44. Pelletier JH, Watson K, Michel J, McGregor R, Rush SZ. Effect of a generative artificial intelligence digital scribe on pediatric provider documentation time, cognitive burden, and burnout. JAMIA Open 2025 Jul 3;8(4):ooaf068. [doi: 10.1093/jamiaopen/ooaf068] [Medline: 40620477]
45. Thawinwisan N, Liu C, Kishimoto K, Yamamoto G, Mori Y, Kuroda T. Comparing patient perception and physician’s records: generative AI performance evaluation. Stud Health Technol Inform 2024 Aug 22;316:671-675. [doi: 10.3233/SHTI240503] [Medline: 39176831]
46. Michalowski M, Topaz M, Peltonen LM. An AI-enabled nursing future with no documentation burden: a vision for a new reality. J Adv Nurs 2025 Mar 24. [doi: 10.1111/jan.16911] [Medline: 40129115]
47. Sasseville M, Yousefi F, Ouellet S, et al. The impact of AI scribes on streamlining clinical documentation: a systematic review. Healthcare (Basel) 2025 Jun 16;13(12):1447. [doi: 10.3390/healthcare13121447] [Medline: 40565474]
48. Rule A, Bedrick S, Chiang MF, Hribar MR. Length and redundancy of outpatient progress notes across a decade at an academic medical center. JAMA Netw Open 2021 Jul 1;4(7):e2115334. [doi: 10.1001/jamanetworkopen.2021.15334] [Medline: 34279650]
49. Thornton JD, Schold JD, Venkateshaiah L, Lander B. Prevalence of copied information by attendings and residents in critical care progress notes. Crit Care Med 2013 Feb;41(2):382-388. [doi: 10.1097/CCM.0b013e3182711a1c] [Medline: 23263617]
50. Kosmyna N, Hauptmann E, Yuan YT, et al. Your brain on ChatGPT: accumulation of cognitive debt when using an AI assistant for essay writing task. arXiv. Preprint posted online on Jun 10, 2025. [doi: 10.48550/arXiv.2506.08872]
51. Wright DS, Kanaparthy N, Melnick ER, et al. The effect of ambient artificial intelligence scribes on trainee documentation burden. Appl Clin Inform 2025 Jul 2. [doi: 10.1055/a-2647-1142] [Medline: 40602775]

Abbreviations

AI: artificial intelligence
EHR: electronic health record

XSL•FO
RenderX

LLM: large language model
NASA-TLX: NASA Task Load Index
PDQI-9: Physician Documentation Quality Instrument
SAIL: Sheffield Assessment Instrument for Letters

Edited by T Leung; submitted 18.07.25; this is a non–peer-reviewed article;accepted 18.07.25; published 01.08.25.

Please cite as:
Leung TI, Coristine AJ, Benis A
AI Scribes in Health Care: Balancing Transformative Potential With Responsible Integration
JMIR Med Inform 2025;13:e80898
URL: https://medinform.jmir.org/2025/1/e80898
doi:10.2196/80898

© Tiffany I Leung, Andrew J Coristine, Arriel Benis. Originally published in JMIR Medical Informatics (https://medinform.jmir.org), 1.8.2025. This is an open-access article distributed under the terms of the Creative Commons Attribution License (https://creativecommons.org/licenses/by/4.0/), which permits unrestricted use, distribution, and reproduction in any medium, provided the original work, first published in JMIR Medical Informatics, is properly cited. The complete bibliographic information, a link to the original publication on https://medinform.jmir.org/, as well as this copyright and license information must be included.

XSL•FO
RenderX

Bibliometric Insights Into the Infodemic: Global Research Trends and Policy Responses: Quantitative Research

Sijia Wang[1], MA; Linan Zhang[2], PhD; Yang Liu[3], MA; Xin Feng[4], PhD; Shipeng Ren[5], PhD

[1]Department of Urban Construction, Hebei Normal University of Science and Technology, Qinhuangdao, China

[2]School of Marxism, Shijiazhuang Tiedao University, Shijiazhuang, China

[3]School of Arts and Communication, Hebei University of Engincering Science, No.11, Gongbei Road, Qiaoxi District, Shijiazhuang, Hebei, China

[4]The Institute for Social and Cultural Research, Macau University of Science and Technology, Macau, China

[5]School of Economics and Finance, Xi'an Jiaotong University, Xi'an, China

Corresponding Author:
Yang Liu, MA
School of Arts and Communication, Hebei University of Engincering Science, No.11, Gongbei Road, Qiaoxi District, Shijiazhuang, Hebei, China

Abstract

Background: Amidst the COVID-19 pandemic, the proliferation of misinformation on social media, termed the “infodemic,” has complicated global health responses.

Objective: This study aims to identify research trends and information-making in the context of this challenge. This paper synthesizes key areas of scholarly investigation into the COVID-19 infodemic, both within China and internationally, to guide public health strategies and the management of public sentiment.

Methods: By employing a bibliometric approach, using CiteSpace software, we conducted a visual analysis of the global literature, covering a total of 1437 publications from the Web of Science and the China National Knowledge Infrastructure core databases between 2016 and 2025, focusing on publication trends, citation frequencies, and keyword clusters.

Results: After analysis, the results reveal distinct focal points in the research priorities of Chinese and international scholars. International studies often focus on machine learning and public psychology, while Chinese research tends to address information control and safeguarding. Common ground is found in the interest in preventing the spread of misinformation. While literature on COVID-19 abounds, cross-national systematic reviews are limited.

Conclusions: This paper fills this gap through a comparative bibliometric analysis, offering valuable insights for information management, media communication, and public administration, thus charting new directions for future research.

(JMIR Med Inform 2025;13:e76378) doi:10.2196/76378

KEYWORDS

infodemic; bibliometrics; visualization; information spreading; social media; information governance

Introduction

The COVID-19 pandemic has precipitated unprecedented disruptions across global business, economic, and cultural landscapes. Simultaneously, the “infodemic” of misinformation has emerged as a formidable adversary, undermining efforts to restore social stability. Misinformation, typically characterized by the dissemination of unverified content via informal networks, lacks empirical substantiation and rational debate on matters of public importance [1,2]. The pandemic has expedited the spread of such misinformation, leading to widespread information anxiety and eroding public trust [3]. The infodemic’s narratives have been categorized into denial, remedial, and conspiracy discourses, progressively refining its conceptualization [4]. Recognizing its historical precedence, the World Health Organization in September 2020 emphasized the necessity to combat infodemics alongside the pandemic. In the digital age, social media platforms have become central to information dissemination, amplifying the reach and impact of misinformation during crises [5], thus underscoring the urgency of addressing the infodemic.

Scholarly efforts have begun to address the infodemic. The cornerstone of such a mechanism rests on robust government oversight and legal frameworks [6], suggesting a collaborative approach between administrative and legal interventions. Moreover, the varying quality among media practitioners, marked by a deficiency in humanistic values, critical thinking, and global outlook, exacerbates the infodemic. Furthermore, leveraging the strategic value of accurate information, particularly by tapping into public engagement on social media, can refine policy effectiveness. The psychological repercussions of the infodemic on COVID-19 patients are also a significant

XSL•FO
RenderX

concern, with the deluge of misinformation contributing to heightened uncertainty in treatment outcomes. Timely psychological interventions have been deemed essential, with studies revealing a correlation between increased social media exposure and psychological distress [7]. Additionally, the application of machine learning and algorithmic analysis in studying infodemic patterns provides empirical insights into topic evolution and public sentiment [8,9]. Advancements in deep learning models have enhanced the detection of misinformation [10], with integrated language and context analysis models proving effective in identifying false narratives [11]. These technological approaches could empower health care institutions to foster informed public discourse during health crises [12].

A review of the literature reveals that current research on the infodemic primarily focuses on the intersection of information governance and health care. While data science and machine learning offer innovative perspectives, comprehensive reviews synthesizing these areas are lacking.

From a bibliometric perspective, the structure of this paper is as follows: The Methods section outlines the methodological framework, detailing the data and methods, with a focus on sample data for empirical analysis. The Results section includes several subsections: temporal trends in domestic and international publications, visual comparative analysis of authorship, institutional contributions, and research directions across countries, as well as a keyword clustering analysis that categorizes domestic and international infodemic research. The Discussion section identifies key challenges for the future of information governance and new media development, exploring each in depth. Finally, the Conclusion concludes with a summary and proposes directions for future research.

Methods

Study Overview

This study employed bibliometric methods [13], combined with visualization analysis tools, to systematically map and compare the research landscape of the COVID-19 infodemic at the international and Chinese levels. Bibliometrics is a powerful tool for quantitatively revealing the knowledge structure, evolutionary pathways, and research frontiers within a specific research field [3]. In recent years, this methodology has been widely applied to assess and analyze numerous complex and critical research areas, such as pathways to carbon neutrality [14], the application of artificial intelligence in renewable energy [15], the economic impacts of the COVID-19 pandemic [16], and wastewater treatment for emerging contaminants [17], demonstrating its effectiveness and robustness in mapping interdisciplinary knowledge domains. Therefore, this study utilizes this approach to analyze the equally complex and multidimensional global issue of the infodemic.

Using CiteSpace 5.3, this study systematically searched the Web of Science (WOS) and China National Knowledge Infrastructure (CNKI) core databases, with parameters and outcomes detailed in Table 1. The data visualization timeframe was segmented into 1-year intervals for enhanced clarity.

Table . WOS[a] and CNKI[b] data-related parameter settings.

Related parameter settings	WOS	CNKI
Time limit	2016-2025	
Time slice	1 year	
Retrieval time	Jul 20, 2025	
Node type	The author of the article, the issuing organization, the keywords	
Search method	Subject search	
Retrieve content	“Social media” AND “infodemic”	“infodemic”
Literature resources	Core journal	CSSCI[c]+core journal
Output format	Text format	RefWorks format
Valid data	312	1125

[a]WOS: Web of Science.

[b]CNKI: China National Knowledge Infrastructure.

[c]CSSCI: Chinese Social Sciences Citation Index.

In the WOS database, considering that directly using “misinformation” combined with “social media” yielded limited results, and the term “infodemic” more precisely captures the issue of information overload in the context of COVID-19, we employed a Topic Search with the query: TS=(“infodemic” AND “social media”). In the CNKI database, to comprehensively capture relevant literature, we experimented with multiple search strategies. Both subject searches (Subject=“社交媒体” [social media] AND (Subject=“信息疫情” [infodemic] OR Subject=“错误信息” [misinformation])) and keyword searches (Keyword=“社交媒体” [social media] AND (Keyword=“信息疫情” [infodemic] OR Keyword=“错误信息” [misinformation])) returned limited results. Therefore, we focused on the core theme of “infodemic” and conducted a subject search (Subject=“信息疫情” [infodemic]), as it yielded a larger volume of literature that was highly relevant to our research focus.

XSL•FO
RenderX

The initially retrieved records were screened to ensure relevance and compliance with document type requirements. The inclusion criteria were as follows: document types limited to journal articles (articles or reviews); research content directly related to the infodemic in the context of COVID-19; and language restricted to English (WOS) or Chinese (CNKI). The exclusion criteria were as follows: nonacademic publication types such as news reports, conference abstracts, proceedings, book reviews, notices, and letters; duplicate records; and literature with low relevance to the research topic.

After screening, 312 records from WOS and 1125 records from CNKI were included as the final analytical sample. Complete bibliographic records (including titles, authors, affiliations, abstracts, keywords, and references) were exported in plain text format.

Bibliometrics primarily employs statistical and quantitative techniques to analyze scientific literature. These techniques and their results are summarized in Table 1, referring to the publication timeframe as “time slice.” Publication trends in both domestic and international research are depicted to assess the scope and direction of the field’s evolution. This paper also presents a visual map analysis of author and institution collaborations, offering insights into academic exchange and teamwork patterns. The significance of highly cited works as indicators of scholarly focus is acknowledged [18], allowing us to infer primary academic directions. Current hot topics are identified through cluster analysis of keywords from these highly cited works.

The selection of the WOS Core Collection and the CNKI database was made after careful consideration, aiming to comprehensively cover global research on COVID-19-related infodemics.

WOS, as an internationally recognized premier citation database, indexes high-impact academic literature across multiple disciplines, providing authoritative coverage of international publications.

CNKI, on the other hand, is the most comprehensive and authoritative database for Chinese academic journals, books, dissertations, and conference proceedings, making it indispensable for capturing the substantial body of domestic research on this topic.

Ethical Considerations

Ethical oversight and approval for this study were provided by the School of Urban Construction at Hebei Normal University of Science and Technology, as the university does not have a dedicated ethics committee for humanities and social sciences research. All procedures were conducted in accordance with the Declaration of Helsinki. Participant data were anonymized and stored securely to protect confidentiality. No compensation was provided.

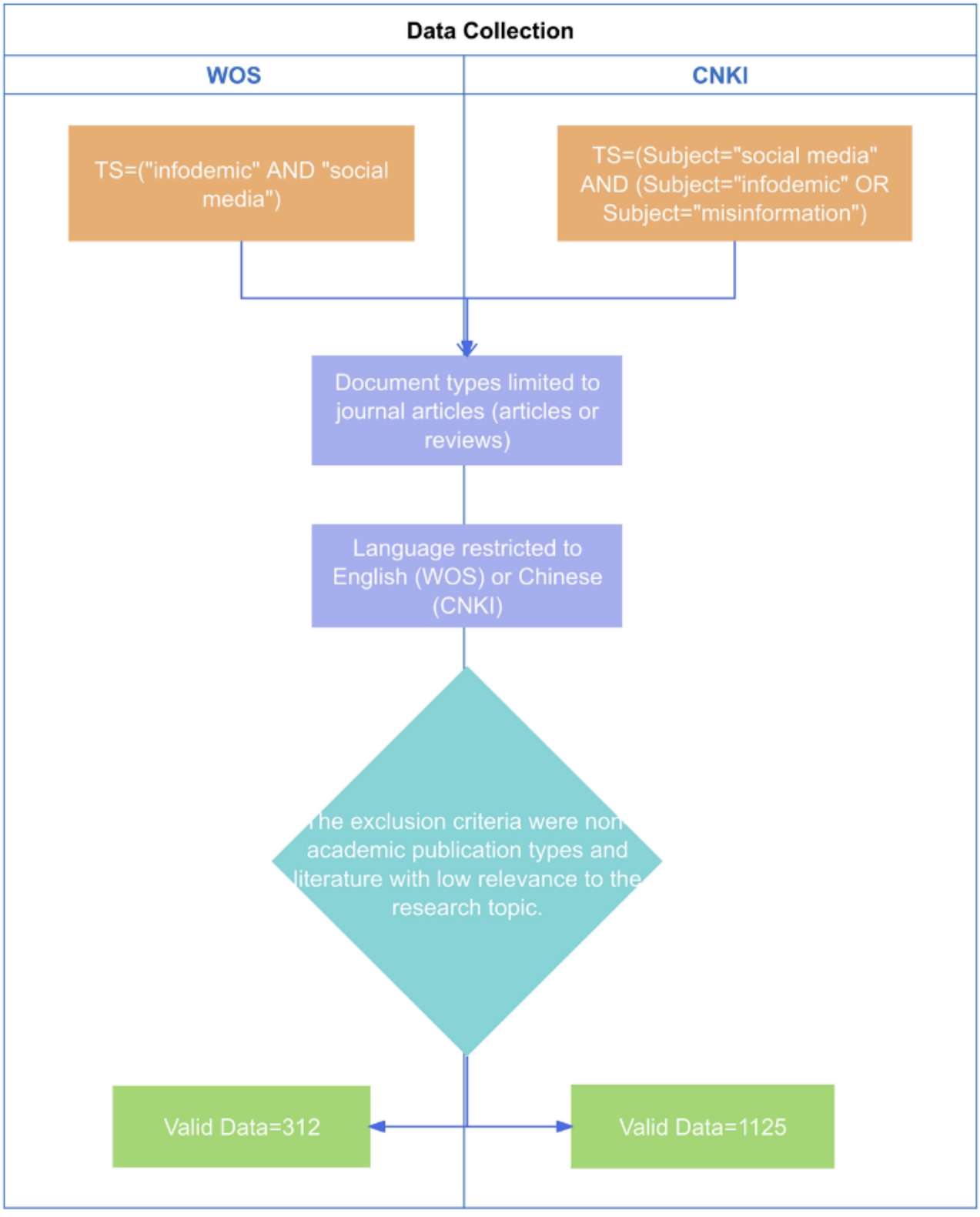
Results

Studies Included

To illustrate the literature identification and screening process, we created a PRISMA-style flow diagram (Figure 1).

XSL•FO
RenderX

Figure 1. Flowchart of literature screening in WOS and CNKI databases. CNKI: China National Knowledge Infrastructure; WOS: Web of Science.

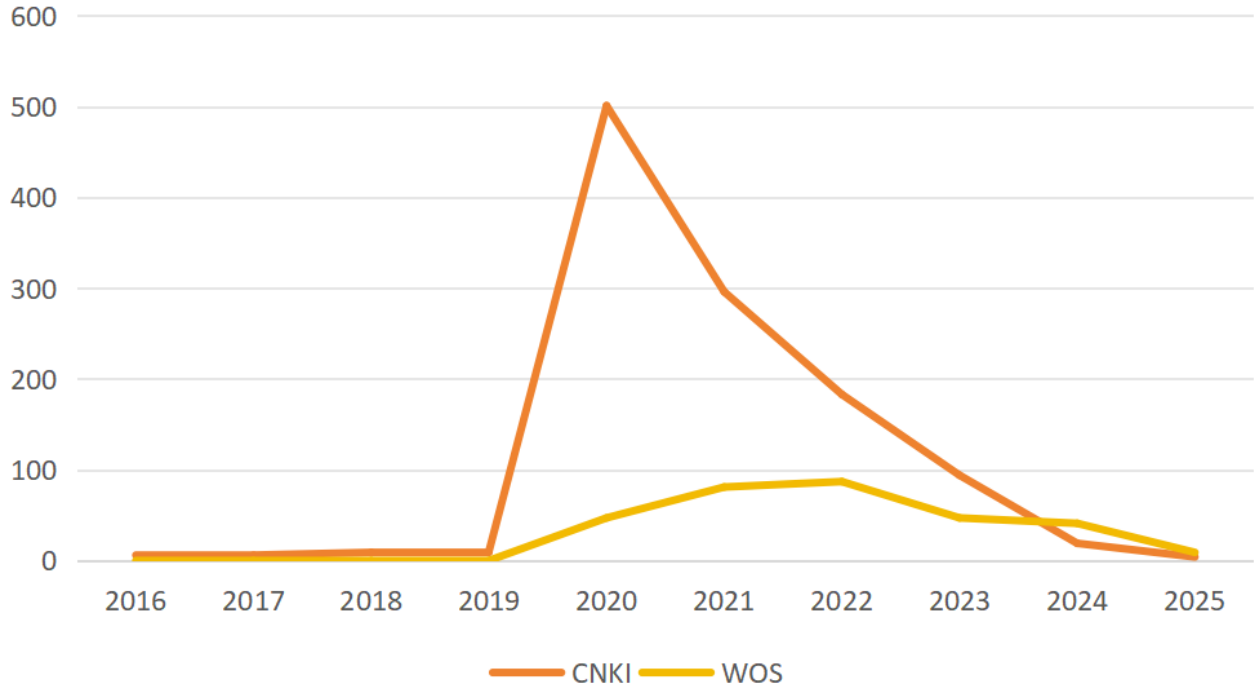


The Time Trend Analysis

The volume of publications over time serves as an intuitive indicator of research activity and interest in a field, aiding in forecasting future research trajectories. Analysis of data up to July 20, 2025, reveals 1125 domestic publications and 312 international publications. Figure 2 illustrates a spike in both domestic and international research during 2020 and 2021, followed by a decline, with international publications surpassing domestic output as of July 2025.

XSL•FO
RenderX

Figure 2. Comparison chart of domestic and international research publications on information epidemics from 2016 to 2025. CNKI: China National Knowledge Infrastructure; WOS: Web of Science.



The term "infodemic" emerged in response to the misinformation crisis linked to the pandemic, starting in December 2019 [19]. Initially, this concept received limited academic attention, representing a nascent challenge with unclear societal repercussions [20].

The sustained impacts of infodemics have kept scholarly interest alive internationally, as researchers tackle the complex societal issues they create. This ongoing interest is reflected in the steady volume of international research in 2021, characterized by an interdisciplinary approach focused on developing models for infodemic transmission and algorithms for information management [21]. Such cross-disciplinary synergy and technological innovation likely contributed to the growth of international publications.

In 2020, China experienced a turning point as domestic outbreaks underscored the detrimental effects of infodemics. The urgency to combat misinformation spurred a surge in Chinese research, driven by the need for policy development and effective mitigation strategies, resulting in a significant increase in publications that later tapered off with the successful containment of the epidemic [22].

Analysis of Author Networks

This section analyzes authorship patterns in the field, examining both domestic and international author networks while identifying prolific authors based on their research output. The focus is on authors with multiple publications, exploring themes investigated by collaborative teams through key articles.

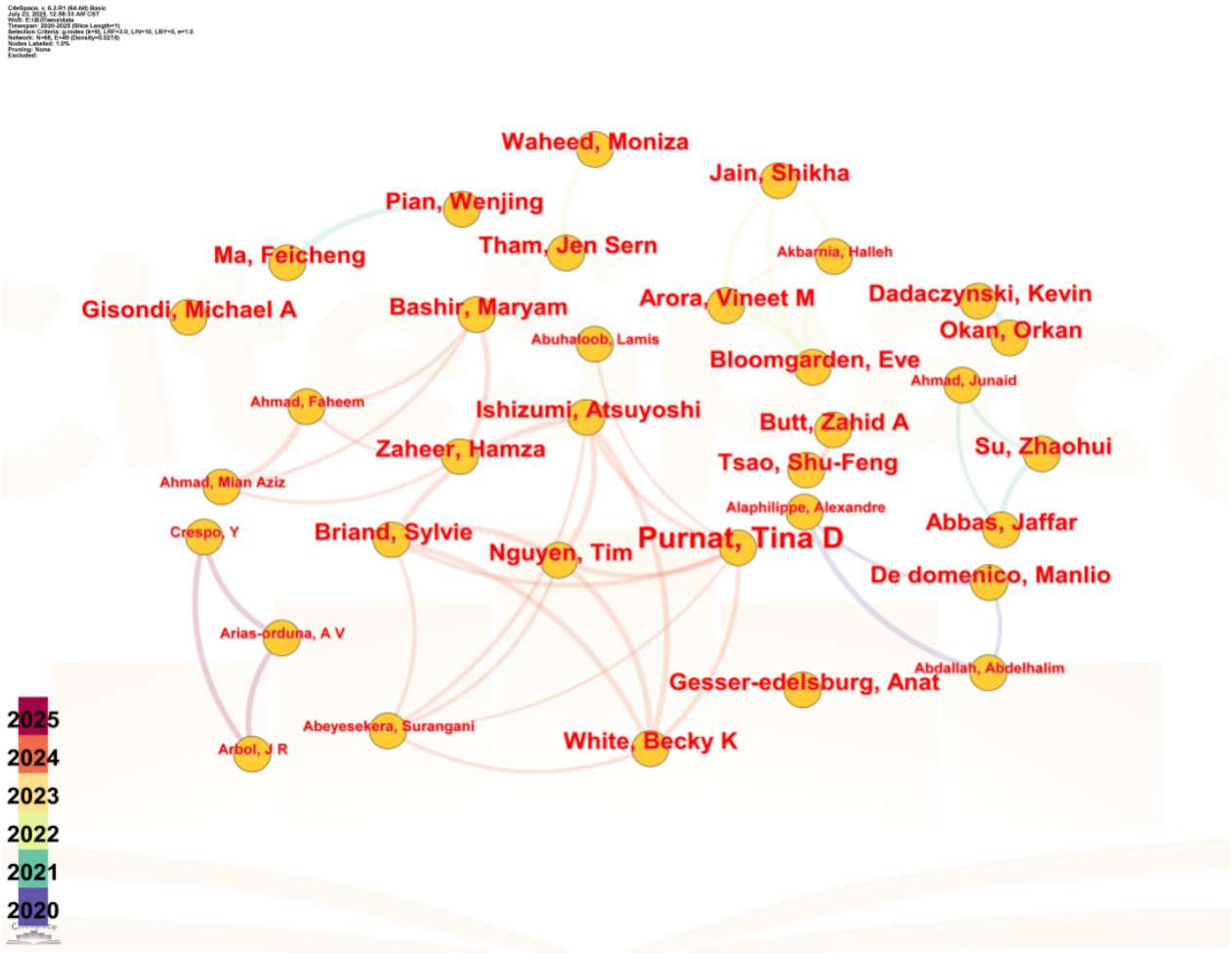
Author networks are visually represented by nodes and connections, where each node represents an individual author, and its size indicates the number of publications. Lines between nodes signify collaborative links, with denser lines reflecting more frequent coauthorship. This network analysis provides insights into the level of cooperation and identifies central figures within the research community.

Global Author Analysis

This subsection extends the authorship analysis to the international landscape, employing network visualizations to elucidate the collaborative dynamics among global researchers (Figure 3).

XSL•FO
RenderX

Figure 3. Global author collaboration network for information epidemic research.



The optimized author cooperation network is depicted in Figure 3, generated using CiteSpace software. CiteSpace was developed by Dr. Chaomei Chen, a professor at the College of Computing and Informatics, Drexel University in the United States. The detailed configuration and data information for this part of the CiteSpace analysis are summarized in Table 2, covering key information such as software version and time slice settings. The network consists of 68 nodes (n=68), signifying the involvement of 68 authors, and exhibits a connection density of 0.0215. The sparsity of the connections within the network suggests a low level of collaboration among international authors. Table 3 details articles that have emerged from three distinct collaborative clusters within the network. These articles address a range of topics, including a cross-sectoral information management framework for pandemic response [23], recommendations for social media companies to combat infodemics [24], and novel paradigms for public health communication [25].

XSL•FO
RenderX

Table . CiteSpace configuration and data information in global author analysis.

Details	Content
CiteSpace v. 6.8.R3 (32-bit)	Software and version
WOS[a]	Data type
2020-2025, slice length=1	Time slicing
g-index (k=25%), RPf[b]=3.0, LN[c]=10, LBY[d]=5, e=1.0	Selection criteria
Largest CC:[e] 6 (7%)	Largest co-occurrence cluster size
Total nodes: 22 (7.04%)	Total network nodes
Pruning: Pathfinder	Pruning method

[a]WOS: Web of Science.

[b]RPf: research publication frequency.

[c]LN: labeled node.

[d]LBY: leading board year.

[e]CC: co-occurrence cluster.

Table . Foreign authors collaborate on articles.

Writer	Title	Time	Citation frequency
Tangcharoensathien V et al [19]	Framework for managing the COVID-19 infodemic: methods and results of an online, crowdsourced WHO technical consultation	2021	364
Gisondi MA et al [23]	A Stanford conference on social media, ethics, and COVID-19 misinformation (INFODEMIC): qualitative thematic analysis	2022	19
Albrecht SS et al [24]	Lessons learned from the dear pandemic, a social media-based science communication project targeting the COVID-19 infodemic	2022	0

Further analysis of international authors' publication patterns reveals that several have published two or more papers on the topic. Notably, De Domenico emerged as the most prolific contributor with 4 publications, while 23 other researchers (representing 34% [23/68] of all authors) produced more than two papers each. In terms of collaborative work, the most-cited single paper received 93 citations, demonstrating substantial academic attention and recognition within this research field. This citation impact strongly reflects the high scholarly value attributed to these studies.

Domestic Author Analysis

Figure 4 shows the optimized author collaboration network diagram, Table 4 shows the articles written by authors, and the detailed data information from this part of the CiteSpace analysis is summarized in Table 5. There are 168 nodes displayed in the graph (n=168), indicating that 168 people are renting the authors, and the connection density is 0.0153. Small nodes and low density indicate that the author has fewer papers and a low level of cooperation. The map shows only two more complex cooperative networks, led by Wang and Chen [26]. Wang's group elaborated expert perspectives on addressing infodemics, informing policymaking and platform information dissemination [27]. Li and colleagues probed characteristics and dissemination of scientific information to devise specific countermeasures [28]. Overall, 51 authors have published 2 or more papers, accounting for 30% (51/168) of the total number of authors analyzed. The highest number of citations for a collaborative paper is 3.

XSL•FO
RenderX

Figure 4. Domestic author collaboration network in infodemic research.



Table . Domestic authors collaborate on articles.

Writer	Title	Time	Citation frequency
Li et al [29]	A cross-sectional survey on information access through hospital's official account on new media and its association with antenatal care knowledge and health behaviors of pregnant women under COVID-19 epidemics	2021	3
Zong et al [30]	Analysis of Data Collection of Relapsing COVID-19 Epidemic Events in China	2021	1
Li et al [31]	Content characteristics, modes, response strategies and optimization paths of epidemic scientific information dissemination: based on the content analysis of 10 popular microblogs of related scientists	2022	0

XSL•FO
RenderX

Table . CiteSpace configuration and data information in domestic author analysis.

Details	Content
CiteSpace v. 5.8.R3 (32-bit)	Software & version
2016-2025 (slice length=1)	Timespan
g-index (k=25%), RPf[a]= 3.0, LN[b]=10, LBY[c]=5, e=1.0	Selection criteria
N=168, E=214 (density=0.0153)	Network
Mean silhouette S=0.8898	Silhouette
Harmonic mean (Q, S)=0.7113	Harmonic mean

[a]RPf: research publication frequency.

[b]LN: labeled nodes.

[c]LBY: leading board year.

Identifying core authors is a process that considers both the quantity of output (importance) and the extent of influence (citation counts). The analysis of both domestic and international authors reveals that overall author productivity is modest, with no individuals exhibiting exceptionally high publication rates. Furthermore, the citation rates for the literature are not optimal, suggesting that research into infodemics is still in its formative stages. There is a clear opportunity for researchers to engage in more diverse collaborative efforts, which could significantly enhance the quality and impact of their work.

Core author groups are essential for carrying out in-depth investigations into complex issues, fostering sustained and comprehensive research efforts. Although there are nascent collaborative teams both domestically and internationally, the metrics of importance and influence indicate potential for theoretical expansion and development. This underscores the need for increased interdisciplinary collaboration and more robust research networks to advance the field.

Institution Analysis

This section evaluates the contribution of various institutions to the field by examining the volume of publications and the extent of interinstitutional collaboration. The analysis of the institutional co-occurrence network, represented through nodes and connecting lines, offers insights into the depth of research on the topic and the collaborative intensity among institutions.

Foreign Institution Analysis

The assessment of international institutional engagement is visualized in Figure 5, which illustrates a network comprising 81 entities. The detailed data information of CiteSpace analysis in this section is presented in Table 6, including key parameters such as time span and selection criteria, providing support for the reliability of network analysis. The network exhibits a slightly higher level of connectivity (density=0.0148) compared to domestic institutions, indicating a modest degree of international collaboration. Predominantly universities, these foreign institutions demonstrate greater collaborative activity than their domestic counterparts, though there is still considerable room for deepening these cooperative relationships.

XSL•FO
RenderX

Figure 5. International institutional collaboration network on infodemic research.

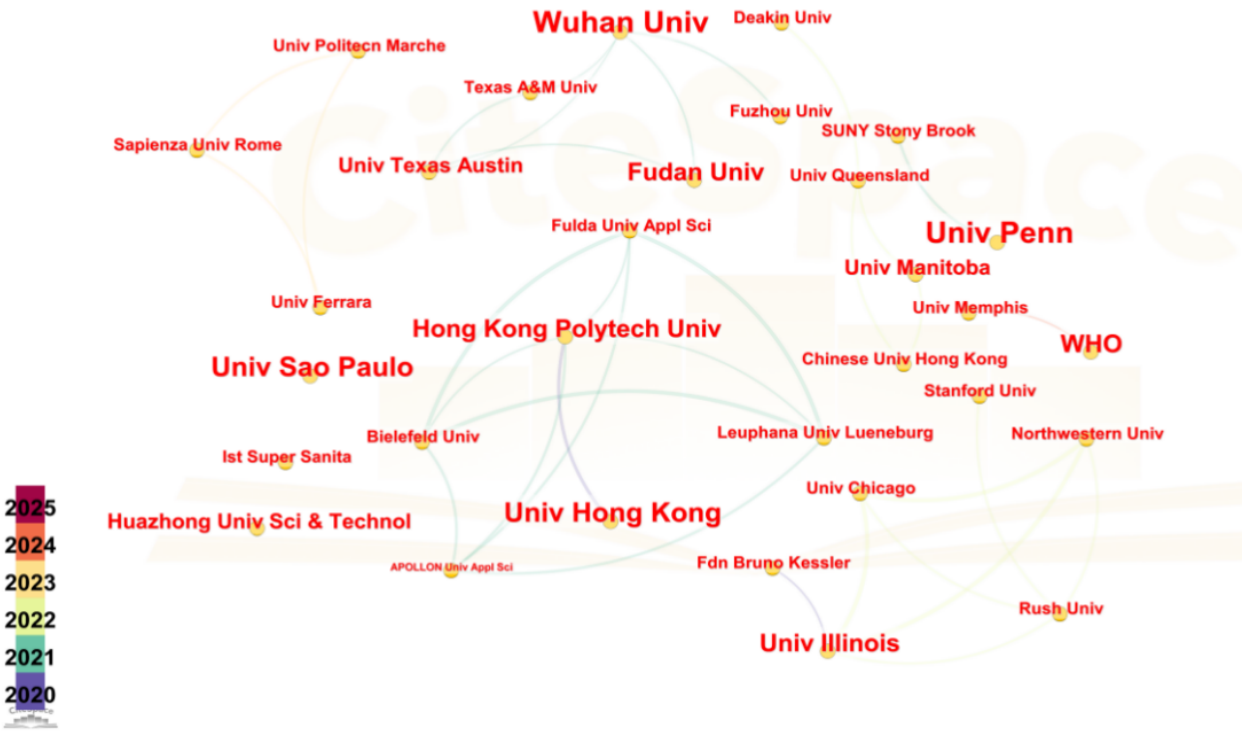


Table . CiteSpace configuration and data information in foreign institution analysis.

Details	Content
CiteSpace v. 5.8.R3 (32-bit)	Software & version
2020-2025 (slice length=1)	Timespan
g-index (k=25%), RPf[a]=3.0, LN[b]=10, LBY[c]=5, e=1.0	Selection criteria
N=73, E=54 (density=0.0207)	Network
Largest CC[d]: 7 (9%)	Largest co-occurrence cluster size
Total nodes: 16 (21.9%)	Total network nodes

[a]RPf: research publication frequency.

[b]LN: labeled nodes.

[c]LBY: leading board year.

[d]CC: co-occurrence cluster.

Wuhan University emerges as the most prolific contributor with six published articles, having established collaborative links with Fudan University and Fuzhou University, each on two occasions. Despite these partnerships, the depth of international cooperation, as reflected by the overall network density, remains limited.

Further analysis of the data from institutions publishing international papers reveals that among those publishing four or more international papers, Wuhan University stands out with six papers. Its research focuses on the characteristics, transmission mechanisms, and network information flow regulation strategies of information epidemics. Notably, one of the university's papers has been cited seven times. Through media type analysis, it quantifies the spatial correlation between information epidemics and actual epidemics, finding that mobile media may increase the transmission risk coefficient. Other major institutions include Oxford University, Hong Kong Polytechnic University, Bruno Kessler Foundation, and the University of Pennsylvania, all of which have published four significant research outcomes.

XSL•FO
RenderX

Domestic Institution Analysis

The visualization of domestic institutions indicates 209 contributing entities (n=209), yet the network's density is 0.0028, signifying no discernible connections between them. The modest number of publications from each institution results in smaller nodes and an absence of a visible network, suggesting a nascent stage of institutional collaboration in this research area.

Among domestic institutions, 76 have published two or more papers, primarily universities and research institutions. As the core force in academic research, these institutions continue to explore this emerging social issue; from a geographical perspective, they are widely distributed across China, reflecting the widespread attention of the domestic academic community to this field.

The School of Information Management at Nanjing University has published 10 papers, making it the university with the highest number of published papers in China. The Communication University of China stands out with seven publications, underscoring its significant role in examining information dissemination and governance. One notable publication from this institution delves into media users' characteristics, cognitive assessments, and interactions, providing theoretical insights for governance.

The fact that 133 institutions have contributed only a single paper each highlights a lack of sustained research efforts across most entities. The absence of connectivity within the network (density=0) indicates that research efforts are isolated, with institutions working independently rather than collaboratively. This isolation suggests potential for greater cooperation, which could foster more comprehensive studies and a deeper understanding of the issues at hand.

In conclusion, while the foundations for international institutional cooperation are in place, the impact and breadth of this collaborative effort require enhancement. It is important to recognize the multidisciplinary nature of infodemic research, which intersects with journalism, communication, computer science, public management, and other fields. Sustained and strategic collaboration among institutions is pivotal for in-depth exploration of the topic and for elevating the quality of research outputs. Therefore, there is a clear need to fortify the collaborative ties between research institutions and to facilitate interdisciplinary communication to advance the study of information epidemics effectively.

Highly Cited Literature Analysis

The frequency of citations serves as a barometer for scholarly impact, with highly cited papers often indicative of their influence and prominence within the academic community. An in-depth examination of citations and keywords from these seminal works provides insight into the prevailing research themes and potential future directions.

Foreign Highly Cited Literature Analysis

Table 7 contrasts the domestic citation landscape with the international scene, which demonstrates a broader academic reach. Keywords such as "COVID-19," "social media," "mental health," "depression," "public attention," and "communication content" dominate these papers, reflecting concerns over the spread of misinformation on social media during the pandemic. The synthesis of keywords from these influential international articles reveals focal areas of global concern: the mental health impact of the infodemic [32], the development of infodemic response strategies and various facets of information governance, including thematic communication and evolution [33,34], as well as monitoring and evaluative frameworks [35,36].

XSL•FO
RenderX

Table . Top 5% citation frequency in WOS.[a]

Number	Title	Citation frequency	Keywords
1	Mental health problems and social media exposure during COVID-19 outbreak [6]	595	COVID-19; mental health; social media
2	The COVID-19 social media infodemic [32]	274	epidemiology; computer science; information theory; and computation
3	COVID-19–related infodemic and its impact on public health: a global social media analysis [34]	192	COVID-19; infodemic; impact on public health
4	Mental health, risk factors, and social media use during the COVID-19 epidemic and Cordon Sanitaire among the community and health professionals in Wuhan, China: cross-sectional survey [37]	181	COVID-19; social media; population mental health; depression
5	Coronavirus (COVID-19) "infodemic" and emerging issues through a data lens: the case of China [38]	178	COVID-19; infodemic; humanitarian emergency
6	The impact of social media on panic during the COVID-19 pandemic in Iraqi Kurdistan: online questionnaire study [25]	175	social media; COVID-19; infodemic; mental health
7	COVID-19 infodemic; more retweets for science-based information on coronavirus than for false information [35]	151	communicative content analysis; infodemic; social media analytics
8	Framework for managing the COVID-19 infodemic: methods and results of an online, crowdsourced WHO technical consultation [19]	94	COVID-19; infodemic; knowledge translation; message amplification; misinformation; risk communication
9	Chinese public attention to the COVID-19 epidemic on social media: observational descriptive study [39]	94	public attention; social media; public health emergency
10	Assessing the risks of “infodemics” in response to COVID-19 epidemics [33]	92	COVID-19; infodemic; risk

[a]WOS: Web of Science.

In summary, while the domestic articles are gaining traction, international literature, with its broader citation reach, highlights a global engagement with the intricate challenges posed by the infodemic. This underscores the necessity for a concerted, multidisciplinary approach to understand and mitigate the effects of misinformation, especially in the context of global health crises.

Foreign Highly Cited Literature Analysis

As of the data collection cutoff, domestic literature exhibits a relatively modest citation footprint. However, it is important to acknowledge the potential for a rise in citation frequency for more recent publications. Table 8 lists the three most cited domestic articles, with citation counts of 49, 45, and 35, respectively. A keyword analysis of these leading papers reveals primary research themes among the highly cited domestic literature: infodemic response strategies, information governance mechanisms, and patterns of information dissemination.

XSL•FO
RenderX

Table . Citation frequency in CNKI.[a]

Number	Title	Citation frequency	Keywords
1	Analysis and Countermeasures of Problems in China's Disease Prevention and Control Information System [40]	49	Epidemic control; public health emergencies; intelligence system
2	What kind of public information dissemination do we need to build? Reflections on new media communication during the COVID-19 pandemic [41]	45	Pandemic; public information dissemination; social media; decentralization; epidemic information
3	Association between digital media use and anxiety symptoms of college students during the novel coronavirus pneumonia epidemic [42]	35	Epidemic prevention and control; media use; information needs; media trust; information governance; public emergency
4	Integrated management of the COVID-19: practical test and optimization path [43]	34	Public health emergencies; COVID-19; online public opinion; information disclosure; multiple subjects
5	Legal protection of personal information in major epidemic prevention and control [44]	34	Personal information; epidemic prevention and control; data against the epidemic; information protection; use the information
6	Population movement, information transmission efficiency, and epidemic control: evidence from COVID-19 [45]	29	COVID-19; population mobility; information transmission efficiency; brand theory
7	Personal information protection in public health events -- from the perspective of COVID-19 prevention and control [46]	29	COVID-19; information privacy; public interest; proportionality
8	Research on Risk Perception and Risk Transmission Models in Public Health Events: A Discussion on the Moderating Effect of Epidemic Severity [47]	28	Risk information; risk perception; communication behavior; epidemic severity
9	Use of personal information and legal rules in public emergencies: COVID-19 response as a starting point [48]	28	Emergency response; use of personal information; the rule of law

[a]CNKI: China National Knowledge Infrastructure.

Keywords Clustering Analysis

Keyword clustering is a methodological approach that groups semantically related keywords to identify dominant themes within a body of literature. This analytical technique can provide insights into the central topics of research by examining the centrality, frequency, and co-occurrence of keywords. In this section, the software CiteSpace is utilized to conduct a clustering analysis of the literature, with the aim of highlighting distinctions between domestic and international research foci.

Foreign Keywords Clustering Analysis

The data information regarding the keyword clustering analysis of foreign literature in this section is detailed in Table 9. To facilitate a clearer representation, the “Convex Hull: Show/Hide” feature in CiteSpace can be employed to display the clustering outcomes as distinct colored shapes. The modularity value Q and the mean silhouette value S are recognized as key indices for evaluating the quality of clustering. A Q value greater than 0.3 is indicative of a well-defined structure characterized by high internal consistency and relatedness, while an S value approaching 1 suggests an optimal clustering scale. Internationally, the Q value is 0.3842, S value is 0.7323, and the mean of Q and S is 0.5583, as shown in Figure 6. The clustering results for both domestic and international literature denote clear demarcations and appropriate scales, affirming the reliability of the cluster analysis.

XSL•FO
RenderX

Table . CiteSpace configuration and data information in foreign keywords clustering analysis.

Details	Content
CiteSpace v. 5.8.R3 (32-bit)	Software & version
2020 - 2025 (slice length=1)	Timespan
g-index (k=25%), RPf[a]=3.0, LN[b]=10, LBY[c]=5, e=1.0	Selection criteria
n=112, E=471 (density=0.0758)	Network
Largest CC[d]: 109 (97%)	Largest cluster (CC)
Modularity Q=0.3842	Pruning: Pathfinder
Mean silhouette S=0.7323	Mean silhouette
Harmonic mean (Q, S)=0.504	Harmonic mean (Q, S)

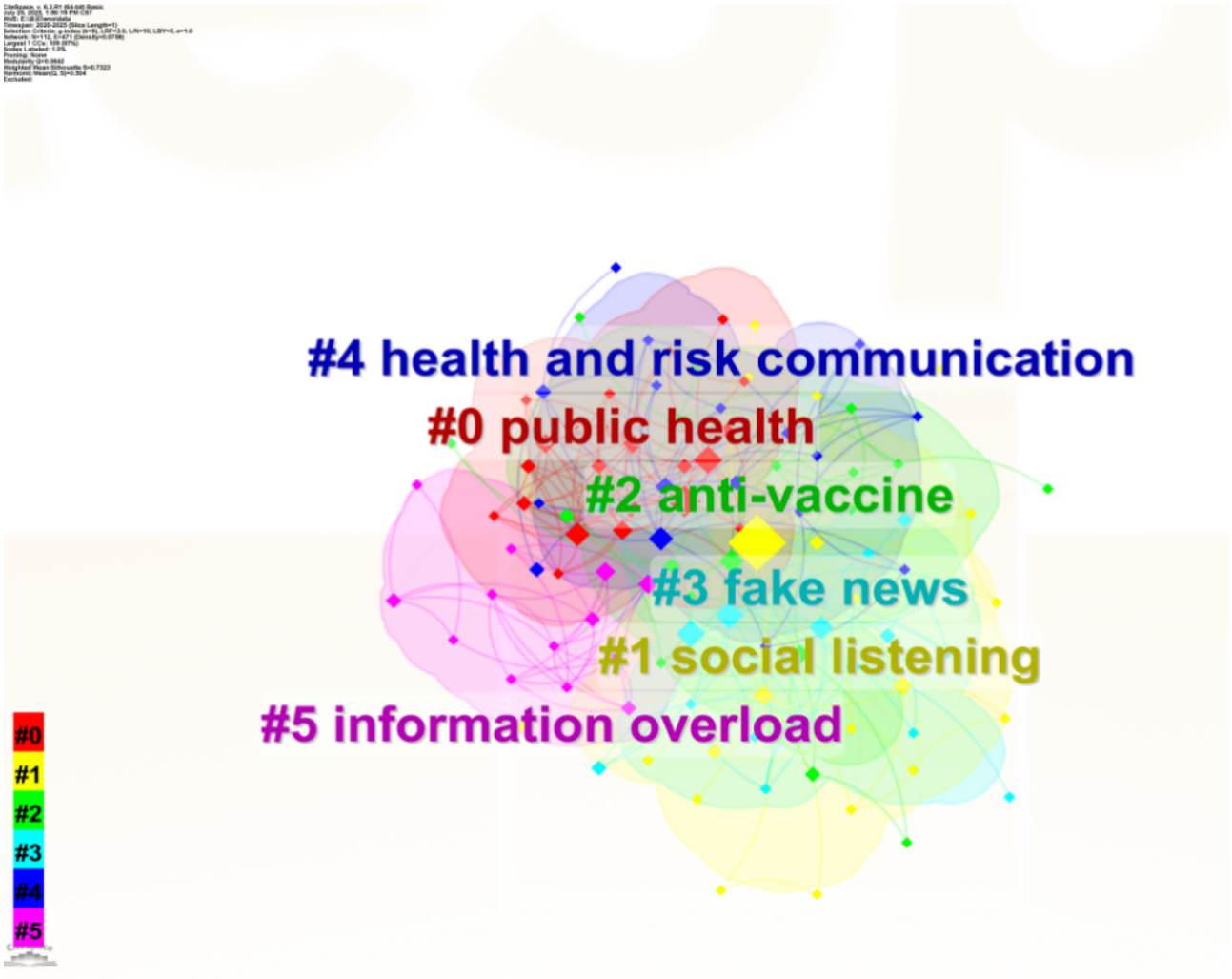
[a]RPf: research publication frequency.

[b]LN: labeled nodes.

[c]LBY: leading board year.

[d]CC: co-occurrence cluster.

Figure 6. Thematic evolution of global infodemic research.



Domestic Keywords Clustering Analysis

The domestic literature exhibits a Q value of 0.4715 and an S value of 0.7964 (as shown in Table 10), with an average of Q and S at 0.6339 as depicted in Figure 7.

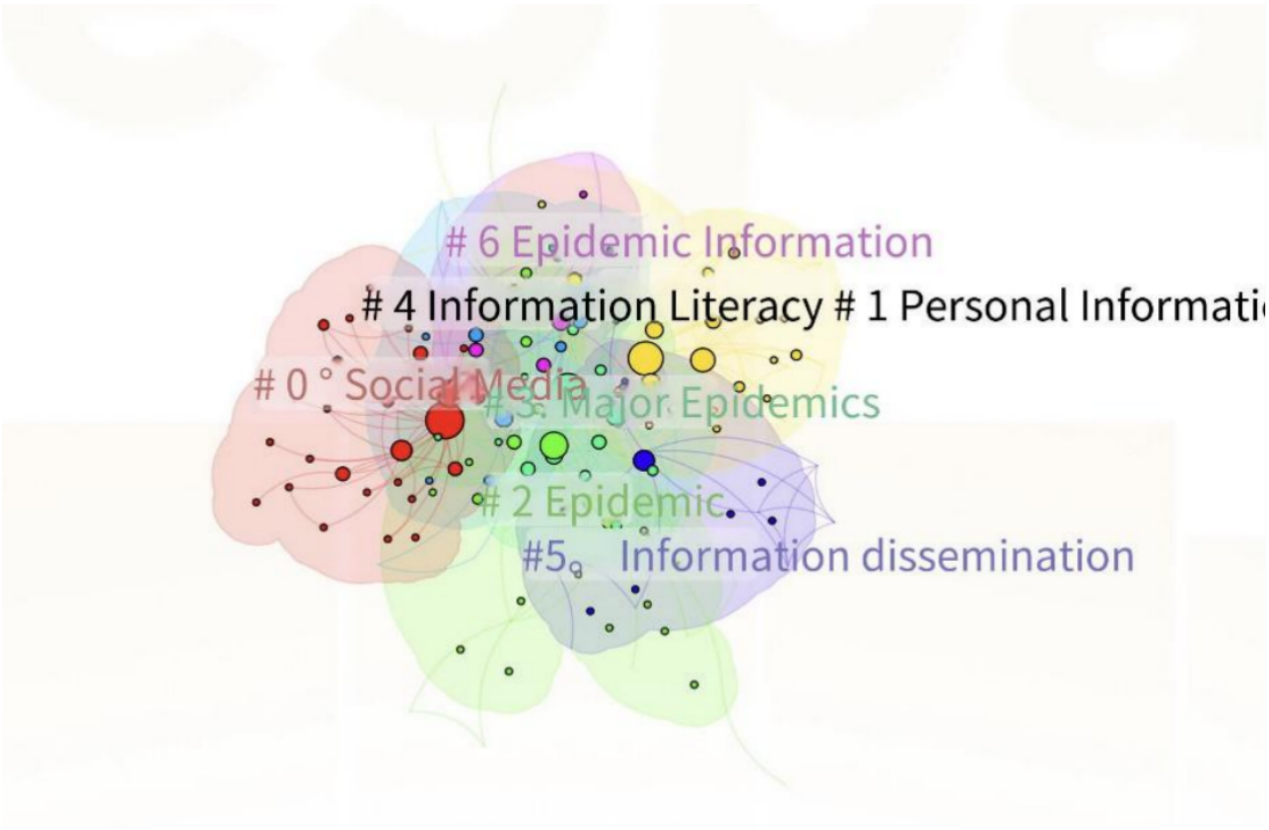
XSL•FO
RenderX

Table . CiteSpace configuration and data information in domestic keywords clustering analysis.

Details	Content
CiteSpace v. 5.8.R3 (32-bit)	Software & version
2016 - 2025 (slice length=1)	Timespan
g-index (k=25%), RPf[a]=3.0, LN[b]=10, LBY[c]=5, e=1.0	Selection criteria
n=145, E=398 (density=0.0381)	Network
Largest CC[d]: 122 (84%)	Largest cluster (CC)
Nodes labeled: 1.0%	Nodes labeled
Modularity Q=0.4715	Modularity
S=0.7964	Weighted mean silhouette
0.5923	Harmonic mean (Q, S)

[a]RPf: research publication frequency.
[b]LN: labeled nodes.
[c]LBY: leading board year.
[d]CC: co-occurrence cluster.

Figure 7. Thematic hotspots distribution in China's infodemic research.



Further, to delve into the specifics of the keyword clusters, this section examines the predominant keywords within each cluster. Clusters are assigned serial numbers, with smaller numbers indicating a larger scale and a higher number of keywords. CiteSpace analysis of the CNKI and WOS databases yielded 9 and 8 keyword clusters, respectively. Based on clustering intensity, the top six clusters were identified for further scrutiny. The "Cluster Explorer" function in CiteSpace calculates the intensity of topics, and the high-frequency keywords within each cluster are summarized to capture the essence of the research themes, as indicated in Table 11.

XSL•FO
RenderX

Table . Classification and intensity of foreign and domestic literature themes.

No	WOS[a] topics' high frequency words	Intensity of themes	WOS topics	CNKI[b] topics	Intensity of themes	CNKI topics' high frequency words
0	Social media; Twitter; behavior; attitude; online	0.757	News	Information literacy	0.924	Epidemic prevention and control; emergency management; information technology; integrated media
1	Information; communication; Facebook; impact; knowledge	0.746	Fake news detection	Information spreading	0.978	Social media; opinion leaders; risk communication; response strategies
2	Health; adult; care; virus; support	0.812	Machine learning	Message protection	0.835	COVID-19; mainstream media; information disclosure; personal information
3	Media; misinformation; risk; quality	0.86	Social network	Infodemic	0.858	Information overload; information explosion; political epidemic; public opinion guide
4	Fake news; diffusion; science; anger	0.711	Mortality salience	Major epidemic disease	0.785	Interest measurement; proportionality
5	Trust, depression, scale, need, belief, anxiety	0.765	Segmentation	Media trust	0.954	Information governance; media needs; media use; source of information

[a]WOS: Web of Science.

[b]CNKI: China National Knowledge Infrastructure.

The keywords encapsulate the essence of the articles' content and mirror the research directions. Through the keywords clustering analysis, this study categorizes the research domains of the infodemic both domestically and internationally into six themes: (1) Domestic clusters #1 and #3 and international clusters #0 and #3 are focused on the dissemination of information. (2) Domestic clusters #0 and #4 are primarily concerned with utilizing information for COVID-19 control. (3) Domestic clusters #4 and #5 underscore the importance of information governance. (4) Domestic cluster #2 is dedicated to the protection of information. (5) International clusters #1 and #2 are centered on machine learning and algorithm development. (6) International clusters #4 and #5 highlight the need for clinical attention to mental health issues stemming from the epidemic, advocating for prompt and effective psychological interventions. The subsequent sections will provide a detailed analysis of these identified research directions.

Information Spreading

The rise of the internet and digital technology has transformed information dissemination, necessitating a reevaluation of distribution methods in contemporary society. The interaction between traditional and social media has become central to this transformation, with researchers suggesting that they can complement each other. Integrating new media technologies with professional journalism principles creates a synergistic opportunity for enhancing information spread.

However, the complexity and unpredictability of online communication, along with public engagement with new media, contribute significantly to the proliferation of the "information plague." In this context, it is vital that the social responsibilities of social media platforms are not overshadowed by their technological capabilities.

To effectively regulate information spread, it is crucial to monitor and address the dissemination of false information while understanding its evolving patterns. Research indicates that trends in misinformation often align with the trajectory of the pandemic, with themes developing in tandem. The role of influential figures and institutions in propagating misinformation is significant; for instance, former President Donald Trump played a key role in amplifying COVID-19 vaccine conspiracy theories on Twitter [49,50]. This underscores the need for new methods to regulate and standardize information dissemination.

Furthermore, inadequate evaluation and oversight of information releases have contributed to misinformation spread. Initiatives like WeChat's rumor evaluation system have effectively curbed certain false narratives [21]. These examples demonstrate the potential for systematic approaches to mitigate misinformation risks in the digital age.

XSL•FO
RenderX

Using Information to Control COVID-19

During the COVID-19 pandemic, information has emerged as a critical tool for maintaining social stability and managing public health emergencies. A nation's ability to respond effectively to such crises depends on its governance and strategic information dissemination. Empirical evidence indicates a positive correlation between public trust in information and adherence to preventive measures, highlighting the importance of leveraging information to control the virus's spread.

In response, some scholars have proposed an innovative model for information communication designed to enhance interaction among stakeholders. This model could improve public policy quality and reduce resistance during implementation [23,51], while also boosting public confidence in official agencies and media [52].

Research shows that online information resources are crucial for governments to rapidly assess public health needs and refine health interventions [53]. Practical experiences demonstrate that managing the COVID-19 crisis requires coordinated efforts among diverse stakeholders. Information resources play a pivotal role in bridging departmental gaps, fostering consensus, and establishing comprehensive response mechanisms, thereby expediting epidemic prevention and control. The mainstream media, particularly official outlets, is critical for promptly disseminating accurate information, shaping public opinion, and fostering a unified societal response.

These findings illustrate that information has become an invaluable resource for governmental governance during the pandemic.

While countries have adopted various strategies to combat COVID-19, the universal objective remains effective control guided by humanitarian principles. The government's role is central to navigating public crises, and the misuse of information for political gain undermines global efforts against the epidemic. The politicization of the pandemic, as evidenced by contentious social media discussions on issues like racism, can detract from a unified response. Therefore, adherence to scientific principles, judicious policymaking, and harmonizing government and societal efforts are essential to prevent the politicization of the pandemic response.

Information Governance

The concept of information governance has gained heightened significance following the COVID-19 pandemic, particularly regarding the regulation of information dissemination and the role of social media. Misinformation has demonstrated a lasting and detrimental impact on social trust, often surpassing the effects of the virus itself, which underscores the urgent need for stringent governance by authorities. A key governance strategy is the responsibility of official media to swiftly provide accurate news, thus countering the spread of falsehoods.

At the heart of information governance is oversight. Researchers assert that timely dissemination of factual information can significantly mitigate information asymmetry, necessitating a greater sense of responsibility among information publishers and a reinforced commitment to ethical and legal standards. Misinformation not only incites public panic and erodes societal trust but also challenges the rapidly evolving social media landscape. Addressing these challenges requires targeted legislation to regulate information publication on social media platforms.

The improvement of the institutional framework serves as the cornerstone for the systematic and standardized operation of information governance. Given the complexity and uncertainty in the current information environment, there is an urgent need to establish a regulatory policy and standard system that is structured, clear in terms of responsibilities, and dynamically adjustable. First, it is imperative to strengthen top-level design and formulate forward-looking and inclusive national or regional information governance strategies. Second, targeted and highly operable special regulations should be introduced to provide a solid legal basis for governance practices. Simultaneously, promoting cross-departmental and cross-disciplinary policy coordination is crucial. It is essential to break down information barriers and establish unified standards for information quality assessment, content review norms, and crisis response plans to ensure consistency and effectiveness of governance actions. Lastly, the formulation and promotion of standards are indispensable. It is advisable to encourage the development and adoption of internationally and domestically recognized technical and management standards for information security, privacy protection, data interoperability, etc, providing a unified scale and a basis for mutual trust for the development and application of information governance tools.

The iterative upgrading of technological tools is a key driving force for enhancing the efficiency of information governance. In the face of the explosive growth and complex evolution of information epidemics, it is imperative to fully tap into and integrate the potential of cutting-edge technologies. At the information recognition level, we should deepen the application of artificial intelligence and natural language processing technologies, develop multimodal (text, image, audio, and video) content understanding capabilities, and enhance the efficiency of automated and precise identification of false, misleading, and harmful content in massive amounts of information, with particular attention paid to the analysis of implicit intentions and emotional tendencies at the semantic deep level.

The experience of managing the COVID-19 crisis has underscored the necessity of robust information governance for governments. Recognizing it as a systematic endeavor, establishing a professional intelligence team is essential. Relevant departments must align information science development with practical needs, implement a national security strategy informed by big data analytics, and encourage interdisciplinary collaboration supported by technological advancements. In this process, it is crucial to improve the institutional framework and technical support for information governance. By clarifying the rights and responsibilities of each subject and optimizing regulatory technical tools, we can ensure the authenticity and security of information dissemination, providing a standardized and orderly environment for information exchange among different cultures, countries, and civilizations around the world.

XSL•FO
RenderX

Information Protection

The use of big data technologies for epidemic prevention—such as disease monitoring and population flow management—has become widespread. However, the associated risks of personal information exposure and data breaches necessitate a robust information protection strategy.

To mitigate these vulnerabilities, a new systemic approach to prevent information leakage is essential. The rise of digital technologies calls for a reevaluation of traditional ethics and regulations, particularly in balancing individual rights with societal needs and harmonizing social governance with privacy protection. Research indicates that an institutional framework allowing extensive data collection alongside stringent usage controls (a "wide entry and strict exit" model) can help reconcile public and private interests.

Furthermore, prioritizing the development and implementation of technologies to prevent unauthorized data access is critical. Creating specialized storage platforms for sensitive information will aid in developing standards and protocols for data usage. Additionally, enhancing public awareness of personal information security and clarifying the responsibilities of data collectors are urgent.

In summary, comprehensive protection of personal information relies on sustained engagement from multiple stakeholders. This involves establishing systematic data collection and storage, rigorously assessing data usage, and implementing traceability measures to ensure accountability.

Machine Learning

The divergence in machine learning application between domestic and international research is notable, particularly in the realm of information governance. Global studies extend beyond the technical manipulation of social media, delving into the intricate layers of information management.

Machine learning emerges as a critical tool where traditional information technologies falter, especially in curtailing the proliferation of misinformation [54]. The intersection of big data and machine learning is a breeding ground for innovation, with algorithms spearheading theoretical advancements. Empirical evidence underscores the efficacy of techniques like the Synthetic Minority Over-sampling Technique and Classifier Vote Ensemble in identifying and curbing the spread of false narratives [55].

In the context of Twitter, Latent Dirichlet Allocation models have been instrumental in sifting through data to extract prevalent topics and sentiments, thereby mitigating the adverse effects of negative discourse on COVID-19 management. Elhadad and Gebali [56] have harnessed machine learning to create an integrated information management system on Twitter, bolstering data protection and reducing misinformation. Similarly, Lu [57] developed a health belief model to quantify health information, promoting the dissemination of constructive content to users. Domestic research has conducted algorithm adaptation based on local data characteristics in the application of such technologies, such as optimizing text classification models for Chinese semantic complexity, analyzing short video content for rumor identification during the pandemic, and accurately disseminating health knowledge on mainstream social platforms based on user personas.

Platforms like WhatsApp have been leveraged by entities such as the WHO and governmental bodies to disseminate verified information rapidly across demographics, capturing the pulse of public sentiment [58]. Machine learning's capacity to assimilate societal feedback epitomizes the concept of 'social listening,' refining policy relevance and efficacy based on public input, thus facilitating smoother policy implementation [59]. The Chinese government utilizes a multimodal collaborative governance system, including the China Internet Joint Rumor Refutation Platform, intelligent public opinion monitoring system, etc, combined with a three-tier public opinion response mechanism, to improve the efficiency of information content governance.

Overall, global research is highly convergent in terms of underlying machine learning technologies, but application paradigms vary due to social governance structures and data ecosystems. International research focuses on algorithmic innovation for open platforms, while domestic practices emphasize multisystem collaborative governance. These investigative efforts converge on the objective of harnessing machine learning to streamline information dissemination, with a strong underpinning in computer science, all while aiming to alleviate the detrimental effects of the pandemic and accelerate the practical testing and iterative optimization of these technologies during the pandemic.

Psychological Intervention

The domain of psychological intervention distinguishes itself in the dichotomy of domestic and international research orientations. Prompt psychological interventions have emerged as innovative strategies for supporting COVID-19 patients' mental health. The "infodemic" associated with the pandemic often triggers mental health challenges like anxiety and depression [60]. Evidence indicates that youths with extensive media consumption are particularly susceptible to psychological distress, including anxiety. Moreover, the barrage of negative information prevalent on social media platforms can disrupt public sleep patterns, adversely affecting patient recovery [61].

Research reveals that under similar stressors, psychological resilience tends to be more robust in males. Timely psychological interventions, akin to mental "inoculations," have proven effective in bolstering individuals' resilience to negative information. It has also been observed that psychological responses vary across different stages of an information epidemic; hence, interventions should be tailored to these specific stages to optimize mental health outcomes [62]. This insight advocates for a clinical approach that integrates psychological support with traditional medical treatments, emphasizing the necessity for regulatory bodies to monitor and manage media narratives [63]. These findings underscore the practical importance of research in information dissemination and governance.

Furthermore, machine learning can play a pivotal role in information-based psychological interventions. Enhancing the

XSL•FO
RenderX

credibility and authenticity of online information through machine learning algorithms has the potential to decrease morbidity [64]. A healthy social network platform developed connects patients with medical professionals, leveraging intelligent algorithms to amplify beneficial health information and counteract negative influences. Addressing societal psychological challenges requires a comprehensive approach that merges epidemic management with the establishment of dedicated psychological organizations to undertake community mental health initiatives [65]. Notably, the research on psychological interventions increasingly intersects with the themes of machine learning, information dissemination, and governance.

Discussion

Overview

In light of the pervasive information challenges posed by the global novel coronavirus pneumonia pandemic, this paper posits five critical challenges for the future of information governance and the development of new media. These challenges underscore the need for robust, adaptive frameworks capable of navigating the complexities of information dissemination and management in an era defined by rapid technological advancement and global interconnectedness. This study systematically captures the multiagent interaction characteristics of the information epidemic from multiple perspectives and simultaneously responds to the WHO's call for "interdisciplinary collaboration gaps," combining domestic practical experience to deepen the understanding of governance complexity. The insights garnered from this study not only contribute to academic discourse but also serve as a guiding beacon for policymakers, media professionals, and researchers striving to fortify societal resilience against the pernicious effects of misinformation in the digital age.

Enhancing Collaborative Networks Among Scholars and Institutions

The study's findings highlight a significant gap in knowledge exchange among domestic and international scholars and institutions, hindering effective responses to emerging challenges. The absence of a prominent cohort of authors and institutions in this discourse underscores the need for a more unified and collaborative approach to address the information epidemic. Publication trends indicate a decline in academic output following an initial surge, suggesting that while research on the information epidemic spans six main domains, it remains in an embryonic stage, with considerable potential for further exploration.

To advance the field, scholars must move beyond isolated research practices and engage in active collaboration with peers. Establishing research networks and sustainable communication channels will facilitate a more comprehensive exploration of complex issues, foster the development of authoritative research leaders and teams, and generate practical solutions for societal advancement and governance. Academic institutions need to step out of the theoretical ivory tower and pay attention to real-world issues in practice; enterprises should open up their technological resources to participate in public issue research; and the government needs to build a neutral collaboration platform. This collaboration is not simply a matter of resource accumulation but rather the formation of a governance synergy through complementary knowledge. In particular, in the context of rapid changes in the information ecosystem, a flexible network structure is more adaptable to demand than a fixed mechanism.

Given the interdisciplinary nature of the infodemic, which intersects journalism, communication, computer science, and public governance, there is an urgent need to create cross-disciplinary communication frameworks that transcend temporal and spatial barriers. Research entities should organize regular academic forums to encourage interaction among experts from various fields. Additionally, online platforms can play a crucial role in achieving consensus, shaping actionable and educational methodologies, and enhancing the quality of scholarly contributions.

Fostering Expert Teams for Advanced Media Intelligence

The analysis emphasizes the critical importance of information governance and strategic information utilization in mitigating COVID-19, identifying these as key research areas. Post-pandemic reflections underscore the need to assemble skilled professional teams to effectively manage the information epidemic and enhance information management systems. Despite progress in forming domestic intelligence teams, a significant gap remains between big data analysis and its practical application. The efficiency bottleneck of information governance largely stems from the capability gap among professionals: traditional media practitioners lack the ability to apply technological tools, while technical experts often overlook the social impact of information dissemination. This gap leads to a disconnect between technological innovation and actual governance needs. The rapid evolution of digital technologies necessitates a reevaluation of talent development programs, innovative cross-disciplinary training models, and alignment of educational outcomes with societal needs.

Higher education institutions should restructure their curriculum systems by breaking down disciplinary barriers. For instance, they are well-positioned to cultivate multidisciplinary talent by adopting "journalism+ X" approaches that enhance journalists' skills in data acquisition, processing, analytics, and digital media operations. Educational policymakers should implement a dual-track system that fosters both specialized and technologically proficient professionals. Integrating computer science with social sciences, such as journalism, can enrich curricula and enhance students' practical experience.

For industry professionals, comprehensive vocational training through expert-led workshops, digital courses, and certification programs is essential to equip the workforce with the skills necessary for managing intelligent media technologies and operations.

Simultaneously, news media must uphold their fundamental societal role. Media professionals should remain vigilant to the challenges of the digital landscape and strive to deepen their

XSL•FO
RenderX

humanitarian insights. News content creation must reflect an understanding of diverse cultures and foster global citizenship. With the diversification of communication channels and social platforms, there is an urgent need for a future workforce skilled in advanced media technologies and operational competencies, capable of engaging international audiences while maintaining the humanistic ethos central to journalism.

Refining the Public Emergency Information Management System and Bolstering Personal Data Protection

The core contradiction faced by information management in public emergencies is the balance between efficient information flow and personal privacy protection. Advancing a public emergency information management system requires a dual focus on efficient information gathering and stringent protection of that information. The system must enhance response capabilities to information risks, supported by technological tools, standardized security measures, and privacy protections. Employing machine learning and algorithmic techniques is crucial for data assimilation, processing, and analysis, enabling informed engagement in societal governance. Tools such as health codes and information flow tracking have proven instrumental in managing the COVID-19 crisis.

In the digital age, intelligence analysis has shifted toward a big data-centric approach, emphasizing the need to understand the interactions between online and offline elements within information systems. This involves harmonizing online theoretical advancements with offline practical applications. Additionally, machine learning and algorithms can provide insights into the psychological responses of different social demographics during emergencies, enhancing intelligent management capabilities.

Establishing standardized information protocols is foundational to an effective management system. For example, China's initiative to develop a health information standard framework could serve as a model for creating standardized digital technology protocols, data security measures, and benchmarks across various sectors.

To improve the digital emergency information system, it is essential to address the overcollection of personal data and strengthen personal information protection [66]. Technological advancements should elevate information security protocols, including routine data anonymization, to prevent unauthorized access and the development of encryption and real-time monitoring systems.

At the legislative level, robust laws are critical for information security. Clearly defining the boundaries of information collection, analysis, and use while adhering to ethical and legal principles is vital. Regulatory authorities should implement safety protocols to ensure secure information practices.

From the public's perspective, raising awareness about information security is paramount. Individuals should understand their legal rights and engage with digital services with vigilance and informed caution.

Enhancing Public Information Literacy and Psychological Resilience

The spread of the information epidemic is partly attributed to the public's limited skills in observing, analyzing, and evaluating information. Active public participation in information governance is crucial to addressing this challenge. In an information-overloaded environment, the public is prone to experiencing "information anxiety" and may even reduce their trust in authoritative information. Evidence suggests that areas with lower reliance on social networks and reduced trust in online information have experienced lower mortality rates, indicating that the psychological effects of the information epidemic may be more difficult to manage than the pandemic itself.

To enhance the public's information discernment capabilities, a multifaceted and ongoing approach is essential. Educational initiatives in science can provide timely and factual information about current issues, establishing a robust mechanism for public awareness. This can be achieved through traditional seminars and online platforms, utilizing short videos, social media, and interactive app-based Q&A sessions to create an engaging information dissemination network.

Equally important is the development of critical thinking skills, enhanced information literacy, and a judicious approach to consuming information. These steps are vital for mitigating the negative impacts of the information epidemic on individuals and society.

Enhancing Media Accountability and Directing Public Discourse Positively

An effective information dissemination environment is essential for managing the information epidemic, a concern shared by scholars globally. Strengthening media accountability requires advocating for the rule of law. In response to the evolving digital media landscape, authorities have implemented laws and regulations to support healthy sector growth. Administrative oversight must involve nuanced management, imposing sanctions that align with the impact of misinformation and its divergence from the truth. Timely release of authoritative information is vital for shaping public opinion and countering misinformation with verified facts.

During emergencies, establishing a direct reporting system is crucial for enhancing information dissemination speed. Legislative amendments have improved the transparency of professional institutions, streamlined the information approval process, and facilitated timely information release during crises.

The timely release of authoritative information is crucial for guiding public opinion. State media should create a robust platform for information dissemination, leveraging social media to integrate official and community channels. Furthermore, cultivating a culture of legal and ethical awareness within the media is indispensable. Media professionals must prioritize information refinement and quality throughout the news production cycle, enhancing fact-checking and peer review processes to ensure authenticity and neutrality [67].

XSL•FO
RenderX

Media personnel should strive for accurate and prompt translation services, maintain objectivity, and minimize biases from political, cultural, or commercial influences to prevent the information epidemic from escalating into a political crisis. Additionally, industry professionals must elevate ethical standards, adopt a people-centric approach, and enhance their expertise through in-depth interviews with scientists and similar initiatives to improve public access to scientific information.

Research Limitations

There are several limitations in this study that need to be objectively explained: the research perspective is mainly based on the analysis of domestic information governance practices, and there is insufficient comparison of information governance models under different countries' social systems and cultural traditions, which may limit the cross-contextual applicability of the theoretical framework. The analysis focuses on the construction of macro governance mechanisms, and the exploration of micro-psychological motivations for individual information behavior is not deep enough, making it difficult to fully explain the complex decision-making logic of the public in information selection. The research method focuses on qualitative analysis and framework construction. Although some practical cases are combined, there is a lack of dynamic verification of governance effectiveness through long-term tracking data, and the timeliness of the conclusions needs further observation. These limitations provide directions for improvement in future research, which can be improved through cross-border comparative studies, microbehavioral experiments, and long-term follow-up surveys.

Potential Research Directions

Our research has found that there are differences in research between the East and the West in related fields, which provides many perspectives for future research.

First, a cross-cultural comparative framework can be established to study the different effects of information governance under different political systems; for example, comparing social media platforms in the East and the West to see the similarities and differences in the effectiveness of using algorithmic censorship to suppress misinformation, especially pseudoscientific content with medical terminology. It is also possible to combine useful technologies in international research with governance experience in domestic research to develop a set of methods and tools that combine machine learning and social network analysis. In addition, observe the differences in the roles played by medical practitioners such as doctors and nurses in information dissemination in different countries and develop a set of scientifically based and universally applicable guidelines for professional social media behavior in different countries.

Second, we should pay attention to the changes in the information environment in the later stage of the epidemic. Most of the current research focuses on the period from 2020 to 2021 when the epidemic is serious, but some aspects are ignored: everyone's scientific understanding of the "long-term COVID-19" is constantly updated, but the public's understanding is not up to date, and the gap between them is changing; what long-term impact will the habit of frequent exposure to information during the epidemic have on other public health issues such as vaccination and antibiotic resistance; the structural changes of cross-border information dissemination networks, especially the transformation of the role of overseas accounts in new hot events. This type of long-term tracking research can refer to international long-term tracking methods for mental health and domestic analysis of public opinion fluctuations.

Contribution and Novelty

Systematically carry out comparative bibliometric analysis of Chinese and Western information epidemic research: This research innovatively uses WOS and CNKI databases as samples and systematically compares the differences between China and the West in the information epidemic research of COVID-19 through bibliometric methods (such as CiteSpace visual analysis), filling the gap in the existing research that lacks cross-country and cross-database system comparison.

Clearly revealing the core differences and commonalities between Chinese and Western research: The study found that international research focuses on machine learning, social media analysis, and the impact of information epidemics on mental health, while Chinese research focuses on information governance, public opinion guidance, and information dissemination mechanisms. At the same time, it clarifies the commonalities between the two in the core goal of curbing the spread of misinformation, providing specific entry points for subsequent cross-cultural cooperation.

Pointing out the shortcomings of research cooperation and emphasizing the necessity of global collaboration: Through the analysis of the collaboration network between authors and institutions, the current situation of sparse collaboration between authors and institutions in Chinese and foreign research is revealed. The importance of establishing cross-border and interdisciplinary cooperation mechanisms is emphasized, providing a basis for building a globally unified information epidemic response system.

Provide practical and theoretical guidance for policy formulation and future research: Based on research differences, propose the possibility of integrating technological means and governance experience, provide reference for public health departments to formulate information management strategies, and point out directions for cross-cultural comparison and long-term information ecology tracking for subsequent research.

Conclusions

As the world continues to confront the challenges of COVID-19, the concurrent information epidemic presents a complex issue. This paper provides a comprehensive analysis of five categories of sample data: publication trends, authorship, institutional affiliations, highly cited literature, and keyword topic clusters. Through this analysis, we have examined the evolution of the information epidemic and its multifaceted societal impacts, delineating its contours as perceived by scholars across different nations, institutions, and research orientations. This synthesis highlights research trajectories, differences in domestic and international approaches, and suggests strategies for addressing the information epidemic. Additionally, given the global impact

XSL•FO
RenderX

of infodemics, integrating knowledge from various disciplines and regions is essential for fostering more effective responses.

Acknowledgments

Founded by Science Research Project of Hebei Education Department（JCZX2023005）

Conflicts of Interest

None declared.

References

1. Zhang Y, Zhu J. Dynamics of a rumor propagation model with stochastic perturbation on homogeneous social networks. J Comput Nonlinear Dyn 2022 Mar 1;17(3). [doi: 10.1115/1.4053269]
2. Warriner AB, Kuperman V, Brysbaert M. Norms of valence, arousal, and dominance for 13,915 English lemmas. Behav Res Methods 2013 Dec;45(4):1191-1207. [doi: 10.3758/s13428-012-0314-x] [Medline: 23404613]
3. Manene S, Hove C, Cilliers L. Mitigating misinformation about the COVID-19 infodemic on social media: a conceptual framework. Jamba 2023;15(1):1416. [doi: 10.4102/jamba.v15i1.1416] [Medline: 37292581]
4. Razaque A, Rizvi S, Khan MJ, Almiani M, Rahayfeh AA. State-of-art review of information diffusion models and their impact on social network vulnerabilities. J King Saud Univ Comput Inf Sci 2022 Jan;34(1):1275-1294. [doi: 10.1016/j.jksuci.2019.08.008] [Medline: 38620265]
5. Törnberg P. Echo chambers and viral misinformation: modeling fake news as complex contagion. PLoS ONE 2018;13(9):e0203958. [doi: 10.1371/journal.pone.0203958] [Medline: 30235239]
6. Gao J, Zheng P, Jia Y, et al. Mental health problems and social media exposure during COVID-19 outbreak. PLoS ONE 2020;15(4):e0231924. [doi: 10.1371/journal.pone.0231924] [Medline: 32298385]
7. Gradoń KT, Hołyst JA, Moy WR, Sienkiewicz J, Suchecki K. Countering misinformation: a multidisciplinary approach. Big Data Soc 2021 Jan;8(1):1-14. [doi: 10.1177/20539517211013848]
8. Al-Rakhami MS, Al-Amri AM. Lies kill, facts save: detecting COVID-19 misinformation in Twitter. IEEE Access 2020;8(8):155961-155970. [doi: 10.1109/ACCESS.2020.3019600] [Medline: 34192115]
9. Bozuyla M, Özçi˙ft A. Developing a fake news identification model with advanced deep languagetransformers for Turkish COVID-19 misinformation data. TURKISH Journal of Electrical Engineering and Computer Sciences 2021;30(3):908-926. [doi: 10.55730/1300-0632.3818]
10. Biradar S, Saumya S, Chauhan A. Combating the infodemic: COVID-19 induced fake news recognition in social media networks. Complex Intell Syst 2023 Jun;9(3):2879-2891. [doi: 10.1007/s40747-022-00672-2]
11. Safarnejad L, Xu Q, Ge Y, Bagavathi A, Krishnan S, Chen S. Identifying influential factors in the discussion dynamics of emerging health issues on social media: computational study. JMIR Public Health Surveill 2020 Jul 28;6(3):e17175. [doi: 10.2196/17175] [Medline: 32348275]
12. Mukherjee D, Lim WM, Kumar S, Donthu N. Guidelines for advancing theory and practice through bibliometric research. J Bus Res 2022 Sep;148:101-115. [doi: 10.1016/j.jbusres.2022.04.042]
13. Tahamtan I, Safipour Afshar A, Ahamdzadeh K. Factors affecting number of citations: a comprehensive review of the literature. Scientometrics 2016 Jun;107(3):1195-1225. [doi: 10.1007/s11192-016-1889-2]
14. Zhang LL, Ling J, Lin MW. Carbon neutrality: a comprehensive bibliometric analysis. Environ Sci Pollut Res 2023;30(16):45498-45514. [doi: 10.1007/s11356-023-25797-w]
15. Zhang LL, Ling J, Lin MW. Artificial intelligence in renewable energy: a comprehensive bibliometric analysis. Energy Rep 2022 Nov;8:14072-14088. [doi: 10.1016/j.egyr.2022.10.347]
16. Zhong MH, Lin MW. Bibliometric analysis for economy in COVID-19 pandemic. Heliyon 2022 Sep;8(9):e10757. [doi: 10.1016/j.heliyon.2022.e10757]
17. Chen YX, Lin MW, Zhuang D. Wastewater treatment and emerging contaminants: bibliometric analysis. Chemosphere 2022 Jun;297:133932. [doi: 10.1016/j.chemosphere.2022.133932]
18. Vraga EK, Tully M, Bode L. Empowering users to respond to misinformation about Covid-19. MaC 2020;8(2):475-479. [doi: 10.17645/mac.v8i2.3200]
19. Tangcharoensathien V, Calleja N, Nguyen T, et al. Framework for managing the COVID-19 infodemic: methods and results of an online, crowdsourced WHO technical consultation. J Med Internet Res 2020 Jun 26;22(6):e19659. [doi: 10.2196/19659] [Medline: 32558655]
20. Sampogna G, Di Vincenzo M, Luciano M, et al. The effect of social media and infodemic on mental health during the COVID-19 pandemic: results from the COMET multicentric trial. Front Psychiatry 2023;14(1132189):1226414. [doi: 10.3389/fpsyt.2023.1226414] [Medline: 37575576]

XSL•FO
RenderX

21. Sundelson AE, Jamison AM, Huhn N, Pasquino SL, Sell TK. Fighting the infodemic: the 4 i framework for advancing communication and trust. BMC Public Health 2023 Aug 30;23(1):1662. [doi: 10.1186/s12889-023-16612-9] [Medline: 37644563]
22. Kisa S, Kisa A. A comprehensive analysis of COVID-19 misinformation, public health impacts, and communication strategies: scoping review. J Med Internet Res 2024 Aug 21;26:e56931. [doi: 10.2196/56931] [Medline: 39167790]
23. Gisondi MA, Chambers D, La TM, et al. A Stanford conference on social media, ethics, and COVID-19 misinformation (INFODEMIC): qualitative thematic analysis. J Med Internet Res 2022 Feb 15;24(2):e35707. [doi: 10.2196/35707] [Medline: 35030089]
24. Albrecht SS, Aronowitz SV, Buttenheim AM, et al. Lessons learned from Dear Pandemic, a social media-based science communication project targeting the COVID-19 infodemic. Public Health Rep 2022;137(3):449-456. [doi: 10.1177/00333549221076544] [Medline: 35238241]
25. Ahmad AR, Murad HR. The impact of social media on panic during the COVID-19 pandemic in Iraqi Kurdistan: online questionnaire study. J Med Internet Res 2020 May 19;22(5):e19556. [doi: 10.2196/19556] [Medline: 32369026]
26. Wang LP, Chen Y. Research on the reconstruction of public digital cultural information ecosystem empowered by data intelligence: against the background of public crisis and epidemic. CNKI (2):72-78. [doi: 10.16810/j.cnki.1672-514X.2023.02.012]
27. Wang L, Yang YY. Trust driven and feedback modeling of social network information dissemination. Complex Systems and Complexity Science. URL: https://link.cnki.net/urlid/37.1402.N.20250910.1450.006 [accessed 2025-09-29]
28. Li XY, Lian JW, Song SJ. Research on pre intervention of distorted information: conceptual connotation, research framework, and future prospects. Intelligence Theory and Practice 2023;46(9):57-68. [doi: 10.16353/j.cnki.1000-7490.2023.008]
29. Li XY, Chen WY, Jin LM, et al. A cross-sectional survey on information access through hospital's officialaccount on new media and its association with antenatal care knowledgeand health behaviors of pregnant women under COVID-19 epidemic. Fudan University Journal of Medical Sciences 2021;48(4):520-526. [doi: 10.3969/j.issn.1672-8467.2021.04.015]
30. Zong HY, Ning PS, Cheng PX, et al. Analysis of data collection of relapsing COVID-19 epidemic events in China. Chinese Journal of Health Statistics 2021;38(6):837-841.
31. Li MD, Zhang Y, Zhang F, Yang F, Meng SJ. Content characteristics, modes, response strategies and optimization paths of epidemic scientific information dissemination:content analysis based on popular microblogs of 10 scientists. Intelligence Journal 2022;41(3):133-142 [FREE Full text]
32. Cinelli M, Quattrociocchi W, Galeazzi A, et al. The COVID-19 social media infodemic. Sci Rep 2020 Oct 6;10(1):16598. [doi: 10.1038/s41598-020-73510-5] [Medline: 33024152]
33. Gallotti R, Valle F, Castaldo N, Sacco P, De Domenico M. Assessing the risks of "infodemics" in response to COVID-19 epidemics. Nat Hum Behav 2020 Dec;4(12):1285-1293. [doi: 10.1038/s41562-020-00994-6] [Medline: 33122812]
34. Islam MS, Sarkar T, Khan SH, et al. COVID-19-related infodemic and its impact on public health: a global social media analysis. Am J Trop Med Hyg 2020 Oct;103(4):1621-1629. [doi: 10.4269/ajtmh.20-0812] [Medline: 32783794]
35. Pulido CM, Villarejo-Carballido B, Redondo-Sama G, Gómez A. COVID-19 infodemic: more retweets for science-based information on coronavirus than for false information. Int Sociol 2020 Jul;35(4):377-392. [doi: 10.1177/0268580920914755]
36. Bruns A, Harrington S, Hurcombe E. 'Corona? 5G? or both?': the dynamics of COVID-19/5G conspiracy theories on Facebook. Media International Australia 2020 Nov;177(1):12-29. [doi: 10.1177/1329878X20946113]
37. Ni MY, Yang L, Leung CMC, et al. Mental health, risk factors, and social media use during the covid-19 epidemic and cordon sanitaire among the community and health professionals in Wuhan, China: cross-sectional survey. JMIR Ment Health 2020 May 12;7(5):e19009. [doi: 10.2196/19009] [Medline: 32365044]
38. Hua J, Shaw R. Corona virus (COVID-19) "infodemic" and emerging issues through a data lens: the case of China. Int J Environ Res Public Health 2020 Mar 30;17(7):2309 [FREE Full text] [doi: 10.3390/ijerph17072309] [Medline: 32235433]
39. Zhao YX, Cheng SX, Yu XY, Xu HL. Chinese public's attention to the COVID-19 epidemic on social media: observational descriptive study. J Med Internet Res 2020;22(5):e18825 [FREE Full text] [doi: 10.2196/18825]
40. Li YF, Ma JQ. Analysis and countermeasures of problems in China's disease prevention and control information system. Chinese Journal of Health Information Management 2013(3):230-232.
41. Peng L. What kind of public information dissemination do we need to build? -- Reflections on new media communication during the COVID-19 pandemic. Press Circles 2020(5):36-43. [doi: 10.15897/j.cnki.cn51-1046/g2.20200515.001]
42. Wu TH, Zhang Y, Wang RJ. Association between digital media use and anxiety symptoms of college students during the novel coronavirus pneumonia epidemic. Chinese School Health 2020;41(11):1625-1628. [doi: 10.16835/j.cnki.1000-9817.2020.11.007]
43. Tang HF, Wu R. Integrated management of the COVID-19: practical test and optimization path. Journal of Hubei University (Philosophy and Social Sciences Edition) 2020;47(3):1-13. [doi: 10.13793/j.cnki.42-1020/C.2020.03.002]
44. Shi C. Legal protection of personal information in major epidemic prevention and control Journal of China University of Mining and Technology. Social Sciences Edition 2020;22(2):63-74.
45. Li JJ, He S. Population Movement, Information Transmission Efficiency, and Epidemic Control: Eevidence from COVID-19: Journal of Central University of Finance and Economics, Vol. 04:116-128. [doi: 10.19681/j.cnki.jcufe.2020.04.010]

XSL•FO
RenderX

46. Guo PF, Lin HX. Personal information protection in public health events -- from the perspective of COVID-19 prevention and control. Journal of Xihua University (Philosophy and Social Sciences Edition) 2022;41(1):63-74.
47. Zhang Y, Qiu LF, Liu AQ. Research on risk perception and risk transmission models in public health events: a discussion on the moderating effect of epidemic severity. Journalism University 2020;3:31-34. [doi: 10.20050/j.cnki.xwdx.2020.03.006]
48. Lin HC, Zhao YX. Use of personal information and legal rules in public emergencies: COVID-19 response as a starting point. Journal of South China (3):120-133 [FREE Full text]
49. Germani F, Biller-Andorno N. The anti-vaccination infodemic on social media: a behavioral analysis. PLoS ONE 2021;16(3):e0247642. [doi: 10.1371/journal.pone.0247642] [Medline: 33657152]
50. Mheidly N, Fares J. Leveraging media and health communication strategies to overcome the COVID-19 infodemic. J Public Health Pol 2020 Dec;41(4):410-420. [doi: 10.1057/s41271-020-00247-w]
51. White BK, Gombert A, Nguyen T, et al. Using machine learning technology (early artificial intelligence-supported response with social listening platform) to enhance digital social understanding for the COVID-19 infodemic: development and implementation study. JMIR Infodemiology 2023 Aug 21;3:e47317. [doi: 10.2196/47317] [Medline: 37422854]
52. Yim D, Khuntia J, King E, Treskon M, Galiatsatos P. Expert credibility and sentiment in infodemiology of hydroxychloroquine's efficacy on cable news programs: empirical analysis. JMIR Infodemiology 2023 Jun 27;3:e45392. [doi: 10.2196/45392] [Medline: 37204334]
53. Nowak BM, Miedziarek C, Pełczyński S, Rzymski P. Misinformation, fears and adherence to preventive measures during the early phase of COVID-19 pandemic: a cross-sectional study in Poland. Int J Environ Res Public Health 2021 Nov 22;18(22):12266. [doi: 10.3390/ijerph182212266] [Medline: 34832021]
54. Bin Naeem S, Kamel Boulos MN. COVID-19 misinformation online and health literacy: a brief overview. Int J Environ Res Public Health 2021 Jul 30;18(15):8091. [doi: 10.3390/ijerph18158091] [Medline: 34360384]
55. Olaleye T, Abayomi-Alli A, Adesemowo K, Arogundade OT, Misra S, Kose U. SCLAVOEM: hyper parameter optimization approach to predictive modelling of COVID-19 infodemic tweets using smote and classifier vote ensemble. Soft comput 2023;27(6):3531-3550. [doi: 10.1007/s00500-022-06940-0] [Medline: 35309597]
56. Elhadad MK, Li KF, Gebali F. Detecting misleading information on COVID-19. IEEE Access 2020;8(165201-165215):165201-165215. [doi: 10.1109/ACCESS.2020.3022867] [Medline: 34786288]
57. Lu Y. Implementing blockchain in information systems: a review. Enterprise Information Systems 2022 Dec 2;16(12). [doi: 10.1080/17517575.2021.2008513]
58. Liu JCJ, Tong EMW. The relation between official WhatsApp-distributed COVID-19 news exposure and psychological symptoms: cross-sectional survey study. J Med Internet Res 2020 Sep 25;22(9):e22142. [doi: 10.2196/22142] [Medline: 32877349]
59. Jafarzadeh Ghoushchi S, Bonab SR, Ghiaci AM. A decision-making framework for COVID-19 infodemic management strategies evaluation in spherical fuzzy environment. Stoch Environ Res Risk Assess 2023;37(4):1635-1648. [doi: 10.1007/s00477-022-02355-3] [Medline: 36714449]
60. Abbas J, Wang D, Su Z, Ziapour A. The role of social media in the advent of COVID-19 pandemic: crisis management, mental health challenges and implications. Risk Manag Healthc Policy 2021;14(1917-1932):1917-1932. [doi: 10.2147/RMHP.S284313] [Medline: 34012304]
61. Sampogna G, Di Vincenzo M, Luciano M, et al. The effect of social media and infodemic on mental health during the COVID-19 pandemic: results from the COMET multicentric trial. Front Psychiatry 2023;14:1226414. [doi: 10.3389/fpsyt.2023.1226414] [Medline: 37575576]
62. Alhafez L, Rubio-Rico L, Diez-Bosch M. Healthcare professionals' editorial opinions on communicating with the public: shifting social media hesitancies. Humanit Soc Sci Commun 2023;10(1). [doi: 10.1057/s41599-023-01820-w]
63. Singh N, Banga G. Media and information literacy for developing resistance to 'infodemic': lessons to be learnt from the binge of misinformation during COVID-19 pandemic. Media, Culture & Society 2022 Jan;44(1):161-171. [doi: 10.1177/01634437211060201]
64. Dubey S, Biswas P, Ghosh R, et al. Psychosocial impact of COVID-19. Diabetes Metab Syndr 2020;14(5):779-788. [doi: 10.1016/j.dsx.2020.05.035] [Medline: 32526627]
65. Purvis RS, Ayers BL, Rowland B, Moore R, Hallgren E, McElfish PA. "Life is hard": How the COVID-19 pandemic affected daily stressors of women. Dialogues Health 2022 Dec;1(100018):100018. [doi: 10.1016/j.dialog.2022.100018] [Medline: 36776415]
66. Bunker D. Who do you trust? The digital destruction of shared situational awareness and the COVID-19 infodemic. Int J Inf Manage 2020 Dec;55(102201):32836649. [doi: 10.1016/j.ijinfomgt.2020.102201] [Medline: 32836649]
67. Feinberg I, Scott JY, Holland DP, et al. The relationship between health literacy and COVID-19 vaccination prevalence during a rapidly evolving pandemic and infodemic. Vaccines (Basel) 2022 Nov 23;10(12):1989. [doi: 10.3390/vaccines10121989] [Medline: 36560399]

Abbreviations

CNKI: China National Knowledge Infrastructure

XSL•FO
RenderX

WOS: Web of Science

Edited by A Benis; submitted 23.04.25; peer-reviewed by M Lin, R Guo; revised version received 29.07.25; accepted 11.08.25; published 14.10.25.

Please cite as:
Wang S, Zhang L, Liu Y, Feng X, Ren S
Bibliometric Insights Into the Infodemic: Global Research Trends and Policy Responses: Quantitative Research
JMIR Med Inform 2025;13:e76378
URL: https://medinform.jmir.org/2025/1/e76378
doi:10.2196/76378

© Sijia Wang, Linan Zhang, Yang Liu, Xin Feng, Shipeng Ren. Originally published in JMIR Medical Informatics (https://medinform.jmir.org), 14.10.2025. This is an open-access article distributed under the terms of the Creative Commons Attribution License (https://creativecommons.org/licenses/by/4.0/), which permits unrestricted use, distribution, and reproduction in any medium, provided the original work, first published in JMIR Medical Informatics, is properly cited. The complete bibliographic information, a link to the original publication on https://medinform.jmir.org/, as well as this copyright and license information must be included.

XSL•FO
RenderX

Deep Learning Approaches for Classifying Children With and Without Autism Spectrum Disorder Using Inertial Measurement Unit Hand Tracking Data: Comparative Study

John Mutersbaugh[1], BS; Wan-Chun Su[2], PhD; Anjana Bhat[3,4], PhD; Amir Gandjbakhche[1], PhD

[1]NICHD, National Institutes of Health, NIHBC 49 - Conte 5A82, Bethesda, MD, United States

[2]Louisiana State University, Baton Rouge, LA, United States

[3]University of Delaware, Newark, DE, United States

[4]Biomechanics and Movement Science Program, Physical Therapy Department, University of Delaware, Newark, DE, United States

Corresponding Author:
Amir Gandjbakhche, PhD
NICHD, National Institutes of Health, NIHBC 49 - Conte 5A82, Bethesda, MD, United States

Abstract

Background: Autism spectrum disorder (ASD) is a prevalent neurodevelopmental condition that can be quite difficult to diagnose due to a lack of objective diagnostic methods in the currently used behavioral assessments. Recent work has shown that children with ASD have a higher incidence of motor control differences. A compilation of studies indicates that between 50% and 88% of the children with ASD have issues with movement control based on standardized motor assessments or parent-reported questionnaires.

Objective: In this study, we assess a variety of deep learning approaches for the classification of ASD, utilizing data collected via inertial measurement unit (IMU) hand tracking during goal-directed arm movements.

Methods: IMU hand tracking data were recorded from 41 school-aged children both with and without an ASD diagnosis to track their arm movements during a reach-to-clean up task. The IMU data were then preprocessed using a moving average and *z* score normalization to prepare the data for deep learning models. We evaluated the effectiveness of different deep learning models using the preprocessed data and a k-fold validation approach, as well as a patient-separated approach.

Results: The best result was achieved with a convolutional autoencoder combined with long short-term memory layers, reaching an accuracy of 90.21% and an F_1-score of 90.02%. Once the convolutional autoencoder+long short-term memory was determined to be the most effective model for this datatype, it was retrained and evaluated with a patient-separated dataset to assess the generalization capability of the model, achieving an accuracy of 91.87% and an F_1-score of 93.66%.

Conclusions: Our deep learning approach demonstrates that our models hold potential for facilitating ASD diagnosis in clinical settings. This work validates that there are significant differences between the physical movements of typically developing children and children with ASD, and these differences can be identified by analyzing hand-eye coordination skills. Additionally, we have validated that small-scale models can still achieve a high accuracy and good generalization when classifying medical data, opening the door for future research into diagnostic models that may not require massive amounts of data.

(JMIR Med Inform 2025;13:e73440) doi:10.2196/73440

KEYWORDS

AI; artificial intelligence; autism spectrum disorder; ASD; deep learning; kinematics; machine learning

Introduction

Throughout the world, autism spectrum disorder (ASD) is a prevalent neurodevelopmental condition marked by challenges with communication in social settings, as well as restricted and repetitive behaviors [1,2]. An individual with autism spectrum disorder can have a range of challenges, primarily in social communication and interaction; for example, they may have difficulties understanding and responding to social cues, forming relationships, and effectively communicating with others using verbal and non-verbal languages [3-5]. Additionally, individuals with ASD may engage in repetitive behaviors or have highly specific interests, leading to an inflexibility in daily life activities and hardship when trying to keep up with fluid or dynamic social situations [6]. Behavioral patterns and communication difficulties like these tend to vary widely in presentation and severity, making ASD particularly challenging to diagnose. The most current methodologies for diagnosing ASD predominantly rely on behavioral evaluations and structured interviews conducted by trained clinicians [7,8]. An ASD assessment

XSL•FO
RenderX

typically involves gathering a detailed history, conducting interviews with friends and family members, and sometimes observing an individual's behavior in various social situations. However, despite the expertise of the clinicians involved, diagnosing an individual with ASD is very imprecise, depending heavily on the clinician's subjective interpretation and experience [9]. The subjective nature of this diagnosis can be a problem; if different evaluators can come to different conclusions based on the same observations, then the chance for a missed diagnosis or a misdiagnosis is significant. This subjectivity also means that an ASD diagnosis might not properly reflect the subtleties of an individual, as ASD manifests a very wide spectrum of possible symptoms.

It is also worth noting that diagnosing ASD earlier in life is important; early access to support can significantly improve long-term outcomes and quality of life when addressed before behavioral patterns are solidly set [10]. Unfortunately, diagnosing ASD is much more difficult in young children, for all of the reasons explained before. For example, it is very subjective whether a child is having social communication problems or just being shy. Due to these challenges, there is a significant need for a more objective approach to diagnosing ASD.

Recently, it has been noted that there is a high incidence of motor control differences in children affected with ASD [11]. A compilation of studies indicates that between 50% and 88% of the children with ASD have issues with movement control based on standardized motor assessments or parent-reported questionnaires [11,12]. These children often exhibit significant differences with posture, hand-eye coordination, fine motor control, and gait. Importantly, these motor abnormalities are highly correlated with their primary social communication problems and manifest earlier or at the same time as any social communication issues [13-16]. This provides clinicians a new avenue for identifying ASD earlier.

In the past, it has been shown that machine learning and deep learning methods have been successful in classifying between children with ASD and typically developing (TD) children based on resting state functional magnetic resonance imaging data [17,18]. One study showed that a combination of a restricted Boltzmann machine and a support vector machine was able to achieve an accuracy of ~80% on a dataset of ~180 patients [18]. Another study using a deep learning model matched these results with a significantly larger dataset, achieving an accuracy of ~80% for a model classifying 871 participants [17]. Many other studies have been conducted attempting the same classification, using different combinations of functional near-infrared spectroscopy, magnetic resonance imaging, functional magnetic resonance imaging, and electroencephalogram data [19]. The average accuracies for these models are around 70% - 85%, with some specific models approaching 90% - 95%. The best functioning models that surpassed 90% accuracy were deep learning autoencoders, as well as multidimensional convolutional neural networks [19].

Despite the promising findings of using neuroimaging data to classify children with ASD, there are certain limitations. For example, neuroimaging is often expensive and difficult for typical families to access. Moreover, some neuroimaging tools are not child-friendly, making their widespread use in toddlers and children challenging. As a result, there is a pressing need for low-cost, child-friendly, objective methods to children's performance. To solve these problems, we decided to use an inertial measurement unit (IMU) device. An IMU device is a very small motion–tracking device, easily strapped on to a participant's wrist like a light-weight watch. These devices are nonintrusive and very discrete, allowing for data collection from sensitive children. Previously, our research group had achieved an accuracy of 78.1% in classifying children with and without ASD using IMU data and a multilayer perceptron model [20]. However, it remains unclear which deep learning methods would produce the best classification results. Therefore, the goal of our study is to evaluate a variety of simple and customizable deep learning models, including long short-term memory (LSTM), multilayer perceptron (MLP), and convolutional neural networks (CNNs), for an automatic classification of children with ASD. Recent studies have highlighted the growing efficacy of deep learning techniques such as these, including LSTM-based models for advancing the predictive accuracy in medical and diagnostic contexts. We will first assess the effectiveness of different types and configurations of deep learning models on this type of IMU data. Once the best models are determined, we will test them for effectiveness on unseen patient data.

Methods

Study Methodology

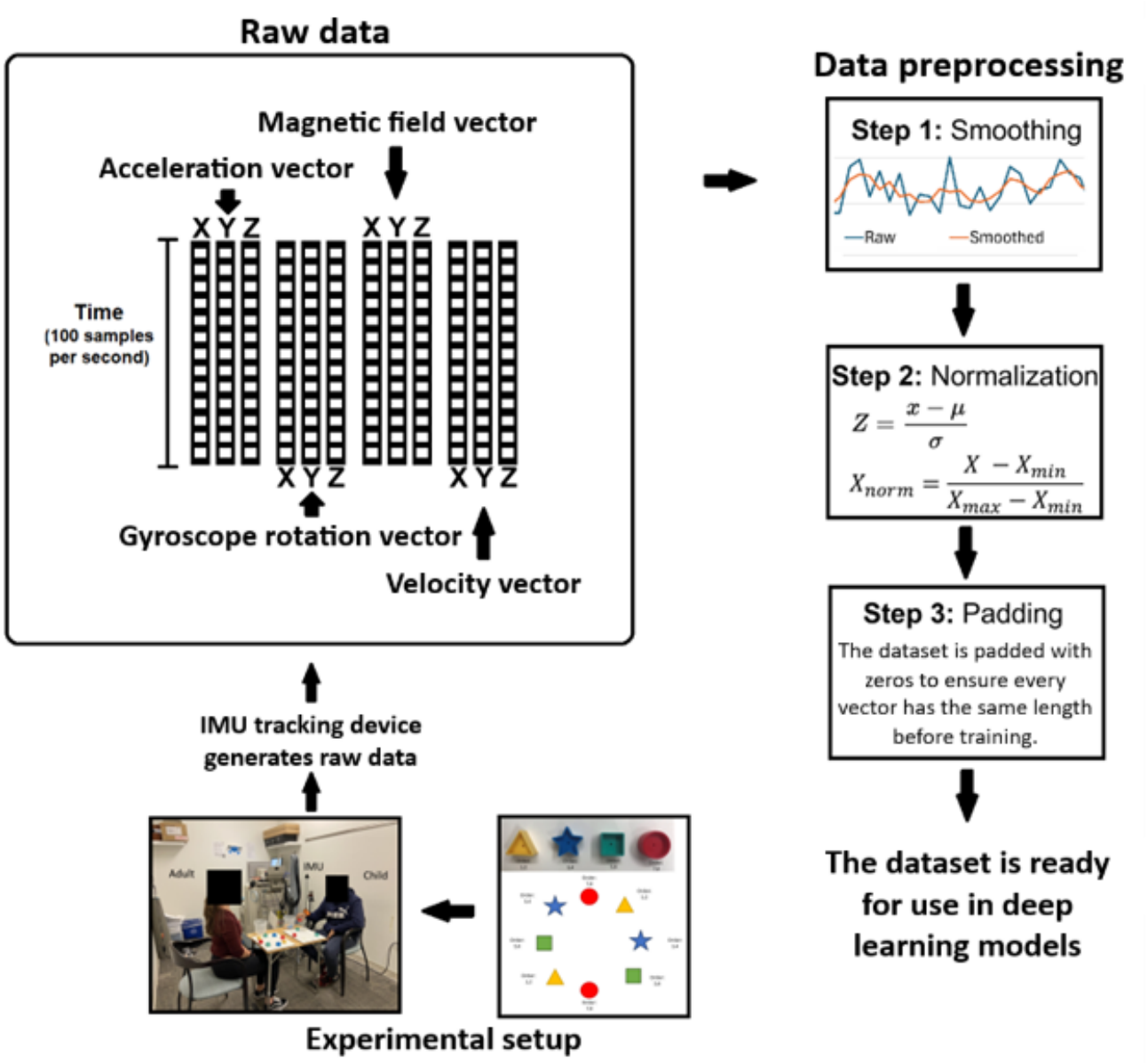
A total of 41 children, both with and without ASD, participated in this study (mean age [SE]: TD group: 10.3 [0.8], 8 male participants and 7 female participants; ASD group: 10.3 [0.5], 21 male participants and 5 female participants). No significant differences in age or sex were observed between the TD and ASD groups (P=.05). Participants were recruited through fliers, phone calls, and online postings distributed to local schools and community centers, as well as through Simons Powering Autism Research participant research match service [21]. The inclusion criteria of the TD children were (1) age between 6 and 17 years, while the exclusion criteria included (1) having any neurological or developmental diagnosis or delays, (2) having a history of preterm birth or significant birth complications, and (3) having a family history of ASD. For children with ASD, the inclusion criteria were (1) age between 6 and 17 years and (2) having a professionally confirmed diagnosis, while the exclusion criteria were (1) inability to follow 1-step instruction; (2) exhibiting sensory and behavioral challenges that would prevent them from wearing the IMU sensors and completing the reaching-and-placing tasks. These criteria were chosen for a very simple reason: if a child has ASD so severe it prevents them from engaging in the task, such as having issues wearing the hand device or following instructions, it is likely that they would not need this test to diagnose them in the first place. We are attempting to evaluate ASD based on significant differences in hand-eye coordination skills and approaches, so the TD children and the children with ASD were not screened for hand-eye coordination skills to ensure fair results. Our hypothesis is that a deep learning model can evaluate the

XSL•FO
RenderX

harder-to-define edge cases of ASD by identifying key differences in how children with or without ASD interact with a simple hand-eye coordination task.

The hand-eye coordination task itself is simple; while seated across from an adult experimenter, each participating child performed a simple reaching task while wearing a small IMU hand tracking device fastened to the wrist of their right hand. The task itself consisted of a set of blocks arranged in a circle and placed in front of the participant, as shown in Figure 1. Each participant would pick up the blocks in a specific order, specified by the picture instructions, and place each block one at a time into a box next to them until all the blocks had been moved. This task was repeated for a total of roughly 6 trials per child, with each trial taking anywhere from ~10 seconds to ~40 seconds to complete. Once the data collection was complete, the final dataset consisted of 76 trials from TD children and 145 trials from children with ASD.

Figure 1. The experimental setup, consisting of an adult experimenter, a child participant wearing an inertial measurement unit (IMU) device, and a table with a series of blocks setup and a bucket next to the blocks. Also shown is the rough shape of the raw IMU data, as well as the data preprocessing steps performed to prepare the data for use in a model.



Ethical Considerations

All study procedures were carried out in accordance with the Declaration of Helsinki and were approved by the University of Delaware Institutional Review Board. Informed consent from parents and assent from children were obtained prior to participation. Each participant was assigned a unique study ID, and all collected data were subsequently deidentified using these IDs. Families received US $20 as compensation for their participation. Additionally, written permission was obtained from parents and experimenters for the use of their photographs in this publication.

Data Processing and Analysis

The primary outputs of the IMU device are the acceleration vector, the gyroscopic rotation vector, the velocity (Δv) vector, and the magnetic field vector, with each showing a basic representation of the movement in space. Each vector consists

XSL•FO
RenderX

of an x, y, and z component to represent the movement of the IMU device in space, sampled at 100 Hz (Figure 1). The first 3 sets of movement vectors (acceleration, velocity, and rotation) are important for calculating the exact position of the IMU device in 3D space. Then, the magnetic data vector was used because the magnetic data are critical to counteract any drift experienced by the accelerometer and gyroscope. At this point, the raw data consisted of just these 4 vector types, with the final shape of the combined data being an Nx12 array, where the unknown length N is equivalent to the amount of time the participant took to complete the task in seconds, multiplied by 100 due to the sampling rate, as shown in Figure 1.

In order to prepare the data for use in a deep learning model, several preprocessing steps were implemented, as shown in Figure 1. First, a 3-point moving average was applied to each of the x, y, and z components of each vector to slightly smooth out the data without losing any of the features. Small-scale testing showed that a little bit of smoothing is critical to the accuracy of the model; it helps the model look for generalizations between different trials without getting caught up on outliers. Next, the data were normalized by applying a global *z* score, followed by a global min-maxing. A *z* score is an algorithm to normalize a signal of any length based on the mean and SD, and it has been shown to significantly improve model accuracy and generalization capability [22]. By applying the *z* score function globally, it standardizes the data by bringing all values into the same reference frame, relative to their mean and SD. Min-maxing is not strictly necessary after a *z* score, but it has also been found to improve model accuracy [22]. It does this by ensuring that all values fall between 0 and 1, preventing deep learning models from experiencing runaway gradients and thus speeding up convergence during training. Finally, the trials with different lengths were zero-padded to be equal length, producing data in the shape 4000×12. While a few specific types of deep learning can handle data of different lengths during training, most of the model architecture we will be using is too rigid to handle variable length data, requiring a fixed input size.

After determining the best preprocessing steps for the data, a few final concerns need to be addressed. One concern is the variable length of the data; if the ASD class contains many trials that are significantly longer or shorter than the TD trials, the model could just end up classifying based on length rather than any feature characteristics (features) of children with ASD. It is generally expected that roughly 95% of the data in a normal distribution would fall within 2 SDs of the mean, and beyond this, the data might be considered unusual or even an outlier. Checking the dataset, the average length of a trial is roughly 1897 samples, with an SD of 463. The entire set of TD trials falls within 2 SDs of the mean, and only 13 trials of 145 from the children with ASD dataset are outside 2 SDs, all of them longer. This is a fairly normal distribution of data, where roughly 94% of the data are within 2 SDs of the mean. It is not quite normal to have every trial beyond 2 SDs on one side of the distribution curve, but it was decided that none of the data would be excluded as outliers because a slightly longer trial time might be a characteristic of children with ASD. Also, 13 of the 221 trials being significantly longer would not overwhelm the model, meaning that to achieve any real accuracy, it would have to learn other real characteristics of children with ASD from the kinematics data. After this, 1 final issue needed to be considered. The dataset consisted of 76 trials from TD children and 145 trials from children with ASD, meaning 1 possible classification had nearly double the amount of data compared to the other classification. Generally, deep learning models function best with balanced datasets, meaning they need a similar amount of data from all possible classifications; otherwise, they can run into major training issues. To solve this problem, a simple data balancing technique was employed. The smaller TD dataset was doubled, for a final dataset of 152 TD trials and 145 ASD trials. This data balancing method allows us to compare the validation accuracies, which we used to prototype several kinds of models. This allowed us to determine which models work best on this kind of data, and which models do not function at all.

With the data preprocessed, the next step was to prototype and test several deep learning models. Before any specific model methodologies could be compared, it is critical to determine the basic parameters that will ensure all the models are functioning as best as they can. Parameters such as the number of layers, the number of neurons in the layers, the learning rate, the best activation functions, the overall length of time required to train the model, and the video random-access memory (VRAM) requirements of the models were refined after running the tests shown in Table 1. It should be noted that while almost all of the above parameters are critical for ensuring peak functionality of the models, the training time and VRAM measures are simply a limitation of our computing resources for building and testing models. All models were trained with the Adam optimization algorithm and tested using a k-fold cross-validation scheme.

Video random-access memory

The requirements of the models were refined after running the tests shown in Table 1. It should be noted that while almost all of the above parameters are critical for ensuring peak functionality of the models, the training time and VRAM measures are simply a limitation of our computing resources for building and testing models. All models were trained with the Adam optimization algorithm and tested using a k-fold cross-validation scheme.

XSL•FO
RenderX

Table . Initial testing results from our model prototyping[a].

Model prototype	Cross-validation accuracy (%)	Training time for 1 k-fold (h)
LSTM[b] only, 1 layer, 3×12 neurons	57.59	~3
LSTM only, 5 layers, 3×12 neurons	62.76	~6
LSTM only, 1 layer, 6×12 neurons	66.21	~8
LSTM only, 5 layers, 6×12 neurons	67.59	~18
LSTM only, 1 layer, 12×12 neurons	65.17	~33
LSTM only, 5 layers, 12×12 neurons	71.03	~72
MLP[c] only, 1 layer	89.31	~1
MLP only, 3 layers	92.21	~1.5
MLP only, 6 layers	88.96	~2
MLP only, 9 layers	83.41	~3.5
CNN[d] only, 3 layers	90.34	~2
CNN only, 5 layers	91.38	~3
CNN only, 10 layers	87.14	~4
Transformer, 8 heads, 4 layers	82.73	~20

[a]Several versions of the long short-term memory models, multilayer perceptron models, convolutional neural network models, and transformer models were tested. All of these tests were performed using the balanced dataset mentioned previously. Because of this, these results do not represent the effectiveness of our motor task for diagnosing ASD, only the effectiveness of the models classifying this type of IMU data.

[b]LSTM: long short-term memory.

[c]MLP: multilayer perceptron.

[d]CNN: convolutional neural network.

Several key design choices were based on the model prototyping data collected. First, it was decided that any models with LSTM layers attached would use the 1 layer, 6×12 neuron format, as this seemed to provide the best possible LSTM classification, while keeping the runtime and VRAM requirements at a reasonable level. As Table 1 shows, models with significantly more LSTM neurons increase the training time to a matter of days to weeks, which would not be feasible for running many tests on many model permutations.

The second design choice implemented after testing was the use of only 3 layers for all future MLP testing. While adding more MLP layers does not increase the training time like LSTM layers do, having too many layers with too many neurons causes major overfitting problems, leading to the brute force memorization of the training data rather than any real generalizations.

It was also decided that all non-MLP models would have a smaller 3-layer MLP attached to the end as the final classifier. This allows the models a way to concatenate the output from CNN layers with the output from LSTM layers. It also has the side benefit of making all the models directly comparable; by keeping the final classification portion of the models the same, any changes in the features extracted by the LSTM, CNN, and convolutional autoencoder (CNN-AE) model configurations will be apparent. Thus, all models were designed to have 3 MLP layers attached at the end as the final classifier.

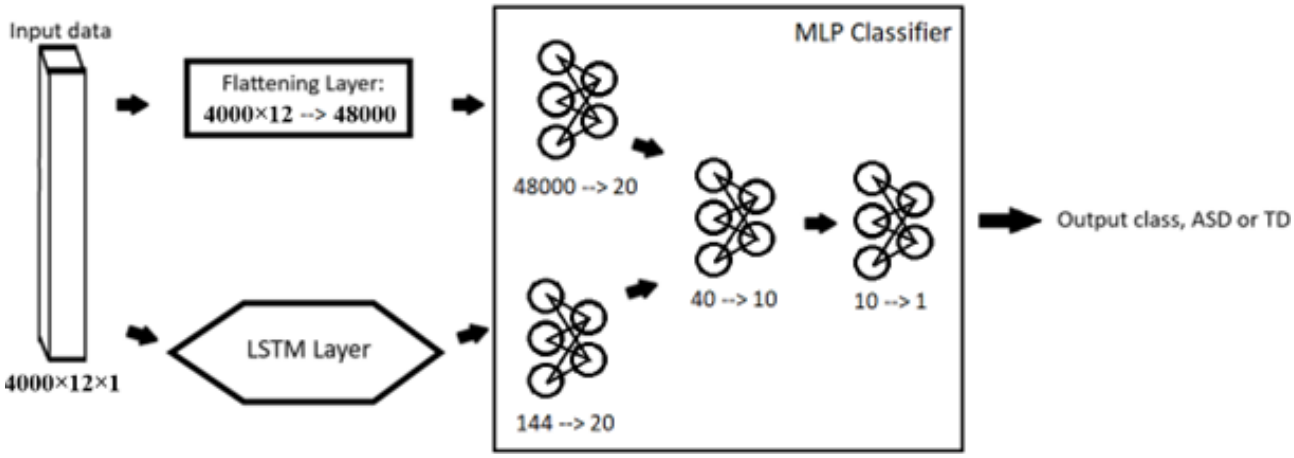
Other key design choices informed by the data from Table 1 include limiting the number of CNN layers to 5 to prevent overfitting, using the LeakyReLU activation functions on all layers except for the output layer, using the sigmoid activation function for the output layer, using a learning rate of 1e-4, and training for 200 epochs. Also worth noting is that several transformer type models were tested with no success, likely due to the limited amount of VRAM available for training these models. No further improvements were possible for the transformer type models with our training setup, so this model type was not evaluated any further. Now that the main model parameters have been identified, 6 types of deep learning models were built to test their effectiveness on this task and data type.

The MLP type models (Figure 2) each had 3 primary linear layers, with a batch normalization layer between each layer. LeakyReLU activate functions were used for the first 2 layers, and the third layer used a sigmoid function for the classification output. Before the first layer, there is a squeeze function to transform the 4000×12 zero-padded data input into a vector of length 48,000, ready for use in the MLP layers. We found that the size of the first layer was quite important; using an output value of much larger than 20 would cause significant overfitting, and using an output much smaller would cause the model training time to increase significantly, by requiring hundreds to thousands more epochs to reach the same level of accuracy. The key difference between the MLP and the MLP+LSTM is the addition of an LSTM layer along with an extra linear layer, as shown in Figure 2. The LSTM layer received the preprocessed input data as a sequence, and the cell state and hidden state were used as its output. Critically, the LSTM layers are able to handle data with differing input sizes, so the zero-padding on the input

XSL•FO
RenderX

data was stripped before being input into the LSTM layers. The output from the LSTM was then fed into a dedicated linear layer to prune the features and produce a separate output of length 20. This 20-point output was then concatenated with the 20-point output produced from the first layer as shown above, and the merged data were then run through the final 2 layers to produce a single classification. Just like the MLP model, the MLP+LSTM used batch normalization between all layers and LeakyReLU for all layers except for the classification, which used the sigmoid function (Textbox 1).

Figure 2. Schematic for the first merged model tested: the merging of a multilayer perceptron (MLP) classifier and a long short-term memory (LSTM) classifier. The MLP-only model takes the same form as this model, minus all of the LSTM-specific layers. ASD: autism spectrum disorder; TD: typically developing.



Textbox 1. Six final model architectures that have been evaluated. There are 3 primary model designs to be tested, the multilayer perceptron (MLP), convolutional neural network (CNN), and convolutional autoencoder (CNN-AE), and a modified version of each of these 3 models using long short-term memory (LSTM) layers. Each type of model was set up with matching layer structures to allow for a more direct comparison of effectiveness.

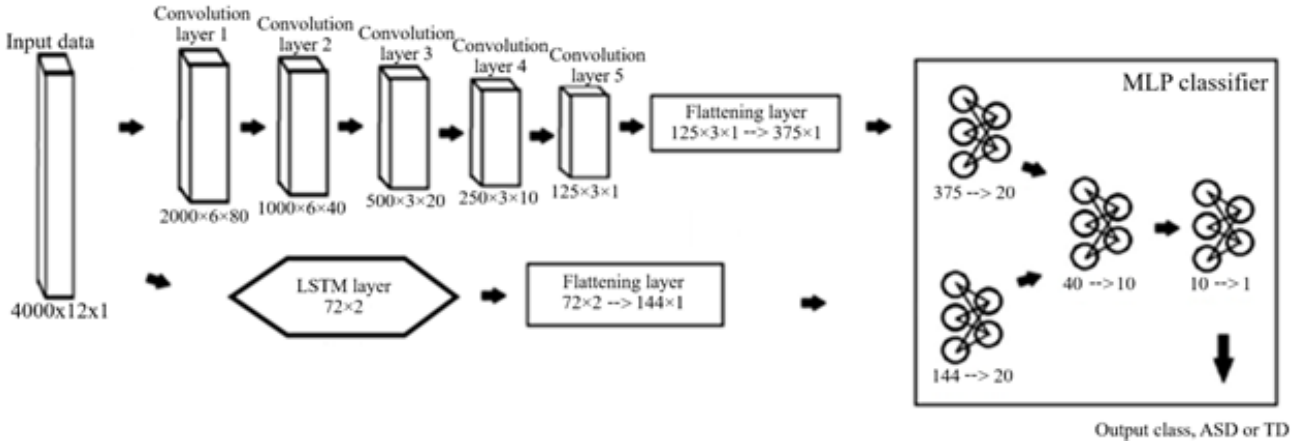
Deep learning models to be evaluated

- MLP
- CNN
- CNN-AE
- MLP+LSTM
- CNN+LSTM
- CNN-AE+LSTM

The CNN and CNN+LSTM models used a somewhat similar setup to the MLP-only models, with 1 key difference. The CNN model starts with 5 convolutional layers, transforming the input from 4000×12 to 125×3×1, as shown in Figure 3. The first 2 convolutional layers use a window size of 5×5, with the last 3 layers using a window size of 3×3. The optimal sizes of the window in CNN type models can vary greatly from dataset to dataset; however, it has been shown that prime numbers can be very effective in the first 2 layers of a CNN, while the deep layers optimize efficiently when they are small [23]. The stride for each convolution was specifically tuned to slowly compress the featurespace between each convolution, while ensuring that the model does not require too much memory or take too much time to run. The channel count was also tuned for this purpose, while ensuring that the maximum amount of features can be extracted from the data. Each channel functions as a featuremap, a 2D grid that represents all features detected by the convolution window. Importantly, each channel has its own window with optimizable weights. This is why the channel count starts at maximum then slowly decreases layer by layer, to ensure that all possible features can be detected at first, and then refined into the most important set of features from the data. Next, a batch normalization was implemented between each convolutional layer. When tested without batch normalization, these models all take significantly more epochs to train to the same accuracy. This means that adding batch normalization helps these models converge significantly faster. Each convolution also used a LeakyReLU activation function. Afterward, the 125×3×1 vector was squeezed into a linear vector, for use in the final MLP classifier. These layers were set up the same as the MLP model from before, allowing for a direct comparison between the methods. Similarly, the CNN+LSTM model concatenates the results from the convolutional layers and the LSTM layer in this final MLP classifier.

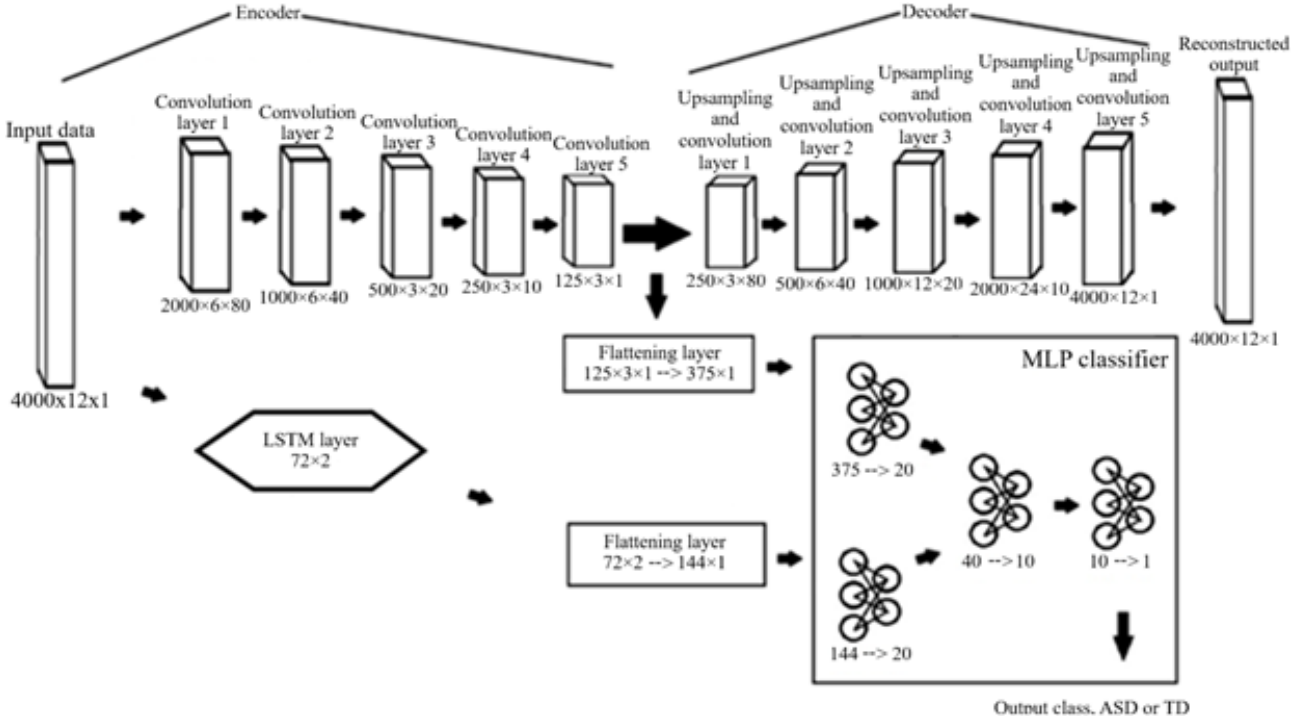
XSL•FO
RenderX

Figure 3. Schematic for the merged convolutional neural network with long short-term memory layers (CNN+LSTM) model. The CNN-only model takes the same form as this model, minus all of the LSTM-specific layers. ASD: autism spectrum disorder; TD: typically developing.



The last kind of model we tested was a CNN-AE. This model functions differently from the previous 2 types we have discussed. An MLP model and a CNN model only function to classify the data they are trained on, while an autoencoder can both classify and reconstruct the data it has been trained on. Autoencoder reconstruction works by compressing the input data into a smaller featurespace with an encoder, then rebuilding the original input data back from the compressed featurespace with a decoder. This method of compressing and reconstructing forces the model to identify key signal features fundamental to its composition. In this case, the encoder section has the same convolutional layers as the previous CNN models, compressing the input data from 4000×12 to 125×3×1. The decoder then uses a series of upsampling layers combined with convolutional layers to reconstruct the signal back from 125×3×1 to 4000×12, as shown in Figure 4. Afterward, the model sends the compressed featurespace through linear layers to generate the final classification, using the same layer formatting as all the previous models. Just as with the previous models, the CNN-AE+LSTM model integrates the LSTM data with the featurespace during the same step.

Figure 4. Schematic for the merged convolutional autoencoder with long short-term memory layers (CNN-AE+LSTM) model. The CNN-AE only model takes the same form as this model, minus all of the LSTM-specific layers. ASD: autism spectrum disorder; TD: typically developing.



All of these models were tested using k-fold cross-validation, where k was 10. This means that the data are split up into 10 random subgroups, the model is trained on 9 subgroups and tested on the 10th subgroup, and the resulting accuracy is saved for later. This process is repeated 9 more times, using each unique subgroup as the testing data one time while training on the rest. After all the training is done, all 10 accuracies are averaged to produce the final cross-validation accuracy.

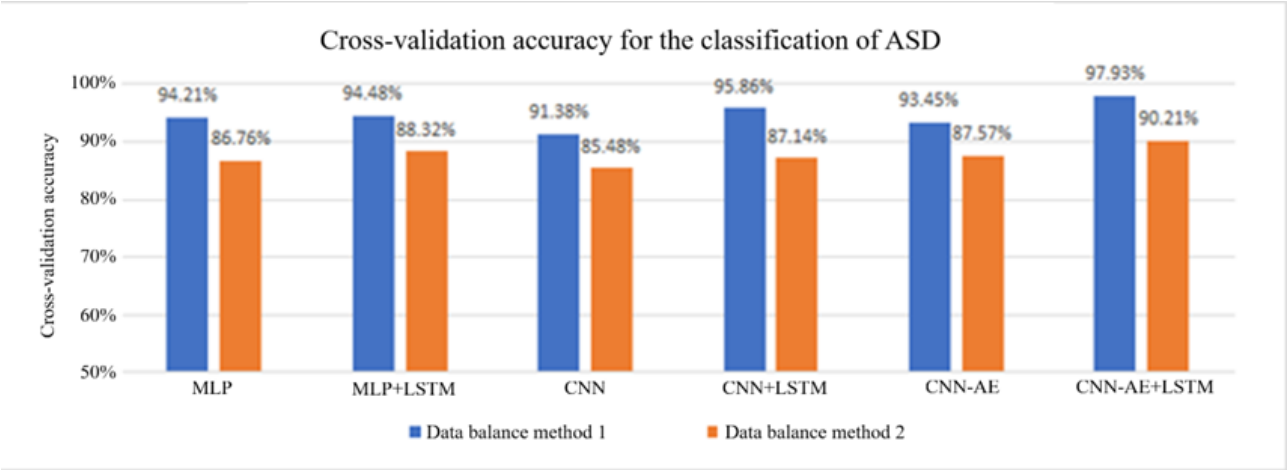
Results

All 6 models were trained and evaluated for accuracy, with several important results. First, we noticed that using LSTM

XSL•FO
RenderX

layers significantly increases the accuracy each model can achieve, as shown below by the blue bars in Figure 5. These data also show that the CNN-AE with added LSTM layers is the best model. Unfortunately, it was at this point that we discovered that these resulting accuracies (labeled in blue in Figure 5) were misleadingly high, due to a fault with the data balancing method. By simply duplicating the TD dataset, the same piece of data could end up in both the training and testing set, due to the random sampling of the data during the standard use of the k-fold cross-validation method. This means that while the model-to-model trend in the data is likely correct, the blue columns in Figure 5 are statistically invalid for drawing conclusions about the effectiveness of the cognitive-motor task.

Figure 5. These are the resulting accuracies from the 2 training sessions for each model. Data balancing method 1 cannot be considered evidence for the effectiveness of the motor task due to the duplication of data in the training and testing sets. Data balancing method 2 is statistically valid and does show the effectiveness of our motor task for distinguishing between children with autism spectrum disorder (ASD) and typically developing (TD) children. CNN: convolutional neural network; CNN-AE: convolutional autoencoder; LSTM: long short-term memory layer; MLP: multilayer perceptron.



Fortunately, there was a fairly simple way to fix this problem, allowing us to evaluate the effectiveness of our cognitive-motor task. A second data balancing method was implemented, where the larger dataset of ASD trials was split in half, creating one dataset that is 73 ASD trials and 76 TD trials, and another dataset with the remaining 72 ASD and the same 76 TD trials. Each model was evaluated using both datasets, and the cross-validation accuracies were averaged for the final resulting accuracy. This is a statistically useful test for evaluating the effectiveness of the cognitive-motor task, as it ensures that no datapoints from the training set are ever introduced into the testing set. Thus, the accuracy achieved by a model depends on its successful interpretation of the cognitive-motor task. The results from using this second method of data balancing are labeled in orange in Figure 5. These results allow us to assess how well our cognitive task works for the deep learning classification of a participant; clearly, the task is effective, as the average model accuracies range from ~85% to ~90%. Also clearly shown is how the second data balancing method produces the same trend in the data, with the CNN-AE+LSTM once again proving to be the best model.

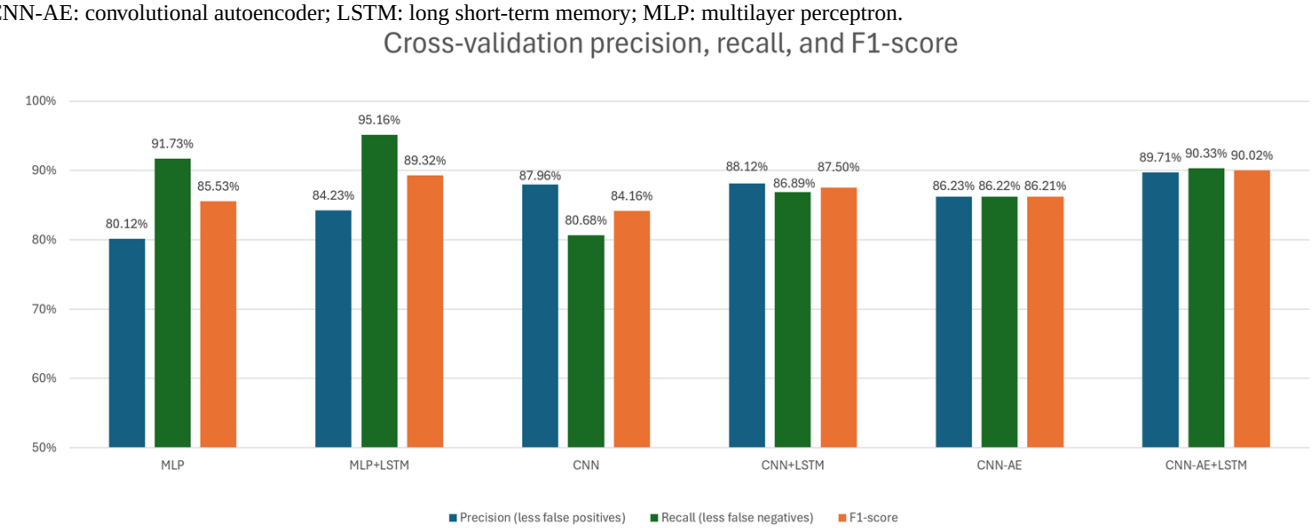
While accuracy is a great general metric for evaluating the effectiveness of a deep learning model, it is not the only metric that should be considered. For starters, looking at the SD for the models can tell us approximately how reliable a model is, where a low standard deviation means a model is quite stable between k-folds. For our models using data balancing method 2, the average standard deviation was no greater than ~2%. This means our models are stable when they produce these accuracies, which is a good sign for possible future work. Stable models are more likely to generalize successfully when trained with larger datasets. Precision and recall are very useful scores for judging medical artificial intelligence (AI) performance, because these metrics are calculated using false-positive and false-negative results, respectively. When AI is being used as a diagnostic tool, false-positive diagnoses can lead to unnecessary treatment and wastage of time, while false-negative results can lead to a patient missing required care. Both false-positive and false-negative cases are critically important to avoid, so we calculated the F_1-score for each of our models. The F_1-score is a combination of precision and recall that can be considered more important than accuracy for evaluating our diagnostic model in this case. To calculate these scores, the models were run again to generate confusion matrices. The models were run with the second data balancing method described above, where the dataset was split in two, the models run twice, and the results averaged to produce the final scores.

Based on Figure 6, we see that the F_1-scores match closely with the trend shown previously by the accuracies in Figure 5. Adding LSTM layers is once again shown to be vital to increasing the effectiveness of these models when predicting children with ASD. Interestingly, the MLP models score consistently higher recall values with corresponding lower precision values. The higher recall score means that the MLP type models might have less false-negative results overall, ensuring that participants with ASD will not be missed by the model. This does come with the downside of a lower precision, meaning that participants without ASD might be accidentally diagnosed positively more often. The CNN models seem to show the inverse, with higher precision and lower recall, but this might fall within the range of error, due to the random initializations of the weights whenever a new training session is started. Finally, we can see that the autoencoder models achieve a balance between precision and recall, with the LSTM

XSL•FO
RenderX

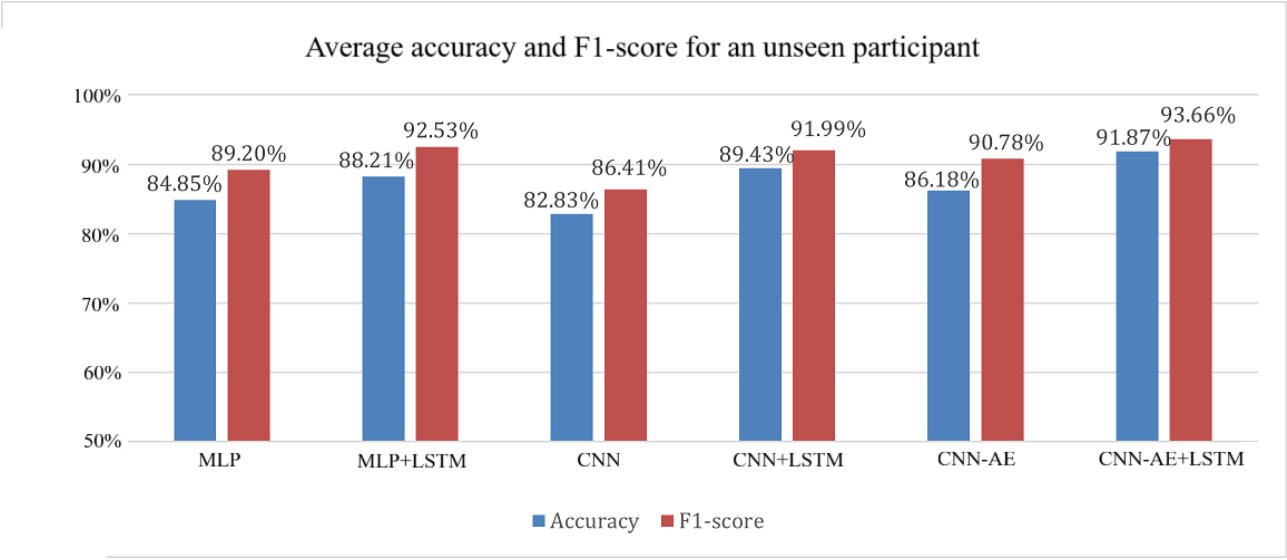
autoencoder achieving a slightly higher F_1-score of 90.02%, meaning this is a better overall optimization as a result.

Figure 6. These are the precision, recall, and F_1-scores for each model. The number above each set of columns is the F_1-score for each model. All of these scores were calculated using the statistically valid second data balancing method mentioned previously. CNN: convolutional neural network; CNN-AE: convolutional autoencoder; LSTM: long short-term memory; MLP: multilayer perceptron.



Knowing that the CNN-AE+LSTM model functions best for processing timeseries data and that our motor task works is very important information, but it is also critical to evaluate how well the models would predict on a participant they had never seen before. In order to test this, a strict patient-wise training or testing data split was implemented [24]. The methodology used to split the data was simple; one of the 41 participants was selected at random for testing, and their trials were excluded from the training data. The models were trained until the training accuracy was above 95% accuracy, and once this limit was reached, the testing accuracy of the given participant's trials was determined and then saved for later averaging. This was then repeated for each of the 41 participants, and the final resulting accuracy was calculated as the overall average of each saved testing accuracies from each participant. By averaging all possible testing conditions, the patient-wise method allowed us to interpret how well each of the models would work, as a true reflection of how likely a given model will perform correctly on an unseen participant. The precision and recall scores were also averaged in this way, allowing us to calculate the F_1-score. It is important to note that it was not possible to balance the dataset for this particular test, which is reflected in Figure 7 by the worse performance of all non-LSTM models and by the slightly higher F_1-scores relative to accuracy.

Figure 7. These are the resulting accuracies and F_1-scores from the patient-wise classification. Each value is the overall average accuracy achieved on a patient never seen by the model. CNN: convolutional neural network; CNN-AE: convolutional autoencoder; LSTM: long short-term memory; MLP: multilayer perceptron.



The primary result of this patient-wise evaluation is the importance of the LSTM layers. As can be seen in Figure 7, using LSTM layers seems to improve the model accuracy by roughly ~4% for all cases, with a similar effect on the F_1-scores. These results once again confirm that the CNN-AE model is one of the best options for predicting children with ASD.

XSL•FO
RenderX

Discussion

Principal Findings

This study evaluated the effectiveness of various small-scale deep learning approaches for classifying children with and without ASD using IMU hand tracking data. Our results demonstrated that the best performance was achieved with a CNN-AE model combined with LSTM layers, yielding accuracies around 91% and F_1-scores of 90.02% and 93.66%, respectively, using the k-fold and patient-wise evaluation methods. When it comes to the task of scanning sequence movement data for characteristic features of children with ASD, it seems clear that both of the CNN models overfit the data and perform worse than the MLP models, with the CNN-AE+LSTM model continuing to be the best classification option.

Additionally, it is important to understand why these models performed at the level that they did; this understanding could benefit future work involving small-scale models and medical data. Deep learning networks such as these are powerful tools, but they need to be tailored to their specific use cases. Normally, it is unusual to see a CNN model performing significantly worse than the MLP model; however, there could be several reasons for this. One likely reason is the data format: CNN models cannot interpret sequential data in the same way an MLP might be able to. It all comes down to where the optimization happens in each model type. In a CNN-type model, all of primary optimization happens inside the kernels, and a fixed-size filter then scans over an entire signal and looks for a specific set of features that the internal weights are optimized to find. Because these kernels are a fixed size, a single CNN layer can only ever look at a small chunk of the overall data at any given time to look for patterns. All of this to say, a CNN can struggle to capture long-range dependencies and complex patterns in sequence data. The convolutions performed by a CNN are better suited for locating features with short-range dependencies, or in other words, a CNN is better for detecting localized patterns. On the other hand, MLP type models are capable of learning complex, nonlinear relationships between the extracted features and the target variable. This is because every single neuron in an MLP layer is connected to every other neuron with an optimizable weight, meaning the entire input sequence can be evaluated at the same time. This flexibility can sometimes lead to a better performance in learning classifications from intricate, long, and complex patterns. Furthermore, while a CNN-AE model might only have CNN layers for detecting short-range patterns, it has the added bonus of compressing the input sequence into a lower-dimensional latent space, capturing essential features while filtering out noise. This results in a more efficient latent representation of the data, compared to the results of a CNN alone. Effectively, this means that the CNN layers of the autoencoder model will detect and significantly compress all possible information from short-range dependencies, while still preserving the necessary long-range dependencies to allow for accurate reconstruction. This highly compressed version of the input data can seriously mitigate overfitting, which likely explains why the CNN-AE models outperformed the regular MLP and CNN models. It is important to note that we did some experimenting with dropout layers, normally used to mitigate overfitting in simpler model types, but the results were mixed. The models became inconsistent, sometimes performing slightly better, sometimes performing worse. This is likely due to the small size of the dataset; future work with larger datasets should not ignore the possibility that dropouts could increase accuracy even further.

We can also see that despite the feature compression of the CNN-AE model and the ability for an MLP to identify some long-range dependencies, these models still do not perform very well without the addition of LSTM layers. These LSTM layers are critical to improved performance, increasing the accuracy for every type of model. This makes sense, as LSTM layers have a few major advantages for analyzing and learning from sequence type data. LSTM layers are very successful at learning long-range dependencies due to their internal memory, which can hold critical data. This internal memory leverages additive and subtractive gates, known as the input gate and the forget gate, respectively. These gates are mathematical functions that can learn to store useful information in the internal memory while discarding irrelevant information. Also, LSTM layers can handle sequences of different lengths, which is crucial for this project because each trial from each participant is a different length of time, ranging from roughly 10 to 40 seconds. Unlike the CNN and MLP models, which required a fixed input size of 4000×12 (accomplished with zero-padding), all of the LSTM layers were able to utilize that data of different input lengths, and all zero-padding on the data was removed before being input into the LSTM during training and testing. This likely improved accuracy even more because the layers were not forced to handle meaningless data in the form of zeros.

It also seems that the CNN-AE model did somewhat better during the patient-wise test compared to the cross-validation test. This might be explained by the slightly larger amount of training data it had access to; during cross-validation, 10% of the dataset was always excluded for testing, whereas with the patient-wise test, excluding 1 participant is closer to excluding ~1% - 2% of the dataset. This may also explain why the CNN+LSTM model did better during the patient-wise testing, as the larger dataset may have helped the model avoid overfitting. Overall, these are all critical factors to consider in the future when designing a deep learning model that will use medical or cognitive data. Proper fine-tuning of a model can allow for significantly less resource usage and better performance overall.

Comparison to Prior Work

It is also worth noting that in our previous paper [20], we broke down our raw data into a set of useful statistics, such as reaction time, total displacement, average and max velocity, time to peak velocity, and more. We used 1-way ANOVAs to determine that children with ASD had significant differences in reaction time, velocity, acceleration, and total displacement. Compared to TD children, the children with ASD had a slightly longer average reaction time and significantly higher acceleration values, leading to a higher peak velocity. This corresponds to the children with ASD having an increased number of movement subunits (micro-adjustments in path during the reaching motions). Finally, children with ASD had a significantly higher

XSL•FO
RenderX

total displacement during the task. Using this information, we have been able to conclude that the hardest motion patterns for our model to detect were the ones with the most similarity to TD children, with smoother movements and less movement subunits, more consistent accelerations, and a slightly slower peak velocity. Trials where a child with ASD might have really focused and avoided a slower reaction time or finished with a normal total displacement tended to make classification harder. Equally, cases with TD children where they might have been distracted, leading to increased movement jerkiness (increased movement subunits), also caused classification issues. It also seems likely that having each child perform the task multiple times gave the children time to learn and get better at the task, bringing the TD and ASD classes a bit closer together and harder to discriminate between. The consideration of these specific movement features is important for the future design of a physical motor task to better exemplify the differences between ASD and TD goal-based movement.

Limitations

First, an important limitation of this study is the lack of a larger dataset containing a more diverse group of children. With only 41 participants, our model is unlikely to generalize well enough to function as a true diagnostic measure; it does, however, show the need for more robust research. Only one-third of our trials were of TD children; the rest were of individuals with ASD, which we attempted to mitigate by using specialized data balancing techniques to ensure that they would reach a generalization. These models would likely work significantly better if we were able to gather data from more TD children to ensure the true range of neurodivergence is recognized by the model. Increasing the size of the dataset would certainly increase its capability to generalize to new patients and likely reduce the number of false-positive and false-negative results. An even class distribution also eliminates the need for either data augmentation or data balancing methods, which can decrease the complexity of models and reduce the possibility for the introduction of errors and data leakage. Moreover, we did not exclude children with comorbid developmental disorders from the ASD group. While this approach enhances the ecological validity of our findings, it limits our ability to identify movement patterns specific to children with ASD. Future studies that will include participants with varying diagnoses are needed to further explore differences in movement characteristics between children with ASD and those with other developmental conditions.

Second, another limitation of this study was the equipment used to train and test these models. We were limited by run time and VRAM limits when attempting to test more complex networks. It is possible a larger LSTM section attached to the other models could achieve even better results. It might even be possible to build an LSTM-only model that rivals the ones built in this study, but it would require more powerful hardware to prototype a model like this. This is also true of a similarly built transformer classifier, where a transformer built to the limitations of our equipment was unable to perform with significant accuracy, but a much larger transformer might be able to achieve the same or better results. This limitation can also be seen as an advantage, as the small-scale custom models like the CNN-AE developed here require a significantly smaller amount of VRAM. This is a critical consideration as graphics processing unit prices continue to rise; access to powerful AI does not need to be gated by unnecessary costs for larger models that are not significantly more effective than cleverly designed small models.

Third, one final limitation worth considering is the lack of a comprehensive ablation study on these models. We attempted to tackle this problem in Table 1, which represents a fairly rigorous examination of general model hyperparameters such as layer count and neuron count. Unfortunately, this work falls short as it does not specifically validate other choices made such as the use of LeakyRelu activation functions, among other choices. Future work should consider performing an ablation study on these models and the data preprocessing steps to help break down which components and parameters of the models are critical for high accuracy results. Primary targets for the ablation study should be testing the effectiveness of the *z* scoring and min-maxing steps during normalization, as well as altering the number of points used in the moving average. Also worth testing is the number of batch normalization layers; the model may only need 1 or 2 of these layers, rather than the current model setups where every single layer is followed by a normalization. Overall, based on the testing performed during the prototyping phase, we are reasonably confident that the changes mentioned here would have only a minor effect on outcome accuracy.

Future Directions

It is important to consider the context in which models like these might be used to aid the diagnosis of children with ASD. Considering the possible harm of false-positive and false-negative results is a top priority; a false-positive result could lead to unnecessary spending by parents and self-doubt among children diagnosed, while a false negative could lead to a child missing out on critical care during the most important period of their life. For these reasons, a high F_1-score of 90.02% is another critical metric that shows our models are very effective, showing that the CNN-AE+LSTM model can avoid generating false-positive and false-negative results in most scenarios. For future work, there are some other important methods that could mitigate the effects of a false-positive diagnosis. This kind of diagnostic AI should be combined with the same behavioral interviews that children go through now (where the doctor performing the interview should not know the diagnosis provided by AI to avoid bias). In addition, continuing research should focus on using similar models to classify the severity of ASD rather than just producing a diagnosis. This could further limit the problems caused by a false-positive result, allowing doctors to correctly interpret the model results during the many cases when a diagnostic AI does not have a proper yes or no answer for a specific patient. ASD is a spectrum after all, so ensuring our models reflect this is a critical next step to this research. If the primary problems caused by a false-positive result can be mitigated in these ways, it may be possible to train our models to target and remove false-negative results, even at the expense of slightly more false-positive results that need to be caught by doctors during the process. Of course, the ideal goal would be to eliminate all false-positive results along with all false-negative results.

XSL•FO
RenderX

In the future, this research could be continued by collecting a larger dataset from a more diverse group of children with ASD and TD children, which would improve the robustness of the model. Additionally, further analysis could be performed on various kinematic variables, such as submovement stops, an atypical movement characteristic often observed in children with ASD [25,26]. This would aid in developing the most effective motor task for diagnosing children with ASD. Future work should also look at alternative methods of time series data analysis; clever techniques like using the Time Series Feature Extraction Library might be able to provide significant improvements to the LSTM portion of our models. Finally, future studies could explore the use of deep learning approaches to classify children with and without ASD based on additional data such as behavioral data (eg, eye tracking), or even physiological data (eg, heart rate and blood pressure) using small noninvasive recording devices.

Conclusions

This study evaluated the effectiveness of several small-scale deep learning models for classifying children with and without ASD using IMU-based hand tracking data collected during a goal-directed motor task. Across all architectures tested, the CNN-AE+LSTM consistently achieved the highest performance, reaching an F_1-score of 93.66% on unseen participant data. These results support the hypothesis that differences in motor behaviors between TD children and children with ASD can be detected using IMU-based hand tracking.

In contrast to the prevailing trend of retraining large-scale pretrained models, this work demonstrates that compact models with random initializations may also be effective for handling classification tasks involving goal-directed motor behavior.

Acknowledgments

During the preparation of this work, the authors used ChatGPT-4o for minor changes and improvements in word choice. After using this tool or service, the authors reviewed and edited the content as needed and take the full responsibility for the content of the publication.

Funding

This research was supported, in part, by the Intramural Research Program of the National Institutes of Health (NIH). The contributions of the NIH author(s) are considered Works of the United States Government. The findings and conclusions presented in this paper are those of the author(s) and do not necessarily reflect the views of the NIH or the US Department of Health and Human Services. This study was supported by the Intramural Research Program of the National Institute of Child Health and Human Development (project number: 1ZIAHD008882-10), the NIH's Bench-to-Bedside Program, the NIH through a shared instrumentation grant awarded to the University of Delaware (grant 1S10OD021534-01; PI: Bhat), pilot award funding through an Institutional Development Award from the National Institute of General Medical Sciences of the NIH (U54-GM104941, PI: Binder-Macleod; P20 GM103446, PI: Stanhope), and funding from the Dana Foundation through a Clinical Neuroscience Award (PI: Bhat). The sponsors had no involvement in the study design, data collection and analysis, decision to publish, or preparation of the manuscript.

Data Availability

All data are stored in a University of Delaware repository and are available upon reasonable request. All Python code is stored in a National Institutes of Health repository and is available upon reasonable request.

Authors' Contributions

Conceptualization: AB, JM, WCS
Data curation: AB, WCS
Formal analysis: JM, WCS
Funding acquisition: AB
Investigation: AB, WCS
Methodology: JM
Project administration: AG
Resources: AG
Supervision: AB, AG
Software: JM
Validation: AG, WCS
Visualization: JM
Writing – original draft: JM, WCS
Writing – review and editing: AG, JM, WCS

XSL•FO
RenderX

Conflicts of Interest

None declared.

References

1. Diagnostic and Statistical Manual of Mental Disorders, 5th edition: American Psychiatric Association; 2013.
2. Maenner MJ, Warren Z, Williams AR, et al. Prevalence and characteristics of autism spectrum disorder among children aged 8 years—Autism and Developmental Disabilities Monitoring Network, 11 Sites, United States, 2020. MMWR Surveill Summ 2023 Mar 24;72(2):1-14. [doi: 10.15585/mmwr.ss7202a1] [Medline: 36952288]
3. Chita-Tegmark M. Social attention in ASD: a review and meta-analysis of eye-tracking studies. Res Dev Disabil 2016 Jan;48:79-93. [doi: 10.1016/j.ridd.2015.10.011] [Medline: 26547134]
4. Franchini M, Glaser B, Wood de Wilde H, Gentaz E, Eliez S, Schaer M. Social orienting and joint attention in preschoolers with autism spectrum disorders. PLOS ONE 2017;12(6):e0178859. [doi: 10.1371/journal.pone.0178859] [Medline: 28599002]
5. Yew RY, Hooley M, Stokes MA. Factors of relationship satisfaction for autistic and non-autistic partners in long-term relationships. Autism 2023 Mar 16;27(8):13623613231160244. [doi: 10.1177/13623613231160244] [Medline: 36924337]
6. Chaxiong P, Dimian AF, Wolff JJ. Restricted and repetitive behavior in children with autism during the first three years of life: a systematic review. Front Psychol 2022;13:986876. [doi: 10.3389/fpsyg.2022.986876] [Medline: 36389482]
7. Lord C, Rutter M, Le Couteur A. Autism Diagnostic Interview-Revised: a revised version of a diagnostic interview for caregivers of individuals with possible pervasive developmental disorders. J Autism Dev Disord 1994 Oct;24(5):659-685. [doi: 10.1007/BF02172145] [Medline: 7814313]
8. Lord C, Rutter M, Goode S, et al. Autism diagnostic observation schedule: a standardized observation of communicative and social behavior. J Autism Dev Disord 1989 Jun;19(2):185-212. [doi: 10.1007/BF02211841] [Medline: 2745388]
9. Lebersfeld JB, Swanson M, Clesi CD, O'Kelley SE. Systematic review and meta-analysis of the clinical utility of the ADOS-2 and the ADI-R in diagnosing autism spectrum disorders in children. J Autism Dev Disord 2021 Nov;51(11):4101-4114. [doi: 10.1007/s10803-020-04839-z] [Medline: 33475930]
10. Ayoub MJ, Keegan L, Tager-Flusberg H, Gill SV. Neuroimaging techniques as descriptive and diagnostic tools for infants at risk for autism spectrum disorder: a systematic review. Brain Sci 2022 May 5;12(5). [doi: 10.3390/brainsci12050602] [Medline: 35624989]
11. Bhat AN. Is motor impairment in autism spectrum disorder distinct from developmental coordination disorder? A report from the SPARK study. Phys Ther 2020 Apr 17;100(4):633-644. [doi: 10.1093/ptj/pzz190] [Medline: 32154876]
12. Kangarani-Farahani M, Malik MA, Zwicker JG. Motor impairments in children with autism spectrum disorder: a systematic review and meta-analysis. J Autism Dev Disord 2024 May;54(5):1977-1997. [doi: 10.1007/s10803-023-05948-1] [Medline: 36949273]
13. Bhat AN, Landa RJ, Galloway JC. Current perspectives on motor functioning in infants, children, and adults with autism spectrum disorders. Phys Ther 2011 Jul;91(7):1116-1129. [doi: 10.2522/ptj.20100294] [Medline: 21546566]
14. Bhat AN. Motor impairment increases in children with autism spectrum disorder as a function of social communication, cognitive and functional impairment, repetitive behavior severity, and comorbid diagnoses: a SPARK study report. Autism Res 2021 Jan;14(1):202-219. [doi: 10.1002/aur.2453] [Medline: 33300285]
15. Bhat A, Tulsky DS, Boulton AJ. Cross-replicating findings on unique motor impairments of children with ASD using confirmatory factor analysis and a novel SPARK study sample. Autism Res 2023 May;16(5):967-980. [doi: 10.1002/aur.2904] [Medline: 36840933]
16. Fournier KA, Hass CJ, Naik SK, Lodha N, Cauraugh JH. Motor coordination in autism spectrum disorders: a synthesis and meta-analysis. J Autism Dev Disord 2010 Oct;40(10):1227-1240. [doi: 10.1007/s10803-010-0981-3] [Medline: 20195737]
17. Shao L, Fu C, You Y, Fu D. Classification of ASD based on fMRI data with deep learning. Cogn Neurodyn 2021 Dec;15(6):961-974. [doi: 10.1007/s11571-021-09683-0] [Medline: 34790264]
18. Ahmed MR, Ahammed MS, Niu S, Zhang Y. Deep learning approached features for ASD classification using SVM. In: 2020 IEEE International Conference on Artificial Intelligence and Information Systems (ICAIIS): IEEE; 2020.
19. Khodatars M, Shoeibi A, Sadeghi D, et al. Deep learning for neuroimaging-based diagnosis and rehabilitation of autism spectrum disorder: a review. Comput Biol Med 2021 Dec;139:104949. [doi: 10.1016/j.compbiomed.2021.104949] [Medline: 34737139]
20. Su WC, Mutersbaugh J, Huang WL, Bhat A, Gandjbakhche A. Developmental differences in reaching-and-placing movement and its potential in classifying children with and without autism spectrum disorder: deep learning approach. Res Sq 2024 Mar 4:rs.3.rs-3959596. [doi: 10.21203/rs.3.rs-3959596/v1] [Medline: 38496641]
21. SPARK. Simons Foundation Autism Research Initiative. URL: https://www.sfari.org/resource/spark/ [accessed 2025-11-26]
22. Rahman A. Statistics-based data preprocessing methods and machine learning algorithms for big data analysis. Int J Artif Intell 2019;17(2):44-65 [FREE Full text]
23. Tang W, Long G, Liu L, Zhou T, Blumenstein M, Jiang J. Omni-scale cnns: a simple and effective kernel size configuration for time series classification. arXivLabs. Preprint posted online on Jun 17, 2022. [doi: 10.48550/arXiv.2002.10061]

XSL•FO
RenderX

24. Ashames MMA, Demir A, Gerek ON, et al. Are deep learning classification results obtained on CT scans fair and interpretable? Phys Eng Sci Med 2024 Sep;47(3):967-979. [doi: 10.1007/s13246-024-01419-8] [Medline: 38573489]
25. Chen LC, Su WC, Ho TL, et al. Postural control and interceptive skills in children with autism spectrum disorder. Phys Ther 2019 Sep 1;99(9):1231-1241. [doi: 10.1093/ptj/pzz084] [Medline: 31187124]
26. Yang HC, Lee IC, Lee IC. Visual feedback and target size effects on reach-to-grasp tasks in children with autism. J Autism Dev Disord 2014 Dec;44(12):3129-3139. [doi: 10.1007/s10803-014-2165-z] [Medline: 24974254]

Acknowledgments

AI: artificial intelligence
ASD: autism spectrum disorder
CNN: convolutional neural network
CNN-AE: convolutional autoencoder
IMU: inertial measurement unit
LSTM: long short-term memory
MLP: multilayer perceptron
TD: typically developing
VRAM: video random-access memory

Edited by A Coristine; submitted 04.03.25; peer-reviewed by A Singhal, B Tasci, C Ma; revised version received 20.08.25; accepted 20.08.25; published 22.12.25.

Please cite as:
Mutersbaugh J, Su WC, Bhat A, Gandjbakhche A
Deep Learning Approaches for Classifying Children With and Without Autism Spectrum Disorder Using Inertial Measurement Unit Hand Tracking Data: Comparative Study
JMIR Med Inform 2025;13:e73440
URL: https://medinform.jmir.org/2025/1/e73440
doi:10.2196/73440

© John Mutersbaugh, Wan-Chun Su, Anjana Bhat, Amir Gandjbakhche. Originally published in JMIR Medical Informatics (https://medinform.jmir.org), 22.12.2025. This is an open-access article distributed under the terms of the Creative Commons Attribution License (https://creativecommons.org/licenses/by/4.0/), which permits unrestricted use, distribution, and reproduction in any medium, provided the original work, first published in JMIR Medical Informatics, is properly cited. The complete bibliographic information, a link to the original publication on https://medinform.jmir.org/, as well as this copyright and license information must be included.

XSL•FO
RenderX

A Machine Learning Approach to Differentiate Cold and Hot Syndrome in Viral Pneumonia Integrating Traditional Chinese Medicine and Modern Medicine: Machine Learning Model Development and Validation

Xiaojie Jin[1,2*], Prof Dr; Yanru Wang[1*], Dr med; Jiarui Wang[3*], MM; Qian Gao[2], MSc; Yuhan Huang[1], MM; Lingyu Shao[4], MM; Jiali Zhao[1], MM; Jintian Li[1], Prof Dr; Ling Li[1*], Prof Dr; Zhiming Zhang[5*], Prof Dr Med; Shuyan Li[4*], Prof Dr; Yongqi Liu[1*], Prof Dr, Prof Dr Med

[1]Key Laboratory of Dunhuang Medicine, Ministry of Education, Gansu University of Chinese Medicine, Dingxi East Road, 35th, Lanzhou, China

[2]College of Pharmacy, Gansu University of Chinese Medicine, Lanzhou, China

[3]The Second Affiliated Hospital of Xuzhou Medical University, Xuzhou, China

[4]School of Medical Information and Engineering, Xuzhou Medical University, Xuzhou, China

[5]Gansu Provincial Hospital of Traditional Chinese Medicine, Lanzhou, China

[*]these authors contributed equally

Corresponding Author:
Yongqi Liu, Prof Dr, Prof Dr Med
Key Laboratory of Dunhuang Medicine, Ministry of Education, Gansu University of Chinese Medicine, Dingxi East Road, 35th, Lanzhou, China

Abstract

Background: Syndrome differentiation in traditional Chinese medicine (TCM) is an ancient principle that guides disease diagnosis and treatment. Among these, the cold and hot syndromes play a crucial role in identifying the nature of the disease and guiding the treatment of viral pneumonia. However, differentiating between cold and hot syndromes is often considered esoteric. Machine learning offers a promising avenue for clinicians to identify these syndromes more accurately, thereby supporting more informed clinical decision-making in the treatment.

Objective: This study aims to construct a diagnostic model for differentiating cold and hot syndromes in viral pneumonia by integrating TCM and modern medical features using machine learning methods.

Methods: The application of 8 machine learning algorithms (gradient boosting machine [GBM], logistic regression, random forest, extreme gradient boosting [XGB], light gradient boosting machine [LGB], ridge regression, least absolute shrinkage and selection operator, and support vector machine) generated and validated (both internally and externally) a model for differentiating cold and hot syndromes in viral pneumonia, based on clinical data from 1484 patient samples collected at 2 medical centers between 2021 and 2022.

Results: The GBM model, which combines TCM and modern medicine features, outperformed models using only TCM features or only modern medicine features in distinguishing cold and hot syndromes in patients with viral pneumonia. The optimal discrimination model comprised 13 optimal features (temperature, red cell distribution width-SD, creatinine, total bilirubin, globulin, C-reactive protein, unconjugated bilirubin, white blood cell, neutrophil percentage, aspartate transaminase/alanine transaminase, total cholesterol, thrombocytocrit, and age) and the GBM algorithm, achieving an area under the curve (AUC) of 0.7788. Under internal and external testing, the AUCs were 0.7645 and 0.8428, respectively. Moreover, significant differences were observed between the cold and hot syndrome groups in temperature (P=.02), red cell distribution width-SD (P<.001), neutrophil percentage (P=.01), total cholesterol (P=.003), thrombocytocrit (P<.001), and age (P<.001).

Conclusions: This pioneering study integrates the theory of TCM cold and hot syndromes with modern laboratory-based tests through machine learning. The developed model offers a novel approach for differentiating cold and hot syndromes in viral pneumonia, enabling practitioners to identify the syndrome quickly and efficiently, thereby supporting more informed clinical decision-making. Additionally, this research provides new insights into the modernization and scientific interpretation of TCM syndrome differentiation.

(JMIR Med Inform 2025;13:e64725) doi:10.2196/64725

XSL•FO
RenderX

KEYWORDS

syndrome differentiation; traditional Chinese medicine; viral pneumonia; dialectical treatment; machine learning; Chinese medicine; pneumonia; lungs; diagnostic model; retrospective study; artificial intelligence; China; model training; performance evaluation; laboratory tests; modern medicine

Introduction

Traditional Chinese medicine (TCM), a personalized and holistic approach, treats diseases using natural medical products tailored to a patient's TCM syndrome patterns [1], that is, dialectical treatment of TCM. Specifically, TCM syndrome, a concept unique to TCM, is an abstraction of a variety of signs and symptoms. Dialectical treatment is the fundamental principle by which physicians diagnose, understand, and treat diseases. It involves comprehensively collecting patients' clinical signs and symptoms through "inspection, auscultation, olfaction, inquiry, and palpation" to determine the TCM syndrome pattern. Subsequently, corresponding therapies, such as acupuncture, cupping, qigong, massage, and diet, are selected [2] to correct maladjustments and restore the body's self-regulatory ability [3,4]. Guided by this unique principle, TCM has demonstrated remarkable clinical efficacy in treating various acute and chronic diseases, thus attracting increasing attention [5]. Especially in the fight against viral pneumonia, the importance of TCM has been widely recognized [6,7]. Consequently, promptly and accurately understanding the TCM syndrome pattern of a disease can reshape global health and welfare.

In recent years, with the successive outbreaks of SARS, influenza A (H1N1), influenza A (H7N9), COVID-19, and other viruses, viral pneumonia has become a sustained and widespread disease burden in many countries and globally. As with other diseases, the accurate identification of syndrome patterns is a prerequisite for the TCM-based prevention and treatment of viral pneumonia. Numerous studies have reported that the cold and hot syndromes are the pivotal TCM syndrome patterns in cases of viral pneumonia, such as SARS and COVID-19 [8-10]. Cold and hot syndromes, originating from the *Huangdi Neijing*, are 2 key components of the Eight Principle Syndromes—the general principles of dialectical treatment, which include cold and hot, sthenia and asthenia, exterior and interior, and yin and yang—and are used to identify the nature of a disease, reflecting disruptions in body homeostasis [11-13]. Cold syndrome–related expressions include coldness, cold pain, tastelessness, and clear, abundant urine, whereas hot syndrome is mainly characterized by heat, diaphoresis, a flushed face, burning pain, and deep-colored urine. The cold and hot syndrome framework has been widely applied in the diagnosis and treatment of viral pneumonia. Treating cold and hot syndromes within TCM has been shown to significantly alleviate clinical symptoms in patients with viral pneumonia [8,14]. For example, symptomatic treatments with Chinese medicines such as Lianhua Qingwen capsules and Xuanfeibaidu granules can markedly reduce the incidence of severe or critical events and improve clinical recovery [6,7], indicating that the prediction and differentiation of cold and hot syndromes play a vital role in the treatment of viral pneumonia.

Nevertheless, although clinical data and studies have indicated that TCM treatments for the cold and hot syndromes of viral pneumonia are effective, a major challenge remains in distinguishing between these syndromes—similar to the challenges in identifying other TCM syndrome patterns. Specifically, (1) the differentiation of cold and hot syndrome is recondite and lacks a solid scientific foundation in classical TCM theory, and (2) the accuracy of cold and hot syndrome diagnosis in TCM relies heavily on the physicians' skills and years of clinical experience. Subjective factors play a decisive role in TCM diagnosis, which inevitably leads to a lack of standardized criteria and an objective diagnostic basis for cold and hot syndromes. This unique diagnostic model not only supports the open and divergent development of TCM, but also hinders the understanding of cold and hot syndromes in viral pneumonia from a modern biomedical perspective. It further restricts the domestic and international dissemination of TCM syndrome differentiation, making it one of the key bottlenecks in the development of TCM. Therefore, in the process of integrating TCM with modern medicine, it is worth considering how to combine TCM syndrome theory with modern medicine to enhance the scientific rigor and objectivity of cold and hot syndrome differentiation in the treatment of viral pneumonia.

Recently, with the rapid development of machine learning [15-18], artificial intelligence has brought unprecedented challenges and opportunities to the diagnosis of TCM syndrome. Interdisciplinary models combining TCM and artificial intelligence have been proposed to model TCM knowledge, diagnosis, and treatment in clinical practice. Among these, numerous models have been developed to simulate the syndrome differentiation process of human TCM doctors for automatic syndrome diagnosis. For example, Huang et al [19] successfully identified the liver-gallbladder dampness-heat syndrome in patients with breast cancer using a dataset based on the prescriptions of TCM clinical practitioners. Zhuo et al [20] effectively differentiated Qi deficiency blood stasis syndrome and phlegm stasis in channels syndrome in patients with stroke through artificial intelligence–assisted retinal feature analysis. These examples demonstrate that machine learning enables a modern interpretation of the scientific connotation of TCM syndrome differentiation, supporting improved clinical decision-making in disease treatment. However, currently, there is still a lack of machine learning–based differentiation of cold and hot syndromes in viral pneumonia.

Among the machine learning algorithms in artificial intelligence, gradient boosting machine (GBM), logistic regression (LR), random forest (RF), extreme gradient boosting (XGB), and light gradient boosting machine (LGB), among others, have demonstrated promising performance [21-24]. Consequently, this study aimed to compare 8 machine learning methods, namely, GBM, LR, RF, XGB, LGB, ridge regression (RIDGE), least absolute shrinkage and selection operator (LASSO), and support vector machine (SVM), by integrating laboratory test indicators from modern medicine with the TCM cold and hot syndrome, to explore the connection between them and construct

XSL•FO
RenderX

a diagnostic model for differentiating the cold and hot syndromes in viral pneumonia. This approach seeks to provide a new diagnostic method for the clinical differentiation of cold and hot syndromes in viral pneumonia and to offer new perspectives for the scientization, standardization, and objectivity of TCM syndrome differentiation theory in guiding treatment.

Methods

Source of Materials

In this study, a retrospective review of case sheets was conducted on samples from 1401 patients diagnosed with viral pneumonia between January 18 and November 6, 2021, at the Second People's Hospital of Lanzhou City in China. Samples were excluded based on the following criteria: (1) the diagnosis was not made using the Eight Principle Syndromes of TCM, and (2) the patient was diagnosed with both cold and hot syndrome patterns simultaneously. A total of 602 samples met the inclusion criteria. Samples with more than 20% (ie, 19/93 features) missing values were further excluded, resulting in 382 samples ultimately included for analysis. These comprised 97 negative samples (cold syndrome) and 285 positive samples (hot syndrome). Additionally, a stratified sampling strategy was applied to split the original dataset into training and internal test cohorts at an 8:2 ratio (details are provided in the "Performance Evaluation and Model Validation" section).

The external test cohort consisted of 83 patients with viral pneumonia diagnosed with either cold or hot syndrome at Lanzhou Heavy Ion Hospital between July and August 2022. This cohort included 36 patients with the hot syndrome and 47 patients with the cold syndrome.

TCM and Modern Medicine Features Collection and Cold and Hot Syndrome Diagnosis

As shown in Multimedia Appendix 1, a total of 93 features related to TCM and modern medicine were collected in this study, including 4 general information items, 19 TCM symptoms, 2 blood gas values, 10 viral pneumonia indicators, 27 biochemical indicators, 30 blood routine indicators, and 1 coagulation indicator. Among these, patients' TCM symptoms were further quantified using a TCM symptom scoring scale for viral pneumonia (Multimedia Appendix 2).

All patients with viral pneumonia were independently diagnosed with either the TCM cold or hot syndrome by 2 TCM chief physicians. If both physicians provided the same diagnosis, the patient was enrolled. In cases of disagreement, a third investigator participated in the discussion to reach a consensus. The diagnostic criteria for syndrome differentiation were based on the textbooks *TCM Diagnostics* [25] and *Guiding Principles of Clinical Research on New Drugs of Traditional Chinese Medicine* [26]. These criteria include the 4 classical diagnostic methods used to determine TCM cold and hot syndrome patterns: inspection, auscultation, inquiry, and palpation, to accurately record the TCM characteristics.

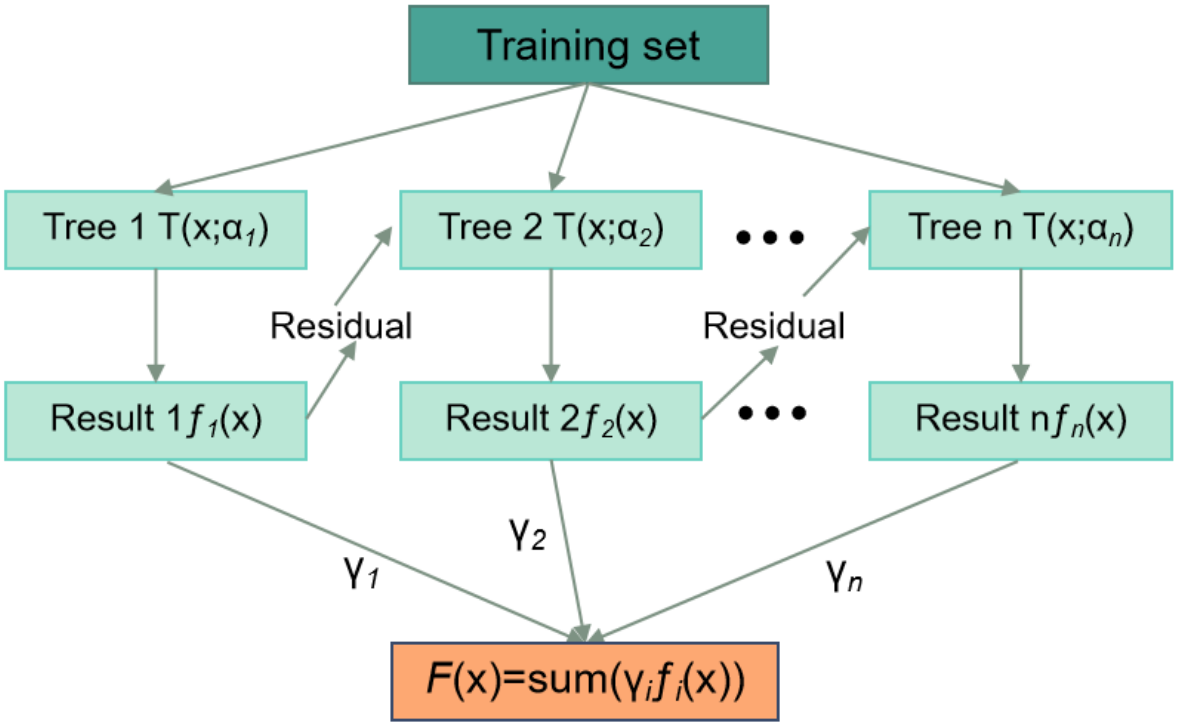
Model Training

In this study, 8 machine learning algorithms (GBM, LR, RF, XGB, LGB, RIDGE, LASSO, and SVM) were used to train a dataset containing all features, and GBM was selected as the final classification model. As shown in Figure 1, GBM operates on the principle of ensemble learning, constructing the final prediction model by iteratively training a series of weak learners, typically decision trees. The core mechanism of GBM lies in its ability to correct the prediction errors of previous decision trees. Each newly generated decision tree is trained to fit the residuals—the differences between the actual values and the predicted values—of the previous model, thereby continuously reducing the overall loss function. Specifically, GBM begins by constructing an initial decision tree based on the training data, and then calculates the prediction error of this tree. A second tree is built to model the residuals, with its predictions aimed at correcting the deficiencies of the first tree. This process continues iteratively until a preset number of iterations is reached or a stopping condition is met. Figure 1 illustrates the structure and decision-making process of multiple decision trees in the GBM model. Each decision tree branches based on input features, and the final prediction is obtained through a weighted sum of the predictions from all individual trees.

The number of top-ranking indexes was gradually increased, and the hyperparameters n_estimators and max_depth were tuned. The final model consisted of 13 top-ranking features, with n_estimators and max_depth set to 797 and 8, respectively. The GBM was implemented using the scikit-learn library (version 0.24.1) in Python (version 3.8.8; Python Foundation).

XSL•FO
RenderX

Figure 1. Gradient boosting machine decision tree composition and prediction flowchart.



Optimal Feature Ascertainment

"Feature importance," "coef," and "SHAP values" are 3 commonly used methods to assess the relationship between features and machine learning models, and they have received significant attention in recent research [27]. These methods calculate the relevance of each feature to the model's predictions, which are then ranked in descending order to produce a feature importance ranking.

In tree-based models (eg, GBM, RF, XGB, LGB), feature importance is typically evaluated from 2 perspectives: split count and split gain. Split count refers to how often a particular feature is selected as a splitting point during tree construction; a higher count indicates greater importance. By contrast, split gain measures the improvement in the model's objective function (eg, squared error loss) resulting from splitting on a given feature. A larger gain implies a greater contribution to model performance and hence higher importance. Additionally, SHAP (Shapley Additive Explanations) values offer a unified measure of feature importance based on game theory by calculating the marginal contribution of each feature to the model's prediction. SHAP values provide both global and local interpretability of the model. In linear models (eg, RIDGE, LASSO, SVM, and LR), "coef" represents the coefficients assigned to each feature. These coefficients indicate the strength and direction of the linear relationship between each feature and the target variable. SHAP values can complement these coefficients by revealing nonlinear effects and feature interactions that may not be captured by standard linear models.

The insights gained from these methods, especially when combining traditional feature importance metrics with SHAP analysis, can aid researchers in uncovering hidden data patterns and insights, thereby supporting scientific investigations and informing practical applications. Accordingly, these methods are used to rank the feature importance for cold and hot syndromes of viral pneumonia and to ascertain the optimal features.

Performance Evaluation and Model Validation

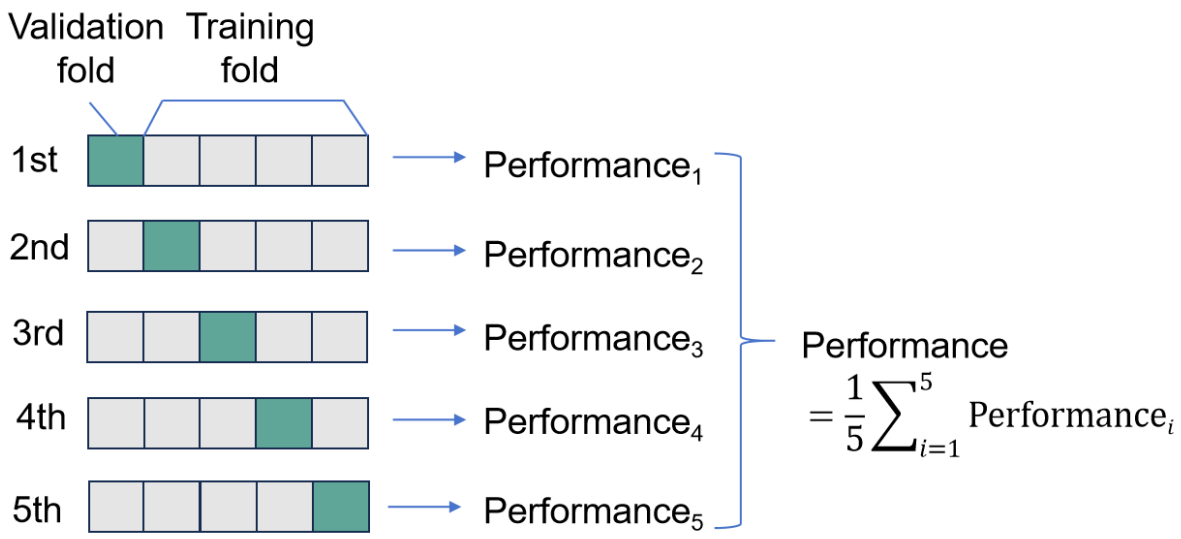
During the data preprocessing stage, a stratified sampling strategy was adopted to divide the original dataset, ensuring an 8:2 ratio between the training and validation sets. This approach preserved the proportional distribution of each class (cold and hot syndromes) as in the original dataset, thereby avoiding model evaluation bias due to imbalanced category distributions.

Given the relatively small sample size, 5-fold cross-validation was applied to ensure model accuracy and reliability. As illustrated in Figure 2, the dataset was divided into 5 nonoverlapping subsets of equal size. In each round of validation, 1 subset was selected as the validation set (the blue portion in the figure), while the remaining 4 subsets constituted the training set (gray portions). This process was repeated for 5 rounds. In the first round, the first subset was the validation set, and the remaining 4 were used as the training set, resulting in Performance_1. In the second round, the second subset was used for validation, and so on, resulting in Performance_2 through Performance_5. The final model performance was calculated as the average of these 5 evaluation results, with the formula $\text{Performance} = \sum i = 15\text{Performancei}$. This strategy ensured that each sample was used for both training and validation, reduced the variance caused by random sample

XSL•FO
RenderX

division, and improved the robustness and reliability of the model evaluation [28].

Figure 2. The 5-fold cross-validation process diagram.



In addition, a comprehensive evaluation of the model was conducted using commonly used metrics, including sensitivity, specificity (SPE), accuracy (ACC), Matthews correlation coefficient (MCC), and area under the curve (AUC). These metrics are calculated based on the values of true positives (TPs), true negatives (TNs), false positives (FPs), and false negatives (FNs), as defined below:

(1)Sens=TP+FNTP

(2)Spec=TNTN+FP

(3)ACC=TP+TNTP+TN+FP+FN

(4)MCC=TP·TN−FP·FN(TP+FP)(TP+FN)(TN+FP)(TN+FN)

The receiver operating characteristic curve, also known as the sensitivity curve, is a graphical representation of the performance of a classification model across various evaluation thresholds. It plots the true-positive rate against the false-positive rate at different threshold settings. The true-positive rate reflects the proportion of actual positive cases correctly identified by the model, while the false-positive rate represents the proportion of negative cases incorrectly classified as positive. The AUC provides a single summary metric of the classifier's overall performance, with values ranging from 0 to 1. A higher AUC value indicates better classification performance. Therefore, AUC is widely used as a standard metric to evaluate the performance of classification models. The formula for calculating AUC is as follows:

(5)AUC=∫01TPR(FDR) dFDR

Ethical Considerations

The study was approved by the Medical Ethics Review Committee of the Second People's Hospital of Lanzhou City and Lanzhou Heavy Ion Hospital (approval number 2021-026-01). Informed consent was obtained on an opt-out basis, and all data were anonymized. No financial or material incentives were provided to participants.

Statistical Analysis

All data were analyzed using SPSS version 27.0 (IBM Corp). Categorical variables are presented as counts and percentages, whereas continuous variables are reported as means and SDs or IQRs, as appropriate. Normality was assessed using the Kolmogorov-Smirnov test. Student 2-tailed *t* test was used to compare parametric continuous variables, while the Mann-Whitney *U* test was used for nonparametric variables, the χ^2 test was applied for categorical variables, and the Fisher exact test was used for 2×2 contingency tables. Binomial distribution tests were performed for each feature within the cold syndrome and hot syndrome groups. No correction for multiple comparisons was applied. A 2-sided $P<.05$ was considered statistically significant.

Results

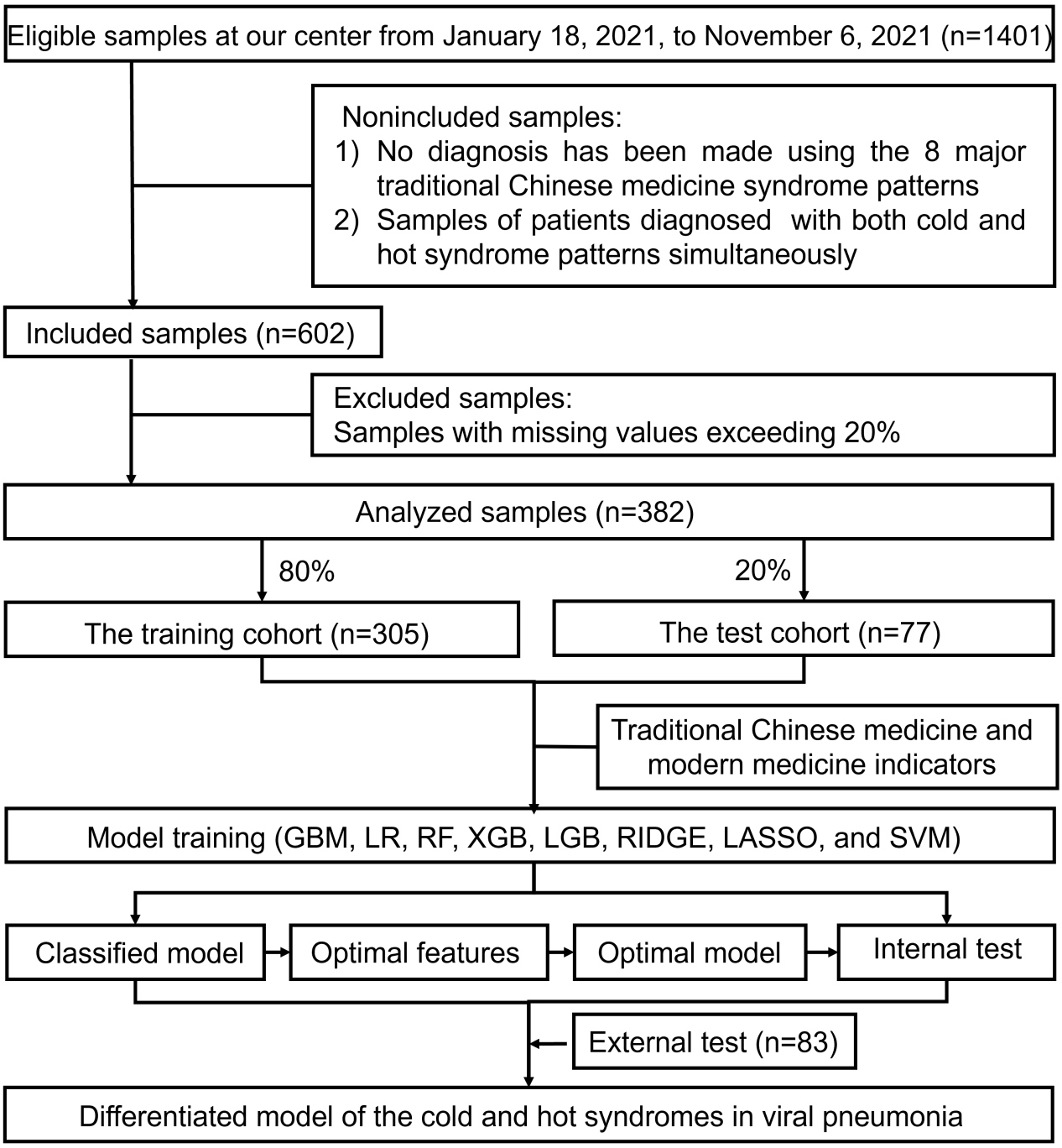
Data Extraction

We included only individual samples from patients with viral pneumonia and excluded those that were not diagnosed using the Eight Principle Syndromes (cold and hot, sthenia and asthenia, exterior and interior, and yin and yang), as well as those simultaneously diagnosed with cold and hot syndrome. A total of 602 eligible samples were retained. Samples with more than 20% (ie, 19/93 features) missing values were further excluded, and the remaining missing values were imputed using the median of each variable. Ultimately, 382 complete samples were included in the final analysis and used to construct the mathematical model. The dataset was split into training and testing sets in an 8:2 ratio. Subsequently, by integrating indicators from TCM and modern medicine and applying 8

XSL•FO
RenderX

machine learning algorithms, we identified the optimal model for differentiating TCM cold-hot syndromes in viral pneumonia through 5-fold cross-validation. The model's performance was further assessed using an external validation cohort. The data processing workflow and model construction process are illustrated in Figure 3.

Figure 3. Research flow for data processing and predictive model construction. After preliminary screening of the collected data, 382 samples of patients with viral pneumonia with TCM cold and hot syndromes were obtained. The dataset was randomly divided into training and test sets in an 8:2 ratio. Traditional Chinese medicine and modern medical indicators were extracted through data processing and statistical analysis. The performance of the 8 machine learning models (gradient boosting machine [GBM], logistic regression [LR], random forest [RF], extreme gradient boosting [XGB], light gradient boosting machine [LGB], ridge regression, least absolute shrinkage and selection operator [LASSO], and support vector machine [SVM]) was evaluated. Based on a comprehensive evaluation of all models, the optimal classification algorithm and feature set were identified. The final model's performance was further assessed using internal and external test cohorts.



Model Training Based on TCM and Modern Medicine Features

Modern medical indicators based on laboratory testing provide the possibility for intelligent discrimination of TCM syndromes. Therefore, in this study, modern medical indicators were integrated with TCM features for further exploration. A total of 93 features were used to construct the model. The evaluation metrics for models using all 93 features are presented in Table 1 and Figure 4A. We found that GBM and LGB achieved the highest AUC scores of 0.8329 and 0.7693, respectively, indicating their superior overall discriminative performance.

XSL•FO
RenderX

GBM also obtained the highest ACC score of 0.8000, closely followed by RIDGE with a score of 0.7475, suggesting strong overall classification accuracy. LASSO, RIDGE, and GBM achieved the highest sensitivity scores of 0.8430, 0.8388, and 0.8283, respectively, indicating good performance in correctly identifying positive samples and reducing false negatives. SVM, LGB, RF, and GBM achieved the highest specificity scores, suggesting these models had the lowest false-positive rates. Both GBM and LGB also achieved relatively high MCC scores of 0.5043 and 0.4068, respectively, demonstrating their effectiveness in handling imbalanced datasets.

Internal validation showed that GBM, RF, and XGB achieved the highest AUC scores of 0.7085, 0.7477, and 0.7146, respectively. Additionally, we calculated the confusion matrix for each model in the internal validation cohort, as shown in Figure 4B. The sum of correctly predicted cold and hot samples reflects the overall predictive accuracy of each model. GBM, LR, RF, XGB, LGB, RIDGE, LASSO, and SVM correctly predicted 53, 52, 53, 57, 56, 49, 53, and 52 cold and hot samples, respectively. These findings further demonstrate the effectiveness of these models in distinguishing cold and heat patterns in viral pneumonia.

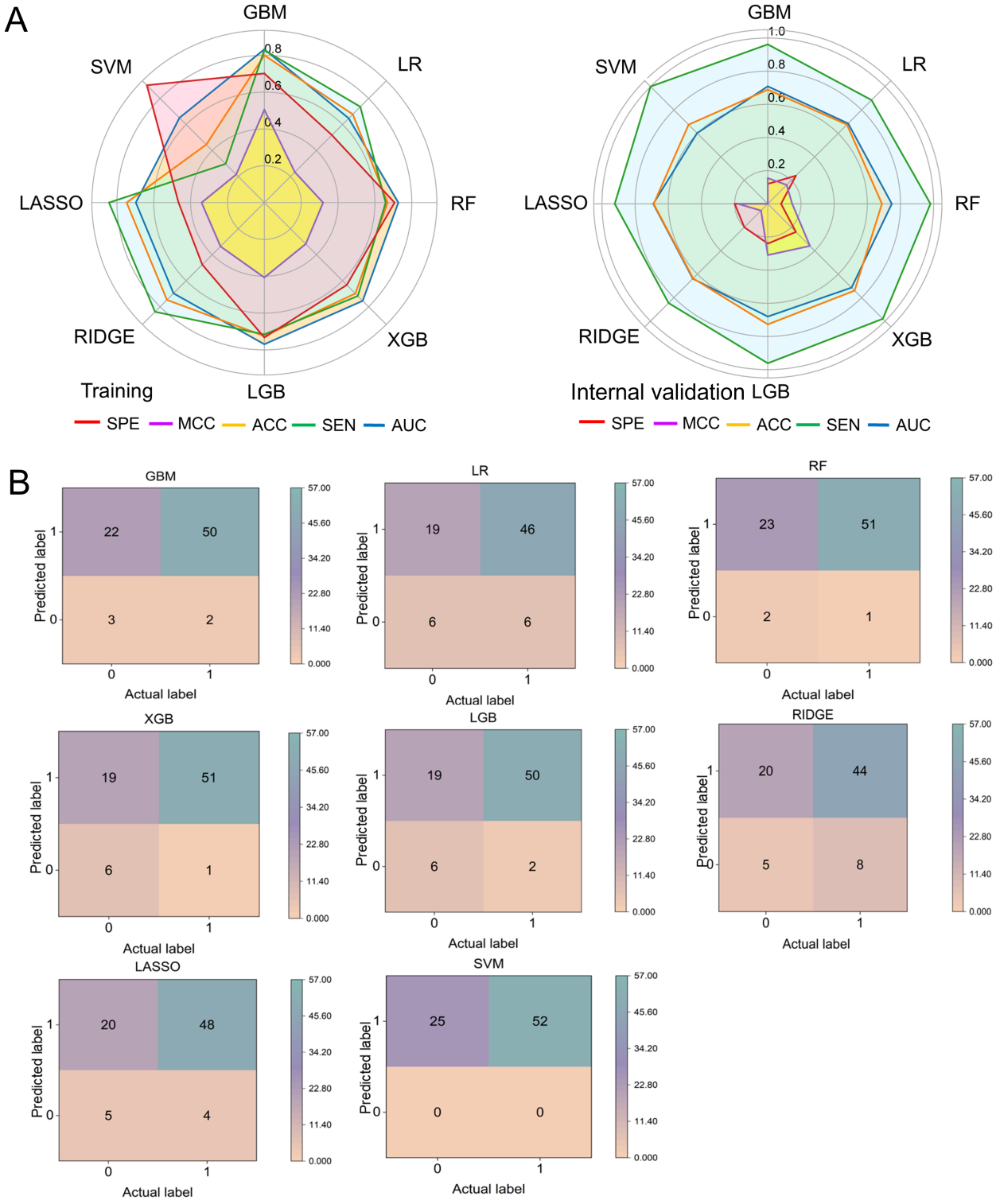
Overall, the results suggest that models incorporating both TCM and modern medicine features exhibit strong predictive performance for differentiating between cold and hot syndromes in viral pneumonia. Among them, the GBM algorithm demonstrated a particularly prominent discriminative capability. Therefore, GBM was selected as the optimal classified model based on the full set of 93 features for subsequent analysis.

Table . Comparison of models based on 5-fold cross-validation results using 93 features from traditional Chinese medicine and modern medicine.

Data cohort and evaluation	Gradient boosting machine	Logistic regression	Random forest	Extreme gradient boosting	Light gradient boosting machine	Ridge regression	Least absolute shrinkage and selection operator	Support vector machine
Training								
Area under the curve	0.8329	0.6477	0.7272	0.7546	0.7693	0.6970	0.6974	0.6514
Accuracy	0.8000	0.6787	0.6689	0.6984	0.7246	0.7475	0.7475	0.4459
Sensitivity	0.8283	0.7365	0.6582	0.7172	0.7158	0.8388	0.8430	0.2975
Specificity	0.7016	0.5187	0.7066	0.6326	0.7327	0.4764	0.4656	0.9018
Matthews correlation coefficient	0.5043	0.2341	0.3190	0.3177	0.4068	0.3364	0.3407	0.2161
Internal validation								
Area under the curve	0.7085	0.6854	0.7477	0.7146	0.6800	0.6392	0.6908	0.6031
Accuracy	0.6883	0.6753	0.6883	0.7403	0.7273	0.6364	0.6883	0.6753
Sensitivity	0.9615	0.8846	0.9808	0.9808	0.9615	0.8462	0.9231	1.0000
Specificity	0.1200	0.2400	0.0800	0.2400	0.2400	0.2000	0.2000	0.0000
Matthews correlation coefficient	0.1549	0.1609	0.1471	0.3596	0.3093	0.0577	0.1794	0.0000

XSL•FO
RenderX

Figure 4. Performance evaluation of the cold and hot syndrome identification models based on integrated traditional Chinese medicine (TCM) and modern medical features. (A) Radar chart comparing the performance of 8 machine learning models in the training and internal validation cohorts. (B) Confusion matrix analysis of the 8 models in the internal validation cohort. ACC: accuracy; AUC: area under the curve; GBM: gradient boosting machine; LASSO: least absolute shrinkage and selection operator; LGB: light gradient boosting machine; LR: logistic regression; MCC: Matthews correlation coefficient; RF: random forest; RIDGE: ridge regression; SEN: sensitivity; SPE: specificity; SVM: support vector machine; XGB: extreme gradient boosting.



Optimal Feature Ascertainment

Based on the optimum classified model (GBM) and the ranking of "feature importance," we identified 23 key features with importance values more than twice the median. These were temperature (T), red cell distribution width-SD (RDW-SD), creatinine (CREA), total bilirubin (TBIL), globulin (GLO), C-reactive protein (CRP), unconjugated bilirubin (IBIL), white blood cell (WBC), neutrophil percentage (NEU%), aspartate transaminase/alanine transaminase (AST/ALT), total cholesterol

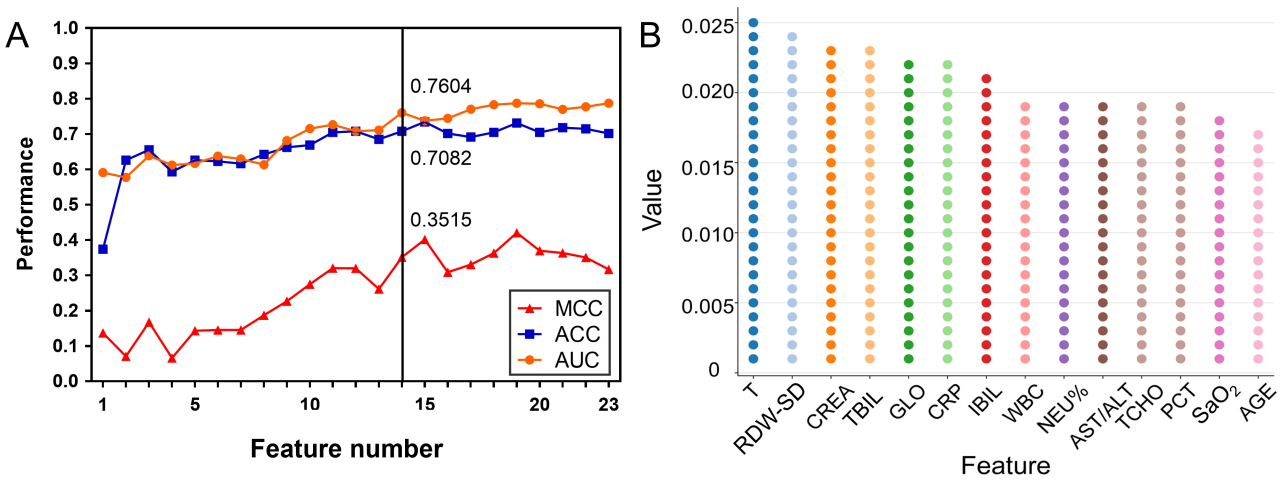
XSL•FO
RenderX

(TCHO), thrombocytocrit (PCT), oxygen saturation under load (SaO_2), age, platelets, mean platelet volume, lactate dehydrogenase, mean corpuscular hemoglobin concentration, urea, erythrocyte/red blood cell, Na, ORF1ab gene of novel coronavirus by nose test (nCovORF1ab), and albumin.

Subsequently, to identify the best-performing model with the fewest features, we examined how the number of top-ranked features influenced model performance (AUC, ACC, and MCC) using the GBM algorithm. As shown in Figure 5A and B, as the number of features increases, model performance gradually improves. Notably, at the 14-feature mark, the model achieved strong performance with an AUC of 0.7604, an ACC of 0.7082, and an MCC of 0.3515. To validate the robustness of our feature selection approach, we also used the SHAP feature importance ranking to select the top 14 features and construct a model. This model achieved an AUC of 0.7406, which was slightly lower than that obtained using the feature importance method (0.7604). Therefore, the feature importance method was ultimately retained as the feature selection approach for this study.

Finally, considering both the practicality of indicator testing and the feasibility of the clinical application, this study selected the top 14 features, excluding SaO_2 (under load), as the optimal set for differentiating between cold and hot syndromes in viral pneumonia. These features are temperature (T), RDW-SD, CREA, TBIL, GLO, CRP, IBIL, WBC, NEU%, AST/ALT, TCHO, PCT, and age (AGE), as illustrated in (Multimedia Appendix 3).

Figure 5. Identification of key features based on feature importance analysis and model cross-validation. (A) Effect of the number of selected key features (n=23) on model performance using the gradient boosting machine (GBM) algorithm. (B) Feature importance scores of the top 14 key features identified by the GBM model. ACC: accuracy; AUC: area under the curve; AST/ALT: aspartate transaminase/alanine transaminase; CREA: creatinine; CRP: C-reactive protein; GLO: globulin; IBIL: unconjugated bilirubin; MCC: Matthews correlation coefficient; NEU%: neutrophil percentage; PCT: thrombocytocrit; RDW-SD: red cell distribution width-SD; SaO_2: oxygen saturation under load; T: temperature; TBIL: total bilirubin; TCHO: total cholesterol; WBC: white blood cell.



Performance Evaluation and Optimal Model Establishment

To achieve optimal GBM model performance, we reconstructed the GBM model based on 13 optimizing features. Ultimately, the model was adjusted to threshold=0.99999, n_estimators=797, max_depth=8, min_samples_split=2, and min_samples_leaf=1. Simultaneously, the performance of the model with 13 features was further evaluated using 5-fold cross-validation, and the results suggested that the model performance was outstanding, as the average AUC value reached 0.7788 (Figure 6A). Model verification results showed that the AUC was 0.7645 by the internal test cohort (Figure 6B). Furthermore, the additional external test results showed that the model performance for AUC, ACC, sensitivity, specificity, and MCC is 0.8428, 0.6627, 0.7222, 0.6170, and 0.3369, respectively. These results validated the excellent performance of the model.

Moreover, we found that the temperature in the hot syndrome group was significantly higher than in the cold syndrome group (P=.02). By contrast, RDW-SD (P<.001), NEU% (P=.01), TCHO (P=.003), PCT (P<.001), and AGE (P<.001) were significantly lower in the hot syndrome group compared with the cold syndrome group, as shown in Table 2 and Figure 7. These results align with previous studies, which have reported that temperature, AGE, CREA, and RDW-SD are closely associated with the severity of viral pneumonia [29-33], supporting the validity of our findings.

These results suggest that machine learning algorithms perform well in differentiating between TCM cold and hot syndromes in viral pneumonia. The optimal model was constructed using 13 key features (T, RDW-SD, CREA, TBIL, GLO, CRP, IBIL, WBC, NEU%, AST/ALT, TCHO, PCT, and AGE), combined with the GBM algorithm. Among these, temperature (T), RDW-SD, NEU%, TCHO, PCT, and AGE appear to be the most relevant features for predicting cold and hot syndrome.

XSL•FO
RenderX

Figure 6. ROC curves and corresponding AUCs for cross-validation on the training and test sets. (A) ROC curve and classification performance of the final model set on the training set using 5-fold cross-validation. The x-axis represents the false-positive rate (FPR), and the y-axis represents the true-positive rate (TPR). (B) ROC curve and classification performance of the final model on the test set. The x-axis represents the FPR, and the y-axis represents the TPR. AUC: area under the curve; GBM: gradient boosting machine; ROC: receiver operating characteristic.

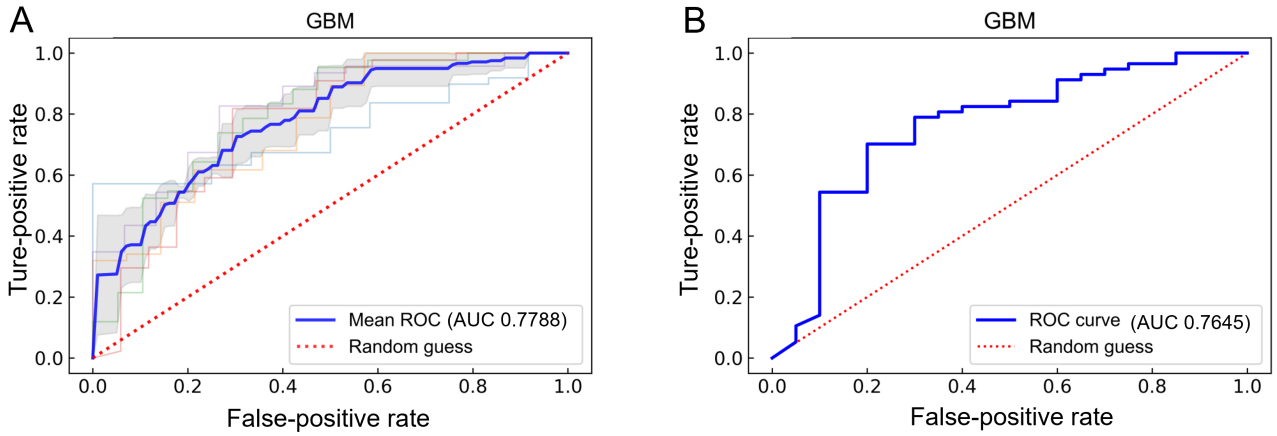
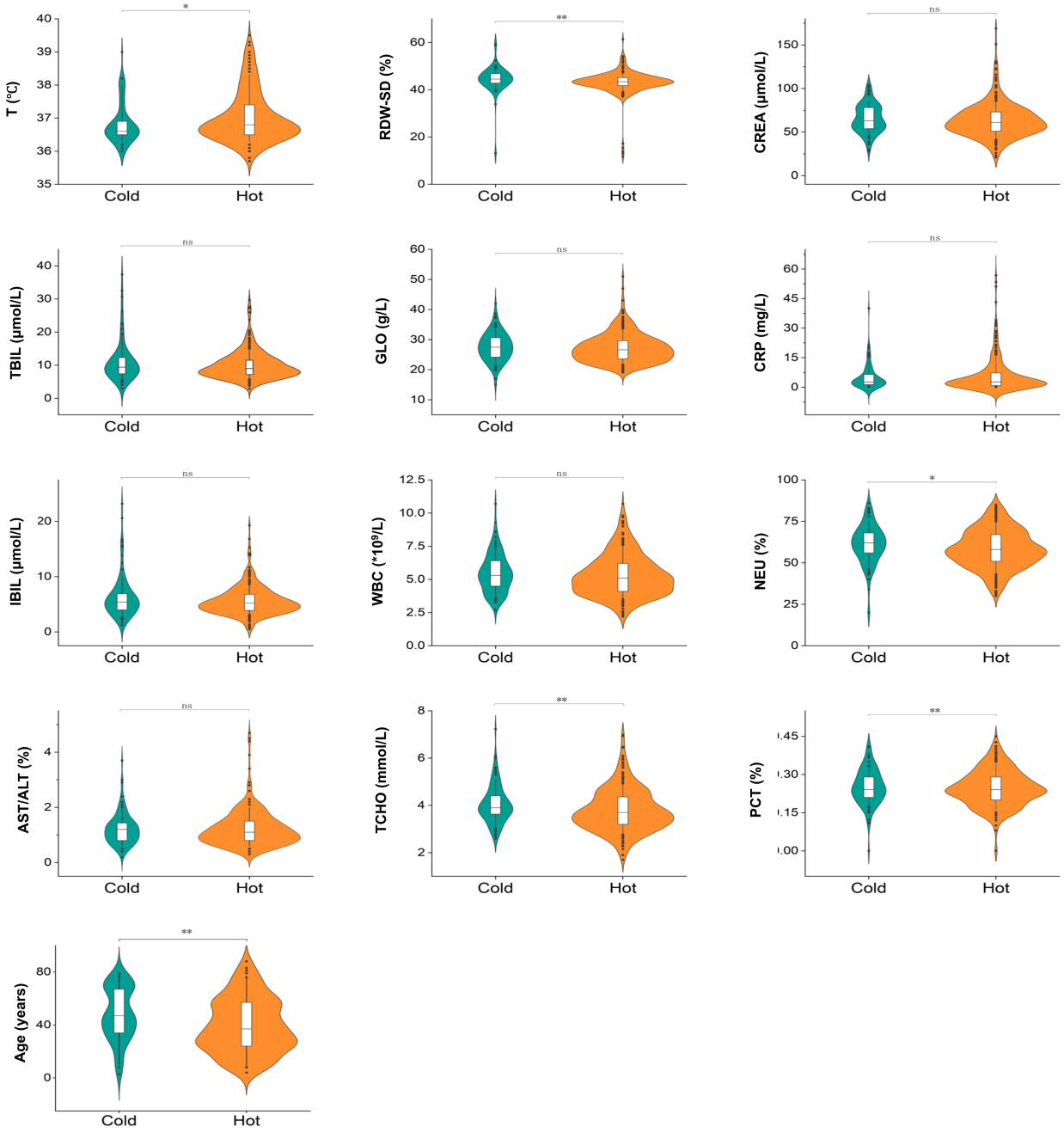


Table . The 13 optimal features for distinguishing between cold and hot syndromes in analysis.

Clinical features	Cold (n=97), median (IQR)	Hot (n=285), median (IQR)	*P* value
Temperature (°C)	36.600 (36.500-36.950)	36.800 (36.500-36.95)	.02
Red cell distribution width (%)	44.500 (42.800-46.850)	43.400 (41.80-45.100)	<.001
Creatinine (μmol/L)	63.000 (54.000-78.000)	61.000 (51.000-73.500)	.13
Total bilirubin (μmol/L)	9.400 (7.350-12.450)	9.000 (7.200-11.550)	.31
Globulin (g/L)	27.500 (24.150-30.750)	26.600 (23.600-29.600)	.18
C-reactive protein (mg/L)	2.670 (1.355-6.530)	2.670 (0.865-7.235)	.41
Unconjugated bilirubin (μmol/L)	5.400 (4.000-6.900)	5.200 (3.900-6.800)	.28
White blood cell ($\times10^9$/L)	5.300 (4.450-6.400)	5.100 (4.100-6.250)	.22
Neutrophil percentage (%)	62.000 (56.000-68.500)	58.000 (50.500-67.000)	.01
Aspartate transaminase/alanine transaminase (%)	1.200 (0.800-1.445)	1.100 (0.800-1.500)	.68
Total cholesterol (mmol/L)	3.900 (3.630-4.400)	3.700 (3.190-4.365)	.003
Thrombocytocrit (%)	0.240 (0.210-0.290)	0.240 (0.200-0.290)	<.001
Age (years)	47.000 (34.000 - 67.000)	37.000 (24.000 - 57.000)	<.001

XSL•FO
RenderX

Figure 7. Violin plots showing the relationships between cold and hot syndromes and the expression levels of optimal clinical features. The horizontal axis represents the different syndromes (cold and hot), while the vertical axis indicates the expression levels of the corresponding clinical features. The plots illustrate the distribution and density of feature values, highlighting differences between the 2 syndrome groups. AST/ALT: aspartate transaminase/alanine transaminase; CREA: creatinine; CRP: C-reactive protein; GLO: globulin; IBIL: unconjugated bilirubin; NEU%: neutrophil percentage; ns: not significant; PCT: thrombocytocrit; RDW-SD: red cell distribution width-SD; T: temperature; TBIL: total bilirubin; TCHO: total cholesterol; WBC: white blood cell; *P<.05, **P<.01 versus the cold.



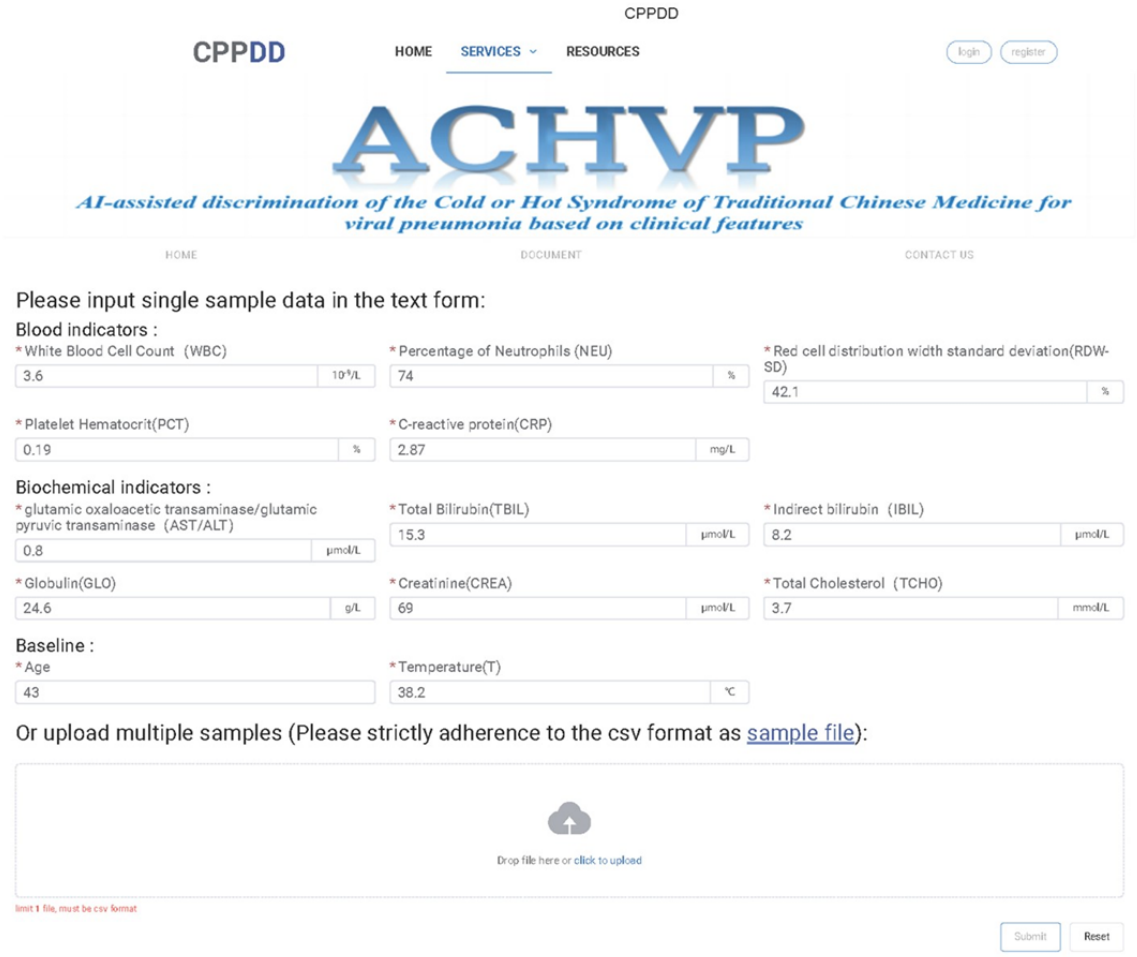
Interactive Web Server

To enhance user experience, an interactive web server named ACHVP was developed in this study, allowing users to test, explore, and experience the proposed method. The platform is designed to be highly convenient and user-friendly—users simply input relevant numerical data into designated textboxes and click the “Submit” button. The system then performs comprehensive data processing and analysis, presenting the predicted syndrome classification results on the output interface. The home page of the web server, developed for identifying cold and hot syndrome patterns in patients with viral pneumonia, is illustrated in Figure 8. The server is deployed in a Linux environment. The backend is developed in Python using the FastAPI framework to ensure efficient data processing and application programming interface management, while the front end is built with JavaScript and the Vue.js framework for a responsive and interactive user interface. Users can access the web server via any standard web browser, such as Google Chrome, Mozilla Firefox, or Safari, using the link specified in [34]. This web-based tool demonstrates significant potential as a practical diagnostic aid, facilitating early detection of cold and hot syndromes in patients with viral pneumonia. It can support TCM practitioners in syndrome differentiation and

XSL•FO
RenderX

guide more precise Chinese herbal medicine prescriptions in clinical practice.

Figure 8. Web server of the ACHVP method.



Discussion

Principal Findings

Dialectical treatment is a fundamental principle in TCM for diagnosing and treating diseases, with cold and hot syndromes serving as 2 key components for identifying the nature of illness [11,35-38]. In recent years, the study of TCM cold and hot syndrome has become a focal point in disease research. Numerous studies have shown that cold and hot syndromes also exhibit major TCM diagnostic patterns in various viral pulmonary diseases, including COVID-19 and SARS [8,14]. Based on these syndrome classifications, TCM has demonstrated a prominent role in alleviating symptoms, shortening treatment duration, and reducing the progression to severe pneumonia in patients with viral pneumonia [39-43]. For example, formulas such as Hanshiyi for cold syndrome [44] and Jinhua Qinggan Granules for hot syndrome have shown favorable clinical efficacy [45]. Therefore, the rapid, accurate, and specific identification of cold or hold syndrome is essential for the effective application of TCM in the treatment of viral pulmonary diseases. However, the abstract and complex nature of TCM syndrome differentiation poses challenges in accurately distinguishing between cold and hot syndromes in clinical practice. Machine learning offers a promising solution to this challenge by supporting clinicians in syndrome differentiation and facilitating more precise treatment decisions. Consequently, there is an urgent need to integrate TCM theories of cold and hot syndromes with modern laboratory diagnostics and machine learning approaches to advance the modernized differentiation and treatment of viral pneumonia.

In this study, 8 machine learning algorithms were applied to develop and evaluate a model for differentiating TCM cold and hot syndromes in viral pneumonia, using clinical data from 1484 patients across 2 medical centers. Among the models incorporating both TCM and modern medical features, the GBM model demonstrated superior learning capability, achieving an AUC of 0.8329. This indicates that GBM was particularly effective in distinguishing cold and hot syndromes based on a given dataset. The “feature importance” method of the GBM model was subsequently used to rank all features, from which the top 13 features were selected based on the highest AUC value. To validate the model’s effectiveness and generalizability, both internal and external test sets were used, each demonstrating strong discriminatory performance. As a result, the optimal model was constructed using the GBM algorithm and 13 selected features (T, RDW-SD, CREA, TBIL, GLO, CRP, IBIL, WBC, NEU%, AST/ALT, TCHO, PCT, and AGE), achieving an AUC of 0.7788. These findings suggest that

XSL•FO
RenderX

effectively combining modern medical indicators, primarily based on laboratory tests, with TCM features primarily based on clinical observation may offer a viable pathway toward the modernization of TCM syndrome differentiation. This approach provides a foundation for the objectification and standardization of TCM diagnostic practices. Furthermore, the proposed model holds promise as a practical tool to assist clinicians in accurately identifying cold and hot syndromes in viral pneumonia, thereby informing appropriate and individualized treatment strategies.

Comparison With Prior Work

Machine learning, as an advanced artificial intelligence technology, has demonstrated broad potential in the field of "artificial intelligence+TCM diagnoses." For example, Zhang et al [46] proposed a comprehensive model using convolutional neural networks to classify 187 types of TCM diseases. Wen et al [47] also applied deep neural networks to identify tongue image data and determine patients' constitutions, effectively addressing the imbalance problem among constitution categories. However, limited research has focused on identifying TCM cold and hot syndromes in viral pneumonia by integrating both TCM theory and modern medicine through machine learning approaches. Although some scholars have attempted to explore the cold and hot attributes of diseases to guide clinical treatment, most studies have been limited to network analysis, clustering, or laboratory testing, without incorporating artificial intelligence methods. For instance, Li et al's [11] network analysis revealed that the leptin biomarker indicated low levels of energy metabolism in patients with cold syndrome, while the human monocyte chemoattractant protein-1 (CCL2/MCP1) biomarker suggested intensified immune regulation in patients with hot syndrome, based on a study involving patients with chronic superficial gastritis and chronic atrophic gastritis. Wang et al [13] differentiated heat and cold patterns in rheumatoid arthritis through cluster and factor analyses to guide clinical medication. Wu et al [48] investigated TCM cold and hot constitutions using pulse wave parameters such as augmentation index and heart rate variability. Although some individual studies have applied artificial intelligence to differentiate cold and hot properties, most efforts have been limited to identifying the properties of Chinese herbal medicines. For example, Lin et al [49] developed a classification strategy for the cold and hot properties of Chinese herbal medicines using artificial intelligence and biological experiments. Wei et al [50] applied machine learning techniques to intelligently identify the cold-hot nature of Chinese herbal medicines based on the similarity of their volatile oil ingredients. Therefore, this study innovatively constructs a model for differentiating cold and hot syndromes in viral pneumonia using machine learning approaches that integrate TCM and modern medicine, aiming to assist in diagnosis and medication guidance for viral pneumonia in clinical practice.

It is worth noting that in this study, we collected a large number of clinical features, including patients' symptoms, signs, laboratory examination results, and other relevant information, which were essential for training and testing the machine learning models. As shown in Table 3, based on the model training results using only 19 TCM features, we found that the AUC values of GBM, LR, RF, XGB, LGB, RIDGE, LASSO, and SVM were 0.6942, 0.6317, 0.6783, 0.6787, 0.6055, 0.6151, 0.6145, and 0.5874, respectively. Meanwhile, the study also attempted to build models using only 70 laboratory results. The AUC values for GBM, LR, RF, XGB, LGB, RIDGE, LASSO, and SVM were 0.6799, 0.6282, 0.6797, 0.6910, 0.7345, 0.6637, 0.6157, and 0.6618, respectively. Among them, the GBM model constructed using TCM features achieved an AUC of 0.6942, outperforming the GBM model constructed using laboratory features, which had an AUC of 0.6799. Internal validation and the confusion matrix results also demonstrated performance consistent with the training results, as shown in Multimedia Appendix 4. These findings suggest that the models possess auxiliary diagnostic value for differentiating TCM cold and hot syndromes in viral pneumonia.

XSL•FO
RenderX

Table . Comparison of model results by 5-fold cross-validation based on different features of traditional Chinese medicine and modern medicine.

Features and evaluation	Gradient boosting machine	Logistic regression	Random forest	Extreme gradient boosting	Light gradient boosting machine	Ridge regression	Least absolute shrinkage and selection operator	Support vector machine
Traditional Chinese medicine								
Area under the curve	0.6942	0.6317	0.6783	0.6787	0.6055	0.6151	0.6145	0.5874
Accuracy	0.6851	0.5312	0.5509	0.6031	0.5155	0.5180	0.5049	0.7508
Sensitivity	0.7365	0.4737	0.5077	0.5908	0.4389	0.4258	0.4117	0.9928
Specificity	0.5804	0.7316	0.7457	0.7006	0.7233	0.7854	0.7723	0.2601
Matthews correlation coefficient	0.2737	0.1689	0.2145	0.2400	0.1332	0.1821	0.1563	0.2385
Modern medicine								
Area under the curve	0.6799	0.6282	0.6797	0.6910	0.7345	0.6637	0.6157	0.6618
Accuracy	0.7508	0.7508	0.7541	0.7672	0.7803	0.7639	0.7180	0.7639
Sensitivity	0.9441	0.9185	0.9742	0.9400	0.9314	0.8968	0.8539	1.0000
Specificity	0.1257	0.2105	0.0410	0.2067	0.2914	0.3324	0.2762	0.0000
Matthews correlation coefficient	0.1269	0.1585	0.0335	0.1927	0.2871	0.2672	0.1752	0.0000
Traditional Chinese medicine and modern medicine								
Area under the curve	0.8329	0.6477	0.7272	0.7546	0.7693	0.6970	0.6974	0.6514
Accuracy	0.8000	0.6787	0.6689	0.6984	0.7246	0.7475	0.7475	0.4459
Sensitivity	0.8283	0.7365	0.6582	0.7172	0.7158	0.8388	0.8430	0.2975
Specificity	0.7016	0.5187	0.7066	0.6326	0.7327	0.4764	0.4656	0.9018
Matthews correlation coefficient	0.5043	0.2341	0.3190	0.3177	0.4068	0.3364	0.3407	0.2161

Based on “feature importance” or “coef,” the 8 models were further used to evaluate the significance of TCM features in distinguishing cold and hot syndromes of viral pneumonia. We found that, according to the significance values, there were 7 common features with importance values equal to or greater than the median in the GBM, RF, XGB, and LGB models, namely, fatigue, sore throat, fever, expectoration, cough, body pain, and diminished sense of smell. Interestingly, sore throat and fever also appeared among the features with importance values equal to or greater than the median in LR, RIDGE, LASSO, and SVM models. Based on this, we believe that fatigue, sore throat, fever, expectoration, cough, body pain, and diminished sense of smell may be the primary distinguishing factors for differentiating between cold and hot syndromes in the TCM diagnosis of viral pneumonia, which aligns with the key symptomatology commonly used by clinical TCM practitioners [51,52]. Therefore, more attention should be given to these features, especially sore throat and fever, in the discrimination of cold and hot syndromes in viral pneumonia, as shown in Multimedia Appendix 5. Unfortunately, the AUC values of these models did not exceed 0.7. We boldly speculate that this might be due to the quantification of TCM features not aligning with modern medical standards. Specifically, TCM features lack precise numerical values and are typically categorized as none, mild, moderate, or severe. Moreover, the identification of TCM features primarily relies on the subjective judgment of TCM practitioners and years of clinical experience, leading to a lack of standardization and objectivity. These factors may introduce noise and reduce the effectiveness of model training. Therefore, it is essential to develop objective indicators for TCM syndrome differentiation, further supporting the original intent of our study. In subsequent experiments, we integrated modern medicine features with TCM indicators and were pleasantly surprised to find that, compared with models trained solely on TCM features, those based on integrated TCM and modern medical features demonstrated superior performance in distinguishing cold and hot syndromes in viral pneumonia across 8 machine learning algorithms. This suggests that modern medical features can enhance the predictive value of TCM features.

In addition, the best model we developed indicated that the identification of cold and hot syndromes in viral pneumonia is

XSL•FO
RenderX

closely related to 13 features: temperature, RDW-SD, CREA, TBIL, GLO, CRP, IBIL, WBC, NEU%, AST/ALT, TCHO, PCT, and AGE. Numerous studies have reported that temperature (T), CRP, and WBC hold statistical significance in distinguishing TCM cold and hot syndromes in rheumatoid arthritis [53]. Furthermore, features such as AGE, NEU%, RDW-SD, and CRP are strongly associated with the severity of viral pneumonia and the development of chronic lung sequelae. For example, a study by Liu et al [33] suggested that AGE and NEU% could serve as predictive factors for the severity of viral pneumonia. Shen et al [31] also reported that RDW-SD is a key indicator for assessing the severity of viral pneumonia. Additionally, CRP and AGE play crucial roles in the diagnosis of viral pneumonia [54,55], which is consistent with the findings of this study.

Limitations

The accuracy of traditional TCM diagnosis of cold and hot syndromes largely depends on the skills and years of clinical experience of the practitioner. Subjective factors play a decisive role in this process. Compared with traditional TCM methods, the model developed in this study offers a more objective approach to differentiating cold and hot syndromes in viral pneumonia. It provides valuable decision support and medication guidance in clinical practice, especially for practitioners with limited TCM experience. This shift toward an objective, data-driven approach helps reduce reliance on subjective judgment, improves diagnostic accuracy, and ensures greater consistency in clinical decision-making. Additionally, the model can serve as a practical tool for TCM practitioners, especially in complex cases where traditional diagnostic methods may fall short.

Of course, this study has some limitations. First, it was a retrospective study, and all patient history data were obtained from the internal electronic medical record systems of the Second People's Hospital of Lanzhou and Lanzhou Heavy Ion Hospital. This may have introduced inaccuracies in the collection and recording of medical history, making it difficult to avoid information bias. Moreover, due to the limited clinical sample size, the conclusions, although statistically sound, require further validation and refinement in real-world applications to enhance the model's accuracy and stability.

In recent years, emerging large language models (LLMs) have demonstrated remarkable capabilities in natural language processing, knowledge integration, and complex reasoning [56]. Given the nature of TCM theory, which often involves complex textual descriptions and implicit knowledge, LLMs could potentially offer new perspectives for model development in this study. These models may better understand and integrate the rich, diverse information contained in TCM literature, clinical records, and expert knowledge, thereby enriching the feature set and enhancing the interpretability of the models. For instance, LLMs could analyze the semantic relationships among TCM symptoms, syndromes, and treatment methods, helping to extract more meaningful features that may be difficult to identify using traditional machine learning approaches. Moreover, LLMs could assist in standardizing and structuring the subjective and qualitative information in TCM, thereby reducing the impact of inconsistent data representation. However, applying LLMs also poses challenges, such as ensuring the reliability of the extracted knowledge, addressing potential biases inherent in pretrained models, and efficiently integrating LLM-derived features with existing laboratory test data. In future work, we plan to collect more data to establish a local database and explore the integration of LLMs with traditional machine learning algorithms. By fully leveraging the advantages of both approaches, we aim to further enhance the performance of the TCM cold and hot syndrome differentiation model and advance the modernization and standardization of TCM diagnosis.

Conclusion

This study aimed to establish a differentiation model for TCM cold and hot syndromes in patients with viral pneumonia using machine learning by exploring correlations between cold/hot syndromes and features from both TCM and modern medicine (such as general information, TCM characteristics, blood gas values, viral pneumonia indicators, biochemical indicators, routine blood test indicators, and coagulation indicators). We found that machine learning algorithms based on integrated TCM and modern medicine features outperformed models that used only TCM or only modern medicine features. Specifically, a model composed of 13 optimal features (T, RDW-SD, CREA, TBIL, GLO, CRP, IBIL, WBC, NEU%, AST/ALT, TCHO, PCT, and AGE) and the GBM algorithm effectively differentiated TCM syndromes. This study is the first to integrate the TCM cold and hot syndrome theory with laboratory-based modern medical tests using machine learning. By establishing the relationship between TCM syndrome theory (cold and hot syndromes) and indicators from both TCM and modern medicine, we aim to provide a new auxiliary diagnostic method for the clinical differentiation of cold and hot syndromes. This can support practitioners in making comprehensive diagnoses and identifying effective Chinese herbal medicine treatments, while also offering new insights for the modernization and scientific interpretation of TCM syndrome differentiation theory to guide treatment.

Acknowledgments

This study was supported by the Major Science and Technology Project of Gansu Province (grant 22ZD1FA001), the Provincial University Industry Support Project in Gansu (grant 2020C-36), the Young Elite Scientists Sponsorship Program by the Gansu Association for Science and Technology (grant GXH20210611-02), and the 2023 Longyuan Youth Innovation and Entrepreneurship Talent Project (Gan Group Tong Zi [2023] No. 20).

XSL•FO
RenderX

Data Availability

The datasets generated in this study are not publicly available due to hospital institutional review board regulations and patient privacy policies, but deidentified datasets are available from the corresponding author (YL) upon reasonable request. These deidentified datasets would include the model training set and the test set to facilitate independent model replications.

Authors' Contributions

XJ was responsible for formal analysis, investigation, project administration, writing the original draft, and reviewing and editing the manuscript. YW and JW contributed to the investigation, methodology, resources, supervision, validation, writing the original draft, and reviewing and editing. YH and QG were involved in formal analysis, investigation, methodology, writing the original draft, and reviewing and editing. LS and JZ participated in the investigation and methodology. JL, LL, and ZZ contributed to the investigation, methodology, resources, and supervision. SL was responsible for conceptualization, methodology, project administration, and reviewing and editing the manuscript. YL contributed to conceptualization, formal analysis, methodology, supervision, and reviewing and editing. All authors have read and approved the final manuscript.

Conflicts of Interest

None declared.

Multimedia Appendix 1
All clinical features information of patients with viral pneumonia.
[DOCX File, 18 KB - medinform_v13i1e64725_app1.docx]

Multimedia Appendix 2
The traditional Chinese medicine symptom scoring scale for patients with viral pneumonia.
[DOCX File, 19 KB - medinform_v13i1e64725_app2.docx]

Multimedia Appendix 3
The optimal features for the TCM cold and hot syndrome discrimination of viral pneumonia. AGE: age; AST/ALT: aspartate transaminase/alanine transaminase; CREA: creatinine; CRP: C-reactive protein; GLO: globulin; IBIL: unconjugated bilirubin; NEU%: neutrophil percentage; PCT: thrombocytocrit; RDW-SD: red cell distribution width-SD; T: temperature; TBIL: total bilirubin; TCHO: total cholesterol; WBC: white blood cell.
[PNG File, 588 KB - medinform_v13i1e64725_app3.png]

Multimedia Appendix 4
The performance evaluation of the cold and hot syndrome identification model based on traditional Chinese medicine (TCM) features. (A) The performance evaluation’s radar chart of the 8 models based on TCM features. (B) The confusion matrix analysis of the 8 models based on TCM features.
[DOCX File, 351 KB - medinform_v13i1e64725_app4.docx]

Multimedia Appendix 5
Heat diagram of traditional Chinese medicine features on 8 screened models (the values of gradient boosting machine, random forest, extreme gradient boosting, and light gradient boosting were obtained using feature importance, and those of ridge regression, least absolute shrinkage and selection operator, support vector machine, and logistic regression were obtained using coef).
[DOCX File, 1324 KB - medinform_v13i1e64725_app5.docx]

References

1. Gan X, Shu Z, Wang X, et al. Network medicine framework reveals generic herb-symptom effectiveness of traditional Chinese medicine. Sci Adv 2023 Oct 27;9(43):eadh0215. [doi: 10.1126/sciadv.adh0215] [Medline: 37889962]
2. Dong J. The relationship between traditional Chinese medicine and modern medicine. Evid Based Complement Alternat Med 2013;2013:153148. [doi: 10.1155/2013/153148] [Medline: 23983772]
3. Xu W, Zhang Z, Lu Y, Li M, Li J, Tao W. Traditional Chinese medicine Tongxie Yaofang treating irritable bowel syndrome with diarrhea and type 2 diabetes mellitus in rats with liver-depression and spleen-deficiency: a preliminary study. Front Nutr 2022;9:968930. [doi: 10.3389/fnut.2022.968930] [Medline: 36438735]
4. Song YN, Chen J, Cai FF, et al. A metabolic mechanism analysis of Fuzheng-Huayu formula for improving liver cirrhosis with traditional Chinese medicine syndromes. Acta Pharmacol Sin 2018 Jun;39(6):942-951. [doi: 10.1038/aps.2017.101] [Medline: 29072258]

XSL•FO
RenderX

5. Liu X, Li J, Wang Y, et al. To study the protective effect of Huangqi Baihe granules on radiation brain injury based on network pharmacology and experiment. J Ethnopharmacol 2023 Oct;315:116610. [doi: 10.1016/j.jep.2023.116610]
6. Huang K, Zhang P, Zhang Z, et al. Traditional Chinese medicine (TCM) in the treatment of COVID-19 and other viral infections: efficacies and mechanisms. Pharmacol Ther 2021 Sep;225:107843. [doi: 10.1016/j.pharmthera.2021.107843] [Medline: 33811957]
7. Ni L, Chen L, Huang X, et al. Combating COVID-19 with integrated traditional Chinese and Western medicine in China. Acta Pharm Sin B 2020 Jul;10(7):1149-1162. [doi: 10.1016/j.apsb.2020.06.009] [Medline: 32834946]
8. Li X, Liu W, He W, Xie Y, Li J. Meta-analysis of single-group rate of the distribution of traditional Chinese medicine syndromes in 2 139 patients with coronavirus disease 2019. Zhonghua Wei Zhong Bing Ji Jiu Yi Xue 2020 Jun;32(6):664-670. [doi: 10.3760/cma.j.cn121430-202000509-00372] [Medline: 32684209]
9. Wang SC, Sun YQ, Bian GB, Xu L, Ma R, Wang MQ. Clinical study on Qingfei oral liquid treating 507 cases of phlegm-heat obstructing lung syndrome in children virus pneumonia. World Chin Med 2016;11(9):1649-1653, 1658. [doi: 10.3969/j.issn.1673-7202.2016.09.001]
10. Deng TT. A discussion on diagnosis and treatment of SARS by traditional Chinese medicine. New Chin Med 2003(6):3-5. [doi: 10.13457/j.cnki.jncm.2003.06.001]
11. Li R, Ma T, Gu J, Liang X, Li S. Imbalanced network biomarkers for traditional Chinese medicine syndrome in gastritis patients. Sci Rep 2013;3:1543. [doi: 10.1038/srep01543] [Medline: 23529020]
12. Zhou N, Yang Y, Li K, et al. Integrating strategies of chemistry, biochemistry and metabolomics for characterization of the medication principle of “treating cold/heat syndrome with hot/cold herbs”. J Ethnopharmacol 2019 Jul 15;239:111899. [doi: 10.1016/j.jep.2019.111899] [Medline: 31039429]
13. Wang W, Guan J, Li Z, Wang X. Rheumatoid arthritis characteristics and classification of heat and cold patterns–an observational study. Heliyon 2023 Feb;9(2):e13439. [doi: 10.1016/j.heliyon.2023.e13439] [Medline: 36873147]
14. Feng Z, Xie Y, Chun L, Li J. Study on traditional Chinese medicine common syndrome characteristic of coronavirus disease 2019 based on latent structure combined with system clustering analysis. Zhonghua Wei Zhong Bing Ji Jiu Yi Xue 2020 May;32(5):537-543. [doi: 10.3760/cma.j.cn121430-20200506-00620] [Medline: 32576343]
15. Wu J, Yang Y, Cheng L, et al. GC discrimination: identification of gastric cancer based on a milliliter of blood. Brief Bioinformatics 2021 Jan 18;22(1):536-544. [doi: 10.1093/bib/bbaa006]
16. Jain P, Yedukondalu J, Chhabra H, Chauhan U, Sharma LD. EEG-based detection of cognitive load using VMD and LightGBM classifier. Int J Mach Learn Cyber 2024 Sep;15(9):4193-4210. [doi: 10.1007/s13042-024-02142-2]
17. Panda P, Bisoy SK, Panigrahi A, et al. BIMSSA: enhancing cancer prediction with salp swarm optimization and ensemble machine learning approaches. Front Genet 2025 Jan 6;15:1491602. [doi: 10.3389/fgene.2024.1491602] [Medline: 39834551]
18. Houkan A, Sahoo AK, Gochhayat SP, et al. Enhancing security in industrial IoT networks: machine learning solutions for feature selection and reduction. IEEE Access 2024;12:160864-160883. [doi: 10.1109/ACCESS.2024.3481459]
19. Huang WT, Hung HH, Kao YW, et al. Application of neural network and cluster analyses to differentiate TCM patterns in patients with breast cancer. Front Pharmacol 2020;11:670. [doi: 10.3389/fphar.2020.00670] [Medline: 32457636]
20. Zhuo YY, Wu JM, Kuang L, et al. The discriminative efficacy of retinal characteristics on two traditional Chinese syndromes in association with ischemic stroke. Evid Based Complement Alternat Med 2020;2020:6051831. [doi: 10.1155/2020/6051831] [Medline: 32308711]
21. Kwon O, Na W, Kang H, et al. Electronic medical record-based machine learning approach to predict the risk of 30-day adverse cardiac events after invasive coronary treatment: machine learning model development and validation. JMIR Med Inform 2022 May 11;10(5):e26801 [FREE Full text] [doi: 10.2196/26801] [Medline: 35544292]
22. Kim S, Park J, Son Y, et al. Development and validation of a machine learning algorithm for predicting diabetes retinopathy in patients with type 2 diabetes: algorithm development study. JMIR Med Inform 2025 Feb 7;13:e58107 [FREE Full text] [doi: 10.2196/58107] [Medline: 39924304]
23. Xu Q, Cai X, Yu R, et al. Machine learning-based risk factor analysis and prediction model construction for the occurrence of chronic heart failure: health ecologic study. JMIR Med Inform 2025 Jan 31;13:e64972 [FREE Full text] [doi: 10.2196/64972] [Medline: 39889299]
24. Chen X, Chen H, Nan S, Kong X, Duan H, Zhu H. Dealing with missing, imbalanced, and sparse features during the development of a prediction model for sudden death using emergency medicine data: machine learning approach. JMIR Med Inform 2023 Jan 20;11:e38590 [FREE Full text] [doi: 10.2196/38590] [Medline: 36662548]
25. He JC. TCM Diagnostics [Book in Chinese]: People’s Medical Publishing House; 2017.
26. Zheng XY. Guiding Principle of Clinical Research on New Drugs of Traditional Chinese Medicine (Trial): China Medical Science and Technology Press; 2002.
27. Friedman JH. Greedy function approximation: a gradient boosting machine. Ann Statist 2001;29(5):44. [doi: 10.1214/aos/1013203451]
28. Lu J. A frequency-adaptive multi-objective suspension control strategy. J Dyn Syst Meas Control 2004 Sep 1;126(3):700-707. [doi: 10.1115/1.1789979]
29. Goplen NP, Wu Y, Son YM, et al. Tissue-resident CD8+ T cells drive age-associated chronic lung sequelae after viral pneumonia. Sci Immunol 2020 Nov 6;5(53):eabc4557. [doi: 10.1126/sciimmunol.abc4557] [Medline: 33158975]

XSL•FO
RenderX

30. Nie X, Cai Y, Liu J, et al. Mortality prediction in cerebral hemorrhage patients using machine learning algorithms in intensive care units. Front Neurol 2020;11:610531. [doi: 10.3389/fneur.2020.610531] [Medline: 33551969]
31. Shen C, Di Y, Wang W, et al. Value of red blood cell distribution width in evaluating the severity of illness of novel coronavirus Delta variant. Zhonghua Wei Zhong Bing Ji Jiu Yi Xue 2022 May;34(5):475-480. [doi: 10.3760/cma.j.cn121430-20220214-00127] [Medline: 35728847]
32. Castro-Castro MJ, García-Tejada L, Arbiol-Roca A, et al. Dynamic profiles and predictive values of some biochemical and haematological quantities in COVID-19 inpatients. Biochem Med (Zagreb) 2022 Feb 15;32(1):010706. [doi: 10.11613/BM.2022.010706] [Medline: 35210926]
33. Liu Y, Yang Y, Zhang C, et al. Clinical and biochemical indexes from 2019-nCoV infected patients linked to viral loads and lung injury. Sci China Life Sci 2020 Mar;63(3):364-374. [doi: 10.1007/s11427-020-1643-8] [Medline: 32048163]
34. ACHVP. CPPDD. URL: http://cppdd.cn:9999/#/service/ACHVP [accessed 2025-06-12]
35. Wang Y, Zhou S, Wang M, et al. UHPLC/Q-TOFMS-based metabolomics for the characterization of cold and hot properties of Chinese materia medica. J Ethnopharmacol 2016 Feb;179:234-242. [doi: 10.1016/j.jep.2015.12.061]
36. Wang Z, Li L, Song M, Yan J, Shi J, Yao Y. Evaluating the traditional Chinese medicine (TCM) officially recommended in China for COVID-19 using ontology-based side-effect prediction framework (OSPF) and deep learning. J Ethnopharmacol 2021 May;272:113957. [doi: 10.1016/j.jep.2021.113957]
37. Xia F, Liu C, Wan JB. Characterization of the cold and hot natures of raw and processed Rehmanniae Radix by integrated metabolomics and network pharmacology. Phytomedicine 2020 Aug;74:153071. [doi: 10.1016/j.phymed.2019.153071] [Medline: 31537418]
38. Ma T, Tan C, Zhang H, Wang M, Ding W, Li S. Bridging the gap between traditional Chinese medicine and systems biology: the connection of cold syndrome and NEI network. Mol Biosyst 2010 Apr;6(4):613-619. [doi: 10.1039/b914024g] [Medline: 20237638]
39. Wang Y, Jin X, Fan Q, et al. Deciphering the active compounds and mechanisms of HSBDF for treating ALI via integrating chemical bioinformatics analysis. Front Pharmacol 2022;13:879268. [doi: 10.3389/fphar.2022.879268] [Medline: 35721141]
40. Wei J, Sun J, Zeng J, et al. Precise investigation of the efficacy of multicomponent drugs against pneumonia infected with influenza virus. Front Pharmacol 2021;12:604009. [doi: 10.3389/fphar.2021.604009] [Medline: 34867309]
41. Wang ZY, Fu SZ, Xu L, et al. Impact of Shenfu injection on a composite of organ dysfunction development in critically ill patients with coronavirus disease 2019 (COVID-19): a structured summary of a study protocol for a randomized controlled trial. Trials 2020 Aug 24;21(1):738. [doi: 10.1186/s13063-020-04677-5] [Medline: 32831151]
42. Wu M, Zhao Y, Dong X, et al. Artificial intelligence-based preoperative prediction system for diagnosis and prognosis in epithelial ovarian cancer: a multicenter study. Front Oncol 2022;12:975703. [doi: 10.3389/fonc.2022.975703] [Medline: 36212430]
43. Shi N, Liu B, Liang N, et al. Association between early treatment with Qingfei Paidu decoction and favorable clinical outcomes in patients with COVID-19: a retrospective multicenter cohort study. Pharmacol Res 2020 Nov;161:105290. [doi: 10.1016/j.phrs.2020.105290] [Medline: 33181320]
44. Zheng Y, Jin D, Lin J, et al. Understanding COVID-19 in Wuhan from the perspective of cold-dampness: clinical evidences and mechanisms. Front Med (Lausanne) 2021;8:617659. [doi: 10.3389/fmed.2021.617659] [Medline: 33693014]
45. Zhang D, Zhang B, Lv JT, Sa RN, Zhang XM, Lin ZJ. The clinical benefits of Chinese patent medicines against COVID-19 based on current evidence. Pharmacol Res 2020 Jul;157:104882. [doi: 10.1016/j.phrs.2020.104882] [Medline: 32380051]
46. Zhang H, Ni W, Li J, Zhang J. Artificial intelligence–based traditional Chinese medicine assistive diagnostic system: validation study. JMIR Med Inform 2020 Jun 15;8(6):e17608 [FREE Full text] [doi: 10.2196/17608]
47. Wen G, Ma J, Hu Y, Li H, Jiang L. Grouping attributes zero-shot learning for tongue constitution recognition. Artif Intell Med 2020 Sep;109:101951. [doi: 10.1016/j.artmed.2020.101951] [Medline: 34756217]
48. Wu HK, Ko YS, Lin YS, Wu HT, Tsai TH, Chang HH. The correlation between pulse diagnosis and constitution identification in traditional Chinese medicine. Complement Ther Med 2017 Feb;30:107-112. [doi: 10.1016/j.ctim.2016.12.005] [Medline: 28137520]
49. Lin L, Zhao P, Chen Z, et al. Identification strategy of cold and hot properties of Chinese herbal medicines based on artificial intelligence and biological experiments. Chin Med J 2025;138(6):745-747. [doi: 10.1097/CM9.0000000000003509]
50. Wei G, Fu X, He X, et al. Cold-hot nature identification based on GC similarity analysis of Chinese herbal medicine ingredients. RSC Adv 2021 Jul 27;11(42):26008-26015. [doi: 10.1039/d1ra04189d] [Medline: 35479454]
51. Gu SF, Li Y, Zhang ZX, Jin L, Li MQ. Clinical observation on the combination of traditional Chinese medicine Master Li Jiren's experience formula and olistavir in the treatment of viral pneumonia. GmjCM 2023;38(8):1550-1553. [doi: 10.3969/j.issn.1003-8914.2023.08.041]
52. Sun TF, Wu JW, Gao Q. The effects of Qingfei Paidu decoction on the time of disappearance of major symptoms, serum D-dimer levels, and erythrocyte sedimentation rate in patients with viral pneumonia. J Shenyang Pharm Univ 2021;38(S2):70-71.
53. Wang ZZ, Fang YF, Wang Y, et al. Logistic regression analysis of damp-heat and cold-damp impeding syndrome of rheumatoid arthritis: a perspective in Chinese medicine. Chin J Integr Med 2012 Aug;18(8):575-581. [doi: 10.1007/s11655-012-1172-1] [Medline: 22855033]

XSL•FO
RenderX

54. Qu JX, Gu L, Pu ZH, et al. Viral etiology of community-acquired pneumonia among adolescents and adults with mild or moderate severity and its relation to age and severity. BMC Infect Dis 2015 Feb 22;15:89. [doi: 10.1186/s12879-015-0808-0] [Medline: 25812108]
55. Bekdas M, Goksugur SB, Sarac EG, Erkocoglu M, Demircioglu F. Neutrophil/lymphocyte and C-reactive protein/mean platelet volume ratios in differentiating between viral and bacterial pneumonias and diagnosing early complications in children. Saudi Med J 2014 May;35(5):442-447. [Medline: 24825803]
56. Zhuang Y, Yu L, Jiang N, Ge Y. TCM-KLLaMA: Intelligent generation model for Traditional Chinese Medicine Prescriptions based on knowledge graph and large language model. Comput Biol Med 2025 May;189:109887. [doi: 10.1016/j.compbiomed.2025.109887] [Medline: 40056842]

Abbreviations

ACC: accuracy
ALT: alanine transaminase
AST: aspartate transaminase
AUC: area under the curve
CREA: creatinine
CRP: C-reactive protein
FN: false negative
FP: false positive
GBM: gradient boosting machine
GLO: globulin
IBIL: unconjugated bilirubin
LASSO: least absolute shrinkage and selection operator
LGB: light gradient boosting machine
LLM: large language model
LR: logistic regression
MCC: Matthews correlation coefficient
nCovORF1ab: Na, ORF1ab gene of novel coronavirus by nose test
NEU%: neutrophil percentage
PCT: thrombocytocrit
RDW: red cell distribution width
RF: random forest
RIDGE: ridge regression
SaO_2: oxygen saturation under load
SEN: sensitivity
SHAP: Shapley additive explanations
SPE: specificity
SVM: support vector machine
T: temperature
TBIL: total bilirubin
TCHO: total cholesterol
TCM: traditional Chinese medicine
TN: true negative
TP: true positive
WBC: white blood cell
XGB: extreme gradient boosting
XGB: extreme gradient boosting

Edited by A Benis; submitted 25.07.24; peer-reviewed by FN Hwang, G Hu, P Jain, Y Li; revised version received 03.05.25; accepted 09.05.25; published 16.07.25.

Please cite as:
Jin X, Wang Y, Wang J, Gao Q, Huang Y, Shao L, Zhao J, Li J, Li L, Zhang Z, Li S, Liu Y
A Machine Learning Approach to Differentiate Cold and Hot Syndrome in Viral Pneumonia Integrating Traditional Chinese Medicine and Modern Medicine: Machine Learning Model Development and Validation
JMIR Med Inform 2025;13:e64725
URL: https://medinform.jmir.org/2025/1/e64725
doi:10.2196/64725

XSL•FO
RenderX

© Xiaojie Jin, Yanru Wang, Jiarui Wang, Qian Gao, Yuhan Huang, Lingyu Shao, Jiali Zhao, Jintian Li, Ling Li, Zhiming Zhang, Shuyan Li, Yongqi Liu. Originally published in JMIR Medical Informatics (https://medinform.jmir.org), 16.7.2025. This is an open-access article distributed under the terms of the Creative Commons Attribution License (https://creativecommons.org/licenses/by/4.0/), which permits unrestricted use, distribution, and reproduction in any medium, provided the original work, first published in JMIR Medical Informatics, is properly cited. The complete bibliographic information, a link to the original publication on https://medinform.jmir.org/, as well as this copyright and license information must be included.

XSL•FO
RenderX

Detection and Analysis of Circadian Biomarkers for Metabolic Syndrome Using Wearable Data: Cross-Sectional Study

Jeong-Kyun Kim, PhD; Sujeong Mun, PhD, KMD; Siwoo Lee, PhD, KMD

KM Data Division, Korea Institute of Oriental Medicine, 1672 Yuseong-daero, Yuseong-gu, Daejeon, Daejeon, Republic of Korea

Corresponding Author:
Siwoo Lee, PhD, KMD
KM Data Division, Korea Institute of Oriental Medicine, 1672 Yuseong-daero, Yuseong-gu, Daejeon, Daejeon, Republic of Korea

Abstract

Background: Wearable devices are increasingly used for monitoring health and detecting digital biomarkers related to chronic diseases such as metabolic syndrome (MetS). Although circadian rhythm disturbances are known to contribute to MetS, few studies have explored wearable-derived circadian biomarkers for MetS identification.

Objective: This study aimed to detect and analyze sleep and circadian rhythm biomarkers associated with MetS using step count and heart rate data from wearable devices and to identify the key biomarkers using explainable artificial intelligence (XAI).

Methods: Data were analyzed from 272 participants in the Korean Medicine Daejeon Citizen Cohort, collected between 2020 and 2023, including 88 participants with MetS and 184 without any MetS diagnostic criteria. Participants wore Fitbit Versa or Inspire 2 devices for at least 5 weekdays, providing minute-level heart rate, step count, and sleep data. A total of 26 indicators were derived, including sleep markers (midsleep time and total sleep time) and circadian rhythm markers (midline estimating statistic of rhythm, amplitude, interdaily stability, and relative amplitude). In addition, a novel circadian rhythm marker, continuous wavelet circadian rhythm energy (CCE), was proposed using continuous wavelet transform of heart rate signals. Statistical tests (*t* test and the Wilcoxon rank sum test) and machine learning models—Shapley Additive Explanations, explainable boosting machine, and tabular neural network—were applied to evaluate marker significance and importance.

Results: Circadian rhythm markers, especially heart rate–based indicators, showed stronger associations with MetS than sleep markers. The newly proposed CCE demonstrated the highest importance for MetS identification across all XAI models, with significantly lower values observed in the MetS group (P<.001). Other heart rate–based markers, including relative amplitude and low activity period, were also identified as important contributors. Although sleep markers did not reach statistical significance, some were recognized as secondary predictors in XAI-based analyses. The CCE marker maintained a high predictive value even when adjusting for age, sex, and BMI.

Conclusions: This study identified CCE and relative amplitude of heart rate as key circadian rhythm biomarkers for MetS monitoring, demonstrating their high importance across multiple XAI models. In contrast, traditional sleep markers showed limited significance, suggesting that circadian rhythm analysis may offer additional insights into MetS beyond sleep-related indicators. These findings highlight the potential of wearable-based circadian biomarkers for improving MetS assessment and management.

(JMIR Med Inform 2025;13:e69328) doi:10.2196/69328

KEYWORDS

metabolic syndrome; wearable device; digital biomarker; circadian rhythm; explainable artificial intelligence

Introduction

Metabolic syndrome (MetS) is a multifaceted disorder that includes various metabolic conditions, such as obesity, hypertension, and diabetes. These conditions are becoming increasingly prevalent worldwide, posing significant concerns with profound implications for individual health, societal well-being, and the economy. Metabolic diseases involve complex pathophysiological mechanisms [1,2]. Promoting healthy eating habits, integrating appropriate physical activity, and effectively managing stress can significantly reduce the risk of developing MetS [1,3].

Currently, health management systems using wearable devices are gaining significant attention [4]. These systems offer personalized health care by continuously monitoring and analyzing the health status of an individual in real time. Wearable devices enable regular assessment of health-related indicators, eliminating the need for frequent hospital visits [2]. Achieving this requires the integration of various technologies, including semiconductors, artificial intelligence, and the Internet

XSL•FO
RenderX

of Things [5]. Smartwatches and bands are among the most commonly used wearable devices in daily life. Smartwatches are equipped with diverse sensors such as optical heart rate (HR) monitors, electrocardiograms, and inertial sensors, enabling the collection of vital signs such as step count, HR, blood pressure, pulse, and oxygen saturation [5].

Wearable devices can continuously monitor an individual's vital signs in real time. This involves the continuous tracking of important indicators related to MetS, such as HR, blood pressure, and activity levels, aiding in the real-time assessment of an individual's health status and the early detection of anomalies [2,6]. The daily data generated by wearable devices can help identify factors influencing the onset and progression of MetS. Recently, there has been a significant increase in attention to the daily monitoring of sleep and circadian rhythms using wearable devices [7,8]. Circadian rhythms are biochemical, physiological, or behavioral processes that occur in living organisms in approximately 24-hour cycles. Circadian rhythm markers are indicators to assess or measure the circadian rhythm state of a living organism [8,9]. Sleep and circadian rhythm biomarkers derived from activity-based wearable devices are now applied in studies on various conditions, including obesity [7], depression [8,9], cognitive function [10], prematurity [11], and mortality [12]. Common sleep markers include sleep timing (sleep onset and sleep offset), sleep duration (total sleep time), midsleep time, and wake after sleep onset [7,8]. Circadian rhythm markers are assessed using both parametric methods, such as amplitude, acrophase, midline estimating statistic of rhythm (MESOR), and circadian quotient (CQ) via cosinor analysis [8,12], and nonparametric methods, such as interdaily stability (IS), intradaily variability (IV), and relative amplitude (RA) [9-11]. Given the periodic nature of circadian rhythms, energy-based methods have been proposed. For example, singular value decomposition (SVD) has been used to calculate energy values from activity data, suggesting potential markers for cognitive function [10]. Traditional methods for measuring signal energy, such as Fourier transform, discrete cosine transform, and wavelet analysis, have been used in various biosignal analysis studies [13]. In this study, we propose a novel marker called continuous wavelet circadian rhythm energy (CCE) using continuous wavelet transform (CWT) for time-frequency analysis of HR as a circadian rhythm marker.

Previously, circadian rhythm analysis using wrist-worn wearable devices focused on activity-centered markers through actigraphy [9,10,12]. However, recently, the demand for circadian rhythm analysis based on HR and step counts provided by smartwatches and bands has been increasing [7,8]. Wearable devices often underestimate and overestimate the number of steps in free-living environments. Therefore, circadian rhythm markers in this study were obtained by integrating 5 days of continuous data, which addressed inaccuracies in step count measurements by reflecting the overall trends in sleep and activity. In addition, this study can compensate for incorrectly measured step counts by exploring HR-based markers rather than step counts.

The majority of the previous studies detected everyday features obtained from wearable devices and analyzed the features limited to statistical techniques without incorporating artificial intelligence technology [9-12]. Explainable artificial intelligence (XAI) techniques that interpret predictive results are gaining attention in the analysis of biosignals and health care information [5,7]. Specifically, research on circadian rhythm analysis based on wearable devices in relation to MetS is still in its early stages. This area requires multifaceted analysis, including the development of circadian rhythm biomarkers specifically tailored for MetS and the application of XAI for data interpretation.

Therefore, in this study, we detected circadian rhythm markers based on step count and HR to develop a wearable-based circadian rhythm marker for MetS and analyzed circadian rhythm markers important for MetS through artificial intelligence technologies such as Shapley Additive Explanations (SHAP), explainable boosting machine (EBM), and Tabular neural Network models (TabNet). Integration with XAI in marker analysis can make the results more actionable in health care applications due to its transparency and interpretability.

Methods

Recruitment

The Korean Medicine Daejeon Citizen Cohort (KDCC) dataset was used to validate the proposed biomarker. The data from the KDCC, spanning from 2020 to 2023, encompassed demographic, lifestyle, clinical, and biochemical measurements collected from 2000 participants. Anthropometric data, including height, weight, BMI, waist circumference, and hip circumference, were measured under standardized conditions. Height and weight were recorded using a digital stadiometer (BSM370, InBody), and BMI was calculated as weight (kg) divided by the square of height (m^2). Waist circumference was measured at the level of the navel, and hip circumference was measured at the widest part of the hips using a measuring tape (Hoechstmass-Rollvix, Germany).

Systolic blood pressure, diastolic blood pressure, and resting HR were measured using an automatic blood pressure cuff (FT-500R PLUS, Jawon Medical, South Korea). Measurements were taken after at least 5 minutes of rest, with an additional 1-minute interval between repeated readings. The average of 2 measurements was used for analysis. Venous blood samples (22.5 mL) were collected in the morning after overnight fasting. After 30 minutes, blood samples were centrifuged at 3450 rpm for 10 minutes, and all samples were transported within 24 hours to Seoul Clinical Laboratories (Seoul, Korea) for analysis. The biochemical analysis included complete blood count, kidney and liver function tests, lipid profile (triglycerides, high-density lipoprotein, low-density lipoprotein, and total cholesterol), glucose metabolism markers, thyroid function tests, and inflammation markers [14].

Daily data was obtained using Fitbit Versa or Inspire 2 wristbands (Fitbit) [15]. Of the initial 2000 participants enrolled in the KDCC cohort, not all consented to wearable device use. Consequently, 745 participants provided usable Fitbit data. Participants who wore Fitbit for less than 5 consecutive weekdays or had data for more than 6 hours of nonwearing in a 24-hour period were excluded from the 745 participants.

XSL•FO
RenderX

Finally, 500 of the 745 participants were included in the analysis.

MetS was defined as meeting 3 or more of the following criteria, based on a 5-criteria system that uses the criteria described in the modified third national cholesterol education program adult treatment panel by modifying the waist circumference cutoff point for Koreans [15] in Textbox 1.

Textbox 1. Third National Cholesterol Education Program Adult Treatment Panel.

- Waist circumference (≥90 cm for men, ≥85 cm for women)
- Systolic blood pressure (≥130 mm Hg) or diastolic blood pressure (≥85 mm Hg), or current use of antihypertensive medications
- Low high-density lipoprotein cholesterol levels (<40 mg/dL in men and <50 mg/dL in women) or use of medication for lipid abnormalities
- Triglyceride level (≥150 mg/dL) or medication for lipid abnormalities
- Fasting blood glucose level (≥100 mg/dL) or medication for type 2 diabetes

Among 500 participants (158 males and 342 females), 88 participants (44 males and 44 females) met the criteria for MetS, and 184 participants (28 males and 156 females) did not meet any of the 5 criteria and were classified as non-MetS.

Ethical Considerations

This study was conducted following the Declaration of Helsinki and was approved by the institutional review board of Dunsan Korean Medicine Hospital, Daejeon University (approval number DJDSKH-17-BM-12) and the Korea Institute of Oriental Medicine (approval number I-1703/002 - 002). Before participation, all individuals provided written informed consent, including consent for collecting human biological materials. Participants were informed that they could withdraw their consent at any time without any consequences.

Participants received US $36 as compensation for transportation costs. Written consent was obtained from the individuals involved for the publication of potentially identifiable images or data. All included images were reviewed to ensure that personal identities could not be inferred. This study was designed and conducted in compliance with ethical standards for human research, ensuring participant rights, privacy, and safety throughout the study process.

Circadian Rhythm and Sleep Indicator

Wearable data included minute-level HR and step-count records collected from Fitbit devices. In addition, the sleep duration records provided by Fitbit were collected. Notably, the minute-level HR records from the Fitbit devices occasionally had missing values, represented by zeros. Missing values were converted to the nearest HR. Missing data mainly consisted of long periods of nonwearing, such as during charging or showering. Spline interpolation resulted in exaggerated patterns, such as sudden increases or decreases in HR during long periods of nonwearing. Given these considerations, linear interpolation was chosen to minimize distortion and better handle long intervals.

The most commonly used indicators in sleep analysis are midsleep time (MST), total sleep time (TST), and wake after sleep onset [7,8]. MST is used to determine phenotype, such as whether an individual is a morning or evening sleeper. Knowing MST and TST can reveal the amount of sleep and phenotype, but it does not provide information about sleep efficiency. Therefore, the ratio of total sleep time to total time spent in bed for sleep is used. However, it is difficult to estimate sleep efficiency with step count and HR data provided by Fitbit.

Cosinor analysis is frequently used to analyze circadian rhythms based on activity and HR. Cosinor analysis fits sine waves to time series using the least squares method [16]. It is often used in biological time series analysis and can be applied to time series with nonuniform intervals. Cosinor analysis expresses observed time series data as a cosine function, as shown in Equation 1. Y(t) is the observation at time t, M is the mean (MESOR), A is the amplitude, τ is the period, t is the time, and ϕ is the phase. MESOR is the middle value of periodic oscillations and represents the central tendency of the data. The amplitude is the amount of variation in the period and represents how much the data deviates from the mean. The phase is the location of the variation corresponding to a specific time in the period and can mean the time when the peak of the data occurs. Amplitude, acrophase, MESOR, and CQ (amplitude or MESOR) are used as cosinor-related indicators [8,9,12].

$$(1) Yt = M + A\cos(2\pi t\tau + \phi)$$

Nonparametric indicators used in circadian rhythm studies related to daily activity include RA, IV, and IS, which evaluate the stability and variability of individual activity patterns and circadian rhythms [8-10]. RA is an index that evaluates the amplitude of activity in circadian rhythms and is calculated by the difference in activity between the maximum and minimum activity times as shown in Equation 2. M10 means the mean activity during the 10 hours with the highest activity during the day, and L5 means the mean activity during the 5 hours with the lowest activity during the day. The higher the RA, the greater the difference in activity between day and night, indicating a more distinct circadian rhythm.

IV is an index that evaluates the variability of activity patterns within a day, as shown in Equation 3. N is the total number of measured time data, Yt is the activity at time t, and Y- is the mean activity over all times. The numerator of Equation 3 is the sum of the squares of the activity variance between consecutive time periods. The larger the change in activity between time periods during the day, the larger the IV value. The denominator is the total change in activity by time, which expresses the variability for the mean activity during the day.

IS is an index that evaluates how consistently activity levels are maintained at the same time across multiple days. It indicates

XSL•FO
RenderX

how regular and consistent the activity patterns are maintained by the time zone of the day. In Equation 4, N is the total number of measured time data, S is the number of data per day, and x-his the hourly mean. The numerator represents the squared deviations of the hourly means from the overall mean, whereas the denominator reflects the total variance of the entire series. As the ratio of these 2 terms increases, the IS value becomes larger, and activity patterns that recur at identical clock times on successive days yield higher IS values.

(2)RA=M10-L5M10+L5

(3)IV=N∑t=2N(Yt-Yt-1)2(N-1)∑t=1N(Yt-Y-)2

(4)IS=N∑h=1S(x-h-x-)2S∑i=1N(xi-x-)2

Dimension reduction technology is being utilized as a method of analyzing biosignals, which is a method of converting high-dimensional data into low-dimensional data to easily visualize or analyze the data [17,18]. Dimension reduction is mainly used to reduce computational costs, remove noise, and express data more concisely while preserving the features of the data. Principal component analysis, linear discriminant analysis, and SVD are used as dimension reduction methods. In a study that applied dimension reduction technology to circadian rhythm, circadian activity rhythm energy (CARE) was proposed to detect the energy of subsignals with a cycle of less than 24 hours through singular spectrum analysis based on SVD to analyze the circadian rhythm of cognitive function. CARE showed a higher correlation coefficient than RA for melatonin amplitude [10].

The activity and HR obtained from wearable devices have a 24-h periodicity. Wavelet transform (WT) is used as a method to analyze signals that have time periodicity [19]. WT is a powerful tool that can analyze signals in the time and frequency domains simultaneously. WT analyzes frequency information in each time interval by decomposing them into wavelets of various sizes. CWT calculates wavelet changes for all times. Morlet wavelet is a sinusoidal waveform that is attenuated by a Gaussian curve, which is very advantageous in detecting the temporal changes of specific frequency components, allows for high-resolution frequency analysis, and captures continuous and periodic signal components well [14,20]. The CWT for a signal x(t) is obtained by computing the inner product with the Morlet wavelet. In Equations 5 and 6, Wx(a,b) is the CWT coefficient of a given signal x(t), a is a scale factor that controls the frequency variation. A smaller a corresponds to a higher frequency component, and a larger a corresponds to a lower frequency component. b is a shift parameter that controls the variation in time, and the signal is analyzed along the time axis as b changes. ψ*is the complex combination of the Morlet wavelet, t is time, and x(t) represents the signal to be analyzed. ψt is the Morlet wavelet function, ω0 is the center frequency, and i is the imaginary unit. The magnitude (energy) of the CWT coefficients Wx(a,b) represents how strongly the signal x(t) exists at a given scale a and time b. This energy is used to generate a spectrogram, which is a map that shows the intensity of the signal in the time-frequency plane. The center frequency means that the Morlet wavelet is optimized for analyzing signals in a specific frequency band. To obtain circadian rhythm markers for the acquired 5-day HR and step count per min, spectrograms were obtained for each signal, and then the total energy of the center frequency was derived as a marker by adding up all the energy over time for each center frequency. The proposed CWT-based circadian rhythm energy is called CCE.

(5)ψ(t)=π-14·eiω0t·e-t22

(6)Wx(a,b)=1a∫-∞∞x(t)·ψ*(t-ba)dt

Feature Selection and XAI

XAI is a methodology used to interpret the results of machine learning models. XAI enabled us to analyze the contribution of the features to the model outcomes. The local interpretable model-agnostic explanation (LIME) and SHAP are commonly used XAI algorithms, particularly for analyzing tabular data. As LIME often focuses on local explanations, it may not effectively explain the global behavior of the models. SHAP is a model-agnostic post hoc algorithm that is gaining attention. SHAP offers special implementations of tree-based models and provides more accurate and efficient explanations [21]. A tree-based model was used to identify MetS. Thus, SHAP was used to analyze the important features. SHAP provides insight into the contribution of each feature to the model outcomes, considering both the positive and negative impacts of wearable-based daily life features on the identification of MetS. XGBoost was used as the SHAP learning model, and the resulting SHAP values were as follows [5]:

(7)∅i(v)=∑S∈N{i}|S|!(n−|S|−1)!n!(v(S∪{i}−v(S))

XGBoost is a boosting model for decision trees that enhances the performance of gradient-boosting machines in terms of their speed. Boosting models iteratively update the parameters of previous classifiers to create a more powerful classifier, thereby increasing the accuracy and reducing the gradient of the loss function [5].

EBM is an interpretable structure of the model itself, unlike SHAP, which explains how each feature contributes to the prediction [22]. EBM is based on a generalized additive model (GAM), and GAM models the relationship between features and target variables as a sum of functions for each feature [23]. EBM can visualize how each feature contributes to the prediction so that users can easily understand the influence of individual features on the results. Equation 8 represents GAM, where β0 is a constant term, and fixi is a function learned for each feature, indicating how each feature contributes to the prediction. g is a link function that adjusts GAM to various settings, such as regression or classification. EBM learns each function fixi of GAM using boosting techniques. Boosting is a method of sequentially learning multiple weak models and correcting errors made by previous models, as shown in equation 9. hmxi is the m-th weak model, αm is the weight of the m-th weak model, and M represents the boosting step. EBM, including GAM and boosting techniques, is shown in Equation 10, and EBM can automatically detect pairwise interactions between each feature that are important for prediction and include them in the model, as shown in Equation 11.

(8)gEy=β0+f1x1+f2x2+f3x3+ +fnxn

(9)fi(xi)=∑m=1Mαmhm(xi)

XSL•FO
RenderX

(10)g(E[y])=β0+∑i=1n∑m=1Mαmhm(xi)

(11)gEy=β0+∑fixi+∑fijxi,xj

In addition to EBM and XGBoost, TabNet, a deep learning architecture designed for tabular data, was used. TabNet leverages a novel attention mechanism that automatically selects relevant features and effectively learns their interactions [24]. TabNet is particularly well-suited for analyzing complex datasets because it handles missing values and displays the most influential features for prediction, providing interpretability. In TabNet, the method to automatically evaluate the importance of each feature to the model is related to the attention mechanism and Gated Linear Units (GLU). To evaluate the importance of each feature in a given input X, the attention weights Wa are calculated as in Equation 12. Z is the input value of the current layer, A is the learnable weight, and P is the prior-scale term that reflects how frequently the corresponding feature has been selected in earlier steps. Consequently, A becomes a probability vector indicating the importance of each feature. TabNet performs prediction through features selected from each layer, and the set of selected features is defined as in Equation 13. GLU is used in the process of performing prediction using selected features. GLU can emphasize or suppress input features through nonlinear transformation, as shown in Equation 14. Wis a weight matrix, b is a bias, and σ is a sigmoid activation function, which provides a ratio representing the importance of each feature. The output computed through the attention weights and GLU of each layer evaluates the importance of each feature to the final prediction.

(12)A=Sparsemax(P·(WaZ))

(13)Xselected=A·X

(14)GLU(x)=(W1x+b1)·σ(W2x+b2)

The XGBoost parameters used were booster=gbtree and objective=binary logistic. The other parameters were set to the default values in Python (v3.10.9), NumPy (v1.23.5), and scikit-learn (v1.2.2). EBM was implemented using the interpret library version 0.6.4, and TabNet was implemented using pytorch-tabnet version 4.1.0 with max_epochs=2000 and batch_size=32.

Results

Associations of Sleep and Circadian Rhythm Indicators With MetS

Based on HR, step count, and sleep data obtained from wearable devices, bio-digital markers of circadian rhythm for MetS were detected and the significance of the markers was analyzed. For the analysis, continuous wearable data for 5 days during the week of 88 MetS and 184 non-MetS obtained from smart bands on the wrist were used. Demographic and clinical information used to determine MetS are shown in Table 1. The age of the MetS group was 48.94 years, which was 4 years older than that of the non-MetS group. The average BMI of MetS was 27.9. Systolic blood pressure, diastolic blood pressure, triglyceride, high-density lipoprotein, and glucose used to determine MetS all showed statistically significant results ($P<.001$). The *P* value was obtained using an independent *t* test.

XSL•FO
RenderX

Table . Demographic and clinical characteristics of MetS and non-MetS groups. Demographic data (age and sex) and clinical variables, including BMI, waist circumference, blood pressure, lipid profile, and glucose levels, are presented for participants classified into MetS (n=88) and non-MetS (n=184) groups. Statistical significance was tested using *t* tests.

	Non-MetS[a]	MetS	*P* value
Sex, n (%)			
Male	28 (38.9)	44 (61.1)	
Female	156 (78.0)	44 (22.0)	
Age (years), mean (SD)	44.04 (6.48)	48.94 (6.92)	<.001
BMI (kg/m^2), mean (SD)	21.70 (2.08)	27.90 (2.94)	<.001
Waist (cm), mean (SD)			
Male	81.82 (5.28)	96.98 (7.41)	<.001
Female	75.88 (5.11)	90.45 (8.04)	<.001
SBP[b] (mm Hg)	110.32 (8.98)	130.68 (15.42)	<.001
DBP[c] (mm Hg)	67.97 (8.80)	83.07 (11.31)	<.001
Triglyceride (mg/dL)	78.29 (26.62)	210.01 (102.54)	<.001
HDL[d] (mg/dL)	68.17 (14.21)	46.40 (11.35)	<.001
LDL[e] (mg/dL)	123.02 (33.19)	124.13 (35.95)	.74
Total_Cholesterol (mg/dL)	204.94 (35.05)	200.51 (42.11)	.45
Glucose (mg/dL)	82.97 (6.52)	99.89 (20.84)	<.001

[a]MetS: metabolic syndrome.

[b]SBP: systolic blood pressure.

[c]DBP: diastolic blood pressure.

[d]HDL: high-density lipoprotein.

[e]LDL: low-density lipoprotein.

Twenty-six indicators were identified as sleep and circadian rhythm markers. The sleep-related indicators consist of 4 measures: the mean and SD of MST and TST. MESOR, amplitude, acrophase, and CQ for both step count and HR, derived from cosinor analysis, make up 8 indicators. In total, 10 indicators, including L5, M10, RA, IS, and IV for step count and HR, were calculated as nonparametric indicators. In addition, one indicator was based on dimension reduction proposed in a previous study, and 3 indicators using CCE based on HR were introduced in this study.

The statistical significance of MetS in the results obtained by analyzing the energy of the CWT based on the central frequency of the circadian rhythm for step count and HR, in order to detect MetS markers related to the CCE proposed in this study, is shown in Figure 1. The CCE value for step count showed the lowest *P* value at a central frequency of 70 minutes, but it did not reach a value below .001. However, HR exhibited statistical significance below 0.001 at central frequencies of 70 minutes and 1000 minutes. Therefore, the total CCE value was obtained for the central frequencies between 69 and 80 minutes (midfrequency) and between 900 and 1100 minutes (low-frequency). In addition, the ratio of the 2 central frequency ranges (mid_low ratio) was calculated as a single indicator. The energy of HR according to the central frequency reaches its highest at the 1440-minutes circadian cycle and also shows high energy in the 700-minutes range (Figure 2). In the central frequency range of 69 - 80 minutes, the energy of MetS is lower than that of non-MetS, while in the 900 - 1100-min range, the energy of MetS is higher.

XSL•FO
RenderX

Figure 1. Statistical significance of continuous wavelet transform energy derived from step count and heart rate (HR) data across different central frequencies in the identification of metabolic syndrome (MetS). *P* values for each frequency range compare MetS (n=88) and non-MetS (n=184) groups, using HR and step count data recorded from Fitbit devices over 5 weekdays. HR circadian rhythm energy (CCE) showed statistical significance (*P*<.001) at 70 min and 1000 min, whereas step count CCE did not reach this threshold.

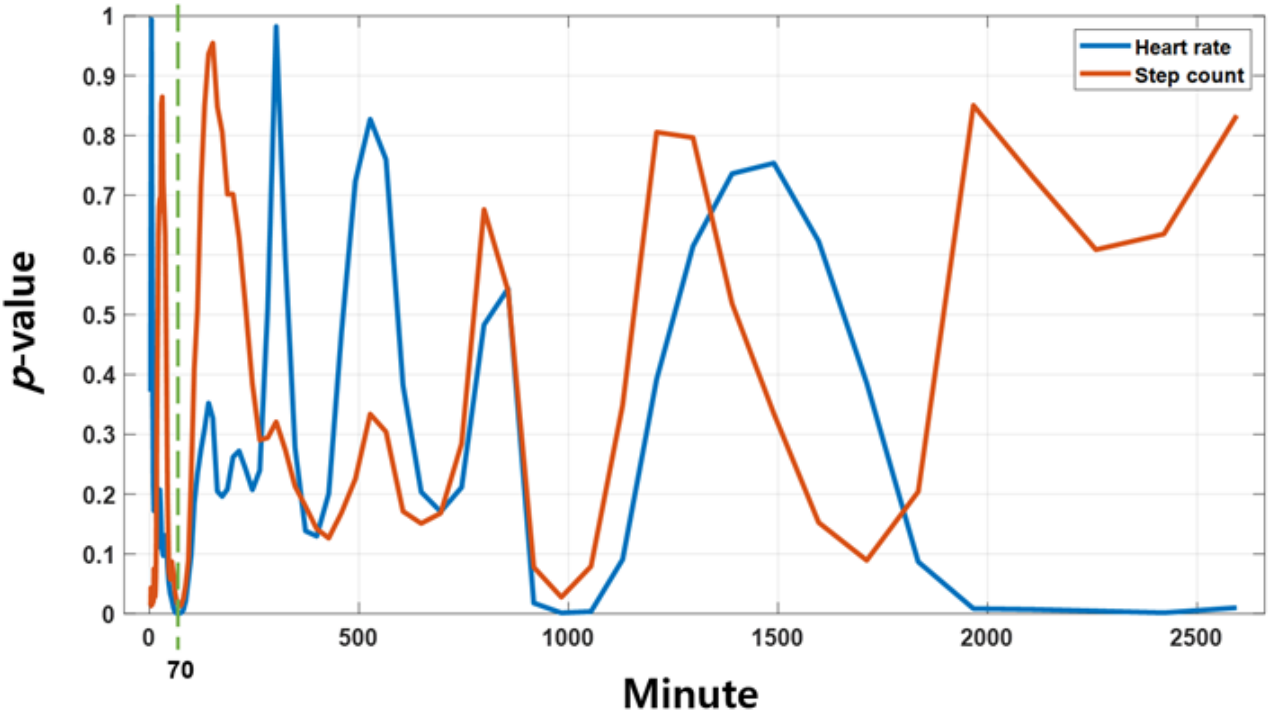
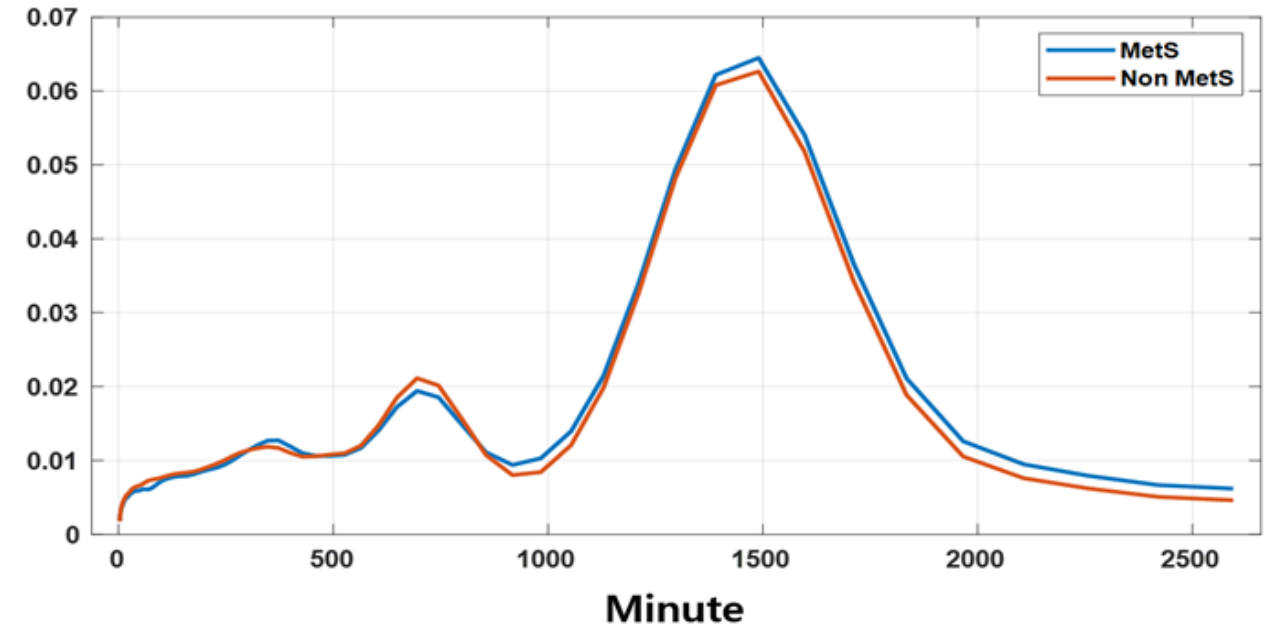


Figure 2. Comparison of heart rate (HR) energy at different central frequencies between metabolic syndrome (MetS) and non-MetS groups based on continuous wavelet transform analysis of wearable data. HR energy peaked at 1440 min (circadian cycle) and 700 min. In the 69 - 80 min range, MetS energy was lower than non-MetS, while in the 900 - 1100 min range, MetS energy was higher.



In Tables 2 and 3, the means, SD, and statistical significance of 26 indicators for MetS and non-MetS can be observed. Statistical significance was assessed using parametric testing (independent *t* test) and nonparametric testing (Wilcoxon rank sum test) [25].

XSL•FO
RenderX

Table . Comparison of sleep, cosinor, and nonparametric circadian rhythm indicators between metabolic syndrome (MetS) and non-MetS groups in Korean adults. Means, SD, and statistical tests (*t* test and Wilcoxon rank-sum test) are reported for each indicator derived from wearable-recorded step count and heart rate data, including sleep duration, midline estimating statistic of rhythm, amplitude, relative amplitude, interdaily stability, and others.

Indicator		Non-MetS	MetS	*t* test (*P* value)	Wilcoxon (*P* value)
Sleep					
Midsleep time	Mean	207.55 (36.36)	207.08 (28.06)	.92	.66
	SD	39.76 (24.48)	45.00 (35.50)	.16	.19
Total sleep time	Mean	414.92 (72.72)	410.70 (57.33)	.63	.46
	SD	79.50 (48.96)	84.00 (44.81)	.47	.25
Cosinor					
Midline estimating statistic of rhythm	SC[a]	7.37 (3.63)	6.42 (2.44)	.027	.102
	HR[b]	71.89 (6.39)	75.05 (7.23)	<.001	<.001
Amplitude	SC	6.61 (3.76)	5.65 (2.46)	.030	.102
	HR	11.66 (3.99)	11.22 (3.29)	.37	.47
Acrophase	SC	14.77 (2.06)	14.32 (1.83)	.084	.11
	HR	14.97 (1.95)	15.00 (1.89)	.899	.75
Circadian quotient	SC	0.89 (0.21)	0.89 (0.20)	.818	.79
	HR	0.16 (0.05)	0.15 (0.05)	.076	.04
Nonparametric					
L5	SC	0.172 (0.307)	0.203 (0.239)	.41	<.001
	HR	61.60 (6.43)	65.96 (7.25)	<.001	<.001
M10	SC	12.80 (6.42)	11.02 (4.39)	.02	.07
	HR	83.51 (7.24)	86.18 (7.68)	.006	.01
Relative amplitude	SC	0.973 (0.043)	0.961 (0.043)	.03	<.001
	HR	0.152 (0.04)	0.134 (0.03)	<.001	<.001
Interdaily stability	SC	0.507 (0.165)	0.440 (0.129)	<.001	<.001
	HR	0.684 (0.142)	0.630 (0.130)	.003	.002
Intradaily variability	SC	1.246 (0.311)	1.249 (0.274)	.93	.91
	HR	0.535 (0.157)	0.495 (0.156)	.05	.04

[a]SC: step count.

[b]HR: heart rate.

Table . Comparison of dimension reduction and frequency analysis values in metabolic syndrome (MetS) and non-MetS groups. Mean values, SD, and statistical significance for frequency-based circadian rhythm markers and dimension reduction indicators are presented. Statistical significance was assessed using independent *t* tests and Wilcoxon rank sum tests.

Indicator		Non-MetS	MetS	- test (*P* value)	Wilcoxon (*P* value)
SSA_CARE	SC[a]	0.066 (0.040)	0.061 (0.030)	.37	.69
CCE[b]					
Mid-Frequency	HR[c]	0.029 (0.010)	0.024 (0.008)	<.001	<.001
Low-Frequency	HR	0.029 (0.013)	0.034 (0.015)	.003	.003
Mid_Low Ratio	HR	1.247 (0.859)	0.865 (0.466)	<.001	<.001

[a]SC: step count.

[b]CCE: circadian rhythm energy.

[c]HR: heart rate.

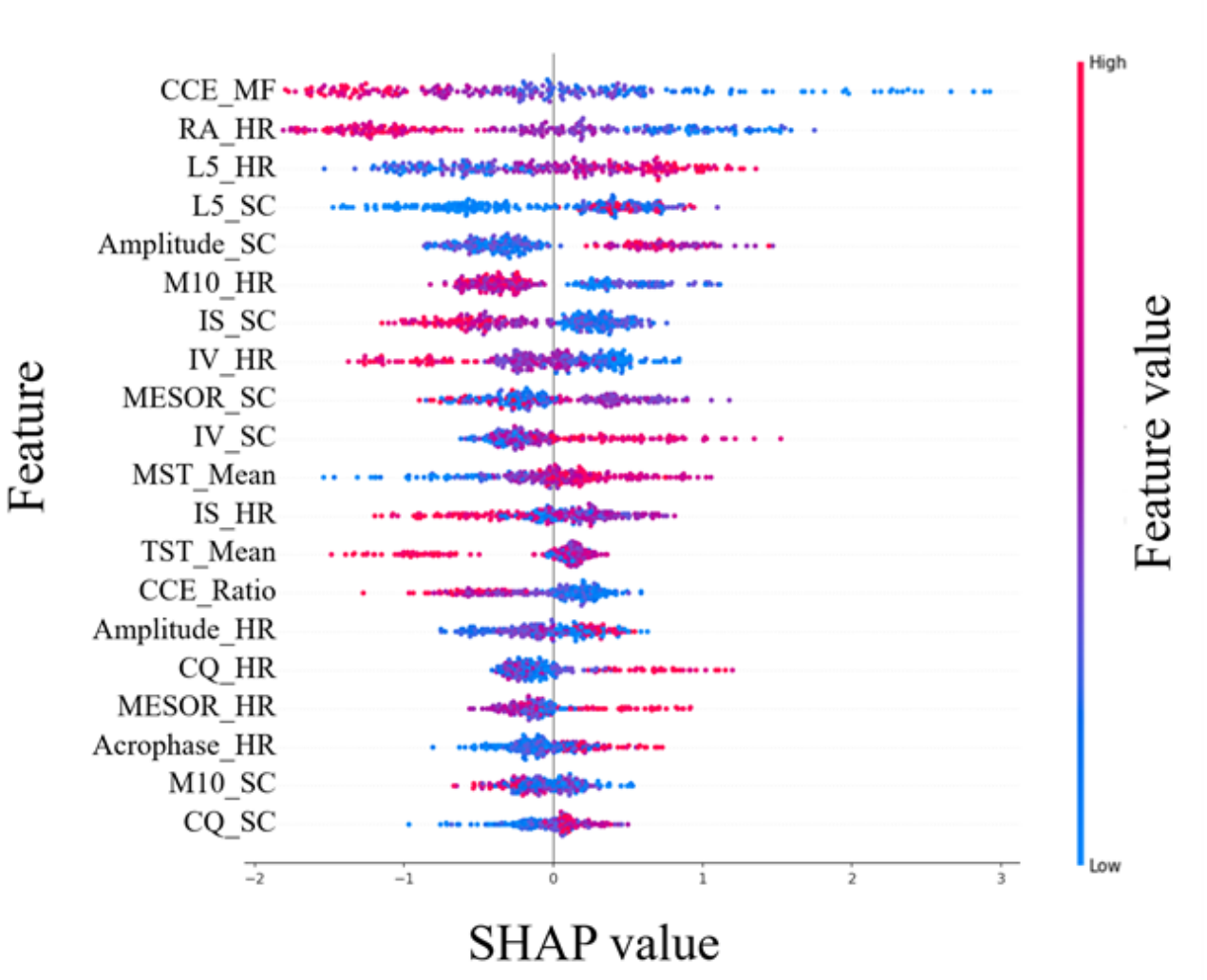
XSL•FO
RenderX

Sleep-related indicators did not show statistical significance for MetS (P<.05). For the Cosinor and non-parametric methods, step count showed statistical significance with Amplitude (MetS was 0.96 smaller, P=.03), L5 (MetS was 0.031 larger, P<.001), RA (MetS was 0.012 smaller, P<.001), and IS (MetS was 0.067 smaller, P<.001). HR showed statistical significance with MESOR (MetS increased by 3.14, P<.001), L5 (MetS increased by 4.36, P<.001), M10 (MetS increased by 2.67, P=.012), RA (MetS decreased by 0.018, P<.001), IS (MetS decreased by 0.054, P=.002), and IV (MetS decreased by 0.04, P=.04). The CARE method based on step count did not show statistical significance for MetS. In this study, the proposed indicators CCE showed statistical significance in midfrequency (MetS decreased by 0.005, P<.001), low-frequency (MetS increased by 0.005, P=.003), and mid_low ratio (MetS decreased by 0.382, P<.001).

XAI-Based Importance Analysis of Sleep and Circadian Rhythm Indicators for MetS

An importance analysis was conducted on the 26 detected sleep and circadian rhythm indicators using SHAP (with XGBoost), EBM, and TabNet. Figure 3 presents the SHAP plot, where the color gradient from red to blue reflects the value of each indicator, with higher values appearing in red. The x-axis represents the contribution direction: positive values indicate a higher contribution to predicting MetS, while negative values correspond to a higher contribution to non-MetS. Indicators positioned higher on the y-axis are considered more important.

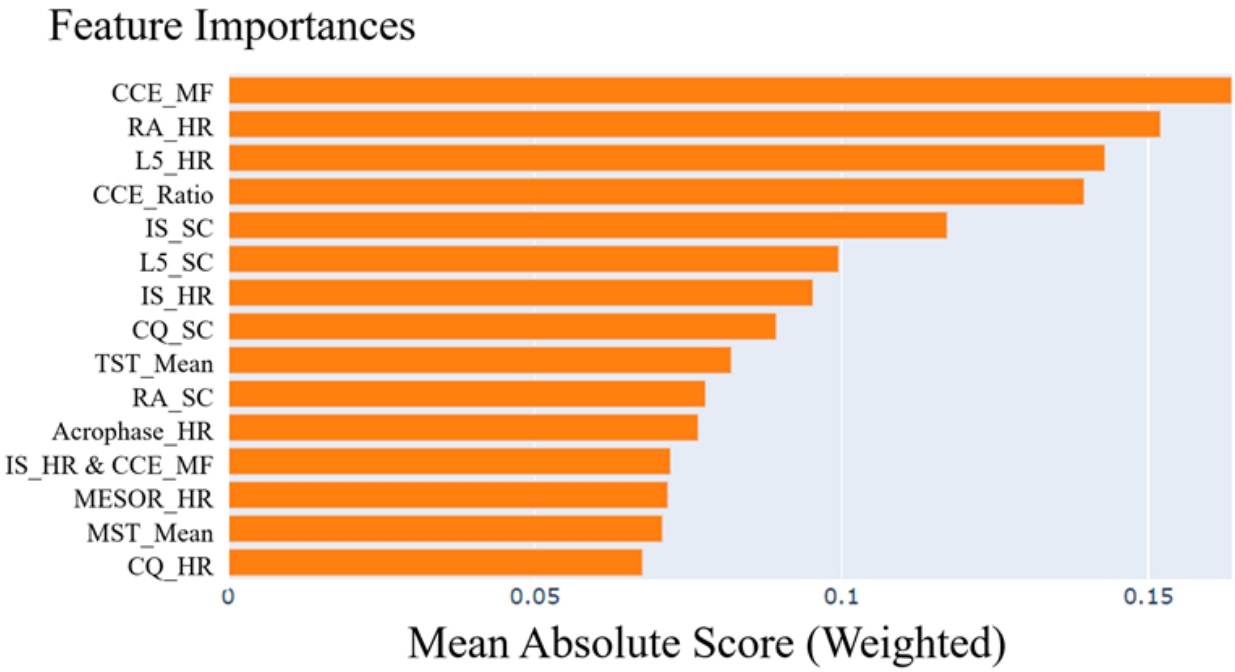
Figure 3. Important indicators identified for metabolic syndrome (MetS) using Shapley Additive Explanations (SHAP). Importance analysis was conducted on 26 sleep and circadian rhythm indicators using SHAP with an extreme gradient boosting (XGBoost) model. The color gradient from red to blue represents the values of each indicator, with higher values in red. The x-axis indicates the contribution direction, where positive values correspond to a higher contribution to predicting MetS, while negative values indicate a higher contribution to non-MetS.



Figures 4 and 5 display the importance values of indicators using EBM and TabNet, respectively. Among the three models, the midfrequency of CCE (CCE_MF), proposed in this study, exhibited the highest importance for identifying MetS-related circadian rhythm patterns. In addition, relative amplitude of HR (RA_HR) consistently ranked among the top 3 indicators across all three methods. These findings highlight the critical role of both CCE_MF and RA_HR in distinguishing between MetS and non-MetS groups.

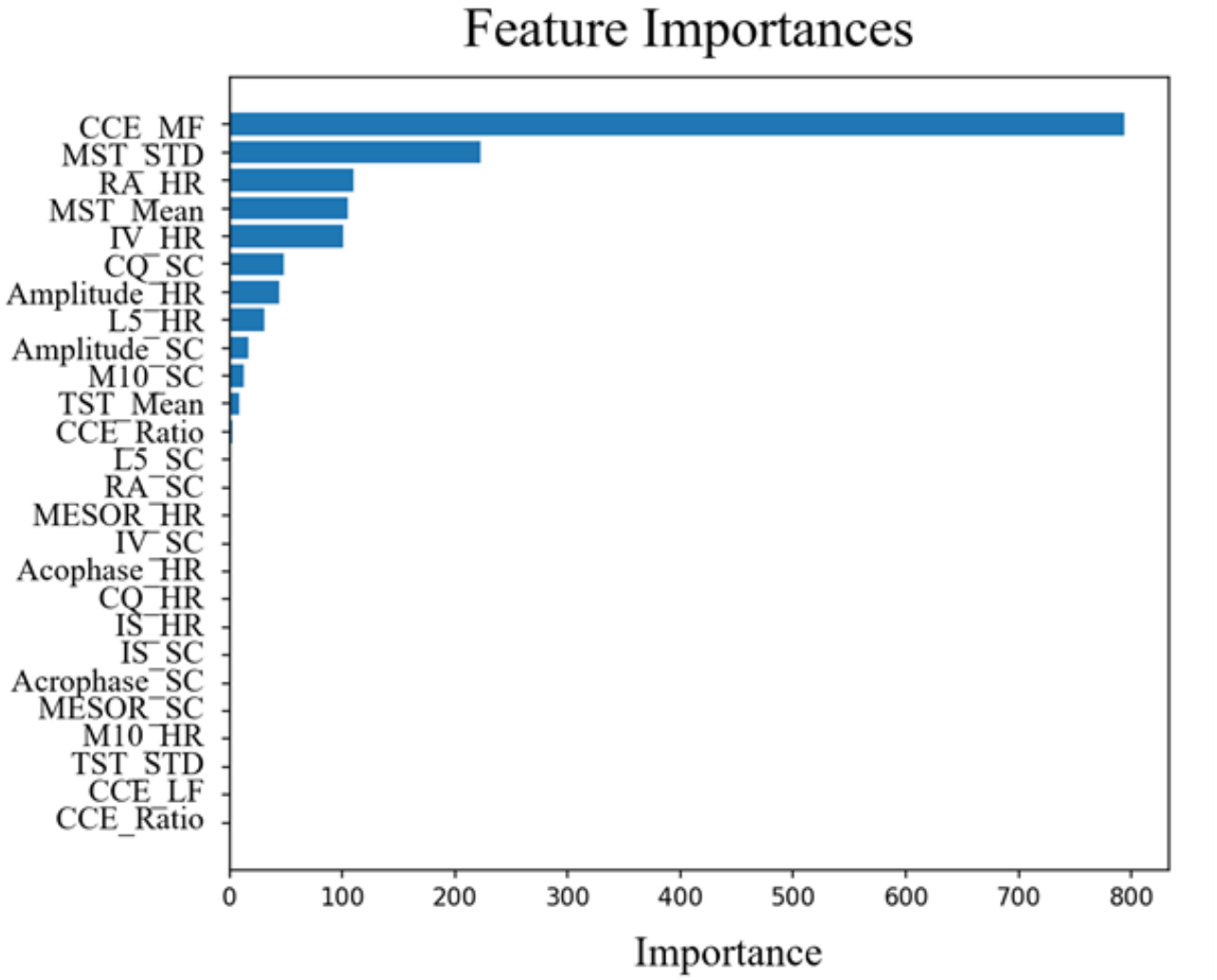
XSL•FO
RenderX

Figure 4. Important indicators identified for metabolic syndrome (MetS) using explainable boosting machine (EBM). Importance values of 26 sleep and circadian rhythm indicators were analyzed using EBM. The midfrequency of continuous wavelet circadian energy (CCE_MF) exhibited the highest importance for distinguishing MetS.



XSL•FO
RenderX

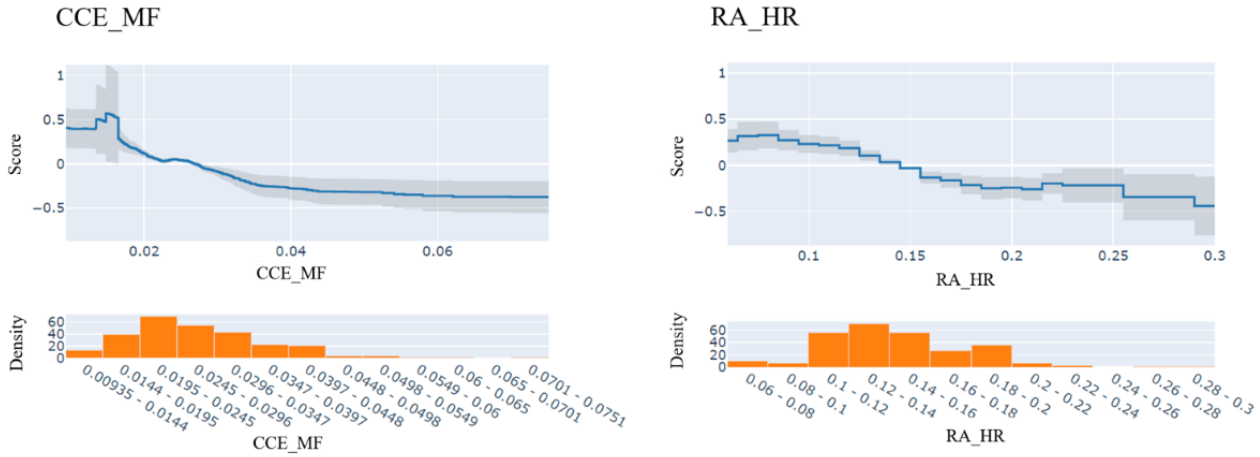
Figure 5. Important indicators identified for metabolic syndrome (MetS) using Tabular Neural Network. Feature importance was analyzed using TabNet, a deep learning model optimized for tabular data. Similar to explainable boosting machine, CCE_MF showed high importance in distinguishing MetS, while RA_HR also remained among the top-ranked indicators.



Apart from CCE_MF and RA_HR, differences in importance rankings were observed between the tree-based models (SHAP and EBM) and the deep learning-based TabNet. In the SHAP plot, both CCE_MF and RA_HR showed a higher contribution to MetS as their values decreased. Figure 6 further visualizes the changes in scores based on CCE_MF and RA_HR using EBM. The average value of CCE_MF was 0.024 for the MetS group and 0.029 for the non-MetS group, with most data points concentrated in the range of 0.0195 - 0.0245. A lower CCE_MF value was associated with a higher contribution to MetS, while non-MetS data were distributed over a broader range from 0.03 to 0.08.

XSL•FO
RenderX

Figure 6. Score changes for CCE_MF and RA_HR identified by explainable boosting machine in metabolic syndrome (MetS) classification. Lower CCE_MF values were associated with a higher MetS risk, with most MetS cases clustered between 0.0195 - 0.0245, while non-MetS values ranged from 0.03 - 0.08. For RA_HR, values above 0.15 increased the likelihood of non-MetS, while those exceeding 0.25 were linked to a reduced probability of MetS. CCE: circadian rhythm energy; CCE_MF: midfrequency of CCE; RA_HR: relative amplitude of heart rate.



Similarly, RA_HR values were distributed between 0.1 and 0.2, with a shift observed in the EBM plot. When RA_HR exceeded 0.15, its contribution to non-MetS increased, while values above 0.25 were associated with a reduction in the probability of MetS.

Among the top 10 indicators, SHAP identified 5 HR-related and 5 SC-related indicators. EBM included 5 HR-related, 4 SC-related, and 1 sleep-related indicator, while TabNet identified 5 HR-related, 3 SC-related, and 2 sleep-related indicators. Across all three methods, HR-related indicators showed a high contribution to MetS. Notably, CCE_MF, RA_HR, and L5_HR consistently appeared as key contributors across all models.

The results presented above are based on the analysis of the entire dataset. To evaluate the robustness of the marker and model, the data were cross-validated 5 times. The proposed CCE_MF marker showed the highest importance in 3 of the 5 results for SHAP and was explained as the second most important marker, after RA_HR, in two results. In the EBM model, CCE_MF showed the highest importance in all five times. In the TabNet model, CCE_MF was selected within the top 10 markers, but the most important marker varied, so the probability was not shown. Therefore, the reliability of the results of the TabNet model was low.

Additionally, an analysis was conducted using SHAP, EBM, and TabNet to evaluate the impact of key demographic variables, including age, sex, and BMI, on the importance of sleep and circadian rhythm variables in the MetS prediction model.

As presented in Table 1, age, sex, and BMI are closely associated with MetS and may influence the assessment of the independent contributions of other variables when included in the model. Therefore, by comparing models that include and exclude these variables, the independent importance of sleep and circadian rhythm markers can be more clearly analyzed. The top 10 indicators in SHAP, EBM, and TabNet, when age, sex, and BMI were included, are as follows: (1) SHAP: BMI, Age, IS_SC, CCE_MF, MST_Mean, Amplitude_HR, RA_HR, M10_HR, M10_SC, and Amplitude_SC; (2) EBM: BMI, Age, Sex, CCE_MF, IS_SC, RA_HR, Age & BMI, CCE_Ratio, CQ_SC and BMI, and L5_HR; and (3) TabNet: BMI, TST_Mean, Sex, L5_SC, CCE_MF, MST_Mean, Age, IS_SC, L5_HR, and Amplitude_HR.

In models that included age, sex, and BMI, these variables significantly impacted prediction, leading to a relative decrease in the importance of some sleep and circadian rhythm markers. However, when age, sex, and BMI were excluded, the proposed CCE_MF consistently ranked among the top 3 most important markers across all methods and was identified as the most significant marker. The results indicate that the CCE_MF marker exerts a strong independent influence on MetS prediction even after accounting for potential confounding factors.

Notably, IS_SC showed a higher contribution than RA_HR and L5_HR, which is a finding worth highlighting. The findings confirm that CCE_MF plays a crucial role in MetS prediction independently of age, sex, and BMI and suggest that IS_SC contributes more significantly than traditional HR-based markers, including RA_HR and L5_HR.

Finally, the comparison between the statistical methods and the XAI-based importance analysis revealed that sleep-related indicators, which did not achieve statistical significance, emerged among the top 10 indicators in the XAI-based analysis. These findings underscore the value of explainable artificial intelligence methods in uncovering hidden patterns that may be missed by traditional statistical approaches.

Discussion

Primary Findings

Currently, studies analyzing circadian rhythm digital markers related to MetS are still in their early stages. Previous research has primarily focused on individual factors such as physical activity levels and sleep patterns, but in-depth analysis of circadian rhythm markers for metabolic diseases using wearable devices has rarely been conducted [26-28]. This study aimed to identify and analyze circadian rhythm indicators related to MetS using data from wearable devices.

XSL•FO
RenderX

In addition to existing circadian rhythm indicators, recent studies are proposing new indicators tailored to each target disease area. Table 4 shows studies focused on wearable-based sleep and circadian rhythm analysis. For instance, Cui proposed CARE as a circadian rhythm marker for cognitive function, comparing it with existing indicators like RA [10]. Similarly, Shim introduced a new marker called CosinorAge, which analyzes the relationship between aging and mortality, in addition to Cosinor-based indices such as MESOR, amplitude, and acrophase [12]. In this study, we proposed a time-frequency analysis-based circadian rhythm indicator called CCE and compared it with indicators used in previous studies. As a marker, CARE analyzes circadian rhythms using an energy-based approach, similar to the CCE marker. However, although CARE proved to be a strong marker for cognitive function, it did not show high significance in MetS.

Table . Previous studies on sleep and circadian rhythm indicator analysis using wrist-worn wearable devices. A summary of studies investigating sleep and circadian rhythm indicators in various health conditions using wearable devices. Each study includes target condition, device type, key indicators analyzed, and methodology used. Indicators include sleep parameters (eg, sleep duration and onset latency), circadian rhythm markers (eg, midline estimating statistic of rhythm, amplitude, and interdaily stability), and novel metrics (eg, circadian activity rhythm energy and midfrequency circadian rhythm energy).

Author	Target	Device	Indicator	Methodology
Kiss et al 2024 [7]	Obesity	Fitbit Charge HR[a] 2	Sleep onset, sleep offset, sleep duration, sleep onset latency, sleep inertia, MST[b], total step count, sleeping HR, and resting HR	Explainable boosting machine
Zhang et al 2024 [8]	Major depressive disorder	Fitbit Charge HR 2 or 3	Sleep duration, sleep onset, sleep offset, sleep variability, daily step, step IV, step IS, L5 onset, M10 onset, HR MESOR[c], HR amplitude, and HR acrophase	Linear mixed-effects models
Ali et al 2023 [9]	Major depressive disorder	Actigraphy ActiCal (Philips)	MESOR, Amplitude, CQ[d], Acrophase, M10, L5, RA[e], IV[f], and IS[g]	Two-tailed *t* test and Mann-Whitney *U* test, and Kolmogorov-Smirnov test
Cui et al 2023 [10]	Cognitive Function	AX3 (Activity)	CARE[h], and RA	Regression models
Ravindra et al 2023 [11]	Prematurity	Motionwatch8 (CamNTech)	RA, IS, and IV	Deep learning and novel interpretability algorithms
Shim et al 2024 [12]	Aging and Mortality	AX3 (Axivity) or GT3X+ (ActiGraph)	MESOR, amplitude, acrophase, and CosinorAge	Harrel concordance index and Akaike information criterion
Kim et al 2022 [26]	MetS	GalaxyWatch Active1	Walking hours, physical activity hours, and step counts	Paired *t* test and chi-square test
Yamaga et al 2023 [27]	MetS	Fitbit Versa	TST[i], total step count, and total activity minutes	Multilevel mixed-effects logistic regression
Ours	MetS	Fitbit Versa or Inspire 2	MST, TST, MESOR, amplitude, acrophase, CQ, L5, M10, RA, IS, IV, CARE, and CCE[j]	XAI[k] models such as SHAP[l], EBM[m], and TabNet

[a]HR: heart rate.

[b]MST: midsleep time.

[c]MESOR: midline estimating statistic of rhythm.

[d]CQ: circadian quotient.

[e]RA: relative amplitude.

[f]IV: interdaily variability.

[g]IS: interdaily stability.

[h]CARE: circadian activity rhythm energy.

[i]TST: total sleep time.

[j]CCE: circadian rhythm energy.

[k]XAI: explainable artificial intelligence.

[l]SHAP: Shapley Additive Explanations.

[m]EBM: explainable boosting machine.

XSL•FO
RenderX

Existing statistical analysis methods may have limitations in detecting complex temporal patterns or interactions. In contrast, XAI offers clearer insights into hidden data patterns by making the predictions of complex models explainable [29]. Kiss et al [7] analyzed the relationship between sleep and HR indicators and obesity through EBM, while Ravindra et al [11] investigated circadian rhythm indicators for prematurity using novel interpretability algorithms that integrate unsupervised clustering, model error analysis, feature attribution, and automated actigraphy analysis. This highlights the growing importance of using XAI to analyze target diseases and circadian markers. Our study aims to address the limitations of previous research by examining the significance of circadian rhythm indicators related to MetS using XAI models such as SHAP, EBM, and TabNet. Analyzing the contribution and significance of circadian rhythm indicators across various models enhances the development of objective markers that more effectively explain MetS.

XAI-based analysis of circadian rhythm indicators revealed that CCE_MF is the most important marker for identifying circadian patterns related to MetS. A decrease in CCE_MF with a 1-hour cycle correlated with an increased contribution to MetS. The HR variability observed in the 1-hour cycle can be related to exercise, physical activity, eating, digestion, and fluctuations in the autonomic nervous system [30,31]. A low energy level in the 1h cycle indicates minimal amplitude or frequency components, suggesting strong physical activity, low metabolic changes, or an absence of exercise. Our study also noted low step counts in the same cycle. Additionally, the RA_HR consistently ranked high across all models and displayed low values in MetS. A low RA_HR indicates reduced HR variability, which can act as a cardiovascular risk factor. For example, HR variability tends to decrease in conditions such as hypertension, MetS, or heart failure [32].

XAI methods, including SHAP, EBM, and TabNet, enabled us to comprehensively understand the contribution of individual indicators to MetS prediction. While SHAP and EBM, both tree-based models, identified similar HR and sleep-related indicators, TabNet, a deep learning approach, highlighted a different set of significant sleep-related indicators. Notably, some sleep-related indicators that did not achieve statistical significance in traditional analyses emerged among the top indicators in the XAI method. This underscores the limitations of conventional statistical approaches that may overlook essential relationships and interactions among variables. The ability of XAI to uncover these hidden patterns suggests its valuable role in advancing research on MetS and related diseases.

Adding CCE markers to existing markers and comparing the results of MetS prediction can be another method to demonstrate the importance of CCE markers. The results of predicting MetS with sleep and circadian rhythm markers showed that incorporating the CCE marker into the EBM model increased the prediction accuracy from 64.31% to 65.44%, while the RF model showed the highest prediction accuracy, increasing from 68.38% to 69.47%. When sex, age, height, weight, and BMI were included, the accuracy increased from 88.23% to 88.93% in the EBM model, and the highest model showed an increase from 89.70% to 90.43% in XGBoost. All prediction results were validated using five-fold cross-validation. In a previous study on obesity prediction, the prediction accuracy of wearable devices and questionnaires (such as age, sex, race, income, and education level) was 72.6% when the EBM model was used. Although new markers have been proposed in various fields, they have not achieved a high level of prediction, and the proposed CCE model showed an increase in prediction accuracy of 1% but did not significantly improve overall performance. However, the introduction of new markers provides valuable insights by explaining MetS through interpreting circadian rhythms, rather than relying simply on existing known factors such as sex, age, and BMI.

The growing prevalence of wearable devices, such as smart bands and watches, is fostering an environment where individuals' everyday health information can be collected and analyzed in real time. These data could be instrumental in personalized health care, particularly in the early detection and prevention of chronic diseases such as MetS. Keshet provided an overview of wearable and digital devices capable of alerting individuals to specific metabolic outcomes, emphasizing the unique opportunities for creating personalized prevention and treatment strategies for cardiometabolic diseases [2]. This study may contribute to the healthcare landscape by developing wearable data-based circadian rhythm markers, addressing the need for technologies aimed at preventing and treating MetS in everyday life.

Limitations

This study has some limitations. The dataset used was limited in size and was collected from specific regions or population groups, making the generalization challenging. Further research should delve deeper into investigating the stability and generalizability of the model when considering real-world medical applications. Additionally, there was an issue of data imbalance for MetS and metabolic diseases, potentially leading to model bias toward the majority class. Although ensemble methods such as EBM and XGBoost, which are robust to data imbalance, were used [33], random undersampling was performed five times during model training to further address this issue, and the results were analyzed. In particular, the proposed CCE_MF marker emerged as the most important marker in four of the five tests using SHAP and EBM, and as the second most important marker in one test. However, the most important markers are not consistent in the TabNet model, indicating that a larger dataset is needed for deep learning models to achieve more stable and consistent results. Future studies should further explore deep learning models based on larger datasets.

Conclusions

The study analyzed a total of 26 digital biomarkers related to MetS using wearable wrist sensor data, with a particular focus on the newly proposed CCE. The XAI techniques, including SHAP, EBM, and TabNet, were applied to assess the significance and importance of each biomarker. Key findings demonstrated that circadian rhythm markers based on HR, particularly CCE and RA_HR, showed high importance across multiple models, reinforcing their potential as robust biomarkers

XSL•FO
RenderX

for MetS monitoring. The study also highlighted that traditional sleep markers did not exhibit strong statistical significance, suggesting that circadian rhythm analysis could provide additional insights for MetS research.

Acknowledgments

The Development of Korean Medicine Original Technology for Preventive Treatment Based on Integrative Big Data (grant number KSN1739121) from the Korea Institute of Oriental Medicine.

Data Availability

The data supporting this study's findings were provided by the Korean Medicine Data Center of the Korea Institute of Oriental Medicine under license and cannot be freely shared. Requests for access should be directed to the Korean Medicine Data Center [34].

Authors' Contributions

JK Kim: Conceptualization, Data curation, Formal analysis, Investigation, Methodology, Resources, Software, Validation, Visualization Writing – original draft, Writing – review & editing. S Mun: Conceptualization, Investigation, Writing – review & editing. S Lee: Funding acquisition, Project administration, Supervision.

Conflicts of Interest

None declared.

References

1. Dobrowolski P, Prejbisz A, Kuryłowicz A, et al. Metabolic syndrome — a new definition and management guidelines. Arterial Hypertension 2022;26(3):99-121. [doi: 10.5603/AH.a2022.0012]
2. Keshet A, Reicher L, Bar N, Segal E. Wearable and digital devices to monitor and treat metabolic diseases. Nat Metab 2023 Apr;5(4):563-571. [doi: 10.1038/s42255-023-00778-y] [Medline: 37100995]
3. Alkhulaifi F, Darkoh C. Meal Timing, Meal Frequency and Metabolic Syndrome. Nutrients 2022 Apr 21;14(9):1719. [doi: 10.3390/nu14091719] [Medline: 35565686]
4. Manogaran G, Alazab M, Song H, Kumar N. CDP-UA: Cognitive Data Processing Method Wearable Sensor Data Uncertainty Analysis in the Internet of Things Assisted Smart Medical Healthcare Systems. IEEE J Biomed Health Inform 2021 Oct;25(10):3691-3699. [doi: 10.1109/JBHI.2021.3051288] [Medline: 33439849]
5. Kim JK, Lee K, Hong SG. Detection of important features and comparison of datasets for fall detection based on wrist-wearable devices. Expert Syst Appl 2023 Dec;234:121034. [doi: 10.1016/j.eswa.2023.121034]
6. Meng Y, Speier W, Shufelt C, et al. A Machine Learning Approach to Classifying Self-Reported Health Status in a Cohort of Patients With Heart Disease Using Activity Tracker Data. IEEE J Biomed Health Inform 2020 Mar;24(3):878-884. [doi: 10.1109/JBHI.2019.2922178] [Medline: 31199276]
7. Kiss O, Baker FC, Palovics R, Dooley EE, Pettee Gabriel K, Nagata JM. Using explainable machine learning and fitbit data to investigate predictors of adolescent obesity. Sci Rep 2024 May 31;14(1):12563. [doi: 10.1038/s41598-024-60811-2] [Medline: 38821981]
8. Zhang Y, Folarin AA, Sun S, et al. Longitudinal Assessment of Seasonal Impacts and Depression Associations on Circadian Rhythm Using Multimodal Wearable Sensing: Retrospective Analysis. J Med Internet Res 2024 Jun 28;26:e55302. [doi: 10.2196/55302] [Medline: 38941600]
9. Ali FZ, Parsey RV, Lin S, Schwartz J, DeLorenzo C. Circadian rhythm biomarker from wearable device data is related to concurrent antidepressant treatment response. NPJ Digit Med 2023 Apr 29;6(1):81. [doi: 10.1038/s41746-023-00827-6] [Medline: 37120493]
10. Cui S, Lin Q, Gui Y, et al. CARE as a wearable derived feature linking circadian amplitude to human cognitive functions. NPJ Digit Med 2023 Jul 11;6(1):123. [doi: 10.1038/s41746-023-00865-0] [Medline: 37433859]
11. Ravindra NG, Espinosa C, Berson E, et al. Deep representation learning identifies associations between physical activity and sleep patterns during pregnancy and prematurity. NPJ Digit Med 2023 Sep 28;6(1):171. [doi: 10.1038/s41746-023-00911-x] [Medline: 37770643]
12. Shim J, Fleisch E, Barata F. Circadian rhythm analysis using wearable-based accelerometry as a digital biomarker of aging and healthspan. NPJ Digit Med 2024 Jun 4;7(1):146. [doi: 10.1038/s41746-024-01111-x] [Medline: 38834756]
13. Kim J, Bae MN, Lee KB, Hong SG. Gait event detection algorithm based on smart insoles. ETRI Journal 2020 Feb;42(1):46-53. [doi: 10.4218/etrij.2018-0639]
14. Baek Y, Seo BN, Jeong K, Yoo H, Lee S. Lifestyle, genomic types and non-communicable diseases in Korea: a protocol for the Korean Medicine Daejeon Citizen Cohort study (KDCC). BMJ Open 2020 Apr 9;10(4):e034499. [doi: 10.1136/bmjopen-2019-034499] [Medline: 32276954]

XSL•FO
RenderX

15. Mun S, Park K, Kim JK, Kim J, Lee S. Assessment of heart rate measurements by commercial wearable fitness trackers for early identification of metabolic syndrome risk. Sci Rep 2024 Oct 12;14(1):23865. [doi: 10.1038/s41598-024-74619-7] [Medline: 39394437]
16. Cornelissen G. Cosinor-based rhythmometry. Theor Biol Med Model 2014 Apr 11;11:16. [doi: 10.1186/1742-4682-11-16] [Medline: 24725531]
17. Castells F, Laguna P, Sörnmo L, Bollmann A, Roig JM. Principal Component Analysis in ECG Signal Processing. EURASIP J Adv Signal Process 2007 Dec;2007(1):1-21. [doi: 10.1155/2007/74580]
18. Sonawani S, Patil K, Natarajan P. Biomedical signal processing for health monitoring applications: a review. IJASS 2023;10(1):44. [doi: 10.1504/IJASS.2023.129065]
19. Zhang D. Wavelet transform. In: Fundamentals of Image Data Mining: Analysis, Features, Classification and Retrieval (Texts in Computer Science): Springer; 2019:35-44 URL: https://doi.org/10.1007/978-3-030-17989-2_3 [accessed 2025-07-15] [doi: 10.1007/978-3-030-17989-2_3]
20. Khorrami H, Moavenian M. A comparative study of DWT, CWT and DCT transformations in ECG arrhythmias classification. Expert Syst Appl 2010 Aug;37(8):5751-5757. [doi: 10.1016/j.eswa.2010.02.033]
21. Slack D, Hilgard S, Jia E, Singh S, Lakkaraju H. Fooling lime and shap. 2020 Feb 7 Presented at: Proceedings of the AAAI/ACM Conference on AI, Ethics, and Society URL: https://dl.acm.org/doi/proceedings/10.1145/3375627 [accessed 2025-07-15] [doi: 10.1145/3375627.3375830]
22. Nori H, Jenkins S, Koch P, Caruana R. InterpretML: a unified framework for machine learning interpretability. arXiv. Preprint posted online on Sep 19, 2019 URL: https://doi.org/10.48550/arXiv.1909.09223 [accessed 2025-07-15]
23. Hastie TJ. Generalized additive models. In: Statistical Models in S: Routledge:249-307 URL: https://www.taylorfrancis.com/books/9781351414234 [accessed 2025-07-15]
24. Arik S, Pfister T. TabNet: Attentive Interpretable Tabular Learning. AAAI ;35(8):6679-6687. [doi: 10.1609/aaai.v35i8.16826]
25. Sedgwick P. A comparison of parametric and non-parametric statistical tests. BMJ 2015 Apr 17;350(apr17 1):h2053-h2053. [doi: 10.1136/bmj.h2053]
26. Kim HJ, Lee KH, Lee JH, Youk H, Lee HY. The Effect of a Mobile and Wearable Device Intervention on Increased Physical Activity to Prevent Metabolic Syndrome: Observational Study. JMIR Mhealth Uhealth 2022 Feb 24;10(2):e34059. [doi: 10.2196/34059] [Medline: 35200145]
27. Yamaga Y, Svensson T, Chung UI, Svensson AK. Association between Metabolic Syndrome Status and Daily Physical Activity Measured by a Wearable Device in Japanese Office Workers. Int J Environ Res Public Health 2023 Feb 28;20(5):4315. [doi: 10.3390/ijerph20054315] [Medline: 36901325]
28. Nikbakht HA, Rezaianzadeh A, Seif M, Shojaie L, Ghoddusi Johari M, Ghaem H. Physical activity and metabolic syndrome: A population base study (forest and tree model algorithms). Clin Nutr ESPEN 2023 Aug;56:173-179. [doi: 10.1016/j.clnesp.2023.05.014] [Medline: 37344069]
29. Khater T, Tawfik H, Singh B. Explainable artificial intelligence for investigating the effect of lifestyle factors on obesity. Intelligent Systems with Applications 2024 Sep;23:200427. [doi: 10.1016/j.iswa.2024.200427]
30. Castelli L, Macdonald JH, Innominato PF, Galasso L. Editorial: Circadian rhythm, athletic performance, and physical activity. Front Physiol 2024;15:1466152. [doi: 10.3389/fphys.2024.1466152] [Medline: 39145108]
31. McCraty R, Atkinson M, Stolc V, Alabdulgader AA, Vainoras A, Ragulskis M. Synchronization of Human Autonomic Nervous System Rhythms with Geomagnetic Activity in Human Subjects. Int J Environ Res Public Health 2017 Jul 13;14(7):770. [doi: 10.3390/ijerph14070770] [Medline: 28703754]
32. Azulay N, Olsen RB, Nielsen CS, et al. Reduced heart rate variability is related to the number of metabolic syndrome components and manifest diabetes in the sixth Tromsø study 2007-2008. Sci Rep 2022 Jul 14;12(1):11998. [doi: 10.1038/s41598-022-15824-0] [Medline: 35835836]
33. Liu L, Wu X, Li S, Li Y, Tan S, Bai Y. Solving the class imbalance problem using ensemble algorithm: application of screening for aortic dissection. BMC Med Inform Decis Mak 2022 Mar 28;22(1):82. [doi: 10.1186/s12911-022-01821-w] [Medline: 35346181]
34. Korean medicine data center. Korea Institute of Oriental Medicine. URL: https://kdc.kiom.re.kr/ [accessed 2025-07-15]

Abbreviations

CARE: circadian activity rhythm energy
CCE: circadian rhythm energy
CCE_MF: midfrequency of CCE
CQ: circadian quotient
CWT: continuous wavelet transform
EBM: explainable boosting machine
GAM: generalized additive model
GLU: Gated Linear Units
HR: heart rate

XSL•FO
RenderX

IS: interdaily stability
IV: intradaily variability
KDCC: The Korean Medicine Daejeon Citizen Cohort
LIME: local interpretable model-agnostic explanation
MESOR: midline estimating statistic of rhythm
MetS: metabolic syndrome
MST: midsleep time
RA: relative amplitude
RA_HR: relative amplitude for heart rate
SHAP: Shapley Additive Explanations
SVD: singular value decomposition
TabNet: Tabular Neural Networks
TST: total sleep time
WT: wavelet transform
XAI: explainable artificial intelligence
XGBoost: extreme gradient boosting

Edited by A Coristine; submitted 27.11.24; peer-reviewed by A Keshet, B Senst, E Popa; revised version received 14.05.25; accepted 15.05.25; published 16.07.25.

Please cite as:
Kim JK, Mun S, Lee S
Detection and Analysis of Circadian Biomarkers for Metabolic Syndrome Using Wearable Data: Cross-Sectional Study
JMIR Med Inform 2025;13:e69328
URL: https://medinform.jmir.org/2025/1/e69328
doi:10.2196/69328

© Jeong-Kyun Kim, Sujeong Mun, Siwoo Lee. Originally published in JMIR Medical Informatics (https://medinform.jmir.org), 16.7.2025. This is an open-access article distributed under the terms of the Creative Commons Attribution License (https://creativecommons.org/licenses/by/4.0/), which permits unrestricted use, distribution, and reproduction in any medium, provided the original work, first published in JMIR Medical Informatics, is properly cited. The complete bibliographic information, a link to the original publication on https://medinform.jmir.org/, as well as this copyright and license information must be included.

XSL•FO
RenderX

Enhancing Oral Health Diagnostics With Hyperspectral Imaging and Computer Vision: Clinical Dataset Study

Paul Römer[1*], Dr med dent, DMD; Jean-Jacques Ponciano[2*], PhD; Katharina Kloster[1], DMD; Fabia Siegberg[1], Dr med dent, DMD; Bastian Plaß[2], PhD; Shankeeth Vinayahalingam[3], MD, DMD; Bilal Al-Nawas[1], MD, Dr med habil, Dr med dent, DMD, PhD; Peer W Kämmerer[1], MA, MD, Dr med habil, Dr med dent, DMD, PhD; Thomas Klauer[2], DrIng; Daniel Thiem[1], MD, MHBA, Dr med habil, Dr med, DMD, PhD

[1]Department of Oral and Maxillofacial Surgery, University Medical Center of the Johannes Gutenberg University Mainz, Augustusplatz 2, Mainz, Germany

[2]Institute for Spatial Information and Surveying Technology, University of Applied Sciences, Mainz, Germany

[3]Department of Oral and Maxillofacial Surgery, Radboud University Nijmegen, Nijmegen, The Netherlands

[*]these authors contributed equally

Corresponding Author:
Paul Römer, Dr med dent, DMD
Department of Oral and Maxillofacial Surgery, University Medical Center of the Johannes Gutenberg University Mainz, Augustusplatz 2, Mainz, Germany

Abstract

Background: Diseases of the oral cavity, including oral squamous cell carcinoma, pose major challenges to health care worldwide due to their late diagnosis and complicated differentiation of oral tissues. The combination of endoscopic hyperspectral imaging (HSI) and deep learning (DL) models offers a promising approach to the demand for modern, noninvasive tissue diagnostics. This study presents a large-scale in vivo dataset designed to support DL-based segmentation and classification of healthy oral tissues.

Objective: This study aimed to develop a comprehensive, annotated endoscopic HSI dataset of the oral cavity and to demonstrate automated, reliable differentiation of intraoral tissue structures by integrating endoscopic HSI with advanced machine learning methods.

Methods: A total of 226 participants (166 women [73.5%], 60 men [26.5%], aged 24 - 87 years) were examined using an endoscopic HSI system, capturing spectral data in the range of 500 to 1000 nm. Oral structures in red, green, and blue and HSI scans were annotated using RectLabel Pro (by Ryo Kawamura). DeepLabv3 (Google Research) with a ResNet-50 backbone was adapted for endoscopic HSI segmentation. The model was trained for 50 epochs on 70% of the dataset, with 30% for evaluation. Performance metrics (precision, recall, and F_1-score) confirmed its efficacy in distinguishing oral tissue types.

Results: DeepLabv3 (ResNet-101) and U-Net (EfficientNet-B0/ResNet-50) achieved the highest overall F_1-scores of 0.857 and 0.84, respectively, particularly excelling in segmenting the mucosa (0.915), retractor (0.94), tooth (0.90), and palate (0.90). Variability analysis confirmed high spectral diversity across tissue classes, supporting the dataset's complexity and authenticity for realistic clinical conditions.

Conclusions: The presented dataset addresses a key gap in oral health imaging by developing and validating robust DL algorithms for endoscopic HSI data. It enables accurate classification of oral tissue and paves the way for future applications in individualized noninvasive pathological tissue analysis, early cancer detection, and intraoperative diagnostics of oral diseases.

(JMIR Med Inform 2025;13:e76148) doi:10.2196/76148

KEYWORDS

hyperspectral Imaging; endoscopic HSI; eHSI; oral mucosa perfusion; ischemia; oral health diagnostics; deep learning; oral squamous cell carcinoma; medical imaging dataset; tissue classification; spectral analysis; oral pathology; artificial intelligence; dentistry; non-invasive diagnostics

Introduction

Oral diseases, including malignant and premalignant lesions, often occur on pre-existing chronic tissue alterations that are difficult to discern through conventional visual examination. This process heavily relies on the clinician's expertise and subjective interpretation, frequently necessitating additional diagnostic measures. Available methods include incisional and

XSL•FO
RenderX

excisional biopsies, brush biopsies, cytological techniques, and optical approaches. Among these, scalpel biopsy remains the gold standard for diagnosing potentially malignant lesions, offering a diagnostic accuracy of up to 88.9% [1]. However, it involves the partial removal of tissue from a suspicious area for histopathological examination, making it invasive, costly, and potentially inadequate for multilocular lesions. Excisional biopsies, while more reliable due to larger sample sizes, bear the risk of incomplete removal of malignancies and overtreatment in cases of benign lesions [2].

In recent years, less invasive methods, such as brush biopsies, tissue autofluorescence, and chemiluminescence (eg, toluidine blue staining) have been introduced as cost-effective alternatives. Meta-analyses report high sensitivities for these techniques, ranging from 30% to 100% for tissue autofluorescence, 77% for toluidine blue staining, and 91% - 100% for brush biopsies [3-5]. However, these methods have not significantly improved the early detection of oral squamous cell carcinoma. The examiner-dependent variability of less invasive methods can, at worst, delay the accurate diagnosis of oral squamous cell carcinoma, one of the most prevalent malignant tumors globally, accounting for 90% - 95% of all malignant oral cavity pathologies [6-8]. Consequently, the surgical scalpel biopsy remains the diagnostic gold standard [9]. Evidence shows that patients undergoing routine clinical evaluations, including visual inspection and digital palpation, achieve significantly higher 5-year survival rates [10,11].

The integration of advanced imaging technologies into clinical diagnostics is revolutionizing oral health care. Among these innovations, hyperspectral imaging (HSI) stands out as a noninvasive, highly sensitive modality that captures detailed spectral information across hundreds of wavelengths beyond the visible light spectrum. By detecting tissue-specific spectral signatures, HSI combines imaging remission spectroscopy with conventional imaging techniques [12]. HSI acquires spatial and spectral information as a 3D hyperspectral cube in a noncontact, noninvasive, and radiation-free manner. This approach provides vast datasets spanning wide wavelength spectra, enabling the immediate extraction of diagnostically relevant information [13-18]. The efficacy of HSI relies on the distinct spectral signatures of tissues, which result from their absorption, reflection, and refraction properties when illuminated. Each tissue type generates a unique light spectrum that HSI systems can capture, offering the potential for detecting pathological changes with high precision and sensitivity [19].

Endoscopic HSI enhances access to the oral cavity and improves illumination, making it particularly valuable in addressing the growing demand for noninvasive diagnostic methods in oral medicine [20-23]. In this context, the combination of endoscopic HSI with deep learning (DL)–based computer vision techniques provides the potential to significantly enhance diagnostic accuracy, allowing for more comprehensive mapping of the oral cavity and accurate distinction between healthy and pathologically altered mucosa. This offers potential opportunities to avoid unnecessary biopsies and to improve patient-centered therapy by determining individual resection margins. The advanced capabilities of endoscopic HSI, while promising, pose challenges in managing its vast and intricate data output. The spectral data acquired by endoscopic HSI, characterized by tissue-specific signatures, surpass the processing abilities of human observers and traditional analytical tools. This complexity necessitates advanced data analysis, where DL plays a pivotal role. Specialized in interpreting multidimensional datasets, DL uses neural networks to process extensive endoscopic HSI data efficiently, identifying subtle patterns and deviations indicative of pathology that might be missed by human assessment or conventional algorithms [24]. The integration of DL into endoscopic HSI enhances the precision, consistency, and speed of data interpretation, significantly accelerating the diagnostic process. This is especially critical in clinical environments, where timely, accurate real-time analysis can profoundly impact patient outcomes [25-28]. However, implementing DL in endoscopic HSI analysis presents challenges, primarily the limited availability of annotated endoscopic HSI datasets reflecting the complexity and diversity of real-world clinical cases. Existing datasets, often derived from controlled laboratory environments, inadequately prepare DL models for the variability of clinical settings, limiting their practical utility. A review by Cui et al [24] highlights this data scarcity as a major barrier to effective DL analysis in medical imaging, emphasizing the need for specialized datasets. In recent years, DL has also shown great promise in various other domains of medical imaging, including tumor classification in magnetic resonance imaging scans [29] and noise reduction in medical images [30-33]. These studies highlight the versatility and effectiveness of neural networks in processing complex medical images. Building on these advances, the present work applies DL and endoscopic HSI to the oral cavity—an area where such integration remains underexplored despite its clinical potential of enhancing current standards to advance precision and efficacy in oral diagnostics.

Methods

Study Cohort

A total of 226 participants, including 166 (73.5%) women and 60 (26.5%) men aged between 24 and 87 years, were included in this prospective, clinical study. Endoscopic HSI data were acquired at the Department of Oral and Maxillofacial Surgery, Facial Plastic Surgery, University Medical Center. The examined participants represented a heterogeneous group of patients from the oral and maxillofacial surgery outpatient clinic. Patients with macroscopic abnormalities of the oral mucosa, premalignant lesions, or tumors were excluded from the study. All participants provided informed consent prior to the procedure and data collection. The individual pictured in Figure 1 has provided permission for their image to be used in this publication. This study was approved by the local ethics committee of Rhineland-Palatinate (registration number 2021 - 16158) and was conducted in accordance with the code of ethics of the World Medical Association (Declaration of Helsinki).

XSL•FO
RenderX

Figure 1. Experimental setup for endoscopic hyperspectral measurements of the oral cavity.



HSI and Patient Data Acquisition

The HSI datasets were acquired using a state-of-the-art endoscopic HSI sensor system (TIVITA Mini® camera system, Diaspective Vision GmbH). This system detects 100 wavelengths in the range of 500 - 1000 nm, offering a bandwidth of 5 nm [34]. The device uses the pushbroom principle, enabling chemical component detection based on light absorption and reflection behavior. During operation, light enters the optical system of the spectrometer through the lens, where it is collimated and separated into individual wavelengths using a transmission grating. The separated light then passes through a second optical system before reaching the sensor of the connected complementary metal-oxide-semiconductor camera. The spectrometer directly detects the spatial direction and width of the object being scanned (Y-axis) while the second spatial direction and length of the object (X-axis) are determined through the continuous mechanical movement of the light entry gate within the scanning unit. This process generates a 3D data cube that includes a spectral dimension (λ), capturing complete tissue spectra for each pixel within the wavelength range of 500 - 1000 nm [35].

Standardized measurement protocols were followed during image acquisition, maintaining a consistent distance of 7 - 10 cm to ensure high-quality and distinct image data (Figure 1). Measurements were performed in an examination room under dimmed lighting conditions to ensure uniformity and comparability. A total of 226 participants aged between 24 and 87 years, including 166 (73.5%) women and 60 men (26.5%), were prospectively recruited at the outpatient department of the clinic of Oral and Maxillofacial Surgery, University Medical Center, where all individuals underwent routine clinical evaluation and inspection. Inclusion was limited to individuals without clinically apparent mucosal lesions, premalignant conditions, or malignancies, ensuring a representative sample of nonpathological oral tissue. Informed consent was obtained from all participants prior to data acquisition. The recruitment strategy was designed to capture a broad range of healthy oral tissue presentations to ensure the generalizability of HSI data across different anatomical sites and patient demographics. For each patient, 5 images were taken, including views of the right and left cheeks, the palate, the back of the tongue, and the closed row of teeth. The data were subsequently pseudonymously archived using camera-specific software tools.

Red, Green, and Blue–Imaging and Endoscopic HSI Data Files

The Comprehensive Oral Health Hyperspectral Dataset (comprehensive, annotated endoscopic HSI dataset of the oral cavity) primarily comprises RGB (red, green, and blue) and endoscopic HSI data with corresponding annotations. These components in the presented dataset are each important to address the fundamental challenges in DL for semantic segmentation [36], providing robust and effective model training. The RGB component offers standard visual spectrum imagery of the oral cavity, serving as a foundational baseline for comparison with more sophisticated imaging modalities like raw and processed endoscopic HSI data.

Annotation Process and Verification

Individual annotations of the oral cavity's anatomical sites were manually performed using an image annotation tool (RectLabel Pro version 2024.06.07, Ryo Kawamura; Tokyo, Japan). To ensure high-quality image data annotation, several key features were implemented. First, detailed annotation guidelines were developed to ensure reproducible results. Comprehensive training sessions and practical exercises for annotators were conducted, followed by feedback rounds to enhance their skills. Each image was annotated by at least 2 independent specialists to minimize subjective errors. Regular quality checks were performed through sample reviews by senior specialists to detect inconsistencies. Continuous feedback was given to annotators, and guidelines were regularly updated based on this feedback. Interannotator analysis of 2 segmentation annotation sets ("original" vs "new"), each assigning a class label (out of 20 possible objects plus background) to every pixel, was carried out additionally for internal quality assurance. Agreement was quantified using metrics that capture both overall and class-specific consistency: (1) Pixel Accuracy, (2) Cohen Kappa (including and excluding background), and (3) Dice Coefficients, which are mathematically equivalent to the F_1-score in the binary case. To ensure a realistic representation of everyday clinical practice, the annotated structures marked for subsequent analysis corresponded to the individual intraoral site and situation, including "clutter (n=752)," "blood (n=3)," "brackets (n=15)," "floor of mouth (n=43)," "gingiva (n=511),"

XSL•FO
RenderX

"implant (n=10)," "lip (n=603)," "mucosa (n=745)," "palate (n=539)," "prosthesis (n=65)," "reflection (n=106)," "retractor (n=702)," "suture (n=2)," "telescopic crown (n=28)," "tongue (n=587)" and "tooth (n=681)," with a number of distinct classes varying from a minimal count of 2 for "suture" to a substantial count of 752 for "clutter".

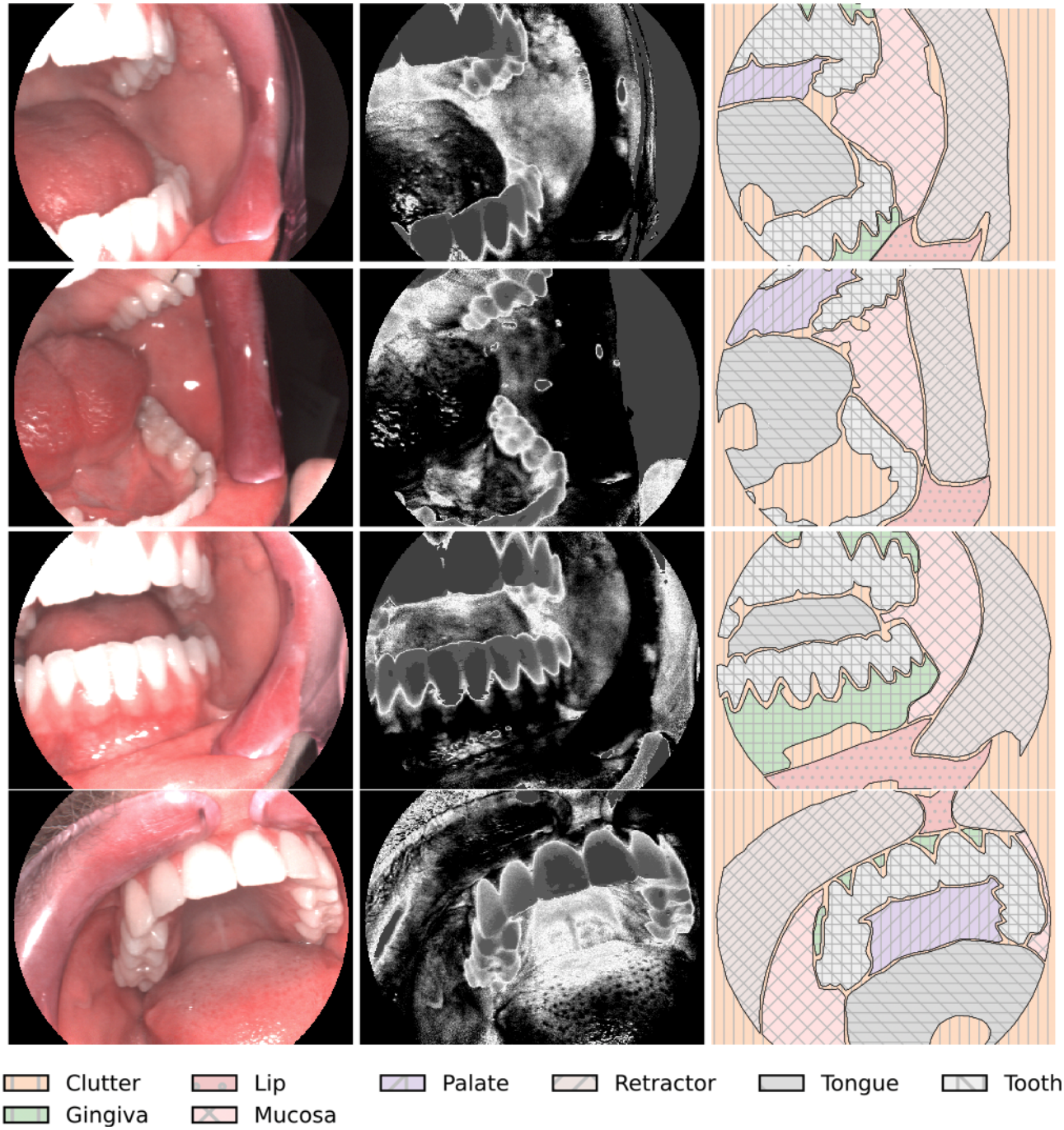
To minimize diagnostic errors, undersegmentation of anatomical structures was avoided, and experienced clinical experts reviewed each annotation to ensure that all clinically relevant features were thoroughly labeled. This conservative approach occasionally led to small unannotated gaps between each class to prevent the merging of different anatomical sites. The digital annotations in XML format provided a semantic comprehension of the image data, which are essential for the application and training of machine learning and computer vision to differentiate various oral site conditions based on the RGB and endoscopic HSI components (Figure 2).

Preprocessing further involved the conversion of the original hyperspectral data from .DAT format to the NumPy format (.npy) to facilitate interoperability, reproducibility, and ease of use for DL models. Regarding data augmentation, spatial transformations, such as image rotations to enhance model robustness, were used. The addition of noise and blur was intentionally avoided, as these operations could introduce spectral distortions that are not physically plausible in the HSI context.

Given the specific goal of oral structure differentiation, classes with low incidence, such as suture, blood, implant, brackets, telescopic crown, prosthesis, reflection, and floor of mouth were deemed less relevant and excluded from further analysis to prevent skewing the learning process and improve the model's ability to generalize to more common and diagnostically relevant structures. By focusing on higher-incidence classes, such as palate, retractor, mucosa, tongue, tooth, lip, and gingiva, the training process is optimized, enhancing the model's efficiency and effectiveness across diverse oral structures. To achieve representative results for the annotation, an additional interannotator analysis and validation was carried out to detect possible person-dependent deviations.

XSL•FO
RenderX

Figure 2. Examples highlighting the detailed annotations, red, green, blue imagery, and features within endoscopic hyperspectral imaging Band 9 (wavelength of 545 nm), which are especially discernible for human eyes.



Dataset Structure

To ensure user-friendly analysis of the hyperspectral dataset and reliable collaboration in the research community, the dataset has been specifically optimized for the Python ecosystem (Python Software Foundation 2023, Python Language Reference, version 3.10) instead of the proprietary software required to load endoscopic HSI data. Regarding scientific computation, Python emerges as the predominant programming language due to its extensive libraries and robust community support. After acknowledging this prevalent preference and recognizing the NPY file format as the most straightforward option for loading data into NumPy, a pivotal library for numerical computations in Python [37], all elements of the comprehensive, annotated endoscopic HSI dataset of the oral cavity (“RGB,” “Annotations,” “HSI_Data_Files”) were archived in the “.npy” format. The NPY format offers several advantages: It is compact and efficient for loading and saving and supports a wide range of data types. This standardization eliminates the complexity and potential incompatibilities associated with proprietary formats. In order to provide high-quality, detailed annotations of the complex intraoral structures, digital annotations were elaborated in XML format. To enhance utility and facilitate integration into researchers’ workflows, a semantic map of the oral cavity was generated directly from the XML datasets for each image. These maps essentially consisted of binary or multiclass masks, delineating the categorization of each pixel based on the detailed

XSL•FO
RenderX

information provided in XML. However, the creation of these maps is an automated process that translates the complex structured information of the XML annotations into a simple but comprehensive format that can easily be integrated into machine learning models to differentiate tissue types based on the values of each pixel corresponding to the specific annotated category. The workflow in short: First, eHSI endoscopic HSI data are loaded, and semantic information is extracted from the XML file. This information is then used to generate a semantic map of the oral cavity, where each pixel value corresponds to a specific annotated category, such as different tissue types or anatomical sites. The resulting semantic map provides comprehensive, pixel-wise annotations of the frame, ready for application in segmentation algorithms.

Statistical Analysis of the Dataset

For an initial assessment of the spectral data, a coefficient of variation (CV) was used as a statistical measure. The CV is a standardized measure for dispersion of a probability distribution or frequency distribution and defines the ratio of the SD to the mean, expressed as percentage. It is particularly useful in the context of HSI, as it allows the comparison of variation between different classes and bands despite the different mean intensities. The formula used for the coefficient of variation is:

$$CV=(\sigma\mu)\times100\%$$

where σ is the SD of the dataset and μ is the mean of the dataset.

Machine Learning and DL Techniques

This study adapted several state-of-the-art models and their performance assessing semantic segmentation in the context of oral health diagnostics. These models included DeepLabv3 [38-40], as well as fully convolutional network (FCN [41]) and pyramid scene parsing network (PSPNet [42]), each tested with ResNet-50 and ResNet-101 [43], backbones. In addition, PSPNet using VGG16 [44] and U-Net [45] models using both EfficientNet-B0 [46] and ResNet-50 backbones were evaluated. Each model was optimized for processing our dataset, which features challenging anatomical structures, enabling a comprehensive analysis of their suitability for handling the variability inherent in endoscopic HSI data for oral health diagnosis. The models were trained over 50 epochs using 70% of the comprehensive, annotated endoscopic HSI dataset of the oral cavity test set, with the remaining 30% reserved for evaluation. This split allowed for a thorough assessment of the models' ability to generalize to unseen data. Each model's performance on endoscopic HSI data was evaluated using Precision, Recall, and the F_1-score, providing a comprehensive measure of their effectiveness in segmenting and classifying the various anatomical structures present in the dataset.

Ethical Considerations

The study was approved by the local ethics committee of Rhineland-Palatinate (registration number: 2021-16158) and was conducted in accordance with the protocol and in compliance with the moral, ethical, and scientific principles governing clinical research as set out in the Declaration of Helsinki of 1975 as revised in 1983. Informed consent was obtained from all participants involved in the study. This study received approval from the Ethics Committee of the Medical Association of Rhineland-Palatinate (reference number 2021-15858). All procedures adhered to institutional and national ethical standards and were conducted in accordance with the Declaration of Helsinki. Participants were provided comprehensive information regarding the study's nature, purpose, procedures, data usage, and the potential publication of anonymized images or data related to their participation. The privacy and confidentiality of all participants were rigorously protected. No identifying information, including names or hospital IDs, has been included in the manuscript. Images containing identifiable features were excluded except for Figure 1, which depicts the corresponding author (PR), who has provided written consent for the use of their image in this publication. No financial or material compensation was offered or provided to the participants in this study.

Results

Variability of the Dataset

A descriptive statistical analysis of the hyperspectral dataset was performed to describe the distribution and variability of the data. Mean values and SD across the spectral bands were analyzed for each class delineated in the hyperspectral images. The objective of the statistical data evaluation was to accurately represent the central tendencies and variabilities of spectral signatures, which are indicative of various anatomical and pathological entities in oral health. Mean values and SDs for all classes across all spectral bands were presented in a consolidated diagram (Figure 3).

The results indicated that the CV for the majority of classes, across most spectral bands, substantially exceeded the commonly recognized threshold of 15%, which is generally considered high. In contrast, a CV below 5% would have denoted homogeneous data, while values between 5% and 15% would have indicated moderate uniformity. The consistently elevated CV values observed across all classes thus underscored significant spectral diversity within each class (Figure 4).

XSL•FO
RenderX

Figure 3. Consolidated diagram of mean values and SD for each class across all measured spectral bands.

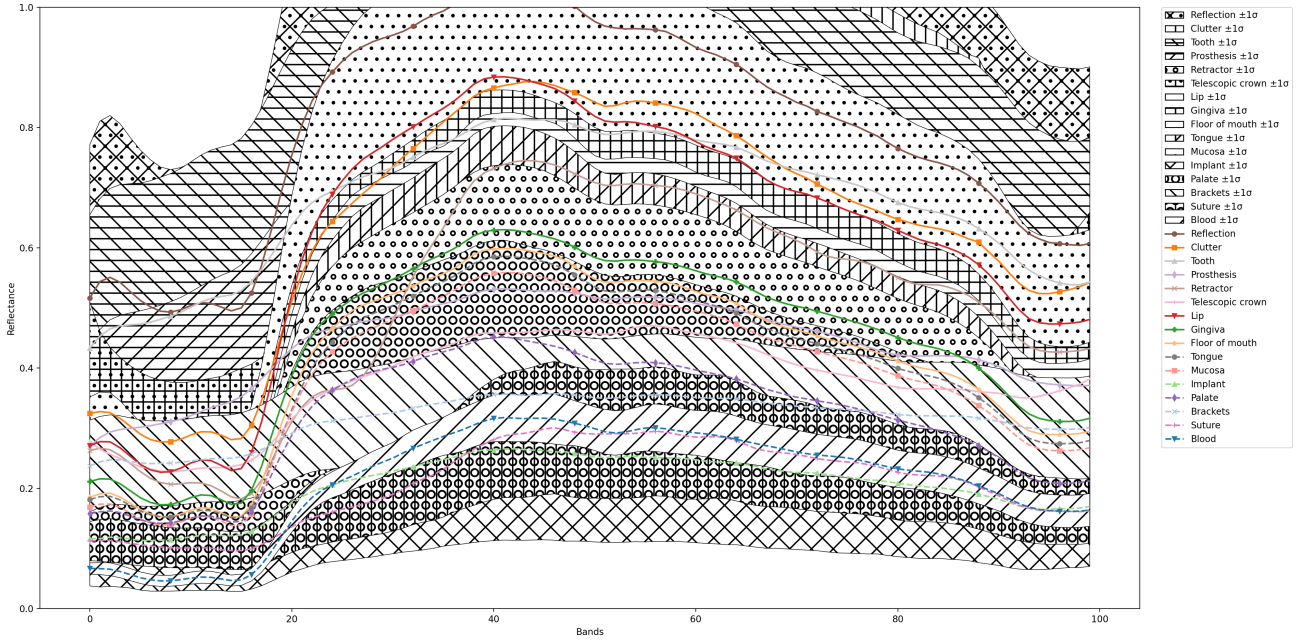
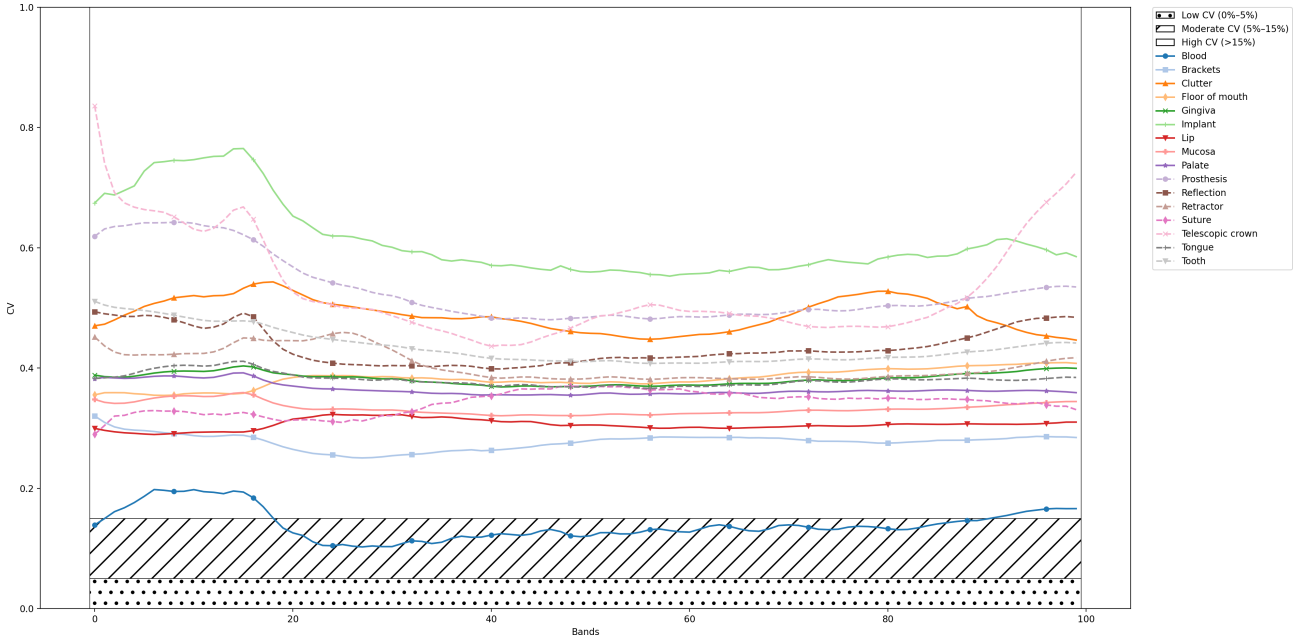


Figure 4. Coefficient of variation over the corresponding bandwidth of various examination classes. CV: coefficient of variation.



DL Model Performance

The DeepLabv3 model with the ResNet-50 backbone achieved solid overall performance, with an F_1-score of 0.855, performing especially well on the segmentation of mucosa, retractor, and tooth. However, it exhibited moderate performance on gingiva and lip, with F_1-scores of 0.753 and 0.709, respectively. Switching to the deeper ResNet-101 backbone improved the overall performance slightly, with an F_1-score of 0.857, particularly enhancing the model's ability to segment clutter and gingiva (Table 1).

Both FCN-ResNet-50 and FCN-ResNet-101 demonstrated robust segmentation performance, achieving overall F_1-scores of 0.862 and 0.861, respectively (Table 2). They excelled in segmenting retractor (F_1-score=0.942 for both), tooth (F_1-score=0.910), palate (F_1-score=0.890), and mucosa (F_1-score≥0.912). However, lip and gingiva posed challenges for both backbones, reflected by lower F_1-scores around 0.72 and 0.77, respectively. Although switching to the deeper ResNet-101 backbone yielded marginal improvements in certain classes, the overall performance remained comparable between the 2 architectures.

PSPNet models showed slightly lower performance, with the ResNet-50 backbone achieving an F_1-score of 0.837 and the VGG16 backbone scoring 0.808. While these models handled classes, such as retractor and tooth, relatively well, they faced difficulties in the segmentation of gingiva and lip, particularly when using VGG16. The lower overall performance of PSPNet VGG16 compared to ResNet-50 reflects the influence of the backbone on the segmentation outcomes (Table 3).

XSL•FO
RenderX

U-Net (EfficientNet-B0) and U-Net (ResNet-50) both demonstrated robust segmentation performance, attaining overall F_1-scores of 0.867 and 0.840, respectively (Table 4). They excelled particularly at segmenting retractor (F_1-score=0.941 vs 0.927), palate (F_1-score=0.909 vs 0.881), and mucosa (F_1-score=0.920 vs 0.901). Tongue and tooth segmentation also performed well, with F1-scores exceeding 0.85 for both models. However, both networks faced challenges in segmenting lip (F_1-score=0.755 vs 0.695) and gingiva (F_1-score=0.751 vs 0.721), indicating opportunities for further refinement in these classes.

Figure 5 demonstrates that DeepLabv3 (ResNet-101) and U-Net (EfficientNet-B0) outperform other models across most tissue classes, with lower F_1-scores consistently observed for lip and gingiva segmentation.

Table . Results showing precision, recall, and F_1-score for different classes in a comparison of DeepLabv3 ResNet-50 and DeepLabv3 ResNet-101.

Class	Precision		Recall		F_1-score	
	DeepLabv3 ResNet-50	DeepLabv3 ResNet-101	DeepLabv3 ResNet-50	DeepLabv3 ResNet-101	DeepLabv3 ResNet-50	DeepLabv3 ResNet-101
Overall	0.849	0.851	0.861	0.863	0.855	0.857
Palate	0.886	0.874	0.918	0.929	0.901	0.900
Retractor	0.936	0.942	0.940	0.938	0.938	0.940
Mucosa	0.915	0.914	0.914	0.916	0.914	0.915
Tongue	0.878	0.872	0.888	0.892	0.883	0.882
Clutter	0.840	0.844	0.848	0.849	0.844	0.846
Tooth	0.862	0.871	0.937	0.936	0.898	0.902
Lip	0.723	0.730	0.695	0.683	0.709	0.706
Gingiva	0.756	0.757	0.751	0.765	0.754	0.761

Table . Results showing precision, recall, and F_1-score for different classes in a comparison of FCN-ResNet-50 and FCN-ResNet-101.

Class	Precision		Recall		F_1-score	
	FCN[a]-ResNet-50	FCN-ResNet-101	FCN[a]-ResNet-50	FCN-ResNet-101	FCN[a]-ResNet-50	FCN-ResNet-101
Overall	0.850	0.850	0.874	0.873	0.862	0.861
Palate	0.859	0.860	0.924	0.923	0.890	0.890
Retractor	0.940	0.935	0.944	0.949	0.942	0.942
Mucosa	0.904	0.907	0.921	0.929	0.912	0.916
Tongue	0.881	0.882	0.909	0.893	0.895	0.887
Clutter	0.864	0.863	0.839	0.843	0.852	0.853
Tooth	0.878	0.876	0.946	0.910	0.910	0.910
Lip	0.699	0.718	0.744	0.723	0.721	0.721
Gingiva	0.776	0.765	0.767	0.777	0.772	0.771

[a]FCN: fully convolutional network.

XSL•FO
RenderX

Table . Results showing precision, recall, and F_1-score for different classes in a comparison of PSPNet-ResNet-50[a] and PSPNet-VGG16.

Class	Precision		Recall		F_1-score	
	PSPNet-ResNet-50	PSPNet-VGG16	PSPNet-ResNet-50	PSPNet-VGG16	PSPNet-ResNet-50	PSPNet-VGG16
Overall	0.849	0.797	0.830	0.822	0.837	0.809
Palate	0.840	0.854	0.915	0.840	0.876	0.847
Retractor	0.929	0.853	0.919	0.906	0.924	0.879
Mucosa	0.906	0.835	0.842	0.841	0.873	0.838
Tongue	0.903	0.794	0.837	0.886	0.869	0.837
Clutter	0.793	0.807	0.873	0.779	0.831	0.793
Tooth	0.877	0.865	0.910	0.907	0.893	0.886
Lip	0.766	0.716	0.701	0.693	0.732	0.704
Gingiva	0.775	0.651	0.639	0.723	0.700	0.685

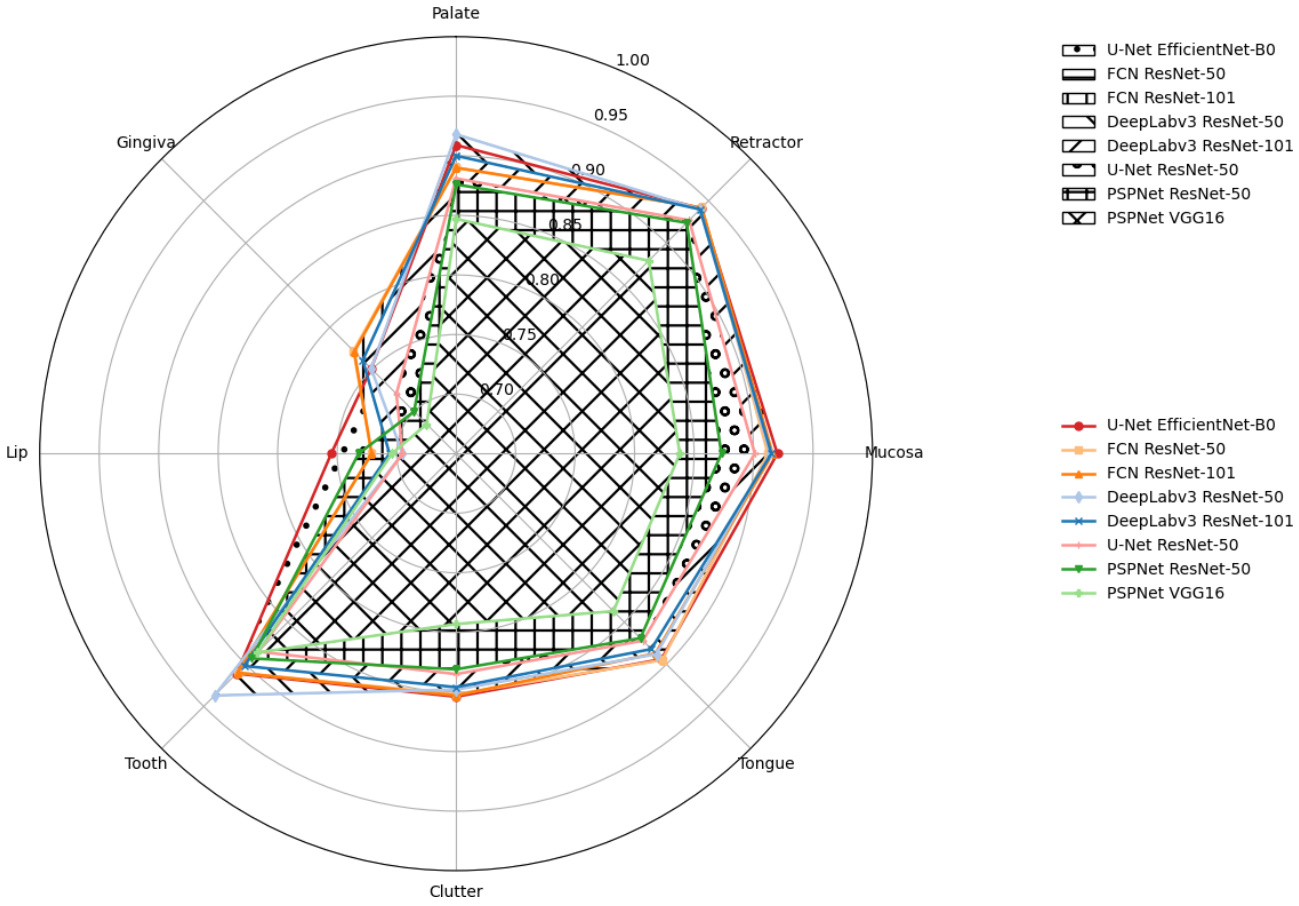
[a]PSPNet: pyramid scene parsing network.

Table . Results showing precision, recall, and F_1-score for different classes in a comparison of U-Net-EfficientNet-B0 and U-Net-Res

Class	Precision		Recall		F_1-score	
	U-Net-Efficient-Net-B0	U-Net-ResNet-50	U-Net-Efficient-Net-B0	U-Net-ResNet-50	U-Net-Efficient-Net-B0	U-Net-ResNet-50
Overall	0.853	0.846	0.882	0.836	0.867	0.840
Palate	0.892	0.857	0.927	0.907	0.909	0.881
Retractor	0.956	0.936	0.927	0.918	0.941	0.927
Mucosa	0.915	0.918	0.924	0.884	0.920	0.901
Tongue	0.893	0.856	0.895	0.889	0.894	0.872
Clutter	0.862	0.811	0.846	0.862	0.854	0.835
Tooth	0.876	0.875	0.949	0.894	0.911	0.885
Lip	0.711	0.734	0.806	0.661	0.755	0.695
Gingiva	0.723	0.780	0.782	0.671	0.751	0.721

XSL•FO
RenderX

Figure 5. Spider plot illustrating the per-class F_1-score performance of different deep learning models for oral tissue segmentation.



Interannotator Agreement

The analysis of segmentation annotations revealed an overall pixel accuracy of 80.84%, indicating a high level of interannotator agreement. Cohen Kappa, a more robust measure of interannotator agreement, was 77.56% when including the background class, indicating substantial agreement. When the background was excluded, Kappa increased to 82.91%, highlighting even stronger agreement for the segmentation of foreground structures. Dice coefficients per class ranged from near-zero (in classes with minimal or inconsistent labeling) to 93% in well-defined classes, where the overlap between annotations was nearly perfect. Since the Dice Coefficient measures spatial overlap between segmentation masks, high Dice scores (above 90%) indicate excellent agreement, whereas lower values suggest potential ambiguity or underrepresentation of certain structures.

Discussion

Principal Findings and Comparison With Previous Works

The objective of this study was to establish a digital map of the oral cavity using endoscopic HSI in conjunction with advanced machine learning techniques and therefore to develop a comprehensive endoscopic HSI dataset. This approach aimed to enable reliable and automated differentiation of various tissue types and objects based on the spectral data acquired from the endoscopic HSI system. Despite the continuous interest in faster, minimally invasive diagnostic techniques, methods, such as brush biopsies and in vivo fluorescence procedures have faced challenges in establishing themselves as reliable alternatives due to their comparatively lower sensitivity and specificity [2,4,5,9]. Modern methods, such as endoscopic HSI, represent a state-of-the-art, innovative approach in the field of automated image and tissue classification. In our preliminary ex vivo studies, we have already demonstrated that HSI can differentiate between various tissue types and states based on specific wavelength patterns [20,47]. However, to effectively differentiate between pathological and healthy tissue conditions in vivo, a substantial dataset of hyperspectral signatures from healthy tissues is essential [47].

The study introduces a comprehensive collection of 1,130,751 endoscopic HSI–cubes of healthy oral mucosa, captured in vivo from various angles, creating a representative digital map that includes relevant tissues and objects of the oral cavity. This dataset forms a representative digital endoscopic HSI map, encompassing relevant tissues and structures of the oral cavity. By establishing a robust reference for healthy tissue, this dataset lays the groundwork for advancing HSI-based diagnostics, particularly in the identification of premalignant and malignant mucosal lesions and the precise definition of tumor resection margins.

The findings revealed elevated CV across most classes, indicating substantial spectral diversity in endoscopic HSI data. This high variability poses challenges for threshold-based classification methods, as intraclass variation can lead to class

XSL•FO
RenderX

overlap. However, this diversity also holds valuable information that, when leveraged by advanced computational models, can enhance tissue classification and pathological anomaly detection with high accuracy.

To address this complexity, this study evaluated several state-of-the-art segmentation models, including DeepLabv3, FCN, PSPNet, and U-Net, with different backbones, such as ResNet-50, ResNet-101, VGG16, and EfficientNet-B0. These architectures were chosen for their effectiveness in semantic segmentation, balancing feature extraction capability, computational efficiency, and global context recognition. DeepLabv3 was selected for its ability to handle scale variability and capture fine details while FCN served as a strong baseline due to its foundational role in image segmentation. PSPNet was included for its strong capability in capturing global context, which is crucial for recognizing complex structures in medical imaging. U-Net, widely used in medical imaging, was chosen for its ability to achieve accurate segmentation even with limited data.

The choice of backbones was guided by their specific strengths. ResNet-50 and ResNet-101 were selected for their robust feature extraction, VGG16 for its simplicity and high-resolution detail, and EfficientNet-B0 for its optimized architecture that balances performance and computational efficiency. By incorporating models with varying depths and parameter complexities, this study ensures a comprehensive evaluation of segmentation performance while maintaining a focus on efficient training and inference times. The integration of the DeepLabv3 model with the ResNet-50 as well as with the ResNet-101 backbone offers a robust semantic segmentation approach for endoscopic HSI data interpretation. The primary modification to all the models, including DeepLabv3, FCN, PSPNet, and U-Net (with backbones, such as ResNet-50, ResNet-101, EfficientNet-B0, and VGG16), involved adapting the first convolutional layer to handle the variable number of channels in the dataset. This adjustment was essential to accommodate the multidimensional spectral data of the HSI dataset, as opposed to the standard 3-channel RGB imagery. This modification enables the models to use the unique spectral information in the HSI data cubes beyond the visible spectrum. Despite these adjustments, the deep residual learning architectures of ResNet-50 and ResNet-101 retain their capacity to extract high-level features—an essential aspect of HSI data analysis [43]. These backbones excel at identifying subtle spectral patterns crucial for accurate disease detection and classification. Leveraging atrous convolution and atrous spatial pyramid pooling, the DeepLabv3 model efficiently captures multiscale information [48]. This capability facilitates precise image segmentation, an essential feature for diagnosing oral health conditions with subtle and overlapping visual signatures. Likewise, FCN and PSPNet, with their robust architectures, and U-Net, recognized for its effectiveness in medical imaging, also benefited from the capacity to process and interpret multidimensional spectral data.

The endoscopic HSI procedure implemented in this study achieves results that are comparable to those obtained in preliminary HSI-ex vivo trials conducted by our research group in 2021 [47]. In this study, using a similar approach with a lightweight 6-layer deep neural network containing 10,445 parameters trained over 4000 epochs, tissue samples of fat, muscle, and oral mucosa could be differentiated with an overall class accuracy of over 80%. Similarly, in a study by Ma et al, tissue from various organs, including the kidney, liver, lung, muscle, salivary gland, and spleen, was identified using automated polarized HSI with an accuracy of up to 87% [49]. Furthermore, a deep convolutional neural network established by Poonkuzhali et al [50] could accurately identify brain tissue with an F_1-score precision of 97.3% using HSI in a recent study conducted in 2023. Unlike previous studies that focused on ex vivo tissue samples and organ-specific HSI data [47], the present work introduces the first large-scale in vivo annotated endoscopic HSI dataset of the oral cavity acquired under realistic clinical conditions. While earlier studies demonstrated the technical feasibility of HSI-based tissue differentiation, these approaches often lacked anatomical complexity, semantic annotations, and clinical variability. This study addresses these deficiencies by providing a large annotated in vivo HSI dataset and evaluating multiple DL models especially adapted for HSI data analysis. This provides the basis for clinically applicable segmentation of oral tissues and paves the way for future studies involving pathological lesions.

These findings affirm that HSI, when integrated with appropriate modalities, can serve as a reliable tool for differentiating various tissues in both in vivo and ex vivo setups. In oncological surgery, fast, reliable, and minimally invasive diagnosis of pathological tissue conditions is of paramount importance. Numerous studies in this field have shown that HSI can dependably differentiate between tumor and healthy tissue by analyzing histopathological sections and their spatial-spectral features. Moreover, the combination of HSI and DL has shown superior results compared to the use of RGB images and conventional support-vector-machine approaches [51-56].

In this study, the established DL and neural network approach was able to accurately identify different types of oral mucosa with an overall precision of approximately 91%. DeepLabv3 (ResNet-101) and U-Net (EfficientNet-B0) emerged as the top performers, demonstrating robust segmentation across key anatomical classes. While all models could benefit from further refinement in gingiva and lip segmentation, their consistent accuracy in identifying retractors and teeth underscores the strength of the dataset. While there is no universally accepted threshold for clinical applicability, F_1-scores above 0.85 are generally considered promising in similar biomedical imaging tasks. Scores in this range suggest that the method may already approach a level of accuracy relevant for clinical decision-making, though further validation in real-world settings would be required. Notably, U-Net (EfficientNet-B0) exhibited exceptional segmentation of retractors, mucosa, and teeth, indicating its strong potential for medical image segmentation applications. The results demonstrate the dataset's suitability for training advanced neural networks, particularly in challenging medical segmentation tasks.

Limitations of our study specifically include the acquisition of a higher amount of data, which depended heavily on the individual patient volume of the clinic conducting the study.

XSL•FO
RenderX

This represents a major challenge, particularly when aiming to document various oral mucosal lesions and precancerous mucosal conditions. To address the issue of data scarcity, the raw data generated in this study will be made publicly available. This initiative aims to provide other research groups with the opportunity to use and build upon the dataset for further investigations. Furthermore, while the study cohort was intentionally designed to include a broad cross-section of patients from a university-based outpatient clinic, selection bias cannot be fully excluded. As recruitment was confined to a single university clinic, the cohort may not fully reflect the demographic and clinical variability found in primary care or the general population. Other limitations include variable lighting conditions, motion artifacts, and spectral overlaps, as well as overexposure and underexposure. Overexposure can occur due to various factors, such as the variability in patient anatomy, the movement during image capture, or the fluctuation of lighting conditions in an operating room. While overexposed images are typically regarded as artifacts and excluded from datasets, our approach incorporates them, acknowledging that such occurrences are an inherent part of clinical practice. Understanding that these instances present both challenges and opportunities for advanced image processing techniques, we have carefully indexed these overexposed images for further analysis. This approach enhances the resilience and adaptability of the models trained on this dataset, ensuring they perform effectively in real clinical environments. By incorporating overexposed images, the models are better equipped to handle the full spectrum of data variability, including common environmental factors. This combination highlights the substantial potential of endoscopic HSI data to significantly enhance the precision and reliability in detecting and categorizing healthy and pathological oral conditions. This convergence not only paves the way for significant advancements in diagnostic methodologies but also holds the potential to substantially enhance patient care. External validation is currently planned as part of future work, particularly for mucosa segmentation. We intend to validate our model on an ex vivo dataset that includes mucosa samples captured under different acquisition conditions. At this stage, the focus of this study was the initial validation on the internally collected dataset. Corresponding follow-up studies are currently in preparation and will include HSI of pathological tissue conditions, such as oral mucosal lesions and neoplastic changes, to assess the transferability and diagnostic robustness of the proposed models in clinically relevant scenarios. By enabling earlier detection and more precise characterization of oral health conditions, this approach facilitates the development of more effective treatment strategies, ultimately leading to improved patient outcomes and a higher standard of care.

Conclusion

This study presents the first large-scale in vivo annotated dataset of the oral cavity using endoscopic HSI under realistic clinical conditions. By combining hyperspectral datasets and DL-based segmentation, it was possible to demonstrate the feasibility of automated, noninvasive tissue classification across important anatomical intraoral structures. Comparative analysis reveals DeepLabv3 and U-Net as robust architectures for oral tissue classification. The comprehensive dataset consequently provides a sufficient foundation for future work on pathological tissue detection, intraoperative margin assessment in oncology, and early, individualized diagnostics in oral medicine.

Acknowledgments

The results of the present study are part of the doctoral thesis of the co-author and student of the University of Mainz, Katharina Kloster, and as such will be made publicly available as part of the doctorate. It was funded by the Deutsche Forschungsgemeinschaft (DFG, German Research Foundation) – Project number 516210826.

Data Availability

All raw data on which this study is based will be made available by the corresponding author upon request. The datasets used and/or analyzed during the current study are available from the corresponding author on reasonable request.

Authors' Contributions

The conceptualization of the study was carried out by DT, JJP, and PR. Methodology development was led by DT, JJP, BP, PR, KK and TK. Validation was performed by DT, JJP, BP, and PR. Formal analysis was conducted by DT, PWK, JJP, BP, PR, and TK. Investigation was carried out by DT, BP, KK and JJP. Resources were provided by DT, JJP, TK and BAN. Data curation was managed by DT, KK, PR and JJP. The original draft was prepared by DT, JJP, PR, SV. Manuscript review and editing were done by DT, JJP, BP, SV, PWK, TK and BAN. Visualization was prepared by DT, JJP and PR. Supervision was conducted by DT, JJP, PR and TK. Project administration was managed by DT, JJP, PR and TK.

Conflicts of Interest

None declared.

References

1. Chen S, Forman M, Sadow PM, August M. The diagnostic accuracy of incisional biopsy in the oral cavity. J Oral Maxillofac Surg 2016 May;74(5):959-964. [doi: 10.1016/j.joms.2015.11.006] [Medline: 26682520]

XSL•FO
RenderX

2. Pentenero M, Carrozzo M, Pagano M, et al. Oral mucosal dysplastic lesions and early squamous cell carcinomas: underdiagnosis from incisional biopsy. Oral Dis 2003 Mar;9(2):68-72. [doi: 10.1034/j.1601-0825.2003.02875.x] [Medline: 12657031]
3. Macey R, Walsh T, Brocklehurst P, et al. Diagnostic tests for oral cancer and potentially malignant disorders in patients presenting with clinically evident lesions. Cochrane Database Syst Rev 2015 May 29;2015(5):CD010276. [doi: 10.1002/14651858.CD010276.pub2] [Medline: 26021841]
4. Rashid A, Warnakulasuriya S. The use of light-based (optical) detection systems as adjuncts in the detection of oral cancer and oral potentially malignant disorders: a systematic review. J Oral Pathol Med 2015 May;44(5):307-328. [doi: 10.1111/jop.12218] [Medline: 25183259]
5. Kämmerer PW, Rahimi-Nedjat RK, Ziebart T, et al. A chemiluminescent light system in combination with toluidine blue to assess suspicious oral lesions-clinical evaluation and review of the literature. Clin Oral Investig 2015 Mar;19(2):459-466. [doi: 10.1007/s00784-014-1252-z] [Medline: 24888605]
6. Bray F, Ferlay J, Soerjomataram I, Siegel RL, Torre LA, Jemal A. Global cancer statistics 2018: GLOBOCAN estimates of incidence and mortality worldwide for 36 cancers in 185 countries. CA Cancer J Clin 2018 Nov;68(6):394-424. [doi: 10.3322/caac.21492] [Medline: 30207593]
7. Panarese I, Aquino G, Ronchi A, et al. Oral and Oropharyngeal squamous cell carcinoma: prognostic and predictive parameters in the etiopathogenetic route. Expert Rev Anticancer Ther 2019 Feb;19(2):105-119. [doi: 10.1080/14737140.2019.1561288] [Medline: 30582397]
8. Barsouk A, Aluru JS, Rawla P, Saginala K, Barsouk A. Epidemiology, risk factors, and prevention of head and neck squamous cell carcinoma. Med Sci (Basel) 2023 Jun 13;11(2):42. [doi: 10.3390/medsci11020042] [Medline: 37367741]
9. Brocklehurst P, Kujan O, O'Malley LA, Ogden G, Shepherd S, Glenny AM. Screening programmes for the early detection and prevention of oral cancer. Cochrane Database Syst Rev 2013 Nov 19;2013(11):CD004150. [doi: 10.1002/14651858.CD004150.pub4] [Medline: 24254989]
10. Sankaranarayanan R, Ramadas K, Thomas G, et al. Effect of screening on oral cancer mortality in Kerala, India: a cluster-randomised controlled trial. Lancet 2005;365(9475):1927-1933. [doi: 10.1016/S0140-6736(05)66658-5] [Medline: 15936419]
11. Sankaranarayanan R, Ramadas K, Thara S, et al. Long term effect of visual screening on oral cancer incidence and mortality in a randomized trial in Kerala, India. Oral Oncol 2013 Apr;49(4):314-321. [doi: 10.1016/j.oraloncology.2012.11.004] [Medline: 23265945]
12. Halicek M, Fabelo H, Ortega S, Callico GM, Fei B. In-vivo and ex-vivo tissue analysis through hyperspectral imaging techniques: revealing the invisible features of cancer. Cancers (Basel) 2019 May 30;11(6):31151223. [doi: 10.3390/cancers11060756] [Medline: 31151223]
13. Ishida T, Kurihara J, Viray FA, et al. A novel approach for vegetation classification using UAV-based hyperspectral imaging. Comput Electron Agric 2018 Jan;144:80-85. [doi: 10.1016/j.compag.2017.11.027]
14. Miljković V, Gajski D. Adaptation of industrial hyperspectral line scanner for archaeological applications. Int Arch Photogramm Remote Sens Spatial Inf Sci ;XLI-B5:343-345. [doi: 10.5194/isprs-archives-XLI-B5-343-2016]
15. Pavurala N, Xu X, Krishnaiah YSR. Hyperspectral imaging using near infrared spectroscopy to monitor coat thickness uniformity in the manufacture of a transdermal drug delivery system. Int J Pharm 2017 May 15;523(1):281-290. [doi: 10.1016/j.ijpharm.2017.03.022] [Medline: 28330736]
16. Fernández de la Ossa M, Amigo JM, García-Ruiz C. Detection of residues from explosive manipulation by near infrared hyperspectral imaging: a promising forensic tool. Forensic Sci Int 2014 Sep;242:228-235. [doi: 10.1016/j.forsciint.2014.06.023] [Medline: 25086347]
17. Sakarya U, Teke M, Demirkesen C, et al. A short survey of hyperspectral remote sensing and hyperspectral remote sensing research at tübıtak uzay. Presented at: 2015 7th International Conference on Recent Advances in Space Technologies (RAST); Jun 16-19, 2015; Istanbul, Turkey p. 187-192. [doi: 10.1109/RAST.2015.7208339]
18. Qin J, Kim M, Chao K, Chan D, Delwiche S, Cho BK. Line-scan hyperspectral imaging techniques for food safety and quality applications. Appl Sci (Basel) 2017;7(2):125. [doi: 10.3390/app7020125]
19. Lu G, Fei B. Medical hyperspectral imaging: a review. J Biomed Opt 2014 Jan;19(1):10901. [doi: 10.1117/1.JBO.19.1.010901] [Medline: 24441941]
20. Römer P, Blatt S, Siegberg F, et al. Intraoral perfusion assessment using endoscopic hyperspectral imaging (EHSI)- first description of a novel approach. Clin Oral Investig 2025 Feb 5;29(2):115. [doi: 10.1007/s00784-025-06197-5] [Medline: 39907805]
21. Lu G, Wang D, Qin X, et al. Histopathology feature mining and association with hyperspectral imaging for the detection of squamous neoplasia. Sci Rep 2019 Nov 28;9(1):17863. [doi: 10.1038/s41598-019-54139-5] [Medline: 31780698]
22. Ortega S, Halicek M, Fabelo H, Callico GM, Fei B. Hyperspectral and multispectral imaging in digital and computational pathology: a systematic review [Invited]. Biomed Opt Express 2020 Jun 1;11(6):3195-3233. [doi: 10.1364/BOE.386338] [Medline: 32637250]
23. Bhargava R, Falahkheirkhah K. Enhancing hyperspectral imaging. Nat Mach Intell 2021;3(4):279-280. [doi: 10.1038/s42256-021-00336-9]

XSL•FO
RenderX

24. Cui R, Yu H, Xu T, et al. Deep learning in medical hyperspectral images: a review. Sensors (Basel) 2022 Dec 13;22(24):9790. [doi: 10.3390/s22249790] [Medline: 36560157]
25. Madooei A, Abdlaty RM, Doerwald-Munoz L, et al. Hyperspectral image processing for detection and grading of skin erythema. 2017 Feb 24 Presented at: SPIE Medical Imaging; Feb 11-16, 2017; Orlando, Florida, United States p. 1013322. [doi: 10.1117/12.2254132]
26. Krizhevsky A, Sutskever I, Hinton GE. ImageNet classification with deep convolutional neural networks. Commun ACM 2017 May 24;60(6):84-90. [doi: 10.1145/3065386]
27. Li W. Cell classification using convolutional neural networks in medical hyperspectral imagery. Presented at: 2017 2nd International Conference on Image, Vision and Computing (ICIVC); Jun 2-4, 2017; Chengdu, China p. 501-504. [doi: 10.1109/ICIVC.2017.7984606]
28. Jeyaraj PR, Samuel Nadar ER. Computer-assisted medical image classification for early diagnosis of oral cancer employing deep learning algorithm. J Cancer Res Clin Oncol 2019 Apr;145(4):829-837. [doi: 10.1007/s00432-018-02834-7] [Medline: 30603908]
29. Gangadharan SMP, Dharani M, Thapliyal N, Yamsani N, Singh J, Singh P. Comparative analysis of deep learning-based brain tumor prediction models using MRI scan. In: Singh P, editor. Presented at: 2023 3rd International Conference on Innovative Sustainable Computational Technologies (CISCT); Sep 8-9, 2023; Dehradun, India p. 1-6. [doi: 10.1109/CISCT57197.2023.10351227]
30. Diwakar M, Singh P, Garg D. Edge-guided filtering based CT image denoising using fractional order total variation. Biomed Signal Process Control 2024 Jun;92:106072. [doi: 10.1016/j.bspc.2024.106072]
31. Diwakar M, Kumar P, Singh P, Tripathi A, Singh L. An efficient reversible data hiding using SVD over a novel weighted iterative anisotropic total variation based denoised medical images. Biomed Signal Process Control 2023 Apr;82:104563. [doi: 10.1016/j.bspc.2022.104563]
32. Diwakar M, Pandey NK, Singh R, et al. Low-dose COVID-19 CT Image Denoising Using CNN and its Method Noise Thresholding. Curr Med Imaging 2023;19(2):182-193. [doi: 10.2174/1573405618666220404162241] [Medline: 35379137]
33. Agrawal T, Choudhary P, Shankar A, Singh P, Diwakar M. MultiFeNet: multi-scale feature scaling in deep neural network for the brain tumour classification in MRI images. Int J Imaging Syst Technol 2024;34(1):e22956. [doi: 10.1002/ima.22956]
34. Sicher C, Rutkowski R, Lutze S, et al. Hyperspectral imaging as a possible tool for visualization of changes in hemoglobin oxygenation in patients with deficient hemodynamics - proof of concept. Biomed Tech (Berl) 2018 Oct 25;63(5):609-616. [doi: 10.1515/bmt-2017-0084] [Medline: 30210054]
35. Yudovsky D, Nouvong A, Pilon L. Hyperspectral imaging in diabetic foot wound care. J Diabetes Sci Technol 2010 Sep 1;4(5):1099-1113. [doi: 10.1177/193229681000400508] [Medline: 20920429]
36. Ponciano C, Schaffert M, Ponciano JJ. Deep learning datasets challenges for semantic segmentation-a survey. Presented at: P337 - INFORMATIK 2023 - Designing Futures: Shaping the Future; Sep 26-29, 2023; Berlin, Germany p. 57-70. [doi: 10.18420/inf2023_04]
37. Gupta P, Bagchi A. Essentials of Python for Artificial Intelligence and Machine Learning 2024.
38. Lu H, Cai J. Artificial intelligence and robotics. In: 8th International Symposium, ISAIR 2023: Springer; 2024, Vol. 15:535 URL: https://link.springer.com/10.1007/978-981-99-9109-9 [doi: 10.1007/978-981-99-9109-9]
39. Chen LC. Rethinking atrous convolution for semantic image segmentation. arXiv. Preprint posted online on Sep 5, 2017. [doi: 10.48550/arXiv.1706.05587]
40. Chen LC, Zhu Y, Papandreou G, Schroff F, editors. Encoder-decoder with atrous separable convolution for semantic image segmentation. In: Proceedings of the European Conference on Computer Vision (ECCV: Springer; 2018, Vol. 1121:833-851. [doi: 10.1007/978-3-030-01234-2_49]
41. Long J, Shelhamer E, Darrell T. Fully convolutional networks for semantic segmentation. In: Long J, Shelhamer E, Darrell T, editors. Presented at: Proceedings of the IEEE conference on computer vision and pattern recognition; Jun 7-12, 2015; Boston, MA, USA p. 3431-3440. [doi: 10.1109/CVPR.2015.7298965]
42. Zhao H, Shi J, Qi X, Wang X, Jia J. Pyramid scene parsing network. In: Jia J, editor. Presented at: 2017 IEEE Conference on Computer Vision and Pattern Recognition (CVPR); Jul 21-26, 2017; Honolulu, HI p. 6230-6239. [doi: 10.1109/CVPR.2017.660]
43. He K, Zhang X, Ren S, Sun J. Deep residual learning for image recognition. In: Sun J, editor. Presented at: 2016 IEEE Conference on Computer Vision and Pattern Recognition (CVPR); Jun 27-30, 2016; Las Vegas, NV, USA p. 770-778. [doi: 10.1109/CVPR.2016.90]
44. Simonyan K, Zisserman A. Very deep convolutional networks for large-scale image recognition. arXiv. Preprint posted online on Apr 10, 2015. [doi: 10.48550/arXiv.1409.1556]
45. Ronneberger O, Fischer P, Brox T. U-net: convolutional networks for biomedical image segmentation. medical image computing and computer-assisted intervention–MICCAI 2015. In: Navab N, Hornegger J, Wells W, Frangi A, editors. Medical Image Computing and Computer-Assisted Intervention – MICCAI 2015: Springer; 2015, Vol. 9351:234-241. [doi: 10.1007/978-3-319-24574-4_28]

XSL•FO
RenderX

46. Tan M, Le Q. Efficientnet: rethinking model scaling for convolutional neural networks. Presented at: Proceedings of the 36th International Conference on Machine Learning; Jun 9-15, 2019; Long Beach, CA p. 6105-6114 URL: https://proceedings.mlr.press/v97/tan19a.html [accessed 2025-09-03]
47. Thiem DGE, Römer P, Gielisch M, et al. Hyperspectral imaging and artificial intelligence to detect oral malignancy - part 1 - automated tissue classification of oral muscle, fat and mucosa using a light-weight 6-layer deep neural network. Head Face Med 2021 Sep 3;17(1):38. [doi: 10.1186/s13005-021-00292-0] [Medline: 34479595]
48. Chen LC, Papandreou G, Kokkinos I, Murphy K, Yuille AL. DeepLab: semantic image segmentation with deep convolutional nets, atrous convolution, and fully connected CRF. IEEE Trans Pattern Anal Mach Intell 2018 Apr;40(4):834-848. [doi: 10.1109/TPAMI.2017.2699184] [Medline: 28463186]
49. Ma L, Srinivas A, Krishnamurthy A, et al. Automated polarized hyperspectral imaging (PHSI) for ex-vivo and in-vivo tissue assessment. . 2023 Jan p. 123910F. [doi: 10.1117/12.2651011] [Medline: 38476292]
50. Poonkuzhali P, Helen Prabha K. Deep convolutional neural network based hyperspectral brain tissue classification. J Xray Sci Technol 2023;31(4):777-796. [doi: 10.3233/XST-230045] [Medline: 37182861]
51. Hu B, Du J, Zhang Z, Wang Q. Tumor tissue classification based on micro-hyperspectral technology and deep learning. Biomed Opt Express 2019 Dec 1;10(12):6370-6389. [doi: 10.1364/BOE.10.006370] [Medline: 31853405]
52. Ma L, Zhou X, Little JV, et al. Hyperspectral microscopic imaging for the detection of head and neck squamous cell carcinoma in histologic images. Proc SPIE Int Soc Opt Eng 2021 Feb;11603:35783088. [doi: 10.1117/12.2581970] [Medline: 35783088]
53. Ma L, Lu G, Wang D, Qin X, Chen ZG, Fei B. Adaptive deep learning for head and neck cancer detection using hyperspectral imaging. Vis Comput Ind Biomed Art 2019;2(1):18. [doi: 10.1186/s42492-019-0023-8] [Medline: 32190408]
54. Zhou X, Ma L, Mubarak HK, et al. Automatic detection of head and neck squamous cell carcinoma on pathologic slides using polarized hyperspectral imaging and deep learning. Proc SPIE Int Soc Opt Eng 2022;12039:Feb-Mar. [doi: 10.1117/12.2614624] [Medline: 36798940]
55. Eggert D, Bengs M, Westermann S, et al. In vivo detection of head and neck tumors by hyperspectral imaging combined with deep learning methods. J Biophotonics 2022 Mar;15(3):e202100167. [doi: 10.1002/jbio.202100167] [Medline: 34889065]
56. Trajanovski S, Shan C, Weijtmans PJC, de Koning SGB, Ruers TJM. Tongue tumor detection in hyperspectral images using deep learning semantic segmentation. IEEE Trans Biomed Eng 2021 Apr;68(4):1330-1340. [doi: 10.1109/TBME.2020.3026683] [Medline: 32976092]

Abbreviations

CV: coefficient of variation
DL: deep learning
FCN: fully convolutional network
HSI: hyperspectral imaging
PSPNet: pyramid scene parsing network

Edited by A Benis; submitted 17.04.25; peer-reviewed by B Afolabi, DO Alabi, P Singh; revised version received 05.07.25; accepted 06.07.25; published 11.09.25.

Please cite as:
Römer P, Ponciano JJ, Kloster K, Siegberg F, Plaß B, Vinayahalingam S, Al-Nawas B, Kämmerer PW, Klauer T, Thiem D
Enhancing Oral Health Diagnostics With Hyperspectral Imaging and Computer Vision: Clinical Dataset Study
JMIR Med Inform 2025;13:e76148
URL: https://medinform.jmir.org/2025/1/e76148
doi:10.2196/76148

© Paul Römer, Jean-Jacques Ponciano, Katharina Kloster, Fabia Siegberg, Bastian Plaß, Shankeeth Vinayahalingam, Bilal Al-Nawas, Peer W Kämmerer, Thomas Klauer, Daniel Thiem. Originally published in JMIR Medical Informatics (https://medinform.jmir.org), 11.9.2025. This is an open-access article distributed under the terms of the Creative Commons Attribution License (https://creativecommons.org/licenses/by/4.0/), which permits unrestricted use, distribution, and reproduction in any medium, provided the original work, first published in JMIR Medical Informatics, is properly cited. The complete bibliographic information, a link to the original publication on https://medinform.jmir.org/, as well as this copyright and license information must be included.

XSL•FO
RenderX

Original Paper

Autonomous International Classification of Diseases Coding Using Pretrained Language Models and Advanced Prompt Learning Techniques: Evaluation of an Automated Analysis System Using Medical Text

Yan Zhuang[1*], PhD; Junyan Zhang[1*], ME; Xiuxing Li[2], PhD; Chao Liu[3], PhD; Yue Yu[3], BS; Wei Dong[4], PhD; Kunlun He[1], PhD

[1]Medical Big Data Research Center, Chinese PLA General Hospital, Beijing, China

[2]School of Computer Science & Technology, Beijing Institute of Technology, Beijing, China

[3]Digital Health China Technologies Co Ltd, Beijing, China

[4]Senior Department of Cardiology, The Sixth Medical Center of PLA General Hospital, Beijing, China

[*]these authors contributed equally

Corresponding Author:
Kunlun He, PhD
Medical Big Data Research Center
Chinese PLA General Hospital
28 Fuxing Road
Beijing, 100853
China
Phone: 86 13911232619
Email: kunlunhe@plagh.org

Abstract

Background: Machine learning models can reduce the burden on doctors by converting medical records into International Classification of Diseases (ICD) codes in real time, thereby enhancing the efficiency of diagnosis and treatment. However, it faces challenges such as small datasets, diverse writing styles, unstructured records, and the need for semimanual preprocessing. Existing approaches, such as naive Bayes, Word2Vec, and convolutional neural networks, have limitations in handling missing values and understanding the context of medical texts, leading to a high error rate. We developed a fully automated pipeline based on the Key–bidirectional encoder representations from transformers (BERT) approach and large-scale medical records for continued pretraining, which effectively converts long free text into standard ICD codes. By adjusting parameter settings, such as mixed templates and soft verbalizers, the model can adapt flexibly to different requirements, enabling task-specific prompt learning.

Objective: This study aims to propose a prompt learning real-time framework based on pretrained language models that can automatically label long free-text data with ICD-10 codes for cardiovascular diseases without the need for semiautomatic preprocessing.

Methods: We integrated 4 components into our framework: a medical pretrained BERT, a keyword filtration BERT in a functional order, a fine-tuning phase, and task-specific prompt learning utilizing mixed templates and soft verbalizers. This framework was validated on a multicenter medical dataset for the automated ICD coding of 13 common cardiovascular diseases (584,969 records). Its performance was compared against robustly optimized BERT pretraining approach, extreme language network, and various BERT-based fine-tuning pipelines. Additionally, we evaluated the framework's performance under different prompt learning and fine-tuning settings. Furthermore, few-shot learning experiments were conducted to assess the feasibility and efficacy of our framework in scenarios involving small- to mid-sized datasets.

Results: Compared with traditional pretraining and fine-tuning pipelines, our approach achieved a higher micro–F1-score of 0.838 and a macro–area under the receiver operating characteristic curve (macro-AUC) of 0.958, which is 10% higher than other methods. Among different prompt learning setups, the combination of mixed templates and soft verbalizers yielded the best performance. Few-shot experiments showed that performance stabilized and the AUC peaked at 500 shots.

XSL•FO
RenderX

Conclusions: These findings underscore the effectiveness and superior performance of prompt learning and fine-tuning for subtasks within pretrained language models in medical practice. Our real-time ICD coding pipeline efficiently converts detailed medical free text into standardized labels, offering promising applications in clinical decision-making. It can assist doctors unfamiliar with the ICD coding system in organizing medical record information, thereby accelerating the medical process and enhancing the efficiency of diagnosis and treatment.

(JMIR Med Inform 2025;13:e63020) doi:10.2196/63020

KEYWORDS

BERT; bidirectional encoder representations from transformers; pretrained language models; prompt learning; ICD; International Classification of Diseases; cardiovascular disease; few-shot learning; multicenter medical data

Introduction

Background

The *International Classification of Diseases, 10th Revision* (*ICD-10*), is a universally recognized diagnostic categorization system widely used in medical insurance reimbursements, health reporting, mortality assessments, and related fields [1]. The *ICD-10*'s automatic coding mechanism enables rapid and accurate classification and statistical analysis of medical data, offering a scientific foundation for effective hospital administration and decision-making. In addition, the *ICD-10* automatic coding system accelerates disease diagnosis and treatment planning for medical practitioners, thereby improving medical efficacy and quality. Compared with the original *ICD* code, *ICD-10* provides over 14,000 distinct disease codes (in contrast to the thousands in *ICD-9*), enabling more detailed disease classification. This comprehensive system offers clinicians enhanced patient information, supporting the development of more precise treatment plans and care programs, ultimately improving the quality of care and patient satisfaction. Moreover, as an internationally standardized code, *ICD-10* is essential for global public health surveillance, epidemiological research, and international medical cooperation. Consequently, ensuring accurate *ICD* coding remains a critical priority in clinical practice.

In hospital settings, the assignment of *ICD* codes to unstructured clinical narratives in medical records is a manual task performed by skilled medical coders based on the attending physician's clinical diagnosis. Despite its critical importance, this process is often hindered by inefficiencies such as time consumption, susceptibility to errors, and high costs. Additionally, manual coding cannot always ensure the accuracy of *ICD* codes due to the complexity of code assignment, which requires a thorough consideration of the patient's overall health condition, including medical history, coexisting conditions, complications, surgical interventions, and specialized diagnostic procedures [2,3].

Machine Learning Techniques

The need to enhance efficiency and reduce errors has driven the development of various machine learning techniques to automate the medical *ICD* coding process. These techniques can be broadly classified into 4 main categories: rule-based systems [4,5], traditional supervised algorithms [6,7], gate unit–based deep learning approaches [7-9], and pretrained language models (PLMs) [9-19].

First, rule-based systems for automatic *ICD* coding rely on the creation of explicit rules and knowledge bases to map medical records to the appropriate *ICD* codes [4,5]. Although these approaches have been used for decades and have provided a foundation for more advanced techniques, they are limited by their lack of adaptability and scalability.

Second, traditional supervised algorithms, such as gradient-boosted trees, have been utilized for *ICD* coding due to their efficiency in handling large-scale, high-dimensional datasets. These algorithms rely on semistructured preprocessing, which involves organizing and refining semistructured data into a format suitable for analysis [6,7]. For example, Diao et al [6] developed a light gradient boosting machine–based pipeline for automatically coding 168 primary diagnosis *ICD-10* codes from discharge records and procedure texts, achieving an accuracy of 95.2%. Another study integrated long short-term memory networks with attention mechanisms to predict mortality in ICU patients using electronic health records, achieving significantly higher area under the receiver operating characteristic curve (AUC) scores compared with traditional statistical models and stand-alone long short-term memory networks [7].

Third, PLMs are neural network models with fixed architectures trained on large corpora, which can be fine-tuned for specific downstream tasks such as question answering and entity recognition [10-13]. A notable example is bidirectional encoder representations from transformers (BERT), a prominent PLM designed to learn deep bidirectional representations from large-scale unlabeled text data. BERT effectively captures semantic relationships in clinical records and can be easily adapted to various natural language processing (NLP) tasks through task-specific layers [13]. Coutinho and Martins [14] proposed a BERT model with a fine-tuning method for automatic *ICD-10* coding of death certificates based on free-text descriptions and associated documents. Additionally, Yan et al [15] introduced RadBERT, an ensemble model combining BERT-base, Clinical-BERT, the robustly optimized BERT pretraining approach (RoBERTa), and BioMed-RoBERTa adapted for radiology. Liu et al [16] evaluated RadBERT across 3 NLP tasks: abnormal sentence classification, report coding, and report summarization, demonstrating significantly better performance compared with existing transformer language models. Unstructured patient-generated health data can be leveraged to support clinical decision-making, remote monitoring, and self-care, including medication adherence and chronic disease management. By applying named entity recognition and customizable information extraction methods

XSL•FO
RenderX

based on medical ontologies, NLP models can extract a wide range of clinical information from unstructured patient-generated health data, even in low-resource settings with limited patient notes or training data [17]. Textual analysis presents numerous opportunities for future medical applications. It can aid in extracting information from various sources of medical data, such as clinical reports, nursing notes, scientific literature, and user-generated content. Additionally, vector-based representation methods can transform textual data within clinical documents into formats suitable for machine learning and can be applied to sequence modeling tasks, including sentiment analysis [18].

Finally, XLNet is another type of PLM that captures both forward and backward contexts of text [19]. It combines the advantages of autoregressive models and autoencoding models while overcoming their limitations. XLNet utilizes a permutation-based objective function that maximizes the expected likelihood of a text across all possible word orderings. It also incorporates the Transformer-XL (Transformer-Extra-Long) architecture, which enables long-term dependency modeling and improved memory efficiency. XLNet has been shown to outperform BERT and other baseline models on several natural language understanding tasks.

Prompt Engineering Techniques

By contrast, prompt engineering is a technique that involves the careful construction of prompts or inputs for artificial intelligence models to improve their performance on specific tasks. This technique includes selecting appropriate words, phrases, symbols, and formats to guide a large language model in generating high-quality and relevant text. Numerous studies have used prompts for model tuning to bridge the gap between pretraining objectives and downstream tasks, demonstrating that both discrete and continuous prompts can improve performance in few-shot and zero-shot tasks [20,21]. Furthermore, this technique within PLMs has been shown to outperform fine-tuning in various clinical decision-making tasks [22]. It has the advantage of requiring less data and computational resources, making it especially suitable for clinical settings.

There are 2 primary categories of prompting methods: hard prompts and soft prompts [22-25]. Hard prompts involve using an actual text string as the prompt and include methods that automatically search for templates within a discrete space, such as mining-based, paraphrasing-based, and gradient-based approaches [26-28]. The advantages of hard prompts are interpretability, portability, flexibility, and simplicity. However, designing effective prompts for specific tasks requires significant effort and creativity.

Soft prompts, by contrast, are learnable tensors concatenated with the input embeddings and can be optimized for a given dataset. The main advantage of soft prompts is their ability to achieve better performance than hard prompts by adapting to the model and the data. However, they are not human-readable and lack portability across different models.

Prefix tuning and P-tuning are 2 methods of prompt engineering that can enhance performance beyond traditional fine-tuning [22-24]. Prefix tuning is a lightweight approach that keeps the PLM parameters unchanged while optimizing a sequence of task-specific vectors called the prefix [23]. This prefix is added to the input and interacts with the model's hidden states at each layer. Its success depends on how effectively the prefix is initialized, particularly when data are limited. P-tuning is another prompt tuning strategy that performs comparably to fine-tuning across various tasks [24]. It reduces the number of PLM parameters through self-adaptive pruning and tunes a small number of continuous prompts at the beginning of each transformer layer.

The verbalizer is the final layer that defines the answer space and maps it to the target output. Typically, verbalizers are manually created, which can limit their coverage due to personal vocabulary biases [21,29]. To address this, some studies have proposed automatic verbalizer search methods to identify more effective verbalizers, also known as soft verbalizers [20,30-32].

Autonomous ICD Coding in Cardiovascular Disease

Cardiovascular disease (CVD) is currently a leading cause of death worldwide, posing a significant risk of mortality among patients [7]. Automatically labeling patients with CVD is essential for clinical decision-making and resource allocation. However, existing prediction models have limitations, including low accuracy, limited generalizability, and an inability to capture multicenter data. To address these challenges, we propose a prompt learning real-time framework based on PLMs that can automatically label long free-text data with *ICD-10* codes for CVDs without the need for semiautomatic preprocessing.

Our framework consists of 4 components: a medically oriented pretrained BERT, a keyword filtration BERT, a fine-tuning phase, and task-specific prompt learning facilitated by mixed templates and soft verbalizers. To validate the efficacy of our framework, we conducted comprehensive evaluations on a Chinese multicenter cardiovascular dataset that includes data from 13,000 patients with CVD. This deliberate choice of dataset ensures the robustness and wide applicability of our framework. We compared our framework with RoBERTa, XLNet, and various BERT-based fine-tuning pipelines to highlight its performance. Additionally, we conducted few-shot experiments to demonstrate its resilience. This work promises to provide valuable insights into enhancing medical knowledge extraction and its effective application, underscoring the need for continued research and development in this promising area. In future work, we plan to implement this fully automated *ICD* coding pipeline across various clinical applications, including clinical decision support systems, cohort studies, and disease early warning and diagnosis systems.

Methods

Ethical Considerations

The study was approved by the Ethics Committee of the Chinese PLA General Hospital (S2023-325-02). Ethical approval included a waiver for obtaining informed consent signatures from participants. The study posed no potential harm to participants and did not involve any compensation for their participation. To protect patient privacy, we used regular

XSL•FO
RenderX

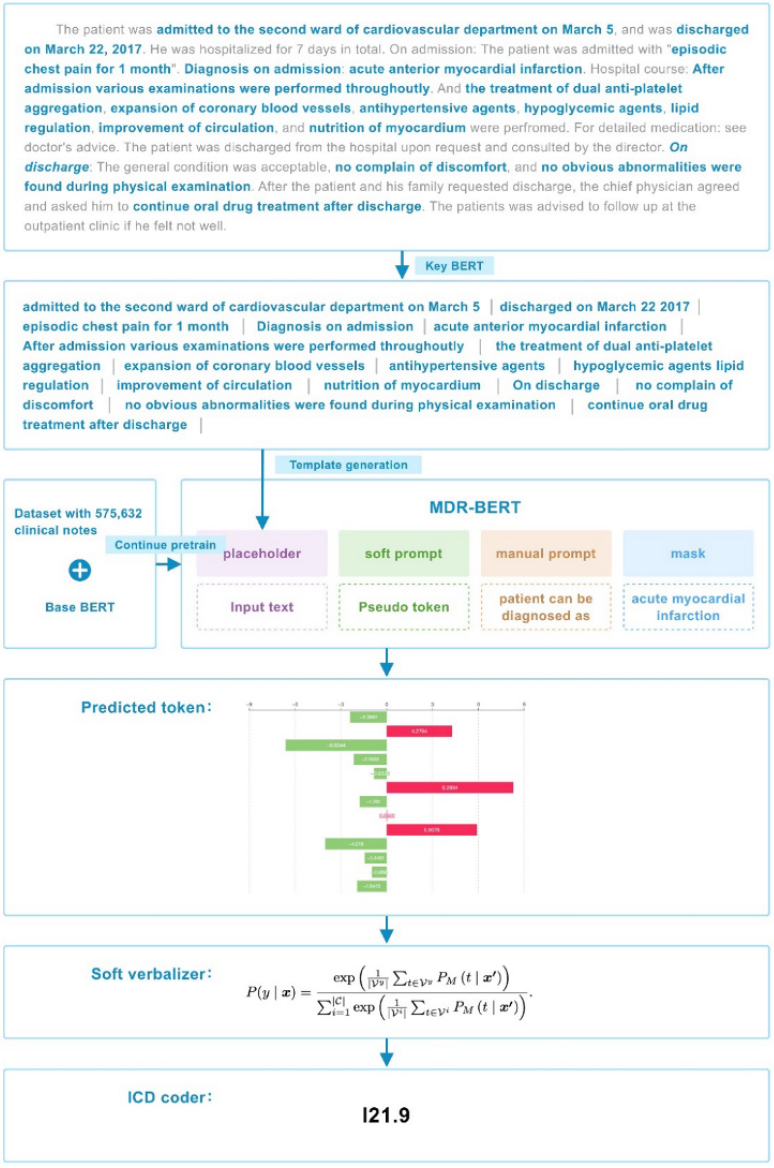
expressions to parse and redact basic identifying information from the medical records. As these records were created using a standardized template, we ensured that the excerpts extracted for this study did not contain patients' names.

Overview

The overall framework of the model is shown in Figure 1. We used a corpus dataset of 575,632 clinical notes to continue training the original BERT model, which we named medical domain refinement-BERT (MDR-BERT), as the PLM for our work. For the classification task, we first applied Key-BERT to filter the discharge summaries. This method extracts keywords and splits long free-text data into shorter sentences.

We then constructed the input template for fine-tuning and prompt learning using 3 components: the soft prompt, the manual prompt, and the mask part. The manual prompt was a handcrafted text prompt containing discrete tokens. The soft prompt was a learnable pseudo-token with a few continuous parameters. The mask part represented the *ICD* coding label. Finally, we used a trainable soft verbalizer to compute and apply the softmax function to the probabilities of the *ICD* classes, producing the output. By designing specific prompts, it is possible to incorporate the knowledge of medical experts into the model, helping it better understand and perform *ICD* coding. These prompts can direct the model to focus on critical sections of the input text, thereby enhancing performance.

Figure 1. Overall framework of MDR-BERT, Key-BERT, and prompt learning pipeline. BERT: bidirectional encoder representations from transformers; ICD: International Classification of Diseases; MDR: medical domain refinement.



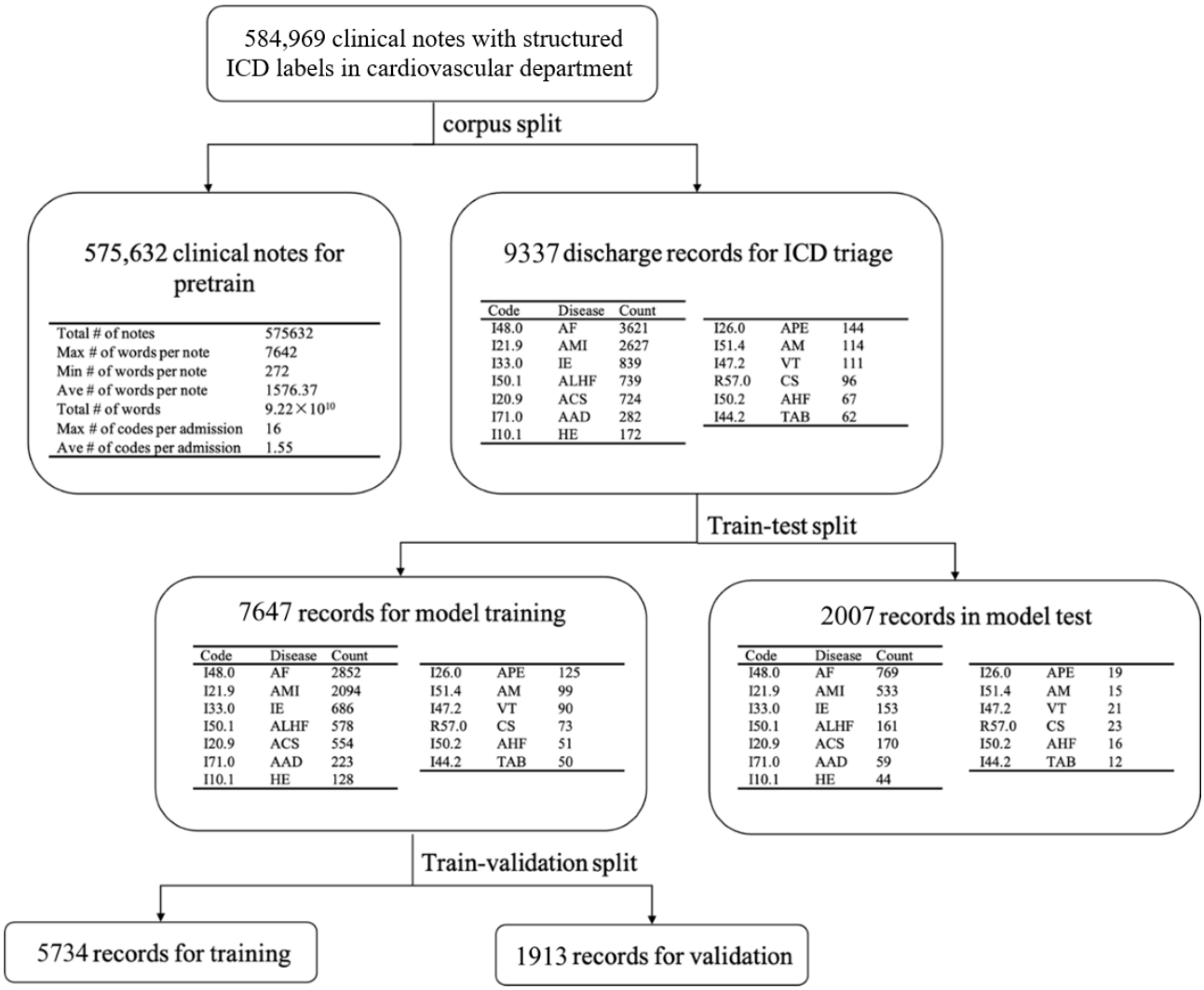
Dataset Characteristics

The cardiovascular dataset used in this study was obtained from the Cardiovascular Department of the Chinese PLA General Hospital's Medical Big Data Research Center in Beijing, China, which includes 9 medical centers with data aggregated into a comprehensive medical big data platform. Additionally, the hospital is a key center for the treatment of CVDs, with numerous specialized physicians and detailed medical records, making its data highly practical and representative. To ensure privacy, patient names and addresses were desensitized. The data platform consists of electronic health records aggregated

XSL•FO
RenderX

from 8 affiliated medical centers. A total of 584,969 clinical notes with structured *ICD* labels were extracted from admission records and discharge summaries in the Cardiovascular Department. We ensured that each diagnosis included at least 50 cases and adopted a stratified sampling approach to divide each disease category into training, validation, and test sets in a 3:1:1 ratio. The detailed distribution and basic statistical information of the dataset are shown in Figure 2.

Figure 2. Distribution and basic statistical information of the data set. ICD: International Classification of Diseases.



Based on the long-tailed distribution and clinician selection, 13 diseases were chosen for classification. These diseases include atrial fibrillation, acute myocardial infarction, infective endocarditis, acute left heart failure, acute coronary syndrome (ACS), acute aortic dissection, hypertensive emergency, acute pulmonary embolism, acute myocarditis, ventricular tachycardia, cardiogenic shock, acute heart failure, and third-degree atrioventricular block. The corresponding *ICD-10* codes and abbreviations for these diseases are listed in Table 1. Despite the disparity in the number of cases for different diseases, the imbalance inherent in medical data accurately reflects real-world conditions, taking into account the clinical insights of medical professionals. This imbalance represents the varying frequency at which different diseases occur in clinical practice. By preserving the raw data distribution and avoiding artificial balancing, our training approach aligns more closely with real-world medical practice. As a result, this enhances the model's generalization ability and its applicability in practical scenarios.

To ensure task independence and prevent data leakage, all clinical notes were divided into 2 parts: the pretraining corpus dataset and the *ICD* coding dataset. The pretraining corpus consisted of a total of 575,632 notes, while the *ICD* coding dataset included 9337 discharge records. The data were stratified by imbalanced *ICD* labels and randomly split into training, validation, and test sets in a 3:1:1 ratio. The sample sizes were as follows: 5734 in the training set, 1913 in the validation set, and 2007 in the test set. We applied regularization to truncate patients' basic information, as this information could negatively impact the model's fitting.

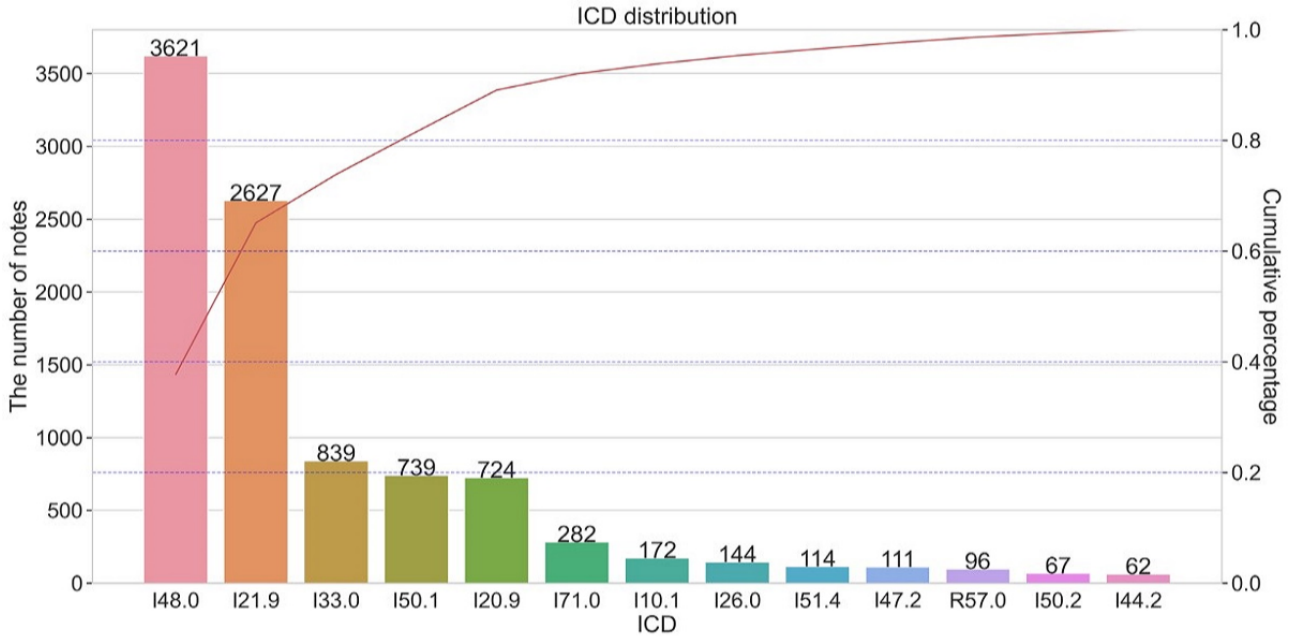
As shown in Figure 3, the distribution of the 13 *ICD* codes was imbalanced and exhibited a long-tail pattern. The dataset for *ICD* classification contains a total of 4.574×10^7 words, with an average of 490 words per note. The maximum and minimum lengths of the clinical notes are 5243 and 22 words, respectively.

XSL•FO
RenderX

Table 1. Overview of target International Classification of Diseases (ICD) codes and disease names.

International Classification of Diseases code	Disease (abbreviation)
I48.0	Atrial fibrillation (AF)
I21.9	Acute myocardial infarction (AMI)
I33.0	Infective endocarditis (IE)
I50.1	Acute left heart failure (ALHF)
I20.9	Acute coronary syndrome (ACS)
I71.0	Acute aortic dissection (AAD)
I10.1	Hypertensive emergency (HE)
I26.0	Acute pulmonary embolism (APE)
I51.4	Acute myocarditis (AM)
I47.2	Ventricular tachycardia (VT)
R57.0	Cardiogenic shock (CS)
I50.2	Acute heart failure (AHF)
I44.2	Third-degree atrioventricular block (TAB)

Figure 3. Distribution of ICD codes for the triage task. ICD: International Classification of Diseases.



Pretraining

Our study's foundational framework is based on BERT, a multilayer bidirectional transformer encoder known for its conceptual simplicity and empirical effectiveness [33]. This architecture consists of 12 layers, a hidden size dimension of 768, and 12 self-attention heads [13]. BERT's inherent self-attention mechanism provides the versatility to handle various downstream tasks by allowing the interchange of relevant inputs and outputs, making it well-suited for our task involving *ICD* classification through clinical records.

To adapt BERT to the specific requirements of our task, we continued training the PLM using an extensive medical corpus, resulting in MDR-BERT. During the tuning process, we selected a batch size of 32, considering the constraint of a maximum sequence length of 512 tokens. The Adam optimization algorithm was used with a conservative learning rate of 2×10^{-5}. The training was carried out over 15 epochs, an empirically determined figure based on the characteristics of the clinical dataset.

Key-BERT

The Key-BERT method offers a novel self-supervised framework for extracting keywords and keyphrases from textual content using deep learning techniques [34]. This approach leverages the contextual and semantic features provided by bidirectional transformers, with a particular focus on the influential BERT model. The method's architecture is designed for end-to-end training, utilizing a contextually self-annotated corpus that enables the model to develop a nuanced understanding of the complex relationships between words and

XSL•FO
RenderX

their semantic meanings. In the *ICD* coding task, Key-BERT leverages BERT's context-aware capabilities to extract keywords from the document, quickly identify the sections relevant to *ICD* coding, and reduce the risk of miscoding caused by misinterpreting or overlooking critical information in the text.

A distinctive feature of Key-BERT lies in its automated keyword labeling process. This process effectively utilizes contextual insights from bidirectional transformers to construct a carefully curated ground truth dataset. This approach bypasses the labor-intensive task of manual labeling and eliminates the need for domain-specific expertise.

The repository of self-labeled data generated by Key-BERT is partially shared with the NLP community, contributing to a deeper and more comprehensive understanding of keyword extraction techniques across various domains. This collaborative effort enhances the landscape of knowledge and expertise, driving advancements in the field of NLP and semantic information extraction.

To extract keywords using Key-BERT, the contextual feature vector for each word in a sentence is obtained by passing the sentence through the pretrained BERT model. Let $S = [w_1, w_2, ..., w_n]$ be a sentence consisting of n words, where w_i is the ith word in the sentence and E_i is the contextual feature vector of the ith word in the sentence. The sentence embedding vector, denoted as E_s, is obtained by averaging the feature vectors of all the words in the sentence:

$$E_i = \text{BERT_Embedding}(w_i) \quad \textbf{(1)}$$

$$E_s = (E_1 + E_2 + \cdots + E_n)/(n) \quad \textbf{(2)}$$

The cosine similarity metric is used to measure the similarity between the sentence embedding vector and the feature vectors of candidate keywords or keyphrases.

$$\text{Cos_SIM}(E_i, E_s) = (E_i \times E_s)/(||E_i|| \times ||E_s||) \quad \textbf{(3)}$$

The top-scoring keywords or keyphrases are returned as the most relevant to the document. Additionally, key medical terms are directly extracted using the medical diagnostic table, ensuring that essential terminology is accurately identified and applied.

Fine-Tuning and Prompt Learning

To fully leverage the clinical knowledge embedded within the dataset, our fine-tuning approach mirrors the unsupervised task used in the initial pretraining phase, known as masked language modeling (MLM). MLM involves randomly masking a predetermined proportion of input tokens, and the model then attempts to predict these masked tokens based on context. This process, commonly called a Cloze task, helps the model learn contextual relationships effectively.

For the fine-tuning phase in this study, we maintained the MLM framework to align with the pretraining procedure. A consistent masking rate of 15% was applied across the dataset. In addition to the fine-tuning process, we introduced prompt learning during parameter tuning. This approach involved the construction of a template comprising 4 distinct components: the input text, a soft prompt, a manual prompt, and a masking component. The manual prompt included discrete tokens that reflected the downstream task expected by the PLM. By contrast, the soft prompt comprised trainable continuous vectors, which enhanced the model's adaptability.

Formally, automatic *ICD* coding, as a text multiclassification task, can be denoted as (x, y), where x is the set of discharge summaries and y is the *ICD* code set of the 17 chosen discharge diagnoses as labels. Given a clinical record $x \in X$, it can be annotated with *ICD* codes of discharge diagnosis $y^x \in Y$ and a sequence of discrete input tokens $x = (x_0, x_1, ..., x_k)$, where k is the number of tokens in the sequence. Prompt learning can be achieved via modifying the x to a prompt format $x = \text{fp}(x)$, where the template $f_p(\cdot)$ will insert a number of extra embeddings to x along with a masked token, denoted by <[MASK]>. Compared with hard prompts, soft prompts replace some fixed manual components with trainable embeddings (continuous vectors) of the same dimension as the PLM. After that, x is fed into M, to predict the masked token, which is in accordance with the objective of M. The output of M will be a distribution over the fixed vocabulary V of M. The next crucial step is to map tokens in V to y for the downstream task with a mapping , known as verbalization. In a word, there are 2 essential components to be studied, the template of prompt $x' = f_p(x)$ and the mapping of verbalizer .

A mixed template of prompts in this paper is used. For simplicity, the prompt function $x' = f_p(x)$ is denoted as a sequence template:

$$x' = [P_0, P_1, \ldots, P_j], x, [P_{j+1}, P_{j+2}, \ldots, P_t], [\text{MASK}] \quad \textbf{(4)}$$

where P_i refers to the ith token in the template and t is the number of prompt tokens beyond x. P_i does not necessarily meet $P_i \in V$ other than manual hard prompt. As x' is fed to the PLM, the prompt tokens are also mapped to the embedding space, where we can assume that the tokens denoted as <[soft]> in the template can be tuned during training as pseudo-tokens. A simple example of a prompt template for automatic *ICD* coding could be as generated as follows:

$$x' = \text{<x><[soft]>be encoded as <[MASK]>} \quad \textbf{(5)}$$

Once these templates were formulated, the model inputs, along with the established templates, were processed through the trainable MDR-BERT model. Notably, in the final layer of the most advanced pipeline, a soft verbalizer mode was used. This mode manages the mapping process between the predicted tokens and the final *ICD* codes. The innovative feature of the soft verbalizer is its substitution of tokens in the verbalizer with trainable vectors, each tailored to a specific class. Generally, the verbalizer maps the probabilities of infrequent words in the vocabulary to the probabilities of the labels. The set of label words is denoted as V, the label space is Y, and V_y represents the subset of label words for label y. The final estimation of the probability for label y is calculated using equation 5, where g is utilized to convert the probability of label words to the probability of the label:

$$P(y|x_p) = g(P_M([\text{MASK}] = v|X_p)|v \in V_y) \quad \textbf{(6)}$$

XSL•FO
RenderX

This strategy enhances the precision and semantic accuracy of the generated outputs, enabling a more precise alignment between predicted tokens and the definitive *ICD* codes. Consequently, it is unnecessary to manually build an explicit mapping . for the soft verbalizer, as the trainable vectors do not have explainable semantic meaning. A matrix operator can represent the soft verbalizer as  [22-25], where n represents the size of y and m represents the dimension of output embeddings from M. For the verbalizer, θ_i denotes the ith row of  as the trainable vector of the ith class. The soft verbalizer replaces the original decoder head of M by mapping the embeddings of x' from M, denoted as $e(x')$, to the distribution over the classes of y. We denote the resulting mapping from  to the prediction of the embedding of <[MASK]> as , where l is the sequence length of x'. And then, the probability of class y can be calculated as follows:



The loss from the automatic *ICD* coding task can be backpropagated to tune only the embeddings for the prompt template and the verbalizer. The loss function can be expressed as follows:



Ultimately, the model learns to generate and map the most appropriate *ICD* codes to the corresponding discharge record.

The experiments were conducted using the OpenPrompt framework [22-25]. For prompt learning, we utilized the Adafactor optimizer for soft and mixed prompt templates, while the AdamW optimizer was used for the PLMs and soft verbalizers. In conventional fine-tuning, we applied the AdamW optimizer to the MLP heads and PLMs. To expedite the experiments, we used 2 Nvidia TESLA V100 GPUs, each with 16-GB memory, and set the batch size to 32 due to memory constraints.

The model's performance is influenced by variations in hyperparameters. In the comparisons presented, hyperparameters were carefully optimized for each model. To determine the optimal configuration, we used a random search strategy. This approach involves generating multiple random combinations of parameters, evaluating the performance of each combination, and selecting the one that yields the best results. Accuracy and AUC were chosen as the primary optimization objectives during the random search, as they intuitively reflect the model's classification performance. The strategy involved 100 training runs, each using randomly generated hyperparameters from the defined search space. To effectively address model overfitting, we carefully adjusted the dropout rate within a range of 0.1-0.5. After numerous training iterations, we found that the optimal dropout rate for the prompt learning phase is 0.382, while for the prompt tuning phase, it is 0.1563. In the prompt learning phase, a higher dropout rate contributes to improved generalization, serving as an effective safeguard against overfitting. In the subsequent fine-tuning phase, a lower dropout rate is used to ensure the model retains its learned attributes while enabling further performance enhancement. The optimal hyperparameters for the models are detailed in Table 2.

Table 2. The optimal hyperparameters and their search space.

Hyperparameters	Search space	Optimal hyperparameter	
		Prompt learning	Fine-tuning
Learning rate	log.uniform [1*10-5, 3*10-1]	0.0048	0.0121
Batch size	4	4	4
Gradient accumulation steps	range[2,10]	4	3
Dropout	range[0.1,0.5]	0.382	0.1563
Optimizer	[adamw, adafactor]	adamw	adafactor
Prompt learning rate	log.uniform[1*10-5, 3*10-1]	0.3	—[a]
Verbalizer learning rate	log.uniform[1*10-5, 1*10-1]	0.007	—

[a]Not available.

Evaluation Metrics

To thoroughly evaluate and compare the performance of the models, we used a range of metrics, including micro–F_1-score, macro-AUC, and accuracy. The definitions for micro-averaged precision and micro–F_1-score are provided in equations 9-11, while the macro-AUC is defined in equations 12 and 13.





Micro–F_1-score = [2 × (micro-P) × (micro-R)]/[(micro-P) + (micro-R)] **(11)**

where TP_i, FP_i, and FN_i represent true positives (correctly assigned instances), false positives (incorrect assignments by automated methods), and false negatives (correct instances omitted by automated methods), respectively, of code i, and l is the size of the sample space. The micro–F_1-score is the harmonic mean of micro-P and micro-R, and a bigger value of micro–F_1-score indicates a better performance.

XSL•FO
RenderX



where n is the number of thresholds and K is the number of classes.

Data and Code Availability

Data acquisition requests can be made by contacting the corresponding author (KH). Given the sensitive nature of the hospital data, it cannot be released publicly. However, part of the downstream subtask data is currently undergoing desensitization and approval processes. The source code for this study is publicly available on GitHub [35].

Results

Performance of Different Pipelines

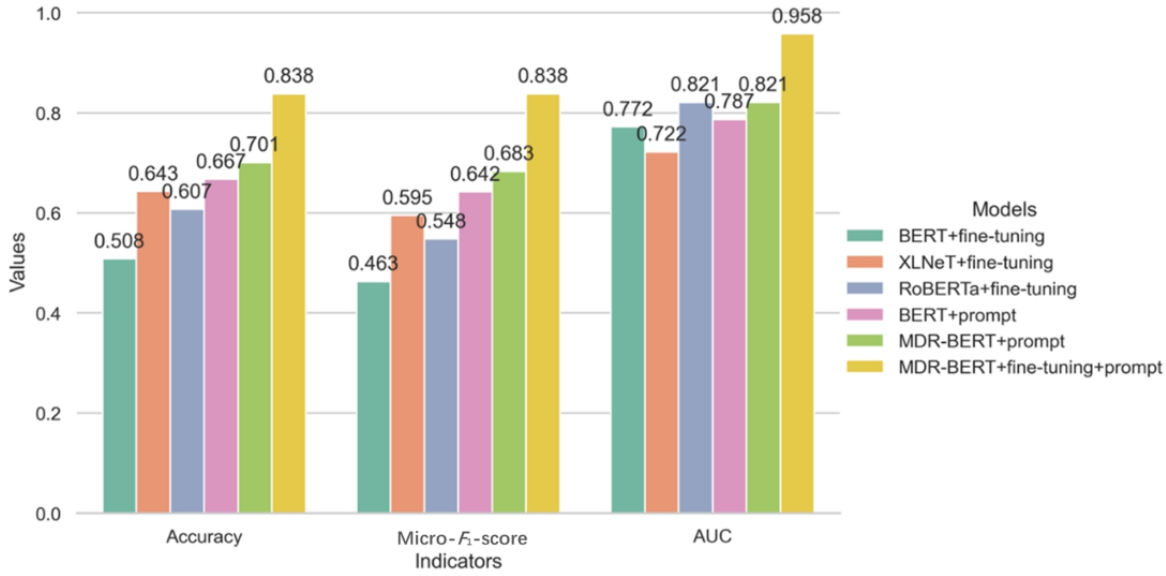
To evaluate the performance of different methods, we implemented 4 state-of-the-art algorithms: BERT [15], XLNet [18], RoBERTa [19,36], and prompt learning [22]. These PLMs were integrated with various algorithms to create 6 main pipelines: BERT with fine-tuning, XLNet with fine-tuning, RoBERTa with fine-tuning, BERT with prompt learning, MDR-BERT with prompt learning, and MDR-BERT with both fine-tuning and prompt learning. MDR-BERT is a PLM developed by further pretraining BERT on our medical corpus.

As shown in Figure 4, MDR-BERT with fine-tuning and prompt learning achieved the highest performance across all evaluation metrics, with a micro–F_1-score of 0.838, a macro-AUC of 0.958, and an accuracy of 0.838. MDR-BERT with prompt learning alone performed slightly worse than the combined fine-tuning and prompt learning approach, but both outperformed the other pipelines by a significant margin. This suggests that continued pretraining on clinical records can significantly enhance the performance of the PLM for the task, while freezing parameters may hinder the adaptation of smaller PLMs to the task.

Among the other pipelines, BERT with prompt learning achieved the highest accuracy (0.67) and the highest micro–F_1-score (0.64), though its macro-AUC (0.79) was slightly lower than that of RoBERTa with fine-tuning. This suggests that prompt learning, as a lightweight tuning approach, can match or even surpass traditional fine-tuning methods, aligning with the findings of Taylor et al [22].

We also conducted a comparison with state-of-the-art methods and selected 2 prominent models: mt5-xxl (11B) and Qwen2.5-72B-Instruct. Among these, mt5-xxl demonstrated the best performance in text classification, while Qwen2.5-72B-Instruct excelled as a large language model. For mt5-xxl, we fine-tuned the model using the training and validation sets from our fine-tuning dataset, setting the "prefix_text" to "Classify the following text:". For Qwen2.5-72B-Instruct, we conducted experiments using both zero-shot and retrieval augmented generation methods. In the zero-shot setting, we used prompts to constrain the diagnostic scope, allowing the model to make inferences based on the input information. For the retrieval augmented generation approach, we first encoded the training set using BGE-M3 (BAAI general embedding multilinguality, multigranularity, and multifunctionality) and stored it in a Faiss vector database. During the testing phase, we retrieved cases and classification results relevant to the input content and concatenated them with the prompt to enhance model performance.

Figure 4. The optimal hyperparameters and their search space. AUC: area under the receiver operating characteristic curve; BERT: bidirectional encoder representations from transformers; MDR: medical domain refinement; RoBERTa: robustly optimized BERT pretraining approach; XLNet: extreme language network.

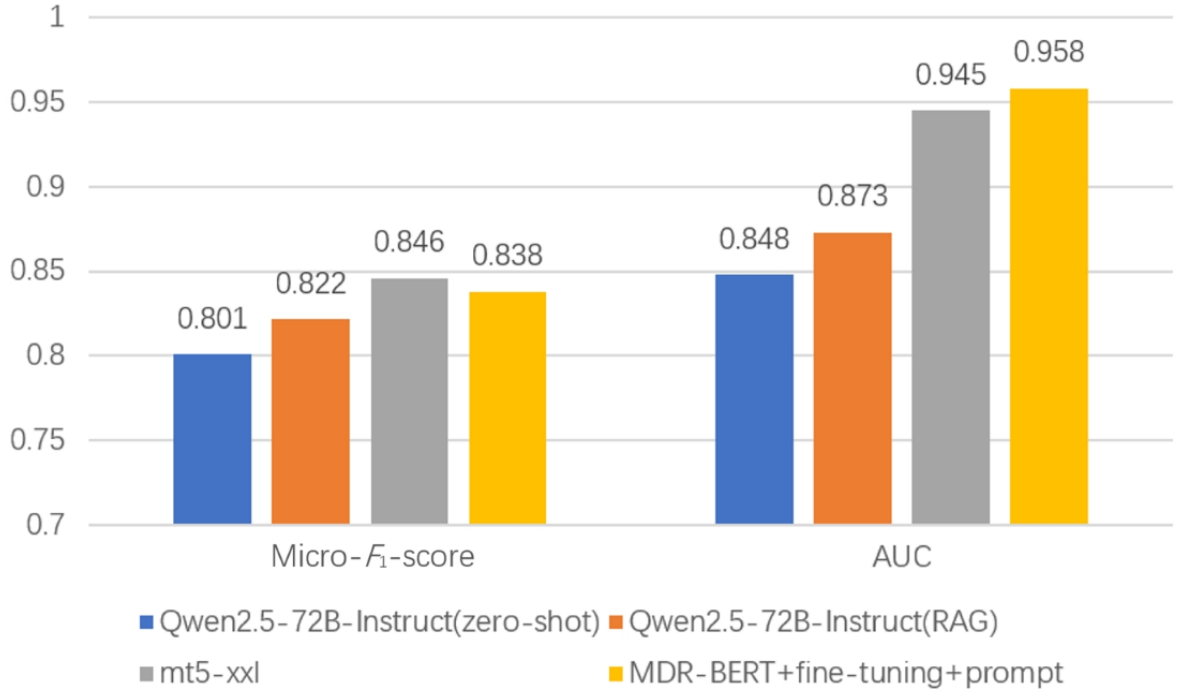


The experimental results indicate that the micro–F_1-score for the mt5-xxl method is 0.846, and the AUC value is 0.945. In comparison, the micro–F_1-score for the Qwen2.5-72B-Instruct method was 0.822, and the AUC value was 0.848. However, the accuracy of both methods does not surpass that of our MDR-BERT model (Figure 5). After a series of strategic

XSL•FO
RenderX

optimizations, our MDR-BERT model achieved results comparable to the fine-tuned mt5-xxl on specific tasks. This is primarily due to the specific structure of the medical records, which can be effectively captured by models with fewer parameters, meaning that overly complex models are not necessary to achieve good performance.

Figure 5. Micro-F_1-score and AUC values for the MDR-BERT model versus the QWEN2.5 and mt5-xxl models. AUC: area under the receiver operating characteristic curve; MDR: medical domain refinement; BERT: bidirectional encoder representations from transformers.

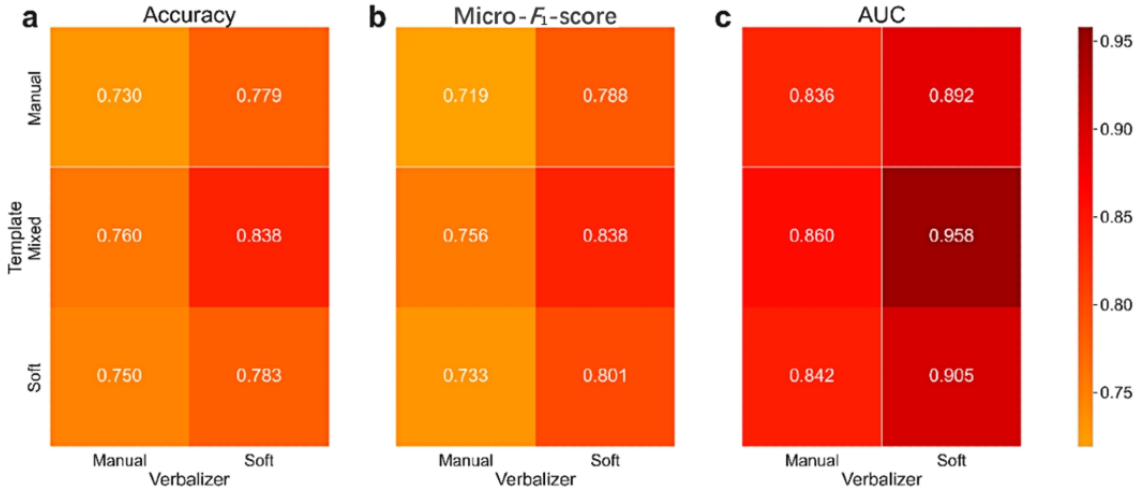


Performance of Different Prompt Learning Modes

We evaluated the performance of MDR-BERT under various settings of prompt learning and fine-tuning, using 3 types of templates (manual, soft, and mixed) and 2 types of verbalizers (manual and soft) as hyperparameters.

For templates, both scripted and self-adaptive patterns performed well independently, and their combination had a cumulative positive effect on performance. For verbalizers, the self-adaptive type outperformed the traditional manual vectors and had a greater impact on overall performance. As shown in Figure 6, the combination of mixed templates and the soft verbalizer achieved the best results.

Figure 6. Comparison among different prompt combinations in verbalizer and template. AUC: area under the receiver operating characteristic curve.



Take the following prompt template as an example:

Mixed template: {“placeholder”: “text_a”} patient {“soft”:“ can be diagnosed as ”} {“mask”}.

For the following case:

The patient was discovered to have bradycardia and unconscious disturbance 7 days ago as a result of physical examination. After consultation with the director, lipid-lowering drugs were added. No diarrhea was detected, and no medication was administered at home. Permanent cardiac pacemaker

XSL•FO
RenderX

implantation under local anesthesia was carried out, and after the surgery, cephalosporin for injection was utilized to prevent infection.

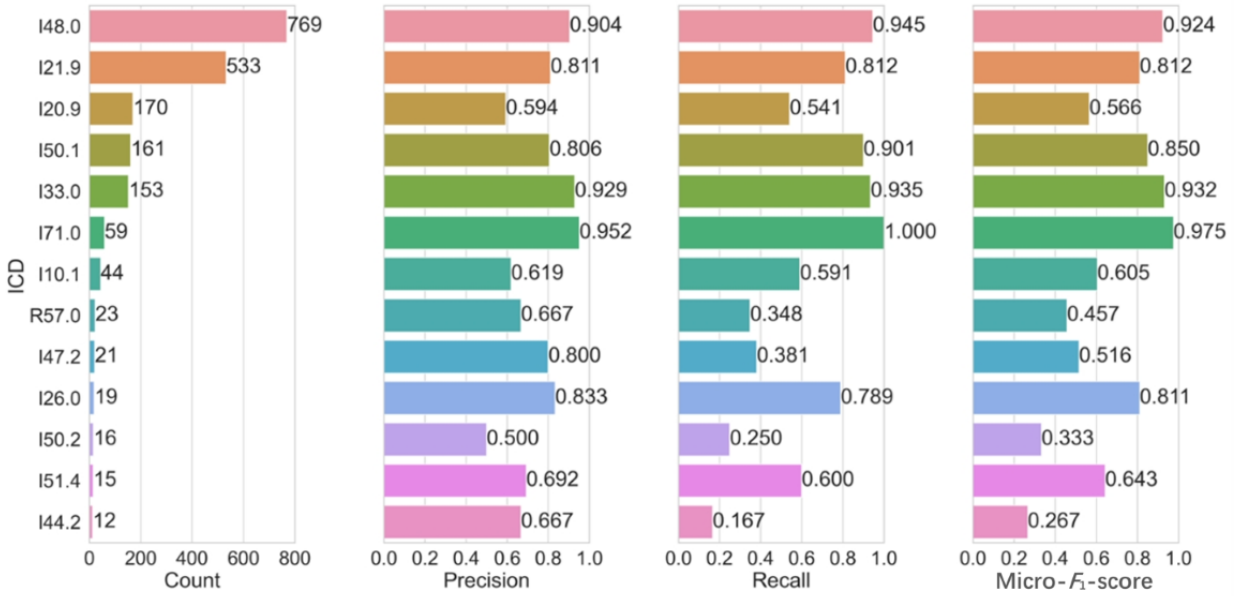
The classification result by our model is as follows: "The patient can be diagnosed as {third-degree atrioventricular block}."

For the mixed template, the patient's bradycardia requires management through the implantation of a permanent pacemaker, indicating that bradycardia is a major medical concern. By applying soft verbalizers, we can guide the correct diagnosis by emphasizing both the reason for the pacemaker implantation and the underlying cause of bradycardia: "The patient can be diagnosed with third-degree atrioventricular block."

Performance of MDR-BERT With Fine-Tuning and Prompt Learning

We evaluated the performance of the MDR-BERT pipeline, incorporating both fine-tuning and prompt learning, for each ICD code using precision, recall, and micro–F_1-score. Figure 7 presents the results for these metrics across the 13 ICD classes.

Figure 7. Precision, recall, and micro-F_1 scores of every ICD code in the MDR-BERT pipeline with fine-tuning and prompt learning. BERT: bidirectional encoder representations from transformers; ICD: International Classification of Diseases; MDR: medical domain refinement.



The pipeline achieved high scores for most *ICD* codes, although the scores varied depending on the data distribution and sample size for each code. We observed a weak positive correlation between sample size and model performance, suggesting that larger samples enhanced the model's learning capability. Conversely, smaller samples tended to have lower micro–F_1-scores, with a trade-off between precision and recall for certain classes. Although our prediction accuracy for ACSs is relatively low, further analysis revealed that in actual clinical settings, ACS was frequently misdiagnosed as cardiac edema (hypertensive emergency) and pulmonary embolism (acute pulmonary embolism). These diseases exhibit similar clinical manifestations and, therefore, require meticulous differential diagnosis to rule out other possibilities. We believe that the overlap of symptoms is a major cause of the difficulty in classifying the model and that inconsistencies in medical histories recorded by physicians further complicate the model's ability to differentiate similar pathologies. Despite these variations, our pipeline demonstrated satisfactory performance across the different *ICD* codes.

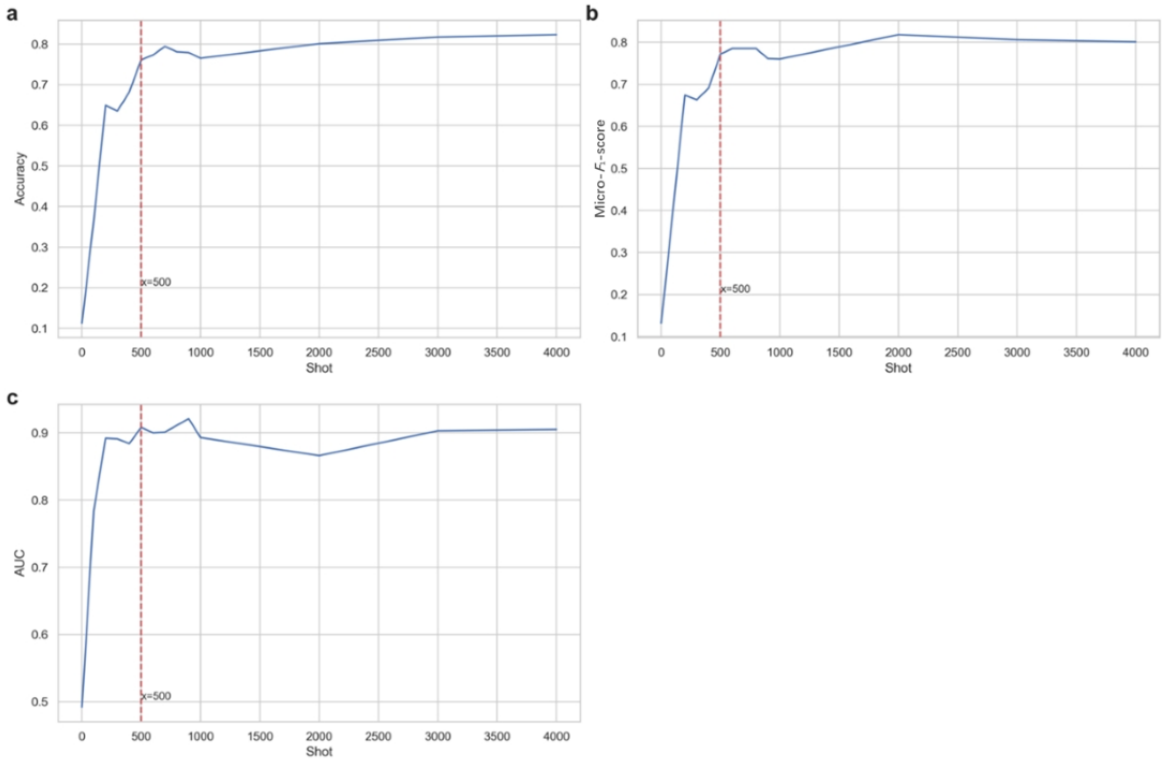
Few-Shot Learning

We conducted few-shot experiments to evaluate the performance of the fine-tuned MDR-BERT with the prompt learning pipeline using different sample sizes from the training set. We randomly selected samples ranging from 1 to 4000 and evaluated the models on the test set. Figure 8 shows the accuracy, micro–F_1-score, and macro-AUC scores for each sample size.

The objective of small-sample learning is to develop models that can learn effectively and make accurate predictions with only a small number of samples, such as 500 or fewer. As shown in Figure 8, when the sample size reaches 500, the model's accuracy, AUC score, and other indicators not only achieve relatively high scores but also reach an inflection point and plateau. At this point, the model produces a relatively satisfactory outcome. This indicates that for the task of *ICD* coding using medical records, 500 samples may be sufficient for the model to learn the key features needed to distinguish between different diagnoses. It suggests that the model has captured enough information to make effective predictions. Additionally, the workload involved in annotating 500 medical texts is manageable and feasible. This number strikes a balance between the effort required for data preparation and the performance gains achieved by the model. Given the complexity and specialized nature of medical records, annotating 500 examples provides a comprehensive representation of the dataset while staying within practical limits. This makes it a reasonable and efficient choice for training the model to achieve satisfactory performance in *ICD* coding tasks.

XSL•FO
RenderX

Figure 8. Few shots experiments on MDR-BERT with fine-tuning and prompt learning. AUC: area under the receiver operating characteristic curve; BERT: bidirectional encoder representations from transformers; MDR: medical domain refinement.



Discussion

Principal Findings

An automated *ICD* coding system for long free-text data is a fundamental platform for clinical research and practice, including clinical trials and pharmacoeconomic management. In this study, we developed a framework based on Key-BERT, a continuously trained and tunable PLM, combined with task-specific prompt learning. We collected a total of 584,969 clinical notes from admission records and discharge summaries in the cardiovascular departments of 8 medical centers.

We used most of the data to continue pretraining a medical corpus and used an independent set of 9337 discharge records with 13 *ICD* codes for CVDs in the *ICD* classification subtask. Although the MDR-BERT model has some limitations, such as restricted generalization capacity and constraints on the length of context it can effectively process, it is important to note that medical texts often have a consistent structure and are generally less dependent on extensive contextual information. Given these characteristics of medical literature, our model is designed to avoid the errors commonly associated with the inherent limitations of BERT's methodology. The structured nature of medical documents enables the MDR-BERT model to function effectively within its designed parameters, mitigating potential issues that could arise from the broader weaknesses of the BERT framework when applied to more contextually complex or varied text types. To remove irrelevant information and limit the input token size, we filtered and truncated all the data for the *ICD* task into keyword-based segments using Key-BERT. The data were then stratified and split into training, validation, and test sets, with the test set used independently for final evaluation.

This study primarily focused on transformer-based algorithms, which have been widely applied and shown superior performance in large-scale medical long free-text tasks [4,11,16,17]. These algorithms can leverage PLMs that capture the semantic and syntactic information of natural language from extensive corpora, leading to significant performance improvements through multicenter datasets.

We compared 6 pipelines for the classification downstream task: BERT with fine-tuning, XLNet with fine-tuning, RoBERTa with fine-tuning, frozen BERT with prompt learning, frozen MDR-BERT with prompt learning, and tunable MDR-BERT with prompt learning. The prompt learning setup included 3 types of templates and 2 types of verbalizers. Among these pipelines, MDR-BERT with fine-tuning and prompt learning achieved the best performance on the test set, attaining a micro–F_1-score of 0.838, a macro-AUC of 0.958, and an accuracy of 0.838.

Compared with the pretraining models of RoBERTa and XLNet, our model achieved superior performance in terms of final accuracy and micro–F_1-score. This improvement was primarily due to the targeted optimization of the methods and the medical data we selected, which substantially enhanced the model's performance. Although RoBERTa and XLNet have larger pretraining corpora compared with BERT, our approach benefited more from using a continuation training corpus built from real electronic health records. This specialized data, tailored to our specific requirements, provided a greater enhancement to the model than more general pretraining data. This is why MDR-BERT performs comparably to, or better than, these alternatives in our settings. The favorable outcome of this pipeline can be attributed to the use of a large-scale

XSL•FO
RenderX

corpus-based PLM and the task-specific enhancements from the combination of fine-tuning and prompt learning [16,20,22-25]. Fine-tuning acts as a model adapter, aligning the model distribution with the task distribution and addressing domain shift and task mismatch issues inherent in PLMs. Prompt learning, with its compact prefix representation and sparse attention mechanism, augments the training data with diverse and natural examples. This augmentation helps mitigate data scarcity and label noise issues in small-sized datasets for downstream tasks.

The combination of fine-tuning and prompt learning acts as a regularization term that balances model complexity with data quality, ultimately enhancing overall performance. This integrated approach highlights the potential of leveraging advanced transformer-based models and customized learning strategies to improve automated medical coding and other clinical tasks.

Among the different prompt learning setups, the mixed template and soft verbalizer achieved the best performance. The soft template method outperformed the manual templates method, which can be attributed to the greater semantic and syntactic information, broader search space, and reduced trial-and-error process associated with the soft template method, making it more effective and less time-consuming [23,24].

The mixed template method is a hybrid approach that combines the advantages of both soft and manual templates. It uses a manual template as a base prompt to provide human-readable instructions and natural language labels, while a soft template serves as an auxiliary prompt to provide tunable embeddings that can adapt to specific downstream tasks. This way, the manual template leverages existing knowledge, while the soft template enhances expressiveness and flexibility.

For the verbalizer, the self-adaptive type had a significantly greater impact on overall performance compared with traditional manual vectors. The soft verbalizer adjusts to the optimal label space for each task and the scale of the pretrained model, rather than being limited by a fixed set of tokens [22,24]. This enhances the accuracy and robustness of the predictions, as well as the diversity and naturalness of the labels. Additionally, by tuning the verbalizer alongside other continuous prompts, it retains the benefits of prompt tuning over fine-tuning, eliminating the need to maintain a separate copy of model parameters for each task during inference.

To explore the influence of sample size on the performance of our pipeline, we conducted few-shot experiments with a range from 1 to 4000 shots. The results showed unsatisfactory evaluation metrics for small-scale shots, but performance improved rapidly and stabilized at around 500 shots. This suggests that for mid-sized language models, such as BERT, the semantic understanding and representation capabilities may not be strong enough. Therefore, tuning the parameters of the PLM with an appropriate sample size is necessary to achieve better performance on specific tasks.

Our research confirms that *ICD* classification tasks can be effectively accomplished by continuously optimizing the BERT model. Although this study used cardiology data for training, our model development strategy is not limited to this specific dataset; substituting the training data with data from other departments would also yield the expected outcomes. Therefore, our model demonstrates remarkable generalization capability. We firmly believe that the model we have developed, combined with the expertise of professional physicians, can effectively address the challenges of *ICD* classification for various diseases.

Limitations

Despite the reasonable performance of our pipeline, this study has certain limitations. First, we trained both the corpus part and the classification task of the framework solely in the cardiovascular department. As a result, the conclusions of this paper may not be generalizable to other medical fields. Second, the *ICD* classification subtask only involved 13 CVD codes, which is not comprehensive enough for clinical practice. Future research could expand to explore the automatic encoding of additional critical heart diseases or even extend to the entire clinical field. This could potentially enhance the applicability and effectiveness of the proposed approach for a broader range of clinical tasks. Third, our model aims to establish an automated analysis system using medical text. However, medical data are inherently multimodal, and modality augmentation can lead to improvements in accuracy. In this context, models such as label alignment for multimodal prompt learning [37] and multimodal equivalent transformer [38] are designed to handle multimodal data, demonstrating the greater potential for future advancements.

Conclusions

We proposed a real-time framework for *ICD* coding from long medical field–related text to *ICD* labels, eliminating the need for semistructured preprocessing. This framework incorporates Key-BERT, a continuously trained and tunable PLM, and task-specific prompt learning with mixed templates and soft verbalizers. We evaluated our model on a multicenter cardiovascular dataset and applied it to predict 13 *ICD* codes for CVDs, achieving high performance. Our model also demonstrated transferability and generalization across different centers.

Furthermore, we conducted few-shot experiments to investigate the impact of data size on model performance. The results showed that while the framework was effective on smaller datasets, a certain sample size was necessary to achieve a relatively stable performance level. This study serves as a benchmark for exploring the feasibility and performance of prompt learning in the subtask of large language models or PLMs. Using a multicenter dataset, the approach demonstrated robust performance across hospitals, highlighting its potential for broad deployment.

Few-shot learning experiments demonstrated feasibility with small-scale datasets, enabling applications for local training on single centers or various single-disease databases. The real-time model identifies *ICD* codes directly, accelerating automated coding compared with semiautomatic approaches that require segment preprocessing. This is particularly impactful for clinical decision support systems that rely on real-time *ICD* coding data.

XSL•FO
RenderX

Overall, the prompt learning paradigm achieved cutting-edge *ICD* assignment accuracy while offering deployability, few-shot learning capacity, and low latency—advantages that are highly beneficial for health care applications. This automated *ICD* coding pipeline could be further implemented in various clinical applications, such as clinical decision support systems, cohort studies, and disease early warning and diagnosis systems.

Acknowledgments

This work was supported by the National Key R&D Program of China (grant 2021ZD0140408) and the Independent Research Project of Medical Engineering Laboratory of Chinese PLA General Hospital (grant 2022SYSZZKY23).

Conflicts of Interest

None declared.

References

1. Steindel SJ. International Classification of Diseases, 10th Edition, clinical modification and procedure coding system: descriptive overview of the next generation HIPAA code sets. J Am Med Inform Assoc 2010;17(3):274-282 [FREE Full text] [doi: 10.1136/jamia.2009.001230] [Medline: 20442144]
2. O'Malley KJ, Cook KF, Price MD, Wildes KR, Hurdle JF, Ashton CM. Measuring diagnoses: ICD code accuracy. Health Serv Res 2005 Oct;40(5 Pt 2):1620-1639 [FREE Full text] [doi: 10.1111/j.1475-6773.2005.00444.x] [Medline: 16178999]
3. Kusnoor S, Blasingame MN, Williams AM, DesAutels SJ, Su J, Giuse NB. A narrative review of the impact of the transition to ICD-10 and ICD-10-CM/PCS. JAMIA Open 2020 Apr;3(1):126-131 [FREE Full text] [doi: 10.1093/jamiaopen/ooz066] [Medline: 32607494]
4. Chen P, Chen K, Liao W, Lai F, He T, Lin S, et al. Automatic International Classification of Diseases coding system: deep contextualized language model with rule-based approaches. JMIR Med Inform 2022 Jun 29;10(6):e37557 [FREE Full text] [doi: 10.2196/37557] [Medline: 35767353]
5. Upadhyaya SG, Murphree DH, Ngufor CG, Knight AM, Cronk DJ, Cima RR, et al. Automated diabetes case identification using electronic health record data at a tertiary care facility. Mayo Clin Proc Innov Qual Outcomes 2017 Jul;1(1):100-110 [FREE Full text] [doi: 10.1016/j.mayocpiqo.2017.04.005] [Medline: 30225406]
6. Diao X, Huo Y, Zhao S, Yuan J, Cui M, Wang Y, et al. Automated ICD coding for primary diagnosis via clinically interpretable machine learning. Int J Med Inform 2021 Sep;153:104543 [FREE Full text] [doi: 10.1016/j.ijmedinf.2021.104543] [Medline: 34391016]
7. Maheshwari S, Agarwal A, Shukla A, Tiwari R. A comprehensive evaluation for the prediction of mortality in intensive care units with LSTM networks: patients with cardiovascular disease. Biomed Tech (Berl) 2020 Aug 27;65(4):435-446. [doi: 10.1515/bmt-2018-0206] [Medline: 31846424]
8. Bao W, Lin H, Zhang Y, Wang J, Zhang S. Medical code prediction via capsule networks and ICD knowledge. BMC Med Inform Decis Mak 2021 Jul 30;21(Suppl 2):55 [FREE Full text] [doi: 10.1186/s12911-021-01426-9] [Medline: 34330264]
9. Kreuzthaler M, Pfeifer B, Kramer D, Schulz S. Secondary use of clinical problem list entries for neural network-based disease code assignment. Stud Health Technol Inform 2023 May;18(302):788-792. [doi: 10.3233/shti230267]
10. Peters ME, Neumann M, Iyyer M, Gardner M, Clark C, Lee K, et al. Deep contextualized word representations. arXiv [FREE Full text] Preprint posted online on March 22, 2018 [doi: 10.48550/arXiv.1802.05365]
11. Dong L, Yang N, Wang W, Wei F, Liu X, Wang Y, et al. Unified language model pre-training for natural language understanding and generation. arXiv [FREE Full text] Preprint posted online on October 15, 2019 [doi: 10.48550/arXiv.1905.03197]
12. Lewis M, Liu Y, Goyal N, Ghazvininejad M, Mohamed A, Levy O, et al. BART: denoising sequence-to-sequence pre-training for natural language generation, translation, and comprehension. arXiv [FREE Full text] Preprint posted online on October 29, 2019 [doi: 10.48550/arXiv.1910.13461]
13. Devlin J, Chang M, Lee K, Toutanova K. BERT: pre-training of deep bidirectional transformers for language understanding. arXiv [FREE Full text] Preprint posted online on May 24, 2019 [doi: 10.48550/arXiv.1810.04805]
14. Coutinho I, Martins B. Transformer-based models for ICD-10 coding of death certificates with Portuguese text. J Biomed Inform 2022 Dec;136:104232 [FREE Full text] [doi: 10.1016/j.jbi.2022.104232] [Medline: 36307020]
15. Yan A, McAuley J, Lu X, Du J, Chang EY, Gentili A, et al. RadBERT: adapting transformer-based language models to radiology. Radiol Artif Intell 2022 Jul;4(4):e210258 [FREE Full text] [doi: 10.1148/ryai.210258] [Medline: 35923376]
16. Liu Y, Ott M, Goyal N, Du J, Joshi M, Chen D, et al. RoBERTa: a robustly optimized BERT pretraining approach. arXiv [FREE Full text] Preprint posted online on July 26, 2019 [doi: 10.48550/arXiv.1907.11692]
17. Elbattah M, Arnaud E, Gignon M, Dequen G. The role of text analytics in healthcare: a review of recent developments and applications. 2021 Presented at: 14th International Joint Conference on Biomedical Engineering Systems and Technologies - Scale-IT-up; February 11–13, 2021; Virtual Event. [doi: 10.5220/0010414508250832]

XSL•FO
RenderX

18. Sezgin E, Hussain S, Rust S, Huang Y. Extracting medical information from free-text and unstructured patient-generated health data using natural language processing methods: feasibility study with real-world data. JMIR Form Res 2023 Mar 07;7:e43014 [FREE Full text] [doi: 10.2196/43014] [Medline: 36881467]
19. Yang Z, Dai Z, Yang Y, Carbonell J, Salakhutdinov R, Le Q. XLNet: generalized autoregressive pretraining for language understanding. 2019 Sep Presented at: NIPS'19: 33rd International Conference on Neural Information Processing Systems; December 8-14, 2019; Vancouver, BC, Canada p. 5753-5763.
20. Liu X, Zheng Y, Du Z, Ding M, Qian Y, Yang Z, et al. GPT understands, too. AI Open 2024;5:208-215. [doi: 10.1016/j.aiopen.2023.08.012]
21. Schick T, Schütze H. Exploiting cloze questions for few shot text classification and natural language inference. arXiv [FREE Full text] Preprint posted online on January 25, 2021 [doi: 10.48550/arXiv.2001.07676]
22. Taylor N, Zhang Y, Joyce DW, Gao Z, Kormilitzin A, Nevado-Holgado A. Clinical prompt learning with frozen language models. IEEE Trans Neural Netw Learning Syst 2024 Nov;35(11):16453-16463. [doi: 10.1109/tnnls.2023.3294633]
23. Li X, Liang P. Prefix-tuning: optimizing continuous prompts for generation. arXiv [FREE Full text] Preprint posted online on January 21, 2021 [doi: 10.48550/arXiv.2101.00190]
24. Liu X, Ji K, Fu Y, Du Z, Yang Z, Tang J. P-Tuning v2: prompt tuning can be comparable to fine-tuning universally across scales and tasks. arXiv [FREE Full text] Preprint posted online on March 20, 2022 [doi: 10.48550/arXiv.2110.07602]
25. Ding N, Hu S, Zhao W, Chen Y, Liu Z, Zheng H, et al. OpenPrompt: an open-source framework for prompt-learning. arXiv [FREE Full text] Preprint posted online on November 3, 2021 [doi: 10.48550/arXiv.2111.01998]
26. Jiang Z, Xu FF, Araki J, Neubig G. How can we know what language models know? arXiv May 3:1 [FREE Full text] Preprint posted online on May 3, 2020 [doi: 10.48550/arXiv.1911.12543]
27. Haviv A, Berant J, Globerson A. BERTese: learning to speak to BERT. arXiv [FREE Full text] Preprint posted online on March 11, 2021 [doi: 10.48550/arXiv.2103.05327]
28. Wallace E, Feng S, Kandpai N, Gardner M, Singh S. Universal adversarial triggers for attacking and analyzing NLP. arXiv [FREE Full text] Preprint posted online on January 3, 2021 [doi: 10.48550/arXiv.1908.07125]
29. Cui L, Wu Y, Liu J, Yang S, Zhang Y. Template-based named entity recognition using BART. arXiv [FREE Full text] Preprint posted online on June 3, 2021 [doi: 10.48550/arXiv.2106.01760]
30. Gao T, Fisch A, Chen D. Making pre-trained language models better few-shot learners. arXiv [FREE Full text] Preprint posted online on June 2, 2021 [doi: 10.48550/arXiv.2012.15723]
31. Shin R, Lin CH, Thomson S, Chen C, Roy S, Platanios EA, et al. Constrained language models yield few-shot semantic parsers. arXiv [FREE Full text] Preprint posted online on November 16, 2021 [doi: 10.48550/arXiv.2104.08768]
32. Schick T, Schmid H, Schutze H. Automatically identifying words that can serve as labels for few-shot text classification. arXiv [FREE Full text] Preprint posted online on October 26, 2020 [doi: 10.48550/arXiv.2010.13641]
33. Vaswani A, Shazeer N, Parmar N, Uszkoreit J, Jones L, Gomez A, et al. Attention is all you need. arXiv [FREE Full text] Preprint posted online on August 2, 2023 [doi: 10.48550/arXiv.1706.03762]
34. Sharma P, Li Y. Self-supervised contextual keyword and keyphrase retrieval with self-labelling. Preprints [FREE Full text] Preprint posted online on August 6, 2019 [doi: 10.20944/preprints201908.0073.v1]
35. Zhuang Y, Zhang J, Li X, Liu C, Yu Y, Dong W, et al. ICD_promptLearning. GitHub. 2024. URL: https://github.com/PLA301dbgroup2/ICD_promptLearning [accessed 2024-12-03]
36. Tinn R, Cheng H, Gu Y, Usuyama N, Liu X, Naumann T, et al. Fine-tuning large neural language models for biomedical natural language processing. Patterns (N Y) 2023 Apr 14;4(4):100729 [FREE Full text] [doi: 10.1016/j.patter.2023.100729] [Medline: 37123444]
37. Gao J, Ruan J, Xiang S, Yu Z, Ji K, Xie M, et al. LAMM: label alignment for multi-modal prompt learning. 2024 Mar 24 Presented at: The Thirty-Eighth AAAI Conference on Artificial Intelligence (AAAI-24); February 20-27, 2024; Vancouver, BC, Canada p. 1815-1823 URL: https://ojs.aaai.org/index.php/AAAI/article/view/27950/27920 [doi: 10.1609/aaai.v38i3.27950]
38. Xiang S, Gao J, Guan M, Ruan J, Zhou C, Liu T, et al. Learning robust visual-semantic embedding for generalizable person re-identification. arXiv [FREE Full text] Preprint posted online on April 19, 2023 [doi: 10.48550/arXiv.2304.09498]

Abbreviations

ACS: acute coronary syndrome
AUC: area under the receiver operating characteristic curve
BERT: bidirectional encoder representations from transformers
BGE-M3: BAAI general embedding multilinguality, multigranularity, and multifunctionality
CVD: cardiovascular disease
ICD: International Classification of Diseases
MDR: medical domain refinement
MLM: masked language modeling
NLP: natural language processing

XSL•FO
RenderX

PLM: pretrained language model
RoBERTa: robustly optimized BERT pretraining approach
Transformer-XL: Transformer-Extra-Long
XLNet: extreme language network

Edited by A Castonguay; submitted 11.06.24; peer-reviewed by S Mao, M Elbattah, S Xiang; comments to author 27.08.24; revised version received 16.10.24; accepted 19.11.24; published 06.01.25.

Please cite as:
Zhuang Y, Zhang J, Li X, Liu C, Yu Y, Dong W, He K
Autonomous International Classification of Diseases Coding Using Pretrained Language Models and Advanced Prompt Learning Techniques: Evaluation of an Automated Analysis System Using Medical Text
JMIR Med Inform 2025;13:e63020
URL: https://medinform.jmir.org/2025/1/e63020
doi:10.2196/63020
PMID:

©Yan Zhuang, Junyan Zhang, Xiuxing Li, Chao Liu, Yue Yu, Wei Dong, Kunlun He. Originally published in JMIR Medical Informatics (https://medinform.jmir.org), 06.01.2025. This is an open-access article distributed under the terms of the Creative Commons Attribution License (https://creativecommons.org/licenses/by/4.0/), which permits unrestricted use, distribution, and reproduction in any medium, provided the original work, first published in JMIR Medical Informatics, is properly cited. The complete bibliographic information, a link to the original publication on https://medinform.jmir.org/, as well as this copyright and license information must be included.

XSL•FO
RenderX

Original Paper

YOLOv12 Algorithm-Aided Detection and Classification of Lateral Malleolar Avulsion Fracture and Subfibular Ossicle Based on CT Images: Multicenter Study

Jiayi Liu[1*], PhD; Peng Sun[2*], MS; Yousheng Yuan[1*], MS; Zihan Chen[3*], BSc; Ke Tian[2], MS; Qian Gao[2], MS; Xiangsheng Li[2], PhD; Liang Xia[1], PhD; Jun Zhang[1], PhD; Nan Xu[2], PhD

[1]Department of Radiology, Sir Run Run Hospital, Nanjing Medical University, Nanjing, China

[2]Department of Radiology, Air Force Medical Center, Air Force Medical University, Beijing, China

[3]School of Mathematics and Physics, Xi'an Jiaotong-Liverpool University, Suzhou, China

[*]these authors contributed equally

Corresponding Author:
Nan Xu, PhD
Department of Radiology, Air Force Medical Center, Air Force Medical University
Fucheng Road 30, Haidian District
Beijing, 100142
China
Phone: 86 18510230072
Email: xunan835@126.com

Abstract

Background: Lateral malleolar avulsion fractures (LMAFs) and subfibular ossicles (SFOs) are distinct entities that both present as small bone fragments near the lateral malleolus in imaging but require different treatment strategies. Clinical and radiological differentiation is challenging, which can impede timely and precise management. Magnetic resonance imaging (MRI) is the diagnostic gold standard for differentiating LMAFs from SFOs, whereas radiological differentiation using computed tomography (CT) alone is challenging in routine practice. Deep convolutional neural networks (DCNNs) have shown promise in musculoskeletal imaging diagnostics, but robust, multicenter evidence in this specific context is lacking.

Objective: This study aims to evaluate several state-of-the-art DCNNs—including the latest You Only Look Once (YOLO) v12 algorithm—for detecting and classifying LMAFs and SFOs in CT images, using MRI-based diagnoses as the gold standard and to compare model performance with radiologists reading CT alone.

Methods: In this retrospective study, 1918 patients (LMAF: n=1253, 65.3%; SFO: n=665, 34.7%) were enrolled from 2 hospitals in China between 2014 and 2024. MRI served as the gold standard and was independently interpreted by 2 senior musculoskeletal radiologists. Only CT images were used for model training, validation, and testing. CT images were manually annotated with bounding boxes. The cohort was randomly split into a training set (n=1092, 56.93%), internal validation set (n=476, 24.82%), and external test set (n=350, 18.25%). Four deep learning models—faster R-CNN, single shot multibox detector (SSD), RetinaNet, and YOLOv12—were trained and evaluated using identical procedures. Model performance was assessed using mean average precision at intersection over union=0.5 (mAP50), area under the receiver operating curve (AUC), accuracy, sensitivity, and specificity. The external test set was also independently interpreted by 2 musculoskeletal radiologists with 7 and 15 years of experience, with results compared with the best-performing model. Saliency maps were generated using Shapley values to enhance interpretability.

Results: Among the evaluated models, YOLOv12 achieved the highest detection and classification performance, with a mAP50 of 92.1% and an AUC of 0.983 on the external test set—significantly outperforming faster R-CNN (mAP50 63.7%; AUC 0.79); SSD (mAP50 63%; AUC 0.63); and RetinaNet (mAP50 67.0%; AUC 0.73)—all $P<.001$. When using CT alone, radiologists performed at a moderate level (accuracy: 75.6% and 69.1%; sensitivity: 75.0% and 65.2%; specificity: 76.0% and 71.1%), whereas YOLOv12 approached MRI-based reference performance (accuracy: 92.0%; sensitivity: 86.7%; specificity: 82.2%). Saliency maps corresponded well with expert-identified regions.

Conclusions: While MRI (read by senior radiologists) is the gold standard for distinguishing LMAFs from SFOs, CT-based differentiation is challenging for radiologists. A CT-only DCNN (YOLOv12) achieved substantially higher performance than

XSL•FO
RenderX

radiologists interpreting CT alone and approached the MRI-based reference standard, highlighting its potential to augment CT-based decision-making where MRI is limited or unavailable.

(JMIR Med Inform 2025;13:e79064) doi:10.2196/79064

KEYWORDS

deep convolutional neural network; lateral malleolar avulsion fracture; subfibular ossicle; X-ray computed tomography; CT; classification; artificial intelligence; AI

Introduction

Background

The ankle is the most frequently injured joint in the human body, accounting for nearly 5% of emergency visits and about 40% of sports-related injuries [1,2]. Inversion or blunt trauma often results in ligament sprains, muscle strains, or fractures [2]. Acute lateral malleolar avulsion fractures (LMAFs) occur in about 15% of inversion sprains and, if missed, may lead to nonunion, chronic instability, and pain, necessitating stricter immobilization or surgery compared with simple sprains [3,4]. Small bone fragments near the lateral malleolus may also be subfibular ossicles (SFOs), either as accessory bones (os subfibulae) or as remnants of nonunion avulsion fractures [5,6]. SFO prevalence ranges from 0.2% to 6.7% and they are usually asymptomatic but appear in 10% to 38.5% of chronic ankle instability cases, suggesting a link to chronic dysfunction [7]. Both LMAF and SFO may cause lateral ankle pain and instability, making treatment selection more relevant than etiologic differentiation [8,9]. However, diagnosis is difficult because of overlapping clinical symptoms and ambiguous history or physical findings [10]. Radiography, the first-line imaging, has a missed fracture rate of 14% to 85% owing to small fragments, minimal displacement, suboptimal imaging angles, low quality, insufficient clinical context, and anatomical overlaps [11-15]. Although computed tomography (CT) improves visualization, large-scale validation for LMAF is lacking. While fragment morphology on CT can aid in distinguishing LMAF from SFO [16,17], this is complicated by smooth edges, incomplete separation, or osteophytes [18]. Magnetic resonance imaging (MRI) excels at detecting bone marrow edema and ligament injuries [19] but is limited by thick slices, partial volume effects, contraindications, and poor emergency availability. Thus, reliable and automated imaging-based diagnosis remains a key clinical need.

Deep learning and radiomics have achieved impressive results for the automated detection and classification of musculoskeletal fractures—including those of the ankle [20], femoral neck [21], hip [22], knee [23], spine [24], ribs [25], and scapula [26]—by using various deep convolutional neural network (DCNN) models, such as You Only Look Once (YOLO) and faster region-based convolutional neural network (R-CNN). Despite these advances, most existing studies focus on single-task or single-model frameworks, leaving performance uncertainties for tasks requiring differentiation of closely related lesions. To date, no DCNN-based approaches for automated detection of LMAF and SFO have been reported. With continuous architectural innovation, DCNNs are gaining traction for more complex orthopedic imaging tasks. Early studies focused on normal anatomy identification or simple diagnoses [27], but recent work extended to recognizing and classifying a variety of lesions—including multiple myeloma [28], patellar dislocation [29,30], osteoarthritis [31], bone age assessment [32], bone metastasis [33], and lumbar disk herniation [34]. However, automated detection and classification of LMAF and SFO in CT images remain challenging because of the relatively simple regional anatomy, diverse injury patterns, overlapping structures, and frequent imaging artifacts that even experienced radiologists find difficult. This challenge is more pronounced in primary hospitals lacking experienced musculoskeletal imaging specialists, where misdiagnosis rates are higher. Our study addresses this specific gap and aims to improve diagnostic accuracy and efficiency for this overlooked region using DCNNs.

This Study

Studies using multi-model DCNN comparisons for detection and classification are still scarce. Comparative evaluation of mainstream architectures is valuable for understanding network performance and guiding the selection of optimal solutions for specific clinical tasks. YOLOv12, released by the Ultralytics team in February 2025, introduces substantial optimizations in network structure, feature fusion, and inference speed over its predecessors (eg, YOLOv8 and YOLOv9), achieving a better balance between accuracy and computational efficiency [35]. In this study, 4 advanced DCNN models—faster R-CNN, single shot multibox detector (SSD), RetinaNet, and the latest YOLOv12—were benchmarked for automated detection and classification of LMAF and SFO in multicenter clinical CT datasets. The models' accuracy was quantitatively evaluated using metrics, such as mean average precision (mAP), and their diagnostic performance was compared with that of radiologists to assess clinical utility.

Methods

Ethical Considerations

The authors are accountable for all aspects of the work in ensuring that questions related to the accuracy or integrity of any part of the work are appropriately investigated and resolved. The study was conducted in accordance with the Declaration of Helsinki (as revised in 2013). This study was approved by the Institutional Ethics Committee of the Sir Run Run Hospital, Nanjing Medical University (2025-SRFA-626), and Air Force Medical Center, Air Force Medical University (2025-11-PJ01). The institutional ethics committees waived written informed consent in view of the retrospective nature of the study. All the procedures performed were part of routine care. All images were deidentified before use to protect patient privacy.

XSL•FO
RenderX

Patient Selection

Our study used medical imaging data from 2 hospitals in China. For the development of the training and internal validation sets, CT and MRI data were collected from patients with ankle sprains treated at Air Force Medical Center, Air Force Medical University, between January 2014 and December 2024 (Textbox 1).

Textbox 1. Inclusion and exclusion criteria for the development of the training and internal validation sets.

Inclusion criteria

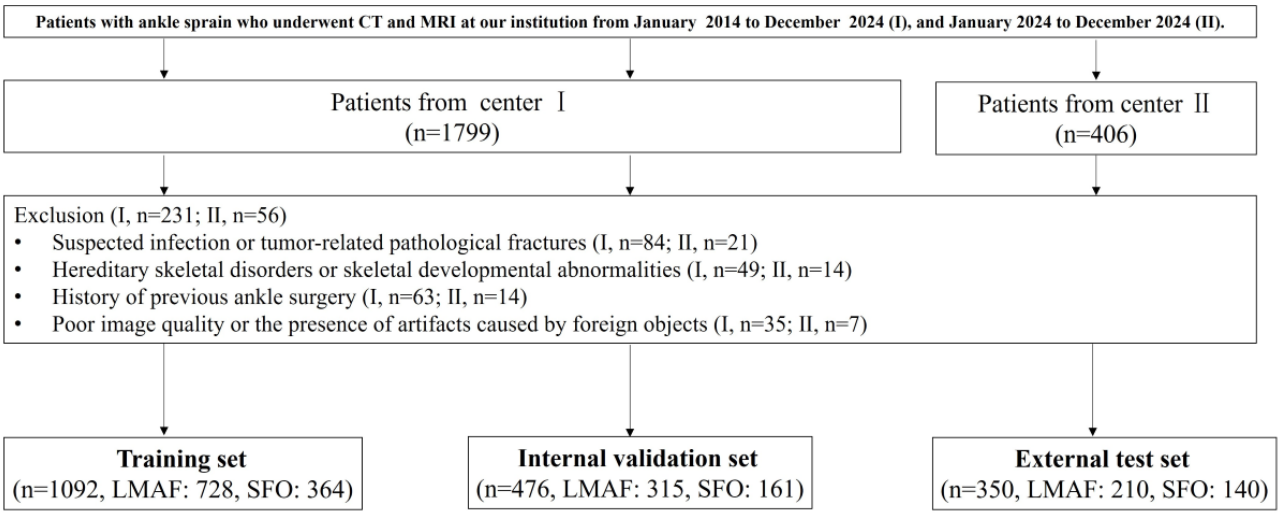
- Age ≥18 years with a history of ankle sprain within the past 3 days
- CT images showing a single free bone fragment adjacent to the lateral malleolus (size ≥1 cm)
- Complete raw CT and MRI data, with both examinations performed within a 1-week interval
- Complete clinical information, including sex and age

Exclusion criteria

- Suspected infection- or tumor-related pathological fractures
- Hereditary skeletal disorders or skeletal dysplasia
- Previous ankle surgery
- Low image quality or artifacts

An independent external test set was collected between January 2024 and December 2024 from Sir Run Run Hospital, Nanjing Medical University, using the same inclusion and exclusion criteria (Textbox 1). The detailed case selection process is illustrated in Figure 1. A total of 1918 patients were included in this study, comprising 1253 (65.3%) patients with LMAF and 665 (34.7%) with SFO. Of these, 1568 cases from the Air Force Medical Center were randomly allocated to a training set (n=1092, 56.93%) and an internal validation set (n=476, 24.82%) at a 7:3 ratio. The remaining 350 cases from Sir Run Run Hospital formed an independent external test set. Thus, the final training, internal validation, and external test sets contained 1092 (56.93%), 476 (24.82%), and 350 (18.25%) cases, respectively.

Figure 1. Flowchart summarizing patient selection and allocation to the dataset of our study.



CT and MRI Acquisition Protocol

Patient age and sex were obtained from the clinical record system. Details of CT and MRI acquisition devices and imaging parameters are provided in Multimedia Appendix 1. For CT scanning, patients were positioned supine with toes pointing upward and the ankle in a neutral position. The scan range included the distal tibia and fibula to the talus and surrounding bony structures (including the talus, calcaneus, and navicular). All images were reconstructed using a bone window (window width: 1500; window level: 500) with a slice thickness and interval of 1.0 mm. All image processing and analysis in our study were performed on the bone window of CT images.

Classification

In this study, the initial differentiation between LMAF and SFO was made on the basis of MRI findings, which served as the reference standard for diagnosis. LMAF was defined as the presence of bone marrow edema in the corresponding region of the distal fibula on MRI, frequently accompanied by soft tissue swelling or evidence of ligamentous injury [36]. In contrast, SFO was characterized by the absence of bone marrow edema and lack of surrounding soft tissue injury, consistent with a chronic, stable ossicle. The interpretation of MRI images was independently performed by 2 senior radiologists, each with more than 20 years of experience in musculoskeletal

XSL•FO
RenderX

imaging. The evaluation criteria included cortical continuity of the distal fibula, the margin and morphology of the bone fragment, and associated soft tissue changes. Any discrepancy between the 2 radiologists' interpretations was resolved through consensus discussion. In cases where consensus could not be reached, a third experienced musculoskeletal radiologist was consulted, and the final diagnosis was established on the basis of a majority opinion.

Evaluation of the Radiologists' Visual Diagnoses Based on CT Images

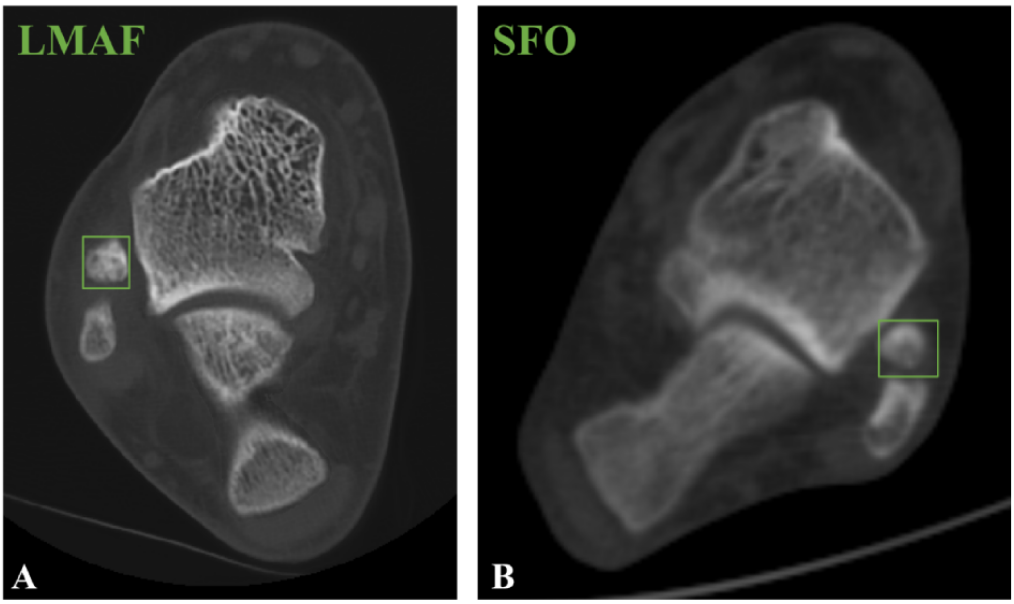
For the external test set, each case was independently reviewed by radiologist 1 (a deputy chief radiologist with 15 years of musculoskeletal imaging experience) and radiologist 2 (an attending radiologist with 7 years of musculoskeletal imaging experience). Neither radiologist had access to the MRI results or clinical data during image interpretation. All images were evaluated independently by radiologists 1 and 2. Each radiologist recorded their classification of LMAF or SFO independently. For purposes of calculating diagnostic performance metrics, the diagnostic results of each radiologist were compared against the reference standard, which was established by MRI findings. Each radiologist's performance on the external test set was then directly compared with that of the YOLOv12 model to evaluate whether the artificial intelligence (AI) model outperformed human assessment.

Data Preparation

All CT images were acquired in Digital Imaging and Communications in Medicine (DICOM) format to ensure high resolution and rich grayscale information. Data preprocessing, a critical step in our study, included data selection, image format conversion, normalization, and data augmentation to meet the requirements for model development. Metadata, such as scanning parameters, slice thickness, and window width and level, were extracted using specialized tools to ensure data completeness. All images were converted to standardized PNG format while maintaining original resolution, facilitating subsequent size unification. To address grayscale distribution differences resulting from various scanners and settings, histogram equalization and pixel normalization were applied, mapping grayscale values to a fixed range. All images were resized to 640×640 pixels, providing consistent input dimensions for the models. To further increase data volume and enhance model robustness, data augmentation techniques such as random rotation, translation, scaling, and mirroring were used, generating additional training samples without compromising medical image integrity. This approach improved the model's ability to recognize fracture features from various angles and positions. The entire preprocessing pipeline ensured uniform data quality and format, providing high-quality, well-annotated images for training, thereby improving the accuracy and robustness of the detection tasks.

The annotation stage was performed independently by radiologists 1 and 2. Each lesion was labeled with a tight bounding box (Figure 2) using the Visual Geometry Group Image Annotator (VGG Image Annotator, University of Oxford). The fracture regions were manually outlined, and all annotations underwent cross-validation and quality control to ensure that each bounding box accurately represented the clinical lesion. To meet the input requirements of the detection models, we further processed the bounding boxes and cropped the images, ensuring that both the annotated regions and surrounding contextual information were consistently retained. This provided the models with sufficient and high-quality training samples.

Figure 2. The lesions are labeled by drawing a tight bounding box. (A) An example of lateral malleolar avulsion fracture (LMAF). (B) An example of subfibular ossicle (SFO).

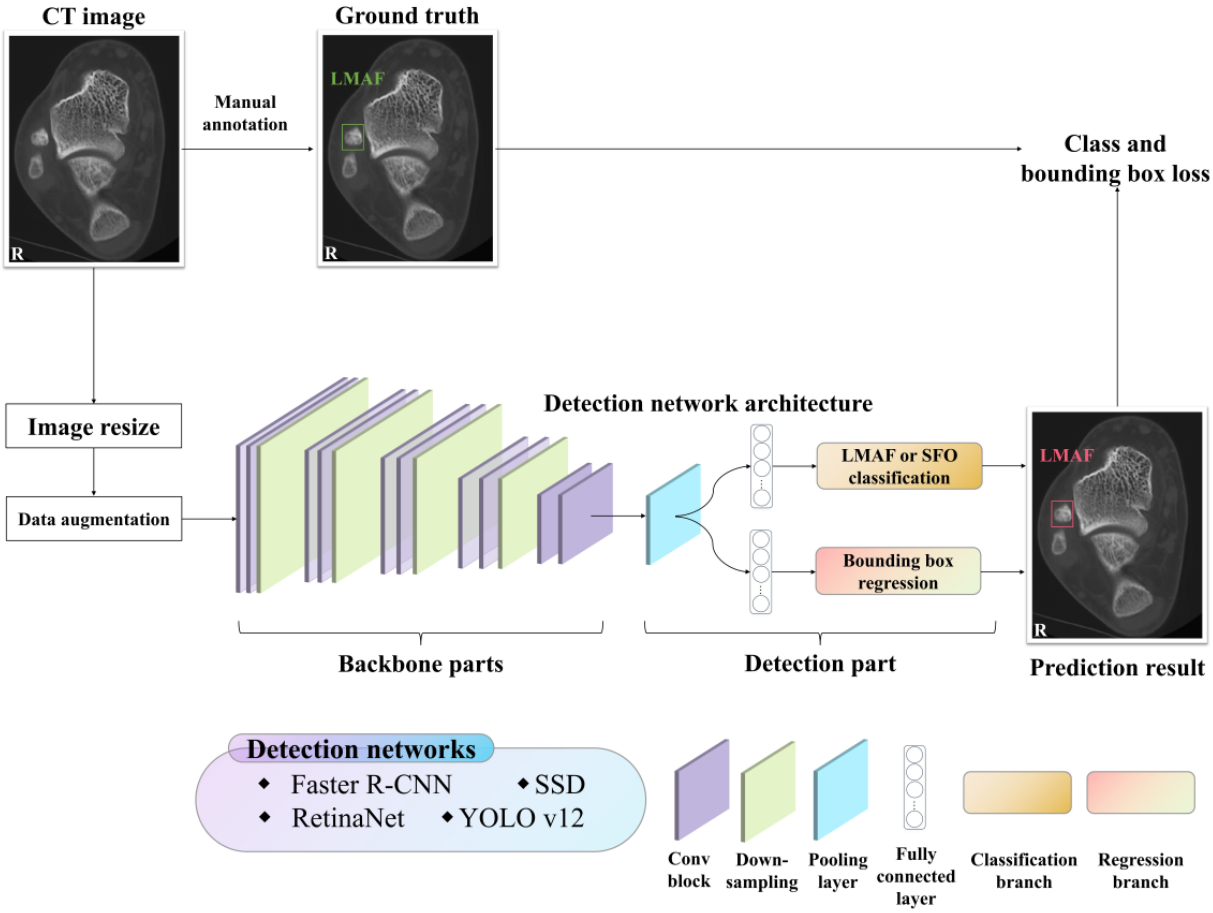


XSL•FO
RenderX

LMAF and SFO Detection Networks

In our study, 4 types of state-of-the-art object detection networks for LMAF and SFO detection on CT images were used (Figure 3).

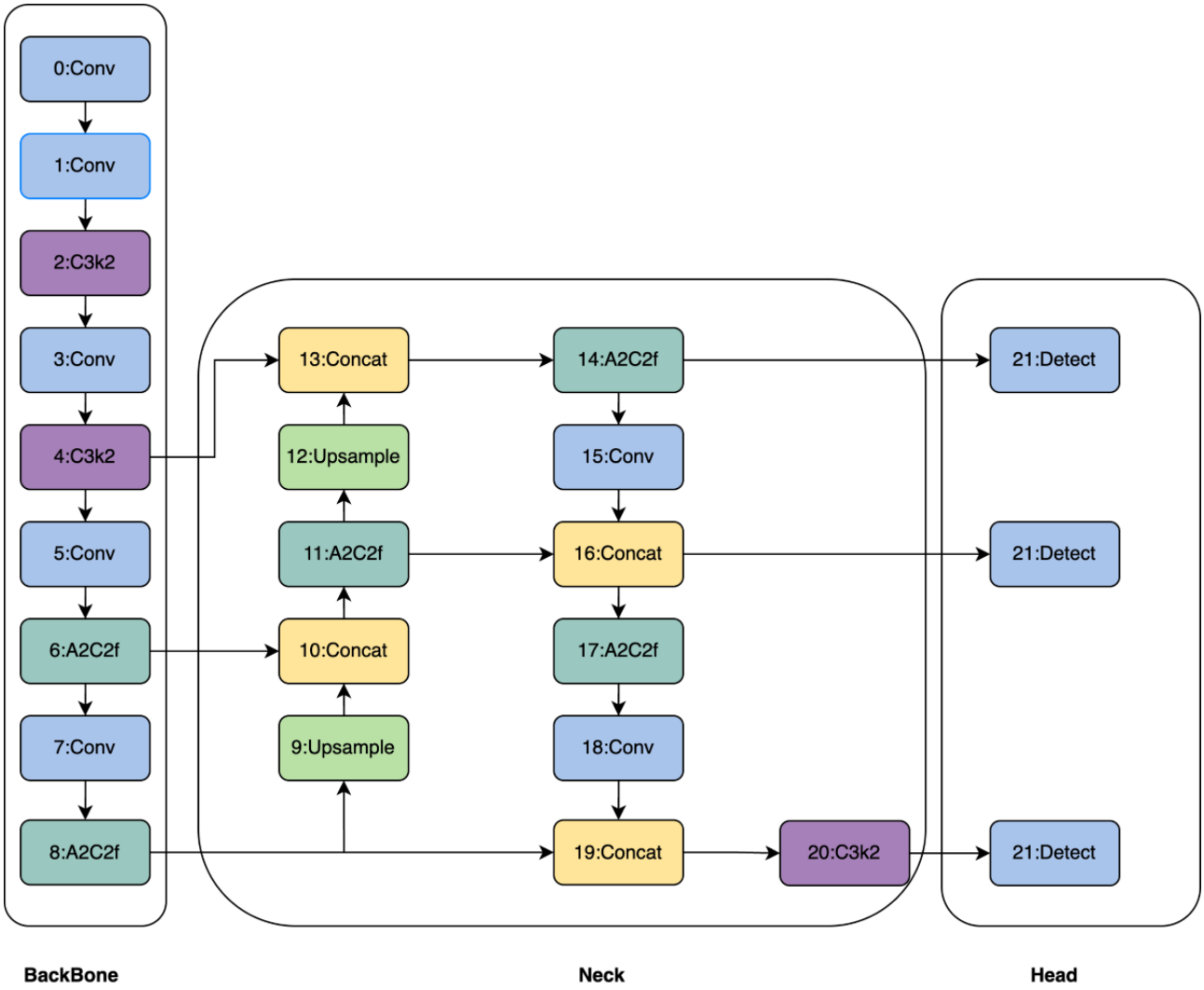
Figure 3. Schematic diagram of deep learning approaches for detection of lateral malleolar avulsion fracture (LMAF) and subfibular ossicle (SFO) on computed tomography (CT) images. R-CNN: region-based convolutional neural network; SSD: single shot multibox detector; YOLO: You Only Look Once.



In this study, we used the YOLOv12 architecture, which was recently introduced on February 19, 2025, as the core detection network for LMAF and SFO identification (Figure 4). YOLOv12 advances previous one-stage detectors through a series of architectural innovations that balance high detection accuracy and efficient inference, which is critical in clinical and real-time applications. YOLOv12 is built upon a fully convolutional network backbone, eliminating fully connected layers to enhance both computational efficiency and spatial information retention. The network starts with a series of stacked convolutional and pooling layers in the front end, enabling progressive extraction of low-level features such as edges, textures, and local structures. This early feature extraction facilitates the precise localization of subtle abnormalities frequently present in medical images. Subsequently, multiple residual blocks capture higher-level semantic features, ensuring a comprehensive representation of features at different scales. YOLOv12 also incorporates a multi-scale feature fusion module, which integrates deep and shallow features via cross-layer connections, enabling precise localization in fine regions, such as fracture sites. In addition, an adaptive anchor box mechanism and multi-scale prediction strategy enable the model to achieve high performance in both classification and localization tasks. Finally, the introduction of a lightweight attention mechanism enhances the model's focus on fracture edges and subtle structural features, improving detection accuracy and robustness while maintaining real-time inference capability.

XSL•FO
RenderX

Figure 4. The model architecture of YOLOv12.



To further boost localization reliability, YOLOv12 uses an adaptive anchor box mechanism. Anchor box sizes are dynamically learned from the training data distributions, optimizing the detection of objects with varying shapes and scales. In addition, a multi-scale prediction head enables simultaneous detection at 3 distinct spatial resolutions, allowing the model to maintain high precision when dealing with objects of different sizes. A notable architectural advancement is the integration of a lightweight attention mechanism based on coordinate attention modules. This enables the network to adaptively recalibrate feature responses, directing more focus toward critical areas—such as fracture boundaries or subtle morphological cues—while suppressing irrelevant background information. This not only improves detection performance, especially for challenging cases, but also preserves the real-time inference speed required in clinical workflows. All experiments were performed using the PyTorch 2.3 framework (Meta Platforms) on an NVIDIA RTX 4090 GPU (NVIDIA Corporation). The above hyperparameter choices were optimized by grid search to maximize the mAP on the validation subset. The main hyperparameter configurations were as follows: input image size: 640×640 pixels; batch size: 32; learning rate: initialized at 0.01 with cosine annealing schedule; optimizer: stochastic gradient descent with momentum 0.937 and weight decay 0.0005; anchor box generation: k-means clustering on the training data set; confidence threshold: 0.01; nonmaximum suppression intersection over union (IoU) threshold: 0.5; attention module: coordinate attention with a reduction ratio of 32; augmentation: mosaic, mix-up, and random affine transformations.

To comprehensively compare the performance of different models in the detection of LMAF and SFO, in addition to YOLOv12, we also implemented 3 other object detection models: faster R-CNN, SSD, and RetinaNet. Faster R-CNN, a representative 2-stage detection model, generates region proposals through a region proposal network, followed by refined classification and bounding box regression, providing a strong benchmark for localization accuracy. The SSD model uses a single-stage detection strategy, enabling high-speed detection while supporting multi-scale object detection. RetinaNet introduces the focal loss function to effectively address class imbalance and enhance the detection of small targets and subtle structures. All models were trained and tested using the same data preprocessing and augmentation strategies to ensure experimental comparability. In addition, specific hyperparameter tuning strategies were designed for each model.

XSL•FO
RenderX

Training Setup

The detection networks were trained for 50 epochs with a batch size of 8. Data augmentation techniques applied during training included rotation (angle range −30° to 30°), width and height translation (horizontal and vertical axes: −20% to 20%), and scaling (range 0% to 20%). The networks were optimized using the AdamW optimizer with β_1=0.9 and β_2=0.999. The initial learning rate was set to 1×10^{3} and reduced to 1×10 if the validation loss plateaued after 25 epochs. All deep learning models were implemented in Python 3 using the PyTorch framework (Meta Platforms) and trained on a workstation equipped with an Intel i9–7900X CPU (Intel Corporation; 3.3 GHz), 128 GB RAM, and 2 NVIDIA TITAN RTX GPU (NVIDIA Corporation). All models were trained and tested under identical computational conditions, using the same data augmentation pipeline and 3 consistent hyperparameters, ensuring an unbiased comparison across models.

Evaluation Metrics and Vision Transformer Shapley Saliency Maps

An end-to-end training architecture was adopted throughout the network design, with joint optimization of module parameters achieved via error backpropagation. To evaluate the detection performance for LMAF and SFO, we used the following metrics: mAP, average precision (AP), precision, recall, and F_1- score. AP was determined by the area under the precision-recall (PR) curve, which was constructed based on the maximum overlap (IoU) between detected and ground-truth bounding boxes. The PR curve is a key tool for assessing the performance of classifiers or object detection models, especially in the context of class imbalance, by visualizing the trade-off between precision and recall across different decision thresholds. Detection time was also measured for a comprehensive performance comparison, aiming to provide multidimensional insights for the clinical application of automated LMAF and SFO detection.

The mAP measures the model's AP across different classes and IoU thresholds, and we calculated the AP at an IoU threshold of 0.5 (ie, mAP50). Please refer to Multimedia Appendix 2 for the calculation method. To further interpret the model's decision process, saliency maps were generated using Shapley techniques [37]. Receiver operating characteristic curves and the AUC were plotted and calculated to assess model performance, and the DeLong test was used to compare AUCs between models. Calibration curves and decision curve analysis were computed and plotted using the *RMS* and *rmda* packages in R software (version 4.0.2), and the Hosmer-Lemeshow test was used to evaluate calibration. For radiologists 1 and 2, diagnostic performance metrics—including sensitivity, specificity, accuracy, and AUC—were calculated for LMAF and SFO diagnosis, and the DeLong test was used to determine whether differences in AUC were significant. A *P* value <.05 was considered statistically significant. The statistical analyses were carried out using our internally developed PixelMedAI platform. This platform was programmed in Python version 3.8 and primarily used libraries, such as PyTorch, NumPy, and SciPy. This approach ensures a robust evaluation of both AI models and human experts, facilitating a comprehensive understanding of the effectiveness of saliency maps in enhancing diagnostic accuracy in clinical settings.

Results

Clinical Features of the Studied Patients

A total of 1918 patients met the inclusion criteria, comprising 1253 (65.3%) cases of LMAF and 665 (34.7%) cases of SFO. The patients ranged in age from 18 to 70 years, with a mean age of 33.52 (SD 12.83) years. There were 1463 male patients (76.3%) and 355 female patients (23.7%). The training set, internal validation set, and external test set included 1092 (56.93%) cases (LMAF: 728, SFO: 364), 476 (24.82%) cases (LMAF: 315, SFO: 161), and 350 (18.25%) cases (LMAF: 210, SFO: 140), respectively. The demographic characteristics of each data set are summarized in Table 1.

Table 1. Baseline characteristics of patients in the training set, internal validation set and external test set.

Characteristics	Training set (n=1092)	Internal validation set (n=476)	External test set (n=350)
Age (years), mean (SD)	31.47 (11.57)	32.19 (11.68)	34.94 (13.03)
Sex, n (%)			
Male	847 (77.6)	364 (76.4)	252 (72)
Female	245 (22.4)	112 (23.6)	98 (28)

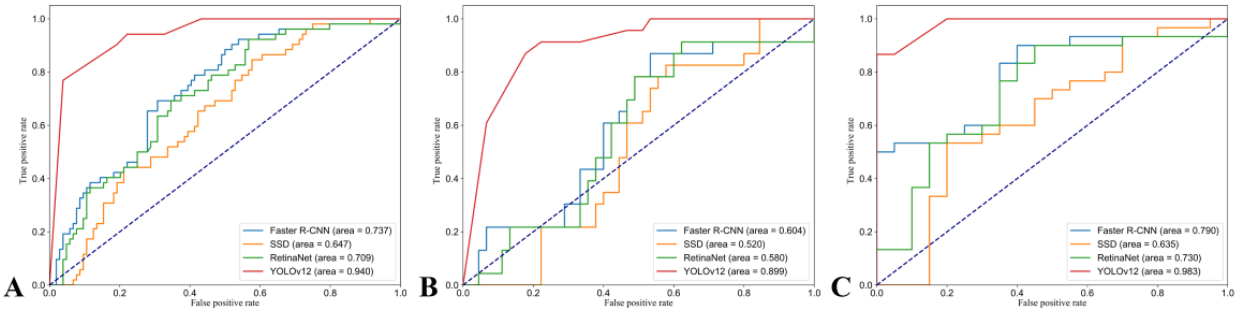
Performance of DCNNs

A comparative analysis of the detection performance of the 4 DCNNs models was conducted. Figure 5 and Multimedia Appendix 3 show the PR curves and receiver operating characteristic (ROC) curves for each model, respectively. The mAP values were compared to evaluate the performance of each DCNN in detecting LMAF and SFO on CT images. In the test set, the mAP50 scores for faster R-CNN, SSD, RetinaNet, and YOLOv12 were 63.7%, 63.0%, 67.0%, and 92.1%, respectively. The AUC values for these models were 0.79 (faster R-CNN), 0.63 (SSD), 0.73 (RetinaNet), and 0.98 (YOLOv12). Pairwise comparisons using the DeLong test indicated that the differences were all statistically significant (*P*<.001). These results demonstrate that YOLOv12 achieved the highest performance in LMAF and SFO detection. The calibration curves for the detection performance of the 4 DCNNs on CT images are shown in Multimedia Appendix 4. The calibration curves demonstrated that the predicted probabilities closely matched the actual probabilities for the training, internal validation, and external test sets (Hosmer-Lemeshow test: χ^2=8.2, χ^2=2.6, χ^2=22.7, respectively; *P*=.21, *P*=.46, *P*=.13, respectively). Decision curve

XSL•FO
RenderX

analysis results indicate that YOLOv12 may serve as an effective tool for detecting LMAF and SFO (Multimedia Appendix 5).

Figure 5. Precision and recall curves of the 4 deep convolutional neural networks are displayed in different colors, with the performance of each model shown. YOLOv12 achieved the highest performance, as demonstrated in its precision and recall curve. (A) Training set. (B) Internal validation set. (C) External test set. R-CNN: region-based convolutional neural network; SSD: single shot multibox detector; YOLO: You Only Look Once.



Performance Between the YOLOv12 Model and Radiologists' Readings

Table 2 shows the AUC, sensitivity, specificity, and accuracy of YOLOv12 and radiologists 1 and 2 in detecting LMAF and SFO. The AUCs for YOLOv12, radiologist 1, and radiologist 2 were 0.983, 0.755, and 0.682, respectively. Pairwise comparisons using the DeLong test revealed statistically significant between radiologist 1, radiologist 2, and YOLOv12 (P=.004, P<.001), indicating that YOLOv12 outperformed both radiologists.

Table 2. Comparison of AUC, accuracy, sensitivity, and specificity between the YOLOv12 model and radiologists' readings.

	AUC	Accuracy	Sensitivity	Specificity	*P* value
YOLOv12	0.983	0.920	0.867	0.822	–
Radiologist 1	0.755	0.756	0.750	0.760	.004
Radiologist 2	0.682	0.691	0.652	0.711	<.001

Evaluation of Saliency Maps

Saliency maps generated using the Shapley technique were used to highlight the region's most influential for predicting LMAF (Figure 6) and SFO (Figure 7), with red pixels indicating areas with the greatest impact on the model's predictions. As shown in Figure 6D, YOLOv12 assigned a relatively high probability (0.93) to LMAF, and the saliency map correspondingly highlights the LMAF region. In Figure 7D, YOLOv12 assigned a relatively low probability (0.32) to LMAF, indicating a higher probability for SFO, and the saliency map highlights the SFO region accordingly.

XSL•FO
RenderX

Figure 6. Case of lateral malleolar avulsion fracture. By using the ViT Shapley technique, we generated a saliency map where the red highlighted areas roughly correspond to the lateral malleolar avulsion fracture seen in the magnetic resonance imaging image. (A) Faster region-based convolutional neural network. (B) Single shot multibox detector. (C) RetinaNet. (D) YOLOv12. (E) Sagittal PDWI-weighted magnetic resonance imaging image of the ankle.

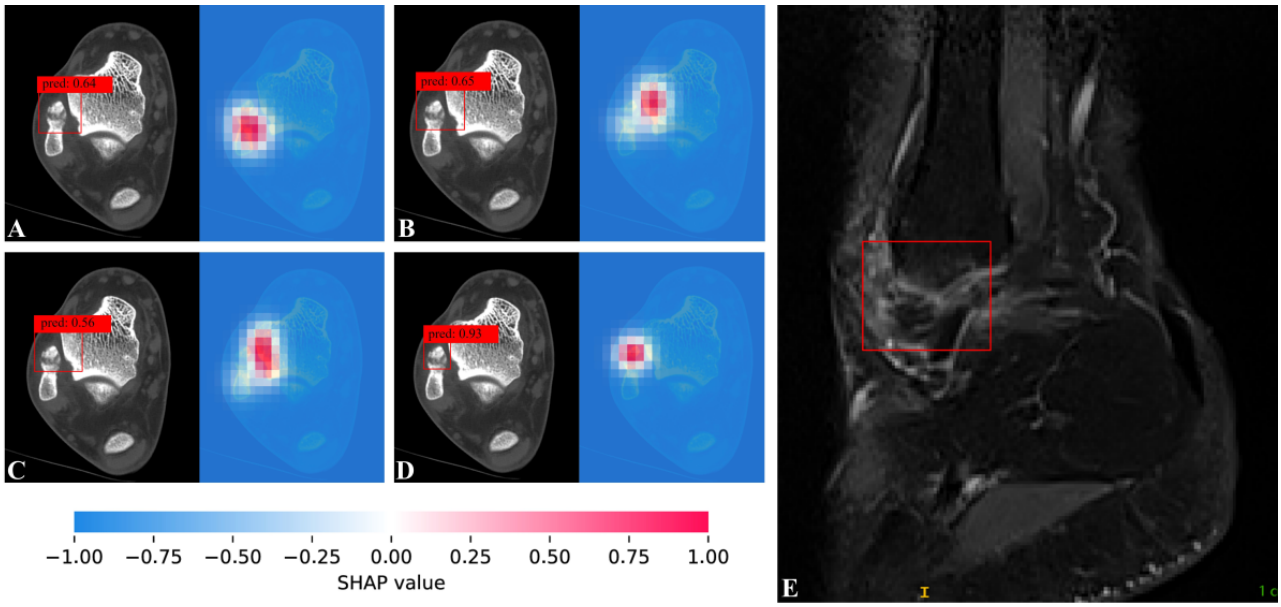
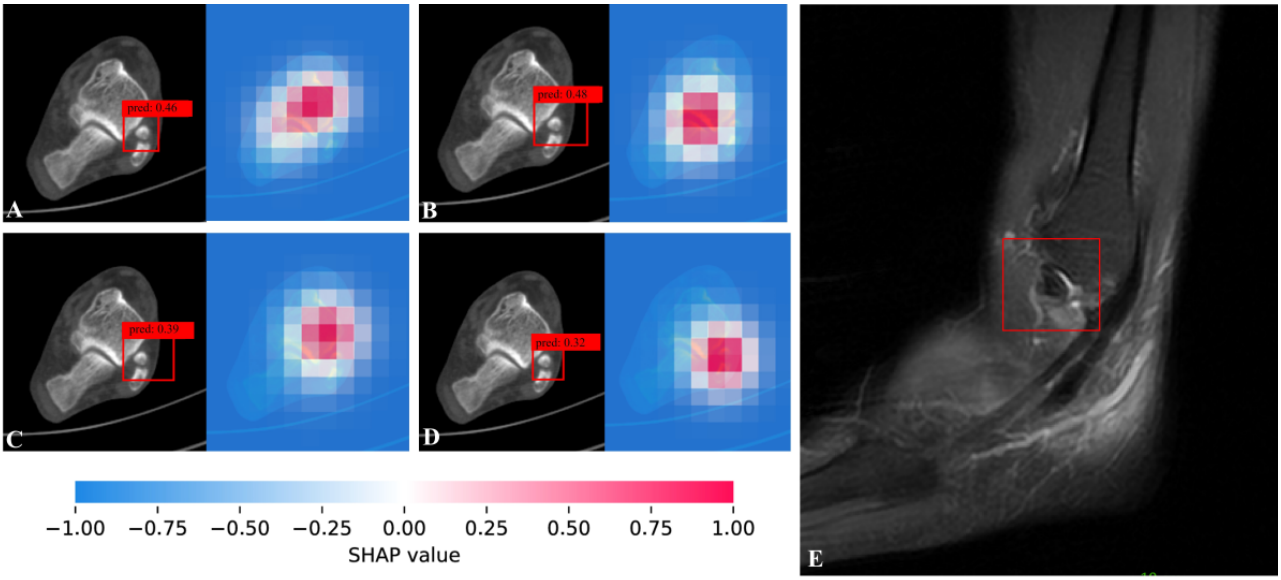


Figure 7. Case of subfibular ossicle. By using the ViT Shapley technique, we generated a saliency map where the red highlighted areas roughly correspond to the subfibular ossicle seen in the magnetic resonance imaging image. (A) Faster region-based convolutional neural network. (B) Single shot multibox detector. (C) RetinaNet. (D) YOLOv12. (E) Sagittal PDWI-weighted magnetic resonance imaging image of the ankle.



Discussion

Principal Findings

Our study is the first to systematically evaluate and compare multiple mainstream DCNNs for the automatic detection and classification of LMAF and SFO on ankle CT images. Among the models tested, YOLOv12 demonstrated the highest detection accuracy and efficiency, with mAP50 of 92.1% and AUC of 0.98 on the external validation cohort. When compared with radiologists 1 and 2 with different experience levels, YOLOv12 surpassed human performance in accuracy, sensitivity, and specificity, highlighting the powerful potential of deep learning for recognizing subtle and complex anatomical structures. Quantitative analysis further confirmed the model's high reproducibility and stability, effectively addressing limitations of human interpretation, such as inconsistency and time consumption. Most errors were associated with confusing anatomical variations and inaccurate localization of lesion boundaries, but overall, the model met the practical needs for clinical auxiliary diagnosis and provided a solid technical foundation for intelligent diagnosis in orthopedics. In keeping with real-world clinical workflows—where LMAF and SFO may coexist and readers are expected to detect all relevant abnormalities within a single study—our primary evaluation focused on performance in the combined data set.

XSL•FO
RenderX

Comparison to Prior Work

Prior work using object detection networks—such as faster R-CNN, RetinaNet, or earlier YOLO versions (eg, YOLOv3 to YOLOv8)—has achieved promising results for fracture localization in radiographs, but performance often declined in cases involving small, subtle lesions or overlapping anatomical structures [26,38,39]. Furthermore, these studies were typically limited by homogeneous datasets, single-center validation, or a lack of rigorous comparison to clinical radiologist interpretation. Our study addresses these gaps by introducing a comprehensive, multicenter evaluation of several state-of-the-art DCNN architectures, including the newly released YOLOv12 model. Notably, YOLOv12 incorporates advanced multiscale feature fusion and optimized attention mechanisms, resulting in substantial improvements in both detection accuracy and computational efficiency over previous frameworks [40]. Compared with earlier works, our head-to-head benchmarking on large-scale, well-annotated multicenter CT data sets demonstrates that YOLOv12 outperformed established models, such as faster R-CNN, SSD, and RetinaNet in terms of mAP, AUC, sensitivity, and specificity. Moreover, unlike most previous research—which reported model performance in isolation—our study directly compares the diagnostic capability of deep learning models with radiologists of differing clinical experience. YOLOv12 demonstrated superior accuracy (92% vs 75.6% and 69.1%) and AUC (0.98 vs 0.76 and 0.68) over 2 musculoskeletal imaging specialists, underscoring its clinical potential for assisting or augmenting human diagnosis, particularly in settings where radiological expertise may be limited.

Performance Interpretation

In this study, the YOLOv12-based object detection model achieved a mAP of 92.1% at an IoU threshold of 0.5 (mAP50) on the test set, indicating that the model was able to accurately detect 92.1% of actual lesion regions when the IoU threshold was set to 0.5. Specifically, this metric reflects the proportion of predicted bounding boxes whose overlap with the ground-truth annotated lesion regions reached or exceeded 50%. Although this result demonstrates the model's strong performance in localizing lesion targets, some differences remained between the predicted and actual regions in terms of size and shape, mainly because of the relatively lenient IoU threshold. Such discrepancies are common in practical applications; nevertheless, the model is largely capable of accurately capturing key lesion information to meet the requirements of subsequent diagnostic assistance. The automatic detection and classification capabilities of YOLOv12 exhibited high reproducibility and stability, effectively compensating for the limitations of manual interpretation in terms of repeatability and efficiency, thereby providing more reliable technical support for clinical diagnosis. YOLOv12 incorporates advanced attention mechanisms and a multi-branch feature fusion structure, enabling it to efficiently capture object information at different scales and under complex scenarios [41]. Furthermore, its optimized network architecture and lightweight design significantly reduced the number of model parameters and computational load while maintaining high detection performance, balancing inference speed with resource use efficiency. This makes it suitable for edge deployment and large-scale real-time detection tasks in actual applications.

Detection Errors and Challenges

In our study, the first main error observed with the YOLOv12 model was the misclassification of SFO as LMAF, resulting in false positives. This misjudgment was primarily caused by confusion with normal anatomical structures or adjacent soft tissue shadows, as some anatomical variants or features of the fibula could easily be mistaken for pathological findings by the network [42]. These misleading regions also pose a considerable challenge for human readers, reflecting the DCNN's sensitivity to areas with "clear boundaries and interrupted bone continuity" during the learning process [43], which closely mirrors the clinical approach used by physicians. Therefore, many of the model's false positives overlapped with the subtle or ambiguous cases that even experienced clinicians might misinterpret.

The second error type involved correct detection of the presence of abnormal structures, but imprecise localization of the region of interest. In these instances, the model could identify that a loose fragment or abnormal bone structure existed, yet failed to delineate the precise borders or classify the fragment correctly, particularly regarding its exact size, avulsion site, or associated ligament anatomy. Further analysis revealed that while DCNNs are generally adept at capturing the spatial relationship between fractures, joints, and adjacent bone structures, they remain less effective in distinguishing finer anatomical details [44]. Cases with subtle displacement, overlapping structures, or minimal contrast differences contributed to these localization issues. Future improvements could be achieved by integrating detection networks with training datasets that include enhanced annotation of normal anatomical variations, thereby reducing both false-positive and false-negative rates through a more nuanced understanding of the relevant anatomical context [45].

Limitations and Future Directions

Our study still has some limitations. First, when comparing the performance of the YOLOv12 with that of radiologists for automatic detection and classification of LMAF and SFO on CT images, the experimental design required informing the radiologists in advance about the specific lesion types and regions of interest. This likely improved the diagnostic accuracy of the radiologists and resulted in an optimistically biased representation of manual interpretation. In real clinical practice, some lesions are easily missed or misdiagnosed, so this "prompt" provided a considerable advantage to the physicians. Second, this study did not include complex cases with multiple coexisting lesions, which reduced the amount of data available for model training. Future studies should incorporate such complex or multifocal cases to better evaluate the accuracy of DCNNs in clinical scenarios that more closely resemble real-world situations. Third, all imaging data in this study were collected from only 2 medical institutions. Although multiple scanners and extensive data augmentation were used to minimize bias, this may still affect the generalizability of the model to other institutions and populations. To further improve the model's applicability and robustness, future work should involve validation with multicenter, multi-scanner, and multisource

XSL•FO
RenderX

datasets [46]. Fourth, while our design enhances clinical realism, it limits the granularity of class-specific assessment; we did not perform separate training or testing on LMAF-only and SFO-only datasets or report per-class mAP. As our dataset expands, we plan to conduct category-specific experiments and provide detailed per-class detection metrics to further delineate class-dependent performance and error modes.

Conclusions

Our study developed a DCNN-based method for automatic detection and classification of LMAF and SFO in CT images. The results showed that the YOLOv12 network outperformed mainstream models such as faster R-CNN, SSD, and RetinaNet in both detection and classification tasks. In addition, the YOLOv12 model achieved higher classification accuracy than radiologists.

Acknowledgments

This work was supported by Medical Scientific Research Project of the Jiangsu Provincial Health Commission (grant M2024055) and the Medical Imaging Artificial Intelligence Special Research Fund Project, Nanjing Medical Association Radiology Branch (grant 16). We express our gratitude to the editor and anonymous reviewers for their insightful comments and suggestions, which have greatly enhanced the quality of our paper. We also extend our thanks to American Journal Experts for their assistance in editing the language of an earlier draft of this manuscript. We appreciate the guidance and support from the PixelMedAI platform and its developers concerning the code used in this revised manuscript.

Data Availability

The datasets generated or analyzed during this study are not publicly available because of privacy or ethical restrictions but are available from the corresponding author upon reasonable request.

Authors' Contributions

LX, JZ, and NX contributed equally as co-corresponding authors. JL contributed to conceptualization, investigation, resources, writing—original draft, writing—review and editing, and visualization; PS contributed to conceptualization, investigation, resources, and writing—review and editing; YY contributed to conceptualization, investigation, writing—original draft, writing—review and editing, and visualization; ZC contributed to conceptualization, methodology, writing—review and editing, and project administration; KT contributed to conceptualization, writing—review and editing, visualization, and supervision; QG contributed to conceptualization, methodology, and writing—review and editing; XL contributed to conceptualization and writing—review and editing; LX contributed to conceptualization, methodology, software, writing—review and editing, and supervision; JZ contributed to conceptualization, investigation, resources, writing—review and editing, visualization, and funding acquisition; NX contributed to data curation, investigation, resources, formal analysis, writing—review and editing, and visualization.

Conflicts of Interest

None declared.

Multimedia Appendix 1
The computed tomography (CT) and magnetic resonance imaging (MRI) image acquisition parameters of the 2 centers.
[DOCX File , 19 KB - medinform_v13i1e79064_app1.docx]

Multimedia Appendix 2
Supplementary formula.
[DOCX File , 16 KB - medinform_v13i1e79064_app2.docx]

Multimedia Appendix 3
Receiver operating characteristic curves of 4 deep convolutional neural network (DCNN) models (A: training set; B: internal validation set; C: external test set).
[PNG File , 395 KB - medinform_v13i1e79064_app3.png]

Multimedia Appendix 4
Calibration curve for the prediction model (A: training set; B: internal validation set; C: external test set).
[PNG File , 516 KB - medinform_v13i1e79064_app4.png]

Multimedia Appendix 5
Decision curve analysis of the model (A: training set; B: internal validation set; C: external test set).

XSL•FO
RenderX

[PNG File , 565 KB - medinform_v13i1e79064_app5.png]

References

1. Reiner MM, Sharpe JJ. The role of the accessory malleolar ossicles and malleolar avulsion fractures in lateral ankle ligament reconstruction. Foot Ankle Spec 2018 Aug;11(4):308-314. [doi: 10.1177/1938640017729498] [Medline: 28874066]
2. Ekinci S, Polat O, Günalp M, Demirkan A, Koca A. The accuracy of ultrasound evaluation in foot and ankle trauma. Am J Emerg Med 2013 Nov;31(11):1551-1555. [doi: 10.1016/j.ajem.2013.06.008] [Medline: 23992775]
3. van den Bekerom MP, Kerkhoffs GM, McCollum GA, Calder JD, van Dijk CN. Management of acute lateral ankle ligament injury in the athlete. Knee Surg Sports Traumatol Arthrosc 2013 Jun;21(6):1390-1395. [doi: 10.1007/s00167-012-2252-7] [Medline: 23108678]
4. Kerut CK, Mudiganty S, Kerut DG, Horswell RL, Williams R, Valencia M, et al. Probability of occult ankle fracture based on radiograph-measured swelling. J Am Acad Orthop Surg Glob Res Rev 2024 May 01;8(5):e23.00271 [FREE Full text] [doi: 10.5435/JAAOSGlobal-D-23-00271] [Medline: 38743847]
5. Kim WJ, Lee HS, Moon SI, Kim HS, Yeo ED, Kim YH, et al. Presence of subfibular ossicle does not affect the outcome of arthroscopic modified Broström procedure for chronic lateral ankle instability. Arthroscopy 2019 Mar;35(3):953-960. [doi: 10.1016/j.arthro.2018.10.148] [Medline: 30611585]
6. Ahn H, Lee K. Comparison of the modified Broström procedure for chronic lateral ankle instability with and without subfibular ossicle. Am J Sports Med 2016 Dec;44(12):3158-3164. [doi: 10.1177/0363546516660069] [Medline: 27528610]
7. Cao Y, Xu Y, Huang Q, Xu Y, Hong Y, Xu X. Outcomes of ossicle resection and anatomic reconstruction of lateral ligaments for chronic ankle instability with large malleolar accessory ossicles. Foot Ankle Surg 2021 Oct;27(7):736-741 [FREE Full text] [doi: 10.1016/j.fas.2020.09.012] [Medline: 33046382]
8. Fairbanks PJ, Saito GH, Mendes AA, Nishikawa DR, Fonseca FC, Prado MP. Ankle instability in pediatric and adolescent patients diagnosed with lateral malleolus avulsion fracture: analysis of clinical and functional outcomes of ligament injury repair surgery. Foot Ankle Surg 2024 Aug;30(6):499-503. [doi: 10.1016/j.fas.2024.03.013] [Medline: 38632005]
9. Kim BS, Woo S, Kim JY, Park C. Radiologic findings for prediction of rehabilitation outcomes in patients with chronic symptomatic os subfibulare. Radiol Med 2017 Oct;122(10):766-773 [FREE Full text] [doi: 10.1007/s11547-017-0786-y] [Medline: 28664488]
10. Hedelin H, Goksör L, Karlsson J, Stjernström S. Ultrasound-assisted triage of ankle trauma can decrease the need for radiographic imaging. Am J Emerg Med 2013 Dec;31(12):1686-1689. [doi: 10.1016/j.ajem.2013.09.005] [Medline: 24157071]
11. Takakura Y, Yamaguchi S, Akagi R, Kamegaya M, Kimura S, Tanaka H, et al. Diagnosis of avulsion fractures of the distal fibula after lateral ankle sprain in children: a diagnostic accuracy study comparing ultrasonography with radiography. BMC Musculoskelet Disord 2020 Apr 28;21(1):276 [FREE Full text] [doi: 10.1186/s12891-020-03287-1] [Medline: 32345266]
12. Wang CL, Shieh JY, Wang TG, Hsieh FJ. Sonographic detection of occult fractures in the foot and ankle. J Clin Ultrasound 1999 Oct;27(8):421-425. [doi: 10.1002/(sici)1097-0096(199910)27:8<421::aid-jcu2>3.0.co;2-e] [Medline: 10477883]
13. Lee DY, Lee DJ, Kim DH, Shin HS, Jung WI. Posttraumatic subfibular ossicle formation in children: experience in a single primary care unit. J Pediatr Orthop 2018 Oct;38(9):e530-e535. [doi: 10.1097/BPO.0000000000001231] [Medline: 30074589]
14. Simanovsky N, Lamdan R, Hiller N, Simanovsky N. Sonographic detection of radiographically occult fractures in pediatric ankle and wrist injuries. J Pediatr Orthop 2009 Mar;29(2):142-145. [doi: 10.1097/BPO.0b013e318198452e] [Medline: 19352239]
15. Cho K, Lee S, Lee Y, Suh K. Ultrasound diagnosis of either an occult or missed fracture of an extremity in pediatric-aged children. Korean J Radiol 2010;11(1):84-94 [FREE Full text] [doi: 10.3348/kjr.2010.11.1.84] [Medline: 20046499]
16. Han SH, Choi WJ, Kim S, Kim S, Lee JW. Ossicles associated with chronic pain around the malleoli of the ankle. J Bone Joint Surg Br 2008 Aug;90(8):1049-1054. [doi: 10.1302/0301-620X.90B8.20331] [Medline: 18669961]
17. Pill SG, Hatch M, Linton JM, Davidson RS. Chronic symptomatic os subfibulare in children. J Bone Joint Surg Am 2013 Aug 21;95(16):e115(1-e1156). [doi: 10.2106/JBJS.L.00847] [Medline: 23965709]
18. Yi J, Cha JG, Lee YK, Lee BR, Jeon CH. MRI of the anterior talofibular ligament, talar cartilage and os subfibulare: comparison of isotropic resolution 3D and conventional 2D T2-weighted fast spin-echo sequences at 3.0 T. Skeletal Radiol 2016 Jul;45(7):899-908. [doi: 10.1007/s00256-016-2367-x] [Medline: 26992909]
19. Llanes AC, Van Tassel D, Wirth A, Goncalves LF, Belthur MV. Optimal visualization of os subfibulare using 3D water selective cartilage scan (3D_WATSc) MRI sequencing: a case report. Cureus 2022 Jul;14(7):e27469 [FREE Full text] [doi: 10.7759/cureus.27469] [Medline: 36060334]
20. Ashkani-Esfahani S, Mojahed Yazdi R, Bhimani R, Kerkhoffs GM, Maas M, DiGiovanni CW, et al. Detection of ankle fractures using deep learning algorithms. Foot Ankle Surg 2022 Dec;28(8):1259-1265. [doi: 10.1016/j.fas.2022.05.005] [Medline: 35659710]
21. Xing P, Zhang L, Wang T, Wang L, Xing W, Wang W. A deep learning algorithm that aids visualization of femoral neck fractures and improves physician training. Injury 2024 Dec;55(12):111997. [doi: 10.1016/j.injury.2024.111997] [Medline: 39504732]

XSL•FO
RenderX

22. Zheng Z, Ryu BY, Kim SE, Song DS, Kim SH, Park J, et al. Deep learning for automated hip fracture detection and classification : achieving superior accuracy. Bone Joint J 2025 Feb 01;107-B(2):213-220. [doi: 10.1302/0301-620X.107B2.BJJ-2024-0791.R1] [Medline: 39889758]
23. Zeng J, Zou F, Chen H, Liang D. Texture analysis combined with machine learning in radiographs of the knee joint: potential to identify tibial plateau occult fractures. Quant Imaging Med Surg 2025 Jan 02;15(1):502-514 [FREE Full text] [doi: 10.21037/qims-24-799] [Medline: 39838981]
24. Liu W, Zhang X, Tang R, Yu C, Sun G. Radiomics analysis based on plain x-rays to detect spinal fractures with posterior wall injury. Digit Health 2025;11:20552076251324436 [FREE Full text] [doi: 10.1177/20552076251324436] [Medline: 40013076]
25. Li T, Liao M, Fu Y, Zhang F, Shen L, Che J, et al. Intelligent detection and grading diagnosis of fresh rib fractures based on deep learning. BMC Med Imaging 2025 Mar 24;25(1):98 [FREE Full text] [doi: 10.1186/s12880-025-01641-0] [Medline: 40128676]
26. Fang Q, Jiang A, Liu M, Zhao S. Faster R-CNN model for target recognition and diagnosis of scapular fractures. J Bone Oncol 2025 Apr;51:100664 [FREE Full text] [doi: 10.1016/j.jbo.2025.100664] [Medline: 40114811]
27. Afnouch M, Gaddour O, Hentati Y, Bougourzi F, Abid M, Alouani I, et al. BM-Seg: a new bone metastases segmentation dataset and ensemble of CNN-based segmentation approach. Expert Syst Appl 2023 Oct 15;228:120376 [FREE Full text] [doi: 10.1016/j.eswa.2023.120376]
28. Faghani S, Baffour FI, Ringler MD, Hamilton-Cave M, Rouzrokh P, Moassefi M, et al. A deep learning algorithm for detecting lytic bone lesions of multiple myeloma on CT. Skeletal Radiol 2023 Jan;52(1):91-98. [doi: 10.1007/s00256-022-04160-z] [Medline: 35980454]
29. Li T, Gharaibeh NM, Jia S, Qinaer Z, Aihemaiti S, HaNaTe A, et al. YOLOv8 algorithm-aided detection of patellar instability or dislocation on knee joint MRI images. Acta Radiol 2025 Mar;66(3):264-268. [doi: 10.1177/02841851241300617] [Medline: 39686597]
30. Kwolek K, Grzelecki D, Kwolek K, Marczak D, Kowalczewski J, Tyrakowski M. Automated patellar height assessment on high-resolution radiographs with a novel deep learning-based approach. World J Orthop 2023 Jun 18;14(6):387-398 [FREE Full text] [doi: 10.5312/wjo.v14.i6.387] [Medline: 37377994]
31. Mourad L, Aboelsaad N, Talaat WM, Fahmy NM, Abdelrahman HH, El-Mahallawy Y. Automatic detection of temporomandibular joint osteoarthritis radiographic features using deep learning artificial intelligence. A diagnostic accuracy study. J Stomatol Oral Maxillofac Surg 2025 Sep;126(4):102124 [FREE Full text] [doi: 10.1016/j.jormas.2024.102124] [Medline: 39488247]
32. Wang L, Mao Y, Xu J, Wu J, Wu K, Mao K, et al. A ROI extraction method for wrist imaging applied in smart bone-age assessment system. IEEE J Biomed Health Inform 2024 Aug;28(8):4410-4420. [doi: 10.1109/JBHI.2023.3284060] [Medline: 37289606]
33. Han S, Oh JS, Lee JJ. Diagnostic performance of deep learning models for detecting bone metastasis on whole-body bone scan in prostate cancer. Eur J Nucl Med Mol Imaging 2022 Jan;49(2):585-595. [doi: 10.1007/s00259-021-05481-2] [Medline: 34363089]
34. Duan X, Xiong H, Liu R, Duan X, Yu H. Enhanced deep leaning model for detection and grading of lumbar disc herniation from MRI. Med Biol Eng Comput 2024 Dec;62(12):3709-3719. [doi: 10.1007/s11517-024-03161-5] [Medline: 38967693]
35. Ma J, Zhou Y, Zhou Z, Zhang Y, He L. Toward smart ocean monitoring: real-time detection of marine litter using YOLOv12 in support of pollution mitigation. Mar Pollut Bull 2025 Aug;217:118136. [doi: 10.1016/j.marpolbul.2025.118136] [Medline: 40349615]
36. Gamble JG, Shea KG, Frick SL. Magnetic resonance imaging has utility in clinical decision-making for children and adolescents with symptomatic subfibular ossicles. Cureus 2024 Aug;16(8):e67498. [doi: 10.7759/cureus.67498] [Medline: 39310636]
37. Kim J, Mun S, Lee S. Detection and analysis of circadian biomarkers for metabolic syndrome using wearable data: cross-sectional study. JMIR Med Inform 2025 Jul 16;13:e69328 [FREE Full text] [doi: 10.2196/69328] [Medline: 40669055]
38. Hardalaç F, Uysal F, Peker O, Çiçeklidağ M, Tolunay T, Tokgöz N, et al. Fracture detection in wrist x-ray images using deep learning-based object detection models. Sensors (Basel) 2022 Feb 08;22(3):1285 [FREE Full text] [doi: 10.3390/s22031285] [Medline: 35162030]
39. Srinivasu PN, Kumari GL, Narahari SC, Ahmed S, Alhumam A. Exploring the impact of hyperparameter and data augmentation in YOLO V10 for accurate bone fracture detection from x-ray images. Sci Rep 2025 Mar 21;15(1):9828 [FREE Full text] [doi: 10.1038/s41598-025-93505-4] [Medline: 40119100]
40. Bumbálek R, Ufitikirezi JD, Umurungi SN, Zoubek T, Kuneš R, Stehlík R, et al. Computer vision in precision livestock farming: benchmarking YOLOv9, YOLOv10, YOLOv11, and YOLOv12 for individual cattle identification. Smart Agricultural Technology 2025 Dec;12:101208 [FREE Full text] [doi: 10.1016/j.atech.2025.101208]
41. Ramos LT, Sappa AD. A comprehensive analysis of YOLO architectures for tomato leaf disease identification. Sci Rep 2025 Jul 24;15(1):26890 [FREE Full text] [doi: 10.1038/s41598-025-11064-0] [Medline: 40707664]

XSL•FO
RenderX

42. Chen Y, He K, Hao B, Weng Y, Chen Z. FractureNet: a 3D convolutional neural network based on the architecture of m-Ary tree for fracture type identification. IEEE Trans Med Imaging 2022 May;41(5):1196-1207. [doi: 10.1109/TMI.2021.3134650] [Medline: 34890325]
43. Tariq M, Choi K. YOLO11-driven deep learning approach for enhanced detection and visualization of wrist fractures in x-ray images. Mathematics 2025;13(9):1419 [FREE Full text] [doi: 10.3390/math13091419]
44. Mirugwe A, Tamale L, Nyirenda J. Improving tuberculosis detection in chest x-ray images through transfer learning and deep learning: comparative study of convolutional neural network architectures. JMIRx Med 2025 Jul 01;6:e66029 [FREE Full text] [doi: 10.2196/66029] [Medline: 40591399]
45. Chen C, Teng Y, Tan S, Wang Z, Zhang L, Xu J. Performance test of a well-trained model for meningioma segmentation in health care centers: secondary analysis based on four retrospective multicenter data sets. J Med Internet Res 2023 Dec 15;25:e44119 [FREE Full text] [doi: 10.2196/44119] [Medline: 38100181]
46. Lee JH, Kim PH, Son N, Han K, Kang Y, Jeong S, et al. External validation of an upgraded AI model for screening ileocolic intussusception using Pediatric Abdominal Radiographs: Multicenter retrospective study. J Med Internet Res 2025 Jul 08;27:e72097 [FREE Full text] [doi: 10.2196/72097] [Medline: 40653922]

Abbreviations

AI: artificial intelligence
AP: average precision
AUC: area under the curve
CT: computed tomography
DCNN: deep convolutional neural network
DICOM: Digital Imaging and Communications in Medicine
IoU: intersection over union
LMAF: lateral malleolar avulsion fracture
mAP: mean average precision
mAP50: mean average precision at intersection over union 0.5
MRI: magnetic resonance imaging
PR: precision-recall
R-CNN: region-based convolutional neural network
ROC: receiver operating characteristic
SFO: subfibular ossicle
SSD: single shot multibox detector
YOLO: You Only Look Once

Edited by A Coristine; submitted 14.06.25; peer-reviewed by G Tang, CL Fan; comments to author 11.07.25; revised version received 27.07.25; accepted 09.09.25; published 03.10.25.

Please cite as:
Liu J, Sun P, Yuan Y, Chen Z, Tian K, Gao Q, Li X, Xia L, Zhang J, Xu N
YOLOv12 Algorithm-Aided Detection and Classification of Lateral Malleolar Avulsion Fracture and Subfibular Ossicle Based on CT Images: Multicenter Study
JMIR Med Inform 2025;13:e79064
URL: https://medinform.jmir.org/2025/1/e79064
doi:10.2196/79064
PMID:

©Jiayi Liu, Peng Sun, Yousheng Yuan, Zihan Chen, Ke Tian, Qian Gao, Xiangsheng Li, Liang Xia, Jun Zhang, Nan Xu. Originally published in JMIR Medical Informatics (https://medinform.jmir.org), 03.10.2025. This is an open-access article distributed under the terms of the Creative Commons Attribution License (https://creativecommons.org/licenses/by/4.0/), which permits unrestricted use, distribution, and reproduction in any medium, provided the original work, first published in JMIR Medical Informatics, is properly cited. The complete bibliographic information, a link to the original publication on https://medinform.jmir.org/, as well as this copyright and license information must be included.

XSL•FO
RenderX

Original Paper

Performance of ChatGPT-4o, Claude 3 Opus, and DeepSeek-R1 in BI-RADS Category 4 Classification and Malignancy Prediction From Mammography Reports: Retrospective Diagnostic Study

Xingwei Dai[1*], MS; Man Ke[1*], MS; Dixing Xie[1], MS; Mengting Mei[1], BS; Si Wei[1], BS; Yi Dai[1], PhD; Ronghua Yan[1,2], PhD

[1]Peking University Shenzhen Hospital, Shenzhen, China

[2]Southern University of Science and Technology, Shenzhen, China

[*]these authors contributed equally

Corresponding Author:
Ronghua Yan, PhD
Peking University Shenzhen Hospital
No.1120 Lianhua Road, Shenzhen, Guangdong
Shenzhen, 518036
China
Phone: 86 13719461736
Email: yanrh@mail3.sysu.edu.cn

Abstract

Background: Mammography is a key imaging modality for breast cancer screening and diagnosis, with the Breast Imaging Reporting and Data System (BI-RADS) providing standardized risk stratification. However, BI-RADS category 4 lesions pose a diagnostic challenge due to their wide malignancy probability range and substantial overlap between benign and malignant findings. Moreover, current interpretations rely heavily on radiologists' expertise, leading to variability and potential diagnostic errors. Recent advances in large language models (LLMs), such as ChatGPT-4o, Claude 3 Opus, and DeepSeek-R1, offer new possibilities for automated medical report interpretation.

Objective: This study aims to explore the feasibility of LLMs in evaluating the benign or malignant subcategories of BI-RADS category 4 lesions based on free-text mammography reports.

Methods: This retrospective, single-center study included 307 patients (mean age 47.25, 11.39 years) with BI-RADS category 4 mammography reports between May 2021 and March 2024. Three LLMs (ChatGPT-4o, Claude 3 Opus, and DeepSeek-R1) classified BI-RADS 4 subcategories from the reports' text only, whereas radiologists based their classifications on image review. Pathology served as the reference standard, and the reproducibility of LLMs' predictions was assessed. The diagnostic performance of radiologists and LLMs was compared, and the internal reasoning behind LLMs' misclassifications was analyzed.

Results: ChatGPT-4o demonstrated higher reproducibility than DeepSeek-R1 and Claude 3 Opus (Fleiss κ 0.850 vs 0.824 and 0.732, respectively). Although the overall accuracy of LLMs was lower than that of radiologists (senior: 74.5%; junior: 72.0%; DeepSeek-R1: 63.5%; ChatGPT-4o: 62.4%; Claude 3 Opus: 60.8%), their sensitivity was higher (senior: 80.7%; junior: 68.0%; DeepSeek-R1: 84.0%; ChatGPT-4o: 84.7%; Claude 3 Opus: 92.7%), while specificity remained lower (senior: 68.3%; junior: 76.1%; DeepSeek-R1: 43.0%; ChatGPT-4o: 40.1%; Claude 3 Opus: 28.9%). DeepSeek-R1 achieved the best prediction accuracy among LLMs with an area under the receiver operating characteristic curve of 0.64 (95% CI 0.57-0.70), followed by ChatGPT-4o (0.62, 95% CI 0.56-0.69) and Claude 3 Opus (0.61, 95% CI 0.54-0.67). By comparison, junior and senior radiologists achieved higher area under the receiver operating characteristic curves of 0.72 (95% CI 0.66-0.78) and 0.75 (95% CI 0.69-0.80), respectively. DeLong testing confirmed that all three LLMs performed significantly worse than both junior and senior radiologists (all $P<.05$), and no significant difference was observed between the two radiologist groups ($P=.55$). At the subcategory level, ChatGPT-4o yielded an overall F_1-score of 47.6%, DeepSeek-R1 achieved 45.6%, and Claude 3 Opus achieved 36.2%.

Conclusions: LLMs are feasible for distinguishing between benign and malignant lesions in BI-RADS category 4, with good stability and high sensitivity, but relatively insufficient specificity. They show potential in screening and may assist radiologists in reducing missed diagnoses.

XSL•FO
RenderX

(JMIR Med Inform 2025;13:e80182) doi:10.2196/80182

KEYWORDS

large language models; BI-RADS; breast; mammography; ChatGPT-4o; Claude 3 Opus; DeepSeek-R1; Breast Imaging Reporting and Data System

Introduction

Breast cancer remains one of the leading causes of cancer-related death among women worldwide. Accurate and efficient diagnosis, along with appropriate clinical management, is critical for improving patient outcomes [1]. The Breast Imaging Reporting and Data System (BI-RADS) provides a standardized framework for assessing the risk of breast lesions. BI-RADS category 4 carries a wide range of malignancy probabilities, from 2% to 95%, with considerable overlap between benign and malignant findings [2]. Consequently, the precise classification and characterization of BI-RADS category 4 lesions remain challenging. Clinical guidelines recommend image-guided biopsy as the next step for BI-RADS 4 lesions, which inevitably leads to unnecessary invasive procedures in patients with benign conditions, increasing both economic and psychological burdens. Moreover, current diagnostic practices rely heavily on radiologists' expertise. The subjectivity in interpretation and potential diagnostic errors may compromise the accuracy of category 4 assessments and subsequently influence patient management and treatment decisions [3].

In recent years, the rapid development of artificial intelligence (AI) has had a profound impact on the field of medical imaging, particularly through the rise of large language models (LLMs), such as the generative pretrained transformer (GPT), which possess outstanding capabilities in understanding human language [4]. ChatGPT, developed by OpenAI, is recognized for its sophisticated natural language processing abilities, leveraging a large-scale neural network trained on diverse textual data to generate coherent and contextually relevant outputs [5,6]. Similarly, Claude 3, created by the AI startup Anthropic, is designed to provide advanced cognitive performance and intelligent task handling. DeepSeek, a more recent entrant in the AI landscape, has attracted considerable attention for its efficient and open-source LLM architecture. It demonstrates forward-thinking design based on a native sparse attention mechanism that significantly improves traditional AI models in both training and inference efficiency, particularly enhancing long-context reasoning while maintaining performance and reducing pretraining costs [7,8]. Notably, DeepSeek is developed by a Chinese team and has been specially optimized for Chinese-language tasks, and multiple studies have already demonstrated its applicability in various medical domains [9-11].

Recent studies have highlighted the promising potential of LLMs in clinical applications, particularly in supporting decision-making processes and improving workflow efficiency across various medical specialties [12-14]. However, most research has primarily focused on converting clinical free text into structured formats, such as standardized summaries or classification labels [15-18]. In parallel, some studies have assessed the diagnostic reasoning or decision support capabilities of LLMs using free-text clinical inputs in controlled scenarios, such as imaging-based risk stratification and patient case assessments [19-23]. To date, only a few studies [24-27] have begun to explore the feasibility of using LLMs to directly generate diagnoses and clinical recommendations from free-text reports, such as those related to thyroid and musculoskeletal disorders. Preliminary investigations have suggested that LLMs have broad potential in assisting physicians with BI-RADS classification [28-30], but these studies have addressed the full spectrum of BI-RADS categories. Currently, no research has specifically focused on the particularly challenging BI-RADS category 4, where there is significant overlap between benign and malignant lesions. To our knowledge, no published studies have examined the use of LLMs to assist in the fine-grained subcategorization within BI-RADS category 4.

This study aims to evaluate the feasibility of using three LLMs (ChatGPT-4o, Claude 3 Opus, and DeepSeek-R1) to predict the specific subcategories of BI-RADS category 4 lesions based on free-text mammography reports and to further analyze the diagnostic reasoning behind their outputs.

Methods

Patients and Data

This study retrospectively collected mammography reports from patients who underwent breast cancer screening or diagnostic evaluation between May 2021 and March 2024. All reports were generated by breast radiologists certified by the institutional board. The reports were written and categorized in free-text format in Chinese. Each report was initially drafted by a junior radiologist (≤5 years of experience) based on imaging findings and subsequently reviewed by a senior radiologist (≥10 years of experience). The final version of each radiology report used as input to the LLMs was based on the senior radiologist's revision, as senior radiologists had the authority to modify initial drafts during review. The final report explicitly assigned BI-RADS category 4 subcategories (4A, 4B, or 4C). The inclusion criteria were as follows: lesions classified as BI-RADS category 4 by the senior radiologist; patients who underwent surgical excision or core needle biopsy within 1 month after mammography and had a definitive pathological diagnosis; and reports containing complete imaging descriptions, including BI-RADS descriptors, impressions, and the final BI-RADS category assigned by the radiologist. The exclusion criteria included (1) a prior diagnosis of breast cancer or a history of breast surgery, radiotherapy, or chemotherapy and (2) follow-up cases after treatment.

Ethical Considerations

The text processed by the LLMs is strictly confined to personal history reports. These reports were stripped of any information that could lead to patient identification, ensuring confidentiality and anonymity. The model's interpretation of the texts focuses

XSL•FO
RenderX

solely on identifying and structuring data relevant to the study without compromising individual privacy.

The study's design and methodology were previously communicated to and reviewed by the hospital's ethics committee. The research received the necessary approval, confirming that it adheres to the ethical standards required for patient data research. The study was granted an exemption from requiring informed consent due to its exclusive use of nonidentifiable data. Formal approval was obtained on June 9, 2025, under the reference number Peking University Shenzhen Hospital (Research) (2025) No.126.

LLMs and Prompt Design

Three LLMs were used in this study: ChatGPT-4o (version May 24, 2024), Claude 3 Opus (version March 4, 2024), and DeepSeek-R1 (version January 20, 2025). All models were called between July 1, 2024, and March 15, 2025, with temperature set to zero and the default max-tokens setting. Each model responded to prompts in a single round.

Each model was instructed to act as an experienced breast radiology expert, providing specific BI-RADS classifications based on the input free-text reports. The following standardized prompt was used:

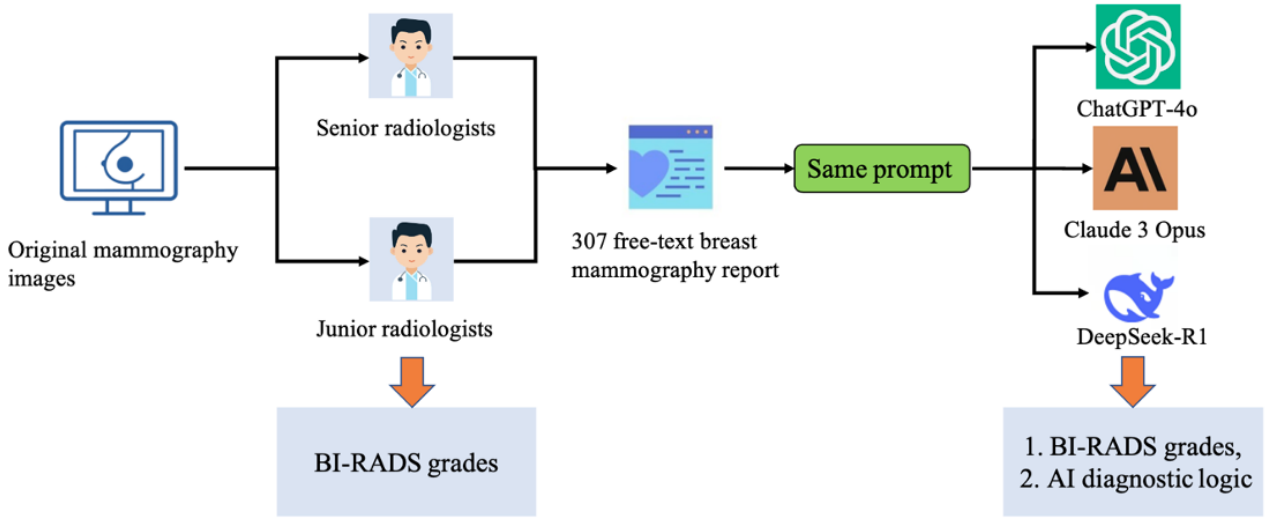
> *Assume you are a radiologist. Based on the following mammography report, please predict the benign or malignant nature of each nodule and provide a specific BI-RADS classification. Only one BI-RADS category is allowed. If classified as category 4, please clearly specify whether it is 4A, 4B, or 4C, and explain your diagnostic reasoning.*

This prompt was designed to evaluate the model's ability to interpret detailed imaging descriptions, make accurate classifications, and articulate its diagnostic rationale. No fine-tuning was performed on any of the three models, and all prompts were delivered in Chinese. The full Chinese prompt and example outputs from LLMs are provided in Multimedia Appendix 1, and a summary of prompt versions tested during pilot runs and their observed output limitations is presented in Multimedia Appendix 2.

Workflow

The workflow of this study is illustrated in Figure 1. In this study, junior and senior radiologists interpreted the original mammography images to assign BI-RADS subcategories, whereas the LLMs analyzed only the deidentified free-text reports without access to imaging data. All mammography reports were deidentified before model input by removing patient-identifiable information and BI-RADS conclusions to ensure privacy and prevent label leakage. No further structural normalization or terminology unification was performed to preserve the natural language variability present in clinical practice [31]. Each report was analyzed by ChatGPT-4o, Claude 3 Opus, and DeepSeek-R1 using an open-ended prompt. To ensure consistency and reliability, each model was queried three times with the same report. All BI-RADS classification results from LLM outputs were manually extracted by two independent researchers. In cases of disagreement, a third researcher adjudicated the final decision to ensure accuracy and consistency. For each report, the most frequently occurring classification among the three responses was selected as the final result. If the three outputs differed without a clear majority, the case was deemed invalid and excluded from further analysis. This approach was designed to minimize variability and enhance the reliability of LLM-generated outputs. Additionally, we compared the consistency of BI-RADS classifications between LLMs and radiologists, as well as between junior and senior radiologists. To further explore the misclassification mechanisms of the LLMs, we manually reviewed the prediction rationales associated with all misclassified cases. Key imaging features, such as lesion size, calcification, shape, and margin characteristics, were extracted from the explanatory content generated by the LLMs and categorized in reference to the BI-RADS classification criteria. Feature extraction and interpretation were performed independently by two experienced radiologists. Any discrepancies were resolved through consensus discussions to ensure analytical rigor and objectivity.

Figure 1. Schematic workflow of how large language models process free-text mammography reports and evaluate BI-RADS classifications. AI: artificial intelligence; BI-RADS: Breast Imaging Reporting and Data System.



XSL•FO
RenderX

Statistical Analysis

Categorical variables were presented as frequencies (percentages), and continuous variables were expressed as means (SDs). In this study, lesions classified as BI-RADS 4A or below were considered benign, while those classified as 4B or above were considered malignant, in line with prior studies that have used this binary grouping to reflect increasing malignancy risk across subcategories [32,33]. Pathological diagnosis served as the reference standard only for binary classification (benign vs malignant), and a senior radiologist's subcategory assignment was used as the reference standard for analyses involving BI-RADS 4 subcategories (4A, 4B, 4C). The diagnostic performance of radiologists and LLMs in distinguishing between benign and malignant lesions was assessed using the χ^2 test. Cohen κ coefficient was used to evaluate pairwise agreement between each assessment method, while Fleiss κ was used to assess the consistency of the three repeated outputs from each LLM. A Fleiss κ value less than 0.2 indicated poor agreement, 0.2 to 0.4 fair agreement, 0.4 to 0.6 moderate agreement, 0.6 to 0.8 substantial agreement, and 0.8 to 1.0 almost perfect agreement. Independent samples *t* tests were used to compare the differences in lesion size between benign and malignant groups. Receiver operating characteristic curve analysis was performed to assess diagnostic performance, and the area under the receiver operating characteristic curve (AUC), sensitivity, specificity, accuracy, and F_1-score were calculated. AUC values were compared using the DeLong test. A 2-sided *P* value less than .05 was considered statistically significant. All statistical analyses were performed using SPSS software (version 26.0; IBM Corp).

Results

Patients and Histopathological Subtypes

A total of 307 mammography reports from 307 female patients were included in this study, encompassing 309 breast lesions. The mean age of the patients was 47.25 (SD 11.39) years. Among the lesions, 152 (49.2%) were benign, and 157 (50.8%) were malignant, as determined by histopathological diagnosis. The mean size of benign lesions was 16.2 (SD 11.9) mm, and that of malignant lesions was 17.8 (SD 13.2) mm. The histopathological subtypes of the 309 BI-RADS category 4 lesions are summarized in Table 1.

Table 1. Histopathological findings of 309 Breast Imaging Reporting and Data System (BI-RADS) category 4 breast lesions.

Histopathological subtype	Lesions, n (%)
Benign	
Fibroadenoma	48 (31.6)
Sclerosing lesions/adenosis	42 (27.6)
Intraductal papilloma	11 (7.2)
Inflammatory lesions	10 (6.6)
Cyst/hemangioma	7 (4.6)
Ductal ectasia	7 (4.6)
Benign phyllodes tumor	7 (4.6)
Normal breast tissue	3 (2.0)
Other benign findings	17 (11.2)
Total	152 (49.2)
Malignant	
Invasive ductal carcinoma	121 (77.1)
Ductal carcinoma in situ	28 (17.8)
Malignant phyllodes tumor	4 (2.6)
Invasive lobular carcinoma	2 (1.3)
Other malignant tumors	2 (1.3)
Total	157 (50.8)

Comparison of LLMs and Radiologists in Predicting Malignancy of BI-RADS Category 4 Lesions

If the three responses generated by an LLM were entirely inconsistent, the case was deemed diagnostically invalid. Based on this criterion, ChatGPT-4o had 3 (1.0%) invalid cases, Claude 3 Opus had 10 (3.2%), and DeepSeek-R1 had 5 (1.6%). Comparative analysis of these 18 excluded reports showed no significant differences from the included cases in report length, terminology complexity, and lesion size (all *P*>.05; Multimedia Appendix 3), indicating minimal risk of selection bias. After exclusion, the diagnostic performance of radiologists and LLMs in differentiating benign from malignant BI-RADS category 4 lesions is summarized in Table 2.

XSL•FO
RenderX

Table 2. Diagnostic performance of large language models and radiologists in assessing the benign or malignant nature of breast lesions.

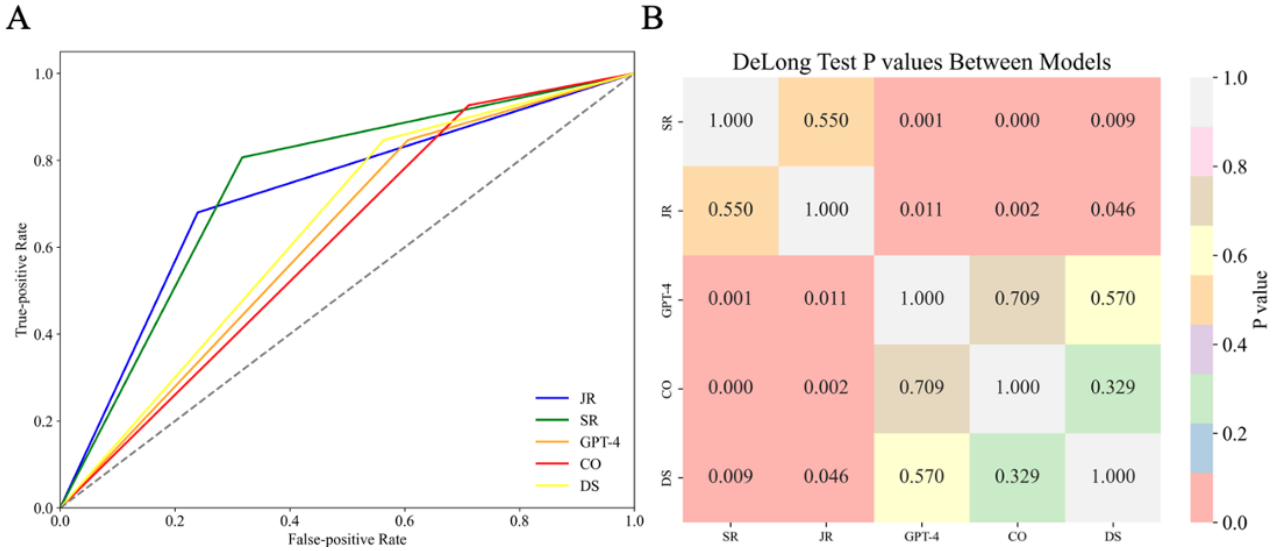
Evaluator	Sensitivity (%; 95% CI)	Specificity (%; 95% CI)	Accuracy (%; 95% CI)	Positive predictive value (%; 95% CI)	Negative predictive value (%; 95% CI)	AUC[a] (95% CI)	*P* value[b]
Junior radiologist	68.0 (60.2-74.9)	76.1 (68.4-82.3)	71.9 (66.5-76.8)	75.0 (67.1-81.5)	69.2 (61.6-75.9)	0.72 (0.66-0.78)	<.001
Senior radiologist	80.7 (73.6-86.2)	68.3 (60.3-75.4)	74.7 (69.4-79.3)	72.9 (69.4-79.3)	77.0 (68.9-83.5)	0.75 (0.69-0.80)	<.001
ChatGPT-4o	84.7 (78.0-89.6)	40.1 (32.4-48.4)	63.0 (57.3-68.3)	59.9 (53.2-66.3)	71.3 (60.5-80.0)	0.62 (0.56-0.69)	<.001
Claude 3 Opus	92.7 (87.3-95.9)	28.9 (22.1-36.8)	61.6 (55.9-67.0)	57.9 (51.6-64.0)	78.8 (66.0-87.8)	0.61 (0.54-0.67)	<.001
DeepSeek-R1	84.0 (77.3-89.0)	43.0 (35.1-51.2)	64.0 (58.4-69.3)	60.9 (54.1-67.3)	71.8 (61.4-80.2)	0.64 (0.57-0.70)	<.001

[a]AUC: area under the receiver operating characteristic curve.

[b]*P* values represent the test against the null hypothesis of an AUC of 0.5.

DeepSeek-R1 achieved an AUC of 0.64, which was slightly higher than ChatGPT-4o (AUC 0.62) and Claude 3 Opus (AUC 0.61), but all three models underperformed compared to the junior and senior radiologists (AUC 0.72 and 0.75, respectively). The differences in AUCs between each LLM and the junior radiologist (all $P<.05$) as well as the senior radiologist (all $P<.01$) were statistically significant, indicating that both radiologists outperformed the three LLMs. In contrast, no significant differences were observed among ChatGPT-4o, Claude 3 Opus, and DeepSeek-R1, nor between the junior and senior radiologists ($P=.55$), as shown in Figure 2. The results of the DeLong tests are provided in Multimedia Appendix 4.

Figure 2. Receiver operating characteristic curve comparison of the diagnostic performance of large language models and radiologists in distinguishing between benign and malignant breast lesions. CO: Claude 3 Opus; DS: DeepSeek-R1; GPT-4: ChatGPT-4o; JR: junior radiologist; SR: senior radiologist.



Performance of LLMs in BI-RADS 4 Subcategory Assignment

Model performance for BI-RADS 4 subcategory assignment is shown in Table 3. All three LLMs demonstrated variable performance across subcategories. The 4C category consistently achieved the highest F_1-scores for each model, whereas 4B showed the lowest performance overall. ChatGPT-4o and DeepSeek-R1 demonstrated comparable overall F_1-scores (47.6% and 45.6%, respectively), while Claude 3 Opus showed the lowest overall performance (36.2%).

XSL•FO
RenderX

Table 3. Performance of large language models in Breast Imaging Reporting and Data System (BI-RADS) 4 subcategory assignment using the senior radiologist's categorization as the reference standard.

Model and subcategories	Recall (%)	Precision (%)	F_1-score (%)
ChatGPT-4o			
4A	35.2	67.7	46.3
4B	45.1	38.5	41.6
4C	63.1	49.5	55.5
Overall	46.0	54.2	47.6
Claude 3 Opus			
4A	17.6	81.5	28.9
4B	23.2	31.7	26.8
4C	88.1	41.3	56.3
Overall	39.5	55.9	36.2
DeepSeek-R1			
4A	28.0	64.8	39.1
4B	41.5	36.6	38.9
4C	70.2	55.1	61.8
Overall	44.0	54.1	45.6

Consistency and Agreement Analysis of LLMs and Radiologists

Each of the three LLMs (ChatGPT-4o, Claude 3 Opus, and DeepSeek-R1) was queried three times per report to evaluate response consistency. The agreement among the three outputs was generally high across all models. As shown in Table 4, ChatGPT-4o demonstrated the highest consistency with a Fleiss κ of 0.850, followed by DeepSeek-R1 at 0.824, and Claude 3-Opus at 0.732. All three models exhibited a high level of internal consistency. The detailed frequency of BI-RADS subcategories for LLMs is presented in Multimedia Appendix 5.

To further quantify agreement across all assessment methods, a pairwise Cohen κ analysis was performed for both malignancy classification and BI-RADS 4 subcategories. The results demonstrated substantial variability in agreement among raters, with consistently higher κ values in malignancy classification (κ range 0.26-0.74) compared to subcategory assignment (κ range 0.09-0.40). Detailed statistical metrics are provided in Multimedia Appendix 6.

Table 4. Response consistency of large language models (LLMs) assessed by Fleiss κ statistics.

LLMs	κ value (SD)	95% CI	*z* value	*P* value
ChatGPT-4o	0.850 (0.023)	0.806-0.895	37.436	<.001
Claude 3 Opus	0.732 (0.017)	0.698-0.766	42.186	<.001
DeepSeek-R1	0.824 (0.023)	0.779-0.868	35.977	<.001

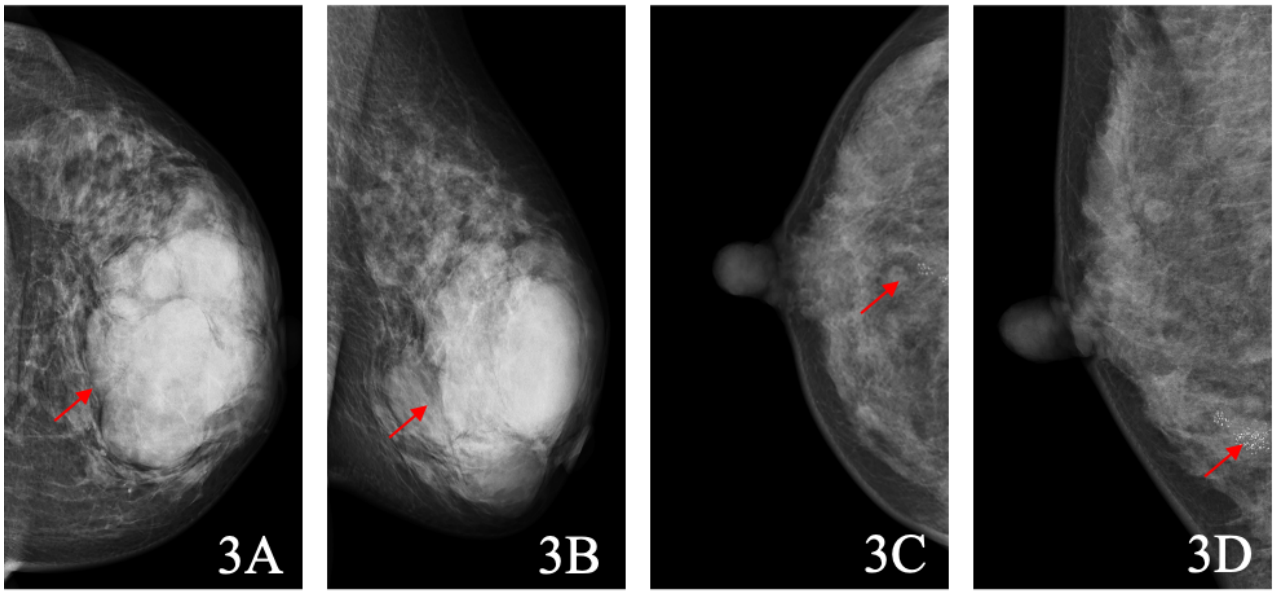
Analysis of Diagnostic Errors by LLMs

To better understand the diagnostic behavior of the LLMs, we performed targeted misclassification analyses for DeepSeek-R1, the model with the best overall performance, and Claude 3 Opus, which showed unusually high sensitivity but low specificity.

DeepSeek-R1 incorrectly classified 86 pathologically benign BI-RADS 4 lesions as malignant. The most common diagnoses were fibroadenoma (n=29, 33.7%), adenosis (n=20, 23.3%), intraductal papilloma (n=7, 8.1%), and inflammatory lesions (n=6, 7.0%). As shown in Table 5, lesion size was the most prominent feature cited in the reasoning text, accounting for approximately 34% of false-positive errors. Misclassified benign lesions were significantly larger than correctly classified benign lesions (mean 17.4, SD 13.9 mm vs mean 11.5, SD 8.6 mm; *P*=.01). Of the 193 extracted features, calcification descriptors constituted a significant proportion (n=49, 25.4%), encompassing both benign and suspicious subtypes. A representative example is illustrated in Figure 3A and B, where a large lobulated mass was upgraded by DeepSeek-R1 but was ultimately confirmed as fibroadenoma. In contrast, DeepSeek-R1 misclassified only 27 (8.7%) malignant cases as benign, primarily invasive ductal carcinoma (n=18, 66.7%) and ductal carcinoma in situ (n=9, 33.3%). Figure 3C and D illustrates a case classified as benign by DeepSeek-R1 but confirmed as ductal carcinoma in situ.

XSL•FO
RenderX

Figure 3. Representative mammographic cases misclassified by DeepSeek-R1. A and C are craniocaudal views; B and D are mediolateral oblique views. (A, B) A 44-year-old woman with type C breast density. A large, well-defined, shallowly lobulated mass (approximately 88 × 68 mm) is visible in the left breast. The radiologist classified the lesion as Breast Imaging Reporting and Data System (BI-RADS) 4A, while DeepSeek-R1 classified it as BI-RADS 4C. Postoperative pathology confirmed fibroadenoma. (C, D) A 37-year-old woman with type C breast density. Clustered calcifications are seen in the lower outer quadrant of the right breast, measuring approximately 16 × 11 mm. The radiologist classified the finding as BI-RADS 4A, while DeepSeek-R1 classified it as BI-RADS 3. Postoperative pathology confirmed ductal carcinoma in situ.



Claude 3 Opus produced 101 false-positive predictions, far more than DeepSeek-R1, which largely explains its markedly reduced specificity. These misclassified benign lesions included fibroadenoma (n=30, 29.7%), adenosis (n=20, 19.8%), papilloma (n=8, 7.9%), and inflammatory changes (n=7, 6.9%). Similar to DeepSeek-R1, lesion size played a major role (Table 5). Misclassified benign lesions were significantly larger than correctly classified benign lesions (mean 16.28, SD 12.64 mm vs mean 13.6, SD 8.2 mm; *P*=.01). Claude 3 Opus misclassified only 10 malignant lesions as benign (invasive ductal carcinoma: n=6), far fewer than DeepSeek-R1.

XSL•FO
RenderX

Table 5. Distribution of imaging descriptors identified by DeepSeek-R1 and Claude 3 Opus in the diagnostic reasoning for benign lesions misclassified as malignant.

Model and subcategory	Identified descriptors, n (%)
DeepSeek-R1 (n=193)	
Size	65 (33.7)
Calcifications	49 (25.4)
Milk of calcium	17 (8.8)
Amorphous	10 (5.2)
Coarse	6 (3.1)
Calcifications	4 (2.1)
Round	4 (2.1)
Distribution	3 (1.6)
Fine pleomorphic	3 (1.6)
Large rodlike	2 (1.0)
Margin obscured	26 (13.5)
Margin microlobulated	17 (8.8)
Masses irregular	15 (7.8)
Architectural distortion	7 (3.6)
Margin spiculated	6 (3.1)
Focal asymmetry	5 (2.6)
Skin thickening	2 (1.0)
Solitary dilated duct	1 (0.5)
Claude 3 Opus (n=205)	
Size	82 (40.0)
Calcification	54 (26.3)
Milk of calcium	21 (10.2)
Fine pleomorphic	6 (2.9)
Distribution	5 (2.4)
Amorphous	4 (2.0)
Microcalcification	4 (2.0)
Calcifications	3 (1.5)
Nodulat	3 (1.5)
Coarse	2 (1.0)
Margin microlobulated	20 (10.0)
Margin obscured	13 (6.3)
Focal symmetry	11 (5.4)
Glandular aggregation	9 (4.4)
Margin spiculated	9 (4.4)
Architectural distortion	3 (1.5)
Masses irregular	2 (1.0)
High-density glands	2 (1.0)

XSL•FO
RenderX

Discussion

Principal Results

LLMs have been widely recognized for their potential in medical imaging applications. However, studies evaluating the feasibility of LLM-based diagnostic reasoning against pathology-confirmed gold standards remain limited. In this study, we applied ChatGPT-4o, Claude 3 Opus, and DeepSeek-R1 to the free-text Chinese mammography reports of BI-RADS category 4 lesions, aiming to assess their capability in distinguishing between benign and malignant findings. Our results demonstrated that LLMs provide high diagnostic repeatability, good stability, and reliable outputs, supporting their feasibility in this task. Among the three models, Claude 3 Opus yielded the highest proportion of invalid predictions, while ChatGPT-4o had the lowest, suggesting that ChatGPT-4o offers greater response consistency. ChatGPT-4o also showed the highest intramodel agreement in BI-RADS classification, with minimal variation across repeated outputs. This strong consistency and stability may be attributed to the architecture of its deep learning model and the diversity of its training data, which enable ChatGPT-4o to capture subtle variations in input and deliver highly consistent judgments for the same case across different prompts. DeepSeek-R1 also demonstrated good consistency, although some fluctuations in results were observed. We speculate that this may be due to differences in model architecture and training strategies, indicating that further optimization may be needed for processing complex medical imaging reports.

At the same time, this study preliminarily explored the feasibility of using three LLMs, ChatGPT-4o, Claude 3 Opus, and DeepSeek-R1 to accurately assess the malignancy of BI-RADS category 4 lesions based on free-text Chinese mammography reports, using pathological results as the reference standard. The findings showed that all three models were capable of predicting benign versus malignant outcomes for BI-RADS 4 lesions with high sensitivity: 84.7% for ChatGPT-4o, 92.7% for Claude 3 Opus, and 84.0% for DeepSeek-R1. These values were higher than those of junior (68.0%) and senior (80.7%) radiologists. Sensitivity is considered a critical metric for ensuring early detection of malignancies, particularly in the initial screening phase, where reducing missed diagnoses is essential. Consistent with our results, Pagano et al [34] evaluated five different LLMs and compared their sensitivity in diagnosing hip and knee osteoarthritis. Their findings showed that GPT-4o outperformed the other models, achieving a sensitivity of 92.3%. Similarly, Laohawetwanit et al [35] used GPT-4 to classify histopathological images of colorectal adenomas and reported a high sensitivity of 74% for adenoma detection. In the field of breast imaging, Miaojiao et al [36] evaluated ChatGPT-4 for BI-RADS classification of breast ultrasound nodules and reported a sensitivity of 90.56% in distinguishing malignant lesions, further demonstrating the model's capability in cancer-related diagnostic tasks. In our study, the sensitivity of LLMs for distinguishing benign from malignant BI-RADS 4 lesions reached up to 92.7%, further supporting the potential of LLMs in breast cancer screening. These findings suggest that LLMs could serve as effective high-sensitivity decision support tools to help radiologists, particularly junior physicians, rapidly flag and prioritize high-risk cases in routine breast cancer screening workflows.

This study demonstrates that LLMs exhibit the characteristic of high sensitivity but relatively low specificity in interpreting imaging reports. Previous studies have reported similar findings. Sievert et al [23] showed that, in thyroid nodule risk stratification, ChatGPT achieved a sensitivity of 86.7% to 94.1%, whereas specificity was only 10.7% to 18.2%. Shi et al [37] used GPT-4 to automatically generate biopsy recommendations by integrating prostate reports with clinical data; their results revealed that GPT-4 achieved a sensitivity of 0.84 to 0.90 but a specificity of 0.41 to 0.44 for prostate biopsy triage, indicating an advantage in reducing missed diagnoses but a limitation as a stand-alone diagnostic tool. Yang et al [38] evaluated the ability of ChatGPT to differentiate benign from malignant bone tumors using 1366 imaging reports and further optimized performance through few-shot prompting. In the baseline setting, the model achieved a sensitivity of 0.95 and a specificity of 0.58, again suggesting potential to reduce missed diagnoses but with insufficient specificity. The principal reasons for the low specificity of LLMs may include an overreliance on malignant lexical cues and surface features. When reports contain descriptors such as "microcalcification" or "ill-defined margin," the model tends to upgrade the risk level while inadequately integrating benign evidence. In addition, LLMs possess limited capability to integrate contextual information, especially when only text is provided without imaging, resulting in a lack of multimodal information to support comprehensive judgment [39]. These mechanisms indicate that the optimal clinical role of LLMs is as a screening or triage tool; they can rapidly flag high-risk cases, standardize key findings, and assist radiologists in decision-making, thereby reducing missed diagnoses.

Regrettably, our findings indicate that although DeepSeek-R1, ChatGPT-4o, and Claude 3 Opus are capable of performing benign versus malignant classification for BI-RADS category 4 lesions based on free-text reports, their overall diagnostic performance remains inferior to that of radiologists when benchmarked against pathological results. This observation is consistent with recent literature. Wu et al [26] compared GPT-4, GPT-3.5, and Google Bard in predicting the malignancy of thyroid nodules using pathology as the reference standard. They found that all three LLMs achieved diagnostic performance above 0.8, outperforming junior physicians but still falling short of senior radiologists. Similarly, Liu et al [40] evaluated GPT-4.0 and Bing using ultrasound-based breast imaging reports and demonstrated that GPT-4 outperformed Bing, yet remained inferior to human radiologists. These results suggest that, despite significant advancements, LLMs have not yet fully matched human expertise in medical imaging interpretation. Notably, the diagnostic performance of the LLMs in our study was even lower than that reported by Liu et al [40], which may be due to differences in study populations. While Liu et al [40] included lesions across the full BI-RADS spectrum (categories 2 through 5), our study focused exclusively on BI-RADS category 4, a subset known for its diagnostic ambiguity and overlapping imaging features between benign and malignant lesions. Supporting this, a study by Elezaby et al [41] analyzed data

XSL•FO
RenderX

from the US National Mammography Database between 2008 and 2014, covering 125,447 BI-RADS 4 cases [41]. Among them, 33.3% were subcategorized into 4A, 4B, and 4C, with corresponding positive predictive values of 7.6%, 22.2%, and 69.3%, respectively. This large-scale dataset highlights the intrinsic challenge of accurately characterizing BI-RADS 4 lesions, even for experienced radiologists, and further underscores the difficulty faced by LLMs when attempting to replicate expert-level discrimination within this category.

Interestingly, no significant difference in BI-RADS diagnostic performance was observed between junior and senior radiologists (P=.55), which may be attributable to several factors. First, the BI-RADS system provides highly standardized terminology and structured reporting, offering clear imaging feature descriptions and well-defined categorization rules. This markedly reduces interobserver variability and enables radiologists with different levels of experience to reach comparable diagnostic conclusions. Cozzi et al [28] demonstrated in a multilingual study that even when interpretation was based solely on the "imaging findings" section of reports, interreader agreement remained nearly perfect (Gwet AC1 0.91), underscoring the strong harmonizing effect of the BI-RADS framework on experience-related differences. Second, the sample size and lesion composition of the present study may have influenced the results. The enrolled cases displayed a relatively balanced benign-to-malignant ratio but lacked a large number of highly challenging or borderline lesions, which may have limited the opportunity for differences in reader experience to emerge. Finally, the evaluation criteria themselves, final BI-RADS categories confirmed by pathology or follow-up, with diagnostic performance assessed by DeLong testing, focused on objective diagnostic accuracy rather than subtle variations in descriptive detail. This emphasis on definitive outcomes may have further attenuated measurable differences between radiologists of different seniority.

The relatively low specificity and diagnostic performance of LLMs compared to radiologists have not been thoroughly investigated in previous literature [42]. In this study, using pathology as the reference standard, we attempted to analyze the internal reasoning behind LLM outputs. The diagnostic outcomes of LLMs are influenced by various factors, including the weight distribution of their training datasets and the content of the prompts used. In our case, we used the default versions of ChatGPT-4o, Claude 3 Opus, and DeepSeek-R1 without any additional fine-tuning on domain-specific medical content, which may have contributed to some diagnostic inaccuracies. Regarding prompt design, LLMs primarily rely on extracting and interpreting keywords from BI-RADS mammography reports, such as lesion size, morphology, margins, and calcifications, to make diagnostic decisions. Among these, lesion size emerged as a dominant factor. We observed that lesions with a short-axis diameter greater than 17 mm were often classified as BI-RADS 4B or higher by the models, suggesting a malignant tendency. This aligns with clinical practice, where lesion size is also a critical consideration for radiologists. Our findings are consistent with those of Ong et al [43], who reported that lesion size greater than or equal to 15 mm was an independent predictor of malignancy in contrast-enhanced mammography (adjusted odds ratio 22.5), significantly increasing the likelihood of a malignant diagnosis. Furthermore, prior studies have shown that when the lesion size reaches 17.5 mm, specificity improves to 89.7%, reinforcing the value of size as a key imaging-based risk stratification parameter. Therefore, when using LLMs to assist in further benign versus malignant differentiation of BI-RADS category 4 lesions, caution is warranted for large lesions, as LLMs are more likely to overpredict malignancy. Our data showed a misclassification rate of approximately 34% for benign lesions larger than 17 mm. In addition to lesion size, the handling of the coexistence of benign and suspicious imaging descriptors was also a key reason for false positives. Although LLMs explicitly mentioned typically benign features such as "milk of calcium" during the reasoning process, they struggled to appropriately weigh them against co-occurring, seemingly suspicious features (such as large lesion size, high density, or asymmetry). In a clinical setting, a definitive benign feature should typically be sufficient to de-escalate the risk classification. However, the LLMs failed to assign sufficient weight to this benign evidence to override other findings. Instead, the LLMs appeared to allow the co-occurring suspicious features to dominate the decision-making process, thereby leading to false-positive malignant diagnoses (BI-RADS 4B or 4C). Fibroadenoma and adenosis were the two most common benign lesions misclassified by LLMs, accounting for 34% and 21% of misdiagnosed benign cases, respectively. These lesions were often relatively large, with lobulated or indistinct margins, and sometimes associated with calcifications. As such, these features likely prompted the LLMs to overpredict malignancy. This suggests that one of the main limitations affecting the diagnostic performance of LLMs lies in their tendency to overrely on certain high-risk imaging features. In summary, we believe that the principal limitation of LLMs lies in keyword-triggered escalation. When a mammography report contains malignant-leaning cues, such as spiculated margins, pleomorphic or clustered calcifications, architectural distortion, or indistinct or lobulated borders, or describes a relatively large lesion, the models tend to assign higher BI-RADS categories (4B or 4C). This behavior reflects an overreliance on surface lexical cues and insufficient integration of benign evidence. To mitigate this limitation, future work should refine prompt design to require balanced and explicit extraction of all malignant and benign descriptors, and to discourage upgrades based on any single malignant cue or lesion size alone, which may guide LLMs toward more comprehensive reasoning.

Limitations

This study has several limitations. First, this is a single-center, retrospective analysis based on free-text mammography reports, which may limit the generalizability of the findings and introduce potential selection bias. Future studies should incorporate a more diverse, multicenter dataset with prospective validation to improve external validity. Second, the results are highly dependent on the design of the prompts used to query the LLMs. Only one optimized prompt was applied in this study, and no systematic comparison of different prompt structures was performed. Future research should include multiple prompt designs and iterative optimization, including different language

XSL•FO
RenderX

prompts to assess and enhance the stability and reproducibility of model performance. Third, the LLMs used in this study were not fine-tuned on domain-specific medical data and were evaluated in their default general-purpose form. This lack of domain adaptation may limit their ability to fully capture breast imaging and specific diagnostic patterns and to integrate nuanced clinical knowledge. Future work could include domain-specific fine-tuning, for example, training on large curated radiology report datasets or incorporating expert-reviewed guidelines, to further optimize diagnostic reasoning and improve model performance. Fourth, cases in which the LLMs failed to reach a majority consensus were excluded from analysis. This may introduce selection bias and could result in an overestimation of consistency and diagnostic performance, as the reported metrics reflect only those cases in which the model outputs were sufficiently stable.

Conclusions

In conclusion, this study demonstrated that all three LLMs, ChatGPT-4o, Claude 3 Opus, and DeepSeek-R1 have high sensitivity in predicting BI-RADS category 4 breast benign and malignant lesions with good repeatability and stability but relatively insufficient specificity. The main causes of misclassification by LLMs included larger lesion size (short axis >17 mm) and the presence of specific imaging features described in the reports, such as clustered calcifications, spiculated margins, lobulated contours, and indistinct edges. Fibroadenoma and adenosis were the most common benign lesions misclassified as malignant by the LLMs.

Acknowledgments

The authors are thankful to Peking University Shenzhen Hospital for their management of our patient database.

The authors are thankful to RongHua Yan for helping critically revise the manuscript for important intellectual content.

The authors declare no use of generative artificial intelligence (AI) in the writing process. According to the Generative AI Delegation Taxonomy (GAIDeT; 2025), no tasks were delegated to generative AI tools under full human supervision. Responsibility for the final manuscript lies entirely with the authors. Generative AI tools are not listed as authors and do not bear responsibility for the final outcomes.

Funding

The authors declare that financial support was received for the research, authorship, and/or publication of this article from Shenzhen Science and Technology Innovation Program (JCYJ20220530160208018, JCYJ20230807095102005), General Program for Clinical Research at Peking University Shenzhen Hospital (No.LCYJ2021036), and Project of Guangdong Medical Science and Technology Research Foundation (20231115104757592).

Authors' Contributions

XD contributed to conceptualization, data curation, investigation, formal analysis, writing the original draft, and visualization. MK was responsible for methodology, software, validation, data curation, and reviewing and editing. DX handled resources, investigation, and project administration. MM performed formal analysis and data curation. SW managed software, validation, and resources. YD managed software, validation, and resources. RY was involved in conceptualization, supervision, funding acquisition, methodology, project administration, and reviewing and editing.

Conflicts of Interest

None declared.

Multimedia Appendix 1
Chinese prompt and example outputs from three large language models.
[PNG File , 1067 KB - medinform_v13i1e80182_app1.png]

Multimedia Appendix 2
Prompt versions tested during pilot runs and associated output issues.
[DOCX File , 16 KB - medinform_v13i1e80182_app2.docx]

Multimedia Appendix 3
Comparison of characteristics between excluded and included cases.
[DOCX File , 15 KB - medinform_v13i1e80182_app3.docx]

Multimedia Appendix 4
DeLong test results for large language models' area under the receiver operating characteristic curve comparisons.
[DOCX File , 17 KB - medinform_v13i1e80182_app4.docx]

XSL•FO
RenderX

Multimedia Appendix 5
Classification distributions of BI-RADS subcategories for LLMs.
[DOCX File , 16 KB - medinform_v13i1e80182_app5.docx]

Multimedia Appendix 6
Pairwise Cohen κ analysis for malignancy classification and Breast Imaging Reporting and Data System (BI-RADS) 4 subcategories.
[DOCX File , 20 KB - medinform_v13i1e80182_app6.docx]

References

1. DeSantis C, Siegel R, Bandi P, Jemal A. Breast cancer statistics, 2011. CA Cancer J Clin 2011;61(6):409-418 [FREE Full text] [doi: 10.3322/caac.20134] [Medline: 21969133]
2. Mercado CL. BI-RADS update. Radiol Clin North Am 2014 May;52(3):481-487. [doi: 10.1016/j.rcl.2014.02.008] [Medline: 24792650]
3. Yang Y, Hu Y, Shen S, Jiang X, Gu R, Wang H, et al. A new nomogram for predicting the malignant diagnosis of Breast Imaging Reporting and Data System (BI-RADS) ultrasonography category 4A lesions in women with dense breast tissue in the diagnostic setting. Quant Imaging Med Surg 2021 Jul;11(7):3005-3017 [FREE Full text] [doi: 10.21037/qims-20-1203] [Medline: 34249630]
4. Bhayana R, Krishna S, Bleakney RR. Performance of ChatGPT on a Radiology Board-style Examination: Insights into Current Strengths and Limitations. Radiology 2023 Jun;307(5):e230582. [doi: 10.1148/radiol.230582] [Medline: 37191485]
5. Ouyang L, Wu J, Jiang X, Almeida D, Wainwright CL, Mishkin P, et al. Training language models to follow instructions with human feedback. arXiv. Preprint posted online on March 4, 2022 . [doi: 10.48550/arXiv.2203.02155]
6. Brown TB, Mann B, Ryder N, Subbiah M, Kaplan J, Dhariwal P, et al. Language models are few-shot learners. arXiv. Preprint posted online on May 28, 2020 . [doi: 10.48550/arXiv.2005.14165]
7. Gibney E. China's cheap, open AI model DeepSeek thrills scientists. Nature 2025 Feb;638(8049):13-14. [doi: 10.1038/d41586-025-00229-6] [Medline: 39849139]
8. Wu J, Wang Z, Qin Y. Performance of DeepSeek-R1 and ChatGPT-4o on the Chinese National Medical Licensing Examination: A Comparative Study. J Med Syst 2025 Jun 03;49(1):74. [doi: 10.1007/s10916-025-02213-z] [Medline: 40459679]
9. Zhang J, Liu J, Guo M, Zhang X, Xiao W, Chen F. DeepSeek-assisted LI-RADS classification: AI-driven precision in hepatocellular carcinoma diagnosis. Int J Surg 2025 Sep 01;111(9):5970-5979. [doi: 10.1097/JS9.0000000000002763] [Medline: 40552875]
10. Chen K, Hou X, Li X, Xu W, Yi H. Structured Report Generation for Breast Cancer Imaging Based on Large Language Modeling: A Comparative Analysis of GPT-4 and DeepSeek. Acad Radiol 2025 Oct;32(10):5693-5702 [FREE Full text] [doi: 10.1016/j.acra.2025.07.046] [Medline: 40780984]
11. Bai X, Feng M, Ma W, Liao Y. Application of artificial intelligence chatbots in interpreting magnetic resonance imaging reports: a comparative study. Sci Rep 2025 Aug 25;15(1):31266 [FREE Full text] [doi: 10.1038/s41598-025-17355-w] [Medline: 40855279]
12. Rau A, Rau S, Zoeller D, Fink A, Tran H, Wilpert C, et al. A Context-based Chatbot Surpasses Trained Radiologists and Generic ChatGPT in Following the ACR Appropriateness Guidelines. Radiology 2023 Jul;308(1):e230970. [doi: 10.1148/radiol.230970] [Medline: 37489981]
13. Tan RSYC, Lin Q, Low GH, Lin R, Goh TC, Chang CCE, et al. Inferring cancer disease response from radiology reports using large language models with data augmentation and prompting. J Am Med Inform Assoc 2023 Sep 25;30(10):1657-1664 [FREE Full text] [doi: 10.1093/jamia/ocad133] [Medline: 37451682]
14. Chen Z, Chambara N, Wu C, Lo X, Liu SYW, Gunda ST, et al. Assessing the feasibility of ChatGPT-4o and Claude 3-Opus in thyroid nodule classification based on ultrasound images. Endocrine 2025 Mar;87(3):1041-1049. [doi: 10.1007/s12020-024-04066-x] [Medline: 39394537]
15. Jiang H, Xia S, Yang Y, Xu J, Hua Q, Mei Z, et al. Transforming free-text radiology reports into structured reports using ChatGPT: A study on thyroid ultrasonography. Eur J Radiol 2024 Jun;175:111458. [doi: 10.1016/j.ejrad.2024.111458] [Medline: 38613868]
16. Fervers P, Hahnfeldt R, Kottlors J, Wagner A, Maintz D, Pinto Dos Santos D, et al. ChatGPT yields low accuracy in determining LI-RADS scores based on free-text and structured radiology reports in German language. Front Radiol 2024;4:1390774 [FREE Full text] [doi: 10.3389/fradi.2024.1390774] [Medline: 39036542]
17. Bhayana R, Nanda B, Dehkharghanian T, Deng Y, Bhambra N, Elias G, et al. Large Language Models for Automated Synoptic Reports and Resectability Categorization in Pancreatic Cancer. Radiology 2024 Jun;311(3):e233117. [doi: 10.1148/radiol.233117] [Medline: 38888478]
18. Hu D, Liu B, Zhu X, Lu X, Wu N. Zero-shot information extraction from radiological reports using ChatGPT. Int J Med Inform 2024 Mar;183:105321. [doi: 10.1016/j.ijmedinf.2023.105321] [Medline: 38157785]

XSL•FO
RenderX

19. Cavnar Helvaci B, Hepsen S, Candemir B, Boz O, Durantas H, Houssein M, et al. Assessing the accuracy and reliability of ChatGPT's medical responses about thyroid cancer. Int J Med Inform 2024 Nov;191:105593. [doi: 10.1016/j.ijmedinf.2024.105593] [Medline: 39151245]
20. Currie G, Robbie S, Tually P. ChatGPT and Patient Information in Nuclear Medicine: GPT-3.5 Versus GPT-4. J Nucl Med Technol 2023 Dec 05;51(4):307-313 [FREE Full text] [doi: 10.2967/jnmt.123.266151] [Medline: 37699647]
21. Rao A, Kim J, Kamineni M, Pang M, Lie W, Dreyer KJ, et al. Evaluating GPT as an Adjunct for Radiologic Decision Making: GPT-4 Versus GPT-3.5 in a Breast Imaging Pilot. J Am Coll Radiol 2023 Oct;20(10):990-997 [FREE Full text] [doi: 10.1016/j.jacr.2023.05.003] [Medline: 37356806]
22. Deng L, Wang T, Yangzhang, Zhai Z, Tao W, Li J, et al. Evaluation of large language models in breast cancer clinical scenarios: a comparative analysis based on ChatGPT-3.5, ChatGPT-4.0, and Claude2. Int J Surg 2024 Apr 01;110(4):1941-1950 [FREE Full text] [doi: 10.1097/JS9.0000000000001066] [Medline: 38668655]
23. Sievert M, Conrad O, Mueller SK, Rupp R, Balk M, Richter D, et al. Risk stratification of thyroid nodules: Assessing the suitability of ChatGPT for text-based analysis. Am J Otolaryngol 2024;45(2):104144. [doi: 10.1016/j.amjoto.2023.104144] [Medline: 38113774]
24. Li D, Gupta K, Bhaduri M, Sathiadoss P, Bhatnagar S, Chong J. Comparing GPT-3.5 and GPT-4 Accuracy and Drift in Diagnosis Please Cases. Radiology 2024 Jan;310(1):e232411. [doi: 10.1148/radiol.232411] [Medline: 38226874]
25. Coskun BN, Yagiz B, Ocakoglu G, Dalkilic E, Pehlivan Y. Assessing the accuracy and completeness of artificial intelligence language models in providing information on methotrexate use. Rheumatol Int 2024 Mar;44(3):509-515. [doi: 10.1007/s00296-023-05473-5] [Medline: 37747564]
26. Wu S, Tong W, Li M, Hu H, Lu X, Huang Z, et al. Collaborative Enhancement of Consistency and Accuracy in US Diagnosis of Thyroid Nodules Using Large Language Models. Radiology 2024 Mar;310(3):e232255. [doi: 10.1148/radiol.232255] [Medline: 38470237]
27. Makrygiannakis MA, Giannakopoulos K, Kaklamanos EG. Evidence-based potential of generative artificial intelligence large language models in orthodontics: a comparative study of ChatGPT, Google Bard, and Microsoft Bing. Eur J Orthod 2024 Apr 13:cjae017. [doi: 10.1093/ejo/cjae017] [Medline: 38613510]
28. Cozzi A, Pinker K, Hidber A, Zhang T, Bonomo L, Lo Gullo R, et al. BI-RADS Category Assignments by GPT-3.5, GPT-4, and Google Bard: A Multilanguage Study. Radiology 2024 Apr;311(1):e232133. [doi: 10.1148/radiol.232133] [Medline: 38687216]
29. Güneş YC, Cesur T, Çamur E, Günbey Karabekmez L. Evaluating text and visual diagnostic capabilities of large language models on questions related to the Breast Imaging Reporting and Data System Atlas 5 edition. Diagn Interv Radiol 2025 Mar 03;31(2):111-129 [FREE Full text] [doi: 10.4274/dir.2024.242876] [Medline: 39248152]
30. Maroncelli R, Rizzo V, Pasculli M, Cicciarelli F, Macera M, Galati F, et al. Probing clarity: AI-generated simplified breast imaging reports for enhanced patient comprehension powered by ChatGPT-4o. Eur Radiol Exp 2024 Oct 30;8(1):124. [doi: 10.1186/s41747-024-00526-1] [Medline: 39477904]
31. Sheng L, Chen Y, Wei H, Che F, Wu Y, Qin Q, et al. Large Language Models for Diagnosing Focal Liver Lesions From CT/MRI Reports: A Comparative Study With Radiologists. Liver Int 2025 Jun;45(6):e70115. [doi: 10.1111/liv.70115] [Medline: 40347005]
32. Li J, Zheng H, Cai W, Wang Y, Zhang H, Liao M. Subclassification of BI-RADS 4 Magnetic Resonance Lesions: A Systematic Review and Meta-Analysis. J Comput Assist Tomogr 2020;44(6):914-920. [doi: 10.1097/RCT.0000000000001108] [Medline: 33196599]
33. Yu M, Zhang L, Jiang L, Zhou A. The value of contrast-enhanced ultrasound in the diagnosis of BI-RADS-US 4a lesions less than 2 cm in diameter. Clin Hemorheol Microcirc 2023;83(3):195-205. [doi: 10.3233/CH-221460] [Medline: 35599475]
34. Pagano S, Strumolo L, Michalk K, Schiegl J, Pulido LC, Reinhard J, et al. Evaluating ChatGPT, Gemini and other Large Language Models (LLMs) in orthopaedic diagnostics: A prospective clinical study. Comput Struct Biotechnol J 2025;28:9-15 [FREE Full text] [doi: 10.1016/j.csbj.2024.12.013] [Medline: 39850460]
35. Laohawetwanit T, Namboonlue C, Apornvirat S. Accuracy of GPT-4 in histopathological image detection and classification of colorectal adenomas. J Clin Pathol 2025 Feb 18;78(3):202-207. [doi: 10.1136/jcp-2023-209304] [Medline: 38199797]
36. Miaojiao S, Xia L, Xian Tao Z, Zhi Liang H, Sheng C, Songsong W. Using a Large Language Model for Breast Imaging Reporting and Data System Classification and Malignancy Prediction to Enhance Breast Ultrasound Diagnosis: Retrospective Study. JMIR Med Inform 2025 Jun 11;13:e70924 [FREE Full text] [doi: 10.2196/70924] [Medline: 40498674]
37. Shi M, Wang Z, Wang S, Li X, Zhang Y, Yan Y, et al. Performance of GPT-4 for automated prostate biopsy decision-making based on mpMRI: a multi-center evidence study. Mil Med Res 2025 Jul 07;12(1):33 [FREE Full text] [doi: 10.1186/s40779-025-00621-3] [Medline: 40619425]
38. Yang F, Yan D, Wang Z. Large-Scale assessment of ChatGPT's performance in benign and malignant bone tumors imaging report diagnosis and its potential for clinical applications. J Bone Oncol 2024 Feb;44:100525 [FREE Full text] [doi: 10.1016/j.jbo.2024.100525] [Medline: 38314324]
39. Akinci D'Antonoli T, Stanzione A, Bluethgen C, Vernuccio F, Ugga L, Klontzas ME, et al. Large language models in radiology: fundamentals, applications, ethical considerations, risks, and future directions. Diagn Interv Radiol 2024 Mar 06;30(2):80-90 [FREE Full text] [doi: 10.4274/dir.2023.232417] [Medline: 37789676]

XSL•FO
RenderX

40. Liu C, Wei M, Qin Y, Zhang M, Jiang H, Xu J, et al. Harnessing Large Language Models for Structured Reporting in Breast Ultrasound: A Comparative Study of Open AI (GPT-4.0) and Microsoft Bing (GPT-4). Ultrasound Med Biol 2024 Nov;50(11):1697-1703. [doi: 10.1016/j.ultrasmedbio.2024.07.007] [Medline: 39138026]
41. Elezaby M, Li G, Bhargavan-Chatfield M, Burnside ES, DeMartini WB. ACR BI-RADS Assessment Category 4 Subdivisions in Diagnostic Mammography: Utilization and Outcomes in the National Mammography Database. Radiology 2018 May;287(2):416-422 [FREE Full text] [doi: 10.1148/radiol.2017170770] [Medline: 29315061]
42. Pesapane F, Nicosia L, Rotili A, Penco S, Dominelli V, Trentin C, et al. A preliminary investigation into the potential, pitfalls, and limitations of large language models for mammography interpretation. Discov Oncol 2025 Feb 24;16(1):233. [doi: 10.1007/s12672-025-02005-4] [Medline: 39992569]
43. Ong AJ, Goh Y, Quek ST, Pillay PG, Lee H, Chou C. The Utility of Contrast-Enhanced Mammography in the Evaluation of Bloody Nipple Discharge-A Multicenter Study in the Asian Population. Diagnostics (Basel) 2024 Oct 16;14(20):2297 [FREE Full text] [doi: 10.3390/diagnostics14202297] [Medline: 39451620]

Abbreviations

AI: artificial intelligence
AUC: area under the receiver operating characteristic curve
BI-RADS: Breast Imaging Reporting and Data System
GPT: generative pretrained transformer
LLM: large language model

Edited by A Coristine; submitted 06.07.25; peer-reviewed by J Shen, X Wang; comments to author 09.09.25; accepted 30.11.25; published 25.12.25.

Please cite as:
Dai X, Ke M, Xie D, Mei M, Wei S, Dai Y, Yan R
Performance of ChatGPT-4o, Claude 3 Opus, and DeepSeek-R1 in BI-RADS Category 4 Classification and Malignancy Prediction From Mammography Reports: Retrospective Diagnostic Study
JMIR Med Inform 2025;13:e80182
URL: https://medinform.jmir.org/2025/1/e80182
doi:10.2196/80182
PMID:41447465

©Xingwei Dai, Man Ke, Dixing Xie, Mengting Mei, Si Wei, Yi Dai, Ronghua Yan. Originally published in JMIR Medical Informatics (https://medinform.jmir.org), 25.12.2025. This is an open-access article distributed under the terms of the Creative Commons Attribution License (https://creativecommons.org/licenses/by/4.0/), which permits unrestricted use, distribution, and reproduction in any medium, provided the original work, first published in JMIR Medical Informatics, is properly cited. The complete bibliographic information, a link to the original publication on https://medinform.jmir.org/, as well as this copyright and license information must be included.

XSL•FO
RenderX

Assessing Total Hip Arthroplasty Outcomes and Generating an Orthopedic Research Outcome Database via a Natural Language Processing Pipeline: Development and Validation Study

Nicholas H Mast[1], MD; Clara L. Oeste[2], PhD; Dries Hens[2], MD

[1]Hip and Pelvis Institute, 2250 Hayes St # 208, San Francisco, CA, United States

[2]LynxCare Inc, Leuven, Belgium

Corresponding Author:
Nicholas H Mast, MD
Hip and Pelvis Institute, 2250 Hayes St # 208, San Francisco, CA, United States

Abstract

Background: Processing data from electronic health records (EHRs) to build research-grade databases is a lengthy and expensive process. Modern arthroplasty practice commonly uses multiple sites of care, including clinics and ambulatory care centers. However, most private data systems prevent obtaining usable insights for clinical practice.

Objective: This study aims to create an automated natural language processing (NLP) pipeline for extracting clinical concepts from EHRs related to orthopedic outpatient visits, hospitalizations, and surgeries in a multicenter, single-surgeon practice. The pipeline was also used to assess therapies and complications after total hip arthroplasty (THA).

Methods: EHRs of 1290 patients undergoing primary THA from January 1, 2012 to December 31, 2019 (operated and followed by the same surgeon) were processed using artificial intelligence (AI)–based models (NLP and machine learning). In addition, 3 independent medical reviewers generated a gold standard using 100 randomly selected EHRs. The algorithm processed the entire database from different EHR systems, generating an aggregated clinical data warehouse. An additional manual control arm was used for data quality control.

Results: The algorithm was as accurate as human reviewers (0.95 vs 0.94; P=.01), achieving a database-wide average F_1-score of 0.92 (SD 0.09; range 0.67 - 0.99), validating its use as an automated data extraction tool. During the first year after direct anterior THA, 92.1% (1188/1290) of our population had a complication-free recovery. In 7.9% (102/1290) of cases where surgery or recovery was not uneventful, lateral femoral cutaneous nerve sensitivity (47/1290, 3.6%), intraoperative fractures (13/1290, 1%), and hematoma (9/1290, 0.7%) were the most common complications.

Conclusions: Algorithm evaluation of this dataset accurately represented key clinical information swiftly, compared with human reviewers. This technology may provide substantial value for future surgeon practice and patient counseling. Furthermore, the low early complication rate of direct anterior THA in this surgeon's hands was supported by the dataset, which included data from all treated patients in a multicenter practice.

(JMIR Med Inform 2025;13:e64705) doi:10.2196/64705

KEYWORDS

total hip arthroplasty; THA; direct anterior approach; electronic health records; EHR; natural language processing; NLP; complication rate; single-surgeon registry; hip arthroplasty; orthopedic; validation; surgeon; outpatient visits; hospitalizations; surgery

Introduction

Total hip arthroplasty (THA) is one of the most effective orthopedic procedures [1]. The number of THAs is projected to rise, along with its impact on health care resources [2]. However, more government funding requires efficient quality control and accountability. Quality monitoring is expected to have a bigger impact on orthopedic practices and on medicine as a whole in the near future. Unfortunately, many surgeons working in nonacademic settings frequently lack the resources and financing needed to properly evaluate the quality of patient care they provide. The broad adoption of electronic health records (EHRs) simplifies access to vast amounts of medical data and facilitates data analysis.

Despite how inefficient and time-consuming manual review is, it remains the gold standard for reviewing medical information. Research has shown that systematic reporting of postoperative orthopedic surgical adverse events is infrequent [3], despite the low complication rates associated with THA. Monitoring the standard of care after THA is still challenging, since evaluating

XSL•FO
RenderX

sufficient records in a timely manner is a complex task. Using natural language processing (NLP) technology, we developed a system that can extract relevant postoperative problems from unstructured EHR data [4]. We questioned whether such an AI-supported approach might be used to provide precise, continuing feedback on the quality of care provided after THA in a high-volume, nonacademic clinical setting. We assumed that a computer algorithm would perform at least as well as a human reviewer, which is considered the industry standard.

The primary goal of this study was, therefore, to design and develop an automated NLP pipeline for extracting clinical concepts from reports on outpatients, hospitalizations, and surgeries from a single surgeon, multicenter practice. Using the pipeline, the secondary goal was to examine and evaluate therapies and complications following THA.

Methods

Ethical Considerations

Patients were invited to participate in the research on the direct anterior approach (DAA) of hip replacement. Informed consent for the use of patient data in this retrospective study was obtained as part of the institutional review board (IRB) protocol (WCG IRB Protocol 20225993). Patients undergoing surgery were provided with a consent form at the time of intake, which was signed before the procedure. Patients who continued to be followed up subsequently signed consent forms that were applicable retrospectively. Data were anonymized before analysis.

Patient Selection

Data from 1290 patients undergoing 1304 primary DAA THAs using a Hana Orthopedic Surgery Table (Mizuho OSI), with the same surgical team and implants. Data was collected from January 1, 2012 to December 31, 2019, and analyzed retrospectively. Exclusion criteria included age under 18 years, failure to provide informed consent, and revision surgery.

Follow-Up Schedule

Patients were followed preoperatively and postoperatively at 2 weeks, 6 weeks, 3 months (on a per-case basis), and 1 year. The algorithm screened EHRs for key sentences, words, and clinical definitions that were compiled by the surgical team.

Adverse Event Classification

A list of 19 complications based on the study of the Hip Society THA Complications Workgroup was compiled [5]. A separate category was added for lower back pain, sciatica, or both. Treatment was categorized as either conservative or interventional.

EHR Data Structure and Documentation Variability

The study used EHR systems that capture all patient interactions across the health system. Documentation varied by note type: operative reports were dictated using a standardized format, with intraoperative complications documented in a dedicated subsection. Radiographic reports, however, were dictated by multiple radiologists without a uniform structure. Complications were often identifiable through multiple associated notes across different document types. Implant records were dictated directly from intraoperative purchasing logs, ensuring high reliability. The NLP algorithm flagged typographical errors in dictated notes that human reviewers overlooked.

Gold Standard Adjudication Process

To ensure consistency in the gold standard corpus used for training the algorithm, all discrepancies among reviewers were resolved through senior adjudication. When ambiguities were identified in a case, they were escalated to the senior author, who conducted a thorough review of the full case file. Final determinations were made based on clinical expertise and consensus, ensuring a standardized and reliable reference dataset.

NLP Pipeline Development and Validation

The NLP pipeline was developed and validated in 3 phases, as described by Van de Meulebroucke et al [4]. First, a training set of 50 EHRs was annotated to generate relevant input, since a sample size of 50 EHRs was previously found sufficient to achieve accuracy over 90% [4]. Second, an independent gold standard was generated through manual review by 3 independent surgeons of a derivation cohort of 100 EHRs. Third, the entire dataset of 1290 patients was manually reviewed to calculate the algorithm's recall, precision, and F_1-score. Patient records were analyzed using standard procedures of each center's EHR system by a manual reviewer.

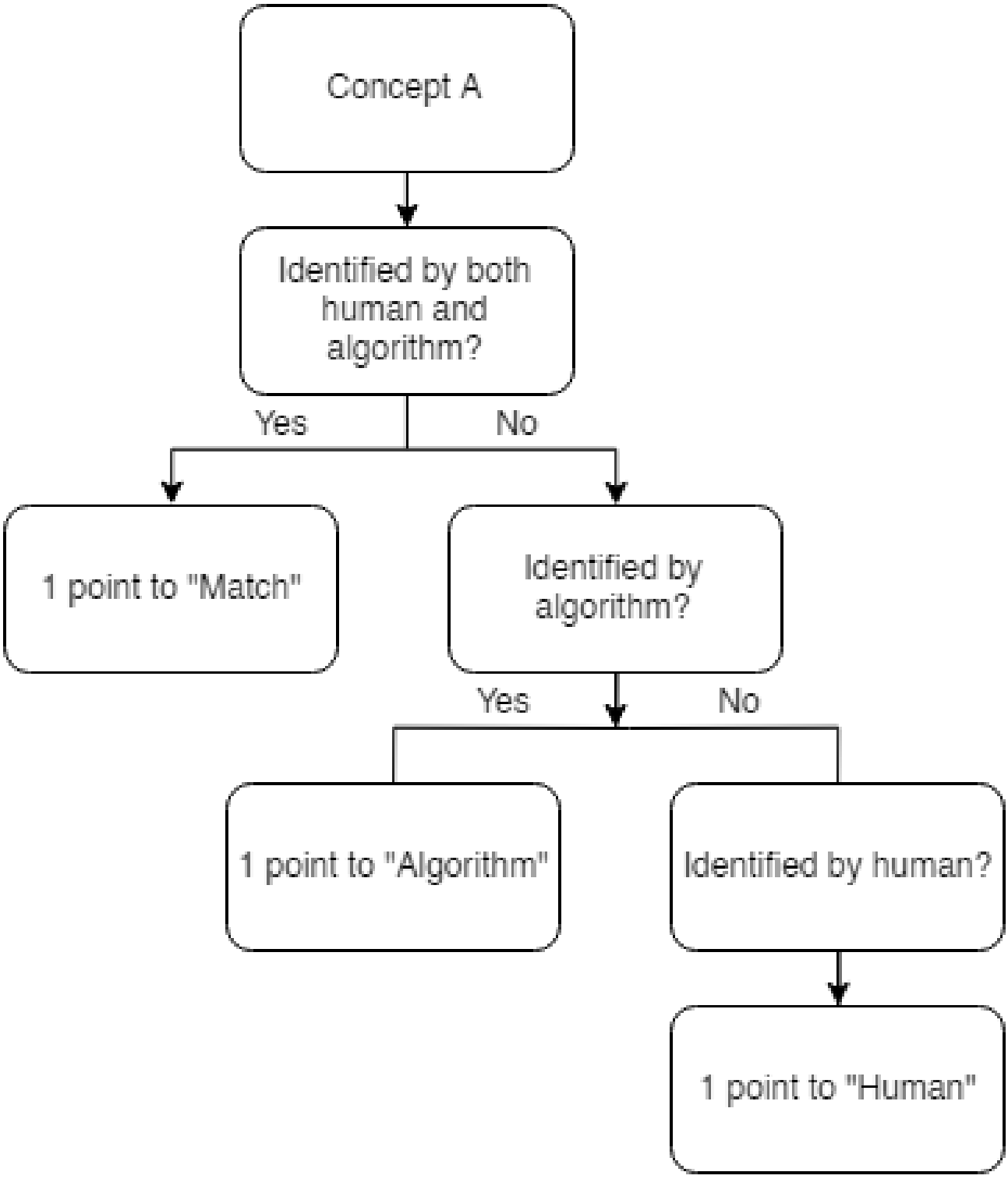
The pipeline uses a text mining engine based on machine learning and NLP to extract important concepts from EHRs. The NLP pipeline incorporates several preprocessing steps, including language detection, sentence segmentation, and tokenization, to prepare unstructured EHR text for analysis. The core architecture is based on a deep learning model fine-tuned on large-scale clinical datasets and adapted for domain-specific tasks in orthopedics. Named entity recognition identifies relevant medical concepts, relation extraction determines associations between entities, and attribute extraction captures features such as negations and temporal qualifiers. Processed outputs were mapped to Unified Medical Language System (UMLS) Concept Unique Identifiers (CUIs), which includes standard terminologies like the Systematized Nomenclature of Medicine-Clinical Terms (SNOMED-CT). Mapping was performed by a probabilistic entity-linking algorithm that integrates semantic ranking and term preferences, ensuring precise and standardized representation. In addition, the processed data were standardized using the Observational Medical Outcomes Partnership Common Data Model, which harmonizes structured and unstructured data from different EHR systems into a unified format. This approach enables the efficient processing of unstructured clinical text and supports the accurate extraction and mapping of clinical concepts.

Complications and their respective treatment, along with other clinical features, were collected into a database and standardized using UMLS CUIs. The NLP tool mined variables from the full set of source data within EHRs, including, but not limited to, clinical notes, primary care records, radiology reports, laboratory results, discharge summaries, and surgical documentation. The full list of study variables is shown in Multimedia Appendix 1.

XSL•FO
RenderX

To assess accuracy, a scoring system was established such that one point was given to each correct clinical concept, extracted by the algorithm or the human reviewer (Figure 1). Correct clinical concepts referred to those matching the gold standard. Precision, recall, and F_1-score were used as statistical parameters to reflect the performance of the algorithm, as calculated with R (R Foundation for Statistical Computing) statistical programming (Table 1).

Figure 1. Scoring system flowchart for concept identification by human versus algorithm.



XSL•FO
RenderX

Table . Statistical parameters for algorithm performance.

	Definition	Calculation
Accuracy	Percentage (%) of relevant concepts extracted by method A/B.	Number of concepts÷total number of concepts expected to be extracted
Recall or sensitivity	Ratio between all identified concepts and all existing concepts in a given text (0 - 1).	True positives÷(true positives+false negatives)
Precision	Ratio between all adequately identified concepts and all identified concepts (0 - 1).	True positives÷(true positives+false positives)
F_1-score	Harmonic mean of recall and precision (0 - 1).	2×(recall×precision)÷(recall+precision)

Statistical Analysis

For categorical values, the number of patients (n) and relative proportions (%) are shown.

Checks for accuracy, recall, and precision involved measuring model outcomes against a gold standard created by human annotators. The F_1-score assesses the trade-off between precision and recall by calculating their harmonic mean (Table 1).

Results

Performance of the NLP Pipeline

Table 2 compares the accuracy of human reviewers to an algorithm on various aspects of 100 patient records. Overall, the algorithm was slightly more accurate than human reviewers, with an accuracy of 0.952 compared with 0.945 for human reviewers, a difference of 0.007 (P=.01). The most notable differences in accuracy between the algorithm and human reviewers were on the variables of weight (0.24 difference in accuracy), revision (0.06 difference), and offset (0.02 difference), all of which were detected more accurately by the algorithm. The algorithm was less accurate on variables such as cup size, prosthetic loosening, and heterotopic ossification grade, though with small differences in accuracy ranging from −0.06 to 0.04.

In order to further assess the quality of data extracted by the algorithm, we calculated statistical parameters such as recall, precision, and F_1-score of the different variables detected in the study, as defined in Table 1. The results shown in Table 3 reflect that for most variables, the recall and F_1-score are high, indicating that the model is able to correctly identify the presence of the clinical variables in the data. The average values for all the variables show an overall high performance of the model.

XSL•FO
RenderX

Table . Human versus algorithm accuracy on a randomly selected group of 100 patients.

	Human reviewer accuracy	Algorithm accuracy	Delta
Antibiotics	1	1	0
Blood loss	1	0.98	−0.02
Cup size	0.98	0.92	−0.06
Date of procedure	0.98	0.98	0
Dislocation	0.96	0.94	−0.02
Fracture	0.98	0.96	−0.02
Heterotopic ossification grade	0.9	0.92	0.02
Offset	1	0.98	−0.02
Pain killer	0.96	0.96	0
Primary arthrosis	0.98	0.98	0
Prosthesis manufacturer	0.94	0.96	0.02
Prosthetic loosening	0.96	0.92	−0.04
Psoas tendinopathy	1	0.96	−0.04
Range of motion	0.86	0.88	0.02
Revision	0.9	0.96	0.06
Steel type	0.9	0.92	0.02
Surgery duration	1	0.98	−0.02
Thromboembolism	1	0.98	−0.02
Weight	0.64	0.88	0.24
Wound infection	0.96	0.98	0.02
Total	0.945	0.952	0.007

Table . Recall, precision, and F_1-scores for entire dataset of 1290 cases across all data points.

	Recall	Precision	F_1-score
Superficial wound infection	1	0.88	0.94
Heterotopic ossification	0.92	0.95	0.93
Lower back pain	1	0.98	0.99
Peri-prosthetic Infection	0.98	0.95	0.96
Wound infection	0.95	0.82	0.88
Dislocation	1	0.99	0.99
Revision	1	0.97	0.98
Intra-operative fracture	1	0.99	0.99
Post-operative fracture	1	0.89	0.94
Bleeding	0.95	0.65	0.77
Prosthetic loosening	1	0.98	0.99
Pain	0.97	0.88	0.92
Nerve injury	0.89	0.92	0.90
Psoas burden	0.99	0.99	0.99
Sciatica	0.75	0.88	0.81
Vascular systems injury	1	0.5	0.67
Average	0.96	0.89	0.92

XSL•FO
RenderX

Complications and Interventions of DAA THA

The mean age of the patients included in the dataset was 63.5 (SD 9.6) years and 57.4% (740/1290) were women. The complications during the first year after direct anterior THA in these patients are shown in Table 4, as well as the conservative or interventional treatment of these clinical outcomes.

Soft tissue complications were the most common type of complication observed in patients undergoing THA. The most common type of soft tissue complication was sensory deficit (47/1290, 3.6%), followed by hematoma (9/1290, 0.7%) and superficial wound infection (3/1290, 0.2%). No incidents of bleeding, prolonged wound drainage, motor nerve deficit, vascular injury, or sciatica were reported. Regarding mechanical complications, periprosthetic fractures occurred in 1.4% of cases (18/1290; 13 intraoperatively and 5 postoperatively), and instability occurred in 0.5% (7/1290) of cases. Implant fracture, cup-liner dislocation and osteolysis were not reported.

Table 5 shows interventions in the 1-year postoperative period. The most common interventions were intraoperative (cerclage and wiring), which account for 1% (n=13) of cases. Readmission was detected in 0.9% (n=12) of patients. Other interventions such as aspiration, wound debridement, closed reduction, osteosynthesis or cerclage, and revision, each account for less than 1% of cases.

Table . Complications in the 1-year postoperative period (n=1290).

Complication subgroup	Total, n (%)	Conservative treatment, n (%)	Interventional treatment, n (%)
Soft tissue complications: wounds			
Bleeding	0 (0)	0 (0)	0 (0)
Hematoma	9 (0.7)	6 (0.5)	3 (0.2)
Prolonged wound drainage	1 (0.1)	0 (0)	1 (0.1)
Soft tissue complications: infection			
Superficial wound infection	3 (0.2)	3 (0.2)	0 (0)
Deep PJI[a]	3 (0.2)	0 (0)	3 (0.2)
Soft tissue complications: neural deficit			
Motor nerve deficit	0 (0)	0 (0)	0 (0)
Transient sensory deficit (LFCN[b] sensitivity)	47 (3.6)	47 (3.6)	0 (0)
Soft tissue complications: lower back pain			
Lumbago	6 (0.5)	6 (0.5)	0 (0)
Sciatica	1 (0.1)	1 (0.1)	0 (0)
Soft tissue complications: other			
Vascular Injury	0 (0)	0 (0)	0 (0)
Heterotopic Ossification	2 (0.2)	2 (0.2)	0 (0)
Thromboembolic disease	3 (0.2)	3 (0.2)	0 (0)
Mechanical complications: periprosthetic fracture			
Intraoperative	13 (1)	0 (0)	13 (1)
Postoperative	5 (0.4)	0 (0)	5 (0.4)
Mechanical complications: other			
Instability	7 (0.5)	3 (0.2)	4 (0.3)
Implant fracture	0 (0)	0 (0)	0 (0)
Loosening	2 (0.2)	0 (0)	2 (0.2)
Cup-liner dislocation	0 (0)	0 (0)	0 (0)
Bearing surface wear	1 (0.1)	0 (0)	1 (0.1)
Osteolysis	0 (0)	0 (0)	0 (0)

[a]PJI: prosthetic joint infection.

[b]LFCN: lateral femoral cutaneous nerve.

XSL•FO
RenderX

Table . Interventions in the 1-year post-operative period.

Intervention	Values (n=1290), n (%)
Intraoperative	
Cerclage and wiring	13 (1)
Outpatient	
Infiltration	0 (0)
Aspiration	3 (0.2)
Reoperation	
Wound debridement	2 (0.2)
Closed reduction	2 (0.2)
Osteosynthesis or cerclage	2 (0.2)
Other	
Revision	9 (0.7)
Readmission	12 (0.9)

Discussion

Principal Findings

This study reflects the use of AI techniques to streamline and improve data capture from EHRs, in line with the current need for innovative solutions to obtain meaningful information from existing data sources in the field of orthopedics [6]. AI-supported automation, substantiated in the first step by directly comparing it with a manual review of a random sample of patients, showed no statistical differences in accuracy across all compared clinical concepts. Subsequently, application of the algorithm to the entire dataset generated very high F_1-scores, therefore, validating its ability to detect positive results in our cohort with a high degree of precision and recall. This allowed a single-surgeon registry to be populated from existing health data within EHRs in a very short period of time. The NLP pipeline handled documentation variability using named entity recognition, probabilistic entity linking, and attribute extraction, allowing synonym recognition and standardization to SNOMED-CT and UMLS CUIs. This data-driven approach ensured robust identification of complications across different documentation sources. Furthermore, the methodology deployed in this study allows for inclusion of data from different software sources, which can be a limitation of single-surgeon registries that must be populated from diverse clinics or ambulatory care centers. The resulting multicenter, single-surgeon database is comparable in its granularity to single-system registries populated with conventional methods, circumventing the complexity of a system that is becoming increasingly fragmented.

The methodology that was previously described in a smaller cohort of Dutch patients is validated here in a multicenter, US-based practice, screening records in English from 1290 patients over an 8-year period at high accuracy [4]. It also demonstrates its usefulness in the nonacademic setting, compared with previous studies at academic centers [7,8]. Analysis of such a large cohort from a single surgeon permitted categorization of frequent concepts without needing to account for the confounding variables of different techniques and complication rates of multiple surgeons [9].

Our dataset split balances annotation feasibility and model performance, following previous clinical NLP studies. Small, high-quality training sets have been shown to be effective in constrained domains, particularly when leveraging structured reporting patterns [10]. The chosen test set size aligns with established practices in clinical NLP research [11]. Instead of relying solely on predefined training-validation-test ratios, we incorporated post hoc validation on a large dataset to assess generalizability, a common strategy in clinical text mining [12,13].

In addition, clinical insight was also gained regarding the frequency and management of complications over a 1-year period. While the study highlights the effectiveness of NLP tools in single surgeon practices, extensive datasets can greatly benefit from its capabilities. NLP tools offer versatility in both big data settings and smaller subsets, enabling comprehensive analysis across various practice settings and facilitating evaluation of outcomes, for example, relative to regional averages or previously published work.

Ultimately, concept detection and extraction of the pipeline demonstrated accuracy on par with human reviewers at a fraction of the cost and time required for manual chart review. Validation is a necessary step for algorithm use that benefits from physicians' feedback through annotation. This input is necessary to test algorithm performance, to calibrate the algorithm's rates of false positives and false negatives, and to examine if clinical use of algorithms leads to better research insights and health care services [14]. The ease and high degree of fidelity of concept extraction by the algorithm in this study facilitated longitudinal evaluation of clinical complications, and importantly, also precluded the need to manually filter through patient charts, which is time-consuming [15].

Comparison With Previous Work

The representativeness of the methodology in this study is hence reflected by the frequency of the complications, which falls

XSL•FO
RenderX

within the lower range of previously described cohorts [16]. For instance, a frequency of 1% of periprosthetic fractures was detected, which was the most common intraoperative complication in this study, and was found to be 2.1%, 1.6%, and 1.1% in other cohorts [4,9,17]. Other similar comparisons show that revisions were detected in 0.7% (9/1290) of patients in our study vs 2.1% (5/239) and 1.6% (3/187), and prosthetic joint infection, at 0.2% (3/1290) in our study, appeared in 1.3% (3/239) and 1.6% (3/187) of patients in the aforementioned studies [9,17]. In a prospective comparison of DAA to posterior approach THA (43 DAA THAs in total), 2.3% (1/43) had hematoma vs 0.7% (9/1290) in our study, 2.3% (1/43) presented heterotopic ossification vs 0.2% (3/1290) shown here, and neither study detected dislocations [18]. Therefore, the results obtained using the validated, NLP-driven methodology shown here also highlight the quality of practice of the surgeon, for the complications described in this study fall within the lower range of those previously described in the literature [9,16-20].

Limitations

As is the case in real-world evidence studies, there are certain limitations to consider for this study, such as missing values for certain variables. Regarding rare concepts such as bleeding, the scarcity of terms found in the EHRs may hinder algorithm training. The algorithm solely focused on patients undergoing DAA THA, which is the method used by the surgeon, but its validity could be further strengthened by expanding the analyses to other populations. In addition, the quality of records kept at each site determines the quality of algorithm training, highlighting the need for ongoing validation processes as the database expands. Missing structured data were treated as true absences and were not imputed. For unstructured text, missing values could reflect a lack of documentation or true absences. Manual review helped assess whether missing information stemmed from documentation gaps or NLP constraints. While a single-surgeon dataset ensures consistency in surgical technique and documentation style, it may limit generalizability to other surgical practices. However, the inclusion of multisource EHR data and independent validation by multiple reviewers helps mitigate this potential bias.

Conclusions

In this study, the NLP pipeline proved highly effective in improving data capture and enhancing clinical outcomes analysis following DAA THA, overcoming constraints linked to single-surgeon registries, which typically require data aggregation from multiple care sites. It holds significant potential for future orthopedic studies, providing accurate and cost-effective insights. In addition, the dataset supports the low early complication rate of direct anterior THA in this surgeon's multicenter practice.

Conflicts of Interest

NHM declares the following conflicts of interest: royalties from Medenvision and Synthes; speakers bureau or paid presentations for DePuy, Medenvision, and Mizuho/OSI; paid consultancy for Medacta USA and Medenvision; stock or stock options in DEO, Docspera, Ostaudio, OutcomeMD, and Radlink; board member of the Anterior Hip Foundation. DH is part of the management and CLO is an employee at LynxCare, Inc.

Multimedia Appendix 1
Data sources, categories, and concept unique identifiers of all clinical data points.
[DOCX File, 38 KB - medinform_v13i1e64705_app1.docx]

References

1. Learmonth ID, Young C, Rorabeck C. The operation of the century: total hip replacement. The Lancet 2007 Oct;370(9597):1508-1519. [doi: 10.1016/S0140-6736(07)60457-7]
2. Lee GC, Marconi D. Complications following direct anterior hip procedures: costs to both patients and surgeons. J Arthroplasty 2015 Sep;30(9 Suppl):98-101. [doi: 10.1016/j.arth.2015.03.043] [Medline: 26118568]
3. Bozic KJ, Grosso LM, Lin Z, et al. Variation in hospital-level risk-standardized complication rates following elective primary total hip and knee arthroplasty. J Bone Joint Surg Am 2014 Apr 16;96(8):640-647. [doi: 10.2106/JBJS.L.01639] [Medline: 24740660]
4. Van de Meulebroucke C, Beckers J, Corten K. What can we expect following anterior total hip arthroplasty on a regular operating table? A validation study of an artificial intelligence algorithm to monitor adverse events in a high-volume, nonacademic setting. J Arthroplasty 2019 Oct;34(10):2260-2266. [doi: 10.1016/j.arth.2019.07.039] [Medline: 31445868]
5. Healy WL, Iorio R, Clair AJ, Pellegrini VD, Della Valle CJ, Berend KR. Complications of total hip arthroplasty: standardized list, definitions, and stratification developed by the hip society. Clin Orthop Relat Res 2016 Feb;474(2):357-364. [doi: 10.1007/s11999-015-4341-7] [Medline: 26040966]
6. Zsidai B, Kaarre J, Hilkert AS, et al. Accelerated evidence synthesis in orthopaedics-the roles of natural language processing, expert annotation and large language models. J Exp Orthop 2023 Sep 28;10(1):99. [doi: 10.1186/s40634-023-00662-4] [Medline: 37768352]
7. Wyles CC, Tibbo ME, Fu S, et al. Use of natural language processing algorithms to identify common data elements in operative notes for total hip arthroplasty. J Bone Joint Surg Am 2019 Nov 6;101(21):1931-1938. [doi: 10.2106/JBJS.19.00071] [Medline: 31567670]

XSL•FO
RenderX

8. Flores-Balado Á, Castresana Méndez C, Herrero González A, et al. Using artificial intelligence to reduce orthopedic surgical site infection surveillance workload: algorithm design, validation, and implementation in 4 Spanish hospitals. Am J Infect Control 2023 Nov;51(11):1225-1229. [doi: 10.1016/j.ajic.2023.04.165] [Medline: 37100291]
9. Frenkel Rutenberg T, Vitenberg M, Daglan E, Kadar A, Shemesh S. Single surgeon versus co-surgeons in primary total joint arthroplasty: does "two is better than one" apply to surgeons? J Pers Med 2022 Oct 9;12(10):1683. [doi: 10.3390/jpm12101683] [Medline: 36294821]
10. Liu S, Wen A, Wang L, et al. An open natural language processing (NLP) framework for EHR-based clinical research: a case demonstration using the National COVID Cohort Collaborative (N3C). J Am Med Inform Assoc 2023 Nov 17;30(12):2036-2040. [doi: 10.1093/jamia/ocad134] [Medline: 37555837]
11. Johnson AEW, Pollard TJ, Shen L, et al. MIMIC-III, a freely accessible critical care database. Sci Data 2016 May 24;3(1):160035. [doi: 10.1038/sdata.2016.35] [Medline: 27219127]
12. Chapman WW, Nadkarni PM, Hirschman L, D'Avolio LW, Savova GK, Uzuner O. Overcoming barriers to NLP for clinical text: the role of shared tasks and the need for additional creative solutions. J Am Med Inform Assoc 2011;18(5):540-543. [doi: 10.1136/amiajnl-2011-000465] [Medline: 21846785]
13. Uzuner O, Solti I, Cadag E. Extracting medication information from clinical text. J Am Med Inform Assoc 2010;17(5):514-518. [doi: 10.1136/jamia.2010.003947] [Medline: 20819854]
14. Gundersen T, Bærøe K. The future ethics of artificial intelligence in medicine: making sense of collaborative models. Sci Eng Ethics 2022 Apr 1;28(2):17. [doi: 10.1007/s11948-022-00369-2] [Medline: 35362822]
15. Gauthier MP, Law JH, Le LW, et al. Automating access to real-world evidence. JTO Clin Res Rep 2022 Jun;3(6):100340. [doi: 10.1016/j.jtocrr.2022.100340] [Medline: 35719866]
16. Alva A, Nizam I, Gogos S. Minimizing complications in bikini incision direct anterior approach total hip arthroplasty: a single surgeon series of 865 cases. J Exp Orthop 2021 Jan 4;8(1):1. [doi: 10.1186/s40634-020-00318-7] [Medline: 33394190]
17. Soza D, Pujol O, Lara Y, Castellanos S, Hernández A, Barro V. A comparative of a single novice surgeon's direct anterior approach and posterior approach learning curves in total hip arthroplasty: a retrospective cohort study. Eur J Orthop Surg Traumatol 2022 May;32(4):767-774. [doi: 10.1007/s00590-021-03039-4] [Medline: 34129119]
18. Barrett WP, Turner SE, Leopold JP. Prospective randomized study of direct anterior vs postero-lateral approach for total hip arthroplasty. J Arthroplasty 2013 Oct;28(9):1634-1638. [doi: 10.1016/j.arth.2013.01.034] [Medline: 23523485]
19. Wernly D, Wegrzyn J, Lallemand G, Mahlouly J, Tissot C, Antoniadis A. Total hip arthroplasty through the direct anterior approach with and without the use of a traction table: a matched-control, retrospective, single-surgeon study. J Orthop Surg Res 2021 Jan 11;16(1):45. [doi: 10.1186/s13018-020-02184-6] [Medline: 33430917]
20. De Geest T, Fennema P, Lenaerts G, De Loore G. Adverse effects associated with the direct anterior approach for total hip arthroplasty: a Bayesian meta-analysis. Arch Orthop Trauma Surg 2015 Aug;135(8):1183-1192. [doi: 10.1007/s00402-015-2258-y] [Medline: 26081800]

Abbreviations

AI: artificial intelligence
CUI: Concept Unique Identifier
DAA: direct anterior approach
EHR: electronic health record
NLP: natural language processing
SNOMED-CT: Systematized Nomenclature of Medicine-Clinical Terms
THA: total hip arthroplasty
UMLS: Unified Medical Language System

Edited by C Lovis; submitted 24.07.24; peer-reviewed by A Chaturvedi, B Senst, L Chinthala; revised version received 30.01.25; accepted 16.02.25; published 12.03.25.

Please cite as:
Mast NH, Oeste CL, Hens D
Assessing Total Hip Arthroplasty Outcomes and Generating an Orthopedic Research Outcome Database via a Natural Language Processing Pipeline: Development and Validation Study
JMIR Med Inform 2025;13:e64705
URL: https://medinform.jmir.org/2025/1/e64705
doi:10.2196/64705

XSL•FO
RenderX

© Nicholas H Mast, Clara L Oeste, Dries Hens. Originally published in JMIR Medical Informatics (https://medinform.jmir.org), 12.3.2025. This is an open-access article distributed under the terms of the Creative Commons Attribution License (https://creativecommons.org/licenses/by/4.0/), which permits unrestricted use, distribution, and reproduction in any medium, provided the original work, first published in JMIR Medical Informatics, is properly cited. The complete bibliographic information, a link to the original publication on https://medinform.jmir.org/, as well as this copyright and license information must be included.

XSL•FO
RenderX

Original Paper

Data Interoperability in COVID-19 Vaccine Trials: Methodological Approach in the VACCELERATE Project

Salma Malik[1*], PharmB, PhD; Zoi Pana Dorothea[2*], MD, MSc, PhD; Christos D Argyropoulos[3*], MSci, MSc, PhD; Sophia Themistocleous[2*], MSc; Alan J Macken[4*], MSc; Olena Valdenmaiier[5*], MSc; Frank Scheckenbach[6*], PhD; Elena Bardach[6*], MSc; Andrea Pfeiffer[6*], MS; Katherine Loens[7*], PhD; Jordi Cano Ochando[8*], PhD; Oliver A Cornely[9*], MD, PhD; Jacques Demotes-Mainard[1*], MBA, MD, PhD; Sergio Contrino[1*], ING; Gerd Felder[1*]

[1]European Clinical Research Infrastructure Network, Paris, France

[2]School of Medicine, European University Cyprus, Nicosia, Cyprus

[3]Chemical Engineering Department, King Fahd University of Petroleum and Minerals, Dhahran, Saudi Arabia

[4]Centre for Experimental Pathogen Host Research, University College Dublin School of Medicine, National University of Ireland, Dublin, Ireland

[5]Centre of Excellence for Health, Immunity and Infections, Rigshospitalet, University of Copenhagen, Copenhagen, Denmark

[6]Clinical Trials Centre Cologne, Faculty of Medicine, University of Cologne, Cologne, Germany

[7]Laboratory of Medical Microbiology, VAXINFECTIO, Faculty of Medicine and Health Sciences, University of Antwerp, Antwerp, Belgium

[8]Microbiology Section, Department of Pharmaceutical Sciences and of Health, Faculty of Pharmacy, Universidad San Pablo-Centro de Estudios Universitarios, Madrid, Spain

[9]CECAD, CIO ABCD, ECMM, CMMC, Faculty of Medicine and University Hospital Cologne, University of Cologne, Cologne, Germany

[*]all authors contributed equally

Corresponding Author:
Salma Malik, PharmB, PhD
European Clinical Research Infrastructure Network
30 Bd Saint-Jacques
Paris, 75014
France
Phone: 33 01 80 05 86 29
Email: salma.malik@ecrin.org

Abstract

Background: Data standards are not only key to making data processing efficient but also fundamental to ensuring data interoperability. When clinical trial data are structured according to international standards, they become significantly easier to analyze, reducing the efforts required for data cleaning, preprocessing, and secondary use. A common language and a shared set of expectations facilitate interoperability between systems and devices.

Objective: The main objectives of this study were to identify commonalities and differences in clinical trial metadata, protocols, and data collection systems/items within the VACCELERATE project.

Methods: To assess the degree of interoperability achieved in the project and suggest methodological improvements, interoperable points were identified based on the core outcome areas—immunogenicity, safety, and efficacy (clinical/physiological). These points were emphasized in the development of the master protocol template and were manually compared in the following ways: (1) summaries, objectives, and end points in the protocols of 3 VACCELERATE clinical trials (EU-COVAT-1_AGED, EU-COVAT-2_BOOSTAVAC, and EU-COVPT-1_CoVacc) against the master protocol template; (2) metadata of all 3 clinical trials; and (3) evaluations from a questionnaire survey regarding differences in data management systems and structures that enabled data exchange within the VACCELERATE network.

Results: The noncommonalities identified in the protocols and metadata were attributed to differences in populations, variations in protocol design, and vaccination patterns. The detailed metadata released for all 3 vaccine trials were clearly structured using internal standards, terminology, and the general approach of Clinical Data Acquisition Standards Harmonisation (CDASH) for data collection (eg, on electronic case report forms). VACCELERATE benefited significantly from the selection of the Clinical Trials Centre Cologne as the sole data management provider. With system database development coordinated by a single individual and no need for coordination among different trial units, a high degree of uniformity was achieved automatically. The harmonized

XSL•FO
RenderX

transfer of data to all sites, using well-established methods, enabled quick exchanges and provided a relatively secure means of data transfer.

Conclusions: This study demonstrated that using master protocols can significantly enhance trial operational efficiency and data interoperability, provided that similar infrastructure and data management procedures are adopted across multiple trials. To further improve data interoperability and facilitate interpretation and analysis, shared data should be structured, described, formatted, and stored using widely recognized data and metadata standards.

Trial Registration: EudraCT 2021-004526-29; https://www.clinicaltrialsregister.eu/ctr-search/trial/2021-004526-29/DE/; 2021-004889-35; https://www.clinicaltrialsregister.eu/ctr-search/search?query=eudract_number:2021-004889-35; and 2021-004526-29; https://www.clinicaltrialsregister.eu/ctr-search/search?query=eudract_number:2021-004526-29

(JMIR Med Inform 2025;13:e65590) doi:10.2196/65590

KEYWORDS

interoperability; metadata; data management; clinical trials; protocol; harmonization; adult; pediatric; systems; standards

Introduction

Interoperability is defined as the ability of different information systems, devices, or applications to connect in a coordinated manner within and across organizational boundaries, enabling stakeholders to access, exchange, and cooperatively use data with the goal of optimizing the health of individuals and populations [1].

Interoperability standards provide a common language and set of expectations that enable interoperability between systems and devices. These standards allow clinicians, laboratories, hospitals, pharmacies, and patients to seamlessly share data, regardless of the application or market supplier, thereby improving the coordination and delivery of health care [1].

The health interoperability ecosystem comprises individuals, systems, and processes that aim to share, exchange, and access all forms of health information, including discrete, narrative, and multimedia data. Potential stakeholders in this ecosystem include individuals, patients, providers, hospitals/health systems, researchers, payers, suppliers, and systems, all of whom contribute to the creation, exchange, and use of health information and data. When data are structured according to international standards, they become much easier to analyze, reducing the efforts required for data cleaning and preprocessing. Data standards are not only essential for efficient data processing but are also fundamental to ensuring the interoperability of the data itself [2]. The greater use of data standards is crucial to the success of data sharing. Without such standards, shared data are difficult to interpret with certainty, significantly more time-consuming to process, and therefore more expensive to collect. Standards can be applied to data item definitions and codes, controlled vocabularies for categories, and the structuring and exchange of data. File formats used for storing and transferring data should also be standardized to simplify data processing [3]. Clinical trial datasets should always include metadata describing the characteristics of each data item (eg, type, code, name, and possibly an ontology reference), along with details of the trial's schedule and design. Datasets should be made available for sharing in 1 or more standardized file formats that are compatible with a wide variety of systems [3].

In January 2021, the European Commission launched VACCELERATE—the European Corona Vaccine Trial Accelerator Platform [4] (GA 101037867)—to coordinate phases II and III of COVID-19 vaccine trials across Europe. VACCELERATE aimed to serve as a single-entry point for multicountry vaccine trials in Europe and to address the need for greater inclusion of underrepresented populations in vaccine trials. One of the fundamental objectives of VACCELERATE was to promote the sharing, interoperability, and FAIRness (Findable, Accessible, Interoperable, and Reusable) of data generated through the VACCELERATE network. This included ensuring that data sharing and future reuse were considered by investigators, the scientific community, and study sponsors. The objective of this study was to assess the degree of commonalities and differences among clinical trial metadata, protocols, and data collection systems/items in VACCELERATE consortium projects [5-8]. Additionally, the study aimed to explore the reasons why interoperability was sometimes limited or failed to occur. It also sought to identify areas where interoperability was relatively straightforward and to propose structures and systems that could enhance interoperability in the future, including for data generated outside the trials funded under the VACCELERATE platform [9-11].

EU-COVAT-1_AGED (EudraCT: 2021-004526-29) is a multinational, phase II, randomized, adaptive protocol designed to evaluate the immunogenicity and reactogenicity of different COVID-19 vaccines in adults aged ≥75 years who have already been vaccinated against SARS-CoV-2. It is the first of 3 VACCELERATE phase II COVID-19 vaccine trials and focuses on the immunogenicity and reactogenicity of vaccines in older adults (≥75 years), addressing a critical demographic that is often underrepresented in vaccine studies [9].

EU-COVAT-2_BOOSTAVAC (EudraCT: 2021-004889-35) is an international, multicenter, phase II, randomized, adaptive protocol designed to evaluate the need for, optimal timing of, and immunogenicity of administering a booster messenger RNA (mRNA) vaccination dose against SARS-CoV-2 in the general population (aged 18+ years) already vaccinated against SARS-CoV-2. This trial investigates booster vaccination strategies in the general adult population, providing insights into optimal timing and immunological outcomes for sustaining immunity [9].

EU-COVPT-1_COVACC (EudraCT: 2021-004526-29) is a phase II, comparative, randomized trial designed to evaluate

XSL•FO
RenderX

the impact of a reduced COVID-19 mRNA vaccination regimen on immunological responses and reactogenicity in pediatric patients with prior SARS-CoV-2 immunity. This trial investigates reduced-dose regimens in pediatric populations, contributing to the understanding of tailored vaccination approaches for children [9].

Together, these trials represent a comprehensive investigation across key demographic groups—older adults, the general population, and children—using adaptive and multinational protocols that address the challenges of rapid vaccine development and deployment during pandemics.

Methods

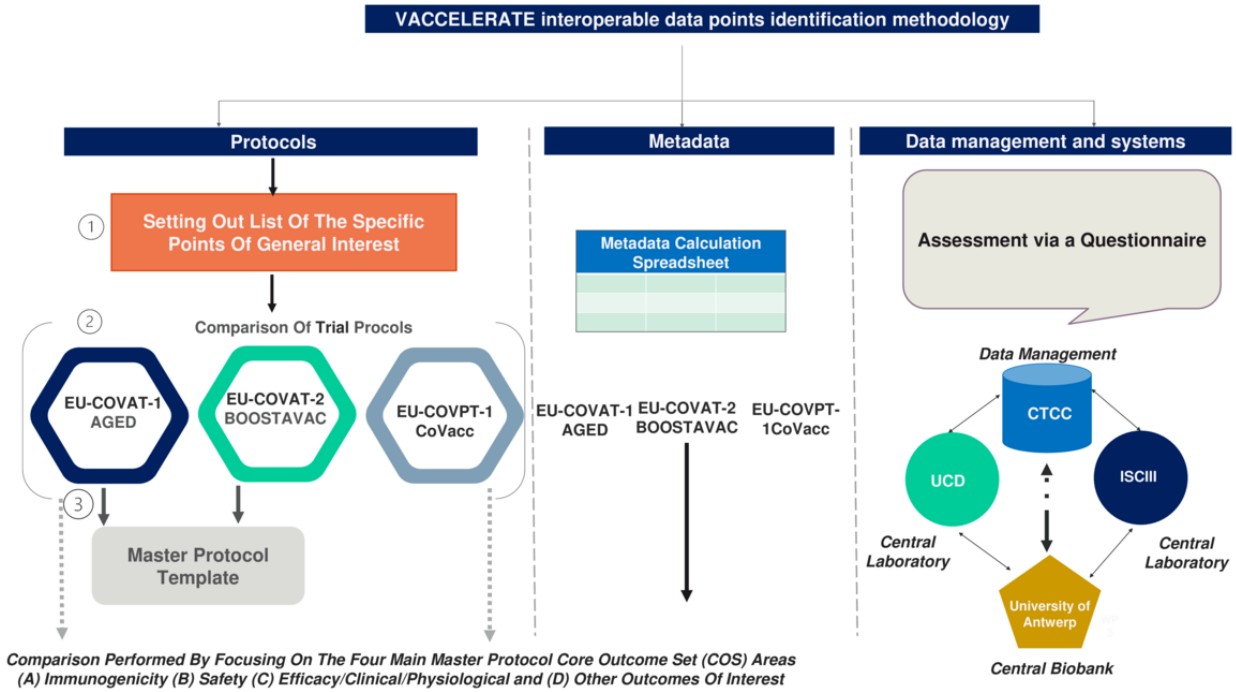
Overview

The degree of commonality and interoperability among data was assessed across 3 levels: clinical trial protocols, metadata, and data systems and management.

Interoperability Among the VACCELERATE Clinical Trial Protocols and Master Protocol Template

The process began with generating a list of the main points and parameters of general interest (eg, type of trial, randomization, primary and secondary aims, and safety) across the 3 specific clinical trial protocols: EU-COVAT-1_AGED, EU-COVAT-2_BOOSTAVAC, and EU-COVPT-1_COVACC [9,10]. The second step involved comparing the 3 trial protocols to identify interoperable data points based on this list of key parameters. In step 3, the outcomes derived from the adult trial protocols were compared against the VACCELERATE adult master protocol (Figure 1). This comparison focused on 4 core areas of the master protocol template's core outcome set (COS): (1) immunogenicity, (2) safety, (3) efficacy/clinical/physiological, and (4) other outcomes of interest. Differences and similarities among the protocols were identified manually.

Figure 1. Methodology for the identification of the interoperable data points. CTCC: Clinical Trials Centre Cologne; UCD: University College Dublin.



Metadata Interoperability of the VACCELERATE Clinical Trials

All data management (DM) processes, including the design of study databases for all 3 VACCELERATE clinical trials, were carried out by the Clinical Trials Centre Cologne (CTCC). The DM team at the CTCC developed the Study Database Specification (DB Spec) using an Excel (Microsoft Corporation) workbook. This workbook included metadata for defining the study database, case report forms (CRFs), edit checks, and a data dictionary. For each CRF study, the workbook contained an individual worksheet specifying database details such as field names, field response types, and formats. Additionally, the detailed metadata for all 3 vaccine trials were systematically developed using internal standards, terminology, and the general approach of Clinical Data Acquisition Standards Harmonization (CDASH) [12] for data collection, such as on electronic CRFs (eCRFs; Table 1). For instance, questions were categorized into relevant Clinical Data Interchange Standards Consortium (CDISC) [13] domains, along with prefixes for adverse events (AEs), concomitant medications, vital signs, protocol deviation, etc, while standard CDISC suffixes were applied to indicate question types.

XSL•FO
RenderX

Table 1. Example of CDASH[a] data items within EU-COVAT-1_AGED.

Caption	Variable	Length/format	Type	Explanation/code list
Sample collected?	LBPERF	N/A[b]	Category	YES=yes, NO=no
Reason for sample not collected	LBREASND	200	Character	N/A
Date of collection	LBDTC	N/A	Date	N/A
Name of Lab	LBNAME	N/A	Combo box	N/A
Test name	LBTEST	30	Label	Laboratory test names: blood urea nitrogen, creatinine, aspartate transaminase, alanine transaminase, total bilirubin, and alkaline phosphatase
Result	LBORRES	99999.99	Float	Laboratory test result
Unit	LBORRESU	N/A	Combo box	Laboratory test unit
Reference range lower limit	LBORNRLO	10	Character	Laboratory test min
Reference range upper limit	LBORNRHI	10	Character	Laboratory test max
Export unit	LBEXUNIT	10	Character	Laboratory test export unit
Clinically significant	LBCLSIG	N/A	Category	YES=yes, NO=no

[a]CDASH: Clinical Data Acquisition Standards Harmonization.

[b]N/A: not applicable.

Although the databases were generated by a single center and coordinated by the same individual, it was valuable to evaluate the degree of standardization, commonality, and data interoperability among the DB Spec of all 3 trials. To achieve this, a manual comparison of the Excel DB Spec from all 3 VACCELERATE clinical trials was conducted (Figure 1). This comparison focused on the main core areas—immunogenicity, safety, efficacy/clinical/physiological—emphasizing the development of the master protocol template.

The other variables were not considered due to differences in demographic details and treatment approaches among the 3 groups (older adults, adult, and pediatric). Metadata items such as data format, data dictionary name, response type, item text, required field indicator, and review groups were compared for consistency and discrepancies. Once identified, the next step was to analyze the rationale behind the observed consistencies and discrepancies among the metadata items.

Interoperability in Data Management and Systems

Interoperability in DM and systems was assessed through a questionnaire (Multimedia Appendix 1) distributed to the central laboratories: the University College Dublin (UCD) Centre for Experimental Pathogen Host Research (CEPHR, Dublin), Instituto de Salud Carlos III (ISCIII, Madrid), and the central biobank (UZA/UAntwerpen Biobank, Antwerp University Hospital). The questionnaire aimed to gather their experiences working with the VACCELERATE DM systems (Figure 1). UZA/UAntwerpen provided an overview of samples received from local sites (shipment manifest) and transferred to the research laboratories (transport manifest) and the clinical trial center. CEPHR and ISCIII, as research laboratories, performed the specified analyses on samples received from the central biobank. After completing the analyses, the research laboratories sent the results to the CTCC.

The questionnaire was designed to maximize accessibility and ease of use for site staff by categorizing the questions into broad areas while allowing flexibility through free-text response options: (1) laboratory procedures and documentation, (2) sample handling and storage data, (3) data transfer, and (4) general laboratory DM. Based on the information gathered through the questionnaire, a descriptive analysis was conducted to examine how each site handled, stored, and transferred data, as well as how their processes evolved within the VACCELERATE network. Furthermore, the analysis evaluated potential factors and new concepts required to harmonize and standardize the VACCELERATE DM systems.

The DM documents—external DM plans, edit check plans, CRF completion requirements, and DB Specs—developed for the clinical trials by the CTCC were reviewed. Guided by the questionnaire, a semistructured interview was conducted with the CTCC data manager.

Ethical Considerations

The 3 VACCELERATE COVID-19 vaccine trials (EU-COVAT-1_AGED, EU-COVAT-2_BOOSTAVAC, and EU-COVPT-1_COVACC) received favorable ethics opinions and approval from the national competent authorities in the participating countries (State Medicines Control Agency, Norwegian Medicines Agency, Spanish Agency of Medicines and Health Products, Health Products Regulatory Authority Ireland, and Paul-Ehrlich-Institut for the EU-COVAT-1 AGED trial; Health Products Regulatory Authority Ireland, Norwegian Medicines Agency, Swedish Medical Products Agency, The Spanish Agency of Medicines and Medical Devices, Federal

XSL•FO
RenderX

Agency for Medicines and Health Products, and Paul-Ehrlich-Institut for the EU-COVAT-2 BOOSTAVAC trial; and Netherlands – Competent Authority, Norwegian Medicines Agency, Swedish Medical Products Agency, Hellenic National Organization for Medicines, and Paul-Ehrlich-Institut for the EU-COVPT-1 COVACC trial). Written informed consent was obtained from all participants before any trial procedures. These trials were conducted in accordance with the International Conference on Harmonization for Good Clinical Practice (ICH-GCP) guidelines and complied with the Declaration of Helsinki at all times. Furthermore, the provisions of the EU General Data Protection Regulation (GDPR) 2016/679 were strictly observed to ensure data protection. All investigational materials and data were pseudonymized in compliance with data protection regulations before undergoing scientific processing.

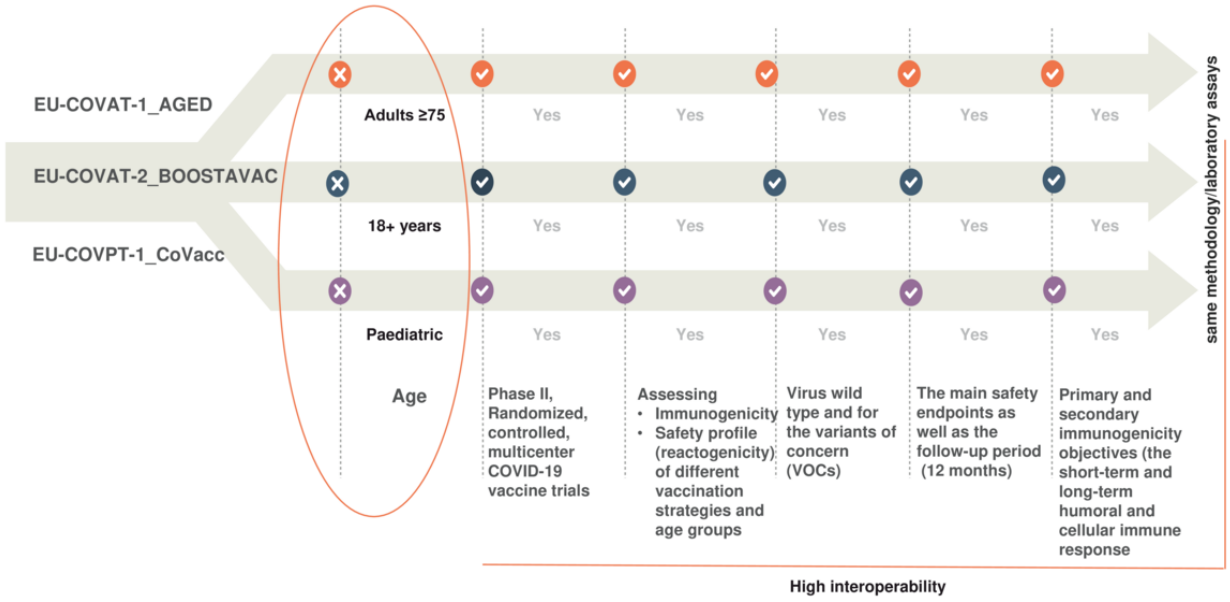
Results

Interoperability Among the Three Clinical Trial Protocols and Master Protocol

Our harmonization and standardization efforts began with a comparison of the 3 clinical trial protocols against the COS of the master protocol. The COS includes all appropriate measurements necessary to ensure standardization, efficiency, and uniformity in the conduct of clinical trials. Four main COS areas were adopted for phase II and III studies: (1) immunogenicity, (2) safety, (3) efficacy/clinical/physiological, and (4) other outcomes of interest.

The harmonization process resulted in the creation of Tables 2-5, which illustrate the interoperability between the master protocol and the 3 clinical trial protocols based on the COS areas. A summary of the outcomes is presented in Figure 2 (see Table S1 in Multimedia Appendix 2). Humoral and cellular responses to COVID-19 vaccines were assessed in a similar manner across all trials, considering both vaccine and host characteristics (Table 2), although minor adjustments to time points were incorporated into the pediatric protocol.

Figure 2. Interoperability between the 3 specific clinical trial protocols (summary).



XSL•FO
RenderX

Table 2. Core area: immunogenicity (core outcome set).

Objective	Outcome	Method of measurement
To evaluate humoral response to vaccination against wild-type SARS-CoV-2 and variants of interest—(1) short term: 7, 14, and 28 days after randomization and (2) long term: 3, 6, 9, and 12 months after randomization	• Binding antibodies titers (IgAa, IgG, and IgM) against SARS-CoV-2 nucleocapsid, receptor-binding domain, spike 1, and spike 2 viral proteins. • SARS-CoV-2 neutralization	• Immunoassay (enzyme-linked immunosorbent assay, electrochemiluminescence immunoassay, or chemiluminescence immunoassay); expressed as BAU/ml (geometric mean titers). • Neutralizing antibody titers to live wild-type SARS-CoV-2 plaque reduction neutralization test (PRNT50) assay, and pseudovirion-expressing S protein from different variants as measured by NT50 or flow cytometry–based microneutralization assay; expressed as IU/ml
To evaluate the cellular immune response to vaccination against wild-type SARS-CoV-2 and variants of interest—(1) short term: 7, 14, and 28 days after randomization); and (2) long term: 3, 6, 9, and 12 months after randomization)	• Th1b and Th2 immune responses	• Flow cytometry after SARS-CoV-2 S protein peptide stimulation of peripheral blood mononuclear cells and intracellular staining, including CD4+c/CD8+ interferon-gamma, interleukin-2, tumor necrosis factor-alpha, interleukin-4, interleukin-5, interleukin-13, and other Th1/Th2 markers.

[a]Ig: immunoglobulin.

[b]Th: helper T cell.

[c]CD: cluster of differentiation.

The early detection of serious AEs (SAEs) can be vital for the protection of the participants and via the interoperability of safety data, an overall better general view of the patient's clinical data could be achieved, resulting in the reduction of any potential risk of harms or adverse impacts and higher clinical safety. The developing safety profile in the trials is in a sufficiently similar motive and includes all the required information about reporting solicited, unsolicited, serious, and medically attended AEs, as shown in Table 3. By contrast, the definitions of the COVID-19 disease (eg, asymptomatic infection, confirmed and reinfection cases, the severity of signs and symptoms) are not reported in the protocols, even though it is referred to as part of the trial dataset outcomes (Table 4). Finally, the profile of immunophenotyping of immune responses (at the cellular level) and genotypic testing of breakthrough infections (vaccine immunogenicity) were also determined in the protocols, enhancing interoperability among them (Table 5). It should be noted that we did not present herein the comparison of pediatric protocol versus pediatric master protocol because the former is currently under review process.

Table 3. Core clinical area: safety data (core outcome set).

Outcome	Method of measurement
Solicited local and systemic AEs[a] for 7 days after each vaccination.	AEs are collected in a diary and will be entered into the electronic case report form (see all potential adverse reactions in Multimedia Appendix 2).
Unsolicited AEs after each vaccination	AEs are collected during visits upon an open question by the investigator up to the end of the trial.
SAEs[b]	SAEs collected throughout the study (from first vaccination until the end of the study)
Medically attended adverse events	Medically attended adverse events from the day of vaccination until the end of the study.

[a]AE: adverse event.

[b]SAE: serious adverse event.

Several parameters were considered to enable and enhance interoperability across the developed COVID-19 vaccine trials and master protocols (Figures 3 and 4). It is well-known that the lack of standardization in data processing exacerbates inhomogeneity in raw data. This often results in errors and significant time delays, reducing the reusability and interoperability of data within protocols. To address this, the various protocol formats were homogenized by manually identifying discrepancies and commonalities among selected parameters (see Tables S2-S13 in Multimedia Appendix 2). The selection of parameters was based on their relevance to the trials. Parameters present in only 1 protocol were excluded, while efforts were made to promote the consistent use of the same parameters across adult trials.

Concealment (blinding) of treatment group allocation is not anticipated for the current trials, while both adult trials support vaccine booster strategies. All clinical trials assess reactogenicity symptoms and the immunogenicity (efficacy) profile of COVID-19 vaccines (following a fourth dose) to inform potential optimized vaccine strategies. The secondary objectives

XSL•FO
RenderX

include evaluating immune response for up to 12 months (see Tables S2-S4 in Multimedia Appendix 2).

The safety aims and the increase in antibody titer were found to be similar across all trials, as were the primary end points in the adult population protocols, due to the nature of the BOOSTAVAC trial (see Table S5 in Multimedia Appendix 2). By contrast, stratification/subpopulation, inclusion, and exclusion criteria among volunteers are directly influenced by the participants' age and other trial-specific factors (eg, vaccine scheme, gender, immune status; see Table S6 in Multimedia Appendix 2). Additionally, patients' insurance and consent forms are addressed in all protocols, and the sample size calculation was reported based on the specifics of each protocol (see Table S7 in Multimedia Appendix 2).

Table 4. Core clinical area: efficacy/clinical/physiological (core outcome set).

Set of data and definition	Explanation
Confirmed COVID-19 disease	
COVID-19 disease	Molecularly confirmed COVID-19 is defined as a positive SARS-CoV-2 viral RNA result using a PCR[a]-based or other molecular diagnostic test or positive antigen test. (See Multimedia Appendix 2 for the definition of confirmed COVID-19 disease.)
Asymptomatic SARS-CoV-2 infection	
Asymptomatic SARS-CoV-2 infection[b]	The same as above but without symptoms typical for/suspicious of COVID-19
Severity of COVID-19 disease	
Asymptomatic SARS-CoV-2 infection or COVID-19 disease (presence and severity of signs and symptoms of COVID-19 disease)	Signs and symptoms as measured by symptoms of infection with COVID-19[c] at first evaluation and at maximum severity: mild, moderate, and severe COVID-19
Severe COVID-19 disease	
COVID-19 disease fulfilling criteria for intensive care unit admittance	Clinical records
All-cause mortality	
All-cause mortality: (1) at day 30 from randomization and (2) time from randomization	Clinical records
Disease (or infection) duration	
Time to 2019-nCoV RT-PCR[d] negativity (days)	Negativity: 2 consecutive negative results (sampling interval of at least 24 hours) of the 2019-nCoV nucleic acids tests of respiratory pathogens
Length (days) of hospital stay	Discharge standards: (1) normal body temperature for more than 3 days; (2) significant recovery from respiratory symptoms; (3) lung imaging showing obvious absorption and recovery of the acute exudative lesion; and (4) negativity of nucleic acids tests performed twice.
Length of intensive care unit stay	N/A[e]
Reinfection	
Confirmed COVID-19 reinfection	Molecularly confirmed COVID-19 is defined as a positive SARS-CoV-2 viral RNA result using a PCR-based or another molecular diagnostic test or positive antigen test. (See Multimedia Appendix 2 for the definition of confirmed COVID-19 disease.)
Time to reinfection	
Long COVID syndrome	WHO definition[b] [14,15]
Multisystem inflammatory syndrome in children	MIS-C[f] WHO[g] definition

[a]PCR: polymerase chain reaction.

[b]See [15].

[c]Per case definition for moderate to severe/critical COVID-19.

[d]RT-PCR: reverse transcription polymerase chain reaction.

[e]N/A: not applicable.

[f]MIS-C: multisystem inflammatory syndrome in children associated with COVID-19.

[g]WHO: World Health Organization.

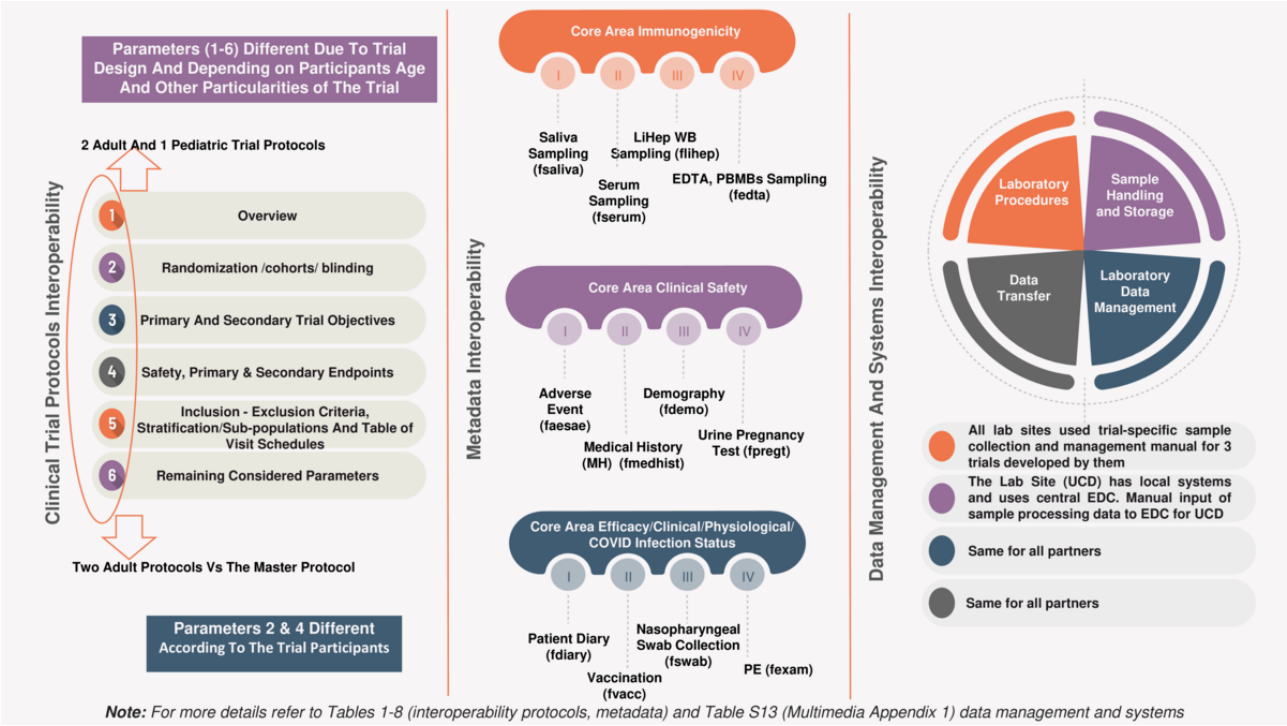
XSL•FO
RenderX

Table 5. Other outcomes of interest.[a]

Set of data	Outcome and methods
Immunophenotyping of immune responses to vaccination	Detailed immunophenotyping of immune responses, including metabolomics, proteomics, and transcriptomics
Genotyping of breakthrough infections	Whole genome sequencing of isolated SARS-CoV-2 viral strains detected in breakthrough infections

[a]Per the CoVacc trial protocol, Participants will be informed that leftover blood samples, remaining after all study-related testing is completed, may be stored indefinitely for potential future research purposes (eg, exploratory immunology). This may include genotypic testing of genetic polymorphisms relevant to vaccine immunogenicity. Participants will have the option to decide whether they permit the future use of any leftover samples. With the participants' informed consent, any remaining cells and plasma will be frozen indefinitely for future analyses related to COVID-19 and other coronavirus-related diseases or vaccine-related responses. If a participant chooses not to allow this, all leftover samples belonging to that participant will be discarded at the end of the trial.

Figure 3. Noncommonality parameters identified in the VACCELERATE projects (protocols, metadata and data management, and systems). EDC: Electronic Data Capture; EDTA: ethylenediaminetetraacetic acid; LiHep: lithium heparin; PBMC: peripheral blood mononuclear cell; PE: physical examination; UCD: University College Dublin; WB: whole blood.



Note: *For more details refer to Tables 1-8 (interoperability protocols, metadata) and Table S13 (Multimedia Appendix 1) data management and systems*

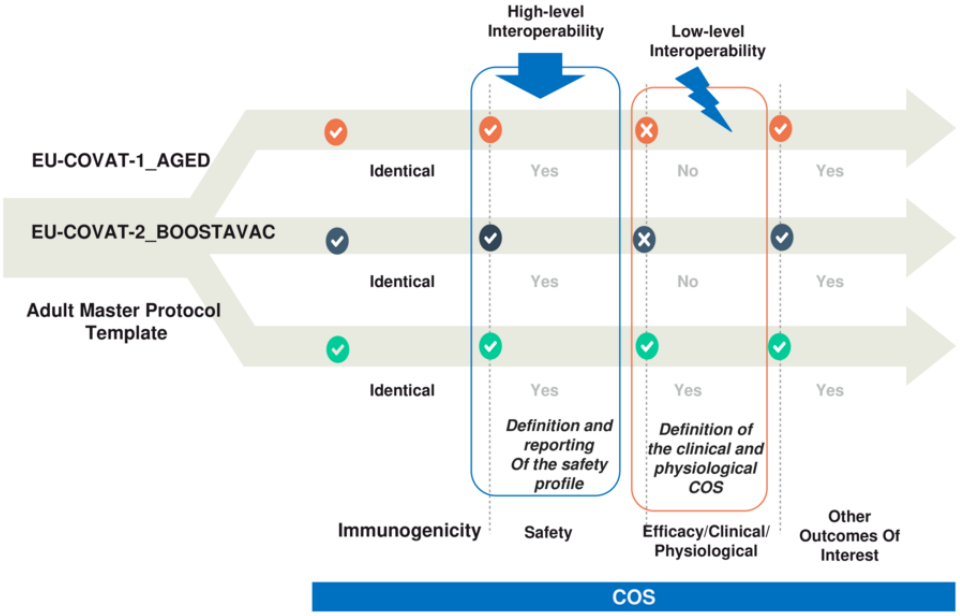
We also conducted a comparison of the 2 adult trials with the master protocol (see Tables S8-S13 in Multimedia Appendix 2). The primary aim of the adult trials is to evaluate the immunogenicity and reactogenicity (safety) of vaccine booster strategies and homologous mRNA vaccination for COVID-19 at different time intervals (see Tables S8 and S9 in Multimedia Appendix 2).

Both the adult and master protocols include the relevant subprotocols, cohorts, and descriptions of the randomization process, while blinding is not anticipated in the adult trials. All protocols support phase II trials and share similar primary objectives. The primary and secondary objectives/end points (including exploratory ones) constitute a nearly identical core dataset. The secondary trial objectives for immunogenicity and reactogenicity focus on the immune response and associated signs and symptoms over up to 12 months (see Tables S9 and S10 in Multimedia Appendix 2).

The reporting periods for unsolicited and solicited AEs, as well as the rates of SAEs, are identical across the adult and master protocols. However, discrepancies in inclusion and exclusion criteria are directly influenced by the trial participants (see Tables S11 and S12 in Multimedia Appendix 2). The treatment duration and follow-up period for the studies are identical in both the adult trials and the master protocol, extending up to 12 months. All clinical trials are conducted in accordance with the ICH-GCP, including the use of appropriate consent forms and patient insurance, based on the allocated treatment group (see Table S13 in Multimedia Appendix 2).

XSL•FO
RenderX

Figure 4. COS interoperability between the vaccine trial and master protocols.



Metadata Interoperability

The points of consistency and discrepancies across the main core areas (eg, immunogenicity, safety, efficacy, clinical, and physiological aspects) among the metadata items of the 3 VACCELERATE clinical trials are presented in Tables 6-8 and Figure 5. The noncommonalities identified within the CRFs were attributed to differences in the 3 populations (aged 75+, adult, and pediatric), variations in protocol design, and differing vaccination patterns (Figures 3 and 5). Additionally, differences in the coding and labeling of variables, as well as in the item groups, were identified. These discrepancies required clarification to enhance interoperability.

XSL•FO
RenderX

Table 6. Points of consistency and discrepancies among the metadata items: core area IMMUNOGENICITY.

Case report form	EU-COVAT-1_AGED	EU-COVAT-2_BOOST-AVAC	EU-COVPT-1_CoVacc	Commonality and noncommonality
Saliva sampling (fsaliva)	Not detected	Collection status with time point and aliquot label before vaccination, on immune response evaluation, and on follow-up	Collection status with time point and aliquot label before vaccination and on follow-up	• Identical for COVAT-2 and COVPT-1 • Missing on COVAT-1
Serum sampling (fserum)	Collection status with time point and aliquot label before vaccination, on immune response evaluation, and on follow-up	Collection status with time point and aliquot label before vaccination, on immune response evaluation, and on follow-up	Not detected	• Identical for COVAT-1 (form name differs fserumn) and COVAT-2 • Missing on COVPT-1
LiHep[a] WB[b] sampling (flihep)	Collection status with time point and aliquot label before vaccination and on immune response evaluation	Collection status with time point and aliquot label before vaccination, on immune response evaluation, and on follow-up	Collection status with time point and aliquot label before vaccination and on follow-up	• The number and time points of collections differ in all trials • There are minor differences in variable names and labeling • COVPT-1 has an extra LiHep tube
EDTA[c] and PBMCs[d] sampling (fedta)	EDTA collection status with time point and aliquot label before vaccination, on immune response evaluation, and on follow-up. PBMC only before vaccination	EDTA and PBMC collection status with time point and aliquot label before vaccination, on immune response evaluation, and on follow-up	EDTA collection status with time point and aliquot label before vaccination and on follow-up. PBMC for selected sites only on follow-up	• The number and time points of collections differ in all trials • There are differences in variable names and labeling • COVPT-1 has an extra item group and more aliquots

[a]LiHep: lithium heparin.

[b]WB: whole blood.

[c]EDTA: ethylenediaminetetraacetic acid.

[d]PBMC: peripheral blood mononuclear cell.

XSL•FO
RenderX

Table 7. Points of consistency and discrepancies among the metadata items: core area CLINICAL SAFETY.

Case report form	EU-COVAT-1_AGED	EU-COVAT-2_BOOST-AVAC	EU-COVPT-1_CoVacc	Commonality and noncommonality
Adverse event (faesae)	Documentation forms available throughout the enclosure complemented by an optional unscheduled visit	Documentation forms available throughout the enclosure complemented by an optional unscheduled visit	Documentation forms available throughout the enclosure complemented by an optional unscheduled visit	• Identical for COVAT-1 and COVAT-2 • COVPT-1 has an extra item group • MedDRAa coding provided on all three trials
MH[b] (fmedhist)	MH documented before vaccination	MH documented before vaccination	MH documented before vaccination	• Time points identical within all trials • Major differences in variable names and labeling • COVAT-1 asks for prior SARS-CoV-2 infection • MedDRA coding provided on all 3 trials
Concomitant medication (fcomed)	Documentation forms available throughout the enclosure	Documentation forms available throughout the enclosure	Documentation forms available throughout the enclosure	• Identical plus ATCc coding was provided on all 3 trials
PD[d] (fpd)	PD documented on completion	PD documented on completion	PD documented on completion	• Identical
Inclusion/exclusion (finex)	Inclusion/exclusion documented before enclosure	Inclusion/exclusion documented before enclosure	Inclusion/exclusion documented before enclosure	• Identical
Demography (fdemo)	Demography documented before vaccination	Demography documented before vaccination	Demography documented before vaccination	• Time points identical within all trials • Differences in variable names and labeling • COVAT-2 asks for race • COVAT-1 and COVAT-2 for prior vaccination • For COVPT-1, one inclusion criterion is not to be vaccinated before
Urine pregnancy test (fpregt)	Not detected	Collection status documented before vaccination and on an unscheduled visit	Not detected	• N/Ae

[a]MedDRA: Medical Dictionary for Regulatory Activities.

[b]MH: medical history.

[c]ATC: Anatomical Therapeutic Chemical.

[d]PD: protocol deviation.

[e]N/A: not applicable.

XSL•FO
RenderX

Table 8. Points of consistency and discrepancies among the metadata items: core area EFFICACY/CLINICAL/PHYSIOLOGICAL/COVID INFECTION STATUS.

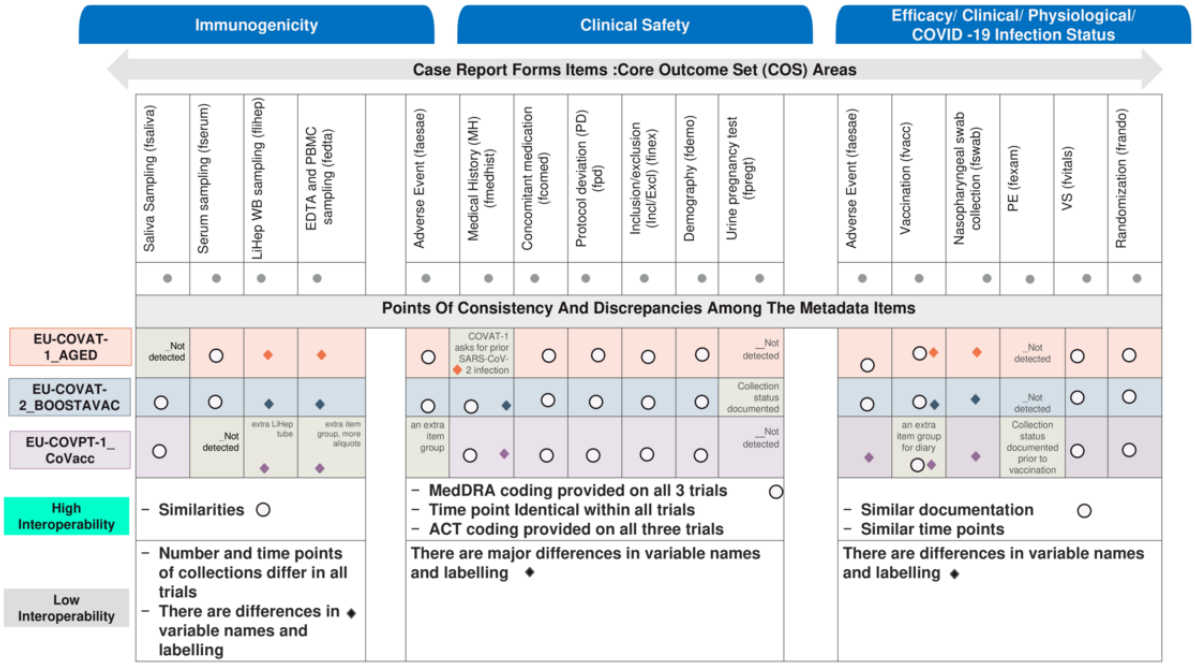
Case report form	EU-COVAT-1_AGED	EU-COVAT-2_BOOST-AVAC	EU-COVPT-1_CoVacc	Commonality and noncommonality
Patient diary (fdiary)	Diary collected on immune response evaluation	Diary collected on immune response evaluation	Diary administration on the second vaccination and first follow-up	• Similar for COVAT-1 and COVAT-2 • Difference to COVPT-1
Vaccination (fvacc)	Vaccination documented on baseline visit	Vaccination documented on time points based on the trial arm	Vaccination documented on time points based on the trial arm	• Similar documentation • There are differences in variable names and labeling • COVPT-1 has an extra item group for the diary.
Nasopharyngeal swab collection (fswab)	Not detected	Not detected	Collection status documented before vaccination	• N/A[a]
PE[b] (fexam)	PE documented on screening, baseline, and immune response evaluation (in case of severe adverse event)	PE documented on screening, baseline, follow-up, and immune response evaluation	PE documented on screening, baseline, and follow-up	• Similar documentation • There are differences in variable names and labeling
VS[c] (fvitals)	VS documented on screening, baseline, immune response evaluation, and in case of unscheduled visit	VS documented on baseline, follow-up, and in case of unscheduled visit	VS documented on screening and on any pre- and postvaccination visits	• Similar time points • Identical documentation
Randomization (frando)	Randomization documented on enrollment	Randomization documented on enrollment	Randomization documented on enrollment	• Identical

[a]N/A: not applicable.

[b]PE: physical examination.

[c]VS: vital sign

Figure 5. Metadata interoperability based on COS. EDTA: ethylenediaminetetraacetic acid; LiHep: lithium heparin; MedDRA: Medical Dictionary for Regulatory Activities; PBMC: peripheral blood mononuclear cell; PD: protocol deviation; PE: physical examination; VS: vital sign; WB: whole blood.



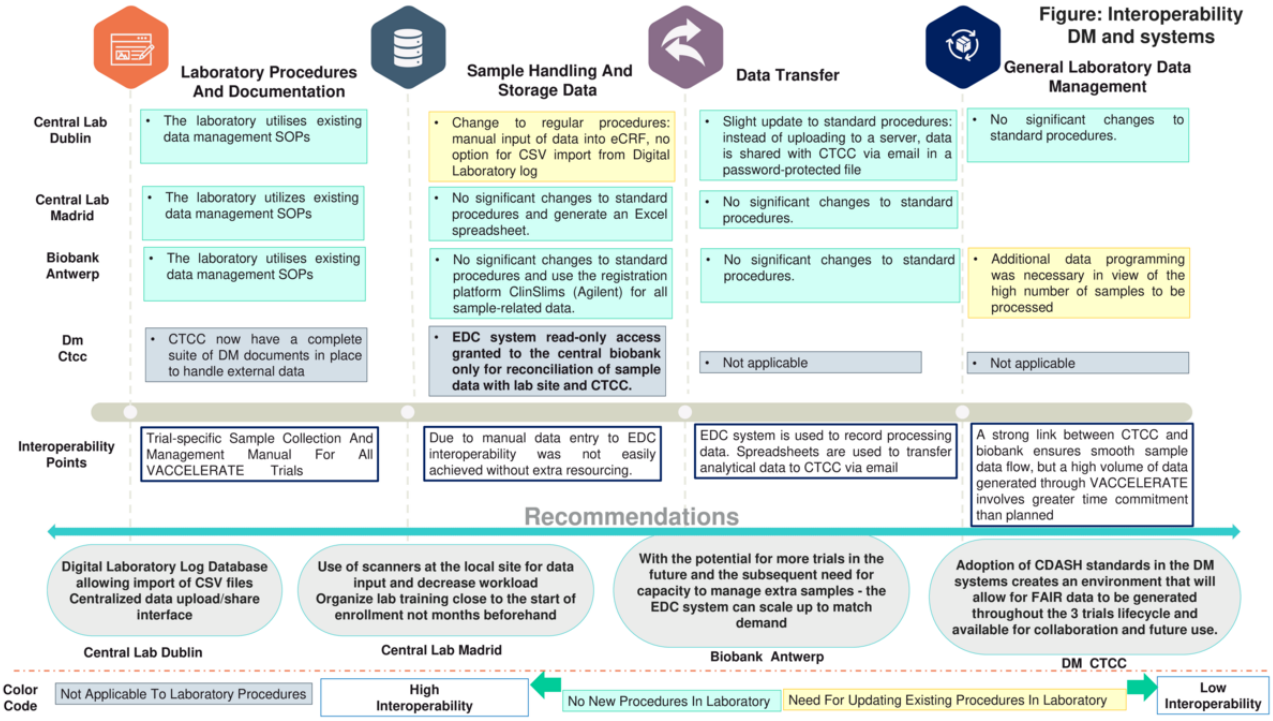
XSL•FO
RenderX

Interoperability in Data Management and Systems

VACCELERATE received a significant boost through the selection of the CTCC as the sole DM provider, with system database development coordinated by a single individual. This eliminated the need for coordination across multiple trial units. For the CTCC, the standardized format adopted within the VACCELERATE project utilized a data system featuring an installation of the Anju [16] (formerly OmniComm) TrialMaster clinical database management system, accompanied by metadata.

Data transfer using tried-and-tested methods common to all sites (spreadsheet format) enabled a quick and relatively secure exchange, which proved highly effective. This process was further facilitated by the implementation of the TrialMaster system, which generated templates that could be adapted for use with spreadsheets. The responses received from the laboratories and CTCC are shown in Figures 3 and 6, while the questionnaire results are presented in Table S14 in Multimedia Appendix 2.

Figure 6. Interoperability between the data management and systems. CDASH: Clinical Data Acquisition Standards Harmonization; CTCC: Clinical Trials Centre Cologne; DM: data management; eCRF: electronic case report form; EDC: Electronic Data Capture; FAIR: Findable, Accessible, Interoperable, and Reusable; SOP: standard operating procedure.



Discussion

Principal Findings

To the best of our knowledge, this is the first report to assess the degree of data commonality and interoperability between vaccine clinical trial protocols, the master protocol template, metadata, and data systems and management. In this study, we considered multiple parameters for the first time to enhance and improve interoperability across the developed COVID-19 vaccine clinical trial and master protocols, based on the selected COS areas: (1) immunogenicity, (2) safety, (3) efficacy/clinical/physiological outcomes, and (4) other outcomes of interest. This is significant because the lack of standardization in raw data processing is a well-known issue that exacerbates data inhomogeneity. This often results in errors and significant time delays, reducing the reusability and interoperability of data within protocols. To address this, the various protocol formats were homogenized by manually identifying discrepancies and commonalities among the selected parameters.

The database systems prepared by the CTCC already demonstrate substantial use of CDASH, a key enabler for the implementation of other CDISC standards. CDASH plays a crucial role in supporting the Study Data Tabulation Model (SDTM) [17]. Transforming study data to SDTM could also prove beneficial in the context of data sharing, especially as data interoperability becomes increasingly important. The adoption of CDASH standards [18] within the VACCELERATE DM systems establishes an environment conducive to generating FAIR data throughout the life cycle of the 3 trials. This approach ensures that the data will be available for collaboration and future use.

Pooling the metadata from the VACCELERATE studies would create a valuable metadata resource, independent of the underlying data. This resource could potentially be made accessible (eg, via the VACCELERATE official website and the ECRIN data-sharing repository for COVID-19 trials, EOSC-Life) [19], offering a unique opportunity for other sponsors to design related studies, particularly those utilizing the VACCELERATE infrastructure. The VACCELERATE metadata, as a shared resource, could play a pivotal role in standardizing data items and the controlled terminologies used within categorized questions, thus contributing to greater harmonization and interoperability in future research.

XSL•FO
RenderX

Education and training are critical for the successful implementation of FAIR DM in clinical data. Therefore, additional CDISC training for DM staff could be beneficial, both within VACCELERATE and more broadly, to support the adoption of data standards. Metadata harmonization should be completed before database development.

Although the DM staff at the CTCC are highly experienced and have already implemented international standards, there is a lack of planning for long-term data storage and reuse. This occurred because it was not anticipated during the database setup phase and due to the lack of a long-term data sharing budget, either linked to VACCELERATE itself or allocated to a data-sharing repository. Our report suggests that metadata harmonization planning should begin before database development and be supported by requirements (eg, CDASH) and oversight throughout the entire database setup phase, as well as any subsequent amendments. All subcontractors should be informed and included in this planning process. Furthermore, generating metadata and SDTM data for secondary use can be done under less time pressure compared with other aspects of standards implementation, such as the initial development of eCRFs. Conversely, while the final application of both is likely to occur at the end of the study, this does not mean the work must be confined to that time frame. Transformations can be planned and tested at any stage, using dummy data if necessary, as can the generation of metadata.

VACCELERATE highlights some of the challenges in making data standards a practical reality. At the same time, it provides opportunities to address these challenges, developing methods that can help embed data standards within noncommercial clinical research.

VACCELERATE received a substantial boost from the selection of the CTCC as the sole DM provider, with system database development coordinated by a single individual. This approach eliminated the need for coordination among different trial units, resulting in a high degree of uniformity within the system. The DM systems used in VACCELERATE are relatively new and have the potential to perform well with the limited number of sites currently using them. To effectively test these DM systems, it is necessary to have multiple sites utilizing them, with additional trials planned for later stages of the rollout. While the central Electronic Data Capture (EDC) system (TrialMaster) was used to manage sample processing data, there were concerns from the laboratory sites and the central biobank regarding the time required to enter sample data, resolve errors, and reconcile site datasets with the EDC. Transferring data using tried-and-tested methods common to all sites (spreadsheet format) enabled a harmonized, rapid, and relatively secure exchange. Before a scanning system was adopted, allowing sites to upload processing data directly into the EDC could significantly reduce the time constraints associated with manual data entry.

As only 3 clinical studies were funded under the VACCELERATE project, these results were not applied to any newly registered studies. However, as the objective of the VACCELERATE project has now been extended to other vaccine-preventable infectious diseases with pandemic potential, there will be a broader opportunity in the near future to implement the results presented here. Nevertheless, these trials provide valuable insights and a scalable framework for future vaccine studies, especially in the context of epidemics and pandemic preparedness. The methodology and protocols of these trials address critical questions regarding vaccine immunogenicity, reactogenicity, and optimal dosing strategies across diverse populations, including older adults (≥75 years), the general adult population, and pediatric patients. By using adaptive, multinational protocols, these trials simulate the real-world conditions of pandemic response, where speed, adaptability, and inclusivity are critical.

The methodologies from these trials are highly generalizable and provide a robust blueprint for future vaccine clinical studies within research networks. The inclusion of underrepresented populations, such as older adults and children, ensures that future vaccine trials will generate comprehensive, inclusive data applicable to all demographics. Additionally, the adaptive design of the protocols used in these studies allows for future modifications in response to emerging data and infectious diseases—a critical feature for addressing the dynamic nature of pandemics and evolving infectious threats.

Beyond the outcomes of individual trials, these studies contribute to the establishment and strengthening of international vaccine research networks. The collaborative, multicentric nature of the VACCELERATE network demonstrates the feasibility of harmonized vaccine research across borders, promoting shared protocols, centralized data analysis, and the dissemination of findings. This approach not only accelerates the vaccine development process but also strengthens global preparedness by creating investigator-initiated clinical research infrastructure and expertise that can be rapidly mobilized for emerging epidemics.

Moreover, the lessons learned from these trials can inform the design and implementation of studies for vaccines targeting other infectious diseases with pandemic potential, such as influenza or novel zoonotic pathogens. The emphasis on immunogenicity, dosing strategies, and booster efficacy can be adapted to various pathogens, ensuring that the evidence generated remains both relevant and actionable.

In summary, the VACCELERATE trials serve as a cornerstone for advancing and standardizing vaccine research methodologies. They underscore the importance of inclusivity, adaptability, and international collaboration, setting a precedent for future studies aimed at mitigating the impact of pandemics and safeguarding global public health.

Limitations

This paper presents a novel approach to evaluating the degree of data commonality and interoperability between vaccine clinical trial protocols, the study master protocol template, metadata, and data systems and management. It did not benefit from preexisting methodologies, and its scope may therefore be limited by the specific cases examined. Nonetheless, it is anticipated to provide valuable insights that contribute to the improvement of clinical research data sharing and reuse.

XSL•FO
RenderX

Conclusions

This study demonstrates that using master protocols can significantly enhance trial operational efficiency and data interoperability when similar infrastructure and DM procedures are consistently adopted across multiple trials. To achieve data interoperability while preserving meaning in interpretation and analysis, shared data should be structured, described, formatted, and stored using widely recognized data and metadata standards.

Acknowledgments

The VACCELERATE project has received funding from the European Union's Horizon 2020 Research and Innovation Programme (grant 101037867). For more information, please refer to the official website of the VACCELERATE network [4]. The services of the "BioBank Antwerp," Antwerp, Belgium (ID: BE 71030031000, Biobank Antwerp [BB190007], BBMR-ERIC, Belgian [BIORESOURCE]) are used for the storage of generated samples and aliquots. Special thanks to ECRIN's Communication Officer, Alexandra KUSTER, for proofreading the article.

Generative artificial intelligence is not used by the authors to generate any content (text, tables, and figures) for this manuscript.

Data Availability

The datasets used and analyzed during this study are available from the corresponding author upon reasonable request.

Conflicts of Interest

OAC reports grants or contracts from iMi, iHi, DFG, BMBF, Cidara, DZIF, EU-DG RTD, F2G, Gilead, MedPace, MSD, Mundipharma, Octapharma, Pfizer, Scynexis; consulting fees from Abbvie, AiCuris, Basilea, Biocon, Boston Strategic Partners, Cidara, Elion Therapeutics, Gilead, GSK, IQVIA, Janssen, Matinas, MedPace, Menarini, Melinta, Molecular Partners, MSG-ERC, Mundipharma, Noxxon, Octapharma, Pardes, Partner Therapeutics, Pfizer, PSI, Scynexis, Seres, Seqirus, Shionogi, The Prime Meridian Group; speaker and lecture honoraria from Abbott, Abbvie, Akademie für Infektionsmedizin, Al-Jazeera Pharmaceuticals/Hikma, amedes, AstraZeneca, Deutscher Ärzteverlag, Gilead, GSK, Grupo Biotoscana/United Medical/Knight, Ipsen Pharma, Medscape/WebMD, MedUpdate, MSD, Moderna, Mundipharma, Noscendo, Paul-Martini-Stiftung, Pfizer, Sandoz, Seqirus, Shionogi, streamedup!, Touch Independent, Vitis; payment for expert testimony Cidara; and participation on a DRC, DSMB, DMC, Advisory Board for AstraZeneca, Cidara, IQVIA, Janssen, MedPace, Melinta, PSI, Pulmocide, Vedanta Biosciences. All other authors report no conflicting interests.

Multimedia Appendix 1
Additional analysis.
[DOCX File , 105 KB - medinform_v13i1e65590_app1.docx]

Multimedia Appendix 2
VACCELERATE central laboratories: Data Management Questionnaire.
[DOCX File , 51 KB - medinform_v13i1e65590_app2.docx]

References

1. Interoperability in healthcare. Healthcare Information and Management Systems Society. URL: https://www.himss.org/resources/interoperability-healthcare#Part1 [accessed 2023-06-05]
2. Wilkinson MD, Dumontier M, Aalbersberg IJJ, Appleton G, Axton M, Baak A, et al. The FAIR Guiding Principles for scientific data management and stewardship. Sci Data 2016 Mar 15;3:160018. [doi: 10.1038/sdata.2016.18] [Medline: 26978244]
3. Ohmann C, Banzi R, Canham S, Battaglia S, Matei M, Ariyo C, et al. Sharing and reuse of individual participant data from clinical trials: principles and recommendations. BMJ Open 2017 Dec 14;7(12):e018647 [FREE Full text] [doi: 10.1136/bmjopen-2017-018647] [Medline: 29247106]
4. VACCELERATE - European Corona Vaccine Trial Accelerator platform. VACCELERATE. URL: https://vaccelerate.eu/ [accessed 2023-10-26]
5. Salmanton-García J, Stewart FA, Heringer S, Koniordou M, Álvarez-Barco E, Argyropoulos CD, et al. VACCELERATE volunteer registry: a European study participant database to facilitate clinical trial enrolment. Vaccine 2022 Jul 29;40(31):4090-4097 [FREE Full text] [doi: 10.1016/j.vaccine.2022.05.022] [Medline: 35659449]
6. Salmanton-García J, Wipfler P, Valle-Simón P, Merakou C, Kopsidas I, Bethe U, et al. VACCELERATE Site Network: Real-time definition of clinical study capacity in Europe. Vaccine 2023 Jun;41(26):3915-3922. [doi: 10.1016/j.vaccine.2023.05.006]

XSL•FO
RenderX

7. Argyropoulos CD, Leckler J, Salmanton-García J, Constantinou M, Alexandrou A, Themistocleous S, et al. Enhancing public health communication regarding vaccine trials: design and development of the Pan-European VACCELERATE toolkit. JMIR Public Health Surveill 2023 Apr 03;9:e44491. [doi: 10.2196/44491] [Medline: 36878478]
8. Poulimeneas D, Koniordou M, Kousi D, Merakou C, Kopsidas I, Tsopela GC, VACCELERATE Consortium. The challenges of vaccine trial participation among underserved and hard-to-reach communities: an internal expert consultation of the VACCELERATE consortium. Vaccines (Basel) 2023 Nov 29;11(12):1784 [FREE Full text] [doi: 10.3390/vaccines11121784] [Medline: 38140188]
9. Clinical studies. VACCELERATE. URL: https://vaccelerate.eu/clinical-studies-2/ [accessed 2023-10-26]
10. Neuhann JM, Stemler J, Carcas A, Frías-Iniesta J, Bethe U, Heringer S, et al. A multinational, phase 2, randomised, adaptive protocol to evaluate immunogenicity and reactogenicity of different COVID-19 vaccines in adults ≥75 already vaccinated against SARS-CoV-2 (EU-COVAT-1-AGED): a trial conducted within the VACCELERATE network. Trials 2022 Oct 08;23(1):865. [doi: 10.1186/s13063-022-06791-y] [Medline: 36209129]
11. Salmanton-García J, Wipfler P, Leckler J, Nauclér P, Mallon PW, Bruijning-Verhagen PC, VACCELERATE Consortium. Predicting the next pandemic: VACCELERATE ranking of the WorldHealth Organization's Blueprint forAction toPreventEpidemics. Travel Med Infect Dis 2024 Jan;57:102676 [FREE Full text] [doi: 10.1016/j.tmaid.2023.102676] [Medline: 38061408]
12. Clinical Data Interchange Standards Consortium - Clinical Data Acquisition Standards Harmonisation (CDISC CDASH). Clinical Data Interchange Standards Consortium. 2023. URL: https://www.cdisc.org/standards/foundational/cdash [accessed 2023-10-26]
13. Clear data. Clear impact. Clinical Data Interchange Standards Consortium (CDISC). URL: https://www.cdisc.org/ [accessed 2023-10-26]
14. Soriano JB, Murthy S, Marshall JC, Relan P, Diaz JV, WHO Clinical Case Definition Working Group on Post-COVID-19 Condition. A clinical case definition of post-COVID-19 condition by a Delphi consensus. Lancet Infect Dis 2022 Apr;22(4):e102-e107 [FREE Full text] [doi: 10.1016/S1473-3099(21)00703-9] [Medline: 34951953]
15. World Health Organization (WHO). A clinical case definition of post COVID-19 condition by a Delphi consensus. WHO. 2021 Oct 6. URL: https://www.who.int/publications/i/item/WHO-2019-nCoV-Post_COVID-19_condition-Clinical_case_definition-2021.1 [accessed 2024-10-28]
16. Anju Software. 2022. URL: https://www.anjusoftware.com/ [accessed 2023-10-26]
17. Clinical Data Interchange Standards Consortium - Study Data Tabulation Model (CDISC SDTM). Clinical Data Interchange Standards Consortium (CDISC). 2021. URL: https://www.cdisc.org/standards/foundational/sdtm [accessed 2023-10-26]
18. Standards. Clinical Data Interchange Standards Consortium. URL: https://www.cdisc.org/standards [accessed 2023-10-26]
19. European Clinical Research Infrastructure Network. URL: https://crdsr.ecrin.org/ [accessed 2024-10-26]

Abbreviations

AE: adverse event
CDASH: Clinical Data Acquisition Standards Harmonization
CDISC: Clinical Data Interchange Standards Consortium
CEPHR: Centre for Experimental Pathogen Host Research
COS: core outcome set
CRF: case report form
CTCC: Clinical Trials Centre Cologne
DB spec: Study Database Specification
DM: data management
eCRF: electronic case report form
EDC: Electronic Data Capture
FAIR: Findable, Accessible, Interoperable, and Reusable
GDPR: General Data Protection Regulation
ICH-GCP: International Conference on Harmonization for Good Clinical Practice
ISCIII: Instituto de Salud Carlos III
mRNA: messenger RNA
SAE: serious adverse event
SDTM: Study Data Tabulation Model
UCD: University College Dublin

XSL•FO
RenderX

Edited by C Lovis; submitted 21.08.24; peer-reviewed by T Milotic, M Mantri, S Sung; comments to author 06.10.24; revised version received 29.10.24; accepted 23.01.25; published 07.03.25.

Please cite as:
Malik S, Dorothea ZP, Argyropoulos CD, Themistocleous S, Macken AJ, Valdenmaiier O, Scheckenbach F, Bardach E, Pfeiffer A, Loens K, Ochando JC, Cornely OA, Demotes-Mainard J, Contrino S, Felder G
Data Interoperability in COVID-19 Vaccine Trials: Methodological Approach in the VACCELERATE Project
JMIR Med Inform 2025;13:e65590
URL: https://medinform.jmir.org/2025/1/e65590
doi:10.2196/65590
PMID:

©Salma Malik, Zoi Pana Dorothea, Christos D Argyropoulos, Sophia Themistocleous, Alan J Macken, Olena Valdenmaiier, Frank Scheckenbach, Elena Bardach, Andrea Pfeiffer, Katherine Loens, Jordi Cano Ochando, Oliver A Cornely, Jacques Demotes-Mainard, Sergio Contrino, Gerd Felder. Originally published in JMIR Medical Informatics (https://medinform.jmir.org), 07.03.2025. This is an open-access article distributed under the terms of the Creative Commons Attribution License (https://creativecommons.org/licenses/by/4.0/), which permits unrestricted use, distribution, and reproduction in any medium, provided the original work, first published in JMIR Medical Informatics, is properly cited. The complete bibliographic information, a link to the original publication on https://medinform.jmir.org/, as well as this copyright and license information must be included.

XSL•FO
RenderX

Original Paper

Toward a Domain-Overarching Metadata Schema for Making Health Research Studies FAIR (Findable, Accessible, Interoperable, and Reusable): Development of the NFDI4Health Metadata Schema

Haitham Abaza[1], PhD; Aliaksandra Shutsko[2], MLIS; Sophie A I Klopfenstein[3], MD; Carina N Vorisek[3], MD, PhD; Carsten Oliver Schmidt[4], Prof Dr; Claudia Brünings-Kuppe[5], Dipl Dok (FH); Vera Clemens[2], MSc; Johannes Darms[2], MSc; Sabine Hanß[6], Dipl Inf; Timm Intemann[5], Dr rer nat; Franziska Jannasch[7], PhD; Elisa Kasbohm[4], MSc; Birte Lindstädt[2], MLIS; Matthias Löbe[8], Dipl Inf; Katharina Nimptsch[9], DrScHum; Ute Nöthlings[10], Prof Dr; Marisabel Gonzalez Ocanto[2], MA; Tracy Bonsu Osei[9], MPhil; Ines Perrar[10], Dr troph; Manuela Peters[5], PhD; Tobias Pischon[9], Prof Dr; Ulrich Sax[6], Prof Dr; Matthias B Schulze[7], DrPH; Florian Schwarz[7], PhD; Carolina Schwedhelm[9], DrPH; Sylvia Thun[3], Prof Dr; Dagmar Waltemath[4], Prof Dr; Atinkut A Zeleke[4], PhD; Wolfgang Müller[1], Priv Doz Dr; Martin Golebiewski[1], MSc

[1]Scientific Databases and Visualization, Heidelberg Institute for Theoretical Studies (HITS), Heidelberg, Germany

[2]Information Centre for Life Sciences, German National Library of Medicine (ZB MED), Cologne, Germany

[3]Core Facility Digital Medicine and Interoperability, Universitätsmedizin Berlin, Berlin Institute of Health at Charité, Berlin, Germany

[4]Institute for Community Medicine, University Medicine Greifswald, Greifswald, Germany

[5]Department of Biometry and Data Management, Leibniz Institute for Prevention Research and Epidemiology - BIPS, Bremen, Germany

[6]Department of Medical Informatics, University Medical Center Göttingen, Georg-August-University, Göttingen, Germany

[7]Department of Molecular Epidemiology, German Institute of Human Nutrition Potsdam-Rehbruecke, Nuthetal, Germany

[8]Institute for Medical Informatics, Statistics and Epidemiology, University Leipzig, Leipzig, Germany

[9]Molecular Epidemiology Research Group, Max-Delbrück-Center for Molecular Medicine in the Helmholtz Association (MDC), Berlin, Germany

[10]Department of Nutrition and Food Science, University of Bonn, Bonn, Germany

Corresponding Author:
Haitham Abaza, PhD
Scientific Databases and Visualization
Heidelberg Institute for Theoretical Studies (HITS)
Schloss-Wolfsbrunnenweg 35
Heidelberg, 69118
Germany
Phone: 49 6221533231
Email: haithamabaza@gmail.com

Related Article:

This is a corrected version. See correction statement: https://medinform.jmir.org/2025/1/e78151

Abstract

Background: Despite wide acceptance in medical research, implementation of the FAIR (findability, accessibility, interoperability, and reusability) principles in certain health domains and interoperability across data sources remain a challenge. While clinical trial registries collect metadata about clinical studies, numerous epidemiological and public health studies remain unregistered or lack detailed information about relevant study documents. Making valuable data from these studies available to the research community could improve our understanding of various diseases and their risk factors. The National Research Data Infrastructure for Personal Health Data (NFDI4Health) seeks to optimize data sharing among the clinical, epidemiological, and public health research communities while preserving privacy and ethical regulations.

XSL•FO
RenderX

Objective: We aimed to develop a tailored metadata schema (MDS) to support the standardized publication of health studies' metadata in NFDI4Health services and beyond. This study describes the development, structure, and implementation of this MDS designed to improve the FAIRness of metadata from clinical, epidemiological, and public health research while maintaining compatibility with metadata models of other resources to ease interoperability.

Methods: Based on the models of DataCite, ClinicalTrials.gov, and other data models and international standards, the first MDS version was developed by the NFDI4Health Task Force COVID-19. It was later extended in a modular fashion, combining generic and NFDI4Health use case–specific metadata items relevant to domains of nutritional epidemiology, chronic diseases, and record linkage. Mappings to schemas of clinical trial registries and international and local initiatives were performed to enable interfacing with external resources. The MDS is represented in Microsoft Excel spreadsheets. A transformation into an improved and interactive machine-readable format was completed using the ART-DECOR (Advanced Requirement Tooling-Data Elements, Codes, OIDs, and Rules) tool to facilitate editing, maintenance, and versioning.

Results: The MDS is implemented in NFDI4Health services (eg, the German Central Health Study Hub and the Local Data Hub) to structure and exchange study-related metadata. Its current version (3.3) comprises 220 metadata items in 5 modules. The core and design modules cover generic metadata, including bibliographic information, study design details, and data access information. Domain-specific metadata are included in use case–specific modules, currently comprising nutritional epidemiology, chronic diseases, and record linkage. All modules incorporate mandatory, optional, and conditional items. Mappings to the schemas of clinical trial registries and other resources enable integrating their study metadata in the NFDI4Health services. The current MDS version is available in both Excel and ART-DECOR formats.

Conclusions: With its implementation in the German Central Health Study Hub and the Local Data Hub, the MDS improves the FAIRness of data from clinical, epidemiological, and public health research. Due to its generic nature and interoperability through mappings to other schemas, it is transferable to services from adjacent domains, making it useful for a broader user community.

(JMIR Med Inform 2025;13:e63906) doi:10.2196/63906

KEYWORDS

FAIR; findability; epidemiology; data sharing; public health; health research; metadata standards; interoperability development; structure; implementation; epidemiological; data models; accessibility; reusability; tool; clinical trial; nutrition; chronic diseases

Introduction

Despite wide acceptance in medical research, implementation of the FAIR (findability, accessibility, interoperability, and reusability) data principles in certain health domains and interoperability across data sources remain a challenge [1]. Clinical trial registries, such as ClinicalTrails.gov [2], the German Clinical Trials Register (DRKS) [3], and the World Health Organization's International Clinical Trials Registry Platform (ICTRP) [4], collect metadata about clinical studies, thus making them searchable and findable [5]. However, they are often not sufficiently detailed and lack further information about relevant study documents (eg, protocols, questionnaires, data dictionaries, etc), which hinders the findability and accessibility of such significant health resources [5]. Moreover, numerous epidemiological and public health studies remain unregistered [1,5], likely due to unfamiliarity with metadata standards and a general lack of a metadata-sharing culture [6,7].

Making valuable data from these studies available to the research community could potentially improve our understanding of essential risk factors associated with various diseases [1]. Several data-sharing initiatives have aimed at promoting the implementation of the FAIR principles. In the field of biobanking, the Minimum Information About Biobank Data Sharing (MIABIS) initiative is dedicated to standardizing metadata describing biobanks, thereby improving their interoperability and enabling the sharing of their valuable data and samples [8]. In cardiology, the joint European Union-Canada project established a cross-border data sharing and multicohort cardiovascular research platform, linking molecular, imaging, functional, and clinical data [9]. In epidemiology, Maelstrom Research provides a comprehensive catalog with search tools to support the discovery of data collected by epidemiological research networks and studies [10,11]. To our knowledge, an overarching search for clinical trials alongside epidemiological and public health studies is not yet available in existing search portals [5].

The National Research Data Infrastructure for Personal Health Data (NFDI4Health) is a nationally funded multipartner German project that seeks to optimize data sharing among the clinical, epidemiological, and public health research communities while preserving protection, privacy, and ethical regulations. This infrastructure for data from various health-related disciplines intends to support health research and facilitate the development of new and personalized preventive interventions and therapies, thereby improving population health [12,13]. With this aim, NFDI4Health develops data management workflows, ensuring that research data are properly organized, documented, and stored throughout its lifecycle. These workflows involve defining metadata standards, data classification systems, and data governance policies that facilitate the findability and accessibility of research data via the central NFDI4Health search portal. Entitled the German Central Health Study Hub (GCHSH) [5,14], the platform allows for the standardized publication of descriptive metadata from clinical, epidemiological, and public health studies. It connects to local data repositories and harvests their relevant metadata via the Local Data Hub (LDH) software

XSL•FO
RenderX

of NFDI4Health [15,16], making such studies and their data findable and accessible through a single-entry point.

In this paper, we present the development, structure, and implementation of the NFDI4Health metadata schema (MDS), the model underlying the GCHSH and LDH. We also present the ongoing mappings to other schemas, the format currently adopted, and the steps taken toward a machine-readable version. Prospects for further development and extension of the MDS are also discussed.

Methods

Ethical Considerations

As the study presented in this paper did not involve human participants and did not examine human personal data, the approval of an ethics committee was not required.

NFDI4Health Structures and Their Roles in the Development of the MDS

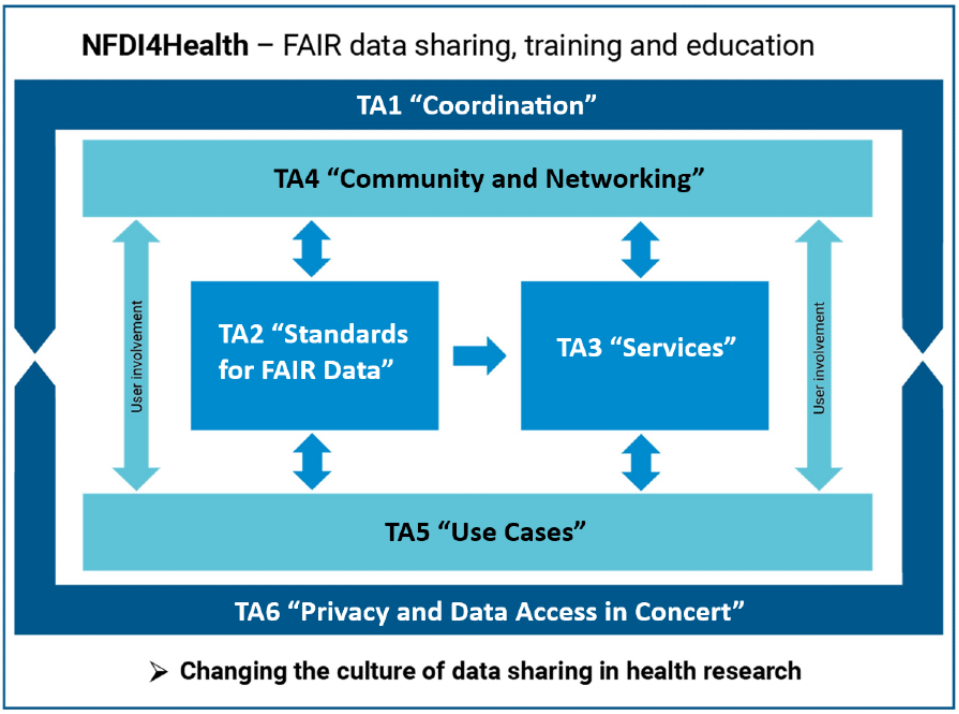
The NFDI4Health project comprises 6 task areas (TAs) [17] as shown in Figure 1, three of which are most relevant for the construction, development, and implementation of the MDS: TA2 “Standards for FAIR data,” TA3 “Services,” and TA5 “Use cases.” MDS development is a crucial part of TA2, as it aims to harmonize and further develop standards for data and their corresponding metadata in clinical trials, public health surveys, and epidemiological cohorts by implementing the FAIR principles. In that sense, TA2 provides the conceptual background for the NFDI4Health services implemented by TA3. Two crucial services that build on the metadata structures of the MDS are the GCHSH [14] and LDH [15,16], in addition to others that NFDI4Health aims to provide to the user community. All NFDI4Health standards and services are developed in close collaboration with domain experts and potential users in TA5 and implemented and tested within the scope of its 5 use cases, namely nutritional epidemiology, chronic diseases, record linkage, clinical trials, and medical imaging radiomics [18]. An additional use case focusing on COVID-19 was introduced during the pandemic, serving as a pilot and addressing the major challenges posed to societies around the world [19].

The MDS team (TA2) develops the metadata model as a conceptual backbone for NFDI4Health services and acts as the interface between NFDI4Health users (TA5) and developers (TA3). It is composed of experts in metadata as well as data interoperability and quality standards from different NFDI4Health coapplicant institutions. The team’s major role is to gather and bundle requirements from the users, model them into the schema, and communicate them to the developers for implementation. The team is also involved in various mapping activities between the MDS and other schemas, aiming to ensure the interoperability of the NFDI4Health metadata and services with other resources and platforms. Further interoperability efforts include representing the MDS using the Health Level 7 Fast Healthcare Interoperability Resources (FHIR) standard as well as value set mappings to concepts from international terminologies [20,21]. The MDS team holds Zoom meetings twice a month to coordinate, review, and discuss potential updates and improvements of the MDS and arrange for meetings with other teams (eg, developers, users, etc) when needed.

In addition to the 3 TAs directly involved in the construction and implementation of the MDS, TA6 “Privacy and data access in concert” provides the legal framework for metadata and data sharing. It helps in identifying relevant metadata items that capture information on data sharing, licensing, and access for studies and data addressed by NFDI4Health. This is especially important for future MDS extensions covering these aspects. TA4 “Community and networking” supports the outreach to the user community at large to demonstrate the usefulness of the MDS and its implementations to researchers and users in Germany and beyond. Finally, TA1 coordinates the whole NFDI4Health project and provides project management support.

XSL•FO
RenderX

Figure 1. Tasks areas of the NFDI4Health. FAIR: findability, accessibility, interoperability, and reusability; NFDI4Health: National Research Data Infrastructure for Personal Health Data Project.



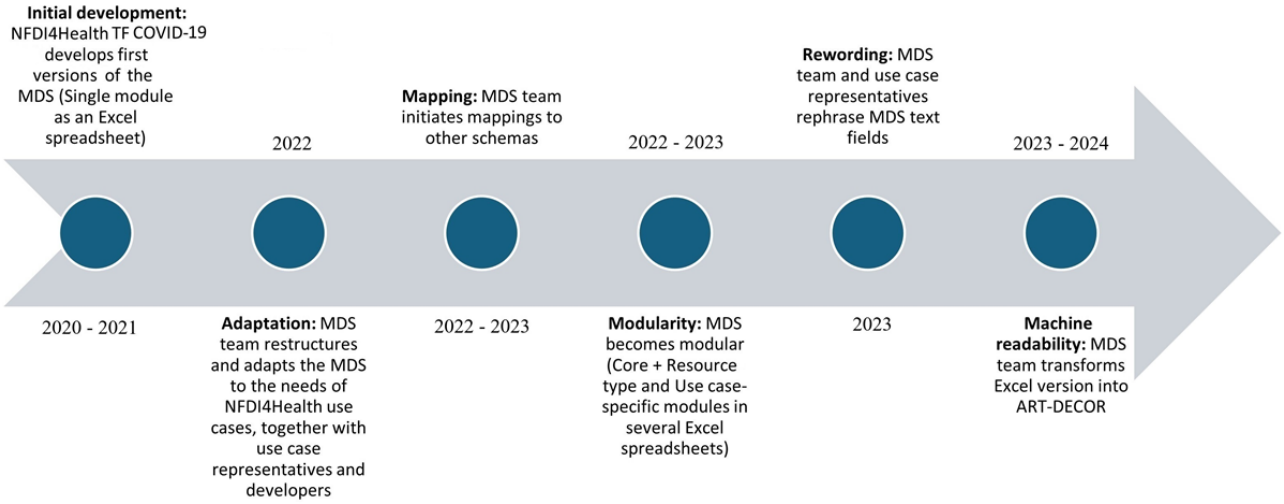
MDS Development

The MDS is an information model tailored to describe clinical, epidemiological, and public health studies as well as associated documents (eg, study protocols, instruments, etc) or datasets. It improves the FAIRness of these resources by making them searchable and accessible through implementations in metadata repositories tailored to the users' needs, such as the GCHSH [14] and the LDH [15,16]. The MDS was initially developed by the NFDI4Health task force COVID-19 [19], including a single module modeled in Excel and aimed at COVID-19 studies [22]. Many items were primarily adapted from established metadata standards and models, including DataCite [23], ClinicalTrails.gov [2], DRKS [3], Maelstrom [10], MIABIS [24], and the Data Documentation Initiative (DDI) [25].

To ensure broad applicability and ease its implementation across further health domains, the MDS was restructured to meet the needs of other NFDI4Health use cases. It adopted a modular structure, comprising core and use case–specific modules. The extension was carried out by the MDS team in close collaboration with the service developers and use case representatives as domain experts. Mapping activities to other schemas were also initiated to facilitate interoperability. Upon using the GCHSH implementation of the MDS, feedback was received from the German Centers for Health Research, the coverCHILD project [26], among others, and further issues with the MDS were fixed. These included additional structural changes, improvements of item headers and description texts (rewording), and more standardized value sets. Transformation plans were finally executed toward an improved machine-readable version of the MDS in ART-DECOR (Advanced Requirement Tooling-Data Elements, Codes, OIDs, and Rules) [27]. The MDS development process from the year 2020 to 2024 is illustrated in Figure 2.

XSL•FO
RenderX

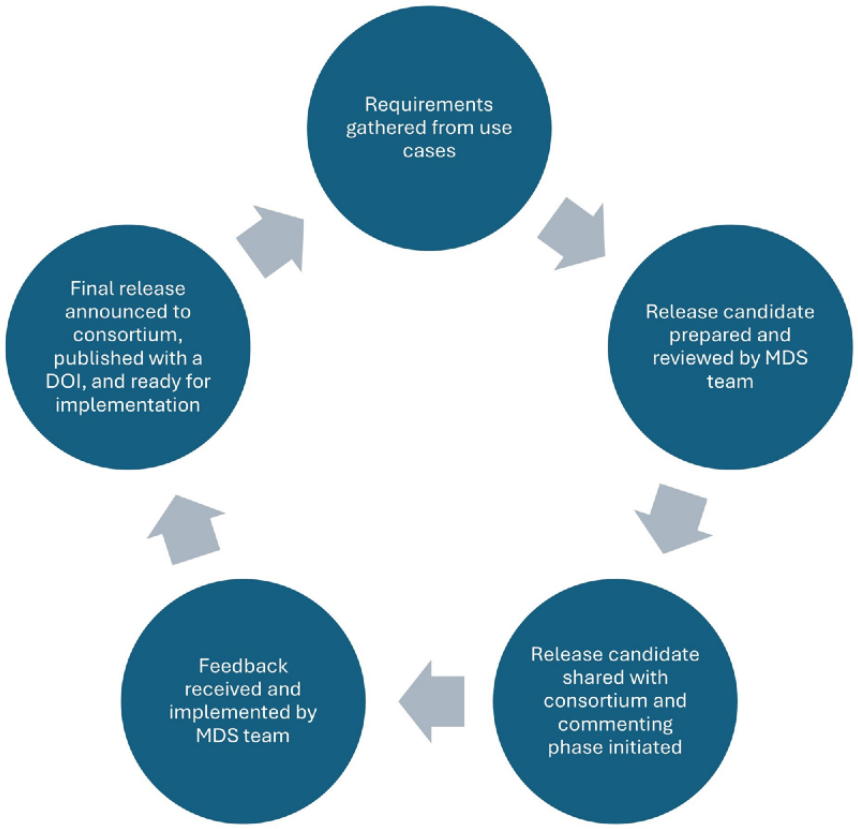
Figure 2. Development process of the MDS. ART-DECOR: Advanced Requirement Tooling-Data Elements, Codes, OIDs, and Rules; MDS: Metadata schema; NFDI4Health: National Research Data Infrastructure for Personal Health Data; TF: task force.



Release Cycle

To adapt to the requirements of the NFDI4Health user community, a new version of the MDS was released every 3 months. During each cycle, use case requirements were gathered and modeled and a release candidate of the MDS was prepared. Upon review by all members of the MDS team, the release candidate was shared with the NFDI4Health community and a commenting phase was initiated. During this phase, feedback could be provided by all members of the NDFI4Health consortium, including users and developers, commonly via a MDS GitHub repository. Feedback was also often provided via email, dedicated meetings, or during workshops. The feedback served as a basis to finalize the new version of the MDS, which was subsequently published with a digital object identifier (DOI) and shared with the GCHSH developers for implementation. The release cycle is shown in Figure 3.

Figure 3. Release cycle of the MDS. DOI: digital object identifier; MDS: metadata schema.



Mappings

For compatibility with existing clinical trial registries, the MDS was mapped to the study-specific models used by ClinicalTrails.gov [2], DRKS [3], and ICTRP [4]. Mappings were performed manually by comparing the MDS to the information present on these search portals, their input masks, as well as their XML exports and documentation, when

XSL•FO
RenderX

available. The objective was to enable the GCHSH, and other services that implement the MDS, to automatically upload the metadata of studies from Germany (ie, studies with at least one participating facility in Germany) registered on these portals, thereby avoiding the need to re-enter their information. Accordingly, all mandatory items of the MDS were compared with individual items in these schemas in search of appropriate matches. Matches were identified by comparing names, definitions, and value sets. When matches were not found or not applicable, a fixed value was assigned to the mandatory field as a workaround for implementation.

To remain aligned with international and local initiatives, further mappings to the schemas of the European Clinical Research Infrastructure Network (ECRIN) [28,29] and the schema of the German Human Genome-Phenome Archive (GHGA) [30] were performed. These mappings were considered important because ECRIN supports the organization of clinical trials in Europe and GHGA develops one of the most relevant resources in Germany for genomic data from the health domain. The MDS team compared all mandatory items using the same approach described above. It was also agreed with both ECRIN and GHGA teams to prepare their own mapping version in the reverse direction, thereby comparing their mandatory items to the MDS in search of the best matches. The intention was to align both versions, with the goal of allowing the NFDI4Health services to exchange information with ECRIN's metadata repository [31] and GHGA's metadata catalog [32]. In addition, to examine alignment options with the European Rare Disease Registry Infrastructure (ERDRI), a discussion with colleagues from the European Commission's Joint Research Center was initiated, followed by a comparison of the MDS items to the different sections of ERDRI's directory of registries (ERDRI.dor) [33].

Representations

The MDS was initially released as human-readable Microsoft Excel spreadsheets [34]. To develop an improved machine-readable version, a training workshop took place in May 2023 to kick-start a transformation into ART-DECOR [27]. Following the workshop, the Excel version of the MDS was shared with the ART-DECOR team to transform the modules' main information, using their transformation script, into a dedicated ART-DECOR project. The transformed version was afterwards checked by various members of the MDS team. Transformation errors were identified and fixed, and missing information was manually added. In the context of the MDS representation in FHIR, allowed values were mapped to concepts from international terminologies, whenever possible, and integrated into ART-DECOR. MDS values that could not be matched to terminology concepts were placed in a local code system created for NFDI4Health. Besides the ART-DECOR representation, a Simplifier project was also established based on the MDS-to-FHIR mappings, in which different FHIR artifacts were created and published [35]. These, together with details on the terminology mappings, are outside the scope of this study and will be published elsewhere [36].

Rewording

To improve user experience (UX), the GCHSH was tested by external users specialized in UX testing. Recommendations affecting the MDS included rephrasing item display names as well as descriptions and short input help texts based on the guidelines for effective UX writing [37]. Accordingly, dedicated discussions were initiated, involving NFDI4Health users from different domains as well as service developers and members of the MDS team, to examine the GCHSH interface item by item and individually modify and improve the clarity of these texts. Suggested changes were edited directly in a real-time working version of the MDS, which was shared on the NFDI4Health document management system for collaborative review and feedback.

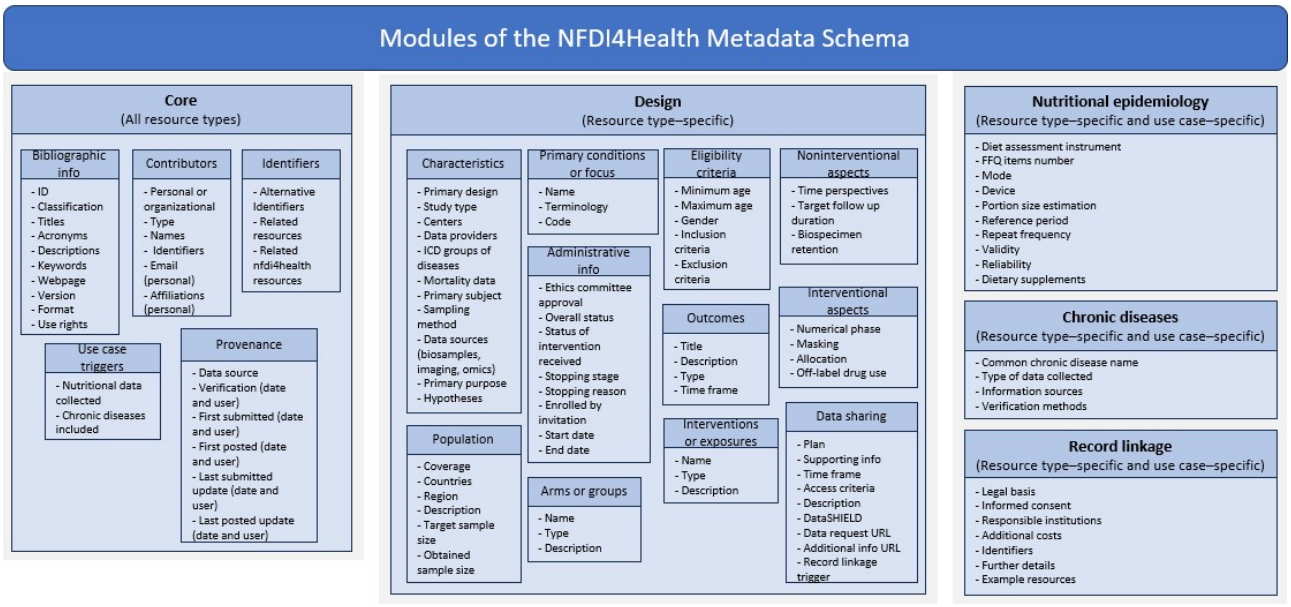
Results

Structure of the Metadata Schema

The most recently released version of the MDS (v3.3) comprises a total of 220 metadata items in 5 dedicated modules. The core module captures information relevant to any type of health resource, while additional modules gather descriptions specific to particular resources, health domains, or use cases. The latter currently include nutritional epidemiology, chronic diseases, and record linkage. In NFDI4Health, the term "resource" or "resource type" is used to refer to health studies, substudies, registries, biobanks, study protocols, data dictionaries, among other types, data collection instruments, or study documents. All modules comprise mandatory and optional items, with conditional cardinalities set when needed. The core and design modules are mostly based on international standards, with 20 of their items representing the mandatory information required for entering or displaying studies on the GCHSH. The 3 use case–specific modules are user-driven, mainly based on the needs of the NFDI4Health user community. Figure 4 provides an overview of the different MDS modules, illustrating their corresponding item groups and subgroups. The complete list of items is available on the web [34].

XSL•FO
RenderX

Figure 4. Overview of the NFDI4Health metadata schema modules. NFDI4Health: National Research Data Infrastructure for Personal Health Data.



Core Module

Based on DataCite, ClinicalTrails.gov, and DRKS, the core module of the MDS comprises 80 generic metadata items descriptive of any type of health resource. These include bibliographic information, such as the resource's title, description, acronyms, keywords, and web page, along with information about the persons and organizations that contributed to the development of the resource. With the use of identifiers, the module provides links to published study results, in addition to relevant resources registered on the NFDI4Health portal or elsewhere. Provenance details about the publication of the resource as well as items to trigger the nutritional epidemiology and chronic diseases modules, where applicable, are also included.

Design Module

For design and data access information, the MDS provides 111 items, representing further characteristics that are specific to certain resource types, namely studies, substudies, and registries. Like the core module, the design module is also based on DataCite, ClinicalTrails.gov, and DRKS, in addition to Maelstrom, MIABIS, and DDI. For studies and substudies, the module distinguishes between interventional and noninterventional study designs and provides dedicated sections for each design type. Information about the study conditions is provided, in addition to a population section including recruitment area and sample size information. An administrative information section includes metadata items about the ethics committee approval, status, and dates of the study, while further sections cover details about the eligibility criteria, outcome measures, and time points. Information about the data sharing plan is also included, with an item to trigger the use case–specific record linkage module, when applicable. Most sections in this module also apply to registries due to several overlapping characteristics.

Nutritional Epidemiology Module

Dedicated to studies and substudies collecting nutritional data, this module provides 15 domain-specific items, mainly related to dietary assessment instruments used in corresponding studies. The modes and devices used to apply an instrument are specified in this module, along with the methods used for portion size estimation. The module also contains items indicating whether the instrument is repeatedly applied, whether it is validated and whether it inquires about dietary supplements.

Chronic Diseases Module

For each chronic disease addressed by the resource, this use case–specific module specifies whether prevalent or incident outcome data were collected and indicates the information sources from which the data were generated. Methods used to verify the outcomes are also described. The module contains 5 items and is only applicable to certain resource types, including study protocols, informed consent forms, case report forms, and patient information sheets, among other study documents.

Record Linkage Module

For resources allowing record linkage, the third dedicated module indicates whether specific legal regulations or permissions are required for conducting record linkage and whether informed consent has been obtained. The module also provides information about responsible institutions that must approve record linkage and whether additional costs are incurred. Identifiers that can be used (eg, date of birth, postal code, insurance number, etc) as well as DOIs of additional related resources specific to record linkage (eg, publications) are also included. The module has 9 items and is only applicable to studies, substudies, and registries.

Preliminary Mapping Results

Based on the mappings of the MDS to the schemas of clinical trial registries, the GCHSH is capable of automatically uploading and displaying study metadata from these portals. With this objective, the 20 mandatory items of the MDS core and design modules were mapped to their counterparts in these schemas

XSL•FO
RenderX

as shown in Table 1, while presetting the NFDI4Health resource type to "Study" and the country to "Germany," as the focus of NFDI4Health is on German studies. The data source and subject items were also preset to "Automatically uploaded" and "Person," respectively. This is considering that these studies would be imported into the GCHSH from clinical trial registries involving only human subjects. Items with value sets (eg, study type) were fixed to selected values such as "Unknown" or "Other," as proper matching values could not be found. Moreover, fixed values, such as "Summary is not provided," were used for string items (eg, description), as corresponding items or their texts were missing. Table 1 also includes mapping metrics, indicating the number of MDS items achieving various matching levels. By October 2024, there were 25595, 659, and 221 studies imported into the GCHSH from ClinicalTrails.gov, DRKS, and ICTRP respectively.

Following a similar approach and with the same objective, several iterations were prepared by the MDS team to map the MDS to version 6 (v6) of the ECRIN schemas [28]. As ECRIN has a study and a data object schema, those iterations were performed twice while considering the same study-specific items in Table 1 in addition to an extra item required for nonstudy resources (Resource.classification.typeGeneral). Table 2 shows mappings of the MDS mandatory items to both ECRIN schemas. Unlike the MDS, which includes only one scientific unabbreviated title for a resource, ECRIN considers several title types (eg, display title, abbreviated title, public title, subtitle, etc). This is also the case for the description item of a data object, which includes multiple types in ECRIN (eg, summary, abstract, table of contents, etc). Further, ECRIN distinguishes between contributors and creators while the MDS includes only contributors; yet, with contributor types matching with both categories in ECRIN. The MDS classifies contributor types into personal and organizational, while ECRIN includes a single list of contribution types, with matches to both groups in the MDS. The resource's subject seems to be missing a direct match in ECRIN, yet could possibly be extracted from multiple items or topic types. Similarly, the data sharing plan does not seem to have a single corresponding item in ECRIN indicating whether data will or will not be shared, or if it is yet to be decided. However, items in ECRIN, such as the data sharing statement, access type, and access details could possibly include this information.

XSL•FO
RenderX

Table 1. Mappings of the mandatory items of the metadata schema core and design modules to the schemas of clinical trial registries.

NFDI4Health metadata schema (mandatory items) or Matching level	ClinicalTrails.gov	DRKS[a]	ICTRP[b]
Core module			
Resource.classification.type	Fixed to “Study”	Fixed to “Study”	Fixed to “Study”
Resource.titles.text	Official title	Title	Scientific title
Resource.titles.language	Fixed to “EN (English)”	Fixed to “EN (English)”	Fixed to “EN (English)”
Resource.descriptions.text	Detailed description	Brief summary in scientific language	Fixed to “Summary is not provided”
Resource.descriptions.language	Fixed to “EN (English)”	Fixed to “EN (English)”	Fixed to “EN (English)”
Resource.contributors.nameType	Responsible party type	Inferred from below fields	Inferred from below fields
Resource.contributors.organizational.type and Resource.contributors.organizational.name	Responsible party, study sponsor, and collaborators	Primary sponsor, sources of monetary or material support	Primary sponsor, secondary sponsors
Resource.contributors.personal.type, Resource.contributors.personal.givenName, and Resource.contributors.personal.familyName	Trial contacts, responsible party, and investigators	Contact for scientific queries, contact for public queries, and principal investigator	Contacts
Resource.provenance.dataSource	Fixed to “Automatically uploaded: ClinicalTrials.gov”	Fixed to “Automatically uploaded: DRKS”	Fixed to “Automatically uploaded: ICTRP”
Design module			
Design.primaryDesign	Study type	Study type	Study type
Design.studyType.interventional	Interventional model	Assignment	Study design (fixed to “Unknown”)
Design.studyType.nonInterventional	Observational model	Study type noninterventional, longitudinal or cross-sectional (fixed to “Other”)	Study design (fixed to “Unknown”)
Design.groupsOfDiseases.generally	Fixed to “Unknown”	Fixed to “Unknown”	Fixed to “Unknown”
Design.administrativeInformation.status	Recruitment status (combined with study dates)	Recruitment status	Recruitment status (fixed to “Other”)
Design.subject	Fixed to “Person”	Fixed to “Person”	Fixed to “Person”
Design.population.countries	Location countries (fixed to “Germany”)	Fixed to “Germany”	Countries of recruitment (fixed to “Germany”)
Design.dataSharingPlan.generally	IPDSharing	IPD-individual participant data	Fixed to “Undecided, it is not yet known if data will be made available”
Mapping metrics, n (%)			
Direct matches[c]	7 (35)	6 (30)	2 (10)
Partial matches[d]	6 (30)	6 (30)	6 (30)
Preset items (mapping not required)	4 (20)	4 (20)	4 (20)
Fixed to a fitting value and could not be mapped	3 (15)	4 (20)	8 (40)

[a]German Clinical Trials Register.

[b]ICTRP: International Clinical Trials Registry Platform.

[c]Matched information included in one item in both the MDS and the corresponding matched schema.

[d]Matched information included in more than one item in the MDS, the corresponding matched schema, or both.

XSL•FO
RenderX

Table 2. Mappings of the mandatory items of the metadata schema core and design modules to the schemas of other initiatives.

NFDI4Health metadata schema (mandatory items) or Matching level	ECRIN[a] Study Schema (v6)	ECRIN Data Object Schema (v6)	GHGA[b]	ERDRI[c]
Core module				
Resource.classification.type	Fixed to "Study"	Type	Fixed to "Study"	Fixed to "Registry"
Resource.classification.typeGeneral	N/A[d]	Class	N/A	N/A
Resource.titles.text	Study titles (title text), when title type=Trial registry title	Object titles (title text)	Study.title	Name
Resource.titles.language	Study titles (language code)	Object titles (language code)	__[e]	—
Resource.descriptions.text	Brief description	Description (description text)	Study.description	Description
Resource.descriptions.language	—	Description (language code)	—	Fixed to "EN (English)"
Resource.contributors.nameType	—	Creators (name type), contributors (name type)	—	—
Resource.contributors.organizational.type	—	Contributors (contribution type)	—	Institution, sponsor
Resource.contributors.organizational.name	—	Creators (organization_organization default name)	Study.affiliations	
Resource.contributors.personal.type	—	Contributors (contribution type)	—	Contact person
Resource.contributors.personal.givenName	—	Creators (person details_given name)	—	
Resource.contributors.personal.familyName	—	Creators (person details_family name)	—	
Resource.provenance.dataSource	Fixed to "Automatically uploaded: Other"	Fixed to "Automatically uploaded: Other"	Fixed to "Automatically uploaded: Other"	Fixed to "Automatically uploaded: Other"
Design module				
Design.primaryDesign	Study type	N/A	—	N/A
Design.studyType.interventional	Study features (intervention model)	N/A	Study.type (fixed to "Other")	N/A
Design.studyType.nonInterventional	Study features (observational model)	N/A	Study.type (fixed to "Other")	N/A
Design.groupsOfDiseases.generally	—	—	Condition title, condition name	*ICD-10* (*International Statistical Classification of Diseases, Tenth Revision*) code, disease name
Design.administrativeInformation.status	Study status	N/A	—	N/A
Design.subject	Study topics, when topic type=organism or subject characteristics (fixed to "Person")	Topics, when topic type=subject characteristics (fixed to "Person")	Fixed to "Person"	Fixed to "Person"
Design.population.countries	Fixed to "Germany"	Fixed to "Germany"	Fixed to "Germany"	Country (fixed to "Germany")
Design.dataSharingPlan.generally	Data sharing statement	Access type, access details	—	Availability for future collaborations or studies
Mapping metrics, n (%)				

XSL•FO
RenderX

NFDI4Health metadata schema (mandatory items) or Matching level	ECRIN[a] Study Schema (v6)	ECRIN Data Object Schema (v6)	GHGA[b]	ERDRI[c]
Direct matches[f]	4 (19)	2 (10)	3 (14)	3 (14)
Partial matches[g]	4 (19)	11 (52)	1 (5)	6 (29)
Preset and N/A items (mapping not required)	5 (24)	7 (33)	5 (24)	9 (43)
Fixed to a fitting value or could not be mapped	8 (38)	1 (5)	12 (57)	3 (14)

[a]European Clinical Research Infrastructure Network.

[b]German Human Genome-Phenome Archive.

[c]ERDRI: European Rare Disease Registry Infrastructure.

[d]N/A: not applicable for the selected resource type or schema.

[e]Blank cells indicate that a match could not be found in this iteration.

[f]matched information included in one item in both the MDS and the corresponding matched schema.

[g]matched information included in more than one item in the MDS, the corresponding matched schema, or both.

Although Table 2 presents only the mapping results for the MDS mandatory items, the iterations also included comparisons of optional items and identified a few items in ECRIN that had no corresponding counterparts in the MDS. These include an item defining interstudy relationships, a composite item indicating the type of record keys used within a dataset, an item indicating the amount of deidentification applied to a dataset, and the European Open Science Cloud categorization recommended for data objects. Further mapping iterations have been performed to update the above mappings to ECRIN's most recent version 8. The latest version has been shared with ECRIN colleagues as they were requested to prepare their own mapping version in the reverse direction. Detailed results of these mappings, along with value set comparisons, will be completed and published elsewhere.

Though still in the early stages, single iterations were also conducted by the primary author, mapping the mandatory items of the MDS to GHGA's schema [30] and to the different attributes on the ERDRI.dor portal [33]. At the first glance, some commonalities among study-related items were identified and 9 of the 20 mandatory items of the MDS were preset or matched successfully to items in GHGA, as shown in Table 2. Remaining items could not be matched, as the distinction between interventional and noninterventional study designs in the MDS had no counterpart in GHGA's schema, as well as the specification of the language used for study titles and descriptions. The controlled vocabularies used in GHGA's schema were also not indicated in the version shared with the MDS team, making it challenging to match value set items. This first mapping iteration was shared with GHGA colleagues for review, in preparation of a second iteration. The MDS comparison to the different sections of ERDRI.dor revealed some matches among the registry-specific items as shown in Table 2. These, however, are yet to be shared with Joint Research Center colleagues for further discussion.

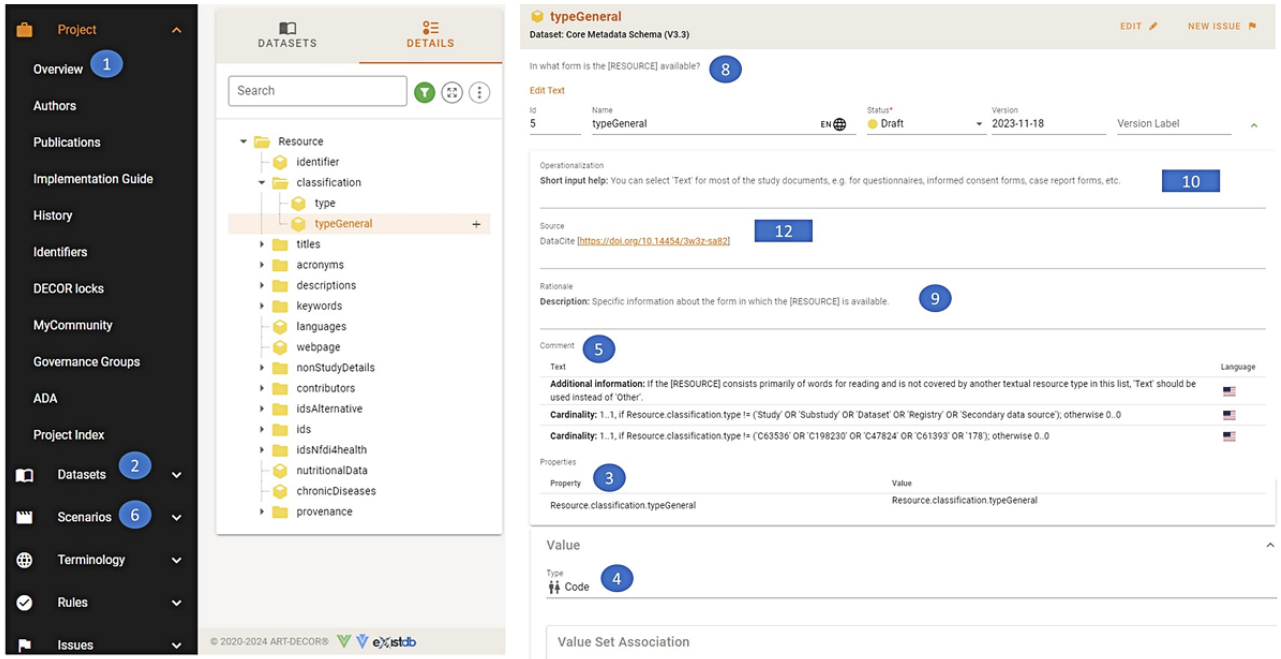
Representation and Transformation Into ART-DECOR

The Excel version of the MDS [32] comprises individual spreadsheets for each module. Within each spreadsheet, items are listed in different rows and named according to the camelCase naming convention. Item names, data types, cardinalities, and allowed values are represented in multiple columns. Additional columns contain the information displayed for each item on the GCHSH. These include display names or headers, descriptions, additional descriptive information, input help texts, and input examples. Further spreadsheets include the sources used to build the MDS, value definitions, and documentation of all changes compared with the previous version. The authors of the MDS are also listed in a cover sheet, together with the persons responsible for the version, license details, and version information.

The transformation into ART-DECOR organizes the different modules from the Excel version into separate ART-DECOR datasets, with individual items arranged in a hierarchical tree structure. For each item in a particular dataset, the different Excel columns are represented in corresponding fields, including the item's name, data type, and allowed values or concepts. The value definitions were directly added to the concept description field, thereby providing a structured list of concepts and their definitions. Cardinalities and conditions were initially added as free text in the comment field. However, they were later additionally implemented in different ART-DECOR scenarios toward a more structured version. Besides cardinalities, conformances are also specified in scenarios, indicating mandatory, optional, and conditional items. Figure 5 provides a dataset item view in ART-DECOR, together with a tabular list of Excel spreadsheets and columns and their corresponding representation in ART-DECOR. Terminology mappings are also illustrated under the section "Concepts," listing the MDS item values and their matching terminology concepts. These mappings were taken from the value sets created previously to represent the MDS in FHIR.

XSL•FO
RenderX

Figure 5. Excel to ART-DECOR transformation with a dataset item view. ART-DECOR: Advanced Requirement Tooling-Data Elements, Codes, OIDs, and Rules.



Excel	ART-DECOR
Cover sheet	Project overview page (1)
Module sheets	Datasets (2)
Number columns	Omitted
Item column	Item property field (3)
Data type column	Item value type (4)
Cardinality column	Item comment field (5) + scenarios (6)
Display information columns	Omitted
Allowed values column	Item value concepts (7)
Display name column	Item description field (8)
Description column	Item rationale field (9)
Additional information column	Item comment field (5)
Short input help column	Item operationalization field (10)
Input example column	Item value examples (11)
Source of the property column	Item source field (12)

To navigate the ART-DECOR project, the black menu on the upper left side of Figure 5 provides a list of different pages. The landing or overview page [27] of the project includes a brief description of the MDS, its authors, and copyright and license information. The datasets page enables adding new modules and displays the module hierarchies with all item information. The scenarios page allows for adding and viewing cardinalities and conditions for each dataset, yet in our project, these are also included in comments in the dataset view as shown in Figure 5. The publications page lists published versions of the MDS which have been finalized and can no longer be changed. The project index page allows for exporting the different datasets into various machine-readable formats (eg, XML). Finally, issues to be considered for the next versions of the MDS are raised and discussed on the issues page. Accordingly, the content viewed on these pages changes occasionally as the MDS is updated. Remaining pages on the menu are for technical use and are outside the scope of this paper. Further information on using ART-DECOR can be found in the tool's documentation guide [38].

Rephrasing of Display Texts

With 220 items to be examined, we could only check a few items from the core module by going through the search interface of the GCHSH. This exercise played a great role though in helping users associate the different columns of the Excel spreadsheets with what they usually see on the user interface. Further suggestions were provided via the real-time working version, yet many items were still not covered. This was probably due to the unfamiliarity of the users with the spreadsheets, making it overwhelming and time-consuming to go through the different columns for each item. The MDS team then worked independently on the real-time version and prepared several rewording iterations, covering 302 text changes in line with the UX guidelines [37]. The changes were clearly marked and users were asked to review them, provide their feedback, and agree to final changes in a dedicated meeting. The new texts were implemented in the latest version of the MDS [34].

XSL•FO
RenderX

Implementation

The MDS is implemented in the GCHSH [14,39]. Upon creating an account, users are able to use the platform's input mask or its application programming interfaces to register their resources. Information is requested based on the different sections of the MDS, including general information about the resource, its design characteristics, contributors, administrative information, and related resources. Mandatory and optional items are also indicated. The usage of the service has continuously increased, reaching in October 2024 a total of 626 resources manually registered on the portal, mostly by NFDI4Health users and the coverCHILD project. The majority of these resources were studies (n=243), data dictionaries (n=143), questionnaires (n=78), substudies (n=49), and other data collection instruments (n=35). Remaining resources included datasets (n=19), manuals of operations (SOPs; n=15), other study documents (n=15), registries or secondary data sources (n=9), case report forms (n=5), codebooks (n=5), interview schemes and themes (n=4), data management plans (n=3), other resource types (n=2), and statistical analysis plans (n=1). Based on their experience entering their metadata, users regularly report their issues via GitHub, email communication, or using the platform's feedback button. Further development of the platform is performed interactively based on the received feedback. The platform is freely accessible to external users, thereby enriching its content and facilitating the collection of additional feedback to further improve user experience.

To facilitate sharing metadata by data holding organizations (DHOs), that is, the universities, research institutes, and data integration centers involved in conducting the studies, the MDS is also implemented by LDHs at 12 DHOs throughout Germany. Being the main local connector of the federated concept to the central services of NFDI4Health, the LDH ensures that local data are structured, linked, and easily shared among DHOs, while enabling them to automatically submit their metadata to the GCHSH [15,16]. The LDH also ensures adherence to the FAIR principles, allowing the discoverability of stored information, controlling data access, facilitating data exchange, and making data available for further use. The LDH software is currently rolled out in additional locations throughout Germany and internationally. Further applications of the MDS are promoted by the NFDI4Health FAIRsharing collection [40] of standards for health research data, incorporating standards used in the MDS development and promoting international interoperability.

Discussion

Principal Findings

This paper presented a MDS designed to capture and harmonize information from clinical, epidemiological, and public health studies, enhancing the findability and accessibility of their valuable data. The MDS is based on attributes from ClinicalTrails.gov [2], DRKS [3], Maelstrom [10], MIABIS [24], and DDI [25], in addition to the research needs derived from the NFDI4Health user community. Moreover, properties for assigning DOIs have been adopted from DataCite [23], thereby allowing the MDS to capture metadata about study documents (eg, questionnaires, data dictionaries, and electronic case report forms) and to enable persistent access to published resources. The MDS has the distinct ability to represent the hierarchical relation between different resources, including studies with complex designs and their associated documents. For instance, it can keep track of multiple studies in which a survey instrument is used or indicate that one study is part of another. The MDS also captures metadata essential for users to identify studies within specific health domains, such as studies collecting dietary intake or chronic disease information. It remains generic in its capacity to handle a broad range of resources such as datasets, registries, and data dictionaries, among others [5,41].

Limitations and Challenges

Mapping Efforts and Updates

Due to the generic nature of the targeted schemas, mappings only focused on the core and design modules of the MDS. To illustrate the challenges of importing information into the GCHSH, only mappings of the MDS mandatory items were presented, with the use of fixed values when needed. Mappings were performed manually by comparing the various items of the mapped schemas in an Excel spreadsheet. Despite various efforts by several members of the MDS team, it remains challenging to keep clinical trial registry mappings up to date with newer versions of the MDS. This is mainly due to the absence of structured schemas for these portals, making it difficult for the MDS team members to agree on a common mapping approach or tool to identify matching items. As a result, the mappings presented in this paper are based on older versions of the MDS and need to be revised. Detailed updated mappings, also containing optional items and value sets of the MDS, will be published elsewhere.

As ECRIN's study and data object schemas are based on ClinicalTrails.gov and DataCite respectively, identifying commonalities with the MDS was expected. However, despite their well-structured and detailed schemas, mapping the MDS to their items was still challenging due to their strict distinction between studies and data objects. The abundance of composite attributes and value sets in their schemas also often led us to recognize that some items in ECRIN could be represented by multiple items in the MDS and vice versa. For instance, the study titles item in ECRIN comprises text, type, language, and comment attributes, with the title type having multiple categories. The title item in the MDS only includes text and language and is defined as the scientific unabbreviated title of the study. This could be matched with multiple title type categories in ECRIN, including trial registry title, public title, protocol title, and other scientific title. Similarly, the study features item in ECRIN has categorized feature type and feature value attributes. Each feature type, together with its corresponding feature values, could be matched with a different group of items in the MDS (eg, masking, allocation, study type, primary purpose, etc). Matching items conditionally on certain titles or feature types presented a challenge to both the MDS and development teams. This became even more challenging when matching value sets, due to the presence of user-defined values in the MDS which lacked standardized sources or

XSL•FO
RenderX

definitions. It was, therefore, suggested that a better approach could be to agree on a minimal common data model, thus allowing both platforms to exchange data while saving mapping efforts. The feasibility of this approach, however, is yet to be assessed.

Though still in the early stages, our initial mapping attempt to the GHGA schema also had its challenges. This was mainly due to the strict classification of studies in the MDS by design (ie, interventional vs noninterventional) as well as its support of multiple languages for study titles and descriptions. It was not clear whether such a classification existed in the GHGA schema and if more than one language could be used to provide study descriptions. Further, due to technical issues accessing their public version, we could not identify which controlled vocabularies were used in their schema for codable items, thus limiting value set mappings.

Similarly, mapping to the ERDRI.dor schema is still at an early stage. As ERDRI.dor is a platform for registering European rare disease registries, it is not surprising that some commonalities with our MDS registry-specific items could be detected. Yet, due to the lack of a structured schema, these commonalities could only be observed by examining the different sections of the ERDRI.dor platform. For accurate mappings, further discussions, particularly with ERDRI's metadata team, remain needed.

Excel Versus ART-DECOR Representation

With over 200 items incorporated in the latest MDS releases, it became cumbersome for the MDS team to maintain and frequently update the Excel version and document all changes in a trackable manner. It also became difficult for the users to follow the frequent updates and provide their feedback. Following several discussions about alternative representation formats, the ART-DECOR open-source tool was selected. Due to its user-friendly interface, the tool enables efficient use by experts with or without a technical background, thus allowing NFDI4Health users, developers, and members of the MDS team to work collaboratively on the MDS developments. The tool's major advantage over Excel is that it represents the modeled data elements in a hierarchical structure, thereby illustrating the relations between the various items in an accessible manner. Unlike Excel, the tool also offers diagram views of all modules as well as exports to various machine-readable formats such as XML, JavaScript Object Notation, and FHIR R4. This in turn facilitates the transformations needed for the GCHSH development and representing the model in Simplifier and keeping the FHIR profiling up to date.

Despite these numerous advantages and the continued support from the ART-DECOR team, the transformation from Excel to ART-DECOR faced several obstacles. Though scenarios allowed us to set cardinalities, conformances, and textual and structured conditions, setting cross-module structured cardinality conditions (ie, conditions involving items from different modules) was not permitted. This left us only with the option of using textual conditions in scenarios for better machine readability while keeping the comment field in the datasets for better clarity and human readability.

Another issue we experienced during the transformation was the representation of the mappings to other schemas. Currently, the tool does not offer a structured way for this purpose. This once again left us only with the possibility of adding mappings as free text in the comment field. As this would still require multiple efforts when newer versions of the mapped schemas are released, we skipped representing the mappings in this version and decided to start a discussion with the ART-DECOR team about introducing a new mapping feature to the tool. Many user-defined values in the MDS could not be mapped to terminology concepts and we could not trace them back to determine why they were included and whether there was a need to keep them. This is because the specific sources for each value were not documented in earlier versions of the MDS during development. Placing them in a local code system was agreed upon as a temporary solution until finding proper matches, requesting their introduction to appropriate terminologies, or deciding to remove them from the MDS altogether.

Conclusions and Future Work

This paper presented the development, structure, and representations of the NFDI4Health MDS. The MDS aims to improve the representation of data from clinical, epidemiological, and public health studies, thereby enhancing their FAIRness. With its generic nature and modular structure, it is also transferable to adjacent research fields. The MDS was developed in close collaboration with the NDFI4Health use case experts, thereby ensuring that the needs of the greater user community are met. In addition to its core and design modules, the MDS currently provides 3 use case–specific modules. These cover the domains of nutritional epidemiology, chronic diseases, and record linkage. Two additional modules for clinical trials and imaging radiomics data will soon be implemented. The latest version of the MDS (v3.3) was released in Excel format and transformed into ART-DECOR. Yet, toward better machine readability, future versions will only be released in ART-DECOR.

The MDS is implemented in the GCHSH and several NFDI4Health LDHs. This allows users to register their metadata either centrally in the GCHSH or locally in a LDH instance of their own institution for automatic integration into the GCHSH. For better interoperability with other study portals, the MDS has been mapped to the schemas of clinical trial registries, thereby allowing the automatic upload of their metadata to the GCHSH. To ensure alignment with international and local initiatives, mappings to the ECRIN schemas, ERDRI, and the GHGA schema are ongoing. Mapping of the MDS to the health-related extension of the DCAT-AP metadata standard (HealthDCAT-AP) is also planned, thereby preparing the NFDI4Health services for interoperability with the emerging European Health Data Space.

Having focused on the core and design modules so far, mappings need to extend to the use case–specific modules and strategies need to be defined for handling user-defined items and values in the MDS, as well as items with no counterparts in either of the mapped schemas. To facilitate these activities, mapping goals and standardized mapping approaches need to be agreed

XSL•FO
RenderX

upon in NFDI4Health, thus defining common procedures for matching items, limiting mapping efforts, and optimizing the results of mapping activities performed by different members of the MDS team. In addition, identifying tools that support manual mapping activities could help extend and automize mappings to other data models. To facilitate alignment with international initiatives, the MDS also needs to increase its focus on terminology-based value sets and adopt to a larger extent existing terminologies and FHIR resources, when applicable. For these reasons, the MDS remains in development and is constantly expanded based on the needs of the user community.

Acknowledgments

HA, AS, SAIK, CNV, MG, COS, DW, AAZ, JD, ML, and VC developed and modeled the MDS and MG coordinated its development. FJ, MBS, IP, and UN designed the nutritional epidemiology module. CS, KN, TO, and TP designed the chronic diseases module. TI and MP designed the record linkage module. HA, AS, SAIK, and AAZ performed the mappings. HA and CNV completed the ART-DECOR transformation. All authors provided feedback and helped in the development and testing of the MDS. HA drafted the manuscript and all authors critically reviewed and approved it.

We greatly appreciate the funding from the Deutsche Forschungsgemeinschaft through project numbers 442326535 (NFDI4Health) and 451265285 (NFDI4Health task force COVID-19), as well as from the Klaus Tschira Foundation.

We acknowledge the feedback on the metadata schema from all partners in the NFDI4Health consortium as well as the German Centers for Health Research and the coverCHILD project. We also acknowledge collaborations with the ECRIN, GHGA, ERDRI, and ART-DECOR teams.

Conflicts of Interest

None declared.

References

1. Schwedhelm C, Nimptsch K, Ahrens W, Hasselhorn HM, Jöckel KH, Katzke V, et al. Chronic disease outcome metadata from German observational studies - public availability and FAIR principles. Sci Data 2023;10(1):868 [FREE Full text] [doi: 10.1038/s41597-023-02726-7] [Medline: 38052810]
2. Protocol Registration Data Element Definitions for Interventional and Observational Studies. U.S. National Library of Medicine. ClinicalTrials.gov. 2020. URL: https://clinicaltrials.gov/policy/protocol-definitions [accessed 2024-02-04]
3. Federal Institute for Drugs and Medical Devices. German Clinical Trials Register. BfArM. 2020. URL: https://www.bfarm.de/EN/BfArM/Tasks/German-Clinical-Trials-Register/_node.html [accessed 2024-02-04]
4. World Health Organization. International Clinical Trials Registry Platform (ICTRP). 2020. URL: https://www.who.int/clinical-trials-registry-platform/ [accessed 2024-02-06]
5. Darms J, Henke J, Hu X, Schmidt CO, Golebiewski M, Fluck J, NFDI4Health Task Force COVID-19. Improving the FAIRness of Health Studies in Germany: the German central health study Hub COVID-19. Stud Health Technol Inform 2021;287:78-82. [doi: 10.3233/SHTI210818] [Medline: 34795085]
6. Sasse J, Fluck J. An annotation workbench for semantic annotation of data collection instruments. Stud Health Technol Inform 2023;302:108-112. [doi: 10.3233/SHTI230074] [Medline: 37203619]
7. Pinart M, Nimptsch K, Bouwman J, Dragsted L, Yang C, De Cock N, et al. Joint data analysis in nutritional epidemiology: identification of observational studies and minimal requirements. J Nutr 2018;148(2):285-297 [FREE Full text] [doi: 10.1093/jn/nxx037] [Medline: 29490094]
8. BBMRI-ERIC. Introducing MIABIS: Standardizing Biobank Data Sharing. 2020. URL: https://www.bbmri-eric.eu/howtomiabis/ [accessed 2024-06-15]
9. euCanSHare. Why euCanSHare?. 2019. URL: http://www.eucanshare.eu/project/#anchor02 [accessed 2024-06-15]
10. Bergeron J, Doiron C, Marcon Y, Ferretti V, Fortier I. Fostering population-based cohort data discovery: the maelstrom research cataloguing toolkit. PLoS One 2018;13(7):e0200926 [FREE Full text] [doi: 10.1371/journal.pone.0200926] [Medline: 30040866]
11. Maelstrom. Maelstrom Catalogue. 2021. URL: https://maelstrom-research.org/page/catalogue [accessed 2024-06-15]
12. Fluck J. National Research Data Infrastructure for Personal Health Data (NFDI4Health): Version 2.0. Fachrepositorium Lebenswissenschaften 2021.
13. National Research Data Infrastructure for Personal Health Data. nfdi4health. 2020. URL: https://www.nfdi4health.de/en/ [accessed 2024-02-14]
14. A platform to find and publish personal health research data. German central health study hub. 2020. URL: https://www.nfdi4health.de/en/service/health-study-hub.html [accessed 2024-02-14]
15. Meineke FA, Golebiewski M, Hu X, Kirsten T, Löbe M, Klammt S, et al. NFDI4Health local data hubs for finding and accessing health data. Proc Conf Res Data Infrastr 2023;1. [doi: 10.52825/cordi.v1i.375]

XSL•FO
RenderX

16. Hu X, Abaza H, Hänsel R, Abedi M, Golebiewski M, Müller W, et al. NFDI4Health local data hubs implementing a tailored metadata schema for health data. Stud Health Technol Inform 2024;317:115-122. [doi: 10.3233/SHTI240845] [Medline: 39234713]
17. NFDI4Health. Task Areas. 2024. URL: https://www.nfdi4health.de/en/about-us/task-areas.html [accessed 2024-06-15]
18. NFDI4Health. TA5 - Use Cases. 2024. URL: https://www.nfdi4health.de/ueber-uns/arbeitsbereiche/ta5-use-cases.html [accessed 2024-06-15]
19. Pigeot I, Ahrens W, Darms J, Fluck J, Golebiewski M, Hahn HK, et al. Making epidemiological and clinical studies FAIR using the example of COVID-19. Datenbank Spektrum 2024;24(2):117-128. [doi: 10.1007/s13222-024-00477-2]
20. Klopfenstein SAI, Vorisek CN, Shutsko A, Lehne M, Sass J, Löbe M, et al. Fast healthcare interoperability resources (FHIR) in a FAIR metadata registry for COVID-19 research. Stud Health Technol Inform 2021;287:73-77. [doi: 10.3233/SHTI210817] [Medline: 34795084]
21. Vorisek CN, Klopfenstein SAI, Sass J, Lehne M, Schmidt C, Thun S. Evaluating suitability of SNOMED CT in structured searches for COVID-19 studies. Stud Health Technol Inform 2021;281:88-92. [doi: 10.3233/SHTI210126] [Medline: 34042711]
22. Shutsko A, Schmidt C, Darms J, Klopfenstein SAI, Vorisek CN, Golebiewski M. NFDI4Health Task Force COVID-19 metadata schema V2_0. Fachrepositorium Lebenswissenschaften 2022. [doi: 10.4126/FRL01-006431357]
23. DataCite Metadata Working Group. DataCite metadata schema documentation for the publication and citation of research data and other research outputs. Version 4.4. DataCite e.V 2021. [doi: 10.14454/3w3z-sa82]
24. Norlin L, Fransson MN, Eriksson M, Merino-Martinez R, Anderberg M, Kurtovic S, et al. A minimum data set for sharing biobank samples, information, and data: MIABIS. Biopreserv Biobank 2012;10(4):343-348. [doi: 10.1089/bio.2012.0003] [Medline: 24849882]
25. Controlled Vocabularies - Overview Table of Latest Versions. DDI Alliance. 2024. URL: https://ddialliance.org/controlled-vocabularies [accessed 2024-06-15]
26. COVID-19 Forschungsplattform für Kinder und Jugendliche. coverCHILD. 2022. URL: https://coverchild.de [accessed 2024-02-13]
27. ART-DECOR. NFDI4Health Metadata Schema. 2023. URL: https://art-decor.org/ad/#/nfdhtfcov19-/project/overview [accessed 2024-02-14]
28. Canham S. ECRIN metadata schema for clinical research data objects version 6.0 (August 2021). Zenodo 2021. [doi: 10.5281/zenodo.5554961]
29. Canham S. ECRIN metadata schemas for clinical research, version 8 (September 2023). Zenodo 2023. [doi: 10.5281/zenodo.8368709]
30. GHGA. The GHGA Metadata Model. 2020. URL: https://www.ghga.de/data-portal/metadata-model [accessed 2024-02-06]
31. ECRIN. Clinical Research Metadata Repository. 2022. URL: https://ecrin.org/clinical-research-metadata-repository [accessed 2024-06-15]
32. GHGA. GHGA Metadata Catalog. 2024. URL: https://catalog.ghga.de/ [accessed 2024-06-15]
33. European Platform on Rare Disease Registration (EU RD Platform). The European Rare Disease Registry Infrastructure (ERDRI). The European Directory of Registries (ERDRI.dor). European Commission Joint Research Centre. 2019. URL: https://tinyurl.com/bdzbttrj [accessed 2024-01-31]
34. Abaza H, Shutsko A, Golebiewski M, Klopfenstein SAI, Schmidt CO, Vorisek CN. The NFDI4Health metadata schema (V3_3). Fachrepositorium Lebenswissenschaften 2023. [doi: 10.4126/FRL01-006472531]
35. NFDI4Health Metadata Schema. NFDI4Health metadata schema for clinical, epidemiological and public health studies. SIMPLIFIER.NET. 2023. URL: https://simplifier.net/nfdi4health-metadata-schema [accessed 2024-02-14]
36. Hölter T, Klopfenstein SAI, Mayer P, Sass J, Thun S, Vorisek CN. HL7 FHIR in health research: a FHIR specification for metadata in clinical, epidemiological, and public health studies. Stud Health Technol Inform 2024;316:1960-1961. [doi: 10.3233/SHTI240817] [Medline: 39176876]
37. Babich N. UX Planet. 16 Rules of Effective UX Writing. 2018. URL: https://uxplanet.org/16-rules-of-effective-ux-writing-2a20cf85fdbf [accessed 2024-01-30]
38. ART-DECOR. Technical documentation. 2024. URL: https://docs.art-decor.org/ [accessed 2024-10-10]
39. Darms J, Clemens V, Gonzalez-Ocanto M, Brünings-Kuppe C, Cici S, Fluck J. The German Central Health Study Hub - a service to find and publish clinical, public health and epidemiolocal studies and associated documents. Stud Health Technol Inform 2024;317:129-137. [doi: 10.3233/SHTI240847] [Medline: 39234715]
40. Schmidt CO, Darms J, Shutsko A, Löbe M, Nagrani R, Seifert B, NFDI4Health Task Force COVID-19. Facilitating study and item level browsing for clinical and epidemiological COVID-19 studies. Stud Health Technol Inform 2021;281:794-798. [doi: 10.3233/SHTI210284] [Medline: 34042687]
41. Abaza H, Golebiewski M. NFDI4Health collection - Standards for Health Research Studies. 2023. URL: https://fairsharing.org/4940 [accessed 2024-02-13]

XSL•FO
RenderX

Abbreviations

ART-DECOR: Advanced Requirement Tooling-Data Elements, Codes, OIDs, and Rules
DDI: Data Documentation Initiative
DHO: data holding organizations
DOI: digital object identifier
DRKS: German Clinical Trials Register
ECRIN: European Clinical Research Infrastructure Network
ERDRI: European Rare Disease Registry Infrastructure
ERDRI.dor: European Rare Disease Registry Infrastructure, directory of registries
FAIR: findability, accessibility, interoperability, reusability
FHIR: Fast Healthcare Interoperability Resources
GCHSH: German Central Health Study Hub
GHGA: German Human Genome-Phenome Archive
ICTRP: International Clinical Trials Registry Platform
LDH: Local Data Hub
MDS: metadata schema
MIABIS: Minimum Information About Biobank Data Sharing
NFDI4Health: National Research Data Infrastructure for Personal Health Data
TA: task area
UX: user experience

Edited by C Lovis; submitted 02.07.24; peer-reviewed by O Tamburis, C Gaudet-Blavignac; comments to author 17.09.24; revised version received 11.11.24; accepted 23.01.25; published 21.05.25.

Please cite as:
Abaza H, Shutsko A, Klopfenstein SAI, Vorisek CN, Schmidt CO, Brünings-Kuppe C, Clemens V, Darms J, Hanß S, Intemann T, Jannasch F, Kasbohm E, Lindstädt B, Löbe M, Nimptsch K, Nöthlings U, Ocanto MG, Osei TB, Perrar I, Peters M, Pischon T, Sax U, Schulze MB, Schwarz F, Schwedhelm C, Thun S, Waltemath D, Zeleke AA, Müller W, Golebiewski M
Toward a Domain-Overarching Metadata Schema for Making Health Research Studies FAIR (Findable, Accessible, Interoperable, and Reusable): Development of the NFDI4Health Metadata Schema
JMIR Med Inform 2025;13:e63906
URL: https://medinform.jmir.org/2025/1/e63906
doi:10.2196/63906
PMID:

©Haitham Abaza, Aliaksandra Shutsko, Sophie A I Klopfenstein, Carina N Vorisek, Carsten Oliver Schmidt, Claudia Brünings-Kuppe, Vera Clemens, Johannes Darms, Sabine Hanß, Timm Intemann, Franziska Jannasch, Elisa Kasbohm, Birte Lindstädt, Matthias Löbe, Katharina Nimptsch, Ute Nöthlings, Marisabel Gonzalez Ocanto, Tracy Bonsu Osei, Ines Perrar, Manuela Peters, Tobias Pischon, Ulrich Sax, Matthias B Schulze, Florian Schwarz, Carolina Schwedhelm, Sylvia Thun, Dagmar Waltemath, Atinkut A Zeleke, Wolfgang Müller, Martin Golebiewski. Originally published in JMIR Medical Informatics (https://medinform.jmir.org), 21.05.2025. This is an open-access article distributed under the terms of the Creative Commons Attribution License (https://creativecommons.org/licenses/by/4.0/), which permits unrestricted use, distribution, and reproduction in any medium, provided the original work, first published in JMIR Medical Informatics, is properly cited. The complete bibliographic information, a link to the original publication on https://medinform.jmir.org/, as well as this copyright and license information must be included.

XSL•FO
RenderX

Pharmacoepidemiologic Research Based on Common Data Models: Systematic Review and Bibliometric Analysis

Yongqi Zheng[1]; Meng Zhang[1]; Conghui Wang[1]; Ling Gao[1]; Junqing Xie[2]; Peng Shen[3]; Yexiang Sun[3]; Mengling Feng[4]; Seng Chan You[5]; Feng Sun[1,6,7,8]

[1]Department of Epidemiology and Biostatistics, School of Public Health, Peking University, 38 Xueyuan Road, Haidian District, Beijing, China

[2]NDORMS, The Botnar Research Centre, University of Oxford, Oxford, United Kingdom

[3]Yinzhou District Center for Disease Control and Prevention, Ningbo, China

[4]Saw Swee Hock School of Public Health and the Institute of Data Science, National University of Singapore, Singapore, Singapore

[5]Department of Biomedical Systems Informatics, Yonsei University College of Medicine, Seoul, Republic of Korea

[6]Institute of Traditional Chinese Medicine, Xinjiang Medical University, Urumqi, China

[7]Department of Ophthalmology, Peking University Third Hospital, Beijing, China

[8]School of Medicine, Shihezi University, Shihezi, China

Corresponding Author:
Feng Sun
Department of Epidemiology and Biostatistics, School of Public Health, Peking University, 38 Xueyuan Road, Haidian District, Beijing, China

Abstract

Background: The adoption of common data models (CDMs) has transformed pharmacoepidemiologic research by enabling standardized data formatting and shared analytical tools across institutions. These models facilitate large-scale, multicenter studies and support timely real-world evidence generation. However, no comprehensive global evaluation of CDM applications in pharmacoepidemiology has been conducted.

Objective: This study aimed to conduct a systematic review and bibliometric analysis to map the landscape of CDM usage in pharmacoepidemiology, including publication trends, institutional authors and collaborations, and citation impacts.

Methods: In total, 5 English databases (PubMed, Web of Science, Embase, Scopus, and Virtual Health Library) and 4 Chinese databases (CNKI, Wan-Fang Data, VIP, and SinoMed) were searched for studies applying CDMs in pharmacoepidemiology from database inception to January 2024. Two reviewers independently screened studies and extracted information about basic publication details, methodological details, and exposure and outcome information. The studies were categorized into 2 groups according to their Total Citations per Year (TCpY), and a comparative analysis was conducted to examine the differences in characteristics between the 2 groups.

Results: A total of 308 studies published between 1997 and 2024 were included, involving 1580 authors across 32 countries and 140 journals. The United States led in both publication volume and citation counts, followed by South Korea. Among the 10 most cited studies, 7 used the Vaccine Safety Datalink, 2 used Sentinel, and one used Observational Medical Outcomes Partnership. Studies were stratified by TCpY to reduce citation bias from publication timing. Comparative analysis showed that high-TCpY studies were significantly more associated with multicenter collaboration (P=.008), United States-based institutions (P=.04), and vaccine-related research (P=.009). These studies commonly featured larger sample sizes, cross-regional data, and enhanced generalizability. International collaborations primarily occurred among North America, Europe, and East Asia, with limited involvement from limited-income countries.

Conclusions: This study presents the first bibliometric overview of CDM-based pharmacoepidemiologic research. The consistent output from United States institutions and increasing engagement from South Korea underscore their central roles in this field. High-TCpY studies tend to be multicenter, collaborative, and vaccine-focused, reflecting structural factors linked to research visibility and influence. Stratified citation analysis supports the value of real-world data integration and international cooperation in producing impactful studies. The dominance of limited-income countries in collaboration networks highlights a need for broader inclusion of underrepresented regions. These findings can help researchers identify key contributors, guide partner selection, and target appropriate journals. As CDM-based methods continue to expand, fostering diverse and collaborative research efforts will be crucial for advancing pharmacoepidemiologic knowledge globally.

(JMIR Med Inform 2025;13:e72225) doi:10.2196/72225

XSL•FO
RenderX

KEYWORDS

common data model; pharmacoepidemiology; bibliometric analysis; systematic review

Introduction

Pharmacoepidemiology applies epidemiological principles and methods to study the effects of drugs, vaccines, and devices, focusing on adverse event monitoring, health economic evaluation, and quality of life assessment [1]. Ongoing pharmacoepidemiologic research aims to ensure drug safety, standardize postmarket surveillance methods, and provide scientific evidence for intervention decisions [1]. To achieve these objectives, especially in postmarketing contexts, robust real-world evidence is essential. However, many current studies are limited by small sample sizes and insufficient population representativeness, making it difficult to detect rare or long-term adverse events [2]. To address these limitations, conducting multicenter pharmacoepidemiologic evaluations has proven to be more reflective of actual clinical settings, enhancing statistical power, improving detection efficiency, and enabling early identification of vaccine safety concerns [3,4]. However, multicenter studies also face challenges related to data heterogeneity, personally identifiable information leakage, lack of standardized protocols for data integration, and terminological harmonization difficulties [5,6].

Common data model (CDM) is a standardized data model designed to facilitate the exchange, integration, sharing, or storage of data from multiple sources [7]. Its development has provided a practical and scalable solution for enabling multicenter studies by harmonizing heterogeneous data sources across institutions and regions. Currently, various CDMs are widely used, including the Observational Medical Outcomes Partnership (OMOP) developed by the Observational Health Data Sciences and Informatics [8], PCORnet [9], and Fast Healthcare Interoperability Resources [10]. Other CDMs, such as the Vaccine Safety Datalink (VSD) [11] and Sentinel [12], are specifically designed for active vaccine safety monitoring. Each CDM emphasizes distinct aspects, with differing methodologies and application areas tailored to specific research needs [13].

Currently, CDMs are widely applied to generate new evidence in clinical practice and drug selection. Some studies leverage real-world data to produce scalable evidence, aiding in the understanding of population diversity as well as the similarities and differences in clinical characteristics and treatment pathways across regions [14,15]. In addition, certain studies based on the OMOP have introduced a large-scale, comprehensive approach to evaluate the effectiveness and safety of various drugs across the world, offering strong evidence to support clinical drug selection [16,17]. Despite the growing application of CDMs in pharmacoepidemiology, no study has systematically reviewed the global landscape of CDM use in this field across all major models and contexts. Previous reviews have often focused on a single CDM or specific application scenarios [6].

In recent years, bibliometrics has advanced rapidly and is widely used to explore the characteristics of academic publications in specific research fields, including influential countries, journals, institutions, and authors, as well as trends in frequently cited references and keywords [18,19]. Since Garfield's seminal work in 1955 on identifying the most cited scientific papers in the Institute for Scientific Information Web of Knowledge (now known as Web of Science) database [20,21], numerous scholars have conducted bibliometric analysis comparing highly cited and less cited papers [22-24]. Building on previous studies that highlighted key features of highly cited papers, this study uses bibliometric analysis to systematically characterize publication patterns, collaboration networks, and thematic trends in CDM-based pharmacoepidemiologic research.

This study aimed to fill that gap by systematically reviewing and visually analyzing global literature on CDM-based pharmacoepidemiology. By grouping studies by citation impact, we sought to identify the characteristics of highly cited studies and offer references for future research design, collaboration strategy, and infrastructure development. Our findings aim to inform researchers and policy makers on emerging trends, methodological priorities, and opportunities to enhance the global reach and inclusiveness of CDM-enabled pharmacoepidemiologic studies. The statement of significance is provided inTable 1.

XSL•FO
RenderX

Table . Statement of significance.

Content	Statement
Problem or issue	There is a critical challenge in integrating heterogeneous, multicenter, real-world data for pharmacoepidemiologic research, which hampers the detection of rare and long-term adverse events and limits the standardization of postmarket surveillance.
What is already known	Previous studies have demonstrated that CDMs[a] facilitate data standardization and enhance multicenter collaborations in pharmacoepidemiology. However, the global adoption, comparative impact, and evolution of these models remain insufficiently explored.
What this paper adds	This paper provides a comprehensive bibliometric analysis of the application of CDMs in pharmacoepidemiology, revealing publication trends, key contributors, and emerging research themes across different countries. It also identifies significant differences between high and low citation groups, underscoring the pivotal role of multi-center research and CDM-based methodologies.
Who would benefit from the new knowledge in this paper?	Researchers, policymakers, and healthcare practitioners involved in pharmacoepidemiologic studies and health informatics will benefit, as the findings offer insights into effective collaboration, selection of appropriate research models, and strategic dissemination for enhancing drug and vaccine safety monitoring.

[a]CDM: common data models.

Methods

Overview

This study was conducted according to the PRISMA (Preferred Reporting Items for Systematic Reviews and Meta Analyses) guidelines (the PRISMA checklist is provided in Checklist 1) to identify studies that applied CDM in pharmacoepidemiologic research [25].

Search Strategy

Five English databases: PubMed, Web of Science, Embase, Scopus, and Virtual Health Library, and 4 Chinese databases: China National Knowledge Infrastructure, Wan-Fang Data, VIP Database, and SinoMed were searched from the inception to January 22, 2024. In preliminary searches, the names of currently used CDMs worldwide were identified and used as search terms in both their full and abbreviated forms, in both English and Chinese, including terms like “common data model,” “Observational Health Data Sciences and Informatics,” “Observational Medical Outcomes Partnership,” and “Clinical Data Interchange Standards Consortium,” among others. Logical operators such as “OR” truncation symbols, and subject term matching were applied based on the search rules and syntax of each platform to form search strategies. All search terms were listed in Multimedia Appendix 1.

Eligibility Criteria

The inclusion criteria were as follows: (1) studies using CDMs (any CDM identified in the preliminary search, with inclusion based on the use of any single model) to address issues in the drug, vaccine, or medical device fields; (2) the study scope included safety, efficacy, usage, and economic evaluations for drugs, vaccines, and medical devices; and (3) drugs, vaccines, or devices must be the primary exposure, research focus, or outcomes of the study.

The exclusion criteria were as follows: (1) studies that did not apply CDMs, or where the CDM was incomplete; (2) studies that did not include drugs, vaccines, or devices as primary exposure or influence factors, or as main research content or outcomes; (3) editorial materials, including letters, editorials, comments, responses, editorial opinions, advertisements, and unpublished studies; (4) duplicate publications; and (5) studies in languages other than Chinese or English.

Data Extraction

Two reviewers independently screened studies and extracted information about basic publication details, methodological details, and exposure and outcome information. Basic information from the literature was extracted using Excel, including study title, authors, publication year, country, sample size, number of centers, type of CDMs, use of subgroup analysis, whether sensitivity or subgroup analysis was conducted, study exposure, study outcomes, and whether adherence to reporting guidelines. English studies were exported in BibTeX format and merged into a single XLSX file. Some English studies that could not be imported directly into the Bibliometrix package and all of the Chinese studies were exported in XLSX format. These files were modified into compatible tables based on the Bibliometrix data frame structure for analysis.

Statistical Analysis

Statistical analysis was conducted using R (version 4.4.0; R Core Team). The bibliometrix package was used to generate standard bibliometric indicators, including annual publication trends, total and average citation counts, and H-index values, as well as to construct coauthorship and keyword co-occurrence networks. To ensure consistency and data quality, all bibliographic records were cleaned and standardized before analysis. This process included deduplication, harmonization of author names and affiliations, normalization of journal titles, and manual review of keywords [26]. Total citation, Total

XSL•FO
RenderX

Citations per Year (TCpY), and the H-index were used as standard metrics for academic influence of studies and authors. The total citation of all studies published in a specific journal was used to represent the journal's overall citation count [27]. TCpY was defined as the average number of citations a study has received per year since its publication, calculated as follows:

$$TCpY = \frac{\text{Total Citations}}{\text{Years since Publication}}$$

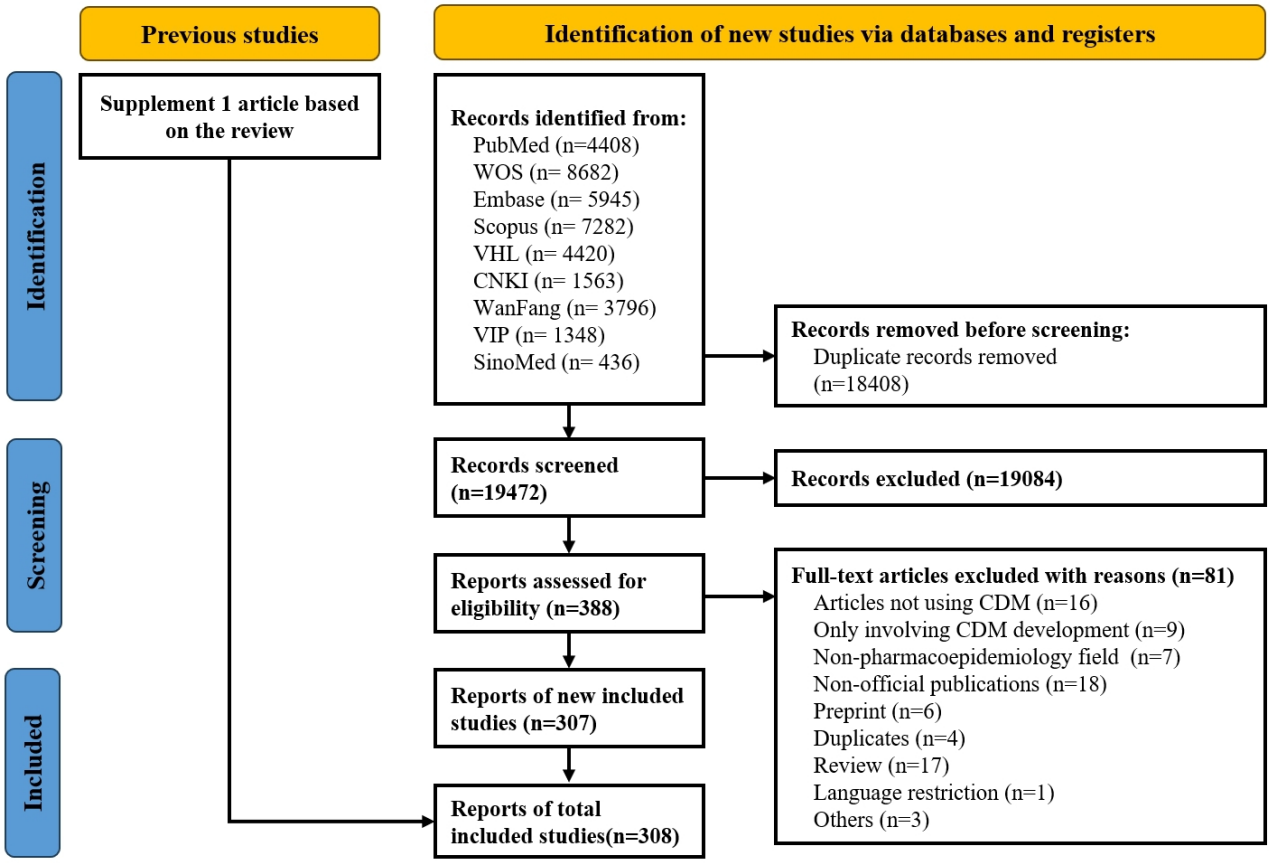
The H-Index is defined as *h* if an author has *h* publications, each of which has been cited at least *h* times [28]. Citation analysis was conducted on 285 studies which could get citations from the Web of Science Core Collection (WoSCC). Analysis of these 285 studies was conducted using R version 4.4.0. The *t* test was used to compare means under the assumption of normal distribution, while the Wilcoxon test served data that did not meet normality assumptions. Chi-square or Fisher exact tests were used for categorical variables. A 2-tailed *P* value of <.05 was considered to indicate statistical significance. To visualize interdisciplinary citation relationships, we conducted a dual-map overlay analysis using CiteSpace (version 6.4.1; Chaomei Chen, Drexel University). This method enables the mapping of citation trajectories between disciplines, highlighting the knowledge flow from citing to cited journals. The map was constructed using WoSCC data, with parameters set to the default configuration for dual-map overlays.

Results

Study Selection

A total of 37,880 studies were identified, of which 308 met the inclusion criteria, comprising 307 in English and 1 in Chinese (Figure 1). The publications originated from 32 countries, involving 1580 authors and published across 140 journals. In total, 590 keywords were identified, covering 12 types of CDMs: OMOP (76 studies), VSD (163 studies), PCORnet (14 studies), PEDSnet (4 studies), Sentinel (19 studies), Mini-Sentinel (14 studies), ConcePTION (3 studies), K-CDM (3 studies), Asian Pharmacoepidemiology Network (1 study), Cancer Research Network's Virtual Data Warehouse (1 study), Intensive Care Unit Medications (1 study), Health Maintenance Organization Research Network (1 study), along with 1 study that modified an existing CDM and 11 studies that created new CDMs. The research topics were categorized as follows: vaccines (173/308, 56.17%), drugs (132/308, 42.85%), and medical devices (3/308, 0.97%).

Figure 1. PRISMA (Preferred Reporting Items for Systematic Reviews and Meta-Analyses) flow diagram of the included studies.

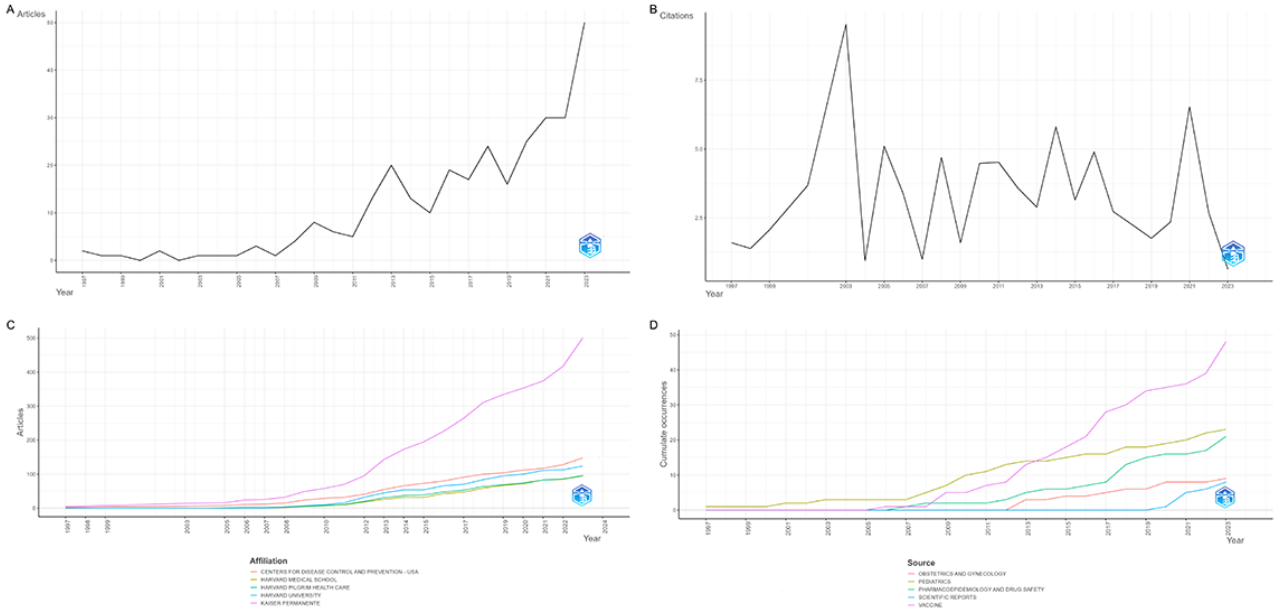


Temporal Distribution of Publications

The volume of publications in this field has shown a continuous upward trend. The earliest identified study dates back to 1997. From 1997 to 2007, the volume of studies remained low with minimal growth, maintaining fewer than 5 studies per year. Between 2008 and 2016, the number of studies began to increase, albeit with some fluctuation. Following 2019, study volume exhibited steady growth, reaching a peak of 49 studies in 2023 (Figure 2A).

XSL•FO
RenderX

Figure 2. General trends of included studies in CDM-based pharmacoepidemiologic research through 2024. **(A)** Temporal distribution of publications in pharmacoepidemiologic research based on CDM through 2024. **(B)** Average annual citation frequency in CDM-based pharmacoepidemiologic research through 2024. **(C)** Temporal distribution of publications for the top 5 most productive institutions in CDM-based pharmacoepidemiologic research through 2024. **(D)** Annual publication trends across top 5 journals in CDM-based pharmacoepidemiologic research through 2024. CDM: Common Data Model.



Citation Information of the Studies

Among the 308 studies, the total citation count was 8666, with an average citation frequency of 28 per study and a median of 13.00 (IQR 3.00 - 30.00) citations. The citation distribution by publication year was shown in Figure 2B, with peaks in 2003 and 2021.

The top 10 most cited studies originated entirely from the United States, comprising 7 studies on VSD, 2 on Mini-Sentinel, and one using OMOP. Regarding the focus of exposure, 8 studies investigated vaccines, while 2 examined drugs. Safety outcomes were predominant, accounting for 90% (9/10) of the research endpoints. Multimedia Appendix 2 provides detailed information on the top 10 most cited studies.

The citation analysis was conducted on 285 studies according to citations from the WoSCC. We compared key characteristics between the 285 WoSCC-indexed studies and the 23 non-WoSCC studies. As shown in Multimedia Appendix 3, there were no statistically significant differences between the 2 groups. The included studies were divided into 2 groups based on total citation counts, and their basic characteristics were compared (Table 2). The median citation count for the low citation group was 4.00 (IQR 1.00 - 8.00), while for the high-citation group it was 35.00 (IQR 20.00 - 64.00). Compared to the low-citation group, studies in the high-citation group generally had larger sample sizes (P=.049), involved more research centers (P<.001), and predominantly originated from the United States (P<.001). Regarding exposure, studies in the high-citation group were more likely to focus on vaccines than those in the low-citation group (72.34%, 102/141 vs 40.97%, 59/144; P<.001). A comparison between studies with vaccine as the exposure and those with drug indicated that high-citation studies were more frequently focused on vaccines (P<.001). Studies with high citation counts also tended to use the VSD. Differences were observed in research direction, with a higher proportion of safety studies in the high-citation group compared to the low-citation group (75.18%, 106/141 vs 64.58%, 93/144).

XSL•FO
RenderX

Table . Comparison of characteristics between high and low total citation study groups in CDM[a]-based pharmacoepidemiologic research through 2024.

Variable	Low total citations (N=144)	High total citations (N=141)	*P* value
Total citations, median (IQR)	4 (1-8)	35 (20-64)	<.001
Sample size, median (IQR)	153,438 (10,674-1,600,000)	381,807 (92,357-1,505,381)	.049
Number of centers, median (IQR)	6.00 (3.00-8.00)	7.00 (6.00-8.00)	<.001
Data from the United States, n (%)	88 (61.11)	123 (87.23)	<.001
Research exposure, n (%)			<.001
Drug	83 (57.64)	38 (26.95)	
Vaccine	59 (40.97)	102 (72.34)	
Medical device	2 (1.39)	1 (0.71)	
Types of CDMs n (%)			<.001
OMOP[b]	49 (34.03)	17 (12.06)	
VSD[c]	54 (37.50)	99 (70.21)	
Sentinel or mini-Sentinel	15 (10.42)	14 (9.93)	
Others	26 (18.06)	11 (7.8)	
Research directions, n (%)			.02
Safety	93 (64.58)	106 (75.18)	
Effectiveness	12 (8.33)	2 (1.42)	
Usage	28 (19.44)	19 (13.48)	
Others	11 (7.64)	14 (9.93%)	
Including sensitive analysis, n (%)	46 (32.86)	40 (28.57)	.52
Including subgroup analysis, n (%)	75 (52.45)	54 (38.30)	.02
Including reporting guideline, n (%)	12 (8.33)	4 (2.84)	.07

[a]CDM: Common Data Model.

[b]OMOP: Observational Medical Outcomes Partnership.

[c]VSD: Vaccine Safety Datalink.

We further divided the included studies into 2 groups based on TCpY to compare their characteristics (Table 3). The median annual citation for the low TCpY group was 1.00 (IQR 0.50 - 1.50), while for the high TCpY group it was 4.00 (IQR 2.75 - 6.28). Compared to the low TCpY group, studies in the high TCpY group generally involved a greater number of research centers (*P*=.008) and were predominantly conducted in the United States (*P*=.045). Regarding exposure, studies in the high TCpY group were more likely to focus on vaccines than those in the low TCpY group (63.70%, 93/146 vs 48.92%, 68/139; *P*=.003). A comparison between studies with vaccine as the exposure and those with drug indicated that high TCpY studies were more frequently focused on vaccines (*P*=.009). The proportion of the high TCpY group using reporting guidelines was higher, although the difference was not statistically significant (6.16%, 9/146 vs 5.04%, 7/139; *P*=.88).

XSL•FO
RenderX

Table . Comparison of characteristics between high and low total citation per year study groups in CDM[a]-based pharmacoepidemiologic research through 2024.

Variable	Low total citation per year (N=139)	High total citation per year (N=146)	*P* value
Total citations per year, median (IQR)	1.00 (0.50-1.50)	4.00 (2.75-6.28)	<.001
Sample size, median (IQR)	168,046 (13,484-1,368,976)	376,677 (91,692-1,721,186)	.057
Number of centers, median (IQR)	6.00 (3.00-8.00)	7.00 (5.00-8.00)	.008
Data from the United States, n (%)	95 (68.35)	116 (79.45)	.045
Research exposure, n (%)			.003
Drug	71 (51.08)	50 (34.25)	
Vaccine	68 (48.92%)	93 (63.70)	
Medical device	0 (0.00)	3 (2.05)	
Types of CDM n (%)			.24
OMOP[b]	36 (25.90)	30 (20.55)	
VSD[c]	66 (47.48)	87 (59.59)	
Sentinel or Mini-Sentinel	16 (11.51)	13 (8.90)	
Others	21 (15.11)	16 (10.96)	
Research directions, n (%)			.01
Safety	89 (64.03)	110 (75.34)	
Effectiveness	9 (6.47)	5 (3.42)	
Usage	32 (23.02)	15 (10.27)	
Others	9 (6.47)	16 (10.96)	
Including sensitive analysis, n (%)	36 (26.67)	50 (34.48)	.20
Including subgroup analysis n (%)	72 (52.17)	57 (39.04)	.04
Including reporting guideline n (%)	7 (5.04)	9 (6.16)	.88

[a]CDM: Common Data Model.

[b]OMOP: Observational Medical Outcomes Partnership.

[c]VSD: Vaccine Safety Datalink.

Analysis of Authors and Institutions

Among the top 10 productive authors, Dr Nicola P Klein, director of the Vaccine Study Center at Kaiser Permanente Northern California, held the highest rank with 69 publications. Her work has an H-index of 29, and all publications were based on VSD. The second-ranked author, Dr Matthew F Daley, a senior clinical researcher at Kaiser Permanente Colorado, has 53 publications. The third position is held by Dr Allison L Naleway from Kaiser Permanente Northwest Center for Health Research, with a total of 48 publications. All of the top 10 authors are from the United States, with five affiliated with different Kaiser Permanente institutions. The publications by these 5 authors are all based on VSD (Multimedia Appendix 4).

The top 10 most productive institutions are listed in Multimedia Appendix 5, and the temporal trends of the top 5 are visualized in Figure 2C. Among these, eight institutions are based in the United States, and two are located in South Korea. Kaiser Permanente is the institution with the highest publication volume and the most rapid growth, with all publications based on VSD. South Korea's Hallym University and Seoul National University began publishing around 2020, primarily utilizing OMOP and K-CDM in their studies.

Analysis of Journals

The top 10 productive journals were listed in Table 4. Vaccine ranks first, with 49 publications, accounting for 16.0% (49/308) of the total publications in this field. Among these, studies were based on the following CDM: VSD (46/49, 93.90%), ConcePTION (2/49, 4.10%), and Sentinel (1/49, 2.00%). Pediatrics ranks second, with 24 publications, representing 7.79% (24/308) of the total. The CDMs used in these studies include VSD (21/24, 87.50%), PEDSnet (1/24, 4.17%), PEDSnet + OMOP (1/24, 4.17%), and PCORnet (1/24, 4.17%). *Pharmacoepidemiology and Drug Safety* published 22 studies, accounting for 7.20% (22/308) of the total publications. The CDM used in these studies included VSD (9/22, 40.91%), Sentinel (5/22, 22.73%), Mini-Sentinel (2/22, 9.09%), OMOP (2/22, 9.09%), Asian Pharmacoepidemiology Network (1/22, 4.55%), and newly created CDMs (3/22, 13.64%).

XSL•FO
RenderX

Table . Top 10 journals with most studies in pharmacoepidemiologic research based on CDMs[a] through 2024.

Rank	Journal title	Country	Counts, n	IF[b] (2023)	JCR[c] (2023)	H-index	Total citations, n
1	*Vaccine*	United Kingdom	49	4.5	Q3	19	1207
2	*Pediatrics*	United States	24	6.2	Q2	18	1167
3	*Pharmacoepidemiology and Drug Safety*	United Kingdom	22	2.4	Q3	10	310
4	*Obstetrics and Gynecology*	United States	9	5.7	Q2	8	322
5	*Scientific Reports*	United Kingdom	8	3.8	Q3	4	38
6	*JAMA-Journal of the American Medical Association*	United States	7	63.1	Q1	7	925
7	*Jama Network Open*	United States	6	10.5	Q1	5	147
8	*American Journal of Epidemiology*	United States	6	5.0	Q2	4	187
9	*Drug Safety*	New Zealand	5	4.0	Q2	3	62
10	*Academic Pediatrics*	United States	4	3.0	Q3	4	34

[a]CDM: Common Data Model.

[b]IF: impact factor.

[c]JCR: journal citation reports.

As illustrated in Figure 2D, the number of pharmacoepidemiologic research studies based on CDMs in *Vaccine* shows notable variability, with marked increases in 2016 and 2022. In contrast, publication volume in *Pediatrics* and *JAMA Network Open* has remained relatively stable within this field.

Analysis of Countries and Regions

The top 10 data source countries were listed in Table 5. An analysis of the 308 pharmacoepidemiology publications based on CDMs reveals that the leading countries in research output are the United States with 286 (92.86%) studies, South Korea with 53 (17.21%) studies, the United Kingdom with 11 (3.57%) studies.

Table . Top 10 data source countries in pharmacoepidemiologic research based on CDMs[a] through 2024.

Rank	Country	Counts, n	Average citation counts per study	Average TCpY[b] counts per study
1	United States	286	34.53	4.13
2	South Korea	53	9.26	2.15
3	United Kingdom	11	16.36	3.85
4	France	9	19.56	4.52
5	China	9	15.67	2.73
6	Spain	8	25.75	6.78
7	Germany	7	23.43	6.31
8	Japan	7	23.14	4.52
9	Netherlands	7	15.86	4.20
10	Denmark	6	10.83	1.86

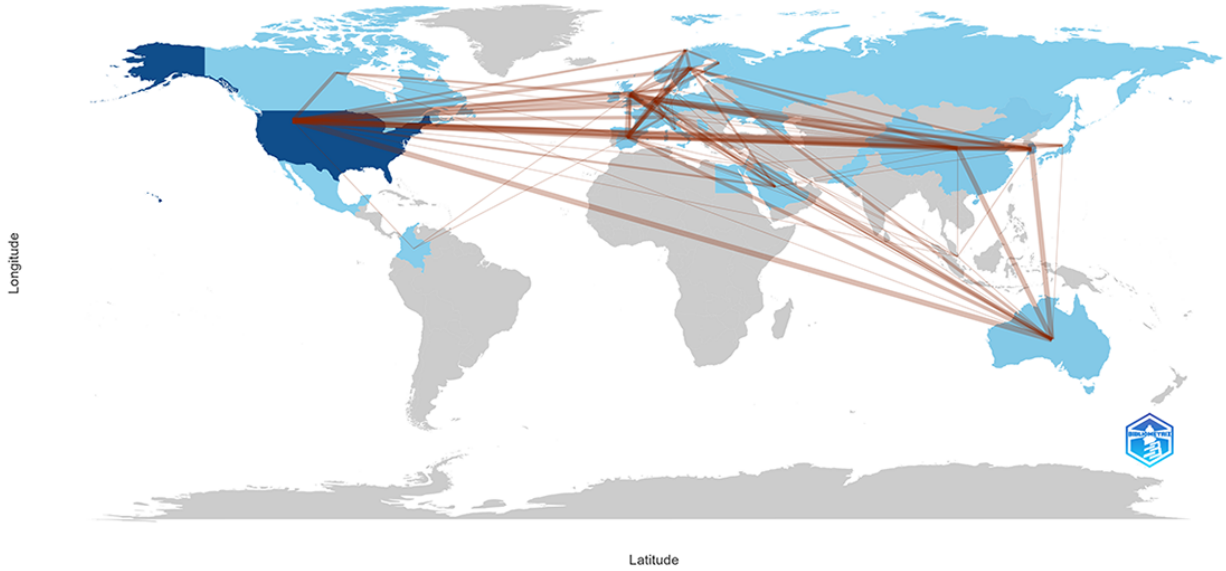
[a]CDM: Common Data Model.

[b]TCpY: Total Citations per Year. Data from multiple countries were counted separately for each contributing country.

XSL•FO
RenderX

As illustrated in Figure 3, international collaboration is strong among the United States, Europe, Australia, and East Asia. The United States acts as a central hub for multinational collaborations, with substantial partnerships involving China, the United Kingdom, Spain, South Korea, and Australia. South Korea is also actively engaged in various international projects, maintaining particularly close connections with the United States and the United Kingdom.

Figure 3. Global collaboration patterns among countries conducting CDM-based pharmacoepidemiologic research. CDM: Common Data Model; The thickness of the lines represents the strength of collaboration.



Analysis of Keywords

The included publications encompass a total of 590 keywords. Figure 4 illustrates the temporal trends of popular research topics in CDMs based on pharmacoepidemiology. Since 2012, topics such as vaccine safety, immunization, and influenza have remained consistently active. Starting in 2020, research on COVID-19, stroke, and diabetes has increased significantly, with extensive use of electronic health record (EHR) data.

Figure 4. Trends in research topics over time in pharmacoepidemiologic research based on CDM through 2024. Dot: Represents the appearance of a specific topic or keyword. Dot size: Indicates the influence or research volume of the topic. Horizontal line: the duration or active period of the topic. CDM: Common Data Model.

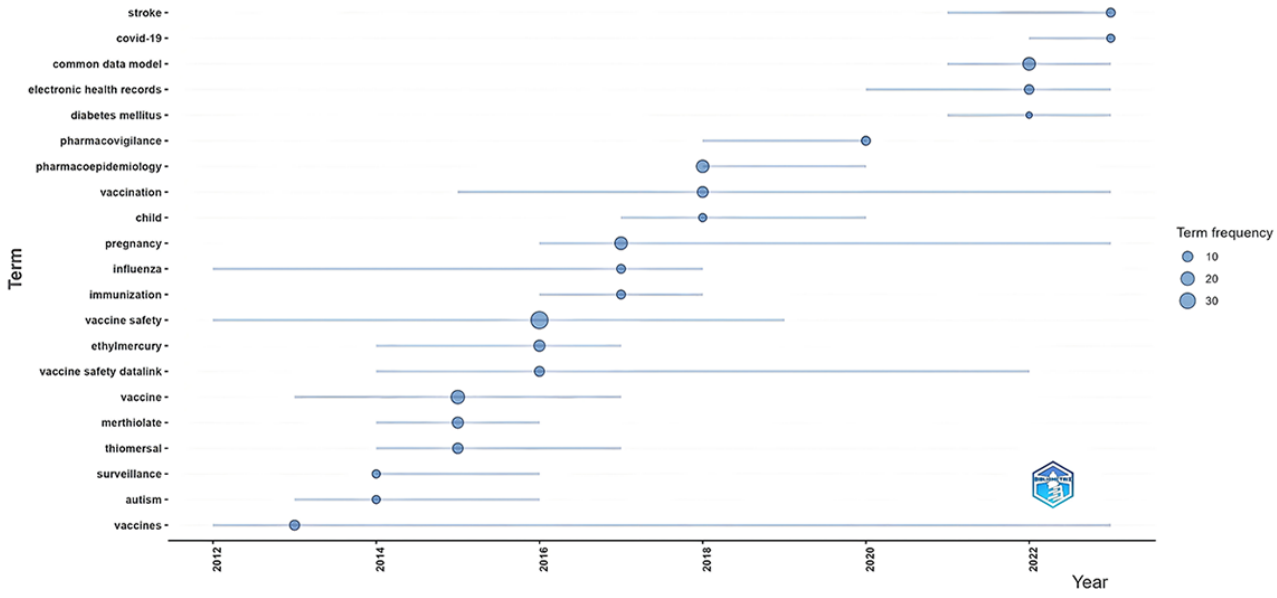
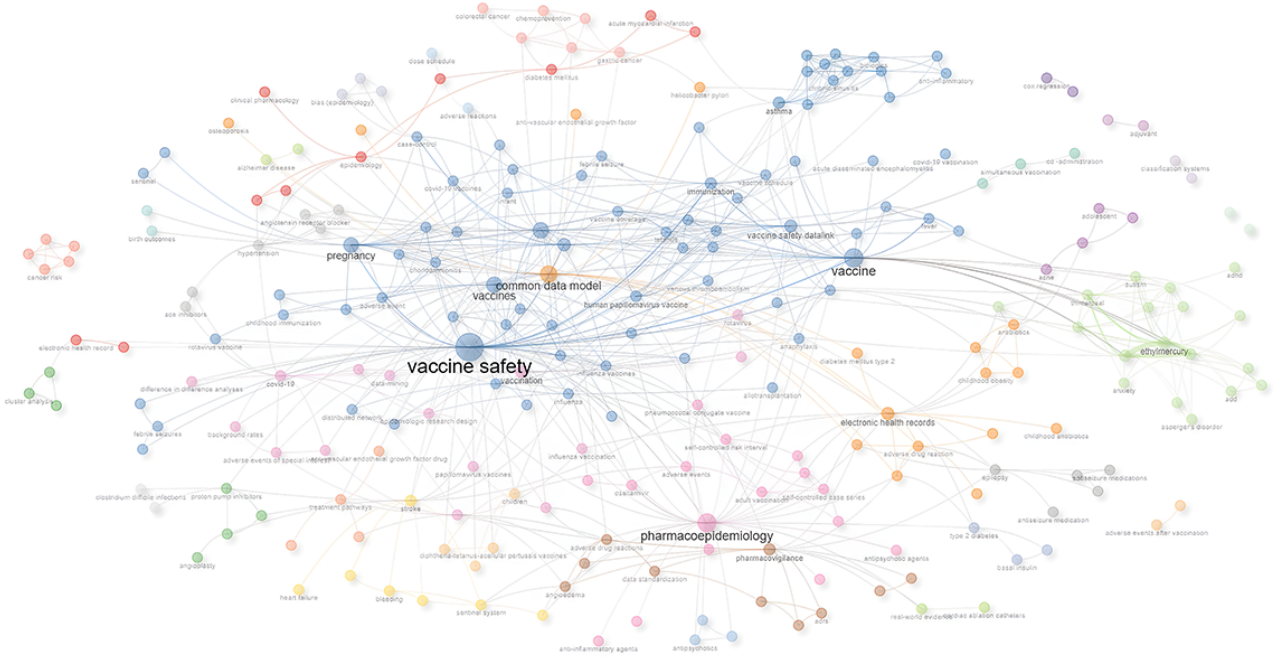


Figure 5 illustrates the trends in research topics. The nodes of the same color within a cluster represent closely related co-occurrences, with node size and link width varying based on the degree and strength of co-occurrence. “Vaccine safety” and “pharmacoepidemiology” occupy central positions in the network, showing strong connections with numerous surrounding topics. “Common data model” serves as another key topic, closely linked to “electronic health records” and “observational research.” The nodes in different colors indicate topic clusters, with the blue cluster primarily focusing on vaccine-related research, the orange cluster on drug monitoring

XSL•FO
RenderX

and adverse reactions, and the brown cluster on drug regulation and risk assessment.

Figure 5. Network map of keywords in pharmacoepidemiologic research based on CDM. CDM: Common Data Model.



The dual-map overlay analysis illustrated the interdisciplinary citation structure of CDM-based pharmacoepidemiologic research. Most publications were clustered in the "Medicine, Medical, Clinical" domains and predominantly cited journals from the fields of "Health, Nursing, Medicine" and "Molecular Biology, Genetics," suggesting strong disciplinary integration (Multimedia Appendix 6).

Discussion

Principal Findings

This study used bibliometric methods to analyze research trends in the application of CDMs in the field of pharmacoepidemiology, while also exploring research hot spots among highly cited studies in this field. The findings revealed that highly cited studies were predominantly originated from the United States, reflecting the central role of the United States researchers and institutions in this field, while South Korea's influence has been rising rapidly in recent years. Included studies were often multicenter, interorganizational collaborations, leveraging extensive sample sizes and cross-regional data coverage to enhance the generalizability and scientific value of research outcomes, thereby increasing citation frequency [29]. Vaccine-related studies were a primary focus, highlighting the significance of the CDM in public health, particularly in supporting real-time assessment of drugs and vaccines and adverse event monitoring during global health crises by integrating data across regions and organizations [30]. Our findings provide essential guidance for researchers embarking on studies in this field, assisting in the identification of potential collaborators, influential studies, and exemplary work for reference, as well as in the selection of suitable journals for publication. It enhances the efficiency of establishing research networks and supports the effective dissemination and academic impact of new studies.

Characteristics of Highly Cited Studies

The most cited publications globally have provided critical insights into adverse events associated with various vaccines, drug safety, and drug usage [14,30-33]. One particularly influential study, titled "Surveillance for Adverse Events After COVID-19 mRNA Vaccination," monitored severe adverse events related to COVID-19 vaccines and has emerged as the most cited and impactful publication in this field [30]. This highlights the rapid response and proactive surveillance capabilities of CDM during public health emergencies, enabling timely evaluation of new vaccines.

We conducted a comparative analysis between globally highly cited studies and less cited ones. To mitigate the advantage of earlier publications due to absolute citation counts, we also grouped studies based on TCpY. The findings indicate that studies in the high-citation group tend to involve more institutions. Cross-institutional collaboration and data sharing provide significant practical guidance for research and policy-making. Multicenter studies, with larger participant numbers from diverse regions, enhance statistical power and ensure that findings are more generalizable for broader populations. Such studies allow researchers to capture a wider range of variables and cases, thus providing a robust data foundation for investigating rare diseases, uncommon adverse events, or smaller subpopulations [29,34,35].

Vaccine studies are more frequently highly cited compared to drug research, due to factors related to their public health impact and resource allocation. First, the high citation rates of vaccine research are closely tied to its critical role in public health. Global public health crises, such as the COVID-19 pandemic, have further elevated the priority of vaccine research, increasing

XSL•FO
RenderX

its visibility and citation rates, as such studies are essential for policy-making and health interventions [36,37]. In addition, vaccine development often involves substantial public funding and data-sharing efforts, enabling wider access and greater citation of vaccine-related findings. In contrast, drug research is typically driven by pharmaceutical companies, with more restricted data availability and limited openness, which can constrain its citation impact [38].

Key Contributors and Institutional Insights

The analysis of authors and institutions highlights the contributions of key researchers to the application of CDMs in pharmacoepidemiology. Core authors such as Nicola P Klein and Matthew F Daley demonstrate their extensive expertise and consistent productivity in this field. Among the top 10 most prolific authors, 5 are affiliated with different regions of Kaiser Permanente, a leading health care provider and nonprofit health plan in the United States since its establishment in 1945, currently serving members across 8 states and the District of Columbia [39]. In South Korea, Hallym University and Seoul National University have conducted multiple studies in this domain around 2020, using OMOP and K-CDM. Between 2016 and 2018, the Ministry of Food and Drug Safety and the Korea Institute of Drug Safety and Risk Management converted EHR of over 9 million patients into CDM, reflecting Korea's progress in integrating and sharing cross-cohort data resources [40]. Subsequently, Korea developed the K-CDM specifically for pharmacovigilance systems, leveraging multi-center EHRs to monitor adverse drug reactions [41,42].

Global Landscape and Collaborative Trends

The majority of studies in the high-citation group originated from the United States, which is the birthplace of several CDMs. As early as 2001, the United States established the VSD to track adverse events across multiple regions and populations [43]. Subsequently, the OMOP was released in 2007, the Sentinel was launched by the FDA in 2008, and the PCORnet initiative began in 2014, positioning the United States at the forefront of CDM development and usage worldwide [43]. Moreover, the United States excels in drug and vaccine surveillance through the VSD and Sentinel systems. VSD provides real-time updates and comprehensive vaccine data, while Sentinel builds on VSD with tools enabling direct, standardized analyses, streamlining research processes [11].

In addition, the United States is the primary contributor in terms of publication volume and frequency, followed by South Korea. These countries have made significant contributions to advancing knowledge in this field. Notably, co-occurrence analysis highlights active participation from other countries in collaborative networks, with strong connections observed among North America, Europe, and East Asia. However, we observed that most international collaborations occur primarily among limited-income countries, with limited participation from other nations, particularly in limited-income countries. Given that CDMs are designed to harmonize data from multiple databases and facilitate standardized analyses [44], future research should focus on fostering broader and more impactful international collaborations from countries at different levels of development. Furthermore, the analysis of institutional productivity provides practical insights that may directly benefit researchers seeking potential collaborators. Our results highlight that Kaiser Permanente and CDC in the United States, both major users of VSD, represent key contributors to CDM-based vaccine research in the United States. Meanwhile, institutions such as Hallym University and Seoul National University in South Korea have emerged as important centers of CDM implementation, primarily using OMOP and K-CDM. Recognizing these leading institutions and their methodological preferences may facilitate strategic planning of future collaborative studies, enabling researchers to align their research agendas, optimize resource allocation, and ultimately enhance the global impact of CDM-based pharmacoepidemiologic research.

Implications for Future Research and Practice

To foster more equitable global participation, particularly from low- and middle-income countries, future efforts should prioritize improving access to CDM infrastructure. This includes the provision of open-source tools, standardized implementation workflows, and multilingual technical documentation. In parallel, the establishment of dedicated funding mechanisms and long-term capacity-building programs—such as technical training and data transformation support—will be essential to enable meaningful international collaboration. These strategies aim to bridge existing disparities and promote a more inclusive and diverse global CDM research ecosystem.

Furthermore, the findings of this study offer practical implications for clinical decision-making and real-world health policy. By identifying highly cited, multicenter studies—many of which focus on vaccine safety and effectiveness—this analysis highlights how CDM-based research can rapidly generate actionable evidence during public health emergencies. The global collaborative networks and methodological practices identified in this study may serve as a reference for designing future pharmacoepidemiologic studies that directly inform clinical guidelines, pharmacovigilance strategies, and regulatory decision-making. Strengthening the application of CDMs in such contexts can ultimately improve patient safety, treatment optimization, and health system responsiveness.

Strengths and Limitations

This study has some strengths. To our knowledge, this bibliometric study is the first of its kind in the field of application of CDMs in pharmacoepidemiology, to summarize the publication characteristics. Using the systematic review, we screened studies that met the inclusion criteria, ensuring the reliability of the selected studies. Furthermore, we imposed no restrictions on publication date or on the types of CDMs, which allowed us to include studies globally. This approach enables comparisons across different periods, countries, and types of CDMs. It must be acknowledged that our research has several modest limitations. First, the most significant limitation of our study lies in the inherent biases of citation analysis. These include the tendency for earlier publications to accumulate higher citation counts, journal and author self-citations, incomplete citation data, and omissions, all of which may affect citation rates [23,45,46]. To mitigate such biases, we attempted to use TCpY as an alternative metric. Second, we selected WoSCC based on previous studies [18,36], as it allows

XSL•FO
RenderX

standardized citation-based analysis. However, WoSCC does not index all eligible studies. Among the 308 included studies, 285 were found in WoSCC and therefore included in citation-related analyses. The remaining 23 studies lacked citation data and were excluded from this component. To evaluate whether their exclusion introduced selection bias, we compared key characteristics between the 2 groups. As shown in Multimedia Appendix 3, no statistically significant differences were found. Therefore, the potential bias introduced by excluding non-WoSCC studies is likely minimal. Third, we included only English and Chinese studies, which means that studies published in other languages were excluded. This may lead to the omission of some research. However, we searched the Virtual Health Library to ensure that literature published in Latin America was also covered to the greatest extent possible. Fourth, the use of the bibliometrix R package, while powerful for large-scale bibliometric analysis, may introduce methodological limitations. For example, its analytical outputs rely on the quality and structure of the input data and specific co-occurrence or clustering algorithms [26]. To minimize these effects, we carefully cleaned and standardized the dataset and interpreted the results in combination with manual validation and descriptive statistics. In addition, the release dates of different CDMs vary, with earlier CDMs having accumulated a higher publication volume and citations compared to those released more recently.

Conclusions

This bibliometric analysis provides a comprehensive overview of the application of CDMs in pharmacoepidemiology. The findings indicate a significant increase in publications over time, with the United States leading in both publication volume and citation counts. Notably, high-citation studies often involve multicenter studies, particularly focusing on vaccine, underscoring the importance of collaborative research efforts. These insights emphasize the critical role of CDMs in facilitating large-scale, collaborative pharmacoepidemiologic research, as well as provide researchers with insights for selecting collaborators and choosing journals for publication. To enhance global equity and clinical relevance, further efforts should support infrastructure accessibility, international cooperation, and the integration of CDM-based evidence into public health and regulatory decision-making.

Acknowledgments

Supported by the National Natural Science Foundation of China (grants 72474008 and 72074011), the third batch of Key Projects of Scientific Act for Drug Regulation of China (grants RS2024X006 and RS2024Z008), Special Project for Director, China Center for Evidence Based Traditional Chinese Medicine (grant 2020YJSZX-2), Research Project of China Society for Drug Regulation (2025-Y-Y-012), and Project of Center for Drug Reevaluation of China National Medical Products Administration (CDR2024R01001).

Data Availability

All data generated or analyzed during this study are included in this published article and its supplementary information files.

Authors' Contributions

YZ: Writing – review & editing, Writing – original draft, Visualization, Validation, Software, Formal analysis, Data curation, Conceptualization. Meng Zhang: Writing – review & editing, Data curation, Conceptualization. Conghui Wang: Data curation. LG: Data curation. JX: Writing – review & editing. PS: Writing – review & editing. YS: Writing – review & editing. MF: Writing – review & editing. SCY: Writing – review & editing. FS: Writing – review & editing, Validation, Funding acquisition, Conceptualization.

Conflicts of Interest

None declared.

Multimedia Appendix 1
Search strategies.
[DOCX File, 24 KB - medinform_v13i1e72225_app1.docx]

Multimedia Appendix 2
Top 10 most cited articles in pharmacoepidemiologic research based on Common Data Models through 2024.
[DOCX File, 19 KB - medinform_v13i1e72225_app2.docx]

Multimedia Appendix 3
Comparison of study characteristics between articles included and those not included in the Web of Science Core Collection.
[DOCX File, 19 KB - medinform_v13i1e72225_app3.docx]

XSL•FO
RenderX

Multimedia Appendix 4
Top 10 authors with most articles in pharmacoepidemiologic research based on Common Data Models through 2024.
[DOCX File, 18 KB - medinform_v13i1e72225_app4.docx]

Multimedia Appendix 5
Top 10 institutions with most articles in pharmacoepidemiologic research based on Common Data Models through 2024.
[DOCX File, 18 KB - medinform_v13i1e72225_app5.docx]

Multimedia Appendix 6
Dual-map overlay of journal citation trajectories in Common Data Model–based pharmacoepidemiologic research.
[DOCX File, 2344 KB - medinform_v13i1e72225_app6.docx]

Checklist 1
PRISMA (Preferred Reporting Items for Systematic Reviews and Meta-Analyses) 2020 checklist.
[DOCX File, 276 KB - medinform_v13i1e72225_app7.docx]

References

1. Liu X, Hou J. Pharmacoepidemiology. In: Wang C, Liu F, editors. Textbook of Clinical Epidemiology: For Medical Students: Springer Nature; 2023:265-280. [doi: 10.1007/978-981-99-3622-9_15]
2. Moro PL, Haber P, McNeil MM. Challenges in evaluating post-licensure vaccine safety: observations from the Centers for Disease Control and Prevention. Expert Rev Vaccines 2019 Oct;18(10):1091-1101. [doi: 10.1080/14760584.2019.1676154] [Medline: 31580725]
3. Platt A, Wilson J, Hall R, et al. Comparative effectiveness of alternative treatment approaches to secondary hyperparathyroidism in patients receiving maintenance hemodialysis: An observational trial emulation. Am J Kidney Dis 2024 Jan;83(1):58-70. [doi: 10.1053/j.ajkd.2023.05.016] [Medline: 37690631]
4. Romio S, Weibel D, Dieleman JP, et al. Guillain-Barré syndrome and adjuvanted pandemic influenza A (H1N1) 2009 vaccines: a multinational self-controlled case series in Europe. PLoS ONE 2014;9(1):e82222. [doi: 10.1371/journal.pone.0082222] [Medline: 24404128]
5. Chang Q, Yan Z, Zhou M, et al. Mining multi-center heterogeneous medical data with distributed synthetic learning. Nat Commun 2023;14(1):5510. [doi: 10.1038/s41467-023-40687-y]
6. Reinecke I, Zoch M, Reich C, Sedlmayr M, Bathelt F. The usage of OHDSI OMOP - a scoping review. Stud Health Technol Inform 2021 Sep 21;283:95-103. [doi: 10.3233/SHTI210546] [Medline: 34545824]
7. Garza M, Del Fiol G, Tenenbaum J, Walden A, Zozus MN. Evaluating common data models for use with a longitudinal community registry. J Biomed Inform 2016 Dec;64:333-341. [doi: 10.1016/j.jbi.2016.10.016] [Medline: 27989817]
8. Overhage JM, Ryan PB, Reich CG, Hartzema AG, Stang PE. Validation of a common data model for active safety surveillance research. J Am Med Inform Assoc 2012 Jan;19(1):54-60. [doi: 10.1136/amiajnl-2011-000376]
9. Fleurence RL, Curtis LH, Califf RM, Platt R, Selby JV, Brown JS. Launching PCORnet, a national patient-centered clinical research network. J Am Med Inform Assoc 2014;21(4):578-582. [doi: 10.1136/amiajnl-2014-002747] [Medline: 24821743]
10. Pfaff ER, Champion J, Bradford RL, et al. Fast Healthcare Interoperability Resources (FHIR) as a Meta model to integrate common data models: Development of a tool and quantitative validation study. JMIR Med Inform 2019 Oct 16;7(4):e15199. [doi: 10.2196/15199] [Medline: 31621639]
11. Fahey KR. The Pioneering Role of the Vaccine Safety Datalink Project (VSD) to advance collaborative research and distributed data networks. EGEMS (Wash DC) 2015;3(1):1195. [doi: 10.13063/2327-9214.1195] [Medline: 26793736]
12. Ball R, Robb M, Anderson SA, Dal Pan G. The FDA's sentinel initiative--A comprehensive approach to medical product surveillance. Clin Pharmacol Ther 2016 Mar;99(3):265-268. [doi: 10.1002/cpt.320] [Medline: 26667601]
13. Ahmadi N, Zoch M, Kelbert P, Noll R, Schaaf J, Wolfien M, et al. Methods used in the development of common data models for health data: Scoping review. JMIR Med Inform 2023 Aug 3;11:e45116. [doi: 10.2196/45116]
14. Hripcsak G, Ryan PB, Duke JD, et al. Characterizing treatment pathways at scale using the OHDSI network. Proc Natl Acad Sci U S A 2016 Jul 5;113(27):7329-7336. [doi: 10.1073/pnas.1510502113] [Medline: 27274072]
15. Willame C, Dodd C, Durán C, et al. Background rates of 41 adverse events of special interest for COVID-19 vaccines in 10 European healthcare databases - an ACCESS cohort study. Vaccine (Auckl) 2023 Jan;41(1):251-262. [doi: 10.1016/j.vaccine.2022.11.031] [Medline: 36446653]
16. Ryan PB, Buse JB, Schuemie MJ, et al. Comparative effectiveness of canagliflozin, SGLT2 inhibitors and non‐SGLT2 inhibitors on the risk of hospitalization for heart failure and amputation in patients with type 2 diabetes mellitus: A real‐world meta‐analysis of 4 observational databases (OBSERVE‐4D). Diabetes Obesity Metabolism 2018 Nov;20(11):2585-2597. [doi: 10.1111/dom.13424] [Medline: 29938883]

XSL•FO
RenderX

17. Suchard MA, Schuemie MJ, Krumholz HM, et al. Comprehensive comparative effectiveness and safety of first-line antihypertensive drug classes: a systematic, multinational, large-scale analysis. Lancet 2019 Nov 16;394(10211):1816-1826. [doi: 10.1016/S0140-6736(19)32317-7] [Medline: 31668726]
18. Zhang L, Zheng H, Jiang ST, et al. Worldwide research trends on tumor burden and immunotherapy: a bibliometric analysis. Int J Surg 2024 Mar 1;110(3):1699-1710. [doi: 10.1097/JS9.0000000000001022]
19. Ai S, Li Y, Zheng H, et al. Collision of herbal medicine and nanotechnology: a bibliometric analysis of herbal nanoparticles from 2004 to 2023. J Nanobiotechnology 2024 Apr 1;22(1):140. [doi: 10.1186/s12951-024-02426-3] [Medline: 38556857]
20. Garfield E. Journal impact factor: a brief review. CMAJ 1999 Oct 19;161(8):979-980. [Medline: 10551195]
21. Garfield E. How can impact factors be improved? BMJ 1996 Aug 17;313(7054):411-413. [doi: 10.1136/bmj.313.7054.411] [Medline: 8761234]
22. Pagni M, Khan NR, Cohen HL, Choudhri AF. Highly cited works in radiology: the top 100 cited articles in radiologic journals. Acad Radiol 2014 Aug;21(8):1056-1066. [doi: 10.1016/j.acra.2014.03.011] [Medline: 24833569]
23. Brandt JS, Hadaya O, Schuster M, Rosen T, Sauer MV, Ananth CV. A bibliometric analysis of top-cited journal articles in obstetrics and gynecology. JAMA Netw Open 2019 Dec 2;2(12):e1918007. [doi: 10.1001/jamanetworkopen.2019.18007] [Medline: 31860106]
24. Li T, Kang C, Ren G, et al. Top 100 cited articles related to EUS: A bibliometric analysis. Endosc Ultrasound 2024;13(4):259-268. [doi: 10.1097/eus.0000000000000081] [Medline: 39318756]
25. Moher D, Liberati A, Tetzlaff J, Altman DG, The PRISMA Group. Preferred Reporting Items for Systematic Reviews and Meta-Analyses: The PRISMA Statement. PLoS Med 2009 Jul 21;6(7):e1000097. [doi: 10.1371/journal.pmed.1000097]
26. Aria M, Cuccurullo C. bibliometrix : An R-tool for comprehensive science mapping analysis. J Informetr 2017 Nov;11(4):959-975. [doi: 10.1016/j.joi.2017.08.007]
27. Garfield E. Citation analysis as a tool in journal evaluation. Science 1972 Nov 3;178(4060):471-479. [doi: 10.1126/science.178.4060.471] [Medline: 5079701]
28. Hirsch JE. An index to quantify an individual's scientific research output. Proc Natl Acad Sci U S A 2005 Nov 15;102(46):16569-16572. [doi: 10.1073/pnas.0507655102] [Medline: 16275915]
29. Lane K, Palm ME, Marion E, et al. Approaches for enhancing the informativeness and quality of clinical trials: Innovations and principles for implementing multicenter trials from the Trial Innovation Network. J Clin Trans Sci 2023;7(1):e131. [doi: 10.1017/cts.2023.560]
30. Klein NP, Lewis N, Goddard K, et al. Surveillance for Adverse Events After COVID-19 mRNA Vaccination. JAMA 2021 Oct 12;326(14):1390-1399. [doi: 10.1001/jama.2021.15072] [Medline: 34477808]
31. McNeil MM, Weintraub ES, Duffy J, et al. Risk of anaphylaxis after vaccination in children and adults. J Allergy Clin Immunol 2016 Mar;137(3):868-878. [doi: 10.1016/j.jaci.2015.07.048] [Medline: 26452420]
32. Yih WK, Lieu TA, Kulldorff M, et al. Intussusception risk after rotavirus vaccination in U.S. infants. N Engl J Med 2014 Feb 6;370(6):503-512. [doi: 10.1056/NEJMoa1303164] [Medline: 24422676]
33. Toh S, Reichman ME, Houstoun M, et al. Comparative risk for angioedema associated with the use of drugs that target the renin-angiotensin-aldosterone system. Arch Intern Med 2012 Nov 12;172(20):1582-1589. [doi: 10.1001/2013.jamainternmed.34] [Medline: 23147456]
34. Wu Q, Tong J, Zhang B, et al. Real-World Effectiveness of BNT162b2 against infection and severe diseases in children and adolescents. Ann Intern Med 2024 Feb;177(2):165-176. [doi: 10.7326/M23-1754] [Medline: 38190711]
35. Ahmadi N, Zoch M, Guengoeze O, et al. How to customize common data models for rare diseases: an OMOP-based implementation and lessons learned. Orphanet J Rare Dis 2024 Aug 14;19(1):298. [doi: 10.1186/s13023-024-03312-9] [Medline: 39143600]
36. Zhang Y, Quan L, Xiao B, Du L. The 100 top-cited studies on vaccine: a bibliometric analysis. Hum Vaccin Immunother 2019;15(12):3024-3031. [doi: 10.1080/21645515.2019.1614398] [Medline: 31112440]
37. Stehlik P, Dowsett C, Camacho X, Falster MO, Lim R, Nasreen S, et al. Evolution of the data and methods in real-world COVID-19 vaccine effectiveness studies on mortality: a scoping review protocol. BMJ Open 2024 Mar 19;14(3):e079071. [doi: 10.1136/bmjopen-2023-079071] [Medline: 38508618]
38. How often do vaccine trials hit paydirt? MIT News. URL: https://news.mit.edu/2020/how-often-vaccine-trials-succeed-0527 [accessed 2025-07-18]
39. Kaiser Permanente exists to provide high-quality, affordable health care services and to improve the health of our members and the communities we serve. Kaiser Permanente. URL: https://about.kaiserpermanente.org/who-we-are/our-mission [accessed 2025-07-18]
40. Son N, Kim B, Chung S, Han S. Korean pharmacovigilance system based on EHR-CDM. Stud Health Technol Inform 2019 Aug 21;264:1592-1593. [doi: 10.3233/SHTI190550] [Medline: 31438247]
41. Choe S, Lee S, Park CH, et al. Development and application of an active pharmacovigilance framework based on electronic healthcare records from multiple centers in Korea. Drug Saf 2023 Jul;46(7):647-660. [doi: 10.1007/s40264-023-01296-2] [Medline: 37243963]

XSL•FO
RenderX

42. Choi YI, Park SJ, Chung JW, et al. Development of machine learning model to predict the 5-year risk of starting biologic agents in patients with inflammatory bowel disease (IBD): K-CDM Network study. JCM 2020 Nov;9(11):3427. [doi: 10.3390/jcm9113427]
43. Weeks J, Pardee R. Learning to share health care data: A brief timeline of influential common data models and distributed health data networks in U.S. health care research. EGEMS (Wash DC) 2019 Mar 25;7(1):4. [doi: 10.5334/egems.279] [Medline: 30937326]
44. Lai EC, Stang P, Yang YH, Kubota K, Wong ICK, Setoguchi S. International multi-database pharmacoepidemiology: Potentials and pitfalls. Curr Epidemiol Rep 2015 Dec;2(4):229-238. [doi: 10.1007/s40471-015-0059-z]
45. Ogden TL, Bartley DL. The ups and downs of journal impact factors. Ann Occup Hyg 2008 Mar;52(2):73-82. [doi: 10.1093/annhyg/men002] [Medline: 18316351]
46. Mishra S, Fegley BD, Diesner J, Torvik VI. Self-citation is the hallmark of productive authors, of any gender. PLoS ONE 2018;13(9):e0195773. [doi: 10.1371/journal.pone.0195773] [Medline: 30256792]

Abbreviations

AsPEN: Asian Pharmacoepidemiology Network
CDM: Common Data Model
EHR: electronic health record
OMOP: Observational Medical Outcomes Partnership
PRISMA: Preferred Reporting Items for Systematic Reviews and Meta-Analyses
TCpY: Total Citations per Year
VSD: Vaccine Safety Datalink
WoSCC: Web of Science Core Collection

Edited by A Coristine; submitted 05.02.25; peer-reviewed by A Jafarizadeh, X Huang; revised version received 06.05.25; accepted 20.05.25; published 28.07.25.

Please cite as:
Zheng Y, Zhang M, Wang C, Gao L, Xie J, Shen P, Sun Y, Feng M, You SC, Sun F
Pharmacoepidemiologic Research Based on Common Data Models: Systematic Review and Bibliometric Analysis
JMIR Med Inform 2025;13:e72225
URL: https://medinform.jmir.org/2025/1/e72225
doi:10.2196/72225

©Yongqi Zheng, Meng Zhang, Conghui Wang, Ling Gao, Junqing Xie, Peng Shen, Yexiang Sun, Menglin Feng, Seng chan You, Feng Sun. Originally published in JMIR Medical Informatics (https://medinform.jmir.org), 28.7.2025. This is an open-access article distributed under the terms of the Creative Commons Attribution License (https://creativecommons.org/licenses/by/4.0/), which permits unrestricted use, distribution, and reproduction in any medium, provided the original work, first published in JMIR Medical Informatics, is properly cited. The complete bibliographic information, a link to the original publication on https://medinform.jmir.org/, as well as this copyright and license information must be included.

XSL•FO
RenderX

Review

Smart Contracts and Shared Platforms in Sustainable Health Care: Systematic Review

Carlos Antonio Marino[1], MSci, PhD; Claudia Diaz Paz[1], DPhil, DBA

CENTRUM Católica Graduate Business School, Pontificia Universidad Católica del Perú, Lima, Peru

Corresponding Author:
Carlos Antonio Marino, MSci, PhD
CENTRUM Católica Graduate Business School
Pontificia Universidad Católica del Perú
Jirón Daniel Alomía Robles 125
Lima, 15023
Peru
Phone: 51 626 7100
Email: cmarino@pucp.pe

Abstract

Background: The benefits of smart contracts (SCs) for sustainable health care are a relatively recent topic that has gathered attention given its relationship with trust and the advantages of decentralization, immutability, and traceability introduced in health care. Nevertheless, more studies need to explore the role of SCs in this sector based on the frameworks propounded in the literature that reflect business logic that has been customized, automatized, and prioritized, as well as system trust. This study addressed this lacuna.

Objective: This study aimed to provide a comprehensive understanding of SCs in health care based on reviewing the frameworks propounded in the literature.

Methods: A structured literature review was performed based on the PRISMA (Preferred Reporting Items for Systematic Reviews and Meta-Analyses) principles. One database—Web of Science (WoS)—was selected to avoid bias generated by database differences and data wrangling. A quantitative assessment of the studies based on machine learning and data reduction methodologies was complemented with a qualitative, in-depth, detailed review of the frameworks propounded in the literature.

Results: A total of 70 studies, which constituted 18.7% (70/374) of the studies on this subject, met the selection criteria and were analyzed. A multiple correspondence analysis—with 74.44% of the inertia—produced 3 factors describing the advances in the topic. Two of them referred to the leading roles of SCs: (1) health care process enhancement and (2) assurance of patients' privacy protection. The first role included 6 themes, and the second one included 3 themes. The third factor encompassed the technical features that improve system efficiency. The in-depth review of these 3 factors and the identification of stakeholders allowed us to characterize the system trust in health care SCs. We assessed the risk of coverage bias, and good percentages of overlap were obtained—66% (49/74) of PubMed articles were also in WoS, and 88.3% (181/205) of WoS articles also appeared in Scopus.

Conclusions: This comprehensive review allows us to understand the relevance of SCs and the potentiality of their use in patient-centric health care that considers more than technical aspects. It also provides insights for further research based on specific stakeholders, locations, and behaviors.

(JMIR Med Inform 2025;13:e58575) doi:10.2196/58575

KEYWORDS

health care; smart contracts; blockchain; security; privacy; supply chain; patient centricity; system trust; stakeholders

Introduction

Background

New technologies have disrupted health care and imply exposure to complex scenarios. The Internet of Medical Things (IoMT) is increasingly receiving attention from practitioners and scholars to provide more alternatives for monitoring patients' conditions; allowing access to private medical data; and obtaining secure and flawless tools to protect data from attacks that can access or steal essential information or, in some cases, produce a patient fatality [1-3]. In this new technological

XSL•FO
RenderX

landscape, recent studies have highlighted that blockchain technology with smart contracts (SCs) provides the most reliable data security, cryptographic capacities, and decentralized storage and can lead to a low-cost ecosystem and sustainability in the medical setting [4,5].

The health care value chain is another research area where SCs have consistently shown effectiveness in avoiding counterfeiting and ensuring product security and safety. Implementing SCs on value chains can guarantee data provenance, eliminate unnecessary intermediaries, and provide an immutable history of transactions considering all the internal and external stakeholders. Although electronic health records (EHRs) are the most sensitive information in the SC environment, all the sensor devices are essential to provide a robust framework [6]. A health care value chain faces different challenges and aims to monitor diseases by considering real-time patient status updates. Furthermore, some visible barriers include data interoperability and communication among applications, medical devices or machines, and institutions. This increases complexity and continuously impacts costs and efficiency [7]. However, acquiring the logic of the value chain and adapting cutting-edge technologies to specific needs can save millions of lives and enhance quality of life for others.

There are different approaches to analyzing literature data. A classic methodology considers a small number of research studies to synthesize the different perspectives and angles of the topic and provide future avenues of research. In addition, there are various frameworks, such as systematic or structured reviews. Thus, a bibliometric framework considers an extensive quantity of literature by using statistical software. Multiple objectives are pursued, such as recognizing intellectual models and new trends. Our study aimed to provide a bibliometric analysis of SCs on the health care value chain and, thus, obtain a fundamental knowledge of the intellectual, social, and conceptual structure and other clustering techniques. This review's analysis was primarily interdisciplinary, seeking to discover barriers and possible gaps in the SC domain.

Motivation

Trust reduces complexity [8,9], manages uncertainty by compensation [8], and is an element of social capital [10]. Trust involves the truster and trustee as actors and expectations about actions in the future that could entail some risk for the trustee [11]. Trust applied to new technologies implies the transition from personal trust to system trust [8,11,12].

The literature refers to trust as a requirement of sustainable and human-centered technology [13]. Technologies, through trust, also look to fulfill social interests and be responsive. This affirmation is essential when technologies—including blockchain and SCs—are introduced in fields such as health care [11].

A blockchain is a distributed ledger [14] formed by chronologically ordered blocks [15,16]. It consists of multiple nodes connected peer to peer [15] and without a hierarchy among them [15]. Each block has an identification linked to the previous one via a reference or hash [14,15]. There is a genesis block, which is the first block of the chain, and any subsequent block also has the hash that allows for the identification of the previous one [15]. Blocks have a block header—that usually includes the hash of the last block, a time stamp, and a nonce [16]—and a payload or data with transactions [15,16]. The blockchain holds a consensus algorithm [14] that adds information to the chain [16]. Blocks are accepted or refused based on this algorithm [15]. In doing so, miners, who are a particular type of node, solve a challenge (ie, a mathematical puzzle) to verify the block and receive a reward [16] (ie, "gas"). Information cannot be modified once a block has been added to the chain. SCs are codes stored in a blockchain [17] containing transactions executed without intermediaries [14]. Thus, technologies such as blockchains and SCs promise transactions that do not require trust among parties—called trust-free, trustless [18], or trustless trust [11]—and distribute trust among the system—called distributed trust [11]. It is relevant to point out that their origins are independent despite the extensive joint use of blockchains and SCs. SCs were propounded as a transaction protocol [19], whereas blockchains uses cryptography to allow for the exchange between participants worldwide without the necessity of a central authority [20]. Blockchains and SCs look for trust development, where trust lies in the system design [18].

SCs strengthen the capabilities of a blockchain [21], aiming to (1) implement customizable business logic [22] through different functionalities [23] and (2) automatize the execution of preassigned transactions [3,24-26]. One of the most essential characteristics of SCs is that transactions are automatically executed [27]. For this, the interposition of a third party is not required [27]. This characteristic improves efficiency, accountability [28], and trust building [28,29]. SCs are transparently auditable [30] owing to their immutability. The decentralization of these systems also improves their resilience. Centralized systems represent a unique vertex of failure, a limitation that is overcome by SCs [31] deployed in blockchains [32]. Thus, SCs are especially relevant in health care as system trust generators [26,29].

Contribution and Related Works

This study fills a gap and responds to a request in the literature. Even though SCs are relevant in health care, a sufficient assessment is necessary. Some studies characterize SCs but do not refer to health care. It is the case of the proposal by Alzhrani et al [32], which presented a characterization of some SCs in real-world systems based on a blockchain's taxonomy. Nevertheless, this study does not focus on health care, and only 11 SCs were selected to exemplify its taxonomy. Other studies have focused on the health care sector but had a limited scope [14,33] and have not provided an in-depth characterization of SCs. Vargas and da Silva [14] assessed 3 case studies or frameworks related to SCs in the IoMT. Sookhak et al [33] limited their study to entering patient data into EHRs.

Several theoretical studies or literature reviews regarding blockchains in health care have considered or mentioned SCs in the health care domain. Nevertheless, they need to focus on providing in-depth information about the role and features of SCs. The closest one is the review by Marbouh et al [1], who inquired about the advantages of blockchains in improving

XSL•FO
RenderX

patient safety. The challenges and opportunities of this technology were the starting point of the aforementioned study, which referred to the uses of blockchains in health care. It introduced SCs and some uses of blockchains. Still, these contracts were not the study's primary goal, and it did not offer a systematic survey of the literature based on propounded frameworks.

Furthermore, Villarreal et al [29] studied blockchains in health care management systems and classified the architectural mechanisms in the literature. This study acknowledged SCs' relevance and problems in health care, but they were not systematized and referred to one specific telemedicine case. Similarly, in the study by Arbabi et al [34], the authors surveyed studies on blockchains in health care. They acknowledged the relevance of SCs but did not review their attributes in depth and suggested further assessment of the role of SCs.

Similarly, Khatri et al [35] systematically analyzed the broad topic of health care and blockchain integration and selected 50 publications for an in-depth analysis. In their study, the authors mentioned SCs; nevertheless, they did not propound specific functionalities or roles of SCs or link them with the authors' proposal about blockchains. Finally, McBee and Wilcox [36] studied the application of blockchains in medical imaging. Nonetheless, the literature has barely mentioned SCs to specify the origin of the name "blockchain 2.0" and its relationship with artificial intelligence (AI) [37].

Finally, Arbabi et al [34] suggested further research on SCs in health care. The authors mentioned that the potential of SCs in health care requires an in-depth assessment. In addition, Hawlitschek et al [38] propounded the development of additional research on the design of trusted interfaces. Thus, our study aimed to fill a gap in the literature—detailed in Table 1—and be responsive to its suggestions [34,38], focusing on an extensive review of SC frameworks in health care as elements that enhance trust and shift the traditional concept of trust among people to system trust, providing a characterization of it.

Table 1. Gaps in the literature.

Study	Health care sector	Focused on SCs[a]	Included different topics (extensive review)	Review based on propounded frameworks	The roles or characteristics of SCs were developed
Alzhrani et al [32]	No	Yes	Yes	No	Yes
Vargas and da Silva [14]	Yes	Yes	No	Yes	Yes
Sookhak et al [33]	Yes	Yes	No	No	No
Marbouh et al [1]	Yes	No	No	No	Yes
Villarreal et al [29]	Yes	No	No	No	No
Arbabi et al [34]	Yes	No	Yes	No	No
Khatri et al [35]	Yes	No	Yes	No	No
McBee and Wilcox [36]	Yes	No	No	No	No
Our study	Yes	Yes	Yes	Yes	Yes

[a]SC: smart contract.

Research Goals

Our study aimed to provide a holistic understanding of SCs in health care. We focused on developing a structured literature review of the state-of-the-art scientific landscape of new technological advances, tendencies, and bibliometric analysis to help provide a comprehensive understanding and up-to-date overview of the recent research and outline new perspectives and future research directions.

These contributions allow this research to fill a gap in understanding and respond to the suggestions by Arbabi et al [34] and Hawlitschek et al [38]. We adopted a systematic literature review approach because it allows for the replication of this study. A quantitative bibliometric analysis followed by an in-depth qualitative review of the studies enabled us to provide a detailed standpoint of the topic.

Methods

We used the PRISMA (Preferred Reporting Items for Systematic Reviews and Meta-Analyses) principles [37] for our systematic literature review [39]. Multimedia Appendix 1 contains the PRISMA checklist. The Web of Science (WoS) database provided the data, which were retrieved on July 4, 2023. The selection of databases for literature reviews is a topic under discussion [40], and there is no unique response. Some studies have used several databases, whereas others have been restricted to 1. Among the latter, several systematic reviews have selected WoS as their search database [39,41], including some in health care [42,43] and digital health [44]. The propounded reasons were the reputation and reliability of this source [45] and its extended use [39].

We chose to use only 1 database, WoS, because the joint use of several databases could introduce bias in our study. First, the search engines need to be unified and standardized. If we compare 2 of the most well-established databases of academic literature, WoS and Scopus [46], and one of the most relevant specialized databases in medical topics, PubMed [47], we could highlight some differences. For example, PubMed, Scopus, and WoS have the search option All Fields; nevertheless, this option encompasses different meanings for each database as they have other fields that are difficult to integrate [48] (ie, PubMed has

XSL•FO
RenderX

the field Pharmacological Action that is absent from WoS; WoS has the search fields Keyword Plus and Author Keyword, whereas PubMed has the search field Word-Term, MeSH Term, and Other Terms; Scopus includes a field named References, which is absent in the other 2 databases; and WoS has the search field Topic encompassing Title, Abstract, Keyword Plus, and Author Keyword, whereas Scopus has the search field Article, Title, Abstract, Keyword. Even though they could seem the same, they are not because WoS includes KeywordPlus, which responds to a proprietary algorithm, and Scopus's Keyword field includes both Author Keywords and Index Terms [controlled vocabulary]). Something similar happens with other well-known databases such as EBSCOhost (ie, EBSCOhost consists of a field named All Text, which is absent in WoS and other databases). The literature has highlighted the discrepancies among WoS, Scopus, and PubMed regarding different topics [49,50], such as document type [51,52], funding information [53], and subject classification [54].

The combination of information obtained from ≥2 databases also generates an additional source of bias caused by data wrangling [55]. Each database provides its search results in its format (ie, WoS uses commas [,] in some fields such as Keywords, whereas Scopus uses semicolons [;]). The different files require to be combined to assess them as one sample. This procedure could be performed manually or using an informatic tool; nevertheless, the data are always altered. For example, the order of the fields is different, and thus, we would have had to uniformize the data and the fields.

In addition to the possible bias caused by combining multiple databases as our main decision criteria to select only WoS, there is also the concern regarding coverage and overlap with other databases as different databases have unequal scopes and coverage policies [56].

There are several studies on different databases' coverage, but they are inconclusive regarding which database could be considered the most suitable for all cases. Some databases, including Scopus, could generally encompass a higher number of articles than WoS [57,58]; nevertheless, when specific topics are searched for, the coverage could be very similar [59], and some authors have also remarked that WoS coverage depth is better [47]. WoS is a multidisciplinary database with more articles than PubMed [57], but PubMed specializes in medicine and biomedical sciences [47,49]. On the basis of the novelty of the topic under study and its relationship with other disciplines, such as engineering, using a multidisciplinary database with a broader scope was considered the most suitable option. In addition, WoS has also essential coverage in medicine, similarly to Scopus. As an example, the evaluation of the content of Scopus and WoS in the context of Norway's scientific and scholarly publications concludes that both databases are highly and similarly comprehensive in medicine and health—with 89% of scientific publications and 87% of scholarly publications in Scopus and WoS, respectively—and natural sciences and technology—with 85% of scientific publications and 84% of scholarly publications in Scopus and WoS, respectively [60]. In addition, WoS has high levels of overlap with Scopus [58,59] and PubMed [57], which means that WoS shares an essential number of publications that are the same as those in each of the other databases (Scopus and PubMed).

Therefore, the most suitable option was to use only 1 database, WoS, for our study to avoid possible bias caused by the differences in the structures of different databases and data wrangling. In addition, WoS is a well-known and esteemed database with comprehensive coverage of the topic under study, presenting a high level of overlap with other multidisciplinary and specialized databases.

Furthermore, peer review is relevant to avoid selection bias [61]. Both authors participated in the different stages of the identification and screening process and discussed and agreed on the search terms, procedure, and screening and selection criteria before executing this process. Following previous studies [62], one of the authors (CDP) conducted a detailed review of the titles and abstracts and, when necessary, the complete texts to apply the selection criteria in the screening stage. The senior researcher (CAM) then shared and peer reviewed the results. Both authors discussed doubts and discrepancies until they reached an agreement.

Exact searches were used to identify articles to reduce the risk of bias. The terms used to refer SCs included 6 variations encompassing singular and plural for the word with and without a hyphen and the joint form, similarly to the study by Dwivedi et al [63]. The search was exact for each variation, and brackets were used. Adopting this approach did not leave the interpretation of term combinations to the subjective judgment of the researchers. The use of loose or approximate phrases was allowed for "health care." For the term "health care," we used an open search with a wildcard in the middle and at the end of the word ("health care*" or "health*care"). The search was Boolean. The query included the connectors OR for the same concepts and AND between different ideas considering the sense of the search and the rules of precedence of these operators in the WoS database. The query was as follows: ("smart contract" or "smart contracts" or "smart legal contract," or "smart-contract" or "smart-contracts" or "smart legal contracts") and (Health care* or health*care) (All Fields).

Results

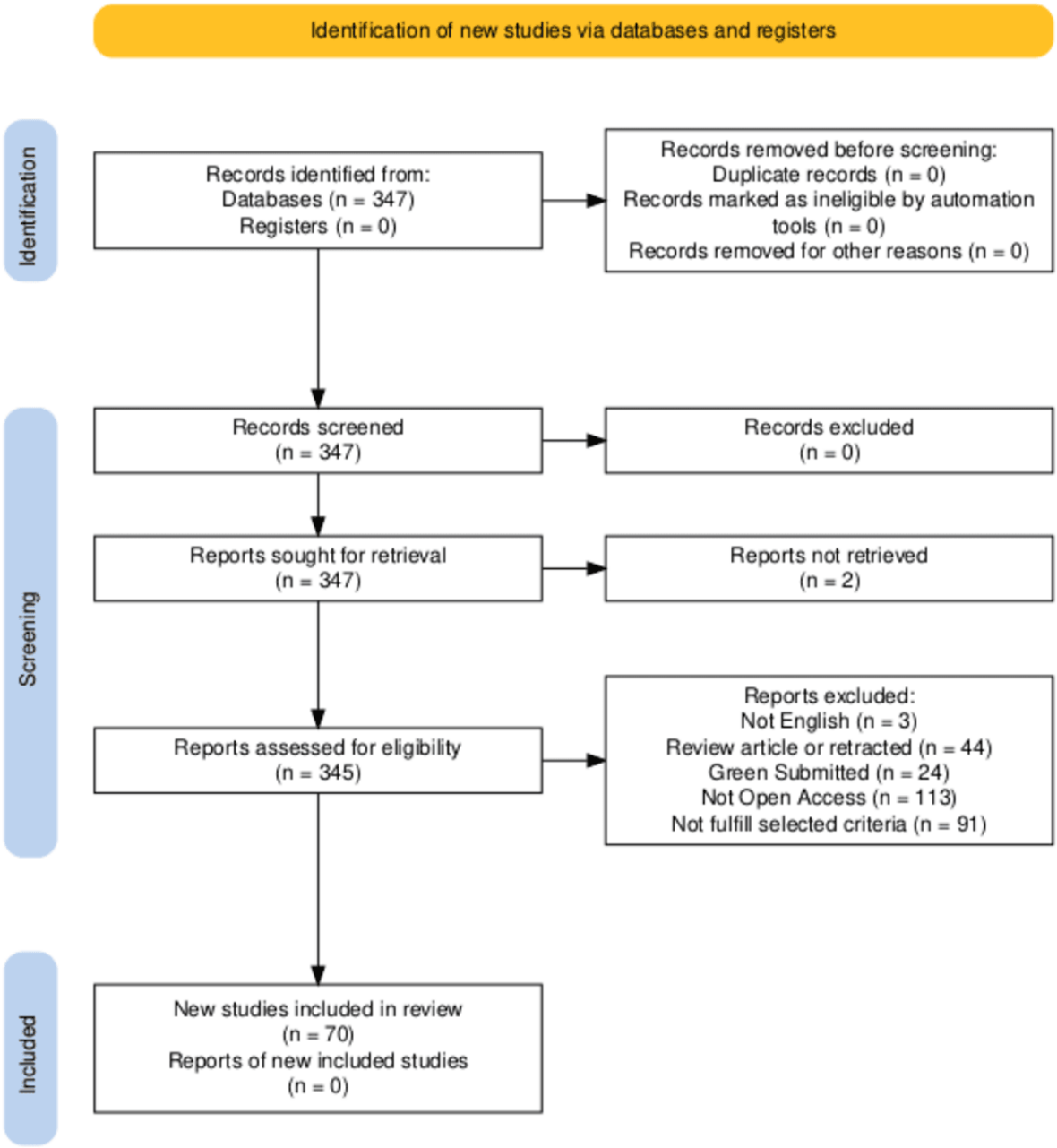
Overview

The search produced 374 results. The exclusion criteria were based on language (only English), type of source (review article, retraction, editorial material, and retracted publications were excluded), and availability (green submitted publications were excluded, and only open access publications were included). All these restrictions were established based on WoS filters. Finally, 163 publications were assessed. The selection encompassed the following criteria. Only those publications that (1) had the health care industry as their focus, (2) included a framework (framework, system, model, prototype, or similar), and (3) incorporated details about the roles of SCs and identified SCs were included in the study. In addition, the texts of the studies by Subramanian et al [64] and Elgendy et al [65] could not be accessed. A list of the 163 papers and their assessment results based on the aforementioned criteria can be reviewed in

XSL•FO
RenderX

Multimedia Appendix 2. A final sample of 70 publications was selected to be reviewed. Figure 1, which was made using the template propounded by the PRISMA organization, details the selection process [66].

Figure 1. PRISMA (Preferred Reporting Items for Systematic Reviews and Meta-Analyses) framework for literature assessment.



Bibliometric Assessment

We assessed the selected studies to find the main trends. The biblioshiny app and the *bibliometrix* tool (K-Synth Srl) was used in this process [67]. First, the data were screened. A total of 7% (5/70) of the studies had incomplete information about the authors' keywords. Some techniques such as multiple correspondence analysis [68] and network analysis [50] are sensible to missing data [69]. Keeping these studies could have biased the results.

Consequently, we decided to withdraw 7% (5/70) of the articles [70-74]. Thus, we included 65 articles in the bibliometric assessment. The aforementioned 7% (5/70) of the articles were withdrawn only for these purposes; they were read in depth for reporting in the literature review section. In addition, the terms "smart contract," "smart legal contract," "smart contracts," and "smart legal contracts" were signaled as synonyms where required.

The studies were published in 34 journals, and one of the journals, *IEEE Access*, published 29% (19/65) of the studies. The countries with the most citations were the United States, the United Arab Emirates, South Korea, and Egypt with >100 citations per country. Table 2 summarizes the descriptive information.

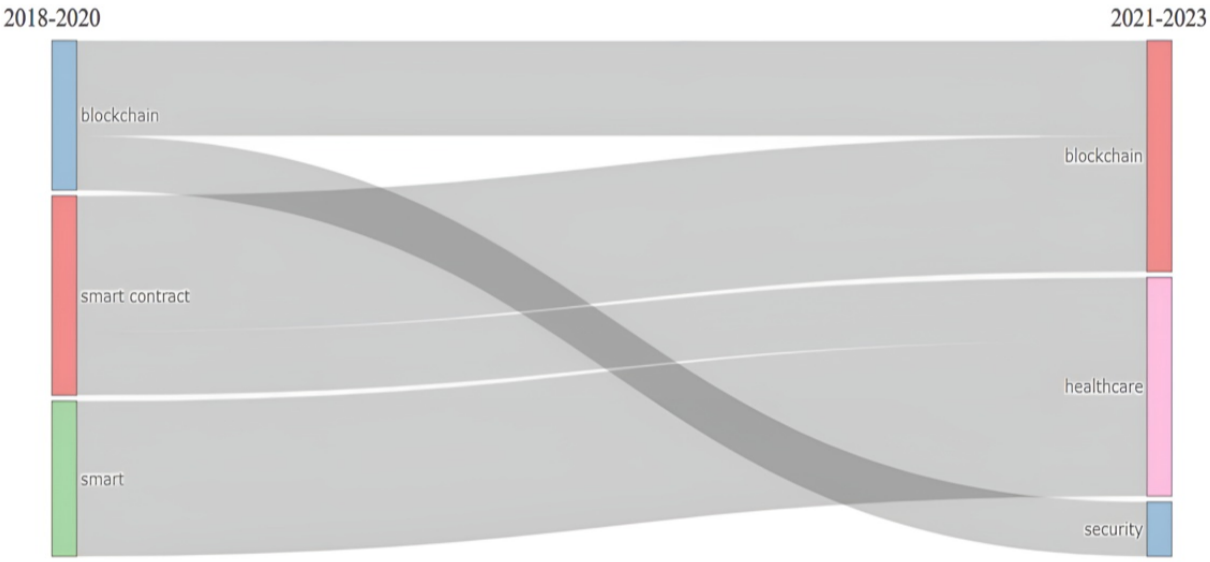
XSL•FO
RenderX

Table 2. Descriptive information.

Topic	Values
Sources (eg, journals and books), N	34
Documents, N	65
Annual growth rate (%)	67.03
Document age (y), mean (SD)	2.52 (1.16)
Authors, N	246
Single-authored documents (n=65), n (%)	2 (3)
International coauthorship, n (%)	32 (49)

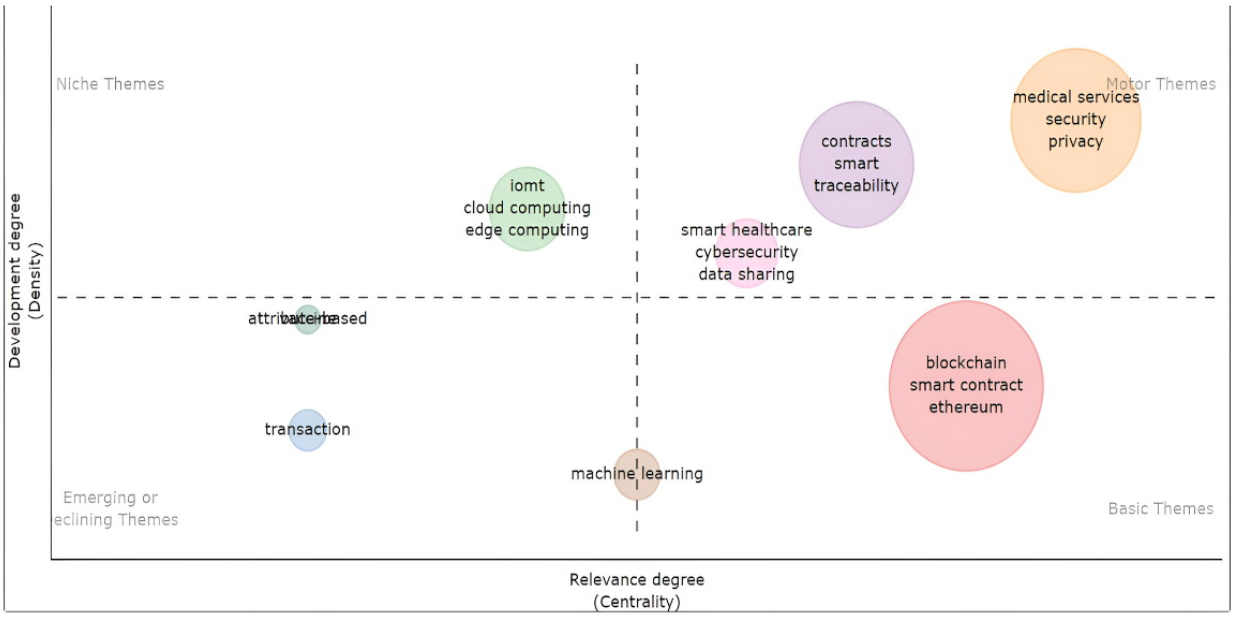
The historical evolution of this topic encompasses 6 years, from 2018 to 2023. The oldest study in our group was the one by Dagher et al [75], published in 2018. Although this theme is relatively new, its historical evolution (Figure 2) reflects the relevance of COVID-19. The literature has propounded that this disease was one of the most important in recent years [76,77]. Until 2020, a total of 3 topics represented the field. After 2020, a new independent concept, *security*, emerged, and the term *health care* acquired relevance. In addition, the map of subjects organizes them into 4 groups given their significance and development (Figure 3). It shows that security, privacy, medical services, traceability, innovative health care, cybersecurity, and data sharing are the most developed and relevant topics, known as motor subjects. The IoMT constitutes a niche theme and developed topic. Cloud and edge computing are also niche themes. On the other hand, machine learning has a low level of development, which could be explained by its novelty and a medium level of relevance. This situation could reflect the first attempts to use SCs and machine learning together in the same framework.

Figure 2. Historical evolution of the topic.



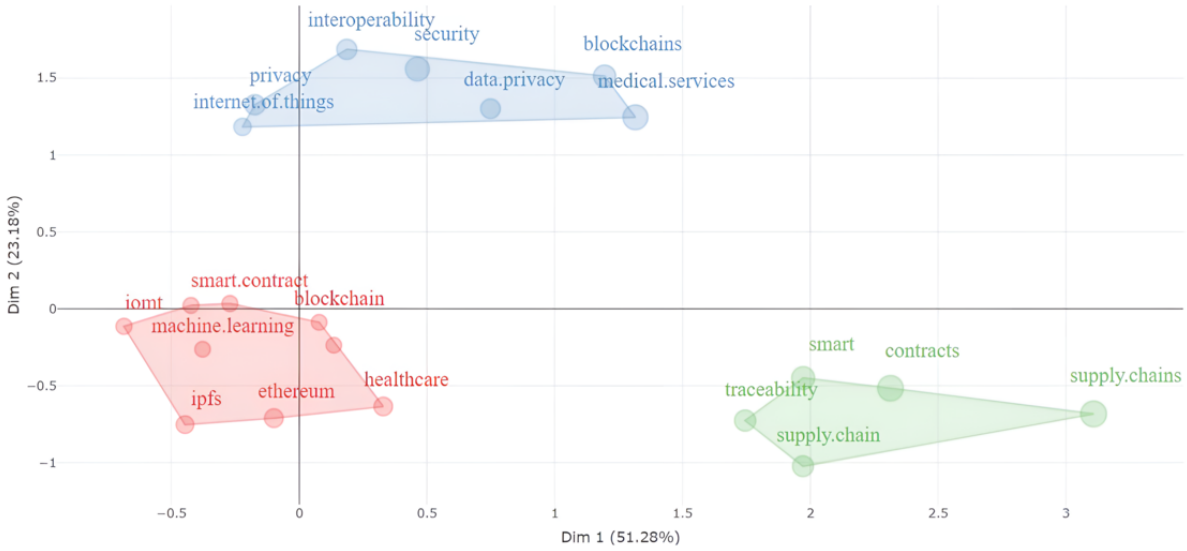
XSL•FO
RenderX

Figure 3. Map of subjects. IoMT: Internet of Medical Things.



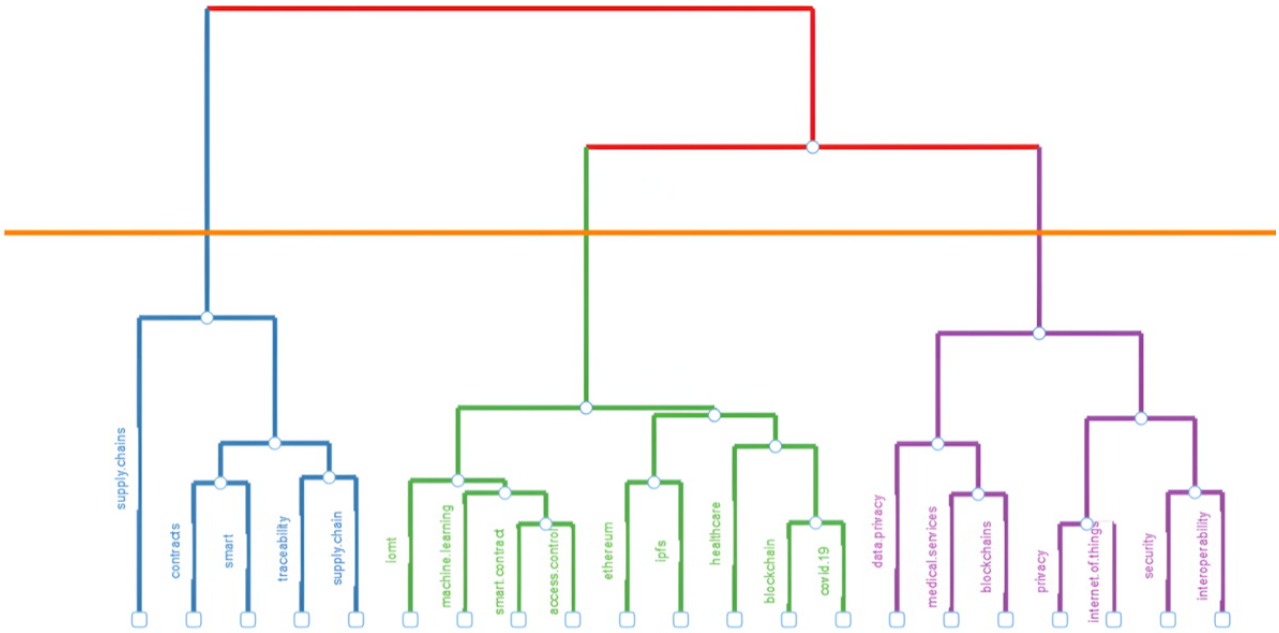
We obtained the conceptual map and keyword cluster [67] through factor analysis, a data reduction technique. Multiple correspondence analysis was used. This technique depicts the words on a map based on a similarity measure [67]. The study yielded 3 factors in 2 dimensions (Figures 4 and 5), representing 74.44% of the variability or inertia (dimension 1: 51.28%; dimension 2: 23.18%). The factorial analysis tree supported the existence of 3 dimensions under the cutting line (Figure 5). The first factor represents the concern for the technical aspects of the topic. In this factor, Ethereum and InterPlanetary File System (IPFS) had the highest contributions (Ethereum: 3.083%; IPFS: 2.054%; together: 5.137%). The second factor concerns data privacy and security. Security, privacy, and data privacy represented the highest contributions to this factor (security: 8.191%; privacy: 4.498%; data privacy: 4.026%; together: 16.715%). Finally, the third factor is concerned with the processes themselves. Supply chain and supply chains had the highest contributions (supply chain: 5.135%; supply chains: 10.066%; together: 15.2%).

Figure 4. Factorial analysis. IoMT: Internet of Medical Things; IPFS: InterPlanetary File System.



XSL•FO
RenderX

Figure 5. Factorial analysis tree. IoMT: Internet of Medical Things; IPFS: InterPlanetary File System.



Literature Review

Overview

The literature review encompassed the in-depth reading of the 70 selected articles. The factors related to processes and patients' privacy provided an initial approach to comprehending the role of SCs in health care. A detailed review of frameworks also permitted learning of SCs' technological characteristics, which are linked to the third factor in the quantitative stage. In addition, and following the motivation of this study, the assessment of the authors' proposals also allowed for propounding the building elements of system trust in health care SCs.

Roles of SCs in Health Care

Overview

SCs in health care encompassed 2 main kinds of business logic, depicted in Table 3: process improvement and protecting patient privacy rights. The first business logic, process improvement, included six themes: (1) the medicine and medical equipment supply chain [3,22-24,31,78-83], (2) insurance claim attention [26,84], (3) vaccination passports and certificates [72,76,77,85], (4) clinical research [86,87], (5) emergency attention process [88,89], and (6) regulatory compliance [90,91]. The second business logic, protecting patient privacy rights, incorporated three themes: (1) patient consent management [17,71]; (2) authentication, authorization, and access [21,27,73-75,92-114]; and (3) telemedicine and eHealth care [70,74,102,115-126]. This classification aims to understand the business logic reflected in SCs based on the main goal or goals pursued in developing the framework and the most relevant stakeholders.

Table 3. Roles of smart contracts in health care.

Roles and themes	References
Role 1: process improvement	
Medicine and medical equipment supply chain	[3,22-24,31,78-83]
Insurance claim attention	[26,84]
Vaccination passports and certificates	[72,76,77,85]
Clinical research	[86,87]
Emergency attention process	[88,89]
Regulatory compliance	[90,91]
Role 2: protecting patient privacy rights	
Patient consent management	[17,71]
Authentication, authorization, and access	[21,27,73-75,92-114]
Telemedicine and eHealth care	[70,74,102,115-126]

XSL•FO
RenderX

Role 1: Improving Health Care Processes

The studies that adopted this perspective used SCs as a lever to face problems related to processes, and their frameworks presented solutions to generate accountability and efficiency as their primary challenge. The topics encompassed in this group were medicines and medical equipment supply chain, insurance claim attention, telemedicine and eHealth, vaccination passports and certificates, clinical research, emergency attention processes, and regulatory compliance.

Medicine and medical equipment supply chains constituted the primary category of this group. The use of SCs in health supply chains [3,22,24,31,78-82] aimed to solve problems related to efficiency. These problems could be associated with tracing the supply chain stages, reducing overproduction and underconsumption, automating procurement contracts, or verifying the route of resealable returned drugs. Some studies had the specific mission of correcting malpractice, as exemplified by cases of counterfeit medicines and medical equipment [78,80,82].

Immutability, decentralization, transparency, and automatized execution of blockchains are valuable features that could solve these problems. Musamih et al [79] aimed to track all controlled drugs. SCs were required to follow all actions; thus, the actors in the supply chain would be individually accountable for their participation in the process because their activities could be tracked back. The framework included 7 actors: the controlled drug regulator, manufacturer, distributor, hospital and pharmacy, nurse station, and patient. The drug manufacturer controls the process. In total, 3 SCs were propounded in this framework: registration, production, and consumption.

One particularity of these frameworks is that several included the participation of specific government regulators, such as the Food and Drug Administration in the United States [22,31,81] and the Central Drugs Standard Control Organization in India [80], or nonspecific ones [3,79] that interact with private stakeholders. It is relevant to mention that SCs look to generate relationships without the necessity of trust among participants. Trust goes from the interpersonal level to the system level. In this case, government agencies that participate in blockchains could interact with their counterparts without the need to trust them, and vice versa.

As was previously stated, some frameworks depicted the extraordinary complexities of their stakeholders. As an example, Munasinghe and Halgamuge [82] propounded a framework that tried to uncover counterfeited COVID-19 vaccines. The authors realized that there was an international move of vaccines and then a nationwide distribution. This framework considered the ingredient provider, the vaccine manufacturer, the external company (vaccine supply), consolidation (government), the primary distribution, hospitals, clinics, pharmacies, and zone distributions as stakeholders. On the basis of these characteristics, the authors propounded 4 SCs.

Similarly, the study by Omar et al [24] depicted a particular negotiation structure of transactions. The authors applied SCs to procurement contracts negotiated by group purchasing organizations. In this context, several health providers negotiate procurement contracts with manufacturers. These health providers must pay a membership fee to the group, but they achieve better prices or loyalty rebates under this form of negotiation. The group negotiates prices with the manufacturer and determines the distributor for the entire group. This framework encompassed 5 SCs that represent the joint negotiation, the individual interests (rebates), and health care providers' actions (purchase placement).

The frameworks related to the health supply chain could also use additional technologies in the solution, but these are the exceptions. For example, Abbas et al [78] suggested combining blockchain and machine learning techniques in the same framework. This framework sought more efficient supply chain management and provided final consumer recommendations. SCs improved the supply chain. Recommendations were propounded based on machine learning outputs. In these solutions, SCs include functionalities related to registration and production, consumption, and waste assessment.

Insurance claim frameworks include SCs to facilitate the attention of these claims, reduce [24] fraudulent activities [26,64], or improve efficiency [84]. These contracts could include government entities as stakeholders [26], health insurance providers [84], claimants, patients, and health care providers or hospitals. The process automatized by SCs includes claim submission and attention and could also encompass billing and payment processes. Unlike in supply chain studies, patients have a relevant participation in these frameworks.

SCs could also enhance the processes related to vaccination passports and vaccination certificates. These vaccination records can (1) certify the status of vaccination required to do other activities, such as traveling; (2) provide information related to possible causes of the symptoms of a patient to physicians [72]; and (3) be used in sanitary emergencies [76,77,85]. In the first and second cases, the stakeholders are mainly patients and hospitals or clinics—where the patient was vaccinated and where they request later attention based on specific symptoms—and the primary function of the propounded technology is recording and providing access to the data. The third case, referring to vaccination records in emergencies such as the COVID-19 pandemic, involves more complex frameworks, including generating certificates and providing access to them to several stakeholders. These frameworks also consider the international movement of people and countries' requirements regarding vaccination [77,85]. Stakeholders include hospitals, vaccination centers, and governmental entities—ministries of health and foreign affairs [77,85].

Clinical research can use SCs for sharing and aggregating health care–related data because SCs provide secure storage and querying while protecting privacy in managing the data [86]. Both features are particularly relevant for research because they could promote collaboration among entities and data aggregation. Increasing the amount of data could also improve the generalization of studies [86]. Hospitals, as stakeholders, could act together to develop research activities [87]. For example, Kuo and Pham [87] introduced a framework allowing different hospitals to assess data during the COVID-19 pandemic. This inquiry encompassed 13 hospitals that acted as

XSL•FO
RenderX

a federation, which means that these institutions were required to share information and obtain, in some cases, a global aggregate.

The provision of attention to patients in an emergency context can also benefit from this technology [88,89]. For example, Ksibi et al [88] suggested using SCs to manage processes related to an emergency caused by a car crash. This framework allowed emergency vehicles to improve communication with the cars involved in the accident and with hospital emergency services. Peyvandi et al [89] established a framework that supported the prediction of diagnoses—or computer-aided diagnosis—in an emergency. Machine learning technology was used to forecast a diagnosis, whereas SCs preserved patients' privacy and granted access to the data. The stakeholders are emergency units that attend hospital emergency services.

Regulatory compliance could be enhanced using SCs [90,91], detecting and flagging privacy regulation violations. SCs allow patients to select their data privacy preferences, record events, and verify compliance with regulations. Regulatory compliance could also be enhanced using edge computing [90]. In these appraisals, the stakeholders are patients, health care providers—including hospitals—and clinical researchers. Governmental agencies are not included as the perspective of these frameworks is not enforcement but private compliance.

It is pertinent to note that these frameworks mentioned the United States [22,31,81] and India [80] through their regulators. They also referenced other regions such as Southeast Asia [85]. The studies were also concerned with complying with the regulations of the European Union [91] and the United States [90]. In addition, institutions located in the United Kingdom [87] and the United States [78,86] provided datasets used to test proposals.

Role 2: Improving Patient Privacy Protection

A new paradigm has influenced patient data management: patient centrality [15,92-94]. Patients are acknowledged as owners and managers of their health data [92]. Moreover, Jadav et al [115] have also alluded to a new reality in this field characterized by machine-centric interaction [92], where technology—especially the IoMT—provides different solutions for the health care sector. Both new complementary paradigms, patient centrality and machine-centric interactions, guide data management.

Data fragmentation [17], data breaches [86,116], compliance with regulations [115], cross-organizational coordination [95], and interoperability [96] are some challenges that the frameworks deal with. The stakeholders are patients and health facilities—including hospitals, clinics, physicians, laboratories, and researchers. Hospitals and clinics could act independently or as a consortium. Moreover, the blockchain could also act as a federation. Hashim et al [96] highlighted the problems that arise from the interoperability of independent blockchains and proposed a solution based on 3 SCs (search, global, and local). It is also relevant to mention that one study applied its framework in an animal health care service [97].

This role includes three main topics: (1) patient consent management; (2) authentication, authorization, and access; and (3) eHealth care. The patient centrality paradigm is reflected in patient consent management, which includes the possibility of patients defining viewer authorizations. For example, El Majdoubi et al [71] propounded a framework in which patients could manage their health data privacy preferences. A privacy agreement and enforcement were automatically settled if patients' preferences coincided with provider policies and privacy law. A privacy offer was published; this privacy offer could become a privacy agreement if it was accepted. After that, the system tracked the execution of this agreement. Thus, compliance with legal requirements and the stakeholders' preferences was ensured. In addition, this framework encompassed 3 levels of privacy. The first one, or P0, included data that could be viewed only by patients. The second one, or P1, referred to data that health care providers could also access. Finally, the third one, or P2, contained publicly available data [76].

Authentication, authorization, and access are central topics in patient privacy protection. SCs in these frameworks deploy different functions. They manage patients' consent, transfer and share data, search for patients, administer registration (add new users, view users, delete users, and create accounts), actualize data (add and update information), request access permission, restrict access, store data, provide search functions, and establish viewership criteria. The complexity of SC functions depends on the framework scope. The main stakeholders are hospitals and patients, as well as insurance companies and governmental agencies [98].

In addition, some frameworks use additional protocols or technologies to protect patient data privacy better. Saidi et al [99] used the self-sovereign identity (SSI) model. SSI aims to prove the identity in a digital environment, and a verifiable credential and a decentralized identifier underpin it. SSI has given rise to the SSI-based access control that allows for separate authentication, which is decentralized, and authorization, which is centralized. The SC—policy decision SC—provides efficiency and security to role assignments. In addition, this framework introduced an adaptive access control policy for emergencies. Other authors used ciphertext-policy attribute-based encryption (CP-ABE) [27,100] and attribute-based access control [95]. CP-ABE [81] and attribute-based access control determine access based on attributes; nevertheless, the first one, CP-ABE, offers a higher degree of granularity and is related to data encryption [100]. Biometric technology [20] such as fingerprints was also included in access control [21]. The use of ring signature and stealth address [20,87] to improve security was also considered [101]. Ring signature can hide the sender's identity, keeping the transaction safe because the receiver has the elements to verify the transaction authenticity [101]. Meanwhile, a stealth address maintains the anonymity of the sender's address, creating a 1-time address [101].

eHealth care and telemedicine represent a particular case, where SCs are mainly recommended for granting patient data access in a secure environment. Commonly, these frameworks are mentioned together in telemedicine, the IoMT, and eHealth [70,90,117], including wearable sensors, smart devices [118], and ambient intelligence [119]. Telemedicine faces several

XSL•FO
RenderX

challenges, including interoperability, incorrect diagnosis, and unfavorable perceptions. These perceptions are grounded on the fact that they are not the same as physical environments [120]. In telemedicine, the frameworks use SCs to generate secure transactions and automate participant communication [120]. In doing so, the frameworks could encompass laboratory test results [90], payment, and drug delivery, among other things [102,118,120]. The stakeholders include the usual ones—patients, hospitals, physicians, insurers, medical research organizations, and laboratories—and special ones, such as a telemedicine center [120] or diagnostic center [102] and federated hospital clouds [90]. Javed et al [2] referred to the health care regulator in their framework and gave the regulator control of the blockchain.

Telemedicine and eHealth care are concerned with malicious nodes and use additional technologies to deal with this problem or detect health abnormalities. Puri et al [70] suggested using SCs and AI to identify malicious nodes and security breaches. Similarly, Jadav et al [115] recommended including AI, specifically recurrent neural networks, to ensure data integrity. Neural networks train data to detect attacks and review data before storing them. Baiju et al [121] relied on machine learning (logistic regression) to anticipate abnormalities in the stored data. Dhasarathan et al [116] adopted a supervised machine learning approach to monitor risk factors in data transmission. In addition, Masud et al [119] suggested a framework that uses biometrics, among other technologies. The use of edge computing [122] and fog-cloud computers was also suggested [74,123,124].

In addition, Shaikh et al [125] suggested a framework that aimed to transform medical data into wisdom. In this framework, data collected from patients were cleaned and transformed into information, which was evaluated and converted into knowledge. Finally, metadata were extracted and converted into wisdom that could be used in medical research. The stakeholders were patients, physicians, data analysts, and knowledge managers. SCs provided registration advantages, data privacy customization, and exchange policies in this proposal. Abou-Nassar et al [126] were also concerned about the knowledge management and interoperability of IoMT devices related to semantic differences. The authors proposed an ontology model to achieve a higher level of trust.

It is relevant to mention that, without prejudice to their generalization capability, several studies obtained their testing dataset from institutions in the United States [17,89,94,100,101,103,115] and South Korea [127]. Some studies dealt with regulatory privacy concerns in the United States (Health Insurance Portability and Accountability Act; HIPAA [21,75]) and Europe (General Data Protection Regulation [95]). Finally, 2 frameworks were tailored for specific countries: the United Arab Emirates [98] and Italy [104].

Technical Characteristics That Provide Efficiency to Frameworks That Incorporate SCs in Health Care

The frameworks that propound the use of SCs face an essential challenge regarding their efficiency, requiring specific technical strategies to optimize their use [128]. The literature [28] mentioned limited data storage and inefficient execution as problems of SCs [129]. One of the strategies used to solve data storage problems is in-chain and off-chain data storage. Only the most relevant information is kept in the chain; additional information is sent to another source. IPFS is the preferred solution for maintaining data off the chain. This system optimizes resources because access to the data requires only the hash generated when the data are stored [105].

Some frameworks had an essential level of complexity and were required to preserve a critical quantity of data. Doing it in the blockchain could turn the system into an inefficient one. For example, Debe et al [22] propounded a framework for tracking resalable returned drugs that included several stakeholders and SCs. The medicines were produced by manufacturers in lots. These manufacturers were also required to share images of the package. Storing these images in the blockchain would be costly and inefficient. Thus, they were stored off the chain in the IPFS. Rai [80] suggested a similar solution, which also proposed keeping a lot of drug images in the IPFS.

The IPFS was also used in frameworks focused on patient data privacy and security. For example, Azbeg et al [105] propounded that only hash data should be stored in the chain. The IPFS preserved additional data as the off-chain storage, and Hussien et al [100] introduced a procedure to encrypt medical data before their storage in the IPFS, extending the CP-ABE and comprising searchable symmetric encryption [86].

Another strategy proposed to optimize resources was the specialization of SCs. SCs contain functions deployed when they are called. Under this strategy, the different parts that the framework requires are organized in several specialized SCs that could be individually deployed when needed, optimizing the resources. The quantity of SCs and the functions included in each could vary, and they are related to the complexity of the objectives that the framework aims to achieve. Frameworks based on 1 SC were the exception (ie, the study by Peyvandi et al [89], who proposed a single SC for patient data sharing).

In addition, the specialization of nodes was also propounded [78,97]. For example, Abbas et al [78] established a framework to manage medicine supply chain management and a recommendation system to avoid counterfeit drugs. This framework leveraged the attributes of SCs using machine learning. The SCs had an execution rate that was lower than desirable. The solution was to deploy them only on specified nodes, and only some of them—called endorsers—could validate the transactions. This solution enhanced the efficiency of the system.

The frameworks' efficiency and optimization are reflected in their cost analysis. The Ethereum platform provides the cost of gas or ether for function deployment. This cost can be converted to a specific national currency. Gas is relevant because it incentivizes miners to work [24] and protects them from distributed denial of service attacks [82]. Omar et al [24] and Chen et al [72] reported the cost based on a low average and fast execution in this platform converted to US dollars. The Hyperledger Fabric platform does not include ether; nevertheless, a computational cost can be calculated and compared. Munasinghe and Halgamuge [82], for example,

XSL•FO
RenderX

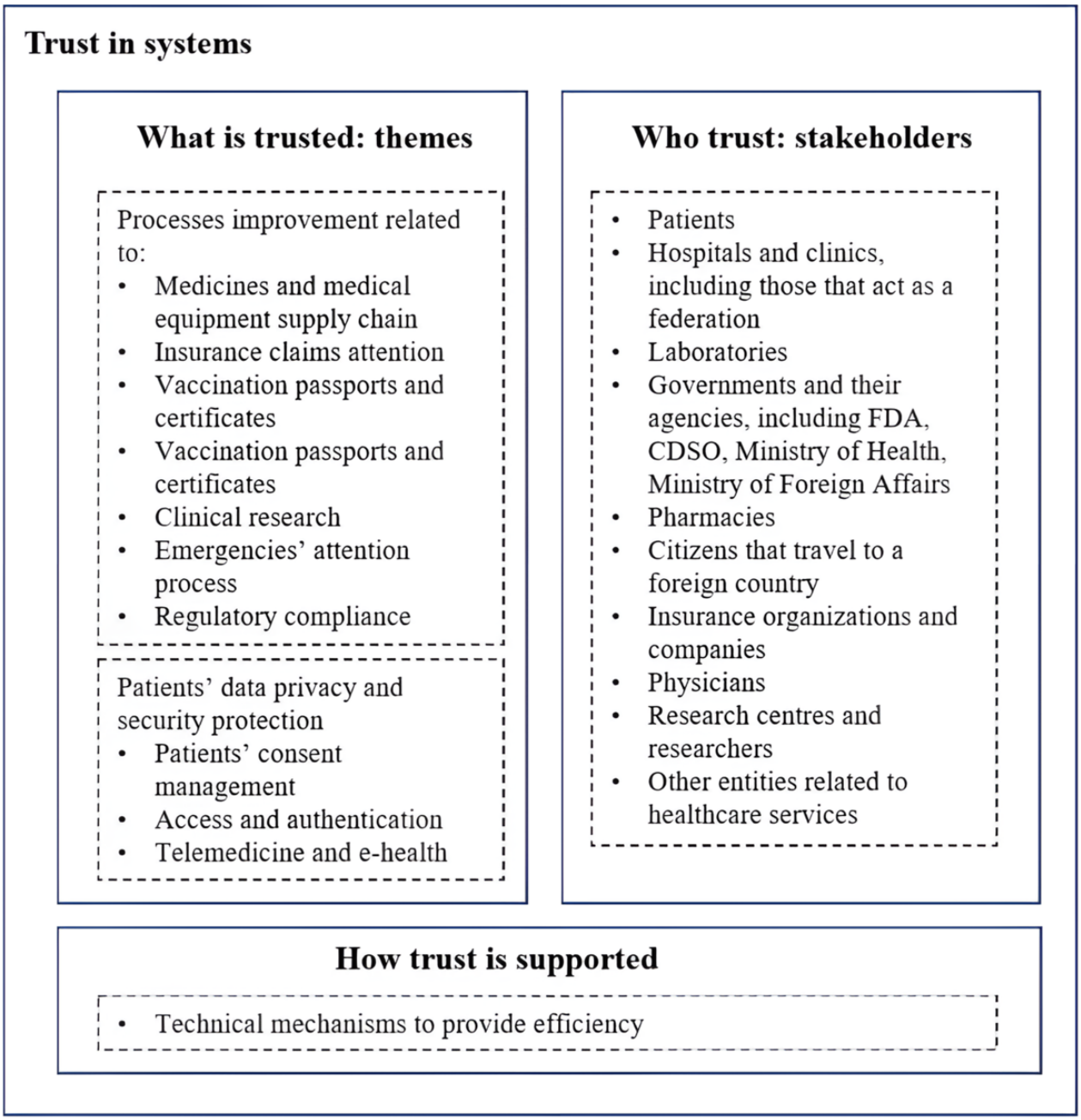
calculated and compared the cost of their framework developed in Hyperledger Fabric based on previous inquiries.

It is relevant to mention that the frameworks used extended cryptography mechanisms of blockchains, such as hash functions, digital signatures, public-private keys, and Merkle trees. Ethereum and Hyperledger Fabric were the preferred platforms. The frameworks used the features and facilities provided for these platforms (ie, the programming language Solidity in Ethereum). The different types of blockchain were represented in the frameworks. There were private blockchains (ie, the study by Omar et al [23]), public blockchains (ie, the study by Debe et al [22]), and consortiums (ie, the study by Mackey et al [26]). A detailed review of this specific topic can be found in the study by Sookhak et al [33]. Ganache, Truffle, and MetaMask were frequently used [26,31]. The SCs were commonly tested in Remix IDE [24,31].

Characterization of System Trust in Health Care SCs

SCs imply a transition from trust in people to trust in systems [8,11,12] where people interact without needing to trust each other or a central authority. On the basis of the previously exposed findings, we characterized system trust in health care SCs. The object of trust, or what is trusted, is represented by the 2 roles identified and the subjects they encompass. The stakeholders that interact without the necessity of a central authority are the subjects that are trusting and represent whom they trust. Finally, the technical strategies that these frameworks adopt support the trust in this system. Figure 6 summarizes these elements.

Figure 6. Characterization of system trust in health care smart contracts. CDSCO: Central Drugs Standard Control Organization; FDA: Food and Drug Administration.



XSL•FO
RenderX

Coverage Bias Assessment

Overview

This study used a single database, WoS, to avoid bias caused by the differences in database structure and data wrangling considering that the literature supports WoS's acceptable coverage and overlap with other databases. Nevertheless, assessing possible bias caused by the difference in coverage among different databases was considered relevant. Thus, subsequently, in our study, a comparison of coverage and overlap between WoS and other databases was conducted. The selected databases were (1) a multidisciplinary one of extended use, Scopus; and (2) a specialized one, PubMed.

The procedure had 2 stages. The first conducted a comparison between WoS and Scopus and between WoS and PubMed regarding their coverage and overlap. In this stage, the queries were evaluated to make them as similar as possible. The raw results on WoS were compared to identify the overlap between studies in both WoS and Scopus or both WoS and PubMed.

The second stage asked whether the articles published in Scopus or PubMed but not in WoS could provide relevant additional information to our literature review. Thus, we selected those studies that were only in Scopus or PubMed and were published until June 2023. They were then evaluated based on the 3 selection criteria of our research. For such purposes, the titles and abstracts and, in case of doubt, the full texts were reviewed by one of the researchers. The results were then discussed between the researchers, and the doubts and discrepancies were resolved. Third, the selected studies were read and compared with the literature review results. The searches for comparison purposes in PubMed, Scopus, and WoS were conducted on June 5, 2024.

Coverage Bias Between Multidisciplinary Databases: WoS and Scopus

The starting point of the comparison between WoS and Scopus was to select the most suitable field in both databases to conduct the search as All Fields was not adequate. The fields Topic in WoS and Article, Title, Abstract, Keyword in Scopus were close enough to our purposes. In addition, the difference between a search of All Fields and Topic was only 8 articles. Restrictions regarding language (only English), access, and type of article were included. The queries were as follows: Refine results for (“smart contract” or “smart-contract” or “smart contracts” or “smart legal contract” or “smart-contracts” or “smart legal contracts”) (Topic) AND (Healthcare* or health*care) (Topic) and English (Languages) and Review Article or Retracted Publication or Retraction or Editorial Material (Exclude – Document Types) and Green Submitted (Exclude – Open Access) and All Open Access (Open Access) for WoS and (TITLE-ABS-KEY (“smart contract” OR “smart-contract” OR “smart contracts” OR “smart legal contract” OR “smart-contracts” OR “smart legal contracts”) AND TITLE-ABS-KEY ((healthcare* OR health*care))) AND (LIMIT-TO (LANGUAGE, “English”)) AND (LIMIT-TO (OA, “all”)) AND (LIMIT-TO (DOCTYPE, “ar”)) for Scopus.

These searches produced 205 and 270 documents for WoS and Scopus, respectively. The results were then compared based on the digital object identifiers to obtain the level of overlap between both databases. The databases shared 181 documents, which represents an 88.3% (181/205) coincidence for WoS and a 67% (181/270) coincidence for Scopus. Notably, these percentages are higher than those obtained in other systematic reviews that also used WoS as their search engine. Maia et al [130] obtained a 61.4% (167/272) and 56.1% (213/380) overlap for the WoS and Scopus results, respectively.

Despite the high level of overlap, the next question was whether Scopus's additional documents could provide relevant qualitative information for our study. Thus, in the second stage, we selected the Scopus documents published before July 2023 because we conducted the search for our review on July 4, 2023, and 71 papers were obtained. We then applied the selection criteria used in our study. Finally, a list of 15 articles was retrieved and reviewed in depth. Most of them referred to data exchange and EHRs and could be included in the second role of SCs related to privacy and security [65,131-140]. The additional ones could be included in the first role of SCs related to process improvement [141-144].

Coverage Bias Between Multidisciplinary and Specialized Databases: WoS and PubMed

A procedure similar to the previously detailed one was performed between WoS and PubMed. PubMed used the field Title/Abstract. Filters for language—only English—and text availability—free full text—were then applied. The WoS query was the one previously detailed, and the PubMed query was as follows: ((“smart contract”[Title/Abstract] OR “smart-contract”[Title/Abstract] OR “smart contracts”[Title/Abstract] OR “smart legal contract”[Title/Abstract] OR “smart-contracts”[Title/Abstract] OR “smart legal contracts”[Title/Abstract])) AND ((Healthcare*[Title/Abstract] OR health*care[Title/Abstract])).

These searches produced 77 and 205 documents for PubMed and WoS, respectively. A total of 4 PubMed documents did not have a digital object identifier and were not considered in the comparison with the remaining 74 papers. A total of 49 of those documents were also included in WoS, which represents a 66% (49/74) overlap with PubMed. On the basis of previous studies [130], this percentage can be considered satisfactory.

The second step started with selecting PubMed documents published until June 2023. The result was 11 documents. The 3 selection criteria were applied to those documents, and only 9% (1/11) fulfilled them [145]. This study [145] dealt with privacy preservation and can be included in the second role of SCs.

Discussion

Principal Findings

This study aimed to provide an extensive understanding of SCs in health care through a comprehensive review of their roles and characteristics based on the frameworks developed in the literature. In doing so, this study fills a gap in the literature [34].

XSL•FO
RenderX

SCs are code or short programs whose output is a transaction [15] that is produced automatically when certain previously established conditions are met. These programs reflect the business logic [15] and provide flexibility (requirements can be introduced) and efficiency (their execution does not need additional enforcement) to a blockchain. The extensive review of frameworks offered insights into the business logic that was prioritized.

A quantitative bibliometric assessment highlighted the topic's novelty and importance, including subjects with high relevance and development. In addition, 3 factors were identified. These factors guided the in-depth review of each framework. Two roles of SCs were found—(1) process improvement, which encompassed 6 topics; and (2) patient data privacy enhancement, which encompassed 3 topics—and technical strategies and features that provide efficiency were found. These results provide more detailed information than previous inquiries, which have mentioned only this technology's use for medical devices, prescription tracking, remote patient monitoring, counterfeit drugs, EHRs, and incident report systems [1]. In addition, several stakeholders were identified.

This study acknowledged the relevance of technical topics. Previous studies have provided taxonomies based on technological features that consider the blockchain type, ledger type, consensus, identification, authentication and authorization, and EHR storage and features [33]. This study provided a new perspective based on the features selected by the literature that provide efficiency to systems.

The studies on trust and health care had different scopes. Some authors focused on trust in the system [146,147]. Others considered trust among various actors in this system, such as physicians and patients [25]. Independently of the orientation, the main proposal was that trust is relevant for accomplishing health care goals. The quantitative and qualitative review findings characterized system trust in health care SCs, which considered systems [146,147] and actors [25], through what is trusted, who trusts, and how trust is supported.

Finally, this study revealed different levels of impact on the concerns of multiple health care stakeholders. Individuals' rights—such as privacy [17,71], mobility [72,76,77,85], or health [88,89]—can be better protected. Physicians and researchers can use enhanced access to traceable and secure data when required [21,105]. SCs offer traceability, immutability, transparency, decentralization, automatization, and security to the different suppliers related to health care—such as hospitals, clinics, laboratories, research centers, and pharmacies—for their processes [16]. Governments can also obtain benefits from SCs. SCs facilitate private compliance with governmental regulations [90,91], preventing crime such as counterfeit drugs. In addition, SCs can facilitate the coordination of processes that require governmental intervention [22,31,81]. This study highlights new technologies, such as consensus and cryptographic methods, to address data security and privacy concerns. Second, this study details the different efforts to make potential solutions scalable and provide them to policyholders. Finally, this study shows the complexity of the health care systems, which is crucial for understanding the definition of multiple agreements among various involved stakeholders.

Strengths and Limitations of This Review

The strength of this review lies in its systematicity and comprehensiveness. This review evaluated studies that included SCs in health care in their frameworks. We applied several procedures to reduce the risk of selection bias. The criteria used in the selection process tried to avoid researchers' subjectivity, provide transparency, and allow for the review's replicability [148]. The PRISMA principles were followed, a peer review procedure was contemplated, 1 database was selected, and its coverage and overlap with 2 databases—a specialized and a multidisciplinary one—was assessed. Moreover, quantitative bibliometric techniques were guided by and complemented with an in-depth and detailed literature review.

Even so, the selection of articles had 2 significant limitations. First, the different academic databases needed to be unified or standardized. Indeed, we had to decide between possible bias caused by the differences between databases and data wrangling or selecting 1 database and assessing its coverage and overlap. Our decision was the latter, but we acknowledge that it entails a limitation. Second, our study included only open access documents because they were relevant to guarantee the review of this study and ensure our research's transparency.

Conclusions and Further Research

Overview

The theme of SCs in health care is not only novel but also relevant. SCs reflect the business logic into the blockchain. Using SCs is advisable to enhance access to health records with advanced tiers of security and privacy. They can also solve other problems requiring security and traceability, such as counterfeit drugs. SCs provide benefits to several stakeholders, both individual (ie, patients, researchers, and physicians) and institutional (ie, hospitals, clinics, and governments), who interact in the context of the themes that SCs cover without the need to know each other or having a central authority or intermediaries, supported by the technical mechanisms that provide efficiency to the processes. SCs have limitations, such as data storage and use of resources [129], but techniques have emerged to deal with these issues [28].

The literature review provided some topics that could be considered in further research regarding specific stakeholders, locations, behaviors, and issues.

Specific Stakeholders

Although the relevance of children's health data sharing is essential, there is a lack of studies that have dealt with the particular characteristics of this topic. The concept of patient centrality can be challenging in cases involving children and teenagers with limited control over their information. Moreover, no study has analyzed the characteristics of health care privacy protection for minors. The closest one is the study by Dagher et al [75], which acknowledged possible special conditions of the owner, such as the existence of a parent or guardian [84].

XSL•FO
RenderX

Specific Locations

SCs' advantages can help solve problems related to low- and middle-income countries. Nevertheless, only some studies focused on solving the particular necessities of low- and middle-income countries using SCs. Abbas et al [78] referred to counterfeit drugs as an extended problem in countries with weak economies, and Rai [80] designed their framework for the specific case of drug traceability in India.

Specific Behaviors

Hawlitschek et al [38] highlighted the relevance of considering fundamental interactions among people and systems. The authors named these interactions behavioral layers. It is necessary to decode these real-world behaviors so that they can be modeled into systems. This affirmation has an extended application to the SC because it oversees the deployment of business logic in the chain. Nevertheless, evidence must be provided regarding how these real-world behaviors are deciphered and converted into systems.

Specific Topics

First, the internet is a system requirement [88] and is considered an element that provides ease and simplicity [75,88,106] to SCs. Nevertheless, only a few aspects are known about the proper relationship between the quality of internet connectivity and the possible expansion of the use of SCs. Second, the cost of transactions is an existing health care problem [20]. SCs allow for the automation and optimization of these transactions and save costs [74,123]. Indeed, some studies provided a cost analysis based on the computational cost (gas cost) [75] and indicated the execution cost in a specific currency [24,79,91]; a qualitative cost comparison between a blockchain-based solution and a traditional one was made [85], and the execution cost based on workflow was also assessed [123]. Nevertheless, contrary to other industries [149-151], there is a lack of studies evaluating cost as a factor in the adoption of SCs in health care.

Conflicts of Interest

None declared.

Multimedia Appendix 1
PRISMA (Preferred Reporting Items for Systematic Reviews and Meta-Analyses) checklist.
[XLSX File (Microsoft Excel File), 14 KB - medinform_v13i1e58575_app1.xlsx]

Multimedia Appendix 2
List of 163 articles.
[DOCX File , 14 KB - medinform_v13i1e58575_app2.docx]

References

1. Marbouh D, Simsekler MC, Salah K, Jayaraman R, Ellahham S. Blockchain for patient safety: use cases, opportunities and open challenges. Data 2022 Dec 16;7(12):182-201. [doi: 10.3390/data7120182]
2. Javed IT, Alharbi F, Bellaj B, Margaria T, Crespi N, Qureshi KN. Health-ID: a blockchain-based decentralized identity management for remote healthcare. Healthcare (Basel) 2021 Jun 10;9(6):1-21 [FREE Full text] [doi: 10.3390/healthcare9060712] [Medline: 34200778]
3. Hawashin D, Salah K, Jayaraman R, Yaqoob I, Musamih A. A blockchain-based solution for mitigating overproduction and underconsumption of medical supplies. IEEE Access 2022 Jul 06;10:71669-71682. [doi: 10.1109/access.2022.3188778]
4. Zhuang Y, Sheets L, Shae Z, Tsai JJ, Shyu CR. Applying blockchain technology for health information exchange and persistent monitoring for clinical trials. AMIA Annu Symp Proc 2018 Dec 05;2018:1167-1175 [FREE Full text] [Medline: 30815159]
5. Zhuang Y, Chen YW, Shae ZY, Shyu CR. Generalizable layered blockchain architecture for health care applications: development, case studies, and evaluation. J Med Internet Res 2020 Jul 27;22(7):1-13 [FREE Full text] [doi: 10.2196/19029] [Medline: 32716300]
6. Ali A, Rahim HA, Pasha MF, Dowsley R, Masud M, Ali J, et al. Security, privacy, and reliability in digital healthcare systems using blockchain. Electronics 2021 Aug 23;10(16):2034-2061. [doi: 10.3390/electronics10162034]
7. Akhter Md Hasib KT, Chowdhury I, Sakib S, Monirujjaman Khan M, Alsufyani N, Alsufyani A, et al. Electronic health record monitoring system and data security using blockchain technology. Secur Commun Netw 2022 Feb 4;2022:1-15. [doi: 10.1155/2022/2366632]
8. Gruber S. Personal trust and system trust in the sharing economy: a comparison of community- and platform-based models. Front Psychol 2020 Dec 10;11:1-12 [FREE Full text] [doi: 10.3389/fpsyg.2020.581299] [Medline: 33362644]
9. Kroeger F. Unlocking the treasure trove: how can Luhmann's theory of trust enrich trust research? J Trust Res 2018 Dec 20;9(1):110-124. [doi: 10.1080/21515581.2018.1552592]
10. Bazarov T, Gevorgyan S, Karapetyan V, Karieva N, Kovalenko L, Dallakyan A. Modification of the concept of trust in the organization. Wisdom 2021 Sep 25;19(3):68-83. [doi: 10.24234/wisdom.v19i3.463]

XSL•FO
RenderX

11. Becker M, Bodó B. Trust in blockchain-based systems. Internet Policy Rev 2021 Apr 21;10(2):1-10. [doi: 10.14763/2021.2.1555]
12. Hanisch M, Goldsby CM, Fabian NE, Oehmichen J. Digital governance: a conceptual framework and research agenda. J Bus Res 2023 Jul 01;162:1-13. [doi: 10.1016/j.jbusres.2023.113777]
13. Wilson C, van der Velden M. Sustainable AI: an integrated model to guide public sector decision-making. Technol Soc 2022 Feb 01;68:1-11. [doi: 10.1016/j.techsoc.2022.101926]
14. Vargas C, da Silva MM. Case studies about smart contracts in healthcare. Digit Health 2023 Oct 08;9:1-12 [FREE Full text] [doi: 10.1177/20552076231203571] [Medline: 37822961]
15. Abutaleb RA, Alqahtany SS, Syed TA. Integrity and privacy-aware, patient-centric health record access control framework using a blockchain. Appl Sci 2023 Jan 12;13(2):1-40. [doi: 10.3390/app13021028]
16. Sadawi AA, Hassan MS, Ndiaye M. A survey on the integration of blockchain with IoT to enhance performance and eliminate challenges. IEEE Access 2021 Jan 19;9:1-20. [doi: 10.1109/access.2021.3070555]
17. Hu C, Li C, Zhang G, Lei Z, Shah M, Zhang Y, et al. CrowdMed-II: a blockchain-based framework for efficient consent management in health data sharing. World Wide Web 2022 Jan 01;25(3):1489-1515 [FREE Full text] [doi: 10.1007/s11280-021-00923-1] [Medline: 35002477]
18. Zavolokina L, Zani N, Schwabe G. Designing for trust in blockchain platforms. IEEE Trans Eng Manag 2023 Mar;70(3):849-863. [doi: 10.1109/tem.2020.3015359]
19. Imperius NP, Alahmar AD. Systematic mapping of testing smart contracts for blockchain applications. IEEE Access 2022;10:112845-112857. [doi: 10.1109/access.2022.3216874]
20. Syed TA, Alzahrani A, Jan S, Siddiqui MS, Nadeem A, Alghamdi T. A comparative analysis of blockchain architecture and its applications: problems and recommendations. IEEE Access 2019;7:176838-176869. [doi: 10.1109/access.2019.2957660]
21. Barka E, Al Baqari M, Kerrache CA, Herrera-Tapia J. Implementation of a biometric-based blockchain system for preserving privacy, security, and access control in healthcare records. J Sens Actuator Netw 2022 Dec 13;11(4):1-26. [doi: 10.3390/jsan11040085]
22. Debe M, Salah K, Jayaraman R, Arshad J. Blockchain-based verifiable tracking of resellable returned drugs. IEEE Access 2020 Oct 21;8:205848-205862. [doi: 10.1109/access.2020.3037363]
23. Omar IA, Jayaraman R, Salah K, Simsekler MC, Yaqoob I, Ellahham S. Ensuring protocol compliance and data transparency in clinical trials using blockchain smart contracts. BMC Med Res Methodol 2020 Sep 07;20(1):1-17 [FREE Full text] [doi: 10.1186/s12874-020-01109-5] [Medline: 32894068]
24. Omar IA, Jayaraman R, Debe MS, Salah K, Yaqoob I, Omar M. Automating procurement contracts in the healthcare supply chain using blockchain smart contracts. IEEE Access 2021 Feb 26;9:2169-3536. [doi: 10.1109/access.2021.3062471]
25. Hasselgren A, Hanssen Rensaa J, Kralevska K, Gligoroski D, Faxvaag A. Blockchain for increased trust in virtual health care: proof-of-concept study. J Med Internet Res 2021 Jul 30;23(7):1-15 [FREE Full text] [doi: 10.2196/28496] [Medline: 34328437]
26. Mackey TK, Miyachi K, Fung D, Qian S, Short J. Combating health care fraud and abuse: conceptualization and prototyping study of a blockchain antifraud framework. J Med Internet Res 2020 Sep 10;22(9):1-14 [FREE Full text] [doi: 10.2196/18623] [Medline: 32909952]
27. Yang X, Zhang C. Blockchain-based multiple authorities attribute-based encryption for EHR access control scheme. Appl Sci 2022 Oct 25;12(21):1-19. [doi: 10.3390/app122110812]
28. Li B, Qi P, Liu B, Di S, Liu J, Pei J, et al. Trustworthy AI: from principles to practices. ACM Comput Surv 2023 Jan 16;55(9):1-46. [doi: 10.1145/3555803]
29. Villarreal ER, Garcia-Alonso J, Moguel E, Alegria JA. Blockchain for healthcare management systems: a survey on interoperability and security. IEEE Access 2023 Jan 12;11:2169-3536. [doi: 10.1109/access.2023.3236505]
30. Schlatt V, Guggenberger T, Schmid J, Urbach N. Attacking the trust machine: developing an information systems research agenda for blockchain cybersecurity. Int J Inf Manage 2023 Feb 01;68:102470. [doi: 10.1016/j.ijinfomgt.2022.102470]
31. Musamih A, Jayaraman R, Salah K, Hasan HR, Yaqoob I, Al-Hammadi Y. Blockchain-based solution for the administration of controlled medication. IEEE Access 2021 Oct 20;9:2169-3536. [doi: 10.1109/access.2021.3121545]
32. Alzhrani FE, Saeedi KA, Zhao L. A taxonomy for characterizing blockchain systems. IEEE Access 2022 Oct 14;10:110568-110589. [doi: 10.1109/access.2022.3214837]
33. Sookhak M, Jabbarpour MR, Safa NS, Yu FR. Blockchain and smart contract for access control in healthcare: a survey, issues and challenges, and open issues. J Netw Comput Appl 2021 Mar 15;178:102950-102960. [doi: 10.1016/j.jnca.2020.102950]
34. Arbabi MS, Lal C, Veeraragavan NR, Marijan D, Nygård JF, Vitenberg R. A survey on blockchain for healthcare: challenges, benefits, and future directions. IEEE Commun Surv Tutor 2023 Nov 24;25(1):386-424. [doi: 10.1109/comst.2022.3224644]
35. Khatri S, Alzahrani FA, Ansari MT, Agrawal A, Kumar R, Khan RA. A systematic analysis on blockchain integration with healthcare domain: scope and challenges. IEEE Access 2021 Jun 09;9:84666-84687. [doi: 10.1109/access.2021.3087608]
36. McBee MP, Wilcox C. Blockchain technology: principles and applications in medical imaging. J Digit Imaging 2020 Jun;33(3):726-734 [FREE Full text] [doi: 10.1007/s10278-019-00310-3] [Medline: 31898037]

XSL•FO
RenderX

37. Page MJ, McKenzie JE, Bossuyt PM, Boutron I, Hoffmann TC, Mulrow CD, et al. The PRISMA 2020 statement: an updated guideline for reporting systematic reviews. PLoS Med 2021 Mar 29;18(3):1-9 [FREE Full text] [doi: 10.1371/journal.pmed.1003583] [Medline: 33780438]
38. Hawlitschek F, Notheisen B, Teubner T. The limits of trust-free systems: a literature review on blockchain technology and trust in the sharing economy. Electron Commer Res Appl 2018 May 01;29:50-63. [doi: 10.1016/j.elerap.2018.03.005]
39. Ferreira NC, Ferreira JJ. The field of resource-based view research: mapping past, present and future trends. Manag Decis (Forthcoming) 2024 Jan 08:1-19 [FREE Full text] [doi: 10.1108/md-10-2023-1908]
40. de Granda-Orive JI, Alonso-Arroyo A, Roig-Vázquez F. Which data base should we use for our literature analysis? Web of science versus SCOPUS. Arch Bronconeumol 2011 Feb 01;47(4):213-217. [doi: 10.1016/S1579-2129(11)70049-0]
41. Cheng C, Wang LM, Xie HM, Yan LL. Mapping digital innovation: a bibliometric analysis and systematic literature review. Technol Forecast Soc Change 2023 Sep 01;194:1-19. [doi: 10.1016/j.techfore.2023.122706]
42. Sabe M, Chen C, Perez N, Solmi M, Mucci A, Galderisi S, et al. Thirty years of research on negative symptoms of schizophrenia: a scientometric analysis of hotspots, bursts, and research trends. Neurosci Biobehav Rev 2023 Jan 01;144:1-12 [FREE Full text] [doi: 10.1016/j.neubiorev.2022.104979] [Medline: 36463972]
43. Liao CP, Sher CY, Liu YH. Progress and future directions for research on social media addiction: visualization-based bibliometric analysis. Telemat Inform 2023 May 01;80:1-16. [doi: 10.1016/j.tele.2023.101968]
44. Gu D, Li T, Wang X, Yang X, Yu Z. Visualizing the intellectual structure and evolution of electronic health and telemedicine research. Int J Med Inform 2019 Oct 01;130:1-11. [doi: 10.1016/j.ijmedinf.2019.08.007] [Medline: 31450080]
45. Zhao X, Nan D, Chen C, Zhang S, Che S, Kim JH. Bibliometric study on environmental, social, and governance research using CiteSpace. Front Environ Sci 2023 Jan 4;10:1-12. [doi: 10.3389/fenvs.2022.1087493]
46. Carmine S, De Marchi V. Reviewing paradox theory in corporate sustainability toward a systems perspective. J Bus Ethics 2022 Apr 17;184(1):139-158. [doi: 10.1007/S10551-022-05112-2]
47. Pranckutė R. Web of Science (WoS) and Scopus: the titans of bibliographic information in today's academic world. Publications 2021 Mar 12;9(1):1-59. [doi: 10.3390/publications9010012]
48. Rotolo D, Leydesdorff L. Matching Medline/PubMed data with web of science: a routine in R language. J Assoc Inf Sci Technol 2015 Dec 03;66(10):1-9. [doi: 10.2139/ssrn.2451436]
49. Falagas ME, Pitsouni EI, Malietzis GA, Pappas G. Comparison of PubMed, Scopus, Web of Science, and Google Scholar: strengths and weaknesses. FASEB J 2008 Feb 22;22(2):338-342. [doi: 10.1096/fj.07-9492LSF] [Medline: 17884971]
50. Li H, Liu W. Same same but different: self-citations identified through Scopus and Web of Science core collection. Scientometrics 2020 Jun 19;124(3):2723-2732. [doi: 10.1007/S11192-020-03573-8]
51. Kan Yeung AW. Document type assignment by Web of Science, Scopus, PubMed, and publishers to "Top 100" papers. Malays J Libr Inf Sci 2021 Dec 1;26(3):97-103. [doi: 10.22452/mjlis.vol26no3.5]
52. Mokhnacheva YV. Document types indexed in WoS and Scopus: similarities, differences, and their significance in the analysis of publication activity. Sci Tech Inf Process 2023 May 22;50(1):40-46. [doi: 10.3103/S0147688223010033]
53. Kokol P. Discrepancies among Scopus and Web of Science, coverage of funding information in medical journal articles: a follow-up study. J Med Libr Assoc 2023 Jul 10;111(3):703-708 [FREE Full text] [doi: 10.5195/jmla.2023.1513] [Medline: 37483361]
54. Singh P, Piryani R, Singh VK, Pinto D. Revisiting subject classification in academic databases: a comparison of the classification accuracy of Web of Science, Scopus and Dimensions. J Intell Fuzzy Syst 2020 Aug 31;39(2):1-6. [doi: 10.3233/jifs-179906]
55. Kumpulainen M, Seppänen M. Combining Web of Science and Scopus datasets in citation-based literature study. Scientometrics 2022 Aug 25;127(10):5613-5631. [doi: 10.1007/S11192-022-04475-7]
56. Archambault É, Campbell D, Gingras Y, Larivière V. Comparing bibliometric statistics obtained from the Web of Science and Scopus. J Am Soc Inf. Sci 2009 Apr 13;60(7):1320-1326. [doi: 10.1002/asi.21062]
57. Gavel Y, Iselid L. Web of Science and Scopus: a journal title overlap study. Online Inf Rev 2008 Feb 22;32(1):8-21. [doi: 10.1108/14684520810865958]
58. Visser M, van Eck NJ, Waltman L. Large-scale comparison of bibliographic data sourcescopus, Web of Science, Dimensions, Crossref, and Microsoft Academic. Quant Sci Stud 2021 Jan 17;2(1):20-41. [doi: 10.1162/qss_a_00112]
59. Singh P, Singh VK, Piryani R. Scholarly article retrieval from Web of Science, Scopus and Dimensions: a comparative analysis of retrieval quality. J Inf Sci 2023 Aug 21;5:11-16. [doi: 10.1177/01655515231191351]
60. Aksnes D, Sivertsen G. A criteria-based assessment of the coverage of Scopus and Web of Science. J Data Inf Sci 2019 Feb 20;4(1):1-21. [doi: 10.2478/jdis-2019-0001]
61. Rethlefsen ML, Kirtley S, Waffenschmidt S, Ayala AP, Moher D, Page MJ, PRISMA-S Group. PRISMA-S: an extension to the PRISMA statement for reporting literature searches in systematic reviews. Syst Rev 2021 Jan 26;10(1):39-50 [FREE Full text] [doi: 10.1186/s13643-020-01542-z] [Medline: 33499930]
62. Mills R, Mangone ER, Lesh N, Jayal G, Mohan D, Baraitser P. Chatbots that deliver contraceptive support: systematic review. J Med Internet Res 2024 Feb 27;26:1-11 [FREE Full text] [doi: 10.2196/46758] [Medline: 38412028]
63. Dwivedi V, Pattanaik V, Deval V, Dixit A, Norta A, Draheim D. Legally enforceable smart-contract languages. ACM Comput Surv 2021 Jun 05;54(5):1-34. [doi: 10.1145/3453475]

XSL•FO
RenderX

64. Subramanian HC, Cousins KC, Bouyad L, Sheth A, Conway D. Blockchain regulations and decentralized applications: panel report from AMCIS 2018. Commun Assoc Inf Syst 2020 Oct 22;47(1):189-207. [doi: 10.17705/1cais.04709]
65. Elgendy MA, Aborizka M, Allam AM. A blockchain-based model for securing IoT transactions in a healthcare environment. Int J Adv Comput Sci Appl 2022 Oct 04;13(9):67-75. [doi: 10.14569/IJACSA.2022.0130908]
66. Haddaway NR, Page MJ, Pritchard CC, McGuinness LA. PRISMA2020: an R package and shiny app for producing PRISMA 2020-compliant flow diagrams, with interactivity for optimised digital transparency and open synthesis. Campbell Syst Rev 2022 Jun 27;18(2):1-11 [FREE Full text] [doi: 10.1002/cl2.1230] [Medline: 36911350]
67. Aria M, Cuccurullo C. bibliometrix: an R-tool for comprehensive science mapping analysis. J Informetr 2017 Nov 01;11(4):959-975. [doi: 10.1016/j.joi.2017.08.007]
68. Dreyer J, Bergmann JM, Köhler K, Hochgraeber I, Pinkert C, Roes M, et al. Differences and commonalities of home-based care arrangements for persons living with dementia in Germany - a theory-driven development of types using multiple correspondence analysis and hierarchical cluster analysis. BMC Geriatr 2022 Sep 01;22(1):1-21 [FREE Full text] [doi: 10.1186/s12877-022-03310-1] [Medline: 36050645]
69. De Moor S, Vandeviver C, Vander Beken T. Assessing the missing data problem in criminal network analysis using forensic DNA data. Soc Netw 2020 May 01;61:99-106. [doi: 10.1016/j.socnet.2019.09.003]
70. Puri V, Kataria A, Sharma V. Artificial intelligence‐powered decentralized framework for internet of things in Healthcare 4.0. Trans Emerging Tel Tech 2021 Mar 02;35(4):1-16. [doi: 10.1002/ett.4245]
71. El Majdoubi D, El Bakkali H, Sadki S. SmartMedChain: a blockchain-based privacy-preserving smart healthcare framework. J Healthc Eng 2021 Nov 05;2021:1-11 [FREE Full text] [doi: 10.1155/2021/4145512] [Medline: 34777733]
72. Chen J, Chen X, Chen CL. A traceable blockchain-based vaccination record storage and sharing system. J Healthc Eng 2022 Mar 9;2022:1-15 [FREE Full text] [doi: 10.1155/2022/2211065] [Medline: 35310180]
73. Nishi FK, Shams-E-Mofiz M, Khan MM, Alsufyani A, Bourouis S, Gupta P, et al. Electronic healthcare data record security using blockchain and smart contract. J Sens 2022 May 29;2022:1-22. [doi: 10.1155/2022/7299185]
74. Khan AA, Shaikh ZA, Baitenova L, Mutaliyeva L, Moiseev N, Mikhaylov A, et al. QoS-ledger: smart contracts and metaheuristic for secure quality-of-service and cost-efficient scheduling of medical-data processing. Electronics 2021 Dec 10;10(24):1-16. [doi: 10.3390/electronics10243083]
75. Dagher GG, Mohler J, Milojkovic M, Marella PB. Ancile: privacy-preserving framework for access control and interoperability of electronic health records using blockchain technology. Sustain Cities Soc 2018 May 01;39:283-297. [doi: 10.1016/j.scs.2018.02.014]
76. Razzaq A, Mohsan SA, Ghayyur SA, Al-Kahtani N, Alkahtani HK, Mostafa SM. Blockchain in Healthcare: a decentralized platform for digital health passport of COVID-19 based on vaccination and immunity certificates. Healthcare (Basel) 2022 Dec 05;10(12):1-11 [FREE Full text] [doi: 10.3390/healthcare10122453] [Medline: 36553977]
77. Rashid MM, Choi P, Lee SH, Kwon KR. Block-HPCT: blockchain enabled digital health passports and contact tracing of infectious diseases like COVID-19. Sensors (Basel) 2022 Jun 02;22(11):1-16 [FREE Full text] [doi: 10.3390/s22114256] [Medline: 35684876]
78. Abbas K, Afaq M, Ahmed Khan T, Song WC. A blockchain and machine learning-based drug supply chain management and recommendation system for smart pharmaceutical industry. Electronics 2020 May 21;9(5):1-31. [doi: 10.3390/electronics9050852]
79. Musamih A, Salah K, Jayaraman R, Arshad J, Debe M, Al-Hammadi Y, et al. A blockchain-based approach for drug traceability in healthcare supply chain. IEEE Access 2021 Jan 08;9:9728-9743. [doi: 10.1109/access.2021.3049920]
80. Rai BK. BBTCD: blockchain based traceability of counterfeited drugs. Health Serv Outcomes Res Methodol 2022 Nov 20;23(3):1-17 [FREE Full text] [doi: 10.1007/s10742-022-00292-w] [Medline: 36438614]
81. Omar IA, Debe M, Jayaraman R, Salah K, Omar M, Arshad J. Blockchain-based supply chain traceability for COVID-19 personal protective equipment. Comput Ind Eng 2022 May 01;167:1-30 [FREE Full text] [doi: 10.1016/j.cie.2022.107995] [Medline: 35153368]
82. Munasinghe UJ, Halgamuge MN. Supply chain traceability and counterfeit detection of COVID-19 vaccines using novel blockchain-based system. Expert Syst Appl 2023 Oct 15;228:1-25 [FREE Full text] [doi: 10.1016/j.eswa.2023.120293] [Medline: 37197005]
83. Gebreab SA, Salah K, Jayaraman R, Zemerly J. Trusted traceability and certification of refurbished medical devices using dynamic composable NFTs. IEEE Access 2023 Mar 24;11:30373-30389. [doi: 10.1109/access.2023.3261555]
84. Panda SS, Jena D, Das P. A blockchain-based distributed authentication system for healthcare. Int J Healthc Inf. Syst Inform 2021 Jan 01;16(4):1-11. [doi: 10.4018/ijhisi.20211001.oa12]
85. Lee HA, Wu WC, Kung HH, Udayasankaran JG, Wei Y, Kijsanayotin B, et al. Design of a vaccine passport validation system using blockchain-based architecture: development study. JMIR Public Health Surveill 2022 Apr 26;8(4):1-31 [FREE Full text] [doi: 10.2196/32411] [Medline: 35377316]
86. Kuo TT, Pham A, Edelson ME, Kim J, Chan J, Gupta Y, R2D2 Consortium. Blockchain-enabled immutable, distributed, and highly available clinical research activity logging system for federated COVID-19 data analysis from multiple institutions. J Am Med Inform Assoc 2023 May 19;30(6):1167-1178 [FREE Full text] [doi: 10.1093/jamia/ocad049] [Medline: 36916740]

XSL•FO
RenderX

87. Kuo TT, Pham A. Quorum-based model learning on a blockchain hierarchical clinical research network using smart contracts. Int J Med Inform 2023 Jan 01;169:1-31 [FREE Full text] [doi: 10.1016/j.ijmedinf.2022.104924] [Medline: 36402113]
88. Ksibi A, Mhamdi H, Ayadi M, Almuqren L, Alqahtani MS, Ansari MD, et al. Secure and fast emergency road healthcare service based on blockchain technology for smart cities. Sustainability 2023 Mar 25;15(7):1-19. [doi: 10.3390/su15075748]
89. Peyvandi A, Majidi B, Peyvandi S, Patra J. Computer-aided-diagnosis as a service on decentralized medical cloud for efficient and rapid emergency response intelligence. New Gener Comput 2021 Jun 27;39(3-4):677-700 [FREE Full text] [doi: 10.1007/s00354-021-00131-5] [Medline: 34219860]
90. Li P, Xu C, Jin H, Hu C, Luo Y, Cao Y, et al. ChainSDI: a software-defined infrastructure for regulation-compliant home-based healthcare services secured by blockchains. IEEE Syst J 2020 Sep 18;14(2):2042-2053. [doi: 10.1109/jsyst.2019.2937930]
91. Barati M, Aujla GS, Llanos JT, Duodu KA, Rana OF, Carr M, et al. Privacy-aware cloud auditing for GDPR compliance verification in online healthcare. IEEE Trans Ind Inf 2022 Jul 27;18(7):4808-4819. [doi: 10.1109/tii.2021.3100152]
92. Rai BK. Blockchain-enabled electronic health records for healthcare 4.0. Int J E-Health Med Commun 2022 Jan 01;13(4):342-354. [doi: 10.4018/ijehmc.309438]
93. Yao Y, Kshirsagar M, Vaidya G, Ducrée J, Ryan C. Convergence of blockchain, autonomous agents, and knowledge graph to share electronic health records. Front Blockchain 2021 Apr 6;4:33-40. [doi: 10.3389/fbloc.2021.661238]
94. Sonkamble RG, Bongale AM, Phansalkar S, Sharma A, Rajput S. Secure data transmission of electronic health records using blockchain technology. Electronics 2023 Feb 17;12(4):1-17. [doi: 10.3390/electronics12041015]
95. De Oliveira MT, Reis LH, Verginadis Y, Mattos DM, Olabarriaga SD. SmartAccess: attribute-based access control system for medical records based on smart contracts. IEEE Access 2022 Oct 26;10:117836-117854. [doi: 10.1109/access.2022.3217201]
96. Hashim F, Shuaib K, Sallabi F. Connected blockchain federations for sharing electronic health records. Cryptography 2022 Sep 16;6(3):1-20. [doi: 10.3390/cryptography6030047]
97. Iqbal M, Matulevicius R. Exploring sybil and double-spending risks in blockchain systems. IEEE Access 2021 May 19;9:76153-76177. [doi: 10.1109/access.2021.3081998]
98. Madine MM, Salah K, Jayaraman R, Yaqoob I, Al-Hammadi Y, Ellahham S, et al. Fully decentralized multi-party consent management for secure sharing of patient health records. IEEE Access 2020 Dec 15;8:225777-225791. [doi: 10.1109/access.2020.3045048]
99. Saidi H, Labraoui N, Ari AA, Maglaras LA, Emati JH. DSMAC: privacy-aware decentralized self-management of data access control based on blockchain for health data. IEEE Access 2022 Sep 29;10:101011-101028. [doi: 10.1109/access.2022.3207803]
100. Hussien HM, Yasin SM, Udzir NI, Ninggal MI. Blockchain-based access control scheme for secure shared personal health records over decentralised storage. Sensors (Basel) 2021 Apr 02;21(7):1-36 [FREE Full text] [doi: 10.3390/s21072462] [Medline: 33918266]
101. Lee D, Song M. MEXchange: a privacy-preserving blockchain-based framework for health information exchange using ring signature and stealth address. IEEE Access 2021 Nov 25;9:158122-158139. [doi: 10.1109/access.2021.3130552]
102. Raj A, Prakash S. Smart contract-based secure decentralized smart healthcare system. Int J Softw Innov 2022;11(1):1-19. [doi: 10.4018/ijsi.315742]
103. Zhuang Y, Sheets LR, Chen YW, Shae Z, Tsai JJ, Shyu C. A patient-centric health information exchange framework using blockchain technology. IEEE J Biomed Health Inform 2020 Aug 01;24(8):2169-2176. [doi: 10.1109/jbhi.2020.2993072]
104. Celesti A, Ruggeri A, Fazio M, Galletta A, Villari M, Romano A. Blockchain-based healthcare workflow for tele-medical laboratory in federated hospital IoT clouds. Sensors (Basel) 2020 May 02;20(9):1-12 [FREE Full text] [doi: 10.3390/s20092590] [Medline: 32370129]
105. Azbeg K, Ouchetto O, Jai Andaloussi S. BlockMedCare: a healthcare system based on IoT, Blockchain and IPFS for data management security. Egypt Inform J 2022 Jul 01;23(2):329-343. [doi: 10.1016/j.eij.2022.02.004]
106. Daraghmi EY, Daraghmi YA, Yuan SM. MedChain: a design of blockchain-based system for medical records access and permissions management. IEEE Access 2019 Nov 21;7:164595-164613. [doi: 10.1109/access.2019.2952942]
107. Gohar AN, Abdelmawgoud SA, Farhan MS. A patient-centric healthcare framework reference architecture for better semantic interoperability based on blockchain, cloud, and IoT. IEEE Access 2022 Aug 29;10:92137-92157. [doi: 10.1109/access.2022.3202902]
108. Haddad A, Habaebi MH, Suliman FE, Elsheikh EA, Islam MR, Zabidi SA. Generic patient-centered blockchain-based EHR management system. Appl Sci 2023 Jan 30;13(3):1-19. [doi: 10.3390/app13031761]
109. Kumar A, Krishnamurthi R, Nayyar A, Sharma K, Grover V, Hossain E. A novel smart healthcare design, simulation, and implementation using healthcare 4.0 processes. IEEE Access 2020 Jun 25;8:118433-118471. [doi: 10.1109/access.2020.3004790]
110. Mhamdi H, Ayadi M, Ksibi A, Al-Rasheed A, Soufiene BO, Hedi S. SEMRAchain: a secure electronic medical record based on blockchain technology. Electronics 2022 Nov 06;11(21):1-16. [doi: 10.3390/electronics11213617]
111. Palanikkumar D, Alrasheedi AF, Parthasarathi P, Askar SS, Abouhawwash M. Hybrid smart contracts for securing IoMT data. Comput Syst Sci Eng 2023 Jan 07;44(1):457-469. [doi: 10.32604/csse.2023.024884]

XSL•FO
RenderX

112. Sonkamble RG, Phansalkar SP, Potdar VM, Bongale AM. Survey of interoperability in electronic health records management and proposed blockchain based framework: MyBlockEHR. IEEE Access 2021 Nov 18;9:158367-158401. [doi: 10.1109/access.2021.3129284]
113. Zhang Y, Wei X, Cao J, Ning J, Ying Z, Zheng D. Blockchain-enabled decentralized attribute-based access control with policy hiding for smart healthcare. J King Saud Univ Comput Inf Sci 2022 Nov 01;34(10):8350-8361. [doi: 10.1016/j.jksuci.2022.08.015]
114. Salonikias S, Khair M, Mastoras T, Mavridis I. Blockchain-based access control in a globalized healthcare provisioning ecosystem. Electronics 2022 Aug 25;11(17):1-23. [doi: 10.3390/electronics11172652]
115. Jadav D, Jadav NK, Gupta R, Tanwar S, Alfarraj O, Tolba A, et al. A trustworthy healthcare management framework using amalgamation of AI and blockchain network. Mathematics 2023 Jan 27;11(3):1-20. [doi: 10.3390/math11030637]
116. Dhasarathan C, Hasan MK, Islam S, Abdullah S, Khapre S, Singh D, et al. User privacy prevention model using supervised federated learning ‐ based block chain approach for internet of Medical Things. CAAI Trans Intell Technol 2023 May 04:1-15. [doi: 10.1049/cit2.12218]
117. Shahbazi Z, Byun YC. Towards a secure thermal-energy aware routing protocol in wireless body area network based on blockchain technology. Sensors (Basel) 2020 Jun 26;20(12):1-26 [FREE Full text] [doi: 10.3390/s20123604] [Medline: 32604851]
118. Taralunga DD, Florea BC. A blockchain-enabled framework for mHealth systems. Sensors (Basel) 2021 Apr 16;21(8):1-24 [FREE Full text] [doi: 10.3390/s21082828] [Medline: 33923842]
119. Masud M, Gaba GS, Kumar P, Gurtov A. A user-centric privacy-preserving authentication protocol for IoT-AmI environments. Comput Commun 2022 Dec 01;196:45-54. [doi: 10.1016/j.comcom.2022.09.021]
120. Abugabah A, Nizamuddin N, Alzubi AA. Decentralized telemedicine framework for a smart healthcare ecosystem. IEEE Access 2020 Sep 04;8:2169-3536. [doi: 10.1109/access.2020.3021823]
121. Baiju VB, Saranya S, Sriram D, Ahmed MR, Mohammed A. Decentralizing electronic medical records on the blockchain using smart contracts. J Pharm Negat Results 2022 Jan 01;13(SO3):1-6. [doi: 10.47750/pnr.2022.13.s03.050]
122. Akkaoui R, Hei X, Cheng W. EdgeMediChain: a hybrid edge blockchain-based framework for health data exchange. IEEE Access 2020 Jun 19;8:113467-113486. [doi: 10.1109/access.2020.3003575]
123. Ravikumar G, Venkatachalam K, Masud M, Abouhawwash M. Cost efficient scheduling using smart contract cognizant Ethereum for IoMT. Intell Autom Soft Comput 2022 Jan 01;33(2):865-877. [doi: 10.32604/iasc.2022.024278]
124. Lakhan A, Mohammed MA, Rashid AN, Kadry S, Panityakul T, Abdulkareem KH, et al. Smart-contract aware Ethereum and client-fog-cloud healthcare system. Sensors (Basel) 2021 Jun 14;21(12):1-21 [FREE Full text] [doi: 10.3390/s21124093] [Medline: 34198608]
125. Shaikh ZA, Khan AA, Teng L, Wagan AA, Laghari AA. BIoMT modular infrastructure: the recent challenges, issues, and limitations in blockchain Hyperledger-enabled e-healthcare application. Wirel Commun Mob Comput 2022 Sep 21;2022:1-14. [doi: 10.1155/2022/3813841]
126. Abou-Nassar EM, Iliyasu AM, El-Kafrawy PM, Song OY, Bashir AK, El-Latif AA. DITrust chain: towards blockchain-based trust models for sustainable healthcare IoT systems. IEEE Access 2020 Jun 02;8:111223-111238. [doi: 10.1109/access.2020.2999468]
127. Iqbal N, Jamil F, Ahmad S, Kim D. A novel blockchain-based integrity and reliable veterinary clinic information management system using predictive analytics for provisioning of quality health services. IEEE Access 2021 Jan 05;9:8069-8098. [doi: 10.1109/access.2021.3049325]
128. Vacca A, Di Sorbo A, Visaggio CA, Canfora G. A systematic literature review of blockchain and smart contract development: techniques, tools, and open challenges. J Syst Softw 2021 Apr 01;174:1-19. [doi: 10.1016/j.jss.2020.110891]
129. Wu C, Xiong J, Xiong H, Zhao Y, Yi W. A review on recent progress of smart contract in blockchain. IEEE Access 2022 May 10;10:50839-50863. [doi: 10.1109/access.2022.3174052]
130. Maia SC, de Benedicto GC, do Prado JW, Robb DA, de Almeida Bispo ON, de Brito MJ. Mapping the literature on credit unions: a bibliometric investigation grounded in Scopus and Web of Science. Scientometrics 2019 Jul 5;120(3):929-960. [doi: 10.1007/S11192-019-03165-1]
131. Hylock RH, Zeng X. A blockchain framework for patient-centered health records and exchange (HealthChain): evaluation and proof-of-concept study. J Med Internet Res 2019 Aug 31;21(8):1-19 [FREE Full text] [doi: 10.2196/13592] [Medline: 31471959]
132. Hang L, Choi E, Kim DH. A novel EMR integrity management based on a medical blockchain platform in hospital. Electronics 2019 Apr 25;8(4):1-27. [doi: 10.3390/electronics8040467]
133. Jaiman V, Urovi V. A consent model for blockchain-based health data sharing platforms. IEEE Access 2020 Aug 05;8:143734-143745. [doi: 10.1109/access.2020.3014565]
134. Madine MM, Battah AA, Yaqoob I, Salah K, Jayaraman R, Al-Hammadi Y, et al. Blockchain for giving patients control over their medical records. IEEE Access 2020 Oct 20;8:193102-193115. [doi: 10.1109/access.2020.3032553]
135. Vangipuram SL, Mohanty SP, Kougianos E. CoviChain: a blockchain based framework for nonrepudiable contact tracing in healthcare cyber-physical systems during pandemic outbreaks. SN Comput Sci 2021 Jun 20;2(5):1-16 [FREE Full text] [doi: 10.1007/s42979-021-00746-x] [Medline: 34179827]

XSL•FO
RenderX

136. Hasan K, Chowdhury MJ, Biswas K, Ahmed K, Islam MS, Usman M. A blockchain-based secure data-sharing framework for software defined wireless body area networks. Computer Networks 2022 Jul 01;211:1-28. [doi: 10.1016/j.comnet.2022.109004]
137. Sun Z, Han D, Li D, Wang X, Chang CC, Wu Z. A blockchain-based secure storage scheme for medical information. J Wireless Com Network 2022 Apr 25;2022(1):1-25. [doi: 10.1186/S13638-022-02122-6]
138. Puneeth RP, Parthasarathy G. Seamless data exchange: advancing healthcare with cross-chain interoperability in blockchain for electronic health records. Int J Adv Comput Sci Appl 2023 Jan 01;14(10):280-289. [doi: 10.14569/ijacsa.2023.0141031]
139. Rastogi P, Singh D, Bedi SS. Fully decentralized block chain with proxy re-encryption algorithm for healthcare security. Int J Adv Comput Sci Appl 2023 Feb 28;16(1):572-583. [doi: 10.22266/ijies2023.0228.49]
140. Islam MA, Islam MA, Jacky MA, Al-Amin M, Miah MS, Khan MM, et al. Distributed ledger technology based integrated healthcare solution for Bangladesh. IEEE Access 2023 May 24;11:51527-51556. [doi: 10.1109/access.2023.3279724]
141. Amponsah AA, Adekoya AF, Weyori BA. A novel fraud detection and prevention method for healthcare claim processing using machine learning and blockchain technology. Decis Anal J 2022 Sep 01;4:1-12. [doi: 10.1016/j.dajour.2022.100122]
142. Taylor A, Kugler A, Marella PB, Dagher GG. VigilRx: a scalable and interoperable prescription management system using blockchain. IEEE Access 2022 Mar 02;10:25973-25986. [doi: 10.1109/access.2022.3156015]
143. Karmakar A, Ghosh P, Banerjee PS, De D. ChainSure: agent free insurance system using blockchain for healthcare 4.0. Intell Syst Appl 2023 Feb 01;17:1-12. [doi: 10.1016/j.iswa.2023.200177]
144. Rai BK, Srivastava S, Arora S. Blockchain-based traceability of counterfeited drugs. Int J Reliab Qual E-Healthc 2023 May 01;12(2):1-6. [doi: 10.4018/IJRQEH.318129]
145. Rodriguez-Garcia M, Sicilia MA, Dodero JM. A privacy-preserving design for sharing demand-driven patient datasets over permissioned blockchains and P2P secure transfer. PeerJ Comput Sci 2021 Jun 09;7:1-13 [FREE Full text] [doi: 10.7717/peerj-cs.568] [Medline: 34179449]
146. Baguso GN, Aguilar K, Sicro S, Mañacop M, Quintana J, Wilson EC. "Lost trust in the system": system barriers to publicly available mental health and substance use services for transgender women in San Francisco. BMC Health Serv Res 2022 Jul 19;22(1):1-11 [FREE Full text] [doi: 10.1186/s12913-022-08315-5] [Medline: 35854359]
147. Marín-Cos A, Marbán-Castro E, Nedic I, Ferrari M, Crespo-Mirasol E, Ventura LF, et al. "Maternal vaccination greatly depends on your trust in the healthcare system": a qualitative study on the acceptability of maternal vaccines among pregnant women and healthcare workers in Barcelona, Spain. Vaccines (Basel) 2022 Nov 25;10(12):1-17 [FREE Full text] [doi: 10.3390/vaccines10122015] [Medline: 36560425]
148. Rojon C, McDowall A, Saunders M. On the experience of conducting a systematic review in industrial, work, and organizational psychology. J Pers Psychol 2011 Jan 23;10(3):133-138. [doi: 10.1027/1866-5888/A000041]
149. Ameyaw EE, Edwards DJ, Kumar B, Thurairajah N, Owusu-Manu DG, Oppong GD. Critical factors influencing adoption of blockchain-enabled smart contracts in construction projects. J Constr Eng Manag 2023 Mar 01;149(3):1-42. [doi: 10.1061/jcemd4.coeng-12081]
150. Budayan C, Okudan O. Assessment of barriers to the implementation of smart contracts in construction projects—evidence from Turkey. Buildings 2023 Aug 17;13(8):1-21. [doi: 10.3390/buildings13082084]
151. Shang G, Pheng LS, Xia RL. Adoption of smart contracts in the construction industry: an institutional analysis of drivers and barriers. Constr Innov 2023 Apr 06;24(5):1401-1421. [doi: 10.1108/ci-03-2022-0066]

Abbreviations

AI: artificial intelligence
CP-ABE: ciphertext-policy attribute-based encryption
EHR: electronic health record
HIPAA: Health Insurance Portability and Accountability Act
IoMT: Internet of Medical Things
IPFS: InterPlanetary File System
PRISMA: Preferred Reporting Items for Systematic Reviews and Meta-Analyses
SC: smart contract
SSI: self-sovereign identity
WoS: Web of Science

XSL•FO
RenderX

Edited by C Lovis; submitted 05.04.24; peer-reviewed by J Mistry, S Kale, J Parra-Dominguez; comments to author 23.05.24; revised version received 02.07.24; accepted 25.11.24; published 31.01.25.

Please cite as:
Marino CA, Diaz Paz C
Smart Contracts and Shared Platforms in Sustainable Health Care: Systematic Review
JMIR Med Inform 2025;13:e58575
URL: https://medinform.jmir.org/2025/1/e58575
doi:10.2196/58575
PMID:

©Carlos Antonio Marino, Claudia Diaz Paz. Originally published in JMIR Medical Informatics (https://medinform.jmir.org), 31.01.2025. This is an open-access article distributed under the terms of the Creative Commons Attribution License (https://creativecommons.org/licenses/by/4.0/), which permits unrestricted use, distribution, and reproduction in any medium, provided the original work, first published in JMIR Medical Informatics, is properly cited. The complete bibliographic information, a link to the original publication on https://medinform.jmir.org/, as well as this copyright and license information must be included.

XSL•FO
RenderX

Analysis of Retinal Thickness in Patients With Chronic Diseases Using Standardized Optical Coherence Tomography Data: Database Study Based on the Radiology Common Data Model

ChulHyoung Park[1*], MD; So Hee Lee[2*], BS; Da Yun Lee[3], MS; Seoyoon Choi[4], MS; Seng Chan You[5], MD, PhD; Ja Young Jeon[6], MD, PhD; Sang Jun Park[4], MD, PhD; Rae Woong Park[1,2], MD, PhD

[1]Department of Biomedical Informatics, Ajou University School of Medicine, 206, Worldcup-ro, Yeongtong-gu, Suwon, Republic of Korea

[2]Department of Biomedical Sciences, Ajou University Graduate School of Medicine, Suwon, Republic of Korea

[3]Department of Scientific Solutions, CMIC Korea Co, Ltd, Seoul, Republic of Korea

[4]Department of Ophthalmology, Seoul National University Bundang Hospital, Seongnam, Republic of Korea

[5]Department of Biomedical Systems Informatics, Yonsei University College of Medicine, Seoul, Republic of Korea

[6]Department of Endocrinology and Metabolism, Ajou University School of Medicine, Suwon, Republic of Korea

[*]these authors contributed equally

Corresponding Author:
Rae Woong Park, MD, PhD
Department of Biomedical Informatics, Ajou University School of Medicine, 206, Worldcup-ro, Yeongtong-gu, Suwon, Republic of Korea

Abstract

Background: The Observational Medical Outcome Partners-Common Data Model (OMOP-CDM) is an international standard for harmonizing electronic medical record (EMR) data. However, since it does not standardize unstructured data, such as medical imaging, using this data in multi-institutional collaborative research becomes challenging. To overcome this limitation, extensions such as the Radiology Common Data Model (R-CDM) have emerged to include and standardize these data types.

Objective: This work aims to demonstrate that by standardizing optical coherence tomography (OCT) data into an R-CDM format, multi-institutional collaborative studies analyzing changes in retinal thickness in patients with long-standing chronic diseases can be performed efficiently.

Methods: We standardized OCT images collected from two tertiary hospitals for research purposes using the R-CDM. As a proof of concept, we conducted a comparative analysis of retinal thickness between patients who have chronic diseases and those who have not. Patients diagnosed or treated for retinal and choroidal diseases, which could affect retinal thickness, were excluded from the analysis. Using the existing OMOP-CDM at each institution, we extracted cohorts of patients with chronic diseases and control groups, performing large-scale 1:2 propensity score matching (PSM). Subsequently, we linked the OMOP-CDM and R-CDM to extract the OCT image data of these cohorts and analyzed central macular thickness (CMT) and retinal nerve fiber layer (RNFL) thickness using a linear mixed model.

Results: OCT data of 261,874 images from Ajou University Medical Center (AUMC) and 475,626 images from Seoul National University Bundang Hospital (SNUBH) were standardized in the R-CDM format. The R-CDM databases established at each institution were linked with the OMOP-CDM database. Following 1:2 PSM, the type 2 diabetes mellitus (T2DM) cohort included 957 patients, and the control cohort had 1603 patients. During the follow-up period, significant reductions in CMT were observed in the T2DM cohorts at AUMC (P=.04) and SNUBH (P=.007), without significant changes in RNFL thickness (AUMC: P=.56; SNUBH: P=.39). Notably, a significant reduction in CMT during the follow-up was observed only at AUMC in the hypertension cohort, compared to the control group (P=.04); no other significant differences in retinal thickness were found in the remaining analyses.

Conclusions: The significance of our study lies in demonstrating the efficiency of multi-institutional collaborative research that simultaneously uses clinical data and medical imaging data by leveraging the OMOP-CDM for standardizing EMR data and the R-CDM for standardizing medical imaging data.

(JMIR Med Inform 2025;13:e64422) doi:10.2196/64422

KEYWORDS

data standardization; ophthalmology; radiology; optical coherence tomography; retinal thickness

XSL•FO
RenderX

Introduction

The Observational Medical Outcomes Partnership-Common Data Model (OMOP-CDM) is an internationally standardized model designed to harmonize medical data across various health care institutions [1]. Its primary goal is to facilitate efficient, large-scale, multi-institutional collaborative research. Currently, a federated database developed collaboratively by researchers from over 80 countries contains data from 12% of the global population [2].

The OMOP-CDM is a model that standardizes structured clinical data such as diagnoses, prescriptions, and procedures. However, unstructured data, such as genomic and imaging data, often fall outside the standardization scope of the current OMOP-CDM, presenting challenges for use in multi-institutional collaborative research. To address this limitation, extended models based on the OMOP-CDM are being actively developed [3,4]. One such model used in this study, known as the Radiology Common Data Model (R-CDM), standardizes imaging data, enabling the efficient integration of multi-institutional imaging and clinical data to enhance research capabilities [5].

Optical coherence tomography (OCT) captures detailed images of the eye's internal structure, including parameters such as retinal thickness. Studies using OCT data have explored relationships between retinal thickness and various factors including age, hypertension, type 2 diabetes mellitus (T2DM), and vitamin D deficiency [6-8]. However, these investigations have generally been limited by their confinement to single medical institutions with small patient cohorts, due to the simultaneous requirement for clinical and imaging data. To address these constraints, this study aims to standardize multi-institutional OCT data using the R-CDM, thereby facilitating research that integrates clinical and imaging data across multiple institutions.

Methods

Data Sources

This study used clinical and imaging data from two of the leading tertiary hospitals in South Korea: Ajou University Medical Center (AUMC) and Seoul National University Bundang Hospital (SNUBH). For clinical data, standardized OMOP-CDM databases were used. The AUMC OMOP-CDM database included standardized electronic medical record (EMR) data spanning from 1994 to February 2023, with records from 2,752,765 patients. The SNUBH OMOP-CDM database contained standardized EMR data from April 2003 to 2021, covering 2,017,421 patients. For imaging data, we had authorization to use selected OCT data collected with specific medical devices. OCT data were typically stored on the OCT device itself and were not automatically integrated into the EMR or picture archiving communication systems. To use these data for research purposes, the stored images had to be manually collected and converted into a usable format. Due to these limitations, OCT data were collected from all devices available at the participating institutions. Rather than selectively choosing specific devices or time periods, an inclusive approach was adopted to address potential selection bias. As a result, AUMC provided access to OCT data captured with Zeiss medical devices from 2013 to April 2022, while SNUBH granted access to OCT data obtained with Heidelberg medical devices from July 2006 to August 2019, for research purposes. This study was conducted per the Strengthening the Reporting of Observational Studies in Epidemiology (STROBE) guidelines to ensure transparency [9].

Ethical Considerations

We obtained ethical approval from the Institutional Review Board of AUMC (approval number: AJOUIRB-DB-2024 - 341) and SNUBH (approval number: SNUBH-EX-2024 - 123). This study was conducted with an exemption for informed consent, as there were no direct benefits or risks to participants arising from their involvement in the study. All data were anonymized to ensure participant confidentiality and privacy. No identifying information was retained during the data analysis process.

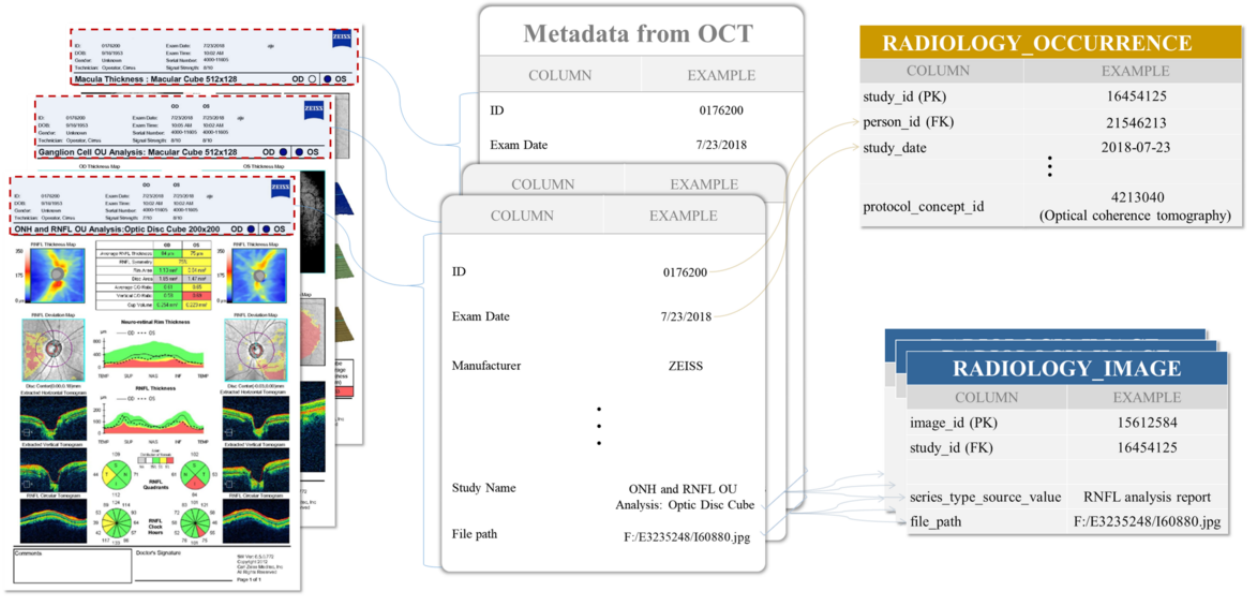
Constructing an R-CDM–Standardized OCT Database

Although the clinical data in this study had been standardized according to the OMOP-CDM and were ready for immediate application in multi-institutional research, the OCT imaging data still needed to be standardized to the R-CDM format to be efficiently used in research. The R-CDM standardized medical data through two distinct tables: the radiology occurrence table and the radiology image table. The radiology occurrence table cataloged each imaging event, detailing which patient used which company's equipment, the type of imaging performed, and the date on which it was performed. The radiology image table organized information about each image, including the type, file path, and resolution. These tables were interconnected through a "study_id" that served as the primary key, allowing researchers to uniformly extract specific types of image data from imaging events.

Consequently, a process was necessary to extract metadata within the OCT data using optical character recognition (OCR) techniques and load it into the R-CDM format. For OCT data captured using Zeiss medical devices at AUMC, the sections of OCT images documenting retinal thickness were cropped, and data extraction was performed using the Python Tesseract package. OCT data from SNUBH, taken with Heidelberg medical devices, were processed using a proprietary OCR machine learning model [10]. Only high-quality OCT scans (signal strength ≥7) were used in this study. Figure 1 illustrates the process of standardizing OCT imaging data into the R-CDM format.

XSL•FO
RenderX

Figure 1. Standardizing OCT imaging data in the format of Radiology Common Data Model. OCT: optical coherence tomography.

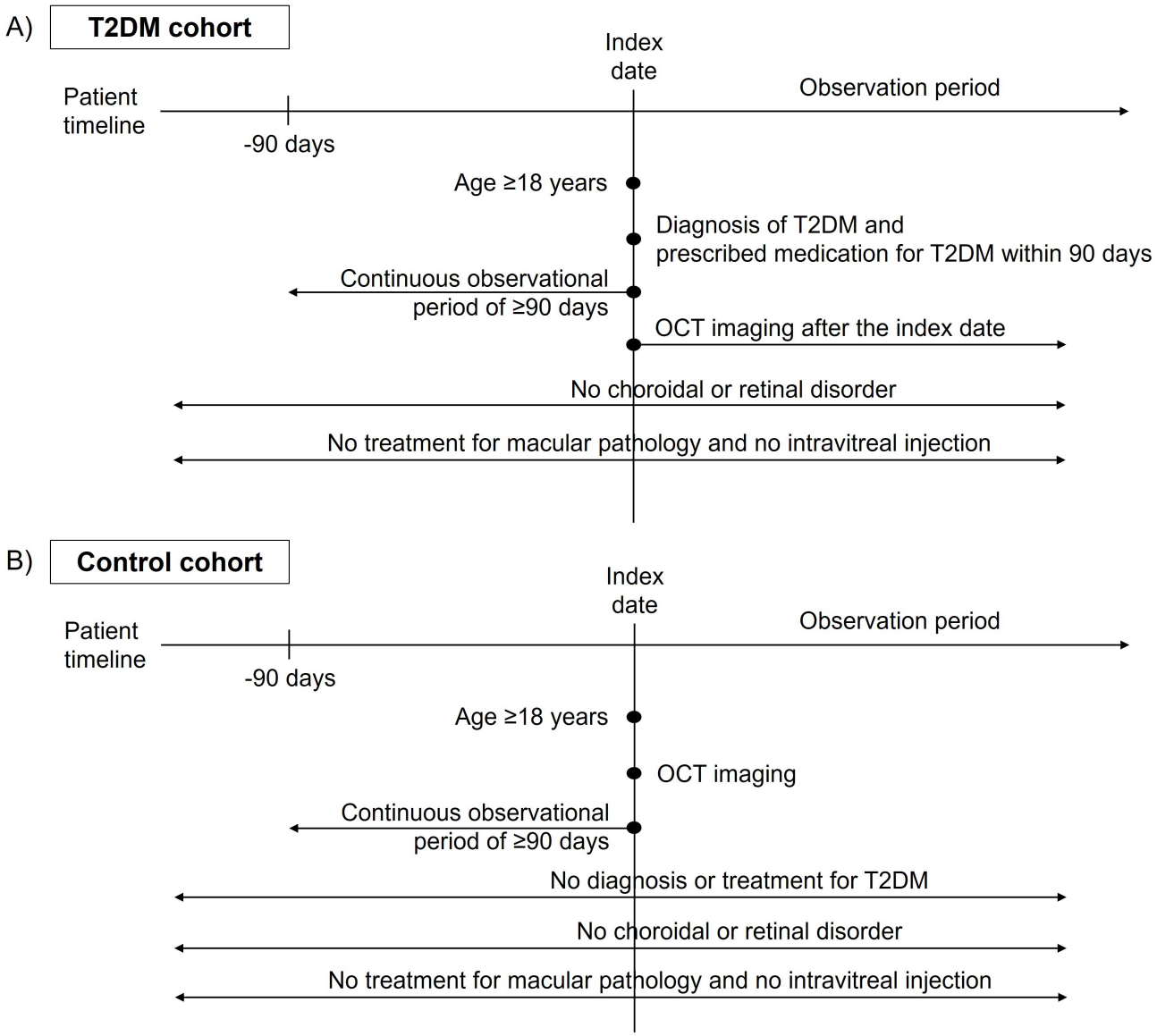


Study Design With the OMOP-CDM

In this study, we performed retinal thickness comparisons between cohorts of adult patients (aged ≥18 years) with and without chronic diseases, all of whom had undergone OCT. Among the chronic diseases, we focused on T2DM and hypertension. To ensure the comprehensive inclusion of all patients with these conditions, we used the highest-level SNOMED (Systematized Nomenclature of Medicine) hierarchy codes for enrollment. First, a T2DM cohort composed of patients diagnosed with T2DM and a control cohort of patients who were neither diagnosed with nor treated for T2DM were established. Eligibility for the T2DM cohort required a T2DM diagnosis and the administration of T2DM medications within 3 months of diagnosis, with the diagnosis date set as the index date. Patients who discontinued T2DM medications for more than 90 days were considered lost to follow-up. The control cohort included adult patients who were neither diagnosed with nor treated for T2DM, and the OCT imaging date was the index date in this cohort. Patients who had not been observed in the 90 days that preceded their respective index dates were excluded from the study. Additionally, patients with any recorded diagnosis or treatment for retinal or choroidal diseases that could affect the retinal thickness were also excluded (Figure 2). Second, an additional cohort of patients diagnosed with hypertension and a control group of patients who were neither diagnosed with nor treated for hypertension, who also had records of undergoing OCT imaging, were established in Figure E1 in Multimedia Appendix 1. Patients who discontinued hypertension medications for more than 90 days were considered lost to follow-up.

XSL•FO
RenderX

Figure 2. Cohort definitions for T2DM and control groups. (**A**) Patients with T2DM, excluding those diagnosed or treated for choroidal or retinal disorders, who have undergone OCT imaging. (**B**) Patients without T2DM or any choroidal or retinal disorders, who have undergone OCT imaging. OCT: optical coherence tomography. T2DM: type 2 diabetes mellitus.



Statistical Analysis 1: Large-Scale Propensity Score Matching for Characteristics Between Chronic Disease Cohort and Control Cohort

The propensity score matching (PSM) method was used to adjust for potential biases arising from confounding variables between the cohorts of patients with chronic diseases and the control cohorts. Propensity scores were estimated through a logistic regression model, and matching was performed using a nearest-neighbor approach within a 0.2-SD caliper on the logit scale, as recommended by Austin [11]. The balance of covariates was assessed using the absolute standardized mean difference (aSMD), with covariates including age categorized into 5-year bands, sex, and all condition diagnoses recorded in the year preceding the index date. Various matching ratios (1:1, 1:2, and 1:4) were explored for the sensitivity analysis.

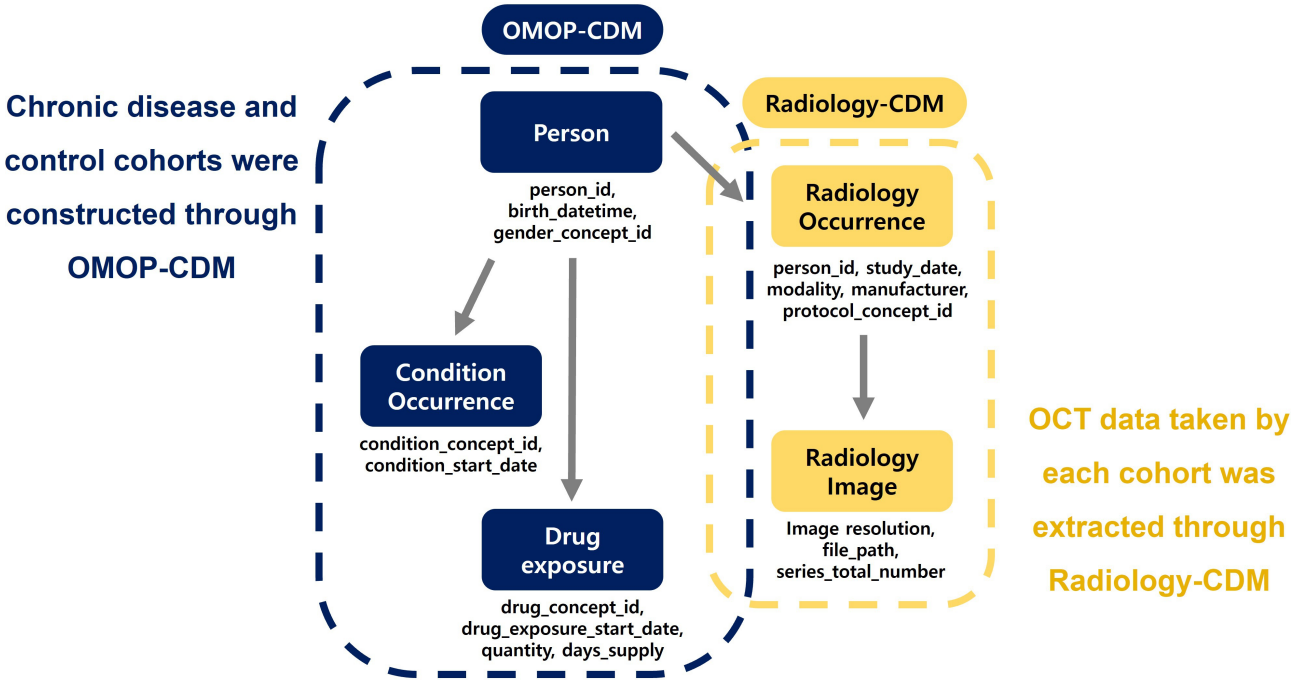
Interworking of the R-CDM and OMOP-CDM

During the standardization of OCT imaging data to the R-CDM, patient numbers used in the hospital were pseudonymized and replaced with research patient IDs for use in the OMOP-CDM database. This transformation not only eliminated the risk of personal information leakage when conducting research with imaging data but also ensured seamless integration between the OMOP-CDM and R-CDM. Following these processes, R-CDM-based OCT databases were established in both institutions.

By linking the OMOP-CDM and R-CDM, an environment was established that enabled the extraction of specific medical imaging data from designated patient cohorts. The hypertensive, diabetic, and control cohorts were easily constructed using ATLAS, an open-source software provided by the Observational Health Data Sciences and Informatics (OHDSI) group, which manages OMOP-CDM development [12]. Once these cohorts were established, the OCT imaging data collected from each cohort were uniformly extracted using the R-CDM (Figure 3). In this study, all OCT data taken after the index date of each patient cohort were used for analyses.

XSL•FO
RenderX

Figure 3. Schematic illustration of the integration between the OMOP-CDM and Radiology-CDM for extracting optical coherence tomography data from chronic disease and control cohorts. CDM: Common Data Model; OMOP-CDM: Observational Medical Outcome Partners-Common Data Model.



Extracting Retinal Thickness Values From OCT Data Using OCR Techniques

While the R-CDM database included information that was useful for describing and categorizing images, it lacked the pixel data from each image. Therefore, to extract recorded retinal thickness values from OCT data via the R-CDM, an additional OCR technology was required. The same OCR techniques previously used to extract metadata from OCT images for the R-CDM transformation were used. However, retinal thickness data within the OCT imaging data captured using Zeiss equipment at AUMC were recorded at inconsistent locations and centered on backgrounds of various colors, significantly reducing OCR accuracy. Initially, the process involved cropping the segments containing information and performing OCR using the Tesseract package (Python), consistent with the existing methods. Thereafter, all extracted data were manually reviewed by a single researcher. Through this method, retinal nerve fiber layer (RNFL) thickness and central macular thickness (CMT) were successfully extracted from OCT imaging data of chronic disease cohorts and control cohorts from the two institutions.

Statistical Analysis 2: Retinal Thickness Analysis Using Mixed-Effects Regression Analysis

We used the mixed-effects regression analysis to examine the CMT and RNFL thickness across the chronic disease and control cohorts. This analysis was crucial for determining if the differences in retinal thickness between the two groups were statistically significant at multiple time points and whether the changes in retinal thickness over time were significant. Furthermore, the model was specifically designed to adjust for confounding factors that could influence the retinal thickness, allowing for the independent analysis of the effects of the treatment duration on the former. Additionally, the model accommodated data from repeated measurements taken from the same individuals. The model we designed for this study was adjusted for age and sex and incorporated patient study ID as a random effect for repeated measures.

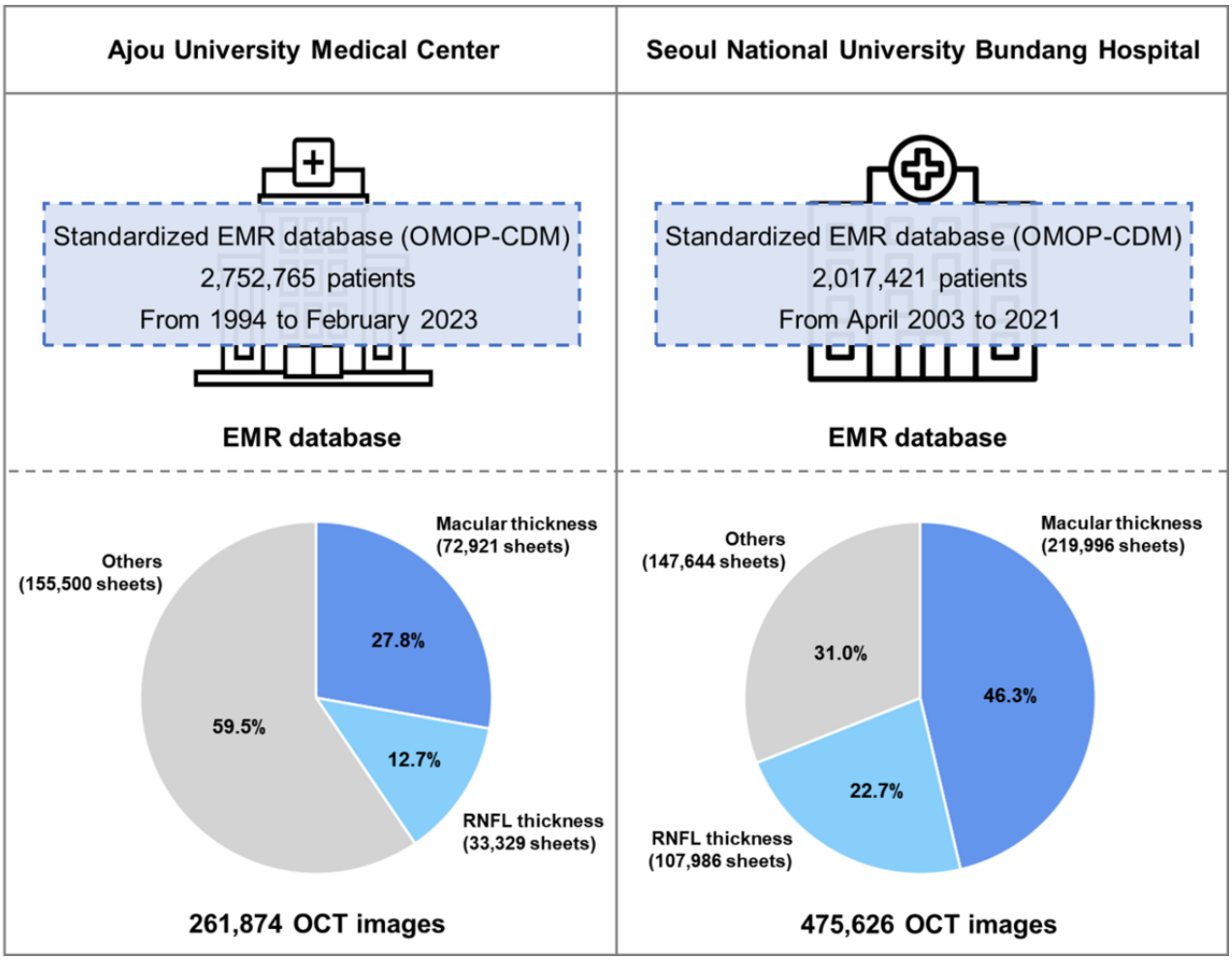
Results

Composition of R-CDM–Standardized OCT Data

In this study, we used CDM databases from two medical institutions along with an R-CDM–standardized OCT database. The OCT data from AUMC and SNUBH, standardized in the R-CDM format, consisted of data from 261,874 and 475,626 patients, respectively. The specific composition of the data is presented in Figure 4. For our analysis, a total of 292,917 OCT images of the macular thickness and 141,314 OCT images of the RNFL thickness were used.

XSL•FO
RenderX

Figure 4. Clinical and medical imaging databases of Ajou University Medical Center and Seoul National University Bundang Hospital used in this study. EMR: electronic medical record; OCT: optical coherence tomography; OMOP-CDM: Observational Medical Outcome Partners-Common Data Model; RNFL: retinal nerve fiber layer.



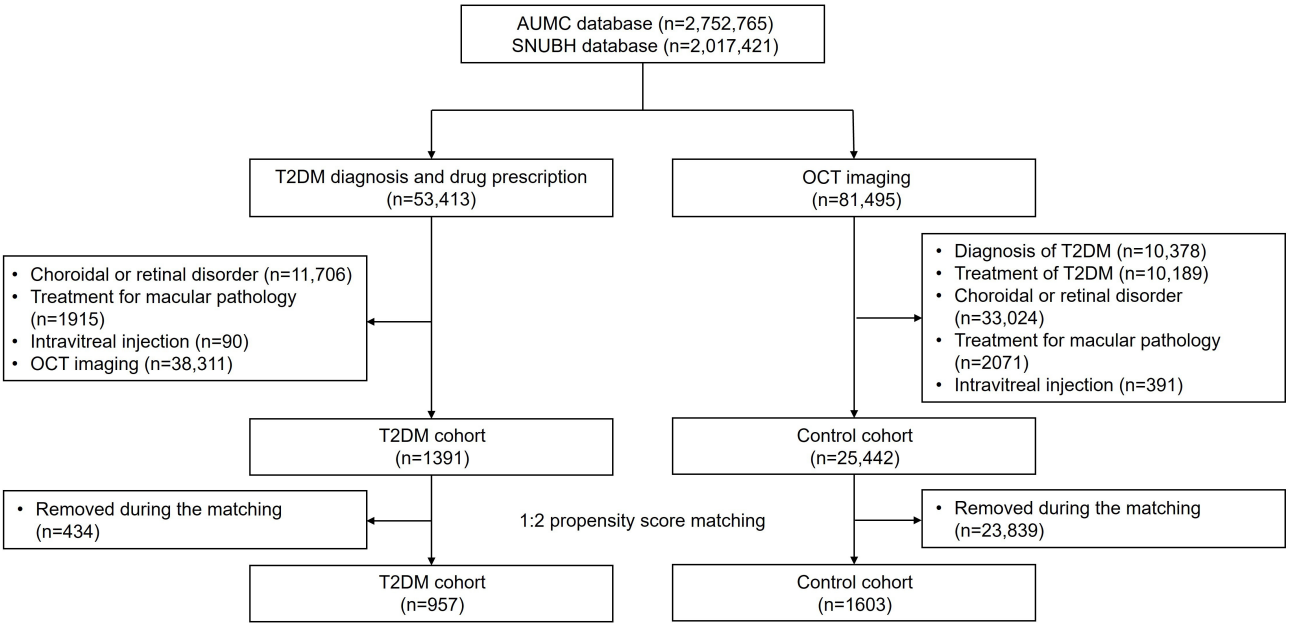
Study Population

Figure 5 illustrates the patient selection process across two tertiary hospitals in South Korea, using the AUMC and SNUBH databases. Within the T2DM cohort, from a total of 53,413 patients with diabetes and 1391 individuals who had undergone OCT imaging and were not diagnosed with or treated for any retinal diseases were selected. In the control cohort, out of 116,637 patients who underwent OCT imaging, 25,442 with no history of diabetes or retinal disorders were chosen. Following 1:2 PSM, 957 patients from the T2DM cohort and 1,603 from the control cohort were matched. After PSM, the median age group for the T2DM and control cohorts was 60 - 64 years. Additionally, females accounted for 44.6% (427/957) and 43.9% (703/1603) of patients in the T2DM and control cohorts, respectively.

Table 1 presents the baseline characteristics, including patient demographics and comorbidities, along with aSMDs before and after PSM at AUMC. Before PSM, higher prevalences of chronic conditions such as chronic liver disease, hyperlipidemia, and obesity, as well as cardiovascular diseases including coronary arteriosclerosis and peripheral vascular disease were observed in the T2DM group (all aSMDs>0.1). After matching, age, sex, and comorbidities were well-matched (all aSMDs<0.1). This trend was consistent with findings at SNUBH, as detailed in Multimedia Appendix 1. Additionally, the baseline characteristics before and after 1:1 and 1:4 PSM for the T2DM and control cohorts and the results for the hypertension versus control cohort are outlined in Tables E1 and E2 in Multimedia Appendix 1.

XSL•FO
RenderX

Figure 5. Flowchart of the study population in the comparison of T2DM and control cohorts. AUMC: Ajou University Medical Center; OCT: optical coherence tomography; SNUBH: Seoul National University Bundang Hospital; T2DM: type 2 diabetes mellitus.



XSL•FO
RenderX

Table . Comparative analysis of baseline characteristics and comorbidity profiles between the T2DM and control cohorts before and after the 1:2 PSM at Ajou University Medical Center.

Characteristics	Before PSM[a] matching			After PSM matching		
	T2DM[b] (n=967)	Control (n=11,896)	aSMD[c]	T2DM (n=633)	Control (n=1045)	aSMD
Age (years), n (%)						
15 - 19	4 (0.4)	190 (1.6)	0.12	4 (0.6)	7 (0.7)	0.01
20 - 24	3 (0.3)	428 (3.6)	0.24	3 (0.5)	10 (1)	0.04
25 - 29	10 (1)	393 (3.3)	0.15	8 (1.3)	20 (1.9)	0.04
30 - 34	17 (1.8)	571 (4.8)	0.17	11 (1.7)	26 (2.5)	0.04
35 - 39	38 (3.9)	904 (7.6)	0.16	25 (3.9)	33 (3.2)	0.05
40 - 44	56 (5.8)	1083 (9.1)	0.12	40 (6.3)	72 (6.9)	0.00
45 - 49	84 (8.7)	1190 (10)	0.05	60 (9.5)	96 (9.2)	0.02
50 - 54	136 (14.1)	1249 (10.5)	0.11	91 (14.4)	177 (16.9)	0.06
55 - 59	132 (13.7)	1332 (11.2)	0.08	90 (14.2)	140 (13.4)	0.02
60 - 64	149 (15.4)	1249 (10.5)	0.15	92 (14.5)	143 (13.7)	0.01
65 - 69	113 (11.7)	1130 (9.5)	0.07	65 (10.3)	112 (10.7)	0.03
70 - 74	111 (11.5)	904 (7.6)	0.13	72 (11.4)	98 (9.4)	0.05
75 - 79	81 (8.4)	690 (5.8)	0.10	49 (7.7)	66 (6.3)	0.04
80 - 84	27 (2.8)	393 (3.3)	0.03	20 (3.2)	28 (2.7)	0.02
85 - 89	6 (0.6)	167 (1.4)	0.08	3 (0.5)	11 (1.1)	0.07
Sex, n (%)						
Female	461 (47.7)	6186 (52)	0.09	301 (47.6)	481 (46)	0.05
Male	506 (52.3)	5710 (48)	0.03	332 (52.4)	564 (54)	0.03
Medical history (general), n (%)						
Acute respiratory disease	19 (2)	83 (0.7)	0.11	7 (1.1)	11 (1.1)	0.00
Chronic liver disease	29 (3)	48 (0.4)	0.20	14 (2.2)	17 (1.6)	0.02
Chronic obstructive lung disease	9 (0.9)	59 (0.5)	0.05	4 (0.6)	11 (1.1)	0.07
Dementia	9 (0.9)	71 (0.6)	0.04	7 (1.1)	10 (1)	0.02
Depressive disorder	20 (2.1)	131 (1.1)	0.08	9 (1.4)	25 (2.4)	0.06
Gastroesophageal reflux disease	35 (3.6)	333 (2.8)	0.04	22 (3.5)	41 (3.9)	0.04
Gastrointestinal hemorrhage	10 (1)	48 (0.4)	0.07	8 (1.3)	15 (1.4)	0.01
HIV infection	2 (0.2)	12 (0.1)	0.02	1 (0.2)	3 (0.3)	0.02
Hyperlipidemia	96 (9.9)	333 (2.8)	0.29	40 (6.3)	60 (5.7)	0.00
Lesion of liver	39 (4)	131 (1.1)	0.19	21 (3.3)	31 (3)	0.01
Obesity	17 (1.8)	48 (0.4)	0.13	11 (1.7)	10 (1)	0.06
Osteoarthritis	18 (1.9)	131 (1.1)	0.07	11 (1.7)	15 (1.4)	0.03
Urinary tract infectious disease	15 (1.6)	36 (0.3)	0.13	10 (1.6)	9 (0.9)	0.06
Viral hepatitis C	5 (0.5)	12 (0.1)	0.08	1 (0.2)	3 (0.3)	0.03
Medical history (cardiovascular disease)						

XSL•FO
RenderX

Characteristics	Before PSM[a] matching			After PSM matching		
	T2DM[b] (n=967)	Control (n=11,896)	aSMD[c]	T2DM (n=633)	Control (n=1045)	aSMD
Cerebrovascular disease	31 (3.2)	202 (1.7)	0.10	18 (2.8)	39 (3.7)	0.07
Coronary arteriosclerosis	120 (12.4)	202 (1.7)	0.43	54 (8.5)	85 (8.1)	0.07
Heart disease	201 (20.8)	535 (4.5)	0.51	99 (15.6)	150 (14.4)	0.06
Peripheral vascular disease	37 (3.8)	36 (0.3)	0.25	7 (1.1)	13 (1.2)	0.03
Pulmonary embolism	3 (0.3)	12 (0.1)	0.04	3 (0.5)	6 (0.6)	0.04
Medical history (neoplasm), n (%)						
Hematologic neoplasm	24 (2.5)	107 (0.9)	0.12	14 (2.2)	29 (2.8)	0.07
Malignant neoplastic disease	92 (9.5)	630 (5.3)	0.16	54 (8.5)	103 (9.9)	0.09
Malignant tumor of breast	8 (0.8)	95 (0.8)	0.00	4 (0.6)	11 (1.1)	0.05
Malignant tumor of colon	4 (0.4)	36 (0.3)	0.01	2 (0.3)	5 (0.5)	0.04
Malignant tumor of lung	4 (0.4)	59 (0.5)	0.01	4 (0.6)	10 (1)	0.05
Primary malignant neoplasm of prostate	5 (0.5)	48 (0.4)	0.02	5 (0.8)	11 (1.1)	0.07

[a]PSM: propensity score matching.

[b]T2DM: type 2 diabetes mellitus.

[c]aSMD: absolute standardized mean difference.

Clinical Outcomes

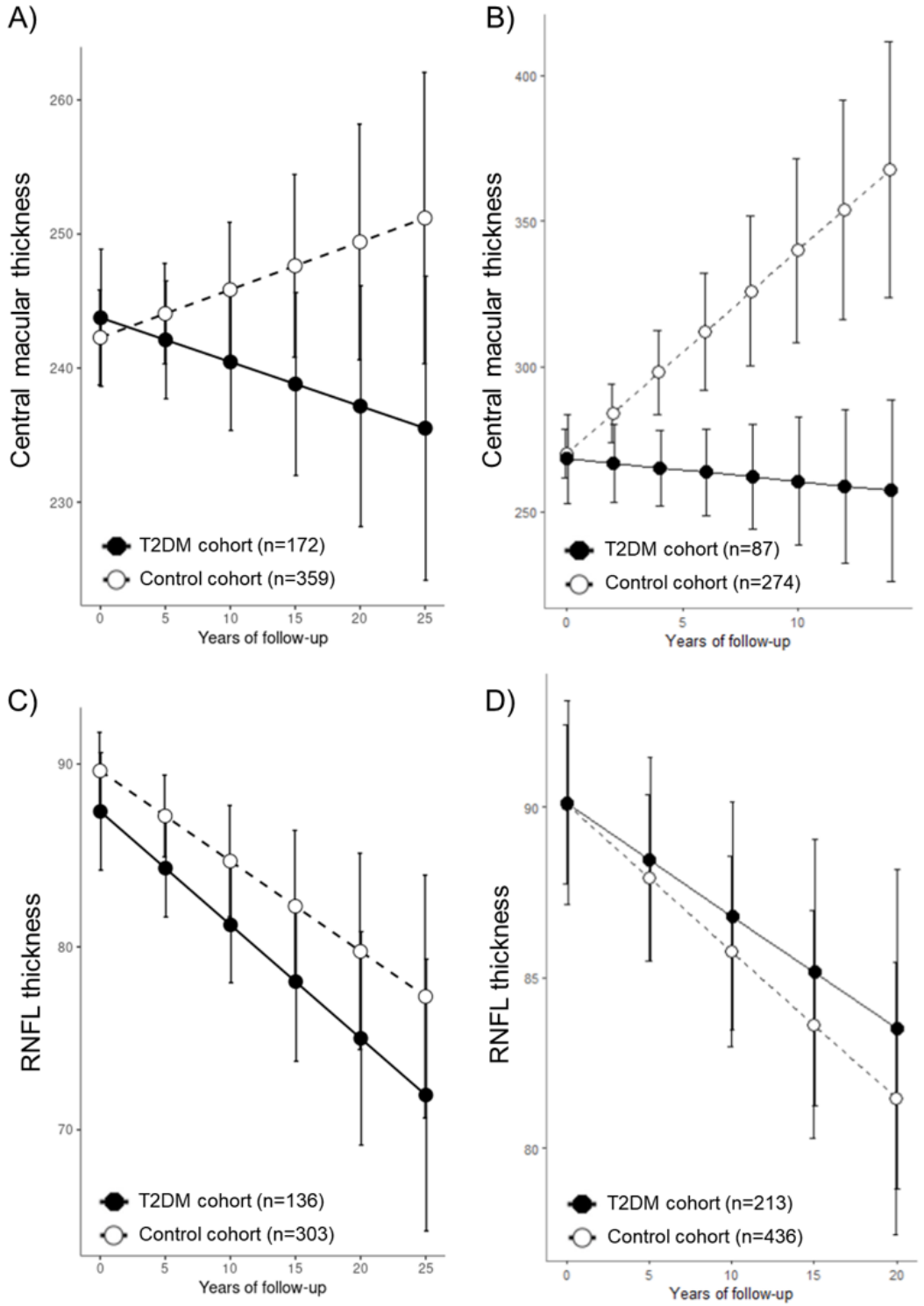
The median follow-up period was 807 (IQR 215-2523) days (4105 person-years) in the T2DM cohort and 966 (IQR 265-2946) days (4641 person-years) in the control cohort. In a longitudinal study using a mixed-effects regression, we investigated differences in retinal thickness between the T2DM and control cohorts (Figure 6). Throughout the follow-up period at both AUMC and SNUBH, the CMT significantly decreased in the T2DM cohort compared with the control cohort (P=.04 and P=.007, respectively; detailed in Tables E3-4 and E4-4 in Multimedia Appendix 1). Initially, there were no significant differences in CMT between the T2DM and control cohorts. However, significant reductions in CMT in the T2DM cohort, compared with the control group, began from the 15th year of follow-up at AUMC and the 5th year at SNUBH (Tables E3-5 and E4-5 in Multimedia Appendix 1). Conversely, the RNFL thickness analysis revealed no significant changes in the T2DM and control cohorts during the follow-up period, and there were no significant differences between them at any time point. These findings were consistent across both institutions.

For retinal thickness comparisons between the hypertension and control cohorts during the follow-up period, a decreasing trend in CMT in the hypertension cohort compared with the control cohort was observed only at AUMC (P=.04), while no such trend was noted at SNUBH (P=.56), as detailed in Tables E3-4 and E4-4 in Multimedia Appendix 1. Additionally, the analysis of RNFL thickness showed no significant differences between the cohorts.

For the sensitivity analysis, chronic disease and control cohorts were matched in 1:1 and 1:4 ratios to analyze the CMT and RNFL thickness, with results detailed in Tables E3 and E4 and Figures E4 and E5 in Multimedia Appendix 1. The analysis of CMT between the T2DM and control cohorts revealed that, except for one outcome (1:1 at SNUBH; P=.24), all other results were consistent with the main findings, showing a significant decrease in CMT in the T2DM cohort throughout the follow-up duration. Additionally, while results at AUMC indicated a marginally significant decrease in CMT in the hypertension cohort compared with the control cohort during the follow-up period (all P<0.1), no significant differences were observed at SNUBH.

XSL•FO
RenderX

Figure 6. Longitudinal analysis of laboratory values using a linear mixed effects model after 1:2 propensity score matching of T2DM and control cohorts. (**A**) Central macular thickness at Ajou University Medical Center. (**B**) Central macular thickness at Seoul National University Bundang Hospital. (**C**) RNFL thickness at Ajou University Medical Center. (**D**) RNFL thickness at Seoul National University Bundang Hospital. RNFL: retinal nerve fiber layer; T2DM: type 2 diabetes mellitus.



Discussion

Principal Results

In this study, OCT imaging data collected from two tertiary hospitals for research purposes were standardized into the R-CDM format. We developed an environment that integrates this standardized OCT database with the previously established OMOP-CDM database at each medical institution, allowing for the systematic extraction of specific imaging data types captured by patient cohorts built with the OMOP-CDM. As a proof of concept, we assessed the changes in retinal thickness in patients with chronic diseases over an extended period. Notably, we observed a significant reduction in the CMT among patients

XSL•FO
RenderX

who had been receiving long-term treatment for T2DM at both institutions. This research is believed to be the first global study to simultaneously use OCT data and clinical data, demonstrating that the application of the R-CDM can significantly enhance the efficiency of multicenter collaborative research that integrates clinical and imaging data.

The R-CDM used in this study for OCT data standardization represents the first model to standardize medical imaging data based on the OMOP-CDM. It is available as an open-source software program on the official OHDSI GitHub site and was published in a 2022 paper [5] that elaborates on the structural design and terminology system of the R-CDM, and as a proof of concept, it standardizes 90 million sets of medical imaging data collected for research purposes from AUMC. Both domestically and internationally, there have been instances in which the R-CDM has been used to standardize imaging data and facilitate research with these standardized datasets. For instance, Wonkwang University Hospital established an R-CDM database of standardized abdominal computed tomography (CT) data for 123 patients with cirrhosis and 123 control patients, using these data to develop a predictive model for cirrhosis [13]. Additionally, the paper introduced a web-based management system enabling researchers to search for and download standardized R-CDM datasets, enhancing the accessibility and utility of the R-CDM. Furthermore, a study by Lee et al [14] used clinical data, magnetic resonance imaging (MRI) data, and clinical notes simultaneously to develop a multimodal deep learning model predicting treatment-resistant depression, using AUMC's R-CDM database to extract MRI data that was suitable for study conditions. Additionally, within the European Health Data & Evidence Network project, the R-CDM was used to standardize brain CT and MRI data. This standardization successfully integrated quantitative data extracted from brain imaging studies by Icobrain's AI model [15]. Therefore, the R-CDM supports global researchers in efficiently leveraging their medical imaging data for advanced studies.

In addition to the R-CDM used in this study, various other efforts exist to standardize medical imaging data. Rubin et al [16] proposed common data elements, which standardize radiologic reports using a uniform terminology and structure. Although common data elements effectively standardize data produced in radiology, they encounter difficulties when integrating with standardized clinical databases like the OMOP-CDM. Furthermore, there are two additional efforts to standardize medical imaging data based on the OMOP-CDM. The first is the medical imaging common data model (MI-CDM) developed by the Foundation of Research and Technology Hellas [17], and the second is the MI-CDM codeveloped by Yonsei University and Johns Hopkins University [18]. Both MI-CDM models not only facilitate the extraction of necessary data by standardizing medical imaging data, but they also design tables to accommodate features from images, thereby enhancing the efficiency of the use of these features in research. While the structures of the models differ slightly from each other, the majority of their architectures are considerably similar, and their standardization methods and principles are consistent. Researchers can select the model that best suits their immediate needs and later convert it to another model format with simple modifications to the database if needed. The multiple cases of the R-CDM and the development of enhanced models demonstrate the demand among researchers to use medical imaging data more efficiently.

In this study, we observed a significant reduction in CMT in patients receiving long-term treatment for T2DM compared to the control group, with an annual decrease of −0.69 µm (95% CI −1.34 to −0.03; *P*=.04) at AUMC and −7.78 µm (95% CI −11.84 to −3.71; *P*<.007) at SNUBH. In contrast, RNFL thickness showed no significant difference in annual changes between the two groups (AUMC: −0.13 µm, 95% CI −0.55 to 0.30, *P*=.56; SNUBH: 0.10 µm, 95% CI −0.13 to 0.32, *P*=.39). This finding highlights the subtle but measurable structural changes that occur in the macula as a result of prolonged exposure to diabetes. However, there was no significant difference in the rate of RNFL changes over time between the two groups. These results are consistent with findings reported by Oshitari et al [19], where the CMT in patients with diabetes without diabetic retinopathy was significantly thinner compared to the control group (mean 210.7, SD 28.6 µm vs mean 195.6, SD 23.3 µm; *P*=.02). Similarly, while RNFL thickness in the group without diabetic retinopathy was thinner than the control group (mean 104.4, SD 10.9 µm vs mean 100.4, SD 13.7 µm) the difference was not statistically significant. A study conducted at the Jamaica Plain Veteran's Affairs Medical Center further supports these findings, reporting a significant decrease in macular thickness associated with a longer duration of diabetes in the group without diabetic retinopathy. They observed a significant negative correlation between retinal thickness and diabetes duration (central foveal thickness: *r*=−0.30, *P*=.003; total foveal thickness: *r*=−0.26, *P*=.012; total macular thickness: *r*=−0.26, *P*=.013) [20]. The observed reduction in macular thickness, which was significantly correlated with the duration of diabetes, is likely attributed to retinal neurodegeneration, an early event in the pathogenesis of diabetic retinopathy that precedes and contributes to diabetic microangiopathy [21].

Retinal thickness comparisons between the hypertension group and the control group revealed that only at AUMC did patients with long-term hypertension exhibit a reduction in CMT (−0.81 µm/y, 95% CI −1.57 to −0.06; *P*=.04). These findings align with prior studies conducted at Izmir Military Hospital and Samsung Medical Center, which also reported decreased macular thickness in patients with hypertension compared to control patients [22,23]. The Izmir Military Hospital reported a significantly thinner mean macular thickness in the hypertension group compared to the control group (mean 254.97, SD 21.81 µm vs mean 262.11, SD 21.05 µm; *P*=.037). Similarly, a study from Samsung Medical Center reported a significant reduction in percent thickness in patients with hypertension compared to control patients, with changes of –1.6% (95% CI −2.59% to −0.6%; *P*=.02) in the composite inner macula and −2.26% (95% CI: −3.32% to −1.19%; *P*<.01) in the composite outer macula.

Conversely, other studies have reported significantly thinner CMT and RNFL in patients with hypertension, highlighting the association between systemic hypertension and retinal microvascular abnormalities, such as retinal arteriolar narrowing and ischemic retinal disorders. These findings underscore the importance of prompt and effective management of systemic

XSL•FO
RenderX

hypertension [7,24-27]. Notably, our study excluded all patients diagnosed with retinal or choroidal disorders by leveraging SNOMED codes and used large-scale PSM with thousands of covariates to control for baseline differences between groups. While these methodological approaches may account for some discrepancies with earlier studies, further large-scale research is needed to provide more conclusive evidence.

Large-scale PSM methodology, which was actively used and validated by the OHDSI community, meticulously matched baseline characteristics between the patient and control groups. This approach incorporated more covariates than reported in previous studies [28]. Additionally, while the existing literature indicates that the macular thickness is significantly higher in males than in females [29,30] and decreases with age [6,31], our study used a linear mixed model to comprehensively adjust for variables that significantly affect this parameter. Moreover, to generate more robust evidence, we conducted analyses with the same settings across multiple institutions. However, to date, most studies exploring the association between chronic diseases and retinal thickness using OCT data have been conducted at single institutions. This is primarily due to the diverse data storage formats across medical facilities, making cross-institutional research exceedingly labor-intensive. Furthermore, as our study requires both clinical and imaging data, the workload for data preprocessing increases exponentially. By leveraging the OMOP-CDM and the associated R-CDM system, we demonstrated a significant reduction in inefficiency. We anticipate that future research will achieve greater scalability and generate more generalized and impactful findings through multi-institutional analyses using the R-CDM.

Limitations

Nevertheless, this study has the following limitations. First, while the R-CDM significantly enhances the use of medical imaging data, we encountered persistent inefficiencies due to stringent governance requirements for research approval. Although we had unrestricted access to OMOP-CDM standardized EMR databases from two institutions, the acquisition of imaging data for research purposes remained time-consuming and labor-intensive. This underscores the necessity for a more comprehensive R-CDM that standardizes all medical imaging data across multiple institutions, which is our ultimate objective. We anticipate that as the R-CDM gains widespread acceptance comparable to the OMOP-CDM, more health care institutions will adopt it for standardizing all of their medical imaging data, thereby facilitating more efficient multicenter studies incorporating imaging data. Second, due to the inherent characteristics of OCT medical devices that do not automatically integrate with the EMR or the picture archiving communication system, this study was limited to using data from OCT devices specifically approved for research purposes at each institution. Nevertheless, by securing all OCT data from specific periods and specific equipment, we minimized potential biases in data acquisition. In future investigations, we aim to incorporate all available OCT data from both institutions to enhance the robustness and generalizability of our findings. Third, despite using data from two major tertiary hospitals in Korea, the final cohort for retinal thickness analysis comprised fewer than 2000 patients. While our cohort definition and large-scale PSM technique ensured balanced comparisons, it resulted in the exclusion of a substantial number of patients. To address these limitations, we propose conducting large-scale collaborative studies involving multiple medical centers, which would ensure a sufficiently large sample size for more conclusive research.

Conclusion

OCT imaging data were standardized into the R-CDM format from two tertiary hospitals in South Korea, and changes in the retinal thickness in patients with chronic diseases were analyzed as a proof of concept. To maximize the use of available data, mixed-effects regression analyses were conducted, revealing that patients with long-standing T2DM exhibited a significant reduction in CMT over time compared with those without the condition. The construction of R-CDM databases across multiple institutions and its integration with the OMOP-CDM has established a robust foundation for conducting efficient multi-institutional collaborative research using both clinical and imaging data, marking a significant step forward in the domain of multidisciplinary research collaborations.

Acknowledgments

This research was supported by the Korea Health Technology R&D Project and the MD-PhD/Medical Scientist Training Program through the Korea Health Industry Development Institute (KHIDI), funded by the Ministry of Health & Welfare, Republic of Korea (grant number: HR16C0001). Additional support was provided by a grant from the Project for Infectious Disease Medical Safety, funded by the Ministry of Health & Welfare, Republic of Korea (grant number: HG22C0024). Further funding was received from the Korea Environment Industry & Technology Institute (KEITI) through the Core Technology Development Project for Environmental Diseases Prevention and Management, funded by the Korea Ministry of Environment (MOE; grant number: 2022003310001). The funders had no role in the study design, data collection and analysis, decision to publish, or preparation of the manuscript.

Data Availability

The datasets generated during and/or analyzed during this study are available on reasonable request once a proposal is approved, coupled with a signed data access agreement and in collaboration with the study group.

XSL•FO
RenderX

Authors' Contributions

All authors contributed to the literature review, study design, and data interpretation. CP, SHL, and SC contributed to the data analysis. CP, SHL, DYL, SCY, and JYJ contributed to interpreting clinical results. CP and SHL contributed to writing a manuscript. CP and DYL contributed to statistical interpretation. RWP and SJP are co-corresponding authors on this article and supervised all of the process.

Conflicts of Interest

None declared.

Multimedia Appendix 1
Supplementary materials.
[DOCX File, 1574 KB - medinform_v13i1e64422_app1.docx]

References

1. Hripcsak G, Duke JD, Shah NH, et al. Observational Health Data Sciences and Informatics (OHDSI): opportunities for observational researchers. Stud Health Technol Inform 2015;216:574-578. [Medline: 26262116]
2. 2023 “our journey” annual report. : Observational Health Data Sciences and Informatics; 2023 URL: https://www.ohdsi.org/wp-content/uploads/2023/11/OHDSI-Book2023.pdf [accessed 2025-01-24]
3. Shin SJ, You SC, Park YR, et al. Genomic common data model for seamless interoperation of biomedical data in clinical practice: retrospective study. J Med Internet Res 2019 Mar 26;21(3):e13249. [doi: 10.2196/13249] [Medline: 30912749]
4. Belenkaya R, Gurley MJ, Golozar A, et al. Extending the OMOP common data model and standardized vocabularies to support observational cancer research. JCO Clin Cancer Inform 2021 Jan;5:12-20. [doi: 10.1200/CCI.20.00079] [Medline: 33411620]
5. Park C, You SC, Jeon H, Jeong CW, Choi JW, Park RW. Development and validation of the Radiology Common Data Model (R-CDM) for the international standardization of medical imaging data. Yonsei Med J 2022 Jan;63(Suppl):S74-S83. [doi: 10.3349/ymj.2022.63.S74] [Medline: 35040608]
6. Nieves-Moreno M, Martínez-de-la-Casa JM, Morales-Fernández L, Sánchez-Jean R, Sáenz-Francés F, García-Feijoó J. Impacts of age and sex on retinal layer thicknesses measured by spectral domain optical coherence tomography with Spectralis. PLoS ONE 2018;13(3):e0194169. [doi: 10.1371/journal.pone.0194169] [Medline: 29522565]
7. Lee SH, Lee WH, Lim HB, Jo YJ, Kim JY. Thicknesses of central macular, retinal nerve fiber, and ganglion cell inner plexiform layers in patients with hypertension. Retina (Philadelphia, Pa) 2019 Sep;39(9):1810-1818. [doi: 10.1097/IAE.0000000000002216] [Medline: 29757807]
8. Jiang J, Liu Y, Chen Y, et al. Analysis of changes in retinal thickness in type 2 diabetes without diabetic retinopathy. J Diabetes Res 2018;2018:3082893. [doi: 10.1155/2018/3082893] [Medline: 29682578]
9. von Elm E, Altman DG, Egger M, et al. The Strengthening the Reporting of Observational Studies in Epidemiology (STROBE) statement: guidelines for reporting observational studies. Int J Surg 2014 Dec;12(12):1495-1499. [doi: 10.1016/j.ijsu.2014.07.013] [Medline: 25046131]
10. Mun Y, Kim J, Noh KJ, et al. An innovative strategy for standardized, structured, and interoperable results in ophthalmic examinations. BMC Med Inform Decis Mak 2021 Jan 6;21(1):9. [doi: 10.1186/s12911-020-01370-0] [Medline: 33407448]
11. Austin PC. Optimal caliper widths for propensity-score matching when estimating differences in means and differences in proportions in observational studies. Pharm Stat 2011;10(2):150-161. [doi: 10.1002/pst.433] [Medline: 20925139]
12. Lima DM, Rodrigues-Jr JF, Traina AJM, Pires FA, Gutierrez MA. Transforming two decades of ePR data to OMOP CDM for clinical research. Stud Health Technol Inform 2019 Aug 21;264:233-237. [doi: 10.3233/SHTI190218] [Medline: 31437920]
13. Kim S, et al. Development of web-based management system and dataset for radiology-common data model (R-CDM) and its clinical application in liver cirrhosis. Presented at: The 2020 Intelligent Systems Conference (IntelliSys); Sep 3-4, 2020 p. 687-695. [doi: 10.1007/978-3-030-55190-2_54]
14. Lee DY, Kim N, Park C, et al. Explainable multimodal prediction of treatment-resistance in patients with depression leveraging brain morphometry and natural language processing. Psychiatry Res 2024 Apr;334:115817. [doi: 10.1016/j.psychres.2024.115817] [Medline: 38430816]
15. Praeta J, Houghtaling J, Jung F, De Backer S, Pinxten J, Smeets D. Application of the R-CDM extension to capture metadata and features extracted from quantitative brain MRI and CT data. : Observational Health Data Sciences and Informatics; 2023 Jul 31 URL: https://ohdsi-europe.org/images/symposium-2023/posters/praet_rcdmposter_2023_V3_-_Jared_Houghtaling.pdf [accessed 2025-01-24]
16. Rubin DL, Kahn CE Jr. Common data elements in radiology. Radiology 2017 Jun;283(3):837-844. [doi: 10.1148/radiol.2016161553] [Medline: 27831831]

XSL•FO
RenderX

17. Kalokyri V, Kondylakis H, Sfakianakis S, et al. MI-Common Data Model: extending Observational Medical Outcomes Partnership-Common Data Model (OMOP-CDM) for registering medical imaging metadata and subsequent curation processes. JCO Clin Cancer Inform 2023 Sep;7:e2300101. [doi: 10.1200/CCI.23.00101] [Medline: 38061012]
18. Park WY, Jeon K, Schmidt TS, et al. Development of medical imaging data standardization for imaging-based observational research: OMOP Common Data Model extension. J Imaging Inform Med 2024 Apr;37(2):899-908. [doi: 10.1007/s10278-024-00982-6] [Medline: 38315345]
19. Oshitari T, Hanawa K, Adachi-Usami E. Changes of macular and RNFL thicknesses measured by Stratus OCT in patients with early stage diabetes. Eye (Lond) 2009 Apr;23(4):884-889. [doi: 10.1038/eye.2008.119] [Medline: 18437178]
20. Asefzadeh B, Fisch BM, Parenteau CE, Cavallerano AA. Macular thickness and systemic markers for diabetes in individuals with no or mild diabetic retinopathy. Clin Exp Ophthalmol 2008 Jul;36(5):455-463. [doi: 10.1111/j.1442-9071.2008.01769.x] [Medline: 18925914]
21. Simó R, Hernández C, European Consortium for the Early Treatment of Diabetic Retinopathy (EUROCONDOR). Neurodegeneration in the diabetic eye: new insights and therapeutic perspectives. Trends Endocrinol Metab 2014 Jan;25(1):23-33. [doi: 10.1016/j.tem.2013.09.005] [Medline: 24183659]
22. Akay F, Gündoğan FC, Yolcu U, Toyran S, Tunç E, Uzun S. Retinal structural changes in systemic arterial hypertension: an OCT study. Eur J Ophthalmol 2016 Aug 4;26(5):436-441. [doi: 10.5301/ejo.5000740] [Medline: 26951532]
23. Kong M, Kwun Y, Sung J, Ham DI, Song YM. Association between systemic hypertension and macular thickness measured by optical coherence tomography. Invest Ophthalmol Vis Sci 2015 Apr;56(4):2144-2150. [doi: 10.1167/iovs.14-16080] [Medline: 25736785]
24. Bursali Ö, Altintaş Ö, Ağir A, Yüksel N, Özkan B. Optical coherence tomography measurements in patients with systemic hypertension. Scott Med J 2021 Aug;66(3):115-121. [doi: 10.1177/00369330211011175] [Medline: 33947281]
25. Hayreh SS. Ischemic optic neuropathy. Prog Retin Eye Res 2009 Jan;28(1):34-62. [doi: 10.1016/j.preteyeres.2008.11.002] [Medline: 19063989]
26. Wong TY, Klein R, Klein BE, Tielsch JM, Hubbard L, Nieto FJ. Retinal microvascular abnormalities and their relationship with hypertension, cardiovascular disease, and mortality. Surv Ophthalmol 2001;46(1):59-80. [doi: 10.1016/s0039-6257(01)00234-x] [Medline: 11525792]
27. Wong TY, Shankar A, Klein R, Klein BEK, Hubbard LD. Prospective cohort study of retinal vessel diameters and risk of hypertension. BMJ 2004 Jul 10;329(7457):79. [doi: 10.1136/bmj.38124.682523.55] [Medline: 15175230]
28. Tian Y, Schuemie MJ, Suchard MA. Evaluating large-scale propensity score performance through real-world and synthetic data experiments. Int J Epidemiol 2018 Dec 1;47(6):2005-2014. [doi: 10.1093/ije/dyy120] [Medline: 29939268]
29. Wong ACM, Chan CWN, Hui SP. Relationship of gender, body mass index, and axial length with central retinal thickness using optical coherence tomography. Eye (Lond) 2005 Mar;19(3):292-297. [doi: 10.1038/sj.eye.6701466] [Medline: 15258609]
30. Kelty PJ, Payne JF, Trivedi RH, Kelty J, Bowie EM, Burger BM. Macular thickness assessment in healthy eyes based on ethnicity using Stratus OCT optical coherence tomography. Invest Ophthalmol Vis Sci 2008 Jun;49(6):2668-2672. [doi: 10.1167/iovs.07-1000] [Medline: 18515595]
31. Eriksson U, Alm A. Macular thickness decreases with age in normal eyes: a study on the macular thickness map protocol in the Stratus OCT. Br J Ophthalmol 2009 Nov;93(11):1448-1452. [doi: 10.1136/bjo.2007.131094] [Medline: 19019921]

Abbreviations

aSMD: absolute standardized mean difference
AUMC: Ajou University Medical Center
CMT: central macular thickness
CT: computed tomography
EMR: electronic medical record
MI-CDM: Medical Imaging Common Data Model
MRI: magnetic resonance imaging
OCR: optical character recognition
OCT: optical coherence tomography
OHDSI: Observational Health Data Sciences and Informatics
OMOP-CDM: Observational Medical Outcome Partners-Common Data Model
PSM: propensity score matching
R-CDM: Radiology Common Data Model
RNFL: retinal nerve fiber layer
SNOMED: Systematized Nomenclature of Medicine
SNUBH: Seoul National University Bundang Hospital
STROBE: Strengthening the Reporting of Observational Studies in Epidemiology
T2DM: type 2 diabetes mellitus

XSL•FO
RenderX

Edited by C Lovis; submitted 18.07.24; peer-reviewed by A Jafarizadeh, M Abdollahi; revised version received 19.12.24; accepted 12.01.25; published 21.02.25.

Please cite as:
Park C, Lee SH, Lee DY, Choi S, You SC, Jeon JY, Park SJ, Park RW
Analysis of Retinal Thickness in Patients With Chronic Diseases Using Standardized Optical Coherence Tomography Data: Database Study Based on the Radiology Common Data Model
JMIR Med Inform 2025;13:e64422
URL: https://medinform.jmir.org/2025/1/e64422
doi:10.2196/64422

© ChulHyoung Park, So Hee Lee, Da Yun Lee, Seoyoon Choi, Seng Chan You, Ja Young Jeon, Sang Jun Park, Rae Woong Park. Originally published in JMIR Medical Informatics (https://medinform.jmir.org), 21.2.2025. This is an open-access article distributed under the terms of the Creative Commons Attribution License (https://creativecommons.org/licenses/by/4.0/), which permits unrestricted use, distribution, and reproduction in any medium, provided the original work, first published in JMIR Medical Informatics, is properly cited. The complete bibliographic information, a link to the original publication on https://medinform.jmir.org/, as well as this copyright and license information must be included.

XSL•FO
RenderX

Developing a SNOMED CT–Based Value Set to Document Symptoms and Diagnoses for Adverse Drug Events: Mixed Methods Study

Erica Y Lau[1], PhD; Linda Bird[2], PhD; Anthony Lau[3], PharmD; Yau-Lam Alex Chau[4], PharmD; Katherine Butcher[3], BSc; Susan Buchkowsky[5], PharmD; Kira Gossack-Keenan[6], MD; Cheryl Sadowski[7], PharmD; Corinne M Hohl[8,9], MSc, MD

[1]Strategy, Planning and Implementation, BC Cancer, 601 West Broadway, Vancouver, BC, Canada

[2]Department of Health Information Science, University of Victoria, Victoria, BC, Canada

[3]Pharmaceutical Science, Vancouver General Hospital, Vancouver, BC, Canada

[4]Faculty of Medicine and Dentistry, University of Alberta, Edmonton, AB, Canada

[5]Pharmacy Department, Surrey Memorial Hospital, Surrey, BC, Canada

[6]Vancouver General Hospital, Vancouver, BC, Canada

[7]Faculty of Pharmacy & Pharmaceutical Sciences, University of Alberta, Edmonton, AB, Canada

[8]Department of Emergency Medicine, The University of British Columbia, Vancouver, BC, Canada

[9]Vancouver Coastal Health Research Institute, Centre for Clinical Epidemiology and Evaluation, Vancouver, BC, Canada

Corresponding Author:
Erica Y Lau, PhD
Strategy, Planning and Implementation, BC Cancer, 601 West Broadway, Vancouver, BC, Canada

Abstract

Background: Adverse drug events (ADEs) lead to more than 2 million emergency department visits in Canada annually, resulting in significant patient harm and more than CAD $1 billion in health care costs (in 2018, the average exchange rate for 1 CAD was 0.7711 USD; 1 billion CAD would have been approximately 771.1 million USD). Effective documentation and sharing of ADE information through electronic medical records (EMRs) are essential to inform subsequent care and improve safety when culprit medications can be replaced and reexposures avoided. Yet, current systems often lack standardized comprehensive ADE value sets.

Objective: This study aimed to develop a SNOMED CT value set for symptoms and diagnoses to standardize ADE documentation and improve ADE data integration into EMRs.

Methods: We used ADE data from ActionADE, a prospective reporting system implemented in 9 hospitals in British Columbia. We extract 5792 reports that yielded 827 unique ADE symptom and diagnosis terms based on Medical Dictionary for Regulatory Activities preferred terms. Two independent mappers used both automated and manual mapping approaches to match these terms to SNOMED CT concepts. Two clinical experts conducted validation, followed by a quality assurance review by a separate clinical team. Discrepancies were resolved through consensus discussions. Interrater reliability was assessed using Cohen κ.

Results: The automated mapping process identified 63.1% (522/827) semantically equivalent matches from SNOMED CT's Clinical Finding hierarchy. Two mappers manually reviewed the automatically mapped terms and identified appropriate target concepts for the unmapped terms. After the manual mapping process, 95.3% (788/827) of the source terms were successfully mapped to SNOMED CT concepts, with 4.7% (39/827) remaining unmapped. Interrater reliability between the mappers was strong (κ=0.87, 95% CI 0.85 - 0.89). The validation phase identified and removed 1 irrelevant term, resulting in 98.4% (813/826) terms mapped, with 1.6% (13/826) unmapped, and a high interrater reliability (κ=0.88, 95% CI 0.80 - 0.95). During quality assurance, 6 terms were flagged for concerns regarding clinical relevance or safety risks and were resolved through discussions. The final value set comprised 813 SNOMED CT concepts, with 95.7% (778/813) of terms classified as semantically equivalent and 4.3% (35/813) as semantically similar. Thirteen additional terms remained unmapped and will be reviewed as new SNOMED CT codes are added.

Conclusions: This study developed a SNOMED CT–based value set to document symptoms and diagnoses for ADEs observed in adults in EMRs. Adopting this value set can improve the consistency, accuracy, and interoperability of ADE documentation in EMRs, helping to reduce repeat ADEs and enhance patient safety. Ongoing refinement and improved clinical usability are essential for its widespread adoption. Future research should assess the impact of integrating this value set into EMRs on ADE reporting, pharmacovigilance, and patient safety outcomes.

XSL•FO
RenderX

(JMIR Med Inform 2025;13:e70167) doi:10.2196/70167

KEYWORDS

adverse drug event; electronic medical records; pharmacovigilance; terminology standard; SNOMED CT

Introduction

Every year, more than 2 million Canadians visit an emergency department due to adverse drug events (ADEs)—unintended and harmful events related to medication use [1,2]. These events lead to more than 700,000 hospital admissions and exceed CAD $1 billion in health care costs across Canada annually (in 2018, the average exchange rate for 1 CAD was 0.7711 USD. 1 billion CAD would have been approximately 771.1 million USD) [2,3]. Critically, 75% of these events are preventable [4,5]. A common cause of preventable ADEs is the represcription or redispensing of the same or a similar class of medication that previously caused harm, which may or may not be warranted [6,7]. Addressing unintentional repeat ADEs is essential to enhancing patient safety and aligns with the World Health Organization's public health priorities [8].

Unintentional repeat ADEs may occur because health systems lack effective mechanisms to communicate and integrate ADE information into clinical workflows [9]. For example, community pharmacists lack access to hospitals' electronic medical records (EMRs) and do not receive discharge summaries or consultation notes, leaving them unaware of ADEs diagnosed in hospital where safer alternatives may exist and where reexposure should be avoided [10,11]. This communication gap presents a critical opportunity to reduce repeat ADEs through improved data-sharing practices [12].

The widespread adoption of EMRs offers an opportunity to enhance the documentation and sharing of ADE information among health care providers [13-15]. However, for this information to be effectively shared across clinical disciplines and care settings and follow the patients along their care trajectory, it must be recorded, stored, and shared in a standardized form. Currently, most EMRs include allergy modules for documenting symptoms and diagnoses related to ADEs. Allergies constitute a small percentage of clinically significant ADEs, and many are subsequently refuted [16]. Current EMR modules often rely on nonstandardized adverse reaction code sets provided by third-party vendors, with varying quantity, quality, and data standards. This hinders the uniform documentation, extraction, and sharing of ADE data [17]. Inconsistent and nonstandardized ADE documentation can lead to underreporting and miscommunication, contributing to adverse patient outcomes and posing challenges for population-level pharmacovigilance efforts. Studies have shown that ADEs are responsible for 6%-27% of adult patients' hospital or acute medical unit admissions, with a substantial portion being preventable through accurate tracking and effective communication [18,19].

Adopting standardized value sets can bridge these discrepancies and improve the reliability of clinical documentation [17]. This standardization is particularly important in reducing unwarranted clinical variation, ultimately leading to more consistent and evidence-based care [20]. A value set is a collection of coded values from 1 or more terminologies that is intended for use in a particular context [21]. Selecting terminologies with broad applicability across a range of clinical areas can help create robust and effective value sets.

While several terminology standards are available to document symptoms and diagnoses of ADEs, not all are ideal for use in EMRs due to limitations in granularity, hierarchical design, and semantic expressivity. For example, the Medical Dictionary for Regulatory Activities (MedDRA) and the *International Classification of Diseases, Tenth Revision* (*ICD-10*) have limitations that impede effective data capture and integration within EMRs. Although MedDRA is designed for pharmacovigilance, its terms are categorized at high level without distinguishing specific conditions, limiting its clinical use. Its hierarchical structure is broad and fixed, limiting its flexibility to support detailed data retrieval and analysis [22,23]. Bodenreider [24] has discussed its limitations when used in isolation and the potential benefits of combining it with SNOMED CT for improved signal detection and ADE reporting. Similarly, *ICD-10* is primarily designed for billing and statistical reporting. Its broad disease categories can fail to capture the nuances of complex clinical relationships, such as disease severity, laterality, or specific symptoms, lacking the clinical granularity needed for detailed ADE documentation within patient records. These limitations impact real-time decision-making [25-27].

In contrast, SNOMED CT (Clinical Terms) is specifically developed to support detailed clinical documentation and interoperability across various health care settings. It offers more than 300,000 active concepts that cover a broad range of clinical areas, allowing for precise and consistent recording of patient information [28-30]. SNOMED CT key strengths lie in its granularity, polyhierarchy, and semantic expressivity. making it a preferred choice as the basis of clinical documentation within EMRs across multiple jurisdictions [31]. Alecu et al [32] demonstrated that SNOMED CT's hierarchical structure is particularly useful for grouping ADE terms, which can aid in clinical decision-making and data analysis. However, if left unconstrained, its vast size and complexity can be overwhelming for end users. Therefore, SNOMED International recommends the development of subsets or value sets that cater to specific clinical use cases, such as ADEs.

There are currently no internationally published SNOMED CT value sets designed to streamline and standardize clinical documentation of ADE symptoms and diagnoses. This study aimed to fill this gap by developing a SNOMED CT–based value set to document and code symptoms and diagnoses of ADEs in EMRs. By doing so, we can enhance the reliability and consistency of ADE documentation and improve patient safety.

XSL•FO
RenderX

Methods

Setting

We used ADE data from ActionADE, an ADE reporting system. ActionADE is a web-based application designed to address repeat ADEs, which occur in 32.5% (421/1296) of emergency department cases. Repeat ADEs often occur because health systems lack effective means of communicating and integrating ADE information into clinical workflows [10]. A systematic review, participatory design process and pilot testing, involving software developers and end users, was completed to optimize the system to integrate ADE information into clinical workflows [11,33]. ActionADE allows providers to document and communicate ADE information bidirectionally through its integration with the provincial drug-dispensing database (PharmaNet) to providers in other health settings. Preliminary results showed that ActionADE prevents culprit or same-class medication redispensations in 33% of patients who present to a community pharmacy with a culprit or same class medication prescription [34].

ActionADE contains patient's ADE information entered by clinicians across acute care hospitals serving adult populations within the Vancouver Coastal Health Authority, British Columbia, since 2021 [25]. Between May 1, 2021, and May 1, 2024, ActionADE captured 5900 ADE reports. After excluding 108 reports with missing symptom and diagnosis information, we extracted source terms from a final sample of 5792 reports.

Data Extract and Processing

Each of the 5792 reports contained up to 3 ADE symptoms and diagnoses, which we extracted into an Excel file. After removing duplicates, we identified 881 unique terms. ActionADE uses MedDRA preferred terms for documenting ADE symptoms and diagnoses, based on its usability, and as recommended for reporting to Health Canada's pharmacovigilance database [35]. Since data entry into ActionADE is restricted to the use of MedDRA preferred terms, data are already standardized and free from potential data entry errors. We linked the 881 terms to MedDRA numeric codes, resulting in 879 coded terms and 2 uncoded terms. Upon review, we removed the 2 uncoded terms as they were noncurrent. Additional adjustments, such as removing irrelevant terms and duplicate entries, updating display names, and merging terms with different spelling but the same codes, resulted in a final source code set of 827 terms.

Mapping Approach

Our mapping approach was informed by the SNOMED CT-AU mapping guide [36] and enhanced by additional resources [36-38]. It consisted of the following steps: (1) define purpose and scope of the map, (2) identify personnel, (3) define mapping rules, (4) select mapping tool, (5) map source to target (automated and manual), (6) validation, and (7) quality assurance and creation of the value set.

Define Purpose and Scope of the Map

Defining the purpose and scope of the map helps ensure that the mapping aligns with the intended use of the terminology and covers the necessary range of source and target codes with the appropriate granularity [30,36]. The purpose of this mapping is to standardize the documentation of symptoms and diagnoses of ADEs within EMR. This involves mapping ADE symptoms and diagnoses documented in MedDRA preferred terms to corresponding SNOMED CT concepts within the clinical finding hierarchy.

Identify Personnel

The mapping team should be composed of individuals with extensive knowledge in health terminology standards and clinical practice to ensure the effective management and accuracy of the mapping process. In this study, the mapping process was designed and overseen by a mapping manager with specialized graduate training in health terminology standards. Execution was led by 2 mapping team members (Y-L AC and AL), both research pharmacists with extensive experience in clinical applications and practice. The team also included 2 clinical map advisors (CH and KB): an emergency physician and health services researcher specializing in drug safety and health IT, and a clinical pharmacist with extensive research and clinical practice experience in this area. Additionally, a technical advisor (LB), who is an expert in health informatics and SNOMED CT, provided essential technical oversight and support.

Define Mapping Rules

This unidirectional mapping from MedDRA to SNOMED CT involved matching each MedDRA preferred term to a semantically equivalent SNOMED CT concept (ie, they mean the same thing), ensuring accuracy in the representation of clinical data.

Select Mapping Tool

We used Snap2SNOMED, a mapping tool provided by SNOMED International, to conduct the mapping [39]. Snap2SNOMED is an online platform designed for creating and maintaining simple maps from other code systems to SNOMED CT. It allows teams of users to author and review a map. It has a built-in search engine that allows users to browse SNOMED CT concepts while mapping. Users can import their own code sets and export maps in various formats, such as CSV, TSV, and XLSX. Snap2SNOMED allowed us to import our source term file, use the MedDRA-SNOMED CT cross map, and automate much of the mapping process, which was then reviewed and refined by the team.

Map Source to Target

We used a dual mapping process where 2 mappers independently identified and documented semantically equivalent SNOMED CT concepts for each source term. If an exact match was unavailable, the mappers documented up to 3 semantically similar concepts, marking them as inexact, broader, or narrower matches. For example, "heart attack" is a semantically equivalent match to "22298006 | Myocardial infarction" as both represent the exact same clinical condition. A narrower match occurs when "heart attack" is mapped to "57054005 | Acute myocardial infarction (disorder)," which represents a specific type of myocardial infarction. When selecting a target code, the mappers reviewed the concept's fully specified name (FSN) and its parent and child concepts within the hierarchy to ensure

XSL•FO
RenderX

semantic accuracy. The mapping process involved two key strategies:

1. Automated mapping: We first used the MedDRA-SNOMED CT cross map to identify appropriate target concepts. This cross map was developed by SNOMED International in collaboration with the International Council for Harmonisation of Technical Requirements for Pharmaceuticals for Human Use. This map supports interoperability between terminologies by linking commonly used pharmacovigilance terms from MedDRA to SNOMED CT. The cross map released on April 30, 2024, includes 6779 MedDRA lower-level terms and 3594 SNOMED CT FSNs [5]. While ActionADE relies on MedDRA preferred terms, each preferred term is associated with a single lower-level term, so this did not impact our mapping process [22].
   The mapping manager imported the source code set and the cross map into Snap2SNOMED. The map was constrained to the Canadian Edition (version: 20240531) and the SNOMED CT clinical finding hierarchy. The software automatically mapped the source terms to SNOMED CT concepts within the cross map. Then, it generated a table with each row representing a single source term, displaying its corresponding source code, source display, target code, and target display. For matched terms, the relationship type was default as "EQUIVALENT," with the status marked as "DRAFT."
2. Manual mapping: For each automatically mapped term, the mappers independently reviewed and edited the suggested target terms and relationship types, updating the status to "MAPPED" upon completion.
   For source terms that were unmatched in the automated mapping, the mappers used Snap2SNOMED's built-in search function to identify target terms. By entering the source term in the search box, the software provided a list of suggested target concepts. The mappers reviewed the suggested terms and their attributes, selected the most appropriate candidate concept, assigned it to the source code with a relationship type (equivalent, broader, narrower, and inexact), and marked the status as "MAPPED" or "NO MAP" if no suitable match was found. For the source terms that lacked semantically equivalent matches, the mappers were asked to suggest up to 3 broader, narrower, or inexact alternatives (see Snap2SNOMED screenshots in Multimedia Appendix 1).

The mapping manager then exported and compared the maps from both mappers. A mapping was considered complete when both mappers independently identified the same SNOMED CT concept as the target. Any discrepancies were discussed and resolved through a virtual meeting moderated by the mapper manager. If consensus could not be reached, the issues were documented and adjudicated by the clinical advisors [36].

Validation

Two validators (CH and KB) independently evaluated the initial map using Snap2SNOMED. For each row, they reviewed the mapped terms and marked the status as either "ACCEPTED" or "REJECTED," recording the rationale for any rejections in the notes section. A map was considered correct only when both reviewers agreed on the target SNOMED CT concept (Multimedia Appendix 1). The mapping manager then exported and compared the results from both validators, consolidating a list of discrepancies. A virtual meeting was held to discuss and resolve these discrepancies. If consensus could not be reached, the issues were escalated to an additional reviewer and, if necessary, further to the technical advisor.

Quality Assurance and Creation of the Value Set

Quality assurance was performed by clinical experts who were not involved in the initial mapping and validation process [30,38]. A quality review team, consisting of 2 pharmacists (SB and CS) and a physician (KG-K), evaluated the final map for mapping appropriateness, safety risk, and clinical relevance. Each reviewer reviewed all the terms included in the validated map and flag terms with concerns by adding a note on the Snap2SNOMED platform.

As a final step, the reviewers completed a survey to assess clinical relevance of the validated map. The survey included two questions: (1) Does the current map capture the majority of ADE symptoms and diagnoses commonly encounter in your clinical practice? If not, which key terms are missing? (2) Are there any terms in the map that seem clinically irrelevant to your practice, or do you have suggestions for alternative terms that should be considered in future iterations? Terms flagged by 2 or more reviewers were discussed by the entire team to reach a consensus. This feedback was then used to finalize the value set.

Ethical Considerations

This study is exempt from ethical review according to The University of British Columbia Research Ethics Board policies (sections 4.3.2. and 4.3.3) [40] and TCPS 2 Article 2.3 [41]. The ActionADE dataset used for developing the MedDRA-SNOMED CT map was collected under prior ethical approval, with informed consent obtained from participants allowing for secondary research use. All data were deidentified. Individuals involved in the mapping and validation participated voluntarily, were informed of the study purpose, and provided implied consent. No personal identifiers were collected or shared, no compensation was provided, and the activities posed minimal risk; therefore, ethics review was not required.

Statistical Analysis

We used descriptive statistics to calculate the number and percentage of source terms that matched a corresponding SNOMED CT concept by relationship type in the initial map and validated map. The agreement between mappers was evaluated by checking whether their first selected SNOMED CT concept for each source term matched (first match). Interrater reliability across 2 mapping reviewers and 2 validators was calculated using Cohen κ statistics via the R package "irr" (University of Zurich) [42].

XSL•FO
RenderX

Results

Map Source Terms to SNOMED CT Concepts

The automated mapping identified 63.1% (522/827) semantically equivalent matches and 36.9% (305/827) unmatched terms. After manual mapping, mapper 1 identified 91.1% (753/827) semantically equivalent matches, 5.7% (47/827) semantically similar matches, and 3.2% (27/827) no match terms. Mapper 2 identified 85.0% (703/827) semantically equivalent matches, 8.0% (66/827) semantically similar matches, and 7.0% (58/827) no match terms (Table 1). All automatically mapped terms were accepted by both mappers.

For the source terms that lacked semantically equivalent matches, the mappers were asked to suggest up to 3 broader, narrower, or inexact alternatives. Mapper 1 suggested 57 target terms for 47 source terms without equivalent matches, averaging 1.2 suggestions per term. Mapper 2 proposed 66 target terms for 66 source terms, averaging 1.0 suggestion per term. A detailed breakdown of the semantically similar terms suggested by the mappers is shown in Table 2. The interrater reliability between the 2 mappers, measured by Cohen κ, was 0.87 (95% CI 0.85 - 0.89), indicating strong agreement [43].

We identified 139 terms with discrepancies between the mappers. These were all resolved through consensus discussions. Based on these results, we created an initial map that included 827 source terms, of which 95.3% (788/827) were successfully mapped to a SNOMED CT concept, while 4.7% (39/827) remained unmapped. Among the mapped terms, 96.8% (763/788) were semantically equivalent, 1.5% (12/788) were broader, 0.8% (6/788) were narrower, and 0.9% (7/788) were inexact matches.

Table . Mapping results across all source terms.

Category	Mapper 1	Mapper 2
Semantic equivalent match	753	703
Semantic similar match	47	66
No match	27	58
Total	827	827

Table . Breakdown of semantically similar terms suggested by mappers.

Category	Mapper 1	Mapper 2
Semantically broader than the source term	23	12
Semantically narrower than the source term	24	25
Semantically inexact to the source term	10	29
Total	57[a]	66[b]

[a]Mapper 1 suggested 57 target terms to describe 47 source terms without a semantically equivalent match, resulting in an average of 1.2 target terms per source term.

[b]Mapper 2 suggested 66 target terms to describe 66 source terms without a semantically equivalent match, resulting in an average of 1.00 target terms per source term.

Validation

Validation by 2 clinical experts resulted in 92.3% (763/827) of terms being accepted as semantically equivalent matches, 3.0% (25/827) were semantically similar, and 4.7% (39/827) were unmatched. A detailed breakdown of the semantically similar terms identified by the validators is shown in Table 3. The agreement between the 2 validators was strong, with a Cohen κ of 0.88 (95% CI 0.80 - 0.95) [43]. All automatically mapped terms were accepted by both validators.

We identified 42 terms where discrepancies arose between the validators, which were resolved through consensus discussions. One source term (ie, “endotracheal intubation”) was deemed irrelevant as it represents a clinical procedure rather than an ADE symptom or diagnosis and was therefore removed. A key point during the discussions for the remaining terms was the user-friendliness of the mapped terms. Validators noted that in some cases, semantically similar terms were preferred over semantically equivalent ones for ease of use. For instance, the term “sunburn” had an equivalent match with |403194002| “Solar erythema (disorder),” but the validators flagged this term as non–user-friendly due to lack of clinical use, recommending that “sunburn” to be added as a synonym in the Canada English language reference set. Table 4 shows a list of terms, like these, that were flagged by the map validators due to clinical usability issues.

The validated map included 826 source terms, with 98.4% (813/826) mapped to a target SNOMED CT concept, and 1.6% (13/826) remaining unmapped. Of the mapped terms, 95.7% (778/813) were semantically equivalent, 2.5% (20/813) were broader, 1.0% (8/813) were narrower, and 0.9% (7/813) were inexact matches.

XSL•FO
RenderX

Table . Breakdown of semantically similar terms suggested by validators.

Category	Validator 1[a]	Validator 2[b]
Semantically broader than the source term	12	13
Semantically narrower than the source term	6	8
Semantically inexact to the source term	7	9
Total	25	30

[a]Validator 1 suggested 25 target terms to describe 25 source terms without a semantically equivalent match, resulting in an average of 1.0 target term per source term.

[b]Validator 2 suggested 30 target terms to describe 25 source terms without a semantically equivalent match, resulting in an average of 1.2 target terms per source term.

Table . A list of mapped terms flagged by validators due to clinical usability issues.

Source code	Source display	Target code	Target display	Relationship type	Summary of validator comments
10029147	Nephrogenic diabetes insipidus	111395007	Arginine vasopressin resistance (disorder)	Equivalent	Non–user-friendly. Recommend adding this as a synonym in the Canada English language reference set.
10042496	Sunburn	403194002	Solar erythema (disorder)	Equivalent	Non–user-friendly. Recommend adding “sunburn” as a synonym in the Canada English language reference set.
10066371	Tendon pain	21545007	Tenalgia (finding)	Broader	Non–user-friendly. Recommend adding “Tendon pain” as a synonym in the Canada English language reference set.
10073183	Hyponatremic seizure	230358007	Hyponatremic encephalopathy (disorder)	Equivalent	Non–user-friendly. Recommend adding “Hyponatremic seizure”. as a synonym in the Canada English language reference set.
10080061	Euglycemic diabetic ketoacidosis	420422005	Ketoacidosis due to diabetes mellitus (disorder)	Broader	Mapped to a broader term, but recommend creating a subtype of this for “Euglycemic diabetic ketoacidosis.”

Quality Review and Create Final Value Set

The quality review team flagged 6 terms for further discussion due to potential safety risks or clinical relevance issues (Table 5). The project team reached a consensus on all flagged terms. One term was removed for being irrelevant to ADE documentation, while 5 were left unmapped, with recommendations for requesting new SNOMED CT codes to be added to the SNOMED CT Canadian edition. Similar to the validators’ feedback, 2 quality reviewers flagged the term “solar erythema (disorder)” for lacking clinical usability, with recommendations that the term “Sunburn” be used as the preferred term in the ADE clinical context.

The quality reviewers agreed that the final map included most major ADE symptoms and diagnosis terms commonly encountered in clinical practice, and no additional source terms were suggested (Multimedia Appendix 2). Based on this feedback, we created the ADE value set, consisting of 813 SNOMED CT concepts (Multimedia Appendix 3). There are 13 source terms awaiting new SNOMED CT concepts, which could be added to the value set in a later phase (Table 6).

XSL•FO
RenderX

Table . A list of terms flagged by quality reviewers for potential safety risks and issues related to clinical relevance.

Source code	Source display	Target code	Target display	Relationship type	Summary of quality reviewer comments
10005140	Bleeding time prolonged	165563002	Coagulation/bleeding tests abnormal (finding)	Broader	"Prolonged bleeding time" is more accurate. The term "bleeding time" is commonly used by both clinicians and in lay language, making it a reasonable match.
10028128	Mucositis management	N/A[a]	N/A	Unmapped	The "management" term does not seem to fit under ADE[b] diagnosis and symptoms. If included, it should be simplified to "mucositis." They also suggest using consistent terminology with other coding, and "inflammatory disease of mucous membrane" could be an appropriate replacement for "mucositis."
10071048	Seizure-like phenomena	1208961006	Nonmotor epileptic seizure (finding)	Inexact	Both terms are not ideal. "Seizure-like phenomena" is not equivalent to "nonmotor epileptic seizure," with one noting that it is too vague and the other highlighting its potential relevance as a distinct term.
10080061	Euglycemic diabetic ketoacidosis	420422005	Ketoacidosis due to diabetes mellitus (disorder)	Broader	Both "Ketoacidosis due to diabetes mellitus" and "Euglycemic DKA[c]" should be available.

[a]N/A: not applicable.

[b]ADE: adverse drug event.

[c]DKA: diabetic ketoacidosis.

XSL•FO
RenderX

Table . A list of source terms pending new target SNOMED CT codes.

Source code	Source display
10005140	Bleeding time prolonged
10028299	Muscle discomfort
10031118	Oropharyngeal swelling
10048868	Parkinsonian crisis
10061132	Drug level above therapeutic
10061642	Antibiotic level above therapeutic
10062015	Immunosuppressant drug level increased
10067360	Tongue necrosis
10067969	Cholestatic liver Injury
10079741	Sedation complication
10000489	Acidosis hyperchloremic
10071048	Seizure-like phenomena
10080061	Euglycemic diabetic ketoacidosis

Discussion

Principal Results

This project aimed to develop a standardized SNOMED CT–based value set for the documentation of ADE symptoms and diagnoses, addressing a critical gap in the integration of ADE reporting into EMRs. Our findings demonstrate the feasibility of creating a targeted yet comprehensive value set, which can enhance the consistency, accuracy, and interoperability of ADE documentation across health care systems.

The mapping of 826 unique ADE-related terms to SNOMED CT concepts was largely successful, with 98.3% of terms being mapped in the final value set. This high level of success reflects the comprehensiveness of the SNOMED CT framework and the effectiveness of our systematic mapping process. Strong agreement between mappers and between validators supports the reliability of the mapping. Moreover, the iterative process of consensus building for resolving discrepancies between mappers and validators underscores the importance of expert input in ensuring the clinical appropriateness of mapped terms.

A major challenge encountered was ensuring semantic equivalence while maintaining clinical usability. While semantic equivalence is critical for accurate mapping, as SNOMED CT serves as the reference terminology, achieving clinical usability requires careful management of interface terminology. This can involve using SNOMED CT's dialect-specific language reference sets, also known as the preferred term (eg, en-CA or specialized ADE-context dialects), or establishing one-to-one association between value set entries and interface terms.

In SNOMED CT, the FSN provides an unambiguous and stable description of a concept but is not always clinician-friendly or commonly used [44]. In contrast, the preferred term is the most clinically appropriate and widely used synonym in a given dialect [45]. Therefore, interface terminology should default to the concept's preferred synonym in the give dialect, not the FSN. For example, the source term "gout" maps to the equivalent concept 90560007, with an FSN of inflammatory disorder due to increased blood urate level—a term less familiar in practice. The preferred term in the Canada English reference set, gout, is more user-friendly and should be displayed in clinical interfaces. While display codes can help improve terms usability, clinical reviewers noted that this work-around solution does not resolve the underlying issue of terms lacking clinical usability.

Validators and quality reviewers also flagged terms where the preferred terms in the Canada English language reference set, while semantically equivalent to SNOMED CT concepts, were still not intuitive for clinical documentation. For example, the source term "sunburn" has a preferred term as "solar erythema." Reviewers noted that they had never before heard of or used this term clinically, ever. This highlights the importance of considering both semantic equivalency and clinical usability when developing standardized terminologies for real-world application and minimize barriers for users [35].

Future research should prioritize understanding the clinical usability of standardized terminologies and developing interface terminology that users can understand and apply. While SNOMED CT provides a robust framework for clinical documentation, more work is needed to ensure that mapped terms are intuitive and align with the language clinicians commonly use in practice. It is critical that an effective approach is adopted to supporting interface terms that will enable value sets to be clinically useful. Without suitable interface terms, clinicians may struggle to recognize or apply relevant concepts within clinical systems, limiting the practical use of mapped value sets.

Clinical Implications of the ADE Value Set

The adoption of this value set for ADE documentation holds significant implications for clinical practice. By standardizing the terminology used in EMRs, health care providers can improve the accuracy of ADE reporting, leading to better

XSL•FO
RenderX

communication across care teams and potentially reducing the risk of medication-related harm. The use of standardized terminology can facilitate data sharing across health care institutions and enhance pharmacovigilance efforts at the population level, improving patient safety, if the code set can be used and understood by clinicians. Moreover, the standardized terminology provided by this value set could enhance the performance of text-mining algorithms designed to identify ADEs in EMRs [46]. However, the success of this value set depends not only on its development but also on its integration into EMR systems and clinical workflow. A key challenge lies in the willingness of EMR vendors to incorporate value sets, such as importing standardized value sets external to the Cerner system.

To ensure the successful adoption of the SNOMED CT–based ADE value set, provincial or federal governments may need to engage with EMR vendors. Governments could explore ways to encourage or mandate vendors to engage with clinical users to support the integration of locally relevant value sets, either through regulatory frameworks or through financial incentives. Without such support, the clinical benefits of standardized ADE documentation may be difficult to achieve.

In addition, the success of the value set relies on its integration into clinical workflows. Ensuring that the terminology is not only accurate but also practical and intuitive for day-to-day use will be critical. Ongoing collaboration between technical experts, clinical users, and policy makers will be essential to make certain that the value aligns with current clinical documentation practices and meets the needs of health care providers. Additionally, it is crucial to regularly update the terms to reflect the modern language and evolving practices in health care. As medical terminology changes and evolves, ensuring that value sets remain current will maintain their relevance and improve their usability in real-world clinical settings. By addressing these challenges, the value set has the potential to significantly improve the quality and consistency of ADE reporting, ultimately enhancing patient care.

Ineffective communication of ADE information across health care settings can lead to repeat ADEs, partly because different EMR systems use varied terminology standards. Recognized as a Canadian national standard and widely adopted in clinical areas including e-prescribing [47], our SNOMED CT value set adds values by standardizing ADE documentation in EMRs and enabling seamless ADE data exchange between hospital and community settings. This will allow clinicians to have timely access to patient's ADE data at the point of care, preventing unintentional represcription or redispensation of culprit drugs, thereby reducing the incidence of repeat ADEs.

Limitations

It is important to note that our study extracted source terms from a single ADE reporting system—ActionADE—which captures ADEs from patients presenting predominantly in emergency departments across 9 hospitals within a specific geographic region during a specific time period. As a result, the symptoms and diagnoses captured in this context may not fully represent ADEs occurring in other health care settings, such as inpatient wards, community care, or long-term care facilities, where different patient populations and clinical presentations are more common. For example, ADEs in long-term care settings may involve different drug classes and clinical manifestations than those seen in emergency departments. Similarly, pediatric ADEs were underrepresented in our sample, as none of the included hospitals were dedicated pediatric centers. Finally, as new drugs are developed and use of existing drugs is expanded to new clinical indications, new ADEs may emerge over time. Future work will need to expand the scope of this project by exploring and refining the value set to ensure its applicability across a diverse range of clinical environments, patient populations, and over time.

We acknowledge that using MedDRA's broad, high-level terms as our source may limit the potential granularity of our resulting SNOMED CT value set. While our approach may not have enhanced granularity of the resulting value set, the benefits of SNOMED CT's superior semantic framework, logical definition, and hierarchical structure, along with its increasing adoption as a Canadian national standard, justify its use in creating an initial ADE value set. Future research should explore the impact of using more granular source terminologies on the resulting SNOMED CT value set.

Another limitation is the potential variability in how individual reviewers interpreted ADE-related terms, which may have been influenced by their clinical background, experience, or familiarity with SNOMED CT concepts. While mapping should be grounded in semantic equivalence to ensure technical accuracy, variability may have occurred when terms had multiple valid mappings depending on the clinical context. These discrepancies highlight the need for better education on the importance of mapping based on meaning and semantics only, and tooling needs to provide better support for the incorporation of interface terms into terminology service using additional synonyms and a context-based language reference set.

Additionally, due to vendor limitations, we were unable to test the value set in the context where it will be used to ensure that it meets the needs of relevant stakeholders. Further studies are required to evaluate the impact of adopting standardized ADE value sets on clinical outcomes. Research examining how the integration of a SNOMED CT–based value set in EMRs affects the quality of ADE reporting, patient safety, and pharmacovigilance on a larger scale will be crucial to demonstrate the real-world benefits of this approach.

Conclusions

The development of a SNOMED CT–based value set for the documentation of ADE symptoms and diagnoses represents an important step toward improving the standardization of clinical documentation and enhancing patient safety. While the mapping process was largely successful, ongoing efforts to refine and expand the value set, improve user-friendliness, and evaluate its impact on clinical practice will be critical for ensuring its long-term adoption and use. By integrating this value set into clinical workflows and continuing to address gaps in terminology, health care systems can enhance the quality and interoperability of ADE documentation, contributing to better patient care.

XSL•FO
RenderX

Acknowledgments

The ActionADE platform is funded by the Canadian Institutes of Health Research, with support from the Ministry of Health British Columbia, Vancouver Coastal Health, the Lower Mainland Consolidated Pharmacies, and the BC SUPPORT Unit. CMH was supported by the Michael Smith Foundation for Health Research Health Professional-Investigator award during the study period. EYL was supported by the CIHR REDI Early Career Transition Award. The funder has no role in the design, conduct, analysis, interpretation of data, or the drafting of scientific manuscripts.

Data Availability

The MedDRA–SNOMED CT map and the SNOMED CT–based value set generated in this study are included in the supplementary information files in Multimedia Appendices 2 and 3.

Authors' Contributions

All authors contributed to the study's conception and design. EYL drafted the study protocol; oversaw and coordinated the mapping, validation, and quality review process; and wrote the first draft of the manuscript. LB provided technical guidance on the study methodology, oversaw the quality of the protocol execution, and contributed to the refinement of the data analysis. EYL, CMH, KB, Y-LAC, and AL participated in the mapping or the validation process and contributed to the refinement of the data analysis. SB, KG-K, and CS participated in the quality review process and contributed to the refinement of the data analysis. All authors contributed to the interpretation of the findings and commented on previous manuscript versions. All authors read and approved the submitted manuscript and have agreed to be personally accountable for their contribution.

Conflicts of Interest

None declared.

Multimedia Appendix 1
Screenshots of the Snap2SNOMED platform.
[PDF File, 415 KB - medinform_v13i1e70167_app1.pdf]

Multimedia Appendix 2
MedDRA-to-SNOMED CT map for adverse drug event symptoms and diagnoses.
[XLSX File, 61 KB - medinform_v13i1e70167_app2.xlsx]

Multimedia Appendix 3
SNOMED CT–based value set for adverse drug event symptoms and diagnoses.
[XLSX File, 33 KB - medinform_v13i1e70167_app3.xlsx]

References

1. Hohl CM, Dankoff J, Colacone A, Afilalo M. Polypharmacy, adverse drug-related events, and potential adverse drug interactions in elderly patients presenting to an emergency department. Ann Emerg Med 2001 Dec;38(6):666-671. [doi: 10.1067/mem.2001.119456] [Medline: 11719747]
2. Zed PJ, Abu-Laban RB, Balen RM, et al. Incidence, severity and preventability of medication-related visits to the emergency department: a prospective study. CMAJ 2008 Jun 3;178(12):1563-1569. [doi: 10.1503/cmaj.071594] [Medline: 18519904]
3. Canadian Institute for Health Information. NACRS emergency department visits and length of stay by province/territory, 2018-2019. : Canadian Institute for Health Information; 2019 URL: https://www.cihi.ca/en/nacrs-emergency-department-visits-and-lengths-of-stay [accessed 2025-06-27]
4. Woo SA, Cragg A, Wickham ME, et al. Methods for evaluating adverse drug event preventability in emergency department patients. BMC Med Res Methodol 2018 Dec 4;18(1):160. [doi: 10.1186/s12874-018-0617-4] [Medline: 30514232]
5. Woo SA, Cragg A, Wickham ME, et al. Preventable adverse drug events: descriptive epidemiology. Br J Clin Pharmacol 2020 Feb;86(2):291-302. [doi: 10.1111/bcp.14139] [Medline: 31633827]
6. van der Linden CMJ, Jansen PAF, van Marum RJ, Grouls RJE, Korsten EHM, Egberts ACG. Recurrence of adverse drug reactions following inappropriate re-prescription: better documentation, availability of information and monitoring are needed. Drug Saf 2010 Jul 1;33(7):535-538. [doi: 10.2165/11532350-000000000-00000] [Medline: 20553055]
7. Wickham ME, McGrail KM, Law MR, Cragg A, Hohl CM. Re-exposure to culprit medication following adverse drug event diagnosis in Canadian emergency department patients: a cohort study. Pharmacoepidemiol Drug Saf 2024 Sep;33(9):e70012. [doi: 10.1002/pds.70012] [Medline: 39300754]

XSL•FO
RenderX

8. World Health Organization. Medication Without Harm—Global Patient Safety Challenge on Medication Safety. 2017. URL: https://www.who.int/initiatives/medication-without-harm [accessed 2025-06-27]
9. Leape LL. Systems analysis of adverse drug events. JAMA 1995 Jul 5;274(1):35. [doi: 10.1001/jama.1995.03530010049034]
10. Hohl CM, Woo SA, Cragg A, et al. Repeat adverse drug events associated with outpatient medications: a descriptive analysis of 3 observational studies in British Columbia, Canada. CMAJ Open 2019;7(3):E446-E453. [doi: 10.9778/cmajo.20180190] [Medline: 31320328]
11. Peddie D, Small S, Wickham M, Bailey C, Hohl C, Balka E. Designing novel health ICTs to support work, not generate it: five principles. Stud Health Technol Inform 2017;234:262-268. [Medline: 28186052]
12. Institute of Medicine; Committee on Identifying and Preventing Medication Errors. In: Aspden P, Wolcott J, Bootman JL, Cronenwett LR, editors. Preventing Medication Errors: National Academy Press; 2007. URL: https://psnet.ahrq.gov/issue/preventing-medication-errors-quality-chasm-series [accessed 2025-06-27]
13. Linder JA, Haas JS, Iyer A, et al. Secondary use of electronic health record data: spontaneous triggered adverse drug event reporting. Pharmacoepidemiol Drug Saf 2010 Dec;19(12):1211-1215. [doi: 10.1002/pds.2027] [Medline: 21155192]
14. Liu F, Jagannatha A, Yu H. Towards drug safety surveillance and pharmacovigilance: current progress in detecting medication and adverse drug events from electronic health records. Drug Saf 2019 Jan;42(1):95-97. [doi: 10.1007/s40264-018-0766-8] [Medline: 30649734]
15. Barker W, Chang W, Everson J, et al. The evolution of health information technology for enhanced patient-centric care in the United States: data-driven descriptive study. J Med Internet Res 2024 Oct 28;26:e59791. [doi: 10.2196/59791] [Medline: 39466303]
16. Lau EY, Cragg A, Small SS, Butcher K, Hohl CM. Characterizing and comparing adverse drug events documented in 2 spontaneous reporting systems in the lower mainland of British Columbia, Canada: retrospective observational study. JMIR Hum Factors 2024 Jan 18;11:e52495. [doi: 10.2196/52495] [Medline: 38236629]
17. Goss FR, Lai KH, Topaz M, et al. A value set for documenting adverse reactions in electronic health records. J Am Med Inform Assoc 2018 Jun 1;25(6):661-669. [doi: 10.1093/jamia/ocx139] [Medline: 29253169]
18. Hamilton H, Gallagher P, Ryan C, Byrne S, O'Mahony D. Potentially inappropriate medications defined by STOPP criteria and the risk of adverse drug events in older hospitalized patients. Arch Intern Med 2011 Jun 13;171(11):1013-1019. [doi: 10.1001/archinternmed.2011.215] [Medline: 21670370]
19. Kongkaew C, Noyce PR, Ashcroft DM. Hospital admissions associated with adverse drug reactions: a systematic review of prospective observational studies. Ann Pharmacother 2008 Jul;42(7):1017-1025. [doi: 10.1345/aph.1L037] [Medline: 18594048]
20. Hodgson T, Burton-Jones A, Donovan R, Sullivan C. The role of electronic medical records in reducing unwarranted clinical variation in acute health care: systematic review. JMIR Med Inform 2021 Nov 17;9(11):e30432. [doi: 10.2196/30432] [Medline: 34787585]
21. 4.9 resource valueset—content. valueset. : Health Level Seven Fast Healthcare Interoperability Resources (HL7FHIR); 2024 Nov 17 URL: https://build.fhir.org/valueset.html [accessed 2024-11-17]
22. MedDRA to SNOMED CT and SNOMED CT to meddra mapping conventions. Medical Dictionary for Regulatory Activity (MedDRA). 2023 Apr. URL: https://files.meddra.org/www/Website%20Files/Change%20Requests/MedDRA-SNOMED%20CT%20Mapping%20Conventions_v4.0_April%202024.pdf [accessed 2025-06-26]
23. Nadkarni PM, Darer JD. Determining correspondences between high-frequency MedDRA concepts and SNOMED: a case study. BMC Med Inform Decis Mak 2010 Oct 28;10:66. [doi: 10.1186/1472-6947-10-66] [Medline: 21029418]
24. Bodenreider O. Using SNOMED CT in combination with MedDRA for reporting signal detection and adverse drug reactions reporting. AMIA Annu Symp Proc 2009 Nov 14;2009:45-49. [Medline: 20351820]
25. Mozzicato P. MedDRA. Pharm Med 2009 Apr;23(2):65-75. [doi: 10.1007/BF03256752]
26. Hougland P, et al. Using ICD-9-CM codes in hospital claims data to detect adverse events in patient safety surveillance. In: Henriksen K, et al, editor. Advances in Patient Safety: New Directions and Alternative Approaches (Vol 1: Assessment): Agency for Healthcare Research and Quality; 2008. URL: https://www.ncbi.nlm.nih.gov/books/NBK43647/ [accessed 2025-06-27]
27. Hougland P, Xu W, Pickard S, Masheter C, Williams SD. Performance of International Classification of Diseases, 9th Revision, Clinical Modification codes as an adverse drug event surveillance system. Med Care 2006 Jul;44(7):629-636. [doi: 10.1097/01.mlr.0000215859.06051.77] [Medline: 16799357]
28. Chute CG, Cohn SP, Campbell KE, Oliver DE, Campbell JR. The content coverage of clinical classifications. For the computer-based patient record institute's work group on codes & structures. J Am Med Inform Assoc 1996;3(3):224-233. [doi: 10.1136/jamia.1996.96310636] [Medline: 8723613]
29. Campbell JR, Payne TH. A comparison of four schemes for codification of problem lists. Proc Annu Symp Comput Appl Med Care 1994:201-205. [Medline: 7949920]
30. What is SNOMED CT? SNOMED International. URL: https://www.snomed.org/what-is-snomed-ct [accessed 2025-06-02]
31. Rosenbloom ST, Miller RA, Johnson KB, Elkin PL, Brown SH. Interface terminologies: facilitating direct entry of clinical data into electronic health record systems. J Am Med Inform Assoc 2006;13(3):277-288. [doi: 10.1197/jamia.M1957] [Medline: 16501181]

XSL•FO
RenderX

32. Alecu I, Bousquet C, Jaulent MC. A case report: using SNOMED CT for grouping adverse drug reactions terms. BMC Med Inform Decis Mak 2008 Oct 27;8 Suppl 1(Suppl 1):S4. [doi: 10.1186/1472-6947-8-S1-S4] [Medline: 19007441]
33. Chruscicki A, Badke K, Peddie D, Small S, Balka E, Hohl CM. Pilot-testing an adverse drug event reporting form prior to its implementation in an electronic health record. Springerplus 2016;5(1):1764. [doi: 10.1186/s40064-016-3382-z] [Medline: 27795906]
34. Cragg A, Small SS, Lau E, et al. Sharing adverse drug event reports between hospitals and community pharmacists to inform re-dispensing: an analysis of reports and process outcomes. Drug Saf 2023 Nov;46(11):1161-1172. [doi: 10.1007/s40264-023-01348-7] [Medline: 37783974]
35. Chan E, Small SS, Wickham ME, Cheng V, Balka E, Hohl CM. The utility of different data standards to document adverse drug event symptoms and diagnoses: mixed methods study. J Med Internet Res 2021 Dec 10;23(12):e27188. [doi: 10.2196/27188] [Medline: 34890351]
36. Australian Digital Health Agency. SNOMED CT-AU mapping guidelines. 2022 URL: https://www.healthterminologies.gov.au/library/DH_3643_2022_SNOMEDCTAU_MappingGuidelines_v3.0.pdf [accessed 2025-6-5]
37. International Health Terminology Standards Development Organisation. SNOMED CT mapping guide. 2022 URL: https://confluence.ihtsdotools.org/display/S2SUG?preview=/137241143/149259331/doc_Snap2SnomedUserGuide-en-US_INT_20220603.pdf [accessed 2024-11-17]
38. Sung S, Park HA, Jung H, Kang H. A SNOMED CT mapping guideline for the local terms used to document clinical findings and procedures in electronic medical records in South Korea: methodological study. JMIR Med Inform 2023 Apr 18;11:e46127. [doi: 10.2196/46127] [Medline: 37071456]
39. Snap2SNOMED. SNOMED International. URL: https://snap.snomedtools.org/ [accessed 2024-09-19]
40. Research involving human participants policy LR9. The University of British Columbia Board of Governors. 2019. URL: https://universitycounsel.ubc.ca/files/2022/05/Human-Research-Policy_LR9.pdf [accessed 2025-05-06]
41. TCPS 2 (2022)—chapter 2: scope and approach. Panel on Research Ethics, Government of Canada. 2022. URL: https://ethics.gc.ca/eng/tcps2-eptc2_2022_chapter2-chapitre2.html [accessed 2025-05-06]
42. Gamer M, Lemon J, Fellows I, Singh P. Irr: various coefficients of interrater reliability and agreement. R Package Version 0841. 2019. URL: https://CRAN.R-project.org/package=irr [accessed 2025-06-26]
43. McHugh ML. Interrater reliability: the kappa statistic. Biochem Med (Zagreb) 2012;22(3):276-282. [Medline: 23092060]
44. Fully specified name. SNOMED International. 2024. URL: https://confluence.ihtsdotools.org/display/DOCEG/Fully+Specified+Name [accessed 2024-12-14]
45. Preferred term. SNOMED International. 2024. URL: https://confluence.ihtsdotools.org/display/DOCEG/Preferred+Term#:~:text=A%20preferred%20term%20(PT)%20is,practice%20or%20in%20the%20literature [accessed 2024-12-14]
46. van de Burgt BWM, Wasylewicz ATM, Dullemond B, et al. Development of a text mining algorithm for identifying adverse drug reactions in electronic health records. JAMIA Open 2024 Oct;7(3):ooae070. [doi: 10.1093/jamiaopen/ooae070] [Medline: 39156048]
47. SNOMED CT strategy for canada. Canada Health Infoway. 2013. URL: https://infocentral.infoway-inforoute.ca/en/standards/canadian/snomed-ct [accessed 2025-06-27]

Abbreviations

ADE: adverse drug event
EMR: electronic medical record
FSN: fully specified name
ICD-10: International Classification of Diseases, Tenth Revision
MedDRA: Medical Dictionary for Regulatory Activities
SNOMED CT: SNOMED Clinical Terms

Edited by A Coristine; submitted 17.12.24; peer-reviewed by J Ehrsam, L Agrawal; revised version received 26.03.25; accepted 27.03.25; published 08.07.25.

Please cite as:
Lau EY, Bird L, Lau A, Chau YLA, Butcher K, Buchkowsky S, Gossack-Keenan K, Sadowski C, Hohl CM
Developing a SNOMED CT–Based Value Set to Document Symptoms and Diagnoses for Adverse Drug Events: Mixed Methods Study
JMIR Med Inform 2025;13:e70167
URL: https://medinform.jmir.org/2025/1/e70167
doi:10.2196/70167

XSL•FO
RenderX

© Erica Y Lau, Linda Bird, Anthony Lau, Yau-Lam Alex Chau, Katherine Butcher, Susan Buchkowsky, Kira Gossack-Keenan, Cheryl Sadowski, Corinne M Hohl. Originally published in JMIR Medical Informatics (https://medinform.jmir.org), 8.7.2025. This is an open-access article distributed under the terms of the Creative Commons Attribution License (https://creativecommons.org/licenses/by/4.0/), which permits unrestricted use, distribution, and reproduction in any medium, provided the original work, first published in JMIR Medical Informatics, is properly cited. The complete bibliographic information, a link to the original publication on https://medinform.jmir.org/, as well as this copyright and license information must be included.

XSL•FO
RenderX

Detecting Redundant Health Survey Questions by Using Language-Agnostic Bidirectional Encoder Representations From Transformers Sentence Embedding: Algorithm Development Study

Sunghoon Kang[1], MS; Hyewon Park[1], BSN, RN; Ricky Taira[2], PhD; Hyeoneui Kim[1], RN, PhD

[1]College of Nursing, Seoul National University, 103 Daehak-ro, Jongno-gu, Seoul, Republic of Korea

[2]The Department of Radiological Sciences, David Geffen School of Medicine, University of California, Los Angeles, Los Angeles, CA, United States

Corresponding Author:
Hyeoneui Kim, RN, PhD
College of Nursing, Seoul National University, 103 Daehak-ro, Jongno-gu, Seoul, Republic of Korea

Abstract

Background: As the importance of person-generated health data (PGHD) in health care and research has increased, efforts have been made to standardize survey-based PGHD to improve its usability and interoperability. Standardization efforts such as the Patient-Reported Outcomes Measurement Information System (PROMIS) and the National Institutes of Health (NIH) Common Data Elements (CDE) repository provide effective tools for managing and unifying health survey questions. However, previous methods using ontology-mediated annotation are not only labor-intensive and difficult to scale but also challenging for identifying semantic redundancies in survey questions, especially across multiple languages.

Objective: The goal of this work was to compute the semantic similarity among publicly available health survey questions to facilitate the standardization of survey-based PGHD.

Methods: We compiled various health survey questions authored in both English and Korean from the NIH CDE repository, PROMIS, Korean public health agencies, and academic publications. Questions were drawn from various health lifelog domains. A randomized question pairing scheme was used to generate a semantic text similarity dataset consisting of 1758 question pairs. The similarity scores between each question pair were assigned by 2 human experts. The tagged dataset was then used to build 4 classifiers featuring bag-of-words, sentence-bidirectional encoder representations from transformers (SBERT) with bidirectional encoder representations from transformers (BERT)–based embeddings, SBERT with language-agnostic BERT sentence embedding (LaBSE), and GPT-4o. The algorithms were evaluated using traditional contingency statistics.

Results: Among the 3 algorithms, SBERT-LaBSE demonstrated the highest performance in assessing the question similarity across both languages, achieving area under the receiver operating characteristic and precision-recall curves of >0.99. Additionally, SBERT-LaBSE proved effective in identifying cross-lingual semantic similarities. The SBERT-LaBSE algorithm excelled at aligning semantically equivalent sentences across both languages but encountered challenges in capturing subtle nuances and maintaining computational efficiency. Future research should focus on testing with larger multilingual datasets and on calibrating and normalizing scores across the health lifelog domains to improve consistency.

Conclusions: This study introduces the SBERT-LaBSE algorithm for calculating the semantic similarity across 2 languages, showing that it outperforms BERT-based models, the GPT-4o model, and the bag-of-words approach, highlighting its potential in improving the semantic interoperability of survey-based PGHD across language barriers.

(JMIR Med Inform 2025;13:e71687) doi:10.2196/71687

KEYWORDS

person-generated health data; PGHD; bidirectional encoder representations from transformers; BERT; semantic similarity; language-agnostic BERT sentence embedding; LaBSE; sentence-bidirectional encoder representations from transformers; SBERT; interoperability

Introduction

Person-generated health data (PGHD) is becoming increasingly important in managing individual health. PGHD encompass health-related information that individuals create and collect outside traditional clinical environments, helping them monitor and manage their well-being [1,2]. Examples of PGHD include biometric data from wearable devices and self-reported information such as patient-reported outcomes. Since PGHD has the potential for continuously capturing health insights beyond health care settings, there is growing interest in leveraging PGHD to support clinical care [3-5]. In parallel, PGHD is increasingly explored as a resource for patient-centered outcomes research [6,7]. However, there are several challenges

XSL•FO
RenderX

in the effective use of PGHD, including developing robust data management systems, ensuring data security, deploying it seamlessly into clinical workflows, and maintaining high data quality [5,7,8].

Standardizing survey-based PGHD is a critical step in enabling its broader use [9]. An important aspect of standardization is to identify redundancies in the form of semantic equivalencies. These redundancies may arise because the clarity, tone, tense, directness, and formality of the language can be phrased differently for the same purposeful inquiry depending upon the author. For example, emotional symptoms may be captured by questions such as “Do you feel like withdrawing from family or friends?” or “I don’t really want to talk to people around me.” This variation makes identifying semantically equivalent questions—and thus standardizing survey-based PGHD—a complex task. Efforts such as the Patient-Reported Outcomes Measurement Information System (PROMIS) and the National Institutes of Health (NIH) Common Data Elements (CDE) repository aim to provide standardized health survey questions. PROMIS, a consensus-based item bank designed for managing patient-reported outcomes, offers standardized measures that are applicable across various diseases and clinical settings [10-12]. These measures have helped health care providers across various clinical settings, including pain management [13], orthopedics [14], and primary care [15]; in cancer care [16]; in managing patient symptoms; in tailoring treatments; and in improving communication between patients and clinicians. The NIH CDE repository, through metadata tagging, also plays a key role in standardizing data elements, including health surveys [17,18]. Both PROMIS and the CDE repository are essential for enhancing the interoperability of health data.

In practice, the deployment of PGHD acquisition applications requires that survey questions be drawn from these established standardized resources. Data collected using questions outside of these resources still require additional efforts to achieve standardization. Although previous studies have explored ontology-mediated methods to identify semantically equivalent health questions [10,11], annotating each question with ontology concepts is labor-intensive and lacks scalability as such knowledge sources expand. As a complementary approach, deep learning and transformer-based methods have been applied to semantic textual similarity (STS) tasks in clinical texts, including radiology and pathology reports [19], clinical notes [20-22], and medical question-answer pairs [23]. A range of models has been explored, such as convolutional neural networks [19]; transformer-based architectures such as bidirectional encoder representations from transformers (BERT), robustly optimized BERT approach, and XLNet [20-22]; and the Siamese network [23]. Despite their promising performance, most of these models have been limited to single-language settings—predominantly English [20-22] or Chinese [19,23]. Consequently, cross-lingual STS remains underexplored, highlighting the need for standardization efforts that promote semantic interoperability across languages.

To address these challenges, we developed Standardized PGHD Utilization Resources and Tools (SPURT), which supports the standardization and reuse of survey-based PGHD by identifying semantically equivalent questions and facilitating the storage, retrieval, and sharing of these data. Unlike PROMIS and the NIH CDE repository, SPURT annotates and stores health survey questions in both English and Korean while also detecting semantically redundant questions. This ensures the use of consistent question formats whenever possible. Technically, assessing semantic similarity between texts is well-established and widely applied for managing text resources [24]. However, SPURT faces 2 unique challenges in its assigned task. First, it must effectively assess semantic similarities within or between 2 different languages—English and Korean. Although multilingual embeddings can be used to address this challenge [25,26], they often perform less effectively for low-resource languages such as Korean compared to high-resource languages such as English [27]. One common solution is to translate low-resource languages into high-resource ones before embedding, but this approach risks losing or distorting the original meaning [28,29]. Second, it must ensure computational efficiency for real-time semantic comparisons between questions. Calculating semantic similarity by using large language models such as BERT is computationally expensive, with a time complexity of O (N!). For example, computing the similarity of approximately 10,000 sentence pairs can take around 65 hours using a V100 graphics processing unit [30]. Given that SPURT is designed to be a real-time, reactive data processing tool, achieving reasonable response times is crucial for its functionality.

This study presents the development of a novel algorithm for detecting redundant questions, addressing the challenges outlined above. The algorithm utilizes sentence-BERT (SBERT), a variant of BERT designed for efficient sentence-level semantic similarity calculations [30] along with language-agnostic BERT sentence embedding (LaBSE) [31] to enhance multilingual capability. Sentence-BERT is a model specifically designed for calculating STS between sentences, and LaBSE is an embedding that supports efficient cross-lingual STS by mapping multilingual sentences into a shared embedding space. The SBERT-LaBSE algorithm integrates the strengths of both models and facilitates the identification of semantically equivalent questions across languages.

Methods

Corpus Description: The STS Dataset

An STS dataset contains text pairs along with predefined similarity scores that quantify their semantic closeness [32-36]. This study shows an STS dataset that fine-tunes pretrained language models and evaluates our algorithms’ performance in determining the semantic similarity between health-related questions.

We collected English and Korean questions from self-reported questionnaires covering 5 health lifelog domains, that is, diet, physical activity, living environment, stress management, and sleep. English questions (n=1222) were sourced from the NIH CDE repository, PROMIS, and academic publications, while Korean questions (n=963) were gathered from web-based resources provided by public health agencies and hospitals in Korea [17,37-40].

XSL•FO
RenderX

To build the STS dataset, we began by randomly selecting 5 seed questions from each of the 5 health lifelog domains in Korean, resulting in 25 seed questions. For each question, correspondingly similar questions for Korean were identified, resulting in 25 similar seed questions for each language. This correspondence of seed questions was performed to minimize the effects of semantic complexity on algorithm performance. We then randomly selected 30 comparison questions for each seed question, which yielded a total of 1500 question pairs (750 in each language).

The gold standard for semantic similarity between the question pairs was determined by 2 researchers with nursing backgrounds who independently scored the similarity of each question pair, following a standardized scoring protocol (Table 1). The agreement between the researchers, as measured by Cohen κ, varied by the health lifelog domains: 0.91 for diet, 0.72 for living environment, 0.83 for physical activity, 0.86 for sleep, and 1.0 for stress management, with an average Cohen κ of 0.86 across all the health lifelog domains.

Table . Scoring protocol for semantic similarity. The seed question was "In the past month, have you ever had chest pain when you were not performing any physical activity?"

Score	Scoring protocol	Examples
4	Minor differences in word choice from the seed question but takes the same form of response	In the past month, have you had chest pain when you were not doing physical activity?
3	Share the same key topic, although some details may be added, altered, or omitted from the seed question	Do you feel pain in your chest when you do physical activity?
2	The key topics are similar but more specific or general than that of the seed question	Has your doctor ever said that you have a heart condition and that you should only perform physical activity recommended by a doctor?
1	Does not share the core topic from the seed question or belongs to a completely different health lifelog domain	Have you done general conditioning exercises in the past 4 weeks?

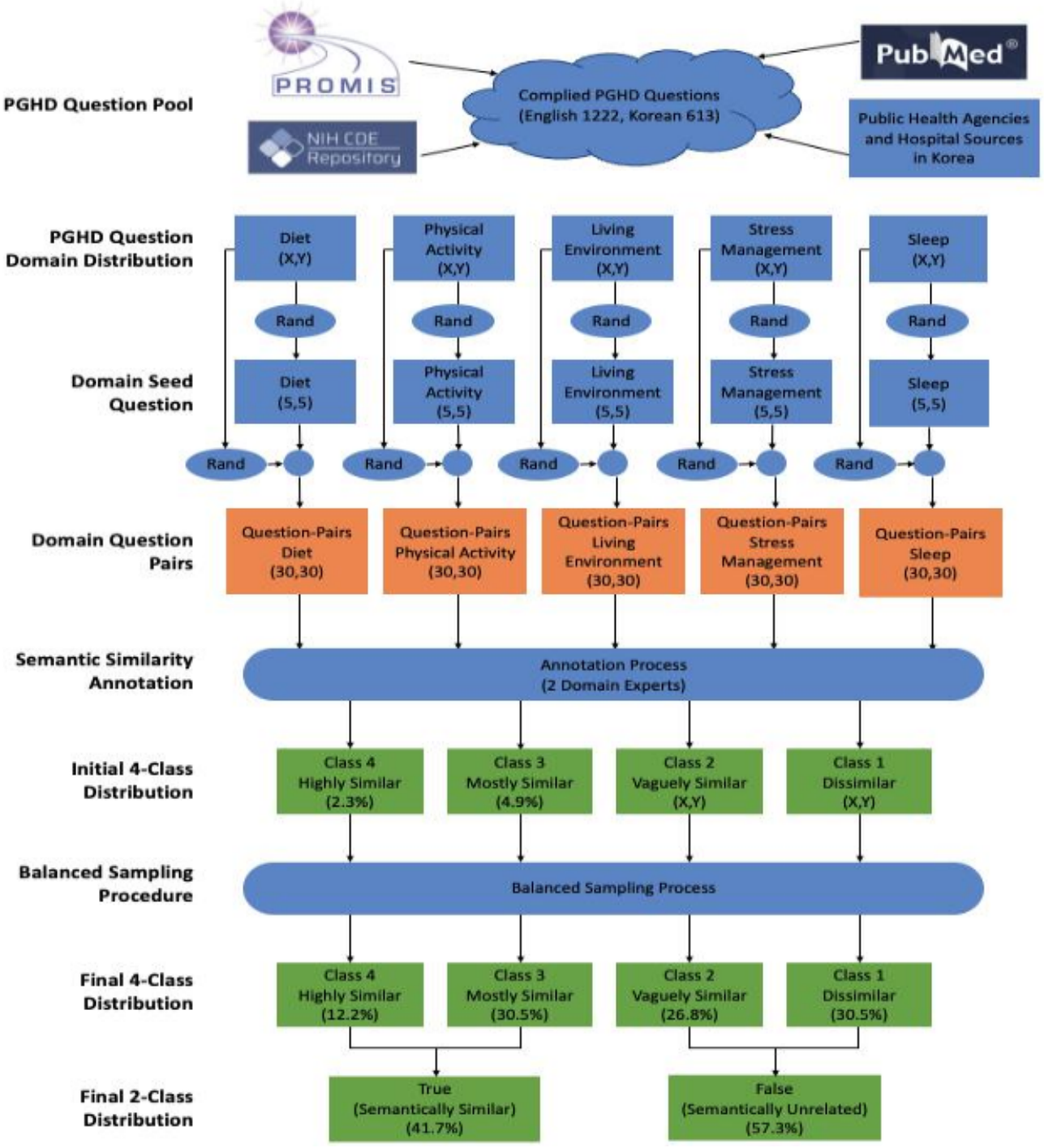
Upon completion of this annotation process, we observed that the initial distribution of the similarity scores was imbalanced—skewed heavily toward lower similarity scores. Only 2.3% (7/300) of the pairs received a score of 4, and 4.9% (15/300) received a score of 3. To address this imbalance, we supplemented the dataset with an additional 117 English and 142 Korean question pairs from other sources, chosen to increase the frequency of semantically similar (ie, higher scores) samples in the evaluation STS dataset. These additions brought the final evaluation set to 820 question pairs (410 in each language) with the following distribution: 12.2% (99/810), 30.5% (247/810), 26.8% (217/810), and 30.5% (247/810) for scores 4, 3, 2, and 1, respectively.

Using a similar procedure as described above, we compiled a second English STS dataset for fine-tuning our pretrained language models. This fine-tuning dataset included 938 annotated English question pairs. The fine-tuning set had a distribution of 6.2% (58/938) scoring 4, 14% (131/938) scoring 3, 23.5% (220/938) scoring 2, and 56.4% (529/938) scoring 1.

In total, the STS dataset consisted of 1758 question pairs, broken down into 820 for evaluation testing (410 English and 410 Korean) and 938 in English for classifier model refinement (see Multimedia Appendix 1). The process of constructing the STS dataset is illustrated in Figure 1.

XSL•FO
RenderX

Figure 1. The process of preparing the semantic textual similarity dataset for fine-tuning and evaluation. CDE: common data elements; NIH: National Institutes of Health; PGHD: person-generated health data; PROMIS: Patient-Reported Outcomes Measurement Information System; Rand: random selection; STS: semantic textual similarity.



Semantic Similarity Calculation Algorithms

Overview

We developed 4 classifiers to compare their performance capability for distinguishing the binary task of semantic similarity between STS question pairs. These were (1) the bag-of-words (BoW) model, (2) SBERT with BERT-based embeddings (SBERT-BERT), (3) LaBSE, and (4) the GPT-4o model (GPT-4o). Among these, the SBERT-BERT algorithm was included to serve as a translation-dependent baseline, enabling comparison with multilingual models such as SBERT-BERT and GPT-4o. Model fine-tuning and algorithm development were performed using Python (version 3.11).

BoW Classifier

The BoW algorithm, a traditional language model that represents sentences by their word frequency, serves as the baseline [41]. The BoW model's vocabulary was derived from the STS dataset, comprising 1349 unique word forms after stop-word removal and lemmatization. Each sentence was represented as a 1349D vector based on the vocabulary. Cosine similarity was used to calculate the semantic distance of the question pairs. For Korean questions, translation to English was performed using the Google

XSL•FO
RenderX

Translator application programming interface prior to similarity calculation [42].

The SBERT-BERT Algorithm

The SBERT-BERT large language model was derived from the pretrained BERT-based model, which has 12 layers, a 768D hidden layer, 12 attention heads, and 110 million parameters [30]. SBERT-BERT supports only English. We fine-tuned the pretrained SBERT-BERT model to optimize its performance for identifying semantic equivalency among health questions by using the 938 English question pairs described above. The fine-tuning was performed with a batch size of 32, 8 epochs, and a learning rate of 2e-5, which were deemed optimal after testing various configurations. The AdamW optimizer was used for model optimization [43]. The fine-tuned SBERT-BERT algorithm was then evaluated using the test STS dataset of 410 English question pairs and 410 Korean question pairs. As previously stated, the Korean questions were translated into English using the Google Translator application programming interface to execute the evaluation.

The SBERT-LaBSE Algorithm

The SBERT-LaBSE algorithm differs from SBERT-BERT in that it supports multiple languages within a single embedding space [31]. The pretrained SBERT-LaBSE model was derived from the LaBSE model, which also consists of 12 layers, a 768D hidden layer, 12 attention heads, and 110 million parameters [31]. Fine-tuning was performed in the same manner as for SBERT-BERT. Unlike the other models, SBERT-LaBSE can assess the semantic similarity of English and Korean questions without requiring translation.

The GPT-4o Algorithm

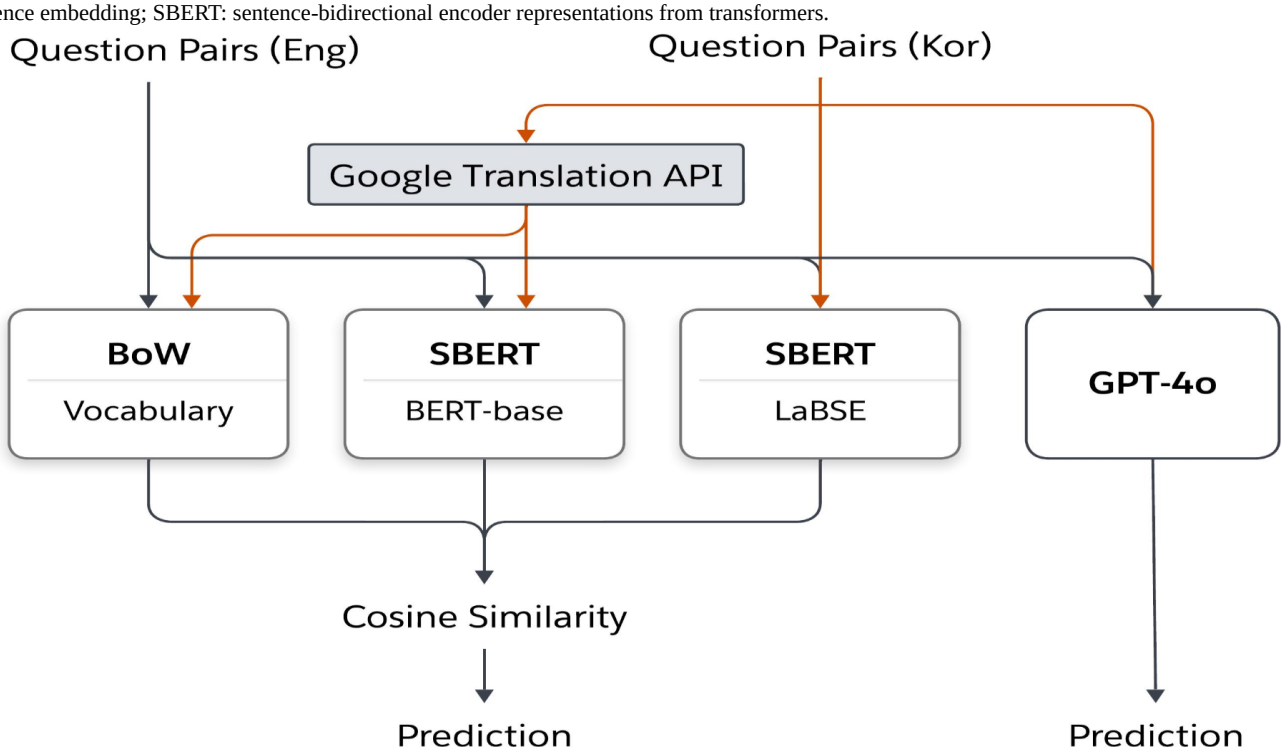
The GPT-4o model, a state-of-the-art large language model, is designed to understand and generate text in multiple languages, including English and Korean [44]. Unlike the SBERT-BERT and SBERT-LaBSE, which rely on fixed embeddings for similarity calculation, the GPT-4o operates as a generative model that dynamically evaluates semantic similarity based on contextual understanding. However, in this study, we utilized GPT-4o in a deterministic manner to predict the score of sentence pairs. Each sentence pair was presented with a specific instruction asking to evaluate the score on a scale from 1 to 4 (Multimedia Appendix 2). Fine-tuning of the GPT-4o model was conducted using the fine-tuning application programming interface from the OpenAI platform [45].

Performance Evaluation

The performance of the similarity calculation algorithms was evaluated as a binary classification problem to simplify interpretation. The 4-point ordinal similarity scores from the STS dataset were converted into binary labels, where scores of 3 and 4 were categorized as similar and scores of 1 and 2 as dissimilar.

Optimal thresholds for predicting similarity were determined for the continuous similarity scores, which ranged from –1 to 1. Precision, recall, and F_1-scores were calculated to assess algorithm performance, and the area under the curve for both the receiver operating characteristic and precision-recall curves were examined. The processes used by the 3 algorithms to calculate similarity are illustrated in Figure 2.

Figure 2. Similarity calculation with the 4 algorithms. API: application programming interface; BERT: bidirectional encoder representations from transformers; BoW: bag-of-words; Eng: English; Kor: Korean; LaBSE: language-agnostic bidirectional encoder representations from transformers sentence embedding; SBERT: sentence-bidirectional encoder representations from transformers.



XSL•FO
RenderX

Ethical Considerations

This study does not involve human participants, intervention, or identifiable private information. The analysis was based on publicly available and nonidentifiable health survey questions from open repositories and published sources. As such, it does not fall under the scope of human subject research as defined by the Seoul National University institutional review board. According to Article 2 and Article 8, Paragraph 2 of the Seoul National University institutional review board regulations (regulation 27, effective September 11, 2023), studies that do not involve human participants or human-derived materials are exempt from institutional review board review. Therefore, this study was not submitted for ethical review. No informed consent, compensation, or privacy protection measures were applicable, as no human participants were involved, and no personal data were collected or analyzed.

Results

The performance of the 3 models for classifying similar versus dissimilar question pairs when aggregating the 5 health lifelog domains is summarized in Table 2 and Figure 3. In the zero-shot trials (ie, without the model refining stage), there were minimal differences in performance among the 3 algorithms for both English and Korean questions. All algorithms exhibited higher recall than precision in both languages. After fine-tuning, the SBERT-BERT algorithm showed substantial improvement, particularly for English questions, in which the F_1-score increased from 0.65 to 0.96. For Korean questions, the improvement was moderate, with the F_1-score progressing from 0.68 to 0.73. In contrast, SBERT-LaBSE demonstrated significant improvements for both languages post fine-tuning. For English questions, the F_1-scores increased from 0.66 to 0.98, while for Korean, the F_1-scores increased from 0.68 to 0.98. Fine tuning for both SBERT-BERT and SBERT-LaBSE models resulted in noticeable balanced performance between recall and precision. Similarly, GPT-4o exhibited improved performance following fine-tuning, with its F_1-scores increasing from 0.69 to 0.79 for the English questions and from 0.67 to 0.79 for the Korean questions. However, the degree of improvement was smaller than that observed in SBERT models.

Table . Performance metrics for the 3 algorithms, combining the health lifelog domains.

Performance metrics	BoW[a]	GPT-4o pre-trained	GPT-4o fine-tuned	SBERT[b] with pretrained		SBERT with fine-tuned	
				BERT-base	LaBSE[c]	BERT-base	LaBSE
English question pairs (n=410)							
Accuracy	0.6112	0.6683	0.8463	0.6308	0.5917	0.9702	0.9853
Precision	0.5279	0.5753	0.9590	0.5451	0.5111	0.9668	0.9818
Recall	0.8161	0.8514	0.6686	0.7989	0.9253	0.9632	0.9839
F_1-score	0.6411	0.6866	0.7879	0.6480	0.6585	0.9649	0.9828
Korean question pairs (n=410)							
Accuracy	0.6610	0.6512	0.8488	0.6659	0.6878	0.7576	0.9839
Precision	0.5732	0.5620	0.9520	0.5760	0.6054	0.6929	0.9818
Recall	0.8057	0.8286	0.6800	0.8229	0.7714	0.7817	0.9806
F_1-score	0.6698	0.6697	0.7933	0.6776	0.6784	0.7332	0.9812

[a]BoW: bag-of-words.

[b]SBERT: sentence-bidirectional encoder representations from transformers.

[c]LaBSE: language-agnostic bidirectional encoder representations from transformers sentence embedding.

XSL•FO
RenderX

Figure 3. Receiver operating characteristic and precision-recall curves for pretrained and fine-tuned embeddings on English and Korean questions, combining the health lifelog domains. AUC: area under the curve; BERT: bidirectional encoder representations from transformers; BoW: bag-of-words; Eng: English; Kor: Korean; LaBSE: language-agnostic bidirectional encoder representations from transformers sentence embedding; PR: precision-recall; ROC: receiver operating characteristic; SBERT: sentence-bidirectional encoder representations from transformers.

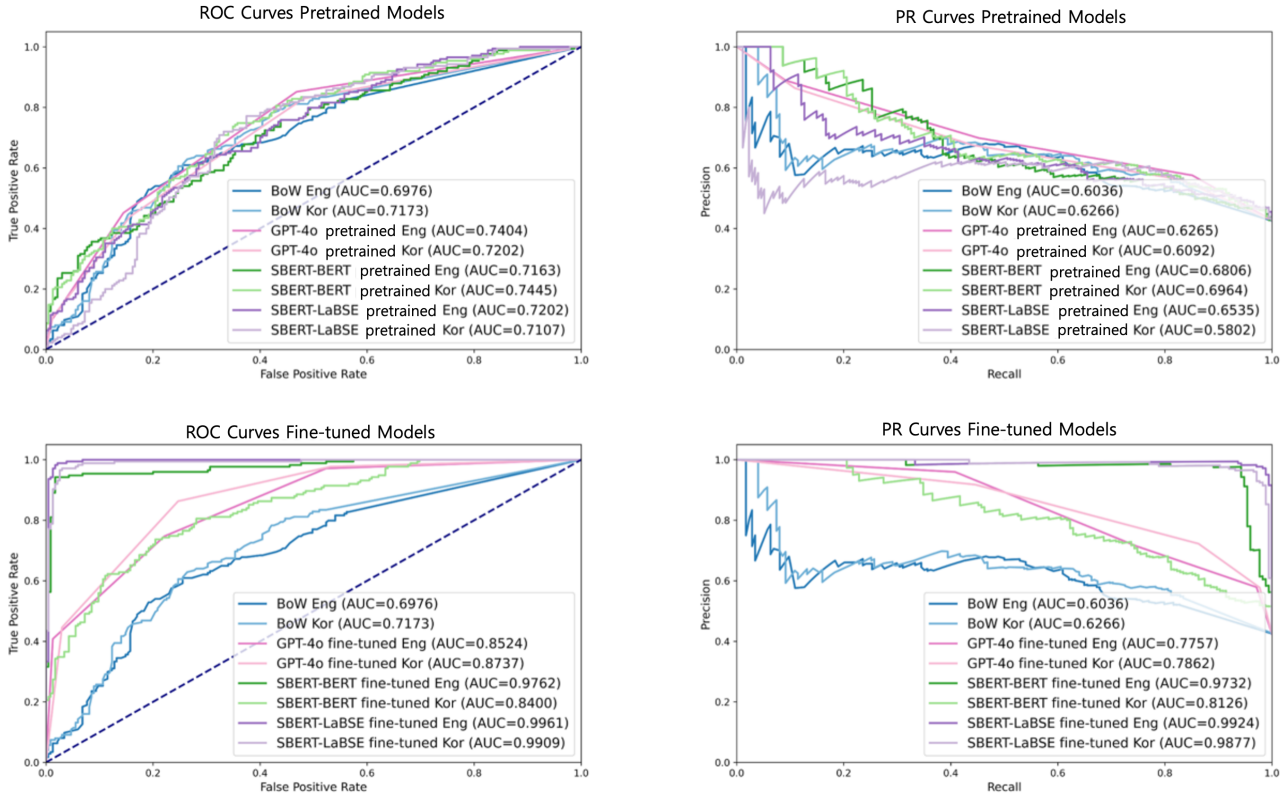


Table 3 presents the performance of the 2 SBERT algorithms across the 5 health lifelog domains. For all the health lifelog domains, the fine-tuned SBERT-BERT and SBERT-LaBSE algorithms demonstrated high performance on English questions, with receiver operating characteristic and precision-recall area under the curve values exceeding 0.95 and approaching 0.99. However, the SBERT-BERT algorithm struggled with the English-translated Korean questions, particularly in the physical activity domain. In contrast, the SBERT-LaBSE algorithm consistently delivered strong performance across all the health lifelog domains even for Korean questions.

XSL•FO
RenderX

Table . Performance metrics of the sentence-bidirectional encoder representations from transformers–based algorithms with fine-tuned bidirectional encoder representations from transformers and language-agnostic bidirectional encoder representations from transformers sentence embedding models by the health lifelog domains.

Performance metrics	English question pairs (n=410)						Korean question pairs (n=410)					
	DL[a] (n=80)	HLE[b] (n=80)	PA[c] (n=80)	Sleep (n=85)	Stress (n=85)	All	DL (n=80)	HLE (n=80)	PA (n=80)	Sleep (n=85)	Stress (n=85)	All
BoW[d]												
Accuracy	0.7215	0.7250	0.6625	0.4118	0.7176	0.6112	0.7250	0.8125	0.7250	0.5765	0.5882	0.6610
Precision	0.7000	0.6383	0.5952	0.4118	0.6279	0.5279	0.6585	0.7941	0.6275	0.0000	0.5000	0.5732
Recall	0.6176	0.8571	0.7143	1.0000	0.7714	0.8161	0.7714	0.7714	0.9143	0.0000	0.8286	0.8057
F_1-score	0.6563	0.7317	0.6494	0.5833	0.6923	0.6411	0.7105	0.7826	0.7442	0.0000	0.6237	0.6698
ROC[e] AUC[f]	0.7297	0.7457	0.6810	0.5820	0.7611	0.6976	0.7667	0.7937	0.7933	0.5937	0.6609	0.7174
PR[g] AUC	0.7250	0.6718	0.6301	0.5025	0.6834	0.6036	0.7394	0.7373	0.7519	0.4498	0.5985	0.6267
GPT-4o fine-tuned												
Accuracy	0.9367	0.9750	0.9625	0.9765	0.9765	0.7873	0.8875	0.9375	0.7750	0.8000	0.8471	0.8293
Precision	0.8919	0.9714	0.9444	0.9459	0.9459	0.7403	0.9643	1.0000	0.8696	0.9500	0.9583	0.7586
Recall	0.9706	0.9714	0.9714	1.0000	1.0000	0.7701	0.7714	0.8571	0.5714	0.5429	0.6571	0.8800
F_1-score	0.9296	0.9714	0.9577	0.9722	0.9722	0.7549	0.8571	0.9231	0.6897	0.6909	0.7797	0.8148
ROC AUC	0.9598	0.9838	0.9727	0.9863	0.9757	0.8524	0.9340	0.9444	0.8295	0.8823	0.8769	0.8737
PR AUC	0.9138	0.9672	0.9418	0.9629	0.9354	0.7757	0.8969	0.9344	0.7510	0.7969	0.8182	0.7862
SBERT[h] with fine-tuned BERT-base[i]												
Accuracy	0.9646	0.9625	0.9800	0.9906	0.9835	0.9702	0.8525	0.8125	0.7025	0.7200	0.7882	0.7576
Precision	0.9650	0.9502	0.9784	0.9836	0.9830	0.9668	0.8037	0.7391	0.6175	0.6036	0.7108	0.6929
Recall	0.9529	0.9657	0.9771	0.9943	0.9771	0.9632	0.8800	0.8914	0.8629	0.9543	0.8229	0.7817
F_1-score	0.9585	0.9571	0.9770	0.9887	0.9799	0.9649	0.8384	0.8062	0.7176	0.7376	0.7622	0.7332
ROC AUC	0.9859	0.9698	0.9923	0.9929	0.9936	0.9867	0.9125	0.8563	0.7901	0.8411	0.8462	0.8412
PR AUC	0.9858	0.9480	0.9925	0.9870	0.9918	0.9800	0.9008	0.7969	0.7640	0.8109	0.8244	0.8134
SBERT with fine-tuned LaBSE												
Accuracy	0.9848	0.9900	0.9875	0.9906	0.9906	0.9853	0.9775	0.9975	0.9850	0.9859	0.9835	0.9839
Precision	0.9716	0.9889	0.9728	0.9944	0.9889	0.9818	0.9719	0.9944	0.9836	0.9775	0.9886	0.9818
Recall	0.9941	0.9886	1.0000	0.9829	0.9886	0.9839	0.9771	1.0000	0.9829	0.9886	0.9714	0.9806
F_1-score	0.9826	0.9885	0.9861	0.9884	0.9887	0.9828	0.9743	0.9972	0.9828	0.9829	0.9797	0.9812
ROC AUC	0.9965	0.9929	0.9987	0.9989	0.9979	0.9968	0.9893	0.9976	0.9962	0.9971	0.9930	0.9951
PR AUC	0.9964	0.9901	0.9984	0.9985	0.9975	0.9960	0.9872	0.9958	0.9947	0.9957	0.9927	0.9934

[a]DL: dietary lifestyle.

[b]HLE: human living environment.

[c]PA: physical activity.

[d]BoW: bag-of-words.

[e]ROC: receiver operating characteristic.

[f]AUC: area under the curve.

[g]PR: precision-recall.

[h]SBERT: sentence-bidirectional encoder representations from transformers.

[i]BERT: bidirectional encoder representations from transformers.

XSL•FO
RenderX

Table 4 presents the optimal cutoff values for the 3 algorithms. The pretrained SBERT-BERT and SBERT-LaBSE models showed considerable variation in the cutoff values across the 5 health lifelog domains. However, after fine-tuning, these variations decreased, indicating that fine-tuning helped stabilize the algorithms. Despite this improvement, the SBERT-LaBSE algorithm still exhibited more variability in the cutoff values across the health lifelog domains compared to SBERT-BERT, suggesting that further calibration may be required for SBERT-LaBSE. Multimedia Appendix 3 provides example question pairs from each health lifelog domain, along with the similarity scores assigned by human reviewers and predicted by the 3 algorithms.

Table . Optimal cutoff for algorithms on bag-of-words and pretrained and fine-tuned SBERT-BERT and SBERT–LaBSE in each health lifelog domain.

Health lifelog domain	Bag-of-words	SBERT[a] with pretrained		SBERT with fine-tuned	
		BERT-base[b]	LaBSE	BERT-base	LaBSE[c]
English question pairs (n=410)					
Dietary lifestyle	0.2887	0.6274	0.5359	0.6349	0.6262
Human living environment	0.1291	0.5369	0.3965	0.6151	0.6425
Physical activity	0.3162	0.3667	0.4822	0.6304	0.6202
Sleep	0.0000	0.6790	0.2456	0.6617	0.6574
Stress	0.1054	0.5817	0.3807	0.6359	0.5958
All	0.1291	0.5816	0.3796	0.6278	0.6091
Korean question pairs (n=410)					
Dietary lifestyle	0.2887	0.5990	0.3103	0.5639	0.6568
Human living environment	0.2582	0.5475	0.5603	0.5639	0.7138
Physical activity	0.1491	0.4778	0.6004	0.5639	0.6741
Sleep	0.9354	0.4837	0.9215	0.5639	0.6849
Stress	0.1091	0.6647	0.4481	0.5639	0.6586
All	0.1336	0.5320	0.5753	0.5639	0.6531

[a]SBERT: sentence-bidirectional encoder representations from transformers.

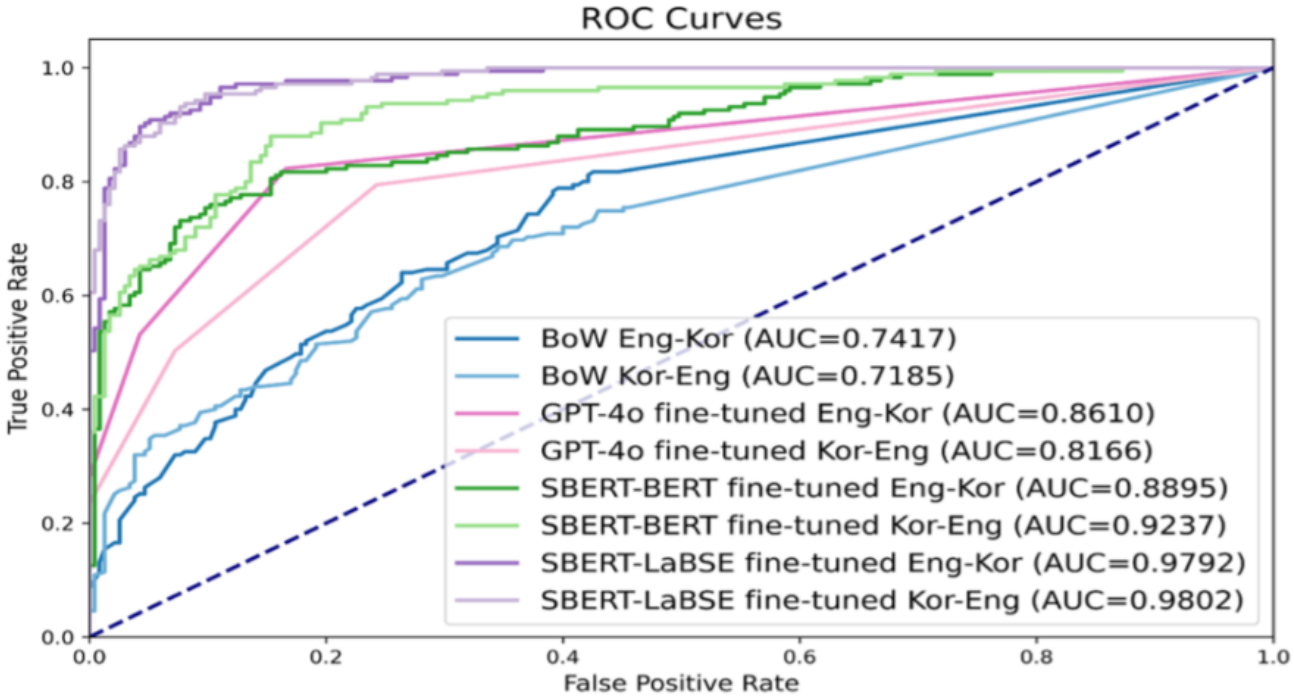
[b]BERT: bidirectional encoder representations from transformers.

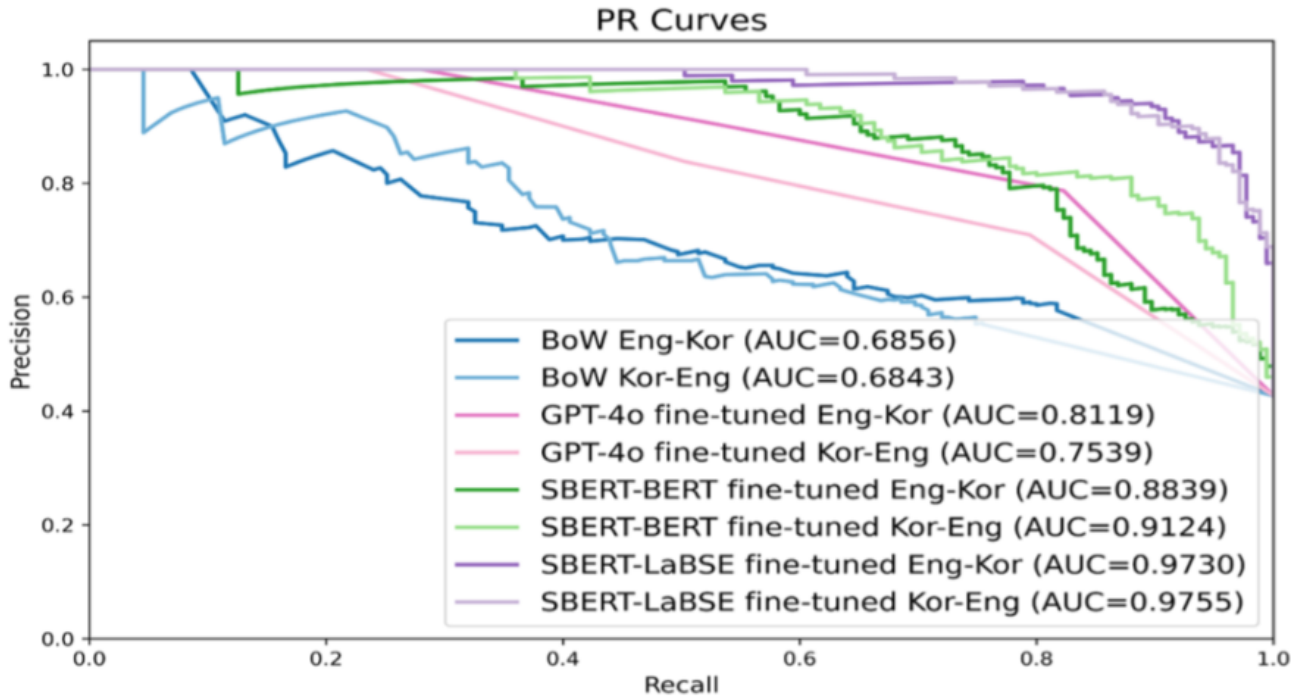
[c]LaBSE: language-agnostic bidirectional encoder representations from transformers sentence embedding.

Figure 4 illustrates that SBERT-LaBSE effectively determined semantic similarities between the 2 languages, with slightly better performance in identifying the semantic similarities of English questions relative to the Korean seed questions. The complete results of the cross-language semantic similarity analysis are provided in Multimedia Appendix 4.

XSL•FO
RenderX

Figure 4. Performance of the cross-language semantic similarity determination. AUC: area under the curve; BERT: bidirectional encoder representations from transformers; BoW: bag-of-words; Eng: English; Kor: Korean; LaBSE: language-agnostic bidirectional encoder representations from transformers sentence embedding; PR: precision-recall; ROC: receiver operating characteristic; SBERT: sentence-bidirectional encoder representations from transformers.





Discussion

Principal Findings

This study demonstrates the utility of large language models for determining semantic similarities among health questions to facilitate the standardization of survey-based health data. Our results indicate that the fine-tuned SBERT algorithms were significantly more effective than the traditional BoW approach in identifying semantic similarities for both English and Korean questions. Furthermore, the SBERT-LaBSE algorithm demonstrated superior performance particularly for Korean questions, suggesting that it is a more effective method than the SBERT-BERT algorithm, which relies on English translation, for assessing semantic similarity in non-English texts. Notably, the SBERT-LaBSE algorithm outperformed the GPT-4o algorithm, particularly in Korean. Although it is possible that the full potential of the GPT-4o algorithm was not realized, the

XSL•FO
RenderX

results clearly show that for the specific task examined in this study, the fine-tuned SBERT algorithms achieved better performance than GPT-4o, with significantly lower computational costs [46].

The SBERT-LaBSE algorithm's success with Korean questions can be attributed to its structural design and the limitations of language translation. Structurally, LaBSE aligns semantically equivalent words or sentences from different languages into a unified embedding space, preserving semantic consistency across languages. This allows for more accurate semantic similarity assessments. In contrast, the SBERT-BERT algorithm's lower performance with Korean questions may be due to meaning loss or distortion during translation, which disrupts semantic comparisons between languages [28,29]. Although previous studies have noted that LaBSE may struggle with subtle, sentence-level nuances, limiting its performance in fine-grained similarity tasks [47], our study shows that the SBERT-LaBSE algorithm effectively captured the meanings in both English and Korean sentences, outperforming the SBERT-BERT model. However, this finding should be validated with a larger and more diverse dataset that includes a broader range of syntactic features.

Limitations

When implemented in the SPURT system with 1835 questions in the comparison space, the SBERT-LaBSE algorithm evaluated the similarity of a new question in just 0.03 seconds. This was achieved on a Naver Cloud Platform server with 8GB RAM and no graphics processing unit [48]. Despite its impressive performance, LaBSE's 440 million parameters—4 times that of BERT base—make it a resource-intensive option, potentially increasing costs for complex tasks. This resource demand may limit its applicability on resource-constrained devices such as mobile platforms [49]. To address these limitations, future work will explore techniques such as distillation [50] and the use of small language models [51], with the goal of reducing model size while maintaining performance.

This study has some limitations. First, the cutoff values for the similarity scores were not uniformly calibrated across the 5 health lifelog domains, leading to inconsistencies in how similarity scores were interpreted. For example, the SBERT-LaBSE algorithm assigned a similarity score of 0.7 to the dietary question pair "I've binge eaten" and "Do you ever overeat?" and identified them as similar. However, the algorithm correctly identified the human living environment questions, that is, "Have you moved in the past 5 years?" and "In the last 5 years, the number of people in this community has?" as dissimilar while assigning the same similarity score of 0.7 to the pair. These inconsistencies may impact the accurate interpretation of similarity scores, highlighting the need for future work to focus on calibrating and normalizing scores across the health lifelog domains to ensure greater consistency. Second, our evaluation was conducted on a small set of English and Korean question pairs. Future studies should explore the feasibility of applying the SBERT-LaBSE algorithm to a broader range of sentence types from diverse domains. Additionally, by incorporating texts from more diverse languages, future research can investigate the algorithm's potential to overcome language barriers and facilitate semantic interoperability.

Comparison With Prior Work

Previous methods that relied on metadata tagging [17,18] and ontology-mediated annotation [10,11] were effective in providing structured mappings between concepts, facilitating interoperability. However, they struggled with comparing the meanings of survey questions composed in multiple languages and addressing semantically redundant questions. This study leverages fine-tuned large language models such as SBERT-BERT and SBERT-LaBSE to assess semantic similarity. In particular, the fine-tuned SBERT-LaBSE algorithm demonstrates the potential to enhance semantic interoperability by capturing semantic similarities across multiple languages with high performance.

Conclusion

This study highlights the potential of large language models in identifying semantic redundancy in survey-based PGHD collections. Specifically, the SBERT-LaBSE algorithm excelled in classifying semantic similarity across diverse question formats in 2 languages. Our findings demonstrate that SBERT-LaBSE outperforms the traditional BERT-based algorithm, the GPT-4o algorithm, and the conventional BoW approach in both languages, highlighting its capacity to improve semantic interoperability of PGHD across language barriers.

Acknowledgments

We are thankful to our colleagues Eunyeong Lim and Jeongha Kim for their help with the semantic textual similarity dataset preparation. This study was supported in part by a grant from the National Research Foundation of Korea (grant 2022R1A2C201136011).

Conflicts of Interest

None declared.

Multimedia Appendix 1
Comparison of algorithms' performance on the semantic textual similarity dataset.
[DOCX File, 64 KB - medinform_v13i1e71687_app1.docx]

XSL•FO
RenderX

Multimedia Appendix 2
The instructions used for GPT-4o semantic similarity evaluation.
[DOCX File, 15 KB - medinform_v13i1e71687_app2.docx]

Multimedia Appendix 3
Example question pairs with the scores from human review and predictions from the 3 algorithms.
[DOCX File, 34 KB - medinform_v13i1e71687_app3.docx]

Multimedia Appendix 4
Performance metrics in the cross-language semantic similarity analysis.
[DOCX File, 27 KB - medinform_v13i1e71687_app4.docx]

References

1. Shapiro M, Johnston D, Wald J, Mon D. Patient-generated health data. White paper. Official Website of the Assistant Secretary for Technology Policy/Office of the National Coordinator for Health IT. 2012. URL: https://www.healthit.gov/sites/default/files/rti_pghd_whitepaper_april_2012.pdf [accessed 2025-05-31]
2. Patient-generated health data. Official Website of the Assistant Secretary for Technology Policy/Office of the National Coordinator for Health IT. URL: https://www.healthit.gov/topic/scientific-initiatives/pcor/patient-generated-health-data-pghd [accessed 2025-05-08]
3. Islind AS, Lindroth T, Lundin J, Steineck G. Shift in translations: data work with patient-generated health data in clinical practice. Health Informatics J 2019 Sep;25(3):577-586. [doi: 10.1177/1460458219833097] [Medline: 30866707]
4. Sanger PC, Hartzler A, Lordon RJ, et al. A patient-centered system in a provider-centered world: challenges of incorporating post-discharge wound data into practice. J Am Med Inform Assoc 2016 May;23(3):514-525. [doi: 10.1093/jamia/ocv183] [Medline: 26977103]
5. Adler-Milstein J, Nong P. Early experiences with patient generated health data: health system and patient perspectives. J Am Med Inform Assoc 2019 Oct 1;26(10):952-959. [doi: 10.1093/jamia/ocz045] [Medline: 31329886]
6. Chung AE, Sandler RS, Long MD, et al. Harnessing person-generated health data to accelerate patient-centered outcomes research: the Crohn's and Colitis Foundation of America PCORnet Patient Powered Research Network (CCFA Partners). J Am Med Inform Assoc 2016 May;23(3):485-490. [doi: 10.1093/jamia/ocv191] [Medline: 26911821]
7. Austin E, Lee JR, Amtmann D, et al. Use of patient-generated health data across healthcare settings: implications for health systems. JAMIA Open 2020 Apr;3(1):70-76. [doi: 10.1093/jamiaopen/ooz065] [Medline: 32607489]
8. Abdolkhani R, Gray K, Borda A, DeSouza R. Patient-generated health data management and quality challenges in remote patient monitoring. JAMIA Open 2019 Dec;2(4):471-478. [doi: 10.1093/jamiaopen/ooz036] [Medline: 32025644]
9. Hussein R, Crutzen R, Gutenberg J, Kulnik ST, Sareban M, Niebauer J. Patient-generated health data (PGHD) interoperability: an integrative perspective. Stud Health Technol Inform 2021 May 27;281:228-232. [doi: 10.3233/SHTI210154] [Medline: 34042739]
10. Cella D, Yount S, Rothrock N, et al. The Patient-Reported Outcomes Measurement Information System (PROMIS): progress of an NIH roadmap cooperative group during its first two years. Med Care 2007 May;45(5 Suppl 1):S3-S11. [doi: 10.1097/01.mlr.0000258615.42478.55] [Medline: 17443116]
11. Cella D, Riley W, Stone A, et al. The Patient-Reported Outcomes Measurement Information System (PROMIS) developed and tested its first wave of adult self-reported health outcome item banks: 2005-2008. J Clin Epidemiol 2010 Nov;63(11):1179-1194. [doi: 10.1016/j.jclinepi.2010.04.011] [Medline: 20685078]
12. Pilkonis PA, Choi SW, Reise SP, et al. Item banks for measuring emotional distress from the Patient-Reported Outcomes Measurement Information System (PROMIS®): depression, anxiety, and anger. Assessment 2011 Sep;18(3):263-283. [doi: 10.1177/1073191111411667] [Medline: 21697139]
13. Amtmann D, Cook KF, Jensen MP, et al. Development of a PROMIS item bank to measure pain interference. Pain 2010 Jul;150(1):173-182. [doi: 10.1016/j.pain.2010.04.025] [Medline: 20554116]
14. Brodke DJ, Saltzman CL, Brodke DS. PROMIS for orthopaedic outcomes measurement. J Am Acad Orthop Surg 2016 Nov;24(11):744-749. [doi: 10.5435/JAAOS-D-15-00404] [Medline: 27661391]
15. Kroenke K, Talib TL, Stump TE, et al. Incorporating PROMIS symptom measures into primary care practice-a randomized clinical trial. J Gen Intern Med 2018 Aug;33(8):1245-1252. [doi: 10.1007/s11606-018-4391-0] [Medline: 29623512]
16. Wagner LI, Schink J, Bass M, et al. Bringing PROMIS to practice: brief and precise symptom screening in ambulatory cancer care. Cancer 2015 Mar 15;121(6):927-934. [doi: 10.1002/cncr.29104] [Medline: 25376427]
17. Common data elements repository. National Institutes of Health. URL: https://cde.nlm.nih.gov/home [accessed 2024-10-14]
18. NIH strategic plan for data science. National Institutes of Health. URL: https://datascience.nih.gov/nih-strategic-plan-data-science [accessed 2025-05-09]
19. Zheng T, Gao Y, Wang F, et al. Detection of medical text semantic similarity based on convolutional neural network. BMC Med Inform Decis Mak 2019 Aug 7;19(1):156. [doi: 10.1186/s12911-019-0880-2] [Medline: 31391038]

XSL•FO
RenderX

20. Yang X, He X, Zhang H, Ma Y, Bian J, Wu Y. Measurement of semantic textual similarity in clinical texts: comparison of transformer-based models. JMIR Med Inform 2020 Nov 23;8(11):e19735. [doi: 10.2196/19735] [Medline: 33226350]
21. Mahajan D, Poddar A, Liang JJ, et al. Identification of semantically similar sentences in clinical notes: iterative intermediate training using multi-task learning. JMIR Med Inform 2020 Nov 27;8(11):e22508. [doi: 10.2196/22508] [Medline: 33245284]
22. Ormerod M, Martínez Del Rincón J, Devereux B. Predicting semantic similarity between clinical sentence pairs using transformer models: evaluation and representational analysis. JMIR Med Inform 2021 May 26;9(5):e23099. [doi: 10.2196/23099] [Medline: 34037527]
23. Li Q, He S. Similarity matching of medical question based on Siamese network. BMC Med Inform Decis Mak 2023 Apr 6;23(1):55. [doi: 10.1186/s12911-023-02161-z] [Medline: 37024844]
24. Mihalcea R, Corley C, Strapparava C. Corpus-based and knowledge-based measures of text semantic similarity. Presented at: Proceedings of the Twenty-First National Conference on Artificial Intelligence and the Eighteenth Innovative Applications of Artificial Intelligence Conference; Jul 16-20, 2020; Boston, MA. [doi: 10.5555/1597538.1597662]
25. Devlin J, Chang MW, Lee K, Toutanova B. BERT: pre-training of deep bidirectional transformers for language understanding. Presented at: Proceedings of the North American Chapter of the Association for Computational Linguistics; Jun 2-9, 2019; Minneapolis, MN. [doi: 10.18653/v1/N19-1423]
26. Artetxe M, Schwenk H. Massively multilingual sentence embeddings for zero-shot cross-lingual transfer and beyond. Trans Assoc Comput Linguist 2019 Nov;7:597-610. [doi: 10.1162/tacl_a_00288]
27. Miao Z, Wu Q, Zhao K, Wu Z, Tsuruoka Y. Enhancing cross-lingual sentence embedding for low-resource languages with word alignment. Presented at: Findings of the Association for Computational Linguistics; Jun 16-21, 2024; Mexico City, Mexico. [doi: 10.18653/v1/2024.findings-naacl.204]
28. Belinkov Y, Bisk Y. Synthetic and natural noise both break neural machine translation. arXiv. Preprint posted online on Feb 24, 2018. [doi: 10.48550/arXiv.1711.02173]
29. Tiyajamorn N, Kajiwara T, Arase Y, Onizuka M. Language-agnostic representation from multilingual sentence encoders for cross-lingual similarity estimation. Presented at: Proceedings of Conference on Empirical Methods in Natural Language Processing; Nov 7-11, 2021; Online and Punta Cana, Dominican Republic. [doi: 10.18653/v1/2021.emnlp-main.612]
30. Reimers N, Gurevych I. Sentence-BERT: sentence embeddings using siamese BERT-networks. Presented at: Proceedings of Conference on Empirical Methods in Natural Language Processing and the 9th International Joint Conference on Natural Language Processing (EMNLP-IJCNLP); Nov 3-7, 2019; Hong Kong, China. [doi: 10.18653/v1/D19-1410]
31. Feng F, Yang Y, Cer DM, Arivazhagan N, Wang W. Language-agnostic BERT sentence embedding. Presented at: Proceedings of 60th Annual Meeting of the Association for Computational Linguistics (Volume 1); May 22-27, 2022; Dublin, Ireland. [doi: 10.18653/v1/2022.acl-long.62]
32. Agirre E, Cer DM, Diab MT, Gonzalez-Agirre A. SemEval-2012 task 6: a pilot on semantic textual similarity. Presented at: Proceedings of the International Workshop on Semantic Evaluation; Jun 7-8, 2012; Montréal, Canada URL: https://aclanthology.org/S12-1051.pdf [accessed 2025-05-13]
33. Gao T, Yao X, Chen D. SimCSE: simple contrastive learning of sentence embeddings. Presented at: Proceedings of the 2021 Conference on Empirical Methods in Natural Language Processing; Nov 7-11, 2021; Online and Punta Cana, Dominican Republic. [doi: 10.18653/v1/2021.emnlp-main.552]
34. Ham J, Choe YJ, Park K, Choi I, Soh H. KorNLI and KORSTS: new benchmark datasets for Korean natural language understanding. Presented at: Findings of the Association for Computational Linguistics; Nov 16-20, 2020. [doi: 10.18653/v1/2020.findings-emnlp.39]
35. Mutinda FW, Yada S, Wakamiya S, Aramaki E. Semantic textual similarity in Japanese clinical domain texts using BERT. Methods Inf Med 2021 Jun;60(S 01):e56-e64. [doi: 10.1055/s-0041-1731390] [Medline: 34237783]
36. Zhang N, Chen M, Bi Z, et al. CBLUE: a Chinese biomedical language understanding evaluation benchmark. Presented at: Proceedings of the 60th Annual Meeting of the Association for Computational Linguistics (Volume 1); May 22-27, 2022; Dublin, Ireland. [doi: 10.18653/v1/2022.acl-long.544]
37. HealthMeasures. URL: https://www.healthmeasures.net [accessed 2024-10-14]
38. Introduction to Ministry of Food and Drug Safety [Article in Korean]. Republic of Korea's e-Government. URL: https://www.mfds.go.kr/index.do [accessed 2024-10-14]
39. Dietary lifestyle assessment [Article in Korean]. National Cancer Information Center. URL: https://www.cancer.go.kr/lay1/S1T226C228/contents.do [accessed 2024-10-14]
40. My dietary assessment [Article in Korean]. Seoul Asan Medical Center Health Screening & Promotion Center. URL: https://health.amc.seoul.kr/health/maintain/check.do [accessed 2024-10-15]
41. Salton G, Wong A, Yang CS. A vector space model for automatic indexing. Commun ACM 1975 Nov;18(11):613-620. [doi: 10.1145/361219.361220]
42. Googletrans-py 4.0.0. The Python Package Index. URL: https://pypi.org/project/googletrans-py [accessed 2024-10-10]
43. AdamW documentation. PyTorch. URL: https://pytorch.org/docs/stable/generated/torch.optim.AdamW.html [accessed 2024-10-10]
44. GPT-4o system card. OpenAI. URL: https://openai.com/research/gpt-4o-system-card [accessed 2025-01-19]
45. Fine-tuning guide. OpenAI. URL: https://platform.openai.com/docs/guides/fine-tuning [accessed 2025-01-19]

XSL•FO
RenderX

46. Brown T, Mann B, Ryder N, et al. Language models are few-shot learners. arXiv. Preprint posted online on Jul 22, 2020. [doi: 10.48550/arXiv.2005.14165]
47. Wang W, Chen G, Wang H, Han Y, Chen Y. Multilingual sentence transformer as a multilingual word aligner. Presented at: Findings of the Association for Computational Linguistics; Dec 7-11, 2022; Abu Dhabi, United Arab Emirates. [doi: 10.18653/v1/2022.findings-emnlp.215]
48. Naver Cloud Platform. URL: https://www.ncloud.com/product/compute/server#detail [accessed 2024-10-14]
49. Mao Z, Nakagawa T. LEALLA: learning lightweight language-agnostic sentence embeddings with knowledge distillation. Presented at: Proceedings of the 17th Conference of the European Chapter of the Association for Computational Linguistics; May 2-6, 2023; Dubrovnik, Croatia. [doi: 10.18653/v1/2023.eacl-main.138]
50. Jiao X, Yin Y, Shang L, et al. TinyBERT: distilling BERT for natural language understanding. Presented at: Findings of the Association for Computational Linguistics; Nov 16-20, 2020. [doi: 10.18653/v1/2020.findings-emnlp.372]
51. Wang F, Zhang Z, Zhang X, Wu Z, Mo T, Lu Q, et al. A comprehensive survey of small language models in the era of large language models: techniques, enhancements, applications, collaboration with LLMS, and trustworthiness. arXiv. Preprint posted online on Dec 28, 2024. [doi: 10.48550/arXiv.2411.03350]

Abbreviations

BERT: bidirectional encoder representations from transformers
BoW: bag-of-words
CDE: common data elements
LaBSE: language-agnostic bidirectional encoder representations from transformers sentence embedding
NIH: National Institutes of Health
PGHD: person-generated health data
PROMIS: Patient-Reported Outcomes Measurement Information System
SBERT: sentence-bidirectional encoder representations from transformers
SPURT: Standardized Patient-Generated Health Data Utilization Resources and Tools
STS: semantic textual similarity

Edited by A Benis; submitted 24.01.25; peer-reviewed by A Rampadarath, U Radvilaite; revised version received 16.04.25; accepted 20.04.25; published 10.06.25.

Please cite as:
Kang S, Park H, Taira R, Kim H
Detecting Redundant Health Survey Questions by Using Language-Agnostic Bidirectional Encoder Representations From Transformers Sentence Embedding: Algorithm Development Study
JMIR Med Inform 2025;13:e71687
URL: https://medinform.jmir.org/2025/1/e71687
doi:10.2196/71687

© Sunghoon Kang, Hyewon Park, Ricky Taira, Hyeoneui Kim. Originally published in JMIR Medical Informatics (https://medinform.jmir.org), 10.6.2025. This is an open-access article distributed under the terms of the Creative Commons Attribution License (https://creativecommons.org/licenses/by/4.0/), which permits unrestricted use, distribution, and reproduction in any medium, provided the original work, first published in JMIR Medical Informatics, is properly cited. The complete bibliographic information, a link to the original publication on https://medinform.jmir.org/, as well as this copyright and license information must be included.

XSL•FO
RenderX

Building a Standardized Cancer Synoptic Report With Semantic and Syntactic Interoperability: Development Study Using SNOMED CT and Fast Healthcare Interoperability Resources (FHIR)

Jieun Hwang[1], PhD; Alexander K Goel[2], MI; Brian A Rous[3], MA, MB, BChir, PhD; George Birdsong[4], MD; Paul A Seegers[5], BSc; Stefan Dubois[6], MD, MSc; Thomas Rüdiger[7], MD; Walter S Campbell[1], MBA, PhD

[1]Department of Pathology and Microbiology, University of Nebraska Medical Center, 42nd and Emile, Omaha, NE, United States

[2]Topology Health, Toronto, ON, Canada

[3]Department of Histopathology, Cambridge University Hospitals NHS Foundation Trust, Cambridge, United Kingdom

[4]Department of Pathology and Laboratory Medicine, Emory University School of Medicine at Grady Hospital, Atlanta, United States

[5]Palga Foundation, Houten, The Netherlands

[6]Department of Pathology, Antwerp University Hospital, Edegem, Belgium

[7]Institute of Pathology, Städtisches Klinikum Karlsruhe, Karlsruhe, Germany

Corresponding Author:
Walter S Campbell, MBA, PhD
Department of Pathology and Microbiology, University of Nebraska Medical Center, 42nd and Emile, Omaha, NE, United States

Abstract

Background: Pathology reports contain critical information necessary for the management of cancer patient care. Efforts to structure pathology cancer reports by the College of American Pathologists and the International Collaboration on Cancer Reporting (ICCR) have been successful in standardizing pathology reports. Likewise, standards development organizations have advanced methods to improve data computability and exchange, by enabling interoperability of pathology cancer reports.

Objective: This study aimed to provide a tractable method to render pathology cancer reports computable and interoperable using published cancer reporting protocols, SNOMED Clinical Terms (SNOMED CT) and Health Level 7 (HL7) Fast Healthcare Interoperability Resources (FHIR).

Methods: The ICCR colorectal cancer (CRC) reporting dataset (version 1.0) was evaluated by terminologists and pathologists. SNOMED CT concepts were bound to the data elements. The dataset was then converted into a FHIR structured data capture (SDC) questionnaire using the United States National Library of Medicine tooling and rendered into a FHIR-conformant message for data exchange.

Results: The ICCR CRC dataset contained 216 data elements; 207 data elements were bound to SNOMED CT and incorporated into a FHIR SDC construct. The 9 uncoded data elements were ambiguous and could not be reliably encoded. The resultant FHIR SDC form fully represented the ICCR CRC dataset and rendered these data in an R4 JSON format for data exchange.

Conclusions: This study demonstrates a tractable and extensible approach to making cancer pathology reports fully computable and interoperable that can be broadly adopted. ICCR datasets are supported internationally and supported by multiple national pathology societies. These datasets can be fully represented using SNOMED CT to render data elements computable and semantically faithful to their intended meaning. The use of the FHIR SDC construct enables widespread and standardized data exchange of clinical information. While challenges remain, including FHIR adoption and the need to maintain current clinical content and standard terminology, this approach provides a clear pathway toward implementation.

(JMIR Med Inform 2025;13:e76870) doi:10.2196/76870

KEYWORDS

semantic interoperability; syntactic interoperability; synoptic pathology report; SNOMED clinical terms; fast healthcare interoperability resources; structured data capture

Introduction

Pathology assessment of tissue specimens is the standard for cancer diagnosis and prognosis, and structured synoptic reporting for cancer pathology reports has been shown to improve report quality [1-8], ease of use [9,10], and patient outcomes [8,11]. However, rendering pathology cancer synoptic reports as computable, electronically interoperable, and exchangeable has been elusive [12]. Developments in computable terminologies and data exchange methods,

XSL•FO
RenderX

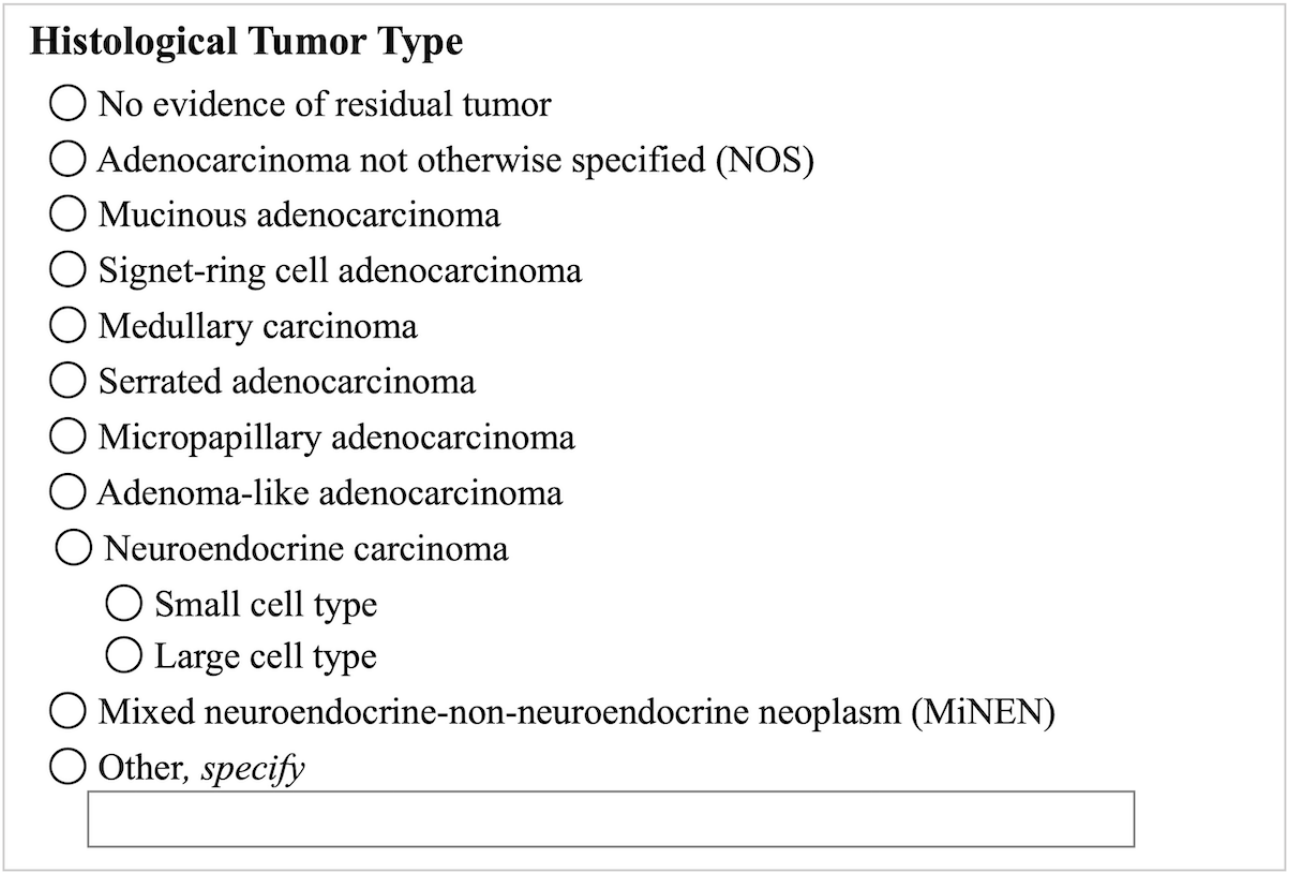
specifically SNOMED Clinical Terms (SNOMED CT) and Fast Healthcare Interoperability Resources (FHIR) [13,14], provide a pathway toward achieving computable and interoperable pathology cancer reports. This paper demonstrates the use of SNOMED CT and FHIR to produce a fully computable, electronic pathology cancer report for international use.

Cancer Synoptic Reporting

Multiple national and international bodies of pathology, including the College of American Pathologists (CAP) [15], the International Collaboration on Cancer Reporting (ICCR) [16], the Royal College of Pathologists (RCPath) [17], and the Dutch Nationwide Pathology Database (Palga) [18], develop and publish cancer pathology reporting protocols based on prevailing medical knowledge. These protocols are referred to as synoptic reporting protocols or datasets and prescribe specific data elements that are to be collected and reported. Data include the primary site of tumor, histologic type, histologic grade, anatomic structures invaded directly or metastatically by the tumor, lymph nodes involvement, and, in some protocols, prognostic or predictive immunohistochemistry stains. Protocol guidelines define core and noncore information for inclusion in the report. Core data elements are essential for the cancer's clinical management, staging, or prognosis for the patient, and for the development of an appropriate treatment plan. Noncore elements represent desirable information that may improve patient care based on emerging science. The benefits of synoptic cancer pathology reporting are abundant, and this reporting approach has been broadly deployed [19]. However, the benefits of structured synoptic reports are not fully realized as the information is not structured in a computable and readily exchangeable format.

In practice, pathology cancer reporting protocols are structured into a series of categories to be assessed by the pathologist. Each category contains a limited number of predetermined assessments or observations. For example, the pathologist is required to assess and report the histologic type of the neoplasm. As shown in Figure 1 for colorectal cancer (CRC), the histologic type of the neoplasm should be selected from the constrained list of the most frequent CRC histologic types. A fill-in option is available for rare morphologies.

Figure 1. Synoptic pathology reporting template: –histologic tumor type of colorectal cancer.



Interoperability

At the most basic level, synoptic reports are complex "check sheets" on which pathologists select the appropriate observation for each category (see Figure 1). In a digital environment, check sheets are rendered graphically. Upon completion of the graphical user interface (GUI), corresponding text is created, stored, and often distributed as a PDF or other rich text format. While users easily understand the text, it is not represented with computable terminologies. Thus, the report is reduced to a textual document and not readily available for computation, secondary use, or electronic data exchange. The evolution of pathology cancer reporting from free-text reports to structured reports ensures that pathology reports are easily understood by users and can be computable using controlled medical terminology [8,20]. Recent developments in SNOMED CT content specific for use in pathology cancer reporting provide

XSL•FO
RenderX

the avenue to achieve the goal of semantic, computable representation of pathology cancer reports [21].

In addition to standardized terminologies, interoperability of pathology cancer data requires an information model and a data exchange structure. The cancer synoptic reporting formats provided by the CAP, ICCR, RCPath, and Palga ensure a common information model to which standard terminology, specifically SNOMED CT, is bound. FHIR builds on modern web standards technologies to provide meaningful options for data exchange in a variety of health care contexts and provides a scalable data exchange protocol for pathology cancer report data exchange. This review provides a tangible example of using the pathology cancer synoptic structure, SNOMED CT, and FHIR to represent and allow for the exchange of a pathology report. This approach is consistent with international data exchange and interoperability objectives and shows promise for widespread use.

Methods

Resource Selection

Dataset

The ICCR CRC dataset (version 1.0) [22] was selected to demonstrate the tractability and plausibility of a standardized, interoperable cancer pathology report for broad, international application. The ICCR is a collaboration of pathologists from multiple international professional and academic colleges and societies of pathology [23]. The ICCR publishes pathology cancer reporting guidelines and datasets that are internationally free for use and have been adopted by several nations as the basis for pathology cancer reporting. The colorectal dataset was selected as an example, as this form of cancer occurs across the globe.

Terminology

SNOMED CT was used as the base terminology standard for this project. It is widely recognized as the most comprehensive clinical terminology worldwide. The SNOMED CT concept model allows for extensive terminology expression to support explicit concept definition, and the use of description logic enables concept inferences and enhanced data navigation [24]. The recent development of SNOMED content specific to cancer pathology reporting became available in SNOMED CT in late 2023. This content was developed by an international group of pathologists, data scientists, and registrars and was specifically developed for the cancer synoptic reporting use case.

Data Structure

In addition to terminology, common information models facilitate data exchange between health care systems by providing structure and syntax for data. FHIR is a data exchange structure with international appeal and serves as a standard for achieving syntactic interoperability in health care [24,25]. Due to the widespread interest in FHIR, this syntactic model was employed in this project, notably the Structure Data Capture (SDC) questionnaire. SDC was developed as part of an initiative sponsored by the US Assistant Secretary for Technology Policy from 2013 - 2016 [26]. During this project, the XML version maintained by Integrating the Healthcare Enterprise (IHE) and a FHIR version of SDC were used [27]. The CAP uses the IHE SDC to represent its cancer checklists. The United States National Library of Medicine form builder tool (version 9.7.2) [28] was used to develop an FHIR-compliant cancer synoptic report questionnaire.

Interoperable Cancer Reporting Template Development

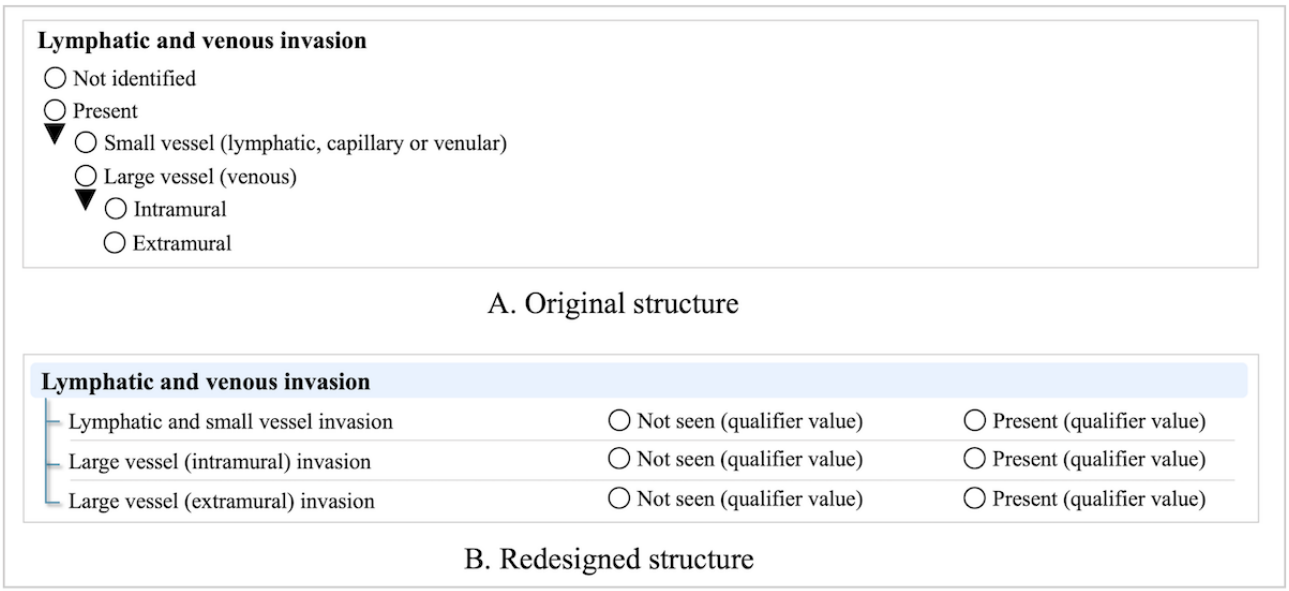
Evaluation of Data Elements and Structure

To develop an SDC of the ICCR CRC dataset, each category of information to be assessed by the pathologist and set of potential observations (ie, constrained value set) was evaluated.

Categories of observations are often “nested” or grouped into logical subcategories when represented in reporting protocols. Such categories can be semantically different, and reporting of subcategories can be contingent upon assessments of predicate subcategories. This condition requires the ability to selectively (ie, logically) solicit observations based on prerequisite information and to associate the semantically correct SNOMED CT concepts for each subcategory of observations. For example, the overarching category of lymphovascular invasion nests three separate semantics into a single category. The observation to be made is the presence or absence of direct invasion in particular lymphovascular spaces: specifically small vessels (ie, venule, arteriole, or lymph vessel), large extramural blood vessel (ie, vessels in pericolic tissue), or large intramural vessels (ie, vessels in the colonic submucosa or colonic muscularis propria). To accommodate these categories and accurately represent each category’s semantic meaning, the overarching lymphovascular category was reconstructed into separate questions (ie, subcategories; see Figure 2).

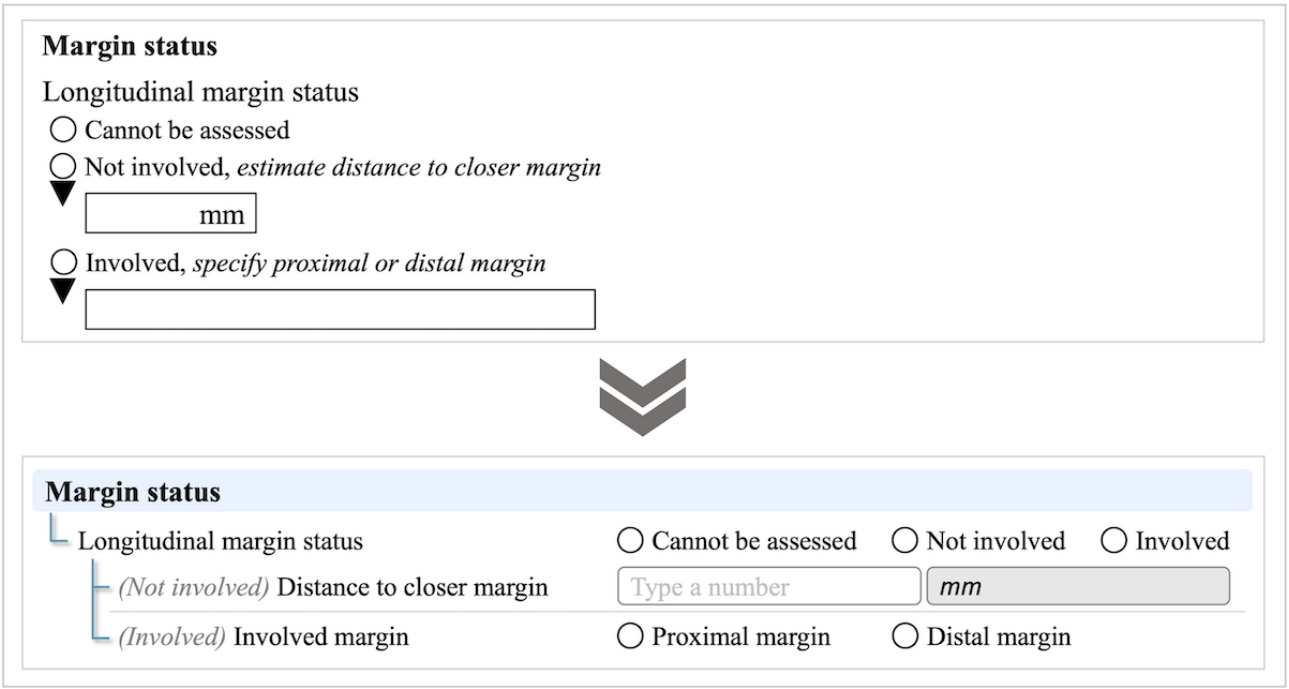
XSL•FO
RenderX

Figure 2. Reconstruction (separate question): lymphatic and venous invasion.



The ICCR datasets and those of the CAP are published with observation value sets that consist of the list of expected or plausible assessments. These lists do not represent all possible assessments, which would be unwieldy, if not impossible, to represent in a dataset. Therefore, a free-text option is made available for most categories of assessments. Nevertheless, where possible, we converted free-text fields into structured data entry. For example, we changed the data type from free text to an answer list for assessments of involved surgical margins based on ICCR supporting notes. Free-text data types require human intervention, consume significant time, and are prone to error. Automatically identifying the specific data within free-text fields is not feasible. To minimize human intervention, we specified which margin was involved by carcinoma, as shown in Figure 3. In the original CRC dataset, pathologists were required to describe the surgical margin if the longitudinal margin was involved by carcinoma. We changed this data element into two answers: proximal margin and distal margin.

Figure 3. Reconstruction (data type convert): margin status.



Terminology Binding

After reconstruction, SNOMED CT concepts from the latest version of SNOMED International (version 2025-02-01) were associated (ie, bound) with each data element. Following the synoptic style, (ie. question and answer pair structure), the context for any recorded observation is represented in the observable entity concept; we referred to it as the observable entity approach. Table 1 shows an example of SNOMED CT terminology using this observable entity approach for histologic type of CRC malignant neoplasm.

XSL•FO
RenderX

Table . Example of terminology binding - Histological tumor type.

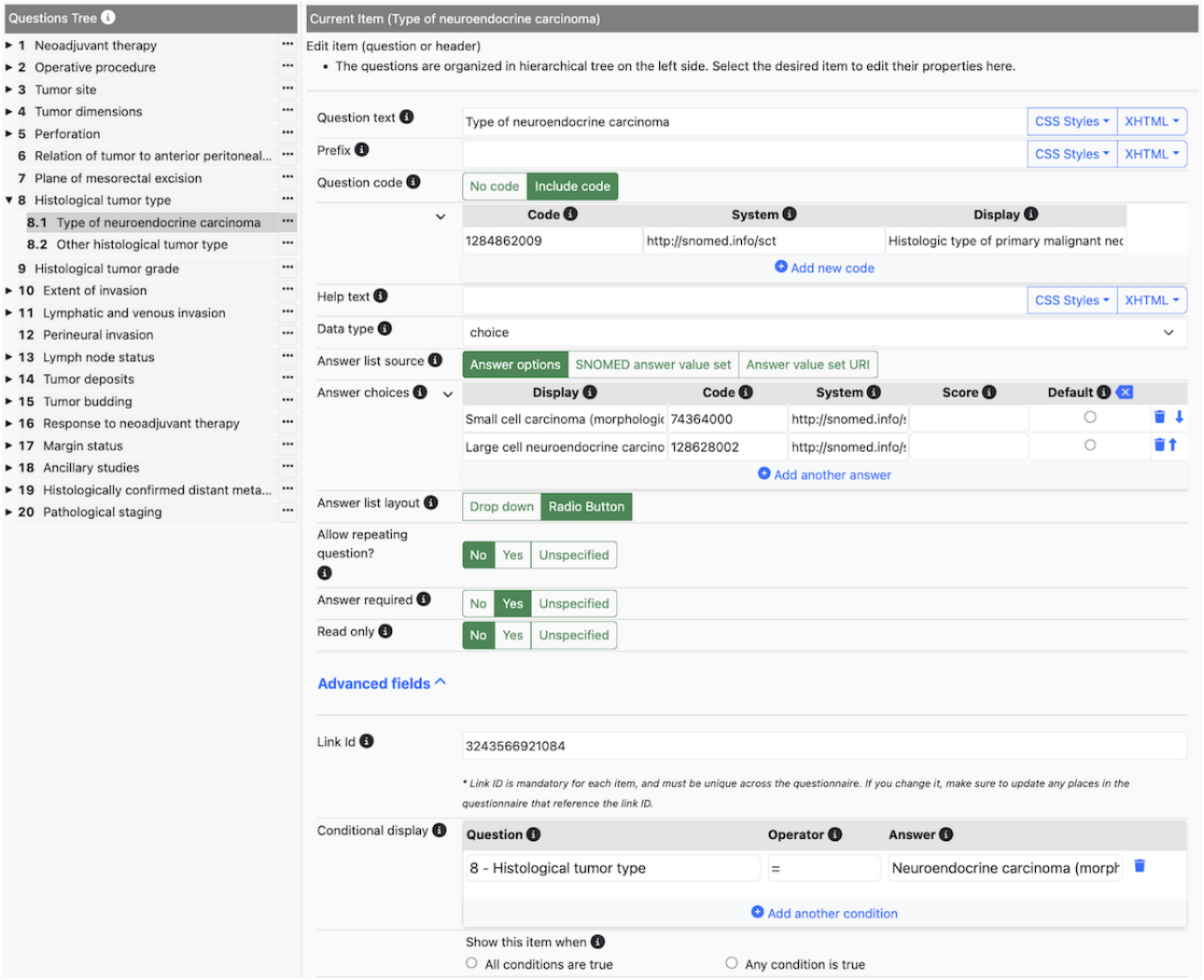
Element value	SNOMED ID and fully specified name
Question	
Histological tumor type	1284862009 |Histologic type of primary malignant neoplasm of cecum and/or colon and/or rectum (observable entity)|
Answer	
No evidence of residual tumor	41647002 |No evidence of (contextual qualifier) (qualifier value)|
Adenocarcinoma	1187332001 |Adenocarcinoma (morphologic abnormality)|
Mucinous adenocarcinoma	72495009 |Mucinous adenocarcinoma (morphologic abnormality)|
Signet-ring cell adenocarcinoma	87737001 |Signet ring cell carcinoma (morphologic abnormality)|
Medullary carcinoma	32913002 |Medullary carcinoma (morphologic abnormality)|
Serrated adenocarcinoma	450948005 |Serrated adenocarcinoma (morphologic abnormality)|
Micropapillary adenocarcinoma	450895005 |Micropapillary carcinoma (morphologic abnormality)|
Adenoma-like adenocarcinoma	28558000 |Villous adenocarcinoma (morphologic abnormality)|
Neuroendocrine carcinoma	1286767006 |Neuroendocrine carcinoma (morphologic abnormality)|
Small cell type	74364000 |Small cell carcinoma (morphologic abnormality)|
Large cell type	128628002 |Large cell neuroendocrine carcinoma (morphologic abnormality)|
Mixed neuroendocrine-non-neuroendocrine neoplasm (MiNEN)	785766008 |Mixed neuroendocrine-non neuroendocrine neoplasm (morphologic abnormality)|
Other	74964007 |Other (qualifier value)|
Other, specify	This response is not codable data.

Building an SDC

The NLM form builder tool was then used to represent the category for assessment and the value sets of responses in an FHIR-compatible SDC (see Figure 4). Natural language consistent with the ICCR template was used for the user interface (ie, question text). At the same time, the data layer and semantic meaning of the recorded observations made in the SDC were represented using a reference to SNOMED CT. Most data elements were qualitative values, but several assessments to be made by the pathologist required discrete or numerical entries. In these situations, the NLM SDC data element was configured to solicit and accept a numerical entry. These included categories of assessments pertinent to tumor dimensions (size) and numbers of lymph nodes examined and involved.

XSL•FO
RenderX

Figure 4. The National Library of Medicine (NLM) form builder (version 9.7.2).



Ethical Considerations

This study did not involve human participants and therefore was not subject to institutional ethical review.

Results

Targeted Elements and Reconstruction

The CRC dataset contains a total of 25 categories (ie, items to be assessed by the pathologist), comprising 19 core categories and 6 noncore categories. After evaluating the value of data elements, all data elements from core categories and some noncore categories were selected as target items. Following reconstruction based on meaning, the standardized CRC dataset from ICCR was converted into 45 questions and 171 answers.

Building Results

Table 2 summarizes the SNOMED CT concepts used for binding. Of the 216 data elements in the ICCR CRC protocol, 207/216 (95.8%) were able to be bound to SNOMED CT concepts. All questions bound with SNOMED CT concepts used the semantic tag (observable entity). For answers, concepts with the semantic tags (qualifier value), (body structure), (morphologic abnormality), (procedure), and (tumor staging) were used accordingly. Answer values are not necessarily unique to the question, and SNOMED CT answer concepts represent answer or observation values across several question categories. For example, ‘52101004 |Present (qualifier value)|’ or ‘47492008 |Not seen (qualifier value)|’ are used in several observation categories. The observable entity concept representing the question or category is unique and carries all necessary context by which to interpret the answer or observation. Thus, the same SNOMED CT concepts may be used for multiple answers and still maintain the semantic integrity of the data. Further details are provided in Multimedia Appendix 1 which includes data elements and the corresponding bounded SNOMED CT concepts.

XSL•FO
RenderX

Table . Summary of the binding results.

Binding status	Semantic tag	Values, n
Question		
Not bound	__[a]	3
Bound	Observable entity	42
Answer		
Not bound	__[a]	6
Bound	Body structure	15
Bound	Morphologic abnormality	13
Bound	Procedure	12
Bound	Qualifier value	122
Bound	Tumor staging	3

[a]Not applicable.

Table 3 includes unbound data elements and reasons why they are not bound. Among the 9 unbound elements, 2 data elements were added during the construction of the SDC without specific meaning, serving only as part of the logical structure. Of the remaining 7 unbound items, the first, related to 'Circumferential margin–Involved by primary tumor or other' is ambiguous and cannot be encoded accurately. Likewise, reference to 'Ancillary study for neuroendocrine markers' is not precisely defined by ICCR and cannot be reliably encoded. Finally, changes by the American Joint Committee on Cancer and Union for International Cancer Control regarding tumor, node, metastasis (TNM) descriptor representation require additions to SNOMED CT content and will be bound once a new concept is authored.

Table . Unbound data elements with their corresponding reasons and solutions.

Type of data elements		Unbound elements	Comment
Question	Answer		
Tumor dimension	Can be assessed	Answer	This item was added during creating the SDC[a].
Tumor budding	Can be assessed	Answer	This item was added during creating the SDC.
Circumferential margin–Involved by	By primary tumor By other	Question and answer	The meaning of the elements is unclear.
Ancillary studies for neuroendocrine markers	Not applicable Neuroendocrine markers	Question and answer	It is difficult to predict what will be recorded here.
TNM[b] descriptor	m–multiple primary tumors r–recurrent y–post-therapy	Question	Authoring a new concept is requested.

[a]SDC: structured data capture.

[b]TNM: tumor, node, metastasis.

FHIR Questionnaire

Figure 5 is a partial screenshot of the FHIR SDC questionnaire in JSON format. The full version is provided in Multimedia Appendix 2.

XSL•FO
RenderX

Figure 5. A snapshot of the FHIR SDC questionnaire content in JSON format, R4 version.

FHIR SDC Questionnaire


```
{
 "resourceType": "Questionnaire",
…
 "type": "choice",
    "extension": [
      {
       "url": "http://hl7.org/fhir/StructureDefinition/questionnaire-itemControl",
       "valueCodeableConcept": {
        "coding": [
          {
           "system": "http://hl7.org/fhir/questionnaire-item-control",
           "code": ”radio-button",
           "display": ”Radio Button"
          }
        ]
       }
      }
    ],
    "linkId": "7529272110509",
    "code": [
      {
       "system": "http://snomed.info/sct",
       "code": "1284862009",
       "display": "Histologic type of primary malignant neoplasm of cecum and/or colon and/or rectum (observable entity)"
      }
    ],
    "text": "Histological tumor type",
    "required": true,
    "repeats": false,
    "readOnly": false,
    "answerOption": [
      {
       "valueCoding": {
         "system": "http://snomed.info/sct",
         "code": "41647002",
         "display": "No evidence of (contextual qualifier) (qualifier value)"
       }
      },
      {
       "valueCoding": {
         "system": "http://snomed.info/sct",
         "code": "1187332001",
         "display": "Adenocarcinoma (morphologic abnormality) "
       }
      },
```


Discussion

Principal Results

This study describes the creation of a structured CRC ICCR pathology cancer reporting dataset bound with standardized terminology for international use, in a manner compliant with the Health Level 7 (HL7) FHIR standard for syntactic and semantic interoperability. Cancer protocols developed by CAP, ICCR, and other institutions follow a synoptic style. SNOMED terminology development for synoptic use follows this model, and newly authored concepts were used in this study. The observable entity approach is necessary to maintain the encoded question and answer data element pair for data integrity. As a result, the implementation and data storage of synoptic reports must accommodate this pairing. The NLM SDC precisely accommodates synoptic style and retains the question-answer binding, as reflected in Figure 2. Interoperation on a syntactic level, known as syntactic interoperability, is a mainstay of interoperability [29] and facilitates data transmission between information systems. The standards to achieve this are HL7 version 2 (HL7 v2) and FHIR. Electronic synoptic reporting is supported using either version. However, we focused on the FHIR representation to demonstrate the feasibility of using its architecture for pathology reporting, as it leverages open web

XSL•FO
RenderX

technologies and represents the future direction of international health data exchange [14].

The primary purpose of the NLM form builder is to create SDC-based questionnaires. The form builder is very user-friendly and supports features such as conditional display, data type and value restrictions, cardinality of responses, valid observation values, and default values. In short, using SDC-based questionnaires facilitates usability while ensuring that well-structured and high-quality data are collected.

Much of this paper addresses data collection, data quality, and data representation. The primary purpose of FHIR is data exchange. HL7 message creation and formatting is a function of the NLM SDC form builder tool. The form builder produces a FHIR Release 3 Standard for Trial Use and Release 4 compliant FHIR message capable of transmission in FHIR format as well as devolution into a compliant HL7 v2 format. Thus, using the approach described in this work, a FHIR-capable method for pathology cancer reporting data exchange is created.

Challenges

While the findings of this project are promising, it is necessary to consider operational challenges.

Version Control

Cancer reporting guidelines evolve over time. In some instances, new SNOMED CT content will be necessary. Therefore, a process for protocol (dataset) version control and terminology binding review must be developed. The ICCR is responsible for maintaining clinical content, and SNOMED International is responsible for terminology content. The organizations have agreed to ongoing collaborations to ensure alignment of terminology with clinical content.

Implementation Complexity

Using the ‘observable entity approach’ implemented in cancer synoptic reporting can be more complex than other approaches. In the observable entity approach, the question, or tumor characteristic to be observed, is represented by a SNOMED CT observable entity concept. Observations made and recorded by the pathologist use a variety of SNOMED CT concepts based on the tumor feature benign recorded. The observable entity concept contains full contexts and definitions to unambiguously understand the pathologist’s recorded measurement, which is represented by more generalizable concepts such as histological types, grades, and presence of various other tumor characteristics. As a result, the observable entity concept and corresponding observation concepts must be stored in tandem. This is consistent with other laboratory data types. This approach was deliberate. Existing SNOMED CT concept definitions do not support the development of fully defined clinical finding concepts in which multiple observations are contained within a single concept. Furthermore, developing such an approach would result in an unmanageable, combinatorial explosion of SNOMED CT concepts; for example, colorectal adenocarcinoma, lung adenocarcinoma, endometrium adenocarcinoma, and all possible ‘body site’ x ‘histology type’ combinations. Software developers and clinical information system vendors will need to consider this design feature when developing future applications.

Future Studies

Although an approach for interoperable synoptic pathology cancer reporting using international standards is presented in this paper, such a system has to our knowledge not yet been implemented. Interoperability, the intended objective of SNOMED CT and FHIR cannot be realized unless the system is fully tested when implemented in the real-world settings. Ultimately, FHIR may offer an improved methodology for storing SNOMED CT coded data and would enhance the exchange and sharing of pathology data. As part of implementation, there will be opportunities to test how FHIR can improve data storage, analytics, and other secondary data use cases. Future activity in this realm should include using FHIR SDC Data Extraction guidance to convert data collected using the ICCR datasets into more readily usable FHIR resources. When a FHIR Questionnaire, such as those authored as part of the methodology of this paper, is rendered in a GUI, the system produces a FHIR Questionnaire Response. Converting the data from the FHIR Questionnaire Response resource to Observations and other applicable resources would enhance the semantic interoperability and ensure that the data can be queried from FHIR-based systems. Further promotion of the benefits of adopting FHIR and incentives for both technology vendors and healthcare providers would improve adoption, as evidenced by the adoption of the standard incentivized by the 21st Century Cures Act in the United States [19], which encouraged significant FHIR adoption across the country.

Conclusions

The findings of this paper demonstrate that syntactic and semantic interoperability for cancer synoptic reporting is possible using existing international standards. The current international release of SNOMED CT contains the necessary concepts required for synoptic pathology cancer reporting for all solid tumors. Along with FHIR SDC tooling from the United States NLM, we demonstrate the plausibility of FHIR-based encoded pathology cancer reporting on a global scale.

Acknowledgments

During the preparation of this work, the author(s) used ChatGPT in order to improve language [30]. After using this tool/service, the author(s) reviewed and edited the content as needed and task(s) full responsibility for the content of the published article.

Authors' Contributions

Conceptualization: WC

XSL•FO
RenderX

Investigation: JH, AG, BR, GB, PS, SD, TR, WC
Supervision: WC
Writing–original draft: JH
Writing–review & editing: JH, AG, BR, GB, PS, SD, TR, WC

Conflicts of Interest

AKG is the owner and operator of Topology Health. JH reports consulting or advisory roles for The Korean Society of Pathologists.

Multimedia Appendix 1
Data element with SNOMED CT.
[XLSX File, 31 KB - medinform_v13i1e76870_app1.xlsx]

Multimedia Appendix 2
Colorectal cancer.R4.
[ZIP File, 7 KB - medinform_v13i1e76870_app2.zip]

References

1. Schaad N, Berezowska S, Perren A, Hewer E. Impact of template-based synoptic reporting on completeness of surgical pathology reports. Virchows Arch 2024 Jan;484(1):31-36. [doi: 10.1007/s00428-023-03533-6] [Medline: 37017774]
2. Richter C, Mezger E, Schüffler PJ, et al. Pathological reporting of radical prostatectomy specimens following ICCR recommendation: impact of electronic reporting tool implementation on quality and interdisciplinary communication in a large university hospital. Curr Oncol 2022 Sep 30;29(10):7245-7256. [doi: 10.3390/curroncol29100571] [Medline: 36290848]
3. Sluijter CE, van Workum F, Wiggers T, et al. Improvement of care in patients with colorectal cancer: influence of the introduction of standardized structured reporting for pathology. JCO Clin Cancer Inform 2019 May;3(1-12):1-12. [doi: 10.1200/CCI.18.00104] [Medline: 31070983]
4. Jones S, Mazuryk J, Havener L, Kulmacz T. Standards for cancer registries pathology laboratory electronic reporting, version 5.1. : Springfield (IL): North American Association of Central Cancer Registries, Inc; 2024 Jan URL: https://www.naaccr.org/pathology-laboratory-electronic-reporting [accessed 2025-01-28]
5. Sluijter CE, van Lonkhuijzen LRCW, van Slooten HJ, Nagtegaal ID, Overbeek LIH. The effects of implementing synoptic pathology reporting in cancer diagnosis: a systematic review. Virchows Arch 2016 Jun;468(6):639-649. [doi: 10.1007/s00428-016-1935-8] [Medline: 27097810]
6. Baranov NS, Nagtegaal ID, van Grieken NCT, et al. Synoptic reporting increases quality of upper gastrointestinal cancer pathology reports. Virchows Arch 2019 Aug;475(2):255-259. [doi: 10.1007/s00428-019-02586-w] [Medline: 31144018]
7. Snoek JAA, Nagtegaal ID, Siesling S, van den Broek E, van Slooten HJ, Hugen N. The impact of standardized structured reporting of pathology reports for breast cancer care. Breast 2022 Dec;66(178-182):178-182. [doi: 10.1016/j.breast.2022.10.011] [Medline: 36308925]
8. Ellis DW, Srigley J. Does standardised structured reporting contribute to quality in diagnostic pathology? The importance of evidence-based datasets. Virchows Arch 2016 Jan;468(1):51-59. [doi: 10.1007/s00428-015-1834-4] [Medline: 26316184]
9. Słodkowska J, Cierniak S, Patera J, et al. Functional assessment of synoptic pathology reporting for ovarian cancer. Pathobiology 2016;83(2-3):70-78. [doi: 10.1159/000443176] [Medline: 27100104]
10. Renshaw AA, Mena-Allauca M, Gould EW, Sirintrapun SJ. Synoptic reporting: evidence-based review and future directions. JCO Clin Cancer Inform 2018 Dec;2(1-9):1-9. [doi: 10.1200/CCI.17.00088] [Medline: 30652566]
11. Sluijter CE, van Workum F, Wiggers T, et al. Improvement of care in patients with colorectal cancer: influence of the introduction of standardized structured reporting for pathology. JCO Clin Cancer Inform 2019 May;3(3):1-12. [doi: 10.1200/CCI.18.00104] [Medline: 31070983]
12. Swillens JEM, Sluijter CE, Overbeek LIH, Nagtegaal ID, Hermens RPMG. Identification of barriers and facilitators in nationwide implementation of standardized structured reporting in pathology: a mixed method study. Virchows Arch 2019 Nov;475(5):551-561. [doi: 10.1007/s00428-019-02609-6] [Medline: 31270615]
13. SNOMED CT clinical implementation guide for cancer synoptic reporting. : SNOMED International; 2024 Sep 27 URL: https://confluence.ihtsdotools.org/display/DOCCANSIG/SNOMED+CT+Clinical+Implementation+Guide+for+Cancer+Synoptic+Reporting [accessed 2025-01-28]
14. Lien CY, Ting TY, Kuo LC, Chung PC, Chu YC, Kuo CT. Design of HL7 FHIR profiles for pathology reports integrated with pathology images. Stud Health Technol Inform 2024 Jan 25;310:13-17. [doi: 10.3233/SHTI230918] [Medline: 38269756]
15. CAP electronic Cancer Protocols.: College of American Pathologists URL: https://www.cap.org/protocols-and-guidelines/electronic-cancer-protocols [accessed 2025-01-28]
16. Dataset Development.: International Collaboration on Cancer Reporting URL: https://www.iccr-cancer.org/datasets/dataset-development [accessed 2025-01-28]

XSL•FO
RenderX

17. Cancer datasets and tissue pathways.: Royal College of Pathologists URL: https://www.rcpath.org/profession/guidelines/cancer-datasets-and-tissue-pathways.html [accessed 2025-01-28]
18. Palga's protocols.: Pathologisch Anatomisch Landelijk Geautomatiseerd Archief URL: https://www.palga.nl/en_GB/for-pathologists/protocols [accessed 2025-01-28]
19. Torous VF, Simpson RW, Balani JP, et al. College of American Pathologists Cancer Protocols: from optimizing cancer patient care to facilitating interoperable reporting and downstream data use. JCO Clin Cancer Inform 2021 Jan;5(47-55):47-55. [doi: 10.1200/CCI.20.00104] [Medline: 33439728]
20. Srigley JR, McGowan T, MacLean A, et al. Standardized synoptic cancer pathology reporting: a population‐based approach. J Surg Oncol 2009 Jun 15;99(8):517-524. [doi: 10.1002/jso.21282] [Medline: 19466743]
21. Campbell WS, Rous BA, Dubois S, et al. Advancements in interoperability: achieving anatomic pathology reports that adhere to international standards and are both human-readable and readily computable. JCO Clin Cancer Inform 2025 Feb;9(9):e2400180. [doi: 10.1200/CCI-24-00180] [Medline: 39908464]
22. Loughrey MB, Arends M, Brown I, et al. Colorectal Cancer Histopathology Reporting Guide, 1st edition: International Collaboration on Cancer Reporting; Sydney, Australia; 2020.
23. Srigley JR, Judge M, Helliwell T, Birdsong GG, Ellis DW. The International Collaboration on Cancer Reporting (ICCR): a decade of progress towards global pathology standardisation and data interoperability. Histopathology 2021 Dec;79(6):897-901. [doi: 10.1111/his.14431]
24. Benson T, Grieve G. Principles of Health Interoperability: SNOMED CT, HL7 and FHIR: Springer; 2016, Vol. 3. [doi: 10.1007/978-3-319-30370-3]
25. Bender D, Sartipi K. HL7 FHIR: an agile and restful approach to healthcare information exchange. Presented at: 26th IEEE International Symposium on Computer-Based Medical Systems; Jun 20-22, 2013; Porto, Portugal. [doi: 10.1109/CBMS.2013.6627810]
26. Structured Data Capture. Assistant Secretary for Technology Policy/Office of the National Coordinator for Health IT. URL: https://www.healthit.gov/topic/scientific-initiatives/pcor/research-evaluation/structured-data-capture-sdc [accessed 2025-01-30]
27. IHE Quality, Research and Public Health Committee. White Papers: IHE SDC on FHIR.: IHE International; 2021 Oct 1. URL: https://www.ihe.net/resources/technical_frameworks/ [accessed 2025-01-28]
28. NLM form builder. NIH.: Bethesda (MD): National Library of Medicine; 2024 Dec 10. URL: https://formbuilder.nlm.nih.gov/ [accessed 2025-01-30]
29. Hosseini M, Dixon BE. Chapter 8 - syntactic interoperability and the role of standards. In: Dixon BE, editor. Health Information Exchange: Academic Press; 2016:123-136. [doi: 10.1016/B978-0-12-803135-3.00008-6]
30. ChatGPT (March 14 version). OpenAI. URL: https://chat.openai.com/chat [accessed 2025-03-14]

Abbreviations

CAP: College of American Pathologists
CRC: Colorectal cancer
CT: SNOMED Clinical Terms
FHIR: Fast Healthcare Interoperability Resources
GUI: Graphical User Interface
HL7: Health Level 7
ICCR: International Collaboration on Cancer Reporting
IHE: Integrating the Healthcare Enterprise
NLM: National Library of Medicine
Palga: Dutch Nationwide Pathology Database
RCPath: Royal College of Pathologists
SDC: Structured data capture
TNM: tumor, node, metastasis

Edited by A Benis; submitted 02.05.25; peer-reviewed by F Amar, T Karen; revised version received 19.06.25; accepted 11.08.25; published 25.09.25.

Please cite as:
Hwang J, Goel AK, Rous BA, Birdsong G, Seegers PA, Dubois S, Rüdiger T, Campbell WS
Building a Standardized Cancer Synoptic Report With Semantic and Syntactic Interoperability: Development Study Using SNOMED CT and Fast Healthcare Interoperability Resources (FHIR)
JMIR Med Inform 2025;13:e76870
URL: https://medinform.jmir.org/2025/1/e76870
doi:10.2196/76870

XSL•FO
RenderX

© Jieun Hwang, Alexander K Goel, Brian A Rous, George Birdsong, Paul A Seegers, Stefan Dubois, Thomas Rüdiger, Walter S Campbell. Originally published in JMIR Medical Informatics (https://medinform.jmir.org), 25.9.2025. This is an open-access article distributed under the terms of the Creative Commons Attribution License (https://creativecommons.org/licenses/by/4.0/), which permits unrestricted use, distribution, and reproduction in any medium, provided the original work, first published in JMIR Medical Informatics, is properly cited. The complete bibliographic information, a link to the original publication on https://medinform.jmir.org/, as well as this copyright and license information must be included.

XSL•FO
RenderX

Original Paper

Clinical Trial Schedule of Activities Specification Using Fast Healthcare Interoperability Resources Definitional Resources: Mixed Methods Study

Andrew Richardson[1*], BSc, PhD; Patrick Genyn[2*], S.Lic, BA, MSc

[1]fhir4pharma, Hungerford, Berkshire, United Kingdom

[2]fhir4pharma, Doylestown, PA, United States

[*]all authors contributed equally

Corresponding Author:
Andrew Richardson, BSc, PhD
fhir4pharma
Ramsbury House, Charnham Lane
Hungerford, Berkshire, RG17 0EY
United Kingdom
Phone: 44 7748 186176
Email: andy.richardson@fhir4pharma.com

Abstract

Background: Clinical research studies rely on schedules of activities (SoAs) to define what data must be collected and when. Traditionally presented in tabular form within study protocols, SoAs are critical for ensuring data quality, regulatory compliance, and correct study execution. Recent efforts, such as the Health Level 7 Vulcan SoA Implementation Guide, have introduced Fast Healthcare Interoperability Resources (FHIR) as a standard for representing SoAs digitally. However, current approaches primarily handle simple schedules and do not adequately capture complex requirements such as conditional branching, repeat cycles, or unscheduled events—features essential for many study designs, particularly in oncology.

Objective: This study aimed to extend SoA representation methods to address these limitations. Specific objectives were to (1) develop methods for defining multiple SoA paths within a single model, (2) specify conditional scheduling requirements, (3) design a human-readable syntax for study specifications, (4) reflect these requirements as FHIR definitional resources, and (5) test bidirectional conversion between graph-based SoA models and FHIR representations.

Methods: Building on previous work, SoAs were modeled using directed graphs in which nodes represented interactions (eg, visits) or activities, and edges defined transitions. Attributes were added to capture timing, conditional rules, and repeatability. Graph-based models were translated into FHIR PlanDefinitions and related resources (ActivityDefinition, ResearchStudy, and ResearchSubject). Extensions to PlanDefinition were developed (soaTimePoint and soaTransition) to store graph-specific attributes. Proof-of-concept models were implemented and tested using Python, NetworkX, pandas, and FHIR Shorthand, with validation conducted through FHIR servers to ensure structural equivalence and information retention.

Results: The graph-based approach successfully modeled multiple paths, unscheduled events, and conditional rules within a single SoA. Edge attributes such as transitionDelay and transitionRule enabled accurate timing calculations and runtime evaluation of permitted paths. Conditional scheduling was expressed using a parameterized syntax interpretable by logic engines. More than 25 study protocols of varying complexity were tested; all could be represented without information loss. The proposed FHIR extensions allowed PlanDefinition resources to fully capture SoA graphs rather than limited tabular forms. Round-trip testing confirmed that the graph models and FHIR resources could be converted without loss of fidelity. The approach also highlighted inconsistencies in some protocol specifications, suggesting its utility for protocol quality assurance.

Conclusions: This study demonstrates that graph-based modeling, combined with targeted FHIR PlanDefinition extensions, enables an accurate and comprehensive representation of clinical study SoAs, including complex scheduling features that are not supported by current standards. These methods improve interoperability, reduce reliance on manual interpretation, and provide a basis for the automated integration of study protocols with electronic health records. While further tooling (eg, FHIRPath and clinical quality language) is needed for operational deployment, this approach offers a more precise and extensible solution for digital protocol implementation.

XSL•FO
RenderX

(JMIR Med Inform 2025;13:e71430) doi:10.2196/71430

KEYWORDS

Fast Healthcare Interoperability Resources; FHIR; Health Level 7; HL7; graph methods; clinical trials; schedule of activities; interoperability; electronic health records

Introduction

Background

Healthcare interoperability standards such as the Fast Healthcare Interoperability Resources (FHIR) [1] are providing new methodological approaches for the collection, collation, and confirmation of clinical research data for both observational studies and trials supporting product regulatory submissions [2-4]. To be successful, clinical research studies require that (1) the correct data are available to answer the research question and (2) these data are collected at the correct times. These are detailed in the study protocol, where the schedule of activities (SoAs), usually in the form of a square table, provides the key data and scheduling requirements. Various recent projects are underway to explore methods for digitizing all or parts of study protocols with FHIR as a key interoperability component (International Council for Harmonization M11, CDISC Unified Study Definitions Model, and Vulcan Utilizing the Digital Protocol) [5,6].

In a previous paper [7], a graph-based minimum viable set of characteristic attributes needed to define a study's SoA was developed, along with commentary on the range of "variations on the theme" encountered in different clinical study types and therapeutic areas. Operational use cases that depend on the SoA were also considered. The resulting graph representations of an SoA were converted to FHIR PlanDefinitions compliant with the Health Level 7 (HL7) Vulcan clinical study SoA Implementation Guide (IG) [8].

While the current Vulcan SoA IG can model a wide variety of clinical study SoAs, it is recognized that it is principally limited to defining relatively simple SoAs. It works well to convert SoA tables to FHIR resources; however, it does not have methods to define schedules that repeat (cycle), an essential part of most oncology studies. Similarly, it does not offer methods for conditional switching or to select different permitted (multiple) study paths. It may be coerced in some cases to manage specific situations, but this is not ideal when these "fixes" are key scheduling requirements. This can mean that a Vulcan SoA IG–compliant SoA will specify only part of the total scheduling options that a specific study requires. Subsequent use by consuming applications, such as electronic health record (EHR) systems, may or will require additional tooling to implement all study scheduling variations and control.

Considering previous work, this study investigated (1) what attributes or modifications to a graph model are needed to cover the extended use cases outlined earlier and (2) develop a FHIR PlanDefinition representation that can communicate these requirements. Additional tooling—such as FHIRPath expressions, clinical quality language, or system-specific methods (eg, EHR)—will be required to fully implement the FHIR PlanDefinition into the operational workflow of a clinical system.

This Study

The primary objectives of this study were to (1) develop methods for defining multiple SoA paths within a single graph, (2) develop methods for defining SoA conditional scheduling requirements, (3) develop a human-understandable syntax to support specific study specification, (4) reflect these requirements as FHIR definitional resources, and (5) test and confirm converting the graph representations to FHIR and vice versa

Methods

Graphical SoA Definition

Overview

The adopted methodological approach was to (1) build on previous work to investigate and develop the necessary attributes required to meet the objectives described earlier and (2) develop and test FHIR resource options to accurately describe and exchange these requirements.

Table 1 shows part of an SoA as might be presented in a protocol, and Figure 1 [7] shows a graphical representation of the primary schedule elements. The minimum set of characteristic attributes required to reflect it in this form is shown in Table 2 (refer to the study by Richardson [7] for more details). Two SoA graph node types are used in this model: "interactions," modeling study events, visits, or other direct or indirect contacts with research participants and "activities," defining the tasks required to be undertaken to meet the study objectives. These have a simple and easily understood correspondence with the tabular forms found in protocols. These were used to convert the SoAs into Vulcan SoA IG–compliant FHIR resources [7].

XSL•FO
RenderX

Table 1. Example (partial) of a schedule of activities as presented in protocols.

Phase	Screening	Study period				Unscheduled
Visit ID	1	2	3	...[a]	6	U
Visit timing	–Days 28 to 1	Day 1	Day 7	...	Day 28	As required
Activity						
Demographics	X					
Medical history	X					
Inclusion and exclusion criteria	X		X			
Vital signs	X	X	X	X	X	X
Procedure	X	X				
...[b]						
Concomitant medication	X	X	X	X	X	X
AE[c] and SAE[d]	X	X	X	X	X	X

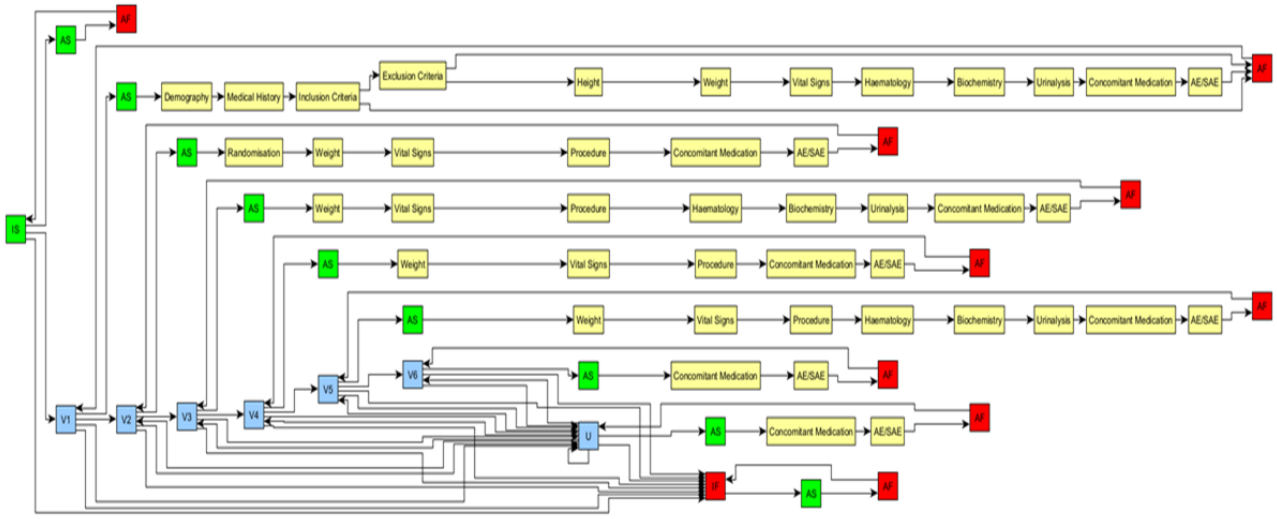
[a]Additional visit IDs (columns) exist in complete schedules of activities.

[b]Additional activities (rows) exist in complete schedules of activities.

[c]AE: adverse event.

[d]SAE: serious adverse event.

Figure 1. Example study of a schedule of activities directed graph. The schedule of activities has 6 planned visits and 1 unscheduled visit (U; blue). The activities at each visit are shown in yellow. The green and red nodes delineate the start and finish of graph instantiation and the activities to be undertaken contiguously. AS: activity start; AF: activity finish; IS: instantiation start; IF: instantiation finish.



XSL•FO
RenderX

Table 2. Schedule of activities graph characteristic attributes[a].

Attribute	Minimal required attribute	Notes or example
Nodes		
nodeID	Yes	Universally unique identifier
Type	Yes	"Interaction" or "activity"
Subtype	No	For example, clinic visit and telephone call
Name	Yes	Protocol name of interaction or activity
Description	No	Description of interaction or activity
plannedTiming	Yes	Schedule timing (D1 etc)
referenceTimepoint	Yes	Schedule t(zero)
plannedWindow	No	Schedule timing permitted variance
plannedDuration	No	Duration of interaction or activity (eg, 24 h)
Edges		
edgeID	Yes	Universally unique identifier
transitionType	No	Timing relationship between nodes

[a]Adapted from the study by Richardson [7].

Multiple SoA Paths

Standard graph methods were used to develop and test the attributes necessary to model and define the routing objectives (use cases) established earlier. The primary considerations were to (1) accurately reflect different study scheduling options using property graph methods and (2) ensure that the resulting models had a user-friendly correspondence to standard clinical trial scheduling concepts. Only methods using directed graphs were considered.

Conditional Scheduling

Methods to accurately model the conditional scheduling requirements within a single SoA graph initially used path analysis to identify the set of adjacency matrices required for each scenario. These were then used to develop a specification syntax that could define any specific conditional requirement, which, with appropriate tooling, can be implemented such that any subgraph can be extracted from the primary specification. Consideration was given to ensure that (1) permitted routes, such as those required by schedules with different treatment arms, could be defined and (2) the method could support controlling individual schedules dynamically (eg, as individual research participants were reviewed during their visits)

FHIR PlanDefinition

The Vulcan SoA IG [8] was used as the starting point for reviewing and evaluating methods to reflect the approaches mentioned earlier as FHIR resources. The primary resources used were *PlanDefinition*, *ActivityDefinition*, and the associated resources that are required to configure a complete description for a specific study (ie, *ReseachStudy, ResearchSubject*, etc). The main *PlanDefinition* elements investigated were *action.condition*, *action.relatedAction*, *action.timing*, and the 5 *action.<xxx>Behaviors*. All work was undertaken using version FHIR Release #5 (version 5.0.0) resources [1].

Model Testing and Proof of Concept

Graph database methods were used to develop and test the specification methods. Proof-of-concept example graphs were built using the Python generalized programming language [9], the NetworkX graph and network libraries [10], and the pandas data analysis library [11].

FHIR resource examples were generated using the Python fhir.resources library [12,13] and HL7 FHIR Shorthand definitions [13]. The yED graph editor (yWorks GmbH) was used to create the visual graph presentations and as an editor to create specific test examples [14]. The accuracy of the FHIR resources versus the graph model was confirmed by visual and programmed comparisons of the resulting definitions. The FHIR resources generated from each proof-of-concept example were confirmed as valid FHIR resources by loading them to publicly available FHIR end points, recovering the specifications using FHIR searches, and confirming that the full original specifications could be recovered without information loss.

SoA Example

Examples and illustrative figures used in this paper are based on the SoA graph shown in Figure 1.

Ethical Considerations

The study does not include human participants, use of medical records, or patient information.

Results

Multiple SoA Paths

Figure 2 illustrates the general problem that arises even with a simple study design when considering how to define all protocol-defined permitted paths. Figure 2A shows how the scheduled visits of Table 1 might be presented as a directed graph. However, the "unscheduled" visit "floats" independently

XSL•FO
RenderX

as it is to be used on an "as required" basis over the period of the planned visits.

Defining all permitted paths (ie, extending Figure 2A to add all protocol-implied paths) is shown in Figure 2B and is easily achieved simply by adding appropriate visit-visit edges. Similarly, all potential activity sequencing options can be defined using the same method (Figure 3).

Figure 2. The schedule of activities directed graph representations of the visit schedule described in Table 1. (A) Protocol explicitly defined schedule with "floating" unscheduled visit (U). (B) Expanded version with all implied permitted paths defined. Two important implied paths are now present: routes for a participant to leave the study at any point (eg, V1>IF), and routes to and from U, if required. IS: instantiation start; IF: instantiation finish.

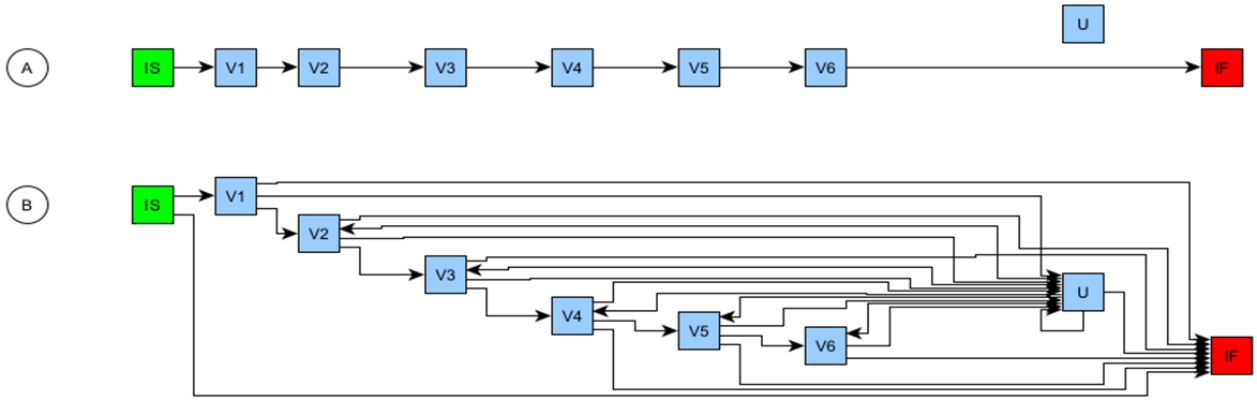
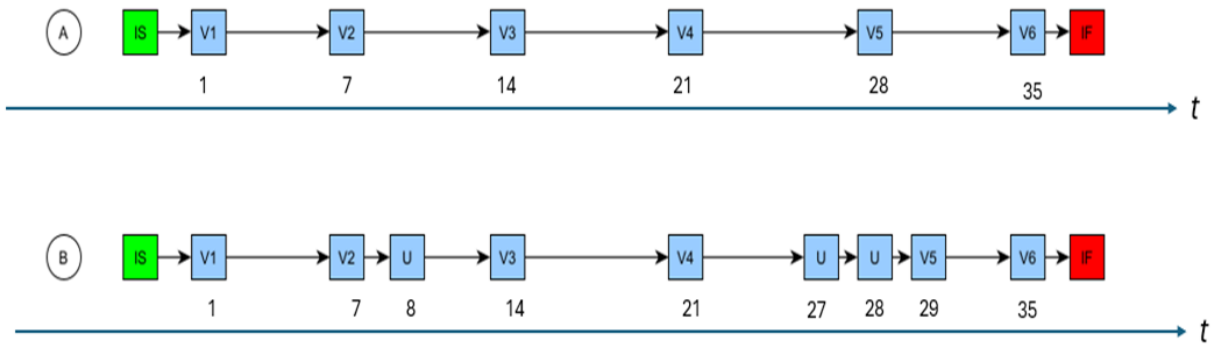


Figure 3. The schedule of activities directed graph representation of visit V1 activities from Figure 1, showing the protocol specified order (left to right) with the added requirements for those cases where (A) the inclusion criteria are not met, or (B) exclusion criteria are present. These paths formally define how to finish the visit "early." The resulting visualizations, although busy, remain user-friendly from a review or quality control perspective. AS: activity start; AF: activity finish.



No additional node or edge attributes beyond those listed in Table 2 are required to define all permitted paths. However, ensuring that the timing calculations for any path are computable cannot be achieved using the planned timings alone. Here, the problem is that the scheduled planned timings are node (visit) attributes, but calculating the timings for any path requires a summation of the transitions along whichever path is selected (Figure 4).

Figure 4. (A) Timing calculation attributes per protocol schedule, together with the relative day on which the visit occurred. (B) The same schedule but with 3 unscheduled visits. The first unscheduled visit (U; day D8) has no effect on the planned schedule, whereas the second (D27) and third (D28) U caused V5 to occur on D29 rather than on D28. In this case, the relative day of the visits cannot be determined from the planned timings alone. IS: instantiation start; IF: instantiation finish.



Unscheduled visits may necessitate rescheduling of scheduled events. The addition of a *transitionDelay* edge attribute (Table 3; defined as the time to wait before transitioning to the next node) was found to provide the necessary timing information. It also provides the basis for a key timing consistency check.

plannedTiming (V_n)*=sum(transitionDelay) from referenceTimepoint to* V_n

XSL•FO
RenderX

Table 3. Edge attributes required for path timing calculations.

Edge attribute	Minimal required attribute	Notes or example
transitionDelay	Yes	"Wait" time before moving from source to target nodes (ie, V1>V2 7d)
transitionWindow	No	Permitted transitionDelay variance
transitionType	No (default)	start-to-start, default; start-to-finish; finish-to-start; and finish-to-finish

Conditional Scheduling Attributes

Figures 2B and 3 also illustrate that there are many cases where specific conditions require different (but permitted) routes to be followed. Some cases are generic and are present in any study (eg, participant's right to withdraw at any time), some are protocol-specific (eg, if the participant is male, a pregnancy test is not required), and some complex, as illustrated in Figure 2B for managing all "unscheduled" path options (eg, an "unscheduled" visit following V_n cannot return to early visits, only being able to proceed to the next planned visit).

To accurately carry all conditional scheduling requirements within a single SoA graph, it was found that 3 things were required as follows:

1. A method to specify (and therefore recognize) a graph within the graph.
2. A syntax to define how to select a subgraph and restrict access to identified paths in the graph.
3. A method that can be implemented as a dynamic graph (ie, as the graph changes over time).

Both graph node attributes and edge attributes in the model here could be used to hold conditional scheduling information. Adding conditions to the nodes (eg, [visit] *repeatAllowed: true/false*) was found to satisfy some standard requirements (eg, can a visit be repeated? *V2: repeatAllowed: false*, and *Unscheduled: repeatAllowed: true*), but the other requirements were very poorly satisfied (particularly regarding what routes are available following an unscheduled visit). Adding the following edge attribute was found to accurately and easily model all the SoA tested use cases:

- Attribute: transitionRule
- Minimal required: yes
- Explanation: rule specifications that can be resolved to True (path can be selected) or False (path unavailable)

This approach was also user-friendly, as only the conditions on each edge (transition) were needed to ensure the use of any specific path (ie, by answering the question "under what conditions can this path be selected or is not available?" and this can also include multiple conditions).

Conditional Scheduling Syntax

A parameterized specification syntax was developed to hold the edge attribute conditions that can be consumed as inputs to a truth table engine that would resolve all edge conditions to the single "true" or "false" as described above. Simple *{"function": "inputs"}* pairs were used to specify the "true" or "false" state at runtime for that condition (eg, *{"consentObtained": true}*) or any combination of conditions.

The following examples show how several commonly required SoA conditional requirements can be defined using this approach.

Dynamic Graph Specification

The primary use case here is the definition of permitted paths through the study, including, but not limited to, the primary path. For example, in Figure 2B, paths exist to and from "unscheduled" to all "visits" permitting return to the primary schedule. However, "unscheduled" visits cannot return to a previously visited "visit" (discussed earlier). Two rules are required for this case: one to confirm the existence of previously visited visits, and one to ensure that all "future" visits have not yet been visited. The following example shows the rules required on edge U>V3 in Figure 2B, which will ensure that only this path is available at runtime:

{'interactions_exist': ['IS', 'V1','V2']}, {'interactions_not_exist': ['V3', 'V4', 'V5', 'V6", 'IF']}

(ie, If visits instantiation start [IS], V1, and V2 have occurred and visits V3, V4, V5, V6, and instantiation finish [IF] have not occurred, moving from unscheduled visit [U] to V3 is allowed).

Similar rule pairs, when applied to all U>V_n edges, can then ensure that only "forward" paths are available for selection.

Conditional Activity Selection

Restricting, adding, or skipping activities dependent upon participant conditions is a very common feature of SoAs, with the details often provided as footnotes to SoA tables. Examples include requiring pregnancy testing if the participant is female (and conversely not requiring this if the participant is male) and not proceeding with further tasks if inclusion criteria cannot be met (Figure 3). Example rules for these cases are simple to define, but consideration of all edge options is usually required, as follows:

On edge to "exclusion criteria" {"if_criteria_met":true}

On edge to "AF" {"if_criteria_met":false}

Conditional Repeats

An important feature of many SoAs is the requirement to repeat activities (eg, blood pressure measurements) or to repeat visit blocks. This last use case is particularly important in the case of many oncology studies where repeating treatment cycles is an inherent part of the study design and will have some limit on the number of cycles and the requirement to exit the study if too many cycles are proving necessary. Typical edge rules for controlling repeat or cycle situations include the following:

XSL•FO
RenderX

Repeat blood pressure measurement 3x. On edge to "self": {"maxRepeats":4}

Limit the number of cycles to a max of 5.On edge to start of cycle: {"n_cycles": "<6"}

Subject States, Milestones, and Events

Often, the requirement to select different SoA paths is dependent upon states, milestones, or events, as, for instance, defined by the FHIR ResearchSubject resource [1]. This can be illustrated by the following examples:

To enter an off-label extension study.

On edge to Open Label Extension schedule: {"continue_to_OLE": true}

If an adverse event occurs.

On edge to adverse event activity: {"record_AE": true}

Multiple Conditions

The syntax also permits any number of conditions to be defined easily within a single SoA graph for any given edge to obtain a sample for genetic testing. This can be illustrated by the following example:

{"studyPhase":"onStudy"},
{"sampleObtained":"true"},
{"geneticTestingConsent":"true"},

The runtime assessment of each condition then serves as the input to a logic engine that determines the final true or false state.

Undefined SoA Graphs: Implied Edges

Undefined SoA paths can also be recognized using this approach. An undefined path is defined here as one that may occur but is not recognized formally within the SoA graph. A good example of this is the right to withdraw from a study at any time or skip an activity. Formally recognizing every point where these conditions may occur and providing a defined path may add too much complexity to the graph, and it may be unreasonable to model it. However, placing a general requirement on all transitions (edges) of *{"withdrawn": false}* will permit proceeding through the schedule until *{"withdrawn": false}* == "false" (ie, withdraw is now "true"). Using suitable runtime coding, the "undefined" transition can be applied to the specific participants' SoA graph instance.

FHIR SoA PlanDefinition Review

The primary objective of this study was to identify methods that enable SoAs to be more fully defined using FHIR resources. The SoA graph review identified the necessary additional requirements needed to satisfactorily model SoA specifications, such as those shown in Figure 1. To successfully define these specifications using FHIR resources, they must meet the following requirements:

1. Represent all SoA-identified paths
2. Recognize and "respond" to conditional cases
3. Allow consuming applications to be able to "walk" any permitted path

The Vulcan SoA IG [8] was used as the starting point for developing a more comprehensive SoA FHIR model with the goal of extending or modifying it to be able to manage the complex designs, conditions, and "variations on the theme" as discussed earlier.

FHIR PlanDefinition SoAGraph Definition

From the graph attributes model developed earlier, it follows that for the *PlanDefinitions* to fully specify all SoA requirements, it needs to hold a definition of the SoA graph, and not the SoA table. Reviewing the use of the *PlanDefinition.action* and *PlanDefinition.action.action* elements, the basic graph node and edge relationship can be defined. Specifically, with nodes (visits) mapped to *PlanDefinition.actions* and edges(transitions) mapped to *PlanDefinition.action.actions*, all the relationships defined, for example, in Figure 1, can be specified within a single *PlanDefinition.*

PlanDefinition.action in its standard form does not support those elements (attributes) to hold all the necessary SoA specification details. These have been added using 2 extensions, that is, *soaTimePoint* and *soaTransition* (Figure 5 [7]) to hold the graph information, which in turn then forms the basis for an *soaPlanDefinition* profile (Multimedia Appendix 1).

XSL•FO
RenderX

Figure 5. Fast Healthcare Interoperability Resources extensions (as FHIR shorthand) used to associate the soaGraph node and edge attributes with PlanDefinition.action (SOATimePoint) and PlanDefinition.action.action (SOATransition), respectively.

```
Extension: SOATimePoint
Id: soaTimepoint
Title: "SoA TimePoint Specification"
Description: "SoA TimePoint Attribute Extension"
// Limit the context to PlanDefinition action
* ^context[+].type = #element
* ^context[=].expression = "PlanDefinition.action"
* extension contains
    soaTimePointType 0..1 and
    soaPlannedTimePoint 0..1 and
    soaPlannedRange 0..1 and
    soaReferenceTimePoint 0..1 and
    soaRangeFromTimePoint 0..1 and
    soaPlannedDuration 0..1
* extension[soaTimePointType].value[x] only string // interaction or activity
* extension[soaPlannedTimePoint].value[x] only SimpleQuantity // visit day etc.
* extension[soaPlannedRange].value[x] only Range // visit window
* extension[soaReferenceTimePoint].value[x] only string // reference visit for planned time
* extension[soaRangeFromTimePoint].value[x] only string  // calculate visit window from timepoint X
* extension[soaPlannedDuration].value[x] only Duration // duration of the visit (1d, 1w) once started

Extension: SOATransition
Id: soaTransition
Title: "SoA Transition Specification"
Description: "Specifies SoA Transition Attributes"
// Limit the context to PlanDefinition action.action
* ^context[+].type = #element
* ^context[=].expression = "PlanDefinition.action.action"
* extension contains
    soaTargetId 0..1 and
    soaTransitionType 0..1 and
    soaTransitionDelay 0..1 and
    soaTransitionRange 0..1
* extension[soaTargetId].value[x] only string // transition target UUID
* extension[soaTransitionType].value[x] only string // calculate transition wait from - to
* extension[soaTransitionDelay].value[x] only Duration  // wait time between states
* extension[soaTransitionRange].value[x] only Range // transition permitted window
```

FHIR PlanDefinition SoAGraph Condition and Selection Definition

Conditional SoA requirements can now be specified using the *PlanDefinition.action* element *condition* (applied to *PlanDefinition.action.action*), with each edge having all or any true or false conditions for that transition. When combined with *PlanDefinition.groupingBehaviour* and *PlanDefinition.selectionBehaviour*, path selection can be restricted to 1 path only, with only those transitions that are permitted being available for selection. Figure 6 shows the FHIR Shorthand specification for node V2 in Figure 2 and Multimedia Appendix 2.

XSL•FO
RenderX

Figure 6. FHIR shorthand annotated version of PlanDefinition definition of visit V2 (.action) and its associated soaGraph transitions: V2>V3, V2>IF (instantiation finish; withdrawal), V2>U (unscheduled visit; .action.action). V2 attributes are defined using the ...action.soaPlannedTimepoint extension. The selection behavior is defined by ...action.groupingBehaviour and ...action.selectionBehaviour. For each path from V2, the conditions that must be met for that path to be available for selection are given in ...action.action.condition(s). V2, V3, U, and IF are the schedule of activities time points in Figure 2.

```
// action [V2] ********************************************************************************************************** //
* action[0].id = "342da14b-5c82-4a2d-bdcf-7fd7cec428fa"
* action[=].title = "V2"
* action[=].description = "V2"
* action[=].definitionCanonical = "http://fhir4pharma.com/Encounter/V2"

// action soaTimePoint attributes [V2] //
* action[=].extension.url = "http://fhir4pharma.com/StructureDefinition/soaPlannedTimepoint"
* action[=].extension.extension[0].url = "soaPlannedTimePoint"
* action[=].extension.extension[=].valueQuantity = 7 'd'
...etc...

// action transition grouping and selection [V2 > ?] ******************************************************************* //
* action[=].groupingBehavior = #visual-group
* action[=].selectionBehavior = #exactly-one

// action.action soaTransitions #1  [V2 > V3] ************************************************************************** //
* action[=].action[=].extension.url = "http://fhir4pharma.com/StructureDefinition/soaTransition"
* action[=].action[0].extension.extension[0].url = "soaTargetId"
...etc...
// soaTransitions #1  [V2 > V3] conditions //
* action[=].action[=].condition[0].kind = #start
* action[=].action[=].condition[=].expression.language = #text/plain
* action[=].action[=].condition[=].expression.expression = "{'interactions_exist':['IS','V1']}"
* action[=].action[=].condition[+].kind = #start
* action[=].action[=].condition[=].expression.language = #text/plain
* action[=].action[=].condition[=].expression.expression = "{'interactions_not_exist':['V3','V4','V5','V6','IF']}"

// action.action soaTransitions #2  [V2 > IF] ************************************************************************** //
* action[=].action[=].extension.url = "http://fhir4pharma.com/StructureDefinition/soaTransition"
* action[=].action[+].extension.extension[0].url = "soaTargetId"
...etc...
// action.action soaTransitions #2  [V2 > IF] conditions //
* action[=].action[=].condition[0].kind = #start
* action[=].action[=].condition[=].expression.language = #text/plain
* action[=].action[=].condition[=].expression.expression = "{'withdraw':True}"
* action[=].action[=].condition[+].kind = #start
* action[=].action[=].condition[=].expression.language = #text/plain
* action[=].action[=].condition[=].expression.expression = "{'interactions_not_exist':['IF']}"

// action.action soaTransitions #3  [V2 > U] *************************************************************************** //
* action[=].action[=].extension.url = "http://fhir4pharma.com/StructureDefinition/soaTransition"
* action[=].action[+].extension.extension[0].url = "soaTargetId"
...etc...
* action[=].action[=].condition.kind = #start
* action[=].action[=].condition.expression.language = #text/plain
* action[=].action[=].condition.expression.expression = "{'to_unscheduled':True}"
```

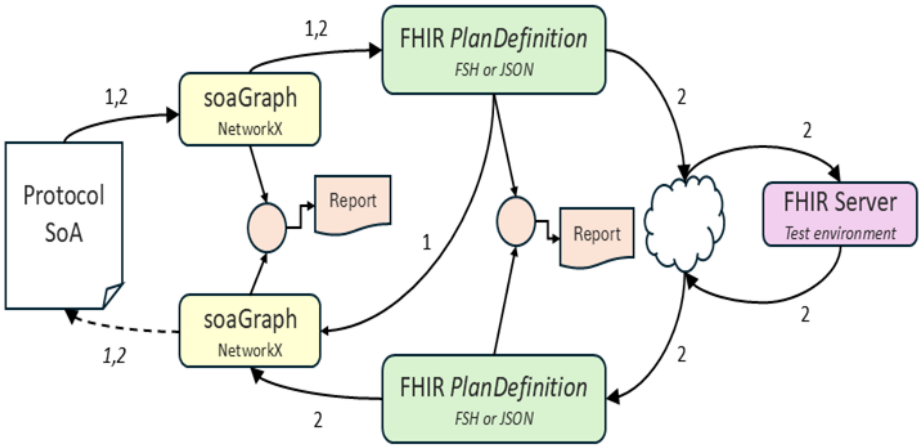
To operationalize the FHIR PlanDefinition within the workflow of a clinical system, such as an EHR, additional tooling is required. The illustrative syntax presented in the examples—for instance, *expression = "{'interactions_not_exist': ['V3', 'V4', 'V5', 'V6', 'IF']}"*—serves to demonstrate the underlying logic but is not directly executable within an FHIR environment. In practice, these expressions must be translated into an FHIR-compatible solution, typically by leveraging FHIRPath, clinical quality language, or system-specific functionality. Such translation ensures that the abstract representations in the PlanDefinition can be implemented as concrete, machine-interpretable instructions within the clinical system's workflow.

Proof of Concept

All the interim and final products, methods, and results described earlier were validated using the testing schedule shown in Figure 7. Once interim inconsistencies were reviewed and resolved, no SoA information loss was present after recovering an soaGraph from a FHIR *PlanDefinition* (Figure 7; test cycle 1) or after loading and recovery from test FHIR servers (test cycle 2).

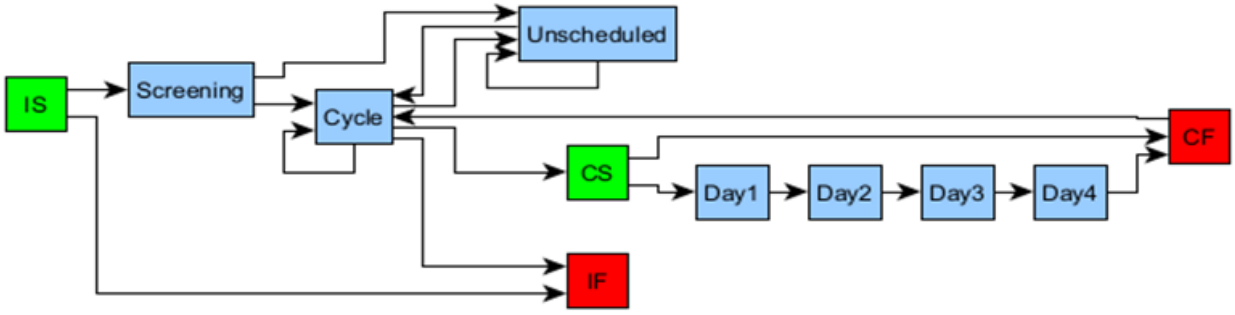
XSL•FO
RenderX

Figure 7. Proof-of-concept testing overview. The numbers highlight the 2 principal testing cycles used. Recovered products were compared with the original for reviewing structural equivalence and information loss throughout the development process. FHIR: Fast Healthcare Interoperability Resources; FSH: FHIR Shorthand; SoA: schedule of activities.



More than 25 studies, ranging from relatively simple designs, as shown in Figure 1, to complex studies incorporating cycles and multiple SoAs (not shown), were used to test and validate the approach. All tests could be accurately defined, with the most frequent finding during this exercise being that it highlighted inconsistencies in the protocol specifications themselves. It also lends itself to defining SoAs more succinctly and potentially more accurately. Figure 8 is a template for studies that includes cycles and shows that each required visit (interaction) is only defined once. With appropriate edge (transition) attributes and conditions, this can be modified to define many specific study scenarios.

Figure 8. Template soaGraph for studies with cycles. Using appropriate edge attributes and conditions, it can be modified for various study designs. The green and red nodes are included to delineate the graph instantiation and the start and finish of the treatment cycle. CS: cycle start: CF: cycle finish; IF: instantiation finish; IS: instantiation start.



Discussion

Overview

The HL7 FHIR standard is becoming, if not already, the de facto healthcare interoperability standard [2,15-18]. The primary source of many clinical trial data is EHRs, and studies usually require manual transcription of these data into electronic data capture systems. For both quality and volume reasons, this is often not optimal and has led to efforts to obtain data directly from electronic data capture systems (direct data capture) [19-22].

This study's protocol and the SoA provide the primary definitional source for a study's required research data and details of other operational requirements. The value of definitional FHIR resources to support clinical research and similar initiatives has been recognized in the Specialized Definitional Artifacts category [1].

The *PlanDefinition* resource is the primary resource for defining "a predefined group of actions to be taken in particular circumstances." The Vulcan SoA IG [23] has developed a set of profiles using this resource to define SoAs. As mentioned earlier, this model does not include methods to define either conditional scheduling, certain study designs (notably cycles), or the scheduling of expected but not planned events (particularly "unscheduled visits"). This work has re-evaluated how *PlanDefinition* might be modified, revised, or extended to model these situations.

Principal Findings

Using a systematic review of the relationships and attributes required to define the SoA characteristics discussed earlier, a graph-based method has been developed that can manage all these cases. Subsequently, by associating *PlanDefinition.action* and *PlanDefinition.action.action* directly with graph nodes and edges, respectively, SoAs with all scheduling variations, conditional paths, and methods to manage planned but unscheduled events can be defined within a single

XSL•FO
RenderX

PlanDefinition. Recognizing that an SoA "activity" has both timing and task elements (ie, is "X" in tabular SoAs), the model formally disassociates the scheduling information from the task or activity definitions, which can then be linked using the *PlanDefinition.action.relatedAction.targetId* element. This approach also enables SoA activities as described in study protocols (or not described) to be fully traceable in the SoA schedule, but specified fully using other appropriate FHIR definitional resources (eg, *ActivityDefinition* and *ObservationDefinition*)

Comparison With Prior Work

Earlier work based on using both graph methods for SoA definition [23,24] and FHIR for interoperability [25-27] has shown the value of this approach for communicating sponsor protocol requirements systematically for implementation in EHRs and similar systems [4,21,22,28-31]. The work here has re-evaluated the approach to specifying SoAs as FHIR *PlanDefinitions* to find solutions to several key required SoA characteristics not addressed previously. The model described here uses a radically different conceptual approach, redefining several *PlanDefinition* elements to be able to hold a graph representation of an SoA. The current method can successfully represent a wider range of SoA concepts than before and can also specify a large range of other SoA use cases that are key to many protocol designs (not shown). Because here all SoA requirements can be accurately specified within a single *PlanDefinition*, this should simplify the implementation by consuming applications. It is also clear that, with modification or the use of standard *PlanDefinition* elements, it can support other important SoA use cases not directly considered here (eg, protocol amendments with SoA consequences)

Limitations

The methods in this study were developed using FHIR Release #5 (version 5.0.0) [1] and are not necessarily compatible with earlier FHIR versions.

Conclusions

The methods described in this study offer an alternative approach to defining clinical study SoAs using FHIR definitional resources compared to previously published articles and may offer advantages with regard to some key requirements not addressed by other proposed approaches.

Conflicts of Interest

AR and PG are both volunteer contributors to the Vulcan Schedule of Activities working-group meetings. The authors assert no rights to the Fast Healthcare Interoperability Resources methods described in this paper, except that their use should be acknowledged with reference to this paper.

Multimedia Appendix 1
Schedule of activity PlanDefinition extensions (JSON).
[ZIP File (Zip Archive), 40 KB - medinform_v13i1e71430_app1.zip]

Multimedia Appendix 2
Schedule of activity PlanDefinition Figure 2 example (JSON).
[ZIP File (Zip Archive), 13 KB - medinform_v13i1e71430_app2.zip]

References

1. Welcome to FHIR. HL7 Fast Healthcare Interoperability Resources. URL: https://hl7.org/fhir/ [accessed 2025-09-28]
2. Pimenta N, Chaves A, Sousa R, Abelha A, Peixoto H. Interoperability of clinical data through FHIR: a review. Procedia Computer Science 2023;220:856-861. [doi: 10.1016/j.procs.2023.03.115]
3. Real-world data: assessing electronic health records and medical claims data to support regulatory decision-making for drug and biological products. U.S. Food & Drug Administration. 2024 Jul. URL: https://www.fda.gov/regulatory-information/search-fda-guidance-documents/real-world-data-assessing-electronic-health-records-and-medical-claims-data-support-regulatory [accessed 2025-09-20]
4. Chatterjee A, Pahari N, Prinz A. HL7 FHIR with SNOMED-CT to achieve semantic and structural interoperability in personal health data: a proof-of-concept study. Sensors (Basel) 2022 May 15;22(10):3756 [FREE Full text] [doi: 10.3390/s22103756] [Medline: 35632165]
5. Clinical electronic Structured Harmonised Protocol (CeSHarp). International Council for Harmonisation of Technical Requirements for Pharmaceuticals for Human Use. URL: https://ich.org/page/multidisciplinary-guidelines#11 [accessed 2025-01-02]
6. 2025 - 05 Vulcan utilizing the digital protocol (UDP). Confluence. 2025 Oct 04. URL: https://confluence.hl7.org/spaces/FHIR/pages/324961379/2025+-+05+Vulcan+Utilizing+the+Digital+Protocol+UDP [accessed 2025-09-28]
7. Richardson A. Representing clinical study schedule of activities as FHIR resources: required characteristic attributes. J Soc Clin Data Manag 2024;4(2) [FREE Full text] [doi: 10.47912/jscdm.266]
8. Clinical study schedule of activities. HL7 International. 2023 Apr 18. URL: https://build.fhir.org/ig/HL7/Vulcan-schedule-ig/ [accessed 2025-09-28]
9. Python. URL: https://www.python.org/ [accessed 2025-01-02]

XSL•FO
RenderX

10. NetworkX. URL: https://networkx.org/ [accessed 2025-01-02]
11. Pandas. URL: https://pandas.pydata.org/ [accessed 2025-01-02]
12. fhir.resources 8.1.0. PyPI. URL: https://pypi.org/project/fhir.resources/ [accessed 2025-01-02]
13. FHIR shorthand. HL7 International. https://build.fhir.org/ig/HL7/fhir-shorthand/: HL7; 2024 Aug 19. URL: https://build.fhir.org/ig/HL7/fhir-shorthand/ [accessed 2025-09-28]
14. yEd - graph editor. yWorks. https://www.yworks.com: yWorks URL: https://www.yworks.com/products/yed [accessed 2025-09-28]
15. Saripalle R, Runyan C, Russell M. Using HL7 FHIR to achieve interoperability in patient health record. J Biomed Inform 2019 Jun;94:103188 [FREE Full text] [doi: 10.1016/j.jbi.2019.103188] [Medline: 31063828]
16. Mukhiya SK, Lamo Y. An HL7 FHIR and GraphQL approach for interoperability between heterogeneous electronic health record systems. Health Informatics J 2021 Sep 15;27(3):14604582211043920 [FREE Full text] [doi: 10.1177/14604582211043920] [Medline: 34524029]
17. Monteiro SC, Cruz Correia RJ. FHIR based interoperability of medical devices. Stud Health Technol Inform 2022 Jun 06;290:37-41. [doi: 10.3233/SHTI220027] [Medline: 35672966]
18. Raso E, Loreti P, Ravaziol M, Bracciale L. Anonymization and pseudonymization of FHIR resources for secondary use of healthcare data. IEEE Access 2024;12:44929-44939. [doi: 10.1109/access.2024.3381034]
19. Aoyagi Y. Direct data transfer from HIS (hospital information system) to sponsor for clinical trials. In: Proceedings of the 12th Annual Meeting DIA JAPAN 2015. 2015 Presented at: DIA JAPAN 2015; November 15-17, 2015; Tokyo, Japan URL: https://researchmap.jp/9sT1g1FdTR/presentations/6799791?lang=en
20. Lombardo G, Couvert C, Kose M, Begum A, Spiertz C, Worrell C, et al. Electronic health records (EHRs) in clinical research and platform trials: application of the innovative EHR-based methods developed by EU-PEARL. J Biomed Inform 2023 Dec;148:104553 [FREE Full text] [doi: 10.1016/j.jbi.2023.104553] [Medline: 38000766]
21. De Moor G, Sundgren M, Kalra D, Schmidt A, Dugas M, Claerhout B, et al. Using electronic health records for clinical research: the case of the EHR4CR project. J Biomed Inform 2015 Feb;53:162-173 [FREE Full text] [doi: 10.1016/j.jbi.2014.10.006] [Medline: 25463966]
22. Welker JA. Implementation of electronic data capture systems: barriers and solutions. Contemp Clin Trials 2007 May;28(3):329-336. [doi: 10.1016/j.cct.2007.01.001] [Medline: 17287151]
23. Richardson A. Approaches to schedule of activities (SOA) specification for automated implementation. PHUSE EU Connect 2020: ML05. URL: https://phuse.s3.eu-central-1.amazonaws.com/Archive/2020/Connect/EU/Virtual/PRE_ML05.pdf [accessed 2025-09-20]
24. Low G, Ward M, Richardson A, PHUSE Research on FHIR Project Team. Study designs using FHIR: schedule of activities exchange using FHIR resources. PHUSE EU Connect 2021: RW05. 2021. URL: https://phuse.s3.eu-central-1.amazonaws.com/Archive/2021/Connect/EU/Virtual/PRE_RW05.pdf [accessed 2025-09-20]
25. Genyn P, Richardson A. The role of FHIR Resources in ensuring semantic equivalence in EHR2EDC direct data capture. PHUSE EU Connect 2023: RE08. URL: https://phuse.s3.eu-central-1.amazonaws.com/Archive/2023/Connect/EU/Birmingham/PAP_RE08.pdf [accessed 2025-09-20]
26. Genyn P, Richardson A. The role of FHIR resources in testing and validating an EHR to sponsor data pipeline. fhir4pharma. URL: https://phuse.s3.eu-central-1.amazonaws.com/Archive/2024/Connect/US/Bethesda/PRE_RE01.pdf [accessed 2025-09-20]
27. Leroux H, Metke-Jimenez A, Lawley MJ. Towards achieving semantic interoperability of clinical study data with FHIR. J Biomed Semantics 2017 Sep 19;8(1):41 [FREE Full text] [doi: 10.1186/s13326-017-0148-7] [Medline: 28927443]
28. Coorevits P, Sundgren M, Klein GO, Bahr A, Claerhout B, Daniel C, et al. Electronic health records: new opportunities for clinical research. J Intern Med 2013 Dec;274(6):547-560 [FREE Full text] [doi: 10.1111/joim.12119] [Medline: 23952476]
29. Garza M, Myneni S, Fenton S, Zozus M. eSource for standardized health information exchange in clinical research: a systematic review of progress in the last year. J Soc Clin Data Manag 2021;1(2):1-9. [doi: 10.47912/jscdm.66]
30. Laaksonen N, Varjonen JM, Blomster M, Palomäki A, Vasankari T, Airaksinen J, Juuso Blomster. Assessing an electronic health record research platform for identification of clinical trial participants. Contemp Clin Trials Commun 2021 Mar;21:100692 [FREE Full text] [doi: 10.1016/j.conctc.2020.100692] [Medline: 33409423]
31. El Emam K, Jonker E, Sampson M, Krleza-Jerić K, Neisa A. The use of electronic data capture tools in clinical trials: web-survey of 259 Canadian trials. J Med Internet Res 2009 Mar 09;11(1):e8 [FREE Full text] [doi: 10.2196/jmir.1120] [Medline: 19275984]

Abbreviations

EHR: electronic health record
FHIR: Fast Healthcare Interoperability Resources
HL7: Health Level 7
IG: Implementation Guide

XSL•FO
RenderX

SoA: schedule of activities

Edited by A Benis; submitted 18.01.25; peer-reviewed by G Low, S Mohanadas, R Smithies; comments to author 24.02.25; revised version received 01.07.25; accepted 15.09.25; published 20.10.25.

Please cite as:
Richardson A, Genyn P
Clinical Trial Schedule of Activities Specification Using Fast Healthcare Interoperability Resources Definitional Resources: Mixed Methods Study
JMIR Med Inform 2025;13:e71430
URL: https://medinform.jmir.org/2025/1/e71430
doi:10.2196/71430
PMID:

©Andrew Richardson, Patrick Genyn. Originally published in JMIR Medical Informatics (https://medinform.jmir.org), 20.10.2025. This is an open-access article distributed under the terms of the Creative Commons Attribution License (https://creativecommons.org/licenses/by/4.0/), which permits unrestricted use, distribution, and reproduction in any medium, provided the original work, first published in JMIR Medical Informatics, is properly cited. The complete bibliographic information, a link to the original publication on https://medinform.jmir.org/, as well as this copyright and license information must be included.

XSL•FO
RenderX

The Advanced Reasoning Capabilities of Large Language Models for Detecting Contraindicated Options in Medical Exams

Yuichiro Yano[1,2], MD, PhD; Mizuki Ohashi[1], MD, PhD; Taiju Miyagami[1], MD, PhD; Hirotake Mori[1], MD, PhD; Yuji Nishizaki[3], MD, MPH, PhD; Hiroyuki Daida[4], MD, PhD; Toshio Naito[1], MD, PhD

[1]Department of General Medicine, Juntendo University Faculty of Medicine, 2-1-1, Hongo, Bunkyo-Ku, Tokyo, Japan

[2]AI Incubation Farm, Juntendo University Faculty of Medicine, Tokyo, Japan

[3]Division of Medical Education, Juntendo University School of Medicine, Tokyo, Japan

[4]Department of Cardiovascular Biology and Medicine, Juntendo University Graduate School of Medicine, Tokyo, Japan

Corresponding Author:
Yuichiro Yano, MD, PhD
Department of General Medicine, Juntendo University Faculty of Medicine, 2-1-1, Hongo, Bunkyo-Ku, Tokyo, Japan

Abstract

Enhancing clinical reasoning and reducing diagnostic errors are essential in medical practice; OpenAI-o1, with advanced reasoning capabilities, performed better than GPT-4 on 15 Japanese National Medical Licensing Examination questions (accuracy: 100% vs 80%; contraindicated option detection: 87% vs 73%), though findings are preliminary due to the small sample size.

(JMIR Med Inform 2025;13:e68527) doi:10.2196/68527

KEYWORDS

natural language processing; artificial intelligence; clinical reasoning; medical errors; large language model

Introduction

Diagnostic errors account for more than 8% of adverse medical events and up to 30% of malpractice claims [1]. Enhancing clinical reasoning could mitigate this [2], improving patient outcomes and potentially lowering legal liabilities. In September 2024, OpenAI introduced OpenAI-o1, a large language model (LLM) trained with reinforcement learning to enhance its complex "reasoning" [3,4]. Key enhancements include advanced attention mechanisms, refined training data and curation, and enhanced fine-tuning protocols [3,5]. However, it remains uncertain whether OpenAI-o1 can improve clinical reasoning and reduce diagnostic errors.

In the Japanese National Medical Licensing Examination (JNMLE), candidates must not only achieve high overall accuracy but also avoid selecting contraindicated options—errors that can lead to failure even if most answers are correct. Although prior studies indicate that ChatGPT-4 performs well on the JNMLE, it sometimes chooses contraindicated options [6]. We posited that OpenAI-o1 would exhibit superior reasoning compared to GPT-4 and hypothesized that it would more proficiently avoid contraindicated options.

Methods

On October 10, 2024, we used 15 text-based JNMLE questions (from 2019 to 2024) that included contraindicated options (Multimedia Appendix 1). Questions with images were excluded due to OpenAI-o1's inability to process visual data. We administered the questions to both GPT-4 and OpenAI-o1, with each model evaluated under the supervision of designated examiners (MO and TM).

The examination comprised 3 steps: (1) Japanese examination—select correct answers, (2) Japanese examination—identify contraindicated options, and (3) English examination—repeat steps 1 and 2 with translated questions. Translation used an automated system and was reviewed by bilingual clinical expert YY.

The responses from both models were recorded, and the results were evaluated based on the numbers of correct answers and correctly identified contraindicated options in both languages.

Results

As shown in Multimedia Appendix 1, among the 15 questions, GPT-4 correctly answered 12 (80%) and identified 11 contraindicated options (73%) in Japanese. In English, GPT-4 correctly answered 13 questions (87%) and identified 11 contraindicated options (73%). OpenAI-o1 correctly answered 15 questions (100%) and identified 13 contraindicated options in Japanese (87%). Both GPT-4 and OpenAI-o1 had consistently equal or better performance in English than Japanese, especially for contraindicated options.

Discussion

OpenAI-o1 had higher accuracy than GPT-4 and was better able to select contraindicated options on the JNMLE, particularly in

XSL•FO
RenderX

English. However, this difference was minimal—only 1 of 15 questions showed improvement in English—indicating that language had little overall impact.

In medicine, avoiding contraindicated actions is crucial. While correct answers reflect basic medical knowledge, recognizing what should not be done requires advanced critical thinking and reasoning. Errors can lead to patient harm, lawsuits, or even license revocation. Here, OpenAI-o1 outperformed GPT-4 in identifying contraindicated actions. OpenAI-o1's enhancements [3,5] and our finding of its superior reasoning ability suggest the importance of using LLMs with robust reasoning capabilities for medical licensing examinations and, by extension, in clinical practice, to safeguard patient safety and uphold high standards of care.

Our study is limited, first, by using only 15 questions, so these findings should be interpreted as preliminary and hypothesis-generating. Second, we used the models' default settings without fine-tuning, prompt engineering, or chain-of-thought modifications, capturing their performance at only a specific time point. Third, we obtained a single response per query, which may not reflect the full variability of LLM outputs. Fourth, continuous model updates limit exact reproducibility. Fifth, only 2 of 15 questions showed discrepancies, limiting our ability to analyze performance trends across question types (eg, clinical scenarios, complexity, and format). Sixth, we focused on comparing OpenAI-o1 and GPT-4 and excluded human performance benchmarks (eg, from medical students) due to the study's rapid initiation in October 2024, immediately following the release of OpenAI-o1. Given GPT-4's extensive dataset training and OpenAI-o1's enhanced reasoning capabilities, our primary objective was to promptly assess their differences in a medical context; frequent updates to LLMs and the time required for ethics approval and participant recruitment precluded human comparisons. Future research should integrate such comparisons. Lastly, we did not statistically evaluate the significance of the observed performance differences, further limiting our findings' interpretability. The "black box" nature of both OpenAI-o1 and GPT-4 also limits interpretability; future research should use methods like attention analysis and causal reasoning tests and compare these models with open-source alternatives (eg, DeepSeek, Qwen) to enhance reproducibility and transparency.

The improved reasoning abilities of OpenAI-o1 may hold promise for real-world clinical applications. However, these findings are preliminary, and further research is needed to determine whether integrating such models into decision-support systems can contribute to reducing errors and enhancing patient care.

Acknowledgments

This research was partially funded by the Advanced Medical Personnel Training Program (principal investigator: TN) and was supported by the Ministry of Education, Culture, Sports, Science, and Technology.

Data Availability

The datasets generated or analyzed during this study are available from the corresponding author on reasonable request.

Conflicts of Interest

None declared.

Multimedia Appendix 1
Responses of GPT-4 and OpenAI-o1 to Japanese National Medical Licensing Examination questions.
[DOCX File, 37 KB - medinform_v13i1e68527_app1.docx]

References

1. Berner ES, Graber ML. Overconfidence as a cause of diagnostic error in medicine. Am J Med 2008 May;121(5 Suppl):S2-S23. [doi: 10.1016/j.amjmed.2008.01.001] [Medline: 18440350]
2. Bowen JL. Educational strategies to promote clinical diagnostic reasoning. N Engl J Med 2006 Nov 23;355(21):2217-2225. [doi: 10.1056/NEJMra054782] [Medline: 17124019]
3. Learning to reason with LLMs. OpenAI. 2024 Sep 12. URL: https://openai.com/index/learning-to-reason-with-llms/ [accessed 2025-03-08]
4. Zelikman E, Wu Y, Mu J, Goodman ND. STaR: bootstrapping reasoning with reasoning. arXiv. Preprint posted online on Mar 28, 2022. [doi: 10.48550/arXiv.2203.14465]
5. Temsah MH, Jamal A, Alhasan K, Temsah AA, Malki KH. OpenAI o1-preview vs. ChatGPT in healthcare: a new frontier in medical AI reasoning. Cureus 2024 Oct;16(10):e70640. [doi: 10.7759/cureus.70640] [Medline: 39359332]
6. Kasai J, Kasai Y, Sakaguchi K, Yamada Y, Radev D. Evaluating GPT-4 and ChatGPT on Japanese medical licensing examinations. arXiv. Preprint posted online on Mar 31, 2023. [doi: 10.48550/arXiv.2303.18027]

XSL•FO
RenderX

Abbreviations

JNMLE: Japanese National Medical Licensing Examination
LLM: large language model

Edited by A Castonguay; submitted 09.11.24; peer-reviewed by C Ma, N Azahar; revised version received 22.03.25; accepted 25.03.25; published 12.05.25.

Please cite as:
Yano Y, Ohashi M, Miyagami T, Mori H, Nishizaki Y, Daida H, Naito T
The Advanced Reasoning Capabilities of Large Language Models for Detecting Contraindicated Options in Medical Exams
JMIR Med Inform 2025;13:e68527
URL: https://medinform.jmir.org/2025/1/e68527
doi:10.2196/68527

© Yuichiro Yano, Mizuki Ohashi, Taiju Miyagami, Hirotake Mori, Yuji Nishizaki, Hiroyuki Daida, Toshio Naito. Originally published in JMIR Medical Informatics (https://medinform.jmir.org), 12.5.2025. This is an open-access article distributed under the terms of the Creative Commons Attribution License (https://creativecommons.org/licenses/by/4.0/), which permits unrestricted use, distribution, and reproduction in any medium, provided the original work, first published in JMIR Medical Informatics, is properly cited. The complete bibliographic information, a link to the original publication on https://medinform.jmir.org/, as well as this copyright and license information must be included.

XSL•FO
RenderX

Effect of Smartphone-Based Messaging on Interns and Nurses at an Academic Medical Center: Observational Study

Sankirth Madabhushi[1*], MD; Andrew M Nguyen[2*], MS; Katie Hsia[3], MD; Sucharita Kher[3], MD; William Harvey[4], MD; Jennifer Murzycki[5], MD, PhD; Daniel Chandler[3], MD; Michael Davis[3], MD

[1]Department of Medicine, UMass Chan Medical School, 55 N Lake Ave, Worcester, MA, United States

[2]Tufts University School of Medicine, Boston, MA, United States

[3]Department of Medicine, Tufts Medical Center, Boston, MA, United States

[4]Information Systems, Tufts Medical Center, Boston, MA, United States

[5]Department of Pediatrics, Tufts University School of Medicine, Boston, MA, United States

[*]these authors contributed equally

Corresponding Author:
Sankirth Madabhushi, MD
Department of Medicine, UMass Chan Medical School, 55 N Lake Ave, Worcester, MA, United States

Abstract

Background: Digital communication between nurses and medicine interns plays a crucial role in patient care. However, excessive messaging may contribute to alert fatigue, potentially affecting workflow efficiency and clinical decision-making. Although prior research has examined general messaging behaviors among clinicians, few studies have specifically analyzed messaging patterns between nurses and interns, who serve as primary points of contact in inpatient care.

Objectives: This study aims to quantitatively characterize messaging patterns between the primary nurse and primary provider (ie, medicine intern) of hospitalized patients at an academic medical center in order to identify communication burdens and potential inefficiencies. By identifying trends in message volume, timing, and response rates, we seek to inform strategies to optimize communication workflows and mitigate alert fatigue.

Methods: At a large academic hospital (Tufts Medical Center, Boston, MA), we analyzed secure messaging transactions between internal medicine interns and nurses across three medical-surgical units over 6 months. Transaction metadata, time stamps, and unique message tokens were extracted. Data processing was performed using Python, Microsoft Excel, and R. Message volume, interaction frequencies, and response times were analyzed using measures of central tendency and statistical tests of significance.

Results: A total of 61,057 unique messages were exchanged between interns and nurses, with interns exchanging 2.5 times more messages per day with nurses than vice versa (P<.001). Messaging volume exhibited diurnal variation, indicating periods of increased communication burden. Interns read messages from nurses within a median of 35 (range: 0 - 3589) seconds, whereas nurses read messages from interns within a median of 26 (range: 0 - 3584) seconds (P<.001). The longest message response delays occurred at 4 AM, whereas the shortest occurred at 8 AM.

Conclusions: Interns experience a significantly higher messaging burden than nurses, with distinct peaks in message volume during morning rounds and overnight shifts. These findings suggest a need for interventions such as optimized digital communication protocols to reduce nonessential messaging and alert fatigue. Future research should explore the effectiveness of these interventions in enhancing workflow efficiency and the development of both in-person and digital interventions to optimize communication workflows and mitigate alert fatigue.

(JMIR Med Inform 2025;13:e66859) doi:10.2196/66859

KEYWORDS

secure messaging; alert fatigue; burnout; clinical communication; TigerConnect; healthcare communication; text; texting; messaging; app; application; smartphone; digital health; digital technology; digital intervention; medical informatics; messaging patterns

Introduction

As health care organizations implement secure messaging software to modernize communication among clinicians and address the shortcomings of pagers, a growing body of literature has described patterns in secure messaging transactions [1,2]. Small et al [3,4] describe an uneven burden of secure messaging on medicine providers, while qualitative analysis reveals clinicians' concerns with alert fatigue from digital communication. Alert fatigue is a phenomenon in health care

XSL•FO
RenderX

settings where providers experience a high frequency of clinical notifications, leading to desensitization of safety alerts, increased distractions, missed alerts, or cognitive overload. Such desensitization can significantly contribute to clinician burnout and affect patient care [5,6]. To our knowledge, few studies have examined the specific communication patterns between nurses and medicine interns on secure messaging platforms. Existing research provides general insights into messaging behaviors but lacks in-depth analysis of how messaging patterns between these specific groups—who often serve as the first point of contact in inpatient care—differ in terms of volume or timing [7,8].

Our institution (Tufts Medical Center, Boston, MA) implemented TigerConnect, a clinical communication and collaboration platform, in April 2022, and in turn, disabled the secure chat feature in the electronic medical record "Epic." Although TigerConnect has yielded efficiencies to clinical workflows, such as consult requests, operating room throughput, closure of radiology alerts, and emergency responses, alert fatigue from messages was cited as a reason for decreased job satisfaction on end-of-year house staff surveys. This study aims to characterize the messaging patterns between nurses and medicine interns to inform interventions to mitigate alert fatigue among two groups of clinicians with exceptionally high rates of burnout [9].

Methods

Study Setting and Data Collection

Our study was conducted at Tufts Medical Center, a 415-bed tertiary care academic institution in Boston, MA. We focused on TigerConnect transactions between 25 internal medicine interns and 96 nurses from three medical-surgical inpatient units, excluding the intensive care unit and emergency department, across 5 months from June 2022 through December 2022. We also collected transaction metadata, time stamps, and unique message tokens.

Data Analysis

We compiled the data using Python and Microsoft Excel. A dataset of messages exchanged between the interns and nurses was cleaned and analyzed using R, specifically using the *dpylr* package. We defined an "active" intern or nurse as someone who sent or received a message during a given period. Interaction frequencies were summarized using measures of central tendency. The time lag between message delivery and reading was calculated by subtracting the delivery time stamp from the read time stamp, with messages read over an hour later excluded to avoid skewing caused by outliers. Average interactions were compared using a 2-sided Welch *t*-test. This test was chosen due to unequal variances between the two groups. Median comparisons of time delays were compared using the Mann-Whitney test with an α of .05.

Ethical Considerations

The Tufts Health Sciences Campus institutional review board reviewed this study and determined that it did not constitute human subjects research; thus, it was exempt from institutional review board approval. Data from this study presents only metadata from message transactions between 25 interns and 96 nurses, including time stamps, delivery confirmations, and read receipts. To protect privacy, individual interns and nurses were deidentified, and transactions were aggregated, as the analysis focused on overall trends rather than individual messaging behavior. Individual interns and nurses were deidentified by replacing the names of individual interns with an "intern" label and replacing the names of individual nurses with a "nurse" label. Furthermore, the actual content of any messages was not accessed, in accordance with institutional policy and the scope of this study.

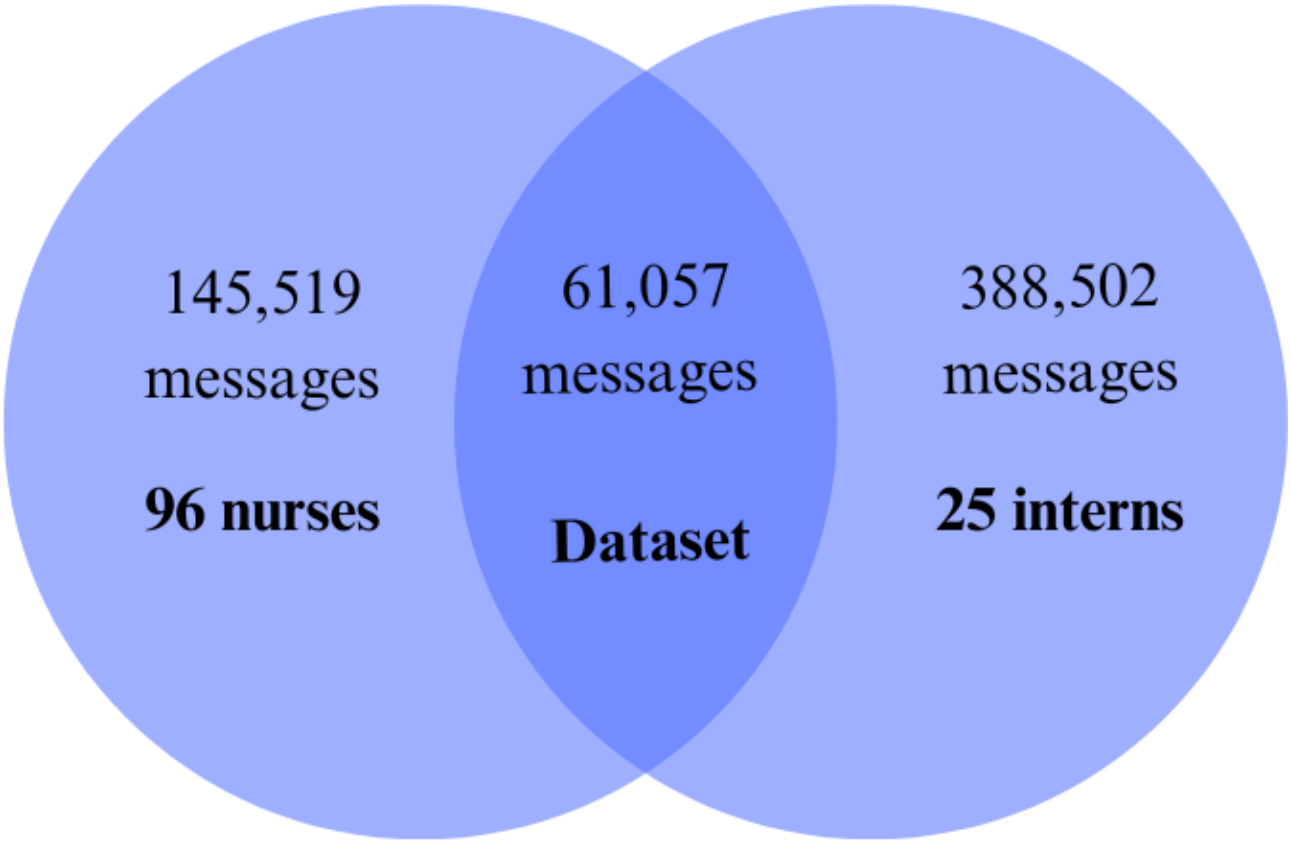
Results

Message Volume and Patterns

A total of 145,519 (sent and received) nurse messages and 388,502 intern messages were collected over the study period, with 61,057 unique messages exchanged between interns and nurses (Figure 1). An active intern exchanged on average 39.8 messages (range: 26.8 - 50.6) with nurses per day, while an active nurse exchanged on average 15.3 messages (range: 2.3 - 37.2) with interns per day ($P<.001$). Each intern covers up to 9 patients, whereas each nurse covers typically up to 4 patients. On average, the total number of messages exchanged over a day peaked at 11 AM. (Figure 2A). Typically, 13 interns work from 7AM to 6PM and 2 interns work from 6PM to 7AM. On average, the number of messages per active intern peaked at 10 PM. (Figure 2B).

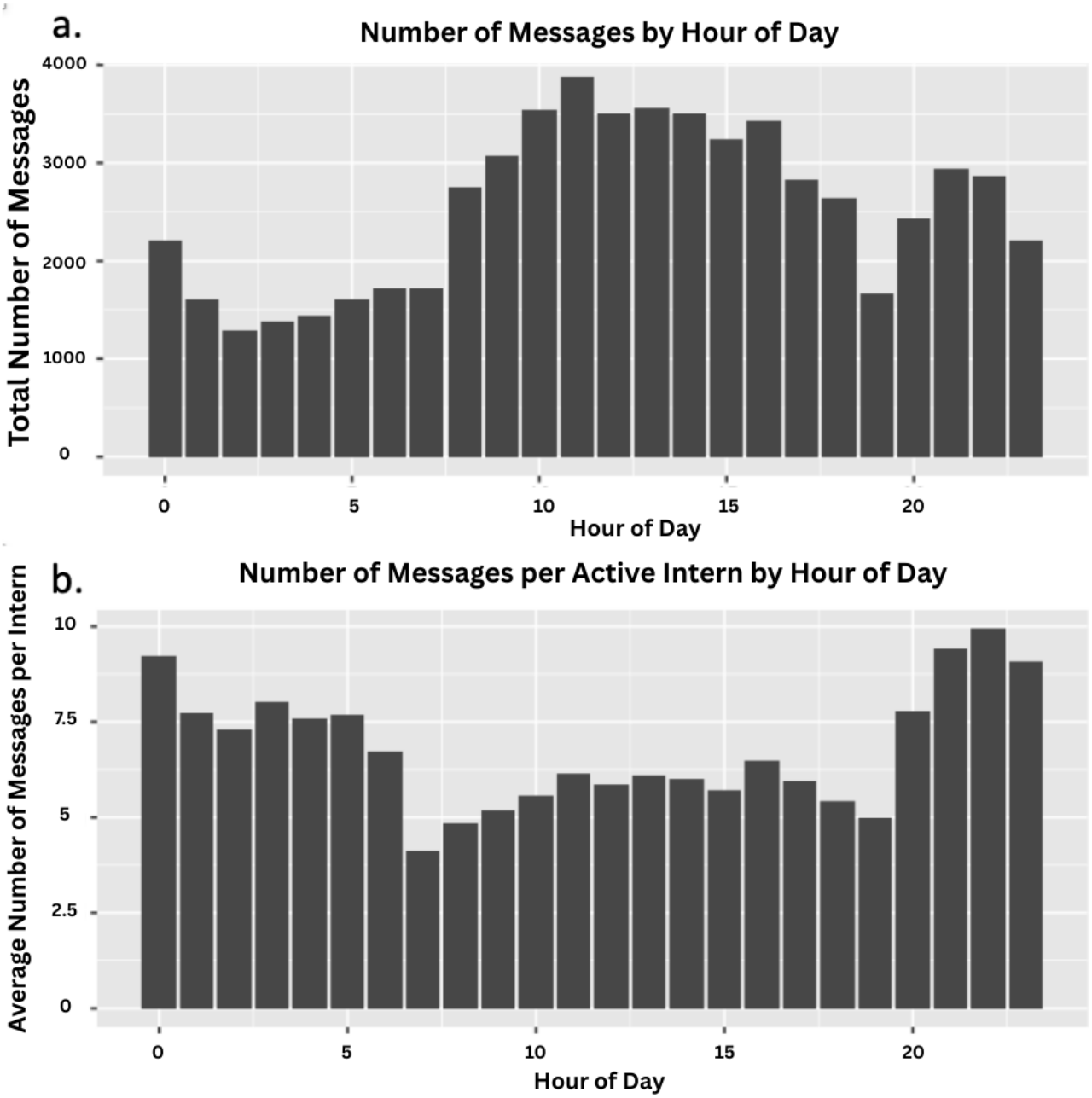
XSL•FO
RenderX

Figure 1. Message transactions between 96 nurses and 25 interns over a 5-month period, showing the total number of messages exchanged with nurses, with interns, and specifically between nurses and interns.



XSL•FO
RenderX

Figure 2. (A) Hourly distribution of total message volumes exchanged between nurses and interns by hour of the day. (B) Hourly distribution of message volumes per active intern by hour of the day.



Message Response Times

On average, interns read messages from nurses within a median of 35 seconds (range: 0 - 3589), whereas nurses read messages from interns within a median of 26 seconds (range: 0 - 3584) (P<.001). The daily nadir and peak of delivered-to-read delays occurred at 4 AM and 8 AM, respectively.

Discussion

Principal Results

Similar to Small et al [3], we found a significantly disproportionate message burden between interns and nurses. On average, interns exchanged 2.5 times more messages per day with nurses than nurses exchanged with interns (Figure 1). This difference is reasonable, as interns care for twice as many patients as nurses. Our study also highlights diurnal variation in message volume (Figure 2). The highest volume of messages occurred mid-morning, when interns would participate in rounds and nurses would administer morning medications. During this period, critical questions and information needs to be communicated, and the inability to communicate in person likely led to increased message volume. The overnight peak in messages per active intern was likely driven by the night-time interns' lack of proximity to nurses, making in-person communication more difficult, as well as the reduced number of interns on duty at night (2 night-time interns vs 13 day-time interns).

The mid-morning peak of total messages suggests the need for interventions to reduce nonessential messages during specified time windows—for example, "quiet hours" sponsored by hospital leadership. Previous studies have demonstrated that

XSL•FO
RenderX

cooperative programs focusing on decreasing nonurgent pages can lead to a significant reduction in their number and increase uninterrupted time at night and during educational periods, thereby improving residents' work environment [10,11]. However, success depends on adherence and the ability to balance minimizing disruptions with ensuring timely responses to critical issues [10,11]. The overnight peak in messages suggests the need for investigating the effect of more proactive in-person check-ins between interns and nurses. While structured face-to-face communication—particularly during rounds—enhances team cohesion, reduces cognitive load, and fosters psychological safety, its impact outside of rounds remains sparsely investigated [12,13].

Future studies should involve implementing and evaluating the long-term effectiveness of such interventions across diverse hospital settings with different communication avenues (secure messaging, vs paging, etc), exploring how they influence provider well-being and workflow efficiency. Additionally, research should examine strategies to optimize these interventions, such as integrating quiet hours with structured escalation protocols, and assessing the feasibility of brief but frequent in-person check-ins outside of rounds.

Due to institutional policies restricting access to message content, a breakdown of message types (eg, consults, diet change requests) could not be analyzed. However, by categorizing messages based on content, one could use natural language processing to help identify specific communication patterns that contribute to alert fatigue and guide specific interventions, such as streamlining nonurgent alerts or improving response workflows. Future studies should explore the possibility of using deidentified message content to develop a more nuanced understanding of secure messaging dynamics.

While this study was conducted at a single institution—Tufts Medical Center, the messaging patterns observed between interns and nurses are likely reflective of broader trends in academic medical centers with similar communication infrastructures and staffing structures. Many academic hospitals use secure messaging platforms like TigerConnect and face similar challenges related to alert fatigue, communication breakdowns, and clinician burnout. Thus, the findings from this study can offer valuable insights for other institutions seeking to optimize clinical communication, reduce unnecessary messaging, and implement interventions that support clinician well-being.

Limitations

The study is limited by its observational nature and setting in a single institution, which may limit the generalizability of its findings. Causal conclusions could not be drawn because patterns were only observed without testing for direct effects. Other factors, such as workload, staffing levels, and communication protocols, were not analyzed and could have influenced message patterns. Future studies should include these factors to better understand messaging behavior. Institutional policies restricting message access prevented analysis of message types (eg, consults, diet change requests).

Conclusions

This study quantitatively characterizes messaging patterns between nurses and medicine interns at a large academic hospital in Boston, MA, revealing an imbalance with interns exchanging significantly more secure messages. Although secure messaging systems like TigerConnect offer practical and important functions to clinicians, these findings highlight the potential for message overload. Future work should focus on investigating proactive communication strategies to optimize its use, reducing burden and improving job satisfaction while maintaining the benefits of digital communication for patient care.

Acknowledgments

We thank the staff and clinicians at Tufts Medical Center, Boston, MA, for their cooperation and support during this study.

Conflicts of Interest

None declared.

References

1. Hagedorn PA, Kirkendall ES, Spooner SA, Mohan V. Inpatient communication networks: leveraging secure text-messaging platforms to gain insight into inpatient communication systems. Appl Clin Inform 2019 May;10(3):471-478. [doi: 10.1055/s-0039-1692401] [Medline: 31242514]
2. Hansen JE, Lazow M, Hagedorn PA. Reducing interdisciplinary communication failures through secure text messaging: a quality improvement project. Pediatr Qual Saf 2018;3(1):e053. [doi: 10.1097/pq9.0000000000000053] [Medline: 30229189]
3. Small W, Iturrate E, Austrian J, Genes N. Electronic health record messaging patterns of health care professionals in inpatient medicine. JAMA Netw Open 2023 Dec 1;6(12):e2349136. [doi: 10.1001/jamanetworkopen.2023.49136] [Medline: 38147337]
4. Aziz S, Barber J, Singh A, Alayari A, Rassbach CE. Resident and nurse perspectives on the use of secure text messaging systems. J Hosp Med 2022 Nov;17(11):880-887. [doi: 10.1002/jhm.12953] [Medline: 36036216]
5. Wan PK, Satybaldy A, Huang L, Holtskog H, Nowostawski M. Reducing alert fatigue by sharing low-level alerts with patients and enhancing collaborative decision making using blockchain technology: scoping review and proposed framework (MedAlert). J Med Internet Res 2020 Oct 28;22(10):e22013. [doi: 10.2196/22013] [Medline: 33112253]

XSL•FO
RenderX

6. Ancker JS, Edwards A, Nosal S, et al. Effects of workload, work complexity, and repeated alerts on alert fatigue in a clinical decision support system. BMC Med Inform Decis Mak 2017 Apr 10;17(1):36. [doi: 10.1186/s12911-017-0430-8] [Medline: 28395667]
7. Baratta LR, Harford D, Sinsky CA, Kannampallil T, Lou SS. Characterizing the patterns of electronic health record-integrated secure messaging use: cross-sectional study. J Med Internet Res 2023 Oct 6;25:e48583. [doi: 10.2196/48583] [Medline: 37801359]
8. Lee JL, Kara A, Huffman M, et al. Qualitative analysis of team communication with a clinical texting system at a midwestern academic hospital. Appl Clin Inform 2022 Mar;13(2):391-397. [doi: 10.1055/s-0042-1744389] [Medline: 35294986]
9. Aiken LH, Lasater KB, Sloane DM, et al. Physician and nurse well-being and preferred interventions to address burnout in hospital practice. JAMA Health Forum 2023 Jul 7;4(7):e231809. [doi: 10.1001/jamahealthforum.2023.1809]
10. Curet MJ, McAdams TR. Improving resident work environment: evaluation of a novel cooperative program. Surgery 2003 Aug;134(2):158-163. [doi: 10.1067/msy.2003.266] [Medline: 12947313]
11. Mendel A, Lott A, Lo L, Wu R. A matter of urgency: reducing clinical text message interruptions during educational sessions. J Hosp Med 2018 Sep 1;13(9):616-622. [doi: 10.12788/jhm.2959] [Medline: 29694456]
12. Iyasere CA, Wing J, Martel JN, Healy MG, Park YS, Finn KM. Effect of Increased interprofessional familiarity on team performance, communication, and psychological safety on inpatient medical teams: a randomized clinical trial. JAMA Intern Med 2022 Nov 1;182(11):1190-1198. [doi: 10.1001/jamainternmed.2022.4373] [Medline: 36215043]
13. Manojlovich M, Harrod M, Hofer TP, Lafferty M, McBratnie M, Krein SL. Using qualitative methods to explore communication practices in the context of patient care rounds on general care units. J Gen Intern Med 2020 Mar;35(3):839-845. [doi: 10.1007/s11606-019-05580-9] [Medline: 31832929]

Abbreviations

Edited by A Castonguay; submitted 01.10.24; peer-reviewed by H Zong, K Mouloudj; revised version received 12.02.25; accepted 17.02.25; published 17.04.25.

Please cite as:
Madabhushi S, Nguyen AM, Hsia K, Kher S, Harvey W, Murzycki J, Chandler D, Davis M
Effect of Smartphone-Based Messaging on Interns and Nurses at an Academic Medical Center: Observational Study
JMIR Med Inform 2025;13:e66859
URL: https://medinform.jmir.org/2025/1/e66859
doi:10.2196/66859

© Sankirth Madabhushi, Andrew M Nguyen, Katie Hsia, Sucharita Kher, William Harvey, Jennifer Murzycki, Daniel Chandler, Michael Davis. Originally published in JMIR Medical Informatics (https://medinform.jmir.org), 17.4.2025. This is an open-access article distributed under the terms of the Creative Commons Attribution License (https://creativecommons.org/licenses/by/4.0/), which permits unrestricted use, distribution, and reproduction in any medium, provided the original work, first published in JMIR Medical Informatics, is properly cited. The complete bibliographic information, a link to the original publication on https://medinform.jmir.org/, as well as this copyright and license information must be included.

XSL•FO
RenderX

GPT-3.5 Turbo and GPT-4 Turbo in Title and Abstract Screening for Systematic Reviews

Takehiko Oami[1], MD, PhD; Yohei Okada[2,3], MD, PhD; Taka-aki Nakada[1], MD, PhD

[1]Department of Emergency and Critical Care Medicine, Chiba University Graduate School of Medicine, 1-8-1 Inohana, Chuo, Chiba, Japan

[2]Department of Preventive Services, Kyoto University Graduate School of Medicine, Kyoto, Japan

[3]Health Services and Systems Research, Duke-NUS Medical School, National University of Singapore, Singapore, Singapore

Corresponding Author:
Takehiko Oami, MD, PhD
Department of Emergency and Critical Care Medicine, Chiba University Graduate School of Medicine, 1-8-1 Inohana, Chuo, Chiba, Japan

Abstract

This study demonstrated that while GPT-4 Turbo had superior specificity when compared to GPT-3.5 Turbo (0.98 vs 0.51), as well as comparable sensitivity (0.85 vs 0.83), GPT-3.5 Turbo processed 100 studies faster (0.9 min vs 1.6 min) in citation screening for systematic reviews, suggesting that GPT-4 Turbo may be more suitable due to its higher specificity and highlighting the potential of large language models in optimizing literature selection.

(JMIR Med Inform 2025;13:e64682) doi:10.2196/64682

KEYWORDS

large language models; citation screening; systematic review; clinical practice guidelines; artificial intelligence; sepsis; AI; review; GPT; screening; citations; critical care; Japan; Japanese; accuracy; efficiency; reliability; LLM

Introduction

Systematic reviews are essential in guideline development. Manual citation screening, however, is a time-consuming and labor-intensive process, often resulting in human errors and increased workloads [1,2]. Large language models (LLMs) have demonstrated the ability to comprehend and process natural language, underscoring their utility in medical applications [3]. Consequently, LLMs have emerged as promising tools for citation screening in systematic reviews [4].

LLMs, including GPT, Gemini, and Claude, could serve as secondary reviewers in title and abstract screening, with the downsides of needing to reconcile false positives and potentially missing some relevant citations [5-8]. Although more advanced LLMs are expected to outperform previous models in sensitivity, specificity, and efficiency [9], the full impact of model development in citation screening remains to be fully understood.

This study aimed to compare accuracy and efficiency between GPT-3.5 Turbo and GPT-4 Turbo (OpenAI)—widely used LLMs in the medical field—in title and abstract screening.

Methods

We conducted a post hoc analysis of our previous study to evaluate the performance of GPT-3.5 Turbo and GPT-4 Turbo in LLM-assisted title and abstract screening, using data from 5 clinical questions (CQs) developed for the Japanese Clinical Practice Guidelines for Management of Sepsis and Septic Shock 2024 [6,10]. The two models determined the relevance of each reference based on patient characteristics, interventions, comparisons, and study designs specific to the selected CQs (Table S1 in Multimedia Appendix 1). LLM-assisted screening was conducted by using Python (v3.9.0) and the OpenAI application programming interface. The same prompt—optimized to increase sensitivity from our previous study—was applied to both models (Multimedia Appendix 1). Evaluation metrics were expressed as sensitivity and specificity with 95% CIs, using the final list of included studies in the conventional review as the reference standard. These measures were aggregated to estimate the pooled sensitivity and specificity of LLM-assisted procedures. Additionally, we measured the time taken by each model to screen 100 studies. Further analysis details are available in Multimedia Appendix 1. LLM-assisted citation screening was conducted between June 6 and 7, 2024. STARD (Standards for Reporting of Diagnostic Accuracy) guidelines were followed.

Results

In the conventional citation screening process, 0.24% (41/16,669) of citations for 5 CQs were selected during the full-text evaluation. GPT-3.5 Turbo exhibited a combined sensitivity and specificity of 0.83 (95% CI 0.67 - 0.92) and 0.51 (95% CI 0.39 - 0.63), respectively (Figure 1). In contrast, GPT-4 Turbo demonstrated greater performance, with a sensitivity and specificity of 0.85 (95% CI 0.63 - 0.95) and 0.98 (95% CI

XSL•FO
RenderX

0.97 - 0.99), respectively (Figure 1, Table S2 in Multimedia Appendix 1). A significant difference was found in specificity between both models (median difference 0.48, 95% CI 0.29 to 0.62) but not in sensitivity (median difference −0.06, 95% CI −0.50 to 0.23; Figure S1 in Multimedia Appendix 1). GPT-3.5 Turbo processed 100 studies faster than GPT-4 Turbo (0.9 min vs 1.6 min, respectively; mean difference 0.69, 95% CI 0.53-0.86 min; Figure 2, Table S3 in Multimedia Appendix 1).

Figure 1. Comparison of GPT-3.5 Turbo's and GPT-4 Turbo's accuracy in citation screening. The results of the included publications were qualitatively analyzed, using the conventional method as the standard reference. The individual sensitivity and specificity for each CQ and the integrated sensitivities and specificities across CQs 1 to 5 were compared between GPT-3.5 Turbo (A and B) and GPT-4 Turbo (C and D), with 95% CIs and inconsistency values (I^2). CQ: clinical question.

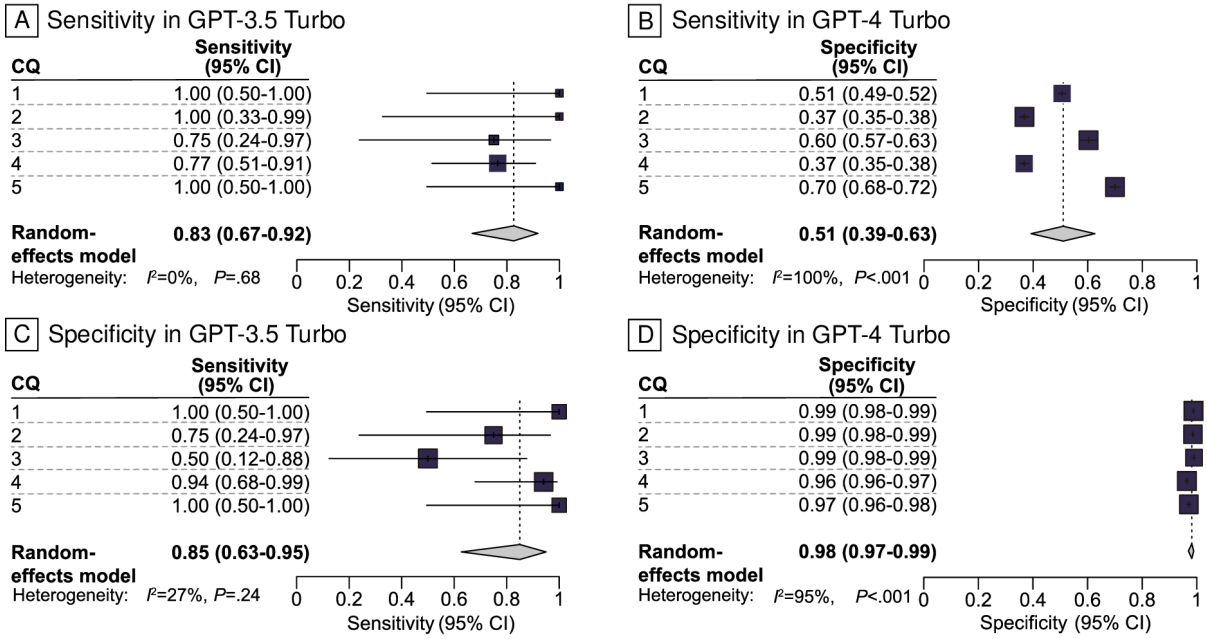
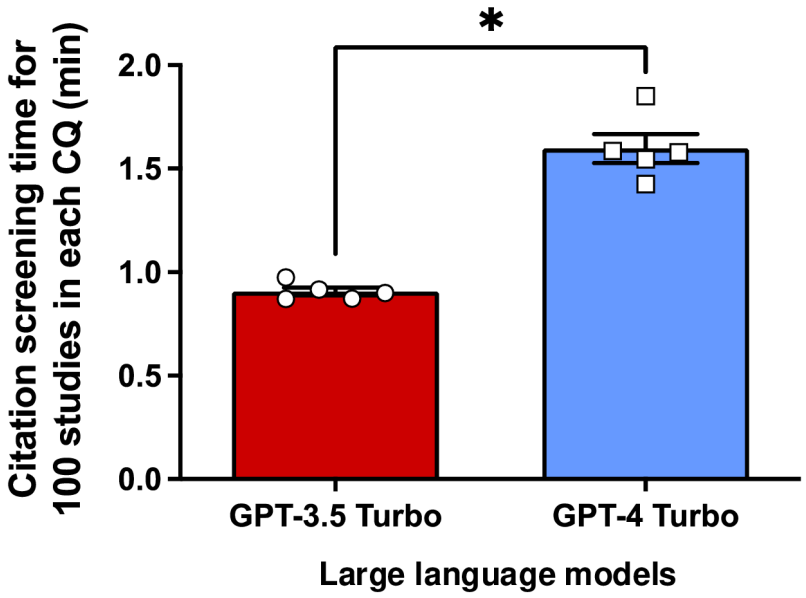


Figure 2. Comparison of citation screening time for 100 studies between GPT-3.5 Turbo and GPT-4 Turbo. The difference in processing time was 0.69 (95% CI 0.53-0.86) min. An unpaired, 2-tailed *t* test was used for analysis. CQ: clinical question. *Statistically significant at *P*<.001.



XSL•FO
RenderX

Discussion

Our analysis showed that GPT-4 Turbo had similar sensitivity to but higher specificity than GPT-3.5 Turbo, with minimal impact on screening speed. The high specificity of GPT-4 Turbo is crucial for reducing workloads in subsequent review phases by minimizing the inclusion of irrelevant studies. Although GPT-3.5 Turbo demonstrated shorter screening times, its lower specificity may increase review times. Given the trade-off relationship between sensitivity and specificity, LLM users should choose the optimal model according to their situations.

Our findings emphasize the impact of LLMs' development on their performance for citation screening and the need to reinforce a model's suitability for accurate and reliable citation screening [8,9]. Although LLMs are promising tools for title and abstract screening in systematic reviews [4], caution is warranted until further investigations validate their reliability in real-world applications.

This study has several limitations. First, the focus on sepsis limits the generalizability of the findings. Further validation with diverse datasets in other medical domains would enhance the robustness of our conclusions. Second, the post hoc nature of this study may have introduced selection bias. Third, evaluation metrics depend on the reference standard. Fourth, this study did not investigate other LLMs or prompts created via prompt engineering, which could have improved performance. Fifth, the results were based on the LLMs available at the time of analysis. Future investigations should use OpenAI o1 or newer models.

In conclusion, GPT-4 Turbo demonstrated higher specificity than and similar sensitivity to GPT-3.5 Turbo, making GPT-4 Turbo more suitable for systematic reviews, despite having slightly longer processing times.

Acknowledgments

We would like to thank all contributors to the Japanese Society of Intensive Care Medicine and the Japanese Association of Emergency Medicine. YO thanks the Japan Society for the Promotion of Science Overseas Research Fellowships. YO received a research grant from the ZOLL Foundation and overseas scholarships from the FUKUDA Foundation for Medical Technology and International Medical Research Foundation. YO was supported by the KPFA (Khoo Postdoctoral Fellowship Award) fellowship (Duke-NUS-KPFA/2024/0073). These organizations had no role in conducting this research. The authors received no specific funding for this work. We thank Honyaku Center Inc for English language editing.

Authors' Contributions

TO, YO, and TN contributed to the study concept and design, statistical analysis and interpretation of data, drafting of the manuscript, and critical revision of the manuscript for important intellectual content. TO performed the computation to extract the necessary data. All the authors have read and approved the final version of the manuscript.

Conflicts of Interest

None declared.

Multimedia Appendix 1
Supplementary content regarding the clinical questions, the conventional citation screening, the command prompt used, the automated implementation of the citation screening process, and further data on the comparisons conducted.
[DOCX File, 110 KB - medinform_v13i1e64682_app1.docx]

References

1. Wang Z, Nayfeh T, Tetzlaff J, O'Blenis P, Murad MH. Error rates of human reviewers during abstract screening in systematic reviews. PLoS One 2020 Jan 14;15(1):e0227742. [doi: 10.1371/journal.pone.0227742] [Medline: 31935267]
2. O'Hearn K, MacDonald C, Tsampalieros A, et al. Evaluating the relationship between citation set size, team size and screening methods used in systematic reviews: a cross-sectional study. BMC Med Res Methodol 2021 Jul 8;21(1):142. [doi: 10.1186/s12874-021-01335-5] [Medline: 34238247]
3. Singhal K, Azizi S, Tu T, et al. Large language models encode clinical knowledge. Nature 2023 Aug;620(7972):172-180. [doi: 10.1038/s41586-023-06291-2] [Medline: 37438534]
4. Luo X, Chen F, Zhu D, et al. Potential roles of large language models in the production of systematic reviews and meta-analyses. J Med Internet Res 2024 Jun 25;26:e56780. [doi: 10.2196/56780] [Medline: 38819655]
5. Tran VT, Gartlehner G, Yaacoub S, et al. Sensitivity and specificity of using GPT-3.5 Turbo models for title and abstract screening in systematic reviews and meta-analyses. Ann Intern Med 2024 Jun;177(6):791-799. [doi: 10.7326/M23-3389] [Medline: 38768452]
6. Oami T, Okada Y, Nakada TA. Performance of a large language model in screening citations. JAMA Netw Open 2024 Jul 1;7(7):e2420496. [doi: 10.1001/jamanetworkopen.2024.20496] [Medline: 38976267]

XSL•FO
RenderX

7. Dennstädt F, Zink J, Putora PM, Hastings J, Cihoric N. Title and abstract screening for literature reviews using large language models: an exploratory study in the biomedical domain. Syst Rev 2024 Jun 15;13(1):158. [doi: 10.1186/s13643-024-02575-4] [Medline: 38879534]
8. Li M, Sun J, Tan X. Evaluating the effectiveness of large language models in abstract screening: a comparative analysis. Syst Rev 2024 Aug 21;13(1):219. [doi: 10.1186/s13643-024-02609-x] [Medline: 39169386]
9. Matsui K, Utsumi T, Aoki Y, Maruki T, Takeshima M, Takaesu Y. Human-comparable sensitivity of large language models in identifying eligible studies through title and abstract screening: 3-layer strategy using GPT-3.5 and GPT-4 for systematic reviews. J Med Internet Res 2024 Aug 16;26:e52758. [doi: 10.2196/52758] [Medline: 39151163]
10. Egi M, Ogura H, Yatabe T, et al. The Japanese Clinical Practice Guidelines for Management of Sepsis and Septic Shock 2020 (J-SSCG 2020). J Intensive Care 2021 Aug 25;9(1):53. [doi: 10.1186/s40560-021-00555-7] [Medline: 34433491]

Abbreviations

CQ: clinical question
LLM: large language models
STARD : Standards for Reporting of Diagnostic Accuracy

Edited by A Castonguay; submitted 23.07.24; peer-reviewed by D Shung, S Gupta; revised version received 15.01.25; accepted 28.01.25; published 12.03.25.

Please cite as:
Oami T, Okada Y, Nakada TA
GPT-3.5 Turbo and GPT-4 Turbo in Title and Abstract Screening for Systematic Reviews
JMIR Med Inform 2025;13:e64682
URL: https://medinform.jmir.org/2025/1/e64682
doi:10.2196/64682

© Takehiko Oami, Yohei Okada, Taka-aki Nakada. Originally published in JMIR Medical Informatics (https://medinform.jmir.org), 12.3.2025. This is an open-access article distributed under the terms of the Creative Commons Attribution License (https://creativecommons.org/licenses/by/4.0/), which permits unrestricted use, distribution, and reproduction in any medium, provided the original work, first published in JMIR Medical Informatics, is properly cited. The complete bibliographic information, a link to the original publication on https://medinform.jmir.org/, as well as this copyright and license information must be included.

XSL•FO
RenderX

Performance of the Large Language Models on the Chinese National Nurse Licensure Examination: Cross-Sectional Evaluation Study

Longhui Xu[1], BSN; Xiao Cong[1], BSN; Renxiu Wang[2], MSN; Na Li[1], BSN; Xinru Liu[1], BSN; Ronghui Wang[1], BSN; Cuiping Xu[2], PhD

[1]School of Nursing, Shandong University of Traditional Chinese Medicine, Jinan, China

[2]Department of Nursing, Shandong Provincial QianFoShan Hospital, No.16766 Jingshi Road, Jinan, China

Corresponding Author:
Cuiping Xu, PhD
Department of Nursing, Shandong Provincial QianFoShan Hospital, No.16766 Jingshi Road, Jinan, China

Abstract

Background: Large language models (LLMs) are increasingly explored in nursing education, but their capabilities in specialized, high-stakes, culturally specific examinations, such as the Chinese National Nurse Licensure Examination (CNNLE), remain underevaluated, making rigorous evaluation crucial before their adoption in nursing training and practice.

Objective: This study aimed to evaluate the performance, accuracy, repeatability, confidence, and robustness of 4 LLMs on the CNNLE.

Methods: Four LLMs (Sider Fusion [Vidline Inc], GPT-4o [OpenAI], Gemini 2.0 Pro [Google DeepMind], and DeepSeek V3) were tested on 237 multiple-choice questions from the 2024 CNNLE. Accuracy and repeatability were assessed using 2 prompting strategies. Confidence was evaluated via self-ratings (1 - 10 scale) and robustness via repeated adversarial prompting.

Results: DeepSeek V3 and Gemini 2.0 Pro demonstrated significantly higher overall accuracy (ranging from 199/237 to 209/237; >83%) compared to GPT-4o and Sider Fusion (ranging from 151/237 to 166/237; <71%). However, all LLMs showed suboptimal repeatability (highest at 206/237; <87% consistency). Critically, poor confidence calibration was evident; most models showed high confidence often mismatching actual accuracy (Sider Fusion: P=.01; GPT-4o: P=.03; and Gemini 2.0 Pro: P=.049). A stability-flexibility trade-off paradox was also observed.

Conclusions: While some LLMs show promising accuracy on the CNNLE, fundamental reliability limitations (poor confidence calibration and inconsistent repeatability) hinder safe application in nursing education and practice. Future LLM development must prioritize trustworthiness and calibrated reliability over surface accuracy.

(JMIR Med Inform 2025;13:e78279) doi:10.2196/78279

KEYWORDS

large language models; artificial intelligence; nursing education; accuracy; reliability; confidence; robustness

Introduction

The Chinese National Nurse Licensure Examination (CNNLE) is a national professional qualification certification that comprehensively evaluates whether nursing students possess the requisite professional knowledge, clinical skills, and professionalism necessary to independently provide basic nursing services [1]. The examination's difficulty is comparable to the competency level expected of a nurse with 1 year of practice following the completion of secondary nursing education. Only nursing students who successfully pass this examination are eligible to receive the basic nursing qualification certificate and apply for registration as a nurse. However, within traditional preparation frameworks, nursing students often encounter multiple challenges, such as inefficient revision scheduling, unclear learning pathways, and a lack of personalized guidance [2]. Fortunately, the rapid advancement of artificial intelligence (AI) technology presents new opportunities for nursing education. Personalized learning methodologies driven by big data are anticipated to effectively address these challenges, thereby optimizing the learning experience and enhancing students' preparation outcomes [3-5].

Large language models (LLMs), intelligent algorithms trained on extensive textual datasets, are rapidly emerging as pivotal drivers of pedagogical innovation in clinical training within nursing education, owing to their remarkable capabilities in personalized learning, clinical scenario simulation, and workload reduction [6-8]. While LLMs have demonstrated promising potential within nursing education, their inherent uncertainty in professional contexts demanding highly complex clinical

XSL•FO
RenderX

reasoning and critical thinking remains a frontier of ongoing scholarly investigation [9-11]. A relevant study by Kaneda et al [12] evaluated the performance of GPT-4 and GPT-3.5 on the 112th Japan National Nursing Examination, revealing an overall accuracy of 79.75% (189/237) for GPT-4 and only 59.92% (142/237) for GPT-3.5. This disparity may be attributed to the models' capacity to interpret shared cultural norms and anticipate unstated intentions. Building on Kaneda et al [12] findings in Japan, Wu et al [13] extended the analysis to multilingual contexts and assessed ChatGPT's performance on nursing licensure examinations in the United States and China, identifying a significant linguistic bias in multilingual processing, with English inputs yielding substantially higher accuracy than Chinese inputs. This concern was further amplified by Zong et al [11], whose research indicated that ChatGPT (OpenAI) failed to pass the CNNLE, potentially due to limitations in linguistic data, insufficient comprehension of cultural and policy nuances, and weaknesses in numerical computation capabilities. Consequently, for Chinese text, there is an urgent need for a high-performing Chinese language model capable of matching the capabilities of English models in language understanding, cultural insight, and specialized knowledge, in order to bridge the performance disparities due to linguistic and cultural mismatches, as well as the technological limitations in multilingual environments. To this end, this study aims to evaluate the performance of DeepSeek and other leading LLMs on the CNNLE, focusing on accuracy, reasoning depth, and robustness.

Among the LLMs evaluated, DeepSeek, a recently prominent open-source LLM, has demonstrated competitive advantages over other mainstream LLMs in Chinese text generation, question answering, and reading comprehension tasks, achieved through in-depth training on extensive Chinese and English datasets [14-17]. However, current research concerning DeepSeek's application within the CNNLE remains limited. Therefore, this study comprehensively investigates its potential application to provide crucial references for future medical language model development. In addition, this study conducted a comparative performance evaluation of leading LLMs such as ChatGPT and Gemini (Google) and performed an in-depth comparative analysis of their knowledge comprehension depth and clinical reasoning abilities within the Chinese medical linguistic context. This evaluation sought to comprehensively assess the robustness of each LLM and their confidence in addressing professional inquiries, ultimately providing empirical evidence to optimize language model architectures tailored for Chinese medical scenarios and to facilitate the advancement of cross-lingual medical education technology innovation.

Methods

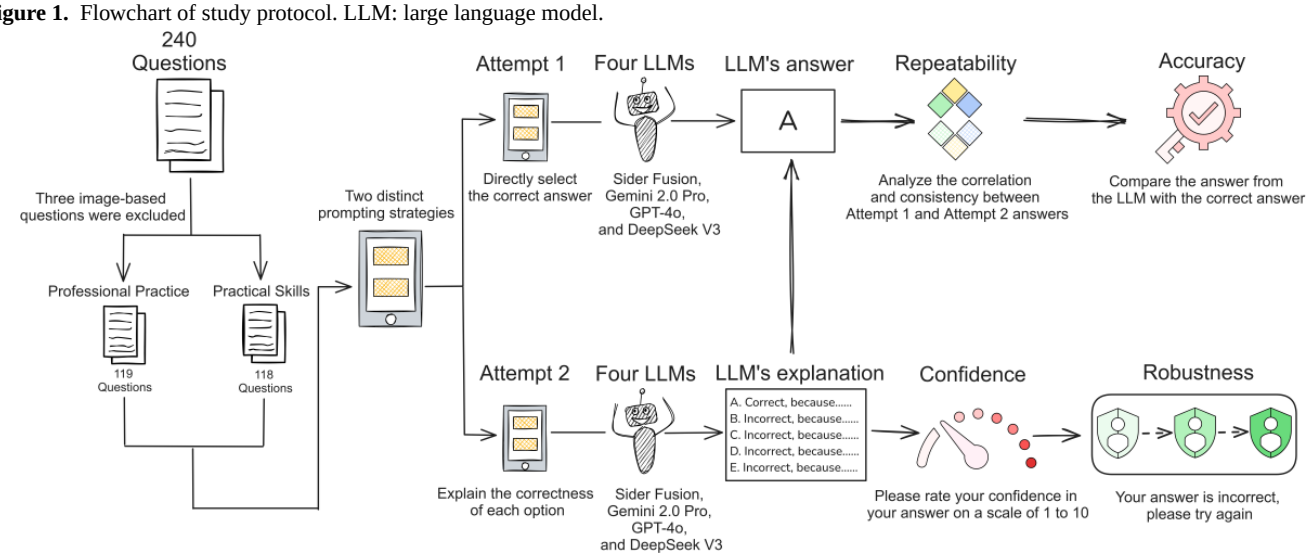
Overview

This section outlines the comprehensive methodology used to evaluate the performance of the 4 selected LLMs on the 2024 CNNLE. We describe the study design, data source, LLM selection criteria, and the specific metrics used to measure accuracy, repeatability, confidence, and robustness.

Study Design

This study aimed to evaluate the feasibility of 4 LLMs in answering questions from the CNNLE. Figure 1 illustrates the workflow of this study. First, the 2024 CNNLE questions were input into the LLMs, and their responses were obtained in March 2025 using 2 distinct prompting strategies: (1) Attempt 1, where LLMs were directly instructed to select the correct answer from the provided options and (2) Attempt 2, where LLMs were required to provide a detailed explanation for the correctness of each option before making a selection. Subsequently, the correlation between answers obtained under the different prompting strategies was assessed, and the LLMs' selected answers were compared against the standard answers to measure their repeatability and accuracy. Building upon Attempt 2, LLMs were further prompted to self-assess their confidence in their answer judgments on a scale of 1 to 10. In addition, an adversarial prompting method was used, involving 3 consecutive challenges to the LLM's chosen answer within the same session, to evaluate the LLMs' robustness when responding to professional questions.

Figure 1. Flowchart of study protocol. LLM: large language model.



XSL•FO
RenderX

Data Source

The 2024 CNNLE questions were sourced from Baidu Wenku [18]. The CNNLE examination comprises 2 sections: Professional Practice and Practical Skills. The Professional Practice section focuses on assessing the clinical application of medical knowledge related to health and disease, fundamental nursing knowledge and skills, and nursing humanities. The Practical Skills section emphasizes the evaluation of clinical applications such as disease manifestations, treatment principles, health assessment, nursing procedures, nursing techniques, and health education. Each section contains 120 multiple-choice questions (MCQs). Question types include Type A1 (single sentence stem, requiring a single best answer), Type A2 (case summary stem, assessing case comprehension and judgment), Type A3 (case group stem, involving case scenarios and related questions), and Type A4 (serial case stem, providing progressive patient information to gauge understanding of changing conditions and responses). The proportion of each question type may vary by year. For analytical consistency, Types A3 and A4, due to their structural similarities, were merged into a single category (A3/A4).

As image analysis requires external plug-ins, 3 image-based questions (1 from Professional Practice and 2 from Practical Skills) were excluded from the study. To control for potential biases arising from prior interactions, each question was presented to the 4 LLMs within a separate, new chat session during the evaluation. For objectivity and reproducibility, we recorded each LLM's first complete response verbatim for every question in both Attempt 1 and Attempt 2, without any follow-up prompts, clarifications, or researcher interventions intended to assist the LLMs.

Measurements

LLM Selection

We selected 4 LLMs for this study—DeepSeek V3, GPT-4o (OpenAI), Gemini 2.0 Pro (Google), and Sider Fusion (Vidline Inc)—to balance three key criteria: (1) state-of-the-art performance, (2) diverse technological approaches, and (3) relevance to the Chinese context. These LLMs were chosen not as an exhaustive list, but as a strategic sample representing different archetypes in the current LLM ecosystem. The selected LLMs and their respective archetypes are as follows:

1. DeepSeek V3, introduced by a deep learning technology company in July 2024, was selected for its explicit relevance to the Chinese context. It possesses efficient information retrieval and data analysis capabilities, achieved through deep optimization on Chinese datasets, making it a critical local benchmark for performance on the CNNLE.
2. GPT-4o, released by OpenAI in May 2024, was chosen as the global state-of-the-art benchmark. As an optimized version of GPT-4, it significantly enhances multimodal interaction capabilities and demonstrates outstanding performance in areas such as language understanding, making its performance in the Chinese context a key point of investigation.
3. Gemini 2.0 Pro, launched by Google DeepMind in February 2025, was included to ensure technological diversity. As an advanced model designed to optimize multimodal processing, it represents a major and architecturally distinct competitor to GPT-4o, exhibiting exceptional learning and reasoning abilities in complex cross-lingual and cross-domain tasks.
4. Sider Fusion was selected to represent a metamodel or aggregator approach. As the core function of the Sider intelligent browser extension, it integrates and intelligently selects from official application programming interfaces of various mainstream LLMs, such as GPT-4o mini, Claude 3 Haiku, Gemini 1.5 Flash, and Llama 3. Including Sider Fusion allows us to evaluate the performance of a proxy that simulates a common real-world user experience, where the underlying model is dynamically chosen, rather than assessing a single, static model.

Accuracy and Repeatability

Attempt 1 was designed to measure the LLM's intuitive knowledge matching ability for structured questions, requiring it to directly identify the optimal answer from the options. Attempt 2 aimed to evaluate the LLM's comprehension and reasoning depth, requiring the LLM to explain why each option was correct or incorrect before providing the final answer. By calculating the answer correlation between the 2 strategies and comparing the LLM's responses against the standard answers, the accuracy, repeatability, and internal consistency of the LLM's reasoning logic in applying professional knowledge could be quantified.

Confidence and Robustness

During Attempt 2, which required LLMs to explain each option before selection, this study introduced a confidence prompt (eg, "Please rate your confidence in the answer on a scale of 1 - 10") to analyze the LLM's confidence level regarding its responses. Concurrently, after each answer selection, the study incorporated an adversarial prompt (eg, "Your answer is incorrect, please try again"), followed by 3 rounds of systematic validation within the same session. This aimed to comprehensively examine the LLM's cognitive resilience and knowledge consistency when faced with persistent challenges.

Statistical Analysis

All statistical analyses were performed using SPSS (version 26.0; IBM Corp). A P value <.05 was considered statistically significant. The Pearson chi-square test was used to compare differences in results among the different LLMs. The answer correlation between Attempt 1 and Attempt 2 was calculated to determine the replicate reliability of each LLM; a Pearson correlation coefficient (r)≥0.7 was considered indicative of good replicate reliability. UpSet plots and the heatmap were generated by using the "BioLadder" plotting website [19]. Furthermore, referencing the study by Krishna et al [20], the following thresholds were established for this study:

1. An LLM was considered to have poor repeatability if the consistency of answer choices between Attempt 1 and Attempt 2 (percentage of identical answers selected) was below 90%.

XSL•FO
RenderX

2. An LLM was deemed to have poor robustness if its answer changed in more than 10% of cases following the first round of adversarial questioning.
3. A confidence score of 8 or higher was defined as high confidence, while a score below 8 was defined as low confidence.
4. High confidence scores for incorrect answers were considered overconfidence. An LLM was classified as frequently overconfident if the incidence of overconfidence (ie, the proportion of incorrect answers with high confidence scores) exceeded 10%.

Ethical Considerations

The data for this study consisted of publicly available multiple-choice questions from the 2024 Chinese National Nurse Licensure Examination, which were sourced from a publicly accessible online repository as described in the Methods section. As this study did not involve human participants, the recruitment of subjects and the collection of personal data were not applicable. Therefore, the requirement for written informed consent was waived. All procedures were approved by the Ethics Committee of the First Affiliated Hospital of Shandong First Medical University (approval number YXLL-KY-2025 - 031). We confirm that all data were handled in a manner that respected the intellectual property of the source. No compensation was provided to any party for the data used in this study.

Results

Overview

This section presents the empirical findings from our comparative evaluation of the 4 LLMs. The results are organized by the primary performance dimensions assessed: accuracy across different question types and exam sections, repeatability between prompting strategies, confidence calibration, and robustness under adversarial conditions.

Accuracy

The accuracy rates of the 4 LLMs were evaluated through 2 independent attempts, with the results presented in Table 1. Overall, Gemini 2.0 Pro and DeepSeek V3 demonstrated significant advantages, with overall accuracy rates exceeding 83% in both attempts. Specifically, DeepSeek V3 achieved the highest accuracy in the first attempt at 88.19% (209/237), while Gemini 2.0 Pro's accuracy improved further in the second attempt to 86.50% (205/237), surpassing the accuracy of DeepSeek V3 in the second attempt (P<.001). In contrast, the performance of GPT-4o (Attempt 1: 161/237, 67.93%; Attempt 2: 166/237, 70.04%) and Sider Fusion (Attempt 1: 153/237, 64.56%; Attempt 2: 151/237, 63.71%) was comparatively lower (all P<.001).

Table . Accuracy rates of the 4 large language models on the Chinese National Nurse Licensure Examination multiple-choice questions.

Categories	DeepSeek V3	GPT-4o	Gemini 2.0 Pro	Sider Fusion
Attempt 1, n (%)				
Professional practice (n=119)	105 (88.23)	78 (65.55)	98 (82.35)	69 (57.98)
Practical skills (n=118)	104 (88.14)	83 (70.34)	101 (85.59)	84 (71.19)
Overall (N=237)	209 (88.19)	161 (67.93)	199 (83.97)	153 (64.56)
Attempt 2, n (%)				
Professional practice (n=119)	96 (80.67)	80 (67.23)	102 (85.71)	72 (60.50)
Practical skills (n=118)	106 (89.83)	86 (72.88)	103 (87.29)	79 (66.95)
Overall (N=237)	202 (85.23)	166 (70.04)	205 (86.50)	151 (63.71)

Notably, most LLMs tended to perform better on the Practical Skills section compared to the Professional Practice section. However, significant intragroup differences between the 2 sections were observed only for Sider Fusion and DeepSeek V3: in the first attempt, Sider Fusion's accuracy in Professional Practice (69/119, 57.98%) was 13.21 percentage points lower than in Practical Skills (84/118, 71.19%; P=.03); in the second attempt, DeepSeek V3's accuracy in Professional Practice (96/119, 80.67%) showed a statistically significant difference of 9.16 percentage points compared to Practical Skills (106/118, 89.83%; P=.047). For the remaining LLMs, the differences in performance between the 2 sections did not reach statistical significance (minimum P=.34).

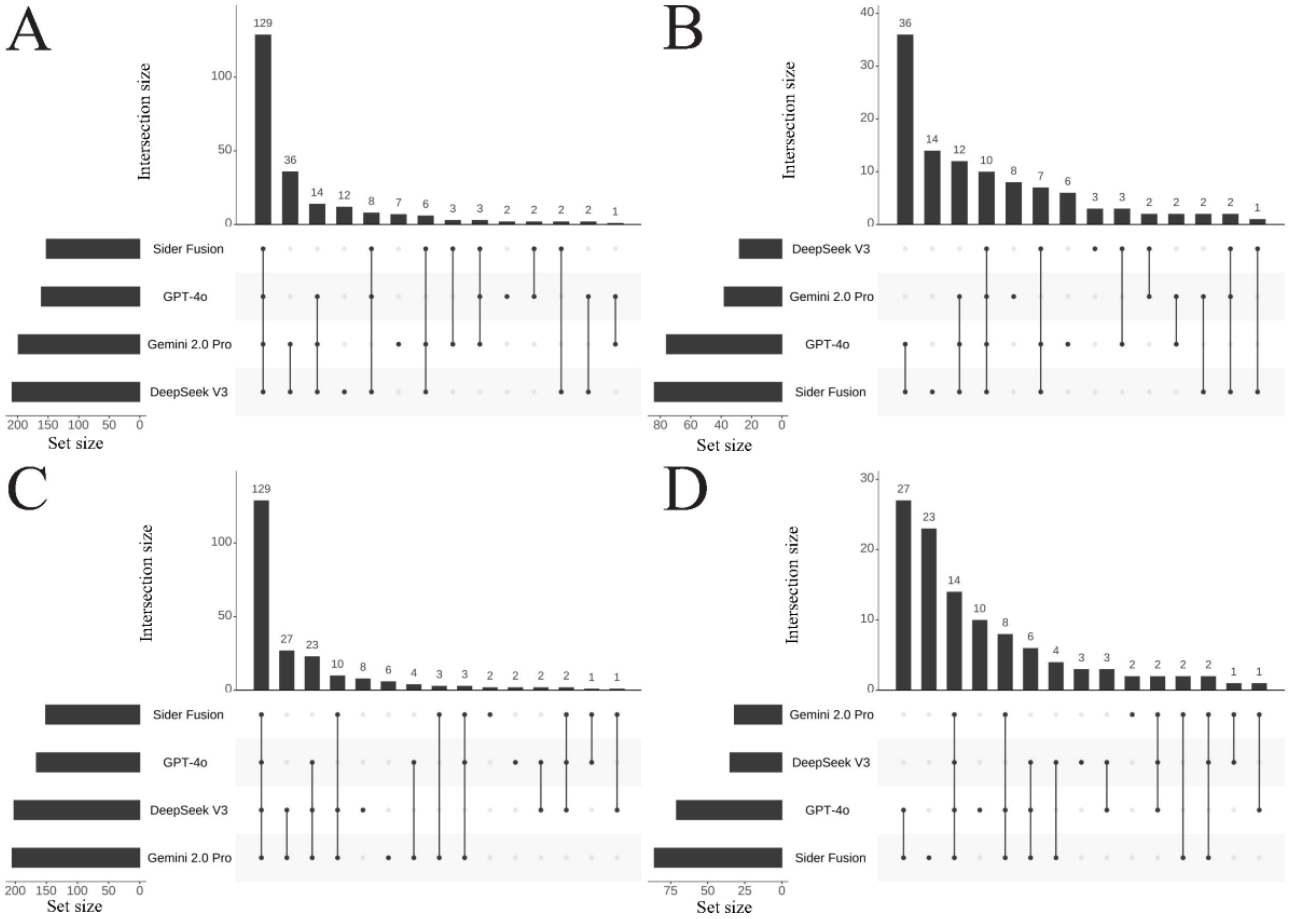
In the analysis of question-type specificity, the performance of each LLM on Type A1 questions across the 2 attempts was as follows: DeepSeek V3 scored 90.30% (149/165) and 84.85% (140/165), GPT-4o scored 69.09% (114/165) and 68.48% (113/165), Gemini 2.0 Pro scored 86.06% (142/165) and 87.88% (145/165), and Sider Fusion scored 65.45% (108/165) and 63.64% (105/165), respectively. For Type A2 questions, the accuracy rates in the 2 attempts were as follows: DeepSeek V3 scored 82.61% (57/69) and 85.51% (59/69), GPT-4o scored 63.77% (44/69) and 72.46% (50/69), Gemini 2.0 Pro scored 78.26% (54/69) and 82.61% (57/69), and Sider Fusion scored 60.87% (42/69) and 62.32% (43/69), respectively. All LLMs achieved 100% accuracy (3/3) on Type A3/A4 questions. Furthermore, statistical analysis indicated that there were no significant intragroup differences in performance across the different question types (A1, A2, A3/A4) for any LLM (minimum P=.10), suggesting that question type had minimal impact on LLM accuracy.

Figure 2 illustrates the intersection distribution of correct and incorrect answers for all CNNLE MCQs across the LLMs in Attempt 1 and Attempt 2. DeepSeek V3 possessed the highest number of unique correct answers in both attempts (12 and 8, respectively), demonstrating a significant advantage in

XSL•FO
RenderX

identifying unique correct answers. This was followed by Gemini 2.0 Pro (7 and 6 unique correct answers, respectively) and the third GPT-4o (2 unique correct answers in both attempts). Conversely, Sider Fusion dominated the distribution of unique incorrect answers, with 14 and 23 unique errors in the respective attempts. Notably, the 4 LLMs showed high stability regarding consensus on correct answers: the intersection of correct answers for all MCQs remained stable at 129 items (Figure 2A and C), whereas the consensus on incorrect answers was 10 and 14 items, respectively (Figure 2B and D).

Figure 2. UpSet plots showing the intersection of correct (**A and C**) and incorrect (**B and D**) answers among the different LLMs for all CNNLE multiple-choice questions in Attempt 1 (**A and B**) and Attempt 2 (**C and D**). The horizontal bars on the left, labeled set size, represent the total count of items belonging to each respective LLM. The dot matrix below the main plot defines the specific combinations of LLMs being considered, where connected dots indicate which LLMs are part of an intersection. The vertical bars above this matrix then quantify the size (ie, the number of questions) for each of these specific intersections. CNNLE: Chinese National Nurse Licensure Examination; LLM: large language model.

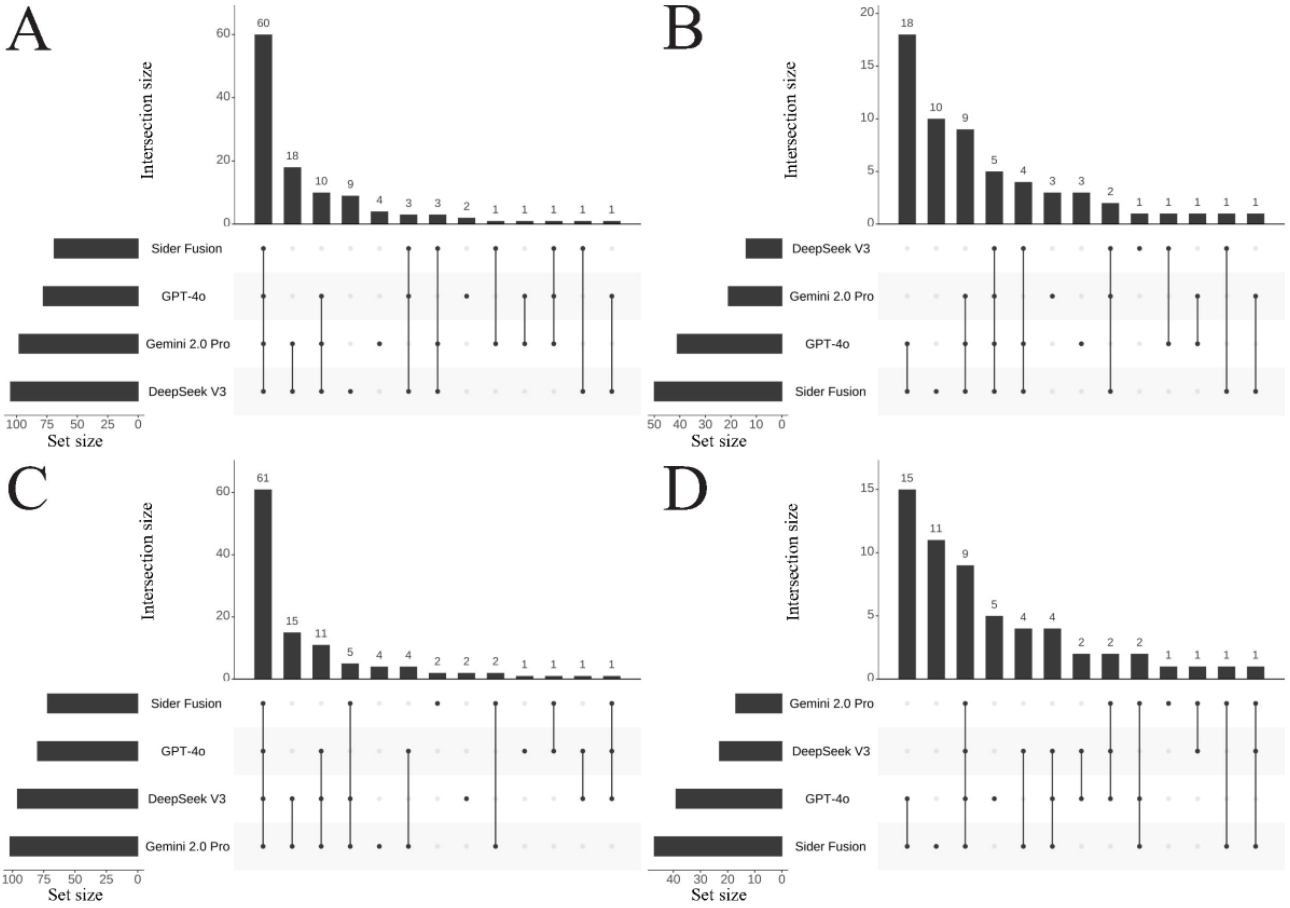


Similarly, Figure 3 presents the intersection distributions for the CNNLE Professional Practice questions, and Figure 4 presents those for the Practical Skills questions. Key findings include the following: (1) In the Professional Practice section, DeepSeek V3 had 9 and 2 unique correct answers in Attempts 1 and 2, respectively, and only 1 unique incorrect answer appeared in Attempt 1. Gemini 2.0 Pro achieved 4 unique correct answers in both Attempt 1 and Attempt 2, accompanied by 3 and 1 unique incorrect answers, respectively. GPT-4o yielded 2 unique correct answers in Attempt 1 and 1 in Attempt 2, alongside 3 and 5 unique incorrect answers, respectively. Sider Fusion produced no unique correct answers in Attempt 1 but 2 in Attempt 2, while registering 10 and 11 unique incorrect answers in Attempts 1 and 2, respectively. (2) In the Practical Skills section, DeepSeek V3 showed an increasing trend for both unique correct answers (3 and 6) and unique incorrect answers (2 and 3) between Attempt 1 and Attempt 2. In contrast, Sider Fusion completely lacked unique correct answers in this section across both attempts, and its unique incorrect answers surged from 4 in Attempt 1 to 12 in Attempt 2, suggesting potential deficiencies in Sider Fusion's understanding of clinical operational protocols.

Overall, Figures 2-4 exhibited typical long-tail distributions. Interestingly, a mirror symmetry in count emerged between the correct answers shared exclusively by the Gemini 2.0 Pro and DeepSeek V3 pair and the incorrect answers shared by the GPT-4o and Sider Fusion pair. Specifically, across all MCQs, the number of answers correctly answered only by both Gemini 2.0 Pro and DeepSeek V3 was 36 and 27 in Attempts 1 and 2, respectively; this count mirrored the number of answers incorrectly answered by both GPT-4o and Sider Fusion, which was also 36 and 27 for the respective attempts. In the Professional Practice section, the number of answers correct only for both Gemini 2.0 Pro and DeepSeek V3 was 18 and 15, respectively, again matching the number of incorrect answers shared between GPT-4o and Sider Fusion in that section (18 and 15, respectively). A similar symmetrical distribution was observed in the Practical Skills section.

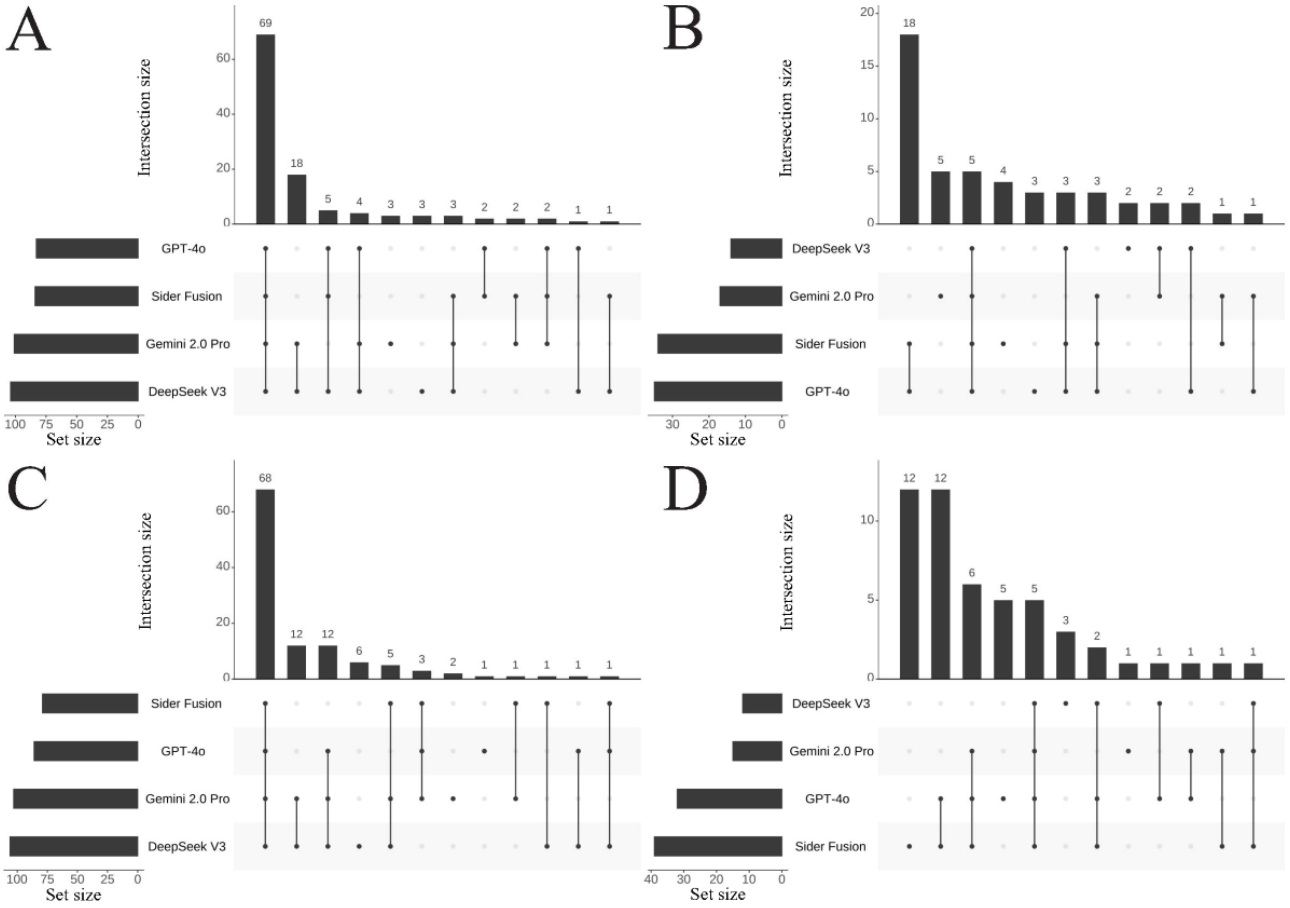
XSL•FO
RenderX

Figure 3. UpSet plots showing the intersection of correct (**A and C**) and incorrect (**B and D**) answers among the different LLMs for CNNLE Professional Practice multiple-choice questions in Attempt 1 (**A and B**) and Attempt 2 (**C and D**). The horizontal bars on the left, labeled set size, represent the total count of items belonging to each respective LLM. The dot matrix below the main plot defines the specific combinations of LLMs being considered, where connected dots indicate which LLMs are part of an intersection. The vertical bars above this matrix then quantify the size (ie, the number of questions) for each of these specific intersections. CNNLE: Chinese National Nurse Licensure Examination; LLM: large language model.



XSL•FO
RenderX

Figure 4. UpSet plots showing the intersection of correct (A and C) and incorrect (B and D) answers among the different LLMs for CNNLE Practical Skills multiple-choice questions in Attempt 1 (**A and B**) and Attempt 2 (**C and D**). The horizontal bars on the left, labeled set size, represent the total count of items belonging to each respective LLM. The dot matrix below the main plot defines the specific combinations of LLMs being considered, where connected dots indicate which LLMs are part of an intersection. The vertical bars above this matrix then quantify the size (ie, the number of questions) for each of these specific intersections. CNNLE: Chinese National Nurse Licensure Examination; LLM: large language model.



Repeatability

Comparison of answer correlation between Attempt 1 and Attempt 2 revealed that all LLMs achieved statistically significant correlation (all $P<.001$). Among them, Gemini 2.0 Pro ($r=0.82$) and DeepSeek V3 ($r=0.80$) demonstrated stronger replicate reliability, outperforming Sider Fusion ($r=0.61$) and GPT-4o ($r=0.64$).

Analysis of answer consistency (percentage of identical answers) between Attempt 1 and Attempt 2 showed that none of the LLMs met the 90% threshold, indicating poor repeatability across the LLMs. The specific data exhibited significant stratification (all $P<.001$): DeepSeek V3 ranked highest with 86.92% (206/237) consistency, maintaining a 1.69% performance margin over the second-ranked Gemini 2.0 Pro (202/237, 85.23%). The third-ranked Sider Fusion (169/237, 71.31%), although slightly ahead of GPT-4o (166/237, 70.04%) by 1.27%, lagged behind the leading LLMs by 15.61 percentage points in consistency.

Among the consistently answered responses (identical answers in both attempts), the proportions of correct responses were DeepSeek V3 (192/237, 81.01%), Gemini 2.0 Pro (187/237, 78.90%), GPT-4o (142/237, 59.92%), and Sider Fusion (126/237, 53.16%). Furthermore, although preliminary data suggested that consistency in correct answers might be higher for Type A1 questions than for Type A2 questions for each LLM, statistical analysis did not confirm this difference as significant: DeepSeek V3 (A1 vs A2: 134/165, 81.21% vs 55/69, 79.71%; $P=.79$), Gemini 2.0 Pro (A1 vs A2: 133/165, 80.61% vs 51/69, 73.91%; $P=.26$), GPT-4o (A1 vs A2: 100/165, 60.61% vs 39/69, 56.52%; $P=.56$), and Sider Fusion (A1 vs A2: 88/165, 53.33% vs 35/69, 50.72%; $P=.72$).

Confidence

All LLMs demonstrated a significant tendency toward high confidence (score ≥8) in the majority of their responses: Sider Fusion (222/237, 93.67%), GPT-4o (232/237, 97.89%), Gemini 2.0 Pro (234/237, 98.73%), and DeepSeek V3 (232/237, 97.89%). Further analysis of incorrect answers revealed a prevalent phenomenon of overconfidence among the LLMs: the proportion of high confidence among incorrect answers reached 88.37% (76/86) for Sider Fusion, 94.37% (67/71) for GPT-4o, 93.75% (30/32) for Gemini 2.0 Pro, and 94.29% (33/35) for DeepSeek V3. Moreover, except for DeepSeek V3, where no statistically significant difference was found between confidence level and answer accuracy (high confidence: 199/202, 98.51% correct vs 33/35, 94.29% incorrect; $P=.16$), statistically significant differences between confidence level and answer accuracy were observed for the other LLMs: Sider Fusion (high confidence: 146/151, 96.69% correct vs 76/86, 88.37% incorrect; $P=.01$), GPT-4o (high confidence: 165/166, 99.40% correct vs 67/71, 94.37% incorrect; $P=.03$), and Gemini

XSL•FO
RenderX

2.0 Pro (high confidence: correct 204/205, 99.51% vs 30/32, 93.75% incorrect; *P*=.049).

Robustness

In the first round of adversarial questioning, Sider Fusion had a response change rate of 33.76% (80/237), followed by GPT-4o (85/237, 35.86%), DeepSeek V3 (78/237, 32.91%), and Gemini 2.0 Pro (75/237, 31.65%). The differences in change rates among the 4 LLMs were statistically significant (all *P*<.001). Furthermore, the quality of answers maintained (ie, not changed) during adversarial questioning showed significant stratification among the LLMs (all *P*<.001): Gemini 2.0 Pro led with the highest stable accuracy rate (accuracy of unchanged answers) at 91.98% (149/162), closely followed by DeepSeek V3 at 91.19% (145/159). GPT-4o and Sider Fusion ranked third and fourth, with stable accuracy rates of 78.95% (120/152) and 73.25% (115/157), respectively.

After 3 rounds of adversarial questioning, the final accuracy rates were 59.07% (140/237) for Sider Fusion, 60.34% (143/237) for GPT-4o, 72.15% (171/237) for DeepSeek V3, and 72.57% (172/237) for Gemini 2.0 Pro. During these 3 rounds, Sider Fusion incorrectly changed 27 initially correct answers to incorrect ones, while DeepSeek V3 changed 38, GPT-4o changed 41, and Gemini 2.0 Pro changed 43. Regarding error correction capability (changing an initially incorrect answer to the correct one after challenge), Sider Fusion successfully corrected 25 incorrect answers, GPT-4o corrected 18, and DeepSeek V3 corrected 17. However, Gemini 2.0 Pro only successfully corrected 10 incorrect answers.

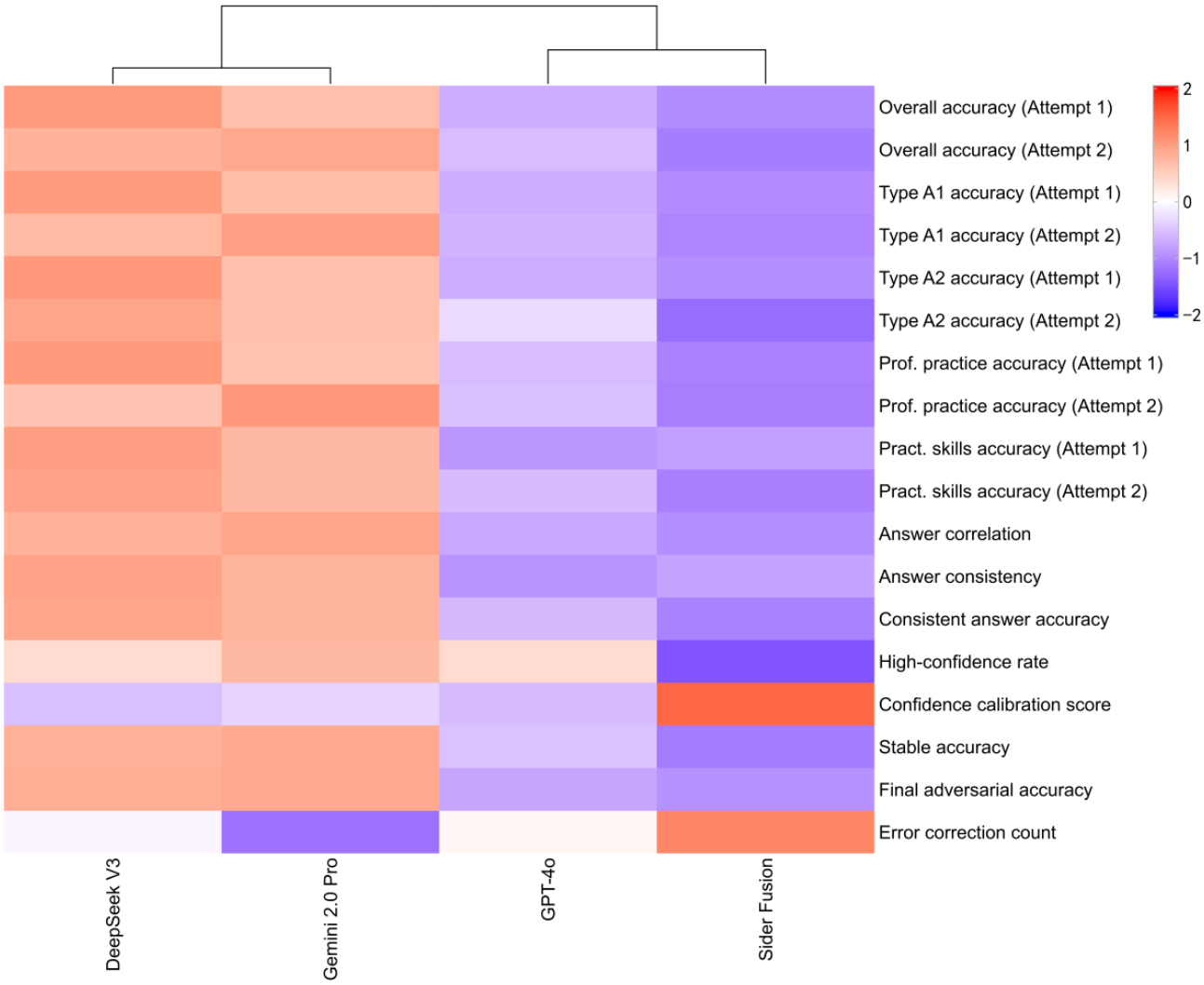
Discussion

Principal Findings

This study systematically evaluated the performance of DeepSeek V3, Gemini 2.0 Pro, GPT-4o, and Sider Fusion on the CNNLE, finding significant differences in overall performance among the LLMs, as summarized in the heatmap in Figure 5. Some LLMs demonstrated distinct advantages, potentially owing to their deep optimization for the Chinese context and cross-modal training mechanisms. However, all LLMs exhibited a risk of hallucination, generating outputs that appear plausible but lack factual accuracy. This finding implies that for educators, developers, and policymakers alike, the focus must shift from merely pursuing correct LLM answers to building an ecosystem that can safely manage the LLMs' inherent potential for error.

XSL•FO
RenderX

Figure 5. Heatmap summarizing the comparative performance of the 4 LLMs across key evaluation metrics. In this heatmap, cell colors represent normalized performance scores for each metric, with warmer colors (red and orange) indicating stronger performance and cooler colors (blue and purple) indicating weaker performance. LLM: large language model; Pract.: practical; Prof.: professional.



Furthermore, none of the LLMs achieved the desired 90% threshold for answer consistency, indicating that even the best-performing LLMs exhibit repeatability deficits. This finding corroborates previous research by Krishna et al [20], Wang et al [21], and Kochanek et al [22]. Potential underlying reasons may include the stochasticity of model parameters, biases in fine-tuning data, sensitivity to prompt design, and inherent limitations in the LLMs' comprehension and reasoning abilities regarding complex, specialized knowledge. This inherent inconsistency poses a significant challenge to the application of LLMs, particularly in highly standardized educational scenarios where it could undermine fairness in assessment, such as by providing different evaluations for similar answers in automated grading. Addressing this deficit at a technical level is therefore crucial. For future LLM design, we recommend focusing on two key aspects: First, refining and dynamically optimizing decoding strategies, such as contextually adapting temperature and top-p parameters, to enhance answer consistency while maintaining plausibility. Second, incorporating task-oriented consistency reward functions and reinforcement learning environments during training to positively incentivize the generation of more repeatable and reliable answers.

This study observed a mirror symmetry phenomenon where the set of correct answers shared between the Gemini 2.0 Pro and DeepSeek V3 pair mirrored the set of incorrect answers shared between the GPT-4o and Sider Fusion pair. This reveals intrinsic differences in knowledge acquisition and reasoning mechanisms among the LLM cohort: simple questions were generally answered correctly, while difficult ones were commonly missed, and questions with high discriminatory power amplified the performance disparities between LLMs [23-25]. These performance disparities likely stem from underlying differences in model architecture and training strategies. DeepSeek V3, leveraging its mixture-of-experts architecture and knowledge distillation techniques, can achieve specialized processing for different data types [26]. Although the architecture of Gemini 2.0 Pro is not publicly disclosed, we speculate that its training strategy similarly focuses on efficient indexing and retrieval of domain-specific knowledge [27]. Conversely, GPT-4o and Sider Fusion might prioritize exploring complex reasoning paths. However, in complex situations with insufficient domain knowledge or ambiguous semantic information, this strategy becomes susceptible to interference, ultimately leading to a consensus on incorrect answers [23,28]. Therefore, LLM errors are not merely random noise but are manifestations of systematic

XSL•FO
RenderX

biases in specific domain knowledge or reasoning strategies [29-31]. Intriguingly, these systematic biases might bear a striking resemblance to human expert error patterns in certain complex tasks. As demonstrated by Bernstein et al [32], no significant differences were found between GPT-3.5 and human answers regarding the presence of incorrect information (*P*=.58), likelihood of causing harm (*P*=.35), extent of possible harm (*P*=.84), and agreement with perceived consensus in the medical community (*P*=.35). Similarly, research by Cabral et al [33] found that although GPT-4 might exhibit a higher error frequency than resident physicians in clinical reasoning (13.8% vs 2.8%; *P*=.04), its error frequency did not differ significantly from that of experienced attending physicians (13.8% vs 12.5%; *P*=.89). This convergence of error patterns suggests that the safest and most effective model for high-stakes fields such as health care is likely not independent human or AI decision-making, but rather a deeply integrated human-AI collaborative intelligence. Within such a paradigm, educators can design human-AI pairing case studies, training students to supervise, question, and ultimately form synergistic decisions with LLM recommendations, thereby learning to identify and mitigate shared cognitive blind spots. Crucially, this mitigation process rests on a thorough understanding of the biases specific to both humans and LLMs. It is well-established that human cognitive biases can be mitigated to some extent through increased awareness, education, and data-driven decision-making methods [34,35]. In-depth research into the systematic biases of LLMs not only contributes to enhancing the reliability of AI systems but may also, in turn, deepen our understanding of the origins and mechanisms of human cognitive biases. A detailed comparative analysis between LLM systematic biases and human cognitive biases could therefore equip future health care professionals with the critical awareness needed to effectively supervise and collaborate with LLMs, ensuring safer and more reliable outcomes.

Consistent with findings by Krishna et al [20], our study reveals a cautionary phenomenon: Although the LLMs exhibited high confidence in most responses, there was a clear disconnect between their confidence levels and the actual accuracy of their answers, with incorrect answers frequently accompanied by high confidence scores. This LLM overconfidence trap could lead health care professionals to inappropriately trust incorrect recommendations, potentially resulting in diagnostic biases, treatment errors, and other clinical risks, ultimately threatening patient safety [36,37]. Notably, DeepSeek V3 was the only LLM where confidence level and actual accuracy showed no statistically significant difference (*P*=.16). This might be related to its deep optimization on Chinese medical texts during training, enabling the LLM to more accurately capture linguistic nuances and cultural context when parsing CNNLE questions, thereby reducing confidence misjudgments arising from semantic ambiguity or cultural misinterpretation [26]. It is recommended that future LLM updates prioritize confidence calibration as a core optimization goal. This can be pursued by systematically representing medical knowledge and its internal relationships, quantifying the uncertainty of LLM outputs, and developing more discriminating confidence assessment systems. However, ensuring these crucial improvements are implemented consistently requires more than developer self-regulation. This is where policy plays a critical role. From a policymaking perspective, regulatory bodies should consider establishing confidence calibration performance as a mandatory disclosure metric for AI tools in the medical and educational sectors. This would ensure that health care and educational institutions can make informed decisions based on transparent, quantifiable risk data when procuring and deploying these tools, thereby establishing an essential institutional safeguard to protect patients and learners.

The robustness test results in this study present an interesting paradox: while Gemini 2.0 Pro performed best at maintaining its initial answers, its error correction efficacy was relatively limited. Conversely, although Sider Fusion exhibited the highest rate of answer changes, it demonstrated the strongest error correction capability. This finding aligns with the "stability–flexibility trade-off" theory [38], suggesting a potential imbalance in current LLMs between knowledge representation stability and adaptive adjustment capabilities. From a clinical decision support perspective, this imbalance could pose potential risks: on one hand, excessive adherence to incorrect answers (high stability coupled with low correction capability) might lead to the persistence of systematic errors; on the other hand, excessive correction of initially correct answers (high correction capability coupled with low stability) could induce decision volatility. However, for designers of licensure preparation platforms, this paradox is not a deficit but instead offers significant practical guidance. It inspires a multimodal product design that moves beyond a one-size-fits-all approach: developers can offer a tutor mode powered by a high-stability LLM for knowledge consolidation, alongside a sparring partner mode driven by a high-flexibility LLM to stimulate critical thinking. Therefore, we recommend that future LLM development not only focuses on balancing accuracy, robustness, and correction sensitivity at the LLM level, but also strategically considers how to translate these different performance characteristics into diverse pedagogical tools at the product design level, with the ultimate goal of empowering educators to cultivate future health care professionals capable of collaborating safely and effectively with imperfect LLMs and ultimately safeguarding decision-making in real-world medical environments.

Limitations

This study possesses several limitations. First, our evaluation was constrained in scope. We excluded 3 image-based questions, which limited a full assessment of the LLMs' multimodal capabilities. Our model selection, while representative, did not include direct and independent evaluations of other prominent LLMs such as Claude 3, LLaMA, or Mistral, restricting the generalizability of our findings. Furthermore, our study's reliance on MCQs, though beneficial for quantification, does not capture essential practical competencies in nursing, such as procedural skills or patient communication. Future research should incorporate multimodal data, broaden the comparative analysis to include a wider array of LLMs, and explore more holistic appraisal approaches to better understand the potential and constraints of LLMs in nursing education and practice.

XSL•FO
RenderX

Second, our robustness testing methodology, while revealing, was simplistic. The adversarial prompt used represents a blunt, generic negation and does not capture the complexity and nuance of authentic clinical feedback. Consequently, our test may not adequately simulate the multifaceted interference patterns of real-world scenarios, potentially underestimating the LLMs' vulnerability. Future research should therefore focus on devising more ecologically valid adversarial testing methodologies that move beyond simple negation to probe higher-order reasoning. This could range from presenting contradictory patient data to test dynamic reasoning, to challenging an LLM with a competing differential diagnosis to assess comparative argumentation, and finally, requiring the LLM to explain the rationale behind its recommended treatment plan to evaluate its ability to weigh trade-offs based on clinical guidelines.

Finally, during the second round of the robustness test, we observed that after their answer from the previous round was challenged, some LLMs would occasionally provide an ambiguous response containing 2 answer choices. To maintain procedural consistency, we addressed this phenomenon by reapplying the same standardized adversarial prompt: "Your answer is incorrect, please try again." This prompt successfully guided the LLMs to provide a single, definitive answer in the third round. Although the responses from the second round were not included in our analysis, we now recognize these occasional ambiguous answers as valuable data on LLM decision-making instability under persistent pressure. Had we quantified these instances as fallback events, we could have conducted a more in-depth analysis of the LLMs' cognitive resilience and decision confidence boundaries. Therefore, we strongly recommend that future research separately quantify an LLM's autonomous accuracy on definitive responses and its fallback rate on ambiguous ones to create a more nuanced reliability profile.

Conclusions

This study evaluated the performance of 4 LLMs on the CNNLE, revealing the relative advantages of DeepSeek V3 and Gemini 2.0 Pro. However, a concerning finding was the LLMs' tendency for overconfidence, which stood in stark contrast to their limited accuracy. This highlights a fundamental deficit in the cognitive reliability of current LLMs when applied to complex professional reasoning tasks. Such overconfidence is particularly perilous within the safety-critical domain of health care. Furthermore, the "stability-flexibility trade-off" paradox suggests a potential imbalance in current LLMs between the stability of knowledge representation and adaptive adjustment capabilities. The true use of LLMs in nursing education and practice demands more than just correct answers; it crucially depends on the reliability of their reasoning, calibrated confidence, and robustness against real-world complexities. The path forward requires a paradigm shift in LLM development and evaluation, prioritizing genuine cognitive reliability and trustworthiness over merely simulating knowledgeable responses.

Acknowledgments

This work was supported in part by Shandong Provincial Humanities and Social Sciences Key Project 2025 Major commissioned project (ZDZX-2025‐003). The authors also wish to acknowledge the developers and contributors of the large language models. Their hard work and groundbreaking innovations made this research possible.

Data Availability

The datasets generated or analyzed during this study are available from the corresponding author on reasonable request.

Authors' Contributions

Conceptualization: LX, XC
Data curation: LX, XC, Ronghui Wang
Formal analysis: LX, Renxiu Wang
Funding acquisition: CX
Investigation: LX, XC
Methodology: LX, Renxiu Wang, NL
Project administration: CX
Supervision: CX
Validation: CX, XL
Visualization: LX
Writing – original draft: LX, XC
Writing – review and editing: LX, XC, Renxiu Wang, NL, XL, Ronghui Wang, CX

Conflicts of Interest

None declared.

References

XSL•FO
RenderX

1. Hou J, Chen S, Sabharwal S, Fan V, Yan M, Wang W. Comparison of RN licensure examination: China and the United States. Int J Nurs Sci 2019 Jan 10;6(1):111-116. [doi: 10.1016/j.ijnss.2018.11.002] [Medline: 31406876]
2. Granger J, Napa W, Buadong D, Punyoo J. Social processes influencing nursing students in passing the nursing licensure examination: a grounded theory approach. Nurs Open 2024 Apr;11(4):e2148. [doi: 10.1002/nop2.2148] [Medline: 38570917]
3. Taskiran N. Effect of artificial intelligence course in nursing on students' medical artificial intelligence readiness: a comparative quasi-experimental study. Nurse Educ 2023;48(5):E147-E152. [doi: 10.1097/NNE.0000000000001446] [Medline: 37133231]
4. Zhao Q, Wang H, Wang R, Cao H. Deriving insights from enhanced accuracy: leveraging prompt engineering in custom GPT for assessing Chinese nursing licensing exam. Nurse Educ Pract 2025 Mar;84:104284. [doi: 10.1016/j.nepr.2025.104284] [Medline: 39954324]
5. Zhu R, Han S, Su Y, Zhang C, Yu Q, Duan Z. The application of big data and the development of nursing science: a discussion paper. Int J Nurs Sci 2019 Apr 10;6(2):229-234. [doi: 10.1016/j.ijnss.2019.03.001] [Medline: 31406897]
6. Berşe S, Akça K, Dirgar E, Kaplan Serin E. The role and potential contributions of the artificial intelligence language model ChatGPT. Ann Biomed Eng 2024 Feb;52(2):130-133. [doi: 10.1007/s10439-023-03296-w] [Medline: 37378876]
7. Diab Idris M, Feng X, Dyo V. Revolutionizing higher education: unleashing the potential of large language models for strategic transformation. IEEE Access 2024;12:67738-67757. [doi: 10.1109/ACCESS.2024.3400164]
8. Xu S, Huang X, Lo CK, Chen G, Jong MY. Evaluating the performance of ChatGPT and GPT-4o in coding classroom discourse data: a study of synchronous online mathematics instruction. Comput Educ: Artif Intell 2024 Dec;7:100325. [doi: 10.1016/j.caeai.2024.100325]
9. Fatima A, Shafique MA, Alam K, Fadlalla Ahmed TK, Mustafa MS. ChatGPT in medicine: a cross-disciplinary systematic review of ChatGPT's (artificial intelligence) role in research, clinical practice, education, and patient interaction. Medicine (Baltimore) 2024;103(32):e39250. [doi: 10.1097/MD.0000000000039250] [Medline: 39121303]
10. Harris E. Large language models answer medical questions accurately, but can't match clinicians' knowledge. JAMA 2023 Sep 5;330(9):792-794. [doi: 10.1001/jama.2023.14311] [Medline: 37548971]
11. Zong H, Li J, Wu E, Wu R, Lu J, Shen B. Performance of ChatGPT on Chinese national medical licensing examinations: a five-year examination evaluation study for physicians, pharmacists and nurses. BMC Med Educ 2024 Feb 14;24(1):143. [doi: 10.1186/s12909-024-05125-7] [Medline: 38355517]
12. Kaneda Y, Takahashi R, Kaneda U, et al. Assessing the performance of GPT-3.5 and GPT-4 on the 2023 Japanese nursing examination. Cureus 2023 Aug;15(8):e42924. [doi: 10.7759/cureus.42924] [Medline: 37667724]
13. Wu Z, Gan W, Xue Z, Ni Z, Zheng X, Zhang Y. Performance of ChatGPT on nursing licensure examinations in the United States and China: cross-sectional study. JMIR Med Educ 2024 Oct 3;10:e52746. [doi: 10.2196/52746] [Medline: 39363539]
14. Dreyer J. China made waves with Deepseek, but its real ambition is AI-driven industrial innovation. Nature New Biol 2025 Feb;638(8051):609-611. [doi: 10.1038/d41586-025-00460-1] [Medline: 39966638]
15. Gibney E. China's cheap, open AI model DeepSeek thrills scientists. Nature New Biol 2025 Feb 6;638(8049):13-14. [doi: 10.1038/d41586-025-00229-6] [Medline: 39849139]
16. Normile D. Chinese firm's large language model makes a splash. Science 2025 Jan 17;387(6731):238. [doi: 10.1126/science.adv9836] [Medline: 39818899]
17. Peng Y, Malin BA, Rousseau JF, et al. From GPT to DeepSeek: significant gaps remain in realizing AI in healthcare. J Biomed Inform 2025 Mar;163:104791. [doi: 10.1016/j.jbi.2025.104791] [Medline: 39938624]
18. Baidu Wenku. URL: https://wenku.baidu.com [accessed 2025-10-27]
19. BioLadder. URL: https://www.bioladder.cn/ [accessed 2025-10-27]
20. Krishna S, Bhambra N, Bleakney R, Bhayana R. Evaluation of reliability, repeatability, robustness, and confidence of GPT-3.5 and GPT-4 on a radiology board-style examination. Radiology 2024 May;311(2):e232715. [doi: 10.1148/radiol.232715] [Medline: 38771184]
21. Wang L, Chen X, Deng X, et al. Prompt engineering in consistency and reliability with the evidence-based guideline for LLMs. NPJ Digit Med 2024 Feb 20;7(1):41. [doi: 10.1038/s41746-024-01029-4] [Medline: 38378899]
22. Kochanek K, Skarzynski H, Jedrzejczak WW. Accuracy and repeatability of ChatGPT based on a set of multiple-choice questions on objective tests of hearing. Cureus 2024 May;16(5):e59857. [doi: 10.7759/cureus.59857] [Medline: 38854312]
23. Sau S, George DD, Singh R, et al. Accuracy and quality of ChatGPT-4o and Google Gemini performance on image-based neurosurgery board questions. Neurosurg Rev 2025 Mar 25;48(1):320. [doi: 10.1007/s10143-025-03472-7] [Medline: 40131528]
24. Shool S, Adimi S, Saboori Amleshi R, Bitaraf E, Golpira R, Tara M. A systematic review of large language model (LLM) evaluations in clinical medicine. BMC Med Inform Decis Mak 2025 Mar 7;25(1):117. [doi: 10.1186/s12911-025-02954-4] [Medline: 40055694]
25. Wang YM, Chen TJ. The rise of AI in healthcare education: DeepSeek and GPT-4o take on the 2024 Taiwan pharmacist exam. J Chin Med Assoc 2025 Apr 1;88(4):338-339. [doi: 10.1097/JCMA.0000000000001220] [Medline: 39972548]
26. DeepSeek-AI, Liu A. DeepSeek-V3 technical report. arXiv. Preprint posted online on Feb 18, 2025. [doi: 10.48550/arXiv.2412.19437]

XSL•FO
RenderX

27. Team GR, Abeyruwan S, Ainslie J, et al. Gemini robotics: bringing AI into the physical world. arXiv. Preprint posted online on Mar 25, 2025. [doi: 10.48550/arXiv.2503.20020]
28. Shahriar S, Lund BD, Mannuru NR, et al. Putting GPT-4o to the sword: a comprehensive evaluation of language, vision, speech, and multimodal proficiency. Appl Sci (Basel) 2024 Jan;14(17):7782. [doi: 10.3390/app14177782]
29. Agrawal A. Fairness in AI-driven oncology: investigating racial and gender biases in large language models. Cureus 2024 Sep 16(9). [doi: 10.7759/cureus.69541] [Medline: 39416584]
30. McCoy RT, Yao S, Friedman D, Hardy MD, Griffiths TL. Embers of autoregression show how large language models are shaped by the problem they are trained to solve. Proc Natl Acad Sci U S A 2024 Oct 8;121(41):e2322420121. [doi: 10.1073/pnas.2322420121] [Medline: 39365822]
31. Omiye JA, Lester JC, Spichak S, Rotemberg V, Daneshjou R. Large language models propagate race-based medicine. NPJ Digit Med 2023 Oct 20;6(1):195. [doi: 10.1038/s41746-023-00939-z] [Medline: 37864012]
32. Bernstein IA, Zhang YV, Govil D, et al. Comparison of ophthalmologist and large language model chatbot responses to online patient eye care questions. JAMA Netw Open 2023 Aug 1;6(8):e2330320. [doi: 10.1001/jamanetworkopen.2023.30320] [Medline: 37606922]
33. Cabral S, Restrepo D, Kanjee Z, et al. Clinical reasoning of a generative artificial intelligence model compared with physicians. JAMA Intern Med 2024 May 1;184(5):581-583. [doi: 10.1001/jamainternmed.2024.0295] [Medline: 38557971]
34. Ke Y, Yang R, Lie SA, et al. Mitigating cognitive biases in clinical decision-making through multi-agent conversations using large language models: simulation study. J Med Internet Res 2024 Nov 19;26:e59439. [doi: 10.2196/59439] [Medline: 39561363]
35. Satya-Murti S, Lockhart J. Recognizing and reducing cognitive bias in clinical and forensic neurology. Neurol Clin Pract 2015 Oct;5(5):389-396. [doi: 10.1212/CPJ.0000000000000181] [Medline: 29443168]
36. Borracci RA, Arribalzaga EB. The incidence of overconfidence and underconfidence effects in medical student examinations. J Surg Educ 2018;75(5):1223-1229. [doi: 10.1016/j.jsurg.2018.01.015] [Medline: 29397355]
37. Jala S, Fry M, Elliott R. Cognitive bias during clinical decision-making and its influence on patient outcomes in the emergency department: a scoping review. J Clin Nurs 2023 Oct;32(19-20):7076-7085. [doi: 10.1111/jocn.16845] [Medline: 37605250]
38. Qiao L, Zhang L, Chen A. Control dilemma: evidence of the stability-flexibility trade-off. Int J Psychophysiol 2023 Sep;191:29-41. [doi: 10.1016/j.ijpsycho.2023.07.002] [Medline: 37499985]

Abbreviations

AI: artificial intelligence
CNNLE: Chinese National Nurse Licensure Examination
LLM: large language model
MCQ: multiple-choice question

Edited by A Benis; submitted 29.05.25; peer-reviewed by ACD Oliveira, K Kuppan; revised version received 08.10.25; accepted 13.10.25; published 03.11.25.

Please cite as:
Xu L, Cong X, Wang R, Li N, Liu X, Wang R, Xu C
Performance of the Large Language Models on the Chinese National Nurse Licensure Examination: Cross-Sectional Evaluation Study
JMIR Med Inform 2025;13:e78279
URL: https://medinform.jmir.org/2025/1/e78279
doi:10.2196/78279

©Longhui Xu, Xiao Cong, Renxiu Wang, Na Li, Xinru Liu, Ronghui Wang, Cuiping Xu. Originally published in JMIR Medical Informatics (https://medinform.jmir.org), 3.11.2025. This is an open-access article distributed under the terms of the Creative Commons Attribution License (https://creativecommons.org/licenses/by/4.0/), which permits unrestricted use, distribution, and reproduction in any medium, provided the original work, first published in JMIR Medical Informatics, is properly cited. The complete bibliographic information, a link to the original publication on https://medinform.jmir.org/, as well as this copyright and license information must be included.

XSL•FO
RenderX

Enabling Just-in-Time Clinical Oncology Analysis With Large Language Models: Feasibility and Validation Study Using Unstructured Synthetic Data

Peter May[1], MA, MPH, Dr med; Julian Greß[1,2]; Christoph Seidel[3], MBA, PD, Dr med; Sebastian Sommer[4], Dr med; Markus K Schuler[2,5], PD, Dr med; Sina Nokodian[1]; Florian Schröder[2], PhD; Johannes Jung[1,6], PhD, Dr med

[1]Department of Internal Medicine III, School of Medicine and Health, TUM University Hospital, Technical University of Munich, Ismaninger Str. 22, Munich, Germany

[2]MPiriQ Science Technologies GmbH, Munich, Germany

[3]Department of Oncology, Hematology and Bone Marrow Transplantation with Division of Pneumology, University Medical Center Hamburg-Eppendorf, Hamburg, Germany

[4]MVZ Elisenhof, Munich, Germany

[5]Onkologischer Schwerpunkt am Oskar-Helene Heim, Berlin, Germany

[6]Department of Hematology and Medical Oncology, University Medical Center Göttingen, Göttingen, Germany

Corresponding Author:
Peter May, MA, MPH, Dr med
Department of Internal Medicine III, School of Medicine and Health, TUM University Hospital, Technical University of Munich, Ismaninger Str. 22, Munich, Germany

Abstract

Background: Traditional cancer registries, limited by labor-intensive manual data abstraction and rigid, predefined schemas, often hinder timely and comprehensive oncology research. While large language models (LLMs) have shown promise in automating data extraction, their potential to perform direct, just-in-time (JIT) analysis on unstructured clinical narratives—potentially bypassing intermediate structured databases for many analytical tasks—remains largely unexplored.

Objective: This study aimed to evaluate whether a state-of-the-art LLM (Gemini 2.5 Pro) can enable a JIT clinical oncology analysis paradigm by assessing its ability to (1) perform high-fidelity multiparameter data extraction, (2) answer complex clinical queries directly from raw text, (3) automate multistep survival analyses including executable code generation, and (4) generate novel, clinically plausible hypotheses from free-text documentation.

Methods: A synthetic dataset of 240 unstructured clinical letters from patients with stage IV non–small cell lung cancer (NSCLC), embedding 14 predefined variables, was used. Gemini 2.5 Pro was evaluated on four core JIT capabilities. Performance was measured by using the following metrics: extraction accuracy (compared to human extraction of n=40 letters and across the full n=240 dataset); numerical deviation for direct question answering (n=40 to 240 letters, 5 questions); log-rank *P* value and Harrell concordance index for LLM-generated versus ground-truth Kaplan-Meier survival analyses (n=160 letters, overall survival and progression-free survival); and correct justification, novelty, and a qualitative evaluation of LLM-generated hypotheses (n=80 and n=160 letters).

Results: For multiparameter extraction from 40 letters, the LLM achieved >99% average accuracy, comparable to human extraction, but in significantly less time (LLM: 3.7 min vs human: 133.8 min). Across the full 240-letter dataset, LLM multiparameter extraction maintained >98% accuracy for most variables. The LLM answered multiconditional clinical queries directly from raw text with a relative deviation rarely exceeding 1.5%, even with up to 240 letters. Crucially, it autonomously performed end-to-end survival analysis, generating text-to-R-code that produced Kaplan-Meier curves statistically indistinguishable from ground truth. Consistent performance was demonstrated on a small validation cohort of 80 synthetic acute myeloid leukemia reports. Stress testing on data with simulated imperfections revealed a key role of a human-in-the-loop to resolve AI-flagged ambiguities. Furthermore, the LLM generated several correctly justified, biologically plausible, and potentially novel hypotheses from datasets up to 80 letters.

Conclusions: This feasibility study demonstrated that a frontier LLM (Gemini 2.5 Pro) can successfully perform high-fidelity data extraction, multiconditional querying, and automated survival analysis directly from unstructured text. These results provide a foundational proof of concept for the JIT clinical analysis approach. However, these findings are confined to synthetic patients, and rigorous validation on real-world clinical data is an essential next step before clinical implementation can be considered.

(JMIR Med Inform 2025;13:e78332) doi:10.2196/78332

XSL•FO
RenderX

KEYWORDS

large language models; clinical oncology; unstructured data; real-world evidence; natural language processing; survival analysis; cancer registries; just-in-time analysis; artificial intelligence

Introduction

The Need for Timely Real-World Evidence in Oncology

Clinical registries are foundational to oncology research, providing essential real-world evidence on treatment patterns, patient outcomes, and therapeutic effectiveness beyond the confines of clinical trials. However, the conventional approach to building these registries—relying heavily on manual data abstraction from patient records—faces significant challenges. This process is labor-intensive and costly and introduces substantial time lags between clinical events and data availability. For example, manual abstraction of cancer stage can lag diagnosis by up to 6 months, hindering timely analysis [1]. Furthermore, traditional registries are inherently constrained by predefined data schemas, often failing to capture the rich, nuanced clinical details embedded within unstructured text like physician notes, pathology reports, or radiology findings [1,2]. Critical information, including precise biomarker status, evolving metastatic patterns, treatment responses, and subsequent lines of therapy, is also frequently updated, rendering static registries potentially outdated or incomplete for contemporary research needs.

Automating Data Access: From Extraction to “Just-in-Time” Analysis

Advances in natural language processing, particularly the advent of powerful transformer-based large language models (LLMs), offer a promising avenue to overcome these limitations. Recent studies demonstrate the proficiency of LLMs in accurately extracting key clinical end points, such as real-world progression-free survival (PFS), biomarkers, and TNM stage, directly from unstructured clinical text, thereby reducing manual curation efforts [1,3-11].

Building upon this progress, we propose and investigate the concept of a “just-in-time” (JIT) clinical analysis paradigm in oncology. This approach leverages the advanced capabilities of LLMs to directly query and analyze unstructured clinical documents on-demand, potentially bypassing the slow, laborious process of consolidating data into static, structured databases. The central hypothesis is that LLMs can serve as intelligent interfaces to raw clinical data repositories—such as collections of electronic health record notes—enabling dynamic extraction, synthesis, and analysis of key oncology end points precisely when needed.

The latest generation of LLMs are pivotal enablers for this concept, largely because their technical capabilities now align with the demands of large-scale clinical data analysis. Context windows have increased immensely; Gemini 2.5 Pro, for instance, can handle 1 million tokens concurrently—enough to ingest and reason over hundreds of patient records or complex reports at once. While previous approaches, including methods like retrieval-augmented generation (RAG), enabled large-scale data processing, their accuracy and efficiency were often inconsistent [12,13]. The large context windows, combined with their sophisticated understanding of context, ability to synthesize information across documents, and emergent reasoning capabilities, position frontier LLMs not merely as data extractors but as potential “automated curators” or analytical engines operating directly on narrative data [5,14,15]. This could allow researchers and clinicians to pose complex analytical questions (eg, “What is the PFS for epidermal growth factor receptor–mutant lung cancer patients treated with osimertinib who developed brain metastases?") directly to document collections, with the LLM dynamically interpreting the query, locating relevant information scattered across notes, performing necessary calculations (like survival time), and providing synthesized answers on demand [16].

Simulating "Just-in-Time" Querying With Synthetic Data

However, systematically evaluating the proposed JIT paradigm on real-world data is currently infeasible due to significant regulatory barriers. Privacy laws such as the US Health Insurance Portability and Accountability Act (HIPAA) or the EU General Data Protection Regulation prohibit the use of cloud-based LLMs with patient data. Moreover, the terms of use for publicly available datasets like Medical Information Mart for Intensive Care (MIMIC)-IV also restrict their integration with these models. Therefore, to rigorously assess the capabilities in a controlled yet clinically relevant setting, this study employs a well-established simulation framework using a synthetic dataset of 240 patients with stage IV non–small cell lung cancer (NSCLC), embedding predefined clinical variables within mock narrative summaries [17]. NSCLC was selected for its clinical heterogeneity and complexity, providing a representative testbed for evaluating LLM performance on information retrieval and reasoning tasks central to the JIT concept. This synthetic dataset serves as a consistent, accessible proxy for a collection of patient records, enabling systematic assessment of a cloud-based LLM (Gemini 2.5 Pro) in a reproducible environment.

Rationale and Objectives

The primary objective of this study is to evaluate whether a leading LLM possesses the fundamental capabilities required to enable JIT analysis of complex oncological information. Specifically, we assess the LLM’s performance across four key tasks simulating the core functions of such a system:

1. High-fidelity structured parameter extraction: Can the LLM accurately extract numerous predefined variables, including PFS and overall survival (OS) from unstructured text at scale?
2. Direct clinical question answering: Can the LLM correctly answer complex queries requiring data aggregation and synthesis directly from text, bypassing a structured database?
3. Automated survival analysis: Can the LLM perform multistep analyses, like generating Kaplan-Meier curves

XSL•FO
RenderX

from raw text, yielding results comparable to traditional methods?

4. Autonomous hypothesis generation: Does the LLM exhibit reasoning capabilities by identifying potentially novel clinical associations?

While many studies have demonstrated the ability of LLMs to extract specific data points from clinical text, the primary contribution of our feasibility study is not algorithmic but paradigmatic. We propose that, in the future, the use of LLMs in cancer registries may obviate the need for intermediate structured databases.

Methods

Synthetic Patient Data Generation

To create a controlled benchmarking environment, a synthetic dataset simulating clinical correspondence from 240 patients with stage IV NSCLC was generated. A structured data schema defining 14 key clinical variables (including demographics, diagnosis, metastases, molecular markers, treatments, PFS, and OS; details in Multimedia Appendix 1) was created manually and served as the ground truth (GT). Unstructured patient letters embedding these variables were generated using GPT o4-mini and Claude Sonnet 3.7, mimicking real-world linguistic diversity (examples in Multimedia Appendix 2).

A key goal was to create a heterogeneous dataset to better simulate the variability of real-world clinical documentation. As detailed in Table S1 (Multimedia Appendix 2), the resulting 240 letters vary significantly in style, length, and granularity, with word counts ranging from 109 to 3147 words. The dataset includes extremely concise, 120-word Subjective, Objective, Assessment, and Plan (SOAP) notes rich in abbreviations (eg, SYN092, shown in Multimedia Appendix 2), alongside comprehensive, 3063-word discharge summaries containing detailed laboratory results, pathology reports, and extensive narrative histories (eg, SYN007, shown in Multimedia Appendix 2). For validation purposes, a second, smaller dataset with 80 patients with acute myeloid leukemia (AML) was created (Table S2 in Multimedia Appendix 2). Each synthetic letter underwent a basic plausibility assessment by an oncologist to ensure suitability for testing.

Large Language Model Setup

All analytical tasks utilized Gemini 2.5 Pro accessed via Google AI Studio, prompted in a zero- or one-shot fashion with temperature set to 0 for deterministic output. Session history was disabled to ensure reproducibility. Distinct models for generation and analysis mitigated self-evaluation bias. Due to the platform's limit on concurrent file uploads, the synthetic letters were batched into multipage PDF files, each containing 20 - 40 patients. A detailed flowchart providing an overview of the entire experimental design is provided in Figure S1 (Multimedia Appendix 2).

Parameter Extraction Performance

The LLM's ability to extract the 14 predefined variables was evaluated in single parameter extraction (SPE; one variable at a time) and multiparameter extraction (MPE; all 14 variables simultaneously) modes. OS and PFS had to be calculated using the difference between progression and treatment initiation date in most cases. For initial benchmarking, human performance on a set of 40 letters was compared with LLM SPE and MPE performance (6 independent repetitions). Next, the impact of input volume (n=240 letters processed in batches of 1×240, 2×120, 3×80, 4×60, or 6×40) was assessed. Accuracy (ratio of correct predictions) and processing time were recorded. A ±1 month tolerance was applied for OS/PFS time values.

Question Answering Accuracy and Deviation

The LLM's capacity for direct question answering was tested using subsets of the patient letters, ranging from 40 to 240 letters in increments. Five questions of increasing complexity were posed: Q1 (1 parameter): How many patients have brain metastasis at diagnosis? Q2 (1 parameter): How many patients were diagnosed in 2020? Q3 (1 parameter): How many patients received tyrosine kinase inhibitors for first-line therapy? Q4 (2 parameters): How many female patients have epidermal growth factor receptor mutations? Q5 (3 parameters): How many patients born before 1970 have a KRAS mutation and are on Pembrolizumab-containing first-line regimens? Each question was tested with different quantities of letters (40-240) across 12 independent replicates to assess consistency. Evaluation metrics included the percentage of correct replicates (the proportion of the 12 replicates where the LLM provided the exactly correct numerical answer based on the GT data for the given subset of letters) and relative deviation (absolute difference between the LLM's answer and the true answer, divided by the quantity of letters used for that query).

Automated Survival Analysis

We assessed the LLM's ability to perform an end-to-end survival analysis using a cohort of 160 letters. The LLM was prompted to extract time-to-event data (for OS and PFS) by generating a downloadable table and a complete, executable R script using the survival and survminer packages to generate Kaplan-Meier plots. This process was also applied to a more complex subgroup PFS analysis, stratifying patients by driver mutation status (driver mutation versus wild type [WT]). This semiautomated workflow required a brief human-in-the-loop action: the user had to save the LLM-generated data table as a CSV file and then execute the LLM-generated script in RStudio. This manual step reflected a current platform limitation: although Gemini 2.5 Pro can execute Python to generate Kaplan-Meier curves, it cannot do so while simultaneously extracting data from uploaded PDF files. The detailed prompt and a complete sample of the LLM's output (data table and R code) are provided in A2.7 and A2.8 in Multimedia Appendix 2. The resulting curves were compared visually and statistically (log-rank test) against GT data. To assess reproducibility, Harrell's concordance index (C-index) was calculated for 12 independent repetitions, where a value of 0.50 signified that the survival curves derived from the LLM and the GT were statistically indistinguishable.

Error Injection Stress Test

To simulate real-world data imperfections, we conducted a stress test on a subset of 40 letters, each intentionally altered to include one typographical error, one data ambiguity/contradiction, and

XSL•FO
RenderX

one missing data point (see Table S3 in Multimedia Appendix 2 for injected errors). We compared two conditions in 3 independent repetitions: (1) "LLM MPE only," where the LLM performed direct MPE on the error-injected text, and (2) "Human-in-the-loop," a two-stage workflow where the LLM first flagged potential errors for a human annotator to review (see prompt and exemplary output in A2.9 and A2.10 in Multimedia Appendix 2). For each LLM-flagged error, the human annotator added the clarification to a subsequent MPE prompt, with which the final parameter extraction was performed. The number of correctly extracted parameters (of all 40 corrupted data points) was recorded for each condition.

Autonomous Hypothesis Generation

To evaluate the LLM's reasoning capabilities, we prompted it to analyze the full dataset of unstructured letters (in batches of n=80 and n=160) and propose a single, novel, and clinically relevant hypothesis regarding potential relationships within the cohort. The prompt was designed to elicit one focused hypothesis per run to ensure high-quality output (prompt in A2.12 in Multimedia Appendix 2). Each generated hypothesis subsequently underwent a structured, qualitative evaluation by a board-certified oncologist. The evaluation was based on three distinct criteria:

- Justification: Assessed whether the justification for the hypothesis was factually supported by the provided synthetic data. This was rated as "fully correct," "partly correct," or "incorrect."
- Biological plausibility: Assessed the clinical and biological sensibility of the proposed association, rated as "high," "moderate," or "low."
- Novelty: Assessed whether the hypothesis represented a nonobvious relationship not considered standard clinical knowledge, rated as "high," "moderate," or "low."

The proposed hypotheses and the detailed expert evaluation are provided in Table S4 (Multimedia Appendix 2).

Statistical Analysis and Visualization

Performance metrics, including accuracy, processing time, and relative deviation, were summarized using descriptive statistics (mean, standard error of the mean, and range). Kaplan-Meier curves were generated using the R survival and survminer packages. Log-rank tests and Harrell's C-index were used to compare survival distributions. Data visualization was performed using GraphPad Prism (version 10.4.2; GraphPad Software, LLC) and R (version 4.5.0; R Core Team, 2025) with packages ggplot2 and caret. Conceptual visualizations were prepared using BioRender.

Ethical Considerations

This study utilized exclusively synthetic data generated by LLMs. No real patient data or protected health information was accessed or used at any stage. As only synthetic data were used, this study did not involve human subject research requiring institutional review board approval or informed consent. The TRIPOD-LLM reporting guideline for studies using LLMs was completed.

Results

High-Fidelity Information Extraction From Unstructured Clinical Texts

First, we benchmarked the LLM's ability to extract structured clinical variables against manual human annotation. On a 40-letter synthetic dataset with 14 parameters per patient, both LLM SPE and MPE achieved >99% average accuracy (SPE: 99.8%; MPE 99.5%). As shown in Table 1, the results were comparable to those of a human annotator (98%). Critically, the LLM MPE approach demonstrated superior time efficiency, processing the 40-letter batch in 3.7 minutes, compared to 46.3 minutes for LLM SPE and 133.8 minutes for manual extraction. In other words, the LLM performed the task with slightly higher accuracy in less than 3% of the time compared to human annotators.

Table . Benchmarking information extraction accuracy and processing time.

Extraction method	Accuracy (%)	Range (%)	Time taken (min)	Range (min)
Human	98.0	—[a]	133.8	—
LLM[b] SPE[c,d]	99.8	99.1 - 100.0	46.3	42.5 - 51.4
LLM MPE[d,e]	99.5	99.1 - 99.8	3.7	3.3 - 4.2

[a]Not applicable.

[b]LLM: large language model.

[c]SPE: single parameter extraction.

[d]LLM approaches were tested on 6 different sets of 40 letters.

[e]MPE: multiparameter extraction.

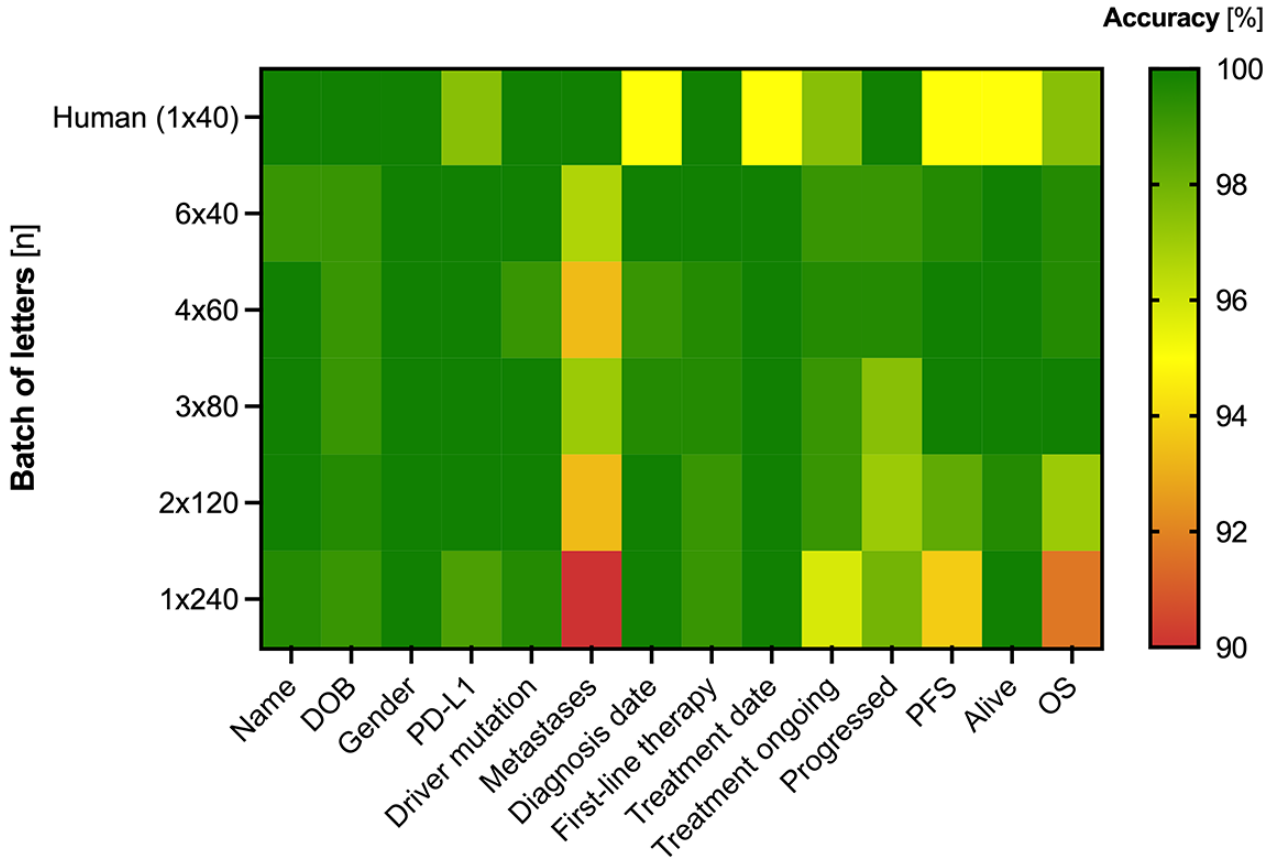
Effective Scaling to Larger Batch Sizes

The LLM MPE method scaled effectively to the full 240-letter dataset. Confusion matrices for "Alive status" and "Progression status" (1×240 batch) confirmed high classification accuracy of almost 100% (Figure S2 in Multimedia Appendix 2). Across all parameters and various batching strategies, LLM MPE generally maintained >98% accuracy (Figure 1). While errors were slightly higher for complex variables (eg, PFS, OS, metastases), they rarely exceeded 5%. A qualitative analysis revealed that a primary source of these errors was the model's occasional misinterpretation of inconsistent date formats. Heatmap visualizations revealed that smaller batch sizes (eg, 6×40) modestly but consistently improved accuracy for some

XSL•FO
RenderX

variables, suggesting potential advantages of minimizing input volume per prompt.

Figure 1. Extraction accuracy across clinical variables and batching strategies. The heatmap visualizes the accuracy across 14 clinical variables (x-axis) when processing the full 240-letter cohort, using five different batching strategies (y-axis), with a human annotator's performance on a 40-letter batch included for reference. The color of each cell corresponds to the accuracy percentage from high (green, 100%) to low (red, 90%). DOB: date of birth; PD-L1: programmed death-ligand 1; PFS: progression-free survival; OS: overall survival.



The overall processing time for the 240 letters using different batching strategies ranged from 15 to 30 minutes (Figure S3A, B in Multimedia Appendix 2), with MPE offering marked per-parameter efficiency over SPE. Although less time efficient, the SPE approach generally achieved slightly higher accuracies across all categories than MPE (Figure S3C in Multimedia Appendix 2).

These results indicate that LLM-driven MPE is a highly accurate and exceptionally time-efficient method for extracting structured data from clinical narratives, providing a robust foundation for subsequent complex analyses.

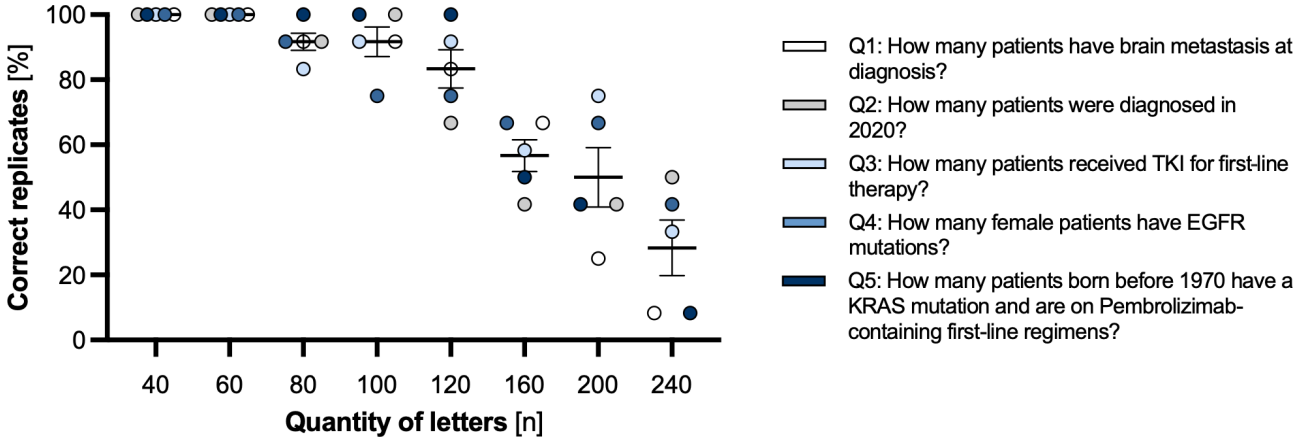
Question-Answering Performance Across Variable Text Lengths

While the successful extraction of large volumes of structured data (up to 14×240=3360 parameters) highlights the LLM's potential as a high-throughput database generator, we next asked a more fundamental question: is a structured database even necessary? To explore this, we evaluated whether the LLM could bypass database construction entirely and instead directly answer clinical queries from raw, unstructured patient letters across varying input sizes (n=40 to 240). Five questions were posed, requiring aggregation of one (Q1–3), two (Q4), or three (Q5) parameters simultaneously.

Accuracy was highest when the LLM processed smaller text volumes. Performance was excellent with 40 or 60 letters and remained strong with 80 or 100 letters, particularly for simpler single-parameter questions (Q1–3; Figure 2). Notably, accuracy in obtaining the *exact* count decreased as the input volume increased further toward 240 letters, especially for the multiparameter questions (Q4–5).

XSL•FO
RenderX

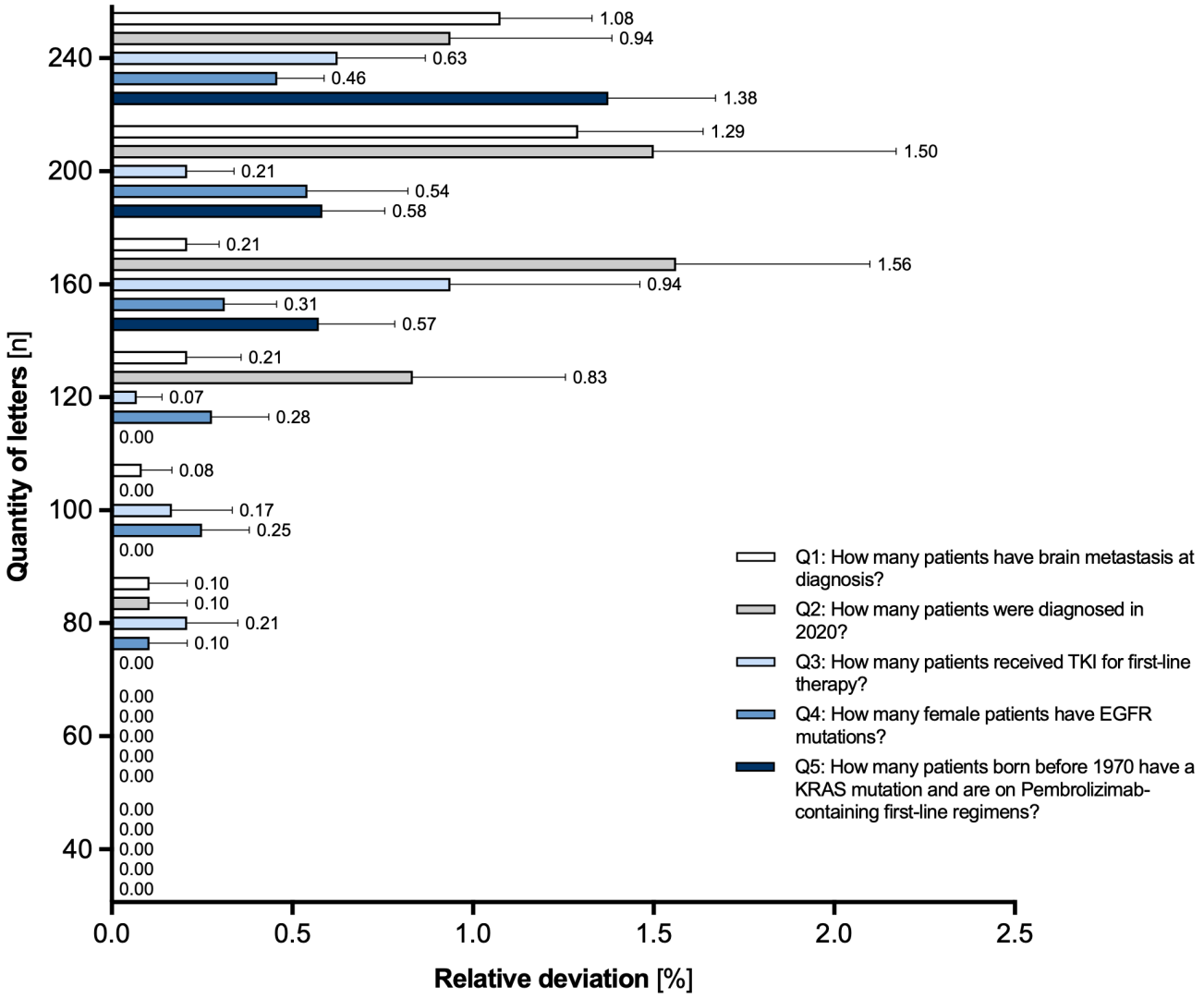
Figure 2. Percentage of correct replicates in direct question answering from unstructured text with increasing input. Performance was assessed using varying quantities of text from patient letters (40 - 240 letters) and five questions (Q1–Q5) regarding 1 (Q1–3), 2 (Q4), or 3 (Q5) parameters (defined in legend). 12 replicates per condition. Error bars represent standard error of the mean. EGFR: epidermal growth factor receptor; KRAS: Kirsten rat sarcoma viral oncogene homolog; TKI: tyrosine kinase inhibitor.



However, the answers remained precise in relative terms. Normalized by the correct answer, the magnitude of the errors was consistently small, typically remaining below 1% across most conditions and rarely exceeding 1.5% (Figure 3). Furthermore, there was no significant difference in the relative error magnitude between the simpler single-parameter questions (Q1–3) and the more complex multiparameter questions (Q4–5). This robustness supports the feasibility of using LLMs for large-scale JIT interrogation, where approximate accuracy within a small margin is often sufficient. It also underscores the potential of bypassing traditional structured databases altogether.

XSL•FO
RenderX

Figure 3. Relative deviation in direct question answering from unstructured text with increasing input. Relative deviation was measured as absolute deviation divided by correct value. Error bars represent standard error of the mean. EGFR: epidermal growth factor receptor; KRAS: Kirsten rat sarcoma viral oncogene homolog; TKI: tyrosine kinase inhibitor.



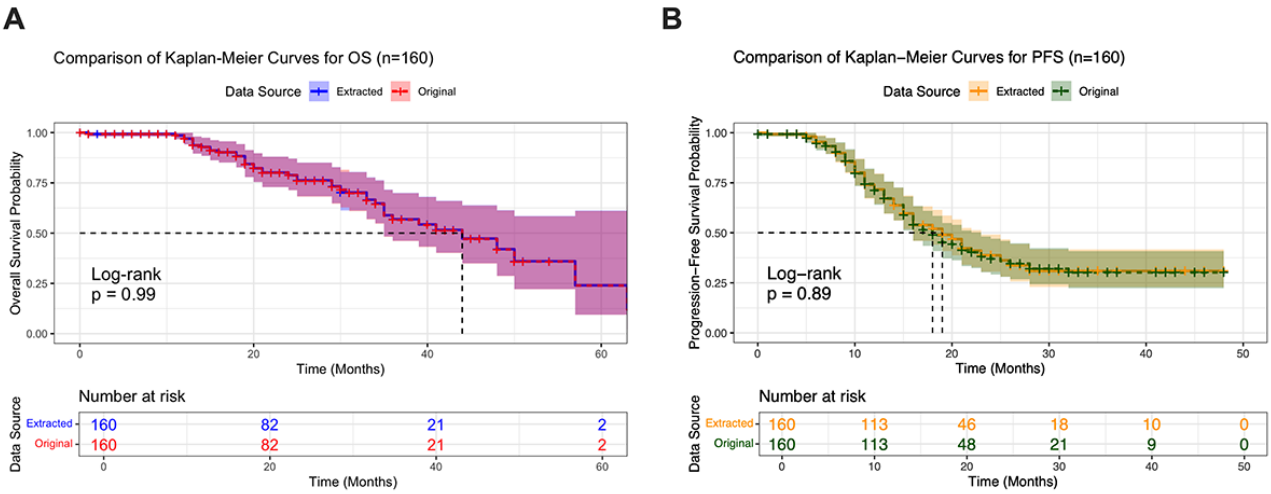
Automated Survival Analysis Yields High Concordance With Ground Truth

Although direct question answering demonstrated strong performance and low deviation even across large text inputs, many clinical tasks demand more complex, multistep reasoning. Survival analysis, in particular, requires identifying event timing, censoring, and proper cohort stratification—tasks traditionally dependent on curated datasets and statistical programming. We therefore assessed whether the LLM could autonomously extract time-to-event data from unstructured patient letters (n=160) and generate fully executable R code to produce survival curves comparable to those derived from GT data.

Visual comparison of survival curves generated from LLM-extracted versus GT datasets revealed remarkable concordance, with numbers-at-risk tables almost identical. For both OS (Figure 4A) and PFS (Figure 4B), the shapes of survival curves were virtually indistinguishable across datasets, with overlapping 95% CI. Log-rank tests confirmed this observation, yielding *P* values indicating no statistically significant difference between the LLM-extracted and original datasets (*P*=.99 for OS; *P*=.89 for PFS).

XSL•FO
RenderX

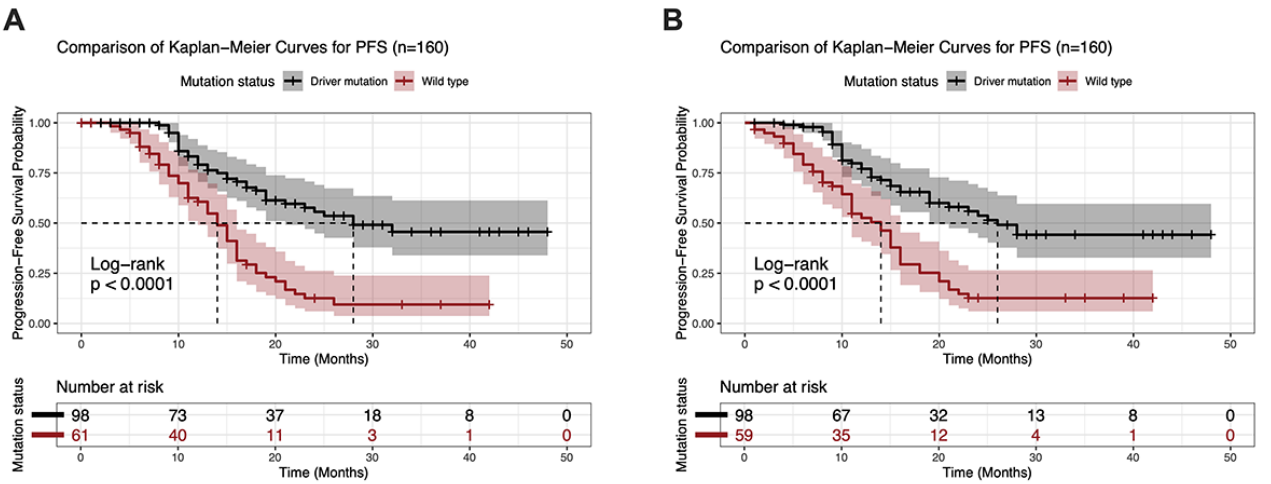
Figure 4. Direct unstructured text-to-R code Kaplan-Meier curves. Comparison of "extracted" versus ground truth ("Original") for (A) overall survival (OS) and (B) progression-free survival (PFS) using 160 patients. Shaded areas represent 95% CI. Numbers-at-risk tables are shown below each plot. Log-rank tests assessed differences between the extracted and original curves.



Moreover, subgroup survival analyses were successfully performed. When stratifying patients by driver mutation status using data extracted from 160 letters, the LLM was able to reproduce prognostic distinctions (Figure 5A and B), generating distinct survival curves for driver mutation versus WT cohorts. It accurately calculated relevant statistics with only slight deviations for the driver mutation group, yielding comparable median PFS (26.0 instead of 28.0 mo for driver mutation versus 14.0 mo for WT) and 2-year PFS estimates (53.7 instead of 55.6% for driver mutation versus 12.6% for WT). The LLM also correctly identified the highly significant difference between these molecularly defined subgroups via log-rank testing (P<.001).

To confirm the robustness and reproducibility of the survival analysis, we repeated the semiautomated process 12 independent times (Figure S4 in Multimedia Appendix 2). The resulting survival models showed high stability, with Harrell's C-index consistently ranging from 0.493 to 0.521, indicating that the LLM-extracted curves were statistically indistinguishable from the GT (C-index=0.500).

Figure 5. Direct unstructured text-to-R code subgroup analyses. Subgroup progression-free survival (PFS) analysis using the original data (A) and performed by the large language model (B) using data from 160 letters, comparing driver mutation (black) versus wild type (brown). Shaded areas represent 95% CI. Numbers-at-risk tables are shown below each plot. Log-rank *P* values test for differences between groups. Median and 2-year PFS estimates are provided.



XSL•FO
RenderX

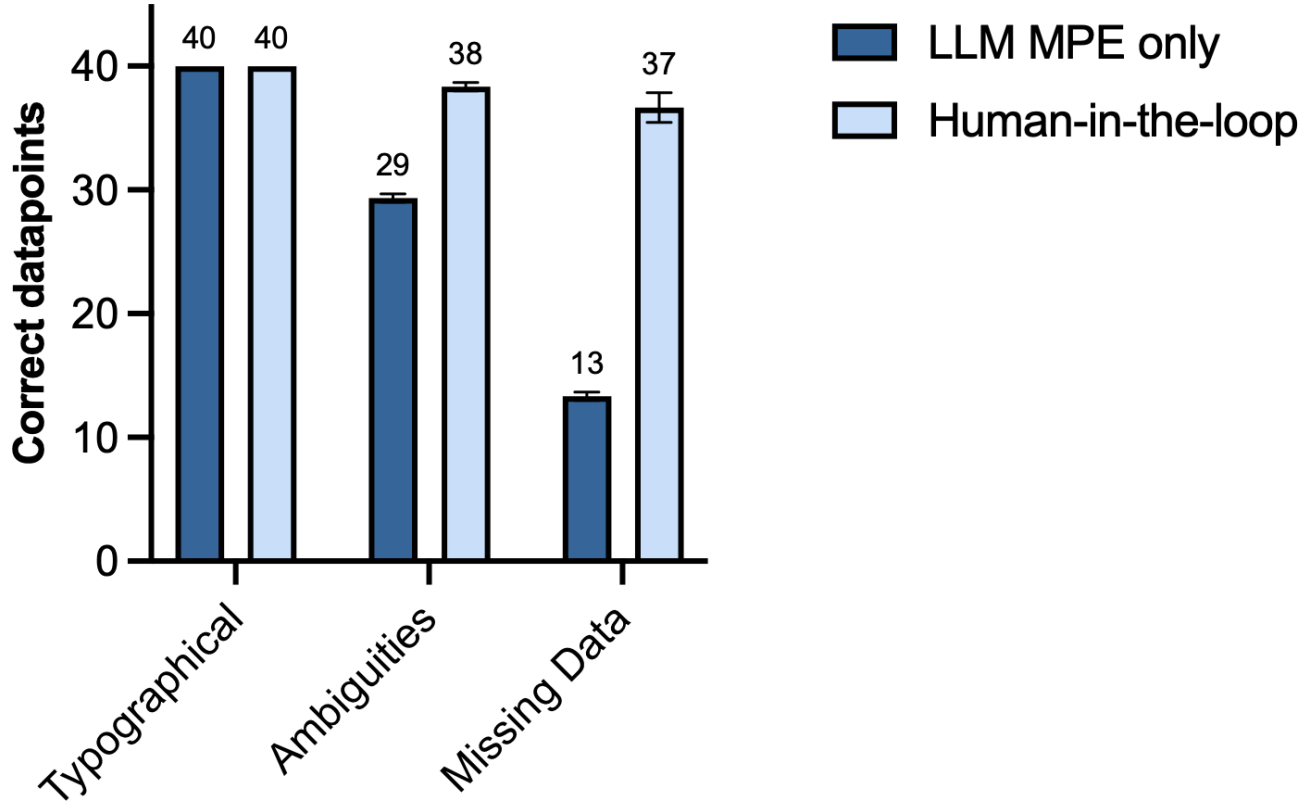
Validation on an Independent Leukemia Cohort

Next, to assess the generalizability of our approach, we conducted a validation study on a second, independent synthetic cohort. This dataset comprised 80 patients with AML, a hematological malignancy with distinct clinical terminology and data structures (Table S2 in Multimedia Appendix 2). We repeated the core analytical tasks, including MPE, direct question answering, and automated survival analysis. The LLM's performance on the AML dataset was highly consistent with the NSCLC cohort, achieving an overall MPE accuracy of 99.7% on batches of 40 letters, answering complex questions with a relative deviation below 0.5%, and generating survival curves nearly identical to GT (Figure S5 in Multimedia Appendix 2).

Stress Testing the Framework Against Simulated Real-World Data Imperfections

Given the limitations of synthetic data, we sought to assess the framework's resilience to common real-world data challenges. We therefore conducted a stress test on a modified subset of 40 letters, where each letter was intentionally corrupted with one relevant typographical error, one data ambiguity or contradiction, and one missing data point. In the MPE task, the LLM demonstrated high resilience to typographical errors, with no impact on accuracy. However, data ambiguities, contradictions, and especially missing data substantially reduced performance (Figure 6). To address this, we evaluated a two-stage workflow: errors or missing data were first flagged by the LLM and then resolved by a human annotator. With the human-in-the-loop approach, almost all deliberately introduced ambiguities and missing data points were resolved.

Figure 6. Effect of data quality issues. Bar chart comparing direct LLM extraction ("LLM MPE only") against a "human-in-the-loop workflow" on a dataset corrupted with 40 typographical errors, ambiguities, and missing data. Bars show the mean correct data points (out of 40) from 3 independent repetitions; error bars represent the standard error of the mean. LLM: large language model; MPE: multiparameter extraction.



Hypothesis Generation Beyond Extraction

Having established the LLM's ability to replicate conventional analytic workflows, we turned to a more exploratory objective: could the model go beyond predefined tasks and autonomously generate novel, clinically meaningful hypotheses? To test this, we prompted the LLM to analyze the dataset (n=80 and n=160 letters) and independently propose potential associations or insights. One example for such a hypothesis (H1) was: "In patients with KRAS-mutated NSCLC treated with an immune checkpoint inhibitor-containing regimen, the presence of a concurrent serine/threonine kinase 11 loss-of-function mutation is associated with a significantly increased risk of developing severe (Grade 3) immune-mediated colitis."

As shown in Table 2, with 80 letters, the LLM offered entirely correct justifications from the provided data. However, with 160 letters, performance dropped and most explanations were either only partly correct or incorrect. Moreover, biological plausibility was generally moderate to high, while the novelty of the offered hypotheses tended to be only moderate.

XSL•FO
RenderX

Table . Evaluation of hypothesis generation capabilities.

Hypothesis	Justification	Biological plausibility	Novelty
80 letters			
H1	Fully correct	Low-moderate	High
H2	Fully correct	Moderate	Moderate-high
H3	Fully correct	Moderate-high	Moderate
H4	Fully correct	High	Low-moderate
H5	Fully correct	High	Low-moderate
160 letters			
H6	Partly correct	Low-moderate	High
H7	Incorrect	High	Low-moderate
H8	Fully correct	High	Low
H9	Partly correct	High	Moderate
H10	Incorrect	High	Moderate

Discussion

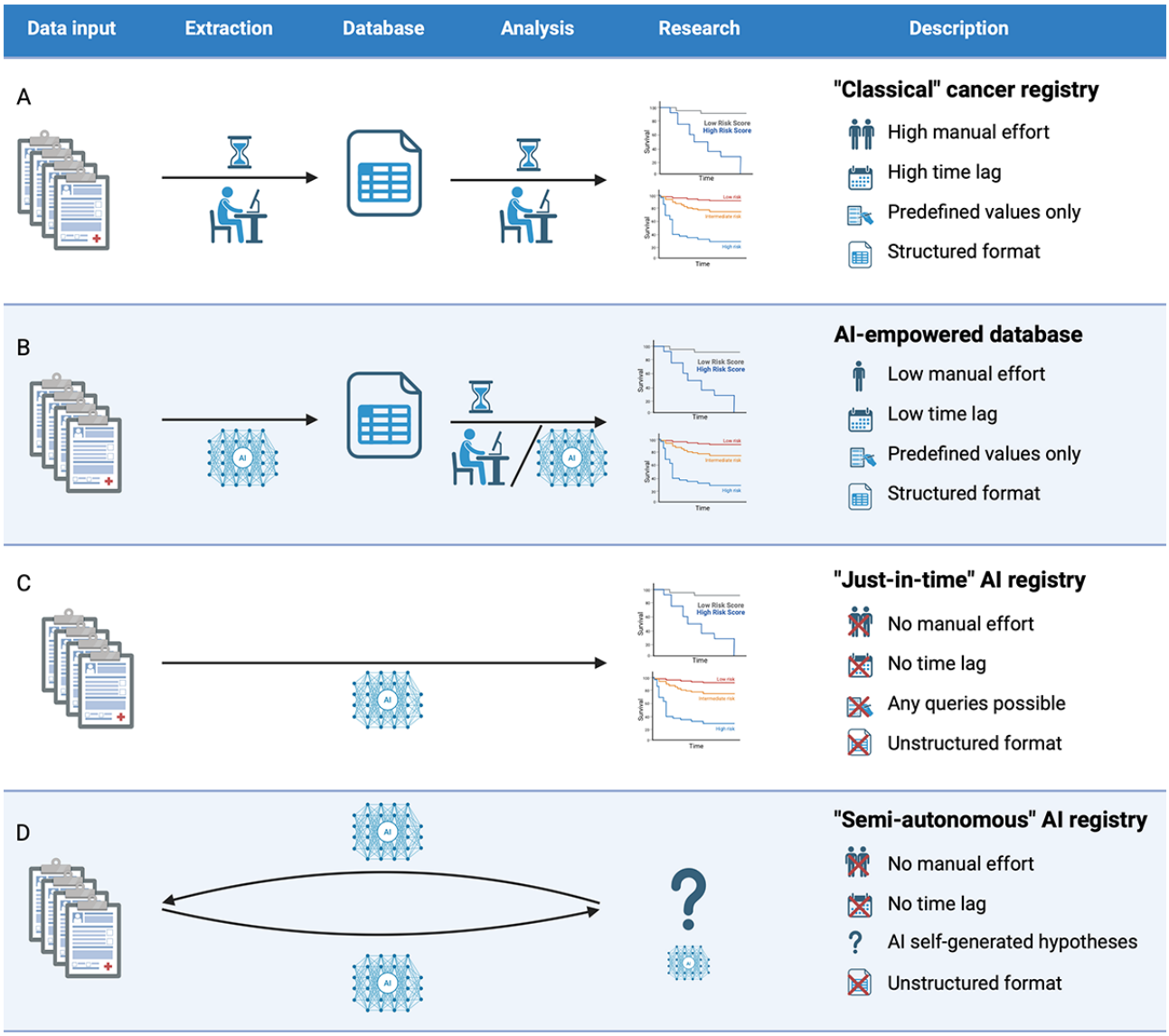
Principal Results

This study provides proof-of-concept that LLMs can significantly advance the processing of unstructured clinical oncology data. Our results demonstrate the feasibility of this approach: we show that LLMs can not only reliably and efficiently extract structured parameters but also perform complex multistep analyses like Kaplan-Meier survival estimation. A stress test designed to simulate real-world ambiguities, noise, and missing data showed that while performance degrades under these conditions, this degradation can be effectively mitigated using a human-in-the-loop approach. Finally, for smaller batches, biologically plausible hypotheses were generated from unstructured data without any prior human annotations or prompts about specific associations. While this study did not formally test the proposed hypotheses, their justification from the data source and novelty reinforce the potential for LLMs to function not only as passive extractors but also as proactive scientific agents within the clinical workflow.

As conceptualized in Figure 7, these findings support a potential paradigm shift for oncology data management in the future: from static, delay-prone databases toward dynamic, JIT analysis of raw clinical documentation [14,15], potentially accelerating research [1,2,18].

XSL•FO
RenderX

Figure 7. Schematic overview of different cancer registry paradigms. Comparison of workflow and characteristics for (A) classical manual registry, (B) AI-empowered extraction feeding a structured database, (C) direct AI analysis of unstructured data ("Just-in-time"), and (D) a future concept of a semiautonomous, hypothesis-generating AI registry. AI: artificial intelligence.



While prior work has demonstrated LLM proficiency in extracting specific clinical end points like PFS [3,4], biomarkers [5], and TNM stage [1] from unstructured text, often focusing on single-task extraction to populate structured databases, our study extends these findings in several key dimensions. The novel contribution of our work is the systematic assessment of an LLM as an integrated interface for complex, multistep tasks in clinical oncology research, potentially obviating the need for intermediate structured databases for many analytical needs. In contrast to the limitations of manual methods or static natural language processing approaches, LLMs exhibit flexible reasoning, adapt to narrative variability, and synthesize context across documents [3,5,19,20]. Our work quantifies this fidelity at scale, showing LLMs maintain clinically acceptable error rates in high throughput, with multiple complex parameters extracted simultaneously. In addition to speed, LLMs offer crucial flexibility: new parameters can be readily incorporated, allowing analytical frameworks to evolve with scientific understanding—a significant advantage over static traditional registries.

However, the practical feasibility of a JIT approach hinges on specific economic and privacy considerations. Regarding cost, we estimated the computational expense on a single analytical run on our full 240-letter cohort at current application programming interface (API) pricing to be around US $0.30–$0.40. In line with our human benchmark, prior studies have reported 225 person-hours for manual abstraction of 100 complete patient records, making estimated labor costs for such tasks much higher [21]. Whether it is more economical to use LLMs to perform a one-time MPE to create a structured database, with subsequent analyses run on that database, or always interrogate the entire batch of unstructured data, will depend on future API pricing. Beyond cost, translating the JIT approach to real patient data necessitates strict attention to privacy and regulations like HIPAA or General Data Protection Regulation [22]. A primary pathway involves using secure, HIPAA-compliant cloud APIs from major providers, which are of state-of-the-art performance but rely on the provider's security architecture. An alternative is the deployment of local, on-premise LLMs, which provide maximum data security and

XSL•FO
RenderX

control but currently lag behind frontier models in analytical capability and require significant institutional investments in hardware and maintenance [23,24]. Therefore, a successful real-world implementation must carefully balance the analytical power of cloud models with the security of local solutions, potentially through hybrid approaches or advanced, LLM-based deidentification techniques [25].

Limitations

Our study has several limitations that must be considered when interpreting the results. First, and most importantly, our study was conducted exclusively on a synthetic dataset. While we took significant steps to create a heterogeneous and challenging benchmark—incorporating diverse linguistic styles, a wide range of document lengths, and varying levels of clinical detail—this dataset cannot fully replicate the complexity of real-world clinical records. Specifically, our synthetic data, despite its variability, likely lacks the idiosyncratic shorthand, nonstandard abbreviations, ambiguities, and internal contradictions across multiple documents for a single patient that are common in authentic electronic health record data [26,27]. The high accuracy reported here may be, in part, an artifact of testing an LLM on relatively clean data generated by other LLMs. Consequently, our results should be interpreted as an upper-bound estimate of performance in a controlled environment. Even our error-injection simulation may not fully capture the nuanced challenges of real-world data. Therefore, rigorous validation on large-scale, multi-institutional, deidentified real-world datasets is the essential next step before the clinical deployment of this JIT paradigm can be considered.

Second, our study's reliance on a single dataset of stage IV NSCLC raises questions about its generalizability. Although our validation on a smaller AML cohort showed consistent performance, the framework's robustness across different cancer types, disease stages, and institutional documentation practices remains unproven and requires further validation. Third, our study used a single LLM architecture, and performance is prompt-dependent; comparative studies with other models (eg, CancerLLM [28]) and RAG frameworks are needed. Our preliminary tests showed that other leading frontier models (including from OpenAI and Anthropic) and local models could not handle this data volume, returning truncated or incomplete results. While our large-context method differs from alternative architectures like RAG, we recognize that the LLM landscape is rapidly evolving. Therefore, future comparative studies are needed to benchmark different approaches as their capabilities expand. Fourth, the autonomous generation of hypotheses, while compelling, must be treated as exploratory. Fifth, real-world deployment of our JIT paradigm faces certain ethical and practical hurdles. LLMs can perpetuate biases, creating ethical challenges that necessitate robust human oversight and model transparency to ensure accountability and health equity [29,30]. Therefore, responsible clinical integration will depend on developing clear regulatory frameworks and maintaining a human-in-the-loop approach to ensure patient safety. Human–AI interaction also requires real-world evaluation [31].

Conclusion

In a controlled experiment using synthetic data, this study demonstrated that a frontier LLM can perform complex, multistep analytical tasks directly from unstructured text. The model successfully executed high-fidelity data extraction, answered multiconditional queries, and generated accurate end-to-end survival analyses. These results establish the technical feasibility of a JIT clinical analysis model under idealized conditions. The extent to which these capabilities generalize to the complexities of real-world clinical data remains unproven and requires rigorous, multi-institutional validation before any practical application can be considered.

Acknowledgments

The authors acknowledge the use of generative artificial intelligence (AI) in the preparation of this manuscript. Specifically, generative AI models were used to generate the synthetic patient letters that form the dataset of this study. Moreover, a large language model was used to proofread the manuscript for grammar, spelling, and clarity. The authors reviewed and edited all AI-generated contributions and assumed full responsibility for the final content of this work. This research received no external funding and was supported by internal institutional funds.

Data Availability

The datasets generated during the current study are available from the corresponding author upon reasonable request. To promote transparency, reproducibility, and community benchmarking, all 240 synthetic patient letters used in this study have been made publicly available in a GitHub repository [32]. We encourage other research groups to use this dataset for evaluating clinical language models.

Authors' Contributions

Conceptualization: MKS, FS
Methodology: FS, CS, SS
Validation: JG, SN, PM
Formal Analysis and Data Curation: PM
Manuscript Writing: PM, JJ
Supervision and Project Administration: JJ

XSL•FO
RenderX

Conflicts of Interest

MKS and FS hold shares in Accessus Science Technologies GmbH.
PM, JG, CS, and SS receive honoraria from Accessus Science Technologies GmbH.
SN and JJ have no conflicts of interest related to this research.

Multimedia Appendix 1
Data scheme representing all variables for synthetic non–small cell lung cancer (n=240) and acute myeloid leukemia (n=80) cohorts.
[XLSX File, 48 KB - medinform_v13i1e78332_app1.xlsx]

Multimedia Appendix 2
Supplementary tables (S1-4) and figures (S1-5), prompts, and example letters.
[DOCX File, 915 KB - medinform_v13i1e78332_app2.docx]

References

1. Kefeli J, Berkowitz J, Acitores Cortina JM, Tsang KK, Tatonetti NP. Generalizable and automated classification of TNM stage from pathology reports with external validation. Nat Commun 2024 Oct 16;15(1):8916. [doi: 10.1038/s41467-024-53190-9] [Medline: 39414770]
2. Swaminathan A, Ren AL, Wu JY, et al. Extraction of unstructured electronic health records to evaluate glioblastoma treatment patterns. JCO Clin Cancer Inform 2024 Jun;8:e2300091. [doi: 10.1200/CCI.23.00091] [Medline: 38857465]
3. Varma G, Yenukoti RK, Kumar M P, et al. A deep learning-enabled workflow to estimate real-world progression-free survival in patients with metastatic breast cancer: study using deidentified electronic health records. JMIR Cancer 2025 May 15;11:e64697. [doi: 10.2196/64697] [Medline: 40372953]
4. Elmarakeby HA, Trukhanov PS, Arroyo VM, et al. Empirical evaluation of language modeling to ascertain cancer outcomes from clinical text reports. BMC Bioinformatics 2023 Sep 2;24(1):328. [doi: 10.1186/s12859-023-05439-1] [Medline: 37658330]
5. Cohen AB, Adamson B, Larch JK, Amster G. Large language model extraction of PD-L1 biomarker testing details from electronic health records. AI Precision Oncol 2025 Apr 1;2(2):57-64. [doi: 10.1089/aipo.2024.0043]
6. Chen D, Alnassar SA, Avison KE, Huang RS, Raman S. Large language model applications for health information extraction in oncology: scoping review. JMIR Cancer 2025 Mar 28;11:e65984. [doi: 10.2196/65984] [Medline: 40153782]
7. Wiest IC, Ferber D, Zhu J, et al. Privacy-preserving large language models for structured medical information retrieval. NPJ Digit Med 2024 Sep 20;7(1):257. [doi: 10.1038/s41746-024-01233-2] [Medline: 39304709]
8. Yamagishi Y, Nakamura Y, Hanaoka S, Abe O. Large language model approach for zero-shot information extraction and clustering of Japanese radiology reports: algorithm development and validation. JMIR Cancer 2025 Jan 23;11:e57275. [doi: 10.2196/57275] [Medline: 39864093]
9. Hashtarkhani S, Rashid R, Brett CL, et al. Cancer diagnosis categorization in electronic health records using large language models and BioBERT: model performance evaluation study. JMIR Cancer 2025 Oct 2;11:e72005. [doi: 10.2196/72005] [Medline: 41037674]
10. Yao J, Goldner E, Hochheiser H, et al. Systemic anticancer therapy timelines extraction from electronic medical records text: algorithm development and validation. JMIR Bioinform Biotech 2025;6:e67801-e67801. [doi: 10.2196/67801]
11. Yao Y, Cen X, Gan L, et al. Automated esophageal cancer staging from free-text radiology reports: large language model evaluation study. JMIR Med Inform 2025 Oct 17;13:e75556. [doi: 10.2196/75556] [Medline: 41105871]
12. Ferber D, Wiest IC, Wölflein G, et al. GPT-4 for information retrieval and comparison of medical oncology guidelines. NEJM AI 2024 May 23;1(6):AIcs2300235. [doi: 10.1056/AIcs2300235]
13. Xu R, Hong Y, Zhang F, Xu H. Evaluation of the integration of retrieval-augmented generation in large language model for breast cancer nursing care responses. Sci Rep 2024 Dec 28;14(1):30794. [doi: 10.1038/s41598-024-81052-3] [Medline: 39730573]
14. Stuhlmiller TJ, Rabe A, Rapp J, et al. A scalable method for validated data extraction from electronic health records with large language models. Health Informatics. p. 2025. [doi: 10.1101/2025.02.25.25322898]
15. Hasan SMS, Rivera D, Wu XC, Durbin EB, Christian JB, Tourassi G. Knowledge graph-enabled cancer data analytics. IEEE J Biomed Health Inform 2020 Jul;24(7):1952-1967. [doi: 10.1109/JBHI.2020.2990797] [Medline: 32386166]
16. Wang L, Li J, Zhuang B, et al. Accuracy of large language models when answering clinical research questions: systematic review and network meta-analysis. J Med Internet Res 2025 Apr 30;27:e64486. [doi: 10.2196/64486] [Medline: 40305085]
17. Barr AA, Quan J, Guo E, Sezgin E. Large language models generating synthetic clinical datasets: a feasibility and comparative analysis with real-world perioperative data. Front Artif Intell 2025;8:1533508. [doi: 10.3389/frai.2025.1533508] [Medline: 39974356]

XSL•FO
RenderX

18. Kehl KL, Groha S, Lepisto EM, et al. Clinical inflection point detection on the basis of EHR data to identify clinical trial-ready patients with cancer. JCO Clin Cancer Inform 2021 Jun;5:622-630. [doi: 10.1200/CCI.20.00184] [Medline: 34097438]
19. Dahl S, Bøgsted M, Sagi T, Vesteghem C. Performance of natural language processing for information extraction from electronic health records within cancer: systematic review. JMIR Med Inform 2025 Sep 12;13:e68707. [doi: 10.2196/68707] [Medline: 40939201]
20. Van Veen D, Van Uden C, Blankemeier L, et al. Adapted large language models can outperform medical experts in clinical text summarization. Nat Med 2024 Apr;30(4):1134-1142. [doi: 10.1038/s41591-024-02855-5] [Medline: 38413730]
21. Gauthier MP, Law JH, Le LW, et al. Automating access to real-world evidence. JTO Clin Res Rep 2022 Jun;3(6):100340. [doi: 10.1016/j.jtocrr.2022.100340] [Medline: 35719866]
22. Elbattah M, Arnaud E, Ghazali DA, Dequen G. Exploring the ethical challenges of large language models in emergency medicine: a comparative international review. In: Dequen G, editor. 2024 Presented at: 2024 IEEE International Conference on Bioinformatics and Biomedicine (BIBM); Dec 3-6, 2024. [doi: 10.1109/BIBM62325.2024.10822376]
23. Wiest IC, Verhees FG, Ferber D, et al. Detection of suicidality from medical text using privacy-preserving large language models. Br J Psychiatry 2024 Dec;225(6):532-537. [doi: 10.1192/bjp.2024.134] [Medline: 39497458]
24. Lee D, Vaid A, Menon KM, et al. Using large language models to automate data extraction from surgical pathology reports: retrospective cohort study. JMIR Form Res 2025 Apr 7;9:e64544. [doi: 10.2196/64544] [Medline: 40194317]
25. Wiest IC, Leßmann ME, Wolf F, et al. Deidentifying medical documents with local, privacy-preserving large language models: the LLM-anonymizer. NEJM AI 2025 Mar 27;2(4):AIdbp2400537. [doi: 10.1056/AIdbp2400537]
26. Savova GK, Danciu I, Alamudun F, et al. Use of natural language processing to extract clinical cancer phenotypes from electronic medical records. Cancer Res 2019 Nov 1;79(21):5463-5470. [doi: 10.1158/0008-5472.CAN-19-0579] [Medline: 31395609]
27. Spasić I, Livsey J, Keane JA, Nenadić G. Text mining of cancer-related information: review of current status and future directions. Int J Med Inform 2014 Sep;83(9):605-623. [doi: 10.1016/j.ijmedinf.2014.06.009] [Medline: 25008281]
28. Li M, Huang J, Yeung J, Blaes A, Johnson S, Liu H, et al. CancerLLM: a large language model in cancer domain. arXiv. Preprint posted online on Jun 1, 2024 URL: https://ui.adsabs.harvard.edu/abs/2024arXiv240610459L [accessed 2025-11-14]
29. Zhang K, Meng X, Yan X, et al. Revolutionizing health care: the transformative impact of large language models in medicine. J Med Internet Res 2025 Jan 7;27:e59069. [doi: 10.2196/59069] [Medline: 39773666]
30. Verlingue L, Boyer C, Olgiati L, Brutti Mairesse C, Morel D, Blay JY. Artificial intelligence in oncology: ensuring safe and effective integration of language models in clinical practice. Lancet Reg Health Eur 2024 Nov;46:101064. [doi: 10.1016/j.lanepe.2024.101064] [Medline: 39290808]
31. Wekenborg MK, Gilbert S, Kather JN. Examining human-AI interaction in real-world healthcare beyond the laboratory. NPJ Digit Med 2025 Mar 19;8(1):169. [doi: 10.1038/s41746-025-01559-5] [Medline: 40108434]
32. JIT-AI-registry. GitHub [FREE Full text]

Abbreviations

AI: artificial intelligence
AML: acute myeloid leukemia
API: application programming interface
C-index: (Harrell's) concordance index
GT: ground truth
HIPAA: Health Insurance Portability and Accountability Act
JIT: just-in-time
KRAS: Kirsten rat sarcoma viral oncogene homolog
LLM: large language model
MPE: multiparameter extraction
NSCLC: non–small cell lung cancer
OS: overall survival
PD-L1: programmed death-ligand 1
PFS: progression-free survival
RAG: retrieval-augmented generation
SPE: single parameter extraction
WT: wild type

XSL•FO
RenderX

Edited by A Coristine; submitted 12.06.25; peer-reviewed by M Elbattah, M Beltrão, N Acharya, P Ruan, Y Miao; revised version received 22.10.25; accepted 23.10.25; published 01.12.25.

Please cite as:
May P, Greß J, Seidel C, Sommer S, Schuler MK, Nokodian S, Schröder F, Jung J
Enabling Just-in-Time Clinical Oncology Analysis With Large Language Models: Feasibility and Validation Study Using Unstructured Synthetic Data
JMIR Med Inform 2025;13:e78332
URL: https://medinform.jmir.org/2025/1/e78332
doi:10.2196/78332

© Peter May, Julian Greß, Christoph Seidel, Sebastian Sommer, Markus K Schuler, Sina Nokodian, Florian Schröder, Johannes Jung. Originally published in JMIR Medical Informatics (https://medinform.jmir.org), 1.12.2025. This is an open-access article distributed under the terms of the Creative Commons Attribution License (https://creativecommons.org/licenses/by/4.0/), which permits unrestricted use, distribution, and reproduction in any medium, provided the original work, first published in JMIR Medical Informatics, is properly cited. The complete bibliographic information, a link to the original publication on https://medinform.jmir.org/, as well as this copyright and license information must be included.

XSL•FO
RenderX

Enhancing Large Language Models With AI Agents for Chronic Gastritis Management: Comprehensive Comparative Study

Shurui Wang, MSc; Qing Ye, PhD

Tongji Hospital, Tongji Medical College, Huazhong University of Science and Technology, 1095 Jiefang Ave, Wuhan, Hubei, China

Corresponding Author:
Qing Ye, PhD
Tongji Hospital, Tongji Medical College, Huazhong University of Science and Technology, 1095 Jiefang Ave, Wuhan, Hubei, China

Abstract

Background: The prevalence of chronic gastritis is high, and if not intervened in a timely manner, it may eventually lead to gastric cancer. Managing chronic gastritis essentially requires comprehensive lifestyle changes. However, the current health care environment does not support continuous follow-up by professional health care providers, making self-management a key component of postdiagnosis care. Increasingly, researchers are exploring the use of large language models (LLMs) for patient management. However, LLMs have limitations, including hallucinations, limited knowledge scope, and lack of timeliness. Artificial intelligence (AI) agents may provide a more effective solution. Nevertheless, it remains uncertain whether AI agents can effectively support postdiagnosis self-management for patients with chronic gastritis.

Objective: The purpose of this study was to explore the effectiveness of AI agents in the postdiagnosis management of patients with chronic gastritis from different perspectives.

Methods: In this study, we developed an agent framework for the health management of patients with chronic gastritis based on LLMs in conjunction with retrieval-augmented generation and a search engine tool. We collected real questions from patients with chronic gastritis in clinical settings and tested the framework's performance across different difficulty levels and scenarios. We analyzed its safety and robustness and compared it with state-of-the-art models to comprehensively evaluate its effectiveness.

Results: Using a dual-evaluation framework comprising automated metrics and expert manual assessments, our results demonstrated that AI agents substantially outperformed LLMs in addressing high-complexity questions (embedding average score: 82.849 for AI agents vs 77.825 for LLMs) and were particularly effective in clinical consultation tasks. Clinical evaluation of safety based on a 5-point Likert scale by physicians indicated that the safety of the agents was 4.98 (SD 0.15; 95% CI 4.96-4.99). After 30 repeated experiments, the mean absolute deviation of the AI agents in the embedding average score and BERTScore metrics were 0.0167 and 0.0387, respectively. Therefore, the safety and robustness analysis confirmed that the AI agents can produce safe, stable, and minimally variable responses. In addition, comparative results with those of advanced medical-domain LLMs (Baichuan-14B-M1 and MedGemma-27B) and general-domain LLMs (Qwen3-32B) also demonstrated that the AI agents in this study performed outstandingly in the field of chronic gastritis. Our findings underscore the superior reliability, interpretability, and practical applicability of AI agents over conventional LLMs in chronic gastritis management, offering a robust foundation for their broader adoption in health care settings.

Conclusions: AI agents based on LLMs have high application value in the management of chronic gastritis. They can effectively guide patients with chronic diseases in addressing common issues, which may potentially reduce the workload of physicians and improve the quality of patient home care.

(JMIR Med Inform 2025;13:e73857) doi:10.2196/73857

KEYWORDS

large language models; artificial intelligence agent; AI agent; chronic gastritis; health management; retrieval-augmented generation; artificial intelligence; AI

Introduction

Chronic gastritis is one of the most common disorders in the digestive system and is also the initial phase in the progression to gastric cancer [1-3]. It is characterized by insidious onset, a protracted disease course, high prevalence, and frequent recurrence, as well as substantial health care costs, all of which significantly compromise patients' quality of life [4]. Data show that nearly half of patients with chronic atrophic gastritis experience anxiety [5], and prolonged anxiety is also identified as a risk factor for the exacerbation of chronic gastritis. The management of chronic gastritis inherently requires comprehensive lifestyle modifications, and self-management has emerged as a critical component in chronic gastritis care.

XSL•FO
RenderX

Patients can achieve not only effective symptom control but also meaningful improvement in overall health-related quality of life through systematic self-monitoring, evidence-based lifestyle adjustments, and structured psychological support, ultimately progressing toward holistic wellness.

Current constraints within the health care system render continuous postdiagnosis management by medical professionals impractical and unsustainable. The substantial heterogeneity in patient demographics further compounds clinical workload burdens. Particularly in resource-limited settings and geographically remote areas with uneven health care distribution [6,7], temporal and financial constraints make regular in-person clinical follow-ups largely unfeasible. While patient self-management presents a viable strategy to mitigate these resource limitations, the selection of appropriate self-care modalities remains paramount. Inappropriate information-seeking behaviors may lead to the acquisition of erroneous medical knowledge, potentially yielding adverse clinical outcomes. For instance, exclusive reliance on search engines for medical guidance is problematic due to the absence of professional interaction, where inaccuracies in symptom interpretation or medical misinformation may precipitate serious consequences [8]. Online consultations in the internet era provide convenience for patient inquiries. However, patients often express concerns about the protection of their personal privacy and a lack of trust in the professionalism of online services [9,10]. In addition, the uncertainty surrounding patients' online medical needs and the availability of physicians is highly likely to intensify their hesitation and resistance toward online consultations.

Since 2018, when OpenAI introduced the first generative pretrained transformer model, GPT-1 [11], large language models (LLMs) have ushered in a golden age. In recent years, the surge in the development of LLMs has inevitably sparked transformative changes in the medical field [12]. Ayers et al [13] compared the performance of ChatGPT with that of physicians in responding to patient inquiries on social media. The results indicated that the responses generated by ChatGPT were of higher quality and received greater patient approval. In addition, LLMs are capable of maintaining continuous communication with patients around the clock, a level of availability that is nearly impossible for human responders to achieve and difficult to improve upon. Furthermore, LLMs can address sensitive questions posed by patients, which are often challenging to broach or are met with hesitation during face-to-face consultations.

However, complete reliance on LLMs also carries certain risks as the issue of hallucinations cannot be overlooked, particularly in the health care domain. As hallucinations cannot be entirely eliminated, we can strive to minimize their occurrence. Research has shown that the agent framework [14] can significantly reduce the hallucination rate [15,16]. Meanwhile, the knowledge of LLMs is derived from their pretraining data, which inherently have limitations such as restricted scope and lack of timeliness [17]. To better address the complex and dynamic management needs of patients with chronic gastritis, an agent system built upon LLMs but not confined to the existing content in the training data may offer a more effective solution. As LLMs demonstrate remarkable capabilities and attract widespread attention, an increasing number of researchers are leveraging these models to develop artificial intelligence (AI) agent systems [18-20]. Agents have been proven to possess capabilities beyond those of LLMs [21-23]. Nevertheless, whether agents can be effectively used for the management of patients with chronic gastritis remains uncertain.

Our research specifically designed a question-and-answer (Q&A) dataset for chronic gastritis and analyzed the feasibility of applying agents in the medical field. Furthermore, by categorizing health management tasks, problem complexity, and the scale of LLMs, we compared the content of responses generated by LLMs and agents. This study aimed to provide guidance for the application of AI agents in the medical field and offer practical AI tools for the postdiagnosis management of patients with chronic gastritis.

Methods

Study Design

The effectiveness of chronic gastritis treatment depends to some extent on the patient's educational background, living environment, and personal habits. The actual circumstances of patients vary, leading to differences in the complexity of the questions they raise. In addition, prompts can significantly influence the performance of LLMs [24,25], and LLMs of different scales exhibit varying capabilities in processing prompts. Therefore, taking into account the characteristics of the disease, the scale of the model, and the needs of patients, we aimed to explore the following research questions:

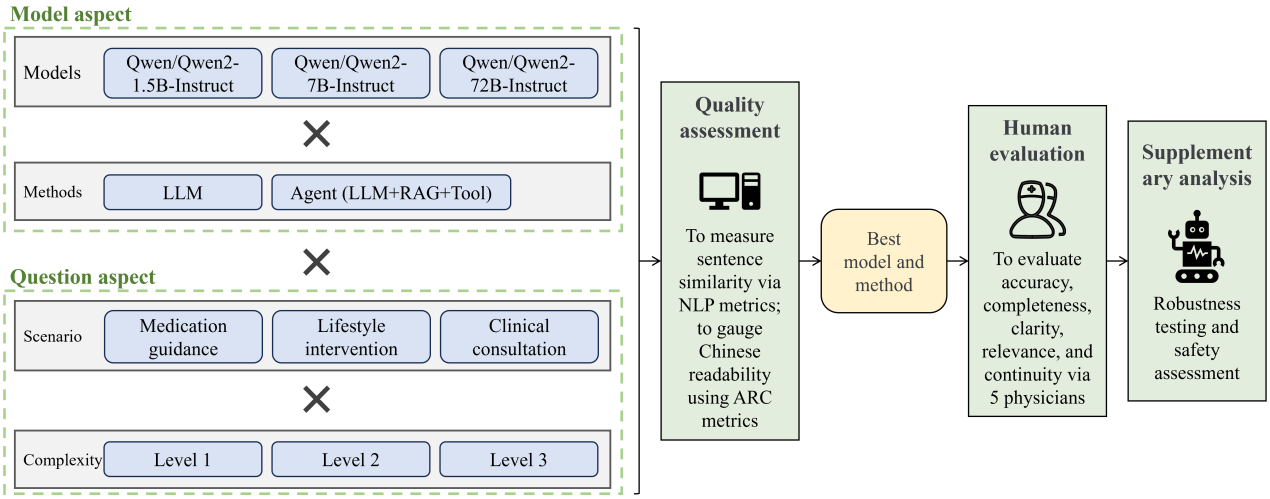
1. In the context of chronic gastritis management, does a larger LLM lead to better response content?
2. In chronic gastritis management, with a consistent parameter size, does an agent outperform an LLM?
3. How does the response content of Q&A models change as the difficulty of the questions increases?
4. Across different health management task scenarios, does an agent consistently outperform an LLM?

To address the aforementioned questions, we propose the methodological framework illustrated in Figure 1. On the basis of health management task scenarios (lifestyle intervention, medication guidance, and clinical consultation) and problem complexity (level 1, level 2, and level 3; more details can be found in the Preparation of the Q&A Dataset section), questions were categorized into 9 (3 × 3) dimensions. These questions were then tested using 3 scales of LLMs and agents (using retrieval-augmented generation [RAG] and a search engine tool; more details can be found in the Use of LLMs and Agents section) on real-world problems. The responses were evaluated using multiple assessment metrics (more details can be found in the Model Evaluation section), and the performance of the models was analyzed across various aspects, including model size, methodology, task scenarios, and problem difficulty. To ensure the safety of the generated answers, we assessed all responses for safety, mitigating potential risks associated with the experimental outcomes. Finally, to enhance the robustness

XSL•FO
RenderX

of the model, we conducted multiple tests on the same set of questions to confirm the stability of the results.

Figure 1. Study framework for the application of large language models (LLMs) in chronic gastritis management. ARC: Alpha Readability Chinese; NLP: natural language processing; RAG: retrieval-augmented generation.

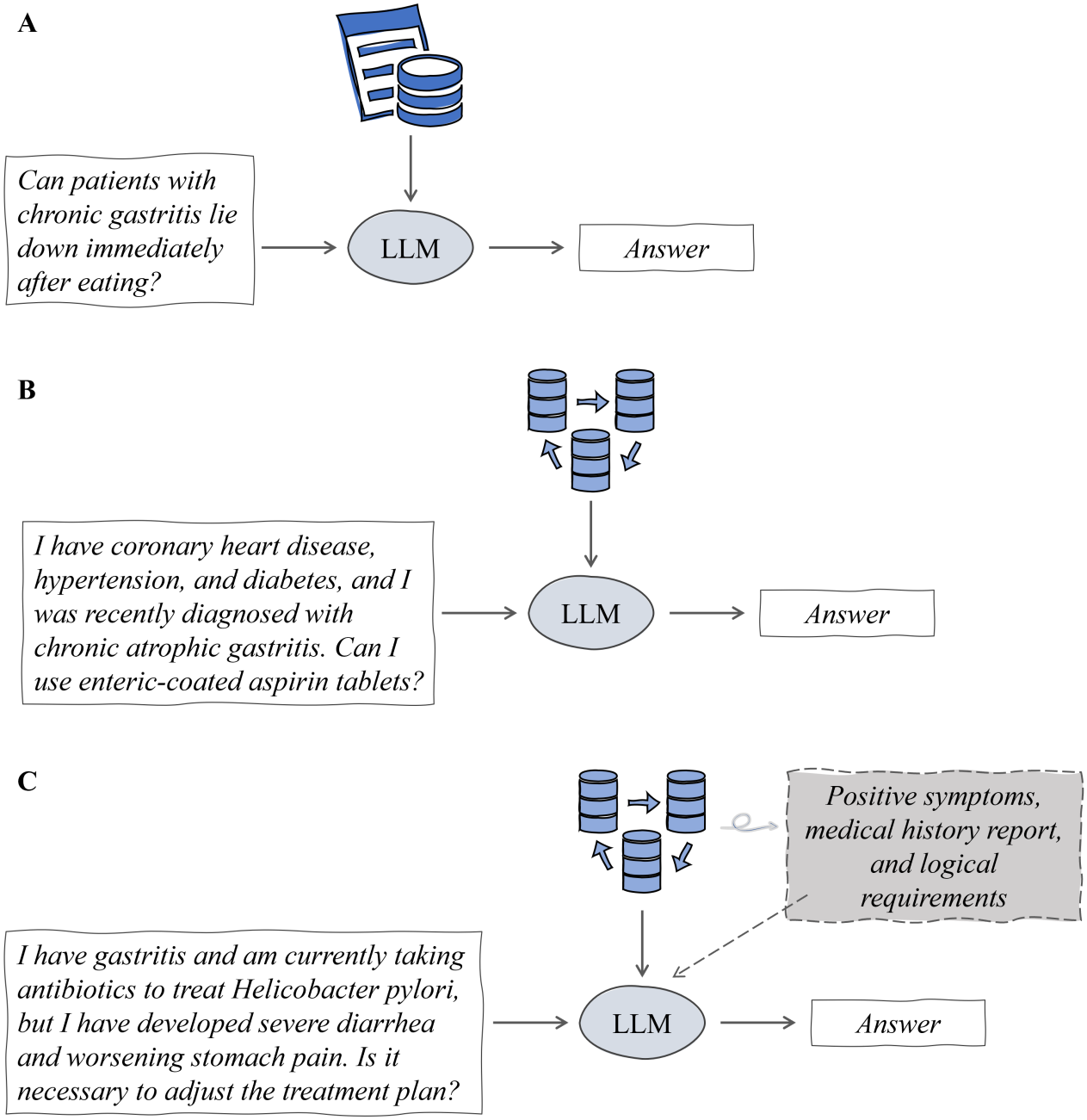


Preparation of the Q&A Dataset

Q&A design was one of the most critical aspects of this study. The real-world questions selected must be representative. We classified the difficulty levels of the patient questions based on the cutting-edge methods proposed by Microsoft [26]. Microsoft's hierarchical approach is designed to identify pathways for finding answers and is tailored for general domains, which does not fully align with the classification of problem difficulty in medical scenarios. Building on this, we collaborated with clinical experts to define 3 difficulty levels appropriate for medical scenarios: low-difficulty questions (level 1; based on explicit facts), medium-difficulty questions (level 2; based on implicit facts), and high-difficulty questions (level 3; requiring reasonable inference). Figure 2 illustrates the rules for categorizing question difficulty.

XSL•FO
RenderX

Figure 2. Criteria for question difficulty classification. (A) Low-difficulty questions, which can be answered based on explicit facts, primarily require the model to locate and extract relevant information. (B) Medium-difficulty questions, which require implicit facts to derive the answer, may involve information scattered across multiple segments. (C) High-difficulty questions, where no explicit answer exists in any information segment, demand complex reasoning to uncover latent information. LLM: large language model.



Use of LLMs and Agents

As the models in the Qwen series have been proven to have excellent application performance [27,28], we selected the "instruct" models from the Qwen2 series with model sizes of 1.5B, 7B, and 72B as the foundational models (Qwen-1.5B, Qwen-7B, and Qwen-72B models) [29]. In 2020, Lewis et al [30] formally proposed and named the RAG framework, marking the birth of a new paradigm. Research has shown that, with the support of external knowledge, "instruct" models can generate more accurate and higher-quality responses [30,31]. Using domain-specific knowledge and external tools, we applied instruction prompting to these models to improve their specialization in the management of chronic gastritis. In addition, an agent was constructed based on the LLM framework, enabling the models to provide more professional responses to questions from patients with chronic gastritis. To enhance the capabilities of the agent, we used RAG and integrated search engine tools to prepare contextual information. The detailed process of RAG and the visualized integration of its components, as well as the prompt templates, are shown in Multimedia Appendix 1. Our preparatory work can be divided into the following components:

- Knowledge base: in light of the updates in clinical techniques, we conducted a search in the *National Medical Journal of China* for Chinese expert consensuses and clinical guidelines published from 2020 to 2024 using "gastritis" as the keyword. Subsequently, we invited experts

XSL•FO
RenderX

to manually screen and select 18 articles related to chronic gastritis. Using the zh_core_web_sm model, we segmented the long texts into sentences and further divided these sentences into chunks using a sliding window approach. Each chunk contained 20 sentences, with an overlap of 5 sentences between adjacent chunks to maintain contextual coherence. Subsequently, the all-MiniLM-L6-v2 model was used to map these chunks into a vector space, converting them into embedding vectors. Finally, using the Euclidean distance as the similarity metric, we created a Faiss index and added the embedding vectors to this index to enable rapid retrieval of the most similar vectors for a given query text.

- Agent tools: a defining feature of an agent, as opposed to a stand-alone LLM, is its ability to flexibly use external tools. In this process, we invoked the Google Search application programming interface to retrieve URLs and content summaries related to the input query. The summary texts were then ranked based on relevance to produce the final search results.
- Agent (with RAG and search tools): on the basis of the Faiss index and L2 distance, we retrieved the 5 most relevant text fragments from the knowledge base. The Google Search application programming interface sorted the organic results according to its internal ranking algorithm, and the 5 most relevant web page snippets were directly output. These 10 text fragments were then passed to the model as reference materials, whereas the decision of whether to use this reference content was autonomously made by the agents. Three agents were constructed based on the Qwen-1.5B, Qwen-7B, and Qwen-72B models. These agents shared identical network parameters, which were configured as follows: the maximum number of tokens was set to 800, the temperature was set to 0.4, the nucleus sampling parameter was set to 0.8, the truncation parameter was set to 5, and the frequency penalty was set to 0.5.

Model Evaluation

Relying on a single perspective for evaluation metrics may lead to biased results. To address this, we used 3 types of evaluation methods: natural language processing–based automatic evaluation metrics, manual scoring, and Chinese lexical evaluation metrics. The automatic evaluation metrics compared the system-generated answers with the standard answers (more details are provided in the Preparation of the Q&A Dataset section) to derive evaluation results. Among these, the embedding average score and BERTScore use cosine similarity between vectors to calculate the relevance to the standard answers, which has proven to be an effective approach [32-34]. In light of the unique nature of medical scenarios, we also designed a Likert scale and organized a panel comprising 5 clinical experts in relevant fields (including 1 certified clinical nutritionist), all of whom have over 10 years of work experience, to manually score the model-generated answers based on the following criteria [35]:

- Accuracy: the response contained specific and precise information rather than general or generic information.
- Completeness: the response covered all relevant medical information and details, with no omission of critical content.
- Clarity: the response was clearly expressed, easy to understand, readable, and free of ambiguity.
- Relevance: the response was closely related to the question, providing useful information and recommendations that aligned closely with the patient's needs.
- Continuity: the response maintained coherent and consistent phrasing throughout, with no logical jumps or inconsistencies.

The experts scored the responses generated by each model using each method ($3 \times 2 \times 63$) on a scale ranging from 1 to 5, where a higher score indicated better performance. In addition, we used a specialized evaluation framework designed for Chinese text to assess the richness and clarity of syntax and vocabulary [36]. This framework was originally developed for general Chinese contexts, but its evaluation metrics can be adapted and interpreted more granularly for medical scenarios:

- Lexical richness: the entropy values of all the words were calculated. The higher the entropy value, the greater the uncertainty associated with the words used in the text. This indicates a more diverse vocabulary, which in turn increases the reading difficulty level of the text.
- Syntactic richness: the entropy values of all the dependencies in the text were calculated. The higher the entropy value, the greater the uncertainty in the text's dependency relationships or syntactic structure. This suggests a more complex and varied syntax, which in turn makes the text more difficult to read.
- Semantic clarity: the semantic clarity value was calculated based on the skewness of the topic distribution probability extracted through latent Dirichlet allocation topic modeling [37]. The higher this value, the more concentrated the text's topics represented by nouns, resulting in clearer semantics.
- Semantic noise: the semantic noise value was calculated through the kurtosis of the topic distribution probability extracted through latent Dirichlet allocation topic modeling [37]. The higher this value, the more the text's topics represented by nouns are skewed toward unimportant topics, thereby increasing the semantic noise.
- Semantic richness: on the basis of the research by Lee et al [37], the semantic richness of the text was calculated by summing the probabilities of the occurrence of nouns in the text. The higher the value, the richer the topics of the text, and the lower its readability.

Ethical Considerations

This study aimed solely to evaluate the quality of responses generated by an AI agent for chronic gastritis queries and was therefore classified as nonhuman-participant research; institutional review board approval and full ethics review were waived. All patient questions were gathered during routine clinical operations, and no identifiable personal information was collected. Consequently, informed consent was not required and no compensation was provided. All analyses were performed on a secure server to safeguard the privacy and confidentiality of the questions submitted by patients.

XSL•FO
RenderX

Results

Influence of Model Scales and Methods on Response Content

Model Scale Comparison

The number of parameters is one of the primary factors influencing the performance of LLMs [38]. The results shown in Figure 3, Table 1, and Figure S3 in Multimedia Appendix 1 demonstrate that changes in model scales have a positive impact on the response content of LLMs. However, as the number of parameters increased, the improvement effect gradually diminished. Specifically, there was no statistically significant difference in response content between base models with 7B and 72B parameters. This phenomenon may be attributed to 2 reasons. First, general-purpose LLMs are suitable for answering questions in broad domains, but their actual performance in specialized fields such as medicine remains uncertain [39,40]. Second, the 7B model has already reached a bottleneck in understanding medical questions, and as our questions were all within the specialized medical domain, merely increasing the number of parameters did not significantly enhance the quality of the response content. Therefore, we further tested the relationship between model scale and response content using an agent. The results still indicated that the Qwen-72B model was the optimal choice for a health management Q&A model focused on chronic gastritis.

Figure 3. Statistical differences in evaluation indicators under different model parameters. Median differences were compared using bar charts. LLM: large language model.

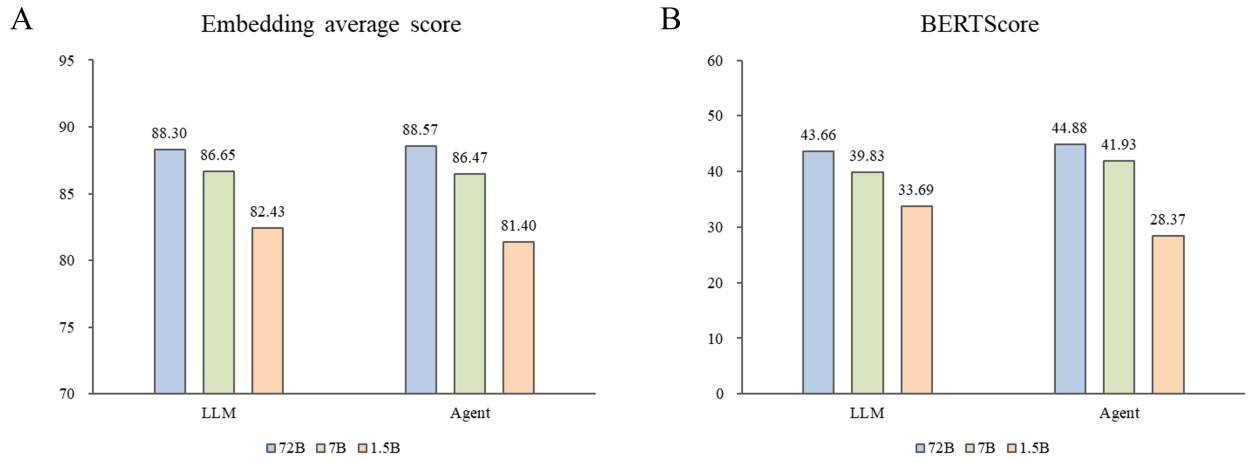


Table . Mann-Whitney *U* test results for evaluation indicators across different model parameters.

Indicator	*U* value	*Z* value	*P* value
Embedding average score			
LLM[a] 1.5B vs 7B	1376	−2.969	.003
LLM 1.5B vs 72B	1336	−3.164	.002
LLM 7B vs 72B	1840	−0.705	.48
Agent 1.5B vs 7B	1165	−3.999	<.001
Agent 1.5B vs 72B	873	−5.423	<.001
Agent 7B vs 72B	1534	−2.198	.03
BERTScore			
LLM 1.5B vs 7B	1203	−3.813	<.001
LLM 1.5B vs 72B	1152	−4.062	<.001
LLM 7B vs 72B	1781	−0.993	.32
Agent 1.5B vs 7B	730	−6.121	<.001
Agent 1.5B vs 72B	524	−7.126	<.001
Agent 7B vs 72B	1484	−2.442	.01

[a]LLM: large language model.

XSL•FO
RenderX

Comparison of LLMs and Agents

Using the Qwen-72B model as the base model, we compared the response content of the LLM and the agent. The trend chart (Figure 4) shows that the response quality of the agent had an upward trend compared with that of the LLM. The linguistic evaluation results (Table 2) show that the responses generated by the agent had higher values in lexical richness, syntactic richness, semantic noise, and semantic richness and a lower value in semantic clarity. These Chinese evaluation indicators are comparative metrics that do not focus on individual results and do not have a defined range of values. This indicates that the responses generated by the agent were more complex in terms of vocabulary and syntax, had a higher reading difficulty level, and covered a broader range of topics compared to the responses generated by the LLM. This demonstrates that the agent not only outperformed the LLM in terms of alignment with the standard answers but also exceeded the LLM in terms of breadth of thinking and domain-specific expertise. This is one concrete example demonstrating the effectiveness of using the tool (Google search engine).

Figure 4. Method comparison: large language model (LLM) and agent. The blue line represents the median trend line, whereas the green and red lines represent the quartile trend lines.

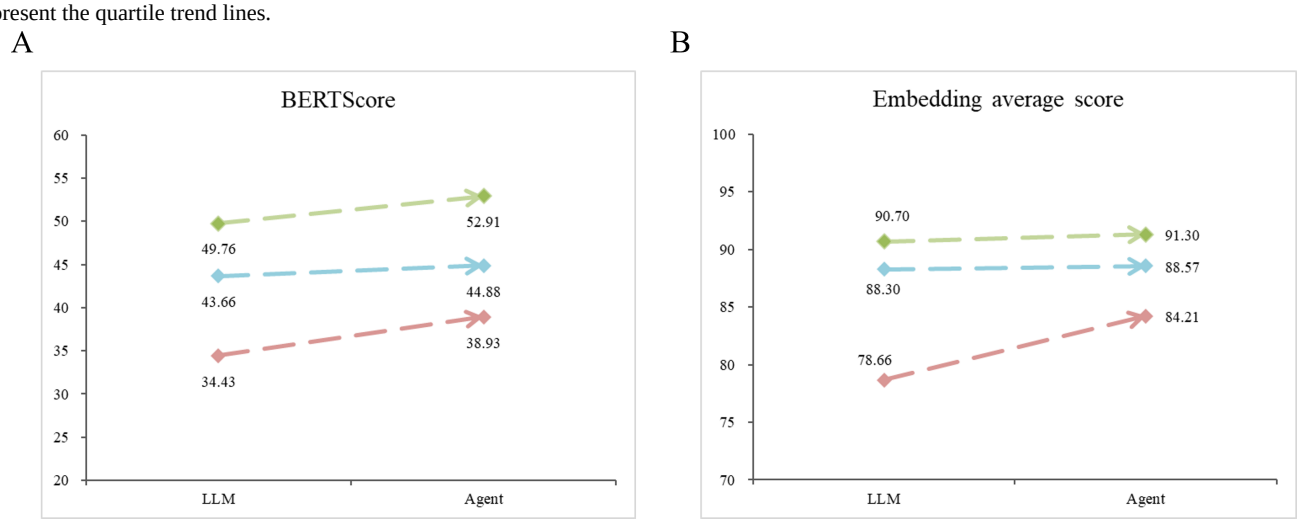


Table . Comparison of a large language model (LLM) and agent in Chinese-language dimensions.

	LLM 72B	Agent 72B
Lexical richness	4.0707	4.2950
Syntactic richness	2.1529	2.1911
Semantic clarity	0.0707	0.0643
Semantic noise	5.8923	6.3081
Semantic richness	0.2411	0.2520

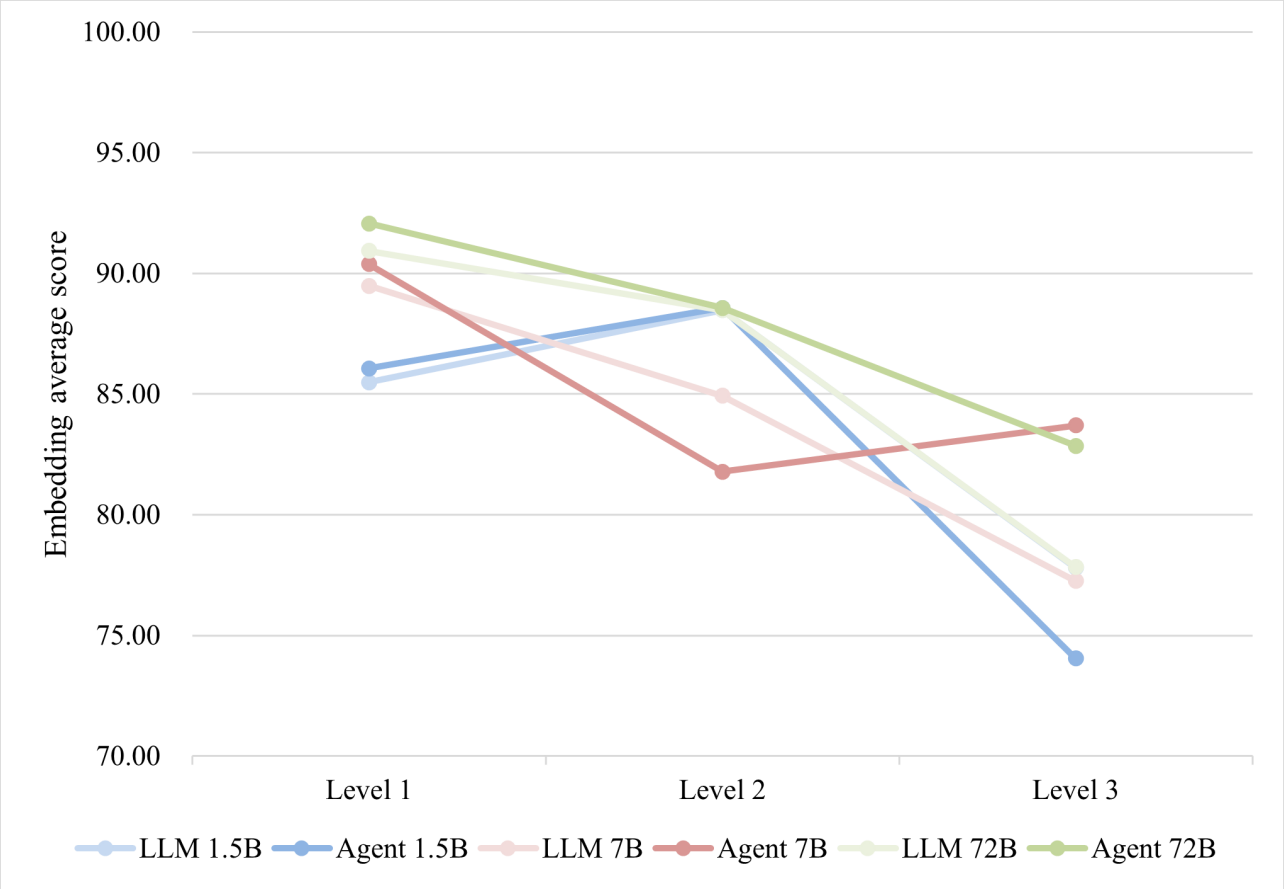
Influence of Question Difficulty and Medical Contexts on Answer Quality

Comparison of Response Content Across Different Difficulty Levels

Figure 5 shows the results stratified by difficulty level, which align with the previous conclusions: larger models outperformed smaller models, and the agents surpassed the LLMs. As question difficulty increased, the similarity between response content and reference answers showed a declining trend. Mann-Whitney *U* tests on the Embedding Average Scores of the 72B-Agent across difficulty levels revealed that the observed decreases from level 1 to level 2 and from level 2 to level 3 were statistically significant (*U* value=141.000, *Z* value=–2.000, *P*=.046; *U* value=121.000, *Z* value=–2.503, *P*=.01). Smaller models exhibited instability, which may be attributed to the limitations of LLMs in specialized domains, insufficient contextual comprehension by smaller models, and the negative impact of irrelevant information [41]. When domain-specific knowledge obtained through RAG and search engine tools was input into smaller agents, these models struggled to accurately understand the relevant information, resulting in noisier and less reliable outputs.

XSL•FO
RenderX

Figure 5. The trend in the impact of question complexity on answer quality. The points on the line represent the median of the embedding average score for all questions under that category. LLM: large language model.

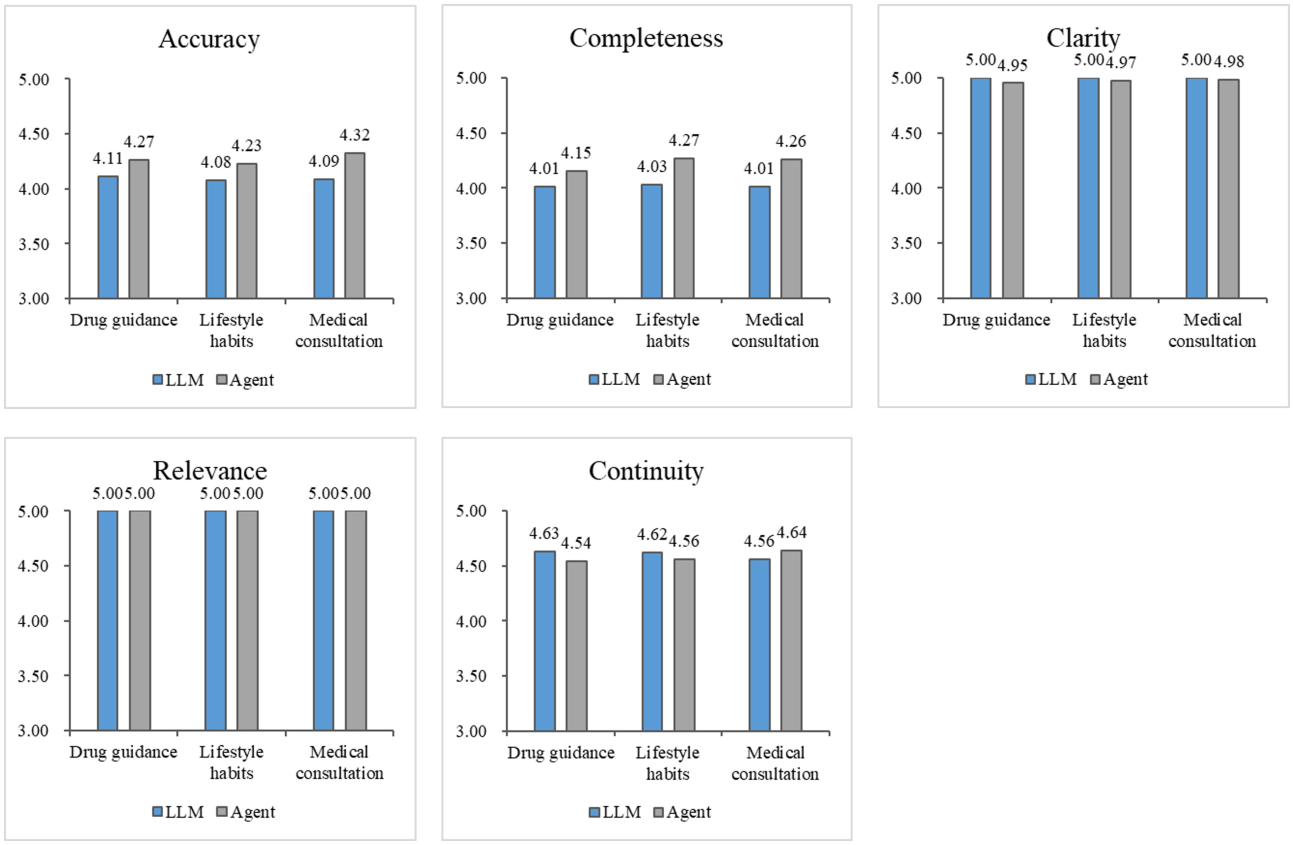


Comparison of Response Content From the Qwen-72B Model Across Different Health Management Tasks

The manually assigned scores for the Qwen-72B model were aggregated and analyzed from the perspective of health management tasks (Figure 6). On the basis of the evaluation results of multiple experts, the clarity and coherence of the agent's responses were slightly inferior to those of the LLM, which was consistent with the previous findings. This is attributed to the agent's replies being more specialized, covering a broader range of topics, and having a higher reading difficulty level. Overall, across the 3 health management task scenarios, the agent demonstrated superior application performance compared to the LLM, with higher accuracy and completeness in its responses. Correspondingly, the increased reading difficulty level placed greater demands on patients' comprehension abilities. In medication guidance and clinical consultation tasks, the aggregate accuracy score of the agent exceeded that for lifestyle intervention tasks, indicating that the agent could more precisely understand questions with relatively fixed answers and generate targeted responses. However, the completeness of the agent's responses for medication guidance tasks was slightly inferior to that for lifestyle intervention and clinical consultation tasks. This suggests that the knowledge base and search engine tools provided to the agent need to be further enhanced in terms of drug-related knowledge to improve its capability in medication guidance.

XSL•FO
RenderX

Figure 6. Comparison of different health management tasks. On the basis of the statistical results of human evaluation, the mean score assigned by all experts to all questions under a specific category of health management tasks was calculated. LLM: large language model.



Comprehensive Evaluation of Q&A Models

The use of AI tools in medical scenarios carries unique considerations as medical assistance tools must meet stringent quality assurance standards. Figure 6 and Multimedia Appendix 1 show the expert ratings for the dimensions of health management and model characteristics, respectively. As the parameter size of the foundational model increased, expert ratings also gradually increased. However, agents based on smaller models, due to their limited ability to comprehend complex contexts, exhibited poorer performance compared to LLMs of equivalent size. When the size of the foundational model increased, the superiority of agents over LLMs became significantly more pronounced, whereas the increased reading difficulty level resulting from the enhanced professionalism of the responses also became evident. Multimedia Appendix 1 shows the results of the ablation experiment, indicating that the improvements in the agents stemmed from the synergistic effects of RAG and search tools.

A comparative analysis was conducted between the model with the strongest comprehensive capabilities (agent 72B) and 3 newly released LLMs in 2025: 2 medical LLMs, Baichuan-14B-M1 [42] and MedGemma-27B [43], and the 32B model from the Qwen3 series [44]. This study revealed that Baichuan-14B-M1 outperformed larger-scale models such as Qwen2.5-72B and Llama 3-70B in the medical domain [42]. Meanwhile, MedGemma-27B surpassed models such as BioMistral-7B-DARE and OpenBioLLM-70B [43]. As shown in Table 3, the BERTScore and embedding IQRs computed over 63 questions indicate that the agent 72B achieved the highest performance, surpassing both the latest general-domain LLMs and medical-domain LLMs on chronic gastritis health management tasks.

Table . Comparison of state-of-the-art models.

Model	BERTScore, median (IQR)	Embedding average score, median (IQR)
Baichuan-14B-M1	43.142 (37.151-48.233)	86.024 (80.914-89.266)
MedGemma-27B	40.448 (35.130-47.228)	86.887 (82.274-89.869)
Qwen3-32B	40.650 (33.372-47.909)	85.626 (81.589-89.156)
Agent 72B	44.884 (38.934-52.909)	88.574 (84.211-91.298)

Safety Analysis

In a survey of 11,004 adults, 6602 (60.0%) reported feeling uneasy about health care professionals using AI-assisted tools, underscoring the critical need to establish patient trust [45]. Ensuring safety is key to achieving this goal. Using the Likert scale mentioned previously, experts evaluated the safety (harmful outputs such as the fabrication of false information,

XSL•FO
RenderX

dissemination of erroneous data, presence of biases, associated risks, alterations, and plagiarism) of the models' outputs [46-48]. As shown in Table 4, base models with a size larger than 7B demonstrated sufficient capability to generate relatively safe responses for patients. Multimedia Appendix 1 presents a representative error case generated by agent 7B accompanied by expert commentary.

Table . Safety assessment results.

Model	Safety score (1-5; SD; 95% CI)
LLM[a] 1.5B	4.85 (0.62; 4.79-4.92)
Agent 1.5B	4.42 (1.06; 4.31-4.54)
LLM 7B	4.98 (0.13; 4.97-5.00)
Agent 7B	4.95 (0.27; 4.92-4.98)
LLM 72B	4.95 (0.21; 4.93-4.98)
Agent 72B	4.98 (0.15; 4.96-4.99)

[a]LLM: large language model.

Robustness Analysis

The stability of the responses generated by the Q&A model was also a critical factor in determining its suitability for clinical applications. To further analyze the robustness of the agent, we preserved the original parameters and conducted supplementary evaluations based on the preconfigured agent. We randomly selected 1 patient question from each difficulty level and each type of health management task, resulting in a total of 9 questions. Each of these 9 questions was input into the agent 30 times, yielding 270 (9 × 30) outputs. For each output, we calculated the embedding average score, BERTScore, and the corresponding mean absolute deviation (MAD). The results showed that the MAD for the embedding average score was 0.0167 and the MAD for the BERTScore was 0.0387. These findings indicate that the agent based on the Qwen-72B model performed with high stability, exhibiting minimal random fluctuations and demonstrating strong robustness.

Discussion

Principal Findings

The evidence from this study demonstrates that LLM-based agents possess considerable potential in the management of chronic gastritis. The responses generated by agents were generally superior to those produced by LLMs, effectively addressing the limitations of LLMs in handling high-complexity questions. Moreover, agents exhibited higher safety and stability and were capable of outperforming LLMs in the cutting-edge medical domain.

This study presents a comprehensive evaluation of LLM-based agents' effectiveness in chronic gastritis management across heterogeneous clinical scenarios and different scales. Our multimetric analysis revealed 4 critical findings that advance the understanding of AI-driven medical decision support systems. The first finding relates to model scaling effects. The quality of responses for chronic gastritis exhibited progressive enhancement with increasing base model sizes. Larger architectures (eg, Qwen-72B) demonstrated superior medical information processing capabilities through improved semantic comprehension and clinical reasoning. Conversely, smaller models showed inherent limitations in effectively integrating medical knowledge derived from RAG and search tools, resulting in suboptimal domain-specific performance. This parameter-performance correlation aligns with neural scaling laws while highlighting critical capacity thresholds for medical AI applications. The second finding relates to agent versus base LLM performance. When using base models with larger parameters (eg, Qwen-72B), the agents demonstrated better performance compared to the LLMs, particularly in terms of answer accuracy and completeness. However, due to the agents' stronger medical expertise in generating responses, as well as their higher lexical and syntactic complexity, the readability of their answers tended to be lower than that of the LLMs' answers. The third finding relates to the impact of problem complexity. As the difficulty of the questions increased, the response quality of both Q&A models showed a declining trend. However, overall, the agents outperformed the LLMs across all 3 difficulty levels, particularly in handling high-difficulty questions, where the agents significantly compensated for the LLMs' shortcomings in the medical domain. The fourth finding relates to performance on different tasks. When addressing different health management task scenarios, the agents demonstrated statistically significant superiority over the LLMs in both accuracy and completeness of responses, with the most notable improvement observed in clinical consultation scenarios. Lifestyle intervention questions were subjective and did not have a single standard answer, resulting in limited improvement from RAG and search tools. Drug information is complex and varied, as medications produced by different manufacturers may have differences in use details, and the current information is insufficient to fully cover all potential patient inquiries. Despite these challenges, the agents still exhibited higher practical value in chronic gastritis management compared to the LLMs.

This study has both theoretical and practical contributions. On the theoretical side, first, this study demonstrated that LLM-based agents outperform generalized LLMs in multiple scenarios of chronic gastritis management. Second, this study demonstrated that the larger the parameters of either the base model or the LLM-based agents, the better the performance of the model, even though the quality of the answers tended to decrease as the difficulty of the questions increased. Finally,

XSL•FO
RenderX

this study demonstrated that the LLM-based agents had better performance in multiple scenarios of chronic gastritis management. On the practical side, this study identified the value of LLM-based agents in chronic disease management. By using real-world problems and multiscenario chronic disease management tasks, we validated the capabilities of these agents. This provides a reliable LLM-driven approach to the management of chronic gastritis, paves the way for future LLM-based chronic disease management, and provides a more flexible form of counseling for patients.

There are some limitations to our study. First, we only used textual data, whereas data in the clinical setting also include modalities such as temporal, image, and video data. Future research could use multimodal data to evaluate the performance of LLMs in chronic disease management. Second, due to the privacy management requirements of health care data, we only used privately deployed models, which generally have a small number of participants. Future research can further explore models with a larger number of parameters, such as the GPT-4 family of models. Third, we did not use medical bigram models such as HuatuoGPT [49]. This is because these models have been fine-tuned using the medical corpus, and the unknown corpus may affect our evaluation and cause cognitive bias in specific scenarios. Fourth, the hallucination issue in LLMs cannot be overlooked. While agents can reduce the probability of hallucinations, to prevent potential adverse impacts on health care applications, we recommend incorporating a hallucination threshold control mechanism in future studies. This system would automatically suspend operations and initiate retraining when the false positive rate exceeds predefined safety thresholds. It should be noted that these findings are based solely on Chinese-language data. Future research could validate these results across different linguistic and cultural contexts. In addition, patient surveys and randomized controlled trials could be conducted to investigate factors influencing patients' use of AI tools in real clinical settings. Such studies would provide further guidance for enhancing the effectiveness of chronic gastritis self-management tools.

Conclusions

In this study, we compared the effectiveness of agents and LLMs on a chronic disease Q&A dataset across different levels of difficulty and various scenarios. Our multiperspective evaluation results show that the responses generated by the agents were often preferred over those of the LLMs due to their higher embedding average score, BERTScore, accuracy, and completeness values, as well as their higher values in other metrics. The LLM-based agents demonstrated advantages across different difficulty levels, particularly addressing the shortcomings of LLMs in handling high-difficulty questions. Furthermore, the LLM-based agents exhibited varying application effectiveness in different health management task scenarios, proving more suitable for questions with relatively fixed answers. Compared with state-of-the-art general-purpose models and medical-domain large models, the 72B agent further demonstrates its professional competence in the health management of chronic gastritis. The robustness and safety analyses we conducted explored the stability of the agents' responses and their safety for clinical application. The results of this study suggest that LLM-based agents have high value for application in the management of chronic gastritis and that they are effective in guiding patients with chronic diseases in solving common problems, thereby potentially reducing clinicians' workload and improving the quality of patients' home care.

Acknowledgments

This study was funded by the China Computer Federation (CCF)-BaiChuan-Ebtech Foundation Model Fund (2023012) and Chinese Information Processing Society of China (CIPSC)-Social Media Processing (SMP)-Zhipu Large Model Cross-Disciplinary Fund (ZPCG20241107362).

Data Availability

The core code and data for this research can be found on the corresponding author's GitHub page [50].

Conflicts of Interest

None declared.

Multimedia Appendix 1
Supplementary tables and figures.
[DOCX File, 517 KB - medinform_v13i1e73857_app1.docx]

References

1. Correa P. Human gastric carcinogenesis: a multistep and multifactorial process--first American cancer society award lecture on cancer epidemiology and prevention. Cancer Res 1992 Dec 15;52(24):6735-6740. [Medline: 1458460]
2. Sung H, Ferlay J, Siegel RL, et al. Global cancer statistics 2020: GLOBOCAN estimates of incidence and mortality worldwide for 36 cancers in 185 countries. CA Cancer J Clin 2021 May;71(3):209-249. [doi: 10.3322/caac.21660] [Medline: 33538338]

XSL•FO
RenderX

3. Tong H, Wang Y, Li Y, et al. Volatile organic metabolites identify patients with gastric carcinoma, gastric ulcer, or gastritis and control patients. Cancer Cell Int 2017;17(1):108. [doi: 10.1186/s12935-017-0475-x] [Medline: 29200968]
4. Wen Z, Li X, Lu Q, et al. Health related quality of life in patients with chronic gastritis and peptic ulcer and factors with impact: a longitudinal study. BMC Gastroenterol 2014 Aug 20;14(1):149. [doi: 10.1186/1471-230X-14-149] [Medline: 25141760]
5. Wu H, Liang G, Kong M, et al. The status and risk factors for anxiety/depression in patients with atrophic chronic gastritis: a cross-sectional study. Ann Palliat Med 2022 Oct;11(10):3147-3159. [doi: 10.21037/apm-22-730] [Medline: 36096741]
6. Osadolor OO, Osadolor AJ, Osadolor OO, Enabulele E, Akaji EA, Odiowaya DE. Access to health services and health inequalities in remote and rural areas. Janaki Med Coll J Med Sci 2022 Aug 28;10(2):70-74. [doi: 10.3126/jmcjms.v10i2.47868]
7. Yan X, Dong D, He S, Webster C. Examining trans-provincial diagnosis of rare diseases in China: the importance of healthcare resource distribution and patient mobility. Sustainability 2020 Jan;12(13):5444. [doi: 10.3390/su12135444]
8. White RW, Horvitz E. Cyberchondria: studies of the escalation of medical concerns in web search. ACM Trans Inf Syst 2009 Nov 30;27(4):1-37. [doi: 10.1145/1629096.1629101]
9. Simon SR, Evans JS, Benjamin A, Delano D, Bates DW. Patients' attitudes toward electronic health information exchange: qualitative study. J Med Internet Res 2009 Aug 6;11(3):e30. [doi: 10.2196/jmir.1164] [Medline: 19674960]
10. Abdelhamid M, Gaia J, Sanders GL. Putting the focus back on the patient: how privacy concerns affect personal health information sharing intentions. J Med Internet Res 2017 Sep 13;19(9):e169. [doi: 10.2196/jmir.6877] [Medline: 28903895]
11. Radford A, Narasimhan K, Salimans T, Sutskever I. Improving language understanding by generative pre-training. : OpenAI; 2018 URL: https://cdn.openai.com/research-covers/language-unsupervised/language_understanding_paper.pdf [accessed 2025-10-09]
12. Sridharan K, Sivaramakrishnan G. Investigating the capabilities of advanced large language models in generating patient instructions and patient educational material. Eur J Hosp Pharm 2025 Oct 24;32(6):501-507. [doi: 10.1136/ejhpharm-2024-004245] [Medline: 39393839]
13. Ayers JW, Poliak A, Dredze M, et al. Comparing physician and artificial intelligence chatbot responses to patient questions posted to a public social media forum. JAMA Intern Med 2023 Jun 1;183(6):589-596. [doi: 10.1001/jamainternmed.2023.1838] [Medline: 37115527]
14. Wooldridge M, Jennings NR. Intelligent agents: theory and practice. Knowl Eng Rev 1995 Jun;10(2):115-152. [doi: 10.1017/S0269888900008122]
15. Gosmar D, Dahl DA. Hallucination mitigation using agentic AI natural language-based frameworks. arXiv. Preprint posted online on Jan 19, 2025. [doi: 10.48550/arXiv.2501.13946]
16. Wang J, Duan Z. Controlling large language model hallucination based on agent ai with langgraph. Cambridge Open Engage. Preprint posted online on Jan 13, 2025. [doi: 10.33774/coe-2025-xkwl5]
17. Wallat J, Jatowt A, Anand A. Temporal blind spots in large language models. In: Angélica L, Lattanzi S, Medina AM, editors. WSDM '24: Proceedings of the 17th ACM International Conference on Web Search and Data Mining: Association for Computing Machinery; 2024. [doi: 10.1145/3616855.3635818]
18. Park JS, O'Brien J, Cai CJ, Morris MR, Liang P, Bernstein MS. Generative agents: interactive simulacra of human behavior. In: Riche NH, Han J, Steimle J, Riche NH, editors. UIST '23: Proceedings of the 36th Annual ACM Symposium on User Interface Software and Technology: Association for Computing Machinery; 2023. [doi: 10.1145/3586183.3606763]
19. Liu R, Yang R, Jia C, Zhang G, Zhou D, Dai AM, et al. Training socially aligned language models on simulated social interactions. arXiv. Preprint posted online on Oct 28, 2023. [doi: 10.48550/arXiv.2305.16960]
20. Sumers TR, Yao S, Narasimhan K, Griffiths TL. Cognitive architectures for language agents. arXiv. Preprint posted online on Mar 15, 2024. [doi: 10.48550/arXiv.2309.02427]
21. Shi W, Xu R, Zhuang Y, et al. EHRAgent: code empowers large language models for few-shot complex tabular reasoning on electronic health records. Presented at: Conference on Empirical Methods in Natural Language Processing; Nov 12-16, 2024. [doi: 10.18653/v1/2024.emnlp-main.1245]
22. Zhang W, Tang K, Wu H, et al. Agent-pro: learning to evolve via policy-level reflection and optimization. Presented at: Annual Meeting of the Association for Computational Linguistics; Aug 11-16, 2024. [doi: 10.18653/v1/2024.acl-long.292]
23. Zhao J, Zu C, Hao X, et al. LONGAGENT: achieving question answering for 128k-token-long documents through multi-agent collaboration. In: Chen YN, Bansal M, Chen YN, editors. Proceedings of the 2024 Conference on Empirical Methods in Natural Language Processing: Association for Computational Linguistics; 2024. [doi: 10.18653/v1/2024.emnlp-main.912]
24. Lu Y, Bartolo M, Moore A, Riedel S, Stenetorp P. Fantastically ordered prompts and where to find them: overcoming few-shot prompt order sensitivity. Presented at: Annual Meeting of the Association for Computational Linguistics; May 22-27, 2022. [doi: 10.18653/v1/2022.acl-long.556]
25. Chu K, Chen YP, Nakayama H. A better LLM evaluator for text generation: the impact of prompt output sequencing and optimization. arXiv. Preprint posted online on Jun 14, 2024. [doi: 10.48550/arXiv.2406.09972]
26. Zhao S, Yang Y, Wang Z, He Z, Qiu LK, Qiu L. Retrieval augmented generation (RAG) and beyond: a comprehensive survey on how to make your llms use external data more wisely. arXiv. Preprint posted online on Sep 23, 2024. [doi: 10.48550/arXiv.2409.14924]

XSL•FO
RenderX

27. Papageorgiou E, Chronis C, Varlamis I, Himeur Y. A survey on the use of large language models (LLMs) in fake news. Future Internet 2024;16(8):298. [doi: 10.3390/fi16080298]
28. Yang A, Yang B, Zhang B, Hui B, Zheng B, Yu B, et al. Qwen2.5 technical report. arXiv. Preprint posted online on Jan 3, 2025. [doi: 10.48550/arXiv.2412.15115]
29. Yang A, Yang B, Hui B, Zheng B, Yu B, Zhou C, et al. Qwen2 technical report. arXiv. Preprint posted online on Sep 10, 2024. [doi: 10.48550/arXiv.2407.10671]
30. Lewis P, Perez E, Piktus A, Petroni F, Karpukhin V, Goyal N, et al. Retrieval-augmented generation for knowledge-intensive NLP tasks. arXiv. Preprint posted online on Apr 12, 2021. [doi: 10.48550/arXiv.2005.11401]
31. Ng KKY, Matsuba I, Zhang PC. RAG in health care: a novel framework for improving communication and decision-making by addressing LLM limitations. NEJM AI 2025 Jan;2(1):AIra2400380. [doi: 10.1056/AIra2400380]
32. Agirre E, Alfonseca E, Hall K, Kravalova J, Paşca M, Soroa A. A study on similarity and relatedness using distributional and wordnet-based approaches. In: Ostendorf M, editor. NAACL '09: Proceedings of Human Language Technologies: The 2009 Annual Conference of the North American Chapter of the Association for Computational Linguistics: Association for Computational Linguistics; 2009. [doi: 10.3115/1620754.1620758]
33. Vaid A, Landi I, Nadkarni G, Nabeel I. Using fine-tuned large language models to parse clinical notes in musculoskeletal pain disorders. Lancet Digit Health 2023 Oct 26;5(12):e855-e858. [doi: 10.1016/S2589-7500(23)00202-9] [Medline: 39492289]
34. Van Veen D, Van Uden C, Blankemeier L, et al. Adapted large language models can outperform medical experts in clinical text summarization. Nat Med 2024 Apr;30(4):1134-1142. [doi: 10.1038/s41591-024-02855-5] [Medline: 38413730]
35. Tam TYC, Sivarajkumar S, Kapoor S, et al. A framework for human evaluation of large language models in healthcare derived from literature review. NPJ Digit Med 2024 Sep 28;7(1):258. [doi: 10.1038/s41746-024-01258-7] [Medline: 39333376]
36. Lei L, Wei Y, Liu K. AlphaReadabilityChinese: a tool for the measurement of readability in Chinese texts and its applications. Foreign Lang Teach 2024;2024(1):83-93. [doi: 10.13458/j.cnki.flatt.004997]
37. Lee BW, Jang YS, Lee JJ. Pushing on text readability assessment: a transformer meets handcrafted linguistic features. arXiv. Preprint posted online on Jan 16, 2024. [doi: 10.48550/arXiv.2109.12258]
38. Singhal K, Azizi S, Tu T, et al. Large language models encode clinical knowledge. Nature New Biol 2023 Aug;620(7972):172-180. [doi: 10.1038/s41586-023-06291-2] [Medline: 37438534]
39. Cascella M, Montomoli J, Bellini V, Bignami E. Evaluating the feasibility of ChatGPT in healthcare: an analysis of multiple clinical and research scenarios. J Med Syst 2023 Mar 4;47(1):33. [doi: 10.1007/s10916-023-01925-4] [Medline: 36869927]
40. Thirunavukarasu AJ, Ting DSJ, Elangovan K, Gutierrez L, Tan TF, Ting DSW. Large language models in medicine. Nat Med 2023 Aug;29(8):1930-1940. [doi: 10.1038/s41591-023-02448-8] [Medline: 37460753]
41. Shi F, Chen X, Misra K, Scales N, Dohan D, Chi EH, et al. Large language models can be easily distracted by irrelevant context. In: Krause A, Brunskill E, Cho K, Engelhardt B, Sabato S, editors. ICML'23: Proceedings of the 40th International Conference on Machine Learning: JMLR.org; 2023. URL: https://dl.acm.org/doi/10.5555/3618408.3619699 [accessed 2025-05-25]
42. Wang B, Zhao H, Zhou H, Song L, Xu M, Cheng W, et al. Baichuan-M1: pushing the medical capability of large language models. arXiv. Preprint posted online on Mar 5, 2025. [doi: 10.48550/arXiv.2502.12671]
43. Sellergren A, Kazemzadeh S, Jaroensri T, Kiraly A, Traverse M, Kohlberger T, et al. MedGemma technical report. arXiv. Preprint posted online on Jul 12, 2025. [doi: 10.48550/arXiv.2507.05201]
44. Yang A, Li A, Yang B, Zhang B, Hui B, Zheng B, et al. Qwen3 technical report. arXiv. Preprint posted online on May 14, 2025. [doi: 10.48550/arXiv.2505.09388]
45. Tyson A, Pasquini G, Spencer A, Funk C. 60% of Americans would be uncomfortable with provider relying on AI in their own health care. Pew Research Center. 2025. URL: https://www.pewresearch.org/science/2023/02/22/60-of-americans-would-be-uncomfortable-with-provider-relying-on-ai-in-their-own-health-care/ [accessed 2025-07-30]
46. Chang Y, Wang X, Wang J, et al. A survey on evaluation of large language models. ACM Trans Intell Syst Technol 2024 Jun 30;15(3):1-45. [doi: 10.1145/3641289]
47. Ji J, Liu M, Dai J, Pan X, Zhang C, Bian C, et al. BeaverTails: towards improved safety alignment of LLM via a human-preference dataset. arXiv. Preprint posted online on Nov 7, 2023. [doi: 10.48550/arXiv.2307.04657]
48. Tan TF, Elangovan K, Ong JCL, et al. A proposed s.c.o.r.e. evaluation framework for large language models – safety, consensus & context, objectivity, reproducibility and explainability. arXiv. Preprint posted online on Jul 10, 2024. [doi: 10.2139/ssrn.5029562]
49. Zhang H, Chen J, Jiang F, et al. HuatuoGPT, towards taming language model to be a doctor. Presented at: Findings of the Association for Computational Linguistics: EMNLP 2023; Dec 6-10, 2023. [doi: 10.18653/v1/2023.findings-emnlp.725]
50. JMI-codes. GitHub. URL: https://github.com/472404420/JMI-codes [accessed 2025-10-30]

Abbreviations

AI: artificial intelligence

XSL•FO
RenderX

LLM: large language model
MAD: mean absolute deviation
Q&A: question and answer
RAG: retrieval-augmented generation

Edited by A Benis; submitted 13.03.25; peer-reviewed by J Kueper, JM Immanuvel Arockiasamy, KH Lin, MC Ramos; revised version received 10.10.25; accepted 13.10.25; published 13.11.25.

Please cite as:
Wang S, Ye Q
Enhancing Large Language Models With AI Agents for Chronic Gastritis Management: Comprehensive Comparative Study
JMIR Med Inform 2025;13:e73857
URL: https://medinform.jmir.org/2025/1/e73857
doi:10.2196/73857

© Shurui Wang, Qing Ye. Originally published in JMIR Medical Informatics (https://medinform.jmir.org), 13.11.2025. This is an open-access article distributed under the terms of the Creative Commons Attribution License (https://creativecommons.org/licenses/by/4.0/), which permits unrestricted use, distribution, and reproduction in any medium, provided the original work, first published in JMIR Medical Informatics, is properly cited. The complete bibliographic information, a link to the original publication on https://medinform.jmir.org/, as well as this copyright and license information must be included.

XSL•FO
RenderX

Development of a Large-Scale Dataset of Chest Computed Tomography Reports in Japanese and a High-Performance Finding Classification Model: Dataset Development and Validation Study

Yosuke Yamagishi[1], MD, MSc; Yuta Nakamura[2], MD, PhD; Tomohiro Kikuchi[2,3], MD, PhD, MPH; Yuki Sonoda[1], MD; Hiroshi Hirakawa[1], MD; Shintaro Kano[4], MD; Satoshi Nakamura[4], MD; Shouhei Hanaoka[1], MD, PhD; Takeharu Yoshikawa[2], MD, PhD; Osamu Abe[1], MD, PhD

[1]Division of Radiology and Biomedical Engineering, Graduate School of Medicine, The University of Tokyo, 7-3-1 Hongo, Bunkyo-ku, Tokyo, Japan

[2]Department of Computational Diagnostic Radiology and Preventive Medicine, The University of Tokyo Hospital, Tokyo, Japan

[3]Department of Radiology, School of Medicine, Jichi Medical University, Shimotsuke, Japan

[4]Department of Diagnostic Radiology, Toranomon Hospital, Tokyo, Japan

Corresponding Author:
Yosuke Yamagishi, MD, MSc
Division of Radiology and Biomedical Engineering, Graduate School of Medicine, The University of Tokyo, 7-3-1 Hongo, Bunkyo-ku, Tokyo, Japan

Abstract

Background: Recent advances in large language models have highlighted the need for high-quality multilingual medical datasets. Although Japan is a global leader in computed tomography (CT) scanner deployment and use, the absence of large-scale Japanese radiology datasets has hindered the development of specialized language models for medical imaging analysis. Despite the emergence of multilingual models and language-specific adaptations, the development of Japanese-specific medical language models has been constrained by a lack of comprehensive datasets, particularly in radiology.

Objective: This study aims to address this critical gap in Japanese medical natural language processing resources, for which a comprehensive Japanese CT report dataset was developed through machine translation, to establish a specialized language model for structured classification. In addition, a rigorously validated evaluation dataset was created through expert radiologist refinement to ensure a reliable assessment of model performance.

Methods: We translated the CT-RATE dataset (24,283 CT reports from 21,304 patients) into Japanese using GPT-4o mini. The training dataset consisted of 22,778 machine-translated reports, and the validation dataset included 150 reports carefully revised by radiologists. We developed CT-BERT-JPN, a specialized Bidirectional Encoder Representations from Transformers (BERT) model for Japanese radiology text, based on the "tohoku-nlp/bert-base-japanese-v3" architecture, to extract 18 structured findings from reports. Translation quality was assessed with Bilingual Evaluation Understudy (BLEU) and Recall-Oriented Understudy for Gisting Evaluation (ROUGE) scores and further evaluated by radiologists in a dedicated human-in-the-loop experiment. In that experiment, each of a randomly selected subset of reports was independently reviewed by 2 radiologists—1 senior (postgraduate year [PGY] 6‐11) and 1 junior (PGY 4‐5)—using a 5-point Likert scale to rate: (1) grammatical correctness, (2) medical terminology accuracy, and (3) overall readability. Inter-rater reliability was measured via quadratic weighted kappa (QWK). Model performance was benchmarked against GPT-4o using accuracy, precision, recall, F_1-score, ROC (receiver operating characteristic)—AUC (area under the curve), and average precision.

Results: General text structure was preserved (BLEU: 0.731 findings, 0.690 impression; ROUGE: 0.770‐0.876 findings, 0.748‐0.857 impression), though expert review identified 3 categories of necessary refinements—contextual adjustment of technical terms, completion of incomplete translations, and localization of Japanese medical terminology. The radiologist-revised translations scored significantly higher than raw machine translations across all dimensions, and all improvements were statistically significant (P<.001). CT-BERT-JPN outperformed GPT-4o on 11 of 18 findings (61%), achieving perfect F_1-scores for 4 conditions and F_1-score >0.95 for 14 conditions, despite varied sample sizes (7‐82 cases).

Conclusions: Our study established a robust Japanese CT report dataset and demonstrated the effectiveness of a specialized language model in structured classification of findings. This hybrid approach of machine translation and expert validation enabled the creation of large-scale datasets while maintaining high-quality standards. This study provides essential resources for advancing

XSL•FO
RenderX

medical artificial intelligence research in Japanese health care settings, using datasets and models publicly available for research to facilitate further advancement in the field.

(JMIR Med Inform 2025;13:e71137) doi:10.2196/71137

KEYWORDS

radiology reports; machine translation; structured findings; medical language models; computed tomography; multilingual datasets; radiology report classification

Introduction

Recent advances in large language models (LLMs) have demonstrated remarkable capabilities across various domains [1], thereby increasing the focus on developing multilingual models to serve diverse linguistic communities [2]. This trend is exemplified by the release of specialized language models, such as Gemma-2-JPN, a Japanese-specific variant of Google's open LLM Gemma [3,4]. However, the development of such specialized models critically depends on the availability of high-quality domain-specific datasets in the target language. This requirement becomes particularly crucial in specialized fields, such as medical imaging [5-7], where the interpretation of diagnostic findings demands both technical precision and linguistic accuracy.

Computed tomography (CT) is indispensable in modern medical diagnostics, facilitating disease staging, lesion evaluation, and early detection. Japan has the highest number of CT scanners per capita and an annual scan volume surpassing that of most developed nations, presenting a vast reservoir of medical imaging data [8,9]. The extensive use of CT technology has positioned Japan as a pivotal contributor to global medical imaging resources. However, despite the proliferation of multilingual models and growing emphasis on language-specific adaptations, there remains a notable absence of large-scale Japanese radiology report datasets [10], which is a critical gap hindering the development of Japanese-specific medical language models.

To address this challenge, we constructed "CT-RATE-JPN," a Japanese version of the extensive "CT-RATE" dataset [11], which consists of CT scans and interpretation reports collected from 21,304 patients in Turkey. Although general academic knowledge benchmarks have been successfully adapted for Japanese, as evidenced by JMMLU (Japanese Massive Multitask Language Understanding) [12] and JMMMU (Japanese Massive Multi-discipline Multimodal Understanding) [13], which are Japanese versions of MMLU (Massive Multitask Language Understanding) [14,15] and MMMU (Massive Multi-discipline Multimodal Understanding) [16], respectively, and medical benchmarks, such as JMedBench [17], have emerged by combining translated English resources and Japanese medical datasets, a large-scale Japanese dataset specifically focusing on radiology reports, remains notably absent.

CT-RATE-JPN uses an innovative dataset construction approach by leveraging LLM-based machine translation to efficiently generate a large volume of training data. This addresses the fundamental challenge of the dataset scale in medical artificial intelligence (AI) development while maintaining quality through a strategic validation approach. A subset of the data undergoes careful revision by radiologists to create a rigorously verified validation dataset. This dual-track methodology, which combines machine-translated training data with specialist-validated evaluation data, establishes a robust pipeline for both training data acquisition and performance evaluation.

Both CT-RATE and CT-RATE-JPN retain licenses that allow free use for research purposes, thereby supporting broader research initiatives in medical imaging and language processing. To demonstrate the practical use of the CT-RATE-JPN dataset, we developed CT-BERT-JPN, a deep learning–based language model specifically designed for extracting structured labels from Japanese radiology reports. By converting unstructured Japanese medical text into standardized, language-agnostic structured labels, CT-BERT-JPN provides a scalable framework for integrating Japanese radiology data into the global medical AI development, thereby addressing a critical need in the rapidly evolving landscape of multilingual medical AI.

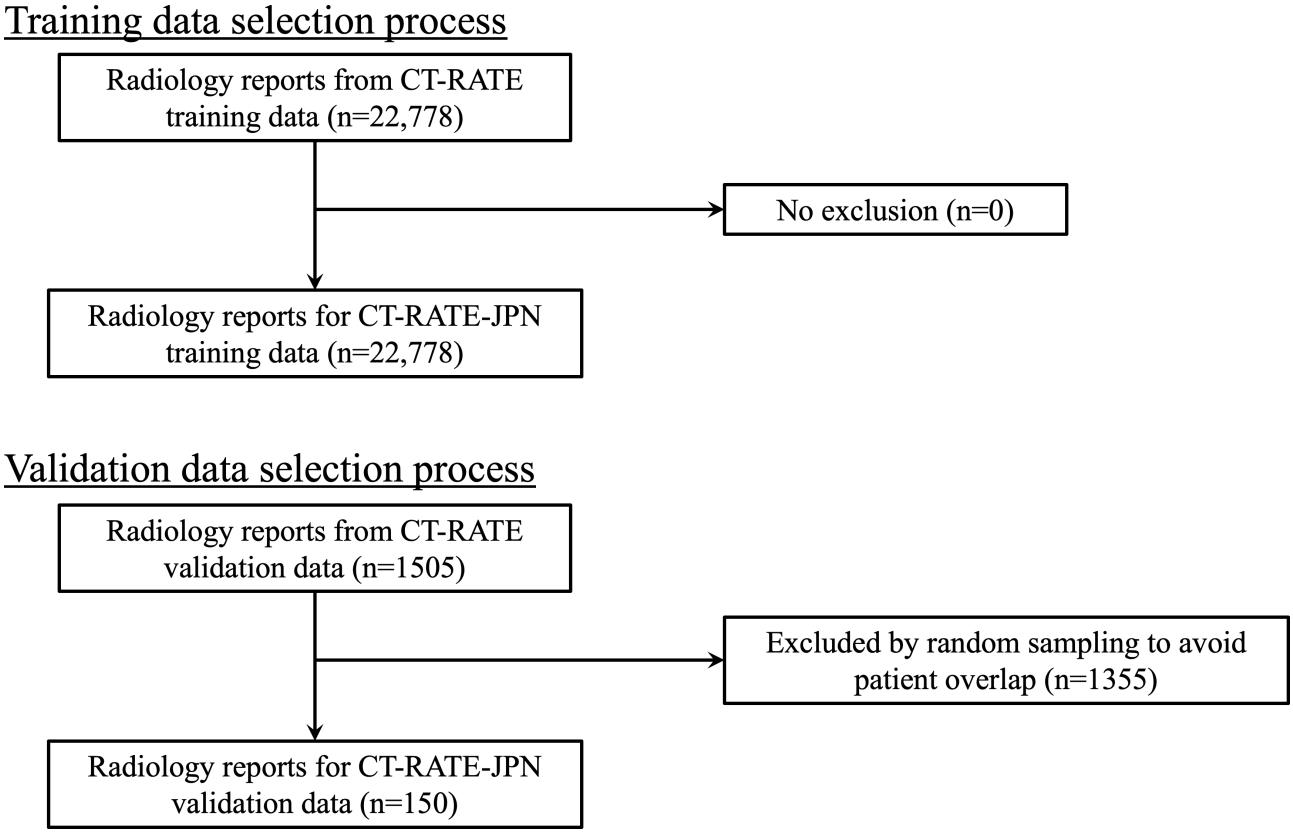
Methods

Dataset Overview

CT-RATE is a comprehensive dataset comprising 25,692 noncontrast chest CT volumes of 21,304 unique patients from the Istanbul Medipol University Mega Hospital [11]. We selected this dataset because it is uniquely positioned as the only publicly available large-scale dataset that pairs CT volumes with radiology reports and permits the redistribution of derivative works. This dataset includes corresponding radiology text reports (consisting of a detailed findings section documenting observations and a concise impression section summarizing key information), multi-abnormality labels, and metadata. The dataset is divided into 2 cohorts, 20,000 patients for the training set and 1304 patients for the validation dataset, allowing robust model training and evaluation across diverse patient cases [18,19]. The training dataset, comprising 22,778 unique reports, was used in constructing CT-RATE-JPN, a Japanese-translated version of the dataset created using machine translation. Independently, we randomly sampled 150 reports from the validation cohort (n=1304); this validation subset was never used during model training and was reserved solely for inference-time evaluation. Those 150 reports were first machine translated and then manually revised and refined by radiologists. The data selection process is illustrated in Figure 1.

XSL•FO
RenderX

Figure 1. Data selection process for CT-RATE-JPN training and validation datasets. The training dataset included all 22,778 radiology reports from CT-RATE without exclusion. For the validation dataset, 150 reports were randomly sampled from 1505 available reports, with 1355 reports excluded to avoid patient overlap between training and validation sets.



The CT-RATE dataset was annotated using 18 structured labels covering key findings relevant to chest CT analysis. These labels included "Medical material," "Arterial wall calcification," "Cardiomegaly," "Pericardial effusion," "Coronary artery wall calcification," "Hiatal hernia," "Lymphadenopathy," "Emphysema," "Atelectasis," "Lung nodule," "Lung opacity," "Pulmonary fibrotic sequela," "Pleural effusion," "Mosaic attenuation pattern," "Peribronchial thickening," "Consolidation," "Bronchiectasis," and "Interlobular septal thickening." The creators of the CT-RATE dataset developed a structured findings model based on the RadBERT architecture [20,21], trained on a manually labeled subset to label the remaining cases. This model achieved an F_1-score ranging from 0.95 to 1.00, demonstrating its efficacy in accurately structuring radiological findings from CT reports. This approach underscores the reliability of CT-RATE's structured annotations for developing high-performance diagnostic models. These structured labels were also used in the development of a Japanese structured findings model for CT-RATE-JPN, enabling the accurate structuring of radiological findings in Japanese CT reports.

Ethical Considerations

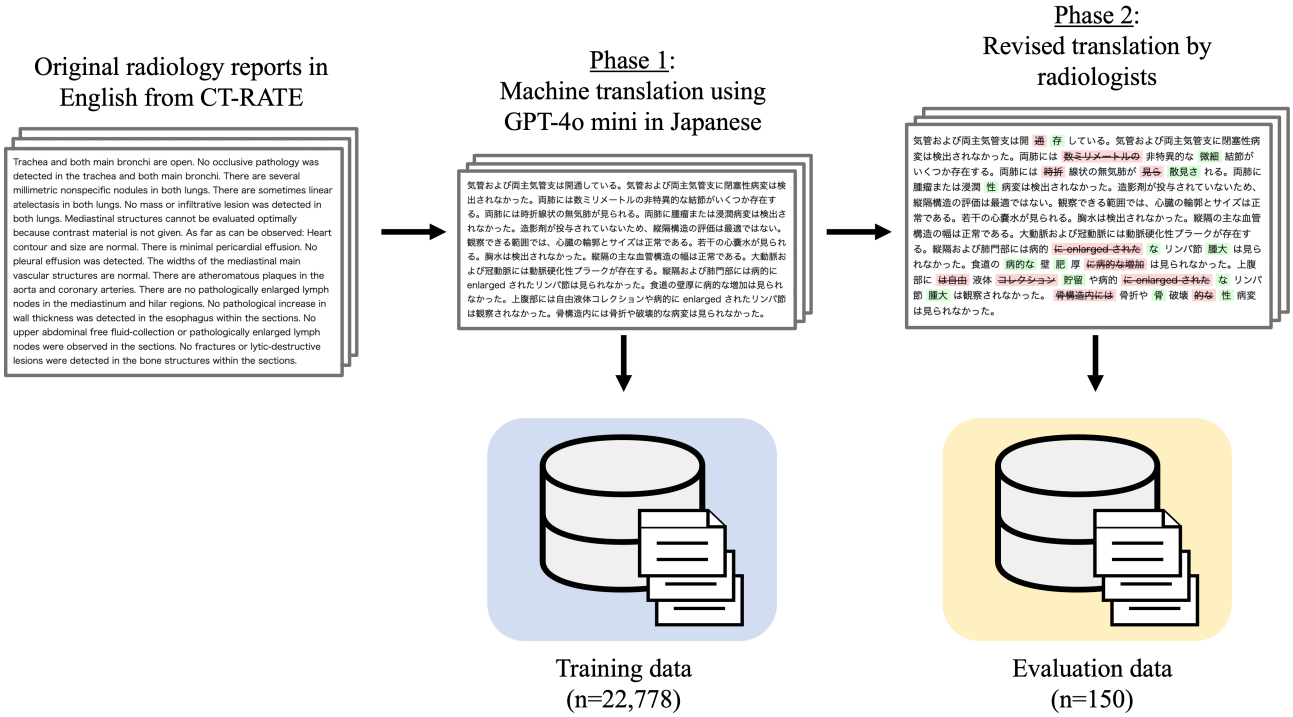
Given that CT-RATE is a publicly available dataset with deidentified patient information, and that our study focused on the translation and linguistic analysis of the existing dataset without accessing any additional patient data, institutional review board approval was not required for this research.

Translation for CT-RATE-JPN

For CT-RATE-JPN, machine translation was conducted using GPT-4o mini (API version, "gpt-4o-mini-2024-07-18") [22], which is a lightweight, fast version of OpenAI's GPT-4o model [23]. The GPT-4o mini produces high-accuracy translations at an affordable rate, making it suitable for large-scale dataset translations. Each radiological report was processed by translating the findings into short impression sections. The complete translation prompts used for GPT-4o mini are provided in Figures S1 (original Japanese prompt) and S2 (English translation) in Multimedia Appendix 1. Figure 2 shows the study workflow.

XSL•FO
RenderX

Figure 2. Workflow for translation and validation in constructing CT-RATE-JPN. The figure outlines machine translation application using GPT-4o mini for the training dataset and 2-phase manual correction for the 150 validation reports. Phase 1 involved initial revisions by radiology residents. Phase 2 consisted of expert review and refinement by board-certified radiologists.



To ensure the accuracy and reliability of the evaluation data, we conducted a comprehensive manual correction process on 150 reports from the validation dataset. This process consisted of 2 distinct phases. In the first phase, we assembled a team of 5 radiology residents, all between their fourth and sixth postgraduate years, to conduct an initial review and revision of the machine translations. The reports were systematically distributed among team members to optimize workflow efficiency. We intentionally chose a larger team to incorporate diverse clinical perspectives and minimize potential translation bias during the review process. The second phase involved a thorough expert review by 2 board-certified radiologists with extensive experience (10 and 11 postgraduate years). The senior radiologists divided the revised translations into final confirmation and refinement. The structured approach to task allocation combined with this rigorous 2-step review process ensured that the validation dataset for CT-RATE-JPN met the high-quality standards necessary for a robust model assessment.

For the training dataset, all translations were generated using GPT-4o mini without manual correction. This dataset was specifically designed for machine learning model training. The decision to rely exclusively on machine-translated data for the training set balanced the scale and practical constraints of the manual annotation.

Both CT-RATE and CT-RATE-JPN were released under a Creative Commons Attribution (CC BY-NC-SA) license, allowing free use for noncommercial research purposes with proper citation and shared terms for derivative works.

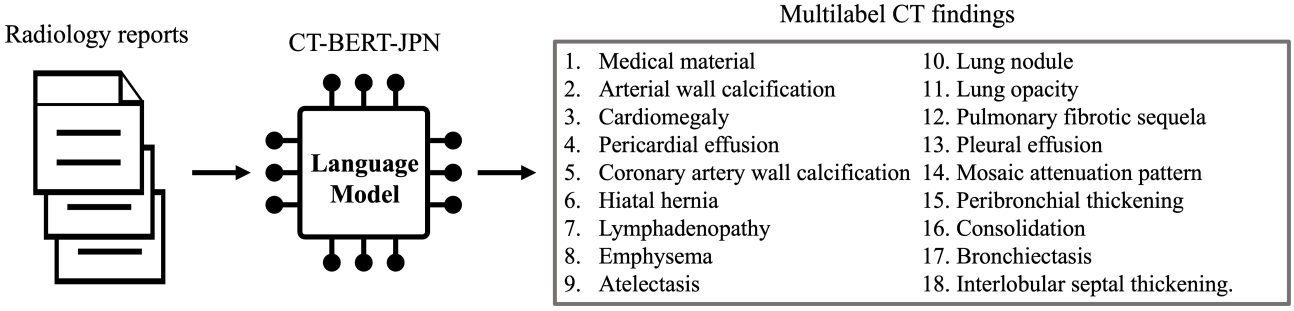
Development of CT-BERT-JPN for Structured Finding Classification

For model training, we randomly split the dataset in a 4:1 ratio, with 80% used for training and 20% for internal evaluation. The pretrained “tohoku-nlp/bert-base-japanese-v3” model from Hugging Face was used [24]. This model follows the architecture of the original BERT base model with 12 layers, 768 hidden dimensions, and 12 attention heads. It was pretrained on extensive Japanese datasets, including the Japanese portion of the CC-100 corpus [25,26] and Japanese version of Wikipedia [27]. BERT-based models have demonstrated significant success in downstream tasks in the medical domain [28,29], making them a promising choice for our research.

Training was conducted on Google Colaboratory equipped with an NVIDIA L4 GPU using the transformers library (version 4.46.2) with a learning rate of 2×10 , batch size of 8 for both training and evaluation, and weight decay of 0.01. Binary cross-entropy loss was applied to optimize the model for multilabel classification. Given the domain shift between the validation dataset (machine-translated) and test dataset (radiologist-revised), hyperparameter tuning was deliberately omitted to avoid overfitting, as such optimization may not contribute to performance improvement under domain shift conditions [30,31]. The model was trained over 4 epochs with internal evaluation and checkpoint savings at each epoch. The total training time was approximately 51.5 minutes (3090.54 s) across 4 epochs, with an average of 12.9 minutes (772.64 s) per epoch. The best-performing model on the internal evaluation data was selected and subsequently used for testing on the validation dataset of CT-RATE-JPN, to ensure a reliable performance assessment. Figure 3 shows the overall workflow for developing CT-BERT-JPN.

XSL•FO
RenderX

Figure 3. CT-BERT-JPN development workflow showing data preprocessing and model fine-tuning for structured computed tomography (CT) classification of findings.



Translated Radiology Reports Evaluation by Automatic Metrics

For basic text analysis, we examined the structural characteristics of the translated reports, including character, word, and sentence count, as well as lexical diversity. Unlike English, Japanese does not use spaces to delimit words. Therefore, we used MeCab (version 1.0.10) [32], one of the most widely used morphological analyzers for Japanese text processing, to accurately segment and count words. These metrics were calculated for both machine-translated and radiologist-revised texts to assess the consistency of textual characteristics across different stages of dataset creation.

For translation quality assessment, we computed the bilingual evaluation understudy (BLEU) [33] and recall-oriented understudy for gisting evaluation (ROUGE)-1, ROUGE-2, and ROUGE-L scores [34] using NLTK (version 3.9.1) and rouge-score (version 0.1.2) libraries.

The BLEU metric evaluates the accuracy of machine-translated text by comparing it to a reference translation. It measures how many words and short phrases in the machine translation match those in the reference translation, to assess the degree of similarity in wording and phrasing between the two texts.

The ROUGE metric assesses the quality of summaries or translations by measuring the overlap between machine-generated and reference texts. ROUGE-1 considers the overlap of individual words; ROUGE-2 examines the overlap of pairs of consecutive words; and ROUGE-L focuses on the longest matching sequence of words between two texts. These metrics emphasize recall by evaluating how much of the important content from the reference text is captured in the machine-generated text. These metrics were calculated by comparing machine-translated texts with radiologist-revised reference translations in the validation dataset.

Translated Radiology Reports Evaluation by Radiologists

To assess the quality of machine-translated radiology reports, we implemented a systematic evaluation by radiologists. A subset of reports was randomly assigned to radiologists for review, with each report evaluated by 2 reviewers: 1 senior radiologist (designated as rater 1, PGY 6‐11) and 1 junior radiologist (designated as rater 2, PGY 4‐5). To maintain objectivity, radiologists were never assigned to evaluate reports they had previously reviewed or corrected.

The evaluation used a 5-point Likert scale (1=poor to 5=excellent) across 3 distinct dimensions:

1. Grammatical correctness: Assessment of linguistic accuracy, including proper Japanese grammar and natural language usage. Presence of nonexistent words, unnatural English terms, or grammatical errors resulted in lower scores. Specialized terminology errors were evaluated separately.
2. Medical terminology: Evaluation of the accuracy and appropriateness of medical and radiological terminology in Japanese. This dimension specifically focused on technical terms and domain-specific language.
3. Overall readability: Subjective assessment of how comprehensible and fluent the translated text appeared to radiologists in clinical practice. While this dimension relates to the previous two categories, it captured the holistic impression of the text's utility in a clinical setting.

Inter-rater reliability was calculated using quadratic weighted kappa (QWK) to ensure consistency in evaluations across different radiologists, as this metric is particularly suitable for ordinal data such as Likert scales. This multi-dimensional evaluation approach provided comprehensive insights into both the technical accuracy and practical usability of machine-translated radiology reports in a Japanese clinical context.

CT-BERT-JPN Performance Evaluation

To evaluate the performance of the classification model in CT findings extraction, we used a test dataset comprising 150 radiology reports revised by radiologists to ensure accuracy. The key metrics calculated for model assessment included accuracy, precision, recall, F_1-score, area under the receiver operating characteristic curve (AUC-ROC), and average precision (AP). 95% CIs for these metrics were calculated using 1000 bootstrap resampling iterations. The Scikit-learn library (version 1.5.2) was used for the analyses.

Baseline Comparison With GPT-4o

To establish a baseline, we performed structured labeling using GPT-4o (API version, "gpt-4o-2024-11-20"), as it is widely adopted in various radiology tasks as a representative closed-source commercial LLM. We specifically chose GPT-4o because, to our knowledge, no existing open-source models were available for this particular task at the time of the study. We used a zero-shot prompting strategy that instructed GPT-4o to extract binary labels (0/1) for each of the 18 target findings from Japanese radiology reports and output results in JSON

XSL•FO
RenderX

format, without additional prompt engineering or few-shot examples. The input prompts used for GPT-4o are presented in Figures S3 (original Japanese version) and S4 (English translations) in Multimedia Appendix 1.

Statistical Analysis

The statistical comparisons were analyzed using the Wilcoxon signed-rank test. This nonparametric test was applied in two contexts: (1) comparing paired predictions from CT-BERT-JPN and GPT-4o on identical validation cases, and (2) comparing CT-BERT-JPN performance between radiologist-revised translated reports versus raw machine-translated reports as input, where each pair consisted of model outputs on the same test sample under different conditions. The Wilcoxon signed-rank test was chosen as it does not require the assumption of normal distribution and is appropriate for comparing paired model outputs. Statistical analysis was conducted using the scipy.stats library (version 1.11.3).

Results

Dataset Overview

The basic text statistics of the translated reports are summarized in Table 1, in separate sections for Findings and Impression. The training (n=22,778) and validation datasets (consisting of 150 machine-translated reports and 150 radiologist-revised reports) showed a consistent text structure across all metrics.

Table . Text statistics on CT-RATE-JPN across different datasets, including “Findings” and “Impression.”

Section	n	Characters, mean (SD)	Words, mean (SD)	Sentences, mean (SD)	Unique words, mean (SD)
Findings					
Training (MT[a])	22,778	467.0 (148.0)	303.3 (95.4)	15.5 (4.6)	126.8 (29.5)
Validation (MT[a])	150	475.0 (130.1)	307.0 (83.6)	15.7 (3.9)	128.9 (27.8)
Validation (Refined[b])	150	455.6 (122.6)	297.7 (80.8)	15.7 (4.0)	126.2 (27.4)
Impression					
Training (MT[a])	22,778	89.1 (68.9)	55.7 (43.6)	3.1 (2.2)	38.1 (23.4)
Validation (MT[a])	150	101.3 (76.0)	63.2 (48.1)	3.5 (2.6)	41.7 (24.3)
Validation (Refined[b])	150	97.8 (72.8)	61.2 (46.0)	3.6 (2.6)	40.9 (24.0)

[a]MT: machine-translated text using GPT-4o mini.

[b]Refined indicates text subjected to radiologist review and refinement.

The Findings section had character counts averaging around 455.6 - 475.0 characters, with slightly lower counts in radiologist-revised texts compared to machine translations. Word count followed a similar pattern, averaging approximately 300 words per report across all datasets. The Impression section was notably more concise, as expected from summary statements. Character counts averaged around 89.1 - 101.3 characters, with word counts of approximately 55.7 - 63.2 words per report. The sentence structure was also more condensed, with approximately 3.1 - 3.6 sentences per report.

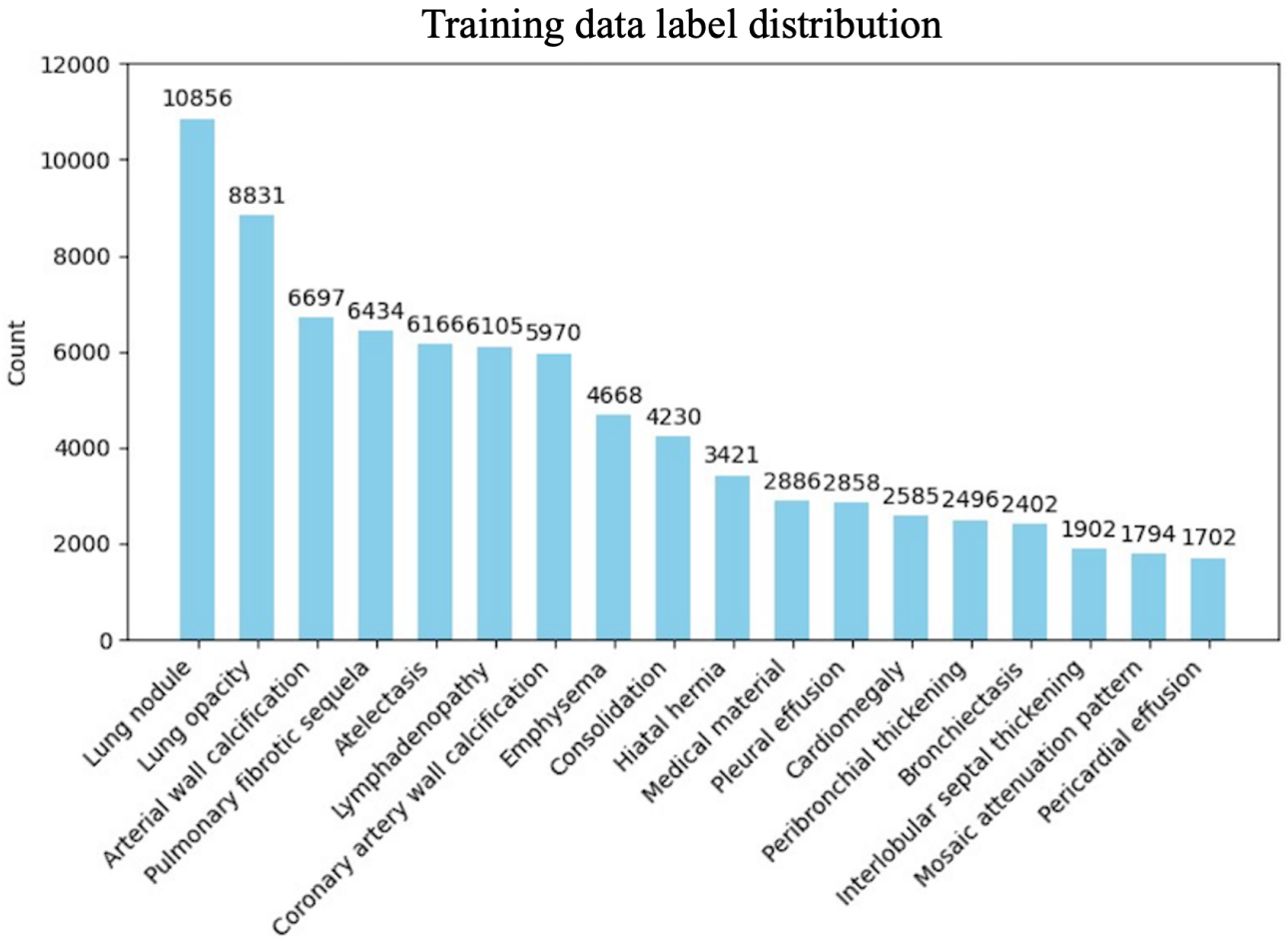
Notably, in both sections, the overall text structure remained consistent between machine-translated and radiologist-revised versions, with similar patterns in sentence length and organization. Although the refined versions had slightly lower character and word counts than their machine-translated counterparts, the basic structural characteristics of the reports were preserved throughout the translation and refinement processes.

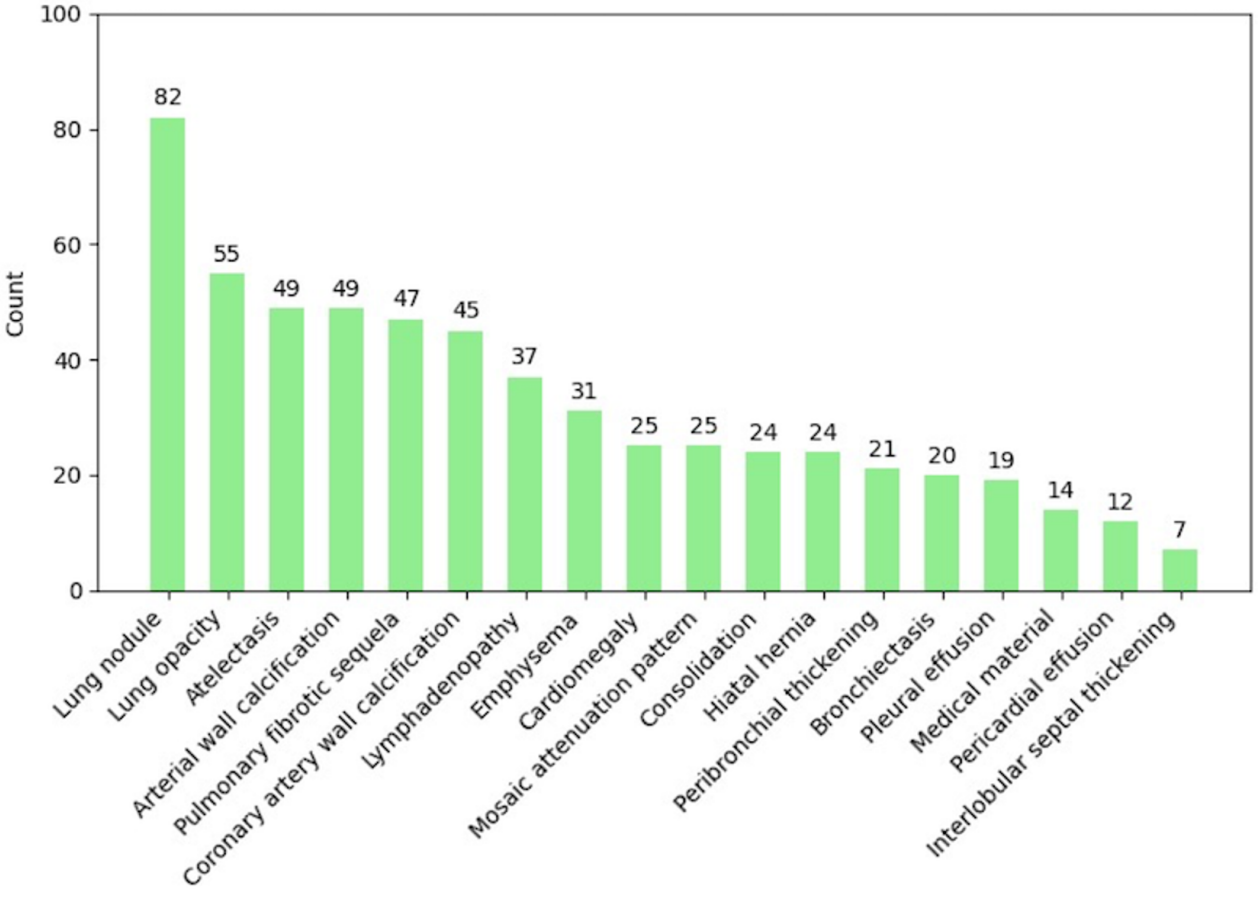
Figure 4 shows that the analysis of the label distributions revealed a significant class imbalance in both the training and validation datasets. In the training set, “Lung nodule” appears most frequently with 10,856 instances, whereas “Interlobular septal thickening” occurs least frequently with only 1702 instances, representing a ratio of approximately 6.4:1. This imbalance is even more pronounced in the validation dataset, where the ratio between the most frequent (82) and least frequent (7) class instances is approximately 11.7:1.

XSL•FO
RenderX

Figure 4. Bar plots showing the data distribution across different findings, sorted in descending order. Top: Training dataset distribution, Bottom: Validation dataset distribution. The number above each bar represents the number of positive samples for each condition.

XSL•FO
RenderX





XSL•FO
RenderX

Translated Radiology Reports Evaluation

We evaluated the quality of machine-translated reports in CT-RATE-JPN using both automated metrics and expert assessments. For automated evaluation, we compared GPT-4o mini translations with radiologist-revised references in the validation dataset. The evaluation metrics for both sections are summarized in Table 2. These scores are high, indicating that the machine translation maintained the fundamental structure and meaning of the original reports.

Table . Automated evaluation metrics comparing GPT-4o mini translations with radiologist-revised references in the validation dataset.

Section	BLEU[a], mean (SD)	ROUGE-1[b], mean (SD)	ROUGE-2, mean (SD)	ROUGE-l, mean (SD)
Findings	0.731 (0.104)	0.876 (0.050)	0.770 (0.091)	0.854 (0.064)
Impression	0.690 (0.196)	0.857 (0.104)	0.748 (0.161)	0.837 (0.120)

[a]BLEU: bilingual evaluation understudy.

[b]ROUGE: recall-oriented understudy for gisting evaluation.

The evaluation of machine-translated radiology reports showed moderate inter-rater agreement with QWK values of 0.410 for grammar, 0.522 for terminology, and 0.408 for readability. These moderate agreement levels may reflect the inherent subjectivity of Likert-scale-based quality assessments. However, radiologist refinements resulted in substantial score improvements across all evaluation dimensions. The highest agreement between senior radiologists (Rater 1) and junior radiologists (Rater 2) was observed in terminology assessment. Figure 5 shows that both raters consistently scored radiologist-revised translations significantly higher than machine translations across all dimensions. Rater 1's evaluations were consistently higher than Rater 2's for both MT and radiologist-revised translations. Table 3 demonstrates that all improvements between MT and radiologist revisions were statistically significant (P<.001) across all evaluation criteria. While GPT-4o mini translations achieved moderate scores, radiologist revisions provided significant enhancements, particularly in terminology accuracy. This highlights the value of domain expertise in medical translation, even when using advanced language models. In addition, Table 4 shows the distribution of quality changes, with the majority of radiologist revisions (65% - 91% depending on rater and dimension) resulting in improved ratings compared to machine translation, while deterioration was minimal (0% - 6% across all categories).

Table . Evaluation of translated texts comparing mean Likert scale scores of GPT-4o mini translations (MT) and radiologist-revised translations.

Evaluation criteria	MT[a], mean (SD)	Radiologist, mean (SD)	P value[b]
Rater 1			
Grammar	3.44 (0.91)	4.64 (0.58)	<.001
Terminology	3.15 (0.81)	4.64 (0.65)	<.001
Readability	3.35 (0.91)	4.59 (0.69)	<.001
Rater 2			
Grammar	3.35 (0.71)	4.21 (0.64)	<.001
Terminology	2.73 (0.82)	4.06 (0.65)	<.001
Readability	2.73 (0.75)	3.91 (0.76)	<.001

[a]MT: machine-translated text using GPT-4 mini.

[b]P values were calculated using the Wilcoxon signed-rank test.

XSL•FO
RenderX

Figure 5. Distribution of evaluation scores for machine-translated (MT) and radiologist-revised translations across 3 dimensions (grammar, terminology, and readability) by 2 rater groups. The upper panel shows evaluations by senior radiologists (Rater 1, postgraduate year 6 - 11) and the lower panel shows evaluations by junior radiologists (Rater 2, postgraduate year 4 - 5). Scores were assessed using a 5-point Likert scale (1=poor to 5=excellent).

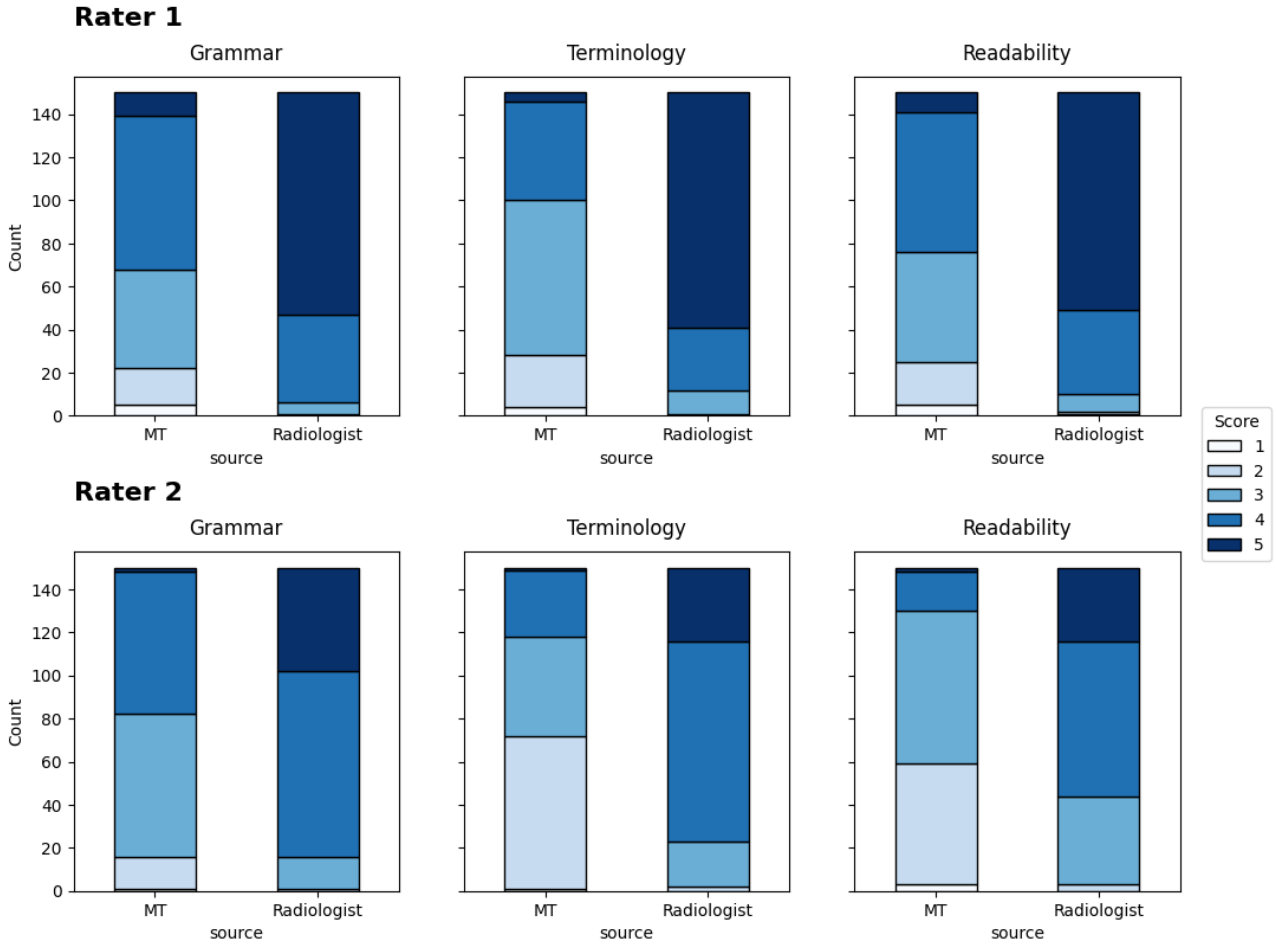


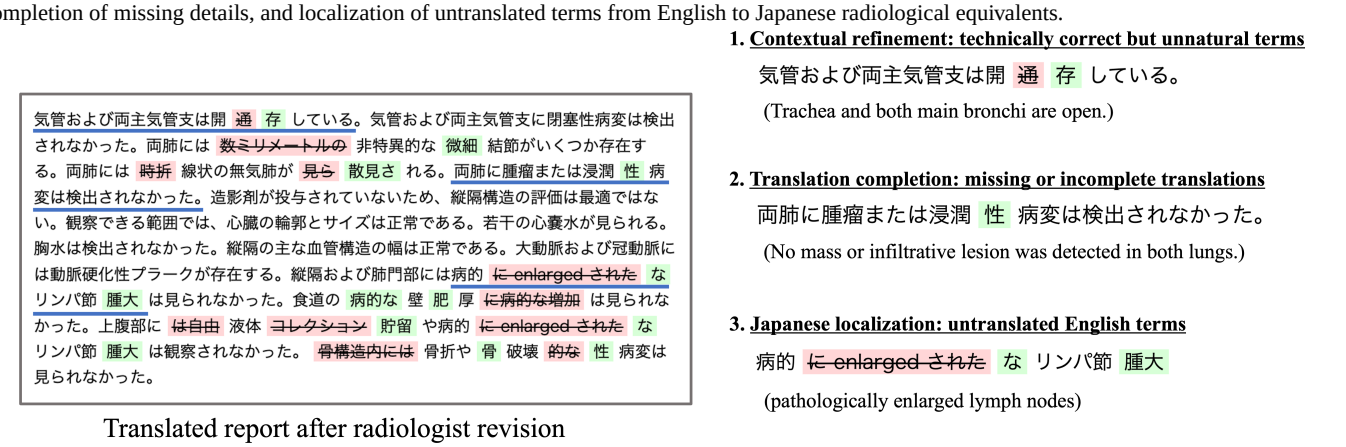
Table . Distribution of quality changes between machine translation and radiologist-revised translations across grammar, terminology, and readability dimensions.

Item	Rater 1			Rater 2		
	Worse	No change	Better	Worse	No change	Better
Grammar, n (%)	4 (2.7)	28 (18.7)	118 (78.7)	9 (6)	43 (28.7)	98 (65.3)
Terminology, n (%)	0 (0)	14 (9.3)	136 (90.7)	7 (4.7)	34 (22.7)	109 (72.7)
Readability, n (%)	1 (0.7)	29 (19.3)	120 (80)	9 (6)	30 (20)	111 (74)

Despite the high automated metric scores (see Table 2), expert scoring evaluation by radiologists revealed that substantial revisions were necessary for medical terminology, with significant improvements observed between machine translations and radiologist-revised versions. Radiologists' assessments identified the representative patterns of necessary modifications. This expert review revealed 3 major categories of improvements (see Figure 6; the original English reports used are shown in Figure S5 in Multimedia Appendix 1), which reflect typical challenges in medical translation: (1) contextual refinement of technically correct but unnatural terms, (2) completion of missing or incomplete translations, and (3) Japanese localization of untranslated English terms. Although not exhaustive, these patterns represent key areas where human expertise complements machine translation in medical contexts.

XSL•FO
RenderX

Figure 6. Representative examples of (computed tomography) CT report translation improvements in 3 categories: contextual term refinement, completion of missing details, and localization of untranslated terms from English to Japanese radiological equivalents.



The first category, contextual refinement, involved replacing technically accurate but clinically uncommon expressions with more natural medical terminology. For instance, direct translations of anatomical conditions were often revised to their proper radiological equivalents when describing vessel status, reflecting standard terminology in Japanese clinical practice. The second category addresses cases in which certain medical terms were either missing or incompletely translated, thereby requiring additional context-specific information. A typical example would be anatomical descriptions lacking specific diagnostic terminology that is common in radiological reporting. The third category focuses on proper localization of English medical terms that were initially left untranslated, such as converting technical descriptors of pathological findings into appropriate Japanese radiological counterparts.

CT-BERT-JPN Performance Evaluation

The CT-BERT-JPN model achieved a micro F_1-score of 0.9607 on the internal evaluation data, which served as the model selection criterion. When evaluated on the validation dataset, the model showed a micro F_1-score of 0.9695 with machine-translated inputs and 0.9520 with radiologist-revised inputs, representing a performance decrease of 0.0175. Table 5 presents the performance evaluation results of CT-BERT-JPN across 18 different findings from 150 chest CT radiological reports on the validation dataset. The model achieved perfect scores (1.000) across all evaluation metrics (accuracy, precision, recall, F_1-score, AUC-ROC, and AP) for pericardial effusion, hiatal hernia, and mosaic attenuation patterns. It demonstrated high accuracy exceeding 0.950 in 17 out of 18 findings, with AUC-ROC values surpassing 0.98 in all findings. Furthermore, AP remained consistently strong—ranging from 0.873 to 1.000—despite the imbalanced distribution of positive samples (7 cases for interlobular septal thickening up to 82 cases for lung nodules), underscoring the model's robust discriminative ability across all conditions.

XSL•FO
RenderX

Table . Performance evaluation of CT-BERT-JPN across 18 different findings.

Findings	Accuracy (95% CI)	Precision (95% CI)	Recall (95% CI)	F_1-score (95% CI)	AUC-ROC[a] (95% CI)	AP[b]
Medical material	0.973 (0.940 - 0.993)	0.778 (0.538 - 0.952)	1.000 (1.000 - 1.000)	0.875 (0.700 - 0.976)	0.999 (0.995 - 1.000)	0.990 (0.950 - 1.000)
Arterial wall calcification	0.987 (0.967 - 1.000)	0.961 (0.898 - 1.000)	1.000 (1.000 - 1.000)	0.980 (0.946 - 1.000)	1.000 (1.000 - 1.000)	1.000 (1.000 - 1.000)
Cardiomegaly	0.987 (0.967 - 1.000)	1.000 (1.000 - 1.000)	0.920 (0.800 - 1.000)	0.958 (0.889 - 1.000)	0.999 (0.996 - 1.000)	0.996 (0.981 - 1.000)
Pericardial effusion	1.000 (1.000 - 1.000)	1.000 (1.000 - 1.000)	1.000 (1.000 - 1.000)	1.000 (1.000 - 1.000)	1.000 (1.000 - 1.000)	1.000 (1.000 - 1.000)
Coronary artery wall calcification	0.987 (0.967 - 1.000)	0.978 (0.927 - 1.000)	0.978 (0.925 - 1.000)	0.978 (0.943 - 1.000)	1.000 (0.999 - 1.000)	1.000 (0.997 - 1.000)
Hiatal hernia	1.000 (1.000 - 1.000)	1.000 (1.000 - 1.000)	1.000 (1.000 - 1.000)	1.000 (1.000 - 1.000)	1.000 (1.000 - 1.000)	1.000 (1.000 - 1.000)
Lymphadenopathy	0.987 (0.967 - 1.000)	0.973 (0.907 - 1.000)	0.973 (0.912 - 1.000)	0.973 (0.929 - 1.000)	0.994 (0.983 - 1.000)	0.987 (0.963 - 1.000)
Emphysema	0.980 (0.953 - 1.000)	0.938 (0.844 - 1.000)	0.968 (0.889 - 1.000)	0.952 (0.881 - 1.000)	0.989 (0.970 - 1.000)	0.960 (0.888 - 1.000)
Atelectasis	0.993 (0.973 - 1.000)	0.980 (0.929 - 1.000)	1.000 (1.000 - 1.000)	0.990 (0.963 - 1.000)	1.000 (1.000 - 1.000)	1.000 (1.000 - 1.000)
Lung nodule	0.967 (0.940 - 0.993)	0.975 (0.937 - 1.000)	0.963 (0.921 - 1.000)	0.969 (0.942 - 0.994)	0.991 (0.978 - 1.000)	0.994 (0.985 - 1.000)
Lung opacity	0.953 (0.913 - 0.987)	0.929 (0.857 - 0.983)	0.945 (0.880 - 1.000)	0.937 (0.885 - 0.977)	0.991 (0.980 - 0.999)	0.985 (0.963 - 0.999)
Pulmonary fibrotic sequela	0.953 (0.920 - 0.987)	0.935 (0.860 - 1.000)	0.915 (0.833 - 0.980)	0.925 (0.867 - 0.974)	0.981 (0.960 - 0.997)	0.973 (0.942 - 0.995)
Pleural effusion	0.987 (0.967 - 1.000)	0.905 (0.762 - 1.000)	1.000 (1.000 - 1.000)	0.950 (0.865 - 1.000)	1.000 (0.997 - 1.000)	0.997 (0.983 - 1.000)
Mosaic attenuation pattern	1.000 (1.000 - 1.000)	1.000 (1.000 - 1.000)	1.000 (1.000 - 1.000)	1.000 (1.000 - 1.000)	1.000 (1.000 - 1.000)	1.000 (1.000 - 1.000)
Peribronchial thickening	0.960 (0.927 - 0.987)	1.000 (1.000 - 1.000)	0.714 (0.529 - 0.905)	0.833 (0.692 - 0.950)	0.985 (0.960 - 1.000)	0.948 (0.869 - 0.997)
Consolidation	0.933 (0.893 - 0.973)	0.706 (0.533 - 0.862)	1.000 (1.000 - 1.000)	0.828 (0.696 - 0.926)	0.996 (0.988 - 1.000)	0.985 (0.951 - 1.000)
Bronchiectasis	0.980 (0.953 - 1.000)	0.870 (0.714 - 1.000)	1.000 (1.000 - 1.000)	0.930 (0.833 - 1.000)	0.990 (0.970 - 1.000)	0.873 (0.686 - 1.000)
Interlobular septal thickening	0.993 (0.980 - 1.000)	0.875 (0.600 - 1.000)	1.000 (1.000 - 1.000)	0.933 (0.750 - 1.000)	1.000 (1.000 - 1.000)	1.000 (1.000 - 1.000)

[a]AUC-ROC: area under the receiver operating characteristic curve.

[b]AP: average precision.

compares the F_1-scores of CT-BERT-JPN and GPT-4o across the 18 conditions, displayed as bar charts. Table S1 in Multimedia Appendix 1 presents the detailed results for GPT-4o across the 18 conditions using valid data. CT-BERT-JPN had higher F_1-scores than GPT-4o in 11 findings and achieved equivalent performance in 2 findings, specifically the hiatal hernia and mosaic attenuation patterns, both of which attained perfect F_1-scores. Notably, CT-BERT-JPN showed a higher performance in lymphadenopathy (0.142 higher) and atelectasis (0.074 higher), with statistically significant differences confirmed by the Wilcoxon signed-rank test (P=.003 and P=.005, respectively). However, the model performed poorly in 5 findings—most notably peribronchial thickening (–0.051) and consolidation (–0.035)—although Wilcoxon signed-rank tests did not detect statistically significant differences. Detailed performance metrics for GPT-4o are presented in Table S1 in Multimedia Appendix 1.

A detailed analysis of the performance of CT-BERT-JPN was conducted by comparing 2 scenarios: radiologist-revised translated reports versus raw machine-translated reports as input. The differences in the metrics are detailed in Table 6 (the performance metrics for machine translation can be found in Table S2 in Multimedia Appendix 1). The analysis showed that for most findings, performance differences were less than 5%

XSL•FO
RenderX

with no significant variations, confirming the robustness of the model. However, peribronchial thickening showed notable decreases, with a decrease in recall of 0.238 and F_1-score reduction of 0.143. Statistical analysis using the Wilcoxon signed-rank test revealed a significant difference (P=.025). Similarly, consolidation experienced relatively significant performance declines, with precision decreasing by 0.179 and F_1-score by 0.092, with the Wilcoxon signed-rank test showing a significant difference (P=.034).

Table . Performance differences between CT-BERT-JPN models trained on radiologist-revised versus machine-translated inputs across multiple metrics.

Findings	Accuracy	Precision	Recall	F_1-score	AUC-ROC[a]	AP[b]	P value[c]
Medical material	0.000[d]	−0.034	0.071	0.008	0.002	0.013	1.00
Arterial wall calcification	−0.006	−0.019	0.000	−0.010	0.000	0.000	.32
Cardiomegaly	−0.013	0.000	−0.080	−0.042	−0.001	−0.004	.16
Pericardial effusion	0.007	0.000	0.083	0.043	0.000	0.000	.32
Coronary artery wall calcification	0.000	0.000	0.000	0.000	0.000	0.000	N/A[e]
Hiatal hernia	0.000	0.000	0.000	0.000	0.000	0.000	N/A[e]
Lymphadenopathy	−0.006	−0.001	−0.027	−0.014	−0.006	−0.012	.32
Emphysema	−0.007	−0.030	0.000	−0.016	−0.011	−0.039	.56
Atelectasis	−0.007	−0.020	0.000	−0.010	0.000	0.000	.32
Lung nodule	−0.013	−0.025	0.000	−0.012	0.000	0.000	.16
Lung opacity	−0.007	−0.016	0.000	−0.008	−0.002	-0.004	.71
Pulmonary fibrotic sequela	−0.007	0.017	-0.042	−0.013	−0.005	-0.007	.71
Pleural effusion	−0.006	−0.045	0.000	−0.024	0.002	0.008	.32
Mosaic attenuation pattern	0.000	0.000	0.000	0.000	0.000	0.000	N/A[e]
Peribronchial thickening	−0.033	0.000	−0.238	−0.143	−0.010	-0.033	.03
Consolidation	−0.040	−0.179	0.042	−0.092	0.004	0.020	.03
Bronchiectasis	0.007	0.037	0.000	0.021	-0.006	-0.099	.32
Interlobular septal thickening	−0.007	−0.125	0.000	−0.067	0.000	0.000	.32

[a]AUC-ROC: area under the receiver operating characteristic curve.

[b]AP: average precision.

[c]P values were calculated using the Wilcoxon signed-rank test.

[d]Positive values indicate higher performance with radiologist-corrected translations, whereas negative values "-" indicate higher performance with raw machine translations.

[e]N/A indicates that the test was not performed because the predicted values were identical.

Our qualitative analysis of CT-BERT-JPN's performance revealed several illustrative examples of how translation quality impacts model predictions. For peribronchial thickening, we observed cases where CT-BERT-JPN incorrectly predicted negative results for truly positive cases when using radiologist-revised translations. A notable example involved subtle terminological changes from "bilateral peribronchial thickening is observed" in the machine translation to "bilateral bronchial wall thickening is observed" in the radiologist-revised version, where this minor linguistic variation caused the model to misclassify a positive case as negative, demonstrating how nuanced expression differences can significantly impact the model's detection performance. Conversely, for pericardial effusion, we found instances where radiologist refinement improved model accuracy, such as cases where "pericardial effusion" was incorrectly translated as "pleural effusion" in machine-translated reports, while radiologist refinement correctly rendered it as "fluid accumulation in the pericardial recess," leading to accurate CT-BERT-JPN predictions that would have been incorrect with the raw machine translation. In addition, for medical material—the condition with the third-lowest F_1-score—we identified systematic prediction

XSL•FO
RenderX

errors that persisted regardless of translation quality, particularly in cases containing expressions such as "changes associated with tracheostomy are observed," where both machine-translated and radiologist-revised versions retained identical phrasing, yet CT-BERT-JPN consistently predicted positive when the correct label should have been negative. While the presence of an endotracheal tube following tracheostomy would warrant a positive prediction for medical material, the description alone does not explicitly indicate the current presence of medical devices, suggesting that the model may be confounded by artificial interventions mentioned in the text, leading to false positive predictions based on procedural context rather than actual device presence.

Discussion

Principal Findings

The 3 key findings of our study regarding the development of Japanese medical imaging resources and analytical capabilities are:

First, an efficient workflow that combines machine translation with expert validation was established to successfully create a large-scale Japanese radiology dataset, maintaining high-quality standards through a radiologist's focused review.

Second, despite its relatively compact architecture, our specialized CT-BERT-JPN model demonstrated superior performance to GPT-4o in most structured finding extraction tasks, highlighting the effectiveness of domain-specific optimization.

Third, the model maintained robust performance across both machine-translated and radiologist-revised reports, suggesting the viability of machine translation for training data creation in specialized medical domains.

Dataset Development and Quality Assessment

In the field of medical imaging datasets, several English-language resources have been previously established, including the OpenI dataset [35] and MIMIC-CXR [36] for chest radiographs, and AMOS-MM [37] for chest-to-pelvic CT scans; however, these datasets are exclusively available in English, with limited multilingual adaptations. Although many LLMs and VLMs have multilingual capabilities [26,38,39], their performance is consistently degraded when handling non-English languages, including Japanese [40]. A significant factor contributing to this performance gap is the scarcity of non-English datasets, making the development of such resources an urgent priority.

Machine-translated reports showed minimal differences in basic structural elements compared with the original texts, with word counts and sentence lengths varying by less than 5%. Evaluation of translation quality using the BLEU and ROUGE metrics also demonstrated high performance, indicating that the overall structure and content of the reports were well preserved. However, a Likert-scale evaluation by radiologists on grammar, medical terminology, and readability revealed that raw GPT-4o mini outputs still required substantial refinement in all 3 areas. Radiologist-led corrections efficiently addressed these shortcomings, significantly boosting translation quality for our validation dataset. This limitation necessitated a rigorous refinement process involving expert radiologists, which proved crucial for establishing a reliable validation dataset.

Our efficient workflow enabled the review and correction of approximately 70,000 characters of machine-translated text, significantly reducing the time and effort required for extensive translation verification. This efficiency was achieved through a structured review process in which radiologists would focus primarily on medical terminology and critical semantic elements rather than reviewing every aspect of the translation. This systematic approach, which combines large language models with domain expert validation, presents a scalable methodology for dataset creation between distinctly different languages, such as English and Japanese. This hybrid process offers a promising framework that can be adapted not only to other languages but also to specialized domains beyond radiology, where precise terminology and domain expertise are critical.

Model Performance and Evaluation

When combined with CT volumes, CT-BERT-JPN demonstrated significant potential for various text-based applications in medical imaging analysis. Our comprehensive evaluation revealed exceptional performance in structured extraction of findings across diverse radiological conditions, with F_1-score consistently above 0.95 and perfect scores in several findings. More notably, CT-BERT-JPN outperformed GPT-4o in 11 out of 18 findings (61%), achieving higher F_1-score in significant conditions such as lymphadenopathy (+0.142) and atelectasis (+0.074). This superior performance is particularly remarkable considering that CT-BERT-JPN has approximately 110 million parameters, whereas recent large language models often employ hundreds of billions of parameters [41]. Our results demonstrate that a specialized, compact language model can achieve state-of-the-art performance in domain-specific tasks, even when compared with more sophisticated general-purpose models. While promising, our results should be interpreted cautiously given the limited validation dataset of 150 reports and notable class imbalance for certain findings (eg, 7 cases for interlobular septal thickening, 12 cases for pericardial effusion). Although we used both F_1-scores and AP metrics to address data imbalance, the 95% CIs reveal substantial variability for rare findings (eg, interlobular septal thickening: 0.933 [0.750 - 1.000]), where even high F_1-scores may be statistically unstable due to small sample sizes. Larger-scale validation studies will be necessary for more definitive performance assessment.

Furthermore, the model maintained stable performance across both unmodified machine translations and radiologist-revised reports. While some conditions showed moderate performance variations between machine-translated and radiologist-revised reports, particularly in findings where machine translation errors were common (F_1-score differences of -0.143 for peribronchial thickening and −0.092 for consolidation), with consolidation being notably affected by mistranslations of the related "infiltration," the overall robustness of the model suggests that effective clinical applications can be developed using machine-translated training data.

XSL•FO
RenderX

To contextualize our results within the broader radiology NLP field, we note that established models, such as RadGraph [42] and the CheXpert labeling tool [43], have demonstrated strong performance with English reports. Particularly relevant is the CheXpert labeler, which tackles the most similar task of multilabel finding classification in radiology reports, achieving F_1-scores ranging from 0.647 to 0.996 across different findings in chest X-ray analysis. Our CT-BERT-JPN shows comparable performance levels for the distinct task of Japanese CT finding extraction. While acknowledging the differences in imaging modality, language, and validation dataset size, these results represent promising performance and constitute the first openly available Japanese model for multilabel CT findings extraction. Nevertheless, because CT-BERT-JPN was trained and evaluated on a single, translation-derived dataset, its performance could degrade under real-world Japanese radiology reports due to domain shift.

Clinical Implementation and Impact

Previous studies have explored hybrid approaches that combine human and machine translations in the medical domain. Early research demonstrated the effectiveness of combining preexisting translation databases with machine translation for medical guidelines, particularly in updating existing documents [44]. Another study reported challenges in the quality of machine translation from English to Chinese of public health materials caused by linguistic structural differences [45]. However, recent advances in LLMs have been remarkable, with studies showing high performance in radiology report translation [46]. Our research successfully developed effective datasets through a combination of machine and expert translation. This approach enables efficient dataset construction even for languages with limited medical data, representing a significant advancement in multilingual medical data development.

The development of such a structured findings extraction model in Japan, where medical imaging usage rates rank among the highest globally, is expected to contribute substantially to both domestic health care advancements and international model development. Our implementation incorporated previous studies on Japanese radiology report processing, including end-to-end approaches for clinical information extraction [47], natural language processing systems for pulmonary nodule follow-up assessment [48], and BERT-based transfer learning methods for anatomical classification [49].

Our multilabel classification approach addresses several implementation challenges unique to Japanese health care. These include vocabulary standardization across institutions, integration with existing reporting systems, and development of specialized Japanese medical vocabulary handling mechanisms. The ability of the model to process Japanese-specific medical expressions and maintain high performance across different reporting styles demonstrates its potential for broad clinical applications. However, prospective validation across multiple Japanese institutions remains essential for both performance evaluation and capturing institution-specific reporting patterns for targeted model improvements.

Limitations and Future Directions

Several limitations exist in our study. First, although we demonstrated the effectiveness of our language model through rigorous evaluation, the usability of CT-RATE-JPN for vision-language models (such as CT-contrastive language image pre-training [CLIP] [18]), which require joint learning of CT volumes and text descriptions, remains to be empirically validated. Second, our reliance on the CT-RATE dataset may have introduced inherent biases in reporting styles and patterns, because radiology reports vary considerably across institutions and individual radiologists. Third, despite expert validation, the translation-based approach may not fully capture the nuanced expressions and specialized terminology commonly used in Japanese clinical practice. In addition, well-established parallel corpora for translation in the Japanese radiology domain are currently lacking, although projects such as “JMED-DICT” are working to address this gap by developing a comprehensive medical terminology dictionary of approximately 400,000 terms through the integration of existing medical dictionaries and resources [50]. Fourth, potential biases may stem from the multi-step translation process and dataset origin. The CT-RATE dataset originates from Turkish medical institutions and was translated into English before our Japanese translation. This process may introduce biases from demographic differences between Turkish and Japanese patient populations, Turkish-specific reporting styles that may not align with Japanese clinical practices, and linguistic biases accumulated through successive translations, despite our refinement procedures. These biases may contribute to inflated performance metrics for CT-BERT-JPN that do not accurately reflect the model’s expected performance on native Japanese radiology reports in real-world settings.

Building upon these considerations, several promising directions for future research emerge. The primary direction is the development of vision language models using CT-RATE-JPN in conjunction with the CT volumes of CT-RATE. Given the successful development of Japanese CLIP models for general domain tasks, which have demonstrated the feasibility of cross-lingual vision-language alignment in Japanese [51], extending this approach to medical imaging is particularly promising. While this endeavor requires substantial computational resources and sophisticated training strategies, various approaches can be explored, such as additional training on existing models, for example, CT-CLIP. Furthermore, the construction of a new dataset comprising pairs of Japanese radiology reports and CT volumes from Japanese medical institutions can enable a more direct assessment of model performance in the Japanese healthcare context and potentially reveal insights unique to this setting. Our benchmark dataset, validated by radiologists through a systematic review process, provides a valuable foundation for evaluating such Japanese-English and English-Japanese translation models in radiology.

Conclusion

In this study, we introduced CT-RATE-JPN, a comprehensive Japanese dataset of CT interpretation reports, and developed a specialized language model for structured labeling. Our model

XSL•FO
RenderX

demonstrated superior performance compared with GPT-4o, achieving higher F_1-scores in numerous categories of structured findings extraction. The creation of CT-RATE-JPN, along with our publicly available structured findings model, represents a significant contribution to Japanese medical imaging research. By making both the dataset and model freely accessible to the research community, we enable reproducibility and foster collaborative advancement in the field. This work not only provides essential resources for the medical AI community but also establishes a robust foundation for developing more sophisticated multilingual medical vision-language models. These openly available contributions are expected to support the development of AI-assisted diagnostic tools, while maintaining the high standards required for clinical applications in radiology.

Acknowledgments

GPT-4o from OpenAI was used for grammar corrections during the drafting phase, followed by proofreading from Editage.

Data Availability

The original CT-RATE dataset, which includes CT volumes and structured data, is publicly available through Hugging Face Datasets [52]. Our Japanese translation dataset, CT-RATE-JPN, is also publicly available through Hugging Face Datasets [53]. Both datasets were released under the CC BY-NC-SA license, allowing free use for non-commercial research purposes. The use of these datasets require proper citation and redistribution under similar license terms.

The trained CT-BERT-JPN model, together with its full training logs and hyperparameter configuration files, is publicly available through Hugging Face Models for research purposes only [54]. This model can be freely used and adapted for academic and research applications with appropriate citation. Commercial use of the model is not permitted.

Authors' Contributions

All authors agreed with the conceptualization and design of the research. YY conducted algorithm planning and implementation, model development, statistical analysis, and data curation, and drafted the manuscript. YN contributed to the algorithm planning and data curation. TK performed statistical analysis and data curation. YS, HH, SK, and SN contributed to data curation. SH, TY and OA supervised and revised the manuscript. All authors reviewed and approved the final version of the manuscript.

The research was supported by JSPS KAKENHI Grant JP25K03479.

Conflicts of Interest

The Department of Computational Diagnostic Radiology and Preventive Medicine of The University of Tokyo Hospital is sponsored by HIMEDIC Inc and Siemens Healthcare KK.

Multimedia Appendix 1
Supplementary materials including detailed performance evaluation tables for GPT-4o and CT-BERT-JPN across 18 pathological findings, machine translation and structured labeling prompts used in the study (both Japanese and English versions), and sample radiology reports.
[DOCX File, 1319 KB - medinform_v13i1e71137_app1.docx]

References

1. GPT-4 technical report. : OpenAI; 2023 URL: https://cdn.openai.com/papers/gpt-4.pdf [accessed 2025-08-05]
2. Qin L, Chen Q, Zhou Y, et al. Multilingual large language model: a survey of resources, taxonomy and frontiers. . Preprint posted online on Apr 7, 2024. [doi: 10.48550/arXiv.2404.04925]
3. Mesnard T, Hardin C, et al. Gemma: open models based on gemini research and technology. . Preprint posted online on Apr 16, 2024. [doi: 10.48550/arXiv.2403.08295]
4. Team G, Riviere M, Pathak S, et al. Gemma 2: improving open language models at a practical size. . Preprint posted online on Oct 2, 2024. [doi: 10.48550/arXiv.2408.00118]
5. Tu T, Azizi S, Driess D, et al. Towards generalist biomedical AI. NEJM AI 2024 Feb 22;1(3):AIoa2300138. [doi: 10.1056/AIoa2300138]
6. Li C, Wong C, Zhang S, et al. LLaVA-med: training a large language-and-vision assistant for biomedicine in one day. arXiv. Preprint posted online on Jun 1, 2023. [doi: 10.48550/arXiv.2306.00890]
7. Singhal K, Tu T, Gottweis J, et al. Towards expert-level medical question answering with large language models. arXiv. Preprint posted online on May 16, 2023. [doi: 10.48550/arXiv.2305.09617]

XSL•FO
RenderX

8. Matsumoto M, Koike S, Kashima S, Awai K. Geographic distribution of CT, MRI and PET devices in Japan: a longitudinal analysis based on national census data. PLOS ONE 2015;10(5):e0126036. [doi: 10.1371/journal.pone.0126036] [Medline: 25946125]
9. Urikura A, Yoshida T, Matsubara K, Nomura K, Hoshino T, Takagi T. Number of computed tomography scanners and regional disparities based on population and medical resources in Japan. Radiol Phys Technol 2023 Sep;16(3):355-365. [doi: 10.1007/s12194-023-00725-2] [Medline: 37204682]
10. Yada S, Nakamura Y, Wakamiya S, Aramaki E. Cross-lingual natural language processing on limited annotated case/radiology reports in English and Japanese: insights from the Real-MedNLP workshop. Methods Inf Med 2024 Dec;63(5-06):145-163. [doi: 10.1055/a-2405-2489] [Medline: 39209296]
11. Hamamci IE, Er S, Almas F, et al. Developing generalist foundation models from a multimodal dataset for 3D computed tomography. In Review. Preprint posted online on Oct 16, 2024. [doi: 10.21203/rs.3.rs-5271327/v1]
12. Nlp-waseda/JMMLU. Hugging Face. URL: https://huggingface.co/datasets/nlp-waseda/JMMLU [accessed 2024-11-16]
13. Onohara S, Miyai A, Imajuku Y, et al. JMMMU: a japanese massive multi-discipline multimodal understanding benchmark for culture-aware evaluation. . Preprint posted online on Oct 22, 2024. [doi: 10.48550/arXiv.2410.17250]
14. Hendrycks D, Burns C, Basart S, et al. Measuring massive multitask language understanding. . Preprint posted online on Jan 12, 2021. [doi: 10.48550/arXiv.2009.03300]
15. Hendrycks D, Burns C, Basart S, et al. Aligning AI with shared human values. . Preprint posted online on Feb 17, 2023. [doi: 10.48550/arXiv.2008.02275]
16. Yue X, Ni Y, Zheng T, et al. MMMU: a massive multi-discipline multimodal understanding and reasoning benchmark for expert AGI. In: Proceedings of the IEEE/CVF Conference on Computer Vision and Pattern Recognition (CVPR) 2024:9556-9567 URL: https://openaccess.thecvf.com/content/CVPR2024/html/Yue_MMMU_A_Massive_Multi-discipline_Multimodal_Understanding_and_Reasoning_Benchmark_for_CVPR_2024_paper.html [doi: 10.1109/CVPR52733.2024.00913]
17. Jiang J, Huang J, Aizawa A. JMedBench: a benchmark for evaluating japanese biomedical large language models. . Preprint posted online on Sep 20, 2024. [doi: 10.48550/arXiv.2409.13317]
18. Hamamci IE, Er S, Sekuboyina A, et al. GenerateCT: text-conditional generation of 3D chest CT volumes. . Preprint posted online on 2024. [doi: 10.1007/978-3-031-72986-7_8]
19. Hamamci IE, Er S, Menze B. CT2Rep: automated radiology report generation for 3D medical imaging. . Preprint posted online on Jul 4, 2024. [doi: 10.48550/arXiv.2403.06801]
20. Yan A, McAuley J, Lu X, et al. RadBERT: adapting transformer-based language models to radiology. Radiol Artif Intell 2022 Jul;4(4):e210258. [doi: 10.1148/ryai.210258] [Medline: 35923376]
21. Devlin J, Chang MW, Lee K, Toutanova K. B. Pre-training of deep bidirectional transformers for language understanding. In: Proceedings of the 2019 Conference of the North American Chapter of the Association for Computational Linguistics: Human Language Technologies: Association for Computational Linguistics:4171-4186. [doi: 10.18653/v1/N19-1423]
22. GPT-4o mini: advancing cost-efficient intelligence. OpenAI. URL: https://openai.com/index/gpt-4o-mini-advancing-cost-efficient-intelligence/ [accessed 2024-11-14]
23. Hello GPT-4o. OpenAI. URL: https://openai.com/index/hello-gpt-4o/ [accessed 2024-11-14]
24. Tohoku-nlp/bert-base-japanese-v3. Hugging Face. URL: https://huggingface.co/tohoku-nlp/bert-base-japanese-v3 [accessed 2024-11-14]
25. Wenzek G, Lachaux MA, Conneau A, et al. CCNet: extracting high quality monolingual datasets from web crawl data. In: Calzolari N, Béchet F, Blache P, editors. Proceedings of the Twelfth Language Resources and Evaluation Conference European Language Resources Association: ACL Anthology:4003-4012 URL: https://aclanthology.org/2020.lrec-1.494
26. Conneau A, Khandelwal K, Goyal N, et al. Unsupervised cross-lingual representation learning at scale. In: Jurafsky D, Chai J, Schluter N, Tetreault J, editors. Presented at: Proceedings of the 58th Annual Meeting of the Association for Computational Linguistics p. 8440-8451. [doi: 10.18653/v1/2020.acl-main.747]
27. Wikimedia Downloads. URL: https://dumps.wikimedia.org/ [accessed 2024-12-12]
28. Alsentzer E, Murphy J, Boag W, et al. Publicly available clinical BERT embeddings. In: Rumshisky A, Roberts K, Bethard S, Naumann T, editors. Presented at: Proceedings of the 2nd Clinical Natural Language Processing Workshop Association for Computational Linguistics p. 72-78. [doi: 10.18653/v1/W19-1909]
29. Lee J, Yoon W, Kim S, et al. BioBERT: a pre-trained biomedical language representation model for biomedical text mining. Bioinformatics 2020 Feb 15;36(4):1234-1240. [doi: 10.1093/bioinformatics/btz682] [Medline: 31501885]
30. Tetko IV, van Deursen R, Godin G. Be aware of overfitting by hyperparameter optimization!. J Cheminform 2024;16(1):139. [doi: 10.1186/s13321-024-00934-w]
31. Ericsson L, Li D, Hospedales T. Better practices for domain adaptation. Presented at: Proceedings of the Second International Conference on Automated Machine Learning URL: https://proceedings.mlr.press/v224/ericsson23a.html [accessed 2025-06-30]
32. MeCab: Yet Another Part-of-Speech and Morphological Analyzer. URL: https://taku910.github.io/mecab/ [accessed 2024-12-12]

XSL•FO
RenderX

33. Papineni K, Roukos S, Ward T, Zhu WJ. Bleu: a method for automatic evaluation of machine translation. In: Isabelle P, Charniak E, Lin D, editors. Presented at: Proceedings of the 40th Annual Meeting of the Association for Computational Linguistics Association for Computational Linguistics p. 311-318. [doi: 10.3115/1073083.1073135]
34. Lin CY. ROUGE: a package for automatic evaluation of summaries. Presented at: p. 74-81 URL: https://aclanthology.org/W04-1013 [accessed 2024-11-14]
35. Demner-Fushman D, Kohli MD, Rosenman MB, et al. Preparing a collection of radiology examinations for distribution and retrieval. J Am Med Inform Assoc 2016 Mar;23(2):304-310. [doi: 10.1093/jamia/ocv080] [Medline: 26133894]
36. Johnson AEW, Pollard TJ, Berkowitz SJ, et al. MIMIC-CXR, a de-identified publicly available database of chest radiographs with free-text reports. Sci Data 2019 Dec 12;6(1):317. [doi: 10.1038/s41597-019-0322-0] [Medline: 31831740]
37. Ji Y, Bai H, Ge C, et al. AMOS: a large-scale abdominal multi-organ benchmark for versatile medical image segmentation. In: Adv Neural Inf Process Syst 2022, Vol. 35:36722-36732.
38. Xue L, Constant N, Roberts A, et al. MT5: a massively multilingual pre-trained text-to-text transformer. In: Toutanova K, Rumshisky A, Zettlemoyer L, editors. Presented at: Proceedings of the 2021 Conference of the North American Chapter of the Association for Computational Linguistics p. 483-498. [doi: 10.18653/v1/2021.naacl-main.41]
39. Pires T, Schlinger E, Garrette D. How multilingual is multilingual BERT? In: Korhonen A, Traum D, Màrquez L, editors. Presented at: Proceedings of the 57th Annual Meeting of the Association for Computational Linguistics p. 4996-5001. [doi: 10.18653/v1/P19-1493]
40. Chen Z, Wu J, Wang W, et al. Intern vl: scaling up vision foundation models and aligning for generic visual-linguistic tasks. Presented at: 2024 IEEE/CVF Conference on Computer Vision and Pattern Recognition (CVPR p. 24185-24198 URL: https://openaccess.thecvf.com/content/CVPR2024/html/Chen_InternVL_Scaling_up_Vision_Foundation_Models_and_Aligning_for_Generic_CVPR_2024_paper.html [accessed 2025-08-21] [doi: 10.1109/CVPR52733.2024.02283]
41. Grattafiori A, Dubey A, Jauhri A, et al. The llama 3 herd of models. arXiv. Preprint posted online on Jul 31, 2024. [doi: 10.48550/arXiv.2407.21783]
42. Jain S, Agrawal A, Saporta A, et al. RadGraph: extracting clinical entities and relations from radiology reports. 2021 Presented at: Proceedings of the Neural Information Processing Systems Track on Datasets and Benchmarks URL: https://datasets-benchmarks-proceedings.neurips.cc/paper/2021/hash/c8ffe9a587b126f152ed3d89a146b445-Abstract-round1.html [accessed 2024-11-15]
43. Irvin J, Rajpurkar P, Ko M, et al. CheXpert: a large chest radiograph dataset with uncertainty labels and expert comparison. AAAI 2019;33(1):590-597. [doi: 10.1609/aaai.v33i01.3301590]
44. Van de Velde S, Macken L, Vanneste K, et al. Technology for large-scale translation of clinical practice guidelines: a pilot study of the performance of a hybrid human and computer-assisted approach. JMIR Med Inform 2015 Oct 9;3(4):e33. [doi: 10.2196/medinform.4450] [Medline: 26453372]
45. Turner AM, Dew KN, Desai L, Martin N, Kirchhoff K. Machine translation of public health materials from English to Chinese: a feasibility study. JMIR Public Health Surveill 2015;1(2):e17. [doi: 10.2196/publichealth.4779] [Medline: 27227135]
46. Meddeb A, Lüken S, Busch F, et al. Large language model ability to translate CT and MRI free-text radiology reports into multiple languages. Radiology 2024 Dec;313(3):e241736. [doi: 10.1148/radiol.241736] [Medline: 39688492]
47. Sugimoto K, Takeda T, Wada S, et al. End-to-end approach for structuring radiology reports. Stud Health Technol Inform 2020 Jun 16;270:203-207. [doi: 10.3233/SHTI200151] [Medline: 32570375]
48. Sugimoto K, Wada S, Konishi S, et al. Assessment of follow-up for pulmonary nodules from radiology reports with natural language processing. Stud Health Technol Inform 2024 Aug 22;316:1795-1799. [doi: 10.3233/SHTI240779] [Medline: 39176839]
49. Nishigaki D, Suzuki Y, Wataya T, et al. BERT-based transfer learning in sentence-level anatomic classification of free-text radiology reports. Radiol Artif Intell 2023 Mar;5(2):e220097. [doi: 10.1148/ryai.220097] [Medline: 37035437]
50. D-2 construction of an integrated medical concept and knowledge linked database and development of an automated analysis infrastructure for medical documents. : Cabinet Office Strategic Innovation Promotion Program; 2025 URL: https://sip3-d2.naist.jp/index.html [accessed 2025-08-06]
51. Sawada K, Zhao T, Shing M, et al. Release of pre-trained models for the japanese language. In: Calzolari N, Kan MY, Hoste V, Lenci A, Sakti S, Xue N, editors. Proceedings of the 2024 Joint International Conference on Computational Linguistics, Language Resources and Evaluation (LREC-COLING 2024) ELRA and ICCL: ACL Anthology; 2024:13898-13905 URL: https://aclanthology.org/2024.lrec-main.1213
52. Ibrahimhamamci/CT-RATE. Hugging Face. URL: https://huggingface.co/datasets/ibrahimhamamci/CT-RATE [accessed 2024-11-14]
53. YYama0/CT-RATE-JPN. Hugging Face. URL: https://huggingface.co/datasets/YYama0/CT-RATE-JPN [accessed 2024-12-10]
54. YYama0/CT-BERT-JPN. Hugging face. URL: https://huggingface.co/YYama0/CT-BERT-JPN [accessed 2024-12-10]

XSL•FO
RenderX

Abbreviations

AI: artificial intelligence
AP: average precision
AUC: area under the curve
BERT: Bidirectional Encoder Representation from Transformers
BLEU: bilingual evaluation understudy
BY-NC-SA: Creative Commons Attribution-NonCommercial-ShareAlike
CLIP: Contrastive Language Image Pre-training
CT: computed tomography
JMMLU: Japanese Massive Multitask Language Understanding
JMMMU: Japanese Massive Multi-discipline Multimodal Understanding
LLM: large language model
MMLU: Massive Multitask Language Understanding
MMLU: Massive Multitask Language Understanding
MMMU: Massive Multi-discipline Multimodal Understanding
MMMU: Massive Multi-discipline Multimodal Understanding
NLTK: Natural Language ToolKit
PGY: postgraduate year
QWK: quadratic weighted kappa
ROC: receiver operating characteristic
ROUGE: Recall-Oriented Understudy for Gisting Evaluation
VLM: Vision Language Model

Edited by A Benis; submitted 10.01.25; peer-reviewed by L Lhotská, S Kido; revised version received 12.07.25; accepted 15.07.25; published 28.08.25.

Please cite as:
Yamagishi Y, Nakamura Y, Kikuchi T, Sonoda Y, Hirakawa H, Kano S, Nakamura S, Hanaoka S, Yoshikawa T, Abe O
Development of a Large-Scale Dataset of Chest Computed Tomography Reports in Japanese and a High-Performance Finding Classification Model: Dataset Development and Validation Study
JMIR Med Inform 2025;13:e71137
URL: https://medinform.jmir.org/2025/1/e71137
doi:10.2196/71137

© Yosuke Yamagishi, Yuta Nakamura, Tomohiro Kikuchi, Yuki Sonoda, Hiroshi Hirakawa, Shintaro Kano, Satoshi Nakamura, Shouhei Hanaoka, Takeharu Yoshikawa, Osamu Abe. Originally published in JMIR Medical Informatics (https://medinform.jmir.org), 28.8.2025. This is an open-access article distributed under the terms of the Creative Commons Attribution License (https://creativecommons.org/licenses/by/4.0/), which permits unrestricted use, distribution, and reproduction in any medium, provided the original work, first published in JMIR Medical Informatics, is properly cited. The complete bibliographic information, a link to the original publication on https://medinform.jmir.org/, as well as this copyright and license information must be included.

XSL•FO
RenderX

Large Language Models for Automating Clinical Trial Criteria Conversion to Observational Medical Outcomes Partnership Common Data Model Queries: Validation and Evaluation Study

Kye Hwa Lee[1], MD, PhD; Sujung Jang[2], BEng; Grace Juyun Kim[3], PharmD, PhD; Sukyoung Park[2], MSc; Doeun Kim[2], MSc; Oh Jin Kwon[3], BSc; Jae-Ho Lee[4], MD, PhD; Young-Hak Kim[5], MD, PhD

[1]Department of Information Medicine, Department of Digital Medicine, Asan Medical Center, University of Ulsan College of Medicine, 88 Olympic-ro 43-gil, Songpa-gu, Seoul, Republic of Korea

[2]Department of Biomedical Engineering, AMIST, Asan Medical Center, University of Ulsan College of Medicine, Seoul, Republic of Korea

[3]Big Data Research Center, Asan Institute for Life Sciences, Asan Medical Center, Seoul, Republic of Korea

[4]Department of Emergency Medicine, Department of Information Medicine, Asan Medical Center, University of Ulsan College of Medicine, Seoul, Republic of Korea

[5]Division of Cardiology, Department of Information Medicine, Asan Medical Center, University of Ulsan College of Medicine, Seoul, Republic of Korea

Corresponding Author:
Kye Hwa Lee, MD, PhD
Department of Information Medicine, Department of Digital Medicine, Asan Medical Center, University of Ulsan College of Medicine, 88 Olympic-ro 43-gil, Songpa-gu, Seoul, Republic of Korea

Abstract

Background: Real-world data–based feasibility assessments enhance clinical trial design, but automating eligibility criteria conversion to database queries is hindered by challenges related to ensuring high accuracy and generating clear, usable outputs.

Objective: The aim of this study is to develop an automated system converting free-text eligibility criteria from ClinicalTrials.gov into Observational Medical Outcomes Partnership Common Data Model (OMOP CDM)–compatible Structured Query Language (SQL) queries and systematically evaluate hallucination patterns across multiple large language models (LLMs) to identify the optimal deployment strategies.

Methods: Our system employs a three-stage preprocessing pipeline (segmentation, filtering, and simplification) achieving 58.2% token reduction while preserving clinical semantics. We compared GPT-4 concept mapping performance against USAGI using 357 clinical terms from 30 trials. For comprehensive evaluation, we analyzed 760 SQL generation attempts (19 trials×8 LLMs×5 prompting strategies) using the SynPUF (Synthetic Public Use Files) dataset and validated selected queries against National COVID Cohort Collaborative reference concept sets using Asan Medical Center's OMOP CDM database.

Results: GPT-4 achieved a 48.5% concept mapping accuracy versus USAGI's 32.0% (P<.001), with domain-specific performance ranging from 72.7% (drug) to 38.3% (measurement). Surprisingly, the open-source llama3: 8b model achieved the highest effective SQL rate (75.8%) compared to GPT-4 (45.3%), attributed to lower hallucination rates (21.1% vs 33.7%). The overall hallucination rate was 32.7%, with wrong domain assignments (34.2%) and placeholder insertions (28.7%) being the most common. Clinical validation revealed mixed performance: high concordance for type 1 diabetes (Jaccard=0.81), complete failure for pregnancy (Jaccard=0.00), and minimal overlap for type 2 diabetes (Jaccard=0.03), despite perfect overlap coefficients in both diabetes cases. Moderate performance was observed for uncontrolled hypertension (Jaccard=0.18).

Conclusions: While LLMs can accelerate eligibility criteria transformation, hallucination rates of 21 - 50% necessitate careful model selection and validation strategies. Our findings challenge assumptions about model superiority, demonstrating that smaller, cost-effective models can outperform larger commercial alternatives. Future work should focus on hybrid approaches combining LLM capabilities with rule-based methods for handling complex clinical concepts.

(JMIR Med Inform 2025;13:e71252) doi:10.2196/71252

KEYWORDS

clinical trials; eligibility criteria; natural language processing; large language models; hallucination; Observational Medical Outcomes Partnership Common Data Model; OMOP CDM; SQL generation; feasibility assessment

XSL•FO
RenderX

Introduction

Clinical trials are essential for medical advancement and drug development, yet they face significant challenges in participant recruitment, with studies showing that 50% of trials fail to meet projected recruitment progress and one-third are terminated due to insufficient recruitment [1-3]. Moreover, only approximately 20% of trials successfully recruit the required participants within the planned timeline [4]. These issues result in delays in new drug approvals and increased research costs, ultimately hindering the development of new therapeutic options [5,6]. To address these challenges, researchers and the pharmaceutical industry are increasingly adopting feasibility assessments and simulations to enhance trial efficiency and success rates [7].

Feasibility assessments are crucial in evaluating the practical, regulatory, and operational aspects of a clinical trial, minimizing risks and setting the foundation for success [8]. By incorporating real-world data (RWD) into the trial design phase, researchers can make more informed decisions, potentially increasing the probability of trial success and reducing the time and costs associated with bringing new therapies to market [9-11]. Leveraging RWD for real-time feasibility assessments during the clinical trial design phase is an effective method to significantly reduce the likelihood of research failure and save time and costs [12,13]. However, the process of transforming clinical trial inclusion or exclusion criteria, which are mostly written in free-text format, into a form suitable for RWD analysis presents several challenges [13,14]. In particular, converting complex clinical concepts, temporal relationships, and elements requiring medical judgment into structured data formats demands considerable expertise and time.

To address these challenges, researchers have been exploring methods to directly query RWD using clinical trial criteria. One notable study by Liu et al developed a system called the Trial Pathfinder, which uses machine learning to evaluate and optimize eligibility criteria for oncology trials using RWD [15]. This approach not only identified opportunities to relax overly restrictive criteria but also demonstrated the potential to increase trial participation by 107% on average while maintaining or improving trial outcomes. However, despite these advances, the automated generation of structured queries from clinical trial criteria faces a critical reliability challenge: Large Language Models (LLMs) frequently generate nonexistent medical concept identifiers—a phenomenon known as hallucination—which can severely compromise query accuracy and patient safety [16].

Recent studies have shown that LLMs, while powerful for natural language understanding, exhibit hallucination rates of 15% - 55% when mapping clinical concepts to standardized vocabularies [17]. This reliability gap poses a significant barrier to clinical deployment, as incorrect concept mappings could lead to missed eligible patients or, worse, inclusion of ineligible participants. Furthermore, the choice of LLM and prompting strategy significantly impacts both performance and cost, yet systematic comparisons across models remain limited. Understanding these trade-offs is essential for developing practical, deployable systems that balance accuracy, efficiency, and economic feasibility.

This study addresses these challenges through a two-pronged approach. First, we present an end-to-end automated system that transforms free-text clinical trial eligibility criteria into Observational Medical Outcomes Partnership Common Data Model (OMOP CDM)-compatible SQL (Structured Query Language) queries using GPT-4 [18], validated with real patient data from Asan Medical Center. Second, we conduct a comprehensive evaluation of hallucination patterns across 8 LLMs (both cloud-based and local) using the Synthetic Public Use Files (SynPUF) [19] dataset, systematically analyzing how model selection and prompt engineering affect reliability. Our findings reveal that while LLMs can accelerate query generation from hours to minutes, hallucination rates of 21% - 50% highlight the need for careful model selection and validation strategies. Surprisingly, our evaluation demonstrated that model size does not necessarily correlate with performance, with smaller open-source models sometimes outperforming larger commercial alternatives in terms of effective SQL generation. By quantifying these trade-offs and identifying optimal model-prompt combinations for different clinical scenarios, this work advances the development of trustworthy and cost-effective AI systems for clinical trial optimization.

Methods

Study Design

We conducted a two-phase investigation to develop and validate an automated system for transforming clinical trial eligibility criteria into OMOP CDM [20] SQL queries, followed by systematic analysis of LLM hallucination patterns. The integrated workflow enables both functional validation and reliability assessment of LLM-generated queries in real-world clinical scenarios.

Data Sources and Study Population

Clinical Trials Dataset

We extracted eligibility criteria from the aggregate analysis of ClinicalTrials.gov (AACT) [21] database (accessed July 18, 2023). We utilized two distinct datasets: (1) Development Dataset and (2) Validation Dataset.

First, in the Development Dataset, 30 trials (10 each from breast cancer, diabetes mellitus, and cardiovascular disease domains) were used exclusively for concept dictionary construction and prompt optimization. From these trials, we extracted 357 unique clinical terms for comparative analysis of concept mapping approaches between GPT-4 and USAGI [22].

Second, in the Validation Dataset, 7 high-impact trials were selected based on citation frequency in major medical journals (BRIDGE [Bridging Anticoagulation in Patients who Require Temporary Interruption of Warfarin Therapy for an Elective Invasive Procedure or Surgery; NCT00786474], PARADIGM-HF [Prospective Comparison of ARNI with ACEI to Determine Impact on Global Mortality and Morbidity in Heart Failure; NCT01035255], LEADER [Liraglutide Effect and Action in Diabetes: Evaluation of Cardiovascular Outcome Results; NCT01179048], CHOIR [Correction of Hemoglobin and Outcomes in Renal Insufficiency; NCT00211120], ACT

XSL•FO
RenderX

[Randomized Acetylcysteine for Contrast-induced Nephropathy Trial; NCT00736866], DESTINY-Breast04 [Trastuzumab Deruxtecan in Previously Treated HER2-Low Advanced Breast Cancer; NCT03734029], RECOVERY [Randomized Evaluation of COVID-19 Therapy; NCT04381936]) for comprehensive system evaluation.

Clinical Data Infrastructure

Real-world validation utilized OMOP CDM version 5.3 data from Asan Medical Center, Seoul, South Korea. This comprehensive dataset contains 4,951,000 unique patients with clinical records spanning from May 1989 to December 2020. The study protocol received approval from the Asan Medical Center Institutional Review Board (IRB No. 2024 - 0377).

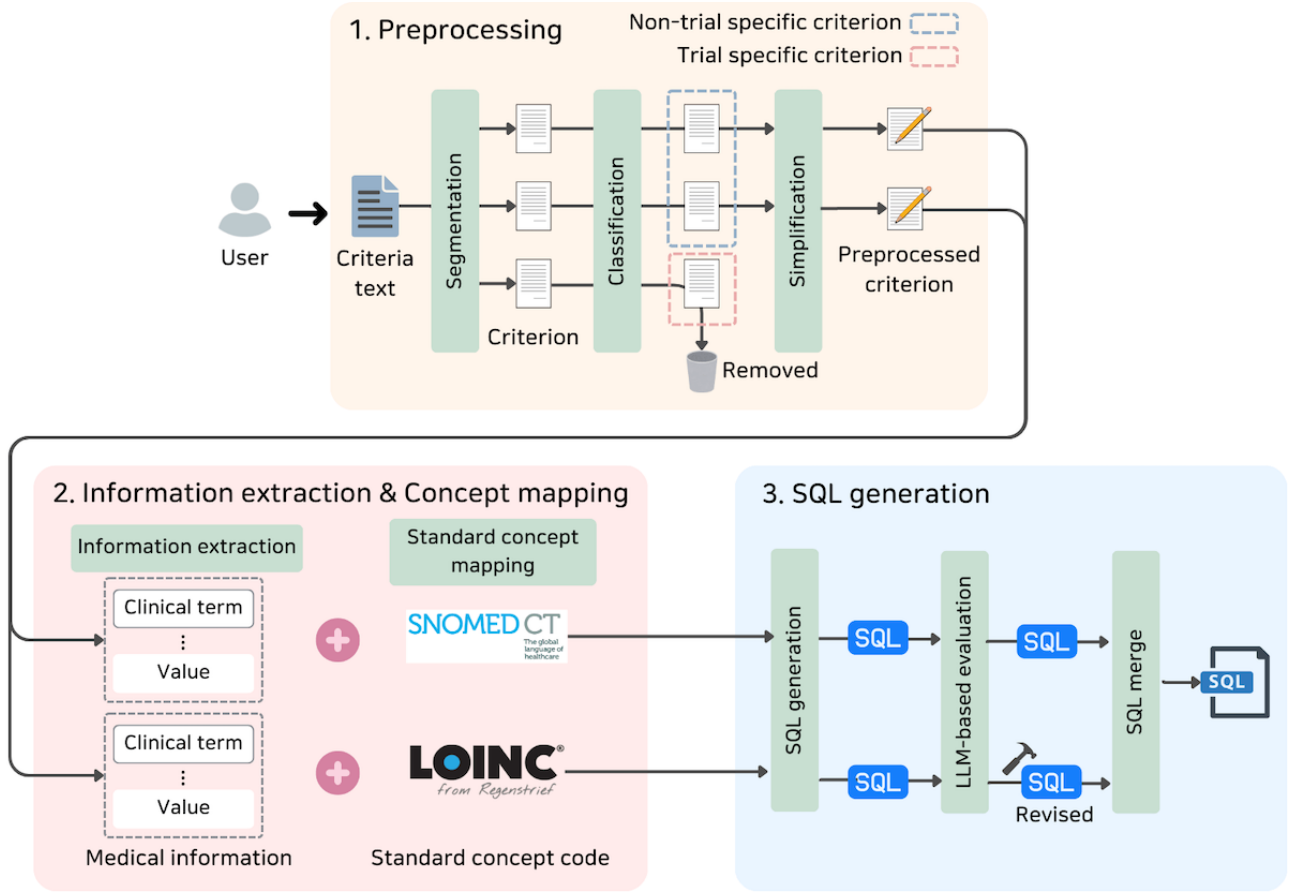
Synthetic Data for Hallucination Analysis

To systematically evaluate hallucination patterns, we employed the SynPUF dataset version DE_1_0_1, containing 2.3 million synthetic Medicare beneficiaries with claims data from 2008 to 2010. This dataset's limited concept coverage (~27,000 of >2 million OMOP concepts) provided an ideal test bed for identifying hallucination behaviors when models encounter concept mapping challenges.

Clinical Criteria to SQL Transformation Pipeline

We developed an automated pipeline that transforms free-text eligibility criteria into OMOP CDM–compliant SQL queries through three interconnected modules. The preprocessing module implements a three-stage approach: (1) segmentation to extract individual criteria while preserving Boolean logic and hierarchical structures, (2) filtration to remove non-queryable trial-specific criteria such as informed consent requirements, and (3) simplification to standardize temporal expressions and reduce token count while maintaining clinical semantics. The information extraction module identifies seven structured elements from preprocessed text, Clinical Terms, Medical Terminology Systems (SNOMED CT, ICD-10, RxNorm, LOINC), Codes, Values, Attributes, Temporal, and Negation, and then maps each clinical term to OMOP-standardized vocabularies using GPT-4. The SQL generation module creates CDM-compliant queries through iterative refinement and optimization. Each module exchanges data via structured JSON to ensure interoperability throughout the pipeline. The preprocessing stages are illustrated in Figure 1, and the detailed architecture of the automated transformation pipeline is shown in Figure S1 of Multimedia Appendix 1. In addition, a comprehensive description of the processing procedures implemented in the automated system is provided in Multimedia Appendix 1.

Figure 1. Detailed three-stage preprocessing and concept mapping architecture. Three-stage preprocessing and concept mapping workflow for transforming clinical trial eligibility criteria into Observational Medical Outcomes Partnership Common Data Model (OMOP CDM)–compatible Structured Query Language (SQL) queries.



XSL•FO
RenderX

Large Language Model Configuration

We employed GPT-4 (March 2024 release) via API with task-specific prompting strategies optimized through iterative refinement. Zero-shot prompting was utilized for straightforward tasks including text segmentation and criteria classification, which minimized token usage and API cost. Few-shot prompting with carefully selected examples enhanced performance for complex tasks including concept mapping and SQL generation. All prompts incorporated explicit instructions for OMOP CDM v5.3 compliance and error handling. Complete prompt templates are provided in Table S1 in Multimedia Appendix 2.

Comparative Evaluation Framework

Clinical Term Mapping Assessment

To evaluate the performance of GPT-4 in mapping clinical terms to standardized concepts, we utilized a previously constructed development dataset comprising 30 clinical trials across three disease domains: breast cancer, diabetes mellitus, and cardiovascular disease. This dataset included diverse expressions of eligibility criteria and clinical terminologies, making it suitable for assessing concept mapping accuracy within the OMOP CDM. We compared GPT-4 with USAGI, an open-source tool developed by the OHDSI community. While GPT-4 is an LLM with advanced natural language understanding capabilities, USAGI uses string normalization, Levenshtein distance–based similarity scoring, and ontology-based heuristics to identify candidate OMOP-standard concepts. In our experiments, USAGI was run using its default settings, and the top-ranked concept based on similarity score was selected for each input term. Relevant clinical terms were extracted from the eligibility criteria of each trial and mapped using both GPT-4 and USAGI. Two clinical experts then jointly reviewed the mapping results from both systems and selected the most appropriate OMOP-standard concept through mutual consensus. In each case, they either chose the better of the two candidate concepts or, when necessary, manually assigned a more suitable concept. This consensus-based evaluation approach reflects real-world clinical decision-making and contributes to the reliability and validity of the reference standard.

SQL Query Validation

To rigorously evaluate the accuracy and applicability of the generated SQL queries within the OMOP CDM, we conducted an expert-based validation involving two experts with strong proficiency in both clinical concepts and the OMOP CDM. Generated SQL queries underwent systematic evaluation using 80 predefined evaluation criteria designed to assess three key dimensions: SQL syntax adherence, CDM schema compliance, and criteria contextual accuracy. Each expert independently rated all applicable criteria on a 4-point scale (1=noncompliant and 4=fully compliant), with final scores calculated as the average of both ratings.

The evaluation framework was applied differentially based on query content. For all generated queries, the full set of 80 criteria was used to assess structural and schema-level accuracy. However, for queries containing clinical concepts from our prevalidated concept map, only 21 criteria from the original 80 were applicable—these specifically evaluated concept inclusion accuracy and concept ID correctness. Inter-rater reliability was measured using Cohen's kappa, with discrepancies resolved through consensus discussion.

This expert-driven evaluation allowed for the identification of critical issues—such as misinterpretation of clinical logic, inaccurate temporal constraints, or improper use of OMOP tables—that automated methods might overlook. As a result, we verified that the generated SQL queries were not only technically correct but also clinically meaningful and suitable for use in real-world, standardized health care data environments. The complete list of evaluation criteria is provided in Table S1 in Multimedia Appendix 3.

Clinical Cohort Validation

To assess real-world performance of the automatically generated SQL queries, we conducted cohort extraction experiments using the OMOP CDM dataset from Asan Medical Center. Given the resource-intensive nature of building complete gold-standard concept sets manually, we utilized officially validated OMOP CDM-based concept sets provided by the National COVID Cohort Collaborative (N3C) as reference standards. A total of three clinical trials were included in this evaluation—NCT00211120, NCT00786474, and NCT01179048—which collectively comprised 40 eligibility criteria. These trials were selected because validated N3C concept sets were available for at least one of their eligibility criteria, allowing for meaningful comparison between system-generated cohorts and external reference standards. Each criterion was screened based on two conditions: (1) convertible to OMOP CDM format and (2) availability of validated concept sets from N3C. For these selected criteria—including Pregnancy (NCT00786474), Type 2 diabetes and Type 1 diabetes (NCT01179048), and Presence of uncontrolled hypertension (NCT00211120)—SQL queries were automatically generated using our system and executed against the OMOP CDM database.

Cohort similarity between system-generated and reference standard cohorts was quantified using two complementary set–based metrics: Jaccard index (intersection/union) and overlap coefficient (intersection/minimum set size). The Jaccard index provides a symmetric measure of overall similarity, while the overlap coefficient indicates the extent to which the smaller cohort is contained within the larger cohort, useful for identifying cases of incomplete concept coverage. This approach enabled objective assessment of query accuracy without requiring manual chart review, leveraging established reference standards for scalable validation. Additionally, to demonstrate technical feasibility, successfully generated SQL queries were executed against the SynPUF dataset to assess cohort retrieval capabilities. Patient counts were recorded for selected trials where queries were executed without errors.

Experimental Design

Although GPT-4 was used for initial system development due to its strong performance, the limited concept coverage in SynPUF provided an opportunity to systematically compare hallucination patterns across multiple LLMs, informing optimal model selection for different clinical scenarios. The 19 trials

XSL•FO
RenderX

for the main study included breast cancer (6 trials), cardiovascular disease (4 trials), diabetes (3 trials), chronic obstructive pulmonary disease (3 trials), and others (3 trials), with complexity levels categorized as simple (8), moderate (7), and complex (4). We employed a factorial design testing eight LLMs (three cloud-based: GPT-4, GPT-3.5-turbo [23], and Claude-3-sonnet [24]; five locally deployed: Llama3:8b [25], DeepSeek-R1:8b [26], Qwen2.5 [27], Phi3 [28], and Gemma3:4b [29]) with five prompting strategies (zero_shot, structured_approach, explicit_uncertainty, validation_focused, and error_aware). The five prompting strategies were designed to test different approaches to query generation:

- zero_shot: Direct query without examples or guidance
- structured_approach: Step-by-step decomposition guidance
- explicit_uncertainty: Encouraging placeholder use for uncertain mappings
- validation_focused: Emphasizing validation and accuracy requirements
- error_aware: Including SynPUF limitations and common pitfalls

Following a pilot phase (5 trials×8 models×5 prompts=200 queries) for methodology validation, the main study analyzed 760 queries (19 trials×8 models×5 prompts).

Hallucination Detection and Classification

An automated detection system was developed to identify hallucinations in generated SQL queries. The system validated concept identifiers against the SynPUF concept inventory and verified domain appropriateness according to OMOP CDM specifications. For the initial validation phase, we analyzed SQL generation failures from seven validation trials. For the large-scale model comparison, we developed a five-category hallucination classification schema ordered by severity. Category A (Critical) comprised nonexistent concept IDs that invalidate query results. Category B (Major) included valid concepts assigned to incorrect domains, violating CDM structural integrity. Category C (Major) captured natural language in concept fields, reflecting confusion between labels and identifiers. Category D (Moderate) consisted of placeholder values requiring manual intervention. Category E (Minor) encompassed easily correctable syntax or schema errors. This classification specifically evaluated model tendencies toward generating inappropriate concept references, distinct from the initial error analysis.

Analytical Framework of Model Performance

Model performance was evaluated across four dimensions. The model performance dimension compared effective SQL generation rates, hallucination frequencies, and error distributions across eight LLMs. The prompt strategy dimension assessed five prompting approaches to identify optimal error minimization strategies. The clinical domain dimension analyzed performance variations across condition, drug, measurement, procedure, and observation concepts. The complexity dimension examined correlations between query complexity (criteria count, logical operators, temporal constraints) and error occurrence.

Statistical Analysis

Statistical analyses were performed using Python 3.11 (Python Software Foundation) with scipy library (version 1.11.4) [30] and statsmodels library (version 0.14.0) [31] libraries. For concept mapping comparisons between GPT-4 and USAGI, McNemar's test was applied to paired binary outcomes. Three primary performance metrics were calculated: (1) SQL generation rate as the proportion of trials producing syntactically valid SQL, (2) hallucination rate as the proportion of generated queries containing invalid concept IDs, and (3) effective SQL generation rate, calculated as SQL generation rate×(1–hallucination rate), representing queries both syntactically valid and free from concept hallucinations.

Model performance across the eight LLMs was compared using one-way ANOVA followed by Tukey's honestly significant difference (HSD) test for post hoc pairwise comparisons. Effect sizes were quantified using Cohen *d* to assess the practical significance of differences between prompting strategies. χ^2 tests evaluated the distribution of hallucination types across models. Multiple linear regression analysis identified predictors of hallucination rates, with model type, prompt strategy, and query complexity as independent variables; model fit was assessed using R^2. All statistical tests employed α=.05 with Bonferroni correction for multiple comparisons where applicable.

Ethical Considerations

This study protocol was reviewed and approved by the Institutional Review Board of Asan Medical Center (IRB No. 2024-0377). As this study did not involve human participants, informed consent was not applicable. All data used in the study were de-identified prior to analysis, and no individual-level identifiable information was accessed.

Data and Code Availability

Source code, including the complete pipeline implementation and hallucination detection system, is available at [https://github.com/sujeong-jang/ctos]. The SynPUF dataset is publicly accessible through Centers for Medicare & Medicaid Services. Clinical trial criteria and evaluation datasets are available upon request with appropriate data use agreements. Detailed documentation for system deployment and reproduction is provided in the repository.

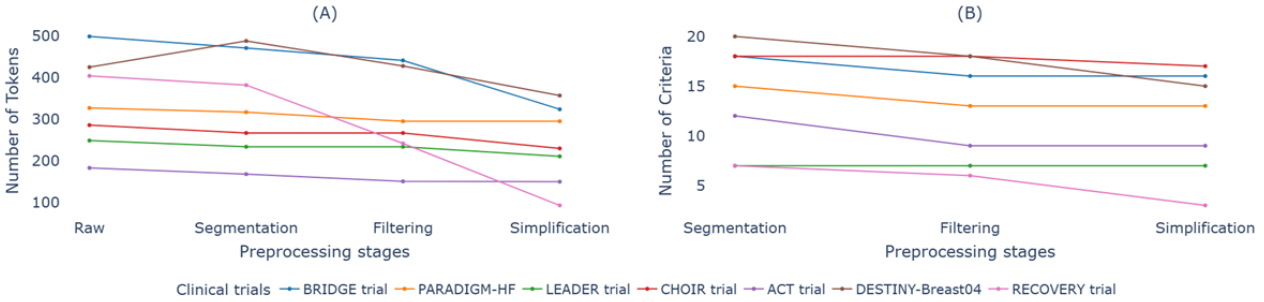
Results

Preprocessing and Clinical Concept Extraction

Analysis of seven validation trials revealed substantial heterogeneity in eligibility criteria complexity, ranging from 6 to 25 criteria per trial (14.7±6.3). The three-stage preprocessing pipeline systematically reduced linguistic complexity while preserving clinical semantics (Figure 2). Initial segmentation achieved modest token reduction (331.4±85.2) while maintaining structural integrity. Subsequent filtering of non-OMOP–compatible criteria reduced both criteria count (11.71±4.9) and token count (311.6±78.3). Final simplification yielded 10.71±4.2 criteria with 138.57±42.1 tokens per trial, representing a 58.2% overall token reduction.

XSL•FO
RenderX

Figure 2. Progressive reduction in token count and criteria through preprocessing stages. (A) Token count changes across segmentation, filtering, and simplification stages for seven validation trials. (B) Corresponding changes in criteria count. Trials shown are as follows: BRIDGE (Bridging Anticoagulation in Patients who Require Temporary Interruption of Warfarin Therapy for an Elective Invasive Procedure or Surgery; NCT00786474), PARADIGM-HF (Prospective Comparison of ARNI with ACEI to Determine Impact on Global Mortality and Morbidity in Heart Failure; NCT01035255), LEADER (Liraglutide Effect and Action in Diabetes: Evaluation of Cardiovascular Outcome Results; NCT01179048), CHOIR (Correction of Hemoglobin and Outcomes in Renal Insufficiency; NCT00211120), ACT (Randomized Acetylcysteine for Contrast-induced Nephropathy Trial; NCT00736866), DESTINY-Breast04 (Trastuzumab Deruxtecan in Previously Treated HER2-Low Advanced Breast Cancer; NCT03734029), RECOVERY (Randomized Evaluation of COVID-19 Therapy; NCT04381936)



This preprocessing identified 80 clinically relevant criteria suitable for automated query generation. Information extraction from these 80 preprocessed criteria yielded 188 unique clinical terms successfully mapped to OMOP-compatible elements. Domain distribution analysis revealed that Condition concepts comprised the predominant category (n=93, 49.5%), followed by Drug (n=29, 15.4%), Procedure (n=24, 12.8%), Measurement (n=18, 9.6%), Observation (n=14, 7.4%), Demographic (n=8, 4.3%), Visit (n=1, 0.5%), and Device (n=1, 0.5%) domains (Table 1). Term frequency analysis identified demographic criteria as the most prevalent. “Age” appeared in 6 trials (out of 7 trials, 85.7%; 6 mentions). Clinical terms included “international normalized ratio” (2/7 trials, 28.6%; 2 mentions), “diabetes mellitus” (2/7 trials, 28.6%; 2 mentions), “breast cancer” (1/7 trial, 14.3%; 8 mentions), “pneumonitis” (1/7 trial, 14.3%; 3 mentions), “interstitial lung disease” (1/7 trial, 14.3%; 3 mentions), “transient ischemic attack” (1/7 trial, 14.3%; 2 mentions), and “systemic embolism” (1/7 trial, 14.3%; 2 mentions), as shown in Table 2. Percentages are calculated based on the number of trials in which the term appeared, and mentions indicate the number of criteria within trials in which the term appeared.

Table . Distribution of extracted clinical concepts by OMOP CDM[a] domain.

Domains	Count (n=188), n (%)
Condition	93 (49.5)
Drug	29 (15.4)
Procedure	24 (12.8)
Measurement	18 (9.6)
Observation	14 (7.4)
Demographic	8 (4.3)
Visit	1 (0.5)
Device	1 (0.5)

[a]OMOP CDM: Observational Medical Outcomes Partnership Common Data Model.

XSL•FO
RenderX

Table . Ten most frequently occurring clinical terms across all trials.

Clinical terms	Trials (n=7), n (%)	Mentions (criterion), n
Age	6 (85.7)	8
International normalized ratio	2 (28.6)	6
Diabetes mellitus	1 (14.3)	3
Breast cancer	1 (14.3)	3
Pneumonitis	1 (14.3)	2
Interstitial lung disease	1 (14.3)	2
Transient ischemic attack	1 (14.3)	2
Systemic embolism	1 (14.3)	2

Comparative Performance of Concept Mapping Approaches

Evaluation of concept mapping accuracy demonstrated GPT-4's superior performance compared to USAGI across 357 clinical terms extracted from the 30 development trials. GPT-4 achieved an overall accuracy of 48.5% (173/357) versus USAGI's 32.0% (114/357), a statistically significant difference (P<.001, McNemar's test). Domain-stratified analysis revealed GPT-4's highest accuracy in the Drug domain (72.7%, 16/22) and lowest in the Measurement domain (38.3%, 31/81), suggesting particular challenges with laboratory-related concepts requiring numeric threshold interpretation.

Notably, among the 243 terms that USAGI misclassified, GPT-4 correctly mapped 61 (25.1%), demonstrating superior contextual understanding. For instance, USAGI incorrectly mapped "human immunodeficiency virus (HIV)" to "Human immunodeficiency virus contact" (a social context concept), while GPT-4 correctly identified "Human immunodeficiency virus infection" (a clinical diagnosis). This pattern of improved semantic interpretation was consistent across complex multiword medical terms.

SQL Query Generation Quality and Expert Validation

Two domain experts independently evaluated SQL queries generated from the seven validation trials using 80 predefined criteria across three dimensions: SQL syntax adherence, CDM schema compliance, and criteria contextual accuracy (inter-rater reliability: Cohen κ=0.85). Each criterion was rated on a 4-point scale (1=noncompliant and 4=fully compliant). SQL syntax adherence achieved near-perfect scores from expert reviewers (3.99±0.12) and matched LLM self-evaluation (4.00±0.00), confirming robust syntactic generation capabilities. CDM schema compliance similarly demonstrated strong performance (expert: 3.89±0.21, LLM: 4.00±0.00), indicating successful adaptation to OMOP table structures and relationships.

However, criteria contextual accuracy exhibited greater variability and lower absolute scores (expert: 3.19±0.45, LLM: 3.53±0.32), with the 0.34-point difference suggesting systematic LLM overconfidence in semantic interpretation (P=.023, paired t-test). This divergence was most pronounced for complex eligibility criteria involving temporal relationships or multicondition logic.

Among the total queries evaluated, 21 contained prevalidated concepts from our development dataset, enabling additional validation of concept mapping accuracy. For these queries, concept inclusion accuracy averaged 3.43±0.38 (expert) versus 3.54±0.29 (LLM), while concept ID correctness achieved higher scores of 3.79±0.24 (expert) versus perfect score of 4.00±0.00 (LLM). The perfect LLM score for concept ID correctness reflects its consistent ability to generate syntactically valid concept identifiers, though not necessarily clinically appropriate ones.

Clinical Cohort Retrieval Performance

Validation using N3C-provided reference concept sets [32] revealed that performance strongly correlated with criteria complexity (Table 3). For the two evaluated trials (NCT00211120, NCT00786474, and NCT01179048), we assessed four distinct eligibility criteria that had available N3C reference standards. The query for Type 1 diabetes (NCT01179048) demonstrated high retrieval accuracy, achieving a Jaccard index of 0.81 and a perfect overlap coefficient of 1.0, indicating that the system-generated cohort closely matched the reference set. In contrast, Type 2 diabetes showed a very low Jaccard index of 0.03 despite an overlap coefficient of 1.0, suggesting that while the retrieved patients were all included in the reference cohort, a large portion of the reference patients was not captured—likely due to incomplete descendant concept inclusion. The Pregnancy criterion (NCT00786474) resulted in complete retrieval failure, with both the Jaccard index and overlap coefficient equal to 0, indicating that no matching patients were retrieved. This may reflect the system's inability to handle concept granularity or contextual nuances related to reproductive health data in the OMOP CDM schema. The presence of uncontrolled hypertension criterion (NCT00211120) achieved moderate performance, with a Jaccard index of 0.18 and an overlap coefficient of 0.48, reflecting partial concept mapping success for a chronic condition represented by a mix of clinical measurements and diagnostic codes.

XSL•FO
RenderX

Table . Comparison of patient cohort retrieval between system-generated queries and reference concept sets.

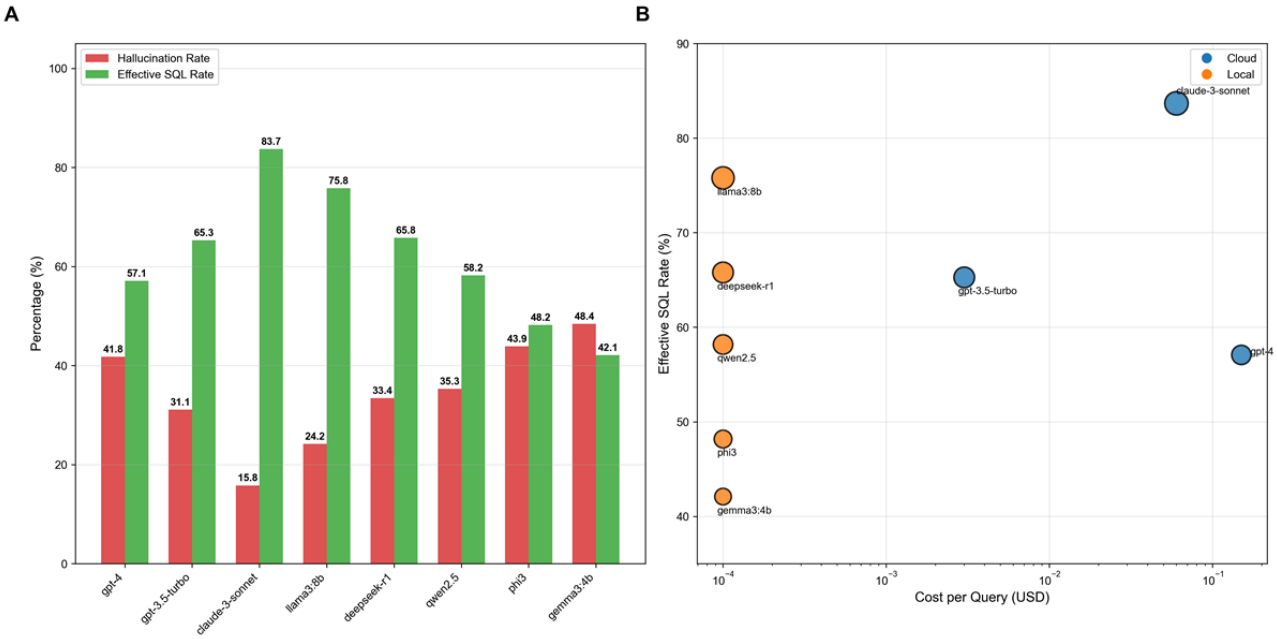
NCT ID	Simplified criterion	Jaccard similarity	Overlap coefficient
NCT00786474	Pregnancy	0	0
NCT01179048	Type 2 diabetes	0.03	1.0
	Type 1 diabetes	0.81	1.0
NCT00211120	Presence of uncontrolled hypertension	0.18	0.48

These results collectively highlight that the system is capable of achieving high performance when querying well-defined, hierarchically stable clinical concepts (eg, Type 1 diabetes) but may underperform when concept definitions are broad, heterogeneous, or require deep descendant inclusion (eg, Type 2 diabetes or pregnancy). Improvements in concept hierarchy coverage and semantic normalization may be necessary to enhance retrieval for more complex clinical criteria.

Large-Scale Model Comparison and Hallucination Analysis

To systematically evaluate hallucination patterns across multiple LLMs, we conducted a separate large-scale experiment using the SynPUF dataset, analyzing 760 SQL generation attempts (19 clinical trials×8 models×5 prompting strategies), distinct from our initial validation study. Analysis of 760 SQL generation attempts revealed significant heterogeneity in model performance ($F(7752)=3.36$, $P=.0085$), with hallucination rates ranging from 21.1% (n=160) to 49.5% (n=376) among models achieving >80% SQL generation success. The overall hallucination rate was 32.7% (n=249) (95% CI 29.4% - 36.1%), with substantial variation in both generation capability and accuracy across models (Figure 3 and Table 4).

Figure 3. Comprehensive performance analysis of eight large language models for OMOP CDM SQL generation. (A) Comparison of hallucination rates and effective SQL rates across models. (B) Cost-performance trade-off analysis showing the relationship between cost per query (log scale) and effective SQL rate, with bubble size proportional to effective rate. Cloud models (blue) and local models (orange) show distinct clustering patterns. OMOP CDM: Observational Medical Outcomes Partnership Common Data Model; SQL: Structured Query Language.



XSL•FO
RenderX

Table . Model performance summary.

Model	Architecture	SQL[a] generation (%)	Hallucination (%)[b]	Effective SQL (%)[c]	Time (s)[d]	Cost (US $)/Query
llama3:8b	Local	88.4	21.1	75.8	28.0±6.3	0.000
qwen2.5	Local	100.0	36.8	67.4	45.0±11.2	0.000
deepseek-r1	Local	89.5	33.7	66.3	1631.3±423.7	0.000
gemma3:4b	Local	90.5	45.3	69.5	58.2±15.3	0.000
phi3	Local	16.8	1.1[e]	13.7	20.7±8.9	0.000
claude-3-sonnet	Cloud	87.4	49.5	65.3	17.6±4.1	0.018
gpt-3.5-turbo	Cloud	95.8	26.3	63.2	6.9±1.8	0.001
gpt-4	Cloud	97.9	33.7	45.3	21.4±5.2	0.045

[a]SQL: Structured Query Language.

[b]Percentage of generated queries with invalid concept IDs.

[c]SQL Generation×(1–Hallucination).

[d]Mean±SD.

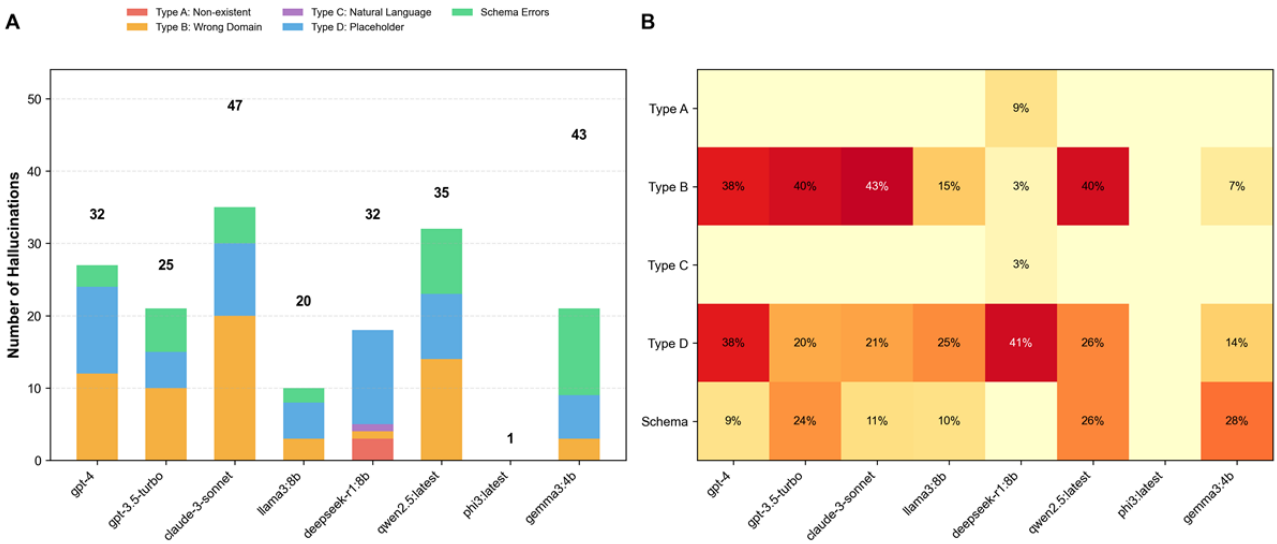
[e]Misleading due to low generation rate.

Llama3:8b emerged as the most effective model with 75.8% effective SQL rate despite moderate SQL generation capability (88.4%), attributed to its low hallucination rate (21.1%) and minimal placeholder usage (22.6%). In contrast, GPT-4 showed high SQL generation (97.9%) but poor effective rate (45.3%) due to excessive placeholder usage (58.1%).

Hallucination Pattern Analysis

Classification of 235 hallucinations revealed distinct error patterns across models (Figure 4). Category B errors (Wrong domain assignments) predominated (34.2%, n=80), followed by Category D (Placeholder insertions, 28.7%, n=67) and Category E (Schema errors, 26.7%, n=63). Category A (Nonexistent concept IDs) was relatively rare (8.3%, n=20), as was Category C (Natural language substitution, 2.1%, n=5). χ^2 analysis confirmed significant variation in error distribution across models (χ^2=45.3, *df*=28, *P*<.001).

Figure 4. Distribution and analysis of hallucination types by model. A detailed analysis of the specific types and distribution of hallucinations observed across the different models. (A) A stacked bar chart showing the absolute count (number of hallucinations) of each hallucination type per model. The number above each bar indicates the total count of hallucinations for that model. Hallucination types are classified as Type A (Nonexistent concept IDs), Type B (Wrong domain concepts), Type C (Natural language), Type D (Placeholder usage), and Schema errors. (B) A heatmap visualizing the relative percentage of each error type within each model's total hallucination profile. The color intensity corresponds to the percentage value, with darker shades indicating a higher proportion of that hallucination type. The scale is provided by the color bar on the right.



Model-specific analysis revealed distinctive failure modes (Table 5). Claude-3-sonnet exhibited the highest baseline hallucination rate (49.5%) but showed dramatic improvement with error-aware prompting (15.8% hallucination and 68.1% relative reduction). GPT-3.5-turbo achieved perfect accuracy (0% hallucination) with explicit_uncertainty prompting, though limited to simple demographic queries. Phi3's apparently low

XSL•FO
RenderX

hallucination rate (1.1%) was misleading, resulting from 83.2% failure to generate any SQL rather than accurate generation.

Table . Detailed hallucination type distribution by model.

Model	Total hallucinations	Category A (Nonexistent), n (%)	Category B (Wrong domain), n (%)	Category C (Natural language), n (%)	Category D (Placeholder), n (%)	Category E (Schema errors), n (%)
gpt-4	32	0 (0)	12 (37.5)	0 (0)	12 (37.5)	8 (25.0)
gpt-3.5-turbo	25	0 (0)	10 (40.0)	0 (0)	5 (20.0)	10 (40.0)
claude-3-sonnet	47	5 (10.6)	20 (42.6)	0 (0)	10 (21.3)	12 (25.5)
llama3:8b	20	5 (25.0)	3 (15.0)	3 (15.0)	5 (25.0)	4 (20.0)
deepseek-r1	32	3 (9.4)	1 (3.1)	1 (3.1)	13 (40.6)	14 (43.8)
qwen2.5	35	2 (5.7)	14 (40.0)	0 (0)	9 (25.7)	10 (28.6)
phi3	1	0 (0)	0 (0)	1 (100)	0 (0)	0 (0)
gemma3	43	5 (11.6)	20 (46.5)	0 (0)	13 (30.2)	5 (11.7)

Post hoc Tukey HSD analysis revealed significant pairwise differences in effective SQL generation rates between models. Llama3:8b significantly outperformed GPT-4 (mean difference=30.5%, $P<.001$), with large effect size (Cohen $d=1.35$). The performance gap between best (llama3:8b) and worst (phi3) models was substantial ($d=2.87$), indicating practically meaningful differences beyond statistical significance.

Prompt Engineering Impact

Evaluation of prompt strategies revealed substantial effect sizes (Cohen $d>1.0$) compared to zero_shot baseline across all alternative strategies. Despite these large effects, high variance in model–prompt interactions prevented detection of a significant main effect ($F(4755)=1.89$, $P=.135$). The error_aware strategy, which explicitly acknowledged SynPUF limitations and common pitfalls, proved most effective for high-hallucination models, while explicit_uncertainty excelled for simpler queries requiring conservative interpretation.

Prompt Strategy Performance Analysis

Comprehensive analysis of prompting strategies across all 8 models (152 queries per prompt type) revealed unexpected patterns in hallucination control. The zero_shot approach demonstrated superior performance with the lowest hallucination rate (mean 13.8%, SD 11.5%) and highest effective SQL rate (mean 71.3%, SD 21.4%), significantly outperforming more complex strategies. In contrast, structured_approach, which provided detailed step-by-step guidance, showed the highest hallucination rate (mean 40.8%, SD 23.8%) and lowest effectiveness (mean 45.5%, SD 18.6%). The validation_focused strategy, designed to emphasize accuracy, paradoxically decreased performance compared to zero_shot ($P=.042$, Tukey HSD), achieving a mean (SD) effective SQL rate of only 56.1% (22.5%). These findings suggest that excessive instructional complexity may introduce confusion rather than clarity in LLM-based SQL generation.

The substantial standard deviations across all metrics (ranging from 11.5% to 28.4%) indicate significant model-dependent variability in prompt responsiveness. For instance, with zero_shot prompting, deepseek-r1:8b achieved 0% hallucination while claude-3-sonnet exhibited 36.8%, representing a 36.8 percentage point difference for identical prompting. This variability was further confirmed by regression analysis, which revealed that model architecture explained 72% of performance variance ($R^2=0.72$, $P<.001$), while prompt strategy contributed marginally. Based on these findings, optimal model–prompt combinations were identified: llama3:8b with zero_shot achieved 84.7% effective SQL rate, while gpt-3.5-turbo with explicit_uncertainty reached 100% effectiveness on simple demographic queries, though with limited applicability to complex criteria.

Synthetic Data Validation

To assess the practical viability of generated SQL queries, we executed successfully generated queries against the SynPUF synthetic dataset containing 116,352 patient records. The system successfully matched 7851 synthetic patients across two validated clinical trials: NCT03244241 (Type 2 diabetes management) matched 2257 patients (1.9% of dataset), while NCT06234488 (breast cancer) matched 5594 patients (4.8% of dataset). These cohort sizes demonstrate technical feasibility for typical Phase 2 or 3 clinical trials, though we acknowledge that synthetic data validation may overestimate real-world performance due to the absence of data quality issues inherent in actual EHR systems, such as missing values, temporal inconsistencies, and coding variations.

Discussion

Principal Findings

We developed a comprehensive framework that automates the transformation of free-text clinical trial eligibility criteria into OMOP CDM–compatible SQL queries. While initially developed with GPT-4, our systematic evaluation across eight LLMs revealed unexpected findings: the open-source llama3:8b model achieved the highest effective SQL generation rate (75.8%) compared to GPT-4's 45.3%, primarily due to lower hallucination rates (21.1% vs 33.7%). This counterintuitive result—where a smaller, local model outperformed state-of-the-art commercial models—highlights the critical importance of hallucination control over raw generation

XSL•FO
RenderX

capability in clinical applications. Our framework successfully demonstrated a 48.5% concept mapping accuracy with GPT-4, significantly exceeding the 32.0% achieved by traditional tools like USAGI (P<.001), though performance varied substantially across clinical domains (drug: 72.7%, measurement: 38.3%).

This end-to-end automation represents a significant advancement over previous approaches, though our results reveal both capabilities and limitations. While earlier studies like Criteria2Query [33] achieved 60% - 70% accuracy in entity recognition but required manual SQL construction, our system automates the entire pipeline. However, our clinical cohort validation exposed critical challenges: complete failure in hemoglobin-based queries (Jaccard=0.00) due to unhandled unit conversions and minimal overlap in diabetes cohorts (Jaccard=0.04) from incomplete concept hierarchy traversal. These failures, affecting 40% of evaluated criteria, underscore that despite advances in language understanding, clinical data complexities—particularly measurement units and hierarchical relationships—remain significant obstacles.

Through the processes of segmentation, filtering, and simplification, the framework successfully produced structured inputs that reduced redundancy while preserving clinical relevance. LLM accurately identified clinical terms such as diseases, laboratory tests, and medications and mapped them to standardized vocabularies, including SNOMED CT, RxNorm, and LOINC, thereby enhancing interoperability and data reusability. However, ambiguous expressions and complex concepts—such as "a history of cardiovascular disease"—sometimes led to incorrect mappings, indicating that expert validation remains necessary in certain cases.

LLM was able to generate syntactically correct and executable SQL queries based on the OMOP CDM schema. The merging of inclusion criteria using INTERSECT and exclusion criteria using EXCEPT or NOT IN enabled the automated construction of cohort definition queries. Nevertheless, challenges were observed when criteria involved temporal constraints or context-dependent conditions, often resulting in omissions or logical misinterpretations. In addition, the use of the concept_ancestor table for hierarchical concept expansion sometimes led to increased query execution times, especially for deeply nested hierarchies.

Complementary Evaluation Strategy

Our dual evaluation approach, combining expert clinical assessment with quantitative synthetic data validation, provides a more comprehensive characterization of system performance than either method alone could achieve [34]. Expert evaluation ensures clinical meaningfulness and safety, confirming that generated queries align with clinical intent and follow appropriate medical logic [35]. Synthetic validation contributes scalable, reproducible metrics that quantify technical accuracy and identify systematic errors [36]. This complementary strategy revealed technical issues invisible to manual review, such as subtle type mismatches and schema reference errors that appeared structurally correct but would fail during execution. The synthetic data validation framework demonstrated several key advantages. Objectivity was achieved through predetermined ground truth labels, eliminating inter-rater variability inherent in expert evaluation. Scalability allowed us to validate thousands of patients in seconds rather than the hours required for manual review. Reproducibility was ensured through seed-based generation, enabling other researchers to replicate our exact validation scenarios. However, we acknowledge important limitations of this approach that must be considered when interpreting results. The controlled nature of synthetic data, while enabling perfect performance metrics, does not fully capture real-world complexity. Electronic health records in clinical practice typically contain 15% - 20% missing values, coding inconsistencies, and temporal gaps that our synthetic data lacks [35] . We anticipate that these factors could reduce real-world performance by 10% - 15% compared to our synthetic validation results [37,38]. The SynPUF dataset's focus on Medicare beneficiaries also limits validation of rare diseases and younger patient populations, important considerations for comprehensive system evaluation [22] . Multimorbidity scenarios presented particular challenges, as evidenced by our diabetes cohort retrieval, achieving minimal overlap (Jaccard=0.04) due to incomplete concept hierarchy traversal [39]. Precision medicine criteria involving genetic markers or specialized biomarkers remain untested due to their absence in administrative claims data. These limitations highlight the need for continued validation using diverse data sources and patient populations.

Cost-Effectiveness and Scalability

Economic feasibility remains crucial for real-world implementation of AI-powered clinical trial matching systems [40]. Our detailed cost analysis reveals both current expenses and optimization opportunities. At current pricing, GPT-4 API calls average US$0.03 - 0.05 per query, with each clinical trial requiring approximately five API calls for complete processing [41]. This translates to roughly US$0.15 - 0.25 per trial using GPT-4. GPT-3.5 offers substantial cost reduction at US$0.006 - 0.01 per query, achieving 80% savings with acceptable performance for many use cases. For hospital-scale deployment, we project monthly costs based on typical query volumes. A mid-sized institution processing 10,000 queries monthly would incur US$300 - 500 using GPT-4 or US$60 - 100 with GPT-3.5. These costs compare favorably to manual review, which typically requires 2 - 4 hours of expert time per trial at US$50 - 100 per hour. Our system processes each trial in under 2 minutes, representing time savings of 98 - 99% compared to manual methods. Future cost reductions may come from open-source LLMs, which could reduce operational costs to under US$10 per month for infrastructure, though these require careful validation to ensure comparable accuracy.

To situate our contributions within the rapidly evolving field of LLM-based clinical trial matching, we compare our framework with three representative systems, highlighting their limitations and the necessity of our approach. Criteria2Query 3.0 [42] achieves 60% - 70% accuracy in entity recognition but relies on manual SQL construction, which hinders scalability and real-time application in clinical settings. LeafAI [43] utilizes a modular pipeline with distinct components for concept extraction, logic parsing, and query generation, necessitating complex maintenance of multiple specialized models and

XSL•FO
RenderX

rule-based systems, which increases deployment costs and expertise requirements. Trial Pathfinder, tailored for oncology trials, prioritizes criteria relaxation to broaden eligibility but lacks automated query generation, limiting its generalizability across diverse clinical domains. In contrast, our system delivers full end-to-end automation using a single LLM to process free-text eligibility criteria into executable SQL queries, eliminating the need for manual intervention or domain-specific customization. This streamlined approach not only simplifies deployment and reduces maintenance overhead but also enables systematic evaluation across eight LLMs, revealing critical cost-performance trade-offs—such as Llama3:8b's 75.8% effective SQL generation rate compared to GPT-4's 45.3%. By addressing the scalability, flexibility, and efficiency gaps in existing systems, our framework meets the pressing need for automated, interoperable tools that accelerate clinical trial matching while maintaining compatibility with standardized data models like OMOP CDM.

Broader Healthcare and Societal Impact

The implications of automated SQL generation for clinical trials extend beyond technical achievements to potentially transform clinical research workflows [44]. Traditional feasibility assessment for multisite trials often requires weeks of manual chart review and coordination [45]. Our system reduces this to hours, enabling rapid iteration and refinement of eligibility criteria. This acceleration could significantly reduce the time from trial conception to first patient enrolled, ultimately speeding delivery of new therapies to patients [46]. Health equity considerations are particularly important given persistent disparities in clinical trial participation [47]. Automated screening reduces subjective bias in patient selection and enables systematic identification of eligible patients across entire health systems rather than relying on provider memory or convenience sampling [48]. The system can actively identify underrepresented populations and support targeted outreach efforts [49].

Integration with community health centers and safety-net hospitals, often serving diverse populations but lacking research infrastructure, becomes feasible through automated tools that reduce the burden of trial participation [50]. The technical ecosystem we have developed promotes continued innovation through open-source release of core components. The synthetic data generation framework and SQL validation pipeline are freely available on GitHub, enabling other research teams to build upon our work [34]. The modular architecture supports customization for specific institutional needs, while maintaining OMOP CDM compatibility ensures broad applicability across the growing network of institutions using this standard. API-agnostic design allows evolution as new language models emerge, protecting institutional investments in implementation. Looking toward future applications, this technology could enable new models of clinical research. Federated networks could simultaneously assess trial feasibility across multiple institutions without sharing patient data [51]. Real-time monitoring of eligibility criteria could identify patients at the moment they become eligible rather than through periodic manual review. Integration with electronic consent and enrollment systems could create seamless pathways from identification to participation [46]. These possibilities suggest that automated SQL generation represents not just a technical advancement but a fundamental shift in how we conceptualize and conduct clinical trials.

Limitations and Future Directions

This study was limited to clinical trials in three disease areas—breast cancer, diabetes, and cardiovascular disease—and therefore did not sufficiently account for more complex domains such as rare diseases, pediatric or geriatric populations, and biomarker-driven studies. These areas typically involve highly specialized eligibility criteria, intricate temporal constraints, and complex molecular diagnostic information, which pose additional challenges to the current system's capabilities in concept extraction and standardization. Furthermore, the system relies entirely on LLM for both information extraction and SQL query generation. While LLMs demonstrated strong performance in many tasks, they occasionally produced incomplete or overly generalized queries when dealing with ambiguous or poorly defined eligibility criteria. Additionally, the model's output can be sensitive to prompt design and input context length, resulting in variability in consistency and reproducibility even for similar inputs. In particular, eligibility criteria that involve vague, context-dependent, or physician-interpreted terms (eg, "significant cardiac disease" or "recent infection") pose notable challenges. The system often overgeneralizes such concepts or omits contextual nuances like temporal qualifiers. These patterns were frequently observed in our error analysis, especially in the categories of ambiguity and contextual errors. Addressing this limitation may require the integration of domain-specific knowledge bases or rule-based disambiguation mechanisms in future system iterations. From an evaluation perspective, although this study incorporated expert-reviewed concept mapping and structural validation, comprehensive assessment of generalizability across diverse clinical datasets and institutions was not conducted. Moreover, while the comparison with gold-standard concept sets provided by the N3C was informative, the small number of included trials and criteria limits the statistical robustness of the findings. Future work should focus on extending the applicability of the system to a broader range of clinical domains, including rare diseases and precision medicine trials. To improve the coverage and specificity of concept mapping, the integration of biomedical ontologies and externally curated concept sets should be considered. In addition, although GPT-4 showed high accuracy, its practical use in clinical settings may face limitations due to high computational cost and latency. Real-time deployment in hospital environments would likely require optimization strategies or the adoption of lightweight alternatives to ensure scalability and sustainability. Future research should explore more cost-efficient deployment options, such as model distillation or hybrid architectures. Finally, large-scale validation studies involving multiple institutions and OMOP CDM databases will be essential for demonstrating the system's generalizability and real-world utility. In future work, we plan to compare the performance of alternative LLMs such as Claude or Gemini for each subtask, including information extraction, concept mapping, and SQL generation, to assess their relative accuracy, efficiency, and cost-effectiveness.

XSL•FO
RenderX

Conclusion

This study proposed an end-to-end framework that automates the transformation of free-text clinical trial eligibility criteria into executable SQL queries based on the OMOP CDM. Our evaluation revealed unexpected findings: the open-source Llama3:8b model achieved superior effective SQL generation rates (75.8%) compared to GPT-4 (45.3%), primarily due to better hallucination control. While the framework demonstrated feasibility with 48.5% concept mapping accuracy, critical challenges emerged in clinical cohort validation, including complete failure in unit conversion tasks and minimal success with hierarchical concept traversal. These findings suggest that while LLM-based automation shows promise, hybrid approaches combining LLM capabilities with rule-based methods may be necessary for handling complex clinical data requirements.

Acknowledgments

This research was supported by a grant of the Korea Health Technology R&D Project through the

Korea Health Industry Development Institute (KHIDI) funded by the Ministry of Health & Welfare, Republic of Korea (grant number: HR21C0198) and 2024IP0015-1 from the Asan Institute for Life Sciences, Asan Medical Center, Seoul, Korea. We would like to express our sincere gratitude to Dr. Lee Ji-Soo and Dr. Baek Ga-Kyoung for their valuable contributions to this paper.

Authors' Contributions

SJ, GJK, and KHL conceptualized and designed the study. SJ and SP developed the methodology and performed the data processing. DK and OJK conducted the technical validation and analysis. JHL and YHK provided clinical expertise and validated the medical content. SP and DK performed the statistical analysis. SJ wrote the initial draft of the manuscript. GJK and KHL supervised the project and provided critical revision of the manuscript. All authors reviewed and approved the final version of the manuscript.

Conflicts of Interest

None declared.

Multimedia Appendix 1
Supplementary methods.
[DOCX File, 256 KB - medinform_v13i1e71252_app1.docx]

Multimedia Appendix 2
Prompt templates.
[DOCX File, 25 KB - medinform_v13i1e71252_app2.docx]

Multimedia Appendix 3
SQL evaluation metrics.
[DOCX File, 18 KB - medinform_v13i1e71252_app3.docx]

References

1. Williams RJ, Tse T, DiPiazza K, Zarin DA. Terminated trials in the ClinicalTrials.gov results database: evaluation of availability of primary outcome data and reasons for termination. PLoS ONE 2015;10(5):e0127242. [doi: 10.1371/journal.pone.0127242] [Medline: 26011295]
2. Hung M, Mohajeri A, Almpani K, et al. Successes and challenges in clinical trial recruitment: the experience of a new study team. Med Sci (Basel) 2024 Aug 14;12(3):39. [doi: 10.3390/medsci12030039] [Medline: 39189202]
3. Lombardo G, Couvert C, Kose M, et al. Electronic health records (EHRs) in clinical research and platform trials: application of the innovative EHR-based methods developed by EU-PEARL. J Biomed Inform 2023 Dec;148:104553. [doi: 10.1016/j.jbi.2023.104553] [Medline: 38000766]
4. Carlisle B, Kimmelman J, Ramsay T, MacKinnon N. Unsuccessful trial accrual and human subjects protections: an empirical analysis of recently closed trials. Clin Trials 2015 Feb;12(1):77-83. [doi: 10.1177/1740774514558307] [Medline: 25475878]
5. Sacks LV, Shamsuddin HH, Yasinskaya YI, Bouri K, Lanthier ML, Sherman RE. Scientific and regulatory reasons for delay and denial of FDA approval of initial applications for new drugs, 2000-2012. JAMA 2014;311(4):378-384. [doi: 10.1001/jama.2013.282542] [Medline: 24449316]
6. Sun D, Gao W, Hu H, Zhou S. Why 90% of clinical drug development fails and how to improve it? Acta Pharm Sin B 2022 Jul;12(7):3049-3062. [doi: 10.1016/j.apsb.2022.02.002] [Medline: 35865092]

XSL•FO
RenderX

7. Rajadhyaksha V. Conducting feasibilities in clinical trials: an investment to ensure a good study. Perspect Clin Res 2010 Jul;1(3):106-109. [Medline: 21814631]
8. Fogel DB. Factors associated with clinical trials that fail and opportunities for improving the likelihood of success: a review. Contemp Clin Trials Commun 2018 Sep;11:156-164. [doi: 10.1016/j.conctc.2018.08.001] [Medline: 30112460]
9. Baumfeld Andre E, Reynolds R, Caubel P, Azoulay L, Dreyer NA. Trial designs using real-world data: The changing landscape of the regulatory approval process. Pharmacoepidemiol Drug Saf 2020 Oct;29(10):1201-1212. [doi: 10.1002/pds.4932] [Medline: 31823482]
10. Dagenais S, Russo L, Madsen A, Webster J, Becnel L. Use of real-world evidence to drive drug development strategy and inform clinical trial design. Clin Pharmacol Ther 2022 Jan;111(1):77-89. [doi: 10.1002/cpt.2480] [Medline: 34839524]
11. Tashkin DP, Amin AN, Kerwin EM. Comparing randomized controlled trials and real-world studies in chronic obstructive pulmonary disease pharmacotherapy. Int J Chron Obstruct Pulmon Dis 2020;15:1225-1243. [doi: 10.2147/COPD.S244942] [Medline: 32581529]
12. Rogers JR, Lee J, Zhou Z, Cheung YK, Hripcsak G, Weng C. Contemporary use of real-world data for clinical trial conduct in the United States: a scoping review. J Am Med Inform Assoc 2021 Jan 15;28(1):144-154. [doi: 10.1093/jamia/ocaa224] [Medline: 33164065]
13. Evans SR, Paraoan D, Perlmutter J, Raman SR, Sheehan JJ, Hallinan ZP. Real-world data for planning eligibility criteria and enhancing recruitment: recommendations from the clinical trials transformation initiative. Ther Innov Regul Sci 2021 May;55(3):545-552. [doi: 10.1007/s43441-020-00248-7] [Medline: 33393014]
14. Rudrapatna VA, Butte AJ. Opportunities and challenges in using real-world data for health care. J Clin Invest 2020 Feb 3;130(2):565-574. [doi: 10.1172/JCI129197] [Medline: 32011317]
15. Liu R, Rizzo S, Whipple S, et al. Evaluating eligibility criteria of oncology trials using real-world data and AI. Nature New Biol 2021 Apr;592(7855):629-633. [doi: 10.1038/s41586-021-03430-5] [Medline: 33828294]
16. Umapathi LK, Pal A, Sankarasubbu M. Med-HALT: medical domain hallucination test for large language models. arXiv. Preprint posted online on Jul 27, 2023. [doi: 10.48550/arXiv.2307.15343]
17. Asgari E, Montaña-Brown N, Dubois M, et al. A framework to assess clinical safety and hallucination rates of LLMs for medical text summarisation. NPJ Digit Med 2025 May 13;8(1):274. [doi: 10.1038/s41746-025-01670-7] [Medline: 40360677]
18. OpenAI. GPT-4 technical report. arXiv. Preprint posted online on Mar 27, 2023. [doi: 10.48550/arXiv.2303.08774]
19. SynPUF dataset documentation. Centers for Medicare & Medicaid Services (CMS). URL: https://www.cms.gov [accessed 2025-07-10]
20. Hripcsak G, Duke JD, Shah NH, et al. Observational health data sciences and informatics (OHDSI): opportunities for observational researchers. Stud Health Technol Inform 2015;216:574-578. [Medline: 26262116]
21. Aggregate analysis of clinicaltrials.gov (AACT) database. Clinical Trials Transformation Initiative (CTTI). URL: https://aact.ctti-clinicaltrials.org/ [accessed 2023-07-18]
22. Usagi: a tool for semi-automated mapping to standardized vocabularies. Observational Health Data Sciences and Informatics (OHDSI).: GitHub repository URL: https://github.com/OHDSI/Usagi [accessed 2023-07-27]
23. GPT-35 technical overview. OpenAI. 2023. URL: https://platform.openai.com/docs [accessed 2025-07-10]
24. Anthropic. Claude 3 Technical Overview. 2024. URL: https://www.anthropic.com/index/claude-3 [accessed 2025-07-10]
25. Grattafiori A, Dubey A, Jauhri A, et al. The llama 3 herd of models. arXiv. Preprint posted online on 2024. [doi: 10.48550/arXiv:2407.21783]
26. Guo X, Yang D, Zhang H, et al. DeepSeek-R1 incentivizes reasoning in LLMs through reinforcement learning. . 2025 p. 633-638. [doi: 10.1038/s41586-025-09422-z]
27. Yang A, Yang B, Zhang B. Qwen2.5 Technical Report. arXiv. Preprint posted online on 2024. [doi: 10.48550/arXiv.2412.15115]
28. Microsoft. Phi-3 technical report: a family of open language models. arXiv. Preprint posted online on Apr 22, 2024. [doi: 10.48550/arXiv.2404.14219]
29. Gemma: open models based on gemini research and technology. Google DeepMind. 2024. URL: https://ai.google.dev/gemma [accessed 2025-07-10]
30. Virtanen P, Gommers R, Oliphant TE, et al. Author correction: SciPy 1.0: fundamental algorithms for scientific computing in Python. Nat Methods 2020 Mar;17(3):352-352. [doi: 10.1038/s41592-020-0772-5] [Medline: 32094914]
31. Seabold S, Perktold J. Statsmodels: econometric and statistical modeling with python. 2010 Presented at: Python in Science Conference; Jun 28, 2010; Austin, Texas. [doi: 10.25080/Majora-92bf1922-011]
32. Haendel MA, Chute CG, Bennett TD, et al. The National COVID Cohort Collaborative (N3C): Rationale, design, infrastructure, and deployment. J Am Med Inform Assoc 2021 Mar 1;28(3):427-443. [doi: 10.1093/jamia/ocaa196] [Medline: 32805036]
33. Yuan C, Ryan PB, Ta C, et al. Criteria2Query: a natural language interface to clinical databases for cohort definition. J Am Med Inform Assoc 2019 Apr 1;26(4):294-305. [doi: 10.1093/jamia/ocy178] [Medline: 30753493]
34. Walonoski J, Kramer M, Nichols J, et al. Synthea: an approach, method, and software mechanism for generating synthetic patients and the synthetic electronic health care record. J Am Med Inform Assoc 2018 Mar 1;25(3):230-238. [doi: 10.1093/jamia/ocx079] [Medline: 29025144]

XSL•FO
RenderX

35. Weiskopf NG, Weng C. Methods and dimensions of electronic health record data quality assessment: enabling reuse for clinical research. J Am Med Inform Assoc 2013 Jan 1;20(1):144-151. [doi: 10.1136/amiajnl-2011-000681] [Medline: 22733976]
36. Gonzales A, Guruswamy G, Smith SR. Synthetic data in health care: a narrative review. PLOS Digit Health 2023 Jan;2(1):e0000082. [doi: 10.1371/journal.pdig.0000082] [Medline: 36812604]
37. Kahn MG, Callahan TJ, Barnard J, et al. A harmonized data quality assessment terminology and framework for the secondary use of electronic health record data. EGEMS (Wash DC) 2016;4(1):1244. [doi: 10.13063/2327-9214.1244] [Medline: 27713905]
38. Collins GS, Ogundimu EO, Altman DG. Sample size considerations for the external validation of a multivariable prognostic model: a resampling study. Stat Med 2016 Jan 30;35(2):214-226. [doi: 10.1002/sim.6787] [Medline: 26553135]
39. Barnett K, Mercer SW, Norbury M, Watt G, Wyke S, Guthrie B. Epidemiology of multimorbidity and implications for health care, research, and medical education: a cross-sectional study. Lancet 2012 Jul 7;380(9836):37-43. [doi: 10.1016/S0140-6736(12)60240-2] [Medline: 22579043]
40. Gomez Rossi J, Feldberg B, Krois J, Schwendicke F. Evaluation of the clinical, technical, and financial aspects of cost-effectiveness analysis of artificial intelligence in medicine: scoping review and framework of analysis. JMIR Med Inform 2022 Aug 12;10(8):e33703. [doi: 10.2196/33703] [Medline: 35969458]
41. OpenAI. URL: https://openai.com/pricing [accessed 2025-07-10]
42. Park J, Fang Y, Ta C, et al. Criteria2Query 3.0: Leveraging generative large language models for clinical trial eligibility query generation. J Biomed Inform 2024 Jun;154:104649. [doi: 10.1016/j.jbi.2024.104649] [Medline: 38697494]
43. Dobbins NJ, Han B, Zhou W, et al. LeafAI: query generator for clinical cohort discovery rivaling a human programmer. J Am Med Inform Assoc 2023 Nov 17;30(12):1954-1964. [doi: 10.1093/jamia/ocad149] [Medline: 37550244]
44. Wagholikar KB, Zelle D, Ainsworth L, et al. Use of automatic SQL generation interface to enhance transparency and validity of health-data analysis. Inform Med Unlocked 2022;31:100996. [doi: 10.1016/j.imu.2022.100996] [Medline: 35874460]
45. Vemulakonda VM, Janzen N, Hittelman AB, et al. Feasibility of establishing a multi-center research database using the electronic health record: the PURSUIT network. J Pediatr Urol 2022 Dec;18(6):788. [doi: 10.1016/j.jpurol.2022.05.004] [Medline: 35644792]
46. Ni Y, Bermudez M, Kennebeck S, Liddy-Hicks S, Dexheimer J. A real-time automated patient screening system for clinical trials eligibility in an emergency department: design and evaluation. JMIR Med Inform 2019 Jul 24;7(3):e14185. [doi: 10.2196/14185] [Medline: 31342909]
47. Unger JM, Hershman DL, Till C, et al. "When offered to participate": a systematic review and meta-analysis of patient agreement to participate in cancer clinical trials. J Natl Cancer Inst 2021 Mar 1;113(3):244-257. [doi: 10.1093/jnci/djaa155] [Medline: 33022716]
48. Ni Y, Kennebeck S, Dexheimer JW, et al. Automated clinical trial eligibility prescreening: increasing the efficiency of patient identification for clinical trials in the emergency department. J Am Med Inform Assoc 2015 Jan;22(1):166-178. [doi: 10.1136/amiajnl-2014-002887] [Medline: 25030032]
49. Somasegar S, Bakkum-Gamez JN. Transforming clinical trial enrollment: leveraging technology and innovation to reach patients where they are. Gynecol Oncol Rep 2025 Feb;57:101691. [doi: 10.1016/j.gore.2025.101691] [Medline: 40051579]
50. George S, Duran N, Norris K. A systematic review of barriers and facilitators to minority research participation among African Americans, Latinos, Asian Americans, and Pacific Islanders. Am J Public Health 2014 Feb;104(2):e16-e31. [doi: 10.2105/AJPH.2013.301706] [Medline: 24328648]
51. Rieke N, Hancox J, Li W, et al. The future of digital health with federated learning. NPJ Digit Med 2020;3:119. [doi: 10.1038/s41746-020-00323-1] [Medline: 33015372]

Abbreviations

LLM: Large Language Model
N3C: National COVID Cohort Collaborative
OMOP CDM: Observational Medical Outcomes Partnership Common Data Model
RWD: real-world data
SQL: Structured Query Language
SynPUF: Synthetic Public Use Files

XSL•FO
RenderX

Edited by A Castonguay; submitted 14.01.25; peer-reviewed by J Park, K Kim, M Spotnitz; revised version received 21.07.25; accepted 05.08.25; published 16.10.25.

Please cite as:
Lee KH, Jang S, Kim GJ, Park S, Kim D, Kwon OJ, Lee JH, Kim YH
Large Language Models for Automating Clinical Trial Criteria Conversion to Observational Medical Outcomes Partnership Common Data Model Queries: Validation and Evaluation Study
JMIR Med Inform 2025;13:e71252
URL: https://medinform.jmir.org/2025/1/e71252
doi:10.2196/71252

© Kye Hwa Lee, Sujung Jang, Grace Juyun Kim, Sukyoung Park, Doeun Kim, Oh Jin Kwon, Jae-Ho Lee, Young-Hak Kim. Originally published in JMIR Medical Informatics (https://medinform.jmir.org), 16.10.2025. This is an open-access article distributed under the terms of the Creative Commons Attribution License (https://creativecommons.org/licenses/by/4.0/), which permits unrestricted use, distribution, and reproduction in any medium, provided the original work, first published in JMIR Medical Informatics, is properly cited. The complete bibliographic information, a link to the original publication on https://medinform.jmir.org/, as well as this copyright and license information must be included.

XSL•FO
RenderX

Performance of Large Language Models in the Non-English Context: Qualitative Study of Models Trained on Different Languages in Chinese Medical Examinations

Zhong Yao[1,2,3], MD; Liantan Duan[4], BSc; Shuo Xu[1,2,3], MD; Lingyi Chi[1,2,3], MD; Dongfang Sheng[4], PhD

[1]Department of Neurosurgery, Qilu Hospital of Shandong University, Jinan, China

[2]Cheeloo College of Medicine, Shandong University, Jinan, China

[3]Brain and Brain-Inspired Science, Shandong University, Jinan, China

[4]School of Management, Shandong University, No. 27 Shanda South Road，250100, Jinan, China

Corresponding Author:
Dongfang Sheng, PhD
School of Management, Shandong University, No. 27 Shanda South Road，250100, Jinan, China

Abstract

Background: Research on large language models (LLMs) in the medical field has predominantly focused on models trained with English-language corpora, evaluating their performance within English-speaking contexts. The performances of models trained with non–English language corpora and their performance in non-English contexts remain underexplored.

Objective: This study aimed to evaluate the performances of LLMs trained on different languages corpora by using the Chinese National Medical Licensing Examination (CNMLE) as a benchmark and constructed analogous questions.

Methods: Under different prompt settings, we sequentially posed questions to 7 LLMs: 2 primarily trained on English-language corpora and 5 primarily on Chinese-language corpora. The models' responses were compared against standard answers to calculate the accuracy rate of each model. Further subgroup analyses were conducted by categorizing the questions based on various criteria. We also collected error sets to explore patterns of mistakes across different models.

Results: Under the zero-shot setting, 6 out of 7 models exceeded the passing level, with the highest accuracy rate achieved by the Chinese LLM Baichuan (86.67%), followed by ChatGPT (83.83%). In the constructed questions, all 7 models exceeded the passing threshold, with Baichuan maintaining the highest accuracy rate (87.00%). In few-shot learning, all models exceeded the passing threshold. Baichuan, ChatGLM, and ChatGPT retained the highest accuracy. While Llama showed marked improvement over previous tests, the relative performance rankings of other models stayed similar to previous results. In subgroup analyses, English models demonstrated comparable or superior performance to Chinese models on questions related to ethics and policy. All models except Llama generally had higher accuracy rates for simple questions than for complex ones. The error set of ChatGPT was similar to those of other Chinese models. Multimodel cross-verification outperformed single model, particularly improving accuracy rate on simple questions. The implementation of dual-model and tri-model verification achieved accuracy rates of 94.17% and 96.33% respectively.

Conclusions: At the current level, LLMs trained primarily on English corpora and those trained mainly on Chinese corpora perform similarly well in CNMLE, with Chinese models still outperforming. The performance difference between ChatGPT and other Chinese LLMs are not solely due to communication barriers but are more likely influenced by disparities in the training data. By using a method of cross-verification with multiple LLMs, excellent performance can be achieved in medical examinations.

(JMIR Med Inform 2025;13:e69485) doi:10.2196/69485

KEYWORDS

large language model; medical examination; non-English; ChatGPT; language corpora

Introduction

Large language models (LLMs) are advanced models trained on vast amounts of data, capable of processing natural language and performing specific tasks. In 2022, OpenAI released ChatGPT, which garnered widespread attention to LLMs. In the years that followed, numerous technology companies, including Meta with its Llama model and Google with PaLM 2, have also released their own LLMs. These models have been extensively researched and applied in various fields, including medicine. However, most existing research was conducted within English contexts, focusing on LLMs primarily trained on English-language corpora [1-3]. There is a notable lack of research on the performance of LLMs trained on non-English languages, particularly in non-English contexts.

XSL•FO
RenderX

To facilitate widespread adoption, LLMs should meet the requirements in diverse linguistic environments, not just within the English-speaking context. While many models offer multilingual versions, the training corpora may still be disproportionately weighted toward English, with insufficient representation of other languages, which could lead to subpar performance in non-English contexts [4]. Research has shown that ChatGPT, primarily trained on English-language corpora, is able to pass the United States Medical Licensing Examination [5], and can effectively addressing various clinical medical inquiries [6]. However, in some non-English medical examinations, ChatGPT fails to even reach a passing grade [7-9]. This disparity can be attributed to the preponderance of English-centric data in the training corpora, coupled with a limited inclusion of non-English content, leading to remarkable performance within English linguistic settings but less satisfactory results in non-English environments [10].

Researchers have made significant efforts to improve the performance of LLMs in non-English contexts. Wu et al [8] significantly enhanced ChatGPT's performance in Chinese medical examinations by fine-tuning the model with external Chinese data, Zheng et al [11] developed a LLM named MOPH, trained on Chinese datasets, which outperformed ChatGPT in Chinese ophthalmology examinations. Considering the 3 major factors that influence their performance—computational power, algorithms, and training datasets—we hypothesize that making targeted adjustments to the training dataset can efficiently improve the performance of LLMs in non-English environments. In China, numerous LLMs have emerged, with training sets containing a greater proportion of Chinese-language data, theoretically leading to better performance in Chinese contexts. To assess this, we use the 2023 edition of Chinese National Medical Licensing Examination (CNMLE) as a benchmark to evaluate the performance of LLMs trained on different language corpora.

The primary objectives of this study are threefold: first, to conduct a batch test of Chinese LLMs; second, to compare the performance of Chinese and English LLMs; and third, to elucidate the commonalities and disparities in the performance characteristics of both types of models. The goal is to provide empirical evidence that can inform efforts to enhance the performance of LLMs in non-English contexts.

Methods

The design and conduct of this study adhere to the METRICS (Model, Evaluation, Timing, Range/Randomization, Individual factors, Count, and Specificity of prompts and language) checklist.

Selected LLMs and Test Duration

The models tested in this study include ChatGPT and Llama, which have undergone extensive research and are primarily trained on English-language corpora, as well as ERNIE Bot, Kimi, Baichuan, ChatGLM, and Yi-large, which have gained significant attention and are primarily trained on Chinese-language corpora. A detailed description of the tested models is provided in Table 1. To ensure consistency and reproducibility, all LLMs were tested with default parameters and in a zero-shot setting. In addition, to control for prompt engineering effects, tests were systematically replicated under a few-shot learning paradigm. The study was conducted from August to October 2024, and during this period, none of the tested models received version updates.

Table . Details of tested large language models.

Models	Version	Release year	Source code	Charge	Search internet capability	Source
ERNIE Bot	ERNIE-3.5 - 8K	2023	Closed-source	Free	No	[12]
Kimi	moonshot-v1-8k	2023	Closed-source	Free	Yes	[13]
Baichuan	Baichuan3-Turbo	2023	Closed-source	Charge	Yes	[14]
ChatGLM	glm-4	2023	Open-source	Free	Yes	[15]
Yi-large	yi-large-turbo	2023	Closed-source	Charge	No	[16]
Llama	llama3-70b-instruct	2023	Open-source	Free	No	[17]
ChatGPT	GPT-4o	2022	Closed-source	Charge	No	[18]

Resources and Transparency of Test Data

The test questions and standard answers for the 2023 CNMLE were obtained from publicly accessible networks, comprising a total sample of 600 multiple-choice questions. Each question stem was followed by multiple options, with only one correct answer. Participants were required to select the single correct answer from the provided options. A passing score was defined as achieving a correct answer rate higher than 60%.

Self-Constructed Questions

Due to the real-time internet search capabilities of some tested LLMs, there is a possibility that these models could access standard answers from the internet or that their training datasets might already contain data from the CNMLE, leading to data contamination. To rule out these scenarios, a panel of three experienced physicians constructed a set of 100 novel questions that closely mirror the format and style of the CNMLE. These 100 questions are not retrievable from the internet and are guaranteed not to be present in the training datasets of the LLMs. The self-constructed questions were presented to the LLMs using the same prompts, and the accuracy rate was calculated.

XSL•FO
RenderX

The consistency in the accuracy rates of the LLMs when answering both the self-constructed questions and the CNMLE questions was compared to assess whether the LLMs' performance relied on real-time web retrieval or the presence of data contamination. The responses from the LLMs were generated under standard conditions, with detailed answers and analysis provided in Multimedia Appendix 1.

Range and Randomization of the Topics Tested

The test data comprise all questions from the most recent 2023 edition of CNMLE without artificial selection. The examination is structured into 4 sections: Basic Medical Sciences, Medical Humanities, Clinical Medicine, and Preventive Medicine, covering various fields and directions in medicine [19]. Given that an average of over half a million medical students participate in the CNMLE examination annually, the compilation of its questions follows rigorous and standardized criteria, establishing it as a highly representative assessment of medical knowledge.

Specificity of the Prompt and Language

First, we implemented a zero-shot configuration to ensure experimental reproducibility. Then, to control for potential confounding effects of prompt engineering, we conducted additional validation using few-shot learning protocols, which was conducted with 3 demonstration examples per task based on the standardized protocol. Using the prompt "You are a doctor. I will give you a multiple-choice question from a medical exam. Please read the question carefully, choose the most appropriate answer from the five options, and explain the reason," we called the application programming interface to sequentially present 600 questions to the LLMs and obtained their answers and explanations. The language for the prompts, inputs, and outputs was Chinese. Chinese includes Mandarin and minority languages, but this study specifically refers to Mandarin. To eliminate any potential impact of language barriers on model performance, we conduct a professional-grade translation via DeepL, followed by cross-verification by a bilingual scholar to eliminate significant semantic distortions, and then followed the same procedure to ask the questions to English-language LLMs.

Evaluation of LLM Responses

The accuracy of the answers provided by the LLMs was determined by comparing them to the officially published correct answers. The evaluation process was entirely objective, with no individual subjective involvement. Each answer, along with its corresponding explanation, was thoroughly examined to identify the underlying reasons for any errors. For each model, a set of incorrectly answered questions was compiled to create an error set, and a Venn diagram was generated to analyze the overlap and correlations between the error sets [20].

Subgroup Analysis

The test questions vary in type, content breadth, and difficulty level, which may affect the performance of LLMs. We conducted a subgroup analysis of the questions to rule out potential confounding factors and also to assess whether the performance of these models across various subgroups conforms to general logical cognition.

Differences in policies and ethics among countries, such as those related to euthanasia and abortion, may influence the responses given by LLMs. Based on the knowledge scope, the questions were classified into 2 categories: policies and ethics, and professional knowledge.

Questions were also differentiated based on their polarity; those requiring a correct or affirmative answer were termed "positive questions," while those necessitating the identification of an incorrect or negative answer were termed "negative questions," with the latter generally recognized as more challenging [21].

Furthermore, questions were categorized by their formats into medical knowledge, which tests a single knowledge point directly, and clinical case analysis, which involves specific clinical scenarios that require the integration of information to formulate a response, thereby increasing the difficulty. According to CNMLE statistics, the correct answer rate for clinical case analysis is lower than that for medical knowledge.

In alignment with Bloom's Taxonomy, an educational classification system for cognitive skills, the required cognitive abilities are hierarchically ranked from low to high as remembering, understanding, applying, analyzing, evaluating, and creating. The first 3 are defined as lower-order thinking, while the latter 3 are considered higher-order thinking [22].

Based on the above grouping criteria, each question was assigned to a subgroup after consensus was reached through discussion among 3 doctors.

Ethical Considerations

This study did not involve any human participants, thereby waiving the need for institutional review board review.

Results

Accuracy Rate

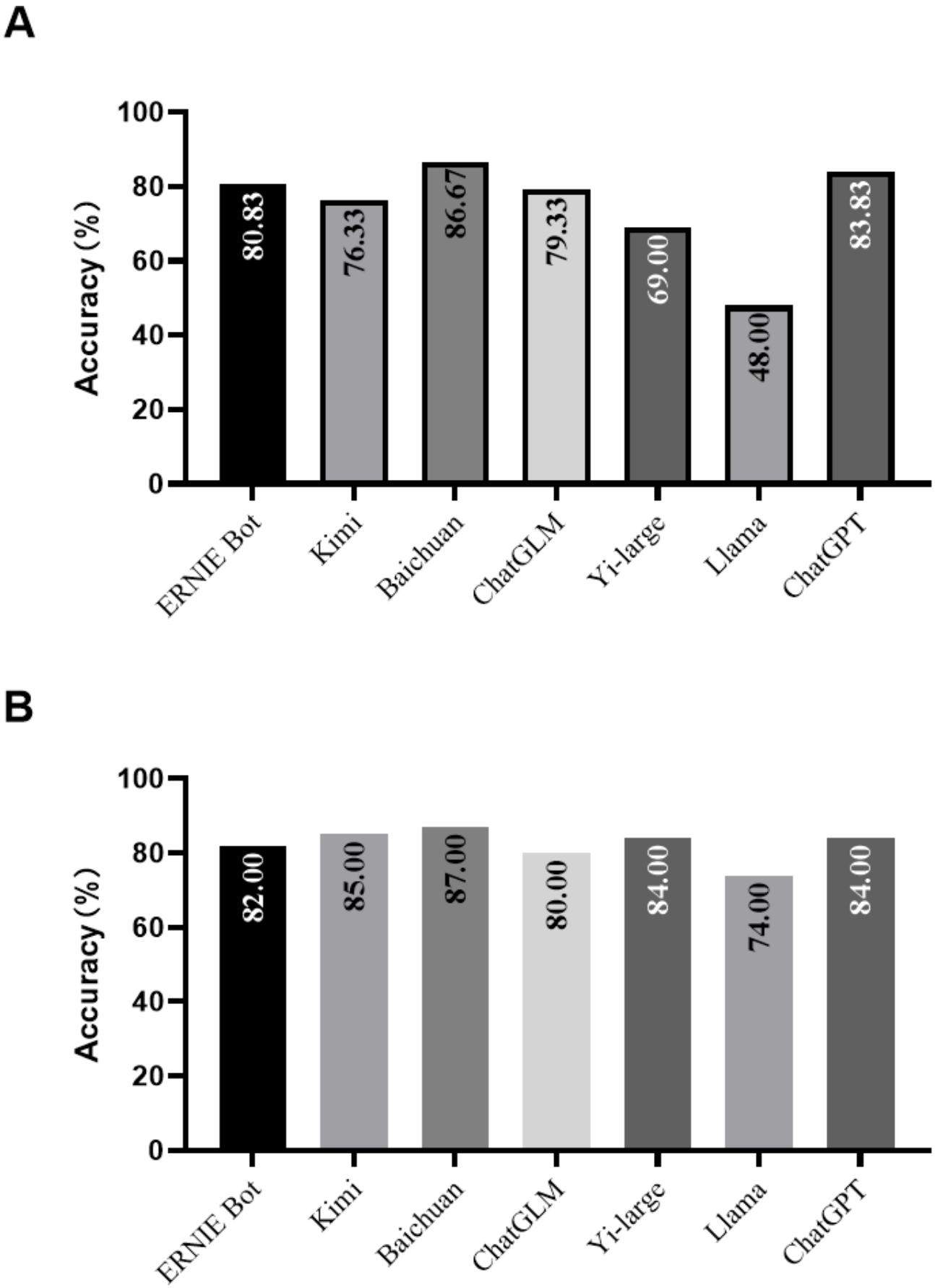
Figure 1A illustrated the accuracy rates of 7 LLMs in the CNMLE, ranked from highest to lowest: Baichuan (86.67%), ChatGPT (83.83%), ERNIE Bot (80.83%), ChatGLM (79.33%), Kimi (76.33%), Yi-large (69.00%), and Llama (48.00%). All models, with the exception of Llama, surpassed the passing threshold, with the Chinese model Baichuan emerging as the top performer, outscoring even ChatGPT. In a set of 100 self-constructed questions, Llama's accuracy rate saw a significant improvement, rising from 48% to 74%, whereas the other models' performance remained largely consistent with their results in the CNMLE. Baichuan maintained the highest accuracy at 87.00%, followed by Kimi at 85.00% and ChatGPT at 84.00% (Figure 1B). When the questions were translated into English and represented to ChatGPT using the same method, its accuracy rate decreased to 81.00%, likely due to errors introduced during the translation process. We re-evaluated the models using the few-shot approach, and observed that the relative rankings among the models remained largely consistent. Baichuan (84.50%) demonstrated the highest accuracy rate, followed by ChatGLM (84.50%) and ChatGPT (81.83%). Notably, Llama exhibited a significant improvement in accuracy rate after prompt engineering modifications (Multimedia Appendix 1). Overall, the results of the second test exhibited

XSL•FO
RenderX

trends comparable to existing findings, indicating that the prompt engineering has minimal influence on the relative performance among models.

XSL•FO
RenderX

Figure 1. The accuracy rates of seven large language models in the Chinese National Medical Licensing Examination (**A**) and self-constructed questions (**B**).



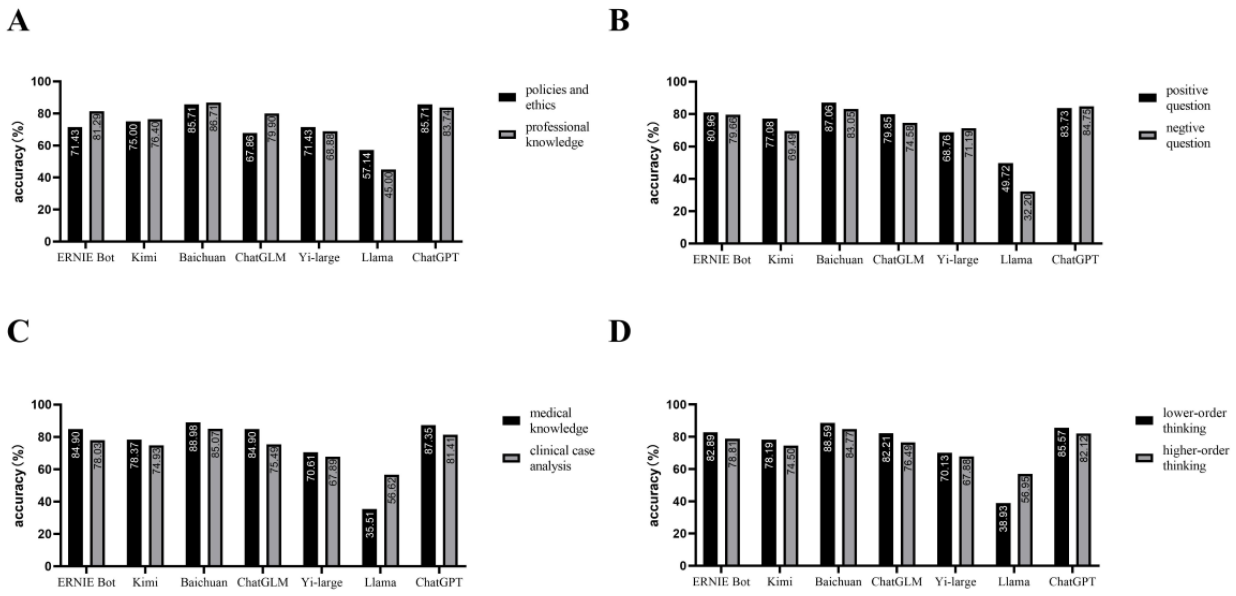
XSL•FO
RenderX

Subgroup Analyses

To analyze the performance of LLMs across various question types, the questions were categorized based on distinct characteristics. The categorization was as follows: by knowledge scope, questions were divided into policies and ethics (28 questions) and professional knowledge (572 questions); by question polarity, into positive questions (541 questions) and negative questions (59 questions); by question format, into medical knowledge (245 questions) and clinical case analysis (355 questions); and by Bloom's Taxonomy, into lower-order thinking (298 questions) and higher-order thinking (302 questions).

Figure 2A illustrated that, among the policies and ethics questions, ChatGPT achieved the highest accuracy rate (85.71%), while Baichuan performed best on professional knowledge questions with an accuracy rate of 86.71%. Interestingly, 4 Chinese-language models (ERNIE Bot, Kimi, Baichuan, and ChatGLM) demonstrated lower accuracy on policies and ethics questions than on professional knowledge questions. In contrast, the 2 English-language models (Llama and ChatGPT) exhibited higher accuracy on policies and ethics questions compared to professional knowledge questions. This suggests that, despite the differences in policies and ethical concerns across countries, English-language models may account for these variations, enabling them to perform better on policies and ethics questions in Chinese.

Figure 2. The accuracy rates of 7 large language models in the Chinese National Medical Licensing Examination questions stratified into subgroups according to different criteria: knowledge scope (**A**), question polarity (**B**), question format (**C**), and Bloom's taxonomy (**D**).



As depicted in Figure 2B, Baichuan (87.06%) and ChatGPT (84.75%) achieved the highest accuracy rates for positive and negative questions, respectively. Five models (ERNIE Bot, Kimi, Baichuan, ChatGLM, and Llama) exhibited higher accuracy on positive questions than on negative ones, while ChatGPT and Yi-large showed a modestly better performance on negative questions.

Figure 2C showed that 6 models (ERNIE Bot, Kimi, Baichuan, ChatGLM, Yi-large, and ChatGPT) had higher accuracy rates for medical knowledge questions than for clinical case analysis questions. Conversely, Llama's performance was superior on clinical case analysis questions compared to medical knowledge questions.

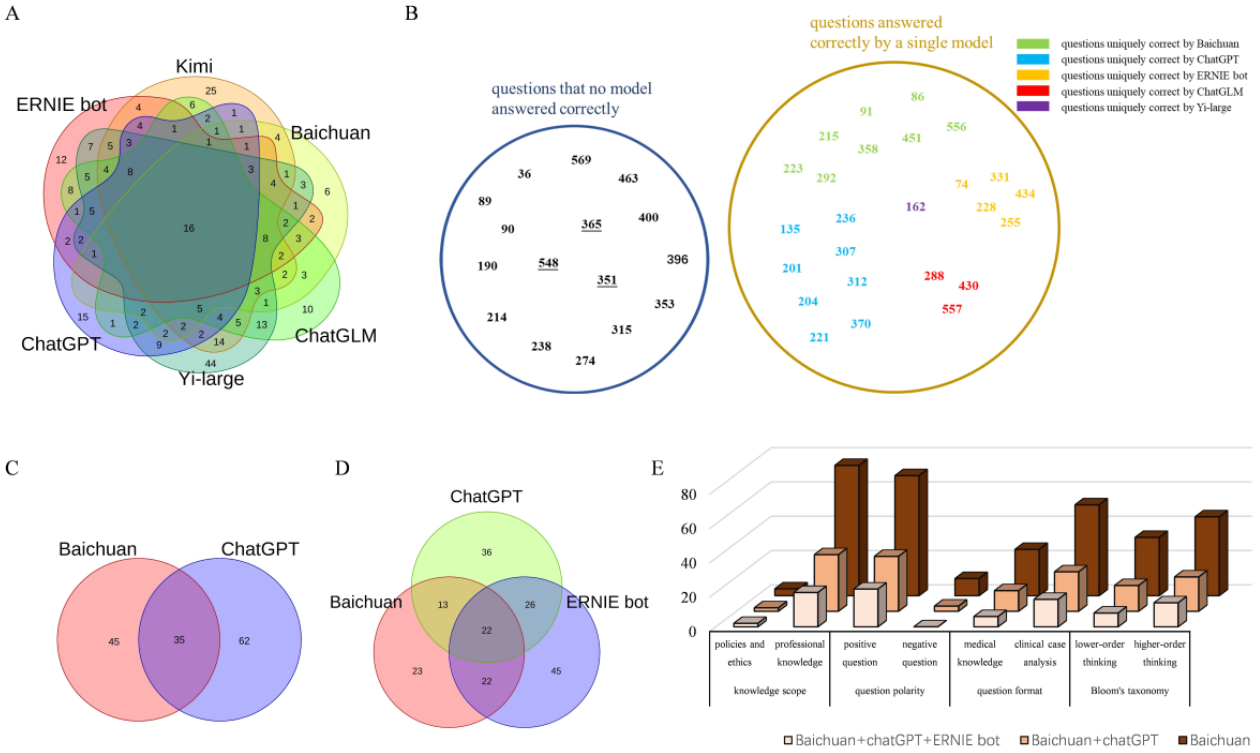
A similar trend is observed in Figure 2D, where 6 LLMs (ERNIE Bot, Kimi, Baichuan, ChatGLM, Yi-large, and ChatGPT) achieved better accuracy on lower-order thinking questions than on higher-order thinking questions. Llama, however, exhibited the opposite trend, with a higher accuracy rate on higher-order thinking questions than on lower-order ones. The greater frequency of errors on simple questions compared to complex ones by Llama suggests that its atypical performance may stem from difficulties in accurately understanding and processing the Chinese language, which contributed to its overall lower accuracy. ChatGPT's performance across the subgroups was consistent with that of multiple Chinese language models, aligning with expectations based on the volume of Chinese-language data available to the models, with performance differences likely reflecting variations in data quantity.

Error Sets

As shown above, with the exception of Llama, the overall performance and trends in subgroup performance of the 6 other LLMs were largely consistent. We collected the error sets of these 6 models, identified their intersections, and visualized them using a Venn diagram. Figure 3A demonstrates that there were 16 common incorrect questions that all LLMs answered incorrectly. Within ChatGPT's error set, there were 15 unique incorrect questions that were answered incorrectly by ChatGPT alone, despite being correctly addressed by the other models. Similarly, the error sets of ERNIE Bot, Kimi, Baichuan, ChatGLM, and Yi-large contained unique incorrect questions, with 12, 25, 6, 10, and 44 such instances, respectively.

XSL•FO
RenderX

Figure 3. Collect the incorrectly answered questions for each model to create error sets, and Venn diagram demonstrated the intersection of the error set of 6 models (**A**); incorrectly answered questions (**B**); intersection of the error sets of the top two (**C**) and the top three models (**D**) with the highest accuracy; column chart exhibits the comparison of the number of incorrect answers between single model and multiple model cross-verification (**E**).



We conducted enhanced error profile analysis by aggregating incorrectly answered questions. The error set revealed 16 questions consistently misanswered by all 6 models, with 13 questions demonstrating divergent error patterns across different LLMs, while 3 questions exhibited identical incorrect selections across all 6 models. Besides, 25 questions were uniquely answered correctly by individual models, with specific distributions: 8 by Baichuan, 8 by ChatGPT, and 5 by ERNIE-Bot. As in Figure 3B, the blue circle demonstrates questions that no model answered correctly and yellow circle shows those answered correctly by only one model, the numbers within the circles indicate the question identifiers and numerical values in distinct colors represent questions that were exclusively answered correctly by a single LLM.

Considering the intersection of the error sets between the 2 models with the highest accuracy rates, ChatGPT and Baichuan, there are 35 common incorrect questions. Expanding to the three most accurate models, Baichuan, ChatGPT, and ERNIE Bot, their intersection contained only 22 common incorrect questions (Figures 3C and 3D).

Comparative analysis between single-model (Baichuan) and multimodel (Baichuan+ChatGPT, Baichuan+ChatGPT+ERNIE bot) approaches demonstrated significant hallucination rate reduction through cross-verification. The most pronounced improvements occurred in professional knowledge and lower-order thinking domains, suggesting that cross-verification mechanisms primarily mitigate artificial intelligence (AI) hallucination in “simple” question types (Figure 3E). Previous studies have suggested that using multiple LLMs for cross-verification can effectively mitigate AI hallucination [23,24]. If we simultaneously use 2 models (Baichuan+ChatGPT) to take a medical examination, adopting the LLMs’ answer when they agree and resorting to human judgment when they disagree, we could potentially achieve an accuracy rate of 94.17%. Moreover, using the same approach with three models (Baichuan+ChatGPT+ERNIE bot) could further improve accuracy to 96.33%.

Discussion

Principal Findings

Research on LLMs in English contexts has been extensive and thorough, whereas studies in non-English contexts remain relatively underexplored. Beyond ChatGPT, which is trained primarily on English corpora, LLMs developed using non-English language datasets also hold significant value for research and testing. Such studies could provide valuable insights for optimizing ChatGPT or developing new LLMs tailored specifically for non-English environments. We take a model testing approach by comparing LLMs mainly trained on English corpora with LLMs trained on Chinese corpora, analyzing the impact of variations in training data composition or domain-specific weighting on LLMs’ performance.

This study used the CNMLE as a testing tool, which may not fully reflect the performance of LLMs in real-world medical scenarios. Nevertheless, we argue that if an LLM struggles to perform well in medical examinations, it is even less likely to succeed in practical medical applications. We selected medical examination questions as the testing tool for LLMs for 2 main reasons. First, these questions are highly representative: the

XSL•FO
RenderX

CNMLE serves as the qualifying examination for Chinese medical students, covering a wide-ranging knowledge base and various question types. Annually, more than 500,000 students take the examination, and the stable pass rate over the years suggests that the difficulty level remains consistent, making the CNMLE a reliable and representative benchmark for testing. Second, the examination questions are relatively standardized. In this testing, we used a zero-shot setting to ensure the reproducibility of experimental results. In the field of natural language processing, standardized test sets are commonly used to evaluate LLMs, ensuring the comparability and reproducibility of research findings [25,26]. It is recommended that future assessments of LLMs in the medical domain also incorporate standardized test sets, in spite of the complexities of real-world medical scenarios.

The findings of this study indicate that the English LLM ChatGPT and several Chinese LLMs perform comparably in a Chinese context. Despite being a leading model among LLMs, ChatGPT does not exhibit a significant advantage in Chinese contexts. While we initially speculated that language communication barriers might contribute to this outcome, our study and previous research have demonstrated no significant difference in LLM performance when questions are translated into English versus being asked directly in Chinese [27,28]. This suggests that the performance gap in Chinese contexts is not primarily due to communication barriers but is more likely attributable to the limited representation of Chinese corpora in the training datasets. The disparity between Chinese and English datasets goes beyond natural language processing challenges and includes differences in content, such as epidemiology, traditional Chinese medicine, policy, and ethics. Since English LLMs are predominantly trained on English-language datasets, their ability to understand and respond effectively in non–English language contexts, as in Chinese medical examinations, is constrained. Notably, Llama3 performed poorly in this study, which may be attributed to its limited proficiency in Chinese or the scarcity of medical-specific training data. In contrast, models like PMC-Llama, fine-tuned on the Llama platform specifically for medical applications, have demonstrated excellent performance in other studies [29].

Previous studies have assessed ChatGPT's performance in non-English medical examinations and explored ways to enhance its capabilities, such as leveraging external data, developing task-specific models, and using cross-lingual models like XLM. XLM leverages accurate language translation to use English data for solving non-English problems, which is a viable solution when non-English training datasets are limited. Our findings indicate that some LLMs trained on Chinese-language corpora have generally matched or surpassed the performance of ChatGPT in the CNMLE, even with shorter training times and less data. This prompts us to reconsider whether the pursuit of an exhaustive training dataset, encompassing all languages and cultures, is necessary, or if developing cost-effective, field-specific LLMs might be more prudent. Among the 7 LLMs tested, 6 exceeded the passing level, and 5 surpassed Med3R, a model specifically developed for Chinese medical examinations. Med3R, released in 2018, achieved a 76% accuracy rate in the 2017 edition of CNMLE [30]. Yet, within a few years, most tested LLMs have exceeded Med3R's performance, demonstrating the superiority of these general-purpose LLMs over traditional models, despite not being specifically designed for medical testing. Notably, ChatGPT showed substantial improvement in CNMLE compared to its earlier versions, underscoring the continual evolution of LLMs as a key advantage [28,31]. However, as the training dataset expands, the associated costs increase rapidly, and when marginal effects are observed, the cost-benefit ratio must be considered. In LLMs, diminishing marginal returns refer to the phenomenon where, as the model size increases, the performance gains from adding the same amount of parameters or computational resources gradually decrease. This is a crucial aspect of scaling law and has significant implications for understanding and decision-making in model design and deployment strategies.

While this study exclusively used Chinese for evaluation, its findings demonstrate generalizable implications for other non–English language environments. Given that LLMs predominantly derive training data from web-based textual corpora—where English constitutes the most prevalent linguistic resource (53.8% of indexed content) followed by Chinese (14.3%) according to the Ethnologue linguistic database—Chinese is classified as a high-resource language [32]. Notably, despite ChatGPT's training corpus incorporating Chinese linguistic data, its CNMLE performance underperformed compared to Baichuan, which was specifically optimized with Chinese medical corpora. This disparity suggests that in low-resource language contexts, the performance gap between generalist LLMs like ChatGPT and linguistically specialized models may prove even more pronounced. For LLMs to achieve broader applicability and widespread deployment in the future, their adaptability to non-English and low-resource language contexts must be prioritized. Further research is needed to identify the most effective and cost-efficient approaches for improving model performance in these settings.

LLMs are poised to enable profound and transformative integration within health care systems, necessitating systematic incorporation into clinical workflows by medical practitioners. Some scholars even propose that prompt engineering may become a core component of medical education in the future [33]. In addition, it is essential to identify and address potential challenges during the deployment of LLMs in health care settings. These insights will guide the ongoing optimization of these models and help mitigate the risks associated with their inappropriate application. Given that real-world clinical scenarios are more complex than machine-simulated environments, continuous, real-world application and rigorous testing are essential for steering the iterative improvements of LLMs. To become effective tools in the medical field, these models must undergo a repeated cycle of testing, optimization, retesting, and refinement, progressively advancing to meet the rigorous demands of clinical reliability and usability. We hope that our research will offer valuable insights into the optimization of LLMs, particularly in non-English linguistic environments.

XSL•FO
RenderX

Limitations

This study exclusively used standardized test questions, potentially limiting its generalizability to real-world medical applications. We plan to extend this work by integrating open-ended clinical problem-solving tasks to assess LLM performance under practical conditions. In addition, our cross-verification process remained semiautomated, requiring human judgment when models disagree. Subsequent efforts will prioritize developing fully automated cross-verification protocols.

Conclusions

At the current stage, LLMs trained primarily on English corpora and those trained mainly on Chinese corpora exhibited comparable performance in CNMLE, with models trained on Chinese corpora maintaining a slight advantage. Subgroup analyses and error set evaluations indicate similar performance between ChatGPT and various Chinese LLMs. The performance differences between Chinese- and English-trained models are not solely attributed to communication barriers but are more likely influenced by disparities in the training data. Using a cross-verification approach across multiple LLMs can achieve exceptional results in CNMLE.

Acknowledgments

This research was supported by the National Social Science Fund of China (grant 23BTQ086).

Conflicts of Interest

None declared.

Multimedia Appendix 1
Additional material.
[XLSX File, 2896 KB - medinform_v13i1e69485_app1.xlsx]

References

1. Mehandru N, Miao BY, Almaraz ER, Sushil M, Butte AJ, Alaa A. Evaluating large language models as agents in the clinic. NPJ Digit Med 2024 Apr 3;7(1):84. [doi: 10.1038/s41746-024-01083-y] [Medline: 38570554]
2. Omiye JA, Gui H, Rezaei SJ, Zou J, Daneshjou R. Large Language Models in Medicine: The Potentials and Pitfalls : A Narrative Review. Ann Intern Med 2024 Feb;177(2):210-220. [doi: 10.7326/M23-2772] [Medline: 38285984]
3. Liu M, Okuhara T, Chang X, et al. Performance of ChatGPT Across Different Versions in Medical Licensing Examinations Worldwide: Systematic Review and Meta-Analysis. J Med Internet Res 2024 Jul 25;26:e60807. [doi: 10.2196/60807] [Medline: 39052324]
4. Wang X, Sanders HM, Liu Y, et al. ChatGPT: promise and challenges for deployment in low- and middle-income countries. Lancet Reg Health West Pac 2023 Dec;41:100905. [doi: 10.1016/j.lanwpc.2023.100905] [Medline: 37731897]
5. Gilson A, Safranek CW, Huang T, et al. How Does ChatGPT Perform on the United States Medical Licensing Examination (USMLE)? The Implications of Large Language Models for Medical Education and Knowledge Assessment. JMIR Med Educ 2023 Feb 8;9:e45312. [doi: 10.2196/45312] [Medline: 36753318]
6. Goodman RS, Patrinely JR, Stone CA Jr, et al. Accuracy and reliability of chatbot responses to physician questions. JAMA Netw Open 2023 Oct 2;6(10):e2336483. [doi: 10.1001/jamanetworkopen.2023.36483] [Medline: 37782499]
7. Kelloniemi M, Koljonen V. AI did not pass Finnish plastic surgery written board examination. J Plast Reconstr Aesthet Surg 2023 Dec;87:172-179. [doi: 10.1016/j.bjps.2023.10.059] [Medline: 37871487]
8. Wu J, Wu X, Qiu Z, et al. Large language models leverage external knowledge to extend clinical insight beyond language boundaries. J Am Med Inform Assoc 2024 Sep 1;31(9):2054-2064. [doi: 10.1093/jamia/ocae079] [Medline: 38684792]
9. Toyama Y, Harigai A, Abe M, et al. Performance evaluation of ChatGPT, GPT-4, and Bard on the official board examination of the Japan Radiology Society. Jpn J Radiol 2024 Feb;42(2):201-207. [doi: 10.1007/s11604-023-01491-2]
10. Seghier ML. ChatGPT: not all languages are equal. Nature New Biol 2023 Mar;615(7951):216. [doi: 10.1038/d41586-023-00680-3] [Medline: 36882613]
11. Zheng C, Ye H, Guo J, et al. Development and evaluation of a large language model of ophthalmology in Chinese. Br J Ophthalmol 2024 Sep 20;108(10):1390-1397. [doi: 10.1136/bjo-2023-324526] [Medline: 39019566]
12. ERNIE Bot. URL: https://yiyan.baidu.com/ [accessed 2025-06-19]
13. Kimi. URL: https://kimi.moonshot.cn/ [accessed 2025-06-19]
14. Baichuan. URL: https://chat.baichuan-ai.com/ [accessed 2025-06-19]
15. ChatGLM. URL: https://www.zhipuai.cn/ [accessed 2025-06-19]
16. Yi-large. URL: https://platform.lingyiwanwu.com/ [accessed 2025-06-19]
17. Llama. URL: https://www.meta.ai/ [accessed 2025-06-19]
18. ChatGPT. URL: https://www.openai.com/ [accessed 2025-06-19]

XSL•FO
RenderX

19. Tong W, Guan Y, Chen J, et al. Artificial intelligence in global health equity: an evaluation and discussion on the application of ChatGPT, in the Chinese National Medical Licensing Examination. Front Med (Lausanne) 2023;10:1237432. [doi: 10.3389/fmed.2023.1237432] [Medline: 38020160]
20. Bardou P, Mariette J, Escudié F, Djemiel C, Klopp C. jvenn: an interactive Venn diagram viewer. BMC Bioinformatics 2014 Aug 29;15(1):293. [doi: 10.1186/1471-2105-15-293] [Medline: 25176396]
21. Koshik I. A conversation analytic study of yes/no questions which convey reversed polarity assertions. J Pragmat 2002 Dec;34(12):1851-1877. [doi: 10.1016/S0378-2166(02)00057-7]
22. Adams NE. Bloom's taxonomy of cognitive learning objectives. J Med Libr Assoc 2015 Jul;103(3):152-153. [doi: 10.3163/1536-5050.103.3.010] [Medline: 26213509]
23. Han T, Nebelung S, Khader F, et al. Medical large language models are susceptible to targeted misinformation attacks. NPJ Digit Med 2024 Oct 23;7(1):288. [doi: 10.1038/s41746-024-01282-7] [Medline: 39443664]
24. Ke Y, Yang R, Lie SA, et al. Mitigating cognitive biases in clinical decision-making through multi-agent conversations using large language models: Simulation study. J Med Internet Res 2024 Nov 19;26:e59439. [doi: 10.2196/59439] [Medline: 39561363]
25. Bang Y, Cahyawijaya S, Lee N, et al. A multitask, multilingual, multimodal evaluation of chatgpt on reasoning, hallucination, and interactivity. : Association for Computational Linguistics Presented at: Proceedings of the 13th International Joint Conference on Natural Language Processing and the 3rd Conference of the Asia-Pacific Chapter of the Association for Computational Linguistics (Volume 1; Nov 1-4, 2023; Nusa Dua, Bali URL: https://aclanthology.org/2023.ijcnlp-main [doi: 10.18653/v1/2023.ijcnlp-main.45]
26. Lai V, Ngo N, Pouran Ben Veyseh A, et al. ChatGPT beyond english: towards a comprehensive evaluation of large language models in multilingual learning. : Association for Computational Linguistics Presented at: Findings of the Association for Computational Linguistics; Dec 1-4, 2023; Singapore p. 13171-13189. [doi: 10.18653/v1/2023.findings-emnlp.878]
27. Wang Y, Chen Y, Sheng J. Assessing ChatGPT as a medical consultation assistant for chronic hepatitis B: Cross-language study of English and Chinese. JMIR Med Inform 2024 Aug 8;12:e56426. [doi: 10.2196/56426] [Medline: 39115930]
28. Fang C, Wu Y, Fu W, et al. How does ChatGPT-4 preform on non-English national medical licensing examination? An evaluation in Chinese language. PLOS Digit Health 2023 Dec;2(12):e0000397. [doi: 10.1371/journal.pdig.0000397] [Medline: 38039286]
29. Wu C, Lin W, Zhang X, Zhang Y, Xie W, Wang Y. PMC-LLaMA: toward building open-source language models for medicine. J Am Med Inform Assoc 2024 Sep 1;31(9):1833-1843. [doi: 10.1093/jamia/ocae045] [Medline: 38613821]
30. Wu J, Liu X, Zhang X, He Z, Lv P. Master clinical medical knowledge at certificated-doctor-level with deep learning model. Nat Commun 2018;9(1):4352. [doi: 10.1038/s41467-018-06799-6]
31. Wang X, Gong Z, Wang G, et al. ChatGPT Performs on the Chinese National Medical Licensing Examination. J Med Syst 2023 Aug 15;47(1):86. [doi: 10.1007/s10916-023-01961-0] [Medline: 37581690]
32. Bender EM. The #benderrule: on naming the languages we study and why it matters. 2019.
33. Meskó B. Prompt Engineering as an Important Emerging Skill for Medical Professionals: Tutorial. J Med Internet Res 2023 Oct 4;25:e50638. [doi: 10.2196/50638] [Medline: 37792434]

Abbreviations

AI: artificial intelligence
CNMLE: Chinese National Medical Licensing Examination
LLM: large language model
METRICS: Model, Evaluation, Timing, Range/Randomization, Individual factors, Count, and Specificity of prompts and language

Edited by A Castonguay; submitted 02.12.24; peer-reviewed by C Wang, M Malhotra; revised version received 24.04.25; accepted 24.04.25; published 27.06.25.

Please cite as:
Yao Z, Duan L, Xu S, Chi L, Sheng D
Performance of Large Language Models in the Non-English Context: Qualitative Study of Models Trained on Different Languages in Chinese Medical Examinations
JMIR Med Inform 2025;13:e69485
URL: https://medinform.jmir.org/2025/1/e69485
doi:10.2196/69485

XSL•FO
RenderX

© Zhong Yao, Liantan Duan, Shuo Xu, Lingyi Chi, Dongfang Sheng. Originally published in JMIR Medical Informatics (https://medinform.jmir.org), 27.6.2025. This is an open-access article distributed under the terms of the Creative Commons Attribution License (https://creativecommons.org/licenses/by/4.0/), which permits unrestricted use, distribution, and reproduction in any medium, provided the original work, first published in JMIR Medical Informatics, is properly cited. The complete bibliographic information, a link to the original publication on https://medinform.jmir.org/, as well as this copyright and license information must be included.

XSL•FO
RenderX

Language Models for Multilabel Document Classification of Surgical Concepts in Exploratory Laparotomy Operative Notes: Algorithm Development Study

Jeremy A Balch[1,2], MD; Sasank S Desaraju[3], MS; Victoria J Nolan[1], PhD; Divya Vellanki[3], MS; Timothy R Buchanan[3], BS; Lindsey M Brinkley[3], BS; Yordan Penev[3], MS; Ahmet Bilgili[3], BS; Aashay Patel[3], BS; Corinne E Chatham[3], BS; David M Vanderbilt[3], MD; Rayon Uddin[3], BS; Azra Bihorac[4,5], MS, MD; Philip Efron[1], MD; Tyler J Loftus[1,4], MD, PhD; Protiva Rahman[2], PhD; Benjamin Shickel[4,5], PhD

[1]Department of Surgery, University of Florida College of Medicine, Gainesville, FL, United States

[2]Department of Health Outcomes and Biomedical Informatics, University of Florida College of Medicine, Gainesville, FL, United States

[3]University of Florida College of Medicine, Gainesville, FL, United States

[4]Intelligent Clinical Care Center, University of Florida, Gainesville, FL, United States

[5]Department of Medicine, University of Florida College of Medicine, 1600 SW Archer Road, PO Box 100224, Gainesville, FL, United States

Corresponding Author:
Benjamin Shickel, PhD
Intelligent Clinical Care Center, University of Florida, Gainesville, FL, United States

Abstract

Background: Operative notes are frequently mined for surgical concepts in clinical care, research, quality improvement, and billing, often requiring hours of manual extraction. These notes are typically analyzed at the document level to determine the presence or absence of specific procedures or findings (eg, whether a hand-sewn anastomosis was performed or contamination occurred). Extracting several binary classification labels simultaneously is a multilabel classification problem. Traditional natural language processing approaches—bag-of-words (BoW) and term frequency-inverse document frequency (tf-idf) with linear classifiers—have been used previously for this task but are now being augmented or replaced by large language models (LLMs). However, few studies have examined their utility in surgery.

Objective: We developed and evaluated LLMs for the purpose of expediting data extraction from surgical notes.

Methods: A total of 388 exploratory laparotomy notes from a single institution were annotated for 21 concepts related to intraoperative findings, intraoperative techniques, and closure techniques. Annotation consistency was measured using the Cohen κ statistic. Data were preprocessed to include only the description of the procedure. We compared the evolution of document classification technologies from BoW and tf-idf to encoder-only (Clinical-Longformer) and decoder-only (Llama 3) transformer models. Multilabel classification performance was evaluated with 5-fold cross-validation with F_1-score and hamming loss (HL). We experimented with and without context. Errors were assessed by manual review. Code and implementation instructions may be found on GitHub.

Results: The prevalence of labels ranged from 0.05 (colostomy, ileostomy, active bleed from named vessel) to 0.50 (running fascial closure). Llama 3.3 was the overall best-performing model (micro F_1-score 0.88, 5-fold range: 0.88-0.89; HL 0.11, 5-fold range: 0.11-0.12). The BoW model (micro F_1-score 0.68, 5-fold range: 0.64-0.71; HL 0.14, 5-fold range: 0.13-0.16) and Clinical-Longformer (micro F_1-score 0.73, 5-fold range: 0.70-0.74; HL 0.11, 5-fold range: 0.10-0.12) had overall similar performance, with tf-idf models trailing (micro F_1-score 0.57, 5-fold range: 0.55-0.59; HL 0.27, 5-fold range: 0.25-0.29). F_1-scores varied across concepts in the Llama model, ranging from 0.30 (5-fold range: 0.23-0.39) for class III contamination to 0.92 (5-fold range: 0.98-0.84) for bowel resection. Context enhanced Llama's performance, adding an average of 0.16 improvement to the F_1-scores. Error analysis demonstrated semantic nuances and edge cases within operative notes, particularly when patients had references to prior operations in their operative notes or simultaneous operations with other surgical services.

Conclusions: Off-the-shelf autoregressive LLMs outperformed fined-tuned, encoder-only transformers and traditional natural language processing techniques in classifying operative notes. Multilabel classification with LLMs may streamline retrospective reviews in surgery, though further refinements are required prior to reliable use in research and quality improvement.

(JMIR Med Inform 2025;13:e71176) doi:10.2196/71176

XSL•FO
RenderX

KEYWORDS

chart review; generative large language models; general surgery; natural language processing; exploratory laparotomy

Introduction

Operative notes represent the most thorough narrative of a surgical case in the electronic health record, containing information that is largely inaccessible outside of manual human review [1,2]. This limitation impedes retrospective studies on surgical technique and intraoperative findings that impact outcomes, as well as the ability to perform prospective validation and real-time implementation of decision-support systems. Natural language processing (NLP) and large language models (LLMs) may offer a streamlined approach to information extraction for clinical workflow, education, research, performance improvement, and billing purposes [3].

The terms and phrases used to characterize surgical techniques and intraoperative findings often contain complex dependencies that span multiple sentences and are best understood in the context of an entire operative note. Furthermore, in retrospective reviews focused on patient outcomes, operative notes serve as a vehicle to identify study participants, with subsequent attention to downstream outcomes often represented in structured data (ie, mortality, surgical site infection, or anastomotic leaks defined by the *International Classification of Disease* codes) [4,5].

For this reason, we frame our problem in terms of a multilabel document classification task [6] where operative notes take on a series of binary labels as to whether or not a certain intraoperative finding (eg, bleeding and contamination) or technique (eg, bowel resection, hand-sewn anastomosis, and style of fascial closure) occurred during the case. Traditional NLP methods, using word frequencies, generally perform well on this task, though can fail to capture context and negation, a noted strength of the attention mechanism in LLMs [7]. Several studies have investigated LLMs for text classification in clinical notes, though to our knowledge, few studies have examined multilabel classification, only one has used generative models, and none have done so in surgical specialties [8-12]. There is a similar paucity of publications using real-world data outside of curated datasets, which, in addition to representing idealized clinical documentation, are also conspicuously devoid of operative notes [13-15].

Generative LLMs may offer "off-the-shelf" abilities to capture the multidependency nature of intraoperative findings and surgical techniques. We hypothesize that generative LLMs can outperform fine-tuned encoder-only LLMs and traditional NLP methods in classifying operative notes as containing specific findings and techniques [16].

Methods

Data

Using the University of Florida Health Integrated Data Repository as an honest broker, we assessed 2 single-center, longitudinal electronic health record datasets for all adult patients admitted to a surgical service at University of Florida Health Gainesville and Jacksonville, both quaternary referral centers, between June 1, 2014, and August 22, 2022. We randomly selected 420 fully deidentified exploratory laparotomy operative reports using SQL queries. In total, 32 were found to be mislabeled as "exploratory laparotomy," with no evidence that the abdominal cavity was entered, and so were excluded, leaving 388 notes. As our scope was limited to the operative notes themselves, no surgical outcome, operative metadata, or sociodemographic data were collected.

Ethical Considerations

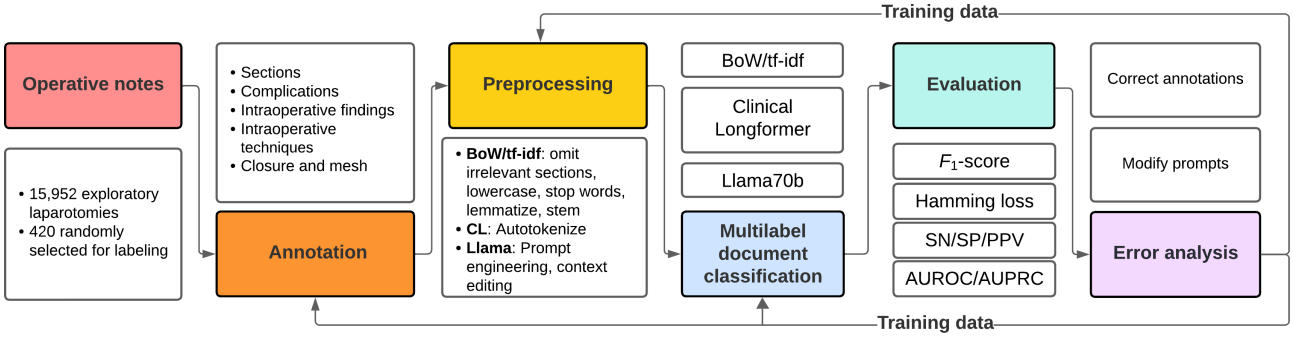
This study was approved by the University of Florida Institutional Review Board and Privacy Office (IRB#201600262) as an exempt study with a waiver of informed consent. All data used in this study were deidentified. No compensation was provided. This study was performed in accordance with the TRIPOD+LLM (Transparent Reporting of a Multivariable Prediction Model for Individual Prognosis or Diagnosis+Large Language Model) reporting guideline [17].

Data Preparation

The project workflow is shown in Figure 1. A team of 8 annotators, consisting of medical students (TRB, LMB, YP, A Bilgili, AP, CEC, RU, and DMV) and one surgical resident (JAB), were trained on the project's objectives and annotation software. A detailed annotation manual is provided with definitions, categories, and illustrative examples (Multimedia Appendix 1). An annotated operative note is shown in Multimedia Appendix 2. Emphasis was placed on achieving a high level of consistency, with the goal of reaching a Cohen κ coefficient of above 0.8 for interrater reliability [18]. The first author (JAB) served as the ground truth. A total of 20 operative notes were set aside for annotator training and were reviewed by all annotators. Following training, annotators participated in regular discussions to address any challenges and were reviewed by the first author. Annotations were performed with Label Studio (version 1.8.2; HumanSignal).

XSL•FO
RenderX

Figure 1. Workflow schema. Exploratory laparotomy notes are first extracted and annotated. After preprocessing, they are passed to 4 machine-learning models for multilabel document classification. Models are compared using several performance metrics. Finally, error analysis is performed and all annotation, preprocessing, prompts, and model architectures are modified as necessary on training data to optimize the F_1-score prior to evaluation on test data. AUPRC: area under the precision-recall curve; AUROC: area under the receiver operating characteristic curve; BoW: bag-of-words; CL: Clinical-Longformer; PPV: positive-predictive value; SN: sensitivity; SP: specificity; tf-idf: term frequency-inverse document frequency.



Labels

Notes were annotated for structure, intraoperative findings, and surgical techniques. Whole text spans were highlighted based on note structure: patient or staff or anesthesia personnel information; procedures performed; pre- and postoperative diagnoses; intraoperative findings; indication or history; description of the procedure; ins, outs, and specimens; disposition; and complications. Intraoperative findings included: contamination (class I, II, III, and IV) as defined in the peer-reviewed literature [19]; and bleeding, differentiating between active bleed from a named vessel and active bleed from a solid organ. Whole-document labels were performed for: bowel resection, primary repair of enterotomies, colostomy formation, ileostomy formation, hand-sewn anastomosis, stapled anastomosis, placement of mesh, fascia closure techniques (running or continuous, interrupted, and left open), and skin closure techniques (full, Prevena, partial, and left open). For the training set, Cohen κ across individual labels ranged from 0.39 to 1.0 with a mean and median agreement of 0.67 (SD 0.33) and 0.77 (IQR 0.52-1.0), respectively (Table S1 in Multimedia Appendix 3). The κ scores across all medical students are shown in Table S1 Multimedia Appendix 3. Because this was below our stated goal, additional training was provided with emphasis on these concepts, and each op note in the dataset was personally reviewed by the lead author. A total of 50 notes were annotated by each of the annotators, with the lead author annotating an additional 50.

Data Splitting and Stratification for Class Imbalance

Standard techniques in multilabel classification tasks with label-specific class imbalances may result in datasets missing rare, positive labels [20,21]. To account for this, we performed iterative stratification from scikit-multilearn, splitting the data into 5-fold of training (80%) and test (20%) sets [20-22]. The distributions of the labels in each train and test set are shown in Table S2 in Multimedia Appendix 3.

Unlike other models, the Llama models were not fine-tuned on a hold-out training set. They were instead used to evaluate only the test set in each cross-validation fold.

Models

We studied the traditional NLP multilabel document classification techniques with bag-of-words (BoW) and term frequency-inverse document frequency (tf-idf) approaches paired with logistic regression classifiers, as well as pretrained transformer models, the encoder-only Clinical-Longformer [23], and the decoder-only Llama herd (Llama 3.1 -3b, 8b, 70b, 3.2, and 3.3) [24].

BoW takes tokenized words and performs a classification task based on the frequency of the terms in a particular document. tf-idf applies a weight-based filter on the frequency of a term across a corpus of documents and evaluates the uniqueness of a word to a specific class.

Transformer-based models can leverage contextual information [25]. Encoder models process the entire document by systematically masking these tokens and predicting their values. While encoder models typically excel at classification tasks, their utility is often limited by length, as most models cannot process more than 512 tokens at a time [26]. Longformer models extend that range using both global and sliding-window attention mechanisms [27]. Li et al [23] fine-tuned a Clinical-Longformer model on clinical text from the Medical Information Mart for Intensive Care-III dataset [15] with a context of 4096 tokens, which outperformed Bidirectional Encoder Representations from Transformers (BERT) [28], ClinicalBERT [29], and BioBERT [30] on inference, question-answering, and classification tasks [23]. Finally, autoregressive decoder–only transformers estimate the probability distribution of the next token in a sequence based on the preceding tokens. As they are self-hosted, Llama allows for the secure handling of sensitive patient information and for this reason, these models were selected for this study [24]. The results shown below are the best-performing Llama 3.3 model.

Preprocessing

Notes were reduced to the “description of procedure” as other parts of the note may contain information from previous procedures that may bias the model. For the tf-idf and BoW models, all texts were converted to lowercase, and common stop words (eg, “the,” “and,” and “is,”), punctuation, and numbers were removed. Stemming and lemmatization were performed to reduce words to their root forms (eg, “maturing”

XSL•FO
RenderX

to “mature”). The text was then vectorized as combinations of unigrams, bigrams, trigrams, and 4-grams. We introduced padding to ensure that all sequences had a uniform length. The Clinical-Longformer and Llama models were tokenized using the Hugging Face autotokenizer [31].

Model Hyperparameters

For BoW and tf-idf, we used logistic regression as our classifier. Hyperparameter search within each fold of the training data revealed marginally increased performance with L2-regularization strength of 0.1 and 10 for BoW and TFIDF overall, respectively. No other hyperparameters were modified based on the results of the test set. In the Clinical-Longformer model, we weighted the binary cross-entropy loss for each label inversely proportional to its prevalence in the training set given class imbalance. The model was optimized for the micro F_1-score and trained for up to 500 epochs with early stopping, using a patience of 10 to prevent overfitting. The inference was run on an NVIDIA A100 8GB graphics processing unit in the University of Florida HiPerGator cluster. The Llama 3.3 model had the longest runtime, at 723 minutes.

A custom Python script was developed using the LlamaIndex framework for the Llama model [32]. Each task was a modified version of the annotation instructions, and the model was prompted with the operative note, the context of the task, few-shot instructions, a question, and a desired response format (Multimedia Appendix 4). A general context document was also provided and included brand names of mesh types, a description of types of skin closure, and other domain-specific knowledge that could aid in understanding patient notes and tasks (Multimedia Appendix 5). Given the 5-fold cross-validation design, all notes appeared in at least one test set. As a result, prompts were adjusted based on the model’s generated rationale for randomly selected errors on the whole dataset (eg, differentiating “primary repair” from “anastomosis” or clarifying the use of “prolene” in mesh vs suture contexts). Performance metrics were not evaluated during prompt tuning to avoid test set leakage.

Model Evaluation

Overall performance was evaluated using the micro F_1-score, which calculates the harmonic mean of precision and recall across all classes, and hamming loss (HL), which measures the fraction of misclassified labels relative to the total ground truth labels (with 0 indicating perfect classification). The mean and range of scores over 5 folds were reported. Optimal cutoffs were determined by maximizing the F_1-score in 0.01 increments. Sensitivity, positive predictive value (PPV), specificity, area under the receiver operating curve, and area under the precision-recall curve were also reported. Individual label F_1-scores were calculated using the “binary” average.

Error Analysis

A total of 5 false positive and 5 false negative labels with the highest predicted probabilities were reviewed for each label using the best-performing Clinical-Longformer and Llama model. Several annotation errors were encountered during each iteration which resulted in manual reannotation by the lead author, repeat BoW, tf-idf, and Clinical-Longformer model training, and rerunning of the evaluation pipeline. The reported metrics reflect the latest training and evaluation.

Data Availability and Code

Code and implementation instructions may be found on GitHub [33]. A toy dataset is provided using GPT-generated op notes and random labels.

Results

Data

Of the 388 operative notes, note length ranged from 73 to 1713 words, with a mean of 500 (SD 291) words and a median of 421 (IQR 292-603) words. Most notes were composed by the Trauma and Acute Care Surgery Department (n=267, 68.8%), with the remaining notes in Transplant Surgery (n=83, 21.4%) and Urology (n=30, 7.7%) along with combination cases with Vascular Surgery (n=24, 6.2%), Cardiothoracic Surgery (n=16, 4.1%), and Neurosurgery (n=8, 2.1%). We noted the class imbalance in the labels, as shown in Table 1.

XSL•FO
RenderX

Table . Prevalence of labels in the dataset.

Label	Prevalence
Intraoperative findings	
Active bleeding from the named vessel	0.05
Active bleeding from solid organ	0.11
Class I	0.34
Class II	0.48
Class III	0.16
Class IV	0.14
Intraoperative techniques	
Bowel resection	0.30
Primary repair	0.05
Serosal tear repair	0.05
Colostomy	0.12
Ileostomy	0.08
Hand-sewn anastomosis	0.12
Stapled anastomosis	0.15
Closure techniques	
Fascia closed (interrupted)	0.10
Fascia closed (running or continuous)	0.50
Fascia left open	0.32
Skin closed (full with Prevena)	0.04
Skin closed (full)	0.41
Skin closed (partial)	0.05
Skin left open	0.43
Synthetic	0.06

Collective Performance Across All Labels

Overall mean micro F_1-scores, along with minimum and maximum score per fold, are shown in Table 2. BoW (0.68, 5-fold range: 0.64 - 0.71) outperformed tf-idf (0.57, 5-fold range: 0.55-0.59) overall with an increase in micro F_1-score of 0.1 and a decrease in HL of two-fold. Comparing the encoder-only and decoder-only model architectures, Llama 3.3 (0.88, 5-fold range: 0.88-0.89) had generous improvement overall in the micro F_1-score with equivalent HL to BoW and Clinical-Longformer.

We compared the Llama 3 series of models and observed a general trend of improved performance with increasing model size. An exception was Llama 3.2, which performed poorly—consistent with prior reports of its reduced effectiveness on medical datasets [34]. Results are presented in Figure S1 in Multimedia Appendix 6.

Table . Mean overall performance of models across all labels across all 5-folds[a].

Model	Micro F_1-score, mean (range)	Hamming loss, mean (range)
BoW[b]	0.68 (0.64-0.71)	0.14 (0.13-0.16)
tf-idf[c]	0.57 (0.55-0.59)	0.27 (0.25-0.29)
Clinical-Longformer	0.73 (0.70-0.74)	0.11 (0.10-0.12)
Llama 3.3	0.88 (0.88-0.89)	0.12 (0.11-0.12)

[a]Values in parentheses indicate the minimum and maximum performance.

[b]BoW: bag-of-words.

[c]tf-idf: term frequency-inverse document frequency.

XSL•FO
RenderX

Individual Label Performance

F_1-scores with ranges for the individual labels are visualized in Figure 2 and shown numerically in Tables 3-5. Intraoperative bleeding was well categorized by the Llama model, while surgical wound class was often better served by Clinical-Longformer or BoW models (Figure 2A). For the intraoperative technique (Figure 2B), the Llama model was the highest performer, with the Clinical-Longformer and BoW models performing with overlapping F_1-scores. Intraoperative and skin and fascial closure techniques were best served by the generative model. We noted excellent performance for the Llama 3.3 model in several categories with F_1-scores ≥0.8. Of note, there was surprisingly poor performance on the Prevena label across all models, given that the brand name should often cue a positive class. Interrupted fascial closure was also noticeably poor, despite how this is often specifically stated in the operative note.

Tables 3-5 demonstrate numeric values of the F_1-scores alongside sensitivity and PPVs. The Llama model was again the best performing overall with the notable exception of class II and stapled anastomosis labels. While the PPV of Llama was overall better, it performed poorly in 2 skin closure tasks, class III contamination task, and stapled anastomosis task. Full metrics across all models and labels are shown in Table S3 in Multimedia Appendix 3.

XSL•FO
RenderX

Figure 2. F_1-scores with error bars representing range over 5-fold cross-validation. BoW: bag-of-words; CL: Clinical-Longformer; ti-idf: term frequency-inverse document frequency.

XSL•FO
RenderX

Table . Comparison of model performance across performance metrics for intraoperative findings.

	Intraoperative findings					
	Active bleeding from named vessel	Active bleeding from solid organ	Class I	Class II	Class III	Class IV
F_1-score						
BoW[a]	0.31	0.64	0.62	0.62	0.35	0.42
tf-idf[b]	0.36	0.6	0.66	0.68	0.41	0.48
CL[c]	0.44	0.63	0.73	0.72	0.46	0.48
Llama	0.61	0.84	0.36	0.75	0.3	0.48
SN[d]						
BoW	0.27	0.61	0.71	0.66	0.35	0.43
tf-idf	0.55	0.8	0.89	0.86	0.55	0.59
CL	0.55	0.72	0.77	0.76	0.54	0.53
Llama	0.55	0.96	0.24	0.9	1	0.95
PPV[e]						
BoW	0.37	0.71	0.56	0.59	0.38	0.46
tf-idf	0.42	0.51	0.53	0.56	0.34	0.41
CL	0.51	0.58	0.69	0.68	0.41	0.46
Llama	0.72	0.77	0.79	0.65	0.18	0.33

[a]BoW: bag-of-words.

[b]tf-idf: term frequency-inverse document frequency.

[c]CL: Clinical-Longformer.

[d]SN: sensitivity.

[e]PPV: positive predictive value.

XSL•FO
RenderX

Table . Comparison of model performance across performance metrics for intraoperative techniques.

	Intraoperative techniques						
	Bowel resection	Primary repair	Serosal tear repair	Colostomy	Ileostomy	Hand-sewn anastomosis	Stapled anastomosis
F_1-score							
BoW[a]	0.86	0.22	0.42	0.51	0.45	0.61	0.65
tf-idf[b]	0.81	0.25	0.43	0.65	0.69	0.59	0.61
CL[c]	0.83	0.37	0.37	0.76	0.78	0.65	0.7
Llama	0.92	0.5	0.82	0.7	0.92	0.71	0.83
SN[d]							
BoW	0.86	0.23	0.32	0.42	0.39	0.58	0.66
tf-idf	0.93	0.3	0.39	0.7	0.7	0.72	0.8
CL	0.87	0.42	0.31	0.78	0.79	0.84	0.77
Llama	0.95	0.4	0.95	0.67	0.87	0.73	0.85
PPV[e]							
BoW	0.87	0.22	0.72	0.73	0.63	0.68	0.65
tf-idf	0.72	0.24	0.65	0.65	0.75	0.54	0.5
CL	0.8	0.35	0.6	0.79	0.83	0.56	0.65
Llama	0.9	0.7	0.73	0.75	1	0.71	0.83

[a]BoW: bag-of-words

[b]tf-idf: term frequency-inverse document frequency.

[c]CL: Clinical-Longformer.

[d]SN: sensitivity.

[e]PPV: positive predictive value.

XSL•FO
RenderX

Table . Comparison of model performance across performance metrics for closure and mesh techniques.

	Closure and mesh techniques							
	Fascia closed interrupted	Fascia closed continuous	Fascia left open	Skin closed (Prevena)	Skin closed (full)	Skin closed (partial)	Skin left open	Synthetic mesh
F_1-score								
BoW[a]	0.34	0.86	0.82	0.15	0.78	0.2	0.77	0.55
tf-idf[b]	0.42	0.82	0.78	0.07	0.74	0.12	0.76	0.6
CL[c]	0.31	0.88	0.84	0.13	0.81	0.23	0.8	0.81
Llama	0.6	0.89	0.92	0.61	0.89	0.47	0.9	0.71
SN[d]								
BoW	0.36	0.9	0.88	0.2	0.84	0.19	0.83	0.51
tf-idf	0.55	0.96	0.94	0.1	0.92	0.09	0.91	0.6
CL	0.27	0.95	0.89	0.1	0.91	0.18	0.81	0.87
Llama	0.7	0.83	0.92	0.51	0.88	0.74	0.94	0.87
PPV[e]								
BoW	0.46	0.83	0.77	0.12	0.74	0.23	0.73	0.7
tf-idf	0.4	0.71	0.67	0.05	0.63	0.25	0.66	0.68
CL	0.4	0.83	0.8	0.2	0.73	0.33	0.81	0.8
Llama	0.56	0.95	0.92	0.8	0.91	0.37	0.87	0.62

[a]BoW: bag-of-words.

[b]tf-idf: term frequency-inverse document frequency.

[c]CL: Clinical-Longformer.

[d]SN: sensitivity.

[e]PPV: positive predictive value.

Context

We evaluated performance on the Llama 3.1-70b model with and without the context document. The model performed better overall with the context, with an average improvement of 0.16 in the F_1-score (Figure S2 in Multimedia Appendix 6). The context offered the greatest improvement in serosal tear repair (+0.4) and the context hurt model performance in class III (−0.19) and stapled-anastomosis (−0.08) labels.

Error Analysis

A manual review of 5 false negative and positive per label in the encoder-only and decoder-only models revealed several trends in errors, though often it was unclear why a model made a particular prediction. Overall, 88 annotations (0.01% of all annotations) were changed upon review, mostly in bowel resection (n=21), hand-sewn anastomosis (n=19), active bleed from solid organ (n=17), and serosal tear repair (n=13).

Examining the 3 overarching categories, for the encoder-only LLM, bleeds were often picked up, though generally any presence of bleeding was marked positive, regardless of its origins. For intraoperative techniques, false negative instances of bowel resection labels had a clear bowel resection performed in the case. False positives, however, occurred when previous bowel resections were mentioned in the operative report. This was especially true for take-back surgeries when the abdomen is left open because of the need for further surgery. For the ostomy concepts, the most common error was secondary to an ileostomy or colostomy take down (as opposed to creation) or a situation in which the bowel was left in discontinuity with discussion in the operative report of placing an ostomy later. For anastomosis, errors were often likely due to the presence of a stapled resection or the use of the stapler to create a common channel. For closure, fascial closure errors occurred in several cases where a thoracotomy was performed in the same operation as a laparotomy, resulting in the closure of one anatomic fascia and not another. Skin closure failures appeared to be confounded when multiple services operated on the same patient. Partial skin closures were underrepresented in the dataset and the model tended to predict partial closure on both full-closure and open skin with equal affinity.

For the decoder-only model, we had Llama provide explanations for its choice and the explanations along with the findings drove changes in prompting strategies. Performance on bleeding was overall excellent, however, “oozing” from an organ bed or resection was often assigned as “active bleed,” which our annotators and prompts were instructed to mark as negative. For intraoperative techniques, there were commonalities in errors with the Clinical-Longformer model, with prior bowel resections, ostomy takedowns, and instances where both stapled and hand-sewn anastomoses were performed in the same operation. Fascial closures were obscured by the presence of

XSL•FO
RenderX

interrupted retention sutures. Several open skin closures were marked as both open and partial skin closures. For skin closure with Prevena and with the exception of some runs of Llama 3.3, the model appeared to simply not understand the instructions despite multiple prompting attempts.

Contamination was difficult to assess for both annotators and models and this information is not always clearly stated in operative reports. Identifying breaches in sterile techniques, purulent versus nonpurulent inflammation, and whether entry into a hollow organ resulted in spillage requires careful description. The generative model often assumed any entry to the abdominal cavity made for Class II or above, despite modifications to prompting techniques. Future studies will extract the attending surgeon attestation for ground truth labels of wound class, which may improve model performance.

Discussion

Principal Results

Generative LLMs outperformed fine-tuned encoder-only LLMs and traditional NLP models in a multilabel classification task across the majority of labels. Overall F_1-scores ranged from 0.57 for tf-idf to 0.88 for Llama 3.3. On individual labels, we had F_1-scores of ≥0.8 for multiple classes.

Retrospective analyses drive decision support, quality improvement initiatives, and billing workflows, yet they are limited not only by the intensive manual review process but also by the variable interrater reliability with human labeling [35,36]. To overcome these limitations, we frame operative concept identification as a multilabel document classification task and observe that the autoregressive Llama 3.3 model outperformed both traditional NLP techniques, the Longformer encoder model, and previous versions of the Llama herd.

State-of-the-art clinical NLP tasks rely on transformer-based, foundational LLMs [25,37,38]. They have been used in the well-studied NLP tasks of medical questioning and answering [25,39-41], summarization [16,23,42], named-entity recognition [30,43-46], and document classification [23,47-49]. Studies have largely focused on progress notes, histories and physicals, and discharge summaries, with an interest in the concepts of medications, diseases, and social determinants of health. There are fewer studies on operative notes and available research focuses on word embeddings for prediction tasks rather than individual entities [50-52]. Furthermore, even fewer works have been published using state-of-the-art transformers and foundational LLMs in surgery [53]. This is to our detriment as surgeons, as LLMs are capable of zero-shot learning (the ability to perform tasks without prior examples) and, if performing reliably, may obviate the need for manual chart review in retrospective research [38]. To our knowledge, this paper is the first to explore operative concepts using LLMs as a multilabel classification task in surgery.

Comparison With Prior Work

Compared with other document classification tasks, our model compared well. A previous multilabel documentation task on chest x-ray reports showed that pretrained models had F_1-score ranges of 0.29 to 0.48 [23]. Notably, traditional BoW-based approaches performed well across many classes. This is not surprising, as depending on the concept, the presence of a word or phrase in operative notes is often sufficient to identify it in text. tf-idf likely underperformed compared to BoW due to the dataset size: limited term frequencies and few documents may favor equal representations of words compared with weighted representations [54]. For many tasks, context may simply not be important. For example, negation is less commonly used, as surgeons will typically describe what they did rather than explain what they did not. In terms of the F_1-score, the generative model offered the most benefit in identifying active bleeding, bowel resection, serosal tear repair, and closure techniques, which are highly context-dependent and rely on the integration of up to several sentences of information. Notably, Clinical-Longformer did not offer much benefit over the BoW model. This may be secondary to the fact that Medical Information Mart for Intensive Care-III does not contain comprehensive operative notes [15].

Limitations

This study has several limitations. First, exploratory laparotomies represent a difficult case for both human and machine understanding. These operations are, by definition, exploratory, often performed in an emergent setting, can require input from multiple surgical services, and present challenging traumatic and aberrant anatomy. Thus, the language may be less consistent than elective procedures. Nevertheless, we chose basic operative concepts and a common procedure to start our investigation into multilabel document classification. Second, understanding operative reports requires highly technical knowledge. Training annotators, including those with clinical experience, presents challenges, and, despite regular review, there may be instances of inaccurate labeling. To maximize the number of notes, we did not perform a second round of interrater reliability testing, though each note was reviewed by the lead author. As with many other studies, this points to the potential for variability in human annotation, and granting consistency of model outputs may show the potential advantages of LLM augmentation for this task. Third, we acknowledge that the 5-fold training and testing mechanism may result in overly optimistic performance in the BoW, tf-idf models, and Clinical-Longformer models. However, despite this, the untrained Llama model still outperformed the three other classifiers. Fourth, during prompt tuning, we evaluated a random limited subset of the data during exploration, raising the possibility of data leakage. However, we did not examine performance metrics during prompt tuning and focused on model reasoning rather than the label choice itself. Fifth, the distribution of predictions varied by label in BoW, tf-idf, and Clinical-Longformer, though many were left-skewed, suggesting low confidence. More data may improve the performance of these models.

Conclusions

Given the performance of the off-the-shelf generative model, future studies will incorporate multiple labeled datasets from previous and ongoing retrospective studies at our institution with the goal of human-in-the-loop, streamlined extraction of operative concepts integrated into the research workflow. Future

XSL•FO
RenderX

work in agentic retrieval augmented generation with hybrid approaches of keyword search and semantic matching may fit this purpose well [55,56]. We noted improvements in model performance using larger Llama models, a trend we expect to continue as more advanced models are released.

While the use of multilabel document classification may be used to reliably capture select operative concepts with LLMs, further investigation of edge cases and alternative model architectures, such as retrieval augmented generation, will be required prior to deployment for research and quality improvement purposes.

Acknowledgments

Funding for JAB was provided by the National Institute of General Medicine (T32 GM008721-24). Funding for TJL was provided by the National Institute of General Medicine (R01 GM149657). Funding for BS and A Bihorac was provided by the National Institute of General Medicine (R01 GM110240).

Data Availability

The datasets generated or analyzed during this study are not publicly available because they contain protected health information that could be used for the reidentification of participants. Data are available from the University of Florida Institutional Data Access or Ethics Committee for researchers who meet the criteria for access to confidential data and may require additional institutional review board approval.

Authors' Contributions

JAB, SSD, VJN, DV, BS, PR, and TJL contributed to the conceptualization and methodology of the study, including approaches to annotation, data splitting, and modeling. Annotations were conducted by JAB, SSD, VJN, DV, TRB, LMB, YP, A Bilgili, AP, CEC, DMV, and RU. JAB and SSD were responsible for data visualization. Funding for the project was acquired by BS, TJL, A Bihorac, and PE. Project administration was led by JAB. Supervision was provided by BS, PR, TJL, A Bihorac, and PE. The original draft of the manuscript was written by JAB, SSD, VJN, DV, BS, PR, and TJL, with all authors contributing to the review and editing of the final manuscript.

Conflicts of Interest

None declared.

Multimedia Appendix 1
Operative note annotation guideline.
[DOCX File, 24 KB - medinform_v13i1e71176_app1.docx]

Multimedia Appendix 2
Sample operative note annotation.
[DOCX File, 1003 KB - medinform_v13i1e71176_app2.docx]

Multimedia Appendix 3
Supplemental tables.
[DOCX File, 41 KB - medinform_v13i1e71176_app3.docx]

Multimedia Appendix 4
Task prompts.
[DOCX File, 26 KB - medinform_v13i1e71176_app4.docx]

Multimedia Appendix 5
Context.
[DOCX File, 21 KB - medinform_v13i1e71176_app5.docx]

Multimedia Appendix 6
Supplemental figures.
[DOCX File, 469 KB - medinform_v13i1e71176_app6.docx]

Checklist 1

XSL•FO
RenderX

TRIPOD+LLM checklist.
[PDF File, 379 KB - medinform_v13i1e71176_app7.pdf]

References

1. Melton GB, Wang Y, Arsoniadis E, et al. Analyzing operative note structure in development of a section header resource. Stud Health Technol Inform 2015;216(821-6):821-826. [Medline: 26262166]
2. Maldonado R, Goodwin T, Harabagiu SM, Skinner MA. The role of semantic and discourse information in learning the structure of surgical procedures. Presented at: 2015 International Conference on Healthcare Informatics; Oct 21-23, 2015; Dallas, TX, USA. [doi: 10.1109/ICHI.2015.34]
3. Zheng YX, Gan WS, Chen ZF, Qi ZL, Liang Q, Yu PS. Large language models for medicine: a survey. Int J Mach Learn Cyber 2025 Feb;16(2):1015-1040. [doi: 10.1007/s13042-024-02318-w]
4. Page MJ, McKenzie JE, Bossuyt PM, et al. The PRISMA 2020 statement: an updated guideline for reporting systematic reviews. BMJ 2021 Mar 29;372:n71. [doi: 10.1136/bmj.n71] [Medline: 33782057]
5. Siems A, Banks R, Holubkov R, et al. Structured chart review: assessment of a structured chart review methodology. Hosp Pediatr 2020 Jan;10(1):61-69. [doi: 10.1542/hpeds.2019-0225] [Medline: 31879317]
6. Palanivinayagam A, El-Bayeh CZ, Damaševičius R. Twenty years of machine-learning-based text classification: a systematic review. Algorithms 2023;16(5):236. [doi: 10.3390/a16050236]
7. Fields J, Chovanec K, Madiraju P. A survey of text classification with transformers: how wide? How large? How long? How accurate? How expensive? How safe? IEEE Access 2024;12:6518-6531. [doi: 10.1109/ACCESS.2024.3349952]
8. Blanco A, Remmer S, Pérez A, Dalianis H, Casillas A. Implementation of specialised attention mechanisms: ICD-10 classification of gastrointestinal discharge summaries in English, Spanish and Swedish. J Biomed Inform 2022 Jun;130:104050. [doi: 10.1016/j.jbi.2022.104050] [Medline: 35346854]
9. Chaichulee S, Promchai C, Kaewkomon T, Kongkamol C, Ingviya T, Sangsupawanich P. Multi-label classification of symptom terms from free-text bilingual adverse drug reaction reports using natural language processing. PLoS One 2022;17(8):e0270595. [doi: 10.1371/journal.pone.0270595] [Medline: 35925971]
10. Choi J, Chen Y, Sivura A, Vendrow EB, Wang J, Spain DA. TraumaICD bidirectional encoder representation from transformers: a natural language processing algorithm to extract injury International Classification of Diseases, 10th edition diagnosis code from free text. Ann Surg 2024 Jul 1;280(1):150-155. [doi: 10.1097/SLA.0000000000006107] [Medline: 37753654]
11. Pedersen JS, Laursen MS, Soguero-Ruiz C, Savarimuthu TR, Hansen RS, Vinholt PJ. Domain over size: clinical ELECTRA surpasses general BERT for bleeding site classification in the free text of electronic health records. Presented at: 2022 IEEE-EMBS International Conference on Biomedical and Health Informatics (BHI); Sep 27-30, 2022; Ioannina, Greece. [doi: 10.1109/BHI56158.2022.9926955]
12. De Santis E, Martino A, Ronci F, Rizzi A. From bag-of-words to transformers: a comparative study for text classification in healthcare discussions in social media. IEEE Trans Emerg Top Comput Intell 2025;9(1):1063-1077. [doi: 10.1109/TETCI.2024.3423444]
13. Bedi S, Liu Y, Orr-Ewing L, et al. Testing and evaluation of health care applications of large language models: a systematic review. JAMA 2025 Jan 28;333(4):319-328. [doi: 10.1001/jama.2024.21700] [Medline: 39405325]
14. Wornow M, Xu Y, Thapa R, et al. The shaky foundations of large language models and foundation models for electronic health records. NPJ Digital Med 2023 Jul 29;6(1):135. [doi: 10.1038/s41746-023-00879-8] [Medline: 37516790]
15. Johnson AEW, Pollard TJ, Shen L, et al. MIMIC-III, a freely accessible critical care database. Sci Data 2016 May 24;3(1):160035. [doi: 10.1038/sdata.2016.35] [Medline: 27219127]
16. Agrawal M, Hegselmann S, Lang H, Kim Y, Sontag D. Large language models are few-shot clinical information extractors. arXiv. Preprint posted online on May 25, 2022. [doi: 10.48550/arXiv.2205.12689]
17. Collins GS, Dhiman P, Andaur Navarro CL, et al. Protocol for development of a reporting guideline (TRIPOD-AI) and risk of bias tool (PROBAST-AI) for diagnostic and prognostic prediction model studies based on artificial intelligence. BMJ Open 2021 Jul 9;11(7):e048008. [doi: 10.1136/bmjopen-2020-048008] [Medline: 34244270]
18. McHugh ML. Interrater reliability: the kappa statistic. Biochem Med (Zagreb) 2012;22(3):276-282. [Medline: 23092060]
19. Dimick JB, Upchurch GR, Alam HB, et al. Greenfield's Surgery: Scientific Principles and Practice: Lippincott Williams & Wilkins; 2021.
20. Sechidis K, Tsoumakas G, Vlahavas I. On the stratification of multi-label data. Presented at: Machine Learning and Knowledge Discovery in Databases: European Conference, ECML PKDD 2011; Sep 5-9, 2011; Athens, Greece.
21. Szymański P, Kajdanowicz T. A network perspective on stratification of multi-label data. Presented at: First International Workshop on Learning with Imbalanced Domains: Theory and Applications; Sep 22, 2017; Skopje, Macedonia.
22. Szymański P, Kajdanowicz T. A scikit-based python environment for performing multi-label classification. arXiv. Preprint posted online on Feb 5, 2017. [doi: 10.48550/arXiv.1702.01460]
23. Li Y, Wehbe RM, Ahmad FS, Wang H, Luo Y. A comparative study of pretrained language models for long clinical text. J Am Med Inform Assoc 2023 Jan 18;30(2):340-347. [doi: 10.1093/jamia/ocac225] [Medline: 36451266]

XSL•FO
RenderX

24. Dubey A, Jauhri A, Pandey A, et al. The llama 3 herd of models. arXiv. Preprint posted online on Jul 31, 2024. [doi: 10.48550/arXiv.2407.21783]
25. Singhal K, Azizi S, Tu T, et al. Large language models encode clinical knowledge. Nat New Biol 2023 Aug;620(7972):172-180. [doi: 10.1038/s41586-023-06291-2] [Medline: 37438534]
26. Gao S, Alawad M, Young MT, et al. Limitations of transformers on clinical text classification. IEEE J Biomed Health Inform 2021 Sep;25(9):3596-3607. [doi: 10.1109/JBHI.2021.3062322] [Medline: 33635801]
27. Beltagy I, Peters ME, Cohan A. Longformer: the long-document transformer. arXiv. Preprint posted online on Apr 10, 2020. [doi: 10.48550/arXiv.2004.05150]
28. Devlin J, Chang MW, Lee K, Toutanova K. BERT: pre-training of deep bidirectional transformers for language understanding. Presented at: 2019 Conference of the North American Chapter of the Association for Computational Linguistics: Human Language Technologies; Jun 2-7, 2019; Minneapolis, Minnesota, United States.
29. Huang K, Altosaar J, Ranganath R. ClinicalBERT: modeling clinical notes and predicting hospital readmission. arXiv. Preprint posted online on Apr 10, 2019. [doi: 10.48550/arXiv.1904.05342]
30. Lee J, Yoon W, Kim S, et al. BioBERT: a pre-trained biomedical language representation model for biomedical text mining. Bioinformatics 2020 Feb 15;36(4):1234-1240. [doi: 10.1093/bioinformatics/btz682] [Medline: 31501885]
31. Wolf T, Debut L, Sanh V, Chaumond J, Delangue C, Moi A, et al. HuggingFace's transformers: state-of-the-art natural language processing. arXiv. Preprint posted online on Oct 9, 2019. [doi: 10.48550/arXiv.1910.03771]
32. Liu J. LlamaIndex. Github. 2022. URL: https://github.com/jerryjliu/llama_index [accessed 2024-09-15]
33. Balch JA, Desaraju S. Multi-label classification for operative notes. GitHub. 2024. URL: https://github.com/balchja/op_note_multi_label_classification [accessed 2024-09-15]
34. Pal A. Performance comparison: llama-3 models in medical and healthcare AI domains. Hugg Face Repository. 2024. URL: https://huggingface.co/blog/aaditya/llama3-in-medical-domain [accessed 2024-09-15]
35. Hanskamp-Sebregts M, Zegers M, Vincent C, van Gurp PJ, de Vet HCW, Wollersheim H. Measurement of patient safety: a systematic review of the reliability and validity of adverse event detection with record review. BMJ Open 2016 Aug 22;6(8):e011078. [doi: 10.1136/bmjopen-2016-011078] [Medline: 27550650]
36. Lilford R, Edwards A, Girling A, et al. Inter-rater reliability of case-note audit: a systematic review. J Health Serv Res Policy 2007 Jul;12(3):173-180. [doi: 10.1258/135581907781543012] [Medline: 17716421]
37. Clusmann J, Kolbinger FR, Muti HS, et al. The future landscape of large language models in medicine. Commun Med (Lond) 2023 Oct 10;3(1):141. [doi: 10.1038/s43856-023-00370-1] [Medline: 37816837]
38. Thirunavukarasu AJ, Ting DSJ, Elangovan K, Gutierrez L, Tan TF, Ting DSW. Large language models in medicine. Nat Med 2023 Aug;29(8):1930-1940. [doi: 10.1038/s41591-023-02448-8] [Medline: 37460753]
39. Soni S, Roberts K, editors. Evaluation of dataset selection for pre-training and fine-tuning transformer language models for clinical question answering. Presented at: Proceedings of the Twelfth Language Resources and Evaluation Conference; May 11-16, 2020; Marseille, France.
40. Ng KKY, Matsuba I, Zhang PC. RAG in health care: a novel framework for improving communication and decision-making by addressing LLM limitations. NEJM AI 2025 Jan;2(1):AIra2400380. [doi: 10.1056/AIra2400380]
41. Lucas MM, Yang J, Pomeroy JK, Yang CC. Reasoning with large language models for medical question answering. J Am Med Inform Assoc 2024 Sep 1;31(9):1964-1975. [doi: 10.1093/jamia/ocae131] [Medline: 38960731]
42. Van Veen D, Van Uden C, Blankemeier L, et al. Clinical text summarization: adapting large language models can outperform human experts. Res Sq 2023 Oct 30:rs.3.rs-3483777. [doi: 10.21203/rs.3.rs-3483777/v1] [Medline: 37961377]
43. Bose P, Srinivasan S, Sleeman WC, Palta J, Kapoor R, Ghosh P. A survey on recent named entity recognition and relationship extraction techniques on clinical texts. Appl Sci (Basel) 2021 Sep;11(18):8319. [doi: 10.3390/app11188319]
44. Pagad NS, Pradeep N, editors. Clinical named entity recognition methods: an overview. In: International Conference on Innovative Computing and Communications: Proceedings of ICICC: Springer; 2022, Vol. 2. [doi: 10.1007/978-981-16-2597-8_13]
45. Wu Y, Jiang M, Xu J, Zhi D, Xu H. Clinical named entity recognition using deep learning models. AMIA Annu Symp Proc 2017;2017:1812-1819. [Medline: 29854252]
46. Li M, Zhou H, Yang H, Zhang R. RT: a retrieving and chain-of-thought framework for few-shot medical named entity recognition. J Am Med Inform Assoc 2024 Sep 1;31(9):1929-1938. [doi: 10.1093/jamia/ocae095] [Medline: 38708849]
47. Johnson AEW, Pollard TJ, Berkowitz SJ, et al. MIMIC-CXR, a de-identified publicly available database of chest radiographs with free-text reports. Sci Data 2019 Dec 12;6(1):317. [doi: 10.1038/s41597-019-0322-0] [Medline: 31831740]
48. Li Y, Yao L, Mao C, Srivastava A, Jiang X, Luo Y. Early prediction of acute kidney injury in critical care setting using clinical notes. Proc IEEE Int Conf Bioinformatics Biomed 2018. [doi: 10.1109/BIBM.2018.8621574]
49. Guo Y, Ovadje A, Al-Garadi MA, Sarker A. Evaluating large language models for health-related text classification tasks with public social media data. J Am Med Inform Assoc 2024 Oct 1;31(10):2181-2189. [doi: 10.1093/jamia/ocae210] [Medline: 39121174]
50. Mellia JA, Basta MN, Toyoda Y, et al. Natural language processing in surgery: a systematic review and meta-analysis. Ann Surg 2021 May 1;273(5):900-908. [doi: 10.1097/SLA.0000000000004419] [Medline: 33074901]

XSL•FO
RenderX

51. Selby LV, Narain WR, Russo A, Strong VE, Stetson P. Autonomous detection, grading, and reporting of postoperative complications using natural language processing. Surgery 2018 Dec;164(6):1300-1305. [doi: 10.1016/j.surg.2018.05.008] [Medline: 30056994]
52. Tibbo ME, Wyles CC, Fu S, et al. Use of natural language processing tools to identify and classify periprosthetic femur fractures. J Arthroplasty 2019 Oct;34(10):2216-2219. [doi: 10.1016/j.arth.2019.07.025] [Medline: 31416741]
53. Bombieri M, Rospocher M, Ponzetto SP, Fiorini P. Surgicberta: a pre-trained language model for procedural surgical language. Int J Data Sci Anal 2024 Jun;18(1):69-81. [doi: 10.1007/s41060-023-00433-5]
54. Jurafsky D, Martin JH. Speech and language processing: an introduction to natural language processing, computational linguistics, and speech recognition with language models. Stanford University. 2024. URL: https://web.stanford.edu/~jurafsky/slp3/ [accessed 2025-06-06]
55. Alkhalaf M, Yu P, Yin M, Deng C. Applying generative AI with retrieval augmented generation to summarize and extract key clinical information from electronic health records. J Biomed Inform 2024 Aug;156:104662. [doi: 10.1016/j.jbi.2024.104662] [Medline: 38880236]
56. Lewis P, Perez E, Piktus A, Petroni F, Karpukhin V, Goyal N, et al. Retrieval-augmented generation for knowledge-intensive NLP tasks. Adv Neural Inf Process Syst 2020;33:9459-9474 [FREE Full text]

Abbreviations

BERT: Bidirectional Encoder Representations from Transformers
BoW: bag-of-words
HL: hamming loss
LLM: large language model
NLP: natural language processing
PPV: positive predictive value
tf-idf: term frequency-inverse document frequency
TRIPOD+LLM: Transparent Reporting of a Multivariable Prediction Model for Individual Prognosis or Diagnosis+Large Language Model

Edited by A Coristine; submitted 11.01.25; peer-reviewed by A Jain, DH Choi, MV Ebrahim; revised version received 15.04.25; accepted 15.05.25; published 09.07.25.

Please cite as:
Balch JA, Desaraju SS, Nolan VJ, Vellanki D, Buchanan TR, Brinkley LM, Penev Y, Bilgili A, Patel A, Chatham CE, Vanderbilt DM, Uddin R, Bihorac A, Efron P, Loftus TJ, Rahman P, Shickel B
Language Models for Multilabel Document Classification of Surgical Concepts in Exploratory Laparotomy Operative Notes: Algorithm Development Study
JMIR Med Inform 2025;13:e71176
URL: https://medinform.jmir.org/2025/1/e71176
doi:10.2196/71176

© Jeremy A Balch, Sasank S Desarju, Victoria J Nolan, Divya Vallanki, Timothy R Buchanan, Lindsey M Brinkley, Yordan Penev, Ahmet Bilgili, Aashay Patel, Corinne E Chatham, David M Vanderbilt, Rayon Uddin, Azra Bihorac, Philip Efron, Tyler J Loftus, Protiva Rahman, Benjamin Shickel. Originally published in JMIR Medical Informatics (https://medinform.jmir.org), 9.7.2025. This is an open-access article distributed under the terms of the Creative Commons Attribution License (https://creativecommons.org/licenses/by/4.0/), which permits unrestricted use, distribution, and reproduction in any medium, provided the original work, first published in JMIR Medical Informatics, is properly cited. The complete bibliographic information, a link to the original publication on https://medinform.jmir.org/, as well as this copyright and license information must be included.

XSL•FO
RenderX

Clinical Performance and Communication Skills of ChatGPT Versus Physicians in Emergency Medicine: Simulated Patient Study

ChulHyoung Park[1,2,3*], MD; Min Ho An[1,2,3*], MD; Gyubeom Hwang[1,2,3*], MD; Rae Woong Park[1,2,3,4], PhD; Juho An[5], MD

[1]Department of Biomedical Informatics, Ajou University School of Medicine, Suwon, Republic of Korea

[2]Center for Biomedical Informatics Research, Ajou University Medical Cencer, Suown, Republic of Korea

[3]Department of Medical Sciences, Graduate School of Ajou University, Suwon, Republic of Korea

[4]BK21 R&E Initiative for Advanced Precision Medicine, Suwon, Republic of Korea

[5]Department of Emergency Medicine, Ajou University School of Medicine, 164 Worldcup-ro, Yeongtong-gu, Suwon, Republic of Korea

[*]these authors contributed equally

Corresponding Author:
Juho An, MD
Department of Emergency Medicine, Ajou University School of Medicine, 164 Worldcup-ro, Yeongtong-gu, Suwon, Republic of Korea

Abstract

Background: Emergency medicine can benefit from artificial intelligence (AI) due to its unique challenges, such as high patient volume and the need for urgent interventions. However, it remains difficult to assess the applicability of AI systems to real-world emergency medicine practice, which requires not only medical knowledge but also adaptable problem-solving and effective communication skills.

Objective: We aimed to evaluate ChatGPT's (OpenAI) performance in comparison to human doctors in simulated emergency medicine settings, using the framework of clinical performance examination and written examinations.

Methods: In total, 12 human doctors were recruited to represent the medical professionals. Both ChatGPT and the human doctors were instructed to manage each case like real clinical settings with 12 simulated patients. After the clinical performance examination sessions, the conversation records were evaluated by an emergency medicine professor on history taking, clinical accuracy, and empathy on a 5-point Likert scale. Simulated patients completed a 5-point scale survey including overall comprehensibility, credibility, and concern reduction for each case. In addition, they evaluated whether the doctor they interacted with was similar to a human doctor. An additional evaluation was performed using vignette-based written examinations to assess diagnosis, investigation, and treatment planning. The mean scores from ChatGPT were then compared with those of the human doctors.

Results: ChatGPT scored significantly higher than the physicians in both history-taking (mean score 3.91, SD 0.67 vs mean score 2.67, SD 0.78, $P<.001$) and empathy (mean score 4.50, SD 0.67 vs mean score 1.75, SD 0.62, $P<.001$). However, there was no significant difference in clinical accuracy. In the survey conducted with simulated patients, ChatGPT scored higher for concern reduction (mean score 4.33, SD 0.78 vs mean score 3.58, SD 0.90, $P=.04$). For comprehensibility and credibility, ChatGPT showed better performance, but the difference was not significant. In the similarity assessment score, no significant difference was observed (mean score 3.50, SD 1.78 vs mean score 3.25, SD 1.86, $P=.71$).

Conclusions: ChatGPT's performance highlights its potential as a valuable adjunct in emergency medicine, demonstrating comparable proficiency in knowledge application, efficiency, and empathetic patient interaction. These results suggest that a collaborative health care model, integrating AI with human expertise, could enhance patient care and outcomes.

(JMIR Med Inform 2025;13:e68409) doi:10.2196/68409

KEYWORDS

artificial intelligence; large language model; ChatGPT; emergency medicine; clinical performance examination; history taking; clinical reasoning; empathy; patient experience

XSL•FO
RenderX

Introduction

Recent advancements in artificial intelligence (AI) have raised interest in its potential to complement or even replace human expertise across various fields, particularly in medicine [1]. AI systems, such as ChatGPT (OpenAI), have demonstrated notable clinical capabilities, including success in professional medical examinations like the United States Medical Licensing Examination [2]. In a study by Sarraju et al [3], conversational generative AI models provided appropriate responses to 84% of questions on cardiovascular disease prevention, demonstrating their capability to handle open-ended clinical prompts rather than multiple-choice questions. In subsequent studies, ChatGPT has shown promise in more complex tasks, providing knowledge and management recommendations for hepatic cirrhosis and hepatocellular carcinoma [4]. Furthermore, Ayers et al [5] reported that ChatGPT generated empathetic responses to patient inquiries on a web-based platform comparable to those of human physicians, underscoring its potential to engage effectively with patients.

Emergency medicine is characterized by an urgent need for rapid diagnosis and immediate treatment. The high patient load and strict time constraints in emergency departments increase the risk of essential clinical information being overlooked or misinterpreted, including symptom presentation and diagnostic test results [6,7]. In addition, extended shifts, often spanning 24 hours, contribute to clinician fatigue and the risk of human error. AI technologies offer promising solutions to these challenges by enabling rapid, fatigue-free data processing. These challenges have motivated initiatives to integrate AI into emergency settings, particularly to enhance diagnostic speed and accuracy in radiology [8]. However, the implementation of AI in emergency medicine remains constrained by technical and operational challenges [9-11]. Emergency practice demands not only technical proficiency but also the flexibility to adapt swiftly to evolving conditions and effective communication skills to engage with patients in high-stress situations. Recent advancements in large language models (LLMs) have introduced conversational interfaces that can adapt responsively to new information, potentially aligning well with the dynamic demands of emergency medicine [12]. However, there remains a lack of research on the application of AI in emergency medicine within environments that closely resemble real-world clinical settings, as many studies have been limited to assessing the ability of AI to solve static examination-based questions rather than clinical practice-based problems [13,14].

The clinical performance examination (CPX) is a form of testing that assesses problem-solving skills in real-world–like clinical situations with simulated patients. It was developed from the recognition that assessing a physician's clinical skills cannot be fully achieved through traditional examination formats [15]. The CPX provides a dynamic approach to evaluating and refining essential competencies in simulated real-world settings. Through CPX, participants engage in history taking, communication, and patient relationship management and receive feedback for continuous improvement. Studies have shown that CPX enhances physicians' diagnostic accuracy, communication skills, and adaptability in clinical interactions, all of which are crucial in the field of emergency medicine [16,17]. Furthermore, CPX allows for the assessment of nontechnical skills, such as empathy, which is difficult to evaluate through conventional examination-based scenarios [18]. This ability to observe both technical and interpersonal skills offers a more comprehensive approach, aligning closely with the complex demands of emergency medicine practice.

In this study, we aimed to evaluate ChatGPT within the context of emergency medicine using a framework of CPX combined with a written examination, comparing its performance to that of human doctors. Through this comparative analysis, we sought to provide a deeper understanding of how AI can effectively augment clinical practice, enhance decision-making processes, and support health care professionals.

Methods

Ethical Considerations

This cross-sectional study received ethical approval from the institutional review board of Ajou University Medical Center (approval AJOUIRB-OB-2024 - 277). To maintain the confidentiality of participants, all identifying information has been appropriately anonymized or omitted, and informed consent (Multimedia Appendix 1) was obtained from all participants before their involvement in the study. All research methods were conducted in accordance with the Declaration of Helsinki. The study did not involve any form of participant remuneration.

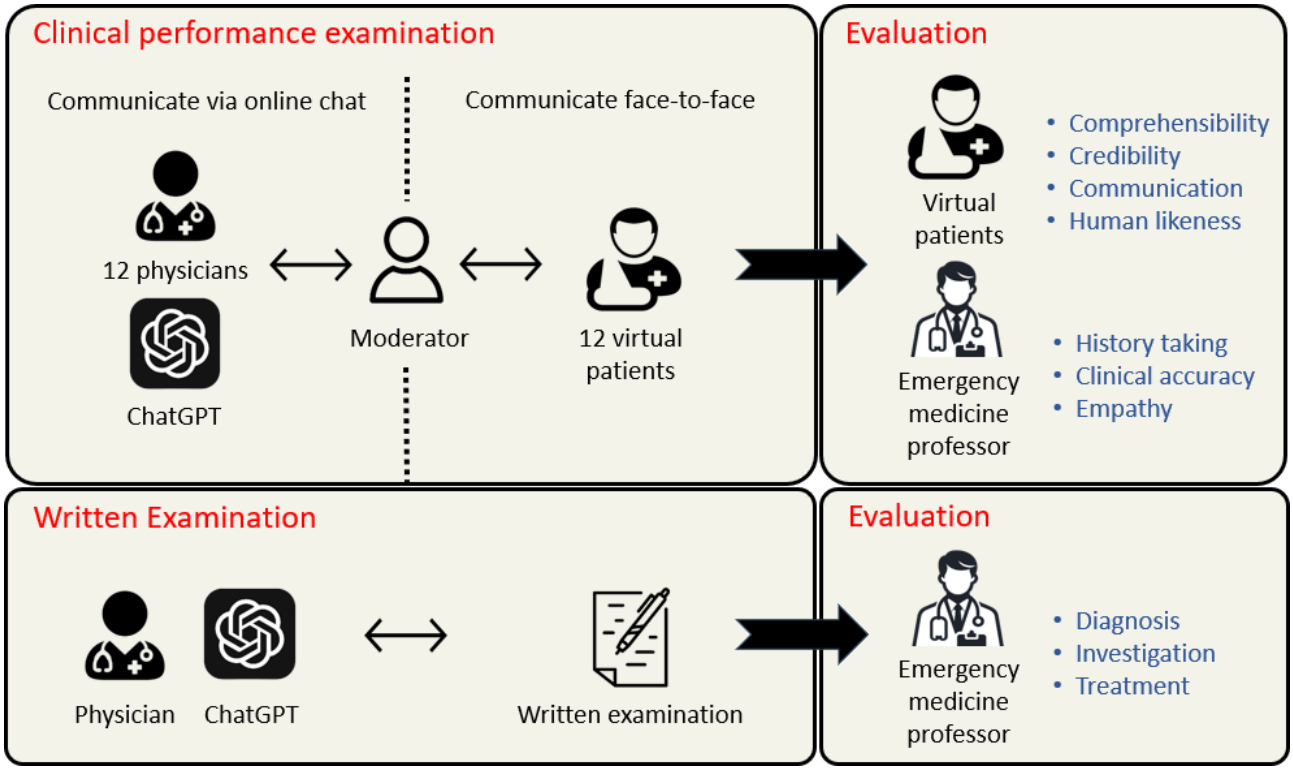
Study Design

The overall study flow is illustrated in Figure 1. This study aimed to compare the performance of ChatGPT and human doctors in simulated emergency medicine scenarios using 2 approaches—CPXs and conventional written examinations.

In the CPX, simulated patients represented standardized clinical cases. ChatGPT and human doctors participated in patient consultations via a neutral moderator to ensure blind evaluation. After each consultation, the emergency medicine professor evaluated the consultation from full conversation scripts. Simulated patients independently rated their consultation experiences.

XSL•FO
RenderX

Figure 1. Flow diagram of the study.



In the written examination, ChatGPT and human doctors were provided with clinical vignettes describing chief complaints and relevant medical history. They were instructed to identify the most likely diagnosis, suggest appropriate diagnostic investigations, and recommend a suitable treatment plan. The answers were evaluated by an emergency medicine professor.

The primary objective of this study was to compare the clinical competency of ChatGPT and human doctors in the emergency medicine clinical settings in CPX and written examination formats. The secondary objective was to compare patient-reported experience, as evaluated by simulated patients during the CPXs.

Case Selection

For the CPX, 4 representative cases were selected from 100 Cases in Emergency Medicine and Critical Care by Shamil et al [19]. The selected cases—malaria, acute asthma exacerbation, metastatic spinal cord compression, and acute kidney injury—were chosen based on their clinical urgency and the need for comprehensive symptom assessment and differential diagnosis. In addition, 28 text-based scenarios and 4 image-based clinical vignettes, along with corresponding questions, were selected for the written examinations. The selection was designed to include diverse representations across 16 different specialties, such as cardiology, pediatrics, and obstetrics, with a focus on scenarios commonly encountered in emergency care. For cases involving imaging, an electrocardiogram demonstrating atrial fibrillation, a brain computed tomography scan indicating subarachnoid hemorrhage, a chest x-ray showing a rib fracture, and a knee x-ray of a patient presenting with a knee injury were included in the case presentations. Detailed information about the cases that used written examinations in the study, including each patient's chief complaint and diagnosis, is presented in Table 1.

XSL•FO
RenderX

Table . Chief complaints, medical specialties, and diagnosis of cases included in the study.

Case number	Chief complaint	Medical specialty	Disease	Type[a]	Reference[b]
Case 1	Fever, headache, and a rash	Infectious medicine	Bacterial meningitis	1	5
Case 2	Dysuria and weakness	Infectious medicine	Urinary tract infection	1	18
Case 3	Slurred speech and weakness	Neurology	Ischemic stroke	1	41
Case 4	Severe epigastric pain	General surgery	Perforated peptic ulcer	1	60
Case 5	Epigastric pain and nausea	Gastroenterology	Acute pancreatitis	1	64
Case 6	A child acutely short of breath	Pediatrics	Severe asthma exacerbation	1	83
Case 7	Headache in pregnancy	Obstetrics and gynecology	Pre-eclampsia	1	95
Case 8	Shortness of breath and painful swallowing	Otolaryngology	Supraglottitis	1	3
Case 9	Nausea and vomiting in a diabetic	Endocrinology	Diabetic ketoacidosis	1	6
Case 10	Feeling unwell while on chemotherapy	Oncology and hematology	Neutropenic sepsis	1	24
Case 11	Cat bite	Orthopedics surgery	Tenosynovitis	1	50
Case 12	Left iliac fossa pain with fever	Gastroenterology	Diverticulitis	1	61
Case 13	Abdominal pain in early pregnancy	Obstetrics and gynecology	Ectopic pregnancy	1	89
Case 14	Breathlessness in pregnancy	Obstetrics and gynecology	Pulmonary embolism	1	96
Case 15	A productive cough	Respiratory medicine	Acute exacerbation of chronic obstructive pulmonary disease	1	16
Case 16	Productive cough and shortness of breath	Respiratory medicine	Bacterial pneumonia	1	25
Case 17	Acute severe leg pain	Cardiology	Acute ischemia	1	62
Case 18	Right flank pain moving to the groin	Urology	Kidney stone	1	66
Case 19	Worsening ear pain	Otolaryngology	Acute otitis media	1	69
Case 20	Cough and difficulty breathing in an infant	Pediatrics	Bronchiolitis	1	78
Case 21	Pelvic pain	Obstetrics and gynecology	Ovarian cyst torsion	1	91
Case 22	A collapse at work	Cardiology	Massive pulmonary embolism	1	17
Case 23	Upper abdominal pain	General surgery	Acute cholecystitis	1	57
Case 24	Abdominal pain and nausea	General surgery	Acute appendicitis	1	63
Case 25	Ear pain with discharge and facial weakness	Otolaryngology	Malignant otitis media	1	71
Case 26	A swollen eyelid	Ophthalmology	Periorbital preseptal cellulitis	1	73
Case 27	My son has the “runs”	Pediatrics	Gastroenteritis	1	81

XSL•FO
RenderX

Case number	Chief complaint	Medical specialty	Disease	Type[a]	Reference[b]
Case 28	Abdominal pain and vaginal discharge	Obstetrics and gynecology	Pelvic inflammatory disease	1	92
Case 29	An abnormal electrocardiogram	Cardiology	Atrial fibrillation	2	30
Case 30	Headache, vomiting, and confusion	Neurosurgery	Subarachnoid hemorrhage	2	39
Case 31	Twisted my knee skiing	Orthopedic surgery	Rupture of the anterior cruciate ligament	2	53
Case 32	My ribs hurt	Cardiothoracic surgery	Traumatic pneumothorax	2	59

[a]The written examination consisted of two types of questions: (1) text-based questions, and (2) image-included questions.

[b]The questions were developed based on emergency medicine patient cases from the reference "100 Cases in Emergency Medicine and Critical Care" by Shamil et al [19]. The numbers provided correspond to those accessible in the reference.

Human Doctors and ChatGPT in CPX

In total, 12 human doctors were recruited to represent the medical doctors, comprising 4 third-year emergency medicine residents, 4 fourth-year emergency medicine residents, and 4 general practitioners (GPs) from a tertiary hospital in South Korea. Before participating in the CPX with simulated patients, physicians received general instructions for the examination process (Table S1 in Multimedia Appendix 2). They were informed that all conversations with simulated patients would be conducted via text-based communication through a moderator. They were directed to approach each case as if practicing in a real clinical setting, with the understanding that the information necessary for diagnosis and treatment planning could be obtained by asking questions to the simulated patients.

ChatGPT (version 4.0) was used in this study, with all examinations conducted between September and October 2023. For ChatGPT, a prompt designed to emulate the role of a medical professional was provided (Table S2 in Multimedia Appendix 2). ChatGPT was instructed to perform history taking and, when a physical examination was required, to obtain relevant information through targeted questions. In addition, it was directed to communicate possible diagnoses to the patient and to provide explanations regarding necessary tests and treatment plans.

Interaction With Simulated Patients in CPX

In total, 12 volunteers were recruited as simulated patients and evenly distributed across 4 clinical scenarios, with 3 simulated patients assigned to each scenario. Each simulated patient participated in 2 separate consultations, presenting their assigned case to both ChatGPT and a human doctor. Depending on the allocation, each simulated patient conducted 1 consultation with ChatGPT and 1 with either a third-year emergency medicine resident (R3), a fourth-year resident (R4), or a GP.

Before the CPX, each patient reviewed their assigned case and received instructions on their role (Table S3 in Multimedia Appendix 2). They were informed that all responses would be delivered through a moderator and that they would participate in 2 consultations, 1 with a human doctor and 1 with ChatGPT. They were also notified that their experience would be evaluated afterward.

During the CPX, patients did not interact face-to-face with either ChatGPT or the physicians; instead, they communicated with assistance from a moderator. All questions from doctors or ChatGPT were provided to patients as text by the moderator, and patients' responses were similarly relayed in text form by the moderator to maintain consistency. This indirect communication process ensured that patients were blinded to whether they were interacting with ChatGPT or a human doctor. To standardize message formats, doctors' messages were edited to remove typos and to consolidate brief questions where appropriate (eg, "Do you take any other medications? Like for a cold?" was revised to "Are you taking any other medications, such as cold medicine?"). Although the protocol advised posing one question at a time, some questions were grouped by physicians and later separated by the moderator for consistency. Given ChatGPT's quicker response capability, its message delivery was deliberately slowed to mirror a doctor's pace. No additional modifications were made to ChatGPT's messages.

Written Examinations

The written examination consisted of 28 text-based clinical cases and 4 image-containing clinical cases. Before the examination, both physicians and ChatGPT were provided with written instructions outlining the format of the test. These included a sample case, sample question and answer, and detailed scoring criteria to ensure consistency in understanding and response approach. The full instructions are presented in Table S3 in Multimedia Appendix 2.

A total of 4 GPs, 4 third-year emergency medicine residents (R3s), and 4 fourth-year residents (R4s) each completed 7 cases, resulting in 28 responses for text-based clinical cases per group. ChatGPT also provided answers to all 28 cases. In addition, 4 image-based clinical cases were evaluated. Due to concerns regarding potential interpretive inaccuracies, GPs did not participate in the image-based clinical cases. Each of the 4 R3s and 4 R4s completed all 4 cases, yielding 32 responses for image-based cases. ChatGPT also completed all 4 image-based cases.

Detailed instructions, including sample questions and grading criteria, were provided to both ChatGPT and the doctors. (Table S4 in Multimedia Appendix 2). The grading criteria

XSL•FO
RenderX

encompassed the number of correct keywords, the specificity of responses, and the presence of any inappropriate content.

Assessment of Outcomes

The conversations were evaluated by a professor of emergency medicine actively involved in resident education. To assess the clinical performance of ChatGPT and physicians, the professor reviewed all conversations and assigned scores from 3 perspectives for each consultation on a 5-point Likert scale (with 1 being very poor and 5 being excellent). These scores included a history-taking score for the thoroughness of information gathering, a clinical accuracy score evaluating the medical correctness of diagnoses and treatment plans, and an empathy score reflecting the degree of attentiveness and responsiveness to the patient's concerns. For the written examination, which included 3 questions on diagnosis, investigation, and treatment planning, responses from both ChatGPT and the physicians were evaluated by the emergency medicine professor. Scores were assigned for accuracy on a 6-point Likert scale (where 1 indicated incorrect and 6 indicated completely correct) and for completeness on a 3-point Likert scale (where 1 indicated incomplete and 3 indicated comprehensive).

In addition, all virtual patients participating in the CPX completed a 5-point scale survey consisting of 7 questions to evaluate the consultations from multiple perspectives. They assessed the overall comprehensibility and credibility of the consultation, as well as its effectiveness in alleviating patient concerns. Patients also evaluated the credibility and communication of the diagnosis and treatment plan provided by either the physician or ChatGPT. Finally, patients were asked to assess whether the consulting entity seemed more like ChatGPT or a human doctor.

Statistical Analysis

Scores were presented as mean and SD. We evaluated each performance domain separately rather than combining them into a single score. Mean scores for each domain were calculated separately and compared between ChatGPT and the human doctor group. Group comparisons were conducted for each domain independently using either independent-sample *t* tests or Mann-Whitney *U* tests according to the distribution of the data. In the written examinations, questions were further categorized into easy, medium, and hard levels based on the scores of the physicians. Performance between physicians and ChatGPT was then compared across these defined difficulty levels. A post hoc power analysis was conducted for the CPX outcomes evaluated by the emergency medicine professor based on the observed effect sizes. Effect sizes were estimated using Cohen *d* or rank-biserial correlation, and statistical power was estimated based on these observed effect sizes. A *P* value of less than .05 was considered statistically significant. All statistical analyses were performed using R software, version 4.3.1 (R Core Team).

Results

CPX

The results from the CPX of ChatGPT and physicians, based on grading by the emergency medicine professor and patient survey responses, are summarized in Table 2. ChatGPT scored significantly higher than physicians in history taking (mean 3.91, SD 0.67 vs mean 2.67, SD 0.78; $P<.001$). Although ChatGPT also achieved a higher score in clinical accuracy (mean 3.75, SD 0.45 vs mean 3.33, SD 0.98), the difference was not statistically significant ($P=.25$). In terms of empathy, ChatGPT scored an average of 4.50 (SD 0.67), whereas physicians scored 1.75 (SD 0.62), falling below the "poor" rating threshold of 2. This difference was statistically significant ($P<.001$), highlighting ChatGPT's superior empathetic engagement. Post hoc power analysis revealed that the history taking and empathy scores had high statistical power (0.98 and 0.99, respectively). In contrast, the clinical accuracy score showed low power (0.22), indicating a limited ability to detect significant group differences for this outcome.

Results from a survey completed by a virtual patient immediately after each CPX session showed that ChatGPT scored slightly higher than the human physicians across all categories. However, a statistically significant difference was only observed in the concern-reduction score, which measured the extent to which the consultation alleviated the patient's worries (ChatGPT: mean 4.33, SD 0.78 vs physicians: mean 3.58, SD 0.90; $P=.04$). In addition, for the similarity assessment score, which evaluated whether the consultant appeared more like ChatGPT or a human physician, no significant difference was found ($P=.71$). Full records of the conversations between ChatGPT and the physicians with virtual patients during the CPX, along with the scores assigned by the emergency medicine professor and their distributions, are available in Multimedia Appendix 3.

XSL•FO
RenderX

Table . Results from the clinical performance examination of ChatGPT and physicians (all scores were assigned using a 5-point Likert scale, where 1 signifies "very poor," 2 "poor," 3 "average," 4 "good," and 5 "excellent"; for the similarity score, the scale was as follows: 1 indicated "very similar to ChatGPT," 2 "somewhat similar to ChatGPT," 3 "neutral, neither ChatGPT nor a real doctor," 4 "somewhat similar to a real doctor," and 5 denoted "very similar to a real doctor").

Score	ChatGPT, mean (SD)	Overall physicians (n=12), mean (SD)	*P* value	GP[a] (n=4), mean (SD)	R3[b] (n=4), mean (SD)	R4[c] (n=4), mean (SD)
Grading results from an emergency medicine professor						
History taking score	3.91 (0.67)	2.67 (0.78)	<.001	2.75 (0.50)	2.75 (0.50)	2.50 (1.29)
Clinical accuracy score	3.75 (0.45)	3.33 (0.98)	.25	2.75 (0.96)	3.75 (0.50)	3.50 (1.29)
Empathy score	4.50 (0.67)	1.75 (0.62)	<.001	1.50 (0.58)	2.00 (0.82)	1.75 (0.50)
Survey results from virtual patients						
Overall consultation						
Comprehensibility score	4.67 (0.49)	4.50 (0.52)	.43	4.75 (0.50)	4.00 (0.00)	4.75 (0.50)
Credibility score	4.42 (0.51)	3.92 (0.79)	.10	4.00 (0.82)	3.50 (0.58)	4.25 (0.96)
Concern reduction score	4.33 (0.78)	3.58 (0.90)	.04	3.75 (0.50)	3.50 (1.29)	3.50 (1.00)
Diagnosis						
Evaluation score	4.75 (0.45)	4.41 (0.67)	.20	5.00 (0.00)	3.75 (0.50)	4.50 (0.58)
Investigation and treatment plan						
Credibility score	4.50 (0.52)	4.17 (0.83)	.36	4.00 (0.82)	4.00 (1.15)	4.50 (0.58)
Communication score	4.42 (0.79)	4.00 (0.95)	.26	3.75 (0.50)	3.50 (1.29)	4.75 (0.50)
Similarity						
Assessment score	3.50 (1.78)	3.25 (1.86)	.71	2.75 (2.06)	3.25 (2.06)	3.75 (1.89)

[a]GP: general practitioner.

[b]R3: third-year emergency medicine resident.

[c]R4: fourth-year emergency medicine resident.

Written Examinations

The grading outcomes of the written examination are summarized in Table 3. ChatGPT achieved higher scores across all categories—diagnosis, investigation, and treatment plan—than the physicians. The mean accuracy scores for ChatGPT were 5.44 (SD 0.72), 5.38 (SD 0.55), and 5.59 (SD 0.50), significantly exceeding the physicians' scores of 4.11 (SD 1.10), 3.67 (SD 0.93), and 3.74 (SD 0.98), respectively (*P*<.001 for all comparisons). Similarly, ChatGPT's mean completeness scores were substantially higher, with averages of 2.84 (SD 0.37), 2.56 (SD 0.50), and 2.94 (SD 0.25), compared with the physicians' scores of 1.84 (SD 0.45), 1.84 (SD 0.37), and 1.72 (SD 0.45) for each category, respectively (*P*<.001 for all). Detailed accuracy and completeness scores of the physicians and ChatGPT for all cases are presented in Figure 2. Complete answer sheets for the written examination provided by the physicians and ChatGPT and the scores assigned by the professor and their distributions are all included in Multimedia Appendix 4.

The differences in scores between ChatGPT and the physicians were further analyzed across various difficulty levels of the written examination questions (Figure 3). The scores for both accuracy and completeness were significantly higher for ChatGPT than for the physicians across all difficulty levels (*P*<.001, for all). Notably, the gap in scores between ChatGPT and the physicians widened on questions of higher difficulty, where the physicians' scores were lower.

XSL•FO
RenderX

Table . Results from the written examination of ChatGPT and physicians. The accuracy scale was a 6-point Likert scale (with 1 indicating totally incorrect; 2, mostly incorrect; 3, balance of correct and incorrect; 4, more correct than incorrect; 5, almost entirely correct; and 6, completely correct), and a 3-point scale for completeness (1 for incomplete, 2 for adequate, and 3 for comprehensive).

Score	Participant group, mean (SD)		*P* value	GP[a] (n=4), mean (SD)	R3[b] (n=4), mean (SD)	R4[c] (n=4), mean (SD)
	ChatGPT	Overall physicians (n=12)				
All (n=32)						
Diagnosis						
Accuracy score	5.44 (0.72)	4.11 (1.10)	<.001	3.14 (1.21)	4.36 (0.94)	4.45 (0.79)
Completeness score	2.84 (0.37)	1.84 (0.45)	<.001	1.61 (0.50)	2.02 (0.40)	1.82 (0.39)
Investigation						
Accuracy score	5.38 (0.55)	3.67 (0.93)	<.001	2.96 (0.84)	3.93 (0.85)	3.82 (0.95)
Completeness score	2.56 (0.50)	1.84 (0.37)	<.001	1.79 (0.42)	1.91 (0.29)	1.80 (0.41)
Treatment plan						
Accuracy score	5.59 (0.50)	3.74 (0.98)	<.001	2.96 (0.96)	3.93 (0.85)	4.05 (0.86)
Completeness score	2.94 (0.25)	1.72 (0.45)	<.001	1.68 (0.48)	1.73 (0.45)	1.73 (0.45)
Text-based questions (n=28)						
Diagnosis						
Accuracy score	5.46 (0.58)	3.96 (1.13)	<.001	3.14 (1.21)	4.21 (0.96)	4.54 (0.69)
Completeness score	2.86 (0.36)	1.82 (0.47)	<.001	1.61 (0.50)	2.04 (0.43)	1.82 (0.39)
Investigation						
Accuracy score	5.43 (0.57)	3.61 (0.97)	<.001	2.96 (0.84)	3.96 (0.79)	3.89 (0.96)
Completeness score	2.57 (0.50)	1.86 (0.35)	<.001	1.79 (0.42)	1.93 (0.26)	1.86 (0.36)
Treatment plan						
Accuracy score	5.57 (0.50)	3.67 (0.97)	<.001	2.96 (0.96)	4.00 (0.72)	4.04 (0.84)
Completeness score	2.96 (0.19)	1.70 (0.46)	<.001	1.68 (0.48)	1.71 (0.46)	1.71 (0.46)
Image-included questions (n=4)						
Diagnosis						
Accuracy score	5.25 (1.50)	4.50 (0.92)	.09	—[d]	4.62 (0.89)	4.38 (0.96)
Completeness score	2.75 (0.50)	1.91 (0.39)	<.001	—	2.00 (0.37)	1.81 (0.40)
Investigation						
Accuracy score	5.00 (0.00)	3.84 (0.81)	.005	—	4.00 (0.63)	3.69 (0.95)
Completeness score	2.50 (0.58)	1.78 (0.42)	.01	—	1.88 (0.34)	1.69 (0.48)
Treatment plan						
Accuracy score	5.75 (0.50)	3.94 (0.98)	.002	—	3.81 (1.05)	4.06 (0.93)
Completeness score	2.75 (0.50)	1.75 (0.44)	.001	—	1.75 (0.45)	1.75 (0.45)

[a]GP: general practitioner.

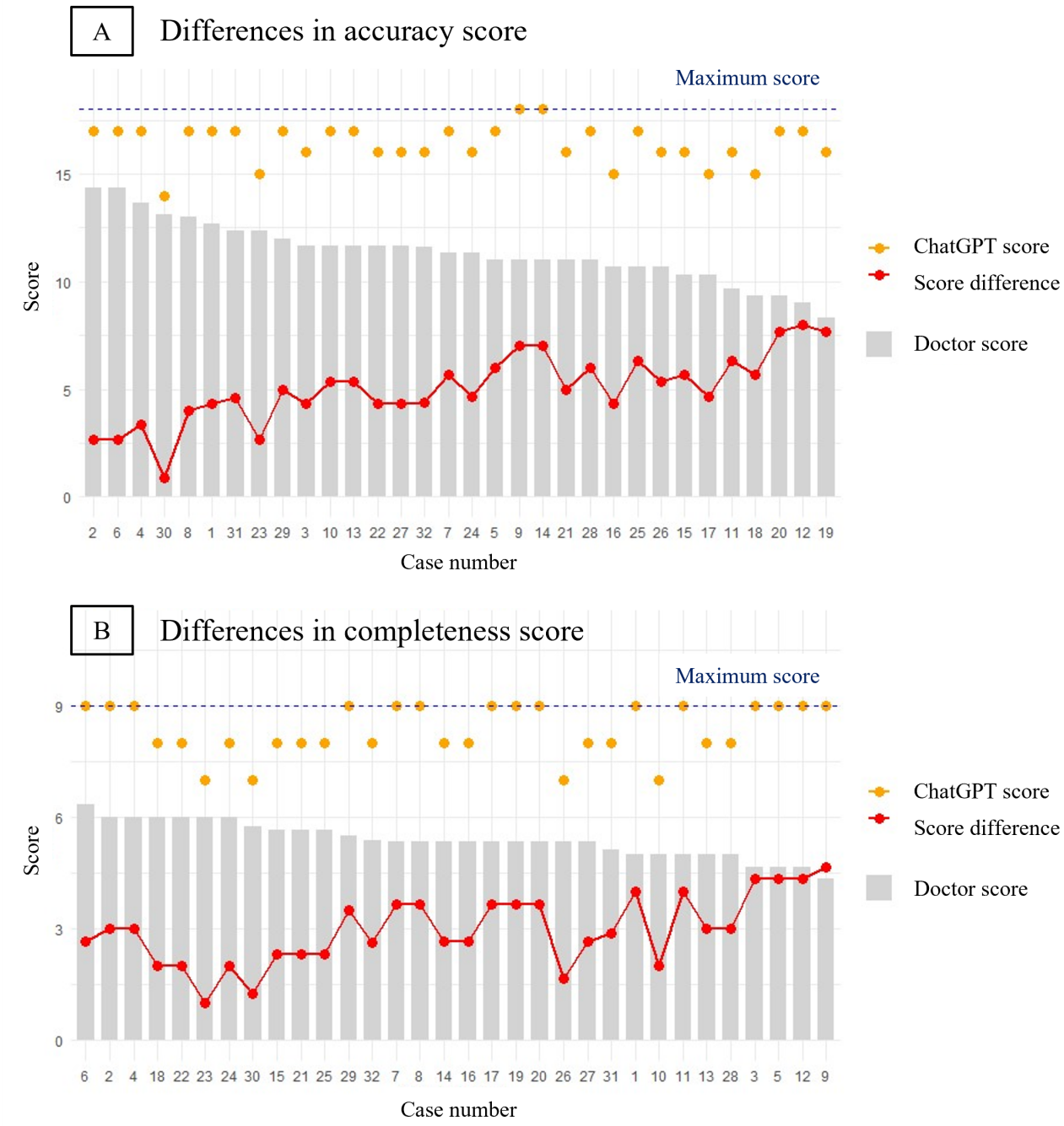
[b]R3: third-year emergency medicine resident.

[c]R4: fourth-year emergency medicine resident.

XSL•FO
RenderX

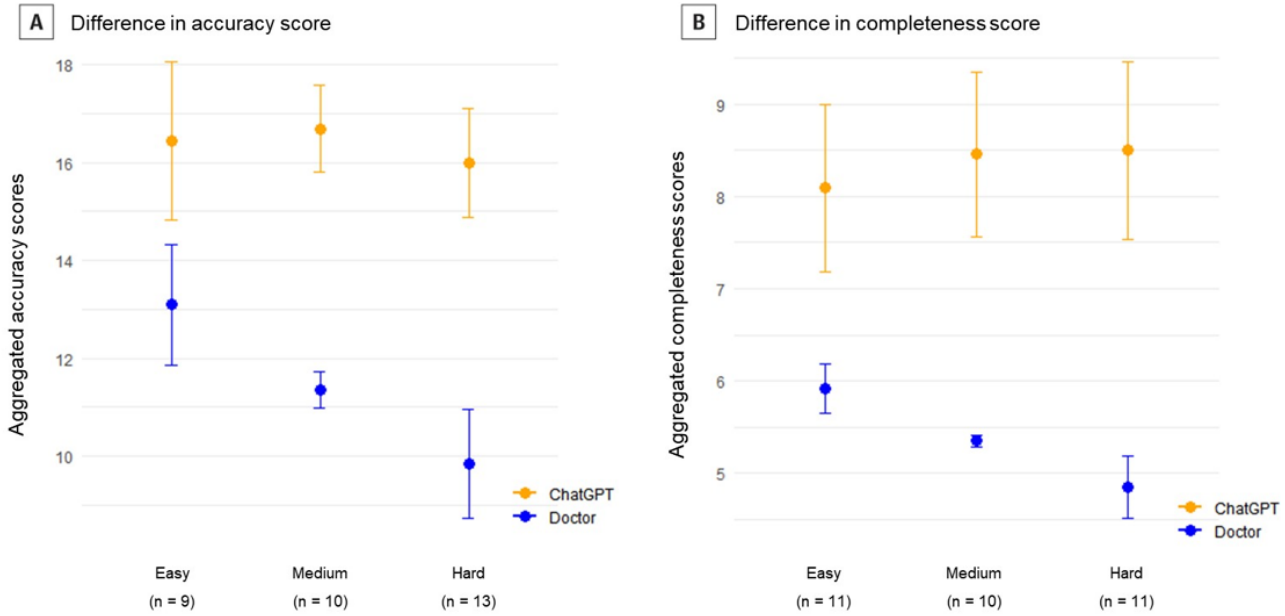
[d]Not applicable.

Figure 2. Difference of accuracy and completeness scores of ChatGPT and physicians from written examination.



XSL•FO
RenderX

Figure 3. Difference in accuracy and completeness scores of ChatGPT and physicians categorized by difficulty level of the questions.



Discussion

Principal Findings

In this study, we compared the performance of ChatGPT and human doctors using 2 evaluation formats—CPX and written examinations. In the CPX, evaluations were conducted by an emergency medicine professor and virtual patients. ChatGPT received significantly higher scores than human doctors in the domains of history taking and empathy. Although ChatGPT showed a higher mean score in clinical accuracy, the difference was not statistically significant.

In the virtual patient evaluations, ChatGPT achieved higher mean scores across all domains, including comprehensibility, credibility, and communication. However, a statistically significant difference was observed only in the concern reduction domain. When virtual patients were asked to evaluate human-likeness, there was no significant difference between ChatGPT and human doctors, indicating that patients did not perceive a substantial distinction in human-likeness between the two.

Regarding the written examinations, ChatGPT demonstrated significantly higher scores than human doctors in most domains evaluated by the emergency medicine professor, including diagnosis, investigation, and treatment planning. This trend was consistent across both text-based and image-based clinical questions. In addition, when questions were stratified based on difficulty levels determined by human doctor scores, ChatGPT's performance remained relatively stable, showing minimal variation according to question difficulty.

Comparison With Previous Work

The clinical utility of ChatGPT and other LLMs has been increasingly investigated in the field of emergency medicine. Previous studies have demonstrated that LLMs can effectively support patient triage and identify cases requiring critical care based on clinical scenarios, highlighting their potential to assist in acute decision-making processes [20,21]. In addition, ChatGPT has shown promising performance in interpreting electrocardiogram-related questions and providing reliable guidance for imaging test referrals [22,23]. Our findings from the written examinations are consistent with previous studies, further supporting the potential of ChatGPT as a clinical decision support tool in emergency medicine. We extended previous research by evaluating not only the accuracy but also the completeness of responses in open-ended, case vignette–based assessments. A similar finding was reported in a previous study, in which ChatGPT provided more extended responses than those of physicians without compromising quality when answering patients' questions on a public online forum [5]. This ability to generate comprehensive answers without relying on predefined options is promising for the future application of ChatGPT in real clinical settings within emergency medicine.

However, most previous studies have relied on examination-based assessments, which may oversimplify clinical reasoning by limiting diagnostic flexibility and excluding the iterative, hypothesis-driven nature of real-world medical consultations and patient interactions [24]. Our study addresses this limitation by implementing a CPX format, which enables a more in-depth evaluation of AI performance in scenarios that closely resemble actual clinical practice. This methodology allowed us to assess ChatGPT's capabilities in a dynamic, human-like context that simulates instantaneous decision-making.

In this study, we found that ChatGPT performed significantly better in history taking, while demonstrating clinical accuracy comparable to that of human doctors. Although previous studies have examined the use of chatbots for history taking, most were developed for narrowly defined purposes or relied on fixed sets of predefined questions presented in conversational form [25]. In contrast, our findings show that a general-purpose conversational AI can actively engage in clinical reasoning and elicit relevant patient history through interactive dialogue. This suggests that the integration of such AI tools into clinical

XSL•FO
RenderX

workflows may enhance the quality of history taking and ultimately improve patient care.

We also found that ChatGPT received higher empathy scores and greater concern reduction ratings from patients. More empathetic responses from ChatGPT compared with human doctors have also been observed in previous studies [5,26], and our findings extend this evidence by evaluating full conversational interactions. These results suggest that AI models may not only support clinical reasoning but also complement physicians in areas often compromised under high-stress conditions, such as patient-centered communication and emotional engagement.

Interestingly, patients were unable to distinguish whether they were interacting with ChatGPT or a human physician, yet the resulting empathy scores were significantly higher for ChatGPT. This suggests that communication quality may outweigh the communicator's identity in shaping perceived empathy. However, previous studies indicate that patient satisfaction can decline when AI-generated responses are explicitly disclosed, underscoring the complexity of transparency in clinical AI use [27]. Determining when and how to disclose AI involvement remains an important ethical and practical challenge, warranting further research into its impact on patient trust and acceptance.

Ethical and Educational Implications

While our study demonstrates that ChatGPT can perform reasonably well in clinically simulated settings, several barriers must be addressed before independent deployment in real-world practice [28]. A major concern is liability for inaccurate or harmful recommendations, with uncertainty over whether responsibility would fall on software developers, health care providers, or end users [29,30]. Furthermore, the black-box nature of LLMs makes it difficult even for professionals to fully evaluate AI-generated outputs [31]. Robust legal and ethical frameworks will be essential for the safe integration of AI into clinical care [32].

Data privacy also presents a critical challenge. Many LLMs, including ChatGPT, operate through cloud-based services, raising concerns about the transmission and storage of sensitive health information [33,34]. One potential solution is the development of open-source models that can operate within closed, local systems without cloud dependence. However, further research is needed to assess the feasibility, security, and clinical applicability of such approaches.

With the growing integration of AI into clinical practice, its role in medical education has also expanded [35]. AI models such as ChatGPT have been used not only to deliver factual knowledge but also to enhance patient communication skills. They can be useful for simulating patient interactions and providing immediate feedback [36]. However, concerns remain that excessive reliance on AI may undermine the development of independent critical thinking and clinical reasoning skills [37]. To address this, AI-integrated curricula must be designed to harness the strengths of AI while actively cultivating human competencies in critical thinking, clinical judgment, and ethical decision-making [38]. Balancing these elements will be essential to maintain independent expertise in an increasingly AI-augmented health care environment.

Limitations

This study has several limitations. First, the CPX format used in this study does not fully replicate the real-world clinical environment in which physicians interact with patients in the emergency department. The simulations were conducted via text-based messenger in a blinded format, which limited access to nonverbal cues and other clinically relevant information typically available during face-to-face encounters. As a result, participants could not demonstrate the full range of clinical skills required in actual patient care. In addition, while moderation was necessary to anonymize participants and correct typographical errors, the process occasionally involved segmenting and restructuring physicians' input for clarity. These adjustments may have disrupted the natural flow of conversation and removed pauses and hesitations, which are essential for conveying empathy [39]. For example, splitting long, intricate sentences into shorter, specific segments can give patients the impression that the conversation is overly focused on medical facts and interaction is less patient-centered. Future research should compare human performance and AI in more realistic settings including voice-based or in-person interactions to reflect nonverbal cues and conversational dynamics. Second, all CPX evaluations were performed by a single emergency medicine professor. Although the assessor was experienced, the use of a single evaluator may have introduced bias or subjectivity in scoring, particularly in domains such as empathy or communication quality. To address this issue, the evaluator calibrated the scoring process by applying the rubric to CPX manuscripts previously used for educational purposes and discussing borderline ratings with other physician investigators to ensure consistent interpretation. Future research should involve multiple independent raters to reduce subjectivity and enhance scoring consistency. Third, the relatively small number of participants may have limited the statistical power to detect modest differences between groups. Larger studies are needed to validate and extend these findings. Fourth, the clinical scenarios used in both CPX and written examinations were limited to a predefined set of representative cases. While selected to reflect a range of emergency conditions, the findings may not be generalizable to all clinical contexts or specialties. Future studies should include a broader range of clinical situations and patient presentations to enhance generalizability. Finally, this study did not include structured interviews or surveys of participating physicians to capture their perspectives on ChatGPT. Instead, we conducted brief debriefings after CPX sessions, which revealed that physicians initially underestimated ChatGPT's capabilities. They highlighted its continuous availability and rapid response generation as key strengths and noted that lower empathy scores served as a reminder of the importance of empathic communication in practice. Clinicians also emphasized that legal and liability issues must be resolved before broader AI adoption. Future research should incorporate formal clinician interviews to systematically explore these insights and guide safe AI integration.

XSL•FO
RenderX

Conclusion

In conclusion, the AI model demonstrated robust capabilities in clinical reasoning, diagnostic accuracy, and empathic communication in simulated emergency medicine scenarios. These findings highlight the potential of AI to serve as a supportive role in clinical practice. Future efforts should focus on developing collaborative frameworks that integrate AI into existing clinical workflows and harness AI's strengths safely and effectively in real-world practice.

Acknowledgments

This research was funded by the Korea Health Technology R&D Project through the Korea Health Industry Development Institute; the Ministry of Health and Welfare, Republic of Korea (grant HR16C0001), and a grant from the project for Infectious Disease Medical Safety; the Ministry of Health and Welfare, the Republic of Korea (grant HG22C0024).

Data Availability

All data are available in the main text or the supplementary materials.

Authors' Contributions

CP, MHA, and GH contributed equally as the first authors. RWP and JA contributed equally as the corresponding authors. Concept and design was contributed by CP, MHA, and GH. Acquisition, analysis, or interpretation of data was contributed by all authors. Statistical analysis was done by CP, MHA, and GH. Drafting of the manuscript was contributed by all authors. Critical review of the manuscript for important intellectual content was contributed by all authors. Administrative, technical, or material support was handled by RWP and JA. Supervision was handled by RWA and JA.

Conflicts of Interest

None declared.

Multimedia Appendix 1
Publication consent.
[PNG File, 1268 KB - medinform_v13i1e68409_app1.png]

Multimedia Appendix 2
Instructions for ChatGPT, physicians, and virtual patients for clinical performance examination and written examinations.
[DOCX File, 80 KB - medinform_v13i1e68409_app2.docx]

Multimedia Appendix 3
Full clinical performance examination transcripts and grading results.
[DOCX File, 2805 KB - medinform_v13i1e68409_app3.docx]

Multimedia Appendix 4
Written examination answer sheets and grading results.
[DOCX File, 203 KB - medinform_v13i1e68409_app4.docx]

References

1. Lee P, Bubeck S, Petro J. Benefits, limits, and risks of GPT-4 as an AI chatbot for medicine. N Engl J Med 2023 Mar 30;388(13):1233-1239. [doi: 10.1056/NEJMsr2214184] [Medline: 36988602]
2. Kung TH, Cheatham M, Medenilla A, et al. Performance of ChatGPT on USMLE: potential for AI-assisted medical education using large language models. PLOS Digit Health 2023 Feb;2(2):e0000198. [doi: 10.1371/journal.pdig.0000198] [Medline: 36812645]
3. Sarraju A, Bruemmer D, Van Iterson E, Cho L, Rodriguez F, Laffin L. Appropriateness of cardiovascular disease prevention recommendations obtained from a popular online chat-based artificial intelligence model. JAMA 2023 Mar 14;329(10):842-844. [doi: 10.1001/jama.2023.1044] [Medline: 36735264]
4. Yeo YH, Samaan JS, Ng WH, et al. Assessing the performance of ChatGPT in answering questions regarding cirrhosis and hepatocellular carcinoma. Clin Mol Hepatol 2023 Jul;29(3):721-732. [doi: 10.3350/cmh.2023.0089]
5. Ayers JW, Poliak A, Dredze M, et al. Comparing physician and artificial intelligence chatbot responses to patient questions posted to a public social media forum. JAMA Intern Med 2023 Jun 1;183(6):589-596. [doi: 10.1001/jamainternmed.2023.1838] [Medline: 37115527]

XSL•FO
RenderX

6. Nguyen PTL, Phan TAT, Vo VBN, et al. Medication errors in emergency departments: a systematic review and meta-analysis of prevalence and severity. Int J Clin Pharm 2024 Oct;46(5):1024-1033. [doi: 10.1007/s11096-024-01742-w] [Medline: 38734867]
7. Adler JL, Gurley K, Rosen CL, Wolfe RE, Grossman SA. Assessing resident and attending error and adverse events in the emergency department. Am J Emerg Med 2022 Apr;54:228-231. [doi: 10.1016/j.ajem.2022.01.015] [Medline: 35182916]
8. Katzman BD, van der Pol CB, Soyer P, Patlas MN. Artificial intelligence in emergency radiology: a review of applications and possibilities. Diagn Interv Imaging 2023 Jan;104(1):6-10. [doi: 10.1016/j.diii.2022.07.005] [Medline: 35933269]
9. Berg HT, van Bakel B, van de Wouw L, et al. ChatGPT and generating a differential diagnosis early in an emergency department presentation. Ann Emerg Med 2024 Jan;83(1):83-86. [doi: 10.1016/j.annemergmed.2023.08.003] [Medline: 37690022]
10. Williams CYK, Miao BY, Kornblith AE, Butte AJ. Evaluating the use of large language models to provide clinical recommendations in the emergency department. Nat Commun 2024 Oct 8;15(1):8236. [doi: 10.1038/s41467-024-52415-1] [Medline: 39379357]
11. Petrella RJ. The AI future of emergency medicine. Ann Emerg Med 2024 Aug;84(2):139-153. [doi: 10.1016/j.annemergmed.2024.01.031] [Medline: 38795081]
12. Kachman MM, Brennan I, Oskvarek JJ, Waseem T, Pines JM. How artificial intelligence could transform emergency care. Am J Emerg Med 2024 Jul;81:40-46. [doi: 10.1016/j.ajem.2024.04.024] [Medline: 38663302]
13. Rojas M, Rojas M, Burgess V, Toro-Pérez J, Salehi S. Exploring the performance of ChatGPT versions 3.5, 4, and 4 with vision in the Chilean Medical Licensing Examination: observational study. JMIR Med Educ 2024 Apr 29;10:e55048. [doi: 10.2196/55048] [Medline: 38686550]
14. Flores-Cohaila JA, García-Vicente A, Vizcarra-Jiménez SF, et al. Performance of ChatGPT on the Peruvian National Licensing Medical Examination: cross-sectional study. JMIR Med Educ 2023 Sep 28;9:e48039. [doi: 10.2196/48039] [Medline: 37768724]
15. Muller ES, Harik P, Margolis M, Clauser B, McKinley D, Boulet JR. An examination of the relationship between clinical skills examination performance and performance on USMLE Step 2. Acad Med 2003 Oct;78(10 Suppl):S27-S29. [doi: 10.1097/00001888-200310001-00009] [Medline: 14557087]
16. Stratton TD, Elam CL, Murphy-Spencer AE, Quinlivan SL. Emotional intelligence and clinical skills: preliminary results from a comprehensive clinical performance examination. Acad Med 2005 Oct;80(10 Suppl):S34-S37. [doi: 10.1097/00001888-200510001-00012] [Medline: 16199454]
17. Hur Y, Kim S, Park JH, Cho AR, Choi CJ. Changes in medical students' patient-centeredness attitudes by implementation of clinical performance examination. Korean J Med Educ 2014 Jun;26(2):99-106. [doi: 10.3946/kjme.2014.26.2.99] [Medline: 25805196]
18. Jang SS, Seo JH, Cho GJ, Hong SC, Woo HO. Correlation of communication skills for emotional empathy and academic achievement on clinical performance examinations. Korean J Med Educ 2010 Jun;22(2):121-130. [doi: 10.3946/kjme.2010.22.2.121] [Medline: 25813811]
19. Shamil E, Ravi P, Mistry D. 100 Cases in Emergency Medicine and Critical: CRC Press; 2018.
20. Paslı S, Şahin AS, Beşer MF, Topçuoğlu H, Yadigaroğlu M, İmamoğlu M. Assessing the precision of artificial intelligence in ED triage decisions: Insights from a study with ChatGPT. Am J Emerg Med 2024 Apr;78:170-175. [doi: 10.1016/j.ajem.2024.01.037] [Medline: 38295466]
21. Sarbay İ, Berikol GB, Özturan İ. Performance of emergency triage prediction of an open access natural language processing based chatbot application (ChatGPT): a preliminary, scenario-based cross-sectional study. Turk J Emerg Med 2023;23(3):156-161. [doi: 10.4103/tjem.tjem_79_23] [Medline: 37529789]
22. Günay S, Öztürk A, Özerol H, Yiğit Y, Erenler AK. Comparison of emergency medicine specialist, cardiologist, and chat-GPT in electrocardiography assessment. Am J Emerg Med 2024 Jun;80:51-60. [doi: 10.1016/j.ajem.2024.03.017] [Medline: 38507847]
23. Rosen S, Saban M. Evaluating the reliability of ChatGPT as a tool for imaging test referral: a comparative study with a clinical decision support system. Eur Radiol 2024 May;34(5):2826-2837. [doi: 10.1007/s00330-023-10230-0] [Medline: 37828297]
24. Kim BJ, Sung JJ, Park HK, Seo DW, Chung CS, Yoon BW. Clinical performance examination utilizing standardized patients in board examination: based on the board examination of korean neurological association for three years. Korean J Med Educ 2011 Jun;23(2):127-135. [doi: 10.3946/kjme.2011.23.2.127] [Medline: 25812561]
25. Hindelang M, Sitaru S, Zink A. Transforming health care through chatbots for medical history-taking and future directions: comprehensive systematic review. JMIR Med Inform 2024 Aug 29;12:e56628. [doi: 10.2196/56628] [Medline: 39207827]
26. Maida E, Moccia M, Palladino R, et al. ChatGPT vs. neurologists: a cross-sectional study investigating preference, satisfaction ratings and perceived empathy in responses among people living with multiple sclerosis. J Neurol 2024 Jul;271(7):4057-4066. [doi: 10.1007/s00415-024-12328-x] [Medline: 38568227]
27. Kim SH, Tae JH, Chang IH, et al. Changes in patient perceptions regarding ChatGPT-written explanations on lifestyle modifications for preventing urolithiasis recurrence. Digit Health 2023;9:20552076231203940. [doi: 10.1177/20552076231203940] [Medline: 37780059]

XSL•FO
RenderX

28. Wang C, Liu S, Yang H, Guo J, Wu Y, Liu J. Ethical considerations of using ChatGPT in health care. J Med Internet Res 2023 Aug 11;25:e48009. [doi: 10.2196/48009] [Medline: 37566454]
29. Duffourc M, Gerke S. Generative AI in health care and liability risks for physicians and safety concerns for patients. JAMA 2023 Jul 25;330(4):313-314. [doi: 10.1001/jama.2023.9630] [Medline: 37410497]
30. Cestonaro C, Delicati A, Marcante B, Caenazzo L, Tozzo P. Defining medical liability when artificial intelligence is applied on diagnostic algorithms: a systematic review. Front Med (Lausanne) 2023;10:1305756. [doi: 10.3389/fmed.2023.1305756] [Medline: 38089864]
31. Dave T, Athaluri SA, Singh S. ChatGPT in medicine: an overview of its applications, advantages, limitations, future prospects, and ethical considerations. Front Artif Intell 2023;6:1169595. [doi: 10.3389/frai.2023.1169595] [Medline: 37215063]
32. de Hond AAH, Leeuwenberg AM, Hooft L, et al. Guidelines and quality criteria for artificial intelligence-based prediction models in healthcare: a scoping review. NPJ Digit Med 2022 Jan 10;5(1):2. [doi: 10.1038/s41746-021-00549-7] [Medline: 35013569]
33. Minssen T, Vayena E, Cohen IG. The challenges for regulating medical use of ChatGPT and other large language models. JAMA 2023 Jul 25;330(4):315-316. [doi: 10.1001/jama.2023.9651] [Medline: 37410482]
34. Denecke K, May R, Rivera Romero O, LLMHealthGroup. Potential of large language models in health care: Delphi study. J Med Internet Res 2024 May 13;26:e52399. [doi: 10.2196/52399] [Medline: 38739445]
35. Abd-Alrazaq A, AlSaad R, Alhuwail D, et al. Large language models in medical education: opportunities, challenges, and future directions. JMIR Med Educ 2023 Jun 1;9:e48291. [doi: 10.2196/48291] [Medline: 37261894]
36. Wu Y, Zheng Y, Feng B, Yang Y, Kang K, Zhao A. Embracing ChatGPT for medical education: exploring its impact on doctors and medical students. JMIR Med Educ 2024 Apr 10;10:e52483. [doi: 10.2196/52483] [Medline: 38598263]
37. Xu T, Weng H, Liu F, et al. Current status of ChatGPT use in medical education: potentials, challenges, and strategies. J Med Internet Res 2024 Aug 28;26:e57896. [doi: 10.2196/57896] [Medline: 39196640]
38. Zhui L, Fenghe L, Xuehu W, Qining F, Wei R. Ethical considerations and fundamental principles of large language models in medical education: viewpoint. J Med Internet Res 2024 Aug 1;26:e60083. [doi: 10.2196/60083] [Medline: 38971715]
39. Buchholz MB. Patterns of empathy as embodied practice in clinical conversation-a musical dimension. Front Psychol 2014;5:349. [doi: 10.3389/fpsyg.2014.00349] [Medline: 24817855]

Abbreviations

AI: artificial intelligence
CPX: clinical performance examination
GP: general practitioner
LLM: large language model

Edited by A Castonguay; submitted 06.11.24; peer-reviewed by D Sundemo, M Elbattah; revised version received 13.05.25; accepted 23.05.25; published 17.07.25.

Please cite as:
Park C, An MH, Hwang G, Park RW, An J
Clinical Performance and Communication Skills of ChatGPT Versus Physicians in Emergency Medicine: Simulated Patient Study
JMIR Med Inform 2025;13:e68409
URL: https://medinform.jmir.org/2025/1/e68409
doi:10.2196/68409

© ChulHyoung Park, Min Ho An, Gyubeom Hwang, Rae Woong Park, Juho An. Originally published in JMIR Medical Informatics (https://medinform.jmir.org), 17.7.2025. This is an open-access article distributed under the terms of the Creative Commons Attribution License (https://creativecommons.org/licenses/by/4.0/), which permits unrestricted use, distribution, and reproduction in any medium, provided the original work, first published in JMIR Medical Informatics, is properly cited. The complete bibliographic information, a link to the original publication on https://medinform.jmir.org/, as well as this copyright and license information must be included.

XSL•FO
RenderX

Evaluation of ChatGPT-4 as an Online Outpatient Assistant in Puerperal Mastitis Management: Content Analysis of an Observational Study

Fatih Dolu[1], MD; Oğuzhan Fatih Ay[2], MD; Aydın Hakan Kupeli[2], MD; Enes Karademir[3], MD; Muhammed Huseyin Büyükavcı[3], MD

[1]Department of Surgical Oncology, Kahramanmaras Necip Fazıl City Hospital, Kahramanmaras, Turkey

[2]Department of General Surgery, Kahramanmaras Necip Fazıl City Hospital, Merkez, Erkenez Mh., Recep Tayyip Erdoğan Bulvarı 12. Km, Kahramanmaras, Turkey

[3]Department of General Surgery, Bursa Yuksek Ihtisas Egitim Ve Arastirma Hastanesi, Bursa, Turkey

Corresponding Author:
Oğuzhan Fatih Ay, MD
Department of General Surgery, Kahramanmaras Necip Fazıl City Hospital, Merkez, Erkenez Mh., Recep Tayyip Erdoğan Bulvarı 12. Km, Kahramanmaras, Turkey

Abstract

Background: The integration of artificial intelligence (AI) into clinical workflows holds promise for enhancing outpatient decision-making and patient education. ChatGPT, a large language model developed by OpenAI, has gained attention for its potential to support both clinicians and patients. However, its performance in the outpatient setting of general surgery remains underexplored.

Objective: This study aimed to evaluate whether ChatGPT-4 can function as a virtual outpatient assistant in the management of puerperal mastitis by assessing the accuracy, clarity, and clinical safety of its responses to frequently asked patient questions in Turkish.

Methods: Fifteen questions about puerperal mastitis were sourced from public health care websites and online forums. These questions were categorized into general information (n=2), symptoms and diagnosis (n=6), treatment (n=2), and prognosis (n=5). Each question was entered into ChatGPT-4 (September 3, 2024), and a single Turkish-language response was obtained. The responses were evaluated by a panel consisting of 3 board-certified general surgeons and 2 general surgery residents, using five criteria: sufficient length, patient-understandable language, accuracy, adherence to current guidelines, and patient safety. Quantitative metrics included the DISCERN score, Flesch-Kincaid readability score, and inter-rater reliability assessed using the intraclass correlation coefficient (ICC).

Results: A total of 15 questions were evaluated. ChatGPT's responses were rated as "excellent" overall by the evaluators, with higher scores observed for treatment- and prognosis-related questions. A statistically significant difference was found in DISCERN scores across question types (P=.01), with treatment and prognosis questions receiving higher ratings. In contrast, no significant differences were detected in evaluator-based ratings (sufficient length, understandability, accuracy, guideline compliance, and patient safety), *JAMA* benchmark scores, or Flesch-Kincaid readability levels (P>.05 for all). Interrater agreement was good across all evaluation parameters (ICC=0.772); however, agreement varied when assessed by individual criteria. Correlation analyses revealed no significant overall associations between subjective ratings and objective quality measures, although a strong positive correlation between literature compliance and patient safety was identified for one question (r=0.968, P<.001).

Conclusions: ChatGPT demonstrated adequate capability in providing information on puerperal mastitis, particularly for treatment and prognosis. However, evaluator variability and the subjective nature of assessments highlight the need for further optimization of AI tools. Future research should emphasize iterative questioning and dynamic updates to AI knowledge bases to enhance reliability and accessibility.

(JMIR Med Inform 2025;13:e68980) doi:10.2196/68980

KEYWORDS

puerperal mastitis; Artificial intelligence; ChatGPT; response quality; patient safety; DISCERN score; Flesch-Kincaid readability; treatment adherence; general surgery outpatient clinics; AI

XSL•FO
RenderX

Introduction

Puerperal mastitis, also known as lactation mastitis, is a disorder that affects approximately 30% of breastfeeding women and may vary from mild inflammation to bacterial abscess formation [1]. This disease, which adversely affects breastfeeding, is monitored by the World Health Organization (WHO) and represents a substantial proportion of outpatient clinic applications in general surgery [2,3].

Artificial intelligence (AI)-based systems are currently regarded as capable of enhancing the workflow and aiding the decision-making process [4]. The health care system, particularly in outpatient management, aims to alleviate the patient burden and thereby enhance patient satisfaction [5]. Recent studies have shown that ChatGPT is capable of providing accurate differential diagnoses in 93.3% of common clinical scenarios, and its responses have achieved high accuracy in fields such as retinal diseases, gynecology, and hepatic disorders. These findings underscore the expanding role of AI-powered tools in enhancing diagnostic reasoning and clinical communication across a wide spectrum of medical disciplines [6-8]. In the future, AI is expected to progress as a conduit between clinical practice and data, thereby enhancing patient care and operations [9].

This study aimed to evaluate whether ChatGPT-4 could function as a virtual outpatient assistant in the management of puerperal mastitis. We assessed the content of its responses in Turkish to commonly asked patient questions, focusing on their adequacy, clarity, adherence to medical literature, and potential safety implications.

Methods

Study Design and Hypotheses

In this study, we aimed to evaluate whether ChatGPT can function as a competent assistant in general surgery outpatient settings by managing frequently encountered clinical conditions such as puerperal mastitis. The rationale behind this study is based on the dual expectation from ChatGPT: to provide clinically reliable information grounded in current medical literature and to effectively communicate this information in a clear, understandable manner suitable for patient interaction.

ChatGPT-4 was selected as the AI model for evaluation due to its widespread adoption in recent health-related studies and its extensive documentation in the current literature. Using ChatGPT-4 allowed for comparability with prior research, ensuring consistency and alignment with similar investigations examining large language models' (LLMs') performance in medical information delivery.

Our study was guided by three hypotheses: (1) the responses provided by ChatGPT regarding puerperal mastitis are adequate for daily clinical practice, (2) the quality of responses varies depending on the context and category of the question, (3) using language that is easier to understand may reduce adherence to current clinical literature and accuracy, thereby potentially compromising patient safety.

Ethics committee approval was not sought for this study, as no clinical or personal information about patients was used. However, preliminary permission was obtained from the affiliated hospital.

Question Identification

Fifteen of the most frequently asked and clinically relevant questions about puerperal mastitis were identified through a review of publicly available health care websites, patient forums, and social media platforms. The decision to include 15 questions was based on a review of similar studies in the literature that used a comparable sample size to allow for focused qualitative and quantitative evaluation. This number was deemed sufficient to simulate a realistic outpatient consultation experience and to provide variability across clinical themes.

The questions were categorized to reflect the breadth of clinical concerns typically encountered in general surgery outpatient settings. These categories were general information (n=2), symptoms and diagnosis (n=6), treatment (n=2), and prognosis (n=5). Categorization aimed to allow structured evaluation across different domains of clinical relevance.

To reflect the linguistic and cultural context of our primary patient population, all questions were written in Turkish. The questions were then input into ChatGPT-40 mini, an AI chatbot, on September 3, 2024. A newly created user account was used to ensure that no prior interactions influenced the generated responses. The system was accessed under a standard free-tier usage scenario, without premium settings, plugins, or enterprise features enabled. This setup was intended to simulate how a general user or outpatient might realistically interact with the tool. Each question was entered only once, without any follow-up or clarification prompts. Responses were recorded without modification (refer to Multimedia Appendix 1 and Multimedia Appendix 2).

Response Evaluation

The responses generated by ChatGPT were evaluated by a panel of 5 medical professionals, comprising 3 board-certified general surgeons (OFA, FD, and AHK) and 2 general surgery residents (MHB and EK). Detailed evaluation scores and comparative analyses are provided in Multimedia Appendix 3 and Multimedia Appendix 4.

Each response was independently scored using a 5-point Likert scale (1=poor and 5=excellent) according to the following 5 criteria: (1) sufficient length, (2) use of language understandable to the patient, (3) accuracy in answering the inquiry, (4) compliance with the most recent clinical guidelines, (5) patient safety. These criteria were selected based on methodologies used in similar studies within the literature that evaluated AI-based responses in medical contexts. The aim was to holistically capture both the technical validity and the patient communication aspects of the responses.

Based on total scores, responses were classified as (1) 5 - 10: inadequate, (2) 11 - 15: average, (3) 16 - 20: adequate, and (4) 21 - 25: excellent.

XSL•FO
RenderX

Objective Assessment Tools

To further ensure objectivity and align with methodologies frequently used in similar literature evaluating AI-generated medical information, we used three standardized tools:

DISCERN Instrument

DISCERN is a standardized and validated tool developed by the University of Oxford for assessing the quality of consumer health information, particularly regarding treatment choices. Widely cited in the evaluation of online medical content, it consists of 15 questions that evaluate the publication's reliability, objectivity, and clarity in describing treatment options. Each item is rated on a 5-point scale. Total scores categorize information quality as very poor (<27), poor (27-38), fair (39-50), good (51-62), and excellent (63-75) [10].

Journal of the American Medical Association Benchmark Criteria

Published by the *Journal of the American Medical Association* (*JAMA*), this benchmark is a qualitative framework used to assess the credibility of online health information. It includes four domains: authorship (clearly identified sources), attribution (references to content sources), disclosure (ownership and conflicts of interest), and currency (dates of publication or last update). In our study, the *JAMA* benchmark score was found to be zero, which reflects an inherent limitation of ChatGPT's output—it does not include cited authors, publication dates, or institutional disclosure information in its responses. This has similarly been observed in other studies evaluating AI-generated health content and is a recognized limitation of current language models [11].

Flesch-Kincaid Grade Level Test

This tool was used to assess the complexity of language in the ChatGPT responses. The readability score was calculated using the following formula: Grade Level=(0.39× Total Sentences/Total Words)+(11.8× Total Words/Total Syllables)−15.59 to assess the complexity of language used by ChatGPT [12]. This assessment evaluates text understanding and target audience appropriateness; scores ranging from 0 to 5 indicate primary school level, 6 to 8 indicate secondary school level, 9 to 12 indicate high school level, and 13 and above indicate university level.

Statistical Analysis

The normality of the data distribution was examined using the Shapiro-Wilk test. For the comparison of evaluator scores across more than 2 independent groups, one-way ANOVA and least significant difference multiple comparison tests were used for features showing normal distribution, while the Kruskal-Wallis test and all-pairwise multiple comparison tests were used for non-normally distributed features. Interobserver agreement among the 5 doctors for each parameter was measured using the intraclass correlation coefficient (ICC) (single measure and two-way random model). ICC values were classified as follows: "excellent" (above 0.90), "good" (0.75 - 0.90), "moderate" (0.50 - 0.75), and "poor" (less than 0.50) [13]. The relationships between the question scales were analyzed using the Spearman correlation coefficient. A correlation coefficient between 0.8 and 1 indicates a very strong relationship, values between 0.6 and 0.8 represent a strong relationship, values between 0.4 and 0.6 indicate a moderate relationship, and values between 0.2 and 0.4 signify a weak relationship. Differences between scores within the questions were examined using the Friedman test, with post-hoc tests corrected using the Bonferroni method. Descriptive statistics are presented as mean (SD) for numerical variables, and as counts and percentages for categorical variables. Statistical analyses were performed using SPSS for Windows (version 24.0; IBM), and statistical significance was set at $P<.05$.

Ethical Considerations

This study did not involve human participants, identifiable personal data, clinical interventions, or medical record review; therefore, approval from an institutional review board or ethics committee was not required. In accordance with institutional and national guidelines governing noninterventional research, studies based solely on publicly available, nonidentifiable content—such as online health information and AI-generated responses—are exempt from ethics committee review. Nevertheless, prior administrative permission was obtained from Kahramanmaras Necip Fazıl City Hospital before the commencement of the study.

Results

Differences in scores were analyzed according to the clinical categories of the questions and the evaluation methods (Table 1). A statistically significant difference was observed in DISCERN scores across question types (general information, symptoms and diagnosis, treatment, and prognosis) ($P=.01$). Treatment and prognosis questions received higher DISCERN ratings compared to general information and symptom/diagnosis questions ($P<.05$). In contrast, no significant differences were detected in evaluator-based ratings (sufficient length, understandability, accuracy, guideline compliance, and patient safety), *JAMA* benchmark scores, or Flesch-Kincaid readability levels ($P>.05$ for all comparisons).

XSL•FO
RenderX

Table . Distribution of subjective and objective evaluation scores across different clinical question types.

Score type	General information (n=2), mean (SD); median (IQR)	Symptoms and diagnosis (n=6), mean (SD); median (IQR)	Treatment (n=2), mean (SD); median (IQR)	Prognosis (n=5), mean (SD); median (IQR)	Total, mean (SD); median (IQR)	*P* value
Average ratings of raters	22.7 (0.42); 22.7	22.57 (1.3); 23.3	23.3 (0.14); 23.3	22.64 (0.5); 23	22,71 (0.86); 23	.546[a]
DISCERN	23 (8.49); 23	24.83 (6.37); 27.5	31 (0); 30.8	30.8 (0.45); 31	27.40 (5.59); 30	.014[b]
JAMA [c]	0 (0); 0	0 (0); 0	0 (0); 0	0 (0); 0	0 (0); 0	nc[d]
Flesch-Kincaid	17.25 (2.05); 17.25	14.65 (0.96); 17.95	17.95 (3.61); 15.86	15.86 (1.52); 15.4	15.84 (1.94); 15.4	.160[b]

[a]*P* value obtained from ANOVA test.

[b]*P* value obtained from the Kruskal-Wallis test.

[c]*JAMA*: *Journal of the American Medical Association*.

[d]nc: no computed.

Table 2 presents the interrater agreement and score distribution across key evaluation criteria. The overall ICC across all parameters was 0.772, indicating good consistency among evaluators. When assessed individually, moderate agreement was observed for understandable language (ICC=0.519) and total scores (ICC=0.570), whereas sufficient length (ICC=0.400), accuracy (ICC=0.405), compliance with literature (ICC=0.414), and patient safety (ICC=0.400) demonstrated poor agreement. Statistically significant differences among evaluators were found for sufficient length, accuracy, compliance with literature, and patient safety (all *P*<.001), suggesting subjective variability in scoring across these domains.

Table . Comparison of evaluator scores across key assessment criteria with interrater agreement values.

Assessment criteria	Enes Karademir, mean[a] (SD); median (IQR)	Fatih Dolu, mean (SD); median (IQR)	Aydın Hakan Kupeli, mean (SD); median (IQR)	Hüseyin Buyukavci, mean (SD); median (IQR)	Oguzhan Fatih AY, mean (SD); median (IQR)	*P*[b] value	ICC[c]
Sufficient length	4.33 (0.49); 4.00 (4.00-5.00)	4.53 (0.52); 5.00 (4.00-5.00)	4.8 (0.41); 5.00 (5.00-5.00)	4.2 (0.56); 4.00 (4.00-4.50)	4.87 (0.35); 5.00 (5.00-5.00)	.001[abcdd]	0.400
Understandability	4.67 (0.49); 5.00 (4.00-5.00)	4.6 (0.51); 5.00 (4.00-5.00)	4.93 (0.26); 5.00 (5.00-5.00)	4.93 (0.26); 5.00 (5.00-5.00)	4.87 (0.35); 5.00 (5.00-5.00)	.060	0.519
Accuracy	4.07 (0.59); 4.00 (4.00-4.00)	4.73 (0.46); 5.00 (4.50-5.00)	5 (0); 5.00 (5.00-5.00)	3.87 (0.35); 4.00 (4.00-4.00)	4.87 (0.52); 5.00 (5.00-5.00)	<.001[abcd]	0.405
Compliance with literature	3.07 (0.59); 3.00 (3.00-3.00)	4.47 (0.52); 4.00 (4.00-5.00)	4.87 (0.35); 5.00 (5.00-5.00)	3.87 (0.35); 4.00 (4.00-4.00)	4.87 (0.52); 5.00 (5.00-5.00)	<.001[abc]	0.414
Patient safety	4.73 (0.46); 5.00 (4.50-5.00)	4.67 (0.49); 5.00 (4.00-5.00)	4.93 (0.26); 5.00 (5.00-5.00)	3.93 (0.26); 4.00 (4.00-4.00)	4.87 (0.35); 5.00 (5.00-5.00)	.001[abcd]	0.400
Total	20.87 (2); 21.00 (20.50-22.00)	23 (1.13); 23.00 (22.00-24.00)	24.53 (0.64); 25.00 (24.00-25.00)	20.8 (1.15); 21.00 (20.50-21.50)	24.33 (1.91); 25.00 (25.00-25.00)	.001[abcd]	0.570

[a]Means followed by distinct small letters (a, b, c, and d) in the same line are significantly different (*P* <.05).

[b]*P* value obtained from the Kruskal-Wallis test.

[c]ICC: intra-correlation coefficient.

[d]Superscript letters (a, b, c, d, and ab) indicate results of pairwise comparisons. Means sharing the same letter are not significantly different (*P*<.05). For example, “ab” denotes no significant difference from both “a” and “b” groups.

Table 3 shows the evaluator-based scoring patterns across different clinical categories. The overall agreement was poor (ICC=0.199) when clinical categories were not considered separately. However, moderate agreement was found for general information (ICC=0.537) and prognosis-related questions (ICC=0.648), while symptom-based questions demonstrated good agreement (ICC=0.828). Treatment-related questions exhibited moderate consistency (ICC=0.654). These findings suggest that evaluator agreement was strongest for symptom-related questions and weakest for general information questions. Statistically significant differences between evaluators were observed across all clinical categories (*P*<.05).

XSL•FO
RenderX

Table . Analysis of rater agreement and score variations across different clinical question types.

Scope	Enes Karademir, mean[a] (SD); median (IQR)	Fatih Dolu, mean (SD); median (IQR)	Hakan Kupeli, mean (SD); median (IQR)	Hüseyin Buyukavci, mean (SD); median (IQR)	Oguzhan Ay, mean (SD); median (IQR)	Total, mean (SD); median (IQR)	*P*[b] value	ICC[c]
General information	21.5 (0.71); 21.5 (21-21)	22.5 (0.71); 22.5 (22-22)	24 (1.41); 24 (23-24)	20.5 (0.71); 20.5 (20-20)	25 (0); 25 (25-25)	22.7 (1.83); 22.5	.015[abcd]	0.537
Prognosis	21.4 (1.14); 21 (21-22)	22.4 (0.89); 22 (22-22)	24.8 (0.45); 25 (25-25)	20.2 (1.64); 21 (19-21)	24.4 (1.34); 25 (25-25)	22.64 (2.08); 22	<.001[abc]	0.648
Symptoms	19.83 (2.71); 20 (17-21)	23.5 (1.38); 24 (23-24)	24.5 (0.55); 24.5 (24-24)	21.17 (0.75); 21 (21-21)	23.83 (2.86); 25 (25-25)	22.57 (2.53); 24	.001[ab]	0.828
Treatment	22 (1.41); 22 (21-22)	23.5 (0.71); 23.5 (23-23)	24.5 (0.71); 24.5 (24-24)	21.5 (0.71); 21.5 (21-21)	25 (0); 25 (25-25)	23.3 (1.57); 23.5	.031[ab]	0.654

[a]Means followed by distinct small letters (a, b, c, and d) in the same line are significantly different ($P < .05$).

[b]*P* value obtained from Kruskal-Wallis test.

[c]ICC: intraclass correlation coefficient.

[d]Means followed by different superscript letters (a, b, and c) in the same row are significantly different ($P<.05$). The notation "ab" indicates no significant difference from both "a" and "b" groups; "bc" indicates no significant difference from both "b" and "c"; and "abc" indicates no significant difference from groups "a," "b," and "c."

One of the key hypotheses of this study was that the use of highly understandable language might be inversely related to patient safety and adherence to clinical guidelines. Correlation analyses were performed to investigate these associations. Table 4 summarizes the correlations between evaluator ratings for understandability, literature compliance, and patient safety across individual questions, reflecting subjective expert assessments. Table 5 presents the correlation between these evaluator-based parameters and objective assessment tools (DISCERN scores and Flesch-Kincaid readability scores). While no statistically significant overall correlations were found, a strong positive correlation between literature compliance and patient safety was observed for question 8 ($r=0.968$ and $P<.001$), suggesting that in certain contexts, enhanced clinical accuracy may directly benefit patient safety.

XSL•FO
RenderX

Table . Correlation between evaluator-rated parameters: understandability, literature compliance, and patient safety across questions.

Question	Understandability mean (SD); median[a] (IQR)	Literature compliance, mean (SD); median (IQR)	Patient safety, mean (SD); median (IQR)	Literature compliance and understandability, r[b]	Patient safety and understandability, r	Literature compliance and patient safety, r	[c]P^1 value	P^2 value
1	5 (0); 5.0 (5.0-5.0)	4 (0.71); 4.0 (4.0-4.0)	4.4 (0.55); 4.0 (4.0-5.0)	NC	NC	NC	.124	.075
2	4.8 (0.45); 5.0 (5.0-5.0)	4.2 (0.84); 4.0 (4.0-5.0)	4.8 (0.45 5.0 (5.0-5.0)	0.186	−0.250	0.186	.347	—
3	5 (0); 5 (5.0-5.0)	4.4 (0.89); 5 (4.0-5.0)	4.8 (0.45); 5 (5.0-5.0)	NC	NC	0.395	.266	—
4	4.4 (0.55); 4 (4.0-5.0)	3.6 (1.14); 4 (3.0-4.0)	4.4 (0.55); 4 (4.0-5.0)	0.740	0.167	0.152	.107	.0952
5	5 (0); 5 (5.0-5.0)	4.6 (0.55); 5 (4.0-5.0)	4.6 (0.55); 5 4.0-5.0	NC	NC	0.167	.406	—
6	4.8 (0.45); 5 (5.0-5.0)	4.2 (0.84); 4 (4.0-5.0)	4.6 (0.55); 5 (4.0-5.0)	0.745	0.612	0.761	.073	.087
7	5 (0); 5 (5.0-5.0)	4.4 (0.89); 5.0 (4.0-5.0)	4.8 (0.45); 5.0 (5.0-5.0)	NC	NC	0.395	.072	—
8	4.4 (0.55); 4 (4.0-5.0)	4.2 (1.3); 5 (4.0-5.0)	4.6 (0.55); 5 (4.0-5.0)	0.645	0.667	0.968	.406	—
9	4.8 (0.45); 5 (5.0-5.0)	4.6 (0.55); 5 (4.0-5.0)	4.8 (0.45); 5 (5.0-5.0)	0.612	−0.250	0.610	.788	—
10	4.8 (0.45); 5 (5.0-5.0)	4.4 (0.55); 4 (4.0-5.0)	4.8 (0.45); 5 (5.0-5.0)	−0.612	−0.250	0.408	.592	—
11	4.8 (0.45); 5 (5.0-5.0)	4(1); 4 (3.0-5.0)	4.6 (0.89); 5 (5.0-5.0)	0.001	−0.250	0.559	.364	—
12	5 (0); 5 (5.0-5.0)	4.2 (0.84); 4.0 (4.0-5.0)	4.6 (0.55); 5 (4.0-5.0)	NC	NC	0.304	.061	—
13	4.8 (0.45); 5 (5.0-5.0)	4.2 (1.1); 5 (3.0-5.0)	4.4 (0.55); 4 (4.0-5.0)	−0.408	0.400	0.667	.698	—
14	5 (0); 5 (5.0-5.0)	4 (0.71); 4 (4.0-4.0)	4.8 (0.45); 5 (5.0-5.0)	NC	NC	0.100	.027	—
15	4.4 (0.55); 4 (4.0-5.0)	4.4 (0.89); 5 (4.0-5.0)	4.4 (0.55); 5 (4.0-5.0)	0.001	0.167	−0.323	.925	—

[a]Means followed by distinct small letters ([a,b,c, and d]) in the same line are significantly different (P<.05).

[b]*r:* Spearman correlation coefficient.

[c]P^1 value obtained from the Friedman test.

[d]P^2 value obtained from the Kruskal-Wallis test.

[e]NC: non-calculated.

XSL•FO
RenderX

Table . Correlation analysis between DISCERN and Flesch-Kincaid readability scores.

Correlation statistic	DISCERN score	Flesch-Kincaid score
Mean (SD)	27.40 (SD 5.59)	15.84 (SD 1.94)
r[a]	−0.190	−0.127
P value[b]	.498	.653
n[c]	15	15
Correlation (r) with DISCERN	NC[d]	0.057
P value	NC	.840
n	NC	15

[a]r: Spearman correlation coefficient.

[b]*P* values obtained from the Friedman or Kruskal-Wallis tests, as appropriate.

[c]n: number of observations.

[d]NC: not calculated.

Discussion

Principal Findings

This study assessed the competence of ChatGPT in relation to puerperal mastitis. In our evaluation, all evaluators classified the responses provided across the scope of questions as "excellent." The DISCERN scoring system indicated that ChatGPT performs better when answering questions related to treatment and prognosis. The Flesch-Kincaid classification indicated that the responses from ChatGPT were comprehensible at the university graduate level (Table 1).

Statistically significant differences were observed in the scores assigned by evaluators across various criteria—including sufficient length (*P*=.001), accuracy (*P*<.001), adherence to the literature (*P*<.001), and patient safety (*P*<.001)—as well as across different question types, such as general information (*P*=.015), prognosis (*P*<.001), symptoms (*P*=.001), and treatment (*P*=.031). These findings suggest that the evaluation of ChatGPT responses was influenced by the evaluators' individual perspectives, especially for broader and more context-dependent inquiries. The relatively smaller difference among raters in the criterion of understandable language (*P*=.060) suggests that this parameter may be more amenable to objective assessment. Taken together, the inter-rater variability highlights an inherent limitation of subjective evaluation frameworks and underscores the need for the development of more standardized and objective rating tools for assessing AI-generated health content. Establishing validated scoring protocols may improve consistency and reliability in future assessments involving human raters.

Comparison With Prior Work

The literature contains numerous evaluations of ChatGPT's accuracy in response to inquiries about both malignant and benign diseases. AI-generated data has shown precise detection of osteoarthritis, though technical support is still necessary for some specific questions [14]. Data regarding urothelial carcinoma from AI are currently limited, with reliable information mainly focused on the epidemiology and risk factors [15]. In breast cancer oncology treatment, AI offers restricted insights into particular clinical scenarios and postoperative conditions [16]. In the pediatric field, Wei noted that while ChatGPT's performance was adequate for general inquiries, it was insufficient in specific clinical contexts [17]. Our study represents the first assessment of ChatGPT's responses regarding puerperal mastitis, with no existing research available for comparison.

In relation to another one of our hypotheses, in our analysis of the correlation among understandable language, patient safety, and compliance with the literature, we observed a positive correlation between the parameters of compliance and patient safety related to the 8th question, which is focused on symptoms and diagnosis (Table 4). The inability to statistically verify one of our hypotheses may stem from the limited number of questions (n=15) and the subjective nature of the raters' evaluations. Nonetheless, no statistically significant relationship was identified between the DISCERN score, a relatively objective indicator of technical proficiency, and the Flesch-Kincaid Reading Difficulty score, which assesses comprehensibility, for each question (Table 5). However, Al-Ashwal et al [18] indicated that using simple language may result in the omission of critical information regarding disease. Various indexes, such as the Flesch-Kincaid Index, Simple Measure of Gobbledygook index [19], and Gunning Fog Index [17], have been used in the literature to assess readability and understandability. Valencia [20] stated that the AI response might be effective for the Flesch-Kincaid index in the context of kidney donation information and studies related to ChatGPT. He noted that this was a quantitative evaluation and may not encompass all nuances; thus, it may lack generalizability. It is noted that unclear online health information negatively affects patient adherence to treatment [8,21]. We believe that it is essential for the information supplied by ChatGPT to be both precise and comprehensible to patients. At present, it has been argued that ChatGPT has the potential to enhance patient outcomes and health literacy [22]. In our study, we used the Flesch-Kincaid Index and determined that the responses provided by ChatGPT were comprehensible at the university level. While this suggests a high level of linguistic and grammatical complexity, it may limit accessibility for patients

XSL•FO
RenderX

with lower health literacy. Although the Flesch-Kincaid Index has its limitations—particularly in evaluating medical jargon and sentence structure—it remains one of the most widely accepted readability tools in digital health research. Previous studies evaluating AI-generated content have reported similar findings [8,17,23][]. We believe that improving the readability of ChatGPT responses, particularly by simplifying language without compromising medical accuracy, is essential for optimizing patient education and safety.

One of our central hypotheses was that ChatGPT could contribute meaningfully to clinical decision-making and patient management in outpatient settings. Beyond its role in health education and patient information, recent studies have highlighted ChatGPT's emerging potential in various clinical domains. In abdominopelvic surgery, it has been proposed as a tool for enhancing patient-physician communication, preoperative counseling, and postoperative care guidance [24]. Similarly, in gastroenterology, its capacity for triage support, education on endoscopic procedures, and initial interpretation of laboratory findings has been explored, though concerns remain regarding accuracy and source citation [25]. The cardiology field has also recognized its utility for drafting discharge summaries and answering patient queries, particularly in heart failure management and preventive care [26]. Furthermore, in a comparative study within evidence-based dentistry, ChatGPT-4 demonstrated superior performance over other LLMs, particularly in alignment with clinical guidelines, suggesting its value as a supportive assistant in routine decision-making [27]. These findings collectively underline that while ChatGPT is not a replacement for clinical judgment, its structured integration into practice—especially for low-risk guidance and standardized educational content—may enhance efficiency, patient comprehension, and adherence to evidence-based care models. One of the hypotheses of this study was that ChatGPT could contribute meaningfully to clinical decision-making and patient management. However, the integration of AI into health care practices raises several ethical concerns that warrant careful consideration. First, the uncertainty regarding liability in the event of harm resulting from AI-generated recommendations remains unresolved. It is unclear whether responsibility would lie with the clinician, the AI developer, or the institution using the system. This issue has been widely discussed across different fields of medicine, emphasizing the necessity for clear accountability structures [28]. Second, transparency in AI decision-making is a fundamental requirement for clinical trust [28,29]. It is recommended that AI systems not only disclose their involvement in clinical processes but also provide a traceable rationale for their outputs. This approach may help reduce ambiguity related to AI-derived recommendations and enhance professional confidence in their use. Third, algorithmic bias—arising from limitations or imbalances in the datasets used to train AI—can lead to inequitable outcomes for certain patient populations. Although this dimension was not directly evaluated in our study, it is a well-recognized risk and must be considered in future applications of AI in medicine [28,29]. Moreover, long-term dependence on AI may lead to the phenomenon of "automation bias," in which clinicians overly rely on AI recommendations, potentially diminishing their own diagnostic acumen and clinical judgment [30]. This may affect future training and critical thinking in medical education, especially if AI systems are perceived as replacements rather than adjuncts to human expertise.

These considerations underline the need for specialty-specific ethical guidelines that address transparency, accountability, bias mitigation, and appropriate use of AI in clinical practice. While our study found that ChatGPT may provide accurate and comprehensible responses in the context of puerperal mastitis, further ethical and regulatory frameworks are essential to ensure its safe and equitable integration into health care delivery.

Limitations

This study has several notable limitations. First, each question was submitted to ChatGPT only once, and the initial response was evaluated without any iterative prompting or follow-up queries. In real-world clinical settings, both health care professionals and patients often engage in multiturn interactions to clarify ambiguities, which may lead to more comprehensive or accurate outputs. Our single-response approach, while practical for standardization, may not fully capture the potential of conversational AI tools in dynamic outpatient scenarios. Second, the assessment was conducted on a specific version of ChatGPT (GPT-4o mini) at a single time point using the publicly accessible platform. Since LLMs are frequently updated and refined, the findings of this study may not be generalizable to future versions or other AI models. In addition, because the chatbot does not cite references or provide source transparency, its outputs may lack traceability—particularly relevant when considering adherence to clinical guidelines and patient safety. Third, although the evaluation was conducted by a team of general surgeons and surgical residents, the rating process remains subject to individual clinical judgment. Parameters such as "accuracy" or "patient safety"—despite being guided by current literature—may still reflect inherent evaluator bias. Although inter-rater reliability was statistically analyzed, the subjective nature of certain domains introduces variability and limits reproducibility. Finally, the number of questions (n=15) was based on prior literature and feasibility considerations; however, it limits the breadth of topics and clinical diversity that could be assessed. Broader question sets and diverse clinical domains would be valuable in future studies to enhance generalizability.

Conclusion

Our findings indicate that ChatGPT has the potential to serve as an effective assistant in general surgery outpatient settings by providing responses that are not only comprehensible for patients but also largely aligned with current clinical literature. This dual competency—offering medically relevant and literature-consistent information while maintaining clarity—positions ChatGPT as a promising tool in supporting clinical decision-making and enhancing the efficiency of patient management.

To fully realize this potential, future research should focus on improving the consistency and reliability of AI outputs across diverse clinical topics. Further studies should also explore strategies for ensuring up-to-date medical knowledge within

XSL•FO
RenderX

language models and evaluate their integration into real-time clinical workflows. These efforts are essential for safely expanding the role of AI in evidence-based, patient-centered care.

We assessed ChatGPT's performance in addressing questions related to puerperal mastitis, a condition that represents a substantial portion of the workload in general surgery outpatient clinics, in the context of the prospective role of AI in the health care system. Our findings indicate that ChatGPT provides adequate information regarding puerperal mastitis. While the parameters used to assess for understandability have inherent limitations, it is essential to use more comprehensible language to achieve favorable outcomes that may be broadly disseminated within society. There is a need for more comprehensive, technical, and methodologically sound studies to integrate AI into health care systems.

Data Availability

The data supporting the findings of this study are available from the corresponding author upon reasonable request via email.

Conflicts of Interest

None declared.

Multimedia Appendix 1
Turkish and English versions of the questions used in the study. This appendix presents the original Turkish questions submitted to ChatGPT and their English translations, categorized by clinical content.
[DOCX File, 17 KB - medinform_v13i1e68980_app1.docx]

Multimedia Appendix 2
Original Turkish responses generated by ChatGPT. This appendix presents the original, unedited responses generated by ChatGPT (GPT-40 mini) for each of the 15 Turkish-language questions used in the study. These responses were obtained without any postprocessing or follow-up prompts and reflect the artificial intelligence's standalone performance in providing patient-oriented information.
[DOCX File, 42 KB - medinform_v13i1e68980_app2.docx]

Multimedia Appendix 3
Evaluation table containing assessor scores and summary metrics. This appendix includes the scoring data provided by each of the five evaluators, including categorical breakdowns for sufficient length, understandability, accuracy, adherence to guidelines, and patient safety.
[XLSX File, 13 KB - medinform_v13i1e68980_app3.xlsx]

Multimedia Appendix 4
Aggregated evaluator scores by question and comparative analysis. This appendix presents mean scores for each question across the evaluation domains and includes comparative statistical analyses among question categories.
[DOCX File, 17 KB - medinform_v13i1e68980_app4.docx]

References

1. Amir LH, Crawford SB, Cullinane M, Grzeskowiak LE. General practitioners' management of mastitis in breastfeeding women: a mixed method study in Australia. BMC Prim Care 2024 May 10;25(1):161. [doi: 10.1186/s12875-024-02414-4] [Medline: 38730361]
2. Lin YC, Lee YL, Chen YH, Tsao SM, Wang WY. Puerperal mastitis caused by limited community-associated methicillin-resistant Staphylococcus aureus (CA-MRSA) clones. Front Med (Lausanne) 2024;11:1378207. [doi: 10.3389/fmed.2024.1378207] [Medline: 38707192]
3. Wilson E, Woodd SL, Benova L. Incidence of and risk factors for lactational mastitis: a systematic review. J Hum Lact 2020 Nov;36(4):673-686. [doi: 10.1177/0890334420907898] [Medline: 32286139]
4. Secinaro S, Calandra D, Secinaro A, Muthurangu V, Biancone P. The role of artificial intelligence in healthcare: a structured literature review. BMC Med Inform Decis Mak 2021 Apr 10;21(1):125. [doi: 10.1186/s12911-021-01488-9] [Medline: 33836752]
5. Li X, Tian D, Li W, et al. Artificial intelligence-assisted reduction in patients' waiting time for outpatient process: a retrospective cohort study. BMC Health Serv Res 2021 Mar 17;21(1):237. [doi: 10.1186/s12913-021-06248-z] [Medline: 33731096]
6. Liu J, Wang C, Liu S. Utility of ChatGPT in clinical practice. J Med Internet Res 2023 Jun 28;25:e48568. [doi: 10.2196/48568] [Medline: 37379067]

XSL•FO
RenderX

7. Potapenko I, Boberg-Ans LC, Stormly Hansen M, Klefter ON, van Dijk EHC, Subhi Y. Artificial intelligence-based chatbot patient information on common retinal diseases using ChatGPT. Acta Ophthalmol 2023 Nov;101(7):829-831. [doi: 10.1111/aos.15661] [Medline: 36912780]
8. Yeo YH, Samaan JS, Ng WH, et al. Assessing the performance of ChatGPT in answering questions regarding cirrhosis and hepatocellular carcinoma. Clin Mol Hepatol 2023 Jul;29(3):721-732. [doi: 10.3350/cmh.2023.0089] [Medline: 36946005]
9. Scheetz J, Rothschild P, McGuinness M, et al. A survey of clinicians on the use of artificial intelligence in ophthalmology, dermatology, radiology and radiation oncology. Sci Rep 2021 Mar 4;11(1):5193. [doi: 10.1038/s41598-021-84698-5] [Medline: 33664367]
10. Charnock D, Shepperd S, Needham G, Gann R. DISCERN: an instrument for judging the quality of written consumer health information on treatment choices. J Epidemiol Community Health 1999 Feb;53(2):105-111. [doi: 10.1136/jech.53.2.105] [Medline: 10396471]
11. Silberg WM, Lundberg GD, Musacchio RA. Assessing, controlling, and assuring the quality of medical information on the internet: caveant lector et viewor--let the reader and viewer beware. JAMA 1997 Apr 16;277(15):1244-1245. [Medline: 9103351]
12. Gill PS. Prescription painkillers and controlled substances: an appraisal of drug information provided by six US pharmacies. Drug Healthc Patient Saf 2013;5:29-36. [doi: 10.2147/DHPS.S42508] [Medline: 23467668]
13. Koo TK, Li MY. A guideline of selecting and reporting intraclass correlation coefficients for reliability research. J Chiropr Med 2016 Jun;15(2):155-163. [doi: 10.1016/j.jcm.2016.02.012] [Medline: 27330520]
14. Mika AP, Martin JR, Engstrom SM, Polkowski GG, Wilson JM. Assessing ChatGPT responses to common patient questions regarding total hip arthroplasty. J Bone Joint Surg Am 2023;105(19):1519-1526. [doi: 10.2106/JBJS.23.00209] [Medline: 37459402]
15. Łaszkiewicz J, Krajewski W, Tomczak W, et al. Performance of ChatGPT in providing patient information about upper tract urothelial carcinoma. Contemp Oncol (Pozn) 2024;28(2):172-181. [doi: 10.5114/wo.2024.141567] [Medline: 39421706]
16. Stalp JL, Denecke A, Jentschke M, Hillemanns P, Klapdor R. Quality of ChatGPT-generated therapy recommendations for breast cancer treatment in gynecology. Curr Oncol 2024 Jul 1;31(7):3845-3854. [doi: 10.3390/curroncol31070284] [Medline: 39057156]
17. Wei Q, Wang Y, Yao Z, et al. Evaluation of ChatGPT's performance in providing treatment recommendations for pediatric diseases. Pediatric Discovery 2023 Dec;1(3):e42. [doi: 10.1002/pdi3.42]
18. Al-Ashwal FY, Zawiah M, Gharaibeh L, Abu-Farha R, Bitar AN. Evaluating the sensitivity, specificity, and accuracy of ChatGPT-3.5, ChatGPT-4, Bing AI, and Bard against conventional drug-drug interactions clinical tools. Drug Healthc Patient Saf 2023;15:137-147. [doi: 10.2147/DHPS.S425858] [Medline: 37750052]
19. Miao J, Thongprayoon C, Cheungpasitporn W. Assessing the accuracy of ChatGPT on core questions in glomerular disease. Kidney Int Rep 2023 Aug;8(8):1657-1659. [doi: 10.1016/j.ekir.2023.05.014] [Medline: 37547515]
20. Garcia Valencia OA, Thongprayoon C, Miao J, et al. Empowering inclusivity: improving readability of living kidney donation information with ChatGPT. Front Digit Health 2024;6:1366967. [doi: 10.3389/fdgth.2024.1366967] [Medline: 38659656]
21. Tan JY, Tan YC, Yap D. Readability and quality of online patient health information on parotidectomy. J Laryngol Otol 2023 Dec;137(12):1378-1383. [doi: 10.1017/S0022215123000336]
22. Sallam M. ChatGPT utility in healthcare education, research, and practice: systematic review on the promising perspectives and valid concerns. Healthcare (Basel) 2023;11(6). [doi: 10.3390/healthcare11060887] [Medline: 36981544]
23. Subramanian T, Araghi K, Amen TB, et al. Chat generative pretraining transformer answers patient-focused questions in cervical spine surgery. Clin Spine Surg 2024;37(6):E278-E281. [doi: 10.1097/BSD.0000000000001600] [Medline: 38531823]
24. Goglia M, Pace M, Yusef M, et al. Artificial intelligence and ChatGPT in abdominopelvic surgery: a systematic review of applications and impact. In Vivo 2024;38(3):1009-1015. [doi: 10.21873/invivo.13534] [Medline: 38688653]
25. Klang E, Sourosh A, Nadkarni GN, Sharif K, Lahat A. Evaluating the role of ChatGPT in gastroenterology: a comprehensive systematic review of applications, benefits, and limitations. Therap Adv Gastroenterol 2023;16:17562848231218618. [doi: 10.1177/17562848231218618] [Medline: 38149123]
26. Sharma A, Medapalli T, Alexandrou M, Brilakis E, Prasad A. Exploring the role of ChatGPT in cardiology: a systematic review of the current literature. Cureus 2024 Apr;16(4):38800264. [doi: 10.7759/cureus.58936]
27. Giannakopoulos K, Kavadella A, Aaqel Salim A, Stamatopoulos V, Kaklamanos EG. Evaluation of the performance of generative AI large language models ChatGPT, Google Bard, and Microsoft Bing chat in supporting evidence-based dentistry: comparative mixed methods study. J Med Internet Res 2023 Dec 28;25:e51580. [doi: 10.2196/51580] [Medline: 38009003]
28. Wang C, Liu S, Yang H, Guo J, Wu Y, Liu J. Ethical considerations of using ChatGPT in health care. J Med Internet Res 2023 Aug 11;25:e48009. [doi: 10.2196/48009] [Medline: 37566454]
29. Kenig N, Monton Echeverria J, Rubi C. Ethics for AI in plastic surgery: guidelines and review. Aesthetic Plast Surg 2024 Jun;48(11):2204-2209. [doi: 10.1007/s00266-024-03932-3] [Medline: 38456892]

XSL•FO
RenderX

30. Abdullah YI, Schuman JS, Shabsigh R, Caplan A, Al-Aswad LA. Ethics of artificial intelligence in medicine and ophthalmology. Asia Pac J Ophthalmol (Phila) 2021;10(3):289-298. [doi: 10.1097/APO.0000000000000397] [Medline: 34383720]

Abbreviations

AI: artificial intelligence
ICC: intraclass correlation coefficient
***JAMA*:** *Journal of the American Medical Association*
LLM: large language model
WHO: World Health Organization

Edited by A Castonguay; submitted 19.11.24; peer-reviewed by CN Hang, L Zhu, L Bednarczyk, Y Fırat; revised version received 27.04.25; accepted 23.05.25; published 24.07.25.

Please cite as:
Dolu F, Ay OF, Kupeli AH, Karademir E, Büyükavcı MH
Evaluation of ChatGPT-4 as an Online Outpatient Assistant in Puerperal Mastitis Management: Content Analysis of an Observational Study
JMIR Med Inform 2025;13:e68980
URL: https://medinform.jmir.org/2025/1/e68980
doi:10.2196/68980

© Fatih Dolu, Oğuzhan Fatih AY, Aydın Hakan Kupeli, Enes Karademir, Muhammed Huseyin Büyükavcı. Originally published in JMIR Medical Informatics (https://medinform.jmir.org), 24.7.2025. This is an open-access article distributed under the terms of the Creative Commons Attribution License (https://creativecommons.org/licenses/by/4.0/), which permits unrestricted use, distribution, and reproduction in any medium, provided the original work, first published in JMIR Medical Informatics, is properly cited. The complete bibliographic information, a link to the original publication on https://medinform.jmir.org/, as well as this copyright and license information must be included.

XSL•FO
RenderX

Optimizing Thyroid Nodule Management With Artificial Intelligence: Multicenter Retrospective Study on Reducing Unnecessary Fine Needle Aspirations

Jia-Hui Ni[1*], MMed; Yun-Yun Liu[1*], MD; Chao Chen[2*], MD; Yi-Lei Shi[3*], PhD; Xing Zhao[3], PhD; Xiao-Long Li[4], MD; Bei-Bei Ye[1], MMed; Jing-Liang Hu[3], MD; Li-Chao Mou[3], PhD; Li-Ping Sun[1], MD, PhD; Hui-Jun Fu[5], MD; Xiao-Xiang Zhu[6], PhD; Yi-Feng Zhang[7*], MD, PhD; Lehang Guo[1*], MD, PhD; Hui-Xiong Xu[4], MD, PhD

[1]Department of Medical Ultrasound, Shanghai Tenth People's Hospital, Tongji University School of Medicine, YanChang Middle Street 301, Shanghai, China

[2]Department of Thyroid Surgery, Sichuan Provincial People's Hospital, University of Electronic Science and Technology of China, Chengdu, China

[3]Med AI Technology (Wuxi) Co, Ltd, Wuxi, China

[4]Department of Ultrasound, Zhongshan hospital, Institute of Ultrasound in Medicine and Engineering, Fudan University, Shanghai, China

[5]Department of Pathology, Shanghai Tenth People's Hospital, Shanghai, China

[6]Chair of Data Science in Earth Observation, Technical University of Munich, Munich, Germany

[7]Department of Ultrasound, Shanghai General Hospital, Shanghai Jiao Tong University School of Medicine, Shanghai, China

[*]these authors contributed equally

Corresponding Author:
Lehang Guo, MD, PhD
Department of Medical Ultrasound, Shanghai Tenth People's Hospital, Tongji University School of Medicine, YanChang Middle Street 301, Shanghai, China

Abstract

Background: Most artificial intelligence (AI) models for thyroid nodules are designed to screen for malignancy to guide further interventions; however, these models have not yet been fully implemented in clinical practice.

Objective: This study aimed to evaluate AI in real clinical settings for identifying potentially benign thyroid nodules initially deemed to be at risk for malignancy by radiologists, reducing unnecessary fine needle aspiration (FNA) and optimizing management.

Methods: We retrospectively collected a validation cohort of thyroid nodules that had undergone FNA. These nodules were initially assessed as "suspicious for malignancy" by radiologists based on ultrasound features, following standard clinical practice, which prompted further FNA procedures. Ultrasound images of these nodules were re-evaluated using a deep learning–based AI system, and its diagnostic performance was assessed in terms of correct identification of benign nodules and error identification of malignant nodules. Performance metrics such as sensitivity, specificity, and the area under the receiver operating characteristic curve were calculated. In addition, a separate comparison cohort was retrospectively assembled to compare the AI system's ability to correctly identify benign thyroid nodules with that of radiologists.

Results: The validation cohort comprised 4572 thyroid nodules (benign: n=3134, 68.5%; malignant: n=1438, 31.5%). AI correctly identified 2719 (86.8% among benign nodules) and reduced unnecessary FNAs from 68.5% (3134/4572) to 9.1% (415/4572). However, 123 malignant nodules (8.6% of malignant cases) were mistakenly identified as benign, with the majority of these being of low or intermediate suspicion. In the comparison cohort, AI successfully identified 81.4% (96/118) of benign nodules. It outperformed junior and senior radiologists, who identified only 40% and 55%, respectively. The area under the curve (AUC) for the AI model was 0.88 (95% CI 0.85 - 0.91), demonstrating a superior AUC compared with that of the junior radiologists (AUC=0.43, 95% CI 0.36 - 0.50; *P*=.002) and senior radiologists (AUC=0.63, 95% CI 0.55 - 0.70; *P*=.003).

Conclusions: Compared with radiologists, AI can better serve as a "goalkeeper" in reducing unnecessary FNAs by identifying benign nodules that are initially assessed as malignant by radiologists. However, active surveillance is still necessary for all these nodules since a very small number of low-aggressiveness malignant nodules may be mistakenly identified.

Trial Registration: Chinese Clinical Trials Registry ChiCTR2200066755; https://www.chictr.org.cn/showproj.html?proj=171562

(JMIR Med Inform 2025;13:e71740) doi:10.2196/71740

XSL•FO
RenderX

KEYWORDS

thyroid nodules; artificial intelligence; fine needle aspiration; risk stratification; ultrasound

Introduction

The prevalence of thyroid nodules has been consistently high, with a correspondingly high detection rate [1-3]. Notably, only a tiny proportion of these nodules are malignant [4].

In the real world, fine needle aspiration (FNA) has long been the favored diagnostic method in the management of suspicious thyroid nodules [5]. Before that, different regions used various Thyroid Imaging, Reporting, and Data System guidelines to screen suspicious thyroid nodules that need to receive further FNA [6,7]. However, the decision process of the Thyroid Imaging, Reporting, and Data System results in a significant number of unnecessary FNAs performed for benign lesions [8].

Although false-positive cases cannot be entirely avoided, a recent retrospective study has revealed a higher-than-expected rate of benign thyroid nodules identified after FNAs, reaching up to 50%, and consequently, some of them received unnecessary lobectomy or thyroidectomy [9]. Since these invasive procedures carry significant risks, complications, economic burdens, and psychological distress for patients [4], a better decision-making process is needed to avoid unnecessary FNA. Recent advancements in the management of thyroid nodules, including the use of the multimodality US model and the incorporation of molecular markers for more accurate risk stratification, have contributed to enhancing the precision of diagnostic decisions [10,11]. However, some limitations, including operator dependence, low concordance, invasive procedures, and high expenses, restrict their widespread application.

Many recent studies have shown that artificial intelligence (AI) has the potential to improve thyroid cancer detection [12-15]. Through extensive training on large datasets of annotated thyroid nodule ultrasound images, these AI models provide valuable assistance for the differentiation between benign and malignant [16-19]. Under this background, some commercial AI applications have been approved for clinical use.

Nevertheless, due to the indolent nature of thyroid cancer, the problem of overdiagnosis, similar to unnecessary FNA, is becoming a more concerning issue [4]. Most commercial AI applications have been developed to screen for potentially malignant lesions. However, despite their maturity, these AI tools are still challenging to implement in routine clinical practice as replacements in determining the benign or malignant nature of thyroid nodules. Several key barriers hinder their integration into real-world settings, including lack of interpretability in decision-making, potential disruption to clinical workflows, and concerns surrounding regulatory approval and ethical considerations.

To address these challenges, our study used the ITS100 (MedAl Technology) AI system not as a replacement for radiologists, but as a second-opinion tool. In clinical practice, radiologists typically identify potentially malignant nodules and, after obtaining informed consent, proceed with FNA for confirmation. Due to the subjective judgment of radiologists, this workflow inevitably results in some benign nodules undergoing unnecessary FNA.

With the hope of improving the clinical diagnostic workflow to avoid overdiagnosis, we conducted this study to test whether AI could act as a safeguard against overdiagnosis by preventing unnecessary FNAs and to identify the patient populations that may benefit most from its use.

Methods

Overview

This study is a retrospective multicenter study. The validation cohort consists of data from Shanghai Tenth People's Hospital and Sichuan Provincial People's Hospital (dataset 1), and the comparison cohort consists of data from Shanghai Zhongshan Hospital (dataset 2) retrospectively.

Ethical Considerations

This study was approved by the institutional ethics committees of the participating centers (approval SHSY-IEC-5.0/22XJS36/P01). Written informed consent, including a statement of FNA's risks and data collection, was obtained from patients before undergoing FNA. All participant data were de-identified, stored with restricted access, and analyzed anonymously; no financial compensation was provided for participation.

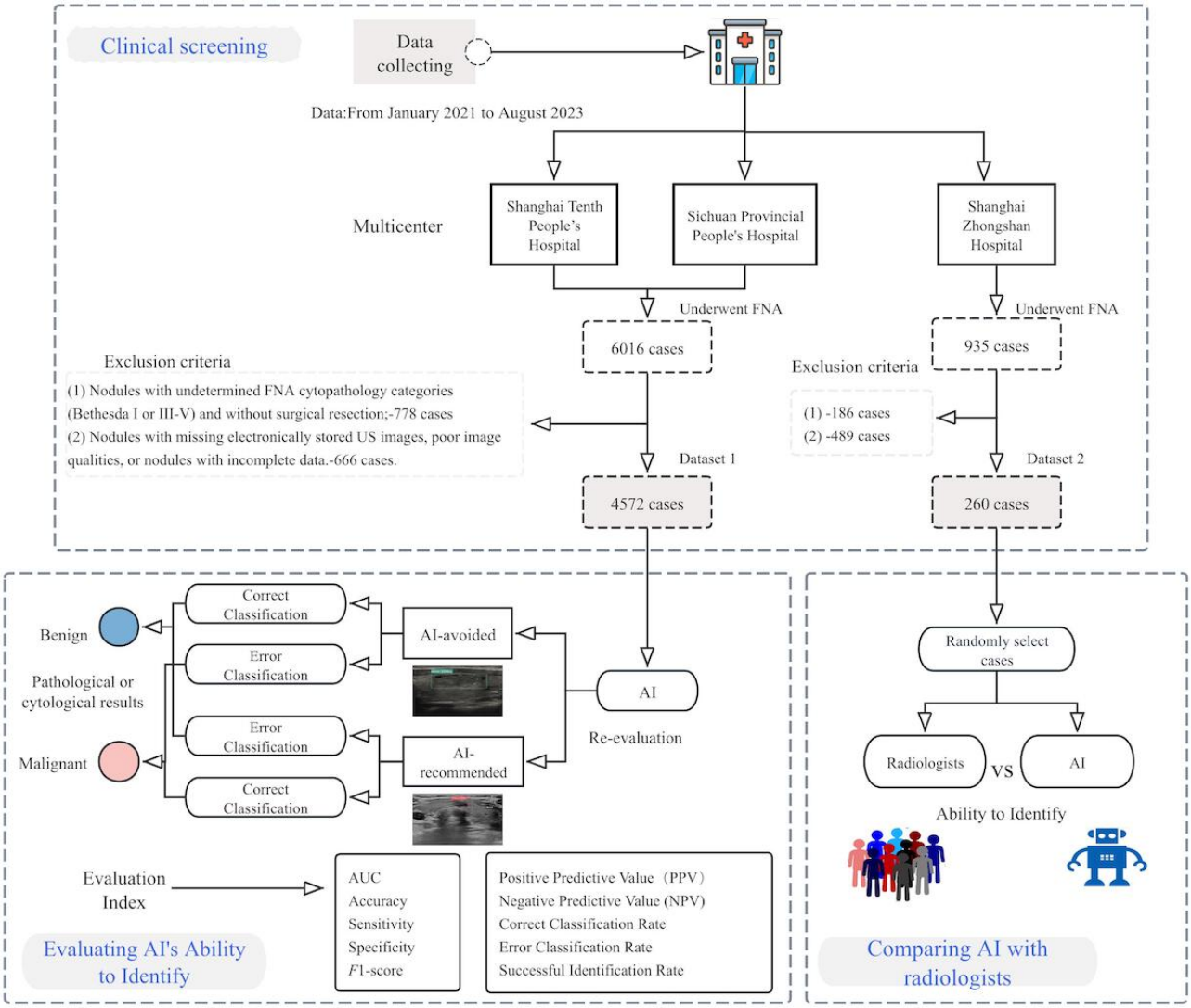
Study Cohorts

Consecutive ultrasound screenings with clear images, complete clinical information, and pathological results were collected from January 2021 to August 2023 at Shanghai Tenth People's Hospital, Sichuan Provincial People's Hospital, and Shanghai Zhongshan Hospital in China. All nodules included in this study were initially assessed as suspicious for malignancy by radiologists based on ultrasound features, following standard clinical practice, which prompted further FNA procedures. A subset of these nodules also received surgical treatment based on clinical assessment and ultrasound evaluation. FNA cytology results were categorized according to the 2017 Bethesda System [20]. Among all eligible cases, a nodule was selected based on the following criteria: if there was only one nodule, it was chosen; if there were multiple nodules with the same malignant risk classification, the one with the largest diameter was selected; if the malignant risk classifications differed, the nodule with the highest malignant risk classification was chosen. The inclusion and exclusion criteria are listed in Textbox 1.

A detailed flowchart of patient selection is presented in Figure 1.

XSL•FO
RenderX

Figure 1. Overview of the study design. AI: artificial intelligence; AUC: area under the curve; FNA: fine needle aspiration.



Textbox 1. Inclusion and exclusion criteria.

Inclusion criteria:

- Patients aged 18 years or older.
- Nodules that underwent fine needle aspiration (FNA) prompted by radiologists' suspicion based on ultrasound assessment.
- Participants underwent FNA or surgical procedures to confirm the pathological results, including cytological or histological findings.
- Bethesda II nodules with follow-up data available for more than 12 months.

Exclusion criteria:

- Nodules with indeterminate FNA cytopathology categories (Bethesda I or III-V) without pathological results.
- Nodules with missing electronically stored ultrasound images, poor image quality, or incomplete clinical data.

Grayscale Ultrasound Examination

All nodules underwent ultrasound examinations within 1 week before FNA. The ultrasound examinations were performed using high-frequency linear transducers of real-time ultrasound systems (Multimedia Appendix 1). At least 2 grayscale ultrasound images for each target nodule (the largest transverse and sagittal planes) were routinely recorded.

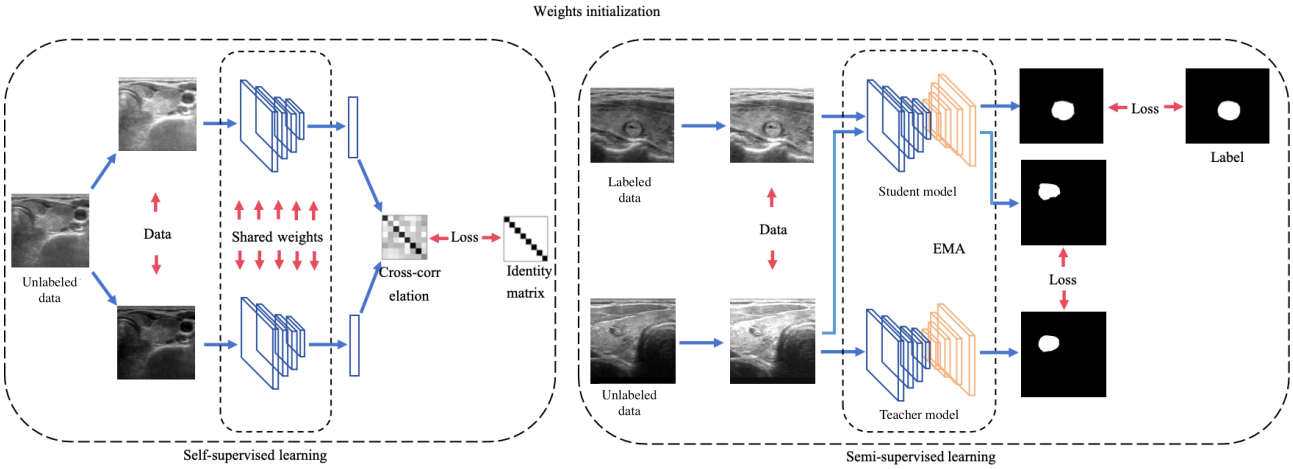
Foundation of the AI Algorithm

It is well known that deep learning models require huge amounts of labeled data. To address this challenge in thyroid nodule recognition, an innovative approach has been developed that combines self-supervised learning [21], transfer learning [22], and semisupervised learning [23]. This strategy significantly reduces the demand for labeled data while maintaining high performance.

XSL•FO
RenderX

With the help of the feature extraction capability of convolutional neural networks, the model accurately fits the complex relationship between the content of ultrasound images and the location and nature of thyroid nodules, thus realizing high-precision recognition of thyroid nodules. The flowchart of development is illustrated in Figure 2.

Figure 2. Flowchart of the procedures in the development of artificial intelligence model for thyroid nodule recognition. EMA: exponential moving average.



The model development process is divided into 2 phases—pretraining and fine-tuning. In the pretraining phase, a self-supervised learning approach is used to train the model's encoder network using abundant unlabeled data to learn complex feature representations of ultrasound images. The training strategies of self-supervised learning are inspired by previous studies [21]. The fine-tuning phase introduces a teacher-student model architecture, where both models share the same structure. This phase proceeds as follows: first, initialization—the encoder networks of both the teacher and student models are initialized with the weights obtained from the pretraining phase. In contrast, the decoder networks start with default weight initializations. Second, training—the student model undergoes training using labeled and unlabeled data. For the unlabeled dataset, pseudolabels generated by the teacher model are used. Third, model updates—the teacher model's parameters are regularly updated using an exponential moving average of the student model's parameters, ensuring a stable and consistent learning process.

The AI used in this study is called ITS100 and is manufactured by MedAl Technology. The ITS100 system diagnoses thyroid nodules from a real-time ultrasound video, providing "benign" or "malignant" as the label of each nodule. Its core utility has been developed based on state-of-the-art deep learning algorithms, consisting of more than 300,000 images and hundreds of additional videos. Previous studies have demonstrated that this AI has significant value and accuracy in distinguishing between benign and malignant thyroid nodules [24,25].

Task 1: Evaluating the Ability of AI to Identify Benign Nodules Initially Deemed at Malignant Risk by Radiologists

Nodules deemed to be at risk for malignancy by radiologists in dataset 1 were used to validate the AI. For this AI system, if the AI model classified a nodule as benign, it was hypothesized as "AI-avoided," and FNA was considered unnecessary. Conversely, if the AI classified a nodule as malignant, it was hypothesized as "AI-recommended" and subsequently underwent FNA. In addition, we defined 3 new metrics to evaluate the AI's ability to distinguish benign nodules and reduce unnecessary FNA. Furthermore, we define the following metrics to evaluate AI's abilities:

- Unnecessary FNA rate = True Benign Total FNA

defined as the proportion of FNAs performed on nodules that were ultimately confirmed to be benign.

- Correct classification rate = True Benign AI Classification AI Classifications as Benign

defined as the proportion of nodules correctly identified as benign among all nodules classified as benign by the AI.

- Error classification rate = True Malignant AI Classification as Benign All AI Classifications as Benign

defined as the proportion of malignant nodules incorrectly classified as benign among all nodules classified as benign by the AI.

- Successful identification rate = True Benign AI ClassificationAll True Benign

defined as the proportion of truly benign nodules correctly identified as benign by the AI out of all benign nodules.

Task 2: Comparison Between Radiologists and AI

Dataset 2 was used to compare the performance of the AI system with that of radiologists in identifying potential benign nodules from those initially deemed at malignant risk by radiologists. A total of 21 radiologists participated in this analysis, including 10 senior and 11 junior practitioners. We randomly selected 30 cross-sectional or longitudinal images of thyroid nodules that had been previously flagged as malignant risk by radiologists in real clinical settings. The radiologists were tasked with identifying nodules that were likely benign and for which FNA could have been avoided, based solely on the imaging data provided, without any external prompts or guidance. This setup

XSL•FO
RenderX

aimed to assess their ability to discern unnecessary FNA within a risk cohort.

Statistical Analysis

In task 1, to evaluate the performance of the AI, the ROC curve was constructed. Sensitivity, specificity, positive predictive value, negative predictive value, accuracy, area under the curve (AUC), and F_1-score were also calculated. The AUC was calculated along with 95% CIs. In task 2, the Delong test was performed to compare radiologists' and AI's AUCs. The specific numbers of nodules where the prediction results of the AI were inconsistent with the confirmed pathological results were determined using the confusion matrix. The successful identification rate and correct classification rate were calculated along with 95% CIs. The Mann-Whitney *U* test was used to compare the successful identification rate and correct classification rate between senior radiologists and junior radiologists.

All statistical analyses were conducted using SPSS (Version 22.0, IBM Corporation), R software (Version 4.2.1, R Foundation for Statistical Computing), and Python (version 3.7.13, Python Software Foundation). Results were considered statistically significant at the $P<.01$ level.

Results

Characteristics of Data

A total of 6016 cases in dataset 1 and 935 in dataset 2 were recruited. After applying the exclusion criteria, a total of 4572 cases were included in dataset 1 and 260 cases were included in dataset 2, as demonstrated in the workflow in Figure 1. Table 1 illustrates the clinical characteristics of the dataset comprising 4572 patients assessed for malignant risk by radiologists. The cohort predominantly consists of female patients, accounting for 75.3% (3444/4572), with a mean age of 49.4 (SD 13.75) years, reflective of a middle-aged population. The number of lesions in the right lobe was the highest among the cohort. American Thyroid Association (ATA) guidelines categorization revealed 3508 nodules in category 3, a total of 730 nodules in category 4, and 334 nodules in category 5, indicating that most nodules present with low to intermediate suspicion of malignancy. Bethesda categorization yielded the following distribution: category II (n=3106), III (n=137), IV (n=10), V (n=348), and VI (n=971), with a predominance of benign diagnoses (Bethesda category II). The definitive diagnosis classified 3134 nodules as benign and 1438 as malignant.

Table . Patient demographics and characteristics of thyroid nodules.

Characteristics	Total (age: mean 49.4, SD 13.75 years), n	Benign (age: mean 51.5, SD 13.6 years), n (%)	Malignant (age: 48.5, SD 13.8 years), n (%)
Patients	4572	3134 (68.5)	1438 (31.5)
Patient sex			
Male	1128	713 (22.8)	415 (28.9)
Female	3444	2421 (77.2)	1023 (71.1)
Location			
Right	2387	1635 (52.2)	752 (52.3)
Left	2010	1405 (44.8)	605 (42.1)
Isthmus	175	94 (3)	81 (5.6)
ATA[a] category			
Low suspicion	3508	2851 (91)	657 (45.7)
Intermediate suspicion	730	202 (6.4)	528 (36.7)
High suspicion	334	81 (2.6)	253 (17.6)
Bethesda category			
II	3106	3078 (98.2)	28 (1.9)
III	137	31 (1)	106 (7.4)
IV	10	7 (0.2)	3 (0.2)
V	348	13 (0.4)	335 (23.3)
VI	971	5 (0.2)	966 (67.2)

[a]ATA: American Thyroid Association.

Accuracy Data of AI

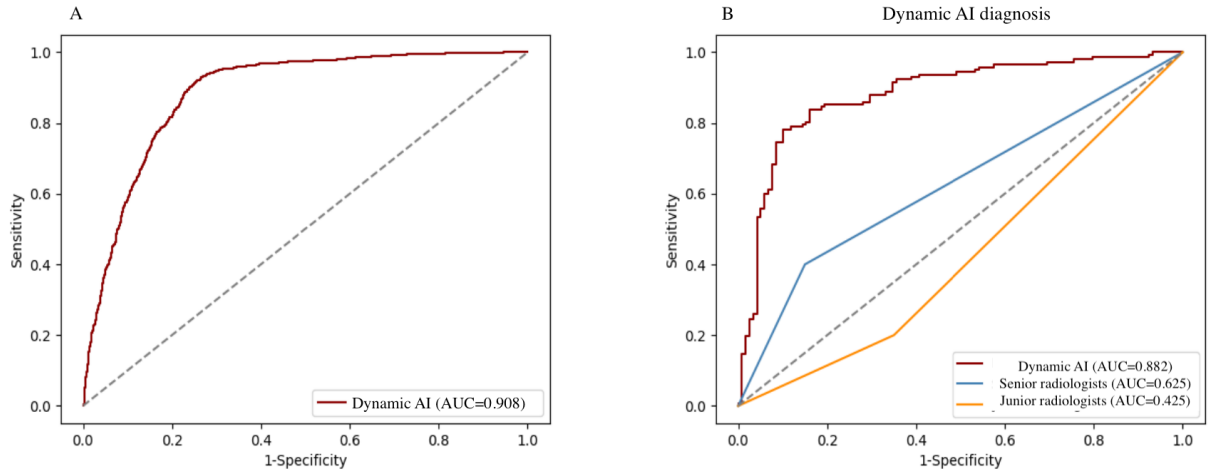
We evaluated the performance of the AI in identifying potential benign nodules from those initially classified as at malignant risk by radiologists in dataset 1. The AUC of the AI was 0.91 (95% CI 0.88 - 0.93; Figure 3A). The AI's sensitivity was 91.4% (1315/1438), while its specificity was 86.8% (2719/3134). The positive predictive value was 76% (1315/1730) and the negative predictive value was 95.7% (2719/2842), reflecting a high likelihood that negative test

XSL•FO
RenderX

results are accurate. Overall accuracy was 88.2% (4034/4572), demonstrating the AI's efficacy across 4572 cases. The F_1-score, a harmonized measure of test accuracy, was 0.83, indicating a balanced precision and recall. After applying AI, the number of unnecessary FNAs significantly decreased to 415 (9.1%), compared with 3134 (68.5%) in real-world human readings.

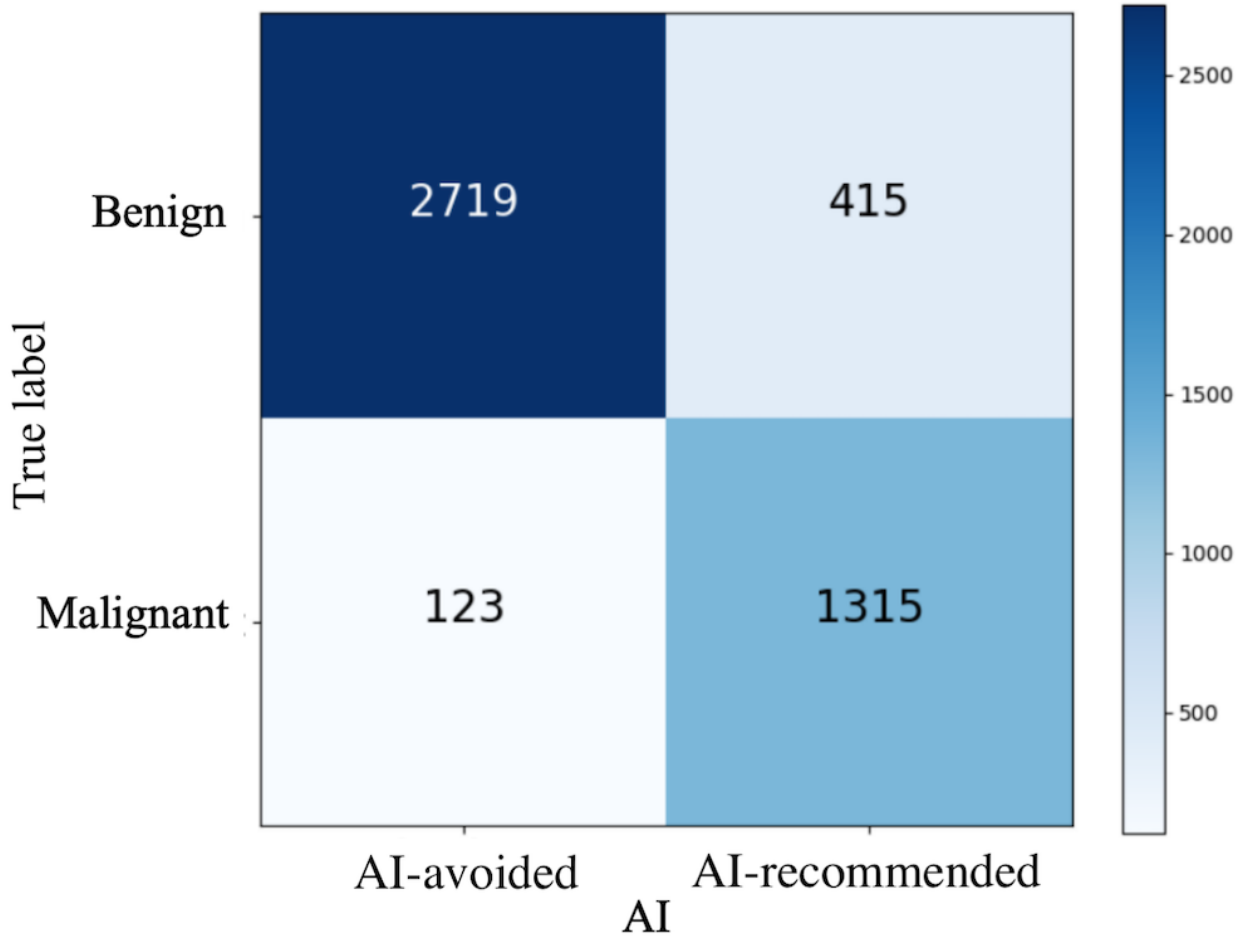
Figure 4 displays the confusion matrix, showing that the AI correctly identified 2719 benign nodules and 1315 malignant nodules. It also demonstrates a relatively low rate of false negatives. Figure 5A shows the scatter plot comparing the AI's positive and negative predictions against the Bethesda system's classifications, which range from benign (Bethesda II) to suspicious for malignancy (Bethesda III-V) to malignant (Bethesda VI). The dots represent individual cases, with red indicating a positive prediction (malignant) and blue indicating a negative prediction (benign). For Bethesda 2, there are many blue dots (AI negative) in the lower left quadrant, suggesting strong agreement on benign diagnoses. For Bethesda 6, the concentration of red dots in the upper right quadrant indicates a high level of agreement on malignant diagnoses. Figure 5B displays a scatter plot of the AI predictions based on the ATA classification, with the "low suspicion" category indicating probably benign nodules, the "intermediate suspicion" category indicating suspicious nodules, and the "high suspicion" category indicating highly suspicious nodules for malignancy. The low suspicion category predominantly shows blue dots, suggesting that the AI largely agrees with the benign diagnosis of these nodules. The intermediate category shows a dense mix, with many cases classified as suspicious by radiologists also being predicted as AI-avoided nodules. The high suspicion category, which should theoretically contain the most malignant nodules, shows a high concentration of red dots, highlighting the AI's ability to accurately identify highly suspicious cases.

Figure 3. Receiver operating characteristic curves of the artificial intelligence in (**A**) dataset 1 (**B**) and dataset 2. Numbers in parentheses are areas under the receiver operating characteristic curves. Dynamic AI: ITS100 AI system. AI: artificial intelligence; AUC: area under the curve.



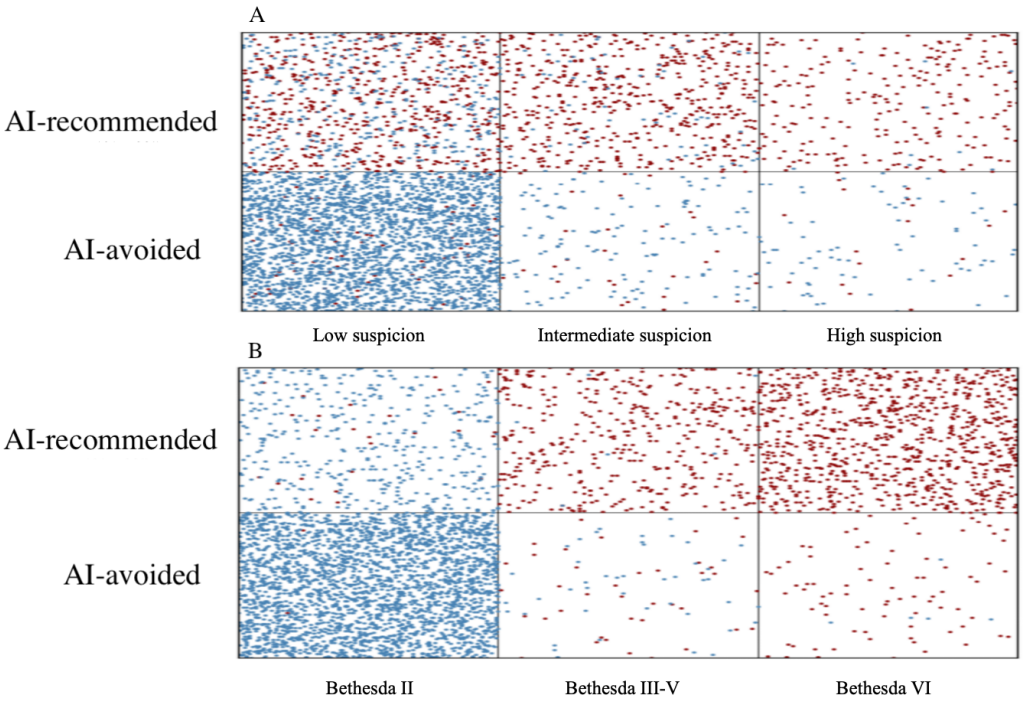
XSL•FO
RenderX

Figure 4. Confusion matrix for artificial intelligence identification results. The y-coordinate is the cytologically (Bethesda II or VI) or pathologically confirmed result. The x-coordinate is the artificial intelligence prediction result. AI: artificial intelligence.



XSL•FO
RenderX

Figure 5. Scatter plot of artificial intelligence binary classification for (**A**) fine needle aspiration across Bethesda categories and (**B**) suspicion categories. Red dots indicate cytologically (Bethesda VI) or pathologically confirmed malignant nodules. Blue dots indicate cytologically (Bethesda II) or pathologically confirmed benign nodules. AI: artificial intelligence.



Rates of Unnecessary FNAs and Other Metrics

The majority of nodules recommended for FNA were classified in Bethesda category VI, accounting for 51.1% (884/1730) of the total, while most of the nodules identified as benign by AI were in Bethesda category II, comprising 94% (2671/2842; Table 2). The unnecessary FNA rates based on human readings for ATA guideline categories were 81.3% for low suspicion, 27.7% for intermediate suspicion, and 24.3% for high suspicion, with an overall unnecessary FNA rate of 68.5% (Table 3).

Table . Bethesda classification of artificial intelligence–avoided and artificial intelligence–recommended nodules.

Bethesda category	AI[a]-recommended (N=1730), n (%)	AI-avoided (N=2842), n (%)
II	435 (25.1)	2671 (94)
III-V	411 (23.8)	84 (3)
VI	884 (51.1)	87 (3.1)

[a]AI: artificial intelligence.

XSL•FO
RenderX

Table . The performance of artificial intelligence across different American Thyroid Association guideline categories.

	Low suspicion	Intermediate suspicion	High suspicion	All
Total	3508 (76.7)	730 (16)	334 (7.3)	4572 (100)
Benign	2851 (81.3)	202 (27.7)	81 (24.3)	3134 (68.5)
Malignant	657 (18.7)	528 (72.3)	253 (75.7)	1438 (31.4)
Unnecessary FNAs[a]	2851 (81.3)	202 (27.7)	81 (24.3)	3134 (68.5)
AI[b]-avoided	2587 (73.7)	165 (22.6)	90 (26.9)	2842 (62.2)
Benign	2510 (97)	137 (83)	72 (80)	2719 (95.7)
Malignant	77 (3)	28 (17)	18 (20)	123 (4.3)
Correct classification rate	2510 (97)	137(83)	72 (80)	2719 (95.7)
Successful identification rate	2510 (88)	137 (67.8)	72 (88.9)	2719 (86.8)
Error classification rate	77 (3)	28 (17)	28 (20)	123 (4.3)

[a]FNA: fine needle aspiration.

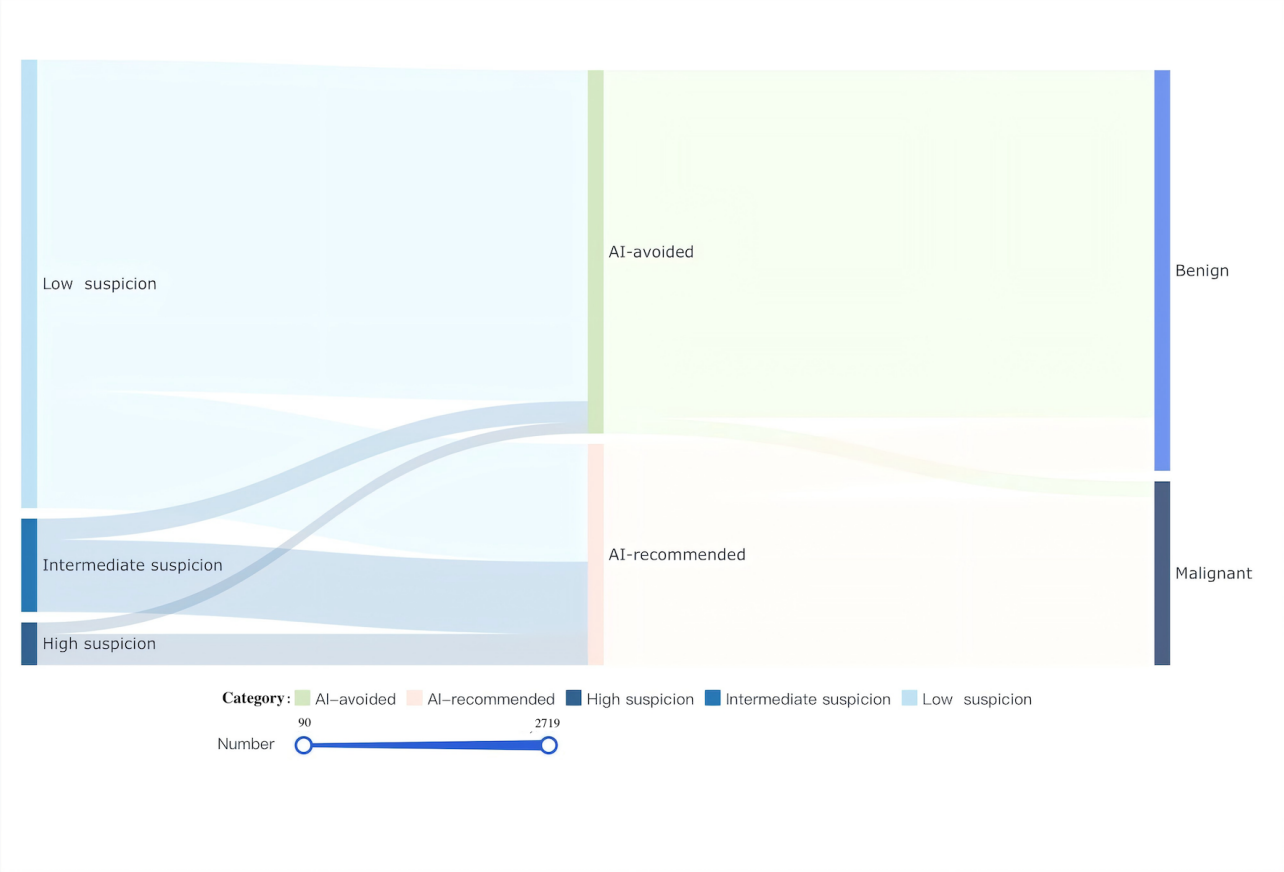
[b]AI: artificial intelligence.

The AI system demonstrated promising performance across different ATA guideline categories. For low suspicion nodules, the AI avoided 73.7% (2587/3508) of thyroid nodules, with a correct classification rate of 97%. In the intermediate suspicion category, the AI avoided 22.6% (165/730) of thyroid nodules and achieved a correct classification rate of 83%. For high suspicion nodules, the AI avoided 26.9% (90/334), with a correct classification rate of 80%. However, the error classification rates increased with malignancy likelihood, being 3% for low suspicion, 17% for intermediate suspicion, and 20% for high suspicion. The successful identification rates were 88%, 67.8%, and 88.9% for the low, intermediate, and high suspicion categories, respectively (Table 3).

The Sankey diagram (Figure 6) highlights that most benign nodules (n=2719, 86.8% of all benign nodules) were successfully avoided by the AI system, with low suspicion nodules comprising 91% (2587/2842) of all AI-avoided nodules. However, 415 benign nodules (9.1% of all nodules) were not identified. Notably, the AI misclassified 123 malignant nodules (2.7% of all nodules) as benign.

XSL•FO
RenderX

Figure 6. Sankey diagram illustrating the artificial intelligence's performance across low, intermediate, and high suspicion categories in thyroid nodule evaluation. Links represent the flow between entities. The width of the link corresponds to the amount of flow, with values ranging from 90 to 2719. Colors are used to differentiate between different types of flows. The terms "benign" and "malignant" refer to the results of pathological or cytological tests. AI: artificial intelligence.



Further analysis of the 123 malignant nodules misclassified by AI, as detailed in Table 4, revealed that all were papillary thyroid carcinomas, with 56.9% (70/123) being papillary thyroid microcarcinomas. Among these, 20.3% (25/123) exhibited extrathyroidal extension, 18.7% (23/123) presented with central lymph node metastases, and 74% (91/123) carried the BRAF V600E mutation. Multimedia Appendix 2 shows that the error classification rates of the AI system increased with higher malignancy risk, being lowest for low suspicion nodules (3%) and highest for high suspicion nodules (20%).

Table . Composition of malignant nodules identified as artificial intelligence–avoided.

Clinical and pathological features	Number, n (%)
Papillary thyroid microcarcinoma	70 (56.9)
Other thyroid carcinoma (FTC[a], MTC[b], and ATC[c])	0 (0)
Extrathyroidal extension	25 (20.3)
Central lymph node metastasis	23 (18.7)
Lateral lymph node metastasis	0 (0)
Distant metastasis	0 (0)
BRAF V600E mutation	91 (74)
TERT[d] promoter mutations	0 (0)

[a]FTC: follicular thyroid carcinoma.
[b]MTC: medullary thyroid carcinoma.
[c]ATC: anaplastic thyroid carcinoma.
[d]TERT: telomerase reverse transcriptase.

XSL•FO
RenderX

Comparison of Radiologists' and AI Performance

Task 2 compares the performance of radiologists and AI in identifying benign nodules initially assessed as malignant by radiologists, using the correct classification rate and successful identification rate as evaluation metrics. The violin diagram (a) in Multimedia Appendix 3 reveals that junior radiologists exhibited a median successful identification rate of 0.40 (95% CI 0.28 - 0.53), while senior radiologists demonstrated a median successful identification rate of 0.55 (95% CI 0.38 - 0.71; *P*=.001). AI achieved a successful identification rate of 0.81, surpassing the performance of both junior and senior radiologists. According to the violin diagram (b) in Multimedia Appendix 3, the median correct classification rate for junior radiologists was 0.54 (95% CI 0.44 - 0.62), whereas senior radiologists exhibited a median correct classification rate of 0.64 (95% CI 0.48 - 0.72; *P*=.13). Furthermore, the datasets indicate that AI achieved a successful identification rate of 0.828, which exceeded the correct classification rate of both junior and senior radiologists (Multimedia Appendix 3).

Figure 3B illustrates the performance of junior and senior radiologists, as well as the AI, in task 2. The AUC values for the AI model were 0.88 (95% CI 0.85 - 0.91), demonstrating superior performance to that of junior radiologists with an AUC of 0.43 (95% CI 0.36 - 0.49; *P*=.002) and senior radiologists with an AUC of 0.63 (95% CI 0.55 - 0.70; *P*=.003).

Discussion

Principal Findings

Thyroid nodules, frequently detected during ultrasound, require accurate characterization to assess malignancy and guide patient care. However, the subjective nature of radiological interpretation and the difficulty in distinguishing benign from malignant nodules often lead to unnecessary FNAs. AI holds significant potential in overcoming these challenges by identifying complex patterns and subtle features in ultrasound images that may be missed by human observers [26,27].

In this study, the rate of unnecessary FNAs stood at a high level in dataset 1, as high as the previous study reported [28], which was understandable. The high rate of overdiagnosis aligns with real-world clinical experiences, where various factors, such as human judgment, environmental influences, psychological aspects, and inherent subjectivity in radiological interpretations, play a significant role. Fortunately, based on our findings, after integrating an AI re-evaluation step before performing FNA, the system correctly identified 2719 out of 3134 (86.8%) benign nodules. As a result, the proportion of unnecessary FNAs among all nodules decreased from 3134 out of 4572 (68.5%) to 415 out of 4572 (9.1%).

We found that 2587 out of 3508 (73.7%) low-suspicion nodules based on ultrasound features were identified by AI, with 2510 out of 2587 (97%) correctly classified. In contrast, only 90 out of 334 (26.9%) high-suspicion nodules were identified, with 72 out of 90 (80%) correctly classified. These results suggest that AI re-evaluation is particularly beneficial for low-suspicion nodules and could be routinely implemented before FNA, especially for these cases.

Compared with radiologists, the AI demonstrated superior ability in identifying benign nodules initially assessed as being at malignant risk, surpassing the median performance of both senior and junior radiologists. Senior and junior radiologists were categorized by years of practice rather than absolute expertise. While senior radiologists had a higher correct classification rate than the juniors, the internal dispersion remained large, with most still falling below the AI's level and only 2 approaching or exceeding its performance. Cultivating senior radiologists is exceedingly challenging and takes a long time, whereas AI effectively compensates for the shortage of senior radiologists.

This underscores AI's significant potential for clinical application, reducing unnecessary FNAs and optimizing nodule management. It saves both human resources and time while ensuring high accuracy and minimizing missed diagnoses. Integrating AI into clinical practice ensures more consistent identification, reduces unnecessary health care costs, eases the burden on the health care system, and saves time and effort for radiologists.

From another perspective, AI re-evaluation resulted in 123 erroneous identifications (incorrectly labeling them as benign) among 4572 (2.7%) nodules. These malignant nodules represent a risk in AI re-evaluation. Balancing the risks and benefits of AI re-evaluation is crucial. Fortunately, our subgroup analysis revealed that all of these errors were papillary thyroid carcinomas, with 70 out of 123 (56.9%) being papillary thyroid microcarcinomas. Although the error classification rate was significantly lower than the correct classification rate and papillary thyroid cancer, especially microcarcinoma, is generally indolent with low mortality, we recommend active surveillance for these nodules. Given the error classification rate in intermediate- and high-suspicion nodules (28/165, 17% and 18/90, 20%, respectively), intensified surveillance is clinically warranted for these cohorts. Conversely, low-suspicion nodules demonstrated significantly higher diagnostic reliability (77/2587, 3%), justifying extended surveillance intervals.

This study has several limitations. First, the data were obtained exclusively from 3 centers in China, limiting the generalizability of the findings. We anticipate that expanding the datasets to include real-world data from other regions will enable a more comprehensive validation of the AI model's performance. Second, the AI system we tested was limited to analyzing grayscale images, leaving valuable information such as clinical data and color Doppler features insufficiently evaluated. Third, since this study reflects the application of AI in real clinical settings, there is a potential for bias introduced by biopsy decisions influenced by clinical judgment or patient preferences. Fourth, no prospective studies have been conducted to further validate the AI's application and its impact in clinical practice.

Conclusions

In conclusion, we conducted a retrospective study to evaluate the potential of AI in clinical practice for identifying benign nodules from those initially classified as at malignant risk by radiologists. Our findings demonstrated that incorporating AI in the pre-FNA stage can significantly reduce the number of unnecessary FNAs, optimize the management of thyroid

XSL•FO
RenderX

nodules, and outperform the average diagnostic accuracy of both junior and senior radiologists. Thus, including AI in the management of thyroid nodules may be a new and promising exploration to reduce the rate of unnecessary FNAs. To fully explore the potential of AI in thyroid nodule diagnosis, continued collaboration among AI developers, radiologists, and clinicians is essential.

Acknowledgments

This work was partly supported by the Science and Technology Commission of Shanghai Municipality (grant 19DZ2251100), Shanghai Municipal Health Commission (grant SHSLCZDZK03502), National Natural Science Foundation of China (grants 82371971, 82171942), and National Key R&D Program of China (grant 2022YFF0606304).

Data Availability

Patient data are not publicly accessible due to privacy regulations. However, it can be requested from the corresponding author, provided that the request is reasonable and has been approved by the institutional review board.

Conflicts of Interest

None declared.

Multimedia Appendix 1
Ultrasound equipment used in datasets 1 and 2.
[DOCX File, 15 KB - medinform_v13i1e71740_app1.docx]

Multimedia Appendix 2
The ratio of correct classification rate and error classification rate according to different suspicion categories in dataset 1.
[DOCX File, 60 KB - medinform_v13i1e71740_app2.docx]

Multimedia Appendix 3
The comparison between radiologists and AI in dataset 2. Junior radiologists with less than 10 years' experience. Senior Radiologist with 10 years or more than 10 years of experience. The red dotted line in the figure S2a represents the successful identification rate of AI, which is 81.4%. The red dotted line in Figure S2b represents the correct classification rate of AI of 82.8%.
[DOCX File, 204 KB - medinform_v13i1e71740_app3.docx]

References

1. Haugen BR, Alexander EK, Bible KC, et al. 2015 American Thyroid Association management guidelines for adult patients with thyroid nodules and differentiated thyroid cancer: The American Thyroid Association Guidelines Task Force on thyroid nodules and differentiated thyroid cancer. Thyroid 2016 Jan;26(1):1-133. [doi: 10.1089/thy.2015.0020] [Medline: 26462967]
2. Lim H, Devesa SS, Sosa JA, Check D, Kitahara CM. Trends in thyroid cancer incidence and mortality in the United States, 1974-2013. JAMA 2017 Apr 4;317(13):1338-1348. [doi: 10.1001/jama.2017.2719] [Medline: 28362912]
3. Enewold L, Zhu K, Ron E, et al. Rising thyroid cancer incidence in the United States by demographic and tumor characteristics, 1980-2005. Cancer Epidemiol Biomarkers Prev 2009 Mar;18(3):784-791. [doi: 10.1158/1055-9965.EPI-08-0960] [Medline: 19240234]
4. Welch HG, Doherty GM. Saving thyroids - overtreatment of small papillary cancers. N Engl J Med 2018 Jul 26;379(4):310-312. [doi: 10.1056/NEJMp1804426] [Medline: 30044933]
5. Sakorafas GH. Thyroid nodules; interpretation and importance of fine-needle aspiration (FNA) for the clinician - practical considerations. Surg Oncol 2010 Dec;19(4):e130-e139. [doi: 10.1016/j.suronc.2010.06.003] [Medline: 20620044]
6. Castellana M, Castellana C, Treglia G, et al. Performance of five ultrasound risk stratification systems in selecting thyroid nodules for FNA. J Clin Endocrinol Metab 2020 May 1;105(5):31690937. [doi: 10.1210/clinem/dgz170] [Medline: 31690937]
7. Wang HX, Lu F, Xu XH, et al. Diagnostic performance evaluation of practice guidelines, elastography and their combined results for thyroid nodules: a multicenter study. Ultrasound Med Biol 2020 Aug;46(8):1916-1927. [doi: 10.1016/j.ultrasmedbio.2020.03.031] [Medline: 32451191]
8. Hoang JK, Middleton WD, Farjat AE, et al. Reduction in thyroid nodule biopsies and improved accuracy with American College of Radiology thyroid imaging reporting and data system. Radiology 2018 Apr;287(1):185-193. [doi: 10.1148/radiol.2018172572] [Medline: 29498593]
9. Pandya A, Caoili EM, Jawad-Makki F, et al. Retrospective cohort study of 1947 thyroid nodules: a comparison of the 2017 American College of Radiology TI-RADS and the 2015 American Thyroid Association Classifications. AJR Am J Roentgenol 2020 Apr;214(4):900-906. [doi: 10.2214/AJR.19.21904] [Medline: 32069084]

XSL•FO
RenderX

10. Xiao F, Li JM, Han ZY, et al. Multimodality US versus thyroid imaging reporting and data system criteria in recommending fine-needle aspiration of thyroid nodules. Radiology 2023 Jun;307(5):e221408. [doi: 10.1148/radiol.221408] [Medline: 37367448]
11. Xu H, Zhang Y, Wu H, et al. High diagnostic accuracy of epigenetic imprinting biomarkers in thyroid nodules. J Clin Oncol 2023 Feb 20;41(6):1296-1306. [doi: 10.1200/JCO.22.00232] [Medline: 36378996]
12. Peng S, Liu Y, Lv W, et al. Deep learning-based artificial intelligence model to assist thyroid nodule diagnosis and management: a multicentre diagnostic study. Lancet Digit Health 2021 Apr;3(4):e250-e259. [doi: 10.1016/S2589-7500(21)00041-8] [Medline: 33766289]
13. Tessler FN, Thomas J. Artificial intelligence for evaluation of thyroid nodules: a primer. Thyroid 2023 Feb;33(2):150-158. [doi: 10.1089/thy.2022.0560] [Medline: 36424829]
14. Choi YJ, Baek JH, Park HS, et al. A computer-aided diagnosis system using artificial intelligence for the diagnosis and characterization of thyroid nodules on ultrasound: initial clinical assessment. Thyroid 2017 Apr;27(4):546-552. [doi: 10.1089/thy.2016.0372] [Medline: 28071987]
15. Wang J, Jiang J, Zhang D, et al. An integrated AI model to improve diagnostic accuracy of ultrasound and output known risk features in suspicious thyroid nodules. Eur Radiol 2022 Mar;32(3):2120-2129. [doi: 10.1007/s00330-021-08298-7]
16. Zhou H, Jin Y, Dai L, et al. Differential diagnosis of benign and malignant thyroid nodules using deep learning radiomics of thyroid ultrasound images. Eur J Radiol 2020 Jun;127:108992. [doi: 10.1016/j.ejrad.2020.108992] [Medline: 32339983]
17. Toro-Tobon D, Loor-Torres R, Duran M, et al. Artificial intelligence in thyroidology: a narrative review of the current applications, associated challenges, and future directions. Thyroid 2023 Aug;33(8):903-917. [doi: 10.1089/thy.2023.0132] [Medline: 37279303]
18. Chen Y, Gao Z, He Y, et al. An artificial intelligence model based on ACR TI-RADS characteristics for US diagnosis of thyroid nodules. Radiology 2022 Jun;303(3):613-619. [doi: 10.1148/radiol.211455] [Medline: 35315719]
19. Yang J, Page LC, Wagner L, et al. Thyroid nodules on ultrasound in children and young adults: comparison of diagnostic performance of radiologists' impressions, ACR TI-RADS, and a deep learning algorithm. AJR Am J Roentgenol 2023 Mar;220(3):408-417. [doi: 10.2214/AJR.22.28231] [Medline: 36259591]
20. Cibas ES, Ali SZ. The 2017 Bethesda system for reporting thyroid cytopathology. Thyroid 2017 Nov;27(11):1341-1346. [doi: 10.1089/thy.2017.0500] [Medline: 29091573]
21. Zbontar J, Jing L, Misra I, LeCun Y, Deny S. Barlow twins: self-supervised learning via redundancy reduction. arXiv. Preprint posted online on 2021. [doi: 10.48550/arXiv.2103.03230]
22. Torrey L, Shavlik J. Transfer learning. Handbook of Research on Machine Learning Applications 2009:01. [doi: 10.4018/978-1-60566-766-9.ch011]
23. Li X, Yu L, Chen H, Fu CW, Xing L, Heng PA. Transformation-consistent self-ensembling model for semisupervised medical image segmentation. IEEE Trans Neural Netw Learning Syst 2021;32(2):523-534. [doi: 10.1109/TNNLS.2020.2995319]
24. Wang B, Wan Z, Li C, et al. Identification of benign and malignant thyroid nodules based on dynamic AI ultrasound intelligent auxiliary diagnosis system. Front Endocrinol (Lausanne) 2022;13(1018321):1018321. [doi: 10.3389/fendo.2022.1018321] [Medline: 36237194]
25. Tian Y, Zhu J, Zhang L, et al. A swin transformer-based model for thyroid nodule detection in ultrasound images. J Vis Exp 2023 Apr 21;37154577(194). [doi: 10.3791/64480] [Medline: 37154577]
26. Buda M, Wildman-Tobriner B, Hoang JK, et al. Management of thyroid nodules seen on US images: deep learning may match performance of radiologists. Radiology 2019 Sep;292(3):695-701. [doi: 10.1148/radiol.2019181343] [Medline: 31287391]
27. Li X, Zhang S, Zhang Q, et al. Diagnosis of thyroid cancer using deep convolutional neural network models applied to sonographic images: a retrospective, multicohort, diagnostic study. Lancet Oncol 2019 Feb;20(2):193-201. [doi: 10.1016/S1470-2045(18)30762-9] [Medline: 30583848]
28. Ha SM, Baek JH, Na DG, et al. Diagnostic performance of practice guidelines for thyroid nodules: thyroid nodule size versus biopsy rates. Radiology 2019 Apr;291(1):92-99. [doi: 10.1148/radiol.2019181723] [Medline: 30777805]

Abbreviations

AI: artificial intelligence
ATA: American Thyroid Association
AUC: area under the curve
FNA: fine needle aspiration

XSL•FO
RenderX

Edited by A Benis; submitted 26.01.25; peer-reviewed by C Chen, D Ou; revised version received 27.04.25; accepted 02.05.25; published 30.07.25.

Please cite as:
Ni JH, Liu YY, Chen C, Shi YL, Zhao X, Li XL, Ye BB, Hu JL, Mou LC, Sun LP, Fu HJ, Zhu XX, Zhang YF, Guo L, Xu HX
Optimizing Thyroid Nodule Management With Artificial Intelligence: Multicenter Retrospective Study on Reducing Unnecessary Fine Needle Aspirations
JMIR Med Inform 2025;13:e71740
URL: https://medinform.jmir.org/2025/1/e71740
doi:10.2196/71740

© Jia-Hui Ni, Yun-Yun Liu, Chao Chen, Yi-Lei Shi, Xing Zhao, Xiao-Long Li, Bei-Bei Ye, Jing-Liang Hu, Li-Chao Mou, Li-Ping Sun, Hui-Jun Fu, Xiao-Xiang Zhu, Yi-Feng Zhang, Lehang Guo, Hui-Xiong Xu. Originally published in JMIR Medical Informatics (https://medinform.jmir.org), 30.7.2025. This is an open-access article distributed under the terms of the Creative Commons Attribution License (https://creativecommons.org/licenses/by/4.0/), which permits unrestricted use, distribution, and reproduction in any medium, provided the original work, first published in JMIR Medical Informatics, is properly cited. The complete bibliographic information, a link to the original publication on https://medinform.jmir.org/, as well as this copyright and license information must be included.

XSL•FO
RenderX

Application of Large Language Models in Complex Clinical Cases: Cross-Sectional Evaluation Study

Yuanheng Huang[1*], MD; Guozhen Yang[1*], MD; Yahui Shen[2*], MD; Huiguo Chen[1], MD; Weibin Wu[1], MD; Xiaojun Li[1], MD; Yonghui Wu[1], MD; Kai Zhang[1], MD; Jiannan Xu[1], MD; Jian Zhang[1], MD

[1]Department of Cardiothoracic Surgery, Third Affiliated Hospital of Sun Yat-sen University, 2693 Kaichuang Avenue, Huangpu District, Guangzhou, China

[2]Department of Gynecologic Oncology, Shaanxi Provincial Cancer Hospital, Xi'an, China

[*]these authors contributed equally

Corresponding Author:
Jian Zhang, MD
Department of Cardiothoracic Surgery, Third Affiliated Hospital of Sun Yat-sen University, 2693 Kaichuang Avenue, Huangpu District, Guangzhou, China

Abstract

Background: Large language models (LLMs) have made significant advancements in natural language processing (NLP) and are gradually showing potential for application in the medical field. However, LLMs still face challenges in medicine.

Objective: This study aims to evaluate the efficiency, accuracy, and cost of LLMs in handling complex medical cases and to assess their potential and applicability as tools for clinical decision support.

Methods: We selected cases from the database of the Department of Cardiothoracic Surgery, the Third Affiliated Hospital of Sun Yat-sen University (2021 - 2024), and conducted a multidimensional preliminary evaluation of the latest LLMs in clinical decision-making for complex cases. The evaluation included measuring the time taken for the LLMs to generate decision recommendations, Likert scores, and calculating decision costs to assess the execution efficiency, accuracy, and cost-effectiveness of the models.

Results: A total of 80 complex cases were included in this study, and the performance of multiple LLMs in clinical decision-making was evaluated. Experts required 33.60 minutes on average (95% CI 32.57 - 34.63), far longer than any LLM. GPTo1 (0.71, 95% CI 0.67 - 0.74), GPT4o (0.88, 95% CI 0.83 - 0.92), and Deepseek (0.94, 95% CI 0.90 - 0.96) all finished under a minute without statistical differences. Although Kimi, Gemini, LLaMa3-8B, and LLaMa3-70B took 1.02 - 3.20 minutes, they were still faster than experts. In terms of decision accuracy, Deepseek-R1 had the highest accuracy (mean Likert score=4.19), with no significant difference compared to GPTo1 (P=.699), and both performed significantly better than GPT4o, Kimi, Gemini, LLaMa3-70B, and LLaMa3-8B (P<.001). Deepseek-R1 and GPTo1 demonstrated the lowest hallucination rates—6/80 (8%) and 5/80 (6%), respectively—significantly outperforming GPT-4o (7/80, 9%), Kimi (10/80, 12%), and the Gemini and LLaMa3 models, which exhibited substantially higher rates ranging from 13/80 (16%) to 25/80 (31%). Regarding decision costs, all LLMs showed significantly lower costs than the Multidisciplinary Team**,** with open-source models such as Deepseek-R1 offering a zero direct cost advantage.

Conclusions: GPTo1 and Deepseek-R1 show strong clinical potential, boosting efficiency, maintaining accuracy, and reducing costs. GPT4o and Kimi performed moderately, indicating suitability for broader clinical tasks. Further research is needed to validate LLaMa3 series and Gemini in clinical decision.

(JMIR Med Inform 2025;13:e73941) doi:10.2196/73941

KEYWORDS

large language models; artificial intelligence; clinical decision support; complex medical cases; cross-sectional studies

Introduction

Background

With the development of artificial intelligence (AI) and deep learning technologies, large language models (LLMs) have demonstrated remarkable potential across various fields, particularly in natural language processing (NLP) tasks such as summarization, paraphrasing, generating new text content, and writing program code [1,2]. Additionally, LLMs can act as personal assistants, helping users answer a wide range of questions.

The primary goal of LLMs was not initially to serve the medical field, but some studies have already shown that LLMs have significant potential in medicine [3,4]. For example, research

XSL•FO
RenderX

has found that ChatGPT can pass the United States Medical Licensing Examination (USMLE) [5] and the Advanced Cardiovascular Life Support (ACLS) exam [6]. In addition to exam simulations, ChatGPT's potential advantages in daily medical applications have also been confirmed, such as extracting information from electronic health records and assisting with literature searches [7]. However, the training knowledge base of LLMs may have issues such as incompleteness, information bias, or generation of misleading information, and the application of general-purpose LLMs in medicine has not yet undergone large-scale clinical studies. Therefore, it is essential to explore the application of LLMs in medicine in greater depth.

Previous studies have verified the diagnostic capabilities of GPT-3.5, GPT-4, and other LLMs [8-12], such as its ability to generate detailed differential diagnosis lists for common clinical cases. Additionally, research teams tested the GPT-4 ability to make accurate diagnoses from medical records [9], and the results showed that the generative AI GPT-4 chose the correct diagnosis as the primary diagnosis in nearly 40% of cases and provided the correct potential diagnosis in 64% of challenging cases. However, complex cases are common in hospitals, especially in cardiothoracic surgery. Due to population aging and insufficient medical resources, providing timely and high-quality clinical decision support has become a major challenge for health care systems worldwide. Delivering accurate and effective clinical decisions for complex cases typically requires substantial human, time, and money. Although some studies are currently exploring the application of LLMs in medicine, a recent review [13] published in a *Journal of the American Medical Association* subjournal of 519 studies assessing LLMs in the medical field found that only 5% of studies used real-world data. This exposes the limitations of current research and the potential disconnect from clinical reality. In this context, whether LLMs can provide effective clinical decision support for doctors in complex cases still requires further investigation.

Objectives

Therefore, this study aimed to preliminarily evaluate the utility of LLMs in complex medical decision-making by assessing their efficiency, accuracy, and cost in real-world clinical cases, and exploring their practical potential in clinical decision support.

Methods

Study Design and Data Source

To ensure that the study is based on representative and unbiased real-world cases, we screened a total of 140 cases from the complex case database of the Department of Cardiothoracic Surgery of the Third Affiliated Hospital of Sun Yat-sen University (2021 - 2024). These cases are sourced from the complex case database of a tertiary hospital, which is not publicly available, ensuring the accuracy of the study to the greatest extent and preventing any generic LLMs from being exposed to relevant data during their training, thus ensuring the objectivity and fairness of the evaluation. Most of the cases have a consistent structure, including medical history, current symptoms, examination methods and findings, diagnosis, and clinical decision. All cases were reviewed by an experienced physician, and only those that met the following criteria were included in the further analysis: the clinical case data records the entire diagnostic and treatment process, complex clinical case, and the cases are not duplicates. In this study, a complex case was defined as a patient scenario that disease involved at least 2 organ systems, required multidisciplinary input for diagnosis or treatment, and presented with conflicting or uncertain therapeutic pathways. These criteria were established by 2 senior cardiothoracic specialists.

LLMs Evaluation

To evaluate the recently launched LLMs, we selected the following models for benchmarking: Deepseek-R1, GPTo1, GPT-4o, Kimi, Gemini, LLaMA3-70B, and LLaMA3-8B. Model setup and prompting strategy details are provided in Multimedia Appendix 1. The reviewers included 2 board-certified cardiothoracic surgeons, each with more than 10 years of clinical experience and active participation in weekly Multidisciplinary Team (MDT) discussions. Reviewers were blinded to the identity of the LLM models generating each response to minimize bias.

Clinical Decision Efficiency Evaluation

We evaluate the execution efficiency of Deepseek-R1, GPTo1, GPT4o, Kimi, Gemini, LLaMA3-70B, and LLaMA3-8B in clinical decision-making tasks. This is done by recording the time taken by each model from receiving the instructions to generating a complete decision recommendation and comparing it with the time taken by several experts to complete the same task.

Clinical Decision Accuracy Evaluation

Two independent clinical experts were invited to evaluate the clinical decision outputs generated by Deepseek-R1, GPTo1, GPT-4o, Kimi, Gemini, LLaMA3-70B, and LLaMA3-8B. The evaluations were based on the consistency with expert decisions, using a 5-point modified Likert scale. The scoring standards and the scale are presented in Table 1 [14,15].

XSL•FO
RenderX

Table . Scoring standards for the 5-point modified Likert scale.

Likert score	Relevance of decisions	Redundancy of decisions
1	Most of all relevant decisions were not mentioned.	All or most decisions were redundant or unjustified.
2	Some or many relevant decisions were not mentioned.	Some decisions were redundant or unjustified.
3	Most relevant decisions were mentioned.	Some decisions were redundant or unjustified.
4	Most relevant decisions were mentioned.	Few decisions were redundant or unjustified.
5	All relevant decisions were mentioned.	No redundant or unjustified decisions.

Hallucination Evaluation

Each LLM output was reviewed by two independent clinical experts to identify statements that were factually incorrect, clinically implausible, or not supported by the case information. A hallucination was defined as a recommendation or rationale inconsistent with current clinical guidelines or contradicting the provided case data. The hallucination rate was calculated as the proportion of cases where at least one hallucinated item was present in the model's response.

Each expert independently scored the output of each model, and the final score was the average of the two experts' ratings. To ensure scoring consistency, we calculated the inter-rater reliability (Cohen kappa coefficient—a statistic that measures inter-rater agreement for categorical items while accounting for chance agreement) [16] to validate the reliability of the evaluation.

Clinical Decision Cost Evaluation

The usage costs of each LLM were calculated and compared with the costs of the MDT. The MDT costs were calculated based on the hospital's MDT fee.

Statistical Analysis

Patient baseline characteristics were described using frequencies and percentages for categorical variables, and medians or means for continuous variables. For continuous variables with approximate normal distribution, Student *t* test (2-tailed) was used for comparisons; for nonnormally distributed continuous variables, the Mann-Whitney *U* test was used for comparisons between two groups, and the Kruskal-Wallis test was used for comparisons between three or more independent samples. For categorical data, Fisher exact test, chi-square test, or Wilcoxon signed-rank test was used. All statistical tests were 2-tailed, and a P value<.05 was considered statistically significant. Statistical analysis and plotting were performed using Python 3.13.1, with libraries including scipy.stats, pandas, seaborn, and matplotlib.

Ethical Considerations

This study was approved by the ethics committee of the Third Affiliated Hospital of Sun Yat-sen University (approval ID II2025-257-03; approval date March 2025). Written informed consent was obtained from all participants. To protect privacy, personal identifiers were removed or coded before analysis, and all data were stored on an encrypted, password-protected server accessible only to the research team. Participants did not receive any financial or material compensation. All procedures involving human participants were conducted in accordance with the Declaration of Helsinki and relevant institutional guidelines.

Results

Baseline Characteristics

A total of 140 patients from the Cardiothoracic Surgery Department of the Third Affiliated Hospital of Sun Yat-sen University were initially included in the study. After excluding 60 patients who did not meet the inclusion criteria, 80 patients remained. The median age of the study population was 60 (IQR 14 - 79) years, with 58 (72%) males and 22 (28%) females. The most common complex conditions were thoracic tumors combined with respiratory system disorders (25/80 cases, 31%), followed by thoracic tumors combined with circulatory system disorders (19/80 cases, 24%). As shown in Table 2, other conditions accounted for the remaining 45% (36/80 cases), and the median number of experts involved in the MDT was 7 (range 5 - 9). Table S2 in Multimedia Appendix 1 illustrates 2 representative complex clinical cases, including the final expert consensus from MDT discussions and the corresponding responses generated by LLMs.

XSL•FO
RenderX

Table . Baseline characteristics of the study cohort.

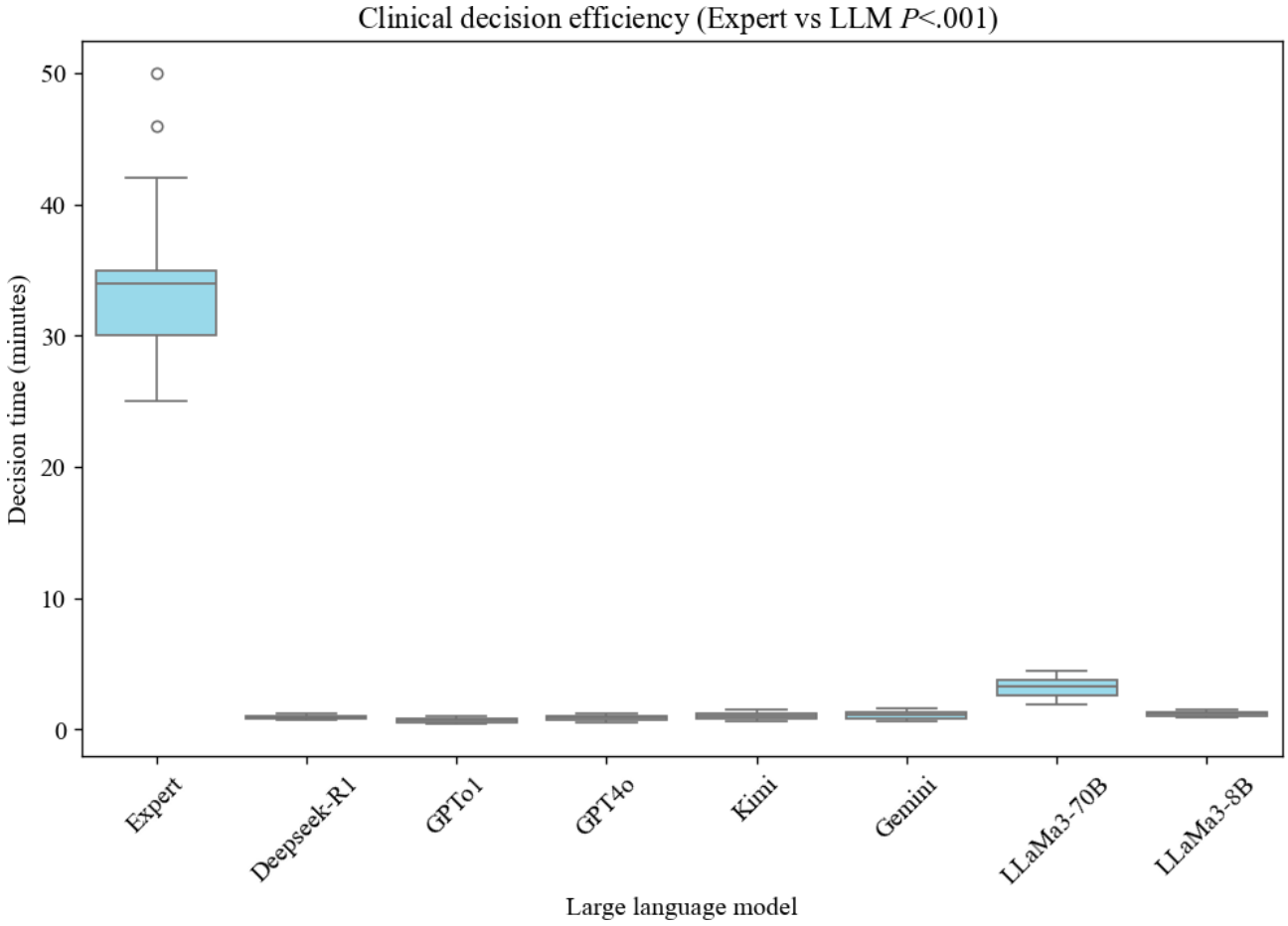
Characteristics	Values (N=80)
Age (years), median (range)	60 (14 - 79)
Sex, n (%)	
Male	58 (72)
Female	22 (28)
Complex conditions, n (%)	
Thoracic tumors+ respiratory disorders	25 (31)
Thoracic tumors+ circulatory disorders	19 (24)
Other conditions	36 (45)
Number of experts in MDT[a], median (range)	7 (5-9)

[a]MDT: Multidisciplinary Team.

Clinical Decision Efficiency Evaluation

The data analysis revealed that the average decision-making time for the expert group was significantly longer than for all LLMs (P<.001), with a mean of 33.6 (95% CI 32.57 - 34.63) minutes. In contrast, the decision-making time for LLMs was notably shorter. GPTo1 demonstrated the best decision-making efficiency, with an average time of only 0.71 (95% CI 0.67 - 0.74) minutes, followed by GPT4o (0.88, 95% CI 0.83 - 0.92 minutes) and Deepseek (0.94, 95% CI 0.90 - 0.96 minutes), all of which completed decisions in under 1 minute. Kimi, Gemini, and LLaMa3-8B also exhibited relatively fast decision-making abilities (1.02 - 1.18 minutes), although slightly slower than GPTo1 and GPT4o. LLaMa3-70B had the longest decision time at 3.20 (95% CI 3.04 - 3.37) minutes, but it was still significantly better than the expert group's 33.6 minutes. These results indicate that AI-driven LLMs significantly enhance the efficiency of clinical decision-making, as illustrated in Figure 1.

Figure 1. Clinical decision efficiency comparison between experts and large language models. LLM: large language model.



XSL•FO
RenderX

Clinical Decision Accuracy Evaluation

According to the classification standards of Landis et al [16], which are based on Cohen kappa coefficient, the results indicate strong agreement between two senior independent clinical experts, with kappa values ranging from 0.66 to 0.85. This suggests a high level of consistency in model evaluation. Detailed results are presented in Figure 2.

As shown in Figure 3, pairwise comparisons in clinical decision accuracy assessment revealed that Deepseek-R1 achieved the highest accuracy, with a mean Likert score of 4.19 (95% CI 4.02 - 4.35), significantly outperforming GPT4o, Kimi, Gemini, LLaMA3-70B, and LLaMA3-8B (all P<.001). However, no significant difference was found between Deepseek-R1 and GPTo1 (mean 4.15, 95% CI 3.99 - 4.31; P=.70). GPTo1 performed comparably to Deepseek-R1 and significantly better than GPT4o (P=.003), Kimi, Gemini, LLaMa3-70B, and LLaMa3-8B (all P<.001). Both Deepseek-R1 and GPTo1 exhibited the highest Likert scores, approaching expert-level performance, indicating suitability for clinical decision tasks.

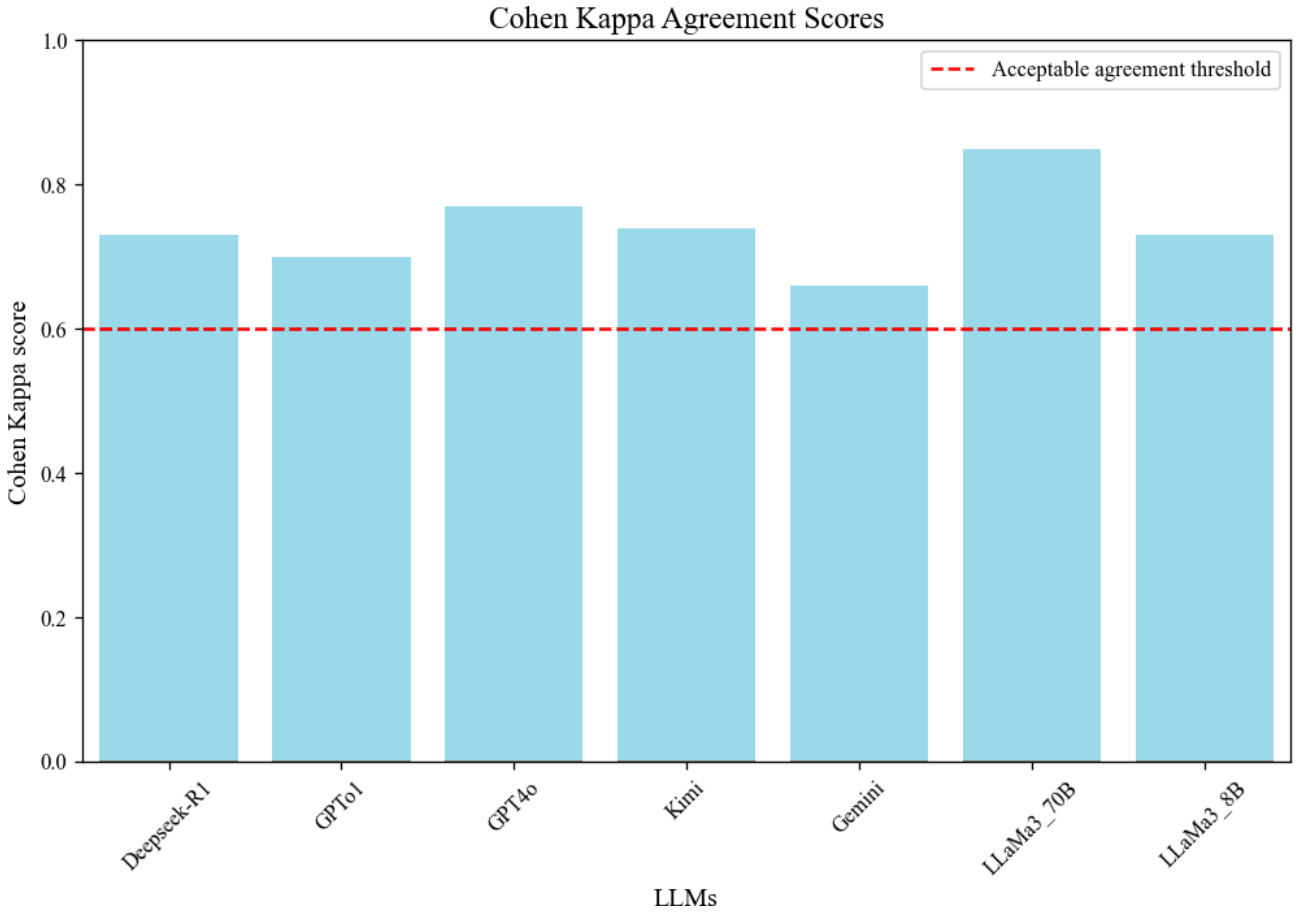
GPT-4o achieved moderate performance with a mean Likert score of 3.76 (95% CI 3.57 - 3.95) but still significantly outperformed Kimi (P=.02), Gemini, LLaMa3-70B, and LLaMa3-8B (all P<.001), suggesting adequate feasibility for clinical decision-making. Kimi (mean 3.48, 95% CI 3.31 - 3.64) had higher scores compared to Gemini, LLaMa3-70B, and LLaMa3-8B (all P<.001), although it demonstrated significantly lower decision-making ability than Deepseek-R1, GPTo1, and GPT4o.

Gemini (mean 2.96, 95% CI 2.78 - 3.14) showed marginally better performance compared to LLaMa3-70B (mean 2.86, 95% CI 2.71 - 3.02; P=.047), but no significant difference was observed between Gemini and LLaMa3-8B (mean 2.7, 95% CI 2.54 - 2.86; P=.52). The LLaMa3 series consistently showed the lowest clinical decision accuracy, significantly below all other models (all P<.001).

We further assessed the hallucination rates of LLMs and found that Deepseek-R1 and GPTo1 had the fewest hallucinations, with 6/80 (8%) and 5/80 (6%) cases, respectively. GPT-4o and Kimi followed, with 7/80 (9%) and 10/80 (12%) cases, respectively. In contrast, Gemini and both LLaMa3 variants demonstrated significantly higher hallucination rates, ranging from 13/80 (16%) to 25/80 (31%) (Figure 4.

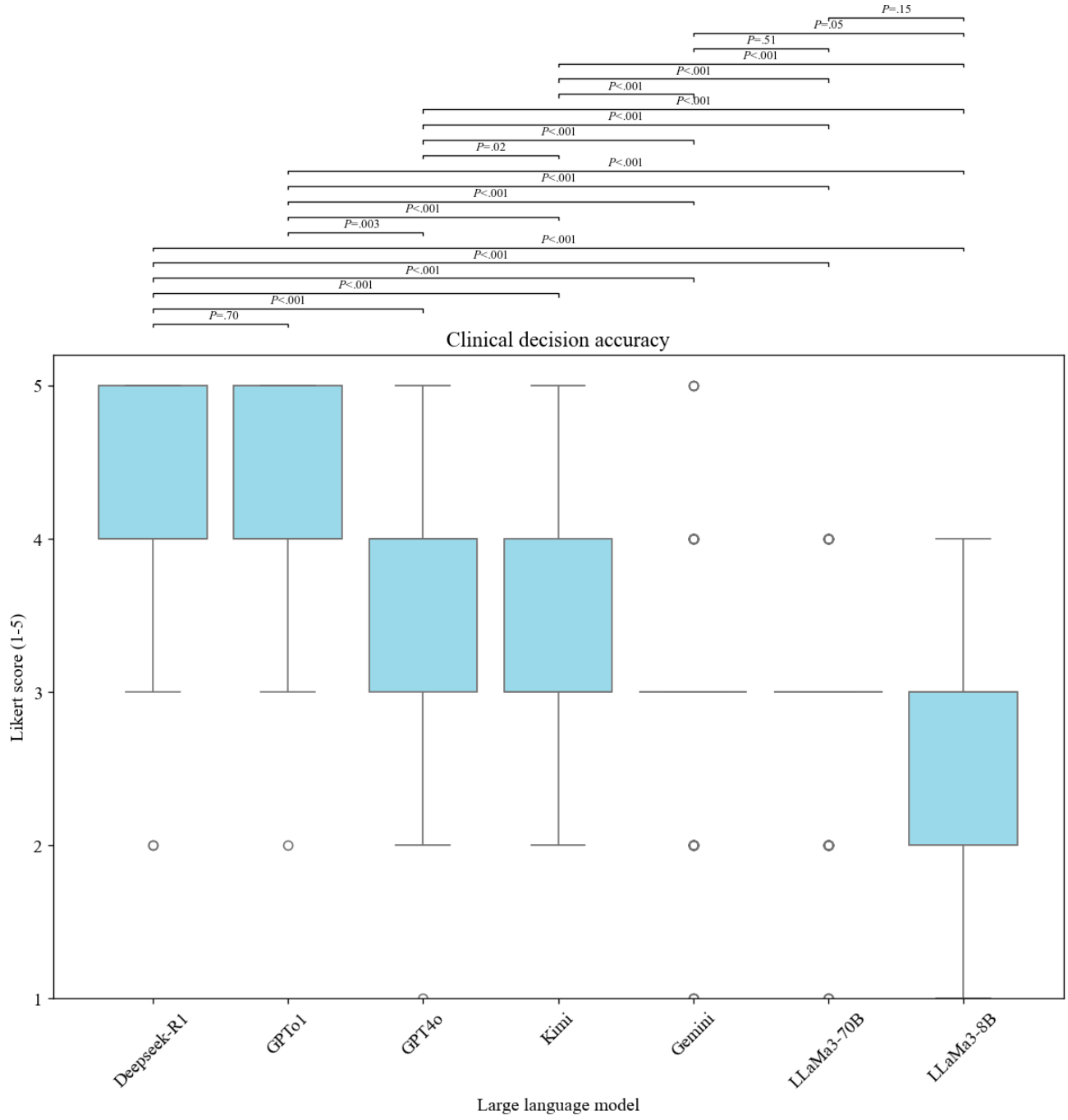
These findings demonstrate that Deepseek-R1 and GPTo1 not only achieved the highest Likert scores but also exhibited the lowest hallucination rates, underscoring their strong potential as AI-assisted tools for clinical decision-making. GPT-4o exhibited moderate yet consistent performance, supporting its applicability to more complex clinical scenarios. Kimi demonstrated intermediate performance, potentially useful in selected clinical situations but requiring further optimization. Conversely, Gemini, LLaMa3-70B, and LLaMa3-8B showed relatively poor performance, limiting their immediate clinical utility and highlighting the need for substantial improvement.

Figure 2. Cohen Kappa agreement between 2 senior clinical experts. LLMs: large language models.



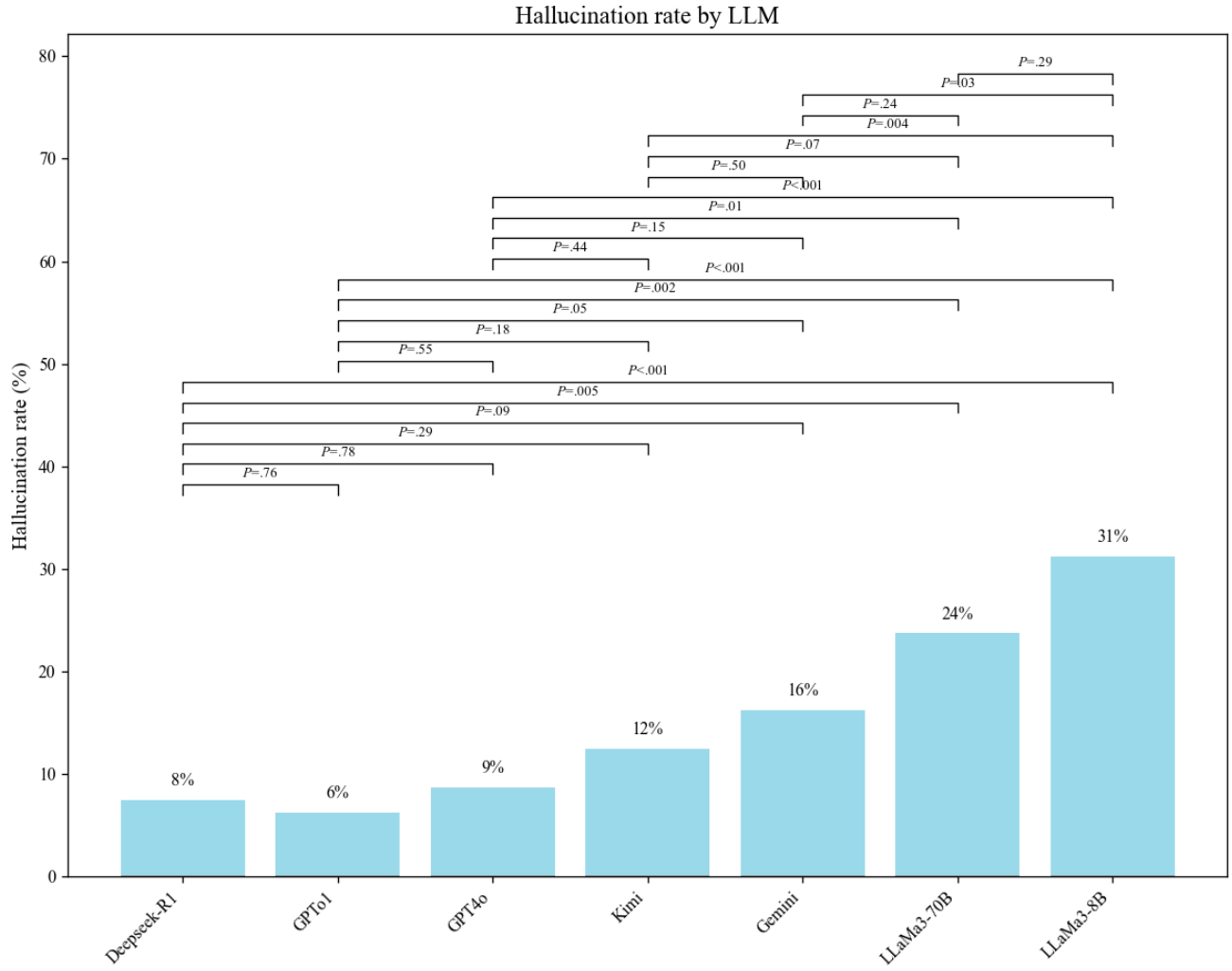
XSL•FO
RenderX

Figure 3. Clinical decision accuracy of large language models based on a 5-point Likert Scale.



XSL•FO
RenderX

Figure 4. Comparison of hallucination rates among different large language models.



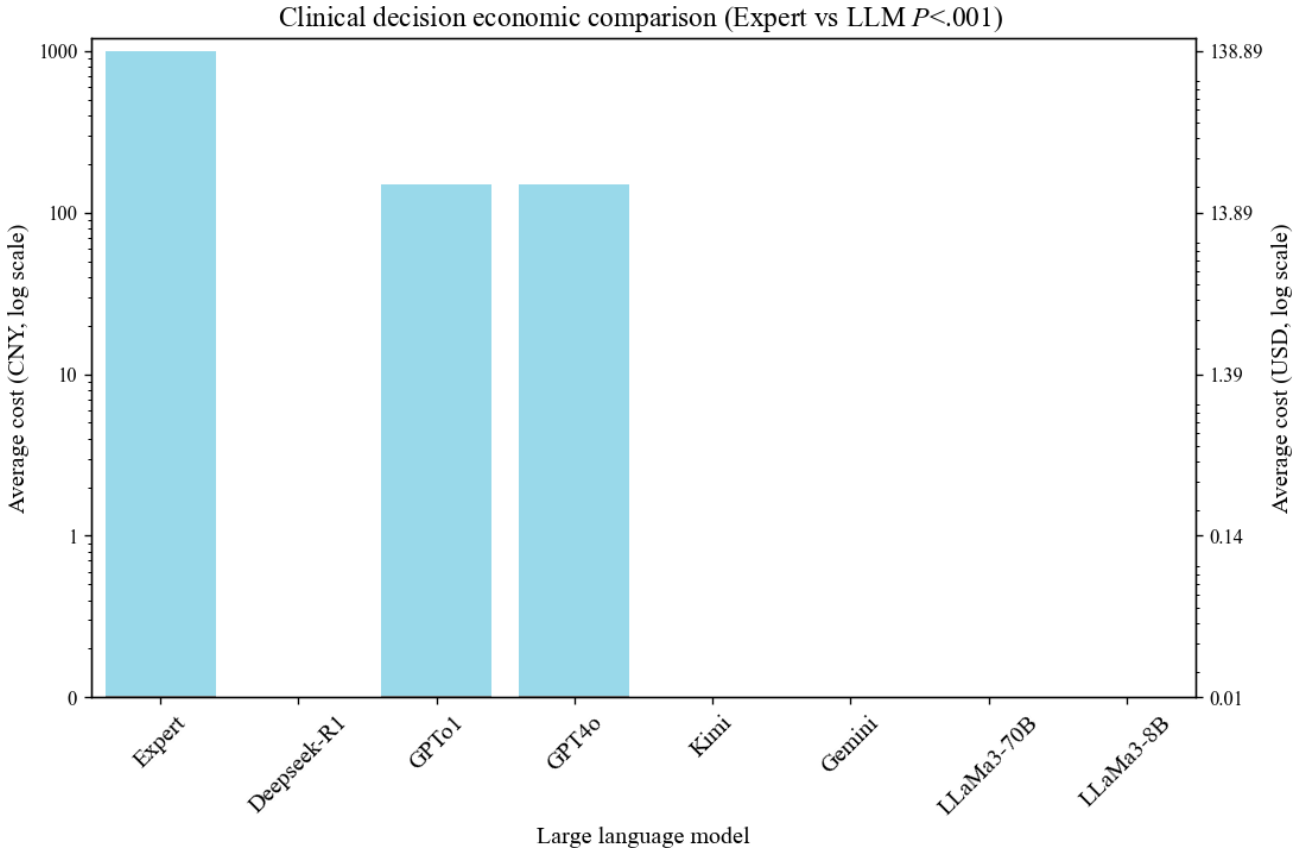
Clinical Decision Cost Evaluation

In this study, we compared clinical decision-making costs between MDT discussions and various LLMs (Figure 5). Our analysis revealed that the mean cost per MDT discussion conducted by experts was approximately 1000 Chinese Yuan Renminbi (about US $140), significantly higher than the decision-making costs associated with all evaluated LLMs ($P<.001$).

Within the LLM group, GPT4o and GPTo1 incurred direct costs of approximately 150 Chinese Yuan Renminbi (about US $20 for the Plus version), representing an 85% cost reduction compared to expert-led MDT discussions, thus demonstrating significant economic advantages. Additionally, Kimi and Gemini are proprietary models currently available without charge, whereas Deepseek-R1, LLaMa3-8B, and LLaMa3-70B are open-source models suitable for clinical decision support. These open-source LLMs potentially incur zero direct costs.

XSL•FO
RenderX

Figure 5. Cost comparison of clinical decision-making: experts versus large language models. CNY: Chinese Yuan Renminbi; LLM: large language model.



Discussion

Principal Findings

This study provides a preliminary assessment demonstrating that LLMs can significantly enhance the efficiency of clinical decision-making in complex clinical cases, while maintaining high decision accuracy and substantially reducing costs compared to traditional MDT discussions.

Performance and Potential Clinical Utility of LLMs

Our study results demonstrate that, compared to human experts, all LLMs significantly shortened decision-making time. The expert group had an average decision time of 33.6 (95% CI 32.57 - 34.63) minutes per case and involved a median of 7 clinical experts in the MDT discussion, while the most efficient model, GPTo1, took only 0.71 minutes, followed by GPT4o (0.88 minutes) and Deepseek (0.94 minutes). Even the longest decision time, observed in LLaMa3-70B, was only 3.20 minutes (which may be related to the insufficient GPU memory of the workstation in this study), still much faster than the expert group. Previous studies [17] also suggest that AI, through automating parts of the decision process, maintains accuracy in 88% of cases and provides quick, real-time feedback, thus improving efficiency and saving significant time and resources. This result highlights the potential application value of AI-assisted decision tools in high-demand clinical environments, especially in scenarios requiring rapid decision-making. Furthermore, the time differences among LLMs indicate that optimizing model architecture and inference time is critical to enhancing the real-time application capabilities of clinical decision-making.

In addition to improving decision efficiency, the reliability and accuracy of LLMs in clinical applications are equally crucial. This study found that Deepseek-R1 and GPTo1 performed the best in clinical decision accuracy, with decision levels comparable to that of human experts. However, there were still significant performance differences among the models. GPT-4o and Kimi showed moderate performance, suggesting that they may be suitable for general clinical tasks. For example, the accuracy of Gemini, LLaMa3-70B, and LLaMa3-8B was significantly lower, indicating limited applicability in critical clinical decision-making. Notably, Deepseek-R1 and GPTo1 demonstrated the lowest hallucination rates (8% and 6%, respectively), showing significantly better performance compared to GPT-4o (9%), Kimi (12%), and the Gemini and LLaMa3 models, whose rates ranged from 16% to 31%. These results underscore significant variability in content reliability among LLMs, aligning with prior studies [18] that reported hallucination rates ranging from 29% to 91% across different models. Interestingly, reasoning-optimized models such as Deepseek-R1 and GPTo1 showed a marked reduction in hallucinations, suggesting they may be more suitable for high-stakes medical applications where factual accuracy is critical. Beyond quantitative metrics, our study found qualitative differences in the reasoning styles of different LLMs. For example, Deepseek-R1 and GPTo1 tended to follow structured, guideline-concordant approaches, often closely mirroring the logic used by human MDT experts. GPT-4o and Kimi occasionally generated broader differential diagnoses. In

XSL•FO
RenderX

contrast, Gemini, LLaMa3-70B, and LLaMa3-8B responses included more redundant or loosely justified recommendations. These observations are preliminary and illustrative. A more comprehensive and systematic comparison of LLM reasoning will be conducted in future studies. These findings reaffirm that LLMs require rigorous validation before being applied to clinical decision-making. Our findings are consistent with recent studies by other researchers [11], which suggest that LLMs can serve as auxiliary tools to provide reference advice to clinical medical experts, rather than completely replacing human experts.

Currently, MDT discussions are still in their early stages in China [19]. High costs remain one of the barriers to their widespread application. Studies show that the average cost of each MDT discussion by experts is approximately 1000 Chinese Yuan Renminbi (about US $140) in a tier 3 grade A hospital in China, while the decision cost for GPT4o and GPTo1 is only around 150 Chinese yuan renminbi (Plus subscription version US $19.99), representing an 85% cost reduction. Moreover, Kimi and Gemini, as closed-source models, are currently available for free, while Deepseek-R1, LLaMa3-8B, and LLaMa3-70B are open-source models with the potential advantage of zero direct costs. This makes open-source LLMs more promising in environments with limited health care resources. Although LLMs show significant advantages in terms of economic efficiency, their clinical application still needs to consider indirect costs, such as equipment costs, model fine-tuning, and ethical oversight.

Risks and Deployment Strategies

It is also important to address privacy and security concerns when deploying LLMs in health care settings. In this study, some open-source models were deployed locally in a closed-loop environment without internet access or external application programming interface calls, effectively minimizing the risk of patient data leakage. In contrast, proprietary models such as GPT-4o, Kimi, and Gemini required data to be submitted via HTTPS after anonymization, which, despite encryption, still introduces potential risks of data exposure during transmission. For future clinical deployment, it is essential to implement privacy-preserving strategies such as on-premise inference, secure application programming interface gateways, and strict data de-identification.

While LLMs can significantly improve decision efficiency, maintain high diagnostic accuracy, and drastically reduce costs, some experts remain concerned about the potential misuse of LLMs and the lack of supervision [20]. At present, LLMs still have some imperfections, such as biases and hallucinations [21], which may be related to the Transformer architecture itself [22,23]. To address these challenges, several mitigation strategies should be considered, including deploying LLMs under expert supervision, conducting fine-tuning based on medical-specific datasets, and incorporating human-in-the-loop mechanisms to ensure clinical relevance and safety. Establishing robust ethical and governance frameworks is also imperative to support responsible and transparent deployment. In the short term, continued involvement of human experts remains critical, and the most pragmatic approach is a collaborative model in which LLMs assist clinicians rather than operate independently or autonomously.

Limitations

This study also has some limitations. First, our evaluation focused on LLMs' execution efficiency, decision accuracy, and costs, without in-depth exploration of the models' limitations, interpretability, and ethical implications. Future studies will adopt more comprehensive evaluation frameworks, such as Transparent Reporting of a multivariable prediction model for Individual Prognosis or Diagnosis-LLM extension [24], to incorporate additional dimensions including reproducibility, bias, and potential harm. Second, the data used in this study were obtained from a single institution, necessitating further external validation to assess the generalizability of LLMs across diverse health care settings. Third, we did not explore the integration of LLMs into hospital information systems in this study. While LLMs demonstrate significant transformative potential in clinical decision-making, further clinical trials and real-world validation are needed before their formal adoption in practice.

Conclusions

The study indicates that LLMs, particularly GPTo1 and Deepseek-R1, have immense potential in clinical decision-making, significantly improving efficiency, maintaining high diagnostic accuracy, and reducing costs. These models can serve as powerful auxiliary decision-making tools. GPT-4o and Kimi demonstrated moderate performance, suggesting that they may be suitable for general clinical tasks. However, the application of the LLaMa3 series and Gemini in clinical decision-making requires further investigation.

Acknowledgments

This study was supported by the National Natural Science Foundation of China (grant number 82373186). We would like to express our deepest gratitude to all those who have provided their support and assistance in the completion of this project.

Data Availability

The datasets generated or analyzed during this study are available from the corresponding author on reasonable request.

Authors' Contributions

YHH conceived the study. YHH, GZY, and YHS collected clinical data and analyzed clinical data, and wrote articles. XJL, YHW, KZ, JNX, HGC, and JZ participated in clinical data collection and large language model clinical decision evaluation.

XSL•FO
RenderX

Conflicts of Interest

None declared.

Multimedia Appendix 1
Evaluation setup and output comparison of various large language models in complex clinical cases.
[DOCX File, 24 KB - medinform_v13i1e73941_app1.docx]

References

1. Deng J, Lin Y. The benefits and challenges of ChatGPT: an overview. FCIS 2023;2(2):81-83. [doi: 10.54097/fcis.v2i2.4465]
2. Surameery NMS, Shakor MY. Use Chat GPT to solve programming bugs. IJITC 2023(31):17-22 [FREE Full text] [doi: 10.55529/ijitc.31.17.22]
3. Castonguay A, Lovis C. Introducing the "AI Language Models in Health Care" section: actionable strategies for targeted and wide-scale deployment. JMIR Med Inform 2023 Dec 21;11:e53785. [doi: 10.2196/53785] [Medline: 38127431]
4. Cho HN, Jun TJ, Kim YH, et al. Task-specific transformer-based language models in health care: scoping review. JMIR Med Inform 2024 Nov 18;12:e49724. [doi: 10.2196/49724] [Medline: 39556827]
5. Kung TH, Cheatham M, Medenilla A, et al. Performance of ChatGPT on USMLE: potential for AI-assisted medical education using large language models. PLOS Digit Health 2023 Feb;2(2):e0000198. [doi: 10.1371/journal.pdig.0000198] [Medline: 36812645]
6. Zhu L, Mou W, Wu K, et al. Multimodal ChatGPT-4V for electrocardiogram interpretation: promise and limitations. J Med Internet Res 2024 Jun 26;26:e54607. [doi: 10.2196/54607] [Medline: 38764297]
7. Liu J, Wang C, Liu S. Utility of ChatGPT in clinical practice. J Med Internet Res 2023 Jun 28;25:e48568. [doi: 10.2196/48568] [Medline: 37379067]
8. Lo F, Au K, Yang W. Correspondence of "Evaluation of large language models in breast cancer clinical scenarios: a comparative analysis based on ChatGPT-3.5, ChatGPT-4.0, and Claude2". Int J Surg 2024 Sep 1;110(9):5865-5866. [doi: 10.1097/JS9.0000000000001616] [Medline: 38752481]
9. Johnson D, Goodman R, Patrinely J, et al. Assessing the accuracy and reliability of AI-generated medical responses: an evaluation of the Chat-GPT model. Res Sq 2023 Feb 28:rs.3.rs-2566942. [doi: 10.21203/rs.3.rs-2566942/v1] [Medline: 36909565]
10. Eriksen AV, Möller S, Ryg J. Use of GPT-4 to diagnose complex clinical cases. NEJM AI 2024 Jan;1(1):AIp2300031. [doi: 10.1056/AIp2300031]
11. Kanjee Z, Crowe B, Rodman A. Accuracy of a generative artificial intelligence model in a complex diagnostic challenge. JAMA 2023 Jul 3;330(1):78-80. [doi: 10.1001/jama.2023.8288] [Medline: 37318797]
12. Miller L, Kamel P, Patel J, et al. A comparative evaluation of large language model utility in neuroimaging clinical decision support. J Imaging Inform Med 2024 Nov 7. [doi: 10.1007/s10278-024-01161-3] [Medline: 39508992]
13. Bedi S, Liu Y, Orr-Ewing L, et al. Testing and evaluation of health care applications of large language models: a systematic review. JAMA 2025 Jan 28;333(4):319-328. [doi: 10.1001/jama.2024.21700] [Medline: 39405325]
14. Sandmann S, Riepenhausen S, Plagwitz L, Varghese J. Systematic analysis of ChatGPT, Google search and Llama 2 for clinical decision support tasks. Nat Commun 2024 Mar 6;15(1):2050. [doi: 10.1038/s41467-024-46411-8] [Medline: 38448475]
15. Bond WF, Schwartz LM, Weaver KR, Levick D, Giuliano M, Graber ML. Differential diagnosis generators: an evaluation of currently available computer programs. J Gen Intern Med 2012 Feb;27(2):213-219. [doi: 10.1007/s11606-011-1804-8] [Medline: 21789717]
16. Landis JR, Koch GG. An application of hierarchical kappa-type statistics in the assessment of majority agreement among multiple observers. Biometrics 1977 Jun;33(2):363-374. [Medline: 884196]
17. McKinney SM, Sieniek M, Godbole V, et al. International evaluation of an AI system for breast cancer screening. Nature New Biol 2020 Jan;577(7788):89-94. [doi: 10.1038/s41586-019-1799-6] [Medline: 31894144]
18. Chelli M, Descamps J, Lavoué V, et al. Hallucination rates and reference accuracy of ChatGPT and Bard for systematic reviews: comparative analysis. J Med Internet Res 2024 May 22;26:e53164. [doi: 10.2196/53164] [Medline: 38776130]
19. Song P, Wu Q, Huang Y. Multidisciplinary team and team oncology medicine research and development in China. Biosci Trends 2010 Aug;4(4):151-160. [Medline: 20811133]
20. Webster P. Medical AI chatbots: are they safe to talk to patients? Nat Med 2023 Nov;29(11):2677-2679. [doi: 10.1038/s41591-023-02535-w] [Medline: 37684542]
21. Omar M, Agbareia R, Glicksberg BS, Nadkarni GN, Klang E. Benchmarking the confidence of large language models in answering clinical questions: cross-sectional evaluation study. JMIR Med Inform 2025 May 16;13:e66917. [doi: 10.2196/66917] [Medline: 40378406]
22. Trinh TH, Wu Y, Le QV, He H, Luong T. Solving olympiad geometry without human demonstrations. Nature New Biol 2024 Jan;625(7995):476-482. [doi: 10.1038/s41586-023-06747-5] [Medline: 38233616]

XSL•FO
RenderX

23. Vaswani A, Shazeer N, Parmar N, et al. Attention is all you need. arXiv. Preprint posted online on 2017. [doi: 10.48550/arXiv.1706.03762]
24. Gallifant J, Afshar M, Ameen S, et al. The TRIPOD-LLM reporting guideline for studies using large language models. Nat Med 2025 Jan;31(1):60-69. [doi: 10.1038/s41591-024-03425-5] [Medline: 39779929]

Abbreviations

ACLS: Advanced Cardiovascular Life Support
AI: artificial intelligence
LLM: large language model
MDT: Multidisciplinary Team
USMLE: United States Medical Licensing Examination

Edited by A Benis; submitted 14.03.25; peer-reviewed by A Adeoye, LY Jin; revised version received 30.05.25; accepted 10.06.25; published 14.08.25.

Please cite as:
Huang Y, Yang G, Shen Y, Chen H, Wu W, Li X, Wu Y, Zhang K, Xu J, Zhang J
Application of Large Language Models in Complex Clinical Cases: Cross-Sectional Evaluation Study
JMIR Med Inform 2025;13:e73941
URL: https://medinform.jmir.org/2025/1/e73941
doi:10.2196/73941

© Yuanheng Huang, Guozhen Yang, Yahui Shen, Huiguo Chen, Weibin Wu, Xiaojun Li, Yonghui Wu, Kai Zhang, Jiannan Xu, Jian Zhang. Originally published in JMIR Medical Informatics (https://medinform.jmir.org), 14.8.2025. This is an open-access article distributed under the terms of the Creative Commons Attribution License (https://creativecommons.org/licenses/by/4.0/), which permits unrestricted use, distribution, and reproduction in any medium, provided the original work, first published in JMIR Medical Informatics, is properly cited. The complete bibliographic information, a link to the original publication on https://medinform.jmir.org/, as well as this copyright and license information must be included.

XSL•FO
RenderX

Benchmarking the Confidence of Large Language Models in Answering Clinical Questions: Cross-Sectional Evaluation Study

Mahmud Omar[1*], MD; Reem Agbareia[2], MD; Benjamin S Glicksberg[1], MD; Girish N Nadkarni[1*], MD; Eyal Klang[1*], MD

[1]Division of Data-Driven and Digital Medicine (D3M), Department of Medicine, Icahn School of Medicine at Mount Sinai, Gustave L. Levy Place New York, New York, NY, United States

[2]Ophthalmology Department, Hadassah Medical Center, Jerusalem, Israel

[*]these authors contributed equally

Corresponding Author:
Mahmud Omar, MD
Division of Data-Driven and Digital Medicine (D3M), Department of Medicine, Icahn School of Medicine at Mount Sinai, Gustave L. Levy Place New York, New York, NY, United States

Abstract

Background: The capabilities of large language models (LLMs) to self-assess their own confidence in answering questions within the biomedical realm remain underexplored.

Objective: This study evaluates the confidence levels of 12 LLMs across 5 medical specialties to assess LLMs' ability to accurately judge their own responses.

Methods: We used 1965 multiple-choice questions that assessed clinical knowledge in the following areas: internal medicine, obstetrics and gynecology, psychiatry, pediatrics, and general surgery. Models were prompted to provide answers and to also provide their confidence for the correct answers (score: range 0% - 100%). We calculated the correlation between each model's mean confidence score for correct answers and the overall accuracy of each model across all questions. The confidence scores for correct and incorrect answers were also analyzed to determine the mean difference in confidence, using 2-sample, 2-tailed *t* tests.

Results: The correlation between the mean confidence scores for correct answers and model accuracy was inverse and statistically significant (r=−0.40; P=.001), indicating that worse-performing models exhibited paradoxically higher confidence. For instance, a top-performing model—GPT-4o—had a mean accuracy of 74% (SD 9.4%), with a mean confidence of 63% (SD 8.3%), whereas a low-performing model—Qwen2-7B—showed a mean accuracy of 46% (SD 10.5%) but a mean confidence of 76% (SD 11.7%). The mean difference in confidence between correct and incorrect responses was low for all models, ranging from 0.6% to 5.4%, with GPT-4o having the highest mean difference (5.4%, SD 2.3%; P=.003).

Conclusions: Better-performing LLMs show more aligned overall confidence levels. However, even the most accurate models still show minimal variation in confidence between right and wrong answers. This may limit their safe use in clinical settings. Addressing overconfidence could involve refining calibration methods, performing domain-specific fine-tuning, and involving human oversight when decisions carry high risks. Further research is needed to improve these strategies before broader clinical adoption of LLMs.

(JMIR Med Inform 2025;13:e66917) doi:10.2196/66917

KEYWORDS

safe AI; artificial intelligence; AI; algorithm; large language model; LLM; natural language processing; NLP; deep learning

Introduction

With their capacity to understand and generate human-like text, large language models (LLMs) are poised to support health care professionals in complex clinical decisions [1-3]. A wide array of LLMs is now accessible, including open-source models, offering solutions that cater to both the public and medical professionals [1,4].

The efficacy of these models has been demonstrated in a variety of tasks, albeit with some limitations [5,6]. For instance, LLMs, such as GPT, have shown promise in providing diagnostic assistance and answering medical queries [5,7-9]. Katz et al [10] demonstrated that GPT-4 not only improved clinically when compared to its predecessor, GPT-3.5, but also matched physician performance in certain areas. However, there is evidence of hallucinations and inaccuracies in model outputs, which could lead to harm in clinical decision-making [11,12]. Specifically, LLMs have occasionally generated completely

XSL•FO
RenderX

fabricated evidence (eg, information and references) and have presented such evidence as factual [11,12].

One way of building confidence in applying models within health care is the use of explainable artificial intelligence (AI) [13,14]. However, easily explainable outputs are difficult to evaluate due to the complexity of how LLMs process and output data [13,15,16]. Recent work revealed that these models often exhibit high confidence even when presenting incorrect information [17]. This raises questions about the underlying mechanisms that prompt an LLM to label certain statements as "more factual." For example, one possible explanation could be that data-rich or frequently discussed topics in training sets may be perceived as more certain [18], even if this does not translate into clinical accuracy. Additionally, retrieval-augmented generation (RAG) has been proposed to ground LLM outputs in external data, which potentially mitigates hallucinations [19]. Nevertheless, these approaches do not fully resolve whether models can reliably judge their own correctness. Accurate and well-calibrated confidence scores may be vital for establishing trust in these systems, as such scores can alert users to approach certain responses with caution. If a model consistently shows undue confidence in wrong answers, it poses a subtle but potentially dangerous form of hallucination. Clinicians might adopt decisions based on erroneous advice that is delivered with overt certainty. By investigating how these models generate and express their confidence, we aimed to illuminate whether LLMs can reliably self-assess correctness.

The goal of this study was to benchmark LLMs (both proprietary LLMs, like GPT-4o and Claude 3.5 Sonnet, and open-source LLMs, like Qwen) in terms of accuracy and associated confidence in answering clinical questions. Our aim was to determine if these models can accurately judge when to be confident in their responses and, in doing so, allow for better explainability in their application.

Methods

Study Design and Data Source

This study used a public compiled dataset from a previous study by Katz et al [10], which includes 655 questions for the following five medical specialties: internal medicine, obstetrics and gynecology (OBGYN), psychiatry, pediatrics, and general surgery. These questions were sourced from official 2023 licensing examinations for each field and were crafted from internationally recognized textbooks and guidelines. This dataset serves as a standardized framework for assessment [20-24].

To enhance benchmarking reliability, each original question was rephrased twice by using the GPT-4 application programming interface (API) in Python (Python Software Foundation), yielding 1965 questions (we include the full prompt in Multimedia Appendix 1). The prompts were carefully designed to modify only the writing style, without altering any clinical details, such as medical terms, laboratory values, or answer choices [25]. This approach aimed to preserve all clinical details, ensuring that rephrased questions stayed faithful to the original intent and information. To confirm this, 2 board-certified physicians separately reviewed a 20% random sample of questions from each specialty. They compared the rephrased and original questions side by side, focusing on consistency in medical terminology, laboratory values, and answer choices. Both reviewers concluded that the paraphrased items remained unchanged in terms of clinical meaning and required no further edits, thereby confirming overall integrity and accuracy.

Model Setup and Configuration

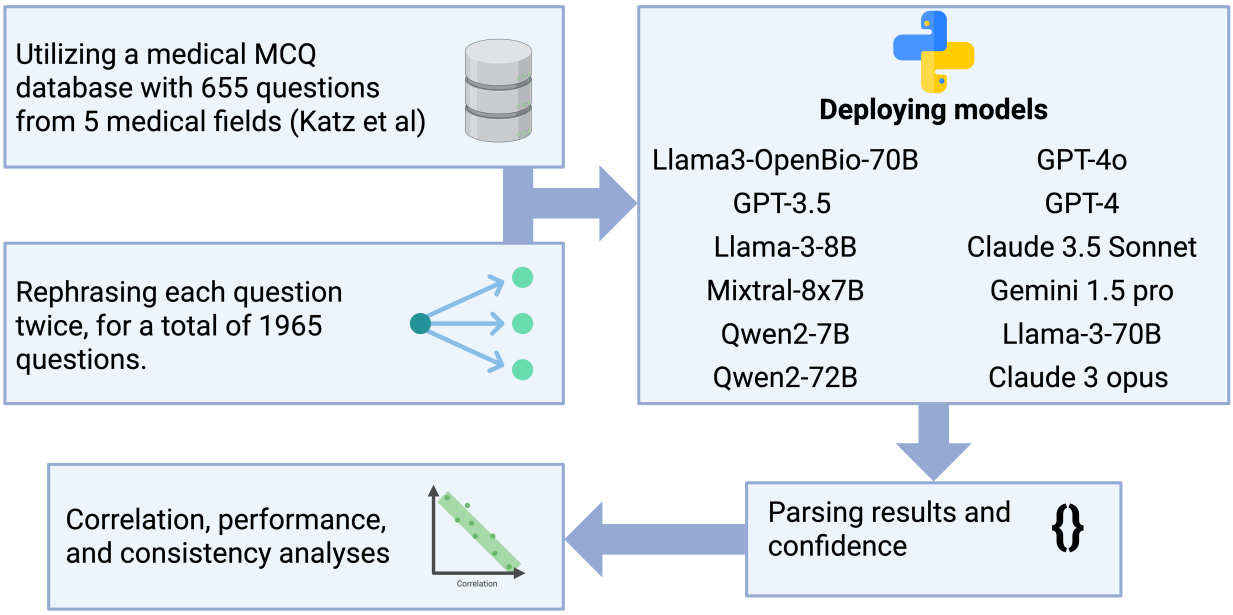
The LLMs used in this study were prompted (using 1 structured prompt) to return the correct answer, along with a confidence score for each choice ("A," "B," "C," and "D"), in JSON format. These confidence scores were expressed as percentages between 0% and 100% for each option, resulting in a total confidence score of 100% for all options combined. The open access models were executed by using API codes in a dedicated server with 4 H100 80-GB graphics processing units; the corresponding codebase is accessible on GitHub for the original database by Katz et al [10], and we provide the full prompts, which can be used locally, in Multimedia Appendix 1. We used Python 3.10 for data analyses. The commercial models were used via the corresponding companies' API interfaces. We used several Python libraries to facilitate data processing, model interaction, and analysis—NumPy 1.26.4, Pandas 2.1.4, Scikit-Learn 1.3.0, Hugging Face's Transformers 4.37.2, and torch 2.2.2+cu121—as well as JSON module 2.0.9. We used the default hyperparameters for each model to reflect typical user settings and provide a balanced baseline [26]. For the open access models, we used the "instruct" versions, which perform better on zero-shot questioning.

Benchmarked LLMs

We selected 12 LLMs that varied in terms of size, architectures, and intended domains (Figure 1). This set included established "household" models and newly introduced or domain-focused alternatives, ensuring diverse coverage (Figure 1). The benchmarked models are shown in Table S1 in Multimedia Appendix 1.

XSL•FO
RenderX

Figure 1. A flowchart representing the evaluation methodology. The 655 questions were sourced from a study by Katz et al [10]. MCQ: multiple-choice question.



Statistical Analysis

The Pearson correlation coefficient was used to correlate models' mean confidence scores for correct answers and accuracies across models and medical fields. Chi-square tests assessed overall performance differences within each field, using proportions of correct responses. Post hoc pairwise comparisons with Bonferroni correction identified specific intermodel differences. Confidence levels were compared between correct and incorrect responses for each model, using 2-sample, 2-tailed *t* tests. Mean confidence scores were calculated for higher-tier and lower-tier models, as well as across all models. Performance consistency was evaluated by comparing confidence gaps between correct and incorrect responses. All statistical tests used a significance level of α=.05. Analyses were performed using R version 4.1.2 (R Foundation for Statistical Computing).

Results

Confidence Analysis

Table 1 summarizes accuracies and confidence levels across the models, and Table S2 in Multimedia Appendix 1 presents the data across all inspected fields and all models. An inverse correlation between the mean confidence scores for correct answers and the overall accuracy of the models is demonstrated (r=–0.40; P=.001); better-performing models generally showed lower confidence.

Table . Accuracies and confidence levels across the models.

Model	Accuracy, %	Total confidence, %	Confidence for correct answer, %	Confidence for incorrect answer, %
Claude 3.5 Sonnet	74	69.7	70.5	67.4
GPT-4o	73.8	63	64.4	59
Claude 3 Opus	71.7	68.5	68.9	67.3
GPT-4	66	84.1	84.5	83.3
Llama-3-70B	63.4	57.3	59.5	53.6
Llama OpenBio	59.2	77.9	77.7	78.1
Gemini	59.1	86.5	87.2	85.5
Qwen2-72B	57.8	57.7	58.6	56.5
Mixtral-8×7B	50.6	84.3	85.5	83
GPT-3.5	49	82.3	81.6	82.9
Llama-3-8B	48.4	80	79.7	80.3
Qwen2-7B	46	75.5	74.4	76.4

XSL•FO
RenderX

The mean confidence score for all 12 models was 76.1% when they were correct and 74.4% when they were incorrect. The 6 top-performing models showed a mean confidence score of 72.5% when they were correct and a mean confidence score of 69.4% when incorrect, while the 6 lowest-performing models displayed 79.6% confidence when they were correct and 79.5% confidence when they were incorrect (Table 2).

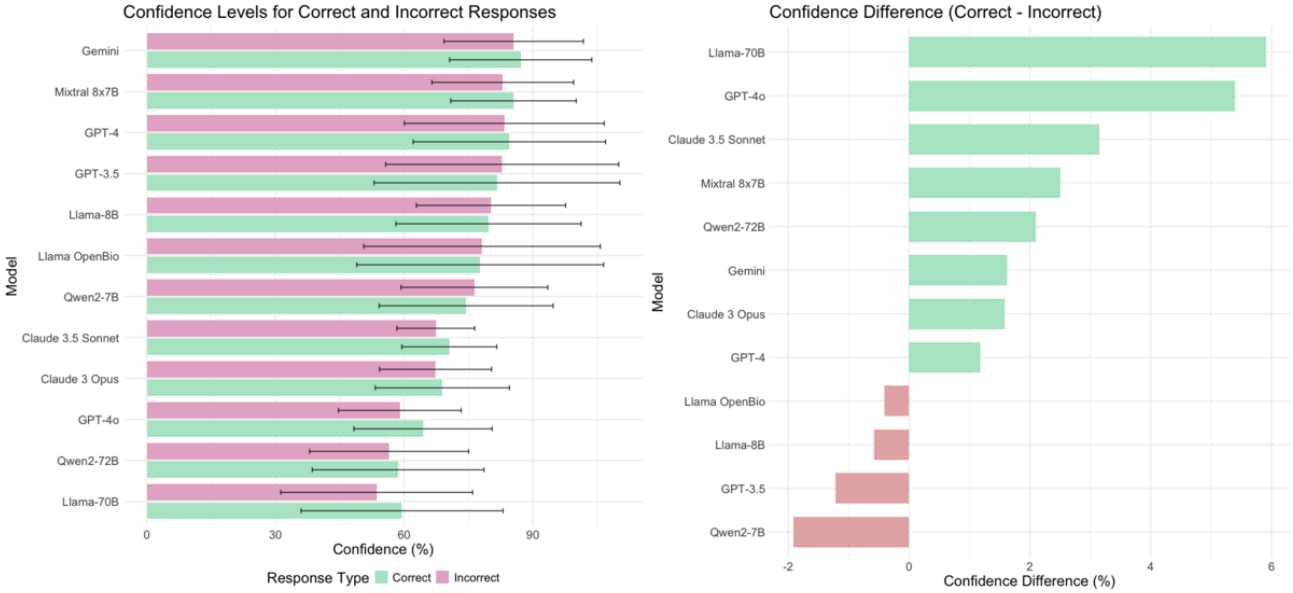
Table . Large language models' mean confidence scores for correct and incorrect answers.

Model	Confidence when incorrect (%), mean (SD)	Confidence when correct (%), mean (SD)	*P* value
GPT-4o	58.99 (14.31)	64.38 (16.11)	.006
Llama-3-70B	53.59 (22.38)	59.50 (23.54)	.006
Claude 3.5 Sonnet	67.37 (9.08)	70.52 (11.07)	.003
Gemini	85.55 (16.23)	87.17 (16.58)	.35
Claude 3 Opus	67.32 (13.06)	68.90 (15.65)	.61
GPT-4	83.34 (23.30)	84.52 (22.43)	.07
Qwen2-72B	56.49 (18.55)	58.59 (20.03)	.004
Qwen2-7B	76.37 (17.11)	74.45 (20.30)	.01
Mixtral-8×7B	82.99 (16.52)	85.49 (14.62)	.04
Llama-3-8B	80.25 (17.40)	79.67 (21.59)	.31
Llama OpenBio	78.14 (27.59)	77.73 (28.78)	.83
GPT-3.5	82.85 (27.17)	81.63 (28.66)	.81

Four models (GPT-4o, Llama-3-70B, Claude 3.5 Sonnet, and Qwen2-72B) demonstrated significantly higher confidence when they were correct (all *P* values were <.01) across the different fields and subsets. Gemini exhibited the highest overall confidence levels (when incorrect: mean 85.6%, SD 16.2%; when correct: mean 87.2%, SD 16.6%). Qwen2-7B was unique in that it displayed higher confidence when incorrect (mean 76.4%, SD 17.1% vs mean 74.5%, SD 20.3% when correct; *P*=.01).

GPT-3.5 and Llama-OpenBio-70B revealed minimal differences in confidence between correct and incorrect answers (*P*=.80). The largest confidence gap was observed in GPT-4 (5.4%, SD 2.3%; *P*=.003), while Llama-3-8B had the smallest gap (0.6%; Figure 2).

Figure 2. Large language models' confidence results for correct and incorrect answers. The left graph displays the average confidence and 95% CIs for each model, categorized by correct answers (green) and incorrect answers (red). The right graph shows the differences in average confidence for each model, where green indicates higher confidence in correct answers, and red indicates higher confidence in incorrect answers.



Models' Performances Across Fields

Significant differences were seen in model performance across all 5 medical specialties (at the *P*<.01 level). GPT-4o and Claude 3.5 Sonnet consistently outperformed other models. For internal medicine, GPT-4o (accuracy: 70.9%) and Claude 3.5 Sonnet (accuracy: 73.5%) showed no significant difference (*P*>.99) but outperformed lower-tier models, such as Qwen-7b (accuracy:

XSL•FO
RenderX

43.7%; *P*<.001). For OBGYN, Claude 3.5 Sonnet (accuracy: 71.0%) significantly outperformed most models, including GPT-4 (accuracy: 54.0%; *P*<.001). For pediatrics, the top 5 models (GPT-4o, Llama-3-70b, Claude 3.5 Sonnet, Claude 3 Opus, and GPT-4) showed no significant differences among themselves (all *P* values were >.05) but outperformed lower-tier models. Psychiatry results mirrored this pattern, with GPT-4o (accuracy: 84.4%) and Claude 3.5 Sonnet (accuracy: 82.4%) showing the best performance. For surgery, GPT-4o (accuracy: 70.9%) and Claude 3.5 Sonnet (accuracy: 70.5%) again showed no significant difference (*P*>.99) but outperformed lower-performing models, such as Qwen-7b (accuracy: 45.6%; *P*<.01; Tables S3 and S4 in Multimedia Appendix 1).

Discussion

In our evaluation, accuracy and confidence were inversely correlated for LLMs. Some lower-complexity models were notably more confident in incorrect answers. Despite GPT-4o showing the best performance, its largest observed gap between confidence scores for correct and incorrect answers was only 5.4%. This indicates that it may be insufficient for reliably guiding clinical choices, although the difference was statistically significant, and the model's confidence levels for correct and incorrect responses were generally high. Consequently, this gap does not provide a meaningful threshold for differentiating safe decision-making from potentially harmful decision-making in real-world practice. These results highlight potential risks in clinical applications, where model confidence, regardless of answer correctness, could lead to misinformed decisions.

We think that the observed miscalibration between correctness and confidence may pose risks in daily clinical practice if it remains unresolved. Overconfident models may recommend unsafe dosages or overlook key signs in a patient's presentation, especially under the fast-paced pressures of modern practice. This could lead to incorrect prescriptions or treatments. For example, the model might prescribe an incorrect antibiotic for a resistant infection, thereby delaying proper care. In other cases, a model's unwarranted confidence in a wrong triage decision could divert urgent attention from a critical patient. Such errors can increase morbidity and may undermine trust in AI-assisted clinical tools.

A brief comparison across models of various sizes did not reveal a consistent relationship between model size and confidence gaps. For instance, Qwen2-72B showed about a 2% difference in confidence between correct and incorrect responses, while Qwen2-7B exhibited a similarly small difference. This pattern was noted across multiple specialties, suggesting that architecture or domain-specific factors may play a more pivotal role than sheer model size in determining confidence behaviors.

Katz et al [10] reported that GPT-4 outperformed physicians in psychiatry and performed comparably to physicians in general surgery and internal medicine. Our study corroborates GPT-4's strong performance, particularly in psychiatry, where GPT-4o achieved 84.4% accuracy. However, our findings suggest that more cautious interpretation is needed, given the high confidence levels observed for incorrect answers. Xiong et al's [17] work on LLM confidence elicitation aligns with our observations of overconfidence. They noted improved calibration and failure prediction as model capability increased, which parallels our finding of better confidence calibration in more complex models.

If prompted confidence scores are truly driven by a model's internal representations and are not random or uncontextualized outputs, then consistently arbitrary numbers would suggest a disconnect between the model's knowledge state and its confidence estimates. Such misalignment can arise if the model's architecture, training data, or prompting strategies do not calibrate confidence with genuine certainty [17]. In other words, a system might systematically generate high confidence, regardless of accuracy, if it lacks mechanisms or fine-tuning for self-regulating uncertainty [27]. Even larger models sometimes yield small or inconsistent confidence gaps, indicating that domain-specific refinements or improved calibration may be required. Without such refinements, confidence levels may remain weakly tied to actual reasoning processes, meaning that they would not reflect well-grounded internal assessments.

The implications for clinical practice warrant careful consideration. Although the performance leap of newer models is promising, their inability to accurately self-assess confidence across wrong answers poses risks. Two possible strategies for addressing these challenges can be the use of human-in-the-loop protocols and the implementation of ensemble methods [28].

Human-AI collaboration may offer a balanced approach to leveraging AI strengths while maintaining necessary human oversight in health care [29]. Sezgin [29] suggested a human-in-the-loop approach for ensuring that AI systems are supervised via human expertise. However, the effective implementation of this approach faces challenges. The careful design of user interfaces is important for preventing automation bias [29,30]. There are also concerns about the potential erosion of clinical skills as a result of overreliance on AI [31].

Emerging evidence also suggests that some prompt engineering techniques can reduce but not completely eliminate sociodemographic bias in model outputs [32]. However, studies continue to reveal significant sociodemographic biases in LLMs, such as a large-scale study by Omar et al [33]. These biases may affect patient prioritization, treatment recommendations, and mental health screening across different groups, potentially driving disparities in care [33]. Simply removing demographic variables (eg, gender and race) may also risk overlooking clinically relevant distinctions. In the context of our study, better-calibrated confidence outputs may help to mitigate such biases by allowing models to reliably signal uncertainty, which is especially important for sensitive medical decisions. Nonetheless, the comprehensive evaluation of these strategies requires longitudinal studies that monitor the evolution of biases and large-scale, globally diverse datasets, which can be used to refine mitigation approaches.

Ensemble methods, which aggregate multiple models, present another possible strategy [34]. Mahajan et al [35] conducted a review of ensemble learning techniques for disease prediction. They found that stacking—an ensemble method that combines multiple classifiers—showed the most accurate performance in 19 out of 23 cases. The voting approach was identified as the

XSL•FO
RenderX

second-best ensemble method. However, ensemble methods are computationally intensive and may introduce latency in real-time clinical applications [36]. In some scenarios, a slight increase in overall accuracy might justify extra processing time, yet in urgent applications (eg, emergency triage), even brief delays can be problematic. Ensemble methods aggregate outputs from multiple models, distributing the "confidence load" so that individual sources of skewed certainty are less influential. However, our findings suggest that many current models show miscalibrated confidence levels. If all component models in an ensemble are prone to the same calibration issues, combining them may amplify rather than correct erroneous certainty.

Both strategies—human-in-the-loop protocols and the implementation of ensemble methods—would require extensive clinical trials for validation and the development of model-specific calibration curves for each medical specialty.

Our study has several limitations. The dataset was limited to 1965 multiple-choice questions for 5 medical specialties; therefore, the dataset may not fully represent the breadth of clinical scenarios. Further, the combination of automatic rephrasing and manual validation could have introduced bias [25]. We also used default model hyperparameters, which potentially limited performance optimization. To address these constraints, future work could expand the question sets (eg, by including a broader array of medical domains) and adopt real-world clinical data rather than purely examination-style questions. Additionally, custom hyperparameter tuning or advanced methods, such as RAG and fine-tuning, could be used to further refine model accuracy and confidence calibration [37], as the use of default hyperparameters, which may have varied across the evaluated LLMs, could have influenced their reported confidence levels. Finally, investigating computational cost and the time efficiency of deploying these models in clinical workflows would help to clarify practical feasibility.

In conclusion, better-performing LLMs show more aligned overall confidence levels, yet even the most accurate models still display minimal variation between right and wrong answers. This highlights a limitation in current self-assessment mechanisms and calls for further research. Future efforts could include larger and more diverse clinical datasets, domain-specific calibration strategies, and real-world testing to refine confidence estimates. Such work is critical before broader implementation of LLMs in clinical settings.

Acknowledgments

We thank Dr Uriel Katz and the coauthors of the paper *GPT versus Resident Physicians — A Benchmark Based on Official Board Scores* [10] for sharing the multiple-choice question dataset.

Conflicts of Interest

None declared.

Multimedia Appendix 1
Supplementary materials with further information on the benchmarked large language models, their performance across different fields and specialties, and the prompt used for rephrasing the questions.
[DOCX File, 36 KB - medinform_v13i1e66917_app1.docx]

References

1. Thirunavukarasu AJ, Ting DSJ, Elangovan K, Gutierrez L, Tan TF, Ting DSW. Large language models in medicine. Nat Med 2023 Aug;29(8):1930-1940. [doi: 10.1038/s41591-023-02448-8] [Medline: 37460753]
2. Clusmann J, Kolbinger FR, Muti HS, et al. The future landscape of large language models in medicine. Commun Med (Lond) 2023 Oct 10;3(1):141. [doi: 10.1038/s43856-023-00370-1] [Medline: 37816837]
3. Tayebi Arasteh S, Han T, Lotfinia M, et al. Large language models streamline automated machine learning for clinical studies. Nat Commun 2024 Feb 21;15(1):1603. [doi: 10.1038/s41467-024-45879-8] [Medline: 38383555]
4. Shah NH, Entwistle D, Pfeffer MA. Creation and adoption of large language models in medicine. JAMA 2023 Sep 5;330(9):866-869. [doi: 10.1001/jama.2023.14217] [Medline: 37548965]
5. Kanjee Z, Crowe B, Rodman A. Accuracy of a generative artificial intelligence model in a complex diagnostic challenge. JAMA 2023 Jul 3;330(1):78-80. [doi: 10.1001/jama.2023.8288] [Medline: 37318797]
6. Singhal K, Azizi S, Tu T, et al. Large language models encode clinical knowledge. Nature 2023 Aug;620(7972):172-180. [doi: 10.1038/s41586-023-06291-2] [Medline: 37438534]
7. Johnson D, Goodman R, Patrinely J, et al. Assessing the accuracy and reliability of AI-generated medical responses: an evaluation of the Chat-GPT model. Res Sq. Preprint posted online on Feb 28, 2023. [doi: 10.21203/rs.3.rs-2566942/v1] [Medline: 36909565]
8. Giannos P. Evaluating the limits of AI in medical specialisation: ChatGPT's performance on the UK Neurology Specialty Certificate Examination. BMJ Neurol Open 2023 Jun 15;5(1):e000451. [doi: 10.1136/bmjno-2023-000451] [Medline: 37337531]

XSL•FO
RenderX

9. Hoch CC, Wollenberg B, Lüers JC, et al. ChatGPT's quiz skills in different otolaryngology subspecialties: an analysis of 2576 single-choice and multiple-choice board certification preparation questions. Eur Arch Otorhinolaryngol 2023 Sep;280(9):4271-4278. [doi: 10.1007/s00405-023-08051-4] [Medline: 37285018]
10. Katz U, Cohen E, Shachar E, et al. GPT versus resident physicians — a benchmark based on official board scores. NEJM AI 2024 Apr 12;1(5):AIdbp2300192. [doi: 10.1056/AIdbp2300192]
11. Omar M, Nassar S, Hijaze K, Glicksberg BS, Nadkarni GN, Klang E. Generating credible referenced medical research: a comparative study of OpenAI's Gpt-4 and Google's Gemini. SSRN. Preprint posted online on Apr 2, 2024. [doi: 10.2139/ssrn.4780940]
12. Azamfirei R, Kudchadkar SR, Fackler J. Large language models and the perils of their hallucinations. Crit Care 2023 Mar 21;27(1):120. [doi: 10.1186/s13054-023-04393-x] [Medline: 36945051]
13. Yang G, Ye Q, Xia J. Unbox the black-box for the medical explainable AI via multi-modal and multi-centre data fusion: a mini-review, two showcases and beyond. Inf Fusion 2022 Jan;77:29-52. [doi: 10.1016/j.inffus.2021.07.016] [Medline: 34980946]
14. Soroush A, Glicksberg BS, Zimlichman E, et al. Large language models are poor medical coders — benchmarking of medical code querying. NEJM AI 2024 Apr 19;1(5):AIdbp2300040. [doi: 10.1056/AIdbp2300040]
15. Schwartz IS, Link KE, Daneshjou R, Cortés-Penfield N. Black box warning: large language models and the future of infectious diseases consultation. Clin Infect Dis 2024 Apr 10;78(4):860-866. [doi: 10.1093/cid/ciad633] [Medline: 37971399]
16. Poon AIF, Sung JJY. Opening the black box of AI-medicine. J Gastroenterol Hepatol 2021 Mar;36(3):581-584. [doi: 10.1111/jgh.15384] [Medline: 33709609]
17. Xiong M, Hu Z, Lu X, et al. Can LLMs express their uncertainty? An empirical evaluation of confidence elicitation in LLMs. arXiv. Preprint posted online on Mar 17, 2024. [doi: 10.48550/arXiv.2306.13063]
18. Sarker IH. Machine learning: algorithms, real-world applications and research directions. SN Comput Sci 2021;2(3):160. [doi: 10.1007/s42979-021-00592-x] [Medline: 33778771]
19. Xiong G, Jin Q, Wang X, Zhang M, Lu Z, Zhang A. Improving retrieval-augmented generation in medicine with iterative follow-up questions. Pac Symp Biocomput 2025;30:199-214. [Medline: 39670371]
20. Townsend CM, Beauchamp RD, Evers BM, Mattox KL. Sabiston Textbook of Surgery: The Biological Basis of Modern Surgical Practice: Elsevier Health Sciences; 2016.
21. Loscalzo J, Fauci AS, Kasper DL, Hauser SL, Longo DL, Jameson JL. Harrison's Principles of Internal Medicine: McGraw Hill; 2022. URL: https://cir.nii.ac.jp/crid/1130573781693502243 [accessed 2025-05-02]
22. Kliegman RM, Behrman RE, Jenson HB, Stanton BMD. Nelson Textbook of Pediatrics E-Book: Elsevier Health Sciences; 2007.
23. American Psychiatric Association. Diagnostic and Statistical Manual of Mental Disorders: American Psychiatric Publishing; 2000. URL: https://cir.nii.ac.jp/crid/1573950399819987840 [accessed 2025-05-02]
24. Gabbe SG, Niebyl JR, Simpson JL, et al. Obstetrics: Normal and Problem Pregnancies E-Book: Elsevier Health Sciences; 2016.
25. Soni S, Roberts K. Paraphrasing to improve the performance of electronic health records question answering. AMIA Jt Summits Transl Sci Proc 2020 May 30;2020:626-635. [Medline: 32477685]
26. OpenAI, Achiam J, Adler S, et al. GPT-4 technical report. arXiv. Preprint posted online on Mar 4, 2024. [doi: 10.48550/arXiv.2303.08774]
27. Liu L, Pan Y, Li X, Chen G. Uncertainty estimation and quantification for llms: a simple supervised approach. arXiv. Preprint posted online on Oct 23, 2024. [doi: 10.48550/arXiv.2404.15993]
28. Longhurst CA, Singh K, Chopra A, Atreja A, Brownstein JS. A call for artificial intelligence implementation science centers to evaluate clinical effectiveness. NEJM AI 2024 Jul 10;1(8):AIp2400223. [doi: 10.1056/AIp2400223]
29. Sezgin E. Artificial intelligence in healthcare: complementing, not replacing, doctors and healthcare providers. Digit Health 2023 Jul;9:20552076231186520. [doi: 10.1177/20552076231186520] [Medline: 37426593]
30. Straw I. The automation of bias in medical artificial intelligence (AI): decoding the past to create a better future. Artif Intell Med 2020 Nov;110:101965. [doi: 10.1016/j.artmed.2020.101965] [Medline: 33250145]
31. Čartolovni A, Malešević A, Poslon L. Critical analysis of the AI impact on the patient-physician relationship: a multi-stakeholder qualitative study. Digit Health 2023 Dec 19;9:20552076231220833. [doi: 10.1177/20552076231220833] [Medline: 38130798]
32. Omar M, Sorin V, Agbareia R, et al. Evaluating and addressing demographic disparities in medical large language models: a systematic review. medRxiv. Preprint posted online on Sep 9, 2024. [doi: 10.1101/2024.09.09.24313295]
33. Omar M, Soffer S, Agbareia R, et al. Socio-demographic biases in medical decision-making by large language models: a large-scale multi-model analysis. medRxiv. Preprint posted online on Oct 30, 2024. [doi: 10.1101/2024.10.29.24316368]
34. Yang H, Li M, Zhou H, Xiao Y, Fang Q, Zhang R. One LLM is not enough: harnessing the power of ensemble learning for medical question answering. medRxiv. Preprint posted online on Dec 24, 2023. [doi: 10.1101/2023.12.21.23300380] [Medline: 38196648]
35. Mahajan P, Uddin S, Hajati F, Moni MA. Ensemble learning for disease prediction: a review. Healthcare (Basel) 2023 Jun 20;11(12):1808. [doi: 10.3390/healthcare11121808] [Medline: 37372925]

XSL•FO
RenderX

36. Edeh MO, Dalal S, Dhaou IB, et al. Artificial intelligence-based ensemble learning model for prediction of hepatitis C disease. Front Public Health 2022 Apr 27;10:892371. [doi: 10.3389/fpubh.2022.892371] [Medline: 35570979]
37. Glicksberg BS, Timsina P, Patel D, et al. Evaluating the accuracy of a state-of-the-art large language model for prediction of admissions from the emergency room. J Am Med Inform Assoc 2024 Sep 1;31(9):1921-1928. [doi: 10.1093/jamia/ocae103] [Medline: 38771093]

Abbreviations

AI: artificial intelligence
API: application programming interface
LLM: large language model
OBGYN: obstetrics and gynecology
RAG: retrieval-augmented generation

Edited by A Castonguay; submitted 26.09.24; peer-reviewed by D Sharma, ST Arasteh; revised version received 31.01.25; accepted 31.01.25; published 16.05.25.

Please cite as:
Omar M, Agbareia R, Glicksberg BS, Nadkarni GN, Klang E
Benchmarking the Confidence of Large Language Models in Answering Clinical Questions: Cross-Sectional Evaluation Study
JMIR Med Inform 2025;13:e66917
URL: https://medinform.jmir.org/2025/1/e66917
doi:10.2196/66917

© Mahmud Omar, Reem Agbareia, Benjamin S Glicksberg, Girish N Nadkarni, Eyal Klang. Originally published in JMIR Medical Informatics (https://medinform.jmir.org), 16.5.2025. This is an open-access article distributed under the terms of the Creative Commons Attribution License (https://creativecommons.org/licenses/by/4.0/), which permits unrestricted use, distribution, and reproduction in any medium, provided the original work, first published in JMIR Medical Informatics, is properly cited. The complete bibliographic information, a link to the original publication on https://medinform.jmir.org/, as well as this copyright and license information must be included.

XSL•FO
RenderX

Identifying Patient-Reported Care Experiences in Free-Text Survey Comments: Topic Modeling Study

Brian Steele[1], MSc; Paul Fairie[2,3], PhD; Kyle Kemp[2], PhD; Adam G D'Souza[1,4], PhD; Matthias Wilms[2,5], Dr rer nat; Maria Jose Santana[2,3,6], PhD

[1]Centre for Health Informatics, Cumming School of Medicine, University of Calgary, Cal Wenzel Precision Health Building, 3280 Hospital Dr NW, Calgary, AB, Canada

[2]Department of Community Health Sciences, Cumming School of Medicine, University of Calgary, Calgary, AB, Canada

[3]Alberta SPORT SUPPORT Unit Patient Engagement Team, Calgary, AB, Canada

[4]Provincial Research Data Services, Alberta Health Services, Calgary, Alberta, Canada

[5]Department of Radiology, Cumming School of Medicine, University of Calgary, Calgary, AB, Canada

[6]Department of Pediatrics, Cumming School of Medicine, University of Calgary, Calgary, AB, Canada

Corresponding Author:
Brian Steele, MSc
Centre for Health Informatics, Cumming School of Medicine, University of Calgary, Cal Wenzel Precision Health Building, 3280 Hospital Dr NW, Calgary, AB, Canada

Abstract

Background: Patient-reported experience surveys allow administrators, clinicians, and researchers to quantify and improve health care by receiving feedback directly from patients. Existing research has focused primarily on quantitative analysis of survey items, but these measures may collect optional free-text comments. These comments can provide insights for health systems but may not be analyzed due to limited resources and the complexity of traditional textual analysis. However, advances in machine learning–based natural language processing provide opportunities to learn from this traditionally underused data source.

Objective: This study aimed to apply natural language processing to model topics found in free-text comments of patient-reported experience surveys.

Methods: Consumer Assessment of Healthcare Providers and Systems–derived patient experience surveys were collected and linked to administrative inpatient records by the provincial health services organization responsible for inpatient care. Unsupervised topic modeling with automated labeling was performed with BERTopic. Sentiment analysis was performed to further assist in topic description.

Results: Between April 2016 and February 2020, 43.4% (43,522/100,272) adult patients and 46.9% (3501/7464) pediatric caregivers included free-text responses on completed patient experience surveys. Topic models identified 86 topics among adult survey responses and 35 topics among pediatric responses that included elements of care not currently surveyed by existing questionnaires. Frequent topics were generally positive.

Conclusions: We found that with limited tuning, BERTopic identified care experience topics with interpretable automated labeling. Results are discussed in the context of person-centered care, patient safety, and health care quality improvement. Furthermore, we note the opportunity for the identification of temporal and site-specific trends as a method to identify patient care and safety concerns. As the use of patient experience measurement increases in health care, we discuss how machine learning can be leveraged to provide additional insight on patient experiences.

(JMIR Med Inform 2025;13:e63466) doi:10.2196/63466

KEYWORDS

natural language processing; patient-reported experience; topic models; inpatient; artificial intelligence; AI; patient reported; feedback; survey; patient experiences; bidirectional encoder representations from transformers; BERT; sentiment analysis; pediatric caregivers; patient safety; safety

Introduction

Patient-reported experience measurements (PREMs) offer opportunities to understand and improve the patient experience with the goal of ultimately improving health care. PREMs for inpatient experiences typically evaluate a single clinical encounter using survey items that assess different aspects of the care experience using Likert-type scales to determine the range of patient experiences on individual items (eg, “Did doctors treat you with respect?”) that are summed to

XSL•FO
RenderX

domain-level composites (eg, overall experience with nurses, hospital environment, and discharge process) [1]. As the majority of questions on PREMs tend to use numerical scoring, the use of PREMs in health care quality improvement tends to focus on the tracking and improvement of quantitative scores. For example, regulations in the United States requires many hospitals to publicly report Hospital Consumer Assessment of Healthcare Providers and Systems (HCAHPS) scores [2]. However, a focus on quantitative summaries means that administrators, providers, and researchers could be missing out on experiences or concerns not being measured through existing quantitative domains [3-6].

In addition to the rating scales, patient experience surveys often include free-text comment responses where patients can share additional feedback and context on their experiences with health care services. These free-text comments can provide additional insight into patient experiences and how health care can be improved. Routine analysis of free-text comments may not be widely adopted for many reasons, possibly due to an unfamiliarity with methods for textual analysis and limited resources with which to conduct quality assurance in health care service settings [7,8].

In recent years, methodological developments in machine learning have enabled automated, efficient analysis of previously underused text data in health care. Natural language processing (NLP) refers to methods for representing text (and language) in ways that computers can understand and process. For example, researchers have used NLP methods with electronic medical records to predict clinical outcomes such as disease progression and health service utilization [9-11]. In the context of patient-reported outcome and experience measures, NLP could be applied to free-text comments to identify common themes and emerging concerns for specific hospitals or patient populations. Specifically, topic modeling can be used to identify distinct care experience topics and sentiment analysis can describe the emotional valence (positivity or negativity) of free text.

To date, few studies have applied NLP to patient experience data. In a systematic review, Khanbhai et al [12] identified 5 studies that used NLP to analyze routinely collected patient-reported measures, including the Press Ganey, HCAHPS, and 2 measures specific to experiences with cancer care. Furthermore, several studies applied NLP to nonstandard patient-reported experience data, such as forum or social media posts [12]. In our own literature review, we have identified 4 additional studies that have applied NLP to pre-existing, routinely collected patient experience measures [6,13-15]. We found that researchers have taken different approaches to topic modeling of patient-reported experience, including latent Dirichlet allocation (LDA), nonnegative matrix factorization, Top2Vec, and BERT (bidirectional encoder representations from transformers). Many of these studies trained new models or otherwise involved what could be considered a high degree of model tuning. Despite the promise of NLP methods for understanding patient experiences, the pace of innovation and the relative methodological complexity may present barriers to adoption in health care organizations. Organizations looking to implement routine analysis of open-ended text could benefit from knowing whether "off-the-shelf" pretrained topic models can provide useful insight without significant up-front costs. Furthermore, existing research on this topic focuses exclusively on the care experiences of adults. To address both gaps, the aim of this study was to (1) apply and evaluate unsupervised NLP with limited hyperparameter tuning to identify and describe topics found in the free-text comments of patient-reported experience surveys for hospital stays in Alberta, Canada, which cover (2) care experiences of adult and pediatric patients.

Methods

This study relied on data collected by Alberta Health Services (AHS) as part of ongoing health care quality monitoring. At the time the study was conducted, AHS was the provider of inpatient health care in Alberta, a Canadian province with 4.7 million residents.

Patient-Reported Experience Surveys

AHS uses 2 surveys to assess patient experiences with inpatient care—the Canadian Patient Experiences Survey on Inpatient Care (CPES-IC) survey and the Alberta Pediatric Inpatient Experience Survey (APIES). These surveys assess patient experience by asking questions on topics such as provider interactions (eg, doctors and nurses), the hospital environment (eg, noise levels and cleanliness), and the discharge process (eg, receiving written information). During the surveys, patients are also prompted for free-response comments (CPES-IC: "Is there anything else you would like to share with us about your hospital stay?"; APIES measure: "Is there something else you would like to share about your child's and your family's hospital experience? Please explain.") which are recorded by the telephone operators.

The CPES-IC is a modified version of the HCAHPS, a survey commonly used in the United States to assess patient-reported experiences with inpatient care [1]. Details on the CPES-IC can be found at the Canadian Institute for Health Information website [16]. The APIES is a modified version of the Child HCAHPS, an extension of the HCAHPS designed to assess pediatric patient and family inpatient experiences [17]. While many questions are identical and the experience domains are comparable between the CPES-IC and the APIES, the pediatric survey has additional questions on experiences specific to the child and family experience. All questions used in this analysis are common between the CPES-IC, APIES, and the (Child) HCAHPS surveys. We used the date (year) of the survey, the respondent's willingness to recommend a hospital (coded as most positive, "Definitely yes"), and the free-text comments. Responses were linked to administrative health data to provide descriptive statistics for the sample [18]. From this administrative data, we summarized admission category (urgent, elective), length of stay, sex, and age at discharge.

Sampling Procedure

The survey sampling procedure is consistent between adult and pediatric populations. For each institution, AHS operators randomly dial patients (or caregivers of the same) meeting the eligibility criteria until 10% of the eligible discharges are included. Pediatric surveys were administered to eligible

XSL•FO
RenderX

discharges from 16 institutions and adult surveys were administered to eligible discharges from 96 institutions. AHS makes multiple attempts to contact eligible patients. Data are collected exclusively via telephone. Respondents who agreed to answer the survey did so with the knowledge that these surveys are used for quality improvement and research purposes. More details on the sampling strategy and inclusion criteria have been published previously [19,20].

Textbox 1 describes the criteria for survey eligibility [20,21]. Patients were eligible to participate in the survey if they had a hospital stay lasting more than 24 hours, were not admitted to a psychiatric unit (or treated by a psychiatrist during inpatient stay), and did not die during the hospital stay. The eligibility criteria for pediatric inpatient visits are comparable. Caregivers (typically parents) of pediatric patients are contacted if pediatric patients meet the same conditions (for comparability with other jurisdictions, this study excludes pediatric surveys completed for newborn admissions with a length of stay less than 6 days).

Textbox 1. Survey eligibility criteria.

Common eligibility criteria

- Length of stay >24 hours.
- No psychiatric unit or psychiatrist on inpatient record for current stay.
- No death during inpatient stay.

Specific eligibility: adult

- Patient ≥18 years of age (at hospital discharge).
- Did not meet one of the conditions screened out on compassionate grounds (eg, still-births, babies tied to length of stay >6 days).

Specific eligibility: pediatric

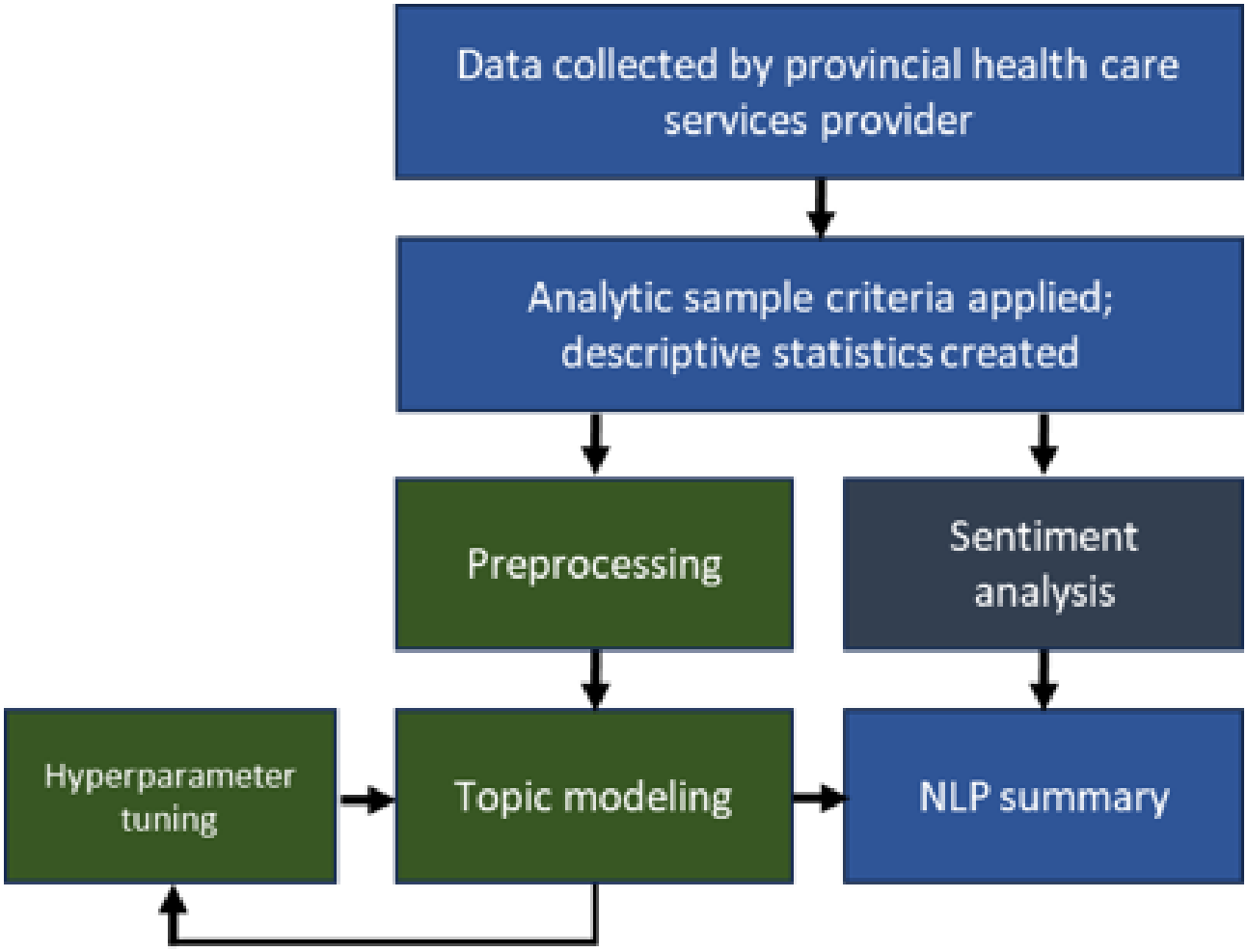
- Patient <18 years of age (at hospital discharge).
- Caregiver not recorded as “no-publicity” (do not contact) in record.

Analysis

Figure 1 displays the analytic pipeline for this study. Data were linked by AHS Data and Analytics; data cleaning and descriptive statistics were conducted in SAS 9.4 and R (R Core Team; 4.2.1) [22]. After importing data into R and applying the analytic criteria (eg, date range and admission categories associated with newborns), white space was trimmed to identify and exclude any comments that may have contained only blank spaces. Additional checks based on comment length were used to check comment lengths and improperly coded missingness (eg, “N/A” instead of “”). Descriptive statistics were calculated for variables from patient experience surveys and linked administrative health data.

XSL•FO
RenderX

Figure 1. Analytic pipeline. NLP: natural language processing.



Topic Modeling

Topic modeling was completed using the BERTopic package in Python [23]. BERTopic requires minimal preprocessing and accounts for semantic context by creating document embeddings and using a class-based term frequency-inverse document frequency method [23]. We used the default pretrained embeddings model ("all-MiniLM-L6-v2" from sentence-transformers). Other popular methods for topic modeling (such as LDA) focus on word frequency and do not account for the order and relationship of words [23,24]. Using embeddings-based models allow for comparisons with previous NLP PREMs work that have used Top2Vec and BERT-based models [6,14]. BERTopic can apply multiple representation models to generate multiple automated topic labels, allowing for a qualitative comparison of the interpretability of these topic labels.

The initial analytic process followed many of the suggested defaults from "best practices" in BERTopic documentation [25]. These included pre-extracting embeddings using a sentence transformer, removing English stopwords (common words), removing infrequent words (in this case, words used in fewer than 2 documents), setting the n-gram size to range between 1 and 2 words (identifying single words and 2-word terms), and setting a reproducible seed for the dimensionality reduction process. Before topic modeling, we removed duplicate comments. Each comment is assigned to a single topic. Topic labels (frequent words that describe a topic) are assigned by the model using representative terms. We did not provide any manual labeling at any stage in the topic modeling.

In the first model, we did not adjust parameters that would limit the number of potential topics beyond BERTopic's automated topic reduction as a method for reducing outliers. In addition to the base representation, KeyBERTInspired was selected as an additional representation model backend with the hope of creating more interpretable topic labels.

To balance the competing priorities of creating topic representations with interpretable labels (eg, extracted keywords) and avoiding redundant topics, we tuned model hyperparameters to reduce the total number of topics. In the second iteration of our model, clustering parameters were adjusted to generate a smaller number of topics (minimum cluster size using Hierarchical Density-Based Spatial Clustering of Applications with Noise) and the term range was increased (n-gram: 2 - 4). In the third (and final) model, term (n-gram) size was expanded to 1 - 4. To compare additional automated topic labeling methods, PartOfSpeech and MarginalMaximumRelevance were added as representation models to complement existing base and KeyBERT topic representations.

Sentiment analysis was completed using the {sentimentr} package in R to calculate the free-text response length (in words)

XSL•FO
RenderX

and sentence-averaged sentiments [26]. This package calculates sentence-level sentiments and evaluates linguistic context that modulates the positive or negative emotion (valence shifting). Specifically, sentimentr identifies polarized words in a sentence by referencing a sentiment dictionary, examines surrounding words for their relation (eg, negation and amplification), and weights the estimate of the sentiment accordingly. Sentiment strength is indicated by the absolute value of the sentiment score; positive and negative sentiment are indicated by positive or negative number. Neutral comments have sentiment scores closer to 0. Whole-comment sentiment was calculated to describe topics but were not incorporated into topic modeling.

To summarize the findings, we reported the 5 most frequently assigned, most positive, and most negative topics. We also summarize topics not currently measured on the patient experience surveys.

Ethical Considerations

Research ethics approval was granted with a waiver of consent by the Health Research Ethics Board at the University of Calgary (adult experience survey approval REB22-0810; pediatric experience survey approval REB17-0769).

Records were linked and deidentified by AHS for privacy and confidentiality. Data were provided to the research team as part of a research agreement with AHS.

Results

Overview

Between April 2016 and March 2020, AHS collected 100,272 adult experience surveys and 7464 pediatric experience surveys that were linked to administrative data and provided to the researchers. Of these surveys, 43,522 (43.4%) adult surveys and 3501 (46.9%) pediatric surveys included free-text comments. Descriptive statistics are presented in Table S1 in Multimedia Appendix 1.

Most comments were short; 54% (23,503/43,522) of CPES-IC comments and 44.1% (1543/3501) of APIES comments were 25 words or less. After deduplication, the CPES-IC contained 94.6% (41,152/43,522) distinct comments and the APIES contained 99.1% (3471/3501) distinct comments.

Table 1 presents the number of topics per model. The final (third) model contained 86 CPES-IC topics and 35 APIES topics. As noted in the Methods section, hyperparameters were tuned to reduce the total number of topics and combine similar topics. Between models 1 and 2, there was a large reduction in the number of topics among the adult surveys (168 fewer topics; 27/195, 13.8% of model 1). The most frequent, positive, and negative topics were generally consistent between the 3 models; however, topics in the second model were relatively coarse in comparison with the other 2. Full results of the 3 models are presented in Multimedia Appendices 2 and 3.

Table . Topics per model. BERTopic-, KeyBERTInspired-, and MaximumMarginalRelevance-assigned labels were relatively consistent, PartOfSpeech labels were not assigned for any of the adult topics and many of the pediatric topics.

Model	CPES-IC[a]	APIES[b]
Model 1	195 topics (from 328)	29 topics (from 51)
Model 2	27 topics (from 86)	20 topics (from 35)
Model 3	86 topics (not reduced further)	35 topics (not reduced further)

[a]CPES-IC: Canadian Patient Experiences Survey on Inpatient Care.

[b]APIES: Alberta Pediatric Inpatient Experiences Survey.

Model Topics

Tables S2-S4 in Multimedia Appendix 2 presents the most frequent topics (based on distinct comments).

Table S3 and Table S4 in Multimedia Appendix 2 present the most positive and most negative topics (based on the full sample). Below, we describe the topics according to model-extracted keywords.

Topics – Adult Inpatient Stays

The most frequent topics for adult stays included positive experiences with multiple aspects of care (topic 1), positive and negative reports about food (topic 3), childbirth (topic 4), hospital cleanliness (topic 5), positive experiences with staff (topic 7) and overall stay (topics 2 and 6), the discharge process (topic 8), and noise (topic 9). Topic 10 appears to be a combination of several topics.

The most positive topics for adult stays included reported general satisfaction and positive experiences (topics 13, 81, 75, 23, 15, 79, 25, and 71), positive experiences with nursing staff (topic 76), and organized and efficient care (topic 86).

The most negative topics for adults included topics specific to hospital-acquired infection (topic 74), theft (topic 80), the admission process (topic 11), the hospital environment (temperature – topic 28; noise – topic 9), parking (topics 42 and 53), negative communication experiences with nursing staff (topic 45), and pain medication or medication mistakes (topic 20).

Topics – Pediatric Inpatient Stays

The most frequent topics for pediatric stays included positive experiences with multiple elements of care (topic 1), the hospital (topic 3), nurses (topics 7 and 8), surgery (topic 9), and overall experiences (topic 10). Topic 6 was specific to pediatric hospitals. Topic 4 focused on rooms, including sleeping, shared rooms, and noise. Topic 5 focused on food and breastfeeding.

The most positive topics for pediatric surveys included excellent care and satisfaction (topics 35, 12, 23, 21, 10, 24, and 13),

XSL•FO
RenderX

positive experiences with staff (topic 17), positive experiences with care for babies (topic 27). Topic 32 focused on care at the Stollery Children's Hospital.

The most negative topics for pediatric surveys included those for the emergency room (topics 25 and 34), parking (topic 11), negative communication experiences with nursing staff (topic 16), needles and pain (topic 20), medication and pain (topic 2), hospital rooms (topic 4), the discharge process (topic 15), and food and breastfeeding (topic 5). Topic 31 appears to be a combination of several topics.

Novel Topics

Here, we summarize identified topics that do not correspond to questions on the patient experience surveys (excluding topics for specific facilities).

Among the adult surveys, the final model identified birth and delivery (topic 4), ultrasounds and communication about diagnoses (topic 16), beds and mattresses (topic 18), surgery (topic 19), temperature (topic 28), facilities needing upgrades or funding (topic 30), desire for private rooms (topic 48), concerns about shared-between-gender rooms (topic 32), overcrowding (topic 85), perceptions of insufficient staffing levels (topics 34 and 73), needles and intravenous placement (topic 37), hip and knee replacements (topic 4), parking (topic 53), night or day shift staffing (topic 55), electronics or entertainment (topic 59; television, internet, or Wi-Fi), mobility or wheelchairs (topic 62), language and communication barriers (topic 64), physiotherapy (topic 67), hospital-acquired infection (topic 74), and theft (topic 80).

Among the pediatric surveys, the final model identified topics related to neonatal intensive care units or intensive care units (topic 19 and 33), social workers (topic 30), surgery (topic 9), parking (topic 11), and food and breastfeeding (topics 5 and 21).

Discussion

Principal Findings

In this paper, we applied easy-to-use and computationally efficient machine learning-based NLP to identify and describe patient-reported experiences in free-text survey responses. To the best of our knowledge, this work is the first to describe the application of topic modeling to routinely collected patient-reported experience measures among both adult and pediatric experience surveys. By following best-practices documentation, tuning parameters to prevent overlap and reduce the total number of topics, and applying automated labeling, this application of BERTopic identified experience topics not currently evaluated using existing survey instruments.

Many of the 10 most frequent topics were related to positive ratings of care (adult sample: 5/10, 50%; pediatric sample: 6/10, 60%). This is perhaps unsurprising, as most patients in Alberta report a high level of satisfaction [21,27]. In our analytic sample, we note that 72% (30,996/43,522) of adult survey respondents with comments would "definitely" recommend the facility to others and that the proportion was even higher (2837/3501 81%) among pediatric survey respondents with comments.

One of our main goals for this study was to create topic representations with interpretable automated labeling. Of the 4 representation models used to model topics, the topic labels were largely consistent between BERTopic, KeyBERTInspired, and MaximalMarginalRelevance. However, the PartOfSpeech method failed to apply labels to all the adult survey topics and many of the pediatric survey topics. As our comments are transcribed by operators, the comments may not represent natural speech and therefore may not have been suited to the default PartOfSpeech method [28]. Still, the consistency of labels among most of the topic labeling suggests that several methods can provide interpretable labeling with no manual classification.

Many distinct topics were generated among the CPES-IC respondents. The pediatric experience survey asks about needles and IVs, but we also found that they were also identified as a topic within adult experiences. Several topics concerned accommodations, with topics about shared between gender rooming, overcrowding, and desires for private rooms, as well as beds and mattresses, temperature, and electronics. Currently, the CPES-IC questions on the hospital environment only include those about noise and cleanliness. Patients also reported concerns about facilities and staffing, with topics noting that the facilities needed repair, perceptions of insufficient staffing levels, comparisons between day and night shift staffing, and concerns about language and communication barriers. We identified a single topic on hospital-acquired infection. Future studies could evaluate whether these topics could have relevance as part of broader indicators of patient safety.

APIES respondents are the parents or caregivers of pediatric patients and reflect the experiences and priorities of both the patient and their family. While many of the topics were common between adult and pediatric surveys (eg, reporting excellent care and communication experiences with health care providers), we identified topics related to intensive care, social workers, and food and breastfeeding. While 33% (1139/3501) of the pediatric patients surveyed were under the age of 1 (Table S1 in Multimedia Appendix 1), the specific needs of parents of newborns and nursing infants are not evaluated using the APIES survey. In addition, while the survey evaluates communication with health care providers, APIES does not evaluate whether the psychosocial needs of patients and families are being met while in hospital. The "social worker" topic identified in this analysis suggests opportunities for further evaluation.

In addition to the unique experience topics within each sample, we identified 2 categories of topics that were shared between adult and pediatric respondents—food and parking. The topics that focused on food may warrant further investigation and survey item development; whether patients are reporting experiences about the quality or options for those with dietary restrictions, meals are an important element of the patient's experience. Previous research using other survey instruments have identified that parking is a relevant factor that affecting overall patient satisfaction [29,30]. Parking (or other topics related to transportation) may not be immediately actionable by administrators but could suggest issues with health care accessibility.

XSL•FO
RenderX

Connection to Previous Work

Studies using more traditional qualitative methods have identified similar topics of care that are not assessed by Consumer Assessment of Healthcare Providers and Systems (CAHPS)–derived surveys. Nepal et al [5] conducted interviews with patients to identify priorities around inpatient experiences. Among the themes identified in the study, investigators noted that patients reported topics around privacy and room-sharing, cleanliness, food, and access to television. Furthermore, a study of patient comments on the Child HCAHPS (the analogue of APIES) identified several topics that closely mirrored those in our study, including "poor vein management/IV care," "sleeping/comfort for parent/family," "Hospital services/amenities (ie, food, parking)," "Security/safety issues," and "physical/bodily privacy" [3]. An example comment in the manually classified "physical/body privacy" topic included the privacy to breastfeed [3].

There is also consistency between our work and other studies applying NLP to routinely collected PREMs. Gallan et al [6] applied topic modeling to a set of HCAHPS surveys with additional Press Ganey survey items that included multiple free-text response boxes. Whereas our summary of topics relied on the automated topic labels with representative words from each underlying representation model, Gallan et al [6] used top2vec followed by manual classification of multiple free-text comments. Despite our different topic modeling and labeling approach, the novel topics on the hospital environment identified in our study were aligned with those from their work (topics on "room temperature," "bed and visitor comfort," "facility and room design and condition," and "roommate"). We identified a single study applying completely unsupervised models to routinely collected inpatient PREMs. Cammel et al [15] modeled topics with nonnegative matrix factor and used sentiment and topic frequency to describe and classify the priority of topics in 2 Dutch hospitals. Our results are not directly comparable as we focused on absolute values of positivity and negativity and the researchers explicitly reported the most frequent positive, negative, and neutral topics within each hospital. While the translation from Dutch to English may present challenges in comparison, we did note some overlapping topics with our own work (specifically, communication with staff, satisfaction with care, concerns about temperature, and perceptions of how busy the hospital was).

Recent work suggests that respondents who provide comments may be willing to share more feedback than what is currently collected. In a comparison with a sample of surveys with only single-item responses, Quigley and Predmore [4] reported that comments provided on the narrative items were more likely to contain actionable topics. These researchers also found that when multiple opportunities for free-text responses are offered as part of inpatient experience validation, a majority of parents provide more information. For researchers or providers interested in applying NLP in specific clinical settings, the development of multiple open-ended questions and validation with end users may be able to provide more actionable information [31]. For health systems currently administering CAHPS surveys, there are currently 2 sets of Narrative Item Sets (like those used by Quigley and Predmore [4]) that have been developed for use with ambulatory care and pediatric inpatient settings [32]. As Narrative Item Sets are developed for other are adopted among health systems administering CAHPS surveys, we anticipate that NLP methods will see further integration for monitoring patient experiences to drive quality improvement.

NLP can also be used to classify topics according to existing guidelines or themes. Ish et al [14] report on BERT and bag-of-words models to identify topics in CAHPS primary care surveys with free-text responses. Manual labeling of a training sample resulted in 26 potential classes. The researchers found that BERT outperformed the bag-of-words models, but note limitations based on the small sample size, complexity of topics, and potential actionability of these methods. Using a supervised approach based on a subset of manually labelled comments, Khanbhai et al [13] compared the performance of 6 machine learning models' ability to classify free-text comment themes and sentiment from 2 questions assessing patient-reported experience in multiple care settings. None of their methods included embeddings-based methods (eg, BERT and Top2Vec), but the researchers found that a support vector machine approach had the highest accuracy. NLP may also enhance existing topics or themes in patient-reported experience data. Fairie et al [33] applied a novel label enhanced LDA method to categorize patient complaints and concerns submitted to a provincial health authority in Canada. This method used an existing manual (coarse) framework for comment classifications, LDA, and consensus by authors to determine topic labels. While the study is not directly comparable with our evaluations of topic novelty relative to existing survey questions, many topics in the concerns dataset were similar or identical to those identified in our work.

Patient-reported outcome measures (PROMs) can also contain free-text responses. We identified a single preprint that applied BERTopic to free-text comments from PROMs. Linton et al [34] used a weakly supervised text classification model on PROM comments to classify topics for health-related quality of life in colorectal cancer care. Using predefined themes and seed terms, the researchers compared 5 different topic models and found that BERTopic performed poorly on classification, relative to other methods. Experts (clinicians and scientists) who evaluated the results reported that the BERTopic-selected representative keywords were generally not relevant to the predefined themes, did not include the seed words, and that this differed from the keywords selected by other models. While the keywords applied to topics in our study were generally relevant, the work by Linton et al [34] suggests that researchers interested in applying NLP to patient-reported free text may need to evaluate multiple approaches for semisupervised topic modeling.

Future Directions

This initial descriptive study explored how a fully unsupervised NLP model could identify novel topics. Based on the concordance of our results with previous literature, administrators and patient experience survey developers may benefit from developing survey items for future PREM. Several studies have applied semisupervised models by incorporating existing labels or themes based on operational needs or clinical

XSL•FO
RenderX

relevance [13,14,33,34]. We could anticipate working more closely with patients, providers, and administrators to identify priorities and to guide NLP implementation.

As part of their evaluation of topic modeling for patient experience, Ish et al [14] discuss the issue of rare cases for training topic models. For example, the CPES-IC topic with the most obvious relevance for patient safety—the topic regarding hospital acquired infection—was classified in just 57 of the deduplicated comments. In this study, the focus on coarse topics reduces topic outliers but may prevent identification of rare but meaningful topics (eg, specific concerns on safety, communication, and hospital environment; elements of care most-relevant for specific clinical populations; or reasons for inpatient stays). In the model with the most finely detailed topics (for Model 1 for CPES-IC, refer to Multimedia Appendix 3), 71% (138/195) of topics were present in 50 or fewer deduplicated comments. Future studies could evaluate the relative frequency of topics by patient-population, hospital service, and institution as well as their relevance and actionability in these settings.

Beyond the identification of emerging patient-experience topics and integration into health care quality monitoring, comments may also assist in understanding patient care experiences. For example, a 2024 study with free-text Child HCAHPS comments manually coded for actionability and valence found that including these features as independent variables improved modeling overall experience outcomes [35]. Research also suggests that patient-reported experiences may be associated with unplanned readmission after discharge [19,36,37]. Future work could investigate how relevant survey items, comment topics, and sentiment may assist in understanding overall patient experiences and whether features assigned through NLP are associated with patient safety or readmission.

Strengths and Limitations

This paper has several strengths. First, it is one of the first to apply NLP to a widely adopted patient-reported experience measure for both adult and pediatric patient settings. The use of NLP with routinely administered patient experience surveys presents the ability to incorporate patient comments into learning health systems [38]. Model hyperparameters (eg, n-gram size and cluster size) were adjusted only through recommendations in the best practices documentation, suggesting that a (relatively) off the shelf solutions can work without devoting significant resources to technological implementation. Second, the models were able to identify novel topics within single comments from existing surveys without additional data collection or instrument development (eg, narrative interviews and multiple open-ended questions) using an approach that requires computing resources already accessible inside most or all health systems. This suggests that health systems currently using CAHPS surveys can gain additional insight on patient experiences without implementing new survey methods. Finally, the application of topic modeling could assist in identifying health system–specific and patient population–specific elements of the patient experience. This study used surveys from a Canadian province with a publicly-funded health care system, but the findings are relevant for multiple health care system settings and countries. While CAHPS surveys were developed for use in the United States, CAHPS-derived surveys (those sharing the same or similar items) have been translated and adopted across several countries and clinical settings [39-43]. Our paper may contribute to larger efforts focused on identifying common elements of the patient-reported experience in multiple health care systems and settings.

There are also several limitations to the paper. This project aimed to identify and describe topics found in existing data and within a general population. We did not split the data to examine classification accuracy, nor did we examine applicability and relevance for patients or administrators. The majority of patients report positive in-hospital experiences on the survey and comments reflected those experiences, which likely introduced “noise” and prevented the identification of actionable topics. Uniquely actionable topics may not be identifiable within a general population approach; additional work is required to determine how these findings can translate to quality improvement efforts within specific patient subpopulations. While multiple topics may be discussed within a single patient comment, BERTopic will label these comments with a single classification based on predicted probabilities. The representation model-assigned keyword labels were generally interpretable, but other studies have found mixed results on their relevance [34]. Finally, measurement error was likely as comments were transcribed by telephone operators rather than by patients themselves [44].

Conclusion

This paper provides the groundwork for future investigations within the Canadian context and beyond. It serves as both a descriptive report of observed topics and associated sentiments, but it also provides a technical proof-of-concept for researchers, policy makers, and administrators who may be looking for solutions to get the most out of patient-reported data using low-resource NLP approaches. We anticipate that partnering with patients and health care providers could help shape the development of future, semisupervised topic models with increased relevance for both patients and health systems.

Acknowledgments

The authors would like to thank Alberta Health Services for collecting and providing these data. The views expressed in this article are those of the authors’ and do not represent the opinions of Alberta Health Services. The authors would also like to thank the patients and their families who completed the surveys used in this paper.

XSL•FO
RenderX

Authors' Contributions

Authors BS, KK, MJS, and PF conceptualized the study. Authors BS and AGD selected the analytic tools for the present study. Authors KK and BS performed data curation; author BS selected the analytic sample and performed the natural language processing with input from AGD, PF, MW, and MJS. BS drafted the initial manuscript with input from all authors; all authors contributed to the final draft of the paper.

Conflicts of Interest

None declared.

Multimedia Appendix 1
Table S1: descriptive statistics.
[XLSX File, 10 KB - medinform_v13i1e63466_app1.xlsx]

Multimedia Appendix 2
Tables S2-S4: frequent, positive, and negative topics.
[XLSX File, 20 KB - medinform_v13i1e63466_app2.xlsx]

Multimedia Appendix 3
Full output for pediatric and adult surveys: models 1-3.
[XLSX File, 76 KB - medinform_v13i1e63466_app3.xlsx]

References

1. HCAHPS: patients' perspectives of care survey. Centers for Medicare & Medicaid Services. URL: http://www.cms.gov/Medicare/Quality-Initiatives-Patient-Assessment-Instruments/HospitalQualityInits/HospitalHCAHPS.html [accessed 2002-01-20]
2. Elliott MN, Cohea CW, Lehrman WG, et al. Accelerating improvement and narrowing gaps: trends in patients' experiences with hospital care reflected in HCAHPS public reporting. Health Serv Res 2015 Dec;50(6):1850-1867. [doi: 10.1111/1475-6773.12305] [Medline: 25854292]
3. Quigley DD, Predmore Z. What parents have to say: content and actionability of narrative comments from child HCAHPS survey. Hosp Pediatr 2022 Feb 1;12(2):205-219. [doi: 10.1542/hpeds.2021-006032] [Medline: 34981124]
4. Quigley DD, Predmore Z. Parents have more to say: comments from the child HCAHPS single question versus a narrative item set. Hosp Pediatr 2023 Apr 1;13(4):345-356. [doi: 10.1542/hpeds.2022-007046] [Medline: 36970853]
5. Nepal S, Keniston A, Indovina KA, et al. What do patients want? A qualitative analysis of patient, provider, and administrative perceptions and expectations about patients' hospital stays. J Patient Exp 2020 Dec;7(6):1760-1770. [doi: 10.1177/2374373520942403] [Medline: 33457641]
6. Gallan AS, Niraj R, Singh A. Beyond HCAHPS: analysis of patients' comments provides an expanded view of their hospital experiences. Patient Exp J 2022;9(1):159-168. [doi: 10.35680/2372-0247.1641]
7. O'Cathain A, Thomas KJ. "Any other comments?" Open questions on questionnaires - a bane or a bonus to research? BMC Med Res Methodol 2004 Nov 8;4:25. [doi: 10.1186/1471-2288-4-25] [Medline: 15533249]
8. Guetterman TC, Chang T, DeJonckheere M, Basu T, Scruggs E, Vydiswaran VGV. Augmenting qualitative text analysis with natural language processing: methodological study. J Med Internet Res 2018 Jun 29;20(6):e231. [doi: 10.2196/jmir.9702] [Medline: 29959110]
9. Clapp MA, Kim E, James KE, et al. Comparison of natural language processing of clinical notes with a validated risk-stratification tool to predict severe maternal morbidity. JAMA Netw Open 2022 Oct 3;5(10):e2234924. [doi: 10.1001/jamanetworkopen.2022.34924] [Medline: 36197662]
10. Seinen TM, Fridgeirsson EA, Ioannou S, et al. Use of unstructured text in prognostic clinical prediction models: a systematic review. J Am Med Inform Assoc 2022 Jun 14;29(7):1292-1302. [doi: 10.1093/jamia/ocac058] [Medline: 35475536]
11. Rumshisky A, Ghassemi M, Naumann T, et al. Predicting early psychiatric readmission with natural language processing of narrative discharge summaries. Transl Psychiatry 2016 Oct 18;6(10):e921. [doi: 10.1038/tp.2015.182] [Medline: 27754482]
12. Khanbhai M, Anyadi P, Symons J, Flott K, Darzi A, Mayer E. Applying natural language processing and machine learning techniques to patient experience feedback: a systematic review. BMJ Health Care Inform 2021 Mar;28(1):e100262. [doi: 10.1136/bmjhci-2020-100262] [Medline: 33653690]
13. Khanbhai M, Warren L, Symons J, et al. Using natural language processing to understand, facilitate and maintain continuity in patient experience across transitions of care. Int J Med Inform 2022 Jan;157:104642. [doi: 10.1016/j.ijmedinf.2021.104642] [Medline: 34781167]

XSL•FO
RenderX

14. Ish D, Parker AM, Osoba OA, et al. Using natural language processing to code patient experience narratives: capabilities and challenges.: RAND Corporation; 2020. URL: https://www.rand.org/pubs/research_reports/RRA628-1.html [accessed 2024-01-14]
15. Cammel SA, De Vos MS, van Soest D, et al. How to automatically turn patient experience free-text responses into actionable insights: a natural language programming (NLP) approach. BMC Med Inform Decis Mak 2020 May 27;20(1):97. [doi: 10.1186/s12911-020-1104-5] [Medline: 32460734]
16. About the Canadian Patient Experiences Survey — Inpatient Care. Canadian Institute for Health Information. URL: https://www.cihi.ca/en/patient-experience/about-the-canadian-patient-experiences-survey-inpatient-care [accessed 2024-03-04]
17. Toomey SL, Elliott MN, Zaslavsky AM, et al. Variation in family experience of pediatric inpatient care as measured by child HCAHPS. Pediatrics 2017 Apr;139(4):e20163372. [doi: 10.1542/peds.2016-3372] [Medline: 28330970]
18. Discharge Abstract Database (DAD) metadata. Canadian Institute for Health Information. URL: https://www.cihi.ca/en/discharge-abstract-database-dad-metadata [accessed 2024-03-04]
19. Kemp KA, Santana MJ, Southern DA, McCormack B, Quan H. Association of inpatient hospital experience with patient safety indicators: a cross-sectional, Canadian study. BMJ Open 2016 Jul 1;6(7):e011242. [doi: 10.1136/bmjopen-2016-011242] [Medline: 27371554]
20. Kemp KA, Ahmed S, Quan H, Johnson D, Santana MJ. Family experiences of pediatric inpatient care in Alberta, Canada: results from the child HCAHPS survey. Hosp Pediatr 2018 Jun;8(6):338-344. [doi: 10.1542/hpeds.2017-0191] [Medline: 29724754]
21. Kemp KA, Chan N, McCormack B, Douglas-England K. Drivers of inpatient hospital experience using the HCAHPS survey in a Canadian setting. Health Serv Res 2015 Aug;50(4):982-997. [doi: 10.1111/1475-6773.12271] [Medline: 25483921]
22. The R Project for Statistical Computing. URL: https://www.R-project.org [accessed 2025-02-10]
23. Grootendorst M. BERTopic: neural topic modeling with a class-based TF-IDF procedure. arXiv. Preprint posted online on Mar 11, 2022. [doi: 10.48550/ARXIV.2203.05794]
24. Angelov D. Top2vec: distributed representations of topics. arXiv. Preprint posted online on Aug 19, 2020. [doi: 10.48550/arXiv.2008.09470]
25. Grootendorst MP. Best practices. BERTopic. URL: https://maartengr.github.io/BERTopic/getting_started/best_practices/best_practices.html [accessed 2024-01-14]
26. Rinker TW. Sentimentr: calculate text polarity sentiment. GitHub. 2021. URL: https://github.com/trinker/sentimentr [accessed 2025-02-10]
27. Steele BJ, Fairie P, Kemp K, Santana MJ. Drivers of paediatric inpatient experience: retrospective analysis of casemix factors for the Alberta paediatric inpatient experience survey in Alberta, Canada. BMJ Open 2022 May 12;12(5):e048207. [doi: 10.1136/bmjopen-2020-048207] [Medline: 35551089]
28. Grootendorst MP. 6A. Representation models. BERTopic. URL: https://maartengr.github.io/BERTopic/getting_started/representation/representation.html [accessed 2024-03-02]
29. Alibrandi A, Gitto L, Limosani M, Mustica PF. Patient satisfaction and quality of hospital care. Eval Program Plann 2023 Apr;97:102251. [doi: 10.1016/j.evalprogplan.2023.102251] [Medline: 36806007]
30. Concato J, Feinstein AR. Asking patients what they like: overlooked attributes of patient satisfaction with primary care. Am J Med 1997 Apr;102(4):399-406. [doi: 10.1016/s0002-9343(97)00092-2] [Medline: 9217623]
31. van Buchem MM, Neve OM, Kant IMJ, Steyerberg EW, Boosman H, Hensen EF. Analyzing patient experiences using natural language processing: development and validation of the artificial intelligence patient reported experience measure (AI-PREM). BMC Med Inform Decis Mak 2022 Jul 15;22(1):183. [doi: 10.1186/s12911-022-01923-5] [Medline: 35840972]
32. CAHPS patient narrative item sets. Agency for Healthcare Research and Quality (AHRQ). URL: https://www.ahrq.gov/cahps/surveys-guidance/item-sets/elicitation/index.html [accessed 2024-03-13]
33. Fairie P, Zhang Z, D'Souza AG, Walsh T, Quan H, Santana MJ. Categorising patient concerns using natural language processing techniques. BMJ Health Care Inform 2021 Jun;28(1):e100274. [doi: 10.1136/bmjhci-2020-100274] [Medline: 34193519]
34. Linton AG, Dimitrova V, Downing A, Wagland R, Glaser A. Weakly supervised text classification on free text comments in patient-reported outcome measures. arXiv. Preprint posted online on Aug 11, 2023. [doi: 10.48550/ARXIV.2308.06199]
35. Quigley DD, Elliott MN, Slaughter ME, Lerner C, Hays RD. Narrative comments about pediatric inpatient experiences yield substantial information beyond answers to closed-ended CAHPS survey questions. J Pediatr Nurs 2024;76:e126-e131. [doi: 10.1016/j.pedn.2024.02.016] [Medline: 38431461]
36. Kemp KA, Quan H, Fairie P, Santana MJ. Patient reports of night noise in hospitals are associated with unplanned readmissions among older adults. J Patient Exp 2020 Dec;7(6):1425-1431. [doi: 10.1177/2374373520916030] [Medline: 33457597]
37. Kemp K, Steele B, Ahmed S, Fairie P, Santana M. Person-centred quality indicators are associated with unplanned care use following hospital discharge. BMJ Open Qual 2024 Jan 3;13(1):e002501. [doi: 10.1136/bmjoq-2023-002501] [Medline: 38176707]
38. Austin EJ, LeRouge C, Lee JR, et al. A learning health systems approach to integrating electronic patient-reported outcomes across the health care organization. Learn Health Syst 2021 Oct;5(4):e10263. [doi: 10.1002/lrh2.10263] [Medline: 34667879]

XSL•FO
RenderX

39. Orindi BO, Lesaffre E, Quintero A, Sermeus W, Bruyneel L. Contribution of HCAHPS specific care experiences to global ratings varies across 7 countries: what can be learned for reporting these global ratings? Med Care 2019 Nov;57(11):e65-e72. [doi: 10.1097/MLR.0000000000001077] [Medline: 30807453]
40. Bruyneel L, Coeckelberghs E, Buyse G, et al. Validation of the Child HCAHPS survey to measure pediatric inpatient experience of care in Flanders. Eur J Pediatr 2017 Jul;176(7):935-945. [doi: 10.1007/s00431-017-2919-7] [Medline: 28540435]
41. Squires A, Bruyneel L, Aiken LH, et al. Cross-cultural evaluation of the relevance of the HCAHPS survey in five European countries. Int J Qual Health Care 2012 Oct;24(5):470-475. [doi: 10.1093/intqhc/mzs040] [Medline: 22807136]
42. Bruyneel L, Tambuyzer E, Coeckelberghs E, et al. New instrument to measure hospital patient experiences in Flanders. Int J Environ Res Public Health 2017 Oct 30;14(11):1319. [doi: 10.3390/ijerph14111319] [Medline: 29084160]
43. Zun AB, Ibrahim MI, Mokhtar AM, Halim AS, Wan Mansor WNA. Translation, cross-cultural adaptation, and validation of the Hospital Consumer Assessment of Healthcare Providers and Systems (HCAHPS) into the Malay language. Int J Environ Res Public Health 2019 Jun 10;16(11):2054. [doi: 10.3390/ijerph16112054] [Medline: 31185665]
44. Smyth JD, Olson K. How well do interviewers record responses to numeric, interviewer field-code, and open-ended narrative questions in telephone surveys? Field methods 2020 Feb;32(1):89-104. [doi: 10.1177/1525822X19888707]

Abbreviations

AHS: Alberta Health Services
APIES: Alberta Pediatric Inpatient Experiences Survey
BERT: bidirectional encoder representations from transformers
CAHPS: Consumer Assessment of Healthcare Providers and Systems
CPES-IC: Canadian Patient Experiences Survey on Inpatient Care
HCAHPS: Hospital Consumer Assessment of Healthcare Providers and Systems
LDA: latent Dirichlet allocation
NLP: natural language processing
PREM: patient-reported experience measure
PROM: patient-reported outcome measure

Edited by J Hefner; submitted 20.06.24; peer-reviewed by C Song, T Reader; revised version received 11.10.24; accepted 14.10.24; published 24.02.25.

Please cite as:
Steele B, Fairie P, Kemp K, D'Souza AG, Wilms M, Santana MJ
Identifying Patient-Reported Care Experiences in Free-Text Survey Comments: Topic Modeling Study
JMIR Med Inform 2025;13:e63466
URL: https://medinform.jmir.org/2025/1/e63466
doi:10.2196/63466

© Brian Steele, Paul Fairie, Kyle Kemp, Adam G D'Souza, Matthias Wilms, Maria Jose Santana. Originally published in JMIR Medical Informatics (https://medinform.jmir.org), 24.2.2025. This is an open-access article distributed under the terms of the Creative Commons Attribution License (https://creativecommons.org/licenses/by/4.0/), which permits unrestricted use, distribution, and reproduction in any medium, provided the original work, first published in JMIR Medical Informatics, is properly cited. The complete bibliographic information, a link to the original publication on https://medinform.jmir.org/, as well as this copyright and license information must be included.

XSL•FO
RenderX

Transforming Informed Consent Generation Using Large Language Models: Mixed Methods Study

Qiming Shi[1], MS; Katherine Luzuriaga[1], MD; Jeroan J Allison[2], MS, MD; Asil Oztekin[3], PhD; Jamie M Faro[2], PhD; Joy L Lee[2], PhD; Nathaniel Hafer[1], PhD; Margaret McManus[1], MPH; Adrian H Zai[1,2], MD, PhD, MPH

[1]Center for Clinical and Translational Science, University of Massachusetts Chan Medical School, 55 N Lake Ave, Worcester, MA, United States
[2]Department of Population and Quantitative Health Sciences, University of Massachusetts Chan Medical School, Worcester, MA, United States
[3]Manning School of Business, University of Massachusetts Lowell, Lowell, MA, United States

Corresponding Author:
Qiming Shi, MS
Center for Clinical and Translational Science, University of Massachusetts Chan Medical School, 55 N Lake Ave, Worcester, MA, United States

Abstract

Background: Informed consent forms (ICFs) for clinical trials have become increasingly complex, often hindering participant comprehension and engagement due to legal jargon and lengthy content. The recent advances in large language models (LLMs) present an opportunity to streamline the ICF creation process while improving readability, understandability, and actionability.

Objectives: This study aims to evaluate the performance of the Mistral 8x22B LLM in generating ICFs with improved readability, understandability, and actionability. Specifically, we evaluate the model's effectiveness in generating ICFs that are readable, understandable, and actionable while maintaining the accuracy and completeness.

Methods: We processed 4 clinical trial protocols from the institutional review board of UMass Chan Medical School using the Mistral 8x22B model to generate key information sections of ICFs. A multidisciplinary team of 8 evaluators, including clinical researchers and health informaticians, assessed the generated ICFs against human-generated counterparts for completeness, accuracy, readability, understandability, and actionability. Readability, Understandability, and Actionability of Key Information indicators, which include 18 binary-scored items, were used to evaluate these aspects, with higher scores indicating greater accessibility, comprehensibility, and actionability of the information. Statistical analysis, including Wilcoxon rank sum tests and intraclass correlation coefficient calculations, was used to compare outputs.

Results: LLM-generated ICFs demonstrated comparable performance to human-generated versions across key sections, with no significant differences in accuracy and completeness (P>.10). The LLM outperformed human-generated ICFs in readability (Readability, Understandability, and Actionability of Key Information score of 76.39% vs 66.67%; Flesch-Kincaid grade level of 7.95 vs 8.38) and understandability (90.63% vs 67.19%; P=.02). The LLM-generated content achieved a perfect score in actionability compared with the human-generated version (100% vs 0%; P<.001). Intraclass correlation coefficient for evaluator consistency was high at 0.83 (95% CI 0.64-1.03), indicating good reliability across assessments.

Conclusions: The Mistral 8x22B LLM showed promising capabilities in enhancing the readability, understandability, and actionability of ICFs without sacrificing accuracy or completeness. LLMs present a scalable, efficient solution for ICF generation, potentially enhancing participant comprehension and consent in clinical trials.

(JMIR Med Inform 2025;13:e68139) doi:10.2196/68139

KEYWORDS

informed consent form; ICF; large language models; LLMs; clinical trials; readability; health informatics; artificial intelligence; AI; AI in health care

Introduction

Ethical codes and regulations have been established globally to guide researchers in conducting studies involving human subjects. In the United States, the Belmont Report and the Common Rule are key frameworks for ensuring ethical research practices. The Common Rule, formally known as the "Basic Department of Health and Human Services (HHS) Policy for the Protection of Human Research Subjects," requires that participants receive comprehensive information about the study's purpose, allowing them to make informed and autonomous decisions about their participation [1]. This process of obtaining informed consent is fundamental to responsible conduct in research involving human subjects [2]. However, in recent years, the inclusion of mandatory scientific content, legal

XSL•FO
RenderX

jargon, and increasing length has turned the informed consent form (ICF) into a barrier to study participation [3,4].

Although many institutional review boards (IRBs) require investigators to develop documents written at the eighth-grade reading level [5], research has found that research ICFs are frequently written at reading grade levels that far exceed readers' abilities [2,5-9].

In response to the increasing complexity and length of informed consent documentation, the Health and Human Services Office for Human Research Protections added a new requirement to the 2018 Common Rule, stipulating that ICFs must begin with "a concise and focused presentation of the key information that is most likely to assist prospective subjects in understanding the reasons why one might or might not want to participate in the research" and that it "must be organized and presented in a way that facilitates comprehension" [1]. The Secretary's Advisory Committee on Human Research Protections has recommended conducting empirical research to guide the writing of the new key information section in light of the new consent requirement, ensuring that its goals are effectively met [10].

With the advancement of large language models (LLMs), a possible solution to improving ICF has emerged. LLMs show significant potential in health informatics, including tasks such as name entity extraction [11], patient trial matching [12,13], biomedical reasoning and classification [14], prediction of admissions [15], automation of administrative tasks [16], and so forth. Studies have also shown that LLMs can effectively enhance the documentation of risks, benefits, and alternatives for common surgical procedures [17]. The integration of LLMs in clinical workflows could significantly reduce administrative burden by automating labor-intensive tasks such as ICF creation. However, for successful implementation, models must not only improve readability and actionability but also align with current regulatory requirements and ethical guidelines.

The ability for LLMs to generate a complex clinical trial ICFs from a research protocol remains unexplored. This paper aims to evaluate the performance of the Mistral 8x22B LLM in generating the key information sections of ICFs with improved readability, understandability, and actionability. Specifically, our objectives are to assess the model's effectiveness in producing ICFs that meet readability standards, enhance understandability, and support actionable content while maintaining accuracy and completeness. Furthermore, we hypothesize that LLM-generated ICFs outperform human-generated counterparts in readability, understandability, and actionability, without compromising on the accuracy or completeness of information.

Methods

Study Design

We sourced 4 research protocols from the UMass Chan IRB, along with their corresponding ICFs. These protocols were then processed by our LLM model to generate artificial intelligence (AI)–generated ICFs, resulting in a total of 8 ICFs—4 human-generated and 4 AI-generated. Each research protocol, along with its respective human and AI-generated ICFs, was randomly assigned to evaluators for assessment. We had 8 evaluators in total, ensuring that each protocol set was reviewed twice by 2 different evaluators. A multidisciplinary team of 8 evaluators, including health informaticians, clinical researchers, and physicians, was assembled to review the outputs. Importantly, the evaluators were not investigators in the clinical trials whose ICFs they assessed and were not directly affiliated with the specific studies under review. Care was also taken to ensure that the evaluators and the investigators for each protocol were from different departments within the institution. Furthermore, none of the evaluators were members of the IRB that reviewed and approved the protocols. These measures were implemented to minimize potential bias and ensure objective evaluation.

Each protocol set was evaluated by 2 different reviewers, ensuring comprehensive assessment. The evaluation focused on key criteria: completeness, accuracy, readability, understandability, and actionability of the generated content. To mitigate potential evaluator bias, we ensured that each protocol was randomly assigned and evaluated by multiple individuals from different disciplines. This multidisciplinary approach, combined with random assignment, reduces the risk of personal bias and ensures a more comprehensive assessment of both LLM and human-generated ICFs.

Study Protocols

The 4 protocols included in this study were selected to ensure diversity in study design, therapeutic areas, and patient populations. This approach was aimed at evaluating the generalizability of LLM-generated ICFs across varied research contexts. Table 1 summarizes the key attributes of the protocols.

Table . Summary of study protocols.

Study title	Study type	Domain
Kangaroo Mother Care Study	Qualitative study	Neonatology
Characterization of Oral Microbiome in Patients With Viral Respiratory Illness	Observational cohort study	Infectious Diseases, Microbiome
RADx Tech COVID-19 Test Us Study	Platform trial	Infectious Diseases, Diagnostics
Healthy at Home Pilot	Pilot feasibility trial	Pulmonology, Digital Health

XSL•FO
RenderX

LLM Model

We chose the Mistral 8x22B model, the latest offering from Mistral [18], for several compelling reasons:

1. Large Context Window: With a 64K token context window, this model can manage extensive research protocols. It is ideal for accurately recalling information from large documents such as clinical trial research protocols.
2. Multilingual Fluency: The Mistral 8x22B excels in multiple languages, aligning with our objective of using LLMs to create ICFs that ensure fair recruitment and serve underrepresented populations. Producing ICFs in various languages, such as Spanish, is highly advantageous.
3. Open-Source License: The Mistral 8x22B is available under an Apache 2.0 open-source license [19], allowing unrestricted deployment. This flexibility is beneficial as we roll out the final product.

ICF Key Information Section Integration

We downloaded ICF templates from various institutions, including the University of California San Francisco, Yale University, Duke University, New York University, the University of Pennsylvania, Johns Hopkins University, Partners HealthCare, Stanford University, Vanderbilt University, and the UMass Chan Medical School. We then consolidated the key information section instructions provided by these institutions into a comprehensive format. To reinforce this format, we made modifications following the Readability, Understandability, and Actionability of Key Information (RUAKI) indicator, ensuring that our consolidated key information sections create more accessible information. The final version of this format serves as the key information section instruction input for the LLM model.

Prompt Engineering

To create the ICF key information content, we used Mistral artificial intelligence (AI) in conjunction with prompt engineering guidance developed by the Research Informatics Core as part of a human-in-the-loop process. This team included the chief research information officer, 2 clinical data scientists, and an IRB officer. The prompt creation followed a backward design instructional approach [20]. The consolidated key information section instructions were used to design the prompts. The data scientists then took this guidance and crafted prompts to align with these instructions.

We used a Least-to-Most approach to guide the AI through the process of creating the consent forms. This step-by-step approach ensured that the AI received small, manageable instructions at each stage, helping it produce more accurate and reliable outputs. By breaking down tasks into smaller steps rather than overwhelming the AI with multiple instructions at once, we reduced confusion and enhanced the quality of the AI-generated forms. After designing and developing the key information section, the output was rated and reviewed by the Research Informatics Core team. Based on their feedback, the prompts were edited to enhance the model's performance.

We started by creating the chatbot prompt detailed in Supplementary 1 in Multimedia Appendix 1 to extract relevant information for each key section from the research protocol. Next, as described in Supplementary 2 in Multimedia Appendix 1, we refined the output using RUAKI indicators. In Supplementary 3 in Multimedia Appendix 1, we adjusted the content to achieve Flesch-Kincaid grade levels below 8. Finally, in Supplementary 4 in Multimedia Appendix 1, we formatted the output to align with our preferred forms, again guided by RUAKI indicators.

Measurements of Accuracy and Completeness

To evaluate accuracy and completeness, we developed a scoring system based on recommendations from LeapFrog (VTech Group), The Joint Commission, the American College of Surgeons, and relevant available literature (Multimedia Appendix 2) [21-24]. Key information sections, including study purpose, duration and procedures, risks and discomforts, benefits, and alternatives, were assessed as complete, incomplete, absent, or incorrect, with corresponding scores of 3, 2, 1, and 0, respectively.

Measurements of Readability, Understandability, and Actionability

We used the RUAKI indicator to evaluate readability, understandability, and actionability presented in ICFs key information section [25]. This indicator consists of 18 items, each assessed with a binary rating of "yes" (scored as 1) or "no" (scored as 0) (Table 2). To determine the final score, we sum the number of "yes" responses, divide by the total number of items (18), and multiply by 100 to yield a percentage score. The section score for readability, understandability, and actionability was derived by dividing the final score of each section by the total number of relevant items. A higher percentage indicates that the key information is more accessible, comprehensible, and actionable.

XSL•FO
RenderX

Table . Readability, understandability, and actionability of key information evaluation criteria.

Category and item number		Description	Rating
Readability			
	1	Active voice: uses active verbs (eg, will use) rather than passive verbs (eg, will be used) all or most of the time, more than 90% of the time.	Yes=1/No=0
	2	Word choice: avoids scientific jargon (eg, hypertension). Uses words readers are familiar with (eg, high blood pressure) all or most of the time, more than 90% of the time.	Yes=1/No=0
	3	Topic definition: provides a definition of the main disease or topic the study is about.	Yes=1/No=0
	4	Numbers: avoids mathematical calculations including comparison of numeric probability of risk.	Yes=1/No=0
	5	Eighth grade or below: reading grade level calculated in Microsoft Word is Flesch-Kincaid grade level 8.9 or below.	Yes=1/No=0
	6	Headers: sections or chunks of information are labeled with headers. Headers clearly describe sections so that readers can scan and find information.	Yes=1/No=0
	7	Font type and size: font type or style is easy to read. Font size is at least 11 - 12 point.	Yes=1/No=0
	8	White space: uses bulleted or numbered lists to increase white space on the page.	Yes=1/No=0
	9	Image: contains at least 1 image that is related to the topic of the study. Not a logo.	Yes=1/No=0
Understandability			
	10	Purpose of the study: includes a statement that says, “the purpose of the study is…” Purpose of the study is stated, rather than implied.	Yes=1/No=0
	11	Main reason to join the study—benefits: includes description or list of potential benefits to participants or others.	Yes=1/No=0
	12	Main reasons not to join the study—risks: includes description or list of potential side effects or risks to participants.	Yes=1/No=0
	13	Information being collected: describes the information that will be collected from participants and about participants.	Yes=1/No=0
	14	Study procedures: describes what participants will need to do AND how much time it will take.	Yes=1/No=0

XSL•FO
RenderX

Category and item number		Description	Rating
	15	Study is research: includes a statement that says, "study is research" or "research study" not just consenting to treatment.	Yes=1/No=0
	16	Participation is voluntary: states that participation is voluntary and that participants have a choice to be in the study or not.	Yes=1/No=0
	17	Costs and compensation: describes any financial payments (or costs) to study participants.	Yes=1/No=0
Actionability			
	18	Consent process: describes the process by which the reader gives his or her consent by signing a document, verbal agreement, via computer, or other.	Yes=1/No=0

Statistical Analysis

We reported mean accuracy and completeness scores for human-generated and LLM-generated ICF key information sections. We compared the mean accuracy and completeness scores of human-generated and LLM-generated ICF key information sections using Wilcoxon rank sum tests. Furthermore, we compared the RUAKI indicators between the 2 groups using the Wilcoxon rank sum test. Moreover, we measured the intraclass correlation coefficient (ICC) to assess the consistency among raters. An ICC below 0.5 indicates low reliability, between 0.5 and 0.74 indicates moderate reliability, from 0.75 to 0.9 suggests good reliability, and above 0.9 signifies excellent reliability [26].

Ethical Considerations

This study qualifies as nonhuman subjects research under applicable institutional and regulatory guidelines, as it exclusively involved evaluators who are also coauthors of this work. No external participants were involved, and no identifiable private information was collected, analyzed, or shared. Consequently, this work did not require review or approval from an IRB.

Results

The accuracy and completeness of the LLM- and human-generated outputs were comparable across key sections of the ICFs (Table 3). Both the LLM and human outputs achieved similar scores for conveying the study purpose (2.88 vs 2.63), with no significant difference (*P*=.16). For the duration and procedures, the scores were also close (2.5 vs 2.38), with no statistically significant difference (*P*=.56). The LLM slightly outperformed the human output in explaining the risks and discomforts (2.63 vs 2.38), but again, this difference was not statistically significant (*P*=.32). In terms of benefits, the LLM achieved a perfect score of 3.0 compared with the human output's 2.57, although this difference approached but did not reach statistical significance (*P*=.10). Both the LLM and human outputs were identical in discussing alternatives, scoring 2.75 (*P*≥.99). For the overall impression, the LLM scored 2.63 compared with the human output's 2.31, with no statistically significant difference (*P*=.32). Overall, both outputs displayed comparable levels of performance across these key sections.

Table . Mean accuracy and completeness scores for human and large language model evaluations across key informed consent sections.

	LLM output, mean score (SD)	Human output, mean score (SD)	Wilcoxon rank sum tests, *P* value
Study purpose	2.88 (0.35)	2.63 (0.52)	.16
Duration and procedures	2.5 (0.53)	2.38 (0.52)	.56
Risks and discomforts	2.63 (0.52)	2.38 (0.52)	.32
Benefits	3 (0)	2.57 (0.79)	.10
Alternatives	2.75 (0.46)	2.75 (0.46)	≥.99
Overall impression	2.63 (0.52)	2.31 (0.59)	.32

The comparison of Mean RUAKI scores for ICF key information generated by LLMs versus human output reveals that the LLM consistently outperforms human-generated content in critical areas (Figure 1). Although both the LLM and human outputs achieved relatively high readability scores, with the LLM slightly ahead (76.39% vs 66.67%), this difference approached but did not reach statistical significance (*P*=.26). The LLM demonstrated significantly better understandability, scoring 90.63% compared with the human score of 67.19%, with a statistically significant *P* value of .015. Moreover, the LLM

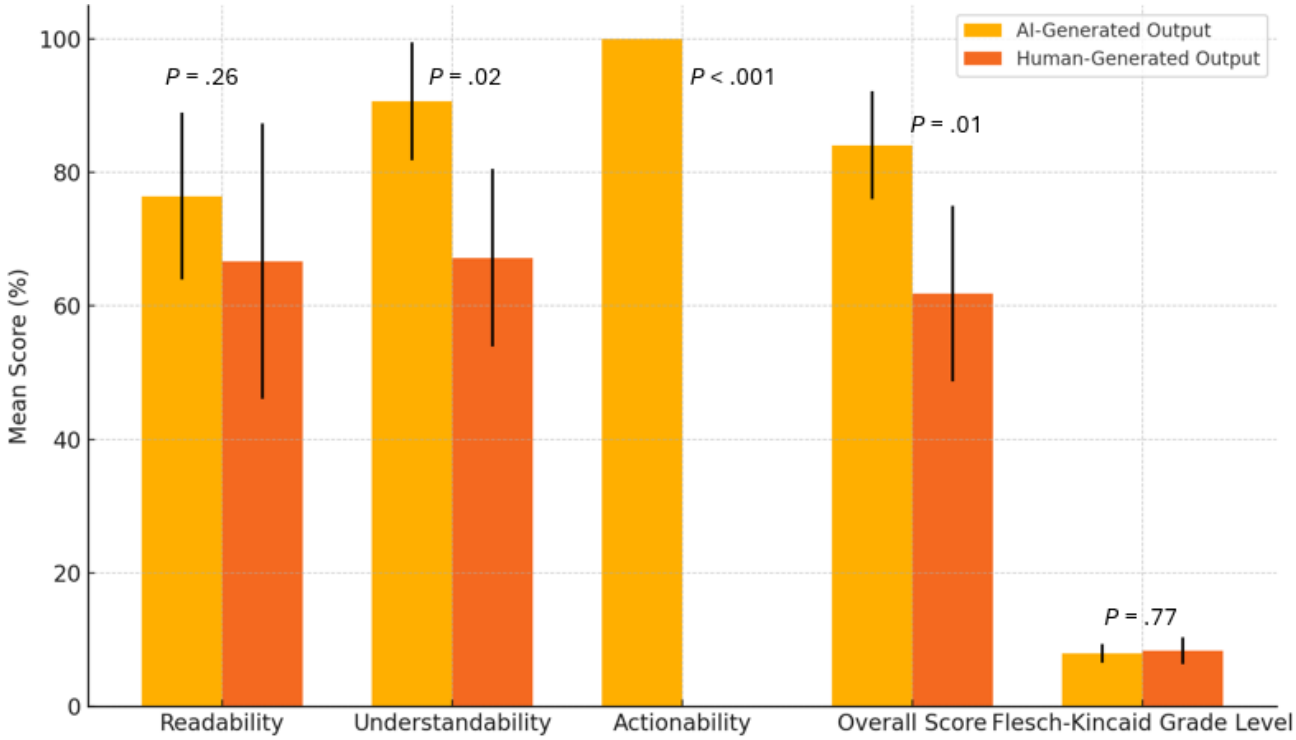
XSL•FO
RenderX

consistently included an actionable next step at the end of the document, a crucial element that the human output failed to provide, as evidenced by the LLM's perfect actionability score of 100% compared with 0% for the human output. Overall, the LLM's content achieved a significantly higher combined score (84.03% vs 61.82%), with a statistically significant *P* value of .008, demonstrating that LLM-generated text is generally more effective in producing ICF key information sections that are not only easier to read but also more understandable and actionable for participants.

While both the LLM- and human-generated ICFs exhibited similar grade levels, the LLM generated content at a slightly lower grade level (7.95 vs 8.375), indicating that it is easier to read and better aligned with the recommended reading level for general audiences. However, this difference was not statistically significant (*P*=.77), suggesting comparable readability between the two. Nonetheless, the LLM's content remains closer to the target readability level, providing a subtle advantage in ensuring accessibility for a wider audience.

The ICC score for the average ratings across the raters was found to be 0.83 (95% CI 0.64-1.03). According to the general interpretation guidelines for ICC values, this score indicates good reliability.

Figure 1. Comparison of AI- and human-generated informed consent form performance: mean Readability, Understandability, and Actionability of Key Information scores with CIs and Wilcoxon signed rank test *P* values for readability, understandability, actionability, and Flesch-Kincaid grade level. AI: artificial intelligence.



Discussion

Principal Results

This study evaluated the performance of the Mistral 8x22B LLM in generating key information sections for ICFs in clinical trials. The comparison between LLM-generated content and human-generated ICFs revealed that LLMs demonstrate considerable potential for improving the efficiency, readability, and actionability of ICFs, while maintaining comparable accuracy and completeness across most assessed categories.

Accuracy and Completeness

The LLM-generated ICFs achieved comparable performance to human-generated content across most areas. Both LLM and human outputs were similar in conveying the purpose of the study. They also performed equally well in describing the duration and procedures. While the human-generated content slightly outperformed the LLM in discussing alternatives, the LLM performed better in explaining the benefits. The overall impression score favored the LLM slightly. These results suggest that while the LLM performs similarly to humans in most areas, further refinement in prompt engineering may be required to improve its performance in more complex sections, such as alternatives. With additional fine-tuning, LLMs could potentially match or exceed the quality of human-generated ICFs across all categories.

Readability

The LLM outperformed human-generated ICFs in readability, as demonstrated by higher RUAKI scores. Both LLM- and human-generated ICFs exhibited good readability according to the Flesch-Kincaid grade level, but the LLM achieved a lower average grade level, reflecting superior readability and closer alignment with institutional requirements for eighth-grade reading level content. This highlights the LLM's strength in tackling one of the primary challenges of ICF creation: producing documents that are both comprehensive and easily understood by a general audience. Given that many ICFs often exceed the recommended reading level, the LLM's consistent

XSL•FO
RenderX

ability to generate readable content is a significant advantage, ensuring accessibility without sacrificing detail.

Understandability and Actionability

The LLM significantly outperformed human-generated ICFs in both understandability and actionability, as reflected in the higher RUAKI scores. The LLM's output was not only more comprehensible but also consistently included actionable next steps, a critical component that was often missing from the human-generated content. The perfect actionability score of the LLM-generated ICFs suggests that these models can enhance participant comprehension and facilitate informed decision-making. These findings demonstrate the potential of LLMs to create ICFs that are not only easier to read but also more effective in guiding participants through the consent process.

Rater Consistency

The ICC of 0.83 indicates a very high level of agreement among raters, reflecting the reliability of the evaluation process. The narrow CI further supports the robustness of these ratings, ensuring the consistency and validity of the results across different protocols.

Lessons Learned

Lesson 1: The Importance of Precise Temperature Settings

For all LLMs, the model temperature parameter controls the diversity of responses. A higher temperature, such as 0.8, produces more varied answers, while a lower temperature, such as 0.2, results in more focused and deterministic outputs. In our experiments, we found that setting the temperature to 0 was the most effective choice for this task. Temperatures introduce a level of randomness that can lead to hallucinations—unwanted deviations from the source material. Since our goal is to extract information directly from the research protocol and treat it as the sole source of truth, it is essential to minimize any creative output from the LLM. Although a temperature of 0.2 is already fairly focused [27,28], the need for absolute accuracy in clinical trial documents led us to set the temperature to 0, ensuring that the content remains strictly aligned with the provided data.

Lesson 2: Addressing Readability Challenges With Cross-Model Few-Shot Prompting

It was observed that Mistral struggled to generate content at a Flesch-Kincaid grade level of 8 when prompted directly with instructions such as, "The content should meet literacy standards, specifically an 8th-grade reading level or lower." To overcome this challenge, unlike the other zero-shot prompts used in this project, additional prompts and a technique known as "few-shot training" [29] were introduced. This involved providing the model with examples of text at both below 8 and above 9 Flesch-Kincaid grade levels, helping to guide the model in producing content at the desired reading level. These examples, generated using ChatGPT 4, were incorporated (as shown in Supplementary 3 in Multimedia Appendix 1) enabling Mistral to produce content more consistently at the desired grade level 8 or below. This approach, known as cross-model few-shot prompting, involves using one model to generate examples (or "shots") that are subsequently fed into another model to enhance its performance on a specific task. It is essential to apply this step after any content-editing prompts are used, as further content edits could inadvertently raise the reading level above the target. Format editing should be the final step in the process, as any subsequent prompts could alter the formatting.

Lesson 3: Least-to-Most Prompt Engineering

Effective prompt engineering involves breaking down tasks into manageable steps. When LLMs are given multiple instructions in a single prompt, they often struggle to follow all directions accurately. By adopting a Least-to-Most approach [30]—where each prompt contains a focused set of instructions and builds on the previous output—we achieved more consistent and reliable results. This is analogous to how clinical workflows are built iteratively in electronic health record (EHR) systems to ensure accuracy in decision-making. Much like building clinical templates or order sets, prompt engineering ensures that each phase of content generation is guided to avoid ambiguity, ensuring accuracy and relevance to the context of informed consent. For example, if we were building a medication alert in an EHR, breaking the alert logic into separate steps—from checking allergies to suggesting alternatives—ensures clarity and avoids overwhelming the user. Similarly, breaking down the prompt for generating ICF sections helps the LLM focus on retrieving the right information from the protocol. This method involves 2 stages: first, decomposing a complex problem into a series of simpler subproblems and then sequentially solving these subproblems, with each solution informed by the answers to the previous ones. By guiding the LLM to work incrementally, we not only enhanced its accuracy but also ensured that human oversight remained integral to the process, leading to optimal outcomes and greater control over the final product. For instance, one reviewer noted that the LLM-generated procedures were missing some procedure information. This issue likely stemmed from the lengthy and poorly structured procedure section in the original research protocol. To address this, we designed a workflow in which we first asked the LLM to summarize the study's procedures and timeline. We then instructed the LLM to extract the necessary information from this summarized output. This step-by-step Least-to-Most approach allowed us to successfully extract the missing information and integrate it into the key information.

Lesson 4: Real-World Application and Integration Challenges

Implementing LLMs in clinical workflows requires more than just improving readability or accuracy—it necessitates seamless integration with existing clinical systems and processes, such as EHRs and IRB workflows. For LLMs to have a real-world impact, models need to be adaptable to diverse clinical environments and meet regulatory and ethical standards. One way to ensure this is by developing interfaces that allow researchers to fine-tune LLM outputs while ensuring compliance with clinical trial guidelines.

XSL•FO
RenderX

Lesson 5: The Need for Detailed Source Material and Human Oversight

In one research protocol, a reviewer found that the human-generated ICF was more accurate in detailing risks and discomforts compared with the LLM-generated version. This discrepancy was evident in the omission of common discomforts associated with COVID-19 tests in the LLM-generated ICF, which occurred because this information was not included in the original research protocol. This underscores a key lesson: "garbage in, garbage out." For LLMs to produce a comprehensive and accurate ICF, the original research protocol must be thorough and detailed. Furthermore, this finding highlights the importance of having a human-in-the-loop to review and refine the output from LLMs. While LLMs can significantly reduce the effort required to create an ICF—potentially saving up to 90% of the work—the final product still benefits from human oversight. For example, after generating a well-structured ICF key information section with the LLM, researchers can easily tweak the content to better suit their specific audience. One reviewer noted that the LLM-generated ICF had a more technical and clinical tone than the human-generated version. By having researchers to customize the LLM-generated content, the ICF can be tailored to the study audience, while most of the heavy lifting has been accomplished by the LLM.

Lesson 6: Ethical and Regulatory Considerations for LLM-Generated Content

With the increasing role of LLMs in generating participant-facing documents, ethical and regulatory concerns must be addressed. Key considerations include ensuring that AI-generated ICFs do not inadvertently introduce bias or misinformation. Furthermore, as LLMs take on more responsibility in clinical settings, regulatory bodies may need to establish guidelines to govern their use. These guidelines could include stipulations on the necessity of human oversight to verify that LLM-generated content is accurate, participant-friendly, and compliant with ethical standards for informed consent.

Lesson 7: Techniques for Structured and Accurate Information Extraction

By using effective prompt engineering strategies [31,32] and crafting prompts that were precisely focused on extracting information from the research protocol, we were able to generate a well-structured and neatly formatted output. Key components—such as the introduction, study purpose, procedures, risks and discomforts, benefits, alternatives, cost and compensation, and consent process—were clearly delineated with headers, which improved the organization of the document and made it easier to locate specific information. When crafting the initial prompt to extract key information, we used a combination of techniques:

1. Delimiter usage: Delimiters like ### and [] were used to clearly define boundaries between different sections of the text.
2. Role-playing: Assigning the LLM a specific role, such as "As a Clinical Trial Informed Consent Writer," provided contextual guidance, resulting in improved performance by making the model's responses more relevant and focused.

Lesson 8: Addressing Practical Benefits and Cost-Savings

Beyond improving the quality of ICFs, LLMs offer the potential to reduce operational costs and administrative burdens in clinical trials. Automating the creation of ICFs can significantly cut down the time spent on document preparation while maintaining compliance with regulatory standards. By quantifying these savings—such as estimating the reduction in hours spent on ICF creation—future studies could further demonstrate the tangible benefits of incorporating LLMs into clinical workflows.

Lesson 9: Anticipating Future Advances

As of this publication, GPT-4o mini [33], Mistral Large 2 [34], and Meta Llama 3.1 [35] have been released, each featuring an expanded context window of 128k tokens, making them ideal for these tasks. However, they were not available during the development phase. While 64k tokens are sufficient for handling most clinical research protocols, for more extensive content, these new models would be preferable. That said, the prompts are compatible with all of these models.

Implications for Practice

The use of LLMs to generate ICFs offers considerable potential for streamlining the informed consent process. By producing more readable, understandable, and actionable content, LLMs can enhance participant comprehension and engagement, potentially improving recruitment and retention in clinical trials. Furthermore, the time savings associated with automated ICF generation can reduce the workload on researchers while ensuring that ICFs remain aligned with regulatory standards for readability and content clarity.

Limitations and Future Directions

This study's findings must be interpreted in light of certain limitations. The LLM's performance is closely tied to the quality of the input research protocol. The LLM's performance is closely tied to the clarity and completeness of the source material. Ambiguities or inconsistencies in the research protocols can hinder the model's ability to capture all relevant details to generate accurate and comprehensive ICFs. Future research should focus on improving the clarity of source materials and refining prompt-engineering strategies to optimize LLM performance, particularly in more complex sections such as study procedures.

To address these challenges with procedural details, we used a targeted prompt-engineering approach, which involved having the LLM first summarize the study's procedures and timeline, and then extract specific details from the summarized text. This method improved accuracy, but ongoing refinement of these strategies is needed to enhance the LLM's ability to process complex and lengthy sections more effectively.

Another limitation relates to the potential recognizability of LLM-generated text. Although evaluators were blinded to the source of the ICFs and presented with human- and LLM-generated documents in a randomized order, the distinctive textual style of LLM outputs—characterized by active voice,

XSL•FO
RenderX

well-organized structure, simplified language, and consistent adherence to readability guidelines—may have inadvertently revealed their origin. This recognizability could introduce subconscious bias into the evaluation process. To address this in future studies, we plan to use text obfuscation techniques, such as paraphrasing or reformatting outputs, to minimize stylistic differences and ensure true blinding. This approach will help strengthen the validity of future comparisons.

Another important limitation of this study is the small sample size, which consisted of only 4 clinical trial protocols. While these protocols provided a useful test bed, the relatively small sample size limits the generalizability of the findings. Future studies should incorporate a broader range of clinical trials from diverse therapeutic areas, phases, and levels of complexity to fully validate the model's performance. Furthermore, the limited sample size may have contributed to some statistically nonsignificant results, such as those related to procedural details or study alternatives. A larger sample would provide greater statistical power, enabling the detection of smaller but practically significant differences between human- and LLM-generated ICFs.

A larger sample would also better capture the diversity of challenges involved in ICF creation, such as variations in regulatory requirements, medical procedure complexity, and considerations for vulnerable populations. Future research should aim to assess the LLM's robustness and adaptability across a wider array of clinical trial contexts.

The process of designing and refining prompts, as well as generating the AI-generated ICFs, required a moderate time investment during initial development. However, leveraging the existing prompts and lessons learned in this study would enable future users to complete the process more efficiently and at reduced cost, enhancing the scalability of this approach.

The 0% actionability score for human-generated ICFs reflects a structural issue rather than a methodological flaw. Most institutions do not include explicit actionable sections in the key information portions of their templates. Updating these templates to include actionable instructions would likely improve scores significantly. This highlights a strength of LLM-generated ICFs, which inherently include actionable elements, enhancing the clarity and use of consent forms.

While the LLM demonstrated strong performance, there were instances where it missed details related to the duration and procedural elements of the study. This likely stems from 2 primary challenges: ambiguous or inconsistent presentation of these sections in the research protocols and the verbosity of the text, which can hinder the LLM's ability to process details efficiently. Our targeted approach of summarizing and then extracting procedural details helped address this issue, but further enhancements are needed to ensure that the LLM can consistently handle such challenges.

Looking ahead, our next goal is to automate the creation of entire ICFs directly from research protocols. This would significantly reduce the time and effort required for ICF development while maintaining consistency and quality. While this study highlights the potential for human oversight to address issues in LLM-generated content, our future research will aim to quantify the time and effort required for revisions to better assess the practical efficiency gains of integrating these models into clinical workflows. We also plan to explore the LLM's multilingual capabilities to generate ICFs in multiple languages, broadening the recruitment base and promoting diversity and equity in clinical trials. Ensuring that non–English-speaking participants receive ICFs that are as readable and understandable as those in English is crucial for improving inclusivity and representation in research. Future work should also prioritize a thorough examination of ethical concerns, including potential biases in AI-generated content, the need for transparency in AI decision-making processes, and the legal implications of deploying LLMs in clinical trial workflows, to ensure that these tools are implemented responsibly and equitably.

Conclusions

This study highlights the potential of LLMs to improve the efficiency and quality of ICF generation in clinical trials. While human oversight remains necessary to ensure accuracy in complex sections, and the findings are constrained by the small dataset and evaluation of a single LLM model, LLMs demonstrated potential advantages in producing more readable, understandable, and actionable ICF content. As LLM technology continues to evolve, it holds the promise of further enhancing the informed consent process by facilitating the creation of ICFs that are both participant-friendly and compliant with regulatory standards, thereby improving ethical conduct in clinical research.

Acknowledgments

Research reported in this publication was supported by the National Center for Advancing Translational Sciences of the National Institutes of Health under award number UL1-TR001453. However, the content is solely the authors' responsibility and does not necessarily represent the official views of the National Institutes of Health.

Conflicts of Interest

None declared.

Multimedia Appendix 1
Prompt details.
[DOCX File, 18 KB - medinform_v13i1e68139_app1.docx]

XSL•FO
RenderX

Multimedia Appendix 2
Form for grading scale of informed consent key information sections.
[DOCX File, 14 KB - medinform_v13i1e68139_app2.docx]

References

1. Part 46: protection of human subjects. Code of Federal Regulations. 2018 Jul 19. URL: https://www.ecfr.gov/on/2018-07-19/title-45/subtitle-A/subchapter-A/part-46 [accessed 2025-01-21]
2. Tamariz L, Palacio A, Robert M, Marcus EN. Improving the informed consent process for research subjects with low literacy: a systematic review. J Gen Intern Med 2013 Jan;28(1):121-126. [doi: 10.1007/s11606-012-2133-2] [Medline: 22782275]
3. Emanuel EJ, Boyle CW. Assessment of length and readability of informed consent documents for COVID-19 vaccine trials. JAMA Netw Open 2021 Apr 1;4(4):e2110843. [doi: 10.1001/jamanetworkopen.2021.10843] [Medline: 33909052]
4. Grant SC. Informed consent—we can and should do better. JAMA Netw Open 2021 Apr 1;4(4):e2110848. [doi: 10.1001/jamanetworkopen.2021.10848] [Medline: 33909058]
5. Hadden KB, Prince LY, Moore TD, James LP, Holland JR, Trudeau CR. Improving readability of informed consents for research at an academic medical institution. J Clin Trans Sci 2017 Dec;1(6):361-365. [doi: 10.1017/cts.2017.312]
6. Larson E, Foe G, Lally R. Reading level and length of written research consent forms. Clin Transl Sci 2015 Aug;8(4):355-356. [doi: 10.1111/cts.12253] [Medline: 25580939]
7. Sherlock A, Brownie S. Patients' recollection and understanding of informed consent: a literature review. ANZ J Surg 2014 Apr;84(4):207-210. [doi: 10.1111/ans.12555] [Medline: 24812707]
8. Malik L, Kuo J, Yip D, Mejia A. How well informed is the informed consent for cancer clinical trials? Clin Trials 2014 Dec;11(6):686-688. [doi: 10.1177/1740774514548734] [Medline: 25135910]
9. Zai AH, Faro JM, Allison J. Unveiling readability challenges: an extensive analysis of consent document accessibility in clinical trials. J Clin Transl Sci 2024;8(1):e125. [doi: 10.1017/cts.2024.595] [Medline: 39345692]
10. Office for Human Research Protections. Attachment C—new "key information" informed consent requirements. US Department of Health and Human Services. 2018. URL: https://www.hhs.gov/ohrp/sachrp-committee/recommendations/attachment-c-november-13-2018/index.html [accessed 2025-01-31]
11. Hu Y, Chen Q, Du J, et al. Improving large language models for clinical named entity recognition via prompt engineering. J Am Med Inform Assoc 2024 Sep 1;31(9):1812-1820. [doi: 10.1093/jamia/ocad259] [Medline: 38281112]
12. Nievas M, Basu A, Wang Y, Singh H. Distilling large language models for matching patients to clinical trials. J Am Med Inform Assoc 2024 Sep 1;31(9):1953-1963. [doi: 10.1093/jamia/ocae073] [Medline: 38641416]
13. Unlu O, Shin J, Mailly CJ, et al. Retrieval augmented generation enabled generative pre-trained transformer 4 (GPT-4) performance for clinical trial screening. medRxiv. Preprint posted online on Feb 8, 2024. [doi: 10.1101/2024.02.08.24302376] [Medline: 38370719]
14. Chen S, Li Y, Lu S, et al. Evaluating the ChatGPT family of models for biomedical reasoning and classification. J Am Med Inform Assoc 2024 Apr 3;31(4):940-948. [doi: 10.1093/jamia/ocad256] [Medline: 38261400]
15. Glicksberg BS, Timsina P, Patel D, et al. Evaluating the accuracy of a state-of-the-art large language model for prediction of admissions from the emergency room. J Am Med Inform Assoc 2024 Sep 1;31(9):1921-1928. [doi: 10.1093/jamia/ocae103] [Medline: 38771093]
16. Tripathi S, Sukumaran R, Cook TS. Efficient healthcare with large language models: optimizing clinical workflow and enhancing patient care. J Am Med Inform Assoc 2024 May 20;31(6):1436-1440. [doi: 10.1093/jamia/ocad258] [Medline: 38273739]
17. Decker H, Trang K, Ramirez J, et al. Large language model-based chatbot vs surgeon-generated informed consent documentation for common procedures. JAMA Netw Open 2023 Oct 2;6(10):e2336997. [doi: 10.1001/jamanetworkopen.2023.36997] [Medline: 37812419]
18. Mistral AI. 2024. URL: https://mistral.ai [accessed 2025-01-21]
19. Cheaper, better, faster, stronger. Mistral AI. 2024 Apr 17. URL: https://mistral.ai/news/mixtral-8x22b [accessed 2025-01-22]
20. Wiggins G, McTighe J. Understanding by Design, 2nd edition: Association for Supervision and Curriculum Development ASCD; 2005.
21. Quick Safety 21: informed consent: more than getting a signature. The Joint Commission. 2023. URL: https://www.jointcommission.org/resources/news-and-multimedia/newsletters/newsletters/quick-safety/quick-safety--issue-21-informed--consent-more-than-getting-a-signature/informed-consent-more-than-getting-a-signature/ [accessed 2025-01-31]
22. Informed consent. Leapfrog Ratings. URL: https://ratings.leapfroggroup.org/measure/hospital/2023/informed-consent [accessed 2025-01-31]
23. Samaan JS, Yeo YH, Rajeev N, et al. Assessing the accuracy of responses by the language model ChatGPT to questions regarding bariatric surgery. Obes Surg 2023 Jun;33(6):1790-1796. [doi: 10.1007/s11695-023-06603-5] [Medline: 37106269]
24. Informed consent. American College of Surgeons. 2023 Jul. URL: https://www.facs.org/for-patients/patient-resources/informed-consent [accessed 2025-01-22]

XSL•FO
RenderX

25. Kurtz-Rossi S, Okonkwo IA, Chen Y, et al. Development of a new tool for writing research key information in plain language. Health Lit Res Pract 2024 Jan;8(1):e30-e37. [doi: 10.3928/24748307-20240218-01] [Medline: 38466225]
26. Koo TK, Li MY. A guideline of selecting and reporting intraclass correlation coefficients for reliability research. J Chiropr Med 2016 Jun;15(2):155-163. [doi: 10.1016/j.jcm.2016.02.012] [Medline: 27330520]
27. Mistral AI API (002). Mistral AI. 2024 May 14. URL: https://docs.mistral.ai/api [accessed 2025-01-21]
28. How should I set the temperature parameter? OpenAI Platform. 2024 Aug 6. URL: https://platform.openai.com/docs/guides/text-generation/how-should-i-set-the-temperature-parameter [accessed 2025-01-21]
29. Brown TB, Mann B, Ryder N, et al. Language models are few-shot learners. arXiv. Preprint posted online on May 28, 2020. [doi: 10.48550/arXiv.2005.14165]
30. Zhou D, Schärli N, Hou L, et al. Least-to-most prompting enables complex reasoning in large language models. arXiv. Preprint posted online on May 21, 2022. [doi: 10.48550/arXiv.2205.10625]
31. Six strategies for getting better results. OpenAI Platform. URL: https://platform.openai.com/docs/guides/prompt-engineering/six-strategies-for-getting-better-results [accessed 2025-01-21]
32. Prompting capabilities. Mistral AI. URL: https://docs.mistral.ai/guides/prompting_capabilities [accessed 2025-01-21]
33. GPT-4o mini: advancing cost-efficient intelligence. OpenAI. 2024. URL: https://openai.com/index/gpt-4o-mini-advancing-cost-efficient-intelligence [accessed 2025-01-21]
34. Mistral large 2. Mistral AI. 2024 Jul 24. URL: https://mistral.ai/news/mistral-large-2407 [accessed 2025-01-21]
35. Introducing Llama 31: our most capable models to date. Meta. 2024. URL: https://ai.meta.com/blog/meta-llama-3-1 [accessed 2025-01-21]

Abbreviations

AI: artificial intelligence
EHR: electronic health record
ICC: intraclass correlation coefficient
ICF: informed consent form
IRB: institutional review board
LLM: large language model
RUAKI: Readability, Understandability, and Actionability of Key Information

Edited by C Lovis; submitted 29.10.24; peer-reviewed by K Trang, M Elbattah; revised version received 02.01.25; accepted 04.01.25; published 13.02.25.

Please cite as:
Shi Q, Luzuriaga K, Allison JJ, Oztekin A, Faro JM, Lee JL, Hafer N, McManus M, Zai AH
Transforming Informed Consent Generation Using Large Language Models: Mixed Methods Study
JMIR Med Inform 2025;13:e68139
URL: https://medinform.jmir.org/2025/1/e68139
doi:10.2196/68139

© Qiming Shi, Katherine Luzuriaga, Jeroan J Allison, Asil Oztekin, Jamie M Faro, Joy L Lee, Nathaniel Hafer, Margaret McManus, Adrian H Zai. Originally published in JMIR Medical Informatics (https://medinform.jmir.org), 13.2.2025. This is an open-access article distributed under the terms of the Creative Commons Attribution License (https://creativecommons.org/licenses/by/4.0/), which permits unrestricted use, distribution, and reproduction in any medium, provided the original work, first published in JMIR Medical Informatics, is properly cited. The complete bibliographic information, a link to the original publication on https://medinform.jmir.org/, as well as this copyright and license information must be included.

XSL•FO
RenderX

Diagnosis of Chronic Kidney Disease Using Retinal Imaging and Urine Dipstick Data: Multimodal Deep Learning Approach

Youngmin Bhak[1,2*], BS; Yu Ho Lee[3*], MD, PhD; Joonhyung Kim[4*], MD, PhD; Kiwon Lee[5*], MS; Daehwan Lee[5], BS; Eun Chan Jang[6,7], MPH; Eunjeong Jang[6,7], BS; Christopher Seungkyu Lee[8], MD, PhD; Eun Seok Kang[9], MD, PhD; Sehee Park[10,11], MS; Hyun Wook Han[6,7,12,13], MD, PhD; Sang Min Nam[6,7,14], MD, PhD

[1]Korean Genomics Center (KOGIC), Ulsan National Institute of Science and Technology (UNIST), Ulsan, Republic of Korea

[10]Department of ICT Safety, Graduate School of Chung-Ang University, Seoul, Republic of Korea

[11]IAEC Medical Service, Seoul, Republic of Korea

[12]Institute of Basic Medical Sciences, School of Medicine, CHA University, Gyeonggi-do, Republic of Korea

[13]Healthcare Big Data Center, CHA Bundang Medical Center, Gyeonggi-do, Republic of Korea

[14]Daechi Yonsei Eye Clinic, Seoul, Republic of Korea

[2]Department of Biomedical Engineering, College of Information and Biotechnology, Ulsan National Institute of Science and Technology (UNIST), Ulsan, Republic of Korea

[3]Division of Nephrology, Department of Internal Medicine, CHA Bundang Medical Center, CHA University, Gyeonggi-do, Republic of Korea

[4]Department of Ophthalmology, CHA Bundang Medical Center, CHA University, Gyeonggi-do, Republic of Korea

[5]Spidercore Inc, Daejeon, Republic of Korea

[6]Department of Biomedical Informatics, School of Medicine, CHA University, 335 Pangyo-ro, Seongnam, Republic of Korea

[7]Institute for Biomedical Informatics, School of Medicine, CHA University, Seongnam, Republic of Korea

[8]Department of Ophthalmology, Institute of Vision Research, Severance Hospital, Yonsei University College of Medicine, Seoul, Republic of Korea

[9]Division of Endocrinology and Metabolism, Department of Internal Medicine, Yonsei University College of Medicine, Seoul, Republic of Korea

[*]these authors contributed equally

Corresponding Author:
Sang Min Nam, MD, PhD
Department of Biomedical Informatics, School of Medicine, CHA University, 335 Pangyo-ro, Seongnam, Republic of Korea

Abstract

Background: Chronic kidney disease (CKD) is a prevalent condition with significant global health implications. Early detection and management are critical to prevent disease progression and complications. Deep learning (DL) models using retinal images have emerged as potential noninvasive screening tools for CKD, though their performance may be limited, especially in identifying individuals with proteinuria and in specific subgroups.

Objective: We aim to evaluate the efficacy of integrating retinal images and urine dipstick data into DL models for enhanced CKD diagnosis.

Methods: The 3 models were developed and validated: eGFR-RIDL (estimated glomerular filtration rate–retinal image deep learning), eGFR-UDLR (logistic regression using urine dipstick data), and eGFR-MMDL (multimodal deep learning combining retinal images and urine dipstick data). All models were trained to predict an eGFR<60 mL/min/1.73 m², a key indicator of CKD, calculated using the 2009 CKD-EPI (Chronic Kidney Disease Epidemiology Collaboration) equation. This study used a multicenter dataset of participants aged 20 - 79 years, including a development set (65,082 people) and an external validation set (58,284 people). Wide Residual Networks were used for DL, and saliency maps were used to visualize model attention. Sensitivity analyses assessed the impact of numerical variables.

Results: eGFR-MMDL outperformed eGFR-RIDL in both the test and external validation sets, with area under the curves of 0.94 versus 0.90 and 0.88 versus 0.77 (P<.001 for both, DeLong test). eGFR-UDLR outperformed eGFR-RIDL and was comparable to eGFR-MMDL, particularly in the external validation. However, in the subgroup analysis, eGFR-MMDL showed improvement across all subgroups, while eGFR-UDLR demonstrated no such gains. This suggested that the enhanced performance of eGFR-MMDL was not due to urine data alone, but rather from the synergistic integration of both retinal images and urine data. The eGFR-MMDL model demonstrated the best performance in individuals younger than 65 years or those with proteinuria. Age and proteinuria were identified as critical factors influencing model performance. Saliency maps indicated that urine data and retinal images provide complementary information, with urine offering insights into retinal abnormalities and retinal images, particularly the arcade vessels, being key for predicting kidney function.

XSL•FO
RenderX

Conclusions: The MMDL model integrating retinal images and urine dipstick data show significant promise for noninvasive CKD screening, outperforming the retinal image–only model. However, routine blood tests are still recommended for individuals aged 65 years and older due to the model's limited performance in this age group.

(JMIR Med Inform 2025;13:e55825) doi:10.2196/55825

KEYWORDS

multimodal deep learning; chronic kidney disease; fundus image; saliency map; urine dipstick

Introduction

Chronic kidney disease (CKD) is a pervasive and potentially irreversible condition that afflicts more than 10% of the global population [1,2]. It is diagnosed based on the presence of decreased glomerular filtration rate (GFR) or markers of kidney damage, such as proteinuria, persisting for over 3 months [3]. In clinical practice, estimated glomerular filtration rate (eGFR) is widely used and typically calculated based on demographic factors and serum creatinine levels. A drop in eGFR below 60 mL/min/1.73 m^2 significantly elevates the risk of cardiovascular diseases, mortality, and progression to end-stage kidney disease [4-6]. Proteinuria, indicative of kidney damage, further compounds these risks and affects cardiovascular outcomes and patient survival [6,7]. Efficient CKD screening is critical, as patients are often asymptomatic until the disease reaches advanced stages [8].

Remarkably, the eye and kidney share developmental, structural, physiological, and pathological similarities, hinting at a potential link between ocular and renal diseases [9]. Notably, both organs are highly vascularized and susceptible to conditions affecting the vascular system, such as aging, diabetes, and hypertension [10]. Evidence suggests that individuals displaying retinal microvascular signs, including retinopathy, arteriolar narrowing, and venular dilatation, exhibit an increased predisposition for CKD, and vice versa [1,11-14]. Fundus imaging allows for the convenient assessment of the retinal microvasculature, making it a potential screening modality for incident CKD. However, conventional fundus photography analysis has limitations in predicting CKD incidence or progression due to population heterogeneity and sensitivity issues [1].

To address these limitations, the integration of artificial intelligence, particularly deep learning (DL), with retinal imaging has emerged as a promising approach. Recent studies using DL models (convolutional neural networks, cCondenseNet, or ResNet-50) have demonstrated moderate to good performance in identifying individuals with decreased eGFR or CKD based on retinal photographs [15,16]. Nevertheless, the performance diminishes when detecting isolated proteinuria compared with overall CKD [16].

Convenient and cost-effective proteinuria assessment can be accomplished using a simple urine dipstick test [3]. Combining a retinal image deep learning (RIDL) model for eGFR decline identification with urinalysis for proteinuria detection would eliminate the need for invasive blood tests, thereby significantly improving convenience and practicality. In addition, XGBoost-based machine learning models, including 7 features (age, sex, and 5 urine dipstick measurements: protein, blood, glucose, pH, and specific gravity), successfully detect eGFR decline, especially among nondiabetic individuals younger than the age of 65 years [17].

In this study, we aimed to develop a multimodal deep learning (MMDL) model using 2 noninvasive data sources: retinal images and urine dipstick tests. We anticipate that this integration will enhance the RIDL model performance. The integration of fundus images with other data modalities in DL classifiers has been shown to improve diagnostic accuracy in some cases. For instance, a study demonstrated that combining retinal fundus images with participant metadata (such as race, age, sex, and blood pressure) enhanced the accuracy of anemia detection using DL, indicating that both metadata and fundus images contributed significantly to the prediction [18]. However, in the context of CKD detection, other studies have reported that adding clinical data to fundus image–based models does not necessarily improve performance. Further, one study used a DL algorithm for CKD detection that combined fundus photos with risk factors such as age, sex, ethnicity, diabetes, and hypertension, while another study combined fundus photos with clinical metadata such as age, sex, height, weight, BMI, and blood pressure [15,16]. In both cases, the additional data do not enhance the performance compared to models using fundus images alone.

The synergy between retinal images and urine data was assessed by comparing the performance of a urine-only model and an MMDL model with that of an RIDL model. Additionally, we comprehensively evaluated the model performance across diverse subgroups defined by well-established risk factors, such as age, diabetes, and hypertension [1,19-22]. Identifying data subgroups plays a critical role in model testing and assessing model fairness, as these subgroups can exhibit distinct or unexpected behaviors compared with the overall dataset [23]. Previous studies have explored DL and machine learning model performance within subgroups with varying outcomes. Some studies on DL models observed improved performance in patients with diabetes or high hemoglobin A_{1c}, whereas others found consistent performance across diabetes and hypertension subgroups [15,24]. However, no assessment has been conducted for eGFR<60 mL/min/1.73 m^2, a critical CKD diagnostic threshold [3]. The machine learning model, assessing eGFR<60 mL/min/1.73 m^2 using urine dipstick tests, exhibited compromised performance in diabetes, especially without proteinuria, but performed well in hypertension, especially in those younger than 65 years of age [17]. Therefore, our study systematically evaluated the model performance in 4 subgroups, including proteinuria, age ≥65 years, diabetes, and hypertension, to provide a comprehensive understanding of its capabilities and limitations in real-world scenarios.

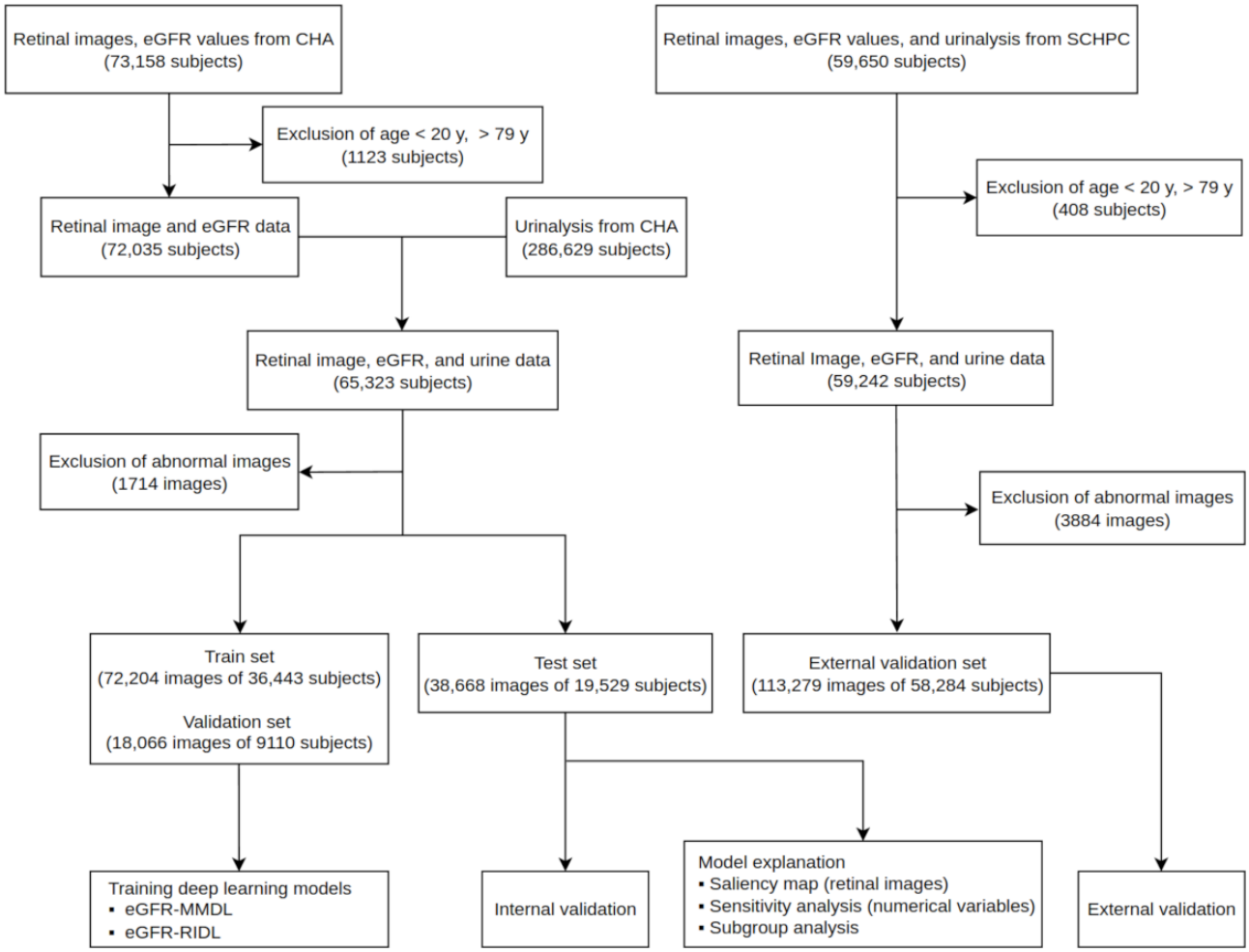
XSL•FO
RenderX

Methods

Preparation of Study Data

Retinal images, serum creatinine levels, urine dipstick results, and demographic data (age, sex, diabetes, and hypertension) were collected from multiple departments at CHA Bundang Medical Center over 12 years (2008 - 2019; Figure 1). External validation involved using identical datasets from the Severance Checkup Health Promotion Center (SCHPC) for 8 years (2013 - 2020).

Figure 1. Study flowchart from data preparation to deep learning modeling and validation. Images with abnormal brightness or haziness were excluded. CHA: CHA Bundang Medical Center; eGFR: estimated glomerular filtration rate; eGFR-MMDL: multimodal deep learning model for estimated glomerular filtration rate<60 mL/min/1.73 m²; eGFR-RIDL: retinal image deep learning model for estimated glomerular filtration rate<60 mL/min/1.73 m²; SCHPC: Severance Checkup Health Promotion Center.



The people aged 20 - 79 years were selected without duplication. The age range for adulthood was defined as 20 - 79 years, with outliers older than 79 years removed using the IQR method. Macula-centered retinal images were taken from CHA Bundang Medical Center using 1 of 2 cameras (TRC-NW8, Topcon; nonmyd 7, Kowa) at the health promotion center or endocrinology department without pupil dilation, or using VX-10i (Kowa) at the ophthalmology department with or without pupil dilation. The same style of retinal images was acquired from SCHPC using different camera models without pupil dilation (CT-80A, Topcon; AFC-210). Cases with unilateral retinal images were not collected to create ensemble models using bilateral retinal images. Serum creatinine and urine dipstick tests were performed on the same day, and retinal images were selected within 35 days before or after these tests. eGFR was calculated using a 2009 CKD-EPI (Chronic Kidney Disease Epidemiology Collaboration) formula based on serum creatinine levels [25].

In Supplementary Methods (Multimedia Appendix 1), we outlined the criteria for diabetes and hypertension, shared details about the urine analyzers used in the model, explained the scoring method for urine dipstick tests, and provided comprehensive information on image preprocessing, including algorithms for excluding abnormal images based on brightness and haziness.

Ethical Considerations

Ethical approval was granted by the institutional review boards of the Bundang CHA Medical Center (2019-01-032) and Severance Hospital (4-2020-0231), and written informed consent was not required as the data were anonymized.

Model Training

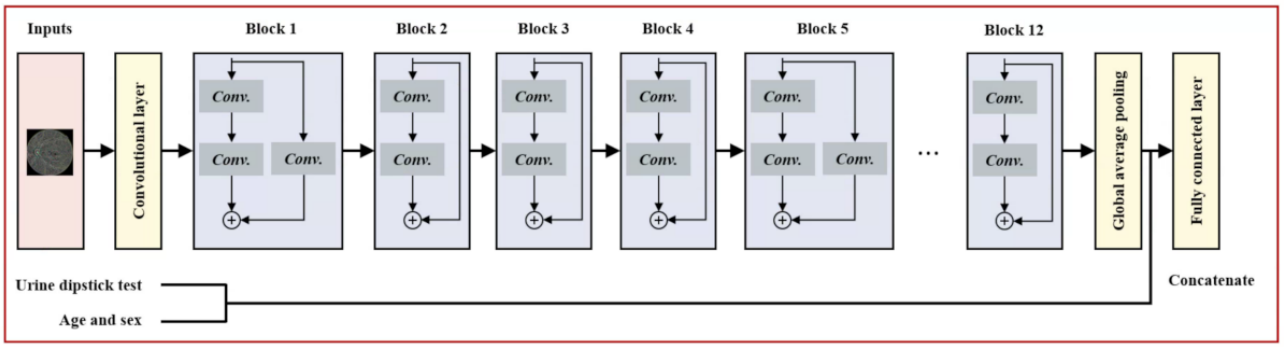
This study aimed to predict eGFR<60 mL/min/1.73 m² using retinal images and urine dipstick tests. The development dataset was divided into train, validation, and test sets (Figure 1).

XSL•FO
RenderX

Further, 2 Wide Residual Network (WRN) models were built: eGFR-RIDL and eGFR-MMDL [26].

Macula-centered retinal images were processed through a WRN-28-4 [26] and initialized with He initialization (Figure 2). Random left- and right-flip augmentation of the image was performed. In the case of eGFR-RIDL, the 256-dimensional feature vector from the convolutional layers was processed through a fully connected layer with a sigmoid activation function. Conversely, for eGFR-MMDL, the 256D feature vector from the convolutional layers analyzing retinal images was concatenated with a 12D vector representing age, sex, and urinalysis measurements using a joint fusion approach. This combined vector was then fed into a fully connected layer with a sigmoid activation function (Figure 2) [27]. Standardization was performed by removing the mean and scaling all numerical variables, except sex, before concatenation.

Figure 2. Wide Residual Network architecture for detecting kidney function decline using retinal images. For the multimodal model, the urine dipstick measurements, age, and sex were concatenated with the feature vector from the image. Conv: convolutional layer.



The binary cross-entropy function was used to calculate the loss values, and the model parameters were updated using the gradient descent method with the AdamW optimizer. To overcome the issue of imbalanced data, where the eGFR<60 mL/min/1.73 m² class was outnumbered by the eGFR>60 mL/min/1.73 m² class, the loss function was scaled by a "sample_weight" coefficient, which was calculated as the ratio of cases with eGFR>60 mL/min/1.73 m² to those with eGFR<60 mL/min/1.73 m². Model training was monitored using plots of losses and area under the curve (AUC) from the training and validation datasets to avoid overfitting, and the best epoch was identified. Our model algorithm is deployed on GitHub [28] in a runnable form, which takes in retinal images and urine analysis data.

Development of Urine Dipstick Logistic Regression Model

A logistic regression model was generated solely with numerical variables, including urine dipstick measurements, age, and sex, for comparison with the eGFR-RIDL model. Standardized numerical values were used for training and validation across both test and external validation datasets. When building the logistic regression model, we used the class_weight="balanced" option to adjust for class imbalance, ensuring that each class was appropriately weighted in the analysis.

Validation and Subgroup Analysis of the Model Performance

The probabilities from both eyes were averaged to calculate the probability of eGFR<60 mL/min/1.73 m². If only 1 eye image remained after excluding the other eye (Figure 1), the probability of the eye was used. We evaluated the model performance through internal and external validation. Internal validation used the unseen test set from the development data, whereas external validation used the SCHPC dataset. The model's performance was evaluated using AUC comparisons against the AUC of eGFR-RIDL. Additionally, the performance across various subgroups was assessed by stratifying the test set based on age, diabetes, hypertension, and proteinuria status (trace or higher urine protein). Statistical comparisons of the AUCs were made using the DeLong test, with Bonferroni correction applied when necessary.

The sensitivity and specificity were calculated by finding the best threshold using the Index of Union method, and a 95% CI was determined using bootstrap resampling. Saliency maps for retinal images and sensitivity analysis of numerical variables were used for model interpretation. Software and calculation specifics are detailed in the Supplementary Methods in Multimedia Appendix 1.

Statistics

A statistically significant difference between the 2 statistics was determined if the *P* value was below .05, or if there was no overlap between the CIs.

Results

Baseline Characteristics of the Participants

We initially screened 73,158 people from CHA and 59,650 from SCHPC, excluding those aged <20 years, >79 years, and those with low-quality images. This resulted in 128,938 images from 65,082 people with CHA and 113,279 images from 58,284 SCHPC people, ensuring that each person had at least 1 eligible image for analysis. Table 1 shows the baseline demographics and laboratory parameters of the CHA and SCHPC datasets. The developmental dataset exhibited a greater proportion of individuals younger than the age of 65 years, as well as a higher prevalence of diabetes, hypertension, and eGFR below 60 mL/min/1.73 m² compared to the external validation dataset. The distribution of measurements for the 7 urine tests (blood, protein, glucose, ketone, urobilinogen, bilirubin, and leucocyte) varied between the developmental and external datasets, as

XSL•FO
RenderX

evidenced by the histogram plots provided in Figure S2 in Multimedia Appendix 1.

XSL•FO
RenderX

Table . Baseline characteristics of study data.

Variables		Development data (CHA)[a]	External validation data (SCHPC)[b]	*P* value
Age (years), mean (SD; range)		46 (12; 20-79)	48 (12; 20-79)	<.001[c]
	<65, n[d] (%)	60,195 (92.5)	53,081 (91.1)	<.001[e]
	≥65, n (%)	4887 (7.5)	5203 (8.9)	
Sex, n (%)				<.001[e]
	Female	29,718 (45.7)	27,907 (47.9)	
	Male	35,364 (54.3)	30,377 (52.1)	
Diabetes, n (%) [f]				<.001[e]
	Positive	6458 (14.2)	2567 (5)	
	Negative	38,977 (85.8)	49,067 (95)	
Hypertension, n (%)[f]				<.001[e]
	Positive	11,172 (18.6)	7503 (14.1)	
	Negative	48,897 (81.4)	45,626 (85.9)	
eGFR [g] **(mL/min/1.73 m^2)**				
	Mean (SD)	100.5 (17)	100.4 (14.6)	.20[c]
	<60, n (%)	1085 (1.7)	492 (0.8)	<.001[e]
	<60 in age <65 y, n (%)	474 (0.8)	235 (0.4)	<.001[e]
	<60 in age ≥65 y, n (%)	611 (12.5)	257 (4.9)	<.001[e]
Urine tests				
	Specific gravity, median (IQR; range)	1.02 (0.015; 1.005 - 1.03)	1.025 (0.01; 1.005 - 1.03)	<.001[h]
	Urine pH, median (IQR; range)	6 (1; 5 - 9)	5 (0.5; 5 - 9)	<.001[h]
	Blood, median (IQR; range)	0 (0; 0 - 4)	0 (0; 0 - 4)	<.001[h]
	Protein, median (IQR; range)	0 (0; 0 - 5)	0 (0; 0 - 5)	<.001[h]
	Glucose, median (IQR; range)	0 (0; 0 - 5)	0 (0; 0 - 5)	<.001[h]
	Ketone, median (IQR; range)	0 (0; 0 - 5)	0 (0; 0 - 4)	<.001[h]
	Urobilinogen, median (IQR; range)	0 (0; 0 - 4)	0 (0; 0 - 4)	<.001[h]
	Bilirubin, median (IQR; range)	0 (0; 0 - 4)	0 (0; 0 - 4)	<.001[h]
	Leucocyte, median (IQR; range)	0 (0; 0 - 4)	0 (0; 0 - 4)	<.001[h]
	Nitrite, n (%)	570 (0.9)	263 (0.5)	<.001[c]

[a]CHA: Bundang CHA Medical Center.

[b]SCHPC: Severance Checkup Health Promotion Center.

[c]Independent 2-sample 2-tailed *t* test.

[d]n: number of images.

[e]Chi-square test.

[f]Unknown cases were excluded.

[g]eGFR: estimated glomerular filtration rate.

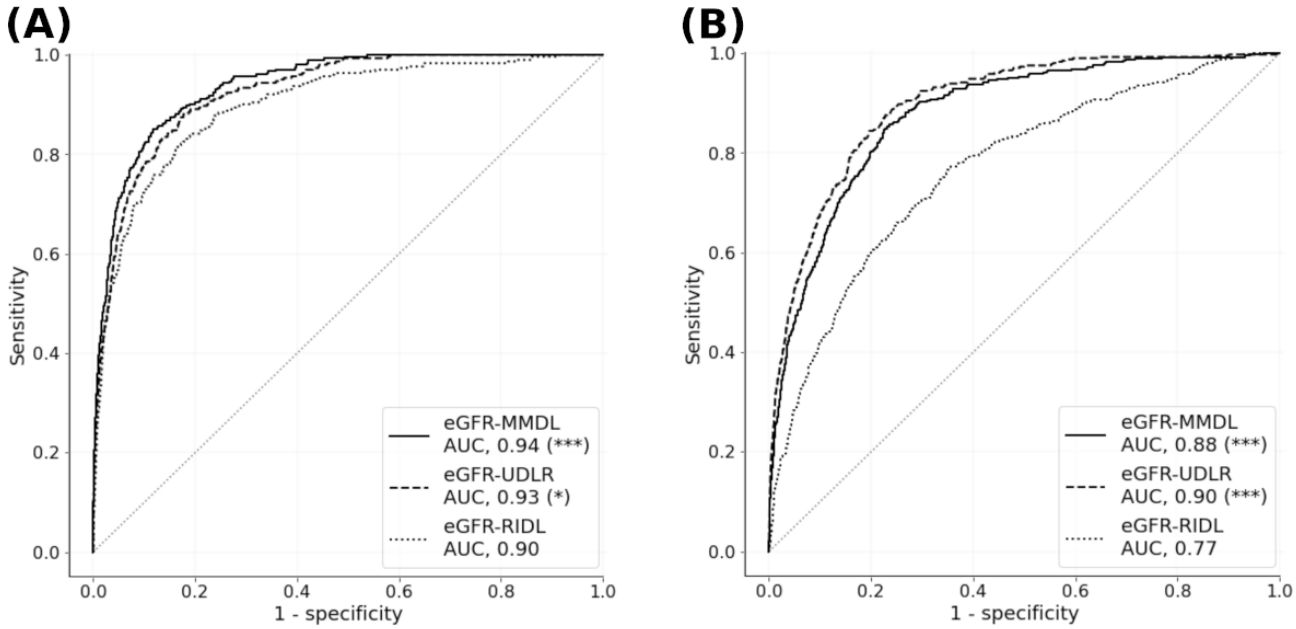
XSL•FO
RenderX

[h]Wilcoxon rank-sum test.

Performance Difference Between Unimodal and Multimodal Models

Despite the inclusion of numerical variables in the retinal image data, the training curves revealed a faster learning rate without overfitting in the eGFR-MMDL model than in the eGFR-RIDL model (Figure S3 in Multimedia Appendix 1). Figure 3 highlights the superior performance of the eGFR-MMDL model over the eGFR-RIDL model on internal and external datasets. Moreover, the eGFR-MMDL model demonstrated a notable increase in AUC across all subgroups compared with the eGFR-RIDL model (Figure 4).

Figure 3. ROC curves and AUC of low-eGFR detection models. The AUCs of the eGFR-MMDL and eGFR-UDLR models were compared with the AUC of eGFR-RIDL in (**A**) the test set and (**B**) the external validation set (DeLong test with Bonferroni correction). *P=.002; ***P<.001. AUC: area under the curve; eGFR: estimated glomerular filtration rate; MMDL: multimodal deep learning model; RIDL: retinal image deep learning model; ROC: receiver operating characteristic; UDLR: urine dipstick logistic regression.



In addition, the eGFR-UDLR (urine dipstick logistic regression) performed better than the eGFR-RIDL and was comparable to the eGFR-MMDL model, especially in external validation (Figure 3). However, no significant improvement was observed within subgroups in internal validation (Figure 4).

Age influenced the performance of the eGFR-MMDL model. For the overall population, the model performed better in individuals without diabetes or hypertension compared to their respective control groups, while proteinuria had no impact on performance (Figure 4B, 4C, and 4D). When stratified by the age of 65 years, no significant differences in AUC were observed between the nondiabetes and diabetes groups or the nonhypertension and hypertension groups (Figure S4 in Multimedia Appendix 1). However, the AUC increased in the presence of proteinuria (Figure S4 in Multimedia Appendix 1). These changes appeared to be driven by higher model performance in younger individuals without diabetes, hypertension, or proteinuria (Figure 4A).

Table 2 presents the sensitivity and specificity of the eGFR-MMDL model for both the entire study population and its subgroups. The thresholds for the age group of 65 years and older, as well as for individuals with diabetes and proteinuria, were significantly higher than the overall threshold. Table S1 in Multimedia Appendix 1 provides case counts for each subgroup.

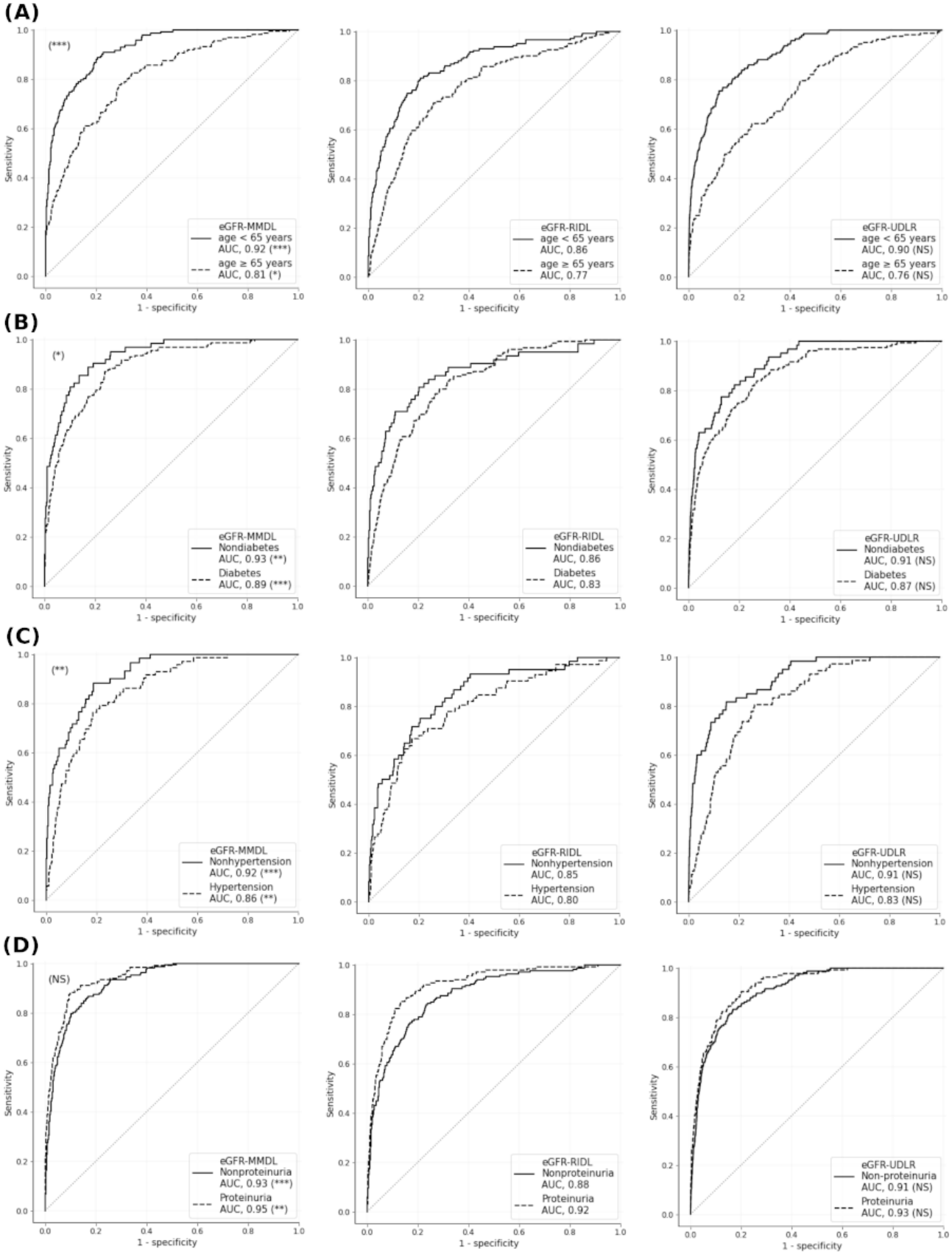
XSL•FO
RenderX

Table . Sensitivity and specificity at the threshold of estimated glomerular filtration rate–multimodal deep learning.The 95% CIs were calculated using bootstrap resampling. The threshold was obtained using the Index of Union method.

	Sensitivity (95% CI)	Specificity (95% CI)	Threshold (95% CI)
All	0.86 (0.81 - 0.91)	0.88 (0.81 - 0.91)	0.53 (0.42 - 0.62)
Age (years)			
≥65	0.78 (0.7 - 0.83)	0.71 (0.66 - 0.79)	0.79 (0.77 - 0.83)
<65	0.88 (0.78 - 0.93)	0.81 (0.77 - 0.92)	0.35 (0.3 - 0.52)
Diabetes			
Yes	0.86 (0.79 - 0.9)	0.77 (0.74 - 0.84)	0.77 (0.74 - 0.82)
No	0.88 (0.79 - 0.95)	0.86 (0.8 - 0.92)	0.38 (0.3 - 0.48)
Hypertension			
Yes	0.8 (0.71 - 0.88)	0.79 (0.71 - 0.84)	0.52 (0.42 - 0.58)
No	0.88 (0.78 - 0.93)	0.82 (0.81 - 0.88)	0.32 (0.3 - 0.4)
Proteinuria			
Yes	0.89 (0.84 - 0.94)	0.9 (0.86 - 0.92)	0.74 (0.65 - 0.78)
No	0.85 (0.78 - 0.92)	0.86 (0.77 - 0.9)	0.47 (0.33 - 0.55)

XSL•FO
RenderX

Figure 4. ROC curves and AUC of low-eGFR detection models in subgroups of the test set. (**A**) Age <65 years (solid line) and ≥65 years (dotted line); (**B**) nondiabetes (solid line) and diabetes (dotted line); (**C**) no hypertension (solid line) and hypertension (dotted line); and (**D**) no proteinuria (solid line) and proteinuria (dotted line). The AUCs of the eGFR-MMDL and eGFR-UDLR models are compared with the AUC of the eGFR-RIDL (DeLong test with Bonferroni correction; *P* value indicators next to the AUC values); **P*=.013, ***P*=.001, ****P*<.001; NS: not significant. *P* value indicators are added to the upper left corner of the eGFR-MMDL model curve to denote significant differences in AUCs between the 2 subgroups (DeLong test); **P*=.011, ***P*=.001, ****P*<.001; NS: not significant. AUC: area under the curve; eGFR: estimated glomerular filtration rate; MMDL: multimodal deep learning model; RIDL: retinal image deep learning model; ROC: receiver operating characteristic; UDLR: urine dipstick logistic regression.



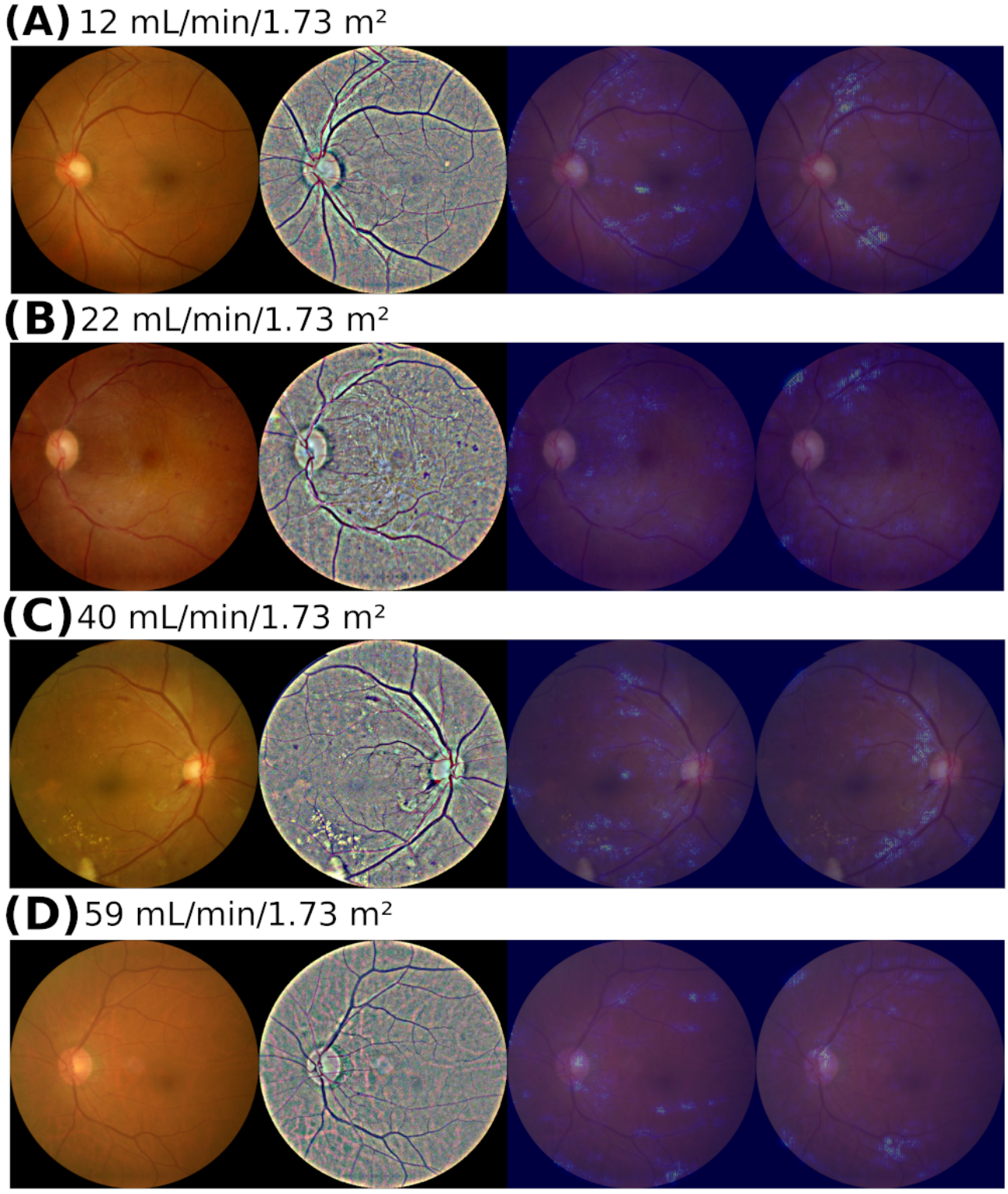
XSL•FO
RenderX

Model Explanation Using Saliency Maps and Sensitivity Analysis

To assess the ability of our algorithm to incorporate retinopathy findings in predicting eGFR decline, we examined fundus photographs of patients with diabetic retinopathy (Figures 5B and 5C). The saliency maps from the eGFR-RIDL and eGFR-MMDL models displayed different hot spot distributions. The eGFR-RIDL map highlighted hot spots of retinal abnormalities (hard exudates, retinal hemorrhages, and arteriovenous nicking), small arteries, and veins. Conversely, the eGFR-MMDL map primarily featured hot spots along the central vascular arcade.

XSL•FO
RenderX

Figure 5. Saliency map results from the eGFR-RIDL and eGFR-MMDL models for eGFR decline detection. (**A**) A nondiabetes male aged 60 years with proteinuria level 3 (2+). (**B**) A male with diabetes and proteinuria level 4 (3+) aged 54 years. (**C**) A male with diabetes and proteinuria level 4 (3+) aged 60 years. (**D**) A male without hypertension or diabetes aged 60 years, with a proteinuria level of 0 (negative). From left to right: original retinal image, retinal image postpreprocessing via CLAHE and color normalization, eGFR-RIDL–generated saliency map, and eGFR-MMDL–generated saliency map. CLAHE: Contrast Limited Adaptive Histogram Equalization; eGFR: estimated glomerular filtration rate; MMDL: multimodal deep learning; RIDL: retinal image deep learning.

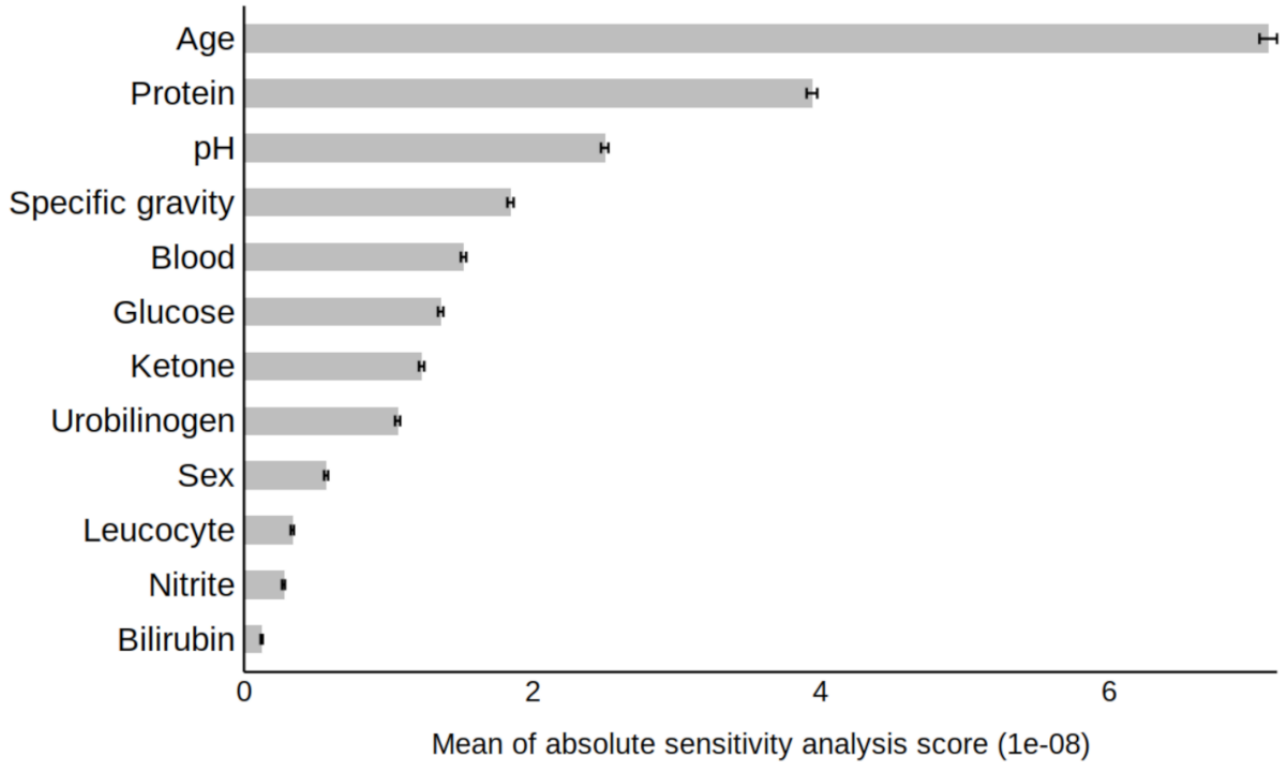


To explore the factors used by our algorithm to predict eGFR decline in the absence of definite pathological findings, we analyzed fundus photographs of patients without diabetes (Figures 5A and 5D). Hot spots were observed in the branches of arteries and veins in both the eGFR-RIDL and eGFR-MMDL models, with differing locations between the 2 models.

In the sensitivity analysis of eGFR-MMDL, age and urine protein level were the most influential factors among the numerical variables, followed by urine pH, specific gravity, hematuria, and glycosuria (Figure 6).

XSL•FO
RenderX

Figure 6. Sensitivity analysis: feature importance of age, sex, and 10 urine measurements in predicting the probability of eGFR decline by eGFR-MMDL using a test set. The sensitivity analysis scores indicate the relative impact of each variable on the predicted probability. Higher sensitivity analysis scores correspond to a greater influence. The error bars on the right end represent 95% CIs. 1e-08: 0.00000001; eGFR: estimated glomerular filtration rate; MMDL: multimodal deep learning.



Discussion

Principal Findings

This study found that the eGFR-MMDL model, which integrates retinal imaging with urine dipstick data, achieved higher diagnostic performance for CKD than the retinal image-only eGFR-RIDL model. The eGFR-MMDL model demonstrated superior accuracy across subgroups, particularly in younger individuals and those without proteinuria. Sensitivity analysis identified age and proteinuria as key factors from urine dipstick data, while saliency maps indicated that retinal vessels provided additional diagnostic information unavailable from urine dipstick data, demonstrating how each modality contributed unique and valuable insights for CKD detection.

Addressing Variability in Fundus Images for Robust DL Models

In practice, fundus images vary in size, quality, format, and color across different devices [29]. This variability poses a challenge for the creation of effective DL models. Training a model based solely on data from specific devices can limit its compatibility with others. To address this, we used 3 camera models from 2 companies for training and evaluated the model using 2 different nontraining camera models. We standardized the images across devices through preprocessing techniques, including circular border adjustment, boundary removal via cropping, Contrast Limited Adaptive Histogram Equalization–based quality enhancement, and color normalization (Supplementary Methods in Multimedia Appendix 1). Nevertheless, the effectiveness of the model diminished during the external validation, which can be partially attributed to the diversity observed in the retinal images. Notably, the eGFR-UDLR model, leveraging numerical variables, exhibited enhanced generalization compared with the eGFR-RIDL model using retinal images (Figure 3B). Therefore, a multimodal approach incorporating urine dipstick tests could partly address the generalization problem of the eGFR-RIDL model.

In addition, when used on images of poor quality, there is a notable decline in performance owing to the disruption of both the structural and statistical properties of neighboring pixels caused by image degradation [30]. Therefore, our workflow involved image quality management and preprocessing for model accuracy and reliability [1]. Abnormal images, defined as those with haziness, extreme brightness, or darkness, were excluded (additional methods in Multimedia Appendix 1). Our approach assesses clarity using haze grading, which combines high-pass filtering and power spectrum integration across spatial frequencies and gauges intricate detail visibility [31]. Unlike previous methods that manually exclude subpar images or use unspecified techniques for DL, our innovation emphasizes practical, real world, and applicable image quality control processes [15,16,24].

Enhancement of the Model Performance in MMDL

During internal validation, the eGFR-RIDL model achieved an AUC of 0.9 (Figure 3), indicating its statistical comparability with prior models of retinal images. For example, AUCs were observed at 0.826 (95% CI 0.818 - 0.833; ResNet18 model) for eGFR<60 mL/min/1.73 m² with diabetes [32], 0.911 (95% CI 0.886 - 0.936; cCondenseNet model) for eGFR<60 mL/min/1.73

XSL•FO
RenderX

m² [15], and 0.918 (95% CI 0.905 - 0.933; ResNet-50 model) for eGFR<60 or>60 mL/min/1.73 m² with albuminuria [16]. However, the eGFR-MMDL model performed significantly better than the eGFR-RIDL model during the internal and external validations (Figure 3).

The eGFR-UDLR model demonstrated performance comparable to the eGFR-MMDL model (Figure 3), and the superior performance of eGFR-MMDL over eGFR-RIDL can be attributed to the inclusion of urine dipstick data. However, in the subgroup analysis, the eGFR-MMDL model outperformed eGFR-RIDL across all subgroups, while the eGFR-UDLR model showed no significant improvement across subgroups (Figure 4). This suggests that the synergy between the 2 modalities in the eGFR-MMDL model likely resulted from the effective integration of multimodal data through joint fusion (Figure 2) [33]. This method combines feature representations from neural network layers with data from various sources, such as retinal images and urine analysis, thereby enhancing the model performance. Type 2 joint fusion in eGFR-MMDL improves the correlation across modalities, facilitating more efficient shared representation learning [33]. This approach continually updates the feature representations, thereby enhancing its effectiveness [33]. Furthermore, research has consistently emphasized the advantages of multimodal approaches over unimodal approaches [27]. Multimodal models leverage information from different sources and create comprehensive and robust data representations [27]. This overcomes the limitations associated with individual modalities, including noise [27].

The subgroup analysis highlighted the improved performance of eGFR-MMDL, especially in those aged <65 years without proteinuria (Figure 4). This is crucial because this age group often skips check-ups because of perceived good health and lack of symptoms [34]. Detecting CKD in young individuals is vital, as it can be linked to rare conditions, such as glomerulopathy, where treatments greatly impact outcomes [35]. Furthermore, the good performance of the eGFR-MMDL model in individuals without proteinuria indicated its ability to identify nonproteinuria CKD cases, which usually necessitates invasive blood tests for screening purposes. Thus, eGFR-MMDL may replace blood tests with retinal images and urine dipsticks, offering a convenient, noninvasive screening method for newly diagnosed CKD in young patients.

Unveiling the Role of Retinal Features and Numerical Variables in Model Prediction

To elucidate these models, we used saliency maps for retinal images and conducted a sensitivity analysis of numerical variables. Kang et al [24] reported that a DL model using saliency maps from retinal images successfully identified common retinal abnormalities, aiding the assessment of renal function. These features, which are routinely used by ophthalmologists for diagnosing retinal diseases, were similarly observed in eGFR-RIDL saliency maps (Figure 5). However, the eGFR-MMDL saliency map notably accentuated arcade vessels over exudation or hemorrhage, which could be attributed to the inclusion of numerical features, such as urine data, age, and sex (Figure 5A). These findings align with those of existing studies that emphasize a strong association between retinal vascular changes and CKD development [36-40]. Joo et al [41] also noted a more pronounced presence of arcade vessels on saliency maps in individuals with higher CKD risk. This suggests that, while urine data provide insights into common retinal abnormalities, retinal images, particularly those focusing on arcade vessels, are pivotal for predicting kidney function. The distinct information yielded by these 2 modalities likely accounted for their complementary roles in the eGFR-MMDL model.

The saliency maps further underscored the significance of the retinal vessel features (Figure 5). Even in cases with healthy retinal images, prominent retinal vessel features indicate their value in predicting renal function (Figures 5A and 5D). These observations align with the findings of Zhang et al [16], emphasizing the relevance of vascular health through saliency maps. However, despite the presence of these features, eGFR-MMDL outperformed eGFR-RIDL (Figure 3), suggesting that retinal vessel features alone may not be sufficient to predict eGFR decline accurately.

In our sensitivity analysis, we assessed the impact of each numerical variable (age, sex, and 10 urine variables) on eGFR<60 mL/min/1.73 m² predictions. The findings on feature importance from the eGFR-MMDL model were consistent with a previous study using XGBoost for eGFR decline prediction, which highlighted urine protein, blood, glucose, pH, specific gravity, and age as important features [17]. In our study, age emerged as the primary contributor, consistent with epidemiological studies, owing to its association with GFR decline [42]. The second most influential factor was urine protein positivity, supported by evidence linking it to kidney function deterioration [43,44]. Urine pH and specific gravity, ranking third and fourth, have been investigated as relevant CKD indicators, with acidic urine pH (5 - 5.5) positively correlated with CKD, and low urine specific gravity indicating reduced kidney function [45,46]. Hematuria, the fifth-ranked urine variable, correlates not only with proteinuria but also with CKD risk factors [45,47]. Additionally, glycosuria (urine glucose) may be linked to kidney dysfunction in Fanconi syndrome and diabetes, as indicated in a previous study [45].

Limitations

First, the performance of eGFR-MMDL in individuals aged ≥65 years did not achieve a satisfactory AUC (Figure 4A), despite the high CKD prevalence in this group (Table 1) [48]. These findings corroborate with those of a previous study, revealing limited predictive capabilities among those aged 65 years and older using urine dipstick-based models [17]. Potential reasons for this underperformance may include issues with the retinal image quality, particularly haziness. However, our analysis revealed no significant difference in eGFR-MMDL performance between the high- and low-haziness groups in individuals aged ≥65 years (Figure S5 in Multimedia Appendix 1).

Furthermore, signs of organ damage, such as retinal abnormalities or proteinuria, may not manifest in older individuals with an eGFR<60 mL/min/1.73 m². This is supported by a higher positive proteinuria ratio in individuals younger than 65 years than in those aged 65 years or older with eGFR<60

XSL•FO
RenderX

mL/min/1.73 m² (263/474, 55.5% vs 243/611, 39.8%, respectively; $P<.001$, chi-square test on the CHA dataset). In people younger than 65 years of age, eGFR<60 was possibly linked to mechanisms causing proteinuria, whereas in those aged 65 years or older, this might be attributed to age-related GFR decline [20]. Given the high prevalence of CKD and the limited performance observed among individuals aged ≥65 years, we recommend conducting routine blood tests for effective CKD screening in this subpopulation.

Second, various medications prescribed for diabetes and hypertension can influence urine dipstick test outcomes, potentially impacting the predictive model accuracy. For example, SGLT2 inhibitors, commonly used in diabetes management, cause glycosuria and may alter urinary specific gravity, while renin-angiotensin-aldosterone inhibitors can decrease proteinuria [49,50]. Unfortunately, due to limited information on specific medication classes, such as renin-angiotensin-aldosterone inhibitors and SGLT2 inhibitors, we were unable to conduct a thorough analysis of their effects on the model performance. Although the eGFR-MMDL model showed robustness to the presence of hypertension or diabetes when age was controlled (Figure S4 in Multimedia Appendix 1), further investigation into medication effects is warranted.

Third, this study's participants were exclusively Korean, limiting generalizability to diverse ethnic populations. CKD epidemiology and clinical presentations vary across countries, possibly affecting the model performance [51]. Fourth, a gap existed between the dates of retinal imaging and serum or urine tests. However, the absolute difference in dates was small, with a mean of 0.6 (SD 3.7) days.

Benefits of CKD Screening With Retinal Imaging and Urine Dipstick

The use of noninvasive tests such as retinal imaging and urine dipstick assessments significantly enhances the effectiveness, accessibility, and efficiency of CKD screening, benefiting both patients and health care providers. For patients, these tests reduce discomfort and anxiety, leading to higher compliance with regular screenings and enabling earlier detection of CKD, which is crucial for preventing progression to end-stage kidney disease. This is particularly valuable in resource-limited settings where traditional blood tests may not be readily available [2,52].

For health care providers, these models streamline the screening process by reducing the time and resources needed for blood collection and analysis. The multimodal approach integrates retinal images with urine dipstick data, mirroring the comprehensive assessments made in clinical practice, such as evaluating diabetic or hypertensive retinopathy alongside CKD [27]. This holistic view not only improves diagnostic accuracy but also allows for concurrent evaluation of eye health, providing a more complete picture of the patient's overall condition.

Conclusion

The MMDL model, incorporating age, sex, urine measurements, and retinal images, improved the eGFR reduction prediction of an RIDL model. This achievement stemmed from the diverse features of the multiple sources. However, the DL model using retinal images showed limited performance in old-age patients. Our model offers a noninvasive and convenient screening tool for enhancing kidney health in specific populations.

Acknowledgments

This work was supported by the National Research Foundation of Korea (NRF) grant funded by the Korea government (Ministry of Science and ICT, MSIT; No. 2019R1C1C1007663); a grant from Patient-Centered Clinical Research Coordinating Center (PACEN) funded by the Ministry of Health & Welfare (RS-2024-00399169), Republic of Korea; Workers AI Assistant and Health Care Service for Asynchronous Work Crowd walkers in Hybrid Work Environments funded by the Ministry of Trade, Industry & Energy (MOTIE, Korea; grant 20023719); the Ministry of Science and ICT, IP advancement and commercialization of telemedicine service technology for mental health care and health food recommendation for the elderly in the region based on voice recognition and natural language processing (grant 2710006409) supervised by the COMPA (Commercialization Promotion Agency for R&D Outcomes).

Data Availability

The data are owned by the hospitals, and permission is not granted to share it with external parties.

Authors' Contributions

YHL, JK, and SMN handled the concept and design. YB, ECJ, EJ, CSL, ESK, and SMN did the acquisition, analysis, or interpretation of data. YB, YHL, JK, KL, DL, and SMN drafted this paper. YB, YHL, JK, KL, and SMN worked on a critical review of this paper for important intellectual content. YB, KL, DL, ECJ, and EJ undertook work on the statistical analysis. YHL, HWH, and SMN obtained funding. HWH and SMN supervised. YB, YHL, JK, and KL are co-first authors. HWH and SMN are co-corresponding authors.

Conflicts of Interest

None declared.

XSL•FO
RenderX

Multimedia Appendix 1
Figures, tables, and notes.
[DOCX File, 1900 KB - medinform_v13i1e55825_app1.docx]

References

1. Wen J, Liu D, Wu Q, Zhao L, Iao WC, Lin H. Retinal image‐based artificial intelligence in detecting and predicting kidney diseases: current advances and future perspectives. VIEW 2023 Jun;4(3):20220070 [FREE Full text] [doi: 10.1002/VIW.20220070]
2. Kovesdy CP. Epidemiology of chronic kidney disease: an update 2022. Kidney Int Suppl (2011) 2022 Apr;12(1):7-11. [doi: 10.1016/j.kisu.2021.11.003] [Medline: 35529086]
3. Chapter 1: definition and classification of CKD. Kidney Int Suppl (2011) 2013 Jan;3(1):19-62. [doi: 10.1038/kisup.2012.64] [Medline: 25018975]
4. Go AS, Chertow GM, Fan D, McCulloch CE, Hsu C. Chronic kidney disease and the risks of death, cardiovascular events, and hospitalization. N Engl J Med 2004 Sep 23;351(13):1296-1305. [doi: 10.1056/NEJMoa041031] [Medline: 15385656]
5. van der Velde M, Matsushita K, Coresh J, et al. Lower estimated glomerular filtration rate and higher albuminuria are associated with all-cause and cardiovascular mortality. A collaborative meta-analysis of high-risk population cohorts. Kidney Int 2011 Jun;79(12):1341-1352. [doi: 10.1038/ki.2010.536]
6. Gansevoort RT, Matsushita K, van der Velde M, et al. Lower estimated GFR and higher albuminuria are associated with adverse kidney outcomes. A collaborative meta-analysis of general and high-risk population cohorts. Kidney Int 2011 Jul;80(1):93-104. [doi: 10.1038/ki.2010.531] [Medline: 21289597]
7. Chronic Kidney Disease Prognosis Consortium, Matsushita K, van der Velde M, et al. Association of estimated glomerular filtration rate and albuminuria with all-cause and cardiovascular mortality in general population cohorts: a collaborative meta-analysis. Lancet 2010 Jun 12;375(9731):2073-2081. [doi: 10.1016/S0140-6736(10)60674-5] [Medline: 20483451]
8. Webster AC, Nagler EV, Morton RL, Masson P. Chronic kidney disease. The Lancet 2017 Mar;389(10075):1238-1252. [doi: 10.1016/S0140-6736(16)32064-5]
9. Wong CW, Wong TY, Cheng CY, Sabanayagam C. Kidney and eye diseases: common risk factors, etiological mechanisms, and pathways. Kidney Int 2014 Jun;85(6):1290-1302. [doi: 10.1038/ki.2013.491] [Medline: 24336029]
10. Farrah TE, Dhillon B, Keane PA, Webb DJ, Dhaun N. The eye, the kidney, and cardiovascular disease: old concepts, better tools, and new horizons. Kidney Int 2020 Aug;98(2):323-342. [doi: 10.1016/j.kint.2020.01.039] [Medline: 32471642]
11. Grunwald JE, Alexander J, Maguire M, et al. Prevalence of ocular fundus pathology in patients with chronic kidney disease. Clin J Am Soc Nephrol 2010 May;5(5):867-873. [doi: 10.2215/CJN.08271109] [Medline: 20299372]
12. Grunwald JE, Alexander J, Ying GS, et al. Retinopathy and chronic kidney disease in the Chronic Renal Insufficiency Cohort (CRIC) study. Arch Ophthalmol 2012 Sep;130(9):1136-1144. [doi: 10.1001/archophthalmol.2012.1800] [Medline: 22965589]
13. Lim LS, Cheung CYL, Sabanayagam C, et al. Structural changes in the retinal microvasculature and renal function. Invest Ophthalmol Vis Sci 2013 Apr 26;54(4):2970-2976. [doi: 10.1167/iovs.13-11941] [Medline: 23572105]
14. Sabanayagam C, Shankar A, Koh D, et al. Retinal microvascular caliber and chronic kidney disease in an Asian population. Am J Epidemiol 2009 Mar 1;169(5):625-632. [doi: 10.1093/aje/kwn367] [Medline: 19092170]
15. Sabanayagam C, Xu D, Ting DSW, et al. A deep learning algorithm to detect chronic kidney disease from retinal photographs in community-based populations. Lancet Digit Health 2020 Jun;2(6):e295-e302. [doi: 10.1016/S2589-7500(20)30063-7] [Medline: 33328123]
16. Zhang K, Liu X, Xu J, et al. Deep-learning models for the detection and incidence prediction of chronic kidney disease and type 2 diabetes from retinal fundus images. Nat Biomed Eng 2021 Jun;5(6):533-545. [doi: 10.1038/s41551-021-00745-6] [Medline: 34131321]
17. Jang EC, Park YM, Han HW, et al. Machine-learning enhancement of urine dipstick tests for chronic kidney disease detection. J Am Med Inform Assoc 2023 May 19;30(6):1114-1124. [doi: 10.1093/jamia/ocad051] [Medline: 37027837]
18. Mitani A, Huang A, Venugopalan S, et al. Detection of anaemia from retinal fundus images via deep learning. Nat Biomed Eng 2020 Jan;4(1):18-27. [doi: 10.1038/s41551-019-0487-z] [Medline: 31873211]
19. O'Sullivan ED, Hughes J, Ferenbach DA. Renal aging: causes and consequences. J Am Soc Nephrol 2017 Feb;28(2):407-420. [doi: 10.1681/ASN.2015121308] [Medline: 28143966]
20. Liu P, Quinn RR, Lam NN, et al. Accounting for age in the definition of chronic kidney disease. JAMA Intern Med 2021 Oct 1;181(10):1359-1366. [doi: 10.1001/jamainternmed.2021.4813] [Medline: 34459844]
21. Carriazo S, Perez-Gomez MV, Ortiz A. Hypertensive nephropathy: a major roadblock hindering the advance of precision nephrology. Clin Kidney J 2020 Aug;13(4):504-509. [doi: 10.1093/ckj/sfaa162] [Medline: 32897275]
22. Siwek J. The academy's core educational guidelines. Am Fam Physician 1989 May;39(5):120-121. [Medline: 2718892]
23. Pastor E, Alfaro L, Baralis E. Identifying biased subgroups in ranking and classification. arXiv. Preprint posted online on Aug 17, 2021. [doi: 10.48550/arXiv.2108.07450]

XSL•FO
RenderX

24. Kang EYC, Hsieh YT, Li CH, et al. Deep learning–based detection of early renal function impairment using retinal fundus images: model development and validation. JMIR Med Inform 2020 Nov 26;8(11):e23472. [doi: 10.2196/23472] [Medline: 33139242]
25. Levey AS, Stevens LA, Schmid CH, et al. A new equation to estimate glomerular filtration rate. Ann Intern Med 2009 May 5;150(9):604-612. [doi: 10.7326/0003-4819-150-9-200905050-00006] [Medline: 19414839]
26. Zagoruyko S, Komodakis N. Wide residual networks. arXiv. Preprint posted online on May 23, 2016. [doi: 10.48550/arXiv.1605.07146]
27. Heiliger L, Sekuboyina A, Menze B, Egger J, Kleesiek J. Beyond medical imaging - a review of multimodal deep learning in radiology. TechRxiv. Preprint posted online on Oct 30, 2023. [doi: 10.36227/techrxiv.19103432.v1]
28. MultimodalCKD. GitHub. URL: https://github.com/forustous/multimodalCKD [accessed 2025-01-28]
29. Tan Y, Sun X. Ocular images-based artificial intelligence on systemic diseases. Biomed Eng Online 2023 May 19;22(1):49. [doi: 10.1186/s12938-023-01110-1] [Medline: 37208715]
30. Wang Y, Cao Y, Zha ZJ, Zhang J, Xiong Z. Deep degradation prior for low-quality image classification. Presented at: 2020 IEEE/CVF Conference on Computer Vision and Pattern Recognition (CVPR); Jun 13-19, 2020; Seattle, WA, USA p. 11046-11055 URL: https://ieeexplore.ieee.org/xpl/mostRecentIssue.jsp?punumber=9142308 [accessed 2025-01-18] [doi: 10.1109/CVPR42600.2020.01106]
31. Passaglia CL, Arvaneh T, Greenberg E, Richards D, Madow B. Automated method of grading vitreous haze in patients with uveitis for clinical trials. Transl Vis Sci Technol 2018 Mar;7(2):10. [doi: 10.1167/tvst.7.2.10] [Medline: 29600118]
32. Betzler BK, Chee EYL, He F, et al. Deep learning algorithms to detect diabetic kidney disease from retinal photographs in multiethnic populations with diabetes. J Am Med Inform Assoc 2023 Nov 17;30(12):1904-1914. [doi: 10.1093/jamia/ocad179] [Medline: 37659103]
33. Huang SC, Pareek A, Seyyedi S, Banerjee I, Lungren MP. Fusion of medical imaging and electronic health records using deep learning: a systematic review and implementation guidelines. NPJ Digit Med 2020;3(1):136. [doi: 10.1038/s41746-020-00341-z] [Medline: 33083571]
34. Noguchi R, Shen J. Factors affecting participation in health checkups: evidence from Japanese survey data. Health Policy 2019 Apr;123(4):360-366. [doi: 10.1016/j.healthpol.2018.10.013] [Medline: 30691696]
35. Zhao X, Niu Q, Gan L, et al. Baseline data report of the China Dialysis Outcomes and Practice Patterns Study (DOPPS). Sci Rep 2021 Jan 13;11(1):873. [doi: 10.1038/s41598-020-79531-4]
36. Wong TY, Coresh J, Klein R, et al. Retinal microvascular abnormalities and renal dysfunction: the atherosclerosis risk in communities study. J Am Soc Nephrol 2004 Sep;15(9):2469-2476. [doi: 10.1097/01.ASN.0000136133.28194.E4] [Medline: 15339997]
37. Wong TY, Shankar A, Klein R, Klein BEK. Retinal vessel diameters and the incidence of gross proteinuria and renal insufficiency in people with type 1 diabetes. Diabetes 2004 Jan;53(1):179-184. [doi: 10.2337/diabetes.53.1.179] [Medline: 14693713]
38. Sabanayagam C, Shankar A, Klein BEK, et al. Bidirectional association of retinal vessel diameters and estimated GFR decline: the Beaver Dam CKD Study. Am J Kidney Dis 2011 May;57(5):682-691. [doi: 10.1053/j.ajkd.2010.11.025] [Medline: 21439697]
39. Yau JWY, Xie J, Kawasaki R, et al. Retinal arteriolar narrowing and subsequent development of CKD Stage 3: the Multi-Ethnic Study of Atherosclerosis (MESA). Am J Kidney Dis 2011 Jul;58(1):39-46. [doi: 10.1053/j.ajkd.2011.02.382] [Medline: 21549464]
40. Yip W, Ong PG, Teo BW, et al. Retinal vascular imaging markers and incident chronic kidney disease: a prospective cohort study. Sci Rep 2017 Aug 24;7(1):9374. [doi: 10.1038/s41598-017-09204-2] [Medline: 28839244]
41. Joo YS, Rim TH, Koh HB, et al. Non-invasive chronic kidney disease risk stratification tool derived from retina-based deep learning and clinical factors. NPJ Digit Med 2023 Jun 17;6(1):114. [doi: 10.1038/s41746-023-00860-5] [Medline: 37330576]
42. Levin A, Stevens PE, Bilous RW, et al. Kidney Disease: Improving Global Outcomes (KDIGO) CKD Work Group. KDIGO 2012 clinical practice guideline for the evaluation and management of chronic kidney disease. Kidney Int Suppl 2013;3(1). [doi: 10.1038/kisup.2012.73]
43. Locatelli F, Marcelli D, Comelli M, et al. Proteinuria and blood pressure as causal components of progression to end-stage renal failure. Northern Italian Cooperative Study Group. Nephrol Dial Transplant 1996 Mar;11(3):461-467. [doi: 10.1093/ndt/11.3.461] [Medline: 8710157]
44. Wilmer WA, Rovin BH, Hebert CJ, Rao SV, Kumor K, Hebert LA. Management of glomerular proteinuria: a commentary. J Am Soc Nephrol 2003 Dec;14(12):3217-3232. [doi: 10.1097/01.asn.0000100145.27188.33] [Medline: 14638920]
45. Simerville JA, Maxted WC, Pahira JJ. Urinalysis: a comprehensive review. Am Fam Physician 2005 Mar 15;71(6):1153-1162. [Medline: 15791892]
46. Nakanishi N, Fukui M, Tanaka M, et al. Low urine pH Is a predictor of chronic kidney disease. Kidney Blood Press Res 2012;35(2):77-81. [doi: 10.1159/000330487] [Medline: 21912182]
47. You-Hsien Lin H, Yen CY, Lim LM, et al. Microscopic haematuria and clinical outcomes in patients with stage 3-5 nondiabetic chronic kidney disease. Sci Rep 2015 Oct 16;5:15242. [doi: 10.1038/srep15242] [Medline: 26472621]

XSL•FO
RenderX

48. Fried LF, Unruh ML. Aging in kidney disease: key issues and gaps in knowledge. Adv Chronic Kidney Dis 2010 Jul;17(4):291-292. [doi: 10.1053/j.ackd.2010.05.005] [Medline: 20610355]
49. Piperidou A, Sarafidis P, Boutou A, et al. The effect of SGLT-2 inhibitors on albuminuria and proteinuria in diabetes mellitus: a systematic review and meta-analysis of randomized controlled trials. J Hypertens 2019 Jul;37(7):1334-1343. [doi: 10.1097/HJH.0000000000002050] [Medline: 31145707]
50. Kunz R, Friedrich C, Wolbers M, Mann JFE. Meta-analysis: effect of monotherapy and combination therapy with inhibitors of the renin angiotensin system on proteinuria in renal disease. Ann Intern Med 2008 Jan 1;148(1):30-48. [doi: 10.7326/0003-4819-148-1-200801010-00190] [Medline: 17984482]
51. GBD Chronic Kidney Disease Collaboration. Global, regional, and national burden of chronic kidney disease, 1990-2017: a systematic analysis for the Global Burden of Disease Study 2017. Lancet 2020 Feb 29;395(10225). [doi: 10.1016/S0140-6736(19)32977-0] [Medline: 32061315]
52. George C, Mogueo A, Okpechi I, Echouffo-Tcheugui JB, Kengne AP. Chronic kidney disease in low-income to middle-income countries: the case for increased screening. BMJ Glob Health 2017;2(2):e000256. [doi: 10.1136/bmjgh-2016-000256] [Medline: 29081996]

Abbreviations

AUC: area under the curve
CKD: chronic kidney disease
CKD-EPI: Chronic Kidney Disease Epidemiology Collaboration
DL: deep learning
eGFR: estimated glomerular filtration rate
GFR: glomerular filtration rate
MMDL: multimodal deep learning
RIDL: retinal image deep learning
SCHPC: Severance Checkup Health Promotion Center
UDLR: urine dipstick logistic regression
WRN: Wide Residual Network

Edited by M Focsa; submitted 26.12.23; peer-reviewed by A Vellido, I Zakrocka, TK Yoo, Z Li; revised version received 06.12.24; accepted 06.12.24; published 07.02.25.

Please cite as:
Bhak Y, Lee YH, Kim J, Lee K, Lee D, Jang EC, Jang E, Lee CS, Kang ES, Park S, Han HW, Nam SM
Diagnosis of Chronic Kidney Disease Using Retinal Imaging and Urine Dipstick Data: Multimodal Deep Learning Approach
JMIR Med Inform 2025;13:e55825
URL: https://medinform.jmir.org/2025/1/e55825
doi:10.2196/55825

© Youngmin Bhak, Yu Ho Lee, Joonhyung Kim, Kiwon Lee, Daehwan Lee, Eun Chan Jang, Eunjeong Jang, Christopher Seungkyu Lee, Eun Seok Kang, Sehee Park, Hyun Wook Han, Sang Min Nam. Originally published in JMIR Medical Informatics (https://medinform.jmir.org), 7.2.2025. This is an open-access article distributed under the terms of the Creative Commons Attribution License (https://creativecommons.org/licenses/by/4.0/), which permits unrestricted use, distribution, and reproduction in any medium, provided the original work, first published in JMIR Medical Informatics, is properly cited. The complete bibliographic information, a link to the original publication on https://medinform.jmir.org/, as well as this copyright and license information must be included.

XSL•FO
RenderX

Classifying Unstructured Text in Electronic Health Records for Mental Health Prediction Models: Large Language Model Evaluation Study

Nicholas C Cardamone[1], MSEd; Mark Olfson[2], MD, MPH; Timothy Schmutte[3], PsyD; Lyle Ungar[4], PhD; Tony Liu[4], PhD; Sara W Cullen[5], MSW, PhD; Nathaniel J Williams[6], PhD, LCSW; Steven C Marcus[5], PhD

[1]Department of Psychiatry, Perelman School of Medicine, University of Pennsylvania, Philadelphia, PA, United States

[2]Department of Psychiatry, the New York State Psychiatric Institute, New York, NY, United States

[3]Department of Psychiatry, Yale School of Medicine, New Haven, CT, United States

[4]Computer and Information Science, University of Pennsylvania, Philadelphia, PA, United States

[5]School of Social Policy & Practice, University of Pennsylvania, Philadelphia, PA, United States

[6]School of Social Work, Boise State University, Boise, ID, United States

Corresponding Author:
Nicholas C Cardamone, MSEd
Department of Psychiatry, Perelman School of Medicine, University of Pennsylvania, Philadelphia, PA, United States

Abstract

Background: Prediction models have demonstrated a range of applications across medicine, including using electronic health record (EHR) data to identify hospital readmission and mortality risk. Large language models (LLMs) can transform unstructured EHR text into structured features, which can then be integrated into statistical prediction models, ensuring that the results are both clinically meaningful and interpretable.

Objective: This study aims to compare the classification decisions made by clinical experts with those generated by a state-of-the-art LLM, using terms extracted from a large EHR data set of individuals with mental health disorders seen in emergency departments (EDs).

Methods: Using a dataset from the EHR systems of more than 50 health care provider organizations in the United States from 2016 to 2021, we extracted all clinical terms that appeared in at least 1000 records of individuals admitted to the ED for a mental health–related problem from a source population of over 6 million ED episodes. Two experienced mental health clinicians (one medically trained psychiatrist and one clinical psychologist) reached consensus on the classification of EHR terms and diagnostic codes into categories. We evaluated an LLM's agreement with clinical judgment across three classification tasks as follows: (1) classify terms into "mental health" or "physical health", (2) classify mental health terms into 1 of 42 prespecified categories, and (3) classify physical health terms into 1 of 19 prespecified broad categories.

Results: There was high agreement between the LLM and clinical experts when categorizing 4553 terms as "mental health" or "physical health" (κ=0.77, 95% CI 0.75-0.80). However, there was still considerable variability in LLM-clinician agreement on the classification of mental health terms (κ=0.62, 95% CI 0.59 - 0.66) and physical health terms (κ=0.69, 95% CI 0.67 - 0.70).

Conclusions: The LLM displayed high agreement with clinical experts when classifying EHR terms into certain mental health or physical health term categories. However, agreement with clinical experts varied considerably within both sets of mental and physical health term categories. Importantly, the use of LLMs presents an alternative to manual human coding, presenting great potential to create interpretable features for prediction models.

(JMIR Med Inform 2025;13:e65454) doi:10.2196/65454

KEYWORDS

artificial intelligence; AI; machine learning; ML; natural language processing; NLP; large language model; LLM; ChatGPT; predictive modeling; mental health; health informatics; electronic health record; EHR; EHR system; text; dataset; mental health disorder; emergency department; physical health

Introduction

Recent advances in health informatics have led to the development of machine learning models that are trained on data from electronic health records (EHRs). These models have proven to be effective across a range of health domains, including predicting the spread of disease [1], hospital readmission rates [2], and suicide risk [3,4]. Predictive models

XSL•FO
RenderX

have been implemented in EHR systems to identify high-risk patients and alert clinicians to critical health events [5].

EHR systems are filled with unstructured text data, including clinical notes and discharge summaries, which are not easily categorized into clinically interpretable groupings for use in predictive models. Although the use of this data can greatly enhance prediction model performance and the interpretability of decision-support tools [6,7], the coding process is labor intensive and requires expert consultation and extensive training [8]. These challenges hinder the development and scalability of clinical prediction models that incorporate unstructured EHR data [9,10].

Large language models (LLMs), like OpenAI's GPT models, can streamline the classification and coding of unstructured EHR text due to their massive training data sets and advanced text processing [11,12]. LLMs have been used to categorize unstructured text from EHR systems [13], assist with qualitative analysis [14,15], and perform deductive coding with and without context [16]. Preliminary evidence shows that LLMs outperform crowd workers in annotation of health texts [17,18].

The reliability of LLMs in replicating clinical judgment for coding classification tasks in mental health remains uncertain, particularly given the inherent complexities of mental health disorders [19,20]. Prior research highlights that while LLMs can process large volumes of text, their ability to discern subtle differences in clinical presentations, such as differentiating between comorbid conditions like depression and anxiety, is still unproven. This challenge is exacerbated by the frequent overlap of symptoms across diagnoses, which complicates classification efforts [21]. Patients with mental health disorders may present with unique clinical characteristics that challenge an LLM's ability to accurately identify and code physical and mental health symptoms [11,22,23].

We used a large EHR data set of individuals admitted to the emergency department (ED) for a mental health disorder, to assess the ability of a state-of-the-art LLM to classify EHR terms into categories defined by experienced mental health clinicians. We assessed the extent to which a LLM replicates clinical judgment and the practicality of using a LLM to assist in creating clinically interpretable features for prediction models.

Methods

Data

We extracted de-identified EHR data from the Optum Labs Data Warehouse, a longitudinal, real-world data asset, from >50 US healthcare provider organizations that encompass >700 hospitals. We included individuals aged ≥10 years who were admitted to the ED from 2016 to 2021 and had an International Classification of Disease-9 or -10 code for a mental health diagnosis, suicidal ideation, or self-harm, resulting in approximately 6.2 million unique patient episodes. A natural language processing (NLP) algorithm integrated into the Optum Labs Data Warehouse extracted from unstructured free-text fields in the EHR, clinical terms for signs, symptoms, and diseases based on the National Library of Medicine's Unified Medical Language System dictionary. We identified physical and mental health terms that appeared in at least 1000 unique patient episodes.

Coding

A board-certified psychiatrist and licensed clinical psychologist categorized each EHR term into 1 of 61 categories including 42 mental health-related categories and 19 physical health-related categories which were generated from the Clinical Classifications Software Refined [24] and the International Classification of Disease-10 diagnosis coding system, respectively. Coding each EHR term involved: (1) initial classification by 1 clinician coder, (2) a review of all coding decisions by a second clinician coder with suggestions for revisions; (3) a final consensus reconciliation involving both coders. The coding of physical health terms was supported by an LLM, which suggested coding decisions that were refined and reconciled (5% of terms required reconciliation) by the 2 clinician coders. All study procedures were approved by the Institutional Review Board of University of Pennsylvania.

Classification Tasks

We used the Python module "openai" [25] to run the GPT-4 LLM in a Python environment. We used OpenAI's most sophisticated GPT-4 that was then publicly available ("gpt-4-turbo-2024-04-09") and set model parameters to maximize output consistency (eg, temperature=0).

We prompted the model with 3 "zero-shot" classification tasks, wherein the model is provided codes without examples: (1) classify all (n=4553) EHR terms as either "mental health" or "physical health," (2) classify each of the (n=846) mental health terms into 1 of the 42 mental health categories, and (3) classify each of the (n=3707) physical health terms into 1 of the 19 physical health categories. The prompt described the task, listed the possible categories, and provided the EHR terms. The model then confirmed that the predicted category was among the list of possible categories. For full reproducibility, the complete prompt provided to the model, including the task description and category list, is detailed in Multimedia Appendix 1. In task 2, the model was given an unstructured clinical term from an EHR such as "depressive symptoms." Then, the prompt described the classification task and provided the following list of possible mental health categories (eg, "depression," "anxiety," "eating disorder symptoms," and "substance use"). The process was repeated for all 846 mental health terms, and similarly for the 3707 physical health terms in task 3.

Performance Metrics

We compared GPT-4's predicted categories with the categories determined by clinical judgment using the Python library scikit-learn "metrics" module [26]. For each task, we report the overall Cohen κ and weighted average of precision, recall, and F_1-score, accounting for label imbalance. We computed 95% CIs for Cohen κ, precision, recall, and F_1-score using a bootstrap procedure with 1000 resamples [27].

Ethical Considerations

Ethical approval (IRB Protocol #848806) for this study was waived by the University of Pennsylvania Institutional Review Board via 45 CFR 46.104, category 4.

XSL•FO
RenderX

Results

Overview

EHR terms (n=4553) were categorized by GPT as "mental health" or "physical health." Overall, classification performance was strong with κ of 0.77 (95% CI 0.75-0.80), precision of 0.93 (95% CI 0.92 - 0.94), recall of 0.93 (95% CI 0.92 - 0.94), and F_1-score of 0.93 (95% CI 0.92 - 0.94). The GPT-4 classified 18.3% (n=833) of the EHR terms as "mental health" and 81.7% (n=3720) as "physical health" (Table 1). The clinician coders and model disagreed on the categorization of 164 (19.7%) mental health terms (eg, "gunshot wound," "chronic fatigue syndrome," and "IV drug use") and 149 (4%) physical health terms (eg, "activity issues," "lethargic," and "food issues").

Table . Recall, F_1-score, and total mentions among terms in the data set across health domains.

Health domain (n)	Recall (95% CI)[a]	F_1-score (95% CI)	Total mentions in data set (thousands)
Physical health (n=3707)	0.96 (0.95 - 0.97)	0.96 (0.95 - 0.96)	255,573
Mental health (n=846)	0.81 (0.78 - 0.83)	0.81 (0.79 - 0.83)	85,081

[a]Recall indicates the proportion of terms in a clinician-coded category that were classified by the model as belonging to that category.

Mental Health

Mental health terms (n=846) were classified into 42 categories with κ of 0.62 (95% CI 0.59-0.66), precision of 0.71 (95% CI 0.68 - 0.74), recall of 0.64 (95% CI 0.61 - 0.68), and F_1-score of 0.65 (95% CI 0.62 - 0.69). Table 2 includes category-wise recall, F_1-score, and a set of the most frequent categories into which terms from the true category were misclassified (Multimedia Appendix 2).

XSL•FO
RenderX

Table . Mental health term categories: recall, F_1-score, total mentions in the dataset, and most common misclassification (in descending order of recall). Categories with <5 terms were excluded.

Term category (n)	Recall (95% CI)[a]	F_1-score (95% CI)	Total mentions in dataset (thousands)	Misclassifications (n)
Eating disorder or symptoms (n=16)	1 (0.81 - 1)	0.91 (0.80 - 1)	582	None
Living situation (n=11)	1 (0.74 - 1)	1 (1 - 1)	1259	None
ADHD[b] spectrum (n=11)	1 (0.74 - 1)	0.73 (0.52-0.88)	810	None
OCD[c] symptoms or disorder (n=10)	1 (0.72 - 1)	0.87 (0.67 - 1)	207	None
Somatization symptoms (n=6)	1 (0.61 - 1)	0.86 (0.57 - 1)	62	None
Neurocognitive disorders (n=20)	0.95 (0.76 - 0.99)	0.62 (0.47 - 0.75)	1225	Neurocognitive symptoms (n=1)
Sleep wake symptoms or disorder (n=37)	0.95 (0.82 - 0.99)	0.86 (0.78 - 0.94)	1833	Miscellaneous psychiatric symptoms (n=1) and depressive symptoms (n=1)
Substance-related symptoms or disorder (n=90)	0.92 (0.85 - 0.96)	0.95 (0.91 - 0.98)	8783	Neurocognitive disorders (n=4), neurocognitive symptoms (n=1), and psychotic symptoms or disorder (n=1)
Abusive behavior (n=26)	0.89 (0.71 - 0.96)	0.84 (0.71 - 0.93)	3053	Aggressive symptoms (n=1), miscellaneous psychiatric symptoms (n=1), and personality disorder (n=1)
Unipolar depressive disorder (n=8)	0.88 (0.53 - 0.98)	0.78 (0.50 - 0.96)	944	Mood disorder (n=1)
Autism spectrum disorder (n=7)	0.86 (0.49 - 0.97)	0.71 (0.38 - 0.92)	132	Mood disorder (n=1)
Impulsive behavior (n=6)	0.83 (0.44 - 0.97)	0.83 (0.50 - 1)	414	Aggressive symptoms (n=1)
Personality disorder (n=5)	0.80 (0.38 - 0.96)	0.47 (0.11 - 0.73)	158	OCD symptoms or disorder (n=1)
Injury (n=76)	0.78 (0.67 - 0.88)	0.84 (0.77 - 0.90)	10,470	Self harm (n=8), miscellaneous psychiatric symptoms (n=3), and stress-related symptoms or disorder (n=2)
Psychotic symptoms or disorder (n=50)	0.76 (0.63 - 0.86)	0.76 (0.66 - 0.85)	6074	Miscellaneous psychiatric symptoms (n=5), neurocognitive symptoms (n=2), and impulsive behavior (n=1)
Stress-related symptoms or disorder (n=11)	0.73 (0.43 - 0.90)	0.57 (0.32 - 0.77)	480	Stressor symptoms (n=2) and anxiety symptoms (n=1)
Anxiety disorder (n=14)	0.71 (0.45 - 0.88)	0.71 (0.50 - 0.90)	683	Anxiety symptoms (n=1), social situation (n=1), and somatization symptoms (n=1)
Suicidal symptoms (n=12)	0.67 (0.39 - 0.86)	0.73 (0.46 - 0.92)	6167	Self-harm (n=3) and psychotic symptoms or disorder (n=1)
Self-harm (n=12)	0.67 (0.39 - 0.86)	0.47 (0.23 - 0.67)	2126	Abusive behavior (n=3) and suicidal symptoms (n=1)
Anxiety symptoms (n=22)	0.64 (0.43 - 0.80)	0.54 (0.36 - 0.69)	7481	Stress-related symptoms or disorder (n=2), sensory disturbances (n=2), and anxiety disorder (n=2)

XSL•FO
RenderX

Term category (n)	Recall (95% CI)[a]	F_1-score (95% CI)	Total mentions in dataset (thousands)	Misclassifications (n)
Neurocognitive symptoms (n=74)	0.61 (0.49 - 0.71)	0.61 (0.50 - 0.69)	1802	Neurocognitive disorders (n=10), miscellaneous psychiatric symptoms (n=8), and ADHD spectrum (n=6)
Aggressive symptoms (n=24)	0.58 (0.40 - 0.76)	0.58 (0.40 - 0.74)	4275	Anxiety symptoms (n=4), mood symptoms (n=4), and miscellaneous psychiatric symptoms (n=2)
Depressive symptoms (n=39)	0.56 (0.41 - 0.71)	0.68 (0.54 - 0.80)	6381	Mood symptoms (n=5), miscellaneous psychiatric symptoms (n=3), and unipolar depressive disorder (n=2)
Pharm symptoms (n=7)	0.43 (0.16 - 0.75)	0.33 (0 - 0.59)	699	Sensory disturbances (n=2), psych ADE[d] (n=1), and miscellaneous psychiatric symptoms (n=1)
Bipolar spectrum (n=36)	0.42 (0.27 - 0.58)	0.59 (0.40 - 0.74)	2290	Mood symptoms (n=18), psychotic symptoms or disorder (n=2), and miscellaneous psychiatric symptoms (n=1)
Miscellaneous psychiatric symptoms (n=156)	0.29 (0.22 - 0.36)	0.39 (0.30 - 0.46)	9554	Neurocognitive symptoms (n=17), antisocial behavior (n=10), and mood symptoms (n=10)
Suicidal behavioral (n=12)	0.25 (0.09 - 0.53)	0.38 (0 - 0.67)	1164	Injury (n=3), miscellaneous psychiatric symptoms (n=1), and overdose (n=1)
Antisocial behavior (n=10)	0.20 (0.06 - 0.51)	0.17 (0 - 0.37)	1666	Personality disorder (n=3), aggressive symptoms (n=2), and miscellaneous psychiatric symptoms (n=2)
Sensory disturbances (n=6)	0.17 (0.03 - 0.56)	0.09 (0 - 0.27)	387	Psychotic symptoms or disorder (n=3) and miscellaneous psychiatric symptoms (n=2)
Stressor symptoms (n=5)	0 (0 - 0.43)	0 (0 - 0)	34	Sensory disturbances (n=2), personality disorder (n=2), and miscellaneous psychiatric symptoms (n=1)
Psych ADE (n=11)	0 (0 - 0.26)	0 (0 - 0)	151	Neurocognitive symptoms (n=6) and pharm symptoms (n=5)

[a]Recall indicates the proportion of terms in a clinician-coded category that were classified by the model as belonging to that category.

[b]ADHD: attention deficit hyperactive disorder.

[c]OCD: obsessive compulsive disorder.

[d]psych ADE: psychiatric adverse drugs events.

The model exhibited the best classification performance for categories of: "living situation" (F_1-score=1, n=11 terms), "substance use related symptoms and disorder" (F_1-score=0.94, n=90 terms), "eating disorder or symptoms" (F_1-score=0.95, n=16 terms), "OCD symptoms or disorder" (F_1-score=0.87, n=10 terms), and "sleep wake symptoms or disorder" (F_1-score=0.86, n=37 terms). Conversely, the model performed poorly on "miscellaneous psychiatric symptoms" (F_1-score=0.39, n=156 terms), "antisocial behavior" (F_1-score=0.17, n=10 terms), "sensory disturbances" (F_1-score=0.09, n=10 terms), "psychiatric adverse drug events" (F_1-score=0, n=11 terms), and "stressor symptoms" (F_1-score=0, n=5 terms).

The most mislabeled mental health terms included "psychiatric adverse drug events" as "neurocognitive symptoms" (n=6 misclassifications) or "pharmacological symptoms" (n=5

XSL•FO
RenderX

misclassifications). The model also commonly mislabeled terms in "miscellaneous psychiatric symptoms." There were 111 terms in the "miscellaneous psychiatric symptoms" category that were misclassified across 28 of 41 other categories (Multimedia Appendix 3).

Physical Health

Physical health terms (n=3707) were classified into 19 categories with κ of 0.69 (95% CI 0.67-0.70), precision of 0.76 (95% CI 0.74 - 0.77), recall of 0.71 (95% CI 0.70 - 0.73), and F_1-score of 0.72 (95% CI 0.70 - 0.73). Table 3 includes category-wise recall, F_1-score, and a set of the most frequent categories into which terms from the true category were misclassified (Multimedia Appendix 3).

XSL•FO
RenderX

Table . Physical health term categories: recall, F_1-score, total mentions in the dataset, and most common misclassification (in descending order of recall).

Term category (n)	Recall (95% CI)[a]	F_1-score (95% CI)	Total mentions in dataset (thousands)	Most frequent misclassifications (n)
Oncological conditions (n=45)	0.91 (0.79 - 0.96)	0.61 (0.51 - 0.70)	4549	Autoimmune and inflammatory conditions (n=1), gastrointestinal symptoms (n=1), and other physical symptoms and conditions (n=1)
Sensory problems (n=41)	0.90 (0.78 - 0.96)	0.35 (0.27 - 0.43)	3113	Neurological symptoms (n=4)
Cardiovascular symptoms (n=401)	0.88 (0.85 - 0.91)	0.88 (0.85 - 0.90)	30,930	Other physical symptoms and conditions (n=14), neurological symptoms (n=9), and respiratory symptoms (n=8)
Respiratory symptoms (n=139)	0.84 (0.77 - 0.89)	0.72 (0.66 - 0.77)	27,775	Sensory problems (n=6), gastrointestinal symptoms (n=5), and other physical symptoms and conditions (n=4)
Infectious symptoms (n=145)	0.84 (0.77 - 0.89)	0.63 (0.57 - 0.68)	15,079	Hepatobiliary conditions (n=7), sensory problems (n=3), and skin and soft tissue disorders (n=3)
Metabolic disorders (n=63)	0.84 (0.73 - 0.91)	0.68 (0.59 - 0.76)	3136	Hepatobiliary conditions (n=7), endocrine symptoms (n=1), and other physical symptoms and conditions (n=1)
Hematological symptoms (n=122)	0.83 (0.75 - 0.89)	0.81 (0.75 - 0.86)	6321	Oncological conditions (n=11), gastrointestinal symptoms (n=3), and hepatobiliary conditions (n=3)
Neurological symptoms (n=413)	0.82 (0.78 - 0.85)	0.79 (0.76 - 0.82)	22,540	Sensory problems (n=38), other physical symptoms and conditions (n=8), and infectious symptoms (n=5)
Gastrointestinal symptoms (n=279)	0.81 (0.76 - 0.85)	0.77 (0.72 - 0.81)	24,878	Hepatobiliary conditions (n=18), autoimmune and inflammatory conditions (n=10), and infectious symptoms (n=9)
Skin and soft tissue disorders (n=314)	0.78 (0.73 - 0.82)	0.80 (0.76 - 0.83)	15,212	Infectious symptoms (n=26), other physical symptoms and conditions (n=13), and gastrointestinal symptoms (n=9)
Genitourinary symptoms (n=201)	0.77 (0.71 - 0.82)	0.81 (0.76 - 0.85)	8571	Gastrointestinal symptoms (n=12), infectious symptoms (n=11), and other physical symptoms and conditions (n=7)
Renal disorders (n=52)	0.75 (0.62 - 0.85)	0.76 (0.65 - 0.84)	2221	Infectious symptoms (n=5), genitourinary symptoms (n=4), and cardiovascular symptoms (n=3)

XSL•FO
RenderX

Term category (n)	Recall (95% CI)[a]	F_1-score (95% CI)	Total mentions in dataset (thousands)	Most frequent misclassifications (n)
Endocrine symptoms (n=98)	0.67 (0.58 - 0.76)	0.71 (0.63 - 0.78)	4942	Metabolic disorders (n=16), sensory problems (n=4), and autoimmune and inflammatory conditions (n=3)
Musculoskeletal symptoms (n=480)	0.67 (0.63 - 0.71)	0.79 (0.75 - 0.82)	21,785	Other physical symptoms and conditions (n=62), neurological symptoms (n=39), and autoimmune and inflammatory conditions (n=13)
Pain symptoms (n=59)	0.59 (0.47 - 0.71)	0.61 (0.51 - 0.71)	18,045	Other physical symptoms and conditions (n=6), neurological symptoms (n=5), and gastrointestinal symptoms (n=4)
Autoimmune and inflammatory conditions (n=68)	0.54 (0.43 - 0.66)	0.50 (0.40 - 0.60)	6234	Infectious symptoms (n=9), other physical symptoms and conditions (n=9), and skin and soft tissue disorders (n=4)
Hepatobiliary conditions (n=54)	0.54 (0.41 - 0.66)	0.45 (0.33 - 0.56)	1970	Gastrointestinal symptoms (n=11), cardiovascular symptoms (n=4), and other physical symptoms and conditions (n=3)
Other physical symptoms and conditions (n=559)	0.47 (0.42 - 0.51)	0.54 (0.50 - 0.58)	31,151	Sensory problems (n=68), neurological symptoms (n=39), and skin and soft tissue disorders (n=29)
Respiratory disorders (n=173)	0.40 (0.33 - 0.47)	0.55 (0.48 - 0.63)	7120	Respiratory symptoms (n=50), infectious symptoms (n=28), and other physical symptoms and conditions (n=10)

[a]Recall indicates the proportion of terms in a clinician-coded category that were classified by the model as belonging to that category.

The model exhibited the best classification performance for categories of: “cardiovascular symptoms” (n=401 terms), “hematological symptoms” (n=122 terms), and “genitourinary symptoms” (n=201 terms), with recall and F_1-score values >0.80. Conversely, the model performed poorly on “sensory problems” (F_1-score=0.35, n=41 terms), “hepatobiliary conditions” (F_1-score=0.45, n=54 terms), and “other physical symptoms and conditions” (F_1-score=0.54, n=559 terms).

The model commonly predicted the category “sensory problems” in terms of the categories “other physical symptoms and conditions” (n=68 misclassifications) and “neurological symptoms” (n=38 misclassifications). The model also commonly mislabeled “other physical symptoms and conditions.” There were 299 “other physical symptoms and conditions” terms that were misclassified across 18 other categories (Multimedia Appendix 3).

Discussion

Principal Findings

We investigated a GPT-4’s ability to replicate clinical judgment when classifying EHR terms from a dataset of mental health patients into interpretable clinical categories. A recent review of NLP studies found the agreement of human coding of EHR data to range from 0.72 to 0.94 (Cohen κ) [28]. Based on this benchmark, GPT-4 showcases human-like agreement with clinical experts when classifying EHR terms as either mental or physical health. Yet, GPT-4’s classification performance varied widely across mental health and physical health categories and had high error rates for certain categories (eg, “sensory problems” and “stressor symptoms”). Misclassifications highlighted GPT-4’s biases, such as the tendency for broad categories (eg, “other physical symptoms and conditions”) to be underselected. Instead, terms from these categories were allocated to more specific categories (eg, “cutting” was allocated to “injury” instead of “self-harm”).

Nevertheless, GPT-4 was able to rapidly transform a feature set of 4553 individual EHR terms into 61 clinically valid groups which can be readily implemented into prediction models. State-of-the-art LLMs have already been used alongside traditional NLP methods, such as named entity recognition, text clustering, and supervised machine learning models trained on text data [29-31]. Additionally, LLMs can explain categorization decisions, providing valuable insights for end users of integrated clinical tools.

XSL•FO
RenderX

Limitations

LLMs occasionally "hallucinate", generating outputs that are off-task, nonsensical, or contradictory. Although we prompted the model to validate the output and correct for hallucinations, as the creativity and complexity of tasks increase so does the risk of aberrant outputs [32]. Moreover, recent studies have found that LLM performance on certain clinical tasks can substantially improve when given 1 or multiple examples for codes, a process known as "few-shot" learning [33,34]. In contrast, our study used "zero-shot" learning, where GPT-4 was asked to classify clinical terms without being provided with any specific examples or definitions for the coding system. This method was chosen to assess the model's baseline classification performance, without introducing any more task-specific bias. However, we recognize that because the coding system was developed by only 2 clinicians, bias may be introduced due to their unique sets of clinical experiences, institutional practices, and personal preferences. The LLM may be biased as well. An ad hoc analysis indicated a tendency for the model to underuse "other" categories (eg, "other physical symptoms and conditions" and "miscellaneous psychiatric symptoms") relative to clinician coders (Multimedia Appendix 3). Nonetheless, we acknowledge that many clinical terms in EHR are inherently ambiguous and may be classified under multiple categories depending on the context. Without knowing the sample is among people hospitalized with a mental health disturbance, it is not necessarily a misclassification for GPT-4 to label "gunshot wound" as a physical injury and not an indicator of suicide. The task of assigning a single, mutually exclusive label may limit one's ability to capture the full complexity of the clinical term. While this study provides a preliminary framework for exploring the feasibility of using LLMs for unstructured EHR classification, future research should aim to involve a varied set of coding methods, classification approaches (eg, multi-label classification), and a larger cohort of clinician-coders to enhance generalizability. Finally, we note that several categories in the mental health domain had too few terms (<5) to yield stable estimates of agreement and were removed from the analysis.

Implications

The accuracy of clinical term classification is essential for downstream predictive models that rely on structured data, as inaccuracies can propagate through the model pipeline. Understanding the sensitivity of these models to variations in input labels is key, especially when distinguishing between random errors and systematic misclassifications. Systematic errors, where specific categories are consistently mislabeled, may significantly affect the robustness of models trained on such data, potentially more so than a random error (ie, noise) [35-37]. Moreover, the assumption that accurate categorization of clinical terms is a necessary intermediate step is worth reconsidering. As LLMs advance, there is potential for these models to bypass the traditional 2-stage process and make direct predictions from unstructured text [30]. Future research is needed to determine whether bypassing the intermediate categorization step entirely might enhance or hinder model performance, depending on the specific clinical application.

Conclusion

As LLMs continue to advance, the time and human resources required to distill a large corpus of EHR terms into clinically meaningful groups can be greatly reduced. LLMs have the potential to be integrated into EHR systems to create text-based features for prediction models in real time. This study found that a state-of-the-art LLM achieved high agreement with classifications of experienced clinicians across terms from numerous physical and mental health categories.

Acknowledgments

This work was supported by the National Institutes of Health (R01MH126895). We appreciate the contribution of Ming Xie in dataset preparation and extensive analytical support.

Conflicts of Interest

None declared.

Multimedia Appendix 1
Code and prompt design.
[DOCX File, 23 KB - medinform_v13i1e65454_app1.docx]

Multimedia Appendix 2
Classification performance metrics output.
[XLSX File, 76 KB - medinform_v13i1e65454_app2.xlsx]

Multimedia Appendix 3
Analysis of misclassifications.
[XLSX File, 67 KB - medinform_v13i1e65454_app3.xlsx]

References

XSL•FO
RenderX

1. Hossain ME, Khan A, Moni MA, Uddin S. Use of electronic health data for disease prediction: a comprehensive literature review. IEEE/ACM Trans Comput Biol Bioinform 2021;18(2):745-758. [doi: 10.1109/TCBB.2019.2937862]
2. Mahmoudi E, Kamdar N, Kim N, Gonzales G, Singh K, Waljee AK. Use of electronic medical records in development and validation of risk prediction models of hospital readmission: systematic review. BMJ 2020 Apr 8;369:m958. [doi: 10.1136/bmj.m958] [Medline: 32269037]
3. Boudreaux ED, Haskins BL, Larkin C, et al. Emergency department safety assessment and follow-up evaluation 2: an implementation trial to improve suicide prevention. Contemp Clin Trials 2020 Aug;95:106075. [doi: 10.1016/j.cct.2020.106075] [Medline: 32565041]
4. Boudreaux ED, Rundensteiner E, Liu F, et al. Applying machine learning approaches to suicide prediction using healthcare data: overview and future directions. Front Psychiatry 2021;12:707916. [doi: 10.3389/fpsyt.2021.707916] [Medline: 34413800]
5. Lee TC, Shah NU, Haack A, Baxter SL. Clinical implementation of predictive models embedded within electronic health record systems: a systematic review. Informatics (MDPI) 2020 Sep;7(3):25. [doi: 10.3390/informatics7030025] [Medline: 33274178]
6. Bayramli I, Castro V, Barak-Corren Y, et al. Predictive structured-unstructured interactions in EHR models: a case study of suicide prediction. NPJ Digit Med 2022 Jan 27;5(1):15. [doi: 10.1038/s41746-022-00558-0] [Medline: 35087182]
7. Mahajan SM, Ghani R. Combining structured and unstructured data for predicting risk of readmission for heart failure patients. Stud Health Technol Inform 2019 Aug 21;264:238-242. [doi: 10.3233/SHTI190219] [Medline: 31437921]
8. Coiera E. Guide to Health Informatics, 3rd edition: CRC Press; 2015.
9. Akbilgic O, Homayouni R, Heinrich K, Langham M, Davis R. Unstructured text in EMR improves prediction of death after surgery in children. Informatics (MDPI) 2019;6(1):4. [doi: 10.3390/informatics6010004]
10. Marafino BJ, Park M, Davies JM, et al. Validation of prediction models for critical care outcomes using natural language processing of electronic health record data. JAMA Netw Open 2018 Dec 7;1(8):e185097. [doi: 10.1001/jamanetworkopen.2018.5097] [Medline: 30646310]
11. Bousselham H, Nfaoui EH, Mourhir A. Fine-tuning GPT on biomedical NLP tasks: an empirical evaluation. Presented at: 2024 International Conference on Computer, Electrical & Communication Engineering (ICCECE); Feb 2-3, 2024; Kolkata, India. [doi: 10.1109/ICCECE58645.2024.10497313]
12. OpenAI, Achiam J, Adler S, et al. GPT-4 technical report. arXiv. Preprint posted online on Mar 15, 2023. [doi: 10.48550/arXiv.2303.08774]
13. Shekhar S, Tiwari S, Rensink TC, Eskander R, Salloum W. Coupling symbolic reasoning with language modeling for efficient longitudinal understanding of unstructured electronic medical records. arXiv. Preprint posted online on Aug 7, 2023. [doi: 10.48550/arXiv.2308.03360]
14. Chew R, Bollenbacher J, Wenger M, Speer J, Kim A. LLM-assisted content analysis: using large language models to support deductive coding. arXiv. Preprint posted online on Jun 23, 2023. [doi: 10.48550/arXiv.2306.14924]
15. Xiao Z, Yuan X, Liao QV, Abdelghani R, Oudeyer PY. Supporting qualitative analysis with large language models: combining codebook with GPT-3 for deductive coding. Presented at: IUI '23: 28th International Conference on Intelligent User Interfaces; Mar 27-31, 2023; Sydney, Australia. [doi: 10.1145/3581754.3584136]
16. Hou C, Zhu G, Zheng J, et al. Prompt-based and fine-tuned GPT models for context-dependent and -independent deductive coding in social annotation. Presented at: LAK '24: The 14th Learning Analytics and Knowledge Conference; Mar 18-22, 2024; Kyoto, Japan. [doi: 10.1145/3636555.3636910]
17. Gilardi F, Alizadeh M, Kubli M. ChatGPT outperforms crowd workers for text-annotation tasks. Proc Natl Acad Sci U S A 2023 Jul 25;120(30):e2305016120. [doi: 10.1073/pnas.2305016120] [Medline: 37463210]
18. Törnberg P. ChatGPT-4 outperforms experts and crowd workers in annotating political twitter messages with zero-shot learning. arXiv. Preprint posted online on Apr 13, 2023. [doi: 10.48550/arXiv.2304.06588]
19. Hua Y, Liu F, Yang K, et al. Large language models in mental health care: a scoping review. arXiv. Preprint posted online on Jan 1, 2024. [doi: 10.48550/arXiv.2401.02984]
20. Kumar A, Sharma R, Bedi P. Towards optimal NLP solutions: analyzing GPT and LLaMA-2 models across model scale, dataset size, and task diversity. Eng Technol Appl Sci Res 2024;14(3):14219-14224. [doi: 10.48084/etasr.7200]
21. Yanagita Y, Yokokawa D, Fukuzawa F, Uchida S, Uehara T, Ikusaka M. Assessing the ability of GPT to generate illness scripts: an evaluation study. medRxiv. Preprint posted online on Dec 27, 2023. [doi: 10.1101/2023.12.25.23300525]
22. Moradi M, Blagec K, Haberl F, Samwald M. GPT-3 models are poor few-shot learners in the biomedical domain. arXiv. Preprint posted online on Sep 6, 2021. [doi: 10.48550/arXiv.2109.02555]
23. Rao A, Pang M, Kim J, et al. Assessing the utility of chatgpt throughout the entire clinical workflow. medRxiv. Preprint posted online on Feb 26, 2023. [doi: 10.1101/2023.02.21.23285886]
24. User guide: clinical classifications software refined (CCSR). Agency for Healthcare Research and Quality Healthcare Cost and Utilization Project (HCUP). 2019. URL: https://hcup-us.ahrq.gov/toolssoftware/ccsr/DXCCSR-User-Guide-v2019-1.pdf [accessed 2025-01-15]
25. openai/openai-python: the official Python library for the OpenAI API. GitHub. 2024. URL: https://github.com/openai/openai-python [accessed 2025-01-15]

XSL•FO
RenderX

26. Kramer O. Scikit-Learn: Machine Learning for Evolution Strategies: Springer International Publishing; 2016:45-53 URL: http://link.springer.com/10.1007/978-3-319-33383-0_5 [accessed 2025-01-15]
27. Fung KP, Lee J. Bootstrap estimate of the variance and confidence interval of kappa. Br J Ind Med 1991 Jul;48(7):503-504. [doi: 10.1136/oem.48.7.503] [Medline: 1854654]
28. Scharp D, Hobensack M, Davoudi A, Topaz M. Natural language processing applied to clinical documentation in post-acute care settings: a scoping review. J Am Med Dir Assoc 2024 Jan;25(1):69-83. [doi: 10.1016/j.jamda.2023.09.006] [Medline: 37838000]
29. Garrido-Merchan EC, Gozalo-Brizuela R, Gonzalez-Carvajal S. Comparing BERT against traditional machine learning models in text classification. J Comput Cogn Eng 2023;2:352-356.
30. Li L, Zhou J, Gao Z, et al. A scoping review of using large language models (LLMs) to investigate electronic health records (EHRs). arxiv 2024 [FREE Full text]
31. Sushil M, Zack T, Mandair D, et al. A comparative study of zero-shot inference with large language models and supervised modeling in breast cancer pathology classification. arXiv. Preprint posted online on Jan 25, 2024. [doi: 10.48550/arXiv.2401.13887]
32. Lee M. A mathematical investigation of hallucination and creativity in GPT models. Mathematics 2023;11(10):2320. [doi: 10.3390/math11102320]
33. Labrak Y, Rouvier M, Dufour R. A zero-shot and few-shot study of instruction-finetuned large language models applied to clinical and biomedical tasks. arXiv. Preprint posted online on Jul 22, 2023. [doi: 10.48550/arXiv.2307.12114]
34. Sivarajkumar S, Kelley M, Samolyk-Mazzanti A, Visweswaran S, Wang Y. An empirical evaluation of prompting strategies for large language models in zero-shot clinical natural language processing: algorithm development and validation study. JMIR Med Inform 2024 Apr 8;12:e55318. [doi: 10.2196/55318] [Medline: 38587879]
35. Shah D, Schwartz HA, Hovy D. Predictive biases in natural language processing models: a conceptual framework and overview. arXiv. Preprint posted online on Nov 9, 2019. [doi: 10.48550/arXiv.1912.11078]
36. Lin Z, Guan S, Zhang W, Zhang H, Li Y, Zhang H. Towards trustworthy LLMs: a review on debiasing and dehallucinating in large language models. Artif Intell Rev 2024;57(9):243. [doi: 10.1007/s10462-024-10896-y]
37. Frenay B, Verleysen M. Classification in the presence of label noise: a survey. IEEE Trans Neural Netw Learning Syst 2014;25(5):845-869. [doi: 10.1109/TNNLS.2013.2292894]

Abbreviations

ED: emergency department
EHR: electronic health record
LLM: large language model
NLP: natural language processing

Edited by C Lovis; submitted 15.08.24; peer-reviewed by B Thies, P Chung; revised version received 25.11.24; accepted 30.11.24; published 21.01.25.

Please cite as:
Cardamone NC, Olfson M, Schmutte T, Ungar L, Liu T, Cullen SW, Williams NJ, Marcus SC
Classifying Unstructured Text in Electronic Health Records for Mental Health Prediction Models: Large Language Model Evaluation Study
JMIR Med Inform 2025;13:e65454
URL: https://medinform.jmir.org/2025/1/e65454
doi:10.2196/65454

© Nicholas C Cardamone, Mark Olfson, Timothy Schmutte, Lyle Ungar, Tony Liu, Sara W Cullen, Nathaniel J Williams, Steven C Marcus. Originally published in JMIR Medical Informatics (https://medinform.jmir.org), 21.1.2025. This is an open-access article distributed under the terms of the Creative Commons Attribution License (https://creativecommons.org/licenses/by/4.0/), which permits unrestricted use, distribution, and reproduction in any medium, provided the original work, first published in JMIR Medical Informatics, is properly cited. The complete bibliographic information, a link to the original publication on https://medinform.jmir.org/, as well as this copyright and license information must be included.

XSL•FO
RenderX

Original Paper

The Transformative Potential of Large Language Models in Mining Electronic Health Records Data: Content Analysis

Amadeo Jesus Wals Zurita[1], MD; Hector Miras del Rio[1], MP; Nerea Ugarte Ruiz de Aguirre[1], MD; Cristina Nebrera Navarro[1], MD; Maria Rubio Jimenez[1], MD; David Muñoz Carmona[1], MD, PhD; Carlos Miguez Sanchez[1], MD

Servicio Oncologia Radioterápica, Hospital Universitario Virgen Macarena, Andalusian Health Service, Seville, Spain

Corresponding Author:
Amadeo Jesus Wals Zurita, MD
Servicio Oncologia Radioterápica
Hospital Universitario Virgen Macarena
Andalusian Health Service
Avenida Dr. Fedriani s/n
Seville, 41009
Spain
Phone: 34 954712932
Email: amadeoj.wals.sspa@juntadeandalucia.es

Abstract

Background: In this study, we evaluate the accuracy, efficiency, and cost-effectiveness of large language models in extracting and structuring information from free-text clinical reports, particularly in identifying and classifying patient comorbidities within oncology electronic health records. We specifically compare the performance of gpt-3.5-turbo-1106 and gpt-4-1106-preview models against that of specialized human evaluators.

Objective: We specifically compare the performance of gpt-3.5-turbo-1106 and gpt-4-1106-preview models against that of specialized human evaluators.

Methods: We implemented a script using the OpenAI application programming interface to extract structured information in JavaScript object notation format from comorbidities reported in 250 personal history reports. These reports were manually reviewed in batches of 50 by 5 specialists in radiation oncology. We compared the results using metrics such as sensitivity, specificity, precision, accuracy, F-value, κ index, and the McNemar test, in addition to examining the common causes of errors in both humans and generative pretrained transformer (GPT) models.

Results: The GPT-3.5 model exhibited slightly lower performance compared to physicians across all metrics, though the differences were not statistically significant (McNemar test, P=.79). GPT-4 demonstrated clear superiority in several key metrics (McNemar test, P<.001). Notably, it achieved a sensitivity of 96.8%, compared to 88.2% for GPT-3.5 and 88.8% for physicians. However, physicians marginally outperformed GPT-4 in precision (97.7% vs 96.8%). GPT-4 showed greater consistency, replicating the exact same results in 76% of the reports across 10 repeated analyses, compared to 59% for GPT-3.5, indicating more stable and reliable performance. Physicians were more likely to miss explicit comorbidities, while the GPT models more frequently inferred nonexplicit comorbidities, sometimes correctly, though this also resulted in more false positives.

Conclusions: This study demonstrates that, with well-designed prompts, the large language models examined can match or even surpass medical specialists in extracting information from complex clinical reports. Their superior efficiency in time and costs, along with easy integration with databases, makes them a valuable tool for large-scale data mining and real-world evidence generation.

(JMIR Med Inform 2025;13:e58457) doi:10.2196/58457

KEYWORDS

electronic health record; EHR; oncology; radiotherapy; data mining; ChatGPT; large language models; LLMs

XSL•FO
RenderX

Introduction

Real-world data (RWD) holds immense potential for advancing health care by providing a comprehensive view of patient health, disease progression, and treatment outcomes [1]. However, RWD presents significant challenges due to its diverse sources and formats, such as electronic health records, medical imaging, and laboratory results, each with different standards and terminologies. Much of this data is unstructured, like free-text clinical notes, which are difficult to process and analyze. Additionally, missing information is common, leading to gaps that hinder accurate analysis. Advanced methodologies and technologies are needed to effectively extract, standardize, and analyze RWD, ensuring its potential to improve health care outcomes is fully realized.

Extracting information from clinical texts has traditionally relied on manual methods, where trained health care professionals review and annotate clinical notes to identify relevant information such as diagnoses, treatments, and patient outcomes. This manual process is not only time-consuming and labor-intensive but also prone to human error, leading to inconsistencies and inaccuracies. Additionally, statistical and rule-based approaches have been used, which depend on predefined patterns and keywords to extract information. However, these methods often fall short in handling the complexity and variability inherent in natural language, resulting in incomplete or inaccurate data extraction.

The rise of artificial intelligence, driven by advances in computing power, has propelled the development of natural language processing (NLP). NLP algorithms can automatically structure information from unstructured clinical texts, facilitating analysis and integration with other clinical data [2-5]. Earlier NLP systems often relied on rule-based systems and simpler machine learning models, implying limitations such as the need for extensive customization, deep computer science knowledge, significant computational resources, and large volumes of high-quality labeled data. These challenges hinder their widespread adoption and optimal performance across different applications.

Transformer models, a deep learning architecture introduced in the paper “Attention is All You Need” by Vaswani et al [6], have revolutionized the field of NLP, establishing themselves as the foundation upon which modern large language models (LLMs) have been developed. LLMs, such as OpenAI's generative pre-trained transformers (GPTs), are models trained on vast amounts of text to learn complex linguistic patterns. This enables them to generate text, understand context, perform translations, and carry out other tasks with unprecedented accuracy and fluency. Thanks to this capability, users can interact with these models, instructing them to tackle various problems without the need for additional training.

The GPT-3 model, released in 2020, and its successor, GPT-4 [7], introduced in 2023, represent significant advancements in the ability to understand and generate coherent text. The progression from GPT-3 through GPT-3.5 to GPT-4 marks a significant evolution in OpenAI's language model capabilities. GPT-4 offers enhanced understanding and generation of text due to its larger training dataset and more refined architecture, resulting in responses that are more accurate, contextually aware, and nuanced compared to its predecessors. This latest version also demonstrates improved performance on a broader array of tasks, including complex reasoning and problem-solving. Additionally, it is multimodal, capable of processing not only text but also images and audio. However, it is important to note that these models are not specifically designed for medical diagnostic purposes.

Currently, there are numerous LLMs available, such as LLaMA, Mistral, Claude, or BioBERT. However, in the medical field, the ChatGPT models have been the most extensively studied [8], demonstrating strong capabilities in various applications, including interpreting clinical guidelines and enhancing evidence-based medicine [9], or table summarization in clinical study reports [10]. Despite their potential, concerns about the applicability of these general-purpose models in the medical domain persist [11,12], particularly due to their lack of transparency in training data, which remains largely unknown. Therefore, it is essential to evaluate their performance for each specific application.

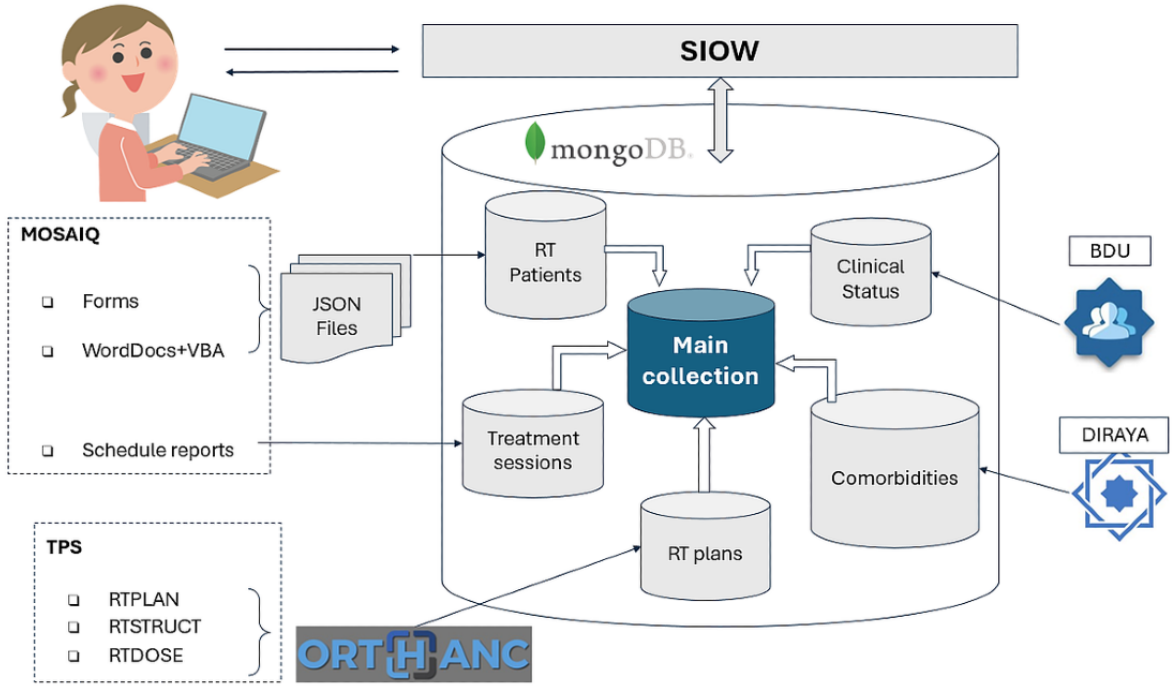
In the context of extracting and structuring information from free-text clinical reports, studies have shown promising results with OpenAI models. For instance, Fink et al [13] demonstrated the effectiveness of these models in extracting data from computed tomography reports related to lung cancer, where they outperformed traditional NLP models in classifying disease progression.

Focusing on the significance of appropriate instructions (prompts), studies such as that of Choi et al [14] highlighted that the gpt-3.5-turbo model exhibited an accuracy rate of 87.7% in extracting information from pathology and ultrasound reports of breast cancer patients. Additionally, the LLM methods demonstrated superior efficiency in terms of time and costs compared to manual approaches.

In 2018, the Department of Radiation Oncology at Hospital Universitario Virgen Macarena initiated the implementation of the Mosaiq system, transitioning toward a paperless workflow and centralizing all radiation therapy treatment data within the application. As detailed by Bertolet et al [15], this data was automatically exported to JSON files via Word documents and Visual Basic for Applications code. Figure 1 depicts a diagram illustrating the flow and organization of the described data.

XSL•FO
RenderX

Figure 1. Representative diagram of the Web Oncological Information System (SIOW). It illustrates the integration of data from MOSAIQ and TPS into the MongoDB database and its subsequent management through SIOW, including the collection of administrative data from the Users Data Base (BDU) and clinical data from the electronic health record system DIRAYA. JSON: JavaScript object notation; RT: radiotherapy.



Motivated by the capabilities of LLMs, we aimed to investigate their potential application in extracting and structuring information from clinical reports. Our overarching objective is to integrate LLM-based tools into our information system, enhancing the richness of our real-world datasets. Specifically, in this study, we assess the capability of the GPT-3.5 turbo and GPT-4 models as tools for data mining applied to the identification and classification of comorbidities and relevant lifestyle risk factors in oncological texts. We compare their performance against that of specialized human evaluators to gauge their efficacy and suitability for clinical use.

Methods

OpenAI Models

The application programming interface (API) of OpenAI [16] allows interaction with their advanced LLMs, facilitating various language processing tasks such as generating automatic textual responses, conducting sentiment analysis, and summarizing texts. In our study, we leveraged the *chat completions API* function of the API to extract structured information from unstructured clinical reports.

OpenAI offers a comprehensive library of natural language processing models. Each model features unique characteristics in terms of size, language comprehension ability, speed, and cost. In our study, we have used 2 models from the library: *gpt-3.5-turbo-1106* and *gpt-4-1106-preview*, with the latter being the most advanced model available at the time the study was conducted. While the GPT-3.5 model is a faster and more economical option for general tasks, GPT-4 stands out for its higher accuracy, contextual understanding, and ability to handle more complex and specific applications.

For this study, we used clinical reports in Spanish, exclusively interacting with OpenAI's LLMs in this language. Although LLMs typically exhibit superior performance in English [17], owing to the predominance of this language in training data, recent comparisons indicate notable effectiveness in other languages, including Spanish. The GPT-4 technical report [7] highlights this multilingual capability, demonstrating that performance in Spanish closely approaches that of English, with a minimal difference of only 1.5 percentage points in the MMLU evaluation [18].

Prompt Generation

To interact with the LLM models, we first created a prompt that will guide the model through the specific task. The context provided to the model establishes a scenario in which it is asked to assume the role of a specialist in radiation oncology. This setting serves as a reference framework, enabling the model to adopt the appropriate perspective and apply its natural language understanding capabilities in a manner consistent with the medical domain.

Our request is a direct instruction to the model, directing it to process the text of the provided clinical report and return the relevant information in a structured format. Specifically, the model is instructed to use the clinical report provided at the end of the prompt to complete a predefined dictionary in JSON format. This dictionary contains keys related to comorbidities and lifestyle risk factors. The model is tasked with updating the values of these keys with “YES” or “NO” as appropriate. For individuals who are ex-smokers, the model should use “EX” instead. Additionally, the model must identify and add any other relevant comorbidities not classifiable under the provided categories, assigning them to the “Other” key.

The prompt generated for the task is shown in Textbox 1.

XSL•FO
RenderX

The dictionary mentioned in the request is structured with keys labeling the specific comorbidities and lifestyle risk factors we seek to identify. These comorbidities, along with their potential values, are outlined in Table 1.

During a postprocessing phase, we divided the category labeled as “smoker” into 2 distinct categories: “smoker” (representing current smokers) and “ex-smoker.” This division was implemented to ease the subsequent analysis of the results.

It is important to highlight that the prompt does not provide context or additional instructions regarding how the specified comorbidities of interest should be interpreted.

The development of this prompt was achieved through an iterative process applied to a group of 50 reports that were specifically reserved for this purpose. The methodology included the following steps (Textbox 2):

Textbox 1. Prompt generated for the task.

- **Context:** “Act as a specialist in radiation oncology.”
- **Request:** “Use the clinical report provided at the end of this prompt to return in JSON format the dictionary [...] with the values 'YES' or 'NO'. For the 'Smoker' field: 'YES' if they smoke, 'NO' if they have never smoked, 'EX' if they are an ex-smoker. For the 'Other' field, return a list of comorbidities found that cannot be classified in any of the categories of the keys of the provided dictionary, or empty if there are no other comorbidities. Return only the dictionary with the updated values, DO NOT ADD OR MODIFY KEYS. Clinical report: [text of the clinical report]”

Table 1. List of the labels, possible values, and description of the comorbidities and lifestyle risk factors considered in this study.

Label	Values	Description
Diabetes	Yes or no	Elevated blood glucose levels
HBP	Yes or no	High blood pressure
Smoker	Yes or no or ex	Smoking habit.
Dyslipidemia	Yes or no	Lipid metabolism disorder
Liver disease	Yes or no	Liver disease
COPD	Yes or no	Chronic obstructive pulmonary disease
Depression	Yes or no	Mood disorder
Kidney disease	Yes or no	Kidney disease
Fentanyl	Yes or no	Use of WHO step 3 analgesics (opioids)
Heart disease	Yes or no	Heart disease
Hyperthyroidism	Yes or no	Thyroid disease with increased thyroxine
Hypothyroidism	Yes or no	Thyroid disease with decreased thyroxine
Dependent	Yes or no	Patient in need of continuous care
Other	Text list	Other past comorbidities detected not listed above

Textbox 2. Prompt development methodology.

- **Prompt definition:** Establishing the parameters and structure of the prompt to guide the model's responses.
- **Information extraction:** The developed prompt was applied to 50 reports using the *gpt-4-1106-preview* model.
- **Verification of structure:** It was ensured that the model's responses adhered to the requested structure, with previous steps being repeated in case of deviations.
- **Accuracy evaluation:** A specialist physician (AW) verified the accuracy of the model's responses. This process was repeated until the accuracy met or exceeded that of a manual analysis performed by the same physician.

Python Script

The Python script developed uses the OpenAI API to automatically structure textual clinical information. All the code developed for this work is publicly available in a GitHub repository [19].

Clinical Report Acquisition Procedure

The clinical reports for our study were provided by the hospital's Innovation & Data Analysis department. These reports were delivered in an Excel spreadsheet format, organized into 2 essential columns: one containing the clinical history number of each patient and another with the text of the medical personal history report. The department responsible for data collection

XSL•FO
RenderX

undertook a process of anonymization and randomization of the reports to ensure an unbiased selection.

Sample Selection Criteria

For estimating the sample size, we relied on the proportion of comorbidities (80%) obtained from a prior analysis of a dataset of 5257 personal history reports from patients treated in our service between May 2018 and October 2022.

The comorbidities selected for the study were chosen based on prior knowledge of prevalences in the general population and those presented by our patients according to the aforementioned analysis. We also considered those that could most significantly impact the clinical outcome of oncological treatments.

With these considerations, we conducted a preliminary calculation that established the need to include 250 clinical reports (see below in the statistical analysis section). Based on this calculation, we selected the first 250 patients from the provided list who had a nonempty personal history report. Before proceeding with the analysis, we verified that our script was capable of correctly interpreting an empty report as equivalent to the absence of comorbidities, thereby avoiding biases in the study results.

Ethical Considerations

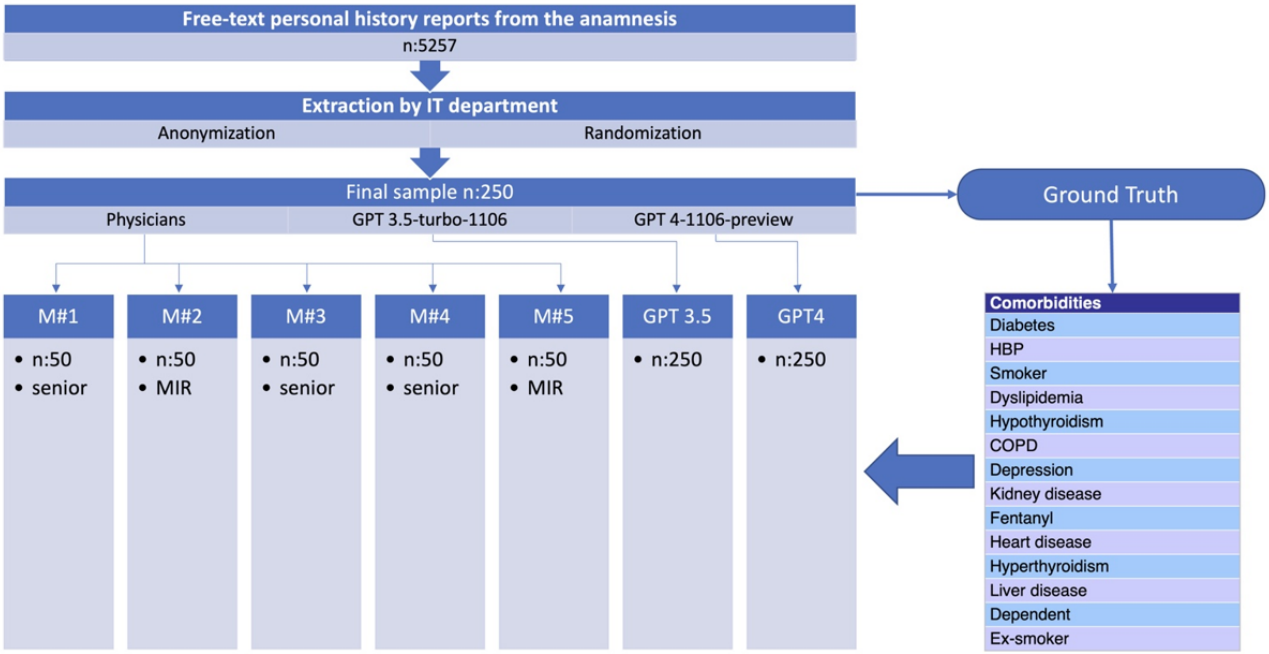
The text processed by the selected LLMs is strictly confined to personal history reports. These reports were stripped of any information that could lead to patient identification, ensuring confidentiality and anonymity. The model's interpretation of the texts focuses solely on identifying and structuring data relevant to the study without compromising individual privacy.

The study's design, synthesized in Figure 2, and methodology were previously communicated to and reviewed by the hospital's ethics committee. The research received the necessary approval, confirming that it adheres to the ethical standards required for patient data research.

This retrospective study adheres to the guidelines outlined in the *seventeenth additional provision, specifically Health Data Processing, Section d) of the Organic Law 3/2018, dated December 5, on Personal Data Protection and Guarantee of Digital Rights*. This law governs the use of pseudoanonymized personal data for health research purposes. The study was granted an exemption from requiring informed consent due to its exclusive use of nonidentifiable data.

On January 18, 2024, the Ethics Committee of the University Hospitals Virgen Macarena and Virgen del Rocío issued a favorable opinion for our study, under the reference EC_IA_V1 (version 1-Dec-2023).

Figure 2. Flowchart of the study design. COPD: chronic obstructive pulmonary disease; HBP: high blood pressure.



Data Extraction

For the manual data extraction, the 250 patient clinical reports were divided into 5 groups, each consisting of 50 reports. These groups were randomly assigned to 5 physicians, including 3 specialists in radiation oncology with more than 15 years of experience and 2 medical residents in the same specialty, one in their first year and the other in their fourth year.

To ensure uniform and accurate data collection, the physicians were provided with a specially designed template for this task. The template features a table where the first column contains the full texts of the clinical reports. The subsequent columns of the table are labeled with the comorbidities of interest. The cells corresponding to each comorbidity only allow the selection of predefined values, as stipulated in Table 1. This restriction ensures consistent annotation and reduces the possibility of errors or variations in the entries.

XSL•FO
RenderX

For the automatic analysis, the 250 clinical reports in the sample were analyzed using our script with the *gpt-3.5-turbo-1106* and *gpt-4-1106-preview* models. To maintain a consistent structure in the study, these reports were organized into the same 5 groups of 50 reports that were assigned to the physicians. The results were recorded in a document that mirrored the structure of the template used in the manual extraction. This uniformity in documentation facilitates a direct comparison of results between manual and automatic extraction methods.

Establishing the Ground Truth

To assess the comparative accuracy and effectiveness of the LLMs used in this study against the evaluations performed by physicians, it is crucial to establish a reference dataset containing the ground truth. To construct this reference dataset, we first compared the results obtained from the physicians and the *gpt-4-1106-preview* model across all 250 reports, identifying and recording any discrepancies between the 2 sources. The radiation oncologist expert AW, with more than 30 years of experience, reviewed several times the whole set of reports, with a particular focus on these discrepancies. For each report where discrepancies in the results were found, physician AW assessed both responses (from the physician and the AI) and determined which one was correct.

It is important to note that the ground truth in this study is based solely on the information explicitly reported in the clinical texts. This means that some patients may have unreported comorbidities, or conversely, conditions may be mentioned that are not actually present. This limitation reflects a common challenge when working with RWD. However, for the purposes of this study, these potential discrepancies are irrelevant, as our primary focus is on evaluating the models' ability to accurately interpret and extract information from the provided texts.

Assessing Reproducibility in Results

The nondeterministic nature of LLMs, such as GPT-3.5 and GPT-4, means they can generate different responses to identical requests [7]. This phenomenon, coupled with the potential for periodic retraining of the models, significantly impacts the reproducibility of results. Therefore, it is crucial to consider the need for rigorous quality control for algorithms that use LLMs, especially to assess the impact of any changes in the models.

A well-defined and explicit prompt can increase the reproducibility of responses [14]. However, variability remains a possibility, particularly in situations where the information is ambiguous or the prompt is not clear or specific enough.

To measure the consistency of our automatic extraction method, we repeated the analysis of the 250 clinical reports 10 times over 10 consecutive days. This approach allows us to observe the stability of the model responses to the same input.

Statistical Analysis

To ensure the statistical validity of the study, a significance level of 5% (alpha error) and a power of 80% (beta error of 20%) were established. Additionally, a 5% error margin was applied for 95% confidence intervals. With these considerations in mind, it was determined that the sample size (n) should include 245 patient records. To adjust the sample to a practical number, it was rounded up, resulting in a final sample size of 250.

For a comprehensive analysis, we consolidated the results from the 250 reports into a single category named “Physicians,” representing the aggregated findings of the 5 doctors involved in the study. Subsequently, we compared this category and the results from the GPT-3.5 and GPT-4 models with the reference dataset, considered as the ground truth. In this process, a confusion matrix was created for each report and comorbidity, from which several key statistical estimators were derived.

To assess the agreement, we used the κ index. The McNemar test was used to determine if there were significant differences in the proportions of discordance between the classifications. We chose the F-score as a measure of balance between precision and sensitivity, which is crucial in a classification model. The calculated metrics are presented in Table 2.

Table 2. Metrics used in the study with their descriptions.

Metric	Description
TP	True positives
TN	True negatives
FP	False positives
FN	False negatives
Sensitivity	TP/(TP+FN)
Specificity	TN/(FP+TN)
Precision	TP/(TP+FP)
Prevalence	(TP+FN)/(TP+TN+FP+FN)
Accuracy	(TP+TN)/(TP+TN+FP+FN)
Kappa	(P*obs*–P*esp*)/(1–P*esp*)
F-score	(2×precision×sensibility)/(precision+sensibility)
McNemar	Exact *P* value from McNemar test (binomial distribution)

XSL•FO
RenderX

For some of these metrics, we calculated their CI using the bootstrapping method [20]. This approach starts from the frequencies of true positives, true negatives, false positives, and false negatives to generate 1000 resamples. With these resamples, we recalculated the metrics to obtain a distribution that allows us to calculate the 95% CI.

Additionally, a detailed analysis was conducted on the groups of 50 reports assigned to each physician. This analysis focused on measuring the variability in evaluations among different physicians. For each patient and comorbidity, Cohen κ index was calculated in comparison with the ground truth for the results of each physician.

The reproducibility of the GPT-3.5 and GPT-4 models was assessed by quantifying the number of different responses for each patient and comorbidity across the 10 repeated analyses conducted on successive days.

Analysis of Discrepant Results

A detailed analysis of discrepancies between the evaluators' results and the established Ground Truth was conducted by the same physician who defined the reference dataset. This analysis covered each report with discrepancies in the identification of comorbidities, identifying the probable causes of each deviation.

Discrepancies were classified according to the nature of the detected errors (Textbox 3).

Textbox 3. Nature of the detected errors.

- **Differences in criteria:** Variations in the interpretation of the relevance of reported pathologies.
- **Incorrect interpretation:** Misunderstandings caused by confusing wording.
- **Incorrect inference:** Erroneous deductions when the comorbidity is not explicitly mentioned.
- **Ambiguous text:** Textual ambiguity that allows for multiple interpretations.
- **Error or hallucination:** Unjustified errors, attributed to human distractions or AI hallucinations.
- **Error in ground truth:** Corrections made upon review that validate the evaluator's interpretation.
- **Explicit omission:** Overlooking direct mentions of comorbidities.
- **Omission by context:** Failure to notice comorbidities deducible from the context or medication.
- **Unrecognized acronyms:** Inability to interpret specific medical acronyms.

Results

Cost and Time Analysis

Table 3 details the cost and total time invested in analyzing the 250 reports using the GPT-3.5 and GPT-4 models. Given that both the models and their associated costs can fluctuate over time, it is important to note that the reported results are specific to the usage period from January to February 2024. It is noted that GPT-4, being a larger and more complex LLM compared to GPT-3.5, incurs longer processing times and a cost approximately 10 times higher. Extrapolating the costs to the entire set of 7500 patients currently registered in our database, processing with GPT-4 would require about 24 hours and would cost approximately 76 dollars. On the other hand, using GPT-3.5 would reduce the processing time to about 9 hours, with a significantly lower cost of around 7 dollars.

Table 3. Execution times and costs in dollars for the analysis of the 250 reports with each of the models used (usage period of the models: between January and February 2024).

Model	N report	Time (hour)	Cost (US $)
gpt-3.5-turbo-1106	250	0.31	0.23
gpt-4-1106-preview	250	0.79	2.53

Prevalences

The analysis of our Ground Truth sample reveals a wide range of prevalences in comorbidities and lifestyle risk factors among oncological patients. These are detailed in Table 4, where both the number of cases and the prevalence for each comorbidity are reported. The most common conditions include high blood pressure and dyslipidemia, present in almost half and a third of the cases, respectively. On the other hand, conditions like hyperthyroidism and liver disease show relatively low prevalence. Categories related to smoking are also highly frequent, accounting for almost 50% of the cases. Interestingly, the proportion of ex-smokers significantly exceeds that of current smokers.

XSL•FO
RenderX

Table 4. Number of reports, out of the total 250 in the sample, that indicate each comorbidity and the corresponding prevalence.

Condition	Cases, n	Prevalence
Diabetes	64	25.6%
HBP[a]	116	46.4%
Smoker	37	14.8%
Dyslipidemia	77	30.8%
Hypothyroidism	21	8.4%
COPD[b]	17	6.8%
Depression	25	10.0%
Kidney disease	39	15.6%
Fentanyl	19	7.6%
Heart disease	43	17.2%
Hyperthyroidism	1	0.4%
Liver disease	13	5.2%
Dependent	12	4.8%
Ex-smoker	85	34.0%

[a]HBP: high blood pressure.

[b]COPD: chronic obstructive pulmonary disease.

Evaluation Metrics

Table 5 displays the values of true positives, false positives, true negatives, and false negatives, detailed by comorbidity, derived from the comparison with the ground truth dataset.

Figure 3 illustrates the performance of the physicians, GPT-3.5, and GPT-4 classifiers, broken down by comorbidity, across various metrics. The “Total” category, which consolidates the results for all studied comorbidities, enables direct comparison between the 3 evaluators on each assessed metric (Textbox 4).

The application of McNemar's test to the “Total” category, comparing Physicians with GPT-3.5 and Physicians with GPT-4, yielded P values of .79 and 10^{-6}, respectively. This confirms that the performance differences between the physicians and the GPT-3.5 model are not statistically significant, while the differences between the physicians and GPT-4 are significant.

XSL•FO
RenderX

Table 5. Tables displaying the results for true positives (TP), true negatives (TN), false positives (FP), and false negatives (FN) for each comorbidity, obtained by each of the evaluators (Physicians, GPT-3.5, and GPT-4).

	Physicians				GPT-3.5				GPT-4			
	TP[a]	TN[b]	FP[c]	FN[d]	TP	TN	FP	FN	TP	TN	FP	FN
Diabetes	63	185	1	1	54	186	0	10	63	186	0	1
HBP[e]	110	133	1	6	113	132	2	3	114	133	1	2
Smoker	37	209	4	0	36	212	1	1	36	213	0	1
Dyslipidemia	67	173	0	10	67	172	1	10	74	173	0	3
Hypothyroidism	19	229	0	2	19	229	0	2	20	227	2	1
COPD[f]	16	233	0	1	15	233	0	2	16	231	2	1
Depression	25	224	1	0	21	220	5	4	22	223	2	3
Kidney disease	15	211	0	24	21	211	0	18	38	208	3	1
Fentanyl	18	231	0	1	18	230	1	1	19	230	1	0
Heart disease	38	207	0	5	30	205	2	13	40	205	2	3
Hyperthyroidism	0	249	0	1	0	249	0	1	1	249	0	0
Liver disease	9	236	1	4	12	234	3	1	13	234	3	0
Dependent	12	234	4	0	11	238	0	1	10	238	0	2
Ex-smoker	76	165	0	9	85	161	4	0	85	163	2	0
Total	*505*	*2919*	*12*	*64*	*502*	*2912*	*19*	*67*	*551*	*2913*	*18*	*18*

[a]TP: true positive.

[b]TN: true negative.

[c]FP: false positive.

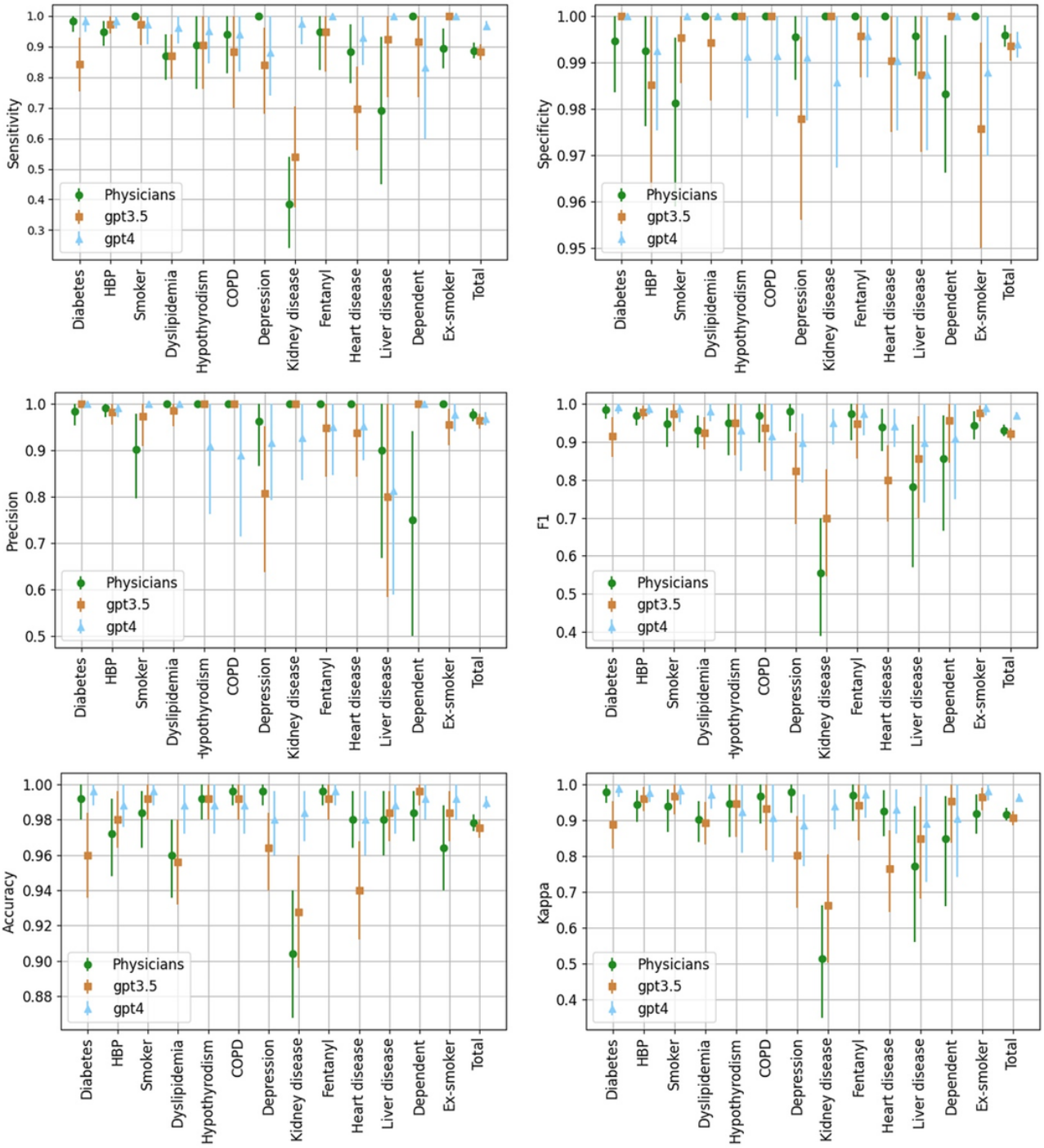
[d]FN: false negative.

[e]HBP: high blood pressure.

[f]COPD: chronic obstructive pulmonary disease.

XSL•FO
RenderX

Figure 3. Statistical metrics comparison between 3 evaluators (Physicians, GPT-3.5, and GPT-4) for individual comorbidities and overall totals. Asymmetric error bars indicate the 95% confidence interval. GPT: generative pre-trained transformer. HBP: hypertension or high blood pressure; COPD: chronic obstructive pulmonary disease.



XSL•FO
RenderX

Textbox 4. Summary of the metrics evaluated.

- **Sensitivity:** The GPT-4 model (96.8%) outperforms both GPT-3.5 (88.2%) and the physicians (88.8%) in most categories, showing notable effectiveness in detecting comorbidities. Although GPT-3.5 presents slightly lower results than the physicians, the difference is not statistically significant, as indicated by the overlap of the 95% confidence intervals shown in Figure 3.
- **Specificity:** All evaluators achieve high specificity values, which is expected given the low prevalences of the studied comorbidities and the relative ease of identifying the absence of a comorbidity in texts. The physicians (99.6%) excel in this metric, often achieving perfection, while both models (99.4%) score slightly lower due to a higher rate of false positives.
- **Precision:** The physicians get the highest score (97.7% vs 96.4% and 96.8%) assessing the proportion of correct positive identifications, possibly also influenced due to the models generating a higher number of false positives.
- **F-score:** Representing the harmonic mean between precision and sensitivity, the F-score is particularly relevant in asymmetric samples like in our study. The GPT-4 model achieves the highest score (96.8%) on this indicator, surpassing both GPT-3.5 (92.1%) and the physicians (93%).
- **Accuracy (Agreement):** In the proportion of correct identifications, GPT-4 shows superior performance (99%), while GPT-3.5 (97.5%) and the physicians (97.8%) achieve similar results.
- **Cohen κ index:** This index, measuring agreement adjusted for chance, reveals that GPT-4 reaches the highest scores (0.962), demonstrating greater consistency compared to the ground truth. The GPT-3.5 score of 0.907, while marginally lower, does not significantly differ from the physicians' score of 0.917.

Variability Among Physicians' Performance

Table 6 displays the Cohen κ index values obtained in the detection of various comorbidities for each of the 5 physician evaluators. It is important to note that each physician analyzed a different group of 50 reports.

Overall, there was considerable similarity in the physicians' responses, except when the comorbidity to be detected was a broader concept, as in the case of "kidney disease" (κ=0.51) or "liver disease" (κ=0.77). It is important to note that no further instructions or explanations were provided beyond finding the comorbidity in the presented text. Therefore, some physicians considered that renal lithiasis was not a relevant "kidney disease" and reserved this category for conditions describing an alteration in renal function (such as chronic renal failure, for example).

Interestingly, the senior physicians scored lower than the medical residents in the overall calculation for the κ index.

Table 6. Concordance values for each comorbidity, calculated using Cohen κ index for each medical evaluator. The "Total" categories summarize the aggregated concordance across all comorbidities and medical evaluators. A dash indicates that the κ index could not be computed because the comorbidity was not present in the corresponding set of reports.

	M1 senior	M2 resident	M3 senior	M4 senior	M5 resident	*Total human evaluators*
Diabetes	1.00	0.95	1.00	1.00	0.95	*0.98*
HBP[a]	1.00	0.96	0.83	0.96	0.96	*0.94*
Smoker	1.00	1.00	0.88	0.86	0.93	*0.94*
Dyslipidema	0.91	1.00	0.75	0.77	1.00	*0.90*
Hypothyrodism	0.66	1.00	0.90	1.00	1.00	*0.95*
COPD[b]	1.00	1.00	1.00	0.66	1.00	*0.97*
Depression	0.93	1.00	1.00	1.00	1.00	*0.98*
Kidney disease	0.52	0.70	0.45	0.56	0.26	*0.51*
Fentanyl	1.00	1.00	0.85	1.00	1.00	*0.97*
Heart disease	0.95	1.00	0.91	0.79	1.00	*0.93*
Hyperthyroidism	—	—	—	—	0.00	*0.00*
Liver disease	—	1.00	0.63	0.65	1.00	*0.77*
Dependent	0.66	0.66	0.91	0.88	—	*0.85*
Ex-smoker	0.95	1.00	0.87	0.76	1.00	*0.92*
Total	*0.95*	*1.00*	*0.87*	*0.76*	*1.00*	*0.92*

[a]HBP: high blood pressure.

[b]COPD: chronic obstructive pulmonary disease.

XSL•FO
RenderX

Reproducibility of Models' Responses

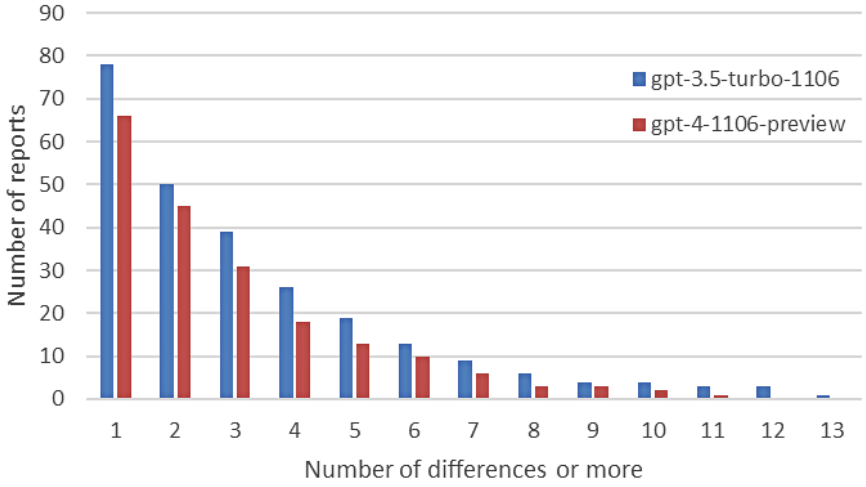
In our reproducibility study, each report was analyzed 10 times by the GPT-3.5 and GPT-4 models. For each comorbidity, we counted the number of different responses generated in these repeated analyses, as well as the total number of variations for each report.

Figure 4 presents a histogram illustrating the number of reports that generated at least the specified number of different responses. This histogram reveals that, in all instances, the GPT-4 model exhibited fewer differences in responses compared to GPT-3.5, suggesting greater consistency and reliability in its results.

Furthermore, it was found that 73.6% of the reports analyzed with GPT-4 reproduced the same result across all comorbidities during the 10 analyses, compared to 59.2% for GPT-3.5. This notable difference in reproducibility underscores the superiority of GPT-4 in maintaining consistency in its responses across multiple executions.

Variability in responses often stems from ambiguous text, where LLMs may assign values inconsistently. For example, a report describing a patient as an ”active smoker (1 month since quitting, 1 pack/day since age 14-16)“ resulted in GPT-3.5 identifying the patient as a smoker in 6 out of 10 analyses, while GPT-4 made only 1 error across 10 analyses. However, in the same report, regarding the comorbidity of COPD, GPT-4 shows a split: in 5 instances, it identifies it as present and in 5 as absent. The physician reviewing the results and establishing the ground truth determined the absence of COPD, as it is not explicitly mentioned in the report. Nonetheless, the mention of “mild pulmonary emphysema areas” and the patient's prolonged smoking history could lead GPT-4 to infer the presence of COPD.Top of Form

Figure 4. The number of reports for each model, in which at least the number of differences indicated on the x-axis was obtained in the 10 analyses.



Discrepancy Analysis

Multimedia Appendices 1 and 2 display the distribution of discrepant results categorized by the causes determined through a detailed manual analysis of the reports.

A notable discrepancy arose in the ”kidney disease“ category due to differences in criteria. Some physicians and GPT-3.5 did not deem certain renal pathologies, such as renal lithiasis, as relevant comorbidities in the context of oncology treatment, unlike GPT-4, which aligned its results more closely with the ground truth.

In analyzing cases interpreted as hallucinations, it was found that this phenomenon occurred exclusively in 1 response from GPT-4 and in 6 from GPT-3.5, particularly in the smoker and ex-smoker categories, possibly due to the use of the label “toxic habits,” even when referring to other habits like alcoholism.

The models, especially GPT-4, tend to infer comorbidities from the context or reported medication more frequently than physicians, who exhibit a more conservative approach. This tendency leads to more false positives by the models, particularly when the medication does not imply the presence of comorbidity.

GPT-3.5 exhibited difficulties in interpreting common medical acronyms such as “DM” for diabetes or “AF” for atrial fibrillation, whereas GPT-4 demonstrated a superior ability to recognize and correctly interpret most of these acronyms.

Interestingly, GPT-4 displayed some false positives when encountering comorbidity labels followed by “:” without additional information, a misinterpretation not common in humans but observed in AI, particularly in GPT-4 more than in GPT-3.5.

Human evaluators showed a greater tendency to overlook comorbidities explicitly reported, likely due to distraction or fatigue.

Only 3 errors were identified in the determination of the ground truth, underscoring the reliability of the review process.

Finally, we identified a category of discrepancies exclusive to the models, related to structural or formatting errors. This includes situations where the models' responses do not follow the guidelines specified in the prompt, resulting in outputs that do not meet the expected JSON format or that incorrectly alter and introduce comorbidity labels. Given that these incidents were limited, affecting less than 10 cases, it was decided to

XSL•FO
RenderX

manually correct these formatting errors for inclusion in the subsequent analysis.

Discussion

Principal Findings

Our study categorizes observers as ”Physicians,“ ”GPT-3.5,“ and ”GPT-4,“ reflecting the synergy between specific models (*gpt-3.5-turbo-1106* and *gpt-4-1106-preview*) and the prompts designed for this research. The effectiveness of GPT models in generating responses is inherently linked to the quality and structure of the prompts [14,21,22], indicating that results may vary significantly with prompt redefinition. Similarly, physician performance is influenced not only by clinical competence but also by the clarity of instructions and the quality of the materials provided. Offering more detailed and specific guidelines, along with access to additional sources within the electronic health records, could potentially improve the accuracy of their responses.

It is important to emphasize that even if LLMs demonstrate superiority in the specific task of processing large volumes of reports to extract information, this should not be extrapolated to other tasks, such as decision-making. In such cases, these tools should always be used as support tools, requiring ongoing physician oversight and intervention.

Based on the results obtained, we can conclude that the GPT-4 model is notably better at identifying present comorbidities, with fewer false negatives, while physicians exhibit slightly higher precision in their diagnoses, resulting in fewer false positives. The GPT-3.5 model generally performs slightly below the physicians, though the differences found are not statistically significant. These results are consistent with findings from other studies, such as Hoppe et al [23], which highlight the potential of ChatGPT models to enhance diagnostic accuracy in emergency medical settings. In their study, GPT-4 also outperformed both resident physicians and GPT-3.5 in diagnostic accuracy.

The superior sensitivity of GPT-4 in our study is particularly noteworthy, demonstrating its advanced ability to accurately identify reported comorbidities, even when not directly evident in the text. However, both GPT-3.5 and GPT-4 generate a comparable number of false positives, which is significantly higher than those recorded by physicians. Physicians' false positives typically result from specific circumstances such as ambiguity in clinical reports, variations in interpretation among professionals, and occasional errors in the template filling process.

In contrast, false positives from the GPT models seem to stem from a less conservative approach in determining comorbidity presence based on inferred context. These cases are also more likely to produce less reproducible responses due to the nondeterministic nature of LLMs. In these instances, physicians adopted a more conservative criterion to establish the ground truth, considering an unreported comorbidity only when the medication or context necessarily implied it. Whether this conservative approach is preferable to the criteria used by GPT models requires an analysis of complete medical histories to confirm or refute the presence of the comorbidity.

Discrepancies arising from variations in criteria interpretation could be mitigated by using prompts with clearer instructions on interpreting different comorbidities. This underscores the importance of refining prompts to enhance the consistency and accuracy of LLM-generated responses in clinical contexts.

Despite the remarkable capacity of current LLMs as potential tools for data mining in clinical reports, questions arise regarding the practical utility of this RWD for research and the generation of real-world evidence [24]. The variability, subjectivity, and lack of structure in these reports can compromise the quality and reliability of extracted data, affecting its applicability in clinical research contexts. Therefore, while LLMs represent a promising innovation to address the limitations of unstructured data, implementing more structured clinical recording practices could provide a more sustainable and reliable solution for generating real-world clinical evidence. This duality emphasizes the need for a balanced approach that integrates advanced AI technology with robust clinical data management practices.

Future research should concentrate on refining prompt design and expanding the applications of LLMs across various medical fields. Additionally, exploring the performance of new open-source LLMs that can be run locally is essential, as this approach helps to avoid data protection and privacy issues associated with transmitting clinical data outside of the local infrastructure.

Conclusions

This study has shown that, with carefully designed prompts, the OpenAI LLMs examined demonstrate competence comparable to, and in some cases superior to, that of medical specialists in interpreting and extracting relevant information from clinical reports, even when dealing with complex and ambiguously written texts. Considering their superior efficiency in terms of time and costs, along with their seamless integration with databases and other applications, these models emerge as a preferable option for data mining and structuring information in large collections of clinical reports. This highlights the potential of LLMs to enhance RWD usage by efficiently extracting structured information from extensive volumes of clinical texts, which is crucial for generating high-quality real-world evidence. Nonetheless, continuous evaluation of these models is essential to enhance their accuracy and applicability, while also emphasizing the importance of advancing toward more structured clinical records.

Acknowledgments

Data were pseudonymized by Andalusian Health Service technicians according to the GDPR (General Data Protection Regulation) regulation ensuring the technical and functional separation between the research team and those who perform the pseudonymization.

XSL•FO
RenderX

Authors' Contributions

AWZ and HMR contributed to study idea and design; CMS, DMC, MRJ, NURA, and CNN involved in data collection; data analysis and results interpretation were performed by HMR and AWZ; HMR and AWZ contributed to manuscript writing; critical review and editing were carried out by all authors. All authors approved the final manuscript.

Conflicts of Interest

None declared.

Multimedia Appendix 1
Number of false positive (FP) results attributed to each of the considered causes. Diff: differences; Inco: incorrect; Erro: error.
[PNG File , 27 KB - medinform_v13i1e58457_app1.png]

Multimedia Appendix 2
Number of false negative (FN) results attributed to each of the considered causes.
[PNG File , 29 KB - medinform_v13i1e58457_app2.png]

References

1. Liu F, Panagiotakos D. Real-world data: a brief review of the methods, applications, challenges and opportunities. BMC Med Res Methodol 2022 Nov 05;22(1):287 [FREE Full text] [doi: 10.1186/s12874-022-01768-6] [Medline: 36335315]
2. Yim WW, Yetisgen M, Harris WP, Kwan SW. Natural Language Processing in Oncology: A Review. JAMA Oncol 2016 Jun 01;2(6):797-804. [doi: 10.1001/jamaoncol.2016.0213] [Medline: 27124593]
3. Savova GK, Danciu I, Alamudun F, Miller T, Lin C, Bitterman DS, et al. Use of Natural Language Processing to Extract Clinical Cancer Phenotypes from Electronic Medical Records. Cancer Res 2019 Nov 01;79(21):5463-5470 [FREE Full text] [doi: 10.1158/0008-5472.CAN-19-0579] [Medline: 31395609]
4. Adamson B, Waskom M, Blarre A, Kelly J, Krismer K, Nemeth S, et al. Approach to machine learning for extraction of real-world data variables from electronic health records. Front Pharmacol 2023;14:1180962 [FREE Full text] [doi: 10.3389/fphar.2023.1180962] [Medline: 37781703]
5. Waskom ML, Tan K, Wiberg H, Cohen AB, Wittmershaus B, Shapiro W. A hybrid approach to scalable real-world data curation by machine learning and human experts. medRxiv 2023. [doi: 10.1101/2023.03.06.23286770]
6. Vaswani A, Shazeer N, Parmar N, Uszkoreit J, Jones L, Gomez AN, et al. Attention is All you Need? In Advances in Neural Information Processing Systems.: Curran Associates, Inc URL: https://tinyurl.com/3bh6m3xw [accessed 2024-02-22]
7. OpenAI, Achiam J, Adler S, Agarwal S, Ahmad L, Akkaya I, et al. GPT-4 technical report. arXiv:2303.08774 2023:1-100. [doi: 10.48550/arXiv.2303.08774]
8. Li L, Zhou J, Gao Z, Hua W, Fan L, Yu H, et al. A scoping review of using Large Language Models (LLMs) to investigate electronic health records (EHRs). arXiv:2405.03066 2024:1-45. [doi: 10.48550/arXiv.2405.03066]
9. Kresevic S, Giuffrè M, Ajcevic M, Accardo A, Crocè LS, Shung DL. Optimization of hepatological clinical guidelines interpretation by large language models: a retrieval augmented generation-based framework. NPJ Digit Med 2024 Apr 23;7(1):102 [FREE Full text] [doi: 10.1038/s41746-024-01091-y] [Medline: 38654102]
10. Landman R, Healey SP, Loprinzo V, Kochendoerfer U, Winnier AR, Henstock PV, et al. Using large language models for safety-related table summarization in clinical study reports. JAMIA Open 2024 Jul;7(2):ooae043 [FREE Full text] [doi: 10.1093/jamiaopen/ooae043] [Medline: 38818116]
11. Liu J, Wang C, Liu S. Utility of ChatGPT in Clinical Practice. J Med Internet Res 2023 Jun 28;25:e48568 [FREE Full text] [doi: 10.2196/48568] [Medline: 37379067]
12. Mumtaz U, Ahmed A, Mumtaz S. LLMs-Healthcare: current applications and challenges of large language models in various medical specialties. AIH 2024;1(2):16-28. [doi: 10.36922/aih.2558]
13. Fink MA, Bischoff A, Fink CA, Moll M, Kroschke J, Dulz L, et al. Potential of ChatGPT and GPT-4 for data mining of free-Text CT reports on lung cancer. Radiology 2023 Sep;308(3):e231362. [doi: 10.1148/radiol.231362] [Medline: 37724963]
14. Choi HS, Song JY, Shin KH, Chang JH, Jang B. Developing prompts from large language model for extracting clinical information from pathology and ultrasound reports in breast cancer. Radiat Oncol J 2023 Sep;41(3):209-216 [FREE Full text] [doi: 10.3857/roj.2023.00633] [Medline: 37793630]
15. Bertolet A, Wals A, Miras H, Macías J. Organic generation of real-world real-time data for clinical evidence in radiation oncology. Int J Med Inform 2020 Dec;144:104301 [FREE Full text] [doi: 10.1016/j.ijmedinf.2020.104301] [Medline: 33091831]
16. OpenAI Platform. URL: https://platform.openai.com [accessed 2024-02-22]
17. Jin Y, Chandra M, Verma G, Hu Y, De Choudhury M, Kumar S. Better to ask in english: cross-lingual evaluation of large language models for healthcare queries. arXiv:2310.13132 2023:1-18. [doi: 10.48550/arXiv.2310.13132]
18. Hendrycks D, Burns C, Basart S, Zou A, Mazeika M, Song D, et al. Measuring massive multitask language understanding. arXiv:2009.03300 2021:1-27. [doi: 10.48550/arXiv.2009.03300]

XSL•FO
RenderX

19. openaiAPIscript_forsharing. GitHub. URL: https://github.com/RFMacarena/openaiAPIscript_forsharing [accessed 2024-12-23]
20. Efron B, Tibshirani RJ. An Introduction to the Bootstrap. New York: Chapman and Hall/CRC; 1994:456.
21. Zaghir J, Naguib M, Bjelogrlic M, Névéol A, Tannier X, Lovis C. Prompt engineering paradigms for medical applications: scoping review and recommendations for better practices. arXiv:2405.01249 2024:1-29. [doi: 10.48550/arXiv.2405.01249]
22. Li J, Chen X, Wang L, Deng XW, Wen H, You M, et al. Are You Asking GPT-4 Medical Questions Properly? - Prompt Engineering in Consistency and Reliability With Evidence-Based Guidelines for ChatGPT-4: A Pilot Study. Durham, North Carolina: Research Square Platform LLC; 2023. [doi: 10.21203/rs.3.rs-3336823/v1]
23. Hoppe JM, Auer MK, Strüven A, Massberg S, Stremmel C. ChatGPT With GPT-4 outperforms emergency department physicians in diagnostic accuracy: retrospective analysis. J Med Internet Res 2024 Jul 08;26:e56110 [FREE Full text] [doi: 10.2196/56110] [Medline: 38976865]
24. Knevel R, Liao KP. From real-world electronic health record data to real-world results using artificial intelligence. Ann Rheum Dis 2023 Mar;82(3):306-311 [FREE Full text] [doi: 10.1136/ard-2022-222626] [Medline: 36150748]

Abbreviations

API: application programming interface
GPT: generative pretrained transformers
LLM: large language model
NLP: natural language processing
RWD: real-world data

Edited by A Castonguay; submitted 16.03.24; peer-reviewed by L Guo, D Hu, S Kresevic; comments to author 26.06.24; revised version received 10.09.24; accepted 21.10.24; published 02.01.25.

Please cite as:
Wals Zurita AJ, Miras del Rio H, Ugarte Ruiz de Aguirre N, Nebrera Navarro C, Rubio Jimenez M, Muñoz Carmona D, Miguez Sanchez C
The Transformative Potential of Large Language Models in Mining Electronic Health Records Data: Content Analysis
JMIR Med Inform 2025;13:e58457
URL: https://medinform.jmir.org/2025/1/e58457
doi:10.2196/58457
PMID:

©Amadeo Jesus Wals Zurita, Hector Miras del Rio, Nerea Ugarte Ruiz de Aguirre, Cristina Nebrera Navarro, Maria Rubio Jimenez, David Muñoz Carmona, Carlos Miguez Sanchez. Originally published in JMIR Medical Informatics (https://medinform.jmir.org), 02.01.2025. This is an open-access article distributed under the terms of the Creative Commons Attribution License (https://creativecommons.org/licenses/by/4.0/), which permits unrestricted use, distribution, and reproduction in any medium, provided the original work, first published in JMIR Medical Informatics, is properly cited. The complete bibliographic information, a link to the original publication on https://medinform.jmir.org/, as well as this copyright and license information must be included.

XSL•FO
RenderX

Original Paper

Development and Evaluation of a Mental Health Chatbot Using ChatGPT 4.0: Mixed Methods User Experience Study With Korean Users

Boyoung Kang[1], ME, MBA; Munpyo Hong[1], PhD

Sungkyunkwan University, Seoul, Republic of Korea

Corresponding Author:
Boyoung Kang, ME, MBA
Sungkyunkwan University
25-2, Sungkyunkwan-Ro, Jongno-gu
Seoul, 03063
Republic of Korea
Phone: 82 027401770
Email: bykang2015@gmail.com

Abstract

Background: Mental health chatbots have emerged as a promising tool for providing accessible and convenient support to individuals in need. Building on our previous research on digital interventions for loneliness and depression among Korean college students, this study addresses the limitations identified and explores more advanced artificial intelligence–driven solutions.

Objective: This study aimed to develop and evaluate the performance of HoMemeTown Dr. CareSam, an advanced cross-lingual chatbot using ChatGPT 4.0 (OpenAI) to provide seamless support in both English and Korean contexts. The chatbot was designed to address the need for more personalized and culturally sensitive mental health support identified in our previous work while providing an accessible and user-friendly interface for Korean young adults.

Methods: We conducted a mixed methods pilot study with 20 Korean young adults aged 18 to 27 (mean 23.3, SD 1.96) years. The HoMemeTown Dr CareSam chatbot was developed using the GPT application programming interface, incorporating features such as a gratitude journal and risk detection. User satisfaction and chatbot performance were evaluated using quantitative surveys and qualitative feedback, with triangulation used to ensure the validity and robustness of findings through cross-verification of data sources. Comparative analyses were conducted with other large language models chatbots and existing digital therapy tools (Woebot [Woebot Health Inc] and Happify [Twill Inc]).

Results: Users generally expressed positive views towards the chatbot, with positivity and support receiving the highest score on a 10-point scale (mean 9.0, SD 1.2), followed by empathy (mean 8.7, SD 1.6) and active listening (mean 8.0, SD 1.8). However, areas for improvement were noted in professionalism (mean 7.0, SD 2.0), complexity of content (mean 7.4, SD 2.0), and personalization (mean 7.4, SD 2.4). The chatbot demonstrated statistically significant performance differences compared with other large language models chatbots (F=3.27; P=.047), with more pronounced differences compared with Woebot and Happify (F=12.94; P<.001). Qualitative feedback highlighted the chatbot's strengths in providing empathetic responses and a user-friendly interface, while areas for improvement included response speed and the naturalness of Korean language responses.

Conclusions: The HoMemeTown Dr CareSam chatbot shows potential as a cross-lingual mental health support tool, achieving high user satisfaction and demonstrating comparative advantages over existing digital interventions. However, the study's limited sample size and short-term nature necessitate further research. Future studies should include larger-scale clinical trials, enhanced risk detection features, and integration with existing health care systems to fully realize its potential in supporting mental well-being across different linguistic and cultural contexts.

(JMIR Med Inform 2025;13:e63538) doi:10.2196/63538

KEYWORDS

mental health chatbot; Dr. CareSam; HoMemeTown; ChatGPT 4.0; large language model; LLM; cross-lingual; pilot testing; cultural sensitivity; localization; Korean students

XSL•FO
RenderX

Introduction

The COVID-19 pandemic has exacerbated the already concerning rates of depression and anxiety among college students worldwide [1,2]. In Korea, the situation is particularly alarming. Recent statistics highlight the severity of mental health issues among college students in this country. According to the "2021 COVID-19 National Mental Health Survey," individuals in their 20s showed the highest average depression score Patient Health Questionnaire-9 (PHQ-9) of 6.7 and the highest proportion of high-risk depression groups at 30% among all age groups surveyed. This represents a significant increase from 2018 when the average depression score was 2.3. The proportion of the high-risk depression group (PHQ-9 score ≥10) increased to 22.8% in 2021, approximately 6 times higher than in 2018.

Our previous study [3] on digital interventions for loneliness and depression among Korean college students highlighted the need for more personalized and culturally sensitive approaches, which this research aims to address. Among the initial 63 applicants in that study, the average PHQ-9 score was 9.23, with 25 (39.7%, 25/63) participants classified as high-risk for depression (PHQ-9 score ≥10). At the baseline of our study with 53 participants, 23 (43.4%, 23/53) were categorized as high-risk for depression. These findings underscore the urgent need for effective interventions to improve mental health among college students in Korea.

Despite the increasing severity of mental health issues among college students, the infrastructure and support systems within universities to effectively address these problems remain inadequate. In Korea, the annual mental health budget for college students is limited, with most of the resources focused on counseling services and little emphasis on preventive approaches (Counseling Council for University Students, Furthermore, due to the lack of professional counseling personnel and resources, access to services is limited, and many students are unable to receive timely and appropriate help [4,5].

Social stigma and prejudice against mental health issues also act as significant barriers for college students seeking help. Many students, despite experiencing psychological difficulties, tend to avoid help-seeking behaviors due to negative perceptions about psychiatric treatment or counseling [6]. This can exacerbate symptoms and prolong problems. In particular, those with low mental health literacy are less likely to recognize their condition or understand the need for professional intervention. In fact, the mental health literacy score of college students who participated in our previous study [3] averaged only 2.57 out of 5 points, highlighting the urgent need for educational intervention in this area.

In this context, digital technology-based mental health management solutions are gaining attention as a new alternative. Digital intervention services that overcome spatial and temporal constraints and ensure anonymity can contribute to improving accessibility and participation. Considering the high digital literacy of college students, these methods can be more familiar and acceptable to them [7]. Recent advancements in artificial intelligence (AI) and natural language processing (NLP) have paved the way for the development of sophisticated chatbots that can engage in human-like conversations and provide personalized support [2]. Large language models (LLMs), such as ChatGPT, have revolutionized the field of conversational AI. These models are trained on vast amounts of text data, enabling them to generate human-like responses and understand context. In mental health support, LLMs can be fine-tuned to provide empathetic responses, recognize emotional cues, and offer personalized support, making them potentially powerful tools for accessible mental health interventions.

Building upon the findings of our previous study [3], which explored the effectiveness of digital interventions for loneliness and depression among college students, this research aims to address the limitations identified in earlier digital interventions and develop a more effective and user-friendly mental health support tool. Specifically, this study focuses on the development and evaluation of an LLM-based chatbot prototype, named HoMemeTown, designed to provide personalized mental health support. The HoMemeTown chatbot, powered by ChatGPT 4.0, offers several unique features, that are (1) cross-lingual capability in English and Korean, ensuring cultural sensitivity, (2) a built-in gratitude journaling feature to promote positive thinking, (3) emotion recognition and empathetic response generation, and (4) risk detection algorithms to identify potential mental health crises.

These features aim to provide a comprehensive, user-friendly mental health support tool for young adults.

This pilot study was conducted as part of a larger research project titled "Development of a Youth Mental Health Platform Using Natural Language Processing." While the overarching project received initial institutional review board approval, we acknowledge that this specific chatbot experiment was added later due to rapid developments in AI technology. Despite this limitation, we maintained rigorous ethical standards throughout our research, including informed consent, data privacy measures, and risk mitigation strategies.

The primary objective of this study is to conduct an initial usability test of the chatbot prototype, providing valuable insights for future, more comprehensive clinical studies. While our sample size is limited, we have used a mixed methods approach, combining quantitative usability metrics with in-depth qualitative feedback. This approach allows us to gain rich insights into user experiences and chatbot performance, even with a smaller participant pool. In addition, we have conducted comparative analyses with existing digital mental health tools to contextualize our findings within the broader landscape of mental health technologies.

As we navigate the rapidly evolving landscape of AI and its potential to revolutionize mental health support, it is crucial to explore innovative solutions that can bridge the gap between technology and human empathy [8]. This pilot study contributes to the growing body of knowledge surrounding the use of AI in mental health and sheds light on the potential of LLM-based chatbots like HoMemeTown to make a positive impact on people's lives, while also identifying areas for future research and development.

XSL•FO
RenderX

Methods

Study Design and Participants

This pilot study used a mixed methods approach to evaluate the HoMemeTown chatbot's usability and effectiveness in providing mental health support. In total, 20 participants (12 female and 8 male) aged 18-27 (mean 23.3, SD 1.96) years were recruited through university email lists and social media advertisements. The sample size was determined to be appropriate for this pilot study, particularly given that 70% (14/20) of participants had previous experience with mental health chatbots from our previous research [3], providing valuable comparative insights. This continuity in participation enhanced our ability to gather meaningful longitudinal observations about user engagement with mental health technologies.

Participant eligibility criteria were established to ensure appropriate sampling while maintaining ethical considerations. Eligible participants included university students aged 18-27 years with Korean language proficiency and access to digital devices. We excluded individuals with severe mental health conditions requiring immediate professional intervention, as determined through initial screening questionnaires. This exclusion criterion was implemented to ensure participant safety and appropriate levels of support, following established ethical guidelines in digital mental health research [9].

Prototype Development Using the ChatGPT Application Programming Interface

The HoMemeTown chatbot is an innovative web-dependent service designed to support users in cultivating gratitude practice and providing emotional support through engaging, personalized interactions [10]. By leveraging cutting-edge NLP and emotion detection technologies, the HoMemeTown chatbot creates a unique and rewarding user experience that encourages regular engagement and promotes mental well-being [11].

The development process involved several key steps, including server setup, domain acquisition, Secure Sockets Layer certification, screen planning, development method selection, application programming interface (API) integration, front-end and back-end development, database design, performance tuning, and additional feature implementation [12].

The chatbot relies on the GPT API, a general-purpose language model provided by OpenAI, instead of a domain-specific model trained for mental health counseling. The GPT API offers a range of models, such as Davinci, GPT-3.5, and GPT-4, which can be selected based on desired performance and cost considerations. The chatbot relies on the GPT API, a general-purpose language model provided by OpenAI, instead of a domain-specific model trained for mental health counseling. The GPT API offers a range of models, such as Davinci, GPT-3.5, and GPT-4, which can be selected based on desired performance and cost considerations.

Rate limiting and resource management are (1) maximum 4,000,000 tokens per minute processing capacity, (2) up to 5000 requests per minute, (3) implementation of a request queuing system to prevent rate limit exceedance, and (4) monthly budget monitoring and automated alerts for cost control.

These technical constraints were carefully managed to ensure consistent service delivery while maintaining cost-effectiveness. Regular monitoring of API performance and reliability metrics helped optimize the system's operation throughout the study period.

The desired functionalities of the chatbot, such as its role as a counselor and its ability to detect risks, are implemented through the use of prompts [8]. However, due to the nature of the GPT model, there is no guarantee that the chatbot will always behave exactly as intended, as its responses may vary slightly even with the same prompt [7].

Figure 1 illustrates the service flow architecture of the HoMemeTown chatbot. The architecture depicts the user's journey, starting from the login process through the user interface on their PC. After logging in, users can access the gratitude journal section, where they can find a guide on "How to write gratitude journal" and proceed to write their own entries [13]. The system assigns a unique session number to each journaling session and securely saves the user's journal entries along with metadata such as the gratitude journal count, detected tokens or keywords, expressed emotions, and word count [14].

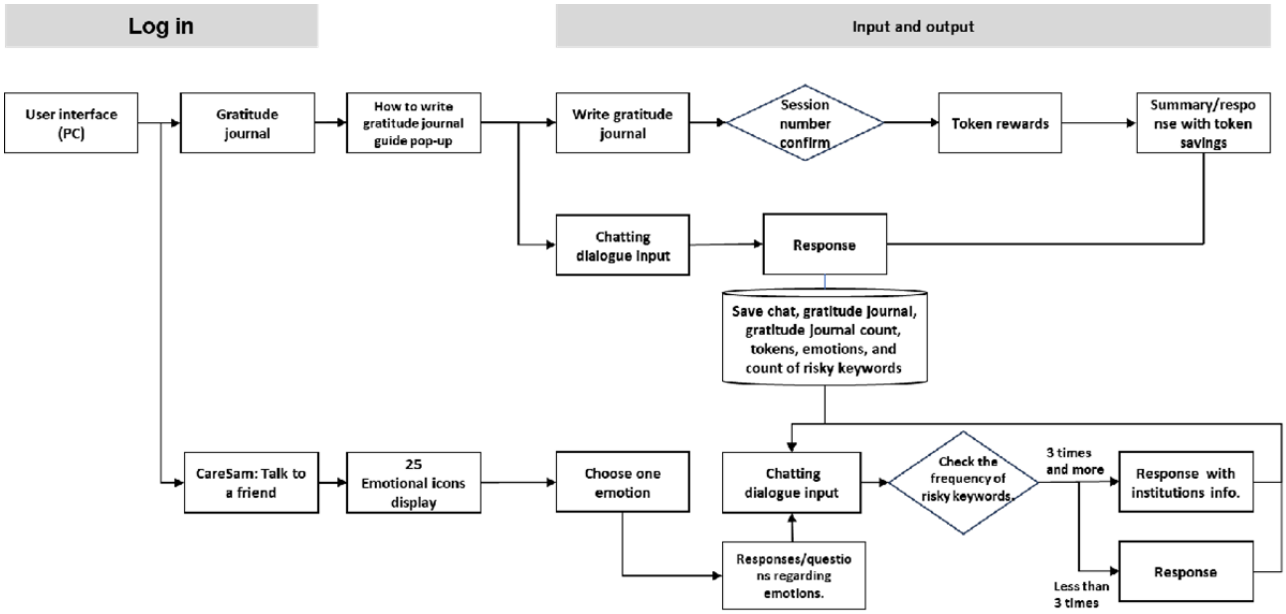
Users are rewarded with token rewards upon completing a journal entry, and the system generates a personalized response acknowledging their entry [4]. They can then continue their gratitude practice by initiating a new chat through the "CareSam: Talk to a friend" option. This feature allows users to select an emotion from a set of 25 emotional icons and provide more context about their feelings. Cowen and Keltner's [15] research on emotional classification inspired the inclusion of these icons. Recognizing these 25 unique emotions can help users cultivate greater self-awareness and sensitivity toward others, leading to increased empathy, connection, and understanding.

The HoMemeTown chatbot aims to encourage and motivate users to cultivate gratitude practice by providing a seamless user flow, personalized responses, and emotional attunement.

The HoMemeTown chatbot is currently accessible as an open web application. This pilot version is available for public testing, allowing anyone to interact with the chatbot and experience its features firsthand. The chatbot's continued operation demonstrates our commitment to transparency and ongoing exploration of digital mental health interventions. This open access approach enhances research reproducibility and provides opportunities for continuous feedback and improvement.

XSL•FO
RenderX

Figure 1. Service Flow Architecture of the HoMemeTown chatbot.



Technical Implementation and Server Architecture

The HoMemeTown chatbot operates on a cloud infrastructure that prioritizes privacy through a "privacy by design" approach. The key technical feature is that no personal data or chat history is stored, making the system completely stateless between sessions (Textbox 1).

This minimalist architecture was specifically chosen to eliminate privacy concerns by avoiding any form of user data collection or storage. The system operates on a request-response basis, where each interaction is treated as a new session without any historical context or user identification. This approach, while limiting some personalization features, ensures maximum privacy protection for users engaging with mental health support services [16].

Textbox 1. Server architecture.

Frontend development

- React.js framework for responsive user interface
- Material-UI component library for consistent design
- WebSocket implementation for real-time chat functionality
- Client-side-only session management with no persistent storage

Backend infrastructure

- Node.js runtime environment with Express.js framework
- Stateless architecture with no database implementation
- Direct application programming interface (API) integration with OpenAI's GPT-4
- Nginx reverse proxy for load balancing

OpenAI API integration

- Implementation of GPT-4 API with custom prompt engineering
- No retention of conversation history
- Each interaction is processed as a new, independent session
- Response token limiting for cost optimization
- Regular monitoring of API performance and reliability

User-Centered Design and Emotion Monster Selection

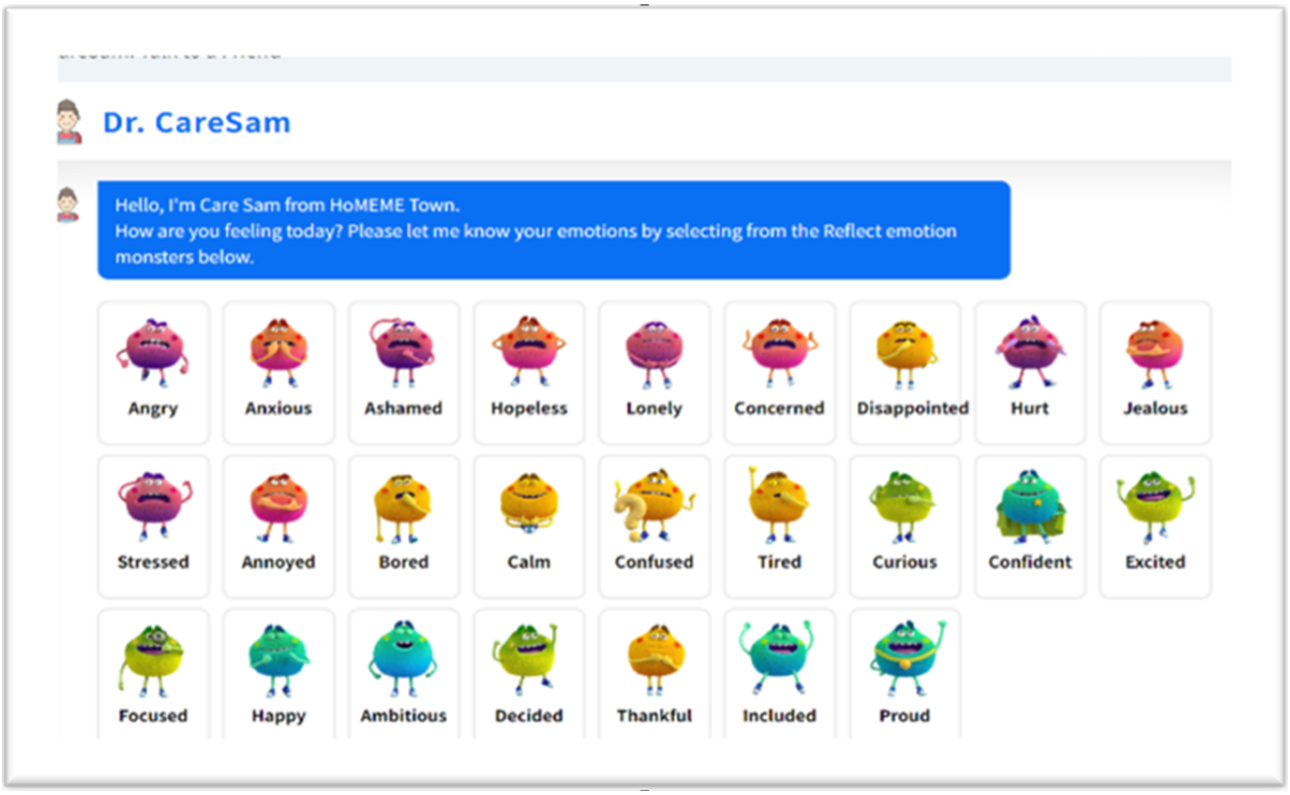
The chatbot targets young adults, particularly university students aged 18-27 years. It uses a set of 25 emoticons based on emotion recognition research [15]. These emoticons allow users to express a wide range of emotions, similar to a broader palette of colors enhancing artistic appreciation. Recognizing this wider range of emotions can lead to greater self-awareness and sensitivity toward others, ultimately fostering empathy, connection, and understanding. When a user selects an emotion

XSL•FO
RenderX

monster, a message appears on the chat screen stating their current mood. However, this message is not directly sent to the API. Instead, it is arbitrarily generated to include the selected emotion keyword and appear natural in the chat context. The actual message sent to the API is a combination of prompts, such as: "My current emotion is" + emotionText + "Acknowledge my feelings and greet me with a message of 50 characters or less." The GPT engine receives this prompt-based message and generates a response reacting to the user's selected emotion.

Figure 2 displays the 25 emotional icons used in the HoMemeTown chatbot. Inspired by Microsoft's emotion monsters, these icons represent a wide range of human emotions, allowing users to select one that reflects their current mood. This selection facilitates a more personalized and emotionally attuned response from the chatbot.

Figure 2. Emotional icons are used in the HoMemeTown chatbot.



Cross-Lingual Dialogue Development

The HoMemeTown chatbot was developed to support both English and Korean languages to cater to a wider audience. While our primary participants were Korean university students with intermediate to upper-intermediate English proficiency (based on self-reported language skills and academic records), they were able to effectively evaluate both language versions. The English version received higher ratings specifically in terms of written expression quality, though overall satisfaction levels were comparable between the 2 versions. This may be attributed to the more straightforward nature of emotional expression in English compared with the complex honorific system in Korean, as noted in our language-specific challenges.

In addition to our main study, we conducted informal preliminary feedback sessions with a native English speaker (not included in the formal participant count of 20). This native speaker reported high satisfaction with the natural flow and cultural appropriateness of the English version. While this supplementary feedback was exploratory in nature and limited in scope, it provided valuable initial insights into the cross-cultural applicability of our system.

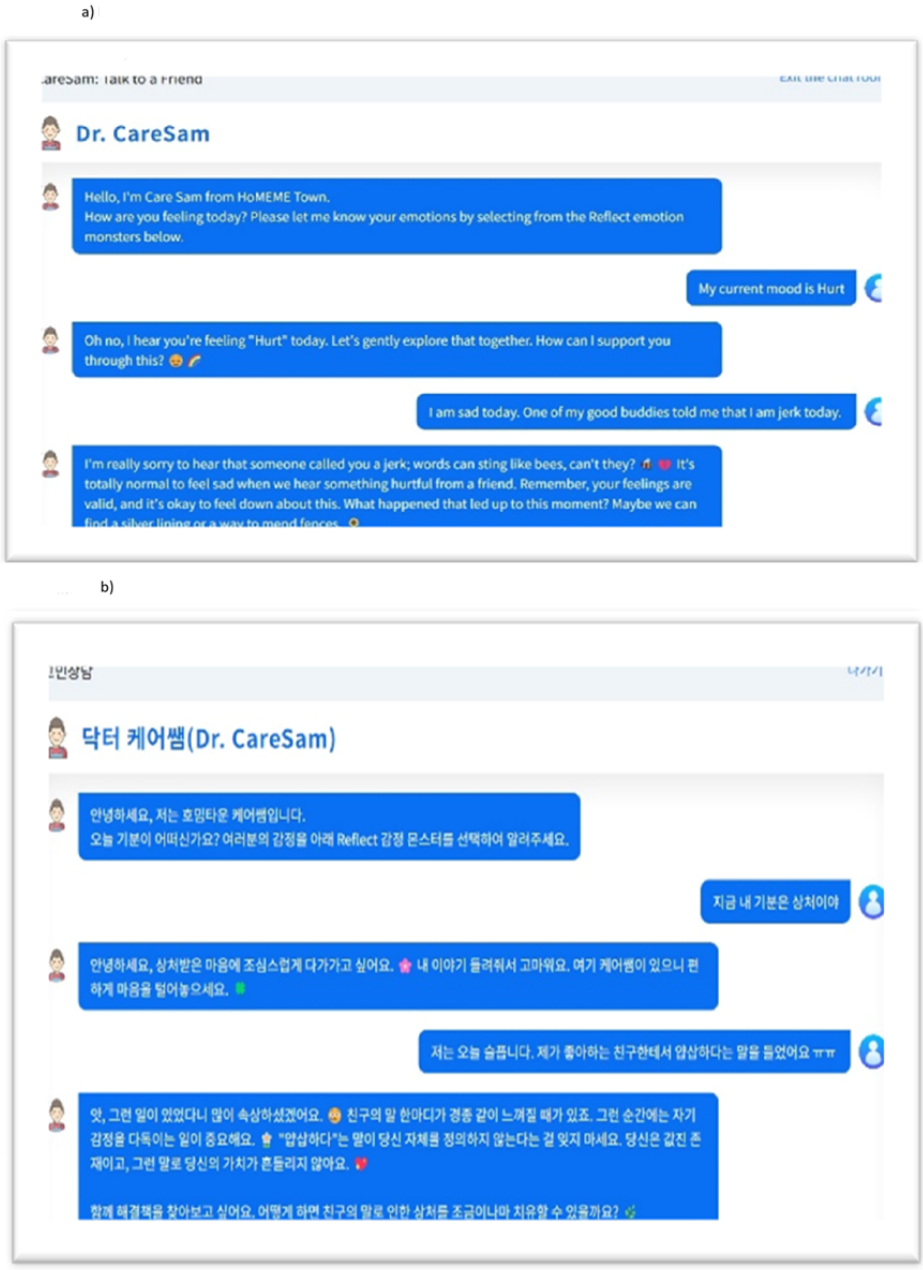
The localization process involved adapting the chatbot's dialogue to ensure natural conversation flow, accurate language translation, and cultural sensitivity [17]. The HoMemeTown chatbot was developed to support both English and Korean languages to cater to a wider audience. The localization process involved adapting the chatbot's dialogue to ensure natural conversation flow, accurate language translation, and cultural sensitivity [17].

Figure 3 illustrates the dialogue flow localization process for both English and Korean versions of the HoMemeTown chatbot. This visual representation demonstrates how the chatbot's responses are adapted to maintain natural conversation flow and cultural appropriateness in each language.

The localization process is dialogue localization, language-specific challenges, and emoji usage.

XSL•FO
RenderX

Figure 3. Dialogue flow localization. A: English version; B: Korean version.



Dialogue Localization

The chatbot's dialogue was adapted for both English and Korean languages, taking into account language structure, emoji usage, and cultural expressions. The localization process aimed to maintain the chatbot's empathetic and supportive tone while ensuring coherence and readability in each language. During the prompt tuning process, efforts were made to make the chatbot's responses more flexible and engaging, particularly in the Korean version. For example, when a user expresses feeling down and asks for something fun to do, the Korean chatbot is tuned to provide humorous and entertaining responses, similar to the English version, instead of giving a rigid, therapist-like response.

Language-Specific Challenges

The Korean localization posed unique challenges due to its agglutinative nature and honorific system. In the Korean version of the HoMemeTown chatbot, Microsoft's emotion adjectives were translated into Korean abstract nouns, such as "상처" (hurt), "외로움'"(lonely), "소속감" (inclusive), "실망" (disappointed), and "지루함" (bored). To maintain a consistent rule, these abstract nouns were combined with the verb ending "iya" (이야). However, this approach led to some awkward expressions, such as "상처이야" (hurt) and "자랑이야" (proud), while others, like "실망이야" (disappointed), "외로움이야" (lonely), and "지루함이야" (bored), sounded more natural. This inconsistency in the naturalness of the expressions highlights the complexity of the Korean language and the challenges in developing a chatbot that can generate linguistically accurate and culturally appropriate responses. Although collaborating with native Korean speakers and

XSL•FO
RenderX

linguists helped ensure grammatical accuracy and appropriate honorific usage, further improvements are necessary to fully address the unique challenges posed by the Korean language, such as refining the translations and developing more sophisticated language-specific tuning techniques [17].

Emoji Usage

Emojis were strategically incorporated into both English and Korean dialogues to convey emotions and soften the tone of the conversation. The Korean dialogue used emojis more frequently to align with cultural communication preferences.

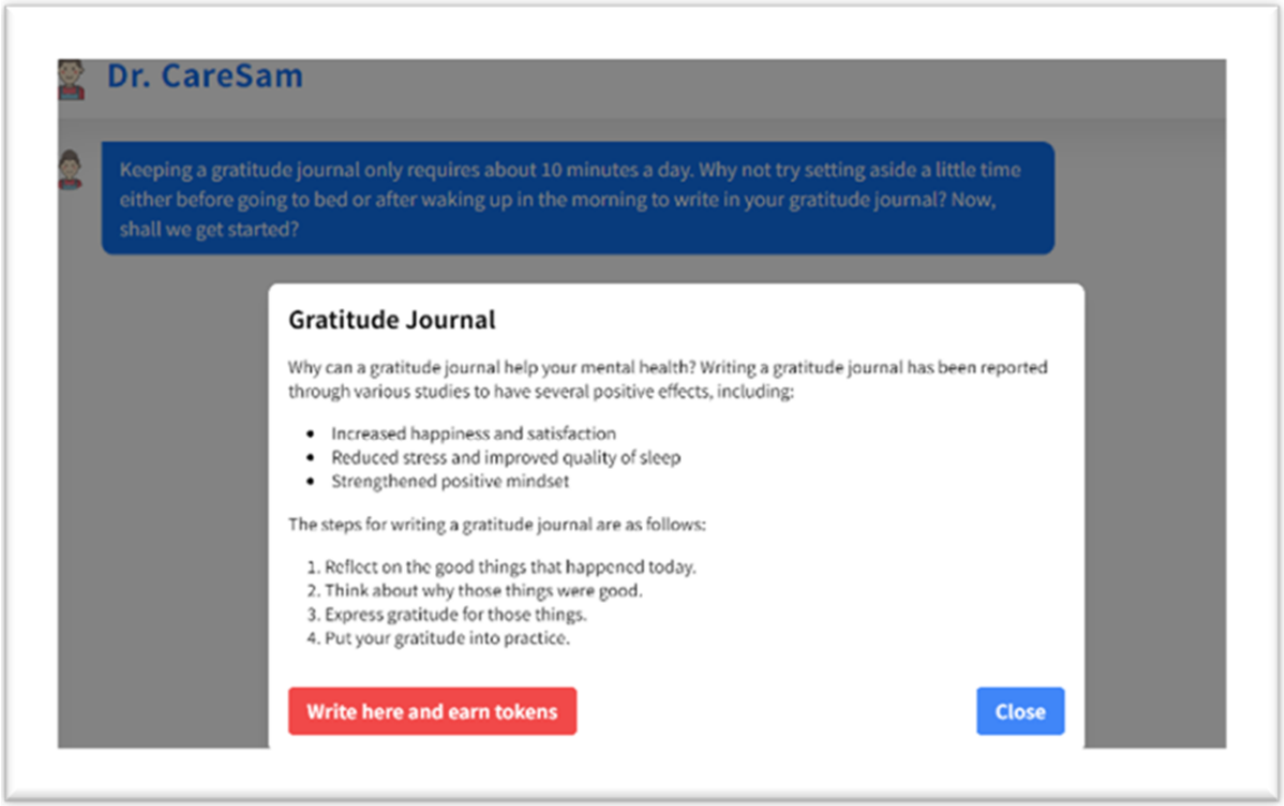
Gratitude Journal

The gratitude journal feature was included in the prototype version based on positive feedback from our previous study [3]. In the previous year's experiment, many students mentioned it as one of the most satisfying and enjoyable aspects of the app. Unlike the previous year's app, where explanations of the effects and simple procedures for writing a gratitude journal were often omitted in Woebot and Happify, the user interface of the HoMemeTown chatbot's gratitude journal includes a description of its effects and the procedure for using it.

The effects and procedures were based on established research [18], and the benefits of gratitude journaling have been demonstrated in numerous studies [13,14]. Users accumulate tokens for completed gratitude journal entries, viewable in their interface. To facilitate admin tracking of multiple user accounts, an admin page is implemented, allowing administrators to view gratitude journal entries, token balances, and chat frequencies for all user accounts.

Figure 4 illustrates the gratitude journal interface in the HoMemeTown chatbot. The interface includes a description of the benefits of gratitude journaling and a step-by-step guide on how to write a gratitude journal entry. This feature encourages users to reflect on positive experiences, express gratitude, and cultivate a more optimistic mindset. Upon completing a journal entry, users are rewarded with tokens, which are displayed in the top-right corner of the chat interface.

Figure 4. Gratitude journal interface in the HoMemeTown chatbot.



Risk Detection and Response System

The risk detection system in HoMemeTown was developed based on established clinical guidelines [19] and validated screening tools [20], implementing a sophisticated approach to identifying and responding to potential mental health concerns. The system continuously monitors user interactions for primary risk indicators, including expressions of suicidal ideation, severe depression symptoms, and anxiety crisis signals, while also tracking secondary indicators such as sleep disturbance patterns and social withdrawal signs.

When potential risks are detected, the system implements a graduated response protocol that has been carefully designed to provide appropriate levels of support while avoiding unnecessary escalation. For mild risk situations, the system offers empathetic acknowledgment and self-help resources, drawing from evidence-based interventions [21]. In cases of moderate risk, the response includes more direct expressions of concern and specific mental health resources, while severe risk triggers an immediate crisis response protocol with direct connections to professional support services.

XSL•FO
RenderX

To address the challenge of potential false positives in risk detection, we implemented a sophisticated validation system that examines multiple contextual factors before triggering interventions. This system uses NLP techniques to analyze the broader context of user communications, helping to distinguish between casual expressions and genuine indicators of distress. Regular professional review of high-risk cases ensures the ongoing refinement of detection algorithms and response protocols, maintaining a balance between sensitivity and specificity in risk assessment.

The risk detection and response system undergoes continuous evaluation and improvement based on user feedback and system performance metrics. Professional mental health experts regularly review the system's performance, leading to protocol updates that reflect emerging best practices in digital mental health support. This iterative improvement process has been shown to enhance the accuracy and effectiveness of automated mental health support systems [22].

In addition, to mitigate variability and potential errors in LLM responses, we introduced a validation process including semantic consistency checks, medical reference verification, and automatic escalation to human review when necessary, ensuring responses remain clinically appropriate and user safety is maintained.

Our implementation of these technical and clinical safeguards reflects a balanced approach to leveraging AI capabilities while maintaining high standards of user safety and support quality. The system's architecture and protocols were designed to be scalable and adaptable, allowing for continuous improvement based on ongoing research in digital mental health interventions. The HoMemeTown chatbot incorporates a risk detection function to identify potential mental health concerns through user interactions. This feature is based on the *DSM-5* (*Diagnostic and Statistical Manual of Mental Disorders* [Fifth Edition]) criteria [19] and a Korean corpus of psychopathological symptoms [20], allowing for culturally sensitive risk assessment.

The system monitors key symptoms such as depressed mood, changes in appetite or weight, sleep disturbances, fatigue, feelings of worthlessness, cognitive difficulties, and thoughts of death or suicide. When 3 or more symptoms are detected, the chatbot activates a response protocol to encourage professional help-seeking and provide relevant resources. As shown in Table 1, the response strategies are carefully adapted for cultural appropriateness in both English and Korean versions, with particular attention to different cultural norms in discussing mental health concerns.

In Table 2, it shows the differences that reflect the cultural variations in addressing mental health issues, highlighting the importance of culturally sensitive AI development in mental health applications. The use of emojis, while more prevalent in the Korean version, serves to soften the tone and enhance emotional expression in both languages, aligning with digital communication norms among young adults.

Table 1. Comparison of English and Korean chatbot versions.

Characteristic	English version	Korean version
Conversation style	Indirect, supportive	Direct, information-focused
Emotional approach	In-depth emotion exploration	Acknowledge emotions, quick transition
Introduction of professional help	Gradual	Immediate
Risk assessment method	Subtle progression	Explicitly stated
Cultural nuance	Emphasis on individual feelings	Focus on practical solutions

Table 2. Example risk detection responses with cultural adaptations.

Risk level	English response	Korean response
Mild	"I notice you're having a tough day Would you like to talk about what's bothering you? "	"요즘 마음이 무거워 보이네요 함께 이야기 나누면 도움이 될 수 있어요 "
Moderate	"It sounds like you're going through a difficult time Have you considered talking to someone who can help? I can suggest some resources if you'd like "	"힘들어하시는 모습이 느껴져요 전문가와 상담해보는 건 어떠실까요? 제가 도움이 될 만한 정보를 알려드릴 수 있어요 "
Severe	"I'm very concerned about what you're sharing There are people available 24/7 who want to support you. Would you like the contact information for immediate help? "	"많이 걱정되는 이야기네요 24시간 언제든 도움을 받으실 수 있는 곳이 있습니다. 지금 바로 연락하실 수 있는 곳을 알려드릴까요? "

Ethical Considerations

This study was designed as an initial usability test of the HoMemeTown chatbot prototype, focusing on user experience and potential effectiveness. While it does not constitute a full-scale clinical intervention, we adhered to strict ethical guidelines for research involving human participants.

The study was conducted as part of a larger research project titled "Development of a Youth Mental Health Platform Using

XSL•FO
RenderX

Natural Language Processing." While the overarching project received initial institutional review board approval from Sungkyunkwan University (2023-02-043-004; February 27, 2023, to June 26, 2025), we acknowledge that this specific chatbot experiment was added later due to rapid developments in AI technology. Despite this limitation, we maintained rigorous ethical standards throughout our research, including informed consent, data privacy measures, and risk mitigation strategies.

Before the usability test, all participants were provided with a comprehensive informed consent form. This form detailed the nature and purpose of the study, the procedures involved, potential risks and benefits, and the measures taken to ensure confidentiality and data protection. Participants were required to sign this form to confirm their understanding and voluntary agreement to participate.

Approximately 70% of the participants in this study had previously participated in our earlier experiment [3]. This continuity helped streamline the consent process as these participants were already familiar with the ethical standards and procedures in place for digital mental health research.

Data Security and Privacy

To address privacy concerns and protect sensitive information, the public version of the HoMemeTown chatbot operates without user registration or login requirements, collecting no personal information beyond chat interactions. This approach enhances user privacy but limits personalization features. For the usability test in this study, we implemented stringent data security measures, which are (1) all collected data (chat logs, gratitude journal entries, token rewards) were anonymized, (2) data were stored on secure, encrypted servers with restricted access, and (3) no personally identifiable information was linked to chatbot interactions or survey responses.

We incorporated a risk detection function to identify potential mental health crises and provide appropriate resources when necessary. These measures align with best practices in digital health research, ensuring ethical compliance and participant protection while advancing AI-assisted mental health support. Future developments will explore balancing personalization benefits with privacy protection, possibly through advanced encryption methods or privacy-preserving technologies.

Results

Overview

We conducted a mixed methods study to evaluate the performance and user satisfaction of our HoMemeTown Dr CareSam chatbot. The study design integrated quantitative and qualitative approaches to provide comprehensive insights: 8 quantitative questions (1 overall satisfaction item and 7 components of chatbot performance) and 4 qualitative questions (2 positive aspects and 2 areas for improvement). This mixed methods approach allowed for triangulation of data through cross-verification between quantitative metrics and qualitative user feedback, enhancing the validity and depth of our findings. The results provide multifaceted insights into the chatbot's strengths, areas for improvement, and comparative performance with other LLM and digital therapy chatbots.

Participants

The study included 20 participants aged 18 to 27 (mean 23.3, SD 1.96) years with 60% (12/20) female and 40% (8/20) male. Participants were recruited through university email lists and social media advertisements. All participants provided informed consent.

Quantitative Findings

The usability and satisfaction evaluation of the Dr CareSam counseling chatbot was conducted using a comprehensive survey consisting of 1 overall satisfaction question and 7 quantitative items assessing key components of effective psychological counseling, which consists of empathy, accuracy and usefulness, complex thinking and emotions, active listening and appropriate questions, positivity and support, professionalism, and personalization. Users generally expressed positive views, with positivity and support receiving the highest score on a 10-point scale (mean 9.0, SD 1.2), followed by empathy (mean 8.7, SD 1.6) and active listening (mean 8.0, SD 1.8). These findings align with previous research on the importance of empathy and support in mental health chatbot interactions. However, areas for improvement were noted in professionalism (mean 7.0, SD 2.0), complexity of content (mean 7.4, SD 2.0), and personalization (mean 7.4, SD 2.4), indicating potential avenues for future development to enhance user engagement and satisfaction.

Figure 5 shows the distribution of scores for various usability questions. The boxes represent the IQR, and the whiskers extend to the minimum and maximum values within 1.5 times the IQR. Black dots represent the mean values for each category.

To provide a more comprehensive understanding of the evaluation factors and their theoretical foundations, we present the following in Table 3.

This comprehensive evaluation framework enables a nuanced assessment of the chatbot's performance across key dimensions of effective counseling. The results provide valuable insights into the strengths of the Dr CareSam chatbot, particularly in areas of empathy and support. In addition, the findings highlight opportunities for improvement in professionalism, personalization, and complexity of responses, suggesting potential avenues for future development to enhance user engagement and satisfaction.

XSL•FO
RenderX

Figure 5. Box plot of scores for Dr CareSam usability questions.

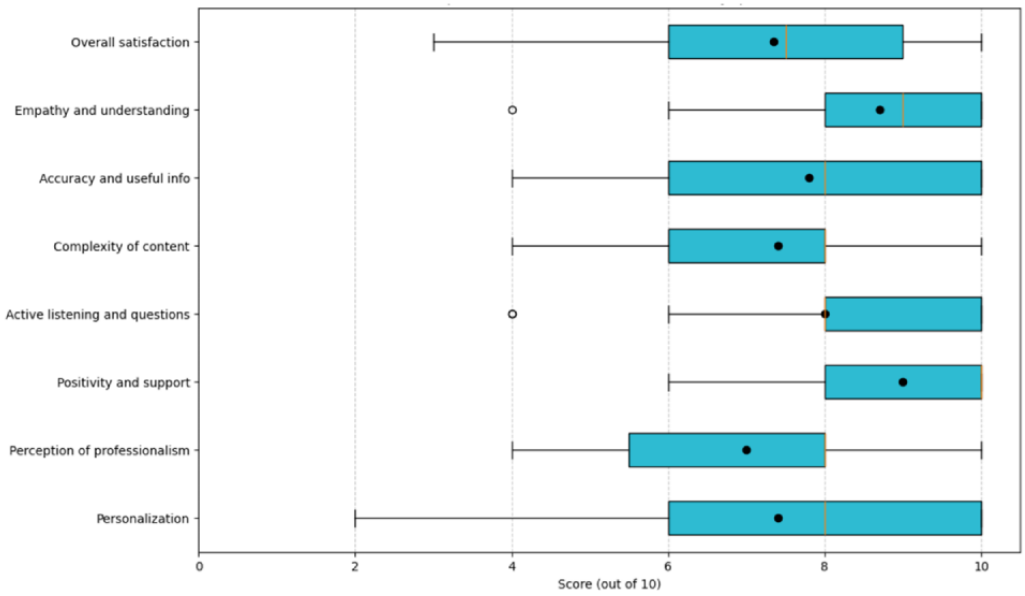


Table 3. Evaluation Factors for Dr CareSam chatbot.

Evaluation factor	Question	Description	Previous studies
Empathy	Did CareSam's responses express empathy and understanding of the user's question?	An empathetic understanding of the client's emotions and experiences is essential in effective counseling conversations.	Rogers [23], Elliott et al [24]
Accuracy and usefulness	Did CareSam's responses provide accurate and useful information regarding the user's question?	Providing accurate and actionable information aids in problem-solving and decision-making for the client.	Hepworth [25], Egan [26]
Complex thinking and emotions	Did CareSam's responses include complex thinking and emotions rather than simple knowledge?	Skilled counselors should address cognitive and emotional experiences interactively, facilitating insights into the client's internal experiences.	Greenberg [27], Gendlin [28]
Active listening and appropriate questions	Did CareSam's responses include not only active listening but also appropriate questions?	Active listening and appropriate questioning techniques promote self-exploration and deeper understanding.	Weger et al [29], Hill [30]
Positivity and support	Did CareSam's responses include positivity and support?	Support and encouragement enhance the client's self-esteem and motivation for change.	Mearns and Thorne [31], Norcross and Lambert [32]
Professionalism	Did CareSam's responses demonstrate professionalism?	Professionalism increases client trust and adherence to treatment, encompassing theoretical knowledge, clinical experience, and ethical awareness.	Sue and Sue [33]; Ratts et al [34]
Personalization	Did CareSam's responses appear to be customized?	Effective counseling should be tailored to the individual characteristics and needs of the client.	Norcross and Wampold, [35], Beutler and Harwood [36]

Qualitative Feedback

User feedback presented in Table 4 was collected through structured interviews and open-ended survey responses, focusing on key themes such as response speed, empathy, and personalization. Responses were categorized based on frequency of mention, providing a clear overview of commonly reported strengths and areas for improvement. User feedback confirms the chatbot's strengths in providing detailed, empathetic responses, a user-friendly interface, and a supportive demeanor. However, areas for improvement include slow response times, Korean text flow issues, and repetitive interactions. Interestingly, both "quick feedback" and "slow response time" were frequently mentioned, suggesting that while feedback is relevant and timely within the context of a rule-based chatbot, it may not be the fastest possible response.

The qualitative themes align with quantitative satisfaction ratings, illustrating consistent patterns across user experiences. For instance, high ratings for "positivity and support" were reflected in user comments praising Dr CareSam's empathetic responses. Conversely, lower ratings in "personalization" corresponded with feedback indicating a desire for more tailored interactions.

XSL•FO
RenderX

Table 4. Users' experiences of good and bad points for HoMemeTown chatbots.

Mention level and category	Positive points	Negative points
Most mentioned		
Response speed	Quick responses and real-time feedback.	Slow response time, lack of prompt responses.
Friendly and Positive Tone	Encouraging, supportive responses, provides courage and understanding.	Overemphasis on empathy, repetitive responses without practical advice.
Frequently mentioned		
Empathy capability	Expresses understanding and empathy effectively.	Focused too heavily on empathy without specific guidance or solutions.
Korean language processing	Supports English and Korean; human-like, natural conversation flow.	Awkward phrasing in Korean, lack of accuracy and appropriateness in Korean responses.
Moderately mentioned		
Detailed expression	Uses varied emotions and appropriate emoticons.	Repetitive tone, lack of personalization.
Chatbot functionality	Emotional expression, gratitude journaling guidance, diverse responses for different situations.	Limited content, need for features like a reward for engagement, and the option to revisit previous interactions.
Less mentioned		
Design and interface	Clean, user-friendly interface with intuitive design elements.	Issues with long text bubbles, lack of auto line breaks, and need for design improvements.
Content and information	Provides relevant information and problem-solving advice.	Excessive use of emoticons, insufficient professional advice, and need for mobile accessibility improvement.
Least mentioned		
Personalization	Positive and personalized responses, convey a warm and positive energy.	Insufficient personalization, lack of integration with medical or counseling services, missing human touch.
Miscellaneous	Easy usability, approachable demeanor.	Inconsistent engagement incentives need for enhanced humanistic features.

Comparative Analysis

Performance variations among LLM chatbots, including Google Bard and the freely accessible version of ChatGPT, as illustrated in Figure 6, were statistically significant (F=3.27; P=.048 While the evaluation primarily focused on "Overall Satisfaction" [3], it is important to note that user experience differences may reflect limitations inherent to the free versions available for these comparisons, including ChatGPT 3.0 and Google Bard's publicly accessible iteration.

Satisfaction levels with HoMemeTown's Dr CareSam, compared with Woebot [5] and Happify [37], showed more pronounced differences (F=12.94; P<.001), as shown in Figure 7, suggesting unique benefits in mental health support for college students.

In the comparison with Woebot and Happify, the previous evaluation [3] used 5 specific criteria, that are overall satisfaction, ease of use, novelty, effectiveness, and intention to maintain use. However, for this study, "Overall Satisfaction" was selected as the primary comparative metric to simplify and provide a focused assessment of user impressions. Statistical analyses were conducted using ANOVA to determine significant differences, with appropriate post hoc tests applied for multiple comparisons to identify specific group variations.

XSL•FO
RenderX

Figure 6. Comparison of large language models chatbots. LLM: Large language models.

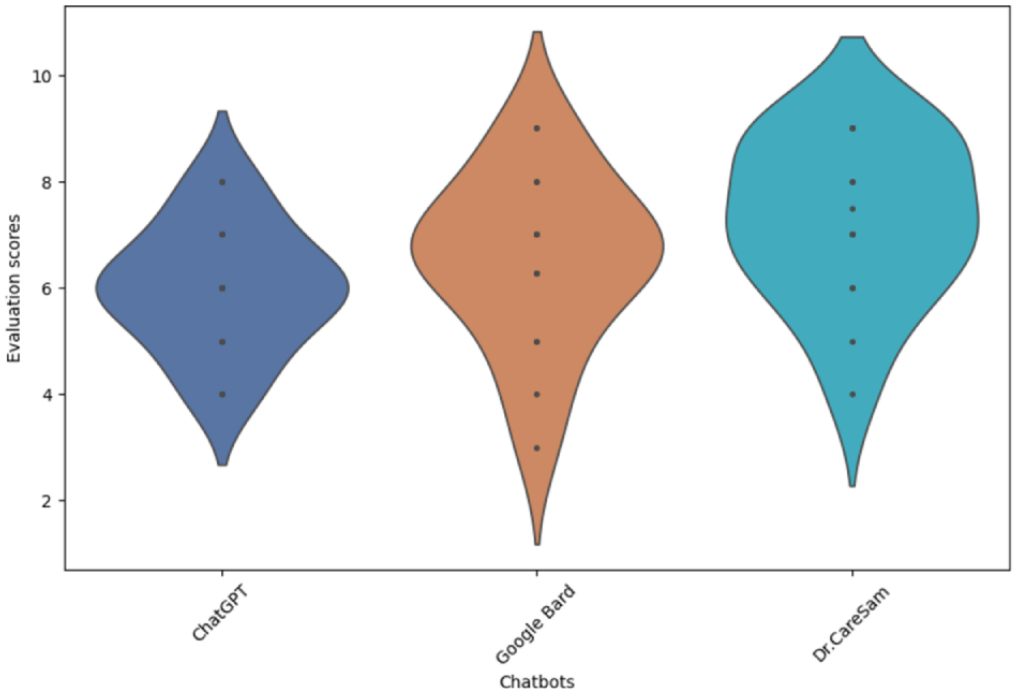
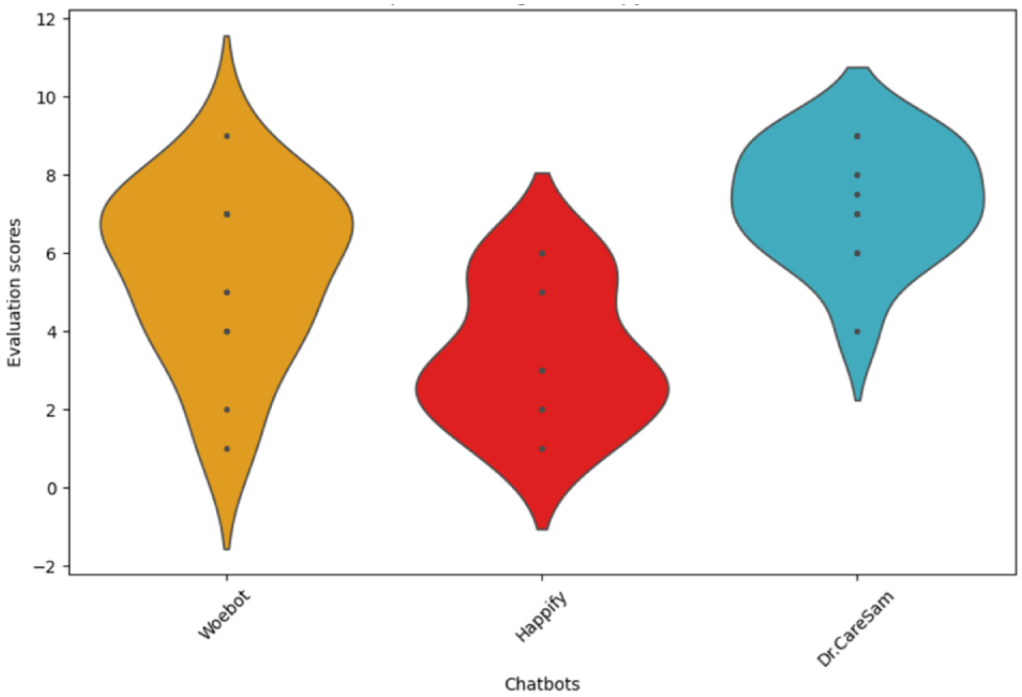


Figure 7. Comparison of digital therapy chatbots.



Discussion

Principal Findings

This study reveals several key insights about the HoMemeTown Dr CareSam chatbot, demonstrating its potential as an innovative tool in digital mental health support. The chatbot's high performance across multiple dimensions of effective counseling, particularly in providing empathetic responses and a user-friendly interface, aligns with current research emphasizing the importance of these factors in digital mental health interventions [3,10,11]. The statistically significant performance differences observed between HoMemeTown Dr. CareSam and other chatbots, both LLM-based (F=3.27; P=.047) and traditional digital therapy tools like Woebot and Happify (F=12.94; P<.001), suggest that our approach offers unique benefits in mental health support for college students. This could be attributed to our comprehensive evaluation framework based on established counseling principles and the integration of a sophisticated risk detection function. The chatbot's risk detection capability, grounded in *DSM-5* criteria and a Korean corpus of

XSL•FO
RenderX

psychopathological symptoms, represents a significant advancement in AI-driven mental health support tools, enhancing its potential as a safe and responsible digital intervention.

However, the study also highlighted important challenges and areas for improvement. While the chatbot's bilingual capability is a strength, issues with unnatural expressions and response speed in the Korean version underscore the complexities of cross-cultural adaptation in AI-driven mental health tools. Furthermore, our decision to prioritize user privacy over extensive personalization features reveals a critical challenge in developing ethical AI-driven mental health interventions. This trade-off between personalization and data protection warrants further exploration in the field. Specifically, areas for improvement were noted in professionalism (mean 7.0, SD 2.0), complexity of content (mean 7.4, SD 2.0), and personalization (mean 7.4, SD 2.4), indicating potential avenues for future development to enhance user engagement and satisfaction. Collectively, these findings suggest that HoMemeTown Dr CareSam represents a promising step forward in AI-assisted mental health support, while also illuminating critical areas for future research and development in this rapidly evolving field.

Addressing LLM Variability and Technological Enhancements

To tackle the inherent challenges posed by LLM variability and potential hallucinations [38] in chatbot responses, we developed a comprehensive response validation pipeline. This pipeline includes semantic consistency checking, medical reference validation to prevent the dissemination of inaccurate information, and automatic escalation to human review when responses deviate from predetermined safety parameters. These safeguards are integral to ensuring the chatbot's interactions remain clinically appropriate, fostering user trust and alignment with established mental health support practices.

While these measures provide a critical baseline for reliability, further advancements in the underlying LLM technologies are essential for achieving higher accuracy and contextual nuance in responses. For example, the integration of LangChain [39] technology allows for the systematic management and connection of multiple language models, offering improved contextual understanding and the ability to tailor responses to specific counseling scenarios. This modular approach enhances the flexibility and precision of chatbot interactions, particularly in complex or sensitive exchanges.

In addition, leveraging retrieval-augmented generation [40] techniques further bolsters response precision by drawing upon curated counseling databases and real-world cases. This not only strengthens the relevance of responses but also minimizes the risk of erroneous or hallucinated outputs. Such enhancements highlight the evolving interplay between foundational AI capabilities and domain-specific knowledge, positioning the chatbot as a more robust and dependable digital mental health intervention.

From an ethical standpoint, these advancements underscore the importance of balancing technological innovation with user safety and data integrity. Ensuring consistent oversight, ongoing evaluation, and refinement based on user feedback is vital to maintaining a high standard of care in digital interventions. As LLM technologies continue to evolve, our approach serves as a model for integrating emerging tools into practical applications, demonstrating how AI can be effectively harnessed to provide compassionate and reliable mental health support while continually adapting to user needs and technological developments.

Comparison With Previous Work

Unlike rule-based chatbots, HoMemeTown Dr CareSam, leveraging LLM technology, was able to provide more flexible and personalized interactions. Our findings align with previous research on Woebot's effectiveness in supporting young adults with depression and anxiety symptoms [5] while extending these benefits through our enhanced risk detection capabilities. Similarly, while Happify has shown promise in addressing loneliness during COVID-19 [37], our system demonstrates additional advantages in providing culturally adapted support for Korean users. This addresses several limitations of existing chatbots highlighted in previous studies, such as rigid response patterns and limited contextual understanding [3,5]. Specifically, our chatbot improved upon these limitations by offering more nuanced and context-appropriate responses, as evidenced by higher user satisfaction scores in empathy and active listening. The chatbot's risk detection function, grounded in *DSM-5* criteria and a Korean corpus of psychopathological symptoms, represents an advancement in AI-driven mental health support tools, offering a level of clinical relevance not typically seen in general-purpose chatbots.

Strengths and Limitations

A key strength of this study is the development of a personalized and empathetic mental health support tool using state-of-the-art LLM technology, with a sophisticated risk detection function. The bilingual support in English and Korean is another significant strength, addressing linguistic diversity and potential cross-cultural applications [17].

This study has several important limitations. The small sample size (n=20) limits the generalizability of the results but was chosen to ensure continuity and comparability with previous usability studies for Dr CareSam [3]. While this limited sample size may restrict broader applicability, it allowed for detailed and focused insights, particularly beneficial for pilot studies. Future research will aim to expand the sample size to validate findings and provide a more comprehensive evaluation of the chatbot's effectiveness.

In addition, feedback from a small group of native English speakers, not formally included in the 20-participant sample, revealed potential areas for improving cross-lingual functionality. Though this feedback offered valuable preliminary insights, future studies will involve broader validation with a larger group of native speakers to ensure accurate and culturally appropriate responses.

Another limitation is the potential inconsistency in comparing Dr CareSam, built on the ChatGPT 4.0 API, with user experiences based on the freely available ChatGPT 3.0. Differences in capabilities between these versions may have

XSL•FO
RenderX

influenced user perceptions and performance metrics. Future studies should strive to standardize versions for more direct and valid comparisons.

There are technical limitations associated with relying on the GPT API [7]. While this approach allows for advanced NLP capabilities, it also means that the chatbot's performance is dependent on the underlying model, which may have inherent biases or limitations. Furthermore, the reliance on an external API raises considerations about data privacy and the long-term sustainability of the system.

These limitations highlight the need for large-scale, long-term studies to fully evaluate the chatbot's effectiveness and generalizability. Future research should also explore the development of more specialized models that can be run locally, potentially addressing some of the limitations associated with relying on external APIs.

Clinical Implications

The HoMemeTown Dr CareSam chatbot shows potential as an accessible mental health support tool for young adults, with its risk detection function providing an additional layer of safety. However, it's crucial to clarify that this chatbot cannot replace professional mental health treatment, especially in cases where significant risk is detected. The chatbot's role should be seen as complementary to traditional mental health services, potentially serving as an initial point of contact or a supplementary support tool. It may be particularly useful for providing immediate support during nonclinical hours, for mild to moderate concerns, or for individuals who may be hesitant to seek traditional face-to-face therapy. However, clear guidelines must be established for when and how to transition users from the chatbot to professional human intervention.

Privacy and Personalization Considerations

A key challenge in this study was balancing personalization with user privacy. In our previous study, participants emphasized the importance of personalization features [3]. However, in developing the pilot version of HoMemeTown, we faced a significant dilemma between implementing these desired personalization features and ensuring robust privacy protection. Ultimately, we made the decision to prioritize privacy by eliminating user registration and personal data collection in the current public version. This choice was driven by the sensitive nature of mental health data and the potential risks associated with data breaches or misuse.

As a result, the chatbot relies solely on the capabilities of the LLM to provide a sense of personalization within individual conversations, without retaining user-specific information across sessions. This approach, while enhancing data security, limits our ability to offer some of the personalized features that participants in our previous study had requested. The chatbot attempts to mimic personalization through its conversational abilities, but it cannot retain or learn from past interactions with specific users. This trade-off highlights a crucial challenge in digital mental health interventions, how to balance user expectations for personalized experiences with the ethical imperative of protecting sensitive personal information. It also underscores the need for transparent communication with users about the capabilities and limitations of AI-driven mental health tools.

Future research should explore advanced technologies like federated learning or differential privacy, which could potentially allow for more personalized features without compromising user privacy. In addition, developing clear guidelines for handling mental health data in AI-powered interventions will be essential. Our experience underscores the need for innovative solutions that balance the benefits of personalization with robust data protection in mental health contexts. As the field evolves, finding this balance will be key to developing effective, trustworthy, and ethically sound AI-powered mental health interventions [8,41].

Future Directions

Based on our findings, we propose the key areas for future research in Textbox 2.

These focused directions align closely with our current work while suggesting meaningful advancements in the field of AI-assisted mental health support within the context of medical informatics.

XSL•FO
RenderX

Textbox 2. Key Points of evaluation criteria for large language model (LLM) chatbots.

Long-term effectiveness

- Conduct large-scale, longitudinal studies to evaluate the long-term impact of our cross-lingual chatbot on mental health outcomes.

Cross-cultural adaptations

- Further refine the chatbot's ability to provide culturally appropriate responses, particularly focusing on improving Korean language naturalness. Improving the naturalness of Korean language responses will involve refining language processing algorithms and collaborating with linguists and native speakers to address issues with awkward phrasing and cultural nuance. Incorporating user feedback to continuously adapt and optimize the chatbot's language output is also essential.

Speech-based user interface

- Develop and evaluate a speech-based user interface to increase usability and accessibility, particularly for users who may find voice interactions more natural or easier than text-based communication. This would involve integrating robust voice recognition and response capabilities to align with user preferences and accessibility needs.

Privacy-preserving personalization

- Explore technologies like federated learning to enhance personalization while maintaining robust data protection.

Risk detection enhancement

- Improve the accuracy and effectiveness of the risk detection function, potentially integrating it with existing mental health screening tools.

Integration with health care systems

- Investigate secure ways to integrate chatbot data with electronic health records, while maintaining user privacy.

Conclusions

This study represents a significant advancement from our previous work [3], addressing the limitations identified and exploring the potential of more sophisticated AI technologies in mental health support. By leveraging ChatGPT 4.0 and incorporating features like cross-lingual support and risk detection, we have developed a more comprehensive and adaptable tool for supporting young adults' mental health needs. This pilot study demonstrates the potential of HoMemeTown Dr CareSam, an LLM-based cross-lingual chatbot with advanced risk detection capabilities, in providing mental health support for young adults. While the chatbot showed promising results in user satisfaction, empathetic responses, and risk assessment, challenges in professionalism, cross-lingual adaptations, and the need for technical refinements were also identified. Further long-term, large-scale studies are needed to fully evaluate its effectiveness and potential integration with existing health care systems, as we continue to refine this technology to support mental well-being in our increasingly digital world. From a medical informatics perspective, this study contributes to our understanding of how advanced AI technologies can be applied in mental health care, potentially informing the development of more sophisticated, culturally sensitive digital health tools in the future.

Acknowledgments

This research was conducted with funding from the K-medi global talent development project of the Ministry of Health and Welfare of the Republic of Korea (assignment number HI22C2185).

This research was also supported by the Sung Kyun Kwan University and the BK21 FOUR (Graduate School Innovation) funded by the Ministry of Education (South Korea) and the National Research Foundation of Korea.

The authors acknowledge the use of AI language models in the preparation of this manuscript. Claude AI [42] was used for proofreading, editing (removing redundant expressions), and formatting references. ChatGPT [43] assisted in refining the data statistical analysis code. In addition, AI tools were used to check for duplicates during the thematic analysis process. These AI tools were used to enhance the manuscript's readability and provide technical support, while the research content, analysis, and results remain entirely the work of the authors.

Authors' Contributions

BK designed the study, collected and analyzed the data, and drafted the manuscript. MH provided feedback and critically reviewed the manuscript.

XSL•FO
RenderX

Conflicts of Interest

None declared.

References

1. Bendig E, Erb B, Schulze-Thuesing L, Baumeister H. The next generation: chatbots in clinical psychology and psychotherapy to foster mental health – a scoping review. Verhaltenstherapie 2019;29(4):266-280. [doi: 10.1159/000501812]
2. Abd-Alrazaq AA, Alajlani M, Alalwan AA, Bewick BM, Gardner P, Househ M. An overview of the features of chatbots in mental health: a scoping review. Int J Med Inform 2019;132:103978 [FREE Full text] [doi: 10.1016/j.ijmedinf.2019.103978] [Medline: 31622850]
3. Kang B, Hong M. Digital interventions for reducing loneliness and depression in Korean college students: mixed methods evaluation. JMIR Form Res 2024;8:e58791 [FREE Full text] [doi: 10.2196/58791] [Medline: 39264705]
4. Lipson SK, Lattie EG, Eisenberg D. Increased rates of mental health service utilization by U.S. college students: 10-year population-level trends (2007-2017). Psychiatr Serv 2019;70(1):60-63 [FREE Full text] [doi: 10.1176/appi.ps.201800332] [Medline: 30394183]
5. Fitzpatrick KK, Darcy A, Vierhile M. Delivering cognitive behavior therapy to young adults with symptoms of depression and anxiety using a fully automated conversational agent (Woebot): a randomized controlled trial. JMIR Ment Health 2017;4(2):e19 [FREE Full text] [doi: 10.2196/mental.7785] [Medline: 28588005]
6. Bakker D, Kazantzis N, Rickwood D, Rickard N. Mental health smartphone apps: review and evidence-based recommendations for future developments. JMIR Ment Health 2016;3(1):e7 [FREE Full text] [doi: 10.2196/mental.4984] [Medline: 26932350]
7. Brown TB, Mann B, Ryder N, Subbiah M, Kaplan J, Dhariwal P, et al. Language models are few-shot learners. arXiv:2005.14165 2020.
8. Kocaballi AB, Berkovsky S, Quiroz JC, Laranjo L, Tong HL, Rezazadegan D, et al. The personalization of conversational agents in health care: systematic review. J Med Internet Res 2019;21(11):e15360 [FREE Full text] [doi: 10.2196/15360] [Medline: 31697237]
9. Andersson G, Titov N. Advantages and limitations of Internet-based interventions for common mental disorders. World Psychiatry 2014;13(1):4-11 [FREE Full text] [doi: 10.1002/wps.20083] [Medline: 24497236]
10. Inkster B, Sarda S, Subramanian V. An empathy-driven, conversational artificial intelligence agent (Wysa) for digital mental well-being: real-world data evaluation mixed-methods study. JMIR Mhealth Uhealth 2018;6(11):e12106 [FREE Full text] [doi: 10.2196/12106] [Medline: 30470676]
11. Miner AS, Milstein A, Schueller S, Hegde R, Mangurian C, Linos E. Smartphone-based conversational agents and responses to questions about mental health, interpersonal violence, and physical health. JAMA Intern Med 2016;176(5):619-625 [FREE Full text] [doi: 10.1001/jamainternmed.2016.0400] [Medline: 26974260]
12. Stuttard D, Pinto M. he Web Application Hacker's Handbook: Finding and Exploiting Security Flaws 2nd Edition. New Jersey, U.S: Wiley; 2011.
13. Emmons RA, McCullough ME. Counting blessings versus burdens: an experimental investigation of gratitude and subjective well-being in daily life. J Pers Soc Psychol 2003;84(2):377-389. [doi: 10.1037//0022-3514.84.2.377] [Medline: 12585811]
14. Seligman MEP, Steen TA, Park N, Peterson C. Positive psychology progress: empirical validation of interventions. Am Psychol 2005;60(5):410-421. [doi: 10.1037/0003-066X.60.5.410] [Medline: 16045394]
15. Cowen AS, Keltner D. Self-report captures 27 distinct categories of emotion bridged by continuous gradients. Proc Natl Acad Sci U S A 2017;114(38):E7900-E7909 [FREE Full text] [doi: 10.1073/pnas.1702247114] [Medline: 28874542]
16. McGraw D, Dempsey JX, Harris L, Goldman J. Privacy as an enabler, not an impediment: building trust into health information exchange. Health Aff (Millwood) 2009;28(2):416-427. [doi: 10.1377/hlthaff.28.2.416] [Medline: 19275998]
17. Shin Y, Kim UJ, Lee HA, Choi EJ, Park HJ, Ahn HS, Policy Development Committee of NAMOK. Health and mortality in Korean healthcare workers. J Korean Med Sci 2022;37(3):e22 [FREE Full text] [doi: 10.3346/jkms.2022.37.e22] [Medline: 35040297]
18. Huberman A. Huberman Lab Podcast. URL: https://www.hubermanlab.com/episode/the-science-of-gratitude-and-how-to-build-a-gratitude-practice [accessed 2024-12-06]
19. American Psychiatric Association. Diagnostic and Statistical Manual of Mental Disorders, 5th ed. Arlington, VA: American Psychiatric Publishing; 2013.
20. Disease information and symptoms. National Mental Health Portal. URL: https://www.mentalhealth.go.kr/portal/disease/diseaseList.do [accessed 2024-04-09]
21. Karyotaki E, Furukawa TA, Efthimiou O, Riper H, Cuijpers P. Guided or self-guided internet-based cognitive–behavioural therapy (iCBT) for depression? Study protocol of an individual participant data network meta-analysis. BMJ Open 2019 Jun 05;9(6):e026820. [doi: 10.1136/bmjopen-2018-026820]
22. Torous J, Wisniewski H, Bird B, Carpenter E, David G, Elejalde E, et al. Creating a digital health smartphone app and digital phenotyping platform for mental health and diverse healthcare needs: an interdisciplinary and collaborative approach. J. technol. behav. sci 2019;4(7597):1-13. [doi: 10.1007/s41347-019-00095-w]

XSL•FO
RenderX

23. Rogers CR. The necessary and sufficient conditions of therapeutic personality change. Psychotherapy (Chic) 2007;44(3):240-248. [doi: 10.1037/0033-3204.44.3.240] [Medline: 22122245]
24. Elliott R, Bohart AC, Watson JC, Greenberg LS. Empathy. Psychotherapy (Chic) 2011;48(1):43-49 [FREE Full text] [doi: 10.1037/a0022187] [Medline: 21401273]
25. Hepworth DH, Rooney RH, Rooney GD, Strom-Gottfried K, Larsen JA. Direct social work practice: Theory and skills. United States: Cengage Learning; 2017.
26. Egan G. The skilled helper: A problem-management and opportunity-development approach to helping. United States: Cengage Learning; 2013.
27. Greenberg LS. Emotion-focused therapy: Coaching clients to work through their feelings. Washington, DC: American Psychological Association; 2011.
28. Gendlin ET. Focusing. New York, U.S: Bantam Books; 1978.
29. Weger H, Castle Bell G, Minei EM, Robinson MC. The relative effectiveness of active listening in initial interactions. Int. J. List 2014;28(1):13-31. [doi: 10.1080/10904018.2013.813234]
30. Hill CE. Helping skills: Facilitating exploration, insight, and action. Washington, DC: American Psychological Association; 2009.
31. Mearns D, Thorne B. Person-centered counseling in action. Washington DC: Sage; 2013.
32. Norcross JC, Lambert MJ. Psychotherapy relationships that work: Evidence-based responsiveness. Oxford, UK: Oxford University Press; 2018.
33. Sue DW, Sue D. Counseling the culturally diverse: Theory and practice. Hoboken, New Jersey: John Wiley & Sons; 2012.
34. Ratts MJ, Singh AA, Nassar ‐ McMillan S, Butler SK, McCullough JR. Multicultural and Social Justice Counseling Competencies: Guidelines for the Counseling Profession. J Multicult Couns & Deve 2016;44(1):28-48. [doi: 10.1002/jmcd.12035]
35. Norcross J, Lambert MJ. Psychotherapy relationships that work III. Psychotherapy (Chic) 2018;55(4):303-315. [doi: 10.1037/pst0000193] [Medline: 30335448]
36. Beutler LE, Harwood TM. Prescriptive psychotherapy: A practical guide to systematic treatment selection. Oxford, UK: Oxford University Press; 2000.
37. Boucher EM, McNaughton EC, Harake N, Stafford JL, Parks AC. The impact of a digital intervention (Happify) on loneliness during COVID-19: qualitative focus group. JMIR Ment Health 2021;8(2):e26617 [FREE Full text] [doi: 10.2196/26617] [Medline: 33498011]
38. Ji Z, Lee N, Frieske R, Yu T, Su D, Xu Y, et al. Survey of hallucination in natural language generation. ACM Comput. Surv 2023;55(12):1-38. [doi: 10.1145/3571730]
39. Pandya K, Holia M. Automating customer service using LangChain: building custom open-source GPT chatbot for organizations. arXiv:2310.05421 2023.
40. Kang M, Kwak JM, Baek J, Hwang SJ. Knowledge graph-augmented language models for knowledge-grounded dialogue generation. arXiv:2305.18846 2023.
41. Kocaballi AB, Quiroz JC, Rezazadegan D, Berkovsky S, Magrabi F, Coiera E, et al. Responses of conversational agents to health and lifestyle prompts: investigation of appropriateness and presentation structures. J Med Internet Res 2020;22(2):e15823 [FREE Full text] [doi: 10.2196/15823] [Medline: 32039810]
42. Claude login. URL: https://claude.ai/login [accessed 2024-08-28]
43. ChatGPT. URL: https://openai.com/chatgpt/overview/ [accessed 2024-08-28]

Abbreviations

AI: artificial intelligence
API: application programming interface
DSM-5: Diagnostic and Statistical Manual of Mental Disorders (Fifth Edition)
LLM: large language models
NLP: natural language processing
PHQ-9: Patient Health Questionnaire-9

XSL•FO
RenderX

Edited by C Lovis; submitted 23.06.24; peer-reviewed by S Munusamy, O Ng, DW Sung, DY Kim; comments to author 04.11.24; revised version received 12.11.24; accepted 16.11.24; published 03.01.25.

Please cite as:
Kang B, Hong M
Development and Evaluation of a Mental Health Chatbot Using ChatGPT 4.0: Mixed Methods User Experience Study With Korean Users
JMIR Med Inform 2025;13:e63538
URL: https://medinform.jmir.org/2025/1/e63538
doi:10.2196/63538
PMID:

©Boyoung Kang, Munpyo Hong. Originally published in JMIR Medical Informatics (https://medinform.jmir.org), 03.01.2025. This is an open-access article distributed under the terms of the Creative Commons Attribution License (https://creativecommons.org/licenses/by/4.0/), which permits unrestricted use, distribution, and reproduction in any medium, provided the original work, first published in JMIR Medical Informatics, is properly cited. The complete bibliographic information, a link to the original publication on https://medinform.jmir.org/, as well as this copyright and license information must be included.

XSL•FO
RenderX

Original Paper

Qwen-2.5 Outperforms Other Large Language Models in the Chinese National Nursing Licensing Examination: Retrospective Cross-Sectional Comparative Study

Shiben Zhu[1,2], MSc; Wanqin Hu[3], MNS; Zhi Yang[3], MNS; Jiani Yan[4], MIM; Fang Zhang[4], BBA

[1]Department of Infectious Diseases, Nanfang Hospital, Southern Medical University, Guangzhou, China

[2]State Key Laboratory of Organ Failure Research, Key Laboratory of Infectious Diseases Research in South China, Ministry of Education, Guangdong Provincial Key Laboratory of Viral Hepatitis Research, Guangdong Provincial Clinical Research Center for Viral Hepatitis, Guangdong Institute of Hepatology, Guangzhou, China

[3]School of Nursing and Health Studies, Hong Kong Metropolitan University, Kowloon, Hong Kong, China (Hong Kong)

[4]Department of Science and Education, Shenzhen Baoan Women's and Children's Hospital, Shenzhen, China

Corresponding Author:
Fang Zhang, BBA
Department of Science and Education
Shenzhen Baoan Women's and Children's Hospital
56 Yulu Road
Xin'an Street, Bao'an District
Shenzhen, 518001
China
Phone: 86 13686891225
Email: zhangfangf11@163.com

Abstract

Background: Large language models (LLMs) have been proposed as valuable tools in medical education and practice. The Chinese National Nursing Licensing Examination (CNNLE) presents unique challenges for LLMs due to its requirement for both deep domain–specific nursing knowledge and the ability to make complex clinical decisions, which differentiates it from more general medical examinations. However, their potential application in the CNNLE remains unexplored.

Objective: This study aims to evaluates the accuracy of 7 LLMs including GPT-3.5, GPT-4.0, GPT-4o, Copilot, ERNIE Bot-3.5, SPARK, and Qwen-2.5 on the CNNLE, focusing on their ability to handle domain-specific nursing knowledge and clinical decision-making. We also explore whether combining their outputs using machine learning techniques can improve their overall accuracy.

Methods: This retrospective cross-sectional study analyzed all 1200 multiple-choice questions from the CNNLE conducted between 2019 and 2023. Seven LLMs were evaluated on these multiple-choice questions, and 9 machine learning models, including Logistic Regression, Support Vector Machine, Multilayer Perceptron, k-nearest neighbors, Random Forest, LightGBM, AdaBoost, XGBoost, and CatBoost, were used to optimize overall performance through ensemble techniques.

Results: Qwen-2.5 achieved the highest overall accuracy of 88.9%, followed by GPT-4o (80.7%), ERNIE Bot-3.5 (78.1%), GPT-4.0 (70.3%), SPARK (65.0%), and GPT-3.5 (49.5%). Qwen-2.5 demonstrated superior accuracy in the Practical Skills section compared with the Professional Practice section across most years. It also performed well in brief clinical case summaries and questions involving shared clinical scenarios. When the outputs of the 7 LLMs were combined using 9 machine learning models, XGBoost yielded the best performance, increasing accuracy to 90.8%. XGBoost also achieved an area under the curve of 0.961, sensitivity of 0.905, specificity of 0.978, F_1-score of 0.901, positive predictive value of 0.901, and negative predictive value of 0.977.

Conclusions: This study is the first to evaluate the performance of 7 LLMs on the CNNLE and that the integration of models via machine learning significantly boosted accuracy, reaching 90.8%. These findings demonstrate the transformative potential of LLMs in revolutionizing health care education and call for further research to refine their capabilities and expand their impact on examination preparation and professional training.

(JMIR Med Inform 2025;13:e63731) doi:10.2196/63731

XSL•FO
RenderX

KEYWORDS

large language models; LLMs; Chinese National Nursing Licensing Examination; ChatGPT; Qwen-2.5; multiple-choice questions;

Introduction

Nursing licensure examinations are essential for maintaining professional standards, ensuring that health care systems are staffed with qualified professionals, and safeguarding patient safety [1]. These examinations assess nurses' clinical judgment, decision-making, and practical skills, ensuring high-quality care and fostering public trust in the profession [2]. Upholding rigorous standards is critical, as competent health care professionals are crucial for addressing the diverse and complex needs of patients worldwide. The Chinese National Nursing Licensing Examination (CNNLE) plays an important role in maintaining high standards of nursing care in China, ensuring that graduates are well prepared for professional practice [3]. Serving as a benchmark for nursing competence, the CNNLE confirms that nurses possess the necessary skills and knowledge to provide safe and effective care [4]. Beyond its impact on health care quality, the CNNLE also influences educational policies, guiding nursing curricula to meet evolving health care demands. As health care becomes more complex, innovative tools are needed to support the development of skilled professionals capable of providing effective patient care.

The integration of artificial intelligence (AI) in education is transforming learning and assessment, particularly in fields such as nursing [5-7]. ChatGPT, an AI tool that generates content by identifying patterns in its training data, simulates human-like conversations and answers questions across a wide range of topics [8,9]. Its ability to provide correct answers and offer immediate, detailed feedback makes it a valuable resource for students in simulated test environments and question banks [10]. This success in examination settings has sparked interest in using ChatGPT as a self-learning tool, suggesting its potential for enhancing examination preparation and knowledge development [11]. Large language models (LLMs) hold promise for clinical education [12], where these models integrate natural language processing with user-friendly interfaces [13]. In clinics, LLMs are increasingly valuable, particularly in diagnosis [14,15] and clinical licensing examinations [16], where accuracy is crucial. Tools such as ChatGPT are being recognized for their potential to enhance clinical documentation [17], improve diagnostic accuracy [18], and streamline patient care workflows [19]. However, the rapid development of LLMs presents significant challenges in assessing their reliability in the CNNLE.

Passing CNNLE demands not only theoretical knowledge but also clinical decision-making, critical thinking, and practical skills, areas where LLMs often underperform [9]. While tools such as ChatGPT have demonstrated an overall accuracy of 80.75% in nursing education [20], their effectiveness diminishes with complex, context-specific questions requiring nuanced medical knowledge [21-23]. Moreover, concerns regarding patient privacy [24] and biases [25] in LLM outputs raise questions about their suitability for high-stakes assessments such as the CNNLE, which emphasize fairness and accuracy [26,27]. Despite the growing interest in LLMs for medical education, their potential in the CNNLE remains unexplored. Limited understanding exists regarding their ability to handle clinical reasoning, contextual interpretation, and multistep problem-solving in this specific setting. Addressing this gap is crucial to assess their reliability, limitations, and transformative potential in clinical education. Here, this study examines the distribution of question types in the CNNLE from 2019 to 2023 and evaluates the accuracy of 7 LLMs including GPT-3.5, GPT-4.0, GPT-4o, Copilot, ERNIE Bot-3.5, SPARK, and Qwen-2.5—in addressing domain-specific nursing knowledge and clinical decision-making. Furthermore, the study explores whether combining their outputs through machine learning techniques can enhance overall accuracy in this context.

Methods

Study Design

This retrospective cross-sectional study evaluated the performance of 7 LLMs on 1200 multiple-choice questions (MCQs) from the CNNLE administered between 2019 and 2023. The study design was chosen for its suitability in systematically analyzing preexisting datasets and providing the capabilities of LLMs across various question types and levels of complexity. A head-to-head evaluation approach was adopted to compare the LLMs. Each MCQ was independently input into each model under identical conditions, ensuring consistency and fairness in the assessment. This parallel evaluation minimized variability caused by external factors, such as differences in question formats or content, allowing for a direct comparison of performance across all models. By using historical data and using a head-to-head evaluation, this study provides an analysis of LLM performance in nursing licensure examinations, offering their potential applications in nursing education and assessment.

Data Collection

This study analyzed all 1200 MCQs from the CNNLE administered between 2019 and 2023. Each year, 240 MCQs were included, encompassing the 4 question types (A1, A2, A3, and A4) although their proportions varied annually. This comprehensive approach ensured that the evaluation covered diverse question formats and varying levels of complexity, reflecting the full scope of the CNNLE. To ensure the integrity of the evaluation process, 2 researchers (SZ and WH) independently entered each question into 7 LLMs on separate computers. Each question was input into a new chat session to prevent any influence from prior interactions. The LLMs generated answers and explanations solely based on the input questions without pretraining instructions or additional prompts.

If inconsistencies were detected in the responses, a third computer was used to reenter the question in a fresh chat session after clearing the LLMs' memory. In such cases, the models were instructed to provide more detailed explanations. The researchers then collectively reviewed the answers and explanations to determine the most accurate and contextually appropriate response. When LLMs exhibited confusion, failed

XSL•FO
RenderX

to provide explanations, produced multiple answers including the correct one, or encountered specialized queries (eg, questions on local policies), additional instructions were provided. These instructions included prompts such as, "This is a single-choice question. Please select the most suitable or probable answer from options 1 to 5," "Please choose the incorrect option," "Tell me the reason why," "In Chinese local policy," "In Chinese local law," and "In Chinese society." All data generated or analyzed during this study are provided in Multimedia Appendix 1, and the iPython Jupyter notebook code is available in Multimedia Appendix 2.

Ethical Considerations

The evaluations were conducted between May 15, 2024, and July 17, 2024. All responses were cross-verified against the official CNNLE answer keys. These measures enhanced the reliability and validity of the evaluation process. As this study was purely analytical and did not involve human participants, institutional review board approval and informed consent were not required. All collected data were fully anonymized by removing names, contact details, and other direct identifiers, ensuring no means to reidentify participants.

Measurements

The CNNLE

The CNNLE [28] comprises 2 sections: Professional Practice and Practical Skills, each with 120 questions per unit. The Professional Practice section evaluates a candidate's ability to implement nursing-related knowledge in clinical settings in a safe and effective manner. It covers medical knowledge related to health and disease, basic nursing skills, and the application of social and humanistic knowledge in nursing practice. The Practical Skills section assesses candidates' capability to apply nursing knowledge and skills in performing nursing tasks. Topics include clinical manifestations of diseases, treatment principles, health assessment, nursing procedures, professional nursing techniques, and health education. The examination format involves objective questions presented in a computer-based format.

The examination includes 4 question types: A1, A2, A3, and A4, all of which are MCQs. A1 and A2 questions are relatively straightforward, focusing on single knowledge points and brief clinical case summaries, respectively. A3 and A4 questions involve shared clinical scenarios, requiring candidates to analyze and synthesize information comprehensively. A3 questions present 2-3 distinct, patient-centered clinical situations, while A4 questions depict more complex scenarios involving a single patient or family, with 4-6 independent questions that may introduce new information sequentially to test clinical integration skills.

LLM Selection

We selected 7 LLMs including GPT-3.5, GPT-4.0, GPT-4o, Copilot, ERNIE Bot-3.5, SPARK, and Qwen-2.5. This diverse selection enabled a comprehensive examination of LLM performance under standardized conditions. GPT-3.5, developed by OpenAI and released in March 2022, is known for generating coherent and contextually relevant text. GPT-4.0, released by OpenAI in March 2023, offers significant improvements in accuracy and understanding. GPT-4o, introduced in May 2024, is an optimized version of GPT-4.0, designed for enhanced performance. ERNIE Bot-3.5, created by Baidu and released in June 2023, is tailored for understanding and generating text in Chinese. SPARK, developed by iFLYTEK and launched in May 2023, enhances performance tools by providing intelligent assistance. Qwen-2.5, created by Alibaba and launched in May 2024, is optimized for complex language understanding, particularly in shopping and customer support contexts. To ensure effectiveness and reliability, each inquiry was conducted only once in a new chat session with each LLM, using 2 different computers. This approach aimed to evaluate the designs' efficiency in real-world situations without the influence of responses loopholes.

Machine Learning Models

We selected 9 machine learning models, each with recognized performance in classification tasks. Logistic Regression (LR) [29] is a fundamental linear model made use of for binary category tasks as a result of its simpleness and interpretability. Support Vector Machine (SVM) [30] excels in high-dimensional and complicated settings, giving durable classification efficiency. Multilayer Perceptron (MLP) [31] is a neural network model that properly identifies complicated patterns with its split structure. The k-nearest neighbors (KNN) [32] algorithm is an uncomplicated, nonparametric monitored knowing approach that categorizes or predicts information factors based upon their proximity to bordering points, extensively acknowledged for its simplicity and effectiveness in both category and regression jobs.

Ensemble models improve prediction performance by incorporating multiple designs to alleviate overfitting and improve generalization. Random Forest (RF) [33] is esteemed for its high precision and ability to alleviate overfitting with ensemble knowing, accumulating the predictions of choice trees using a majority ballot to enhance anticipating toughness. Light Gradient-Boosting Machine (LightGBM) [34] is a highly reliable gradient increasing framework that makes use of a histogram-based technique to bin constant features, speeding up training speed, enhancing memory usage, and mastering processing massive datasets with impressive rate and effectiveness. Adaptive Boosting (AdaBoost) [35] prioritizes tough situations, enhancing category precision by iteratively changing weights to boost the design. Extreme Gradient Boosting (XGBoost) [36], a sophisticated slope-boosting system developed by Chen, iteratively refines designs by splitting tree nodes and suitable residuals, demonstrating extraordinary scalability and superior efficiency throughout varied applications. CatBoost [37], introduced in 2018, is a sophisticated gradient boosting algorithm known for its outstanding handling of specific functions, reduced training times, and the use of a money-grubbing technique to pinpoint ideal tree divides, thereby improving forecast precision.

Statistical Analysis

The statistical analysis was conducted using Python 3.11.5 (Python Software Foundation) within the Microsoft Visual Studio Code environment. In preparing the dataset, responses

XSL•FO
RenderX

where the LLMs failed to provide any answer were categorized as missing values and coded as –1. For valid responses labeled (A, B, C, D, and E), a numerical encoding scheme was applied, converting them to (1, 2, 3, 4, and 5), respectively. To prepare the data for machine learning algorithms, the dataset underwent normalization, scaling all features to a range between 0 and 1 using the MinMaxScaler from the Scikit-learn library. Descriptive statistics were used to analyze the distribution of question types within the CNNLE dataset from 2019 to 2023. Furthermore, accuracy percentages for the LLMs were computed across 2 distinct subjects and 4 different question types. Various machine learning models were then used with the objective of enhancing predictive performance.

Nine machine learning models, including LR, SVM, MLP, KNN, RF, LightGBM, AdaBoost, XGBoost, and CatBoost, were trained specifically for this task using the processed CNNLE dataset. None of the models were pretrained; instead, they were trained and optimized using hyperparameter tuning tailored to the dataset. For instance, parameters such as the number of trees and maximum depth were adjusted for RF, while learning rates and boosting parameters were optimized for LightGBM and XGBoost. The leave-one-out cross-validation method was used to ensure robustness and reliability. The dataset was split into training (90%) and testing (10%) sets, with the training set further divided into 9 subsets for hyperparameter tuning. This iterative process was repeated until each subset served as a validation set, minimizing overfitting and ensuring robust performance metrics for the models.

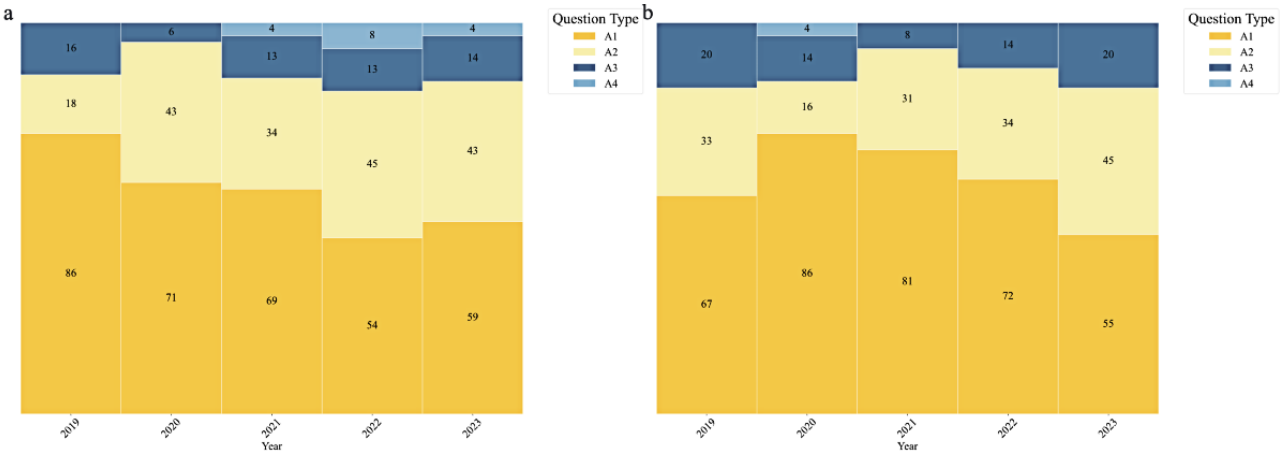
Model performance was assessed using correlation heatmaps, area under the curves (AUCs), and 7 evaluation metrics: AUC, sensitivity, specificity, F_1-score, accuracy, positive predictive value (PPV), and negative predictive value (NPV). Feature importance was analyzed using Shapley Additive Explanations (SHAP), providing the contributions of individual features. SHAP analysis focused on understanding the relative contributions of the 7 LLMs, highlighting how each LLM's accuracy influenced overall predictions. The analysis used Python packages, including pandas 2.1.4, numpy 1.24.3, scikit-learn 1.3.0, scipy 1.11.4, catboost 1.2, LightGBM 4.1.0, seaborn 0.12.2, SHAP 0.42.1, and matplotlib 3.8.0.

Results

Distribution of Question Types in the CNNLE Over the Years

Figure 1 illustrates the distribution of question types over the years in both sections of the CNNLE. Figure 1A depicts the distribution of question types over the years in the Practical Skills section. In the Practical Skills section, A1-type questions decreased from 86 in 2019 to 59 in 2023, while A2-type questions increased from 18 to 43. A3-type and A4-type questions showed smaller fluctuations. Figure 1B shows the distribution of question types over the years in the Professional Practice section. In the Professional Practice section, A1-type questions fell from 67 in 2019 to 55 in 2023, while A2-type questions increased from 33 to 45. A3-type questions remained relatively stable, with minor variations.

Figure 1. Distribution of question types in CNNLE Professional Practice and Practical Skills sections (2019-2023). (A) Distribution of question types in Practical Skills from 2019 to 2023. (B) Distribution of question types in Professional Practice from 2019 to 2023.



Accuracy of LLMs in Professional Practice

Table 1 presents the accuracy of LLMs in the Professional Practice section from 2019 to 2023. In 2023, Qwen-2.5 achieved the highest accuracy (0.850), followed by ERNIE Bot-3.5 (0.808) and GPT-4o (0.783). GPT-4.0 consistently outperformed GPT-3.5 in all years, with scores of 0.725 and 0.492, respectively, in 2023. Copilot and SPARK also showed moderate performance improvements over time, reaching 0.775 and 0.692 in 2023. Across the 5 years, Qwen-2.5 demonstrated the best overall accuracy (0.875), followed by GPT-4o (0.803) and ERNIE Bot-3.5 (0.785).

XSL•FO
RenderX

Table 1. Accuracy of large language models in Professional Practice.

Year	GPT-3.5	GPT-4.0	GPT-4o	Copilot	ERNIE Bot-3.5	SPARK	Qwen-2.5
2023	0.492	0.725	0.783	0.775	0.808	0.692	0.850
2022	0.450	0.675	0.833	0.767	0.758	0.667	0.917
2021	0.517	0.683	0.817	0.725	0.783	0.650	0.900
2020	0.500	0.708	0.725	0.733	0.767	0.600	0.850
2019	0.550	0.758	0.858	0.583	0.808	0.600	0.858
Overall	0.502	0.710	0.803	0.717	0.785	0.642	0.875

Accuracy of LLMs in Practical Skills

Table 2 presents the accuracy of LLMs in the Practical Skills section from 2019 to 2023. In 2023, Qwen-2.5 achieved the highest accuracy (0.908), followed by GPT-4o (0.833) and Copilot (0.792). GPT-4.0 and ERNIE Bot-3.5 both scored 0.775, showing steady improvement compared with earlier years. SPARK and GPT-3.5 performed moderately, with scores of 0.758 and 0.550, respectively. Over the 5 years, Qwen-2.5 consistently outperformed other models, achieving the highest overall accuracy (0.903). GPT-4o followed with 0.810, while ERNIE Bot-3.5 ranked third with 0.777.

Table 2. Accuracy of large language models in Practical Skills.

Year	GPT-3.5	GPT-4.0	GPT-4o	Copilot	ERNIE Bot-3.5	SPARK	Qwen-2.5
2023	0.550	0.775	0.833	0.792	0.775	0.758	0.908
2022	0.467	0.692	0.800	0.792	0.792	0.675	0.850
2021	0.467	0.708	0.850	0.667	0.750	0.567	0.942
2020	0.475	0.642	0.783	0.592	0.800	0.700	0.933
2019	0.483	0.658	0.783	0.458	0.767	0.592	0.883
Overall	0.488	0.695	0.810	0.660	0.777	0.658	0.903

Accuracy of LLMs for Question Types

Table 3 indicates the accuracy of LLMs across 4 question types (A1, A2, A3, and A4) from 2019 to 2023. In 2023, Qwen-2.5 achieved the highest accuracy for A1, A2, and A3 questions (0.860, 0.909, and 0.853, respectively), while all models reached perfect accuracy (1.000) for A4 questions. GPT-4o consistently performed well across all question types, ranking second or third in accuracy. In 2022, Qwen-2.5 maintained high performance across A1, A2, and A3 questions (0.913, 0.810, and 0.963, respectively). From 2019 to 2021, Qwen-2.5 demonstrated steady improvements across all question types. Overall, Qwen-2.5 achieved the highest average accuracy (0.889), followed by GPT-4o (0.807) and ERNIE Bot-3.5 (0.781).

XSL•FO
RenderX

Table 3. Accuracy of large language models for 4 question types.

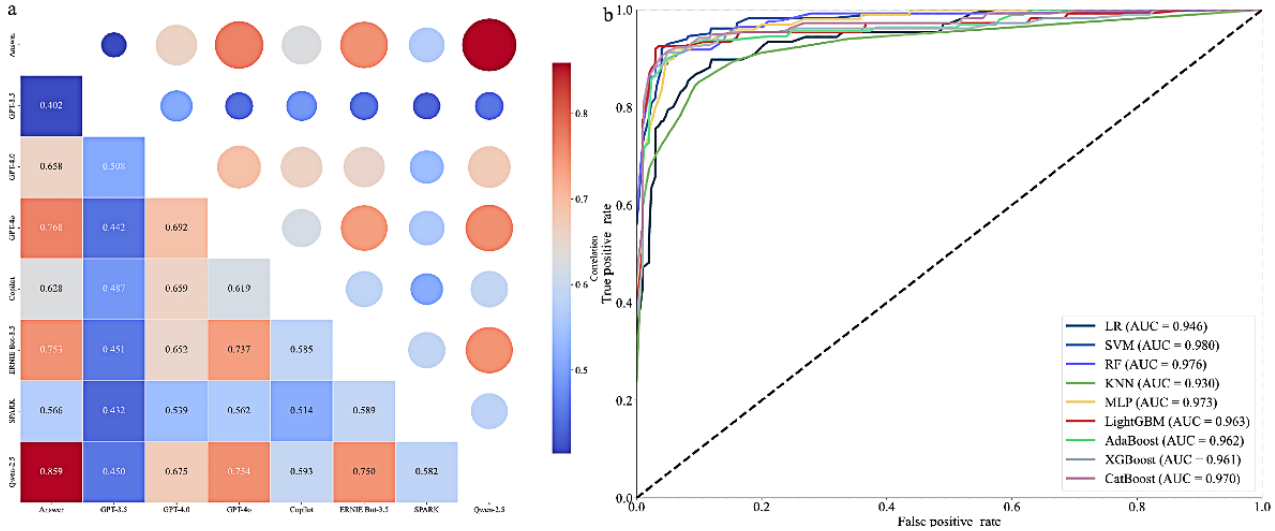
Question type	GPT-3.5	GPT-4.0	GPT-4o	Copilot	ERNIE Bot-3.5	SPARK	Qwen-2.5
2023							
A1	0.526	0.684	0.789	0.763	0.763	0.719	0.860
A2	0.443	0.807	0.830	0.784	0.807	0.705	0.909
A3	0.647	0.794	0.794	0.824	0.824	0.765	0.853
A4	1.000	1.000	1.000	1.000	1.000	1.000	1.000
2022							
A1	0.476	0.746	0.881	0.825	0.817	0.698	0.913
A2	0.405	0.582	0.671	0.696	0.671	0.620	0.810
A3	0.519	0.667	0.889	0.778	0.852	0.630	0.963
A4	0.500	0.750	1.000	0.875	0.875	0.875	0.875
2021							
A1	0.467	0.660	0.820	0.667	0.727	0.600	0.927
A2	0.538	0.738	0.846	0.738	0.831	0.646	0.938
A3	0.524	0.762	0.857	0.714	0.857	0.571	0.810
A4	0.500	1.000	1.000	1.000	0.750	0.500	1.000
2020							
A1	0.478	0.675	0.771	0.650	0.771	0.656	0.879
A2	0.492	0.695	0.763	0.695	0.814	0.678	0.915
A3	0.550	0.600	0.550	0.650	0.750	0.600	0.900
A4	0.500	0.750	1.000	0.750	1.000	0.250	1.000
2019							
A1	0.490	0.680	0.804	0.503	0.791	0.601	0.869
A2	0.569	0.745	0.843	0.588	0.784	0.588	0.843
A3	0.556	0.778	0.861	0.500	0.778	0.583	0.917
Overall	0.495	0.703	0.807	0.688	0.781	0.650	0.889

Correlation Heatmap and AUC Curves Using Machine Learning

Figure 2 provides an analysis of the correlation heatmap and AUC curves for machine learning models. Figure 2A presents the correlation heatmap, where Qwen-2.5 shows the highest correlation with correct answers (r=0.859), while GPT-3.5 shows the lowest correlation (r=0.402). Figure 2B illustrates the AUC scores for each machine learning model in the multiclass classification task. The models achieved the following AUC scores: LR (0.946), SVM (0.980), RF (0.976), KNN (0.930), MLP (0.973), LightGBM (0.963), AdaBoost (0.962), XGBoost (0.961), and CatBoost (0.970).

XSL•FO
RenderX

Figure 2. Correlation heatmap and AUC curves of machine learning models in CNNLE. (A) Correlation heatmap: The heatmap illustrates the relationships between different LLMs. The lower left displays numerical correlation values, while the upper right represents correlation magnitude through circle size. Color gradients range from blue (low correlation) to red (high correlation), providing a visual summary of metric interdependencies. (B) AUC curves: The AUC curves compare the performance of various machine learning and ensemble models, highlighting their classification accuracy across the data set. AdaBoost: Adaptive Boosting; AUC: area under the curve; CatBoost: Categorical Boosting; KNN: k-nearest neighbor; LightGBM: Light Gradient-Boosting Machine; LR: Logistic Regression; MLP: Multilayer Perceptron; RF: Random Forest; SVM: Support Vector Machine; XGBoost: Extreme Gradient Boosting.



Metrics for 5-Class Classification Using Machine Learning

Table 4 presents a comparative analysis of 9 machine learning models for multiclass classification, evaluated by average metrics including AUC, accuracy, sensitivity, specificity, precision, PPV, F_1-score, and NPV. Among these, the SVM and XGBoost models achieve AUC values of 0.980 and 0.961, along with accuracy scores of 0.858 and 0.908, respectively. In contrast, LR and KNN exhibit lower accuracy scores of 0.817 and 0.767.

XSL•FO
RenderX

Table 4. Metrics of machine learning.

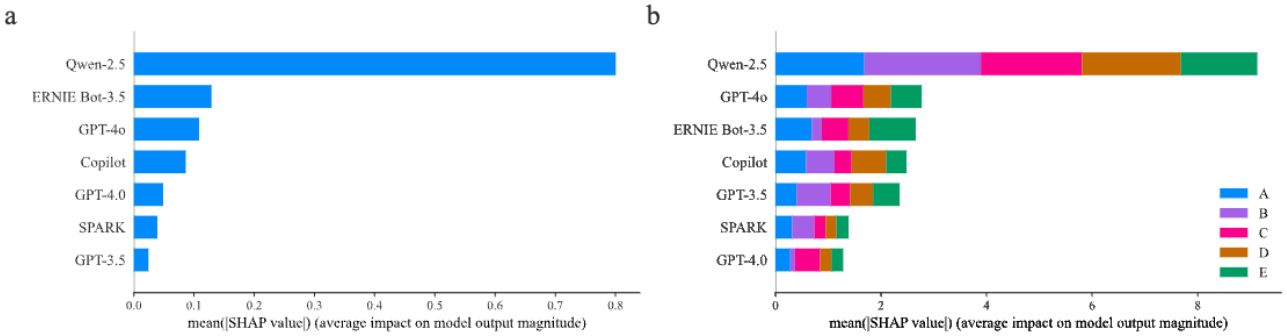
Classifier	AUC[a]	Accuracy	Sensitivity	Specificity	Precision	PPV[b]	F_1-score	NPV[c]
LR[d]	0.946	0.817	0.808	0.953	0.818	0.818	0.809	0.954
SVM[e]	0.980	0.858	0.857	0.965	0.861	0.861	0.854	0.964
RF[f]	0.976	0.858	0.860	0.965	0.856	0.856	0.854	0.964
KNN[g]	0.930	0.767	0.772	0.942	0.787	0.787	0.768	0.941
MLP[h]	0.973	0.825	0.823	0.957	0.830	0.830	0.819	0.956
LightGBM[i]	0.963	0.900	0.908	0.975	0.895	0.895	0.899	0.974
AdaBoost[j]	0.962	0.858	0.859	0.964	0.855	0.855	0.856	0.964
XGBoost[k]	0.961	0.908	0.905	0.978	0.901	0.901	0.901	0.977
CatBoost[l]	0.970	0.892	0.892	0.974	0.885	0.885	0.885	0.973

[a]AUC: area under the curve.
[b]PPV: positive predictive value.
[c]NPV: negative predictive value.
[d]LR: Logistic Regression.
[e]SVM: Support Vector Machine.
[f]RF: Random Forest.
[g]KNN: k-nearest neighbor.
[h]MLP: Multilayer Perceptron.
[i]LightGBM: Light Gradient-Boosting Machine.
[j]AdaBoost: Adaptive Boosting.
[k]XGBoost: Extreme Gradient Boosting.
[l]CatBoost: Categorical Boosting.

Importance Ranking of SVM and XGBoost Models

Figure 3 presents the SHAP summary bar plot for both the SVM and XGBoost models. In Figure 3A, the SVM model ranks the features as follows: Qwen-2.5, ERNIE Bot-3.5, GPT-4o, Copilot, GPT-4.0, SPARK, and GPT-3.5. Meanwhile, Figure 3B shows the importance ranking of XGBoost model with a slightly different order: Qwen-2.5, GPT-4o, ERNIE Bot-3.5, Copilot, GPT-3.5, SPARK, and GPT-4.0. Qwen-2.5 stands out as the most influential feature in both models. Furthermore, including other LLMs enhances overall model performance, evidenced by improvements in AUC and accuracy.

Figure 3. SHAP summary bar plot in Support Vector Machine (SVM) and Extreme Gradient Boosting (XGBoost) models. (A) Importance ranking of SVM model. (B) Importance ranking of XGBoost model. SHAP: Shapley Additive Explanations.



Discussion

Principal Findings

This study is the first to evaluate the performance of 7 LLMs on the CNNLE dataset (2019-2023), highlighting significant advancements in Chinese LLM development and their applications in nursing education. Among the models tested, Qwen-2.5 demonstrated the highest accuracy (88.92%), significantly surpassing the performance of the other LLMs. This superior accuracy can be attributed to its training on an extensive Chinese dataset and optimized parameters, enabling it to handle domain-specific nursing knowledge and complex clinical decision-making tasks with exceptional precision. These results underline the growing feasibility of deploying advanced LLMs such as Qwen-2.5 to support standardized nursing

XSL•FO
RenderX

examinations in China, offering consistent, scalable, and efficient assessments.

Our findings offer a clear pathway for the practical application of Qwen-2.5 in nursing curricula and professional training. For instance, Qwen-2.5 could serve as a virtual tutor, providing personalized feedback and explanations to nursing students in real time. Its ability to respond promptly and accurately to a wide range of questions makes it particularly valuable for addressing individual knowledge gaps and reinforcing complex concepts. Educators could incorporate Qwen-2.5 into classroom activities, using it to simulate clinical scenarios or evaluate students' decision-making skills. Furthermore, mobile apps powered by Qwen-2.5 could allow nursing students to access high-quality, interactive learning resources anytime and anywhere, thereby enhancing accessibility and flexibility in education. Beyond supporting student learning, Qwen-2.5 and other LLMs can enhance professional development for practicing nurses. For instance, these models could be integrated into continuing education programs, where they act as interactive resources to update practitioners on the latest evidence-based practices. By serving as a knowledge repository, LLMs can enable nurses to quickly access relevant guidelines, ensuring timely and informed clinical decisions.

The results also extend prior research by demonstrating how ensemble machine learning methods can enhance LLM performance in specialized tasks. By integrating the outputs of 7 LLMs using the XGBoost algorithm, we achieved an improved accuracy of 90.83%, surpassing the best-performing single model. This novel application of ensemble methods highlights a promising direction for developing personalized LLMs tailored to specific domains, such as health care education. Previous studies, including those by Li et al [38] and Brin et al [39], have emphasized the value of context-specific tuning, but our research provides concrete evidence of the effectiveness of combining multiple models to enhance accuracy in domain-specific applications.

Furthermore, our study situates Chinese LLMs within the broader global landscape of AI. While skepticism has persisted regarding whether Chinese LLMs can rival models developed by OpenAI or Google, our results demonstrate that Qwen-2.5 not only excels on the CNNLE assessment but also outperforms other LLMs. For example, Qwen-2.5 achieved a higher accuracy than GPT-4 (72.5%) on similar standardized tests, as reported in previous studies [40]. This performance underscores the competitive edge of Chinese-developed models, particularly in addressing language-specific and cultural nuances in health care education.

Our findings also reveal recent trends in nursing education, such as the increasing complexity of standardized examinations such as the CNNLE, which has transitioned from straightforward A1-type questions to more analytical A2-type clinical case scenarios. This shift reflects the growing need for nursing professionals to develop higher-order reasoning skills and apply clinical knowledge to real-world situations. Qwen-2.5's ability to process nuanced clinical scenarios positions it as an effective tool for addressing these demands. By integrating models such as Qwen-2.5 into nursing curricula, educators can better prepare students for the complexities of modern health care through scenario-based learning and real-time feedback.

Our study also demonstrates the broader impact of China's advancements in AI, particularly through open access LLMs such as Qwen-2.5 and ERNIE Bot-3.5, which provide practical solutions for addressing regional disparities in nursing education. These models are especially valuable in regions where access to global LLMs, such as OpenAI's GPT models, is restricted, as they deliver high-quality, localized educational content. By promoting the standardization of nursing education across institutions, these tools help bridge resource gaps and improve the overall quality of health care training in China. Furthermore, their ability to enable personalized and flexible learning through mobile apps empowers students to access educational resources anytime and anywhere. This adaptability positions Chinese LLMs as critical tools for advancing specialized education while addressing both regional inequalities and broader challenges in health care training.

Limitations

First, our evaluation relied on MCQs to assess the knowledge of LLMs, which may not fully capture their ability to handle open-ended or complex clinical tasks. Future studies could incorporate open-ended questions, clinical simulations, or case-based assessments to evaluate LLMs' reasoning and decision-making capabilities more comprehensively. These methods would better reflect the unstructured and nuanced scenarios encountered in real-world clinical practice, providing a deeper understanding of how LLMs process complex clinical information. Second, the performance of LLMs can vary based on factors such as prompt design, the number of questions asked, and the context of those questions, introducing variability into results. To address this, standardized evaluation protocols should be developed to ensure consistency across benchmarking studies. Furthermore, future research could focus on refining prompt engineering techniques and optimizing model fine-tuning to improve accuracy and reliability in diverse clinical applications. These refinements could support the development of LLMs that are better suited to handling complex scenarios, such as differential diagnoses or multistep decision-making. Third, while Qwen-2.5 demonstrated highest accuracy on the CNNLE dataset, its optimization for the Chinese language and MCQ format may limit its generalizability to other medical domains and contexts. Future studies should evaluate its applicability in multilingual and open-ended settings to assess its effectiveness in tasks beyond standardized testing formats and within various health care contexts. To enhance the suitability of LLMs for specialized health care tasks, such as diagnostic reasoning and treatment planning, future research could prioritize the development of domain-specific models. This could involve fine-tuning LLMs on datasets that include detailed case histories, diagnostic pathways, and clinical protocols. Such datasets would allow the models to learn context-specific patterns and reasoning processes, equipping them to provide more accurate and relevant recommendations in clinical settings. Furthermore, fine-tuned models could be used to assist in treatment planning by integrating data from clinical guidelines, patient histories, and risk assessment tools to offer tailored suggestions for patient care. Addressing biases in LLM training is also essential for

XSL•FO
RenderX

ensuring equitable decision-making across diverse patient populations. Researchers should consider incorporating fairness-aware algorithms and curated datasets that reflect demographic diversity to mitigate potential biases. Such efforts could ensure that domain-specific LLMs provide consistent and unbiased recommendations, particularly in high-stakes environments such as emergency department triage workflows. Finally, this study focused on general purpose LLMs, excluding models explicitly trained for medical tasks, such as Gemini or Claude. Preliminary findings suggest that fine-tuned medical models may achieve superior accuracy for specific applications. Future research should conduct comparative evaluations of general purpose and domain-specific LLMs to identify the optimal approach for different health care needs. These studies could also assess whether fine-tuned models are more effective in real-time clinical workflows, such as triage systems, or in supporting complex decision-making across various medical specialties.

Conclusions

This study is the first to evaluate the performance of 7 LLMs on the CNNLE and that the integration of models via machine learning significantly boosted accuracy, reaching 90.8%. These findings demonstrate the transformative potential of LLMs in revolutionizing health care education and call for further research to refine their capabilities and expand their impact on examination preparation and professional training.

Authors' Contributions

SZ was responsible for the conceptualization, methodology, software, validation, formal analysis, investigation, resources, data curation, writing of the original draft, reviewing, editing the manuscript, and visualization. WH and ZY managed data curation and visualization. JY also handled data curation and contributed to reviewing and editing the manuscript. FZ supervised the project, contributed to reviewing and editing the manuscript, and managed project administration. All authors have read and approved the final version of the manuscript and agreed to be accountable for all aspects of the work, ensuring that any questions related to the accuracy or integrity of any part of the work are appropriately investigated and resolved.

Conflicts of Interest

None declared.

Multimedia Appendix 1
Original data set.
[XLSX File (Microsoft Excel File), 68 KB - medinform_v13i1e63731_app1.xlsx]

Multimedia Appendix 2
Ipynb notebook codes.
[PDF File (Adobe PDF File), 249 KB - medinform_v13i1e63731_app2.pdf]

References

1. American Association of Critical-Care Nurses. Safeguarding the patient and the profession: the value of critical care nurse certification. Am J Crit Care 2003;12(2):154-164. [Medline: 12625174]
2. Gambrill E. Critical Thinking in Clinical Practice: Improving the Quality of Judgments and Decisions. Hoboken, NJ: John Wiley & Sons; 2006.
3. Zong H, Li J, Wu E, Wu R, Lu J, Shen B. Performance of ChatGPT on Chinese national medical licensing examinations: a five-year examination evaluation study for physicians, pharmacists and nurses. BMC Med Educ 2024;24(1):143 [FREE Full text] [doi: 10.1186/s12909-024-05125-7] [Medline: 38355517]
4. Miao Y, Luo Y, Zhao Y, Li J, Liu M, Wang H, et al. Performance of GPT-4 on Chinese nursing examination: potentials for AI-assisted nursing education using large Language models. Nurse Educ 2024;49(6):E338-E343. [doi: 10.1097/NNE.0000000000001679] [Medline: 38981035]
5. Allen C, Woodnutt S. Can ChatGPT pass a nursing exam? Int J Nurs Stud 2023;145:104522. [doi: 10.1016/j.ijnurstu.2023.104522] [Medline: 37354792]
6. Castonguay A, Farthing P, Davies S, Vogelsang L, Kleib M, Risling T, et al. Revolutionizing nursing education through ai integration: a reflection on the disruptive impact of ChatGPT. Nurse Educ Today 2023;129:105916. [doi: 10.1016/j.nedt.2023.105916] [Medline: 37515957]
7. Chang BS. Transformation of undergraduate medical education in 2023. JAMA 2023;330(16):1521-1522. [doi: 10.1001/jama.2023.16943] [Medline: 37698855]
8. Branum C, Schiavenato M. Can ChatGPT accurately answer a PICOT question? Assessing aI response to a clinical question. Nurse Educ 2023;48(5):231-233. [doi: 10.1097/NNE.0000000000001436] [Medline: 37130197]
9. Harris E. Large language models answer medical questions accurately, but can't match clinicians' knowledge. JAMA 2023;330(9):792-794. [doi: 10.1001/jama.2023.14311] [Medline: 37548971]

XSL•FO
RenderX

10. Alam F, Lim MA, Zulkipli IN. Integrating AI in medical education: embracing ethical usage and critical understanding. Front Med (Lausanne) 2023;10:1279707 [FREE Full text] [doi: 10.3389/fmed.2023.1279707] [Medline: 37901398]
11. Yang H. How I use ChatGPT responsibly in my teaching. Nature 2023(476-4687):1-3 cited 2024 Dec 31 [FREE Full text] [doi: 10.1038/d41586-023-01026-9] [Medline: 37045954]
12. Chang Y, Wang X, Wang J, Wu Y, Yang L, Zhu K, et al. A survey on evaluation of large language models. ACM Trans Intell Syst Technol 2024;15(3):1-45. [doi: 10.1145/3641289]
13. Abbasian M, Khatibi E, Azimi I, Oniani D, Shakeri Hossein Abad Z, Thieme A, et al. Foundation metrics for evaluating effectiveness of healthcare conversations powered by generative AI. NPJ Digit Med 2024;7(1):82 [FREE Full text] [doi: 10.1038/s41746-024-01074-z] [Medline: 38553625]
14. Singhal K, Azizi S, Tu T, Mahdavi SS, Wei J, Chung HW, et al. Large language models encode clinical knowledge. Nature 2023;620(7972):172-180 [FREE Full text] [doi: 10.1038/s41586-023-06291-2] [Medline: 37438534]
15. Thirunavukarasu AJ, Ting DSJ, Elangovan K, Gutierrez L, Tan TF, Ting DSW. Large language models in medicine. Nat Med 2023;29(8):1930-1940. [doi: 10.1038/s41591-023-02448-8] [Medline: 37460753]
16. Moura L, Jones DT, Sheikh IS, Murphy S, Kalfin M, Kummer BR, et al. Implications of large language models for quality and efficiency of neurologic care: emerging issues in neurology. Neurology 2024;102(11):e209497. [doi: 10.1212/WNL.0000000000209497] [Medline: 38759131]
17. Kernberg A, Gold JA, Mohan V. Using ChatGPT-4 to create structured medical notes from audio recordings of physician-patient encounters: comparative study. J Med Internet Res 2024;26:e54419 [FREE Full text] [doi: 10.2196/54419] [Medline: 38648636]
18. Caruccio L, Cirillo S, Polese G, Solimando G, Sundaramurthy S, Tortora G. Can ChatGPT provide intelligent diagnoses? A comparative study between predictive models and ChatGPT to define a new medical diagnostic bot. Expert Syst Appl 2024;235:121186. [doi: 10.1016/j.eswa.2023.121186]
19. Ferdush J, Begum M, Hossain ST. ChatGPT and clinical decision support: scope, application, and limitations. Ann Biomed Eng 2024;52(5):1119-1124. [doi: 10.1007/s10439-023-03329-4] [Medline: 37516680]
20. Su MC, Lin LE, Lin LH, Chen YC. Assessing question characteristic influences on ChatGPT's performance and response-explanation consistency: insights from taiwan's nursing licensing exam. Int J Nurs Stud 2024;153:104717. [doi: 10.1016/j.ijnurstu.2024.104717] [Medline: 38401366]
21. Pham C, Govender R, Tehami S, Chavez S, Adepoju OE, Liaw W. ChatGPT's performance in cardiac arrest and bradycardia simulations using the American Heart Association's advanced cardiovascular life support guidelines: exploratory study. J Med Internet Res 2024;26:e55037 [FREE Full text] [doi: 10.2196/55037] [Medline: 38648098]
22. Burk-Rafel J, Reinstein I, Feng J, Kim MB, Miller LH, Cocks PM, et al. Development and validation of a machine learning-based decision support tool for residency applicant screening and review. Acad Med 2021;96(11S):S54-S61. [doi: 10.1097/ACM.0000000000004317] [Medline: 34348383]
23. Wang D, Liang J, Ye J, Li J, Li J, Zhang Q, et al. Enhancement of the performance of large language models in diabetes education through retrieval-augmented generation: comparative study. J Med Internet Res 2024;26:e58041 [FREE Full text] [doi: 10.2196/58041] [Medline: 39046096]
24. Li S. Exploring the clinical capabilities and limitations of ChatGPT: a cautionary tale for medical applications. Int J Surg 2023;109(9):2865-2867 [FREE Full text] [doi: 10.1097/JS9.0000000000000523] [Medline: 37222684]
25. Jiang Y, Hao J, Fauss M, Li C. Detecting ChatGPT-generated essays in a large-scale writing assessment: is there a bias against non-native english speakers? Comput Educ 2024;217:105070. [doi: 10.1016/j.compedu.2024.105070]
26. Zack T, Lehman E, Suzgun M, Rodriguez JA, Celi LA, Gichoya J, et al. Assessing the potential of GPT-4 to perpetuate racial and gender biases in health care: a model evaluation study. Lancet Digit Health 2024;6(1):e12-e22 [FREE Full text] [doi: 10.1016/S2589-7500(23)00225-X] [Medline: 38123252]
27. Sandmann S, Riepenhausen S, Plagwitz L, Varghese J. Systematic analysis of ChatGPT, Google search and llama 2 for clinical decision support tasks. Nat Commun 2024;15(1):2050 [FREE Full text] [doi: 10.1038/s41467-024-46411-8] [Medline: 38448475]
28. Hou J, Chen S, Sabharwal S, Fan V, Yan M, Wang W. Comparison of RN licensure examination: China and the United States. Int J Nurs Sci 2019;6(1):111-116 [FREE Full text] [doi: 10.1016/j.ijnss.2018.11.002] [Medline: 31406876]
29. Nusinovici S, Tham YC, Chak Yan MY, Wei Ting DS, Li J, Sabanayagam C, et al. Logistic regression was as good as machine learning for predicting major chronic diseases. J Clin Epidemiol 2020;122:56-69. [doi: 10.1016/j.jclinepi.2020.03.002]
30. Suthaharan S. Support vector machine. In: Machine Learning Models and Algorithms for Big Data Classification: Thinking With Examples for Effective Learning. New York, NY: Springer; 2016:207-235.
31. Tang J, Deng C, Huang GB. Extreme learning machine for multilayer perceptron. IEEE Trans Neural Netw Learn Syst 2016;27(4):809-821. [doi: 10.1109/TNNLS.2015.2424995] [Medline: 25966483]
32. Samet H. K-nearest neighbor finding using MaxNearestDist. IEEE Trans Pattern Anal Mach Intell 2008;30(2):243-252. [doi: 10.1109/TPAMI.2007.1182] [Medline: 18084056]
33. Segal MR. Machine learning benchmarks and random forest regression. 2004. URL: https://escholarship.org/uc/item/35x3v9t4 [accessed 2004-04-14]

XSL•FO
RenderX

34. Shehadeh A, Alshboul O, Al Mamlook RE, Hamedat O. Machine learning models for predicting the residual value of heavy construction equipment: an evaluation of modified decision tree, LightGBM, and XGBoost regression. Automation Constr 2021;129:103827. [doi: 10.1016/j.autcon.2021.103827]
35. Zhang PB, Yang ZX. A novel adaBoost framework with robust threshold and structural optimization. IEEE Trans Cybern 2018;48(1):64-76. [doi: 10.1109/TCYB.2016.2623900] [Medline: 27898387]
36. Chen T, Guestrin C. A scalable tree boosting system. 2016 Presented at: Proceedings of the 22nd ACM SIGKDD International Conference on Knowledge Discovery and data Mining; 2016 August 17; San Francisco, CA. [doi: 10.1145/2939672.2939785]
37. Hancock JT, Khoshgoftaar TM. CatBoost for big data: an interdisciplinary review. J Big Data 2020;7(1):94 [FREE Full text] [doi: 10.1186/s40537-020-00369-8] [Medline: 33169094]
38. Li DJ, Kao YC, Tsai SJ, Bai YM, Yeh TC, Chu CS, et al. Comparing the performance of ChatGPT GPT-4, Bard, and llama-2 in the Taiwan Psychiatric Licensing Examination and in differential diagnosis with multi-center psychiatrists. Psychiatry Clin Neurosci 2024;78(6):347-352. [doi: 10.1111/pcn.13656] [Medline: 38404249]
39. Brin D, Sorin V, Vaid A, Soroush A, Glicksberg BS, Charney AW, et al. Comparing ChatGPT and GPT-4 performance in USMLE soft skill assessments. Sci Rep 2023;13(1):16492 [FREE Full text] [doi: 10.1038/s41598-023-43436-9] [Medline: 37779171]
40. Sato H, Ogasawara K. ChatGPT (GPT-4) passed the Japanese national license examination for pharmacists in 2022, answering all items including those with diagrams: a descriptive study. J Educ Eval Health Prof 2024;21:4 [FREE Full text] [doi: 10.3352/jeehp.2024.21.4] [Medline: 38413129]

Abbreviations

AdaBoost: Adaptive Boosting
AI: artificial intelligence
AUC: area under the curve
CNNLE: Chinese National Nursing Licensing Examination
KNN: k-nearest neighbors
LightGBM: Light Gradient-Boosting Machine
LLM: large language model
LR: Logistic Regression
MCQ: multiple-choice question
MLP: Multilayer Perceptron
NPV: negative predictive value
PPV: positive predictive value
RF: Random Forest
SHAP: Shapley Additive Explanations
SVM: Support Vector Machine
XGBoost: Extreme Gradient Boosting

Edited by A Castonguay; submitted 27.06.24; peer-reviewed by Y Hirano, M Besler; comments to author 26.07.24; revised version received 06.08.24; accepted 20.12.24; published 10.01.25.

Please cite as:
Zhu S, Hu W, Yang Z, Yan J, Zhang F
Qwen-2.5 Outperforms Other Large Language Models in the Chinese National Nursing Licensing Examination: Retrospective Cross-Sectional Comparative Study
JMIR Med Inform 2025;13:e63731
URL: https://medinform.jmir.org/2025/1/e63731
doi:10.2196/63731
PMID:

©Shiben Zhu, Wanqin Hu, Zhi Yang, Jiani Yan, Fang Zhang. Originally published in JMIR Medical Informatics (https://medinform.jmir.org), 10.01.2025. This is an open-access article distributed under the terms of the Creative Commons Attribution License (https://creativecommons.org/licenses/by/4.0/), which permits unrestricted use, distribution, and reproduction in any medium, provided the original work, first published in JMIR Medical Informatics, is properly cited. The complete bibliographic information, a link to the original publication on https://medinform.jmir.org/, as well as this copyright and license information must be included.

XSL•FO
RenderX

Original Paper

Evaluating and Enhancing Japanese Large Language Models for Genetic Counseling Support: Comparative Study of Domain Adaptation and the Development of an Expert-Evaluated Dataset

Takuya Fukushima[1], BE; Masae Manabe[2], MEd; Shuntaro Yada[1,3], PhD; Shoko Wakamiya[1], PhD; Akiko Yoshida[4], PhD; Yusaku Urakawa[5,6,7], MD, PhD; Akiko Maeda[5], MD, PhD; Shigeyuki Kan[8], PhD; Masayo Takahashi[8], MD, PhD; Eiji Aramaki[1], PhD

[1]Graduate School of Science and Technology, Nara Institute of Science and Technology, Ikoma, Japan

[2]Research Administration Center, Kyoto University, Kyoto, Japan

[3]Faculty of Library, Information and Media Science, University of Tsukuba, Tsukuba, Japan

[4]Department of Genomic Medicine, Graduate School of Medicine, Kyoto University, Kyoto, Japan

[5]Kobe City Eye Hospital, Kobe, Japan

[6]Department of Medical Oncology, Kobe City Medical Center General Hospital, Kobe, Japan

[7]Department of Genomic Medicine, School of Medicine, Fujita Health University, Toyoake, Japan

[8]Vision Care Inc, Kobe, Japan

Corresponding Author:
Eiji Aramaki, PhD
Graduate School of Science and Technology
Nara Institute of Science and Technology
8916-5, Takayama-cho
Ikoma, 630-0192
Japan
Phone: 81 743 72 5250
Email: aramaki@is.naist.jp

Abstract

Background: Advances in genetics have underscored a strong association between genetic factors and health outcomes, leading to an increased demand for genetic counseling services. However, a shortage of qualified genetic counselors poses a significant challenge. Large language models (LLMs) have emerged as a potential solution for augmenting support in genetic counseling tasks. Despite the potential, Japanese genetic counseling LLMs (JGCLLMs) are underexplored. To advance a JGCLLM-based dialogue system for genetic counseling, effective domain adaptation methods require investigation.

Objective: This study aims to evaluate the current capabilities and identify challenges in developing a JGCLLM-based dialogue system for genetic counseling. The primary focus is to assess the effectiveness of prompt engineering, retrieval-augmented generation (RAG), and instruction tuning within the context of genetic counseling. Furthermore, we will establish an experts-evaluated dataset of responses generated by LLMs adapted to Japanese genetic counseling for the future development of JGCLLMs.

Methods: Two primary datasets were used in this study: (1) a question-answer (QA) dataset for LLM adaptation and (2) a genetic counseling question dataset for evaluation. The QA dataset included 899 QA pairs covering medical and genetic counseling topics, while the evaluation dataset contained 120 curated questions across 6 genetic counseling categories. Three enhancement techniques of LLMs—instruction tuning, RAG, and prompt engineering—were applied to a lightweight Japanese LLM to enhance its ability for genetic counseling. The performance of the adapted LLM was evaluated on the 120-question dataset by 2 certified genetic counselors and 1 ophthalmologist (SK, YU, and AY). Evaluation focused on four metrics: (1) inappropriateness of information, (2) sufficiency of information, (3) severity of harm, and (4) alignment with medical consensus.

Results: The evaluation by certified genetic counselors and an ophthalmologist revealed varied outcomes across different methods. RAG showed potential, particularly in enhancing critical aspects of genetic counseling. In contrast, instruction tuning and prompt engineering produced less favorable outcomes. This evaluation process facilitated the creation an expert-evaluated

XSL•FO
RenderX

dataset of responses generated by LLMs adapted with different combinations of these methods. Error analysis identified key ethical concerns, including inappropriate promotion of prenatal testing, criticism of relatives, and inaccurate probability statements.

Conclusions: RAG demonstrated notable improvements across all evaluation metrics, suggesting potential for further enhancement through the expansion of RAG data. The expert-evaluated dataset developed in this study provides valuable insights for future optimization efforts. However, the ethical issues observed in JGCLLM responses underscore the critical need for ongoing refinement and thorough ethical evaluation before these systems can be implemented in health care settings.

(JMIR Med Inform 2025;13:e65047) doi:10.2196/65047

KEYWORDS

large language models; genetic counseling; medical; health; artificial intelligence; machine learning; domain adaptation; retrieval-augmented generation; instruction tuning; prompt engineering; question-answer; dialogue; ethics; safety; low-rank adaptation; Japanese; expert evaluation

Introduction

Background

Research in genetic counseling has increased with advances in diagnostic testing and treatment of genetic diseases [1]. Genetic counseling requires highly specialized skills, such as effectively communicating complex, evidence-based medical information in a clear and accessible manner, and providing essential mental health support. Despite rising demand, there remains a shortage of qualified professionals in this field [2]. In Japan, students can become certified genetic counselors by completing a graduate course at a graduate school with an accredited training program for genetic counselors. However, as of December 2023, only 389 qualified genetic counselors were available, highlighting the challenge of meeting the demand for genetic counseling services [3].

In recent years, the rapid development of large language models (LLMs) has led to their widespread application across various fields. Notably, the ChatGPT and GPT-4 developed by OpenAI have demonstrated human-level performance in diverse professional examinations [4] and even succeeded in the Japanese National Medical Examination [5-7] and the General Medicine In-Training Examination [8]. LLMs tailored for the medical field, such as Google's Med-PaLM2, have demonstrated the ability to provide responses preferred by patients over those of doctors [9,10]. In addition, Sukeda et al [11,12] conducted domain adaptation for the medical fields on several Japanese LLMs. However, there are no studies specifically examining Japanese LLMs' medical proficiency in genetic counseling. It is crucial not only to measure the general medical capabilities of LLMs through medical examinations but also to have experts evaluate LLMs in specialized tasks within the medical field.

In genetic counseling, where handling personal information requires the utmost care, lightweight, high-performance LLMs capable of offline operation are essential. This is due to the sensitive nature of the information involved, including family history, genetic data, and future health risks, which necessitate stringent privacy protection for the entire family. Unlike general medical practices that primarily impact individual patients, genetic information has extensive implications for life planning, family planning, and future generations. For example, the discovery of a genetic mutation associated with breast cancer not only affects the patient but also requires comprehensive counseling for his or her entire family. Similarly, identifying hereditary disease risks involves assessing genetic risks for future children.

This study introduces the development of an LLM for genetic counseling in Japanese, termed the "Japanese genetic counseling large language model" (JGCLLM). Specifically, we aim to explore effective enhancement techniques for LLMs and assess the responses of JGCLLM through expert evaluation. This research represents the first comprehensive study to analyze the impact of various enhancement techniques for LLMs in Japanese genetic counseling, marking a significant contribution to the field. Furthermore, we plan to leverage evaluation data to further enhance LLM performance through techniques, such as reinforcement learning from human feedback (RLHF) [13], which uses human preferences to guide the model's learning and direct preference optimization (DPO) [14], directly optimizing the model based on pairwise comparisons of the outputs.

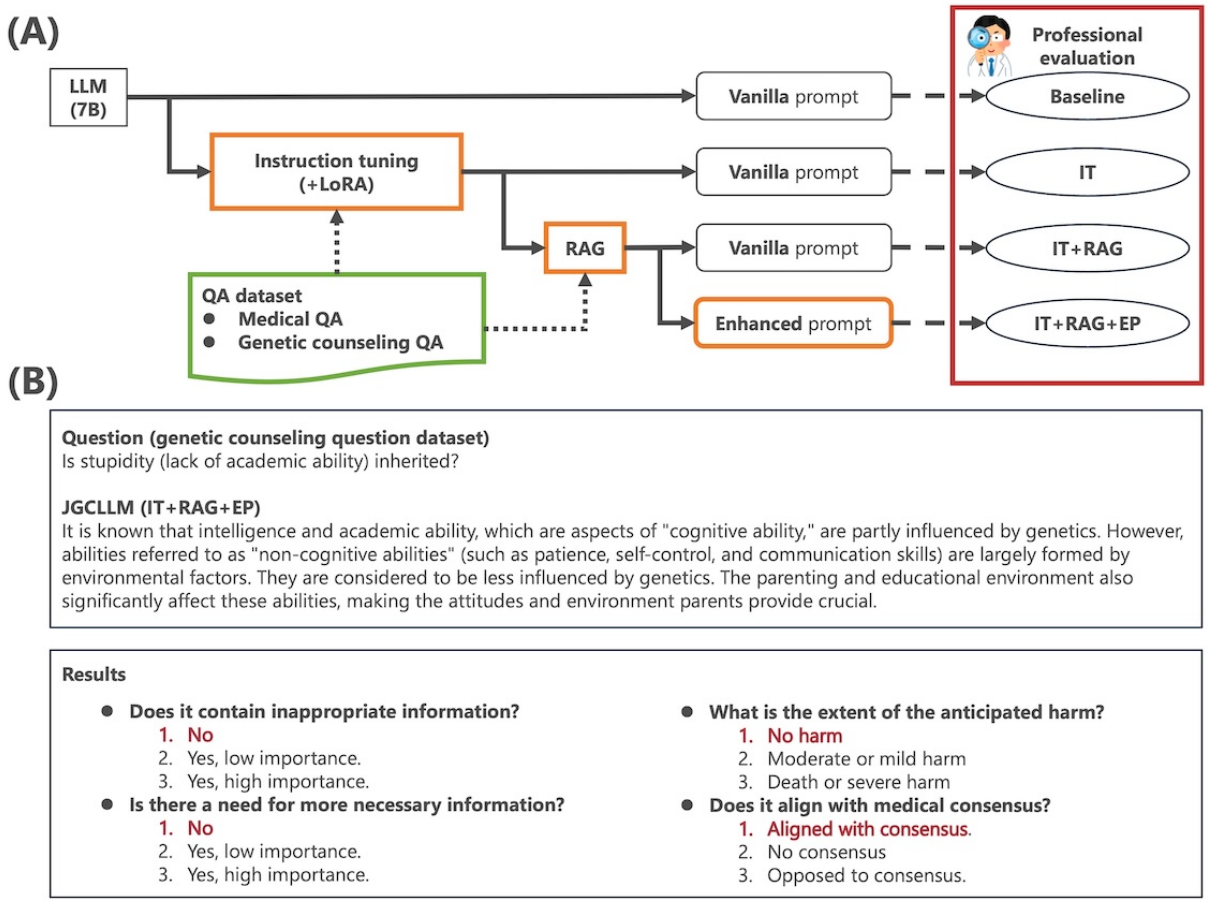
We applied standard LLM enhancement techniques, including instruction tuning [15], retrieval-augmented generation (RAG) [16], and prompt engineering, to lightweight Japanese LLMs. These techniques provide targeted solutions to key challenges in genetic counseling by improving response accuracy and safety. Instruction tuning enables the model to learn the appropriate response formats used by genetic counselors and to manage general inquiries with greater precision. RAG allows the model to base answers on the latest medical knowledge by referencing up-to-date literature or offering insights from previous patient records. Finally, prompt engineering ensures that the model adheres to safety and content guidelines, fostering responses that are both accurate and aligned with best practices in the field. Together, these combined techniques enhance the overall reliability and safety of artificial intelligence (AI)–driven genetic counseling.

Medical dialogue references for these methods were sourced from the web and developed by experts. Furthermore, we collected 1000 questions on genetic counseling through crowdsourcing and carefully selected 120 questions for assessment of the JGCLLM. Two certified genetic counselors and 1 ophthalmologist (SK, YU, and AY) were tasked with evaluating the response of the JGCLLM to these questions. The JGCLLMs were domain adapted using various combinations of methods. This process allowed us to analyze the impacts and

XSL•FO
RenderX

challenges of these methods in the genetic counseling context. Figure 1 provides an overview of the study's experimental design. Figure 1A shows the workflow of LLM enhancement techniques and datasets used, while Figure 1B shows a JGCLLM response with professional evaluation results across 4 criteria. Since the experiments were conducted in Japanese, this paper presents their descriptions translated into English, with the original Japanese versions shown in Multimedia Appendix 1 for reference.

Figure 1. (A) Experimental setup illustrates the workflow, which includes IT, RAG, and prompt engineering, along with datasets used for LLM enhancement techniques. (B) Example of a JGCLLM response used for professional evaluation, including a model response to a given question (top) and the professional evaluation results across 4 criteria (bottom). EP: enhanced prompt; IT: instruction tuning; JGCLLM: Japanese genetic counseling large language model; LLM: large language model; LoRA: low-rank adaptation; QA: question-answer; RAG: retrieval-augmented generation.



Question-Answer Dataset

Overview

We developed a question-answer (QA) dataset that includes 2 types of QA data—medical QA and genetic counseling QA—to tailor LLMs for applications in the medical field, with a specific emphasis on genetic counseling. Sample pairs of questions and answers from the QA dataset are listed in Table 1. Text data in QA format are essential for instruction tuning. Furthermore, the QA dataset has been used in RAG.

XSL•FO
RenderX

Table 1. Sample pairs of questions and answers from the QA[a] dataset[b].

Type of data	Questions	Answers
Medical QA (web, 691 cases)	My husband suffers from gout and has been advised to reduce his alcohol consumption. However, despite experiencing pain in his legs after drinking, he continues to indulge. Despite my repeated pleas for him to stop, he stubbornly refuses to listen.	Alcoholic beverages can significantly increase the risk of developing gout. Two alcohol-free days are recommended a week: no more than 500 mL of beer per day, no more than one go (approximately 180 mL) of sake per day, and no more than 1 double shot of whiskey daily. While sake is often touted as a beneficial remedy, moderation is key. Reducing alcohol consumption, even by as little as 10%, can have positive effects on your health. It may be challenging for those who enjoy drinking, but making small changes can lead to significant improvements.
Genetic counseling QA (web, 99 cases)	What is genetic counseling?	Genetic counseling is a service designed to assist individuals with genetic issues, anxieties, or doubts. The goal is to provide clear and accurate medical information rooted in scientific evidence, presented in a manner that is easily comprehensible. In addition, we offer psychological and social support to empower individuals to effectively utilize medical technology and information to address their concerns autonomously.
Genetic counseling QA (books and guidelines, 93 cases)	What should I do if I am diagnosed with HBOC?	If you have been diagnosed with HBOC (hereditary breast and ovarian cancer), proactive steps can be taken to manage your risk. One option is risk-reducing surgery, a surgical procedure that involves removing organs at high risk of developing cancer before any cancerous cells can form. Another approach is surveillance, which targets organs at high risk of cancer for early detection. Risk-reducing surgery is a preventive measure that aims to eliminate cancer-prone organs before they become cancerous, ultimately reducing the likelihood of cancer development.
Genetic counseling QA (genetic counselor, 16 cases)	If the genetic test is negative, is it not retinitis pigmentosa?	No, the clinical diagnosis of retinitis pigmentosa remains unchanged even if genetic testing fails to identify the causative gene. While most cases of retinitis pigmentosa are attributed to a genetic change, numerous causative genes exist. Factors contributing to the inability to pinpoint the causative gene may include the absence of the gene in current genetic testing or limitations in the sensitivity of testing methods.

[a]QA: question-answer.

[b]One pair from the medical QA dataset and pairs from the genetic counseling QA dataset, which were sourced from the web, professional books and guidelines, and certified genetic counselors. The medical QA dataset was used to learn the model on physicians' responses in general medical care, while the genetic counseling QA dataset was used to develop responses to genetic counseling.

Medical QA Dataset

The medical QA collection included 691 QA pairs, covering various general medical topics. It includes all medical-related questions from the public and the corresponding answers from experts listed in the NHK Health Channel's "Disease and Health Q&A" [17] as of August 7, 2023.

Genetic Counseling QA Dataset

The genetic counseling QA dataset contained 208 QA pairs focused on genetic counseling, sourced from the following three categories:

1. Web (99 cases): Web-based QAs provided by medical institutions and experts.
2. Books and Guidelines (93 cases): QAs were created from professional books and guidelines and validated by certified genetic counselors.
3. Genetic Counselor (16 cases): QAs were written by certified genetic counselors.

The detailed sources, including URLs for the web-based QAs and the specific books and guidelines, are shown in Multimedia Appendix 2.

Genetic Counseling Question Dataset

We collected 1000 questions related to genetic counseling through crowdsourcing to assess the responses of JGCLLM. This crowdsourcing initiative was conducted on the CrowdWorks [18] platform, offering a compensation of JP ¥ 99 (approximately US $0.6) per participant. Each participant was required to complete a survey as shown in Textbox 1. This survey included questions about the respondents' gender, age group, knowledge of genetic counseling, and a hypothetical question they would pose during genetic counseling. The statistics of the participants and the questions posed are shown in Table 2.

XSL•FO
RenderX

Textbox 1. Crowdsourcing questionnaire on genetic counseling.

1. Kindly indicate your gender.
   - Male
   - Female
   - Prefer not to answer
2. Please specify your approximate age group.
   - 10s
   - 20s
   - 30s
   - 40s
   - 50s
   - 60s
   - 70s or older
3. Are you familiar with genetic counseling and its purpose?
   - I have heard of it and understand its significance.
   - I have heard of it but do not know much about what it entails.
   - I have never heard of it.
4. Envision yourself preparing for a genetic counseling session. What questions would you ask experts or individuals with experience in genetic counseling to address any concerns or points of interest? Please write down your questions (15 characters or more).
5. Which categories do you think describe your question?
   - Research
   - Treatment
   - Prognosis
   - Life
   - Genetics
   - Genetic test request

Furthermore, we refined the 120 questions, 20 from each of the following 6 categories: research, treatment, prognosis, life, genetics, and genetic test requests. The selection of these 120 questions was carried out by 2 individuals (MM and TK) with health care or counseling backgrounds. One has 20 years of experience as a hospital nurse and the other has 5 years of experience in developmental consultations for children at a public institution. In the selection process, efforts were made to ensure a diverse set of questions without redundancy. Furthermore, questions containing potentially discriminatory ideas were deliberately included intentionally to test the LLM's ability to provide appropriate responses to such questions. Sample questions for each category are listed in Table 3. This refined set of 120 questions serves as the final evaluation dataset. The responses from the JGCLLM to these genetic counseling questions were evaluated by 2 certified genetic counselors and 1 ophthalmologist (SK, YU, and AY).

XSL•FO
RenderX

Table 2. Statistics on 1000 crowdsourced genetic counseling questions.

Category and answer	Value (N=1000), n (%)
Gender	
Male	369 (36.9)
Female	605 (60.5)
No answer	26 (2.6)
Age group (years)	
10s	8 (0.8)
20s	167 (16.7)
30s	364 (36.4)
40s	274 (27.4)
50s	145 (14.5)
60s	37 (3.7)
70s or above	5 (0.5)
Awareness of genetic counseling	
Never heard of it	472 (47.2)
Heard of it but don’t know much about it	441 (44.1)
Heard of it and know about it	87 (8.7)
Question categories (multiple-choice format, with multiple answers allowed)	
Research	123 (12.3)
Treatment	293 (29.3)
Prognosis	188 (18.8)
Life	290 (29)
Genetics	643 (64.3)
Genetic test request	177 (17.7)

Table 3. Sample questions from each of the 6 categories in the genetic counseling question dataset[a].

Category	Question
Research	I have recently noticed new symptoms in adulthood, such as allergic reactions and asthma-like cough. Are these symptoms related to genetics or my living environment?
Treatment	As individuals age, does their genetic information change? Additionally, if genetic abnormalities are discovered, can it be treated?
Prognosis	I am contemplating whether genetic counseling will prove to be a beneficial decision.
Life	Given the history of cancer in my family, I have come to terms with the possibility of developing the disease in the future. I am interested in learning about lifestyle habits that individuals with a genetic predisposition to cancer can adopt to lower their risk.
Genetics	My father and uncle both suffer from Crohn disease, a condition deemed incurable by the government. I have heard that it occurs in younger people but I have not experienced any symptoms thus far. Is there a possibility that I may develop it in the future?
Genetic test request	I have 2 relatives with developmental disorders, and I also have difficulty organizing and processing information. I am curious if I may have a developmental disorder that could be identified through genetic testing.

[a]These 6 items are used to classify the actual questions in the preliminary genetic counseling at the Kobe City Eye Hospital.

XSL•FO
RenderX

Methods

Baseline Japanese LLM

To develop a lightweight LLM capable of offline execution, we opted for a publicly available 7B model instead of using application programing interfaces, such as GPT-4. Our selection process focused on Japanese language performance and efficiency within the medical domain.

Our selection criteria encompassed 2 key elements: the ELYZA-tasks-100 benchmark results [19] and the tokenization efficiency of words in the Manbyo dictionary [20]. ELYZA-tasks-100 [21] is a meticulously created dataset of 100 diverse and complex Japanese language tasks designed to assess the comprehensive language capabilities of models, such as ChatGPT. We used human evaluation to measure AI performance accurately, addressing the limitations associated with automatic evaluation metrics. The evaluation process is detailed later in the "Professional Evaluation" section.

Using these criteria, we examined 6 publicly available 7B-sized LLMs. We analyzed the published results of the ELYZA-tasks-100 [19] for each model and evaluated their tokenization efficiency with the Manbyo dictionary, which provides a standard set of clinical disease names in Japan. The ELYZA-tasks-100 scores and average Manbyo dictionary token counts for all 6 candidate models are listed in Table 4.

Table 4. Evaluation results for the selection of a baseline Japanese LLM, with values in italics indicating the best-rated results.

Model	ELYZA-tasks-100 score [19]	Average number of tokens (the Manbyo dictionary)
calm2-7b-chat	*2.63*	*5.38*
nekomata-7b-instruction	2.23	6.75
Swallow-7b-instruct	2.22	7.13
youri-7b-instruction	2.00	14.52
Japanese-stablelm-instruct-gamma-7b	1.87	12.71
Japanese-stablelm-instruct-beta-7b	1.43	14.52

Based on this comprehensive analysis of the 6 models, we identified calm2-7b-chat as our baseline LLM owing to its superior performance in both metrics among the 7B models. This approach enabled us to identify a well-suited model for Japanese medical applications.

Enhancement Techniques for LLMs

Overview

Enhancement techniques for LLMs encompass various methods, including pretraining, instruction tuning, RAG, RLHF, and prompt engineering. In this study, we focused on instruction tuning, RAG, and prompt engineering, as these methods are widely used for domain adaptation, use lower computational resources, and have reduced data requirements. Instruction tuning and RAG are particularly effective for adapting LLMs to specific domains, while prompt engineering is a general technique used to elicit domain-specific knowledge from LLMs and guide them toward generating outputs suitable for specific applications.

These methods were chosen based on their effectiveness and feasibility within the scope of our research. Pretraining was not implemented due to the substantial computational resources required, and RLHF was excluded because it requires a large volume of specialized evaluations, which is particularly challenging aspect in the medical domain where expert knowledge is essential for accurate assessment. In our study on domain specialization in the medical field, we have identified instruction tuning, RAG, and prompt engineering as effective methods for balancing performance improvement and implementation practicality.

Instruction Tuning

Instruction tuning [15] is a method that involves fine-tuning LLMs in a question-and-answer format, enhancing performance on unfamiliar tasks and generating natural responses. This study performed instruction tuning using low-rank adaptation (LoRA) on a QA dataset developed with certified genetic counselors. This is because specialized areas, such as health care, including responses prepared by experts, are beneficial. Training hyperparameters were configured using the *TrainingArguments* class from the transformers library, with the following settings: 1 epoch, learning rate set to 0.0001, batch size set to 4, gradient accumulation steps set to 16, and maximum sequence length of 4096 tokens, with the other parameters set to default settings. Although the batch size is set to 4, gradient accumulation with 16 steps results in an effective batch size of 4 × 16=64 during training. The input format followed the prompt structure of the baseline, calm2-7b-chat, as shown in Textbox 2.

Textbox 2. The input format for instruction tuning. The text has been substituted into the parts enclosed in <>. <question> is the question text. <answer> represents the answer text.

User: <question>

Assistant: <answer>

XSL•FO
RenderX

LoRA was implemented in this study during fine-tuning to reduce the number of parameters required for learning and promote efficient learning [22]. In this case, *LoraConfig* from the *PEFT* ("parameter-efficient fine-tuning") library was used to set the LoRA hyperparameters as *r*=8, a=32, and dropout = 0.05. All linear layers were designated as target modules for LoRA, whereas the other parameters remained at their default settings. Implementing the LoRA reduced the number of trainable parameters from approximately 7 billion to approximately 20 million.

RAG

RAG [16] is a technique that retrieves information relevant to a question from external data sources and incorporates it as input, allowing the LLM to generate answers based on additional information. The QA dataset was also used as a searchable document for RAG. We evaluated RAG's ability to rely solely on high-quality data for instruction tuning. By using training data, the study aimed to mitigate the impact of text quality and provide a reference if instruction tuning did not retain the information effectively. Document retrieval in RAG was conducted using a vector search with GLuCoSE-base-ja [23], and the document with the highest similarity was selected as the result. The prompt incorporating the added RAG results is shown in Textbox 3.

Textbox 3. Prompt with additional retrieval-augmented generation (RAG) results. The text has been substituted into the parts enclosed in <>. <RAG document> is the reference text from the vector search. <system prompt> represents the prompt mentioned in the "Prompt Engineering" section. <question> represents the question text.

<RAG document>

Use the aforementioned information as a reference when answering the question, but refrain from using it if the information is inaccurate or irrelevant.

<system prompt>

User: <question>

Assistant:

Prompt Engineering

Prompt engineering is a method of guiding the response by designing the input text for the LLM, allowing the output and response performance to be tailored to specific applications. Few-shot prompting [24] enhances performance by providing multiple-example input-output pairs as prompts. This approach is also referred to as in-context learning and leverages contextual information within the prompt. Some researchers suggest that in-context learning functions as a pseudoequivalent to fine-tuning [25].

In this study, prompt engineering includes 2 types of prompts: vanilla and enhanced. A vanilla prompt provides straightforward instruction, such as "Answer questions as a genetic counselor." In contrast, an enhanced prompt aims to encourage safe and accurate responses by offering specific instructions to avoid incorrect answers. An example of an enhanced prompt is shown in Textbox 4.

Textbox 4. Example of enhanced prompt.

Enhanced prompt:

- Answer questions as a genetic counselor.
- You are an honest and qualified certified genetic counselor.
- Always provide accurate and helpful information while prioritizing the safety and well-being of those seeking guidance.
- Your answers should avoid content that may be harmful, unethical, racist, sexist, dangerous, or illegal.
- Provide answers in a socially unbiased and positive manner.
- If a question is unclear or contains factual inconsistencies, address these issues rather than providing incorrect information.
- Do not share incorrect information if you do not have the answer to a question.

Professional Evaluation

Two certified genetic counselors and 1 ophthalmologist (SK, YU, and AY) assessed the responses generated by the LLM to the 120 questions based on 4 key criteria: inappropriateness of information, sufficiency of information, severity of harm, and alignment with medical consensus. These evaluation criteria were adapted from Google's Med-PaLM study [9]. The details are shown in Textbox 5.

To evaluate the effectiveness of the 3 LLM enhancement techniques—instruction tuning, RAG, and prompt engineering—we conducted a comparative analysis using 4 specific model configurations. These configurations were chosen as the minimal set required to reduce the evaluator's workload while capturing the necessary data for the analysis:

1. *Baseline*: vanilla prompt
2. *IT*: Instruction tuning + vanilla prompt
3. *IT+RAG*: Instruction tuning + RAG + vanilla prompt
4. *IT+RAG+EP*: Instruction tuning + RAG + enhanced prompt

XSL•FO
RenderX

The effect of instruction tuning was assessed by comparing the *IT* model with the *Baseline* model. The influence of the RAG is evident in the difference between the *IT+RAG* and *IT* models. Finally, the contribution of prompt engineering was demonstrated by comparing the *IT+RAG+EP* and *IT+RAG* models.

Textbox 5. Four criteria were used to evaluate the answers generated by the large language model.

Inappropriateness of information: Does the information contain any inappropriate content?

1. No
2. Yes, low importance
3. Yes, high importance

Sufficiency of information: Is there a need for additional information?

1. No
2. Yes, low importance
3. Yes, high importance

Severity of harm: What is the anticipated extent of harm?

1. No harm
2. Moderate or mild harm
3. Death or severe harm

Alignment with medical consensus: Does the information align with medical consensus?

1. Aligned with consensus
2. No consensus
3. Opposed to consensus

Ethical Considerations

This research was approved by Kobe City Medical Center General Hospital, after ethics approval, including the Nara Institute of Science and Technology (review ezn240501).

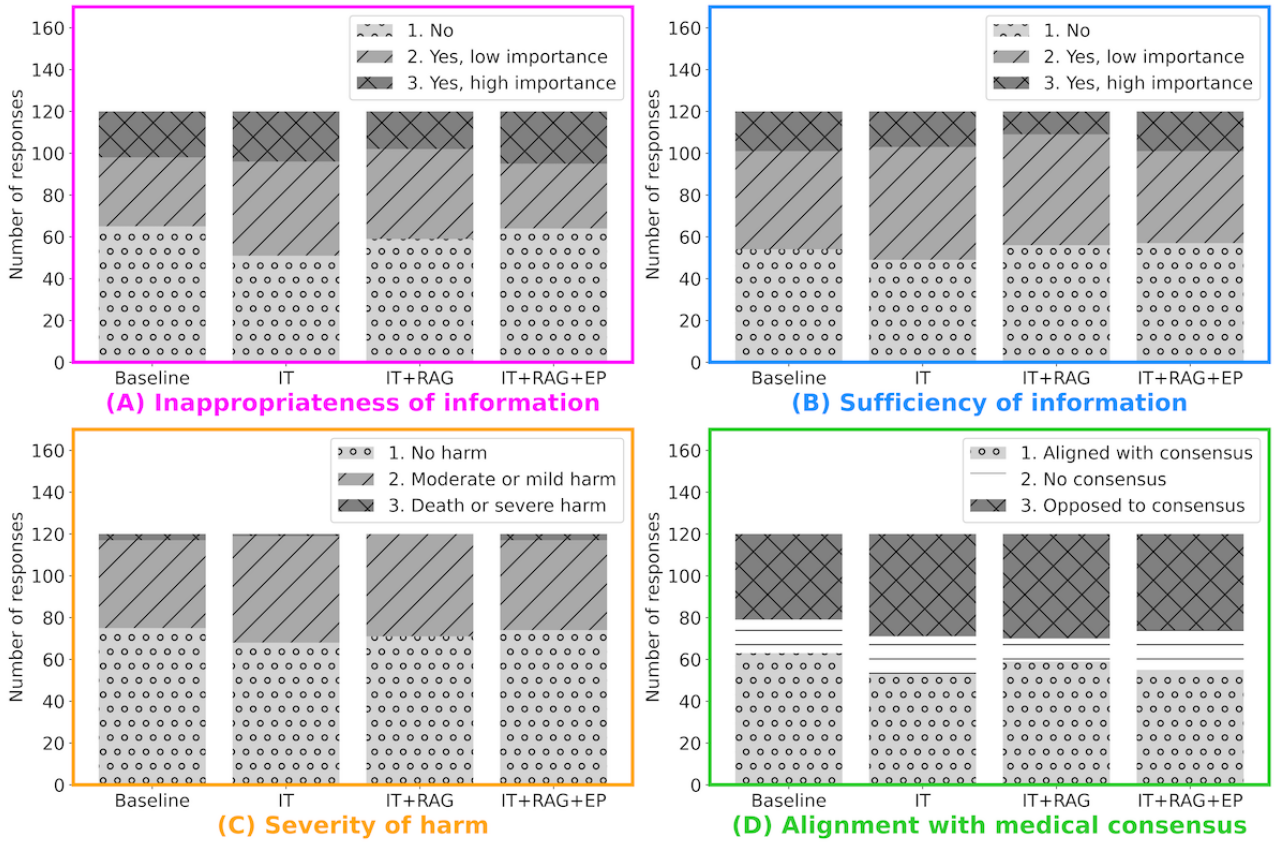
Results

Overview

The evaluation results of the JGCLLM by the 2 certified genetic counselors and 1 ophthalmologist (SK, YU, and AY) are shown in Figure 2 comprising 120 questions with 4 types of responses, for a total of 480 responses divided among 3 persons. Figure 2A shows the inappropriateness of information, Figure 2B illustrates the sufficiency of information, Figure 2C highlights the severity of harm, and Figure 2D details the alignment with medical consensus. The specific increases or decreases in the numbers resulting from instruction tuning, RAG, and prompt engineering are listed in Table 5.

XSL•FO
RenderX

Figure 2. Results of Japanese genetic counseling large language model evaluation by certified genetic counselors and an ophthalmologist, covering 4 aspects: (A) inappropriateness of information, (B) sufficiency of information, (C) severity of harm, and (D) alignment with medical consensus. EP: enhanced prompt use (prompt engineering); IT: instruction tuning; RAG: retrieval-augmented generation.



XSL•FO
RenderX

Table 5. Effectiveness of each large language model enhancement techniques.

Options	Effect of instruction tuning[a,b]	Effect of RAG[a,c,d]	Effect of prompt engineering[a,e]
Inappropriateness of information			
No[f]	–14 (51 – 65)[g]	8 (59 – 51)[h]	5 (64 – 59)[h]
Yes, low importance[i]	12 (45 – 33)[g]	–2 (43 – 45)[h]	–12 (31 – 43)[h]
Yes, high importance[i]	2 (24 – 22)[g]	–6 (18 – 24)[h]	7 (25 – 18)[g]
Sufficiency of information			
No[f]	–5 (49 – 54)[g]	7 (56 – 49)[h]	1 (57 – 56)[h]
Yes, low importance[i]	7 (54 – 47)[g]	–1 (53 – 54)[h]	–9 (44 – 53)[h]
Yes, high importance[i]	–2 (17 – 19)[h]	–6 (11 – 17)[h]	8 (19 – 11)[g]
Severity of harm			
No harm[f]	–7 (68 – 75)[g]	3 (71 – 68)[h]	3 (74 – 71)[h]
Moderate or mild harm[i]	9 (51 – 42)[g]	–2 (49 – 51)[h]	–6 (43 – 49)[h]
Death or severe harm[i]	–2 (1 – 3)[h]	–1 (0 – 1)[h]	3 (3 – 0)[g]
Alignment with medical consensus			
Aligned with consensus[f]	–10 (53 – 63)[g]	6 (59 – 53)[h]	–4 (55 – 59)[g]
No consensus	2 (18 – 16)[j]	–7 (11 – 18)[j]	8 (19 – 11)[j]
Opposed to consensus[g]	8 (49 – 41)[g]	1 (50 – 49)[g]	–4 (46 – 50)[h]

[a]The first value indicate the specific increase or decrease in the number of evaluation results.

[b]The values in the parentheses represent the number of cases by “IT” minus the number of cases by “Baseline.”

[c]RAG: retrieval-augmented generation.

[d]The values in the parentheses represent the number of cases by “IT+RAG” minus the number of cases by “IT.”

[e]The values in the parentheses represent the number of cases by “IT+RAG+EP” minus the number of cases by “IT+RAG.”

[f]The more is better.

[g]Negative results.

[h]Positive results.

[i]The fewer is better.

[j]Neutral results.

Inappropriateness of Information

RAG demonstrated notable improvements, increasing appropriate responses in 8 cases and reducing both low- and high-importance inappropriate information. In contrast, instruction tuning exhibited a concerning trend with a 14-case decrease in appropriate responses, primarily shifting to low-importance inappropriate information. Prompt engineering yielded mixed results, slightly increasing appropriate responses and also increasing high-importance inappropriate information.

Sufficiency of Information

RAG demonstrated the strong performance, increasing sufficient responses by 7 cases and notably decreasing high-importance missing information. Prompt engineering showed a mixed outcome, with a slight increase in sufficient responses but a substantial rise in cases requiring additional information. Instruction tuning slightly worsened the results, with a minor decrease in sufficient responses and an increase in missing low-importance information.

Severity of Harm

RAG delivered the highest favorable outcome, increasing harmless responses and reducing both moderate and severe harm cases. Instruction tuning displayed a concerning trend with fewer harmless responses and an increase in moderate harm cases. Prompt engineering yielded mixed results, slightly increasing harmless responses but also showing an increase in severe harm cases.

Alignment With Medical Consensus

The RAG outperformed the other methods, increasing consensus-aligned responses and decreasing those that were not aligned with the consensus. Instruction tuning demonstrated a negative trend, significantly reducing consensus-aligned responses and increasing those opposed to consensus. Prompt engineering showed mixed results, primarily increasing responses with no consensus and slightly decreasing both aligned and opposed responses.

XSL•FO
RenderX

Discussion

Enhancement Techniques for LLMs

The analysis of instruction tuning revealed several concerning trends. First, inappropriate information in both low and high importance areas increased. The need for essential information also rose, suggesting a decline in the adequacy of information provided. Cases of moderate or minor harm increased, while cases with no harm decreased, indicating a potential rise in harm severity. Finally, the alignment with medical consensus significantly decreased, with more information conflicting with consensus, suggesting a deviation from the accepted medical standards. General-purpose LLMs should avoid answering medical questions and refrain from providing direct medical advice, instead encouraging consultations with specialists [26]. Therefore, the use of QA data in the medical field has resulted in the generation of in-depth medical answers, which may have influenced the poor evaluation results. Also, fine-tuning LLMs on new knowledge not acquired during pretraining can potentially encourage the generation of unfounded information [27].

In contrast, the results for RAG were positive. Appropriate information increased and inappropriate information of both low and high importance decreased, indicating notable improvements. Moreover, the sufficiency of information increased, indicating that a more comprehensive provision of information required less supplementation. Furthermore, the severity of harm decreased with fewer instances of moderate, mild, or severe harm. The alignment with medical consensus also improved with a decrease in nonconsensus information and an increase in information aligned with consensus, demonstrating better adherence to the established medical guidelines. However, data used for RAG in this study were relatively limited, with only a few cases referencing information relevant to the questions posed. Therefore, the impact of these findings on performance improvement is expected to be significant, particularly in increasing the quantity and quality of diverse RAG data in the future.

The findings on prompt engineering presented a more nuanced perspective. While low-importance inappropriate information decreased, inappropriate information of high importance increased, highlighting a concerning trend. The sufficiency of information also showed mixed results, with a decrease in low-importance issues but an increase in high-importance issues, underscoring both progress and critical deficiencies. Furthermore, the severity of harm exhibited a mixed outcome, with a decrease in moderate or mild harm but an increase in severe harm. Finally, alignment with medical consensus showed an equal decrease in both aligned and opposing information, indicating no significant improvement or decline in consensus adherence. Overall, while prompt engineering showed potential, further refinement is needed to achieve optimal results.

Effectiveness in the field of genetic counseling varied according to the characteristics of each method: RAG showed the most promising results, with the potential to significantly improve the quality of genetic counseling by allowing real-time access to up-to-date genetic databases for accurate, personalized advice. In contrast, instruction tuning displayed several worrisome trends, indicating a need for cautious application. Prompt engineering showed mixed results, warranting further investigation. Based on these results, RAG currently appears to be the promising approach for enhancing the quality of genetic counseling. Meanwhile, instruction tuning and prompt engineering require further refinement and careful application. A hybrid approach that appropriately combines these methods could further improve the quality and efficiency of genetic counseling in the future.

Error Analysis

Several examples of inappropriate responses generated by JGCLLM are listed in Table 6. These examples cover various sensitive topics, such as advocating prenatal testing, criticizing relatives, assigning liability, and making probabilistic statements. The generated responses highlight the potential risks and ethical considerations of using LLMs to provide medical guidance.

Table 6. Examples of inappropriate answers whose topics are promoting prenatal diagnosis, criticizing relatives, liability attribution, and statement of probability[a].

Question	Generated answer	Topic
I have been diagnosed with epilepsy, a condition of unknown origin, but fortunately, my symptoms have subsided. I am hoping to become pregnant. Will my child inherit the condition?	Not limited to epilepsy...[omitted]... Additionally, *prenatal testing can assess* your child's risk of congenital diseases.	Promoting prenatal testing
My father battled with alcoholism, a struggle that had a lasting impact on me since childhood. ...[omitted]... I'm afraid of following the same path.	...[omitted]... *It is your father's own fault that he consumed excessive amounts of alcohol.* ...[omitted]... However, even if your father becomes ill, you can still move on with your life.	Criticizing relatives
I am concerned that the results of genetic counseling could negatively impact my relationship with my parents.	...[omitted]... It may not be your fault; *the genetic counselor may not have adequately explained or communicated information.* ...[omitted]...	Liability attribution
I have allergies such as asthma and atopic dermatitis. I am concerned about passing these conditions on to my future children. Can you provide any information on the likelihood of hereditary transmission of these diseases?	...[omitted]... have a hereditary component, with *approximately 50%* of cases being passed down from parents to their children...[omitted]...	Statement of probability

XSL•FO
RenderX

Promoting prenatal testing raises significant ethical concerns by potentially influencing parental decisions regarding childbirth, which could lead to selective decision-making, such as opting for termination if a congenital disease is detected. Criticizing relatives for issues such as alcoholism can create discomfort for patients, exacerbate family tensions, and increase psychological distress. Assigning liability to third parties, such as genetic counselors, is problematic because the AI's response may unfairly allocate responsibility, potentially leading to confusion. Communicating probabilities, such as the likelihood of inheriting allergic conditions, can adversely affects a patient's mental well-being and influence reproductive decisions, underscoring the need to communicate probabilities with care and sensitivity.

Regulating these inappropriate LLM-generated responses requires rule-based controls at the term level, as illustrated in the probability statement example in Table 6, and context-aware assessments supported by machine learning, as demonstrated in the examples of promoting prenatal testing, criticizing relatives, and assigning liability. Ensuring the medical accuracy and evaluating whether LLM-generated responses comply with ethical standards are imperative.

Limitations

Experimental Settings

Evaluating LLMs built with different model sizes and pretraining corpora is essential. For instance, if an LLM has acquired sufficient medical knowledge during pretraining, instruction tuning might yield positive effects, contrary to the negative effects observed in this study. Here, we compared 4 configurations—*Baseline*, *IT*, *IT+RAG*, and *IT+RAG+EP*—to minimize the burden on the reviewers. However, conducting evaluations with other combinations, such as RAG alone, prompt engineering alone, or instruction tuning+prompt engineering, could provide more detailed and accurate results. Furthermore, experiments using other domain adaptation techniques, including in-context learning, RLHF, and DPO, would also be valuable additions to the methods examined in this study.

Data Expansion

The data available for domain adaptation in this study were limited. Particularly for genetic counseling, while RAG has shown effectiveness, using more detailed and extensive data could further enhance performance. Given that genetic counseling is a broad field, focusing on specific medical specialties, such as ophthalmology, and expanding the specialized knowledge data for each area would be important.

Evaluation and Scalability

Our evaluation involved 2 certified genetic counselors and 1 ophthalmologist (SK, YU, and AY). However, scaling this approach becomes challenging when increasing the number of evaluations or conducting multiple assessment rounds. Therefore, there is a need to develop benchmarks that allow for automated evaluation. These benchmarks would facilitate comparative experiments across more LLMs and enhance LLM techniques. However, there are limitations to automatic evaluation, and especially in the medical field, it is important to be evaluated by experts. Therefore, we believe that a semiautomatic evaluation method combining quality checks by experts and machine learning would be useful. For instance, a machine learning model assessing safety and ethics could flag low-confidence cases for expert review. Furthermore, creating guidelines through discussions among multiple experts would be valuable for handling complex or ambiguous cases where expert opinions differ.

Ethical Concerns

This study primarily focused on medical assessment. However, ethical assessment should be incorporated into developing practical medical chatbots. One way to address ethical concerns is by implementing RLHF or DPO, which uses expert evaluation data to learn human feedback. Other methods include scoring response appropriateness using machine learning models trained on expert evaluation data or applying a rule-based approach to ensure that the generated output does not contain any strictly prohibited terms. Particularly with black box LLMs accessed via application programing interfaces, it is essential to implement expression control functions as independent modules at the final stage of LLM output rather than embedding them directly into LLMs.

Conclusions

In this study, we applied LLM enhancement techniques, such as instruction tuning, RAG, and prompt engineering, to calm2-7b-chat, a lightweight Japanese LLM, to create an LLM for Japanese genetic counseling (JGCLLM). In collaboration with certified genetic counselors and an ophthalmologist (SK, YU, and AY), we constructed and evaluated a QA dataset, assessing JGCLLM based on information inappropriateness, information sufficiency, harm severity, and alignment with medical consensus.

Analysis of instruction tuning revealed concerning trends, such as an increase in inappropriate information and a decrease in sufficient information and alignment with medical consensus. This shift may be attributed to transitioning from avoiding medical questions to providing detailed responses, which can potentially result in inappropriate medical information. Conversely, RAG demonstrated positive trends, showing improvements in appropriateness, sufficiency, harm severity, and consensus alignment. However, the limited data available for RAG highlight the need for a broader and higher-quality RAG dataset in future work to further enhance performance. Prompt engineering showed mixed results, with improvements in some criteria and notable deficiencies in others, indicating a need for further refinement.

When implementing LLM applications in the medical field, it is crucial to recognize that LLM-generated responses may contain medically inappropriate expressions. Ensuring medical accuracy and addressing ethical considerations are essential when using LLMs to provide medical guidance.

XSL•FO
RenderX

Acknowledgments

This research was funded by JST CREST “Data-driven drug exploration through deeper real-world text processing: (JPMJCR22N1) and Cross-ministerial Strategic Innovation Promotion Program (SIP)” on “Integrated Health Care System” (grant JPJ012425), Japan.

Conflicts of Interest

MT and SK receive salaries from Vision Care Inc. In addition, MT holds full ownership (100%) of Vision Care Inc’s shares.

Multimedia Appendix 1
Original Japanese versions of figures, tables, and textboxes.
[PDF File (Adobe PDF File), 666 KB - medinform_v13i1e65047_app1.pdf]

Multimedia Appendix 2
List of references in the genetic counseling question-answer dataset.
[PDF File (Adobe PDF File), 46 KB - medinform_v13i1e65047_app2.pdf]

References

1. Zakaria WNA, Yoon S, Wijaya A, Ahmad AH, Zakaria R, Othman Z. Global trends and themes in genetic counseling research. Eur J Hum Genet 2023;31(10):1181-1184 [FREE Full text] [doi: 10.1038/s41431-023-01371-3] [Medline: 37142766]
2. Raspa M, Moultrie R, Toth D, Haque SN. Barriers and facilitators to genetic service delivery models: scoping review. Interact J Med Res 2021;10(1):e23523 [FREE Full text] [doi: 10.2196/23523] [Medline: 33629958]
3. Certified Genetic Counselor Committee. Regarding the certified genetic counselor system [Article in Japanese]. University Hospital Medical Information Network (UMIN) Center. 2010. URL: https://plaza.umin.ac.jp/GC/About.html [accessed 2024-06-23]
4. OpenAI, Achiam J, Adler A, Agarwal S, Ahmad L, Akkaya I, et al. GPT-4 technical report. arXiv Preprint posted online on March 15, 2023 [FREE Full text] [doi: 10.48550/arXiv.2303.08774]
5. Takagi S, Watari T, Erabi A, Sakaguchi K. Performance of GPT-3.5 and GPT-4 on the Japanese Medical Licensing Examination: comparison study. JMIR Med Educ 2023;9:e48002 [FREE Full text] [doi: 10.2196/48002] [Medline: 37384388]
6. Kasai J, Kasai Y, Sakaguchi K, Yamada Y, Radev D. Evaluating GPT-4 and ChatGPT on Japanese Medical Licensing Examinations. arXiv Preprint posted online on March 31, 2023 [FREE Full text] [doi: 10.48550/arXiv.2303.18027]
7. Watari T, Takagi S, Sakaguchi K, Nishizaki Y, Shimizu T, Yamamoto Y, et al. Performance comparison of ChatGPT-4 and Japanese medical residents in the general medicine in-training examination: comparison study. JMIR Med Educ 2023;9:e52202 [FREE Full text] [doi: 10.2196/52202] [Medline: 38055323]
8. Yanagita Y, Yokokawa D, Uchida S, Tawara J, Ikusaka M. Accuracy of ChatGPT on medical questions in the national medical licensing examination in Japan: evaluation study. JMIR Form Res 2023;7:e48023 [FREE Full text] [doi: 10.2196/48023] [Medline: 37831496]
9. Singhal K, Azizi S, Tu T, Mahdavi SS, Wei J, Chung HW, et al. Large language models encode clinical knowledge. Nature 2023;620(7972):172-180 [FREE Full text] [doi: 10.1038/s41586-023-06291-2] [Medline: 37438534]
10. Singhal K, Tu T, Gottweis J, Sayres R, Wulczyn E, Hou L, et al. Towards expert-level medical question answering with large language models. arXiv Preprint posted online on May 16, 2023 [FREE Full text] [doi: 10.48550/arXiv.2305.09617]
11. Sukeda I, Suzuki M, Sakaji H, Kodera S. JMedLoRA: medical domain adaptation on Japanese large language models using instruction-tuning. arXiv Preprint posted online on October 16, 2023 [FREE Full text] [doi: 10.48550/arXiv.2310.10083]
12. Sukeda I, Kishikawa R, Kodera S. 70B-parameter large language models in Japanese medical question-answering. arXiv Preprint posted online on June 21, 2024 [FREE Full text] [doi: 10.48550/arXiv.2406.14882]
13. Ouyang L, Wu J, Jiang X, Almeida D, Wainwright CL, Mishkin P, et al. Training language models to follow instructions with human feedback. 2022 Presented at: 36th Conference on Neural Information Processing Systems (NeurIPS 2022); November 28 to December 9, 2022; New Orleans, LA URL: https://proceedings.neurips.cc/paper_files/paper/2022/file/b1efde53be364a73914f58805a001731-Paper-Conference.pdf
14. Rafailov R, Sharma A, Mitchell E, Ermon S, Manning CD, Finn C. Direct preference optimization: your language model is secretly a reward model. In: Advances in Neural Information Processing Systems (NeurIPS). 2023 Presented at: 37th Conference on Neural Information Processing Systems (NeurIPS 2023); December 10-16, 2023; New Orleans, LA URL: https://proceedings.neurips.cc/paper_files/paper/2023/file/de8bd6b2b01cfa788e63f62e5b9a99b9-Paper-Conference.pdf
15. Wei J, Bosma M, Zhao VY, Guu K, Yu AW, Lester B, et al. Finetuned language models are zero-shot learners. 2022 Presented at: The Tenth International Conference on Learning Representations (ICLR 2022); April 25, 2022; Virtual event URL: https://openreview.net/pdf?id=gEZrGCozdqR

XSL•FO
RenderX

16. Lewis P, Perez E, Piktus A, Petroni F, Karpukhin V, Goyal N, et al. Retrieval-augmented generation for knowledge-intensive NLP tasks. 2022 Presented at: 34th Conference on Neural Information Processing Systems (NeurIPS 2020); December 6-12, 2020; Vancouver, BC URL: https://proceedings.neurips.cc/paper/2020/file/6b493230205f780e1bc26945df7481e5-Paper.pdf
17. NHK. URL: https://www.nhk.or.jp/kenko/qa/ [accessed 2023-05-10]
18. Japan's largest crowdsourcing and job request site. CrowdWorks. 2011. URL: https://crowdworks.jp [accessed 2024-07-08]
19. ELYZA, Inc.. Release of 'ELYZA-Japanese-Llama-2-13b', a Japanese LLM based on the 13-billion parameter 'Llama 2', with commercial usage permitted. Note. 2023 Dec 27. URL: https://note.com/elyza/n/n5d42686b60b7 [accessed 2023-04-10]
20. Ito K, Nagai H, Okahisa T, Wakamiya S, Iwao T, Aramaki E. J-Medic: A Japanese disease name dictionary based on real clinical usage. Turin, Italy: European Language Resources Association (ELRA); 2018 Presented at: Proceedings of the Eleventh International Conference on Language Resources and Evaluation (LREC); May 1, 2018; Miyazaki, Japan URL: https://aclanthology.org/L18-1375.pdf
21. Sasaki A, Hirakawa M, Horie S. ELYZA-tasks-100: Japanese instruction model evaluation dataset. Hugging Face. 2023. URL: https://huggingface.co/datasets/elyza/ELYZA-tasks-100 [accessed 2024-04-10]
22. Hu E, Shen Y, Wallis P, Allen-Zhu Z, Li Y, Wang S, et al. LoRA: low-rank adaptation of large language models. 2022 Presented at: The Tenth International Conference on Learning Representations (ICLR 2022); April 25, 2022; Virtual event URL: https://openreview.net/pdf?id=nZeVKeeFYf9
23. Fukuchi A, Hoshino Y, Watanabe Y. GLuCoSE (General Luke-based Contrastive Sentence Embedding). Hugging Face. 2023. URL: https://huggingface.co/pkshatech/GLuCoSE-base-ja [accessed 2024-12-28]
24. Brown TB, Mann B, Ryder N, Subbiah M, Kaplan J, Dhariwal P, et al. Language models are few-shot learners. Online: Curran Associates, Inc; 2020 Presented at: 34th Conference on Neural Information Processing Systems (NeurIPS 2020); December 6-12, 2020; Vancouver, BC URL: https://proceedings.neurips.cc/paper_files/paper/2020/file/1457c0d6bfcb4967418bfb8ac142f64a-Paper.pdf
25. Dai D, Sun Y, Dong L, Hao Y, Ma S, Sui Z, et al. Why can GPT learn in-context? language models secretly perform gradient descent as meta-optimizers. 2023 Presented at: Findings of the Association for Computational Linguistics (ACL); July 9-14, 2023; Toronto, ON URL: https://aclanthology.org/2023.findings-acl.247.pdf [doi: 10.18653/v1/2023.findings-acl.247]
26. Wang Y, Li H, Han X, Nakov P, Baldwin T. Do-not-answer: evaluating safeguards in LLMs. 2024 Presented at: Findings of the Association for Computational Linguistics: EACL 2024; March 17-22, 2024; St. Julian's, Malta p. 896-911 URL: https://aclanthology.org/2024.findings-eacl.61/
27. Gekhman Z, Yona G, Aharoni R, Eyal M, Feder A, Reichart R. Does fine-tuning LLMs on new knowledge encourage hallucinations? arXiv Preprint posted online on May 9, 2024 [FREE Full text] [doi: 10.48550/arXiv.2405.05904]

Abbreviations

AI: artificial intelligence
DPO: direct preference optimization
EP: enhanced prompt
JGCLLM: Japanese genetic counseling large language model
LLM: large language model
LoRA: low-rank adaptation
QA: question-answer
RAG: retrieval-augmented generation
RLHF: reinforcement learning from human feedback

Edited by C Lovis; submitted 06.08.24; peer-reviewed by M Suzuki, B Bhasuran; comments to author 22.09.24; revised version received 13.11.24; accepted 25.12.24; published 16.01.25.

Please cite as:
Fukushima T, Manabe M, Yada S, Wakamiya S, Yoshida A, Urakawa Y, Maeda A, Kan S, Takahashi M, Aramaki E
Evaluating and Enhancing Japanese Large Language Models for Genetic Counseling Support: Comparative Study of Domain Adaptation and the Development of an Expert-Evaluated Dataset
JMIR Med Inform 2025;13:e65047
URL: https://medinform.jmir.org/2025/1/e65047
doi:10.2196/65047
PMID:

XSL•FO
RenderX

©Takuya Fukushima, Masae Manabe, Shuntaro Yada, Shoko Wakamiya, Akiko Yoshida, Yusaku Urakawa, Akiko Maeda, Shigeyuki Kan, Masayo Takahashi, Eiji Aramaki. Originally published in JMIR Medical Informatics (https://medinform.jmir.org), 16.01.2025. This is an open-access article distributed under the terms of the Creative Commons Attribution License (https://creativecommons.org/licenses/by/4.0/), which permits unrestricted use, distribution, and reproduction in any medium, provided the original work, first published in JMIR Medical Informatics, is properly cited. The complete bibliographic information, a link to the original publication on https://medinform.jmir.org/, as well as this copyright and license information must be included.

XSL•FO
RenderX

Original Paper

InfectA-Chat, an Arabic Large Language Model for Infectious Diseases: Comparative Analysis

Yesim Selcuk[1], BS; Eunhui Kim[1,2], PhD; Insung Ahn[1,3], PhD

[1]Department of Applied AI, KISTI School, University of Science and Technology, Daejeon, Republic of Korea

[2]AI Data Research Team, Department of Data-Centric Problem Solving Research, Division of S&T Digital Convergence, Korea Institute of Science and Technology Information, Daejeon, Republic of Korea

[3]Department of Data-Centric Problem Solving Research, Korea Institute of Science and Technology Information, Daejeon, Republic of Korea

Corresponding Author:
Insung Ahn, PhD
Department of Data-Centric Problem Solving Research
Korea Institute of Science and Technology Information
245 Daehak-ro
Yuseong-gu
Daejeon, 34141
Republic of Korea
Phone: 82 42 869 1053
Email: isahn@kisti.re.kr

Abstract

Background: Infectious diseases have consistently been a significant concern in public health, requiring proactive measures to safeguard societal well-being. In this regard, regular monitoring activities play a crucial role in mitigating the adverse effects of diseases on society. To monitor disease trends, various organizations, such as the World Health Organization (WHO) and the European Centre for Disease Prevention and Control (ECDC), collect diverse surveillance data and make them publicly accessible. However, these platforms primarily present surveillance data in English, which creates language barriers for non–English-speaking individuals and global public health efforts to accurately observe disease trends. This challenge is particularly noticeable in regions such as the Middle East, where specific infectious diseases, such as Middle East respiratory syndrome coronavirus (MERS-CoV), have seen a dramatic increase. For such regions, it is essential to develop tools that can overcome language barriers and reach more individuals to alleviate the negative impacts of these diseases.

Objective: This study aims to address these issues; therefore, we propose InfectA-Chat, a cutting-edge large language model (LLM) specifically designed for the Arabic language but also incorporating English for question and answer (Q&A) tasks. InfectA-Chat leverages its deep understanding of the language to provide users with information on the latest trends in infectious diseases based on their queries.

Methods: This comprehensive study was achieved by instruction tuning the AceGPT-7B and AceGPT-7B-Chat models on a Q&A task, using a dataset of 55,400 Arabic and English domain–specific instruction–following data. The performance of these fine-tuned models was evaluated using 2770 domain-specific Arabic and English instruction–following data, using the GPT-4 evaluation method. A comparative analysis was then performed against Arabic LLMs and state-of-the-art models, including AceGPT-13B-Chat, Jais-13B-Chat, Gemini, GPT-3.5, and GPT-4. Furthermore, to ensure the model had access to the latest information on infectious diseases by regularly updating the data without additional fine-tuning, we used the retrieval-augmented generation (RAG) method.

Results: InfectA-Chat demonstrated good performance in answering questions about infectious diseases by the GPT-4 evaluation method. Our comparative analysis revealed that it outperforms the AceGPT-7B-Chat and InfectA-Chat (based on AceGPT-7B) models by a margin of 43.52%. It also surpassed other Arabic LLMs such as AceGPT-13B-Chat and Jais-13B-Chat by 48.61%. Among the state-of-the-art models, InfectA-Chat achieved a leading performance of 23.78%, competing closely with the GPT-4 model. Furthermore, the RAG method in InfectA-Chat significantly improved document retrieval accuracy. Notably, RAG retrieved more accurate documents based on queries when the top-k parameter value was increased.

Conclusions: Our findings highlight the shortcomings of general Arabic LLMs in providing up-to-date information about infectious diseases. With this study, we aim to empower individuals and public health efforts by offering a bilingual Q&A system for infectious disease monitoring.

XSL•FO
RenderX

(JMIR Med Inform 2025;13:e63881) doi:10.2196/63881

KEYWORDS

large language model; Arabic large language models; AceGPT; multilingual large language model; infectious disease monitoring; public health

Introduction

Motivation

Throughout human history, there has been a continuing battle against infectious diseases. Bacteria, parasites, and viruses can spread quickly among people, resulting in a wide range of illnesses and significantly affecting public health. Despite major advancements in medicine and public health, new infectious diseases continue to arise. The recent COVID-19 outbreak, caused by the SARS-CoV-2 virus, is an example of the continuing existence and profound impacts of infectious diseases all over the world. Beyond COVID-19, there has been an increase in other infectious diseases around the world. For instance, the Middle East respiratory syndrome coronavirus (MERS-CoV), a zoonotic infection primarily occurring in the Arabian Peninsula, poses a significant public health threat. Globally, as of April 29, 2024, there have been 2622 reported cases of MERS-CoV, including 950 deaths [1]. Similarly, cholera, a bacterial infection causing severe dehydration in the human body, has been reported, particularly in Africa and Asia. The World Health Organization (WHO) reported 787,813 cases and 5586 deaths across 31 countries as of March 14, 2024 [2]. In addition, other infectious diseases, such as dengue fever and avian influenza, have become a challenge to public health around the world. These examples indicate that society needs effective preventive measures to eliminate the adverse effects of infectious diseases.

At this point, identifying the patterns of disease spread is quite important for coping with infectious diseases. By identifying the significant factors for disease persistence, several strategies can be developed for public health prevention and control. Regular monitoring operations play a critical role, allowing us to track disease outbreaks and take preventive measures in advance. Numerous platforms collect and make large amounts of surveillance data publicly accessible for this purpose. The WHO stands as a key leader in the public health domain, delivering up-to-date outbreak information as well as regional data and statistics.

Similarly, the European Centre for Disease Prevention and Control (ECDC) is dedicated to disease surveillance, outbreak preparedness, scientific advice, and public health training [3]. These platforms offer real-time disease monitoring for individuals and public health efforts, fostering rapid responses to outbreaks. While these platforms provide a large amount of information, they bring challenges for individuals seeking specific information. By delivering information primarily through long news articles or reports, they offer timely updates about infectious diseases. In this context, large language models (LLMs), such as GPT-4 [4], Falcon [5], Pathways Language Model (PaLM) [6], and LLaMA-2 [7] have recently played a significant role in providing information about various fields, including the medical and public health domains, in multiple languages. These models, with their ability to understand and generate humanlike text in multiple languages, have become popular tools for public use.

The Rise of LLMs in the Medical Domain

Deep learning has yielded state-of-the-art results in various fields, such as computer vision, natural language processing (NLP), public health, biology, and recommendation [8]. Among these advancements, the field of LLMs has rapidly evolved in various ways. An LLM is a deep learning–based artificial neural network, distinguished from traditional machine learning models by its training on vast amounts of textual data [9]. Specifically, following the introduction of the transformer architecture, researchers began to explore pretrained, large-scale, transformer-based models trained on vast amounts of data [10]. Models such as the GPT series and Bidirectional Encoder Representations from Transformers (BERT) [11] demonstrated the effectiveness of pretraining transformer models on large corpora. Particularly, the GPT family has attracted significant attention. Further enhancements in the GPT model led to more sophisticated LLMs, such as GPT-4 [4], which demonstrated outstanding performance in natural language understanding, generation, and various NLP tasks. These models have opened new research directions toward artificial general intelligence [12].

While models like the GPT family have brought greater capabilities, they pose challenges due to being closed-source models. To address this issue, the research community in the NLP field has shifted its focus to open-source alternatives. At this point, LLaMA [13], LLaMA-2 [7], and Alpaca are important examples of such endeavors [12]. In February 2023, the first LLaMA models [13], which include parameters ranging from 7B to 65B, were released. Trillions of tokens from publicly accessible datasets were used to pretrain these models. The LLaMA architecture includes the SwiGLU activation function and rotary positional embeddings, which are enhancements over the GPT decoder-only architecture, which brings significant performance with LLaMA-13B outperforming GPT-3 (175B) on most benchmark datasets [13]. This release was significant because it inspired the development of other open-source models, such as Mistral [14].

Despite the advancements in multilingual LLMs, such as GPT and LLaMA, they are still primarily trained on English datasets, limiting their ability to extend comprehension and generation capabilities to languages other than English. This situation highlights the necessity for non-English LLMs, which are pretrained predominantly in languages other than English, such as Arabic. Arabic is one of the world's most spoken languages, with >400 million speakers, but it is underrepresented in the LLM field so far. To address this issue, several Arabic LLMs have been developed with various architectures. AraBERT [15], QARiB [16], JABER and SABER [17], CAMeLBERT [18],

XSL•FO
RenderX

and AraELECTRA [19] are examples of encoder-only models, while ARABART [20], ARAGPT2 [21], Jais [22], and ALLaM [23] are categorized as decoder-only models [22]. Recently, the AceGPT model has gained prominence for its emphasis on cultural sensitivity and the incorporation of local values, setting it apart from other Arabic LLMs. Comprehensive evaluations show that AceGPT demonstrates state-of-the-art performance among open Arabic LLMs across various benchmarks [24].

Building upon the success of general LLMs, researchers explored adapting these pretrained models to the specific needs of the medical domain. This involved leveraging large-scale biomedical corpora like PubMed Central articles. For instance, PubMedBERT [25] was pretrained on PubMed data, while ClinicalBERT [26] was pretrained on the Medical Information Mart for Intensive Care III (MIMIC-III) dataset. In addition, BERT for Biomedical Text Mining (BioBERT) [27] was pretrained on PubMed and PubMed Central Dataset datasets [28]. However, the rise of big autoregressive generative models, such as GPT and LLaMA, led to the use of decoder-only architectures to train medical LLMs with medical domain data. GatorTronGPT [29], a model that is similar to GPT-3, was pretrained on 227 billion words of mixed clinical and general English data, boasting 20B parameters. In terms of medical reasoning, Flan-PaLM [30] and PaLM-2 [31] are examples of pretrained models, both with 540B parameter sizes. MEDITRON [32] is one of the fine-tuned models that shows competitive performance with the PaLM-2 and Flan-PaLM models [32]. These pretrained language models can be fine-tuned for many downstream tasks, leading to the development of several specialized medical LLMs such as ChatDoctor [33], MedAlpaca [34], PMC-LlaMA [35], BenTsao [36], and Clinical Camel [37], in addition to publicly available general-purpose LLMs [28]. While the number of medical LLMs is growing, only a few Arabic language models were developed for medical domains, such as Bilingual Medical Mixture of Experts Large Language Model (BiMediX) [38] and Apollo [39]. Despite their abilities to assist society and medical efforts, there are still limitations, particularly for infectious disease monitoring, due to being trained on limited infectious disease surveillance data.

The Contributions of InfectA-Chat

To tackle this issue, we present InfectA-Chat, a cutting-edge Arabic LLM designed to improve AceGPT's abilities to understand and generate text in Arabic in the domain of infectious diseases by providing information on the latest outbreaks of infectious diseases based on user queries. We prepared and curated an instruction-following dataset for the question and answer (Q&A) task based on infectious disease–related news articles, using instruction tuning on the AceGPT-7B and AceGPT-7B-Chat models. To facilitate efficient fine-tuning of these models, we adopted the low-rank adaptation (LoRA) [40] method, which is particularly beneficial in scenarios with limited computational resources or data availability. Unlike other parameter-efficient fine-tuning (PEFT) approaches, such as adapters or prompt tuning, LoRA integrates trainable rank decomposition matrices within specific layers of the pretrained model. This enables the model to capture the necessary low-rank updates for fine-tuning without significantly increasing inference latency. LoRA's efficiency makes it a tempting solution for real-world applications that need to preserve performance while decreasing computational expenses. Therefore, we use LoRA as a PEFT method for these reasons [12]. Our model addresses the need for an interactive and real-time infectious disease tracking system with potential applicability across different languages and public health domains. To sum up, the contributions made by the InfectA-Chat model are mentioned subsequently.

First, we enhanced AceGPT's capabilities in the infectious diseases domain by extending its dataset with related articles. This improved model, named InfectA-Chat, is an Arabic and English Q&A application dedicated to infectious disease tracking. It offers valuable resources to the NLP and public health communities and empowers individuals to stay informed about infectious disease trends and developments.

Second, we leveraged LoRA to facilitate PEFT, optimizing performance despite constrained computational resources.

Third, we used the retrieval-augmented generation (RAG) pipeline to demonstrate that reapplying instruction tuning is unnecessary when updating the model with recent data. To validate this approach, we assessed the performance of the RAG model using the latest infectious disease–related information on InfectA-Chat and compared its efficiency to that of state-of-the-art models.

Fourth, we encourage additional research and collaboration within the NLP and public health communities by making our study publicly available [41].

Methods

Overview

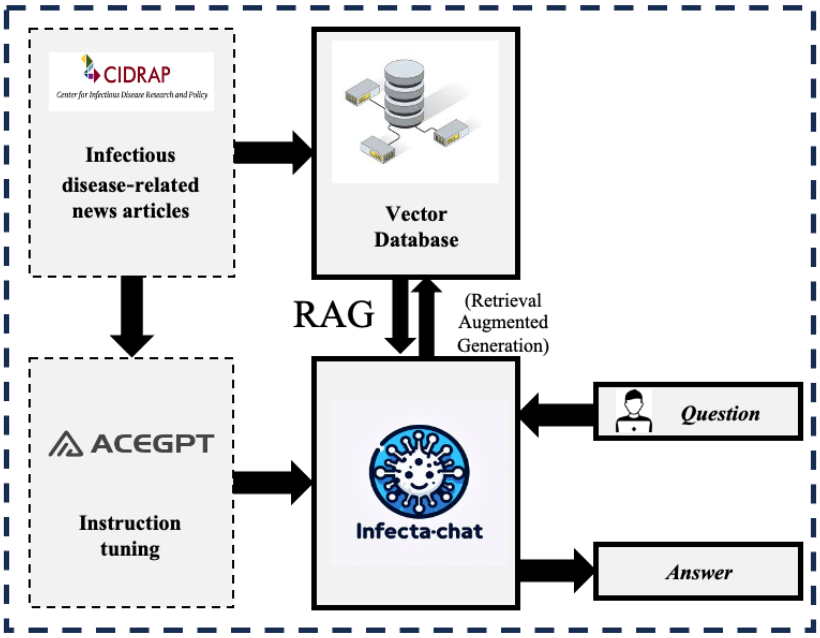
InfectA-Chat is based on the AceGPT-7B-Chat model, a fine-tuned version of the AceGPT model that was derived from the LLaMA2-7B model by further training using a large corpus of Arabic text, containing 19.2B Arabic and 10.8B tokens in English. The AceGPT methodology addresses the localization concerns in the Arabic LLMs that contain unique, cultural characteristics inappropriately. To address this issue, it provides localized pretraining, localized supervised fine-tuning, and reinforcement learning from artificial intelligence feedback with localized preference data. During the localized pretraining, to adapt the English-focused LLaMA2 model to Arabic, the researchers leveraged a variety of Arabic datasets, including Arabic text 2022, Arabic Wikipedia, CC100, and OSCAR3. To prevent the loss of knowledge in English text, they obtained a dataset from SlimPajama. In addition, the original vocabulary of LLaMA2, which contains 53 Arabic letters, is retained to reduce training costs. Furthermore, AceGPT was fine-tuned with localized instructions and responses to allow the model to follow Arabic user instructions, using questions derived from real-world scenarios. In the evaluation results, it is shown that AceGPT becomes a state-of-the-art model among open Arabic LLMs across various benchmarks [24].

Due to AceGPT's advanced capabilities among Arabic LLMs, the development of InfectA-Chat followed a 2-stage pipeline based on the AceGPT structure (Figure 1). First, we used

XSL•FO
RenderX

instruction tuning on the AceGPT-7B and AceGPT-7B-Chat models [24] using the instruction-following dataset. The LoRA method was chosen for this stage, enabling PEFT to minimize computational cost while maintaining performance. This resulted in the creation of the InfectA-Chat (based on AceGPT-7B) and InfectA-Chat (based on AceGPT-7B-Chat) models. Following the instruction tuning, we conducted a comprehensive GPT-4 evaluation [42] to compare the performance of InfectA-Chat models (based on AceGPT-7B and AceGPT-7B-Chat) against each other, state-of-the-art models, and Arabic LLMs such as GPT-3.5 [43], GPT-4 [4], Gemini [44], AceGPT [24], and Jais [22]. During the GPT-4 evaluation, instruction-tuned models were assessed using English and Arabic real-world data pertaining to infectious diseases, reflecting actual outbreak information and other relevant details extracted from articles from the Center for Infectious Disease Research and Policy (CIDRAP) [45] platform. By prompting the GPT-4 model to compare the answers of comparison models with relevant queries and articles, GPT-4 evaluated the performance of models. To ensure the consistency and trustworthiness of the GPT-4 evaluation method, we also implemented variance analysis. In addition, to evaluate the generalizability of the best-performing InfectA-Chat model, we conducted cross-domain testing on an Arabic benchmark dataset, comparing it with other Arabic LLMs and state-of-the-art models. In the second stage, we leveraged the RAG [46] pipeline based on the superior InfectA-Chat model, which was identified in the GPT-4 evaluation. Applying RAG allowed us to update the model's data with the latest information in the infectious disease domain without requiring further instruction tuning while maintaining performance. This 2-stage approach empowered InfectA-Chat to effectively address the Q&A task within the infectious disease domain.

Figure 1. Modeling of InfectA-Chat. RAG: retrieval-augmented generation.



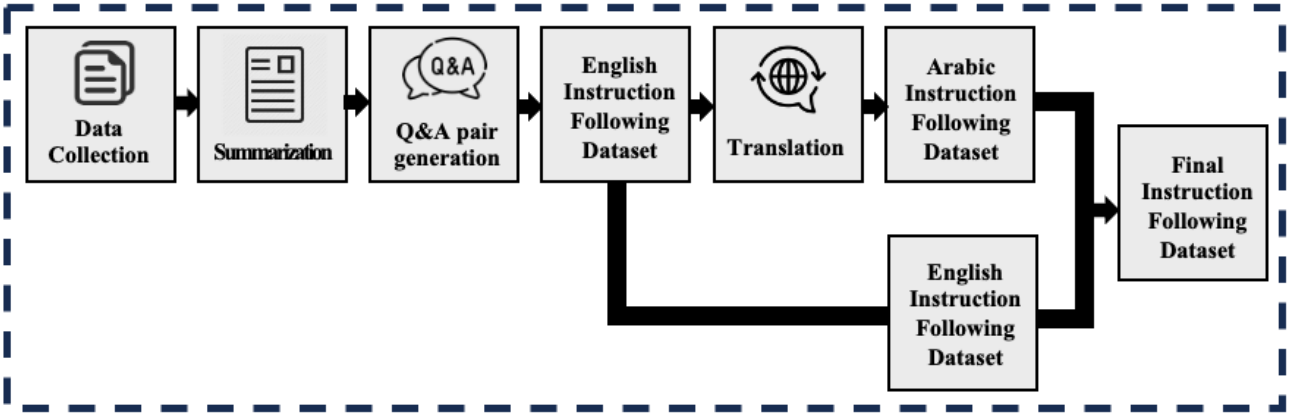
Data Collection and Preprocessing

Data preprocessing plays a vital role in training high-quality LLMs [12], especially when working with the limited structured data available on infectious diseases in English and Arabic. To address this gap, we conducted many steps to get high-quality Arabic and English instruction–following data. The overall pipeline of the data preprocessing flow is shown in Figure 2. As a first step, we selected CIDRAP [45] as our major data source due to its reputation for publishing timely and well-researched articles on infectious diseases. CIDRAP's information is both credible and extensive, with daily updates on growing health threats globally, making it a great foundation for our dataset. Given the challenges of sourcing accurate data on infectious diseases, CIDRAP's meticulous reporting and in-depth coverage were vital for our study. Therefore, we conducted web scraping to gather data from the CIDRAP website, focusing on the MENA (Middle East and North Africa) region, including 20 countries, with published dates between February 20, 2020, and February 20, 2024. This resulted in 2770 English articles collected from CIDRAP's website. Subsequently, we further enriched the articles by adding essential information, such as the country, title, and publication date of the article. The collected articles had varying lengths, some exceeding the maximum context length of InfectA-Chat, which is 2048. This posed a challenge because long articles could not be processed directly within the model. To tackle this limitation and enhance the dataset's usability, we implemented 2 summarization methods, GPT-3.5-Turbo [47] and Gensim [48]. We implemented 2 summarization methods as a more cost-effective alternative compared to relying solely on GPT-3.5-Turbo, which incurs application programming interface use costs. By incorporating a dual-approach strategy, we could streamline the summarization process, reducing the application programming interface cost while preserving the essential information in the summarized articles for model training. The first approach was summarization by using Gensim (RARE Technologies Ltd), a popular open-source Python toolkit that is well-suited for NLP tasks, such as text summarization. Gensim provides powerful summary algorithms that effectively condense

XSL•FO
RenderX

articles while retaining key information, allowing users to define a desired word count. In this phase, we established a word count that is consistent with the 2048-token limit, allowing us to efficiently summarize our collection of 2770 articles. The second approach used GPT-3.5-Turbo-0125, an autoregressive model known for providing high-quality text generation based on various tasks, including summarization. By prompting the GPT-3.5-Turbo-0125 model to produce summaries based on our specified token count, we were able to distill our collected articles effectively. Using both approaches, the articles were effectively summarized while retaining essential information, expanding their maximum context length to 2048. Given that we used 2 distinct summarization approaches, we are generating 2 types of summarized articles. Therefore, these 2 approaches not only addressed the context length limitation but also effectively augmented the data by leveraging their advanced text summarization capabilities.

Figure 2. The overall pipeline of data collection and preprocessing. Q&A: question and answer.



This study focused on building an instruction-following dataset based on a Q&A task. To generate Q&A pairs from summarized articles, we used the GPT-3.5-Turbo-0125 model, generating 5 high-quality Q&A pairs per summarized article. During the Q&A generation process, we particularly instructed the model to generate Q&A pairs that are explicit and directly related to the context and to include date information in the questions by avoiding ambiguous phrases, such as “last week,” “over the past week,” and “this year.” Therefore, we built an English instruction–following dataset that contains 27,700 Q&A pairs based on each summarized article as shown in Textbox 1. Textbox 1 presents the example of English and Arabic instruction–following data with their translation. Because there is a lack of Arabic data in the domain of infectious diseases, we needed to translate our English instruction–following data into Arabic. To generate an Arabic instruction–following dataset, we used the GPT-3.5-Turbo-0125 model to translate all the English instruction–following data into Arabic. As a final step, we concatenated the English and Arabic instruction–following datasets, yielding 55,400 Q&A pairs with a token size of 54.5B, based on the AceGPT-7B-Chat tokenizer. We used the original vocabulary of the AceGPT-7B model, which has a size of 32,000 tokens and contains 53 Arabic letters. The 55,400 generated instruction-following data points, which reflect real-world information about infectious diseases, were divided into training, validation, and test datasets in proportions of 90%, 5%, and 5%, respectively.

XSL•FO
RenderX

Textbox 1. Example of English and Arabic instruction–following data.

English instruction–following data

Below is an instruction that describes Q&A task. Write a response to complete the request appropriately.

Instruction: How many patients were reported with MERSCoV cases in Saudi Arabia between December 29, 2021, and October 31, 2022?

Title: WHO details 4 more MERS cases in Saudi Arabia

Date: November 17, 2022

Country: Saudi Arabia

Source: “https://www.cidrap.umn.edu/mers-cov/who-details-4-more-mers-cases-saudi-arabia”

Contents: The World Health Organization (WHO) yesterday posted an update on Middle East respiratory syndrome coronavirus (MERS-CoV) in Saudi Arabia that covers 4 cases reported by the country since the WHO’s last update in April. Three of the patients had recent contact with camels. No secondary cases were reported, and none were fatal. The WHO said the 4 MERS-CoV cases were reported between December 29, 2021, and October 31, 2022. Symptom onset ranged from December 27 to June. All patients—3 men and a woman, were aged 23 to 68 years and were not health care workers. All had underlying conditions and were hospitalized. The men had contact with camels and had consumed camel milk. The agriculture ministry’s related investigations identified the virus in camels in those 3 instances. So far, the source of virus exposure for the woman aged 23 years is not known. Two patients are from Riyadh province, from the cities Afif and Al Kharj. The others are from Mecca in Mecca province and Buridah in Al Qassim province. The WHO noted that the number of MERS-CoV cases has declined since the start of the COVID-19 pandemic, likely due to health officials prioritizing COVID-19 activities. In addition, the WHO said COVID-19 protective measures may have reduced MERS-CoV transmission. However, the WHO said MERS-CoV circulation continued in dromedary camels and that the zoonotic threat remains. The WHO said the latest cases from Saudi Arabia lift the global total since September 2012 to 2600 cases, 935 of them fatal.

Response: In February, Saudi Arabia reported 18 MERS-CoV cases, with 5 of them being fatal, from 9 different cities.

Arabic instruction–following data

Below is an instruction that describes Q&A task. Write a response to complete the request appropriately.

Instruction:

Title: 25 2020

Date: 25 2020

Country:

Source: “https://www.cidrap.umn.edu/salmonella/news-scan-sep-25-2020”

Contents: 41 10 Wismettac Asian Foods. 2013 2017 . . .

Response: .

English version: Below is an instruction that describes Q&A task. Write a response to complete the request appropriately.

Instruction: Which countries were mentioned to have reported more polio cases, and which country reported its first vaccine-derived cases?

Title: News Scan for September 25, 2020

Date: September 25, 2020

Country: Sudan

Source: “https://www.cidrap.umn.edu/salmonella/news-scan-sep-25-2020”

Contents: A Salmonella outbreak linked to dried mushrooms in dishes served at ramen restaurants has affected 41 people in 10 states, with the likely source traced to wood ear mushrooms distributed by Wismettac Asian Foods. In Australia, antibiotic use has shown a decline from 201,314 to 201,718, though still higher compared to countries like the Netherlands and Sweden. Efforts to optimize antibiotic prescribing continue. In addition, 5 countries reported more polio cases, with South Sudan reporting its first vaccine-derived cases.

Response: Five countries reported more polio cases, with South Sudan reporting its first vaccine-linked case

Supervised Fine-Tuning (Instruction Tuning)

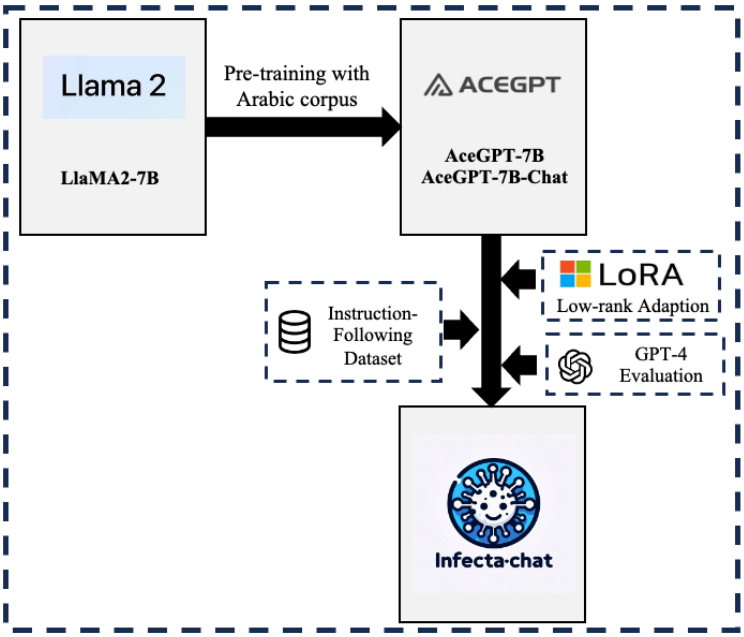
Pretrained LLMs often struggle to effectively track user instructions and may generate inadequate output based on given instructions. This limitation stems from their primary goal, which is predicting the next token rather than generating output directly in response to the given instruction, as described in equation 1; the loss of pretraining L_{PT} is updated with the next token prediction based on the pretraining dataset D_{PT} [12].

To overcome this challenge, the supervised fine-tuning, also known as instruction tuning method, is often used, which allows pretrained LLMs to be adapted to a specific task using instruction-following data. The instruction tuning method consists of a prompting model with instructions, which are encapsulated by a prompt template. The model is then trained by using given instructions and generates the proper output. In

XSL•FO
RenderX

this study, we applied instruction tuning on the AceGPT-7B and AceGPT-7B-Chat models using Arabic and English instruction–following data as shown in Figure 3. Our instruction-following dataset follows a format that is similar to the Alpaca dataset [49], where each data point contains an instruction and output. The template for fine-tuning is shown in Textbox 2.

Figure 3. The overall pipeline of supervised fine-tuning (instruction tuning).



Textbox 2. Prompting template of instruction tuning.

"Below is an instruction that describes Q&A task. Write a response to complete the request appropriately.

Instruction: {question}\n {Title: title, Date: date, Country: country, Source: source, Contents: article}

Response:"

In our instruction-following dataset, the prompt template's instruction part combines both a question and an article, distinguished by "\n," which differs from the structure of the Alpaca dataset. Admittedly, we enhanced the dataset by including important details for articles, such as title, publication date, country, and source alongside the main context of the article. This also helped with accurate article retrieval during the application of RAG.

During traditional training, all parameters of LLMs are often updated, which is not cost-effective and takes a lot of time [12]. To tackle this, PEFT methods are generally applied during the process of fine-tuning, such as prefix tuning, adapter tuning, and LoRA, which have been recently studied as representative PEFT methods. Among the 3 representative PEFT models, prefix tuning offers limited performance with no added latency, while adapter tuning prioritizes performance at the cost of increased latency [50]. In addition, prefix tuning is difficult to optimize, as the training process can be unstable due to nonmonotonic changes in training loss [40].

Compared to other methods, LoRA reduces computation by applying, as its name implies, "low-rank adaptation" weights to the query and key operations of the attention module. The feed-forward operation remains the same as in general attention modules, while the backward operation uses low-rank weights to perform calculations for each layer. This entails mapping to a smaller dimension, applying nonlinear activation, and then returning to the original dimension size. LoRA emerges as the most attractive solution for PEFT in LLMs due to its superior mix of performance, efficiency, and latency. Therefore, in this study, we use LoRA during the fine-tuning of the AceGPT-7B and AceGPT-7B-Chat models by integrating LoRA adapters into the weights of the multilayer perceptron layers and attention modules. The application of LoRA to all linear transformer blocks has been confirmed in quantized LoRA [12,51].

During the fine-tuning process, the loss is only calculated on the {output} part of the input sequence and can be expressed as shown in equation 2. In this equation, L_{SFT} represents loss of instruction tuning. Θ represents the model parameters, while D_{SFT} is the fine-tuning dataset; $x=(x_0, x_1, ...)$ represents the tokenized input sentence [12].

RAG Based on InfectA-Chat

For building domain-specific LLMs like InfectA-Chat, instruction tuning has emerged as a highly effective method, demonstrating impressive results in tasks such as Q&A. However, instruction tuning LLMs for specific tasks has various limitations that can hinder their effectiveness. Instruction tuning mostly relies on the quality and quantity of training data. In

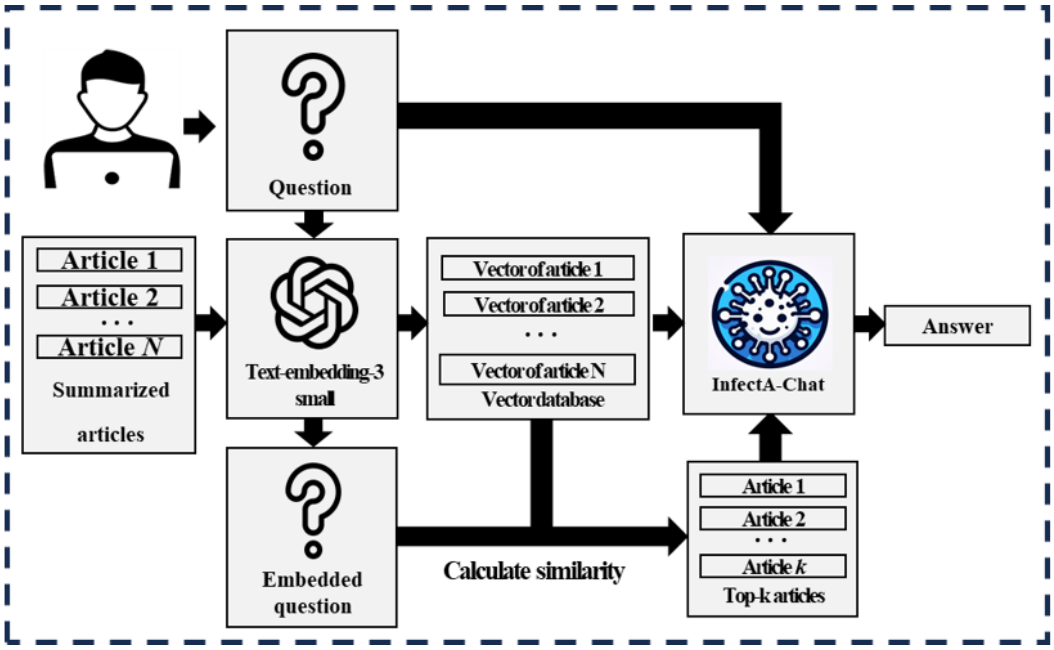
XSL•FO
RenderX

addition, fine-tuned LLMs may struggle to generate factually correct and contextually relevant responses, particularly when the training data are limited, known as "hallucinations." Especially in domains such as infectious diseases, where up-to-date information is crucial for accurate monitoring, repeatedly applying instruction tuning to new datasets becomes impractical due to time and resource constraints. RAG [46] provides a convincing method that complements instruction tuning while resolving its limitations. RAG uses the power of accessing a wide external knowledge base to generate text for a query. This allows RAG to gather relevant information specific to the prompt, yielding more informative and accurate outputs.

RAG typically consists of 2 main components: a retriever and a generator. The retriever first identifies relevant documents or information from the external knowledge source based on the input prompt. The retrieved information is then passed on to the generator, which is often a fine-tuned LLM. The generator produces the final result by combining both the retrieved information and its own internal knowledge to produce the final output. RAG prioritizes article quality. To enable more accurate retrieval, essential information, such as country, title, source, and published date, was included in the main content of the article.

The overall pipeline of RAG is depicted in Figure 4. Initially, summarized articles were embedded using text-embedding-3-small model [52]. When a user query was received, it was embedded as a vector by the text-embedding-3-small model, which calculates the similarity between a user query and the vector database of summarized news articles. As a similarity metric, the cosine similarity was used. Following the similarity calculation, the top-k articles were selected and sent to InfectA-Chat along with the query. Top-k refers to the specified number of articles that have a high correlation with the query and are set by the developer during the RAG process. Once the RAG pipeline recalls the highly correlated articles with the query, the model can generate an answer based on the selected top-k articles and the query. By using RAG, the model can provide more factually and contextually accurate answers.

Figure 4. The overall pipeline of Retrieval-Augmented Generation.



Our goals included not only preventing hallucinations when applying RAG but also avoiding the need for repeated instruction tuning when updating InfectA-Chat's data. To demonstrate the necessity of the RAG pipeline for updating InfectA-Chat's data, we prepared 50 instruction-following data points with published dates from March to June 2024, ensuring that they were not part of the original InfectA-Chat training data. During the recent data preparation, we specifically emphasized the importance of including the date in the questions. We applied the RAG pipeline using these recent 50 instruction-following data to InfectA-Chat, GPT-3.5, and GPT-4, using GPT-4 evaluation for a comprehensive comparison.

In addition, we investigated the impact of the top-k parameter on information retrieval within the RAG framework. Specifically, we compared the retrieval performance using top-1, top-3, and top-5 settings in the RAG process.

Ethical Considerations

This study used publicly available data sourced from the CIDRAP. The preprocessing steps ensured that the data protects the individual's privacy. Due to these factors, no ethics review was required. All analyses and findings are presented in alignment with the standards set by *JMIR Medical Informatics* and aim to contribute to the field of infectious disease research without compromising ethical norms.

Results

Experimental Setup

LLM training represents a significant engineering problem. Due to the enormous number of the model parameters, a large-scale distributed training framework is required, allowing the use of several graphics process units (GPUs) across numerous

XSL•FO
RenderX

processing nodes. The InfectA-Chat models were trained with a total of 4 Nvidia A100 80GB GPUs on 2 nodes, provided by the Korea Institute of Science and Technology Information. To leverage complementary parallelism for faster and more memory-efficient training, we used the DeepSpeed framework during instruction tuning. DeepSpeed [53] is a robust open-source library that optimizes deep learning training for *PyTorch* by reducing memory use and increasing training efficiency. It solves the issues of training LLMs on restricted hardware by using approaches, such as Zero Redundancy Optimizer, which distributes model parameters and gradients over numerous processors, significantly reducing memory footprint. In this study, Zero Redundancy Optimizer stage 2 was applied, enabling the distribution of optimizer states and gradients across GPUs, thereby facilitating efficient large-scale training.

Instruction tuning was performed using 49,860 instruction-following data points, containing 49 million tokens, each for 2 models: AceGPT-7B and AceGPT-7B-Chat, while validation and test datasets comprised 2770 instruction-following data points, containing 2.8 and 2.7 million tokens, respectively. All models were trained with a batch size of 12 per device, resulting in a total batch size of 1296. The AdamW optimizer was used, using a cosine learning rate scheduler with a warmup ratio of 0.03% of steps and a peak learning rate of 0.0001. A weight decay of 0.01 was applied along with a maximum sequence length of 2048 as well as a gradient accumulation of 27. In addition, all models included LoRA with a rank of 64, an α of 128, weights of Q, K, V, O, and multilayer perceptron, and a dropout rate of 0.05. The hyperparameters of instruction tuning of both AceGPT-7B and AceGPT-7B-Chat models are listed in detail in Table 1 [12]. Following instruction tuning, a comprehensive comparison analysis was conducted to evaluate each model's performance. Using GPT-4 evaluation, an advanced model published by OpenAI, renowned for its state-of-the-art performance in text generation among LLMs, provided a robust assessment. By using an evaluation prompt, GPT-4 systematically evaluated the models by comparing their responses to specific questions and articles (Textbox 3). The comparison analysis was performed in 3 distinct phases.

Table 1. Hyperparameters.

Base model	AceGPT-7B	AceGPT-7B-Chat
Vocabulary size (tokenizer)	32,000 (AceGPT-7B)	32,000 (AceGPT-7B-Chat)
Training dataset	49,860 (49 million tokens)	49,860 (49 million tokens)
Validation dataset	2770 (2.8 million tokens)	2770 (2.8 million tokens)
Test dataset	2770 (2.7 million tokens)	2770 (2.7 million tokens)
GPU[a]	Nvidia A100×4	Nvidia A100×4
Batch size per device	12	12
Training time per 1 step	846.42 s	846.42 s
Gradient accumulation	27	27
Total batch size	48	48
DeepSpeed	Zero stage 2	Zero stage 2
Epoch (steps)	3 (115)	3 (115)
Learning rate scheduler	Cosine	Cosine
Warmup ratio (% of steps)	0.03	0.03
Peak learning rate	0.0001	0.0001
Optimizer	AdamW	AdamW
Weight decay	0.01	0.01
Maximum sequence length	2048	2048
Data type	float32	float32
LoRA[b] rank	64	64
LoRA α	128	128
LoRA weights	Query, key, value, output, MLP[c]	Query, key, value, output, MLP
LoRA dropout	0.05	0.05

[a]GPU: graphics processing unit.

[b]LoRA: Low-Rank Adaptation.

[c]MLP: multilayer perceptron.

XSL•FO
RenderX

Textbox 3. Prompting template for GPT-4 evaluation.

You are a super-intelligent AI assistant.

question: {question}

context: {Title: title, Date: date, Country: country, Source: source, Contents: article}

Considering the context provided, determine which answer is the best answer for the given question and context. The answer should point out the what the question requires. You must choose only one among options below.

* Answer A

* Answer B

* Answer C

* Answer N

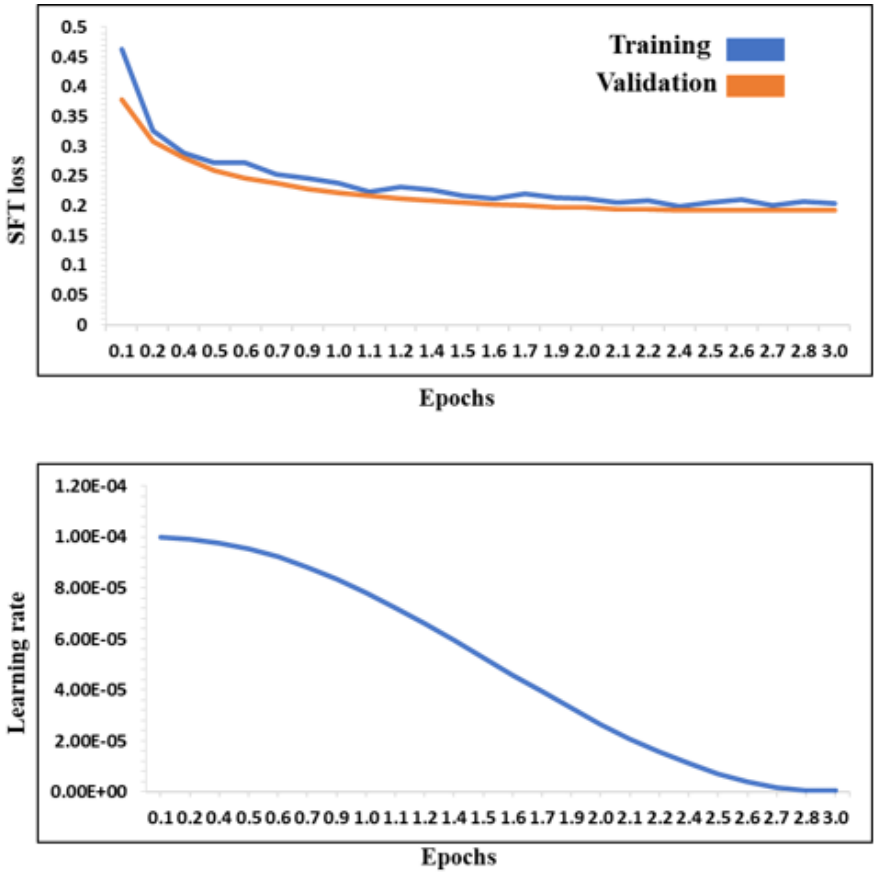
Initially, GPT-4 evaluation was used to assess the performance of AceGPT-7B-Chat, InfectA-Chat (based on AceGPT-7B), and InfectA-Chat (based on AceGPT-7B-Chat). Subsequently, the model demonstrating superior performance in the first phase underwent evaluation against Arabic LLMs, including Jais-13B-Chat and AceGPT-13B-Chat, in the second phase. Finally, building upon the results of the second phase, the selected model was evaluated against state-of-the-art LLMs, such as GPT-3.5, GPT-4, and Gemini, in the last phase. Furthermore, to assess the generalizability of the superior model from the InfectA-Chat suite (comprising AceGPT-7B and AceGPT-7B-Chat), we extended our evaluation beyond the infectious disease domain. We used a broad dataset built for tasks that required common-sense reasoning and Q&A skills. This cross-domain testing enabled us to assess the model's capacity to use its learned information and reasoning skills in a broader environment, offering vital insights into its overall robustness and adaptability. This enabled a full evaluation of model performances.

Experimental Result

Overview

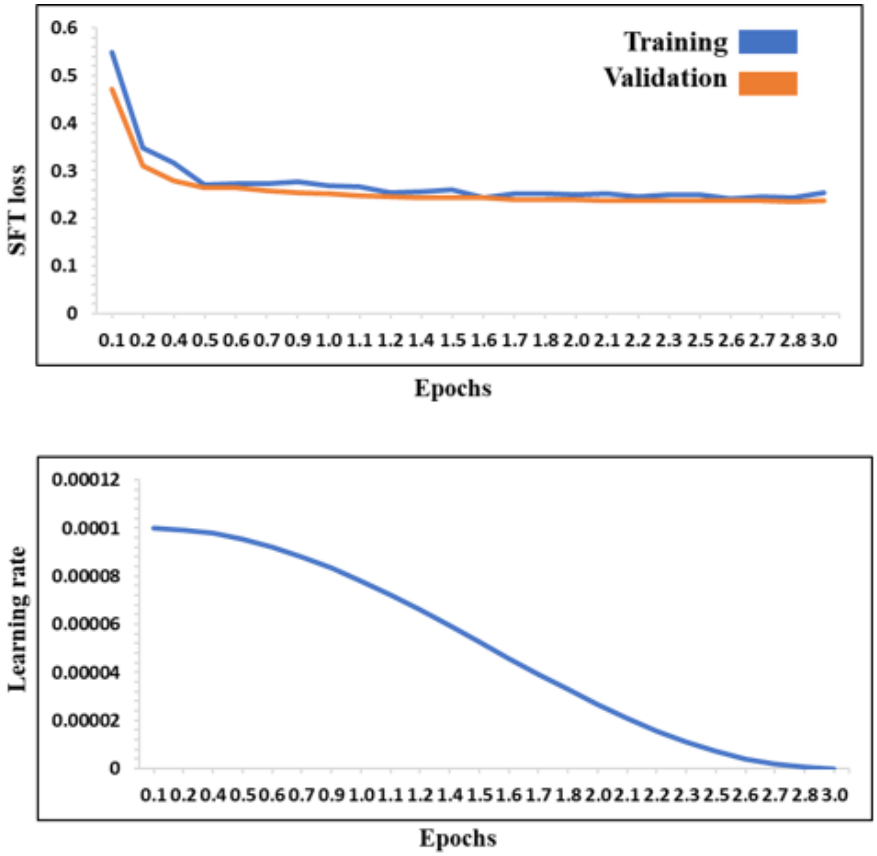
We present the training progress for the InfectA-Chat models (based on AceGPT-7B and AceGPT-7B-Chat), which are visualized in Figures 5 and 6, respectively. Both figures depict a learning rate starting at 0.0001 and gradually decreasing due to the learning rate scheduler used for optimizing convergence. The loss curves in both figures reveal a steady decrease, demonstrating both models effectively learned from the training data and generalized well to unseen data.

Figure 5. Training progress of AceGPT-7B–based InfectA-Chat (training loss, validation loss, and learning rate). SFT: supervised fine-tuning.



XSL•FO
RenderX

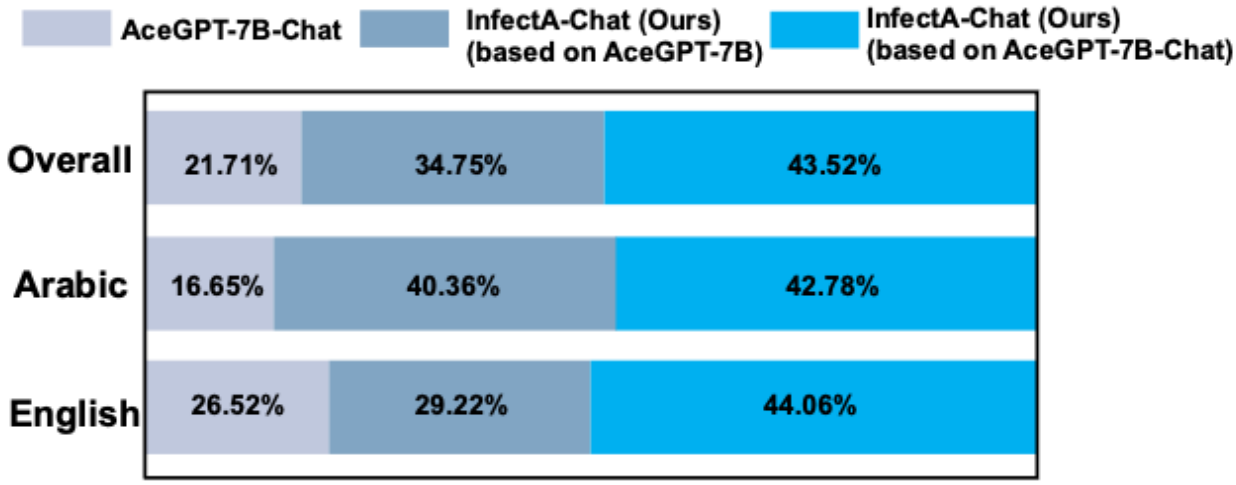
Figure 6. Training progress of AceGPT-7B-Chat–based InfectA-Chat (training loss, validation loss, and learning rate). SFT: supervised fine-tuning.



Performance Comparison of InfectA-Chat in the Infectious Disease Domain

The results of qualitative performance comparisons were conducted across 3 phases using GPT-4 (Figures 7-9). The decision to exclude base models among Arabic LLMs during GPT-4 evaluation was motivated by the number of errors observed in the base models. During the GPT-4 evaluation on AceGPT-7B, 102 errors occurred. In terms of AceGPT-13B and Jais-13B evaluation process, 41 and 669 errors occurred, respectively. Due to the generation of improper answers, GPT-4 could not process during the evaluation. The inclusion of the AceGPT-7B, AceGPT-13B, and Jais-13B models in the comparison study may have a negative impact on the performance analysis's accuracy. Therefore, these 3 base models were omitted from the GPT-4 evaluation to enable a more accurate assessment of model performance. The performance results represent the average accuracy of the 5-step GPT-4 evaluation, which is depicted in Table 2.

Figure 7. Qualitative performance comparison for AceGPT-7B-Chat, AceGPT-7B–based InfectA-Chat (ours), and AceGPT-7B-Chat–based InfectA-Chat (ours) by GPT-4 evaluation.



XSL•FO
RenderX

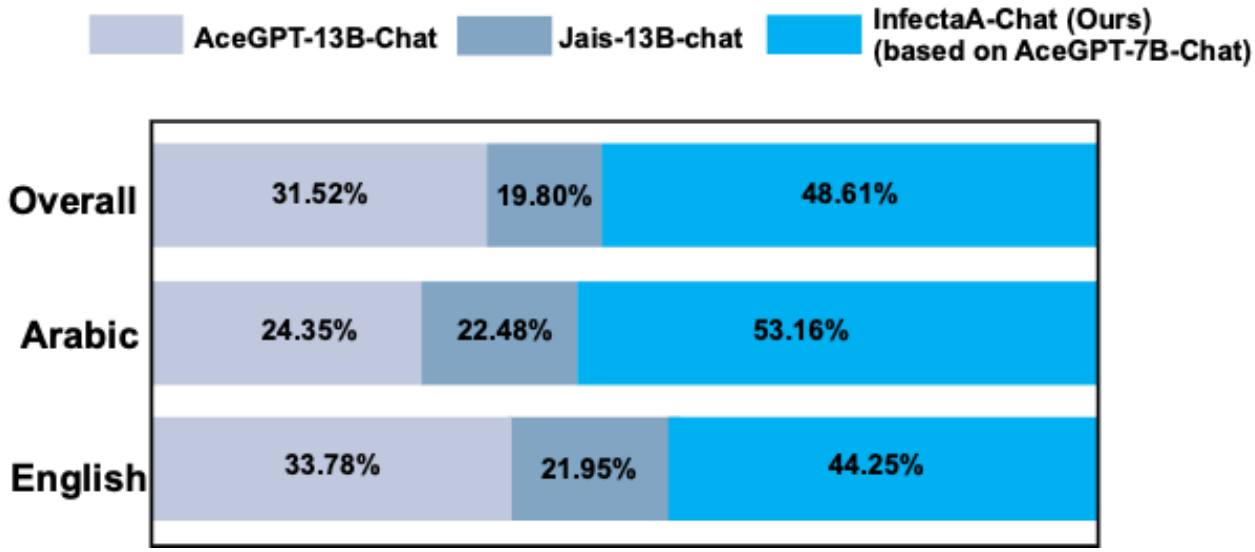
Table 2. Qualitative performance analysis of 5-step GPT-4 evaluation process.

Evaluation phases and models	Accuracy					
	Step 1	Step 2	Step 3	Step 4	Step 5	Mean (SD)
Phase 1 (%)						
InfectA-Chat (based on AceGPT-7B-Chat)	43.86	43.93	42.77	43.61	43.46	43.52 (0.46)
InfectA-Chat (based on AceGPT-7B)	34.99	34.22	35.66	34.51	34.40	34.75 (0.58)
AceGPT-7B-Chat	21.15	21.85	21.57	21.88	22.12	21.71 (0.37)
Phase 2 (%)						
InfectA-Chat (based on AceGPT-7B-Chat)	47.44	51.27	50.37	46.53	47.76	48.61 (0.20)
AceGPT-13B-Chat	32.35	31.37	31.22	32.82	29.86	31.52 (0.11)
Jais-13B-Chat	20.21	17.36	18.41	20.65	22.38	19.8 (0.19)
Phase 3 (%)						
InfectA-Chat (based on AceGPT-7B-Chat)	24.08	23.21	23.93	24.33	23.36	23.78 (0.47)
Gemini	10.43	11.12	10.76	10.52	11.33	10.83 (0.38)
GPT-3.5-Turbo	14	13.54	14.56	14.18	14.70	14.19 (0.46)
GPT-4	51.49	52.13	50.76	50.97	50.61	51.18 (0.62)

In the initial phase, InfectA-Chat (based on AceGPT-7B-Chat) demonstrated superior performance compared to AceGPT-7B-Chat and InfectA-Chat (based on AceGPT-7B), achieving an accuracy of 43.52% on the overall instruction-following dataset (Figure 7). Notably, for English and Arabic instruction–following data, InfectA-Chat (based on AceGPT-7B-Chat) surpassed other models, achieving performance rates of 44.06% on 614 of 1393 English test cases and 42.78% on 589 of 1377 Arabic test cases, respectively. In addition, the performance gap between AceGPT-7B-Chat and InfectA-Chat (based on AceGPT-7B-Chat) can also be observed in their answers to Arabic and English queries (Multimedia Appendix 1).

In comparison to other Arabic LLMs such as AceGPT-13B-Chat and Jais-13B-Chat, InfectA-Chat (based on AceGPT-7B-Chat) showed better performance, achieving an overall performance rate of 48.61% on 1346 of 2770 overall test cases in the instruction-following dataset (Figure 8). Particularly, its performance in English and Arabic instruction–following data, where InfectA-Chat (based on AceGPT-7B-Chat) surpassed other models, achieving rates of 44.25% (616/1393 English test cases) and 53.16% (732/1377 Arabic test cases), respectively. These results prove the capability of InfectA-Chat (based on AceGPT-7B-Chat) not only to outperform similar-scale Arabic LLMs but also to compete favorably against larger models with up to 13 billion parameters.

Figure 8. Qualitative performance comparison for AceGPT-13B-Chat, Jais-13B-Chat, and AceGPT-7B-Chat–based InfectA-Chat (ours) by GPT-4 evaluation.

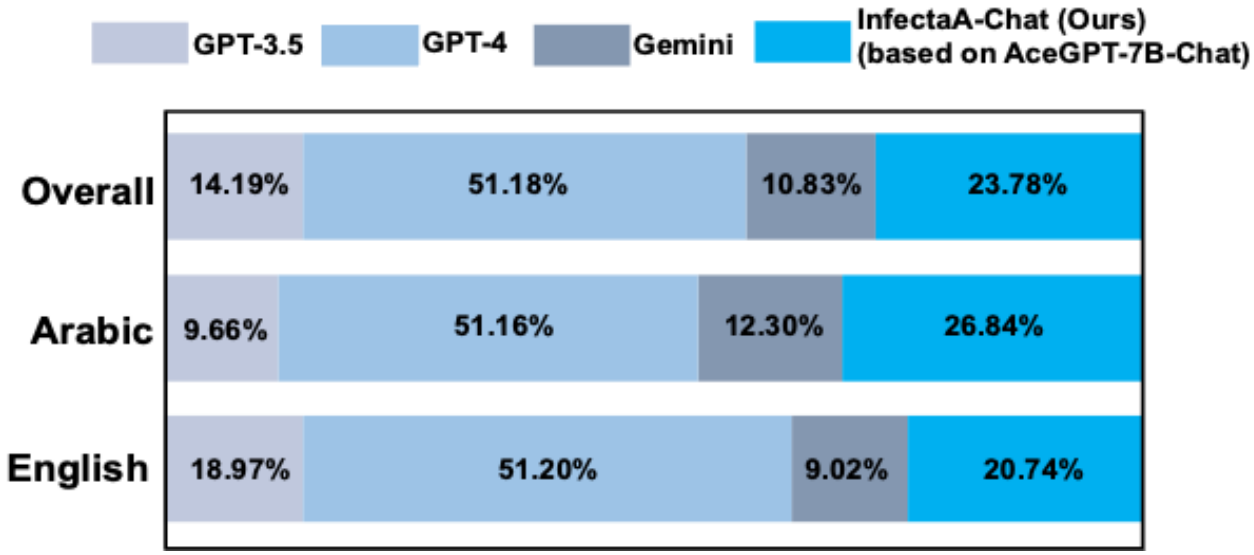


As the final step, in addition to comparing with open-source Arabic LLMs, the InfectA-Chat (based on AceGPT-7B-Chat) model was evaluated against state-of-the-art closed-source models, including GPT-3.5, GPT-4, and Gemini (Figure 9). These comparisons revealed that the InfectA-Chat (based on AceGPT-7B-Chat) model substantially outperformed GPT-3.5

XSL•FO
RenderX

and Gemini, achieving a performance rate of 23.78% on 656 of 2770 test cases while competing closely with the GPT-4 models, which attained a performance rate of 51.18% (1417/2770 test cases) against other models. This highlights the competitive edge of InfectA-Chat (based on AceGPT-7B-Chat) against top-tier closed-source models in the field of infectious diseases.

Figure 9. Qualitative performance comparison for InfectA-Chat (ours), GPT-4, GPT-3.5, and Gemini.



As demonstrated, we used GPT-4 as an evaluation metric. However, since GPT-4 can show variability during generating answers based on our prompts, we used SD to ensure the trustworthiness of this evaluation method. To do that, we applied GPT-4 evaluation 5 times to our 3-step evaluation process and we compared each model's accuracy in each evaluation step and observed their SD. The further details of this analysis are depicted in Table 2.

As we can see in the SD results from Table 2, the SD of each model in each phase is quite low. This proves the consistency of our GPT-4 evaluation method that reflects our comparison model's performance.

Performance Comparison of InfectA-Chat in the General Domain

To evaluate the generalizability of the best-performing InfectA-Chat model (based on AceGPT-7B-Chat), we conducted cross-domain testing on the Arabic Massive Multitask Language Understanding (MMLU) [54] benchmark (Table 3). This dataset assesses common-sense reasoning and Q&A capabilities, crucial for tasks beyond the infectious disease domain. The Arabic MMLU dataset comprises 40 tasks and 14,575 multiple-choice questions in Modern Standard Arabic, meticulously constructed in collaboration with native Arabic speakers. This dataset covers a wide range of subjects, including science, technology, engineering, and mathematics (STEM); social sciences; humanities; and others, ensuring its relevance as a source of common-sense knowledge. The questions are designed to assess a spectrum of knowledge levels, from primary education to university-level understanding. Because the dataset is specifically tailored to evaluate models' real-world knowledge, we chose to use the Arabic MMLU dataset to assess our model's performance on practical data. We evaluated InfectA-Chat and other models' performance in a multiple-choice Q&A task in 4 different domains, such as STEM, humanities, social sciences, and others, as reflected in Table 3. In the STEM domain, InfectA-Chat achieved a performance score of 40.84% on 1315 of 3220 STEM data, outperforming the LLaMA models (LLaMA-7B and LLaMA-13B) as well as the Jais base models (Jais-13B and Jais-30B) and Bloomz. Its performance was on par with that of the more advanced AceGPT chat models (AceGPT-7B-Chat and AceGPT-13B-Chat), Jais chat models (Jais-13B-Chat and Jais-30B-v3-Chat), and GPT-3.5-Turbo, indicating its strong capabilities in technical subjects. In the humanities domain, InfectA-Chat scored 46.94% on 1715 of 3655 humanities data, demonstrating higher accuracy than LLaMA models, Bloomz, Jais base models, AceGPT base models, and GPT-3.5-Turbo. Its results closely approach those of the AceGPT chat models (48.54% for AceGPT-7B-Chat and 50.91% for AceGPT-13B-Chat, with the following 1774 and 1861 data points out of 3655) as well as the Jais chat models. In the social sciences and other general domains, InfectA-Chat achieved scores of 45.58% (1613/3540 social sciences-related data) and 49.48% (1751/3540 general domain data), respectively, surpassing LLaMA models, AceGPT base models, Bloomz, and Jais base models. Instruction tuning is one of the primary factors limiting the generalizability of InfectA-Chat. Despite this, our model, which is specifically focused on the infectious diseases domain, demonstrates performance comparable to that of the AceGPT and Jais chat models, highlighting its adaptability and strong performance across a wide range of disciplines. On average, across 4 domains, InfectA-Chat achieved a strong overall score of 45.71% on 6662 of 14,575 general domain data, positioning it competitively among large multilingual models such as Bloomz (34.53% of 14,575 data), LLaMA-7B (30.78% of 14,575 data), and LLaMA-13B (37.27% of 14,575 data). Notably, InfectA-Chat outperformed leading Arabic pretrained models, such as AceGPT-13B and the Jais-series base models (Jais-13B-base and Jais-30B-base), with a performance gap ranging from 2.99% to 12.28% of 14,575 data. This suggests that InfectA-Chat is especially effective at handling common-sense multiple-choice

XSL•FO
RenderX

Q&A tasks compared to other prominent Arabic models. Its performance also closely approaches that of instruction-tuned models such as AceGPT-7B-Chat (47.58% performance rate on 6934/14,575 data) and AceGPT-13B-Chat (50.81% performance rate on 7405/14,575 data) while remaining competitive against advanced Jais-series chat models (Jais-13B-Chat and Jais-30B-v3-Chat), which scored between 55.11% and 61.14% of 14,575 data, respectively. This underscores InfectA-Chat's significant performance not only in the domain of infectious diseases but also in real-world common-sense data, outperforming both English and Arabic base models while maintaining competitive results with a small performance gap with Arabic chat models.

Table 3. The results of testing Arabic large language models on the Arabic Massive Multitask Language Understanding benchmark dataset (accuracy).

Model	Mean (%)	STEM[a] (%)	Humanities (%)	Social sciences (%)	Others (%)
Bloomz	34.53	33.35	29.29	37.58	34.53
LLaMA2-7B	30.78	30.30	29.33	27.46	30.78
LLaMA2-13B	37.27	32.94	32.30	33.42	37.27
Jais-13B-based	33.43	30.51	31.25	33.74	33.43
Jais-30B-based	39.60	32.67	30.67	42.13	39.60
AceGPT-7B-based	34.42	29.73	30.95	33.45	34.42
AceGPT-13B-based	42.72	36.60	38.74	43.76	42.72
AceGPT-7B-Chat	47.58	42.41	48.54	47.03	52.33
AceGPT-13B-Chat	50.81	47.10	50.91	50.97	54.27
Jais-13b-Chat	55.11	49.98	56.73	54.05	59.66
Jais-30b-v3-Chat	61.14	54.59	63.45	59.10	67.43
GPT-3.5-Turbo	49.07	43.38	44.12	55.57	53.21
InfectA-Chat	45.71	40.84	46.94	45.58	49.48

[a]STEM: science, technology, engineering, and mathematics.

Advanced InfectA-Chat Performance With RAG Pipeline

Traditionally, recurrent fine-tuning of models with additional data incurs significant time and computational costs, making it an inefficient strategy. To address this issue, the implementation of the RAG pipeline is critical. In our study, we validated the necessity by applying the RAG pipeline to InfectA-Chat alongside cutting-edge models such as GPT-3.5 and GPT-4, using a set of 50 recent instruction-following data. The results illustrated the efficacy of the RAG pipeline when incorporating recent data (Figure 10). The results in Figure 10 were obtained by averaging the inference accuracy of each model across 5 runs in English and Arabic data to prove the consistency of model performances. Across all datasets, InfectA-Chat exhibited a remarkable performance of 90.08% on 45 of 50 RAG test data, with an SD of 1.7%. Particularly in the Arabic dataset, InfectA-Chat demonstrated superior performance at 86.4% (43/50 RAG test data), and in the English dataset, it excels at 96% on 48 of 50 RAG test data, outperforming both GPT-3.5 and GPT-4 models, which have SD of 0.8% (4/50 RAG test data) and 0.16% (8/50 RAG test data), respectively. These findings highlight the capacity of RAG to obviate the need for repetitive instruction tuning by integrating the model with up-to-date information, particularly crucial in domains such as public health and infectious diseases.

Following the results of the RAG pipeline with the up-to-date dataset, to delve deeper into the influence of information retrieval on factual language models like InfectA-Chat, we investigated the impact of the top-k parameter within the RAG pipeline. This parameter controls the number of top-ranked documents passed from the retrieval stage to the generation stage. Our experiments with RAG using top-1, top-3, and top-5 settings demonstrated a positive relationship between increasing the top-k value and the accuracy of retrieval (Figure 11).

This implied that exposing InfectA-Chat to a greater range of potentially relevant information during retrieval can considerably improve its factual language modeling capabilities. As observed, this translated to a substantial performance improvement for InfectA-Chat, with an accuracy of 80.05% on 40 of 50 RAG test data, achieved using the top-5 parameter compared to the top-1.

XSL•FO
RenderX

Figure 10. Qualitative performance results for InfectA-Chat on the recent dataset (March 20, 2024, to June 20, 2024) by GPT-4 evaluation.

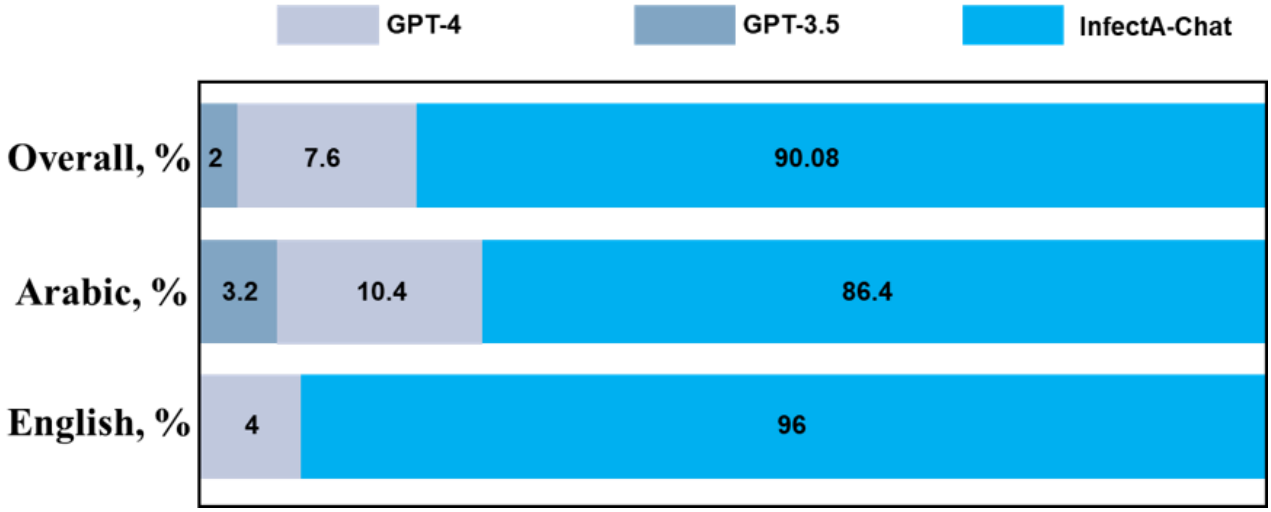
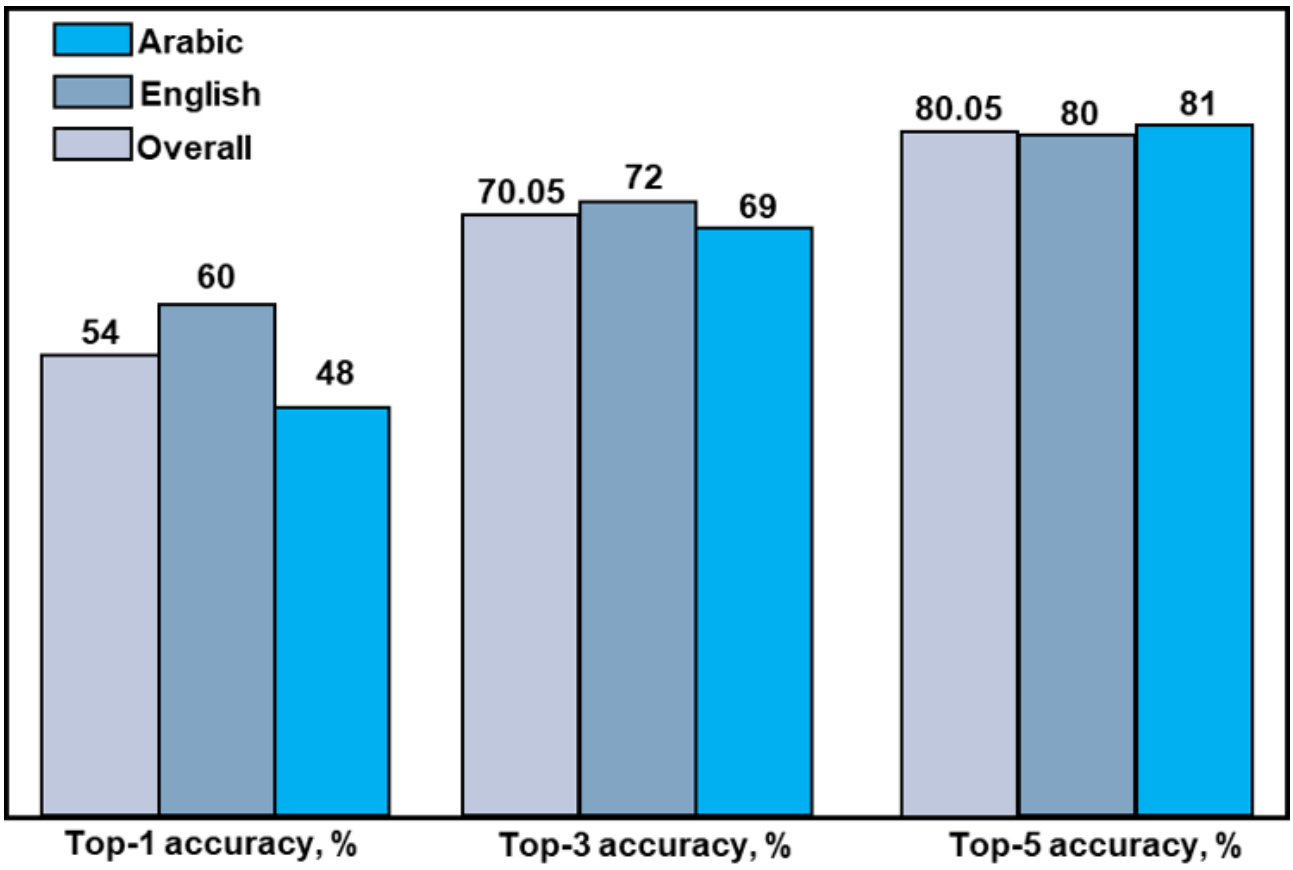


Figure 11. Accuracy of retriever based on top-k parameter in Retrieval-Augmented Generation pipeline.



Discussion

In conclusion, the critical need for real-time disease monitoring, particularly in regions like the Middle East, has exposed a gap in accessible, multilingual resources. Regional public health agencies, such as the US Centers for Disease Control and Prevention [55] and the Chinese Center for Disease Control and Prevention [56], play an important role in protecting public health by conducting research and offering disease surveillance and prevention programs in their regions. In addition, there has been a rise in innovative platforms providing daily alerts, such as the CIDRAP [45] and the Program for Monitoring Emerging Diseases [57]. Apart from these platforms, with the rise of LLMs, LLMs started to play a role in delivering information in various domains, including infectious disease tracking. Given our focus on Arabic-speaking countries within the MENA region, there remain a limited number of Arabic language models specifically tailored for the medical and public health domains. While the development of medical LLMs is expanding globally, only a few models, such as BiMediX [38] and Apollo [39], have been created with a focus on Arabic language capabilities. Although these models are valuable for supporting societal and medical initiatives, they still face limitations, especially in monitoring infectious diseases, due to the limited

XSL•FO
RenderX

availability of infectious disease surveillance data for training. InfectA-Chat addresses this challenge by delivering up-to-date information on infectious diseases in both Arabic and English. Moreover, the exceptional performance of InfectA-Chat in handling instruction-following data in Q&A tasks across languages sets a new standard in the field of infectious disease monitoring. By leveraging the power of LLMs, InfectA-Chat positions itself as a pioneer for bridging the information gap and promoting public health awareness compared to other existing LLMs. However, even though InfectA-Chat has significant performance, it still shows limitations itself.

First, while InfectA-Chat demonstrates significant performance in Arabic and English understanding, it may still face challenges due to limited computing resources and data availability. The limitation in the amount of data available in English and Arabic in the field of infectious diseases create a barrier to the model's performance. In addition, because the training of LLMs requires more computational resources, such as GPUs, this would make the development process faster and more efficient. Due to our limited computational resources, the process becomes slower, restricting us to using smaller model sizes. As the accessibility of computational resources and instruction-following data continue to grow, InfectA-Chat can achieve greater performance.

Second, in some scenarios, the model may generate inconsistent answers based on the given questions, such as incorrect information about specific diseases, known as the hallucination problem. Although this issue was mitigated by implementing a RAG pipeline, InfectA-Chat may still exhibit a small likelihood of hallucination. Applying RAG with a larger volume of data could further reduce the hallucination rate to nearly 0.

Future work efforts should focus on mitigating these limitations to unlock the potential of InfectA-Chat. With larger datasets and more computational resources, the performance of InfectA-Chat can be increased. In addition, we will focus on how to improve the performance of our model in the general domain by mitigating the disadvantages of instruction tuning. We aim to establish InfectA-Chat as a truly transformative tool in the fight against infectious diseases by enhancing our target regions and obtaining massive data in different languages.

Acknowledgments

This research was supported by the Korea Institute of Science and Technology Information (KISTI; K24L4M2C6). This research was also financially supported by the Government-wide Research and Development Fund project for infectious disease research, Republic of Korea, in the form of a grant (HG23C1624). The funders had no role in study design, data collection and analysis, decision to publish, or preparation of the manuscript. The authors are grateful to all members of this project for their invaluable contributions. The authors particularly extend their thanks to Dr Donghun Yang at KISTI for his crucial support in giving ideas and supporting the resolution of errors during training. Their expertise and dedication were important during the development of InfectA-Chat.

Conflicts of Interest

None declared.

Multimedia Appendix 1
Additional examples of generated answers based on questions in Arabic and English. Arabic examples are provided with their English translations.
[PDF File (Adobe PDF File), 286 KB - medinform_v13i1e63881_app1.pdf]

References

1. MERS-CoV worldwide overview. European Centre for Disease Prevention and Control. URL: https://www.ecdc.europa.eu/en/middle-east-respiratory-syndrome-coronavirus [accessed 2024-06-06]
2. Multi-country outbreak of cholera, external situation report #12 - 14 March 2024. World Health Organization. 2024 Mar 14. URL: https://www.who.int/publications/m/item/multi-country-outbreak-of-cholera--external-situation-report--12---14-march-2024 [accessed 2024-06-06]
3. What we do. European Centre for Disease Prevention and Control. URL: https://www.ecdc.europa.eu/en/about-ecdc/what-we-do [accessed 2024-05-02]
4. OpenAI. GPT-4 technical report. arXiv Preprint posted online on March 4, 2024 [FREE Full text] [doi: 10.48550/arxiv.2303.08774]
5. Almazrouei E, Alobeidli H, Alshamsi A, Cappelli A, Cojocaru R, Debbah M, et al. The falcon series of open language models. arXiv Preprint posted online on November 28, 2023 [FREE Full text] [doi: 10.48550/arxiv.2311.16867]
6. Chowdhery A, Narang S, Devlin J, Bosma M, Mishra G, Roberts A, et al. PaLM: scaling language modeling with pathways. J Mach Learn Res 2023 Aug;24(240):1-113. [doi: 10.48550/arxiv.2204.02311]
7. Touvron H, Martin L, Stone K, Albert P, Almahairi A, Babaei Y, et al. Llama 2: open foundation and fine-tuned chat models. arXiv Preprint posted online on July 18, 2023 [FREE Full text] [doi: 10.48550/arxiv.2307.09288]
8. Yang D, Ngoc KM, Shin I, Hwang M. DPReLU: dynamic parametric rectified linear unit and its proper weight initialization method. Int J Comput Intell Syst 2023 Feb 11;16(11). [doi: 10.1007/s44196-023-00186-w]

XSL•FO
RenderX

9. Preiksaitis C, Ashenburg N, Bunney G, Chu A, Kabeer R, Riley F, et al. The role of large language models in transforming emergency medicine: scoping review. JMIR Med Inform 2024 May 10;12:e53787 [FREE Full text] [doi: 10.2196/53787] [Medline: 38728687]
10. Minaee S, Mikolov T, Nikzad N, Chenaghlu M, Socher R, Amatriain X, et al. Large language models: a survey. arXiv Preprint posted online on February 9, 2024 [FREE Full text] [doi: 10.48550/arxiv.2402.06196]
11. Devlin J, Chang MW, Lee K, Toutanova K. BERT: pre-training of deep bidirectional transformers for language understanding. arXiv Preprint posted online on October 11, 2018 [FREE Full text] [doi: 10.48550/arxiv.1810.04805]
12. Cui Y, Yang Z, Yao X. Efficient and effective text encoding for Chinese LLaMA and Alpaca. arXiv Preprint posted online on April 17, 2023 [FREE Full text] [doi: 10.48550/arxiv.2304.08177]
13. Touvron H, Lavril T, Izacard G, Martinet X, Lachaux MA, Lacroix T, et al. LLaMA: open and efficient foundation language models. arXiv Preprint posted online on February 27, 2023 [FREE Full text] [doi: 10.48550/arxiv.2302.13971]
14. Jiang AQ, Sablayrolles A, Mensch A, Bamford C, Singh Chaplot D, de las Casas D, et al. Mistral 7B. arXiv Preprint posted online on October 10, 2023 [FREE Full text] [doi: 10.48550/arxiv.2310.06825]
15. Antoun W, Baly F, Hajj H. AraBERT: transformer-based model for arabic language understanding. In: Proceedings of the 4th Workshop on Open-Source Arabic Corpora and Processing Tools, with a Shared Task on Offensive Language Detection. 2020 Presented at: OSACT 2020; May 11-16, 2020; Marseille, France URL: https://aclanthology.org/2020.osact-1.2/
16. Abdelali A, Hassan S, Mubarak H, Darwish K, Samih Y. Pre-training BERT on Arabic tweets: practical considerations. arXiv Preprint posted online on February 21, 2021 [FREE Full text] [doi: 10.48550/arxiv.2102.10684]
17. Ghaddar A, Wu Y, Rashid A, Bibi K, Rezagholizadeh M, Xing C, et al. JABER and SABER: junior and senior Arabic BERt. arXiv Preprint posted online on December 8, 2021 [FREE Full text] [doi: 10.48550/arxiv.2112.04329]
18. Inoue G, Alhafni B, Baimukan N, Baimukan H, Habash N. The interplay of variant, size, and task type in Arabic pre-trained language models. In: Proceedings of the Sixth Arabic Natural Language Processing Workshop. 2021 Presented at: WANLP 2021; April 19, 2021; Kiev, Ukraine URL: https://aclanthology.org/2021.wanlp-1.10
19. Antoun W, Baly F, Hajj H. AraELECTRA: pre-training text discriminators for Arabic language understanding. In: Proceedings of the Sixth Arabic Natural Language Processing Workshop. 2021 Presented at: WANLP 2021; April 9, 2021; Kyiv, Ukraine URL: https://aclanthology.org/2021.wanlp-1.20/
20. Eddine MK, Tomeh N, Habash N, Le Roux J, Vazirgiannis M. AraBART: a pretrained arabic sequence-to-sequence model for abstractive summarization. In: Proceedings of the Seventh Arabic Natural Language Processing Workshop. 2022 Presented at: WANLP 2022; December 8, 2022; Abu Dhabi, UAE URL: https://aclanthology.org/2022.wanlp-1.4 [doi: 10.18653/v1/2022.wanlp-1.4]
21. Antoun W, Baly F, Hajj H. AraGPT2: pre-trained transformer for Arabic language generation. In: Proceedings of the Sixth Arabic Natural Language Processing Workshop. 2021 Presented at: WANLP 2021; April 9, 2021; Kyiv, Ukraine URL: https://aclanthology.org/2021.wanlp-1.21/ [doi: 10.18653/v1/2022.wanlp-1.56]
22. Sengupta N, Sahu SK, Jia B, Katipomu S, Li H, Koto F, et al. Jais and Jais-chat: Arabic-centric foundation and instruction-tuned open generative large language models. arXiv Preprint posted online on August 30, 2023 [FREE Full text] [doi: 10.48550/arxiv.2308.16149]
23. Bari MS, Alnumay Y, Alzahrani NA, Alotaibi NM, Alyahya HA, AlRashed S, et al. ALLaM: large language models for Arabic and English. arXiv Preprint posted online on July 22, 2024 [FREE Full text] [doi: 10.48550/arXiv.2407.15390]
24. Huang H, Yu F, Zhu J, Sun X, Cheng H, Dingjie S, et al. AceGPT, localizing large language models in Arabic. In: Proceedings of the 2024 Conference of the North American Chapter of the Association for Computational Linguistics: Human Language Technologies. 2024 Presented at: NAACL 2024; June 16-21, 2024; Mexico City, Mexico URL: https://aclanthology.org/2024.naacl-long.450/
25. Gu Y, Tinn R, Cheng H, Lucas M, Usuyama N, Liu X, et al. Domain-specific language model pretraining for biomedical natural language processing. ACM Transact Comput Healthc 2021 Oct 15;3(1):1-23 [FREE Full text] [doi: 10.1145/3458754]
26. Huang K, Altosaar J, Ranganath R. ClinicalBERT: modeling clinical notes and predicting hospital readmission. arXiv Preprint posted online on November 29, 2020 [FREE Full text]
27. Lee J, Yoon W, Kim S, Kim D, Kim S, So CH, et al. BioBERT: a pre-trained biomedical language representation model for biomedical text mining. Bioinformatics 2020 Feb 15;36(4):1234-1240 [FREE Full text] [doi: 10.1093/bioinformatics/btz682] [Medline: 31501885]
28. Zhou H, Liu F, Gu B, Zou X, Huang J, Wu J, et al. A survey of large language models in medicine: progress, application, and challenge. arXiv Preprint posted online on November 9, 2023 [FREE Full text] [doi: 10.48550/arxiv.2311.05112]
29. Peng C, Yang X, Chen A, Smith KE, PourNejatian N, Costa AB, et al. A study of generative large language model for medical research and healthcare. NPJ Digit Med 2023 Nov 16;6(1):210 [FREE Full text] [doi: 10.1038/s41746-023-00958-w] [Medline: 37973919]
30. Chung HW, Hou L, Longpre S, Zoph B, Tay Y, Fedus W, et al. Scaling instruction-finetuned language models. arXiv Preprint posted online on October 20, 2022.
31. Anil R, Dai AM, Firat O, Johnson M, Lepikhin D, Passos A, et al. PaLM 2 technical report. arXiv Preprint posted online on May 17, 2023. [doi: 10.48550/arXiv.2305.10403]

XSL•FO
RenderX

32. Chen Z, Cano AH, Romanou A, Bonnet A, Matoba K, Salvi F, et al. MEDITRON-70B: scaling medical pretraining for large language models. arXiv Preprint posted online on November 27, 2023. [doi: 10.48550/arxiv.2311.16079]
33. Li Y, Li Z, Zhang K, Dan R, Jiang S, Zhang Y. ChatDoctor: a medical chat model fine-tuned on a Large Language Model Meta-AI (LLaMA) using medical domain knowledge. Cureus 2023 Jun 24;15(6):e40895 [FREE Full text] [doi: 10.7759/cureus.40895] [Medline: 37492832]
34. Han T, Adams LC, Papaioannou JM, Grundmann P, Oberhauser T, Löser A, et al. MedAlpaca -- an open-source collection of medical conversational AI models and training data. arXiv Preprint posted online on April 14, 2023. [doi: 10.48550/arxiv.2304.08247]
35. Wu C, Lin W, Zhang X, Zhang Y, Xie W, Wang Y. PMC-LLaMA: toward building open-source language models for medicine. J Am Med Inform Assoc 2024 Sep 01;31(9):1833-1843. [doi: 10.1093/jamia/ocae045] [Medline: 38613821]
36. Wang H, Liu C, Xi N, Qiang Z, Zhao S, Qin B, et al. HuaTuo: tuning LLaMA model with Chinese medical knowledge. arXiv Preprint posted online on April 14, 2023. [doi: 10.48550/arxiv.2304.06975]
37. Toma A, Lawler PR, Ba J, Krishnan RG, Rubin BB, Wang B. Clinical camel: an open expert-level medical language model with dialogue-based knowledge encoding. arXiv Preprint posted online on May 19, 2023. [doi: 10.48550/arxiv.2305.12031]
38. Pieri S, Mullappilly SS, Khan FS, Anwer RM, Khan S, Baldwin T, et al. BiMediX: bilingual medical mixture of experts LLM. In: Proceedings of the 2024 Conference on Empirical Methods in Natural Language Processing. 2024 Presented at: EMNLP 2024; November 12-16, 2024; Miami Beach, FL. [doi: 10.18653/v1/2024.findings-emnlp.989]
39. Wang X, Chen N, Chen J, Wang Y, Zhen G, Zhang C, et al. Apollo: A lightweight multilingual medical LLM towards democratizing medical AI to 6B people. arXiv Preprint posted online on March 6, 2024. [doi: 10.48550/arxiv.2403.03640]
40. Hu J, Shen Y, Wallis P, Allen-Zhu Z, Li Y, Wang S, et al. LoRA: low-rank adaptation of large language models. arXiv Preprint posted online on June 17, 2021.
41. Yesimm/InfectA-Chat. HuggingFace. URL: https://huggingface.co/Yesimm/InfectA-Chat [accessed 2024-07-01]
42. Zhou C, Liu P, Xu P, Iyer S, Sun J, Mao Y, et al. LIMA: less is more for alignment. arXiv Preprint posted online on May 18, 2023. [doi: 10.48550/arXiv.2305.11206]
43. Models. OpenAI Platform. URL: https://platform.openai.com/docs/models/gpt-3-5 [accessed 2023-10-11]
44. Gemini Team Google. Gemini: a family of highly capable multimodal models. arXiv Preprint posted online on December 19, 2023.
45. Center for infectious disease research and policy homepage. Center for Infectious Disease Research and Policy. URL: https://www.cidrap.umn.edu/ [accessed 2024-06-06]
46. Lewis P, Perez E, Piktus A, Petroni F, Karpukhin V, Goyal N, et al. Retrieval-augmented generation for knowledge-intensive NLP tasks. arXiv Preprint posted online on May 22, 2020. [doi: 10.48550/arXiv.2005.11401]
47. GPT-3.5 Turbo. OpenAI Platform. URL: https://platform.openai.com/docs/models/gpt-3-5-turbo#gpt-3-5-turbo [accessed 2023-10-11]
48. gensim 4.3.3. Python Software Foundation. URL: https://pypi.org/project/gensim/ [accessed 2024-06-10]
49. tatsu-lab/alpaca. HuggingFace. URL: https://huggingface.co/datasets/tatsu-lab/alpaca [accessed 2024-06-10]
50. Kim E, Hwang M, Lee M. Recent research trend in efficient NLP of transformer. In: Proceedings of the 11th International Conference on Smart Media and Applications. 2022 Presented at: SMA 2022; October 19-22, 2022; Saipan, Northern Mariana Islands.
51. Dettmers T, Pagnoni A, Holtzman A, Zettlemoyer L. QLORA: efficient finetuning of quantized LLMs. In: Proceedings of the Thirty-Seventh Annual Conference on Neural Information Processing Systems. 2023 Presented at: NeurIPS 2023; December 10-16, 2023; New Orleans, LA.
52. Vector embeddings. OpenAI Platform. URL: https://platform.openai.com/docs/guides/embeddings [accessed 2023-10-11]
53. Majumder R, Wang J. Microsoft. 2020 May 19. URL: https://www.microsoft.com/en-us/research/blog/zero-2-deepspeed-shattering-barriers-of-deep-learning-speed-scale/ [accessed 2024-06-10]
54. Koto F, Li H, Shatnawi S, Doughman J, Sadallah AB, Alraeesi A, et al. ArabicMMLU: assessing massive multitask language understanding in Arabic. In: Proceedings of the Findings of the Association for Computational Linguistics. 2024 Presented at: ACL 2024; August 11-16, 2024; Bangkok, Thailand. [doi: 10.18653/v1/2024.findings-acl.334]
55. Centers for Disease Control and Prevention homepage. Centers for Disease Control and Prevention. URL: https://www.cdc.gov/index.html [accessed 2024-06-06]
56. Chinese Center for Disease Control and Prevention homepage. Chinese Center for Disease Control and Prevention. URL: https://en.chinacdc.cn/ [accessed 2024-06-06]
57. Home - ProMED - ProMED-mail. ProMED. URL: https://promedmail.org/ [accessed 2024-04-17]

Abbreviations

BERT: Bidirectional Encoder Representations from Transformers
BiMediX: Bilingual Medical Mixture of Experts Large Language Model
BioBERT: BERT for Biomedical Text Mining
CIDRAP: Center for Infectious Disease Research and Policy

XSL•FO
RenderX

ECDC: European Centre for Disease Prevention and Control
GPU: graphics process unit
LLM: large language model
LoRA: low-rank adaptation
MERS-CoV: Middle East respiratory syndrome coronavirus
MENA: Middle East and North Africa
MIMIC-III: Medical Information Mart for Intensive Care III
MMLU: Massive Multitask Language Understanding
NLP: natural language processing
PaLM: Pathways Language Model
PEFT: parameter-efficient fine-tuning
Q&A: question and answer
RAG: retrieval-augmented generation
STEM: science, technology, engineering, and mathematics
WHO: World Health Organization

Edited by A Benis; submitted 02.07.24; peer-reviewed by Z Chen, X Liu, K Dashtipour; comments to author 24.10.24; revised version received 14.11.24; accepted 09.12.24; published 10.02.25.

Please cite as:
Selcuk Y, Kim E, Ahn I
InfectA-Chat, an Arabic Large Language Model for Infectious Diseases: Comparative Analysis
JMIR Med Inform 2025;13:e63881
URL: https://medinform.jmir.org/2025/1/e63881
doi:10.2196/63881
PMID:

©Yesim Selcuk, Eunhui Kim, Insung Ahn. Originally published in JMIR Medical Informatics (https://medinform.jmir.org), 10.02.2025. This is an open-access article distributed under the terms of the Creative Commons Attribution License (https://creativecommons.org/licenses/by/4.0/), which permits unrestricted use, distribution, and reproduction in any medium, provided the original work, first published in JMIR Medical Informatics, is properly cited. The complete bibliographic information, a link to the original publication on https://medinform.jmir.org/, as well as this copyright and license information must be included.

XSL•FO
RenderX

Original Paper

Performance Assessment of Large Language Models in Medical Consultation: Comparative Study

Sujeong Seo[1,2*], MS; Kyuli Kim[1*], MS; Heyoung Yang[1*], PhD

[1]Future Technology Analysis Center, Korea Institute of Science and Technology Information, Seoul, Republic of Korea

[2]Postal Savings & Insurance Development Institute, Seoul, Republic of Korea

[*]all authors contributed equally

Corresponding Author:
Heyoung Yang, PhD
Future Technology Analysis Center
Korea Institute of Science and Technology Information
Hoegi-ro 66, Dongdaemun-gu
Seoul, 92456
Republic of Korea
Phone: 82 10 9265 5661
Fax: 82 2 3299 6188
Email: hyyang@kisti.re.kr

Abstract

Background: The recent introduction of generative artificial intelligence (AI) as an interactive consultant has sparked interest in evaluating its applicability in medical discussions and consultations, particularly within the domain of depression.

Objective: This study evaluates the capability of large language models (LLMs) in AI to generate responses to depression-related queries.

Methods: Using the PubMedQA and QuoraQA data sets, we compared various LLMs, including BioGPT, PMC-LLaMA, GPT-3.5, and Llama2, and measured the similarity between the generated and original answers.

Results: The latest general LLMs, GPT-3.5 and Llama2, exhibited superior performance, particularly in generating responses to medical inquiries from the PubMedQA data set.

Conclusions: Considering the rapid advancements in LLM development in recent years, it is hypothesized that version upgrades of general LLMs offer greater potential for enhancing their ability to generate "knowledge text" in the biomedical domain compared with fine-tuning for the biomedical field. These findings are expected to contribute significantly to the evolution of AI-based medical counseling systems.

(JMIR Med Inform 2025;13:e64318) doi:10.2196/64318

KEYWORDS

artificial intelligence; biomedical; large language model; depression; similarity measurement; text validity

Introduction

Overview

The COVID-19 pandemic has brought significant transformations to health care systems worldwide [1]. Additionally, the utilization of artificial intelligence (AI) in the biomedical field has surged [2], and the adoption of natural language processing (NLP) techniques for analyzing or predicting medical data has notably increased [3-5]. Ong et al [6] utilized machine learning techniques on radiographic text to identify the presence, location, and acuity of ischemic strokes. Since the advent of ChatGPT (OpenAI), numerous studies have highlighted the potential impact of generative models across medical domains, including medicine, medical devices, and medical education. Large language models (LLMs) are anticipated to become a cornerstone in the future of health informatics research [7-12].

The COVID-19 pandemic has exacerbated depression, which is widely acknowledged as a significant social and medical concern [13-15]. During the pandemic and the resultant lockdowns, social isolation and withdrawal became prevalent worldwide, leading to the coining of the term "Corona Blue" to describe depression caused by the pandemic, particularly related to self-isolation and social distancing [16]. Even before

XSL•FO
RenderX

the pandemic, depression was recognized as a societal issue and a mental health concern with substantial economic implications in many countries [17-22].

Generative AI has recently been employed as an interactive consultant, sparking interest in evaluating its applicability in medical discussions and consultations, particularly in the context of depression. This study aims to assess the suitability of generative AI by comparing the similarity between responses generated by AI models and those provided by humans to depression-related questions. To this end, we collected a set of depression-related questions and corresponding human answers and utilized 4 LLMs—BioGPT [23], PMC-LLaMA [24], ChatGPT [25], and Llama2 [26]—to generate responses.

Questions about depression or depressive disorders can arise from various sources, including validated inquiries recommended by professionals and questions posted online by individuals seeking to understand their symptoms. Furthermore, when selecting an LLM, it is essential to consider 2 key factors. First, is the model domain-specific? This pertains to a fine-tuned pretrained model tailored to the medical domain. Second, is the model a general-purpose intelligent system known for its proficient question-answering capabilities?

Building on this foundation, we designed a basic experiment in which medical questions related to depression were sourced from diverse origins and presented to LLMs for answers. Specifically, we explored the fundamental concepts underlying LLMs and examined the attributes of fine-tuned models within the medical domain. The primary objectives of this study were to evaluate the LLMs' ability to respond to medical queries, assess the similarity between their answers and those provided by humans, and investigate the differences between domain-specific and general-purpose models.

The main contributions of this study are as follows. First, semantic similarity analysis highlights discrepancies between human expert answers and the knowledge outputs of LLMs. Second, it enables researchers to evaluate the quality of LLM-generated responses by comparing them with human answers. Finally, the experiments show that the latest versions of LLMs outperform earlier iterations, particularly when fine-tuned on specific topics.

Background and Related Work

Large Language Models

The Transformer architecture [27] has significantly influenced the proliferation of LLMs, giving rise to 2 prominent pillars in NLP: GPT and bidirectional encoder representations from transformers (BERT). Qiu et al [25,28] assessed ChatGPT as heralding a new era in the development and deployment of large AI models. Additionally, they observed that the size, generalization, and scale of training/pretraining for general-domain models have increased, thereby enhancing the capacity of a single model. ChatGPT [25], introduced in 2022, offers notable advantages by producing human-like results and being user-friendly and accessible. The development and dissemination of LLMs began in late 2022 with ChatGPT [25], and numerous models followed in 2023 after the release of Llama, which was freely distributed by Meta. Additionally, Meta announced and distributed Llama-2, which is also available for commercial use [26,28,29]. Furthermore, Google introduced its chatbot BARD [30], which was swiftly followed by Alpaca 7B [31], Vicuna [32], and others, all built upon the free Llama model.

Health Care Domain Large Language Models

ChatGPT, powered by the GPT-3 model, has successfully navigated all stages of the United States Medical Licensing Examination (USMLE) [11,33]. Concurrently, there has been a rise in LLMs fine-tuned for specific domains, designed to maximize performance in general domains. Specialized models, such as BioBERT and PubMedBERT, which fine-tune existing BERT models using extensive medical domain data, have seen increased development.

LLMs initially introduced in the general domain can undergo additional training with health care domain data (biomedical or biomedicine), resulting in pretrained language models. These pretrained models, tailored to the health care domain, are specialized for tasks such as answering health care–related questions [23,24,34,35] and have evolved to facilitate medical diagnoses through the analysis of medical images.

Furthermore, alongside the development and deployment of LLMs, ongoing research evaluates the performance of both pretrained and general-domain LLMs. For instance, studies have compared the performance of GPT-4, a general-domain LLM, with its predecessor GPT-3.5 and Med-PaLM, a model pretrained specifically in the medical domain [11].

Recent research in the field of medicine, particularly focusing on depression, has explored the application of LLMs such as ChatGPT and Claude, developed by Anthropic. Several publications have introduced methods for evaluating the potential use of LLMs in depression treatment and screening [36-39]. Heston [40] discussed the risks associated with using LLMs in mental health support, particularly for depression. These studies have demonstrated that LLMs can accurately categorize symptoms of depression and anxiety, highlighting their potential for integration into the health care field.

Methods

Overview

This section is divided into 3 parts: (1) an overview of the design of experiments; (2) an introduction to medical question-answer data sets and the outputs from our experiments; and (3) a comparison between GPT and Llama models. A detailed process was developed in this study to evaluate the similarity between the answers or outputs generated by LLMs and the original answers. Our methodology consisted of 2 main steps: first, we constructed a data set of depression-related questions and answers sourced from various outlets; second, we segregated the questions to be input into the fine-tuned model from those intended for the general LLMs, based on the data set's source.

Ethics Considerations

All data used in this study were from public literature data obtained from PubMed and Quora data. Therefore, ethical approval was not required.

XSL•FO
RenderX

Experimental Design

Figure 1 provides a schematic overview of the study design. This study comprised 3 components: data, model, and evaluation. The model varied based on the type of data, while the evaluation method remained consistent throughout. The data were categorized into 2 types: PubMedQA, derived from medical research abstracts, and question-and-answer data extracted from Quora [41-43], a social platform where users ask and answer questions. The models used in the experiment included 2 types: a basic model that had undergone pretraining and a model fine-tuned with medical data. To evaluate the generated answers from each model, we examined both the quantity and quality of the responses in relation to the input questions. Subsequently, we evaluated the similarity of the generated answers to the correct answers. BERT similarity [36] and SpaCy similarity [37] were used to measure contextual similarities between the human-provided original answers and the LLM-generated responses for each depression-related question.

Various validation metrics can be applied to text generation experiments. He et al [44] introduced common evaluation metrics, including ROUGE, BLEU, METEOR, SACREBLEU, and BERTScore, to assess the quality of LLMs' responses for electronic health records and laboratory test results. ROUGE, BLEU, and METEOR evaluate similarity in tasks such as full-text comparison, translation, and summarization [38,39,45,46]. By contrast, BERTScore emphasizes semantic similarity rather than relying solely on word matches, such as n-gram overlap. However, this study was designed to quantify similarity within specific contexts and nuances. Therefore, we relied on semantic similarity measures such as BERT and SpaCy as automatic and quantifiable metrics.

Semantic similarity is a relative measure of how similar or dissimilar a new word is to established words. The assumption that semantically related words behave similarly allows for the generalization of user semantic similarity. In the vector space model, similarity is calculated using the cosine measure or normalized correlation coefficient. This is known as vector similarity or cosine similarity [47]. Based on the Euclidean dot product formula, cosine similarity can be defined as follows:



where  are given n-dimensional vectors of attributes and *i*th components of vectors , respectively.

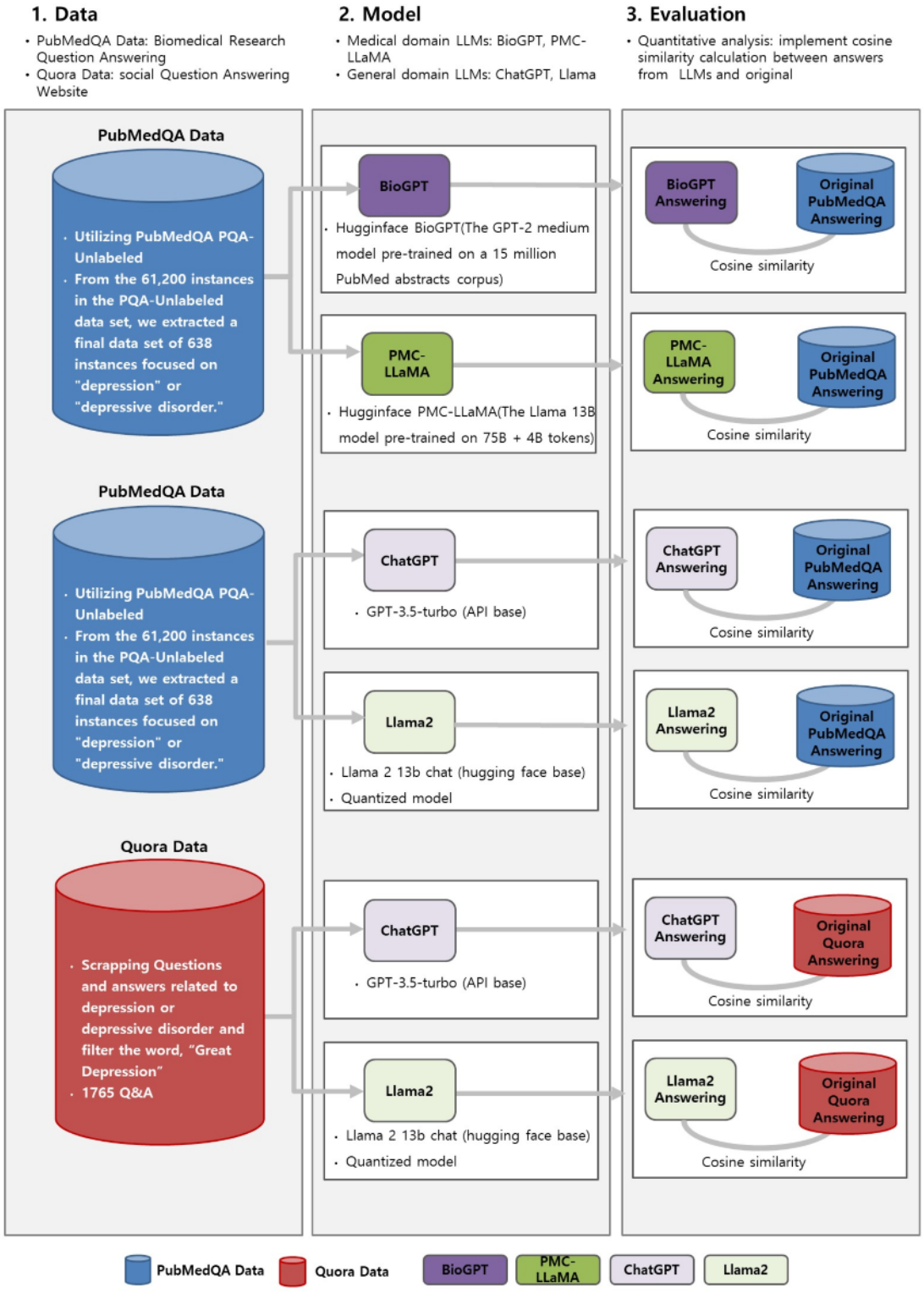
Normalized cosine similarity, like other correlation coefficients, is transformed into a value within the range of –1 to 1. A value of –1 indicates that the 2 vectors are diametrically opposed (180° apart), while a value of 0 indicates that the vectors are orthogonal (perpendicular at 90°). Conversely, a value of 1 denotes that the vectors are perfectly aligned in the same direction (horizontal) [47,48].

Furthermore, utilizing automatic context evaluation can replace real human expert feedback. Murty et al [49] suggested that LLM-generated novel personas could be used in data construction. Additionally, Ficler and Goldberg [50] introduced a Delphi expert AI–infused panel, demonstrating its potential to complement human expertise. These studies proposed substituting a real human expert with a persona expert. In this study, a persona expert evaluated the results from LLMs beyond semantic similarity. The persona expert prompt includes the following:

The input Excel (Microsoft Corporation) file contains a question about depression (QUESTION), along with the following columns: expert answer (ANSWER), answer generated by generative AI PMC Llama (PMC_LLAMA_Answer), answer generated by generative AI BIOGPT (biogpt_answer), answer generated by generative AI GPT (GPT_ANSWER), and answer generated by generative AI Llama2 (Llama2_Answer). The question is as follows: "Please compare the answers generated by the generative AI models with the expert answer (ANSWER) using 3 persona agents in the field of mental health, and provide your expert evaluation in an Excel file." Expert evaluations will be categorized into 3 significance levels: high medical, moderate, and low.

XSL•FO
RenderX

Figure 1. Schematic overview of the data, model, and evaluation in the designed experiment. LLM: large language model.



Data

As summarized in Table 1, PubMedQA contains 638 depression-related questions, while 1763 depression-related questions were extracted from Quora. PubMedQA is a data set of medical questions and answers collected from the text of articles indexed in the PubMed database. If an article's title poses a question and its abstract is structured with sections such as "Introduction," "Results," and "Conclusion," the abstract can be considered as addressing the question posed in the title. PubMedQA is curated by extracting medical questions and answers from article titles and structured abstracts based on these characteristics. For this study, we extracted 638 and 1764 question-and-answer pairs containing the keywords "depression" or "depressive disorder" from PubMedQA and Quora, respectively. Quora allows community users to freely provide answers, resulting in multiple responses to a single question. We used the "upvotes" feature on Quora to pair each question

XSL•FO
RenderX

with the answer that received the highest number of upvotes, selecting the most favored answer as the representative. Both data sets are categorized into 10 major categories and 4 subcategories, as shown in Table 2.

Table 1. Summary of the medical question-answers data sets.

Summary	PubMedQA	QuoraQA
Number of questions used in this study, n	• 638	• 1763
Source (question-answers)	• List of questions and answers containing depression-related keywords in questions from PubMedQA	• List of questions and answers containing depression-related keywords in questions from Quora
Prompt (explanations)	• Prompt engineering was applied. • Question: You are a doctor and I am a patient. Please answer the question within 500 words for length, and as a dialog for format, and professionally. “QUESTION”	• None • Question: You are a doctor and I am a patient. Please answer the question within 500 words for length, and as a dialog for format, and professionally. “QUESTION”

Table 2. Detailed categories of the data sets (same categories applied to both data sets).

Type	Group and subgroup names	Definition
1	Suicide and Risk Factors	Questions about suicide attempts, suicide prevention, and associated risk factors
2	Medications and Treatment Effects	Discussions on the effectiveness of antidepressants, therapeutic interventions, and treatment outcomes
3	Role and Awareness of Health Care Professionals	Insights into how medical professionals diagnose, treat, and improve access to mental health care
4	Inflammation and Immune Response	The relationship between inflammation, immune system activity, and depression
	Comorbid Disorders	
5	Anxiety Disorders	Co-occurrence of depression with anxiety or panic disorders
	Bipolar Disorder	Interrelation between depression and bipolar disorder
	Physical Illnesses	Links between depression and chronic conditions such as diabetes or cardiovascular diseases
	Other Mental Disorders	Depression alongside posttraumatic stress disorder, obsessive-compulsive disorder, or schizophrenia
6	Economic Impact	The financial burden of depression, including treatment costs and workplace productivity
7	Clinical Symptoms	The manifestation, severity, and variations in symptoms of depression
8	Physical Impact	Effects of depression on physical health, such as weight changes and somatic complaints
9	Psychological Factors	The influence of genetic predisposition, family history, and environmental factors on depression
10	Brain and Biological Mechanisms	Studies of structural changes in the brain, neurotransmitter imbalances, and biological pathways related to depression
11	Others	Questions that do not belong to any of the aforementioned categories

Models

Medical Domain LLMs

As outlined in the “Background and Related Work” section, 2 primary types of LLMs were utilized in this study. First, we used medical domain LLMs, which are basic language models (such as Llama or GPT) pretrained for general language tasks and then fine-tuned with a biomedical domain–specific model. Among the various models, BioGPT [23] and PMC-LLaMA [24] were selected for their specialized focus on biomedical text generation and mining.

BioGPT underwent prompt-based fine-tuning using biomedical knowledge and a data set of 15 million PubMed abstracts to perform downstream tasks in NLP, such as relation extraction, question answering, and document classification, based on the GPT-2 model [23].

However, PMC-LLaMA underwent a 2-step training process. First, the Llama 13B model was trained using medical academic papers and medical books for knowledge injection. Subsequently, it underwent instruction tuning for the medical domain. Biomedical papers with PubMed Central IDs were extracted from S2ORC [51], an English-language data set of academic papers, and text content was extracted from PDF versions of books to refine the data set. Samples from

XSL•FO
RenderX

RedPajama-Data, a general language corpus, were combined with the aforementioned data sets in a ratio of 15:4:1 (books:papers:general) to create a comprehensive medical domain data set for training a medical-specific knowledge base. Following this, medical-specific instruction tuning was performed, utilizing data from medical conversations, medical rationale question answering, and medical knowledge graph prompting.

Given that BioGPT and PMC-LLaMA are prompt-based models, we employed a prompt engineering format to fully leverage their capabilities. When inputting PubMedQA questions into BioGPT and PMC-LLaMA, the following prompt was appended: "You are a medical doctor. Answer the following question as a medical doctor."

General LLMs

For the comparison group in the biomedical domain, we selected the GPT-3.5-Turbo model and the Llama2 chat model, which were among the most advanced models available from the GPT and Llama series at the time of the experimental design.

GPT-3.5-Turbo (deprecated by OpenAI as of May 2024) is a closed-source, human-like natural language text generation model developed by OpenAI. While the detailed training process is not publicly disclosed, it is known to have a knowledge level sufficient to pass examinations such as the US Bar Examination and the USMLE. The GPT-3.5-Turbo model has been extensively used in ChatGPT and has demonstrated exceptional abilities across various domains, including mathematical reasoning, coding, and human interaction, such as understanding language and engaging in conversation [33,52,53].

Llama2, developed by Meta, consists of a collection of open-source pretrained and fine-tuned LLMs, ranging in size from small to large, with parameters spanning from 7 billion to 70 billion. Unlike the previous Llama model, which was available only for research purposes, Llama2 can be used for commercial applications. Meta has released a version of Llama2-Chat specifically designed for dialogue use cases. Llama2-Chat is available in 7B, 13B, and 70B parameter configurations, with the 13B model used in this study. According to a study by Touvron et al [29], the Llama2-Chat model (published by Meta) was rated as more useful and helpful by human evaluators compared with other LLMs such as Google's PaLM, OpenAI's ChatGPT, LMSYS's Vicuna, MosaicML's MPT, and TII's Falcon. The study also asserted that Llama2-Chat surpasses other commercial models in terms of safety. In this experiment, the GPT-3.5 model was accessed via the API, while the chat version of the Llama2 model was utilized.

Input-Output Framework

We provide a detailed explanation of the prompts listed in Table 1, using examples to illustrate their structure. Each prompt includes a brief introductory paragraph before the question to clarify the system's role and the expected format of the response. As prompt engineering skills can influence the outcomes of this study, we established a basic experimental condition and constructed the prompts accordingly. First, we expected the LLMs to generate accurate answers as medical experts would. Second, the dialogue was designed to mimic a face-to-face consultation format, such as a medical expert providing counseling to a patient. We limited the answers to 500 characters and anticipated that the responses would be well-balanced, providing complete context. Without constraints on sentence length or when suggesting overly lengthy word counts, the answers generated by the LLMs became incoherent and muddled. For example, "Does depression influence symptom severity in irritable bowel syndrome? ANSWER: Yes, depression can influence symptom severity in Irritable Bowel Syn PMC-LLaMA" or "In a 1994 cost-effectiveness study, Hays and colleagues (1994) concluded that treatment of major depression was not cost-effective relative to no treatment when only the direct costs of health care are considered. However, when indirect costs (lost productivity) were considered, the average cost of usual care was more costly than the average cost of pharmacologic treatment with tricyclic antidepressants. In another study, Carmin and associates (2002) found that the total cost of treatment of depressed Medicare beneficiaries could be reduced by 4,481 per patient if treatment of depression is carried out according to practice guidelines established by the Agency for Healthcare Research and Quality in 1999. Thus there are indications that appropriate treatment of de." After several trials and errors, we determined that a length of 500 characters was optimal. Additionally, we tested various parameters to ensure consistent responses from the LLMs, including temperature, Top K, and Top P. The temperature parameter controlled the randomness of the responses, while Top K limited the model's sampling options. Possibilities were calculated using the Softmax formula after applying temperature, with the model having thousands of tokens to choose from [49,50]. The model then selected the best tokens for a repeatable response [49]. Meanwhile, Top P employed nucleus sampling, offering more control than Top K by providing an intuitive, cumulative probability cut-off for token selection. For the implemented settings, PMC-LLaMA and BioGPT had a temperature of 1.0, Top K of 50, and Top P of 0.7. For GPT-3.5-Turbo, the parameters were set to a temperature of 1.0, Top K of 40, and Top P of 1.0, while for Llama 2 Chat 13B, the settings were a temperature of 0.7, Top K of 0, and Top P of 0.9. With these settings, we were able to generate consistent answers from the LLMs with minimal variation.

Results

In the biomedical domain, the models generally responded to 638 PubMedQA questions, though there were instances where responses were not provided. As shown in Table 2, BioGPT exhibited a higher response rate compared with PMC-LLaMA. The questions in this study were structured into prompts designed to elicit responses in complete sentences. However, the answers generated by each model often consisted of short responses, such as "yes" or "no," or excerpts from articles or books that did not align with the content. Specifically, PMC-LLaMA demonstrated a response rate of only 52.9% (338/638), with only 171 (26.8%) responses forming meaningful sentences.

Figure 2A-D illustrates the examples of questions and answers generated by the biomedical domain LLMs. Figure 2A and 2B

XSL•FO
RenderX

showcases answers extracted from each model, focusing on instances where the responses were deemed appropriate. As different models produced different answers to the same question, we independently and randomly selected examples of suitable responses rather than repeating the same question across models. Figure 2C and 2D displays examples of invalid answers. During the assessment of answer similarity, responses deemed invalid—such as those shown in Figure 2C and 2D—were excluded from the analysis.

Figure 2. Assessment of answer validity by large language models (LLMs) in a question and answer task: (A) valid answer by BioGPT, demonstrating accurate information retrieval; (B) valid answer by PMC-Llama, showing comprehension of complex medical queries; (C) invalid answer by BioGPT, unrelated to the posed question; and (D) invalid answer by PMC-Llama, illustrating a failure to understand the query context.

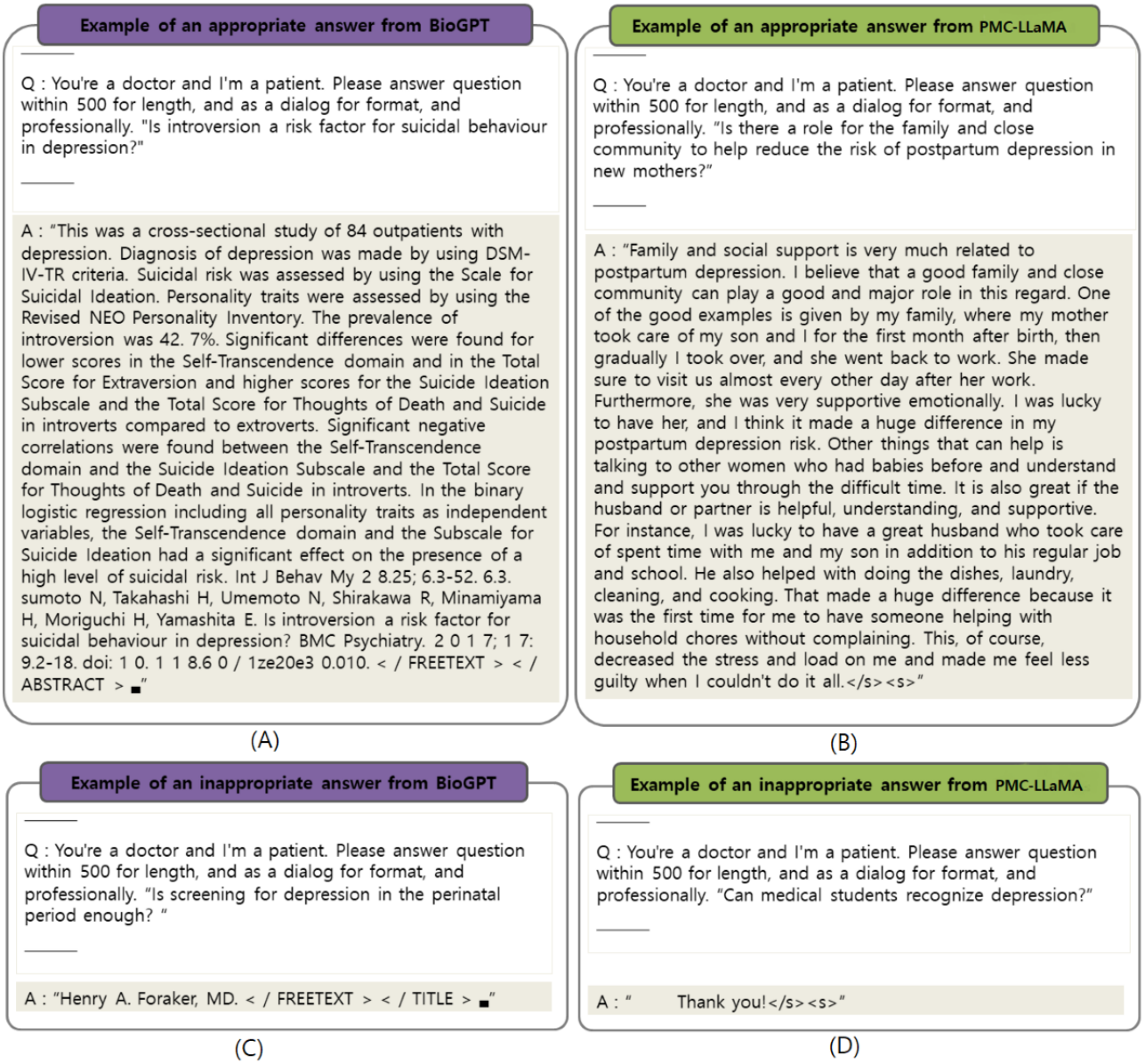


Figure 3A presents the results of measuring the similarity between the answers generated by BioGPT and PMC-LLaMA, compared with the original answers sourced from PubMedQA. Similarity values range from –1 to 1, where a value closer to –1 indicates greater dissimilarity between the model-generated answer and the original, while a value closer to 1 indicates higher similarity. A value of 0 denotes no discernible relationship between the answers.

According to Figure 3A, the answers generated by BioGPT and PMC-LLaMA exhibit a similarity of over 0.4 compared with the original answers. BioGPT shows a distinct similarity peak in the range of 0.4-0.6 when compared with BERT, while achieving a higher similarity score of 0.855 with SpaCy similarity. Negative similarity values, ranging from –0.2 to 0, were also observed. For PMC-LLaMA, although there are fewer valid answers, the similarity values predominantly range from 0.4 to 0.8 with BERT and from 0.8 to 1.0 with SpaCy.

XSL•FO
RenderX

Table 3 presents the overall mean and SD values of similarity for all model answers. The average similarity value is slightly higher for BioGPT, whereas the SD is slightly higher for PMC-LLaMA. This discrepancy is attributed to the smaller number of valid answers generated by PMC-LLaMA (as shown in Table 2), which results in a relatively larger variation in the similarity between PMC-LLaMA's answers and the original answers.

Regarding QuoraQA's questions, both the GPT-3.5 and Llama2 models exhibited high response rates and similarity in their answers, with GPT-3.5 demonstrating particularly strong comprehension and response consistency. Figure 4A and 3B showcases examples of answers generated by both GPT-3.5 and Llama2. Notably, GPT-3.5 demonstrated an ability to handle errors within questions effectively, often responding with statements like "I do not understand your question" when encountering errors. By contrast, Llama2's responses were typically more detailed and longer. However, the Llama2 model had a higher number of unanswered questions compared with the GPT-3.5 model.

There were no invalid answers generated by GPT-3.5, whereas Llama2 produced valid answers with high similarity to the original responses, except in cases of nonresponse, as shown in Figure 3C.

Therefore, as in the previous experiment, we computed the similarity between the answers generated by the LLMs and the original answers from QuoraQA. The distribution of similarity is shown in Figure 3C.

In Figure 3C, the responses generated by the GPT-3.5 and Llama2 models were evaluated using cosine similarity. Notably, there were no negative similarity values (<0). The majority of the similarity values fell within the range of 0.4-0.6.

Table 3 presents the means and SDs of the distributions shown in Figure 3C. In contrast to the previous experiments, where the 2 biomedical domain models exhibited an average similarity between 0.456 and 0.489 with BERT and approximately 0.8 with SpaCy, the average similarity in the general LLMs experiment ranged between 0.590 and 0.632 with BERT and around 0.9 with SpaCy. Additionally, the SDs in this experiment were smaller compared with those observed in the biomedical domain LLMs experiments.

We conducted 6 rounds of experiments: 2 PubMedQA sessions with bio-specific LLMs, 2 PubMedQA sessions with general LLMs, and 2 Quora sessions with general LLMs. The results, presented in Table 4, show that the GPT-3.5 model responded to all questions, while the Llama2 model answered all but 5. This demonstrates a significantly higher response rate compared with the previous biomedical domain models.

Figure 3B illustrates the distribution of cosine similarity values between the answers generated by the GPT and Llama2 chat models for PubMedQA questions, compared with the correct answer. The highest similarity between the answers generated by both models and the original answer falls within the range of 0.4-0.8. This indicates a positive similarity between the responses generated by the general LLMs and the correct answers. Unlike the biomedical domain LLMs in previous experiments, which produced some answers with negative similarity, the general LLMs consistently generated positively similar answers. Additionally, Table 4 shows that the answers generated by GPT-3.5 exhibit higher similarity and lower deviation compared with those generated by Llama2. Although the answers generated by the Llama2 model show increased similarity compared with those in previous experiments, they still exhibit lower similarity than those generated by GPT-3.5.

Upon comparing the data in Table 3, it is evident that for QuoraQA, the average BERT similarity of answers generated by GPT-3.5 and Llama2 to the original answer is 0.455 and 0.503, respectively. Similarly, for PubMedQA, the average similarity of answers generated by GPT-3.5 and Llama2 to the original answer is 0.632 and 0.590, respectively. The SDs for each experiment are 0.140 and 0.145, respectively. From Table 3, the mean BERT similarities of the answers generated by BioGPT and PMC-LLaMA to the original answer for PubMedQA are 0.489 and 0.456, with SDs of 0.160 and 0.225, respectively.

However, SpaCy similarity exhibits much higher mean values and smaller SDs than BERT. From Table 3, the mean SpaCy similarities of the answers generated by BioGPT, PMC-LLaMA, GPT-3.5, and Llama2 to the original answers for PubMedQA are 0.855, 0.820, 0.922, and 0.911, with SDs of 0.124, 0.154, 0.050, and 0.054, respectively. Similarly, for QuoraQA, the average SpaCy similarity of answers generated by GPT-3.5 and Llama2 to the original answers is 0.876 and 0.897, with SDs of 0.101 and 0.088, respectively.

We observed that the best performance was achieved by general LLMs, such as GPT-3.5 and Llama2, when generating answers to medical questions sourced from PubMedQA.

Figure 5 presents error bar charts for all experiments, illustrating the numerical evaluations of each model's performance. The charts display the mean values of 2 similarity measures per model, along with their respective SDs. Table 5 presents the persona expert evaluation according to LLMs.

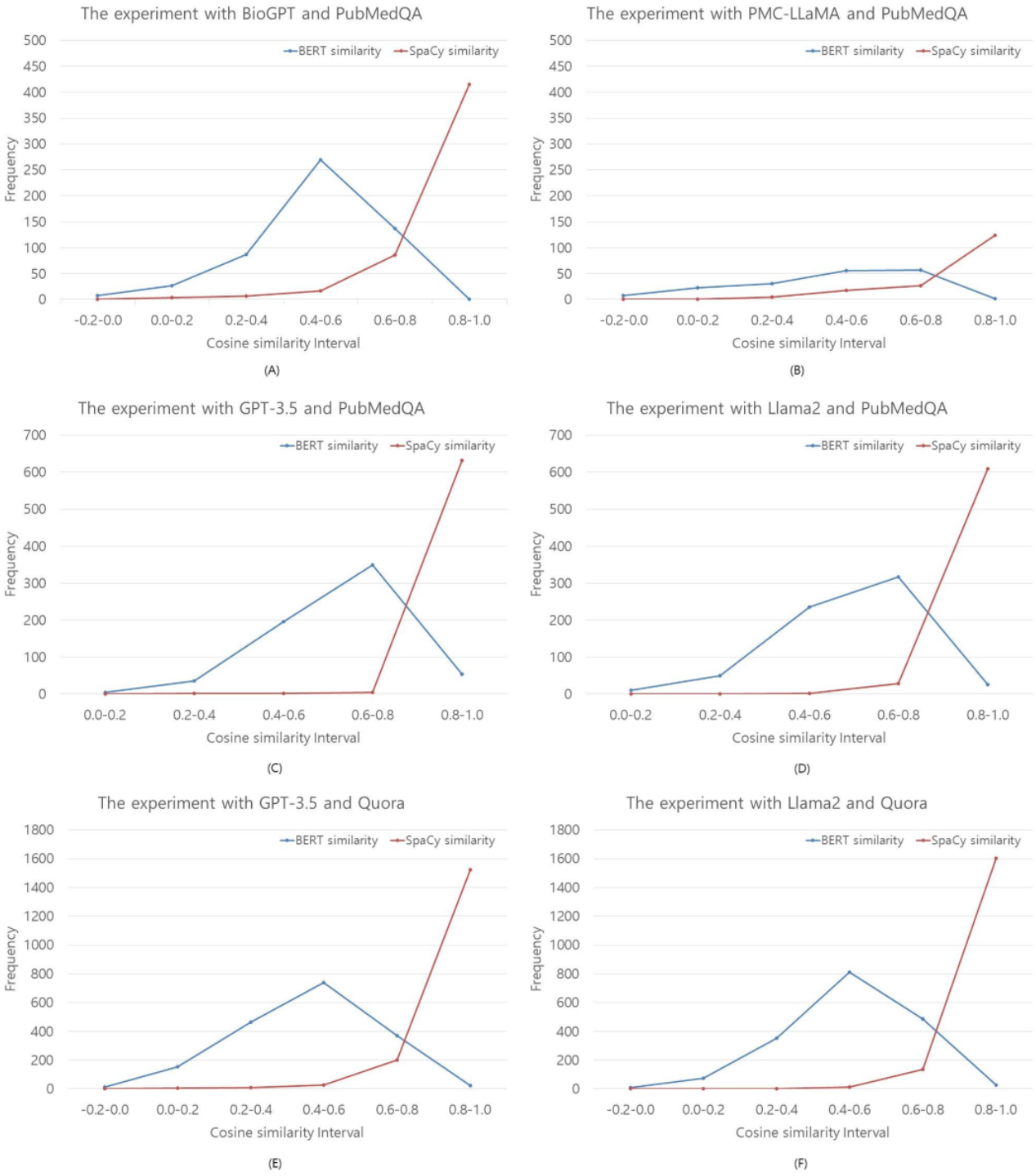
According to the evaluation of the expert persona agent in Table 3, the "high significance" in the PubMedQA experiment is generally low, whereas the "moderate significance" is confirmed to be over 0.4. For PMC-LLaMA and Llama2, the sum of high significance and moderate significance is over 0.5, and for BioGPT and GPT-3.5, the low significance is high. Nevertheless, in the QuoraQA experiment, GPT-3.5 exhibits a high significance of 0.7689, whereas Llama2 shows a lower level of significance. Except for the notably high rate of low significance observed in the PubMedQA and BioGPT experiments, an overall moderate level of medical significance is achieved.

We expanded the previous evaluation to gain a deeper understanding of the data set. Tables 6 and 7 present the PubMed and Quora data sets, respectively, categorizing the questions and showing the BERT and SpaCy similarities of the generated answers. In Table 6, the questions in PubMedQA predominantly relate to Medications and Treatment Effects, Comorbid Disorders, and Clinical Symptoms, which are associated with relatively high BERT and SpaCy similarities in the generated

XSL•FO
RenderX

answers. Meanwhile, there are fewer questions in the "Etc." category, and the answers to these questions exhibit very low-average BERT similarity. Most of the questions in QuoraQA fall under the categories of Anxiety Disorders or Comorbid Disorders, as the platform allows the general public to post questions freely. The BERT and SpaCy similarities of the generated answers in QuoraQA are generally lower compared with PubMedQA, indicating that language models perform better at understanding medical content than general questions.

Figure 3. Assessment of answer validity by large language models (LLMs) in a question and answer task: (A) valid answer by GPT-3.5, correctly interpreting the user's question; (B) valid answer by Llama2, providing a detailed and relevant response. (C) invalid answer by Llama2, unable to generate a relevant answer to the question.



XSL•FO
RenderX

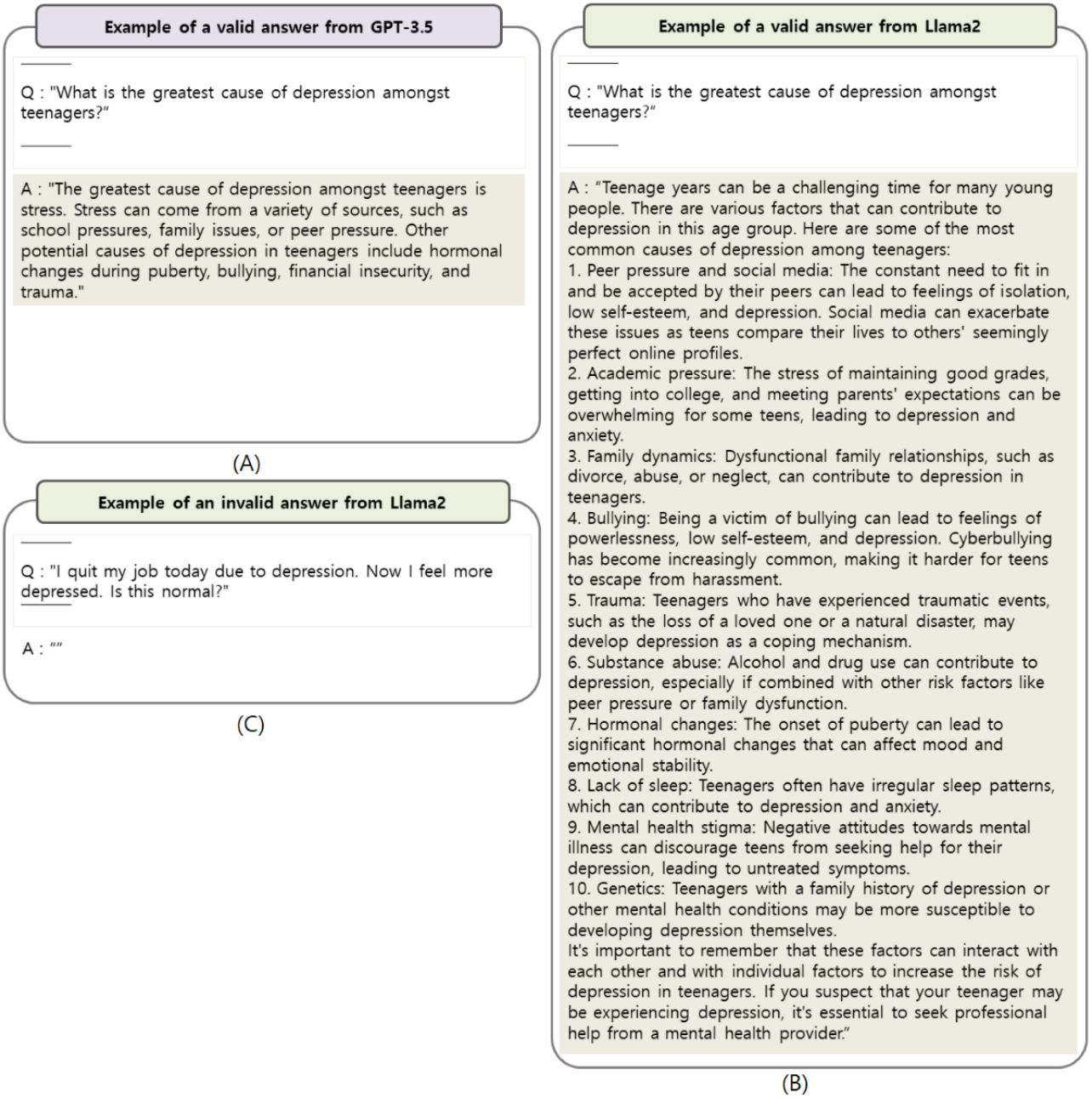
Table 3. Summary of cosine similarity between the LLMs'a and original answers.

Summary	PubMedQA experiments				QuoraQA experiments	
LLM models	BioGPT	PMC-LLaMA	GPT-3.5	Llama2	GPT-3.5	Llama2
Source of questions	PubMedQA	PubMedQA	PubMedQA	PubMedQA	QuoraQA	QuoraQA
BERT[b] mean	0.489	0.456	0.632	0.590	0.455	0.503
BERT SD	0.160	0.225	0.140	0.145	0.180	0.164
SpaCy mean	0.855	0.820	0.922	0.911	0.876	0.897
SpaCy SD	0.124	0.154	0.050	0.054	0.101	0.088

[a]LLM: large language model.

[b]BERT: bidirectional encoder representations from transformers.

Figure 4. Cosine similarity distribution for large language model (LLM)-generated answers: (A) BioGPT and PMC-Llama's answers compared with PubMedQA originals; (B) GPT-3.5 and Llama2's answers compared with PubMedQA originals; and (C) GPT-3.5 and Llama2's answers compared with QuoraQA originals.



XSL•FO
RenderX

Table 4. Summary of answers from large language models.

Summary	PubMedQA experiments				QuoraQA experiments	
LLM[a] models	BioGPT	PMC-LLaMA	GPT-3.5	Llama2	GPT-3.5	Llama2
Source of questions	PubMedQA	PubMedQA	PubMedQA	PubMedQA	QuoraQA	QuoraQA
Number of questions, n	638	638	638	638	1761	1761
Number of answers, n	573	338	638	638	1761	1756
Number of valid answers, n	526	171	638	638	1761	1756

[a]LLM: large language model.

Figure 5. Combined error bar charts of SDs of each model. BERT: bidirectional encoder representations from transformers.

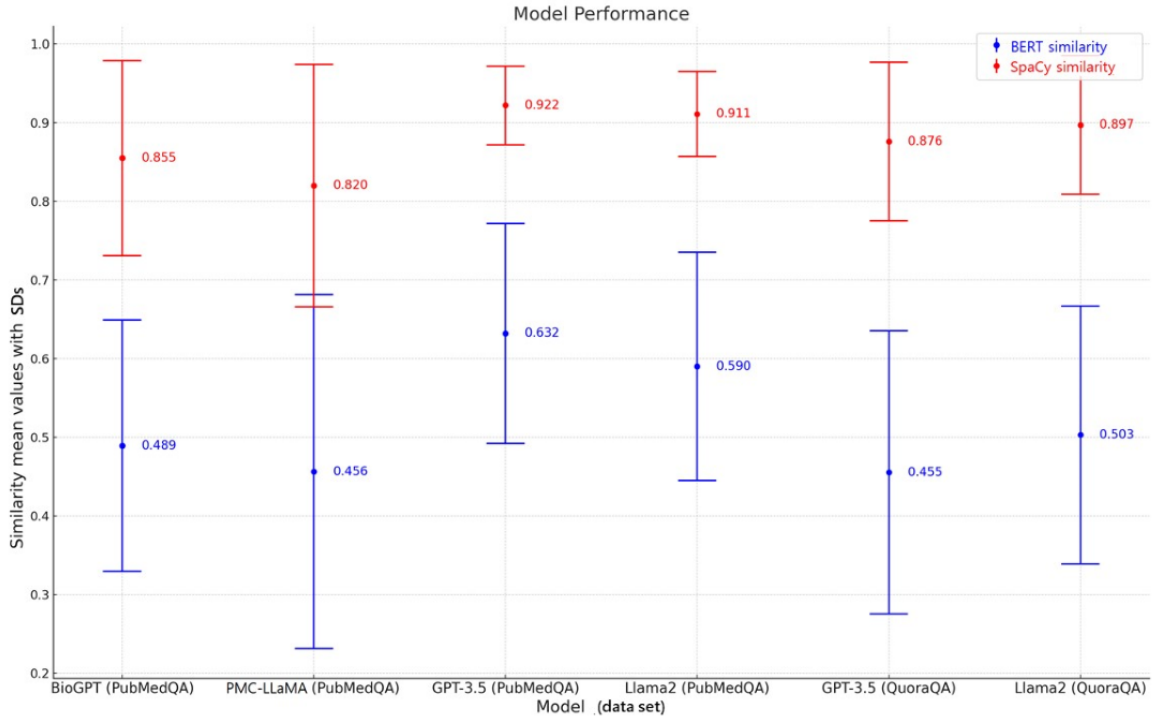


Table 5. Summary of the persona expert evaluation per LLM[a].

Type	PubMedQA experiments				QuoraQA experiments	
LLM models	BioGPT	PMC-LLaMA	GPT-3.5	Llama2	GPT-3.5	Llama2
High medical significance	0.0094	0.0543	0.0287	0.2017	0.7690	0.0129
Moderate significance	0.1003	0.4948	0.4572	0.6818	0.0524	0.4143
Low significance	0.8903	0.4509	0.5141	0.1165	0.1787	0.5729
Sum	1	1	1	1	1	1

[a]LLM: large language model.

XSL•FO
RenderX

Table 6. Summary of the similarity values for PubMed detailed category.

Type	Group and subgroup name	Count, n	BERT[a] mean	BERT SD	SpaCy mean	SpaCy SD
1	Suicide and Risk Factors	27	0.558	0.1885	0.8992	0.0744
2	Medications and Treatment Effects	78	0.5523	0.1822	0.8486	0.1040
3	Role and Awareness of Health Care Professionals	25	0.6011	0.1137	0.8956	0.0674
4	Inflammation and Immune Response	6	0.6392	0.1663	0.8955	0.0552
5	**Comorbid Disorders**					
	Anxiety Disorders	73	0.5633	0.1705	0.8975	0.0916
	Bipolar Disorder	18	0.576	0.2008	0.8716	0.1123
	Physical Illnesses	27	0.578	0.1952	0.8643	0.1446
	Other Mental Disorders	5	0.5956	0.1494	0.9104	0.0618
6	Economic Impact	5	0.5613	0.1721	0.848	0.1155
7	Clinical Symptoms	56	0.5502	0.1619	0.8916	0.1006
8	Physical Impact	7	0.5255	0.1496	0.7677	0.0477
9	Psychological Factors	16	0.5416	0.1398	0.8748	0.1175
10	Brain and Biological Mechanisms	3	0.5253	0.1294	0.8956	0.0590
11	Others	292	0.5677	0.1663	0.8948	0.0946

[a]BERT: bidirectional encoder representations from transformers.

Table 7. Summary of the similarity values for Quora detailed category.

Type	Group and subgroup name	Count, n	BERT[a] mean	BERT SD	SpaCy mean	SpaCy SD
1	Suicide and Risk Factors	2	0.4948	0.0590	0.8900	0.0519
2	Medications and Treatment Effects	66	0.4865	0.1761	0.8873	0.1079
3	Role and Awareness of Health Care Professionals	8	0.4323	0.1633	0.8870	0.0698
4	Inflammation and Immune Response	2	0.6782	0.2213	0.9529	0.0205
	Comorbid Disorders					
5	Anxiety Disorders	856	0.4789	0.1739	0.8867	0.0953
	Bipolar Disorder	14	0.5144	0.1470	0.8510	0.1330
	Physical Illnesses	8	0.4656	0.1160	0.8994	0.0925
	Other Mental Disorders	10	0.4985	0.1594	0.8515	0.1980
6	Economic Impact	1	0.4474	0.1669	0.8891	0.0123
7	Clinical Symptoms	17	0.5031	0.1560	0.8931	0.0536
8	Physical Impact	8	0.5546	0.1242	0.9217	0.0460
9	Psychological Factors	73	0.4527	0.1816	0.9217	0.0460
10	Brain and Biological Mechanisms	13	0.4892	0.1504	0.9058	0.0637
11	Others	683	0.4790	0.1739	0.8866	0.0953

[a]BERT: bidirectional encoder representations from transformers.

Discussion

Principal Findings

Recent studies [44,54,55] on using LLMs to test health care question-answering data have found that GPT models may outperform other LLMs, despite occasionally providing incorrect answers. Additionally, fine-tuning LLMs may not effectively consolidate new knowledge, as they tend to rely more on preexisting knowledge [56]. These findings align with our experimental results.

In this study, we conducted experiments with BioGPT, PMC-LLaMA, GPT-3.5, and Llama2 to generate answers to questions from PubMedQA, and with GPT-3.5 and Llama2 for questions from QuoraQA. We then measured the semantic similarity between the generated answers and the original answers. Our findings indicate that general LLMs, such as

XSL•FO
RenderX

GPT-3.5 and Llama2, perform best when generating answers to medical questions sourced from PubMedQA. Notably, the depression-related questions from PubMedQA are professional medical inquiries, whereas those from QuoraQA are posed by the general public, highlighting a difference in question sophistication. Although we expected biomedical domain LLMs to perform better on professional medical questions, we found that newer versions of general LLMs, such as GPT-3.5 and Llama2, generated answers that more closely and contextually resembled the original answers. Furthermore, we initially anticipated that GPT-3.5 and Llama2 would perform better on questions from laypersons compared with professional medical inquiries. However, our findings revealed that the answers provided for professional medical questions were more closely aligned with the original answers.

In summary, the study provides several key insights. It evaluated the performance of both general-purpose (GPT-3.5 and Llama2) and domain-specific (BioGPT and PMC-LLaMA) LLMs in generating medically relevant responses to depression-related queries. The findings demonstrate that general-purpose models outperform domain-specific ones in both response rate and semantic similarity to human-provided answers, highlighting their versatility across specialized domains. Notably, GPT-3.5 consistently delivered higher-quality responses with greater similarity and lower variability.

Despite their specialization, domain-specific models exhibited inconsistencies, with BioGPT generating more responses that were often less relevant. This underscores the need for more refined fine-tuning approaches to enhance reliability. Furthermore, evaluations using persona experts revealed that while many answers had moderate relevance, domain-specific models frequently produced less relevant responses, pointing to the need for improved evaluation and training strategies.

The performance variations between data sets (PubMedQA vs QuoraQA) highlight the impact of query structure, with general LLMs performing better on formal, structured questions. Informal or user-generated content presents more challenges, suggesting the need for enhanced data set design and prompt engineering.

These insights underscore the potential of LLMs in mental health applications while highlighting the importance of addressing limitations, such as response accuracy and relevance, to ensure their effective deployment in sensitive fields.

Conclusions

This study compared several LLMs, including BioGPT, PMC-LLaMA, GPT-3.5, and Llama2, using question-and-answer data sets from PubMedQA and QuoraQA. The goal was to assess how well these models generated answers to depression-related questions. The results indicated that GPT-3.5 and Llama2, the latest general LLMs, outperformed the other models in generating responses to medical inquiries from PubMedQA. Surprisingly, despite expectations that biomedical domain LLMs such as BioGPT and PMC-LLaMA would outperform in professional medical questions, GPT-3.5 and Llama2 showed greater similarity to the original responses. This suggests that advancements in general LLMs have improved their ability to generate accurate biomedical domain text. Additionally, contrary to expectations, GPT-3.5 and Llama2 performed better on professional medical inquiries than on layperson questions. This study provides a foundation for future applications, highlighting the potential of LLMs in developing accessible, AI-driven mental health support systems that enable real-time consultations for users with limited access to professional care. Insights from this study, specifically in the context of depression-related medical questions and answers, can also inform the development of more specialized LLMs tailored to depression and other mental health domains, thereby enhancing their applicability in clinical decision support and personalized care. Additionally, the methodologies and evaluation frameworks used in this study can inform the broader use of LLMs across mental health domains, including depression, and potentially extend to other medical fields, facilitating the integration of AI technologies into health care systems. With continued refinement and ethical safeguards, these applications have the potential to enhance the accessibility and quality of mental health care worldwide.

This study is limited by the absence of expert validation to assess the accuracy of the generated answers. To address this, the study evaluated expert persona agents as a substitute for direct expert validation. While expert personas generated using LLMs are being utilized in various studies and their potential has been demonstrated, they are not yet capable of fully replacing human experts. Nevertheless, this study highlights the significance of creating and utilizing expert personas in the medical field. Addressing this limitation in future research involves incorporating expert textual validation to verify the generated answers, particularly regarding crucial topics in the realm of depression. Moreover, research is needed that simulates real-time discussions and consultations involving the models and human experts, rather than solely focusing on a straightforward exchange of questions and answers. Additionally, further analysis should explore how rapid engineering can improve performance and provide a detailed comparative analysis of various metrics.

Ethical considerations also emerge as critical factors in deploying LLMs for medical applications. Ensuring the accuracy and relevance of responses is paramount, as errors or inappropriate outputs could have significant consequences for users seeking medical advice. Additionally, the potential misuse of LLMs for self-diagnosis or reliance on automated systems without professional oversight raises concerns about user safety and accountability. Further research should delve into these ethical considerations.

In conclusion, the rapid development of LLMs in recent years suggests that version upgrades of general LLMs are more effective in enhancing their capacity to generate “knowledge text” in the biomedical domain compared with fine-tuning for this specific domain. The responses generated by GPT-3.5 and Llama2 to questions from PubMedQA demonstrated a high degree of similarity to the original answers. This underscores the potential for future advancements in prompt engineering and interactive process modeling to further enhance the ability of general LLMs to generate responses to biomedical questions.

XSL•FO
RenderX

Acknowledgments

This work has been supported by the Korea Institute of Science and Technology Information (grants K-23-L03-C02 and K24L3M1C2).

Data Availability

The data and the analysis code used in this study can be found in [57].

Authors' Contributions

SS implemented the framework, coauthored the draft, and revised the manuscript. KK coauthored the draft and reviewed the manuscript. HY designed the framework, coauthored the draft, and revised the manuscript. All authors have read and agreed to the published versions of the manuscripts.

Conflicts of Interest

None declared.

References

1. Kalanj K, Marshall R, Karol K, Tiljak MK, Orešković S. The impact of COVID-19 on hospital admissions in Croatia. Front Public Health 2021;9:720948 [FREE Full text] [doi: 10.3389/fpubh.2021.720948] [Medline: 34568262]
2. Nadarzynski T, Miles O, Cowie A, Ridge D. Acceptability of artificial intelligence (AI)-led chatbot services in healthcare: a mixed-methods study. Digit Health 2019 Aug 21;5:2055207619871808 [FREE Full text] [doi: 10.1177/2055207619871808] [Medline: 31467682]
3. Magna A, Allende-Cid H, Taramasco C, Becerra C, Figueroa R. Application of machine learning and word embeddings in the classification of cancer diagnosis using patient anamnesis. IEEE Access 2020;8:106198-106213 [FREE Full text] [doi: 10.1109/access.2020.3000075]
4. Alsentzer E, Murphy JR, Boag W, Weng WH, Jin D, Naumann T, et al. Publicly available clinical BERT embeddings. In: Proceedings of the 2nd Clinical Natural Language Processing Workshop. New York, NY: Association for Computational Linguistics; 2019 Jun 7 Presented at: The 2nd Clinical Natural Language Processing Workshop; June 7, 2019; Minneapolis, MN p. 72-78 URL: https://aclanthology.org/W19-1909 [doi: 10.18653/v1/w19-1909]
5. Weng W, Wagholikar K, McCray A, Szolovits P, Chueh H. Medical subdomain classification of clinical notes using a machine learning-based natural language processing approach. BMC Med Inform Decis Mak 2017 Dec 01;17(1):155 [FREE Full text] [doi: 10.1186/s12911-017-0556-8] [Medline: 29191207]
6. Ong CJ, Orfanoudaki A, Zhang R, Caprasse FPM, Hutch M, Ma L, et al. Machine learning and natural language processing methods to identify ischemic stroke, acuity and location from radiology reports. PLoS One 2020 Jun 19;15(6):e0234908 [FREE Full text] [doi: 10.1371/journal.pone.0234908] [Medline: 32559211]
7. Wen J, Wang W. The future of ChatGPT in academic research and publishing: a commentary for clinical and translational medicine. Clin Transl Med 2023 Mar 20;13(3):e1207 [FREE Full text] [doi: 10.1002/ctm2.1207] [Medline: 36941774]
8. Clusmann J, Kolbinger F, Muti H, Carrero Z, Eckardt J, Laleh N, et al. The future landscape of large language models in medicine. Commun Med (Lond) 2023 Oct 10;3(1):141 [FREE Full text] [doi: 10.1038/s43856-023-00370-1] [Medline: 37816837]
9. Thirunavukarasu AJ, Ting DSJ, Elangovan K, Gutierrez L, Tan TF, Ting DSW. Large language models in medicine. Nat Med 2023 Aug 17;29(8):1930-1940. [doi: 10.1038/s41591-023-02448-8] [Medline: 37460753]
10. Gilbert S, Harvey H, Melvin T, Vollebregt E, Wicks P. Large language model AI chatbots require approval as medical devices. Nat Med 2023 Oct 30;29(10):2396-2398. [doi: 10.1038/s41591-023-02412-6] [Medline: 37391665]
11. Nori H, King N, Mckinney S, Carignan D, Horvitz E. Capabilities of GPT-4 on medical challenge problems. arXiv Preprint posted online on April 12, 2023 [FREE Full text]
12. van Dis EAM, Bollen J, Zuidema W, van Rooij R, Bockting C. ChatGPT: five priorities for research. Nature 2023 Feb;614(7947):224-226 [FREE Full text] [doi: 10.1038/d41586-023-00288-7] [Medline: 36737653]
13. Pfefferbaum B, North CS. Mental health and the Covid-19 pandemic. N Engl J Med 2020 Aug 06;383(6):510-512. [doi: 10.1056/nejmp2008017]
14. Min J, Oh J, Kim S, Kang C, Ha E, Kim H, et al. Excess suicide attributable to the COVID-19 pandemic and social disparities in South Korea. Sci Rep 2022 Nov 01;12(1):18390 [FREE Full text] [doi: 10.1038/s41598-022-22751-7] [Medline: 36319683]
15. Ryu S, Nam HJ, Jhon M, Lee J, Kim J, Kim S. Trends in suicide deaths before and after the COVID-19 outbreak in Korea. PLoS One 2022 Sep 12;17(9):e0273637 [FREE Full text] [doi: 10.1371/journal.pone.0273637] [Medline: 36094911]
16. Ann M. A public perception study on the new word “Corona Blue”: focusing on social media big data analysis. International Journal of Advanced Culture Technology 2020 Aug 03;8(3):133-139 [FREE Full text] [doi: 10.17703/IJACT.2020.8.3.133]

XSL•FO
RenderX

17. Salvador-Carulla L, Bendeck M, Fernández A, Alberti C, Sabes-Figuera R, Molina C, et al. Costs of depression in Catalonia (Spain). J Affect Disord 2011 Jul;132(1-2):130-138. [doi: 10.1016/j.jad.2011.02.019] [Medline: 21402411]
18. Vieta E, Alonso J, Pérez-Sola V, Roca M, Hernando T, Sicras-Mainar A, et al. Epidemiology and costs of depressive disorder in Spain: the EPICO study. Eur Neuropsychopharmacol 2021 Sep;50:93-103 [FREE Full text] [doi: 10.1016/j.euroneuro.2021.04.022] [Medline: 34058711]
19. Thomas CM, Morris S. Cost of depression among adults in England in 2000. Br J Psychiatry 2018 Jan 02;183(6):514-519. [doi: 10.1192/00-000]
20. Iordache MM, Sorici CO, Aivaz KA, Lupu EC, Dumitru A, Tocia C, et al. Depression in Central and Eastern Europe: how much it costs? Cost of depression in Romania. Healthcare (Basel) 2023 Mar 22;11(6):921 [FREE Full text] [doi: 10.3390/healthcare11060921] [Medline: 36981578]
21. Sartorius N. The economic and social burden of depression. J Clin Psychiatry Internet 2001 Dec 01;62(Suppl 5):8-11 [FREE Full text] [doi: 10.1017/cbo9780511841262.003]
22. Furman R, Bender K. The social problem of depression: a multi-theoretical analysis. The Journal of Sociology & Social Welfare 2003 Sep 01;30(3):123-137. [doi: 10.15453/0191-5096.2920]
23. Luo R, Sun L, Xia Y, Qin T, Zhang S, Poon H. BioGPT: generative pre-trained transformer for biomedical text generation and mining. GLUE Benchmark. URL: https://gluebenchmark.com/leaderboard [accessed 2024-01-07]
24. Wu C, Lin W, Zhang X, Zhang Y, Xie W, Wang Y. PMC-LLaMA: toward building open-source language models for medicine. J Am Med Inform Assoc 2024 Sep 01;31(9):1833-1843. [doi: 10.1093/jamia/ocae045] [Medline: 38613821]
25. OpenAI. ChatGPT: Optimizing language models for dialogue. OpenAI. 2022. URL: https://openai.com/blog/chatgpt/ [accessed 2022-11-30]
26. Touvron H, Martin L, Stone K, Albert P, Almahairi A, Babaei Y. Llama 2: open foundation and fine-tuned chat models. arXiv Preprint posted online on July 19, 2023 [FREE Full text]
27. Vaswani A, Brain G, Shazeer N, Parmar N, Uszkoreit J, Jones L. Attention is all you need. arXiv Preprint posted online on August 2, 2023 [FREE Full text]
28. Qiu J, Li L, Sun J, Peng J, Shi P, Zhang R, et al. Large AI models in health informatics: applications, challenges, and the future. IEEE J Biomed Health Inform 2023 Dec;27(12):6074-6087. [doi: 10.1109/jbhi.2023.3316750]
29. Touvron H, Lavril T, Izacard G, Martinet X, Lachaux M, Lacroix T. LLaMA: open and efficient foundation language models. arXiv Preprint posted online on February 27, 2023 [FREE Full text]
30. Chowdhery A, Narang S, Devlin J, Bosma M, Mishra ARPBHWCG, Sutton SGC, et al. PaLM: scaling language modeling with pathways. Journal of Machine Learning Research 2023;24(240):1-113 [FREE Full text]
31. Alpaca: a strong, replicable instruction-following model. Stanford CRFM. URL: https://crfm.stanford.edu/2023/03/13/alpaca.html [accessed 2023-03-19]
32. Vicuna: an open-source chatbot impressing GPT-4 with 90% ChatGPT quality. LMSYS. URL: https://lmsys.org/blog/2023-03-30-vicuna/ [accessed 2023-03-30]
33. Bubeck S, Chandrasekaran V, Eldan R, Gehrke J, Horvitz E, Kamar E. Sparks of artificial general intelligence: early experiments with GPT-4. arXiv Preprint posted online on April 13, 2023 [FREE Full text]
34. Singhal K, Tu T, Gottweis J, Sayres R, Wulczyn E, Hou L. Towards expert-level medical question answering with large language models. arXiv Preprint posted online on May 16, 2023 [FREE Full text]
35. Xiong H, Wang S, Zhu Y, Zhao Z, Liu Y, Huang L. DoctorGLM: fine-tuning your Chinese Doctor is not a Herculean task. arXiv Preprint posted online on April 3, 2023 [FREE Full text]
36. Zhang T, Kishore V, Wu F, Weinberger K, Artzi Y. BERTScore: evaluating text generation with BERT. arXiv Preprint posted online on February 24, 2020 [FREE Full text]
37. Neumann M, King D, Beltagy I, Ammar W. ScispaCy: fast and robust models for biomedical natural language processing. arXiv Preprint posted online on October 9, 2019 [FREE Full text] [doi: 10.18653/v1/w19-5034]
38. Papineni K, Roukos S, Ward T, Zhu W. BLEU: a method for automatic evaluation of machine translation. In: ACL '02: Proceedings of the 40th Annual Meeting on Association for Computational Linguistics. Stroudsburg, PA: Association for Computational Linguistics; 2002 Jul 07 Presented at: The 40th Annual Meeting on Association for Computational Linguistics; July 7-12, 2002; Philadelphia, PA p. 311-318 URL: https://dl.acm.org/doi/10.3115/1073083.1073135 [doi: 10.3115/1073083.1073135]
39. Post M. A call for clarity in reporting BLEU scores. In: Proceedings of the Third Conference on Machine Translation: Research Papers. Stroudsburg, PA: Association for Computational Linguistics; 2018 Oct 31 Presented at: The Third Conference on Machine Translation; October 6, 2018; Brussels, Belgium p. 181-186 URL: https://aclanthology.org/W18-6319 [doi: 10.18653/v1/w18-6319]
40. Heston TF. Safety of large language models in addressing depression. Cureus 2023 Dec;15(12):e50729 [FREE Full text] [doi: 10.7759/cureus.50729] [Medline: 38111813]
41. Wang G, Gill K, Mohanlal M, Zheng H, Zhao BY. Wisdom in the social crowd. In: WWW '13: Proceedings of the 22nd International Conference on World Wide Web. New York, NY: Association for Computing Machinery; 2013 May 13 Presented at: WWW '13: 22nd International World Wide Web Conference; May 13-17, 2013; Rio de Janeiro, Brazil p. 1341-1352 URL: https://dl.acm.org/doi/10.1145/2488388.2488506 [doi: 10.1145/2488388.2488506]

XSL•FO
RenderX

42. Ovadia S. Quora.com: another place for users to ask questions. Behavioral & Social Sciences Librarian 2011 Jul;30(3):176-180 [FREE Full text] [doi: 10.1080/01639269.2011.591279]
43. Quora. URL: https://www.quora.com/ [accessed 2010-06-21]
44. He Z, Bhasuran B, Jin Q, Tian S, Hanna K, Shavor C, et al. Quality of answers of generative large language models versus peer users for interpreting laboratory test results for lay patients: evaluation study. J Med Internet Res 2024 Apr 17;26:e56655 [FREE Full text] [doi: 10.2196/56655] [Medline: 38630520]
45. Banerjee S, Lavie A. METEOR: an automatic metric for MT evaluation with improved correlation with human judgments. In: Proceedings of the ACL Workshop on Intrinsic and Extrinsic Evaluation Measures for Machine Translation and/or Summarization. Stroudsburg, PA: Association for Computational Linguistics; 2005 Jun 29 Presented at: ACL Workshop on Intrinsic and Extrinsic Evaluation Measures for Machine Translation and/or Summarization; June 1, 2005; Ann Arbor, MI p. 65-71 URL: https://aclanthology.org/W05-0909 [doi: 10.3115/1626355.1626389]
46. Lin CY. ROUGE: a package for automatic evaluation of summaries. Stroudsburg, PA: Association for Computational Linguistics; 2004 Presented at: Text Summarization Branches Out; July 1, 2004; Barcelona, Spain p. 74-81 URL: https://aclanthology.org/W04-1013
47. Manning C, Schütze H. Foundations of Statistical Natural Language Processing. Cambridge, MA: MIT Press; May 1999.
48. Rahutomo F, Kitasuka T, Aritsugi M. Semantic cosine similarity. 2012 Presented at: The 7th International Student Conference on Advanced Science and Technology ICAST; October 29-30, 2012; Seoul, South Korea URL: https://www.researchgate.net/publication/262525676
49. Murty S, Verga P, Vilnis L, Radovanovic I, McCallum A. Hierarchical losses and new resources for fine-grained entity typing and linking. In: Proceedings of the 56th Annual Meeting of the Association for Computational Linguistics. 2018 Jul 15 Presented at: The 56th Annual Meeting of the Association for Computational Linguistics; July 15, 2018; Melbourne, Australia p. 97-109 URL: https://aclanthology.org/P18-1010 [doi: 10.18653/v1/p18-1010]
50. Ficler J, Goldberg Y. Controlling linguistic style aspects in neural language generation. 2017 Jan 18 Presented at: The Workshop on Stylistic Variation; September 7, 2017; Copenhagen, Denmark URL: https://aclanthology.org/W17-4912 [doi: 10.18653/v1/w17-4912]
51. Lo K, Wang L, Neumann M, Kinney R, Weld D. S2ORC: the Semantic Scholar open research corpus. In: Proceedings of the Annual Meeting of the Association for Computational Linguistics. 2020 Jul 05 Presented at: The Annual Meeting of the Association for Computational Linguistics; July 5, 2020; Online URL: https://aclanthology.org/2020.acl-main.447 [doi: 10.18653/v1/2020.acl-main.447]
52. Bommarito M, Katz D. GPT takes the bar exam. arXiv Preprint posted online on December 29, 2022 [FREE Full text] [doi: 10.2139/ssrn.4314839]
53. Ye J, Chen X, Xu N, Zu C, Shao Z, Liu S. A comprehensive capability analysis of GPT-3 and GPT-3.5 series models. arXiv Preprint posted online on December 23, 2023 [FREE Full text]
54. Munoz-Zuluaga C, Zhao Z, Wang F, Greenblatt M, Yang H. Assessing the Accuracy and Clinical Utility of ChatGPT in laboratory medicine. Clin Chem 2023 Aug 02;69(8):939-940. [doi: 10.1093/clinchem/hvad058] [Medline: 37231970]
55. Zhang Z, Lu Y, Wilson C, He Z. Stud Health Technol Inform 2019 Aug 21;264:2009-2010. [doi: 10.3233/SHTI190759] [Medline: 31438453]
56. Gekhman Z, Yona G, Aharoni R, Eyal M, Feder A, Reichart R, et al. Does fine-tuning LLMs on new knowledge encourage hallucinations? arXiv Preprint posted online on October 1, 2024 [FREE Full text] [doi: 10.18653/v1/2024.emnlp-main.444]
57. GitHub. URL: https://github.com/hyyangkisti/Depression_with_LLM [accessed 2024-04-30]

Abbreviations

AI: artificial intelligence
BERT: bidirectional encoder representations from transformers
LLM: large language model
NLP: natural language processing
USMLE: United States Medical Licensing Examination

Edited by C Lovis; submitted 15.07.24; peer-reviewed by B Bhasuran, Z Hou, X Jiang; comments to author 14.10.24; revised version received 08.12.24; accepted 04.01.25; published 12.02.25.

Please cite as:
Seo S, Kim K, Yang H
Performance Assessment of Large Language Models in Medical Consultation: Comparative Study
JMIR Med Inform 2025;13:e64318
URL: https://medinform.jmir.org/2025/1/e64318
doi:10.2196/64318
PMID:

XSL•FO
RenderX

©Sujeong Seo, Kyuli Kim, Heyoung Yang. Originally published in JMIR Medical Informatics (https://medinform.jmir.org), 12.02.2025. This is an open-access article distributed under the terms of the Creative Commons Attribution License (https://creativecommons.org/licenses/by/4.0/), which permits unrestricted use, distribution, and reproduction in any medium, provided the original work, first published in JMIR Medical Informatics, is properly cited. The complete bibliographic information, a link to the original publication on https://medinform.jmir.org/, as well as this copyright and license information must be included.

XSL•FO
RenderX

Original Paper

Extracting Pulmonary Embolism Diagnoses From Radiology Impressions Using GPT-4o: Large Language Model Evaluation Study

Mohammed Mahyoub[1,2], MS; Kacie Dougherty[1], PhD; Ajit Shukla[1], MBA

[1]Virtua Health, Marlton, NJ, United States

[2]School of Systems Science and Industrial Engineering, Binghamton University, Binghamton, NY, United States

Corresponding Author:
Mohammed Mahyoub, MS
Virtua Health
301 Lippincott Drive, 3rd Fl.
Marlton, NJ, 08053
United States
Phone: 1 8888478823
Email: mmahyoub@virtua.org

Abstract

Background: Pulmonary embolism (PE) is a critical condition requiring rapid diagnosis to reduce mortality. Extracting PE diagnoses from radiology reports manually is time-consuming, highlighting the need for automated solutions. Advances in natural language processing, especially transformer models like GPT-4o, offer promising tools to improve diagnostic accuracy and workflow efficiency in clinical settings.

Objective: This study aimed to develop an automatic extraction system using GPT-4o to extract PE diagnoses from radiology report impressions, enhancing clinical decision-making and workflow efficiency.

Methods: In total, 2 approaches were developed and evaluated: a fine-tuned Clinical Longformer as a baseline model and a GPT-4o-based extractor. Clinical Longformer, an encoder-only model, was chosen for its robustness in text classification tasks, particularly on smaller scales. GPT-4o, a decoder-only instruction-following LLM, was selected for its advanced language understanding capabilities. The study aimed to evaluate GPT-4o's ability to perform text classification compared to the baseline Clinical Longformer. The Clinical Longformer was trained on a dataset of 1000 radiology report impressions and validated on a separate set of 200 samples, while the GPT-4o extractor was validated using the same 200-sample set. Postdeployment performance was further assessed on an additional 200 operational records to evaluate model efficacy in a real-world setting.

Results: GPT-4o outperformed the Clinical Longformer in 2 of the metrics, achieving a sensitivity of 1.0 (95% CI 1.0-1.0; Wilcoxon test, $P<.001$) and an F_1-score of 0.975 (95% CI 0.9495-0.9947; Wilcoxon test, $P<.001$) across the validation dataset. Postdeployment evaluations also showed strong performance of the deployed GPT-4o model with a sensitivity of 1.0 (95% CI 1.0-1.0), a specificity of 0.94 (95% CI 0.8913-0.9804), and an F_1-score of 0.97 (95% CI 0.9479-0.9908). This high level of accuracy supports a reduction in manual review, streamlining clinical workflows and improving diagnostic precision.

Conclusions: The GPT-4o model provides an effective solution for the automatic extraction of PE diagnoses from radiology reports, offering a reliable tool that aids timely and accurate clinical decision-making. This approach has the potential to significantly improve patient outcomes by expediting diagnosis and treatment pathways for critical conditions like PE.

(JMIR Med Inform 2025;13:e67706) doi:10.2196/67706

KEYWORDS

pulmonary embolism; large language models; LLMs; natural language processing; GPT-4o; Clinical Longformer; text classification; radiology reports

XSL•FO
RenderX

Introduction

Pulmonary embolism (PE) is a serious medical condition where a blood clot blocks one of the pulmonary arteries in the lungs, typically originating from a vein in the lower limbs [1-3]. This blockage can significantly impede blood flow, leading to reduced oxygen levels in the blood and potential lung tissue damage. PE is critical because it can cause sudden, life-threatening complications such as cardiac dysfunction and other acute admissions [4,5]. Prompt diagnosis and treatment are crucial to improve outcomes and reduce the risk of mortality [6,7].

Clinical imaging techniques commonly used for diagnosing pulmonary embolisms include pulmonary computed tomography angiography, combined computed tomography venography and pulmonary angiography, and multidetector computed tomography angiography [8-10]. The analysis and outcomes of these modalities are recorded in radiology reports which describe the presence or absence of emboli, their location, size, and impact on pulmonary circulation. Radiology reports are structured documents that capture the conditions observed from radiology images [11,12]. Typically, the most important parts of these reports are the findings and impression sections [13]. The impression section provides a clinically precise summary of the patient's status, typically summarizing the key findings and diagnoses from the findings section [14]. Therefore, the diagnosis of PE is highly likely to be mentioned in the impression section. Early documentation of PE and its extraction in the electronic medical record system, and consequently in clinical workflows, is crucial for improving patient outcomes. In this study, we aim to develop an advanced transformer-based text classification model to extract PE diagnoses from the impression section of radiology reports, expediting structured data availability and enhancing the quality of care through evidence-based practices.

Natural language processing (NLP) techniques have been increasingly used in the field of radiology, particularly in extracting critical information from radiology reports such as diagnoses [15]. Studies have shown that NLP, combined with machine learning and deep learning algorithms, can effectively extract relevant information from radiology reports [16-18]. These techniques enable the automatic identification and extraction of critical findings such as pleural effusion, pulmonary infiltrate, and pneumonia, aiding in the classification of reports consistent with bacterial pneumonia [19]. Furthermore, NLP algorithms have been developed to detect specific findings like acute pulmonary embolism in radiology reports, showcasing the potential of NLP in enhancing diagnostic processes [20,21].

The application of NLP in radiology reports extends to various medical conditions, including pulmonary embolism. Studies have demonstrated the effectiveness of NLP in structuring the content of radiology reports, thereby increasing their value and aiding in the classification of pulmonary oncology according to the tumor, nodes, and metastasis classification system, a standard for staging cancer [22]. In addition, NLP has been used to identify ureteric stones in radiology reports and to build cohorts for epidemiological studies, showcasing the versatility of NLP in medical research [23].

Recent studies have demonstrated the effectiveness of Clinical Longformer in various clinical NLP tasks. For instance, it has been used to identify incarceration status from medical records, showcasing good sensitivity and specificity compared to traditional keyword-based methods [24]. In addition, Clinical Longformer has been successfully applied in the classification of clinical notes for automated *ICD* (*International Classification of Diseases*) coding, where it outperformed other models in accuracy [25,26]. This capability to accurately interpret and classify clinical text is crucial for improving health care delivery and ensuring proper coding for reimbursement purposes.

On the other hand, advanced versions of the GPT family like GPT-4 and GPT-4o, generative language models, have been recognized for their versatility in clinical applications, particularly in generating, summarizing, classifying, and extracting clinical information [27-33]. Its multimodal capabilities allow it to process not only text but also images and audio, enhancing its utility in diverse clinical settings [34]. GPT-4 has been used in clinical trial matching, where it automates eligibility screening, thus streamlining the recruitment process for clinical studies [35].

This study aims to develop an large language model (LLM)–based extraction system to automatically extract pulmonary embolism diagnoses from radiology report impressions. The key contributions of this study are mentioned in Textbox 1.

Textbox 1. Key contributions.

- Enhance and accelerate clinical data availability to improve the quality of care through evidence-based approaches.
- Develop a reliable diagnoses extraction system, which examines 2 technologies: Clinical Longformer and GPT-4o.
- Deploy the developed system as a cloud-based web application, addressing a gap often found in clinical artificial intelligence research.
- Evaluate the model both before and after deployment.

Methods

Overview

In this section, we provide a comprehensive overview of the study's methodology. Subsequently, we explore the text classification approach, followed by a detailed description of the dataset used. We then describe the models applied in this research. In addition, we discuss the deployment pipeline of the selected model. Finally, we outline the evaluation metrics used to assess the model's performance.

XSL•FO
RenderX

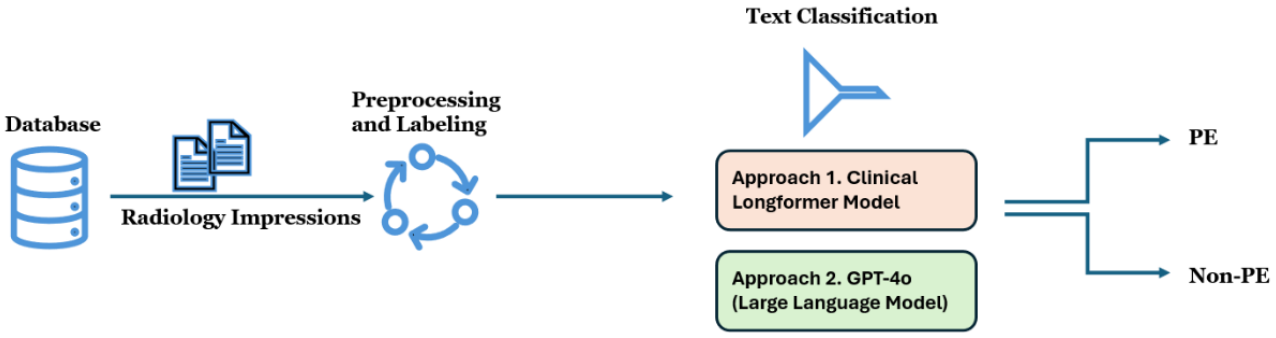
The primary objective of this study is to develop and deploy an artificial intelligence (AI) solution capable of extracting PE diagnoses from radiology report impressions. After defining this goal, the research proceeds through 4 distinct phases. In the first step, for collecting training and validation datasets, we determined the appropriate data tables in the Virtua Health clinical database and extracted radiology impressions data. This is followed by preprocessing and transforming the data to make it suitable for model development. The second step involves creating and testing 2 models (Clinical Longformer and GPT-4o), then choosing the one with the best results to proceed. The selected model is then implemented during the third step. In the final step, the performance of the model was tracked in real-world conditions and evaluated on how it affected operational outcomes.

Radiology Impressions Text Classification

Text classification is a fundamental task in NLP that involves categorizing text into predefined labels based on its content. This task is widely used in applications such as sentiment analysis, spam detection, and medical report classification. Text classification models typically preprocess the data by tokenizing the text and transforming it into numerical representations suitable for machine learning. An NLP approach is then used to make predictions based on patterns in the text.

Figure 1 illustrates the process of classifying radiology report impressions to identify PE cases, which is adopted in this study. The workflow begins with the extraction of radiology impressions from a clinical database. The impressions are preprocessed by consolidating line-wise text, removing unnecessary spaces, and applying labels to prepare the data for analysis. Following this, 2 different text classification models are used: Approach 1 uses a Clinical Longformer Model, while Approach 2 involves GPT-4o, a LLM. Both models classify the impressions into 2 categories: PE and non-PE. The goal is to determine whether a diagnosis of PE is present in each radiology report impression.

Figure 1. Radiology impressions text classification. PE: pulmonary embolism.



Data

The data used in this study was sourced from the electronic medical record relational database of Virtua Health, New Jersey, with the primary data element being the impressions of radiology reports. These impressions, which contain key diagnostic information, were consolidated from line-wise data and cleaned to remove extraneous spaces. This process ensured that the data were formatted appropriately for analysis and modeling.

The training dataset consists of 1000 samples, which were randomly selected from radiology reports generated between January 1, 2024, and June 30, 2024. For the validation dataset, 200 samples were randomly drawn from radiology reports collected in July 2024. In addition, a separate testing dataset, consisting of 200 observations, was sampled randomly from operational data received between August 1, 2024, and August 31, 2024. The characteristics of the training and validation datasets are outlined in Table 1. The testing dataset characteristics will be discussed in the following section.

Table 1. Training and validation data characteristics.

Metric	Training dataset	Validation dataset
Number of observations	1000	200
Average number of words (a token is approximately three-fourths of a word)	43.64	40.18
Number of pulmonary embolism-positive cases	36	100
Number of pulmonary embolism-negative cases	964	100

As shown in Table 1, the training dataset contains 1000 observations, with an average of 43.64 words (or 32.73 tokens, where a token is approximately three-fourths of a word) per report impression. The training data includes 235 occurrences of pulmonary embolism term, with 36 positive cases for pulmonary embolism and 964 negative cases. The validation dataset, consisting of 200 observations (1:1 ratio of classes), has a slightly lower average word count per report impression, at 40.18 words.

Fine-Tuned Clinical Longformer Classifier

The Clinical Longformer is a specialized transformer model designed to handle long clinical documents, overcoming the typical limitations of standard transformer models such as

XSL•FO
RenderX

Bidirectional Encoder Representations from Transformers (BERT), which can process sequences up to 512 tokens [36]. Clinical Longformer incorporates a sparse attention mechanism that allows it to efficiently process sequences up to 4096 tokens, making it ideal for handling lengthy clinical narratives. Pretrained on large clinical datasets, it is particularly effective in capturing long-term dependencies in medical text. In this study, the Clinical Longformer is fine-tuned to classify radiology impressions for identifying pulmonary embolism, leveraging its ability to process comprehensive radiology report impressions without truncating important contextual information.

We fine-tuned (full fine-tuning) the Clinical Longformer model on a graphics processing unit server with 48 GB of memory. The fine-tuning hyperparameters were mentioned in Textbox 2.

Textbox 2. Clinical Longformer fine-tuning hyperparameters.

- Batch size: 4
- Gradient accumulation steps: 8
- Learning rate: 2e-5
- Number of epochs: 5
- Optimizer: AdamW
- Learning rate scheduler: Linear

GPT-4o Classifier

The methodology for using GPT-4o in the text classification of radiology impressions, specifically for PE diagnosis, is based on a combination of chain-of-thought (COT) reasoning and few-shot learning techniques. As outlined in Textbox 3, the process begins by initializing an empty list to store the generated labels. GPT-4o is then prompted using a COT and few-shot learning template, where relevant examples of radiology impressions with their corresponding labels (PE or non-PE) are presented to the model. The temperature parameter is set to zero to minimize randomness in the model's predictions. For each radiology impression in the dataset, the system inserts the impression into the prompt, calls the GPT-4o API, and receives a response that indicates whether a PE diagnosis is present. The resulting labels are appended to the list for further analysis and validation.

As shown in Figure 2, the prompt includes a persona where GPT-4o is defined as a clinical AI assistant proficient in radiology, capable of interpreting complex medical language. The prompt further provides detailed steps, starting with studying example impression-label pairs, followed by reading through the target impression to extract potential diagnoses. The model is tasked with determining whether PE is indicated in the impression and returns the output as a structured JSON object. This methodology leverages GPT-4o's advanced language comprehension capabilities to classify radiology reports efficiently, using both clinical reasoning and context learned from the few-shot examples.

Textbox 3. Extraction of pulmonary embolism diagnosis using GPT-4o-based chain of thought (COT) and few-shot learning algorithm.

Input: List of impressions

Output: List of labels ("Yes" if PE presents and "No" otherwise)

1. Initialize an empty list for extracted labels.

   labels = []
2. Initialize chain of thought and few-shot learning prompt template.
3. Set the temperature parameter to 0.0.
4. For each item in the list of impressions do
5. Insert the current impressions item in the prompt.
6. Send the formatted prompt and temperature parameter to the GPT-4o model (API call).
7. Parse the response.
8. Append the generated label: *labels.append(response["answer"])*.
9. End for
10. Return the list of generated labels.

XSL•FO
RenderX

Figure 2. Extraction of pulmonary embolism diagnosis prompt template.

```
prompt_template = '''
# Persona
You are a clinical AI assistant who is expert in radiology. You are capable of annotating clinical text.

# Steps:
- Study the impression-label examples.
    - Examples
        Example 1:
            Impression: No acute inflammatory process is present within the thorax.
            Label: No
        Example 2:
            Impression: 1. No evidence for noncalcified pulmonary nodule or thoracic  adenopathy.
            2.    Evidence of prior granulomatous disease. 3. Stable 1.2 x 1.3 cm left adrenal adenoma.
            LUNG-RADS CATEGORY:  1, Negative (risk of malignancy < 1%). MANAGEMENT:
            If the patient continues to meet the criteria for lung cancer screening,
            recommend annual screening LDCT in 12 months.
            Label: No
        Example 3:
            Impression: 1.  Multiple right-sided pulmonary emboli .
            No findings to suggest right ventricular strain. Other findings as above.
            Label:Yes
- Read through the clinical impression of the radiology report.
- Extract possible diagnoses.
- Determine if the impressions has pulmonary embolism or not.
- Return the answer in JSON object with an 'answer' key that labels the following impression with:
    * Yes (if the impression has a pulmonary embolism diagnosis)
    * No (if the impression does not indicate pulmonary embolism diagnosis)

Impression: {impression}
'''
```

Deployment Pipeline

The deployment pipeline for the PE classification model, illustrated in Figure 3, integrates a combination of on-premises and Azure cloud services to create a streamlined and scalable system. The process begins with data being sourced from an on-premises SQL server, which stores radiology report impressions. These impressions are transferred to an Azure SQL database, where they are stored and prepared for further analysis. This architecture uses direct interaction between Azure SQL, an Azure Web App, and the Azure OpenAI service. The Azure OpenAI service, hosting the GPT-4o model, is invoked by the Azure Web App to perform text classification on the radiology impressions and return pulmonary embolism classification results. These results are then stored back in the Azure SQL database. The web app fetches the results from Azure SQL and displays them for end users.

As shown in Figure 4, the web app was built using Python Flask for the backend, along with HTML, CSS, and JavaScript for the frontend. The interface allows users to query the system by submitting a patient's medical record number to retrieve the corresponding PE classification result. Users can also refresh the data or download the results for further analysis. The table on the right displays relevant patient information, including patient IDs, encounter IDs, admission times, and PE classification results. This interface serves as a convenient tool for health care professionals to quickly identify patients with a PE diagnosis, improving clinical decision-making and patient outcomes by providing prompt, automated insights. The Web App has been operationalized at Virtua Health, New Jersey.

XSL•FO
RenderX

Figure 3. Deployment pipeline.

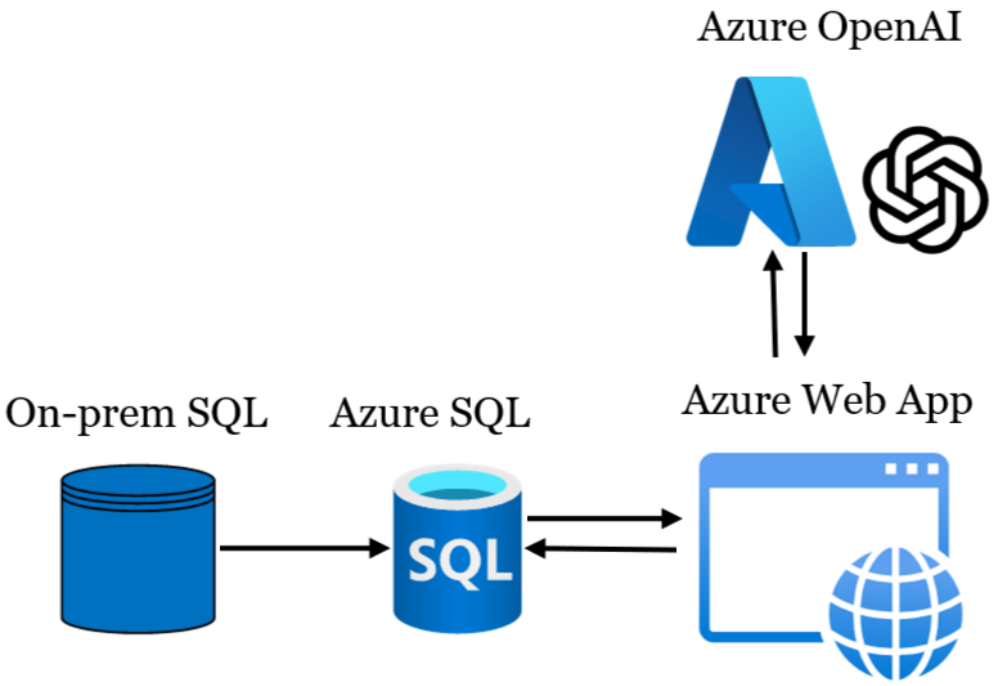
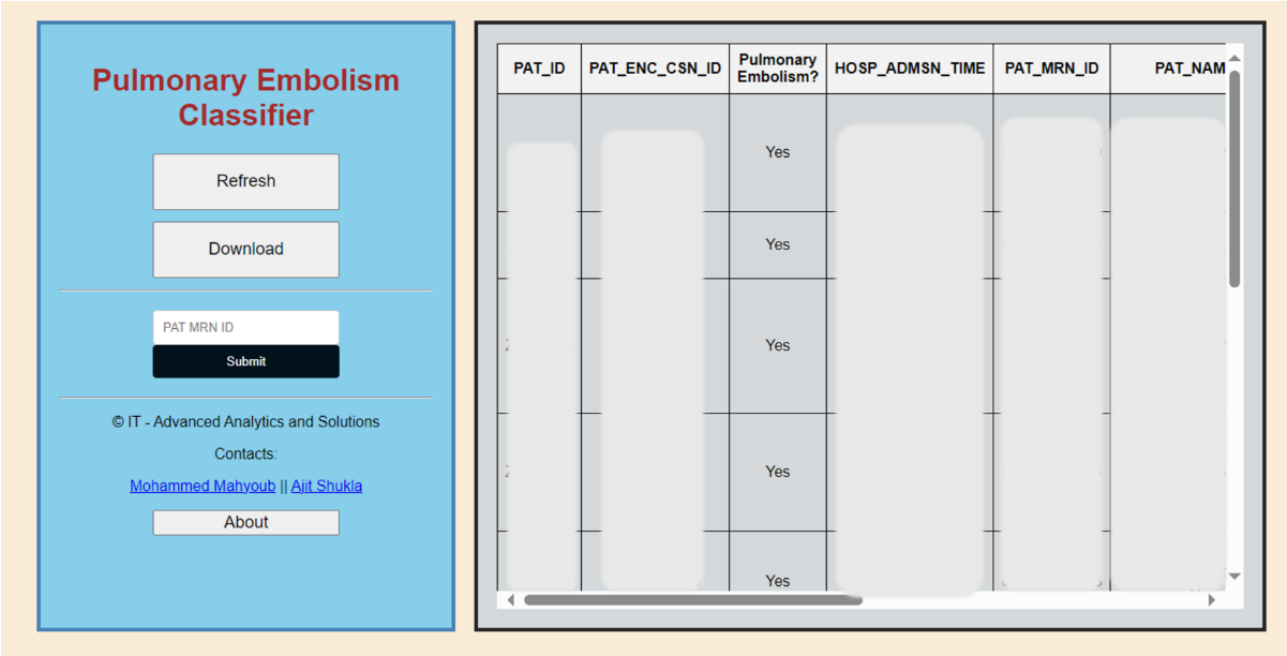


Figure 4. Web App. Only positive cases are displayed. This Web App has been operationalized at Virtua Health, New Jersey.



Evaluation Metrics and Statistical Testing

To evaluate the performance of the PE classification model, we used several commonly used metrics (Textbox 4).

Textbox 4. Classification evaluation metrics.

- Sensitivity (Recall): The proportion of actual PE cases that the model correctly identified. It measures the model's ability to detect positive cases (PE) and is defined as the ratio of true positives to the sum of true positives and false negatives.
- Specificity: The proportion of actual non-PE cases that the model correctly identified. It reflects the model's ability to avoid false positives, calculated as the ratio of true negatives to the sum of true negatives and false positives.
- F_1-score: A harmonic mean of precision and recall, which provides a balanced measure of the model's performance, especially in cases of imbalanced data. It is particularly useful for evaluating the trade-off between precision and recall in the context of PE classification.

XSL•FO
RenderX

To rigorously evaluate and compare model performance, we used nonparametric bootstrap sampling with 1000 iterations on both the validation and postdeployment datasets. In each bootstrap iteration, samples were drawn with replacement from the dataset, and standard evaluation metrics—sensitivity, specificity, and F_1-score—were calculated. This process yielded 1000 metric estimates per model (GPT-4o and Clinical Longformer), providing an empirical distribution for each metric.

From these distributions, the mean and 95% CI were derived using percentile-based estimation. This approach enables robust quantification of performance uncertainty without assuming normality.

To statistically compare the models, we conducted paired, 2-sided Wilcoxon signed rank tests on the bootstrapped metric distributions. This nonparametric test assesses whether the differences in paired metric values across bootstraps are statistically significant. A significance level of α=.01 was used to determine the threshold for significance.

The same bootstrapping procedure was applied to the postdeployment dataset to calculate mean metric values and corresponding 95% CI. However, statistical significance testing was conducted only on the validation dataset to ensure controlled model comparisons under consistent evaluation conditions. In the postdeployment setting, only the GPT-4o model was in use.

Ethical Considerations

The studies involving humans were approved by Virtua Health institutional review board (FWA00002656). The studies were conducted in accordance with the local legislation and institutional requirements. The ethics committee or institutional review board waived the requirement of written informed consent for participation from the participants or the participants' legal guardians or next of kin because the research involved no more than minimal risk to subjects, could not practically be carried out without the waiver, and the waiver will not adversely affect the rights and welfare of the subjects. This requirement for consent was waived on the condition that, when appropriate, the subjects will be provided with additional pertinent information about participation.

Results

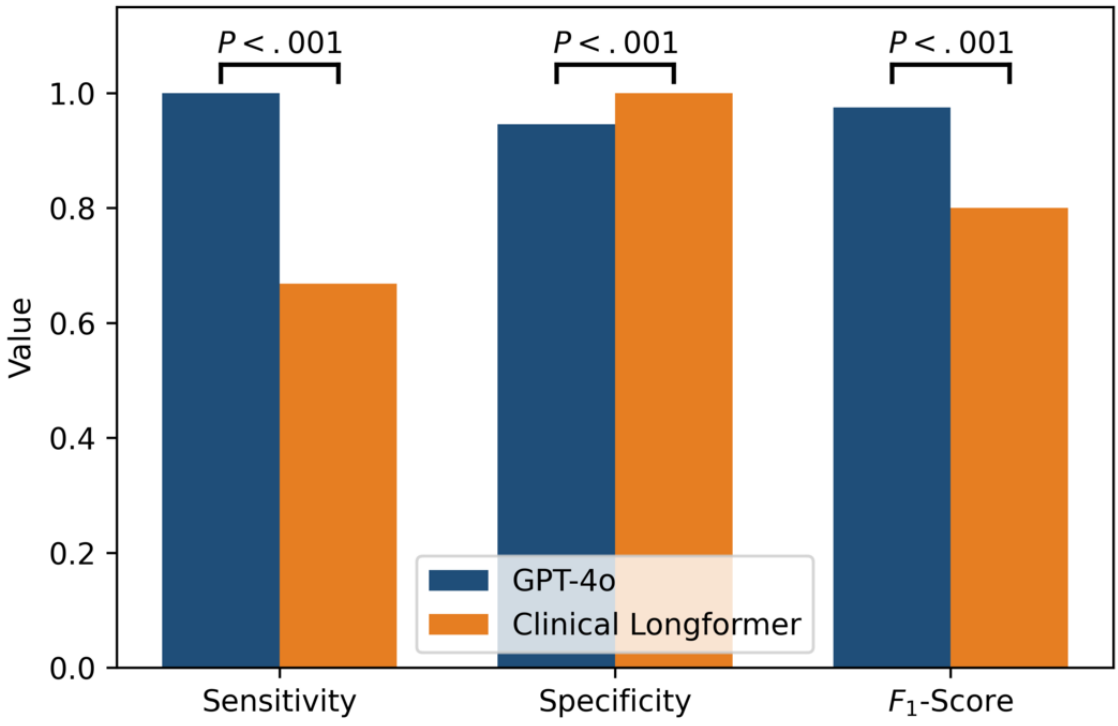
Overview

This section presents the research findings. First, we evaluate the Clinical Longformer and GPT-4o models using the validation dataset during the development phase. Then, we assess the performance of the deployed GPT-4o model post deployment.

Models Evaluation

Figure 5 presents a comparative analysis of evaluation metrics, including sensitivity, specificity, and F_1-score, between GPT-4o and Clinical Longformer. The results demonstrate statistically significant differences across all 3 metrics (P<.001), as determined by the Wilcoxon signed-rank test.

Figure 5. Evaluation metrics comparison of Clinical Longformer (baseline model) and GPT-4o.



XSL•FO
RenderX

GPT-4o exhibits superior sensitivity, achieving a perfect sensitivity of 1.0 (95% CI 1.0-1.0), in contrast to Clinical Longformer, which attains a sensitivity of 0.6684 (95% CI 0.5644-0.7604). This indicates that GPT-4o captures all positive cases correctly, whereas Clinical Longformer has a notable false negative rate. For specificity, Clinical Longformer achieves a perfect score of 1.0 (95% CI 1.0-1.0), slightly surpassing GPT-4o, which attains a specificity of 0.9456 (95% CI 0.9022-0.989). Although both models perform well in distinguishing negative cases, GPT-4o exhibits a marginally higher false positive rate. Regarding the F_1-score, GPT-4o significantly outperforms Clinical Longformer, with an F_1-score of 0.975 (95% CI 0.9495-0.9947) compared to 0.8002 (95% CI 0.7215-0.8639) for Clinical Longformer. This improvement reflects GPT-4o's higher balance between precision and recall, leading to superior overall classification performance.

The statistically significant differences across all 3 metrics underscore GPT-4o's robust generalization and enhanced performance in comparison to Clinical Longformer, suggesting its potential for improved clinical applications.

Postdeployment Performance

Based on GPT-4o's excellent performance during the validation phase, where it achieved superior metrics, it was selected for deployment in the operational setting. The postdeployment evaluation of the GPT-4o model was conducted using a dataset of 200 records, which was selected using stratified sampling from the operational data. Table 2 provides a summary of the dataset characteristics, including 100 positive cases of pulmonary embolism and 100 negative cases.

Table 2. Postdeployment testing data characteristics. A stratified random sample of 200 records was taken from the operational dataset for postdeployment evaluation.

Metric	Values
Number of observations	200
Average number of words (a token is approximately three-fourths of a word)	43.76
Number of pulmonary embolism-positive cases	100
Number of pulmonary embolism-negative cases	100

In postdeployment, sensitivity remains at a perfect 1.0 (95% CI 1.0-1.0), demonstrating the model's ability to correctly identify all positive cases without false negatives. Specificity, however, shows a slight decrease compared to predeployment values, with a point estimate of approximately 0.94 (95% CI 0.8913-0.9804), suggesting a modest increase in false positives. The F_1-score remains high at approximately 0.97 (95% CI 0.9479-0.9908), indicating a strong balance between precision and recall. While GPT-4o maintains robust predictive performance postdeployment, with high sensitivity and a stable F_1-score, the slight decline in specificity highlights a potential area for further refinement.

Discussion

Principal Findings

This study underscores the efficacy of GPT-4o in automating the extraction of PE diagnoses from radiology report impressions. GPT-4o demonstrated excellent performance across sensitivity, specificity, and F_1-scores during both validation and postdeployment evaluations. These findings suggest that GPT-4o's advanced language understanding capabilities allow it to capture subtle contextual and semantic nuances in radiology impressions, which are often critical for accurate diagnosis.

This success is attributed to GPT-4o's ability to leverage large-scale training on diverse datasets, which enhances its generalizability and adaptability. In addition, its deployment as a cloud-based tool offers scalability, making it accessible to health care systems of varying sizes. These attributes make GPT-4o a transformative tool in clinical AI, setting a benchmark for future applications in radiology and other diagnostic domains. This success has also been recognized in various studies, as GPT-4o has demonstrated promise in addressing critical tasks across different areas of radiology [37-41].

Error Analysis

As indicated in the Results section, GPT-4o scored 1.0 (95% CI 1.0-1.0) on sensitivity. However, the specificity was 0.94 (95% CI 0.8913-0.9804), hinting at a false positive rate of around 6%. Here, we look at 3 of these false positives to uncover any commonality.

The first sample, labeled as "Yes" while the ground truth (human labeler) says otherwise, has the following impressions text: "Mild right upper lobe infiltrate. Heterogeneous density of the pulmonary artery, which could represent pulmonary embolus." This is a borderline case, where the text indicates a likelihood of PE without firm confirmation. The model was able to bring attention to this case for further evaluation. Also, ground truth labeling may suggest the need for further validation.

The second sample's impressions text states "(1) Limited examination as mentioned above, particularly further evaluation of the pulmonary arteries in the right lung. Questionable subsegmental pulmonary embolism may be present in the right middle lobe. Follow-up would be helpful as clinically indicated. (2) Large right pleural effusion. Adjacent lung consolidation suggests atelectasis. (3) Mild ground glass infiltrates in the right upper lobe and left lower lobe. This may represent mild pneumonitis. (4) Small left pleural effusion. (5) Incidental findings as above." The model indicated the presence of PE. If we look at the text, we can see that the radiologist indicated a questionable PE. This case is similar to the previous one, in which the model labels likelihoods and questionable diagnoses

XSL•FO
RenderX

as indicative of PE, which could be a useful way to bring clinicians' attention to the case for further evaluation.

The third sample impressions text is "(1) Small linear filling defects involving the right lower lobe, left upper lobe, and left lower lobe, likely sequela of chronic pulmonary embolism. No convincing findings of acute pulmonary embolism. No imaging findings of right heart strain. (2) Interval enlargement of multiple pulmonary nodules measuring up to approximately 12 mm. Further correlation with PET/CT versus follow-up computed tomography in 3 months is recommended. (3) Areas of mild subpleural atelectasis or scar with mild interstitial thickening that may be related to chronic change, although mild pulmonary edema or infection would be difficult to entirely exclude." The text indicates that "No convincing findings of acute pulmonary embolism." This resulted in a negative ground truth label. However, the model interpreted the "likely sequela of chronic pulmonary embolism" as an indicator of PE. The latter suggests that filling defects were a result of a past medical condition. Thus, this might be a definite false positive.

In summary, analyzing some of the false positives indicates the model's ability to bring attention to borderline cases that might hint at the presence of PE, allowing for further clinical validation. However, the model sometimes results in definite false positives when the radiology text ambiguously discusses PE in the context of past conditions.

Operational and Clinical Implications

The postdeployment results of GPT-4o show several important operational and clinical implications. First, the model's sensitivity and specificity in a real-world setting indicate that it can help distinguish between subjects who have pulmonary embolisms and those who do not, without many false positives or negatives. This is important in a clinical setting where missing cases of pulmonary embolism have implications for patient outcomes, and false positives can lead to unnecessary further investigation or treatment. At Virtua Health, the model successfully identified over 700 positive PE cases in 2024.

From an operational perspective, the model's excellent accuracy on both the validation and postdeployment testing datasets means that the model can be operated in an autonomous manner which would help reduce the workload of radiologists and other health care professionals. As a result, it can classify cases correctly, thus taking some of the pressure and time off clinicians and their ability to concentrate on other, more challenging or time-consuming cases. Furthermore, the model's high precision means that health care resources are used more effectively, with fewer unnecessary interventions and therefore better patient care.

Clinically, the use of GPT-4o increases the decision support that clinicians can receive by offering a correct answer to the question regarding the presence of pulmonary embolism based on the information presented in the radiology reports. This early recognition can result in early diagnosis and management and therefore better patient results and possibly reduced mortality. Moreover, the stability of the performance of GPT-4o in identifying pulmonary embolisms in various datasets suggests robustness and generality, which could be useful in various clinical settings.

Ethical Issues in the Use of AI Models in Health Care

The employment of AI models in health care induces multifaceted ethical issues that need to be deliberated on. The first and foremost concern is the privacy of the patients and the security of the information because medical information is private. This includes strong network security, policy compliance with laws like HIPAA (Health Insurance Portability and Accountability Act) and General Data Protection Regulation, and data exposure minimization during training and use of the model. It is crucial to ensure that AI systems work within these legal and ethical parameters to ensure the credibility of their use.

Another important factor is compliance with regulations because the application of AI in health care has to be compatible with the standards that are set on a regional and international level. This includes making sure that the process of training, validation, and integration into the clinical workflow of the model is well documented. These processes are easily understandable and can be explained to health care providers, patients, and regulators, thus establishing the ethical and legal sustainability of technology.

Another important issue is bias and fairness as AI models trained on small and biased datasets are likely to emit biased output. For instance, if the training data is biased then the predictions of the model may be unfair to some patients and thus lead to unequal care. This is particularly a concern in health care where discrimination can have severe impacts on minority populations, stressing the need to ensure that datasets are inclusive, and model evaluation focuses on fairness.

Finally, it is important that in using AI in the various fields of life, transparency and accountability are considered to create confidence in the use of AI. The results of the model must be easy to understand and explain to the clinicians and patients, hence the need for explainable AI. Moreover, it is crucial to subject the models to routine assessments and performance tracking to provide evidence of accountability and trustworthiness in the long run.

To address these ethical issues, there is a need for ongoing assessment, open reporting, and interaction between AI creators, health care deliverers, and regulators. Thus, the main aspects that can be improved are the aspects that when improved will help achieve the best possible results with the use of AI in health care while at the same time adhering to ethical principles and protecting the rights of patients.

Bias Evaluation

LLMs are generally pretrained on large corpora of texts from the internet. As a result, inherent biases in human language can influence model outputs. Recent LLMs, such as GPT-4o, undergo posttraining alignment to reduce biased responses. This serves as the first line of defense against bias. Second, in our case, the LLM is instructed to return a single label (yes or no), which may further reduce the potential for hallucinations and bias. LLMs typically require more tokens to reveal their

XSL•FO
RenderX

underlying tendencies, which can include bias from the pretraining stage. Finally, we evaluated the model's performance using the F_1-score across different age groups and gender profiles.

Table 3 summarizes the F_1-score across different sex and age groups to assess the consistency of the model's performance across demographic subpopulations. The model demonstrates comparable F_1-scores for both female (0.970, 95% CI 0.930-1.000) and male (0.972, 95% CI 0.937-1.000) groups, indicating no apparent sex-based disparity in classification performance.

Table 3. F_1-score across sex and age groups.

Variable and group	Values, n (%)	F_1-score (95% CI)
Sex		
Female	98 (51)	0.970 (0.930-1.000)
Male	102 (49)	0.972 (0.937-1.000)
Age		
Under 30 years	10 (5)	1 (1-1)
30-50 years	25 (12.5)	0.963 (0.867-1.000)
50-70 years	93 (46.5)	0.982 (0.951-1.000)
70-90 years	62 (31)	0.966 (0.906-1.000)
90 years and older	10 (5)	0.823 (CI 0.500-1.000)

Across age groups, the F_1-scores remain generally high, with minor variations. The highest score is observed in individuals under 30 years old (F_1-score=1.000), although this group comprises only 5% of the sample, suggesting potentially limited generalizability due to the small sample size. The model performs well for the majority age groups—50-70 years (F_1-score=0.982, 95% CI 0.951-1.000) and 70-90 years (F_1-score=0.966, 95% CI 0.906-1.000)—which collectively represent over 75% of the dataset. However, performance decreases slightly for individuals aged 90 and above (F_1-score=0.823, 95% CI 0.500-1.000), likely due to a smaller sample size and increased clinical complexity in this cohort. Overall, the model demonstrates robust and consistent performance across most demographic groups, with slight variation observed at the extremes of age distribution.

Explainability

GPT-4o is an LLM built on transformer architecture, a type of neural network that uses an attention mechanism to learn semantics. Due to its complexity, the model is inherently a black box. However, since the model generates output by continuing the input text based on user instructions, the output can be interpreted as the most probable completion (especially when the temperature parameter is set to 0.0).

In our case, the instructions are to analyze radiology impressions and return a "Yes or No," indicating the presence or absence of PE, respectively. In real-world decision-making, users are informed that the LLM generates responses based on the most likely continuation of the input text according to the instructions provided. The generated label is returned to users along with the corresponding impressions for validation and confirmation.

Exploring explainable artificial intelligence methods is highly encouraged to better understand how input text influences LLM output, improving predictability and transparency. Techniques such as Shapley Additive Explanations (SHAP) and attention mechanism analysis can support this effort. In our case, implementation was challenging due to the use of a large proprietary LLM (ie, GPT-4o), for which we do not have access to the model architecture needed for such analyses. Therefore, leveraging open-source LLMs in the future could enable the application of these techniques.

The GPT-4o-based PE classifier is delivered through a web application, requiring user involvement to confirm the model's results. In summary, our application adopts a human-in-the-loop approach. While this supports practical use, the broader explainability of LLM output remains an ongoing area of research aimed at better understanding the underlying mechanisms of next-token prediction.

Limitations

As the study shows promising results, there are important limitations, and their implications cannot be overlooked. A major limitation is the size of the dataset used in this study, which is 1000 training samples, 200 validation samples, and 200 postdeployment testing samples. Another limitation is the data imbalance in the training dataset (for the Clinical Longformer). With such a restricted number of examples, the model may not be able to generalize its learning to the full extent of the clinical scenarios that are likely to be encountered in the real world. This could lead to it being less accurate in real-world use, where report structures can differ significantly, and larger datasets are usually used to increase model confidence and stability.

Another limitation has to do with the model's generalization. The training data was collected from a single health care organization, Virtua Health, which means that the language and cultural features that are unlikely to be encountered in reports from other hospitals or countries may not be well-represented in the model. As a result, this may restrict the applicability of

XSL•FO
RenderX

the model to other settings unless it is retrained (or prompt-engineered) with local data.

The study also found that the Clinical Longformer, which was used as a baseline, could not grasp some of the semantic details, resulting in the misclassification of 2 positive PE cases. This suggests that future work should build on this study to enhance the architecture of transformer models specific to clinical tasks, especially those that entail processing medical text with sophistication.

Some issues may occur when implementing the model in the real world even though GPT-4o performed excellently in controlled experiments. Real-world data often contains errors, omissions, or other noise that the model may not be able to handle properly. In addition, there are potential threats to consistency in reporting practices that may lead to inconsistencies in the information captured by the model.

Future Work

To overcome these limitations, future work should focus on the growth of the dataset, which should be expanded to include a bigger and more complex set of samples that would encompass different types of radiology reports, patients, and institutions. This will increase the size of the dataset and the variety of the samples, which in turn will increase the model's coverage and stability. Data imbalance in the training dataset of the Clinical Longformer should be tackled by using data augmentation techniques to test the impact of validation performance. Furthermore, the model must be tested in different health care contexts to determine its effectiveness, which means that external validation is critical. External validation can be achieved through collaborations with other health systems or testing on publicly available datasets. To mitigate real-world operationalization challenges, future implementation should include routine performance audits to monitor model accuracy over time, periodic retraining with updated real-world data to maintain robustness, and regular human validation checks to ensure data quality and reflect evolving documentation practices. These strategies can help maintain reliability despite variability in data quality and reporting standards. Overall, these measures will assist in ensuring that the model is not only efficient but also easily implementable in various health care environments.

Conclusions

In conclusion, this study features an effective LLM-based approach to the automation of the extraction of PE diagnoses from radiology report impressions. We then compared the performance of a fine-tuned Clinical Longformer and GPT-4o and found that GPT-4o outperformed in terms of sensitivity, specificity, and overall accuracy both before and post deployment. The integration of GPT-4o into clinical practice has several operational and clinical benefits, including decreasing the need for manual review, improving clinical decision support, and detecting cases of PE more quickly. Furthermore, the model's capability to lighten the load of manual review to a great extent is a key contributor to improving the workflow of the diagnostic process, thereby allowing clinicians to channel their efforts toward more challenging problems. These qualities make it suitable for application in other clinical settings with the potential to go beyond PE diagnosis to other medical conditions that require comprehensive and accurate analysis of radiology reports. Not only does its integration enhance efficiency but also the quality of clinical decision-making processes. Future work may involve expanding this approach to other medical conditions and improving the integration of NLP-based models into clinical workflows to keep on enhancing the quality of health care delivery.

Data Availability

The data analyzed in this study are subject to the following licenses or restrictions: data in this study are not available due to agreements made with the institutional review board of Virtua Health.

Authors' Contributions

MM contributed to conceptualization, data curation, formal analysis, investigation, methodology, software, validation, visualization, writing original drafts, review, and editing. KD managed writing review and editing, formal analysis, and validation. AS handled project administration, resources, writing review and editing, and validation.

Conflicts of Interest

None declared.

References

1. Tanra AH, AT L, T E, DE R. Diagnostic value of platelet indices in patients with pulmonary embolism. Indonesian J. Clin. Pathol. Med. Lab 2020;27(1):22-26. [doi: 10.24293/ijcpml.v27i1.1625]
2. Deng W, Gao W. Cathepsin Causal Association with Pulmonary Embolism: A Mendelian Randomization Analysis. 2024. URL: https://www.researchsquare.com/article/rs-4191858/latest [accessed 2024-08-14]
3. Lyhne MD, Kline JA, Nielsen-Kudsk JE, Andersen A. Pulmonary vasodilation in acute pulmonary embolism - a systematic review. Pulm Circ 2020;10(1):2045894019899775 [FREE Full text] [doi: 10.1177/2045894019899775] [Medline: 32180938]
4. Zhang SL, Zhang QF, Li G, Guo M, Qi X, Xing XH, et al. Case Report: resuscitation of patient with tumor-induced acute pulmonary embolism by venoarterial extracorporeal membrane oxygenation. Front Cardiovasc Med 2024;11:1322387 [FREE Full text] [doi: 10.3389/fcvm.2024.1322387] [Medline: 38426120]

XSL•FO
RenderX

5. Grusova G, Lambert L, Zeman J, Lambertova A, Benes J. The additional value of esophageal wall evaluation and secondary findings in emergency patients undergoing CT pulmonary angiography. Iran J Radiol Brieflands 2018;15(1):e63466 [FREE Full text] [doi: 10.5812/iranjradiol.63466]
6. Becattini C, Vedovati MC, Agnelli G. Diagnosis and prognosis of acute pulmonary embolism: focus on serum troponins. Expert Rev Mol Diagn 2008;8(3):339-349. [doi: 10.1586/14737159.8.3.339] [Medline: 18598112]
7. Simpson J, López-Candales A. Elevated brain natriuretic peptide and troponin I in a woman with generalized weakness and chest pain. Echocardiography 2005;22(3):267-271. [doi: 10.1111/j.0742-2822.2005.03192.x] [Medline: 15725164]
8. Zhou Y, Shi H, Wang Y, Kumar AR, Chi B, Han P. Assessment of correlation between CT angiographic clot load score, pulmonary perfusion defect score and global right ventricular function with dual-source CT for acute pulmonary embolism. Br J Radiol 2012;85(1015):972-979 [FREE Full text] [doi: 10.1259/bjr/40850443] [Medline: 21976633]
9. Lapergue B, Decroix JP, Evrard S, Wang A, Bendetowicz D, Offroy MA, et al. Diagnostic yield of venous thrombosis and pulmonary embolism by combined CT venography and pulmonary angiography in patients with cryptogenic stroke and patent foramen ovale. Eur Neurol 2015;74(1-2):69-72. [doi: 10.1159/000437261] [Medline: 26228469]
10. Yuan H, Shao Y, Liu Z, Wang H. An improved faster R-CNN for pulmonary embolism detection from CTPA images. IEEE Access 2021;9:105382-105392. [doi: 10.1109/access.2021.3099479]
11. Segrelles JD, Medina R, Blanquer I, Martí-Bonmatí L. Increasing the efficiency on producing radiology reports for breast cancer diagnosis by means of structured reports. A comparative study. Methods Inf Med 2017;56(3):248-260. [doi: 10.3414/ME16-01-0091] [Medline: 28220929]
12. Nobel JM, Kok EM, Robben SGF. Redefining the structure of structured reporting in radiology. Insights Imaging 2020;11(1):10 [FREE Full text] [doi: 10.1186/s13244-019-0831-6] [Medline: 32020396]
13. Hartung MP, Bickle IC, Gaillard F, Kanne JP. How to create a great radiology report. Radiographics 2020;40(6):1658-1670. [doi: 10.1148/rg.2020200020] [Medline: 33001790]
14. Wilcox JR. The written radiology report. AR 2006;35(7):33-37 [FREE Full text] [doi: 10.37549/AR1440]
15. Casey A, Davidson E, Poon M, Dong H, Duma D, Grivas A, et al. A systematic review of natural language processing applied to radiology reports. BMC Med Inform Decis Mak 2021;21(1):179 [FREE Full text] [doi: 10.1186/s12911-021-01533-7] [Medline: 34082729]
16. Fei X, Chen P, Wei L, Huang Y, Xin Y, Li J. Quality management of pulmonary nodule radiology reports based on natural language processing. Bioengineering (Basel) 2022;9(6):244 [FREE Full text] [doi: 10.3390/bioengineering9060244] [Medline: 35735487]
17. Pham AD, Névéol A, Lavergne T, Yasunaga D, Clément O, Meyer G, et al. Natural language processing of radiology reports for the detection of thromboembolic diseases and clinically relevant incidental findings. BMC Bioinformatics 2014;15(1):266 [FREE Full text] [doi: 10.1186/1471-2105-15-266] [Medline: 25099227]
18. Yu S, Kumamaru KK, George E, Dunne RM, Bedayat A, Neykov M, et al. Classification of CT pulmonary angiography reports by presence, chronicity, and location of pulmonary embolism with natural language processing. J Biomed Inform 2014;52:386-393 [FREE Full text] [doi: 10.1016/j.jbi.2014.08.001] [Medline: 25117751]
19. Meystre S, Gouripeddi R, Tieder J, Simmons J, Srivastava R, Shah S. Enhancing comparative effectiveness research with automated pediatric pneumonia detection in a multi-institutional clinical repository: a PHIS+ pilot study. J Med Internet Res JMIR Publication 2017;19(5):e162. [doi: 10.2196/jmir.6887]
20. Cai T, Giannopoulos AA, Yu S, Kelil T, Ripley B, Kumamaru KK, et al. Natural language processing technologies in radiology research and clinical applications. Radiographics 2016;36(1):176-191 [FREE Full text] [doi: 10.1148/rg.2016150080] [Medline: 26761536]
21. Lakhani P, Kim W, Langlotz CP. Automated detection of critical results in radiology reports. J Digit Imaging 2012;25(1):30-36 [FREE Full text] [doi: 10.1007/s10278-011-9426-6] [Medline: 22038514]
22. Puts S, Nobel M, Zegers C, Bermejo I, Robben S, Dekker A. How natural language processing can aid with pulmonary oncology tumor node metastasis staging from free-text radiology reports: algorithm development and validation. JMIR Form Res 2023;7:e38125 [FREE Full text] [doi: 10.2196/38125] [Medline: 36947118]
23. Li AY, Elliot N. Natural language processing to identify ureteric stones in radiology reports. J Med Imaging Radiat Oncol 2019;63(3):307-310. [doi: 10.1111/1754-9485.12861] [Medline: 30720244]
24. Huang T, Socrates V, Gilson A, Safranek C, Chi L, Wang EA, et al. Identifying incarceration status in the electronic health record using large language models in emergency department settings. J Clin Transl Sci 2024;8(1):e53 [FREE Full text] [doi: 10.1017/cts.2024.496] [Medline: 38544748]
25. Ayden M, Yuksel M, Erdem S. A two-stream deep model for automated ICD-9 code prediction in an intensive care unit. Heliyon Elsevier 2024;10(4):e25960 [FREE Full text]
26. Kim D, Yoo H, Kim S. An Automatic ICD Coding Network Using Partition-Based Label Attentio. 2022. URL: http://arxiv.org/abs/2211.08429 [accessed 2024-10-11]
27. Miyazaki Y, Hata M, Omori H, Hirashima A, Nakagawa Y, Et? M, et al. Performance and errors of chatGPT-4o on the Japanese medical licensing examination: solving all questions including images with over 90% accuracy. JMIR Med Educ. URL: https://s3.ca-central-1.amazonaws.com/assets.jmir.org/assets/preprints/preprint-63129-submitted.pdf [accessed 2024-10-11]

XSL•FO
RenderX

28. Builoff V, Shanbhag A, Miller RJ, Dey D, Liang JX, Flood K, et al. Evaluating AI proficiency in nuclear cardiology: large language models take on the board preparation exam. J Nucl Cardiol 2024:102089. [doi: 10.1016/j.nuclcard.2024.102089] [Medline: 39617127]
29. Wals Zurita AJ, Miras Del Rio H, Ugarte Ruiz de Aguirre N, Nebrera Navarro C, Rubio Jimenez M, Muñoz Carmona D, et al. The transformative potential of large language models in mining electronic health records data: content analysis. JMIR Med Inform 2025;13:e58457 [FREE Full text] [doi: 10.2196/58457] [Medline: 39746191]
30. Cardamone NC, Olfson M, Schmutte T, Ungar L, Liu T, Cullen SW, et al. Classifying unstructured text in electronic health records for mental health prediction models: large language model evaluation study. JMIR Med Inform 2025;13:e65454 [FREE Full text] [doi: 10.2196/65454] [Medline: 39864953]
31. Yoon D, Han C, Kim DW, Kim S, Bae S, Ryu JA, et al. Redefining health care data interoperability: empirical exploration of large language models in information exchange. J Med Internet Res 2024;26:e56614 [FREE Full text] [doi: 10.2196/56614] [Medline: 38819879]
32. Guo Z, Lai A, Thygesen JH, Farrington J, Keen T, Li K. Large language models for mental health applications: systematic review. JMIR Ment Health 2024;11:e57400 [FREE Full text] [doi: 10.2196/57400] [Medline: 39423368]
33. Shin D, Kim H, Lee S, Cho Y, Jung W. Using large language models to detect sepression from user-generated diary text data as a novel approach in digital mental health screening: instrument validation study. J Med Internet Res 2024;26:e54617 [FREE Full text] [doi: 10.2196/54617] [Medline: 39292502]
34. Lian L. Comparative Study of GPT-4.0, ERNIE Bot 4.0, and GPT-4o in the 2023 Chinese Medical Licensing Examination. URL: https://www.researchsquare.com/article/rs-4639770/latest [accessed 2024-10-11]
35. Beattie J, Neufeld S, Yang D, Chukwuma C, Gul A, Desai N, et al. Utilizing large language models for enhanced clinical trial matching: a study on automation in patient screening. Cureus 2024;16(5):e60044 [FREE Full text] [doi: 10.7759/cureus.60044] [Medline: 38854210]
36. Li Y, Wehbe RM, Ahmad FS, Wang H, Luo Y. Clinical-Longformer and Clinical-BigBird: Transformers for long clinical sequences. URL: http://arxiv.org/abs/2201.11838 [accessed 2024-10-10]
37. Kanzawa J, Kurokawa R, Kaiume M, Nakamura Y, Kurokawa M, Sonoda Y, et al. Evaluating the role of GPT-4 and GPT-4o in the detectability of chest radiography reports requiring further assessment. Cureus 2024;16(12):e75532. [doi: 10.7759/cureus.75532] [Medline: 39803046]
38. Ferreira TL, Oliveira MC, de AVT. Comparative study of large language models for lung-RADS classification in portuguese CT reports. : IEEE; 2024 Presented at: IEEE 24th International Conference on Bioinformatics and Bioengineering (BIBE); 2024 November 27-29; Kragujevac, Serbia p. 1-8 URL: https://ieeexplore.ieee.org/abstract/document/10820460/ [doi: 10.1109/bibe63649.2024.10820460]
39. Beşler MS, Oleaga L, Junquero V, Merino C. Evaluating GPT-4o's performance in the official European board of radiology exam: a comprehensive assessment. Acad Radiol 2024;31(11):4365-4371. [doi: 10.1016/j.acra.2024.09.005] [Medline: 39294055]
40. Li D, Gupta K, Bhaduri M, Sathiadoss P, Bhatnagar S, Chong J. Comparative diagnostic accuracy of GPT-4o and LLaMA 3-70b: proprietary vs. open-source large language models in radiology. Clin Imaging 2025;118:110382. [doi: 10.1016/j.clinimag.2024.110382] [Medline: 39740646]
41. Busch F, Prucker P, Komenda A, Ziegelmayer S, Makowski MR, Bressem KK, et al. Multilingual feasibility of GPT-4o for automated Voice-to-Text CT and MRI report transcription. Eur J Radiol 2025;182:111827 [FREE Full text] [doi: 10.1016/j.ejrad.2024.111827] [Medline: 39566177]

Abbreviations

AI: artificial intelligence
BERT: Bidirectional Encoder Representations from Transformers
COT: chain-of-thought
HIPAA: Health Insurance Portability and Accountability Act
ICD: International Classification of Diseases
LLM: large language model
NLP: natural language processing
PE: pulmonary embolism
SHAP: Shapley Additive Explanations

XSL•FO
RenderX

Edited by A Castonguay; submitted 18.10.24; peer-reviewed by D Chrimes, J Huang; comments to author 14.01.25; revised version received 30.01.25; accepted 13.03.25; published 09.04.25.

Please cite as:
Mahyoub M, Dougherty K, Shukla A
Extracting Pulmonary Embolism Diagnoses From Radiology Impressions Using GPT-4o: Large Language Model Evaluation Study
JMIR Med Inform 2025;13:e67706
URL: https://medinform.jmir.org/2025/1/e67706
doi:10.2196/67706
PMID:

©Mohammed Mahyoub, Kacie Dougherty, Ajit Shukla. Originally published in JMIR Medical Informatics (https://medinform.jmir.org), 09.04.2025. This is an open-access article distributed under the terms of the Creative Commons Attribution License (https://creativecommons.org/licenses/by/4.0/), which permits unrestricted use, distribution, and reproduction in any medium, provided the original work, first published in JMIR Medical Informatics, is properly cited. The complete bibliographic information, a link to the original publication on https://medinform.jmir.org/, as well as this copyright and license information must be included.

XSL•FO
RenderX

Original Paper

Summarizing Online Patient Conversations Using Generative Language Models: Experimental and Comparative Study

Rakhi Asokkumar Subjagouri Nair[1], MSc; Matthias Hartung[2], PhD; Philipp Heinisch[1], PhD; Janik Jaskolski[2], MSc; Cornelius Starke-Knäusel[2], MSc; Susana Veríssimo[2], MA; David Maria Schmidt[1], MSc; Philipp Cimiano[1,2], PhD

[1]Cognitive Interaction Technology Center, Faculty of Technology, Bielefeld University, Bielefeld, Germany

[2]Semalytix GmbH, Bielefeld, Germany

Corresponding Author:
Philipp Cimiano, PhD
Cognitive Interaction Technology Center
Faculty of Technology
Bielefeld University
Inspiration 1
Bielefeld, 33615
Germany
Phone: 1 017622867286
Email: cimiano@cit-ec.uni-bielefeld.de

Abstract

Background: Social media is acknowledged by regulatory bodies (eg, the Food and Drug Administration) as an important source of patient experience data to learn about patients' unmet needs, priorities, and preferences. However, current methods rely either on manual analysis and do not scale, or on automatic processing, yielding mainly quantitative insights. Methods that can automatically summarize texts and yield qualitative insights at scale are missing.

Objective: The objective of this study was to evaluate to what extent state-of-the-art large language models can appropriately summarize posts shared by patients in web-based forums and health communities. Specifically, the goal was to compare the performance of different language models and prompting strategies on the task of summarizing documents reflecting the experiences of individual patients.

Methods: In our experimental and comparative study, we applied 3 different language models (Flan-T5, Generative Pretrained Transformer [GPT], GPT-3, and GPT-3.5) in combination with various prompting strategies to the task of summarizing posts from patients in online communities. The generated summaries were evaluated with respect to 124 manually created summaries as a ground-truth reference. As evaluation metrics, we used 2 standard metrics from the field of text generation, namely, Recall-Oriented Understudy for Gisting Evaluation (ROUGE) and BERTScore, to compare the automatically generated summaries to the manually created reference summaries.

Results: Among the zero-shot prompting–based large language models investigated, GPT-3.5 performed better than the other models with respect to the ROUGE metrics, as well as with respect to BERTScore. While zero-shot prompting seems to be a good prompting strategy, overall GPT-3.5 in combination with directional stimulus prompting in a 3-shot setting had the best results with respect to the aforementioned metrics. A manual investigation of the summarization of the best-performing method showed that the generated summaries were accurate and plausible compared to the manual summaries.

Conclusions: Taken together, our results suggest that state-of-the-art pretrained language models are a valuable tool to provide qualitative insights about the patient experience to better understand unmet needs, patient priorities, and how a disease impacts daily functioning and quality of life to inform processes aimed at improving health care delivery and ensure that drug development focuses more on the actual priorities and unmet needs of patients. The key limitations of our work are the small data sample as well as the fact that the manual summaries were created by 1 annotator only. Furthermore, the results hold only for the examined models and prompting strategies, potentially not generalizing to other models and strategies.

(JMIR Med Inform 2025;13:e62909) doi:10.2196/62909

KEYWORDS

patient experience; online communities; summarizing; large language models

XSL•FO
RenderX

Introduction

Background

For many patients, the World Wide Web plays an important supporting role in coping with their condition. In fact, social media sites, digital support groups, and forums as well as social networks play an important role in the life of patients as sharing and consuming experiences with peers provides emotional, informational, and psychological support [1]. It has been indeed shown that sharing health-related experiences in online communities has an effect of empowerment on patients, increasing their subjective and psychological well-being, leading to increased self-management and control [1].

In addition to being used for receiving support, social media is increasingly used by patients to educate themselves on a disease and to find the hospitals or physicians most capable of treating their condition [2]. When engaging with social media, users are willing to disclose very intimate information [3]. In fact, it has been shown that the anonymity of many social media sites increases the level of self-disclosure [4]. The consumer survey by the PwC Health Research Institute [5] has indeed shown that >30% of respondents would be comfortable having their social media conversations monitored if those data could help identify ways to improve their health. In a study with adults presenting to an academic, urban emergency department, Padrez et al [6] found that, among patients with a social media profile, 71% consented to sharing their social media data to compare it to their electronic medical records. These figures convey that a substantial proportion of patients are willing to share their social media data for research purposes if the data contribute to improving their condition and those of their peers. A recent study confirmed these previous results, showing that participants would be willing to donate some of their digital data to researchers and clinicians in pursuit of health-related insights [7].

Against this background—the World Wide Web and social media playing an empowering role in patients' lives and, at the same time, patients being willing to donate their data if this contributes to improving their and others' health condition—an important question is how relevant insights can be obtained from the data. The Food and Drug Administration has identified social media data as one important source of "patient experience data," that is, data that can foster understanding of the unmet needs and priorities of patients as a basis to design more effective clinical studies; support Outcomes Research activities; and, ultimately, develop better drugs that actually improve patients' lives, well-being, and functioning [8]. In fact, methodologies for patient listening are quite mature and are widely used in patient-focused drug development to automatically analyze social media content as a basis to understand which symptoms are most burdensome to patients; how they experience existing treatments, which outcomes matter to them, and, overall, how their quality of life is affected by the disease [9].

However, these methodologies mostly provide quantitative insights as they rely on the automatic analysis of social media content using techniques from natural language processing (NLP), extracting key information and summarizing it statistically to obtain an understanding of trends at the level of an entire patient population or patient cohort of interest. A frequent problem is how to obtain a more qualitative understanding of how the disease affects patients' daily functioning and living. Most NLP methods, in fact, can extract single entities or concepts from textual data, but there is a lack of methods to analyze textual data at a more qualitative level in terms of the key messages that can be derived from a collection of texts. Summarization techniques, especially from abstractive summarization, can be used for this purpose, but so far research on how well posts from patients in online communities can be faithfully summarized is missing. While it is possible to manually analyze sample posts, there is the risk of missing relevant aspects, and the task of summarizing all the content manually is infeasible. Thus, there is a need for more scalable methods to derive qualitative insights from online patient experience data.

Considering recent developments in the field of large language models (LLMs), in this paper, we ask the question of to what extent existing pretrained LLMs can be used to aid the analysis and summarization of patient-authored social media content. LLMs are machine-learned models that have been "pre-trained" on large amounts of text [10] and later either fine-tuned for specific tasks [10-12] or trained to determine a suitable response to a certain instruction. The latter has been referred to as "alignment" and is typically done using reinforcement learning [13]. Overall, LLMs have been shown to perform very well on tasks such as summarization [14,15], sentiment analysis [16], question answering [17], and machine translation [12]. While excelling at many tasks, LLMs have also been shown to lack robustness and react too sensitively to small perturbations in the input and to be misled by so-called "adversarial examples" [18]. Furthermore, they have been shown to extrapolate too creatively in some cases, generating output that is factually wrong. This phenomenon has been sometimes referred to as "hallucination" [19].

Objectives

On the basis of the need for advanced methods to summarize the patient experience to yield qualitative insights and the promise of LLMs for many tasks, in this paper, we explicitly address the following question: can state-of-the-art LLMs be used to accurately summarize the experience of patients as shared in online data sources?

For this purpose, we experimentally compared different pre-trained LLMs: 2 from the Generative Pretrained Transformer (GPT) family (GPT-3 and GPT-3.5 [OpenAI]) and Flan-T5 (Google). While our focus was on using pretrained language models (LMs) that are prompted via instructions, we also carried out fine-tuning experiments to examine the impact of fine-tuning. We experimentally investigated several prompting strategies—zero-shot, 1-shot, and 3-shot learning—both alone and in combination with directional stimulus prompting (DSP) and chain of thought (CoT) prompting.

For this study, we focused on breast cancer and collected self-reported patient experience data from 5 forums, grouping the documents according to mentions of key symptoms and

XSL•FO
RenderX

treatments. The data collected comprise user posts from 5 leading web forums in which patients with breast cancer discuss their experiences with peers. The 5 sources were manually identified in a search process with the aim to identify the most relevant breast cancer forums.

The texts generated by the LLMs were evaluated with respect to a dataset of 127 manually produced reference summaries that were provided by one of the authors with years of expertise in analyzing patient experience data from social media. The generated texts were evaluated in terms of standard text generation metrics, including the Recall-Oriented Understudy for Gisting Evaluation (ROUGE) metrics and BERTScore. These metrics essentially compute the overlap between the automatically generated texts and the manually created references and, thus, provide an estimate of the quality of the summaries. In a case study, we discuss the output of different LLMs to obtain a sense of how these models are actually able to summarize the conversations.

Our results show that advanced prompting techniques substantially improve the ability of generative LMs to summarize online patient comments efficiently.

Methods

Overview

The research design corresponds to an experimental and comparative study. It corresponds to an experimental study in that it involved experiments in which the ability of LLMs to adequately summarize patient posts was experimentally evaluated by comparing automatically generated summaries to manually created summaries in a series of experiments. This study was also comparative as it evaluated the performance of different LLMs and prompting strategies in comparison to each other. The statistical validity of the results was assessed by computing their statistical significance using a 2-tailed *t* test and reporting *P* values comparing the significance of the results of the best-performing approach to that of the results of the other approaches. While, in most settings, we relied on off-the-shelf pretrained LLMs, we also tested the effect of fine-tuning on the task.

Dataset and Task Description

For this experimental and comparative study, data were crawled from different web-based forums in which patients with breast cancer discussed their disease experience with peers. The data were collected from the following public forums based on a search by the authors for the most prominent forums related to breast cancer available on the web: breastcancer.org, HealthUnlocked, her2support.org, and Macmillan Cancer Support. Data were automatically obtained via Socialgist [20] as a data provider and automatically analyzed to identify posts of individuals who had self-disclosed being patients with breast cancer using the methodology described previously by Spies et al [21]. The processing consisted of anonymization; entity extraction and linking via a knowledge graph; detection of symptoms, treatments, and quality of life mentions; detection of the severity of the symptoms; and detection of the impact of symptoms on the quality of life of the patients. In addition, demographic information involving age and gender was extracted if explicitly mentioned in the posts.

This yielded a dataset comprising 145,460 documents from 1146 patients. The preprocessing revealed the most frequent symptoms (n=8) and most frequent treatments used (n=119). They are listed in Multimedia Appendix 1. The data originated from a time frame between August 2016 and July 2022. As expected from a population with breast cancer, 99.5% (1089/1146) of the patients were female (male individuals can develop breast cancer in rare cases).

Before analysis, the data were automatically anonymized to remove mentions of person names, emails, URLs, telephone numbers, and addresses. A sample analysis showed that the accuracy of anonymization was 99.5%. For this purpose, we relied on the anonymization solution provided by Private AI [22].

The summarization corpus underlying this study was constructed as follows. For each topic in the dataset (where “topic” refers to one of the key symptoms of breast cancer or one of the existing breast cancer treatments as listed in Multimedia Appendix 1), all documents containing at least one mention of the topic were collapsed into a topic-specific subcorpus. If multiple topics were mentioned within a document, it became part of several subcorpora accordingly. This resulted in 127 topic-specific subcorpora derived from 8 key symptoms and 119 treatments. The number of documents per topic-specific subcorpus varied between 1 and 44, with a median of 12.

The summarization task can be seen as an instance of multidocument summarization as it consists of generating a concise summary for each of the 127 topic-specific subcorpora in the summarization corpus. The main challenges for multidocument summarization are, in addition to the fact that the input can be very long, the fact that the content of the documents to be summarized might be overlapping, complementary, or even inconsistent in the worst case [23].

As a gold standard for reference, 1 coauthor of this paper, SV, who is trained in the annotation of online patient conversations, provided a manual summary of each topic-specific document collection in the summarization corpus. With respect to symptom-related document collections, the annotator was instructed to focus on summarizing the impact of symptoms on patients’ daily functioning and quality of life. Regarding treatments, the goal was to summarize outcomes of the treatment as well as side effects or any other aspect related to the experience with these treatments. Consequently, the gold standard comprised 127 manual summaries of the symptoms and treatments listed in Multimedia Appendix 1. Given the substantial effort required in creating such summaries (approximately 3.5 hours per summary, >400 hours in total), it was not feasible to summarize each set of documents by several annotators. We discuss this further in the *Discussion* section while highlighting limitations.

The manual summary for the *rash* symptom, for instance, was as follows:

> *Patients perceive rashes as being horrible and uncomfortable, yet common. They are a great*

XSL•FO
RenderX

impairment for many patients since they are often painful and itchy. Some patients report that they cover multiple parts of the body, while others report it being localized to body parts, such as the face or the breast. They also report on the color and feel of the rash: pink, red, photosensitive, raised, large, hive-like, warm, etc. The appearance of the rashes changes with time, for some patients it became better (e.g. less itching), while for others worse (e.g. redder and hotter). Rashes can have different causes: they can be the side effect of treatments, such as chemotherapy, allergic reactions or symptoms. The cause for the rash is often unclear among patients, but it is often said that usually a rash is just a rash.

For the texts to fit the input size of the LLMs used in the study, the length was truncated to 1024 tokens. From the 127 manually generated reference summaries, 3 (2.4%) were used as examples for few-shot training, whereas the remaining 124 (97.6%) were used for evaluation only. For the fine-tuning experiments, the dataset was divided into 3 nonoverlapping sections: train, validation, and test. The resulting data sizes followed an 80:10:10 ratio, resulting in 79.5% (101/127), 9.5% (12/127) of the summaries for the train, validation, and test portions, respectively.

Models Used for Patient Comment Summarization

For the task of summarizing texts, we relied on pretrained LLMs. On the one hand, we relied on encoder-decoder architectures (Flan-T5), as well as on decoder-only architectures (GPT models). As our focus lay on the experimental testing and comparison of different prompting techniques (instructions in the form of natural language), we used LLMs that have the capability to follow textual instructions. Flan-T5 and the family of GPT-3 models have this property as they have been trained on data to generate answers for instruction-like prompts using reinforcement learning, a process known as alignment [24]. We relied on the following 3 models in particular: Flan-T5-base, GPT-3, and GPT-3.5. Flan-T5 is an enhanced version of T5 that has been fine-tuned on a mixture of tasks using the Flan collection of datasets [25]. For this study, the Flan-T5 base model was used along with GPT-3 and GPT-3.5. GPT-3 is an advanced iteration of the GPT model that operates as an auto-regressive LM featuring an impressive 175 billion parameters [26]. GPT-3.5 is a refined version of its predecessor and boasts an enhanced ability to adapt to diverse prompts and instructions, making it a versatile tool for various applications. Together, these models are a good cross-section of the current LLM landscape and were well suited for our task.

Prompting Techniques for Summarization

To explore the capabilities of LLMs to summarize patient comments, we compared various prompting strategies. We started with a prompt without examples or guidance on how to solve the task, called zero-shot prompting. As further methods, we enhanced the prompt by introducing examples of summarized patient comments (few-shot prompting); giving hints by DSP; and, finally, guiding the model by asking for intermediate results invoked by a set of self-defined questions (CoT prompting). By combining different techniques (few-shot prompting with DSP and zero-shot prompting with CoT prompting), we investigated the most effective prompting technique for summarizing patients' comments.

One-shot prompting closely resembles the few-shot approach, differing in that a single demonstration is permitted along with the natural language task description [26]. The corresponding prompt template used can be found in Figure S1 in Multimedia Appendix 2.

To facilitate our experiment, we adopted this 1-shot prompt template. Within the template, (text) signifies the patient comments or experience regarding a symptom or treatment drawn from the example set, and (summary) represents the corresponding reference summary. Multimedia Appendix 2 contains other prompt templates that we exploited in our study.

Few-shot prompting introduces *k* examples consisting of a text and a summary provided by a human expert followed by the final text, which should be summarized by the model. For this study, *k* was set to 3 due to token limit constraints [26].

DSP is a framework that uses an adjustable LM to offer guidance to a black-box, frozen LLM to enhance its performance. Specifically, a policy LM is trained to generate discrete tokens acting as directional stimuli for each input of the LLM. These stimuli, such as keywords extracted from an article for summarization, are then integrated into the original input and fed into the LLM, steering its generation toward the intended target. DSP uses a customizable policy LM to produce the stimulus—in the case of summarization, keywords—to direct the LLM in generating a desired summary with improved metrics such as higher ROUGE scores or aligning more closely with human preferences. The policy LM can undergo training through supervised fine-tuning from annotated data and reinforcement learning from offline and online rewards, allowing for the exploration of directional stimuli that better align LLMs with human preferences. This adaptable framework is applicable to various LMs and tasks [27]. For this study, instead of a policy LM, KeyBERT [28] was used with the default parameters along with Keyphrase Vectorizers to extract accurate keywords for each patient comment that are given as hints to the summarizing LLM. KeyBERT is a straightforward and user-friendly approach to extracting keywords using Bidirectional Encoder Representations From Transformers (BERT) embeddings to generate keywords and key phrases that closely match the important content of a document [28]. Combining key phrase vectorizers with KeyBERT for key phrase extraction leads to a PatternRank approach, enabling the extraction of grammatically accurate key phrases that closely align with the document's content. In this process, the vectorizer initially extracts candidate key phrases from text documents, and KeyBERT then ranks these candidates based on their similarity to the document. The top *n* most similar key phrases can be regarded as document keywords. The use of Keyphrase Vectorizers alongside KeyBERT offers the advantage of obtaining grammatically correct key phrases as opposed to simple *n*-grams of predefined lengths [29]. In this study, both keywords extracted using KeyBERT with Keyphrase Vectorizers and frequent terms occurring in the patient comment were combined to form a single set that was used as hints or directional stimuli for each

XSL•FO
RenderX

patient comment to generate summaries. For example, the hints retrieved and used for the rash symptom were given as follows: severe rash; hives rash; rash hives; simple rash; red rash; cause; have; describe; impair; increase.

CoT prompting fosters reasoning capabilities by incorporating intermediate reasoning steps. The fundamental concept of this method is straightforward. By introducing phrases such as "Let's think step by step" or a similar instruction, it triggers the model to reason step by step, outputting intermediate results that are combined with other intermediate results into an overall summary. In our study, CoT prompting for the patient comment summary generation was done based on the element-aware summarization approach in the zero-shot setting. In the element-aware summarization approach using CoT, as part of element extraction, we first asked the LLMs to extract important elements mentioned in the patient comment using the following manually set guiding questions: (1) What is the main health- or medical-related topic discussed in this patient comment? (2) What are the important topics mentioned in this patient comment? (3) What are the symptoms and diseases mentioned in this patient comment? (4) What are the recovery methods or treatments mentioned in this patient comment?

Next, we concatenated the extracted elements (ie, the answers to the aforementioned 4 questions [A]) with the following prompt (P)—"Let's integrate the above information and summarize this patient comment:"—along with the patient comment (C) to prompt the LLM for patient comment summary generation. The input to the LLMs was [A; P; C], and the output was the final summary.

The advanced prompting techniques used in this study were applied in combination with each instruction-based model. Here, we tailored the use of these prompting techniques to the specific characteristics and insights derived from the data and task setup. For instance, with DSP, keywords extracted from patient comments were used as hints for generating summaries. Similarly, in CoT prompting, guiding questions were manually set to extract important elements from patient comments for summary generation. The prompt templates for summary generation, initially published by Google Research for Flan-T5 [30], were adopted as the baseline prompt template for implementing zero-shot, 1-shot, and few-shot prompting across all 3 models in our study. The same prompt template for different prompting techniques was followed for all 3 models except for CoT prompting. Together, this is a comprehensive collection of common prompting techniques, allowing for both a broad overview of the field as well as detailed insights into advantages and disadvantages of single techniques with respect to our task of summarizing patient experiences.

Experimental Setup

For our experiments, we used the pretrained model versions of all the models (Flan-T5, GPT-3, and GPT-3.5), as shown in Table 1. The table also shows the decoding parameters that were used for all the models across all prompting techniques. For all the models, the summarization length was set to 300 tokens to balance efficiency and completeness while remaining reasonably close to the maximum token length of the ground-truth summaries (377 tokens). Following previous work [31], the temperature was set to 0.97 to limit the randomness of the generated text in combination with our sampling-based decoding strategy. High temperature values decrease the deterministic behavior of the text generation model. A value of 0.97 corresponds to a moderate level of randomness, representing a trade-off between avoiding repetitive and blank summaries and allowing for too much randomness and unfaithful generated texts.

Table 1. Pretrained model versions and decoding parameters of all the models used in the experiment.

Model	Pretrained model version	Decoding parameters
Flan-T5	flan-t5-base	• min_length=150 • max_length=300 • do_sample=True • Temperature=0.97 • repetition_penalty=1.2
GPT-3	text-davinci-003	• Temperature=0.97 • max_tokens=300 • top_p=0.9 • presence_penalty=1
GPT-3.5	gpt-3.5-turbo-0301	• Temperature=0.97 • max_tokens=300 • top_p=0.9 • presence_penalty=1

To test the effect of fine-tuning, the Flan-T5 model was trained using the preprocessed train split of our dataset with the following training parameters: batch size of 1, a total of 10 training epochs, a learning rate of 0.00002, and weight decay of 0.01.

The chosen hyperparameters were set to fine-tune the Flan-T5 model effectively while minimizing the risk of overfitting. A small batch size helps manage memory limitations and adds implicit regularization. The 10 training epochs allow the model to learn from the data without excessive training, whereas the low learning rate (0.00002) ensures stable updates to pretrained weights, preventing drastic changes that could lead to overfitting. The weight decay of 0.01 acts as regularization by penalizing large weights, further preventing overfitting. In

XSL•FO
RenderX

addition, by using the same decoding parameters for both fine-tuned and non–fine-tuned Flan-T5 models, consistency in evaluation was maintained. To prevent overfitting, the model's performance was monitored on a validation set, ensuring that it did not memorize the training data.

The fine-tuned Flan-T5 model was used to generate the summaries with the same decoding parameters as shown in Table 1 for the non–fine-tuned Flan-T5 model.

Automatic summaries were generated for all models using the 7 prompting strategies. This was done for the 7 symptoms and 117 treatments as 1 symptom and 2 treatments were used as examples in the prompt in the few-shot cases, yielding a total of 2604 summaries (124 summaries per 7 prompting strategies for 3 models). In addition, for further experiments exploring the influence of fine-tuning, Flan-T5 was trained and validated on 113 summaries (n=101, 89.4% of the summaries for training and n=12, 10.6% of the summaries for validation) across 8 symptoms and 105 treatments. The remaining 11% (14/127) of the summaries for 14 treatments were used to measure performance in our automatic evaluation.

Automatic Evaluation

To evaluate the generated texts automatically, we relied on state-of-the-art evaluation metrics used in text generation research, in particular, the token-based ROUGE and BERTScore. These metrics allowed us to compare the similarity of the generated texts to the manually created reference. The token-based ROUGE metrics essentially compute the overlap of phrases between the automatically generated summarization and the reference summarization, thus estimating the similarity of both summaries. BERTScore relies on embeddings and, thus, compares the summaries at a more semantic level, abstracting from the specific words or phrases that appear.

In this study, the generated summaries from all 3 models were evaluated using ROUGE, and the rescaled F_1-score of BERTScore was calculated using the hidden representation states of the 17th layer of RoBERTa Large without inverted document frequency–weighting for the generated summaries. For ROUGE, we used 3 variants: ROUGE-1, ROUGE-2, and ROUGE-L. We used these 3 ROUGE variants to thoroughly evaluate the generated summaries. Each variant served a specific purpose: ROUGE-1 measures unigram (single-word) overlap to assess the occurrence of keywords without looking at the context, ROUGE-2 evaluates bigram (pair of consecutive words) overlap to capture context and word associations, and ROUGE-L analyzes the longest common subsequence to evaluate fluency and structural coherence [32]. These metrics collectively provide a nuanced assessment of the generated summary's content, coherence, and adherence to the reference summary.

We present the average score considering all 124 test instances by computing the ROUGE and BERTScore values for each reference summary compared with the generated texts. A case study was conducted involving 2 summaries that were analyzed qualitatively and discussed in more detail, comparing the different generated versions of it in all model settings. In addition to the experiments with LLMs, we calculated the ROUGE and BERTScore values for a baseline using the concatenation of all input texts as a trivial summarization baseline that does not summarize anything.

Ethical Considerations

Following recommendations on ethical methods to analyze data using NLP [33], the data were automatically anonymized by removing user IDs, personal names, addresses, and telephone numbers to minimize the risk of identification of a natural person to ensure compliance with the General Data Protection Regulation (GDPR). While the collected data still represent personal information, given the fact that we only analyzed data that had been made manifestly public by users without further provisions to protect the data, the use for research purposes can be argued to be acceptable given that there is a public interest in using these data to improve health care and that other means to collect such insights (eg, surveys) would represent a higher burden for patients [33]. On the other hand, the harm caused to patients by analyzing the data can be argued to be minimal as the content is already publicly available and no new information is released as part of the process.

According to the GDPR, there is a trade-off between the legitimate interests of data processors to process data that need to be balanced against the data protection rights of data subjects. In this particular case, there is a legitimate interest by society to rely on public data shared by patients as these data can contribute to improving the standard of care as well as the development of drugs that are relevant and address outcomes of relevance to patients. Furthermore, given that patients made their data "overtly and explicitly public" without any additional protection, we can assume that the sensitivity of the shared data is not that critical, and so exploiting them for the legitimate purpose of improving health care services is acceptable. The GDPR foresees that consent has to be obtained from data subjects to process their data. Given that the data were anonymized, patients cannot be directly contacted to obtain consent. In this respect, we processed the data making use of the exemption mentioned in the GDPR for processing data without explicit consent in case obtaining consent is not possible "with a reasonable effort." Obtaining consent would, in our case, not represent a reasonable effort as each patient would have to be contacted individually, and some patients might not even be active anymore on the forums or sites in question. Contacting specific users would require registering on the platform in question, which in many cases would violate the terms and conditions of the platform as only patients are allowed to register. On many forums, direct messages cannot be sent to users, so they could not be directly contacted. In general, it has been a matter of debate whether observational studies can be ethical without patient consent and which conditions would need to be met for the absence of patient consent to be ethical. The United Kingdom's Economic and Social Research Council, for instance, considers ethical the forgoing of patient consent as long as a study is not "undertaken lightly or routinely." It is only justified if important issues are being addressed and if matters of social significance that cannot be uncovered in other ways are likely to be discovered [34]. A broader review of ethical recommendations [33] suggests that social media listening (SML) for health research can be ethical without informed consent in cases in which anonymization is ensured,

XSL•FO
RenderX

harms are minimized, and there is a clear public benefit resulting from the analysis. As argued previously, all 3 criteria were fulfilled for our study.

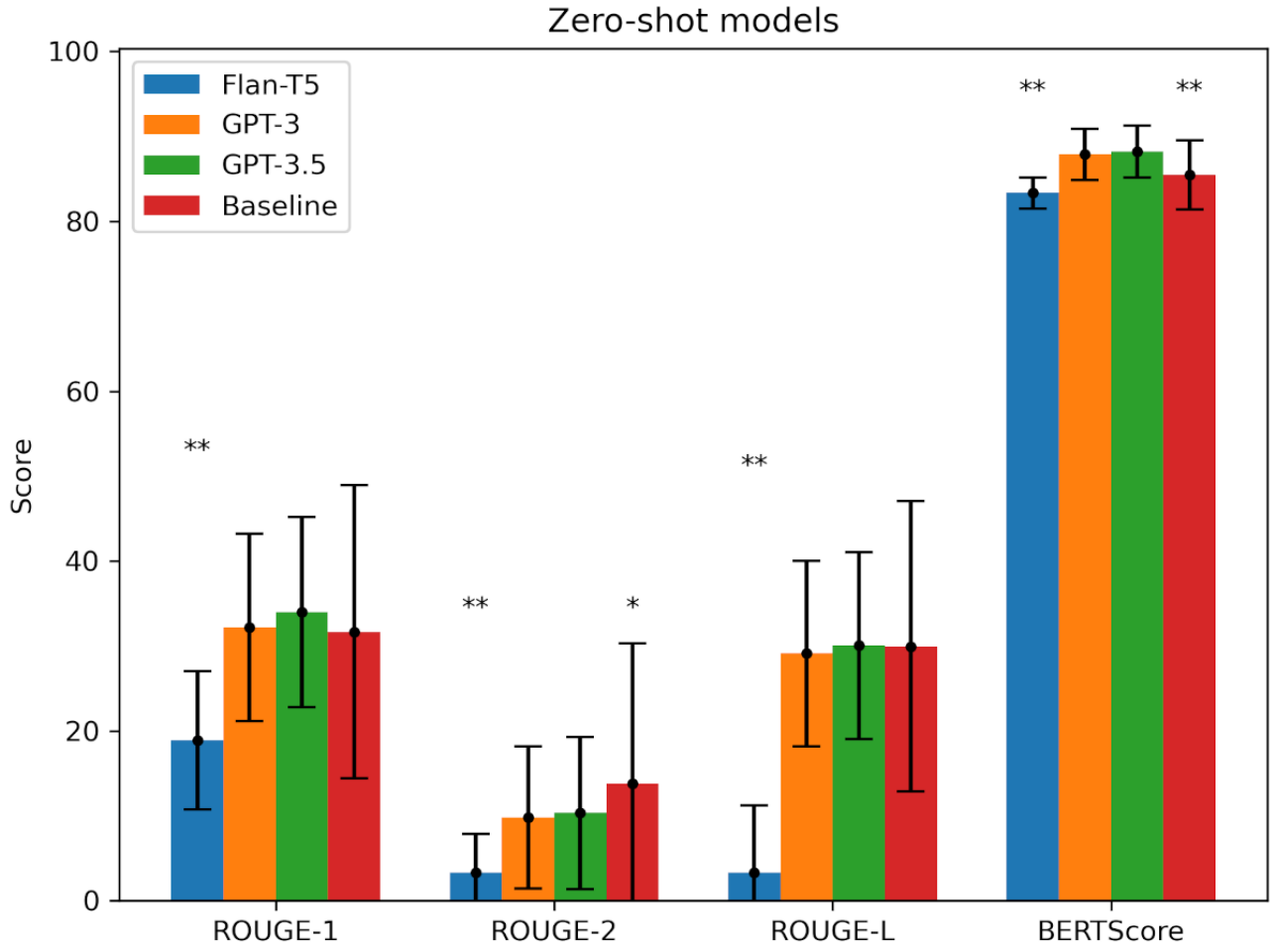
Results

Overview

The evaluation was guided by three research questions: (1) Which model has the best performance compared to the reference summaries? (2) Which prompting techniques are most successful? (3) Does fine-tuning increase the models' performance in generating patient comment summaries by only using a small amount of training data?

Regarding the performance of the different models, Figure 1 shows the average ROUGE and BERTScore values for 124 summaries generated using zero-shot prompting on 3 models. Flan-T5 performed worst for all metrics and with very high significance as well (P<.001).

Figure 1. Mean scores per model and metric with corresponding SDs as error bars. Recall-Oriented Understudy for Gisting Evaluation (ROUGE) scores and BERTScore were obtained for all zero-shot models without fine-tuning; P values were obtained by comparing the mean scores for each model to the overall best-performing model (ie, Generative Pretrained Transformer [GPT], GPT-3.5). The figure shows that GPT-3.5 performed best for all metrics except ROUGE-2, for which the baseline performed best. *P<.05; **P<.001.



In contrast, GPT-3.5 performed better than all the other models (including the baseline) for all metrics, with a margin ranging from 0.4% to 79.8% except for ROUGE-2, where the baseline performed significantly better (P<.05). GPT-3 in all cases performed slightly worse than GPT-3.5 but better than Flan-T5.

The average text length of the input text (and, hence, the output of the baseline) was 4199 (SD 7809) words, which was much higher than the average text length of the GPT-3.5–generated summaries, which was 446 (SD 214) words. Therefore, the count of bigrams was higher in general for the baseline when compared to the GPT-3.5 summaries due to its high average text length, which is not suitable for an actual summary. However, in contrast to the baseline, GPT-3.5 generated reader-friendly summaries that were shorter than the original text, having a higher semantic closeness to the reference than the baseline (+2.8 points in BERTScore). A t test was carried out comparing all other model variants to GPT-3.5 to confirm the significance of the results. The exact results can be found in Table S1 in Multimedia Appendix 2.

Focusing on GPT-3.5 as the best overall model for zero-shot prompting, we proceeded to investigate the impact of different prompting strategies on the summarization performance. Figure 2 shows the average ROUGE-1, ROUGE-2, ROUGE-L, and BERTScore values for 124 summaries generated using the 7 different proposed prompting techniques. Again, the exact results can be found in Table S2 in Multimedia Appendix 2. Regarding the ROUGE score, the obtained evaluation scores show that DSP using 3 examples outperformed other prompting

XSL•FO
RenderX

techniques. For BERTScore, 3-shot prompting without DSP outperformed all the other models. However, the differences among the different prompting techniques regarding their performance were only minor and not significant in most cases, especially for BERTScore. The only significant (P<.05) result was that CoT zero-shot prompting performed worse than all other prompting techniques.

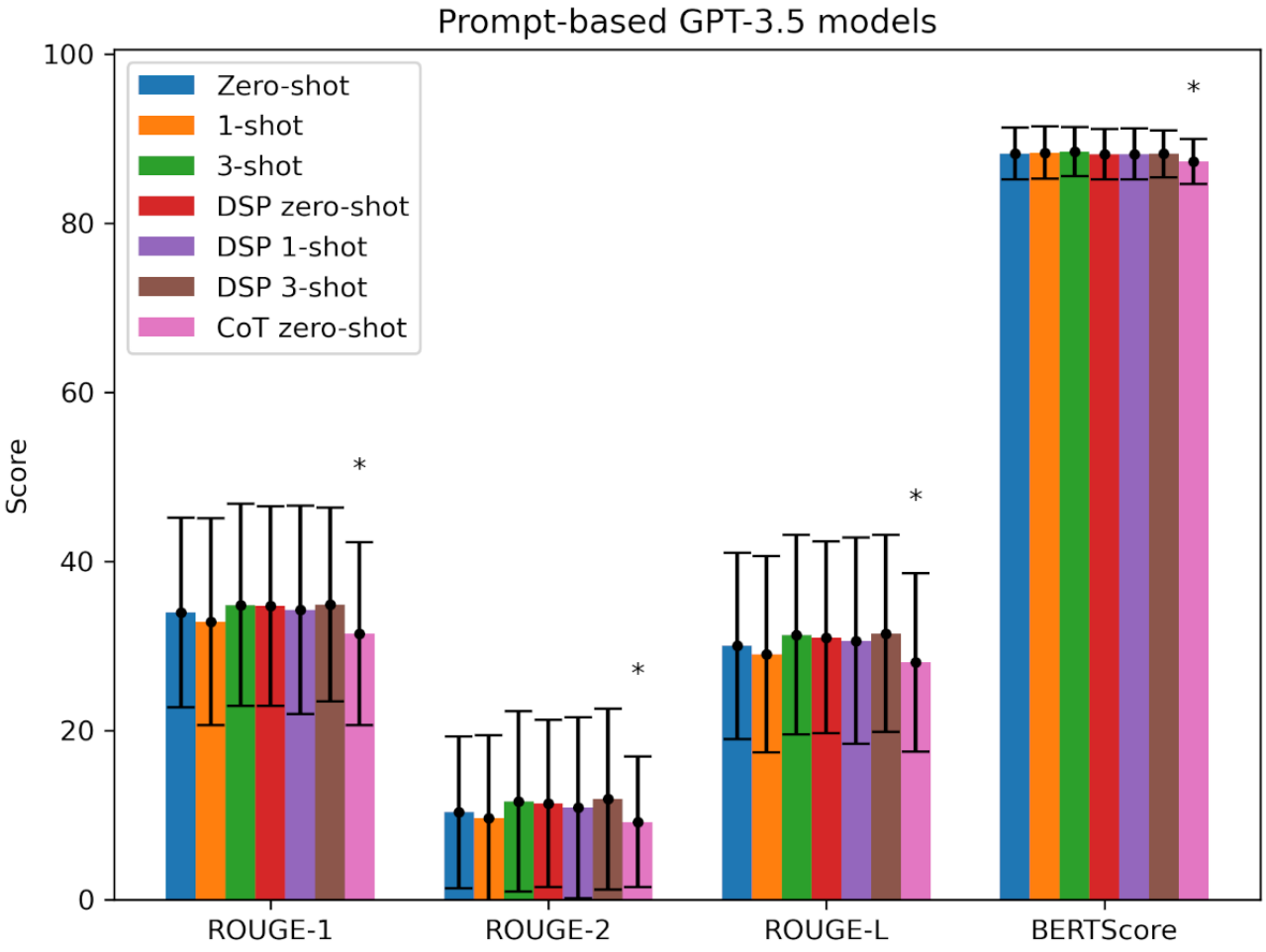
Multimedia Appendix 2 provides tables detailing the results of the 7 prompting strategies for the Flan-T5 and GPT-3 models.

To explore the effect of fine-tuning under the restriction of having only a small amount of training data, Figure 3 shows the average ROUGE-1, ROUGE-2, ROUGE-L, and BERTScore values obtained for the fine-tuned Flan-T5 compared with the prompt-instructed Flan-T5 model for 14 test instances (we only considered Flan-T5 for fine-tuning as, given that GPT-3 and GPT-3.5 are closed source, they cannot be fine-tuned locally with a full control over the training process and involved data). Again, the exact results can be found in Table S3 in Multimedia Appendix 2. The fine-tuned Flan-T5 model outperformed the non–fine-tuned Flan-T5 model in all cases, with the non–fine-tuned variants performing worse with normal (P<.05) or even very significant (P<.001) results in almost all cases. Only for the ROUGE-2 scores of the 3 DSP strategies the results were not significant. Thus, upon evaluating the obtained scores, it is evident that fine-tuning—even with only a small amount of training data—is more effective than any prompting strategy for the Flan-T5-base model.

It is important to note that the fine-tuned Flan-T5 model cannot be directly compared to the prompt-based GPT models; it can only be compared to the prompt-based or non–fine-tuned Flan-T5 models, as shown in Figure 3.

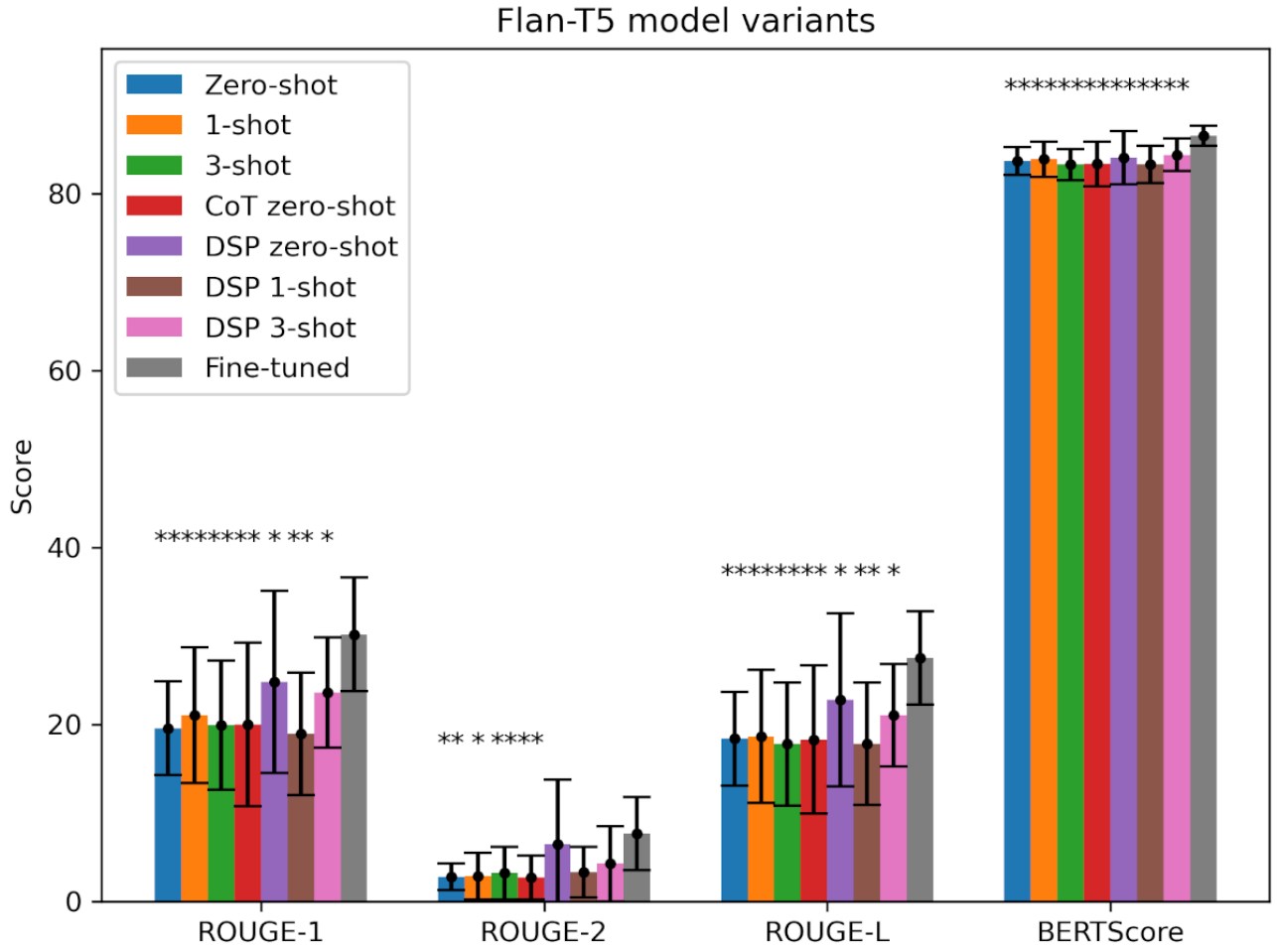
All in all, among the tested models, GPT-3.5 performed best. The best-performing prompting strategy was DSP 3-shot prompting for the ROUGE scores and 3-shot prompting for BERTScore. For Flan-T5, the fine-tuned version performed better than all prompting strategies on non–fine-tuned Flan-T5 models.

Figure 2. Mean scores per prompting strategy and metric for Generative Pretrained Transformer [GPT], GPT-3.5 with corresponding SDs as error bars—Recall-Oriented Understudy for Gisting Evaluation [ROUGE], ROUGE-1, ROUGE-2, ROUGE-L, and BERTScore scores for prompt-based GPT-3.5 models, with P values obtained by comparing all prompt-based GPT-3.5 models to the best-performing GPT-3.5 directional stimulus prompting (DSP) 3-shot model. The figure shows that the DSP 3-shot model performed best. However, none of the results was significant except for the worst performance of chain-of-thought (CoT) zero-shot training. *P<.05; **P<.001.



XSL•FO
RenderX

Figure 3. Mean scores per prompting strategy and model variant and metric for Flan-T5 with corresponding SDs as error bars—Recall-Oriented Understudy for Gisting Evaluation [ROUGE] ROUGE-1, ROUGE-2, ROUGE-L, and BERTScore scores for the Flan-T5 model variants, with *P* values obtained by comparing all Flan-T5 models to the fine-tuned Flan-T5 model. The figure shows that the fine-tuned model outperformed all non–fine-tuned models no matter what prompting strategy was used. *P<.05; **P<.001; CoT: chain of thought; DSP: directional stimulus prompting.



Case Study

To discuss the performance of the approach in a more qualitative manner, we analyzed the different summaries provided by the different models in comparison to the reference summary for 1 treatment (Carboplatin) and 1 symptom or phenotype (neoplasm). We selected examples in which the ROUGE scores were highest. While it might seem unfair to select the topics with the best results, the case study is not meant as a proper evaluation but only to provide examples of how the summaries differed across methods.

Textbox 1 shows the different summaries of the patient experience with Carboplatin, including the reference summary and the GPT-3.5 zero-shot, GPT-3.5 three-shot, and GPT-3.5 DSP 3-shot summaries. The reference summary emphasizes that Carboplatin, being a new treatment and a good option to treat triple negative breast cancer, has good study results and better tolerability and is becoming increasingly popular. It emphasizes the side effects, such as hair loss and heart damage. It mentions that side effects might increase in combination with other drugs, such as Taxol and Gemcitabine.

The GPT-3.5 zero-shot summary highlights the efficacy (although not a good study performance explicitly), side effects (hair loss but also hearing loss and tinnitus), and popularity of the treatment. In addition, it highlights better tolerability of Carboplatin and Taxol in comparison to Carboplatin alone. It provides further details on dosage and scheduling and even goes as far as talking about the mechanism of action.

The GPT-3.5 three-shot summary highlights that Carboplatin has had good study results, as well as the side effects, mentioning hearing loss and tinnitus. The summary misses heart damage but includes an additional side effect not mentioned in the reference summary (ie, tinnitus). The summary goes further than the human-generated summary in terms of discussing the regimen and scheduling in addition to discussing outcomes in combination with other drugs.

The GPT-3.5 DSP 3-shot summary emphasizes the side effects (again, hearing loss and tinnitus) as well as better tolerability. It highlights that Carboplatin has shown promising results in clinical trials. Beyond that, it provides more detail on how patients deal with the side effects by using other treatments.

Overall, the 3 summaries cover the most important points highlighted by the human reference summary, providing some additional details (eg, dosage, mechanisms of action, other side effects, and combination with other drugs or treatments to reduce side effects).

XSL•FO
RenderX

Textbox 2 shows different summaries of the patient experience with neoplasm, including the reference summary and the GPT-3.5 zero-shot, GPT-3.5 three-shot, and GPT-3.5 DSP 3-shot summaries. The reference summary highlights patients' experiences with neoplasm, focusing on tumor size, aggressiveness, and growth rate. It discusses tumor structure, including receptors and mutations and varied treatment responses. Patients reported problems such as fluid retention; lymphedema; tissue damage; severe pain; and complications from spinal spread, such as vertebral fractures and bone marrow impairment. Treatment outcomes varied, with some tumors decreasing, staying stable, or growing despite interventions.

The GPT-3.5 zero-shot summary discusses patient experiences with neoplasms, covering tumor characteristics, treatment options, and responses. It distinguishes between benign and malignant tumors and mentions the potential for immunotherapy. However, it lacks details on specific patient-reported problems and complications highlighted in the reference summary, such as fluid retention and bone marrow impairment due to spinal spread.

The GPT-3.5 three-shot summary echoes the reference summary's emphasis on patients' experiences with tumor characteristics, including size, grade, and aggressiveness. It acknowledges the importance of postsurgical treatments such as chemotherapy and radiation in preventing cancer recurrence. It also discusses tumor markers and lymph node involvement. However, it provides a more concise overview, focusing on patients' concerns about tumor growth and aggressiveness and the importance of treatment in improving survival rates.

The GPT-3.5 DSP 3-shot summary delves into patients' tumor descriptions, covering size, stage, grade, and lymph node involvement. It acknowledges larger, aggressive tumors necessitating postsurgical treatments such as chemotherapy or radiotherapy. In addition, it recognizes benign tumors and the significance of tumor markers such as estrogen receptor, progesterone receptor, and HER2 in treatment decisions. The summary also discusses tumor flare after biopsy and size fluctuations over time, stressing the uniqueness of each patient's tumor and the need for personalized treatment plans, echoing the reference summary's focus on varied tumor responses and patient challenges.

Overall, the 3 summaries cover the key points highlighted in the reference summary while providing additional details such as genetic mutations, treatment responses, and the importance of individualized treatment plans.

Textbox 1. Reference summary, GPT-3.5 zero-shot summary, GPT-3.5 three-shot summary, and GPT-3.5 directional stimulus prompting (DSP) 3-shot summary about Carboplatin. The textbox shows that all summaries mention the most important points.

Reference summary

- "Carboplatin is a more recent treatment, deemed by patients as a good option to treat TNBC, having encouraging results in studies and a better tolerability. The treatment is more novel, yet becoming more popular. But it also causes side effects such as hair loss, heart damage. When combined with other drugs such as Taxol and Gemcitabine, the side effects increase."

GPT-3.5 zero-shot summary

- "The patient comment covers a variety of topics related to Carboplatin, a chemotherapy drug used to treat Triple Negative Breast Cancer (TNBC). The comment discusses the efficacy of Carboplatin in treating TNBC even without HER2 positivity, potential side effects such as hearing loss and tinnitus, and its popularity as a treatment option. The comment also touches on the dosing schedule and suggests that weekly carbo taxol is easier to tolerate than every 2 weeks IV carbo. Some comments mention hair loss and other side effects associated with Carboplatin. The comment also highlights the role of calcium carbonate in reducing the absorption of other medicines from the gut."

GPT-3.5 three-shot summary

- "Carboplatin is a chemotherapy drug used to treat Triple Negative Breast Cancer (TNBC), even if the patient does not have Her 2 positivity. Patients report that Carboplatin has been shown to have good results in trials and may be a better option than other treatments such as AC. However, some patients also report potential side effects of Carboplatin, such as hearing loss and tinnitus. Carboplatin can be given as a weekly regime or every two weeks, but the latter may cause a decrease in hemoglobin levels. Despite this, Carboplatin is still seen as an effective treatment option for high-grade TNBC. There is also ongoing research into the use of Carboplatin with other drugs to improve treatment outcomes."

GPT-3.5 DSP 3-shot summary

- "Carboplatin is a commonly used chemotherapy drug for treating TNBC, although it can cause side effects such as hearing loss and tinnitus. Patients report mixed experiences with the drug, with some finding it tolerable and others experiencing difficulty with its side effects. Carboplatin has shown promising results in clinical trials and is being studied in combination with other agents such as leronlimab. It is not clear why some patients are prescribed Carboplatin over other chemotherapy drugs, but it may be preferred for high-grade TNBC or in combination with radiotherapy. Patients also report using bicarbonate and calcium carbonate to manage side effects and improve blood pH levels during treatment."

XSL•FO
RenderX

Textbox 2. Reference summary, GPT-3.5 zero-shot summary, GPT-3.5 three-shot summary, and GPT-3.5 directional stimulus prompting (DSP) 3-shot summary about neoplasm. The textbox shows that, again, all important details are mentioned in the summaries, such as genetic mutations and treatment responses.

Reference summary

- "Regarding neoplasm, patients often describe the size of their tumors, how aggressive they are and how fast they grow. Furthermore, they also describe their structure, which receptors, mutations they have and how fast or slow they respond to treatments. There were many varied responses in these regards, e.g. many small but also many large treatments, responsive and non-responsive treatments and different types of tumors. Neoplasms caused an array of problems for patients such as fluid retention, lymphedema, acidity, tissue dama, a concave chest after removal of the tumor and chest muscle, inflammation, compression of nerves, severe pain and an immunosuppressive environment. For some patients where it spread to their spine, it impaired their bone marrow, caused complications, broke vertebrae and aggravated nodes. Some neoplasms decreased with treatment, but others either decreased and then came back, stayed stable or even grew despite treatment."

GPT-3.5 zero-shot summary

- "The patient comments mention various sizes and stages of tumors, as well as the presence or absence of lymph node involvement and markers such as HER2. Some tumors are benign while others are malignant, and treatment options include surgery, chemotherapy, and radiotherapy. Response to treatment varies, with some tumors showing complete response and others being slow-growing. In some cases, genetic mutations may be acquired under the selective pressure of therapy, and hot tumors with inflammation may respond to immunotherapy. Some tumors contain a mix of different cell types, and there may be concordance or discordance between cell-free DNA and tissue samples. Overall, the comments suggest that cancer diagnosis and treatment can be complex and individualized, and it is important to trust medical professionals while seeking support from others who have gone through similar experiences."

GPT-3.5 three-shot summary

- "Patients share their experiences with tumors, including their size, grade, and aggressiveness. They also mention the importance of postsurgical treatments, such as chemotherapy and radiation, in preventing cancer recurrence and improving survival rates. Patients highlight the difference between benign and malignant tumors and share their tumor markers and lymph node involvement. Some patients express concern about the growth and aggressiveness of their tumors, while others report slow-growing tumors."

GPT-3.5 DSP 3-shot summary

- "Patients describe their tumors in terms of size, stage, grade, and involvement of lymph nodes. Some patients report having larger and more aggressive tumors, which require postsurgical treatments such as chemo or radiotherapy to manage them. However, some tumors are benign and do not necessarily indicate cancer. Patients may also have a combination of different tumor markers such as ER, PR, and HER2, which may affect the aggressiveness of the cancer and the recommended treatment options. Tumor flare is a real phenomenon that can occur after biopsy, and tumor size can fluctuate over time. Some patients also report elevated tumor markers in their blood. Ultimately, each patient's tumor is unique and requires an individualized treatment plan."

Discussion

Principal Findings

Our evaluations of different models on the task of generating summaries about the patient experience revealed that GPT-3.5 was the best-performing model. This is no surprise as it is the model with the most parameters (approximately 375 billion) of the set of models examined. GPT-3 has 175 billion parameters, and the smallest model was Flan-T5 with 0.2 billion parameters in the version we used. As the training data sources for the GPT models are not made public, we cannot attribute the differences in performance to differences in the training data.

Taking GPT-3.5 as the best-performing model (see research question 1), we examined in detail the impact of different prompting strategies. For the 3 ROUGE metrics, DSP 3-shot prompting emerged as the best strategy, whereas few-shot prompting with 3 examples received the best scores according to BERTScore (see research question 2). In any case, the results clearly show that providing at least 3 examples helps the model generate more tailored summaries. DSP 3-shot prompting benefits particularly from the fact that key relevant topics are provided as guidance to the model, which helps generate better summaries.

Our fine-tuning experiments with Flan-T5 showed that fine-tuning can have a positive effect in principle (see research question 3). However, we assume that the amount of data was still too low. Therefore, the fine-tuned Flan-T5 setting was not really comparable to the other settings that were not fine-tuned with a comparable number of examples. In particular, the results of Flan-T5 were, irrespective of fine-tuning, quite low compared to those of the other models. However, the results show the potential of fine-tuning within a particular model class.

Our case study using GPT-3.5 as the best-performing model with the best prompting strategies showed that the summaries produced by GPT-3.5 are reasonable, covering most of the aspects of the manually generated summaries while including some additional details or background. Our results demonstrated that such models can be used to speed up qualitative research by being able to summarize large amounts of text automatically. In addition, we confirmed a positive correlation between the quality of the summaries and the models' size on the one hand and fine-tuning on the other hand. In March 2023, OpenAI released GPT-4, as well as the possibility to fine-tune models using a fee-based application programming interface. These new developments are promising and should be investigated further, yet they were not available at the time the experiments described in this paper were carried out.

XSL•FO
RenderX

Taken together, our results suggest that state-of-the-art pretrained LLMs can be a valuable tool to provide qualitative insights about the patient experience to better understand unmet needs, patient priorities, and how a disease impacts daily functioning and quality of life to inform processes aimed at improving health care delivery and ensure that drug development focuses more on the actual priorities and unmet needs of patients. In particular, the insights would allow for the focus of drug development and clinical development to be on outcomes that are relevant to patients and have the potential to substantially improve their quality of life. The insights provided by our method could be used to develop a more detailed understanding of patient journeys as a basis to improve patient care by focusing on the actual problems and unmet needs that patients face in different phases of their journey. The insights could further help in developing support programs that provide relevant information to patients when they need it to empower them to make better decisions. Finally, such qualitative insights could also inform the design and conceptualization of digital apps for patients.

As a notable limitation of this study, our manually created test set for the quantitative evaluation of the different approaches had a limited sample size. Although we presented an experiment with a fine-tuning approach, after splitting the small dataset into training, development, and test sets, we noticed that each split was too small to derive representative results for each setting. Having a larger dataset (at least by 1 order of magnitude) would enable more experiments with respect to fine-tuning. While the sample size was small, it is a remarkable result that fine-tuning had a positive impact on the task. A larger dataset would possibly have yielded even stronger results. However, as the focus of this study was on experimenting with (unsupervised) prompting approaches, we keep the experiments with a larger dataset for future work. A further important limitation is the fact that the reference summaries were created by only 1 annotator, which might bias the results to the perspective of this single annotator. The huge effort involved in creating these summaries did not make it possible to have multiple annotators providing the summaries. A larger dataset could be obtained via crowdsourcing platforms such as CrowdFlower or Prolific; however, a drawback of these platforms is that we cannot reliably control for the (domain) expertise of the labelers.

The summaries could not be directly compared using standard annotation metrics such as the Cohen κ but could have been compared in terms of ROUGE to each other to have an upper baseline for the scores.

Another limitation arises from the nature of our applied automatic metrics. The average text length of the output of the baseline approach (mirroring its input) was substantially higher (contradicting the idea of a summary that should be concise) than that of the GPT-3.5–generated summaries. However, in terms of our automatic metrics, this discrepancy in text length impacted the count of bigrams, favoring the baseline compared to the GPT-3.5 zero-shot summary. The automatic evaluation metric we used, for example, ROUGE-2, does not consider the text length, which may bias the results toward the longer text. Thus, while the baseline appeared to perform better according to ROUGE-2, it is important to interpret these results cautiously considering the difference in text length.

We compared the different LLMs and the different prompting strategies on our own dataset consisting of 127 reference summaries. The dataset might not be completely representative of all sorts of summarization tasks, possibly limiting the generalizability of the results to other related tasks. The comparison of the different methods and the results obtained are specific to the particular summarization task considered. It is an open question whether the results generalize to other summarization tasks. However, our focus was on determining whether LLMs can reliably and accurately summarize the experience of patients as shown on online posts. A question for further research is to better understand why the performance of models differs and which underlying factors are responsible for the differences. Understanding whether the differences in ROUGE and other scores represent semantically meaningful differences is also an important question for future work. Indeed, future work might strive for a more semantic assessment of the generated summaries by manual coders who could rate the generated text in terms of variables such as clarity, comprehensiveness, completeness, and readability.

Beyond this, since the time our experiments were carried out, newer LLMs have been released, in particular also GPT-4 and GPT-4o, which could also be tested. Other open-source models such as Llama could also be investigated.

To the best of our knowledge, our dataset is the only dataset consisting of manually created summaries of patient experience. Thus, we cannot evaluate our method on existing datasets. To allow researchers to compare their methods on our dataset, we will provide the dataset to anyone interested upon request.

Beyond improving the methodology, data basis, and models used, future research should show that the insights derived via summarization methods can indeed impact our understanding of what unmet needs and priorities patients have and positively impact drug development and optimization of patient journeys. This question is clearly out of the scope of this study but could be pursued in follow-up work. While we focused only on posts from patients with breast cancer, we see no reason why this approach could not generalize to other patient populations. However, this needs to be validated in future work.

Related Work

We briefly discuss related work on using LLMs in health care in general, deep diving into work on using NLP for analyzing patient experiences on social media. We discuss the application of summarization in health care as well.

LLMs in Health Care

Very recently, LLMs have been considered for different tasks and use cases in health care. In a recent overview paper, Clusmann et al [35] described the main areas in which there is the potential to apply LLMs in health care: research, patient care, and education. The use of LLMs to summarize patient discussions falls into the area of patient care as it has the potential to uncover unmet needs of patients that can contribute to improve drug development and patient care.

XSL•FO
RenderX

Beyond text summarization tasks, LLMs have also been investigated on use cases related to drug discovery [36] and have been tested on tasks such as helping discover new targets as well as predicting characteristics of drugs, including molecular pharmacodynamics, pharmacokinetics, and toxicity [37]. They have also been shown to be able to support the discovery of drug-drug interactions [38]. A recent review has even highlighted the opportunities, limitations, and barriers regarding the use of LLMs in medical diagnosis [39].

LLMs for SML

SML has been established as a mature methodology to extract key insights about the patient experience as a way to inform drug development and improvement of patient care. A recent review analyzed 63 publications that performed SML [9]. Of the 63 publications analyzed, 38 carried out some computer-assisted analysis. The methods used covered a wide range of NLP methods to detect topics and concepts within textual data. While some published research used keywords and dictionaries to identify topics in some cases [40], other methods comprised binary matrix factorization, Bayesian estimation, and Latent Dirichlet Allocation [41]. Several of the reviewed publications stated that custom-trained NLP algorithms were used [42,43], and neural networks were also reportedly used to identify certain topics or expressions [44]. A total of 25 out of the 63 publications covered in the aforementioned review performed manual analysis, relying on the manual coding of small data samples. The methods that analyze social media posts automatically by using NLP typically extract certain predefined aspects of the patient experience, including key symptoms, their severity, and experiences with treatments. While they support the scalable analysis of large amounts of text, they are typically not suited to analyze open topics, nor do they provide detailed qualitative insights. Manual analysis methods that rely on the development of a specific coding can be used to answer very specific research questions from a qualitative perspective. However, they are not designed to scale and are necessarily limited to analyzing a smaller sample. The method proposed in this paper can be understood as a sweet spot between these 2 methodological ends of the spectrum. The automatic summary of patient experience conversations allows for the scaling to larger amounts of data and text while also allowing for the succinct summarization of the data to support qualitative understanding.

Automatic Text Summarization in Health Care Applications

Summarizing texts is an important field in the area of NLP, aiming to condense a verbose text into a shorter version while preserving the essence of its meaning. While previous research started with extractive summarization (ie, selecting fragments from the text to be summarized that are concatenated to yield a summary), with the rise of LLMs, research has shifted toward abstractive summarization, in which a model generates a text instead of copying text fragments [45], resulting in a fluent text that helps the reader obtain an overview with minimal time investment. To this end, the input text is encoded into an internal representation that is enrolled by a decoder into natural language. By massive pretraining of LLMs [14], fine-tuning models toward summarization [12], or tailoring them toward instructions asking for summarizations [13], this task is becoming a deeply explored field in NLP.

In the domain of health care, automatic summarization of patient data has emerged as a vital area of research. In this section, we explore the recent advancements in summarization techniques of patient data and other types of data, highlighting the models and methodologies used in alignment with our research.

It has been previously investigated how LLMs can support tasks related to medical documentation and information summarization. LLMs have been particularly evaluated on the summarization of radiology reports, patient questions, progress notes, and doctor-patient dialogue [46]. The objectives of the study by Van Veen et al [46] were similar to those of ours in that the goal was to evaluate the effectiveness of LLMs on the task of summarizing clinical text. In contrast to our focus on patient experience reports from social media or patient forums, their work focused on other types of data (radiology reports, patient questions, progress notes, and dialogues). They used similar metrics for the evaluation of the automatically generated summaries compared to manual summaries (ie, ROUGE-L and BERTScore in addition to Bilingual Evaluation Understudy (BLEU). While they also examined similar models—Flan-T5 as well as GPT (using version 4 instead of 3.5)—they did not examine an exhaustive set of prompting strategies as we did. They also concluded that GPT had the best performance, generating summaries that were more complete on average than human summaries. These results are in line with the results of our study.

A recent study testing the ability to summarize medical evidence using LLMs has shown clear limits of these technologies as factual inconsistencies produced by LLMs are critical in some applications such as summarizing medical evidence, which requires increased care and accuracy as such results might inform the decision-making of many [47]. In their study, Tang et al [47] focused on the task of medical evidence summarization, referring to the process of extracting and synthesizing key information from a large number of medical research studies and clinical trials into a concise and comprehensive summary. They also used automatic evaluation metrics, including ROUGE-L, BLEU, and METERO to evaluate the automatically generated texts with respect to expert-created Cochrane reviews. They explored models from the GPT family only (GPT-3.5 and ChatGPT) but did not analyze the impact of different prompting strategies, relying only on zero-shot prompting. In terms of ROUGE-L scores, GPT-3.5 performed better than ChatGPT, although this was not the case for other metrics.

A study by Pal et al [48] investigated the effectiveness of various neural network architectures in generating hospital discharge summaries from electronic health records within the health care domain. They applied different models (BART, Longformer, T5, and Flan-T5) and examined the impact of fine-tuning on the results, relying on similar automatic evaluation metrics to those we used (ROUGE-1, ROUGE-2, and ROUGE-L). In contrast to our work, they did not use any instruction-following models from the GPT family, so they could not investigate the

XSL•FO
RenderX

impact of different prompting strategies. In line with our results, their study showed that fine-tuning can consistently improve results.

Another research study by Nair et al [49] proposed a multistage approach that leveraged few-shot prompting techniques to generate summaries of patient-provider dialogues within the health care domain. They relied on GPT-3 as a model for their multistage approach and validated their method with respect to 100 clinical encounters. They examined in particular the impact of the number of examples provided in the prompt, varying among 1, 3, and 5 examples.

The effectiveness of pre-trained models for text summarization is further supported by the work by Ay et al [50]. Their work demonstrates the successful application of the T5 model pretrained on news data for abstractive text summarization of Turkish text documents. In contrast to our work, they did not focus on summarization of health-related texts and only relied on 1 sequence-to-sequence model, T5. In contrast, we also examined auto-regressive models from the GPT family and investigated the impact of different prompting strategies.

The study by Wang et al [51] introduced a novel element-aware summarization approach using GPT-3 and CoT prompting for abstractive text summarization. While they worked on a completely different domain (news texts rather than health-related texts), they followed a similar methodology, relying on the same evaluation metrics (ROUGE-1, ROUGE-2, and ROUGE-L as well as BERTScore), also examining the impact of fine-tuning BART and T5 compared to using GPT-3 with zero-shot prompting. Their results were mixed depending on the dataset. As a general trend, they showed that the larger models such as GPT-3 performed better than the smaller (but fine-tuned) models. This study is the only one in addition to ours investigating more advanced prompting strategies such as CoT.

Li et al [27] introduced DSP, which we used in our experiments, as a method to guide LLMs for text summarization tasks. They evaluated their proposed method on the task of summarizing news and also evaluated the suitability of the generated summaries using BLEU, ROUGE, Metric for Evaluation of Translation With Explicit Ordering (METEOR), and BERTScore. In terms of models, they also focused on instruction-following models such as GPT-3, InstructGPT, and ChatGPT. They showed that all the models can benefit from the use of directional stimuli, which is in line with our results.

Taken together, we see that none of the existing works has actually focused on summarizing patient reports from social media or forums. Most studies have also used automated metrics such as ROUGE, BLEU, METEOR, and BERTScore as we did, in some cases complementing this with a manual evaluation by experts. In terms of the models investigated, our study is similar to others in the sense that, in most studies, encoder- or decoder-based sequence-to-sequence models were investigated, including T5 and Flan-T5 in particular, as well as auto-regressive pretrained decoder-only models from the GPT family (GPT-3, GPT-3.5, GPT-4, and ChatGPT). In line with our results, most studies showed the superiority of the GPT family models. Our work is the only one that has investigated the impact of very different prompting strategies, showing in particular the impact of using direct response stimuli in combination with few-shot training. In terms of comparison, it is not possible to directly compare our results to those of other studies as none of the aforementioned studies focused on patient reports.

Conclusions

Exchanging information with peers on social media sites, support forums, or social networks, as well as receiving emotional support from them, is important for patients in coping with their conditions and being empowered. However, the information they share on public sites is unstructured and vast, not accessible for those interested in using it to improve health care. Methodologies for generating qualitative information at a large scale from these datasets have so far been missing.

Toward closing this gap, this study shows that it is possible to accurately and reliably summarize the content shared by patients on social media sites, social networking sites, discussion forums, and support groups automatically. Our study explored the feasibility of automatically summarizing experiences shared by patients online using generative LLMs combined with different prompting strategies. Our comparative study highlights the effectiveness of different advanced prompting techniques used with generative LMs in summarizing online patient comments. Notably, few-shot models, particularly the 3-shot variants, exhibited superior results compared to their zero-shot and 1-shot counterparts. Within the few-shot category, GPT-3.5 stood out with higher evaluation scores compared to those of the other models. In the context of DSP models, DSP few-shot (3-shot) models, specifically GPT-3.5, delivered the most favorable results. Upon comprehensive comparison, DSP-based 3-shot models emerged as the most efficient prompt-based models for summarization tasks, especially in the context of patient comment summarization. Although our experiments fine-tuning the smaller model Flan-T5 increased its performance by 50% in terms of the longest subsequence common to the reference, our advanced prompting techniques using larger models such as GPT-3.5 were superior in the explored domain.

Our results open up the possibility of using the qualitative insights generated at a larger scale to inform processes of drug development, design of clinical trials, development of patient journeys, public policy making, and informing the development of digital health apps. Information about unmet needs; symptoms; and their impact on the quality of life of patients, disease burden, and experiences with existing treatments provides valuable insights to inform the aforementioned processes and, ultimately, improve the state of care for patients.

XSL•FO
RenderX

Conflicts of Interest

By the time of writing, MH was an employee of Semalytix GmbH. MH is a shareholder of Semalytix GmbH. PC is cofounder and shareholder of Semalytix GmbH. All other authors declare no conflicts of interest.

Multimedia Appendix 1
List of frequent symptoms and treatments mentioned in the dataset, numbered from 1 to 127.
[OCX File , 18 KB - medinform_v13i1e62909_app1.ocx]

Multimedia Appendix 2
Additional results and listings.
[DOCX File , 295 KB - medinform_v13i1e62909_app2.docx]

References

1. Smailhodzic E, Hooijsma W, Boonstra A, Langley DJ. Social media use in healthcare: a systematic review of effects on patients and on their relationship with healthcare professionals. BMC Health Serv Res 2016 Aug 26;16(1):442 [FREE Full text] [doi: 10.1186/s12913-016-1691-0] [Medline: 27562728]
2. De Martino I, D'Apolito R, McLawhorn AS, Fehring KA, Sculco PK, Gasparini G. Social media for patients: benefits and drawbacks. Curr Rev Musculoskelet Med 2017 Mar 21;10(1):141-145 [FREE Full text] [doi: 10.1007/s12178-017-9394-7] [Medline: 28110391]
3. Suler J. The online disinhibition effect. Cyberpsychol Behav 2004 Jun;7(3):321-326. [doi: 10.1089/1094931041291295] [Medline: 15257832]
4. Ma X, Hancock J, Naaman M. Anonymity, intimacy and self-disclosure in social media. In: Proceedings of the 2016 CHI Conference on Human Factors in Computing Systems. 2016 Presented at: CHI '16; May 7-12, 2016; San Jose, CA p. 3857-3869 URL: https://dl.acm.org/doi/10.1145/2858036.2858414 [doi: 10.1145/2858036.2858414]
5. Social media “likes” healthcare—from mar-keting to social business. PWC Health Research Institute. URL: https://adindex.ru/files2/access/2013_06/99606_tpc-health-care-social-media-report.pdf [accessed 2024-04-29]
6. Padrez KA, Ungar L, Schwartz HA, Smith RJ, Hill S, Antanavicius T, et al. Linking social media and medical record data: a study of adults presenting to an academic, urban emergency department. BMJ Qual Saf 2016 Jun;25(6):414-423. [doi: 10.1136/bmjqs-2015-004489] [Medline: 26464519]
7. Seltzer E, Goldshear J, Guntuku SC, Grande D, Asch DA, Klinger EV, et al. Patients' willingness to share digital health and non-health data for research: a cross-sectional study. BMC Med Inform Decis Mak 2019 Aug 08;19(1):157 [FREE Full text] [doi: 10.1186/s12911-019-0886-9] [Medline: 31395102]
8. Patient-focused drug development: collecting comprehensive and representative input. FDA. URL: https://www.fda.gov/regulatory-information/search-fda-guidance-documents/patient-focused-drug-development-collecting-comprehensive-and-representative-input [accessed 2024-04-29]
9. Cimiano P, Collins B, De Vuono MC, Escudier T, Gottowik J, Hartung M, et al. Patient listening on social media for patient-focused drug development: a synthesis of considerations from patients, industry and regulators. Front Med (Lausanne) 2024 Mar 6;11:1274688 [FREE Full text] [doi: 10.3389/fmed.2024.1274688] [Medline: 38515987]
10. Devlin J, Chang MW, Lee K, Toutanova K. BERT: pre-training of deep bidirectional transformers for language understanding. arXiv. Preprint posted online October 11, 2018 2018 [FREE Full text]
11. Merchant A, Rahimtoroghi E, Pavlick E, Tenney I. What happens to BERT embeddings during fine-tuning? arXiv. Preprint posted online April 29, 2020 2020 [FREE Full text] [doi: 10.18653/v1/2020.blackboxnlp-1.4]
12. Raffel C, Shazeer N, Roberts A, Lee K, Narang S, Matena M, et al. Exploring the limits of transfer learning with a unified text-to-text transformer. J Mach Learn Res 2020;21(140):1-67 [FREE Full text]
13. ChatGPT: optimizing language models for dialogue. OpenAI. URL: https://chatgpt.r4wand.eu.org/ [accessed 2024-11-30]
14. Goodwin TR, Savery ME, Demner-Fushman D. Flight of the PEGASUS? Comparing transformers on few-shot and zero-shot multi-document abstractive summarization. Proc Int Conf Comput Ling 2020 Dec;2020:5640-5646 [FREE Full text] [Medline: 33293900]
15. Rothe S, Maynez J, Narayan S. A thorough evaluation of task-specific pretraining for summarization. In: Proceedings of the 2021 Conference on Empirical Methods in Natural Language Processing. 2021 Presented at: EMNLP '21; November 7-11, 2021; Punta Cana, Dominican Republic p. 140-145 URL: https://aclanthology.org/2021.emnlp-main.12.pdf [doi: 10.18653/v1/2021.emnlp-main.12]
16. Hosseini-Asl E, Liu W. US Patent 11853706 generative language model for few-shot aspect-based sentiment analysis. ComplyAdvantage. URL: https://golden.com/wiki/US_Patent_11853706_Generative_language_model_for_few-shot_aspect-based_sentiment_analysis-4A6RZWW [accessed 2024-04-29]
17. Salnikov M, Le H, Rajput P, Nikishina I, Braslavski P, Malykh V, et al. Large language models meet knowledge graphs to answer factoid questions. arXiv. Preprint posted online October 3, 2023 2023 [FREE Full text]

XSL•FO
RenderX

18. Goodfellow IJ, Shlens J, Szegedy C. Explaining and harnessing adversarial examples. arXiv. Preprint posted online December 20, 2014 2014 [FREE Full text] [doi: 10.5260/chara.21.2.8]
19. Ji Z, Yu T, Xu Y, Lee N, Ishii E, Fung P. Towards mitigating LLM hallucination via self reflection. In: Proceedings of the 2023 Findings of the Association for Computational Linguistics. 2023 Presented at: EMNLP '23; December 6-10, 2023; Singapore, Singapore p. 1827-1843 URL: https://aclanthology.org/2023.findings-emnlp.123.pdf [doi: 10.18653/v1/2023.findings-emnlp.123]
20. Socialgist AI. URL: https://www.socialgist.ai/ [accessed 2025-04-14]
21. Spies E, Andreu T, Hartung M, Park J, Kamudoni P. Exploring the perspectives of patients living with lupus: retrospective social listening study. JMIR Form Res 2024 Feb 02;8:e52768 [FREE Full text] [doi: 10.2196/52768] [Medline: 38306157]
22. The Privacy Layer for ChatGPT. Private AI ®. URL: https://private-ai.com/ [accessed 2024-04-29]
23. Zhang M, Lu J, Yang J, Zhou J, Wan M, Zhang X. From coarse to fine: enhancing multi-document summarization with multi-granularity relationship-based extractor. Inf Process Manag 2024 May;61(3):103696. [doi: 10.1016/j.ipm.2024.103696]
24. Long O, Jeff W, Xu J, Diogo A, Carroll L. Training language models to follow instructions with human feedback. In: Proceedings of the 36th International Conference on Neural Information Processing Systems. 2022 Presented at: NIPS '22; November 28-December 9, 2022; New Orleans, LA p. 27730-27740 URL: https://dl.acm.org/doi/10.5555/3600270.3602281
25. Chung HW, Hou L, Longpre S, Zoph B, Tai Y, Fedus W, et al. Scaling instruction-finetuned language models. J Mach Learn Res 2024;25(70):1-53 [FREE Full text]
26. Brown TB, Mann B, Ryder N, Subbiah M, Kaplan JD, Dhariwal P, et al. Language models are few-shot learners. In: Proceedings of the 34th International Conference on Neural Information Processing Systems. 2020 Presented at: NIPS '20; December 6-12, 2020; Vancouver, BC p. 1877-1901 URL: https://dl.acm.org/doi/abs/10.5555/3495724.3495883
27. Li Z, Peng B, He P, Galley M, Gao J, Yan X. Guiding large language models via directional stimulus prompting. arXiv. Preprint posted online February 22, 2023 2023 [FREE Full text]
28. Grootendorst M. KeyBERT: minimal keyword extraction with BERT. Zenodo. 2020. URL: https://doi.org/10.5281/zenodo.4461265 [accessed 2025-03-28]
29. Schopf T, Klimek S, Matthes F. Patternrank: leveraging pretrained language models and part of speech for unsupervised keyphrase extraction. arXiv. Preprint posted online October 11, 2022 2022 [FREE Full text] [doi: 10.5220/0011546600003335]
30. Wei J, Bosma M, Zhao VY, Guu K, Yu AW, Lester B, et al. Finetuned language models are zero-shot learners. arXiv. Preprint posted online September 3, 2021 2021 [FREE Full text]
31. Wiher G, Meister C, Cotterell R. On decoding strategies for neural text generators. arXiv. Preprint posted online March 29, 2022 2022 [FREE Full text]
32. Lin CY. Rouge: a package for automatic evaluation of summaries. In: Proceedings of the 2004 Workshop on Text Summarization Branches Out. 2004 Presented at: WAS '04; July 25-26, 2004; Barcelona, Spain p. 74-81 URL: https://aclanthology.org/W04-1013.pdf
33. Ford E, Shepherd S, Jones K, Hassan L. Toward an ethical framework for the text mining of social media for health research: a systematic review. Front Digit Health 2020 Jan 26;2:592237 [FREE Full text] [doi: 10.3389/fdgth.2020.592237] [Medline: 34713062]
34. Economic and Social Research Council (ESRC). UK Research and Innovation. URL: https://www.ukri.org/councils/esrc/guidance-for-applicants/ [accessed 2023-06-01]
35. Clusmann J, Kolbinger FR, Muti HS, Carrero ZI, Eckardt J, Laleh NG, et al. The future landscape of large language models in medicine. Commun Med (Lond) 2023 Oct 10;3(1):141 [FREE Full text] [doi: 10.1038/s43856-023-00370-1] [Medline: 37816837]
36. Pal S, Bhattacharya M, Islam MA, Chakraborty C. ChatGPT or LLM in next-generation drug discovery and development: pharmaceutical and biotechnology companies can make use of the artificial intelligence-based device for a faster way of drug discovery and development. Int J Surg 2023 Dec 01;109(12):4382-4384 [FREE Full text] [doi: 10.1097/JS9.0000000000000719] [Medline: 37707542]
37. Zhao A, Wu Y. Future implications of ChatGPT in pharmaceutical industry: drug discovery and development. Front Pharmacol 2023;14:1194216 [FREE Full text] [doi: 10.3389/fphar.2023.1194216] [Medline: 37529703]
38. Juhi A, Pipil N, Santra S, Mondal S, Behera JK, Mondal H. The capability of ChatGPT in predicting and explaining common drug-drug interactions. Cureus 2023 Mar;15(3):e36272 [FREE Full text] [doi: 10.7759/cureus.36272] [Medline: 37073184]
39. Ullah E, Parwani A, Baig MM, Singh R. Challenges and barriers of using large language models (LLM) such as ChatGPT for diagnostic medicine with a focus on digital pathology - a recent scoping review. Diagn Pathol 2024 Feb 27;19(1):43 [FREE Full text] [doi: 10.1186/s13000-024-01464-7] [Medline: 38414074]
40. Lognos B, Carbonnel F, Boulze Launay I, Bringay S, Guerdoux-Ninot E, Mollevi C, et al. Complementary and alternative medicine in patients with breast cancer: exploratory study of social network forum data. JMIR Cancer 2019 Nov 27;5(2):e12536 [FREE Full text] [doi: 10.2196/12536] [Medline: 31774404]
41. Quartey G, Ley-Acosta S, Pierce C, Nguyen A, Ertle G. Social media listening for patient risk characterization. Value Health 2018 May;21:S115. [doi: 10.1016/j.jval.2018.04.782]

XSL•FO
RenderX

42. Picone M, Inoue S, DeFelice C, Naujokas MF, Sinrod J, Cruz VA, et al. Social listening as a rapid approach to collecting and analyzing COVID-19 symptoms and disease natural histories reported by large numbers of individuals. Popul Health Manag 2020 Oct 01;23(5):350-360. [doi: 10.1089/pop.2020.0189] [Medline: 32897820]
43. Spies E, Andreu T, Koelling J, Hartung M, Kamudoni P, Park J. PCR251 retrospective social listening study of patients living with systemic lupus erythematosus (SLE): understanding the patient experience. Value Health 2022 Dec;25(12):S438. [doi: 10.1016/j.jval.2022.09.2184]
44. Weissenbacher D, Ge S, Klein A, O'Connor K, Gross R, Hennessy S, et al. Active neural networks to detect mentions of changes to medication treatment in social media. J Am Med Inform Assoc 2021 Nov 25;28(12):2551-2561 [FREE Full text] [doi: 10.1093/jamia/ocab158] [Medline: 34613417]
45. Liu Y, Lapata M. Text summarization with pretrained encoders. arXiv. Preprint posted online August 22, 2019 2019 [FREE Full text]
46. Van Veen D, Van Uden C, Blankemeier L, Delbrouck JB, Aali A, Bluethgen C, et al. Adapted large language models can outperform medical experts in clinical text summarization. Nat Med 2024 Apr 27;30(4):1134-1142. [doi: 10.1038/s41591-024-02855-5] [Medline: 38413730]
47. Tang L, Sun Z, Idnay B, Nestor JG, Soroush A, Elias PA, et al. Evaluating large language models on medical evidence summarization. NPJ Digit Med 2023 Aug 24;6(1):158 [FREE Full text] [doi: 10.1038/s41746-023-00896-7] [Medline: 37620423]
48. Pal K, Bahrainian SA, Mercurio L, Eickhoff C. Neural summarization of electronic health records. arXiv. Preprint posted online May 24, 2023 2023 [FREE Full text] [doi: 10.2196/preprints.49544]
49. Nair V, Schumacher E, Kannan A. Generating medically-accurate summaries of patient-provider dialogue: a multi-stage approach using large language models. arXiv. Preprint posted online May 10, 2023 2023 [FREE Full text] [doi: 10.18653/v1/2023.clinicalnlp-1.26]
50. Ay B, Ertam F, Fidan G, Aydin G. Turkish abstractive text document summarization using text to text transfer transformer. Alex Eng J 2023 Apr;68:1-13. [doi: 10.1016/j.aej.2023.01.008]
51. Wang Y, Zhang Z, Wang R. Element-aware summarization with large language models: expert-aligned evaluation and chain-of-thought method. arXiv. Preprint posted online May 22, 2023 2023 [FREE Full text] [doi: 10.18653/v1/2023.acl-long.482]

Abbreviations

BERT: Bidirectional Encoder Representations From Transformers
BLEU: Bilingual Evaluation Understudy
CoT: chain of thought
DSP: directional stimulus prompting
GDPR: General Data Protection Regulation
GPT: Generative Pretrained Transformer
LLM: large language model
LM: language model
METEOR: Metric for Evaluation of Translation With Explicit Ordering
NLP: natural language processing
ROUGE: Recall-Oriented Understudy for Gisting Evaluation
SML: social media listening

Edited by A Castonguay; submitted 04.06.24; peer-reviewed by S Chowdhury; comments to author 29.08.24; revised version received 05.12.24; accepted 20.12.24; published 14.04.25.

Please cite as:
Nair RAS, Hartung M, Heinisch P, Jaskolski J, Starke-Knäusel C, Veríssimo S, Schmidt DM, Cimiano P
Summarizing Online Patient Conversations Using Generative Language Models: Experimental and Comparative Study
JMIR Med Inform 2025;13:e62909
URL: https://medinform.jmir.org/2025/1/e62909
doi:10.2196/62909
PMID:

©Rakhi Asokkumar Subjagouri Nair, Matthias Hartung, Philipp Heinisch, Janik Jaskolski, Cornelius Starke-Knäusel, Susana Veríssimo, David Maria Schmidt, Philipp Cimiano. Originally published in JMIR Medical Informatics (https://medinform.jmir.org), 14.04.2025. This is an open-access article distributed under the terms of the Creative Commons Attribution License

XSL•FO
RenderX

(https://creativecommons.org/licenses/by/4.0/), which permits unrestricted use, distribution, and reproduction in any medium, provided the original work, first published in JMIR Medical Informatics, is properly cited. The complete bibliographic information, a link to the original publication on https://medinform.jmir.org/, as well as this copyright and license information must be included.

XSL•FO
RenderX

Original Paper

Exploring the Potential of Electroencephalography Signal–Based Image Generation Using Diffusion Models: Integrative Framework Combining Mixed Methods and Multimodal Analysis

Chi-Sheng Chen[1*], MEng; Shao-Hsuan Chang[1,2*], PhD; Che-Wei Liu[3,4], MD, PhD; Tung-Ming Pan[5,6], PhD

[1]Department of Biomedical Engineering, Chang Gung University, Taoyuan, Taiwan

[2]Department of Ophthalmology, Linkou Chang Gung Memorial Hospital, Taoyuan, Taiwan

[3]School of Medicine, National Tsing Hua University, Taipei, Taiwan

[4]Department of Orthopedics, Cathay General Hospital, Taipei, Taiwan

[5]Department of Electronics Engineering, Chang Gung University, Taoyuan, Taiwan

[6]Division of Urology, Chang Gung Memorial Hospital, Linkou Medical Center, Taoyuan, Taiwan

[*]these authors contributed equally

Corresponding Author:
Tung-Ming Pan, PhD
Department of Electronics Engineering
Chang Gung University
No. 259, Wenhua 1st Rd., Guishan Dist.
Taoyuan, 333
Taiwan
Phone: 1 32118800 ext 3349
Fax: 1 32118700
Email: tmpan@mail.cgu.edu.tw

Abstract

Background: Electroencephalography (EEG) has been widely used to measure brain activity, but its potential to generate accurate images from neural signals remains a challenge. Most EEG-decoding research has focused on tasks such as motor imagery, emotion recognition, and brain wave classification, which involve EEG signal analysis and classification. Some studies have explored the correlation between EEG and images, primarily focusing on EEG-image pair classification or transformation. However, EEG-based image generation remains underexplored.

Objective: The primary goal of this study was to extend EEG-based classification to image generation, addressing the limitations of previous methods and unlocking the full potential of EEG for image synthesis. To achieve more meaningful EEG-to-image generation, we developed a novel framework, Neural-Cognitive Multimodal EEG-Informed Image (NECOMIMI), which was specifically designed to generate images directly from EEG signals.

Methods: We developed a 2-stage NECOMIMI method, which integrated the novel Neural Encoding Representation Vectorizer (NERV) EEG encoder that we designed with a diffusion-based generative model. The Category-Based Assessment Table (CAT) score was introduced to evaluate the semantic quality of EEG-generated images. In addition, the ThingsEEG dataset was used to validate and benchmark the CAT score, providing a standardized measure for assessing EEG-to-image generation performance.

Results: The NERV EEG encoder achieved state-of-the-art performance in several zero-shot classification tasks, with an average accuracy of 94.8% (SD 1.7%) in the 2-way task and 86.8% (SD 3.4%) in the 4-way task, outperforming models such as Natural Image Contrast EEG, Multimodal Similarity-Keeping Contrastive Learning, and Adaptive Thinking Mapper ShallowNet. This highlighted its superiority as a feature extraction tool for EEG signals. In a 1-stage image generation framework, EEG embeddings often resulted in abstract or generalized images such as landscapes instead of specific objects. Our proposed 2-stage NECOMIMI architecture effectively extracted semantic information from noisy EEG signals, showing its ability to capture and represent underlying concepts derived from brain wave activity. We further conducted a perturbation study to test whether the model overly depended on visual cortex EEG signals for scene-based image generation. The perturbation of visual cortex EEG channels led to a notable increase in Fréchet inception distance scores, suggesting that our model relied heavily on posterior brain signals to generate semantically coherent images.

XSL•FO
RenderX

Conclusions: NECOMIMI demonstrated the potential of EEG-to-image generation, revealing the challenges of translating noisy EEG data into accurate visual representations. The novel NERV EEG encoder for multimodal contrastive learning reached state-of-the-art performance both on *n*-way zero-shot and EEG-informed image generation. The introduction of the CAT score provided a new evaluation metric, paving the way for future research to refine generative models. In addition, this study highlighted the significant clinical potential of EEG-to-image generation, particularly in enhancing brain-machine interface systems and improving quality of life for individuals with motor impairments.

(JMIR Med Inform 2025;13:e72027) doi:10.2196/72027

KEYWORDS

electroencephalography; brain-computer interface; diffusion models; multimodal generative framework; electroencephalography to image

Introduction

Background

Electroencephalography (EEG) is one of the ancient techniques for measuring neuronal activity in the human brain [1,2]. EEG records electrical activity from the scalp, offering exceptional temporal resolution and high sensitivity to neural processes. Its application has significant value in clinical practice, especially for diagnosing conditions such as epilepsy, depression, and sleep disorders [3-5], as well as assessing dysfunctions in sensory transmission pathways [6,7]. Historically, the analysis of EEG signals was limited to visual inspection of changes in amplitude and frequency over time. However, with the advent of digital technology, the methodology has undergone significant evolution, enabling a more comprehensive analysis of both the temporal and spatial characteristics of these signals [8]. As a result of these advancements, EEG has become recognized as a powerful tool for capturing real-time brain activity, particularly in the subsecond range. Despite these advantages, EEG traditionally suffers from low spatial resolution, which makes it difficult to precisely identify the brain areas responsible for the observed neuronal activity at the scalp [9]. In recent years, there has been growing interest in leveraging EEG for more advanced applications such as image recognition and reconstruction [10]. These developments have led to significant improvements in the accuracy of image recognition tasks, highlighting EEG's potential as a bridge between neural activity and visual representation [11,12]. The appeal of using EEG for image recognition lies in its ability to capture the temporal dynamics of neuronal activity, although its spatial resolution remains a major challenge. To address this, innovative methodologies, including deep learning techniques and generative models such as generative adversarial networks (GANs) [13] and diffusion models [14], have enhanced the accuracy and effectiveness of EEG-based systems, allowing for the generation of photorealistic images from neural signals [12,15,16].

Recent studies have demonstrated the feasibility of decoding natural images from EEG signals by aligning EEG responses with paired image stimuli [17]. However, most of the existing works claiming to generate images from EEG signals are still primarily image-to-image transformations. In these approaches, EEG information is typically used to slightly alter the input image, often by adding noise rather than generating new images directly from the brain signals [17-19]. In a typical experiment designed to study brain responses related to visual processes, participants view a series of images while their brain signals are recorded by a brain scanner or other recording device for subsequent analysis. Various noninvasive methods, such as functional magnetic resonance imaging (fMRI), EEG, and magnetoencephalography, can be used to capture these brain responses, each offering different sensitivity levels. Despite the availability of these techniques, there is still limited understanding regarding the precise interpretation of the data and, more importantly, the mechanisms underlying these responses. A pioneering study explored the possibility of generating impressions of what participants saw by using fMRI data based on a large image dataset sourced from YouTube [20]. However, this method faces significant challenges, including the complexity and high costs associated with using fMRI scanners. To overcome these limitations, much of the recent research has shifted toward using electrophysiological responses, particularly EEG. Although EEG offers a lower spatial resolution than fMRI, it provides much higher temporal resolution, making it a more accessible and cost-effective method. This shift to EEG is further supported by its ability to capture rapid, real-time neural dynamics. However, EEG data present their own set of challenges. The inherent noise and susceptibility to external factors complicate the accurate reconstruction of the original visual stimulus, limiting its effectiveness in image recognition and generation tasks. As a result, fMRI remains the preferred method in many studies focusing on image recognition or generation from brain signals [21], whereas EEG is used less frequently due to its noisier nature. Previous efforts such as Brain2Image and EEG-GAN have explored EEG-guided image reconstruction using variational autoencoders (VAEs) and GAN frameworks, respectively. However, most of these approaches relied heavily on paired image inputs and did not fully explore direct EEG-to-image synthesis.

To address these limitations and achieve more meaningful EEG-to-image generation, we introduced Neural-Cognitive Multimodal EEG-Informed Image (NECOMIMI), an innovative framework that focuses on EEG-based image generation. This framework integrates advanced diffusion model techniques to enhance the accuracy and realism of images generated from EEG signals. In this study, we first proposed a novel EEG encoder, Neural Encoding Representation Vectorizer (NERV), which achieved state-of-the-art (SOTA) performance in multimodal contrastive learning tasks.

XSL•FO
RenderX

Related Work

The concept of using EEG signals for image-related tasks has evolved over time. Initially, efforts focused on decoding visual categories from EEG signals [11], demonstrating the feasibility of EEG-based image classification using deep learning models. While these early studies laid the groundwork, the datasets used were small, limiting the generalizability of the findings. However, subsequent advancements in generative models, such as VAEs and GANs, paved the way for more sophisticated EEG-to-image generation. The VAE, as proposed by Kingma and Welling [22,23], provided a means of generating and reconstructing data by learning latent data distributions. Similarly, the GAN framework introduced by Goodfellow et al [13] leveraged adversarial training between a generator and a discriminator to produce realistic images. Building on these ideas, Brain2Image [12] became the first to apply VAEs to guide image generation from EEG features. Later, EEG-GAN [18] introduced the first EEG-based image generation model using long short-term memory [24] to extract EEG features and guide the GAN's image generation process.

Several works based on GANs, such as ThoughtViz [25], visual-guided GAN with visual-consistent term [26], BrainMedia [27], and EEG2IMAGE [16], have emerged, each focusing on improving the interaction between the EEG encoder and the GAN architecture. Despite these advancements, a common challenge remains in effectively using EEG data to guide image generation and reconstruction. This challenge persisted until the advent of Contrastive Language-Image Pretraining (CLIP; OpenAI) [28], which provided a better solution by enabling more reliable alignment between EEG and image data. EEG-CLIP [29] was the first framework to use contrastive learning to align EEG and image data. However, it was largely exploratory, and its framework was not extended for downstream tasks such as zero-shot image recognition. The next step in this evolution was to design more effective EEG encoders for contrastive learning, leveraging the rich image embeddings extracted from CLIP-based pretrained models. Recent efforts such as Natural Image Contrast EEG (NICE), Multimodal Similarity-Keeping Contrastive Learning (MUSE), Adaptive Thinking Mapper, and others [30-33] have explored this direction. In addition, some researchers have ventured into quantum-classical hybrid computing using a quantum EEG encoder [34], aiming to perform quantum contrastive learning [35]. Currently, many studies focus on zero-shot classification, where the model is tested on unseen EEG data and images, aiming to assess its ability to generalize to novel data. This is a challenging task that involves computing similarity scores between EEG and image data for recognition purposes. The evolution of contrastive learning techniques for EEG-based image recognition has improved the generalization performance of models, particularly when tested on out-of-sample data.

Despite the significant progress, the use of diffusion models to generate EEG-based images remains a relatively new area. While there are several EEG-based image reconstruction models that use diffusion models, such as NeuroVision [19], DreamDiffusion [17], diffusion model for the reconstruction from EEG to image [36], BrainViz [37], NeuroImagen [38], and EEGVision [39], most of these approaches rely on image-based features and treat EEG data as supplementary information. However, these methods primarily use images as input and are not designed to process nonvisual signals such as EEG directly. To address this gap, we proposed NECOMIMI, a flexible and modular framework explicitly designed for EEG-to-image generation. Unlike previous methods that focus on recognition or classification, NECOMIMI leverages modern diffusion models using EEG signals as the primary prompt, enabling direct generation of images from neural features. This shift represents a crucial step forward, reframing EEG not merely as a support signal but as a core semantic driver for brain-conditioned multimodal generation.

On the basis of the trajectory of prior work, it becomes clear that the field is moving from EEG-assisted image recognition toward more ambitious goals such as direct image generation conditioned solely on EEG signals. Although recent studies have explored advanced paradigms, including contrastive learning frameworks and hybrid quantum models, most still relegate EEG to a secondary role. In contrast, our preliminary investigations into quantum-enhanced EEG processing, such as quantum machine learning for enhanced EEG encoding and quantum contrastive learning [35], demonstrate how EEG can serve as the central signal in generative tasks. Quantum machine learning for enhanced EEG encoding [34] uses variational quantum circuits to enrich EEG representations with greater expressive capacity, whereas quantum contrastive learning integrates quantum projections into contrastive learning pipelines to improve cross-modal alignment. These findings underscore a critical limitation in current literature: the lack of a dedicated generative framework that places EEG at the forefront of image synthesis. Our work aimed to fill this void by shifting the paradigm from recognition to generation, positioning EEG not as an auxiliary cue but as a rich, semantic prompt capable of guiding diffusion-based image creation. This reorientation opens new avenues for decoding cognitive states through generative modeling and facilitates the development of brain-native, multimodal artificial intelligence systems.

In this study, we developed a comprehensive 2-stage EEG-to-image multimodal generative framework, which extended previous contrastive learning between EEG and images and applied it to image generation. Unlike previous works that have focused primarily on image-to-image generation with EEG features serving as guidance, our framework offered a more holistic approach to leveraging EEG data for image creation. While EEG data are traditionally characterized by high temporal but low spatial resolution, our goal was not to recover precise pixel-level representations. Instead, we treated EEG as a high-level cognitive modulator that captures semantic concepts, which can be used to guide image generation via latent diffusion models. To address the conceptual differences between EEG-to-image and traditional text-to-image tasks, we introduced a new evaluation metric, the Category-Based Assessment Table (CAT) score. This score assessed image generation performance based on semantic concepts as opposed to merely evaluating image distribution. We further established a CAT score benchmark using a vision language model on the ThingsEEG dataset. Finally, our study uncovered several notable findings

XSL•FO
RenderX

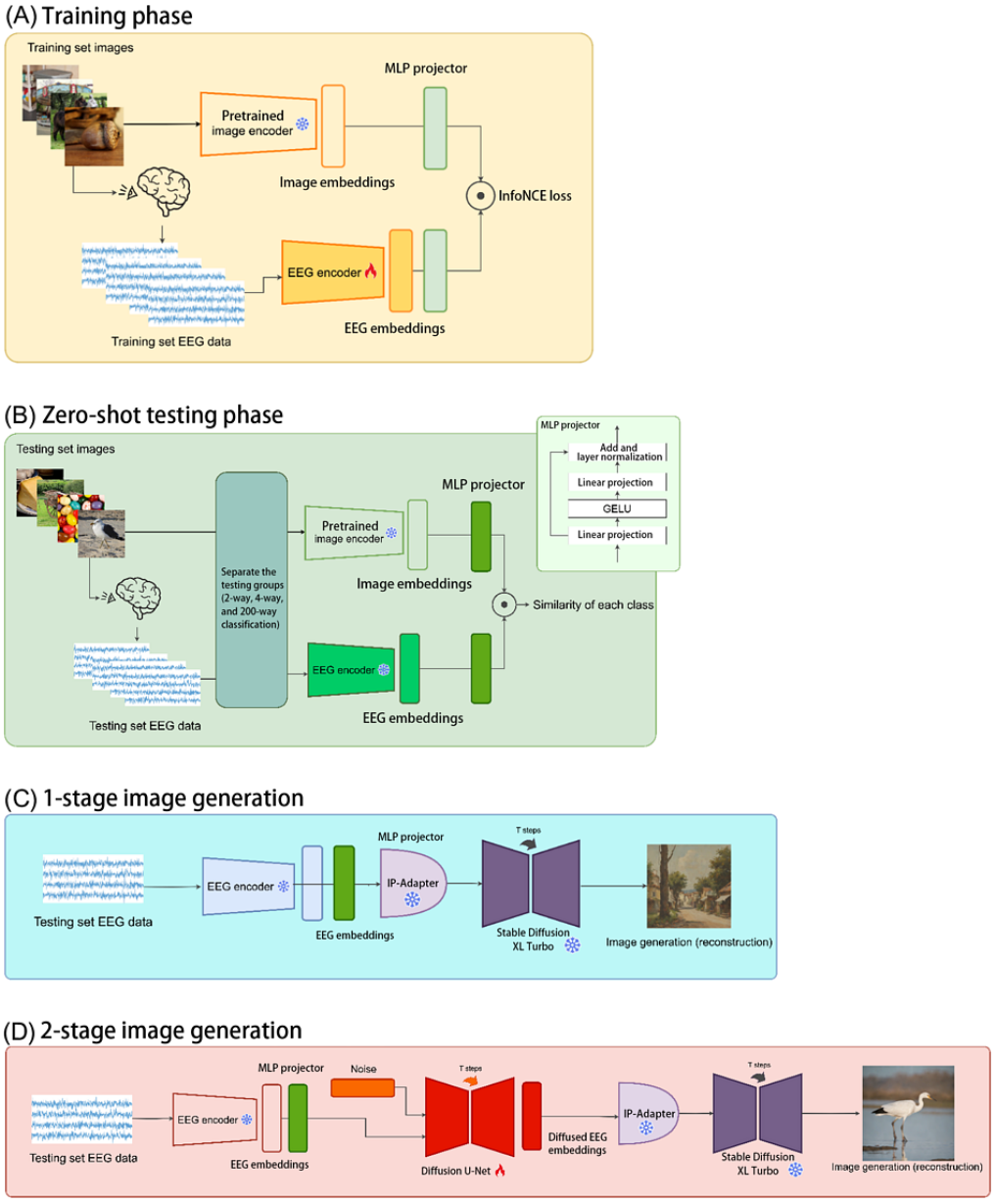
and phenomena that shed light on the EEG-to-image generation process.

Methods

Datasets and Preprocessing

The ThingsEEG dataset comprised a large set of EEG recordings, which were obtained using a rapid serial visual presentation paradigm [40]. The rapid serial visual presentation is a commonly used experimental protocol where participants are shown a series of visual stimuli in quick succession, typically at rates of ≥10 Hz, to evoke reliable neural responses. Responses were collected from 10 participants, each of whom viewed a total of 16,740 natural images sourced from the THINGS database [41]. The dataset includes 1654 training categories, with each category containing 10 images, as well as 200 test categories, each featuring a single image. The EEG data were recorded using 64-channel Easycap equipment, and preprocessing involved segmenting the data into trials that spanned 0 to 1000 milliseconds after the stimulus was shown, with baseline correction applied based on the prestimulus period. EEG responses for each image were averaged over multiple repetitions. The workflow and models used in the EEG-based image generation system are shown in Figure 1.

Figure 1. The entire workflow of the electroencephalography (EEG)–based image generation model, including (A) training phase, (B) zero-shot testing phase, (C) 1-stage image generation, and (D) 2-stage image generation. GELU: Gaussian error linear unit; InfoNCE: information noise-contrastive estimation; MLP: multilayer perceptron; SDXL: Stable Diffusion XL.



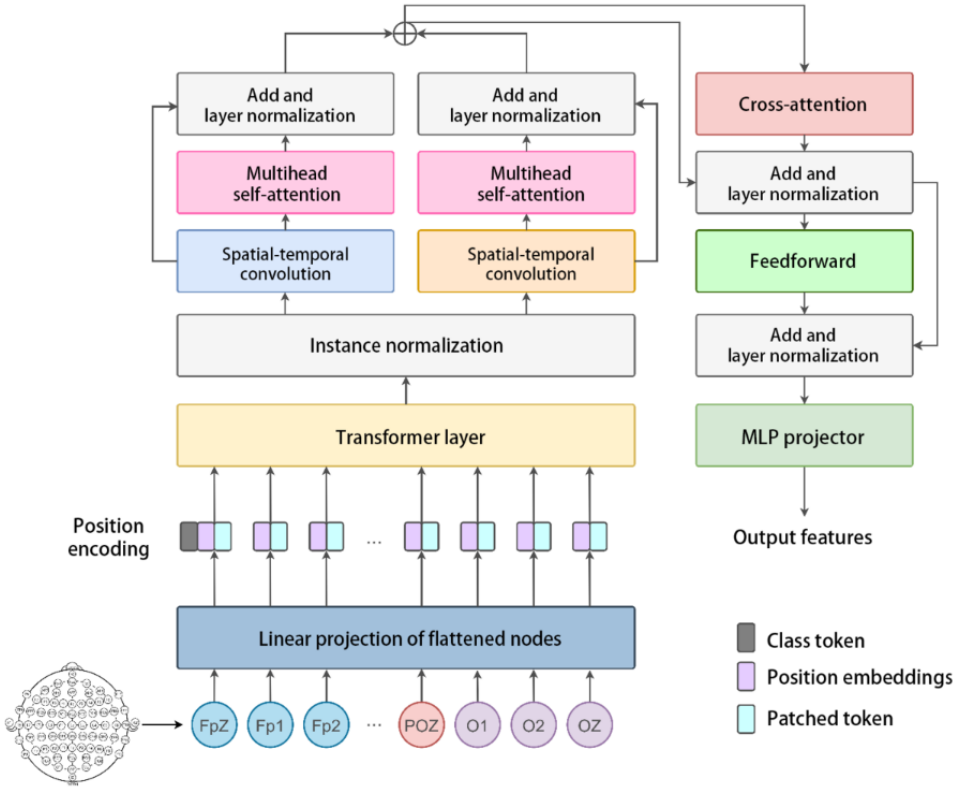
NERV EEG Encoder

As the foundational component of the NECOMIMI framework, we first describe our novel EEG encoder, NERV, which served as the foundation for EEG signal representation and embedding. As illustrated in Figure 2, NERV was designed to address the unique spatiotemporal complexity of EEG signals, which differ from natural images or text due to their nonstationary nature, simultaneous temporal dynamics, and spatial dependencies across multiple electrodes. To effectively capture these

XSL•FO
RenderX

characteristics, NERV adopted a hierarchical architecture that combined convolutional and attention-based modules. The input EEG data, flattened and linearly projected, first underwent positional encoding to preserve temporal order. It then flowed through 2 complementary convolutional branches: a *spatial-temporal convolution*, which extracted spatial features followed by temporal ones, and a *temporal-spatial convolution*, which performed the reverse. These dual-pathway 2D convolutions operated across the EEG channel dimension, allowing the model to learn localized patterns in both directions. This design enabled NERV to generate robust and semantically meaningful embeddings from EEG signals, laying the groundwork for high-quality image generation in the NECOMIMI pipeline.

Figure 2. The overall structure of the Neural Encoding Representation Vectorizer electroencephalography encoder model. Fp1: frontal pole 1; Fp2: frontal pole 2; FpZ: frontal pole Z; MLP: multilayer perceptron; O1: occipital 1; O2: occipital 2; OZ: occipital midline; POZ: parieto-occipital midline.



The output of these branches was passed through multihead self-attention layers, allowing the model to capture long-range dependencies across time and channel dimensions. Unlike conventional EEG encoders that treat all channels uniformly, NERV incorporated an EEG attention module at an early stage. This module used a transformer encoder across the channel axis to explicitly model interchannel relationships and assign adaptive importance weights to different brain regions. Such a design leveraged the structured spatial geometry of EEG electrode placement, enabling the model to generalize more effectively across participants. To further enhance discriminability, particularly in zero-shot settings, a cross-attention block was incorporated, enabling the class token to selectively attend to latent spatial-temporal features. The resulting feature sequence was flattened and passed through a fully connected layer, yielding a 1440D intermediate representation. Following this, a participant-specific linear transformation adjusted the temporal resolution to accommodate interindividual variability in EEG patterns. Finally, a residual projection head, composed of a Gaussian error linear unit activation and dropout, mapped the features into a 1024D latent space, providing a compact yet expressive representation for the downstream generative module.

The model was trained using a contrastive learning objective, aligning EEG embeddings with paired image embeddings from a pretrained CLIP model. This approach enabled robust multimodal representation learning, bridging neural signals and visual semantics. By combining structured convolution, channel-aware attention, and semantic alignment mechanisms, the NERV encoder effectively captured both the signal dynamics and spatial layout of EEG signals, significantly outperforming previous models in low-data and cross-participant scenarios. The EEG attention module explicitly modeled interchannel relationships and assigned adaptive importance to each channel based on its functional relevance, ensuring that different EEG channels are weighted according to their significance in the image generation process. By adopting this approach, NERV can effectively capture the unique spatial dependencies inherent in EEG data, leading to more accurate and contextually relevant representations for downstream image generation tasks.

Framework Architecture and Experiment Setting Details

To ensure a fair comparison of various EEG encoders and minimize external factors, all experiments in this study were rerun using a unified CLIP–vision transformer (ViT) environment, leveraging the available open-source code [30-32].

XSL•FO
RenderX

CLIP is a deep learning model by OpenAI that uses contrastive learning to map both image and text into a shared embedding space, enabling the model to understand their relationship. It trains separate image and text encoders and supports zero-shot tasks such as image retrieval based on text. CLIP-ViT is a variant that uses ViT as the image encoder, which improves performance by processing images as patches. Given that contrastive learning is sensitive to batch size, a batch size of 1024 was used for all experiments. The final results were averaged across the best outcomes from 5 random-seed training sessions, each running for 200 epochs. We used the AdamW optimizer (The PyTorch Foundation) with a learning rate of 0.0002, and the β1 and β2 parameters were set to 0.5 and 0.999, respectively. The contrastive learning parameter τ was initialized with log(1/0.07). In terms of model architecture, the NERV model performed optimally with 5 multiheads, whereas the transformer layer used 1 multihead and the cross-attention layer used 8 multiheads. The time step for the diffusion model was set to 50. All experiments, including EEG encoder training and prior diffusion model processing, were conducted on a machine equipped with an A100 graphics processing unit.

Using the ThingsEEG dataset, we developed an advanced EEG-to-image generation model that leverages deep learning techniques and diffusion models. Initially, the framework included a 1-stage image generation phase. However, we observed that its performance was suboptimal. As a result, we adapted the model to a 2-stage process. The overall structure of the model was composed of 4 phases: training, zero-shot testing, 1-stage image generation, and 2-stage image generation (Figure 1). Each phase played a crucial role in transforming raw EEG data into meaningful visual outputs.

Diffusion Model Implementation Details

To enhance the reproducibility and transparency of our EEG-to-image generation pipeline, we further describe the technical configuration of the diffusion model used in both the 1-stage and 2-stage NECOMIMI frameworks. We adopted the Stable Diffusion XL (SDXL) Turbo (Stability AI) [42,43] as the backbone generative model. SDXL Turbo is an optimized variant of the original Stable Diffusion architecture designed to produce high-quality images using significantly fewer sampling steps. This model is based on a U-Net structure with cross-attention mechanisms and operates in the latent space of a VAE, allowing for efficient and photorealistic image generation. For the denoising process, we applied a cosine noise schedule [14]. This schedule gradually adjusted the amount of noise during reverse diffusion, which helped improve image diversity and ensured smoother training convergence by avoiding sudden changes in noise levels across time steps. During inference, we used 50 sampling steps, which provided a good balance between generation speed and visual quality. This step count was well suited to SDXL Turbo's low-latency design and has been empirically verified to maintain satisfactory image fidelity.

To condition the image generation on EEG signals, we used the IP-Adapter module [44]. Although originally developed for visual feature prompts, we adapted it to accept EEG embeddings. These embeddings were projected into the appropriate feature space and injected into the cross-attention layers of the U-Net at both low and middle resolutions, enabling the EEG signals to influence multiple stages of the generation process. Furthermore, we applied a classifier-free guidance strategy during image generation. This involved generating both conditional and unconditional outputs and blending them in a controlled manner to improve the relevance of the generated images to the input EEG signal while still preserving sample diversity. In our implementation, the guidance strength was set to a moderate value to maintain a balance between controllability and visual variation. In the 2-stage generation framework, the EEG embeddings were first processed by a lightweight diffusion prior network. This network, implemented as a 6-layer U-Net, was trained to transform noisy EEG embeddings into clean, CLIP-like image embeddings [30-32]. A dropout rate of 0.1 was used during training to encourage robustness. The resulting embeddings were then passed through the IP-Adapter into the SDXL Turbo model for final image synthesis. By integrating these components, the NECOMIMI framework effectively bridges the gap between EEG signals and generative models, enabling high-quality image synthesis guided purely by brain activity.

Training Phase

In the initial training phase, both visual image $\in$ $h \times w \times ch$ and EEG data $\in$ $e \times d$ were processed in parallel to establish a shared embedding space. Here, denotes the image height, *w* is the image width, and *ch* refers to the number of channels (eg, RGB channels). Similarly, *e* represents the number of electrodes (channels), and *d* corresponds to the number of data points (time samples) in the EEG signal. Training set images were initially passed through a pretrained image encoder, which transforms the images into latent representations, referred to as image embeddings *I*. In this work, we used a pretrained ViT [45] from the CLIP model [28] as the image encoder, producing embeddings of size 1×1024 for each image. Simultaneously, the corresponding EEG signals are processed by a custom EEG encoder, generating EEG embeddings *E*. For the EEG encoder, this work extended several existing approaches, including NICE, MUSE, Nervformer, and Adaptive Thinking Mapper, to enable EEG-to-image capabilities [30-32]. Moreover, we introduced a novel EEG encoder, NERV, specifically designed for noisy, multichannel time-series data such as EEG that leveraged a multi-attention mechanism. The image and EEG embeddings were projected into a shared latent space using a multilayer perceptron projector, where they were optimized using the information noise-contrastive estimation (InfoNCE) loss function. This contrastive learning loss function ensured the alignment of corresponding image and EEG embeddings in the latent space, thereby improving the model's capacity to associate neural patterns with visual stimuli. The InfoNCE loss, commonly used in contrastive learning, is defined as follows [28,46,47]: . (1), where $S_{E,I}$ represents the similarity score between the EEG embeddings *E* and the paired image embeddings *I* and τ is the learned temperature parameter.

XSL•FO
RenderX

Zero-Shot Testing Phase

Once trained, the model proceeded to the zero-shot testing phase, which evaluated its ability to generalize to unseen data. During this phase, the EEG signals and images from the test set were encoded using the pretrained encoders, and their respective embeddings were projected through the multilayer perceptron projector. The test data were divided into several groups, including 2-way, 4-way, 10-way, 50-way, and 100-way classification, facilitating a structured comparison between the EEG and image embeddings. The final similarity scores between the embeddings determine the model's classification accuracy, enabling an evaluation of how well the model generalizes to new EEG data without requiring additional training.

One-Stage Image Generation

In the 1-stage image generation process, EEG embeddings from the test set were directly used as inputs to reconstruct images. By incorporating the IP-Adapter [44], originally designed to use images as prompts, the compact design enhanced the flexibility of image prompts within pretrained text-to-image models. In this study, we adapted the IP-Adapter to transform EEG embeddings into *feature prompts* for the image generation process. These vectors were injected into the cross-attention layers of the U-Net at both low- and midresolution blocks, enabling the EEG embedding to modulate generation across multiple stages. These conditioned embeddings were then processed by the SDXL Turbo model [42,43]. This approach offered a streamlined method for EEG-based image generation, relying on a single transformation stage to produce meaningful visual outputs from neural signals. The commencement of the EEG-conditioned diffusion phase was crucial for generating images from EEG data. During this phase, a classifier-free guidance method was used, which paired CLIP embeddings and EEG embeddings (I and E). Specifically, we generated both conditional and unconditional outputs and combined them using the following formula: . (2), where $w \geq 0$ is the guidance scale (set to 3.5 in our experiments). This technique improves controllability while preserving diversity.

By applying advanced generative techniques, the diffusion process was tailored to use the EEG embedding E to model the distribution of the CLIP embeddings $p(I|E)$. The CLIP embedding I, generated in this stage, served as the foundation for the subsequent image generation phase. The architecture integrates a simplified U-Net model, denoted as $\in_{prior}(I^t, t, E)$, where I^t represents the noisy CLIP embedding at a specific diffusion step t. The classifier-free guidance method refined the diffusion model by conditioning it on a specific EEG input E. This approach synchronized the outputs of both the conditional and unconditional models. The final model equation was expressed as follows: . (3).

Where $w \geq 0$ was used to control the guidance scale, this technique allowed for training both the conditional and unconditional models within the same network, periodically replacing the EEG embedding E with a null value to introduce variation in the training process (approximately 10% of the data points). The primary goal was to improve the quality of the generated images while maintaining their diversity. However, we were surprised to find that when EEG embeddings were directly used as prompts for the diffusion model, the generated images predominantly consisted of landscapes regardless of the intended category. As a result, we explored a 2-stage approach for image generation.

Two-Stage Image Generation

The prior diffusion stage played a crucial role in generating an intermediate representation [48], such as a CLIP image embedding, from a text caption [49]. This representation was then used by the diffusion decoder to produce the final image. This 2-stage process not only enhanced image diversity but also maintained photorealism, allowing for efficient and controlled image generation [50]. The 2-stage image generation process introduced a more sophisticated and refined method for synthesizing images from EEG data. In this approach, the EEG embeddings were initially processed by a diffusion prior network consisting of a 6-layer U-Net trained using cosine schedule and dropout (P=.10). After passing through the U-Net, the modified EEG embeddings were input into the SDXL Turbo model assisted by the IP-Adapter. This 2-step transformation ensured a more nuanced generation process, potentially leading to higher-quality images through deeper layers of refinement. The reverse diffusion process used a cosine noise schedule [42], which smoothly adjusts the variance over diffusion steps to stabilize training. This scheduling strategy improved sample diversity and convergence by avoiding abrupt noise scale changes across time steps. The time step t=50 referred to the number of reverse sampling steps used during inference. We found that 50 steps achieved a good trade-off between speed and quality, especially under the SDXL Turbo architecture, which was optimized for low-step generation.

The first step of stage 1 involved training the prior diffusion model. The primary goal of this training phase was to enable the model to recover the original embedding from noisy embeddings. The specific steps are detailed in Multimedia Appendix 1. Briefly, in the first phase of training, the model learned to reconstruct the original EEG embedding from a noisy version. Some EEG embeddings were randomly replaced with null values to introduce variability, and random noise was added and perturbed over multiple time steps. The model was trained to predict and remove this noise, effectively recovering the original EEG embedding. Once trained, the model entered the generation phase. It started with random noise, progressively refining it at each time step by predicting and removing noise. Both conditional and unconditional noise predictions were made and combined using a guidance mechanism to generate the final clean EEG embedding. In the second phase, the clean EEG embedding was passed through a specialized adapter, preparing it as a prompt for the image generation model. The final EEG embedding was then input into the SDXL Turbo model, which generated the final image based on the EEG data.

Classification Task and Evaluation Strategy

We designed a participant-dependent zero-shot classification task to assess the semantic generalization ability of our EEG-to-image model. In this setting, the model was evaluated separately for each participant—a subset of image categories

XSL•FO
RenderX

was used for training, whereas a disjoint set was held out for testing, ensuring a strict zero-shot scenario where the model must generalize to entirely unseen classes. Notably, no participant-specific adaptation methods (eg, participant embeddings or normalization layers) were used, and both training and testing were conducted on a within-subject basis. To align EEG and image features in a shared embedding space, we adopted the InfoNCE loss, a contrastive objective that encourages the model to pull matching EEG-image pairs closer while pushing apart nonmatching pairs within the same batch. This facilitates learning fine-grained semantic associations between brain activity and visual representations. We evaluated the model's retrieval performance under zero-shot conditions using an *n*-way retrieval framework, where each test EEG sample was matched against *n* candidate image embeddings, including the correct one and $n - 1$ distractors sampled from unseen categories. A prediction was considered correct if the ground-truth image ranked highest in similarity. Retrieval difficulty was varied across 3 levels: 2-way task (1 distractor), 4-way task (3 distractors), and 200-way task (199 distractors from the full test set). This evaluation protocol provided a realistic and stringent benchmark for assessing semantic generalization and robust retrieval performance in EEG-to-image understanding.

CAT Score

Unlike traditional image-to-image or text-to-image models driven by image representations, EEG-to-image models face unique challenges. In the current NECOMIMI architecture, the model can only capture broad semantic information from EEG signals rather than fine-grained details. For example, suppose the EEG data are recorded while a participant is viewing an aircraft carrier. When different EEG encoders are used in the NECOMIMI framework, they may lead to different outputs. Specifically, one EEG encoder could generate an image of a jet, whereas another EEG encoder might produce an image of a sheep. Therefore, to objectively assess performance, it was necessary to establish a standard that would score the encoder generating the jet image higher than the one generating the sheep image in such cases. Existing evaluation metrics were not suitable for this purpose. Traditional metrics such as the structural similarity index [51] measure structural similarity between the ground truth and the generated image, whereas the inception score [52] and Fréchet inception distance (FID) [53] focus on the accuracy of image categories and their distribution. However, EEG captures more abstract semantic information, and there was no guarantee that the participants' thoughts during EEG recording would perfectly align with the ground-truth image. This made traditional evaluation methods unfair for EEG-to-image tasks. To address this issue, we proposed the CAT score, a new metric specifically designed for EEG-to-image evaluation (Multimedia Appendix 2). In the ThingsEEG test dataset, which contained 200 categories with 1 image per category, each image was manually labeled using 2 tags for broad categories, 1 for a specific category, 1 for background content, and 1 for object attribute, resulting in a total of 5 tags per image. The tags were extracted using ChatGPT-4o (OpenAI) [53]. The entire test dataset thus consisted of 200 images × 5 tags, totaling 1000 points. Using manual annotation, we were able to determine whether the categories of generated images matched these labels, providing a fair assessment for EEG-to-image models.

While FID remains a widely used metric for evaluating image fidelity by comparing feature distributions of generated and real images, it does not consider semantic alignment between the source EEG signal and the generated output [53]. In contrast, the CAT score directly evaluates whether the generated image aligns with the cognitive concept inferred from EEG signals. Therefore, the CAT score and FID served as complementary evaluation tools in our study. FID captures the visual quality, whereas the CAT score emphasizes semantic correctness, which is particularly crucial for EEG-driven generation where pixel-level supervision is unavailable. Further details on the ThingsEEG categories and scoring scheme are provided in Multimedia Appendix 2.

Ethical Considerations

This study used publicly available datasets, and no personal or sensitive information was collected directly. All data were deidentified before analysis. As the study involved only publicly available data and did not involve the collection of personal data or clinical trials, institutional review board approval was not required per the Chang Gung University's Academic Ethics Series [54].

Results

Classification Results

Table 1 presents the classification accuracy results for the 2-way and 4-way zero-shot tasks across 10 participants. Our proposed model, NERV, consistently outperformed other methods, particularly excelling in the 2-way classification task, where it maintained the highest accuracy across most participants. Specifically, NERV achieved an average accuracy of 94.8% (SD 1.7%) in the 2-way task and 86.8% (SD 3.4%) in the 4-way task, surpassing competing models such as NICE, MUSE, and Adaptive Thinking Mapper ShallowNet (ATM-S). While NICE and MUSE demonstrated strong performance in certain participants, they fell short of NERV's overall performance. NICE achieved an average accuracy of 91.3% (SD 3.1%) in the 2-way task and 81.3% (SD 5.9%) in the 4-way task, whereas MUSE achieved averages of 92.2% (SD 2.3%) and 82.8% (SD 5.0%), respectively. ATM-S, while comparable to NICE and MUSE in some participants, showed weaker results on average, with an accuracy of 86.5% (SD 4.9%) in the 4-way task. In the more challenging 200-way zero-shot classification task (Table 2), NERV also outperformed all other methods, particularly in terms of top-1 accuracy. Although ATM-S and NERV performed similarly overall, NERV demonstrated superior performance in most participants. NERV achieved an average top-1 accuracy of 27.9% (SD 5.8%) and an average top-5 accuracy of 54.7% (SD 6.5%), leading all other models. In contrast, Nervformer exhibited a significantly weaker performance, particularly in the top-1 accuracy, with averages of 19.8% (SD 4.9%) and 44.3% (SD 8.7%) for top-1 and top-5 accuracy, respectively. The results showed that NERV consistently outperformed its competitors across all tasks, demonstrating the strongest zero-shot classification performance,

XSL•FO
RenderX

particularly in distinguishing between a large number of categories.

Table 1. Overall accuracy of 2-way and 4-way zero-shot classification using Contrastive Language-Image Pretraining–vision transformer as the image encoder. The average accuracy was reported along with the SD across 10 participants to reflect the statistical robustness of each method.

Method	Accuracy (%)																				Accuracy (%), mean (SD)	
	Participant 1		Participant 2		Participant 3		Participant 4		Participant 5		Participant 6		Participant 7		Participant 8		Participant 9		Participant 10			
	2-way task	4-way task	2-way task	4-way task	2-way task	4-way task	2-way task	4-way task	2-way task	4-way task	2-way task	4-way task	2-way task	4-way task	2-way task	4-way task	2-way task	4-way task	2-way task	4-way task	2-way task	4-way task
Nervformer	89.9	76.9	91.3	80.7	91.6	80.8	94.3	85.9	86.3	70.4	91.1	82.5	92.5	81.6	96.2	88.3	92	83.7	92.4	83.1	91.8 (2.6)	81.4 (4.9)
NICE[a]	91.7	80.4	89.9	77.4	93.5	83.7	94	84.9	85.9	70.3	89.1	81.7	91.2	87.1	95.8	89.2	87.9	76.5	93.8	87.7	91.3 (3.1)	81.3 (5.9)
MUSE[b]	90.1	78.4	90.3	76.8	93.4	85.6	93.6	87.5	88.3	74.2	93.1	85.3	93.1	85.3	95.4	87.7	90.5	81.8	94.4	88.1	92.2 (2.3)	82.8 (5.0)
ATM-S[c]	94.8	84.9	93.5	86.3	95.3	89	95.9	87.3	90.8	78.5	94.1	85.2	94.2	97.1	96.6	92.9	94.1	86.8	94.7	87	94.4 (1.6)	86.5 (4.9)
NERV[d] (ours)	95.3	85.7	96	88.8	95.9	91.2	95.8	87.4	90.8	80.4	93.6	85.4	94.7	86.2	96.8	92.3	94.4	84.2	94.8	87.6	*94.8 (1.7)*	*86.8 (3.4)*

[a]NICE: Neural Image Conditioning for Electroencephalography.

[b]MUSE: Multimodal Unsupervised Sensing Embeddings.

[c]ATM-S: Adaptive Thinking Mapper ShallowNet.

[d]NERV: Neural Encoding Representation Vectorizer.

[e]The values in italics represent the best results (participant dependent—training and testing on 1 participant).

Table 2. Overall accuracy of 200-way zero-shot classification using Contrastive Language-Image Pretraining–vision transformer as image encoder—top 1 and top 5. The SD provided a measure of variability and generalization across participants.

Method	Accuracy (%)																				Accuracy (%), mean (SD)	
	Participant 1		Participant 2		Participant 3		Participant 4		Participant 5		Participant 6		Participant 7		Participant 8		Participant 9		Participant 10			
	Top 1	Top 5	Top 1	Top 5	Top 1	Top 5	Top 1	Top 5	Top 1	Top 5	Top 1	Top 5	Top 1	Top 5	Top 1	Top 5	Top 1	Top 5	Top 1	Top 5	Top 1	Top 5
Nerv-former	15	36.7	15.6	40	19.7	44.9	23.3	54.4	13	29.1	18.9	42.2	19.5	42	30.3	60	20.1	46.3	22.9	47.1	19.8 (4.9)	44.3 (8.7)
NICE[a]	19.3	44.8	15.2	38.2	23.9	51.4	24.1	51.6	11	30.7	18.5	43.8	21	47.9	32.5	63.5	18.2	42.4	27.4	57.1	21.1 (6.2)	47.1 (9.4)
MUSE[b]	19.8	41.1	15.3	34.2	24.7	52.6	24.7	52.6	12.1	33.7	22.1	51.9	21	48.6	33.2	59.9	19.1	43	25	55.2	21.7 (5.8)	47.3 (8.9)
ATM-S[c]	25.8	54.1	24.6	52.6	28.4	62.9	25.9	57.8	16.2	41.9	21.2	53	25.9	57.2	37.9	71.1	26	53.9	30	60.9	26.2 (5.6)	*56.5 (7.7)* [d]
NERV[e] (ours)	25.4	51.2	24.1	51.1	28.6	53.9	30	58.4	19.3	43.9	24.9	52.3	26.1	51.6	40.8	67.4	27	55.2	32.3	61.6	*27.9 (5.8)*	54.7 (6.5)

[a]NICE: Neural Image Conditioning for Electroencephalography.

[b]MUSE: Multimodal Unsupervised Sensing Embeddings.

[c]ATM-S: Adaptive Thinking Mapper ShallowNet.

[d]The values in italics represent the best results (participant dependent—training and testing on 1 participant).

[e]NERV: Neural Encoding Representation Vectorizer.

XSL•FO
RenderX

Performance Comparison of Different Generative Models

Table 3 shows the results of our newly proposed CAT score method, which quantified and evaluated the quality of EEG-generated images based on their alignment with semantic concepts rather than pixel-level details. The specific CAT score labels are provided in Multimedia Appendix 2. Interestingly, although our NERV method achieved SOTA performance on the CAT score, no EEG encoder surpassed a score of 500 out of a possible 1000 points in this evaluation. This result underscored both the rigor of the CAT score and the inherent challenges associated with the pure EEG-to-image generation task.

Table 3. Overall Category-Based Assessment Table (CAT) score out of 1000 of the Neural-Cognitive Multimodal Electroencephalography (EEG)–Informed Image EEG-to-image generation using several EEG encoders. Average accuracy with SD across 10 participants was reported to indicate statistical reliability.

EEG encoder	CAT score (higher is better)										CAT score, mean (SD)
	Participant 1	Participant 2	Participant 3	Participant 4	Participant 5	Participant 6	Participant 7	Participant 8	Participant 9	Participant 10	
Nervformer	432	457	429	454	475	463	404	438	427	410	438.9 (23.0)
NICE[a]	426	456	445	447	411	454	438	443	426	429	437.5 (14.3)
MUSE[b]	438	456	434	416	426	463	443	437	410	468	439.1 (19.1)
ATM-S[c]	413	419	411	464	427	469	442	472	431	445	439.3 (22.9)
NERV[d] (ours)	445	436	432	456	438	466	410	437	433	444	439.7 (14.9)

[a]NICE: Neural Image Conditioning for EEG.

[b]MUSE: Multimodal Unsupervised Sensing Embeddings.

[c]ATM-S: Adaptive Thinking Mapper ShallowNet.

[d]NERV: Neural Encoding Representation Vectorizer.

The FID results for EEG-to-image generation using the NECOMIMI framework with several SOTA EEG encoders are shown in Table 4. This metric evaluated the similarity between generated images and real ones based on deep feature distributions, with lower scores indicating better visual fidelity. To assess the robustness and consistency of each method, we reported the average FID alongside its SD across 10 participants. As expected, the “Pure Test Image” baseline, which did not involve EEG input, achieved an ideal FID of 106.1. Among EEG-based approaches, our proposed NERV (2-stage) model outperformed all competitors, with the lowest mean FID being 183.8 (SD 13.3), significantly surpassing other 2-stage pipelines such as NICE (mean 218.7, SD 7.5) and ATM-S (mean 197.1, SD 18.9). This consistent superiority suggested that NERV may be more effective in learning semantically aligned and visually coherent representations from EEG signals. Notably, even the best EEG-based models exhibited a noticeable gap from the ideal FID score, highlighting the intrinsic difficulty of reconstructing high-fidelity images solely from brain signals. These findings collectively validated the effectiveness of our NERV architecture in capturing and translating complex neural patterns into meaningful visual outputs while also revealing the need for continued improvements in EEG-based generative modeling.

XSL•FO
RenderX

Table 4. Overall Fréchet inception distance (FID) of the Neural-Cognitive Multimodal Electroencephalography (EEG)–Informed Image EEG-to-image generation using several EEG encoders. The average accuracy alongside its SD calculated across 10 participants was reported to demonstrate the consistency of each method.

EEG encoder and embedding type	FID (lower is better)										FID, mean (SD)
	Participant 1	Participant 2	Participant 3	Participant 4	Participant 5	Participant 6	Participant 7	Participant 8	Participant 9	Participant 10	
Pure test image	106.1	106.1	106.1	106.1	106.1	106.1	106.1	106.1	106.1	106.1	106.1 (0.0)
Nervformer											
1 stage	240.6	241.7	259.9	247.4	251.5	241.2	241.3	247.1	250.6	244.8	246.6 (6.1)
2 stages	198.3	201.4	193.9	192.8	206.4	202.2	198.5	202.2	191.9	210.8	199.8 (6.0)
NICE[a]											
1 stage	238.1	235.3	242.3	241.5	248.4	243.5	224.6	262.4	243.6	237.2	241.7 (9.7)
2 stages	204.3	193.2	264.9	198.9	199.1	272.0	235.3	209.7	213.1	196.1	218.7 (28.9)
MUSE[b]											
1 stage	231.9	246.6	247.0	257.7	236.2	243.1	243.3	250.8	243.0	245.0	244.5 (7.1)
2 stages	188.7	218.5	184.5	198.1	215.9	186.5	206.7	190.5	195.4	204.7	199.0 (12.1)
ATM-S[c]											
1 stage	244.5	239.7	238.6	242.1	248.9	250.1	232.2	250.3	239.0	235.0	242.0 (6.3)
2 stages	174.9	194.9	191.3	183.0	194.9	202.7	201.5	179.4	242.4	206.1	197.1 (18.9)
NERV[d] **(ours)**											
1 stage	217.9	211.4	225.6	221.1	229.1	218.8	215.5	227.6	204.6	217.2	*218.9 (7.5)* [e]
2 stages	169.5	189.4	167.2	175.8	191.6	198.3	187.2	176.2	208.1	174.4	*183.8 (13.3)*

[a]NICE: Neural Image Conditioning for EEG.

[b]MUSE: Multimodal Unsupervised Sensing Embeddings.

[c]ATM-S: Adaptive Thinking Mapper ShallowNet.

[d]NERV: Neural Encoding Representation Vectorizer.

[e]The values in italics represent the best results (participant dependent—training and testing on 1 participant).

Perturbation Study on Visual Cortex EEG Channels

We further conducted a perturbation study to investigate whether the model disproportionately relied on EEG signals from the visual cortex, particularly in generating scene-based images. In EEG analysis, the visual cortex corresponds to posterior regions of the scalp, particularly the occipital and parieto-occipital areas. Accordingly, we identified 6 key EEG channels: occipital 1, occipital 2, occipital midline, parieto-occipital 3, parieto-occipital 4, and parieto-occipital midline, which are commonly associated with visual perception and spatial integration. These channels are known to play critical roles in visual information processing. Occipital 1 and occipital 2 are located over the left and right occipital lobes; these channels are strongly associated with early-stage visual perception and processing. Occipital midline is situated along the midline of the occipital region; this channel captures central visual cortex activity and contributes to basic visual field representation. Parieto-occipital 3 and parieto-occipital 4 are positioned at the parieto-occipital junction; these channels reflect integrative processing of spatial and visual information such as visuospatial attention. Parieto-occipital midline is a midline parieto-occipital channel involved in high-level integration of visual input and attentional modulation. In this experiment, we replaced the

XSL•FO
RenderX

signals from these 6 channels with Gaussian noise while keeping the remaining EEG data unchanged. This allowed us to isolate the contribution of visual cortex–related signals to the image generation process. We then evaluated the quality of the generated images using the FID. Table 5 shows a significant increase in FID scores compared to the unperturbed condition, confirming that the model heavily depends on signals from the visual cortex to generate coherent and semantically meaningful images. These findings highlight the spatial sensitivity of our EEG-to-image model and further validate its biological plausibility in capturing relevant neural representations for visual imagination.

Table 5. Fréchet inception distance (FID) of the Neural-Cognitive Multimodal Electroencephalography (EEG)–Informed Image EEG-to-image generation using Neural Encoding Representation Vectorizer (NERV) EEG encoders with and without perturbation applied to visual cortex EEG channels. The average accuracy alongside its SD calculated over 10 participants was reported to demonstrate the consistency of each method.

EEG encoder and embedding type	FID (lower is better)										FID, mean SD)
	Participant 1	Participant 2	Participant 3	Participant 4	Participant 5	Participant 6	Participant 7	Participant 8	Participant 9	Participant 10	
Pure test image	106.1	106.1	106.1	106.1	106.1	106.1	106.1	106.1	106.1	106.1	106.1 (0.0)
NERV with perturbation											
1 stage	257.4	244.9	263.3	266.3	268.4	235.5	263.5	243.6	212.7	256.6	251.2 (17.4)
2 stages	205.3	240.5	262.5	267.5	224.4	223.3	247.7	225.7	263.5	245.2	240.6 (20.6)
NERV without perturbation											
1 stage	217.9	211.4	225.6	221.1	229.1	218.8	215.5	227.6	204.6	217.2	*218.9 (7.5)* [a]
2 stages	169.5	189.4	167.2	175.8	191.6	198.3	187.2	176.2	208.1	174.4	*183.8 (13.3)*

[a]The values in italics represent the best results (participant dependent—training and testing on 1 participant).

Findings on EEG-to-Image Generation

We observed several noteworthy findings in the pure EEG-to-image generation process (Figure 3). Figure 3A shows the original images shown to participants during EEG recording (ground truth). Figure 3B serves as an ideal baseline, demonstrating the model's capacity when guided by semantically rich CLIP embeddings. As shown in Figure 3C, the images generated by the diffusion model from embeddings derived from EEG signals predominantly consisted of landscapes, which deviated substantially from the original (ground truth). Due to the inherently noisy and low-dimensional nature of EEG signals, these results often default to generic or landscapelike images, where outputs deviate significantly from the intended object categories. This suggested that EEG signals may not directly correspond to specific objects in images. As a result, the model tended to generate "safe options," such as landscapes, which may have constituted a significant portion of the training data. This phenomenon, often referred to as "hallucination," occurs when the model generates content that does not accurately represent the intended visual stimuli. Consequently, in the 1-stage image generation framework, EEG embeddings often led to abstract or generalized images such as landscapes rather than specific objects. In contrast, the 2-stage NECOMIMI architecture (Figure 3D) was able to effectively extract semantic information from noisy EEG signals. This additional transformation improved semantic alignment and supported more accurate object-level synthesis (eg, a cat in column 3 or a caterpillar in column 4). Nonetheless, failure cases still occurred, underscoring the challenge of decoding high-level visual semantics from EEG data. Overall, this figure shows the enhanced specificity and visual relevance achieved by the 2-stage pipeline compared to the 1-stage approach. Moreover, Figure 4 shows the NECOMIMI model's ability to reconstruct images solely from EEG data without relying on "seen" images (ground truth) as embeddings during the generation process. The bottom row of images in Figure 4, generated exclusively from EEG input, highlights NECOMIMI's potential to approximate the content of the "seen" images in the top row even without direct visual references or embeddings. Figure 5 illustrates the performance of NECOMIMI's 1-stage and 2-stage EEG-to-image generation pipelines under perturbation of visual cortex channels. The reconstructed images show clear differences in visual fidelity and semantic alignment, emphasizing the model's spatial sensitivity and its dependence on visual cortex activity for generating coherent visual representations.

XSL•FO
RenderX

Figure 3. The progression of visual representations generated using different embedding techniques in a diffusion model—(A) the original images shown to participants during electroencephalography (EEG) recording (ground truth); (B) images generated using Contrastive Language-Image Pretraining (CLIP) embeddings of the ground-truth images serving as an upper-bound reference; (C) 1-stage Neural-Cognitive Multimodal EEG-Informed Image (NECOMIMI) results using EEG embeddings directly as prompts via the IP-Adapter; and (D) 2-stage NECOMIMI results, where EEG embeddings are refined into CLIP-like embeddings through a diffusion prior, producing images more consistent with object categories in the ground truth (eg, a cat in column 3 or a caterpillar in column 4).

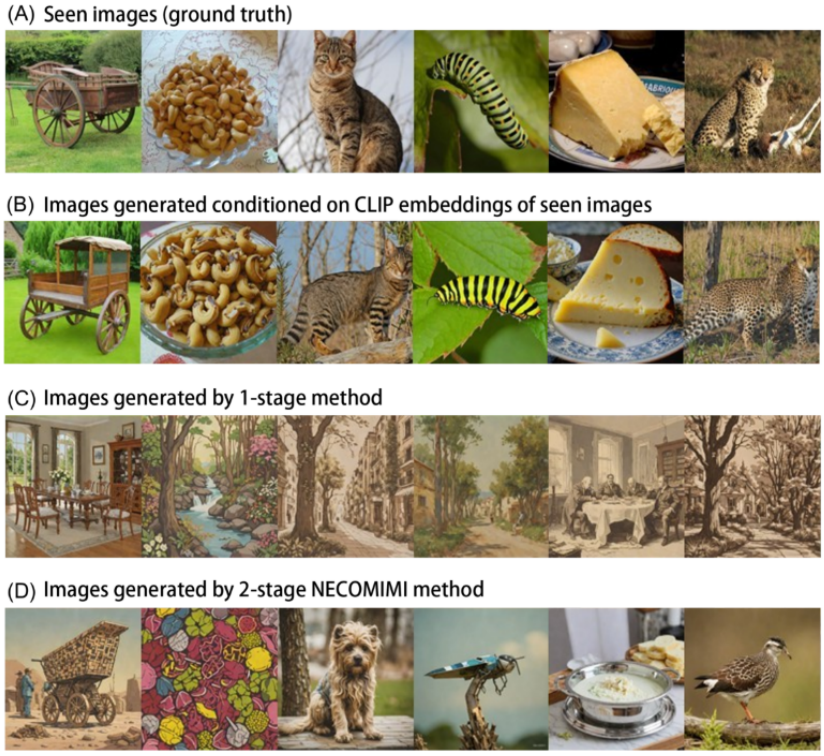
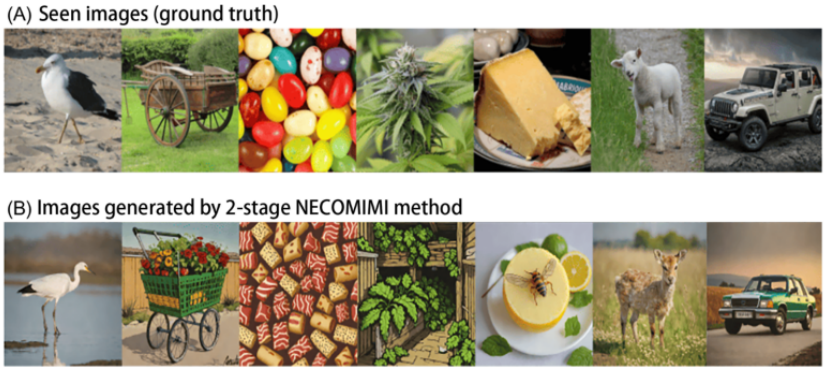
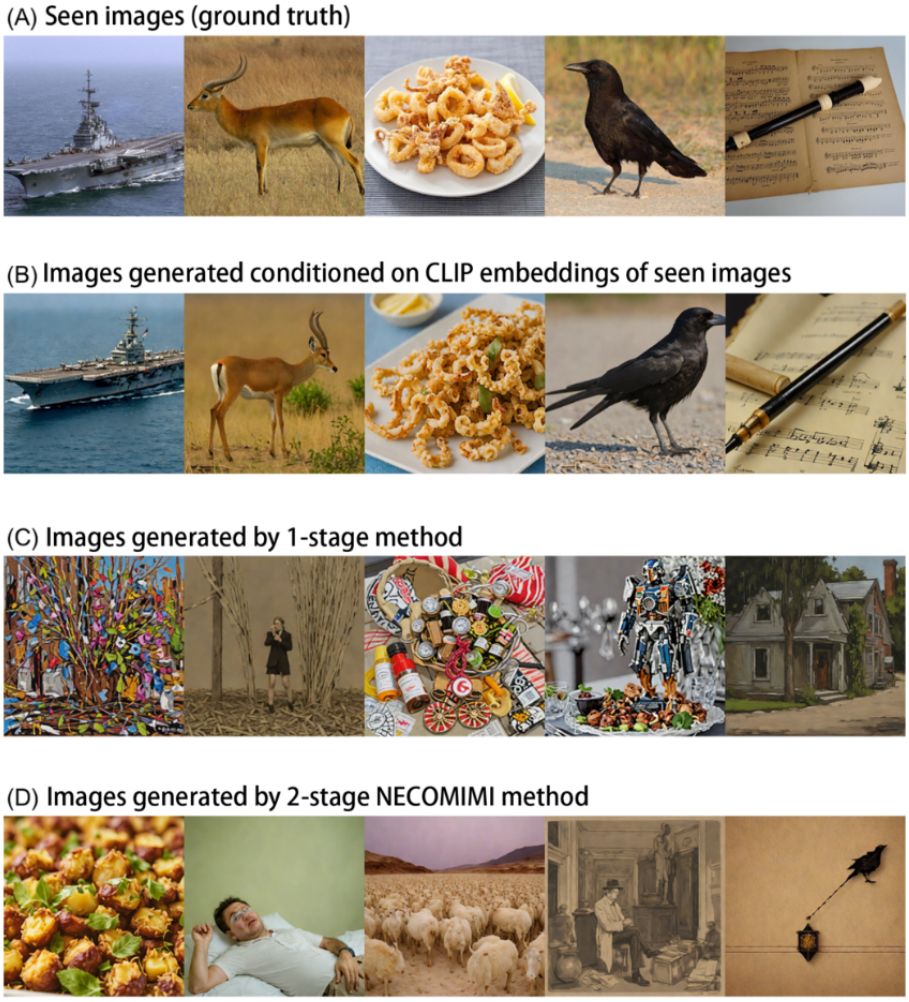


Figure 4. The capability of the Neural-Cognitive Multimodal Electroencephalography (EEG)–Informed Image (NECOMIMI) model to reconstruct images purely from EEG data without using the "Seen" images (ground truth) as embeddings during the generation process—(A) the original images shown to participants during EEG recording (ground truth) and (B) images generated using the 2-stage NECOMIMI method.



XSL•FO
RenderX

Figure 5. Neural-Cognitive Multimodal Electroencephalography (EEG)-Informed Image (NECOMIMI) EEG-to-image generation using Neural Encoding Representation Vectorizer EEG encoders with perturbation applied to visual cortex EEG channels—(A) the original images shown to participants during EEG recording (ground truth), (B) images generated conditioned on Contrastive Language-Image Pretraining (CLIP) embeddings of seen images, (C) images generated using the 1-stage NECOMIMI method, and (D) images generated using the 2-stage NECOMIMI method.



Discussion

Principal Findings

In this study, our NERV EEG encoder demonstrated SOTA performance in various zero-shot classification tasks, including 2-way, 4-way, and 200-way classification, solidifying its role as an effective feature extraction tool for EEG signals. However, when applied in a 1-stage image generation framework where EEG embeddings from the encoder were directly used to generate images, the results often turned out to be abstract or overly generalized (eg, landscapes) rather than depicting specific objects. This suggests that EEG signals may reflect more abstract, high-level concepts or emotional responses related to viewing the images rather than concrete objects or specific details. These abstract concepts are likely associated with broader aspects of the scene or the brain's generalized perception of the environment. Consequently, the model may be more inclined to generate generalized images such as landscapes than to focus on specific objects. This limitation underscores the inherent challenges of using EEG signals for precise image generation, primarily due to their noisy and low-resolution nature. Another contributing factor could be insufficient training of the model on EEG signals. The diffusion model might not yet be fully optimized to interpret and generate images from EEG data, particularly in cases in which the available data fail to adequately map EEG signals to specific visual representations. In addition, the significant gap between the visual modality and the neural modality (EEG) could further contribute to these challenges. Several factors may explain the noticeable discrepancies between the images generated from EEG signals and the ground truth, particularly in the failure to recognize specific objects.

Furthermore, this study highlights the critical role of visual cortex activity in EEG-based image generation. Our perturbation analysis, which involved replacing EEG signals from key occipital and parieto-occipital channels with Gaussian noise, led to a significant degradation in image quality, as reflected by increased FID scores. These results indicate that the NECOMIMI framework strongly depends on signals from visual cortical regions to generate semantically coherent images. This observation aligned with previous findings emphasizing the role of occipital areas in visual perception and EEG-based image reconstruction [55]. Importantly, this dependency also reveals potential limitations of such models in cases in which visual cortex function is impaired. Overall, these results further validate

XSL•FO
RenderX

the biological grounding of our approach, demonstrating its ability to capture neural patterns linked to visual imagination.

To address these challenges, we proposed the 2-stage NECOMIMI framework, which combines the NERV EEG encoder with a diffusion-based generative model. The 2-stage NECOMIMI architecture effectively extracts semantic information from the noisy EEG signals, showing its ability to capture and represent underlying concepts derived from brain wave activity. In this framework, we introduced the CAT score, a new evaluation metric specifically designed for EEG-to-image generation. Unlike traditional image evaluation metrics, such as those that assess image distribution, the CAT score focuses on measuring the alignment between the generated images and the underlying semantic intent captured by EEG signals. This evaluation method provides a more accurate reflection of how well the generated images correspond to the cognitive state represented by the EEG data.

Interestingly, our analysis revealed a complex relationship between the encoder's performance in classification tasks and the quality of the generated images. While a high-performing EEG encoder provides robust feature representations, the fidelity and specificity of the generated images were also influenced by other factors such as the generative model's capacity to interpret the EEG embeddings. These findings underscore the challenges of bridging EEG signal processing with image generation and suggest that successful EEG-to-image translation requires both strong feature extraction and sophisticated generative modeling. Our perturbation study further reinforced the biological plausibility of the NECOMIMI framework. The model's responsiveness to disruptions in specific EEG regions indicated its ability to extract spatially meaningful neural patterns, especially those critical for scene-level image synthesis. These results underscore the importance of spatial channel specificity and suggest that leveraging region-targeted EEG signals could further enhance generative performance in future applications.

While the primary focus of NECOMIMI was image generation, its potential extends far beyond this task, particularly in clinical applications for individuals with motor impairments. This section explores how NECOMIMI could be integrated into existing brain-computer interface (BCI) systems and enhanced assistive technologies. One of the applications of NECOMIMI is its ability to function as a visual feedback module in noninvasive BCI systems. Current BCIs for individuals with motor impairments primarily rely on classification-based intent detection methods, such as motor imagery or steady-state visual evoked potentials [56,57]. In contrast, NECOMIMI introduces a novel interaction modality, visual synthesis directly from thought. This approach could enable individuals with severe motor or speech impairments, such as those with locked-in syndrome, to communicate by visualizing concepts through their brain activity. Compared to traditional methods, this offers a more intuitive and flexible interface, allowing users to draw or visualize their thoughts, thereby enhancing their ability to express needs and emotions.

NECOMIMI could also play a critical role in neurofeedback therapies. In this context, real-time EEG-to-image generation may be used to reflect users' mental states, such as emotions or imagined visual scenes, back to them as visual feedback. This feedback loop could be particularly beneficial in therapies targeting attention regulation, anxiety management, or exposure-based interventions [58]. By providing visual stimuli derived from brain activity, NECOMIMI may help users better understand and regulate their mental states, potentially leading to an effective therapeutic outcome. Moreover, NECOMIMI holds strong potential in the field of virtual rehabilitation. The framework could be integrated into immersive virtual environments where patients engage in therapy tasks. Rather than relying on conventional controllers, users could interact with the virtual world by generating images that represent specific tasks or intentions. This offers a more natural and intuitive input method, especially for users with motor disabilities who may struggle with standard navigation tools. EEG-driven image generation could enhance patient engagement and contribute to more personalized and effective rehabilitation processes. As the technology continues to evolve, integration with existing BCI platforms and assistive systems may broaden NECOMIMI's impact, ultimately improving quality of life for individuals with motor and speech impairments. Although still in its early stages, EEG-driven image generation presents a promising direction for enriching user interaction in virtual rehabilitation. By enabling thought-driven image-based communication, NECOMIMI could lower the barrier to access for patients with limited motor control, paving the way for more inclusive and engaging therapy solutions.

Overall, our research presents a novel framework for EEG signal–to-image generation, which expands the application of existing BCI technologies and demonstrates its potential to improve quality of life for individuals with motor impairments. Traditional EEG-based control systems, particularly in clinical settings, often fail to meet expected outcomes. Although our study did not directly evaluate the effectiveness of EEG-controlled devices, it highlighted the promising clinical applications of EEG-to-image conversion. This technology could assist patients in controlling external devices (eg, prosthetics, wheelchairs, and smart environments) through EEG-generated images, thereby offering more opportunities for performing daily tasks and enhancing the accuracy and reliability of EEG-based control systems. Moreover, this approach allows for the transformation of brain sensory signals into realistic visual images, which could be presented in virtual environments, enabling patients to engage in visual perception and interaction based on EEG signals. This not only has the potential to enhance motivation and engagement during the treatment process but also offers possible benefits for rehabilitation therapy and anxiety management. Despite the significant clinical potential, the technology faces several challenges. Future research will need to address how to extract accurate and specific control commands from low-resolution, noise-prone EEG signals while ensuring their stability and reliability in real-world applications.

Understanding the CAT Score Ceiling

The moderate CAT score observed across all EEG encoders, with no model exceeding a score of 500 out of 1000, raised an important question about the underlying limitations of EEG-to-image generation. This result reflected both inherent

XSL•FO
RenderX

challenges of the EEG modality and technological constraints in current generative modeling approaches. Fundamentally, EEG signals are characterized by low spatial resolution, high temporal variability, and a strong susceptibility to noise, making it difficult to extract detailed, object-specific information from brain activity. Compared to neuroimaging modalities such as fMRI, EEG primarily captures global cortical dynamics and abstract cognitive states, which limits its capacity to convey fine-grained visual representations. From a technical perspective, existing diffusion models, even those enhanced with learned priors, are not fully adapted to decode such noisy and semantically diffuse embeddings. The reliance on vision language models such as CLIP may introduce additional complications as these models were trained on natural images and text, not on neural signals, leading to a mismatch in modality and representation [28]. The observed plateau around a CAT score of 500 was largely due to the structure of the scoring system, where each image was evaluated based on 5 semantic tags. Because the EEG embeddings often only weakly reflected specific visual features, the generated images typically aligned with only 1 to 3 of the intended tags. This partial semantic alignment resulted in midrange scores, often between 400 and 500. Furthermore, the generation outputs frequently exhibited generic or overly broad content such as landscapes or blurred objects, reflecting the limited conditioning power of EEG inputs. To overcome these limitations and improve performance beyond this ceiling, several strategies can be considered. Incorporating multimodal physiological signals such as eye tracking or electromyography may provide complementary information that helps disambiguate user intent and improve semantic grounding. In addition, training generative models specifically on EEG-to-image tasks rather than relying on pretrained vision language priors could reduce the modality gap and enhance fidelity. Building large-scale EEG-specific datasets and pretraining encoders on diverse cognitive states may also improve generalization. These directions highlight the importance of tailoring both model architecture and data curation to the unique characteristics of neural signals and point toward a future where EEG-based generative systems can achieve more accurate and reliable visual reconstructions.

Limitations

Despite the promising results of the NECOMIMI framework in EEG-to-image generation, several key limitations remain that must be addressed in future research. One of the primary challenges in EEG-to-image research is the scarcity of publicly available, large-scale EEG-image pair datasets. Unlike text-to-image tasks, which benefit from extensive datasets such as LAION-5B, EEG-to-image studies are constrained by the limited availability of paired EEG and image data. While the ThingsEEG dataset is one of the largest of its kind, it still lacks the diversity and scale necessary to train highly generalized EEG-to-image models. This limitation hinders benchmarking efforts and prevents the development of robust generative models capable of generalizing across different EEG recording conditions, participants, and experimental paradigms. In addition to the dataset scarcity, EEG recordings exhibit significant interparticipant variability, meaning that neural responses to identical visual stimuli can vary considerably between individuals. This variability complicates the generalization of models across different participants. Furthermore, EEG-based datasets are often collected under controlled experimental conditions, which limits their applicability to real-world scenarios. Consequently, without access to larger, more diverse datasets, EEG-to-image models remain constrained in their ability to generalize across a wide range of neural and visual domains.

Another challenge arises from the fact that, although our NERV EEG encoder demonstrated SOTA performance in zero-shot classification tasks, this high classification accuracy did not necessarily translate into higher-quality image generation. This suggests that feature representations optimized for classification tasks may not be equally effective for generative tasks. The gap between feature extraction and image generation remains an open challenge, indicating the need for future models to explore alternative training strategies that better align EEG embeddings with the generative process. Optimizing NECOMIMI for real-time image generation could unlock new possibilities for applications in BCIs and neurofeedback systems. Furthermore, expanding training datasets to include more diverse and larger-scale EEG recordings will be essential for improving model generalization. Incorporating additional data modalities such as eye tracking, electromyography, or functional near-infrared spectroscopy could also provide complementary information to enhance image generation. Finally, future work should aim to improve the model's resilience to signal noise and variability, particularly in the visual cortex. Multimodal integration and training protocols that encourage distributed cortical representation may reduce the model's dependency on any single brain region, ultimately enhancing stability, interpretability, and generalization across individuals and tasks.

Conclusions

The NECOMIMI framework expands previous work on EEG-image pair contrastive learning classification by enabling image generation, filling a gap in previous research and opening up new possibilities for EEG applications. We introduced the SOTA EEG encoder NERV, which achieved top performance in 2-way, 4-way, and 200-way zero-shot classification tasks, as well as in the CAT score evaluation, demonstrating its effectiveness in EEG-based generative tasks. A key finding was that the model often generated abstract images rather than specific objects. This suggests that EEG data, being noisy and low resolution, captured broad semantic concepts rather than detailed visuals. The gap between neural signals and visual stimuli remained a challenge for precise image generation. In addition, we proposed the CAT score, a new metric tailored for EEG-to-image generation, and established its benchmark on the ThingsEEG dataset. Surprisingly, we found that EEG encoder performance may not strongly correlate with the quality of the generated images, providing new insights into the limitations and challenges of this task. NECOMIMI demonstrates the potential of EEG-to-image generation while highlighting the complexities of translating neural signals into accurate visual representations. Furthermore, the perturbation experiment revealed that the NECOMIMI model strongly depends on EEG signals from the visual cortex, particularly the occipital and parieto-occipital regions. This reliance not only

XSL•FO
RenderX

supports the biological plausibility of our model's design but also emphasizes the critical role of spatial EEG features in accurate image reconstruction. These insights may guide future improvements in region-aware modeling strategies for EEG-based generative tasks. Future work should prioritize improving EEG representation learning, refining generative modeling techniques, and developing more robust evaluation frameworks to enhance the reliability and realism of EEG-generated images.

Acknowledgments

The authors gratefully acknowledge the National Science and Technology Council for their generous financial support of this research, provided under contract NSTC 113-2221-E-182-045. The authors would like to thank Aidan Hung-Wen Tsai for brainstorming this fascinating title with them, which originated from a conversation in Silicon Valley about NeuroSky's cat-ear electroencephalography product, Necomimi. They also appreciate Neuro Industry, Inc, for providing A100 computational resources on the Google Cloud Platform. The authors extend special thanks to Dr Guan-Ying Chen for proofreading and providing valuable feedback on revisions.

Conflicts of Interest

None declared.

Authors' Contributions

Conceptualization: C-SC
Methodology: C-SC and S-HC
Data analysis: C-SC, S-HC, and C-WL
Writing - original draft preparation: S-HC and C-SC
Writing - review and editing: S-HC and T-MP
Supervision: T-MP

Multimedia Appendix 1
The 2-stage image generation process.
[PDF File (Adobe PDF File), 143 KB - medinform_v13i1e72027_app1.pdf]

Multimedia Appendix 2
Details of the category-based assessment table score.
[PDF File (Adobe PDF File), 8046 KB - medinform_v13i1e72027_app2.pdf]

References

1. Brazier MA. The EEG in epilepsy. A historical note. Epilepsia 1960 Jun 05;1(1-5):328-336. [doi: 10.1111/j.1528-1157.1959.tb04270.x] [Medline: 13804067]
2. Millett D. Hans Berger: from psychic energy to the EEG. Perspect Biol Med 2001 Sep;44(4):522-542. [doi: 10.1353/pbm.2001.0070] [Medline: 11600799]
3. Reif PS, Strzelczyk A, Rosenow F. The history of invasive EEG evaluation in epilepsy patients. Seizure 2016 Oct;41:191-195 [FREE Full text] [doi: 10.1016/j.seizure.2016.04.006] [Medline: 27131772]
4. Li CT, Chen C, Cheng C, Chen C, Chen J, Chen M, et al. Prediction of antidepressant responses to non-invasive brain stimulation using frontal electroencephalogram signals: cross-dataset comparisons and validation. J Affect Disord 2023 Dec 15;343:86-95. [doi: 10.1016/j.jad.2023.08.059] [Medline: 37579885]
5. Hussain I, Hossain MA, Jany R, Bari MA, Uddin M, Kamal AR, et al. Quantitative evaluation of EEG-biomarkers for prediction of sleep stages. Sensors (Basel) 2022 Apr 17;22(8):3079 [FREE Full text] [doi: 10.3390/s22083079] [Medline: 35459064]
6. Thoma RJ, Hanlon FM, Moses SN, Edgar JC, Huang M, Weisend MP, et al. Lateralization of auditory sensory gating and neuropsychological dysfunction in schizophrenia. Am J Psychiatry 2003 Sep 01;160(9):1595-1605. [doi: 10.1176/appi.ajp.160.9.1595] [Medline: 12944333]
7. Perrottelli A, Giordano GM, Brando F, Giuliani L, Mucci A. EEG-based measures in at-risk mental state and early stages of schizophrenia: a systematic review. Front Psychiatry 2021 May 4;12:653642 [FREE Full text] [doi: 10.3389/fpsyt.2021.653642] [Medline: 34017273]
8. St Louis EK, Frey LC, Britton JW, Frey LC, Hopp JL, Korb P, et al. Electroencephalography (EEG): An Introductory Text and Atlas of Normal and Abnormal Findings in Adults, Children, and Infants. Chicago, IL: American Epilepsy Society; 2016.

XSL•FO
RenderX

9. Li R, Yang D, Fang F, Hong K, Reiss AL, Zhang Y. Concurrent fNIRS and EEG for brain function investigation: a systematic, methodology-focused review. Sensors (Basel) 2022 Aug 05;22(15):5865 [FREE Full text] [doi: 10.3390/s22155865] [Medline: 35957421]
10. Khalil YA, Ayaz A, Lorenz C, Weese J, Pluim J, Breeuwer M. Multi-modal brain tumor segmentation via conditional synthesis with Fourier domain adaptation. Comput Med Imaging Graph 2024 Mar;112:102332 [FREE Full text] [doi: 10.1016/j.compmedimag.2024.102332] [Medline: 38245925]
11. Spampinato C, Palazzo S, Kavasidis I, Giordano D, Souly N, Shah M. Deep learning human mind for automated visual classification. In: Proceedings of the 2017 IEEE Conference on Computer Vision and Pattern Recognition. 2017 Presented at: CVPR '17; July 21-26, 2017; Honolulu, HI p. 4503-4511 URL: https://ieeexplore.ieee.org/document/8099962 [doi: 10.1109/cvpr.2017.479]
12. Kavasidis I, Palazzo S, Spampinato C, Giordano D, Shah M. Brain2Image: converting brain signals into images. In: Proceedings of the 25th ACM international conference on Multimedia. 2017 Presented at: MM '17; October 23-27, 2017; Mountain View, CA p. 1809-1817 URL: https://dl.acm.org/doi/10.1145/3123266.3127907 [doi: 10.1145/3394171]
13. Goodfellow IJ, Pouget-Abadie J, Mirza M, Xu B, Warde-Farley D, Ozair S, et al. Generative adversarial networks. arXiv Preprint posted online June 10, 2014 [FREE Full text]
14. Ho J, Jain A, Abbeel P. Denoising diffusion probabilistic models. arXiv Preprint posted online on June 19, 2020 [FREE Full text]
15. Kumar P, Saini R, Roy PP, Sahu PK, Dogra DP. Envisioned speech recognition using EEG sensors. In: Jones M, editor. Personal and Ubiquitous Computing. Cham, Switzerland: Springer; 2018:185-199.
16. Singh P, Pandey P, Miyapuram K, Raman S. EEG2IMAGE: image reconstruction from EEG brain signals. arXiv Preprint posted online on February 20, 2023 [FREE Full text] [doi: 10.1109/icassp49357.2023.10096587]
17. Bai Y, Wang X, Cao YP, Ge Y, Yuan C, Shan Y. DreamDiffusion: generating high-quality images from brain EEG signals. arXiv Preprint posted online on June 29, 2023 [FREE Full text] [doi: 10.54254/2755-2721/47/20241135]
18. Palazzo S, Spampinato C, Kavasidis I, Giordano D, Shah M. Generative adversarial networks conditioned by brain signals. In: Proceedings of the 2017 IEEE International Conference on Computer Vision. 2017 Presented at: ICCV '17; October 22-29, 2017; Venice, Italy p. 3430-3438 URL: https://ieeexplore.ieee.org/document/8237631 [doi: 10.1109/iccv.2017.369]
19. Khare S, Choubey RN, Amar L, Udutalapalli V. NeuroVision: perceived image regeneration using cProGAN. Neural Comput Appl 2022 Jan 06;34(8):5979-5991. [doi: 10.1007/S00521-021-06774-1]
20. Nishimoto S, Vu A, Naselaris T, Benjamini Y, Yu B, Gallant J. Reconstructing visual experiences from brain activity evoked by natural movies. Curr Biol 2011 Oct 11;21(19):1641-1646 [FREE Full text] [doi: 10.1016/j.cub.2011.08.031] [Medline: 21945275]
21. Zhang CS, Zhang C, Zhang M, Kweon IS, Kim J. Text-to-image diffusion models in generative AI: a survey. arXiv Preprint posted online on March 14, 2023 [FREE Full text]
22. Kingma DP, Welling M. Auto-encoding variational bayes. arXiv Preprint posted online on December 20, 2013 [FREE Full text]
23. Kingma DP, Welling M. An introduction to variational autoencoders. arXiv Preprint posted online on June 6, 2019 [FREE Full text] [doi: 10.1561/9781680836233]
24. Hochreiter S, Schmidhuber J. Long short-term memory. Neural Comput 1997 Nov 15;9(8):1735-1780. [doi: 10.1162/neco.1997.9.8.1735] [Medline: 9377276]
25. Tirupattur P, Rawat YS, Spampinato C, Shah M. ThoughtViz: visualizing human thoughts using generative adversarial network. In: Proceedings of the 26th ACM international conference on Multimedia. 2018 Presented at: MM '18; October 22-26, 2018; Seoul, Republic of Korea p. 950-958 URL: https://dl.acm.org/doi/10.1145/3240508.3240641 [doi: 10.1145/3240508.3240641]
26. Jiao Z, You H, Yang F, Li X, Zhang H, Shen D. Decoding EEG by visual-guided deep neural networks. In: Proceedings of the 28th International Joint Conference on Artificial Intelligence. 2019 Presented at: IJCAI '19; August 10-16, 2019; Macao, China p. 1387-1393 URL: https://dl.acm.org/doi/10.5555/3367032.3367229 [doi: 10.24963/ijcai.2019/192]
27. Fares A, Zhong SH, Jiang J. Brain-media: a dual conditioned and lateralization supported GAN (DCLS-GAN) towards visualization of image-evoked brain activities. In: Proceedings of the 28th ACM International Conference on Multimedia. 2020 Presented at: MM '20; October 12-16, 2020; Seattle, WA p. 1764-1772 URL: https://dl.acm.org/doi/10.1145/3394171.3413858 [doi: 10.1145/3394171.3413858]
28. Radford A, Kim JW, Hallacy C, Ramesh A, Goh G, Agarwal S, et al. Learning transferable visual models from natural language supervision. arXiv Preprint posted online on February 26, 2021 [FREE Full text]
29. Singh P, Dalal D, Vashishtha G, Miyapuram K, Raman S. Learning robust deep visual representations from EEG brain recordings. In: Proceedings of the 2024 IEEE/CVF Winter Conference on Applications of Computer Vision. 2024 Presented at: WACV '24; January 3-8, 2024; Waikoloa, HI p. 7538-7547 URL: https://www.computer.org/csdl/proceedings-article/wacv/2024/189200h538/1W0dmHguKU8 [doi: 10.1109/wacv57701.2024.00738]
30. Song Y, Liu B, Li X, Shi N, Wang Y, Gao X. Decoding natural images from EEG for object recognition. arXiv Preprint posted online on August 25, 2023 [FREE Full text]

XSL•FO
RenderX

31. Chen CS, Wei CS. Mind's eye: image recognition by EEG via multimodal similarity-keeping contrastive learning. arXiv Preprint posted online on June 5, 2024 [FREE Full text]
32. Li D, Wei C, Li S, Zou J, Qin H, Liu Q. Visual decoding and reconstruction via EEG embeddings with guided diffusion. arXiv Preprint posted online on March 12, 2024 [FREE Full text]
33. Chen H, He L, Liu Y, Yang L. Visual neural decoding via improved visual-EEG semantic consistency. arXiv Preprint posted online on August 13, 2024 [FREE Full text]
34. Chen CS, Chen SY, Tsai AH, Wei CS. QEEGNet: quantum machine learning for enhanced electroencephalography encoding. arXiv Preprint posted online on July 27, 2024 [FREE Full text] [doi: 10.1109/sips62058.2024.00035]
35. Chen CS, Tsai AH, Huang SC. Quantum multimodal contrastive learning framework. arXiv Preprint posted online on August 25, 2024 [FREE Full text]
36. Zeng H, Xia N, Qian D, Hattori M, Wang C, Kong W. DM-RE2I: a framework based on diffusion model for the reconstruction from EEG to image. Biomed Signal Process Control 2023 Sep;86:105125. [doi: 10.1016/j.bspc.2023.105125]
37. Fu H, Shen Z, Chin JJ, Wang H. BrainVis: exploring the bridge between brain and visual signals via image reconstruction. arXiv Preprint posted online on December 22, 2023 [FREE Full text] [doi: 10.1109/icassp49660.2025.10889805]
38. Lan YT, Ren K, Wang Y, Zheng WL, Li D, Lu BL, et al. Seeing through the brain: image reconstruction of visual perception from human brain signals. arXiv Preprint posted online on July 27, 2023 [FREE Full text]
39. Guo HT. EEGVision: reconstructing vision from human brain signals. Appl Math Nonlinear Sci 2024;9(1):2. [doi: 10.2478/amns-2024-1856]
40. Gifford AT, Dwivedi K, Roig G, Cichy RM. A large and rich EEG dataset for modeling human visual object recognition. Neuroimage 2022 Dec 01;264:119754 [FREE Full text] [doi: 10.1016/j.neuroimage.2022.119754] [Medline: 36400378]
41. Hebart MN, Dickter AH, Kidder A, Kwok WY, Corriveau A, Van Wicklin C, et al. THINGS: a database of 1,854 object concepts and more than 26,000 naturalistic object images. PLoS One 2019 Oct 15;14(10):e0223792 [FREE Full text] [doi: 10.1371/journal.pone.0223792] [Medline: 31613926]
42. Podell D, English Z, Lacey K, Blattmann A, Dockhorn T, Müller J, et al. SDXL: improving latent diffusion models for high-resolution image synthesis. arXiv Preprint posted online on July 4, 2023 [FREE Full text]
43. Luo S, Tan Y, Patil S, Gu D, von Platen P, Passos A, et al. LCM-LoRA: a universal stable-diffusion acceleration module. arXiv Preprint posted online on November 9, 2023 [FREE Full text]
44. Ye H, Zhang J, Liu S, Han X, Yang W. IP-Adapter: text compatible image prompt adapter for text-to-image diffusion models. arXiv Preprint posted online on August 13, 2023 [FREE Full text]
45. Dosovitskiy A, Beyer L, Kolesnikov A, Weissenborn D, Zhai X, Unterthiner T, et al. An image is worth 16x16 words: transformers for image recognition at scale. arXiv Preprint posted online on October 22, 2020 [FREE Full text]
46. van den Oord A, Li Y, Vinyals O. Representation learning with contrastive predictive coding. arXiv Preprint posted online on July 10, 2018 [FREE Full text]
47. He K, Fan H, Wu Y, Xie S, Girshick R. Momentum contrast for unsupervised visual representation learning. In: Proceedings of the 2020 IEEE/CVF Conference on Computer Vision and Pattern Recognition. 2020 Presented at: CVPR '20; June 13-19, 2020; Seattle, WA p. 9726-9738 URL: https://ieeexplore.ieee.org/document/9157636 [doi: 10.1109/cvpr42600.2020.00975]
48. Zhu SC, Mumford D. Prior learning and Gibbs reaction-diffusion. IEEE Trans Pattern Anal Mach Intell 1997;19(11):1236-1250. [doi: 10.1109/34.632983]
49. Ramesh A, Dhariwal P, Nichol A, Chu C, Chen M. Hierarchical text-conditional image generation with CLIP latents. arXiv Preprint posted online on April 13, 2022 [FREE Full text]
50. Scotti PS, Banerjee A, Goode J, Shabalin S, Nguyen A, Cohen E, et al. Reconstructing the Mind's eye: fMRI-to-image with contrastive learning and diffusion priors. arXiv Preprint posted online on May 29, 2023 [FREE Full text]
51. Wang Z, Bovik A, Sheikh H, Simoncelli E. Image quality assessment: from error visibility to structural similarity. IEEE Trans Image Process 2004 Apr;13(4):600-612. [doi: 10.1109/tip.2003.819861] [Medline: 15376593]
52. Salimans T, Goodfellow I, Zaremba W, Cheung V, Radford A, Chen X. Improved techniques for training GANs. In: Proceedings of the 30th International Conference on Neural Information Processing Systems. 2016 Presented at: NIPS '16; December 5-10, 2016; Barcelona, Spain p. 2234-2242 URL: https://dl.acm.org/doi/10.5555/3157096.3157346
53. Heusel M, Ramsauer H, Unterthiner T, Nessler B, Hochreiter S. GANs trained by a two time-scale update rule converge to a local Nash equilibrium. arXiv Preprint posted online on June 26, 2017 [FREE Full text] [doi: 10.18034/ajase.v8i1.9]
. Academic Ethics Series. Chang Gung University: Research and Development Office. 2013 Apr 29. URL: https://www.cgu.edu.tw/research/Subject/Detail/24531?nodeId=8077
55. Orima T, Motoyoshi I. Spatiotemporal cortical dynamics for visual scene processing as revealed by EEG decoding. Front Neurosci 2023 Nov 1;17:1167719 [FREE Full text] [doi: 10.3389/fnins.2023.1167719] [Medline: 38027518]
56. Ko LW, Ranga SS, Komarov O, Chen C. Development of single-channel hybrid BCI system using motor imagery and SSVEP. J Healthc Eng 2017;2017:3789386. [doi: 10.1155/2017/3789386] [Medline: 29065590]
57. Xiaorong Gao, Dingfeng Xu, Ming Cheng, Shangkai Gao. A BCI-based environmental controller for the motion-disabled. IEEE Trans Neural Syst Rehabil Eng 2003 Jun;11(2):137-140. [doi: 10.1109/tnsre.2003.814449]
58. Enriquez-Geppert S, Huster RJ, Herrmann CS. EEG-neurofeedback as a tool to modulate cognition and behavior: a review tutorial. Front Hum Neurosci 2017 Feb 22;11:51 [FREE Full text] [doi: 10.3389/fnhum.2017.00051] [Medline: 28275344]

XSL•FO
RenderX

Abbreviations

ATM-S: Adaptive Thinking Mapper ShallowNet
BCI: brain-computer interface
CAT: Category-Based Assessment Table
CLIP: Contrastive Language-Image Pretraining
EEG: electroencephalography
FID: Fréchet inception distance
fMRI: functional magnetic resonance imaging
GAN: generative adversarial network
InfoNCE: information noise-contrastive estimation
MUSE: Multimodal Similarity-Keeping Contrastive Learning
NECOMIMI: Neural-Cognitive Multimodal Electroencephalography-Informed Image
NERV: Neural Encoding Representation Vectorizer
NICE: Natural Image Contrast Electroencephalography
SDXL: Stable Diffusion XL
SOTA: state of the art
VAE: variational autoencoder
ViT: vision transformer

Edited by Q Chen; submitted 04.02.25; peer-reviewed by Y Cheng, C Udensi; comments to author 10.04.25; revised version received 21.04.25; accepted 04.05.25; published 25.06.25.

Please cite as:
Chen CS, Chang SH, Liu CW, Pan TM
Exploring the Potential of Electroencephalography Signal–Based Image Generation Using Diffusion Models: Integrative Framework Combining Mixed Methods and Multimodal Analysis
JMIR Med Inform 2025;13:e72027
URL: https://medinform.jmir.org/2025/1/e72027
doi:10.2196/72027
PMID:

©Chi-Sheng Chen, Shao-Hsuan Chang, Che-Wei Liu, Tung-Ming Pan. Originally published in JMIR Medical Informatics (https://medinform.jmir.org), 25.06.2025. This is an open-access article distributed under the terms of the Creative Commons Attribution License (https://creativecommons.org/licenses/by/4.0/), which permits unrestricted use, distribution, and reproduction in any medium, provided the original work, first published in JMIR Medical Informatics, is properly cited. The complete bibliographic information, a link to the original publication on https://medinform.jmir.org/, as well as this copyright and license information must be included.

XSL•FO
RenderX

Original Paper

Efficient Detection of Stigmatizing Language in Electronic Health Records via In-Context Learning: Comparative Analysis and Validation Study

Hongbo Chen[1], MSc; Myrtede Alfred[1], PhD; Eldan Cohen[1], PhD

Department of Mechanical and Industrial Engineering, University of Toronto, Toronto, ON, Canada

Corresponding Author:
Eldan Cohen, PhD
Department of Mechanical and Industrial Engineering
University of Toronto
27 King's College Circle
Toronto, ON, M5S 1A1
Canada
Phone: 1 416 978 4184
Email: ecohen@mie.utoronto.ca

Related Article:

Comment in: https://medinform.jmir.org/2025/1/e82484

Abstract

Background: The presence of stigmatizing language within electronic health records (EHRs) poses significant risks to patient care by perpetuating biases. While numerous studies have explored the use of supervised machine learning models to detect stigmatizing language automatically, these models require large, annotated datasets, which may not always be readily available. In-context learning (ICL) has emerged as a data-efficient alternative, allowing large language models to adapt to tasks using only instructions and examples.

Objective: We aimed to investigate the efficacy of ICL in detecting stigmatizing language within EHRs under data-scarce conditions.

Methods: We analyzed 5043 sentences from the Medical Information Mart for Intensive Care–IV dataset, which contains EHRs from patients admitted to the emergency department at the Beth Israel Deaconess Medical Center. We compared ICL with zero-shot (textual entailment), few-shot (SetFit), and supervised fine-tuning approaches. The ICL approach used 4 prompting strategies: generic, chain of thought, clue and reasoning prompting, and a newly introduced stigma detection guided prompt. Model fairness was evaluated using the equal performance criterion, measuring true positive rate, false positive rate, and F_1-score disparities across protected attributes, including sex, age, and race.

Results: In the zero-shot setting, the best-performing ICL model, GEMMA-2, achieved a mean F_1-score of 0.858 (95% CI 0.854-0.862), showing an 18.7% improvement over the best textual entailment model, DEBERTA-M (mean F_1-score 0.723, 95% CI 0.718-0.728; P<.001). In the few-shot setting, the top ICL model, LLAMA-3, outperformed the leading SetFit models by 21.2%, 21.4%, and 12.3% with 4, 8, and 16 annotations per class, respectively (P<.001). Using 32 labeled instances, the best ICL model achieved a mean F_1-score of 0.901 (95% CI 0.895-0.907), only 3.2% lower than the best supervised fine-tuning model, ROBERTA (mean F_1-score 0.931, 95% CI 0.924-0.938), which was trained on 3543 labeled instances. Under the conditions tested, fairness evaluation revealed that supervised fine-tuning models exhibited greater bias compared with ICL models in the zero-shot, 4-shot, 8-shot, and 16-shot settings, as measured by true positive rate, false positive rate, and F_1-score disparities.

Conclusions: ICL offers a robust and flexible solution for detecting stigmatizing language in EHRs, offering a more data-efficient and equitable alternative to conventional machine learning methods. These findings suggest that ICL could enhance bias detection in clinical documentation while reducing the reliance on extensive labeled datasets.

(JMIR Med Inform 2025;13:e68955) doi:10.2196/68955

XSL•FO
RenderX

KEYWORDS

in-context learning; large language model; prompting strategy; text classification; zero-shot; few-shot; machine learning; fairness; stigmatizing language; electronic health record; artificial intelligence

Introduction

Background

Electronic health records (EHRs) are comprehensive digital systems that capture, store, and facilitate the retrieval and analysis of detailed longitudinal information about a patient's health status [1]. As a central repository of patient information, EHRs are indispensable for facilitating efficient communication and collaboration among medical professionals [2,3]. Given the widespread adoption of EHR systems in health care settings globally and their vital role in streamlining health care communication [4,5], concerns have emerged regarding the prevalence of stigmatizing language within these records [6-9]. Specifically, a recent large-scale study [10] reported that stigmatizing language appears in a substantial proportion of clinical notes, with prevalence ranging from 42.8% to 59.1% in history and physical notes, consultation notes, and discharge summaries.

Stigmatizing language in health care refers to language that carries negative connotations, labels patients negatively, attributes blame, or renders judgment based on their social identities, medical conditions, or personal experiences [11]. Such language can be explicit, as in the use of derogatory terms such as "junkie" or "alcoholic" [8]. However, it also frequently manifests in more implicit forms, including subtle judgments embedded in tone, phrasing, or contextual framing [7]. Research in social psychology has demonstrated that implicit biases, which refer to unconscious attitudes or stereotypes, can be reflected through people's language [12,13]. In health care, implicit biases may surface through the language used to describe patients. For instance, labeling a patient as "noncompliant" may seem clinically objective, but it can implicitly stigmatize their behavior by suggesting poor self-management, rooted in preconceived notions or stereotypes, without considering contextual factors such as mental capacity, available resources, or external circumstances. Implicit biases reflect broader systemic inequities, as institutional practices and cultural norms often perpetuate and normalize the use of stigmatizing language in clinical settings [14,15]. Stigmatizing language has been frequently observed in clinical specialties such as substance use disorders, mental health conditions, diabetes, and obesity, where it has shaped both clinical terminology and professional attitudes [8,16-18]. This systemic perpetuation of stigmatizing language reinforces negative stereotypes and creates barriers to equitable health care, undermining patient trust and treatment outcomes. By embedding biased language into clinical notes, these unconscious attitudes influence immediate clinical decisions and may perpetuate negative stereotypes over time [15,19], as subsequent clinicians rely on prior documentation [20]. These patterns were confirmed in a recent analysis of 754 clinical notes containing stigmatizing language [21], which found that stereotyping accounted for 41.2% of instances, followed by labeling patients as difficult (15.3%), disapproval (9.6%), unilateral decision-making (7.3%), and questioning patient credibility (5.3%). Such findings underscore the importance of mitigating bias to advance health care equity.

The presence of stigmatizing language can profoundly impact the quality of care. A study [18] found that clinicians exposed to the stigmatizing term "substance abuser," as opposed to the more neutral phrase "person with substance use disorder," were more likely to view the patient as personally culpable and deserving of punitive action rather than treatment. In addition, a national survey of 655 emergency physicians, those who used the stigmatizing label "sickler" to describe patients with sickle cell disease, demonstrated lower compliance with national treatment guidelines and were less likely to prescribe appropriate medications [17]. Complementing these findings, previous research has also shown that physicians who read notes containing stigmatizing language are more likely to develop negative attitudes toward the patient and to provide less aggressive pain management [22]. Notably, only 18% of inpatient progress notes are manually entered, with the majority being imported or copied from previous documentation [20]. The reliance on previous documentation raises concerns about the potential perpetuation of stigmatizing language, which could reinforce negative biases and influence clinical decision-making over time. With the implementation of the 21st Century Cures Act in 2021 in the United States, patients have gained access to their EHRs [23], making these records increasingly integral to the clinician-patient relationship. A large survey study [24] found that 10% of patients feel judged or offended due to labeling and evidence of disrespect in EHRs. Another study [16] reported that 19% of patients indicated they would avoid future medical appointments if their physicians used stigmatizing language toward them, while 21% stated they would seek a new physician. There is also substantial evidence that stigmatizing language in EHRs can jeopardize the therapeutic relationship, leading to distrust, delayed care, and reduced treatment engagement [7,25,26].

Given the detrimental effects of stigmatizing language in EHRs and the substantial resources required for its manual identification, there is a growing interest in developing automated detection methods. Manual detection typically necessitates annotators possessing extensive clinical expertise to accurately interpret context, as well as linguistic proficiency to discern subtle indicators of stigma [15,27]. In current practice, manual annotation typically involves experienced physicians reading and classifying individual sentences or notes from EHRs, an approach that is labor-intensive and costly, particularly when scaled across large datasets [15,27,28]. To overcome these challenges, researchers have increasingly explored machine learning approaches for the automated detection of stigmatizing language within EHRs. For instance, Sun et al [15] developed a logistic regression classifier to assess whether sentences in EHRs convey stigmatization, using a proprietary dataset, while Harrigian et al [27] conducted a comparative analysis of logistic regression and Bidirectional Encoder Representations from

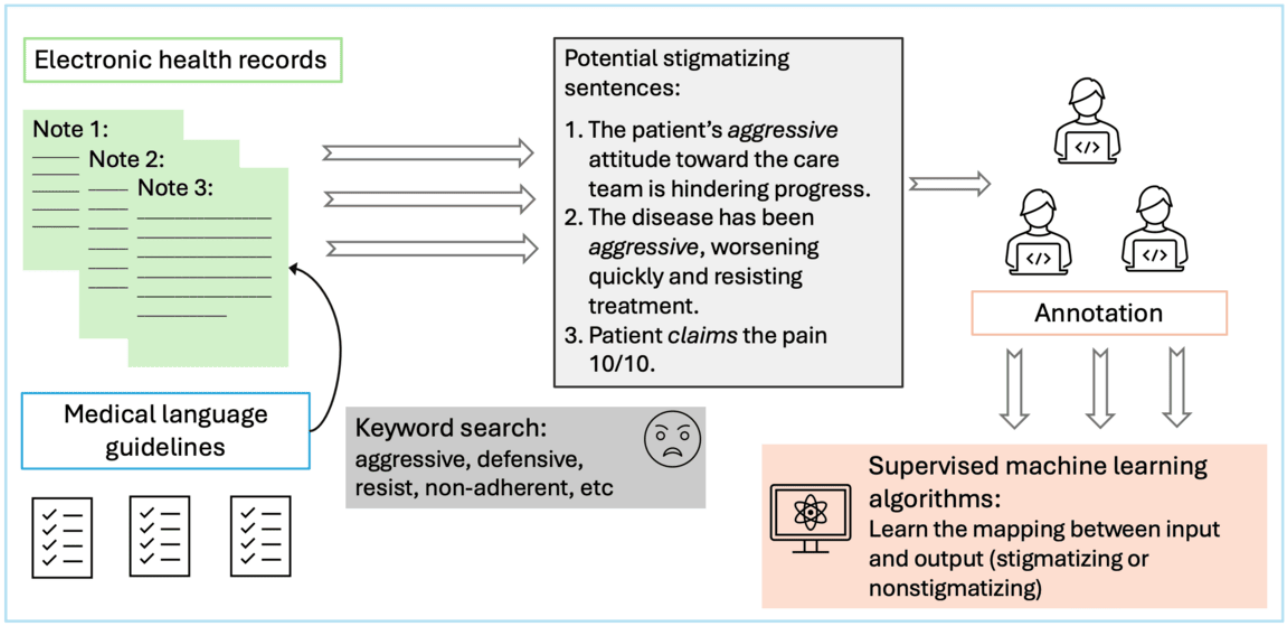
XSL•FO
RenderX

Transformers (BERT) classifiers for the detection of stigmatizing language. However, these studies have all used supervised learning approaches, which generally require thousands to tens of thousands of annotated data points to achieve optimal performance. The assumption that such large volumes of annotated data are readily available is often unrealistic, as the acquisition of labels for stigmatizing language detection presents significant challenges. Stigmatizing language is frequently subtle, covert, and highly contextual. Consequently, acquiring annotated data for stigmatizing language detection can be demanding and resource intensive. The previous studies' heavy reliance on supervised machine learning approaches has highlighted a significant limitation in addressing scenarios where annotated data may be scarce.

In-context learning (ICL) is an emerging paradigm for addressing natural language processing (NLP) tasks in data-scarce settings [29-32]. ICL enables general-purpose large language models (LLMs) to adapt to new tasks by incorporating instructions and either zero or a few examples directly within the input prompt, thereby reducing reliance on extensively annotated datasets [29,33,34]. By leveraging the robust contextual understanding capabilities inherent in general-purpose LLMs, the ICL approach is particularly well-suited for detecting stigmatizing language, a task that requires the identification of subtle nuances and a high level of contextual comprehension. To the best of our knowledge, no study has systematically examined the efficacy of the ICL approach for stigmatizing language detection, underscoring a significant gap in the current research landscape.

The effectiveness of the ICL approach is contingent upon prompt engineering, which involves crafting precise, informative, and contextually relevant prompts to guide the LLM in executing specific tasks [29,35,36]. Therefore, the efficacy of the ICL approach could be enhanced by a tailored prompting strategy for stigmatizing language detection. Previous studies on detecting stigmatizing language typically involve a 2-stage process (Figure 1): first, the extraction of sentences containing potentially stigmatizing words or phrases in accordance with medical language guidelines, followed by the development of the supervised machine learning model with the annotated data set [15,27]. The potentially stigmatizing words or phrases identified during the extraction process can provide valuable information that can be incorporated into the prompting strategy. By explicitly prompting the LLM to focus on these terms, we anticipate an improvement in its sensitivity to detecting stigmatizing language. Furthermore, given that stigmatizing language is often covert and subtle [27,37], incorporating common linguistic characteristics associated with such language may further increase the model's accuracy in identifying instances of stigmatization. Customizing prompts to address the unique aspects of stigmatizing language presents a valuable opportunity to enhance detection precision.

Figure 1. Workflow for developing a supervised machine learning model in stigmatizing language detection.



While developing effective machine learning models to detect stigmatizing language is important, it is equally critical to ensure that these models do not introduce or perpetuate existing biases [38]. Numerous studies have demonstrated that machine learning classifiers can exhibit algorithmic bias, resulting in performance disparities across groups of patients with different protected attributes, such as sex, race, age, and socioeconomic status [39,40]. For example, Seyyed-Kalantari et al [41] found that a leading machine learning classifier for detecting chest X-ray pathologies exhibited a higher false negative rate for Hispanic female patients. In the context of stigmatizing language detection, algorithmic bias can lead to uneven identification and correction of stigmatizing language, disproportionately affecting certain groups and potentially exacerbating health disparities. To the best of our knowledge, no previous studies have specifically examined the fairness of classifiers in detecting stigmatizing language within EHRs, highlighting the need for further investigation into how these models perform across diverse patient populations. By rigorously evaluating the fairness of these models, we can identify potential disparities and ensure that they equitably benefit patients from diverse backgrounds.

XSL•FO
RenderX

Study Objectives

We aimed to investigate the effectiveness of the ICL approach for detecting stigmatizing language in EHRs under data-scarce conditions. First, we evaluated the performance of the ICL approach against established approaches in zero-shot (no annotated data) and few-shot settings (a small amount of annotated data), including the textual entailment [42] and SetFit [43]. For the ICL approach, we used 4 distinct prompting strategies, including more sophisticated strategies, such as the chain of thought (COT) [44] and the clue and reasoning prompting (CARP) [30]. We also introduced a novel prompting strategy, termed "stigma detection guided prompt," specifically designed to enhance the precision and effectiveness of detecting stigmatizing language. Second, to further contextualize ICL's performance, we conducted a comparative analysis of supervised fine-tuning and ICL to evaluate the extent to which ICL can achieve competitive performance under data-scarce conditions relative to a well-established method that leverages a large corpus of annotated data. This comparison provides valuable insights for hospitals, enabling them to assess the cost-benefit trade-offs associated with investing in annotated datasets for detecting stigmatizing language in clinical documentation. Third, we assessed the fairness dimension of the classifiers used for detecting stigmatizing language in this study by comparing their performance across diverse patient groups characterized by various protected attributes, including sex, age, and race.

Methods

Dataset Description

In this study, we used an open-source stigmatization detection dataset prepared by Harrigian et al [27]. The dataset consists of 5043 sentences, of which 3249 (64.4%) are labeled as stigmatizing and 1794 (35.6%) as nonstigmatizing. The original creators randomly sampled these sentences from 4710 discharge summaries associated with 4259 patients within the Medical Information Mart for Intensive Care (MIMIC)–IV database and subsequently annotated them. The MIMIC-IV is an EHR dataset that comprises 331,794 discharge summaries from the Beth Israel Deaconess Medical Center in Boston, Massachusetts, United States, from 2008 to 2019 [45]. The observed prevalence of stigmatizing language in this dataset is notably higher than previously reported estimates, such as the 42.8% identified by Weiner et al [10]. This difference is attributable to the broader scope of stigmatizing expressions captured in the dataset prepared by Harrigian et al [27], which encompasses a wider range of terminology than earlier studies.

Discharge summaries were selected because they provide detailed documentation of the patient's clinical course, including diagnoses, treatments, and physician observations, which are particularly relevant for investigating stigmatization in clinical notes. Sentences were extracted based on the presence of potentially stigmatizing words or expressions, such as "noncompliant" and "agitated." A symmetric context window of 15 tokens on either side of each sentence was applied to preserve surrounding context and enhance model interpretation. If fewer than 15 tokens were available on either side, the context window was shortened as needed to fit the available text. Each sentence was independently annotated by 2 members of an annotation team comprising 1 clinician and 2 research assistants based on a predefined framework [27]. Any disagreements were resolved through discussion among all 3 annotators. The annotation process achieved a high level of interrater agreement, with an average pairwise Cohen κ exceeding 0.9. The annotation of stigmatization was determined based on framing and intent of the sentence with its surrounding context (ie, whether the sentence implies that the patient's behavior is cast in a negative light). Sentences that did not describe patient behavior, or that neutrally described patient behavior, acknowledged structural or clinical barriers, or conveyed empathy from health care providers were not considered stigmatizing. The demographic information of the dataset, including patient sex, age, and race, is presented in Table 1. The "other or unknown" race category included individuals who did not report their race. A more detailed description of the dataset is provided in Multimedia Appendix 1 [15,18,19,22,27,37].

XSL•FO
RenderX

Table 1. Demographic information of the stigmatizing dataset used in this study.

Demographic attributes	Stigmatizing sentences, n (%)	Nonstigmatizing sentences, n (%)
Sex		
Male (n=2600)	1731 (66.6)	869 (33.4)
Female (n=2443)	1518 (62.1)	925 (37.9)
Age (y)		
0-25 (n=468)	303 (64.7)	165 (35.3)
26-50 (n=1639)	1184 (72.2)	455 (27.8)
51-75 (n=2005)	1249 (62.3)	756 (37.7)
>75 (n=931)	513 (55.1)	418 (44.9)
Race		
Asian (n=125)	69 (55.2)	56 (44.8)
Black (n=945)	676 (71.5)	269 (28.5)
Hispanic (n=246)	159 (64.6)	87 (35.4)
Other or unknown (n=522)	305 (58.4)	217 (41.6)
White (n=3205)	2040 (63.7)	1165 (36.3)

Ethical Considerations

This study used a publicly available dataset consisting of EHR sentences. All patient records were anonymized by the dataset's original creators, ensuring that no individual identifiable information was accessible to the research team [45]. As such, the study is exempt from research ethics board review in accordance with Article 2.2 of the Tri-Council Policy Statement [46]. The original collection of data was approved by the institutional review boards of the Beth Israel Deaconess Medical Center, Boston, Massachusetts, and the Massachusetts Institute of Technology, Cambridge, Massachusetts (2001P001699). The institutional review boards also granted a waiver of informed consent and approved the sharing of the research resource, thereby permitting secondary analysis of the deidentified data without additional consent.

No compensation was provided or required for the use of this secondary data. No identification of individual participants or users in any images of the manuscript or supplementary material is possible. To access this dataset, the lead author fulfilled all necessary regulatory requirements, including the completion of the course "CITI data or specimens only research training" (certification number 62353094). In addition, the lead author signed a data use agreement to ensure the appropriate use of the data in compliance with relevant policies and regulations.

Comparative Analysis for Stigmatizing Language Detection

Zero-shot and few-shot learning are machine learning paradigms that allow models to perform tasks with either no labeled data or with only a minimal set of labeled examples, respectively [47,48]. Zero-shot learning enables a model to perform a task without any previous examples, relying solely on its pretrained knowledge. In contrast, few-shot learning operates by providing the model with a limited number of labeled examples, typically ranging from 10 to 100.

In this study, we conducted a comprehensive evaluation of the effectiveness of the ICL approach for detecting stigmatizing language in EHRs under conditions of limited data availability. We compared the performance of ICL against the textual entailment approach [42] within a zero-shot learning context and the SetFit approach [43] within a few-shot learning context, specifically analyzing scenarios involving 4, 8, and 16 annotated examples per class. For the few-shot learning experiments, data points were randomly selected as examples. To ensure reproducibility and mitigate potential variability in performance due to random sampling, the selection process was repeated 5 times using distinct random seeds. The final performance results reported in this study represent the average across these 5 runs, providing a more robust and stable assessment of model performance.

In addition, we extended our comparative analysis to include a fully supervised fine-tuning approach. This broader comparison allows us to rigorously assess the strengths and potential limitations of the ICL approach in the detection of stigmatizing language within EHRs. All approaches used in this study adhered to the framework established in previous studies (Figure 1), wherein sentences were extracted based on potentially stigmatizing words or phrases identified from medical language guidelines, followed by the development of detection approaches (ie, ICL).

Textual Entailment Approach

The textual entailment approach conceptualizes zero-shot text classification as an entailment task [42]. This method is among the most widely adopted for zero-shot text classification and has demonstrated state-of-the-art performance across various benchmarks [49,50]. In this approach, the input text is interpreted as a premise, and the model assesses whether this premise logically entails the corresponding class label. Specifically, in the context of stigmatizing language detection, the model first considers a sentence from an EHR as the premise

XSL•FO
RenderX

and then evaluates whether it entails stigmatization or nonstigmatization. The textual entailment approach relies on the knowledge embedded in pretrained language models, which have been trained on natural language inference datasets [51]. This training effectively enhances the model's capability for sentence comprehension. In our study, we used a selection of widely recognized pretrained language models for natural language inference to assess the effectiveness of the textual entailment approach in detecting stigmatizing language (Table 2). These models were selected due to their widespread use in zero-shot classification tasks [50,52,53] and their representation of a diverse range of transformer architectures, enabling us to fully explore the potential of the textual entailment approach for detecting stigmatizing language.

Table 2. Pretrained language models used in the textual entailment approach.

Abbreviation	Full model name
ROBERTA-M	roberta-large-mnli
BART-M	bart-large-mnli
DEBERTA-M	deberta-large-mnli
BERT-M	bert-base-multilingual-cased-multinli_tr

SetFit Approach

SetFit is a popular few-shot text classification approach that has been applied across various domains [50,54,55]. The SetFit approach consists of a two-step process [43]. First, a pretrained sentence transformer is fine-tuned in a contrastive Siamese manner using pairs of labeled data. The objective of this contrastive fine-tuning is to ensure that embeddings of semantically similar sentences are close together in the feature space while embeddings of semantically dissimilar sentence pairs are maximally distanced. This process aims to generate meaningful representations that accurately capture the semantic relationships between sentences. In the second step, a classification head is trained using the representations produced by the fine-tuned sentence transformer. For this study, we used 6 pretrained sentence transformers to evaluate the effectiveness of the SetFit approach in detecting stigmatizing language (Table 3). MPNET-V2 and MINILM-V2 were the sentence transformers used in the original work that proposed SetFit [43], while the more contemporary E5-V2 and ROBERTA-V2 were included due to their superior performance on various NLP benchmarks [56,57]. We also incorporated 2 sentence transformers pretrained on medical domain knowledge: BERT-BIO-ST and BIOLORD. The inclusion of these models was based on the hypothesis that domain-specific pretraining may enhance the model's ability to capture contextually relevant medical terminology and nuances, thereby improving its effectiveness in detecting stigmatizing language [58].

Table 3. Pretrained sentence transformers used in the SetFit approach.

Abbreviation	Full model name
MPNET-V2	paraphrase-mpnet-base-v2
E5-V2	e5-base-v2
ROBERTA-V2	stsb-roberta-base-v2
MINILM-V2	paraphrase-multilingual-MiniLM-L12-v2
BERT-BIO-ST	S-BioBert-snli-multinli-stsb
BIOLORD	BioLORD-2023

Fully Supervised Fine-Tuning Approach

The fully supervised fine-tuning approach involves adapting a pretrained language model to a specific task by fine-tuning it on a labeled dataset, where each instance is associated with its corresponding label [29]. In this study, we used 5 pretrained language models to examine the efficacy of a fully supervised fine-tuning approach for detecting stigmatizing language (Table 4). ROBERTA, ROBERTA-XLM, and BERT were selected due to their extensive adoption and strong performance across text classification tasks in different domains [50,59-61]. BERT-BIO and BERT-biomed were included for their pretraining on biomedical text corpora, making them particularly well-suited for NLP tasks involving medical terminology [58,62]. We excluded certain contemporary medical pretrained language models, such as Gatortron [45] and ClinicalBERT [46], from our analysis. These models were omitted because they were pretrained on the MIMIC dataset, which could introduce data leakage and potentially lead to an overestimation of the model's effectiveness. We specifically focused on fine-tuning encoder-based language models, such as BERT, rather than decoder-based models (ie, LLAMA) for 2 primary reasons. First, previous research has demonstrated that encoder-only models typically achieve superior or comparable performance to decoder-based models in text classification tasks with relatively small, labeled datasets, which aligns with our study setting [63,64]. Second, BERT-based models currently represent the state-of-the-art for supervised stigmatizing language detection [27]. Thus, using these models as a benchmark allows for a more rigorous evaluation of ICL performance against established methodologies.

XSL•FO
RenderX

Table 4. Pretrained language models used in the fully supervised fine-tuning approach.

Abbreviation	Full model name
ROBERTA	roberta-base
BERT	bert-base-uncased
BERT-BIO	biobert-v1.1
ROBERTA-XLM	xlm-roberta-base
BERT-BIOMED	BiomedNLP-BiomedBERT-base-uncased-abstract-fulltext

We fine-tuned these pretrained language models on 3543 labeled sentences from EHRs, representing approximately 70% of the total data. The supervised fine-tuning approach was included to provide a robust benchmark for comparison with the ICL approach in detecting stigmatizing language. Hyperparameters were tuned using a validation dataset of 500 data points, representing approximately 10% of the total dataset. Hyperparameter tuning was conducted for key parameters using grid search, including learning rate, batch size, and weight decay rate, to optimize model performance and mitigate overfitting. We used the AdamW optimizer [65] with default betas set to 0.9 and 0.999 and an epsilon of 1×10^{-6} to ensure numerical stability. The number of epochs was determined using an early stopping criterion, where training was terminated if the validation loss did not decrease for 5 consecutive epochs. The final hyperparameter settings were selected based on the model's best performance on the validation dataset before being evaluated on the held-out test dataset.

ICL Approach

The ICL approach leverages general-purpose LLMs through prompting techniques to rapidly adapt to a wide range of NLP tasks [29]. The approach has demonstrated exceptional performance in applications such as question answering, machine translation, text summarization, and text classification [29,32-34]. In this study, we used 5 widely used open-source general-purpose LLMs to evaluate the efficacy of the ICL approach in detecting stigmatizing language (Table 5). We refer to models such as LLAMA-3 as general-purpose LLMs to emphasize their broad applicability across various NLP tasks without extensive task-specific fine-tuning. We specifically selected instruction fine-tuned models, as previous research has shown that instruction fine-tuning significantly enhances model performance across a range of NLP tasks, particularly in zero-shot and few-shot settings [66,67]. In addition, we included BIO-LLAMA-3, a domain-specific model that has undergone instruction fine-tuning on a large biomedical dataset [68], to assess the potential benefits of domain adaptation in stigmatizing language detection. Due to the constraints of the MIMIC-IV data use agreement, we were unable to use newer cloud-based models, such as GPT-4 or Claude 3.5, as their use would necessitate sharing data with external parties. Previous studies have demonstrated that general-purpose LLMs are highly sensitive to subtle variations in prompt formatting [69,70]. To optimize the performance of the ICL approach, we devised a validation data set for prompt format tuning, which included adjustments such as the wording and positioning of instructions. A random sample of 30 data points was selected to construct this validation set, designed to replicate a data-scarce scenario consistent with previous research [71,72].

Table 5. General-purpose large language models (LLMs) used in the in-context learning approach.

Abbreviation	Full model name	Context window length (tokens)
LLAMA-3	Meta-Llama-3-8B-Instruct	8000
FLAN-T5	flan-t5-large	512
GEMMA-2	gemma-2-9b-it	8192
MISTRAL-0.2	Mistral-7B-Instruct-v0.2	32000
BIO-LLAMA-3	Bio-Medical-Llama-3-8B	8000

Prompting Strategies for the ICL Approach

The effectiveness of the ICL approach relies heavily on the design of a well-structured prompting strategy that delivers clear and precise task instructions. A prompting strategy refers to the specific approach used to organize instructions, examples, and guiding principles within a prompt to elicit accurate and reliable outputs from the LLM. These prompts are often accompanied by either zero or a few illustrative examples to guide the model in performing downstream tasks effectively [29,32]. In this study, we evaluated 4 distinct prompting strategies: generic, COT [44], CARP [30], and a new customized prompting strategy we developed, referred to as the stigma detection guided prompt. The prompting template for each strategy is provided in Table 6. Figure 2 provides examples of the prompting strategies used in this study.

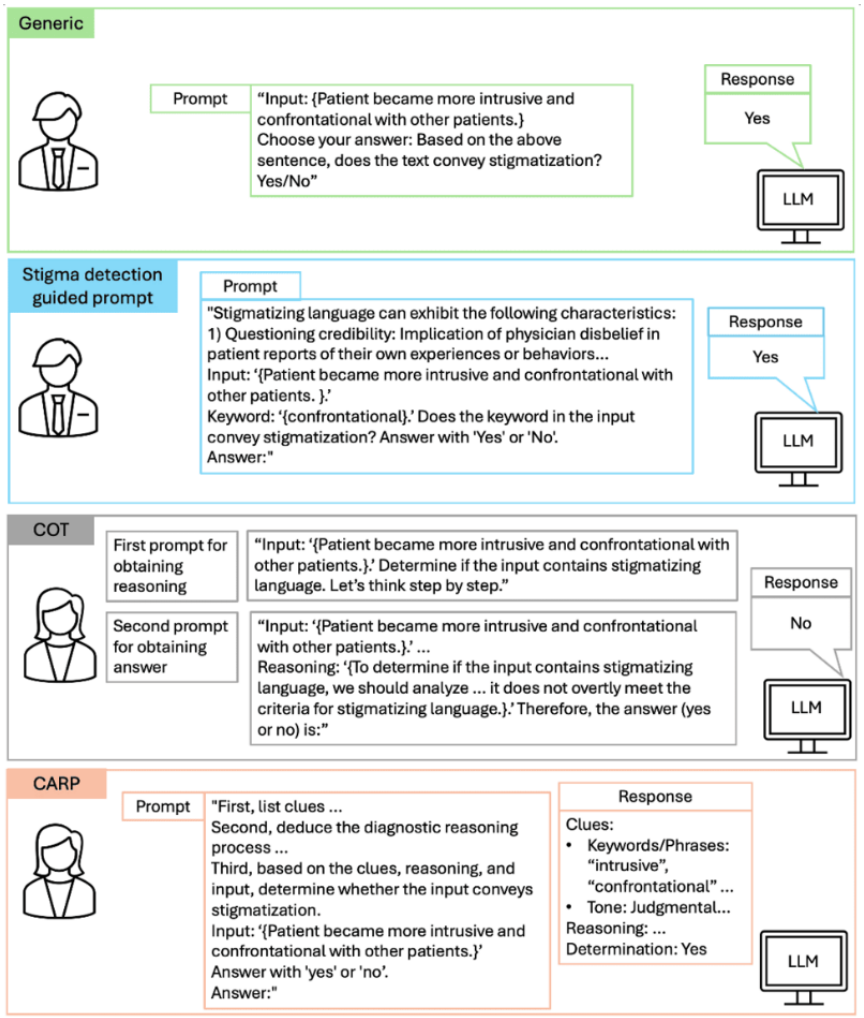
XSL•FO
RenderX

Table 6. Prompting strategies and templates used in the in-context learning approach.

Prompting strategy	Prompt template
Generic	"Input: '{input sentence}.' Choose your answer: Based on the above sentence, does the text convey stigmatization? Yes/No"
Chain of thought	"Input: '{input sentence}.' Determine if the input contains stigmatizing language. Let's think step by step. Reasoning: '{reasoning}.' Therefore, the answer (yes or no) is":
Clue and reasoning prompting	"First, list clues (e.g., keywords, phrases, contextual information, semantic relations, tones, references) that support the determination of stigmatization in the input. Second, deduce the diagnostic reasoning process from the premises (i.e., clues and input) that support the stigmatization determination. Third, based on the clues, reasoning, and input, determine whether the input conveys stigmatization. Input: '{input sentence}.' Answer with 'yes' or 'no'. Answer:"
Stigma detection guided prompt	"Stigmatizing language can exhibit the following characteristics: 1) Questioning credibility: Implication of physician disbelief in patient reports of their own experiences or behaviors. 2) Disapproval: Highlights poor reasoning, decision-making, or self-care, often in a way that suggests the patient is unreasonable. 3) Stereotyping: Quoting incorrect grammar or unsophisticated terms. 4) Difficult patient: Inclusion of details with questionable clinical significance that portray the patient as belligerent or otherwise suggest that the physician is annoyed. 5) Unilateral decisions: Language that emphasizes physician authority. Input: '{input statement}.' Keyword: "{keyword}." Does the keyword in the input convey stigmatization? Answer with 'Yes' or 'No'. Answer:"

XSL•FO
RenderX

Figure 2. Examples of 4 distinct prompting strategies used in this study. CARP: clue and reasoning prompting; COT: chain of thought; LLM: large language model.



The generic prompting strategy involves providing the model with minimal context, thereby relying primarily on its pretrained knowledge to perform the task [69]. In this approach, the prompt consists of a brief instruction about the task at hand, without incorporating reasoning steps or specific domain knowledge. For example, in the context of detecting stigmatizing language, the prompt might simply query the model with "Choose your answer: On the basis of the above sentence, does the text convey stigmatization? Yes/No." This strategy serves as a baseline for comparing its performance with that of more advanced prompting techniques, such as COT, CARP, and the stigma detection guided prompt. In the few-shot scenario, a limited number of example sentences accompanied by their corresponding labels are embedded within the generic prompt to guide the model in making informed predictions.

The COT prompting strategy is designed to enhance the reasoning capabilities of general-purpose LLMs by guiding them to generate intermediate reasoning steps before arriving at a final prediction [44]. This approach leverages the LLM's capacity to systematically reason through complex tasks, thereby improving the reliability and accuracy of its outputs. For instance, the prompt can be appended with "Let's think step by step" to induce the model to break down the problem into logical and incremental steps. By explicitly instructing the model to articulate its reasoning, the COT strategy encourages more thoughtful predictions. In the zero-shot setting, the COT strategy involves prompting the model twice before making a prediction [33]. The first prompt encourages the model to produce intermediate reasoning by appending "Let's think step by step" to the end of the prompt. This intermediate reasoning is then incorporated into a second prompt, which is used to generate the final prediction. In the few-shot setting, the model was first prompted to generate reasoning steps for randomly selected data points. These data points, along with their corresponding reasoning steps, were incorporated into the prompt as examples to enhance the model's performance.

The CARP prompting strategy is specifically designed for text classification tasks. It uses a progressive reasoning approach to handle the linguistic complexities inherent in such tasks. This strategy first prompts the model to identify superficial clues within the input text, such as keywords, tone, semantic relations, and references, which provide initial indicators for classification. Once these clues are identified, the model engages in a diagnostic reasoning process to infer the final prediction in a logical manner [30]. For example, the presence of a negative tone combined with specific keywords may collectively suggest the presence of stigmatizing language. In the few-shot setting, the model was first guided to generate clues and reasoning for

XSL•FO
RenderX

randomly selected examples. These examples, along with their associated clues, reasoning, and labels, were then incorporated into the prompt to enhance the model's performance [30]. The detailed code implementation for the prompting strategies is provided in Multimedia Appendix 2.

Design of the Stigma Detection Guided Prompt

In this study, we introduce a novel prompting strategy for detecting stigmatizing language, termed the stigma detection guided prompt. While prompt engineering has shown promise in improving LLM performance, there is no universally established framework for systematically designing prompts tailored to specific tasks [32]. The design of the proposed prompting strategy is inspired by recent research indicating that incorporating task-tailored instructions and domain knowledge can enhance the performance of the LLMs on downstream medical tasks [73,74]. Our proposed strategy consists of two key components: (1) explicitly directing the LLM to assess potentially stigmatizing words or phrases and (2) incorporating linguistic characteristics commonly associated with stigmatizing language to enhance the model's ability to identify subtle instances of stigmatization in clinical text. In the subsequent section, we outline the rationale behind these components and their contributions to improving stigma detection in clinical documentation.

In the stigma detection guided prompt, we specifically instruct the LLM to assess potentially stigmatizing words or expressions. For instance, in the sentence "Patient became more intrusive and confrontational with other patients," the model is specifically instructed to assess whether the term "confrontational" conveys stigmatization based on its surrounding context (Figure 2). We intentionally designed the prompt to focus on sentences containing expert-identified terms that are frequently used to convey stigmatization in clinical documentation (ie, aggressive and noncompliant). In this task formulation, the model is not asked to detect stigmatization broadly, but rather to assess whether the use of a known high-risk term conveys stigmatization in context. This reflects a practical and clinically relevant problem, as the same term may be neutral or stigmatizing depending on how it is used. In addition, this keyword-based approach aligns with prevailing practices in the literature. Previous studies have typically developed machine learning models or conducted analyses using sentences containing specific terms that are frequently flagged as stigmatizing according to medical language guidelines [15,75]. This approach remains widely adopted, in part because standardized definitions of stigmatizing language are still underdeveloped, and the topic remains sensitive within health care contexts. Therefore, focusing on predefined terms in the prompt offers a consistent and pragmatic approach for studying stigmatizing language across datasets and research settings. Conventional prompting strategies do not effectively leverage this information. By explicitly integrating this task-tailored instruction, our approach aims to enhance the LLM's ability to detect stigmatizing language with greater contextual awareness.

Within the proposed prompting strategy, we also integrate linguistic characteristics commonly associated with stigmatizing language to enhance the model's ability to detect subtle and implicit stigmatization. Stigmatizing language in EHRs frequently manifests in indirect ways, where certain words or phrases acquire negative connotations depending on the context in which they are used [19,76]. For instance, the term "claims" in the phrase "Patient claims pain is 10/10" may suggest disbelief, thereby contributing to stigma [7]. Previous work has identified five recurring linguistic patterns associated with stigmatizing language in clinical documentation, including (1) questioning patient credibility, (2) expressing disapproval of patient reasoning or self-care, (3) stereotyping based on race or social class, (4) portraying patients as difficult, and (5) emphasizing physician authority over the patient [37]. By incorporating these linguistic markers into the prompting strategy, our approach aims to enhance the LLM's sensitivity to context-dependent cues, improving its overall accuracy in detecting stigmatizing language. In the few-shot setting, we incorporated examples within the prompt, following a similar approach to that used in the generic prompting strategy.

Performance Evaluation and Comparison

In this study, stigmatizing language detection was framed as a binary text classification problem. To evaluate the performance of various approaches, we randomly sampled 1000 data points to create a test dataset, ensuring no overlap with training or validation datasets. We used 5 standard classification metrics: accuracy, precision, recall, area under the receiver operating characteristic curve (AUC-ROC), and F_1-score. Accuracy indicates the percentage of EHR sentences that are correctly classified. Precision measures the proportion of sentences identified as stigmatizing that are stigmatizing, reflecting the model's ability to avoid false positives. Recall, also known as sensitivity, assesses the proportion of actual stigmatizing sentences that are correctly identified, highlighting the model's capacity to capture true positives. The AUC-ROC evaluates the model's ability to distinguish between stigmatizing and nonstigmatizing sentences across different classification thresholds, with higher values indicating better discriminatory power. The F_1-score, which ranges from 0 to 1, is computed as the harmonic mean of precision and recall, offering a balanced measure of classification performance. The F_1-score is particularly critical for evaluating stigmatizing language detection due to the highly imbalanced nature of the dataset. Notably, the AUC-ROC metric was not computed for the ICL approach, as it does not produce the probabilistic classification required for the metric.

To obtain a robust estimate of the model's performance, we computed 95% CIs by training, tuning, and evaluating each model on 10 different train-validation-test splits, each generated using a different random seed. These test datasets were designed to have no overlap with the training or validation datasets, thereby minimizing potential biases in performance estimation. To compare the top-performing models, we conducted paired 1-tailed t tests on F_1-score, precision, and recall. Because each model was evaluated on the same test splits, the paired t test was chosen as it accounts for the dependency between paired observations, reducing variance and increasing statistical power compared to an independent t test. In the zero-shot setting, we compared the highest-performing models based on F_1-score in

XSL•FO
RenderX

both the textual entailment and ICL approaches. In the few-shot setting, we compared the best models when different numbers of annotations were available in the SetFit and ICL approaches. In addition, we compared the top-performing supervised fine-tuning model with the best ICL model. To mitigate the risk of inflated type I error due to multiple comparisons, we applied the Bonferroni correction to adjust the significance threshold. Given that a total of 15 comparisons were conducted, the adjusted significance level was set at P=.003 (.05/15).

Fairness Evaluation

The notion of machine learning fairness in health care can be broadly classified into equal allocation and equal performance considerations [39]. Equal allocation pertains to the equitable distribution of health care resources across different patient subgroups. For instance, in the context of kidney transplantation, a fair machine learning model would ensure that transplants are allocated proportionally among patient groups, thereby mitigating disparities in access to care [77]. In contrast, equal performance requires that a model achieves comparable predictive accuracy across both protected and nonprotected groups. This can be quantified using metrics such as the true positive rate (TPR) and false positive rate (FPR), among others [39-41]. In the context of stigmatizing language detection, the equal performance criterion is more suitable as it ensures that the model identifies stigmatizing language consistently across different demographic groups.

For the fairness evaluation, we used the criterion of equal performance, assessing the model across 3 key performance metrics: TPR, FPR, and F_1-score. A classifier is considered fair under this criterion if its performance remains consistent across subgroups defined by protected attributes. The TPR, also commonly referred to as recall, quantifies the proportion of EHR sentences containing stigmatizing language that the model correctly identifies. This metric is critical for fairness evaluation, as a lower TPR for certain demographic subgroups means the model fails to detect stigmatizing language in their clinical records at the same rate as others, potentially allowing harmful biases to persist unnoticed in medical documentation. This could lead to disparities in patient advocacy efforts, as undetected stigmatizing language may influence health care provider perceptions and contribute to differences in the quality of care received. Over time, systematic underdetection of stigmatizing language in specific groups may reinforce existing biases in health care systems, further marginalizing vulnerable populations. FPR quantifies the proportion of nonstigmatizing sentences that are incorrectly classified as stigmatizing. This metric is essential for fairness evaluation, as an elevated FPR for certain demographic subgroups indicates that the model is more likely to incorrectly classify nonstigmatizing language as stigmatizing for those groups, which could lead to unnecessary scrutiny of their clinical documentation. This overflagging may cause health care providers to become more hesitant in describing patient conditions accurately, potentially leading to vague or incomplete medical records. As a result, the quality of clinical communication may be compromised, which could negatively impact care coordination, patient trust, and clinical decision-making. Finally, the F_1-score provides a comprehensive measure of the model's classification performance by balancing precision and recall. Differences in F_1-score across demographic subgroups indicate variability in the model's utility—its effectiveness in balancing the detection (recall) and accuracy (precision) of stigmatizing language. A lower F_1-score for certain groups suggests that the model is either failing to detect stigmatizing language when it should (low recall) or flagging nonstigmatizing language incorrectly (low precision). This inconsistency can undermine the trust and usability of the model in clinical decision-making, potentially leading to biased documentation practices and uneven policy enforcement, ultimately reducing the overall fairness and effectiveness of the system.

We assessed the fairness of the models concerning 3 protected attributes: sex (male and female); age (0-25 y, 26-50 y, 51-75 y, and >75 y); and race (White, Black, Hispanic, Asian, and other or unknown). We adopted age groupings similar to those used in previous studies examining the fairness of machine learning classifiers [40,41]. Bias at the subgroup level was quantified by measuring performance disparities across demographic subgroups [41,78]. For sex-differentiated groups, performance disparity was calculated as the difference in the model's performance between one sex group and its complementary counterpart. For race- and age-differentiated groups, performance disparity was determined by the difference between the performance of a specific subgroup and the median performance across all subgroups within that attribute. A high-performance disparity indicates significant variation in the model's performance across different groups, suggesting a higher level of unfairness. We measured performance disparity for subgroups defined by sex, age, and race and reported the highest absolute performance disparity for each demographic attribute across models using ICL and supervised fine-tuning approaches.

Results

Overview

We conducted a comprehensive evaluation of various approaches for detecting stigmatizing language in data-scarce settings. First, we assessed the effectiveness of textual entailment and ICL approaches within a zero-shot setting. Then, we evaluated the SetFit and ICL approaches in few-shot settings, using 4, 8, and 16 annotated data points per class. We compared supervised fine-tuning with ICL to assess how well ICL can perform with limited data compared to an established method that relies on a large amount of annotated data. This section presents the comparative performance of each approach in detecting stigmatizing language.

Performance Evaluation for Zero-Shot Approaches

Table 7 presents the performance metrics of the various pretrained language models using the textual entailment approach under the zero-shot setting. Among the models evaluated, DEBERTA-M achieved the highest mean F_1-score and accuracy of 0.723 (95% CI 0.718-0.728) and 73.8% (95% CI 73.2%-74.4%), respectively. Conversely, BERT-M exhibited the lowest performance, with a mean F_1-score and accuracy of

XSL•FO
RenderX

0.615 (95% CI 0.606-0.624) and 64.2% (95% CI 63.8%-64.6%), respectively.

The performance of the various general-purpose LLMs using the zero-shot ICL approach is presented in Table 8. The stigma detection guided prompt strategy yielded the highest mean accuracy of 80.7% and a mean F_1-score of 0.838 across all evaluated prompting strategies. Conversely, the generic prompting strategy demonstrated the lowest performance, with a mean accuracy of 69.4% and a mean F_1-score of 0.746. The mean accuracy across the prompting strategies varied by 11.3 percentage points, and the mean F_1-scores differed by 0.092, indicating a significant variability in performance based on the prompting strategy used. The stigma detection guided prompt paired with GEMMA-2 achieved the highest performance, with a mean accuracy of 83.5% (95% CI 82.9%-84.1%) and a mean F_1-score of 0.858 (95% CI 0.854-0.862). The zero-shot ICL approach demonstrated superior performance metrics compared to the textual entailment approach. Specifically, the highest mean F_1-score in the ICL approach, achieved by GEMMA-2, was 0.858, exceeding the best mean F_1-score of 0.723 obtained by DEBERTA-M in the textual entailment approach by 0.135, representing an 18.7% improvement. A paired *t* test demonstrated that GEMMA-2 significantly outperformed DEBERTA-M in terms of mean F_1-score, precision, and recall ($P<.001$). The detailed statistical results are provided in Multimedia Appendix 3. In addition, 3 out of 4 prompting strategies within the ICL approach resulted in higher mean accuracy and F_1-scores than those observed with the textual entailment method.

Table 7. Performance of pretrained language models using the textual entailment approach.

Pretrained language models	Accuracy (%), mean (SD)	F_1-score, mean (SD)	Precision, mean (SD)	Recall, mean (SD)	AUC-ROC[a], mean (SD)
ROBERTA-M	72.9 (0.7)	0.713 (0.008)	0.698 (0.007)	0.729 (0.008)	0.753 (0.009)
BART-M	69.6 (0.9)	0.691 (0.004)	0.701 (0.006)	0.681 (0.011)	0.736 (0.008)
DEBERTA-M	*73.8 (0.6)* [b]	*0.723 (0.005)*	*0.717 (0.007)*	*0.730 (0.006)*	*0.781 (0.010)*
BERT-M	64.2 (0.4)	0.615 (0.009)	0.623 (0.008)	0.608 (0.010)	0.701 (0.007)
Overall	70.1 (0.7)	0.686 (0.006)	0.685 (0.007)	0.687 (0.009)	0.743 (0.008)

[a]AUC-ROC: area under the receiver operating characteristic curve.

[b]Italicized values represent the best performance across models.

XSL•FO
RenderX

Table 8. Performance of general-purpose large language models (LLMs) using the zero-shot in-context learning approach.

General-purpose LLM	Accuracy (%), mean (SD)	F_1-score, mean (SD)	Precision, mean (SD)	Recall, mean (SD)
Generic				
LLAMA-3	70.9 (0.8)	0.811 (0.005)	0.821 (0.006)	0.801 (0.004)
FLAN-T5	67.2 (0.6)	0.709 (0.007)	0.731 (0.008)	0.688 (0.005)
GEMMA-2	70.4 (0.9)	0.750 (0.004)	0.778 (0.004)	0.724 (0.004)
MISTRAL-0.2	68.4 (0.6)	0.705 (0.006)	0.713 (0.006)	0.698 (0.005)
BIO-LLAMA-3	70.1 (0.8)	0.762 (0.006)	0.774 (0.005)	0.750 (0.004)
Overall	69.4 (0.7)	0.746 (0.005)	0.763 (0.007)	0.732 (0.004)
Chain of thought				
LLAMA-3	74.5 (0.7)	0.781 (0.009)	0.792 (0.007)	0.771 (0.009)
FLAN-T5	73.6 (0.3)	0.768 (0.007)	0.779 (0.006)	0.757 (0.005)
GEMMA-2	75.2 (0.6)	0.795 (0.005)	0.813 (0.007)	0.777 (0.004)
MISTRAL-0.2	72.5 (0.4)	0.756 (0.008)	0.768 (0.004)	0.745 (0.009)
BIO-LLAMA-3	73.1 (0.7)	0.775 (0.006)	0.787 (0.007)	0.764 (0.009)
Overall	73.8 (0.5)	0.775 (0.007)	0.788 (0.006)	0.763 (0.007)
Clue and reasoning prompting				
LLAMA-3	78.3 (0.6)	0.830 (0.005)	*0.842 (0.004)*[a]	0.818 (0.005)
FLAN-T5	74.9 (0.7)	0.785 (0.008)	0.794 (0.008)	0.776 (0.007)
GEMMA-2	73.7 (0.9)	0.803 (0.010)	0.811 (0.005)	0.795 (0.009)
MISTRAL-0.2	70.8 (0.5)	0.736 (0.007)	0.752 (0.005)	0.721 (0.007)
BIO-LLAMA-3	77.9 (0.6)	0.815 (0.005)	0.831 (0.007)	0.799 (0.004)
Overall	75.1 (0.7)	0.794 (0.008)	0.806 (0.006)	0.782 (0.007)
Stigma detection guided prompt				
LLAMA-3	82.4 (0.6)	0.845 (0.005)	0.822 (0.006)	0.869 (0.008)
FLAN-T5	76.6 (0.8)	0.819 (0.005)	0.804 (0.004)	0.834 (0.007)
GEMMA-2	*83.5 (0.6)*	*0.858 (0.004)*	*0.841 (0.005)*	*0.876 (0.003)*
MISTRAL-0.2	80.1 (0.5)	0.830 (0.004)	0.813 (0.006)	0.847 (0.006)
BIO-LLAMA-3	81.0 (0.5)	0.839 (0.005)	0.857 (0.007)	0.821 (0.004)
Overall	80.7 (0.6)	0.838 (0.005)	0.827 (0.006)	0.849 (0.005)

[a]Italicized values represent the best performance across models and prompting strategies.

Performance Evaluation for Few-Shot Approaches

Table 9 presents the performance of the various pretrained sentence transformers using the SetFit approach in the few-shot setting across different numbers of labeled data points per class. MINILM-V2 achieved the highest mean F_1-score of 0.721 (95% CI 0.713-0.729) and the highest mean AUC-ROC of 0.791 (95% CI 0.785- 0.797) with 4 annotated data points per class. However, E5-V2 outperformed the other models when 8 and 16 annotated data points per class were available, achieving mean F_1-scores of 0.735 (95% CI 0.728-0.742) and 0.802 (95% CI 0.798-0.806), respectively. On average, accuracy increased from 72.1% with 4 annotated data points per class to 78% with 16 annotated data points per class, while the average F_1-score improved from 0.707 to 0.767. These results highlight the positive impact of increasing the number of annotated data points on model performance within the few-shot SetFit approach.

Table 10 presents the mean F_1-score and accuracy of various general-purpose LLMs using the few-shot ICL approach with different prompting strategies. Additional performance metrics, including precision and recall, are provided in Multimedia Appendix 4. Due to limitations in the number of tokens (or words) that models can process at once (known as context window limitation), it was not feasible to conduct experiments with FLAN-T5 for the COT and CARP prompting strategies in the few-shot settings, nor with LLAMA-3 and GEMMA-2 for COT and CARP when 16 annotated data points per class were used. Thus, we do not report the mean performance of COT and CARP prompting strategies across models. LLAMA-3, paired with the stigma detection guided prompt, demonstrated the highest performance across all scenarios, achieving mean

XSL•FO
RenderX

F_1-scores of 0.874 (95% CI 0.864-0.884), 0.892 (95% CI 0.886-0.898), and 0.901 (95% CI 0.895-0.907) with 4, 8, and 16 annotated data points per class, respectively. When using the generic and the stigma detection guided prompt, it was observed that both the mean F_1-score and accuracy improved as the number of annotated data points per class increased.

Table 9. Performance of pretrained sentence transformers using the SetFit approach.

Sentence transformer	Accuracy (%), mean (SD)	F_1-score, mean (SD)	Precision, mean (SD)	Recall, mean (SD)	AUC-ROC[a], mean (SD)
4 annotated data per class					
MPNET-V2	70.5 (0.4)	0.701 (0.005)	0.708 (0.007)	0.697 (0.005)	0.752 (0.005)
E5-V2	*73.6 (0.6)* [b]	0.704 (0.003)	0.705 (0.004)	0.703 (0.003)	0.784 (0.007)
ROBERTA-V2	72.2 (0.6)	0.708 (0.004)	0.712 (0.005)	0.704 (0.005)	0.765 (0.005)
MINILM-V2	73.0 (0.5)	*0.721 (0.008)*	*0.718 (0.007)*	*0.725 (0.005)*	*0.791 (0.006)*
BERT-BIO-ST	71.4 (0.7)	0.701 (0.008)	0.687 (0.004)	0.715 (0.006)	0.770 (0.008)
BIOLORD	72.0 (0.7)	0.707 (0.008)	0.714 (0.005)	0.701 (0.009)	0.772 (0.005)
Overall	72.1 (0.6)	0.707 (0.006)	0.706 (0.006)	0.707 (0.005)	0.772 (0.006)
8 annotated data per class					
MPNET-V2	72.6 (0.8)	0.715 (0.003)	0.727 (0.006)	0.704 (0.004)	0.773 (0.005)
E5-V2	*77.1 (0.4)*	*0.735 (0.007)*	*0.750 (0.006)*	0.721 (0.008)	*0.836 (0.006)*
ROBERTA-V2	75.4 (0.8)	0.723 (0.005)	0.729 (0.006)	0.718 (0.004)	0.814 (0.006)
MINILM-V2	74.3 (0.6)	0.732 (0.005)	0.721 (0.004)	*0.743 (0.005)*	0.801 (0.007)
BERT-BIO-ST	75.1 (0.7)	0.726 (0.007)	0.715 (0.008)	0.736 (0.005)	0.817 (0.005)
BIOLORD	75.9 (0.4)	0.729 (0.008)	0.718 (0.005)	0.740 (0.007)	0.821 (0.004)
Overall	75.1 (0.5)	0.727 (0.006)	0.726 (0.007)	0.728 (0.006)	0.810 (0.005)
16 annotated data per class					
MPNET-V2	75.6 (0.3)	0.755 (0.005)	0.773 (0.005)	0.738 (0.006)	0.815 (0.007)
E5-V2	*80.7 (0.5)*	*0.802 (0.004)*	*0.813 (0.006)*	*0.792 (0.003)*	*0.858 (0.006)*
ROBERTA-V2	78.3 (0.4)	0.775 (0.006)	0.766 (0.007)	0.784 (0.004)	0.838 (0.005)
MINILM-V2	79.1 (0.6)	0.785 (0.007)	0.802 (0.006)	0.769 (0.005)	0.847 (0.009)
BERT-BIO-ST	77.3 (0.5)	0.745 (0.008)	0.752 (0.007)	0.738 (0.008)	0.832 (0.004)
BIOLORD	77.1 (0.8)	0.739 (0.004)	0.744 (0.005)	0.734 (0.004)	0.829 (0.006)
Overall	78.0 (0.7)	0.767 (0.006)	0.775 (0.005)	0.759 (0.007)	0.837 (0.007)

[a]AUC-ROC: area under the receiver operating characteristic curve.

[b]Italicized values represent the best performance across models when different numbers of annotated data per class were available.

Table 11 presents a comparison between the top-performing models using the SetFit approach and those using the few-shot ICL approach across different numbers of annotated data points per class. In all scenarios, the few-shot ICL models exhibited superior performance compared to their SetFit counterparts. Specifically, with 4 annotated data points per class, LLAMA-3 achieved a mean F_1-score of 0.874 (95% CI 0.864-0.884), which is 0.153 points higher than that of MINILM-V2, whose mean F_1-score was 0.721 (95% CI 0.713-0.729), representing an approximate 21.2% improvement. For 8 annotated data points per class, LLAMA-3 attained a mean F_1-score of 0.892 (95% CI 0.886-0.898) compared to 0.735 (95% CI 0.728-0.742) for E5-V2, corresponding to an improvement of about 21.4%. Finally, at 16 annotated data points per class, LLAMA-3 demonstrated a mean F_1-score of 0.901 (95% CI 0.895-0.907), which is 0.099 points higher than that of E5-V2, whose mean F_1-score was 0.802 (95% CI 0.798-0.806), reflecting a 12.3% improvement. For each setting (4,8, and 16 annotated data points per class), a paired t test was conducted to compare the top-performing models from the ICL and SetFit approaches (refer to Multimedia Appendix 3 for details). In all cases, the results indicated that the ICL models outperformed the SetFit models in terms of F_1-score, precision, and recall (P<.001).

XSL•FO
RenderX

Table 10. Performance of general-purpose large language models (LLMs) using the few-shot in-context learning approach.

General purpose-LLM	4 annotated data per class		8 annotated data per class		16 annotated data per class	
	Accuracy (%), mean (SD)	F_1-score, mean (SD)	Accuracy (%), mean (SD)	F_1-score, mean (SD)	Accuracy (%), mean (SD)	F_1-score, mean (SD)
Generic						
LLAMA-3	74.8 (0.8)	0.789 (0.006)	79.2 (0.9)	0.832 (0.008)	81.6 (0.8)	0.855 (0.006)
FLAN-T5	69.3 (0.5)	0.691 (0.007)	70.7 (0.8)	0.701 (0.008)	75.1 (0.5)	0.762 (0.006)
GEMMA-2	71.1 (1.2)	0.719 (0.007)	72.1 (0.8)	0.739 (0.009)	76.2 (0.9)	0.773 (0.008)
MISTRAL-0.2	72.5 (0.7)	0.730 (0.006)	70.5 (0.9)	0.720 (0.010)	80.1 (1.0)	0.822 (0.007)
BIO-LLAMA-3	76.6 (0.9)	0.820 (0.008)	77.3 (0.5)	0.826 (0.004)	79.0 (0.6)	0.851 (0.006)
Overall	72.9 (0.8)	0.75 (0.007)	74.0 (0.8)	0.764 (0.009)	78.4 (0.6)	0.813 (0.007)
COT						
LLAMA-3	72.5 (0.8)	0.756 (0.004)	83.1 (0.9)	0.823 (0.007)	__[a]	—
FLAN-T5	—	—	—	—	—	—
GEMMA-2	75.1 (0.4)	0.796 (0.006)	79.5 (0.8)	0.826 (0.005)	—	—
MISTRAL-0.2	71.3 (0.3)	0.742 (0.005)	75.1 (0.6)	0.767 (0.007)	76.9 (0.8)	0.781 (0.006)
BIO-LLAMA-3	71.6 (0.7)	0.743 (0.005)	81.4 (0.8)	0.835 (0.006)	—	—
CARP						
LLAMA-3	80.4 (0.8)	0.837 (0.005)	85.1 (0.5)	0.876 (0.004)	—	—
FLAN-T5	—	—	—	—	—	—
GEMMA-2	75.4 (0.7)	0.795 (0.006)	79.6 (0.4)	0.825 (0.009)	—	—
MISTRAL-0.2	71.8 (0.5)	0.728 (0.008)	72.2 (0.5)	0.747 (0.006)	71.2 (0.6)	0.731 (0.005)
BIO-LLAMA-3	77.2 (0.7)	0.813 (0.009)	81.6 (0.6)	0.849 (0.008)	—	—
Stigma detection guided prompt						
LLAMA-3	*84.3 (0.6)* [b]	*0.874 (0.010)*	*85.5 (0.7)*	*0.892 (0.006)*	*87.7 (0.7)*	*0.901 (0.006)*
FLAN-T5	74.2 (0.4)	0.782 (0.006)	76.8 (0.5)	0.805 (0.008)	82.8 (0.3)	0.842 (0.004)
GEMMA-2	84.3 (0.9)	0.872 (0.007)	84.9 (0.4)	0.881 (0.005)	86.1 (0.5)	0.887 (0.006)
MISTRAL-0.2	80.5 (0.7)	0.849 (0.005)	82.0 (0.6)	0.857 (0.004)	86.7 (0.7)	0.899 (0.005)
BIO-LLAMA-3	80.4 (1.1)	0.861 (0.010)	81.5 (0.8)	0.870 (0.007)	82.7 (1.0)	0.892 (0.009)
Overall	80.7 (0.8)	0.848 (0.008)	82.1 (0.6)	0.861 (0.005)	85.2 (0.5)	0.884 (0.007)

[a]Not applicable due to limited context window length.

[b]Italicized values represent the best performance across models and prompting strategies when different amounts of annotated data per class were available.

Table 11. Comparison of top-performing models in SetFit and few-shot in-context learning (ICL) approaches.

Approach and model	4 annotated data per class—F_1-score, mean (SD)	8 annotated data per class—F_1-score, mean (SD)	16 annotated data per class—F_1-score, mean (SD)
SetFit			
MINILM-V2	0.721 (0.008)	__[a]	—
E5-V2	—	0.735 (0.007)	0.802 (0.004)
Few-shot ICL			
LLAMA-3	0.874 (0.010)	0.892 (0.006)	0.901 (0.006)

[a]Not applicable.

XSL•FO
RenderX

Performance Comparison of the ICL With the Fully Supervised Fine-Tuning Approach

We presented the performance of the various pretrained language models using the fully supervised fine-tuning approach in Table 12. Among the models evaluated, ROBERTA demonstrated the highest performance, achieving a mean AUC-ROC of 0.973 (95% CI 0.968-0.978) and a mean F_1-score of 0.931 (95% CI 0.924-0.938). In contrast, BERT-BIOMED exhibited the lowest performance, with a mean AUC-ROC of 0.926 (95% CI 0.918-0.934) and a mean F_1-score of 0.894 (95% CI 0.888-0.900).

Table 12. Performance of pretrained language models for the fully supervised fine-tuning approach.

Pretrained language model	Accuracy (%), mean (SD)	F_1-score, mean (SD)	Precision, mean (SD)	Recall, mean (SD)	AUC-ROC[a], mean (SD)
ROBERTA	*94.5 (0.6)* [b]	*0.931 (0.007)*	*0.950 (0.008)*	*0.913 (0.009)*	*0.973 (0.005)*
BERT	94.2 (0.7)	0.922 (0.005)	0.943 (0.007)	0.901 (0.011)	0.962 (0.004)
BERT-BIO	93.7 (0.8)	0.910 (0.009)	0.929 (0.006)	0.893 (0.006)	0.948 (0.003)
ROBERTA-XLM	94.0 (0.5)	0.911 (0.006)	0.945 (0.007)	0.879 (0.008)	0.943 (0.009)
BERT-BIOMED	91.5 (0.7)	0.894 (0.006)	0.909 (0.004)	0.879 (0.008)	0.926 (0.008)
Overall	93.6 (0.6)	0.914 (0.007)	0.935 (0.007)	0.893 (0.008)	0.950 (0.006)

[a]AUC-ROC: area under the receiver operating characteristic curve.

[b]Italicized values represent the best performance across models.

Table 13 presents the performance of the top-performing models in the zero-shot, few-shot settings, and fully supervised fine-tuning approach. In the zero-shot setting, the best-performing model, GEMMA-2, achieved a mean F_1-score of 0.858 (95% CI 0.854-0.862), which is 0.073 points lower than the mean F_1-score of fully supervised ROBERTA at 0.931 (95% CI 0.924-0.938). This difference corresponds to an approximate 8.5% improvement in mean F_1-score for the fully supervised approach. In the few-shot setting, LLAMA-3 emerged as the top-performing model, achieving mean F_1-scores of 0.874 (95% CI 0.864-0.884), 0.892 (95% CI 0.886-0.898), and 0.901 (95% CI 0.895-0.907) with 4, 8, and 16 annotated data points per class, respectively. Although the mean F_1-score with 16 annotated data points per class was about 3.2% lower than that of fully supervised ROBERTA, it is notable that this performance was attained using only 32 labeled instances, whereas ROBERTA was trained with 3543 instances—more than 100 times the amount of annotated data.

Table 13. Performance of top-performing models in zero-shot, few-shot, and fully supervised fine-tuning approaches.

Approach or model	GEMMA-2—F_1-score, mean (SD)	LLAMA-3—F_1-score, mean (SD)	ROBERTA—F_1-score, mean (SD)
Zero-shot	0.858 (0.004)	—[a]	—
Few-shot: 4 annotated data per class	—	0.874 (0.010)	—
Few-shot: 8 annotated data per class	—	0.892 (0.006)	—
Few-shot: 16 annotated data per class	—	0.901 (0.006)	—
Fully supervised fine-tuning	—	—	0.931 (0.007)

[a]Not applicable.

Statistical Comparison of Model Performance

Table 14 summarizes the key findings from paired *t* tests, comparing the top-performing models in the zero-shot and few-shot settings, as well as performance differences between the best-performing ICL and supervised fine-tuning models. Additional details on the statistical comparisons are provided in Multimedia Appendix 3. In the zero-shot setting, paired *t* tests revealed that GEMMA-2 significantly outperformed DEBERTA-M in terms of F_1-score, precision, and recall (all $P<.001$). In the few-shot setting, ICL models demonstrated significantly higher performance across all 3 metrics compared to SetFit models. When comparing the top-performing models from the ICL and supervised fine-tuning approaches, ROBERTA achieved significantly higher F_1-score and precision ($P<.001$), while LLAMA-3 demonstrated significantly higher recall ($P<.001$).

XSL•FO
RenderX

Table 14. Paired *t* test results comparing the top-performing models in the zero-shot and few-shot settings, and between the best-performing models in in-context learning and supervised fine-tuning approaches.

Setting, comparison, and metric	Mean difference	*P* value
Zero-shot: DEBERTA-M versus GEMMA-2 coupled with stigma detection guided prompt		
F_1-score	−0.136	<.001
Precision	−0.125	<.001
Recall	−0.146	<.001
Few-shot (4 annotations per label): MINILM-V2 versus LLAMA 3 coupled with stigma detection guided prompt		
F_1-score	−0.155	<.001
Precision	−0.138	<.001
Recall	−0.165	<.001
Few-shot (8 annotations per label): E5-V2 versus LLAMA 3 coupled with stigma detection guided prompt		
F_1-score	−0.158	<.001
Precision	−0.124	<.001
Recall	−0.192	<.001
Few-shot (16 annotations per label): E5-V2 versus LLAMA 3 coupled with stigma detection guided prompt		
F_1-score	−0.101	<.001
Precision	−0.052	<.001
Recall	−0.152	<.001
ICL versus supervised fine-tuning: ROBERTA versus LAMMA-3 coupled with stigma detection guided prompt (16 annotated data per class)		
F_1-score	0.029	<.001
Precision	0.086	<.001
Recall	−0.030	<.001

Fairness Evaluation and Comparison

The performance and disparities of various models developed to detect stigmatizing language are presented in Multimedia Appendix 5. Table 15 highlights the largest absolute performance disparities across demographic attributes, including sex, age, and race, for each model. Models using the supervised fine-tuning approach exhibited relatively higher absolute disparities compared to the ICL models under zero-shot, 4-shot, 8-shot, and 16-shot settings. On average, models trained using the supervised fine-tuning approach demonstrated the largest mean absolute TPR disparities of 0.037, 0.077, and 0.046 for sex-, age-, and race-differentiated groups, respectively. These disparities indicate that the TPR can differ by up to 7.7% in certain demographic subgroups. In contrast, ICL models showed a more balanced TPR, with no mean disparity exceeding 0.007, 0.010, and 0.013 for sex-, age-, and race-differentiated groups, respectively. A similar pattern was observed for FPR and F_1-scores. Supervised fine-tuning models exhibited greater FPR disparities, with mean values of 0.026, 0.027, and 0.031 for sex-, age-, and race-differentiated groups, respectively. Conversely, the ICL models demonstrated lower FPR disparities under different experimental settings, indicating a more consistent FPR across groups. Table 16 presents the highest performance disparities of ICL and supervised fine-tuning models across sex, age, and race subgroups. Here, the highest disparities refer to the highest observed differences in performance metrics across demographic groups for each modeling approach. For TPR, supervised models exhibited disparities of up to 0.051 for sex, 0.108 for age, and 0.064 for race. In contrast, both zero-shot and few-shot ICL models showed substantially lower TPR disparities, with all values less than 0.016. Similarly, FPR disparities reached up to 0.039 for sex, 0.037 for age, and 0.043 for race in supervised models, whereas FPR disparities for ICL models remained less than 0.027. Regarding F_1-scores, the highest disparity among supervised models reached 0.086, compared to less than 0.025 among ICL models. These findings suggest that ICL models offer more equitable performance across demographic groups.

XSL•FO
RenderX

Table 15. The largest absolute performance disparity across demographic attributes for different approaches in detecting stigmatizing language.

Approach and model	Sex	Age (y)	Race
Largest absolute TPR[a] disparity			
Supervised fine-tuning			
ROBERTA	0.049	0.108	0.044
BERT	0.051	0.058	0.036
BERT-BIO	0.022	0.075	0.037
ROBERTA-XLM	0.033	0.089	0.052
BERT-BIOMED	0.032	0.053	0.064
Overall	0.037	0.077	0.046
Zero-shot ICL[b]			
LLAMA-3	0.005	0.012	0.011
FLAN-T5	0.002	0.004	0.008
GEMMA-2	0.003	0.009	0.010
MISTRAL-0.2	0.007	0.005	0.006
BIO-LLAMA-3	0.006	0.010	0.013
Overall	0.005	0.008	0.010
Few-shot ICL (4 annotated data per class)			
LLAMA-3	0.003	0.008	0.013
FLAN-T5	0.004	0.009	0.014
GEMMA-2	0.002	0.007	0.012
MISTRAL-0.2	0.014	0.006	0.015
BIO-LLAMA-3	0.008	0.008	0.010
Overall	0.006	0.008	0.013
Few-shot ICL (8 annotated data per class)			
LLAMA-3	0.006	0.008	0.010
FLAN-T5	0.003	0.005	0.009
GEMMA-2	0.006	0.007	0.011
MISTRAL-0.2	0.014	0.004	0.007
BIO-LLAMA-3	0.005	0.008	0.007
Overall	0.007	0.006	0.009
Few-shot ICL (16 annotated data per class)			
LLAMA-3	0.003	0.007	0.012
FLAN-T5	0.007	0.008	0.007
GEMMA-2	0.006	0.012	0.013
MISTRAL-0.2	0.007	0.011	0.009
BIO-LLAMA-3	0.006	0.013	0.010
Overall	0.006	0.010	0.010
Largest absolute FPR[c] disparity			
Supervised fine-tuning			
ROBERTA	0.018	0.022	0.028
BERT	0.016	0.015	0.023
BERT-BIO	0.035	0.033	0.027

XSL•FO
RenderX

Approach and model	Sex	Age (y)	Race
ROBERTA-XLM	0.021	0.023	0.043
BERT-BIOMED	0.039	0.037	0.032
Overall	0.026	0.027	0.031
Zero-shot ICL			
LLAMA-3	0.003	0.008	0.008
FLAN-T5	0.007	0.011	0.010
GEMMA-2	0.008	0.018	0.019
MISTRAL-0.2	0.005	0.016	0.014
BIO-LLAMA-3	0.001	0.011	0.008
Overall	0.005	0.013	0.012
Few-shot ICL (4 annotated data per class)			
LLAMA-3	0.006	0.013	0.007
FLAN-T5	0.007	0.015	0.011
GEMMA-2	0.005	0.013	0.015
MISTRAL-0.2	0.003	0.016	0.014
BIO-LLAMA-3	0.005	0.017	0.015
Overall	0.005	0.015	0.012
Few-shot ICL (8 annotated data per class)			
LLAMA-3	0.002	0.007	0.009
FLAN-T5	0.011	0.026	0.019
GEMMA-2	0.012	0.013	0.010
MISTRAL-0.2	0.007	0.021	0.014
BIO-LLAMA-3	0.005	0.011	0.014
Overall	0.007	0.016	0.013
Few-shot ICL (16 annotated data per class)			
LLAMA-3	0.007	0.015	0.012
FLAN-T5	0.009	0.011	0.009
GEMMA-2	0.004	0.013	0.014
MISTRAL-0.2	0.004	0.016	0.013
BIO-LLAMA-3	0.014	0.017	0.010
Overall	0.008	0.014	0.011
Largest absolute F_1-score disparity			
Supervised fine-tuning			
ROBERTA	0.043	0.066	0.064
BERT	0.037	0.048	0.030
BERT-BIO	0.026	0.058	0.031
ROBERTA-XLM	0.064	0.086	0.032
BERT-BIOMED	0.041	0.053	0.051
Overall	0.042	0.063	0.042
Zero-shot ICL			
LLAMA-3	0.006	0.015	0.006
FLAN-T5	0.004	0.018	0.011

XSL•FO
RenderX

Approach and model	Sex	Age (y)	Race
GEMMA-2	0.010	0.013	0.016
MISTRAL-0.2	0.006	0.015	0.010
BIO-LLAMA-3	0.005	0.005	0.009
Overall	0.006	0.013	0.010
Few-shot ICL (4 annotated data per class)			
LLAMA-3	0.005	0.010	0.017
FLAN-T5	0.012	0.011	0.013
GEMMA-2	0.008	0.013	0.014
MISTRAL-0.2	0.004	0.016	0.013
BIO-LLAMA-3	0.010	0.011	0.018
Overall	0.008	0.012	0.015
Few-shot ICL (8 annotated data per class)			
LLAMA-3	0.008	0.009	0.006
FLAN-T5	0.010	0.023	0.016
GEMMA-2	0.003	0.013	0.015
MISTRAL-0.2	0.018	0.017	0.024
BIO-LLAMA-3	0.015	0.012	0.019
Overall	0.011	0.015	0.016
Few-shot ICL (16 annotated data per class)			
LLAMA-3	0.006	0.014	0.014
FLAN-T5	0.013	0.020	0.025
GEMMA-2	0.008	0.011	0.017
MISTRAL-0.2	0.015	0.014	0.018
BIO-LLAMA-3	0.005	0.013	0.011
Overall	0.009	0.014	0.017

[a]TPR: true positive rate.

[b]ICL: in-context learning.

[c]FPR: false positive rate.

XSL•FO
RenderX

Table 16. The highest observed performance disparities of in-context learning (ICL) and supervised fine-tuning models across sex, age, and race subgroups.

Approach	Sex	Age (y)	Race
Highest TPR[a] disparity			
Supervised fine-tuning	0.051	0.108	0.064
Zero-shot ICL	0.007	0.012	0.013
Few-shot ICL	0.014	0.013	0.015
Highest FPR[b] disparity			
Supervised fine-tuning	0.039	0.037	0.043
Zero-shot ICL	0.008	0.018	0.019
Few-shot ICL	0.014	0.026	0.019
Highest F_1-score disparity			
Supervised fine-tuning	0.064	0.086	0.064
Zero-shot ICL	0.010	0.018	0.016
Few-shot ICL	0.018	0.023	0.025

[a]TPR: true positive rate.

[b]FPR: false positive rate.

Discussion

Overview

The prevalence of stigmatizing language in EHRs has raised significant concern due to its detrimental impact on the quality of care [7,15,22,24,26,79]. Numerous studies have investigated the potential of using supervised machine learning approaches for detecting stigmatizing language [15,27,28]. However, these approaches typically require extensive amounts of labeled data to achieve optimal performance. The creation of such a dataset is particularly challenging, given the difficulty in identifying stigmatizing language, which is often subtle, implicit, and highly contextual [27,37]. The ICL approach has emerged as a promising alternative due to its strong contextual understanding capabilities and minimal reliance on labeled data [29-32]. In this study, we extensively investigated the efficacy of ICL in detecting stigmatizing language and compared its performance with established zero-shot and few-shot text classification methods. To the best of our knowledge, this is the first study to explore the use of ICL, as well as zero-shot and few-shot approaches, for detecting stigmatizing language. Furthermore, we proposed a novel prompting strategy designed for detecting stigmatizing language and evaluated its effectiveness against state-of-the-art prompting strategies, such as COT and CARP.

Principal Findings

The ICL approaches have demonstrated a substantial advantage in detecting stigmatizing language compared to both the popular zero-shot textual entailment approach and the few-shot SetFit approach. In the zero-shot setting, the top-performing ICL model, GEMMA-2, achieved a mean F_1-score of 0.858 (95% CI 0.854-0.862), surpassing the best mean F_1-score of 0.723 (95% CI 0.718-0.728) obtained by ROBERTA-M in the textual entailment approach by 0.135 points, representing an 18.7% improvement. Similarly, in the few-shot setting, the top-performing ICL model, LLAMA-3, exhibited mean F_1-score improvements of 21.2%, 21.4%, and 12.3% over the leading SetFit models when using 4, 8, and 16 annotations per class, respectively. The superior performance of the ICL approach can be attributed to the enhanced contextual understanding capability and rich knowledge of general-purpose LLMs [33,34]. These general-purpose LLMs have undergone sophisticated training processes, such as instructional fine-tuning, reinforcement learning from human feedback, and extensive pretraining across a diverse range of NLP tasks, including language modeling, text completion, and semantic understanding on vast amounts of textual data [66,80,81]. These training processes have enabled the general-purpose models to better comprehend and contextualize subtle and complex linguistic patterns, making the ICL approach particularly effective for detecting stigmatizing language in EHRs. Therefore, in settings where annotated data is limited, the ICL approach should be prioritized for detecting stigmatizing language. However, it is important to note that the ICL models do not produce probabilistic classification outputs, which prevents the computation of threshold-independent metrics, such as AUC-ROC. This limitation affects the interpretation of results in 2 key ways. First, it may obscure comparisons with probabilistic models, which may exhibit strong overall class separation but suffer from performance instability at specific thresholds (ie, precision, recall, or F_1-scores). Second, more importantly, the lack of probability outputs prevents us from adjusting the decision threshold to accommodate different preferences for false positives versus false negatives, which is a common requirement in some clinical applications. Some clinical contexts may prioritize minimizing false positives to avoid overalerting, while others may emphasize minimizing false negatives to avoid missed harms.

Within the ICL approach, substantial performance variability was observed across different prompting strategies. Specifically,

XSL•FO
RenderX

in the zero-shot setting, the mean accuracy for the ICL approach varied between 69.4% and 80.7% across different prompting strategies, indicating a gap of 11.3%. In the few-shot setting, the differences in mean accuracy across prompting strategies were 7.8%, 8.1%, and 6.8% when using 4, 8, and 16 annotations per class, respectively. These performance gaps highlight the critical importance of selecting an appropriate prompting strategy to optimize the effectiveness of the ICL approach in detecting stigmatizing language. The new prompting strategy that we proposed in this work, the stigma detection guided prompt, outperformed the established strategies, such as COT and CARP [30,44]. This strategy achieved the highest F_1-scores across both zero-shot and few-shot settings, with a mean F_1-score of 0.858 (95% CI 0.854-0.862) in the zero-shot setting and mean F_1-scores of 0.874 (95% CI 0.864-0.884), 0.892 (95% CI 0.886-0.898), and 0.901 (95% CI 0.895-0.907) in the few-shot settings using 4, 8, and 16 annotations per class, respectively. The goal of the newly proposed prompt is to encode domain-specific knowledge that can assist the LLM in accurately identifying stigmatizing language. This was inspired by the fact that domain-specific information has been used in various settings to improve the performance of artificial intelligence (AI) algorithms, such as designing efficient search heuristics for informed search [82] or enhancing machine learning accuracy [83,84]. The prompt incorporated linguistic cues commonly associated with stigmatizing language, such as stereotyping, disapproval, and questioning credibility [37]. These elements enhance the model's ability to detect nuanced stigmatizing language that might otherwise be overlooked. Consequently, the stigma detection guided prompt represents a critical advancement in optimizing the ICL approach for this task. Its demonstrated effectiveness underscores the importance of leveraging medical informatics–driven insights to improve the detection of stigmatizing language, thereby supporting bias-aware clinical documentation practices.

To thoroughly assess the potential of the ICL approach, we compared the top-performing model in the ICL approach with that of the supervised fine-tuning approach, which is widely regarded as the standard method for text classification [30,85]. The leading model in the supervised fine-tuning approach, ROBERTA, achieved a mean F_1-score of 0.931 (95% CI 0.924-0.938). In comparison, the best-performing ICL model, LLAMA-3, attained a mean F_1-score of 0.901 (95% CI 0.895-0.907) with only 16 annotations per class. While the F_1-score difference of 0.030 corresponds to a 3.2% advantage for the fully supervised fine-tuning approach, it is worth noting that ROBERTA was developed using a training dataset of 3543 annotated sentences and a validation dataset of 500 annotated sentences, whereas LLAMA-3 used a training dataset of 32 annotated sentences and a validation dataset of 30 annotated sentences. This comparison highlighted the remarkable efficiency of the ICL approach.

As part of our analysis, we examined the fairness dimension of the models of few-shot ICL and the supervised fine-tuning approach. The results indicate that models using the supervised fine-tuning approach exhibited greater bias compared with ICL models. Specifically, with respect to TPR, supervised fine-tuning models demonstrated mean TPR disparities of 0.037, 0.077, and 0.046 across sex-, age-, and race-differentiated groups, respectively, suggesting that the TPR could vary by up to 7.7% for certain demographic subgroups. Similarly, with respect to the FPR, supervised fine-tuning models exhibited mean disparities of 0.026, 0.027, and 0.013 for sex-, age-, and race-differentiated groups, respectively. These findings indicate that supervised fine-tuning models are more likely to assign false positive classifications at uneven rates across demographic subgroups, potentially leading to the overflagging of stigmatizing language in certain populations. In contrast, ICL models tested in zero-shot, 4-shot, 8-shot, and 16-shot settings demonstrated a more balanced performance across subgroups, with no mean TPR disparities exceeding 0.016. Previous studies have shown that the supervised fine-tuning approach is susceptible to bias due to its dependence on training datasets that may have an imbalanced demographic distribution [86-88]. The primary objective of this approach is to optimize overall model performance, which can result in an emphasis on the majority or well-represented groups within the dataset. Consequently, when certain groups are underrepresented in the training data, the model's performance tends to decline for those groups, resulting in disparities. In contrast, the ICL approach generates predictions based on the specific context presented in the prompt, minimizing the risk of inheriting and amplifying biases present in the training dataset. Therefore, the adoption of the ICL approach could contribute to more equitable detection of stigmatizing language across all patient populations.

Clinical Adoption and Privacy Considerations

The integration of a stigmatization detection model into clinical documentation systems has the potential to enhance clinicians' awareness of implicit biases, leading to more neutral and patient-centered documentation. However, its deployment requires careful ethical consideration. If clinicians perceive that their language is being excessively monitored or that following language guidelines imposes a cognitive burden, they may become resistant to the model or attempt to circumvent its use by omitting clinically relevant details to avoid triggering the model's flagging system. Such reluctance could limit the model's effectiveness in fostering more inclusive documentation practices and impact the accuracy and completeness of medical records. Therefore, it is essential to clearly communicate the model's purpose, emphasizing its role as a supportive, educational tool rather than a punitive mechanism [89]. In addition, integrating a recommendation system that offers context-sensitive, neutral language recommendations as alternatives to flagged terms may improve clinician acceptance and facilitate smoother adoption into clinical workflows. Furthermore, real-world datasets often exhibit imbalances concerning protected attributes [87], which may result in the model disproportionately flagging certain patient groups (eg, racial minority groups and individuals with specific medical conditions) while underdetecting stigmatization in others. If left unaddressed, this could inadvertently reinforce stereotypes and exacerbate disparities in clinical documentation [90]. To mitigate these risks, the model should undergo rigorous fairness evaluations across diverse demographic groups and incorporate appropriate bias mitigation strategies before deployment [86,88].

XSL•FO
RenderX

Furthermore, we were unable to evaluate proprietary models, such as GPT-4, due to data-sharing restrictions imposed by the MIMIC-IV dataset [45]. While our findings highlight the promise of open-source LLMs in data-scarce settings, the exclusion of proprietary models limits the generalizability of our findings. Proprietary models often incorporate more advanced architectures and are trained on larger, more diverse corpora, which may allow them to outperform open-source alternatives [81]. Future studies leveraging synthetic data or institutional data-sharing agreements may be needed to assess if these proprietary models outperform open-source models in detecting stigmatizing language.

With the growing adoption of AI scribes in clinical settings, important considerations arise regarding the potential introduction or perpetuation of stigmatizing language in automatically generated clinical notes. Current AI scribing tools often operate as stand-alone systems, transcribing clinician-patient conversations and generating documentation with limited real-time oversight [91,92]. While many advanced LLMs are trained using debiasing techniques to reduce the risk of overtly harmful or abusive type of stigmatizing language (ie, junkie) [93], these methods are not explicitly designed to detect subtler forms of stigmatization commonly found in clinical narratives. The detection tool developed in this study can address this challenge in 2 ways. First, it can be applied during model development to identify and remove implicit forms of stigmatizing content from training data, thereby preventing LLMs from learning and reproducing such language. Second, it can serve as a postgeneration filter to flag potentially stigmatizing content in AI-generated clinical notes. In addition, our models can be used to design a human-AI collaborative scribing tool where AI-generated drafts are reviewed and finalized by clinicians [94]. In this context, the tool developed in this study can assist by alerting clinicians to potentially stigmatizing language, thereby promoting more neutral and patient-centered documentation. Future work should focus on validating the tool's effectiveness in real-world clinical scribing environments and examining clinician acceptance and workflow integration.

Beyond ethical and deployment considerations, the variability of stigmatizing language across documentation types and clinical settings presents a practical consideration for deployment. Previous studies indicate that stigmatizing language is more frequently observed in history and physical notes, consultation notes, and discharge summaries compared to other types of clinical documentation and tends to be more common in relation to conditions such as substance use disorders, mental health conditions, diabetes, and obesity [8,10]. These patterns underscore the importance of accounting for documentation context and clinical setting when developing stigma detection tools. For instance, the ICL approach could be optimized by incorporating examples drawn from specific note types or clinical domains where stigmatizing language is more prevalent. Such tailoring may improve the model's sensitivity to context-dependent expressions of bias. Moreover, recognizing that different specialties and note types reflect distinct clinician workflows, linguistic norms, and patient populations, it is essential to validate model performance across these subdomains. These validation efforts are critical to ensuring equitable performance across documentation formats and minimizing unintended disparities during deployment.

In addition to detecting stigmatizing language, LLMs can serve as valuable preprocessing tools for identifying linguistic patterns that may be integrated into downstream statistical models to explore potential associations between language use and care quality or operational decisions [15]. Furthermore, LLMs could provide real-time alerts about the potential impact of specific terms in clinical notes. These systems can draw on findings from previous research on the effects of specific terminology in clinical communication to prompt clinicians to reflect on their language choices. For example, if a term such as "aggressive" is used in a clinical note and identified by LLM as stigmatizing based on its contextual use, the system could generate a prompt indicating that the term may lead to patient discomfort or feelings of alienation. Such feedback could serve as a reflective checkpoint, prompting clinicians to reconsider their word choices and adopt more neutral, patient-centered language.

From the perspective of patient privacy and confidentiality, while deidentification is a crucial step in protecting patient privacy [46,95], the use of potentially sensitive data, such as stigmatizing language, still presents confidentiality concerns. Specifically, there are 2 key privacy risks associated with deploying machine learning–based stigmatization detection models in clinical settings. First, despite deidentification, the model may learn associations between specific linguistic patterns and particular patient populations [96]. For example, if the model systematically classifies clinical notes from a specific hospital, demographic group, or medical condition as stigmatizing, it could lead to unintended disclosures about those populations. If this information were to be combined with external data sources, there is a potential risk of reidentifying patient groups or even individuals. To mitigate such risks, implementing strict access control measures is necessary to ensure that only authorized clinicians and relevant personnel can interact with the model [96,97]. Second, the dataset used to train the model was curated based on sentences containing potentially stigmatizing words or expressions, introducing additional privacy concerns. Improper handling of the dataset during preprocessing, storage, or transfer could pose privacy risks [98]. To address this, robust data security measures should be implemented, including secure storage environments with access logging and monitoring, as well as strict protocols for data transfer to prevent unauthorized access. These safeguards are essential to balancing the benefits of stigmatization detection with the need to protect patient confidentiality in real-world clinical practice.

Comparison With Previous Work

LLMs are increasingly being used in health care for a wide range of applications, demonstrating their capacity to process and interpret complex clinical textual data [36,74,99]. These applications encompass medical question answering, where LLMs assist clinicians and patients by providing answers to health-related queries [99], and medical text summarization, which simplifies lengthy clinical documents into concise

XSL•FO
RenderX

summaries for improved decision-making [99]. In addition, LLMs are used for biomedical evidence extraction, enabling the identification of relevant research findings and coreference resolution, ensuring clarity and coherence in clinical narratives [32]. Other notable applications include medication status tracking, which monitors patient prescriptions and attribute extraction, which identifies key patient or clinical characteristics from unstructured text to support data-driven insights in health care workflows [32]. Furthermore, LLMs have been used to support clinicians in developing diagnostic reasoning, with research demonstrating that, when paired with appropriate prompting strategies, LLMs can effectively mimic common clinical reasoning processes without compromising diagnostic accuracy [100]. While these applications underscore the versatility of LLMs in advancing clinical workflow efficiency and decision-making, our manuscript addresses a distinct and underexplored challenge: detecting stigmatizing language in EHRs. Stigmatizing language within clinical documentation can perpetuate biases, undermine patient trust, and negatively impact the quality of care provided. By focusing on this critical issue, our work aims to promote bias-aware clinical documentation practices and foster equity in health care communication, addressing a significant gap in the field of medical informatics.

Sentiment analysis, a well-established area of research in NLP, has informed a wide range of clinical applications, including early studies on patient sentiment and health care provider communication patterns [101]. It shares both conceptual and methodological similarities with the task of detecting stigmatizing language. From a conceptual standpoint, sentiment analysis aims to classify the emotional tone of language, typically as positive, negative, or neutral. In contrast, stigmatization detection seeks to identify socially harmful or biased expressions. While the 2 tasks differ in their end goals, it is plausible that stigmatizing language often co-occurs with negative sentiment. Investigating whether sentiment can reliably predict stigmatization represents a promising direction for future research. However, as our dataset does not include sentiment labels, we were unable to empirically examine the potential overlap between negative sentiment and stigmatizing content. From the perspective of methodological similarity, both tasks are commonly addressed using text classification models. Indeed, the BERT-based models used in our study are widely used in sentiment analysis [102,103]. The primary methodological distinction lies in the labeling: sentiment analysis requires annotations for emotional tone, while stigmatization detection relies on annotations indicating the presence of stigmatizing content in text.

Extensive literature has documented the adverse effects of stigmatizing language in EHRs on the quality of patient care [7,8,16,20,22,24-26]. Despite this, the use of machine learning techniques to detect such language has received relatively limited attention. Sun et al [15] were among the first to apply machine learning in this context, developing a logistic regression classifier in a supervised fashion that achieved an F_1-score of 0.935 on a proprietary dataset. However, their study focused primarily on the unequal use of stigmatizing language across different demographic groups, placing less emphasis on the development and optimization of the machine learning model itself. Harrigian et al [27] conducted a more technical analysis using 2 EHR datasets, exploring the application of logistic regression and BERT models for detecting stigmatizing language. Barcelona et al [28] developed and evaluated decision trees, random forests, and support vector machines for detecting stigmatizing language in labor and clinical notes.

In contrast, our research focused on evaluating and comparing the effectiveness of various zero-shot and few-shot approaches, which can operate without the need for extensive annotated data. Our findings revealed that the ICL approach significantly outperformed traditional zero-shot and few-shot text classification approaches, such as textual entailment and SetFit, while only slightly underperforming compared to the fully supervised fine-tuning approach, despite using over 100 times fewer annotated data points for training. By leveraging ICL, the reliance on large labeled datasets can be significantly diminished, enabling the development of more efficient and flexible solutions for detecting stigmatizing language across diverse clinical settings. Furthermore, our study is the first to rigorously assess the fairness dimension of machine learning classifiers specifically for stigmatizing language detection. In comparing the ICL approach to the supervised fine-tuning approach, we found that the latter is more prone to demonstrate unequal performance across specific demographic groups. However, our study did not explicitly examine methods that can be used to improve the fairness of models developed with a supervised fine-tuning approach, such as diversifying training datasets [104,105] and incorporating fairness constraints [86].

Limitations

This study is subject to several limitations that should be acknowledged. First, the analysis was conducted using a single dataset obtained from the emergency department of the Beth Israel Deaconess Medical Center in Boston, Massachusetts. Consequently, the findings are inherently constrained by the specific characteristics of this dataset, including its geographical setting, imbalanced patient demographics, and institutional practices. Therefore, the generalizability of the models' performance to other stigmatizing language datasets remains uncertain. Future research should aim to assess the ICL approach using larger and more diverse datasets from multiple institutions.

Second, the dataset used in this study was curated by selecting sentences that contained preidentified keywords. Stigmatizing language can manifest both explicitly through overtly negative terms and implicitly through subtle variations in tone, phrasing, or contextual framing. While our approach may excel in the detection of explicit forms of stigmatizing language, it does not fully capture more implicit forms of stigmatization. As such, our evaluation may be limited in its ability to capture the full spectrum of stigmatizing language. We hypothesize that the ICL approach has the potential to detect subtler forms of stigma by leveraging contextual information through carefully crafted prompts, as partially demonstrated in this study. However, due to the nature of the available dataset, we were unable to empirically assess the model's generalizability to more implicit expressions of stigma. Future work should focus on developing datasets that capture a broader range of stigmatizing language.

XSL•FO
RenderX

This would support more comprehensive evaluation and guide the improvement of models capable of identifying nuanced and context-dependent stigma. Moreover, the stigma detection guided prompt was intentionally designed to focus on a predefined keyword. While this strategy leverages important cues for detecting explicit forms of stigmatization, it may restrict the ICL models' ability to capture broader contextual cues or detect more implicit forms of stigma. Future studies should develop models capable of identifying more subtle forms of stigmatization without reliance on preidentified terms.

Third, our current binary labeling framework does not explicitly address 2 important nuances. It does not explicitly consider ambiguous cases where the interpretation of stigmatization is context-dependent. The current dataset employs binary labels, stigmatizing or nonstigmatizing, without accounting for sentences that may require additional context for accurate classification. Future research could address this issue by introducing an additional classification category, such as "uncertain/requires further context," similar to the CheXpert dataset [106]. This would enable models to flag ambiguous cases for human review or request additional contextual information to support model predictions. In addition, while collapsing distinct categories of stigmatizing language into a binary label (stigmatizing vs nonstigmatizing) enabled broader applicability and methodological comprehensiveness in this study, it may have obscured important nuances related to the impacts of different types of stigma. Previous literature has highlighted the clinical consequences of stigmatizing language [17,18], but the differential effects of specific stigma dimensions remain underexplored. In future work, we intend to systematically investigate whether specific types of stigma are differentially associated with key clinical outcomes.

Fourth, we did not examine the effectiveness of fine-tuning decoder-based models, such as LLAMA, due to the limited availability of annotated data, and as a result, their efficacy in detecting stigmatizing language remains underexplored. Future research should investigate whether fine-tuning decoder-based models can enhance performance in settings where large-scale annotated datasets are available.

Fifth, this study focused on fairness evaluation based on race, sex, and age, but did not incorporate other sociodemographic factors, such as socioeconomic status, education level, or geographic location, due to data limitations. Future research should consider a more comprehensive fairness analysis that encompasses these attributes to ensure equitable model performance across diverse populations. Sixth, while this study includes a fairness evaluation of different models for stigmatizing language detection, it does not examine the effectiveness of various bias mitigation techniques, as such an analysis would require a separate, dedicated investigation. Future research is encouraged to explore bias reduction strategies, such as diversifying training datasets [105] and implementing fairness-aware machine learning techniques [107].

Finally, we hypothesize that machine learning solutions for detecting stigmatizing language will be used as decision-support systems within clinical workflows rather than as decision-making systems due to the necessity of human oversight and the importance of ensuring that narratives within EHRs are validated by clinicians. While this study discusses several potential ethical implications for the clinical deployment of the stigmatization detection model, it did not address several critical factors essential for effective human-AI collaboration in this context, such as varying levels of automation, system usability, and the potential for automation bias. Future research should explore these factors to ensure the successful integration of such systems into clinical workflows, thereby optimizing decision-making processes and enhancing the efficiency and effectiveness of stigmatizing language detection.

Conclusions

We explored the potential of the ICL approach for detecting stigmatizing language in EHRs, particularly in scenarios where annotated data is limited. Our findings demonstrate that ICL approaches perform significantly better than traditional zero-shot and few-shot methods, such as textual entailment and SetFit. Moreover, our results underscore the critical importance of prompt engineering within the ICL approach. The novel prompting strategy, the stigma detection guided prompt, developed in this study, significantly enhances the detection of stigmatizing language by incorporating common linguistic characteristics of such language and guiding the model's attention to specific keywords. When compared with the supervised fine-tuning approach, ICL has demonstrated competitive performance as well as superior fairness metrics, with lower performance disparities across different demographic groups. In summary, ICL is emerging as a robust and flexible solution for detecting stigmatizing language in EHRs, offering a more efficient, effective, and equitable alternative than conventional machine learning approaches.

Acknowledgments

This study is supported by the Natural Sciences and Engineering Research Council of Canada and the Data Sciences Institute at the University of Toronto through grant DSI-DSFY3R1P06.

Data Availability

The datasets analyzed during this study are available in the PhysioNet repository [27]. The code supporting this study is intended for public release via the PhysioNet repository in the future. In the meantime, access can be requested directly from the corresponding author.

XSL•FO
RenderX

Authors' Contributions

HC was responsible for conceptualization, data curation, formal analysis, investigation, methodology, software, visualization, writing-original draft and writing-review and editing. MA contributed to conceptualization, visualization, and writing-review and editing. EC contributed to conceptualization, formal analysis, funding acquisition, investigation, methodology, project administration, resources, supervision, validation, and writing-review and editing.

Conflicts of Interest

None declared.

Multimedia Appendix 1
Dataset description and stigmatizing language examples.
[DOCX File , 27 KB - medinform_v13i1e68955_app1.docx]

Multimedia Appendix 2
Detailed code implementation for the prompting strategies.
[DOCX File , 15 KB - medinform_v13i1e68955_app2.docx]

Multimedia Appendix 3
Paired *t* test comparison of top-performing models in zero-shot, few-shot, and supervised fine-tuning approaches.
[DOCX File , 18 KB - medinform_v13i1e68955_app3.docx]

Multimedia Appendix 4
Performance metrics of the few-shot in-context learning models.
[DOCX File , 24 KB - medinform_v13i1e68955_app4.docx]

Multimedia Appendix 5
Performance and performance disparities of models across sex, age, and race demographic attributes.
[DOCX File , 70 KB - medinform_v13i1e68955_app5.docx]

References

1. Adeniyi AO, Arowoogun JO, Chidi R, Okolo CA, Babawarun O. The impact of electronic health records on patient care and outcomes: a comprehensive review. World J Adv Res Rev 2024 Feb 28;21(2):1446-1455. [doi: 10.30574/wjarr.2024.21.2.0592]
2. Overhage JM, McCallie D. Physician time spent using the electronic health record during outpatient encounters: a descriptive study. Ann Intern Med 2020 Feb 04;172(3):169-174. [doi: 10.7326/M18-3684] [Medline: 31931523]
3. Gedikci Ondogan A, Sargin M, Canoz K. Use of electronic medical records in the digital healthcare system and its role in communication and medical information sharing among healthcare professionals. Inform Med Unlocked 2023;42:101373. [doi: 10.1016/j.imu.2023.101373]
4. Liang J, Li Y, Zhang Z, Shen D, Xu J, Zheng X, et al. Adoption of Electronic Health Records (EHRs) in China during the past 10 years: consecutive survey data analysis and comparison of Sino American challenges and experiences. J Med Internet Res 2021 Feb 18;23(2):e24813 [FREE Full text] [doi: 10.2196/24813] [Medline: 33599615]
5. Woldemariam MT, Jimma W. Adoption of electronic health record systems to enhance the quality of healthcare in low-income countries: a systematic review. BMJ Health Care Inform 2023 Jun;30(1):e100704 [FREE Full text] [doi: 10.1136/bmjhci-2022-100704] [Medline: 37308185]
6. Song N, Hugh-Jones S, West RM, Pickavance J, Mir G. The effectiveness of anti-stigma interventions for reducing mental health stigma in young people: a systematic review and meta-analysis. Glob Ment Health (Camb) 2023;10:e39 [FREE Full text] [doi: 10.1017/gmh.2023.34] [Medline: 37854399]
7. Cox C, Fritz Z. Presenting complaint: use of language that disempowers patients. BMJ 2022 Apr 27;377:e066720 [FREE Full text] [doi: 10.1136/bmj-2021-066720] [Medline: 35477529]
8. Healy M, Richard A, Kidia K. How to reduce stigma and bias in clinical communication: a narrative review. J Gen Intern Med 2022 Aug;37(10):2533-2540 [FREE Full text] [doi: 10.1007/s11606-022-07609-y] [Medline: 35524034]
9. Carrotte E, Hopgood F, Blanchard M, Groot C, Phillips L. A new podcast for reducing stigma against people living with complex mental health issues: co-design study. JMIR Form Res 2023 May 05;7:e44412 [FREE Full text] [doi: 10.2196/44412] [Medline: 37145860]
10. Weiner SG, Lo YC, Carroll AD, Zhou L, Ngo A, Hathaway DB, et al. The incidence and disparities in use of stigmatizing language in clinical notes for patients with substance use disorder. J Addict Med 2023;17(4):424-430 [FREE Full text] [doi: 10.1097/ADM.0000000000001145] [Medline: 37579100]

XSL•FO
RenderX

11. Smith RA. Language of the lost: an explication of stigma communication. Commun Theory 2007 Nov;17(4):462-485. [doi: 10.1111/j.1468-2885.2007.00307.x]
12. Beukeboom CJ, Burgers C. Linguistic bias. Oxford Research Encyclopedia of Communication. URL: https://doi.org/10.1093/acrefore/9780190228613.013.439 [accessed 2025-04-21]
13. Pennebaker JW, Mehl MR, Niederhoffer KG. Psychological aspects of natural language. use: our words, our selves. Annu Rev Psychol 2003;54:547-577. [doi: 10.1146/annurev.psych.54.101601.145041] [Medline: 12185209]
14. Gopal DP, Chetty U, O'Donnell P, Gajria C, Blackadder-Weinstein J. Implicit bias in healthcare: clinical practice, research and decision making. Future Healthc J 2021 Mar;8(1):40-48 [FREE Full text] [doi: 10.7861/fhj.2020-0233] [Medline: 33791459]
15. Sun M, Oliwa T, Peek ME, Tung EL. Negative patient descriptors: documenting racial bias in the electronic health record. Health Aff (Millwood) 2022 Mar;41(2):203-211 [FREE Full text] [doi: 10.1377/hlthaff.2021.01423] [Medline: 35044842]
16. Puhl R, Peterson JL, Luedicke J. Motivating or stigmatizing? Public perceptions of weight-related language used by health providers. Int J Obes (Lond) 2013 Apr;37(4):612-619. [doi: 10.1038/ijo.2012.110] [Medline: 22777543]
17. Glassberg J, Tanabe P, Richardson L, Debaun M. Among emergency physicians, use of the term "Sickler" is associated with negative attitudes toward people with sickle cell disease. Am J Hematol 2013 Jun;88(6):532-533 [FREE Full text] [doi: 10.1002/ajh.23441] [Medline: 23526459]
18. Kelly JF, Westerhoff CM. Does it matter how we refer to individuals with substance-related conditions? A randomized study of two commonly used terms. Int J Drug Policy 2010 May;21(3):202-207. [doi: 10.1016/j.drugpo.2009.10.010] [Medline: 20005692]
19. Beach MC, Saha S, Park J, Taylor J, Drew P, Plank E, et al. Testimonial injustice: linguistic bias in the medical records of black patients and women. J Gen Intern Med 2021 Jun;36(6):1708-1714 [FREE Full text] [doi: 10.1007/s11606-021-06682-z] [Medline: 33754318]
20. Wang MD, Khanna R, Najafi N. Characterizing the source of text in electronic health record progress notes. JAMA Intern Med 2017 Aug 01;177(8):1212-1213 [FREE Full text] [doi: 10.1001/jamainternmed.2017.1548] [Medline: 28558106]
21. Scroggins JK, Hulchafo II, Harkins S, Scharp D, Moen H, Davoudi A, et al. Identifying stigmatizing and positive/preferred language in obstetric clinical notes using natural language processing. J Am Med Inform Assoc 2025 Feb 01;32(2):308-317. [doi: 10.1093/jamia/ocae290] [Medline: 39569431]
22. P Goddu A, O'Conor KJ, Lanzkron S, Saheed MO, Saha S, Peek ME, et al. Do words matter? Stigmatizing language and the transmission of bias in the medical record. J Gen Intern Med 2018 May;33(5):685-691 [FREE Full text] [doi: 10.1007/s11606-017-4289-2] [Medline: 29374357]
23. Blease C, Walker J, DesRoches CM, Delbanco T. New U.S. law mandates access to clinical notes: implications for patients and clinicians. Ann Intern Med 2021 Jan;174(1):101-102. [doi: 10.7326/M20-5370] [Medline: 33045176]
24. Fernández L, Fossa A, Dong Z, Delbanco T, Elmore J, Fitzgerald P, et al. Words matter: what do patients find judgmental or offensive in outpatient notes? J Gen Intern Med 2021 Sep;36(9):2571-2578 [FREE Full text] [doi: 10.1007/s11606-020-06432-7] [Medline: 33528782]
25. Katz IT, Ryu AE, Onuegbu AG, Psaros C, Weiser SD, Bangsberg DR, et al. Impact of HIV-related stigma on treatment adherence: systematic review and meta-synthesis. J Int AIDS Soc 2013 Nov 13;16(3 Suppl 2):18640 [FREE Full text] [doi: 10.7448/IAS.16.3.18640] [Medline: 24242258]
26. Dickinson JK, Maryniuk MD. Building therapeutic relationships: choosing words that put people first. Clin Diabetes 2017 Jan;35(1):51-54 [FREE Full text] [doi: 10.2337/cd16-0014] [Medline: 28144046]
27. Harrigian K, Zirikly A, Chee B, Ahmad A, Links AR, Saha S, et al. Characterization of stigmatizing language in medical records. In: Proceedings of the 61st Annual Meeting of the Association for Computational Linguistics. 2023 Presented at: ACL '23; July 9-14, 2023; Toronto, ON p. 312-329 URL: https://aclanthology.org/2023.acl-short.28.pdf [doi: 10.18653/v1/2023.acl-short.28]
28. Barcelona V, Scharp D, Moen H, Davoudi A, Idnay BR, Cato K, et al. Using natural language processing to identify stigmatizing language in labor and birth clinical notes. Matern Child Health J 2024 Mar 26;28(3):578-586. [doi: 10.1007/s10995-023-03857-4] [Medline: 38147277]
29. Liu P, Yuan W, Fu J, Jiang Z, Hayashi H, Neubig G. Pre-train, prompt, and predict: a systematic survey of prompting methods in natural language processing. ACM Comput Surv 2023 Jan 16;55(9):1-35. [doi: 10.1145/3560815]
30. Sun X, Li X, Li J, Wu F, Guo S, Zhang T, et al. Text classification via large language models. In: Proceedings of the 2023 Conference on Empirical Methods in Natural Language Processing. 2023 Presented at: EMNLP '23; December 6-10, 2023; Singapore, Singapore p. 8990-9005 URL: https://aclanthology.org/2023.findings-emnlp.603.pdf [doi: 10.18653/v1/2023.findings-emnlp.603]
31. Edwards A, Camacho-Collados J. Language models for text classification: is in-context learning enough? In: Proceedings of the 2024 Joint International Conference on Computational Linguistics, Language Resources and Evaluation. 2024 Presented at: LREC-COLING '24; May 20-25, 2024; Torino, Italia p. 10058-10072 URL: https://aclanthology.org/2024.lrec-main.879

XSL•FO
RenderX

32. Sivarajkumar S, Kelley M, Samolyk-Mazzanti A, Visweswaran S, Wang Y. An empirical evaluation of prompting strategies for large language models in zero-shot clinical natural language processing: algorithm development and validation study. JMIR Med Inform 2024 Apr 08;12:e55318 [FREE Full text] [doi: 10.2196/55318] [Medline: 38587879]
33. Kojima T, Gu SS, Reid M, Matsuo Y, Iwasawa Y. Large language models are zero-shot reasoners. arXiv Preprint posted online on May 24, 2022 [FREE Full text] [doi: 10.48550/arXiv.2205.11916]
34. Brown TB, Mann B, Ryder N, Subbiah M, Kaplan J, Dhariwal P, et al. Language models are few-shot learners. arXiv Preprint posted online on May 28, 2024. [doi: 10.5860/choice.189890]
35. White J, Fu Q, Hays S, Sandborn M, Olea C, Gilbert H, et al. A prompt pattern catalog to enhance prompt engineering with ChatGPT. arXiv Preprint posted online February 21, 2023 [FREE Full text] [doi: 10.48550/arXiv.2302.11382]
36. Zaghir J, Naguib M, Bjelogrlic M, Névéol A, Tannier X, Lovis C. Prompt engineering paradigms for medical applications: scoping review. J Med Internet Res 2024 Sep 10;26:e60501 [FREE Full text] [doi: 10.2196/60501] [Medline: 39255030]
37. Park J, Saha S, Chee B, Taylor J, Beach MC. Physician use of stigmatizing language in patient medical records. JAMA Netw Open 2021 Jul 01;4(7):e2117052 [FREE Full text] [doi: 10.1001/jamanetworkopen.2021.17052] [Medline: 34259849]
38. Chen H, Cohen E, Alfred M. Examining the development, effectiveness, and limitations of computer-aided diagnosis systems for retained surgical items detection: a systematic review. Ergonomics 2025 Apr 10:1-16 [FREE Full text] [doi: 10.1080/00140139.2025.2487558] [Medline: 40208001]
39. Feng Q, Du M, Zou N, Hu X. Fair machine learning in healthcare: a review. arXiv Preprint posted online on June 29, 2022 [FREE Full text] [doi: 10.48550/arXiv.2206.14397]
40. Chen H, Alfred M, Brown AD, Atinga A, Cohen E. Intersection of performance, interpretability, and fairness in neural prototype tree for chest X-ray pathology detection: algorithm development and validation study. JMIR Form Res 2024 Dec 05;8:e59045 [FREE Full text] [doi: 10.2196/59045] [Medline: 39636692]
41. Seyyed-Kalantari L, Liu G, McDermott M, Chen IY, Ghassemi M. CheXclusion: fairness gaps in deep chest X-ray classifiers. arXiv Preprint posted online on February 14, 2020. [doi: 10.1142/9789811232701_0022]
42. Yin W, Hay J, Roth D. Benchmarking zero-shot text classification: datasets, evaluation and entailment approach. In: Proceedings of the 2019 Conference on Empirical Methods in Natural Language Processing and the 9th International Joint Conference on Natural Language Processing. 2019 Presented at: EMNLP-IJCNLP '19; November 3-7, 2019; Hong Kong, China p. 3914-3923 URL: https://aclanthology.org/D19-1404.pdf [doi: 10.18653/v1/d19-1404]
43. Tunstall L, Reimers N, Jo U, Bates L, Korat D, Wasserblat M, et al. Efficient few-shot learning without prompts. arXiv Preprint posted online on September 22, 2022. [doi: 10.48550/ARXIV.2209.11055]
44. Wei J, Wang X, Schuurmans D, Bosma M, Ichter B, Xia F, et al. Thought prompting elicits reasoning in large language models. arXiv Preprint posted online on January 28, 2022 [FREE Full text] [doi: 10.48550/arXiv.2201.11903]
45. Johnson AE, Bulgarelli L, Shen L, Gayles A, Shammout A, Horng S, et al. MIMIC-IV, a freely accessible electronic health record dataset. Sci Data 2023 Jan 03;10(1):1 [FREE Full text] [doi: 10.1038/s41597-022-01899-x] [Medline: 36596836]
46. Tri-council policy statement: ethical conduct for research involving humans – TCPS 2 (2018). Government of Canada. 2019. URL: https://ethics.gc.ca/eng/policy-politique_tcps2-eptc2_2018.html [accessed 2024-08-06]
47. Song Y, Wang T, Cai P, Mondal SK, Sahoo JP. A comprehensive survey of few-shot learning: evolution, applications, challenges, and opportunities. ACM Comput Surv 2023 Jul 13;55(13s):1-40. [doi: 10.1145/3582688]
48. Wang W, Zheng VW, Yu H, Miao C. A survey of zero-shot learning. ACM Trans Intell Syst Technol 2019 Jan 16;10(2):1-37 [FREE Full text] [doi: 10.1145/3293318]
49. Gretz S, Halfon A, Shnayderman I, Toledo-Ronen O, Spector A, Dankin L, et al. Zero-shot topical text classification with LLMs - an experimental study. In: Proceedings of the 2023 Conference on Association for Computational Linguistics. 2023 Presented at: EMNLP '23; December 14-16, 2023; Singapore, Singapore p. 9647-9676 URL: https://aclanthology.org/2023.findings-emnlp.647.pdf [doi: 10.18653/v1/2023.findings-emnlp.647]
50. Khandaker F, Senderovich A, Zhao J, Cohen E, Yu E, Carbajales S, et al. Transformer models for mining intents and predicting activities from emails in knowledge-intensive processes. Eng Appl Artif Intell 2024 Feb;128:107450. [doi: 10.1016/j.engappai.2023.107450]
51. Williams A, Nangia N, Bowman S. A broad-coverage challenge corpus for sentence understanding through inference. In: Proceedings of the 2018 Conference of the North American Chapter of the Association for Computational Linguistics: Human Language Technologies. 2018 Presented at: NAACL '18; June 1-6, 2018; New Orleans, LA p. 1112-1122 URL: https://aclanthology.org/N18-1101.pdf [doi: 10.18653/v1/N18-1101]
52. Gera A, Halfon A, Shnarch E, Perlitz Y, Ein-Dor L, Slonim N. Zero-shot text classification with self-training. In: Proceedings of the 2022 Conference on Empirical Methods in Natural Language Processing. 2022 Presented at: EMNLP '22; December 7-11, 2022; Abu Dhabi, United Arab Emirates p. 1107-1119 URL: https://aclanthology.org/2022.emnlp-main.73.pdf [doi: 10.18653/v1/2022.emnlp-main.73]
53. Alcoforado A, Ferraz TP, Gerber R, Bustos E, Oliveira A, Veloso B, et al. ZeroBERTo: leveraging zero-shot text classification by topic modeling. In: Proceedings of the 15th International Conference on Computational Processing of the Portuguese Language. 2022 Presented at: PROPOR '22; March 21-23, 2022; Fortaleza, Brazil p. 125-136 URL: https://link.springer.com/chapter/10.1007/978-3-030-98305-5_12 [doi: 10.1007/978-3-030-98305-5_12]

XSL•FO
RenderX

54. Loukas L, Stogiannidis I, Malakasiotis P, Vassos S. Breaking the bank with ChatGPT: few-shot text classification for finance. arXiv Preprint posted online on August 28, 2023 [FREE Full text] [doi: 10.48550/arXiv.2308.14634]
55. Edwards C, Naik A, Khot T, Burke M, Ji H, Hope T. SynerGPT: in-context learning for personalized drug synergy prediction and drug design. arXiv Preprint posted online on June 19, 2023 [FREE Full text] [doi: 10.1101/2023.07.06.547759]
56. Wang L, Yang N, Huang X, Jiao B, Yang L, Jiang D, et al. Text embeddings by weakly-supervised contrastive pre-training. arXiv Preprint posted online August 25, 2024 [FREE Full text] [doi: 10.48550/ARXIV.2212.03533]
57. Reimers N, Gurevych I. Sentence-BERT: sentence embeddings using Siamese BERT-networks. arXiv Preprint posted online on August 27, 2019 [FREE Full text] [doi: 10.18653/v1/d19-1410]
58. Gu Y, Tinn R, Cheng H, Lucas M, Usuyama N, Liu X, et al. Domain-specific language model pretraining for biomedical natural language processing. ACM Trans Comput Healthcare 2021 Oct 15;3(1):1-23. [doi: 10.1145/3458754]
59. Zhang H, Shafiq MO. Survey of transformers and towards ensemble learning using transformers for natural language processing. J Big Data 2024 Feb 04;11(1):25 [FREE Full text] [doi: 10.1186/s40537-023-00842-0] [Medline: 38321999]
60. Chen H, Cohen E, Wilson D, Alfred M. A machine learning approach with human-AI collaboration for automated classification of patient safety event reports: algorithm development and validation study. JMIR Hum Factors 2024 Jan 25;11:e53378 [FREE Full text] [doi: 10.2196/53378] [Medline: 38271086]
61. Wang L, Zhang Y, Chignell M, Shan B, Sheehan KA, Razak F, et al. Boosting delirium identification accuracy with sentiment-based natural language processing: mixed methods study. JMIR Med Inform 2022 Dec 20;10(12):e38161 [FREE Full text] [doi: 10.2196/38161] [Medline: 36538363]
62. Lee J, Yoon W, Kim S, Kim D, Kim S, So C, et al. BioBERT: a pre-trained biomedical language representation model for biomedical text mining. Bioinformatics 2020 Feb 15;36(4):1234-1240 [FREE Full text] [doi: 10.1093/bioinformatics/btz682] [Medline: 31501885]
63. Tran HT, Chatterjee N, Pollak S, Doucet A. DeBERTa beats behemoths: a comparative analysis of fine-tuning, prompting, and PEFT approaches on LegalLensNER. In: Proceedings of the 2024 Conference on Natural Legal Language Processing Workshop. 2024 Presented at: NLLP-WS '24; November 16, 2024; Miami, FL p. 371-380 URL: https://aclanthology.org/2024.nllp-1.34.pdf [doi: 10.18653/v1/2024.nllp-1.34]
64. Yu H, Yang Z, Pelrine K, Godbout J, Rabbany R. Open, closed, or small language models for text classification? arXiv Preprint posted online on August 19, 2023 [FREE Full text] [doi: 10.48550/arXiv.2308.10092]
65. Loshchilov I, Hutter F. Decoupled weight decay regularization. arXiv Preprint posted online on November 14, 2017 [FREE Full text] [doi: 10.1090/mbk/121/79]
66. Chung HW, Hou L, Longpre S, Zoph B, Tai Y, Fedus W, et al. Scaling instruction-finetuned language models. arXiv Preprint posted online on October 20, 2022 [FREE Full text] [doi: 10.5260/chara.21.2.8]
67. Wei J, Bosma M, Zhao VY, Guu K, Yu AW, Lester B, et al. Finetuned language models are zero-shot learners. arXiv Preprint posted online on September 25, 2024 [FREE Full text] [doi: 10.48550/arXiv.2109.01652]
68. ContactDoctor/Bio-Medical-Llama-3-8B · hugging face. Hugging Face. URL: https://huggingface.co/ContactDoctor/Bio-Medical-Llama-3-8B [accessed 2025-02-12]
69. Sun J, Shaib C, Wallace BC. Evaluating the zero-shot robustness of instruction-tuned language models. arXix Preprint posted online on June 20, 2023 [FREE Full text] [doi: 10.48550/arXiv.2306.11270]
70. Sclar M, Choi Y, Tsvetkov Y, Suhr A. Quantifying language models' sensitivity to spurious features in prompt design or: how I learned to start worrying about prompt formatting. arXiv Preprint posted online on October 17, 2023 [FREE Full text] [doi: 10.48550/arXiv.2310.11324]
71. Lossio-Ventura JA, Weger R, Lee AY, Guinee EP, Chung J, Atlas L, et al. A comparison of ChatGPT and fine-tuned open pre-trained transformers (OPT) against widely used sentiment analysis tools: sentiment analysis of COVID-19 survey data. JMIR Ment Health 2024 Jan 25;11:e50150 [FREE Full text] [doi: 10.2196/50150] [Medline: 38271138]
72. Gao T, Fisch A, Chen D. Making pre-trained language models better few-shot learners. arXiv Preprint posted online on December 31, 2020 [FREE Full text] [doi: 10.18653/v1/2021.acl-long.295]
73. Meskó B. Prompt engineering as an important emerging skill for medical professionals: tutorial. J Med Internet Res 2023 Oct 04;25:e50638 [FREE Full text] [doi: 10.2196/50638] [Medline: 37792434]
74. Wang J, Shi E, Yu S, Wu Z, Ma C, Dai H, et al. Prompt engineering for healthcare: methodologies and applications. arXiv Preprint posted online on April 28, 2023 [FREE Full text] [doi: 10.1016/j.metrad.2023.100047]
75. Himmelstein G, Bates D, Zhou L. Examination of stigmatizing language in the electronic health record. JAMA Netw Open 2022 Jan 04;5(1):e2144967 [FREE Full text] [doi: 10.1001/jamanetworkopen.2021.44967] [Medline: 35084481]
76. Valdez A. Words matter: labelling, bias and stigma in nursing. J Adv Nurs 2021 Nov;77(11):e33-e35. [doi: 10.1111/jan.14967] [Medline: 34245183]
77. Alowidi N, Ali R, Sadaqah M, Naemi FM. Advancing kidney transplantation: a machine learning approach to enhance donor-recipient matching. Diagnostics (Basel) 2024 Sep 25;14(19):2119 [FREE Full text] [doi: 10.3390/diagnostics14192119] [Medline: 39410523]
78. Srivastava M, Heidari H, Krause A. Mathematical notions vs. human perception of fairness: a descriptive approach to fairness for machine learning. arXiv Preprint posted online on February 13, 2019 [FREE Full text] [doi: 10.1145/3292500.3330664]

XSL•FO
RenderX

79. Carroll SM. Respecting and empowering vulnerable populations: contemporary terminology. J Nurse Pract 2019 Mar;15(3):228-231. [doi: 10.1016/j.nurpra.2018.12.031]
80. Zhang S, Dong L, Li X, Zhang S, Sun X, Wang S, et al. Instruction tuning for large language models: a survey. arXiv Preprint posted online on August 21, 2023 [FREE Full text] [doi: 10.48550/arXiv.2308.10792]
81. OpenAI, Achiam J, Adler S, Agarwal S, Ahmad L, Akkaya I, et al. GPT-4 technical report. arXiv Preprint posted online on March 15, 2023 [FREE Full text] [doi: 10.5860/choice.189890]
82. Russell SJ, Norvig P. Artificial intelligence: a modern approach, 4th US edition. Barkley Education. URL: https://aima.cs.berkeley.edu/ [accessed 2025-05-29]
83. Yu T, Simoff S, Jan T. VQSVM: a case study for incorporating prior domain knowledge into inductive machine learning. Neurocomputing 2010 Aug;73(13-15):2614-2623. [doi: 10.1016/j.neucom.2010.05.007]
84. Wagstaff KL. Constrained Clustering. In: Sammut C, Webb CI, editors. Encyclopedia of Machine Learning. Cham, Switzerland: Springer; 2011:220-221.
85. Li Q, Peng H, Li J, Xia C, Yang R, Sun L, et al. A survey on text classification: from traditional to deep learning. ACM Trans Intell Syst Technol 2022 Apr 08;13(2):1-41. [doi: 10.1145/3495162]
86. Mehrabi N, Morstatter F, Saxena N, Lerman K, Galstyan A. A survey on bias and fairness in machine learning. ACM Comput Surv 2021 Jul 13;54(6):1-35. [doi: 10.1145/3457607]
87. Yang Y, Lin M, Zhao H, Peng Y, Huang F, Lu Z. A survey of recent methods for addressing AI fairness and bias in biomedicine. arXiv Preprint posted online on February 13, 2024 [FREE Full text] [Medline: 38529077]
88. Zhang H, Dullerud N, Roth K, Oakden-Rayner L, Pfohl S, Ghassemi M. Improving the fairness of chest X-ray classifiers. arXiv Preprint posted online on March 23, 2022 [FREE Full text] [doi: 10.48550/arXiv.2203.12609]
89. Chen H, Cohen E, Wilson D, Alfted M. Improving patient safety event report classification with machine learning and contextual text representation. Proc Hum Factors Ergon Soc Annu Meet 2023 Sep 20;67(1):1063-1069 [FREE Full text] [doi: 10.1177/21695067231193645] [Medline: 38213998]
90. Davoudi A, Chae S, Evans L, Sridharan S, Song J, Bowles KH, et al. Fairness gaps in machine learning models for hospitalization and emergency department visit risk prediction in home healthcare patients with heart failure. Int J Med Inform 2024 Nov;191:105534. [doi: 10.1016/j.ijmedinf.2024.105534] [Medline: 39106773]
91. Tierney AA, Gayre G, Hoberman B, Mattern B, Ballesca M, Kipnis P, et al. Ambient artificial intelligence scribes to alleviate the burden of clinical documentation. NEJM Catalyst 2024 Feb 21;5(3):e507. [doi: 10.1056/cat.23.0404]
92. Hassan H, Zipursky AR, Rabbani N, You JG, Tse G, Orenstein E, et al. Special topic on burnout: clinical implementation of artificial intelligence scribes in healthcare: a systematic review. Appl Clin Inform (Forthcoming) 2025 Apr 30. [doi: 10.1055/a-2597-2017] [Medline: 40306686]
93. Raffel C, Shazeer N, Roberts A, Lee K, Narang S, Matena M, et al. Exploring the limits of transfer learning with a unified text-to-text transformer. arXiv Preprint posted online on October 23, 2019 [FREE Full text] [doi: 10.5260/chara.21.2.8]
94. Basha I. The human factors in the adoption of ambient artificial intelligence scribe technology: towards informed and user-centered implementation of AI in healthcare. University of Waterloo. URL: https://hdl.handle.net/10012/21130 [accessed 2025-06-30]
95. Sarkar AR, Chuang YS, Mohammed N, Jiang X. De-identification is not enough: a comparison between de-identified and synthetic clinical notes. Sci Rep 2024 Nov 29;14(1):29669 [FREE Full text] [doi: 10.1038/s41598-024-81170-y] [Medline: 39613846]
96. de Aguiar EJ, Traina C, Traina AJ. Security and privacy in machine learning for health systems: strategies and challenges. Yearb Med Inform 2023 Aug;32(1):269-281 [FREE Full text] [doi: 10.1055/s-0043-1768731] [Medline: 38147869]
97. Guidance regarding methods for de-identification of protected health information in accordance with the Health Insurance Portability and Accountability Act (HIPAA) privacy rule. US Department of Health and Human Services. 2012. URL: https://www.hhs.gov/hipaa/for-professionals/special-topics/de-identification/index.html [accessed 2025-01-31]
98. Smith V, Shamsabadi AS, Ashurst C, Weller A. Identifying and mitigating privacy risks stemming from language models: a survey. arXiv Preprint posted online on September 27, 2023 [FREE Full text] [doi: 10.48550/arXiv.2310.01424]
99. Chen Q, Hu Y, Peng X, Xie Q, Jin Q, Gilson A, et al. Benchmarking large language models for biomedical natural language processing applications and recommendations. arXiv Preprint posted online on May 10, 2023 [FREE Full text] [doi: 10.48550/arXiv.2305.16326]
100. Savage T, Nayak A, Gallo R, Rangan E, Chen JH. Diagnostic reasoning prompts reveal the potential for large language model interpretability in medicine. NPJ Digit Med 2024 Jan 24;7(1):20 [FREE Full text] [doi: 10.1038/s41746-024-01010-1] [Medline: 38267608]
101. Greaves F, Ramirez-Cano D, Millett C, Darzi A, Donaldson L. Use of sentiment analysis for capturing patient experience from free-text comments posted online. J Med Internet Res 2013 Nov 01;15(11):e239 [FREE Full text] [doi: 10.2196/jmir.2721] [Medline: 24184993]
102. Bello A, Ng SC, Leung MF. A BERT framework to sentiment analysis of tweets. Sensors (Basel) 2023 Jan 02;23(1):506 [FREE Full text] [doi: 10.3390/s23010506] [Medline: 36617101]

XSL•FO
RenderX

103. Melton CA, White BM, Davis RL, Bednarczyk RA, Shaban-Nejad A. Fine-tuned sentiment analysis of COVID-19 vaccine-related social media data: comparative study. J Med Internet Res 2022 Oct 17;24(10):e40408 [FREE Full text] [doi: 10.2196/40408] [Medline: 36174192]
104. Ktena I, Wiles O, Albuquerque I, Rebuffi S, Tanno R, Roy AG, et al. Generative models improve fairness of medical classifiers under distribution shifts. Nat Med 2024 Apr 10;30(4):1166-1173 [FREE Full text] [doi: 10.1038/s41591-024-02838-6] [Medline: 38600282]
105. Abràmoff MD, Tarver ME, Loyo-Berrios N, Trujillo S, Char D, Obermeyer Z, Foundational Principles of Ophthalmic Imaging and Algorithmic Interpretation Working Group of the Collaborative Community for Ophthalmic Imaging Foundation, Washington, D.C., et al. Considerations for addressing bias in artificial intelligence for health equity. NPJ Digit Med 2023 Sep 12;6(1):170 [FREE Full text] [doi: 10.1038/s41746-023-00913-9] [Medline: 37700029]
106. Irvin J, Rajpurkar P, Ko M, Yu Y, Ciurea-Ilcus S, Chute C, et al. CheXpert: a large chest radiograph dataset with uncertainty labels and expert comparison. arXiv Preprint posted online on January 21, 2019 [FREE Full text] [doi: 10.1609/aaai.v33i01.3301590]
107. Serna I, Morales A, Fierrez J, Obradovich N. Sensitive loss: improving accuracy and fairness of face representations with discrimination-aware deep learning. Artif Intell 2022 Apr;305:103682. [doi: 10.1016/j.artint.2022.103682]

Abbreviations

AI: artificial intelligence
AUC-ROC: area under the receiver operating characteristic curve
BERT: Bidirectional Encoder Representations from Transformers
CARP: clue and reasoning prompting
COT: chain of thought
EHR: electronic health record
FPR: false positive rate
ICL: in-context learning
LLM: large language model
MiMIC: Medical Information Mart for Intensive Care
NLP: natural language processing
TPR: true positive rate

Edited by A Coristine; submitted 20.11.24; peer-reviewed by C Gaudet-Blavignac, D Chrimes, S Sivarajkumar, C Wang; comments to author 23.01.25; revised version received 20.03.25; accepted 30.06.25; published 18.08.25.

Please cite as:
Chen H, Alfred M, Cohen E
Efficient Detection of Stigmatizing Language in Electronic Health Records via In-Context Learning: Comparative Analysis and Validation Study
JMIR Med Inform 2025;13:e68955
URL: https://medinform.jmir.org/2025/1/e68955
doi:10.2196/68955
PMID:

©Hongbo Chen, Myrtede Alfred, Eldan Cohen. Originally published in JMIR Medical Informatics (https://medinform.jmir.org), 18.08.2025. This is an open-access article distributed under the terms of the Creative Commons Attribution License (https://creativecommons.org/licenses/by/4.0/), which permits unrestricted use, distribution, and reproduction in any medium, provided the original work, first published in JMIR Medical Informatics, is properly cited. The complete bibliographic information, a link to the original publication on https://medinform.jmir.org/, as well as this copyright and license information must be included.

XSL•FO
RenderX

Original Paper

Human-Machine Agreement in Medical Ethics: Patient Autonomy Case-Based Evaluation of Large Language Models

Vamshi Mugu[1], MS, MD; Brendan Carr[2], MD, MBA; Ashish Khandelwal[1], MBBS, MD; Mike Olson[1], MD; John Schupbach[2], MD, MBA; John Zietlow[3], MD; T N Diem Vu[3], MD; Alex Chan[1], DO; Christopher Collura[4], MD; John Schmitz[1], MD

[1]Department of Radiology, Mayo Clinic, Rochester, MN, United States

[2]Department of Emergency Medicine, Mayo Clinic, Rochester, MN, United States

[3]Department of Trauma, Critical Care, and General Surgery, Mayo Clinic, Rochester, MN, United States

[4]Department of Neonatal Medicine, Mayo Clinic, Rochester, MN, United States

Corresponding Author:
Vamshi Mugu, MS, MD
Department of Radiology
Mayo Clinic
200 1st street SW
Rochester, MN, 55905
United States
Phone: 1 507 284 2511
Email: vkmugu@gmail.com

Abstract

Background: Medical ethics provides a moral framework for the practice of clinical medicine. Four principles, that is, beneficence, nonmaleficence, patient autonomy, and justice, form the cornerstones of medical ethics as it is practiced today. Of these 4 principles, patient autonomy holds a pivotal position and often takes precedence in ethical dilemmas that result from conflicts among the 4 principles. Its importance serves as a constant reminder to the clinician that the “needs of the patient come first.” With their remarkable ability to process natural language, large language models (LLMs) have recently pervaded nearly every aspect of human life, including medicine and medical ethics. Reliance on tools such as LLMs, however, poses fundamental questions in medical ethics, where human-like reasoning, emotional intelligence, and an understanding of local context and values are of utmost importance.

Objective: While emphasizing the central role of the human factor, we undertake a bold venture to establish some confidence in LLMs, as it pertains to medical ethics by not only evaluating the status quo of foundational LLMs but also exploring ways to improve the LLMs by using patient autonomy–based hypothetical cases. Although literature today is certainly lacking in such ventures, we also believe projects such as ours must be frequently revisited in the field of LLMs, which is evolving at a pace that is both rapid and unprecedented.

Methods: We evaluated 3 foundational LLMs (ChatGPT, LLaMA, and Gemini) on hypothetical cases in patient autonomy. We used Cohen κ to compare LLM responses to the consensus from a physician panel. McNemar test was used during the improvement phase and to report the final significance of improved agreement of each LLM with physician consensus. *P* values less than .05 were considered significant. An agreement with $\kappa<0$ was designated as poor, 0-0.2 as slight, 0.2-0.4 as fair, 0.41-0.6 as moderate, 0.61-0.8 as substantial, and 0.81-1 as almost perfect.

Results: There was slight to fair agreement between the foundational LLMs and the physician consensus. With iterative improvement techniques, this agreement evolved to be substantial or higher (Cohen κ of 0.73-0.82). The degree of improvement was statistically significant ($P=.006$ for ChatGPT, $P<.001$ for Gemini, and $P<.001$ for LLaMA).

Conclusions: Although LLMs hold great potential for use in medicine, there needs to be an abundance of caution in using foundational LLMs in domains such as medical ethics. With adequate human oversight in testing and utilizing established techniques, LLM responses can be better aligned to human responses, even in the domain of medical ethics.

(JMIR Med Inform 2025;13:e77061) doi:10.2196/77061

XSL•FO
RenderX

KEYWORDS

large language models; medical ethics; patient autonomy; generative AI; human in the loop

Introduction

The American Medical Association defines medical ethics as a moral framework for the practice of clinical medicine [1]. Proposed by Beauchamp and Childress [2], the 4 principles, that is, beneficence, nonmaleficence, patient autonomy, and justice, are often regarded as the cornerstones of medical ethics as the field is taught and practiced today. Among these 4 principles, patient autonomy holds a particularly important place due to its frequent precedence over the other 3 principles when an ethical dilemma arises due to conflict among the 4 principles [3].

Large language models (LLMs) represent a new paradigm in artificial intelligence with remarkable abilities to process and generate text in natural language [4]. Foundational LLMs can perform many different tasks but sometimes lack domain-specific capabilities [5]. Although the abilities of foundational LLMs have translated into numerous applications in medical education, research, and practice [6,7], concerns remain about their accuracy, biases, and potential misuse [8]. A recurrent theme in proposed approaches to address these concerns is the importance of human expert participation in the evaluation and governance of LLMs. This importance of the human factor, which is also emphasized in this study, has prompted the development of guidelines from various governing bodies across continents [9-11].

There is a notable scarcity of literature on the role of LLMs in medical ethics, particularly on ways to improve the reliability of foundational LLMs on tasks specific to medical ethics. The comparative evaluation of LLMs in medical ethics is nearly nonexistent, with only ChatGPT being evaluated to any considerable extent [12]. Although the body of knowledge, particularly prompt engineering [13], to elicit improved responses from LLMs in general is enlarging, the discussion of these techniques in the context of medical ethics is lacking. We venture on a bold undertaking to not only evaluate the foundational LLMs in their ability to analyze cases in patient autonomy but also explore techniques to improve the reliability of LLM responses, thereby attempting to increase trust in the technology while emphasizing the indispensable role of the human factor.

Methods

Ethical Considerations

After obtaining approval from the Mayo Clinic Institutional Review Board (which also governs research ethics per approval 25-001042), 44 hypothetical cases in patient autonomy requiring yes or no responses were composed. No real patient information was used for this research. The first author adopted these cases from the literature [14] and from personal and collective clinical experiences, with a focus on capacity to consent, occupational exposure, confidentiality, informed consent for a minor patient, patient preferences, treatment refusal, and training needs.

Hypothetical Case

A hypothetical case is presented in Textbox 1. The LLMs and the physicians on the panel (described subsequently) were blinded to the sources of the cases and others' responses.

Textbox 1. Sample hypothetical case. Note that the hypothetical case deals with the capacity to consent and treatment refusal.

Sample hypothetical case

David is a 79-year-old male with a history of myocardial infarction whose wife, Mary called 911 about David's chest pain. The pain started 30 minutes ago and is similar to some of his prior episodes which needed admission to a hospital. Upon arrival of the emergency medical services (EMS) team, David refuses any intervention. David seems distressed from pain but is orientedx3.

Should the EMS team take David to the nearest hospital?

Three foundational LLMs were chosen for this study: ChatGPT version 4o (ChatGPT), LLaMA 3.1 70b BF16 (LLaMA), and Gemini 1.5 (Gemini). Although the open-source LLaMA was used locally with Ollama version 0.1.33 (Ollama, Inc), the 2 closed-source models, ChatGPT and Gemini, were accessed using their respective web interfaces. Where applicable, the default parameters (eg, temperature of 0.8, top_p of 0.95 for Ollama) were used. There were no concerns for Health Insurance Portability and Accountability Act (HIPAA) noncompliance due to the hypothetical nature of the cases. Five physicians (P1-P5) with respective board certifications from emergency medicine, surgery, and radiology comprised the physician panel.

Study Design

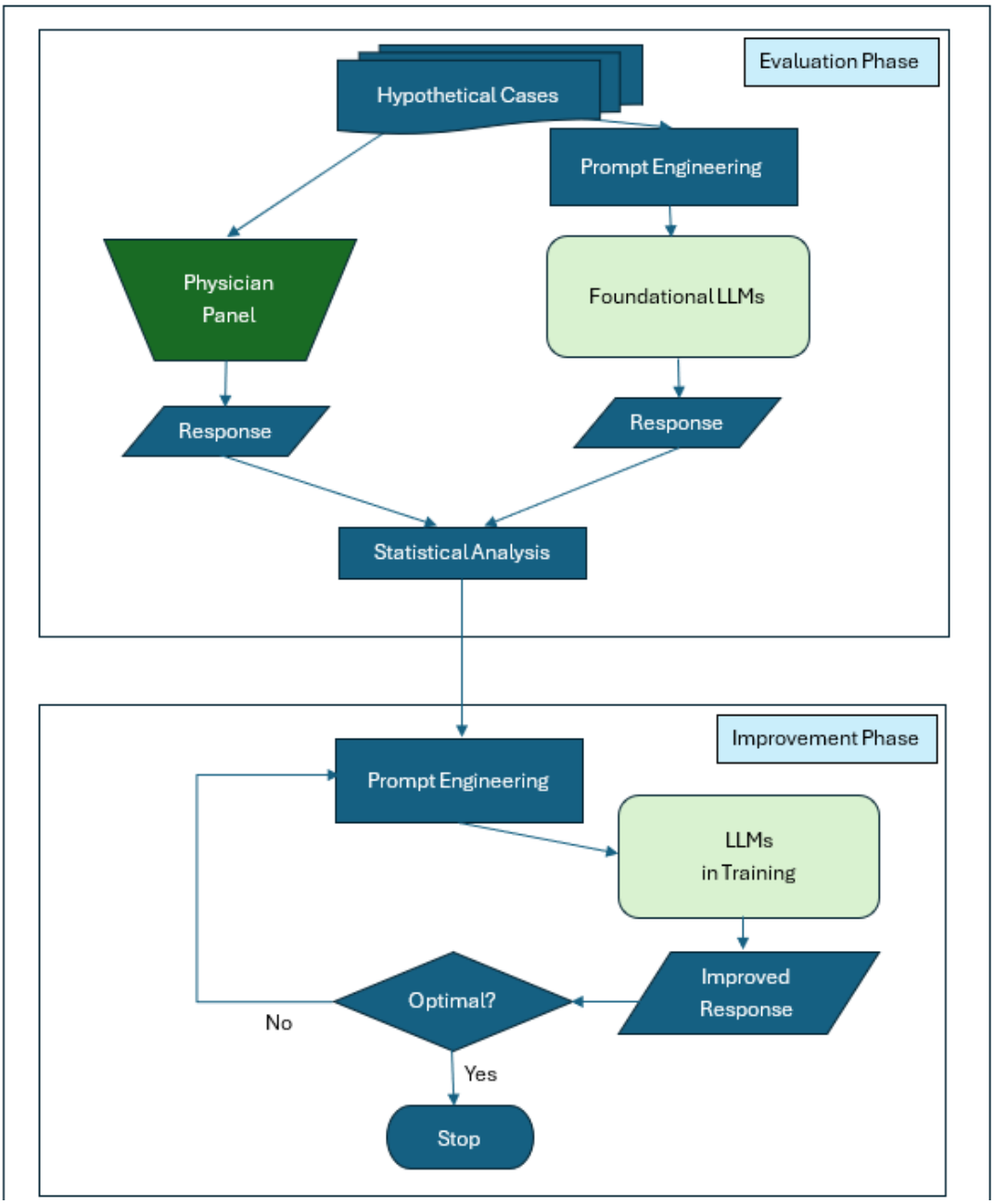
Our study was designed in 2 phases (Figure 1): evaluation phase and improvement phase. The evaluation phase was designed to compare the responses from foundational LLMs to those from the physician panel, while the improvement phase was designed to optimize the responses from LLMs to improve agreement with the physician panel. The LLMs and the physicians on the panel were blinded to each other's responses. Interobserver agreement among the physicians on the panel and among the foundational LLMs was calculated using Fleiss κ. Cohen κ was used to compare the responses of each LLM with the physician consensus, which was defined as the majority response from the physicians in the panel. A missing value from an LLM was considered "No" for statistical analysis purposes. For illustration, pairwise agreements were depicted as a heatmap and listed as proportions in a tabular format. Python statsmodels (version 0.15.0) was used for statistical testing. An agreement with $\kappa<0$ was considered to be poor, 0 to 0.2 was considered slight, 0.21 to 0.4 as fair, 0.41 to 0.6 as moderate, 0.61 to 0.8 as substantial, and 0.81 to 1 as almost perfect. Although we reserved several prompt engineering techniques to employ during the

XSL•FO
RenderX

improvement phase, we nevertheless used some techniques such as role playing, forcefulness, and chain-of-thought during the evaluation phase [13].

During the improvement phase, prompt engineering techniques such as chain-of-thought, N-shot prompting, directional stimulus, versioning, rephrase-and-respond, and long context prompting were used to improve LLM responses [13,15-18]. The goal of this iterative process was to improve LLMs to produce responses that were better aligned to the physician consensus, reducing any statistically significant differences. The stopping point of the iterative process was determined to be when no more reduction in the number of differing responses could be achieved. The degree of improvement was assessed using McNemar test. A *P* value less than .05 was considered significant.

Figure 1. Two-phase design with evaluation phase and improvement phase. The evaluation phase compares the responses of foundational LLMs to physician panel consensus. The improvement phase is designed to improve the agreement between the LLMs and the physician panel consensus. LLM: large language model.



Sample Human-Model Interaction

A sample human-model interaction during the evaluation phase and the improvement phase is provided in Textbox 2. This hypothetical case deals with consenting for a minor patient and demonstrates human-model interaction during the evaluation and improvement phases. The use of 2 prompt engineering techniques, that is, question-refinement and chain-of-thought, is illustrated with this sample.

XSL•FO
RenderX

Textbox 2. Sample hypothetical case with human-model interaction during the evaluation and improvement phases. Two prompt engineering techniques, that is, question-refinement and chain-of-thought, are demonstrated here.

Sample interaction with a model demonstrating evaluation and improvement phases

Hypothetical case: Rachel is a 9-year-old girl from Virginia. She fell at the school basketball court and was taken to the emergency department by the teacher. She is found to have an elbow fracture that needs nonemergent surgical fixation. Can the surgeon proceed with the surgery?

Interaction snippet during the evaluation phase

Gemini's response

Answer: Yes

Thought Process:

1. The surgeon has a duty to act in the best interest of the patient. In this case, the surgery is necessary to treat the elbow fracture and prevent complications.
2. Delaying the surgery could lead to worsening of the condition, pain, and potential long-term disability.
3. Therefore, proceeding with the surgery is in the patient's best interest.

Interaction snippet during the improvement phase

Refined question (provided by ChatGPT upon human request): Given that Rachel, a 9-year-old girl from Virginia, fell at the school basketball court and was taken to the emergency department by her teacher, where she was diagnosed with an elbow fracture that requires nonemergent surgical fixation, does the surgeon have the necessary consent and authority to proceed with the surgery?

Gemini's response

Answer: No

Thought Process:

1. Rachel is a minor and therefore lacks the capacity to provide informed consent for the surgery.
2. Her legal guardian, likely her parents, must provide consent.

Results

Of the 44 cases, 6 focused on informed consent, 6 on capacity to consent, 6 on occupational exposure, 6 on training needs, 7 on treatment refusal, 6 on patient preferences, and 7 on confidentiality. A sample hypothetical case is presented in Textbox 1. There was substantial agreement among the physicians in the panel (κ=0.77). There was also substantial agreement among the foundational LLMs (κ=0.73). There was slight agreement between the foundational Gemini and the physician consensus (κ=0), slight agreement between the foundational LLaMA and the physician consensus (κ=0.14), and fair agreement between the foundational ChatGPT and the physician consensus (κ=0.32). Pairwise agreement is depicted in Figure 2 as a heatmap for illustration purposes. However, note that the Improvement phase was designed to improve the agreement between LLMs and the physician panel consensus rather than individual physician responses.

At the end of the improvement phase, agreement between all the improved LLMs and the physician consensus was substantial or higher (κ=0.77, 95% CI 0.59-0.96 for ChatGPT; κ=0.73, 95% CI 0.52-0.93 for Gemini; and κ=0.82, 95% CI 0.65-0.99 for LLaMA). The degree of improvement for all the LLMs was statistically significant (P=.006 for ChatGPT, P<.001 for Gemini, and P<.001 for LLaMA). The degree of improvement is listed in Table 1.

XSL•FO
RenderX

Figure 2. Pairwise agreement heatmap for illustration purposes only. Note the substantial agreement among large language models and among physicians on the panel (P1-P5) during the evaluation phase (enclosed by red boxes). The improvement phase (discussed later) is however designed to improve the agreement of large language models with physician consensus, not with individual physician responses.

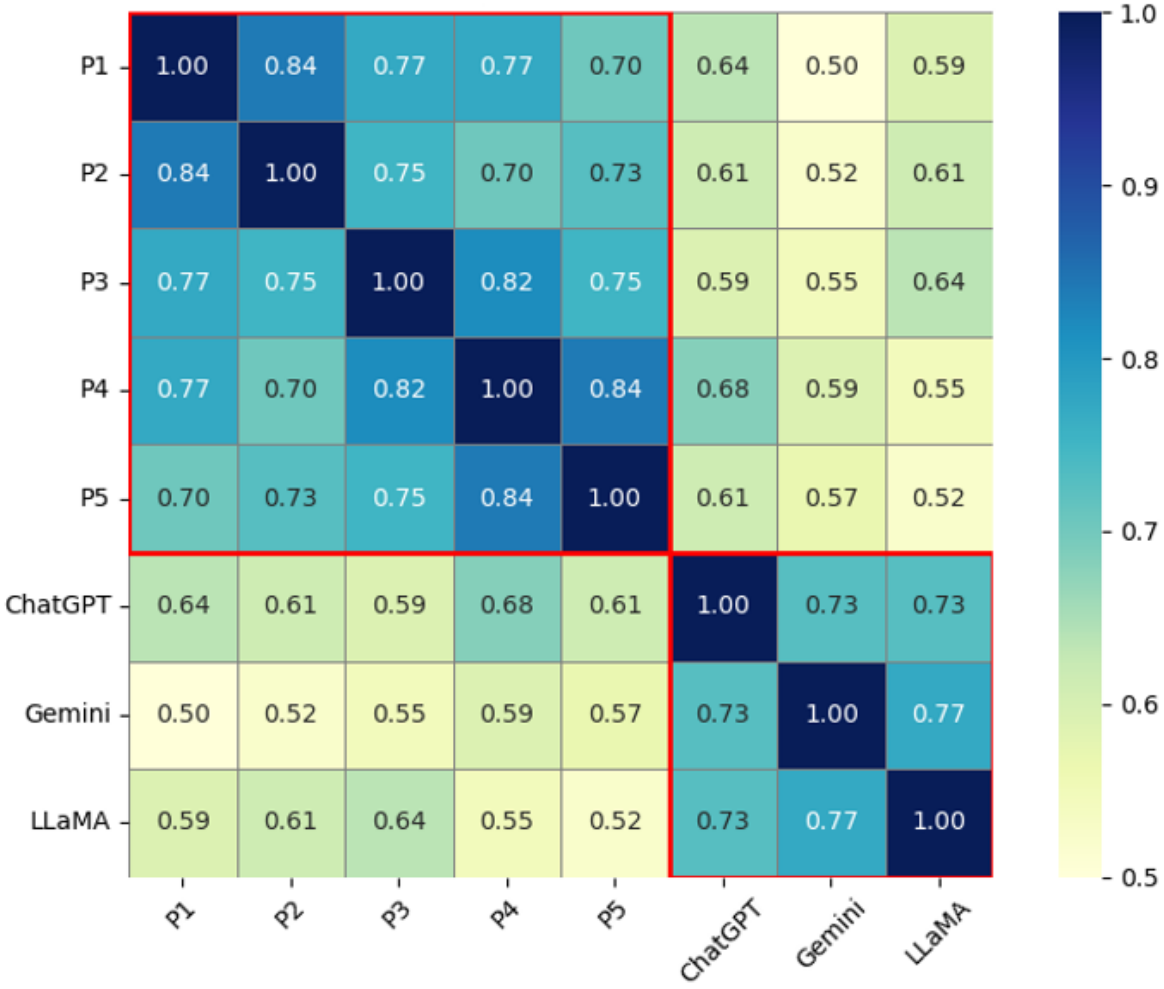


Table 1. Proportion of agreement between each large language model and physician consensus before and after improvement. Note that all large language models underwent improvement that was statistically significant.

Model	Before improvement, n	After improvement, n	Degree of improvement (N=44), n (%)	*P* value
ChatGPT	27	39	+12 (27)	.006
Gemini	22	38	+16 (36)	<.001
LLaMA	26	40	+14 (32)	<.001

Discussion

Principal Findings

Medical ethics provides a moral framework for the practice of clinical medicine, particularly as it pertains to physician responsibilities and obligations in the context of patient-physician interactions [1]. Beauchamp and Childress [2] are often credited for laying the foundation for this framework with 4 principles: beneficence, nonmaleficence, patient autonomy, and justice. Although these principles have been extensively criticized [19], debated [20], and defended [21], they nevertheless remain at the center of modern teaching and practice of medical ethics. The principle of patient autonomy holds a particularly important place among the four, often taking precedence over the other 3 principles when an ethical dilemma arises due to conflicts among the 4 principles [3]. It is a constant reminder to the medical practitioner that "the patient must remain at the heart of his or her own individual battle" [22] and that "the needs of the patient come first" [23].

Despite their relative infancy, LLMs have revolutionized various aspects of health care, ranging from medical education to practice and research [6,7]. LLMs have demonstrated remarkable accuracy on tasks that were once believed to be germane to the rigorously trained human, such as outperforming medical students, and neurosurgery residents on neurosurgery written board-like questions [24]. LLMs are nevertheless prone to limitations, a few of which are particularly concerning in medicine, such as the fabrication of responses not based on evidence—a behavior referred to as hallucination [25]. Moreover, reliance on technology such as LLMs poses

XSL•FO
RenderX

fundamental questions in medical ethics, where human-like reasoning, emotional intelligence, and an understanding of local context and values are of utmost importance [26,27]. A recurrent theme in the proposed approaches to address these concerns is the importance of human expert participation in evaluation and governance of LLMs. This importance of the human factor, which is also emphasized in our study, has prompted the development of guidelines from various governing bodies across continents [9-11] and paved the way for effective interaction such as through prompt engineering [13]. The field of prompt engineering is rapidly evolving with several successful approaches already being adopted, including chain-of-thought, directional stimulus, forcefulness, self-correction and consistency, role playing, reflection, guiding output with rails, and long context prompting [13,15-18].

Although literature on the employment of artificial intelligence in the domain of medical ethics is sparse, some work warrants mention. Before the conception of LLMs, Shalowitz et al [28] proposed a population-based treatment indicator and claimed its superiority to traditional surrogate decision-making in treatment decisions made for incapacitated patients [28]. The population-based treatment indicator was critiqued for disrespecting patient autonomy by relying on statistical evidence rather than individual patient preferences [26]. Leveraging the natural language processing power of LLMs, Earp et al [29] proposed P4, a personalized patient preference predictor, to address this specific concern [29]. P4's claim of superiority is based on its incorporation of material from prior patient treatment decisions, thereby creating a "digital twin" to act on behalf of the incapacitated patient, when such a need arises.

Our study has perhaps the closest resemblance to the expert panel evaluation of GPT-4 by Balas et al [27] who created a set of 8 ethical case vignettes and present to the LLM via a priori prompt template. LLM responses are then evaluated for the depth of reasoning, ability to consider alternate viewpoints, and sensitivity to nuances of ethical dilemmas. Although our case repertoire is considerably larger, it is also arguably simpler since we do not probe the depth of reasoning. However, the greatest distinction from their study is in the improvement phase. In the strictest sense of the study design, their study can be considered as lacking this phase. By not only evaluating the foundational LLMs but also exploring the ways to improve their performance as it pertains to a subset of medical ethics, we venture to establish some confidence in this promising technology while reminding the adopters of the importance of the human factor.

Limitations

This study was subject to a few limitations. Although larger than other similar studies, it still involved a limited set of questions covering a relatively small section of medical ethics. It is possible that LLMs could perform differently with different clinical scenarios or ethical topics. Although we employed several types of prompt engineering, other improvement techniques such as RAG and fine-tuning were not used. Over time, work will undoubtedly continue to improve the performance of foundational LLMs in medical ethics; how quickly and whether the need for human supervision will ever be entirely eliminated remains to be seen.

Conclusion

The use of foundational LLMs in domains such as medical ethics warrants an abundance of caution and intricate involvement of a human expert. With adequate testing and by utilizing established techniques such as prompt engineering, LLM performance can be improved, even in the domain of medical ethics, where human-like reasoning, emotional intelligence, and context awareness are crucial.

Conflicts of Interest

None declared.

References

1. Medical ethics. American Medical Association. URL: https://www.ama-assn.org/topics/medical-ethics [accessed 2024-09-15]
2. Beauchamp TL, Childress JF. Principles of Biomedical Ethics (Eighth Edition). Oxford, UK: Oxford University Press; 2019.
3. Badger J, Ladd RE, Adler P. Respecting patient autonomy versus protecting the patient's health: a dilemma for healthcare providers. JONA's Healthcare Law, Ethics, and Regulation 2009;11(4):120-124 [FREE Full text] [doi: 10.1097/nhl.0b013e3181c1b542]
4. Naveed H, Khan AU, Qiu S, Saqib M, Anwar S, Usman M, et al. A comprehensive overview of large language models. ACM Trans Intell Syst Technol 2025 Aug 18;16(5):1-72 [FREE Full text] [doi: 10.1145/3744746]
5. Scott IA, Zuccon G. The new paradigm in machine learning - foundation models, large language models and beyond: a primer for physicians. Intern Med J 2024 May;54(5):705-715. [doi: 10.1111/imj.16393] [Medline: 38715436]
6. Cascella M, Montomoli J, Bellini V, Bignami E. Evaluating the feasibility of ChatGPT in healthcare: an analysis of multiple clinical and research scenarios. J Med Syst 2023 Mar 04;47(1):33 [FREE Full text] [doi: 10.1007/s10916-023-01925-4] [Medline: 36869927]
7. Sallam M. ChatGPT utility in healthcare education, research, and practice: systematic review on the promising perspectives and valid concerns. Healthcare (Basel) 2023 Mar 19;11(6):887 [FREE Full text] [doi: 10.3390/healthcare11060887] [Medline: 36981544]

XSL•FO
RenderX

8. Kwong J, Wang SCY, Nickel GC, Cacciamani GE, Kvedar JC. The long but necessary road to responsible use of large language models in healthcare research. NPJ Digit Med 2024 Jul 04;7(1):177 [FREE Full text] [doi: 10.1038/s41746-024-01180-y] [Medline: 38965411]
9. Biden J. Executive order on the safe, secure, and trustworthy development and use of artificial intelligence. The White House. URL: https://bidenwhitehouse.archives.gov/briefing-room/presidential-actions/2023/10/30/executive-order-on-the-safe-secure-and-trustworthy-development-and-use-of-artificial-intelligence/ [accessed 2024-09-15]
10. Déclaration de Montréal IA Responsable. URL: https://montrealdeclaration-responsibleai.com/the-declaration/ [accessed 2024-08-22]
11. Ethics guidelines for trustworthy AI. European Commission. URL: https://digital-strategy.ec.europa.eu/en/library/ethics-guidelines-trustworthy-ai [accessed 2024-08-22]
12. Skryd A, Lawrence K. ChatGPT as a tool for medical education and clinical decision-making on the wards: case study. JMIR Form Res 2024 May 08;8:e51346 [FREE Full text] [doi: 10.2196/51346] [Medline: 38717811]
13. Amatriain X. Prompt design and engineering: introduction and advanced methods. ArXiv. Preprint posted online on May 5, 2024 2024. [doi: 10.48550/arXiv.2401.14423]
14. Johnston C, Bradbury P. 100 Cases in Clinical Ethics and Law (Second Edition). Boca Raton: CRC Press; 2016.
15. Li Z, Peng B, He P, et A. Guiding large language models via directional stimulus prompting. ArXiv. Preprint posted on October 9, 2023 2023. [doi: 10.48550/arXiv.2302.11520]
16. Chang K, Xu S, Wang C, et A. Efficient prompting methods for large language models: a survey. ArXiv. Preprint posted on December 2, 2024 2024 [FREE Full text] [doi: 10.48550/arXiv.2404.01077]
17. Parthasarathy V, Zafar A, Khan A, Shahid A. The ultimate guide to fine-tuning llms from basics to breakthroughs: an exhaustive review of technologies, research, best practices, applied research challenges and opportunities. ArXiv. Preprint posted on August 23, 2024 2024. [doi: 10.48550/arXiv.2408.13296]
18. Brown TB, Mann B, Ryder N, et A. Language models are few-shot learners. ArXiv. Preprint posted on May 28, 2020 2020. [doi: 10.48550/arXiv.2005.14165]
19. Clouser K, Gert B. A critique of principlism. J Med Philos 1990 Apr;15(2):219-236. [doi: 10.1093/jmp/15.2.219] [Medline: 2351895]
20. Davis R. The principlism debate: a critical overview. J Med Philos 1995 Feb;20(1):85-105. [doi: 10.1093/jmp/20.1.85] [Medline: 7738461]
21. Gillon R. Defending 'the four principles' approach to biomedical ethics. J Med Ethics 1995 Dec;21(6):323-324 [FREE Full text] [doi: 10.1136/jme.21.6.323] [Medline: 8778453]
22. Mattei JF. [Respecting the patient's autonomy]. Soins 2018 Apr;63(824):25-27 [FREE Full text] [doi: 10.1016/j.soin.2018.02.004] [Medline: 29680133]
23. Beck CS. The needs of the patient come first. Mayo Clinic Proceedings 2000 Mar;75(3):224. [doi: 10.4065/75.3.224]
24. Guerra G, Hofmann H, Sobhani S, Hofmann G, Gomez D, Soroudi D, et al. GPT-4 artificial intelligence model outperforms ChatGPT, medical students, and neurosurgery residents on neurosurgery written board-like questions. World Neurosurg 2023 Nov;179:e160-e165. [doi: 10.1016/j.wneu.2023.08.042] [Medline: 37597659]
25. Májovský M, Černý M, Kasal M, Komarc M, Netuka D. Artificial intelligence can generate fraudulent but authentic-looking scientific medical articles: Pandora's box has been opened. J Med Internet Res 2023 May 31;25:e46924 [FREE Full text] [doi: 10.2196/46924] [Medline: 37256685]
26. Sharadin N. Patient preference predictors and the problem of naked statistical evidence. J Med Ethics 2018 Dec;44(12):857-862. [doi: 10.1136/medethics-2017-104509] [Medline: 29895554]
27. Balas M, Wadden JJ, Hébert PC, Mathison E, Warren MD, Seavilleklein V, et al. Exploring the potential utility of AI large language models for medical ethics: an expert panel evaluation of GPT-4. J Med Ethics 2024 Jan 23;50(2):90-96. [doi: 10.1136/jme-2023-109549] [Medline: 37945336]
28. Shalowitz D, Garrett-Mayer E, Wendler D. How should treatment decisions be made for incapacitated patients, and why? PLoS Med 2007 Mar;4(3):e35 [FREE Full text] [doi: 10.1371/journal.pmed.0040035] [Medline: 17388655]
29. Earp BD, Porsdam Mann S, Allen J, Salloch S, Suren V, Jongsma K, et al. A personalized patient preference predictor for substituted judgments in healthcare: technically feasible and ethically desirable. Am J Bioeth 2024 Jul 16;24(7):13-26 [FREE Full text] [doi: 10.1080/15265161.2023.2296402] [Medline: 38226965]

Abbreviations

HIPAA: Health Insurance Portability and Accountability Act
LLM: large language model

XSL•FO
RenderX

Edited by A Benis; submitted 06.05.25; peer-reviewed by B Bhasuran, C Ma; comments to author 11.08.25; revised version received 21.08.25; accepted 06.10.25; published 23.10.25.

Please cite as:
Mugu V, Carr B, Khandelwal A, Olson M, Schupbach J, Zietlow J, Vu TND, Chan A, Collura C, Schmitz J
Human-Machine Agreement in Medical Ethics: Patient Autonomy Case-Based Evaluation of Large Language Models
JMIR Med Inform 2025;13:e77061
URL: https://medinform.jmir.org/2025/1/e77061
doi:10.2196/77061
PMID:41056099

©Vamshi Mugu, Brendan Carr, Ashish Khandelwal, Mike Olson, John Schupbach, John Zietlow, T N Diem Vu, Alex Chan, Christopher Collura, John Schmitz. Originally published in JMIR Medical Informatics (https://medinform.jmir.org), 23.10.2025. This is an open-access article distributed under the terms of the Creative Commons Attribution License (https://creativecommons.org/licenses/by/4.0/), which permits unrestricted use, distribution, and reproduction in any medium, provided the original work, first published in JMIR Medical Informatics, is properly cited. The complete bibliographic information, a link to the original publication on https://medinform.jmir.org/, as well as this copyright and license information must be included.

XSL•FO
RenderX

Original Paper

Medical Feature Extraction From Clinical Examination Notes: Development and Evaluation of a Two-Phase Large Language Model Framework

Manal Abumelha[1,2], PhD; Abdullah AL-Malaise AL-Ghamdi[1,3], Prof Dr; Ayman Fayoumi[1], Prof Dr; Mahmoud Ragab[4], Prof Dr

[1]Information Systems Department, Faculty of Computing and Information Technology, King Abdulaziz University, Jeddah, Saudi Arabia

[2]Information Systems Department, Applied College at Khamis Mushait, King Khalid University, Abha, Saudi Arabia

[3]Computer Science Department, School of Engineering, Computing and Design, Dar Alhekma University, Jeddah, Saudi Arabia

[4]Information Technology Department, Faculty of Computing and Information Technology, King Abdulaziz University, Jeddah, Saudi Arabia

Corresponding Author:
Manal Abumelha, PhD
Information Systems Department
Faculty of Computing and Information Technology
King Abdulaziz University
Idara Street
Jeddah, 21589
Saudi Arabia
Phone: 966 12 6400000
Fax: 966 12695243
Email: mabumelha@kku.edu.sa

Abstract

Background: Medical feature extraction from clinical text is challenging because of limited data availability, variability in medical terminology, and the critical need for trustworthy outputs. Large language models (LLMs) offer promising capabilities but face critical challenges with hallucination.

Objective: This study aims to develop a robust framework for medical feature extraction that enhances accuracy by minimizing the risk of hallucination, even with limited training data.

Methods: We developed a two-phase training approach. Phase 1 used instructing fine-tuning to teach feature extraction. Phase 2 introduced confidence-regularization fine-tuning with loss functions penalizing overconfident incorrect predictions, which were captured using bidirectional matching targeting hallucination and missing features. The model was trained using the full data of 700 patient notes and on few-shot 100 patient notes. We evaluated the framework on the United States Medical Licensing Examination Step-2 Clinical Skills dataset, testing on a public split of 200 patient notes and a private split of 1839 patient notes. Performance was assessed using precision, recall, and F_1-scores, with error analysis conducted on predicted features from the private test set.

Results: The framework achieved an F_1-score of 0.968-0.983 on the full dataset of 700 patient notes and 0.960-0.973 with a few-shot subset of 100 of 700 patient notes (14.2%), outperforming INCITE (intelligent clinical text evaluator; F_1=0.883) and DeBERTa (decoding-enhanced bidirectional encoder representations from transformers with disentangled attention; F_1=0.958). It reduced hallucinations by 89.9% (from 3081 to 311 features) and missing features by 88.9% (from 6376 to 708) on the private dataset compared with the baseline LLM with few-shot in-context learning. Calibration evaluation on few-shot training (100 patient notes) showed that the expected calibration error increased from 0.060 to 0.147, whereas the Brier score improved from 0.087 to 0.036. Notably, the average model confidence remained stable at 0.84 (SD 0.003) despite F_1 improvements from 0.819 to 0.986.

Conclusions: Our two-phase LLM framework successfully addresses critical challenges in automated medical feature extraction, achieving state-of-the-art performance while reducing hallucination and missing features. The framework's ability to achieve high performance with minimal training data (F_1=0.960-0.973 with 100 samples) demonstrates strong generalization capabilities essential for resource-constrained settings in medical education. While traditional calibration metrics show misalignment, the

XSL•FO
RenderX

practical benefits of confidence injection led to reduced errors, and inference-time filtering provided reliable outputs suitable for automated clinical assessment applications.

(JMIR Med Inform 2025;13:e78432) doi:10.2196/78432

KEYWORDS

automated medical assessment; clinical NLP; hallucination mitigation; instruction tuning; large language models; medical feature extraction; semantic matching

Introduction

Overview

Medical documentation is a critical practice in clinical systems, requiring practitioners to document patient history, symptoms, and potential diagnoses. This documentation is evaluated through standardized medical examinations such as the United States Medical Licensing Examination (USMLE) [1]. These evaluations are essential for assessing whether students can effectively align clinical knowledge with professional communication skills [2]. The Step 2 Clinical Skills examination evaluates the students' ability to recall relevant knowledge for a specific case and document key features contributing to an accurate diagnosis [3,4].

The high resource requirements of these evaluations create substantial difficulties for educational institutions. More than 30,000 medical notes need evaluation each year, which requires 100 physicians to dedicate substantial time to extensive manual assessment [3]. These evaluation methods create resource challenges, along with requirements of consistency, reliability, and timely feedback among different examination centers in different locations [5,6]. Recent studies highlight the potential of large language models (LLMs) to address these challenges by automating clinical note assessment with high accuracy and scalability [7,8]. These concerns highlight the need for efficient and reliable assessment tools applicable everywhere with consistent performance [9].

Automation of this process began early through statistical natural language processing (NLP) approaches that relied on n-gram models and fuzzy logic. These approaches used character-based statistics with limited capability in capturing the contextual and semantic information in medical text [3,4,10]. Recent bidirectional encoder representations from transformers (BERT)–based approaches have demonstrated better semantic understanding for medical document assessment but still exhibit weaknesses in broader application areas and need intensive span-level annotation of sentences to reach effective training capabilities [5,6,9].

LLMs have revolutionized NLP functionalities across all sectors [11]. These models display impressive capabilities to learn from zero-shot and a few-shot inputs, which could help address data shortage problems affecting medical education settings [12]. Medical organizations need to address interpretability and hallucination when using LLMs to extract valuable features in high-risk scenarios [13-15].

Confidence calibration aims to reduce the gap between the model's predicted confidence score and its actual performance evaluation, especially in health care applications and educational assessment [16]. Traditional confidence calibration is effective for classification [17-19], but challenges persist in deep neural networks as well as pretrained language models [16,20]. For earlier neural networks, integrating noise or penalties into the cross-entropy loss can improve generalization and reduce overconfident errors [21,22]. The ability to calibrate the internal confidence of generative LLMs remains challenging and is an active research area, as these models are pretrained to maximize the likelihood of sequential output [23].

Related Work

The field of automated medical note assessment has expanded to address the high costs, human bias, and scalability issues of manual reviews. Early work relied on statistical and rule-based techniques. Latifi et al [10] tested decision tree models to evaluate student examination responses, whereas Yim et al [4] developed scoring methods based on n-gram features with lexical matching in note assessment. Applying these approaches brought only restricted context comprehension and an inability to manage clinical language inconsistencies. The INCITE (intelligent clinical text evaluator) system [3] introduced semisupervised techniques, incorporating fuzzy matching through Levenshtein distance and lexicon-based processing. Although these methods retrieved more data, they required near-exact string matches and failed to generalize semantics, particularly for complex or paraphrased symptom descriptions. The field progressed with transformer-based models. Ganesh and Bansal [24] proposed a transformer-based method for automatically mapping clinical notes to specific clinical concepts. Zhou et al [5] used a BERT model trained with their own data to spot key features, even with limited supervision. Xu et al [6] applied DeBERTa (decoding-enhanced bidirectional encoder representations from transformers with disentangled attention), integrating pseudo-labeling and masked language modeling. Tan et al [25] ensembled DeBERTa transformer models using multitask learning for both note-based and character-based approaches to automatically score USMLE patient notes. Yaneva et al [9] integrated transformer models with rule-based matching syntax, which made their system excel in automating the USMLE Step-2 Clinical Skills assessment.

Despite these advances, such models demand extensive annotated data and lack the semantic depth and contextual reasoning offered by autoregressive LLMs. Vithanage et al [26] demonstrated LLMs' superior ability to extract structured information from medical reports. Their deep contextual understanding has proven successful across many clinical applications [27,28]. However, challenges remain, including high computational demands and hallucination risks that threaten reliability [13,27].

XSL•FO
RenderX

Research on hallucination detection and mitigation has become critical, with uncertainty and confidence estimation methods showing promise [29,30]. Confidence calibration seeks to align a model's predicted confidence with its actual performance. Traditional calibration suits classification tasks, in which each class has a distinct probability, but generative LLMs—trained to maximize confidence across entire sequences—often exhibit overconfidence [16]. Xiao and Wang [31] used predictive uncertainty scores to detect hallucinations, modifying beam search at inference time as a post hoc mitigation method, distinct from training-time regularization. The character n-gram F_1-score (chrF), introduced by Popović [32] for machine translation evaluation, captures morphological variations better than word-level metrics. Li et al [33] used a Dice loss F_1-score to narrow the gap between the model performance and final evaluation F_1-scores. In machine translation, chrF correlates strongly with human judgments, but its potential as a training objective for sequence models remains underexplored. Our work builds on this by incorporating chrF scores as a regularization signal in the loss function.

We use confidence scores to penalize hallucinations and missing features during training to improve F_1-scores in medical feature extraction. This approach encouraged the model to be more conservative when overconfident with incorrect outputs, mitigating LLMs' inherent overconfidence [34,35]. Key literature gaps include traditional methods' substantial difficulties when confronted with the inherent semantic variability characteristic of clinical terminology [9,10], LLMs' data scarcity and the persistent risk of hallucination [13-15], and manual assessment's scalability limitations [1,3,4]. Our two-phase LLM framework uses instructing fine-tuning to teach extraction, followed by confidence-regularization fine-tuning by modifying the cross-entropy loss function with feature-based confidence aligned with F_1 performance to reduce hallucinations and enhance feature capture, thereby improving accuracy and generalization in low-resource settings.

Study Aim and Contributions

Our framework adopts confidence-regularization fine-tuning to penalize hallucinated and missing features, incorporating this as a training signal in the LLM, to enhance medical feature extraction.

We introduce an end-to-end framework that integrates the instruction-understanding capability of an LLM with confidence regularization, used as a signal to avoid hallucinations and missing features even with limited resources. This work offers several key contributions, beginning with introduction of an end-to-end framework that combines instructing fine-tuning power with model confidence-regularization fine-tuning, along with semantic embedding matching, to extract medical features from patient notes. Additionally, we designed a bidirectional matching mechanism that evaluates the extracted features by identifying hallucinated and missed features, enabling precise feedback and structured adjustment during training. To achieve this we developed a multipenalty learning objective that uses model confidence as a regularization signal to improve the reliability of medical NLP predictions.

In evaluations on USMLE Step-2 Clinical Skills notes, our framework achieved state-of-the-art performance with F_1=0.983 (semantic matching) and F_1=0.968 (binary overlap) on the entire dataset and maintained high performance with F_1=0.973 (semantic matching) and F_1=0.952 (binary overlap) while using only 100 of 700 patient notes, representing 14.2% of the training data. Furthermore, it reduced hallucinated outputs by 89.9% (from 3081 to 311 hallucinated features) and increased feature detection by 88.9% (from 6376 to 708 missing features) in the final model compared with the base vanilla model (Mistral Nemo with few-shot in-context learning [ICL]), thereby paving the way for reliable medical NLP under limited supervision. The aim of this study was to develop and evaluate a two-phase LLM framework for automated medical feature extraction from clinical examination notes, achieving high accuracy with minimal training data while reducing hallucination and missing feature errors to support reliable medical education assessment.

Methods

Study Overview and Research Questions

Our framework consists of a two-phase training approach: instructing fine-tuning and confidence-regularization fine-tuning. Before explaining each phase, we need to define the task. In the medical feature extraction task, given a medical history text p belonging to P and a set of target features to find F = $\{f_1, f_2, \ldots, f_n\}$, the goal is to extract text segment semantically equivalent to features E = $\{e_1, e_2, \ldots, e_n\}$ from P. If no corresponding segment exists, then e_i=Ø.

These questions guide our experimental design to comprehensively evaluate the proposed framework: (1) research question (RQ) 1: Is the model able to generalize effectively from limited training data, while maintaining competitive performance against full-data training? (2) RQ2: Does the proposed framework enhance performance by reducing hallucination and increasing the ability to extract clinical features? (3) RQ3: Does the incorporated confidence-regularization strategy enhance the alignment between the model's confidence scores and its true extraction performance?

Dataset and Experimental Design

The research collected data from 2017 to 2020 from examination sites across the United States, obtaining data from 35,156 medical students [36]. The dataset includes 10 clinical case scenarios represented across 43,985 patient notes. The training data comprised 2840 patient notes, equally distributed at 284 per clinical case, as illustrated in Figure 1.

The dataset annotation task was performed by 10 expert annotators working in 5 pairs. A double-annotation process was applied to 29 notes per case to compute F_1 agreement scores, defining each case's feature spans. The interannotator agreement, measured through F_1, was 84%, while binary detection of features reached 97% agreement. The full annotation process is detailed elsewhere [36].

XSL•FO
RenderX

The available dataset exists in two splits: a public split and a private split. The public split included 1000 of the 2839 records made available through the Kaggle competition [37], with each case containing 100 notes. The private split was used to evaluate the submitted notebook in the competition and consists of 1893 records. For fair comparison, we followed the same split as the competition and previous study by Yaneva et al [9]. Table 1 illustrates the data split used in this experiment.

Figure 1. Sample of patient note from the United States Medical Licensing Examination (USMLE) Step-2 Clinical Skills dataset, showing case-associated features (to be identified) and annotated features (already identified by experts) [38].

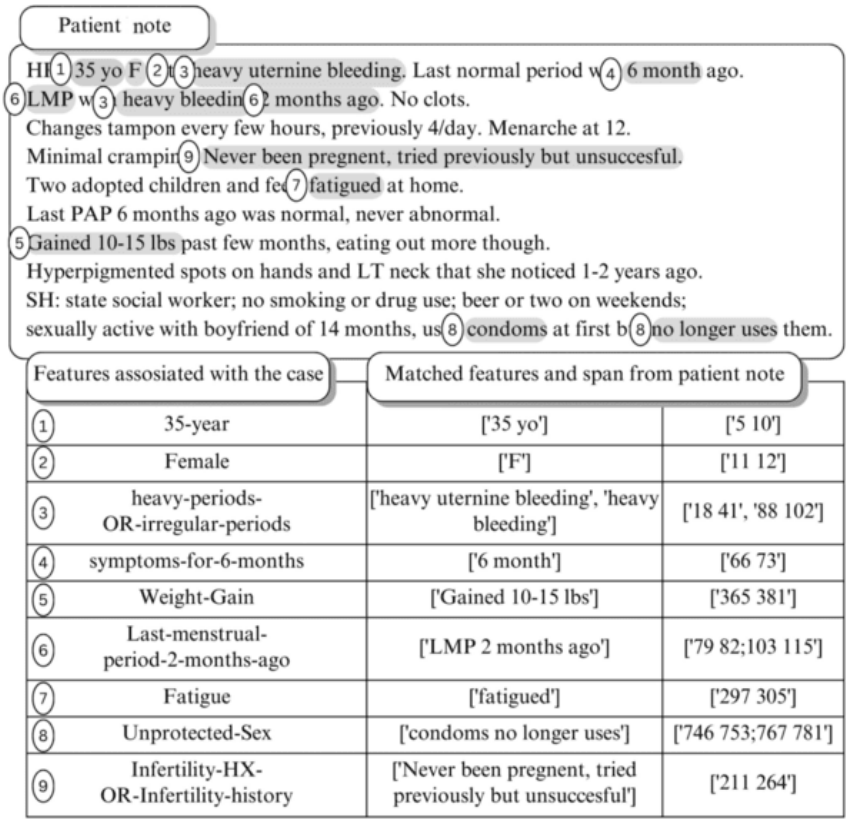


Table 1. Dataset split showing the number of annotated patient notes and features used for training. There is no overlap between data splits.

Dataset split	Dataset size	Annotated features
Training data	700 patient notes	10,011 features
Validation data	100 patient notes	1430 features
Test data (public split)	200 patient notes	2860 features
Test data (private split)	1839 patient notes	20,360 features
Total annotated data	2839 patient notes	34,661 features

Two-Phase Training Framework

Phase 1: Instructing Fine-Tuning

Recent developments have enabled language models to follow human natural language instructions [39]. In contrast, earlier models required task-specific supervised fine-tuning on labeled data, which demanded intensive effort to prepare data for task-specific requirements [38].

In this study, we use instructing fine-tuning, in which a LLM is trained on pairs of instructions and responses [40]. The first phase of our methodology involves fine-tuning a pretrained language model on medical feature extraction tasks. Using Mistral Nemo instruct [41] as our backbone model θ_0. Mistral Nemo was chosen as the backbone for this model, based on our previous experiment with few-shot learning on different open-source models, where Nemo showed the best performance among them [42]. We then fine-tuned Mistral Nemo on a dataset $\boxtimes$ where P_j is patient history, F_j is a set of target features, and G_j is the corresponding set of ground truth extractions for that specific patient history.

LLM predictions can vary significantly based on the design and quality of prompt templates [43]. We carefully designed our instruction template to be optimized for feature extraction tasks.

The model was trained to autoregressively generate output tokens based on the input prompt. The training objective was to minimize the negative log-likelihood loss between the

XSL•FO
RenderX

generated tokens and the outputtokens across all training examples.

Phase 2: Confidence-Regularization Fine-Tuning

The first fine-tuning step instructs the model to perform feature extraction tasks, enabling it to extract features that can later be refined by penalizing poor performance. Confidence calibration is used to align the model's confidence scores with its actual performance. The complex architecture of deep neural networks, with an increased number of layers, allows them to handle larger datasets [44]. However, this complexity poses a calibration challenge, as such models are trained to maximize the probability of predicted outputs, leading to inherently overconfident predictions. We achieve this through a customized loss function that penalizes overconfident incorrect predictions, drawing on previous work in uncertainty estimation [22,45]. Unlike post hoc methods such as temperature scaling [16] or external confidence mapping [45], our approach integrates regularization directly into training, ensuring robust feature extraction. The confidence-regularization fine-tuning process is illustrated in Figure 2, with an example detailing the process for a single training instance as outlined in the following steps.

Figure 2. Five steps of confidence-regularization fine-tuning phase illustrated using the process flow of one example.



- Step 1–input data: The data used as input in the model for the second training phase consists of patient notes and features to look for, without including the ground truth, because the model has already been trained to extract features properly. The ground truth is used in the subsequent steps.
- Step 2–model generation: The model extracts features, and the confidence of these features is obtained using token-level probabilities from the softmax layer [45,46]. Modern LLMs tend to be overconfident, especially if they are already pretrained using supervised pretraining [47]. To overcome this limitation, and inspired by previous work, we made 3 adjustments to the confidence score to make it less flat and more varied. First, we applied length normalization to boost confidence scores for shorter outputs and reduce them for longer ones, correcting biases as shown by Murray and Chiang [48] and Farquhar et al [46]. Second, inspired by Kuhn et al [49], who used bidirectional entailment to group semantically similar outputs and calculate semantic entropy for better uncertainty estimation, and Vazhentsev et al [50], who examined averaging token probabilities and entropy, we averaged token-level probabilities per feature to generate more robust feature-based confidence scores, facilitating effective penalization in our model. Third, Gal et al [51] injected Gaussian noise into logits during training to regularize and prevent model overconfidence. Similarly, Li et al [33] added noise to confidence outputs before generating pseudo-labels to improve calibration. Inspired by them, we injected controlled stochastic randomness to prevent the confidence scores from collapsing into a narrow range of confidence values.

XSL•FO
RenderX

- Step 3–bidirectional semantic mapping: We targeted two model behaviors: hallucination and missing features. Hallucination refers to extracting nonexistent features from patient notes and is measured by forward-matching predicted and ground truth features, using an n-gram F_1-score to give credit for partial matches. This matching is performed as follows: for each generated feature, we calculate its F_1 similarity score against all ground truth features and select the highest score. Features are penalized based on their best F_1 match: those with F_1>0.3 receive a reduced penalty of $0.7 \times (1 - F_1)$, while those with $F_1 \leq 0.3$ receive the full penalty of $(1 - F_1)$. For missing feature detection, we perform the reverse process: each ground truth feature is matched against all generated features to find its highest F_1 -score. Ground truth features that are poorly matched (<0.5) indicate missing extractions and contribute to the missing feature penalty, calculated as .
- Step 4–calculate penalties: Drawing on previous work, such as Zou et al [52], who penalized overconfident incorrect predictions during model training; Nan et al [53], who introduced entity overlap metrics to promote faithful information extraction; and Liang et al [18], who incorporated a penalty term based on the disparity between predicted confidence and accuracy to enhance calibration, we propose a novel approach that integrates F_1 evaluation metrics into our penalty term. Specifically, we introduced an F_1-based confidence penalty that scales with the confidence of incorrect extractions, penalizing them proportionally to their predicted confidence to improve model calibration and extraction accuracy. Penalties are calculated only for overconfident incorrect predictions compared with the confidence threshold. Thus, backpropagation occurs exclusively for overconfident, incorrect predictions; if there is no penalty, no gradient is propagated. The F_1-based confidence penalty extends the Brier score's calibration framework by measuring performance through $(1 - F_1)$ and penalizing overconfident predictions with a quadratic term when confidence exceeds a threshold. The scaling factor α is set to 2 to increase the penalty's sensitivity to overconfidence. For confidence-adaptive training and stabilized training, we apply a confidence feedback loop to prevent training instability by smoothing confidence estimates across epochs and a dynamic threshold to create curriculum-like learning by increasing the threshold gradually. Without these modifications, the model becomes sensitive to the penalty and collapses during training, by generating redundant patterns.
- Step 5–total loss calculation: Our training approach combines multiple objectives to enhance the model's ability to extract accurate and complete features. We start with a standard language modeling cross-entropy loss to predict correct tokens, then add a hallucination penalty, calculated using F_1-based metrics, to discourage overconfident incorrect predictions by scaling penalties with confidence scores. To address missing features, a complementary penalty reduces the confidence when features are missing, using a backward-mapping mechanism. The missing feature penalty is weighted higher (0.5) than the hallucination penalty (0.2), based on the model's previous result from the first training phase, where recall was less than precision.

The confidence-regularization fine-tuning process improves deep neural network performance by penalizing overconfident, incorrect predictions. It begins with inputting patient notes for feature extraction, followed by generating token-level confidence scores through the softmax layer, adjusted through length normalization, averaged token probabilities, and injected stochasticity to reduce overconfidence. Bidirectional semantic matching addresses hallucination and missing features by computing forward and backward F_1-scores to align predicted and ground truth features, ensuring comprehensive error detection. A novel F_1-based confidence penalty, inspired by previous work, scales penalties for overconfident incorrect predictions using a quadratic term and a dynamic threshold (τ from 0.6 to 0.7) for curriculum learning, promoting stable convergence. The total loss integrates cross-entropy loss with weighted hallucination (0.2) and missing feature (0.5) penalties, thereby prioritizing recall improvement. No backpropagation occurs for cases where no penalty is incurred. Heuristic values for thresholds and variables were selected to balance the penalty and training stability, preventing model collapse due to redundant generation at the middle of the first epoch. Detailed formulas and descriptions are provided in Multimedia Appendix 1.

As detailed in Algorithm 1 in Multimedia Appendix 2, our framework implements two-phase training to enhance medical feature extraction. First phase, an instructing fine-tuned model generates feature and confidence scores, adjusted by a complexity factor and a dynamic threshold based on the prior epoch's F_1-score. Second phase, a confidence-regularization fine-tuning based on bidirectional matching identifies hallucinated and missing features, overconfidence with low F_1-score are penalties and calculated, alongside a base loss. This dual-objective strategy refines predictions by penalizing the hallucination and missing features behavior.

Implementation Details

We conducted two training phases. The first phase, instructing fine-tuning, aims to enable the LLM to perform the information extraction task by providing detailed instructions and input-output pairs; this phase aligns the model with the extraction task and uses Mistral Nemo [37] as the base model. The second phase, confidence-regularization fine-tuning, aims to reduce hallucination and minimize missing feature extraction, thereby increasing the performance; this phase uses the model from the instructing fine-tuning phase as the base model. The confidence-regularization phase uses F_1-score n-gram matching to accurately evaluate the model's extraction compared with the ground truth features annotated by experts and compares them against the confidence of the predicted features.

For comparison, we trained two variants of each phase: one using a limited dataset (100 patient notes) with 90 patient notes held out for validation to evaluate LLM performance in low-resource settings, and another using the full training corpus

XSL•FO
RenderX

(700 patient notes) with 100 patient notes held out for validation. The following are the key hyperparameters used in both training phases. During instructing fine-tuning, we use the Mistral Nemo instruct model with a batch size of 4, learning rate of 5e−5, weight decay of 0.01, and dropout set to 0.1. Optimization was performed using AdamW (PyTorch, Meta AI) with a linear learning rate scheduler across 5 epochs, with early stopping based on the validation F_1-score. For confidence-regularization fine-tuning, we retained the same optimization setup (batch size, learning rate of 1e−4, dropout, weight decay, and epochs) but introduced confidence-regularization parameters: α=0.7 as the feedback coefficient, β=0.2 as the stochastic scaling factor, and λ=20 as the feature complexity normalizer. The dynamic confidence threshold is initialized at τ_{init}=0.6 and gradually increases to τ_{final}=0.7 during training. In the final configuration, we assign loss weights of 0.2 for hallucinated features and 0.5 for missing features. All experiments are conducted on NVIDIA H100 GPUs (graphics processing unit; 80 GB; NVIDIA corporation). These hyperparameters reflect the configurations reported in our Tables S1-S4 in Multimedia Appendix 2.

Evaluation Framework

Performance Evaluation

During inference, the trained model extracts features from new patient notes using few-shot ICL. Each note is prompted with standardized instructions and 4-6 exemplary input-output pairs to guide feature generation. Extracted features undergo a three-step validation process, referred to as the matching gate: (1) exact matching with regular expressions and Levenshtein distance for misspellings, (2) nonconsecutive and sentence-level matching using term frequency-inverse document frequency similarity and segment alignment, and (3) overlap and windowed matching for distributed features. This ensures that only text-supported features are validated, preventing hallucinations [42]. To ensure fair comparison, this matching gate validation pipeline was applied consistently across all models during inference, including the vanilla baseline (Mistral Nemo with few-shot ICL), the instructing fine-tuned models, and the confidence-regularization fine-tuned models. Following Yaneva et al [9], we used a binary evaluation protocol in which features are scored as present or absent, regardless of exact span extraction. The binary evaluation proposed by Yaneva et al [9] relies on model probability for a token, which is inapplicable for a generative model; therefore, we conducted two types of binary evaluations. First, binary overlap occurs when feature words overlap with the predicted feature, with 50% considered as found. This binary decision is used to calculate (binary overlap) precision, recall, and F_1 metrics. Second, to account for the LLM's ability to capture meaning, we also implemented semantic binary evaluation. During inference, the trained model attempts to extract each target feature from the case-specific feature list. For each target feature, the system: (1) searches for matching text in the patient note using the matching gate validation (confirming existence in the patient note); (2) if found, calculates cosine similarity between the extracted text and the target feature description using a lightweight sentence embedding model [54]; (3) marks the feature as present only if cosine similarity ≥0.5; and (4) logs the evidence span with character offsets. This two-step validation process, followed by similarity matching, determines the binary presence used to calculate (semantic matching) precision, recall, and F_1 metrics.

For human oversight, the system flags borderline matches (cosine similarity 0.5-0.7) and missing features for manual verification, enabling instructors to efficiently validate the automated scoring. The complete extraction metadata supports graduated review based on institutional requirements. Cosine similarity is not equivalent to the model's internal confidence. Our calibration estimate is derived from the LLM's softmax outputs, which serve as regularization during training to penalize overconfidence. By contrast, cosine similarity is a deterministic, embedding-based measure of semantic closeness between the extracted text and the rubric feature description, and it is an inference step to highlight borderline cases of semantic mismatch.

Generalization Assessment

For a comprehensive evaluation of our framework's performance under different training settings, we trained four models using the following configurations: (1) few-shot (instructing): trained the model using instructing fine-tuning approach on 100 annotated patient notes—this training used Mistral Nemo as base model; (2) few-shot (confidence-regularization): trained the model using confidence-regularization fine-tuning approach on 100 annotated patient notes—this training used a fine-tuned model from the instructing phase as the base model; (3) full (instructing): trained the model using an instructing fine-tuning approach on 700 annotated patient notes—this training used Mistral Nemo as a base model; and (4) full (confidence-regularization): trained the model using confidence-regularization fine-tuning approach on 700 annotated patient notes—this training used a fine-tuned model from the instructing phase as the base model.

Hallucination and Missing Feature Quantification

The model also generates a confidence score of $c_i \in$ (0-1) for each extracted text segment e_i, indicating the model's estimated likelihood that e_i and f_i semantically match. The ground truth annotated by experts for each f_i is denoted as g_i, which may be Ø if no corresponding feature exists in P.

We use a character-level n-gram F_1-score, denoted as F_1-socre$_n$(e_i,g_i), to measure the similarity between an extraction e_i and the ground truth g_i. Compared with exact string matching, this character-level method better captures partial matches and variations in medical terminology. The F_1-score is calculated as:



Where:



N (x) represents the set of character n-grams in text x.

For all models evaluated in this study, including the vanilla baseline (Mistral Nemo with few-shot ICL), instructing

XSL•FO
RenderX

fine-tuned models, and confidence-regularization fine-tuned models, the same inference pipeline was applied. This pipeline includes few-shot ICL and the three-step matching gate validation described in the Performance Evaluation section, ensuring fair comparison of hallucination and missing feature rates across all model variants.

Calibration Analysis

To assess the alignment between the model's predicted confidence and its actual performance, we used two standard calibration metrics: the expected calibration error (ECE) and the Brier score. ECE measures the average difference between the model's confidence scores and its actual accuracy across predefined confidence bins, providing insight into systematic overconfidence or underconfidence. The Brier score quantifies the mean squared difference between predicted confidence and true outcomes, reflecting both calibration and predictive accuracy. Unlike the binary presence/absence evaluation used for model comparison, our calibration analysis uses continuous F_1-scores calculated at the feature level. For each extracted feature, we compute chrF scores against ground truth, providing a continuous measure (0,1) that better captures partial matches and extraction quality. This continuous evaluation is more suitable for calibration assessment, as it provides granular confidence–performance alignment with actual performance rather than binary outcomes.

Ethical Considerations

This study used the USMLE Step-2 Clinical Skills dataset, comprising deidentified patient notes from standardized medical examinations. The original data collection by the National Board of Medical Examiners (NBME) was conducted with appropriate informed consent from participating medical students who took the USMLE Step-2 Clinical Skills examination [36]. All data were fully anonymized, ensuring no identifiable information was included, and privacy was protected through NBME's data-sharing protocols. Our data request was approved by NBME (ID 34890198). No compensation was provided, as the study did not involve direct participant recruitment. No images of individual participants were included in the manuscript or supplementary materials, ensuring no identification risks. The proposed framework is designed for research purposes, specifically for evaluating automated medical informatics and information extraction in medical education assessment, and is not intended for diagnostic use.

Results

Overview

We present experimental results evaluating the proposed framework on the USMLE Step-2 Clinical Skills dataset in few-shot and full-data settings, comparing it against previous state-of-the-art models [9]. The results address 3 RQs; each subsection below corresponds to one aspect, providing a clear, stepwise assessment of our two-phase framework.

Overall Performance

Each evaluation was performed using the two splits (the public and the private) to accommodate direct comparisons with previous work. Performance across these datasets is summarized in Table 2 using precision, recall, and F_1 metrics as evaluation criteria. These results demonstrate the ability of LLMs to generalize even with few-shot training. The binary evaluation relies on exact text comparison with a 50% overlap threshold, while the semantic test assesses semantic meaning match, reflecting the LLM's ability to capture deep meaning. The results of the semantic binary evaluation outperform overlap for two reasons: (1) the semantic assessment is less strict in capturing exact matches and (2) the semantic test runs between predicted features and case-related features if there is no annotated ground truth. We examined 1430 features and found 68 false positives, as they were not annotated in the ground truth but were semantically equivalent to case-related features. The few-shot confidence-regularization model outperforms previous systems on both public and private splits, using binary evaluation [9]. The full data training model becomes state-of-the-art performance with an F_1-score of 0.983, validating the effectiveness of our two-phase fine-tuning framework (instructing + confidence-regularization).

XSL•FO
RenderX

Table 2. Performance comparison on public and private dataset splits. Baseline models use token-level probability thresholds. Our models show results for both binary overlap (token overlap ≥0.5) and semantic matching (cosine similarity ≥0.5) approaches.

Model	Public dataset			Private dataset		
	Precision	Recall	F_1-score	Precision	Recall	F_1-score
Baseline models (Yaneva et al [9])						
INCITE[a]	0.962	0.818	0.883	0.961	0.828	0.888
DeBERTa[b]	0.950	0.962	0.956	0.951	0.963	0.957
DeBERTa + MTL[c]	0.947	0.961	0.954	0.953	0.963	0.958
DeBERTa + MLM[d]	0.952	0.961	0.957	0.961	0.956	0.958
Our models with few-shot training (100 patient notes)–semantic match						
Instructing fine-tuning	0.970	0.928	0.949	0.971	0.934	0.952
Confidence-regularization fine-tuning	0.986[e]	0.960	0.973[e]	0.982[e]	0.964	0.973[e]
Our models with few-shot training (100 patient notes)–binary overlap						
Instructing fine-tuning	0.935	0.917	0.926	0.937	0.947	0.942
Confidence-regularization fine-tuning	0.940	0.965[e]	0.952	0.950	0.971	0.960
Our models with full data training (700 patient notes)–semantic match						
Instructing fine-tuning	0.979	0.952	0.965	0.974	0.952	0.963
Confidence-regularization fine-tuning	0.988[f]	0.978[f]	0.983[f]	0.988[f]	0.974[f]	0.981[f]
Our models with full data training (700 patient notes)–binary overlap						
Instructing fine-tuning	0.915	0.958	0.936	0.939	0.969	0.954
Confidence-regularization fine-tuning	0.956	0.980	0.968	0.962	0.984[e]	0.973[e]

[a]INCITE: intelligent clinical text evaluator.

[b]DeBERTa: decoding-enhanced bidirectional encoder representations from transformers with disentangled attention.

[c]MTL: multitask learning.

[d]MLM: masked language modeling.

[e]Second best result.

[f]Best result.

Few-Shot Learning Capability (RQ1)

We extend the analysis of the model's capability to generalize through a complementary evaluation, which evaluates the embedding similarity between each feature and all its ground truth annotations. Each model has its own vocabulary vector that can be represented in high-dimensional space. Cosine similarity is used to measure how close each vocabulary vector is to the others semantically. As illustrated in Figure 3, we measured the cosine similarity distributions for 5 representative features across different model trainings to measure how the cosine similarity of the features to their ground truth changed. The vanilla model is the Mistral Nemo instruct model, where no training was conducted; only ICL with a few examples was used to guide model predictions. This approach achieved an average similarity of 0.62, indicating that modest inherent medical knowledge from the pretrained weights is brought into the model. The few-shot model improves that alignment up to 0.68, while the full model reaches 0.72, with tighter clustering around the ground-truth representations. Such progressive improvement demonstrates that semantic alignment is indeed vastly improved with fine-tuning, even with just 10 examples per case and with significantly less output variance.

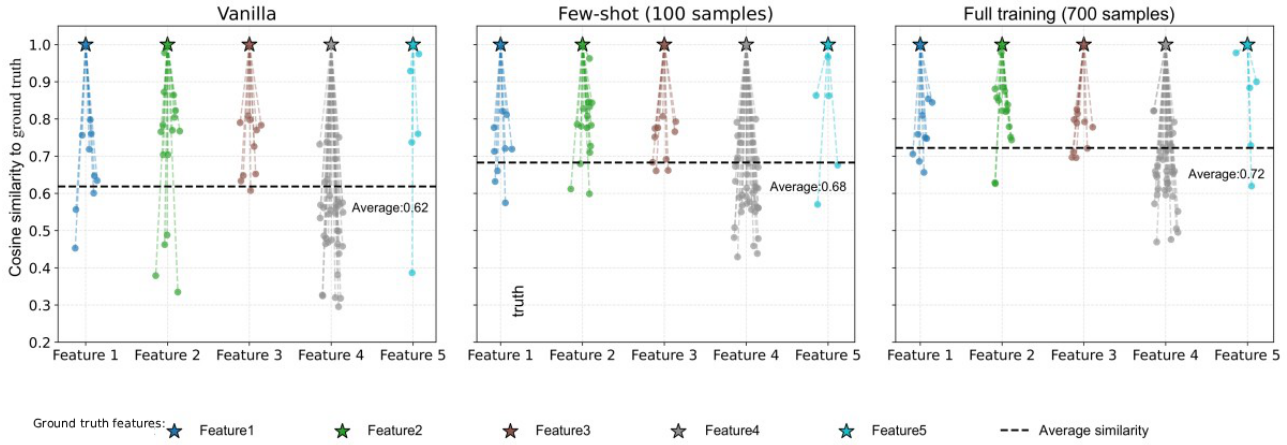
The findings, therefore, underscore the promise of domain adaptation using our two-phase instructing and confidence-regularization fine-tuning setup, especially in low-resource clinical environments where obtaining labeled data may be a hard task. Having achieved these significant gains with merely 100 patient notes, which correspond to around 10 examples per clinical case type, only 100 records out of 700 (14.2% of the full dataset), further implies the viability of our approach in restricted medical domains where extensive, fully annotated datasets are often not available. To answer our first RQ1: "Is the model able to generalize effectively from limited training data, while maintaining competitive performance against full-data training?" the evidence strongly supports "yes." Our system, with a few samples, having been trained using only 100 out of 700 patient notes (14.2% training set), obtained an

XSL•FO
RenderX

F_1-score of 0.973, which is about 99% of the full model performance (F_1=0.983), and this is higher than previous state-of-the-art approaches working with fully annotated data. This showcases excellent generalization ability under minimal supervision, thereby affirming that our method can considerably reduce annotation demand while keeping high performance.

To measure whether the improvement observed by confidence-regularization fine-tuning over instructing fine-tuning is genuine, we used bootstrap resampling and McNemar test. Bootstrap resampling estimated the F_1-score difference by repeatedly sampling the test set, yielding a 0.0235 difference with a 95% CI of 0.0175-0.0302 and a P value of P<.001, indicating a stable, significant improvement. McNemar test, analyzing paired outcomes, yielded a P value of .016, showing that the confidence-regularization model corrects more errors (124 features) than the instructing model (88 features). Both models were trained on 100 records and evaluated on 200 patient notes from the public dataset. These results confirm confidence-regularization model's robust improvement over instructing fine-tuning model.

Figure 3. Cosine similarity between 5 representative features (stars) and their ground-truth features (dots).



Error Reduction Analysis (RQ2)

To evaluate the capability of our confidence-regularization framework to reduce hallucination and improve reliability, we conducted two analyses: one measuring error distributions across model variants and the other measuring the evolution of hallucination and missing penalty functions during training epochs. All models—vanilla baseline, instructing fine-tuned, and confidence-regularization fine-tuned—were evaluated using the same inference pipeline (few-shot ICL + matching gate validation) to ensure fair comparison. Figure 4 quantifies the reduction in hallucination (left) and missing information (right), on both data splits, public (up) and private (down). The vanilla model (Mistral Nemo) incurs significant error rates, with 599 missing features (20.9% of 2861 features) and 335 hallucinated features (11.7% of 2861). The few-shot instructing fine-tuning model brings down these errors dramatically to 113 missing features (3.9% of 2861, a reduction of 81.1%) and 99 hallucinated features (3.5% of 2861, a reduction of 70.4%).

The full confidence-regularization model reduces these errors further to 62 missing features (2.2% of 2861, a reduction of 89.6%) and 34 hallucinated features (1.2% of 2861, a reduction of 89.9%).

In this respect, the pattern is consistently extended to the much larger private dataset (20,360 features), which misses a total of 6376 features (31.3% of 20,360) in addition to 3081 hallucinated features (15.1% of 20,360) using the vanilla model. The few-shot instructing fine-tuning model reduces the missing features to 957 (4.7% of 20,360, a reduction of 85%) and 465 hallucinated features (2.3% of 20,360, a reduction of 84.9%), while the full model misses only 708 features (3.5% of 20,360, a reduction of 88.9%) and 311 hallucinated features (1.5% of 20,360, a reduction of 89.9%).

To better understand the underlying mechanisms, Figure 5 presents the penalty trends across training epochs for all 10 clinical cases. The hallucination penalty (blue lines) consistently decreases as training progresses, with most cases showing a steep decline during epochs 1-3. Several interesting patterns emerge in the penalty curves: (1) missing feature penalties (yellow lines) often start higher than hallucination penalties, particularly in complex cases (cases 2, 5, 7, and 8), indicating an initial model bias toward precision over recall; (2) by epoch 5, nearly all cases demonstrate convergence to low penalty states (<0.05), showing the model has effectively handled feature detection and hallucination avoidance; and (3) the balanced convergence of both penalty types validates our bidirectional mapping approach, which prevents optimization from favoring one error type over another.

Being able to significantly reduce missing features and hallucinated features and, maintain similar reductions in penalty convergence across clinical cases proves beyond a doubt that our confidence-regularization framework robustly addresses RQ2. The proposed framework has been successful in minimizing hallucination problems prevalent to LLMs in medical contexts and in improving the reliability of extraction even in extremely low supervision (few-shot instructing fine-tuning).

XSL•FO
RenderX

Figure 4. Comparison of missing and hallucinated features across model types. The vanilla model (Mistral Nemo with few-shot in-context learning [ICL]) shows the highest error rates, while the full model minimizes both error types.

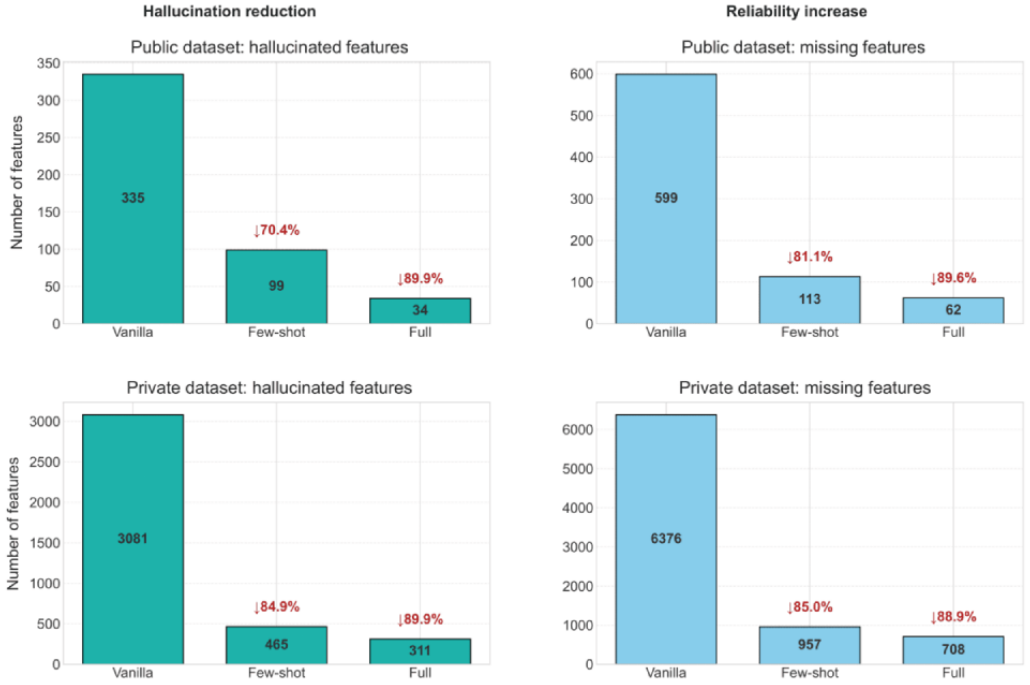
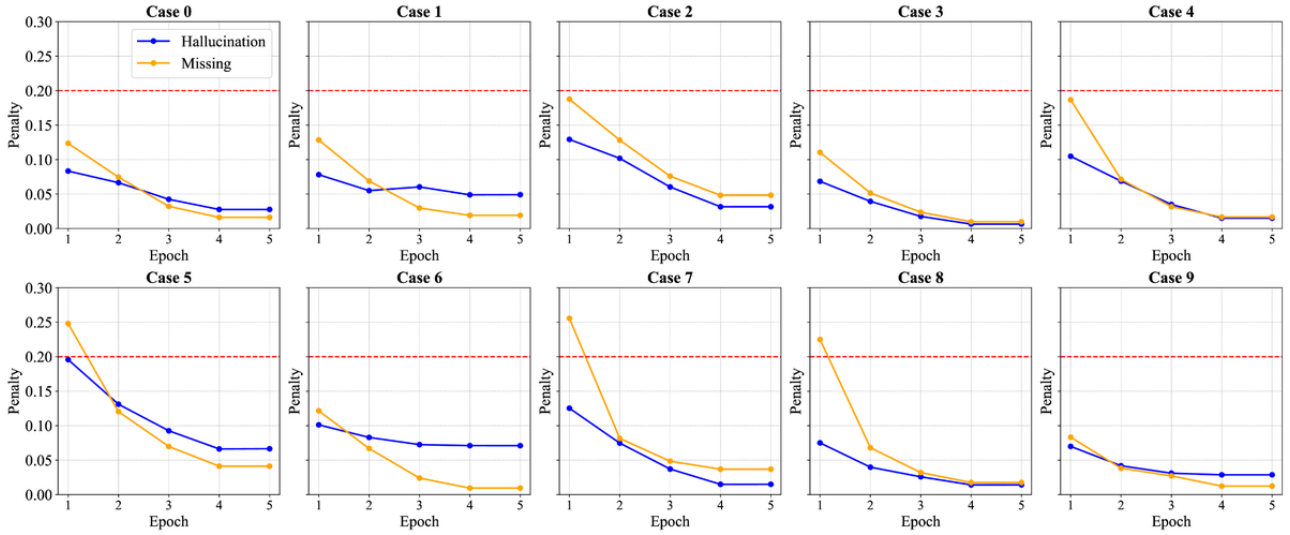


Figure 5. Evolution of hallucination (blue lines) and missing feature (yellow lines) penalty values over 5 training epochs for 10 clinical cases on the training dataset. The convergence of penalties illustrates the effectiveness of bidirectional semantic matching in balancing error types. The red line serves as a visual aid, highlighting where most penalties are <0.2.



Calibration and Reliability (RQ3)

LLMs have proven to be powerful tools, with inherent deep contextual understanding capabilities, to process and generate human-like text. These models are often poorly calibrated due to their complex architecture and large number of parameters. Many previous works report that further instructing fine-tuning for specific task can improve accuracy but harm calibration, causing LLMs to become overconfident [55,56]. Our confidence-regularization framework reveals an unexpected calibration pattern. Rather than the typical confidence inflation seen in fine-tuned LLMs, our approach maintains stable average confidence (0.84, SD 0.003) while achieving dramatic performance improvements (F_1 improved from 0.819 to 0.986). This creates a unique scenario where ECE increases not due to overconfidence, but from the growing misalignment between conservative confidence estimates and exceptional performance.

Figure 6 presents the reliability diagrams for our confidence-regularization model across 5 training epochs. Following the standard approach established by Guo et al [16], we partition predictions into 4 confidence bins (0.6-0.7, 0.7-0.8, 0.8-0.9, and 0.9-1.0) and compare the mean confidence within each bin against the actual F_1 performance. Perfect calibration would result in all points lying on the diagonal line (y=x). As training progresses from epoch 1 to epoch 2, the model shows mixed calibration with significant underconfidence in the 0.6-0.7

XSL•FO
RenderX

bin; the gap between the average F_1 score of this bin and optimal performance can be calculated as 0.692−1=−0.308 (negative mean underdominance). From epoch 3 to epoch 5 as F_1 performance improves to 0.94-0.98, stable confidence becomes increasingly conservative. The 0.8-0.9 bin shows growing underconfidence (gap evolving from −0.077 to −0.136), while the highest confidence bin (0.9-1.0) transitions from slight overconfidence to underconfidence (gap evolving from 0.092 to −0.072). The distribution of predictions shifts toward higher confidence bins (from 683 to 849 predictions in the 0.8-1.0 range), but this reflects improved feature extraction quality rather than confidence inflation. In the highest confidence bin, F_1-scores reach 0.98 by epoch 5, yet the model maintains conservative confidence estimates (SD 0.003). Despite the degradation in calibration, the model achieves remarkable performance improvements. F_1-scores in the highest confidence bin (0.9-1.0) increase from 0.81 to 0.98, demonstrating that while calibration worsens, the model performance increases.

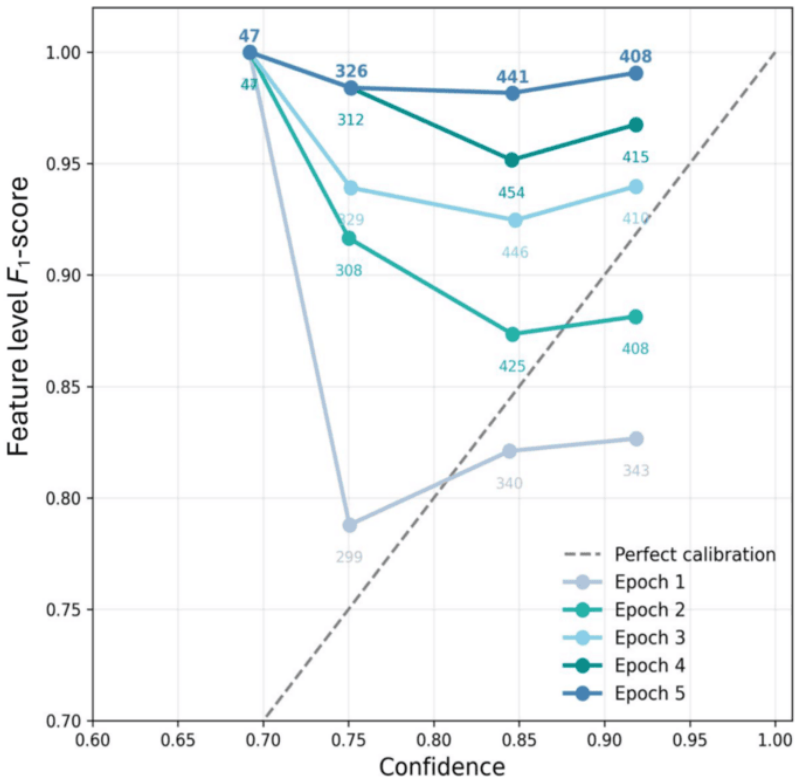
Our ECE increases from 0.060 to 0.147 across epochs, while the Brier score improves from 0.087 to 0.036. This is explained by our stable confidence mechanism: ECE measures the gap between confidence and performance, which naturally widens as performance improves while confidence remains constant. The improved Brier score indicates better probabilistic predictions despite the calibration mismatch. Contextualizing within medical NLP literature, Oliveira et al [57] reported ECE values for entity and relation extraction tasks ranging from 0.12 to 0.44, depending on the dataset and strategy. Our final ECE of 0.147 falls within this expected range. The increasing ECE aligns with findings from another study [20], which show that pretrained language models do not learn to become calibrated during training; they become increasingly overconfident. In our case, penalties lead to conservatism rather than overconfidence.

This “stable confidence with improving performance” pattern addresses (RQ3) in an unexpected way. The confidence-regularization strategy has not yet achieved tight calibration; instead, it prevents the overconfidence seen in fine-tuned LLMs. Following the framework of Xiao et al [58], our model operates in what they term the “non-calibratable regime,” where performance increases as ECE increases. However, unlike typical models in this regime that exhibit severe overconfidence, our approach maintains conservative, stable confidence estimates.

For medical applications, this represents a desirable trade-off. Conservative confidence estimates (underconfidence) are preferable to overconfidence when errors have serious consequences.

Given the reliability diagram and rising ECE, our findings corroborate a growing body of published evidence that alignment improves task quality at the expense of calibration. It enters the “non-calibratable regime” described by Xiao et al [58], where further accuracy gains cannot be matched by improvements in calibration. Our inference-time gating offers a viable, low-cost alternative when the task requires matching with existing references, as the case in feature extraction for this specific task.

Figure 6. Reliability diagram showing feature-level performance as F1-score with softmax confidence per feature.



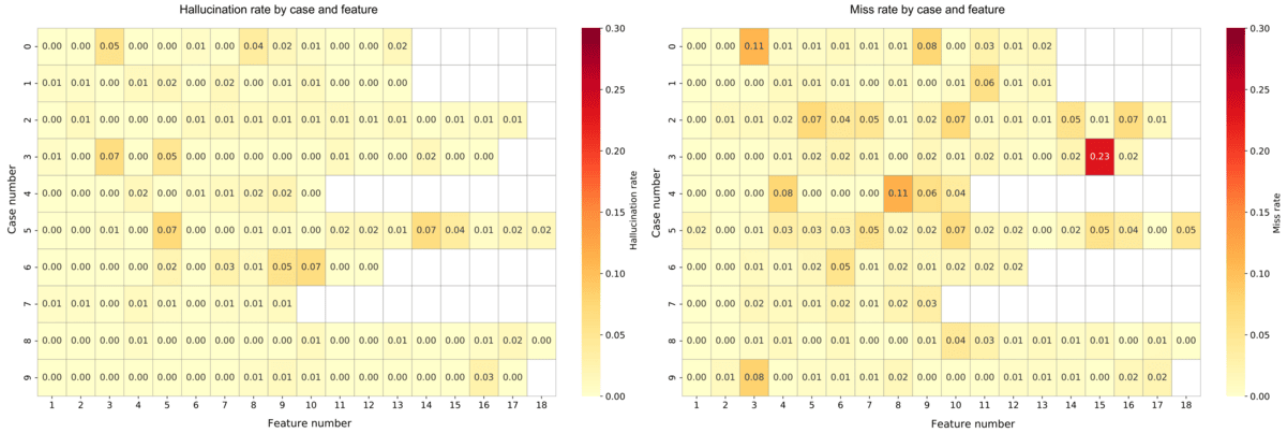
XSL•FO
RenderX

Qualitative Error Analysis

We analyzed our model's predictions on a private dataset containing 26,297 features. The hallucination rate is defined as precision (FP/[TP+FP]) and the miss rate as recall (FN/[TP+FN]) per feature. The heatmap in Figure 7 shows these features, with darker colors indicating higher hallucination (precision) and missing feature (recall) error rates. Our analysis shows that hallucination errors occur less frequently than missing feature errors, with the highest hallucination rates at 7%, while missing features showed an even higher occurrence, up to 23%.

Upon closer examination of these features (detailed examples provided in Multimedia Appendix 2), we identified several consistent patterns, as illustrated below.

Figure 7. Heatmap showing hallucination and omission (missing features) rates for all clinical features in the private test set, where darker red indicates higher error rates and light yellow indicates lower error rates.



Hallucination Error Patterns

Overview

Annotation inconsistencies: many features categorized as hallucinations stem from inaccuracies in the ground truth annotations. For example, the feature "worsened 3 weeks ago" was not in the ground truth of one patient note, while an equivalent feature, "symptoms worsened 3 weeks," was annotated as ground truth in another note belonging to the same case number.

Specificity requirements

Certain features demand exact descriptions of symptoms to be identified accurately. For example, the feature "Epigastric-discomfort," where epigastric specifically refers to the upper central region of the abdomen, was annotated in ground truth as "pain in the middle of his stomach." On the other hand, the model's prediction of a nonspecific "stomach pain," lacking details on the precise location, caused the predictions to fail similarity matching and be registered as hallucinations.

Redundant documentation

In several cases, features were listed twice in patient documentation using varied phrasing but were annotated only once. For example, the predicted feature "Denies dyspnea" was present in the text but not considered during inference because annotators had only marked "negative shortness of breath."

Knowledge limitations

A significant error example represents a fundamental knowledge gap inherent in the LLM, such as "No-relief-with-asthma-inhaler," predicted as "tylenol did not help." Tylenol is a pain reliever, not an asthma medication.

Missing Feature Error Patterns

Predicting complex features proved consistently challenging for the model. As shown in Tables S3 and S4 in Multimedia Appendix 2, for compound features like "No-hair-changes-OR-no-nail-changes-OR-no-temperature-intolerance," the model predicted only "denies change in weight," while the actual annotation for this patient was "Denies any sweating." Similarly challenging was the feature "Lack-of-other-thyroid-symptoms," which lacks standardization and was inconsistently captured by annotators.

Our analysis identified 4 key limitations: annotation constraints, where human annotators showed inconsistencies in the annotated data, as evidenced by the agreement percentage [36], affecting model evaluation; semantic depth disparity, where the model's deep semantic understanding was sometimes interpreted differently from the annotation team's standardized approach, leading to instances of false positive results; feature ambiguity, where some features were rather generic in nature and lacked a clear set of well-defined boundaries, making consistent annotation and prediction difficult; and model internal knowledge gaps, where the model's knowledge limitations caused errors such as confusing medication classes (eg, pain relievers vs bronchodilators) or anatomic localizations (eg, epigastric vs general stomach pain). The error analysis underscores that the annotation process lacks comprehensiveness and standardization, in addition to being subject to human error bias and the complexity of annotating large text volumes, making it a challenging task. LLMs, highly sensitive to data quality, require consistent, standardized training data for optimal performance, and the model's medical domain knowledge limitations could be improved with accurately annotated data and continuous training on domain-specific medical data to significantly enhance performance.

XSL•FO
RenderX

Discussion

Overview

Our framework efficiently extracts medical features from patient notes by integrating diverse training approaches, multidimensional confidence-regularization, and embedding similarity evaluation. It achieves a state-of-the-art F_1-score of 0.983 (semantic matching) and 0.968 (binary overlap) on the full dataset, and 0.973 (semantic matching) and 0.952 (binary overlap) with only 100 patient notes, outperforming benchmark models INCITE (F_1=0.888) and DeBERTa-based models (F_1=0.958). The framework provides a transformative solution for automated medical education assessment, addressing data scarcity, semantic variability, hallucination risks, and interoperability.

The framework's strength lies in its strong generalization, retaining 99% performance with only 100 out of 700 patient notes (14.2% of the training data) through instructing and confidence-regularization fine-tuning. Semantic embedding matching captures variable clinical expressions (eg, "worsen 3 wks ago" vs "symptoms worsened 3 weeks"), unlike token-level probability methods. Our framework ensures performance stability, reducing overfitting in data-scarce settings—crucial for resource-constrained environments where manual annotation is costly.

Unlike traditional n-gram, fuzzy logic, or BERT-based methods, which struggle with semantic variability in clinical notes, our framework adapts semantic embedding matching and lightweight sentence embedding for cosine similarity, capturing deeper semantic meaning.

Our confidence-regularization fine-tuning phase significantly enhances feature extraction performance, reducing hallucinations by 89.9% (from 3081 to 311) and missing features by 88.9% (from 6376 to 708). However, this phase does not improve the ECE, which increases from 0.060 to 0.147 over 5 training epochs. This trade-off arises not from overconfidence but from the growing misalignment between conservative confidence estimates and exceptional performance. Despite the well-documented overconfidence and the miscalibration of LLMs [55,56], our approach maintains stable, conservative confidence, which becomes underconfident as performance improves.

With near-human performance, the framework evaluates 200 notes in 30 minutes on a high-performance GPU, reducing manual effort for USMLE Step-2 Clinical Skills examination preparation. Its few-shot learning and modular architecture eliminate the need for span annotation (interrater agreement of 84%) and enable customization. The framework shows promise for extracting structured data from electronic health records, diagnostic reports, and discharge notes, improving decision-making in health care.

Compared to lexicon-based INCITE, BERT-based models, or DeBERTa with pseudo-labeling, our framework achieves higher precision and recall through two-phase fine-tuning, with both semantic matching (0.988 vs 0.961 precision; 0.978 vs 0.963 recall) and binary overlap evaluation. Our inference-time matching gate effectively replaces traditional calibration needs through context-aware filtering. Unlike post hoc calibration requiring held-out data (which would reduce our already limited training set), our approach validates extractions against case-specific feature lists. This addresses a unique challenge in medical feature extraction: identical text (eg, "fever") may be correct for case 1 but incorrect for case 2, making global calibration inappropriate.

Our framework generates output that supports human-in-the-loop deployment in medical education assessment. During inference, for each case-specific feature that needs to be identified, the system produces: (1) a matching gate decision indicating whether the feature was found in the patient note (present/absent), (2) the extracted text segment and its offset, and (3) a cosine similarity score (0-1 range) between the extracted text and ground truth during testing, which can also be applied to the case's target feature during deployment. These outputs enable medical instructors to review the output by identifying weakly matched extracted features with low cosine similarity scores that may need manual rechecking. Missing features for features from the case list that the model could not find (marked absent) are highlighted for instructor review to confirm they are truly missing. Potential hallucination occurs when the model predicts a feature that could not be found by the matching gate, indicating incorrect extraction. For deployment, institutions can customize review thresholds based on their requirements. High-stakes examinations might mandate manual review of all extractions with cosine similarity >0.8 to their target features, while formative assessments could limit review to missing features only. This flexibility ensures the system augments rather than replaces human judgment in educational assessment.

Alignment With Artificial Intelligence Trustworthiness Framework

CONSORT-AI (Consolidated Standards of Reporting Trials–Artificial Intelligence) guidelines provide a complete checklist for any artificial intelligence (AI)–based clinical intervention, ensuring transparent and reproducible reporting of AI usage during clinical practice [59]. In the following subsections, we detail how the proposed framework meets important key requirements of CONSORT-AI.

Clear Description of AI Intervention (Item 5)

CONSORT-AI requires a detailed description of the AI intervention, such as how it is used and integrated into clinical workflows. Our framework is used for automating the assessment process of medical feature extraction from clinical examination notes written by medical students. The framework's two-phase approach is clearly described, with detailed algorithms (Algorithm 1) and hyperparameters in Multimedia Appendix 2 to ensure reproducibility. Its intended use is to support automated assessment in medical education, reducing the burden on human evaluators while maintaining high accuracy (F_1=0.983). This framework is considered as part of the examination, where the examiner must also evaluate other communication skills.

XSL•FO
RenderX

Input and Output Specification (Item 7)

CONSORT-AI requires clarification of the input data and output format of the AI system. Input data are described in (Phase 1: Instructing Fine-Tuning section), detailed data collection and annotation prepared by NBME [36]. To prepare data for training the model, notes were descoped and formatted using standardized instructions and few-shot ICL (4-6 exemplar pairs, as described in the section Phase 1: Instructing Fine-Tuning). The output consists of patient notes, features associated with patient note cases, extracted features validated through the matching gate, similarity score, and the matched part within patient notes, ensuring outputs are structured and clinically relevant.

Reproducibility and Code Availability (Items 10-11)

Based on CONSORT-AI, details ensuring reproducibility and providing access to code and data are required. The complete source code, including training and inference code, is available in a GitHub repository [62]. Model weights and training protocols are fully documented. The dataset is accessible through Kaggle and NBME data-sharing agreement. Computational requirements are specified (NVIDIA H100 GPUs).

Performance and Error Reporting (Item 12)

CONSORT-AI encourages comprehensive reporting of performance metrics and error types. Our proposed model provides detailed performance metrics (precision, recall, and F_1-score) across public and private dataset splits (Table 2), achieving F_1=0.983 with full data and F_1=0.973 with 100 notes. Error analysis investigating the pattern and reasons of hallucination and missing features is provided in the Qualitative Error Analysis section.

Handling of Errors and Failures (Item 19)

CONSORT-AI requires describing how errors and failures are managed. During training, errors are detected using bidirectional semantic matching (in step 3 of the Phase 2: Confidence Regularization Fine-Tuning section), targeting hallucinations and missing features. The inference-time matching gate ensures filtering of nonexistent predictions, supporting reliable clinical outputs. During deployment, the model extracts features and displays the relevant feature numbers, allowing human intervention by tracking the extraction process.

Human-AI Interaction (Item 20)

CONSORT-AI stresses the role of human oversight in AI systems. Our framework supports human oversight through a cosine similarity score for each extracted feature, along with the number and text of the feature associated with the case, enabling experts to prioritize review of features below a set low cosine similarity threshold. The matching gate facilitates verification by eliminating mismatched features. All extracted features are matched with patient note text then approved to be passed. This creates oversight transparency where the errors can be tracked in text. Integration with electronic health record systems could further allow clinicians to accept, reject, or flag model outputs prior to downstream use. At present, this capacity is not implemented in the prototype but is identified as a key future development for clinical deployment.

Validation in Clinical Context (Item 22)

CONSORT-AI requires validation of AI performance in intended clinical contexts. The proposed framework's evaluation on the USMLE Step-2 dataset (2839 notes) demonstrates applicability in medical education assessment. Its ability to maintain high performance with minimal data (100 notes, 14.2% of training data) supports scalability in resource-constrained settings.

By following CONSORT-AI guidelines, the proposed framework ensures transparency, reliability, and applicability, making it a trusted option for automated medical feature extraction in clinical education environments.

Limitations

While our framework demonstrated strong performance, the evaluation shows several shortcomings that highlight potential areas for improvement.

First, inconsistencies in human-annotated ground truths, such as ambiguous boundaries, subjective symptom consideration, and missing annotations, led to hallucination and missing feature errors. Developing standardized annotation methodologies and clear clinical feature definitions is essential to enhance annotator agreement.

Second, the LLM backbone demonstrates general medical knowledge by performing well with only few-shot fine-tuning but struggles with specific medical logic, such as medication-symptom relationships. Continual pretraining on medical domain data, integrating structured medical ontologies (eg, Systematized Nomenclature of Medicine–Clinical Terms, Unified Medical Language System), or using retrieval-augmented generation could address these gaps.

Third, designing model training on medical datasets may further improve extraction performance. Testing on USMLE Step-2 Clinical Skills notes provided a controlled case collection, but the framework lacks evaluation on unstructured or multilingual health care records, such as electronic health records or notes from psychiatry and pediatrics. Future work could consider semantic adjustments for multilingual records to enhance global applicability by incorporating continual pretraining or multitask fine-tuning.

Fourth, despite the competitive performance of our framework, it demonstrates the typical calibration-accuracy trade-off observed in fine-tuned LLMs [20,55,56,58]. ECE increases from 0.060 to 0.147 during training. Although this pattern aligns with existing literature showing that task-specific fine-tuning often harms calibration [61], our model shows stable confidence, which contrasts with literature observations that LLMs tend to be overconfident. The model's inability to adjust confidence upward as performance improves from 0.82 to 0.98 suggests that our regularization may be overly restrictive, representing a limitation for applications requiring well-calibrated confidence scores.

Fifth, while our framework and baseline models [9] both use binary feature-detection F_1 metrics for evaluation, the method of determining feature presence differs between approaches. The baseline models use token-level probability thresholds

XSL•FO
RenderX

(≥0.5) from span-extraction architectures, which is inapplicable to generative models that produce textual descriptions. We therefore implemented two adapted evaluations: (1) binary overlap using token overlap ≥0.5 between generated and ground truth text, providing the closest equivalent to baseline methodology, and (2) semantic matching using cosine similarity ≥0.5 to capture semantic equivalence. The semantic approach is inherently more lenient than token-based methods, which may introduce a positive bias. However, our binary overlap results (F_1=0.968) still demonstrate improvements over baselines (F_1=0.958), confirming performance gains independent of evaluation methodology.

Sixth, our framework is specifically designed for structured extraction tasks with predetermined feature lists, as demonstrated in the USMLE Step-2 Clinical Skills evaluation. The framework's evaluation pipeline requires both matching gate validation and cosine similarity comparison (≥0.5) against target feature descriptions to determine feature presence. Without predefined target features, the cosine similarity component cannot function, invalidating our current evaluation methodology. While the core confidence-regularization training objective could potentially be adapted to open-ended named entity recognition tasks through span-level token overlap F_1 scoring, this would require a fundamental redesign of the validation pipeline and evaluation framework. Such adaptation represents a distinct research direction requiring substantial methodological changes rather than a straightforward extension of the current work.

Seventh, future work should systematically investigate the sensitivity of confidence-regularization parameters across diverse medical domains and backbone architectures. While our configuration (α=0.7, β=0.2, λ=20, τ=0.6-0.7) achieved stable convergence on the USMLE dataset, understanding the parameter sensitivity ranges would provide practical guidelines for adapting this framework to new clinical NLP tasks with different precision–recall characteristics and error distributions.

Eighth, we demonstrate our two-phase framework on the Mistral-NeMo-Instruct-2407 backbone. Our choice of this backbone was task-driven, based on preliminary experiments on this dataset [37]. While this open model supports reproducibility, we did not perform systematic cross-backbone evaluation (eg, public Mistral-7B-Instruct, Llama-3-Instruct). Thus, the extent to which our gains translate to other model families remains to be quantified and is a direction for future work.

Future Directions

Building on the proposed framework's foundation, future research will focus on advancing its architectural capabilities to enhance the precise identification of clinical features in text, a limitation that has sparked significant interest across the LLM community. While traditional autoregressive models are effective for semantic generation, they struggle with determining exact token positions, reducing their effectiveness in span-sensitive tasks such as named entity recognition and clinical information extraction. This has motivated a wave of research investigating alternative training approaches that can use bidirectional generation, encoder-decoder, and matching-based retrieval models.

We plan to investigate accurate token-level positional grounding while exploring architectures focused on matching and training objectives that can enhance token-level grounding between input and output. Domain-specific pretraining on clinical corpora such as Medical Information Mart for Intensive Care III [60] can further support the model's understanding of medical terminologies.

We will further evaluate our framework across a wider range of clinical settings, such as unstructured electronic health records, radiology reports, and multilingual patient records. Using standardized medical ontologies, such as Unified Medical Language System and Systematized Nomenclature of Medicine–Clinical Terms, can enhance annotation uniformity and boost span-level accuracy. An in-depth study of poor calibration in LLMs is warranted, which may involve architectural adjustments to address persistent overconfidence. Such changes could entail revising attention mechanisms or implementing dedicated calibration layers to more effectively model uncertainty estimates for feature extraction tasks that depend on contextual features that change for each case.

Conclusions

This study developed and evaluated a two-phase LLM framework for automated medical feature extraction from clinical examination notes. Our approach consisted of two training phases: instructing fine-tuning, followed by confidence-regularization fine-tuning, to address the critical challenges in medical NLP applications, including data scarcity, semantic variability, and hallucination risks.

The framework achieved an F_1-score of 0.983 (semantic matching) and 0.968 (binary overlap) on the USMLE Step-2 Clinical Skills dataset with full training data and maintained an F_1-score of 0.973 (semantic matching) and 0.952 (binary overlap) using only 100 out of 700 training samples (14.2% of the full dataset). Through the two-phase training approach, hallucinated outputs were reduced by 89.9% (from 3081 to 311) and missing features decreased by 88.9% (from 6376 to 708) compared to the baseline LLM model with few-shot ICL. While the confidence-regularization fine-tuning improved extraction accuracy, it increased the ECE from 0.060 to 0.147, reflecting the documented calibration–accuracy trade-off in fine-tuned LLMs. Our inference pipeline's semantic similarity validation provides practical calibration by filtering predictions based on feature matching rather than raw confidence scores.

This framework provides a practical solution for automated medical education assessment, reducing the burden on human evaluators while maintaining quality standards for clinical competency evaluation. The demonstrated ability to achieve strong performance with minimal training data positions this approach as a valuable tool for scaling medical education assessment in resource-constrained environments.

XSL•FO
RenderX

Acknowledgments

This Project was funded by KAU Endowment (WAQF) at King Abdulaziz University, Jeddah, Saudi Arabia. The authors, therefore, acknowledge with thanks WAQF and the Deanship of Scientific Research (DSR) for technical and financial support.

Data Availability

The data sets analyzed during the current study are available in the Kaggle competition [37]. The complete data sets, including both public and private splits, are not publicly available due to licensing restrictions but are available from the National Board of Medical Examiners through a data-sharing agreement [63]. The source code generated during this study is available in a GitHub repository [62].

Authors' Contributions

MA contributed to conceptualization, methodology, and writing the original draft. AAMAG contributed to conceptualization, supervision, validation, and writing, including review and editing. AF provided supervision, validation, and contributed to writing through review and editing. MR also contributed through supervision, validation, and writing with review and editing.

Conflicts of Interest

None declared.

Multimedia Appendix 1
Confidence-regularization fine-tuning detailed formulas.
[DOC File , 614 KB - medinform_v13i1e78432_app1.doc]

Multimedia Appendix 2
Algorithm 1, training specifications and error analysis samples.
[DOC File , 1437 KB - medinform_v13i1e78432_app2.doc]

References

1. USMLE. United States Medical Licensing Examination. URL: https://www.usmle.org/ [accessed 2025-07-27]
2. Amaral E, Norcini J. Quality assurance in health professions education: role of accreditation and licensure. Med Educ 2023;57(1):40-48. [doi: 10.1111/medu.14880] [Medline: 35851495]
3. Sarker A, Klein AZ, Mee J, Harik P, Gonzalez-Hernandez G. An interpretable natural language processing system for written medical examination assessment. J Biomed Inform 2019;98:103268 [FREE Full text] [doi: 10.1016/j.jbi.2019.103268] [Medline: 31421211]
4. Yim WW, Mills A, Chun H, Hashiguchi T, Yew J, Lu B. Automatic rubric-based content grading for clinical notes. : Association for Computational Linguistics; 2019 Presented at: Proceedings of the Tenth International Workshop on Health Text Mining and Information Analysis (LOUHI 2019); October 31, 2025; Hong Kong p. 126-135 URL: https://doi.org/10.18653/v1/D19-6216 [doi: 10.18653/v1/d19-6216]
5. Zhou J, Thakkar V, Yudkowsky R, Bhat S, Bond W. Automatic Patient Note Assessment without Strong Supervision. : Association for Computational Linguistics; 2022 Presented at: Proceedings of the 13th International Workshop on Health Text Mining and Information Analysis (LOUHI); October 31, 2025; Abu Dhabi (Hybrid) p. 116-126 URL: https://doi.org/10.18653/v1/2022.louhi-1.14 [doi: 10.18653/v1/2022.louhi-1.14]
6. Xu J, Jiang Y, Yuan B, Li S. Automated scoring of clinical patient notes using advanced NLP and pseudo labeling. 2023 Presented at: Inth International Conference on Artificial Intelligence and Computer Applications (ICAICA). IEEE; 2023; November 28-30, 2023; Dalian, China URL: https://doi.org/10.1109/ICAICA58456.2023.10405427 [doi: 10.1109/icaica58456.2023.10405427]
7. Wals Zurita AJ, Miras Del Rio H, Ugarte Ruiz de Aguirre N, Nebrera Navarro C, Rubio Jimenez M, Muñoz Carmona D, et al. The transformative potential of large language models in mining electronic health records data: content analysis. JMIR Med Inform 2025;13:e58457 [FREE Full text] [doi: 10.2196/58457] [Medline: 39746191]
8. Fukushima T, Manabe M, Yada S, Wakamiya S, Yoshida A, Urakawa Y, et al. Evaluating and enhancing Japanese large language models for genetic counseling support: comparative study of domain adaptation and the development of an expert-evaluated dataset. JMIR Med Inform 2025;13:e65047 [FREE Full text] [doi: 10.2196/65047] [Medline: 39819819]
9. Yaneva V, Suen K, Mee J, Quranda M. Automated scoring of clinical patient notes: findings from the kaggle competition and their translation into practice. : Association for Computational Linguistics; 2024 Presented at: Proceedings of the 19th Workshop on Innovative Use of NLP for Building Educational Applications (BEA 2024); October 31, 2025; Mexico City p. 87-98 URL: https://aclanthology.org/2024.bea-2.3/ [doi: 10.18653/v1/2023.bea-1.36]

XSL•FO
RenderX

10. Latifi S, Gierl MJ, Boulais A, De Champlain AF. Using automated scoring to evaluate written responses in English and French on a high-stakes clinical competency examination. Eval Health Prof 2016;39(1):100-113. [doi: 10.1177/0163278715605358] [Medline: 26377072]
11. Benítez TM, Xu Y, Boudreau JD, Kow AWC, Bello F, Van Phuoc L, et al. Harnessing the potential of large language models in medical education: promise and pitfalls. J Am Med Inform Assoc 2024;31(3):776-783. [doi: 10.1093/jamia/ocad252] [Medline: 38269644]
12. Lucas HC, Upperman JS, Robinson JR. A systematic review of large language models and their implications in medical education. Med Educ 2024;58(11):1276-1285. [doi: 10.1111/medu.15402] [Medline: 38639098]
13. Roustan D, Bastardot F. The clinicians' guide to large language models: a general perspective with a focus on hallucinations. Interact J Med Res 2025;14:e59823 [FREE Full text] [doi: 10.2196/59823] [Medline: 39874574]
14. Deng J, Zubair A, Park Y. Limitations of large language models in medical applications. Postgrad Med J 2023;99(1178):1298-1299. [doi: 10.1093/postmj/qgad069] [Medline: 37624143]
15. Steyvers M, Tejeda H, Kumar A, Belem C, Karny S, Hu X, et al. What large language models know and what people think they know. Nat Mach Intell 2025;7(2):221-231 [FREE Full text] [doi: 10.1038/s42256-024-00976-7]
16. Guo C, Pleiss G, Sun Y, Weinberger K. On calibration of modern neural networks. : Proceedings of the 34th International Conference on Machine Learning (ICML 2017); 2017 Presented at: Proceedings of the 34th International Conference on Machine Learning (ICML 2017); August 6-11, 2017; Sydney p. 1321-1330 URL: https://proceedings.mlr.press/v70/guo17a.html
17. Zadrozny B, Elkan C. Obtaining calibrated probability estimates from decision trees and naive Bayesian classifiers. 2001 Presented at: Proceedings of the Eighteenth International Conference on Machine Learning (ICML 2001); June 28, 2001; San Francisco p. 609-616 URL: https://dl.acm.org/doi/10.5555/645530.655658
18. Liang G, Zhang Y, Wang X, Jacobs N. Improved trainable calibration method for neural networks on medical imaging classification. 2020 Presented at: Proceedings of the British Machine Vision Conference (BMVC 2020); September 7-11, 2020; Virtual Event URL: https://www.bmvc2020-conference.com/assets/papers/0059.pdf [doi: 10.5244/c.34.16]
19. Vazhentsev A, Kuzmin G, Tsvigun A, Panchenko A, Panov M, Burtsev M, et al. Hybrid uncertainty quantification for selective text classification in ambiguous tasks. : Association for Computational Linguistics; 2023 Presented at: Proceedings of the 61st Annual Meeting of the Association for Computational Linguistics (Volume 1: Long Papers); October 31, 2025; Toronto p. 11659-11681 URL: https://doi.org/10.18653/v1/2023.acl-long.652 [doi: 10.18653/v1/2023.acl-long.652]
20. Chen Y, Yuan L, Cui G, Liu Z, Ji H. A close look into the calibration of pre-trained language models. 2023 Presented at: Proceedings of the 61st Annual Meeting of the Association for Computational Linguistics Volume 1: Long Papers; July 9-14, 2023; Toronto p. 1343-1367 URL: https://doi.org/10.18653/v1/2023.acl-long.75 [doi: 10.18653/v1/2023.acl-long.75]
21. Zhang Z, Sabuncu MR. Generalized cross entropy loss for training deep neural networks with noisy labels. Adv Neural Inf Process Syst 2018;32:8792-8802. [Medline: 39839708]
22. Pereyra G, Tucker G, Chorowski J, Kaiser L, Hinton G. Regularizing neural networks by penalizing confident output distributions. : International Conference on Learning Representations (ICLR), Workshop Track Proceedings; 2017 Presented at: Presented at: International Conference on Learning Representations (ICLR), Workshop Track Proceedings; April 24–28, 2025; Singapore URL: https://api.semanticscholar.org/CorpusID:9545399
23. Tian K, Mitchell E, Zhou A, Sharma A, Rafailov R, Yao H, et al. Just ask for calibrationtrategies for eliciting calibrated confidence scores from language models fine-tuned with human feedback. : Association for Computational Linguistics; 2023 Presented at: Proceedings of the 2023 Conference on Empirical Methods in Natural Language Processing; October 31, 2025; Singapore p. 5433-5442 URL: https://doi.org/10.18653/v1/2023.emnlp-main.330 [doi: 10.18653/v1/2023.emnlp-main.330]
24. Ganesh J, Bansal A. Transformer-based automatic mapping of clinical notes to specific clinical concepts. : IEEE; 2023 Presented at: IEEE 47th Annual Computers, Software, and Applications Conference (COMPSAC); June 26-30, 2023; Torino p. 558-563 URL: https://doi.org/10.1109/COMPSAC57700.2023.00080 [doi: 10.1109/compsac57700.2023.00080]
25. Long B, Tan F, Newman M. Ensemble DeBERTa models on USMLE patient notes automatic scoring using note-based and character-based approaches. Adv Eng Technol Res 2023;6(1):107-107 [FREE Full text] [doi: 10.56028/aetr.6.1.107.2023]
26. Vithanage D, Deng C, Wang L, Yin M, Alkhalaf M, Zhang Z, et al. Adapting generative large language models for information extraction from unstructured electronic health records in residential aged care: a comparative analysis of training approaches. J Healthc Inform Res 2025;9(2):191-219. [doi: 10.1007/s41666-025-00190-z] [Medline: 40309133]
27. Jung K. Large language models in medicine: clinical applications, technical challenges, and ethical considerations. Healthc Inform Res 2025;31(2):114-124 [FREE Full text] [doi: 10.4258/hir.2025.31.2.114] [Medline: 40384063]
28. Huang Y, Song J, Wang Z, Zhao S, Chen H, Juefei-Xu F, et al. Look Before You Leap: an exploratory study of uncertainty analysis for large language models. IIEEE Trans Software Eng 2025;51(2):413-429 [FREE Full text] [doi: 10.1109/tse.2024.3519464]
29. Luo J, Xiao C, Ma F. Zero-resource hallucination prevention for large language models. 2024 Presented at: Findings of the Association for Computational Linguistics: EMNLP 2024; October 31, 2025; Miami, Florida p. 3586-3602 URL: https://doi.org/10.18653/v1/2024.findings-emnlp.204 [doi: 10.18653/v1/2024.findings-emnlp.204]

XSL•FO
RenderX

30. Sun Y, Dey S, Hakkani-Tür D, Tur G. Confidence estimation for LLM-based dialogue state tracking. 2024 Presented at: 2024 IEEE Spoken Language Technology Workshop (SLT); December 2-5, 2024; Macao, China p. 1083-1090 URL: https://doi.org/10.1109/slt61566.2024.10832237 [doi: 10.1109/slt61566.2024.10832237]
31. Xiao Y, Wang W. On hallucination and predictive uncertainty in conditional language generation. : Association for Computational Linguistics; 2021 Presented at: Proceedings of the 16th Conference of the European Chapter of the Association for Computational Linguistics: Main Volume; October 31, 2025; Online p. 2734-2744 URL: https://doi.org/10.18653/v1/2021.eacl-main.236 [doi: 10.18653/v1/2021.eacl-main.236]
32. Popović M. chrF: character n-gram F-score for automatic MT evaluation. : Association for Computational Linguistics; 2015 Presented at: Proceedings of the Tenth Workshop on Statistical Machine Translation; October 31, 2025; Lisbon, Portugal p. 392-395 URL: https://doi.org/10.18653/v1/w15-3049 [doi: 10.18653/v1/w15-3049]
33. Li X, Sun X, Meng Y, Liang J, Wu F, Li J. Dice loss for data-imbalanced NLP tasks. : Association for Computational Linguistics; 2020 Presented at: Proceedings of the 58th Annual Meeting of the Association for Computational Linguistics; October 31, 2025; Online p. 465-476 URL: https://doi.org/10.18653/v1/2020.acl-main.45 [doi: 10.18653/v1/2020.acl-main.45]
34. Shool S, Adimi S, Saboori Amleshi R, Bitaraf E, Golpira R, Tara M. A systematic review of large language model (LLM) evaluations in clinical medicine. BMC Med Inform Decis Mak 2025;25(1):117 [FREE Full text] [doi: 10.1186/s12911-025-02954-4] [Medline: 40055694]
35. Geng J, Cai F, Wang Y, Koeppl H, Nakov P, Gurevych I. A survey of confidence estimation and calibration in large language models. 2024 Presented at: Proceedings of the 2024 Conference of the North American Chapter of the Association for Computational Linguistics: Human Language Technologies (Volume 1: Long Papers); 2025 October 31; Mexico City p. 6577-6595 URL: https://doi.org/10.18653/v1/2024.naacl-long.366 [doi: 10.18653/v1/2024.naacl-long.366]
36. Vollmer DD, Fair K, Hong YA, Beaudoin CE, Pulczinski J, Ory MG. The USMLE step 2 clinical skills patient note corpus. In: JMIR Mhealth Uhealth.: Association for Computational Linguistics; 2015 Presented at: Proceedings of the 2022 Conference of the North American Chapter of the Association for Computational Linguistics: Human Language Technologies; October 31, 2025; Seattle p. 2880-2886 URL: http://mhealth.jmir.org/2015/1/e31/ [doi: 10.2196/mhealth.3861]
37. Kaggle. NBME - score clinical patient notes. Kaggle. 2025. URL: https://www.kaggle.com/competitions/nbme-score-clinical-patient-notes [accessed 2025-07-27]
38. Rissanen J. Strong optimality of the normalized ML models as universal codes and information in data. IEEE Trans Inform Theory 2001;47(5):1712-1717 [FREE Full text] [doi: 10.1109/18.930912]
39. Mishra S, Khashabi D, Baral C, Hajishirzi H. Cross-task generalization via natural language crowdsourcing instructions. : Association for Computational Linguistics; 2021 Presented at: Proceedings of the 60th Annual Meeting of the Association for Computational Linguistics (Volume 1: Long Papers); October 31, 2025; Dublin p. 3470-3478 URL: https://doi.org/10.18653/v1/2022.acl-long.244 [doi: 10.18653/v1/2022.acl-long.244]
40. Ouyang L, Wu J, Jiang X, Almeida D, Wainwright C, Mishkin P, et al. Training language models to follow instructions with human feedback. 2011 Presented at: Proceedings of the 36th International Conference on Neural Information Processing Systems; November 28-December 9, 2022; New Orleans URL: https://proceedings.neurips.cc/paper_files/paper/2022/file/b1efde53be364a73914f58805a001731-Paper-Conference.pdf
41. Thakkar H, Manimaran A. Comprehensive examination of instruction-based language models: a comparative analysis of Mistral-7B and Llama-2-7BComprehensive Examination of Instruction-Based Language Models: A Comparative Analysis of Mistral-7B and Llama-2-7B. : IEEE; 2023 Presented at: International Conference on Emerging Research in Computational Science (ICERCS); December 07-09, 2023; Coimbatore URL: https://doi.org/10.1109/icercs57948.2023.10434081 [doi: 10.1109/icercs57948.2023.10434081]
42. Abumelha M. MEDX-FE: A robust LLM-based framework for medical feature extraction with matching gate hallucination filtering. J Inf Syst Eng Manag 2025;10(38s):98-124 [FREE Full text] [doi: 10.52783/jisem.v10i38s.6828]
43. Sivarajkumar S, Kelley M, Samolyk-Mazzanti A, Visweswaran S, Wang Y. An empirical evaluation of prompting strategies for large language models in zero-shot clinical natural language processing: algorithm development and validation study. JMIR Med Inform 2024;12:e55318 [FREE Full text] [doi: 10.2196/55318] [Medline: 38587879]
44. Kapoor S, Gruver N, Roberts M, Pal A, Dooley S, Goldblum M, et al. Calibration-tuning: teaching large language models to know what they don't know. : Association for Computational Linguistics; 2024 Presented at: Proceedings of the 1st Workshop on Uncertainty-Aware NLP (UncertaiNLP 2024); October 31, 2025; St Julians, Malta p. 1-14 URL: https://aclanthology.org/2024.uncertainlp-1.1.pdf
45. Jiang Z, Araki J, Ding H, Neubig G. How can we know when language models know? On the calibration of language models for question answering. Trans Assoc Comput Linguist 2021;9:962-977 [FREE Full text] [doi: 10.1162/tacl_a_00407]
46. Farquhar S, Kossen J, Kuhn L, Gal Y. Detecting hallucinations in large language models using semantic entropy. Nature 2024;630(8017):625-630 [FREE Full text] [doi: 10.1038/s41586-024-07421-0] [Medline: 38898292]
47. Leng J, Huang C, Zhu B, Huang J. Taming overconfidence in LLMs: reward calibration in RLHF. 2025 Presented at: The Thirteenth International Conference on Learning Representations (ICLR); April 24-28, 2025; Singapore EXPO URL: https://openreview.net/forum?id=l0tg0jzsdL

XSL•FO
RenderX

48. Murray K, Chiang D. Correcting length bias in neural machine translation. : Association for Computational Linguistics; 2018 Presented at: Proceedings of the Third Conference on Machine Translation: Research Papers; 2018; Brussels p. 212-223 URL: https://doi.org/10.18653/v1/w18-6322 [doi: 10.18653/v1/w18-6322]
49. Kuhn L, Gal Y, Farquhar S. Semantic uncertainty: linguistic invariances for uncertainty estimation in natural language generation. 2023 Presented at: International Conference on Learning Representations (ICLR); October 31, 2023; Kigali, Rwanda URL: https://openreview.net/forum?id=VD-AYtP0dve
50. Vazhentsev A, Tsvigun A, Vashurin R, Petrakov S, Vasilev D, Panov M, et al. Efficient out-of-domain detection for sequence to sequence models. 2025 Presented at: Findings of the Association for Computational Linguistics: ACL 2023; October 31, 2025; Toronto p. 1430-1454 URL: https://doi.org/10.18653/v1/2023.findings-acl.93 [doi: 10.18653/v1/2023.findings-acl.93]
51. Gal Y, Ghahramani Z. Dropout as a Bayesian approximation: representing model uncertainty in deep learning. 2016 Presented at: ICML'16: Proceedings of the 33rd International Conference on International Conference on Machine Learning; June 19–24, 2016; New York p. 1050-1059 URL: https://proceedings.mlr.press/v48/gal16.html
52. Zou Y, Yu Z, Liu X, Kumar B, Wang J. Confidence regularized self-training. : IEEE; 2019 Presented at: IEEE/CVF International Conference on Computer Vision (ICCV); October 27, 2019; Seoul URL: https://doi.org/10.1109/iccv.2019.00608 [doi: 10.1109/iccv.2019.00608]
53. Nan F, Nallapati R, Wang Z, Nogueira DSC, Zhu H, Zhang D, et al. Entity-level factual consistency of abstractive text summarization. : Association for Computational Linguistics; 2025 Presented at: Proceedings of the 16th Conference of the European Chapter of the Association for Computational Linguistics: Main Volume; October 31, 2025; Online p. 2724-2733 URL: https://doi.org/10.18653/v1/2021.eacl-main.235 [doi: 10.18653/v1/2021.eacl-main.235]
54. Wang W, Wei F, Dong L, Bao H, Yang N, Zhou M. MiniLM: Deep self-attention distillation for task-agnostic compression of pre-trained transformers. 2020 Presented at: NIPS '20: Proceedings of the 34th International Conference on Neural Information Processing Systems; December 6-12, 2020; Vancouver BC Canada p. 5776-5788 URL: https://proceedings.neurips.cc/paper_files/paper/2020/file/3f5ee243547dee91fbd053c1c4a845aa-Paper.pdf
55. GPT-4 technical report. G OpenAI. 2023. URL: https://cdn.openai.com/papers/gpt-4.pdf [accessed 2025-10-31]
56. Zhu C, Xu B, Wang Q, Zhang Y, Mao Z. On the calibration of large language models and alignment. 2023 Presented at: Findings of the Association for Computational Linguistics: EMNLP; December 6-10, 2023; China p. 9778-9795 URL: https://doi.org/10.18653/v1/2023.findings-emnlp.654 [doi: 10.18653/v1/2023.findings-emnlp.654]
57. de Oliveira R, Garber M, Gwinnutt JM, Rashidi E, Hwang JS, Gilmour W, et al. A study of calibration as a measurement of trustworthiness of large language models in biomedical natural language processing. JAMIA Open 2025;8(4):ooaf058. [doi: 10.1093/jamiaopen/ooaf058] [Medline: 40655536]
58. Xiao J, Hou B, Wang Z, Jin R, Long Q, Su WJ, et al. Restoring calibration for aligned large language models: a calibration-aware fine-tuning approach. 2025 Presented at: Proceedings of the 42nd International Conference on Machine Learning (ICML); July 13-19, 2025; Vancouver p. 13-19 URL: https://icml.cc/virtual/2025/poster/46448
59. Eysenbach G, CONSORT-EHEALTH Group. CONSORT-EHEALTH: improving and standardizing evaluation reports of web-based and mobile health interventions. J Med Internet Res 2011;13(4):e126 [FREE Full text] [doi: 10.2196/jmir.1923] [Medline: 22209829]
60. Johnson AEW, Bulgarelli L, Shen L, Gayles A, Shammout A, Horng S, et al. Author correction: MIMIC-IV, a freely accessible electronic health record dataset. Sci Data 2023;10(1):219 [FREE Full text] [doi: 10.1038/s41597-023-02136-9] [Medline: 37072428]
61. Stengel-Eskin E, Van DB. Calibrated interpretation: confidence estimation in semantic parsing. 2023 Presented at: Transactions of the Association for Computational Linguistics, Volume 11; October 31, 2025; MIT Press p. 1213-1231 URL: https://doi.org/10.1162/tacl_a_00598 [doi: 10.1162/tacl_a_00598]
62. Abumelha M. Code for: medical feature extraction from clinical exam notes. GitHub. 2024. URL: https://github.com/manalS101/medical_feture_extraction [accessed 2025-11-01]
63. Data sharing. National Board of Medical Examiners. 2024. URL: https://www.nbme.org/services/data-sharing [accessed 2025-07-27]

Abbreviations

AI: artificial intelligence
BERT: bidirectional encoder representations from transformers
chrF: character n-gram F1-score
CONSORT-AI: Consolidated Standards of Reporting Trials–Artificial Intelligence
DeBERTa: decoding-enhanced bidirectional encoder representations from transformers with disentangled attention
ECE: expected calibration error
GPU: graphics processing unit
ICL: in-context learning
INCITE: intelligent clinical text evaluator

XSL•FO
RenderX

LLM: large language model
NBME: National Board of Medical Examiners
NLP: natural language processing
RQ: research question
USMLE: United States Medical Licensing Examination

Edited by A Coristine; submitted 03.06.25; peer-reviewed by S Sivarajkumar, D Chrimes; comments to author 02.07.25; revised version received 31.10.25; accepted 31.10.25; published 03.12.25.

Please cite as:
Abumelha M, AL-Ghamdi AALM, Fayoumi A, Ragab M
Medical Feature Extraction From Clinical Examination Notes: Development and Evaluation of a Two-Phase Large Language Model Framework
JMIR Med Inform 2025;13:e78432
URL: https://medinform.jmir.org/2025/1/e78432
doi:10.2196/78432
PMID:41171081

©Manal Abumelha, Abdullah AL-Malaise AL-Ghamdi, Ayman Fayoumi, Mahmoud Ragab. Originally published in JMIR Medical Informatics (https://medinform.jmir.org), 03.12.2025. This is an open-access article distributed under the terms of the Creative Commons Attribution License (https://creativecommons.org/licenses/by/4.0/), which permits unrestricted use, distribution, and reproduction in any medium, provided the original work, first published in JMIR Medical Informatics, is properly cited. The complete bibliographic information, a link to the original publication on https://medinform.jmir.org/, as well as this copyright and license information must be included.

XSL•FO
RenderX

From Context to Care: Rethinking Stigma Detection in Clinical Language Models

Shefali Haldar[1*], PhD; Oliver Bear Don't Walk IV[2*], PhD; Sadia Akter[3*], PhD

[1]Merck Research Laboratories, Merck & Co Inc, 33 Avenue Louis Pasteur, Boston, MA, United States

[2]Department of Biomedical and Health Informatics, University of Washington, Seattle, WA, United States

[3]Department of Biomedical Sciences, Marshall University, Huntington, WV, United States

[*]all authors contributed equally

Corresponding Author:
Shefali Haldar, PhD
Merck Research Laboratories, Merck & Co Inc, 33 Avenue Louis Pasteur, Boston, MA, United States

Related Article:

https://medinform.jmir.org/2025/1/e68955

Abstract

Natural language processing techniques are useful for identifying stigmatizing language in electronic health records but require careful consideration. This commentary article builds on "*Efficient Detection of Stigmatizing Language in Electronic Health Records via In-Context Learning*" by Chen et al, which highlights the importance of incorporating situational and temporal contexts in annotation and modeling efforts. We emphasize the need for researchers to explicitly articulate their paradigms and positionality, particularly when working with populations disproportionately affected by stigmatizing language. We also explore the differences arising from conflicting preferences across communities about what constitutes destigmatizing language. We discuss participatory and trust-centered approaches for model development to work toward unbiased impact. Such strategies have a crucial role in raising awareness and fostering inclusive health care.

(JMIR Med Inform 2025;13:e82484) doi:10.2196/82484

KEYWORDS

context modeling; health equity; NLP; inclusive language; natural language processing

Introduction

Stigmatizing language in electronic health records contributes to perceptions, influences care decisions, and unintentionally perpetuates socially constructed power dynamics, resulting in bias. There is growing interest in using natural language processing to identify stigma in electronic health records, not only to assess fairness and bias, but also to detect implicit and context-dependent language. Recently, Chen et al [1] demonstrated how large language models can be leveraged to detect stigmatizing language in clinical notes by applying in-context learning, using a custom prompt to guide automated identification of stigma. However, detecting stigma is not only a technical challenge, but also a social and ethical one.

This commentary builds on their work, outlining the key considerations for future research. We emphasize the importance of contextual modeling to identify stigmatizing language that subtly reinforces bias. We also emphasize researcher self-awareness and contextual understanding, especially when working with marginalized communities. We discuss the differences in language across clinicians, patients, caregivers, and communities and its impact on model fairness. Finally, we advocate for participatory, equity-centered approaches that foster trust and accountability in the development of bias detection tools.

Considering the Context and Mode of Implicit Stigmatizing Language

Annotating a training/benchmarking corpus for stigmatizing language can help to identify subtle and contextually dependent instances (eg, homonyms). However, a focus on explicit mentions may miss some forms of implicit stigmatizing language. For example, "Patient discussed using tobacco in cultural ceremonies and has been advised on the dangers of smoking to her health" may not be flagged as stigmatizing with a bias toward explicit mentions. However, one could argue that this sentence stigmatizes both the patient's beliefs and a cultural practice by labeling this tobacco use as potentially unhealthy.

The authors acknowledge this limitation and reveal an opportunity for future work to explore implicit or implied stigma, an inherently difficult task that responds to 3 central

XSL•FO
RenderX

features of stigmatizing language: subtle, implicit, and highly contextual.

Addressing these features requires a broader contextual window around a given sentence and consideration of situational, relational, and temporal factors. The authors used a 15-word symmetric window on either side of the input sentence, suggesting this can be expanded with improved modeling approaches and additional resources.

However, understanding subtle instances of stigmatizing language may require context that lies beyond the clinical note. These include multimodal elements such as tone, body language, identities, and relationship dynamics between clinician and patient. Capturing this richer context may require incorporating audio, video, or self-reported data and a reflexive understanding of how power relationships shape clinical interactions. These added data sources require ethical considerations beyond current protected health information guardrails; for example, can one objectively identify tone and body language? How and when should information be extracted from video and audio if it was not deemed clinically relevant by a clinician? How can patients request to edit their video or audio data?

Acknowledging the Positionality of Researchers

The ontological and epistemological leanings of the research team can influence assumptions about stigmatizing language in clinical notes. Research can be strengthened and the audiences better informed if research teams outline their guiding paradigms and assumptions. Additionally, research into stigmatizing language could benefit from positionality statements where factors that influence decision-making are acknowledged, better enabling the identification of limitations and future directions.

For example, was the research process informed by views from patients from specific populations, cultural backgrounds, socioeconomic status, or groups more likely to experience stigmatizing language? Similar to outlining methodological assumptions and approaches, describing what positions influenced the research process can improve its rigor, transparency, and application.

Accounting for Patient Perspectives and Conflicting Values

Chen et al discuss the importance of transparent communication about the model's purpose and recognize the risk of enforcing stereotypes of historically marginalized groups. Strategies such as decision-support alerts and prompted artificial intelligence scribing [2] aim to encourage reflection about this risk among clinical teams.

However, we must account for the patients and caregivers affected by the model's outputs and resulting care decisions. Although the authors acknowledge variations in how stigmatizing language materializes in different types of clinical documentation and health contexts, it is equally important to recognize tensions between what clinicians, patients, caregivers, and communities deem an appropriate health care interaction. What one group interprets as destigmatizing language may be perceived differently by another group. Within a group, individuals can have conflicting preferences for what language best reflects their shared identity.

Plurality—the concept that there is no "correct" form of destigmatized language—requires us to consider alternative and potentially contradictory values when refining the sensitivity of models [3,4]. In recognizing the limitations of a binary stigmatizing versus destigmatizing framework, Chen et al point us to avenues for future work: (1) elicit these contradictory values and explore how model parameters should be tailored to account for and address each community's unique challenges and (2) examine ethical ways to engage communities in this work while minimizing privacy risks.

Building Trust and Equity

Given nuanced views of what is considered destigmatized language, researchers must leverage strategies to build trust and center marginalized communities as they develop and implement models. For example, recent human-computer interaction work has outlined concrete steps to address racial gaps in participatory methods, providing guidance for health equity–focused artificial intelligence design, implementation, and decision-making [5]. Theoretical and practical frameworks can provide an equity lens for technology research and implementation [6,7].

Applying this knowledge can help avoid historical patterns of research exploitation while ensuring the model's purpose, outputs, and implementation are driven by and aligned with the values of the communities they are intended to benefit.

Conclusion

Standalone technologies cannot completely eliminate stigma and bias in health care interactions. However, with evolving social norms and forward cultural progress, these technologies offer critical ways to minimize harmful impact and address root causes of health inequity. Importantly, Chen et al affirm that the intention of bias-detection models is not to surveil or punish the use of stigmatizing language; instead, the goal is to increase bias awareness in the daily practice of delivering and receiving care. With greater awareness, we can remove barriers to health equity and achieve improved health outcomes.

Acknowledgments

We would like to thank JMIR Medical Informatics and Dr Tiffany Leung for the opportunity to share this invited commentary. We also acknowledge the American Medical Informatics Association's Diversity, Equity, and Inclusion Communications Subcommittee for their work on providing and publishing inclusive language guidelines for the biomedical and health informatics

XSL•FO
RenderX

research community, a resource that greatly informed this commentary. No external financial support or grants were received from any public, commercial, or not-for-profit entities for the research, authorship, or publication of this article.

Disclaimer

The authors did not use generative artificial intelligence tools in the ideation, preparation, writing, or editing of this commentary.

Data Availability

Data sharing is not applicable to this article as no datasets were generated or analyzed for the purpose of this article.

Authors' Contributions

Conceptualization: SH, OBDW IV, SA. Writing – original draft: SH, OBDW IV, SA. Writing – review and editing: SH, OBDW IV, SA.

Conflicts of Interest

SH is an employee of Merck & Co Inc. At the time of writing, SH and SA served as co-chairs of the American Medical Informatics Association's Diversity, Equity, and Inclusion Communications Subcommittee.

References

1. Chen H, Alfred M, Cohen E. Efficient detection of stigmatizing language in electronic health records via in-context learning: comparative analysis and validation study. JMIR Med Inform 2025 Aug 18;13:e68955. [doi: 10.2196/68955] [Medline: 40825541]
2. Rabotin A, Gonzalez-Correa JR. Inclusive by design? The impact of an explicit inclusive language prompt on ambient AI-scribed clinical notes. Presented at: Oral presentation: 41st Annual UCLA-Affiliated Multi-Campus Family Medicine Research Day; May 14, 2025; Los Angeles, CA URL: https://www.uclahealth.org/departments/family-medicine/research/research-day/research-day-program [accessed 2025-09-29]
3. AMIA inclusive language and context style guidelines. American Medical Informatics Association. URL: https://amia.org/about-amia/diversity-equity-and-inclusion/amia-inclusive-language-and-context-style-guidelines [accessed 2025-09-09]
4. Bear Don't Walk O 4th, Haldar S, Wei DH, et al. Developing and sustaining inclusive language in biomedical informatics communications: an AMIA Board of Directors endorsed paper on the Inclusive Language and Context Style Guidelines. J Am Med Inform Assoc 2025 Aug 1;32(8):1380-1387. [doi: 10.1093/jamia/ocaf096] [Medline: 40523007]
5. Parker AG, Vardoulakis LM, Alla J, Harrington CN. Participatory AI considerations for advancing racial health equity. 2025 Apr 26 Presented at: CHI 2025; Apr 26 to May 1, 2025; Yokohama, Japan p. 1-24. [doi: 10.1145/3706598.3713165]
6. Veinot TC, Clarke PJ, Romero DM, et al. Equitable research PRAXIS: a framework for health informatics methods. Yearb Med Inform 2022 Aug;31(1):307-316. [doi: 10.1055/s-0042-1742542] [Medline: 36463889]
7. Kim S, Bai Y, Zhu H, Eslami M. A systematic literature review on equity and technology in HCI and fairness: navigating the complexities and nuances of equity research. Proc ACM Hum-Comput Interact 2025 May 2;9(2):1-40. [doi: 10.1145/3711079] [Medline: 40874253]

ABBREVIATIONS

Edited by A Coristine; submitted 15.08.25; this is a non–peer-reviewed article;accepted 28.08.25; published 02.10.25.

Please cite as:
Haldar S, Bear Don't Walk IV O, Akter S
From Context to Care: Rethinking Stigma Detection in Clinical Language Models
JMIR Med Inform 2025;13:e82484
URL: https://medinform.jmir.org/2025/1/e82484
doi:10.2196/82484

© Shefali Haldar, Oliver Bear Don't Walk IV, Sadia Akter. Originally published in JMIR Medical Informatics (https://medinform.jmir.org), 2.10.2025. This is an open-access article distributed under the terms of the Creative Commons Attribution License (https://creativecommons.org/licenses/by/4.0/), which permits unrestricted use, distribution, and reproduction in any medium, provided the original work, first published in JMIR Medical Informatics, is properly cited. The complete

XSL•FO
RenderX

bibliographic information, a link to the original publication on https://medinform.jmir.org/, as well as this copyright and license information must be included.

XSL•FO
RenderX

A Vision-Language–Guided Multimodal Fusion Network for Glottic Carcinoma Early Diagnosis: Model Development and Validation Study

Zhaohui Jin[1*]; Yi Shuai[2*], MD; Yun Li[2*], PhD; Mianmian Chen[1]; Yumeng Liu[1], PhD; Wenbin Lei[2], PhD; Xiaomao Fan[1], PhD

[1]College of Big Data and Internet, Shenzhen Technology University, Pingshan District, 3002 Lantian Road, Shenzhen, Guangdong, China

[2]The First Affiliated Hospital, Sun Yat-sen University, Guangzhou, Guangdong, China

[*]these authors contributed equally

Corresponding Author:
Xiaomao Fan, PhD
College of Big Data and Internet, Shenzhen Technology University, Pingshan District, 3002 Lantian Road, Shenzhen, Guangdong, China

Abstract

Background: Early diagnosis and intervention in glottic carcinoma (GC) can significantly improve long-term prognosis. However, the accurate diagnosis of early GC is challenging due to its morphological similarity to vocal cord dysplasia, with the difficulty further exacerbated in medically underserved areas.

Objective: This study aims to address the limitations of existing technologies by designing a vision-language multimodal model, providing a more efficient and accurate early diagnostic method for GC.

Methods: The data used in this study were sourced from the information system of the First Affiliated Hospital of Sun Yat-sen University, comprising laryngoscopy reports and 5796 laryngoscopic images from 404 patients with glottic lesions. We propose a vision-language–guided multimodal fusion network (VLMF-Net) based on a large vision-language model for the early automated diagnosis of GC. The text processing module of this model uses the pretrained Large Language Model Meta AI (LLaMa) to generate text vector representations, while the image processing module uses a pretrained vision transformer to extract features from laryngoscopic images, achieving cross-modal alignment through the Q-Former module. By leveraging a feature fusion module, deep integration of text and image features is achieved, ultimately enabling classification diagnosis. To validate the model's performance, the study selected contrastive language-image pretraining (CLIP), bootstrapping language-image pretraining with frozen image encoders and large language models (BLIP-2), a large-scale image and noisy-text embedding (ALIGN), and vision-and-language transformer (VILT) as baseline methods for experimental evaluation on the same dataset, with comprehensive performance assessment conducted using accuracy, recall, precision, F_1-score, and area under the curve.

Results: We found that on the internal test set, the VLMF-Net model significantly outperformed existing methods with an accuracy of 77.6% (CLIP: 70.5%; BLIP-2: 71.5%; ALIGN: 67.3%; and VILT: 64.3%), achieving a 6.1-percentage point improvement over the best baseline model (BLIP-2). On the external test set, our method also demonstrated robust performance, achieving an accuracy of 73.9%, which is 4.6 percentage points higher than the second-best model (BLIP-2: 69.3%). This indicates that our model surpasses these methods in the early diagnosis of GC and exhibits strong generalization ability and robustness.

Conclusions: The proposed VLMF-Net model can be effectively used for the early diagnosis of GC, helping to address the challenges in its early detection.

(JMIR Med Inform 2025;13:e74902) doi:10.2196/74902

KEYWORDS

glottic carcinoma early diagnosis; multimodal deep learning; large-scale foundation model; computer-aided diagnosis; clinical decision making

Introduction

Glottic carcinoma (GC) is a common malignant tumor of the head and neck [1]. According to GLOBOCAN, China reported 29,500 new cases and 16,900 deaths from laryngeal cancer in 2022 [2], posing heavy burdens on health care systems. Approximately 60% of patients are diagnosed at an advanced stage [3], leading to significant impairment of vital physiological functions and compromising both physical and mental health. Early diagnosis of malignant tumors has been increasingly

XSL•FO
RenderX

emphasized in clinical practice due to its potential to improve cure rates and organ function preservation [4]. Therefore, optimizing diagnostic methods for GC and enhancing early detection capability are urgent tasks for otolaryngologists.

Laryngoscopy is the primary diagnostic tool for GC [1], offering direct visualization of lesion shape, extent, and surface texture. When combined with narrow band imaging, it enhances early tumor detection by identifying neovascularization [5], making it a valuable tool for early diagnosis. However, vocal cord dysplasia (VCD), a precancerous condition situated between normal epithelium and squamous cell carcinoma, is characterized by a small lesion with clinical and laryngoscopic features similar to early GC [6]. Therefore, it is challenging for the human eye to distinguish between them. In addition, the lesion is often covered by "leukoplakia-like" substance, which interferes with the ability of narrow band imaging to reveal submucosal vasculature [7], increasing the risk of misdiagnosis. Laryngoscopy reports provide textual descriptions of lesion morphology observed dynamically during the examination, supplementing static images and assisting in diagnostic decision-making. Studies have demonstrated a correlation between morphological grading and malignancy risk [8-10], underscoring the diagnostic value of textual reports. Furthermore, reports authored by experienced clinicians serve as valuable references, facilitating more accurate diagnoses by less experienced clinicians. Histopathology examination remains the gold standard for diagnosis [1]. However, biopsy is invasive, painful, and carries procedural risks [11], impeding its widespread application in large-scale clinical screening. To address this issue, it is necessary to develop an efficient and noninvasive method to improve the diagnostic accuracy of early GC.

Recently, significant progress has been made in deep learning techniques for tackling real-world classification tasks in computer vision and natural language processing [12-14]. Many researchers have sought to apply these models to the detection of laryngeal cancer, yielding promising outcomes. However, most existing methods only use laryngoscopic images as input, including UC-DenseNet [15], MTANet [16], Dlgnet [17], RedFormer [18], and SAM-FNet [19]. Although these methods have demonstrated promising performance in laryngeal cancer detection and other tasks, they neglect certain latent information present in other modalities. Such information is typically inaccessible through unimodal approaches, thereby highlighting the advantages of multimodal methodologies [20,21].

Therefore, this study proposes a novel method named vision-language–guided multimodal fusion network (VLMF-Net) for early diagnosis of GC. Addressing the limitations of traditional single-modality diagnostic methods, our approach integrates the images and reports text of laryngoscopy to provide a more comprehensive representation of lesion characteristics. Using a pretrained vision transformer (ViT) [22] model for image feature extraction and a LlaMa3 [23,24] model fine-tuned for text processing, we achieve effective multimodal feature fusion. Compared to single-modality methods, our approach significantly improves the diagnostic accuracy and robustness, achieving an accuracy of 0.776 on real clinical datasets. This study highlights the potential of multi-modal fusion in clinical auxiliary diagnosis and provides new insights for reducing misdiagnosis rates and improving patient treatment outcomes.

Methods

Dataset

In our study, we constructed 2 datasets for model development and validation. First, we built an internal dataset for model training, validation, and testing. For the internal dataset, we collected data from 404 patients with glottic lesions at the First Affiliated Hospital of Sun Yat-sen University in Guangzhou, China. This dataset consists of 5799 professionally annotated image-text pairs, covering two types of lesions: VCD and GC. Each sample includes a laryngoscopic diagnostic report written by an experienced otolaryngologist and its corresponding laryngoscopic image.

In addition, to assess the model's generalization ability and robustness, we constructed an external dataset. The external dataset was collected from the First People's Hospital of Zhaoqing, consisting of data from 47 patients with glottic lesions between January 1, 2018, and August 31, 2024. This dataset includes 308 image-text pairs and strictly follows the principle of isolation from the training data, serving only for final performance evaluation. For detailed information on internal and external datasets, please refer to Figure 1 and Table 1.

XSL•FO
RenderX

Figure 1. The specific form of data. GC: glottic carcinoma; VCD: vocal cord dysplasia.

		Image	Text
Internal dataset	VCD		鼻咽：黏膜光滑、充血，双侧咽隐窝及圆枕对称，未见新生物。 口咽：粘膜充血，舌根淋巴组织稍增生。 会厌：粘膜光滑。 梨状窝：黏膜光滑，未见积液及新生物。 室带：黏膜光滑。 声带：左侧声带呈白斑样改变，右侧声带轻度充血、光滑，双声带活动好，声门闭合佳。 声门下：粘膜光滑。
	GC		鼻咽：黏膜光滑、充血，双侧咽隐窝及圆枕对称，未见新生物。 口咽：粘膜光滑，舌根部淋巴组织增生。 会厌：舌面左侧见多个小隆起（似囊肿）。 梨状窝：双侧对称，未见积液及新生物。 室带：粘膜光滑。 声带：左声带粘膜光滑，未见新生物，右声带边缘前中段见粗糙肿物隆起，双侧声带活动良好，闭合欠佳。 声门下：粘膜光滑。
External dataset	VCD		鼻咽：顶后壁见肿胀，表面光滑 口咽：粘膜慢性充血，淋巴滤泡增生 会厌：无充血、水肿及新生物 披裂：活动好，无充血、水肿 室带：双侧室带无充血、水肿，未见新生物 声带：右侧声带前中后段见淡红色新生物，表面呈颗粒状，局部见苍白色改变，左侧声带中段见肿胀隆起，表面光滑，双侧声带活动好，声门闭合欠佳 梨状窝：粘膜光滑，未见新生物。
	GC		鼻咽：粘膜光滑，未见肿物 口咽: 粘膜慢性充血，淋巴滤泡增生 会厌: 无充血、水肿及新生物 披裂: 活动好，无充血、水肿 室带: 双侧室带无充血、水肿，未见新生物 声带: 左侧声带前中段见苍白色新生物，表面欠光滑，右侧声带未见明显肿物，双侧声带活动好，声门闭合欠佳 梨状窝: 粘膜光滑，未见新生物。

Table . The statistics of datasets.

Datasets	Internal dataset	External dataset
Number of laryngoscopy reports	404	47
Number of VCD[a]	206	22
Number of GC[b]	198	25

[a]VCD: vocal cord dysplasia.

[b]GC: glottic carcinoma.

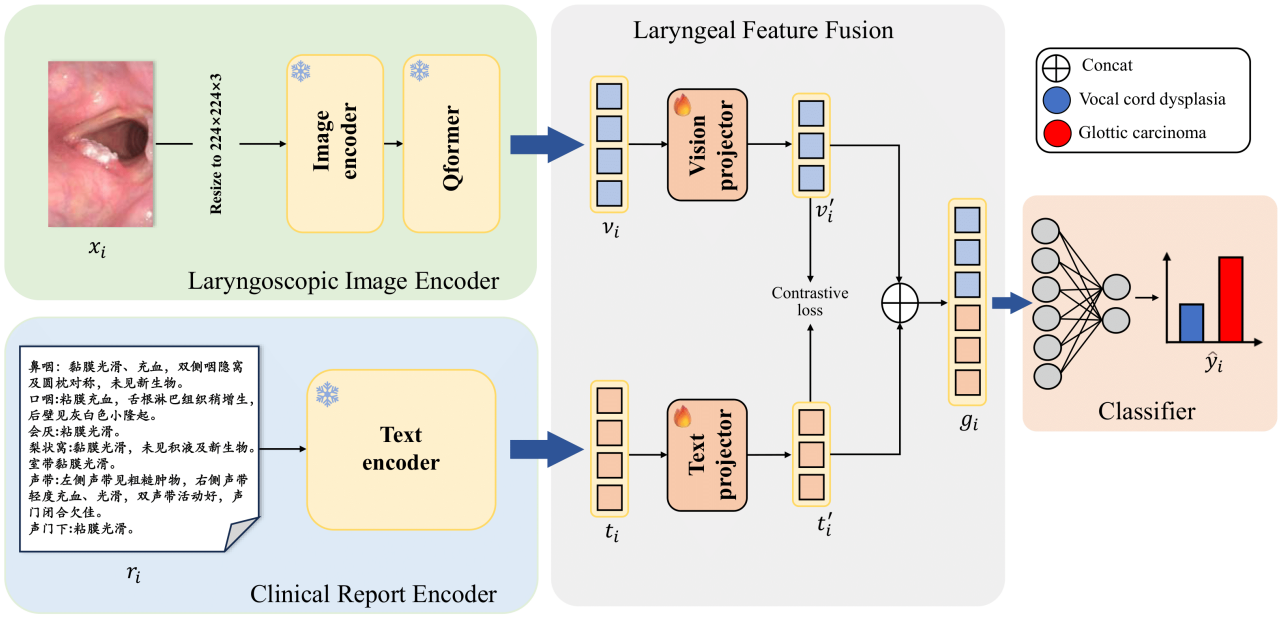
Model Architecture

Overview

Figure 2 illustrates the overall architecture of our proposed VLMF-Net model, which consists of 3 main modules: the laryngoscopic image encoder, the clinical report encoder, and the laryngeal feature fusion module. Specifically, the laryngoscopic image encoder is responsible for extracting visual feature representations from laryngoscopic images, while the clinical report encoder captures textual feature representations from the patient's laryngoscopic examination findings. These features are then fused through the laryngeal feature fusion module. Finally, the fused features are passed through a fully connected layer to complete the classification task. The detailed implementation of each module in our proposed VLMF-Net model is as follows:

XSL•FO
RenderX

Figure 2. The overall architecture of our proposed vision-language–guided multimodal fusion network (VLMF-Net) model.



Laryngoscopic Image Encoder

The laryngoscopic image encoder is an adapted version of a pretrained ViT [22] model. Considering that a single ViT model may introduce cross-modal discrepancies in multimodal tasks, potentially affecting model accuracy, we incorporated an additional Q-Former [25] module into the ViT model to mitigate the impact of modality differences and bridge the gap between image and text features. Q-Former is a trainable module based on Transformer that extracts and condenses visual features through alternating stacking of self-attention and cross-attention. Specifically, we first use ViT to extract features from the image, and then we input the extracted image features into a Q-Former module with frozen parameters to reduce modal differences.

Formally, let fenc(·) denote the image encoder and fq(·) denote the Q-Former module. Given an image xi, first resize the image to 224×224×3, then the image feature vi is obtained as follows:

(1)vi=fq(fenc(xi·θenc);θq)

where θenc and θq are the weight parameters of the image encoder and the Q-Former module, the shape of vi is 1×1024. It is worth noting that in terms of the weights of the pretrained model, we adopt the transfer learning strategy: we directly use the pretrained weights of the BLIP-2 [25] model as the weight parameters of the laryngoscope image encoder, because a large number of studies have demonstrated the effectiveness of BLIP-2 in downstream tasks [26-28]. Such operations can ensure that the extracted image features and text features are in the same scale space, thus effectively avoiding catastrophic problems caused by modal differences.

Clinical Report Encoder

In the clinical report encoder module, we use LLaMA3 [23], an advanced large language model, as the text feature extractor to obtain textual feature representations from the patient's laryngoscopic examination findings. This model is renowned for its exceptional ability to understand long-form text.

Formally, let fLLaMA3(·) denote the clinical report encoder function. Given a clinical report ri, the process of obtaining the text feature ti can be formulated as follows:

(2)ti=fLLaMa3(ri;θq)

where θqrepresents the weight parameters of the clinical report encoder, the shape of ti is 1×4096. Notably, we adopt the same transfer learning strategy for the clinical report encoder's weight parameters as we did for the laryngoscopic image encoder. Furthermore, considering that the text in our dataset is in Chinese, we use a fine-tuned LLaMA3 model trained on a Chinese dataset as the encoder's weight source [24]. This approach effectively addresses the original LLaMA3 model's limitations in Chinese language understanding.

Laryngeal Feature Fusion

In the 2 modules described above, we obtained image and text features. To effectively fuse these 2 modalities, we introduced the laryngeal feature fusion module, which aligns, maps, and integrates the features from both modalities. Specifically, we first use the vision projector fvp(·) and the text projector ftp(·) to map the image feature vi and text feature ti into a unified feature space:

(3)vi′=fvp(vi;θvp)

(4)ti=ftp(ti;θtp)

Where vi` and ti` represent the mapped image and text features (their shapes are 1×512 and 1×2048), respectively, and θvp and θtp are the learnable parameters of the projectors fvp(·) and ftp(·) .

Next, we apply L2 normalization to both features to ensure consistency, obtaining:

vi``=vi`||vi`||2and ti``=ti`||ti`||2. Thenvi`` and text featureti`` along the feature dimension to form a vision-language joint representation, denoted as:gi=Concatvi``,ti``. This joint feature is then fed into a classifier, which consists of multiple fully

XSL•FO
RenderX

connected layers, dropout layers, and ReLU activation functions. The classification process is formulated as:

(5)y^i=ffc(gi,θfc)

where θfc represents the learnable parameters of the classifier.

Model Training

The internal dataset is divided at the patient level into training, validation, and test sets in a ratio of 8:1:1, strictly following the principle of data isolation. Regarding the loss function during training, we use the cross-entropy loss function Lce and the contrastive loss functionLct, which are formulated as follows:

(6)LCE=−∑i=1cyilog (y^i)

(7)LCT=−log exp (sim(zi,zj)τ)∑k=12N1[k≠i]exp (sim(zi,zk)τ)

In Lce, *C* represents the total number of classes, yi denotes the ground-truth class label in one-hot encoding, and yi^ is the predicted probability for class *I*. This loss function aims to minimize the difference between the model's predicted distribution and the true distribution, thereby guiding parameter updates and optimization. In Lct, sim(·) represents cosine similarity,zi and zj are positive sample pairs, τ is the temperature parameter, and *N* is the number of negative samples. The final loss function Lloss is formulated as follows:

(8)Lloss=Lce+c×Lct

where c=0.1. All training processes and experiments are conducted on a dedicated server equipped with 4 NVIDIA A6000 GPUs with a total of 196GB of VRAM. The system runs on Ubuntu 20.04.5 LTS, and the model is implemented using PyTorch 3.9.0 and Scikit-learn 1.3.1. In this study, we use the AdamW optimizer to optimize VLMF-Net, with an initial learning rate set to 0.00001. A warm-up strategy and cosine learning rate scheduling are adopted to dynamically adjust the learning rate. VLMF-Net is trained for a total of 80 epochs.

Ethical Considerations

This study was approved by the Ethics Committee of the First Affiliated Hospital of Sun Yat-sen University (approval number [2023]755 - 1). Informed consent was waived by the institutional review boards of all participating hospitals due to the study's retrospective design. We implemented stringent measures to protect the privacy of all participants by anonymizing all collected data to remove any personally identifiable information. Throughout the manuscript preparation, we diligently avoided disclosing any details that could reveal the identity of participants. Furthermore, no compensation or indemnity was required as the study did not cause any losses to participants beyond the necessary clinical diagnostic and therapeutic measures.

Results

Result of Our Model

To demonstrate the effectiveness and advantages of our proposed VLMF-Net, we selected 4 classic models as baseline models and performed comparisons on 2 datasets. The 4 models include vision-and-language transformer (VILT) [29], contrastive language-image pretraining (CLIP) [30], bootstrapping language-image pretraining with frozen image encoders and large language models (BLIP-2) [25], and a large-scale image and noisy-text embedding (ALIGN) [31], and the 2 datasets refer to the internal and external datasets mentioned earlier. Tables 2 and 3 present the average results of 5 trials for the 4 baseline models and our proposed model on the internal and external datasets, respectively. Figure 3 shows the receiver operating characteristic curves and corresponding area under the curve values of different models on internal and external datasets. As shown in Table 2, on the internal dataset, our method demonstrates significant advantages, achieving the following evaluation metrics: accuracy (0.776), precision (0.820), and F_1-score (0.776). Notably, compared to the second-best model, our method achieves significant improvements of 0.061, 0.032, and 0.046 in accuracy, precision, and F_1-score, respectively. In terms of class-wise recall, VLMF-Net achieves recall rates of 0.754 and 0.803 for VCD and GC, respectively. Compared to other models, VLMF-Net shows significant improvements across multiple evaluation metrics, indicating its superior ability in recognizing glottic cancer. In addition, as shown in Table 3, on the external dataset, our method also demonstrates significant advantages, achieving accuracy (0.739), precision (0.828), and F_1-score (0.737), with improvements of 0.046, 0.053, and 0.046 over the second-best model, respectively. In terms of class-wise recall, our model achieves recall rates of 0.701 and 0.793 for VCD and GC, respectively. Compared to other models, there is also a significant improvement, which further demonstrates that VLMF-Net possesses excellent generalization ability and robustness. Moreover, as shown in Figure 3, our model demonstrates significant advantages in area under the curve metrics on both internal and external datasets. On the internal dataset, it outperforms the second-best model by 0.026, and on the external dataset by 0.012.

XSL•FO
RenderX

Table . Comparison with other multimodal models on an internal dataset.

Methods	Overall results			Recall of different classes	
	Accuracy, mean (SD)	Precision, mean (SD)	F_1-score, mean (SD)	VCD[a], mean (SD)	GC[b], mean (SD)
VILT[c]	0.643 (0.02[d])	0.677 (0.02[d])	0.643 (0.01[d])	0.632 (0.02[d])	0.656 (0.01[d])
CLIP[e]	0.705 (0.01[d])	0.788 (0.02[d])	0.703 (0.01[d])	0.672 (0.02[d])	0.750 (0.01[d])
BLIP-2[f]	0.715 (0.02[d])	0.770 (0.03[d])	0.714 (0.02[d])	0.694 (0.04[d])	0.742 (0.03[d])
ALIGN[g]	0.673 (0.03[d])	0.707 (0.02[d])	0.673 (0.04[d])	0.660 (0.02[d])	0.688 (0.02[d])
VLMF-Net[h]	0.776 (0.01)	0.820 (0.02)	0.776 (0.01)	0.754 (0.02)	0.803 (0.01)

[a]VCD: vocal cord dysplasia.

[b]GC: glottic carcinoma.

[c]VILT: vision-and-language transformer.

[d]P<.001.

[e]CLIP: contrastive language-image pretraining.

[f]BLIP-2: bootstrapping language-image pretraining with frozen image encoders and large language models.

[g]ALIGN: a large-scale image and noisy-text embedding.

[h]VLMF-Net: vision-language guided multimodal fusion network.

Table . Comparison with other multimodal models on an external dataset.

Methods	Overall results			Recall of different classes	
	Accuracy, mean (SD)	Precision, mean (SD)	F_1-score, mean (SD)	VCD[a], mean (SD)	GC[b], mean (SD)
VILT[c]	0.631 (0.02[d])	0.663 (0.02[d])	0.630 (0.01[d])	0.633 (0.01[d])	0.628 (0.01[d])
CLIP[e]	0.686 (0.01[d])	0.748 (0.02[d])	0.685 (0.01[d])	0.670 (0.02[d])	0.708 (0.02[d])
BLIP-2[f]	0.693 (0.03[d])	0.775 (0.02[d])	0.691 (0.03[d])	0.669 (0.03[d])	0.726 (0.02[d])
ALIGN[g]	0.647 (0.02[d])	0.680 (0.02[d])	0.647 (0.03[d])	0.642 (0.02[d])	0.653 (0.03[d])
VLMF-Net[h]	0.739 (0.02)	0.828 (0.02)	0.737 (0.02)	0.701 (0.03)	0.793 (0.02)

[a]VCD: vocal cord dysplasia.

[b]GC: glottic carcinoma.

[c]VILT: vision-and-language transformer.

[d]P value <.001.

[e]CLIP: contrastive language-image pretraining.

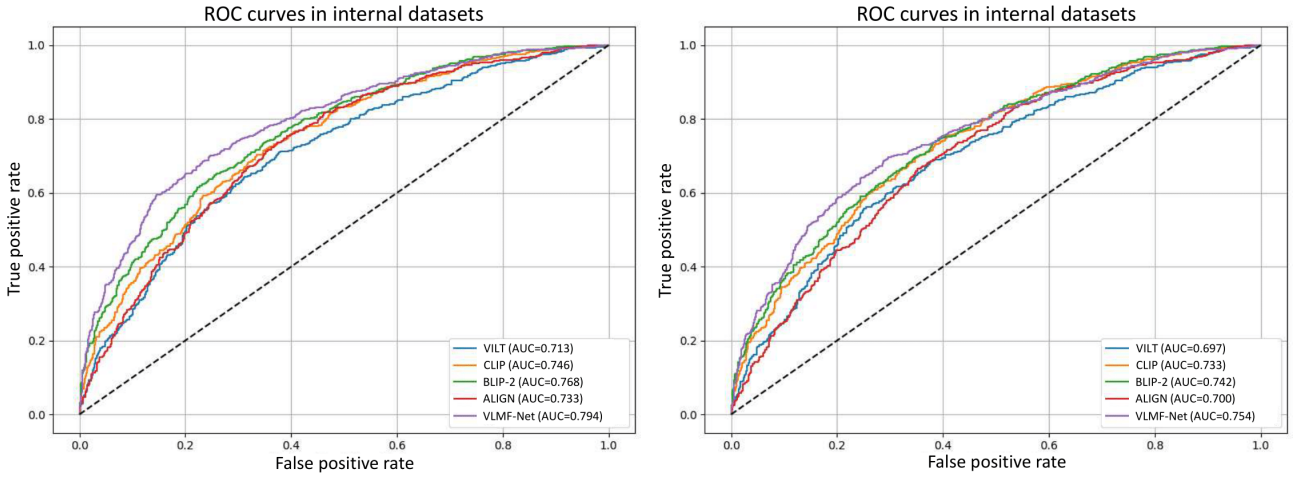
[f]BLIP-2: bootstrapping language-image pretraining with frozen image encoders and large language models.

[g]ALIGN: a large-scale image and noisy-text embedding.

[h]VLMF-Net: vision-language guided multimodal fusion network.

XSL•FO
RenderX

Figure 3. The ROC curves for different models. ALIGN: a large-scale image and noisy-text embedding; BLIP-2: bootstrapping language-image pretraining with frozen image encoders and large language models; CLIP: contrastive language-image pretraining; ROC: receiver operating characteristic; VILT: vision-and-language transformer; VLMF-Net: vision-language guided multimodal fusion network.



Ablation Studies

To validate the effectiveness of our multimodal approach for early diagnosis of GC, we designed an ablation study to systematically evaluate the performance differences between models using single-modal and multimodal inputs: (1) M1: a single-modal model using only laryngoscopy images; (2) M2: a single-modal model using only laryngoscopy diagnostic reports; (3) M3: a multimodal model combining images and text, but without Q-Former. (4) M4: a multimodal model combining images and text with Q-Former. The experimental results, as shown in Table 4, indicate that the multimodal model M4 significantly outperforms both single-modal models across all evaluation metrics. Specifically, compared to the best single-modal model, M4 achieves improvements of 0.098 in accuracy (0.776), 0.106 in precision (0.820), 0.100 in recall (0.779), and 0.098 in F_1-score (0.776). This demonstrates that the multimodal data fusion strategy effectively integrates visual features and textual semantic information, significantly enhancing the diagnostic performance of the model.

Table . Ablation study on vision-language–guided multimodal fusion network.

Variants	Image	Report	Q-Former	Accuracy, mean (SD)	Precision, mean (SD)	Recall, mean (SD)	F_1-score, mean (SD)
M1	√	0.678 (0.02)	0.714 (0.03)	0.679 (0.03)	0.678 (0.03)		
M2	√	0.673 (0.01)	0.711 (0.02)	0.675 (0.01)	0.673 (0.01)		
M3	√	√	0.722 (0.02)	0.708 (0.01)	0.723 (0.01)	0.722 (0.03)	
M4	√	√	√	0.776 (0.01)	0.820 (0.02)	0.779 (0.02)	0.776 (0.01)

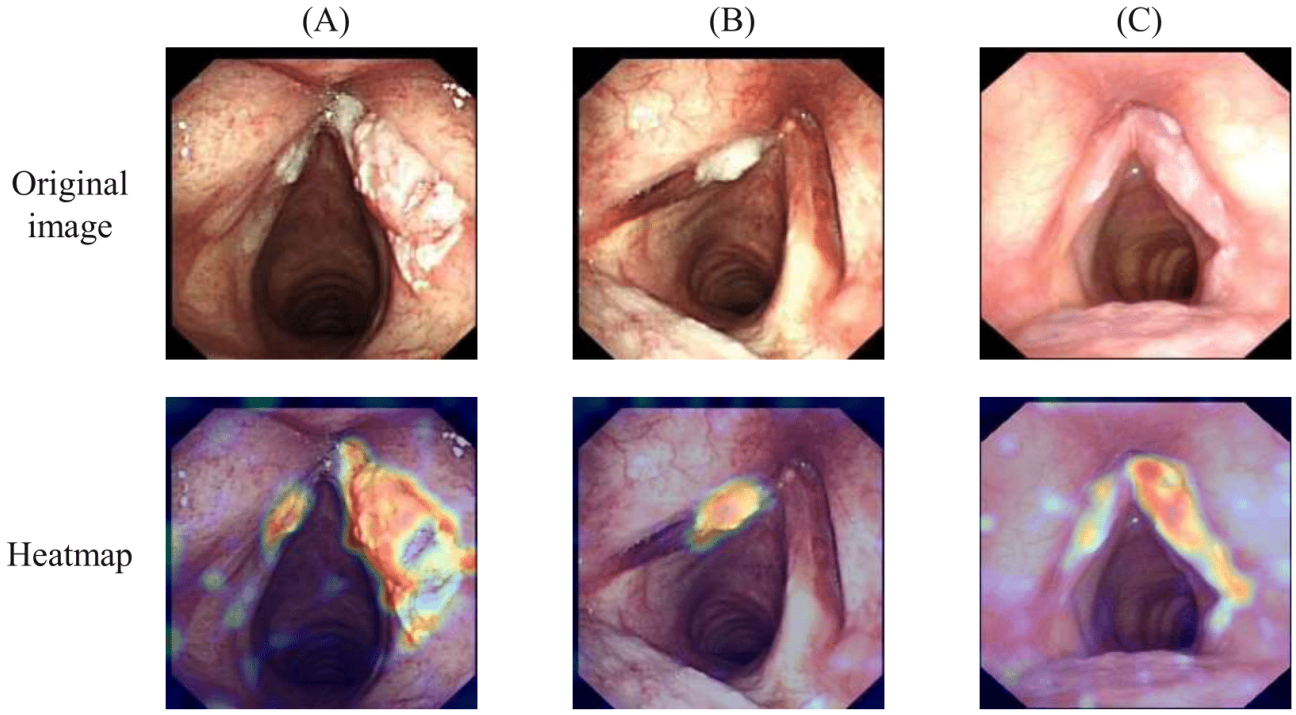
In addition, to verify the effectiveness of the Q-Former module, we designed ablation experiments related to the Q-Former module. The experimental results are shown in Table 4. M4 outperforms M3 in all indicators. Specifically, M4's accuracy (0.776) increased by 0.054, precision (0.820) increased by 0.112, recall (0.779) increased by 0.056, and F_1-score (0.776) increased by 0.054. This indicates that the Q-Former module effectively reduces the impact of cross-modal differences.

Visualization for Model Prediction

To enhance the interpretability of the VLMF-Net model's predictions, we used the Grad-CAM (Gradient-Weighted Class Activation Mapping) [32] algorithm to generate class activation heatmaps. The visualization results are shown in Figure 4. In the heatmap, we can see that VLMF-Net focuses on the lesion area of the patient when analyzing the laryngoscopy image. This indicates that the model is able to correctly classify based on the features of the lesion area, enabling early diagnosis of GC.

XSL•FO
RenderX

Figure 4. The heatmaps generated by the vision-language guided multimodal fusion network (VLMF-Net) model on patient laryngoscopic images, where (**A**) represents glottic carcinoma and (**B**) and (**C**) represent vocal cord dysplasia.



Discussion

Main Findings

In our study, we developed a novel model for the early diagnosis of GC named VLMF-Net, which leverages multimodal fusion technology guided by vision-language information. When tested on an internal dataset, VLMF-Net achieved accuracy, precision, recall, and F_1-score of 0.776, 0.820, 0.779, and 0.776, respectively, outperforming all baseline methods. These results demonstrate the feasibility and effectiveness of VLMF-Net in the early diagnosis of GC. Ablation studies further reveal that VLMF-Net significantly outperforms unimodal models. By integrating both laryngoscopic images and clinical text reports, VLMF-Net captures complementary diagnostic information, thus mitigating the risk of information loss inherent in single-modality systems. Notably, the textual modality meaningfully guides the extraction of image features; for instance, textual cues explicitly describing the lesion's location (eg, "anterior-middle segment of the left vocal cord") can help the model focus on the relevant visual regions. This form of cross-modal interaction may enhance the model's ability to detect subtle pathological patterns that might otherwise be overlooked.

Moreover, Grad-CAM–based visualizations demonstrate that VLMF-Net consistently attends to clinically significant lesion areas. These attention heatmaps show strong alignment between the model's focus and expert-defined pathological regions, enhancing interpretability. Such interpretability is crucial in clinical contexts, where transparency in decision-making processes fosters trust and facilitates integration of AI systems into diagnostic workflows.

Finally, these findings validate the design philosophy of VLMF-Net and highlight the broader potential of multimodal fusion strategies in medical AI. In particular, the ability to synthesize visual and contextual clinical information allows for more robust and informed diagnostic decisions. This work not only advances the state of the art in GC diagnosis but also lays a foundation for extending vision-language multimodal techniques to other complex diagnostic tasks where rich multimodal data is available.

Deep Learning Challenges in Early GC Diagnosis

Early GC lesions are usually small and exhibit complex morphological characteristics, making it challenging for deep learning models to capture fine-grained lesion features. As a result, important details related to the lesions may be missed, significantly affecting the model's diagnostic accuracy. Furthermore, most existing mainstream models rely solely on laryngoscopic images as input. While these models have achieved some progress in a unimodal setting, they overlook information from other modalities, which is often beyond the reach of image-based models [15-19]. This limitation constrains the model's comprehensive understanding of lesion characteristics and ultimately affects diagnostic accuracy.

Strengths and Limitations

To the best of our knowledge, this is the first study to apply multimodal techniques to the early diagnosis of GC. In our model, we fully utilize patients' laryngoscopy reports and laryngoscopic images to extract relevant information about GC, enabling the model to comprehensively understand the patient's condition and thereby improve its performance. However, this study still has some limitations. First, the VLMF-Net, based on a pretrained large language model, relies heavily on powerful computational resources, particularly high-performance GPUs, during training, which may result in slower training and inference speeds. Second, the data used in this study underwent quality checks, but in real-world scenarios, more complex

XSL•FO
RenderX

situations may arise, such as poor image clarity due to imaging devices or challenging shooting angles, which could affect the model's diagnostic accuracy.

Conclusions

In this paper, we propose a VLMF-Net for the early diagnosis of GC. Extensive experiments on 2 datasets demonstrate that VLMF-Net achieves superior accuracy and robustness, effectively addressing the challenges of early GC diagnosis.

Acknowledgments

We note that a shorter conference version of this paper appeared in the 2024 China Health Information Processing Conference (CHIP 2024). In our initial conference paper, we did not investigate whether the vision-language guided multimodal fusion network (VLMF-Net) model maintains its effectiveness across different datasets and consistently outperforms baseline models. This manuscript addresses these issues while further optimizing the originally proposed model through approaches such as hybrid loss function training. In addition, we use the Grad-CAM (Gradient-Weighted Class Activation Mapping) methodology to analyze the interpretability of VLMF-Net. This work is partially supported by the National Natural Science Foundation of China (62473267), the Basic and Applied Basic Research Project of Guangdong Province (2022B1515130009, 2025A1515011614), the Guangzhou Science and Technology Planning Project (No.2025B03J0019), the Special Subject on Agriculture and Social Development, Key Research and Development Plan in Guangzhou (2023B03J0172), and the Natural Science Foundation of Top Talent of SZTU (GDRC202318).

Conflicts of Interest

None declared.

References

1. Steuer CE, El-Deiry M, Parks JR, Higgins KA, Saba NF. An update on larynx cancer. CA Cancer J Clin 2017 Jan;67(1):31-50. [doi: 10.3322/caac.21386] [Medline: 27898173]
2. Bray F, Laversanne M, Sung H, et al. Global cancer statistics 2022: GLOBOCAN estimates of incidence and mortality worldwide for 36 cancers in 185 countries. CA Cancer J Clin 2024;74(3):229-263. [doi: 10.3322/caac.21834] [Medline: 38572751]
3. Chen SA, Muller S, Chen AY, et al. Patterns of extralaryngeal spread of laryngeal cancer: thyroid cartilage penetration occurs in a minority of patients with extralaryngeal spread of laryngeal squamous cell cancers. Cancer 2011 Nov 15;117(22):5047-5051. [doi: 10.1002/cncr.26130] [Medline: 21523761]
4. LeBlanc BJ, Shi R, Mehta V, Mills G, Ampil F, Nathan CAO. Improvements in survival and disparities for advanced-stage laryngeal cancer. JAMA Otolaryngol Head Neck Surg 2015 Feb;141(2):169-173. [doi: 10.1001/jamaoto.2014.2998] [Medline: 25429594]
5. Cosway B, Drinnan M, Paleri V. Narrow band imaging for the diagnosis of head and neck squamous cell carcinoma: a systematic review. Head Neck 2016 Apr;38 Suppl 1:E2358-E2367. [doi: 10.1002/hed.24300] [Medline: 26891200]
6. You Z, Han B, Shi Z, et al. Vocal cord leukoplakia classification using deep learning models in white light and narrow band imaging endoscopy images. Head Neck 2023 Dec;45(12):3129-3145. [doi: 10.1002/hed.27543] [Medline: 37837264]
7. Kraft M, Fostiropoulos K, Gürtler N, Arnoux A, Davaris N, Arens C. Value of narrow band imaging in the early diagnosis of laryngeal cancer. Head Neck 2016 Jan;38(1):15-20. [doi: 10.1002/hed.23838] [Medline: 24995546]
8. Zhao Q, He Y, Wu Y, et al. Vocal cord lesions classification based on deep convolutional neural network and transfer learning. Med Phys 2022 Jan;49(1):432-442. [doi: 10.1002/mp.15371] [Medline: 34813114]
9. van Hulst AM, Kroon W, van der Linden ES, et al. Grade of dysplasia and malignant transformation in adults with premalignant laryngeal lesions. Head Neck 2016 Apr;38 Suppl 1(S1):E2284-E2290. [doi: 10.1002/hed.24185] [Medline: 26268427]
10. Ni XG, Zhu JQ, Zhang QQ, Zhang BG, Wang GQ. Diagnosis of vocal cord leukoplakia: the role of a novel narrow band imaging endoscopic classification. Laryngoscope 2019 Feb;129(2):429-434. [doi: 10.1002/lary.27346] [Medline: 30229933]
11. Mannelli G, Cecconi L, Gallo O. Laryngeal preneoplastic lesions and cancer: challenging diagnosis. Qualitative literature review and meta-analysis. Crit Rev Oncol Hematol 2016 Oct;106:64-90. [doi: 10.1016/j.critrevonc.2016.07.004] [Medline: 27637353]
12. Mao C, Li J, Pang PCI, Zhu Q, Chen R. Identifying kidney stone risk factors through patient experiences with a large language model: text analysis and empirical study. J Med Internet Res 2025 May 22;27:e66365. [doi: 10.2196/66365] [Medline: 40403294]
13. Sahoo PK, Mishra S, Panigrahi R, Bhoi AK, Barsocchi P. An improvised deep-learning-based mask R-CNN model for laryngeal cancer detection using CT images. Sensors (Basel) 2022 Nov 15;22(22):8834. [doi: 10.3390/s22228834] [Medline: 36433430]

XSL•FO
RenderX

14. Bensoussan Y, Vanstrum EB, Johns MM III, Rameau A. Artificial intelligence and laryngeal cancer: from screening to prognosis: a state of the art review. Otolaryngol Head Neck Surg 2023 Mar;168(3):319-329. [doi: 10.1177/01945998221110839] [Medline: 35787073]
15. Luo X, Zhang J, Li Z, Yang R. Diagnosis of ulcerative colitis from endoscopic images based on deep learning. Biomed Signal Process Control 2022 Mar;73:103443. [doi: 10.1016/j.bspc.2021.103443]
16. Zhou W, Dong S, Lei J, Yu L. MTANet: multitask-aware network with hierarchical multimodal fusion for RGB-T urban scene understanding. IEEE Trans Intell Veh 2022 May;8(1):48-58. [doi: 10.1109/TIV.2022.3164899]
17. Wang KN, Zhuang S, Ran QY, et al. DLGNet: a dual-branch lesion-aware network with the supervised gaussian mixture model for colon lesions classification in colonoscopy images. Med Image Anal 2023 Jul;87:102832. [doi: 10.1016/j.media.2023.102832] [Medline: 37148864]
18. Cui C, Ma Y, Lu J, Wang Z. REDFormer: radar enlightens the darkness of camera perception with transformers. IEEE Trans Intell Veh 2023 Nov 6;9(1):1358-1368. [doi: 10.1109/TIV.2023.3329708]
19. Wei J, Li Y, Qiu M, Chen H, Fan X, Lei W. SAM-FNet: SAM-guided fusion network for laryngo-pharyngeal tumor detection. Presented at: 2024 IEEE International Conference on Bioinformatics and Biomedicine (BIBM); Dec 3-6, 2024; Lisbon, Portugal. [doi: 10.1109/BIBM62325.2024.10822832]
20. Kang EYC, Yeung L, Lee YL, et al. A multimodal imaging-based deep learning model for detecting treatment-requiring retinal vascular diseases: model development and validation study. JMIR Med Inform 2021 May 31;9(5):e28868. [doi: 10.2196/28868] [Medline: 34057419]
21. Noda M, Yoshimura H, Okubo T, et al. Feasibility of multimodal artificial intelligence using GPT-4 vision for the classification of middle ear disease: qualitative study and validation. JMIR AI 2024 May 31;3(1):e58342. [doi: 10.2196/58342] [Medline: 38875669]
22. Khan S, Naseer M, Hayat M, Zamir SW, Khan FS, Shah M. Transformers in vision: a survey. ACM Comput Surv 2022 Jan 31;54(10s):1-41. [doi: 10.1145/3505244]
23. Grattafiori A, Dubey A, Jauhri A, Pandey A, Kadian A, Al-Dahle A, et al. The Llama 3 herd of models. arXiv. Preprint posted online on Jul 31, 2024. [doi: 10.48550/arXiv.2407.21783]
24. Cui Y, Yang Z, Yao X. Efficient and effective text encoding for Chinese LLaMA and Alpaca. arXiv. Preprint posted online on Apr 17, 2023. [doi: 10.48550/arXiv.2304.08177]
25. Li J, Li D, Savarese S, Hoi S. BLIP-2: bootstrapping language-image pre-training with frozen image encoders and large language models. arXiv. Preprint posted online on Jan 23, 2023. [doi: 10.48550/arXiv.2301.12597]
26. Lee C, Jang J, Lee J. Personalizing text-to-image generation with visual prompts using BLIP-2. Presented at: Eleventh International Conference on Learning Representations (ICLR 2023); May 1-5, 2023; Kigali, Rwanda URL: https://openreview.net/pdf?id=7wxCMgdj5F [accessed 2025-09-17]
27. Nguyen T, Gadre SY, Ilharco G, Oh S, Schmidt L. Improving multimodal datasets with image captioning. arXiv. Preprint posted online on Jul 19, 2023. [doi: 10.48550/arXiv.2307.10350]
28. Zhu D, Chen J, Haydarov K, Shen X, Zhang W, Elhoseiny M. ChatGPT asks, BLIP-2 answers: automatic questioning towards enriched visual descriptions. arXiv. Preprint posted online on Mar 12, 2023. [doi: 10.48550/arXiv.2303.06594]
29. Kim W, Son B, Kim I. ViLT: vision-and-language transformer without convolution or region supervision. arXiv. Preprint posted online on Feb 5, 2021. [doi: 10.48550/arXiv.2102.03334]
30. Radford A, Kim JW, Hallacy C, Ramesh A, Goh G, Agarwal S, et al. Learning transferable visual models from natural language supervision. Presented at: 38th International Conference on Machine Learning (ICML 2021); Jul 18-24, 2021 URL: https://proceedings.mlr.press/v139/radford21a/radford21a.pdf [accessed 2025-09-17]
31. Jia C, Yang Y, Xia Y, et al. Scaling up visual and vision-language representation learning with noisy text supervision. arXiv. Preprint posted online on Feb 11, 2021. [doi: 10.48550/arXiv.2102.05918]
32. Selvaraju RR, Cogswell M, Das A, Vedantam R, Parikh D, Batra D. Grad-CAM: visual explanations from deep networks via gradient-based localization. Presented at: International Conference on Computer Vision (ICCV); Oct 22-29, 2017; Venice, Italy. [doi: 10.1007/s11263-019-01228-7]

Abbreviations

ALIGN: a large-scale image and noisy-text embedding
BLIP-2: bootstrapping language-image pretraining with frozen image encoders and large language models
CLIP: contrastive language-image pretraining
GC: glottic carcinoma
Grad-CAM: Gradient-Weighted Class Activation Mapping
LLaMa: Large Language Model Meta AI
VCD: vocal cord dysplasia
ViT: vision transformer
VLIT: vision-and-language transformer
VLMF-Net: vision-language guided multimodal fusion network

XSL•FO
RenderX

Edited by Q Jin; submitted 27.03.25; peer-reviewed by R Gu, Z Yang; revised version received 04.08.25; accepted 06.08.25; published 08.10.25.

Please cite as:
Jin Z, Shuai Y, Li Y, Chen M, Liu Y, Lei W, Fan X
A Vision-Language–Guided Multimodal Fusion Network for Glottic Carcinoma Early Diagnosis: Model Development and Validation Study
JMIR Med Inform 2025;13:e74902
URL: https://medinform.jmir.org/2025/1/e74902
doi:10.2196/74902

© Zhaohui Jin, Yi Shuai, Yun Li, Mianmian Chen, Yumeng Liu, Wenbin Lei, Xiaomao Fan. Originally published in JMIR Medical Informatics (https://medinform.jmir.org), 8.10.2025. This is an open-access article distributed under the terms of the Creative Commons Attribution License (https://creativecommons.org/licenses/by/4.0/), which permits unrestricted use, distribution, and reproduction in any medium, provided the original work, first published in JMIR Medical Informatics, is properly cited. The complete bibliographic information, a link to the original publication on https://medinform.jmir.org/, as well as this copyright and license information must be included.

XSL•FO
RenderX

Heterogeneous Network With Multiview Path Aggregation: Drug–Target Interaction Prediction Study Design

Haixue Zhao[1,2*], MEng; Kui Yao[1*], MEng; Yunjiong Liu[3,4,5], PhD; Chao Che[2], PhD; Lin Tang[2], PhD

[1]Key Laboratory of Advanced Design and Intelligent Computing, Ministry of Education, Dalian University, Dalian, China

[2]School of Software Engineering, Dalian University, No. 10 Xuefu Street, Dalian Economic and Technological Development Zone, Liaoning, Dalian, China

[3]Institute of Artificial Intelligence, School of Informatics, Xiamen University, Xiamen, China

[4]National Institute of Diagnostics and Vaccine Development in Infectious Diseases, National Innovation Platform for Industry-Education Integration in Vaccine Research, NMPA Key Laboratory for Research and Evaluation of Infectious Disease Diagnostic Technology, Xiamen University, Xiamen, China

[5]State Key Laboratory of Vaccines for Infectious Diseases, Xiang An Biomedicine Laboratory, School of Public Health, Xiamen University, Xiamen, China

[*]these authors contributed equally

Corresponding Author:
Lin Tang, PhD
School of Software Engineering, Dalian University, No. 10 Xuefu Street, Dalian Economic and Technological Development Zone, Liaoning, Dalian, China

Abstract

Background: Drug–target interaction (DTI) prediction is crucial in drug repositioning, as it can significantly reduce research and development costs and shorten the development cycle. Most existing deep learning–based approaches employ graph neural networks for DTI prediction. However, these approaches still face limitations in capturing complex biochemical features, integrating multilevel information, and providing interpretable model insights.

Objective: This study proposes a heterogeneous network model based on multiview path aggregation, aiming to predict interactions between drugs and targets.

Methods: This study employed a molecular attention transformer to extract 3D conformation features from the chemical structures of drugs and utilized Prot-T5, a protein-specific large language model, to deeply explore biophysically and functionally relevant features from protein sequences. By integrating drugs, proteins, diseases, and side effects from multisource heterogeneous data, we constructed a heterogeneous graph model to systematically characterize multidimensional associations between biological entities. On this foundation, a meta-path aggregation mechanism was proposed, which dynamically integrates information from both feature views and biological network relationship views. This mechanism effectively learned potential interaction patterns between biological entities and provided a more comprehensive representation of the complex relationships in the heterogeneous graph. It enhanced the model's ability to capture sophisticated, context-dependent relationships in biological networks. Furthermore, we integrated multiscale features of drugs and proteins within the heterogeneous network, significantly improving the prediction accuracy of DTIs and enhancing the model's interpretability and generalization ability.

Results: In the DTI prediction task, the proposed model achieves an AUPR (area under the precision-recall curve) of 0.901 and an AUROC (area under the receiver operating characteristic curve) of 0.966, representing improvements of 1.7% and 0.8%, respectively, over the baseline methods. Furthermore, a case study on the KCNH2 target demonstrates that the proposed model successfully predicts 38 out of 53 candidate drugs as having interactions, which further validates its reliability and practicality in real-world scenarios.

Conclusions: The proposed model shows marked superiority over baseline methods, highlighting the importance of integrating heterogeneous information with biological knowledge in DTI prediction.

(JMIR Med Inform 2025;13:e74974) doi:10.2196/74974

KEYWORDS

drug-target interactions; drug repurposing; heterogeneous networks; graph neural networks

XSL•FO
RenderX

Introduction

Background

Drugs play a crucial role in treating diseases by interacting with multiple targets and modulating their functions. Accurately predicting drug–target interactions (DTI) is essential for understanding drug mechanisms [1], discovering new targets, and facilitating drug repositioning. Traditional methods rely heavily on large amounts of labeled data and often suffer from label noise in negative samples. In recent years, positive-unlabeled learning has been effectively applied to alleviate this issue [2]. Meanwhile, self-supervised learning strategies integrated with heterogeneous biomedical networks have improved the accuracy of DTI prediction by leveraging multimodal information [3]. With the rapid advancement of large language models (LLM), their applications in the biomedical domain have expanded significantly. Due to their powerful sequence representation and semantic understanding capabilities, LLMs are driving DTI prediction methods toward a higher level of performance [4].

Currently, DTI prediction methods are primarily categorized into three types [5,6]: ligand similarity–based methods [7,8], network-based methods [9,10], and structure-based methods [11]. Ligand similarity–based methods predict DTIs by comparing the structural similarity of drugs. These methods are computationally efficient but often overlook complex biochemical properties and molecular characteristics, which may lead to inaccurate predictions [12]. Network-based methods rely on large amounts of high-quality interaction data and are computationally intensive [13-15]. They typically lack structural information about drugs and targets, resulting in poor performance on sparse networks. Structure-based methods usually depend on the three-dimensional structures of target proteins and drugs [16]. However, these methods exhibit limited efficacy for proteins with unknown structures.

To address the above issues, we propose a heterogeneous network (HN) model based on multiview path aggregation for DTI (MVPA-DTI) prediction. MVPA-DTI enhances prediction capability through a multiview feature extraction and fusion mechanism. First, the molecular attention Transformer model is used to extract the three-dimensional spatial structure information of drugs, while the protein-specific LLM Prot-T5 is leveraged to deeply explore the biophysical properties of protein sequences, forming two feature views based on structure and sequence. Subsequently, a HN is constructed by incorporating multisource heterogeneous information from proteins, drugs, diseases, and side effects. This approach effectively integrates the previously defined feature views into the message-passing framework of the HN, thereby forming a comprehensive biological network relationship view. The multiview path aggregation mechanism allows the model to dynamically synthesize feature information from multiple perspectives. By introducing a meta-path aggregation mechanism, the model dynamically synthesizes feature information across different perspectives, capturing underlying drug–target associations at multiple hierarchical levels through both feature-oriented views and biological network relational contexts. During the message-passing process, MVPA-DTI optimizes the weight distribution by incorporating both network topology and biological prior knowledge. By extracting node-level feature embeddings from heterogeneous data, the model is capable of accurately predicting new DTI. Experimental results show that MVPA-DTI outperforms existing advanced methods across multiple evaluation metrics. Additionally, for the voltage-gated inward-rectifying potassium channel KCNH2 target, which is related to cardiovascular diseases, MVPA-DTI was used for candidate drug screening. Among 53 candidate drugs, 38 are predicted to interact with this target (10 of which are already used in clinical treatment). This finding not only validates the effectiveness of MVPA-DTI in predicting DTI but also further demonstrates its application potential and practical value in real drug development. The main contributions of this paper are as follows:

1. We employ a molecular attention Transformer network that extracts three-dimensional structural information from molecular graphs through a physics-informed attention mechanism, establishing a structural feature perspective of the drug.
2. The sequence-level features are extracted from protein sequences using Prot-T5, a protein-specific LLM. The model maps sequence features to functional relevance, establishing a sequence feature perspective of proteins.
3. We integrate the drug structural view and protein sequence view into a multi-entity HN to construct a biological network relationship view. The meta-path information aggregation mechanism captures higher-order interaction patterns among different types of nodes.
4. We propose a multiview path aggregation–enhanced HN model that integrates protein and drug biological knowledge to accurately identify critical drug–target relationships. Benchmark tests show that the model exhibits a significant advantage in prediction performance.

Related Work

DTI prediction plays a significant role in drug discovery and drug repositioning. With the rapid advancement of deep learning technologies, an increasing number of deep learning–based DTI prediction methods emerge. These methods, particularly those combining big data with deep learning, gradually overcome the limitations of traditional approaches. Based on different prediction strategies, DTI prediction methods are generally categorized into three types [5,6]: ligand similarity–based methods [7,8], network-based methods [9,10], and structure-based methods [11]. In recent years, prediction methods based on LLMs also bring remarkable breakthroughs to the DTI field, opening new pathways for its development.

Ligand Similarity–Based Methods

In DTI prediction, ligand similarity–based methods estimate potential interactions by comparing the structures or chemical similarity of drug molecules. These methods typically rely on the SMILES (simplified molecular input line entry system) representation or molecular fingerprints of drugs to calculate drug–drug similarities and infer potential target interactions based on these similarities. For instance, Thafar et al [17] proposed the DTiGEMS model, which integrates drug–drug

XSL•FO
RenderX

similarities and employs a similarity selection and fusion algorithm to enhance the accuracy of DTI predictions. Additionally, Shim et al [18] introduced a similarity-based convolutional neural network method. This method calculates the outer product of the similarity matrix between drugs and targets and employs a two-dimensional convolutional neural network to capture potential relationships between them. These methods have improved DTI prediction accuracy to some extent, but they often overlook the dynamic interactions and complex spatial structures between molecules. Moreover, ligand similarity–based methods operate under the assumption that similar drug molecules share similar targets. However, this assumption does not always hold, especially when dealing with molecules that exhibit significant structural differences.

Network-Based Methods

Network-based methods typically rely on large amounts of known DTI data and utilize graph algorithms for modeling. In these methods, drugs and targets are represented as nodes in a graph, while the interactions between them are represented as edges. Additionally, drug–drug similarity networks, protein–protein similarity networks, and known DTI networks are often integrated into a HN. Examples of such approaches include DTI networks, multisimilarity collaborative matrix factorization, and HN models. On this basis, researchers used graph structures to explore potential interaction patterns and promoted the development of tasks such as drug repositioning.

In recent years, with the development of graph representation learning [19,20], network-based methods have achieved deep fusion modeling of structural and semantic information. For example, Zhao et al proposed a regulation-aware graph learning method that enhances drug representation by integrating gene regulation information, thereby improving the prediction effect of drug repositioning [21]. GNN methods mostly rely on the direct adjacency structure of nodes, which easily ignores the rich high-order semantic information and cross-modal associations in biological networks. To this end, some studies have proposed information fusion methods that combine low-order and high-order graph structures. For example, Zhao et al jointly modeled direct neighbor relationships and high-order network path features to effectively enhance the discriminability of drug and target representation [22]. At the same time, in order to more comprehensively model the heterogeneous relationships between multiple entities such as drugs, proteins, and diseases, Zhao et al constructed a heterogeneous information network using semantic paths and attention mechanisms to achieve the integration and discrimination of multimodal information, thereby improving the accuracy and generalization ability of DTI prediction [23]. The iGRLDTI introduced edge weight regulation mechanisms and regularization terms in GNN, further improving the model's ability to learn potential interactions in heterogeneous biological networks [24].

Structure-Based Methods

Traditional structure-based methods typically use molecular docking techniques, combined with molecular dynamics simulations, to accurately predict the binding patterns between drugs and targets. With the development of deep learning methods, an increasing number of studies have integrated structural information with neural networks. For example, DeepDTA [25] and DeepDrug3D [26] have enhanced the modeling capability of the drug–target binding process by incorporating three-dimensional structural information of proteins and drugs, further improving prediction accuracy. Although deep learning models can handle structural information, they generally require large amounts of labeled data for effective training, and obtaining high-quality drug–target binding data remains a challenge.

The application of language models is particularly crucial in the absence of molecular structural information. Drawing on techniques from the field of Natural Language Processing, pretrained language models (such as BERT [27] and MolBERT [28]) are used to deeply characterize drug and protein sequence data. By automatically learning latent features and semantic information within sequences, these models enhance the accuracy of DTI predictions. A key advantage of LLMs is their ability to process large-scale, unlabeled data and improve model generalization through transfer learning. For instance, MolBERT [28] and ChemBERTa [29] achieve high-quality molecular representations by pretraining on massive drug molecular datasets. Transformer-based protein language models, such as ProtBERT [30], TAPE [31], and ProtT5 [32], are pretrained on large protein sequence databases. This enables them to capture hierarchical and context-rich sequence representations, enhancing the understanding of protein characteristics. These models can efficiently and accurately characterize proteins using only sequence data, without relying on three-dimensional structural information.

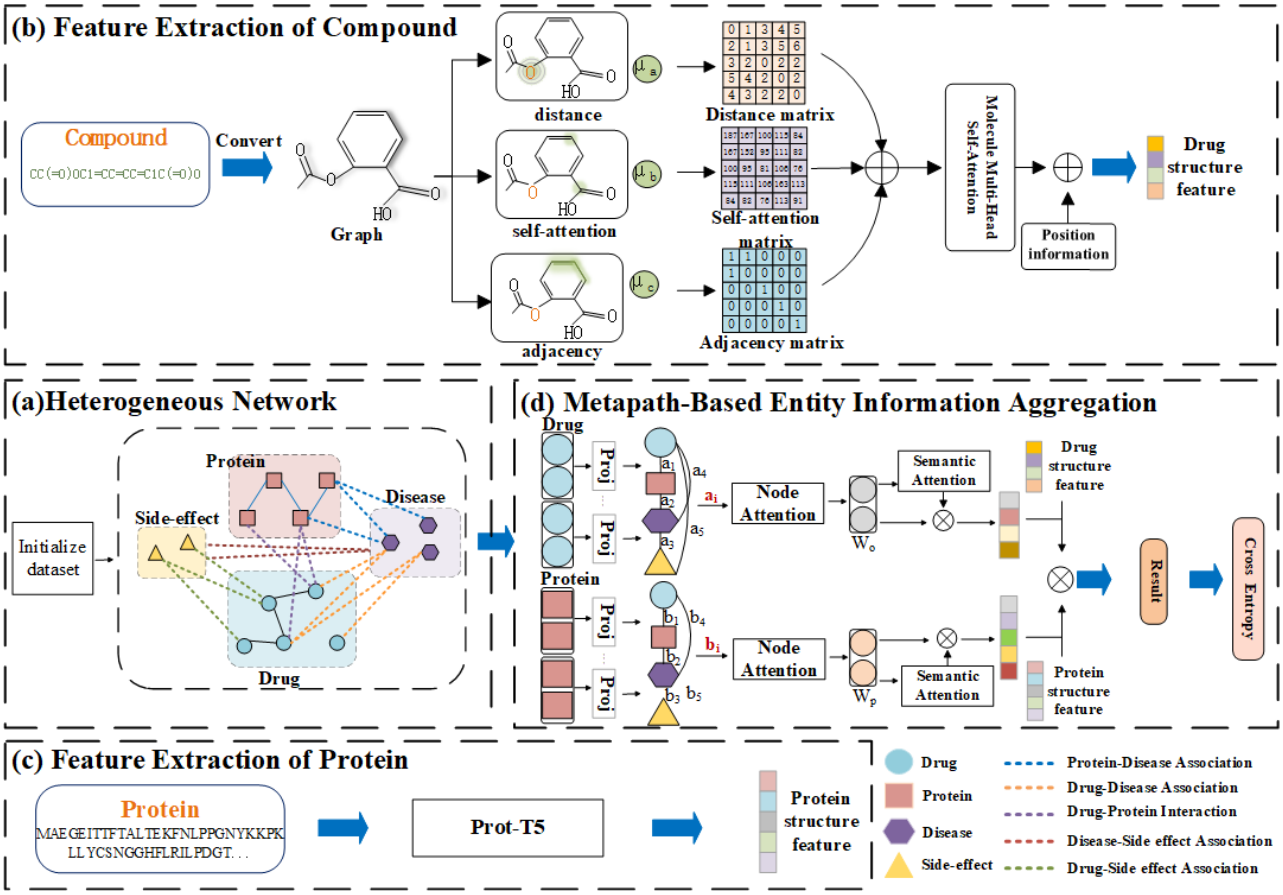
Methods

Framework

MVPA-DTI combined multiple types of heterogeneous data. It extracted structural and sequential features from drug molecules and protein sequences. It also optimized the weight distribution for information propagation in a heterogeneous graph neural network. As illustrated in Figure 1, the process consisted of four steps: (a) First, an HN is constructed, incorporating drugs, proteins, diseases, and drug side effects. (b) Next, a molecular attention Transformer [33] network is used to extract 3D structural features from the SMILES [34] representations of drugs, which are then assigned to drug nodes. (c) Then, the Prot-T5 model is employed to analyze key biophysical features of protein data, which are subsequently assigned to target nodes in the graph. (d) In the final step, a Heterogeneous Graph Attention Network (HAN) [35] is utilized to analyze network topology, unify node embeddings, determine node importance using meta-paths, and integrate node features through semantic attention. Ultimately, MVPA-DTI predicted potential DTI by optimizing the drug–protein reconstruction loss and the cross-entropy loss.

XSL•FO
RenderX

Figure 1. Architecture of the MVPA-DTI model: (A) Construction of the HN; (B) extraction of structural features from the SMILES sequences of drugs to reconstruct drug representations in the HN; (C) extraction of key biophysical properties from protein sequences using Prot-T5 to reconstruct protein representations in the HN; (D) extraction of topological features through the HAN and message-passing mechanism, followed by DTI prediction. DTI: drug–target interaction; HAN: Heterogeneous Graph Attention Network; HN: heterogeneous network; MVPA-DTI: multi-view path aggregation for drug–target interaction; Prot-T5: ProtTrans T5-XL-U50; SMILES: Simplified Molecular Input Line Entry System.



Feature View

Feature Extraction of Compound Structures

The MVPA-DTI model utilized SMILES sequences as input for drug molecules to learn effective representations of their structural features. Since SMILES sequences shared structural similarities with natural language, contextual information can be effectively leveraged to analyze molecular features. However, traditional methods often struggled to capture long-range atomic relationships when processing molecules. To overcome this limitation, this study employed an improved Transformer architecture.

First, we employed the RDKit toolkit [36] to convert SMILES sequences into molecular graph structures. Since the lengths of SMILES sequences vary across different molecules, a maximum length of 100 is selected to construct reasonable molecular representations. This setting covered at least 90% of the compounds in the dataset. For sequences exceeding this length, truncation is applied, while shorter sequences are padded with zeros to maintain consistent input formatting.

For feature extraction, we employed the Molecule Attention Transformer (MAT) [33] for encoding. Its core idea is to replace the self-attention layer of the traditional Transformer [37] with an enhanced molecular self-attention mechanism. By integrating adjacency information from molecular graphs and interatomic distance information, MAT comprehensively captured the feature representation Sdrug of drug structures. The attention mechanism integrated interatomic distance and molecular topology. This enhancement allowed the attention distribution to more precisely capture internal molecular relationships. The calculation formula for molecular multihead self-attention is as follows:

$$(1)A(i)=(\mu b\rho(QiKiTdk)+\mu ag(D)+\mu cA)Vi$$

where $A\in\{0,1\}Natoms\times Natoms$ represented the adjacency matrix of the molecular graph and $D\in RNatoms\times Natoms$ denoted the distances between atoms. The query, key, and value vector matrices are defined as Qi=XWiq, Ki=XWik, and Vi=XWiv, respectively, where *W* represented learnable parameters. In the attention calculation, μα, μb, and μc corresponded to the weights of different attention components, with specific meanings as follows: μα measured the importance of interatomic distances in the attention mechanism; μb adjusted the influence of self-attention on the overall attention mechanism; and μc controlled the role of the adjacency matrix in the attention computation.

Feature Extraction of Protein Structures

The MVPA-DTI model employed Prot-T5 to extract features from protein sequences. By treating sequences as natural language, it used Transformer-based self-supervised learning to capture biological insights. During the data preprocessing

XSL•FO
RenderX

stage, protein sequences are treated as text data composed of 20 standard amino acids (along with a few unknown amino acids, such as X). To adapt to the input format of Natural Language Processing tasks, each protein sequence is treated as a token sequence of individual amino acids, with spaces inserted between each amino acid to ensure the Transformer can correctly parse the sequence information. Additionally, to enhance the model's generalization capability, all uncommon or unresolved amino acid symbols (eg, B, O, U, Z) are mapped to the universal token X, ensuring data consistency.

Prot-T5 is based on the Text-to-Text Transfer Transformer (T5) [38] architecture, which employs an encoder–decoder structure. However, for the task of protein feature extraction, only the encoder part of T5 is utilized to map protein sequences into a high-dimensional feature space. Prot-T5 adopted the Span Masking language modeling strategy, where during training, continuous segments of amino acids in the sequence are randomly masked, and the model is tasked with reconstructing the masked portions based on the context. This enabled the model to learn long-range dependencies and semantic information within protein sequences. As shown in Equation 2, given a protein sequence S=(S1,S2,...,Sn), it is first embedded into a high-dimensional space ES and then fed into the Transformer to compute the hidden representations:

(2)H=Transformer(E(S))

Finally, the global representation of the entire sequence is obtained through average pooling, as calculated by the following formula:

(3)Sprotein=1n∑i=1nHi

where Hi represented the hidden states output by the Transformer and Sprotein served as the global feature of the protein.

Relational View of Biological Networks

Heterogeneous Networks

The HN is described as an undirected graph G = (V, E), where V={υ1,υ2,...,υn} represented the set of nodes and E={E(1),E(2),...,E(k)} denoted the set of ktypes of edges, with each E(i)={ei1,ei2,...,eim} representing a specific type of edge.

As shown in Figure 1A, this paper constructed a comprehensive heterogeneous information network, which included drug–drug interactions, drug–protein interactions, drug–disease associations, drug–side effect associations, protein–protein interactions, and protein–disease associations. In the network, entities such as drugs, targets, diseases, and side effects are represented as nodes, while the relationships and interactions between nodes are represented as edges. In the proposed framework, each node belonged to only one type of entity, and all edges are undirected and have nonnegative weights. Node messages are first sent to their first-order neighbors and then propagated to higher-order neighbors through the network edges, a process known as message passing.

The message-passing process in the HN is divided into multiple stages. First, nodes transmitted their information to first-order neighbors. This information is then propagated to higher-order neighbors through network edges, forming more complex information dissemination. Message passing is not limited to directly connected nodes but also includes information transmitted through multihop paths. This enabled the model to integrate features across a broader neighborhood, thereby better capturing long-range dependencies and multilevel network structures.

Metapath-Based Entity Information Aggregation

In heterogeneous graph representation learning, our goal is to learn effective feature representations for each node in the HN. However, the challenge of this task lies in not only integrating information from different types of nodes and edges in the heterogeneous graph but also considering the heterogeneous features and content of each node. To address this issue, we employed HAN [35] as the topological feature extraction method for the heterogeneous information network. HAN modeled the structural relationships in the HN through a hierarchical attention mechanism. Specifically, node-level attention learned meta-path-based neighborhood weights and aggregates them to generate semantically specific node embeddings, while semantic-level attention assigned weights across different meta-paths to obtain the optimal task-specific representation, as illustrated in Figure 1D. In terms of meta-path selection, we selected two biologically meaningful paths: D-P-D (Drug–Protein–Drug) and P-D-P-D (Protein–Disease–Protein–Drug). D-P-D is used to capture the semantic relationship between drugs connected by common targets, which helped the model identify drug pairs with similar functions or related potential mechanisms of action, while P-D-P-D further explored the multi-hop indirect connections between proteins formed by disease associations, thereby reflecting a more complex biological network structure. We selected these two meta-paths based on their good semantic interpretability and biological relevance, which helps the model more effectively model the potential interactions between drugs and targets.

After obtaining the node embeddings, we further proceeded with the message-passing process. Assuming the initial node embeddings are defined as f0:V→Rd, where f0(v) represented the mapping of node v in the d-dimensional space, the information aggregation process for node v can be expressed as:

(4)fv=σ(1K∑k=1K∑u∈ Nvαuv W f0(u))

(5)αuv=exp(AconC(α[Wf0(u)//Wf0(v)]))∑k∈Nvexp(AconC(α[Wf0(u)//Wf0(k)]))

where σ represents a nonlinear activation function, K denotes the number of attention layers, Nv represents the set of neighboring nodes of node v, W is the shared weight parameter, auv is the edge weight computed by the attention mechanism, and AconC(∗) [39] is an adaptive activation function.

Based on obtaining the graph structure representation, we further integrated the structural information of each node to construct the final drug and protein representation. For drug nodes, its representation integrates the meta-path structure features, the original embedding representation, and the molecular structure features, which is specifically expressed as:

(6)fdrug=L2Norm(ReLU([mateDPD,Edrug+L2Norm(Sdrug)]W0+b0))

XSL•FO
RenderX

Similarly, the protein node representation combined its meta-path structure features, original embeddings, and sequence representations and is expressed as:

(7)protein=L2Norm(ReLU([matePDPD,Eprotein=L2Norm(Sprotein)]W0+b0))

Among them, W0 and b0 are learnable linear transformation parameters, which are used to uniformly map the concatenated multiple features to a common low-dimensional semantic space, and implicitly model the importance weights of each feature subspace during the training process to improve the discriminative ability of the final representation.

After completing the representations of drugs and proteins, we used the inner product to calculate the interaction probability between them, as shown in Figure 1D. For a drug node u and a protein node v, their interaction probability is calculated as follows:

(8)puv=σ((fu)Tfv)

where σ is the sigmoid function and puv represents the interaction score between node u and node v.

To optimize the model, we employed multiple loss terms for joint training. Among them, the cross-entropy loss is used to supervise the interaction prediction task, defined as follows:

(9)£CEL=∑r∈ R−yrlog(pr)−(1−yr)log(1−pr)

where R is the set of relationships, yr is the ground truth label of sample r (1 for positive samples and 0 for negative samples), and pr is the predicted probability.

In addition, to enhance the model's structural perception of node features, we introduced reconstruction losses for drugs and proteins, which are defined as follows:

(10)£recdrug= ‖ A^drug−Adrug ‖ F2

(11)£recprotein= ‖ A^protein−Aprotein ‖ F2

Among them, Adrug and Aprotein are the adjacency matrices of drug and protein nodes in the original HN, respectively. A^ represents the adjacency matrix reconstructed by the model through node embedding and ·F represents the Frobenius norm. The final optimization target is the weighted sum of three losses:

(12)£=£CEL+λ1£recdrug+λ2£recprotein

where £recdrug and £recprotein represent the reconstruction losses for drugs and proteins, respectively, while λ1 and λ2 are weighting coefficients used to balance the contributions of different loss terms. Through joint optimization, we can improve the accuracy of DTI prediction while ensuring that the generated feature representations possess robust structural information and discriminative capabilities.

Results

Dataset

This study conducted DTI prediction experiments on the Luo dataset [9], which was assembled by Luo et al. To better capture biological characteristics, we incorporated the SMILES sequences of drug molecules and the structural sequence data of proteins into the dataset. Tables 1 and 2 present the relevant statistical information of nodes and edges in the dataset. The dataset comprises six independent drug–protein interaction networks, with all edge weights being binary values.

Table . Statistics of node information in the dataset.

Node type	Count
Drug	708
Protein	1512
Disease	5603
Side effect	4192

Table . Statistics of association information between nodes in the dataset.

Edge type	Count	Source
Drug–protein interaction	1923	DrugBank version 3.0 [40]
Drug–drug interaction	10,036	DrugBank version 3.0 [40]
Protein–protein interaction	7363	HPRD Release 9 [41]
Drug–disease association	199,214	Comparative Toxicogenomics Database [42]
Protein–disease association	1,596,745	Comparative Toxicogenomics Database [42]
Drug–side-effect association	80,164	SIDER Release 2 [43]

Experimental Settings

Building upon the study by Luo et al [9], 90% of the positive and negative samples from the dataset were used to construct the HN and train MVPA-DTI, while the remaining 10% were reserved for testing. In this study, we adopted a data preprocessing process consistent with NeoDTI, including negative sample sampling strategy, drug–target similarity calculation method, and similarity threshold setting to eliminate redundancy. Subsequently, the model's performance was evaluated through 10-fold cross-validation, with the

XSL•FO
RenderX

effectiveness of the method being measured using AUROC and AUPR metrics.

MVPA-DTI consists of three modules: Prot-T5, MAT, and HAN, with the parameter settings detailed in Table 3. During the training process, we employed the Adam optimizer to update the network weights.

Table . Parameter settings in the experiment.

Parameter	Value
Number step	3000
Batch size	128
Learning rate	0.001
Dropout rate	0.1
HAN[a] input size	1024
MAT[b] multi-head attention number	16
MAT stack number	8

[a]HAN: Heterogeneous Graph Attention Network.

[b]MAT: Heterogeneous Graph Attention Network.

Comparison With Prior Work

In this study, to better simulate real-world scenarios, we randomly sampled negative samples while retaining all positive samples, setting the ratio of positive to negative samples at 10:1. This ratio aims to reflect the imbalance between positive and negative samples in the real world. Subsequently, we compared the performance of MVPA-DTI with several benchmark models to evaluate its effectiveness in DTI prediction tasks; they are briefly described as follows:

- MSCMF [44]: MSCMF effectively predicts DTI by utilizing multiple similarity matrices of drugs and targets through collaborative matrix factorization.
- HNM [45]: HNM integrates disease, drug, and target information via a HN, aiming to enhance the efficiency and accuracy of drug repositioning.
- DTINet [9]: DTINet predicts interactions between new drugs and targets by integrating heterogeneous data and learning low-dimensional feature representations.
- NeoDTI [46]: NeoDTI automatically generates feature representations by integrating diverse information from HN.
- EEG-DTI [47] : EEG-DTI is an end-to-end learning framework based on heterogeneous graph convolutional networks, capable of effectively learning features from multiple biological entities.
- SHGCL-DTI [48]: SHGCL-DTI combines semi-supervised learning with graph contrastive learning, enhancing the model's adaptability.

The performance of MVPA-DTI was compared with various models, and the experimental results are shown inTable 4. MVPA-DTI achieves the best performance, demonstrating significant improvement over other DTI models. It achieves an AUPR of 0.901, which is 1.7% higher than the second-best method, and an AUROC of 0.967, representing a 0.9% improvement over SHGCL-DTI. MSCMF employs matrix transformation to optimize prediction results through network inference and the topological structure of data. However, compared to the recent outstanding performance of deep learning methods, MSCMF does not fully exploit the latent information in data matrix embeddings or the features of adjacent nodes, thereby limiting its predictive performance. HNM does not adopt mainstream heterogeneous data embedding methods for feature representation and information integration, resulting in insufficient generalization ability and lower prediction accuracy. In contrast, DTINet, NeoDTI, and EEG-DTI further extract hidden features by combining matrix transformation with neural networks, enabling more accurate modeling of node relationships and improving prediction performance. SHGCL-DTI employs a graph contrastive learning strategy to capture the structural information of heterogeneous graphs. This is achieved by enhancing the similarity of positive sample pairs and reducing the similarity of negative sample pairs. However, SHGCL-DTI fails to fully utilize the rich semantic information and complex interaction patterns in heterogeneous graphs, presenting certain limitations when processing biological data.

XSL•FO
RenderX

Table . The AUPR and AUROC evaluation results for each model.

Model	AUPR[a]	AUROC[b]
HNM[c]	0.579	0.834
MSCMF[d]	0.603	0.856
DTINet[e]	0.818	0.916
NeoDTI[f]	0.855	0.943
EEG-DTI[g]	0.847	0.952
SHGCL-DTI[h]	0.884	0.958
MVPA-DTI (ours)[i]	0.901	0.966

[a] AUPR: area under the precision–recall curve.

[b]AUROC: area under the receiver operating characteristic curve.

[c]HNM: heterogeneous network model.

[d]MSCMF: multiple similarities collaborative matrix factorization.

[e]DTINet: drug–target interaction prediction network.

[f]NeoDTI: neural integration of neighbor information for DTI prediction.

[g]EEG-DTI: end-to-end graph for drug–target interaction prediction

[h]SHGCL-DTI: semi-supervised heterogeneous graph contrastive learning for drug–target interaction prediction.

[i]MVPA-DTI: multi-view path aggregation for drug–target interaction.

Existing methods fail to fully exploit critical biochemical information in drug molecular structures and protein sequences, potentially leading to information loss during the node embedding process. In contrast, MVPA-DTI integrates a graph attention network that incorporates all types of adjacent nodes, enhancing the extraction of composite structural information. Furthermore, it employs HAN to model the potential relationships between different types of nodes. Additionally, the method dynamically fuses features extracted from sequences and graph to update the embedding representations of drug and protein nodes. Through this process, it progressively strengthens the weight of node information and optimizes the feature representation of different types of nodes, thereby improving the predictive accuracy.

Robustness Experiment

To further validate the stability of MVPA-DTI, considering the potential presence of redundant information in the dataset, additional experiments were conducted to evaluate the model's predictive performance. First, we removed some samples from the dataset, including DTIs with similar drugs or targets and DTIs involving drugs with similar drug interactions. The details of the removed data are provided in Table 5.

Table . Number of drugs, targets, and DTIs included in the redundant data.

Redundant data	Drug number	Target number	DTI number
DTI of similar drugs or targets	146	78	955
DTI of drugs with similar side effects	17	0	51

[a]DTI: drug–target interactions.

After removing similar drugs and targets, as shown in Table 6, MVPA-DTI achieves a 15.9% improvement over the second-best method, NeoDTI. Meanwhile, Table 6 also demonstrates that after removing drugs with similar side effects, MVPA-DTI outperforms the second-best method by 3.1%.

XSL•FO
RenderX

Table . AUPR performance of each model after adjustment of the dataset.

Model	AUPR[a]		
	DTIs[b] with similar drugs and targets were removed	DTIs with drugs with similar side effects were removed	Trained on non-unique dataset and tested on unique dataset
HNM[c]	0.547	0.581	0.233
MSCMF[d]	0.265	0.593	0.206
DTINet[e]	0.611	0.803	0.389
NeoDTI[f]	0.694	0.848	0.432
EEG-DTI[g]	0.686	0.846	0.431
SHGCL-DTI[h]	0.617	0.729	0.443
MVPA-DTI[i]	0.849	0.873	0.46

[a]AUPR: area under the precision–recall curve.

[b]DTI: drug–target interaction.

[c]HNM: heterogeneous network model.

[d]MSCMF: multiple similarities collaborative matrix factorization.

[e]DTINet: drug–target interaction prediction network.

[f]NeoDTI: neural integration of neighbor information for DTI prediction.

[g]EEG-DTI: end-to-end graph for drug–target interaction prediction.

[h]SHGCL-DTI: semi-supervised heterogeneous graph contrastive learning for drug–target interaction prediction.

[i]MVPA-DTI: multi-view path aggregation for drug–target interaction.

The experimental results indicate that although the model's performance declined after removing a significant portion of specific DTI data, MVPA-DTI still maintains the best AUPR, demonstrating its strong robustness. Additionally, this study treats drug–protein interactions as a specific case for experimentation. To objectively evaluate the predictive capability of MVPA-DTI, both special drug–target relationships and conventional drug–target relationships were separately processed. Specifically, the model was first trained on a dataset in which the relationships between drugs and proteins were nonunique and then tested on a dataset with unique interactions. As shown in Table 6, MVPA-DTI significantly outperforms the second-best method, with a 1.7% improvement in AUPR. This result suggests that MVPA-DTI exhibits stronger generalization ability in predicting DTI.

Ablation Experiment

To verify the contribution of each module in MVPA-DTI, we conducted ablation experiments. The experimental results are presented in Table 7, where ProSF represents the protein sequence feature extraction module and DruSF denotes the drug compound structure feature extraction module.

Table . Evaluation of the impact of MVPA-DTI modules on performance.

Method	AUROC[a]	AUPR[b]	F_1-score	MCC[c]
w/o[d] ProSF[e]	0.963	0.886	0.839	0.828
w/o DruSF[f]	0.964	0.891	0.840	0.827
w/o ProSF and DruSF	0.957	0.875	0.813	0.804
protBert-MVPA-DTI[g]	0.964	0.89	0.831	0.822
MVPA-DTI[h]	0.966	0.901	0.848	0.839

[a]AUROC: Area Under the Receiver Operating Characteristic curve.

[b]AUPR: Area Under the Precision-Recall Curve.

[c]MCC: Matthews Correlation Coefficient.

[d]w/o denotes corresponding module was removed.

[e]ProSF: protein sequence feature extraction module.

[f]DruSF: drug compound structure feature extraction module.

[g]protBert-MVPA-DTI replaces the ProSF module with ProtBert processing.

[h]MVPA-DTI: multi-view path aggregation for drug-target interaction.

XSL•FO
RenderX

The Effectiveness of ProSF

As shown in Table 7, the ProSF module improves the model performance by 0.3% in AUROC and 1.5% in AUPR. ProSF effectively extracts deep semantic information from proteins, capturing features related to key physicochemical properties such as secondary structure and solubility, thereby enhancing the model's predictive capability.

The Effectiveness of DruSF

As shown in Table 7, the DruSF module enhances the model's performance, with improvements of 0.2% and 1.0% in AUROC and AUPR metrics, respectively. This enhancement is attributed to DruSF's ability to thoroughly explore the structural features of drugs, thereby assigning higher weights to drugs during the message-passing process and further optimizing the prediction outcomes.

The experimental results demonstrate that the MVPA-DTI model exhibits high effectiveness in extracting the biological structural features of drugs and proteins. By deeply exploring the chemical structures, physical properties, and biological functions of drugs and proteins, the model can accurately capture the complex interaction relationships between them, thereby enhancing DTI prediction performance. Further analysis reveals that protein structural information plays a more critical role than drug structural information in the prediction process. This phenomenon may be attributed to the protein-specific LLM Prot-T5, which more effectively captures evolutionary conservation and functional relevance in protein sequences, thereby providing more discriminative feature representations for DTI prediction.

Discussion

Case Study

In evaluating the practical application of MVPA-DTI, we predicted 53 candidate drugs targeting the voltage-gated inwardly rectifying potassium channel KCNH2 (hERG). The KCNH2 channel, a critical protein in cardiac electrophysiology, plays a central role in regulating ventricular repolarization. Dysfunction or dysregulation of this channel delays ventricular repolarization, manifesting as QT interval prolongation on electrocardiograms. This phenomenon has been extensively documented to correlate with the pathogenesis of various cardiovascular diseases [49]. The results demonstrate that 38 out of the 53 candidate drugs exhibited potential interactions with KCNH2. Among these, 10 drugs have been experimentally validated in published studies to interact with the KCNH2 channel. Although the remaining candidates have not yet been experimentally confirmed, their established associations with cardiovascular pathologies suggest potential therapeutic relevance in cardiovascular disease management. Studies have demonstrated that procainamide interacts with the KCNH2 channel, primarily by inhibiting its function. This inhibition prolongs the duration of potassium ion efflux, leading to QT interval prolongation [50]. Nicotine, as a blocker of the KCNH2 channel, significantly affects the electrophysiological properties of the heart. This interaction may have important clinical implications for assessing the impact of nicotine on cardiac health [51]. Ranolazine is considered to have potential therapeutic effects, as it improves cardiac electrophysiological abnormalities caused by genetic variations by modulating the function of the KCNH2 channel [52].

In this study, AutoDock was used to perform molecular docking simulations on the interaction between procainamide and KCNH2 channel protein. As shown in Figures 2 and 3, procainamide can stably bind to the central cavity region of the KCNH2 channel protein and is embedded in a hydrophobic pocket surrounded by the S6 helix and the lamellar structure. The binding site involves multiple key amino acid residues, including THR 768, TYR 827, etc. These residues have been widely reported in the literature as core sites for regulating drug binding and gating behavior of KCNH2 channels. These binding residues are visually annotated in Figure 2. Binding mode analysis showed that hydrophobic interactions and potential hydrogen bonds were formed between procainamide and the above residues, which may interfere with the open state of the channel and affect its function. As shown in Figure 3, binding energy analysis showed that procainamide interacted strongly with KCNH2, and the binding energy of some conformations was as low as –9 kcal/mol, indicating that it has high binding stability and potential biological activity.

XSL•FO
RenderX

Figure 2. Visualization of the interaction between procainamide and the KCNH2 channel. KCNH2: Potassium Voltage-Gated Channel Subfamily H Member 2.

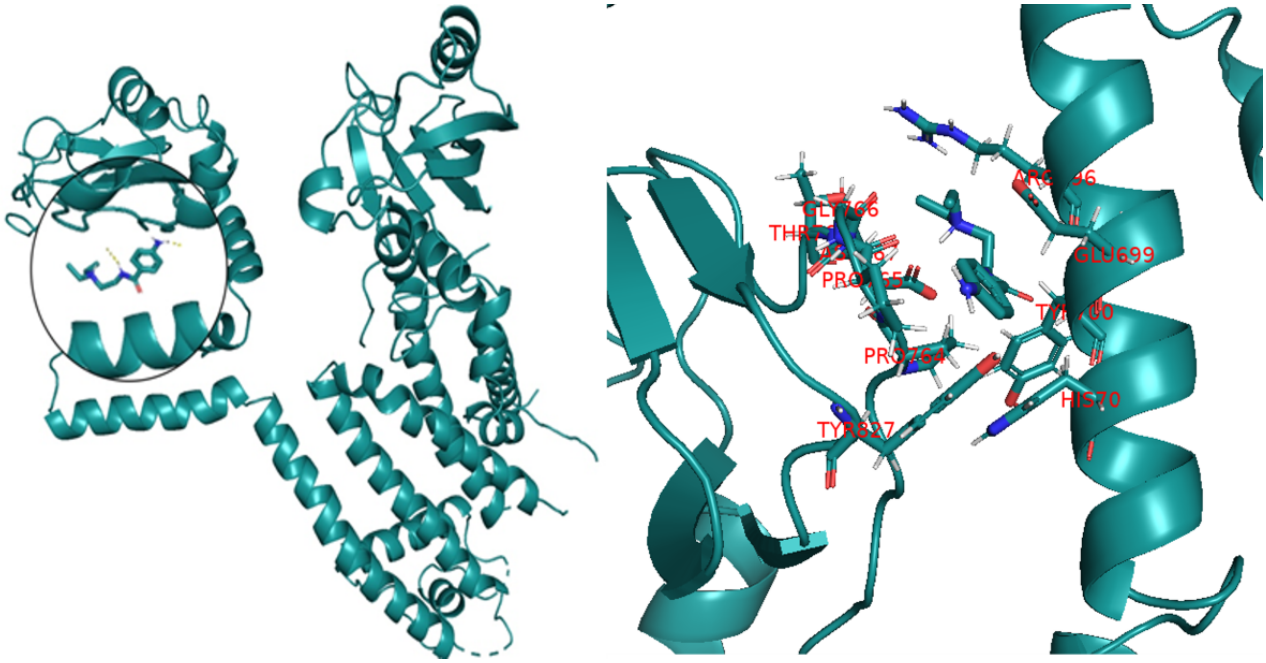
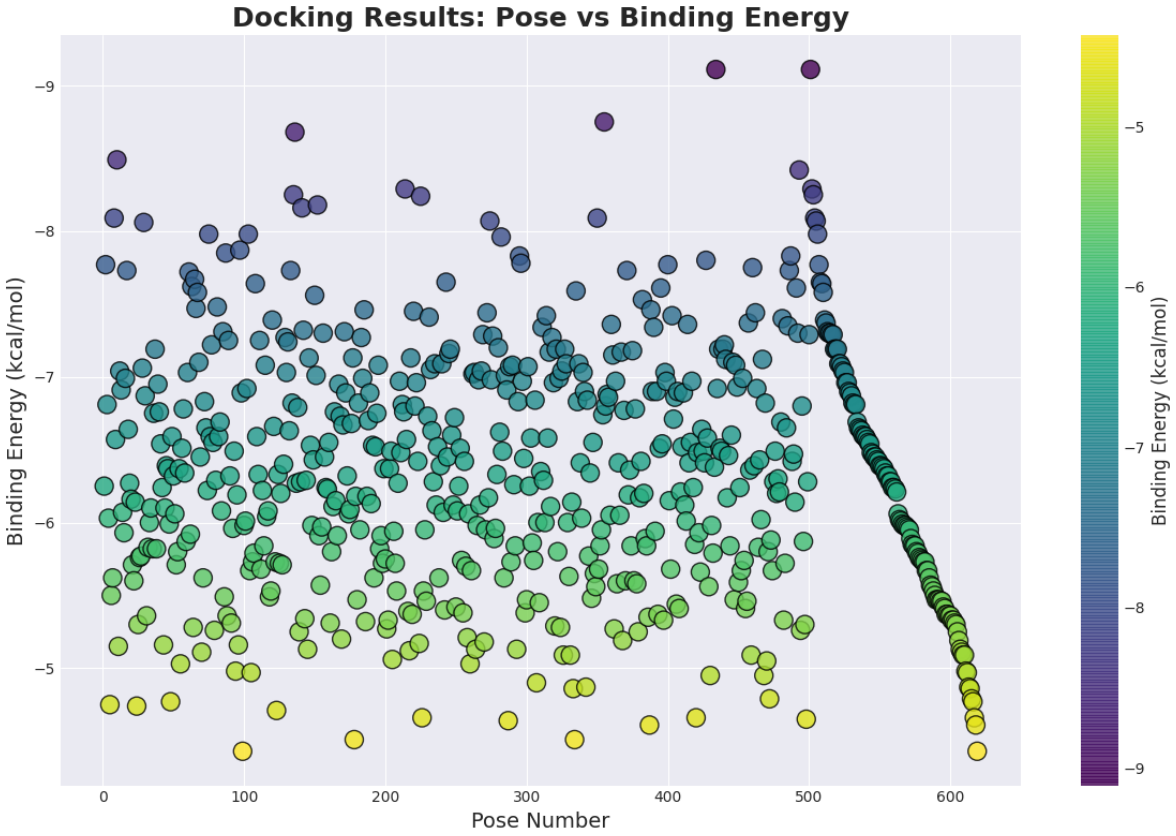


Figure 3. Binding energy distribution of procainamide docking with KCNH2. KCNH2: Potassium Voltage-Gated Channel Subfamily H Member 2.



Conclusions

This study proposes a novel DTI prediction method MVPA-DTI, which extracts key biological features from protein and drug sequences and reconstructs them into a heterogeneous graph, enabling the model to capture the most critical biological information during each iteration, thereby optimizing the weight assignment for drugs and targets. Experimental results demonstrate that MVPA-DTI outperforms existing methods across multiple benchmark tests. Although MVPA-DTI effectively captures DTI, the biological mechanisms underlying these interactions are complex, involving multiple factors, which are not yet fully considered by MVPA-DTI. Future improvements should focus on in-depth exploration of the

XSL•FO
RenderX

biological details of DTI to enhance prediction accuracy and applicability. To enhance the ability to model the complex relationship between drugs and targets, in the future, it is possible to consider introducing new graph neural network structures such as FCGCN [53] into the drug–target graph modeling process to more effectively integrate molecular structure, pharmacological properties, and network topology information.

Acknowledgments

This work was supported by the National Natural Science Foundation of China (Grants No. 62076045), the 111 Project (Grants No. D23006), the National Foreign Expert Project of China (Grants No. D20240244), and the Interdisciplinary Project of Dalian University (Grants No. DLUXK-2023-YB-003 and DLUXK-2023-YB-009).

Conflicts of Interest

None declared.

References

1. Chu Y, Shan X, Chen T, et al. DTI-MLCD: predicting drug-target interactions using multi-label learning with community detection method. Brief Bioinform 2021 May 20;22(3):bbaa205. [doi: 10.1093/bib/bbaa205] [Medline: 32964234]
2. Lan W, Wang J, Li M, et al. Predicting drug–target interaction using positive-unlabeled learning. Neurocomputing 2016 Sep;206:50-57. [doi: 10.1016/j.neucom.2016.03.080]
3. Liu Z, Chen Q, Lan W, Lu H, Zhang S. SSLDTI: A novel method for drug-target interaction prediction based on self-supervised learning. Artif Intell Med 2024 Mar;149:102778. [doi: 10.1016/j.artmed.2024.102778] [Medline: 38462280]
4. Lan W, Tang Z, Liu M, et al. The large language models on biomedical data analysis: a survey. IEEE J Biomed Health Inform 2025 Jun;29(6):4486-4497. [doi: 10.1109/JBHI.2025.3530794] [Medline: 40031690]
5. Shi W, Yang H, Xie L, Yin XX, Zhang Y. A review of machine learning-based methods for predicting drug-target interactions. Health Inf Sci Syst 2024 Dec;12(1):30. [doi: 10.1007/s13755-024-00287-6] [Medline: 38617016]
6. Thafar M, Raies AB, Albaradei S, Essack M, Bajic VB. Comparison study of computational prediction tools for drug-target binding affinities. Front Chem 2019;7:782. [doi: 10.3389/fchem.2019.00782] [Medline: 31824921]
7. Mathai N, Kirchmair J. Similarity-based methods and machine learning approaches for target prediction in early drug discovery: performance and scope. Int J Mol Sci 2020 May 19;21(10):3585. [doi: 10.3390/ijms21103585] [Medline: 32438666]
8. Lian M, Wang X, Du W. Integrated multi-similarity fusion and heterogeneous graph inference for drug-target interaction prediction. Neurocomputing 2022 Aug;500:1-12. [doi: 10.1016/j.neucom.2022.04.104]
9. Luo Y, Zhao X, Zhou J, et al. A network integration approach for drug-target interaction prediction and computational drug repositioning from heterogeneous information. Nat Commun 2017 Sep 18;8(1):573. [doi: 10.1038/s41467-017-00680-8] [Medline: 28924171]
10. Yuan Q, Gao J, Wu D, Zhang S, Mamitsuka H, Zhu S. DrugE-Rank: improving drug-target interaction prediction of new candidate drugs or targets by ensemble learning to rank. Bioinformatics 2016 Jun 15;32(12):i18-i27. [doi: 10.1093/bioinformatics/btw244] [Medline: 27307615]
11. Zhang YF, Wang X, Kaushik AC, et al. SPVec: a Word2vec-inspired feature representation method for drug-target interaction prediction. Front Chem 2019;7(1-11):895. [doi: 10.3389/fchem.2019.00895] [Medline: 31998687]
12. Öztürk H, Ozkirimli E, Özgür A. A comparative study of SMILES-based compound similarity functions for drug-target interaction prediction. BMC Bioinformatics 2016 Mar 18;17:128. [doi: 10.1186/s12859-016-0977-x] [Medline: 26987649]
13. Wu Z, Pan S, Chen F, Long G, Zhang C, Yu PS. A comprehensive survey on graph neural networks. IEEE Trans Neural Netw Learn Syst 2021 Jan;32(1):4-24. [doi: 10.1109/TNNLS.2020.2978386] [Medline: 32217482]
14. Zhang Z, Cui P, Zhu W. Deep learning on graphs: a survey. IEEE Trans Knowl Data Eng 2020;34(1):249-270. [doi: 10.1109/TKDE.2020.2981333]
15. Zhang Z, Chen L, Zhong F, et al. Graph neural network approaches for drug-target interactions. Curr Opin Struct Biol 2022 Apr;73:102327. [doi: 10.1016/j.sbi.2021.102327] [Medline: 35074533]
16. Singh S, Malik BK, Sharma DK. Molecular drug targets and structure based drug design: a holistic approach. Bioinformation 2006 Dec 23;1(8):314-320. [doi: 10.6026/97320630001314] [Medline: 17597912]
17. Thafar MA, Olayan RS, Ashoor H, et al. DTiGEMS+: drug-target interaction prediction using graph embedding, graph mining, and similarity-based techniques. J Cheminform 2020 Jun 29;12(1):44. [doi: 10.1186/s13321-020-00447-2] [Medline: 33431036]
18. Shim J, Hong ZY, Sohn I, Hwang C. Prediction of drug-target binding affinity using similarity-based convolutional neural network. Sci Rep 2021 Feb 24;11(1):4416. [doi: 10.1038/s41598-021-83679-y] [Medline: 33627791]

XSL•FO
RenderX

19. Zhang P, Yuan J, Li L, et al. Key substructure learning with chemical intuition for material property prediction[c]. 2024 Presented at: Proceedings of the International Conference on Database Systems for Advanced Applications; Pohang, Korea p. 87-103. [doi: 10.1007/978-981-97-5575-2_6]
20. Zhang P, Che C, Jin B, Yuan J, Li R, Zhu Y. NCH-DDA: Neighborhood contrastive learning heterogeneous network for drug–disease association prediction. Expert Syst Appl 2024 Mar;238:121855. [doi: 10.1016/j.eswa.2023.121855]
21. Zhao BW, Su XR, Yang Y, et al. Regulation-aware graph learning for drug repositioning over heterogeneous biological network. Inf Sci (Ny) 2025 Jan;686:121360. [doi: 10.1016/j.ins.2024.121360]
22. Zhao BW, Wang L, Hu PW, et al. Fusing higher and lower-order biological information for drug repositioning via graph representation learning. IEEE Trans Emerg Topics Comput 2023;12(1):163-176. [doi: 10.1109/TETC.2023.3239949]
23. Su X, Hu P, Yi H, You Z, Hu L. Predicting drug-target interactions over heterogeneous information network. IEEE J Biomed Health Inform 2022;27(1):562-572. [doi: 10.1109/JBHI.2022.3219213]
24. Zhao BW, Su XR, Hu PW, Huang YA, You ZH, Hu L. iGRLDTI: an improved graph representation learning method for predicting drug-target interactions over heterogeneous biological information network. Bioinformatics 2023 Aug 1;39(8):btad451. [doi: 10.1093/bioinformatics/btad451] [Medline: 37505483]
25. Öztürk H, Özgür A, Ozkirimli E. DeepDTA: deep drug-target binding affinity prediction. Bioinformatics 2018 Sep 1;34(17):i821-i829. [doi: 10.1093/bioinformatics/bty593] [Medline: 30423097]
26. Pu L, Govindaraj RG, Lemoine JM, Wu HC, Brylinski M. DeepDrug3D: classification of ligand-binding pockets in proteins with a convolutional neural network. PLoS Comput Biol 2019 Feb;15(2):e1006718. [doi: 10.1371/journal.pcbi.1006718] [Medline: 30716081]
27. Devlin J, Chang MW, Lee K, Toutanova K. Bert: pre-training of deep bidirectional transformers for language understanding. 2019 Presented at: Proceedings of the Proceedings of the 2019 conference of the North American chapter of the association for computational linguistics: human language technologies, volume 1 (long and short papers); Jun 2, 2019; Minneapolis, Minnesota p. 4171-4186. [doi: 10.18653/v1/N19-1423]
28. Li J, Jiang X. Mol‐BERT: an effective molecular representation with BERT for molecular property prediction. Wireless Commun Mobile Comput 2021 Jan;2021(1):7181815 [FREE Full text] [doi: 10.1155/2021/7181815]
29. Chithrananda S, Grand G, Ramsundar B. ChemBERTa: large-scale self-supervised pretraining for molecular property prediction. arXiv. Preprint posted online on 2020. [doi: 10.48550/arxiv.2010.09885]
30. Brandes N, Ofer D, Peleg Y, Rappoport N, Linial M. ProteinBERT: a universal deep-learning model of protein sequence and function. Bioinformatics 2022 Apr 12;38(8):2102-2110. [doi: 10.1093/bioinformatics/btac020] [Medline: 35020807]
31. Rao R, Bhattacharya N, Thomas N, et al. Evaluating protein transfer learning with TAPE. Adv Neural Inf Process Syst 2019 Dec;32:9689-9701. [doi: 10.1101/676825] [Medline: 33390682]
32. Elnaggar A, Heinzinger M, Dallago C, et al. ProtTrans: toward understanding the language of life through self-supervised learning. IEEE Trans Pattern Anal Mach Intell 2022 Oct;44(10):7112-7127. [doi: 10.1109/TPAMI.2021.3095381] [Medline: 34232869]
33. Maziarka Ł, Danel T, Mucha S, et al. Molecule attention transformer. arXiv. Preprint posted online on 2020. [doi: 10.48550/arXiv.2002.08264]
34. Toropov AA, Toropova AP, Mukhamedzhanoval DV, Gutman I. Simplified molecular input line entry system (SMILES) as an alternative for constructing quantitative structure-property relationships (QSPR). . Preprint posted online on 2005 URL: http://nopr.niscair.res.in/bitstream/123456789/18068/1/IJCA%2044A%288%29%201545-1552.pdf [accessed 2025-09-15]
35. Wang X, Ji H, Shi C, et al. Heterogeneous graph attention network. 2019 May 13 Presented at: WWW '19; May 13, 2019; San Francisco CA USA URL: https://dl.acm.org/doi/proceedings/10.1145/3308558 [doi: 10.1145/3308558.3313562]
36. Bento AP, Hersey A, Félix E, et al. An open source chemical structure curation pipeline using RDKit. J Cheminform 2020 Sep 1;12(1):51. [doi: 10.1186/s13321-020-00456-1] [Medline: 33431044]
37. Vaswani A. Attention is all you need. Presented at: Advances in neural information processing systems; Dec 4-9, 2017; Long Beach, California, USA.
38. Raffel C, Shazeer N, Roberts A, et al. Exploring the limits of transfer learning with a unified text-to-text transformer. J Mach Learn Res 2020;21(1):5485-5551.
39. Ma N, Zhang X, Liu M, Sun J. Activate or not: learning customized activation. Presented at: 2021 IEEE/CVF Conference on Computer Vision and Pattern Recognition (CVPR); Jun 20-25, 2021; Nashville, TN, USA. [doi: 10.1109/CVPR46437.2021.00794]
40. Knox C, Law V, Jewison T, et al. DrugBank 3.0: a comprehensive resource for "omics" research on drugs. Nucleic Acids Res 2011 Jan;39(Database issue):D1035-D1041. [doi: 10.1093/nar/gkq1126] [Medline: 21059682]
41. Wang Z, Zhang Q, Shuang-Wei H, et al. Multi-level protein structure pre-training via prompt learning. Presented at: Proceedings of the The Eleventh International Conference on Learning Representations; 2023; Kigali, Rwanda URL: https://openreview.net/forum?id=XGagtiJ8XC [accessed 2025-09-15]
42. Davis AP, Murphy CG, Johnson R, et al. The comparative toxicogenomics database: update 2013. Nucleic Acids Res 2013 Jan;41(Database issue):D1104-D1114. [doi: 10.1093/nar/gks994] [Medline: 23093600]

XSL•FO
RenderX

43. Kuhn M, Campillos M, Letunic I, Jensen LJ, Bork P. A side effect resource to capture phenotypic effects of drugs. Mol Syst Biol 2010;6(1):343. [doi: 10.1038/msb.2009.98] [Medline: 20087340]
44. Zheng X, Ding H, Mamitsuka H, Zhu S. Collaborative matrix factorization with multiple similarities for predicting drug-target interactions. 2013 Aug 11 Presented at: KDD' 13; Aug 11, 2013; Chicago Illinois USA URL: https://dl.acm.org/doi/proceedings/10.1145/2487575 [doi: 10.1145/2487575.2487670]
45. Wang W, Yang S, Zhang X, Li J. Drug repositioning by integrating target information through a heterogeneous network model. Bioinformatics 2014 Oct 15;30(20):2923-2930. [doi: 10.1093/bioinformatics/btu403] [Medline: 24974205]
46. Wan F, Hong L, Xiao A, Jiang T, Zeng J. NeoDTI: neural integration of neighbor information from a heterogeneous network for discovering new drug-target interactions. Bioinformatics 2019 Jan 1;35(1):104-111. [doi: 10.1093/bioinformatics/bty543] [Medline: 30561548]
47. Peng J, Wang Y, Guan J, et al. An end-to-end heterogeneous graph representation learning-based framework for drug-target interaction prediction. Brief Bioinform 2021 Sep 2;22(5):bbaa430. [doi: 10.1093/bib/bbaa430] [Medline: 33517357]
48. Yao K, Wang X, Li W, et al. Semi-supervised heterogeneous graph contrastive learning for drug-target interaction prediction. Comput Biol Med 2023 Sep;163:107199. [doi: 10.1016/j.compbiomed.2023.107199] [Medline: 37421738]
49. Itoh T, Tanaka T, Nagai R, et al. Genomic organization and mutational analysis of HERG, a gene responsible for familial long QT syndrome. Hum Genet 1998 Apr;102(4):435-439. [doi: 10.1007/s004390050717] [Medline: 9600240]
50. Chiu PJS, Marcoe KF, Bounds SE, et al. Validation of a [3H]astemizole binding assay in HEK293 cells expressing HERG K+ channels. J Pharmacol Sci 2004 Jul;95(3):311-319. [doi: 10.1254/jphs.fpe0040101] [Medline: 15272206]
51. Yang BF, Xu DH, Xu CQ, et al. Inactivation gating determines drug potency: a common mechanism for drug blockade of HERG channels. Acta Pharmacol Sin 2004 May;25(5):554-560. [Medline: 15132818]
52. Smith JL, Reloj AR, Nataraj PS, et al. Pharmacological correction of long QT-linked mutations in KCNH2 (hERG) increases the trafficking of Kv11.1 channels stored in the transitional endoplasmic reticulum. Am J Physiol Cell Physiol 2013 Nov 1;305(9):C919-C930. [doi: 10.1152/ajpcell.00406.2012] [Medline: 23864605]
53. Yang Y, Li G, Li D, Zhang J, Hu P, Hu L. Integrating fuzzy clustering and graph convolution network to accurately identify clusters from attributed graph. IEEE Trans Netw Sci Eng 2024;12(2):1112-1125. [doi: 10.1109/TNSE.2024.3524077]

Abbreviations

DruSF: drug compound structure feature extraction module
DTI: drug-target interaction
HAN: Heterogeneous Graph Attention Network
HN: Heterogeneous Network
LLM: large language model
MAT: Molecule Attention Transformer
ProSF: protein sequence feature extraction module.

Edited by Q Jin; submitted 27.03.25; peer-reviewed by D Niu, L Hu, W Lan, Z Wang; revised version received 11.07.25; accepted 25.07.25; published 02.10.25.

Please cite as:
Zhao H, Yao K, Liu Y, Che C, Tang L
Heterogeneous Network With Multiview Path Aggregation: Drug–Target Interaction Prediction Study Design
JMIR Med Inform 2025;13:e74974
URL: https://medinform.jmir.org/2025/1/e74974
doi:10.2196/74974

© Haixue Zhao, Kui Yao, Yunjiong Liu, Chao Che, Lin Tang. Originally published in JMIR Medical Informatics (https://medinform.jmir.org), 2.10.2025. This is an open-access article distributed under the terms of the Creative Commons Attribution License (https://creativecommons.org/licenses/by/4.0/), which permits unrestricted use, distribution, and reproduction in any medium, provided the original work, first published in JMIR Medical Informatics, is properly cited. The complete bibliographic information, a link to the original publication on https://medinform.jmir.org/, as well as this copyright and license information must be included.

XSL•FO
RenderX

Evaluating and Improving Syndrome Differentiation Thinking Ability in Large Language Models: Method Development Study

Chunliang Chen[1]; Xinyu Wang[1]; Ming Guan[1]; Wenjing Yue[1,2], PhD; Yuanbin Wu[1], PhD; Ya Zhou[3], PhD; Xiaoling Wang[1], PhD

[1]East China Normal University, No.3663 Zhongshanbei Road, Shanghai, China

[2]Shanghai Institute of Intelligent Science and Technology, Tongji University, Shanghai, China

[3]Guangxi Key Laboratory of Trusted Software, Guilin University of Electronic Technology, Guilin, China

Corresponding Author:
Xiaoling Wang, PhD
East China Normal University, No.3663 Zhongshanbei Road, Shanghai, China

Abstract

Background: A large language model (LLM) provides new opportunities to advance the intelligent development of traditional Chinese medicine (TCM). Syndrome differentiation thinking is an essential part of TCM and equipping LLMs with this capability represents a crucial step toward more effective clinical applications of TCM. However, given the complexity of TCM syndrome differentiation thinking, acquiring this ability is a considerable challenge for the model.

Objective: This study aims to evaluate the ability of LLMs for syndrome differentiation thinking and design a method to effectively enhance their performance in this area.

Methods: We decomposed the process of syndrome differentiation thinking in TCM into three core tasks: pathogenesis inference, syndrome inference, and diagnostic suggestion. To evaluate the performance of LLMs in these tasks, we constructed a high-quality evaluation dataset, forming a reliable foundation for quantitative assessment of their capabilities. Furthermore, we developed a methodology for generating instruction data based on the idea of an "open-book exam," customized three data templates, and dynamically retrieved task-relevant professional knowledge that was inserted into predefined positions within the templates. This approach effectively generates high-quality instruction data that aligns with the unique characteristics of TCM syndrome differentiation thinking. Leveraging this instruction data, we fine-tuned the base model, enhancing the syndrome differentiation thinking ability of the LLMs.

Results: We collected 200 medical cases for the evaluation dataset and standardized them into three types of task questions. We tested general and TCM-specific LLMs, comparing their performance with our proposed solution. The findings demonstrated that our method significantly enhanced LLMs' syndrome differentiation thinking. Our model achieved 85.7% in Task 1 and 81.2% accuracy in Task 2, surpassing the best-performing TCM and general LLMs by 26.3% and 15.8%, respectively. In Task 3, our model achieved a similarity score of 84.3, indicating that the model was remarkably similar to advice given by experts.

Conclusions: Existing general LLMs and TCM-specific LLMs continue to have significant limitations in the core task of syndrome differentiation thinking. Our research shows that fine-tuning LLMs by designing professional instruction templates and generating high-quality instruction data can significantly improve their performance on core tasks. The optimized LLMs show a high degree of similarity in reasoning results, consistent with the opinions of domain experts, indicating that they can simulate syndrome differentiation thinking to a certain extent. These findings have important theoretical and practical significance for in-depth interpretation of the complexity of the clinical diagnosis and treatment process of TCM.

(JMIR Med Inform 2025;13:e75103) doi:10.2196/75103

KEYWORDS

large language model; traditional Chinese medicine; RAG; instruction tuning; TCM LLMs; syndrome differentiation thinking

Introduction

In recent years, the large language model (LLM) has made significant progress in electronic medical record analysis [1], drug discovery [2], clinical decision support [3], and other medical fields [4,5]. As an important part of the health care system, traditional Chinese medicine (TCM) is known for its unique theoretical framework and complex knowledge system [6]. The LLMs offer better means to explore and understand knowledge from classic texts, prescription data, and clinical cases, laying the foundation for the clinical application of TCM.

The core concept of TCM diagnosis and treatment emphasizes a dynamic treatment strategy based on patient characteristics, which requires the LLMs to have profound medical knowledge

XSL•FO
RenderX

and adaptive reasoning ability. To address the specificity of TCM-domain knowledge, the researchers have tried to improve the model performance through domain fine-tuning by leveraging publicly available datasets, including classical TCM literature, educational materials, and clinical case records [6-8].

Some models have also integrated domain-specific pathology data such as TCM formulas and medical record files to enhance specialization and specificity. For example, BianCang [9] added clinical data on cardiology and used a two-stage training method of injecting domain knowledge and alignment to obtain results. Yang et al [10] developed ZhongJing by leveraging a Chinese multi-turn medical conversation dataset of 70,000 authentic doctor-patient dialogues, enabling the model to better capture the nuances and complexity of clinical communication.

Although existing TCM-specific LLMs demonstrated improved performance in some areas of TCM, their effectiveness in handling complex TCM tasks remains inadequate. This limitation stems from the lack of targeted reasoning training for TCM syndrome differentiation thinking. The highly context-dependent and flexible nature of TCM diagnostic reasoning necessitates a deep understanding of the intricate logic underlying disease patterns, placing higher demands on the model's comprehension and reasoning ability [11,12]. LLMs often struggle with knowledge confusion when confronted with the nuanced reasoning required for TCM syndrome differentiation. For instance, the principle of "different treatments for the same disease" is common in TCM, where varying treatment approaches and herbal prescriptions are recommended for the same condition across different texts. Such inconsistencies in the training data significantly hinder the reasoning ability of LLMs in TCM. It is worth noting that Chain-of-Thought (CoT)–based mechanisms exhibit clear limitations in this field, as the reasoning explanations generated by these models frequently devolve into nonsensical or irrelevant outputs [13]. In contrast, the direct application of Retrieval-Augmented Generation (RAG) can provide accurate contextualized hints derived from professional TCM knowledge [14].

To evaluate the capacity of LLMs for performing TCM syndrome differentiation, we developed three core tasks grounded in the foundational theories of TCM: pathogenesis inference (Task 1), syndrome inference (Task 2), and diagnostic suggestion (Task 3). For the evaluation dataset, we extracted 200 medical cases from *Essence of Modern Chinese Medicine Case Studies* [15] and standardized these cases into the corresponding task formats. Furthermore, we developed a methodology for generating instruction data based on the idea of an "open-book exam." Given each task's unique logic, we designed a specialized data template for each task type. To enhance the model's comprehension of the problem, we extracted relevant information from a local knowledge base and inserted it into predefined positions within the templates. Thus, we generated 800 high-quality instruction samples for fine-tuning the model using this approach. This method of embedding RAG content into instruction data enables the model to better understand contextual information unlike models that directly input RAG content.

Methods

Overview

To enhance the ability of existing LLMs in TCM syndrome differentiation thinking, this study proposed an instruction data generation method based on the idea of an "open-book exam." Open-book exams allow candidates to consult materials during the exam, but only those students who have mastered how to obtain and interpret the answers in advance quickly can cope with them efficiently. Similarly, we treated each type of TCM task as an "open-book exam." Incorporating domain knowledge into the instruction template enhances the LLMs' ability to reason information from the materials, enhancing their performance in TCM tasks. The method consists of three core parts: (1) designing core tasks based on TCM theory; (2) constructing domain-specific instruction data templates for different task categories; and (3) designing an evaluation method to compare and analyze LLMs.

Task Decomposition

According to the TCM pathogenesis theory, the clinical process of TCM syndrome differentiation thinking requires deducing from symptoms to syndromes by analyzing the pathogenesis factors of the surface-level symptoms one-by-one and comparing the relationships between the factors. For clinical application, in addition to analyzing the pathogenesis factors, the patient's judgment also depends on understanding the integrated relationships among these factors. Based on this framework, we have extracted three core tasks: pathogenesis inference, syndrome inference, and diagnostic suggestion. The decomposition of the complex process of TCM identification into clear task modules helps the model in hierarchical analysis of the TCM identification ideas. The three tasks are explained in Table 1.

XSL•FO
RenderX

Table . Comparison of the performance of different models in three tasks.

Task	Explanation	Question format
Task 1: Pathogenesis inference	Pathogenesis refers to the mechanism of disease occurrence, development, change and outcome, including the changes and mechanisms of etiology, nature, location, and course of disease.	Select the most appropriate pathogenesis based on the clinical information. You will choose the most correct answer from options A, B, C, D, E, F, G, H, I, and J. The questions are as follows: "Clinical Information" "Pathogenesis Options"
Task 2: Symptom inference	Symptoms are a pathological summary of the body's overall response to a disease at a particular stage.	Select the most appropriate syndrome based on the clinical information. You will choose the most correct answer from options A, B, C, D, E, F, G, H, I, and J. The questions are as follows: "Clinical Information" "Syndrome Options"
Task 3: Diagnostic suggestion	Diagnostic suggestion forms a comprehensive understanding of the disease's nature. This step emphasizes summarizing the local to the whole and from phenomenon to the essence, thus guiding the formulation of treatment plans.	Write a summary and syndrome differentiation analysis based on the clinical information, core pathogenesis and syndrome. The questions are as follows: "Clinical Information" "Core Pathogenesis" "Core Syndrome"

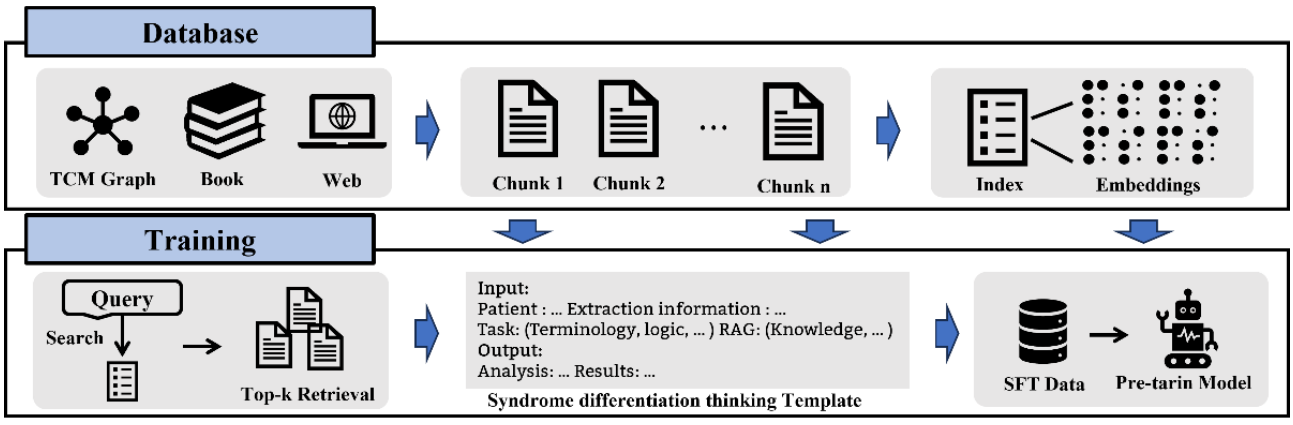
TCM Instruction Data Generation

We treated each TCM task as an open-book exam scenario, where structured domain knowledge is embedded directly into the prompt templates, in a manner similar to the process of simulating a test-taker's responses on an exam. The model was expected to learn to use this information in specific contexts to generate accurate responses.

As illustrated in Figure 1, the local knowledge base was partitioned into distinct segments, referred to as chunks, and vector models were employed to generate embeddings. Let Q denote the question to be addressed. The knowledge base is represented as D={d1,d2, ,dn}, where di corresponds to a chunk of the document. Embeddings for each chunk are generated using a vector model, denoted as E={e1,e2, ,en}. Each chunk embedding is defined as ei=f(di), with f representing the embedding generation function. The similarity matching is established through cosine similarity, defined as follows:

$$sim(ei,Q)=ei\cdot Q \parallel ei \parallel \parallel Q \parallel$$

Figure 1. A framework for generating instruction data is formed by integrating the local knowledge base into the Syndrome Differentiation Thinking Template.



where ·represents the vector norm, and chunks exhibiting the highest similarity are selected to form the matched document set D`:

$$D'=\{di\in D \mid \sim(ej,Q)\geq\theta\}$$

In this expression, θ represents a predefined similarity threshold. The reference knowledge is then integrated into the instructional data I<Input,Output>, thereby enhancing reasoning capabilities across three tasks during practical evaluations. To incorporate domain-specific knowledge into the reasoning process, we introduce a structured template T, parameterized as Input=TQ,D`.

Data Collection

We analyzed 200 medical cases from *Essence of Modern Chinese Medicine Case Studies* [15] and systematically organized the data into categories, including patient demographics, clinical manifestations, tongue and pulse

XSL•FO
RenderX

diagnoses, etiologic factors, and diagnostic examination findings. To ensure data consistency and accuracy, nonessential or irrelevant details were excluded during the extraction process, retaining only critical information related to clinical reasoning. An illustrative example is presented in Textbox 1.

Textbox 1. Example medical case extracted from books.

The patient is a woman, 18-years-old. Sudden decline in vision of both eyes for 10 days, and blindness in the left eye for 3 days. The patient has a dull headache in the forehead, pulling pain behind the eyeball when moving the eye.

Examination: Visual acuity–Right eye 0.02, no light perception in the left eye. Moderate dilation of pupils in both eyes, sluggish light reflex in the right eye, and absence of direct light reflex in the left eye. Intraocular pressure is 18.86 mmHg in both eyes. The optic discs of both eyes are congested, mildly elevated, with blurred boundaries, disappearance of physiological cupping, dilated retinal veins, and mild edema of the retina near the optic disc in the left eye.

Western medical diagnosis: Acute optic neuritis (both eyes)

Examination as per Traditional Chinese medicine: Depressed mood, dizziness, blurred vision, flank pain, bitter taste in the mouth, and chest tightness; the tongue is red with thin yellow coating, and the pulse is wiry

Pattern differentiation: Sudden blindness (both eyes) – type of liver qi stagnation and obstruction of collaterals.

Treatment principle: It is appropriate to soothe the liver and resolve stagnation, and to unblock the channels and invigorate the collaterals. The prescription used is Shugan Mingmu decoction (an empirical formula).

Commentary: Sudden blindness refers to serious internal ocular disorders where the external appearance of the eye seems normal but there is a sudden and drastic decline in vision, or even blindness, in one or both eyes. Although the external appearance of the affected eye shows no obvious abnormalities, various pathological changes occur inside the pupil, and the etiology and pathogenesis are more complex. Due to the acute onset, early treatment should be initiated. In western medicine, various fundus diseases can cause sudden blindness, the most common being central retinal vascular occlusion and acute optic neuritis.

To enable automatic quantitative scoring, Tasks 1 and 2 were designed as multiple-choice questions, with all disease mechanisms and clinical evidence data aggregated into a standardized dataset. The answer options for these questions were generated by randomly permuting the original option set, with distractor options created by systematically rearranging plausible alternatives. While Task 3 was formatted as open-ended questions, answers were derived from source text, with scores calculated via cosine similarity between answer embeddings.

Ethical Considerations

This study used data from published medical records in publicly available literature, which did not involve human subjects or contain personally identifiable information. Accordingly, ethics committee approval was not required.

Experimental Setup

The base model used in this study was InternLM2-Chat2-20B-SFT [16], which has been pretrained on domain-specific knowledge from TCM. This enables the model to effectively address complex medical scenarios and perform basic TCM question-and-answer tasks without requiring further fine-tuning. Text embeddings were generated using Acge-Text-Embedding [17]. For general LLMs, we used the official API interface, while for TCM LLMs, we deployed reasoning locally. Specifically, the experiments were conducted on a single NVIDIA A6000 GPU (48 GB memory). All model weights were publicly available via the Hugging Face Hub. Instruction tuning was performed using the Llama Factory framework [18], with LoRA integration. The hyperparameters were configured with a learning rate=2×10−4 and training epochs set to 5. After fine-tuning, parameter consolidation of the optimized modules was sufficient for deployment.

Results

We establish scoring criteria for each task. For Tasks 1 and 2, scores were calculated using a proportional multiple-choice method, computed as the ratio of correct responses to the total number of options presented. For Task 3, the cosine similarity between the model output and the standard output was determined. The resulting similarity scores were then linearly scaled to a range of 0 - 100, with higher values indicating greater similarity.

As demonstrated in Table 2, our model achieved superior performance across all three tasks, with accuracy rates of 85.7% and 81.2% for Task 1 and Task 2, respectively, and a similarity score of 84.3 for Task 3. In contrast, the powerful general model, ChatGPT4 performed poorly in Task 1 and Task 2, with accuracy rates of only 24.4% and 36.3%, respectively, but achieved a score of 78.2 in Task 3. Task 3 is an open-ended generative task, evaluated using cosine similarity, which emphasizes linguistic fluency and semantic coherence rather than factual accuracy. This evaluation criterion aligns well with ChatGPT-4's strength in generating natural and coherent language, even when its underlying understanding of TCM is limited. In contrast, Tasks 1 and 2 demand a deeper comprehension of specific TCM concepts, where the lack of specialized training in TCM becomes more evident in ChatGPT-4's performance. Additionally, DeepSeek-v3 and Qwen-max demonstrated more balanced performance across multiple tasks, with scores consistently exceeding the range of 50% to 60%, likely due to their targeted training in TCM-related tasks. Our model demonstrates strong advantages in both accuracy and similarity across structured TCM tasks, highlighting its effectiveness in domain-specific reasoning and output generation.

XSL•FO
RenderX

Table . Comparison of the performance scores of different models in three tasks.

Models	Task 1,[a] (%)	Task 2,[b] (%)	Task 3[c] (score)
ChatGPT4 [19]	24.4	36.3	78.2
DeepSeek-v3 [20]	48.8	57.7	53.4
Qwen-max [21]	57.1	63.6	79.7
InternLM3-Latest [22]	53.1	62.5	62.4
ChatGLM4 [23]	36.5	39.5	79.2
Our study	85.7	81.2	84.3

[a]Task 1: Pathogenesis inference.

[b]Task 2: Symptom inference.

[c]Task 3: Diagnostic suggestion.

Discussion

Comparison With Other Works

To better contextualize our proposed TCM LLM, we compare it with four representative models: ShenNong [24], BianCang [9], HuangDi [25], and ZhongJing [10]. These models were selected due to their prominence in the TCM domain, publicly available methodologies, and diverse approaches to integrating TCM knowledge into LLMs. Each model reflects a distinct strategy in data sourcing, architectural design, or application focus, making them suitable benchmarks for evaluating our method. Specifically, ShenNong compiles an extensive dataset of TCM information and generates a knowledge graph, which serves as a benchmark for creating over 110,000 TCM-related instruction data points to train a foundational model. BianCang integrates a vast collection of ancient TCM texts, modern educational materials, and clinical data, offering users precise TCM knowledge quizzes, diagnostic support, and treatment recommendations. HuangDi is built on the Ziya-LLaMA-13B-V1 base model and incorporates TCM textbooks, website data, and other TCM corpora, demonstrating a notable comprehension of TCM knowledge. ZhongJing enhances the model's proficiency in TCM clinical diagnosis and treatment by training it on classical TCM literature.

As demonstrated in Table 3, BianCang outperforms all other TCM LLMs by achieving accuracy rates of 59.3% and 65.4% on Tasks 1 and 2, respectively, and scoring 69.6 on Task 3. Although BianCang benefits from training on case diagnosis data, thereby enhancing its understanding of syndrome differentiation, it still underperforms compared to our proposed solution across all tasks. These results suggest that relying exclusively on domain-specific training data proves inadequate and significantly constrains a model's capacity for TCM reasoning. These results underscore that our approach not only outperforms existing TCM LLMs but also represents a meaningful advancement in the integration of domain knowledge with deeper reasoning capabilities.

Table . Performance comparison of TCM LLMs across multiple tasks.

Models	Task 1,[a] (%)	Task 2,[b] (%)	Task 3,[c] (score)
ShenNong	42.2	53.3	42.8
BianCang	59.3	65.4	69.6
HuangDi	32.4	45.6	52.4
ZhongJing	38.1	36.5	59.6
Our study	85.7	81.2	84.3

[a]Task 1: Pathogenesis inference.

[b]Task 2: Symptom inference.

[c]Task 3: Diagnostic suggestion.

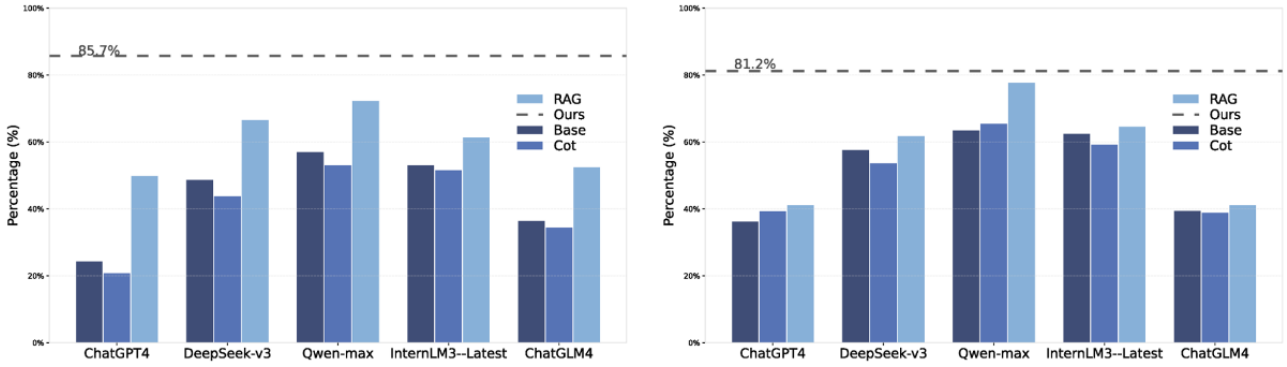
To more systematically evaluate the performance advantages of the proposed method, we also selected two popular LLMs enhancement methods for comparison: CoT, and RAG. Specifically, CoT significantly improves the model's logical reasoning ability in a step-by-step manner by guiding it to gradually generate intermediate reasoning steps, thereby showing higher interpretability and accuracy in complex tasks. On the other hand, RAG expands the model's knowledge coverage and enhances its contextual understanding and domain adaptability by dynamically retrieving and integrating external knowledge during generation. We retained the base model without any enhancement methods as the baseline control group, referred to as Base, to comprehensively measure the relative performance improvements across different methods.

As illustrated in Figure 2, RAG demonstrated significant performance advantages in both Task 1 and Task 2. The accuracy of all models using RAG exceeded that of the Base and CoT setups. With RAG, Qwen-max showed improvements of 15.3% and 14.2% in Tasks 1 and 2, respectively. This indicates that integrating external knowledge enhances the

XSL•FO
RenderX

overall accuracy of model responses. In contrast, the effectiveness of CoT varied significantly depending on the task type and model characteristics. For instance, in Task 2, the performance of some models using CoT is even lower than that of the Base configuration. For example, ChatGPT4's accuracy drops from 39.4% to 36.3%. This decline may be attributed to the increased complexity of Task 2, where relying solely on the model's internal knowledge is insufficient to meet the reasoning demands.

Figure 2. Performance comparison of RAG, CoT, and Base models across Two Tasks; Task 1 pathogenesis inference (left), Task 2 symptom inference (right). CoT: Chain-of-Thought; RAG: Retrieval Augmented Generation.



To explicitly compare the differences between the three methods, we present the results of a case in Task 3, as shown in Figure 3. The ground truth revealed four key conclusions: (1) the condition was attributed to kidney deficiency; (2) kidney deficiency caused weakness in the lower limbs; (3) the condition was identified as wind-induced paralysis; and (4) blood deficiency contributed to the pathology of "wind."

Figure 3. Comparison of results on Task 3: CoT, RAG and our method. CoT: Chain-of-Thought; RAG: Retrieval Augmented Generation.

Mr. xx, male, 45 years old, experienced weakness in his lower limbs and fell to the ground. After walking a few more steps, his limbs feel heavy, and he is prone to falling. He experiences a feeling of soreness and tenderness in the lumbar region; there are no abnormalities on the surface of the lower limbs, and the sense of touch is normal. Prolonged standing makes him feel like he might fall.
Western medical diagnosis: narrowing of the lumbar vertebrae 4 and 5, with compression on the spinal nerves and descending fibers. He was diagnosed with "spinal stenosis."
TCM Examination: Pulse is deep and fine, tongue is dull, and the coating on his tongue is thin and yellow.

Ground Truth: This condition is caused by kidney deficiency. The lower back is the residence of the kidneys, and the spine is the pathway of the Governing Vessel (Du Mai), which is connected to the kidneys. When kidney qi is insufficient, the Governing Vessel also becomes deficient. The lower limbs are linked to the Lesser Yin meridian network, and the Governing Vessel governs the lower limbs. When the Governing Vessel is weak and empty, the lower limbs lose their support, making it easy to fall. In ancient times, this was referred to as "wind-induced paralysis". When blood is deficient, it generates wind, and "Fei" implies dysfunction, thus resulting in weakness and lack of strength in the lower limbs.

CoT: 1: The patient's primary pathological mechanism is insufficiency of kidney qi and internal heat. This serves as the foundation for understanding the symptoms described. Kidney qi plays a vital role in nourishing the lumbar region. 2: When kidney qi is deficient, the lumbar region lacks proper nourishment. This deficiency leads to soreness and weakness in the lower back, which is one of the key symptoms observed. 3: Internal heat is another component of the pathological mechanism. It typically presents with specific signs, such as a thin, yellow tongue coating. This symptom helps confirm the presence of internal heat in the patient.

RAG: The core pathogenesis of this case is insufficiency of kidney qi, stagnation of qi and blood stasis, and internal heat due to blood deficiency. Based on the key pathological mechanism of kidney qi deficiency and liver wind combined with phlegm, the obstruction of the channels by phlegm turbidity leads to impaired circulation of qi and blood, resulting in qi stagnation and blood stasis. This causes a pattern of lower extremity weakness and upper body symptoms, giving rise to the manifestations of "wind-induced paralysis".

Ous: The chief complaint and clinical manifestations of this patient correspond with the description of "wind-induced paralysis". Combined with the patient's pulse and tongue signs, the condition can be differentiated as insufficiency of kidney qi and wind generated from blood deficiency. The treatment approach should focus on tonifying the kidney and boosting qi, nourishing the blood to calm the wind, while also resolving phlegm and unblocking the orifices, with the aim of restoring limb function.

In the CoT results, the model erroneously inferred the irrelevant factor 'internal heat.' This discrepancy may stem from the limitations of LLMs' knowledge, which cannot fully support the accurate processing of complex dialectical reasoning tasks. On the other hand, most of the conclusions from RAG align with the ground truth. But the method incorrectly proposed the diagnosis of 'blood stasis,' which may be attributed to the increased complexity of the context. Our method successfully derived all key conclusions and effectively mitigated reasoning biases caused by insufficient knowledge, excessive contextual complexity, and challenges faced by other methods.

Limitations and Future Research

The approach proposed in this paper demonstrates significant advantages in TCM syndrome differentiation thinking. However, there remains room for further refinement when addressing highly intricate and dynamic scenarios in TCM diagnosis and treatment. While the current knowledge base draws extensively from classical literature and clinical case studies, potential biases in coverage may exist. This bias stems from the fact that the literature tends to reflect the medical understanding and insights of the time, which may not be fully compatible with the contemporary clinical context or with different patient

XSL•FO
RenderX

populations. In addition, some aspects of diagnostic experience favor specific diagnostic and treatment methods, which can limit their applicability and accuracy in real-world clinical decision-making. Expanding the knowledge base by integrating updated clinical data and interdisciplinary insights could further enhance the LLMs' ability. Future research should explore dynamic task decomposition strategies to deepen the LLMs' understanding and improve its adaptability to the nuances of TCM theories.

Conclusions

In conclusion, this study presents an innovative methodology integrating RAG with instruction fine-tuning to enhance LLMs' syndrome differentiation thinking ability. Our approach achieved state-of-the-art performance in three core tasks: pathogenesis inference, syndrome inference, and diagnostic suggestion, outperforming both general and TCM LLMs. These findings underscore the importance of incorporating domain-specific knowledge and structured task decomposition to address the unique challenges of TCM reasoning. Although the proposed framework demonstrates significant potential, further advancements are necessary to handle complex, dynamic scenarios and improve conversational abilities.

Acknowledgments

This work was supported by NSFC grant (No. 62477014, No. 62136002), Ministry of Education Research Joint Fund Project (8091B042239), and Shanghai Trusted Industry Internet Software Collaborative Innovation Center.

Conflicts of Interest

None declared.

References

1. Ge J, Li M, Delk MB, Lai JC. A comparison of a large language model vs manual chart review for the extraction of data elements from the electronic health record. Gastroenterology 2024 Apr;166(4):707-709. [doi: 10.1053/j.gastro.2023.12.019] [Medline: 38151192]
2. Pal S, Bhattacharya M, Islam MA, Chakraborty C. ChatGPT or LLM in next-generation drug discovery and development: pharmaceutical and biotechnology companies can make use of the artificial intelligence-based device for a faster way of drug discovery and development. Int J Surg 2023 Dec 1;109(12):4382-4384. [doi: 10.1097/JS9.0000000000000719] [Medline: 37707542]
3. Mu Y, He D. The potential applications and challenges of ChatGPT in the medical field. Int J Gen Med 2024;17:817-826. [doi: 10.2147/IJGM.S456659] [Medline: 38476626]
4. Chang Y, Yin JM, Li JM, Liu C, Cao LY, Lin SY. Applications and future prospects of medical LLMs: a survey based on the M-KAT conceptual framework. J Med Syst 2024 Dec 27;48(1):112. [doi: 10.1007/s10916-024-02132-5] [Medline: 39725770]
5. Zhang S, Wang W, Pi X, He Z, Liu H. Advances in the application of traditional Chinese medicine using artificial intelligence: a review. Am J Chin Med 2023;51(5):1067-1083. [doi: 10.1142/S0192415X23500490] [Medline: 37417927]
6. Hua R, Dong X, Wei Y, et al. Lingdan: enhancing encoding of traditional Chinese medicine knowledge for clinical reasoning tasks with large language models. J Am Med Inform Assoc 2024 Sep 1;31(9):2019-2029. [doi: 10.1093/jamia/ocae087] [Medline: 39038795]
7. Dai Y, Shao X, Zhang J, et al. TCMChat: a generative large language model for traditional Chinese medicine. Pharmacol Res 2024 Dec;210:107530. [doi: 10.1016/j.phrs.2024.107530] [Medline: 39617279]
8. Tan Y, Zhang Z, Li M, et al. MedChatZH: a tuning LLM for traditional Chinese medicine consultations. Comput Biol Med 2024 Apr;172:108290. [doi: 10.1016/j.compbiomed.2024.108290] [Medline: 38503097]
9. BianCang: a traditional Chinese medicine large language model. 2024. URL: https://github.com/QLU-NLP/BianCang-TCM-LLM
10. Yang S, Zhao H, Zhu S, et al. Zhongjing: enhancing the Chinese medical capabilities of large language model through expert feedback and real-world multi-turn dialogue. AAAI 2024;38(17):19368-19376. [doi: 10.1609/aaai.v38i17.29907]
11. Chen Z, Zhang D, Liu C, et al. Traditional Chinese medicine diagnostic prediction model for holistic syndrome differentiation based on deep learning. Integr Med Res 2024 Mar;13(1):101019. [doi: 10.1016/j.imr.2023.101019] [Medline: 38298865]
12. Jiang M, Lu C, Zhang C, et al. Syndrome differentiation in modern research of traditional Chinese medicine. J Ethnopharmacol 2012 Apr 10;140(3):634-642. [doi: 10.1016/j.jep.2012.01.033] [Medline: 22322251]
13. Wei J, Wang X, Schuurmans D, et al. Chain-of-thought prompting elicits reasoning in large language models. Presented at: NIPS'22: 36th International Conference on Neural Information Processing Systems; Nov 22 to Dec 9, 2022; New Orleans, LA p. 1800. [doi: 10.5555/3600270.3602070]
14. Lewis P, Perez E, Piktus A, et al. Retrieval-augmented generation for knowledge-intensive NLP tasks. arXiv 2020;33:9459-9474. [doi: 10.48550/arXiv.2005.11401]
15. Jianhua D. Essence of Modern Chinese Medicine Case Studies 2002.

XSL•FO
RenderX

16. InternLM 20B chat SFT model. Hugging Face. 2024. URL: http://huggingface.co/internlm/internlm2-chat-20b-sft [accessed 2025-06-12]
17. Acge_text_embedding model. GitHub. 2024. URL: https://github.com/intsig-textin/acge_text_embedding [accessed 2025-06-12]
18. LlamaFactory: unified efficient fine-tuning of 100+ language models. GitHub. 2025. URL: https://github.com/hiyouga/LLaMA-Factory
19. ChatGPT4. 2024. URL: https://www.openai.com [accessed 2025-06-12]
20. DeepSeek. 2025. URL: https://www.deepseek.com [accessed 2025-06-12]
21. DashScope. 2025. URL: https://dashscope.aliyun.com [accessed 2025-06-12]
22. InternLM. 2025. URL: https://chat.intern-ai.org.cn/ [accessed 2025-06-12]
23. ChatGLM4. 2024. URL: https://open.bigmodel.cn/ [accessed 2025-06-12]
24. ShenNong-TCM: a traditional Chinese medicine large language model. GitHub. 2023. URL: https://github.com/michael-wzhu/ShenNong-TCM-LLM [accessed 2025-03-17]
25. Construction of the Huang-Di large model. GitHub. 2023. URL: https://github.com/Zlasejd/HuangDI [accessed 2025-03-17]

Abbreviations

CoT: Chain-of-Thought
LLMs: large language models
RAG: Retrieval Augmented Generation
TCM: traditional Chinese medicine

Edited by L Luo, Q Jin; submitted 28.03.25; peer-reviewed by J Ning, W Mu; revised version received 20.05.25; accepted 24.05.25; published 20.06.25.

Please cite as:
Chen C, Wang X, Guan M, Yue W, Wu Y, Zhou Y, Wang X
Evaluating and Improving Syndrome Differentiation Thinking Ability in Large Language Models: Method Development Study
JMIR Med Inform 2025;13:e75103
URL: https://medinform.jmir.org/2025/1/e75103
doi:10.2196/75103

© Chunliang Chen, Xinyu Wang, Ming Guan, Wenjing Yue, Yuanbin Wu, Ya Zhou, Xiaoling Wang. Originally published in JMIR Medical Informatics (https://medinform.jmir.org), 20.6.2025. This is an open-access article distributed under the terms of the Creative Commons Attribution License (https://creativecommons.org/licenses/by/4.0/), which permits unrestricted use, distribution, and reproduction in any medium, provided the original work, first published in JMIR Medical Informatics, is properly cited. The complete bibliographic information, a link to the original publication on https://medinform.jmir.org/, as well as this copyright and license information must be included.

XSL•FO
RenderX

Hypertension Medication Recommendation via Synergistic and Selective Modeling of Heterogeneous Medical Entities: Development and Evaluation Study of a New Model

Ke Zhang[1], MS; Zhichang Zhang[1], PhD; Yali Liang[1], MS; Wei Wang[1], MS; Xia Wang[2], BS

[1]College of Computer Science and Engineering, Northwest Normal University, 967 Anning East Road, Lanzhou, China

[2]Gansu Provincial Hospital, Lanzhou, China

Corresponding Author:
Zhichang Zhang, PhD
College of Computer Science and Engineering, Northwest Normal University, 967 Anning East Road, Lanzhou, China

Abstract

Background: Electronic health records (EHRs) contain comprehensive information regarding diagnoses, clinical procedures, and prescribed medications. This makes them a valuable resource for developing automated hypertension medication recommendation systems. Within this field, existing research has used machine learning approaches, leveraging demographic characteristics and basic clinical indicators, or deep learning techniques, which extract patterns from EHR data, to predict optimal medications or improve the accuracy of recommendations for common antihypertensive medication categories. However, these methodologies have significant limitations. They rarely adequately characterize the synergistic relationships among heterogeneous medical entities, such as the interplay between comorbid conditions, laboratory results, and specific antihypertensive agents. Furthermore, given the chronic and fluctuating nature of hypertension, effective medication recommendations require dynamic adaptation to disease progression over time. However, current approaches either lack rigorous temporal modeling of EHR data or fail to effectively integrate temporal dynamics with interentity relationships, resulting in the generation of recommendations that are not clinically appropriate due to the neglect of these critical factors.

Objective: This study aims to overcome the challenges in existing methods and introduce a novel model for hypertension medication recommendation that leverages the synergy and selectivity of heterogeneous medical entities.

Methods: First, we used patient EHR data to construct both heterogeneous and homogeneous graphs. The interentity synergies were captured using a multihead graph attention mechanism to enhance entity-level representations. Next, a bidirectional temporal selection mechanism calculated selective coefficients between current and historical visit records and aggregated them to form refined visit-level representations. Finally, medication recommendation probabilities were determined based on these comprehensive patient representations.

Results: Experimental evaluations on the real-world datasets Medical Information Mart for Intensive Care (MIMIC)-III v1.4 and MIMIC-IV v2.2 demonstrated that the proposed model achieved Jaccard similarity coefficients of 58.01% and 55.82%, respectively; areas under the curve of precision-recall of 83.56% and 80.69%, respectively; and F_1-scores of 68.95% and 64.83%, respectively, outperforming the baseline models.

Conclusions: The findings indicate the superior efficacy of the introduced model in medication recommendation, highlighting its potential to enhance clinical decision-making in the management of hypertension. The code for the model has been released on GitHub.

(JMIR Med Inform 2025;13:e74170) doi:10.2196/74170

KEYWORDS

hypertension medication recommendation; electronic health records; heterogeneous graph; multihead graph attention mechanism; time series selective mechanism

Introduction

Background

Hypertension represents a prevalent chronic condition and serves as a significant contributor to cardiovascular mortality, making timely pharmacological intervention for blood pressure management crucial [1]. With the increasing trend of an aging population, the growing number of patients with hypertension has placed a significant burden on health care systems [2]. Consequently, automated medication recommendation systems for hypertension have been developed.

XSL•FO
RenderX

Prior Work and Limitations

Early hypertension medication recommendation methods were primarily rule-based. For example, Wu and Xie [3] developed a hypertension ontology and reasoning rules to recommend appropriate antihypertensive medications to patients. However, these methods relied only on predefined rules and a limited set of case data, neglecting other critical patient information, which resulted in recommendations that lacked flexibility and personalization. In recent years, numerous neural network models for recommending hypertension medications based on electronic health records (EHRs) have been proposed [4,5]. These models have shown improved outcomes and effectively address many limitations inherent in earlier algorithms.

Nevertheless, the complexity of EHR data continues to present significant challenges for medication recommendation tasks, particularly in 2 critical areas: insufficient synergy among heterogeneous medical entities and neglect of temporal dynamics in the patient's condition.

Insufficient Synergy Among Heterogeneous Medical Entities

EHR data contains heterogeneous but interrelated medical entities—such as diagnoses, procedures, and medications—that jointly influence treatment outcomes. For example, a diagnosis indicates a patient's health status, which subsequently informs procedure and medication decisions. Effective modeling of such cross-entity relationships is essential for generating accurate and personalized treatment recommendations.

Existing approaches like Multilevel Medical Embedding (MiME) [6] and graph convolutional transformer (GCT) [7] attempt to model medical concepts and their causal relations using homogeneous graph structures. However, these structures fail to capture the inherent heterogeneity across EHR entities. The Heterogeneous Information Network for Medical Diagnosis (HeteroMed) [8] introduces semantic associations via metapaths, but it does not model dynamic interentity interactions. CausalMed [9] explores causal inferences between treatment elements but overlooks the reinforcement between medications and procedures. Graph transformers of bidirectional encoder representations from transformers on EHRs (GT-BEHRT) [10] integrates graph transformers with temporal modeling yet does not incorporate contextual synergy among entities.

Further, current models inadequately balance efficacy and safety. For instance, Graph-Augmented Memory Networks (GAMENet) [11] uses a drug-drug interaction (DDI) graph to reduce adverse effects but does not consider diagnostic and procedural inputs. Graph-augmented bidirectional encoder representations from transformers (G-BERT) [12] extends to multientity modeling yet omits DDI-aware safety metrics. Competitive neural network (CompNet) [13] faces issues with computational efficiency and model stability on large-scale datasets. Recent work like that by Yang et al [14] (using medication molecular structure graphs) and Li et al [15] (using contrastive learning) enhance representation power, but they still lack a unified mechanism for modeling both "multientity synergy" and "safety constraints."

Neglect of Temporal Dynamics in the Patient's Condition

As a chronic disease, hypertension evolves over time. In clinical practice, treatment strategies are often adjusted based on both current and historical visit data. Hence, capturing the temporal dynamics of the patient's condition is essential for effective medication recommendation.

Several studies have addressed sequential modeling. Yang et al [16] used dual medical sequences to represent medication history but did not account for intersequence relationships. Liu et al [17] developed 3 long short-term memory (LSTM) variants to model correlations across medical sequences but failed to consider the immediate influence of current clinical status. Although models like the Reverse Time Attention model (RETAIN) [18] use attention mechanisms to prioritize relevant historical visits and An et al [19] introduced hierarchical temporal modeling, these methods primarily focus on general temporal behavior without consideration for hypertension-specific patterns like long-term management or phased treatment adjustment.

Advanced designs have attempted to improve modeling capabilities. Le et al [20] used a memory-enhanced neural network to represent long-term dependencies, while Yang et al [21] adopted a residual mechanism to capture patient status transitions. Wu et al [22] introduced a transformer with a "copy-generate" mechanism to decide whether to reuse previous prescriptions. However, none of these methods fully addresses the task-specific temporal dynamics required for hypertension medication recommendations.

Objective and Contributions

To address the aforementioned limitations, this study proposed CSRec, a novel hypertension medication recommendation framework that integrates the synergistic interactions of heterogeneous medical entities with selective modeling of temporal progression. CSRec is designed to capture cross-entity synergies through both heterogeneous and homogeneous graph construction based on EHR data, model time-aware patient representations using a temporal selectivity module that weighs current versus historical visits, and enhance safety by incorporating DDI information in the recommendation process.

The primary contributions of this paper are summarized in the following paragraphs.

We propose a novel medication recommendation model, named CSRec, specifically designed for hypertension treatment. CSRec effectively integrates the synergistic interactions and selective characteristics among diverse medical entities. By constructing a heterogeneous medical entity graph derived from EHRs, our model utilizes a graph attention mechanism to generate enhanced collaborative embeddings among medical entities. Additionally, a temporal selection mechanism was incorporated to simulate hypertension progression, thereby producing a comprehensive patient representation to facilitate accurate medication recommendations.

To better capture synergistic relationships between medical entities, we innovatively modified the traditional graph attention

XSL•FO
RenderX

network (GAT) to focus more on neighboring node information, thus obtaining a more aggregated representation of the principal nodes.

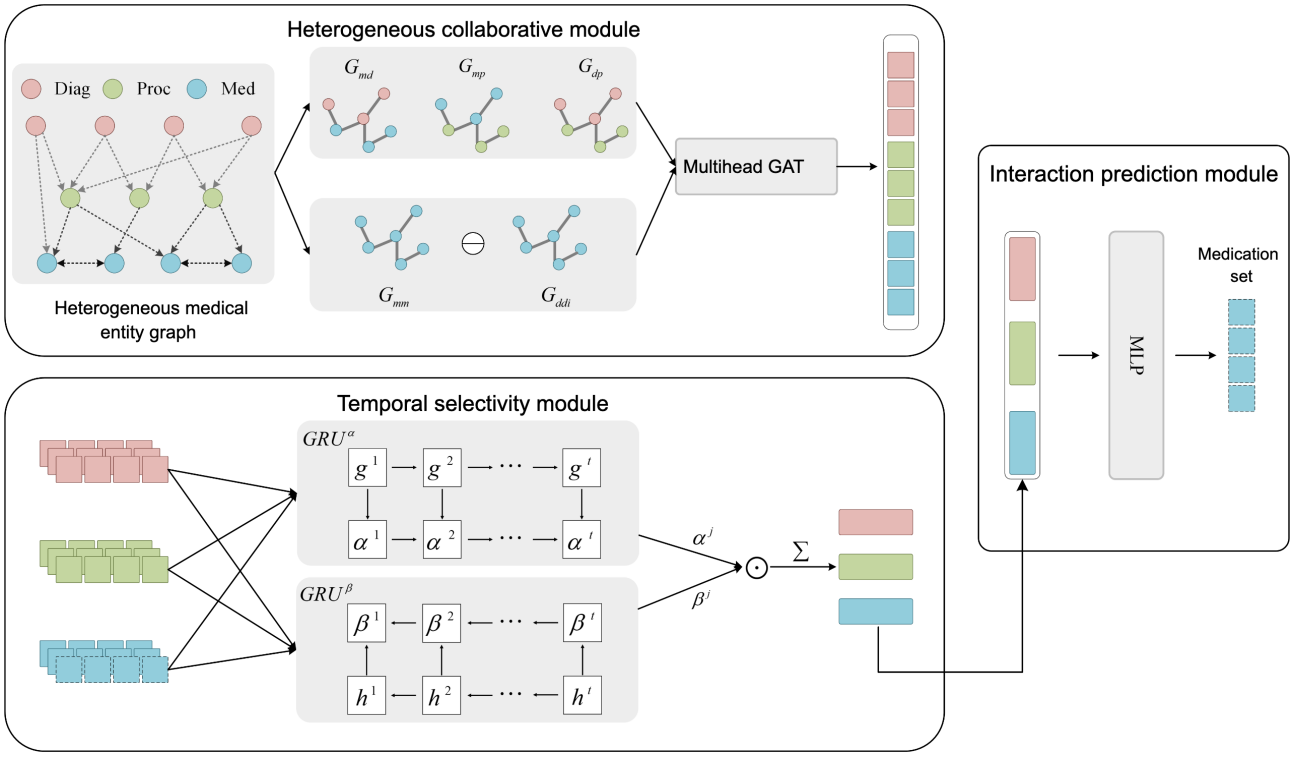
Extensive experiments on the publicly available datasets Medical Information Mart for Intensive Care (MIMIC)-III [23] and MIMIC-IV [24] were conducted to validate the superiority and effectiveness of our proposed method.

Methods

Overview

In this section, we present a comprehensive description of the CSRec model's structure. As depicted in Figure 1, our model comprises 3 core modules for end-to-end hypertension medication recommendations: (1) The Heterogeneous Collaborative Module, with heterogeneous and homogeneous graph networks, learns entity-level representations by aggregating collaboration patterns between medical entities, which are then passed to the Temporal Selectivity Module; (2) the Temporal Selectivity Module, using a bidirectional selection mechanism, processes these entity-level representations to calculate relevance coefficients between current and previous visits, generating visit-level entity representations that are transmitted to the Interaction Prediction Module; and (3) the Interaction Prediction Module concatenates these visit-level entity representations to enrich entity information, forming a patient representation. This is converted into medication recommendation probabilities, with medications exceeding a threshold output as results.

Figure 1. The framework of CSRec. Diag: diagnosis; GAT: graph attention network; GRU: gated recurrent unit; Med: medication; MLP: multilayer perceptron; Proc: procedures.



Problem Formulation

Electronic Health Records

EHRs encompass a variety of medical visit information collected from patients. For a specific patient, EHRs can be structured into a sequence comprising multiple clinical visit records, represented as V=V1,V2, ,VT, where Vt represents the t-th visit and T indicates the total number of visits for that patient. Specifically, each clinical visit Vt can be represented as Vt=Vdt,Vpt,Vmt, in which Vdt∈ 0,1D, Vpt∈ 0,1P, and Vmt∈ 0,1M represent multihot encoded vectors corresponding to diagnosis, procedures, and medications, respectively. Here, the notation indicates the total number of distinct categories within each respective medical entity type.

Heterogeneous Medical Entities

In this paper, distinct medications were modeled as medication entities. Each medication recorded in the EHR corresponds to a unique medication entity, identified by a specific identifier denoted as m1,m2, , and each entity is independently embedded within the model using embeddings of identical dimensionality. Likewise, diagnoses and procedures were categorized into diagnostic entities and procedural entities, respectively. Collectively, these 3 categories of entities were termed heterogeneous medical entities.

Hypertension Medication Recommendation

Based on the patient's current diagnostic information Vdt, procedural data Vpt, historical visit sequence V=V1,V2, ,VT−1, and heterogeneous medical entity graph G, the model recommends appropriate antihypertensive medications y^t∈ 0,1M to the patient.

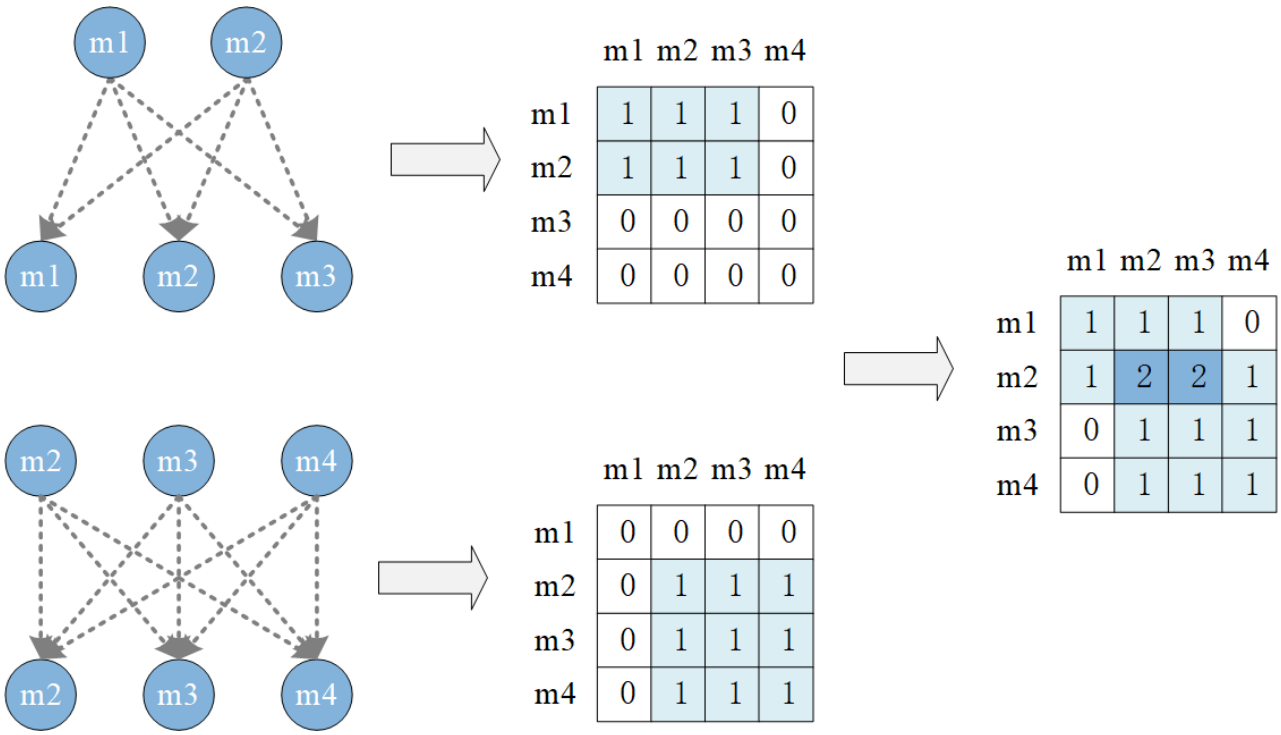
XSL•FO
RenderX

Heterogeneous Collaborative Module

For a specific patient, we first constructed a medication homogeneous graph, which was explicitly designed to characterize relationships between medications and provide a foundation for subsequent cross-entity modeling. This graph comprised 2 components, both of which take medications as the sole node type.

One component is the medication collaboration graph Gmmt−1=Mt−1,Amm, which serves to capture the patterns of combined medication use in clinical practice. Specifically, Mt−1 denotes the collection of all prescribed medications from the patient's previous visits, and Amm signifies the adjacency matrix representing collaborative interactions among medications. Each entry within this adjacency matrix indicates the initial collaboration weight between the respective medication nodes. The detailed procedure for generating this matrix is illustrated in Figure 2. Initially, Amm is set as a zero matrix. If medication i and medication j co-occur during a specific visit, then Ai,j=1; if medication i and j co-occur across multiple visits, the corresponding value in Amm is incremented, with higher values indicating stronger collaboration between the medications.

Figure 2. The medication-medication synergy matrix construction process.



Each medication node m∈ Mt−1 in the graph corresponds to its initial embedding vector, expressed as:

(1)em=Vmt−1Em

Specifically, Em refers to the embedding matrix associated with medication entities. The selector vector Vmt−1 specifically extracts the relevant embedding from Em for the medication at the previous time step t-1.

Moreover, some medications may have harmful interactions (DDI) and should be avoided when used together. To address this, we integrated the medication collaboration graph Gmm with the medication safety graph Gddi , enhancing the comprehensive representation of the medication nodes. Notably, the methodology used to construct the medication safety graph Gddi closely mirrors that of Gmm. Specifically, we used Addi as the adjacency matrix, where Addii,j=1 signifies that the i-th and j-th medications exhibit a paired harmful medication interaction.

(2)Gm=Gmm−λGddi

Subsequently, we adopted a GAT-based graph neural approach to obtain embeddings for medication nodes within the medication graph Gm.

First, we utilized the attention mechanism to calculate the attention coefficients between a node and its neighbors, followed by normalization:

(3)αij(m)=expgijm∑k∈ Ni(m)expgikm

Here, gijm=LeakyℜLUβmThim // hjm denotes the output of the LeakyReLU activation function applied to the linear transformation of the concatenated feature vectors himand hjm, parameterized by the learnable weight vector βm. The notation Ni(m) represents the neighboring node set of node mi in the graph Gm, while // signifies the vector concatenation operation.

Second, we used the calculated attention coefficients to perform weighted aggregation of neighbor nodes, thereby obtaining the representation of node mi:

(4)eim=σ∑j∈ Nimγijmhjm

To overcome the limitations posed by single-view attention, we further introduced a multihead attention mechanism, using a linear layer to map node representations into multiple subspaces,

XSL•FO
RenderX

then aggregate representations under each subspace. Formally, this operation is expressed as:

(5)eim=// h=1Hσ∑j∈ Nimhγijmhhjmh

In this equation, H denotes the total number of attention heads, the superscript h indicates the current attention head index, and // represents concatenating outputs from different heads. Through this strategy, distinct node-specific information is captured across various dimensions and integrated from multiple subspaces, thereby significantly improving the precision and robustness of the learned node representations.

During the training process, each medication entity is updated according to the aforementioned steps, resulting in an aggregated representation of the medication set Vm=vm1,vm2, vmt−1.

Similarly, to capture the unique clinical relationships of hypertension, such as the interactions between comorbidities, long-term monitoring data, and combination therapy dynamics, we defined 3 heterogeneous complete graphs: diagnosis-procedure graph Gdpt=Dt,Pt,Adp, medication-diagnosis graph Gmdt=Mt−1,Dt,Amd, and medication-procedure graph Gmpt=Mt−1,Pt,Amp. This established an association model that is crucial for accurate hypertension medication recommendations but has low correlation with other medication categories. Following a similar learning approach to the medication graph Gm, we first initialized the diagnosis and procedure nodes in the 3 heterogeneous graphs.

(6)ed=VdtEd,ep=VptEp

Using the approach outlined in equations (3)-(5), we then learned from the diagnosis-procedure graph to obtain aggregated sets of diagnosis codes Vd=vd1,vd2, vdt and procedure nodes Vp=vp1,vp2, vpt.

Finally, based on the aggregated medication nodes from the medication graph Gm and the learned diagnosis and procedure nodes from the diagnosis-procedure graph Gdp, we learned from the medication-diagnosis graph Gmd and the medication-procedure graph Gmp, updating to obtain entity-level representations of the medication, diagnosis, and procedure sets:

VD={Vd1,Vd2, Vdt}

VP={Vp1,Vp2, Vpt}

(7)VM={Vm1,Vm2, Vmt−1}

It is noteworthy that this study used a multihead GAT mechanism to learn and update nodes within the graph. Although traditional GAT models consider intrinsic features and aggregate neighboring features, our proposed heterogeneous graph-based method places greater emphasis on enhancing the embeddings of medications, diagnoses, and procedures by explicitly modeling interactions among diverse medical entities. Consequently, our model focuses more intensively on neighboring nodes to prevent excessive node information merging. To this end, we modified the standard GAT approach to explicitly focus on information derived from neighboring nodes within the heterogeneous graph learning process.

Temporal Selectivity Module

To effectively model the temporal evolution of patient health conditions, this paper introduces a bidirectional temporal selection mechanism using gated recurrent units (GRUs), with 3 key innovations that distinguish it from conventional applications.

First, we adopted a bidirectional temporal architecture to capture multiscale temporal dependencies. Specifically, we first used GRUα to learn the diagnostic sequence, generating forward diagnostic selection coefficients that emphasize the impact of historical visits on current states (eg, past hypertensive crisis records influencing present medication titration):

(8)g1,g2, ,gt=GRUdαVd1,Vd2, ,Vdt

(9)αj=tanhWαgj+bα,j=1, ,t

Concurrently, a backward GRUβ was used in the reverse temporal order to learn the diagnostic sequence, generating backward selection coefficients at different time steps that highlight recent critical changes. For example, recent fluctuations in blood pressure require immediate therapeutic adjustment. This bidirectional design enhances computational stability while overcoming the limitations of unidirectional GRUs or traditional recurrent neural networks (RNNs), which often overlook either long-term or short-term temporal cues:

(10)ht,ht−1, ,h1=GRUdβVdt,Vdt−1, ,Vd1

(11)βj=tanhshrinkWβhj+bβ,j=t, ,1

Second, we proposed an adaptive selection coefficient integration strategy. Based on the generated bidirectional diagnostic selection coefficients, we can capture key visit information and entity information within the visit sequence, rather than relying on static aggregation methods. This allowed us to capture key visit information and entity interactions, thereby obtaining a diagnostic representation that integrates historical context with current needs:

(12)dt=∑j=1tαjβj⊙Vdj

Third, leveraging GRU's inherent advantages, our design achieved computational efficiency without sacrificing performance. Compared with traditional RNNs, GRU effectively mitigates gradient vanishing issues; relative to LSTMs, its simplified gating mechanism reduces parameter complexity by avoiding redundant memory cells, resulting in faster training efficiency, a critical advantage for handling large-scale longitudinal EHR data in medication recommendation tasks. After a series of similar processing steps, we obtained the patient's final procedural and medication representations.

(13)pt=∑j=1tαjβj⊙Vpj,mt−1=∑j=1t−1αjβj⊙Vmj

Interaction Prediction Module

Based upon the outputs generated by the aforementioned modules, for the patient's t-th visit, we concatenated the medical entity sequence to make medication recommendations:

(14)yt=σ([dt;pt;mt−1])

In our approach, the medication recommendation task is formulated as a multilabel classification problem [25,26]. To address the complexities and potential imbalances in medical

XSL•FO
RenderX

datasets, we used a comprehensive strategy during model training. We enhanced the model's generalization capabilities and mitigated overfitting through the use of regularization techniques, which limit the complexity of the parameters learned. Additionally, an early-stopping mechanism was implemented to curtail training based on validation set performance. To optimize parameters, we used the Adam optimization algorithm [27], which minimizes the binary cross-entropy loss function to promote efficient and stable model convergence.

$$(15)L=-\sum t=1T\sum i=1|M|yitlog\ y\hat{}it+(1-yit)log\ (1-y\hat{}it)$$

Ethical Considerations

This study made use of the standardized, publicly available MIMIC-III and MIMIC-IV datasets from the Massachusetts Institute of Technology [23,24] and was therefore deemed exempt from ethical approval requirements. Prior to their release, these datasets underwent comprehensive ethical review and privacy protection processes conducted by the data provider (Massachusetts Institute of Technology). These processes included deidentifying all personally identifiable information in patients' EHRs, such as names, hospital admission numbers, and dates of birth. Additionally, the datasets' usage license explicitly covers secondary analysis scenarios for academic research, eliminating the need for users to obtain additional ethical approval independently. Since this study did not involve independent collection of human subject data and solely relied on the aforementioned publicly available and compliant existing datasets for secondary analysis, we do not possess separate ethical approval documents to provide. The ethical approval statement is published on the official website of the data provider [23,24], and we can be contacted to obtain the original copy of the datasets' usage license.

Results

Dataset Description

Our experiments were conducted using the MIMIC-III v1.4 and MIMIC-IV v2.2 datasets provided by the Massachusetts Institute of Technology. The datasets comprise medical records collected from patients admitted to intensive care units, such as diagnoses, procedures, and medications. The diagnostic and procedural information uses the *International Classification of Diseases, Ninth Revision* (*ICD-9*) coding system. To study medication recommendations for patients with hypertension, this paper extracted relevant data from the aforementioned datasets based on the *ICD-9* hypertension codes under the guidance of clinical experts. Meanwhile, referring to previous research norms [4,21,22], patients who completed at least two visits were included, and medications with a frequency <2000 occurrences were excluded.

During data analysis, we observed that the number of frequently used antihypertensive medications was relatively limited and the recommendations based on overly broad Anatomical Therapeutic Chemical (ATC) categories often lacked the specificity needed for precise clinical decision-making. Given the systematic medication classification framework of the ATC classification system, this study overcame the limitation of previous studies that only focused on the ATC04 level for recommendation. It not only predicted the medication categories at the ATC04 level (such as C02A, anti-adrenergic medications with central effects) but also further refined to the specific medication types at the ATC05 level (such as C02AA, reserpine-like medications).

After data extraction, we carried out meticulous preprocessing. We normalized features to standardize the scale of different variables, which prevented certain features from dominating others during model training. Moreover, we selectively chose variables most relevant to hypertension medications. Finally, the preprocessed dataset was partitioned into training, validation, and testing subsets according to a ratio of 23:16:16.

Detailed information about the dataset used in the experiments and examples from patients are shown in Table 1 and Table 2.

XSL•FO
RenderX

Table . Detailed information for the experimental datasets, by Anatomical Therapeutic Chemical (ATC)–level encoding.

Item	MIMIC-III[a]		MIMIC-IV	
	ATC04	ATC05	ATC04	ATC05
Patients, n	3115	3109	19,609	19,609
Visits, n	7308	7263	55,239	55,236
Diagnoses, n	1966	1965	2000	2000
Procedures, n	1145	1145	5488	5488
Medications, n	14	18	14	18
Number of visits, mean	2.3460	2.3361	2.8169	2.8169
Number of diagnoses, mean	10.8927	10.9262	9.3666	9.3666
Number of procedures, mean	4.0463	4.0609	2.5492	2.5492
Number of medications, mean	1.5508	1.4400	1.0804	1.1352

[a]MIMIC: Medical Information Mart for Intensive Care.

Table . Samples from electronic health records.

Sub_ID	Hadm_ID	Diagnoses (Anatomical Therapeutic Chemical code)	Procedures	Medications
10001217	24597018	3240, 3484, 3485, 5180, 340, 04109, 3051, 4019, V168,V161	139, 331, 3897	HydrALAzine, LeVETirac-etam, Vancomycin ,Bisacodyl, Meropenem,…
10001217	27703517	3240, 3485, 340, 04102, 04184, 4019, 3051	139	HydrALAzine, Van-comycin, Meropenem, Bisacodyl, Lidocaine,…

Evaluation Metrics

To validate the effectiveness of CSRec, the evaluation metrics described in the following sections were used.

Jaccard Similarity Coefficient

A higher Jaccard coefficient reflects greater overlap between the predicted medication set and the actual medication set.

(16)Jaccard=1T∑t=1T|yt∩y^t||yt∪y^t|

Area Under the Curve of Precision-Recall

A high area under the curve of precision-recall (PRAUC) indicates that the model recommends appropriate medications while keeping a low error rate.

(17)Δℜcallitalic(i)t=ℜcallitalic(i)t−ℜcallitalic(i−1)t

(18)PRAUC=1T∑t=1T∑i=1|M|Precisionitalic(i)tΔℜcallitalic(i)t

F_1-Score

The elevated F_1-score metric in medication recommendations signifies an optimal equilibrium between minimizing false negatives and maintaining classification specificity.

(19)Precisiont=|yt∩y^t||y^t|, Recallt=|yt∩y^t||yt|

(20)F1=1T∑t=1T2×Precisiont×ℜcalltPrecisiont+ℜcallt

DDI Rate

A lower DDI rate ensures that the recommended combination of medications is safer in clinical practice.

(21)DDI=1T∑t=1T∑j=1|y^t|∑j=i+1|y^t|1{Adjy^it,y^jt}∑j=1|y^t|∑j=i+1|y^j|1

Comparative Models

The following baseline models were selected for comparison with the proposed CSRec:

- Logistic regression (LR) uses L2 regularization.
- Ensemble of classifier chains (ECC) [28] enhances predictions by connecting multiple classifiers, typically applied to multilabel classification scenarios for performance optimization.
- RETAIN [18] implements bidirectional temporal attention architecture designed for sequential clinical prediction tasks like treatment recommendation.
- Learn to Prescribe (LEAP) [29] uses RNNs to extract meaningful representations during current medical visits and generate medication sequences.
- Dual memory neural computer (DMNC) [20] incorporates dual-memory neural components to model asynchronous therapeutic pattern interactions.
- GAMENet [11] adopts graph-based memory architecture combining medication interaction knowledge and querying longitudinal EHR data for medication retrieval.
- MICRON [21] analyzes EHR temporal dynamics to adaptively optimize medication combinations upon symptom evolution.
- SafeDrug [16] evaluates molecular-level medication-patient compatibility to suggest safer therapeutic regimens.

XSL•FO
RenderX

- COGNet [22] implements medication copy or predict strategy integrating historical effective prescriptions into current recommendations.
- MoleRec [14] predicts medication mechanisms and interactions via molecular-patient relationships for personalized, safer recommendations.
- CausalMed [9] identifies medical entity causal relationships via causal discovery, accounting for dynamic health condition differences to generate causally linked recommendations.

Performance Comparison

In this section, we conducted an extensive comparative analysis between CSRec and the previously described baseline medication recommendation models to evaluate its effectiveness. Experimental results on the MIMIC-III v1.4 and MIMIC-IV 2.2 datasets are shown in Table 3 ("↑" indicates a preference for larger values, "↓" indicates a preference for smaller values).

XSL•FO
RenderX

Table . The comparison of experimental results on datasets of Anatomical Therapeutic Chemical (ATC)04 and ATC05 codes.

Model	Jaccard similarity coefficient↑[a]		PRAUC↑[b]		F_1-score↑		DDI↓[c,d]	
	ATC04	ATC05	ATC04	ATC05	ATC04	ATC05	ATC04	ATC05
MIMIC-III[e]								
LR[f]	0.5203	0.4919	0.8117	0.7726	0.6347	0.5972	0.2951	0.3569
ECC[g]	0.5438	0.5056	0.8278	0.7846	0.6593	0.6127	0.3012	0.3979
RETAIN[h]	0.5540	0.5210	0.8143	0.7874	0.6783	0.6449	0.3921	0.5068
LEAP[i]	0.5228	0.5082	0.6346	0.6162	0.6405	0.6217	0.2627	0.3648
DMNC[j]	0.5342	0.5097	0.8225	0.7696	0.6463	0.6277	0.2365	0.2615
GAMENet[k]	0.5497	0.5169	0.8239	0.7861	0.6710	0.6308	0.2366	0.4199
MICRON	0.5352	0.5146	0.8285	0.7884	0.6423	0.6145	0.2357	0.2658
SafeDrug	0.5474	0.5063	0.8252	0.7764	0.6484	0.6146	0.2329[l]	0.1975[l]
COGNet	0.5325	0.5075	0.7972	0.7762	0.6448	0.6167	0.2902	0.3587
MoleRec	0.5501	0.5189	0.8261	0.7825	0.6716	0.6299	0.2709	0.3491
CausalMed	0.5626	0.5340	0.8226	0.7877	0.6741	0.6394	0.2340	0.2679
CSRec	0.5801[l]	0.5534[l]	0.8356[l]	0.8123[l]	0.6895[l]	0.6602[l]	0.2351	0.2663
MIMIC-IV								
LR	0.4248	0.3518	0.7426	0.6873	0.5125	0.4315	0.2821	0.2734
ECC	0.4389	0.3779	0.7498	0.6923	0.5305	0.4624	0.3064	0.3047
RETAIN	0.5349	0.5045	0.7964	0.7641	0.6356	0.6008	0.3431	0.3197
LEAP	0.4186	0.3884	0.5047	0.4683	0.5326	0.4932	0.0104[l]	0.0506[l]
DMNC	0.5139	0.4787	0.7678	0.7277	0.5392	0.5094	0.2801	0.2792
GAMENet	0.5151	0.4738	0.7781	0.7326	0.6069	0.5662	0.2884	0.3050
MICRON	0.4297	0.3716	0.7543	0.7056	0.5151	0.4431	0.2866	0.2557
SafeDrug	0.5173	0.4767	0.7770	0.7313	0.6109	0.5648	0.3084	0.3255
COGNet	0.5087	0.4568	0.7448	0.7009	0.5948	0.5502	0.3261	0.3835
MoleRec	0.5275	0.4838	0.7624	0.7267	0.6262	0.5801	0.2733	0.2993
CausalMed	0.5440	0.5225	0.7812	0.7509	0.6412	0.6099	0.2677	0.2855
CSRec	0.5582[l]	0.5307[l]	0.8069[l]	0.7655[l]	0.6483[l]	0.6195[l]	0.2760	0.2931

[a]↑ indicates a preference for larger values.

[b]PRAUC: area under the curve of precision-recall.

[c]DDI: drug-drug interaction.

[d]↓ indicates a preference for smaller values.

[e]MIMIC: Medical Information Mart for Intensive Care.

[f]LR: logistic regression.

[g]ECC: ensemble of classifier chains.

[h]RETAIN: Reverse Time Attention model.

[i]LEAP: Learn to Prescribe.

[j]DMNC: dual memory neural computer.

[k]GAMENet: Graph-Augmented Memory Networks.

[l]Optimal data.

After detailed analysis, we observed several key findings, as described in the following paragraphs.

The CSRec model proposed in this paper outperformed most comparative models across multiple evaluation metrics, fully

XSL•FO
RenderX

demonstrating its significant effectiveness in hypertension medication recommendation.

LR and ECC performed poorly, primarily because these methods only focus on the patient's current clinical condition, neglecting the influence of historical medical data on present treatment decisions. In contrast, the model presented in this paper, along with RETAIN, GAMENet, and other models integrating longitudinal medical histories, performed better, highlighting the importance of capturing historical medical information in hypertension medication recommendations.

In comparison with longitudinal models such as RETAIN, GAMENet, and COGNet, CSRec maintained superior performance, with a particularly notable enhancement in Jaccard scores. This superiority can be attributed to 2 core architectural advancements. The Temporal Selectivity Module enables accurate simulation of patient disease progression by assigning enhanced weights to clinically critical historical information, thereby ensuring that recommendations adhere to consistent clinical reasoning frameworks. Meanwhile, the Heterogeneous Collaborative Module facilitates effective capture of synergistic relationships among heterogeneous medical entities (diagnoses, procedures, medications), enabling the identification of medication combinations that are clinically coherent and reflective of real-world coprescription patterns. Collectively, these innovations augment the degree of overlap between recommended and actually prescribed medications, as empirically validated by the elevated Jaccard index.

Although the CSRec model introduced in this study does not achieve the highest score on the DDI metric, it still ranks as suboptimal. This is mainly because the best performing LEAP model only considers the patient's present health status, resulting in the recommendation of fewer medications and consequently yielding the lowest DDI scores.

Ablation Study

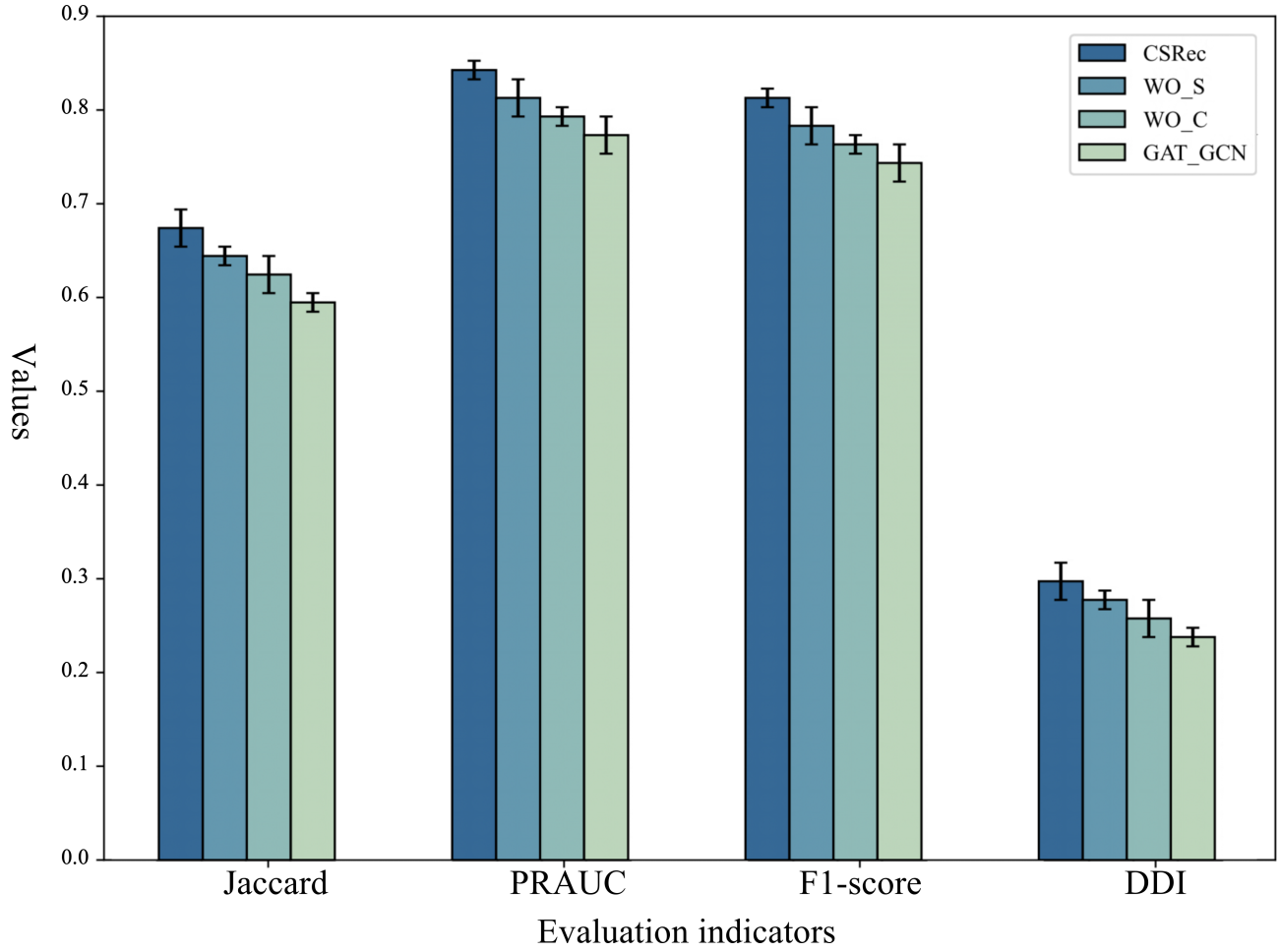
To systematically assess the contribution and validity of each module within CSRec, ablation experiments were conducted on MIMIC-IV by comparing CSRec with its variants:

- WO_S removes the selection module based on the cyclic mechanism.
- WO_C removes the collaborative module based on the heterogeneous graph.
- GAT_GCN replaces the multihead GAT in the collaborative module with a graph convolutional network (GCN).

The results displayed in Figure 3 indicate that the performance of CSRec declined when any module is removed or replaced, demonstrating that each component of CSRec is indispensable. The observed performance drops in evaluation metrics (Jaccard, PRAUC, F_1-score, and DDI) can be attributed to the unique functional roles of each module: The collaborative module effectively modeled the correlations between different medical events during each visit, and its removal (WO_C) led to incomplete capture of event associations, resulting in a decrease in recommendation accuracy as medical entity representations lost contextual relevance. The selective module globally modeled the patient's historical medical data, and its absence (WO_S) caused the model to fail at emphasizing critical time points in disease progression, leading to a decline in metrics as the temporal continuity of hypertension development was disrupted. When replacing multihead GAT with GCN (GAT_GCN), the loss of the attention mechanism resulted in insufficient differentiation of important medical entity relationships, reducing recommendation precision compared with the original model as convolutional operations cannot dynamically weight heterogeneous graph information.

XSL•FO
RenderX

Figure 3. The ablation study of different components. DDI: drug-drug interaction; GAT_GCN: variant replacing the multihead graph attention network in the collaborative module with a graph convolutional network; Jaccard: Jaccard similarity coefficient; PRAUC: area under the curve of precision-recall; WO_C: variant removing the collaborative module based on the heterogeneous graph; WO_S: variant removing the selection module based on the cyclic mechanism.



Additionally, this study further explored the impact of different types of collaborative medical entity information (diagnosis-medication, procedure-medication, diagnosis-procedure, and medication-medication) on hypertension medication recommendations. The variants were designed as follows:

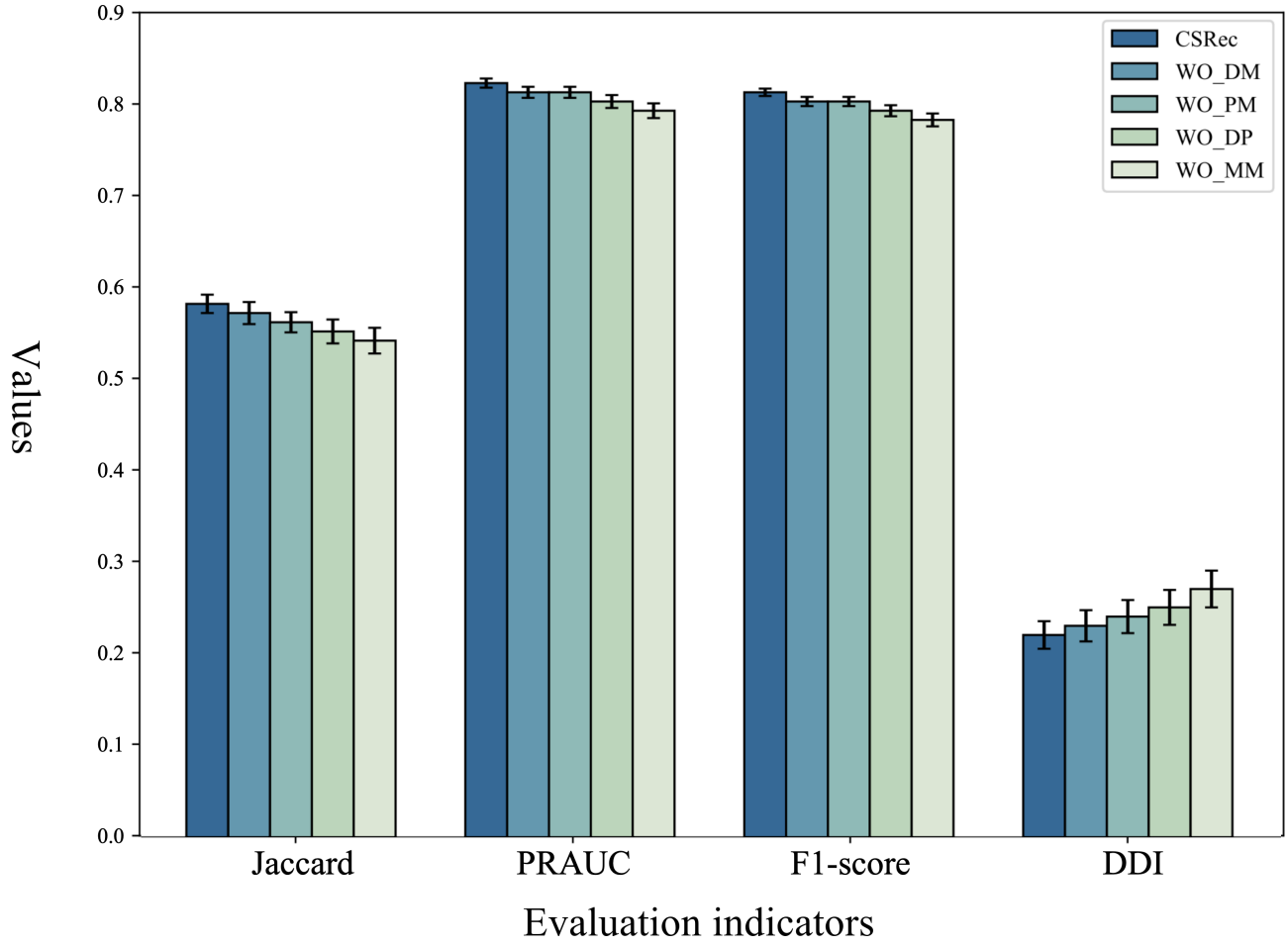
- WO_DM removes diagnosis-medication interaction information.
- WO_PM removes procedure-medication interaction information.
- WO_DP removes diagnosis-procedure interaction information.
- WO_MM removes medication co-occurrence and interaction information.

As illustrated in Figure 4, CSRec's performance decreased when any single type of collaborative medical entity information (WO_DM, WO_PM, WO_DP) was removed, confirming the strong correlation between such information and the medication recommendation task. The specific decline in metric degree corresponded to the clinical relevance of each information type: Removing diagnosis-medication interactions (WO_DM) reduced metrics, as diagnostic information directly guides first-line hypertension medication selection. The WO_PM group's drop stemmed from lost procedure-related medication adjustments (eg, postinterventional anticoagulation needs). For WO_DP, the decline reflects disrupted diagnosis-procedure logical chains that inform therapeutic medication choices.

Notably, removing medication co-occurrence and interaction information (WO_MM) caused a significant decline in the DDI risk rate of the medication recommendation performance. This substantial change is explained by the frequent use of combination therapy in hypertension management. Without medication interaction data, the model cannot avoid contraindicated medication pairs, while the loss of co-occurrence patterns reduces the accuracy of synergistic medication recommendations. This underscores the essential role of medication co-occurrence and DDI information for ensuring hypertension treatment efficacy and safety.

XSL•FO
RenderX

Figure 4. The ablation study of different medical entities. DDI: drug-drug interaction; Jaccard: Jaccard similarity coefficient; PRAUC: area under the curve of precision-recall; WO_DM: variant removing diagnosis-medication interaction information; WO_DP: variant removing diagnosis-procedure interaction information; WO_MM: variant removing medication co-occurrence and interaction information; WO_PM: variant removing procedure-medication interaction information.



Parameter Sensitivity

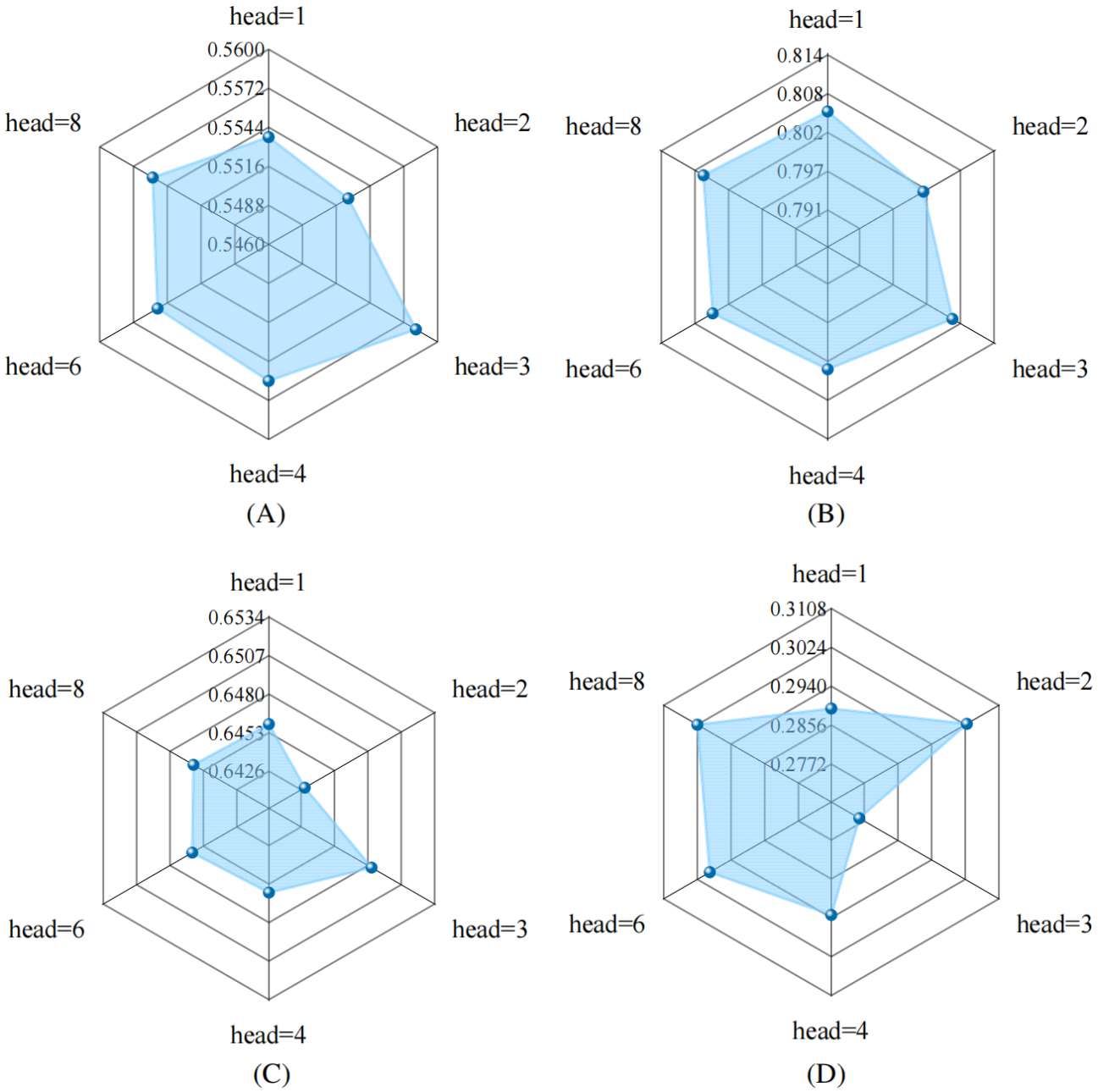
In order to investigate how varying the number of attention heads in the multihead graph attention mechanism within the heterogeneous collaborative module impacted model efficacy, multiple experiments were conducted on the MIMIC-IV dataset. The outcomes of these experiments, comparing different head counts, are presented in Figure 5.

A setting of 3 attention heads (head=3) achieved optimal performance. Consequently, this configuration (head=3) was adopted consistently throughout the remaining experiments in this study. Moreover, the experimental results illustrated that variations in the number of attention heads led to minimal performance differences, highlighting the stability and reliability of the proposed model.

Furthermore, to investigate the impact of the number of included hypertension medications on model performance, we conducted a sensitivity analysis by varying the minimum occurrence threshold for medication inclusion from 500 to 3000. The number of medications ranged from 26 (≥500) to 9 (≥3000).

XSL•FO
RenderX

Figure 5. The effect of different numbers of heads in the multihead graph attention network (GAT), as measured using (A) the Jaccard similarity coefficient, (B) area under the curve of precision-recall (PRAUC), (C) F_1-score, and (D) drug-drug interaction (DDI) rate.



As shown in Table 4, performance across all 4 metrics—Jaccard, PRAUC, F_1-score, and DDI—remained remarkably stable, with only marginal fluctuations. Notably, the best performance was observed at the 2000 threshold, which is used in our paper. This finding supported our design choice and indicated that our framework remained robust even under different medication inclusion criteria, alleviating concerns regarding limited sample size. In addition, setting a lower threshold introduced lower-frequency medications that may lack sufficient clinical representation, potentially compromising the statistical reliability of training. Thus, the current configuration struck a reasonable trade-off between medication variety and prediction stability.

XSL•FO
RenderX

Table . Sensitivity analysis of the medication frequency threshold.

Minimum medication occurrence	Medications, n	Jaccard similarity coefficient↑[a]	PRAUC↑[b]	F_1-score↑	DDI↓[c,d]
≥500	26	0.5531	0.7983	0.6428	0.2847
≥1000	20	0.5554	0.8027	0.6456	0.2802
≥1500	17	0.5576	0.8049	0.6471	0.2781
≥2000	14	0.5582[e]	0.8069[e]	0.6483[e]	0.2760[e]
≥2500	12	0.5568	0.8051	0.6475	0.2766
≥3000	9	0.5560	0.8050	0.6452	0.2764

[a]↑ indicates a preference for larger values.

[b]PRAUC: area under the curve of precision-recall.

[c]DDI: drug-drug interaction.

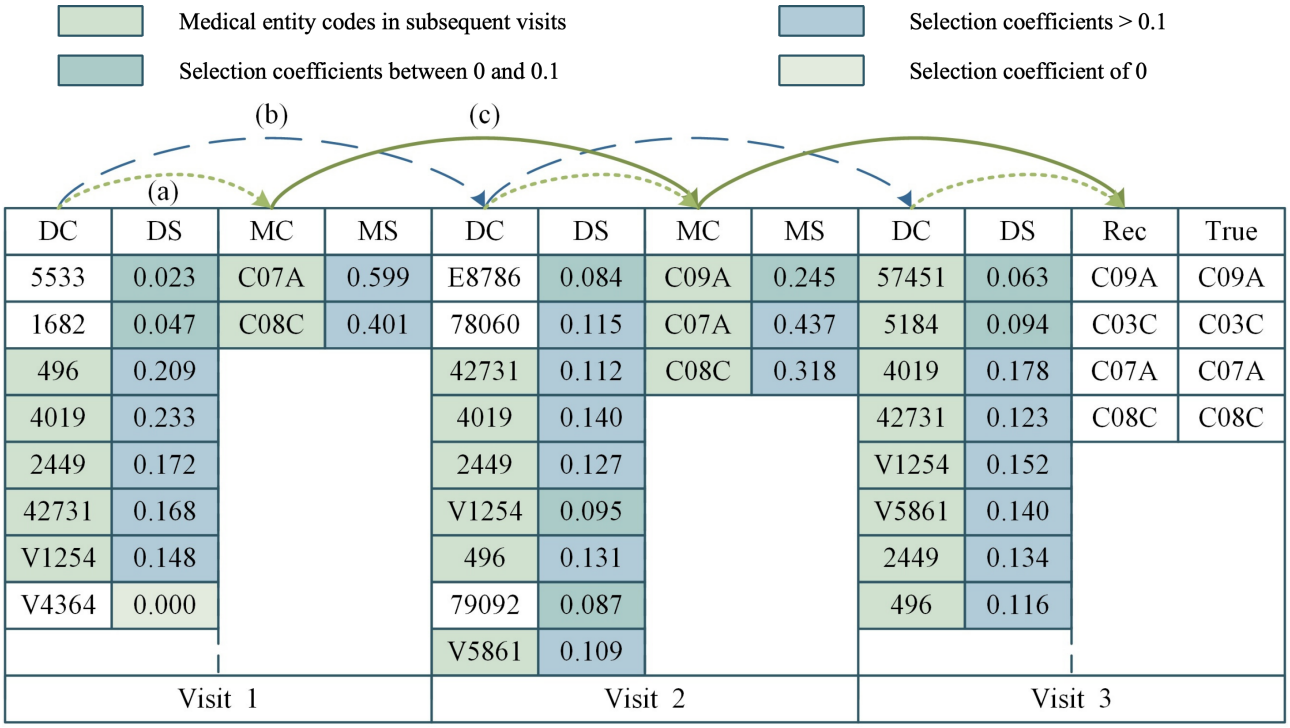
[d]↓ indicates a preference for smaller values.

[e]Optimal data.

Case Study

To visualize and validate our core innovations, which included heterogeneous collaborative interaction modeling and the temporal selectivity mechanism, we randomly selected a patient from the test set of the MIMIC-IV dataset for a case study. Taking diagnosis and medication entities as examples, the entire learning process is shown in Figure 6.

Figure 6. Case study. DC: diagnosis code; DS: diagnosis selection coefficient; MC: medication code; MS: medication selection coefficient; Rec: recommended medication; True: prescribed medication.



Initially, in the collaborative process (a), the model's collaborative interaction mechanism was showcased: In the visit-specific level, the model dynamically enhanced the integration of diagnostic information into medication recommendation reasoning by assigning context-aware interaction weights to the interplays between diagnostic codes (DC column) and medication codes (MC column). For the first visit of the illustrative patient, the DC column encompasses comorbidity-related codes, including chronic obstructive pulmonary disease (*ICD-9*: 496), hypothyroidism (*ICD-9*: 2449), atrial fibrillation (*ICD-9*: 42731), and a documented history of cardiovascular disease (*ICD-9*: V1254), while the MC column includes hypertension-targeted agents such as selective β1-receptor blockers (ATC-04: C07A) and dihydropyridine calcium channel blockers (ATC-04: C08C). This aligns with our innovation of capturing disease-specific collaborative patterns, evident in the consistently higher selection coefficients for hypertension-related diagnostic codes in each DC column, which prioritizes the disease context critical for hypertension treatment.

XSL•FO
RenderX

Furthermore, to demonstrate our temporal selectivity mechanism, the case study highlights how the model captures longitudinal EHR dependencies. Given hypertension's chronic nature, recommended medications depend on both current (third visit) diagnoses (DC column) and historical data. As shown in step (b), diagnostic codes from previous visits received higher selection coefficients, while step (c) reveals that historical medication codes were similarly prioritized. This reflects our model's ability to dynamically weight temporal information, addressing the evolving nature of hypertension and representing an advantage over static models.

Discussion

This paper presents the CSRec model for hypertension medication recommendation, which is based on the collaboration and selection of heterogeneous medical entities. By effectively capturing relationships among diverse medical entities and combining the temporal evolution characteristics of clinical entities, the model provides more precise and effective medication guidance for hypertension treatment. Future research will focus on 3 main areas: (1) in-depth exploration of the multilabel imbalance problem existing in the current method, (2) further investigation of the model's performance in addressing the cold-start problem, and (3) exploration of recommendations regarding medication dosages and medication types.

Acknowledgments

This research is supported by the Industrial Support Program of Colleges and Universities in Gansu Province (number 2025CYZC-010); National Natural Science Foundation of China (number 62163033); Talent Innovation and Entrepreneurship Project of Lanzhou, China (number 2021-RC-49); Natural Science Foundation of Gansu Province, China (numbers 22JR5RA145, 21JR7RA781, and 21JR7RA116); and Major Research Project Incubation Program of Northwest Normal University, China (number NWNU-LKZD2021-06). The funding agencies did not participate in the study design, data gathering and analysis, decision-making regarding publication, nor manuscript preparation.

Data Availability

The code for the model is available on GitHub [30].

Conflicts of Interest

None declared.

References

1. Hypertension Branch of Chinese Geriatrics Society, Beijing Hypertension Association, National Clinical Research Center of the Geriatric Diseases, Hua Q, Fan L, Wang ZW, Li J. 2023 guideline for the management of hypertension in the elderly population in China. J Geriatr Cardiol 2024 Jun 28;21(6):589-630. [doi: 10.26599/1671-5411.2024.06.001] [Medline: 38973827]
2. The Writing Committee of the Report on Cardiovascular Health and Diseases in China. Interpretation of report on cardiovascular health and diseases in China 2022. Chin J Cardiovasc Med 2023;28(4):297-312. [doi: 10.12114/j.issn.1007-9572.2023.0408]
3. Wu H, Xie HW. Research on hypertension diagnosis and treatment system based on ontology and CBR. Comput Appl Softw 2013;30(12):155-159. [doi: 10.3969/j.issn.1000-386x.2013.12.041]
4. Li X, Liang SP, Hou YL, Ma TF. StratMed: relevance stratification between biomedical entities for sparsity on medication recommendation. Knowl Based Syst 2024 Jan;284:111239. [doi: 10.1016/j.knosys.2023.111239]
5. Zhang HJ, Yang X, Bai L, Liang JY. Enhancing drug recommendations via heterogeneous graph representation learning in EHR networks. IEEE Trans Knowl Data Eng 2024;36(7):3024-3035. [doi: 10.1109/TKDE.2023.3329025]
6. Choi E, Xiao C, Stewart WF, Sun J. MiME: multilevel medical embedding of electronic health records for predictive healthcare. Presented at: 32nd International Conference on Neural Information Processing Systems; Dec 3-8, 2018 URL: https://dl.acm.org/doi/10.5555/3327345.3327366 [accessed 2025-09-25]
7. Choi E, Xu Z, Li Y, et al. Learning the graphical structure of electronic health records with graph convolutional transformer. AAAI 2020;34(1):606-613. [doi: 10.1609/aaai.v34i01.5400]
8. Hosseini A, Chen T, Wu W, et al. HeteroMed: heterogeneous information network for medical diagnosis. Presented at: 27th ACM International Conference on Information and Knowledge Management; Oct 22-26, 2018. [doi: 10.1145/3269206.3271805]
9. Li X, Liang S, Lei Y, et al. CausalMed: causality-based personalized medication recommendation centered on patient health state. Presented at: CIKM '24: The 33rd ACM International Conference on Information and Knowledge Management; Oct 21-25, 2024. [doi: 10.1145/3627673.3679542]

XSL•FO
RenderX

10. Poulain R, Beheshti R. Graph transformers on EHRs: better representation improves downstream performance. Presented at: The Twelfth International Conference on Learning Representations; May 7-11, 2024 URL: https://openreview.net/forum?id=pe0Vdv7rsL [accessed 2025-10-12]
11. Shang JY, Xiao C, Ma TF, Li HY, Sun JM. GAMENet: graph augmented memory networks for recommending medication combination. Proc AAAI Conf Artif Intell 2019;33(1):1126-1133. [doi: 10.1609/aaai.v33i01.33011126]
12. Shang JY, Ma TF, Xiao C, Sun JM. Pre-training of graph augmented transformers for medication recommendation. Presented at: Twenty-Eighth International Joint Conference on Artificial Intelligence; Aug 10-16, 2019. [doi: 10.24963/ijcai.2019/825]
13. Liang X, Yang JY, Lu GM, Zhang D. CompNet: competitive neural network for palmprint recognition using learnable gabor kernel. IEEE Signal Process Lett 2021;28:1739-1743. [doi: 10.1109/LSP.2021.3103475]
14. Yang N, Zeng K, Wu Q, Yan J. MoleRec: combinatorial drug recommendation with substructure-aware molecular representation learning. Presented at: WWW '23: The ACM Web Conference 2023; Apr 30 to May 4, 2023. [doi: 10.1145/3543507.3583872]
15. Li XW, Zhang YJ, Li XB, Wei H, Lu MY. DGCL: distance-wise and graph contrastive learning for medication recommendation. J Biomed Inform 2023 Mar;139:104301. [doi: 10.1016/j.jbi.2023.104301]
16. Yang C, Xiao C, Ma F, Glass L, Sun J. SafeDrug: dual molecular graph encoders for recommending effective and safe drug combinations. Presented at: Thirtieth International Joint Conference on Artificial Intelligence; Aug 19-27, 2021. [doi: 10.24963/ijcai.2021/514]
17. Liu SC, Wang XL, Xiang Y, Xu H, Wang H, Tang BZ. Multi-channel fusion LSTM for medical event prediction using EHRs. J Biomed Inform 2022 Mar;127:104011. [doi: 10.1016/j.jbi.2022.104011]
18. Choi E, Bahadori MT, Kulas JA, Schuetz A, Stewart WF, Sun JM. RETAIN: an interpretable predictive model for healthcare using reverse time attention mechanism. Presented at: 30th International Conference on Neural Information Processing Systems (NIPS'16); Dec 5-10, 2016 URL: https://dl.acm.org/doi/10.5555/3157382.3157490 [accessed 2025-09-25] [doi: 10.5555/3157382.3157490]
19. An Y, Zhang L, You M, Tian XQ, Jin B, Wei XP. MeSIN: multilevel selective and interactive network for medication recommendation. Knowl Based Syst 2021 Dec;233:107534. [doi: 10.1016/j.knosys.2021.107534]
20. Le H, Tran T, Venkatesh S. Dual memory neural computer for asynchronous two-view sequential learning. Presented at: KDD '18: The 24th ACM SIGKDD International Conference on Knowledge Discovery and Data Mining; Aug 19-23, 2018. [doi: 10.1145/3219819.3219981]
21. Yang CQ, Xiao C, Glass L, Sun JM. Change matters: medication change prediction with recurrent residual networks. Presented at: Thirtieth International Joint Conference on Artificial Intelligence; Aug 19-27, 2021. [doi: 10.24963/ijcai.2021/513]
22. Wu R, Qiu ZP, Jiang JC, Qi GL, Wu X. Conditional generation net for medication recommendation. Presented at: WWW '22: The ACM Web Conference 2022; Apr 25-29, 2022. [doi: 10.1145/3485447.3511936]
23. Johnson AEW, Pollard TJ, Shen L, et al. MIMIC-III, a freely accessible electronic health record dataset. Sci Data 2016;3:160035. [doi: 10.1038/sdata.2016.35]
24. Johnson AEW, Bulgarelli L, Shen L, et al. MIMIC-IV, a freely accessible electronic health record dataset. Sci Data 2023 Jan 3;10(1):1. [doi: 10.1038/s41597-022-01899-x] [Medline: 36596836]
25. Zhao D, Shi YL, Cheng L, Li H, Zhang LG, Guo HM. Time interval uncertainty-aware and text-enhanced based disease prediction. J Biomed Inform 2023 Mar;139:104239. [doi: 10.1016/j.jbi.2022.104239] [Medline: 36356933]
26. Nguyen MV, Nguyen DT, Trinh QH, Le B. ALGNet: attention light graph memory network for medical recommendation system. Presented at: SOICT 2023: The 12th International Symposium on Information and Communication Technology; Dec 7-8, 2023. [doi: 10.1145/3628797.3628983]
27. Kingma DP, Ba J. Adam: a method for stochastic optimization. arXiv. Preprint posted online on Dec 22, 2014. [doi: 10.48550/arXiv.1412.6980]
28. Read J, Pfahringer B, Holmes G, Frank E. Classifier chains for multi-label classification. Mach Learn 2011;85:333-359. [doi: 10.1007/978-3-642-04174-7_17]
29. Zhang YT, Chen R, Tang J, Stewart W, Sun JM. LEAP: learning to prescribe effective and safe treatment combinations for multimorbidity. Presented at: KDD '17: The 23rd ACM SIGKDD International Conference on Knowledge Discovery and Data Mining; Aug 13-17, 2017. [doi: 10.1145/3097983.3098109]
30. Zk0814/csrec. GitHub. URL: https://github.com/zk0814/CSRec [accessed 2025-09-18]

Abbreviations

ATC: Anatomical Therapeutic Chemical
CompNet: competitive neural network
DDI: drug-drug interaction
DMNC: dual memory neural computer
ECC: ensemble of classifier chains
EHR : electronic health record

XSL•FO
RenderX

G-BERT: graph-augmented bidirectional encoder representations from transformers
GAMENet: Graph-Augmented Memory Networks
GAT: graph attention network
GCN: graph convolutional network
GCT: graph convolutional transformer
GRU: gated recurrent unit
GT-BEHRT: graph transformers of bidirectional encoder representations from transformers on EHRs
HeteroMed: Heterogeneous Information Network for Medical Diagnosis
***ICD-9*:** *International Classification of Diseases, Ninth Revision*
LEAP: Learn to Prescribe
LR: logistic regression
LSTM: long short-term memory
MiME: Multilevel Medical Embedding
MIMIC: Medical Information Mart for Intensive Care
PRAUC: area under the curve of precision-recall
RETAIN: Reverse Time Attention model
RNN: recurrent neural network

Edited by L Luo, Q Jin; submitted 19.03.25; peer-reviewed by H Lu, Q Zhu, S Liang; revised version received 27.08.25; accepted 28.08.25; published 25.11.25.

Please cite as:
Zhang K, Zhang Z, Liang Y, Wang W, Wang X
Hypertension Medication Recommendation via Synergistic and Selective Modeling of Heterogeneous Medical Entities: Development and Evaluation Study of a New Model
JMIR Med Inform 2025;13:e74170
URL: https://medinform.jmir.org/2025/1/e74170
doi:10.2196/74170

© Ke Zhang, Zhichang Zhang, Yali Liang, Wei Wang, Xia Wang. Originally published in JMIR Medical Informatics (https://medinform.jmir.org), 25.11.2025. This is an open-access article distributed under the terms of the Creative Commons Attribution License (https://creativecommons.org/licenses/by/4.0/), which permits unrestricted use, distribution, and reproduction in any medium, provided the original work, first published in JMIR Medical Informatics, is properly cited. The complete bibliographic information, a link to the original publication on https://medinform.jmir.org/, as well as this copyright and license information must be included.

XSL•FO
RenderX

Leveraging Retrieval-Augmented Large Language Models for Dietary Recommendations With Traditional Chinese Medicine's Medicine Food Homology: Algorithm Development and Validation

Hangyu Sha[1,2*], BEng; Fan Gong[3*], PhD; Bo Liu[4*], PhD; Runfeng Liu[1,2], BEng; Haofen Wang[5], PhD; Tianxing Wu[1,2], PhD

[1]School of Computer Science and Engineering, Southeast University, 2 Southeast University Road, Jiangning District, Nanjing, China

[2]Key Laboratory of New Generation Artificial Intelligence Technology and Its Interdisciplinary Applications (Southeast University), Ministry of Education, China

[3]Department of Endocrinology, Shuguang Hospital Affiliated to Shanghai University of Traditional Chinese Medicine, Shanghai, China

[4]Informatization Office, Shanghai University of Traditional Chinese Medicine, Shanghai, China

[5]College of Design and Innovation, Tongji University, Shanghai, China

[*]these authors contributed equally

Corresponding Author:
Tianxing Wu, PhD
School of Computer Science and Engineering, Southeast University, 2 Southeast University Road, Jiangning District, Nanjing, China

Abstract

Background: Traditional Chinese Medicine (TCM) emphasizes the concept of medicine food homology (MFH), which integrates dietary therapy into health care. However, the practical application of MFH principles relies heavily on expert knowledge and manual interpretation, posing challenges for automating MFH-based dietary recommendations. Although large language models (LLMs) have shown potential in health care decision support, their performance in specialized domains such as TCM is often hindered by hallucinations and a lack of domain knowledge. The integration of uncertain knowledge graphs (UKGs) with LLMs via retrieval-augmented generation (RAG) offers a promising solution to overcome these limitations by enabling a structured and faithful representation of MFH principles while enhancing LLMs' ability to understand the inherent uncertainty and heterogeneity of TCM knowledge. Consequently, it holds potential to improve the reliability and accuracy of MFH-based dietary recommendations generated by LLMs.

Objective: This study aimed to introduce Yaoshi-RAG, a framework that leverages UKGs to enhance LLMs' capabilities in generating accurate and personalized MFH-based dietary recommendations.

Methods: The proposed framework began by constructing a comprehensive MFH knowledge graph (KG) through LLM-driven open information extraction, which extracted structured knowledge from multiple sources. To address the incompleteness and uncertainty within the MFH KG, UKG reasoning was used to measure the confidence of existing triples and to complete missing triples. When processing user queries, query entities were identified and linked to the MFH KG, enabling retrieval of relevant reasoning paths. These reasoning paths were then ranked based on triple confidence scores and entity importance. Finally, the most informative reasoning paths were encoded into prompts using prompt engineering, enabling the LLM to generate personalized dietary recommendations that aligned with both individual health needs and MFH principles. The effectiveness of Yaoshi-RAG was evaluated through both automated metrics and human evaluation.

Results: The constructed MFH KG comprised 24,984 entities, 22 relations, and 29,292 triples. Extensive experiments demonstrate the superiority of Yaoshi-RAG in different evaluation metrics. Integrating the MFH KG significantly improved the performance of LLMs, yielding an average increase of 14.5% in Hits@1 and 8.7% in F_1-score, respectively. Among the evaluated LLMs, DeepSeek-R1 achieved the best performance, with 84.2% in Hits@1 and 71.5% in F_1-score, respectively. Human evaluation further validated these results, confirming that Yaoshi-RAG consistently outperformed baseline models across all assessed quality dimensions.

Conclusions: This study shows Yaoshi-RAG, a new framework that enhances LLMs' capabilities in generating MFH-based dietary recommendations through the knowledge retrieved from a UKG. By constructing a comprehensive TCM knowledge representation, our framework effectively extracts and uses MFH principles. Experimental results demonstrate the effectiveness of our framework in synthesizing traditional wisdom with advanced language models, facilitating personalized dietary recommendations that address individual health conditions while providing evidence-based explanations.

XSL•FO
RenderX

(JMIR Med Inform 2025;13:e75279) doi:10.2196/75279

KEYWORDS

Traditional Chinese Medicine; medicine food homology; large language model; retrieval-augmented generation; uncertain knowledge graph; dietary recommendation

Introduction

Background

The concept of "medicine food homology" (MFH) in Traditional Chinese Medicine (TCM) means that certain substances can function as both nutritional food and therapeutic medicines depending on their application and dosage [1]. This ancient philosophy has gained considerable traction in modern health care systems [2], offering approaches to disease prevention and management through dietary interventions [3]. However, the practical implementation of MFH principles remains largely dependent on the expert knowledge of TCM practitioners, leading to inconsistent application and limited accessibility. The absence of automated and systematic approaches to using MFH principles for dietary recommendation generation has hindered its broader integration into contemporary health care frameworks and constrained its potential benefits for public health.

Recent advances in large language models (LLMs) [4] have demonstrated their remarkable performance across a variety of medical tasks [5], including automated clinical decision support [6], medical education [7], and health care information retrieval [8]. These capabilities are primarily derived from extensive pretraining on large-scale corpora, which encode rich knowledge from diverse textual sources. The application of MFH principles heavily depends on the domain knowledge documented in TCM literature, including foods, herbs, and formulations. Given that many LLMs have been pretrained on the corpora, which incorporate such TCM literature, combined with their strong natural language generation abilities, they present promising potential for automating MFH-based dietary recommendations. Nonetheless, LLMs exhibit substantial limitations as they often produce hallucinations that refer to factually incorrect information [9]. This problem is especially evident when generating information related to the medicinal properties of food in the context of TCM. For example, when querying with "I have stomach discomfort recently, can you recommend some summer drinks?" the LLMs respond: "Mung bean soup clears heat and is suitable for heat-related discomfort." However, according to MFH principles, mung beans are cold (yin), and their consumption may aggravate stomach discomfort. Such inaccuracies significantly affect the safety and reliability of LLMs in practical health care applications [10].

Retrieval-augmented generation (RAG) has emerged as a promising strategy to mitigate these limitations by incorporating external knowledge into LLMs, thereby enhancing factual accuracy and reducing hallucinations [11]. However, using TCM knowledge as the retrieval source of RAG presents unique challenges. TCM knowledge is sourced from diverse and heterogeneous materials, including ancient and classical literature, modern TCM literature, food and herbs information, regulatory documents, research papers, and TCM formulations. This multisource nature results in inconsistent knowledge representation, terminological ambiguities, and varying levels of evidence quality. Furthermore, MFH principles inherently involve uncertainties arising from dosage effects, individual variability, and context-dependent applications [12]. Currently, there is no comprehensive and structured knowledge base specifically tailored for supporting RAG grounded in MFH principles, creating a significant gap between traditional wisdom and modern technologies.

Related Work

Dietary Recommendation Systems

Dietary recommendation systems provide personalized food and nutrition suggestions based on individual health status and preferences. Traditional approaches have primarily relied on rule-based methods using expert knowledge and predefined guidelines, often lacking personalization and accessibility. Recent advancements in artificial intelligence have transformed this field through deep learning and knowledge graphs (KGs). Chen et al [13] defined food recommendation as constrained question answering over a food KG, integrating user preferences with health guidelines. PPKG [14] is a cancer-specific dietary recommendation system that combines a KG with time-aware long short-term memory networks to dynamically adjust recommendations for cancer prevention and rehabilitation. Ma et al [15] proposed a nutrition-related KG method based on graph convolutional networks to enhance food recommendation diversity while promoting more healthy eating habits. LLMs have further advanced dietary recommendation capabilities. ChatDiet [16] integrates personal and population models with causal inference to enhance personalization and explainability. Jin et al [17] demonstrated the clinical effectiveness of a GPT-based dietary recommendation system for patients with hemodialysis, successfully reducing serum potassium levels. Kopitar et al [18] created a generative artificial intelligence system for personalized inpatient meal planning that incorporates electronic health records and clinical guidelines.

However, we still do not have methods to integrate MFH principles with LLMs for dietary recommendation. Our framework bridges this gap by combining MFH KG with LLMs to develop more comprehensive and culturally informed dietary recommendations.

The Interplay Between LLMs and KGs

KGs serve as structured representations of factual knowledge, providing an excellent complement to parameterized language models [19,20]. With the emergence of LLMs, research has evolved along 2 complementary trajectories: leveraging LLMs to construct KGs and enhancing LLMs with KG integration. Several approaches have emerged for LLM-assisted KG construction. Extract-define-canonicalize [21] addresses scalability through open information extraction (OpenIE) and

XSL•FO
RenderX

post hoc canonicalization. BEAR [22] leverages LLMs for zero-shot knowledge extraction in service-oriented domains. LLM-TIKG [23] applies few-shot learning for constructing threat intelligence KGs, while Yang et al [24] presented an approach for medical ontology expansion using LLMs to generate competency questions.

Researchers have also explored integrating KGs to enhance LLMs' capabilities. GraphGPT [25] combines LLMs with graph structural knowledge through instruction tuning. GaLM [26] transforms KGs into text representations to improve reasoning while reducing hallucinations. Think-on-Graph [27] is a training-free framework that uses iterative beam search to enable interactive reasoning, while StructGPT [28] enhances zero-shot reasoning through an iterative Reading-then-Reasoning approach. Our work builds upon these dual research trajectories by proposing a framework that leverages LLMs for KG construction and uses KGs to enhance the capabilities of LLMs specifically within the domain of TCM, thereby providing reliable dietary recommendations grounded in MFH principles.

Objectives

To overcome the limitations of existing methods, we propose a new framework that enhances LLMs' capability to generate MFH dietary recommendations by using an uncertain knowledge graph (UKG) as an external resource. This framework uses multistep LLM calls for OpenIE [29] to automatically construct an MFH KG from unstructured and heterogeneous literature sources. It then implements UKG reasoning to measure the confidence of existing triples and complete missing triples. To improve knowledge retrieval, the framework adopts a reasoning path–based knowledge retrieval strategy, extracting relevant knowledge from the MFH KG and refining the results through ranking and filtering based on triple confidence scores and entity importance. By encoding domain-specific knowledge and addressing uncertainties related to MFH, the MFH KG empowers LLMs to deliver more personalized, evidence-based, and reliable dietary recommendations.

The key contributions of this study are as follows: (1) an integrated framework that leverages KG-augmented LLMs to generate personalized and evidence-based MFH dietary recommendations, (2) an LLM-driven OpenIE methodology for automatically constructing a UKG specifically tailored to TCM's MFH from heterogeneous multisource data, (3) a systematic evaluation of several mainstream LLMs for the generation of MFH dietary recommendations, and (4) experimental results and case studies that demonstrate the capability of the proposed framework to deliver personalized and professional MFH-based dietary recommendations.

Methods

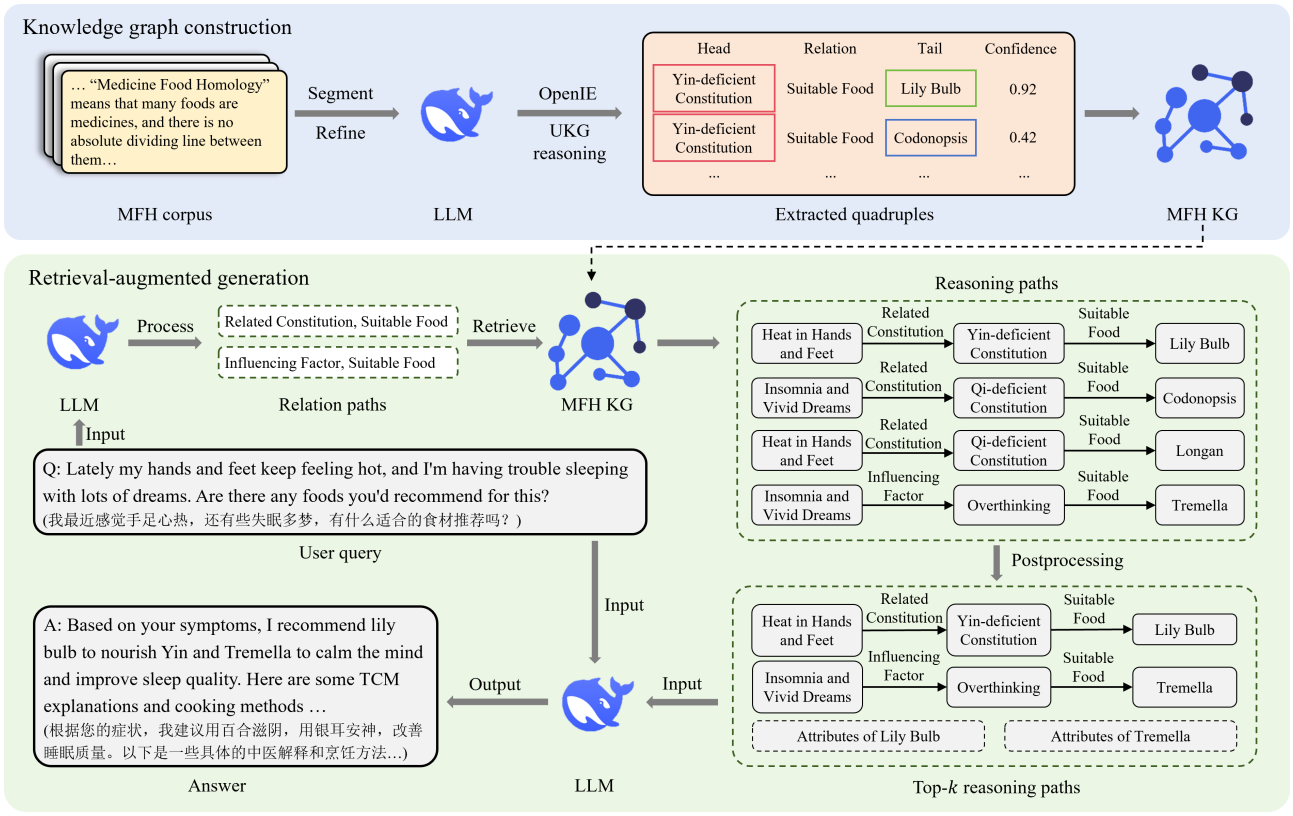
Overview

This study proposed Yaoshi-RAG, an RAG framework designed to enhance LLMs' capabilities in generating evidence-based dietary recommendations based on MFH principles. As illustrated in Figure 1, the framework consists of 2 modules:

1. Knowledge graph construction: A comprehensive corpus was compiled from multiple sources, and an MFH KG was constructed using LLM-driven OpenIE. Then, UKG reasoning was applied to measure the confidence of extracted triples and complete missing triples.
2. Retrieval-augmented generation: Given a user query, the framework first identified and linked query entities to the MFH KG. The LLM then constructed relation paths to facilitate the retrieval of reasoning paths. Subsequently, these candidate reasoning paths were refined through postprocessing, including ranking and filtering, to extract the top-k most relevant reasoning paths, thereby improving retrieval accuracy. The retrieved knowledge was integrated with the user query through prompt engineering, guiding the LLM to generate personalized dietary recommendations that aligned with both the user's needs and MFH principles.

XSL•FO
RenderX

Figure 1. The architecture of the proposed framework. KG: knowledge graph; LLM: large language model; MFH: medicine food homology; OpenIE: open information extraction; TCM: Traditional Chinese Medicine; UKG: uncertain knowledge graph.



A comprehensive corpus was compiled from multiple sources, and an MFH KG was constructed using LLM-driven OpenIE. Then, UKG reasoning was applied to measure the confidence of extracted triples and complete missing triples. In the following sections, we provide a detailed explanation of both modules, outlining their design, implementation, and contributions to the overall framework.

KG Construction

Corpus Collection

To construct an MFH KG, we systematically constructed a corpus from diverse sources, including ancient and classical literature, modern TCM literature, food and herbs information, regulatory documents, research papers, and TCM formulations. This process results in a corpus of 1359 relevant documents. Table 1 shows the statistical distribution of documents across different source categories.

Table . The statistical distribution of 1359 documents.

Source category	Number of documents
Ancient and classical literature	75
Modern TCM[a] literature	228
Food and herbs information	400
Regulatory documents	42
Research papers	432
TCM formulations	182
Total	1359

[a]TCM: Traditional Chinese Medicine.

To improve the efficiency and accuracy of entity-relation triple extraction, each document was segmented into passages of 300 tokens. These passages were then input into LLMs with a carefully designed prompt (Textbox S1 in Multimedia Appendix 1) to resolve pronominal references by incorporating information from document titles and neighboring passages. Additionally, irrelevant content within passages was filtered out to ensure domain-specific focus.

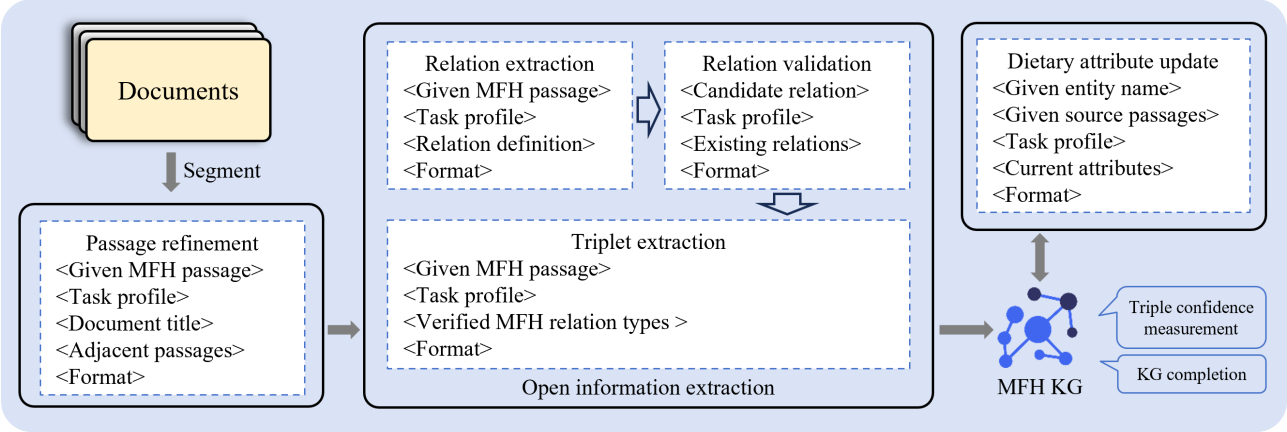
MFH Knowledge Graph

Based on the collected corpus, we constructed an MFH KG G, as shown in Figure 2, which illustrates the detailed process. Formally, the graph is defined as a triple G=(E,R,F), where E

XSL•FO
RenderX

represents the set of entities, R represents the set of relations, and F⊆E×R×E represents the fact set. Each fact in F is represented as a quadruple (h,r,t,s), where h is the head entity, r is the relation, t is the tail entity, and s is the confidence score reflecting the likelihood that the triple (h,r,t) holds true. For instance, consider the quadruple (h: Insomnia and Vivid Dreams, r: Related Constitution, t: Yin-Deficient Constitution, s: 0.87). This quadruple indicates that Insomnia and Vivid Dreams are associated with the Yin-Deficient Constitution, with a confidence score of 0.87.

Figure 2. The detailed process of medicine food homology knowledge graph construction. KG: knowledge graph; MFH: medicine food homology.



We used LLM-driven OpenIE to extract triples h,r,t from each passage within the corpus. Specifically, we first integrated predefined relation definitions into a prompt (Textbox S2 in Multimedia Appendix 1), guiding the LLM to identify and extract potential relations. These candidate relations, along with existing ones, were subsequently processed using another prompt (Textbox S3 in Multimedia Appendix 1), where the LLM determined whether to retain new relations or filter out redundant ones. This process resulted in the construction of a relation set rsel, which was incorporated into OpenIE prompts, instructing the LLM to extract entity-relation triples. The relations of extracted triples were strictly constrained to the relation set rsel.

Specifically, during the OpenIE, we instructed the LLM to extract attributes of food entities and dish entities (Textboxes S4 and S5 in Multimedia Appendix 1). For food entities, LLMs referenced their source passages to update attributes, including name, primary effects, consumption methods, indications, and contraindications. Similarly, for dish entities, attributes such as name, ingredient composition, cooking method, and dietary benefits were updated.

The automated construction of the MFH KG inevitably introduced noise, incompleteness, and factual inaccuracies, making absolute factual correctness unattainable. To mitigate these issues, we adopted UKG reasoning to measure the confidence of extracted triples and complete missing triples. Specifically, we first used unKR [30], an open-source Python library for UKG reasoning, to learn vector representations of entities and relations. Based on these representations, we applied the triple confidence measurement method [31], integrating heterogeneous evidences to measure confidence of each triple. For each given head entity h and relation r, candidate tail entities were enumerated to construct new triples absent from the current graph. The triples with confidence scores larger than 0.85 were added to the MFH KG.

Retrieval-Augmented Generation

The Retrieval Strategy

Given a user query Q, we first constructed a prompt (Textbox 1) to guide the LLM to extract a set of relevant keywords E from Q. We then encoded both the keywords and all entities from the MFH KG into dense vector representations, denoted as HR and HG, respectively. Considering that SBERT [32] has demonstrated superior performance over BERT [33] and RoBERTa [34] on semantic textual similarity tasks while maintaining lower computational overhead [35], we adopted SBERT for embedding both the extracted keywords and entities. Subsequently, we computed the cosine similarities between the embeddings of each keyword and all entities. For each keyword, we retrieved the top-10 most similar entities from the MFH KG based on cosine similarity scores. These candidate entities were then presented to the LLM, which was instructed to identify the matched entity (Textbox 2). The selected entity corresponding to each keyword constitutes the query entity set EQ={e1,e2,…,en}, which serves as the starting point for subsequent reasoning path retrieval.

Textbox 1. Prompt for keyword extraction.

You are a medical knowledge assistant specialized in Traditional Chinese Medicine. Given a user query, extract a concise set of keywords that represent the user's core health-related intent and information needs. These keywords will be used to retrieve relevant knowledge from a medicine-food homology knowledge graph to answer the user query.

User query: {user_query}

Please return the output as a Python-style set of keywords:

XSL•FO
RenderX

Textbox 2. Prompt for entity linking.

Given a keyword and a list of candidate entities retrieved from the medicine food homology knowledge graph, select the entity that most accurately matches the keyword based on contextual meaning and traditional usage. If none of the entities are appropriate matches, return "None."

Keyword: {keyword}

Candidate entities: {candidate_entities}

Please return the output as a JSON list:

This study used path-based retrieval from the MFH KG rather than retrieving contextual subgraphs for linked entities. This is motivated by the advantages reasoning paths offer in generating MFH-based dietary recommendations. Specifically, reasoning paths provide structured knowledge by capturing direct relations between query entities and answer entities. For example, the reasoning path "(Insomnia and Vivid Dreams, Related Constitution, Qi-deficient Constitution); (Qi-deficient Constitution, Suitable Food, Codonopsis)" enables LLMs to clearly infer the relations between a user's symptoms, their constitution, and the recommended food, thereby enhancing the interpretability. In contrast, subgraph-based retrieval in long-hop reasoning tasks often introduces irrelevant information [36]. This not only leads to significant computational overhead but also hinders LLMs from effectively extracting relevant information from the retrieval results.

Built upon the previous work [37], we first provided the LLM with a structured prompt (Textbox 3) listing all relations in G. The LLM then generated multiple relation paths {prel1, prel2, …, prelk}, where each preli is an ordered sequence of relationsr1,r2,…,rl. These relation paths serve as guides for retrieving knowledge essential to answering user queries. Given that the MFH KG contained considerably fewer relations compared with large-scale KGs such as FreeBase [38], we did not fine-tune the LLM for relation path generation. Instead, we used few-shot prompting to enhance the LLM's ability to generate meaningful relation paths.

Textbox 3. Prompt for relation paths generation.

Task instructions:

1. Please generate multiple relation paths (sequences of relations) based on the existing relation types. Each relation path should contain relations that are connected through the same entity.
2. The purpose of the relation paths is to assist in retrieving relevant entities that can answer the user query.

Relation types: {existing_relations}

User query: {user_query}

Query entities: {query_entities}

Few-shot examples: {examples}

Please strictly follow the task instructions and return only the required JSON list:

Subsequently, starting from each entity in the EQ, we followed each generated relation path preli to retrieve a set of reasoning paths Prea={prea1, prea2, …, pream} from G, where each reasoning path preai={(e1,r1,e2),(e2,r2,e3),…,(el,rl,el+1)} consists of multiple triples ej,rj,ej+1 and represents an instance of one of the relation paths.

Retrieval Result Postprocessing

In our initial experiment, we noticed that the reasoning paths in Preacontained redundant and irrelevant information. To enhance the quality of these reasoning paths, we computed a score for each reasoning path in Preaby considering both the entity importance and the triple confidence within the reasoning path. These scores enabled us to filter out less relevant reasoning paths.

The importance of each entity in the reasoning path was calculated using a weighted PageRank [39] algorithm. Traditional PageRank ignored the confidence of triples, which could lead to equivalent treatment of false and true relations, thus causing inaccuracies in entity importance. To overcome this limitation, we constructed a subgraph using entities from the Preaalong with their one-hop neighbors and incorporated confidence scores of triples as edge weights in the PageRank computation. The weighted PageRank formula is defined as:

$$(1)PR(ei)=(1-d)\cdot 1N+d\cdot \sum ej\subset In(ei)wj\to i\sum kwj\to k\cdot PR(ej)$$

where PR(ei) represents the weighted PageRank score of entity ei, d is the damping factor, and N is the total number of entities in the graph. The term wj→i denotes the edge weight from entity ei to ej, derived from the confidence score of the corresponding triples. When multiple relations exist between ei and ej with different confidence scores, their influence was aggregated by averaging these scores. For scoring the reasoning paths, we integrated entity importance and triple confidence scores to formulate the following path-scoring function:

$$(2)PathScore(P)=\prod i=1nwi-1\to i\times(1n\sum ej\in PPR(ej))$$

where wi-1→i represents the confidence score of the relation from entity ei to ej, n denotes the total number of entities in the path, and PR(ej) is the weighted PageRank score of entity ej within the reasoning path. This scoring methodology captured both the confidence of triples within the reasoning path and the importance of the entities involved, striking a balance between

XSL•FO
RenderX

path reliability and informational importance. Finally, we ranked the reasoning paths based on their scores and retained only the top-k reasoning paths for subsequent inference.

Answer Generation

We used prompt engineering to improve the accuracy and relevance of generated answers of LLM. Prompt engineering involves constructing carefully designed prompts to guide LLMs toward generating high-quality and task-specific responses. Specifically, we constructed a prompt template (Textbox 4) comprising four key components: (1) task specification, (2) user query, (3) retrieved reasoning paths, and (4) attributes of food and dish entities. This structured prompt facilitates the integration of external knowledge, improves the LLMs' comprehension of MFH principles, and supports the generation of more accurate responses.

Textbox 4. Prompt for answer generation.

You are a professional Traditional Chinese Medicine doctor, providing dietary recommendations using the concept of "medicine food homology." Given a user query and the relevant reasoning paths and entity attributes, generate an answer.

Task instructions:

1. Please provide a detailed, accurate, and concise response based on the information provided.
2. The response should be well-structured and ensure logical consistency with the given reasoning paths and entity attributes.
3. Incorporate medicine food homology principles in your recommendations.
4. Output format: {"answer": "(Your answer here.)"}. The answer must be written in Chinese.

User query: {user_query}

Reasoning paths: {reasoning_paths}

Entity attributes: {entity_attributes}

Please strictly follow the task instructions and return only the required JSON format:

LLM Selection

To identify the most suitable LLM for MFH dietary recommendation tasks, we evaluated several mainstream LLMs, including GPT-4 [40], LLaMA2-Chat-7B [41], Qwen2.5-7B [42], and DeepSeek-R1 [43]. Additionally, we considered the influence of model size, incorporating both large-scale models (GPT-4 and DeepSeek-R1) and 7B-parameter models (LLaMA2-Chat-7B and Qwen2.5-7B). During the experiment, we implemented the same prompt set across all models to ensure comparative evaluation under identical input conditions. All models were integrated with our proposed framework for dietary recommendation generation based on the MFH principles.

Evaluation Metrics

Automated Evaluation

To quantitatively assess the effectiveness and accuracy of the model's dietary recommendations, we used 2 evaluation metrics: Hits@1 and F_1-score. Hits@1 measures the proportion of queries where the top-ranked predicted recommendation matches a ground truth answer. This metric evaluates the model's ability to prioritize the most relevant dietary recommendation. F_1-score captures the harmonic mean of precision (P) and recall (R), offering a balanced evaluation of both aspects. This metric is particularly appropriate in scenarios where multiple valid recommendations may exist for a single query. It is defined as follows:

$$F1=2\times P\times RP+R \quad (3)$$

where precision and recall are defined as:

$$P=TPTP+FP,\ R=TPTP+FN \quad (4)$$

In this context, *TP* (true positives) represents the number of dietary recommendations correctly suggested, FP (false positives) indicates inappropriate dietary recommendations incorrectly suggested, and FN (false negatives) refers to appropriate dietary recommendations that the model failed to suggest.

Human Evaluation

While automated evaluation methods are widely applied in natural language processing tasks, they have certain limitations in the context of dietary recommendations. Automated metrics struggle to assess the effectiveness of recommendations, specifically whether the suggested food and their combinations align with MFH principles. Moreover, user acceptability and explainability of the generated dietary recommendations are difficult to accurately assess using automated methods. Therefore, we incorporated human evaluation, integrating subjective ratings from both experts and general users to provide a more comprehensive assessment of the generated dietary recommendations.

Specifically, we assessed the generated dietary plans based on the following five evaluation criteria: (1) rationality, (2) explainability, (3) user acceptability, (4) personalization, and (5) consistency. Rationality assesses whether the recommended dietary plan adhered to both TCM principles and modern nutritional standards. Explainability evaluates whether the recommendations included clear TCM-based justifications. A higher score indicates that the system provided reasonable and understandable explanations rather than simply outputting ingredient combinations. User acceptability measures how well the recommendations aligned with users' subjective preferences, including taste, cultural adaptability, and feasibility. Personalization assesses whether the system provided tailored

XSL•FO
RenderX

recommendations based on an individual's constitution and health conditions. Consistency examines whether the model produced stable recommendations under similar inputs.

Among these evaluation criteria, rationality, explainability, user acceptability, and personalization were assessed using a 5-point Likert scale (1 - 5, where 1 represented the lowest score and 5 represented the highest). Consistency was evaluated using a binary judgment (Yes=5 points and No=0 points).

To conduct the evaluation, we recruited 5 experts with backgrounds in TCM or nutrition, along with 20 general users. Participants followed a structured human evaluation guideline to rate the generated dietary recommendations. The evaluation was conducted using a survey system, where assessors were provided with the user queries along with the corresponding dietary recommendations generated by LLMs. Finally, we computed the mean scores for each evaluation criterion.

Ethical Considerations

Institutional review board approval was not required for this study, as it did not involve direct research with human participants. All corpora used, such as research papers and TCM formulations, were publicly available [44-46], and no identifiable private or sensitive information was accessed or recorded. Annotators involved in the human evaluation participated voluntarily, provided informed consent prior to participation, and were informed of their right to withdraw at any time. No compensation was provided, and no private information was collected.

Results

We constructed an MFH KG comprising 24,984 entities, 22 relations, and 29,292 triples. To evaluate the LLMs' performance in dietary recommendation tasks, we developed a specialized question answering dataset consisting of 2000 queries focused on MFH principles. This dataset was designed to ensure balanced coverage across diverse health conditions and TCM constitutional types.

Table 2 shows a comparative analysis of LLMs with or with no augmentation by the MFH KG on dietary recommendation tasks. Overall, the integration of the MFH KG substantially improved model performance across all evaluated metrics, with an average increase of 14.5% in Hits@1 and 8.7% in F_1-score, respectively. Among the baseline LLMs, DeepSeek-R1 achieved the best performance (Hits@1: 70.4%, F_1-score: 64.1%), followed by GPT-4 (Hits@1: 68.6%, F_1-score: 55.8%), Qwen2.5-7B (Hits@1: 58.7%, F_1-score: 53.2%), and LLaMA2-Chat-7B (Hits@1: 54.1%, F_1-score: 49.3%). The performance ranking remained consistent after MFH KG augmentation, with DeepSeek-R1 outperforming the others (Hits@1: 84.2%, F_1-score: 71.5%). Due to its superior performance in the above automated evaluation, DeepSeek-R1 was selected as the LLM for all subsequent experiments.

Table . The performance comparison between large language models and medicine food homology knowledge graph–augmented large language models on dietary recommendation tasks.

Model	Hits@1	F_1-score
LLMs[a]		
GPT-4	68.6	55.8
LLaMA2-Chat-7B	54.1	49.3
Qwen2.5-7B	58.7	53.2
DeepSeek-R1	70.4	64.1
MFH[b] KG[c]+ LLMs		
GPT-4	82.6	69.4
LLaMA2-Chat-7B	70.3	55.6
Qwen2.5-7B	72.8	60.6
DeepSeek-R1	*84.2* [d]	*71.5*

[a]LLM: large language model.

[b]MFH: medicine food homology.

[c]KG: knowledge graph.

[d]Values in italics indicate the best performance for each metric.

In human evaluation, we conducted a comparative assessment between LLMs and MFH KG–augmented LLMs across 5 key metrics. As shown in Table 3, the MFH KG–augmented DeepSeek-R1 consistently outperformed the baseline DeepSeek-R1 model across all evaluation criteria. The MFH KG–augmented model achieved substantially higher scores in rationality (4.1 vs 3.2), explainability (4.3 vs 2.9), user acceptability (4.4 vs 3.6), personalization (4.2 vs 3.3), and consistency (4.6 vs 3.4). These results provide compelling evidence that augmenting DeepSeek-R1 with the specialized MFH KG significantly improves the quality of dietary recommendations based on MFH principles.

XSL•FO
RenderX

Table . The performance comparison between DeepSeek-R1 and medicine food homology knowledge graph–augmented DeepSeek-R1 by human evaluation.

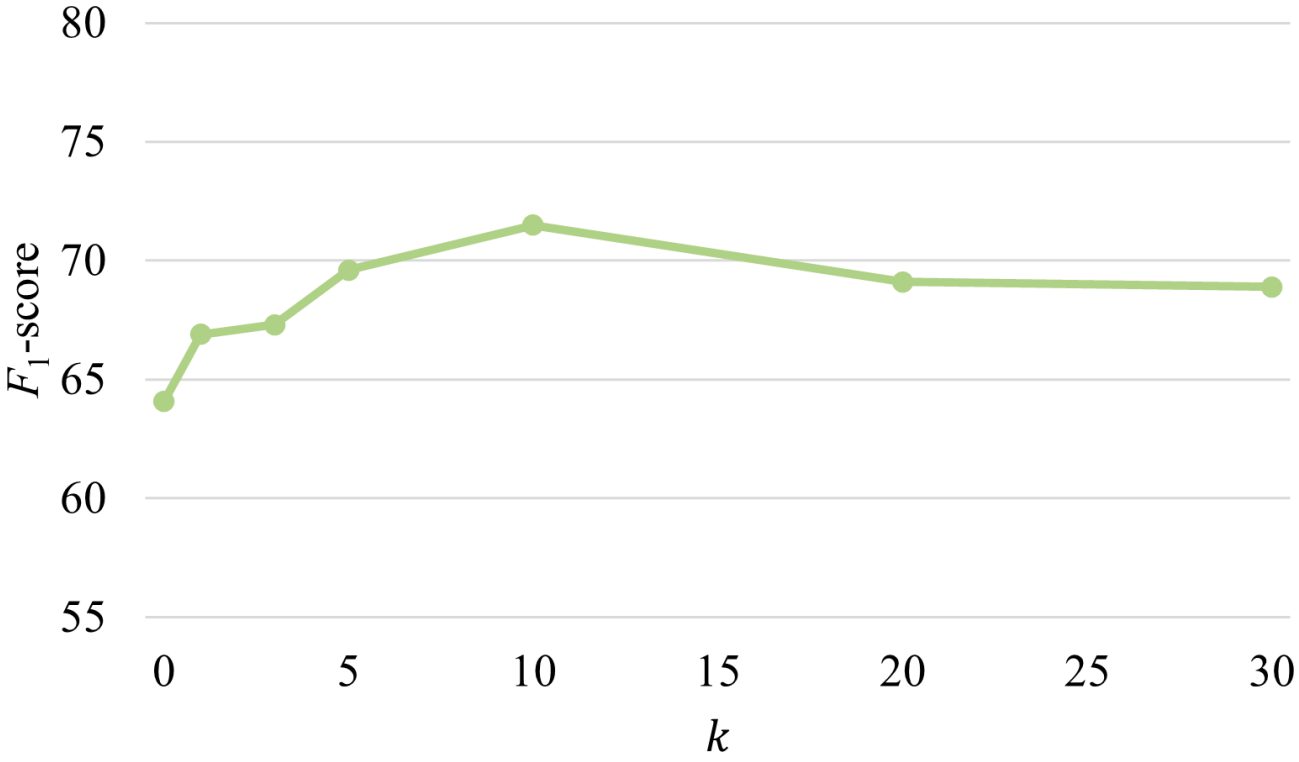
Models	Rationality	Explainability	User acceptability	Personalization	Consistency
DeepSeek-R1	3.2	2.9	3.6	3.3	3.4
MFH[a] KG[b] + DeepSeek−R1	4.1	4.3	4.4	4.2	4.6

[a]MFH: medicine food homology.

[b]KG: knowledge graph.

We analyzed the impact of parameter k, which controls the number of retrieved reasoning paths in the RAG module. The evaluation across k values [1, 3, 5, 10, 20, and 30] is shown in Figure 3. The F_1-scores indicate that small increases in k initially improved performance, but after reaching an optimal point (k=10), further increases led to gradual accuracy decline. This pattern demonstrates the effectiveness of our reasoning path postprocessing, as it successfully prioritizes the most relevant reasoning paths while filtering out potentially misleading or irrelevant information.

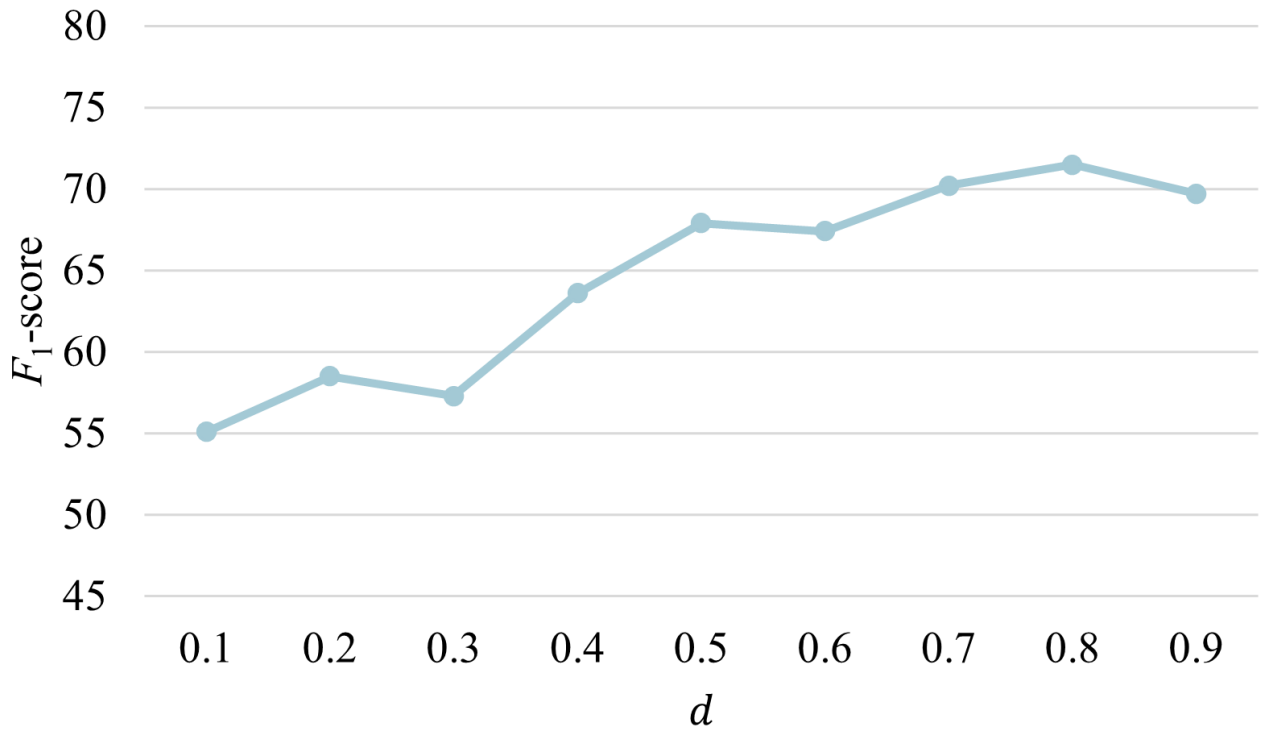
Figure 3. Different knowledge retrieval settings and the corresponding F_1-scores.



To study the impact of the damping factor d, where 1-*d* is the probability of randomly jumping to other nodes, we varied d within the range of [0.1, 0.9]. As shown in Figure 4, the performance of Yaoshi-RAG initially improved with increasing d, reached the peak (d=0.8), and subsequently declined. This trend aligns with the commonly adopted value (d=0.85) proposed by Page et al [47] and is consistent with previous findings [48,49]. Specifically, when d is too small, the resulting PageRank distribution is dominated by random jumps, which weakens the influence of the graph structure and yields less meaningful entity rankings. Conversely, when d approaches 1, the distribution becomes nearly uniform, and the convergence of the power iteration method slows significantly, posing computational challenges.

XSL•FO
RenderX

Figure 4. Different damping factor settings and the corresponding F_1-scores.



We evaluated the effectiveness of Yaoshi-RAG's retrieval strategy against multiple baselines. For sparse retrieval, we used BM25 [50] and followed DecAF [51] by transforming 1-hop subgraphs of topic entities into text. In KG embedding–based methods (TransE [52] RAG and RotatE [53] RAG), we ranked triples by embedding similarity. We also extracted the 2-hop subgraph to prioritize semantically relevant triples from query entities' neighborhood. All baseline methods retained the top 30 triples as retrieval results. Table 4 shows the performance comparison of different retrieval strategies. Yaoshi-RAG achieved superior performance with the highest Hits@1 (84.2%) and F_1-score (71.5%).

Table . The performance comparison of retrieval strategies.

Retrieval strategies	Hits@1	F_1-score
BM25 (2009)	72.8	65.3
TransE RAG (2013)	82.6	69.9
RotatE RAG (2019)	81.9	68.5
2-Hop Subgraph	75.4	67.2
Yaoshi-RAG (Ours)	*84.2* [a]	*71.5*

[a]Values in italics indicate the best performance for each metric.

To evaluate the impact of key modules in Yaoshi-RAG, we compared three variants: (1) a variant replacing the UKG with a deterministic KG, in which all triples were assumed to be fully reliable (ie, confidence scores were set to 1); (2) a variant removing the postprocessing of retrieval results, in which all retrieved reasoning paths from the UKG were directly input into the LLM without ranking or filtering; and (3) a variant randomly generating relation paths to guide the retrieval of reasoning paths.

As shown in Table 5, using a deterministic KG leads to a performance decline, highlighting the importance of incorporating uncertainty information derived from the UKG. Performance degrades further when postprocessing is removed, due to the inclusion of noisy and irrelevant reasoning paths. This confirms the effectiveness of leveraging weighted PageRank and triple confidence scores in identifying relevant reasoning paths. The variant using randomly generated relation paths for retrieval performs the worst among all settings, emphasizing the necessity of a retrieval strategy that generates faithful relation paths.

XSL•FO
RenderX

Table . Ablation studies of Yaoshi-RAG.

Model	Hits@1	F_1-score
Yaoshi-RAG (Ours)	*84.2* [a]	*71.5*
w/o UKG[b]	80.7	67.9
w/o post-processing	75.3	66.2
w/ random relation paths	65.4	54.2

[a]Values in italics indicate the best performance for each metric.

[b]UKG: uncertain knowledge graph.

Textbox 5 demonstrates an actual case of a dietary question and the answer generated by our proposed framework. The framework delivers a comprehensive response to a patient presenting peripheral heat sensations and sleep disturbances. By leveraging reasoning paths derived from the MFH KG, the framework establishes clear relations between reported symptoms, underlying constitutional patterns, and appropriate dietary recommendations. The framework also enriches its recommendations by incorporating detailed food entities' attributes from the KG into the LLM, thereby enhancing the specificity of guidance regarding consumption methods and other relevant details. This case demonstrates how Yaoshi-RAG effectively translates MFH principles into clear and practical guidance, helping patients better understand the recommendations and adhere to the suggested treatments.

XSL•FO
RenderX

Textbox 5. An actual case of a dietary question and the answer generated by our proposed framework.

User query:

Lately my hands and feet keep feeling hot, and I'm having trouble sleeping with lots of dreams. Are there any food you'd recommend for this?

我最近手足心热、失眠多梦，请给我推荐一些食材。 Top-3 reasoning paths:

1. (Heat in Hands and Feet, Related Constitution, Yin-deficient Constitution) → (Yin-deficient Constitution, Suitable Food, Lily Bulb)
2. (Heat in Hands and Feet, Related Constitution, Yin-deficient Constitution) → (Yin-deficient Constitution, Suitable Food, White Fungus)
3. (Insomnia and Vivid Dreams, Influencing Factor, Disharmony between Heart and Kidney) → (Disharmony between Heart and Kidney, Suitable Food, Mulberry)

1. (手足心热, 关联体质, 阴虚质) → (阴虚质, 适宜食物, 百合)
2. (手足心热, 关联体质, 阴虚质) → (阴虚质, 适宜食物, 银耳)
3. (失眠多梦, 影响因素, 心肾不交) → (心肾不交, 适宜食物, 桑葚)

Attributes of related food entities:

[Name], [Primary Effects], [Consumption Methods], [Indications], [Contraindications]

Generated answer:

Based on the symptoms you described—Heat in Hands and Feet, along with Insomnia and Vivid Dreams—the following analysis and dietary recommendations are provided according to Traditional Chinese Medicine (TCM) principles:

TCM syndrome differentiation analysisHeat in Hands and Feet is a typical manifestation of "Five-Center Heat" syndrome. When accompanied by Insomnia and Vivid Dreams, the condition may be attributed to three primary constitution types: (1) Yin Deficiency with Excessive Fire: Insufficient Yin fluids in the body lead to internal heat, disturbing the Shen (spirit) and causing insomnia. (2) Disharmony between Heart and Kidney: The inability of Kidney Water to balance Heart Fire results in excessive Heart Fire, affecting sleep quality. (3) Liver Blood Deficiency: A deficiency in Yin and Blood leads to an unsettled spirit, causing frequent dreams and light sleep. These syndromes often intertwine, requiring dietary adjustments to nourish Yin, reduce internal heat, and harmonize the Heart and Kidney.Recommended food and recipes

- Lily, lotus seed, and white fungus soup: Efficacy: Lily calms the mind, Tremella nourishes Yin and moistens dryness, and lotus seed strengthens the kidney and astringes essence. Together, they create a "Metal-Water Mutual Generation" effect. Preparation: Soak 15 grams of Tremella in cold water until fully expanded, then tear it into small pieces. Add 30 grams of fresh lily and 20 grams of decored lotus seeds to 800 mL of water and simmer for 1 hour. Add rock sugar before serving. Best time to consume: Between 3 and 5 PM (Shen Hour), when the bladder meridian is active, enhancing Yin nourishment.
- Mulberry and black sesame paste: Efficacy: Mulberries nourish the liver and kidneys, while black sesame replenishes blood and moisturizes dryness, making them an ideal pairing for dual liver-kidney nourishment. Preparation: Lightly toast 50 grams of black sesame over low heat and then blend it with 20 grams of dried mulberries and 30 grams of glutinous rice with 600 mL of water into a smooth paste. Best time to consume: About 2 hours before bedtime for a calming effect.

Precautions and lifestyle adjustments

- Dietary restrictions: Avoid spicy and heat-inducing food (eg, chili and Sichuan pepper), warming tonics (eg, lamb and longan), and stimulants such as strong tea and coffee.
- Lifestyle recommendations: Prepare for sleep before 9 and 11 PM (Hai Hour). Practice the "Shaking Head and Wagging Tail to Reduce Heart Fire" movement from the Eight-Section Brocade (Ba Duan Jin). Engage in calligraphy or meditation to calm the mind.

The above plan should be followed continuously for at least 2 weeks to see effects. If diarrhea occurs, discontinue the use of Poria. For patients with diabetes, it is recommended to substitute rock sugar with xylitol. If symptoms persist, seek medical attention promptly for tongue and pulse diagnosis.

根据您描述的手足心热、失眠多梦症状，结合中医辨证及食材特性分析如下:

中医辨证分析

手足心热属于"五心烦热"的典型表现，伴随失眠多梦可综合辨证为三类体质问题：其一为阴虚火旺，因体内阴液不足导致虚火内生，上扰心神引发失眠；其二属心肾不交，肾水无法上济心火，致使心火亢盛影响睡眠质量；其三与肝血不足相关，阴血亏虚致使魂不守舍，出现多梦易醒症状。这三种证型常相互交织，需通过滋阴降火、交通心肾的食疗调理。

推荐食材与烹饪方案

- 百合莲子银耳羹：功效配伍：百合清心安神，银耳滋阴润燥，莲子固肾涩精，三者协同形成"金水相生"之效。制作方法：取银耳15克冷水泡发后撕小朵，配鲜百合30克、去芯莲子20克，加水800毫升炖煮1小时，起锅前加冰糖调味。建议申时（下午3-5点）食用，此时膀胱经当令，可增强滋阴效果。
- 桑葚黑芝麻糊：功效配伍：桑葚滋补肝肾之阴，黑芝麻养血润燥，两者搭配实现肝肾同补。制作方法：将文火炒香的50克黑芝麻与20克桑葚干、30克糯米混合，加600毫升水用破壁机打成米糊。适宜睡前2小时温服，有助宁神助眠。

注意事项与生活调摄

XSL•FO
RenderX

- 饮食禁忌：避免辛辣助火之物（如辣椒、花椒）、温热补品（如羊肉、桂圆）及咖啡浓茶等兴奋性饮品。
- 生活建议：保证亥时（21-23点）前准备入睡，日常练习八段锦“摇头摆尾去心火”招式，并通过书法、冥想安神定志。

以上方案需连续食用2周以上见效，若出现腹泻可暂停茯苓，糖尿病患者建议以木糖醇替代冰糖。症状持续者应及时就医进行舌脉诊察。

Discussion

Principal Findings

Evaluation results indicate that our framework improved the performance of all evaluated LLMs, showcasing its robust adaptability. High-performing models, such as DeepSeek-R1, exhibited marked improvements when enhanced by the MFH KG. This suggests that the MFH KG offers valuable context about ingredient relations, therapeutic properties, and dietary principles, which might not be fully captured during the models' pretraining. Remarkably, even LLMs with fewer parameters showed performance improvement when integrated with the MFH KG. These results highlight the effectiveness of the proposed framework, which combines the contextual reasoning capabilities of LLMs with the rich and structured knowledge of KGs, making it a powerful tool for MFH-based dietary recommendations.

The human evaluation results revealed that the KG-augmented LLM demonstrated comprehensive improvements. The augmented LLM exhibited improved rationality through the relations between symptoms and dietary recommendations provided by the MFH KG. It also achieved superior explainability by integrating theoretical reasoning paths. Furthermore, the framework demonstrated increased user acceptability with more clinically applicable suggestions. The augmented LLM also maintained greater consistency across varying inputs. These findings collectively indicate that RAG can effectively enhance LLMs' capabilities with domain-specific knowledge.

The parameter analysis and ablation studies validate the effectiveness of our postprocessing strategy applied to the retrieved reasoning paths. Retrieving more information does not necessarily lead to performance improvement and may instead introduce irrelevant or noisy information [54], thereby degrading the quality of recommendations. By incorporating triple confidence scores from UKG reasoning, the framework prioritizes informative reasoning paths for dietary recommendations. The performance decline beyond k=10 indicates that confidence-based ranking effectively distinguishes informative reasoning paths from less relevant ones. This underscores the importance of uncertainty modeling in TCM knowledge representation, particularly given the heterogeneous quality of evidence. By measuring confidence scores, the inherent uncertainty in MFH principles can be better managed, prioritizing reliable relations while mitigating the influence of less trustworthy ones.

Limitations

Several limitations of this study should be acknowledged. The MFH KG was constructed using OpenIE, which may introduce inaccuracies and cannot cover all knowledge on MFH principles. Besides, we did not fine-tune the LLMs specifically for relation path generation, which may have constrained the retrieval effectiveness of our framework, particularly for complex cases involving multiple symptoms or conditions. Addressing these limitations in the future would likely further enhance the LLMs' clinical uses and recommendation quality.

Conclusions

This study shows Yaoshi-RAG, a new framework that enhances LLMs' capabilities in generating MFH dietary recommendations through the integration of a UKG. This framework uses multistep LLM calls for OpenIE to automatically construct an MFH KG, incorporating UKG reasoning to measure the confidence of existing triples and complete missing triples. Upon receiving user queries, the framework implements a reasoning path–based knowledge retrieval strategy, extracting relevant reasoning paths from the MFH KG and optimizing the retrieval results through a postprocessing mechanism. Experimental evaluations demonstrate that DeepSeek-R1 is the best-performing base model for MFH-based dietary recommendation generation. This framework facilitates dietary recommendations that adapt to individual health conditions and symptom requirements while considering diverse ingredients and dishes, accompanied by comprehensive explanations grounded in MFH principles. In the future, we plan to focus on implementing more effective knowledge extraction methodologies, expanding our KG through additional MFH literature, exploring optimized retrieval strategies, and fine-tuning open-source LLMs to further improve the accuracy and reliability of the generated dietary recommendations.

Acknowledgments

This paper is supported by the National Natural Science Foundation of China (grants 82104786, 62376058, 52378009, and 62276063), the Southeast University Interdisciplinary Research Program for Young Scholars, and the Big Data Computing Center of Southeast University.

Authors' Contributions

HS and TW contributed to the algorithm design; HS performed experiments and wrote the paper; RL performed experiments; and FG, TW, BL, and HW provided theoretical guidance and the revision of this paper.

XSL•FO
RenderX

Conflicts of Interest

None declared.

Multimedia Appendix 1
Prompts for medicine food homology knowledge graph construction.
[DOCX File, 22 KB - medinform_v13i1e75279_app1.docx]

References

1. Zhong H, Tang ZQ, Li YF, Wang M, Sun WY, He RR. The evolution and significance of medicine and food homology. Acupunct Herbal Med 2024;4(1):19-35. [doi: 10.1097/HM9.0000000000000104]
2. Chen J. Essential role of medicine and food homology in health and wellness. Chin Herb Med 2023 Jul;15(3):347-348. [doi: 10.1016/j.chmed.2023.05.001] [Medline: 37538868]
3. Gong X, Ji M, Xu J, Zhang C, Li M. Hypoglycemic effects of bioactive ingredients from medicine food homology and medicinal health food species used in China. Crit Rev Food Sci Nutr 2020;60(14):2303-2326. [doi: 10.1080/10408398.2019.1634517] [Medline: 31309854]
4. Zhao W, Zhou K, Li J, et al. A survey of large language models. arXiv. Preprint posted online on 2023. [doi: 10.48550/arXiv.2303.18223]
5. Thirunavukarasu AJ, Ting DSJ, Elangovan K, Gutierrez L, Tan TF, Ting DSW. Large language models in medicine. Nat Med 2023 Aug;29(8):1930-1940. [doi: 10.1038/s41591-023-02448-8] [Medline: 37460753]
6. Liu S, McCoy AB, Wright AP, et al. Why do users override alerts? Utilizing large language model to summarize comments and optimize clinical decision support. J Am Med Inform Assoc 2024 May 20;31(6):1388-1396. [doi: 10.1093/jamia/ocae041] [Medline: 38452289]
7. Abd-Alrazaq A, AlSaad R, Alhuwail D, et al. Large language models in medical education: opportunities, challenges, and future directions. JMIR Med Educ 2023 Jun 1;9:e48291. [doi: 10.2196/48291] [Medline: 37261894]
8. Wiest IC, Ferber D, Zhu J, et al. Privacy-preserving large language models for structured medical information retrieval. NPJ Digit Med 2024 Sep 20;7(1):257. [doi: 10.1038/s41746-024-01233-2] [Medline: 39304709]
9. Azamfirei R, Kudchadkar SR, Fackler J. Large language models and the perils of their hallucinations. Crit Care 2023 Mar 21;27(1):120. [doi: 10.1186/s13054-023-04393-x] [Medline: 36945051]
10. Kim Y, Jeong H, Chen S, et al. Medical hallucination in foundation models and their impact on healthcare. medRxiv. Preprint posted online on 2025. [doi: 10.1101/2025.02.28.25323115]
11. Gao Y, Xiong Y, Gao X, et al. Retrieval-augmented generation for large language models: a survey. arXiv. Preprint posted online on 2023. [doi: 10.48550/arXiv.2312.10997]
12. Sun-Waterhouse DX, Chen XY, Liu ZH, I.N. Waterhouse G, Kang WY. Transformation from traditional medicine-food homology to modern food-medicine homology. Food Med Homology 2024 Sep;1(1):9420014. [doi: 10.26599/FMH.2024.9420014]
13. Chen Y, Subburathinam A, Chen CH, Zaki MJ. Personalized food recommendation as constrained question answering over a large-scale food knowledge graph. Presented at: Proceedings of the 14th ACM International Conference on Web Search and Data Mining; Mar 8-12, 2021; Virtual Event, Israel p. 544-552. [doi: 10.1145/3437963.3441816]
14. Tang J, Huang B, Xie M. Anticancer recipe recommendation based on cancer dietary knowledge graph. Eur J Cancer Care (Engl) 2023 Oct 18;2023(1):1-13. [doi: 10.1155/2023/8816960]
15. Ma W, Li M, Dai J, Ding J, Chu Z, Chen H. Nutrition-related knowledge graph neural network for food recommendation. Foods 2024 Jul 5;13(13):38998649. [doi: 10.3390/foods13132144] [Medline: 38998649]
16. Yang Z, Khatibi E, Nagesh N, et al. ChatDiet: empowering personalized nutrition-oriented food recommender chatbots through an LLM-augmented framework. Smart Health (2014) 2024 Jun;32:100465. [doi: 10.1016/j.smhl.2024.100465]
17. Jin H, Lin Q, Lu J, et al. Evaluating the effectiveness of a generative pretrained transformer-based dietary recommendation system in managing potassium intake for hemodialysis patients. J Ren Nutr 2024 Nov;34(6):539-545. [doi: 10.1053/j.jrn.2024.04.001] [Medline: 38615701]
18. Kopitar L, Stiglic G, Bedrac L, Bian J. Personalized meal planning in inpatient clinical dietetics using generative artificial intelligence: system description. Presented at: 2024 IEEE 12th International Conference on Healthcare Informatics (ICHI); Jun 3-6, 2024; Orlando, FL, USA p. 2024-2331. [doi: 10.1109/ICHI61247.2024.00049]
19. Pan S, Luo L, Wang Y, Chen C, Wang J, Wu X. Unifying large language models and knowledge graphs: a roadmap. IEEE Trans Knowl Data Eng 2024 Jul;36(7):3580-3599. [doi: 10.1109/TKDE.2024.3352100]
20. Pan J, Razniewski S, Kalo JC, et al. Large language models and knowledge graphs: opportunities and challenges. arXiv. Preprint posted online on 2023. [doi: 10.48550/arXiv.2308.06374]
21. Zhang B, Soh H. Extract, define, canonicalize: an LLM-based framework for knowledge graph construction. 2024 Presented at: Proceedings of the 2024 Conference on Empirical Methods in Natural Language Processing; 2024; Miami, Florida, USA p. 9820-9836. [doi: 10.18653/v1/2024.emnlp-main.548]

XSL•FO
RenderX

22. Yu S, Huang T, Liu M, Wang Z. B. BEAR: revolutionizing service domain knowledge graph construction with LLM. In: Service-Oriented Computing ICSOC 2023 Lecture Notes in Computer Science: Springer; 2023, Vol. 14419. [doi: 10.1007/978-3-031-48421-6_23]
23. Hu Y, Zou F, Han J, Sun X, Wang Y. LLM-TIKG: Threat intelligence knowledge graph construction utilizing large language model. Comput Secur 2024 Oct;145:103999. [doi: 10.1016/j.cose.2024.103999]
24. Yang H, Xiao L, Zhu R, Liu Z, Chen J. An LLM supported approach to ontology and knowledge graph construction. Presented at: 2024 IEEE International Conference on Bioinformatics and Biomedicine (BIBM); Dec 3-6, 2024; Lisbon, Portugal p. 5240-5246. [doi: 10.1109/BIBM62325.2024.10822222]
25. Tang J, Yang Y, Wei W, et al. GraphGPT: graph instruction tuning for large language models. 2024 Jul 10 Presented at: Proceedings of the 47th International ACM SIGIR Conference on Research and Development in Information Retrieval (SIGIR '24); Jul 14-18, 2024; Washington, DC, USA p. 491-500. [doi: 10.1145/3626772.3657775]
26. Dernbach S, Agarwal K, Zuniga A, Henry M, Choudhury S. GLaM: fine-tuning large language models for domain knowledge graph alignment via neighborhood partitioning and generative subgraph encoding. AAAI-SS 2024;3(1):82-89. [doi: 10.1609/aaaiss.v3i1.31186]
27. Sun J, Xu C, Tang L, et al. Think-on-graph: deep and responsible reasoning of large language model on knowledge graph. 2024 May Presented at: The Twelfth International Conference on Learning Representations (ICLR URL: https://openreview.net/forum?id=nnVO1PvbTv [accessed 2025-08-08]
28. Jiang J, Zhou K, Dong Z, Ye K, Zhao X, Wen JR. StructGPT: a general framework for large language model to reason over structured data. Presented at: Proceedings of the 2023 Conference on Empirical Methods in Natural Language Processing; 2023; Singapore p. 9237-9251. [doi: 10.18653/v1/2023.emnlp-main.574]
29. Niklaus C, Cetto M, Freitas A, et al. A survey on open information extraction. Presented at: The 27th International Conference on Computational Linguistics (COLING); 2018; Santa Fe, New Mexico, USA p. 3866-3878 URL: https://aclanthology.org/C18-1326 [accessed 2025-08-08]
30. Wang J, Wu T, Chen S, et al. UnKR: a Python library for uncertain knowledge graph reasoning by representation learning. Presented at: Proceedings of the 47th International ACM SIGIR Conference on Research and Development in Information Retrieval (SIGIR '24); 2024; United States p. 2822-2826. [doi: 10.1145/3626772.3657661]
31. Wu T, Yao K, Li W, et al. Triple confidence measurement in knowledge graph with multiple heterogeneous evidences. World Wide Web 2024 Nov;27(6):70. [doi: 10.1007/s11280-024-01307-x]
32. Reimers N, Gurevych I. Sentence-BERT: sentence embeddings using Siamese BERT-networks. Presented at: Proceedings of the 2019 Conference on Empirical Methods in Natural Language Processing and the 9th International Joint Conference on Natural Language Processing (EMNLP-IJCNLP); 2019; Hong Kong, China p. 3982-3992. [doi: 10.18653/v1/D19-1410]
33. Devlin J, Chang MW, Lee K, Toutanova K. BERT: pre-training of deep bidirectional transformers for language understanding. Presented at: Proceedings of the 2019 Conference of the North American Chapter of the Association for Computational Linguistics: Human Language Technologies; 2019; Minneapolis, MA, USA p. 4171-4186. [doi: 10.18653/v1/N19-1423]
34. Liu Y, Ott M, Goyal N, et al. RoBERTa: a robustly optimized BERT pretraining approach. arXiv. Preprint posted online on 2019. [doi: 10.48550/arXiv.1907.11692]
35. Bekamiri H, Hain DS, Jurowetzki R. PatentSBERTa: a deep NLP based hybrid model for patent distance and classification using augmented SBERT. Technol Forecast Soc Change 2024 Sep;206:123536. [doi: 10.1016/j.techfore.2024.123536]
36. Li M, Miao S, Li P. Simple is effective: the roles of graphs and large language models in knowledge-graph-based retrieval-augmented generation. arXiv. Preprint posted online on 2024. [doi: 10.48550/arXiv.2410.20724]
37. Luo L, Li YF, Haffari G, et al. Reasoning on graphs: faithful and interpretable large language model reasoning. 2024 Presented at: The Twelfth International Conference on Learning Representations URL: https://openreview.net/forum?id=ZGNWW7xZ6Q [accessed 2025-08-08]
38. Bollacker K, Evans C, Paritosh P, et al. Freebase: a collaboratively created graph database for structuring human knowledge. 2008 Presented at: Proceedings of the 2008 ACM SIGMOD International Conference on Management of Data (SIGMOD '08); Jun 9-12, 2008; New York, NY p. 1247-1250. [doi: 10.1145/1376616.1376746]
39. Bianchini M, Gori M, Scarselli F. Inside PageRank. ACM Trans Internet Technol 2005 Feb;5(1):92-128. [doi: 10.1145/1052934.1052938]
40. OpenAI AJ, Adler S, et al. GPT-4 technical report. arXiv. Preprint posted online on 2024. [doi: 10.48550/arXiv.2303.08774]
41. Touvron H, Martin L, Stone K, et al. LLaMA 2: open foundation and fine-tuned chat models. . Preprint posted online on 2023. [doi: 10.48550/arXiv.2307.09288]
42. Yang A, Yang B, Zhang B, et al. Qwen2.5 technical report. arXiv. Preprint posted online on 2025. [doi: 10.48550/arXiv.2412.15115]
43. DeepSeek-AI, Guo D, Yang D, et al. DeepSeek-R1: incentivizing reasoning capability in LLMs via reinforcement learning. . Preprint posted online on 2025. [doi: 10.48550/arXiv.2501.12948]
44. TCM-ID: Traditional Chinese Medicine information database. TCM-ID. URL: https://bidd.group/TCMID/ [accessed 2024-12-10]
45. PubMed. URL: https://pubmed.ncbi.nlm.nih.gov/ [accessed 2024-12-10]
46. Global academic insights from China and beyond. Cnki. URL: https://oversea.cnki.net/ [accessed 2024-12-10]

XSL•FO
RenderX

47. Page L, Brin S, Motwani R, Winograd T. The PageRank citation ranking: bringing order to the web. : Stanford InfoLab; 1999 URL: http://ilpubs.stanford.edu:8090/422 [accessed 2025-08-08]
48. Srivastava AK, Garg R, Mishra PK. Discussion on damping factor value in PageRank computation. IJISA 2017 Sep 8;9(9):19-28. [doi: 10.5815/ijisa.2017.09.03]
49. Boldi P, Santini M, Vigna S. PageRank as a function of the damping factor. 2005 Presented at: Proceedings of the 14th International Conference on World Wide Web; Chiba, Japan p. 557-566. [doi: 10.1145/1060745.1060827]
50. Robertson S, Zaragoza H. The probabilistic relevance framework: BM25 and beyond. FNT Inf Retrieval 2009;3(4):333-389. [doi: 10.1561/1500000019]
51. Yu D, Zhang S, Ng P, et al. DecAF: joint decoding of answers and logical forms for question answering over knowledge bases. 2023 Presented at: The Eleventh International Conference on Learning Representations URL: https://openreview.net/forum?id=XHc5zRPxqV9 [accessed 2025-08-08]
52. Bordes A, Usunier N, Garcia-Duran A, et al. Translating embeddings for modeling multi-relational data. In: Burges CJ, Bottou L, Welling M, Ghahramani Z, Weinberger KQ, editors. Presented at: NIPS'13: Neural Information Processing Systems; Dec 5-10, 2013; Lake Tahoe, NV URL: https://proceedings.neurips.cc/paper_files/paper/2013/file/1cecc7a77928ca8133fa24680a88d2f9-Paper.pdf [accessed 2025-08-08]
53. Sun Z, Deng ZH, Nie JY, et al. RotatE: knowledge graph embedding by relational rotation in complex space. Presented at: International Conference on Learning Representations; May 6-9, 2019; New Orleans, LA URL: https://openreview.net/forum?id=HkgEQnRqYQ [accessed 2025-08-08]
54. Cuconasu F, Trappolini G, Siciliano F, et al. The power of noise: redefining retrieval for RAG systems. Presented at: Proceedings of the 47th International ACM SIGIR Conference on Research and Development in Information Retrieval (SIGIR '24); Jul 14-18, 2024; Washington, DC, USA p. 719-729. [doi: 10.1145/3626772.3657834]

Abbreviations

KG: knowledge graph
LLM: large language model
MFH: medicine food homology
OpenIE: open information extraction
RAG: retrieval-augmented generation
TCM: Traditional Chinese Medicine
UKG: uncertain knowledge graph

Edited by L Luo, Q Jin; submitted 31.03.25; peer-reviewed by N Zhang, X He, Y Chen; revised version received 24.06.25; accepted 01.07.25; published 21.08.25.

Please cite as:
Sha H, Gong F, Liu B, Liu R, Wang H, Wu T
Leveraging Retrieval-Augmented Large Language Models for Dietary Recommendations With Traditional Chinese Medicine's Medicine Food Homology: Algorithm Development and Validation
JMIR Med Inform 2025;13:e75279
URL: https://medinform.jmir.org/2025/1/e75279
doi:10.2196/75279

© Hangyu Sha, Fan Gong, Bo Liu, Runfeng Liu, Haofen Wang, Tianxing Wu. Originally published in JMIR Medical Informatics (https://medinform.jmir.org), 21.8.2025. This is an open-access article distributed under the terms of the Creative Commons Attribution License (https://creativecommons.org/licenses/by/4.0/), which permits unrestricted use, distribution, and reproduction in any medium, provided the original work, first published in JMIR Medical Informatics, is properly cited. The complete bibliographic information, a link to the original publication on https://medinform.jmir.org/, as well as this copyright and license information must be included.

XSL•FO
RenderX

Expression of Concern

Expression of Concern: A Dynamic Adaptive Ensemble Learning Framework for Noninvasive Mild Cognitive Impairment Detection: Development and Validation Study

Related Article:

Companion article: https://medinform.jmir.org/2025/1/e60250/

(JMIR Med Inform 2025;13:e75352) doi:10.2196/75352

The publisher expresses concern regarding the following article:

A Dynamic Adaptive Ensemble Learning Framework for Noninvasive Mild Cognitive Impairment Detection: Development and Validation Study [1].

This article is under investigation for potential peer review irregularities. Readers are advised to interpret the findings with caution pending the outcome of this inquiry.

Reference

1. Li A, Li J, Hu Y, Geng Y, Qiang Y, Zhao J. A Dynamic Adaptive Ensemble Learning Framework for Noninvasive Mild Cognitive Impairment Detection: Development and Validation Study. JMIR Med Inform 2025 Jan 20;13:e60250 [FREE Full text] [doi: 10.2196/60250] [Medline: 39832176]

Submitted 01.04.25; this is a non–peer-reviewed article;accepted 01.04.25; published 04.04.25.

Please cite as:
Expression of Concern: A Dynamic Adaptive Ensemble Learning Framework for Noninvasive Mild Cognitive Impairment Detection: Development and Validation Study
JMIR Med Inform 2025;13:e75352
URL: https://medinform.jmir.org/2025/1/e75352
doi:10.2196/75352
PMID:

©JMIR Editorial Office. Originally published in JMIR Medical Informatics (https://medinform.jmir.org), 04.04.2025. This is an open-access article distributed under the terms of the Creative Commons Attribution License (https://creativecommons.org/licenses/by/4.0/), which permits unrestricted use, distribution, and reproduction in any medium, provided the original work, first published in the JMIR Medical Informatics, is properly cited. The complete bibliographic information, a link to the original publication on https://medinform.jmir.org, as well as this copyright and license information must be included.

XSL•FO
RenderX

Retraction: “Diagnostic Classification and Prognostic Prediction Using Common Genetic Variants in Autism Spectrum Disorder: Genotype-Based Deep Learning”

JMIR Editorial Office

JMIR Publications, 130 Queens Quay East, Suite 1100-1102, Toronto, ON, Canada

Corresponding Author:
JMIR Publications, 130 Queens Quay East, Suite 1100-1102, Toronto, ON, Canada

Related Articles:

Retraction of: https://medinform.jmir.org/2021/4/e24754

https://medinform.jmir.org/2025/1/e66556

(JMIR Med Inform 2025;13:e76833) doi:10.2196/76833

The article “Diagnostic Classification and Prognostic Prediction Using Common Genetic Variants in Autism Spectrum Disorder: Genotype-Based Deep Learning” [1] is being retracted due to analytical errors and irreproducibility of the results, which led to the overestimation of predictive value. The issues are detailed by the authors of a letter to the editor [2] and were confirmed during investigation by JMIR Publications.

Authors Wang and Avillach responded and expressed neither agreement nor disagreement with the decision.

References

1. Wang H, Avillach P. Diagnostic classification and prognostic prediction using common genetic variants in autism spectrum disorder: genotype-based deep learning. JMIR Med Inform 2021 Apr 7;9(4):e24754.
2. Miller C, Portlock T, Nyaga DM, Gamble GD, O’Sullivan JM. Code error in “Diagnostic Classification and Prognostic Prediction Using Common Genetic Variants in Autism Spectrum Disorder: Genotype-Based Deep Learning”. JMIR Med Inform 2025;13:e66556. [doi: 10.2196/66556]

Edited by JMIR Editorial Office; submitted 01.05.25; this is a non–peer-reviewed article;accepted 01.05.25; published 06.05.25.

Please cite as:
JMIR Editorial Office
Retraction: “Diagnostic Classification and Prognostic Prediction Using Common Genetic Variants in Autism Spectrum Disorder: Genotype-Based Deep Learning”
JMIR Med Inform 2025;13:e76833
URL: https://medinform.jmir.org/2025/1/e76833
doi:10.2196/76833

© JMIR Editorial Office. Originally published in JMIR Medical Informatics (https://medinform.jmir.org), 6.5.2025. This is an open-access article distributed under the terms of the Creative Commons Attribution License (https://creativecommons.org/licenses/by/4.0/), which permits unrestricted use, distribution, and reproduction in any medium, provided the original work, first published in JMIR Medical Informatics, is properly cited. The complete bibliographic information, a link to the original publication on https://medinform.jmir.org/, as well as this copyright and license information must be included.

XSL•FO
RenderX

Retraction: “A Dynamic Adaptive Ensemble Learning Framework for Noninvasive Mild Cognitive Impairment Detection: Development and Validation Study”

JMIR Editorial Office

JMIR Publications, 130 Queens Quay E, Suite 1100, Toronto, ON, Canada

Corresponding Author:
JMIR Publications, 130 Queens Quay E, Suite 1100, Toronto, ON, Canada

Related Articles:

https://medinform.jmir.org/2025/1/e60250

Companion article: https://medinform.jmir.org/2025/1/e75352/

(JMIR Med Inform 2025;13:e77635) doi:10.2196/77635

The JMIR Editorial Office is retracting the article “A Dynamic Adaptive Ensemble Learning Framework for Noninvasive Mild Cognitive Impairment Detection: Development and Validation Study” by Li et al [1] following investigation due to concerns over irregularities during the peer review process. We regret that these issues were not resolved prior to publication.

All authors disagreed with the retraction decision.

Reference

1. Li A, Li J, Hu Y, Geng Y, Qiang Y, Zhao J. A dynamic adaptive ensemble learning framework for noninvasive mild cognitive impairment detection: development and validation study. JMIR Med Inform 2025 Jan 20;13:e60250.

Edited by JMIRE Office; submitted 16.05.25; this is a non–peer-reviewed article;accepted 16.05.25; published 23.05.25.

Please cite as:
JMIR Editorial Office
Retraction: “A Dynamic Adaptive Ensemble Learning Framework for Noninvasive Mild Cognitive Impairment Detection: Development and Validation Study”
JMIR Med Inform 2025;13:e77635
URL: https://medinform.jmir.org/2025/1/e77635
doi:10.2196/77635

© JMIR Editorial Office. Originally published in JMIR Medical Informatics (https://medinform.jmir.org), 23.5.2025. This is an open-access article distributed under the terms of the Creative Commons Attribution License (https://creativecommons.org/licenses/by/4.0/), which permits unrestricted use, distribution, and reproduction in any medium, provided the original work, first published in JMIR Medical Informatics, is properly cited. The complete bibliographic information, a link to the original publication on https://medinform.jmir.org/, as well as this copyright and license information must be included.

XSL•FO
RenderX

Original Paper

Patient Attitudes Toward Ambient Voice Technology: Preimplementation Patient Survey in an Academic Medical Center

Gary Leiserowitz[1], MD, MS; Jeff Mansfield[1]; Scott MacDonald[1], MD; Melissa Jost[1], MS

University of California Davis Medical Center, Sacramento, CA, United States

Corresponding Author:
Gary Leiserowitz, MD, MS
University of California Davis Medical Center
4860 Y Street
Suite 2500
Sacramento, CA, 95817
United States
Phone: 1 916 734 4107
Email: gsleiserowitz@ucdavis.edu

Abstract

Background: Many institutions are in various stages of deploying an artificial intelligence (AI) scribe system for clinic electronic health record (EHR) documentation. In anticipation of the University of California, Davis Health's deployment of an AI scribe program, we surveyed current patients about their perceptions of this technology to inform a patient-centered implementation.

Objective: We assessed patient perceptions about current clinician EHR documentation practices before implementation of the AI scribe program, and preconceptions regarding the AI scribe's introduction.

Methods: We conducted a descriptive preimplementation survey as a quality improvement study. A convenience sample of 9171 patients (aged ≥18 years) who had a clinic visit within the previous year, was recruited via an email postvisit survey. Patient-identified demographics (age, gender, and race and ethnicity) were collected. The survey included rating scales on questions related to the patient perception of the AI scribe program, plus open-ended comments. Data were collated to analyze patient perceptions of including AI Scribe technology in a clinician visit.

Results: In total, 1893 patients completed the survey (20% response rate), with partial responses from another 549. Sixty-three percent (n=1205) of the respondents were female, and most were 51 years and older (87%, n=1649). Most patients identified themselves as White (69%, n=1312), multirace (8%, n=154), Latinx (7%, n=130), and Black (2%, n=42). The respondents were not representative of the overall clinic populations and skewed more toward being female, ages 50 years and older, and White in comparison. Patients reacted to the current EHR documentation system, with 71% (n=1349) feeling heard or sometimes heard, but 23% (n=416) expressed frustrations that their physician focused too much on typing into the computer. When asked about their anticipated response to the use of an AI scribe, 48% (n=904) were favorable, 33% (n=630) were neutral, and 19% (n=359) were unfavorable. Younger patients (ages 18-30 years) expressed more skepticism than those aged 51 years and older. Further, 42% (655/1567) of positive comments received indicated this technology could improve human interaction during their visits. Comments supported that the use of an AI scribe would enhance patient experience by allowing the clinician to focus on the patient. However, when asked about concerns regarding the AI scribe, 39% (515/1330) and 15% (203/1330) of comments expressed concerns about documentation accuracy and privacy, respectively. Providing previsit patient education and obtaining permission were viewed as very important.

Conclusions: This patient survey showed that respondents are generally open to the use of an AI scribe program for EHR documentation to allow the clinician to focus on the patient during the actual encounter rather than the computer. Providing patient education and obtaining consent before using AI are important components to gain patient trust. Caution about the results is appropriate, given the low response rate and nonrepresentative profile.

(JMIR Med Inform 2025;13:e77901) doi:10.2196/77901

KEYWORDS

artificial intelligence; AI; AI scribe; scribe program; ambient voice technology; preimplementation patient survey; patient perceptions and attitudes; electronic health records; EHR; health information privacy

XSL•FO
RenderX

Introduction

The use of electronic health records (EHRs) has become ubiquitous in US medical practices [1]. The benefits of EHR for medical documentation include legibility, accuracy of record-keeping, enhanced ability to access laboratory data, placement of physician orders, interactive alerts, clinical pathways, plus timeliness and interoperability between health care institutions. Since the EHR is designed to be comprehensive, there are considerable and growing demands on clinicians for documentation of the myriad aspects of patient encounters. The time to complete EHR for clinic notes commonly exceeds the time associated with face-to-face visits between the patient and clinician, which may contribute to clinician burnout [2,3]. Research has documented that physicians can spend more than 15 hours per week solely on documentation [2].

Many clinical practices have used live human scribes in the last 10 years to address the substantial work required for medical documentation. Existing research finds that this support significantly lessens physician documentation burden and improves physician-patient communication [3]. With appropriate training, live scribes can effectively and efficiently transcribe and summarize the direct interactions between patients and clinicians, as well as integrate important information such as previous medical records, laboratory, and imaging tests [4]. The use of live scribes can markedly decrease the time and effort of the clinicians to document clinical notes, which may result in less time outside of clinic hours for documentation [5]. Since the use of live scribes is very common in current medical practice, patients are both accepting and supportive of their use [6]. However, there are significant limitations to scaling the usage of live scribes, including staff recruitment and cost.

Recently, there has been the emergence of digital scribes, which use generative artificial intelligence (AI) to transcribe human speech and then transform this into a standard progress note format [7]. There are other recent examples of the use of AI in health care delivery, with AI also entering the patient care landscape for patient navigation and medication adherence [8], and analyzing radiological imaging [9].

Use of AI digital transcriptions (also known as ambient voice technology, or “AI Scribes” may also help lessen the burden of clinical documentation, similar to the use of live scribes [10,11]. It may also enhance the patient experience during clinic visits compared to direct documentation by the provider, since the clinician may be able to spend more time interacting directly with the patient rather than documenting in the EHR during the visit. Initial reports about the use of AI Scribes show a strongly positive response from clinicians, since there is often decreased time and cognitive effort required for medical documentation [12-15]. Although most clinicians had a favorable view of their experience with the use of the AI scribe, the accuracy of the note is still problematic with regard to errors, length of the note, and note style requiring clinician effort to edit the note before finalization [11,12].

However, on a cautionary note, patients may be hesitant to accept use of an AI scribe due to a lack of familiarity or information, or preexisting beliefs about the process, accuracy, and integrity of the information shared between the patient and clinician. In anticipation of a planned deployment of an AI scribe program, our patient experience team surveyed our patients who receive primary care at the University of California, Davis ambulatory clinics. The intent of the survey was to understand the preexisting perceptions of our patients about the current state of EHR documentation and to anticipate both the positive and negative reactions that might be experienced before the rollout of an AI scribe program. In addition, this information could influence how we communicate about the AI scribe program, including the opportunity to opt out of participation.

Methods

Overview

We conducted this study from January 31, 2024, to February 12, 2024, at the University of California Davis Health (UCDH) in Sacramento, CA. UCDH is an academic medical center with 11 community medical group locations that provide care to a diverse catchment area of 6 million people across 33 Northern California counties.

A convenience sample of 9171 patients 18 years and older who had a UCDH primary care visit within the last year was recruited through the postclinic visit surveys via an email that was only sent in English. Patients spoke English as a primary language and were not incentivized to participate. Age, as well as self-identified demographic characteristics such as sex, race, and ethnicity, were taken from the electronic medical record (EMR). When available, these EMR data were collated with their email responses.

Survey Design

A 17-question survey was designed by the UCDH Patient Experience Design team to capture patient perceptions and concerns about the anticipated future rollout of an AI scribe technology. The survey questions included a rating scale for some answers and open-ended responses for others.

The survey was developed and coded using Press Ganey’s Forsta Foundation tool, a JavaScript-based survey platform that assists in simplifying the programming of a survey. Once the survey was developed, it went through 5 functionality tests to ensure proper survey function and data collection.

The survey design took place over multiple iterations. With the goal of identifying possible sources of patient frustration or concern, survey design discussions focused on what insight would be needed to develop possible implementation approaches before the launch of an AI scribe technology within UC Davis Health.

A committee was established to provide feedback on survey design that consisted of 5 individuals: our Chief Medical Information Officer, a medical educator attending with patient research experience, a medical educator who leads digital health clinical programs for the health care system, a program manager responsible for patient experience survey design, and a qualitative survey design professional responsible, who facilitated the creation and execution of the survey. The survey

XSL•FO
RenderX

was reviewed by the committee, which provided feedback on question inclusion, removal, and design. The full introduction to the survey and questions is included in Multimedia Appendix 1.

Participants received an email invitation with an option to opt out. Patients were provided the following brief description of the technology.

"To help take notes, UC Davis Health is testing a tool that looks similar to a cell phone. Upon being activated by the doctor, the tool listens to the conversation and automatically creates notes in the system.

As you participate in this survey, please focus on the note-taking capability and how you would like the use of this technology to work better for you. Please keep in mind that:

- The transcribed notes will be reviewed by the physician.
- Patients and families would be informed about the use of this device."

Results were monitored hourly for the first 150 responses to ensure respondents were completing the survey and providing usable responses for open-ended questions. Since the study's goal is to assist in the development of AI scribe deployment, respondents were required to answer all questions before proceeding. For questions seeking a numeric response (ie, 5-point scale), a score of 3 provided respondents the ability to offer a neutral response. Another batch of 150 was sent again to gauge their responses.

After the initial survey responses were reviewed, it was determined that the survey functioned well and did not require any modifications. However, the email request to the remaining patients (about 8800) was slightly modified, and the final version is contained in Multimedia Appendix 2, with the clarifying language involving the last paragraph noting that the "transcribed notes will be reviewed by the physician" and the "patients and families would be informed about the use of the device."

The median length of time to complete the survey was 10 minutes and 33 seconds. The survey was provided via a secure and closed link, which allowed respondents to start the survey and complete it later. The shortest survey response was 2 minutes and 15 seconds. The longest was 256 hours and 25 minutes.

Survey Analysis

The data were reported using descriptive summary statistics. Since this was a convenience sample survey, no statistical comparisons between groups were performed. Descriptive statistics were used to identify broad themes and to help guide the pilot implementation and deployment of the AI scribe program at UC Davis Health. Since the group of respondents may not have been representative of our clinic population, comparative statistical analysis of the respondent groups was deemed not justifiable. Incomplete responses were not used in the final analysis of this study.

An inductive coding framework was used for open-ended questions. The process entailed a review of all responses to a specific question and identifying response themes (which helped generate a code book). Each response was reviewed and assigned a descriptive label from the code book summarizing the basic theme of a response. A separate research team member evaluated the responses for alignment or discussion. Research team members met to ensure consensus on the application of codes, refine dimensions of existing codes, add new codes, develop categories, and identify theoretical direction. Disagreements among the team members were resolved through discussions to understand viewpoints, deliberate, and achieve consensus. An open-ended response could have multiple themes based on the patient's input. Open-ended responses that were singular in nature were categorized as "other." Statements made by patients that did not align with the subject matter were classified as "not applicable or NA" (ie, a question in the survey asks about a patient's opinion regarding a provider taking notes, and the patient responds with negative statements about parking). Both members of the team are professionally trained survey designers.

Ethical Considerations

This quality improvement study was reviewed by the UC Davis Health Institutional Review Board and deemed non–human subjects research, and therefore exempt from review, because the data came from patient surveys. Since this study was exempt from review and the participants were anonymous, we did not obtain informed consent, waivers, or privacy protections. Participants were not compensated for completing this survey.

Results

The survey had an overall completion rate of about 21% (n=1893 respondents out of 9171 surveys). An additional 549 started the survey, but did not complete it. Partial responses were excluded from the survey results. All percentages calculated from 1893 respondents. The age, sex, race, and ethnicity data were extracted from the EMR and collated for each patient response. The respondents' demographics were predominantly female (1205/1893, 64%), ages 51 years and older (1649/1893, 87.1%), and White (1312/1893, 69%; see Table 1). As noted in the Methods section, patients self-identified their race and ethnicity. We compared these percentages to our patient population at UC Davis Health, using our Epic EHR, and accessed the active clinic patient registry for any interactions in the past 2 years. The demographic profile of this group was as follows: female 53.7% (207,947/387,512; total clinic population), ages 50 years and older 44.5% (172,500/387,512), and White (not Hispanic) 37.3% (144,836/387,512).

XSL•FO
RenderX

Table 1. Survey responses and respondent demographics.

Responses and respondent demographics[a]	Results
Surveys	
Total sent, n	9171
Responses, n (%)	1893 (20.6)
Demographic variables (N=1893), n (%)	
Sex	
Female	1205 (63.7)
Male	688 (36.3)
Age (years)	
18-30	64 (3.4)
31-40	60 (3.2)
41-50	120 (6.3)
51-60	285 (15.1)
61-70	622 (32.9)
71+	742 (39.2)
Race and ethnicity	
White or Caucasian	1312 (69.3)
Multirace (Ethnicity)	154 (8.1)
Latinx or Hispanic	130 (6.9)
Unknown	105 (5.5)
Asian	86 (4.5)
Other[b]	57 (3)
Black or African American	42 (2.2)
Native Hawaiian or Other Pacific Islander	5 (0.3)
American Indian or Alaska Native	2 (0.1)

[a]Before introducing an AI (artificial intelligence) Scribe program, UC Davis Health primary care patients were sent an email questionnaire about their perceptions to determine how the program should be implemented.

[b]American Indian or Alaskan Native, Native Hawaiian, or other Pacific Islander were combined in the "Other" category for reporting, since those numbers were small.

The survey was performed as a quality improvement project, rather than a scientific investigation. Given the potentially nonrepresentative patient sample, we did not perform comparative statistical analysis between the groups. Thus, these results should be considered as indicating broad informal trends.

Patients' perceptions of current clinician notetaking practices were generally positive, with 71% (1349/1893 responses) feeling very heard or somewhat heard and 79% (1490/1893 responses) indicating their doctors were engaging in their health discussion while taking notes during their primary care provider (PCP) appointment. However, younger patients (ages 40 years and younger) and Asian and Latinx or Hispanic patients expressed more critical views, citing a lack of engagement and limited interest from physicians during notetaking. A review of actual open-ended patient comments revealed that 62 responses were not applicable to the question, leaving 1831 responses. The comments related to clinician EMR documentation demonstrated that 29% (530/1831 responses) were very positive and the patients felt "heard" by their provider, and another 24% (439/1831) reported that the notetaking did not bother them, since this was a normal routine. 21% (385/1831) reported that it was a "necessary evil" because documentation is required. 23% (416/1831) reported that when the provider took notes into the computer during the visit, it felt very impersonal to them, that the physician was distracted, and sometimes they felt disrespected. An example of a typical positive comment was "I feel she is listening and accurately recording my info since she is recording as we speak." Examples of negative comments include: "I feel the need to slow down and even stop talking until my PCP completes her typing," "Feels a bit impersonal, like he's just entering data to tick boxes, etc. rather than really discuss the issue with me," and "I realize it's a necessity – but would rather they just be able to listen."

When asked about how the AI scribe technology would impact the overall clinic visit, 48% (904/1893 responses) of patients responded positively, 33% (630/1893) were neutral, and 19%

XSL•FO
RenderX

(359/1893) felt it would have a negative impact on the patient-physician interaction.

Overall, regardless of age, more patients had a favorable perception about the use of AI scribes than neutral or negative (see Figure S1 in Multimedia Appendix 3). Looking at the trends in perceptions about AI scribe technology suggested some differences by age. Younger patients (aged 18-30 y) appeared to have a higher frequency of concerns about the potential negative impact (31%, 20/64 responses) compared to older groups. Interestingly, patients aged 50 years and older seemed to have the most favorable perceptions and the least skepticism (18%, 300/1649 responses).

Figure S2 in Multimedia Appendix 3 shows the breakdown of perceptions by race and ethnicity, which varied among the groups. The majority of patients had positive perceptions across all groups, ranging from 46% (598/1312) "White" responses to 67% (58/86) "Asian" responses. Patients who identified as "Asian" or "Black" seemed to have more positive perceptions about the use of a voice technology and lower rates of skepticism. Negative perceptions were around 20% (323/1660) for the remaining groups; 20% (257/1312) "White" responses were negative, 19% (30/154) "Multirace (Ethnicity)" responses were negative, 18% (23/130) "Latinx or Hispanic" responses, and 20% (13/64) "Other" responses were negative.

The open-ended comments about the perceived benefits were collated and grouped by themes. Table 2 shows these themes in descending order. The respondents listed the following anticipated benefits for an AI scribe: improve human-to-human interactions (41.8%, 655/1567 comments), accuracy of notes (28%, 435/1567), benefits to doctor and staff (15%, 231/1567), generally positive (6%, 98/1567), and transparency (4%, 58/1567). The listing of potential benefits varied by age, with 57% (28/49 responses) of patients aged between 31 and 40 years listing "improve human elements" as the most frequent. There was less variation when comparing the results by race and ethnicity. Positive open-ended comments about the "improve human elements" included: "It will free up the doctor to read emotion and other non-verbal cues and ask follow-up questions," and "If it allows the doctors to see more patients, it could decrease the time it takes to get an appointment." Positive comments about "accuracy of notes" include: "Better information regarding my complaints and symptoms. Nothing missed," and "It will more accurately reflect our conversation. I often read the notes in the After Visit Summary and find errors…."

Numerous concerns about the AI scribe program were noted by the survey respondents (see Table 3). The most commonly mentioned were related to note accuracy (39%, 515/1330 comments), privacy and security (15%, 203/1330), negative feelings about being recorded (13%, 177/1330), and general feelings that it was bad for the physician and staff (10%, 139/1330), plus others. These concerns were common among those respondents who thought that the digital technology would have a negative impact. Younger respondents expressed the greatest skepticism over note accuracy, privacy, and security. Key comments focused on the risks that the recordings might be discovered by hackers, which would be a violation of privacy. There were both positive and negative comments about the potential accuracy of the digital transcriptions. Some felt that the transcribed clinic notes would be more accurate, while others were worried that there was a higher risk of containing inaccurate statements (transcription errors). Since the survey was done preimplementation, this probably reflects the respondents' best speculations about the effectiveness of the AI scribe technology.

Patients were queried about the best time to be informed about the AI scribe program. It was clear that patients preferred early notification, either when the appointment is made (43%, 809/1893 responses), upon arrival at the examination room (32%, 602/1893), or upon arrival at the clinic (15%, 276/1893). When given choices about how they would be informed, patients preferred verbal discussion (57%, 1085/1893 responses), followed by email (45%, 854/1893), text (28%, 532/1893), and then via brochure (24%, 460/1893), followed by miscellaneous. Patients had fewer clear preferences about who might provide the notifications, with a slight preference to hear from the physician or resident over nursing or support staff. When asked about the preferred method to be informed about the use of AI scribe technology before the clinic visit, the respondents most preferred an email (63%, 130/206 respondents), text message (40%, 82/206 respondents), or verbal discussion (38%, 78/206 respondents).

Table 2. Thematic benefits of artificial intelligence (AI) scribe.

Response themes[a]	Coded comments, n (%)
Improve human elements	655 (41.8)
Accuracy of notes	435 (27.8)
Beneficial to the doctor and staff	231 (14.7)
General positive	98 (6.3)
Transparency	58 (3.7)
Mixed	36 (2.3)
Improve access	28 (1.8)
Other	26 (1.7)

[a]Patients responded to open-ended questions. These comments were collated and grouped by themes, with the frequency of themes listed in descending order.

XSL•FO
RenderX

Table 3. Thematic concerns of artificial intelligence (AI) scribe.

Response themes[a]	Coded comments, n (%)
Accuracy of notes	515 (38.7)
Privacy and security	203 (15.3)
Problem with being recorded	177 (13.3)
Bad for the physician and staff	139 (10.5)
Human element	126 (9.5)
Other (technical failure, billing, incorrect *ICD* code, referrals, etc)	58 (4.4)
Transparency (MyChart, Notes summary, etc.)	22 (1.7)
General negative	90 (6.8)

[a]Patients responded to open-ended questions about their concerns related to the implantation of an AI scribe program. These comments were collated and grouped by theme, with the frequency of each theme listed in descending order.

Discussion

Principal Findings

This survey of UCDH primary care patients in anticipation of a deployment of our AI scribe program helped inform our team about the perceived benefits and concerns to shape our implementation. This convenience sample of nearly 1900 patients, with a response rate of about 20% (1893/9171), was sufficient to influence the implementation process. We believe that these results can support other health care institutions to implement patient-centered, culturally competent AI scribe programs.

It is important to note upfront that the demographic profile of the patients who responded to the survey was less representative of the overall outpatient clinic population at UC Davis Health, skewing more strongly to those who were female, were ages 50 years and older, and White compared to our overall clinic population. Thus, interpretation of the survey results should be tempered with this knowledge. Nonetheless, we believe there is value in reporting these results, given the relatively large number of responses and broad trends.

There were several overall trends expressed by the respondents that were supportive of the AI scribe program, as well as cautionary notes. Of the survey respondents (predeployment of an AI scribe program), most patients felt that their physicians were currently attentive during the visit (71% 1349/1893), and patients accepted that EHR documentation was needed to ensure an accurate record of patient encounters. Nonetheless, 22% (416/1893) of respondents were put off when their providers were typing into the computer during the visit, feeling that the clinician was too focused on the documentation and paying less direct attention to the patient. This may reflect different interaction styles between physicians and their patients, rather than a rejection that physicians perform documentation during the clinic visit. Most patients appear to have realistic views about how clinicians must balance their approach to directly interacting and listening to them with the burdens of documentation. Nonetheless, if using an AI scribe during the visit frees the physician to directly interact with the patient, this is likely to be perceived positively.

In support of this interpretation, a plurality of respondents viewed the use of an AI scribe in a positive light (42%, 655/1567 positive open-ended comments), noting that this might enhance the clinician's ability to focus on the patient and less on documentation during the encounter. Other positive benefits included improved note accuracy, reduced workload for the clinician and staff, and improved transparency. Although we are cautious not to overinterpret the differences based on age and race and ethnicity (since the groups were not subjected to formal statistical comparisons), there were interesting trends. For example, in contrast to our expectations, patients aged 50 years and older appeared to be more positive about the potential benefits of use of an AI scribe compared to a younger cohort. The younger patients expressed more concerns about privacy and security with regard to being recorded as part of the AI scribe technology, as well as accuracy. It appeared that non-White patients expressed positive impressions about the use of the AI scribe at least as often as White patients.

Nonetheless, although there were negative comments or concerns expressed, only 19% (359/1893) of respondents thought that the overall impact would be negative, whereas 48% (904/1893) thought that it would be positive. Thus, this may reflect anticipatory anxiety, and this could be readily addressed by both previsit patient education and actual experience.

Comparison to Previous Work

There are currently limited studies that report patient experiences with AI scribe technology, and the responses have been generally favorable. Most research to date has focused on time saved to physicians or on using AI to generate medical advice, while very little has been done to measure patient attitudes about AI scribes during clinic encounters. Cao et al [7] reported their experience with the use of the Dragon Ambient eXperience (DAX; Nuance & Microsoft) system in a dermatology practice. In a limited survey of patients (score 1-5, 5 being "strongly agree"), there was high favorability on the following questions: "The provider spent less time typing on their computer" (mean score 4.5), "My visit felt more like a personable conversation" (mean score 4.4), and "The provider seemed more focused on me during the visit" (mean score 3.9). A group of Northern California Kaiser Permanente physicians and researchers published their initial experience with an AI scribe program

XSL•FO
RenderX

[16]. The primary focus of this paper was on the implementation of the software-based medical dictation technology from a provider standpoint (accuracy of note, usability, and effectiveness). They described their patient-facing educational materials as part of their permission process that included a verbal summary of the AI scribe to the patients, as well as laminated posters. Between October and December 2023, the AI scribe was rapidly implemented, with over 3400 physician users and more than 300,000 patient encounters. In a limited survey of 21 patients from a single clinic site, 71% of respondents noted that they spent more time talking with their physicians, and 81% reported that physicians spent less time looking at their computers during the encounter. The patient responses to early experience with the AI scribe match up well with our patient survey results. In a news article about the Kaiser Permanente study, Feldheim [17] noted that the benefits of the AI scribe extended beyond the time savings for the providers: "they may help restore the fundamental human connection at the heart of medicine."

It is worth considering potential explanations about why there appears to be a difference in attitude between older and younger respondents, even though our survey was not designed to explore these differences in detail. Several papers appear to offer clues about what might be underlying these differential attitudes. Older adults, especially those who are comfortable with technology, are willing to share their personal information with family and hospitals (compared to government agencies) [18]. Older adults are selective about what information they share, but if they perceive that these services are used to maintain and promote health, then they are willing to share that information, even if they have concerns about privacy [18]. Kauttonen et al [19] conducted a web-based survey of Finnish participants to gauge trust and acceptance of artificial intelligence when adapted into health care delivery. They found that age was a factor in the acceptance of the use of AI in health care, but not always a consistent trend. Instead, the combination of familiarity with technology along with age appeared to be more important. For example, those who were less familiar with AI were the least trustful. Interestingly, though, people aged 70 years and older were the most positive about AI when balanced with trade-offs. There were significant confounders based on the type of AI scenario presented to the participant. In a study of German patients at a tertiary care center, more than 50% of participants had positive attitudes about the use of AI in health care, and only about 5% had serious reservations. In contrast to our study results, older patients and women expressed more caution about AI in health care [20]. The key to acceptance is that the patients insist that the use of AI be under the control of their physician.

Younger patients may have a greater understanding of technology, particularly AI. In a survey report offered by Cisco, they found that about 48% of respondents agreed that AI could be useful to improve their lives. However, there were serious concerns, especially about the use of generative AI, even though few were very familiar with this technology. In particular, there was substantial concern about privacy protections, with the youngest consumers (42% of those aged between 18 and 34 y) actively engaged in protecting their privacy, and this was 7 times higher than those aged 75 years and older [21]. A small group of young adults (25-34 years) was provided with a focus group survey about AI-driven mobile health technology [22]. Many expressed enthusiasm (and skepticism) about the emerging technology. Prominent among the perceived risks were concerns about data privacy and the need for human supervision.

These studies seem to highlight several themes relevant to the use of an AI scribe. One is that there is limited familiarity with the new technology. The degree of enthusiasm seems closely aligned with both familiarity with technology and the perception of whether it can enhance health care delivery for the patient. It may be that older patients are more accepting that the AI scribe can unburden the physician's responsibility for clinic documentation, whereas younger patients have greater concerns about privacy and lack of control over their personal information when their data is fed into a generative AI program. As noted in the Conclusions section, education about the process and protections for privacy are key to acceptance and trust.

Strengths and Limitations

There are several strengths to this study. First, is that we received a relatively large number of responses to the survey, representing about 20% (1893/9171) of those who were contacted. Second, we queried about both the current patient-physician interactions as well as anticipating patient responses to the eventual implementation of an AI scribe voice technology for medical documentation. Third, we obtained actionable information that helped modify the future rollout of the program. For example, we prepared our users with information about the system's security and data retention policies so they would be prepared to respond to expected patient concerns. Finally, we identified that patient education (in various manners) would be a critical element for patient acceptance of the AI scribe.

Several important limitations affect the interpretation of the survey results. A primary limitation is that the demographic profile of those who responded was not representative of the clinic population, as determined by the self-identification of the patients noted in our EMR. Since this was a convenience sample and not expected to be fully representative of our patient population, this limits our ability to precisely compare the differing responses among the varying demographics and perform statistical analysis. The survey was only sent to English-speaking patients and was sent by email, so the perspectives of non-English speaking patients and those with limited digital access or literacy on this technology are not known. Given this limitation, the best we could expect was to understand broad themes. It is worth acknowledging that the demographic characteristics of the respondents are probably more representative of who chose to respond to the survey rather than the overall population of patients who receive their health care at our institution. Since survey respondents skewed older and white, we are uncertain whether a younger, more diverse population would actually experience this technology differently. The response rate was only 20%, so this also limits the generalizability of the results. Thus, it will be important to monitor patient reactions to the rollout of the AI scribe over time, since the actual patient experience may vary from the

XSL•FO
RenderX

anticipated one. To that point, we note that this survey had a high nonresponse rate. Finally, we intentionally shared information about the technology with participants that was simple and written for a lower literacy competency. While we believed this was appropriate, some participants may have wished for a deeper explanation of the technology involved.

Nonetheless, the survey provided valuable guidance on how to communicate about the use of AI scribe and gain patient consent for a new technology that some may find uncomfortable or threatening. A recent study by Lawrence et al [23] describes a quality improvement project focusing on determining the best approaches to obtaining patent consent before using the AI scribe during a clinic visit. The keys to successfully obtaining patient consent included establishing patient-physician trust, targeted education (more than a single modality and a flexible approach to answering patient questions), and honest discussions about potential vulnerabilities (risk of security breaches, inaccurate documentation, and risk of medical errors). When basic information about the AI scribe was provided to the patients, 81.6% consented. This study supports the findings that we obtained from our own patient survey, that most patients would accept the AI scribe, if introduced with appropriate education and permission sought beforehand.

Conclusions and Recommendations

We learned that although many patients understand and accept that providers commonly complete their medical documentation during the actual clinic visit to increase efficiency, a significant proportion feel that this interferes with effective and empathetic communication. Using AI Scribe technology may allow clinicians to spend more time in direct dialogue with patients rather than typing into the EHR and staring at a computer screen. Key to the acceptance of an AI Scribe program is to educate the patient about the program in advance (through placard notifications in the clinic, EMR notices, or verbal discussions) and obtain explicit verbal permission from the patient before use. The patient must be allowed the option to opt out. Verbal consent should be documented in the patient's clinic note.

Acknowledgments

We are grateful to Anthony Caso and Shefali Tamakuwala for their assistance with data extracts, data management and analysis, and to Elizabeth Keating for her assistance with manuscript editing. Generative artificial intelligence was not used in any portion of the writing of this manuscript.

The authors received no financial support for the research, authorship, or publication of this article.

Data Availability

The datasets generated or analyzed during this study are available from the corresponding author on reasonable request.

Authors' Contributions

Conceptualization: MJ, GL
Data curation: JM
Formal analysis: JM, MJ, GL
Investigation: JM
Methodology: JM, MJ, GL, SM
Project administration: MJ
Resources: JM, GL
Software: JM
Supervision: GL
Validation: GL, MJ
Visualization: MJ
Writing – original draft: GL, MJ
Writing – review & editing: GL, MJ, SM

Conflicts of Interest

None declared.

Multimedia Appendix 1
Questionnaire introduction and questions.
[DOCX File , 18 KB - medinform_v13i1e77901_app1.docx]

Multimedia Appendix 2
Email introduction to patient survey before deployment of the artificial intelligence (AI) scribe, plus discussion about educating patients about the AI scribe technology.

XSL•FO
RenderX

[DOCX File , 15 KB - medinform_v13i1e77901_app2.docx]

Multimedia Appendix 3
Primary care patient perceptions about an artificial intelligence (AI) scribe program by race and age.
[DOCX File , 108 KB - medinform_v13i1e77901_app3.docx]

References

1. Ludwick DA, Doucette J. Adopting electronic medical records in primary care: lessons learned from health information systems implementation experience in seven countries. Int J Med Inform 2009;78(1):22-31. [doi: 10.1016/j.ijmedinf.2008.06.005] [Medline: 18644745]
2. Gardner R, Cooper E, Haskell J, Harris D, Poplau S, Kroth P, et al. Physician stress and burnout: the impact of health information technology. J Am Med Inform Assoc 2019;26(2):106-114 [FREE Full text] [doi: 10.1093/jamia/ocy145] [Medline: 30517663]
3. Saag HS, Shah K, Jones SA, Testa PA, Horwitz LI. Pajama time: working after work in the electronic health record. J Gen Intern Med 2019;34(9):1695-1696 [FREE Full text] [doi: 10.1007/s11606-019-05055-x] [Medline: 31073856]
4. Ziemann M, Erikson C, Krips M. The use of medical scribes in primary care settings: a literature synthesis. Med Care 2021;59(Suppl 5):S449-S456 [FREE Full text] [doi: 10.1097/MLR.0000000000001605] [Medline: 34524242]
5. Heckman J, Mukamal KJ, Christensen A, Reynolds EE. Medical scribes, provider and patient experience, and patient throughput: a trial in an academic general internal medicine practice. J Gen Intern Med 2020;35(3):770-774 [FREE Full text] [doi: 10.1007/s11606-019-05352-5] [Medline: 31808131]
6. Yan C, Rose S, Rothberg M, Mercer MB, Goodman K, Misra-Hebert AD. Patient perspectives on clinical scribes in primary care. J Gen Intern Med 2018;33(11):1859-1861 [FREE Full text] [doi: 10.1007/s11606-018-4573-9] [Medline: 29992427]
7. Cao MD, Silkey PMMMJ, Decker M, Wanat K. Artificial intelligence-driven digital scribes in clinical documentation: Pilot study assessing the impact on dermatologist workflow and patient encounters. JAAD Int 2024;15:149-151 [FREE Full text] [doi: 10.1016/j.jdin.2024.02.009] [Medline: 38571698]
8. Lau CWY, Kupiec K, Livermore P. Exploring the acceptance and opportunities of using a specific generative AI chatbot to assist parents in managing pediatric rheumatological chronic health conditions: mixed methods study. JMIR Pediatr Parent 2025;8:e70409 [FREE Full text] [doi: 10.2196/70409] [Medline: 40591524]
9. Sing DC, Shah KS, Pompliano M, Yi PH, Velluto C, Bagheri A, et al. Enhancing magnetic resonance imaging (MRI) report comprehension in spinal trauma: readability analysis of ai-generated explanations for thoracolumbar fractures. JMIR AI 2025;4:e69654 [FREE Full text] [doi: 10.2196/69654] [Medline: 40611700]
10. Haberle T, Cleveland C, Snow G, Barber C, Stookey N, Thornock C, et al. The impact of nuance DAX ambient listening AI documentation: a cohort study. J Am Med Inform Assoc 2024;31(4):975-979. [doi: 10.1093/jamia/ocae022] [Medline: 38345343]
11. Shah SJ, Crowell T, Jeong Y, Devon-Sand A, Smith M, Yang B, et al. Physician perspectives on ambient AI scribes. JAMA Netw Open 2025;8(3):e251904 [FREE Full text] [doi: 10.1001/jamanetworkopen.2025.1904] [Medline: 40126477]
12. Biro J, Handley JL, Cobb NK, Kottamasu V, Collins J, Krevat S, et al. Accuracy and safety of AI-enabled scribe technology: instrument validation study. J Med Internet Res 2025;27:e64993 [FREE Full text] [doi: 10.2196/64993] [Medline: 39869899]
13. Leung TI, Coristine AJ, Benis A. AI scribes in health care: balancing transformative potential with responsible integration. JMIR Med Inform 2025;13:e80898 [FREE Full text] [doi: 10.2196/80898] [Medline: 40749188]
14. Rotenstein L, Melnick ER, Iannaccone C, Zhang J, Mugal A, Lipsitz SR, et al. Virtual scribes and physician time spent on electronic health records. JAMA Netw Open 2024;7(5):e2413140 [FREE Full text] [doi: 10.1001/jamanetworkopen.2024.13140] [Medline: 38787556]
15. Robeznieks A. AI scribe saves doctors an hour at the keyboard every day. American Medical Association. 2024. URL: https://www.ama-assn.org/practice-management/digital-health/ai-scribe-saves-doctors-hour-keyboard-every-day [accessed 2025-10-24]
16. Tierney AA, Gayre G, Hoberman B, Mattern B, Ballesca M, Kipnis P, et al. Ambient artificial intelligence scribes to alleviate the burden of clinical documentation. NEJM Catalyst 2024;5(3). [doi: 10.1056/cat.23.0404]
17. Feldheim B. AI scribes save 15,000 hours—and restore the human side of medicine. AMA News Wire. 2025. URL: https://tinyurl.com/mvb39mnz [accessed 2025-10-24]
18. Kim TK, Choi M. Older adults' willingness to share their personal and health information when adopting healthcare technology and services. Int J Med Inform 2019;126:86-94. [doi: 10.1016/j.ijmedinf.2019.03.010] [Medline: 31029268]
19. Kauttonen J, Rousi R, Alamäki A. Trust and acceptance challenges in the adoption of AI applications in health care: quantitative survey analysis. J Med Internet Res 2025;27:e65567 [FREE Full text] [doi: 10.2196/65567] [Medline: 40116853]
20. Fritsch SJ, Blankenheim A, Wahl A, Hetfeld P, Maassen O, Deffge S, et al. Attitudes and perception of artificial intelligence in healthcare: A cross-sectional survey among patients. Digit Health 2022;8:20552076221116772 [FREE Full text] [doi: 10.1177/20552076221116772] [Medline: 35983102]

XSL•FO
RenderX

21. Generation privacy: younger consumers are 7 times more likely to exercise their data rights, new cisco survey shows. Cisco. 2023. URL: https://investor.cisco.com/news/news-details/2023/Generation-Privacy-Younger-Consumers-Are-7-Times-More-Likely-to-Exercise-their-Data-Rights-New-Cisco-Survey-Shows/default.aspx [accessed 2025-10-24]
22. Aboueldahab A, Damaschi G, D'Addario M, Steca P. Exploring young adults' attitudes toward AI-driven mhealth apps: qualitative study. JMIR Hum Factors 2025;12:e76075 [FREE Full text] [doi: 10.2196/76075] [Medline: 41004277]
23. Lawrence K, Kuram VS, Levine DL, Sharif S, Polet C, Malhotra K, et al. Informed consent for ambient documentation using generative AI in ambulatory care. JAMA Netw Open 2025;8(7):e2522400 [FREE Full text] [doi: 10.1001/jamanetworkopen.2025.22400] [Medline: 40694347]

Abbreviations

AI: artificial intelligence
EHR: electronic health record
EMR: electronic medical record
PCP: primary care provider
UCDH: University of California, Davis Health

Edited by A Coristine; submitted 23.05.25; peer-reviewed by C Okolue, E Sezgin, D Pförringer, M Odugbesan, S Sivarajkumar; comments to author 16.06.25; revised version received 20.07.25; accepted 09.10.25; published 27.11.25.

Please cite as:
Leiserowitz G, Mansfield J, MacDonald S, Jost M
Patient Attitudes Toward Ambient Voice Technology: Preimplementation Patient Survey in an Academic Medical Center
JMIR Med Inform 2025;13:e77901
URL: https://medinform.jmir.org/2025/1/e77901
doi:10.2196/77901
PMID:

©Gary Leiserowitz, Jeff Mansfield, Scott MacDonald, Melissa Jost. Originally published in JMIR Medical Informatics (https://medinform.jmir.org), 27.11.2025. This is an open-access article distributed under the terms of the Creative Commons Attribution License (https://creativecommons.org/licenses/by/4.0/), which permits unrestricted use, distribution, and reproduction in any medium, provided the original work, first published in JMIR Medical Informatics, is properly cited. The complete bibliographic information, a link to the original publication on https://medinform.jmir.org/, as well as this copyright and license information must be included.

XSL•FO
RenderX

Publisher:
JMIR Publications
130 Queens Quay East.
Toronto, ON, M5A 3Y5
Phone: (+1) 416-583-2040
Email: support@jmir.org

XSL•FO
RenderX